TRANSACTIONS

OF THE

AMERICAN INSTITUTE

OF

ELECTRICAL ENGINEERS

VOLUME 69

1950

PART I

PUBLISHED BY THE

AMERICAN INSTITUTE OF ELECTRICAL ENGINEERS

33 WEST 39TH STREET

NEW YORK 18, N. Y., U. S. A.

COPYRIGHT 1950
BY THE
AMERICAN INSTITUTE OF ELECTRICAL ENGINEERS

Printed in the United States of America by
The Mack Printing Company, Easton, Pa.

TRANSACTIONS

OF THE

AMERICAN INSTITUTE

OF

ELECTRICAL ENGINEERS

VOLUME 69

1950

PART II

PUBLISHED BY THE

AMERICAN INSTITUTE OF ELECTRICAL ENGINEERS
33 WEST 39TH STREET
NEW YORK 18, N. Y., U. S. A.

COPYRIGHT 1950
BY THE
AMERICAN INSTITUTE OF ELECTRICAL ENGINEERS

Printed in the United States of America by
The Mack Printing Company, Easton, Pa.

AIEE Transactions Index for 1950

(Complete Index for Parts I and II of Volume 69)

1. Technical Subject Index

Accelerators, Ignitron Converters for High Energy Particle. Boyer, Marcum....1110–14
Accelerators, Ignitron Pulse Equipment for Particle. Herskind, Hudson....992–6
Accounting System, Fundamentals of the Automatic Telephone Message. Messar....255–68; disc. 269
Accuracy Counter-Type Tachometer, A New High-. Berry, Beattie....686–90; disc. 690
Accuracy Performance of the Selsyn Generator Control Transformer System, Static. Kronacher....645–54; disc. 653
Adjuster, Differential Relay Sensitivity. Headley....1203–05; disc. 1209
Air Circuit Breaker with 50,000 Ampere Interrupting Capacity at 600 Volts A-C, New Low-Voltage. Horn, Mikos....1654–7; disc. 1657
Air Circuit Breakers, An Air Delayed Selective Overcurrent Tripping Device for Low-Voltage. Tremblay, Horn....1649–53
Air Gaps, Dielectric Recovery Characteristics of Power Arcs in Large. McCann, Conner, Ellis....616–24; disc. 624
(Air Transportation) An Environment-Free 120-Volt D-C High Performance Limit Switch. Steelnagel....1280–93
(Air Transportation) Analogue Techniques for Turbojet Thrust Instrumentation. Van Valkenburg, Matthews....1342–6
(Air Transportation) Dynamic Characteristics of Carbon Pile Voltage Regulators. Mills....1347–52; disc. 1352
(Air Transportation) The Design of Reactors for Radio Interference Filters. Knudson....1294–8
Aircraft D-C Circuit Breakers for 28 and 120 Volts. Beall, Reifschneider....1283–8
Aircraft D-C System, Transient Analysis of a Voltage-Regulated. Scorgie....1318–23
Aircraft Electric Motors Need Test Equipment. Ross....1359–64
Aircraft Engine Failure at Take-off, Automatic Feathering—To Reduce the Hazard of. Kershaw....1328–34
Aircraft Inverter, An Amplistat Regulator Applied to a 5-Kva 400-Cycle. Morgan, Walley....1243–8; disc. 1248
Aircraft Manufacturer's Viewpoint, Aluminum Conductors from an. Schumacher....1335–41
Aircraft, Tracking Radio Noise on. Owen....1249–52
Aircraft, Wide Speed Range A-C Electric Systems for. James, Judkins, Mershon....1353–8; disc. 1358
Alco-GE 4,500-Horsepower Gas-Turbine Electric Locomotive, The. Morey....504–07
Allocation of the Capacity Benefits Resulting from Interconnecting Two or More Generating Systems, The Determination and. Watchorn....1180–6
A-C Components, The Extension of Amplistat Performance by. Morgan, Ogle, Wattenberger....986–91
A-C Electric Systems for Aircraft, Wide Speed Range. James, Judkins, Mershon....1353–8; disc. 1358
A-C Generators, Design Calculations for. Ginsberg....1274–80; disc. 1280
A-C Generators with Suddenly Applied Loads, Regulation of. Part II. Harder, Cheek, Clayton....395–405; disc. 405
(Part I—1944)
A-C Lead Networks for Servomechanisms, Improvements in the Characteristics of. McDonald....293–300
A-C Series Motors—A Design Method. Chang, Karr....1257–61; disc. 1261
A-C Servo Systems with Compensation for Carrier Frequency Changes, Phase Lead for. Notthoff....285–91; disc. 291
A-C Turbine Generators, Liquid Cooling of. Part II. Fechheimer....165–71; disc. 171
(Part I—1947)
Alternator, Variable Speed Drive Constant Frequency. Gould, Krupotich....745–7; disc. 747
Alternators, Symmetrical Short Circuits on Saturated. Mikhail....1554–62
Aluminum Conductors from an Aircraft Manufacturer's Viewpoint. Schumacher....1335–41
Aluminum Industry, The Theory of the Current Transductor and Its Application in the. Specht, Wagner....441–52; disc. 452
American Gas and Electric Company—Corona, Radio Influence, and Other Factors, Progress Report on Tidd 500-Kv Test Project of the. Sporn, Monteith....891–7; disc. 897
American Gas and Electric Company System, Selection, Design, and Operation of Power Transformers on. Lane, Gross, Pugh....786–93; disc. 793
Ampere Interrupting Capacity at 600 Volts A-C, New Low-Voltage Air Circuit Breaker with 50,000. Horn, Mikos....1654–7; disc. 1657
Amplidyne-Controlled Log Carriage Drive. Vincent....1124–9; disc. 1129
Amplifier Frequency Control, A Magnetic. Johnson, Schafer....613–15
Amplifiers, An Analysis of Transients and Feedback in Magnetic. Johnson, Latson....604–11; disc. 611
Amplifiers, An Analysis of Transients in Magnetic. VerPlanck, Finzi, Beaumariage....498–503
Amplifiers, Determination of Steady-State Performance of Self-Saturating Magnetic. Smith....1309–17
Amplifiers, General Characteristics of Magnetic. Finzi, Beaumariage....919–27
Amplifiers, Response Time of Magnetic. Harder, Horton....1130–8; disc. 1138
Amplistat Performance by A-C Components, The Extension of. Morgan, Ogle, Wattenberger....986–91
Amplistat Regulator Applied to a 5-Kva 400-Cycle Aircraft Inverter, An. Morgan, Walley....1243–8; disc. 1248
Anacom—Electric Analog, Computer, New Techniques on the. Harder, Carleton....547–56
Analog Computer, New Techniques on the Anacom—Electric. Harder, Carleton....547–56
Analogue Computer for Flight Simulation, A Generalized. Hall....308–20
Analogue Computer for Multicomponent Fractionation Calculations. Goels, Calvert....97–103
Analogue Computer Using the Photo Cell as a Nonlinear Element, An Electric. Koenig....1606–11
Analogue Techniques for Turbojet Thrust Instrumentation. Van Valkenburg, Matthews....1342–6
Analogue, Transients in Coupled Inductance-Capacitance Circuits Analyzed in Terms of a Rolling-Ball. Magnuson....1525–30
Analogues in the Study of Transmission Line Vibration, Use of Techniques from Electrical. Lummis, Klopfenstein....1676–80
Analysis of a Voltage-Regulated Aircraft D-C System, Transient. Scorgie....1318–23
Analysis of Synchronous Machine Short Circuits. Camburn, Gross....671–8; disc. 678
Analysis of Transients and Feedback in Magnetic Amplifiers. Johnson, Latson....604–11; disc. 611
Analysis of Transients in Magnetic Amplifiers, An. VerPlanck, Finzi, Beaumariage....498–503
Analytical Study of Turbine Generator Rotor Ventilation, An Experimental and. Fechheimer....1563–9
Analyzed in Terms of a Rolling-Ball Analogue, Transients in Coupled Inductance-Capacitance Circuits. Magnuson....1525–30
Analyzer Solution of Complex Problems, Special Devices Aid Differential. Cook, Kirchmayer, Weygandt....1365–70; disc. 1370
Analyzing and Synthesizing Contactor Servomechanisms, A Frequency Response Method for. Kochenburger....270, 83; disc. 283
Apparatus Against Lightning, Evaluation of Lightning-Arrester Lead Length and Separation in Coordinated Protection of. Carpenter, Johnson, Saline....933–41; disc. 941
Apparatus, Quick and Accurate Production Testing on Large D-C. Baldwin, Barnhart....136–8
Application and Handling of Very Large Power Transformers on the System of the Bonneville Power Administration. Stevens....158–63; disc. 163
Application of Electronic Motor Drives to Printing Presses. Johnson, Stacey....816–19
Application of Power Transformers, Selection and. Seelye....830–3
Application of Transformer Differential Protection, Theory and. McKenna....1197–1202
Applications to Bonneville Power Administration System, Microwave. Stevens, Stringfield....1088–99
Arcs in Large Air Gaps, Dielectric Recovery Characteristics of Power. McCann, Conner, Ellis....616–24; disc. 624
Armature Circuit Inductance, Measurement and Calculation of D-C Machine. Snively, Robinson....1228–35; disc. 1235
Armature Windings, Current in Equalizer Connections of D-C Machine. Linville, Strang....1219–26; disc. 1226
Armatures, Solderless Commutator Joints for High Temperature Operation of Railway Traction. Reed....638–41
Arrester Location with Transformer Insulation Level, Co-ordination of Lightning. Winske, Bias....964–73; disc. 973
Arrester Protective Levels and Transformer Insulation, Margins Between Lightning. Vogel....110–12; disc. 112
Arrester Standard, New Lightning. Stewart, Defandorf....525–6
Arresters as a Criterion for Insulation Levels, Lightning. Rorden....84–91; disc. 91
Aspects of Community Dial Office Equipment, General. Burkett....1540–3
Aspects of Lightning Surges on Power Systems and Their Suppression, Some. Kaneff....1544–9
Audible Noise of Power Transformers. Gordy....45–50; disc. 50
Audio Noise in Transformers in Residential and Commercial Areas. Baugh....121–6; disc. 126
Audio Multiplexing Equipment with High Stability Carrier Supply, A Low Noise and Distortion. Beale....1028–37; disc. 1037
Audio Noise Investigation, Harmonic Index—A Tool for Transformer. Mutschler, Madden....115–18; disc. 118
Automatic Control of Ignitron Rectifier Stations. Cham, Derr....801–11; disc. 811
Automatic Control of Metal-Clad Switchgear Serving Oil Refinery Motors During Power System Disturbances. Horsfall, Thompson, Mills, Bobo....1600–03; disc. 1603
Automatic Feathering—To Reduce the Hazard of Aircraft Engine Failure at Take-off. Kershaw....1328–34
Automatic Telephone Message Accounting System, Fundamentals of the. Messar....255–68; disc. 269
Automatic Telephone Systems, The Universal Director in Strowger. Ostline....1080–7
Auxiliaries of the Consolidated Edison System, Thrust Bearing Problems and Their Solution on Turbine-Generator Units and. Driscoll, Otten....1642–7; disc. 1647
Auxiliary System, Bus Transfer Tests on 2,300-Volt Station. Johnson, Thompson....386–90; disc. 390

B

Ball Analogue, Transients in Coupled Inductance-Capacitance Circuits Analyzed in Terms of a Rolling-. Magnuson....1525–30
Band Transformers for Linear Electronic Circuits, The Design of Broad-. Lord....1005–10
Bandwidth, The Direct Measurement of. Ammerman....27–31
Basic Design Considerations, Underground Conduit for Electric Power Systems—Fundamentals and. Watkins....1532–90; disc. 1590
Basic Impulse Insulation Levels for High-Voltage Systems, Proposed. Clem, Meador, Rudge, Powell....953–60; disc. 960
Basic Patterns for Arrangement of Electric Power Systems for Steel Mills. Finison....54–9; disc. 59
(Basic Sciences) Classification of the Reference Frames of a Synchronous Machine. Kron....720–7
(Basic Sciences) Steady-State Waves on Transmission Lines. Waidelich....1521–4
(Basic Sciences) The Calculation of the Capacitance of Coaxial Cylinders of Rectangular Cross-Section. Anderson....728–31
(Basic Sciences) Transients in Coupled Inductance-Capacitance Circuits Analyzed in Terms of a Rolling-Ball Analogue. Magnuson....1525–30
(Basic Sciences) Transpositions and the Calculation of Inductance from Geometric Mean Distances. Boast....1531–4
Basic Theory Underlying Bell System Facilities Capacity Tables. Gracey....238–43; disc. 243
Bearing Problems and Their Solution on Turbine-Generator Units and Auxiliaries of the Consolidated Edison System, Thrust. Driscoll, Otten....1642–7; disc. 1647
Bell System Facilities Capacity Tables, Basic Theory Underlying. Gracey....238–43; disc. 243
Benefits Resulting from Interconnecting Two or More Generating Systems, The Determination and Allocation of the Capacity. Watchorn....1180–6

Beta Rays, Noncontacting Thickness Gauge Using. Clapp, Bernstein....488–90
Board for Steam-Electric Generating Plants, Centralized Control. Lowe, Hodgkins....1396–9; disc. 1399
Boiler-Turbine-Generator Units, Centralized Control Desirable for Single. Lind, Geiger....1176–9
Bonneville Power Administration, Applic a and Handling of Very Large Power Transformers on the System of the. Stevens....158–63; disc. 163
Bonneville Power Administration Relaying and Reclosing Program, The. Diemond, Wylie....1039–46; disc. 1046
Bonneville Power Administration System, Microwave Applications to. Stevens, Stringfield....1088–99
Boulder 287.5-Kv Transmission Lines, Thirteen-Year Lightning Performance of. Blakeslee, Kanouse....796–9; disc. 800
Brake Magnets, The Operating Speed of D-C. Ryan, Spitler....1253–7
Breaker, A New 69-Kv Oil-Blast Circuit. Rietz, Balentine....416–23; disc. 423
Breaker, Development and Testing of an Improved High-Voltage, High-Capacity Impulse Circuit. Rietz....15–25; disc. 25
Breaker with 50,000 Ampere Interrupting Capacity at 600 Volts A-C, New Low-Voltage Air Circuit. Horn, Mikos....1654–7; disc. 1657
Breakers, An Air Delayed Selective Overcurrent Tripping Device for Low-Voltage Air Circuit. Tremblay, Horn....1649–53
Breakers for 5,000,000- to 10,000,000-Kva Interrupting Capacity, High-Voltage Oil Circuit. Leeds, Friedrich....70–6; disc. 76
Breakers for 28 and 120 Volts, Aircraft D-C Circuit. Beall, Reifschneider....1283–8
Bridge, A Direct Reading High-Voltage Capacitance. Foley....692–8; disc. 698
Bridge, Resistance Wire Strain Gauges as Elements of the Wheatstone. Petrucelly....742–4
Bridge River Hydroelectric Development, The. Ingledow, Steede....845–54
Bridges, Power Factor Measurements on Polyphase and Multiconductor Cable Using Single-Phase. Greenfield....680–5; disc. 685
Broad-Band Transformers for Linear Electronic Circuits, The Design of. Lord....1005–10
Buck-Boost Voltage Regulator on Steady-State Power Limit, Effect of. Concordia....380–4; disc. 384
Buildings for Small Communities, Dial Telephone Central Office. Reese, Roys....1535–9
Bureau of Reclamation, Relaying Practices and Economical Switching Station Arrangements of the. Morgan, Worth....865–70; disc. 870
Burner Safety Devices, Flame Detectors for Domestic Fuel. Deubel....220–5
Bus Enclosures, Induced Currents in High-Capacity. Killian....1388–95; disc. 1395
Bus Transfer Tests on 2,300-Volt Station Auxiliary System. Johnson, Thompson....586–90; disc. 590
Bushing-Type Current Transformers, A New Line of Orthomagnetic. Farr....424–8
Bushing-Type Current Transformers for Metering Purposes, A Survey of. Camilli....429–40

C

Cable-Connected Equipment, Surge Protection of. Witzke, Bliss....527–38; disc. 539
Cable, Development of Improved Luminous Sign. Roehmann, Greenfield....350–5; disc. 355
Cable Ducts and Duct Assemblies, Heat Transfer Study on Power. Greebler, Barnett....357–64; disc. 364
Cable Manholes, Critical Inside Dimensions for Power. Halfmann....1576–80; disc. 1580
Cable Using Single-Phase Bridges, Power Factor Measurements on Polyphase and Multiconductor. Greenfield....680–5; disc. 685
Cables, A Two-Channel Carrier Telegraph System for Short Submarine. Newell, Cramer....61–5
Cables and a Surrounding Pipe or Duct Wall, The Thermal Resistance Between. Buller, Neher....342–7; disc. 347
Cables, Terminal Risers for Solid-Type Impregnated Paper. Del Mar....1592–7; disc. 1597
Calculation of D-C Machine Armature Circuit Inductance, Measurement and. Snively, Robinson....1228–35; disc. 1235
Calculation of Inductance from Geometric Mean Distances, Transpositions and the. Boast....1531–4
Calculation of the Capacitance of Coaxial Cylinders of Rectangular Cross-Section, The. Anderson....728–31
Calculations, Analogue Computer for Multicomponent Fractionation. Coels, Calvert....97–103
Calculations for A-C Generators, Design. Ginsberg....1274–80; disc. 1280
Calculations of Single-Phase Induction Motors, Suggested Improvements in the Performance. Thacker, Gopalakrishna....1–6; disc. 6
Calibrating Watt-Hour Meters, A New Device for. Robison, Wickham....732–4
Capacitance Bridge, A Direct Reading High-Voltage. Foley....692–8; disc. 698
Capacitance Circuits Analyzed in Terms of a Rolling-Ball Analogue, Transients in Coupled Inductance-. Magnusson....1525–30
Capacitance of Coaxial Cylinders of Rectangular Cross-Section, The Calculation of the. Anderson....728–31
Capacity at 600 Volts A-C, New Low-Voltage Air Circuit Breaker with 50,000 Ampere Interrupting. Horn, Mikos....1654–7; disc. 1657
Capacity Benefits Resulting from Interconnecting Two or More Generating Systems, The Determination and Allocation of the. Watchorn....1180–6
Capacitance Bus Enclosures, Induced Currents in High-. Killian....1388–95; disc. 1395
Capacity by the Probability Method, Determination of Reserve. Calabrese....1681–8; disc. 1688
Capacity, High-Voltage Oil Circuit Breakers for 5,000,000- to 10,000,000-Kva Interrupting. Leeds, Friedrich....70–6; disc. 76
Capacity Low-Voltage Power Fuse, A New High-Interrupting. Schuck....770–6; disc. 776
Carbon Pile Voltage Regulators, Dynamic Characteristics of. Mills....1347–52; disc. 1352
Carriage Drive, Amplidyne-Controlled Log. Vincent....1124–9; disc. 1129
Carrier Channel, Simulation Supervisory Control, Telemetering and Communication on Single-Frequency. Derr, Wren, Kresser....1115–21; disc. 1121
Carrier Current Test Equipment and Its Application, Modern. Brinton....777–80
Carrier Frequency Changes, Phase Lead for A-C Servo Systems with Compensation for. Northoff....285–91; disc. 291
Carrier Supply, A Low Noise and Distortion Audio Multiplexing Equipment with High Stability. Beale....1028–37; disc. 1037
Carrier System for Telephone Lines of Short or Medium Length, An Improved Transmitted. Brodie....1501–04
Carrier Telegraph System for Short Submarine Cables, A Two-Channel. Newell, Cramer....61–5
Carrier Telephone System, A Medium-Haul. Smith....1505–12
Carrier Telephone System, A Simplified 48-Channel. Erickson....1493–1500
Carrier-Type Servomechanism, Integral Controller for Use in. Cosgriff....1379–83
Cell as a Nonlinear Element, An Electric Analogue Computer Using the Photo. Koenig....1606–11
Central Control Rooms, Design and Operation of. Borgel....598–602; disc. 602
Central Office Buildings for Small Communities, Dial Telephone. Reese, Roys....1535–9
Centralized Control Board for Steam-Electric Generating Plants. Lowe, Hodgkins....1396–9; disc. 1399
Centralized Control Desirable for Single Boiler-Turbine-Generator Units. Lind, Geiger....1176–9
Centralized Instrumentation and Controls for Steam Electric Power Stations. Mallory....591–6; disc. 596
Changes, Investigation and Elimination of Unusual Vibration in the Field on a Large Single-Phase Frequency. Ballantyne, Allen, Baudry....1264–72; disc. 1272
Changes, Phase Lead for A-C Servo Systems with Compensation for Carrier Frequency. Northoff....285–91; disc. 291
Changes Produced by Single-Phase Loads, Effect of Three-Phase Motor Loads on Voltage. Fawcett, Fisher, Helm....1467–72
Channel Carrier Telegraph System for Short Submarine Cables, A Two-. Newell, Cramer....61–5
Channel Carrier Telephone System, A Simplified 48-. Erickson....1493–1590
Channel for Voice Communication, Relaying, Telemetering, and Supervisory Control, Field Testing a Microwave. Pattison, Reagan, Leyland, Gunter....945–51; disc. 951
Channel, Multistation Supervisory Control, Telemetering and Communication on Single-Frequency Carrier. Derr, Wren, Kresser....1115–21; disc. 1121
Characteristics of A-C Lead Networks for Servomechanisms, Improvements in the. McDonald....293–300
Characteristics of Carbon Pile Voltage Regulators, Dynamic. Mills....1347–52; disc. 1352
Characteristics of Magnetic Amplifiers, General. Finzi, Beaumariage....919–27
Characteristics of Power Arcs in Large Air Gaps, Dielectric Recovery. McCann, Conner, Ellis....616–24; disc. 624
Characteristics of Some Magnetic-Fluid Clutch Servomechanisms. Parziale, Tilton....150–7
(Chemical) Design and Control of Ferroalloy Furnaces. Andreae....557–62
(Chemical) Electric Equipment and Operation of Graphitizing Furnaces. Cole....563–6
(Chemical) Electrode Control and Associated Operating Mechanisms. Hauff....567–70; disc. 570
Circuit Breaker, A New 69-Kv Oil Blast. Rietz, Balentine....416–23; disc. 423
Circuit Breaker, Development and Testing of an Improved High-Voltage, High-Capacity Impulse. Rietz....15–25; disc. 25
Circuit Breaker with 50,000 Ampere Interrupting Capacity at 600 Volts A-C, New Low-Voltage Air. Horn, Mikos....1654–7; disc. 1657
Circuit Breakers, An Air Delayed Selective Overcurrent Tripping Device for Low-Voltage Air. Tremblay, Horn....1649–53
Circuit Breakers for 5,000,000 to 10,000,000-Kva Interrupting Capacity, High-Voltage Oil. Leeds, Friedrich....70–6; disc. 76
Circuit Breakers for 28 and 120 Volts, Aircraft D-C. Beall, Reifschneider....1283–8
Circuit Inductance, Measurement and Calculation of D-C Machine Armature. Snively, Robinson....1228–35; disc. 1235
Circuit Transformers, Control. Frank, Hauck....1376–8
Circuits, Analysis of Synchronous Machine Short. Camburn, Gross....671–8; disc. 678
Circuits Analyzed in Terms of a Rolling-Ball Analogue, Transients in Coupled Inductance-Capacitance. Magnusson....1525–30
Circuits Between Community Dial Offices, Simplified Subscriber Toll Dialing for Low-Rate Low-Density Toll. Brooke, Blackhall, Blashfield....1417–20
Circuits of the Shaded-Pole Motor with Space Harmonics, Equivalent. Kron....735–41
Circuits on Saturated Alternators, Symmetrical Short. Mikhail....1554–62
Circuits, The Design of Broad-Band Transformers for Linear Electronic. Lord....1005–10
Clampers in Video Transmission. Doba, Rieke....477–87
Class-H Material for the Insulation of Traction Motor Field Coils, A New-Resilient. Reed, Tyner....1158–61
Classification of the Reference Frames of a Synchronous Machine. Kron....720–7
Clutch Servomechanisms, Characteristics of Some Magnetic-Fluid. Parziale, Tilton....150–7
Coaxial Cylinders of Rectangular Cross-Section, The Calculation of the Capacitance of. Anderson....728–31
Coefficients for Hydrogen-Cooled Rotating Electric Machines, Surface Heat-Transfer. Snell, Norris, Buckland....174–85; disc. 185
Coefficients of Synchronous Machines and Their Application, Spring and Damping. Kilgore, Whitney....226–9; disc. 229
Coils, A New Resilient Class-H Material for the Insulation of Traction Motor Field. Reed, Tyner....1158–61
Combined Phase and Ground Distance Relaying. New....37–42; disc. 42
Commercial Areas, Audio Noise in Transformers in Residential and. Baugh....121–6; disc. 126
(Committee Report) A Method of Estimating Lightning Performance of Transmission Lines. (50-163)....1187–95; disc. 1195
(Committee Report) Maximum Short-Circuit Current of D-C Motors and Generators. (50-23)....146–9
(Committee Report) Protection of Electronic Power Converters. (50-133)....813–29
(Committee Report) Sensitive Ground Protection. (50-70)....473–5; disc. 475
Committees and Officers for 1950–51....1717–36
(Communication) A Frequency Response Method for Analyzing and Synthesizing Contactor Servomechanisms. Kochenburger....270–83; disc. 283
(Communication) A Medium-Haul Carrier Telephone System. Smith....1505–12
(Communication) A New Electronic Telegraph Regenerative Receiver. Ostendorf....32–6; disc. 36
(Communication) A Printing Telegraph Tape-to-Page Translator. Frost....79–83
(Communication) An Improved Transmitted Carrier System for Telephone Lines of Short or Medium Length. Brodie....1501–04
(Communication) Basic Theory Underlying Bell System Facilities Capacity Tables. Gracey....238–43; disc. 243
(Communication) Crossbar Tandem System. Collis....997–1004
(Communication) Dial Telephone Central Office Buildings for Small Communities. Reese, Roys....1535–9
(Communication) Fundamentals of the Automatic Telephone Message Accounting System. Meszar....255–68; disc. 269
(Communication) General Aspects of Community Dial Office Equipment. Burkett....1540–3
(Communication) Interexchange Tandem Trunking in the Los Angeles Metropolitan Area. Pfeiffer....1071–9
Communication on Single-Frequency Carrier Channel, Multistation Supervisory Control, Telemetering and. Derr, Wren, Kresser....1115–21; disc. 1121
Communication, Relaying, Telemetering, and Supervisory Control, Field Testing a Microwave Channel for Voice. Pattison, Reagan, Leyland, Gunter....945–51; disc. 951

(Communication) Simplified Subscriber Toll Dialing for Low-Rate Low-Density Toll Circuits Between Community Dial Offices. Brooke, Blackhall, Blashfield 1417–20
(Communication) The Number 5 Crossbar Dial Telephone Switching System. Korn, Ferguson 244–54
(Communication) The Universal Director in Strowger Automatic Telephone Systems. Outline 1080–7
Communities, Dial Telephone Central Office Buildings for Small. Reese, Roys 1535–9
Community Dial Office Equipment, General Aspects of. Burkett 1540–3
Community Dial Offices, Simplified Subscriber Toll Dialing for Low-Rate Low-Density Toll Circuits Between. Brooke, Blackhall, Blashfield 1417–20
Commutation, Resistance. Olsen ..... 1207–15; disc. 1215
Complex Problems, Special Devices Aid Differential Analyzer Solution of. Cook, Kirchmayer, Weygandt ..... 1365–70; disc. 1370
Components, The Extension of Amplistat Performance by A-C. Morgan, Ogle, Wattenberger 986–91
Computer for Flight Simulation, A Generalized Analogue. Hall 308–20
Computer for Multicomponent Fractionation Calculations, Analogue. Geels, Calvert 97–105
Computer, New Techniques on the Anacom—Electric Analog. Harder, Carleton 547–56
Computer Using the Photo Cell as a Nonlinear Element, An Electric Analogue. Koenig 1606–11
(Computing Devices) An Electronic Simulator for Nonlinear Servomechanisms. Edwards, Johnson ..... 300–06; disc. 306
Commutator Joints for High Temperature Operation of Railway Traction Armatures, Solderless. Reed 638–41
Concepts of Thyratron Deionization Time, Statistical Nature and Physical. Romanowitz, Dow 368–79
Conditions, Ice Testing of Outdoor Disconnecting Switches to Simulate Field. Owens ..... 1488–91; disc. 1491
Conductors from an Aircraft Manufacturer's Viewpoint, Aluminum. Schumacher 1335–41
Conduit for Electric Power Systems—Fundamentals and Basic Design Considerations, Underground. Watkins ..... 1582–90; disc. 1590
Confinement, Transformer Noise and Its. McLean ..... 1409–15; disc. 1415
Connected Equipment, Surge Protection of Cable-Witzke, Bliss ..... 527–38; disc. 539
Connected Saturable Reactor with Control Source of Comparatively High Impedance, Series-. Storm 1299–1309
Connected Saturable Reactor with Control Source of Comparatively Low Impedance, Series. Storm 756–65
Connections for Phase Relays, A Study of Directional Element. Sonnemann ..... 1438–50; disc. 1450
Connections of D-C Machine Armature Windings, Current in Equalizer. Linville, Strang ..... 1219–26; disc. 1226
Conductors for Operation Above 230 Kv, Desert Measurements of Corona Loss on. Peterson, Cozzens, Carroll ..... 872–8; disc. 878
Consideration of Requirements and Limitations of Relaying and High-Speed Reclosing on Long and Heavily Loaded Transmission Lines. Parks, Brownlee ..... 103–07; disc. 107
Considerations, Transformer Sound Level. Maslin ..... 1142–5; disc. 1145
Considerations, Underground Conduit for Electric Power Systems—Fundamentals and Basic Design. Watkins ..... 1582–90; disc. 1590
Consolidated Edison System, Thrust Bearing Problems and Their Solution on Turbine-Generator Units and Auxiliaries of the. Driscoll, Otten ..... 1642–7; disc. 1647
Constant Frequency Alternator, Variable Speed Drive. Gould, Krupotich ..... 745–7; disc. 747
Constant Using the Susceptance Variation Principle, An Improved Method of Measuring Dissipation Factor and Dielectric. Miller, Whelan 491–7
Contactor Servomechanisms, A Frequency Response Method for Analyzing and Synthesizing. Kochenburger ..... 270–83; disc. 283
Continuous Scavenging System for Hydrogen-Cooled Generators. Snell, Grobel 1625–36
Contributing Factors in Determining the Ratings of Power Transformers for Use on the Systems of the Hydro-Electric Power Commission of Ontario. Fleming, Lotimer ..... 1658–62; disc. 1662
Control, A Magnetic Amplifier Frequency. Johnson, Schafer 613–15
Control and Associated Operating Mechanisms, Electrode. Hanff ..... 567–70; disc. 570
Control Board for Steam-Electric Generating Plants, Centralized. Lowe, Hodgkins ..... 1396–9; disc. 1399
Control Circuit Transformers. Frank, Hauck 1376–8
Control Desirable for Single Boiler-Turbine-Generator Units, Centralized. Lind, Geiger 1176–9
Control for Tube Testing, High-Voltage Rectifier Equipment and. Durand 909–12
Control of Ferroalloy Furnaces, Design and. Andreae 557–62
Control of Gas Turbines for Power Generation. Hoffmann, Mellor, Starkey ..... 1637–41; disc. 1641
Control of Ignitron Rectifier Stations, Automatic. Cham, Derr ..... 801–11; disc. 811
Control of Large D-C Motors Supplied from Ignitron Rectifiers. Livingston 205–10
Control of Metal-Clad Switchgear Serving Oil Refinery Motors During Power System Disturbances, Automatic. Hornall, Thompson, Mills, Bobo ..... 1600–03; disc. 1603
Control Rooms, Design and Operation of Central. Borgel ..... 598–602; disc. 602
Control Source of Comparatively High Impedance, Series-Connected Saturable Reactor with. Storm 1299–1309
Control Source of Comparatively Low Impedance, Series-Connected Saturable Reactor with. Storm 756–65
Control System for a 4,500-Horsepower Gas-Turbine Electric Locomotive. Warrick 508–13
Control System Synthesis by Root Locus Method. Evans 66–9
Control, Telemetering and Communication on Single-Frequency Carrier Channel, Multistation Supervisory. Derr, Wren, Kresser ..... 1115–21; disc. 1121
Control Transformer System, Static Accuracy Performance of the Selsyn Generator. Kronacher ..... 645–53; disc. 653
Controlled Log Carriage Drive, Amplidyne-. Vincent ..... 1124–9; disc. 1129
Controller for Use in Carrier-Type Servomechanisms, Integral. Cosgriff 1379–83
Controls for Steam Electric Power Stations, Centralized Instrumentation and. Mallory ..... 591–6; disc. 596
Converters for High Energy Particle Accelerators, Ignitron. Boyer, Marcum 1110–14
Converters, Protection of Electronic Power. (Committee Report) 813–29
Cooled Generators at Elevated Gas Pressures, Loading of Hydrogen-. Snell ..... 186–99; disc. 199
Cooled Generators, Continuous Scavenging System for Hydrogen-. Snell, Grobel 1625–36
Cooled Rotating Electric Machines, Surface Heat-Transfer Coefficients for Hydrogen-. Snell, Norris, Buckland ..... 174–85; disc. 185
Cooling of A-C Turbine Generators, Liquid. Part II. Fechheimer ..... 165–71; disc. 171 (Part I–1947)
Co-ordination of Lightning Arrester Location with Transformer Insulation Level. Witzke, Bliss ..... 964–73; disc. 973
Cores, Single-Phase Power Transformer Formed. Gordy, Somerville 1384–7
Corona Loss on Conductors for Operation Above 230 Kv, Desert Measurements of. Peterson, Cozzens, Carroll ..... 872–8; disc. 878
Corona, Radio Influence, and Other Factors, Progress Report on Tidd 500-Kv Test Project of the American Gas and Electric Company— Sporn, Monteith ..... 891–7; disc. 897
Counter-Type Tachometer, A New High-Accuracy. Berry, Beattie ..... 686–90; disc. 690
Coupled Inductance-Capacitance Circuits Analyzed in Terms of a Rolling-Ball Analogue, Transients in. Magnusson 1525–30
Critical Inside Dimensions for Power Cable Manholes. Halfmann ..... 1576–80; disc. 1580
Cross-Section, The Calculation of the Capacitance of Coaxial Cylinders of Rectangular. Anderson 728–31
Crossbar Dial Telephone Switching System, The Number 5. Korn, Ferguson 244–54
Crossbar Tandem System. Collis 997–1004
Current in Equalizer Connections of D-C Machine Armature Windings. Linville, Strang ..... 1219–26; disc. 1226
Current of D-C Motors and Generators, Maximum Short-Circuit. (Committee Report) 146–9
Current Test Equipment and Its Application, Modern Carrier. Brinton 777–80
Current Transductor and Its Application in the Aluminum Industry, The Theory of the. Specht, Wagner ..... 441–52; disc. 452
Current Transformers, A New Line of Orthomagnetic Bushing-Type. Farr 424–8
Current Transformers, A Primary Method of Measuring the Ratio and Phase Angle of. Brownlee 459–60
Current Transformers for Metering Purposes, A Survey of Bushing-Type. Camilli 429–40
Currents, Effect of Frequency on Perception. Daniel, Mansfield 1162–8
Currents in High-Capacity Bus Enclosures, Induced. Killian ..... 1388–95; disc. 1395
Customer's Premises, Protective Grounding of Electrical Installations on. Schirmer 657–9
Cylinders of Rectangular Cross-Section, The Calculation of the Capacitance of Coaxial. Anderson 728–31

D

Damping Coefficients of Synchronous Machines and Their Application, Spring and. Kilgore, Whitney ..... 226–9; disc. 229
Damping Torque at Low Speeds, Synchronous Machine. Concordia 1550–3
Deionization Time, Statistical Nature and Physical Concepts of Thyratron. Romanowitz, Dow 368–79
Delayed Selective Overcurrent Tripping Device for Low-Voltage Air Circuit Breakers, An Air. Tremblay, Horn 1649–53
Desert Measurements of Corona Loss on Conductors for Operation Above 230-Kv. Peterson, Cozzens, Carroll ..... 872–8; disc. 878
Design and Control of Ferroalloy Furnaces. Andreae 557–62
Design and Operation of Central Control Rooms. Borgel ..... 598–602; disc. 602
Design and Operation of Power Transformers on American Gas and Electric Company System, Selection. Lane, Gross, Pugh ..... 786–93; disc. 793
Design and Test on Electronic Exciter Supplied from Common Shaft-Driven Generator. Colsiaco, Johnson, Reilly ..... 328–35; disc. 335
Design as Applied to Polyphase Induction Motors, A Method of Total. Crouse 1434–7
Design Calculations for A-C Generators. Ginsberg ..... 1274–80; disc. 1280
Design Considerations, Underground Circuit for Electric Power Systems—Fundamentals and Basic. Watkins ..... 1582–90; disc. 1590
Design, Information Theory Applied to System. Tuller 1612–14
Design, Light Steel Tower Line. Osipovich ..... 1513–17; disc. 1517
Design Method, A-C Series Motors—A. Chang, Karr ..... 1257–61; disc. 1261
Design of a 3-Phase Transformer, Economical. Ciganek ..... 1371–4; disc. 1374
Design of Broad-Band Transformers for Linear Electronic Circuits, The. Lord 1005–10
Design of Log-Scale D-C Indicating Instruments, Principles of. Stimson, Taylor 101–15
Design of Reactors for Radio Interference Filters, The. Knudson 1294–8
Designers, Quiet Transformer Installations—A Problem for Both Equipment and Substation. Mendenhall, Taylor ..... 1148–52; disc. 1152
Detectors for Domestic Fuel Burner Safety Devices, Flame. Deubel 220–5
Determination and Allocation of the Capacity Benefits Resulting from Interconnecting Two or More Generating Systems, The. Watchorn 1180–6
Determination of Effective Oil Temperature in a Transformer. Beavers ..... 703–08; disc. 708
Determination of Reserve Capacity by the Probability Method. Calabrese ..... 1681–8; disc. 1688
Determination of Steady-State Performance of Self-Saturating Magnetic Amplifiers. Smith 1309–17
Development and Testing of an Improved High-Voltage, High-Capacity Impulse Circuit Breaker. Rietz ..... 15–23; disc. 25
Development of Fluid Mappers, The Further. Moore 1615–24
Development of Improved Luminous Sign Cable. Roehmann, Greenfield ..... 350–5; disc. 355
Development of Preferred Voltage Ratings for Transformers. St. Clair, Jalonack ..... 1049–59; disc. 1059
Development of the Standard for Neutral Grounding Devices. Clem 976–9
Development, The Bridge River Hydroelectric. Ingledow, Steede 845–54
Device for Calibrating Watt-Hour Meters, A New. Robison, Wickham 732–4
Device for Low-Voltage Air Circuit Breakers, An Air Delayed Selective Overcurrent Tripping. Tremblay, Horn 1649–53
Device for Metal-Clad Switchgear, A New Grounding and Testing. Krida, McCurry ..... 407–12; disc. 412
Devices Aid Differential Analyzer Solution of Complex Problems, Special. Cook, Kirchmayer, Weygandt ..... 1365–70; disc. 1370
Devices, Development of the Standard for Neutral Grounding. Clem 976–9
Devices, Flame Detectors for Domestic Fuel Burner Safety. Deubel 220–5
Dial Office Equipment, General Aspects of Community. Burkett 1540–3
Dial Telephone Central Office Buildings for Small Communities. Reese, Roys 1535–9
Dial Telephone Switching System, The Number 5 Crossbar. Korn, Ferguson 244–54
Dialing for Low-Rate Low-Density Toll Circuits Between Community Dial Offices, Simplified Subscriber Toll. Brooke, Blackhall, Blashfield 1417–20
Dielectric Constant Using the Susceptance Variation Principle, An Improved Method of Measuring Dissipation Factor and. Miller, Whelan 491–7
Dielectric Recovery Characteristics of Power Arcs in Large Air Gaps. McCann, Conner, Ellis ..... 616–24; disc. 624

Differential Analyzer Solution of Complex Problems, Special Devices Aid. Cook, Kirchmayer, Weygandt.....1365–70; disc. 1370
Differential Protection, Theory and Application of Transformer. McKenna.....1197–1202
Differential Relay Sensitivity Adjuster. Headley.....1203–05; disc. 1205
Digital Recording and Telemetering. The Metrotype System of. Foster.....543–6; disc. 546
Dimensions for Power Cable Manholes, Critical Inside. Halfmann.....1576–80; disc. 1580
D-C Apparatus, Quick and Accurate Production Testing on Large. Baldwin, Barnhart.....136–8
D-C Brake Magnets, The Operating Speed of. Ryan, Spitler.....1253–7
D-C Circuit Breakers for 28 and 120 Volts, Aircraft. Beall, Reifschneider.....1283–8
Direct-Current Dynamos, Transient Response of. Koenig.....139–44; disc. 144
D-C High Performance Limit Switch, An Environment-Free 120-Volt. Stuelpnagel.....1289–93
D-C Indicating Instruments, Principles of Design of Log-Scale. Stimson, Taylor.....1011–15
D-C Machine Armature Circuit Inductance, Measurement and Calculation of. Snively, Robinson.....1228–35; disc. 1235
D-C Machine Armature Windings, Current in Equalizer Connections of. Linville, Strang.....1219–26; disc. 1226
D-C Motor Drives, Rectifier Equipment for Electronic. Mulhern, Crawford.....211–15
D-C Motors and Generators, Maximum Short-Circuit Current. (Committee Report).....146–9
D-C Motors Supplied from Ignitron Rectifiers, Control of Large. Livingston.....205–10
D-C System, Transient Analysis of a Voltage-Regulated Aircraft. Scorgie.....1318–23
Direct Measurement of Bandwidth, The. Ammerman.....27–31
Direct Reading High-Voltage Capacitance Bridge, A. Foley.....692–8; disc. 698
Directional Element Connections for Phase Relays, A Study of. Sonnemann.....1438–50; disc. 1450
Director in Stroger Automatic Telephone Systems, The Universal. Outline.....1080–7
Directors, Report of the Board of.....1690–1716
Disconnecting Switches to Simulate Field Conditions, Ice Testing of Outdoor. Owens.....1488–91; disc. 1491
Dissipation Factor and Dielectric Constant Using the Susceptance Variation Principle, An Improved Method of Measuring. Miller, Whelan.....491–7
Distance Power Transmission, Long-. Crary.....834–40; disc. 840
Distance Relaying, Combined Phase and Ground. New.....37–42; disc. 42
Distances, Transpositions and the Calculation of Inductance from Geometric Mean. Boast.....1531–4
Distortion Audio Multiplexing Equipment with High Stability Carrier Supply, A Low Noise and. Beale.....1028–37; disc. 1037
Disturbances, Automatic Control of Metal-Clad Switchgear Serving Oil Refinery Motors During Power System. Horsfall, Thompson, Mills, Bobo.....1600–03; disc. 1603
Domestic Fuel Burner Safety Devices, Flame Detectors for. Deutsch.....220–5
Drive, Amplidyne-Controlled Log Carriage. Vincent.....1124–9; disc. 1129
Drive Constant Frequency Alternator, Variable Speed. Gould, Krupotich.....745–7; disc. 747
Drives, Rectifier Equipment for Electronic D-C Motor. Mulhern, Crawford.....211–15
Drives to Printing Presses, Application of Electronic Motor. Johnson, Stacey.....216–19
Dry-Type Insulation for Instrument Transformers, A New. Pfuntner, Franck, D'Entremont.....453–8
Duct Wall, The Thermal Resistance Between Cables and a Surrounding Pipe or. Buller, Neher.....342–7; disc. 347
Ducts and Duct Assemblies, Heat Transfer Study on Power Cable. Greebler, Barnett.....357–64; disc. 364
Dynamic Characteristics of Carbon Pile Voltage Regulators. Mills.....1347–52; disc. 1352
Dynamos, Transient Response of Direct-Current. Koenig.....139–44; disc. 144

E

Economical Design of a 3-Phase Transformer. Ciganek.....1371–4; disc. 1374
Economical Switching Station Arrangements of the Bureau of Reclamation, Relaying Practices and. Morgan, World.....865–70; disc. 870
Effect of Buck-Boost Voltage Regulator on Steady-State Power Limits. Concordia.....380–4; disc. 384
Effect of Frequency on Perception Currents. Dalziel, Mansfield.....1162–8
Effect of Three-Phase Motor Loads on Voltage Changes Produced by Single-Phase Loads. Faucett, Fisher, Helm.....1467–72
Effects of Supply Line Unbalance on the Filtered Output Ripple of Polyphase Rectifiers. Hooper, McAdie.....766–70
Electric Analog Computer, New Techniques on the Anacom—. Harder, Carleton.....547–56
Electric Analogue Computer Using the Photo Cell as a Nonlinear Element, An. Koenig.....1606–11
Electric Equipment and Operation of Graphitizing Furnaces. Cole.....563–6
Electric Equipment for a Gas-Turbine Electric Locomotive, Rotating. Cohn.....514–18
Electric Equipment for Heavy-Media Separation Process. Bean, Blind.....1421–9
Electric Fences—Their Hazards, Types, Regulations, and Safe Application. Dalziel.....8–15
Electric Generating Plants, Centralized Control Board for Steam-. Lowe, Hodgkins.....1396–9; disc. 1399
Electric Locomotive, Control System for a 4,500-Horsepower Gas-Turbine. Warrick.....508–13
Electric Locomotive, The Alco-GE 4,500-Horsepower Gas-Turbine. Morey.....504–07
Electric Machines, Surface Heat-Transfer Coefficients for Hydrogen-Cooled Rotating. Snell, Norris, Buckland.....174–85; disc. 185
Electric Motors Need Test Equipment, Aircraft. Ross.....1359–64
Electric Power Stations, Centralized Instrumentation and Controls for Steam. Mallory.....591–6; disc. 596
Electric Power Systems for Steel Mills, Basic Patterns for Arrangement of. Finison.....54–9; disc. 59
Electric Power Systems—Fundamentals and Basic Design Considerations, Underground Conduit for. Watkins.....1582–90; disc. 1590
Electric Systems for Aircraft, Wide Speed Range A-C. James, Judkins, Mershon.....1353–8; disc. 1358
Electrical Analogues in the Study of Transmission Line Vibration, Use of Techniques from. Lemmis, Klopfenstein.....1676–80
Electrical Hazards to Farm Stock. Buchanan.....654–6
Electrical Installations on Customer's Premises, Protective Grounding of. Schirmer.....657–9
Electrical Instrumentation in Medical Research. Benjamin, Hale, Carstensen, Tompkins.....1324–7
Electrification, Rectifier-Type Motive Power for Railroad. Hibbard, Whittaker, Ames.....519–23; disc. 523
Electrode Control and Associated Operating Mechanisms. Hanff.....567–70; disc. 570
Electronic Circuits, The Design of Broad-Band Transformers for Linear. Lord.....1005–10
Electronic D-C Motor Drives, Rectifier Equipment for. Mulhern, Crawford.....211–15
Electronic Excitation and Regulation of Electric Generators as Compared to Conventional Methods, Excitation Improvement—. Phillips, Lambert, Pattison.....338–40; disc. 340
Electronic Exciter Supplied from Common Shaft-Driven Generator, Design and Test on. Colaiaco, Johnson, Reilly.....328–35; disc. 335
Electronic Motor Drives to Printing Presses, Application of. Johnson, Stacey.....216–19
Electronic Power Converters, Protection of. (Committee Report).....813–29
Electronic Simulator for Nonlinear Servomechanisms, An. Edwards, Johnson.....300–06; disc. 306
Electronic Telegraph Regenerative Receiver, A New. Ostendorf.....32–6; disc. 36
(Electronics) A Magnetic Amplifier Frequency Control. Johnson, Schafer.....613–15
(Electronics) An Analysis of Transients and Feedback in Magnetic Amplifiers. Johnson, Latson.....604–11; disc. 611
(Electronics) An Analysis of Transients in Magnetic Amplifiers. VerPlanck, Finzi, Beaumariage.....498–503
(Electronics) Determination of Steady-State Performance of Self-Saturating Magnetic Amplifiers. Smith.....1309–17
(Electronics) General Characteristics of Magnetic Amplifiers. Finzi, Beaumariage.....919–27
(Electronics) High-Voltage Ignitron Rectifiers. Mulhern.....913–18
(Electronics) High-Voltage Rectifier Equipment and Control for Tube Testing. Durand.....909–12
(Electronics) Ignitron Converters for High Energy Particle Accelerators. Boyer, Marcum.....1110–14
(Electronics) Ignitron Pulse Equipment for Particle Accelerators. Herskind, Hudson.....992–6
(Electronics) Response Time of Magnetic Amplifiers. Harder, Horton.....1130–8; disc. 1138
(Electronics) Series-Connected Saturable Reactor with Control Source of Comparatively High Impedance. Storm.....1299–1309
(Electronics) Series Connected Saturable Reactor with Control Source of Comparatively Low Impedance. Storm.....756–65
(Electronics) Statistical Nature and Physical Concepts of Thyratron Deionization Time. Romanowitz, Dow.....368–79
(Electronics) The Direct Measurement of Bandwidth. Ammerman.....27–31
(Electronics) The Further Development of Fluid Mappers. Moore.....1615–24
Element, An Electric Analogue Computer Using the Photo Cell as a Nonlinear. Koenig.....1606–11
Element Connections for Phase Relays, A Study of Directional. Sonnemann.....1438–50; disc. 1450
Elements, Stability of Servomechanisms with Linearly Varying. Kirby.....1662–7; disc. 1667
Elimination of Unusual Vibration in the Field on a Large Single-Phase Frequency Changer, Investigation and. Ballantyne, Allen, Baudry.....1264–72; disc. 1272
Enclosures, Induced Currents in High-Capacity Bus. Killian.....1388–95; disc. 1395
Energized Systems, Measurement of Insulation Resistance on. Brancato, McClinton.....1238–42
Energy Particle Accelerators, Ignitron Converters for High. Boyer, Marcum.....1110–14
Engine Failure at Take-off, Automatic Feathering—To Reduce the Hazard of Aircraft. Kershaw.....1328–34
Environment-Free 120-Volt D-C High Performance Limit Switch, An. Stuelpnagel.....1289–93
Equalizer Connections of D-C Machine Armature Windings, Current in. Linville, Strang.....1219–26; disc. 1226
Equipment, Aircraft Electric Motors Need Test. Ross.....1359–64
Equipment and Control for Tube Testing, High-Voltage Rectifier. Durand.....909–12
Equipment and Its Application, Modern Carrier Current Test. Brinton.....777–80
Equipment and Operation of Graphitizing Furnaces, Electric. Cole.....563–6
Equipment and Substation Designers, Quiet Transformer Installations—A Problem for Both. Mendenhall, Taylor.....1148–52; disc. 1152
Equipment for a Gas-Turbine Electric Locomotive, Rotating Electric. Cohn.....514–18
Equipment for Electronic D-C Motor Drives, Rectifier. Mulhern, Crawford.....211–15
Equipment for Heavy-Media Separation Process, Electric. Bean, Blind.....1421–9
Equipment for Particle Accelerators, Ignitron Pulse. Herskind, Hudson.....992–6
Equipment General Aspects of Community Dial Office. Burkett.....1540–3
Equipment, Surge Protection of Cable-Connected. Wrake, Bliss.....527–38; disc. 539
Equipment with High Stability Carrier Supply, A Low Noise and Distortion Audio Multiplexing. Beale.....1028–37; disc. 1037
Equivalent Circuits of the Shaded-Pole Motor With Space Harmonics. Kron.....735–41
Evaluation of Lightning-Arrester Lead Length and Separation in Co-ordinated Protection of Apparatus Against Lightning. Carpenter, Johnson, Saline.....933–41; disc. 941
Excitation Experience at Grand Coulee, Hydroelectric Generator. Killgore, Holmdahl.....855–60
Excitation Improvement—Electronic Excitation and Regulation of Electric Generators as Compared to Conventional Methods. Phillips, Lambert, Pattison.....338–40; disc. 340
Excitation System Performance with Motor-Driven Exciters. Mellor, Temoshok.....321–7
Exciter Supplied from Common Shaft-Driven Generator, Design and Test on Electronic. Colaiaco, Johnson, Reilly.....328–35; disc. 335
Exciters, Excitation System Performance with Motor-Driven. Mellor, Temoshok.....321–7
Expansion of the System of the Southern California Edison Company. Kroneberg.....861–4
Experience at Grand Coulee, Hydroelectric Generator Excitation. Killgore, Holmdahl.....855–60
Experiences with Resonant Grounding in a Large 34.5-Kv System, Practical. Brown, Gross.....1401–06; disc. 1406
Experimental and Analytical Study of Turbine Generator Rotor Ventilation, An. Fechheimer.....1563–9
Extension of Amplitat Performance by A-C Components, The. Morgan, Ogle, Wattenberger.....986–91

F

Facilities Capacity Tables, Basic Theory Underlying Bell System. Gracey.....238–43; disc. 243
Factor and Dielectric Constant Using the Susceptance Variation Principle, An Improved Method of Measuring Dissipation. Miller, Whelan.....491–7
Factor Measurements on Polyphase and Multiconductor Cable Using Single-Phase Bridges, Power. Greenfield.....680–5; disc. 685
Factors in Determining the Ratings of Power Transformers for Use on the Systems of the Hydro-Electric Power Commission of Ontario, Contributing. Fleming, Lotimer.....1658–62; disc. 1662
Failure at Take-off, Automatic Feathering—To Reduce the Hazard of Aircraft Engine. Kershaw.....1328–34
Failures of Rubber Insulation Caused by Soil Microorganisms. Blake, Kitchin, Pratt.....748–54; disc. 754

Farm Stock, Electrical Hazards to. Buchanan....654–6
Fatigue Life of Steel Strand, Vibration and. Little, MacMillan, Majercak.....1473–8; disc. 1478
Feathering—To Reduce the Hazard of Aircraft Engine Failure at Take-off, Automatic. Kershaw...1328–34
Feedback in Magnetic Amplifiers, An Analysis of Transients and. Johnson, Latson.....604–11; disc. 611
Fences—Their Hazards, Types, Regulations, and Safe Application, Electric. Dalziel.....8–15
Ferroalloy Furnaces, Design and Control of. Andreae 557–62
Field Coils, A New Resilient Class-H Material for the Insulation of Traction Motor. Reed, Tyner.....1158–61
Field Conditions, Ice Testing of Outdoor Disconnecting Switches to Simulate. Owens..1488–91; disc. 1491
Field Testing a Microwave Channel for Voice Communication, Relaying, Telemetering, and Supervisory Control. Pattison, Reagan, Leyland, Gunter.....G945–51; disc. 951
Filter Output Ripple of Polyphase Rectifiers, Effects of Supply Line Unbalance on the. Hooper, McAdie 766–70
Filters, The Design of Reactors for Radio Interference. Knudson.....1294–8
5,000-Kva Underground Substation, A. Sinnott. .....882–9; disc. 889
Flame Detectors for Domestic Fuel Burner Safety Devices. Deubel.....220–5
Flight Simulation, A Generalized Analogue Computer for. Hall.....308–20
Fluid Clutch Servomechanisms, Characteristics of Some Magnetic-. Parziale, Tilton.....150–7
Fluid Mappers, The Further Development of. Moore 1615–24
Flux Induction Heating, Transverse. Baker.....711–19
Formed Cores, Single-Phase Power Transformer. Gordy, Somerville.....1384–7
Fractionation Calculations, Analogue Computer for Multicomponent. Goetz, Calvert.....97–103
Frames of a Synchronous Machine, Classification of the Reference. Kron.....720–7
Frequencies, Indicating Instruments at the Servomechanism. Pritchett, Saunders.....980–5
Frequency Alternator, Variable Speed Drive Constant. Gould, Krupovich.....745–7; disc. 747
Frequency Carrier Channel, Multistation Supervisory Control, Telemetering, and Communication on Single-. Derr, Wren, Kreuzer..1115–21; disc. 1121
Frequency Changer, Investigation and Elimination of Unusual Vibration in the Field on a Large Single-Phase. Ballantyne, Allen, Baudry.....1264–72; disc. 1272
Frequency Changes, Phase Lead for A-C Servo Systems with Compensation for Carrier. Notthoff.....285–91; disc. 291
Frequency Control, A Magnetic Amplifier. Johnson, Schafer.....613–15
Frequency on Perception Currents, Effect of. Dalziel, Mansfield.....1162–8
Frequency Response Method for Analyzing and Synthesizing Contactor Servomechanisms, A. Kochenburger.....270–83; disc. 283
Fuel Burner Safety Devices, Flame Detectors for Domestic. Deubel.....220–5
Fundamentals and Basic Design Considerations, Underground Conduit for Electric Power Systems—. Watkins.....1582–90; disc. 1590
Fundamentals of the Automatic Telephone Message Accounting System. Mestar....255–68; disc. 269
Furnaces, Design and Control of Ferroalloy. Andreae 557–62
Furnaces, Electric Equipment and Operation of Graphitizing. Cole.....563–6
Fuse, A New High-Interrupting Capacity Low-Voltage Power. Schuck.....770–6; disc. 776

G

Gaps, Dielectric-Recovery Characteristics of Power Arcs. McCann, Conner, Ellis.....616–24; disc. 624
Gaps for Voltage Measurement, The Irradiation of Spark. Hardy, Craggs.....584–90
Gas Pressures, Loading of Hydrogen-Cooled Generators at Elevated. Snell.....186–99; disc. 199
Gas-Turbine Electric Locomotive, Control System for a 4,500-Horsepower. Warrick.....508–13
Gas-Turbine Electric Locomotive, Rotating Electric Equipment for a. Coho.....514–18
Gas-Turbine Electric Locomotive, The Alco-GE 4,500-Horsepower. Morey.....504–07
Gas Turbines for Power Generation, Control of. Hoffmann, Mellor, Starkey.....1637–41; disc. 1641
Gauge Using Beta Rays, Noncontacting Thickness. Clapp, Bernstein.....488–90
Gauges as Elements of the Wheatstone Bridge, Resistance Wire Strain. Petrucelly.....742–4
General Aspects of Community Dial Office Equipment. Burkett.....1540–3
General Characteristics of Magnetic Amplifiers. First, Beaumariage.....919–27
GE 4,500-Horsepower Gas-Turbine Electric Locomotive, The Alco-. Morey.....504–07
Generalized Analogue Computer for Flight Simulation, A. Hall.....308–20
Generating Plants, Centralized Control Board for Steam-Electric. Lowe, Hodgkins.....1396–9; disc. 1399
Generating Stations, The Choice of Main Power Transformers for. Dillow, Butler.....781–5; disc. 785
Generating Systems, The Determination and Allocation of the Capacity Benefits Resulting from Interconnecting Two or More. Watchorn.....1180–6
Generation, Control of Gas Turbines for Power. Hoffmann, Mellor, Starkey.....1637–41; disc. 1641
Generator Control Transformer System, Static Accuracy Performance of the Selsyn. Kronacher.....645–53; disc. 653
Generator, Design and Test on Electronic Exciter Supplied from Common Shaft-Driven. Colaiaco, Johnson, Reilly.....328–35; disc. 335
Generator Excitation Experience at Grand Coulee, Hydroelectric. Killgore, Holmdahl.....855–60
Generator Rating of Induction Motors. Smith..129–35
Generator Rotor Ventilation, An Experimental and Analytical Study of Turbine. Fechheimer..1563–9
Generator Units and Auxiliaries of the Consolidated Edison System, Thrust Bearing Problems and Their Solution on Turbine-. Driscoll, Otten.....1642–7; disc. 1647
Generator Units, Centralized Control Desirable for Single Boiler Turbine. Lind, Geiger.....1176–9
Generators as Compared to Conventional Methods, Excitation Improvement—Electronic Excitation and Regulation of Electric. Phillips, Lambert, Pattison .....338–40; disc. 340
Generators at Elevated Gas Pressures, Loading of Hydrogen-Cooled. Snell.....186–99; disc. 199
Generators, Continuous Scavenging System for Hydrogen-Cooled. Snell, Grobel.....1625–36
Generators, Design Calculations for A-C. Ginsberg .....1274–80; disc. 1280
Generators, Liquid Cooling of A-C Turbine. Part II. Fechheimer.....165–71; disc. 171 (Part I–1947)
Generators, Maximum Short-Circuit Current of D-C Motors and. (Committee Report).....146–9
Generators with Suddenly Applied Loads, Regulation of A-C. Part II. Harder, Cheek, Clayton.....395–405; disc. 405 (Part I–1944)
Geometric Mean Distances, Transpositions and the Calculation of Inductance from. Boast.....1531–4
Georges Phenomenon—Induction Motors with Unbalanced Rotor Impedances, The. Garbarino, Gross.....1569–74; disc. 1574
Gradient Meter, A Voltage. Tremaine, Cheek.....633–7; disc. 637
Grand Coulee, Hydroelectric Generator Excitation Experience at. Killgore, Holmdahl.....855–60
Graphitizing Furnaces, Electric Equipment and Operation of. Cole.....563–6
Ground Distance Relaying, Combined Phase and. New .....37–42; disc. 42
Ground Protection, Sensitive. (Committee Report) .....473–5; disc. 475
Grounding and Testing Device for Metal-Clad Switchgear, A New. Krida, McCurry..407–12; disc. 412
Grounding Devices, Development of the Standard for Neutral. Clem.....976–9
Grounding in a Large 34.5-Kv System, Practical Experiences with Resonant. Brown, Gross.....1401–06; disc. 1406
Grounding of Electrical Installations on Customer's Premises, Protective. Schirmer.....657–9

H

Harmonic Index—A Tool for Transformer Audio Noise Investigation. Mutschler, Madden.....115–18; disc. 118
Harmonics, Equivalent Circuits of the Shaded-Pole Motor with Space. Kron.....735–41
Haul Carrier Telephone System, A Medium-. Smith 1505–12
Hazard of Aircraft Engine Failure at Take-off, Automatic Feathering—To Reduce the. Kershaw.....1328–34
Hazards to Farm Stock, Electrical. Buchanan....654–6
Hazards, Types, Regulations, and Safe Application, Electric Fences—. Dalziel.....8–15
Heat-Transfer Coefficients for Hydrogen-Cooled Rotating Electric Machines, Surface. Snell, Norris, Buckland.....174–85; disc. 185
Heat Transfer Study on Power Cable Ducts and Duct Assemblies. Grezebler, Barnett..357–64; disc. 364
Heating, Transverse Flux Induction. Baker.....711–19
Heavy-Media Separation Process, Electric Equipment for. Bean, Blind.....1421–9
High-Accuracy Counter-Type Tachometer, A New. Berry, Beattie.....686–90; disc. 690
High-Capacity Bus Enclosures, Induced Currents in. Killian.....1368–95; disc. 1395
High Interrupting Capacity Low-Voltage Power Fuse, A New. Schuck.....770–6; disc. 776
High-Speed Reclosing on Long and Heavily Loaded Transmission Lines, Consideration of Requirements and Limitations of Relaying and. Parks, Brownlee .....103–07; disc. 107
High Voltage Capacitance Bridge, A Direct Reading. Foley.....692–8; disc. 698
High-Voltage, High-Capacity Impulse Circuit Breaker, Development and Testing of an Improved. Riers .....15–25; disc. 25
High-Voltage Ignitron Rectifiers. Mulhern.....913–18
High-Voltage Oil Circuit Breakers for 3,000,000 to 10,000,000-Kva Interrupting Capacity. Leeds, Friedrich.....70–6; disc. 76
High-Voltage Rectifier Equipment and Control for Tube Testing. Durand.....909–12
High-Voltage Systems, Proposed Basic Impulse Insulation Levels for. Clem, Meador, Rudge, Powell .....953–60; disc. 960
High-Voltage Transmission Lines, Relay Protection for Medium Length. Kinghorn.....461–5; disc. 465
Hook-On Method, Power Measurement by the. Corson, Nylander.....699–702
Horn-Gap Switches, Interrupting Ability of. Andrews, Janes, Anderson.....1016–24; disc. 1025
Horsepower Gas-Turbine Electric Locomotive, Control System for a 4,500-. Warrick.....508–13
Horsepower Gas-Turbine Electric Locomotive, The Alco-GE 4,500-. Morey.....504–07
Hydroelectric Development, The Bridge River. Ingledow, Steede.....845–54
Hydroelectric Generator Excitation Experience at Grand Coulee. Killgore, Holmdahl.....855–60
Hydroelectric Power Commission of Ontario, Contributing Factors in Determining the Ratings of Power Transformers for Use on the Systems of the. Fleming, Lotimer.....1658–62; disc. 1662
Hydroelectric Power Plants, Underground. Gaiger.....1169–75
Hydroelectric Power Stations in Sweden, Underground. Rusck, Westerberg.....928–32
Hydrogen-Cooled Generators at Elevated Gas Pressures, Loading of. Snell.....186–99; disc. 199
Hydrogen-Cooled Generators, Continuous Scavenging System for. Snell, Grobel.....1625–36
Hydrogen-Cooled Rotating Electric Machines, Surface Heat-Transfer Coefficients for. Snell, Norris, Buckland.....174–85; disc. 185

I

Ice Testing of Outdoor Disconnecting Switches to Simulate Field Conditions. Owens.....1488–91; disc. 1491
Ignitron Converters for High Energy Particle Accelerators. Boyer, Marcum.....1110–14
Ignitron Pulse Equipment for Particle Accelerators. Herskind, Hudson.....992–6
Ignitron Rectifier Stations, Automatic Control of. Cham, Derr.....801–11; disc. 811
Ignitron Rectifiers, Control of Large D-C Motors Supplied From. Livingston.....205–10
Ignitron Rectifiers, High-Voltage. Mulhern....913–18
Impedance Repeater, A Negative. Merrill.....1461–6
Impedance, Series-Connected Saturable Reactor with Control Source of Comparatively High. Storm 1899–1309
Impedance, Series-Connected Saturable Reactor with Control Source of Comparatively Low. Storm.....756–65
Impedances, The Georges Phenomenon—Induction Motors with Unbalanced Rotor. Garbarino, Gross.....1569–74; disc. 1574
Impregnated Paper Cables, Terminal Risers for Solid-Type. Del Mar.....1593–7; disc. 1597
Improved Luminous Sign Cable, Development of. Roehmann, Greenfield.....350–5; disc. 355
Improved Method of Measuring Dissipation Factor and Dielectric Constant Using the Susceptance Variation Principle, An. Miller, Whelan.....491–7
Improved Reclosing Relay, An. Goff.....1480–4; disc. 1484
Improved Transmitted Carrier System for Telephone Lines of Short or Medium Length, An. Brodie 1501–04
Improvement—Electronic Excitation and Regulation of Electric Generators as Compared to Conventional Methods, Excitation. Phillips, Lambert, Pattison .....338–40; disc. 340
Improvements in the Characteristics of A-C Lead Networks for Servomechanisms. McDonald..293–300
Improvements in the Performance Calculations of Single-Phase Induction Motors, Suggested. Thacker, Gopalakrishna.....1–6; disc. 6
Impulse Circuit Breaker, Development and Testing of an Improved High-Voltage, High-Capacity. Riers .....15–25; disc. 25

Impulse Insulation Levels for High-Voltage Systems, Proposed Basic. Clem, Meador, Rudge, Powell ....953–60; disc. 960
Impulse Measurements by Repeated-Structure Networks. Dawes, Thomas, Drought....571–80; disc. 580
Incremental Losses in Power Transmission Networks, Total and. Ward, Eaton, Hale...626–31; disc. 631
Index—A Tool for Transformer Audio Noise Investigation, Harmonic. Mutschler, Madden....115–18; disc. 118
Indicating Instruments at the Servomechanisms Frequencies. Pritchett, Saunders....980–5
Indicating Instruments, Principles of Design of Log-Scale. Stimson, Taylor....1011–15
Induced Currents in High-Capacity Bus Enclosures. Killian....1388–95; disc. 1395
Inductance-Capacitance Circuits Analyzed in Terms of a Rolling-Ball Analogue, Transients in Coupled. Magnusson....1525–30
Inductance from Geometric Mean Distances, Transpositions and the Calculation of. Boast....1531–4
Inductance, Measurement and Calculation of D-C Machine Armature Circuit. Snively, Robinson ....1228–35; disc. 1235
Inductances of Synchronous Machines, Per-Unit. Kirschbaum....231–8
Induction Heating, Transverse Flux. Baker....711–19
Induction Motors, A Method of Total Design as Applied to Polyphase. Crouse....1434–7
Induction Motors, Generator Rating of. Smith....129–35
Induction Motors, Suggested Improvements in the Performance Calculations of Single-Phase. Thacker, Gopalakrishna....1–6; disc. 6
Induction Motors with Unbalanced Rotor Impedances, The Georges Phenomenon—. Garbarino, Gross ....1569–74; disc. 1574
(Industrial) Basic Patterns for Arrangement of Electric Power Systems for Steel Mills. Finison....54–9; disc. 59
Industry, The Theory of the Current Transductor and Its Application in the Aluminum. Specht, Wagner ....441–52; disc. 452
Information Theory Applied to System Design. Tuller 1612–14
Inside Dimensions for Power Cable Manholes, Critical. Halfmann....1576–80; disc. 1580
Installations—A Problem for Both Equipment and Substation Designers, Quiet Transformer. Mendenhall, Taylor....1148–52; disc. 1152
Installations on Customer's Premises, Protective Grounding of Electrical. Schirmer....657–9
Instrument Transformers, A New Dry-Type Insulation for. Pfuntner, Franck, D'Entremont....453–8
Instrumentation, Analogue Techniques for Turbojet Thrust. Van Valkenburg, Matthews....1342–6
Instrumentation and Controls for Steam Electric Power Stations, Centralized. Mallory...591–6; disc. 596
Instrumentation in Medical Research, Electrical. Benjamin, Hale, Carstensen, Tompkins....1324–7
(Instruments) A Direct Reading High-Voltage Capacitance Bridge. Foley....692–8; disc. 698
(Instruments) A New High-Accuracy Counter-Type Tachometer. Berry, Beattie....686–90; disc. 690
(Instruments) A Voltage Gradient Meter. Tremaine, Cheek....633–7; disc. 637
Instruments at the Servomechanism Frequencies, Indicating. Pritchett, Saunders....980–5
(Instruments) Noncontacting Thickness Gauge Using Beta Rays. Clapp, Bernstein....488–90
Instruments, Principles of Design of Log-Scale D-C Indicating. Stimson, Taylor....1011–15
(Instruments) Resistance Wire Strain Gauges as Elements of the Wheatstone Bridge. Petrucelly..742–4
(Instruments) The Metrotype System of Digital Recording and Telemetering. Foster....543–6; disc. 546
(Instruments) The Theory of the Current Transductor and Its Application in the Aluminum Industry. Specht, Wagner....441–52; disc. 452
(Insulated Conductors) Development of Improved Luminous Sign Cable. Roehmann, Greenfield ....350–5; disc. 355
(Insulated Conductors) Heat Transfer Study on Power Cable Ducts and Duct Assemblies. Greebler, Barnett....357–64; disc. 364
(Insulated Conductors) The Thermal Resistance Between Cables and a Surrounding Pipe or Duct Wall. Buller, Neher....342–7; disc. 347
Insulation Caused by Soil Microorganisms, Failures of Rubber. Blake, Kitchin, Pratt..748–54; disc. 754
Insulation for Instrument Transformers, A New Dry-Type. Pfuntner, Franck, D'Entremont....453–8
Insulation Level, Co-ordination of Lightning Arrester Location with Transformer. Witzke, Bliss....964–73; disc. 973
Insulation Levels for High-Voltage Systems, Proposed Basic Impulse. Clem, Meador, Rudge, Powell ....953–60; disc. 960
Insulation Levels, Lightning Arresters as a Criterion for. Rorden....84–91; disc. 91
Insulation, Margins Between Lightning Arrester Protective Levels and Transformer. Vogel....110–12; disc. 112
Insulation of Traction Motor Field Coils, A New Resilient Class-H Material for the. Reed, Tyner....1158–61
Insulation Resistance on Energized Systems, Measurement of. Brancato, McClinton....1238–42
Integral Controller for Use in Carrier-Type Servomechanisms. Cosgriff....1379–83
Interconnecting Two or More Generating Systems, The Determination and Allocation of the Capacity Benefits Resulting from. Watchorn....1180–6
Interexchange Tandem Trunking in the Los Angeles Metropolitan Area. Pfeiffer....1071–9
Interference Filters, The Design of Reactors for Radio. Knudson....1294–8
Interrupting Ability of Horn-Gap Switches. Andrews, Jahn, Anderson....1016–24; disc. 1025
Interrupting Capacity at 600 Volts A-C, New Low-Voltage Air Circuit Breaker with 50,000 Ampere. Horn, Mikos....1654–7; disc. 1657
Interrupting Capacity, High-Voltage Oil Circuit Breakers for 5,000,000 to 10,000,000-Kva. Leeds, Friedrich....70–6; disc. 76
Interrupting Capacity Low-Voltage Power Fuse, A New High. Schuck....770–6; disc. 776
Inverter, An Amplistat Regulator Applied to a 5-Kva 400-Cycle Aircraft. Morgan, Walley....1243–8; disc. 1248
Investigation and Elimination of Unusual Vibration in the Field on a Large Single-Phase Frequency Changer. Ballantyne, Allen, Baudry....1264–72; disc. 1272
Investigation, Harmonic Index—A Tool for Transformer Audio Noise. Mutschler, Madden....115–18; disc. 118
Irradiation of Spark Gaps for Voltage Measurement, The. Hardy, Craggs....584–90

J

Joints for High Temperature Operation of Railway Traction Armatures, Solderless Commutator. Reed....638–41

L

(Land Transportation) A New Resilient Class-H Material for the Insulation of Traction Motor Field Coils. Reed, Tyner....1158–61
(Land Transportation) Control System for a 4,500-Horsepower Gas-Turbine Electric Locomotive. Warrick....508–13
(Land Transportation) Locomotive Wheel-Slip and Wheel-Lock Protection. Smith....1154–7
(Land Transportation) Rectifier-Type Motive Power for Railroad Electrification. Hibbard, Whittaker, Ames....519–23; disc. 523
(Land Transportation) Rotating Electric Equipment for A Gas-Turbine Electric Locomotive. Coho..514–18
(Land Transportation) Solderless Commutator Joints for High Temperature Operation of Railway Traction Armatures. Reed....638–41
(Land Transportation) The Alco-GE 4,500 Horsepower Gas-Turbine Electric Locomotive. Morey..504–07
Lead for A-C Servo Systems with Compensation for Carrier Frequency Changes, Phase. Nothoff ....285–91; disc. 291
Lead Length and Separation in Co-ordinated Protection of Apparatus Against Lightning, Evaluation of Lightning-Arrester. Carpenter, Johnson, Saline ....933–41; disc. 941
Lead Networks for Servomechanisms, Improvements in the Characteristics of A-C. McDonald....293–300
Level Considerations, Transformer Sound. Maslin. ....1142–5; disc. 1145
Level, Co-ordination of Lightning Arrester Location with Transformer Insulation. Witzke, Bliss....964–73; disc. 973
Levels and Transformer Insulation, Margins Between Lightning Arrester Protective. Vogel....110–12; disc. 112
Levels for High-Voltage Systems, Proposed Basic Impulse Insulation. Clem, Meador, Rudge, Powell ....953–60; disc. 960
Levels, Lightning Arresters as a Criterion for Insulation. Rorden....84–91; disc. 91
Life of Steel Strand, Vibration and Fatigue. Little, MacMillan, Majerczak....1473–8; disc. 1478
Light Steel Tower Line Design. Osipovich....1513–17; disc. 1517
Lightning-Arrester Lead Length and Separation in Co-ordinated Protection of Apparatus Against Lightning, Evaluation of. Carpenter, Johnson, Saline....933–41; disc. 941
Lightning Arrester Location with Transformer Insulation Level, Co-ordination of. Witzke, Bliss....964–73; disc. 973
Lightning Arrester Protective Levels and Transformer Insulation, Margins Between. Vogel....110–12; disc. 112
Lightning Arrester Standard, New. Stewart, Defandorf....525–6
Lightning Arresters as a Criterion for Insulation Levels. Rorden....84–91; disc. 91
Lightning Performance of Boulder 287.5-Kv Transmission Lines, Thirteen-Year. Blakeslee, Kanouse ....796–9; disc. 800
Lightning Performance of Transmission Lines, A Method of Estimating. (Committee Report)....1187–95; disc. 1195
Lightning Surges on Power Systems and Their Suppression, Some Aspects of. Kaneff....1544–9
Limit, Effect of Buck-Boost Voltage Regulator on Steady-State Power. Concordia..380–4; disc. 384
Limit Switch, An Environment-Free 120-Volt D-C High Performance. Stuelpnagel....1289–93
Limitations of Relaying and High-Speed Reclosing on Long and Heavily Loaded Transmission Lines, Consideration of Requirements and. Parks, Brownlee....103–07; disc. 107
Line Design, Light Steel Tower. Osipovich....1513–17; disc. 1517
Line Protection of Short Lines of the Metropolitan Area of a Typical System, Transmission-. Marter ....468–71; disc. 471
Line Vibration, Use of Techniques from Electrical Analogues in the Study of Transmission. Lummis, Klopfenstein....1676–80
Linear Electronic Circuits, The Design of Broad-Band Transformers for. Lord....1005–10
Linearly Varying Elements, Stability of Servomechanisms with. Kirby....1662–7; disc. 1667
Lines, A Method of Estimating Lightning Performance of Transmission. (Committee Report)....1187–95; disc. 1195
Lines, Consideration of Requirements and Limitations of Relaying and High-Speed Reclosing on Long and Heavily Loaded Transmission. Parks, Brownlee ....103–07; disc. 107
Lines of Short or Medium Length, An Improved Transmitted Carrier System for Telephone. Brooke 1501–04
Lines, Relay Protection for Medium Length High-Voltage Transmission. Klaghorn....461–5; disc. 465
Lines, Steady-State Waves on Transmission. Waidelich....1521–4
Lines, Thirteen-Year Lightning Performance of Boulder 287.5-Kv Transmission. Blakeslee, Kanouse....796–9; disc. 800
Liquid Cooling of A-C Turbine Generators. Part II. Fechheimer....165–71; disc. 171
(Part I–1947)
Load for Testing Rectifiers, Synthetic. Tetherow..642–4
Loading in Sealed Transformers, Variations of Tank Pressure with Transformer. Tipton....1669–73; disc. 1673
Loading of Hydrogen-Cooled Generators at Elevated Gas Pressures. Snell....186–99; disc. 199
Loads on Voltage Changes Produced by Single-Phase Loads, Effect of Three-Phase Motor. Faucett, Fisher, Helm....1467–72
Loads, Regulation of A-C Generators with Suddenly Applied. Part II. Harder, Cheek, Clayton....395–405; disc. 405
(Part I–1944)
Local Wire Video Television Networks. Nebel..1451–60
Lock Protection, Locomotive Wheel-Slip and Wheel-Smith....1154–7
Locomotive, Control System for a 4,500-Horsepower Gas-Turbine Electric. Warrick....508–13
Locomotive, Rotating Electric Equipment for a Gas-Turbine Electric. Coho....514–18
Locomotive, The Alco-GE 4,500-Horsepower Gas-Turbine Electric. Morey....504–07
Locomotive Wheel-Slip and Wheel-Lock Protection. Smith....1154–7
Locus Method, Control System Synthesis by Root. Evans....66–9
Log Carriage Drive, Amplidyne-Controlled. Vincent ....1124–9; disc. 1129
Log-Scale D-C Indicating Instruments, Principles of Design of. Stimson, Taylor....1011–15
Long-Distance Power Transmission. Crary....834–40; disc. 840
Los Angeles Metropolitan Area, Interexchange Tandem Trunking in the. Pfeiffer....1071–9
Los Angeles, Power System Planning in the City of. Williams, Kanouse....900–07; disc. 907
Loss on Conductors for Operation Above 230 Kv, Desert Measurements of Corona. Peterson, Cozzens, Carroll....872–8; disc. 878
Losses in Power Transmission Networks, Total and Incremental. Ward, Eaton, Hale..626–31; disc. 631
Low Impedance, Series-Connected Saturable Reactor with Control Source of Comparatively. Storm 756–65
Low Speeds, Synchronous Machine Damping Torque at. Concordia....1550–3

Low-Voltage Air Circuit Breaker with 50,000 Ampere Interrupting Capacity at 600 Volts A-C, New. Horn, Mikos....1654–7; disc. 1657
Low-Voltage Air Circuit Breakers, An Air Delayed Selective Overcurrent Tripping Device for. Tremblay, Horn....1649–53
Low-Voltage Power Fuse, A New High-Interrupting Capacity. Shuck....770–6; disc. 776
Luminous Sign Cable, Development of Improved. Roehmann, Greenfield....350–5; disc. 355

M

Machine Armature Circuit Inductance, Measurement and Calculation of D-C. Snively, Robinson....1228–35; disc. 1235
Machine Armature Windings, Current in Equalizer Connections of D-C. Linville, Strang....1219–26; disc. 1226
Machine, Classification of the Reference Frames of a Synchronous. Kron....720–7
Machine Damping Torque at Low Speeds, Synchronous. Concordia....1550–3
Machine Short Circuits, Analysis of Synchronous. Camburn, Gross....671–8; disc. 678
Machines and Their Application, Spring and Damping Coefficients of Synchronous. Kilgore, Whitney....226–9; disc. 229
Machines, Per-Unit Inductances of Synchronous. Kirschbaum....231–4
Machines, Power Reactance for Salient-Pole Synchronous. Mikhail....235–8
Machines, Surface Heat-Transfer Coefficients for Hydrogen-Cooled Rotating Electric. Snell, Norris, Buckland....174–85; disc. 185
Magnetic Amplifier Frequency Control, A. Johnson, Schafer....613–15
Magnetic Amplifiers, An Analysis of Transients and Feedback in. Johnson, Latson....604–11; disc. 611
Magnetic Amplifiers, An Analysis of Transients in. VerPlanck, Finzi, Beaumariage....498–503
Magnetic Amplifiers, Determination of Steady-State Performance of Self-Saturating. Smith....1309–17
Magnetic Amplifiers, General Characteristics of. Finzi, Beaumariage....919–27
Magnetic Amplifiers, Response Time of. Harder, Horton....1130–8; disc. 1138
Magnetic-Fluid Clutch Servomechanisms, Characteristics of Some. Parziale, Tilton....150–7
Magnets, The Operating Speed of D-C Brake. Ryan, Spitler....1253–7
Main Power Transformers for Generating Stations, The Choice of. Dillow, Butler....781–5; disc. 785
Manholes, Critical Inside Dimensions for Power Cable. Halfmann....1576–80; disc. 1580
Manufacturer's Viewpoint, Aluminum Conductors from an Aircraft. Schumacher....1335–41
Mappers, The Further Development of Fluid. Moore....1615–24
Margins Between Lightning Arrester Protective Levels and Transformer Insulation. Vogel....110–12; disc. 112
Maximum Short-Circuit Current of D-C Motors and Generators. (Committee Report)....146–9
Mean Distances, Transpositions and the Calculation of Inductance from Geometric. Boast....1531–4
Measurement and Calculation of D-C Machine Armature Circuit Inductance. Snively, Robinson....1228–35; disc. 1235
Measurement by the Hook-on Method, Power. Corson, Nylander....699–702
Measurement of Bandwidth, The Direct. Ammerman....27–31
Measurement of Insulation Resistance on Energized Systems. Brancato, McClinton....1238–42
Measurement, The Irradiation of Spark Gaps for Voltage. Hardy, Craggs....584–90
Measurements by Repeated Structure Networks, Impulse. Dawes, Thomas, Drought....571–80; disc. 580
Measurements of Corona Loss on Conductors for Operation Above 230 Kv, Desert. Peterson, Cozzens, Carroll....872–8; disc. 878
Measurements on Polyphase and Multiconductor Cable Using Single-Phase Bridges, Power Factor. Greenfield....680–5; disc. 685
Measuring Dissipation Factor and Dielectric Constant Using the Susceptance Variation Principle, An Improved Method of. Miller, Whelan....491–7
Measuring the Ratio and Phase Angle of Current Transformers, A Primary Method of. Brownlee....459–60
Mechanisms, Electrode Control and Associated Operating. Hanff....567–70; disc. 570
Media Separation Process, Electric Equipment for Heavy-. Bean, Blind....1421–9
Medical Research, Electrical Instrumentation in. Benjamin, Hale, Carstensen, Tompkins....1324–7
Medium-Haul Carrier Telephone System, A. Smith....1505–12
Megacycles, Microwave Systems for 960 and 2,000. Rector, Sutter....1100–08; disc. 1108
Message Accounting System, Fundamentals of the Automatic Telephone. Meszar....255–68; disc. 269
Metal-Clad Switchgear, A New Grounding and Testing Device for. Krida, McCurry....407–12; disc. 412
Metal-Clad Switchgear Serving Oil Refinery Motors During Power System Disturbances, Automatic Control of. Horsfall, Thompson, Mills, Bobo....1600–03; disc. 1603
(Metal) Electric Equipment for Heavy-Media Separation Process. Bean, Blind....1421–9
Meter, A Voltage Gradient. Tremaine, Cheek....633–7; disc. 637
Metering Purposes, A Survey of Bushing-Type Current Transformers for. Camilli....429–40
Meters, A New Device for Calibrating Watt-Hour. Robison, Wickham....732–4
Method, Control System Synthesis by Root Locus. Evans....66–9
Method, Determination of Reserve Capacity by the Probability. Calabrese....1681–8; disc. 1688
Method for Analyzing and Synthesizing Contactor Servomechanisms, A Frequency Response. Kochenburger....270–83; disc. 283
Method of Estimating Lightning Performance of Transmission Lines, A. (Committee Report)....1187–95; disc. 1195
Method of Measuring Dissipation Factor and Dielectric Constant Using the Susceptance Variation Principle, An Improved. Miller, Whelan....491–7
Method of Measuring the Ratio and Phase Angle of Current Transformers, A Primary. Brownlee....459–60
Method of Total Design as Applied to Polyphase Induction Motors, A. Crouse....1434–7
Method, Power Measurement by the Hook-On. Corson, Nylander....699–702
Metropolitan Area of a Typical System, Transmission-Line Protection of Short Lines of the. Marter....468–71; disc. 471
Metrotype System of Digital Recording and Telemetering, The. Foster....543–6; disc. 546
Microorganisms, Failures of Rubber Insulation Caused by Soil. Blake, Kitchin, Pratt....748–54; disc. 754
Microwave Applications to Bonneville Power Administration System. Stevens, Stringfield....1088–99
Microwave Channel for Voice Communication, Relaying, Telemetering, and Supervisory Control, Field Testing a. Pattison, Reagan, Leyland, Gunter....945–51; disc. 951
Microwave Systems for 960 and 2,000 Megacycles. Rector, Sutter....1100–08; disc. 1108
Mills, Basic Patterns for Arrangement of Electric Power Systems for Steel. Finison....54–9; disc. 59
Modern Carrier Current Test Equipment and Its Application. Brinton....777–80
Motive Power for Railroad Electrification, Rectifier-Type. Hibbard, Whittaker, Ames....519–23; disc. 523
Motor-Driven Exciters, Excitation System Performance with. Mellor, Temoshok....321–7
Motor Drives, Rectifier Equipment for Electronic D-C. Mulhern, Crawford....211–15
Motor Drives to Printing Presses, Application of Electronic. Johnson, Stacey....216–19
Motor Field Coils, A New Resilient Class-H Material for the Insulation of Traction. Reed, Tyner....1158–61
Motor Loads on Voltage Changes Produced by Single-Phase Loads, Effect of Three-Phase. Faucett, Fisher, Helm....1467–72
Motor with Space Harmonics, Equivalent Circuits of the Shaded-Pole. Kron....735–41
Motors—A Design Method, A-C Series. Chang, Karr....1257–61; disc. 1261
Motors, A Method of Total Design as Applied to Polyphase Induction. Crouse....1434–7
Motors and Generators, Maximum Short-Circuit Current of D-C. (Committee Report)....146–9
Motors During Power System Disturbances, Automatic Control of Metal-Clad Switchgear Serving Oil Refinery. Horsfall, Thompson, Mills, Bobo....1600–03; disc. 1603
Motors, Generator Rating of Induction. Smith....129–35
Motors Need Test Equipment, Aircraft Electric. Ross....1359–64
Motors, Suggested Improvements in the Performance Calculations of Single-Phase Induction. Thacker, Gopalakrishna....1–6; disc. 6
Motors Supplied from Ignitron Rectifiers, Control of Large D-C. Livingston....205–10
Motors with Unbalanced Rotor Impedances, The Goerges Phenomenon—Induction. Garbarino, Gross....1562–74; disc. 1574
Multicomponent Fractionation Calculations, Analogue Computer for. Goela, Calvert....97–103
Multiconductor Cable Using Single-Phase Bridges, Power Factor Measurements on Polyphase and. Greenfield....680–5; disc. 685
Multiplexing Equipment with High Stability Carrier Supply, A Low Noise and Distortion Audio. Beale....1028–37; disc. 1037
Multistation Supervisory Control, Telemetering, and Communication on Single-Frequency Carrier Channel. Derr, Wren, Kresser....1115–21; disc. 1121

N

Nature and Physical Concepts of Thyratron Deionization Time, Statistical. Romanowitz, Dow....368–79
Negative Impedance Repeater, A. Merrill....1461–6
Networks for Servomechanisms, Improvements in the Characteristics of A-C Lead. McDonald....293–300
Networks, Impulse Measurements by Repeated Structure. Dawes, Thomas, Drought....571–80; disc. 580
Networks, Local Wire Video Television. Nebel....1451–60
Networks, Total and Incremental Losses in Power Transmission. Ward, Eaton, Hale....626–31; disc. 631
Neutral Grounding Devices, Development of the Standard for. Clem....976–9
Neutral Potentials, Rural. Waghorne....660–3; disc. 663
New Lightning Arrester Standard. Stewart, Defandorf....525–6
New Line of Orthomagnetic Bushing-Type Current Transformers, A. Farr....424–8
New 69-Kv Oil Blast Circuit Breaker, A. Rietz, Balentine....416–23; disc. 423
New Techniques on the Anacom—Electric Analog Computer. Harder, Carleton....547–56
Noise and Distortion Audio Multiplexing Equipment with High Stability Carrier Supply, A Low. Beale....1028–37; disc. 1037
Noise and Its Confinement, Transformer. McLean....1409–15; disc. 1415
Noise in Transformers in Residential and Commercial Areas, Audio. Baugh....121–6; disc. 126
Noise Investigation, Harmonic Index—A Tool for Transformer Audio. Mutschler, Madden....115–18; disc. 118
Noise of Power Transformers, Audible. Gordy....45–50; disc. 50
Noise on Aircraft, Tracking Radio. Owen....1249–52
Noncontacting Thickness Gauge Using Beta Rays. Clapp, Bernstein....488–90
Nonlinear Element, An Electric Analogue Computer Using the Photo Cell as a. Koenig....1606–11
Nonlinear Servomechanisms, An Electronic Simulator for. Edwards, Johnson....300–05; disc. 306
Number 5 Crossbar Dial Telephone Switching System, The. Korn, Ferguson....244–54

O

Office Buildings for Small Communities, Dial Telephone Central. Reese, Roys....1535–9
Office Equipment, General Aspects of Community Dial. Burkett....1540–3
Officers and Committees for 1950–51....1717–36
Offices, Simplified Subscriber Toll Dialing for Low-Rate Low-Density Toll Circuits Between Community Dial. Brooke, Blackhall, Blashfield....1417–20
Oil Blast Circuit Breaker, A New 69-Kv. Rietz, Balentine....416–23; disc. 423
Oil Circuit Breakers for 5,000,000 to 10,000,000-Kva Interrupting Capacity, High-Voltage. Leeds, Friedrich....70–6; disc. 76
Oil Refinery Motors During Power System Disturbances, Automatic Control of Metal-Clad Switchgear Serving. Horsfall, Thompson, Mills, Bobo....1600–03; disc. 1603
Oil Temperature in a Transformer, Determination of Effective. Beavers....703–08; disc. 708
Oil, Transformers. Treanor, Raab....1060–70; disc. 1070
Operating Mechanisms, Electrode Control and Associated. Hanff....567–70; disc. 570
Operating Speed of D-C Brake Magnets, The. Ryan, Spitler....1253–7
Operation of Central Control Rooms, Design and. Borgel....598–602; disc. 602
Operation of Graphitizing Furnaces, Electric Equipment and. Cole....563–6
Operation of Power Transformers on American Gas and Electric Company System, Selection, Design, and. Lane, Gross, Pugh....786–93; disc. 793
Operation of Railway Traction Armatures, Solderless Commutator Joints for High Temperature. Reed....638–41
Orthomagnetic Bushing-Type Current Transformers, A New Line of. Farr....424–8
Outdoor Disconnecting Switches to Simulate Field Conditions, Ice Testing of. Owens....1488–91; disc. 1491
Overcurrent Tripping Device for Low-Voltage Air Circuit Breakers, An Air Delayed Selective. Tremblay, Horn....1649–53

P

Paper Cables, Terminal Risers for Solid-Type Impregnated. Del Mar.....1592-7; disc. 1597
Particle Accelerators, Ignitron Converters for High Energy. Boyer, Marcum.....1110-14
Particle Accelerators, Ignitron Pulse Equipment for. Herskind, Hudson.....992-6
Patterns for Arrangement of Electric Power Systems for Steel Mills, Basic. Finison.....54-9; disc. 59
Per-Unit Inductances of Synchronous Machines. Kirschbaum.....231-4
Perception Currents, Effect of Frequency on. Dalziel, Mansfield.....1162-8
Performance by A-C Components, The Extension of Amplistat. Morgan, Ogle, Wattenberger...986-91
Performance Calculations of Single-Phase Induction Motors, Suggested Improvements in the. Thacker, Gopalakrishna.....1-6; disc. 6
Performance of Low-Voltage, An Environment-Free 120-Volt D-C High. Stuelpnagel.....1289-93
Performance of Boulder 287.5-Kv Transmission Lines, Thirteen-Year Lightning. Blakeslee, Kanouse.....796-9; disc. 800
Performance of Self-Saturating Magnetic Amplifiers, Determination of Steady-State. Smith.....1309-17
Performance of the Selsyn Generator Control Transformer System, Static Accuracy. Kronacher.....645-53; disc. 653
Performance of Transmission Lines, A Method of Estimating Lightning. (Committee Report).....1187-95; disc. 1195
Performance with Motor-Driven Exciters, Excitation System. Mellor, Temoshok.....321-7
Phase and Ground Distance Relaying, Combined. New.....37-42; disc. 42
Phase Angle of Current Transformers, A Primary Method of Measuring the Ratio and. Brownlee.....459-60
Phase Lead for A-C Servo Systems with Compensation for Carrier Frequency Changes. Nottbolf.....285-91; disc. 291
Phase Relays, A Study of Directional Element Connections for. Sonnemann.....1438-50; disc. 1450
Phenomenon—Induction Motors with Unbalanced Rotor Impedances, The Goerges. Garbarino, Gross.....1569-74; disc. 1574
Photo Cell as a Nonlinear Element, An Electric Analogue Computer Using the. Koenig.....1606-11
Physical Concepts of Thyratron Deionization Time, Statistical Nature and. Romanowitz, Dow.....368-79
Pile Voltage Regulators, Dynamic Characteristics of Carbon. Mills.....1347-52; disc. 1352
Pipe or Duct Wall, The Thermal Resistance Between Cables and a Surrounding. Buller, Neher.....342-7; disc. 347
Planning in the City of Los Angeles, Power System. Williams, Kanouse.....900-07; disc. 907
Plants, Centralized Control Board for Steam-Electric Generating. Lowe, Hodgkins...1396-9; disc. 1399
Plants, Underground Hydroelectric Power. Gisiger.....1169-75
Pole Motor with Space Harmonics, Equivalent Circuits of the Shaded-. Kron.....735-41
Pole Synchronous Machines, Potier Reactance for Salient. Mikhail.....235-8
Polyphase and Multiconductor Cable Using Single-Phase Bridges, Power Factor Measurements on. Greenfield.....680-5; disc. 685
Polyphase Induction Motors, A Method of Total Design as Applied to. Crouse.....1434-7
Polyphase Rectifiers, Effects of Supply Line Unbalance on the Filtered Output Ripple of. Hooper, McAdie.....766-70
Potentials, Rural Neutral. Waghorne...660-3; disc. 663
Potier Reactance for Salient-Pole Synchronous Machines. Mikhail.....235-8
Power Arcs in Large Air Gaps, Dielectric Recovery Characteristics of. McCann, Conner, Ellis.....616-24; disc. 624
Power Cable Ducts and Duct Assemblies, Heat Transfer Study on. Greebler, Barnett.....357-64; disc. 364
Power Cable Manholes, Critical Inside Dimensions for. Halfmann.....1576-80; disc. 1580
Power Converters, Protection of Electronic. (Committee Report).....813-29
Power Factor Measurements on Polyphase and Multiconductor Cable Using Single-Phase Bridges. Greenfield.....680-5; disc. 685
Power for Railroad Electrification, Rectifier-Type Motive. Hibbard, Whittaker, Ames...519-23; disc. 523
Power Fuse, A New High Interrupting Capacity Low-Voltage. Schuck.....770-6; disc. 776
(Power Generation) Bus Transfer Tests on 2,300-Volt Station Auxiliary System. Johnson, Thompson.....386-90; disc. 390
Power Generation, Control of Gas Turbines for. Hoffmann, Mellor, Starkey.....1637-41; disc. 1641
(Power Generation) Design and Operation of Central Control Rooms. Borgel.....597-602; disc. 602
(Power Generation) Design and Test on Electronic Exciter Supplied from Common Shaft-Driven Generator. Colalaco, Johnson, Reilly...328-35; disc. 335
(Power Generation) Excitation Improvement—Electronic Excitation and Regulation of Electric Generators as Compared to Conventional Methods. Phillips, Lambert, Pattison.....338-40; disc. 340
(Power Generation) Excitation System Performance with Motor-Driven Exciters. Mellor, Temoshok.....321-7
(Power Generation) Hydroelectric Generator Excitation Experience at Grand Coulee. Killgore, Holmdahl.....855-60
(Power Generation) Induced Currents in High-Capacity Bus Enclosures. Killian.....1388-95; disc. 1395
(Power Generation) Regulation of A-C Generators with Suddenly Applied Loads. Part II. Harder, Cheek Clayton...395-405; disc. 405 (Part I-1944)
(Power Generation) The Bridge River Hydroelectric Development. Ingledow, Steede.....845-54
Power Limit, Effect of Buck-Boost Voltage Regulator on Steady-State. Concordia.....380-4; disc. 384
Power Measurement by the Hook-On Method. Corson, Nylander.....698-702
Power Plants, Underground Hydroelectric. Gisiger.....1169-75
Power Stations, Centralized Instrumentation and Controls for Steam Electric. Mallory...591-6; disc. 596
Power Stations in Sweden, Underground Hydroelectric. Ruseck, Westerberg.....928-32
Power System Disturbances, Automatic Control of Metal-Clad Switchgear Serving Oil Refinery Motors During. Horsfall, Thompson, Mills, Bobo.....1600-03; disc. 1603
Power System Planning in the City of Los Angeles. Williams, Kanouse.....900-07; disc. 907
Power Systems and Their Suppression, Some Aspects of Lightning Surges on. Kaneff.....1544-9
Power Systems for Steel Mills, Basic Patterns for Arrangement of Electric. Finison.....54-9; disc. 59
Power Systems—Fundamentals and Basic Design Considerations, Underground Conduit for Electric. Watkins.....1582-90; disc. 1590
Power Transformer Formed Cores, Single-Phase. Gordy, Somerville.....1384-7
Power Transformers, Audible Noise of. Gordy.....45-50; disc. 50
Power Transformers for Generating Stations, The Choice of Main. Dillow, Butler.....781-5; disc. 785
Power Transformers for Use on the Systems of the Hydro-Electric Power Commission of Ontario, Contributing Factors in Determining the Ratings of. Fleming, Lotimer.....1658-62; disc. 1662
Power Transformers on American Gas and Electric Company System, Selection, Design, and Operation of. Lane, Gross, Pugh.....786-93; disc. 793
Power Transformers on the System of the Bonneville Power Administration, Application and Handling of Very Large. Stevens.....158-63; disc. 163
Power Transformers, Selection and Application of. Seelye.....830-3
Power Transmission, Long-Distance. Crary.....834-40; disc. 840
Power Transmission Networks, Total and Incremental Losses in. Ward, Eaton, Hale...626-31; disc. 631
Practical Experiences with Resonant Grounding in a Large 34.5-Kv System. Brown, Gross.....1401-06; disc. 1406
Practices and Economical Switching Station Arrangements of the Bureau of Reclamation, Relaying. Morgan, World.....865-70; disc. 870
Premises, Protective Grounding of Electrical Installations on Customer's. Schirmer.....657-9
Presses, Application of Electronic Motor Drives to Printing. Johnson, Stacey.....216-19
Pressure with Transformer Loading in Sealed Transformers, Variations of Tank. Tipton.....1669-73; disc. 1673
Pressures, Loading of Hydrogen-Cooled Generators at Elevated Gas. Snell.....186-99; disc. 199
Primary Method of Measuring the Ratio and Phase Angle of Current Transformers, A. Brownlee.....459-60
Principle, An Improved Method of Measuring Dissipation Factor and Dielectric Constant Using the Susceptance Variation. Miller, Whelan.....491-7
Principles of Design of Log-Scale D-C Indicating Instruments. Stimson, Taylor.....1011-15
Printing Presses, Application of Electronic Motor Drives to. Johnson, Stacey.....216-19
Printing Telegraph Tape-to-Page Translator, A. Frost.....79-83
Probability Method, Determination of Reserve Capacity by the. Calabrese.....1681-8; disc. 1688
Problems and Their Solution on Turbine-Generator Units and Auxiliaries of the Consolidated Edison System, Thrust Bearing. Driscoll, Otten.....1642-7; disc. 1647
Problems, Special Devices Aid Differential Analyzer Solution of Complex. Cook, Kirchmayer, Weygandt.....1365-70; disc. 1370
Process, Electric Equipment for Heavy-Media Separation. Bean, Blind.....1421-9
Production Testing on Large D-C Apparatus, Quick and Accurate. Baldwin, Barnhart.....136-8
Program, The Bonneville Power Administration Relaying and Reclosing. Diemond, Wylie.....1039-46; disc. 1046
Progress Report on Tidd 500-Kv Test Project of the American Gas and Electric Company—Corona, Radio Influence, and Other Factors. Sporn, Monteith.....891-7; disc. 897
Proposed Basic Impulse Insulation Levels for High Voltage Systems. Clem, Meador, Rudge, Powell.....953-60; disc. 960
Protection for Medium Length High-Voltage Transmission Lines, Relay. Kinghorn...461-5; disc. 465
Protection, Locomotive Wheel-Slip and Wheel-Lock. Smith.....1154-7
Protection of Apparatus Against Lightning, Evaluation of Lightning-Arrester Lead Length and Separation in Co-ordinated. Carpenter, Johnson, Saline.....933-41; disc. 941
Protection of Cable-Connected Equipment, Surge. Witzke, Bliss.....527-38; disc. 539
Protection of Electronic Power Converters. (Committee Report).....813-29
Protection of Short Lines of the Metropolitan Area of a Typical System, Transmission-Line. Marter.....468-71; disc. 471
Protection, Sensitive Ground. (Committee Report).....473-5; disc. 475
Protection, Theory and Application of Transformer Differential. McKenna.....1197-1202
(Protective Devices) Co-ordination of Lightning Arrester Location with Transformer Insulation Level. Witzke, Bliss.....964-73; disc. 973
(Protective Devices) Development of the Standard for Neutral Grounding Devices.....976-9
(Protective Devices) Lightning Arresters as a Criterion for Insulation Levels. Rorden.....84-91; disc. 91
(Protective Devices) New Lightning Arrester Standard. Stewart, Defandorf.....525-6
(Protective Devices) Practical Experiences With Resonant Grounding in a Large 34.5-Kv System. Brown, Gross.....1401-06; disc. 1406
Protective Grounding of Electrical Installations on Customer's Premises. Schirmer.....657-9
Protective Levels and Transformer Insulation, Margins Between Lightning Arrester. Vogel.....110-12; disc. 112
Pulse Equipment for Particle Accelerators, Ignitron. Herskind, Hudson.....992-6

Q

Quiet Transformer Installations—A Problem for Both Equipment and Substation Designers. Mendenhall, Taylor.....1148-52; disc. 1152

R

Radio Influence, and Other Factors, Progress Report on Tidd 500-Kv Test Project of the American Gas and Electric Company—Corona. Sporn, Monteith.....891-7; disc. 897
Radio Interference Filters, The Design of Reactors for. Knudson.....1294-8
Radio Noise on Aircraft, Tracking. Owen.....1249-52
Railroad Electrification, Rectifier-Type Motive Power for. Hibbard, Whittaker, Ames...519-23; disc. 523
Railway Traction Armatures, Solderless Commutator Joints for High Temperature Operation of. Reed.....638-41
Range A-C Electric Systems for Aircraft, Wide Speed. James, Judkins, Merahon.....1353-8; disc. 1358
Rate Low-Density Toll Circuits Between Community Dial Offices, Simplified Subscriber Toll Dialing for Low-. Brooke, Blackhall, Blashfield.....1417-20
Rating of Induction Motors, Generator. Smith...129-35
Ratings for Transformers, Development of Preferred Voltage. St. Clair, Jalonack...1049-59; disc. 1059
Ratings of Power Transformers for Use on the Systems of the Hydro-Electric Power Commission of Ontario, Contributing Factors in Determining the. Fleming, Lotimer.....1658-62; disc. 1662
Ratio and Phase Angle of Current Transformers, A Primary Method of Measuring the. Brownlee.....459-60
Rays, Noncontacting Thickness Gauge Using Beta. Clapp, Bernstein.....488-90
Reactance for Salient-Pole Synchronous Machines, Potier. Mikhail.....235-8
Reactor with Control Source of Comparatively High Impedance, Series-Connected Saturable. Storm.....1299-1309
Reactor with Control Source of Comparatively Low Impedance, Series Connected Saturable. Storm.....756-65
Reactors for Radio Interference Filters, The Design of. Knudson.....1294-8

Reading High-Voltage Capacitance Bridge, A Direct. Foley ..... 692–8; disc. 698
Receiver, A New Electronic Telegraph Regenerative. Ostendorf ..... 32–6; disc. 36
Reclosing on Long and Heavily Loaded Transmission Lines, Consideration of Requirements and Limitations of Relaying and High-Speed. Parks, Brownlee ..... 103–07; disc. 107
Reclosing Program, The Bonneville Power Administration Relaying and. Diemond, Wylie ..... 1039–46; disc. 1046
Reclosing Relay, An Improved. Goff ..... 1480–4; disc. 1484
Recording and Telemetering, The Metrotype System of Digital. Foster ..... 543–6; disc. 546
Recovery Characteristics of Power Area in Large Air Gaps, Dielectric. McCann, Conner, Ellis ..... 616–24; disc. 624
Rectangular Cross-Section, The Calculation of the Capacitance of Coaxial Cylinders of. Anderson 728–31
Rectifier Equipment and Control for Tube Testing, High-Voltage. Durand 909–12
Rectifier Equipment for Electronic D-C Motor Drives. Mulhern, Crawford 211–13
Rectifier Stations, Automatic Control of Ignitron. Cham, Derr ..... 801–11; disc. 811
Rectifier-Type Motive Power for Railroad Electrification. Hibbard, Whittaker, Ames. 519–23; disc. 523
Rectifiers, Control of Large D-C Motors Supplied from Ignitron. Livingston 205–10
Rectifiers, Effects of Supply Line Unbalance on the Filtered Output Ripple of Polyphase. Hooper, McAdie 766–70
Rectifiers, High-Voltage Ignitron. Mulhern 913–18
Rectifiers, Synthetic Load for Testing. Tetherow 642–4
Reference Frames of a Synchronous Machine, Classification of the. Kron 720–7
Refinery Motors During Power System Disturbances, Automatic Control of Metal-Clad Switchgear Serving Oil. Horsfall, Thompson, Mills, Bobo ..... 1600–03; disc. 1603
Regenerative Receiver, A New Electronic Telegraph. Ostendorf ..... 32–6; disc. 36
Regulated Aircraft D-C System, Transient Analysis of a Voltage-. Scorgie 1318–23
Regulation of A-C Generators with Suddenly Applied Loads. Part II. Harder, Cheek, Clayton ..... 395–405; disc. 405
(Part I–1944)
Regulation of Electric Generators as Compared to Conventional Methods, Excitation Improvement—Electronic Excitation and. Phillips, Lambert, Pattison ..... 338–40; disc. 340
Regulations, and Safe Application, Electric Fences—Their Hazards, Types. Dalziel 8–15
Regulator Applied to a 5-Kva 400-Cycle Aircraft Inverter, An Amplistat. Morgan, Walley ..... 1243–8; disc. 1248
Regulator on Steady-State Power Limit, Effect of Buck-Boost Voltage. Concordia ..... 380–4; disc. 384
Regulators, Dynamic Characteristics of Carbon Pile Voltage. Mills ..... 1347–52; disc. 1352
Regulators, Stability of Voltage. Bothwell ..... 1430–3; disc. 1433
Relay, An Improved Reclosing. Goff ..... 1480–4; disc. 1484
Relay Protection for Medium Length High-Voltage Transmission Lines. Kingborn ..... 461–5; disc. 465
Relay Sensitivity Adjuster, Differential. Headley ..... 1203–05; disc. 1205
(Relay) Transmission-Line Protection of Short Lines of the Metropolitan Area of a Typical System. Marter ..... 468–71; disc. 471
Relaying and High-Speed Reclosing on Long and Heavily Loaded Transmission Lines, Consideration of Requirements and Limitations of. Parks, Brownlee ..... 103–07; disc. 107
Relaying and Reclosing Program, The Bonneville Power Administration. Diemond, Wylie ..... 1039–46; disc. 1046
Relaying, Combined Phase and Ground Distance. New ..... 37–42; disc. 42
Relaying Practices and Economical Switching Station Arrangements of the Bureau of Reclamation. Morgan, World ..... 865–70; disc. 870
Relaying Telemetering, and Supervisory Control, Field Testing a Microwave Channel for Voice Communication. Pattison, Reagan, Leyland, Gunter ..... 945–51; disc. 951
Relays, A Study of Directional Element Connections for Phase. Sonnemann ..... 1438–50; disc. 1450
(Relays) Sensitive Ground Protection. (Committee Report) ..... 473–5; disc. 475
(Relays) Theory and Application of Transformer Differential Protection. McKenna 1197–1202
Repeated Structure Networks, Impulse Measurements by. Dawes, Thomas, Drought ..... 571–80; disc. 580
Repeater, A Negative Impedance. Merrill 1461–6
Report of the Board of Directors 1690–1716
Report on Tidd 500-Kv Test Project of the American Gas and Electric Company—Corona, Radio Influence, and Other Factors, Progress. Sporn, Monteith ..... 691–7; disc. 897
Requirements and Limitations of Relaying and High-Speed Reclosing on Long and Heavily Loaded Transmission Lines, Consideration of. Parks, Brownlee ..... 103–07; disc. 107
Research, Electrical Instrumentation in Medical. Benjamin, Hale, Carstensen, Tompkins 1324–7
Reserve Capacity by the Probability Method, Determination of. Calabrese ..... 1681–8; disc. 1688
Residential and Commercial Areas, Audio Noise in Transformers in. Baugh ..... 121–6; disc. 126
Resistance Between Cables and a Surrounding Pipe or Duct Wall, The Thermal. Buller, Neher ..... 342–7; disc. 347
Resistance Commutation. Olney ..... 1207–15; disc. 1215
Resistance on Energized Systems, Measurement of Insulation. Brancato, McClinton 1238–42
Resilient Class-H Material for the Insulation of Traction Motor Field Coils, A New. Reed, Tyner 1158–61
Resistance Wire Strain Gauges as Elements of the Wheatstone Bridge. Petruccelly 742–4
Resonant Grounding in a Large 34.5-Kv System, Practical Experiences with. Brown, Gross ..... 1401–06; disc. 1406
Response Method for Analysing and Synthesizing Contactor Servomechanisms, A Frequency. Kochenburger ..... 270–83; disc. 283
Response of Direct-Current Dynamos, Transient. Koenig ..... 139–44; disc. 144
Response Time of Magnetic Amplifiers. Harder, Hurton ..... 1130–8; disc. 1138
Risers for Solid-Type Impregnated Paper Cables, Terminal. Del Mar ..... 1592–7; disc. 1597
River Hydroelectric Development, The Bridge. Ingledow, Steede 845–54
Rolling-Ball Analogue, Transients in Coupled Inductance-Capacitance Circuits Analysed in Terms of a. Magnusson 1525–30
Rooms, Design and Operation of Central Control. Borgel ..... 598–602; disc. 602
Root Locus Method, Control System Synthesis by. Evans 66–9
Rotating Electric Equipment for a Gas-Turbine Electric Locomotive. Cobo 514–18
Rotating Electric Machines, Surface Heat-Transfer Coefficients for Hydrogen-Cooled. Snell, Norris, Buckland ..... 174–85; disc. 185
(Rotating Machinery) A-C Series Motors—A Design Method. Chang, Karr ..... 1257–61; disc. 1261
(Rotating Machinery) An Experimental and Analytical Study of Turbine Generator Rotor Ventilation. Fechheimer 1563–9
(Rotating Machinery) Design Calculations for A-C Generators. Ginsberg ..... 1274–80; disc. 1280
(Rotating Machinery) Loading of Hydrogen-Cooled Generators at Elevated Gas Pressures. Snell ..... 186–99; disc. 199
(Rotating Machinery) Measurement of Insulation Resistance on Energized Systems. Brancato, McClinton 1238–42
(Rotating Machinery) Quick and Accurate Production Testing on Large D-C Apparatus. Baldwin, Barnhart 136–8
(Rotating Machinery) Resistance Commutation. Olney ..... 1207–15; disc. 1215
(Rotating Machinery) Spring and Damping Coefficients of Synchronous Machines and Their Application. Kilgore, Whitney ..... 226–9; disc. 229
(Rotating Machinery) Symmetrical Short Circuits on Saturated Alternators. Mikhail 1554–62
(Rotating Machinery) Transient Response of Direct-Current Dynamos. Koenig ..... 139–44; disc. 144
(Rotating Machinery) Variable Speed Drive, Constant Frequency Alternator. Gould, Krupotich ..... 745–7; disc. 747
Rotor Impedances, The Goerges Phenomenon—Induction Motors with Unbalanced. Garbarino, Gross ..... 1569–74; disc. 1574
Rotor Ventilation, An Experimental and Analytical Study of Turbine Generator. Fechheimer 1563–9
Rubber Insulation Caused by Soil Microorganisms, Failures of. Blake, Kitchin, Pratt ..... 748–54; disc. 754
Rural Neutral Potentials. Waghorne ..... 660–3; disc. 663

S

Safety Devices, Flame Detectors for Domestic Fuel Burner. Deubel 220–5
(Safety) Effect of Frequency on Perception Currents. Dalziel, Mansfield 1162–8
(Safety) Electric Fences—Their Hazards, Types, Regulations, and Safe Application. Dalziel 8–15
(Safety) Electrical Hazards to Farm Stock. Buchanan 654–6
(Safety) Protective Grounding of Electrical Installations on Customer's Premises. Schirmer 657–9
(Safety) Rural Neutral Potentials. Waghorne ..... 660–3; disc. 663
Salient-Pole Synchronous Machines, Potier Reactance for. Mikhail 235–8
Saturable Reactor with Control Source of Comparatively High Impedance, Series-Connected. Storm 1299–1309
Saturable Reactor with Control Source of Comparatively Low Impedance, Series Connected. Storm 756–65
Saturated Alternators, Symmetrical Short Circuits on. Mikhail 1554–62
Saturating Magnetic Amplifiers, Determination of Steady-State Performance of, Self. Smith 1309–17
Scale, D-C Indicating Instruments, Principles of Design of Log-. Stimson, Taylor 1011–15
Scavenging System for Hydrogen-Cooled Generators, Continuous. Snell, Grobel 1625–36
Sealed Transformers, Variations of Tank Pressure with Transformer Loading in. Tipton ..... 1669–73; disc. 1673
Selection and Application of Power Transformers. Seelye 830–3
Selection, Design, and Operation of Power Transformers on American Gas and Electric Company System. Lane, Gross, Fugh ..... 786–93; disc. 793
Selective Overcurrent Tripping Device for Low-Voltage Air Circuit Breakers, An Air Delayed. Trembley, Horn 1649–53
Selsyn Generator Control Transformer System, Static Accuracy Performance of the. Kronacher ..... 645–53; disc. 653
Sensitive Ground Protection. (Committee Report) ..... 473–5; disc. 475
Sensitivity Adjuster, Differential Relay. Headley ..... 1203–05; disc. 1205
Separation Process, Electric Equipment for Heavy-Media. Bean, Blind 1421–9
Series-Connected Saturable Reactor with Control Source of Comparatively High Impedance. Storm 1299–1309
Series Connected Saturable Reactor with Control Source of Comparatively Low Impedance. Storm 756–65
Series Motors—A Design Method, A-C. Chang, Karr ..... 1257–61; disc. 1261
Servo Systems with Compensation for Carrier Frequency Changes, Phase Lead for A-C. Notthoff ..... 285–91; disc. 291
Servomechanism Frequencies, Indicating Instruments at the. Pritchett, Saunders 980–5
Servomechanisms, A Frequency Response Method for Analysing and Synthesizing Contactor. Kochenburger ..... 270–83; disc. 283
Servomechanisms, An Electronic Simulator for Nonlinear. Edwards, Johnson ..... 300–06; disc. 306
Servomechanisms, Characteristics of Some Magnetic-Fluid Clutch. Parziale, Tilton 150–7
Servomechanisms, Improvements in the Characteristics of A-C Lead Networks for. McDonald 293–300
Servomechanism, Integral Controller for Use in Carrier-Type. Cosgriff 1379–83
Servomechanisms with Linearly Varying Elements, Stability of. Kirby ..... 1662–7; disc. 1667
Shaded-Pole Motor with Space Harmonics, Equivalent Circuits of the. Kron 735–41
Shaft-Driven Generator, Design and Test of Electronic Exciter Supplied from Common. Colaizzo, Johnson, Reilly ..... 328–35; disc. 335
Short-Circuit Current of D-C Motors and Generators, Maximum. (Committee Report) 146–9
Short Circuits, Analysis of Synchronous Machine. Camburn, Gross ..... 671–6; disc. 678
Short Circuits on Saturated Alternators, Symmetrical. Mikhail 1554–62
Short Lines of the Metropolitan Area of a Typical System, Transmission-Line Protection of. Marter ..... 468–71; disc. 471
Sign Cable, Development of Improved Luminous. Roehmann, Greenfield ..... 350–5; disc. 355
Simplified 48-Channel Carrier Telephone System, A. Erickson 1493–1500
Simplified Subscriber Toll Dialing for Low-Rate Low-Density Toll Circuits Between Community Dial Offices. Brooke, Blackhall, Blashfield 1417–20
Simulation, A Generalized Analogue Computer for Flight. Hall 308–20
Simulator for Nonlinear Servomechanisms, An Electronic. Edwards, Johnson ..... 300–06; disc. 306
Single-Phase Frequency Changer, Investigation and Elimination of Unusual Vibration in the Field on a Large. Ballantyne, Allen, Baudry ..... 1264–72; disc. 1272
Single-Phase Induction Motors, Suggested Improvements in the Performance Calculations of. Thacker, Gopalakrishna ..... 1–6; disc. 6
Single-Phase Loads, Effect of Three-Phase Motor Loads on Voltage Changes Produced by. Faucett, Fisher, Helm 1467–72
Single-Phase Power Transformer Formed Cores. Gordy, Somerville 1384–7
Soil Microorganisms, Failures of Rubber Insulation Caused by. Blake, Kitchin, Pratt ..... 748–54; disc. 754

Solderless Commutator Joints for High Temperature Operation of Railway Traction Armatures. Reed for. Del Mar 638–41
Solid-Type Impregnated Paper Cables, Terminal Risers for. Del Mar ..... 1592–7; disc. 1597
Solution of Complex Problems, Special Devices Aid Differential Analyzer. Cook, Kirchmayer, Weygandt ..... 1365–70; disc. 1370
Some Aspects of Lightning Surges on Power Systems and their Suppression. Kaneff 1544–9
Sound Level Considerations, Transformer. Maslin ..... 1142–5; disc. 1145
Source of Comparatively High Impedance, Series-Connected Saturable Reactor with Control. Storm 1299–1309
Source of Comparatively Low Impedance, Series-Connected Saturable Reactor with Control. Storm 756–65
Southern California Edison Company, Expansion of the System of the. Kroneberg 861–4
Spark Gaps for Voltage Measurement, The Irradiation of. Hardy, Craggs 584–90
Special Devices Aid Differential Analyzer Solution of Complex Problems. Cook, Kirchmayer, Weygandt ..... 1365–70; disc. 1370
Speed Drive Constant Frequency Alternator, Variable. Gould, Krupotich ..... 745–7; disc. 747
Speed of D-C Brake Magnets, The Operating. Ryan, Spitler 1253–7
Speed Range A-C Electric Systems for Aircraft, Wide. James, Judkins, Mershon ..... 1353–8; disc. 1358
Speeds, Synchronous Machine Damping Torque at Low. Concordia 1550–3
Spring and Damping Coefficients of Synchronous Machines and Their Application. Kilgore, Whitney ..... 226–9; disc. 229
Stability of Servomechanisms with Linearly Varying Elements. Kirby ..... 1662–7; disc. 1667
Stability of Voltage Regulators. Bothwell ..... 1430–3; disc. 1433
Standard for Neutral Grounding Devices, Development of the. Clem 976–9
Standard, New Lightning Arrester. Stewart, Defandorf 525–6
State Waves on Transmission Lines, Steady-. Waudelich 1521–4
Static Accuracy Performance of the Selsyn Generator Control-Transformer System. Kronacher ..... 645–53; disc. 653
Station Arrangements of the Bureau of Reclamation, Relaying Practices and Economical Switching. Morgan, World ..... 865–70; disc. 870
Station Auxiliary System, Bus Transfer Tests on 2,300-Volt. Johnson, Thompson ..... 386–90; disc. 390
Stations, Automatic Control of Ignitron Rectifier. Chaney, Derr ..... 801–11; disc. 811
Stations, Centralized Instrumentation and Controls for Steam Electric Power. Mallory ..... 591–6; disc. 596
Stations, The Choice of Main Power Transformers for Generating. Dillow, Butler ..... 781–5; disc. 785
Statistical Nature and Physical Concepts of Thyratron Deionization Time. Romanowitz, Dow 368–79
Steady-State Performance of Self-Saturating Magnetic Amplifiers, Determination of. Smith 1309–17
Steady-State Power Limit, Effect of Buck-Boost Voltage Regulator on. Concordia ..... 380–4; disc. 384
Steady-State Waves on Transmission Lines. Waudelich 1521–4
Steam-Electric Generating Plants, Centralized Control Board for. Lowe, Hodgkins ..... 1396–9; disc. 1399
Steam Electric Power Stations, Centralized Instrumentation and Controls for. Mallory ..... 591–6; disc. 596
Steel Mills, Basic Patterns for Arrangement of Electric Power Systems for. Finison ..... 54–9; disc. 59
Steel Strand, Vibration and Fatigue Life of. Little, MacMillan, Majercak ..... 1473–8; disc. 1478
Steel Tower Line Design, Light. Osipovich ..... 1513–17; disc. 1517
Strain Gauges as Elements of the Wheatstone Bridge, Resistance Wire. Petrucelly 742–4
Strand, Vibration and Fatigue Life of Steel. Little, MacMillan, Majercak ..... 1473–8; disc. 1478
Strowger Automatic Telephone Systems, The Universal Director in. Ostline 1080–7
Structure Networks, Impulse Measurements by Repeated. Dawes, Thomas, Drought ..... 571–80; disc. 580
Study of Directional Element Connections for Phase Relays, A. Sonnemann ..... 1438–50; disc. 1450
Study of Transmission Line Vibration, Use of Techniques from Electrical Analogues in the. Lummis, Klopfenstein 1676–80
Study of Turbine Generator Rotor Ventilation, An Experimental and Analytical. Fechheimer 1563–9
Study on Power Cable Ducts and Duct Assemblies, Heat Transfer. Greebler, Barnett ..... 357–64; disc. 364
Submarine Cables, A Two-Channel Carrier Telegraph System for Short. Newell, Cramer 61–5
Subscriber Toll Dialing for Low-Rate Low-Density Toll Circuits Between Community Dial Offices, Simplified. Brooke, Blackhall, Blashfield 1417–20
Substation, A 5,000-Kva Underground. Sinnott ..... 882–9; disc. 889
Substation Designers, Quiet Transformer Installations—A Problem for Both Equipment and. Mendenhall, Taylor ..... 1148–52; disc. 1152
Suddenly Applied Loads, Regulation of A-C Generators with. Part II. Harder, Cheek, Clayton ..... 395–405; disc. 405
(Part I—1944)
Suggested Improvements in the Performance Calculations of Single-Phase Induction Motors. Thacker, Gopalakrishna ..... 1–6; disc. 6
Supervisory Control, Field Testing a Microwave Channel for Voice Communication, Relaying, Telemetering and. Pattison, Reagan, Leyland, Gunter ..... 945–51; disc. 951
Supervisory Control, Telemetering, and Communication on Single-Frequency Carrier Channel, Multistation. Derr, Wren, Kresser ..... 1115–21; disc. 1121
Supply, A Low Noise and Distortion Audio Multiplexing Equipment with High Stability Carrier. Beale ..... 1028–37; disc. 1037
Supply Line Unbalance on the Filtered Output Ripple of Polyphase Rectifiers, Effects of. Hooper, McAdie 766–70
Surface Resistance Coefficients for Hydrogen-Cooled Rotating Electric Machines. Snell, Norris, Buckland ..... 174–85; disc. 185
Surge Protection of Cable-Connected Equipment. Witzke, Bliss ..... 527–38; disc. 539
Surges on Power Systems and Their Suppression, Some Aspects of Lightning. Kaneff 1544–9
Survey of Bushing-Type Current Transformers for Metering Purposes, A. Camilli 429–40
Sweden, Underground Hydroelectric Power Stations in. Ruack, Westerberg 928–32
Switch, An Environment-Free 120-Volt D-C High Performance Limit. Stuelpnagel 1289–93
Switches, Interrupting Ability of Horn-Gap. Andrews, Janes, Anderson ..... 1016–24; disc. 1025
Switches to Simulate Field Conditions, Ice Testing of Outdoor Disconnecting. Owens ..... 1488–91; disc. 1491
Switchgear, A New Grounding and Testing Device for Metal-Clad. Krida, McCurry ..... 407–12; disc. 412
(Switchgear) A New High Interrupting Capacity Low-Voltage Power Fuse. Schuck ..... 770–6; disc. 776
(Switchgear) A New 69-Kv Oil Blast Circuit Breaker. Rietz, Balentine ..... 416–23; disc. 423
(Switchgear) An Air Delayed Selective Overcurrent Tripping Device for Low-Voltage Air Circuit Breakers. Tremblay, Horn 1649–53
(Switchgear) Development and Testing of an Improved High-Voltage, High-Capacity Impulse Circuit Breaker. Rietz ..... 15–25; disc. 25
Switchgear Serving Oil Refinery Motors During Power System Disturbances, Automatic Control of Metal-Clad. Horsfall, Thompson, Mills, Bobo ..... 1600–03; disc. 1603
Switching Station Arrangements of the Bureau of Reclamation, Relaying Practices and Economical. Morgan, World ..... 865–70; disc. 870
Switching System, The Number 5 Crossbar Dial Telephone. Korn, Ferguson 244–54
Symmetrical Short Circuits on Saturated Alternators. Mikhail 1554–62
Synchronous Machine, Classification of the Reference Frames of a. Kron 720–7
Synchronous Machine Damping Torque at Low Speeds. Concordia 1550–3
Synchronous Machine Short Circuits, Analysis of. Cauburn, Gross ..... 671–8; disc. 678
Synchronous Machines and Their Application, Spring and Damping Coefficients of. Kilgore, Whitney ..... 226–9; disc. 229
Synchronous Machines, Per-Unit Inductances of. Kirschbaum 231–4
Synchronous Machines, Potier Reactance for Salient-Pole. Mikhail 235–8
Synthesis by Root Locus Method, Control System. Evans 66–9
Synthesizing Contactor Servomechanisms, A Frequency Response Method for Analyzing and. Kochenburger ..... 270–82; disc. 283
Synthetic Load for Testing Rectifiers. Tetherow 642–4
System, A Medium-Haul Carrier Telephone. Smith 1505–12
System, A Simplified 48-Channel Carrier Telephone. Erickson 1493–1500
System, Bus Transfer Tests on 2,300-Volt Station Auxiliary. Johnson, Thompson ..... 386–90; disc. 390
System, Crossbar Tandem. Collis 997–1004
System Design, Information Theory Applied to. Tuller 1612–14
System Disturbances, Automatic Control of Metal-Clad Switchgear Serving Oil Refinery Motors During Power. Horsfall, Thompson, Mills, Bobo ..... 1600–03; disc. 1603
System for a 4,500-Horsepower Gas-Turbine Electric Locomotive, Control. Warrick 508–13
System for Hydrogen-Cooled Generators, Continuous Scavenging. Snell, Grobel 1625–36
System for Short Submarine Cables, A Two-Channel Carrier Telegraph. Newell, Cramer 61–5
System for Telephone Lines of Short or Medium Length, An Improved Transmitted Carrier. Brodie 1501–04
System, Fundamentals of the Automatic Telephone Message Accounting. Mezzar ..... 255–68; disc. 269
System of Digital Recording and Telemetering, The Metrotype. Foster ..... 543–6; disc. 546
System of the Southern California Edison Company, Expansion of the. Kroneberg 861–4
System Performance with Motor-Driven Exciters, Excitation. Mellor, Temoshok 321–7
System Planning in the City of Los Angeles, Power. Williams, Kanouse ..... 900–07; disc. 907
System, Practical Experiences with Resonant Grounding in a Large 34.5-Kv. Brown, Gross ..... 1401–06; disc. 1406
System, Static Accuracy Performance of the Selsyn Generator Control Transformer. Kronacher ..... 645–53; disc. 653
System Synthesis by Root Locus Method, Control. Evans 66–9
System, The Number 5 Crossbar Dial Telephone Switching. Korn, Ferguson 244–54
System, Transient Analysis of a Voltage-Regulated Aircraft D-C. Scorgie 1318–23
Systems and Their Suppression, Some Aspects of Lightning Surges on Power. Kaneff 1544–9
Systems for Aircraft, Wide Speed Range A-C Electric. James, Judkins, Mershon ..... 1353–8; disc. 1358
Systems for 960 and 2,000 Megacycles, Microwave. Rector, Sutter ..... 1100–08; disc. 1108
Systems for Steel Mills, Basic Patterns for Arrangement of Electric Power. Finison ..... 54–9; disc. 59
Systems—Fundamentals and Basic Design Considerations, Underground Conduit for Electric Power. Watkins ..... 1582–90; disc. 1590
Systems, Measurement of Insulation Resistance on Energized. Brancato, McClinton 1238–42
Systems, Proposed Basic Impulse Insulation Levels for High-Voltage. Clem, Meador, Rudge, Powell ..... 953–60; disc. 960
Systems, The Determination and Allocation of the Capacity Benefits Resulting from Interconnecting Two or More Generating. Watchorn 1180–6
Systems, The Universal Director in Strowger Automatic Telephone. Ostline 1080–7
Systems with Compensation for Carrier Frequency Changes, Phase Lead for A-C Servo. Notthoff ..... 285–91; disc. 291

T

Tables, Basic Theory Underlying Bell System Facilities Capacity. Gracey ..... 238–43; disc. 243
Tachometer, A New High-Accuracy Counter-Type. Berry, Beattie ..... 686–90; disc. 690
Take-off, Automatic Feathering—To Reduce the Hazard of Aircraft Engine Failure at. Kershaw 1328–34
Tandem System, Crossbar. Collis 997–1004
Tandem Trunking in Los Angeles Metropolitan Area, Interexchange. Pfeiffer 1071–9
Tank Pressure with Transformer Loading in Sealed Transformers, Variations of. Tipton ..... 1669–73; disc. 1673
Tape-to-Page Translator, A Printing Telegraph. Frost 79–83
Techniques for Turbojet Thrust Instrumentation, Analogue. Van Valkenburg, Matthews 1342–6
Techniques from Electrical Analogues in the Study of Transmission Line Vibration, Use of. Lummis, Klopfenstein 1676–80
Techniques on the Anacom—Electric Analog Computer, New. Harder, Carleton 547–56
Telemetering, The Metrotype System of Digital Recording and. Foster ..... 543–6; disc. 546
Telegraph Regenerative Receiver, A New Electronic. Ostendorf ..... 32–6; disc. 36
Telegraph System for Short Submarine Cables, A Two-Channel Carrier. Newell, Cramer 61–5
Telegraph Tape-to-Page Translator, A Printing. Frost 79–83
Telemetering and Communication on Single-Frequency Carrier Channel, Multistation Supervisory Control. Derr, Wren, Kresser ..... 1115–21; disc. 1121
Telemetering, and Supervisory Control, Field Testing a Microwave Channel for Voice Communication, Relaying. Pattison, Reagan, Leyland, Gunter ..... 945–51; disc. 951
Telephone Central Office Buildings for Small Communities, Dial. Reese, Roys 1535–9
Telephone Lines of Short or Medium Length, An Improved Transmitted Carrier System for. Brodie 1501–04
Telephone Message Accounting System, Fundamentals of the Automatic. Mezzar ..... 255–68; disc. 269
Telephone Switching System, The Number 5 Crossbar Dial. Korn, Ferguson 244–54
Telephone System, A Medium-Haul Carrier. Smith 1505–12
Telephone System, A Simplified 48-Channel Carrier. Erickson 1493–1500

Telephone Systems, The Universal Director in Stroweger Automatic. Carline.....1080–7
(Television) Clampers in Video Transmission. Doba, Rieke.....477–87
Television Networks, Local Wire Video. Nebel...1451–60
Temperature in a Transformer, Determination of Effective Oil. Beavers.....703–08; disc. 708
Temperature Operation of Railway Traction Armatures, Solderless Commutator Joints for High. Reed.....638–41
Terminal Risers for Solid-Type Impregnated Paper Cables. Del Mar.....1592–7; disc. 1597
Test Equipment, Aircraft Electric Motors Need. Ross.....1359–64
Test Equipment and Its Application, Modern Carrier Current. Brinton.....777–80
Test on Electronic Exciter Supplied from Common Shaft-Driven Generator, Design and. Colaiaco, Johnson, Reilly.....328–35; disc. 335
Testing a Microwave Channel for Voice Communication, Relaying, Telemetering, and Supervisory Control, Field. Pattison, Reagan, Leyland, Gunter.....945–51; disc. 951
Testing Device for Metal-Clad Switchgear, A New Grounding and. Krida, McCurry.....407–12; disc. 412
Testing, High-Voltage Rectifier Equipment and Control for Tube. Durand.....909–12
Testing of an Improved High-Voltage, High-Capacity Impulse Circuit Breaker, Development and. Rietz.....15–25; disc. 25
Testing of Outdoor Disconnecting Switches to Simulate Field Conditions, Ice. Owens..1488–91; disc. 1491
Testing on Large D-C Apparatus, Quick and Accurate Production. Baldwin, Barnhart.....136–8
Testing Rectifiers, Synthetic Load for. Tetherow..642–4
Tests on 2,300-Volt Station Auxiliary System, Bus Transfer. Johnson, Thompson...386–90; disc. 390
Theory and Application of Transformer Differential Protection. McKenna.....1197–1202
Theory Applied to System Design, Information. Tuller.....1612–14
Theory of the Current Transductor and Its Application in the Aluminum Industry, The. Specht, Wagner.....441–52; disc. 452
Theory Underlying Bell System Facilities Capacity Tables, Basic. Gracey.....238–43; disc. 243
(Therapeutics) Electrical Instrumentation in Medical Research. Benjamin, Hale, Carstensen, Tompkins.....1324–7
Thermal Resistance Between Cables and a Surrounding Pipe or Duct Wall. Buller, Neher..342–7; disc. 347
Thickness Gauge Using Beta Rays, Noncontacting. Clapp, Bernstein.....488–90
Thirteen-Year Lightning Performance of Boulder 287.5-Kv Transmission Lines. Blakeslee, Kanouse.....796–9; disc. 800
Three-Phase Motor Loads on Voltage Changes Produced by Single-Phase Loads, Effect of. Faucett, Fisher, Helm.....1467–72
Three-Phase Transformer, Economical Design of a. Ciganek.....1371–4; disc. 1374
Thrust Bearing Problems and Their Solution on Turbine-Generator Units and Auxiliaries of the Consolidated Edison System. Driscoll, Otten.....1642–7; disc. 1647
Thrust Instrumentation, Analogue Techniques for Turbojet. Van Valkenburg, Matthews...1342–6
Thyratron Deionization Time, Statistical Nature and Physical Concepts of. Romanowitz, Dow...368–79
Tidd 500-Kv Test Project of the American Gas and Electric Company—Corona, Radio Influence, and Other Factors, Progress Report on. Sporn, Monteith.....891–7; disc. 897
Time of Magnetic Amplifiers, Response. Harder, Horton.....1130–8; disc. 1138
Time, Statistical Nature and Physical Concepts of Thyratron Deionization. Romanowitz, Dow...368–79
Toll Dialing for Low-Rate Low-Density Toll Circuits Between Community Dial Offices, Simplified Subscriber. Brooke, Blackhall, Blashfield.....1417–20
Tool for Transformer Audio Noise Investigation, Harmonic Index—A. Mutschler, Madden.....115–18; disc. 118
Torque at Low Speeds, Synchronous Machine Damping. Concordia.....1550–3
Total and Incremental Losses in Power Transmission Networks. Ward, Eaton, Hale...626–31; disc. 631
Total Design as Applied to Polyphase Induction Motors, A Method of. Crouse.....1434–7
Tower Line Design, Light Steel. Osipovich.....1513–17; disc. 1517
Tracking Radio Noise on Aircraft. Owen.....1249–52
Traction Armatures, Solderless Commutator Joints for High Temperature Operation of Railway. Reed.....638–41
Traction Motor Field Coils, A New Resilient Class-H Material for the Insulation of. Reed, Tyner.....1158–61
Transductor and Its Application in the Aluminum Industry, The Theory of the Current. Specht, Wagner.....441–52; disc. 452
Transfer Coefficients for Hydrogen-Cooled Rotating Electric Machines, Surface Heat. Snell, Norris, Buckland.....174–85; disc. 185
Transfer Study on Power Cable Ducts and Duct Assemblies, Heat. Greebler, Barnett...357–64; disc. 364
Transfer Tests on 2,300-Volt Station Auxiliary System, Bus. Johnson, Thompson.....386–90; disc. 390
Transformer Audio Noise Investigation, Harmonic Index—A Tool for. Mutschler, Madden.....115–18; disc. 118
Transformer, Determination of Effective Oil Temperature in a. Beavers.....703–08; disc. 708
Transformer Differential Protection, Theory and Application of. McKenna.....1197–1202
Transformer, Economical Design of a 3-Phase. Ciganek.....1371–4; disc. 1374
Transformer Formed Cores, Single-Phase Power. Gordy, Somerville.....1384–7
Transformer Installations—A Problem for Both Equipment and Substation Designers, Quiet. Mendenhall, Taylor.....1148–52; disc. 1152
Transformer Insulation Level, Coordination of Lightning Arrester Location with. Witzke, Blin.....964–73; disc. 973
Transformer Insulation, Margins Between Lightning Arrester Protective Levels and. Vogel.....110–12; disc. 112
Transformer Insulation in Sealed Transformers, Variations of Tank Pressure with. Tipton.....1669–73; disc. 1673
Transformer Noise and Its Confinement. McLean.....1409–15; disc. 1415
Transformer Oil. Treanor, Raab..1060–70; disc. 1070
Transformer Sound Level Considerations. Maslin.....1142–5; disc. 1145
Transformer System, Static Accuracy Performance of the Selsyn Generator Control. Kronacher.....645–53; disc. 653
Transformers, A New Dry-Type Insulation for Instrument. Pfuntner, Franck, D'Entremont.....453–8
Transformers, A New Line of Orthomagnetic Bushing-Type Current. Farr.....424–8
Transformers, A Primary Method of Measuring Ratio and Phase Angle of Current. Brownlee...459–60
Transformers, Audible Noise of Power. Gordy.....45–50; disc. 50
Transformers, Control Circuit. Frank, Hauck...376–8
Transformers, Development of Preferred Voltage Ratings for. St. Clair, Jalonack...1049–59; disc. 1059
Transformers for Generating Stations, The Choice of Main Power. Dillow, Butler.....781–5; disc. 785
Transformers for Linear Electronic Circuits, The Design of Broad-Band. Lord.....1005–10
Transformers for Metering Purposes, A Survey of Bushing-Type Current. Camilli.....429–40
Transformers for Use on the Systems of the Hydro-Electric Power Commission of Ontario, Contributing Factors in Determining the Ratings of Power. Fleming, Lotimer.....1658–62; disc. 1662
Transformers in Residential and Commercial Areas, Noise Control for. Baugh.....121–6; disc. 126
Transformers on American Gas and Electric Company System, Selection, Design, and Operation of Power. Lane, Gross, Pugh.....786–93; disc. 793
Transformers on the System of the Bonneville Power Administration, Application and Handling of Very Large Power. Stevens.....158–63; disc. 163
Transformers, Selection and Application of Power. Seelye.....830–3
Transient Analysis of a Voltage-Regulated Aircraft D-C System. Scorgie.....1318–23
Transient Response of Direct-Current Dynamos. Koenig.....139–44; disc. 144
Transient and Feedback in Magnetic Amplifiers, An Analysis of. Johnson, Latson...604–11; disc. 611
Transients in Coupled Inductance-Capacitance Circuits Analyzed in Terms of a Rolling-Ball Analogue. Magnuson.....1525–30
Transients in Magnetic Amplifiers, An Analysis of. VerPlanck, Finzi, Beaumariage.....408–503
Translator, A Printing Telegraph Tape-to-Page. Frost.....79–83
Transmission, Clampers in Video. Doba, Rieke..477–87
(Transmission) Dielectric-Recovery Characteristics of Power Arcs in Large Air Gaps. McCann, Conner, Ellis.....616–24; disc. 624
(Transmission) Expansion of the System of the Southern California Edison Company. Kroneberg...861–4
(Transmission) Interrupting Ability of Horn-Gap Switches. Andrews, Janes, Anderson.....1016–24; disc. 1025
(Transmission) Light Steel Tower Line Design. Osipovich.....1513–17; disc. 1517
Transmission-Line Protection of Short Lines of the Metropolitan Area of a Typical System. Marter.....468–71; disc. 471
Transmission Lines, Control Vibration, Use of Techniques from Electrical Analogues in the Study of. Lummis, Klopfenstein.....1676–80
Transmission Lines, A Method of Estimating Lightning Performance of. (Committee Report).....1187–95; disc. 1195
Transmission Lines, Consideration of Requirements and Limitations of Relaying and High-Speed Reclosing on Long and Heavily Loaded. Parts, Brownlee.....103–07; disc. 107
Transmission Lines, Relay Protection for Medium Length High-Voltage. Kinghorn..461–5; disc. 465
Transmission Lines, Steady-State Waves on. Waidelich.....1521–4
Transmission Lines, Thirteen-Year Lightning Performance of Boulder 287.5-Kv. Blakeslee, Kanouse.....796–9; disc. 800
Transmission, Long-Distance Power. Crary.....834–40; disc. 840
Transmission Networks, Total and Incremental Losses in Power. Ward, Eaton, Hale...626–31; disc. 631
(Transmission) Progress Report on Tidd 500-Kv Test Project of the American Gas and Electric Company—Corona, Radio Influence, and Other Factors. Sporn, Monteith.....891–7; disc. 897
(Transmission) Some Aspects of Lightning Surges on Power Systems and Their Suppression. Kaneff.....1644–9
Transmitted Carrier System for Telephone Lines of Short or Medium Length, An Improved. Brodie.....1501–04
(Transportation, Air) Aircraft D-C Circuit Breakers for 28 and 120 Volts. Beall, Reifschneider...1283–8
(Transportation, Air) Aircraft Electric Motors Need Test Equipment. Ross.....1359–64
(Transportation, Air) Aluminum Conductors from an Aircraft Manufacturer's Viewpoint. Schumacher.....1335–41
(Transportation, Air) An Amplistat Regulator Applied to a 5-Kva 400-Cycle Aircraft Inverter. Morgan, Wall...1243–6; disc. 1248
(Transportation, Air) An Environment-Free 120-Volt D-C High Performance Limit Switch. Stuelpnagel.....1289–93
(Transportation, Air) Analogue Techniques for Turbojet Thrust Instrumentation. Van Valkenburg, Matthews.....1342–6
(Transportation, Air) Automatic Feathering—To Reduce the Hazard of Aircraft Engine Failure at Take-off. Kershaw.....1328–34
(Transportation, Air) Dynamic Characteristics of Carbon Pile Voltage Regulators. Mills.....1347–52; disc. 1352
(Transportation, Air) The Design of Reactors for Radio Interference Filters. Knudson.....1294–8
(Transportation, Air) Transient Analysis of a Voltage-Regulated Aircraft D-C System. Scorgie..1318–23
(Transportation, Air) Wide Speed Range A-C Electric Systems for Aircraft. James, Judkins, Mershon.....1353–6; disc. 1358
(Transportation, Land) A New Resilient Class-H Material for the Insulation of Traction Motor Field Coils. Reed, Tyner.....1158–61
(Transportation, Land) Locomotive Wheel-Slip and Wheel Lock Protection. Smith.....1154–7
Transpositions and the Calculation of Inductance from Geometric Mean Distances. Boast.....1531–4
Transverse Flux Induction Heating. Baker.....711–19
Tripping Device for Low-Voltage Air Circuit Breakers, An Air Delayed Selective Overcurrent. Tremblay, Horn.....1649–53
Trunking in the Los Angeles Metropolitan Area, Interexchange Tandem. Pfiffer.....1071–9
Tube Testing, High-Voltage Rectifier Equipment and Control for. Durand.....909–12
Turbine Electric Locomotive, Control System for a 4,500-Horsepower Gas-. Warrick.....506–13
Turbine Electric Locomotive, Rotating Electric Equipment for a Gas-. Cobo.....514–18
Turbine Electric Locomotive, The Alco-GE 4,500-Horsepower Gas-. Morey.....504–07
Turbine Generator Rotor Ventilation, An Experimental and Analytical Study of. Fechheimer.....1563–9
Turbine-Generator Units and Auxiliaries of the Consolidated Edison System, Thrust Bearing Problems and Their Solution on. Driscoll, Otten.....1642–7; disc. 1647
Turbine Generator Units, Centralized Control Desirable for Single Boiler. Lind, Geiger.....1176–9
Turbine Generators, Liquid Cooling of A-C. Part II. Fechheimer.....165–71; disc. 171
(Part I–1947)
Turbines for Power Generation, Control of Gas. Hoffmann, Mellor, Starkey.....1637–41; disc. 1641
Turbojet Thrust Instrumentation, Analogue Techniques for. Van Valkenburg, Matthews.....1342–6
Two-Channel Carrier Telegraph System for Short Submarine Cables, A. Newell, Cramer.....61–5
Type Servomechanisms, Integral Controller for Use in Carrier-. Cogriff.....1379–83

U

Unbalance on the Filtered Output Ripple of Polyphase Rectifiers, Effects of Supply Line. Hooper, McAdie.....766–70

Unbalanced Rotor Impedances, The Georges Phenomenon—Induction Motors with. Garbarino, Gross .....1569–74; disc. 1574
Underground Conduit for Electric Power Systems—Fundamentals and Basic Design Considerations. Watkins.....1582–90; disc. 1590
Underground Hydroelectric Power Plants. Gisiger 1169–75
Underground Hydroelectric Power Stations in Sweden. Ruck, Westerberg.....928–32
Underground Substation, A 5,000-Kva. Sinnott.....882–9; disc. 889
Units and Auxiliaries of the Consolidated Edison System, Thrust Bearing Problems and Their Solution on Turbine-Generator. Driscoll, Otten.....1642–7; disc. 1647
Units, Centralized Control Desirable for Single Boiler-Turbine-Generator. Lind, Geiger.....1176–9
Universal Director in Strowger Automatic Telephone Systems, The. Outline.....1080–7

V

Variable Speed Drive, Constant Frequency Alternator. Gould, Krupotich.....745–7; disc. 747
Variation Principle, An Improved Method of Measuring Dissipation Factor and Dielectric Constant Using the Susceptance. Miller, Whelan.....491–7
Variations of Tank Pressure with Transformer Loading in Sealed Transformers. Tipton.....1669–73; disc. 1673
Ventilation, An Experimental and Analytical Study of Turbine Generator Rotor. Fechheimer.....1563–9
Vibration and Fatigue Life of Steel Strand. Little, MacMillan, Majercak.....1473–8; disc. 1478
Vibration in the Field on a Large Single-Phase Frequency Changer, Investigation and Elimination of Unusual. Ballantyne, Allen, Baudry.....1264–72; disc. 1272
Vibration, Use of Techniques from Electrical Analogues in the Study of Transmission Line. Lummis, Klopfenstein.....1676–80
Video Television Networks, Local Wire. Nebel.....1451–60
Video Transmission, Clampers in. Dobs, Ricke.....477–87
Viewpoint, Aluminum Conductors from an Aircraft Manufacturer's. Schumacher.....1335–41
Voice Communication, Relaying, Telemetering, and Supervisory Control, Field Testing a Microwave Channel for. Pattison, Reagan, Leyland, Gunter.....945–51; disc. 951
Voltage Changes Produced by Single-Phase Loads, Effect of Three-Phase Motor Loads on. Faucett, Fisher, Helm.....1467–72
Voltage Gradient Meter, A. Tremaine, Check.....633–7; disc. 637
Voltage Measurement, The Irradiation of Spark Gaps for. Hardy, Craggs.....584–90
Voltage Power Fuse, A New High Interrupting Capacity Low-. Schuck.....770–6; disc. 776
Voltage Ratings for Transformers, Development of Preferred. St. Clair, Jalonack.....1049–59; disc. 1059
Voltage-Regulated Aircraft D-C System, Transient Analysis of a. Scorgie.....1318–23
Voltage Regulator on Steady-State Power Limit, Effect of Buck-Boost. Concordia.....380–4; disc. 384
Voltage Regulators, Dynamic Characteristics of Carbon Pile. Mills.....1347–52; disc. 1352
Voltage Regulators, Stability of. Bothwell.....1430–3; disc. 1433
Volts, Aircraft D-C Circuit Breakers for 28 and 120. Beall, Reifschneider.....1283–8

W

Wall, The Thermal Resistance Between Cables and a Surrounding Pipe or Duct. Buller, Neher.....342–7; disc. 347
Watt-Hour Meters, A New Device for Calibrating. Robison, Wickham.....732–4
Waves on Transmission Lines, Steady-State. Waidelich.....1521–4
Wheatstone Bridge, Resistance Wire Strain Gauges as Elements of the. Petruccelly.....742–4
Wheel-Slip and Wheel-Lock Protection, Locomotive. Smith.....1154–7
Wide Speed Range A-C Electric Systems for Aircraft. James, Judkins, Mershon.....1353–8; disc. 1358
Windings, Current in Equalizer Connections of D-C Machine Armature. Linville, Strang.....1219–26; disc. 1226
(Wire Communication) A Negative Impedance Repeater. Merrill.....1461–6
Wire Strain Gauges as Elements of the Wheatstone Bridge, Resistance. Petruccelly.....742–4
Wire Video Television Networks, Local. Nebel.....1451–60

2. Author Index

Abetti, P. A. Disc.....539, 580, 974, 1027
Ackermann, O. Disc.....624
Adler, H. A.; K. H. Wadleigh. Disc.....1580
Alexanderson, W. F. W.; D. C. Prince, C. H. Willis. Disc.....843
Allen, J. E.; W. M. H. Ballantyne, R. A. Baudry. Investigation and Elimination of Unusual Vibration in the Field on a Large Single-Phase Frequency Changer. (50-199)....1264–72; disc. 1273
Ames, E. W.; L. J. Hibbard, C. C. Whittaker. Rectifier-Type Motive Power for Railroad Electrification. (50-81).....519–23; disc. 523
Ammerman, Charles R. The Direct Measurement of Bandwidth. (50-5).....27–31
Anderson, George M. The Calculation of the Capacitance of Coaxial Cylinders of Rectangular Cross-Section. (50-115).....728–31
Anderson, G. M.; W. Caywood, Jr. Disc.....1667
Andersson, M. A.; F. E. Andrews, L. R. Janes. Interrupting Ability of Horn-Gap Switches. (50-161).....1016–24; disc. 1027
Andreae, F. V. Design and Control of Ferroalloy Furnaces. (50-86).....557–62
Andrews, F. E.; W. H. Hatch. Disc.....541
Andrews, F. E.; L. R. Janes, M. A. Andersson. Interrupting Ability of Horn-Gap Switches. (50-161).....1016–24; disc. 1027
Asbury, C. E. Disc.....466, 471
Asbury, C. E.; C. W. Fredericksen. Disc.....1121
Attura, George M. Disc.....291

B

Baker, M. A. Disc.....1235
Baker, Robert M. Transverse Flux Induction Heating. (50-113).....711–19
Baldwin, M. J.; H. D. Barnhart. Quick and Accurate Production Testing on Large D-C Apparatus. (50-21).....136–8
Balentine, C. J.; E. B. Rietz. A New 69-Kv Oil Blast Circuit Breaker. (50-61).....416–23; disc. 423
Ballantyne, W. M. H.; J. E. Allen, R. A. Baudry. Investigation and Elimination of Unusual Vibration in the Field on a Large Single-Phase Frequency Changer. (50-199).....1264–72; disc. 1273
Barnes, H. C. Disc.....1485
Barnett, Guy F.; P. Greebler. Heat Transfer Study on Power Cable Ducts and Duct Assemblies. (50-55).....357–64; disc. 366
Barnhart, H. D.; M. J. Baldwin. Quick and Accurate Production Testing on Large D-C Apparatus. (50-21).....136–8
Baudry, R. A.; W. M. H. Ballantyne, J. E. Allen. Investigation and Elimination of Unusual Vibration in the Field on a Large Single-Phase Frequency Changer. (50-199).....1264–72; disc. 1273
Baugh, C. E. Audio Noise in Transformers in Residential and Commercial Areas. (50-19).....121–6; disc. 127
Beale, F. S. A Low Noise and Distortion Audio Multiplexing Equipment with High Stability Carrier Supply. (50-162).....1028–37; disc. 1037
Beall, B. S., III; P. J. Reifschneider. Aircraft D-C Circuit Breakers for 28 and 120 Volts. (50-202).....1283–8
Bean, J. J.; K. A. Blind. Electric Equipment for Heavy-Media Separation Process. (50-230)..1421–9
Beattie, C. L.; T. M. Berry. A New High-Accuracy Counter-Type Tachometer. (50-109).....686–90; disc. 691
Beattie, C. S. Disc.....1026
Beattie, C. S.; S. C. Killian. Disc.....1491
Beaumariage, D. C.; L. A. Finzi. General Characteristics of Magnetic Amplifiers. (50-148)..919–27
Beaumariage, D. C.; D. W. VerPlanck, L. A. Finzi. An Analysis of Transients in Magnetic Amplifiers. (50-76).....498–503
Beavers, Martin F. Determination of Effective Oil Temperature in a Transformer. (50-112).....703–08; disc. 710
Beck, E. Disc.....113, 541, 942, 962
Beck, E.; A. M. Opasht. Disc.....92
Beckwith, Sterling. Disc.....185
Bellaschi, P. L. Disc.....92, 163, 897
Benjamin, J. Malvern, Jr.; J. Hale, E. L. Carstensen, H. E. Tompkins. Electrical Instrumentation in Medical Research. (50-209).....1324–7
Bernstein, S.; C. W. Clapp. Noncontacting Thickness Gauge Using Beta Rays. (50-73).....488–90
Berry, T. M.; C. L. Beattie. A New High-Accuracy Counter-Type Tachometer. (50-109).....686–90; disc. 691
Bishop, E. A. Disc.....414
Blackburn, J. L.; S. L. Goldsborough. Disc.....1047
Blackhall, J. M.; E. Brooke, W. H. Blashfield. Simplified Subscriber Toll Dialing for Low-Rate Low-Density Toll Circuits Between Community Dial Offices. (50-227).....1417–20
Blake, Joel W. Disc.....1641
Blake, John T.; D. W. Kitchin, O. S. Pratt. Failures of Rubber Insulation Caused by Soil Microorganisms. (50-121).....748–54; disc. 755
Blakeslee, T. M.; E. L. Kanouse. Thirteen-Year Lightning Performance of Boulder 287.5-Kv Transmission Lines. (50-130).....796–9; disc. 800
Blankmeyer, W. H. Disc.....1108
Blashfield, W. H.; E. Brooke, J. M. Blackhall. Simplified Subscriber Toll Dialing for Low-Rate Low-Density Toll Circuits Between Community Dial Offices. (50-227).....1417–20
Blind, K. A.; J. J. Bean. Electric Equipment for Heavy-Media Separation Process. (50-230)..1421–9
Bliss, T. J.; R. L. Witzke. Co-ordination of Lightning Arrester Location with Transformer Insulation Level. (50-153).....964–73; disc. 974
Bliss, T. J.; R. L. Witzke. Surge Protection of Cable-Connected Equipment. (50-83)..527–38; disc. 539
Bliss, T. J.; R. L. Witzke. Disc.....943
Blomqvist, E. A. Disc.....126
Blume, A. E.; R. W. Votaw. Disc.....653
Boast, W. B. Transpositions and the Calculation of Inductance from Geometric Mean Distances. (50-246).....1531–4
Bobo, P. O.; R. T. Horsfall, K. N. Thompson, R. W. Mills. Automatic Control of Metal-Clad Switchgear Serving Oil Refinery Motors During Power System Disturbances: (50-261)..1600–03; disc. 1603
Borgel, B. F. Design and Operation of Central Control Rooms. (50-92).....598–602
Bostwick, Myron A. Disc.....1450
Bothwell, Frank E. Stability of Voltage Regulators. (50-231).....1430–3; disc. 1433
Boyer, J. L.; C. R. Marcum. Ignitron Converters for High Energy Particle Accelerators. (50-174).....1110–14
Brancato, E. L.; J. Cybulski. Disc.....144
Brancato, E. L.; A. T. McClinton. Measurement of Insulation Resistance on Energized Systems. (50-194).....1238–42
Bretch, Edward. Disc.....7
Brinton, R. L. Modern Carrier Current Test Equipment and Its Application. (49-211).....777–80
Brodie, G. H. An Improved Transmitted Carrier System for Telephone Lines of Short or Medium Length. (50-241).....1501–04
Brooke, Eric; J. M. Blackhall, W. H. Blashfield. Simplified Subscriber Toll Dialing for Low-Rate Low-Density Toll Circuits Between Community Dial Offices. (50-227).....1417–20
Brooks, G. E. Disc.....1485, 1604
Bross, R. B. Disc.....1235
Brown, Harold H. Disc.....1406
Brown, Harold H.; E. T. B. Gross. Practical Experiences with Resonant Grounding in a Large 34.5-Kv System. (50-224).....1401–06; disc. 1407
Brownlee, Allan L. A Primary Method of Measuring the Ratio and Phase Angle of Current Transformers. (50-67).....459–60
Brownlee, W. R. Disc.....631
Brownlee, W. R.; J. A. Elzi. Disc.....391
Brownlee, W. R.; C. E. Parks. Consideration of Requirements and Limitations of Relaying and High-Speed Reclosing on Long and Heavily-Loaded Transmission Lines. (50-16)....103–07; disc. 109
Buchanan, W. B. Electrical Hazards to Farm Stock. (50-104).....654–6
Buchanan, W. B. Disc.....663
Buckland, Mrs. B. O.; R. H. Norris. Disc.....347
Buckland, Mrs. B. O.; D. S. Snell, R. H. Norris. Surface Heat-Transfer Coefficients for Hydrogen-Cooled Rotating Electric Machines. (50-29).....174–85; disc. 185
Buller, F. H. Disc.....365
Buller, F. H.; J. H. Neher. The Thermal Resistance Between Cables and a Surrounding Pipe or Duct Wall. (50-52).....342–7; disc. 349
Burkett, Albert. General Aspects of Community Dial Office Equipment. (50-249).....1540–3
Burkhalter, A. H. Disc.....603
Burrell, R. W. Disc.....347, 364
Butler, J. W.; N. E. Dillow. The Choice of Main Power Transformers for Generating Stations. (50-128).....781–5

C

Calabrese, G. Determination of Reserve Capacity by Probability Method. (50-280)..1681–8; disc. 1688
Callander, D. W. Disc.....1662
Calvert, J. F.; G. W. Goelz. Analogue Computer for Multicomponent Fractionation Calculations. (50-15).....97–103
Camburn, Robert D.; E. T. B. Gross. Analysis of Synchronous Machine Short Circuits. (50-37).....671–8; disc. 678

Camilli, G. A Survey of Bushing-Type Current Transformers for Metering Purposes. (50-63)....429–40
Carleton, J. T.; B. L. Harder. New Techniques on the Anacom—Electric Analog Computer (50-85)....547–56
Carlson, K. W. Disc....1352, 1358
Carothers, B. M. Disc....413
Carpenter, T. J.; I. B. Johnson, L. E. Saline. Evaluation of Lightning-Arrester Lead Length and Separation in Co-ordinated Protection of Apparatus Against Lightning. (50-150)....933–41; disc. 941
Carroll, Joseph S.; W. S. Peterson, B. Cozzens. Desert Measurements of Corona Loss on Conductors for Operation Above 230 Kv. (50-141)....872–8; disc. 880
Carstensen, Edwin L.; J. M. Benjamin, Jr., J. Hale, H. E. Tompkins. Electrical Instrumentation in Medical Research. (50-209)....1324–7
Caywood, William, Jr.; G. M. Anderson. Disc....1667
Cham, E. J.; W. A. Derr. Automatic Control of Ignitron Rectifier Stations. (50-131)..801–11; disc. 812
Chang, S. S. L.; J. H. Karr. A-C Series Motors—A Design Method. (50-198)....1257–61; disc. 1262
Cheek, R. C.; E. L. Harder, J. M. Clayton. Regulation of A-C Generators with Suddenly Applied Loads. Part II. (50-58)....395–405; disc. 406
(Part I–1944)
Cheek, R. C.; R. L. Tremaine. A Voltage Gradient Meter. (50-98)....633–7; disc. 637
Chipman, J. F. Disc....414
Ciganek, Ladislav. Economical Design of a 3-Phase Transformer. (50-216)....1371–4; disc. 1375
Clapp, C. W.; S. Bernstein. Noncontacting Thickness Gauge Using Beta Rays. (50-73)....488–90
Clayton, J. M.; E. L. Harder, R. C. Cheek. Regulation of A-C Generators with Suddenly Applied Loads. Part II. (50-58)....395–405; disc. 406
(Part I–1944)
Clem, J. E. Development of the Standard for Neutral Grounding Devices. (50-154)....976–9
Clem, J. E.; J. R. Meador, W. J. Rudge, A. H. Powell. Proposed Basic Impulse Insulation Levels for High-Voltage Systems. (50-152)....953–60; disc. 963
Cobb, E. E. Disc....385
Cohn, O. C. Rotating Electric Equipment for a Gas-Turbine Electric Locomotive. (50-79)....514–18
Colaiaco, A. F.; A. A. Johnson, J. E. Reilly. Design and Test on Electronic Exciter Supplied from Common Shaft-Driven Generator. (50-50)....328–35; disc. 336
Cole, Edward R. Electric Equipment and Operation of Graphitizing Furnaces. (50-87)....564–6
Collis, R. E. Crossbar Tandem System. (50-158)....997–1004
Concordia, C. Effect of Buck-Boost Voltage Regulator on Steady-State Power Limit. (50-57)....380–4; disc. 384
Concordia, Charles. Synchronous Machine Damping Torque at Low Speeds. (50-252)....1550–3
Conner, J. E.; G. D. McCann, H. M. Ellis. Dielectric Recovery Characteristics of Power Arcs in Large Air Gaps. (50-96)....616–24; disc. 624
Cook, A. C.; L. K. Kirchmayer, C. N. Weygandt. Special Devices Aid Differential Analyzer Solution of Complex Problems. (50-215)....1365–70; disc. 1370
Cooper, R. J. Disc....1484
Cornelius, H. A. Disc....539
Corson, A. J.; A. L. Nylander. Power Measurement by The Hook-On Method. (50-111)....699–702
Cosgriff, R. L. Integral Controller for Use in Carrier-Type Servomechanisms. (50-219)....1379–83
Cozzens, Bradley; W. S. Peterson, J. S. Carroll. Desert Measurements of Corona Loss on Conductors for Operation Above 230 Kv. (50-141)....872–8; disc. 880
Craggs, J. D.; D. R. Hardy. The Irradiation of Spark Gaps for Voltage Measurement. (50-90)..584–90
Cramer, C. H.; E. L. Nowell. A Two-Channel Carrier Telegraph System for Short Submarine Cables. (50-10)....61–5
Crary, S. B. Long-Distance Power Transmission. (50-135)....834–40; disc. 843
Crawford, S. N.; M. J. Mulhern. Rectifier Equipment for Electronic D-C Motor Drives. (50-33)..211–15
Crouse, C. H. A Method of Total Design as Applied to Polyphase Induction Motors. (50-232)..1434–7
Cybulski, John. Disc....1235
Cybulski, J.; E. L. Branzato. Disc....144

D

Dalziel, Charles F. Electric Fences—Their Hazards, Types, Regulations, and Safe Application. (50-2)....8–15
Dalziel, Charles F.; T. H. Mansfield. Effect of Frequency on Perception Currents. (50-184)..1162–8
Dawes, C. L.; C. H. Thomas, A. B. Drought. Impulse Measurements by Repeated-Structure Networks. (50-89)....571–80; disc. 580
Dawson, E. J. Disc....1590
deBellis, A. M. Disc....77
Defandorf, F. M.; H. R. Stewart. New Lightning Arrester Standard. (50-82)....525–6
de Koning, Th. Disc....172, 201
Del Mar, W. A. Terminal Risers for Solid-Type Impregnated Paper Cables. (50-258)....1592–7; disc. 1597
Del Mar, Wm. A. Disc....685, 1580, 1590
D'Entremont, F. R.; R. R. Pfuntner, R. E. Franck. A New Dry-Type Insulation for Instrument Transformers. (50-66)....453–8
Derr, W. A.; E. J. Cham. Automatic Control of Ignitron Rectifier Stations. (50-131)..701–11; disc. 812
Derr, W. A.; T. C. Wren, J. V. Kresser. Multi-station Supervisory Control, Telemetering and Communication on Single-Frequency Carrier Channel. (50-175)....1115–21; disc. 1122
Deubel, Justin A. Flame Detectors for Domestic Fuel Burner Safety Devices. (50-35)....220–5
Diemond, Clifford C.; D. L. Wylie. The Bonneville Power Administration Relaying and Reclosing Program. (50-164)....1039–46; disc. 1047
Dillow, N. E.; J. W. Butler. The Choice of Main Power Transformers for Generating Stations. (50-128)....781–5
Doba, S., Jr.; J. W. Rieke. Clampers in Video Transmission. (50-72)....477–87
Dornhoefer, W. J. Disc....1138
Dovjikov, A. Disc....384
Dow, W. G.; H. A. Romanowitz. Statistical Nature and Physical Concepts of Thyratron Deionization Time. (50-56)....368–79
Driscoll, E. G. Disc....1590
Driscoll, John M.; H. C. Otten. Thrust Bearing Problems and Their Solution on Turbine-Generator Units and Auxiliaries of the Consolidated Edison System. (50-270)....1642–7
Drought, A. B.; C. L. Dawes, C. H. Thomas. Impulse Measurements by Repeated Structure Networks. (50-89)....571–80; disc. 580
Durand, S. R. High-Voltage Rectifier Equipment and Control for Tube Testing. (50-145)....909–12

E

Eager, G. S., Jr. Disc....355
Eaton, J. R.; J. B. Ward, H. W. Hale. Total and Incremental Losses in Power Transmission Networks. (50-97)....626–31; disc. 631
Edwards, Charles M.; E. C. Johnson, Jr. An Electronic Simulator for Nonlinear Servomechanisms. (50-47)....300–06; disc. 306
Ein, S. Disc....59
Ellis, H. M.; G. D. McCann, J. E. Conner. Dielectric Recovery Characteristics of Power Arcs in Large Air Gaps. (50-96)....616–24; disc. 624
Elst, J. A.; W. R. Brownlee. Disc....391
Engineering Staff of Anaconda Wire and Cable Company. Disc....879, 898
Erickson, L. G. A Simplified 48-Channel Carrier Telephone System (50-240)....1493–1500
Evans, O. D. Disc....1478, 1517
Evans, Walter R. Control System Synthesis by Root Locus Method. (50-11)....66–9

F

Farr, John W. A New Line of Orthomagnetic Bushing-Type Current Transformers. (50-62)....424–8
Faucett, M. A.; M. Fischer, Jr., M. S. Helm. Effect of Three-Phase Motor Loads on Voltage Changes Produced by Single-Phase Loads. (50-236)....1467–72
Fechheimer, Carl J. An Experimental and Analytical Study of Turbine Generator Rotor Ventilation. (50-256)....1563–9
Fechheimer, Carl J. Liquid Cooling of A-C Turbine Generators. Part II. (50-28)....165–71; disc. 171
(Part I–1947)
Fechheimer, Carl J. Disc....185
Ferguson, J. G.; F. A. Korn. The Number 5 Crossbar Dial Telephone Switching System. (50-41)..244–54
Finison, Harvey J. Basic Patterns for Arrangement of Electric Power Systems for Steel Mills. (50-9)....54–9; disc. 60
Finzi, L. A. Disc....611, 942
Finzi, L. A.; D. C. Beaumariage. General Characteristics of Magnetic Amplifiers. (50-148)..919–27
Finzi, L. A.; D. W. VerPlanck, D. C. Beaumariage. An Analysis of Transients in Magnetic Amplifiers. (50-76)....498–503
Fischer, E. G. Disc....126
Fischer, H. D., Jr. Disc....1478
Fisher, M., Jr.; M. A. Faucett, M. S. Helm. Effect of Three-Phase Motor Loads on Voltage Changes Produced by Single-Phase Loads. (50-236)....1467–72
Fleming, D. B.; J. S. Lodmer. Contributing Factors in Determining the Ratings of Power Transformers for Use on the Systems of the Hydro-Electric Power Commission of Ontario. (50-273)....1658–62
Floyd, G. D. Disc....77
Foley, A. H. A Direct Reading High-Voltage Capacitance Bridge. (50-110)....692–8; disc. 698
Foster, G. E. The Metrotype System of Digital Recording and Telemetering. (50-84)....543–6
Fountain, L. L. Disc....471
Franck, R. E.; R. A. Pfuntner, F. R. D'Entremont. A New Dry-Type Insulation for Instrument Transformers. (50-66)....453–8
Frank, Jerome M.; A. J. Hauck. Control Circuit Transformers. (50-217)....1376–8
Franklin, Paul W. Disc....1217, 1226, 1280
Frederickson, C. W. Disc....43
Frederickson, C. W.; C. E. Asbury. Disc....1121
Freeman, Stephen, Jr. Disc....1575
Friedrich, R. E.; W. M. Leeds. High-Voltage Oil Circuit Breakers for 5,000,000 to 10,000,000-Kva Interrupting Capacity. (50-12)....70–6; disc. 77
Friend, O. A. Disc....269
Frost, A. E. A Printing Telegraph Tape-to-Page Translator. (50-13)....79–83
Fugill, A. P. Disc....50

G

Garbarino, Harold L.; E. T. B. Gross. The Goerges Phenomenon—Induction Motors with Unbalanced Rotor Impedances. (50-255)..1569–74; disc. 1574
Garin, A. N. Disc....794
Gartner, C. M. Disc....690
Garrett, K. S. Disc....1399
Gay, F. W. Disc....392
Geiger, J. M.; J. A. Lind. Centralized Control Desirable for Single Boiler-Turbine-Generator Units. (50-187)....1176–9
George, E. K. Disc....631
Ginsberg, David. Design Calculations for A-C Generators. (50-201)....1274–80; disc. 1281
Glaiger, Paul E. Underground Hydroelectric Power Plants. (50-186)....1169–75
Glover, H. A. Disc....1025
Goelz, G. W.; J. F. Calvert. Analogue Computer for Multicomponent Fractionation Calculations. (50-15)....97–103
Goff, L. E. An Improved Reclosing Relay. (50-238)....1480–4; disc. 1486
Goldman, J. E. Disc....51
Goldsborough, S. L. Disc....43
Goldsborough, S. L.; J. L. Blackburn. Disc....1047
Goldsmith, L. M. Disc....1604
Gopalakrishna, H. V.; M. S. Thacker. Suggested Improvements in the Performance Calculations of Single-Phase Induction Motors. (50-1)....1–6; disc. 7
Gordy, F. D. Audible Noise of Power Transformers. (50-8)....45–50; disc. 53
Gordy, T. D. Disc....126, 1145, 1152, 1415
Gordy, T. D.; G. G. Somerville. Single-Phase Power Transformer Formed Cores. (50-220)....1384–7
Gould, G. G.; E. Krupotich. Variable Speed Drive Constant Frequency Alternator. (50-119)....745–7; disc. 747
Gracey, A. L. Basic Theory Underlying Bell System Facilities Capacity Tables. (50-40)....238–43
Graff, J. M. Disc....413
Greebler, Paul. Disc....348
Greebler, Paul; G. F. Barnett. Heat Transfer Study on Power Cable Ducts and Duct Assemblies. (50-55)....357–64; disc. 366
Greenfield, E. W. Power Factor Measurements on Polyphase and Multiconductor Cable Using Single-Phase Bridges. (50-107)..680–5; disc. 685
Greenfield, E. W. Disc....1597
Greenfield, E. W.; L. F. Roehmann. Development of Improved Luminous Sign Cable. (50-53)....350–5; disc. 356
Grobel, L. P.; D. S. Snell. Continuous Scavenging System for Hydrogen-Cooled Generators. (50-268)....1625–36
Gross, Eric T. B. Disc....452, 476, 793, 870, 1205
Gross, Eric T. B.; H. H. Brown. Practical Experiences with Resonant Grounding in a Large 34.5-Kv System. (50-224)....1401–06; disc. 1407
Gross, Eric T. B.; R. D. Camburn. Analysis of Synchronous Machine Short Circuits. (50-37)....671–8; disc. 679
Gross, Eric T. B.; H. L. Garbarino. The Goerges Phenomenon—Induction Motors with Unbalanced Rotor Impedances. (50-255)..1569–74; disc. 1574
Gross, I. W.; F. A. Lane, P. S. Pugh. Selection, Design, and Operation of Power Transformers on American Gas and Electric Company System. (50-129)....786–93; disc. 795
Gunter, F. B.; D. R. Pattison, M. E. Reagan, S. C. Leyland. Field Testing a Microwave Channel for Voice Communication, Relaying, Telemetering, and Supervisory Control. (50-151)....945–51; disc. 952

H

Hadley, N. L. Disc. 776
Hagenguth, J. H. Disc. 582, 942, 1195
Hale, H. W.; J. B. Ward, J. R. Eaton. Total and Incremental Losses in Power Transmission Networks. (50-97) 626–31; disc. 631
Hale, John; J. M. Benjamin, Jr., E. L. Carstensen, H. E. Tompkins. Electrical Instrumentation in Medical Research. (50-209) 1324–7
Halfmann, Edward S. Critical Inside Dimensions for Power Cable Manholes. (50-256) 1576–80; disc. 1580
Hall, Albert C. A Generalized Analogue Computer for Flight Simulation. (50-48) 308–20
Halperin, Herman. Disc. 199, 1070
Hanff, E. A. Electrode Control and Associated Operating Mechanisms. (50-88) 567–70; disc. 570
Harder, E. L. Disc. 541
Harder, E. L.; J. T. Carleton. New Techniques on the Anacom—Electric Analog Computer. (50-85) 547–56
Harder, E. L.; R. C. Cheek, J. M. Clayton. Regulation of A-C Generators with Suddenly Applied Loads. Part II. (50-58) 395–405; disc. 406
(Part I—1944)
Harder, E. L.; W. F. Horton. Response Time of Magnetic Amplifiers. (50-177) 1130–8; disc. 1141
Hardy, D. R.; J. D. Craggs. The Irradiation of Spark Gaps for Voltage Measurement. (50-90) 584–90
Harrison, A. M. Disc. 1236
Hartzell, H. W. Disc. 973
Hatch, W. H.; F. E. Andrews. Disc. 541
Hatcher, C. T. Disc. 1580
Hauck, A. J.; J. M. Frank. Control Circuit Transformers. (50-217) 1376–8
Hayford, B. I. Disc. 413
Headley, C. L. Differential Relay Sensitivity Adjuster. (50-190) 1203–05; disc. 1205
Heberlein, G. E. Disc. 1025
Helm, M. S.; M. A. Faucett, M. Fisher, Jr. Effect of Three-Phase Motor Loads on Voltage Changes Produced by Single-Phase Loads. (50-236) 1467–72
Herskind, C. C. Disc. 523
Herskind, C. C.; J. E. Hudson. Ignitron Pulse Equipment for Particle Accelerators. (50-157) 992–6
Heumann, G. W. Disc. 1575
Hibbard, L. J.; C. C. Whittaker, E. W. Ames. Rectifier-Type Motive Power for Railroad Electrification. (50-81) 519–23; disc. 523
Hickernell, L. F. Disc. 1598
Hill, A. W. Disc. 423
Hinton, C. B. Disc. 1407
Hodgkins, R. L.; H. L. Lowe. Centralized Control Board for Steam-Electric Generating Plants. (50-223) 1396–9; disc. 1399
Hoffmann, D. C.; A. G. Mellor, N. E. Starkey. Control of Gas Turbines for Power Generation. (50-269) 1637–41
Holm, J. G. Disc. 840
Holmdahl, N. G.; C. L. Killgore. Hydroelectric Generator Excitation Experience at Grand Coulee. (50-137) 855–60
Hooper, C. K.; C. H. McAdie. Effects of Supply Line Unbalance on the Filtered Output Ripple of Polyphase Rectifiers. (50-125) 766–70
Horn, M. E.; J. J. Mikos. New Low-Voltage Air Circuit Breaker with 50,000 Ampere Interrupting Capacity at 600 Volts A-C. (50-272) 1654–7; disc. 1657
Horn, M. E.; B. G. Tremblay. An Air Delayed Selective Overcurrent Tripping Device for Low-Voltage Air Circuit Breakers. (50-271) 1649–53
Horstfall, R. T.; K. N. Thompson, R. W. Milk, P. O. Bobo. Automatic Control of Metal-Clad Switchgear Serving Oil Refinery Motors During Power System Disturbances. (50-261) 1600–03; disc. 1603
Horstman, C. C. Disc. 51
Horton, W. F.; E. L. Harder. Response Time of Magnetic Amplifiers. (50-177) 1130–8; disc. 1141
Howard, S. B.; W. A. McMorris, J. R. Meador. Disc. 95
Hudson, J. E.; C. C. Herskind. Ignitron Pulse Equipment for Particle Accelerators. (50-157) 992–6
Hunt, Lloyd F. Disc. 475
Hunter, E. M. Disc. 540
Hvizd, Andrew, Jr. Disc. 710

I

Ingledow, T.; J. H. Steede. The Bridge River Hydroelectric Development. (50-136) 845–54

J

Jalonack, H. M.; H. P. St. Clair. Development of Preferred Voltage Ratings for Transformers. (50-166) 1049–59
James, H. B. Disc. 1248
James, H. B.; R. P. Judkins, C. L. Mershon. Wide Speed Range A-C Electric Systems for Aircraft. (50-276) 1353–8; disc. 1358
James, W. Gordon. Disc. 164
Janes, L. R.; F. E. Andrews, M. A. Anderson. Interrupting Ability of Horn-Gap Switches. (50-161) 1016–24; disc. 1027
Jeanne, P. A. Disc. 108, 523
Johnson, A. A.; A. P. Colaiacco, J. E. Reilly. Design and Test on Electronic Exciter Supplied from Common Shaft-Driven Generator. (50-50) 328–35; disc. 336
Johnson, A. A.; H. A. Thompson. Bus Transfer Tests on 2,300-Volt Station Auxiliary System. (50-59) 386–90; disc. 393
Johnson, E. Calvin, Jr.; C. M. Edwards. An Electronic Simulator for Nonlinear Servomechanisms. (50-47) 300–06; disc. 306
Johnson, I. B. Disc. 973
Johnson, I. B.; T. J. Carpenter, L. E. Saline. Evaluation of Lightning Arrester Lead Length and Separation in Co-ordinated Protection of Apparatus Against Lightning. (50-150) 933–41; disc. 941
Johnson, I. B.; L. E. Saline. Disc. 94
Johnson, J. A.; E. M. Stacey. Application of Electronic Motor Drives to Printing Presses. (50-34) 216–19
Johnson, L. J.; H. G. Schafer. A Magnetic Amplifier Frequency Control. (50-95) 613–15
Johnson, Walter C. Disc. 1138
Johnson, Walter C.; F. W. Latson. An Analysis of Transients and Feedback in Magnetic Amplifiers. (50-94) 604–11; disc. 611
Jones, J. W. Disc. 1272
Judkins, R. P.; H. B. James, C. L. Mershon. Wide Speed Range A-C Electric Systems for Aircraft. (50-276) 1353–8; disc. 1358

K

Kaneff, S. Some Aspects of Lightning Surges on Power Systems and Their Suppression. (50-250) 1544–9
Kanouse, E. L.; T. M. Blakslee. Thirteen-Year Lightning Performance of Boulder 287.5-Kv Transmission Lines. (50-130) 796–9; disc. 800
Kanouse, E. L.; A. L. Williams. Power System Planning in the City of Los Angeles. (50-144) 900–07; disc. 908
Karr, J. H.; S. S. L. Chang. A-C Series Motors—A Design Method. (50-198) 1257–61; disc. 1262
Kaufmann, R. H. Disc. 776
Kennedy, L. F. Disc. 475
Kershaw, Wilfred L. Automatic Feathering—To Reduce the Hazard of Aircraft Engine Failure at Take-off. (50-210) 1328–34
Kidder, A. H. Disc. 348
Kilbourne, C. E.; D. S. Snell. Disc. 171
Kilgore, Lee A.; E. C. Whitney. Spring and Damping Coefficients of Synchronous Machines and Their Application. (50-36) 226–9; disc. 229
Killgore, C. L.; N. G. Holmdahl. Hydroelectric Generator Excitation Experience at Grand Coulee. (50-137) 855–60
Killian, S. C. Induced Currents in High-Capacity Bus Enclosures. (50-222) 1388–95; disc. 1395
Killian, S. C. Disc. 1026
Killian, S. C.; C. S. Beattie. Disc. 1491
Kimbark, Edward W. Disc. 678
Kinghorn, J. H. Relay Protection for Medium Length High-Voltage Transmission Lines. (50-68) 461–5; disc. 465
Kinghorn, J. H. Disc. 1604
Kinghorn, J. H.; F. M. Porter. Disc. 340
Kirby, M. J. Stability of Servomechanisms with Linearly Varying Elements. (50-274) 1662–7; disc. 1667
Kirchmayer, L. K. Disc. 631
Kirchmayer, L. K.; A. C. Cook, C. N. Weygandt. Special Devices Aid Differential Analyzer Solution of Complex Problems. (50-215) 1365–70; disc. 1370
Kirschbaum, H. S. Per-Unit Inductances of Synchronous Machines. (50-38) 231–4
Kitchin, Donald W.; J. T. Blake, O. S. Pratt. Failures of Rubber Insulation Caused by Soil Microorganisms. (50-121) 748–54; disc. 755
Klopfenstein, A.; J. Lummis. Use of Techniques from Electrical Analogues in the Study of Transmission Line Vibration. (50-278) 1676–80
Klumb, Ray K. Disc. 889
Knudson, L. I. The Design of Reactors for Radio Interference Filters. (50-204) 1294–8
Kochenburger, Ralph J. A Frequency Response Method for Analyzing and Synthesizing Contactor Servomechanisms. (50-44) 270–83; disc. 283
Koenig, Eldo C. An Electric Analogue Computer Using the Photo Cell as a Nonlinear Element. (50-263) 1606–11
Koenig, H. E. Transient Response of Direct-Current Dynamos. (50-22) 139–44; disc. 145
Korn, F. A.; J. G. Ferguson. The Number 5 Crossbar Dial Telephone Switching System. (50-41) 244–54
Kouwenhoven, W. B. Disc. 685
Kresser, J. V.; W. A. Derr, T. C. Wren. Multistation Supervisory Control, Telemetering and Communication on Single-Frequency Carrier Channel. (50-175) 1115–21; disc. 1122
Krida, H.; E. T. McCurry. A New Grounding and Testing Device for Metal-Clad Switchgear. (50-60) 407–12; disc. 414
Kron, Gabriel. Classification of the Reference Frames of a Synchronous Machine. (50-114) 720–7
Kron, Gabriel. Equivalent Circuits of the Shaded-Pole Motor with Space Harmonics. (50-117) 735–41
Kronacher, G. Static Accuracy Performance of the Selsyn Generator Control-Transformer System. (50-103) 645–53; disc. 653
Kroneberg, A. A. Expansion of the System of the Southern California Edison Company. (50-138) 861–4
Krupotich, F.; G. G. Gould. Variable Speed Drive Constant Frequency Alternator. (50-119) 745–7; disc. 747
Kulman, F. E. Disc. 754

L

Lambert, W. H.; A. H. Phillips, D. R. Pattison. Excitation Improvement—Electronic Excitation and Regulation of Electric Generators as Compared to Conventional Methods. (50-51) 338–40; disc. 340
Lansman, Gerald. Disc. 306
Lane, F. A.; I. W. Grow, P. S. Pugh. Selection, Design and Operation of Power Transformers on American Gas and Electric Company System. (50-129) 786–93; disc. 795
Langstaff, H. A. P. Disc. 335
Larson, N. G. Disc. 546
Latson, Frank W.; W. C. Johnson. An Analysis of Transients and Feedback in Magnetic Amplifiers. (50-94) 604–11; disc. 611
Lebell, D. Disc. 1370
Lee, J. R. Disc. 570
Leeds, W. M. Disc. 25
Leeds, W. M.; R. E. Friedrich. High-Voltage Oil Circuit Breakers for 5,000,000 to 10,000,000-Kva Interrupting Capacity. (50-12) 70–6; disc. 77
LeVesconte, Lester B. Disc. 785
Leyland, S. C.; D. R. Pattison, M. E. Reagan, F. B. Gunter. Field Testing a Microwave Channel for Voice Communication, Relaying, Telemetering, and Supervisory Control. (50-151) 945–51; disc. 952
Lind, J. A.; J. M. Geiger. Centralized Control Desirable for Single Boiler-Turbine-Generator Units. (50-187) 1176–9
Linders, J. R. Disc. 475
Linville, T. M.; D. P. Strang. Current in Equalizer Connections of D-C Machine Armature Windings. (50-192) 1219–26; disc. 1227
Little, J. C.; D. G. MacMillan, J. V. Majercak. Vibration and Fatigue Life of Steel Strand. (50-237) 1473–8; disc. 1479
Livingston, O. W. Control of Large D-C Motors Supplied from Ignitron Rectifiers. (50-32) 205–10
Lord, H. W. The Design of Broad-Band Transformers for Linear Electronic Circuits. (50-159) 1005–10
Lotimer, J. S.; D. B. Fleming. Contributing Factors in Determining the Ratings of Power Transformers for Use on the Systems of the Hydro-Electric Power Commission of Ontario. (50-273) 1658–62
Lowe, H. L.; R. L. Hodgkins. Centralized Control Board for Steam-Electric Generating Plants. (50-223) 1396–9; disc. 1399
Lowerison, Cort. Disc. 108
Lummis, Jordan. Disc. 1518
Lummis, J.; A. Klopfenstein. Use of Techniques from Electrical Analogues in the Study of Transmission Line Vibration. (50-278) 1676–80

M

MacCarthy, D. D. Disc. 942
MacLeod, D. R. Disc. 523
MacMillan, D. G.; J. C. Little, J. V. Majercak. Vibration and Fatigue Life of Steel Strand. (50-237) 1473–8; disc. 1479
Macpherson, R. H. Disc. 107
Madden, T. F.; W. H. Muschler, Jr. Harmonic Index—A Tool for Transformer Audio Noise Investigation. (50-18) 115–18; disc. 120
Magnuson, P. C. Transients in Coupled Inductance-Capacitance Circuits Analyzed in Terms of a Rolling-Ball Analogue. (50-245) 1525–30

Majercak, J. V.; J. C. Little, D. G. MacMillan. Vibration and Fatigue Life of Steel Strand. (50-257) ....1473–8; disc. 1479
Mallory, B. C. Centralized Instrumentation and Control for Steam Electric Power Stations. (50-91) 591–6
Mansfield, Thomas H.; C. F. Dalziel. Effect of Frequency on Perception Currents. (50-184) .1162–8
Marcum, C. R.; J. L. Boyer. Ignitron Converters for High Energy Particle Accelerators. (50-174) 1110–14
Marter, W. E. Transmission-Line Protection of Short Lines of the Metropolitan Area of a Typical System. (50-69) ....468–7; disc. 472
Martin, E. R. Disc. 1281
Maslin, A. J. Transformer Sound Level Considerations. (50-170) ....1142–5; disc. 1147
Maslin, A. J. Disc. 1153
Mason, V. V. Disc. 199, 364
Mathews, C. A. Disc. 471
Matthews, N. W.; E. S. Van Valkenburg. Analogue Techniques for Turbojet Thrust Instrumentation. (50-212) 1342–6
McAdie, C. H.; C. K. Hooper. Effect of Supply Line Unbalance on the Filtered Output Ripple of Polyphase Rectifiers. (50-125) 766–70
McCann, G. D.; J. E. Conner, H. M. Ellis. Dielectric Recovery Characteristics of Power Arcs in Large Air Gaps. (50-96) ....616–24; disc. 624
McClinton, A. T.; E. L. Brancato. Measurement of Insulation Resistance on Energized Systems. (50-194) 1238–42
McConnell, A. J. Disc. 465
McCreary, Harold J. Disc. 36
McCurry, E. T.; H. Krida. A New Grounding and Testing Device for Metal-Clad Switchgear. (50-60) ....407–12; disc. 414
McDonald, Donald. Improvements in the Characteristics of A-C Lead Networks for Servomechanisms. (50-46) 293–300
McKenna, George W. Theory and Application of Transformer Differential Protection. (50-189) 1197–1202
McLean, Corbett. Transformer Noise and Its Confinement. (50-225) ....1409–15; disc. 1415
McMorris, W. A. Disc. 941, 974
McMorris, W. A.; S. B. Howard, J. R. Meador. Disc. 95
Meador, J. R. Disc. 941, 973
Meador, J. R.; J. E. Clem, W. J. Rudge, A. H. Powell. Proposed Basic Impulse Insulation Levels for High-Voltage Systems. (50-152) ....953–60; disc. 963
Meador, J. R.; W. A. McMorris, S. B. Howard. Disc. 95
Mellor, A. G.; D. C. Hoffmann, N. E. Starkey. Control of Gas Turbines for Power Generation. (50-269) 1637–41
Mellor, A. G.; M. Temoshok. Excitation System Performance with Motor-Driven Exciters. (50-49) 321–7
Mellor, A. G.; M. Temoshok. Disc. 390
Mendenhall, I. S.; F. L. Taylor. Quiet Transformer Installations—A Problem for Both Equipment and Substation Designers. (50-179) ....1148–52; disc. 1153
Merrill, J. L., Jr. A Negative Impedance Repeater. (50-235) 1461–6
Mershon, C. L.; H. B. James, R. P. Judkins. Wide Speed Range for A-C Electric Systems for Aircraft. (50-276) ....1353–8; disc. 1358
Mesner, John. Fundamentals of the Automatic Telephone Message Accounting System. (50-42) 255–68
Mikhail, Saad L. Potier Reactance for Salient-Pole Synchronous Machines. (50-39) 235–8
Mikhail, Saad L. Symmetrical Short Circuits on Saturated Alternators. (50 253) 1554–62
Mikos, J. J.; M. E. Horn. New Low-Voltage Air Circuit Breaker with 50,000 Ampere Interrupting Capacity at 600 Volts A-C. (50-272) ....1654–7; disc. 1657
Miller, C. Frank; F. G. Whelan. An Improved Method of Measuring Dissipation Factor and Dielectric Constant Using the Susceptance Variation Principle. (50-74) 491–7
Miller, R. H. Disc. 951, 1037, 1108
Mills, Robert L. Dynamic Characteristics of Carbon Pile Voltage Regulators. (50-213) ....1347–52; disc. 1352
Mills, R. W.; R. T. Horsfall, K. N. Thompson, P. O. Bobo. Automatic Control of Metal-Clad Switchgear Serving Oil Refinery Motors During Power System Disturbances. (50-261) ....1600–03; disc. 1603
Monteith, A. C.; P. Sporn. Progress Report on Tidd 500-Kv Test Project of the American Gas and Electric Company—Corona, Radio Influence, and Other Factors. (50-143) ....891–7; disc. 899
Moore, A. D. The Further Development of Fluid Mappers. (50-267) 1615–24
Morey, A. H. The Alco-GE 4,500-Horsepower Gas-Turbine Electric Locomotive. (50-77) 504–07
Morgan, F. D.; L. H. Rahlen. Disc. 1395
Morgan, R. E.; H. M. Ogle, V. J. Wattenberger. The Extension of Amplistat Performance by A-C Components. (50-156) 986–91
Morgan, R. E.; J. A. Walley. An Amplistat Regulator Applied to a 5-Kva 400-Cycle Aircraft Inverter. (50-195) ....1243–8; disc. 1248
Morgan, W. A. Disc. 108, 841, 907
Morgan, W. A.; R. W. World. Relaying Practices and Economical Switching Station Arrangements of the Bureau of Reclamation. (50-140) ....865–70; disc. 871
Morgan, W. A.; R. W. World. Disc. 1046
Morton, W. B. Disc. 1492
Mulhern, M. J. High-Voltage Ignitron Rectifiers (50-146) 913–18
Mulhern, M. J.; S. N. Crawford. Rectifier Equipment for Electronic D-C Motor Drives. (50-33) ..211–15
Murphy, B. R. Disc. 1518
Murray, C. S. Disc. 52, 118, 1146
Mutschler, W. H., Jr.; T. F. Madden. Harmonic Index—A Tool for Transformer Audio Noise Investigation. (50-18) ....115–18; disc. 120

N

Naef, Otto. Disc. 26, 637, 879
Nagel, G. A. Disc. 405
Narbutovskih, Paul. Disc. 708
Nau, Robert H. Disc. 76, 1657
Nebel, C. N. Local Wire Video Television Networks. (50-234) 1451–60
Neher, J. H. Disc. 365
Neher, J. H.; F. H. Buller. The Thermal Resistance Between Cables and a Surrounding Pipe or Duct Wall. (50-52) ....342–7; disc. 349
New, Warren C. Combined Phase and Ground Distance Relaying. (50-7) ....37–42; disc. 44
Newell, E. L.; C. H. Cramer. A Two-Channel Carrier Telegraph System for Short Submarine Cables. (50-10) 61–5
Noest, John G. Disc. 384, 391, 405
Norris, R. H.; Mrs. B. O. Buckland. Disc. 347
Norris, R. H.; D. S. Snell, B. O. Buckland. Surface Heat-Transfer Coefficients for Hydrogen-Cooled Rotating Electric Machines. (50-29) ....174–85; disc. 185
Nottheff, Arthur P., Jr. Phase Lead for A-C Servo Systems with Compensation for Carrier Frequency Changes. (50-45) ....285–91; disc. 292
Nylander, A. L.; A. J. Corson. Power Measurement by the Hook-On Method. (50-111) 699–702

O

Ogle, H. M.; R. E. Morgan, V. J. Wattenberger. The Extension of Amplistat Performance by A-C Components. (50-156) 986–91
Olney, Frank D. Resistance Commutation. (50-191) ....1207–15; disc. 1217
Olney, Frank D. Disc. 690
Opsahl, A. M. Disc. 113, 539, 941, 960
Opsahl, A. M.; E. Beck. Disc. 92
Osipovich, A. A. Light Steel Tower Line Design. (50-243) ....1513–17; disc. 1519
Ottendorf, B., Jr. A New Electronic Telegraph Regenerative Receiver. (50-6) ....32–6; disc. 36
Ostline, J. E. The Universal Director in Strowger Automatic Telephone Systems. (50-169) ..1080–7
Otten, H. C.; J. M. Driscoll. Thrust Bearing Problems and Their Solution on Turbine-Generator Units and Auxiliaries of the Consolidated Edison System. (50-270) 1642–7
Owen, T. B. Tracking Radio Noise on Aircraft. (50-196) 1249–52
Owens, J. B. Ice Testing of Outdoor Disconnecting Switches to Simulate Field Conditions. (50-239) ....1488–91; disc. 1491

P

Packer, L. C. Disc. 1261
Park, J. H. Disc. 581
Parker, Wayne A. Disc. 1508
Parks, C. E.; W. R. Brownlee. Consideration of Requirements and Limitations of Relaying and High-Speed Reclosing on Long and Heavily-Loaded Transmission Lines. (50-16) ....103–07; disc. 109
Parmakian, John. Disc. 1273
Paratale, A. J.; P. D. Tillson. Characteristics of Some Magnetic-Fluid Clutch Servomechanisms. (50-24) 150–7
Pattison, D. R.; A. H. Phillips, W. H. Lambert. Excitation Improvement—Electronic Excitation and Regulation of Electric Generators as Compared to Conventional Methods. (50-51) ..338–40; disc. 340
Pattison, D. R.; M. E. Reagan, S. C. Leyland, F. B. Gunter. Field Testing a Microwave Channel for Voice Communication, Relaying, Telemetering, Supervisory Control. (50-151) ..945–51; disc. 952
Pearce, C. T. Disc. 1272
Peck, R. R. Disc. 1152
Peterson, W. S.; B. Comrent, J. S. Carroll. Desert Measurements of Corona Loss on Conductors for Operation Above 230 Kv. (50-141) ....872–8; disc. 880
Petrucelly, Vincent J. Resistance Wire Strain Gauges as Elements of the Wheatstone Bridge. (50-118) 732–4
Pfieffer, W. F. Interexchange Tandem Trunking in the Los Angeles Metropolitan Area. (50-168) 1071–9
Pfuntner, R. A.; R. E. Franck, F. R. D'Entremont. A New Dry-Type Insulation for Instrument Transformers. (50-66) 453–8
Philbrick, George A. Disc. 283
Phillips, A. H.; W. H. Lambert, D. R. Pattison. Excitation Improvement—Electronic Excitation and Regulation of Electric Generators as Compared to Conventional Methods. (50-51) ..338–40; disc. 340
Porter, F. M. Disc. 201
Porter, F. M.; J. H. Kinghorn. Disc. 340
Povey, E. H. Disc. 698
Powell, A. H.; J. E. Clem, J. R. Meador, W. J. Rudge. Proposed Basic Impulse Insulation Levels for High-Voltage Systems. (50-152) ....953–60; disc. 963
Powers, R. C. Disc. 1280
Pratt, Orison S.; J. T. Blake, D. W. Kitchin. Failures of Rubber Insulation Caused by Soil Microorganisms. (60-121) ....748–54; disc. 755
Prince, D. C.; W. F. W. Alexanderson, C. H. Willis. Disc. 843
Prior, C. H. Disc. 842
Pritchett, Wilson S.; R. M. Saunders. Indicating Instruments at the Servomechanism Frequencies. (50-155) 980–5
Puchatein, A. F. Disc. 1215, 1261
Pugh, P. S.; F. A. Lane, I. W. Gross. Selection, Design, and Operation of Power Transformers on American Gas and Electric Company System. (50-129) ....786–93; disc. 795

R

Raab, E. L.; E. D. Treanor. Transformer Oil. (50-165) ....1060–70; disc. 1070
Rademacher, L. B.; W. L. Teague. Disc. 539
Ramsaur, O. Disc. 466
Reagan, M. E.; D. R. Pattison, S. C. Leyland, F. B. Gunter. Field Testing a Microwave Channel for Voice Communication, Relaying, Telemetering, Supervisory Control. (50-151) ..945–51; disc. 952
Rector, R. V.; W. E. Sutter. Microwave Systems for 960 and 2,000 Megacycles. (50-171) ....1100–08; disc. 1108
Reed, J. R. Solderless Commutator Joints for High Temperature Operation of Railway Traction Armatures. (50-100) 638–41
Reed, J. Ross; J. J. Tyner. A New Resilient Class-H Material for the Insulation of Traction Motor Field Coils. (50-182) 1158–61
Reese, F. E.; E. C. Roys. Dial Telephone Central Office Buildings for Small Communities. (50-248) 1535–9
Reifschneider, P. J.; B. S. Beall, III. Aircraft D-C Circuit Breakers for 28 and 120 Volts. (50-202) 1283–8
Reilly, J. E.; A. P. Colaiacco, A. A. Johnson. Design and Test on Electronic Exciter Supplied from Common Shaft-Driven Generator. (50-50) ....328–35; disc. 346
Rice, Berton S. Disc. 907
Rieke, J. W.; S. Doba, Jr. Clampers in Video Transmission. (50-72) 477–87
Rietz, E. B. Development and Testing of an Improved High-Voltage, High-Capacity Impulse Circuit Breaker. (50-3) ....15–25; disc. 26
Rietz, E. B.; C. J. Balentine. A New 69-Kv Oil Blast Circuit Breaker. (50-61) ....416–33; disc. 423
Robertson, Lawrence M. Disc. 1406
Robinson, Paul B.; H. D. Snively. Measurement and Calculation of D-C Machine Armature Circuit Inductance. (50-193) ....1228–35; disc. 1237
Robison, H. F.; W. H. Wickham. A New Device for Calibrating Watt-Hour Meters. (50-116) ..732–4
Roehmann, L. F. Disc. 523
Roehmann, L. F.; E. W. Greenfield. Development of Improved Luminous Sign Cable. (50-53) ....350–5; disc. 356
Romanowitz, H. A.; W. O. Dow. Statistical Nature and Physical Concepts of Thyratron Deionization Time. (50-56) 368–79
Rorden, Harold L. Lightning Arresters as a Criterion for Insulation Levels. (50-14) ....84–91; disc. 95
Rosch, S. J. Disc. 356
Rose, H. A. Disc. 1129
Ross, I. E. Aircraft Electric Motors Need Test Equipment. (50-277) 1359–64
Ross, M. D.; R. A. Towne. Disc. 199
Roys, E. C.; F. D. Reese. Dial Telephone Central Office Buildings for Small Communities. (50-248) 1535–9

Rudge, W. J.; J. E. Clem, J. R. Meador, A. H. Powell. Proposed Basic Impulse Insulation Levels for High-Voltage Systems. (50-152)...953–60; disc. 963
Ruhlen, L. H.; F. D. Morgan. Disc....1395
Ruck, Ake; G. Westerberg. Underground Hydroelectric Power Stations in Sweden. (50-149)...928–32
Ryan, J. E.; T. M. Spitler. The Operating Speed of D-C Brake Magnets. (50-197)....1253–7

S

St. Clair, H. P. Disc....77
St. Clair, H. P.; H. M. Jalonack. Development of Preferred Voltage Ratings for Transformers. (50-166)....1049–59
Saline, L. E. Disc....973
Saline, L. E.; T. J. Carpenter, I. B. Johnson. Evaluation of Lightning-Arrester Lead Length and Separation in Co-ordinated Protection of Apparatus Against Lightning. (50-150)...933–41; disc. 941
Saline, L. E.; I. B. Johnson. Disc....94
Saunders, Robert M.; W. S. Pritchett. Indicating Instruments at the Servomechanism Frequencies. (50-155)....980–5
Schafer, H. G.; L. J. Johnson. A Magnetic Amplifier Frequency Control. (50-95)....613–15
Schirmer, A. H. Protective Grounding of Electrical Installations on Customer's Premises. (50-105)....657–9
Schirmer, P. W. Disc....1122
Schuck, C. L. A New High Interrupting Capacity Low-Voltage Power Fuse. (50-127)...770–6; disc. 776
Schumacher, W. W. Aluminum Conductors from an Aircraft Manufacturer's Viewpoint. (50-211)....1335–41
Scorgie, Donald G. Transient Analysis of a Voltage-Regulated Aircraft D-C System. (50-208)...1318–23
Seelye, Howard P. Selection and Application of Power Transformers. (50-134)....830–3
Seelye, Howard P. Disc....1059
Shepherd, R. V. Disc....229
Sheppard, R. Disc....1647
Sherrard, E. S. Disc....1352, 1358
Siegel, Ralph. Disc....811
Sinnott, Joseph F. A 5,000-Kva Underground Substation. (50-142)....882–9; disc. 890
Smith, Edward J. Determination of Steady-State Performance of Self-Saturating Magnetic Amplifiers. (50-206)....1309–17
Smith, E. P. Disc....1226
Smith, H. B. Disc....631
Smith, Howard H. A Medium-Haul Carrier Telephone System. (50-242)....1505–12
Smith, Otto J. M. Generator Rating of Induction Motors. (50-20)....129–35
Smith, R. M. Locomotive Wheel-Slip and Wheel-Lock Protection. (50-181)....1154–7
Smith, R. M. Disc....1491
Snell, D. S. Loading of Hydrogen-Cooled Generators at Elevated Gas Pressures. (50-30)....186–99; disc. 202
Snell, D. S.; L. P. Grobel. Continuous Scavenging System for Hydrogen-Cooled Generators. (50-268)....1625–36
Snell, D. S.; C. E. Kilbourne. Disc....171
Snell, D. S.; R. H. Norris, B. O. Buckland. Surface Heat-Transfer Coefficients for Hydrogen-Cooled Rotating Electric Machines. (50-29)....174–85; disc. 185
Snively, H. D.; P. B. Robinson. Measurement and Calculation of D-C Machine Armature Circuit Inductance. (50-193)....1228–35; disc. 1237
Snyder, F. L. Disc....793
Somerville, G. G.; T. D. Gordy. Single-Phase Power Transformer Formed Cores. (50-220)....1384–7
Sonnemann, W. K. A Study of Directional Element Connections for Phase Relays. (50-233)....1438–50; disc. 1450
Specht, T. R. Disc....1416
Specht, T. R.; R. N. Wagner. The Theory of the Current Transductor and Its Application in the Aluminum Industry. (50-64)...441–52; disc. 452
Spitler, T. M.; J. E. Ryan. The Operating Speed of D-C Brake Magnets. (50-197)....1253–7
Sporn, Philip; A. C. Monteith. Progress Report on Tidd 500-Kv Test Project of the American Gas and Electric Company—Corona, Radio Influence, and Other Factors. (50-143)....891–7; disc. 899
Stacey, E. M.; J. A. Johnson. Application of Electronic Motor Drives to Printing Presses. (50-34)...216–19
Starcke, O. A. Disc....952
Starkey, N. E.; D. C. Hoffmann, A. G. Mellor. Control of Gas Turbines for Power Generation. (50-269)....1637–41
Starr, E. C. Disc....91, 112
Steede, J. H.; T. Ingledow. The Bridge River Hydroelectric Development. (50-136)....845–54
Stein, G. M. Disc....1374
Stevens, Richard F. Application and Handling of Very Large Power Transformers on the System of the Bonneville Power Administration. (50-26)....158–63; disc. 163
Stevens, R. F.; T. W. Stringfield. Microwave Applications to Bonneville Power Administration System. (50-170)....1088–99
Stewart, H. M. Disc....1603
Stewart, H. R.; F. M. Defandorf. New Lightning Arrester Standard. (50-82)....525–6
Stimson, Allen; C. F. Taylor. Principles of Design of Log-Scale D-C Indicating Instruments. (50-160)....1011–15
Storm, H. F. Series-Connected Saturable Reactor with Control Source of Comparatively High Impedance. (50-205)....1299–1309
Storm, H. F. Series-Connected Saturable Reactor with Control Source of Comparatively Low Impedance. (50-123)....756–65
Strang, D. P.; T. M. Linville. Current in Equalizer Connections of D-C Machine Armature Windings. (50-192)....1219–26; disc. 1227
Streifus, C. A. Disc....1486
Streifus, C. A.; F. Von Roeschlaub. Disc....42
Stringfield, T. W.; R. F. Stevens. Microwave Applications to Bonneville Power Administration System. (50-170)....1088–99
Stuelpnagel, Thomas R. An Environment-Free 120-Volt D-C High-Performance Limit Switch. (50-203)....1289–93
Suhr, F. W. Disc....6
Sutter, Carl. Disc....1406
Sutter, W. E.; R. V. Rector. Microwave Systems for 960 and 2,000 Megacycles. (50-171)....1100–08; disc. 1108

T

Taylor, C. F.; A. Stimson. Principles of Design of Log-Scale D-C Indicating Instruments. (50-160)....1011–15
Taylor, D. W. Disc....392
Taylor, F. L.; I. S. Mendenhall. Quiet Transformer Installations—A Problem for Both Equipment and Substation Designers. (50-179)....1148–52; disc. 1153
Taylor, Hugh M., Jr. Disc....1433
Teague, William L. Disc....94
Teague, W. L.; L. B. Rademacher. Disc....539
Temoshok, M. Disc....899
Temoshok, M.; A. G. Mellor. Excitation System Performance with Motor-Driven Exciters. (50-49)....321–7
Temoshok, M.; A. G. Mellor. Disc....390
Tetherow, C. L. Synthetic Load for Testing Rectifiers. (50-102)....642–4
Thacker, M. S.; H. V. Gopalakrishna. Suggested Improvements in Performance Calculations of Single-Phase Induction Motors. (50-1)....1–6; disc. 7
Thomas, C. H.; C. L. Dawes, A. B. Drought. Impulse Measurements by Repeated Structure Networks. (50-89)....571–80; disc. 580
Thomas, M. A. Disc....1574
Thompson, A. T. Disc....581
Thompson, H. A.; A. A. Johnson. Bus Transfer Tests on 2,300-Volt Station Auxiliary System. (50-59)....386–93; disc. 393
Thompson, K. N.; R. T. Horsfall, R. W. Mills, P. O. Bobo. Automatic Control of Metal-Clad Switchgear Serving Oil Refinery Motors During Power System Disturbances. (50-261)..1600–03; disc. 1603
Tilles, Abe. Disc....800, 878
Tilton, P. D.; A. J. Parzale. Characteristics of Some Magnetic-Fluid Clutch Servomechanisms. (50-24)....150–7
Tipton, E. W. Variations of Tank Pressure with Transformer Loading in Sealed Transformers. (50-275)....1669–73; disc. 1673
Tomlinson, C. M. Disc....269
Tompkins, Howard E.; J. M. Benjamin, Jr., J. Hale, E. L. Carstensen. Electrical Instrumentation in Medical Research. (50-209)....1324–7
Towne, R. A.; M. D. Ross. Disc....199
Treanor, E. D.; E. L. Raab. Transformer Oil. (50-165)....1060–70; disc. 1070
Tremaine, R. L.; R. C. Cheek. A Voltage Gradient Meter. (50-98)....633–7; disc. 637
Tremblay, B. G.; M. E. Horn. An Air Delayed Selective Overcurrent Tripping Device for Low-Voltage Air Circuit Breakers. (50-271)....1649–53
Trickey, P. H. Disc....747
Tuller, W. G. Information Theory Applied to System Design. (50-266)....1612–14
Tyner, J. J.; J. Ross Reed. A New Resilient Class-H Material for the Insulation of Traction Motor Field Coils. (50-182)....1158–61

V

Valentine, C. E. Disc....384
Van Ness, B., Jr. Disc....1272
Van Valkenburg, E. S.; N. W. Matthews. Analogue Techniques for Turbojet Thrust Instrumentation. (50-212)....1342–6
VerPlanck, D. W.; L. A. Finzi, D. C. Beaumariage. An Analysis of Transients in Magnetic Amplifiers. (50-76)....498–505
Vikoren, O. B. Disc....412
Vincent, W. D. Amplidyne-Controlled Log Carriage Drive. (50-176)....1124–9; disc. 1129
Vogel, F. J. Margins Between Lightning Arrester Protective Levels and Transformer Insulation. (50-17)....110–12; disc. 114
Vogel, F. J. Disc....1673
Von Roeschlaub, F.; C. A. Streifus. Disc....42
Von Voigtlander, F. Disc....119
Votaw, R. W.; A. E. Blume. Disc....653

W

Wadleigh, K. H.; H. A. Adler. Disc....1580
Waghorne, J. H. Rural Neutral Potentials. (50-106)....660–3
Wagner, C. F. Disc....961
Wagner, H. H. Disc....1673
Wagner, R. N.; T. R. Specht. The Theory of the Current Transductor and Its Application in the Aluminum Industry. (50-64)...441–52; disc. 452
Waidelich, D. L. Steady-State Waves on Transmission Lines. (50-244)....1521–4
Walley, J. A.; R. E. Morgan. An Amplistat Regulator Applied to a 5-Kva 400-Cycle Aircraft Inverter. (50-195)....1243–8; disc. 1248
Ward, J. B.; J. R. Eaton, H. W. Hale. Total and Incremental Losses in Power Transmission Networks. (50-97)....626–31; disc. 631
Warrick, T. J. Control System for a 4,500-Horsepower Gas-Turbine Electric Locomotive. (50-78)...508–13
Watchorn, C. W. The Determination and Allocation of the Capacity Benefits Resulting from Interconnecting Two or More Generating Systems. (50-188)....1180–6
Watchorn, C. W. Disc....1688
Watkins, E. G. Underground Conduit for Electric Power Systems—Fundamentals and Basic Design Considerations. (50-257)....1582–90; disc. 1590
Wattenberger, V. J.; R. E. Morgan, H. M. Ogle. The Extension of Amplistat Performance by A-C Components. (50-156)....986–91
Webb, R. L. Disc....391
Wentz, E. C. Disc....452
West, C. P. Disc....602, 1399
Westerberg, G.; A. Ruack. Underground Hydroelectric Power Stations in Sweden. (50-149)....928–32
Weygandt, C. N.; A. C. Cook, L. K. Kirchmayer. Special Devices Aid Differential Analyzer Solution Complex Problems. (50-215)..1365–70; disc. 1370
Whelan, Frederick G.; C. F. Miller. An Improved Method of Measuring Dissipation Factor and Dielectric Constant Using the Susceptance Variation Principle. (50-74)....491–7
Whitehead, E. R. Disc....1196
Whitney, E. C. Disc....405
Whitney, Eugene C.; L. A. Kilgore. Spring and Damping Coefficients of Synchronous Machines and Their Application. (50-36)....226–9; disc. 229
Whittaker, C. C.; L. J. Hibbard, E. W. Ames. Rectifier-Type Motive Power for Railroad Electrification. (50-81)....519–23; disc. 523
Wickham, W. H.; H. F. Robison. A New Device for Calibrating Watt-Hour Meters. (50-116)...732–4
Wilder, Willard S. Disc....475
Wilkinson, R. I. Disc....243
Williams, A. L.; E. L. Kanouse. Power System Planning City of Los Angeles. (50-144)..900–07; disc. 908
Willis, C. H.; W. F. W. Alexanderson, D. C. Prince. Disc....843
Wiseman, R. J. Disc....348, 365, 754, 1580, 1591, 1598
Witzke, R. L.; T. J. Bliss. Co-ordination of Lightning Arrester Location with Transformer Insulation Level. (50-153)....964–73; disc. 974
Witzke, R. L.; T. J. Bliss. Surge Protection of Cable-Connected Equipment. (50-83)..527–38; disc. 539
Witzke, R. L.; T. J. Bliss. Disc....943
Wolfe, W. A. Disc....44, 1406
World, R. W. Disc....475
World, R. W.; W. A. Morgan. Relaying Practices and Economical Switching Station Arrangements of the Bureau of Reclamation. (50-140)....865–70; disc. 871
World, R. W.; W. A. Morgan. Disc....1046
Wortman, H. B. Disc....540
Wren, T. G.; W. A. Derr, J. V. Kresser. Multistation Supervisory Control, Telemetering and Communication on Single-Frequency Carrier Channel. (50-175)....1115–21; disc. 1122
Wyatt, Kenneth S. Disc....754
Wylie, Donald L.; C. C. Diemond. The Bonneville Power Administration Relaying and Reclosing Program. (50-164)....1039–46; disc. 1047

Z

Zadeh, L. A. Disc....1668

Preface

The 1950 TRANSACTIONS (volume 69) of the American Institute of Electrical Engineers will be published in two parts.

Part I contains technical program papers and related discussions presented at the

Winter General Meeting, New York, N. Y., January 30–February 3, 1950.

Part II of the 1950 volume will contain approved papers and related discussions presented at the following meetings:

North Eastern District Meeting, Providence, R. I., April 26–28, 1950.
Great Lakes District Meeting, Jackson, Mich., May 11–12, 1950.
Summer and Pacific General Meeting, Pasadena, Calif., June 12–16, 1950.
Middle Eastern District Meeting, Baltimore, Md., October 3–5, 1950.
Fall General Meeting, Oklahoma City, Okla., October 23–27, 1950.

Full correlation of all material in this volume has been accomplished by means of the multi-entry index beginning on page 664. Reference to any of the several subject entries for a technical paper will lead directly to the paper and to any published discussion on that paper.

The original number assigned each paper by the Technical Program Committee is given in the author index.

Statements and opinions given in papers and discussions published in TRANSACTIONS are the expressions of contributors for which the American Institute of Electrical Engineers assumes no responsibility.

Part II of Volume 69 is expected to be available for distribution early in 1951.

Suggested Improvements in the Performance Calculations of Single-Phase Induction Motors

M. S. THACKER
FELLOW AIEE

H. V. GOPALAKRISHNA
NONMEMBER AIEE

THREE methods have been presented so far—the cross-field theory, the revolving-field theory and the system of symmetrical components—of calculating the performance of the split-phase and capacitor types of single-phase induction motors. In these analytical solutions either an arbitrary distribution of core-loss between the main and the cross-fields is suggested or the angle of hysteretic lag between the flux and the magnetomotive force is neglected and correction for core-loss made in the numerical calculations by treating it as if it were a friction loss. The subtraction of the total core-loss assumed constant at all loads from the rotor output is not justified theoretically though fair results are obtained ordinarily. It also is noticed that in the development of maximum torque equations the speed at which the maximum rotor input occurs is considered to be the same as the speed at which maximum power is developed and quite likely, safe results may not be obtained in all cases. In the present paper a complete and accurate analysis is provided for the solution of single-phase induction motor performance characteristics based on a paper by F. W. Suhr.[1]

Symbols and Factors

V_m = main phase rms volts
V_s = start phase rms volts
V_m^+ = positive sequence component of V_m
V_m^- = negative sequence component of V_m
V_s^+ = positive sequence component of V_s
V_s^- = negative sequence component of V_s
I_m = main phase rms amperes
I_s = start phase rms amperes
I_m^+ = positive sequence component of I_m
I_m^- = negative sequence component of I_m
I_s^+ = positive sequence component of I_s
I_s^- = negative sequence component of I_s
I_{2m}^+ = positive sequence component of M phase secondary current referred to primary current
I_{2m}^- = negative sequence component of M phase secondary current referred to primary current
I_{2s}^+ = positive sequence component of S phase secondary current referred to primary current
I_{2s}^- = negative sequence component of S phase secondary current referred to primary current
Z_m^+ = total positive sequence impedance of M phase
Z_m^- = total negative sequence impedance of M phase
Z_s^+ = total positive sequence impedance of S phase
Z_s^- = total negative sequence impedance of S phase
X_{1m} = reactance of M phase primary winding
R_{1m} = resistance of M phase primary winding

$$a = \frac{\text{effective conductors of } S \text{ phase}}{\text{effective conductors of } M \text{ phase}}$$

$$= a'\sqrt{\frac{X_s}{X_m}},\ a' \text{ being a constant}$$

a^2R_{1s} = primary resistance of S phase
a^2X_{1s} = primary leakage reactance of S phase
R_c = capacitor resistance
X_c = capacitor reactance
R_2 = equivalent M phase secondary resistance referred to primary winding
X_2 = equivalent M phase secondary reactance referred to primary winding
Z_2^{+1} = apparent secondary positive sequence impedance of M phase
Z_2^{-1} = apparent secondary negative sequence impedance of M phase
R_2^{+1} = apparent positive sequence M phase secondary resistance
X_2^{+1} = apparent positive sequence M phase secondary reactance
R_2^{-1} = apparent negative sequence M phase secondary resistance
X_2^{-1} = apparent negative sequence M phase secondary reactance
R_φ = resistance representing core loss when connected in series with X_φ

$$= \frac{\text{core loss}}{i_m^2}$$

X_φ = equivalent M phase mutual or magnetizing reactance
X = ideal short circuit reactance of motor ($R_2 = 0$)

$$= X_{1m} + X_2\frac{X_\varphi}{X_\varphi + X_2}$$

$X_0 = X_\varphi + X_{1m}$ = reactance of the primary winding with the secondary open circuited

$$K_\varphi = \sqrt{K_r} = \frac{X_\varphi}{X_0} = \sqrt{\frac{X_0 - X}{X_0}}$$

used only when $X_{1m} = X_2$

$i_m = \dfrac{V_m}{X_0}$ = primary current with the secondary open
T = internal torque developed in synchronous watts
= rotor input
P = power output in watts
$F + W$ = watts, friction, and windage
Pulley output $= P - (F + W)$
S = speed as a fraction of synchronism

$$s = \frac{\text{slip rpm}}{\text{synchronous rpm}} = 1 - \frac{\text{actual speed}}{\text{synchronous speed}} = 1 - S$$

Basic Assumptions

1. Squirrel cage rotor.
2. Sine wave distributions of the magnetomotive force and uniform air gap permeances.
3. Sinusoidal voltages and currents.
4. Space quadrature of main and start phases.
5. Same effective resistance of rotor at frequencies fs and $f(2-s)$.

Paper 50-1, recommended by the AIEE Rotating Machinery Committee and approved by the AIEE Technical Program Committee for presentation at the AIEE Winter General Meeting, New York, N. Y., January 30–February 3, 1950. Manuscript submitted August 23, 1948; made available for printing October 31, 1949.

M. S. THACKER and H. V. GOPALAKRISHNA are with the Indian Institute of Science, Bangalore, India.

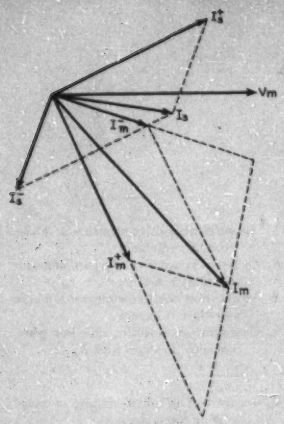

Figure 1. Graphical representation of positive and negative sequence current components in a split-phase motor

Theory

Consider a stator having two windings M (main) and S (start) separated in space by 90 electrical degrees. Let I_m and I_s be the vectors representing the effective values of the currents $|I_m|$ and $|I_s|$ in the two windings. It is obvious that

$$|I_m| = a|I_s|$$

where

$$a = \frac{\text{effective conductors in } S \text{ phase}}{\text{effective conductors in } M \text{ phase}}$$

The currents I_m and I_s may be resolved into two balanced components of opposite phase order, Figures 1 and 2, such that

$$I_m = I_m^+ + I_m^- \tag{1}$$

$$I_s = I_s^+ + I_s^- \tag{2}$$

It is understood that all vectors are assumed to rotate in an anticlockwise direction in accordance with the standard convention. The sequence is determined not by any differences in direction of rotation but by the order in which the vectors pass any fixed position. I_m^+ is called as the positive sequence component and I_m^- as the negative sequence component. It is seen clearly that

$$I_s^+ = j\frac{I_m^+}{a} \tag{3}$$

$$I_s^- = -j\frac{I_m^-}{a} \tag{4}$$

Now equation 2 becomes

$$I_s = j\frac{I_m^+}{a} - j\frac{I_m^-}{a} \tag{5}$$

Operating on equation 5 by ja

$$jaI_s = -I_m^+ + I_m^- \tag{6}$$

and adding to equation 1 gives

$$I_m^- = \frac{I_m + jaI_s}{2} \tag{7}$$

Subtracting equation 6 from equation 1 results

$$I_m^+ = \frac{I_m - jaI_s}{2} \tag{8}$$

The equivalent circuits of the M phase of a single-phase induction motor having a primary impedance of $R_{1m}+jX_{1m}$ are shown in Figure 3(A). By combining the positive sequence secondary impedance, $R_2/s+jX_2$, with the magnetizing impedance, $R_\varphi+jX_\varphi$, of the positive sequence, equivalent circuit the apparent secondary impedance can be written as

$$Z_2^{+1} = \frac{1}{\dfrac{1}{\dfrac{R_2}{s}+jX_2} + \dfrac{1}{R_\varphi+jX_\varphi}} = R_2^{+1} + jX_2^{+1} \tag{9}$$

where the apparent secondary positive sequence resistance

$$R_2^{+1} = \left(\frac{R_2}{s}R_\varphi - X_2X_\varphi\right)\left(\frac{R_2}{s}+R_\varphi\right) + \frac{\left(\dfrac{R_2}{s}X_\varphi + X_2R_\varphi\right)(X_2+X_\varphi)}{\left(\dfrac{R_2}{s}+R_\varphi\right)^2 + (X_2+X_\varphi)^2} \tag{10}$$

and the apparent secondary positive sequence reactance

$$X_2^{+1} = \left(\frac{R_2}{s}X_\varphi + X_2R_\varphi\right)\left(\frac{R_2}{s}+R_\varphi\right) - \frac{\left(\dfrac{R_2}{s}R_\varphi - X_2X_\varphi\right)(X_2+X_\varphi)}{\left(\dfrac{R_2}{s}+R_\varphi\right)^2 + (X_2+X_\varphi)^2} \tag{11}$$

By combining the negative sequence secondary impedance

$$\frac{R_2}{2-s} + jX_2$$

with the magnetizing impedance, $R_\varphi+jX_\varphi$, of the negative sequence equivalent circuit the apparent secondary negative sequence can be written as

$$Z_2^{-1} = \frac{1}{\dfrac{1}{\dfrac{R_2}{2-s}+jX_2} + \dfrac{1}{R_\varphi+jX_\varphi}} = R_2^{-1} + jX_2^{-1} \tag{12}$$

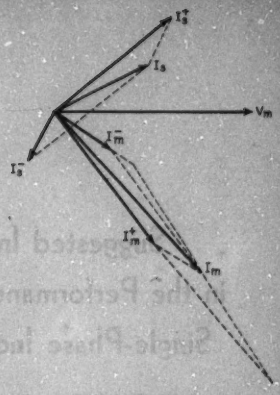

Figure 2. Graphical representation of positive and negative sequence current components in a capacitor motor

where the apparent secondary negative sequence resistance

$$R_2^{-1} = \left(\frac{R_2}{2-s}R_\varphi - X_2X_\varphi\right)\left(\frac{R_2}{2-s}+R_\varphi\right) + \frac{\left(\dfrac{R_2}{2-s}X_\varphi + X_2R_\varphi\right)(X_2+X_\varphi)}{\left(\dfrac{R_2}{2-s}+R_\varphi\right)^2 + (X_2+X_\varphi)^2} \tag{13}$$

and the apparent secondary negative sequence reactance

$$X_2^{-1} = \left(\frac{R_2}{2-s}X_\varphi + X_2R_\varphi\right)\left(\frac{R_2}{2-s}+R_\varphi\right) - \frac{\left(\dfrac{R_2}{2-s}R_\varphi - X_2X_\varphi\right)(X_2+X_\varphi)}{\left(\dfrac{R_2}{2-s}+R_\varphi\right)^2 + (X_2+X_\varphi)^2} \tag{14}$$

so that, the total positive sequence impedance of M phase

$$Z_m^+ = (R_{1m} + R_2^{+1}) + j(X_{1m} + X_2^{+1}) \tag{15}$$

and the total negative sequence impedance of M phase

$$Z_m^- = (R_{1m} + R_2^{-1}) + j(X_{1m} + X_2^{-1}) \tag{16}$$

The single-phase equivalent circuits for the S phase are shown in Figure 3(B). In the equivalent circuits the primary impedance, $a^2R_{1s}+ja^2X_{1s}$, is in series with an external impedance. The rotor quantities previously referred to the M phase will have to be multiplied now by the square of the transformation ratio. The apparent secondary impedance of the S phase, therefore, differs from the M phase by a^2. Hence, in the general case of a capac-

itor motor the total positive sequence impedance of S phase

$$Z_s^+=(R_s+a^2R_{1s}+a^2R_2^{+1})+j(-X_s+a^2X_{1s}+a^2X_2^{+1}) \quad (17)$$

and the total negative sequence impedance of S phase

$$Z_s^-=(R_s+a^2R_{1s}+a^2R_2^{-1})+j(-X_s+a^2X_{1s}+a^2X_2^{-1}) \quad (18)$$

The voltages V_m and V_s applied across the phases M and S respectively may be resolved into two balanced components of opposite phase order. When both positive and negative sequence voltages are applied simultaneously, the currents of the two sequences do not react upon each other; they may be computed separately. Thus

$$V_m=V_m^++V_m^-=I_m^+Z_m^++I_m^-Z_m^- \quad (19)$$

$$V_s=V_s^++V_s^-=I_s^+Z_s^++I_s^-Z_s^- \quad (20)$$

In single-phase motors the same voltage is impressed across both M and S phases, that is, $V_s \equiv V_m$. The resolution of the impressed voltage across M and S phases into positive and negative sequence components is illustrated in Figures 4 and 5. Equation 20 becomes

$$V_m=I_s^+Z_s^++I_s^-Z_s^- \quad (21)$$

From equations 3 and 4 this is

$$V_m=j\frac{I_m^+}{a}Z_s^+-j\frac{I_m^-}{a}Z_s^- \quad (22)$$

The positive and negative sequence currents of the main winding are determined from equations 19 and 22, so that

$$I_m^+=V_m\left[\frac{Z_s^--jaZ_m^-}{Z_m^+Z_s^-+Z_m^-Z_s^+}\right] \quad (23)$$

$$I_m^-=V_m\left[\frac{Z_s^++jaZ_m^+}{Z_m^+Z_s^-+Z_m^-Z_s^+}\right] \quad (24)$$

The main phase current being the vector sum of $I+_m{}^+$ and $I_m{}^-$ is

$$I_m=V_m\left[\frac{(Z_s^++Z_s^-)+ja(Z_m^+-Z_m^-)}{Z_m^+Z_s^-+Z_m^-Z_s^+}\right] \quad (25)$$

The start phase current computed from equations 23, 24, and 5 is

$$I_s=V_m\left[\frac{(Z_m^++Z_m^-)+j\left(\frac{Z_s^-}{a}-\frac{Z_s^+}{a}\right)}{Z_m^+Z_s^-+Z_m^-Z_s^+}\right] \quad (26)$$

By Figure 6 and equations 25 and 26, the line current

$$I_L=I_m+I_s$$

$$=V_m\frac{(Z_m^++Z_m^-+Z_s^++Z_s^-)+j\left(aZ_m^+-aZ_m^-+\frac{Z_s^-}{a}-\frac{Z_s^+}{a}\right)}{Z_m^+Z_s^-+Z_m^-Z_s^+}$$

$$=p-jq \quad (27)$$

The power factor is given by

$$\frac{p}{\sqrt{p^2+q^2}}$$

The application of Kirchoff's laws to the loops of the equivalent circuits in Figure 3(A) will give the relationship between the secondary currents and the component currents of the main phase current. Thus

$$I_{2m}^+=\frac{R_\varphi+jX_\varphi}{\left(\frac{R_2}{s}+jX_2\right)+(R_\varphi+jX_\varphi)}I_m^+ \quad (28)$$

and

$$I_{2m}^-=\frac{R_\varphi+jX_\varphi}{\left(\frac{R_2}{2-s}+jX_2\right)+(R_\varphi+jX_\varphi)}I_m^- \quad (29)$$

It is true that

$$|I_{2s}^+|=\left|\frac{I_{2m}^+}{a}\right| \quad (30)$$

$$|I_{2s}^-|=\left|\frac{I_{2m}^-}{a}\right| \quad (31)$$

Since the phase orders of the positive-sequence and negative-sequence currents are opposite, the torques due to these currents are opposite. Therefore the total internal torque is

$$T=T^+-T^-$$

$$=|I_{2m}^+|^2\frac{R_2}{s}+|I_{2s}^+|^2a^2\frac{R_2}{s}-|I_{2m}^-|^2\frac{R_2}{2-s}-|I_{2s}|^2a^2\frac{R_2}{2-s} \quad (32)$$

Now, from equations 28 and 29 it is clear that

$$|I_{2m}^+|^2\frac{R_2}{s}=\frac{R_\varphi^2+X_\varphi^2}{\left(\frac{R_2}{s}+R_\varphi\right)^2+(X_2+X_\varphi)^2}|I_m^+|^2\frac{R_2}{s} \quad (33)$$

and

$$|I_{2m}^-|^2\frac{R_2}{2-s}=\frac{R_\varphi^2+X_\varphi^2}{\left(\frac{R_2}{2-s}+R_\varphi\right)^2+(X_2+X_\varphi)^2}|I_m^-|^2\frac{R_2}{2-s} \quad (34)$$

Equations 33 and 34 in conjunction with equations 30 and 31 give

$$T=2\left[\frac{R_\varphi^2+X_\varphi^2}{\left(\frac{R_2}{s}+R_\varphi\right)^2+(X_2+X_\varphi)^2}|I_m^+|^2\frac{R_2}{s}-\frac{R_\varphi^2+X_\varphi^2}{\left(\frac{R_2}{2-s}+R_\varphi\right)^2+(X_2+X_\varphi)^2}|I_m^-|^2\frac{R_2}{2-s}\right] \quad (35)$$

synchronous watts

The power output is

$$P=T(1-s) \text{ watts} \quad (36)$$

Subtracting the friction and windage losses yields

$$\text{Pulley output}=T(1-s)-(F+W) \text{ watts} \quad (37)$$

$$\text{Pulley output}=\frac{112.7}{\text{synchronous rpm}}[T(1-s)-(F+W)] \text{ ounce-feet} \quad (38)$$

$$\text{Efficiency}=\frac{T(1-s)-(F+W)}{|V_mp|} \quad (39)$$

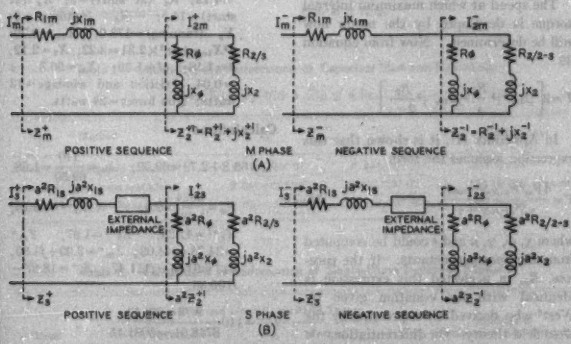

Figure 3. Equivalent circuits of a single-phase induction motor

External impedance: for capacitor motor $=R_c-jX_c$; for split-phase motor $=0$

With the quadrature circuit open under running conditions as in capacitor start and split-phase motors: $I_m^+=I_m^-$ and $I_s^+=-I_s^-$

The value of the resistance R_φ representing the core loss included in the equivalent circuits is

$$R_\varphi = \frac{\text{Core loss}}{i_m^2} = \frac{\text{Core loss}}{\left[\dfrac{V_m}{X_\varphi + X_{1m}}\right]^2} \tag{40}$$

The foregoing equations are directly applicable to capacitor motors. An example is worked out in Appendix I.

The split-phase and capacitor-start motors will have the auxiliary winding disconnected when running so that

$$I_s = 0 \tag{41}$$

From equation 2

$$I_s^+ = -I_s^- \tag{42}$$

And from equations 7 and 8

$$I_m^+ = \frac{I_m}{2} = I_m^- \tag{43}$$

These conditions are illustrated in Figure 3 and by the vector diagram of Figure 7. Equation 19 expressing the relation between the applied voltage and the currents flowing for a given slip reduces to

$$\begin{aligned} V_m &= I_m^+(Z_m^+ + Z_m^-) \\ &= I_m^+[(R_{1m} + R_2^{+1}) + j(X_{1m} + X_2^{+1}) + \\ &\qquad (R_{1m} + R_2^{-1}) + j(X_{1m} + X_2^{-1})] \\ &= 2I_m^+\left[\left(R_{1m} + \frac{R_2^{+1} + R_2^{-1}}{2}\right) + \right. \\ &\qquad \left. j\left(X_{1m} + \frac{X_2^{+1} + X_2^{-1}}{2}\right)\right] \end{aligned} \tag{44}$$

Therefore

$$|I_m^+| = \frac{\dfrac{V_m}{2}}{\sqrt{\left(R_{1m} + \dfrac{R_2^{+1} + R_2^{-1}}{2}\right)^2 + \left(X_{1m} + \dfrac{X_2^{+1} + X_2^{-1}}{2}\right)^2}} = |I_m^-| \tag{45}$$

The internal torque expressed by the equation 35 gets modified to

$$T = 2R_2(R_\varphi^2 + X_\varphi^2)|I_m^+|^2 \times \left[\frac{1}{\left\{\left(\dfrac{R_2}{s} + R_\varphi\right)^2 + (X_2 + X_\varphi)^2\right\}s} - \frac{1}{\left\{\left(\dfrac{R_2}{2-s} + R_\varphi\right)^2 + (X_2 + X_\varphi)^2\right\}(2-s)}\right] \text{ synchronous watts} \tag{46}$$

and is equal to the power input to the rotor.

The power output

$$P = T(1-s) \text{ watts} \tag{47}$$

$$\text{Pulley output} = T(1-s) - (F + W) \text{ watts} \tag{48}$$

$$= \frac{112.7}{\text{synchronous rpm}} \times [T(1-s) - (F + W)] \text{ ounce-feet} \tag{49}$$

As the starting winding is disconnected the line current = main phase current = $2I_m^+$, so that

$$|I_L| = \frac{V_m}{\sqrt{\left(R_{1m} + \dfrac{R_2^{+1} + R_2^{-1}}{2}\right)^2 + \left(X_{1m} + \dfrac{X_2^{+1} + X_2^{-1}}{2}\right)^2}} \tag{50}$$

The power factor is

$$\frac{R_{1m} + \dfrac{R_2^{+1} + R_2^{-1}}{2}}{\sqrt{\left(R_{1m} + \dfrac{R_2^{+1} + R_2^{-1}}{2}\right)^2 + \left(X_{1m} + \dfrac{X_2^{+1} + X_2^{-1}}{2}\right)^2}} \tag{51}$$

The input is the product of the impressed voltage and the in-phase component of the line current, found by multiplying equations 50 and 51. Thus

$$\text{Input} = \frac{V_m^2\left(R_{1m} + \dfrac{R_2^{+1} + R_2^{-1}}{2}\right)}{\left(R_{1m} + \dfrac{R_2^{+1} + R_2^{-1}}{2}\right)^2 + \left(X_{1m} + \dfrac{X_2^{+1} + X_2^{-1}}{2}\right)^2} \tag{52}$$

$$\text{Efficiency} = \frac{\text{Pulley output (equation 48)}}{\text{Input (equation 52)}} \tag{53}$$

A sample calculation is shown in Appendix II.

The speed at which maximum internal torque is developed by the motor now will be determined. Now from equation 32

$$T = 2\left[|I_{2m}^+|^2 \frac{R_2}{s} - |I_{2m}^-|^2 \frac{R_2}{2-s}\right]$$

In Appendix III, it is shown that this expression assumes the form

$$T = \frac{4V_m^2 R_2(\chi S^3 + \omega S)}{\gamma S^4 + \mu S^2 + \epsilon} \tag{54}$$

where χ, ω, γ, μ and ϵ could be computed from the motor constants. If the core-loss, R_φ, is neglected this expression is identical with the equation given by West[6] who derived his expression by the cross field theory. On differentiation,

$$\frac{dT}{dS} = 4V_m^2 R_2 \times \frac{S^4(-\gamma\chi) + S^2(\mu\chi - 3\gamma\omega) + S^2(3\chi\epsilon - \mu\omega) + \epsilon\omega}{(\gamma S^4 + \mu S^2 + \epsilon)^2}$$

The speed corresponding to maximum internal torque is obtained by equating the numerator to zero.

That is,

$$S^4(-\gamma\chi) + S^2(\mu\chi - 3\gamma\omega) + S^2(3\chi\epsilon - \mu\omega) + \epsilon\omega = 0 \tag{55}$$

As only even powers of S exist the equation is of the third degree in S^2 which can be solved easily.

The power output is given by

$$P = TS = 4V_m^2 R_2 \frac{(\chi S^4 + \omega S^2)}{\gamma S^4 + \mu S^2 + \epsilon} \tag{56}$$

Differentiating

$$\frac{dP}{dS} = 8V_m^2 R_2 S \frac{(\mu\chi - \gamma\omega)S^4 + 2\chi\epsilon S^2 + \omega\epsilon}{(\gamma S^4 + \mu S^2 + \epsilon)^2}$$

$S = 0$ indicates that the power output is zero at standstill. The biquadratic expression in the numerator, equated to zero gives the speed for maximum power output.

That is

$$(\mu\chi - \gamma\omega)S^4 + 2\chi\epsilon S^2 + \omega\epsilon = 0 \tag{57}$$

The maximum or breakdown power output is calculated easily. This is shown in Appendix IV.

Appendix I

These are the running performance calculations on a capacitor start and run motor for the same motor for which constants are given in Morrill's paper[13] with some additional items as given by Puchstein and Lloyd[8]. The values for this 4-pole 1/4-horsepower 110-volt motor are

$R_{1m} = 2.02$; $a^2R_{1s} = 1.18^2 \times 5.12 = 7.13$; $R_2 = 4.12$; R_e (at start) $= 3$; X_e (at start) $= 14.5$; R_e (running) $= 9$; X_e (running) $= 172.0$; $X_{1m} = 2.79$; $a^2X_{1s} = 1.18^2 \times 2.31 = 3.22$; $X_2 = 2.12$; $a = 1.18$; $a^2 = 1.39$; $X_m = 66.8$; $s = 0.04$. Friction and windage $= 13$ watts; Iron losses $= 24$ watts.

Calculations

$X_0 = 66.8 + 2.79 = 69.59$; $i_m = \dfrac{110}{69.59} = 1.58$;

$R_\varphi = \dfrac{6624}{1.58^2} = 9.6$; $R_2^{+1} = 32.76$;

$X_2^{+1} = 41.23$; $R_2^{-1} = 1.97$; $Z_m^+ = 34.78 + j44.02$; $Z_m^- = 3.99 + j4.89$; $Z_s^+ = 61.67 - j111.47$; $Z_s^- = 18.87 - j165.86$;

$$I_m^- = 110\frac{9.73 - j70.43}{8748.61 - j5081.15}$$

$$I_m^+ = 110\frac{24.64 - j170.57}{8748.61 - j5081.15}$$

$$I_m = I_m^+ + I_m^- = 1.64 - j2.08 = 2.65/-51°47'$$

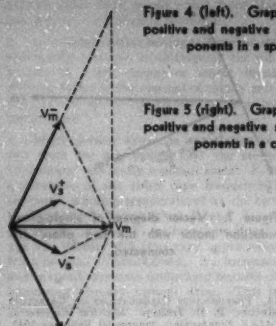

Figure 4 (left). Graphical representation of positive and negative sequence voltage components in a split-phase motor

Figure 5 (right). Graphical representation of positive and negative sequence voltage components in a capacitor motor

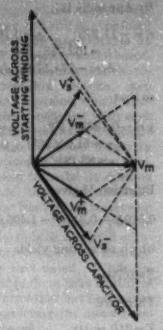

$$I_s = \frac{j}{a}(I_m^+ - I_m^-) = 0.729 + j0.582$$
$$= 0.933\angle 38°36'$$

$$|I_m^+|^2 = 110^2 \times 0.00029$$
$$|I_m^-|^2 = 110^2 \times 0.00005$$

$T = 186.8$ synchronous watts
Pulley putput $= 186.8\,(1-0.04) - 13$
$= 166$ watts

Appendix II

Machine data are taken from the example given by Puchstein and Lloyd[4] for a single-phase induction motor, 1/6 horsepower, 110 volts, 6 poles, 60 cycles. In the symbols of this paper

$R_{1m} = 3.95$; $R_3 = 3.7$; $X = 9.72$; $K_r = 0.862$; $(F+W) = 9$ watts

Performance Calculations

$$K_r = \frac{X_0 - X}{X_0}$$

Therefore

$X_0 = 70.4$; $X_\varphi = \sqrt{K_r X_0} = 65.35$; $X_{1m} = X_3 = 5.05$; $i_m = 1.565$; $R_\varphi = 12$; $R_3^{+1} = 32.1$; $R_3^{-1} = 1.40$; $X_3^{+1} = 39.30$; $X_3^{-1} = 4.70$.

Substituting in equation 46

$T = 123.93$ synchronous watts
Pulley output $= 123.93 \times 0.97 - 9 = 111.2$ watts.

From equation 50 $|I_L| = 3.23$; from equation 51 $\cos\varphi = 0.61$; and from equation 53 efficiency $= 0.514$.

Appendix III

This demonstrates the calculation of the total internal torque of a capacitor-start or split-phase motor.

Equation 32 can be put down as a function of S thus

$$T = 2[\varphi(S) - \varphi(-S)] \text{ where } S = 1 - s$$

$$\varphi(S) = |I_{3m}^+|^2 \frac{R_3}{1-S}$$
$$= \left| I_m + \frac{R_3^{+1} + jX_3^{+1}}{\frac{R_3}{1-S} + jX_3} \right|^2 \frac{R_3}{1-S}$$
$$= \left| \frac{V_m}{Z_m^+ + Z_m^-} \frac{R_3^{+1} + jX_3^{+1}}{\frac{R_3}{1-S} + jX_3} \right|^2 \frac{R_3}{1-S}$$
$$= \left| \frac{V_m}{(2R_{1m} + 2jX_{1m} + R_3^{+1} + jX_3^{+1} + R_3^{-1} + jX_3^{-1})} \times \frac{R_3^{+1} + jX_3^{+1}}{\frac{R_3}{1-S} + jX_3} \right|^2 \frac{R_3}{1-S}$$
$$= \left| \frac{V_m}{2R_{1m} + 2jX_{1m} + \frac{1}{\frac{1}{\frac{R_3}{1-S} + jX_3} + \frac{1}{R_\varphi + jX_\varphi}} + \frac{1}{\frac{1}{\frac{R_3}{1+S} + jX_3} + \frac{1}{R_\varphi + jX_\varphi}}} \times \frac{\frac{1}{\frac{1}{\frac{R_3}{1-S} + jX_3} + \frac{1}{R_\varphi + jX_\varphi}}}{\frac{R_3}{1-S} + jX_3} \right|^2 \frac{R_3}{1-S}$$
$$= \left| \frac{V_m(D + CS)B}{AD^2 + 2BED - S^2F} \right|^2 R_3(1-S)$$

where

$A = 2R_{1m} + 2jX_{1m}$
$B = R_\varphi + jX_\varphi$
$C = R_\varphi + jX_\varphi + jX_3$
$D = R_\varphi + jX_\varphi + jX_3 + R_3$
$E = R_3 + jX_3$
$F = AC^2 + 2jBCX_3$

Grouping real and imaginary components yields

$$V_m^2 R_3 \left| \frac{(Se_1 + f_1) + j(Sg_1 + h_1)}{(S^2a_1 + b_1) + j(S^3c_1 + d_1)} \right|^2 (1-S)$$

where

$a_1 = 2R_{1m}[(X_3 + X_\varphi)^2 - R_\varphi^2] + 4R_\varphi X_{1m}(X_3 + X_\varphi) + 2X_3R_\varphi \times (X_3 + 2X_\varphi)$

$b_1 = 2R_{1m}[(R_3 + R_\varphi)^2 - (X_3 + X_\varphi)^2] - 4X_{1m}(R_3 + R_\varphi)(X_3 + X_\varphi) + 2R_\varphi(R_3^2 - X_3^2 - 2X_3X_\varphi) + 2R_3(R_\varphi^2 - X_\varphi^2 - 2X_3X_\varphi)$

$c_1 = (2X_3X_\varphi - 4R_{1m}R_\varphi)(X_3 + X_\varphi) - 2R_\varphi^2(X_{1m} + X_3) + 2X_{1m}(X_3 + X_\varphi)^2$

$d_1 = 2X_{1m}[(R_3 + R_\varphi)^2 - (X_3 + X_\varphi)^2] + 4R_{1m}(R_3 + R_\varphi)(X_3 + X_\varphi) + 2X_\varphi(R_3^2 - X_3^2 - X_3X_\varphi) + 4R_3R_\varphi(X_3 + X_\varphi) + X_3R_\varphi^2$

$e_1 = R_\varphi^2 - X_\varphi^2 - X_3X_\varphi$
$f_1 = R_\varphi^2 + R_3R_\varphi - X_\varphi^2 - X_3X_\varphi$

Table I. Calculating the Performance of Capacitor Start and Run Motor

Motor Running With a Slip of 4 Per Cent

Method	I_m	I_s	Net Output
Double revolving field (Morrill)	$2.47\angle -59°3'$	$0.948\angle 38°45'$	177 watts
Cross field (Puchstein and Lloyd)	$2.64\angle -58°30'$	$0.954\angle 39°0'$	177 to 179.8 watts
Symmetrical components	$2.65\angle -51°47'$	$0.933\angle 38°36'$	166 watts

Table II. Calculations of Performance of Single-Phase Induction Motor

Item	Puchstein and Lloyd Cross Field Theory: Method I	Puchstein and Lloyd Cross Field Theory: Method II	Method of Symmetrical Components
Slip	0.03	0.03	0.03
Line current	3.16 amperes	3.03 amperes	3.23 amperes
Power factor	0.595	0.619	0.61
Output	117.8 watts	118.8 watts	111.2 watts
Efficiency	0.586	0.578	0.514

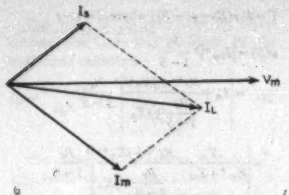

Figure 6. Vector relationships in a capacitor motor

$$g_1 = 2X_\varphi R_\varphi + X_2 R_\varphi$$
$$h_1 = 2X_\varphi R_\varphi + X_2 R_\varphi + R_2 X_\varphi$$

The expression may be written down in the form

$$V_m^2 R_3 \left[\frac{(Se_1+f_1)^2+(Sg_1+h_1)^2}{(S^2a_1+b_1)^2+(S^2c_1+d_1)^2} \right](1-S)$$

$$= \frac{V_m^2 R_3 [S^3(-c_1^2-g_1^2)+ S^2(c_1^2+g_1^2-2e_1f_1-2g_1h_1)+ S(2e_1f_1+2g_1h_1-f_1^2-h_1^2)+f_1^2+h_1^2]}{S^4(a_1^2+c_1^2)+S^3(2a_1b_1+2c_1d_1)+ b_1^2+d_1^2}$$

Finally the expression assumes the form

$$\varphi(S) = V_m^2 R_2 \frac{\chi S^3+\psi S^2+\omega S+\eta}{\gamma S^4+\mu S^3+\epsilon}$$

and

$$\varphi(-S) = V_m^2 R_2 \frac{-\chi S^3+\psi S^2-\omega S+\eta}{\gamma S^4+\mu S^3+\epsilon}$$

where

$$\chi = -c_1^2-g_1^2$$
$$\psi = c_1^2+g_1^2-2e_1f_1-2g_1h_1$$
$$\omega = 2e_1f_1+2g_1h_1-f_1^2-h_1^2$$
$$\eta = f_1^2+h_1^2$$
$$\gamma = a_1^2+c_1^2$$
$$\mu = 2a_1b_1+2c_1d_1$$
$$\epsilon = b_1^2+d_1^2.$$

This gives

$$T = \frac{4V_m^2 R_2[\chi S^3+\omega S]}{\gamma S^4+\mu S^3+\epsilon}$$

Appendix IV

This is an example of maximum rotor input and maximum power output calculations. Machine data are taken from the example by Veinott[7] for a single-phase induction motor, 110 volts, 4 poles, 60 cycles. In the notations of this paper

$R_{1m}=3.8$; $R_3=4.65$; $X_\varphi=X_\psi+X_{1m}=110$; $X=X_{1m}+K_pX_2=8.3$; $K_p=0.964$; $X_{1m}=X_2$ (assumption); Core loss $=19$ watts; Friction and windage $=10$ watts.

Then

$X_{1m}=X_1=4.23$; $X_\varphi=105.77$; $i_m=1$; $R_\varphi=19$.

By Appendix III,

$e_1=-11{,}273$; $g_1=4{,}100$; $a_1=15{,}962$; $c_1=162{,}918$; $f_1=-11{,}185$; $h_1=4{,}501$; $b_1=-274{,}576$; $d_1=-113{,}078$.

so that

$\chi=-0.1439\times10^9$; $\omega=0.1436\times10^9$; $\gamma=51.9\times10^4$; $\mu=-124.3\times10^9$; $\epsilon=88.18\times10^9$.

Equation 55 gives

$$0.519S^3-0.317S^2-1.406S^2+0.8818=0$$

which on solving yields

$$S=0.794$$

Therefore

$T=310$ watts

From equation 57

$$0.1043S^4-0.2538S^3+0.1266=0$$

resulting in $S=0.8367$ as against 0.81 given by Veinott[7] and 0.817 given by Puchstein and Lloyd.[6] From equation 56 $P=253.5$. The net mechanical power at the rotor shaft (253.5 watts) minus watts due to friction and windage $=243.5$ as against 242 watts of Veinott's result.

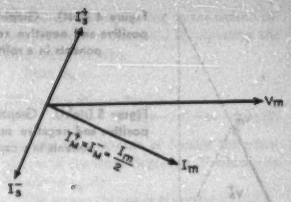

Figure 7. Vector diagram of single-phase induction motor with the start phase disconnected

References

1. Symmetrical Components as Applied to the Single Phase Induction Motor, F. W. Suhr. *Electrical Engineering* (*AIEE Transactions*), volume 64, September 1945, pages 651–66.

2. Analysis of Unsymmetrical Machines, W. V. Lyon, Charles Kingsley. *Electrical Engineering* (*AIEE Transactions*), volume 55, May 1936, pages 471–76.

3. The Apparent-Impedance Method of Calculating Single-Phase-Motor Performance, W. J. Morrill. *Electrical Engineering* (*AIEE Transactions*), volume 60, December 1941, pages 1037–41.

4. Discussion, C. R. Boothby. *AIEE Transactions*, volume 48, April 1929, pages 629–30.

5. Single Phase Induction Motors, W. J. Branson. *AIEE Transactions*, volume 31, part 2, 1912, pages 1749–87.

6. The Cross-Field Theory of Alternating-Current Machines, H. R. West. *AIEE Journal*, volume 45, part 1, 1926, pages 160–66.

7. Performance Calculations on Induction Motors, C. G. Veinott. *AIEE Transactions*, volume 51, September 1932, pages 743–54.

8. Single-Phase Induction-Motor Performance, A. F. Puchstein, T. C. Lloyd. *Electrical Engineering* (*AIEE Transactions*), volume 56, October 1937, pages 1277–84.

9. The Cross-Field Theory of the Capacitor Motor, A. F. Puchstein, T. C. Lloyd. *Electrical Engineering* (*AIEE Transactions*), volume 60, February 1941, pages 58–61.

10. The Design of Fractional Horsepower Induction Motors, N. F. T. Saunders. *Journal*, Institution of Electrical Engineers (London, England), volume 85, number 502, August 1939.

11. Single-Phase Induction-Motor Performance Calculation, F. S. Himebrook. *Electrical Engineering* (*AIEE Transactions*), volume 60, February 1941, pages 55–58.

12. The Revolving Field Theory of the Capacitor Motor, W. J. Morrill. *AIEE Transactions*, volume 48, April 1929, pages 614–29.

13. Segregation of Losses in Single Phase Induction Motors, C. G. Veinott. *Electrical Engineering* (*AIEE Transactions*), volume 54, December 1935, pages 1302–06.

14. Performance Calculations on Capacitor Motors, P. H. Trickey. *Electrical Engineering* (*AIEE Transactions*), volume 60, February 1941, pages 73–76.

15. Design of Capacitor Motors for Balanced Operation, P. H. Trickey. *AIEE Transactions*, volume 51, September 1932, pages 780–84.

16. The Equal-Volt-Ampere Method of Designing Capacitor Motors, P. H. Trickey. *Electrical Engineering* (*AIEE Transactions*), volume 60, November 1941, pages 990–92.

17. Current Loci for the Capacitor Motor, T. C. McFarland. *Electrical Engineering* (*AIEE Transactions*), volume 61, March 1942, pages 152–56.

18. Fundamental Theory of the Capacitor Motor, W. C. Specht. *AIEE Transactions*, volume 48, April 1929, pages 607–13.

19. The Condenser Motor, B. F. Bailey. *AIEE Transactions*, volume 48, April 1929, pages 596–606.

20. Method of Symmetrical Co-ordinates Applied to the Solution of Polyphase Networks, C. L. Fortescue. *AIEE Transactions*, volume 37, part 2, 1918, pages 1027–1115.

21. Principles of Alternating-Current Machinery (book), R. R. Lawrence. McGraw-Hill Book Company, Inc., New York, N. Y., third edition, 1940.

22. Theory of Alternating-Current Machinery (book), A. S. Langsdorf. McGraw-Hill Book Company, Inc., New York, N. Y., fifth edition, 1940.

23. Fractional Horsepower Electric Motors (book), C. G. Veinott. McGraw-Hill Book Company, Inc., second edition, 1948.

24. Electric Circuits, Theory and Application (book), O. G. C. Dahl. McGraw-Hill Book Company, Inc., New York, N. Y., first edition, 1938.

25. Symmetrical Components (book), C. F. Wagner, R. D. Evans. McGraw-Hill Book Company, Inc., New York, N. Y., first edition, 1933.

Discussion

F. W. Suhr (General Electric Company, Fort Wayne, Ind.): In the first half of this paper the authors have closely followed the earlier work of this discusser. They have introduced the innovation of including the core loss as an equivalent resistance (R_φ) in series with the magnetizing reactance (X_φ). To the practical motor designer this refinement does not seem to be justified for these reasons:

1. Core loss is (in part at least) a loss subtractive from rotor output.

2. Harmonic torques and load losses (which are not too well known) cause a

greater error than would result from this refinement in calculation technique.

3. It is doubtful that testing techniques are sufficiently accurate to distinguish the difference in rotor output or stator input whether based on the concept of totally subtractive core loss or the method proposed by the authors.

4. Much greater errors in calculation result from the assumption that the motor "constants" are really constant since: R_1 is a function of the rotor cage frequencies; the exact winding temperatures at the test load are rarely known, thus R_1 and R_2 are not exact; X_1 and X_2 are functions of leakage flux density and thus vary appreciably from no load to breakdown; X_ϕ increases as the speed decreases under load because of increasing primary voltage drop. This is due to desaturation of the main flux paths.

Solution of the maximum theoretical internal torque and power output in terms of speed, as given by the authors' equations 55 and 56 respectively, does not appear to be of real practical value for these reasons;

1. In their collapsed or "short hand" forms they appear to be fairly simple. But a great deal of calculation labor is involved in working out the derived "constants" $\gamma, X_1, \mu, a, \omega$. While an arithmetic solution of a cubic equation is possible, it can hardly be called "easy."

Even a designer of only very limited experience will soon learn at what value of slip he can expect maximum torque to occur. By making about three assumptions as to the value of slip in the breakdown region he can calculate the torques and by plotting torque against slip (or speed) he can arrive at the proper value. This is a very simple calculation which would consume only a fraction of the time that would be required to perform the operations called for by the authors' equations. Many designers have semiempirical formulas for break-down torque which are quite simple.

2. The same reasons given previously for not using the R_ϕ apply equally well here.

While I have not checked all of the algebraic manipulations involved in deriving the authors' equations 55 and 56, I do not doubt their mathematical precision for the assumed conditions. When rotor resistance for the low-frequency forward field differs from rotor resistance for the high-frequency backward field or when X_1, X_2, and X_ϕ vary with the amount of current drawn by the motor, then the assumptions are no longer valid. The simpler, but less elegant, method of assuming the slip and then applying resistance and reactance values that obtain at this condition will yield more accurate results.

Edward Bretch (Century Electric Company, St. Louis, Mo.): In the January 1950 issue of Electrical Engineering,[1] the following observation is noted: "When a comprehensive practical engineering problem must be solved, however, the first, and perhaps the most important task is to make the necessary and proper assumptions to reduce the complexity of the problem to make its solution possible."

The subject of single-phase squirrel-cage motor theory has been and still is a confused subject, due to the early assumptions on which the pioneer theories were based. Thacker and Gopalakrishna mention the rotating-field and cross-flux theories, each based on different assumptions, which theories are not altogether consistent with each other or with actual test results. It appears that 50 or 60 years ago when the "necessary and proper assumptions to reduce the complexity of the problem to make its solution possible" were made, there was not sufficient basic knowledge from which to develop consistent assumptions. These pioneer theories appear to have been accepted without regard to the correctness of the assumptions on which they were based. While the mathematics applied to them have kept pace with the times, no attention has been given to exploring and correcting the assumption on which they are based.

B. G. Lamme[2] did make an exploration into the physics of the rotating field theory and sums up as follows: "Such a set or unit has certain characteristics which are so similar to those of the usual single-phase motor that on first consideration one would assume them to be identical. However, a more careful study of the individual operating conditions shows that the similarity is a general one and a number of decided discrepancies are found." On the other hand, no test has so far been cited which verifies the basic assumption of the rotating field theory, namely that two equal constant fluxes rotating at equal speed in opposite directions combine vectorially into a single-phase alternating flux.

While Mr. Suhr may have improved on the mathematics applied to the problem by the use of symmetrical components, it seems that his method is still fundamentally based on the same assumption which Mr. Lamme found by actual test to be inconsistent.

As to the cross-flux assumptions, this theory assumes that the cross flux varies directly with rotor speed, equals the main flux at synchronism, and continues to increase directly with rotor speed above synchronism. At one time the writer addressed the late Dr. A. S. McAllister who was an outstanding advocate of the cross-flux theory, inquiring as to how this increased cross flux above synchronism could be tested and verified. He suggested that the rotor of a single-phase motor be driven above synchronism and the cross flux measured by voltage induced in a second stator winding placed in space quadrature with the main stator winding. However, this test shows that while the cross flux is approximately equal to the main flux at synchronism, it is not proportional to rotor speed but more nearly inversely proportional to slip, since it decreases as slip increased both above and below synchronism. When Dr. McAllister was shown these results he expressed surprise but had no explanation for the discrepancy between the theory and test results.

Steinmetz,[3] some years after the rotating field and cross flux theories were established, proposed another theory which appears to be more logical and to represent more accurately than the pioneer theories the actual actions within the single-phase squirrel-cage motor. This, briefly, is his theory: "In a single-phase motor, one of the two superimposed quadrature fields is excited by the primary current and the other by the secondary currents carried into the quadrature position by the rotation of the secondary." While, so far as known, he never developed this theory in detail, it appears to be well worth exploring. Likewise, it is felt that the basic assumptions on which the pioneer single-phase theories were based should also be given some further attention. In solving engineering problems, correct assumptions are just as important as correct mathematics.

References

1. Design Problems for Engineering Education, T. M. Linville, K. B. McEachron, Jr. *Electrical Engineering*, January 1950, pages 29–33.

2. A Physical Conception of the Operation of the Single-Phase Induction Motor, B. G. Lamme. *AIEE Transactions*, volume XXXVII, 1918, part I, pages 627–702.

3. Theoretical Elements of Electrical Engineering, C. P. Steinmetz. McGraw-Hill Book Company (New York, N. Y.), 1918, page 309.

M. S. Thacker and H. V. Gopalakrishna: Mr. Suhr's comments are correct. There are many other limitations in the analysis. Admittedly, the ultimate design method is the one which takes into account all of the variables, but provision for all the variables in the equations results in the most complicated formulae. From the practical point of view, there is a large measure of evidence to show that the average values assumed for the less important so-called constants will yield the operating characteristics which are in substantial agreement with the test results. The paper was presented with a view to giving a clear concept of the inter-relationships in the motor and to develop the desired degree of accuracy in the equations which form the basis of our other paper.[1]

The comments of Mr. Bretch in trying to overthrow the principal theories are based on misinterpretation of experimental observation and theoretical deductions. Mr. Puchstein, in his letter to the editor, has very ably thrashed out all the issues raised in the discussion.[2] Experimental results do affirm that a nonrotating field is present in the air gap when two oppositely-rotating fluxes are produced by two equal 3-phase windings placed in the same slots but connected in series. Theory also proves that the cross-field will be in direct proportion to the speed only if the main flux is constant. The figures in Table II of the letter[2] afford conclusive proof that the voltage induced in the starting winding plotted against speed has the same shape as predicted by the theory. The pioneer theories have withstood the test of time and practice. Although new investigations are essential to progress, there is hardly any basis for associating the scheme visualized by Steinmetz and so far not translated into concrete process with our method of analyzing the performance of the single-phase induction motor.

References

1. Design of Auxiliary Circuits of Single Phase Induction Motors, M. S. Thacker, H. V. Gopalakrishna. *AIEE Transactions*, volume 68, part II, 1949, pages 1373–79.

2. Letter to the Editor, A. F. Puchstein. *Electrical Engineering*, volume 66, February 1947, pages 208–10.

Electric Fences—Their Hazards, Types, Regulations, and Safe Application

CHARLES F. DALZIEL
MEMBER AIEE

SUSTAINED purchases of 400,000 electric fence controllers per year by American farmers substantiate the fact that the electric fence is a practical and valuable aid to modern farming. These devices have been accepted, not only in this country but also in foreign countries, including Australia, Canada, and the countries of Europe. That this general acceptance is substantial is evident from Danish estimates that the number of electric fence controllers now in use exceeds 100,000; the number of farms in Denmark is approximately 210,000.

Since the primary objective of the electric fence is to control farm animals by subjecting them to a powerful shock when they contact the fence wire, human beings will be similarly affected, and attention must be given to controlling the shock intensity so that it will be harmless to both man and beast. This objective has been achieved in approved* electric fence controllers. Approved electric fence controllers are safe, effective, and economical. They are the result of over ten years' experience in the field and in the laboratory.

The electric fence consists of one or more bare wires, such as ordinary galvanized wire or barbed wire, insulated from ground, which are energized from a device called a controller. An animal or human touching the wire completes the circuit to ground thereby receiving a painful but harmless shock. The wire is strung on insulators supported by lightweight poles at a vertical distance about three-quarters of the height of the animal. Where animals of different sizes are to be controlled in the same enclosure, two or more wires, placed at different levels, are used. In cases where poor grounding conditions predominate, such as in sandy or very dry soil, effectiveness can be improved by installing a ground wire about six inches from the ungrounded energized wire or wires.

The idea of utilizing electric shock as a means of controlling animals appeals to the imagination. Application appears so simple that many laymen have constructed homemade devices with disastrous results. Much concern has been given to effectiveness by these laymen and far too little concern has been given to electric shock hazards. Novices, such as radio amateurs, garage mechanics, and ambitious farmers, have resorted to various schemes, by far the most dangerous being the use of the ungrounded side of the 120-volt lighting circuit protected only by fuses or by $7^1/_2$ to 100 watt electric lamps. Such means may give fair results during ordinary conditions, poor results during conditions of high grounding resistance, and numerous fatalities to both humans and animals during good grounding conditions. Other dangerous homemade gadgets currently in use involve radio transformers and neon sign transformers. Fatalities are of serious concern. Lack of effectiveness of these homemade devices has done much to discourage the use of electric fences in general. These unfortunate instances have done much to discourage both scientific development and application. The homemade gadget has given the electric fence its bad reputation as an executioner of humans and animals. Estimates place the yearly toll between 10 to 15 humans, while animal fatalities are said to be in the hundreds. In contrast to the continuing number of fatalities caused by unauthorized devices, the approved electric fence controller continues to maintain an almost zero fatality record.

The electrical profession, alert to new and useful applications of electricity, is much concerned over the continuing number of fatalities resulting from nonapproved fences. The continuing number of serious accidents is of special importance in connection with present efforts to complete the electrification of all farms in the country. This expansion must be accompanied with sound technical advice and adequate supervision up to the point of ultimate utilization. Construction of dangerous homemade electric gadgets must be discouraged; use of unauthorized appliances and devices must be discontinued. That these misapplications are often not apparent or remote from the ordinary paths of electrical engineers presents a challenge which must be accepted.

During the 13 years that the author has followed electric fencing but two human deaths involving commercial electric fence controllers have come to his attention. These occurred near Toppenish, Wash.[1] in 1937, and Pixley, Calif.[2] in 1944. Recently two independent searches by attorneys have located but two lawsuits involving electric fence accidents in which opinions have been filed in American state and federal appellate courts in the last ten years. One case concerned injury to a human being,[3] the other, the death of a mule.[4] Both litigations involved electric fences energized from homemade electric fence controllers.

Like all mechanical devices, the elec-

* Approved means approved by the Underwriters' Laboratories, Inc., Industrial Commission of Wisconsin, or other institutions of similar standing.

Paper 50-2, recommended by the AIEE Safety Committee and approved by the AIEE Technical Program Committee for presentation at the AIEE Winter General Meeting, New York, N. Y., January 30–February 3, 1950. Manuscript submitted April 4, 1949; made available for printing October 28, 1949.

CHARLES F. DALZIEL is Professor of Electrical Engineering, University of California, Berkeley, Calif.

The author wishes to acknowledge and thank O. H. Marchal, Directeur d'Administration, Ministere du Combustible et de l'energie, Bruxelles, Belgium, for his kindness in supplying much of the information regarding European practice. Acknowledgment also is given to various electric fence controller manufacturers for their co-operation in supplying information used in the preparation of this paper.

Table I. Electric Fence Industry

Taken from United States Census "Facts for Industry"

Year	Number Mfgrs. Reporting	Total Sales	
		Number Controllers	Value
1945	20	306,879	$2,834,349
1944	23	399,779	3,525,566
1943	23	440,102	3,267,416
1942		385,641	2,470,422

tric fence is not without its shortcomings. Stock must be trained to respect it. Small animals are difficult to fence electrically. Remote fences are hard to keep in operating condition. Brush and vegetation must be kept off the energized wires. Although a well-designed controller will handle 15 or more miles of fence, regardless of the length of the fence wire, unsatisfactory results may be experienced in places where the top soil is very dry, or during a heavy fog or light rain when the insulators are contaminated. The shock delivered by the fence should be more powerful and hence electric fencing should be more successful when used on irrigated lands, or in localities which receive summer rains in contrast to similar installations on the dry farms of the west or southwest.

Although not recommended for a property line fence or to restrain wild or ferocious animals, the electric fence is a valuable supplement to the conventional fence. It is cheaper and easier to erect. It provides a convenient movable barrier for controlling grazing. The ease with which the electric fence can be moved permits the subdivision of pasture land on which animals can graze progressively, thereby giving maximum efficiency in the use of the land for grazing. It has been found to be a valuable aid in the summer grazing of forest lands. When used in conjunction with the conventional fence it reduces maintenance by discouraging animals from riding down, pawing, gnawing, nuzzling, or uprooting permanent structures. The electric stock prod is a closely related application of the principles of the electric fence. Stock prods are valuable aids in the handling of animals in stock yards, slaughter houses, loading racks, and so forth.

The fundamental requirements of an electric fence are that it shall be effective and safe. The shock during poor grounding conditions, such as when an animal is standing on relatively dry ground, must be sufficiently powerful to repel him. On the other hand, the shock must be harmless to a child under all conditions. For example, an extreme case might be one in which the electrified wire was grasped with wet hands while the child was standing in a salt marsh. These two highly essential requirements of effectiveness and safety present difficult technical problems.

Because of the wide variation in the physical condition of individuals, it is impossible to design an electric fence which will be safe for all humans. The press contains frequent accounts of fatalities ascribed to heart failure caused by overexcitement, intense emotion, fear, or shock (that is, shock to the nervous system and not electric shock). For such susceptible persons, it is possible that contact with any electric circuit which permits currents only slightly in excess of the threshold of sensation might result in fatality. This possibility must be recognized, and in spite of what may be done to develop a safe electric fence, an occasional death is to be expected due to casual contact involving electric currents known to be safe for most normal individuals. Death in such cases should be considered due to shock and not to the primary effects of electric current.

All intermittent controllers impress a short shock which is followed by an off period during which time it is assumed that a human will release himself from the circuit. It must be recognized that failure to break contact with the fence wire may dangerously increase the hazard attending the use of these devices.

Many of the essential characteristics of electric fencing have not yet been determined. Neither the maximum shock safe for a small child nor the minimum shock required to control animals is known with certainty. The resistance between feet and ground and between the point of contact and the fence wire may vary from 1,000 to 2,000 ohms to values approaching infinity. Leakage resistance between the fence wire and ground due to wet dirty insulators is subject to wide variations, possibly from 10,000 to 20,000

Table II. Manufacturers and Distributors of Approved Electric Fence Controllers

Industrial Commission of Wisconsin, April 28, 1948

Babson Brothers
Chicago, Ill.
Badger Electric Fence Company
Appleton, Wisc.
Brown Fence and Wire Company
Cleveland, Ohio
Bussey Pen Prod. Company
Chicago, Ill.
Coast to Coast Stores
Minneapolis, Minn.
Co-operative G. L. F. Farm Supplies
Ithaca, N. Y.
Cussins and Fearn Company
Columbus, Ohio
Diller Electric Manufacturing Company
Kokomo, Ind.
Dayton Electric Company
Chicago, Ill.
Electric Service Systems
Minneapolis, Minn.
Electric Timed Products Company
Chicago, Ill.
Electrite Fence Company
Whitewater, Wisc.
Farmers' Engineering and Manufacturing Company
Pittsburgh, Pa.
Gamble Stores, Inc.
Minneapolis, Minn.
Globe Electric Fence Company
Milwaukee, Wisc.
Globe Machine and Manufacturing Company
Albert Lea, Minn.
Guaranteed Products Corporation
Wellington, Ohio
Guard-it Manufacturing Company
Chicago, Ill.
Hot Wire Company
Milwaukee, Wisc.
Hovey-Hayes Company
Kansas City, Mo.
Ives Engineering Laboratories
Chicago, Ill.
Kingston Products Corporation
Kokomo, Ind.
Lionel Corporation
Irvington, N. J.
Montgomery Ward and Company
Chicago, Ill.
National Co-operatives
Chicago, Ill.
Northern Signal Company
Milwaukee, Wisc.
Parker-McCrory Manufacturing Company
Kansas City, Mo.
Prime Manufacturing Company
Milwaukee, Wisc.
Reynolds Electric Company
Chicago, Ill.
Roberts Electric Fence Company
Waukesha, Wisc.
Sampsell Time Control Company
Spring Valley, Ill.
Sears Roebuck and Company
Chicago, Ill.
Sentinel Electric Fence Control Company
Cincinnati, Ohio
Southern States Co-operative
Richmond, Va.
Spiegel, Inc.
Chicago, Ill.
L. H. Underwood and Company
Mount Vernon, Ohio
Western Auto Supply
Kansas City, Mo.

Table III. Manufacturers and Distributors of Approved Electric Fence Controllers

Underwriters' Laboratories, Inc., May, 1948

Betz and Sons
Celina, Ohio
Kingston Products Corporation
Kokomo, Ind.
Parker-McCrory Manufacturing Company
Kansas City, Mo.
Prime Manufacturing Company
Milwaukee, Wisc.
Sears Roebuck and Company
Chicago, Ill.

ohms to infinity. However, in spite of this situation, electric fencing with approved controllers is giving satisfactory, economical, and safe service.

Patents covering electric fences date back to 1863, and several were issued between 1863 and 1934, the date generally regarded as the beginning of the electric fence industry. The magnitude of the electric fence industry at the present time in this country is evident from Table I, in which the number of manufacturers, number of units sold, and the dollar value, are given for the years 1942–1945. These data were taken from the United States Census "Facts for Industry." The year 1945 is the last for which figures are available. Manufacturers and distributors of electric fence controllers approved by the Industrial Commission of Wisconsin, dated April 28, 1948, are given in Table II, and a similar list approved by the Underwriters' Laboratories as of May 1948, are given in Table III.

It is interesting to note that most of the electric fence manufacturers are specialty houses or manufacturers of agricultural equipment; the large electrical manufacturers not having entered this field. The ready acceptance of electric fencing, following its commercial appearance in this country in 1934, resulted in some 200 manufacturers in 1938. Although many have not survived, only a fraction of the firms now engaged in the manufacture of controllers produce approved devices. Many concerns, especially the smaller ones, continue to manufacture controllers without formal compliance with any recognized safety code. In this regard it is indeed fortunate that the mortality rate is as low as it appears to be.

Types of Electric Fence Controllers

Types of electric fence controllers and required electrical characteristics are given in Table IV, wherein are summarized for comparative study, the essential output limitations of the three United States safety codes and similar regulations in effect in Finland, Denmark, Great Britain, France, and Sweden. Emphasis will be given to practices in this country, as only limited information is available regarding foreign developments. Although this procedure is necessitated by the lack of detailed information from foreign countries, it is believed that coverage of the subject should be satisfactory since electric fencing was in use here several years before it spread abroad. Foreign references state that the United States codes served as a basis for deliberation in all countries which have enacted legislation, and that all controllers fall into the four basic types covered by the National Electrical Safety Code.

Electric fence controllers may be classified in one of several ways, such as according to power supply, intended installation, and whether the output is continuous or intermittent. The power supply may be commercial alternating current or batteries (dry cells or storage battery). The controller may be designed for indoor or outside installation. The output may be noninterrupted, or it may consist of periodic impulses. Most commercial controllers are of the intermittent type.

Intermittent controllers may be provided with tapped transformer windings to permit adapting the output to various field conditions. A selector switch or several output terminals may be provided. Certain manufacturers claim that effectiveness is improved during conditions of high grounding resistance by operating at maximum voltage and reduced current,

Table IV. Regulations Pertaining to Electric Fences

Output Limitations	United States: Industrial Commission of Wisconsin	United States: Underwriters' Laboratories	United States: National Bureau of Standards	Europe: Finland	Europe: Denmark	Europe: Great Britain	Europe: France	Europe: Sweden	Europe: C.E.E**
Inductive Discharge Type									
Quantity of electricity per impulse, millicoulombs, maximum	3.0	4.0	3.0	3.0	3.0	3.0	3.0	2.5	2.5
Impulse current, crest milliamperes, maximum	500	Pulse duration at 300 ma not to exceed 0.00030 sec.	500			500	500		300
Current at 0.1 second, milliamperes, maximum	0	5*	10	0	0	0	10	5	5
Interval between impulses, seconds, minimum	0.75	0.75	0.75	0.75	0.75	0.75	0.75		
Impulses per second, maximum								1.2	1.16
Capacity Discharge Type									
Quantity of electricity per impulse, millicoulombs, maximum	3.0	4.0	3.0		3.0	3.0	3.0	2.5	2.5
Impulse current, crest milliamperes, maximum	500	Pulse duration at 300 ma not to exceed 0.00030 sec.	500			500	500		300
Current at 0.1 second, milliamperes, maximum	10	5*	10		0	10	10	5	5
Noninterrupted type									
Sustained current, milliamperes, maximum	5.0		3.0				3.0	2.5	0.5
Intermittent type									
Sustained current, milliamperes, maximum			0.0			5.0		2.5	0.5
Interval between impulses, seconds, minimum		0.75	0.75		0.75		0.75		
Impulses per second maximum								1.2	1.16
Intermittent A-C Output Type				NA		NA			
Quantity of electricity per impulse, millicoulombs, maximum					3.0			2.5	2.5
Impulse current, rms milliamperes, maximum	25.0	Current = −350t + 75 (t = 0.03 to 0.20 sec.)	25.0				25.0		
Duration of impulse, seconds, maximum	0.1	0.2	0.1		0.1		0.1		0.1
Interval between impulses, seconds, minimum		0.90			0.75		1.0		
Impulses per second, maximum	1.0		1.0					1.2	1.16
Continuous Type	NA	NA		NA		NA		NA	NA
Sustained current, rms milliampere, maximum			8.0		5.0		8.0		

Notes: Output current and quantity measured with load conditions which will result in maximum output. In no case shall the load, including instruments, be less than 500 ohms.
NA = Not authorized.
* = Measured at 0.2 second.
** Proposed European Standard.

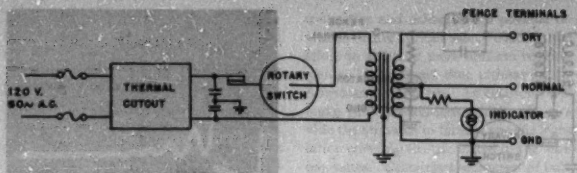

Figure 1. Schematic diagram of an a-c intermittent electric fence controller

while during conditions of high leakage current, lower voltage and maximum current produce better results. Since the electric shock hazard depends solely upon the output current or quantity, and not voltage, the output limitations given in Table IV must not be exceeded under any conditions.

The chief electrical characteristics of the four types of controllers will be discussed in the paragraphs immediately following:

Intermittent A-C Output Type. The intermittent a-c controller consists of a high reactance transformer which is periodically energized from the 120-volt lighting circuit by an electrically-operated rotary or oscillating interrupter. Figure 1 gives a schematic diagram for such a controller. An oscillogram of the output from a commercial controller is shown in Figure 2.

A typical commercial intermittent a-c electric fence controller is shown in Figure 3. Depending upon the manufacturer, the output consists of 2 to 12 cycles of sine wave applied frequency, the first cycle or two of which may be asymmetrical. The open circuit voltage rarely exceeds 2,500 rms volts. The input circuit must be protected with a thermal cut-out arranged to disconnect the unit from the source should the interrupted contacts stop in a closed position or should a jumper be placed across the interrupted contacts (to protect against tampering). To protect the fence against transformer insulation failure it is required that the primary and secondary windings be placed on separate core legs so arranged that insulation failure will be to a grounded metallic barrier. One side of the output circuit, transformer core, and housing are connected to a common terminal and connected to an effective ground.

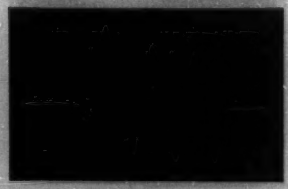

Figure 2. Oscillogram from an a-c intermittent electric fence controller

500-ohm noninductive resistor load

Inductive-Discharge Type. The inductive impulse controller is essentially an induction coil which is periodically energized from a low voltage d-c source by an electrically-operated rotating or oscillating interrupter. The output is similar to that produced by a jump spark ignition coil. The open-circuit voltage may exceed 10,000 crest volts. The d-c source may be rectified alternating current or supplied from batteries. Battery controllers are usually designed to operate three to five months between changes of dry cells or recharge of the storage battery. Some of these units are provided with a switch to permit operation on either batteries or 120 volts of alternating current which is transformed and rectified to battery voltage. A schematic diagram of a combination inductive impulse controller which may be energized from either 120 volts of alternating current or batteries is given in Figure 4. Figure 5 is an oscillogram showing the characteristic output wave form, and Figure 6 is a commercial unit.

A-c operated inductive impulse controllers must be protected with a thermal cutout, or equivalent device, and the steady current limited to 25 milliamperes, unless the construction inherently limits the maximum steady current under any condition, such as that caused by failure of the transformer or current interrupter, to 3 to 5 milliamperes. The 60-cycle trap in the output circuit of Figure 4 illustrates one method of complying with this requirement.

A battery compartment is usually provided in the controller housing for dry cell operated controllers, thereby making the unit entirely self-contained. Since the unit may be installed without regard to the availability of central station power, this type has been very popular and has enjoyed the greatest volume of sales.

Capacity-Discharge Type. The commercial capacity discharge controller is an intermittent device. The output of the capacity discharge controller is similar to the inductive-impulse type, except that transients caused by contact chatter are absent. The device consists of a moderate voltage rectifier which builds up a charge on a storage capacitor. When the voltage on the capacitor reaches a predetermined value, a trigger tube ionizes and suddenly discharges the capacitor through the primary of a pulsing transformer, the output of which is impressed between the fence wire and ground. This controller possesses the advantage of having no moving mechanical parts. However, it is costly, and at present it is of lesser importance in the highly competitive market.

A typical circuit diagram and an oscillogram taken from a capacity discharge controller are given in Figures 7 and 8 respectively. The storage capacitor is denoted by $C1$; $C2$ is a small blocking condenser, and V_1 is the trigger tube. Since the trigger tube remains conducting only during the discharge of $C1$, sustained current in the output is negligible. The circuit is essentially that of a relaxation oscillator, the frequency being fixed by resistance R.

An earlier and much simpler type of capacity discharge controller operated on the principle of energizing the fence wire directly from the charge stored in a capacitor. The essential elements were a high-voltage rectifier and a resistance input filter. The initial current in the discharge was limited to a safe value by a resistor in the output circuit; a second resistor in the rectifier circuit limited the

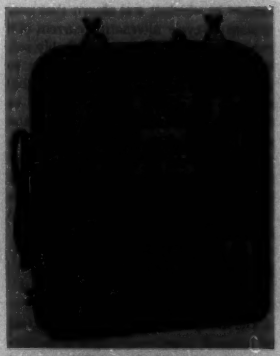

Figure 3. Typical commercial a-c intermittent electric fence controller

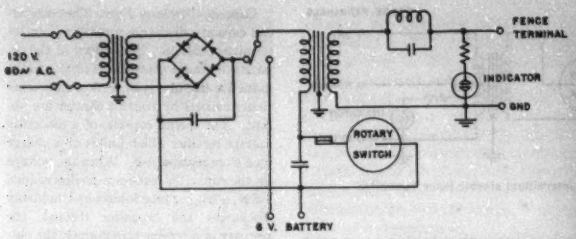

Figure 4. Schematic diagram of a combination inductive impulse electric fence controller

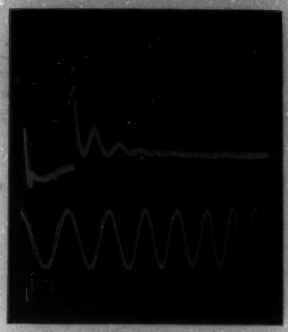

Figure 5. Oscillogram from a combination inductive impulse electric fence controller operated on 120 volts alternating current

Timing wave 100 cycles per second, 500-ohm noninductive resistor load

sustained output current. Although this type gave satisfactory results when the fence insulation resistance was high, it was found that the fence insulator leakage currents during ordinary conditions lowered the potential on the capacitor and seriously reduced the effectiveness of the electric fence. This type of controller has practically disappeared because of the serious reduction in effectiveness during slightly adverse operating conditions.

Continuous Type. The continuous electric fence controller is the simplest type, and consists of a high reactance transformer. Since no off period is provided, it is mandatory that the output current be sufficiently curtailed to permit a person to release accidental grasp of the fence wire by using muscles directly affected by the current. The maximum authorized current for the continuous electric fence is 8 milliamperes rms.

The continuous electric fence was popular in the early years of electric fencing. The electric shock hazard from such a device was pointed out by the author in his publications on let-go currents[44] in which it was shown that continuous 60-cycle alternating current of 8 rms milliamperes, although probably safe for normal men, would be dangerous to women and children. Since it is highly doubtful that lower currents would be effective in controlling animals, several concerns manufacturing continuous a-c electric fence controllers stopped production shortly after publication of these findings. To the best of the author's knowledge, the continuous type is no longer being marketed in this country.

Legislation Concerning Electric Fence Controllers

The number of fatalities due to contact with electric fences involving both humans and animals in the late 1930's reached such proportions as to constitute a problem of public safety. As a result, committees composed of representatives from agriculture, the electrical profession, and local, state, and federal agencies were organized to evaluate technical requirements and formulate safety regulations. The results of this effort produced three safety codes. These are General Orders on Electric Fences, Industrial Commission of Wisconsin, 1938; Standard for Electric Fence Controllers, Underwriters' Laboratories, 1939; and Safety Rules for Electric Fences, Part 6, Fifth Edition, National Electrical Safety Code, 1940.

Agricultural interests, much concerned with this problem, adopted in June, 1941, the following:

"WHEREAS loss of life has resulted from improper designs and installations of electric fencing equipment, and

"WHEREAS the National Bureau of Standards, the Underwriters' Laboratories, and several states have codes or standards for electric fence equipment which, so far as known, are safe, and

"WHEREAS a number of farmers, unmindful of the danger, are using various types of unapproved systems, which are believed to hazard human life, therefore be it

"RESOLVED that the American Society of Agricultural Engineers urge that greater efforts be made by the various interested agencies to further warn the public of the dangers involved in the use of such unapproved electric fence devices and installations, and that the Secretary of the Society be instructed to send copies of this resolution to the proper agencies of public regulation in each state."

Application and enforcement of these standards varies greatly in the several states. The Wisconsin statute provides that "every day during which any person, persons, corporation, or any official, agent, or employee thereof, shall fail to observe and comply with any order of the Commission. . . shall constitute a separate and distinct violation of such order, or of such sections, as the case may be." The Bureau of Labor, State of Oregon, requires compliance with the Underwriters' Standard. The Public Utilities Commission, State of Idaho, adopted Safety Rules for Electric Fences on August 15, 1940.

Although no specific legislation covering electric fences has been enacted by the State of California, such matters fall within the jurisdiction of the Department of Industrial Relations, Division of Industrial Safety. It is required that all appliances shall be of approved type. The Division will usually accept equipment and devices which have been approved by the Underwriters' Laboratories, United States Bureau of Standards, United States Bureau of Mines, and other institutions of recognized standing. The Division has jurisdiction only when employed labor is involved, with the exception of domestic servants, on federal reservations, and where the law delegates

Figure 6. Typical combination inductive impulse electric fence controller 120 volts alternating current or 6 volts direct current

other agencies. To date the Division has issued no list of approved controllers, yet electric fence controllers are available in stores throughout the state, and tens of thousands of electric fences are in daily use.

In the past there has been much heated discussion regarding the differences in the three codes. This controversy in technical circles has been unfortunate in that undoubtedly it has deterred adoption of any code in many states, and has created difficult problems for those individuals charged with enforcement in those states where regulations were in effect. As a result the average farmer, residing in a state not having specific legislation on electric fences and desiring to install an electric fence, has been left largely to his own resources. It is probable that he has been guided more by advertising than by the fact that a particular device carried or did not carry a certificate of approval. That construction of homemade controllers is still being considered by farmers is evident from the fact that during the period this paper was in preparation, the author received two requests for information regarding the construction of homemade controllers from persons on the eastern seaboard.

Just before the outbreak of World War II, the American Standards Association authorized the formation of a Sectional Committee on Electric Fences (*C-69*) to study the entire situation. Activity was suspended during the war, and the committee is still in the formative stages. However, it is anticipated that organization will be completed in 1950. In the interim, the National Bureau of Standards is setting up a committee on Test Methods and Apparatus in an endeavor to standardize methods of test and the instruments used to make them. It is anticipated that the Sectional Committee will review the accomplishments of this committee and deliberate on possible revisions of the various safety codes in the effort to arrive at more uniform requirements. It is hoped that ultimately the American Standards Association will make recommendations which will provide the stimulus to initiate specific legislation covering electric fences in the various states. Certainly the interest of public safety demands that this potentially hazardous device be controlled by specific enforceable regulations in all states, and thus put an end to the present unsatisfactory conditions which prevail over much of the country.

The almost zero mortality record of the past ten years in this country with approved electric fence controllers suggests that present regulations might be relaxed somewhat with resulting increase in effectiveness. With the single exception of the continuous a-c fence, Safety Rules for Electric Fences, National Electrical Safety Code, Part 6, Fifth Edition, paragraph *640D*, a reasonable compromise for a uniform code might consider the most liberal provisions of the three codes with advantageous results and without materially increasing the electric shock hazard.

Electric Fencing in Foreign Countries

Only limited information is available regarding electric fencing in foreign countries; however, recent inquiry indicates substantial interest in the subject. Although incomplete, Table V presents a list of standards, issuing authorities, and addresses both in this country and abroad. As mentioned previously, Table IV contains a summary of comparative output limitations. With the exception of the Underwriters' Standard, the similarity of the various codes is somewhat unexpected as one would hardly expect such substantial agreement between peoples otherwise having so many divergent viewpoints. Since similar studies comparing test methods and construction specifications would be of only limited interest, these will not be included here.

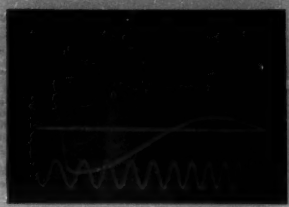

Figure 8. Oscillogram from a capacity discharge electric fence controller

Timing wave 10,000 cycles per second, 500-ohm noninductive resistor load

New regulations now are being issued in Norway. Previously, the output limitations for battery-operated controllers corresponded to the Danish regulations and a-c controllers were prohibited. Danish engineers have expressed much concern over the possibility that the high-voltage output might cause insulation breakdown of the transformer and thus permit the fence to become energized directly from the power circuit. This is of increased importance in Europe, since 220-volt lighting circuits are in general use. In contrast to American and French requirements that one side of the output circuit, transformer core, and controller housing be connected to the ground terminal, the regulations in Norway, Sweden, and Denmark require that both output terminals be insulated from the housing. In this case the protective ground for the housing and unenergized components is provided by the supply conduit. This requirement is intended to reduce high-voltage stresses should the controller ground become defective. In addition, all a-c operated controllers are limited to 5,000 crest volts on open circuit.

The opinion is held by many that battery-operated electric fence controllers are inherently safer than controllers energized from commercial power sources. This opinion is undoubtedly based on the possibility that insulation failure might cause the fence wire to become electrified without proper restraint. The various safety codes require that the primary and secondary windings of all a-c controller power transformers be placed on separate core legs, or otherwise separated, so that in case of failure of insulation the break-

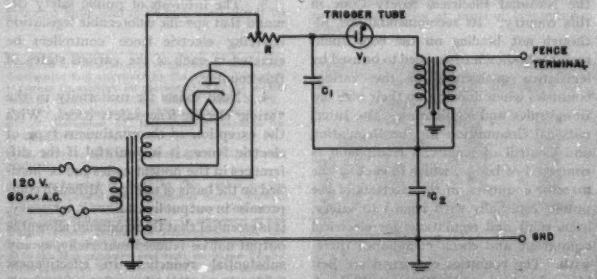

Figure 7. Schematic diagram of a capacity discharge electric fence controller

Table V. Electric Fence Regulations

Name of Standard	Organization	When Issued
General Orders on Electric Fences	Industrial Commission of Wisconsin, Madison, Wisc.	October 6, 1938
Standard for Electric Fence Controllers	Underwriters' Laboratories, Inc., Chicago, Ill.	1st Ed. Sept. 1939 2nd Ed. June 1948
Safety Rules for Electric Fences, National Electrical Safety Code, Part 6, Fifth Edition	U. S. Dept. of Commerce, National Bureau of Standards, Washington, D. C.	April 17, 1940
Bestemmelser for Spaendingsgivere Til Elektriske Hegn	Elektricitetsradet, Gothersgade 100, Copenhagen, Denmark	1st Ed. April 1940 2nd Ed. Dec. 1942 3rd Ed. March 1945 4th Ed. Oct. 1946
Elektriska Stangel for Betesmarker; Elektriska Inspektoratets Meddelande	Elektriska Inspektoratet, Nalmerinkeu, Helsingfors, Finland	February 1945
Battery Operated Electric Fences; British Standard 1222	British Standards Institution, 28 Victoria Street, London, S. W. 1, England	1945
Regles A'. Appliquer Pour L'Execution Et L'Entretien Des Clotures Electriques	L'Union Technique des Syndicate de L'Electricite, 54 Avenue Marceau, Paris, France	May 6, 1946
Bestammelser For Utforlande Och Provning Af Elstangselapparateur	Svenska Elektriska Materielkontrollanstalen, Stockholm, Sweden	May 1947
Specifications for Electric Fence Controllers	Dansk Elektroteknish Komite, Vesterbrogade, Copenhagen, Denmark	Oct. 15, 1948
Regulations	Norges Elektriske Materiellkontroll, Oslo, Norway	1948

down will be to a grounded metallic barrier. In addition, high potential dielectric tests, and safety cutouts or fuses are specified. It is generally recognized that lightning is the chief cause of insulation failure in well constructed controllers. Although separate lightning arresters connected to separate grounds provide the best protection, protective gaps or equivalent devices are provided in some controllers. This practice is highly recommended as an additional precaution. The importance of obtaining an effective ground must be emphasized. A low resistance ground is essential for protection against lightning, as well as insulation failures in general. In addition a good ground permits delivery of the maximum output, and thus assures maximum effectiveness in controlling animals. Possibly the opinion that battery controllers are inherently safer than a-c operated devices is also based upon the idea that the energy available from any device designed to operate from batteries which last three to five months cannot be very hazardous. While the author appreciates the logic behind this reasoning, such argument obviously fails if a manufacturer, oblivious to safety requirements, produces a device based on effectiveness only. In this connection it is pertinent to mention that in 1944 a human fatality occurred in Canada due to contact with an electric fence energized from a homemade controller supplied from a 6-volt battery. It is the author's opinion that when safety code requirements are followed, and the device is properly installed, the a-c operated electric fence controller should present no more of a hazard than other electrically-operated farm devices or household appliances.

To date, the Canadian Standards Association has refrained from taking definite action on electric fence matters; however, the electrical inspection departments of some of the provinces have approved battery-operated units. Nor has the Standards Association of Australia issued regulations, but it is reported that battery-operated controllers are finding increased use. Presumably local specifications are based on the British Standard for battery-operated electric fences.

The most recent action concerning electric fencing was that proposed at Copenhagen, Denmark. On October 15, 1948, the International Commission for the Regulation and Control of Electrical Equipment (CEE) adopted tentative Specifications for Electric Fence Controllers. The regulations adopted by this body, which was formerly known as Installations Fragons-Kommission (IFK), constitute the European counterpart of the National Electrical Safety Code in this country. Its recommendations, although not binding on the constituent member bodies, are intended to be used by legislative authorities in the various countries when drawing up their own national rules and regulations. The International Commission for the Regulation and Control of Electrical Equipment is composed of bodies, which in each of the member countries, in the interests of the public, especially with regard to safety, issue rules and regulations for electrical equipment and check compliance therewith. The countries concerned are Belgium, Czechoslovakia, Denmark, Finland, France, Hungary, Netherlands, Norway, Poland, Sweden, Switzerland, and the United Kingdom.

This new European tentative standard places the most rigid output limitations so far adopted. The effect of reduced shock intensity, particularly with regard to reduction of the impulse crest is of concern, since it is highly probable that these reduced limits will be incorporated in future revisions of the standards in the various member countries. The proposed standards were not accompanied by any comments relating to the reason for the downward revision of allowable current and quantity outputs. Possibly climatic conditions are more favorable in Europe, as normally precipitation occurs somewhat more evenly distributed throughout the year than in many sections of this country. The resulting improved grounding conditions may permit effective control with lower shock intensity than that believed essential for satisfactory operation in this country.

Almost without exception, the most serious adverse criticism of California farmers regarding electric fencing concerns effectiveness. Farmers desire a more powerful shock so that effectiveness may be better maintained during adverse operating conditions. Should the lower limits as proposed by the International Commission for the Regulation and Control of Electrical Equipment be adopted in this country, the value of electric fencing to the American farmer might be seriously jeopardized.

Conclusions

1. The approved electric fence is a safe, effective, and economical aid to modern farming.

2. Homemade electric fence controllers are responsible for the continuing electrocution of both human beings and animals. The use of such controllers should be prohibited by law.

3. The interests of public safety demand that specific enforceable legislation covering electric fence controllers be enacted in each of the various states of this country.

4. Need exists for uniformity in the various electric fence safety codes. With the exception of the continuous type of electric fence, it is doubtful if the differences in the present codes can be justified on the basis of safety. Although compromise in output limitations is necessary, it is essential that the maximum allowable output not be reduced materially, as any substantial reduction in effectiveness might jeopardize the value of electric fencing.

References

1. Electric Shock as it Pertains to the Electric Fence. *Bulletin of Research* (Underwriters' Laboratories, Inc., New York, N. Y.), number 14, December 1939, pages 45–50.

2. Electrocution by Electric Fence Controller, Charles F. Dalziel. *Agricultural Engineering* (St. Joseph, Mich.), number 8, volume 25, August 1944, page 308.

3. Case v. Peterson, Supreme Court of Washington. *Pacific Reporter*, P 2nd Series, volume 136, 1943, pages 192–96.

4. McMullen v. McClunney, Court of Appeal of Louisiana. *Southern Reporter*, So. 2nd Series, 1945, pages 658–61.

5. Effect of Frequency on Let-Go Currents, Charles F. Dalziel, Eric Ogden, Curtis E. Abbott, *Electrical Engineering* (*AIEE Transactions*), volume 62, December 1943, pages 745–50.

6. Effect of Wave Form on Let-Go Currents, Charles F. Dalziel. *Electrical Engineering* (*AIEE Transactions*), volume 62, December 1943, pages 739–44.

No Discussion

Development and Testing of an Improved High-Voltage, High-Capacity Impulse Circuit Breaker

E. B. RIETZ
ASSOCIATE AIEE

Synopsis: In October 1947, F. A. Lane and B. W. Wyman[1] described before the Institute the switchgear equipment developed for the Tidd High-Voltage Test Line. This equipment included a low oil content impulse-type circuit breaker rated 10,000,000 kva at 360 kv. The unit described at that time was part of an over-all development program of higher capacity switchgear equipments which will be needed to control and protect properly the rapidly expanding power systems of this country. This paper describes the development of the high-capacity impulse-type circuit breaker to be used in these equipments, both at existing transmission voltages and at the higher transmission voltages projected for the future. In addition, it presents substantiating laboratory and field test data indicating the ample margin of safety possessed by this circuit breaker to meet any requirements the future might dictate.

THE unprecedented expansion in electric load growth during and since the war has made it necessary for most power systems to operate close to their ultimate installed capacity, and many systems have had to be operated closer to their transient stability limit than would formerly have been considered good practice. Moreover, there is every indication that this rate of growth will continue for some time in the future. The result has been a tremendous increase in installed and planned generating capacity, with proportionate increases in paralleling transmission lines and greater interconnections between systems. Larger blocks of power than ever before are being transmitted over longer distances than ever before at existing transmission voltages, and the transmission of still larger blocks at higher voltages is being considered for the future.

Such an expansion in the power systems of this country cannot occur without placing new requirements on the high-voltage circuit breakers and switchgear used to control and protect these systems against short circuits.

Some of the new circuit breaker requirements are

1. The development of much higher interrupting capacities at existing transmission voltages.

2. The development of higher voltage ratings for use on the higher voltage transmission systems now under consideration.

3. The development of higher continuous current ratings.

4. The development of shorter reclosing times to permit reclosure as soon as the flashover paths are deionized. Present evidence indicates these times may be appreciably shorter than the present standard reclosing times of 20 cycles.

5. The development of circuit breakers with consistently short arcing times over the entire interrupting current range. This is increasingly important with the higher interrupting capacity circuit breakers contemplated, as the majority of faults they will interrupt may be some distance out on a line, and therefore less than 25 per cent of the interrupting rating of the circuit breaker.

6. The development of circuit breakers which do not restrike when interrupting the capacitive charging current of long transmission lines to eliminate the possibility of generating overvoltage surges which may cause line flashovers.

7. As the circuit breaker design determines, in large part, the design of the total station, its development must be co-ordinated with the over-all station so that it provides the best protection and switching at both a minimum first cost, and a minimum operating cost.

Of all the known types of high-voltage circuit breakers which might be developed to meet these requirements, the impulse-type low oil content circuit breaker had the most impressive test and operating

Figure 1. Original design of impulse-type low oil content circuit breaker in service on 287-kv transmission system between Hoover Dam and Los Angeles

Cross-blast interrupting contacts in small diameter horizontal porcelain insulators at top with piston housing in center to provide impulse blast action. Both pistons and contacts are operated by a vertical operating rod in center column. Vertical porcelain columns at either end enclose cascade-type current transformers

[1] Paper 50-3, recommended by the AIEE Switchgear Committee and approved by the AIEE Technical Program Committee for presentation at the AIEE Winter General Meeting, New York, N. Y., January 30–February 3, 1950. Manuscript submitted November 15, 1948; made available for printing October 28, 1949.

E. B. Rietz is with the General Electric Company, Philadelphia, Pa.

Acknowledgment is given by the author to the personnel of the American Gas and Electric Service Corporation, who made possible connection to the Tidd High Voltage Test Line; to personnel of the United States Bureau of Reclamation and the Bonneville Power Administration, who made possible the high-capacity field tests at Grand Coulee Switchyard; to W. F. Skeats and T. R. Coggeshall, who furnished many of the ideas incorporated in the design; and to E. J. Olsen, who aided in the factory and field tests.

Figure 2. 138-kv low oil content impulse-type circuit breaker as manufactured in 1935 having four sets of series contacts in horizontal porcelain insulators with impulse oil blast piston located at right end. Cascade-type current transformers located in vertical porcelain column at either end

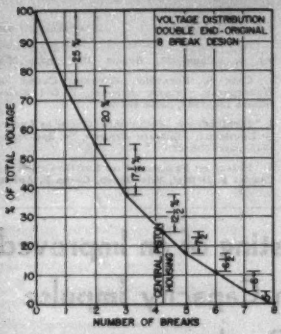

Figure 4. Per cent distribution of total voltage between eight breaks uniformly spaced on original 287-kv impulse interrupter

Note the effect of large central piston whose capacitance increases voltage across 4 breaks on high side and decreases voltage across four breaks on low side. First break is most highly stressed with 25 per cent of voltage

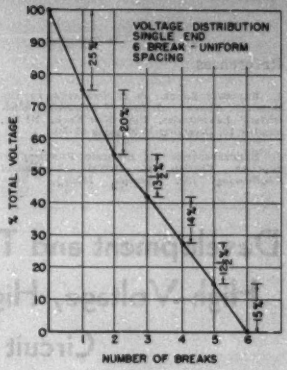

Figure 5. Per cent distribution of total voltage between six breaks uniformly spaced with piston housing moved to end

First break is most highly stressed with 25 per cent of total voltage

record. On the basis of this record, it was selected for development.

The impulse low oil content circuit breaker is not new. Fourteen years of outstanding operating experience have been obtained on the first impulse-type low oil content circuit breakers since they were placed in service on the 287-kv transmission line between Hoover Dam and Los Angeles. These circuit breakers were described before the Institute in June 1935.[2] As they were developed primarily to obtain high-speed fault isolation to increase the transient stability limit of that line, they had an interrupting time of 3 cycles. This was considered extremely high speed interruption at that time when most standard tank-type high-voltage circuit breakers had interrupting times of 8 cycles or longer. Besides increasing the system stability limit, the high speed fault interruption obtained with this type of circuit breaker resulted in reduced conductor damage at the point of fault, negligible voltage dips on the system, and negligible contact maintenance on the circuit breaker itself.

The design of these circuit breakers was a radical departure from standard tank-type high-voltage circuit breakers. The interrupters, instead of being submerged in large tanks of oil, were enclosed in small horizontal porcelain insulators. This construction eliminated over 90 per cent of the 15,000 gallons of oil required in tank-type circuit breakers and reduced the weight of the circuit breaker by more than one-half. Figure 1 shows one of these circuit breakers installed on the 287-kv Hoover Dam transmission line. Major savings were made possible with this circuit breaker in the cost of oil, and in the elimination of extensive oil-handling, filtering, and storage equipment.

Extremely high-speed arc interruption was obtained in these circuit breakers by using eight sets of cross-blast contacts located in the horizontal porcelain insulators. These contacts were divided into two groups of four, and separated in the center by two impulse pistons, one supplying a cross-blast of oil to each group.

Unlike tank-type circuit breakers, whose blast pressure is generated by the arc itself, and therefore varies with the current in the arc, these impulse circuit

Figure 6. Per cent distribution of total voltage between six breaks nonuniformly spaced to provide optimum distribution. First three breaks stressed almost uniformly

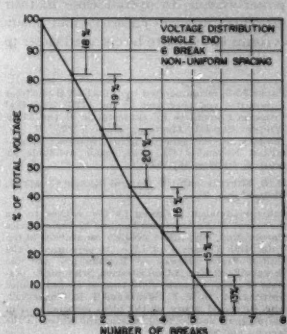

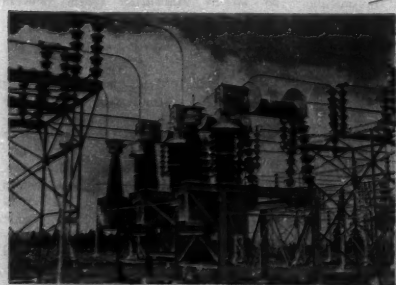

Figure 3. 230-kv low oil content impulse-type circuit breaker in service at J. D. Ross Substation of Bonneville Power System

Five sets of cross-blast contacts are located in horizontal interrupting unit with impulse oil blast piston located at upper right end. Eye-bolt current transformers replace cascade types of original designs

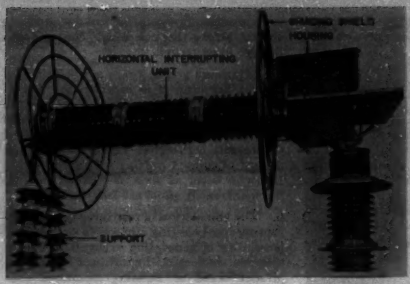

Figure 7. Horizontal interrupting unit of newly developed 360-kv low oil content circuit breaker

Six sets of series cross-blast contacts are enclosed in inner thick wall herkolite tube which carries entire weight of unit. Porcelain insulating shells are spaced concentrically around outside of herkolite tube as weather shields and are connected together by flexible metallic sylphons which prevent any load being transmitted to porcelains. Impulse oil blast piston which supplies oil blast to contacts is located in housing at ends. Large shielding rings at either end of interrupter improve distribution of voltage between various breaks

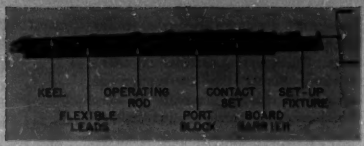

Figure 9. Complete 6-break contact assembly removed from interrupter for inspection on factory floor

Figure 10. Comparison of mechanism frame sizes between older type 230-kv spring-operated mechanism and new smaller 360-kv compressed-air operated mechanisms

breakers generated their blast pressure by the central piston, whose action was independent of the current being interrupted. Consistently short arcing times therefore were obtained whether interrupting either light load current or heavy short circuit currents. Special tests showed these circuit breakers to have extremely wide margins of safety above their rated interrupting capacity, both as regards voltage-interrupting ability and current-interrupting ability. Low oil content impulse circuit breakers of similar designs also were developed for other voltages soon afterwards. Figure 2 shows a 138-kv circuit breaker which is essentially one-half of the 287-kv circuit breaker with the operating rod in one of the vertical porcelain columns along with the cascade current transformer. The interrupting unit of this circuit breaker had four breaks, and its impulse piston was located at one end. With this arrangement, more uniform voltage distribution between the various breaks was obtained even with voltage shields omitted than was possible on the 287-kv circuit breaker, as a result of the elimination of the large piston housing in the center of the interrupter. The improved voltage distribution obtained with the impulse piston located at the end of the interrupter instead of the middle resulted in a 230-kv design with only five breaks, with the most highly stressed break having less voltage across it than the 8-break design at 287 kv. Figure 3 shows a 230-kv circuit breaker in service at the J. D. Ross Substation of the Bonneville Power System, in which external-type current transformers were used to replace the internal cascade transformers of earlier designs.

Although lower cost tank-type circuit breakers were used for the larger percentage of high-voltage switching applications between 1934 and the present time, large numbers of impulse-type circuit breakers have been installed in loca-

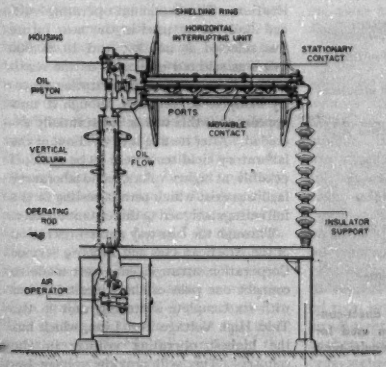

Figure 8. Cross section of complete single-pole of 360-kv impulse-type circuit breaker rated 10,000,000 kva showing six sets of cross-blast contacts in horizontal interrupting unit at top whose cross oil blast action is supplied by impulse piston in housing at left end

Both contacts and piston are driven through vertical operating rod directly connected to high-speed closing piston at bottom

Figure 11. Typical contact closing and contact opening curve showing the smooth high-speed closing action obtained with the air-operated mechanism

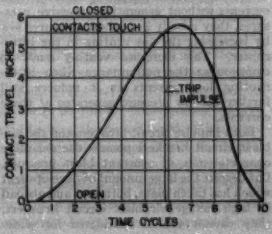

tions which demanded the utmost in interrupting performance over the entire range of interrupting currents, or where restriking during the interruption of capacitance charging currents of long transmission lines had to be eliminated, or where the reduction in maintenance oil-handling equipment, or fire hazard justified the higher cost of this type of circuit breaker.

Selection for Future Development

When it became evident some time ago, that circuit breakers for much higher interrupting capacities and higher voltage would be required in the near future, all the various established types of circuit breakers were reviewed to determine which type should be developed. By checking the impulse-type circuit breaker with other types against the list of requirements set forth earlier in this paper, it can be seen that the impulse circuit breaker best fulfills these requirements:

1. From the standpoint of interrupting ability, experience to date has shown no upper limit to the capacity for which impulse circuit breakers can be designed. Laboratory tests early showed that the 2,500,000-kva and 3,500,000-kva ratings which were assigned to previous designs did not represent anything near their actual interrupting capacity. This was born out by field tests at Grand Coulee Dam in 1947, when a 230-kv impulse circuit breaker installed in 1945 interrupted short circuits up to 6,700,000 kva without signs of distress, and gave every indication that it could have interrupted appreciably more, had more been available at that time.[4,5] Neither on line-charging currents nor on short-circuit currents did the circuit breaker exceed its rated 3.0-cycle interrupting time.

At the higher interrupting capacities under consideration, the extremely short arcing time of the impulse circuit breaker not only keeps the line damage at the point of fault to a minimum, but also reduces oil carbonization within the circuit breaker to a very low value. Moreover, as the range of currents to be interrupted from minimum to maximum becomes ever greater, the fundamental advantage of the constant blast pressure in the impulse circuit breaker assumes ever increasing importance. Although tank-type interrupters which generate their own blast pressure by the current in the arc can be developed to interrupt high currents without generating excessive pressures, they usually keep these pressures low by increasing the gas venting in the interrupter. This increased venting tends to compromise the performance when interrupting low currents as it reduces still further the low pressure generated at these currents.

Both impulse circuit breakers and the air-blast circuit breakers possess the desirable characteristics of constant blast pressure, but despite the large amount of development which has taken place, both here and abroad in high-voltage air blast circuit breakers, they cannot yet be considered for widespread application for the extremely high capacities, or high voltages required in the immediate future, whereas years of outstanding performance stand behind the impulse-type circuit breaker for voltages from 138 to 287 kv.

2. For higher voltages, one of the primary advantages of the impulse-type circuit breaker over the tank-type circuit breaker is its tremendous reduction in the quantity of oil required. As the diameter of the tank in tank-type circuit breakers must increase with voltage to maintain adequate clearance between the interrupters and the side wall of the tank, the difference in the quantity of oil required becomes tremendous at the higher voltages. Also, the usual loop arrangement of the interrupter, and the grounded steel tank surrounding them in the tank-type circuit breaker make good voltage distribution between the various breaks very difficult.

3. As higher continuous current ratings are required at the higher voltages under consideration for the future, the impulse-type circuit breaker has two distinct advantages over other types of circuit breakers. First, its contact stroke from the fully closed to the fully open position is only 25 to 35 per cent that of the tank-type circuit breakers; second, it has no heavy current-carrying crosshead. Both of these features reduce the energy required to produce the high-speed operation required. The reduction in contact stroke in the impulse circuit breaker is made possible by the improved voltage distribution between the series breaks by their straight line arrangement and by the elimination of the grounded steel tank.

4. As the original impulse circuit breakers antedated the advent of high-speed reclosing, they were operated by a mechanism which required several seconds to recharge before reclosing could take place. A complete new mechanism was therefore necessary to meet the requirement of high-speed reclosing. With this new mechanism provided, however, much faster reclosing times are possible with impulse circuit breakers than with tank-type circuit breakers for the expenditure of the same amount of energy, because of the reduced weight of contacts, the reduction in operating linkage, and the shorter stroke through which contacts and linkage must travel.

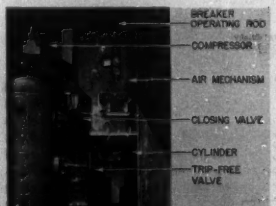

Figure 12. Simplicity of the new direct-connected piston-type air mechanism used for high-speed operation of 360-kv impulse-type circuit breaker

5. Minimum arcing times at all values of current are insured in impulse-type circuit breakers by the positive blast action of the impulse piston which starts simultaneously with the contacts. A substantial blast of oil pressure is therefore available before the instant of contact parting. As interruption then can occur as soon as current zero arrives, extremely short arc lengths result.

6. The elimination of restriking when interrupting line-charging current to prevent the possibility of generating overvoltage surges assumes increased importance with the present trend of building minimum cost transmission lines with reduced insulation levels. This is particularly true at 230 kv and above. The positive blast action of the impulse-type circuit breaker forces fresh oil between the contacts at the same rate whether the circuit breaker is interrupting line charging currents, or interrupting heavy short circuit currents. Therefore, no restriking can occur.

7. The impulse-type circuit breaker simplifies over-all station design by eliminating extensive oil handling, filtering, and storage equipment. Its reduced weight simplifies foundations, particularly when the station is located on marshy or filled ground, or close to river beds. The framework of the circuit breaker also may be used to support the overhead structure for mounting disconnecting switches, current transformers, or lightning arresters to simplify arrangement layouts.

Development of Improved Impulse Circuit Breaker

The first step in the development of higher-capacity higher-voltage impulse circuit breakers was the building of an experimental circuit breaker of the highest voltage and highest interrupting capacity then considered likely to be required in the next 5-to-10 year period. The interrupting and reclosing time were to be the shortest which would be required at any location. The maximum operating voltage likely to be used in the near future was selected as 360 kv, and 10,000,000 kva was selected originally as the maximum kilovolt-ampere interrupting capacity likely to be required, though it now appears that this will be substantially exceeded. After testing it to the limit of the laboratory, field tests were to be made, if possible, at higher values, as no laboratory facilities exist which permit testing to the full ratings assigned to this circuit breaker.

Through the courtesy and co-operation of the American Gas and Electric Service Corporation, arrangements were made to connect one pole of this circuit breaker with its complete switching unit to the Tidd High Voltage Test Line, which has the highest operating voltage in the country. This will provide voltage be-

havior data under actual field conditions.

Through the courtesy and co-operation of the United States Bureau of Reclamation, a second pole of this circuit breaker was given short-circuit interrupting tests at Grand Coulee Dam, which has the largest concentration of short circuit capacity of any location in the country.

The development of a higher-voltage higher-capacity impulse circuit breaker divided itself into two main categories.

1. The development of a higher voltage interrupter which also would be capable of interrupting the maximum current required of the new circuit breaker.

2. The development of a new high speed mechanism capable of reclosing in 10 cycles or less.

Higher Voltage Impulse-Type Interrupter

The fundamental oil blast equation stating the maximum rate of rise of recovery voltage a circuit breaker can interrupt equals the oil velocity multiplied by oil dielectric strength is simpler to calculate for the impulse-type interrupter than for any other known type, because the velocity of the oil from the impulse piston does not vary with the current in the arc. The number of breaks required for any given voltage is determined by the uniformity of the voltage distribution between breaks. In the original 287 kv impulse circuit breaker, with its large piston housing in the middle, the distribution of voltage between the eight breaks with one end grounded is shown in Figure 4. It will be noted that 25 per cent of the total voltage appears across the first break. The later 138- and 230-kv circuit breakers, however, with their piston housings located at the end of the interrupter showed considerably better voltage distribution, so that the latter arrangement was selected for higher voltage development. As the distribution of voltage between breaks is extremely difficult to calculate, a scale model interrupter was made up in which the number and spacing of the breaks could be varied as well as the size and shape of the shielding rings at the ends. This model showed that with six breaks uniformly spaced, and with enlarged shielding rings at the ends, the voltage distribution curve shown in Figure 5 could be obtained. Here, with only six breaks the voltage across the most highly stressed breaks is also 25 per cent, or the same as with the eight breaks in the 287-kv arrangement. The spacing of the six breaks was then varied nonuniformly by increasing the spacing between the center breaks giving

Figure 13. Single pole of 360-kv low oil content impulse circuit breaker set up for test in high power short circuit testing laboratory

a greatly improved voltage distribution which is shown in Figure 6. With this arrangement of breaks, it will be noted that the six breaks could be operated at 360 kv with the same voltage stress appearing across the worst break as in the original 8-break design, as can be seen from the following:

$$25 \text{ per cent of } \frac{287}{\sqrt{3}} = 41.6 \text{ kv}$$

$$20 \text{ per cent of } \frac{360}{\sqrt{3}} = 41.7 \text{ kv}$$

Although single break tests had shown this voltage to be extremely conservative for one break, it was decided on the basis of the large amount of excellent operating data obtained on previous designs, that this voltage should be retained for 360 kv. At 230 kv, considerably smaller shielding rings are used to reduce phase spacing. With these smaller shielding rings and somewhat poorer voltage distribution, five interrupting breaks are used.

Due to the increased length of the horizontal interrupting units which would increase the bending moment on the horizontal porcelains if they were rigidly mounted, the design of the horizontal unit was modified so that the porcelain insulators act merely as a rain shield. The entire weight of the interrupting unit and porcelains is carried on a thick-walled internal herkolite liner tube which forms the interrupting chamber. This herkolite tube has annular spacing rings around it to support the porcelain shells. Short oil-tight sylphons are then used to obtain an oil-tight joint between the porcelains, as shown in Figure 7. Figure 8, which is a cross-sectional view of the entire circuit breaker unit, shows the details of the contacts and impulse piston, with arrows indicating the flow of the oil blast out in the lower half of the herkolite tube and up between each set of contacts which part directly beneath ports in a horizontal dividing baffle. As each set of contacts and port forms a jet for the release of the oil pressure beneath the baffle, extremely high oil velocities are obtained between the contacts.

For contact inspection purposes, only the small volume of oil in the central herkolite tube, 90 gallons, in the 360-kv interrupter and 70 gallons in the 230-kv interrupter, need be drained before sliding the entire contact assembly out for inspection. The oil used for insulation between the outside of the herkolite tube and porcelain shell is isolated. Therefore, it need not be drained as it is not subject to arcing. Figure 9 shows a 360-kv contact assembly removed for inspection on the factory floor.

The contacts and blast piston are operated by a heavy insulation rod traveling up through the vertical operating column. The operating rod is carried through a mercury seal at the bottom of the vertical column which prevents leakage of oil. As in the horizontal unit, the vertical porcelain shells take none of the circuit breaker load, but merely act as rain shields with the inner thick-walled herkolite tube supporting the entire circuit breaker. As neither the vertical nor horizontal shells carry load, they are not subject to strain or vibration. Should they be broken accidentally, however, the oil inside the herkolite tubes would not be lost, and the circuit breaker could still be operated under emergency conditions until repairs could be made.

New High-Speed Reclosing Mechanism

The spring-type mechanism used on earlier impulse circuit breakers was not designed for high-speed reclosing. It was replaced, therefore, on the new circuit breaker by an air mechanism to obtain the highest possible reclosing speed. By locating this mechanism directly below the vertical operating rod, no linkage, cams, rollers, cranks, or gears were required. The piston used to close the circuit breaker was directly connected to the bottom of the vertical operating rod, as shown in Figure 8. The opening springs used to open the circuit breaker then were located at the far end of the horizontal interrupter at the other end of the contacts. A high-speed valve admits air to the top of the piston to close the circuit breaker. As it travels downward and

Figure 14. Complete single-phase switching unit shortly after assembly at Brilliant, Ohio for connection to Tidd High Voltage Test Line sponsored by the American Gas and Electric Company, showing construction of overhead structure for supporting disconnecting switches, through-type sealed bushings with current transformers and Thyrite lightning arresters

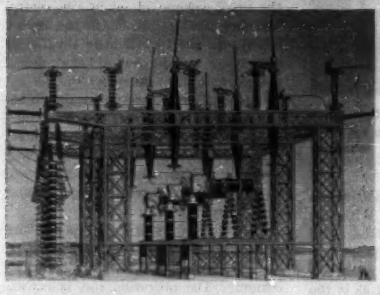

Figure 14(A). Artist's conception of complete triple-pole 360-kv switching unit including impulse circuit breaker motor-operated isolating switches with through-type sealed bushings and Thyrite-type lightning arresters

closes the contacts, it compresses the opening springs at the far end of the interrupter. When the circuit breaker is completely closed, a high-speed latch drops into position on top of the piston. When tripped, the springs at the far end of the interrupter open the circuit breaker. This arrangement has the important operating advantage of keeping all rods and links in the circuit breaker continually in tension, both during the closing and opening operations of the circuit breaker. Appreciably faster trip-free operation is obtained when closing on a fault than is possible with most circuit breakers whose operating rods are in compression in one direction and therefore cannot reverse their contacts until all lost motion, pin play, and deflections first are reversed. Immediate reversal, however, is possible with this mechanism. The reduction in mechanism size obtained by substituting the air mechanism for the old type spring mechanisms can be seen by referring to Figure 10, which shows the framework of one of the large spring mechanisms beside three frameworks of the small air mechanism. The low mass of the contact parts permits an easy control of the opening and closing speed. Figure 11 shows a typical closing and opening curve of the new circuit breaker.

The simplicity of the direct-connected assembled mechanism can be seen in Figure 12. Each pole is equipped with its own individual operator as it has been found that simultaneous operation of the three poles of high-voltage circuit breakers can be achieved reliably in this manner. Besides simplifying the circuit breaker construction and operation, individual pole mechanisms also make possible either single-pole or triple-pole reclosing without addition of extra mechanisms or linkages.

Laboratory Tests on 360-Kv Unit With Six Breaks

Figure 13 shows one pole of the 360-kv circuit breaker set up for test in the General Electric Company's high power, short circuit testing laboratory at Schenectady. The following data illustrate the results of the tests made on this unit.

1. Operating Times
   - Closing time = 8 cycles (250 pounds per square inch)
   - Contacts part = 1.5 cycles
   - Fully open = 5 cycles
   - Reclosing time = 8 cycles
2. Operating Speed
   - Closing = 9 feet per second at point of contact touching
   - Opening = 12 feet per second average for first 2 inches after contacts part
3. Life Tests
   - 1,000 reclosing operations
   - 1,000 trip-free operations
   - 1,000 close and open operations

   No faulty operations were observed during tests, and inspection after tests showed all circuits breaker and mechanism parts in excellent condition.
4. 60-Cycle High-Potential Tests—Rated 1-Minute Withstand = 590 kv
   620 kv (5 per cent over rating) withstood with circuit breaker open and closed.
5. $1^1/_2$ by 40 Microsecond Impulse Tests—Rated 1,300 kv
   - Maximum withstand test; Positive circuit breaker closed, 1,375 kv; circuit breaker open, 1,407 kv
   - Maximum withstand test; Negative circuit breaker closed, 1,650 kv; circuit breaker opened 1,550 kv
6. Interrupting Tests
   Table I lists a few representative interrupting tests made in the high power laboratory. The maximum voltage at which interrupting tests were made on the single-pole circuit breaker was 264 kv which is appreciably in excess of 210 kv which is phase voltage for 360 kv.

Connection to Tidd High-Voltage Test Line at Brilliant, Ohio

Following the laboratory tests, a single-pole unit was shipped to Brilliant, Ohio, and connected to the Tidd High Voltage

Table I. Single-Phase Interrupting Tests—High-Power Laboratory

Six Breaks—Light Piston

Line Voltage, Kilovolts	Current in Amperes, Rms: Max. Loop	Current in Amperes, Rms: Initial in Arc	Interrupting Time Trip Impulse to Interruption, cycles
264*	1,410	1,400	2.0
264†	850	760	2.6
264*	1,400	1,350	2.1
264†	850	750	3.0
264*	1,310	1,120	2.2
264†	1,220	1,050	2.2
264*	1,410	1,240	1.8
264†	850	820	2.3
264*	1,420	1,200	2.2
264†	1,090	950	2.5
264*	1,420	1,220	2.3
264†	1,320	1,000	3.0
264*	1,420	1,240	2.4
264†	980	860	2.3
264*	1,420	1,220	2.4
264†	900	810	2.7
132*	2,600	2,500	1.9
132†	2,500	2,100	1.8
132*	2,700	2,700	2.0
132†	1,630	1,630	2.2
132*	2,700	2,300	1.7
132†	2,300	1,940	1.6
132*	2,600	2,200	2.1
132†	2,200	1,800	2.7
132*	2,500	2,100	2.1
132†	2,600	2,100	2.3
14.5*	23,000	21,000	1.7
14.5†	17,400	15,400	1.6
14.5*	24,000	20,000	1.3
14.5†	17,600	15,900	1.9
14.5*	23,000	23,000	1.3
14.5†	21,000	18,500	1.5
14.5*	21,000	17,800	1.8
14.5†	13,800	13,700	1.6
14.5*	25,000	20,000	1.5
14.5*	19,600	17,700	1.5
14.5*	28,000	23,000	2.0
14.5†	25,000	22,000	1.8
14.5*	25,000	23,000	1.8
14.5†	14,800	13,400	1.7
14.5*	25,000	25,000	1.4
14.5†	14,600	13,400	1.7
14.5*	25,000	25,000	1.9
14.5†	21,000	18,800	1.8
14.5*	25,000	23,000	1.5
14.5†	17,400	15,200	1.8

* Open.
† + Instantaneous + Close-Open.

Test Line, sponsored by the American Gas and Electric Service Corporation. Figure 14 shows the assembly of the complete switching unit with its overhead structure supporting the disconnecting switches, through-type sealed bushings with current transformers and thyrite lightning arresters. The unit will be left on the line for extended periods through various types of weather before the test can be considered complete.

Tests at Grand Coulee Dam

A second pole unit of the circuit breaker was sent to Grand Coulee Dam for high-capacity short circuit tests on the 230-kv bus to which one, four, and eight 108,000-kw generators could be connected, plus three or six transmission lines. As two additional generators had been installed since the 1947 field tests on an earlier design impulse circuit breaker when 6,700,000 kva was obtained, it was expected that higher short-circuit currents would be obtained on these tests. The tests were scheduled during two weekends with the following objectives:

1. To determine the interrupting per-

Table II. Single-Phase Line Switching Tests at Grand Coulee

Five Breaks—Heavy Piston

Series A Test Number	Connection	Miles of Line	Charging Current, Amperes	Time in Cycles: Interrupting	Time in Cycles: Arcing
1*	On System	100	78	1.95	0.12
2*		100	77	1.75	0.04
3†		100	77		
4*		200	151	1.95	0.14
5*		200	151	1.85	0.13
6†		200	151		
7*		300		No Record	
8*		300	184	201	0.37
9†		300	184		
10*	Isolated	382	240	1.80	0.07
11*		382	230	1.80	0.05
12†		382	240		
13*		382	360	2.00	0.25
15†		382	340		
16*		300	165	2.00	0.50
17*		300	165	2.00	0.50
18†		300	165		
19*		200	129	2.2	0.45
20*		200	127	1.8	0.10
21†		200	130		
25*	On System	100		No Record	
26*		100		No Record	
27†		100	78		
				Average 1.93	

All tests at 238 kv.
No restrikes were obtained on any of these tests.
* Open.
† Closed.

Figure 15. One pole of the 360-kv impulse type low oil content circuit breaker set up test in Grand Coulee switchyard

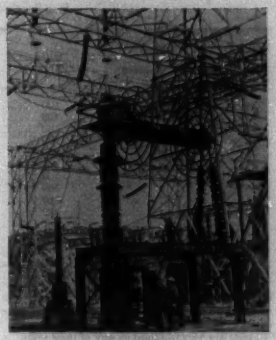

Table III. Single-Phase Fault Tests at Grand Coulee

Six and Five Breaks—Heavy Piston

Series B Test Number	Bussing Arrangement	Duty Cycle	Line Voltage, Kilovolts	Interrupted Current, Amperes Rms	Equivalent 3-Phase Megavolt-Amperes Interrupted	Interrupting Time, Cycles	Reclosing Time, Cycles
Six breaks							
01	1 Generator	Open	238			2.1	
02		Close Open	238			3.0	
1	4 Generators and 3 Lines	Open	238			2.8	
2		Close Open	238			2.9	
3-A		Open	238	Current transformer		2.5	
3-B		+Instantaneous +Close Open	238	partially grounded		2.8	12.9
4		Open	238	current measure-		2.5	
5		Close Open	238	ment inaccurate		2.6	
6	8 Generators and 3 Lines	Open	238	12,630	5,220	2.2	
7-A		Close Open**	238	17,600	7,270	3.3	
7-B		+15 Seconds +Close Open	238	12,500	5,160	2.8	
8-A		Open	238	13,800	5,700	2.2	
8-B		+Instantaneous +Close Open**	238	17,630	7,280	3.4	13.0
Five breaks							
9	4 Generators and 3 Lines	Open	238	7,800	3,220	2.5	
10		Close Open	238	8,200	3,380	2.8	
11-A		Open	238	9,700	4,000	2.3	
11-B		+Instantaneous +Close Open	238	8,200	3,380	3.3	12.5
12		Open	238	12,400	5,120	2.6	
13		Close Open	238	12,500	5,160	3.1	
14-A		Open	238	14,000	5,780	2.4	
14-B		+Instantaneous +Close Open	238	13,300	5,500	2.8	13.0
16	8 Generators and 6 Lines	Open**	238	19,500	8,050	2.2	
16R1		Open**	238	12,950	5,350	2.6	
16R2		Open**	238	13,200	5,450	2.6	
16R3		Open**	238	9,750	4,020	2.1	
17*		Open +Instantaneous +Close	238	13,300	5,480	2.7	12.4
18*		Open +Instantaneous +Close	238	14,900	6,150	2.5	12.8

* All faults solid single-phase-to-ground except Numbers 17 and 18 which were arcing ground faults.
** Tests which were pretripped.

Table IV. Single-Phase Line Switching Tests at Grand Coulee

Four Breaks—Light Piston

Series C Test Number	Connection	Miles of Line	Charging Current, Amperes	Time in Cycles: Interrupting	Time in Cycles: Arcing
1*	On System	100	86	2.3**	1.0
2*		100	84	1.5	0.2
3†		100	84		
4*		200	150	1.5	0.3
5*		200	150	2.0**	0.8
6†		200	153		
				Average 1.8	

All tests at 241 kv.
* Open.
† Closed.
** Restrike on these tests. Interrupting time read to end of restrike.

Table V. Single-Phase Line Switching Tests at Grand Coulee

Five Breaks—Light Piston

Series F Test Number	Connection	Miles of Line	Charging Current, Amperes	Time in Cycles: Interrupting	Time in Cycles: Arcing
1*	On System	100	82	1.3	0.05
2*		100	82	1.5	0.3
3†		100	129		
4*		200	148	1.6	0.3
5*		200	150	1.5	0.2
6*		200	150	1.3	0.2
7*		300	176	1.5	0.3
8*		300	183	1.4	0.2
9*		300	180	1.7	0.5
10*		382	240	1.5	0.2
11*		382	240	1.4	0.1
12*		382	240	1.8	0.1
13*	Isolated	300	161	1.7	0.4
14*		300	166	1.6	0.3
15†		300	170	1.4	0.2
				Average 1.4	

All tests at 241 kv.
No restrikes were obtained on any of these tests.
* Open.
† Closed.

formance of the complete 360-kv circuit breaker with six breaks.

2. To obtain sufficient interrupting data to determine the design of the 230-kv, 10,000,000-kva circuit breakers which are to be installed in the new switchyard on the other side of Grand Coulee Dam.

For this latter objective, provisions were made to short circuit first one break then two breaks in the 6-contact interrupter as a 230-kv circuit breaker would not require six breaks.

It was realized that the simple short circuiting of one and two breaks without changing the spacing of the other contacts or shielding rings would upset the ideal voltage distribution obtained with all six breaks. Tests made on this basis would be extremely conservative. Also, the port openings associated with shorted breaks were not plugged so that part of the blast pressure was lost through these ports; this also added to the conservativeness of the tests. Information also was desired on two weights of blast pistons, one a so-called light piston and the other a so-called heavy piston. Tests with two weights were desired to determine the effect, if any, which could be detected upon interruption by the slightly greater tendency of the light piston to slow down in the middle of a current loop, caused by the arc directly across the port entrances. The tests showed no noticeable difference in performance other than somewhat slower mechanical operation with the heavy piston.

The test set-up was similar to that used for the previous series, and is described in

Figure 18. Condition of one of the stationary contacts after fault tests on impulse circuit breaker with light piston. Condition represents 18 fault tests, 10 of which were made at full capacity of Grand Coulee switchyard

Figure 16. Condition of one of the stationary contacts after fault tests on impulse circuit breaker with heavy piston. Seven of the 13 fault operations were made at full capacity of Grand Coulee switchyard

Figure 17. Condition of one of the moving contacts after fault tests on impulse circuit breaker with heavy piston. Seven of the 13 fault operations were made at full capacity of Grand Coulee switchyard

Figure 19. One of moving contacts after fault tests on impulse circuit breaker with light piston. Condition represents 18 fault tests, 10 of which were made at full capacity of Grand Coulee switchyard

Table VI. Single-Phase Fault Tests at Grand Coulee

Five and Four Breaks—Light Piston

Series D Test Number	Bussing Arrangement	Duty Cycle	Line Voltage, Kilovolts	Interrupted Current, Amperes Rms	Equivalent 3-Phase Megavolt-Amperes Interrupted	Interruption Time, Cycles	Reclosing Time, Cycles
Five breaks							
01	1 Generator	Open	234	4,320	1,760	2.2	
02		Close Open	234	3,670	1,500	2.4	
1	4 Generators and 3 Lines	Open	234	8,000	3,250	2.3	
2		Close Open	234	6,760	2,750	2.3	
3-A		Open	234	9,100	3,700	1.8	
3-B		+Instantaneous +Close Open	234	9,000	3,660	2.4	11.3
4	8 Generators and 6 Lines	Open	234	13,800	5,600	1.8	
5		Close Open	234	15,900	6,450	2.5	
6-A		Open	234	15,800	6,420	1.9	
6-B		+Instantaneous +Close Open	234	16,800	6,830	2.5	11.2
7-A		Close Open	234	15,300	6,220	2.6	
7-B		+15 Seconds +Close Open**	234	17,100	6,950	2.4	
8-R		Open**	234	19,300	7,850	1.9	
8-B		+Instantaneous +Close Open**	234	11,900	4,840	2.8	10.5
8R1-A		Open**	234	21,350†	8,680	2.0	
8R1-B		+Instantaneous +Close Open**	234	12,500	5,080	2.6	8.6
Four breaks							
9	4 Generators and 3 Lines	Open	231	8,450	3,400	2.4	
10		Close Open	231	9,660	3,900	2.4	
11-A		Open	231	8,200	3,300	2.0	
11-B		+Instantaneous +Close Open	231	9,150	3,680	2.4	8.5
12	8 Generators and 6 Lines	Open	231	13,650	5,470	2.3	
13		Close Open	231	14,900	5,980	2.3	
14-A		Open	231	12,200	4,900	2.3	
14-B		+Instantaneous +Close Open	231	13,650	5,470	2.4	8.8
15-A		Close Open	231	14,100	5,660	2.7	
15-B		+15 Seconds +Close Open**	231	18,600	7,460	2.9	
16-A		Open	231	14,900	5,980	2.2	
16-B		+Instantaneous +Close Open**	231	12,800	5,140	2.6	8.5
17*		Open +Instantaneous +Close	231	17,000	6,820	2.0	9.7
18*		Open +Instantaneous +Close	231	13,100	5,260	1.8	8.6

* All faults solid single-phase-to-ground except Numbers 17 and 18 which were arcing ground faults.

** Tests which were pretripped.

† Single-current loop.

detail in the paper, Field Tests for Development of 10,000,000-kva 230-kv Oil Circuit Breakers for Grand Coulee Dam Power Plant by C. L. Killgore and W. H. Clagett.[4] Figure 15 shows one pole of the 360-kv impulse-type low-oil content circuit breaker set up for test in Grand Coulee switchyard.

All faults were single-line-to-ground on *A* phase only, and were applied directly to the switchyard ground mat. Pretripping of the test circuit breaker was used to obtain maximum fault current in the arc by taking advantage of the rapid current decrement due to the effect of subtransient reactance during the first one or two cycles of fault current. Faults were applied for the opening tests by using as a closing circuit breaker the same impulse circuit breaker tested during the spring of 1947.

Test Results at Grand Coulee Dam

Five series of tests were made in two weekends. In the first series, Series *A*, Table II, five breaks were used with the heavy impulse piston. This series consisted of 23 tests interrupting the charging currents of from 100 to 328 miles of line. There were no restrikes on any test, and the maximum interrupting time was 2.2 cycles with an average of 1.93 cycles. Arcing times varied from 0.04 to 0.5 cycle.

In the first part of the next series of tests which were short-circuit interrupting tests, Series *B*, Table III, all six breaks were used. Thirteen tests, ranging from 500 to 7,280 megavolt amperes were obtained. One reclosing test set for 13-cycle reclosing time was obtained. Figures 16 and 17 show the contacts after the first part of this series. For the last part of the series, one outer end break was short circuited and 14 tests were made varying from 3,220 to 8,050 megavolt amperes. Ten of the tests were made at full capacity some of which were duty cycles. The last two tests were reclosing tests on arcing ground faults with the circuit breaker set for 13-cycle reclosing. In neither of these did the arcing ground reignite.

In the next series of tests, Series *C*, Table IV, the heavy piston was replaced by the light piston. A new contact unit was installed, and the two outer breaks were shorted out which gave very poor voltage distribution on the remaining four breaks. This series consisted of six line-charging and line-dropping tests on 100-mile and 200-mile line lengths. As restrikes occurred on two of the interruptions, indicating overstressing of one set of contacts, testing on this arrangement was discontinued.

In the next series of tests, Series *F*, Table V, the short circuit was removed from one of the sets of contacts, and 15 line-charging and dropping tests were made on line lengths from 100 to 382 miles with the light piston. Again there were no restrikes, and the maximum interrupting time was reduced to 1.7 cycles with arcing times varying from 0.05 to 0.5 cycle.

The next series, Series *D*, Table VI, was made on the same arrangement (five breaks and light piston), but were short-circuit interrupting tests. Eighteen tests were made from 500 to 8,680 megavolt amperes with interrupting times from 1.8 to 2.8 cycles. Ten of these were at full capacity including a standard close-open +15 second+close-open duty cycle, and three reclosing duty cycles with reclosing times down to 8.6 cycles. There was no disturbance evident, and the contacts were in good condition after tests. Figures 18 and 19 show the contacts. The last of this series was made with an additional break again short circuited leaving four breaks. Fourteen tests were made with duties varying from 3,400 to 7,460 megavolt amperes. The interrupting times varied from 1.8 to 2.9 cycles. Ten tests

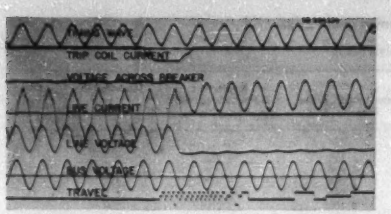

Figure 20. Oscillogram of test number 11, series *F*, showing the interruption of charging current of 382 miles of 230-kv transmission line by low oil content impulse circuit breaker using five breaks and light piston with lines connected to system

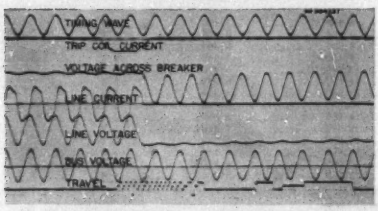

Figure 21. Oscillogram of test number 13, series *F*, showing interruption of line charging current of 300 miles of line by impulse breaker with five breaks and light piston with lines isolated from system

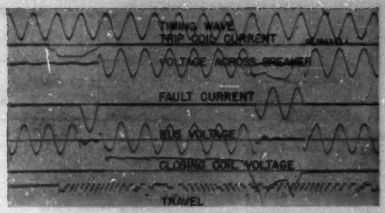

Figure 22. Oscillogram of test number 8R1, series *D*, showing reclosing fault duty on low oil content impulse circuit breaker at Grand Coulee switchyard interrupting 8,700,000 kva on first operation with 2 cycles interrupting time and reclosing 8.6 cycles

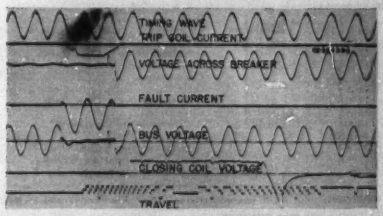

Figure 23. Oscillogram of test number 17, series *D*, showing interruption of arcing ground fault followed by successful reclosing without re-establishment of arcing fault in 9.7 cycles with low oil content impulse circuit breaker. Interrupting duty on this test was approximately 6,800,000 kva with total de-energized time 7.7 cycles

were made at full capacity, including a standard close-open+15 second+close-open duty cycle, and instantaneous reclosing duty cycles with the circuit breaker set for 8.5-cycle reclosing. The last two full capacity tests were made with arcing grounds, one with 8.6-cycle reclosing time, and in neither did reignition of the flashover occur. The de-energized time of the fault was 6.8 cycles. There was no disturbance during the tests, and after the test the contacts were in excellent condition.

Summary of Test Results

These tests indicated no difference in arc interrupting performance between light and heavy pistons. As faster opening, closing, and reclosing times are obtained with the light piston, it will be used in future designs. With the light piston, no interrupting times exceeded 2.9 cycles, either in factory tests or field tests.

Ultra-high speed reclosing tests up to 8,680,000 kva were obtained with 8.6 cycles reclosing which, so far as is known by the author, has not been duplicated on any other type of circuit breaker. Arcing ground tests showed no tendency for re-establishment of a high capacity flashover on an insulator string in the station after a dead time of only 6.8 cycles. It cannot be assumed from this test that the same successful reclosing time would have been obtained if capacitive coupling had been present. The field performance of the circuit breaker on single-phase line-to-ground tests up to an equivalent of 8,680,000 kva at 230 kv indicated it could have handled 10,000,000 kva with ease. As these tests duplicate high power laboratory tests at lower voltage almost exactly up to this value, it also may be assumed that tests up to 25,000 amperes also would duplicate laboratory tests at 25,000 amperes, which would result in an interrupting capacity in excess of 10,000,000 kva. An equivalent interrupting current at 360 kv on the 6-break design would result in an interrupting capacity of over 15,000,000 kva.

No restriking was obtained even when switching 382 miles of line with five breaks despite the poor voltage distribution obtained with one break in a 6-break unit short circuited. Restriking was en-

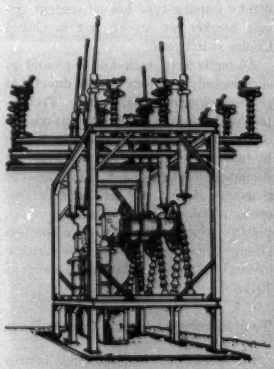

Figure 24. Artist's conception of one of the nine complete switching units being built for new switchyard at Grand Coulee Dam with supporting structure for disconnecting switches, through-type bushings, and current transformers mounted directly on circuit breaker framework

countered, however, with four breaks, though it probably would not have been if better voltage distribution between breaks could have been obtained on the sample unit which had some breaks short-circuited. To be conservative, however, five breaks were selected for the 10,000,000-kva circuit breakers being built for the new switchyard at Grand Coulee Dam.

Figure 24 shows an artist's view of one of the nine complete switching units being built for this application using impulse circuit breakers with the overhead disconnecting switches and current transformer structure carried directly on top of the circuit breaker frame.

Conclusions

For higher interrupting capacities at existing transmission voltages and for higher voltages, the impulse-type low-oil-content circuit breaker has a number of important advantages. Laboratory and field tests for 10,000,000-kva designs at 230 and 360 kv have been made, showing it capable of meeting without exception, all the requirements desirable in a circuit breaker for the protection of the higher capacity power systems of the future.

References

1. Switchgear Equipment for Tidd High Voltage Test Line, F. A. Lane, B. W. Wymer. *AIEE Transactions*, volume 66, 1947, pages 1619–21.

2. Circuit Breakers for Boulder Dam Line, D. C. Prince. *AIEE Transactions*, volume 54, 1935, pages 366–72.

3. Special Tests on Impulse Circuit Breakers, W. F. Skeats. *AIEE Transactions*, volume 55, 1936, pages 710–17.

4. Field Tests for Development of 10,000,000-Kva, 230-Kv Oil Circuit Breakers for Grand Coulee Power Plant, C. L. Killgore, W. H. Clagett. *AIEE Transactions*, volume 67, part I, 1948, pages 271–83.

5. Unusual Performance of Standard 230-Kv Impulse and Tank-Type Oil Circuit Breakers on Field Tests, E. B. Rietz. *AIEE Transactions*, volume 67, part I, 1948, pages 367–70.

Discussion

W. M. Leeds (Westinghouse Electric Corporation, East Pittsburgh, Pa.): The low-oil-content impulse-type circuit breaker appeared 15 years ago as a challenge to the conventional dead-tank construction for the highest voltage circuit breaker ratings. The excellence of its original design is indicated by the relatively few modifications that have been made since, the principal improvement disclosed in this paper being the substitution of a modern pneumatic mechanism suitable for rapid reclosing in place of the earlier motor-wound spring-type operator.

In spite of its generally satisfactory performance record, the impulse circuit breaker has failed in all these years to supplant the reliable steel-tank circuit breaker. In fact, the manufacturers of the impulse circuit breaker, recognizing its limited field of application to special high-voltage and high-interrupting capacity installations, brought out recently a completely new and redesigned line of conventional dead-tank circuit breakers for voltages up to 230 kv. Furthermore, reports from England indicate that throughout Europe where the low-oil-content circuit breakers have found wide-spread usage, the trend now is definitely away from this construction in favor of air-blast circuit breakers for even the highest voltage ratings.

Over ten years ago, a 138-kv low-oil-content porcelain-clad circuit breaker was designed and built in this country.[1] An experimental unit was tested successfully to more than 2,000,000 kva on a large 230-kv power system, but limited applicability in competition with standard circuit breakers made it inadvisable to use this design commercially. To avoid an obviously undesirable situation in the industry of having three entirely different types of high-voltage circuit breaker construction for identical ratings, it is necessary now to consider carefully whether this reappearance of the low-oil-content circuit breaker actually represents a new lease on life to fill requirements impossible to meet with the other types, or whether it is only an interim design destined eventually to be superseded.

The disadvantages of inherently high cost and unsuitability for inclusion of current transformers and potential taps within the circuit breaker structure are pointed out in the paper. The mounting of separate through-type bushings in the overhead structure to provide for necessary current transformers involves additional steel work that may or may not fit into a particular station layout. Claims of improved interrupting performance in comparison with conventional dead-tank circuit breakers may apply in the case of certain older designs which require low-ohmic resistors to bolster up their erratic operation. However, the most modern multiflow interrupters equipped with auxiliary oil-flow pistons are restrike-free when opening line-charging current, and are capable of interrupting the highest interrupting capacities required by industry without particularly heavy mechanism loading.

While the inertia of the moving parts of the impulse circuit breaker may be less than the corresponding steel-tank design, it is evident that very powerful springs must be necessary to drive the impulse pistons against the back-pressure of the heaviest short-circuit currents since each pole of the circuit breaker is provided with a separate operating mechanism, any one of which is large enough to close all three poles of a conventional circuit breaker.

The statement has been made before and is repeated again in this paper that "the velocity of the oil does not vary with the current in the arc." No satisfactory data has been presented to substantiate such a statement, and in fact other discussion in the paper definitely indicates that the opposite is true. For instance, in explaining the reasons for testing with either a light or a heavy piston, it is admitted that there is a "slightly greater tendency of the light piston to slow down in the middle of a current loop, caused by the arc directly across the port entrances." The observation that there was no appreciable effect on the interrupting performance on a particular series of tests does not change the fact that a temporary slowing up of the oil velocity does take place during the arcing period. The possibility of the piston even backing up due to excessive arc pressure is recognized by the provision of a check valve in the flow channel between the piston and the contacts. It would be interesting to know whether any tendency to stall the piston would also result in slowing down the contact motion.

The use of horizontal insulating surfaces between live parts under oil generally has been considered undesirable because of the possibility of creepage breakdown due to the presence of carbon particles settling out of oil that has been subjected to arcing. I should like to ask the author whether impulse circuit breakers have ever been used in tie-line positions between two systems that have operated for a time out-of-synchronism subjecting the circuit breaker to a low-frequency potential difference of twice normal voltage.

It is gratifying to see such a large amount of test data from both laboratory and field tests included in the paper. Repeated testing is, of course, the best guarantee of reliable performance. However, it is unfortunate that in verifying a multibreak device in the laboratory, the old method of extrapolation to higher powers should still be used, that is, interrupting at rated voltage low currents amounting to only a fraction of the circuit breaker rating, and then interrupting rated short-circuit current at only a fraction of the rated voltage. For instance, the 25,000-ampere interruptions of Table I would be much more convincing if cleared by one break only. (From Figure 6, the most highly stressed break in a 360-kv circuit breaker will have to handle 20 per cent of the line-to-ground voltage, or 42 kv). Instead, all six breaks in series were used to open a 14.5-kv circuit which is less than 1/14 of rated voltage. The arcing times at this low voltage were only two-thirds of the times at 264 kv, indicating that the performance shown can hardly be considered representative of what the circuit breaker would do at full voltage and full power.

As an example of what would seem to be a more justifiable extrapolation, I should like to mention recent laboratory tests on a steel-tank high-voltage circuit breaker equipped with 360-kv multiflow grid interrupters. Short-circuit currents of 17,200 amperes at 88 kv, 12,100 amperes at 110 kv, and 11,000 amperes at 132 kv across one-half of the pole unit were interrupted successfully in less than 3 cycles, representing direct tests at the appropriate voltage and current equivalent to 3-phase faults of 8,000,000 to 9,000,000 kva at line voltages of 305, 380,

and 460 kv respectively. This would seem to indicate that the steel-tank circuit breaker is not yet an extinct species.

REFERENCE

1. THE VERTICAL FLOW INTERRUPTER AND ITS APPLICATION TO OIL-POOR CIRCUIT INTERRUPTERS, B. P. Baker, *AIEE Transactions*, volume 60, 1941, pages 440–45.

Otto Naef (American Gas and Electric Service Corporation, New York, N. Y.): In the description of the interrupter, it is stated that the velocity of the oil from the impulse piston does not vary with the current in the arc. This statement seems to me to require some clarification. The back pressure generated by the arc undoubtedly tends to retard the movement of the impulse piston, whereas, it may add to or subtract from the force which opens the contacts, depending on how the design is worked out. The velocity of the oil flow and the opening speed of the circuit breaker is a function of both influences, as well as of the kind of coupling, rigid or flexible, between impulse piston and contacts. Some more detailed information on this point will be appreciated, as it will help to estimate the performance of the circuit breaker under conditions of unusual severity in excess of the circuit breaker rating.

Figure 6 of the paper shows an improved voltage distribution between six breaks nonuniformly spaced. Provided the lengths of individual breaks vary, it would appear that this voltage distribution is only obtained in the fully open position of the contacts and not at the moment of arc extinction.

With other types of circuit breakers, trouble has been caused by the formation of leakage paths on horizontal insulating surfaces rendered semiconductive by deposits of carbon. It has therefore been considered sound practice to arrange insulating surfaces only vertically between parts which are continuously at different potentials. In the impulse circuit breaker, the insulating tube and the plate carrying the ports are in a horizontal position and under continuous voltage stress when the circuit breaker is open.

Although the production of carbon and sludge is undoubtedly much smaller than in older circuit breakers and the contacts are normally closed, which removes the stress, it will be interesting to learn whether tests have been made to determine the intervals in which these parts must be cleaned.

E. B. Rietz: I would remind Mr. Leeds that most of the questions raised in his discussion are familiar to us, and probably better realized because of the many years that we have been making impulse circuit breakers. When he speaks of the failure of this circuit breaker to supplant the tank-type circuit breaker, it is still possible that this can be due to the fact that the low-oil-content-type of circuit breaker is still ahead of its time and is not recognized in its rightful position. Certainly, there are economic limitations. We are striving to overcome them and feel that considerable progress has been made in the last few years.

There are still the three general types of circuit breaker for this field. The question of whether a low-oil-content circuit breaker or a compressed-air circuit breaker will be the circuit breaker of the future is still unknown. Both circuit breakers have similar structures and have somewhat the same limitations. However, the oil circuit breaker is self-contained in the sense that a reliable source of air is not required for interruption. Likewise, there is more experience with this type of circuit breaker. It also would seem that the known susceptibility of air-blast circuit breakers to high voltage recovery rates is not a serious problem with the oil circuit breaker.

I would question the limited applicability of a low-oil-content impulse circuit breaker because for many years these were used interchangeably with tank-type circuit breakers. When furnished without a complete switching unit, they are just as applicable as far as we can see. Indeed, they are just as applicable as any air-blast circuit breaker which Mr. Leeds seems to prefer.

The desirable operating characteristics of the impulse circuit breaker on line switching has not been equaled by any tank-type circuit breaker as far as the published literature shows. The impulse circuit breaker has no restrikes, while as far as we have been able to observe tank-type circuit breakers do have restrikes, but they can be controlled so as not to give rise to abnormal overvoltages.

The reference to oil velocity in the paper is intended to stress the fact that regardless of the current to be interrupted, there is always the same oil velocity previous to the drawing of the arc. Mr. Leeds is quite right that there may be a hesitation of the oil piston on high duties. The use of both light and heavy pistons on the field tests was to observe the effect. It was observed that the interrupting performance was equally satisfactory with the light piston on which there was some hesitation. The contact design is such that this is no effect on the opening speed of the contacts, therefore, it does not affect the interrupting performance.

Special precautions have been taken to obtain maximum creepage between the series contacts to provide adequate insulation across the horizontal interrupting unit. It should be remembered that the contact parts are located on the underside of the board and are actually spaced away from the board. Therefore, the creepage paths are much larger than I believe generally expected.

Some 16 years of experience with 60 to 70 circuit breakers would seem to indicate that this feature has been adequately covered in the design.

We do not question the fact that a tank-type circuit breaker is still in the picture for this class of service. We merely intend to point out that the low-oil-content impulse circuit breaker should be considered in future thinking as it appears to have advantages which will ultimately cause it to supplant tank-type circuit breakers.

Mr. Naef's discussion covers a number of the same points referred to above and I think requires no further comments.

The Direct Measurement of Bandwidth

CHARLES R. AMMERMAN
ASSOCIATE AIEE

EVER since the field of communications had its beginning, the width of the band of frequencies that could be passed by any piece of equipment has been important. Advances in the field have put more rigorous demands on the fidelity of response of some systems, consequently requiring greater pass-bands and at the same time progress has demanded that other systems become more and more selective with an appropriate limitation of pass-band. Notwithstanding, the specification of bandwidth is not standard, nor has its measurement been greatly simplified.

Traditional methods of bandwidth measurement are based on somewhat arbitrary specifications, for example, the frequency difference between the high and low frequencies at which the single-tone response provides half the power corresponding to the frequency of maximum response. Other definitions of bandwidth or cut-off frequency are used in special cases whenever they seem appropriate. The lack of standardization in this matter creates confusion which is only now being resolved by the concept of equivalent bandwidth. A review of this concept is given to facilitate discussion of the measuring instruments described.

The Concept of Bandwidth

In consideration of band-pass devices, it is often convenient to think of an ideal frequency response curve. The response would be uniform between the cut-off frequencies, and zero above and below the cut-off frequencies. Figure 1(A) represents such an ideal case. Here f_1 is the low-frequency cut-off, f_2 is the high-frequency cut-off, and A_0 is the amplification of the device in the pass band. (In this discussion amplification will be considered the magnitude of the ratio of the output voltage to the input voltage.) In the ideal case there can be no doubt about the meaning of the term bandwidth; it is simply f_2-f_1.

Figure 1(B) represents a generalized response curve of the type often found in actual practice. The amplification, instead of being either A_0 or zero, is some function of frequency, $A(f)$. There are no real cut-off frequencies, because the amplification approaches zero rather slowly at both extremes. The amplification A_0, also is somewhat indefinite. Often $A(f)$ has a broad maximum, which usually is designated the amplification. Even if the maximum is sharp, as in a tuned network, the amplification is taken as the maximum value of $A(f)$. If $A(f)$ is rather irregular, it may possibly be desirable to use a different definition of A_0, but for the purposes of this paper A_0 will be defined as the maximum value of $A(f)$.

The specification of bandwidth of this network is more difficult. Previous methods have followed the procedure of deciding how much variation of $A(f)$ is significant and placing the frequency limits at these points, for example f_a and f_b. (Half-power points are often used.) Since the determination of significant variation usually is subjective, this is not so satisfactory. Another important point in the specification of bandwidth arises in connection with the acceptance of noise by a receiver. The bandwidth of the receiver determines the noise power in the output, and consequently affects the signal-to-noise ratio. This fact makes it especially important to consider noise in defining bandwidth.

For all these reasons it is desirable to specify bandwidth in terms of the ideal response shape of Figure 1(A) which is equivalent to the practical response shape of Figure 1(B). This equivalence is based on the power output resulting from a random noise input.

Random Noise

Random noise, fluctuation noise, or "white" noise has a constant power density spectrum. That is, it is composed of equal components of voltage of all phases and frequencies. A random noise may be produced in several ways, all of them exploiting the randomness of certain electronic phenomena. Shot noise and thermal agitation noise are examples; other sources of noise will be discussed later, but the point is that a noise can be produced having a uniform spectrum at least over a range sufficiently wide for most measuring purposes.

Mathematically random noise can be written

$$\begin{aligned} e = {} & E \sin[\omega_0 t+\varphi_0] + E \sin[(\omega_0+\Delta\omega)t+\varphi_1] + \\ & E \sin[(\omega_0+2\Delta\omega)t+\varphi_2] + \\ & E \sin[(\omega_0+3\Delta\omega)t+\varphi_3] \ldots\ldots + \\ & E \sin[(\omega_0-\Delta\omega)t+\varphi_{-1}] + \\ & E \sin[(\omega_0-2\Delta\omega)t+\varphi_{-2}] + \\ & E \sin[(\omega_0-3\Delta\omega)t+\varphi_{-3}] \ldots\ldots \quad (1) \end{aligned}$$

where E is the magnitude of one of the harmonic components (all equal), $\Delta\omega$ is the radian frequency difference between components, and φ_n is a completely random phase angle.

A very thorough discussion of the statistical character of random noise has been written by S. O. Rice,[2] while E. B. Moullin[3] presents the physical side of many noise phenomena.

Equivalent Bandwidth

The equivalence of the practical and ideal networks regarding response to random noise or uniform power spectrum is developed by equating the noise power outputs. If a single tone of voltage E and frequency f be impressed on a practical net-

Paper 50-5, recommended by the AIEE Joint Subcommittee on Electronic Instruments and approved by the AIEE Technical Program Committee for presentation at the AIEE Winter General Meeting, New York, N. Y., January 30-February 3, 1950. Manuscript submitted October 31, 1949; made available for printing November 21, 1949.

CHARLES R. AMMERMAN is with the Electrical Engineering Department, Pennsylvania State College, State College, Pa.

Appreciation is expressed to Dr. V. M. Albers and Dr. A. H. Waynick for their interest and aid in this problem.

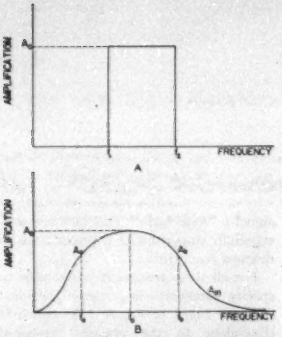

Figure 1. (A) Frequency response of idealized band pass network. (B) Frequency response of practical network

work, the output power will be $E^2A_{(f)}^2/R_1$ where R_1 is the termination of the network. Also n single tones will produce a voltage of

$$\sum^{n} E_n^2 A_{(f)}^2/R_1$$

A noise spectrum will have an infinite number of equal components and the power output will be

$$P_0 = \int_0^{\infty} \frac{E^2 A_{(f)}^2}{R_1}\, df \qquad (2)$$

The ideal network will be similar except that the integral will be zero between 0 and f_1 and between f_2 and ∞, and between f_1 and f_2 the amplification is A_0. For this case

$$P_0 = \int_{f}^{f_2} \frac{E^2 A_0^2}{R_1}\, df \qquad (3)$$

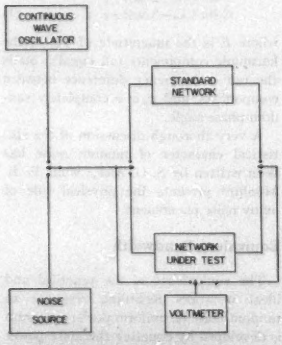

Figure 2. Block diagram of apparatus used for direct measurement of bandwidth

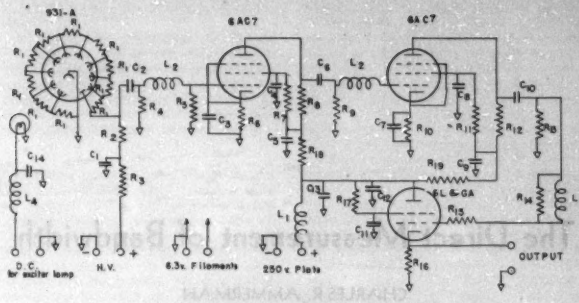

Figure 3. Schematic wiring diagram of noise generator

R_1 = 39,000 ohms	R_{13} = 12,000 ohms	C_6 = 0.0003 microfarad
R_2 = 12,000 ohms	R_{14} = 4,700 ohms	C_7 = 0.1 microfarad
R_3 = 10,000 ohms	R_{15} = 47 ohms	C_8 = 0.1 microfarad
R_4 = 22,000 ohms	R_{16} = 1,250 ohms	C_9 = 0.1 microfarad
R_5 = 3,300 ohms	R_{17} = 9,200 ohms	C_{10} = 0.0003 microfarad
R_6 = 650 ohms	R_{18} = 4,700 ohms	C_{11} = 0.1 microfarad
R_7 = 55,000 ohms	R_{19} = 4,700 ohms	C_{12} = 0.1 microfarad
R_8 = 6,900 ohms	C_1 = 0.1 microfarad	C_{13} = 8.0 microfarads
R_9 = 12,000 ohms	C_2 = 0.00025 microfarad	C_{14} = 0.001 microfarad
R_{10} = 150 ohms	C_3 = 0.1 microfarad	L_1 = 10 henrys
R_{11} = 55,000 ohms	C_4 = 0.1 microfarad	L_2 = peaking coil
R_{12} = 6,900 ohms	C_5 = 0.1 microfarad	L_4 = 250 millihenrys

A_0 for the ideal network is equal to A_0, or the maximum value of $A_{(f)}$, for the practical network.

Equating the power outputs and eliminating E and R_1 which are not functions of frequency and are the same for both networks

$$\int_0^{\infty} A^2_{(f)} df = \int_{f_1}^{f_2} A_0^2 df = A_0^2(f_2 - f_1) \qquad (4)$$

Hence the two networks are equivalent if

$$(f_2 - f_1) = \int_0^{\infty} \frac{A_{(f)}^2\, df}{A_0^2} \qquad (5)$$

That is, $f_2 - f_1$ is the equivalent bandwidth of the practical network.

To determine equivalent bandwidth using this definition it is necessary to perform the integration of the squared frequency response curve. This can be accomplished in three general ways.

First, of course, the integration can be accomplished mathematically if the mathematical form of $A_{(f)}$ is known and if the integration can be carried out. One example of this is a pentode supplying a parallel resistance-capacitance circuit with essentially constant current. Mathematical evaluation of equation 5 gives bandwidth $= 1/(4RC)$. For more complicated cases the difficulty of this process becomes excessive.

A graphical-mechanical method can be used to perform the integration. A graph of $A_{(f)}^2$ is plotted, point by point, using data obtained with a continuous wave signal. The area then is found by counting squares or using a planimeter. The effective bandwidth is this area divided by the maximum value of $A_{(f)}^2$. This system is used widely but is tedious and time-consuming, and herein lies its disadvantage.

The third general method is to set up the unknown network and compare its noise power output to that of a standard network. By properly doing this, the bandwidth may be measured directly. The block diagram showing the needed apparatus is shown in Figure 2. The continuous wave variable frequency oscillator and the noise source are arranged so that the input to the two networks will be the same. The voltmeter reads the output voltage of either network using either source. The voltmeter must be suitable for the measurement of noise voltages; that is, its frequency range must be sufficient to encompass all components in the output of either network and its indication must be proportional to power or rms voltage.

If a certain noise voltage E_i is applied to standard network, the voltmeter reading will be

$$E_{os}^2 = E_i^2 A_{os}^2 BW_s \qquad (6)$$

E_i is the noise input voltage; A_{os} is the maximum amplification of the standard, and BW_s is the bandwidth of the stand-

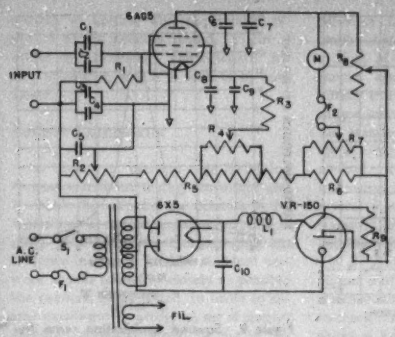

Figure 4. Schematic wiring diagram of voltmeter

R_1 = 1 megohm
R_2 = 100 ohms
R_3 = 500 ohms
R_4 = 10,000 ohms
R_5 = 4,800 ohms
R_6 = 25 ohms
R_7 = 200 ohms
R_8 = 2,000 ohms
R_9 = 2,000 ohms
F_1 = 1-ampere fuse
F_2 = 1/200-ampere fuse
S_1 = Single-pole, single-throw switch
M = 100-microampere d-c meter
C_1 = 0.0005 microfarad
C_2 = 0.01 microfarad
C_3 = 0.0005 microfarad
C_4 = 0.01 microfarad
C_5 = 25 microfarads
C_6 = 0.0005 microfarad
C_7 = 0.5 microfarad
C_8 = 0.0005 microfarad
C_9 = 0.5 microfarad
C_{10} = 8 microfarads
L_1 = 10 henrys
Transformer: 100-volt primary
250–0–250 volt secondary
6.3-volt secondary

ard. If the same noise voltage is applied to the network being tested, the voltmeter reading will be

$$E_{os}^2 = E_i^2 A_{os}^2 BW_x \tag{7}$$

Here A_{os} is the maximum amplification of the unknown and BW_x is the bandwidth of the unknown. The ratio of these is

$$\frac{E_{os}^2}{E_{ss}^2} = \frac{A_{os}^2 BW_s}{A_{ss}^2 BW_x} \tag{8}$$

Solving for the bandwidth of the unknown

$$BW_x = \frac{E_{os}^2}{E_{ss}^2} \frac{A_{ss}^2}{A_{os}^2} BW_s \tag{9}$$

The ratio A_{os}^2/A_{ss}^2 is the ratio of the voltmeter readings of the two networks using for each network the frequency of maximum amplification (input voltage constant). The ratio E_{os}^2/E_{ss}^2, as in equation 9, is the ratio of voltmeter readings with equal noise voltages. BW_s is calculated by the graphical-mechanical means outlined above.

General requirements for the measuring equipment having been set, consideration now will be given to the specific items of equipment. Each of the units shown in Figure 2 is discussed separately; connection and switching is accomplished by a coupler-comparator unit.

Noise Generator

There are many suitable sources of noise, each having its own peculiar advantages and disadvantages. The ultimate choice of the noise source will probably be a matter of convenience and availability, and in this case a noise generator from a modulator for a radar jamming set used by the armed forces proved to be the most convenient starting point. Certain modifications were made to make it more useful, and the complete circuit is shown in Figure 3.

The photoelectric cathode, secondary-emission multiplier tube is a source of fairly high-level noise. Noise in a photoelectric diode is similar to the shot noise in a temperature-limited diode. The rms noise current is[1]

$$I = \sqrt{2eI_{dc}\Delta f} \text{ amperes}/\sqrt{\text{cycle}} \tag{10}$$

where e is the charge on an electron, I_{dc} is the average current, and Δf is the bandwidth. This noise is amplified and slightly augmented in the multiplier sections.[5] Consider a type *931-A* tube with a current amplification of 10^6 and a maximum d-c anode current of 10^{-8} amperes at rated conditions. The photocathode current is therefore 10^{-9} amperes at rated conditions, and the noise component in the photocathode current is

$$I = 5.6 \times 10^{-18} \text{ amperes}/\sqrt{kc}$$

This is amplified by 10^6 and slightly increased, so that this may produce a noise current of 6×10^{-8} amperes/$\sqrt{kc}$ in the anode circuit. Suppose the anode load resistance is 3,000 ohms; this will produce a noise voltage of 18 millivolts per $\sqrt{kc}$. Very little amplification is necessary to make this useful for present purposes. The circuit in Figure 3 shows two stages of video amplification and a cathode follower output stage.

The frequency range of this generator is important. The high-frequency response of the video amplifiers is good to nearly 4 megacycles. The low frequency response is poor, particularly because of the coupling circuit between the *931-A* and the *6AC7*, for which the 3-decibel point is approximately 42 kc. This did not constitute a serious objection in the work done in this case; however, it is felt that a noise generator with uniform

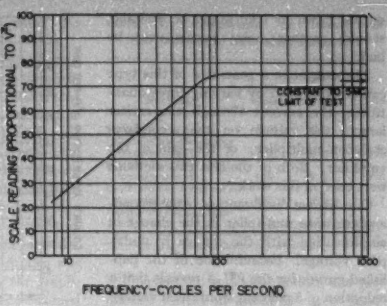

Figure 6 (right). Frequency response of voltmeter

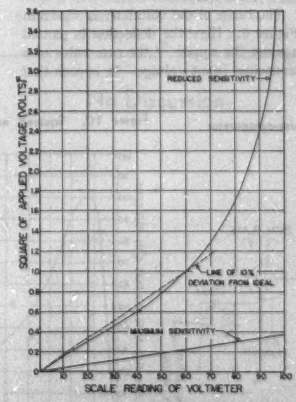

Figure 5. Calibration curves of voltmeter with sinusoidal input voltage

output down to 1 kc would be desirable should another noise source ever be built.

The output in a generator of this type can be controlled by varying three quantities: the current through the exciter lamp; the voltage on the secondary-emission multiplier; or the gain of the amplifier. Both of the first two methods were used in this work.

One distinct disadvantage of the secondary emission multiplier is the change in amplification with the change in multiplier voltage. Examination of the published curves for the *931-A* reveals that a reduction of 5 per cent from rated voltage results in a reduction of 30 per cent from rated amplification. Close control of anode voltage during a test is therefore necessary.

Continuous Wave Generator

Any signal generator with frequency range including the frequencies of maximum response of standard and unknown networks, and having sufficient output voltage, may be used here.

Voltmeter

A voltmeter of wide frequency range, reading rms values (or proportional to the average power) must be used in this setup. In the voltmeter constructed, use is made of the nonlinear region of the grid voltage-plate current characteristics. By proper selection of the operating range, a characteristic is obtained such that the meter deflection is proportional to the square of the input voltage.

The instrument is based on a square-law voltmeter described by J. R. Ragazzini and B. R. Boymel.[4] A few minor changes were incorporated, and the circuit is shown in Figure 4.

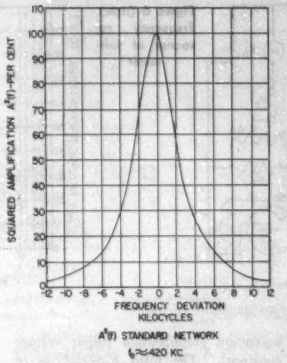

Figure 8. Squared amplification versus frequency for standard network

The criterion for square-law operation is that the grid voltage-plate current curve shall be expressible by the equation

$$I_p = I_o + aE_g + bE_g^2 \tag{11}$$

The simplest way to locate this region is to make use of a mutual conductance bridge.

$$g_m = \frac{\partial I_p}{\partial E_g} = a + bE_g \tag{12}$$

If g_m is plotted against E_g, the region where the graph is a straight line will be the region where equation 11 is satisfied. Since it is reasonable to expect negative variations as great as positive variations, the grid bias is set in the middle of this region. For the tube used, a bias of -1.7 volts is necessary.

The range of the voltmeter is shown in Figure 5. Here the deflection is plotted against the square of the rms value of a sinusoidal input voltage. It is seen that

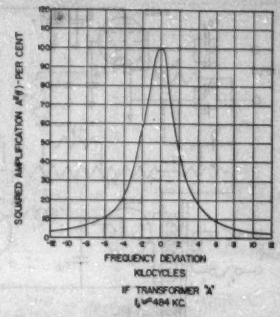

Figure 9. Squared amplification versus frequency for one intermediate-frequency transformer tested

deviation from square law increases slowly. It was felt that a 10 per cent deviation at the peaks would not be detrimental; in that case the range of the instrument is approximately 1.0 volt rms sine wave or 1.4 volts peak. If the voltmeter is operated at maximum sensitivity and approximately midscale the rms voltage is approximately 0.44 volt compared to 1.4 volts peak allowable.

The probability of the absolute value of instantaneous noise voltage exceeding a value r times the rms value is given by[5]

$$p = 1 - erf\left(\frac{r}{\sqrt{2}}\right) \tag{13}$$

where *erf* is the error function. If $r = 1.4/0.44$; $p = 0.00146$.

That is, the noise voltage will exceed the voltmeter range only approximately 1/700 of the time. It is felt that serious error is not caused by neglecting these peaks.

It is required that the voltage response be uniform over a range at least broad

Figure 7. Schematic wiring diagram of coupler-comparator

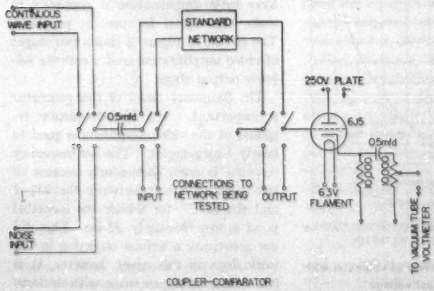

Figure 10. Squared amplification versus frequency for network of resistors and capacitors

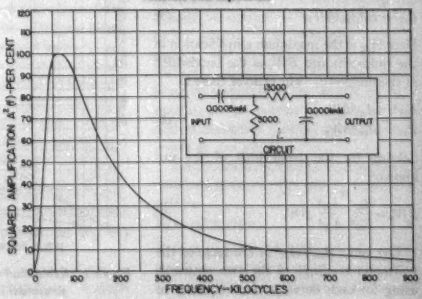

enough to include any appreciable response in the network tested. Figure 6 shows the frequency characteristic for this voltmeter, and it is seen to be adequate.

Coupler Comparator

In order to perform the switching necessary without undue confusion, and to couple the output of the network to the voltmeter, a coupler comparator unit is used. The complete schematic diagram is shown in Figure 7. The standard network should match as closely as possible the network being tested, in order to assure maximum accuracy. A set of plug-in standard networks would be highly desirable.

The input to the network is low-impedance and the output is high-impedance. If the network is designed for other terminations, these terminations can be taken into account and proper impedances used when the network is connected to the input and output terminals.

It is possible to use a fiducial mark on the voltmeter and calibrate a potentiometer gain control in the coupler comparator to read the ratios A_{as}^2/A_{cs}^2 and E_{as}^2/E_{ac}^2. It is necessary in that case to be most careful of capacitive loading of the potentiometer to prevent modification of the high-frequency characteristics as gain is changed.

Experimental Results

The experimental work done with this apparatus consists of measuring the bandwidth of several networks directly, and comparing this result with the bandwidth obtained by actually plotting the $A_{(f)}^2$ curve of each network and using the graphical-mechanical method.

Most of the networks measured were simple double-tuned Intermediate-frequency transformers. One transformer of rugged mechanical design was selected as the standard, and its bandwidth was found by the graphical-mechanical method. The $A_{(f)}^2$ curve of this network is shown in Figure 8. Using this standard, several other Intermediate-frequency transformers and one network of resistors and capacitors were measured directly. The $A_{(f)}^2$ curve of each network also was plotted and the bandwidth by the graphical-mechanical method was determined to check on the direct method. Figure 9 shows a typical $A_{(f)}^2$ curve for one of the intermediate-frequency transformers tested. Figure 10 shows the $A_{(f)}^2$ curve and the circuit of a resistance-capacitance filter tested. Table I gives the statistics of these tests and shows that the agreement is very good. No attempt to go beyond two significant figures was made because of the limitations of the equipment at hand.

Conclusions

From the foregoing data it can be seen that the measurement of equivalent bandwidth directly is possible. The percentage difference between the values of bandwidth obtained by this method and by the graphical-mechanical method are quite small.

If this equipment were to be used for routine or versatile measurements of filter bandwidths, certain obvious improvements could be made. The equipment needed, however, is relatively simple and straightforward.

Table I. Comparison of Results of Measurement of Equivalent Bandwidth

Network	f_o, Kilocycles	Bandwidth, Kilocycles Graph*	Bandwidth, Kilocycles Direct
Standard	420	7.6	
Intermediate-frequency transformer A	484	5.8	5.8
Intermediate-frequency transformer B	420	7.6	7.6
Intermediate-frequency transformer C	500	4.8	4.7
Resistance-capacitance network	65	240	220

* By the graphical-mechanical method.

This method could be used for the production testing of filters to check bandwidth within tolerances, or for the laboratory testing of miscellaneous networks of which bandwidth is an important parameter. Refinements of this method may possibly be developed which would make possible the testing, as a 4-terminal network, a complete system, such as a radio receiver or a telephone cable circuit.

References

1. Spontaneous Current Fluctuations in Various Conductors, W. Schottky. *Annalen der Physik* (Leipzig, Germany), volume 57, 1918, pages 541–67.

2. Mathematical Analysis of Random Noise, S. O. Rice. *Bell System Technical Journal* (New York, N. Y.), volume 23, July 1944, pages 282–332; volume 24, January 1945, pages 46–156.

3. Spontaneous Fluctuations of Voltage (book), E. B. Moullin. Clarendon Press, Oxford, England, 1938.

4. A Square Law Vacuum Tube Voltmeter, J. R. Ragazzini, B. R. Boymel. *Review of Scientific Instruments* (New York, N. Y.), volume 11, October 1940, pages 312–14.

5. The Secondary Emission Multiplier, V. K. Zworykin, G. A. Morton, L. Malter. *Proceedings*, Institute of Radio Engineers (New York, N. Y.), volume 24, March 1936, pages 351–75.

6. The Distribution of Amplitude with Time in Fluctuation Noise, V. D. Landon. *Proceedings*, Institute of Radio Engineers (New York, N. Y.), volume 29, February 1941, pages 50–55.

No Discussion

A New Electronic Telegraph Regenerative Receiver

B. OSTENDORF, JR.
MEMBER AIEE

Synopsis: An all-electronic device for removing distortion from start-stop teletypewriter signals is described. The circuit utilizes a sine wave oscillator for timing and binary counters for synchronization. It provides low output distortion, high tolerance to input distortion, hit-reduction, transmission of steady-space break signals, and regeneration of one element-length of stop time. It features quick change of speed and code, use of office battery power, and reduction of routine maintenance to one adjustment. Over a year's experience has been obtained with about 100 of these units.

THE growing use of teletypewriter service has brought about an increasing need for regeneration. Operating speeds have tended to become higher, more multibranched long-haul circuits are being used and it has become desirable to allow greater latitude in the maintenance of receivers and other apparatus. These factors cause an increase of signal distortion along the transmission path and a loss of tolerance to distortion at the receiving end of the path. Where the signal distortion is excessive, a regenerative repeater (or even several regenerative repeaters) connected along the circuit may be the best economic answer, and is frequently the only answer to the problem.

Relative to the age of telegraphy itself, the regenerative repeater is a new device. Its use became possible only after the adoption of the printing telegraphy system, and in its first form it utilized the mechanical distributor which also was employed in sending and receiving apparatus. This repeater[1] satisfactorily achieved its major objective; but, with rotating brushes, regular and frequent maintenance is essential to successful operation. To avoid the disadvantages of brush and commutator maintenance, a repeater was developed which used cam-driven contacts for the essential timing of the output signals.[2] The cam-type repeater reduced maintenance time to two or three man hours per month (per 1-way repeater) and has been used widely since 1936.

More recently, at least ten more or less "electronic" regenerative repeaters[3,4,5] have been designed, here and abroad. In each of these, it is the timing circuits which set the style of the complete repeater. The nonmechanical timing methods include resistance-capacitance phase shift oscillators, inductance-capacitance oscillators, free-running and 1-shot multivibrators, gas tube relaxation oscillators, and inductance-capacitance delay networks. All of these methods have been used and each has certain advantages, and possibly disadvantages, as regards economy, stability, size, weight, and maintenance.

The repeater here described is an all-electronic device known as the *143A* regenerative repeater. It was designed specifically to meet the requirements imposed by Bell System teletypewriter service. A number of these repeaters have shown satisfactory performance in commercial service for over a year.

In any semisynchronous or start-stop regenerative repeater, two timing functions are required: character timing and element timing. Character timing synchronizes the receiver by responding to only the initial transition of each coded character. Element timing determines the instant of occurrence for the transitions of the code selecting elements in the reformed output signals.

Paper 50-6, recommended by the AIEE Telegraph Systems Committee and approved by the AIEE Technical Program Committee for presentation at the AIEE Winter General Meeting, New York, N. Y., January 30–February 3, 1950. Manuscript submitted November 2, 1949; made available for printing November 21, 1949.

B. Ostendorf, Jr., is with the Bell Telephone Laboratories, Inc., New York, N. Y.

Principal Circuits

A block diagram of the *143A* regenerative repeater is shown in Figure 1. Element timing in this repeater is generated by a start-stop inductance-capacitance oscillator whose frequency is such that one cycle of sine wave is produced for each element of the code.

Character timing is accomplished by a 3-stage binary-type counting circuit which counts the number of cycles of the oscillation and stops the oscillator when the proper number of cycles has been generated.

Reforming of the output signals is done by a modulating circuit and a flip-flop circuit. The modulating circuit combines voltages from the input signals with impulses from the element timing circuit, and applies impulses selectively to either the left or right grid of the flip-flop circuit which will then follow the sense of the input signals—minus their distortion.

The oscillator is started by the input signal start element. Impulses derived from the sine wave are then applied to the character timing and transmission circuits where the signals are regenerated.

Circuit Description

The details of circuit operation are illustrated by the functional schematic, Figure 2. The general layout is the same as that of the block diagram. Secondary apparatus such as grid bias resistors, by-pass capacitor and vacuum tube heaters are not shown. The voltage wave shapes are approximately those which would be viewed on an oscilloscope, with the letters *A* to *H* indicating points of identical time. This drawing is perhaps best understood by studying the various parts in the following sequence:

Oscillator Control

This is a 2-input circuit which causes the oscillator to start conditionally when

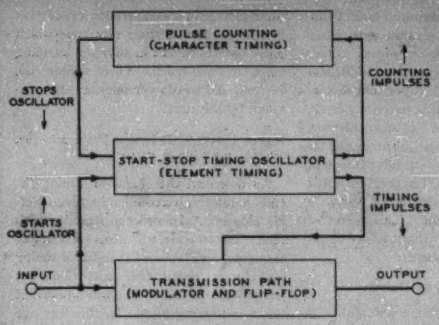

Figure 1. Block diagram of principal circuits—143A regenerative repeater

the input becomes spacing, and holds the oscillator in the running condition after the counting circuits are started.

Inductance-Capacitance Oscillator

To avoid signal distortion, it is necessary that the oscillator start and stop without transients. Transientless starting is effected by applying a direct current through the inductance and approximately zero voltage across the capacitor during the idle period between characters. When the source of this holding current is cut off upon receipt of a start signal, the current in the inductance must then flow into the tuning capacitor. The capacitor then charges sinusoidally. The direct current becomes the peak value of the alternating current and the peak voltage is initially

$E_m = I\sqrt{L/C}$ volts

The voltage peaks of subsequent cycles are kept equal to the peak value of the first cycle by adjusting the feedback energy to just balance the resonant circuit losses. Stopping transients are avoided by stopping at the exact end of a cycle, at which time the alternating current is just equal to, and in the same direction as, the reapplied direct current.

Square Wave Generator

The connection to the modulator circuit is used to supply positive impulses for the selecting or input-sampling function. These impulses (derived through series capacitors) are centered with respect to an undistorted input signal element, and consequently allow a maximum displacement of either end of the element with respect to the start transition.

Modulators

The lower triode is biased so that only the positive impulses which occur during marking elements will be amplified. The upper triode is similarly biased, but it receives inverted input signals so that only the positive impulses which occur during spacing elements will be amplified.

Output Flip-Flop

By its holding action, this circuit converts the transient information contained in the selecting impulses into d-c square waves bearing the information of the input signals and the timing of the locally-generated impulses.

Cathode Follower

This is a power output stage.

Initial Counting Impulse

The same modulator impulse which samples the input start element also is used to generate the first counting impulse. The modulator pulse (dotted line) is amplified by the count recognizer circuit and applied to the first counter (via dotted line) which is caused to flip.

Counting Circuits

When the left triode of a counter circuit flips to the conducting (negative plate) condition, the impulse thus generated flips the succeeding counter in either direction. In the idle condition the three left triodes have positive plates and therefore the action of the initial counting impulse is to flip all the counters in rapid succession. Seven subsequent negative impulses from the square wave generator are required before the idle condition of the three counters again is reached.

Count Recognizer

After transmitting the initial counting impulse, this tube remains cut off as long as one or more of the count voltages is negative. When the three count voltages are again positive (idle condition, time H) the count output voltage applied to the oscillator control circuit will act to stop the oscillator, provided the input signal is marking at the same time. If the input is not marking (as in the case of a stop signal shortened to less than the length of a unit element) the oscillator will not be stopped, but will continue for another 7-cycle count.

Marking Ensuring Circuit

This tube provides a conductive link between input and output during the idle condition. It therefore prevents a spacing output signal in the presence of a steady marking input signal, as might otherwise occur, for example, when power is first applied to the repeater.

Advantages

This repeater affords the following advantages in line with the general requirements:

Low Maintenance

The general rise in maintenance cost per man-hour is well known. This repeater is designed to require negligible routine maintenance for itself, and to permit a reduction in maintenance requirements for all other transmission apparatus, including teletypewriters, in circuits using the repeater.

The regenerator units usually are operated 24 hours per day. Specially designed vacuum tubes and regulated office filament battery provide a tube life measured in years, while the other apparatus represents a good compromise between reliability and first cost. The first use of these repeaters was in an installation of 40 units. Troubles of all kinds during the first year averaged one per four months per repeater and represented a maintenance time improvement of almost six to one over that of the counterpart mechanical regenerative repeaters. Analysis of the trouble reports indicates that no failures have resulted from circuit design inadequacies. Most recurrent failures have been caused by capacitors whose temperature rating was exceeded by the high ambient temperatures which resulted when the maximum number of regenerator units were mounted on a single bay. These troubles have since been eliminated (at a small increase in first cost) by changing to condensers of higher temperature rating.

Only one routine adjustment is necessary to take care of vacuum tube aging: adjustment of the oscillator stop current. All other functions, including tuning, are independent of tube characteristics during the life of the tube. Tuning and oscillator feedback are factory adjustments.

Compactness

Because of the increased number of regenerated telegraph circuits, required floor space and weight of the repeater are important. The circuit is fully electronic and uses miniature tubes, pigtail resistors, and so forth. This, together with the simple timing device, enables 34 1-way regenerator units to be accommodated in a standard $11^1/_2$-foot 19-inch relay rack bay. Each unit weighs 13 pounds. A single unit is shown in Figure 3.

Tolerance to Distortion

The width of an element sampling impulse is less than one per cent of the width of a signal element. (All percentages are in terms of a whole element.) The impulses are timed to be in the exact center of an undistorted incoming signal element; accordingly any transition of the input signals may be displaced up to $49^1/_2$ per cent without causing an error. Tuning inaccuracies reduce this tolerance but experience indicates that 45 per cent is a reliable minimum under field conditions.

Stability

Over a range of 55 degrees Fahrenheit, temperature compensation of the tuning capacity keeps the maximum output distortion under 2 per cent in most cases (4 per cent, in one case out of six). Over a period of one or two years, an additional drift of not more than 3 per cent distortion, or one-half per cent frequency error, caused by aging of the coil and capacitor, is anticipated. The aging error can be removed at any time by an adjustment of the capacity and the temperature error can be removed by allowing a warm-up time before adjustment. This degree of stability is obtained without resort to expensive tuning components.

Use of Office Battery Power

Power supply of +130, −130, and −24 volts is used for the repeater. These voltages are available from power plants having battery reserve which are normally provided in offices where the repeater will be used. Use of the office battery power rather than rectified commercial alternating-current avoids service interruptions which would result from failure of the commercial a-c supply.

Rapid Change of Operating Speed

Speed is controlled by a switch which selects a preadjusted tuning capacity for each desired speed. The possibility of a rapid change in speed permits a reduction in the number of spare repeaters which must be maintained in an office handling more than one speed. Three speeds—60, 75, and 100 words per minute—are provided by this unit.

Rapid Change Between Five and Six Unit Selecting Code

As described the character timing circuit operates with a code having five selecting elements. In order to function with teletypesetter code, which has six selecting elements, a resistance-capacitance timing and clamper circuit (one twin-triode, not shown) can be added to eliminate one of the counting impulses. In this way one extra cycle of sine wave will be generated before the counting circuit comes to a stop. When the additional circuit components are provided, switching between five and six unit code is done simply by removing or inserting associated vacuum tube. No adjustment is necessary.

Reduction of Line Hits

In 2-condition signaling such as telegraphy, sporadic changes in condition

Figure 2. Functional schematic—*143A* regenerative repeater

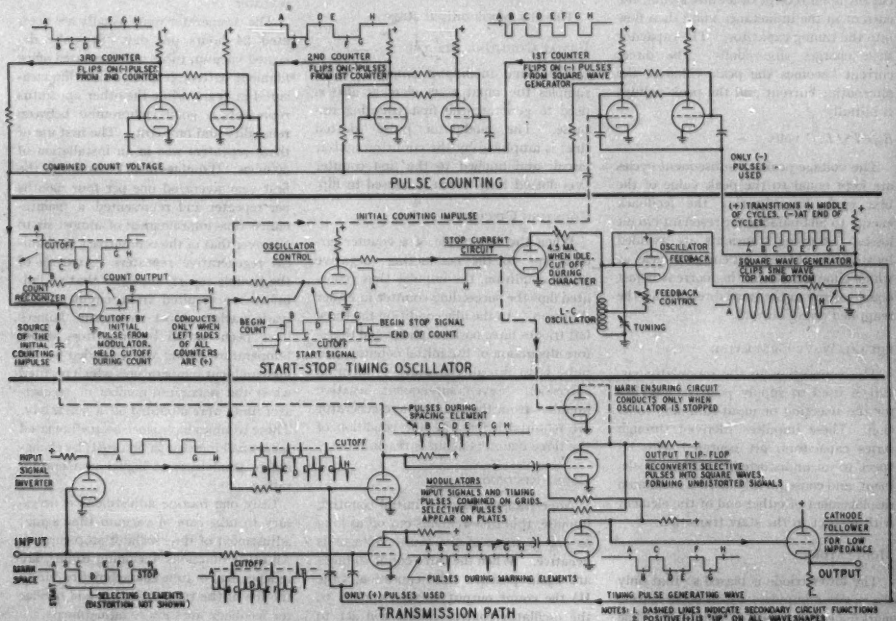

during a mark or space signal are called hits. A regenerative repeater will eliminate hits which do not occur during the sampling impulse with the following important exception: A spacing hit during a stop element or idle period will act the same as an incoming start signal. Unless the hit is extremely short, it will cause the repeater to begin its cycle of operation. This is actually the worst sort of hit since it may put a start-stop system out of synchronism for many characters, particularly if the signals go through several pieces of start-stop synchronized apparatus. Electronic regenerative repeaters tend to be very susceptible to this trouble because of their rapidity of response. One type of mechanical regenerator which now is being used requires about two milliseconds to unlatch, whereas an electronic trigger device ordinarily will act in a few microseconds.

This repeater eliminates most of the susceptibility to false unlatching by not starting the synchronizing action of the character timing circuit until one-half element after the beginning of a code character—that is, at the time of selection of the start pulse. The effect is then that a hit of less than 11 milliseconds (one-half element at a speed of 60 words per minute) will not unlatch the repeater. The sine wave oscillator will begin a cycle but will return to steady state soon after the end of the hit.

Steady Space or Mark

When a steady mark is being received, the same conditions which stop the oscillator also actuate a circuit which is paralleled with the output circuit and insures a marking output signal. This avoids complete dependence upon the holding action of the output flip-flop tube, and is required for a number of minor reasons not covered here.

When a steady space is being received, the oscillator never stops and the mark-restoring circuit just mentioned is never actuated. Accordingly, a series of uninterrupted spacing selections is made. Retransmission of an uninterrupted space is valuable when break circuits or timing circuits are connected on the line, or when manual Morse signals must go through the repeater.

Partial Regeneration of the Stop Element

Because of its indefinite length, the stop element of a start-stop signal cannot be regenerated; or, more accurately, the interval between two start transitions—that is, character length—cannot be regenerated. Even with automatic signals where the characters are all of the same length, the stop element cannot be regenerated in the true sense, because there must be some amount of time provided, however small, for the regenerator to come to rest in order for it to operate on a start-stop basis and permit some variation in the speed of the teletypewriter transmitters.

Since it is not regenerated, the stop element may suffer cumulative distortions, especially in circuits having more than one regenerated section in tandem. Transmission circuits having long time constants, speed errors, and fortuitous effects contribute to changing the character length, with a consequent fortuitous lengthening or shortening of succeeding stop elements. Properly, a regenerative repeater should limit the shortness of a stop element being retransmitted, to prevent cumulative shortening to the point of failure.

This limiting action is best applied when the code system used has a stop period longer than the other elements. In this case the repeater regenerates the first element length of stop period in the same way as any other element is regenerated. When a foreshortened stop pulse is received, the timing oscillator does not stop but, after causing selection of a 1-element stop period, proceeds with timing of the next character. Recycling of the character timing circuit is not affected by the failure to stop, since character timing is merely a matter of counting the proper number of cycles for the second character after finishing the count of the first.

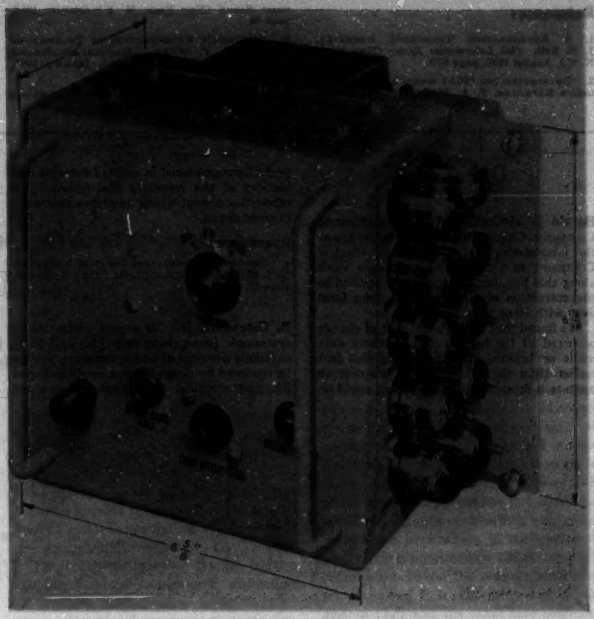

Figure 3. *143A* regenerative repeater

System Application

The regenerative repeater being discussed was designed concurrently with a new hub-type method of multibranch operation. The repeater itself is simply a 1-way device, but when incorporated with the new hub transmission system, each branch or spoke (one at a time) may send through the single 1-way regenerator unit to all the other stations, thereby making efficient use of the regenerator. The hub-coupling circuits, one of which is associated with each branch, are voltage-operated devices and may be driven directly from the output of a vacuum tube circuit; consequently neither input nor output relays are required in the regenerative repeater. An additional saving in first cost, maintenance, and space results

References

1. A Regenerative Telegraph Repeater, J. H. Bell. *Bell Laboratories Record* (New York, N. Y.), August 1930, page 570.

2. Developing the 106A1 Regenerative Telegraph Repeater, T. A. McCann. *Bell Laboratories Record* (New York, N. Y.), October 1938, page 45.

3. Electronic Regeneration of Teleprinter Signals, H. F. Wilder. *Electrical Engineering* (*AIEE Transactions*), volume 65, January 1946, pages 34–40.

4. An Electronic Regenerative Repeater for Teletypewriter Signals, R. B. Hesra. *AIEE Transactions*, volume 66, 1947, pages 904–11.

5. An Electronic Regenerative Repeater for 7/2 Unit Start-Stop Telegraph Signals, R. O. Carter, L. K. Wheeler, A. C. Frost. *Journal*, Post Office Electrical Engineers (London, England), January 1949, page 222.

Discussion

Harold J. McCreary (Automatic Electric Company, Chicago, Ill.): Some years ago at the laboratories of the Automatic Electric Company in Chicago we did some work along this line, but it specifically applied to the correction of dial pulses on long farm lines with 10 or 12 parties.

We found that the greatest rate of change occurred at the instant dial contacts were made or broken, and that using this fact rather than the magnitude of current to operate a repeater, the dial pulses could be perfectly reproduced in spite of extreme distortions of the incoming dial pulses. We received a patent which describes this work in some detail.[1]

Reference

1. Distortion Correcting Impulse Repeater, H. J. McCreary, United States Patent 2,422,309, June 17, 1947.

B. Ostendorf, Jr.: If signal distortion is systematic (comprising only bias and characteristic distortion) and is constant, it may be removed by designing the combination of line and terminal equipment to have the desired variation of loss and phase with frequency. This is called equalization. Adding a derivative, as described by Mr. McCreary, is one method of equalization which will reduce bias and negative characteristic distortion (systematic shortening of shorter elements, either marking or spacing, in a train of coded signals).

Where the distortion is variable or includes a fortuitous component such as is caused by interference, signal perfection can be restored only by regeneration. Regeneration provides a more general treatment for distortion: foreknowledge of the type and amount of distortion is not required.

Combined Phase and Ground Distance Relaying

WARREN C. NEW
ASSOCIATE AIEE

A NEW relaying system is described herein providing complete phase and ground distance relaying protection for transmission lines, which features a reduction in the necessary equipment over the 6 directional-reactance-distance relay system usually applied where three relays are connected to protect against 3-phase, phase-to-phase, and double-phase-to-ground faults, and three relays are connected to protect against single-phase-to-ground faults. The reduction in equipment is achieved by causing the directional element of the ground-reactance relay to perform the double duty of detecting faults of a phase nature as well as faults of a ground nature. This new system also offers the advantage of providing complete phase and ground protection without the use of objectionable switching arrangements heretofore used to select the faulted-phase current or potential.

The combined system is effected by adding to the basic directional-reactance-distance relay for ground fault protection a reactance relay which operates with the directional-fault-detecting element of the ground relay to provide the phase-fault protection.

Description

The basic directional-reactance-distance relay for ground-fault protection is composed of a directional-impedance starting unit having a circular impedance characteristic which passes through the origin on an R and X diagram, an ohm unit having a pure reactance characteristic, and a transfer relay to change the ohm unit calibration, thus providing a second zone in ohmic reach. The added reactance relay includes an ohm unit having a reactance characteristic, and a transfer relay for changing its calibration. Since the directional-impedance starting unit of the ground relay will respond to all faults within its zone of reach, it can be used in conjunction with the phase ohm units to provide phase-fault protection as well as with the ground ohm units providing ground-fault protection.

The complete relaying system for the combined phase-and-ground protection of 3-phase transmission lines includes three directional-reactance-distance relays, one per phase, for the ground relaying; and three reactance relays, one per phase, for the phase relaying; two timing relays, one each for the phase and ground relaying; an auxiliary relay for blocking the ground trip circuits; and an auxiliary current transformer.

The timer is described completely in an AIEE paper.[1] Both timers are started by the impedance starting units of the ground relays when a fault occurs and they control the tripping time in accordance with the operation of the phase and ground ohm units. Two timers are provided so that proper time co-ordination can be made with other portions of the system, especially where different times of tripping are required for phase faults compared to ground faults.

The auxiliary blocking relay consists of three telephone relays which are used to prevent the ground ohm units from tripping on all except single-phase-to-ground faults. One blocking telephone relay is associated with each phase.

The auxiliary current transformer is used to compensate for the mutual effect of the ground current and also for the current in neighboring or parallel lines. This current compensation is effected by supplying the relays with enough of the residual current of the protected line and of any nearby or parallel lines to offset the extra potential caused by the mutual effect of the ground current and neighboring line current.

In certain cases, some variation in ground distance measurement is introduced by arc resistance especially where there is an appreciable phase angle difference between the generated potentials behind the two ends of the line. This variation would not lead to incorrect operation with normal settings using the current compensation described above. Potential compensation might be used to correct the error resulting from out-of-phase generated potentials, but also it introduces a similar error which may cause just as much variation in measurement. This error is produced by the phase angle difference between the zero sequence current supplied from the relay end of the system (I_0') and the total zero sequence current in the fault (I_0). For example, if the fault occurs near a transformer having a grounded neutral, I_0 may be considerably more lagging than I_0' which may pass through considerable line and ground resistance, hence the error may be quite large.

Choice of Potential versus Current Compensation

The problem of potential versus current compensation has long been considered in the application of ground distance relays. In measuring the distance to a single-phase-to-ground fault, two approaches may be considered: the actual measurement of the zero sequence impedance by separating it from the positive and negative sequence impedances through the use of filters or other

Paper 50-7, recommended by the AIEE Relays Committee and approved by the AIEE Technical Program Committee for presentation at the AIEE Winter General Meeting, New York, N. Y., January 30–February 3, 1950. Manuscript submitted October 31, 1949; made available for printing November 21, 1949.

WARREN C. NEW is with the General Electric Company, Philadelphia, Pa.

The author gratefully acknowledges the technical advice and assistance rendered by Mr. A. R. van C. Warrington of the General Electric Company, Philadelphia, Pa.

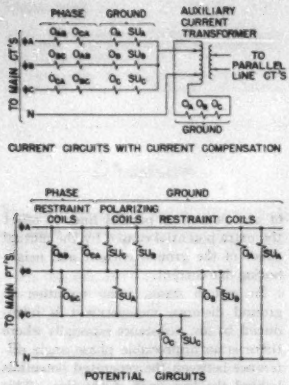

Figure 1. Current and potential connections to the relay using current compensation

separating circuits; or the measurement of phase quantities with residual or zero sequence quantities added to correct for the effects of induction, double end feed, and so forth. Voltage compensation lends itself particularly well to the first approach, while current compensation lends itself to the second approach.

The use of zero sequence quantities alone through potential compensation has the disadvantage of requiring the relay to operate on very small quantities so that the torque produced is very small. Such a relay is beset by various ills induced by its extreme sensitivity, such as transient operation, contact rebound, and so forth. The voltage restraint applied to the relay is little more than half the line-to-neutral voltage since the potential compensation is applied to reduce the phase-to-neutral voltage. Voltage compensation is most useful where there is a large amount of reactive current transfer over the protected line section or where the phase angle difference between the generated potentials behind the two ends of the line section is large. Potential compensation has been described completely elsewhere.[2]

The use of phase quantities with zero sequence correction through current compensation offers the advantage of a higher torque relay. The potential restraint applied here is the full line-to-neutral voltage. Special precautions must be taken, however, to insure that all the necessary corrections are made.

Applied Compensation

To use a high-torque relay, the method of current compensation was selected for this relaying system. This current compensation corrects the phase quantities applied to the relay for the effects of mutual induction between the line and ground and between two lines which are mutually coupled. The complete derivation of the mathematical equations are shown in Appendix I.

The resulting current (I_R) and potential (V_R) applied to the relay are as follows, where the primed values represent line quantities of the protected section towards the fault, I_0'' is the zero sequence current and Z_m the mutual impedance coefficient of a parallel line, I_{res}' is the residual current of the protected line, I_{res}'' is the residual current of the parallel line, and I_aR_a is the voltage drop due to the arc.

$$V_R = I'Z_1' + I_0'(Z_0' - Z_1') + I_0''Z_m + I_aR_a$$

which is the phase-to-neutral voltage of the line.

$$I_R = I' + K'I_{res}' + K''I_{res}''$$

The quantities K' and K'' are explained in Appendix I. Figure 1 shows schematically how these quantities are supplied to the relays.

The relay therefore measures the positive phase sequence impedance of the protected line section, Z_1', plus an error term. A reactance relay will only be affected by the reactance or j component of this error term. The error term is

$$\frac{3R_a}{2\dfrac{I_1'}{I_1} + \dfrac{I_0'}{I_0}\dfrac{Z_0'}{Z_1'} + \dfrac{I_0''}{I_0}\dfrac{Z_m}{Z_1'}}$$

where

R_a = the resistance of the arc.

Neglecting the effect of mutual induction, the error term can be expressed as

$$\frac{3R_a}{2\dfrac{Z_1}{Z_{1R}} + \dfrac{Z_0'}{Z_1'}\dfrac{Z_0}{Z_{0R}}}$$

where

Z_{1R} and Z_{0R} = the sequence impedances on the relay side of the fault.

If the denominator of this latter error impedance term is real, there will be no error. Many lines approach this condition if the neutrals are solidly grounded since the various impedances are of approximately the same power factor and on short lines the phase angle between the generation at the two ends of the line will be small. Similarly if the two neutrals are both grounded through fairly large and equal resistances, the error will also be small.

Overreach will be more likely to occur when

1. The generation on the relay side of the fault is leading the generation on the far side of the fault (I_1' leads I_1).

2. The impedances on the relay side of the fault, either positive or zero sequence, are leading the impedances on the far side of

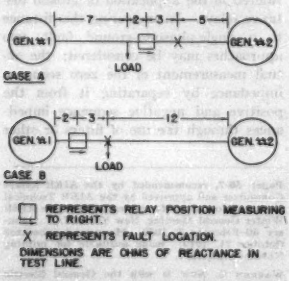

Figure 2. Test arrangement to determine errors resulting from arc resistance, earth resistance, and load current

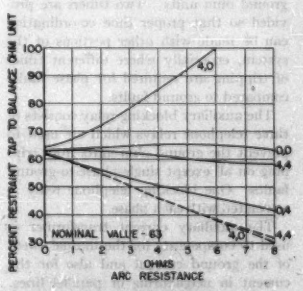

Figure 3. Effect of arc resistance with double-end-feed and various neutral grounding resistances (Case A)

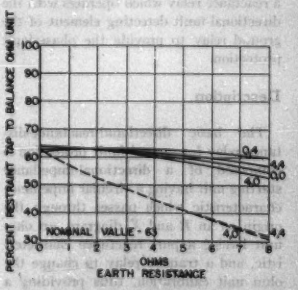

Figure 4. Effect of earth resistance with double-end-feed and various neutral grounding resistances (Case A)

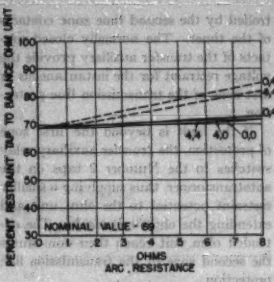

Figure 5. Effect of arc resistance with double-end-feed and various neutral grounding resistances (Case B)

the fault (Z_{1R} leads Z_1, or Z_{0R} leads Z_0).

3. The zero sequence impedance of the protected line is more lagging than the positive sequence impedance (Z_1' leads Z_0').

4. The zero sequence current of a parallel line is more lagging than the zero sequence current of the protected line (I_0 leads I_0'').

5. The mutual impedance of a parallel line is more lagging than the positive sequence impedance of the protected line (Z_1' leads Z_m).

Since tripping of the ground ohm units on all except single-phase-to-ground faults is prevented by the auxiliary blocking relay, the errors resulting from 3-phase, phase-to-phase, and double-phase-to-ground faults need not be considered here. These faults are all cleared by the operation of the phase ohm units. Figures 2, 3, 4, 5, and 6 show the magnitude of the errors under various conditions of arc resistance, earth resistance, and neutral grounding resistance for single-phase-to-ground faults.

Figure 2 shows the nature of the test

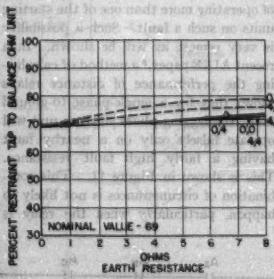

Figure 6. Effect of earth resistance with double-end-feed and various neutral grounding resistances (Case B)

setup using an artificial transmission line that was used to determine the curves of Figures 3, 4, 5, and 6 illustrating the nature and magnitude of the error resulting from various conditions of arc resistance, earth resistance, neutral grounding resistance and load current during single-phase-to-ground faults. The first of the two numbers indicated on each curve is the neutral grounding resistance in ohms at the relay end of the system, and the second figure the opposite end. The broken line curves represent conditions where load current is flowing in addition to relay fault current. In Case *A* the load current used was 125 per cent of the relay fault current, and in Case *B* the load current was 50 per cent of the fault current. Figures 3 and 4 are for Case *A* and Figures 5 and 6 are for Case *B*. Values above the nominal value on each curve represent overreaching. Overreaching is the increase of the relay reach beyond its calculated value so that the relay tends to trip for faults within a longer part of the protected line.

Starting Unit

In this phase and ground distance relaying scheme a unit must be provided to determine first, that fault conditions actually exist and second, to determine if the fault is in the tripping direction. These functions are performed by the directional-impedance starting unit of the basic reactance-distance relay.

The starting unit is a 4-pole induction cup unit. The side poles are energized by the quadrature voltage to produce the polarizing flux. The back pole is energized by the phase-to-neutral voltage of the protected phase to produce the restraining flux. The front pole is energized by the line current of the protected phase to produce a directional torque dependent upon the phase angle between the current and the polarizing voltage. Figure 7 shows the schematic connections for the starting unit.

The starting unit will pick up when the restraining torque equals the operating torque. The equation for this condition is

$$TE_AE_{BC}\sin\beta = 550I_AE_{BC}\cos(\alpha - 30 \text{ degrees})$$

where T is the voltage restraint tap setting, β is the angle by which E_A leads E_{BC}, and α is the angle by which the current I_A leads the quadrature voltage E_{BC}.

For a 3-phase fault, $\beta = 90$ degrees, and $\alpha = (90 \text{ degrees} - \phi)$ where ϕ is the phase angle of the line. The relay will then

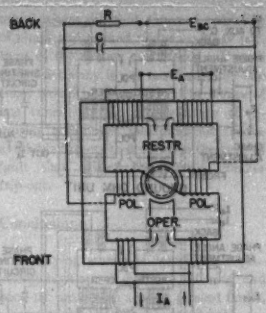

Figure 7. Schematic connection of the directional-impedance starting unit

pick up when the current is equal to

$$\frac{TE_A}{550\cos(60 \text{ degrees} - \phi)}$$

With a 100 per cent tap setting and a voltage E_A of $115/\sqrt{3} = 66.4$ volts, the pickup current will be 12 amperes at a phase angle of 60-degree lag. Typical variation of pickup current with phase angle and tap setting is shown in Figure 8. Pickup currents for other types of faults can all be determined from the basic equation shown above.

Normally, the setting of the starting unit is not required to be particularly accurate and it is sufficient to assume for all faults that with 115 volts phase-to-phase at its terminals and tap settings of 100 per cent, the relay will have a mini-

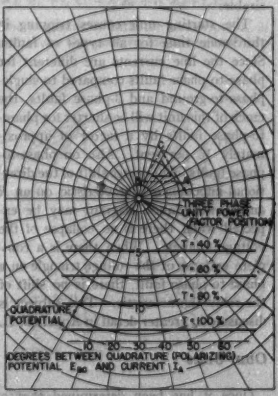

Figure 8. Typical current pick-up characteristics of the directional-impedance starting unit (current values apply to 3-phase faults)

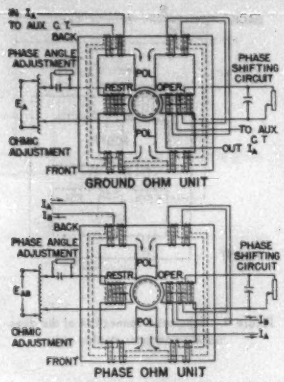

Figure 9. Schematic connections of the ground and phase ohm measuring units

mum pickup of 12 amperes at the maximum torque angle of 60-degree lag. The operating or directional torque closes the relay contacts when the fault current is in the tripping direction and of a sufficient magnitude to overcome the voltage-restraining torque. The operating torque on 3-phase faults is a maximum for fault currents lagging by 60 degrees, and is reliable down to one per cent voltage with secondary current from 5 to 60 amperes. The voltage restraining torque is a maximum under balanced 3-phase conditions which exist normally and during power swings when operation would be undesirable.

The starting unit causes tripping in third-zone time for all types of faults. Since the line currents are different for phase-to-phase faults compared to single-phase-to-ground and 3-phase faults, the reach of this unit will be shorter for phase-to-phase faults by a factor of approximately 15 per cent. Also on phase-to-phase faults, a 30-degree shift of the directional-impedance characteristic on an R and X impedance diagram may be expected when there is no collapse of the voltage triangle. When there is a complete collapse of the voltage triangle on a phase-to-phase fault, there is no shift of the relay characteristic. This subject is discussed in greater detail in Appendix II.

Ohm Units

Once it has been determined that a fault condition actually exists, a unit must be provided to measure accurately the distance to that fault and decide whether or not the fault lies within the tripping zone. This function is performed by the ohm units which are reactance measuring units.

The ohm units of both the ground relays and the phase relays are 4-pole induction cup units. The front and back poles each have two current coils which produce a polarizing flux proportional to the sum of currents supplied to them. The right-hand pole has two current coils to produce the operating flux which is also proportional to the sum of the two currents supplied. The flux in the right-hand pole is made to lag its current by about 90 degrees by means of a phase-shifting winding.

The left-hand pole has a potential coil which produces the restraining flux. The schematic connections for the phase and ground ohm units are shown in Figure 9. The operating theory and torque equations for these units are explained in a previous paper.[1]

The ground ohm units are supplied with a phase current in one current winding and the compensating current from the auxiliary current transformer in the other current winding. The left-hand or restraint pole is supplied with the phase-to-neutral voltage through a tapped autotransformer which allows adjustment of the restraint in one per cent steps.

The phase ohm units are supplied with two phase currents, one in each current winding. The left-hand or restraint pole is supplied with the phase-to-phase voltage between the two phase currents supplied to the current windings. This voltage is supplied through a tapped autotransformer which also allows adjustment of the restraint in one per cent steps.

The phase and ground ohm units will measure the same reactance within ±2 per cent over a range of 2 to 40 amperes secondary current with any power factor obtainable on a transmission line. The minimum voltage during fault conditions imposes no practical limitations on the accuracy of the ohm unit. Measurements are accurate within ±2 per cent down to 1 volt for a one-half ohm phase-to-neutral measuring unit.

Ohm Unit Transfer Auxiliary

The ground and phase ohm units are each provided with a telephone relay known as the ohm unit transfer auxiliary (OX). This transfer relay provides the second step of transmission line protection by means of a switching arrangement which changes the amount of voltage restraint supplied to the ohm units. The operation of this transfer auxiliary is controlled by the second time zone contacts of the timer. The normally closed contacts of the transfer auxiliary provide the voltage restraint for the instantaneous or first zone of the transmission line protection.

If the fault is beyond the first zone of protection, the transfer auxiliary relay switches to the Number 2 taps on the autotransformer, thus supplying a smaller restraint potential to the ohm unit and extending the ohm unit reach. The extended ohm unit reach then constitutes the second zone of the transmission line protection.

Auxiliary Blocking Relay

The auxiliary blocking relay contains three telephone relays, A_A, A_B, and A_C, which are used to prevent the ground ohm units from tripping on all except single-phase-to-ground faults. One blocking telephone relay is associated with each phase. The contacts of the telephone relays are arranged in the trip circuits so that they may be used to provide this tripping selection.

This arrangement provides 3-step protection on single-phase-to-ground faults. This is accomplished by connecting a normally open contact of the protected phase-blocking relay in series with a normally closed contact from each of the other two phase-blocking relays. Blocking is then accomplished for all faults except single-phase-to-ground faults. Figure 10 shows this arrangement of contacts in phase A of the trip circuits. It can be seen that tripping will be blocked when two or more phases are involved in a particular fault.

When the auxiliary blocking relays are connected so as to block the tripping of the ground ohm units on all except bona-fide single-phase-to-ground faults, some thought must be given to the possibility of operating more than one of the starting units on such a fault. Such a possibility is very remote as will be shown. In a recent AIEE paper,[3] a method of calculating the performance of distance relays shows that for a single-phase-to-ground fault, the lagging-phase starting unit will operate falsely only on a nearby fault having a fairly high fault resistance. This is shown in Figure 11. This combination of circumstances is not likely to happen, particularly when the relay is

Figure 10. Blocking relay contact arrangement for phase A

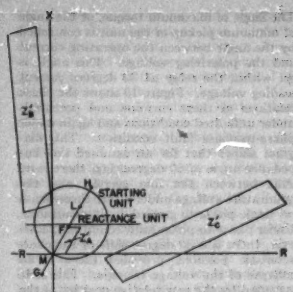

Figure 11. Impedance seen by ground relays during a phase *A*-to-ground fault

located close to a generating source. Such a fault, however, most likely will be cleared by the phase relays since the impedance will fall into their tripping zone as is shown by Figure 12.

Operation of the D-C Control Circuits

Referring to the elementary connection diagram in Figure 13, the sequence of operation of the d-c control circuits may be explained. A single-phase-to-ground fault on phase *A* will operate the starting unit *SU* which will in turn operate the auxiliary blocking relay A_A and start the timing unit *TU* through its auxiliary relay *TX*. The trip circuit for phase *A* will then be complete up to the ground-ohm-unit contacts O_ϕ. If the fault is within the first zone of reach of the ground ohm unit, that unit of course will operate and trip the circuit breaker through the first zone ground targets T_{1G}. If the fault is

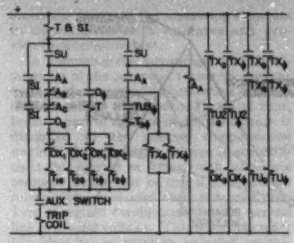

Figure 13. Circuit breaker control circuits for phase *A*

beyond the first zone reach, after the timer has operated the *TU*2 contacts, the ohm unit transfer auxiliary will operate and change the ohm unit calibration by applying a smaller potential restraint. If the fault lies within the second zone of reach, the ohm unit will operate and trip the circuit breaker through the second zone ground target T_{2G}. If the fault is beyond the second zone reach, then when the timer has operated its TU_ϕ contact, the circuit breaker will be tripped by the starting unit contact *SU* through the third zone target T_ϕ.

The phase ohm units operate in much the same manner as the ground ohm units, since they work in conjunction with a separate auxiliary transfer relay and separate timer. The difference is the a-c connections of the phase ohm units allowing them to operate on different line quantities.

A separate timer is provided for the phase trip circuits as well as the ground trip circuits so as to provide close time selectivity with the relaying on other portions of the system. It is especially useful where different times of operation of phase and ground relays on other portions of the system are desired. If such close selectivity is not required, only one timer would be necessary. The choice of one timer has the disadvantage of requiring a different interpretation of the available targets to determine the type of fault that caused the circuit breaker trip-out.

Conclusions

A relaying scheme is described for providing high-speed distance relaying and back-up protection against ground faults, so combined with high-speed distance relaying and back-up protection against phase faults that a minimum of relays are used. Current compensation is applied requiring the minimum of auxiliary equipment with the least adjustment.

Appendix I

The distance relay being used to measure single-phase-to-ground faults is supplied with phase-to-neutral voltage. The left part of Figure 14 shows the distribution of sequence currents and potentials on a typical system under single-phase-to-ground fault conditions. This figure does not take into consideration the phase angle of the various voltage drops at the fault, but simply uses these drops as scalar quantities. The actual vector diagram of such a fault condition would be as shown to the right of Figure 14, where it is seen how the various drops may be projected on the phase-to-neutral generated voltage, E_g. Referring to Figure 14, the phase-to-neutral voltage is V_R and is equal to

$$= I_1'Z_1' + I_1'Z_s' + I_1'Z_s' + I_0'Z_m + I_aR_a$$

where quantities with the subscripts 1, 2, and 0 are the positive, negative, and zero

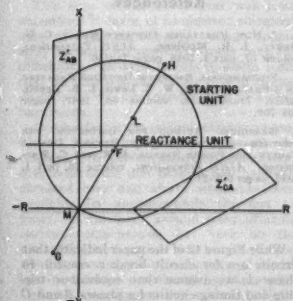

Figure 12. Impedance seen by phase relays during a phase *A*-to-ground fault ($Z_{BC}' = \infty$)

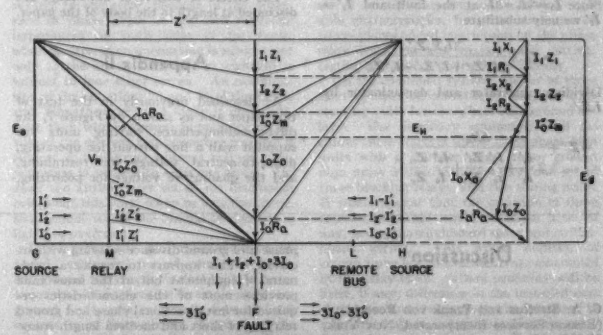

Figure 14. Distribution and phase relations of sequence potentials during a single-phase-to-ground fault (for the faulted phase only)

sequence quantities, respectively; primed values represent quantities of the protected line section. I_0'' is the zero sequence current in a parallel line which has a mutual coupling with the protected line and Z_m is the zero sequence mutual coupling coefficient of such a parallel line. I_aR_a is the voltage drop due to the arc.

In order to use phase quantities, these must be separated and since we usually assume that $Z_1' = Z_2'$ we may substitute

$$V_R = I_1'Z_1' + I_2'Z_2' + I_0'Z_0' - I_a'Z_1' + I_0'Z_0' + I_0''Z_m + I_aR_a$$
$$= I'Z_1' + I_0'(Z_0' - Z_1') + I_0''Z_m + I_aR_a$$

Dividing this voltage by Z_1' gives the current necessary to measure Z_1' in a distance relay having a phase-to-neutral voltage restraint.

$$I = I' + I_0'\left[\frac{Z_0' - Z_1'}{Z_1'}\right] + I_0''\frac{Z_m}{Z_1'} + \frac{I_aR_a}{Z_1'} \text{ or}$$
$$= I' + K'I_{res}' + K''I_{res}'' + \frac{I_aR_a}{Z_1'}$$

where I_{res}' and I_{res}'' are the residual currents of the protected line and parallel line, respectively, and

$$K' = \frac{Z_0' - Z_1'}{3Z_1'} \text{ and } K'' = \frac{Z_m}{3Z_1'}$$

Since the actual arc current cannot be measured, the relay is supplied with the phase current, a portion K' of the residual current of the protected line, and a portion K'' of the residual current of a parallel line. The impedance seen by the relay with this current and the phase-to-neutral voltage will then be

$$Z \text{ relay} = \frac{[I'Z_1' + I_0'(Z_0' - Z_1') + I_0''Z_m + I_aR_a]Z_1'}{I'Z_1' + I_0'(Z_0' - Z_1') + I_0''Z_m}$$
$$= Z_1' + \frac{I_aR_aZ_1'}{I'Z_1' + I_0'(Z_0' - Z_1') + I_0''Z_m}$$
$$= Z_1' + \frac{I_aR_aZ_1'}{(I_1' + I_1' + I_0' - I_0')Z_1' + I_0'Z_0' + I_0''Z_m}$$

Since $I_a = 3I_0 = 3I_1$ at the fault and $I_1' \approx I_1'$ we may substitute

$$= Z_1' + \frac{3I_1R_aZ_1'}{2I_1'Z_1' + I_0'Z_0' + I_0''Z_m}$$

Dividing numerator and denominator by I_1Z_1'

$$= Z_1' + \frac{3R_a}{2\frac{I_1'}{I_1} + \frac{I_0'}{I_0}\frac{Z_0'}{Z_1'} + \frac{I_0''}{I_0}\frac{Z_m}{Z_p}}$$

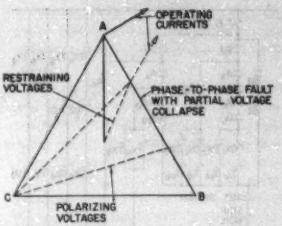

Figure 15. Phase relations of currents and potentials supplied to the phase-A starting unit

The second term of this equation then is the impedance error resulting from a single-phase-to-ground fault as seen by the relay. In the case of the reactance relay, the error becomes the j component of the error impedance.

With short lines or heavily interconnected systems, the phase angle difference between the currents supplied to the fault from the relay end of the system (I_1', I_0') and the total fault currents (I_1, I_0) will be small and these currents will be inversely proportional to the system impedances. The ratio

$$C = \frac{I_1'}{I_1} = \frac{Z_1}{Z_{1R}}$$

can then be used to express the impedance error in other terms.

Similarly

$$C_0 = \frac{I_0'}{I_0} = \frac{Z_0}{Z_{0R}}$$

where Z_{1R} and Z_{0R} are the sequence impedances on the relay side of the fault.

Neglecting the effect of mutual induction, the error then becomes:

$$\text{error} = j \text{ component of } \frac{3R_a}{2\frac{Z_1}{Z_{1R}} + \frac{Z_0'}{Z_1'}\frac{Z_0}{Z_{0R}}}$$

The effects of this error impedance are discussed at length in the body of the paper.

Appendix II

As described previously in the text of this paper and as shown by Figure 7, the directional-impedance starting units are supplied with a line current for operating, phase-to-neutral voltage for restraining, and the quadrature voltage for polarizing. The angle of maximum torque, or the angle of minimum pickup of the unit is controlled by the angle between the operating current and the polarizing voltage. This angle is set within the relay at 30 degrees current leading voltage. Figure 15 shows the phase relations of these currents and potentials under unfaulted conditions and again under phase-to-phase fault condition. This diagram shows that for an assumed line impedance angle of 60 degrees lag, there is no shift between the line current and the quadrature voltage under either three-phase or single-phase-to-ground fault conditions. Under phase-to-phase fault conditions, however, there is a 30 degree shift of the characteristic possible, provided there is no collapse of the voltage triangle. This shift is caused by the new relative position of the fault current with respect to the polarizing voltage. The phase-to-phase fault current will lag the phase-to-phase voltage causing its flow by the line impedance angle or 60 degrees lag as assumed previously. This factor requires that to achieve the maximum torque angle position, the line impedance angle would have to be 90 degrees lag. Thus the relay characteristic is shifted to 90 degrees lag. As the voltage triangle collapses under the phase-to-phase fault, the shift of the characteristic becomes smaller until at complete collapse, the characteristic returns to its original position.

There also is a small change in the reach of the directional-impedance starting units under different fault conditions. During 3-phase and single-phase-to-ground fault conditions, there is available a phase-to-neutral voltage to cause a certain line current to flow through the line impedance of a single conductor. During phase-to-phase fault conditions there is available a phase-to-phase voltage to cause a certain line current to flow through twice the line impedance of a single conductor. It is obvious that the line current will not be the same for the two conditions, the phase-to-phase fault conditions producing about 85 per cent of the former current. A smaller current indicates a larger impedance and this has the effect of reducing the reach of the starting unit on phase-to-phase faults by a factor of 15 per cent.

References

1. A New Reactance Distance Relay, C. G. Dewey, J. R. McGlynn. *AIEE Transactions*, volume 67, part I, 1948, pages 743–46.

2. Fundamental Basis for Distance Relaying on 3-Phase Systems, W. A. Lewis, L. S. Tippett. *AIEE Transactions*, volume 66, 1947, pages 694–700.

3. Graphical Method for Estimating the Performance of Distance Relays During Faults and Power Swings, A. R. van C. Warrington. *AIEE Transactions*, volume 68, part I, 1949, pages 608–21.

Discussion

C. A. Streifus and **Frank von Roeschlaub** (Ebasco Services Incorporated, New York, N. Y.): Mr. New presents in a complete and concise form the description of and technical background applying to this combination of phase and ground distance relaying without carrier. This appears to require a minimum of equipment but at the same time provides most of the characteristics required for fast directional phase and ground relaying of short and medium length transmission lines carrying relatively small quantities of power either for line-fault operation or during transient swing conditions.

While Figure 13 of the paper indicates that circuits are for circuit breaker control fo phase A, we assume that equivalent trip ping and timing circuits for phases B and C are connected between the positive lead and the auxiliary switch in parallel with phase A tripping circuits.

In Figures 11 and 12, it appears that this combination of relays does not provide third

zone backup protection for faults occurring in the direction opposite to that in which the relays are pointed. This region, however, is covered by the second or third zone of similar relays at the opposite terminal of the line section under protection.

Figures 11 and 12 indicate further that the characteristic impedance of the reactance and starting units for both phase and ground relays adequately cover the fault zone areas for phase and ground faults for relatively short lines carrying small amounts of power. Because of the breadth of the starting unit circle in a direction perpendicular to the line impedance characteristic on the conventional *R-X* diagram, if the relays are applied on long lines or on short lines near the electrical center between systems, there may be false tripping during some transient swing conditions when large quantities of power are flowing and especially for the condition when this power is in a direction opposite to that in which the relays are pointed. This combination of conditions, however, is rare.

Although not mentioned in the paper, problems associated with distance relaying on a 3-terminal line exist similarly in the application of these relays, namely, sequential clearing of circuit breakers is required and impedance viewed by a certain relay on a 3-terliminal line may be relatively high during a fault condition because of the fault current supplied from the third terminal.

S. L. Goldsborough (Westinghouse Electric Corporation, Newark, N. J.): The combined phase and ground relaying combination described by Mr. New does not seem to offer anything new in the way of phase relaying or ground relaying. Apparently the only new feature is the combination whereby one starter element per phase is required to function on both phase faults and ground faults.

In regard to the phase relaying it is noted that the distance measuring element now is supervised by a starter element which was discarded several years ago. It is recalled that several years ago the reactance phase relay employed a modified impedance supervising element which was energized by fault current and both faulted and unfaulted phase voltages.

This type of starter element was later abandoned in favor of an element energized only on fault current and voltage apparently in order to overcome some inherent difficulties. In view of this it would seem that the return to the former type of starter element in the new combination is a step backwards.

In considering the ground relaying a number of interesting points come up. In employing the current compensation method it is to be noted that nothing new has been obtained over and above what has been available for approximately the last 15 years. A reactance ground relay utilizing current compensation has been on the market for this length of time but its application has been very limited because of fundamental troubles occasioned by the starter element operating on line current. Nothing has been done in the described combination to overcome the fundamental limitations of current compensation other than the rather drastic reduction in the "reach" of starter element which, of course, seriously limits the ability of the measuring elements to accommodate fault resistance and provide backup protection.

In discussing the advantages and disadvantages of the potential versus the current method of compensation the author makes a rather puzzling statement. He states that, because part of the line to neutral voltage is discarded in the voltage compensation method, the remaining voltage is not sufficient to operate a relay with adequate torque. This might be true if three ground relays were used and their potential coils were energized continuously on the normal line to ground voltage. This is possibly what Mr. New has in mind in bringing up this point. However, the use of three normally energized relays would certainly not be an efficient way of employing voltage compensation. The use of zero sequence quantities in voltage compensation naturally suggests the use of one reactance measuring element with a phase selector in the potential circuits. With a potential switching device it is, of course, not necessary nor desirable to leave the potential circuits energized continuously and, therefore, it is obvious that the amount of line to ground voltage is immaterial. A normal and desirable energy level can be maintained in a relay regardless of the value of input voltage as long as the relay does not have to withstand a higher continuous voltage. Such a relay was described in October 1948 before the Institute[1] and it is, therefore, difficult to conceive of any engineering reason why the author has brought up the point.

The author points out that current compensation is subject to error where there is a phase angle difference between the generated potentials behind the two ends of the lines. It is claimed that this error would normally be inconsequential. It also is pointed out that voltage compensation avoids this particular error but introduces another error which may be just as large. It would seem that this is not a fair comparison of current and voltage compensation since it implies that current compensation is subject to only one error and voltage compensation is subject to another equally deleterious error. This is not at all the case, as would be apparent, if the author also had given the equation covering voltage compensation. Voltage compensation is subject to one error, because of the difference in phase angle of the zero sequence impedances on both sides of the fault, whereas current compensation is subject not only to the above error but in addition is subject to four other errors. An examination of the equations 23 and 25 of the Lewis and Tippett paper[2] will make it quite evident that where mutual inductance is involved the current compensation method is subject to five errors whereas voltage compensation is subject to only one error. Indeed the author later on in his discussion brings out this point when he lists the conditions under which the reactance element is liable to overreach.

It is felt that the chief impediment to the general successful use of combined phase and ground relaying is the fact that, in order to prevent false operation on single-phase-to-ground faults where there is flow of fault current on all three phases, the reach of the starter must be drastically restricted. It is noted that all the diagrams given show the starter element circle reaching approximately only twice as far as the instantaneous zone. This certainly does not allow the first zone element to accommodate much arc resistance. This limitation applies even more to the second element since the diagrams clearly show that a normal second element setting of twice the first zone setting could not be attained even if fault resistance were zero. On the same basis it is evident that a suitable backup setting for the third zone is impossible.

It also should be noted that the starter element is an uncompensated element and is, therefore, subject to all the errors in distance measurement which must be removed from the distance measuring elements. In other words, even if we assume no fault resistance whatever, it would be impossible to depend on correct relay operation when set according to the diagrams shown.

A further point is that, by combining the phase and ground starter elements, the restrictions dictated by ground fault conditions also are placed on the phase relays thus impairing the flexibility of phase distance relaying.

In view of the foregoing points it seems evident that the elimination of one starter element per phase in the combined phase and ground relay equipment described is hardly worthwhile.

References

1. A New Distance Ground Relay, S. L. Goldsborough. *AIEE Transactions*, volume 67, part II, 1948, pages 1442–47.
2. See reference 2 of the paper.

C. W. Frederickson (Commonwealth Services Inc., Jackson, Mich.): The use of distance ground relays has been rather limited in the past, no doubt due largely to the complexity of the numerous elements and the resultant high cost. On the other hand, distance phase relays have been universally accepted for transmission line protection. The combined phase and ground distance relay system proposed in the paper does not appear to reduce materially the number of elements required from those necessary for a separate phase and ground distance relay system. Moreover, the proposed common use of one set of starting units, having variable characteristics, by phase and ground relays places added restrictions on the phase relay operation and makes relay setting, testing and maintenance more difficult.

On the combined system, one set of three starting units is eliminated by using the same starting units for the phase and ground relays. The necessary equipment still includes three starting units, three phase-ohm units with a transfer relay, three ground ohm units with a transfer relay, one set of three blocking relays, and two timing units. It would appear that the omission of three starting elements would result in little, if any, saving in switchboard space and switchboard wiring. This would depend, of course, upon how the elements are assembled in the relay cases. There probably will be little, if any, difference in the installed cost of the combined relay system as compared to a separate phase and ground distance relay system.

It is noted that the starting units selected for this relay system are similar to, if not the

same as, those formerly used in GCX distance relays. These starting units are subject to change due to the collapse of the voltage triangle on phase to phase faults. As explained in a previous paper[1] the old type starting unit was replaced in the GCX relay because the variable characteristic made it susceptible to tripping on power swings. The size of the starting unit circle is a measure of the load carrying ability of the relay. Since it becomes necessary to increase the reach of this unit to assure clearing of line to line faults in the third zone, the load ability of the relay will be reduced correspondingly. Both of these facts make this starting unit undesirable for phase relaying.

The use of the same starting unit by the combined phase and ground relay system also may adversely affect the load carrying ability of the relay. As is stated in the paper and in a previous paper,[2] distance ground relaying must necessarily be of the reactance type due to the possibility of considerable arc resistance. On the GCX ground relays, zones 1 and 2 measure reactance, but it should be noted that zone 3 (starting unit) has an impedance characteristic. The reach of the starting unit should be sufficient to assure clearing ground faults with considerable arc resistance in the third zone. This means that on some applications the required reach of the starting unit may of necessity be so great that the load carrying ability of the relay may be materially reduced.

The combined phase and ground system does not seem to lend itself to testing or maintenance of individual elements while retaining partial circuit protection. The removal of any starting unit for maintenance or testing would render the associated phase and ground relay useless and would permit the other two ground relays to function incorrectly unless they also were removed from service. On the other hand, with separate phase and ground schemes the removal of a phase starting unit would render just that phase relay inoperative while the removal of any ground starting unit would render that ground relay inoperative and permit the other two ground relays to function incorrectly.

The setting of the relays on this combined system would be more difficult than setting of separate phase and ground relay. The setting of the starting unit might be rather critical, if not impossible, in certain applications due to the variable characteristics of this unit, the effect of arc resistance and the desired load requirements of the circuit.

It is not clear from Figure 13 of the paper how zone 3 trips for ground faults. This could be accomplished by connecting a $TU3_g$ contact from the common connection between A_g and O_g contacts to the trip wire.

REFERENCES

1. See reference 1 of the paper.
2. See reference 2 of the paper.

W. A. Wolfe (Kansas Gas and Electric Company, Wichita, Kan.): This is a most interesting paper. It describes an improvement in phase and ground distance relaying achieved by combining in one element for each phase, the starting unit for phase and ground faults. Heretofore each phase and ground relay has had its own starting unit,

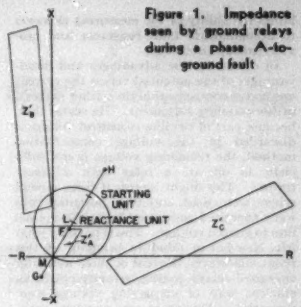

Figure 1. Impedance seen by ground relays during a phase A-to-ground fault

a total of six for a 3-phase line. The result is considerable simplification in the control circuits and also a reduction in current and potential transformer burdens.

I agree with the author that in most cases current compensation is to be preferred over potential compensation. One reason, not mentioned, is that for a relay system using potential compensation, the zero sequence reactance of the line must be accurately determined in order to set the relay correctly. Although the zero sequence impedance is used in setting the compensation of current compensated relays, the required accuracy is not as great. In current compensated relays, the positive sequence reactance which can be calculated to a higher degree of accuracy than zero sequence reactance, is the most important quantity.

This paper is valuable for another reason, in it the errors inherent in distance ground relaying are discussed and evaluated for the first time. As the author shows, for systems having solidly grounded neutral, which are probably the majority, the errors are such that they need cause no hesitation in applying distance protection for ground faults.

Warren C. New: Messrs. Frederickson, Streifus, von Roeschlaub, and Goldsborough in their discussions have pointed out that the starting units have variable characteristics which make them susceptible to false tripping due to power swings. It is true that a similar starting unit, in use for 15 years for phase distance relaying, was replaced in 1948[1] by a unit less susceptible to operation on power swings. However, as pointed out by Streifus and von Roeschlaub, the combination of conditions requiring less susceptibility to power swings is rare. Furthermore, the combined phase and ground distance relaying scheme described in this paper was designed primarily for subtransmission line applications where heavy line loadings or stability problems are not a serious factor.

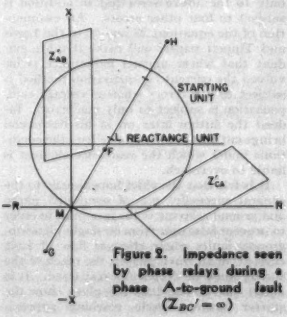

Figure 2. Impedance seen by phase relays during a phase A-to-ground fault ($Z_{BC}' = \infty$)

Mr Goldsborough in his discussion questioned the ability of starting units of the unfaulted phases to perform correctly during a single-phase-to-ground fault. The ground distance relaying in use for the past ten years has used the same starting unit as this new system employs. While it is possible to imagine system conditions under a nearby phase-to-ground fault where the starting unit of an unfaulted phase may operate, no such false operations have been reported on the many relays that now are in use. Further, a system study and calculations made for a proposed application of this combined system reveals that at the station with the largest amount of fault current on the unfaulted phases, with load current added, and with a generous increase of starting unit reach, the starting unit had ample margin to preclude the possibility of false blocking for a ground fault in the tripping direction of the relays.

Apparently from the discussions received, there is some misunderstanding resulting from the way in which Figures 11 and 12 of the paper were drawn. These figures were discovered to be slightly incorrect and not entirely clear. For the reader's benefit, these figures have been clarified and are shown in the discussion as Figures 1 and 2. It should be noted that the scales for the two figures are not the same, Figure 1 using a reduced scale. As the discussers have pointed out, the third zone should adequately cover the protected line section and the next adjacent line section as is indicated in the redrawn figures.

The current compensation errors on heavily interconnected systems or on loop systems having a single source easily resolve into a single small error (determined by Z_0'/Z_1', see Appendix 1 of the paper) with homogeneous systems or possibly three small errors with nonhomogeneous systems. The five errors that are possible with the current compensation method as pointed out by Mr. Goldsborough are all small for typical transmission systems. This is shown by the error curves where it also is obvious that with solidly grounded systems or systems grounded through equal resistances the errors are small and in many cases negligible. Further, as Mr. Wolfe points out in his discussion, in applying the current compensated relay, it is not required that the zero sequence line impedance be known to nearly as great an accuracy as is required in applying potentially compensated relays.

It is believed that this combined system is a forward step in distance relaying since the economical aspects of the system make possible the application of phase and ground distance relaying to subtransmission line systems where it previously had not been economically justified.

REFERENCE

1. See reference 1 of the paper.

Audible Noise of Power Transformers

T. D. GORDY
MEMBER AIEE

Synopsis: In the past few years, much emphasis has been put on audible noise of power transformers. Control of noise levels of such transformers without seriously affecting other important characteristics of the transformers is an important challenge to manufacturers. Sources of audible noise in power transformers, its attenuation and transmission, and the effect on designs are considered. Some characteristics of such noise are presented and methods of reducing noise levels are discussed. Power transformer noise problems confronting the manufacturer of such apparatus are discussed in relation to the over-all transformer design.

TRENDS in power system design require installations of large power transformers in thickly populated areas. These trends have been brought about by increasing capacities of existing stations and by transforming power closer to the ultimate customer than has been done in the past.[1] As a result, power transformer manufacturers have been asked to build low noise level designs for these installations. Simultaneous with these new requirements being placed on them, manufacturers have been developing new materials, processes, and material applications; and to advance the art, certain of these improvements are being incorporated in designs. The manufacturer then finds himself faced with the problem of designing for low noise levels and, at the same time, improving his product in quality, cost, and dependability. The way in which these two parts of the problem are related will be shown in this paper.

Sources of Noise

Transformers are becoming more complex because of their requirements, and no longer can the only source of transformer noise be considered magnetostriction. Even though magnetostriction is still recognized as one important driving source of audio noise, there are other sources, such as resonant parts or structures, vibrations at core gaps and joints, vibrations caused by interaction between core and coils, and vibrations of the coil conductors carrying current, which may result in noise generation or aid in noise transmission.

Magnetostriction

Magnetostriction may be defined as the change of dimensions of a magnetic material under magnetic stimulus. This is the only source of vibration in the core that is a property of the material, and true evaluation of this property can be obtained only with a d-c stimulus. D-c magnetostriction measurements may be made,[2] and results are similar to d-c flux-density-field-intensity data[2,3] in that a singly valued relation between magnetostriction and flux density is obtained on the initial magnetization of the sample. A loop is obtained if the flux density is increased, then decreased. Magnetostrictive characteristics are dependent upon the surface of the sample, the strain in the sample, and the heat treatment of the sample. Chemical composition of the steel also affects magnetostriction. Variation of d-c magnetostriction of transformer core steel with flux density in general follows a concave curve of three different types: (a), (b), and (c) of Figure 1, or, much less often, a convex curve (d) of Figure 1. Curves of Figure 1 are for the initial magnetization of the sample. If the flux density is varied through positive and negative values of flux, starting with an initially unmagnetized sample, the singly-valued curve goes into a loop as shown in Figure 2. Both the singly-valued curves and the loop show a nonlinear relation between magnetostriction and flux density. This nonlinearity requires harmonics in magnetostriction if flux density is varied sinusoidally.

In making a-c magnetostriction tests, factors other than the material in the sample may affect the shape of the a-c magnetostriction-flux density curve. Measurements of a-c magnetostriction have been made,[4] and a-c loops are similar to the d-c loop of Figure 2. If, however, the peak a-c flux density be increased to where it approaches saturation, the a-c loop becomes very much distorted, as shown in Figure 3. Again, vibration harmonics are generated; and since small sections of core laminations in joint regions are at very high flux densities during parts of the flux cycle, high-frequency components of vibration will exist around these sections.

Not only is the magnitude of magnetostriction important, but also the shape of the curve or loop is equally as important because of the harmonic phenomena involved. Even though one core material may have less magnetostriction magnitude than a second material, it may cause more effective noise emission than the second material unless its frequency distribution is confined to the fundamental and low harmonics.

Volume magnetostriction is another type of magnetostriction, but up to the present time, it is believed that it plays a negligible part in causing audio noise. In this type of magnetostriction, change in volume is considered instead of change in a linear dimension.

Gaps and Joints

Cores of power transformers usually are built by stacking many thin laminations into a structure. Necessarily, these laminations have junctions, joints, and gaps of one type or another through which flux must pass. Most such joints have overlapping regions in which the flux is divided between the parallel iron and air paths. Division of flux between the paths

Paper 50-8, recommended by the AIEE Transformers Committee and approved by the AIEE Technical Program Committee for presentation at the AIEE Winter General Meeting, New York, N. Y., January 30–February 3, 1950. Manuscript submitted October 7, 1949; made available for printing November 21, 1949.

T. D. Gordy is with the General Electric Company, Pittsfield, Mass.

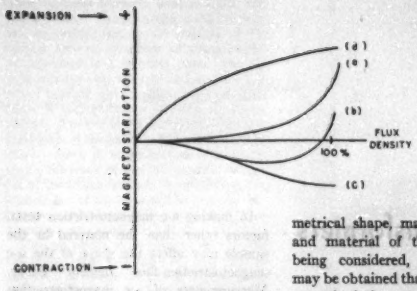

Figure 1. Shapes of d-c magnetostriction versus flux density for transformer core steel

Curves (a), (b), (c) representative shapes
Curve (d) less frequent shape

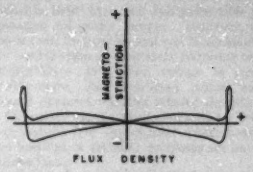

Figure 3. A-c magnetostriction loop of transformer core steel at peak flux density near saturation

varies throughout the cycle because of the variable iron permeability. Also, flux distribution in the corner sections of plate-type cores is nonuniform.[6] Across these gaps or joints in the core exists a force at each instant during the cycle that varies as the square of the instantaneous flux density. These forces tend to vibrate the leg and yoke sections of the core, thus becoming a source of noise.

If these regions had only fundamental flux in them, only a vibration and noise frequency of twice the core excitation frequency would be obtained. That is, if only 60-cycle sinusoidal flux were in the joint region, only 120-cycle vibrations would exist. However, with flux distortion and variable permeability in the joint regions, harmonics of the vibration and noise fundamental will be generated, and this in turn is emitted from the transformer, as will be shown later.

Resonating Parts

Most all materials which are built into a transformer have, either themselves or as a structure, mass and spring characteristics. This is true for the core, tank, radiator tubes, junction boxes, control cabinets, and so forth. Also, to some extent, there is a damping component associated with the mass and spring characteristics. Depending upon the geometrical shape, mass, elastic properties, and material of the part or structure being considered, resonant frequencies may be obtained that fall on or near one or several of the component vibration frequencies being supplied by the core. If damping is not sufficient, vibrations of these parts may be large enough to contribute to the transformer noise. Core vibrations have been described by Fahnoe;[6] if resonance of cooling tubes and other components exists, it may be necessary to modify the structure.

Although most of these resonating parts do not in themselves contain sources such as magnetostriction, they may, if not properly designed, be driven by other sources and amplify or easily transmit certain frequencies that would otherwise not be detected so easily. When a transformer has one of its major components, such as a tank wall, in resonance, the slope of the noise level versus excitation voltage curve is very small—much under the usual 2-to-3-decibel change in noise for a 10-per cent change in voltage.

Coils and Interaction Between Core and Coils

When current flows in a transformer winding, forces are exerted on the conductors and winding supports. An exaggerated case of such forces is the forces that occur when a transformer is short-circuited. However, at normal current densities used in power transformer designs, noise emitted by the coils due to their carrying load current is not enough to be appreciable. If the transformer must be designed for exceptionally low noise level, noise due to the coils may then become a source that cannot be neglected.

Similar to the coil noise, noise caused by vibrations due to forces between the coil and core and clamps is negligibly small in normal designs.

Fans and Pumps

Another source of noise which is not related to the transformer proper is the external cooling equipment. This equipment may be fans, pumps, or unit coolers. Usually, this equipment is mounted external to the transformer tank. Fans are mounted on radiator tubes or headers and, therefore, are a source of noise from one to several feet out from the tank. As will be shown later, the frequency spectra of fans and coolers are quite different from that of the transformer itself.

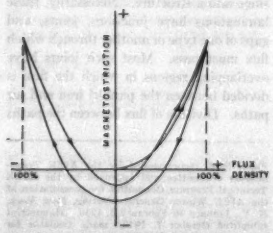

Figure 2. Representative d-c magnetostriction loop of transformer core steel

Damping Mechanisms

Vibrations caused by core displacement may be damped in three principal ways: damping in the core structure; damping in structural and metallic parts other than the core and coils; and damping in insulation. Complexity of the conventional power transformer structure makes it very difficult to segregate and evaluate these various types of damping.

In the core, steel itself may be damping. Part of this damping will be associated with the loss of energy associated with elastic vibration. In ferromagnetic materials these losses are generally larger than in nonmagnetic materials and may be interpreted in terms of other magnetic phenomena. Part of the damping in steel is due to eddy currents excited by the change of induction of the specimen as a whole, resulting from strain occurring during vibration. Still another type of damping is that caused by local changes of magnetization brought about by strain of vibration and accompanied by irreversible

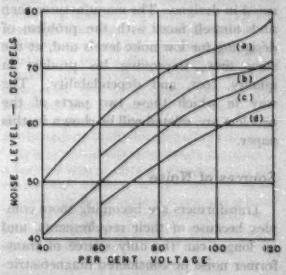

Figure 4. Variation of noise level with excitation

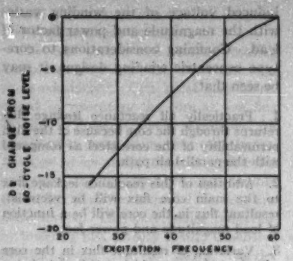

Figure 5 (left). Variation of noise level with excitation frequency

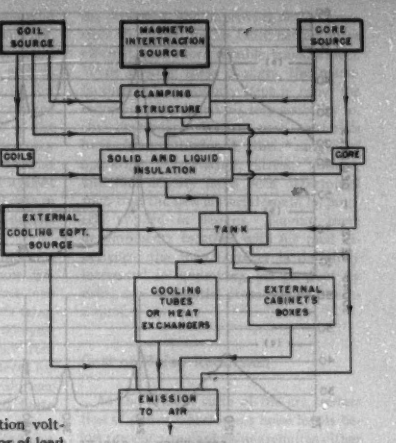

Figure 6 (right). Block diagram of transformer noise circuit

displacement of the boundaries between domains. Damping by interstitial impurities within the iron crystal lattice may be caused by mechanical movement of the sample structure. Damping in core laminations is mostly a problem in metallurgy and physics; and until the various types are evaluated by these fields of science, the transformer design engineer cannot make much use of these characteristics.

Vibrations in structural parts such as clamps, tanks, braces, and so forth, are damped by energy loss related to elastic vibration. Some damping is present in layer and major insulations of the coils. However, all of the damping present in these parts of the transformer is not sufficient to reduce the noise emitted from a noisy core and coil structure to a value low enough to effect appreciable noise reduction. Also, the degree to which this type of damping is effective varies from design to design and is, therefore, not easily predicted and utilized in the design for noise reduction purposes.

Characteristics of Transformer Noise

Power transformer noise level is dependent not only upon the transformer itself, but also upon conditions imposed upon the transformer. Excitation voltage, magnitude and power factor of load current, and noise sources external to the transformer proper are some of these imposed factors affecting the total emitted noise from a transformer installation.

Variation of Sound Level with Excitation Voltage

Under no-load conditions, the variation of sound level with excitation voltage is dependent upon the type of core and core steel used in the core, as well as the operating flux density for which the transformer was designed. Given a design with a certain core material, the change in sound level per per cent change in excitation voltage will vary as the excitation voltage is changed. This is shown by Figure 4; curves (a) and (b) are for one type of core using two different steels; curves (c) and (d) are for two different cores of another type but using the same steel as curve (b). Curves (a) and (b) show a range of decibel versus per cent voltage slope from 0.55 to 0.12, depending upon the per cent voltage being considered. The corresponding range for curves (c) and (d) is 0.38 to 0.16. Around 100 per cent voltage, the change in noise level change is between 0.2 and 0.3 decibel per per cent change in voltage.

Curves of Figure 4 are for 60-cycle excitation; change in noise level for frequencies lower than 60 cycles is shown by Figure 5. The decrease in noise level with frequency is due to lowering the fundamental noise frequency and all of its harmonics. Necessarily, total noise level would be decreased because of the 40-decibels weighting characteristics specified by the standards for noise meters.[7]

Variation of Sound Level with Load

Present audio noise standards for transformers[8] specify that noise tests be made at 100 per cent excitation voltage with no-load on the transformer. In operation of the transformer, the problem still remains to determine what noise level the transformer will have under load if no-load noise level of the unit is known.

The degree to which load changes noise level is mostly dependent upon the way in which flux of the core is affected by load. Obviously, the type of core, type of windings, and winding arrangement must be considered. Also, in most cases, the noise level of the transformer is determined by the highest flux density in the core if as much as half of the total core steel operates at this high flux density. The problem then reduces to one of determining the variation of core flux density with load.

Basic transformer theory shows that

Table I. Representative Frequencies Present in Noise Emitted from 60-Cycle Transformers Rated from 750 to 37,500 Kva

Frequency Component	Decibel Level of Components Transformer A	B	C	D	E	F	G	H	I
120	39.5	44.5	45.5	82.5	59.5	67.0	49.5	73.0	60.5
240	55.0	44.0	56.5	74.0	65.0	62.5	60.5	55.0	51.5
360	35.0	55.5	47.0	76.5	57.0	53.5	54.0	59.5	54.0
480	52.5	55.0	44.5	75.0	57.0	49.0	47.5		53.5
600	36.0	47.0	36.5	69.0	52.5	49.5	42.0	53.5	50.0
720	45.5	48.0	39.5	66.5	54.0	47.0	45.5		47.0
840	43.0			66.0		57.0	47.5		
960	46.0		41.5	61.0	42.0	52.0	50.0	59.5	48.0
1,080	48.5			60.5	40.0	53.5	46.5	60.0	44.0
1,200	53.5	56.0	54.0	64.5	40.0		55.5	52.5	39.5
1,320	44.0			60.5	40.0				
1,440	43.0				51.5				
1,560	36.5								
1,680	40.5				43.0				
1,800	36.5				43.5			52.5	

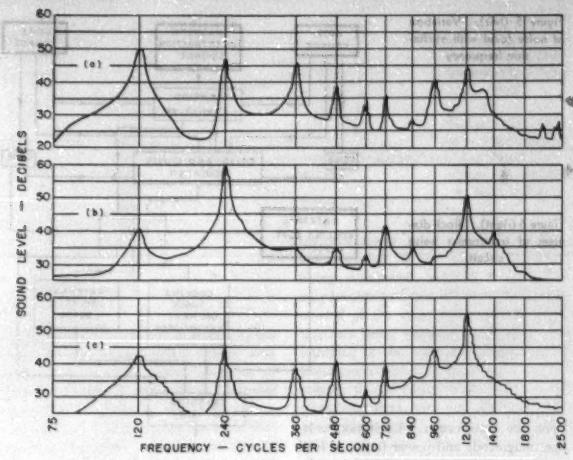

Figure 7. Representative recording of frequencies in transformer noise

(a) 120-cycle component predominant; total measured noise level = 55.2 decibels
(b) 240-cycle component predominant; total measured noise level = 59.0 decibels
(c) 1,200-cycle component predominant; total measured noise level = 56.0 decibels

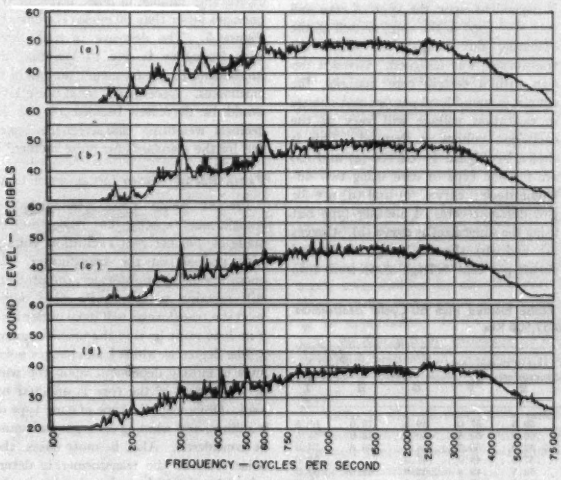

Figure 8. Recordings of representative frequency spectra for transformer cooling fan

(a) Zero degrees from fan axis; total noise level = 65.2 decibels
(b) 30 degrees from fan axis; total noise level = 64.8 decibels
(c) 45 degrees from fan axis; total noise level = 63.0 decibels
(d) 90 degrees from fan axis; total noise level = 55.5 decibels

induced voltage of the winding varies with the magnitude and power factor of load. Confining considerations to core-type concentric winding designs, it may be seen that:

1. Practically all reactance leakage flux returns through the core because of the high permeability of the core steel as compared with the parallel air path.

2. Addition of this reactance leakage flux to the main core flux will be vectorial; resultant flux in the core will be a function of load magnitude and power factor.

3. Variation of resultant flux in the core will depend upon which winding is being excited and which winding is connected to the load; that is, inside or outside winding as primary or secondary.

4. Resultant core flux will depend upon whether input or output voltage is maintained constant.

It is seen, therefore, that variation of noise level with load is closely related to the transformer design in a manner similar to regulation and must be considered as another characteristic dependent upon other specified characteristics.

Magnitude of noise level change may be as high as that corresponding to the core flux density being increased by the full reactance flux. For example, if the inside winding be excited, constant output voltage be maintained on the winding, a load of 10-per cent power factor lagging be supplied, and the reactance of the transformer be 10 per cent, change in noise level would be between two and three decibels. This would be an extreme case and for higher power factor loads with the inside winding as secondary, no change in noise level would be detected. Change in noise level because of load variation is, therefore, in the order of two to three decibels at the most and may vary all the way down to zero.

Noise Transmission and Reduction

Transmission of vibration and sound from the various sources to final emission to air is through a very complex 3-dimensional network. The simplified block diagram of Figure 6 shows the complexity of the circuit. Sources are shown in heavy blocks and direction of transmission is shown by arrow heads. Three sources are inside the tank and feed through the various components into the tank. On the tank another source, external cooling equipment, is added. From the tank, transmission may be directly to the air or through cooling tubes or heat exchangers and cabinets, then to air.

Even though transmission of vibration and noise in a transformer is very complicated, the diagram of Figure 6 shows the various locations either inside or out-

side of the tank at which noise suppression measures may be taken.

The core source and external cooling equipment source are the important ones to be considered. Core noise may be reduced by operating the core at low flux density. Present steels available for transformer cores have magnetic characteristics which make them desirable for operation at flux densities considerably above flux densities required for very low noise levels. Therefore, noise reduction by lowering flux density is very expensive besides giving rise to larger, heavier transformers. Another method of reducing core noise would be to eliminate gaps or joint sections. This may be done in small transformers,[9] but in power transformers it is necessary to use cores built up of many laminations instead of a continuously wound core. Still another method to reduce core noise would be to use core steel that has no magnetostriction at any part of the operating flux density cycle. Such a material, having this and other necessary characteristics, is not available to the transformer manufacturer at the present time.

Introduction of noise barriers inside the transformer tank is the only alternative for appreciably reducing noise transmission through the liquid insulation. This is, in effect, introducing high acoustic impedances in the transmission paths. Such barriers can be built, but they require additional space and weight, both of which should be held to a minimum in a well-balanced, economical design. Such additions, for acoustic reasons only, are necessarily expensive.

Fan or cooler noise may be reduced by either using special design, low-noise-level fans which have reduced cooling capacities, or by reducing the operating speeds of standard transformer cooling fans. Reducing fan speed 50 per cent may give noise reductions as high as 30 decibels. To cool transformers with such fans, it is necessary to use many more of them than would be used if they were operated at their standard speeds. Again, this noise reduction is expensive.

Frequencies of Noise

Necessary for noise reduction studies of power transformers are the frequencies present in emitted transformer noise. Frequency composition of emitted noise varies from position to position around a transformer, but by analyzing several positions around the transformer, the important frequencies with which to be concerned may be determined.

The simplest and most accurate method of obtaining and recording component frequencies is to put the output of the sound level meter into an analyzer and recorder. The recorded trace then is a plot of sound level in decibels versus frequency, such as that shown in Figure 7. Traces of this figure are for transformers without cooling fans, and rated 1,000 kva. Peaks of the various component frequencies then may be read. Summation of the component frequencies then may be checked against the sound level meter reading. All data in this paper were taken with the 40-decibel weighting scale.

In Table I are tabulated frequencies for several transformers to show how frequency composition varies from one transformer to another. From this tabulation, it may be seen that, for 60-cycle supply voltage, a range in frequency from 120 to 1,200 cycles must be considered for noise reduction purposes. Transformer noise is characterized by peaked finite frequencies; whereas most fan noises have a large component of broad-band noise, as shown in Figure 8. Although peaks may be present in fan noise, a large part of the noise of most transformer cooling fans is contributed by broad-band noise.

Design Characteristics and Requirements

The primary purpose of a power transformer is to transform energy from one circuit at one potential level to another circuit at another potential level. In some cases, more than two circuits are tied in by the transformer. Depending upon the application of the unit, a few or many specific requirements must be met by the design. Impedances may be specified, efficiencies may be specified, a certain regulation may be required, floor space and total weight may be a limiting factor, shipping dimensions and weight are limitations, temperature limits must be observed, and core and copper losses must meet specified values. These and many more similar characteristics determine the degree of flexibility available to the designer. Because of these varied and interrelated functional characteristics, the designer must consider the design as a whole. One particular requirement cannot be designed for, without considering its effect on other requirements.

The increasing importance of transformer noise imposes another constraint on the transformer design.

Simultaneous with the imposition of more requirements being placed upon the design, the manufacturer has been developing new materials, new manufacturing processes, and improving design practices to enable him to build better, more efficient, and more reliable transformers. While making these changes, the manufacturer has constantly kept in mind the requirements of, and his responsibility to, the customer. Where new materials have been introduced, their ranges of operating temperature, stress, voltage, and flux density have been determined such that the new material would be properly applied in designs. Having these developments together with his past experience, the manufacturer is definitely interested in improving his product by using new materials, processes, and techniques.

Cost of Noise Reduction

At the present state of the art, reduction of power transformer noise levels below present standard values requires either a reduction in operating flux densities or introduction of acoustic impedances in one or more of the transmission paths. Such impedances may be internal or external to the transformer tank. Either of these reduction methods is expensive and places handicaps on the designer. Lowering noise levels of cooling equipment requires either slow-speed standard fans or redesigned low-noise-level fans which are not as efficient on cooling as present standard fans. Either of these methods is expensive. Therefore, noise level reductions of the transformer itself are expensive and may necessitate cost increases of power transformers.

The other alternative for obtaining low-noise-level transformer installations is to build walls, barriers, or enclosures around the transformer. This method sometimes requires cooling equipment for the installation, is difficult to arrange for incoming and outgoing voltage lines, and, to a certain extent, imposes fire protection and repair handicaps. In metropolitan or residential areas, such measures may have to be used, but at stations remote from such areas or in noisy areas, present standard transformer noise levels would be satisfactory. It appears that installations requiring very low noise levels should be considered as special installations.

Whether extra expense required to obtain a low-noise-level transformer installation be put into the transformers themselves or in walls, barriers, and structures is a matter of which method is less costly. Operators and manufacturers will have to work together to obtain the most desirable solution which probably will vary with the installation.

Conclusions

Characteristics of power transformer audio noise vary from one design to another, but the more important characteristics, such as variations with excitation voltage, load, frequencies present, and size of transformer, are fairly well established. Increased importance of transformer noise requires the manufacturer to be very much aware of these characteristics because of the interrelation between audio noise and other characteristics.

For special installations, low-noise-level transformers may be designed and built, but they are costly. The other alternative of building enclosures around transformers also is expensive and disadvantageous in other respects. For such installations, the best compromise can best be worked out by the operator balancing costs, advantages, and disadvantages of the two possible methods. Either method will increase cost over that of a standard transformer, but such cost may have to be borne for particular locations.

References

1. Transformer Audio Noise Problems on an Electric Power System, C. S. Murray. *AIEE Transactions*, volume 68, part 1, 1949, pages 740–47.

2. Magnetostriction Made Visible, S. C. Leonard. *General Electric Review* (Schenectady, N. Y.), volume 45, number 11, November 1942, pages 637–41.

3. Magnetostriction Phenomena, W. D. Williams. *General Electric Review* (Schenectady, N. Y.), volume 45, number 3, March 1942, pages 161–63.

4. New Techniques in Measurement of Magnetostriction, J. K. Mickelson. *General Electric Review* (Schenectady, N. Y.), volume 51, number 11, November 1948, pages 24–27.

5. Influence of the Core Form Upon the Iron Losses of Transformers, O. M. Stein. *AIEE Transactions*, volume 67, part 1, 1948, pages 95–100.

6. A Study of Sound Levels of Transformers, H. Fahnoe. *Electrical Engineering* (*AIEE Transactions*), volume 60, June 1941, pages 277–83.

7. Tentative American Standard: Sound Level Meters for Measurement of Noise and Other Sounds, *Z24.3*. American Standards Association (New York, N. Y.), 1944.

8. Standards for Transformers. *Publication 42-132*, National Electrical Manufacturers Association (New York, N. Y.), 1948, pages 33–34.

9. The Wound-Core Distribution Transformer, E. D. Trembor. *Electrical Engineering* (*AIEE Transactions*), volume 57, November 1938, pages 622–25.

Discussion

A. P. Fugill (The Detroit Edison Company, Detroit, Mich.): Mr. Gordy's paper represents one viewpoint on the subject of quiet transformers which, I believe, is rather typical of the manufacturing companies. Other papers at the session present the typical user's viewpoint. As I interpret these views, most manufacturers believe that no large segment of the transformer-buying industry needs transformers much quieter than the present ones, and, if quieter transformers are needed, they will cost more. Some utility users know the transformers they have been receiving under the present noise limits are not quiet enough for many installations, and believe that quieter transformers could be obtained with little or no increase in cost, if sufficient attention were given to the noise factor in transformer design and manufacture. The natural conclusion is that the present National Electrical Manufacturers Association standard limits for noise in transformers should be changed, but the manufacturers would like to raise them and the users would like to lower them. If the limits are raised too high, the installations where quietness is essential will carry a disproportionate amount of the cost, and, if they are lowered too far, installations where quietness is of no importance will be penalized.

A number of points have been brought out which, though important, are subordinate to the main point at issue, which is the determination of the proper set of noise limits to serve the best interests of the whole industry. For instance, complaints have been made against the present sound level meter. We must realize that we have an impossible task if we try to make a meter which will match the sound perception characteristics of even a million people, each one of whom differs not only from the others but from himself at different times and under different conditions. Certainly we should try to improve our measuring equipment, but the present sound level meter is entirely adequate to differentiate between a transformer which will cause trouble and one which will not, if only the requirements are known. The greatest variable is not in the meter, but in the people who live next door to our substations.

The techniques of measurement seem to be causing some concern. The location of the microphone, the effect of the ambient, and the weighting network to be used are important. Perhaps the present methods and standards can be improved upon in the light of modern knowledge. But the use of a different weighting uetwork in the meter will not make the transformer being measured any quieter, nor will it point the way to an economical design for a quiet transformer.

More important than either of these factors is the basic research into the causes of noise in transformers and the development of inherently quiet designs. In time, we may discover how to design a quieter transformer without the proportionate increase in cost. But even this problem does not rate top priority. Though some may disagree, I believe the present knowledge is sufficient to produce transformers which will meet most of the present needs of industry. The question is not so much whether we can obtain quieter transformers but rather whether that is the economical way to obtain the quietness we need.

Since about 1939 all manufacturers have been designing to meet the limits imposed by NEMA standards. Perhaps a look at their performance in terms of the transformers which have been received by The Detroit Edison Company may be helpful in determining the proper noise limits. In considering these data, note that The Detroit Edison Company has been using noise specifications since 1937 and had been stressing quietness in transformers for several years before that.

The curves shown in Figure 1 of the discussion were obtained from the measurement of noise on 252 transformers from 500 to 10,000 kva, mostly 24,000/4,800 volt, which we received during the period from 1916 through 1949. They cover virtually all the transformers in this class that we have purchased. The results are plotted in terms of deviation from the present NEMA standard limits in order to fit all sizes into the same curve. The curve used is essentially a cumulative distribution curve by which the percentage of transformers that equal or exceed a given noise level can be read directly. We have classified all transformers, regardless of size or manufacturer, into three age groups. The dashed curve covers 96 transformers received in the years 1916 through 1930, during which time there were no noise specifications in use. Practically no transformers were purchased in the years 1931–1936, so the solid-line curve is for the 61 transformers received from 1937 through 1942, during the period when noise specifications were in use and before the influence of the war was felt and different core materials were used. Very few transformers were purchased in the years from 1943 through 1946. The dotted curve covers the 95 transformers received from 1947 through 1949, the post-war years when newer core materials were available, and situations resulting from production during the war may have had an influence. From these curves, you will note that in the 1916–1930 period, 70 per cent of the transformers received did not meet the present specification limits. That is no indictment of the manufacturers, of course, because the present specification limits did not exist in that period. For the 1937–1942 period, 13 per cent of the transformers received were over specification limits. This is a very appreciable improvement, when compared with the upper curve, but possibly not such remarkable performance when you remember that the specification limit was set up as a maximum figure with no intended tolerance. In the 1947–1949 period, however, 33 per cent of the transformers received were over specification limits, a very definite backward step. This is the situation which raises the present concern over noise limits.

From this evidence, and similar findings by other utility companies, it is clear that a rather significant proportion of modern transformers is not meeting even the present NEMA standard limits. Furthermore, it has been our experience, substantiated by the experience of others, that even transformers which meet the present limits are much too noisy for some installa-

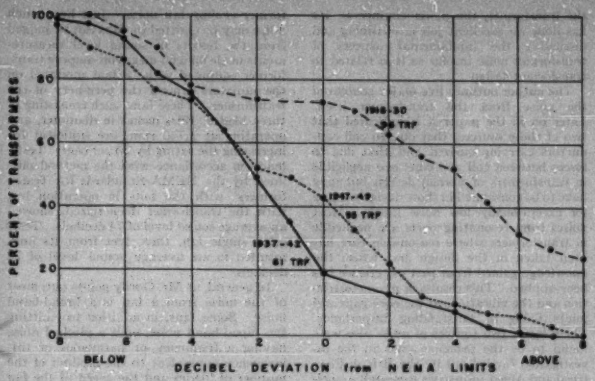

Figure 1. Percentage of transformers measured (500–10,000 kva) that equaled or exceeded indicated sound levels

tions, and remedial measures must be applied at considerable cost.

Since there is such a divergence of opinion, however, it is important, before any change is made in these limits, that additional information be obtained from all segments of the industry—manufacturers, utility users, and industrial users. Three questions need to be answered, and only after the answers are obtained will we be sure that we have solved the problem in such a way that the lowest cost to the industry will result. First, what sound level limits are really needed, if due regard is given to the average situation as well as the extreme ones? This is a job for the users, not the manufacturers, and the users who have no noise problems are just as important as those who have. Second, how does the true cost of the transformer vary with the sound level, if the designer gives the noise factor equal status with such other design factors as reliability, weight, and losses? Third, what is the cost of the remedial measures external to the transformer, which can be used to make the transformer acceptable? These facts are not easy to obtain and they vary over a wide range. But a thorough-going investigation on a wide front, with an earnest effort on the part of all concerned, will go a long way towards establishing the optimum values of sound level limits for transformers.

J. E. Goldman (Westinghouse Research Laboratories, East Pittsburgh, Pa.): It is apparent from Mr. Gordy's paper that noise in transformers is a very complicated phenomenon and to understand it quantitatively requires the solution of complex mechanical, electrical, and magnetic problems. One of the principal, although by no means exclusive, magnetic problems that arises is that of magnetostriction. A full discussion of the fundamental aspects of magnetostriction and its measurement by this writer is on the agenda of the magnetic symposium tomorrow. There are, however, a few points pertinent to Mr. Gordy's paper that it may be well to bring up here.

It is correctly pointed out that the only true measure of the macroscopic magnetostriction is by means of d-c measuring techniques. This is because the vibration measured under a-c excitation may include amplified components due to mechanical resonance of the whole or a part of a sample but which may be different if the sample geometry is changed. In this connection it is to be noted that in a transformer core the core resonances and local resonances merely amplify the effects normally produced by excitation forces which are necessarily magnetic in origin; resonance in itself we do not believe to be a source of vibration as implied by Mr. Gordy. An individual sample when measured under a-c excitation is essentially a small transformer core with the same mechanical and magnetic complexities. Moreover, most existing methods of measurement under a-c excitation that we know of introduce measuring errors that may tend to exaggerate a given harmonic of the magnetostriction spectrum. For example, most piezoelectric crystals have resonances between 600 and 1,000 cycles. Use of a crystal pickup in an a-c magnetostriction measurement may, therefore, tend to exaggerate the higher harmonics and change both the amplitude and shape of the curve completely.

The term macroscopic magnetostriction was employed in order to distinguish it from the more fundamental magnetostrictive lattice distortion of the unit cell which we shall call the microscopic or spontaneous magnetostriction. The latter is a basic property of the magnetic material that depends primarily on the composition of the alloy and can be measured only by an involved set of magnetostriction measurements on single crystals in various crystal directions. The former is measured by noting the change in dimensions of the sample in a given direction; its magnitude is conditioned largely by the crystal and domain orientation. Nonrandomness of the distribution of the domain direction such as may be achieved by cold rolling can bring the measured macroscopic magnetostriction down to a very low value in a material that normally has a large basic microscopic magnetostriction. Such is, in fact, largely the situation with cold rolled oriented sheet steels.

This suggests an important shortcoming in the methods used by many manufacturers and employed by Mr. Gordy in interpreting the influence of magnetostriction on transformer noise. The measurements of the magnetostriction are macroscopic and often show that the material changes its dimensions to only a minor extent. Yet, had the measurements been made in other than the direction of normal magnetization, the magnitude of the magnetostriction may be significantly larger and the shape of the $\Delta l/l$ versus B curve perceptibly different. In a transformer core, there are regions where the flux is not in the direction of the sheet. This is particularly true in the neighborhood of the joint but is to some extent prevalent throughout the iron circuit. In these regions, therefore, the magnetostriction and resulting vibration can be quite large in a direction transverse to the direction of flux.

The usual measurement of magnetostriction on sheet steel samples gives no indication of the magnitude of this type of magnetostriction. In point of fact, the latter is quite large for oriented sheet steels in which we are accustomed to viewing the magnetostriction as being small. This also is to some extent true of the silicon steels with high silicon content.

The question of coil noise is one that often comes up for discussion and has been raised by Mr. Gordy. It has been our experience that coils do not contribute measurably to the total noise of the transformer. Many tests over an extended period of time in which cores were first tested with only a skeleton winding and later as assembled with the coils and finally under operating conditions in the field seem to substantiate this viewpoint.

In general, the complex problem of transformer noise has been treated quite adequately by Mr. Gordy and he should be commended for introducing many aspects of the subject that are of more than casual importance but that have been somehow neglected in previous discussions of this subject.

C. C. Horstman (Westinghouse Electric Corporation, Sharon, Pa.): Mr. Gordy has presented a very excellent paper covering the factors involved in the design and use of power transformers with regard to sound level. It is certainly true that in order to reduce the cost and improve the quality of power transformers the manufacturer has to design to use higher operating inductions. These higher operating inductions are made possible with the better core materials available today, but unfortunately, full usage of these higher inductions is incompatible with sound level reduction unless further development takes place.

The author, in his paper, makes a very good listing of the sources of noise, and we certainly agree that mechanical vibration sources are as important as magnetostriction. It is to be noted that resonance is not strictly a driving force, but is an amplifying

agent for noise. We have found that excessive noise due to resonance can be largely eliminated by designing specifically to avoid the fundamental frequency and its multiples in our various structures. It also may be pointed out that the effect of resonance reducing the slope of the curve of sound level with voltage as described by Mr. Gordy may or may not be true because it depends on the particular harmonic which is driving the resonant part, the amplitude of which usually varies with the induction.

The author's comments on core joint influence are very good. We have found that butt joints in wound cores perform very well, even in large sizes, provided the joint surfaces are bound together sufficiently well to eliminate simple joint vibration. We certainly concur that flux distribution in the joint is a very important factor influencing sound level.

In the author's discussion of damping mechanisms he refers to damping in the core steel itself. It is not clear whether or not this is a process by which the magnetostriction is reduced. We know, in general, that the better the magnetic properties of the core material the lower its inherent basic magnetostriction. This to me would preclude the damping or lowering of magnetostriction vibration of the core steel by effects, such as strain or lattice impurity, causing harm to the magnetic characteristics. It is true that information on these causes and effects is meager and requires further study.

It is quite another situation though in regard to vibration of the structural parts, such as tanks, braces, clamps, and so forth. Here improvement has been accomplished, by proper design, to effectively reduce sound level by effective means of core clamping, bracing, and mounting.

The author has summed up the requirements for sound level reduction and its probable influence on cost very well. It may be pointed out that the use of internal barriers is very complex and expensive. The problem of adequate cooling without making the transformer unnecessarily large is encountered at once because it must be remembered that while the barrier will insulate against sound transmission, it is as equally effective in preventing heat transmission to the oil or cooling medium. It also is to be noted that cooling oil pipes or ducts, where they come out through the barrier, present a design problem to avoid the transmission of sound energy to the outside along these avenues. It also should be pointed out that the very nature of such devices as internal barriers makes successful operation in hot oil over an extended service life very doubtful.

It is very evident that at this stage of development the operators and manufacturers will have to work closely together to obtain the best solution, which, as the author points out, will probably vary with the installation. It cannot be overemphasized that a decrease in operating induction is an expensive solution to lower sound levels.

C. S. Murray (Consolidated Edison Company of New York, Inc., New York, N. Y.): Mr. Gordy is to be commended on outlining the sources of transformer noise in a language that can be understood by those using the transformer, the power engineers. He has done an excellent job in outlining and discussing the fundamental aspects of transformer noise insofar as it is related to transformer design.

The author outlines five major sources of the noise from the transformer itself. Later on in the paper it is indicated that two of these sources, that due to coil conductors carrying current and that due to forces between coil and core, are negligible in transformers of normal design but may have to be considered in those designs calling for exceptionally low noise levels. Most noises from resonating parts are negligible in transformers where reasonable care has been taken in the design and where the knowledge gained from past experience has been applied. This results in magnetostriction and the vibrations at the core gaps and joints being of outstanding importance. These latter two sources of noise also were found to be the principle ones in the investigation carried out by the British Electrical and Allied Industries Research Association in the late 1930's.

Mr. Gordy points out the importance of the shape of the magnetostriction loop because of the harmonic phenomena involved. This is of the utmost importance to the user since the higher frequency noises are radiated more efficiently from the core and the human ear is much more sensitive to them. Therefore, if a steel could be found having a shape for the loop which would result in only the lower frequencies of noise being set up, the loudness of the noise radiated would be reduced and the loudness of the noise would decrease more rapidly with increase of distance from the transformer.

The author discusses noise due to the core gaps and joints but does not point out how the transformer designer attempts to decrease it. The question is raised as to whether a greater problem exists here other than properly designed core clamping.

There is still another source of noise in those transformers equipped with tap changing under load equipment using a series transformer. With the tap changer in the full-buck or full-boost position, the average sound level of the transformer may be as much as 4 to 5 decibels above that value when the tap changer is in the neutral position. The design of the series transformer must not be overlooked.

Transformers have been received from manufacturers wherein mechanical noises, some high pitched and others low pitched, have been emitted. In some cases, either loose or unequal tightening of the radiator tube bracing bands have allowed the tubes to vibrate against the bands. In other cases, the fan control conduit was run too close to the tubes which vibrated against it. In the case of these noises, the transformer designer may have taken care of them on the drawing board, but it never reached the finished product.

Location of these local noises and their elimination could only be made in the field after the transformer was energized. If this noise had not been attended to immediately it could have been the basis for a noise complaint and, as I have stated elsewhere, once a complaint arises, a series of noise complaints usually follow because the complainant is made noise conscious.

The paper points out the problem of transformer cooling fan noise. Just how much noise may be emitted by fans can be judged from the results of sound level measurements made on a 60-megavolt-ampere transformer equipped with 18 fans mounted on the radiators around the periphery of the transformer. These fans, each consisting of three blades, $19^1/_2$ inches in diameter, and operating at 1,750 rpm, are sufficient for increasing the rating by 25 per cent. Tests, made in accordance with the method outlined by the NEMA Standards for Transformers[1] with the fans in operation but with the transformer deenergized, showed an average sound level of 74 decibels. Tests on a single fan, three feet from its hub, resulted in an average sound level of 73 decibels.

In general, as Mr. Gordy points out, most of the noise from a fan is a broad-band noise. Some fans, in addition to emitting the broad-band noise, emit a pitched noise having a frequency or harmonics of this frequency equivalent to the product of the number of blades and the speed of the fan in revolutions per second. This pitched noise might be objectionable in some installations unless it becomes masked by the transformer noise. Fan designs resulting in an appreciable component of pitched noise should be avoided for quiet transformer installations.

In addition to the noise characteristics of the individual fan, the mounting of the fans must be considered not only in regard to efficient cooling but also in regard to the noise. Tests have been made on a transformer which indicate that the noise attributed to the fans may be greater with the transformer energized than with it deenergized. Tests on another transformer show an increase in sound level for some of the component frequencies present in the transformer noise and introduction of higher harmonic frequencies due to the operation of the fans. Yet, the results of tests made on an individual fan in the laboratory do not account for the change in the components of the noise emitted by the installation.

In those installations having transformers with triple ratings the fan problem may be minimized by obtaining the first step in increased rating by means of forced-oil cooling instead of forced air as is the present practice. The load curve for the particular installation may permit the use of the second step, that is forced oil-forced air, only during the day time when higher ambient noise levels usually exist. However, if the transformer is installed in a tie feeder where the second step may be necessary at any time, the fan noise remains a problem.

The author describes a method of obtaining a measure of the component frequencies around the transformer. If he wishes to imply that it is more accurate to record the output of the analyzer, I disagree with him. The mere recording of a value will not change the accuracy of the value measured. There are advantages in recording when making tests in the vicinity of the transformer, one of them being that if the audio band is scanned a complete plot of the transformer components is available right there on the job. It is simpler to look at a plot of values rather than a large number of figures. However, at distances remote from the transformer there may be more disadvantages in recording particularly if the audio band is scanned. Transformer noise

remote from a transformer varies in magnitude and, if the analyzer is driven through a transformer frequency at the time when this component is a minimum, the recorded value will not be a proper one. It would be necessary to record each particular important frequency over a period to obtain the proper values. Then, again, the operator, while recording is in progress, must mark the chart when extraneous noises occur which contain the frequency being recorded. When a peculiar value is noted on the chart the question often arises as to whether an extraneous noise existed and the operator failed to mark the chart.

In Table I is listed the component frequencies of some transformer noises. In my experience with distribution and power transformers the component frequencies from 120 to 480 cycles have generally been of the major importance. However, the results for the transformer identified as "B" show the outstanding component to be 1,200 cycles. The use of such a transformer should be avoided even in a location where only a fair degree of quietness is desirable. The question is raised as to whether this noise has not resulted from improper core clamping.

The reduction of transformer noise by means external to the transformer is costly as the power engineer well knows and as the author also recognizes in his paper. In the past, most installations have been made quiet by means external to the transformer. In the last few years, however, many users have begun to feel that an economically quiet transformer can only result by a reduction in the noise at its source. This may mean the use of steel having proper magnetostrictive properties together with the application of the knowledge available to the transformer designer.

Reference

1. See reference 8 of the paper.

T. D. Gordy: Mr. Fugill considers the major problem as that of determining a set of noise limits that will serve the best interests of the whole industry. He points out phases of the problem which must be solved by the manufacturers. We, as a manufacturer, are working on the basic causes of transformer noise and development of quiet designs. However, satisfactory improvements in noise level must be obtained without seriously handicapping other important functional characteristics of the transformer. Introduction of cold-rolled steel into power transformers has resulted in lighter, more efficient and smaller transformers. Possibly, manufacturers have used cold-rolled steel prematurely so far as noise level is concerned, but other improvements, such as reductions in core loss, exciting current, weight, and dimensions, have been passed on to the users.

The curves presented by Mr. Fugill indicate that transformer levels were higher during 1947–1949 than during 1937–1942. In the period 1947–1949, however, manufacturers were under several handicaps. Increased output, serious shortages of some materials, new and partially-trained technical and factory personnel, and loss of continuity of development during the war were handicaps that would allow shipment of transformers that might exceed noise specification limits. Also, margins between test values and specification limit values were decreased. Conditions existing in 1947–1949 are not so prevalent now, and an improvement in meeting specification limits on the part of the manufacturer should be realized.

Mr. Murray's comments on change in noise level with tap position on tap-changing transformers using series transformers are certainly justified. Depending upon the relative kilovolt-ampere ratings of the main and series transformers, effect of excitation on the series transformer may be anywhere from negligible to 4 or 5 decibels. However, whether the series transformer is or is not excited at no load depends upon the particular design under consideration, and present standards specify only no-load noise level. Revision of the standards should include the effect of the series transformer.

Properly designed core clamping is only one factor in minimizing core gap and joint noise. Type of joint, location of the joint region in the magnetic circuit, and flux distributions in joint regions are other factors which affect gap and joint noise. Developments along these lines have shown improvements not only in noise, but also in core loss and exciting current.

Radiator tube bracing bands, control conduit, and other similar parts of the transformer cause undesirable noise emission as Mr. Murray has observed. These items may be checked in the engineering and drafting stage and again when the transformer receives factory tests, but some parts still vibrate after installation. Careful inspection of the installation must be made in addition to inspections made at the factory. Even though the vibrations may not be serious so far as transformer life and functional operation are concerned, they may be annoying to an observer. This, together with the discussion of fan noise given by Mr. Murray, shows the importance of the psychological part of noise evaluation.

Mr. Murray is correct in stating that recording values of component frequencies does not increase the accuracy of the value being measured. Recordings have the advantages discussed by Mr. Murray, and they also give a permanent record that may be reproduced.

Transformer "B" of Table I was selected as a representative unit of a particular type and kilovolt-amperes. A 1,200-cycle predominant component was not unique for the particular unit of Table I. Investigation of that type and kilovolt-amperes of transformer has not shown that the high-frequency component was caused by improper core clamping.

As Mr. Horstman states, harmonic composition of the driving force varies with induction. However, if sufficient power at any induction is available to maintain resonance, and if resonance is an important contributing force, the slope of the noise-level-voltage curve will be decreased. As a specific example, a transformer was found to have serious resonance of some parts at 120 cycles. Total average noise levels measured at various percent voltages were:

Per Cent Voltage	Noise Level, Decibels
90	71.7
95	72.0
100	72.1
105	72.6
110	73.1

Variation of noise level with per cent voltage is much less than the normal value of 0.3 decibel per per cent change in voltage. As has been pointed out by Mr. Horstman and Mr. Murray,[1] designing specifically to avoid fundamental frequency and its multiples will considerably reduce resonance.

In the paper, various types of damping that could exist in the core steel were mentioned but not discussed in detail. How these types of damping affect magnetostriction was not stated. As the paper states, damping in core laminations is a metallurgical physics problem which requires further study. Therefore, Mr. Horstman's question of whether or not damping reduces magnetostriction must await additional study.

Mr. Goldman's discussion of magnetostriction is most timely, because magnetostriction is an important source of noise. Short treatment of magnetostriction in the paper was intentional because, as Mr. Goldman's discussion shows, complete treatment of magnetostriction is in itself enough material for another paper. Studies of basic metallurgical physics problems should include details brought out by Mr. Goldman, but such findings must be put into a form that may be used by the engineer before they are fully utilized in the transformer designs. Magnetostriction as used in the paper determines vibrations of the leg and yoke members as whole vibrating bodies. Noise resulting from spontaneous magnetostriction may or may not be as important as that resulting from macroscopic magnetostriction; experimental evaluation of the relative magnitudes of noise from the two types of magnetostriction is needed.

Discussions by Mr. Horstman and Mr. Goldman agree with the paper on the complexity of the transformer noise problem. Users, as represented by Mr. Fugill and Mr. Murray, require quieter transformers without excessive cost. Obviously, a compromise must be reached, and it is only through close co-operation between manufacturers and users that a satisfactory solution will be otained. This was recommended in the paper and in three of the discussions. Although the manufacturer is faced with a difficult problem, developments under way show promise and are encouraging, and it is reasonable to expect a satisfactory solution will be obtained.

Reference

1. See reference 1 of the paper

Basic Patterns for Arrangement of Electric Power Systems for Steel Mills

HARVEY J. FINISON
MEMBER AIEE

THE steel mill power systems to be discussed in this paper may be as small as about 15,000 kw installed capacity and may approach or even exceed a capacity of 200,000 kw. If the steel mill has blast furnaces and coke ovens with waste fuel available, part of this capacity will be from turbine generators. Where possible there will be a tie to the electrical utility; and in many mills all of the electric power is provided by the electrical utility.

The utilization voltages for the steel mill usually will include 440 volts, 2,300 volts, and 6,600 or 13,200 volts for the large motors or furnaces. Generation will usually be at 6,900 or 13,800 volts, although some older 2,300-volt machines are still in service. Formerly there was only limited use of voltages above 6,900 but there is an increasing need for higher transmission voltages. These include 22, 33, and 69 kv.

Steel mill power systems are somewhat different than those for other industries:

1. The systems are usually larger in capacity than for most other industries.
2. There are large unit loads—large motors and electric furnaces.
3. There are large fluctuations in load.
4. The location of generating capacity is dictated by availability of waste gas fuel rather than by electric load requirements.
5. There is severe exposure to dust and dirt.

Paper 50-9, recommended by the AIEE Industrial Power Systems Committee and approved by the AIEE Technical Program Committee for presentation at the AIEE Winter General Meeting, New York, N. Y., January 30–February 3, 1950. Manuscript submitted April 15, 1949; made available for printing November 22, 1949.

HARVEY J. FINISON was Application Engineer, Industrial Engineering Divisions, General Electric Company, Schenectady, N. Y., at the time this paper was prepared. He now is Assistant Chairman, Electrical Engineering Research, Armour Research Foundation, Chicago, Ill.

Steel Mill Installation Problems

To maintain adequate insulation levels for outdoor structures and over head lines, it is usual to provide insulation levels above actual system voltage and to clean insulators at least once a year, although some require cleaning every three months. Cleaning is expensive and must be accomplished at a time when the parts being cleaned can be taken out of service. Additional circuits or busses may be required in order that those being cleaned may be conveniently taken out of service; or economic compromises may dictate the acceptance of reduced reliability during the cleaning operation.

Substantial freedom from frequent maintenance cleaning can be obtained for the steel mill power system by these methods:

1. Use of metal-enclosed switchgear installed in air-conditioned rooms where necessary.
2. Use of insulated power cable rather than open overhead lines.
3. Use of cable or enclosed bus connection to all transformers.

These methods also improve safety since the entire power system may be enclosed in grounded metal.

Cable

Underground cable gives freedom from adverse weather or other operating conditions, good protection from accidental disturbance, and permits compact construction in and around buildings. It is desirable for steel mill systems although for many areas underground construction is a handicap. For these areas, aerial cable has many advantages:

1. Virtual elimination of lightning problems.
2. Ability to construct a line close to or even hung from building structures.
3. Elimination of insulator cleaning.
4. Improved safety.

For aerial cable overinsulation is not required, since the steel mill service has little more serious effects than service in any other industry. Additional savings in lightning arresters, reduced space and congestion at the power house and other terminations, and the reduced main-

Table I. Ratings of Circuit Breakers Applicable to Steel Mill Systems

List Applies to Circuit Breakers Used in Metal-Enclosed Equipments and Includes Only Those Most Frequently Applicable

Interrupting Rating in 3-phase, Thousands of Kilovolt-Amperes at Rated Voltage	Voltage: Rating, Kilovolts	Voltage: Minimum Operating Kilovolt-Amperes at Rated Kilovolt-Amperes	Current Ratings: Continuous at 60 Cycles	Current Ratings: Momentary in Rms Total Amperes	Interrupting Rating in Rms Total Amperes: At Rated Voltage	Interrupting Rating in Rms Total Amperes: Maximum Rating
500*	15	6.6	1,200 2,000	80,000	20,000	44,000
1,000	15	10.5 9.7	1,200 3,000	90,000 100,000	40,000 40,000	55,000 60,000
1,500	15	10.8	2,000 4,000	130,000	60,000	80,000
1,000	34.5	19.3	1,200	60,000	17,000	30,000
1,500	34.5	21.6	1,200 3,000	70,000	25,000	40,000

* Oilless mange-blast vertical lift. All others are air-blast station type.

Figure 1 (Left). Typical installation of metal-clad switchgear with oilless-type current circuit breakers in a motor room in a steel plant

(Right). Station-type switchgear with air blast circuit breaker of 1,000-megavolt-ampere interrupting rating

tenance make aerial cable compare favorably in cost with open overhead lines.

Switchgear

The economics of switchgear application will be a major factor in selection of voltage levels and in the arrangement of the steel mill electric power system. A summary of the characteristics of the types of circuit breakers that will be considered is given in Table I. Only indoor types with steel enclosures are included in this list since these will permit obtaining a safe reliable system with freedom from the frequent insulator cleaning required for outdoor types in steel mill areas. The 500-megavolt-ampere interrupting rating circuit breaker listed is of typical metal-clad construction and of the oilless type. See Figure 1. The 1,000- and 1,500-megavolt-ampere circuit breakers listed are station-type switchgear in steel cubicles and of air-blast type of operation. Figure 1 (left) shows a typical installation.

System without Current Limiting Reactors

Consider that a steel mill electric power system is solidly tied together without use of reactors to limit short-circuit currents, and assume that the system is in a small area so that impedance of interconnecting lines may be neglected. What is the maximum system capacity that may be connected into such a solidly tied system without exceeding the short-circuit ratings of the different circuit breakers?

Figure 2 shows the assumed constants used for calculating the short-circuit currents to obtain the answer to this question. Included are generators and motor loads of typical capacity and reactance. Frequently part or even all of the capacity here represented as a generator may be a tie to an electrical utility; where the tie is through a transformer, the reactance value shown would still be representative. Where the utility tie is direct to a main power station at the steel mill voltage level this may not be a good assumption, since there may be little impedance to limit the fault current delivered by the electrical utility system.

Figure 3 shows the results of calculations to determine short-circuit currents for systems of various capacities by methods described in references 1, 2, and 3. Shown in Figure 3(A) is the momentary current rating required of circuit breakers to be used on the system. Figure 3(B) shows the interrupting duty in megavolt-amperes. Shown at the right of each chart is the corresponding rating of circuit breakers selected from Table I. The size of the circuit breaker is designated in terms of its interrupting rating in megavolt-amperes. These charts will give the maximum system capacity that can be allowed for each of the circuit breaker ratings shown.

For example, what is the largest system capacity at 6,900 volts that can be allowed for 500-megavolt-ampere switchgear? Figure 3(A) shows that a system capacity of 38,000 kva will give a momentary short circuit current of 80,000 amperes, the maximum rating of the 500-megavolt-ampere switchgear. Figure 3(B) shows that 500-megavolt-amperes interrupting rating would permit application on a system up to 45,000 kva.

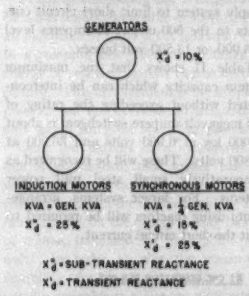

Figure 2. Constants of steel mill power system assumed for short-circuit calculations

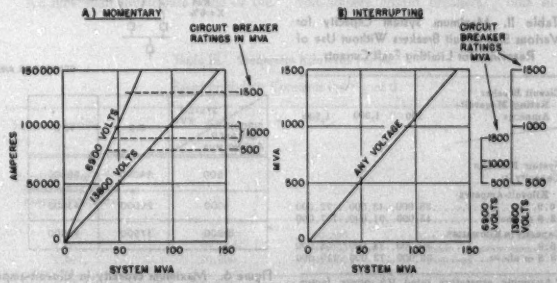

Figure 3. Results of short-circuit calculations on typical system with no impedance in tie circuits

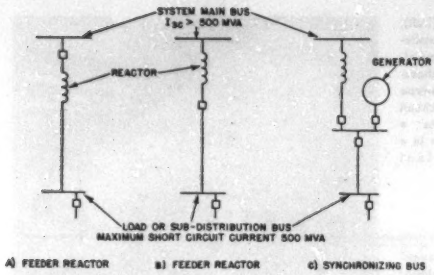

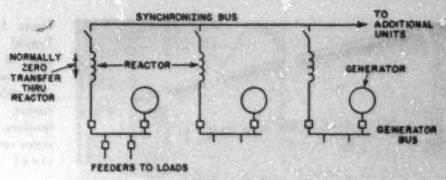

Figure 4 (left). Use of reactors to limit short-circuit current

Figure 5 (above). Typical synchronizing bus arrangement

For this example the momentary short-circuit current is the limiting factor and the maximum system capacity permissible for the 500-megavolt-amperes switchgear would be 38,000 kva.

Similar maximum system capacities for the other circuit breaker ratings are summarized in Table II. For 13,800 volts and above the momentary duties do not approach the momentary rating of the switchgear and interrupting duty is the limiting application consideration. The more limited ability to expand power systems at 6,900 volts as compared with 13,800 volts and higher is emphasized by Table II.

These statements do not mean that for systems smaller than the limits listed in Table II it would be possible to arrange the system without consideration of the arrangements that would be required by expansion beyond those limits. It should be the objective to arrange the system in such a manner that it can be conveniently expanded as may be required by any future needs.

Short-Circuit Level at Loads

In a steel mill there will be appreciable utilization equipment and considerable distribution at either the 6,600- or 13,200-volt level. For switching load and distribution circuits 500-megavolt-amperes metal-clad switchgear is now, and is likely to continue to be, the most popular switchgear.

In general, it will be found uneconomical to use higher than 500,000 kva interrupting capacity circuit breakers for this service and there appears to be no requirements indicating that a higher capacity will be required. Therefore, we must consider an arrangement of a power supply system to limit short-circuit currents to the 500-megavolt-amperes level at 6,900- or 13,800-volt busses.

Table II shows that the maximum system capacity which can be interconnected without exceeding the rating of 500-megavolt-ampere switchgear is about 30,000 kw at 6,900 volts and 36,000 at 13,800 volts. These will be recognized as comparatively small steel mill power systems. For larger systems, arrangements using reactors will be required to limit the short-circuit current.

Table II. Maximum System Capacity for Various Size Circuit Breakers Without Use of Reactance for Limiting Fault Currents

Circuit Breaker Rating, Megavolt-Amperes	500	1,000	1,500
System Kilovolts Capacity in			
Kilovolt-Amperes			
6.9	38,000	43,000	72,000
13.8 or above	45,000	91,000	137,000
Capacity in Kilowatts*			
6.9	30,000	34,000	58,000
13.8 or above	36,000	73,000	110,000

* Assuming generators rated 0.8 power factor. Figures are rounded.

Use of Reactors to Limit Fault Currents

Figures 4(A) and 4(B) show arrangements using feeder reactors. In Figure 4(A) the reactor is shown on the load side of the feeder circuit breaker and hence the feeder circuit breaker must have a suitable rating to interrupt the full available short-circuit current. In Figure 4(B) with the reactor on the bus side of the circuit breaker, economies could be realized in the feeder circuit breaker rating but the reactor represents an undesirable exposure of the bus and does not lend itself to good physical arrangement of the switchgear. Figure 4(C) shows a typical synchronizing bus arrangement with a reactor between the synchronizing bus and the generator bus. This arrangement gives a more direct path for flow of power from supply to load and provides a number of advantages over feeder reactors: lower kilowatt loss; lower kilovar loss; better voltage; permits low capacity feeder circuit breakers (low cost and less space); and usually fewer reactors and hence less space in the powerhouse.

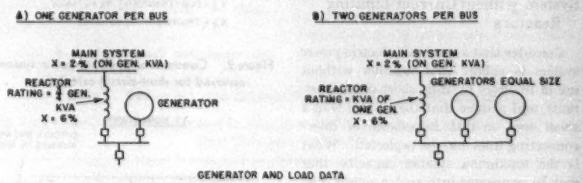

GENERATOR AND LOAD DATA

CIRCUIT BREAKER RATING MVA \ SYSTEM KV	6.9	13.8
500	24000	25000
1000	26000	43000
15000	37500	72000

CIRCUIT BREAKER RATING MVA \ SYSTEM KV	6.9	13.8
500	26000	27000
1000	29000	55000
1500	40000	83000

Figure 6. Maximum capacity in kilovolt-amperes that may be connected to one bus in synchronizing bus arrangement

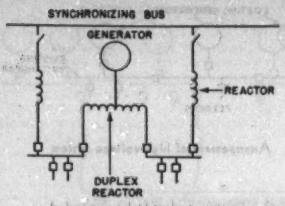

Figure 7. Use of a duplex reactor to divide the capacity of a large generator between two busses

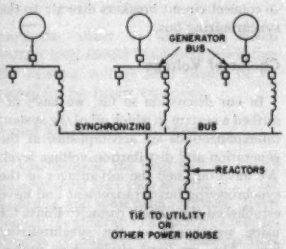

Figure 8. Method of connecting to utility or other powerhouse

In the normal synchronizing bus arrangement best performance is obtained when the load requirements and generator capacity are fairly closely matched so that there is normally little power or reactive transfer across the reactance tie to the synchronizing bus.

In response to load changes, the no load voltage of the generator may be raised or lowered by action of its voltage regulator to maintain substantially constant voltage on the bus for all load conditions.

In the feeder reactor arrangement all current must pass through the reactor and some voltage variation will be experienced as the load magnitude and power factor vary. Wide fluctuations in load and the starting of large motors may make this a serious consideration for steel mills.

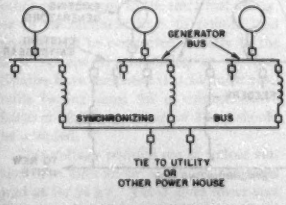

Figure 9. Circuit breakers connected directly to synchronizing bus

Figure 10. Geographical plan of typical steel mill areas

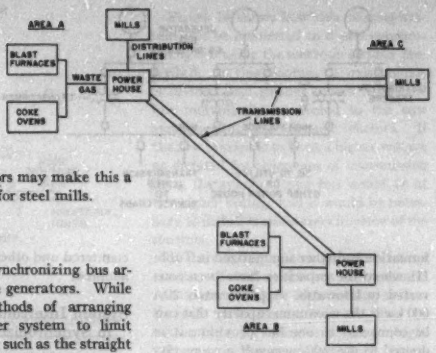

Synchronizing Bus

Figure 5 shows a synchronizing bus arrangement with three generators. While there are other methods of arranging reactance in a power system to limit short-circuit currents, such as the straight bus or ring bus with sectionalizing reactors, the synchronizing bus gives superior performance in almost every respect.

By far the outstanding advantage of the synchronizing bus arrangement is the unit simplicity or unit organization obtained for the system. This feature contributes the following benefits: ease of understanding, and ease of expanding the system.

In the synchronizing bus arrangement, each bus section is capable of operating as an independent unit, yet it is simply tied to a common bus where interchange of energy or reactive current can be accomplished. This arrangement is the simplest possible for the operator to understand and makes for good operating practices.

Once the pattern of a synchronizing bus is established, new busses can be added without greatly affecting the fault current on any of the existing busses. The fault current on the synchronizing bus is, of course, increased for each additional unit. In order to give the maximum flexibility for future expansion, it is usually desirable to make the momentary current rating of the bus considerably above that which is actually required for the installation as currently planned.

We now shall investigate some of the boundaries of application of a synchronizing bus arrangement with regard to system capacity and the capacity connected to each generator bus. We must first determine the approximate maximum amount of generating capacity that can be connected to each generator bus. A portion of this capacity might be a utility tie if the utility supply is the normal supply for the load connected to the bus. Figure 6 shows one arrangement with one generator on the bus and another with two equal size generators per bus. It is assumed that it would be undesirable to use a reactor in the tie to the synchronizing bus in excess of approximately 6 per cent based on maximum kilovolt-amperes expected to be transmitted through the reactor.

A multiple number of generators on the bus has the advantage that if one is out of service, a smaller amount of power and reactive current may be transmitted across the reactor and hence voltage under abnormal conditions will be better.

Shown in Figure 6 are tables giving the maximum permissible kilovolt-ampere capacity for 500, 1,000, and 1,500-megavolt-ampere circuit breakers. This in-

Table III. Generator Kilowatts Per Bus

Based on System Constants Per Figure 6

System Kilovolts / Circuit Breaker Interrupting Rating, Megavolt-Amperes	6.9	13.8	
500	20,000*	20,000	Use without feeder reactors
1,000	20,000*	40,000	Feeder reactors normally required
1,500	30,000	60,000	

* Capacity figures are rounded. Calculations gave 19,200 kw for 500 megavolt-ampere and 20,700 for 1,000 megavolt-ampere circuit breakers at 6.9 kv.

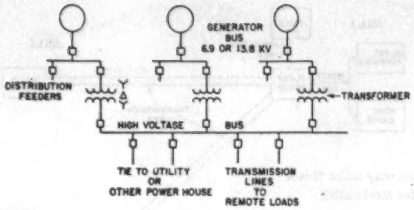

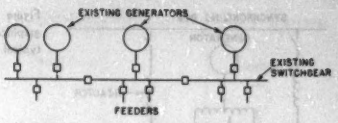

Figure 11 (left). Arrangement of high-voltage system

Figure 13 (above). Existing system to be expanded

formation is further summarized in Table III where the capacities have been converted to kilowatts. Approximately 20,000 kw is the maximum capacity that can be connected to one bus providing it is desired to use 500-megavolt-ampere circuit breakers on that bus and to avoid use of feeder reactors. Additional capacity can be connected to one bus providing larger circuit breakers are used and providing feeder reactors are added in the feeder or subdistribution circuits. There appears to be little advantage in using circuit breakers of 1,000 megavolt-amperes at 6,900 volts, and hence either 500-megavolt-ampere or 1,500-megavolt-amperes circuit breakers would be used at 6,900 volts. It should be recognized that heavy short-circuit currents at the 1,500-megavolt-ampere level at 6,900 volts may impose serious problems in keeping the thermal and mechanical ability of all parts of the system sufficiently high to withstand the short-circuit currents until they are cleared by the circuit breakers.

The maximum of 20,000 kw per generator bus does not imply that generators of larger than 20,000 kw could not be used with 500-megavolt-ampere switchgear. Figure 7 shows how the capacity of one generator may be divided between two busses by use of a duplex reactor.[4] However, it is doubtful if there are many requirements for this arrangement. Normally, higher voltage systems will be required when large generators are encountered and other arrangements will be adopted.

System Interconnections to Synchronizing Bus

In the synchronizing bus scheme it is usually desired to approximately balance the generating capacity with its corresponding load and normally there is little transfer through the reactor. Interconnections, such as a tie to an electrical utility or a tie to another power station, may not closely relate to any of the individual loads. Hence they should be connected to the synchronizing bus as shown in Figure 8. Circuit breakers are ordinarily required in order to protect the tie lines or tie transformers. Reactors are necessary to limit the fault current to the rating of the circuit breakers.

In some cases it may be desired to eliminate these reactors and connect larger circuit breakers directly to the synchronizing bus, Figure 9. Here a limit on the size to which the system can grow has been imposed by the rating of the circuit breakers connected to the synchronizing bus. Table IV gives the maximum system capacity that can be achieved without exceeding the rating of certain size circuit breakers when connected to the synchronizing bus. At a voltage of 13.8 kv or above and with 1,500-megavolt-ampere circuit breakers, a total system capacity of 200,000 kw can be achieved. At 6,900 volts the limit is 110,000 kw. For larger systems it would not be possible to connect circuit breakers directly to the synchronizing bus.

Choice of Voltage

In our discussion so far, we have described a system in which all of the system interconnections are accomplished at the generation and distribution voltage level. We have outlined the advantages of the synchronizing bus arrangement and have established the system capacity limits for using switchgear on the synchronizing bus. Also, we have obtained an understanding of the approximate amount of generating capacity that can be connected to each generator bus.

This information would be directly applicable to a system having approximately the geographical plan shown in Figure 10 for Area A. In this case the powerhouse is located close to the blast furnaces and all electric loads are in the same area. System voltage would be either 6,900 or 13,800. The 6,900-volt level would give the lower cost for the large motors. The 13,800-volt level would give lower cost for the distribution lines and switchgear (due to lower current). The higher voltage also permits use of circuit breakers directly connected to a synchronizing bus on larger systems than would be possible at 6,900 volts.

These factors must be evaluated for the

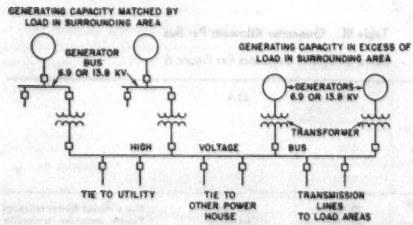

Figure 12. Method of connecting generators not supplying local loads

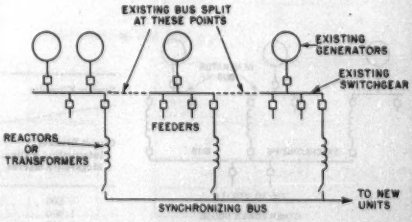

Figure 14. Method of expansion by subdivision of existing system and connection to synchronizing bus

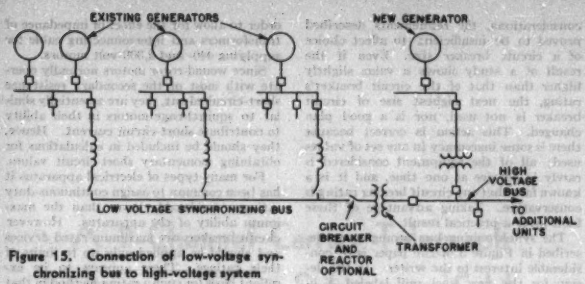

Figure 15. Connection of low-voltage synchronizing bus to high-voltage system

particular plant to determine which voltage level should be adopted or whether the existing voltage level should be retained for the future expansion.

Need for Higher Voltages

Now suppose the steel mill comprises an additional area such as Area B similar to Area A and some distance away. Even though the generators at each area may be capable of supplying the load in that area, it may be desirable to tie the two systems together in order to reduce the total requirements for reserve capacity. The requirement for interconnecting the two powerhouses with transmission lines brings a desire for a higher voltage in order to reduce the cost and losses for the transmission line.

Let us add an additional area such as Area C to our steel plant and assume that this area incorporates only steel working capacity and hence is an electric load with no power-generating facilities. Now, the only way to supply this is by a transmission line and if the distance is great, there is a definite need for use of higher voltage for lower cost, lower losses, and lower voltage regulation.

Figure 11 shows a method of interconnecting the system at a higher system voltage with the synchronizing bus arrangement. Each generator bus is connected to the tie or synchronizing bus through a transformer. The tie to the other powerhouse, to the electrical utility, or to transmission lines to remote load areas would be connected directly to the high voltage synchronizing or tie bus. Studies have indicated that for most steel mills having need for a voltage above 6,900 or 13,800, a voltage of 33 kv should be adopted.

This voltage permits use of indoor station-type switchgear at almost the same cost as for 22 kv. Yet it gives lower cost for transmission lines. A higher voltage will require use of outdoor structures and usually will not give lower transmission line cost except for very large systems requiring transfer of appreciable power.

In some cases it may be desirable to adopt a utility transmission voltage where a tie is made to the utility, although this may mean an outdoor structure at higher than 33 kv and higher interrupting rating for switchgear.

At 33 kv with indoor-station type switchgear an interrupting rating of 1,500 megavolt-ampere will usually be best.

In some instances the power supply capacity at one of the powerhouses may considerably exceed the load in that area due to the availability of waste fuel. Generators not matched by local load should be connected directly to the high-voltage bus through transformers, as shown in Figure 12.

Expansion of Existing Systems

The arrangements which have been described may be used not only for new systems but also for modernization or expansion of existing systems. Figure 13, with a number of generators connected to a straight bus, is typical. The addition of new capacity may increase the short-circuit duty above the rating of the existing switchgear.

Table IV. Maximum System Generating Capacity in Kw for Circuit Breakers on Synchronizing Bus

System Kilovolts	6.9	13.8 or above
Circuit Breaker Rating, Megavolt-Amperes		
500	70,000	70,000
1,000	80,000	140,000
1,500	110,000	210,000

Calculation based on system shown by Figure 6.

Figure 14 shows how this existing system can be connected to a new synchronizing bus using the methods already prescribed. In this diagram the existing bus is divided into smaller busses with each bus individually connected to the new synchronizing bus through reactors. If the new system is to be at a higher voltage as dictated by economies of transmission lines, the synchronizing bus would be at the higher voltage and it would be necessary to install transformers in place of the reactors.

If the existing system is broken into a number of individual bus sections and each connected to a high-voltage system through transformers, the cost may be rather high for transformers and high-voltage switchgear. Where both the existing and the new high-voltage system have load and capacity that match and each has reserve capacity, it may be acceptable to form a low-voltage synchronizing bus and connect it to the high-voltage bus through a single transformer, as shown in Figure 15.

References

1. System Short-Circuit Currents, W. M. Hanna, H. A. Travers, C. F. Wagner, C. A. Woodrow, W. F. Skeats. *Electrical Engineering (AIEE Transactions)*, volume 60, September 1941, pages 877–81.

2. Simplified Calculation of Fault Currents, AIEE Committee Report. *Electrical Engineering (AIEE Transactions)*, volume 61, October 1942, pages 1133–35.

3. Revisions Made to Simplified Calculations of Fault Currents. *Electrical Engineering*, February 1944, page 65.

4. The Duplex Reactor and Its Application, E. G. Merrick. *General Electric Review* (Schenectady, N. Y.), September 1944.

Discussion

S. Ein (Armco International Corporation, Chicago, Ill.): The matter contained in the paper can be used with considerable profit by power and steel mill engineers. The author has used an approach which is different from the usual one as far as the writer knows. The following discussion is not critical of the paper but is an elaboration of some points of interest to the writer.

It has been the writer's experience in several steel mills on which he had made many short-circuit studies that the proportion shown in Table I of the discussion exists between synchronous motors and generators.

Induction motors are not included by the writer in short-circuit studies. With few exceptions, the induction motors connected directly to the 13,800- and 6,900-volt busses discussed in the paper are wound-rotor motors. This type of motor operates with the external resistance of the slip regulator in the rotor circuit. Reports by one of the larger electrical motor manufacturers, based on tests, show that wound-rotor motors have

Table 1. Steel Mill Motors and Generators

Steel Mill	Synchronous Motors, Kva	Generation, Kva	Proportion, Per Cent
L*	57,100	108,700	53
R*	176,000	314,000	56
S**	57,700	93,800	62
Total	290,800	516,500	56
Paper			25

*L and R are very large steel mills now in existence and interconnected electrically.
**S is a small steel mill in the planning stage.

such a fast decrement that these motors can be neglected when momentary current is concerned.

This is not true where squirrel-cage induction motors are concerned if connected to the 13,800- and 6,900-volt busses. However, this type of motor is usually of such small size that if used at these voltages the cross-section of the coils becomes small and the coils will not withstand full-voltage starting and, in some cases, reduced-voltage starting. Therefore, the motors are used at 2,300 and 460 volts. This requires transformers which introduces reactance between the motors and the fault, and with the reactance of the lines on either side of the transformer, the momentary current is reduced to such an extent that neglect of the contribution of the motors to the fault causes only a comparatively small error when compared to the total duty. This reduction is partially compensated for by the increase in short-circuit kilovolt-amperes resulting from neglect of small reactances of short lines, busses, current transformers, and such minor items.

In short-circuit studies of motors conducted since 1935 in accordance with these considerations, the refinements described proved to be insufficient to affect choice of a circuit breaker size. Even if the result of a study shows a value slightly higher than that of the circuit breaker's rating, the next highest size of circuit breaker is not used, nor is a good plan changed. This action is correct because there is some inaccuracy in any set of values used; all of the equipment considered is rarely in service at one time, and it is a known fact that any circuit breaker rating is conservative. Taking advantage of these facts gives a practical result.

The synchronizing bus arrangement described in Figure 5 of the paper is of considerable interest to the writer. In the design for the new steel mill labeled *S* in Table I of the discussion, the original plan called for a continuous power station bus with 1,500,000-kva station-type circuit breakers and feeder reactors. The writer suggested a synchronizing bus which permitted the use of 500,000-kva metal-clad circuit breakers and eliminated the need for the feeder reactors. This latter plan, similar to Figure 5 of the paper, was adopted with a consequent prospective large monetary saving.

H. J. Finison: Mr. Ein's comments on the paper are very much appreciated. The availability of information on motor loads as supplied by Mr. Ein is very helpful for general systems studies of the type described in my paper. A discussion of the other comments by Mr. Ein follows.

In the study described in the paper, the subtransient reactance of induction motors was assumed to be 0.25 per unit which is higher than most high-speed induction motors. This assumption was made in order to allow for the effect of impedance of transformers and interconnecting cable for supplying 440- and 2,300-volt motors.

Since wound-rotor motors normally operate with most of the secondary resistance short-circuited out, they are essentially similar to squirrel-cage motors in their ability to contribute short-circuit current. Hence, they should be included in calculations for obtaining momentary short-circuit values.

For many types of electrical apparatus it has been common to assign continuous-duty ratings considerably lower than the maximum ability of the apparatus. However circuit breakers are maximum rated devices and should be applied only up to limits of their ratings. There appears to be excellent basis for such a rating method in that it permits the allocation of any safety margins by the person making the application.

Too often where ratings are not assigned at the maximum, safety margins may be adopted by both the designer and the system engineer. However, the system engineer must recognize his responsibility for not exceeding the maximum ratings assigned by the designer.

On low-voltage systems some reduction from calculated fault currents might be expected due to busses, connections, and so forth, which are not included in the calculation.

On high-voltage systems the effect of these will be relatively small, and it is possible that errors in data on machines and circuit impedance may be in a direction to give higher than calculated fault currents. Thus the system engineer can achieve true safety only by applying circuit protective equipment on systems where the available short-circuit current does not exceed the manufacturer's assigned ratings.

A 2-Channel Carrier Telegraph System for Short Submarine Cables

E. L. NEWELL
MEMBER AIEE

C. H. CRAMER
MEMBER AIEE

Synopsis: A new 2-channel carrier telegraph system for short submarine telegraph cables is described. Developed specifically for the Western Union Key West—Havana cables, about 100 nautical miles in length and with attenuations up to 80 decibels at 1,000 cycles per second, it utilizes standard land-line frequency-modulation channel terminal equipment and provides excellent 50-cycle telegraph transmission on both channels without appreciably degrading the physical circuits. Depending upon the facilities available the carrier may be operated either as a metallic or a ground-return circuit.

THE narrow useful frequency spectrum on submarine telegraph cables restricts the use of frequency-division methods of channelization. This is evident when it is noted that, of the transatlantic cables, the nonloaded types have attenuations of about 100 decibels at 15 to 20 cycles per second and the loaded cables have attenuations of the same order at 100 cycles. Where channelization is desirable on long cables use is made of electromechanical time-division multiplex methods.

The submarine telegraph cable network also includes cables of shorter lengths, ranging down to 100 nautical miles or less, which serve as connecting links in long circuits or provide direct traffic facilities such as those to or between islands. The connecting links originally were, and in some cases still are, operated at the speeds of the related long cable sections and thus below their potential signaling capacities. The direct facilities have been more fully developed under the compulsion of increasing traffic loads.

In recent years signal-shaping amplifiers have been installed rather generally on the connecting cables of some cable systems, making higher physical-circuit operating speeds available. As a result channels of separate long cables may be combined for transmission on the connecting links through use of modern time-division multiplex methods, involving devices such as the channel repeater.

Low frequency carrier circuits also are in use on a number of short cables in various cable systems. The limited use of carrier in the Western Union cable plant includes one early installation in which the cable is 326 nautical miles in length; the physical circuit can be operated at dot frequencies up to 30 cycles; the superposed circuit, in one direction only, with a carrier frequency of 90 cycles, is operated at a speed of 31 cycles. Another application of carrier, to which further reference is made in this paper, involves cables about 100 nautical miles in length and provides a 1-way channel with a carrier frequency of 300 cycles and an operating speed of 35 cycles.

Although the traffic requirements prevailing from time to time have been satisfied in the manner outlined previously, present utilization of the useful frequency spectrum of the short cables cannot be regarded as efficient. Consideration of means for attaining optimum efficiency inevitably leads to time-division multiplex methods. Because of mechanical limitations the multiplex system long in use on land-line and cable d-c telegraph circuits is not suitable for the high speeds implied. Perfection of electronic time-division systems, currently under intense development for radio applications, may well provide the ultimate solution at the bottom of the frequency spectrum also. In the meantime modern frequency-division methods and equipment, already in an advanced stage of development, are available and a recent carrier installation on the Western Union Key West—Havana cables has yielded a substantial increase in message capacity.

The Key West—Havana Cables

Western Union wire facilities to Cuba consist of three single-core submarine cables between Key West and Havana, each about 100 nautical miles in length. The physical circuits are operated as ground-return polar differential duplexes. Because of the high cable attenuation, the receiving terminals utilize the principle of the well-known Gulstadt vibrating relay to insure adequate sensitivity for the low-level received signals. The normal assignments are 3-channel multiplex circuits.

For some years the physicals were supplemented with two 1-way southbound carrier channels, each having a carrier frequency of 300 cycles per second and utilizing amplitude modulation. One channel was superposed on two of the cables as a metallic circuit, the second as a ground-return circuit on the third cable. The high attenuation of the cables and the state of the carrier art when the original system was installed made it impracticable to provide additional channels through the use of higher frequencies.

Recently a need for additional telegraph facilities to Cuba became evident. In view of improvements in carrier telegraphy it was decided to undertake the development of a new system which would provide two 2-way channels of higher transmission quality. The type *C-3* carrier system resulting from that development, and described in this paper, was installed at Key West and Havana in the early part of 1949.

Paper 50-10, recommended by the AIEE Telegraph Systems Committee and approved by the AIEE Technical Program Committee for presentation at the AIEE Winter General Meeting, New York, N. Y., January 30–February 3, 1950. Manuscript submitted October 19, 1949; made available for printing November 22, 1949.

E. L. NEWELL and C. H. CRAMER are with the Western Union Telegraph Company, New York, N. Y.

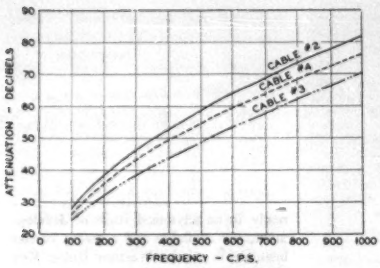

Figure 1 (left). Attenuation of Key West—Havana cables

Figure 2 (right). Sending-end impedance of Key West — Havana cables, Key West end

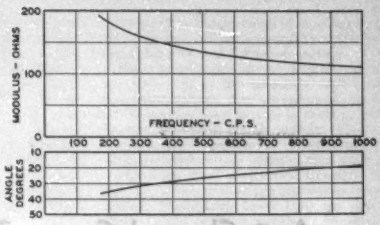

Table I. Characteristics of Key West—Havana Cables

Cable	Length Nautical Miles	*Major Core Types	Total Resistance Ohms	Total Capacity Microfarads
2 KZ-HVA	105	107/140	988	31.2
3 KZ-HVA	98	160/166	675	35.2
4 KZ-HVA	96	130/130	775	30.5
Key West Undergrounds	0.89		23	0.15
Havana Undergrounds	4.44		70	2.0

* Pounds per nautical mile of copper and gutta percha.

Carrier System Requirements

When this project was initiated, traffic considerations required that the proposed carrier system should:

1. Provide two 2-way channels, each suitable for 35-cycle multiplex operation or for teleprinter operation.

2. Permit operation of the physical circuits as 3-channel multiplexes with the existing differential duplex equipment or as 4-channel multiplexes with resistance-bridge duplex circuits and signal-shaping amplifiers.

3. Be capable of operation as a metallic circuit over any two of the three cables, thus providing some protection against cable failure.

Cable Characteristics

The three Key West—Havana cables, *2, 3,* and *4 KZ-HVA*, are single-core, nonloaded cables lying about ten miles apart over most of their length. Each cable is a composite of several different types of cable. The general characteristics are given in Table I.

The receiving earth in all cases is carried back from the office through the underground to the cable hut at the beach on a conductor paired with the cable conductor.

The attenuation and impedance characteristics of the three cables, including the undergrounds, are shown in Figures 1 and 2. The attenuation characteristic of any two cables taken as a metallic circuit may be approximated by averaging the values of the selected cables. With attenuations of 38 to 46 decibels at 300 cycles, and 70 to 82 decibels at 1,000 cycles, these cables approach the attenuation characteristics of 16-gauge paper-lead cable. The total attenuation is about three times that encountered in a typical land-line carrier section. As a metallic circuit, the conductors of the submarine section are unbalanced and unpaired, conditions which, in a land-line carrier system, usually result in intolerable interference levels but are here largely offset by the shielding effect of the sea water.

Description of Carrier System

The *C-3* carrier system is shown schematically in Figure 3. It utilizes the frequency-modulation channel terminals[1] standardized by Western Union and widely installed in the land-line carrier systems.

The channel terminal comprises two units, one a sending-receiving filter panel, and the second a transceiver which combines the electronic transmitting and receiving functions. Standard mid-channel frequencies are used, 375 and 525

Figure 3. Block diagram of carrier system terminal

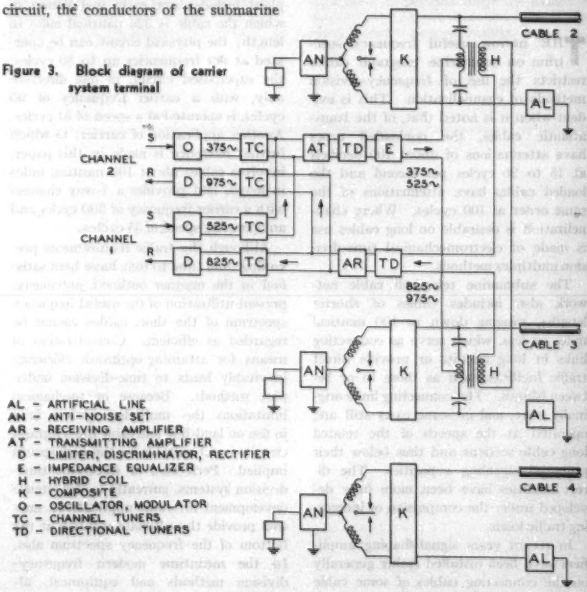

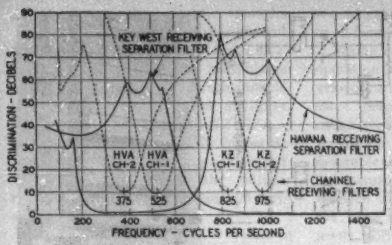

Figure 4 (left). Receiving filter characteristics

Figure 6 (right). Frequency characteristics of composites and antinoise sets

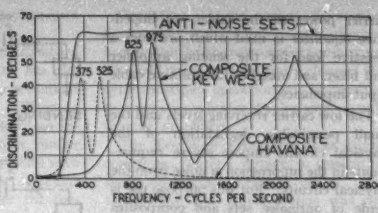

cycles for southbound transmission, and 825 and 975 cycles for northbound transmission. The channels have a bandwidth of 80 cycles and are spaced at 150-cycle intervals, with one channel omitted to facilitate directional separation. Frequency modulation of the transmitted carrier is accomplished by raising and lowering the mid-channel frequency 35 cycles to send spacing and marking impulses, respectively. This type of channel terminal is designed for operation at a maximum dot frequency of 35 cycles per second in land-line installations where two or more carrier systems may be operated in tandem. In such cases, the additive effects of successive channel filters narrow the channel bandwidth and thus limit the maximum signaling speed. The present application involves only a single carrier section and the channel bandwidth is sufficient under these conditions for a dot frequency of 50 cycles per second provided other factors, such as interference levels, are favorable.

Figure 5. System power levels

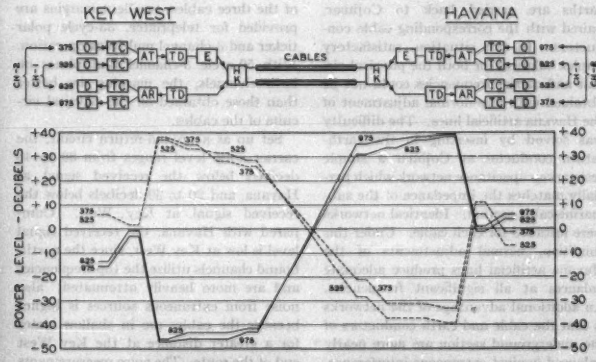

The channel terminals as used in the *C-3* system are standard in most respects. Minor wiring modifications in the transceivers adapt them to the power supplies at Key West and Havana and discard the half-duplex and repeater facilities which are not required in this instance. In the standard channel terminal, the sending and receiving channel carrier frequencies are alike while in the *C-3* system the sending and receiving frequencies differ.

Other components of the *C-3* system are: the hybrid coils which couple the carrier equipment to the cables, and the receiving amplifier, both of standard land-line type; sending amplifier, directional separation filters, impedance equalizer, antinoise set and composite, and leg circuit equipment, all of special design.

Directional separation of the channels is secured in part by frequency discrimination and to a lesser degree by the duplex balancing action of the hybrid coils. With different channel frequencies in the two directions, some directional discrimination is provided by the channel filters. The additional frequency discrimination required is obtained by the use of separation filters with cutoff in the 150-cycle guard band, located between the northbound and southbound channel frequencies. Characteristics of the channel receiving filters and the receiving separation filters are shown in Figure 4. The characteristics of the corresponding sending filters are generally similar. With cable attenuation up to 80 decibels, it is necessary to provide a total maximum discrimination of 110 decibels between sending and receiving channels to maintain crosstalk interference at 30 decibels below the received signal level. Under practical operating conditions, the discrimination resulting from the balanced hybrid coil arrangement may not be more than 10 decibels. The discrimination supplied by the channel filters amounts to about 80 decibels, nominally leaving 20 decibels to be provided by the separation filters. However, the channel filters do not protect the receiving amplifier, common to both channels, against overload by the sending frequencies and their modulation products. As shown in the system power level chart, Figure 5, the sending power level is high, about plus 38 decibels per channel or a total of 42 decibels (referred to zero power level of 1.0 milliwatt) and for that reason the separation filters must actually provide discrimination of some 60 decibels.

To provide the high sending carrier level, the transmitting amplifier has greater gain and power output than the corresponding amplifier standard in the land-line system. It consists of two push-pull stages, with three *25C6* tubes in parallel on each side of the output stage, and delivers 17 watts. By using about 20 decibels of combined voltage and current feedback, the total harmonic distortion is limited to one per cent and most of this is at frequencies outside the pass bands of the channel filters.

The cable capacitance combined with the capacitors used to couple the carrier system to the cables result in a highly reactive sending-end impedance at carrier frequencies. For efficient transfer of

carrier power to the cables, an impedance equalizer is used which provides a resistive load for the sending amplifier and filter, and matches the reactive cable input impedance.

The low carrier receiving levels and the small permissible degradation of the physical circuits impose severe requirements in the suppression of noise from the physical circuits. For this purpose use is made of antinoise sets and composites having the characteristics shown in Figure 6. The anti-noise sets are low-pass filters in the apexes of the physical circuits with cutoff at about 200 cycles and providing discrimination of over 60 decibels against carrier-frequency components of the physical circuit signals. The composites provide maximum discrimination against the physical circuit signals at the frequencies of the carrier channels. A total discrimination of over 100 decibels is thus obtained while the insertion loss in the physical circuits for frequencies below 150 cycles is less than three decibels. Corresponding values in land-line circuits are 50 decibels and 10 decibels.

High frequency noise components are generated by the motion of the armatures of the receiving relays of the physical circuits. This noise, unless suppressed, may overload the carrier receiving amplifier. The band-pass separation filter at Havana provides the necessary suppression, which, however, is lacking in the high-pass separation filter at Key West. At that terminal the suppression is accomplished by including in the composites an attenuation section centered at about 2,150 cycles.

In the land-line system, relays for transmitting and receiving have been eliminated in the channel terminals and the transceivers function entirely electronically with single-current telegraph impulses in the leg circuits. This simplification became practicable in the domestic telegraph plant with the vast expansion of carrier operation and the concurrent decline in d-c grounded and metallic facilities. Circuit extensions at Key West and Havana are not yet compatible with such simplification, and the *C-3* system includes intermediate relays in both the sending and receiving legs so that leg-circuit operation may be either single-current or polar. As shown in Figure 7, each leg circuit is provided with sounder and key and means for connecting a teleprinter for monitoring purposes. Jacks in the leg and intermediate relay circuits permit the insertion of a meter for measurements of current and signal bias.

While the *C-3* system is designed primarily for operation on a metallic circuit, it is evident that in the event of interruption of two of the three cables, ground-return operation on the remaining cable is greatly to be desired. Networks simulating the cable and artificial line impedances are provided at each terminal and arranged to be substituted for the second cable to maintain proper impedance relations for ground-return operation.

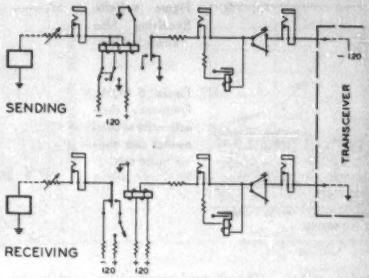

Figure 7 (above). Schematic of telegraph leg circuits

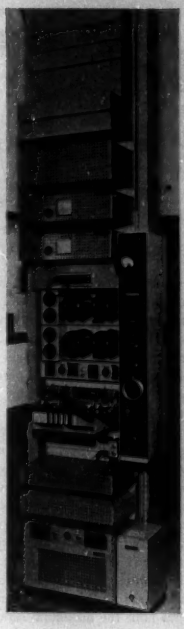

Figure 8 (right). Havana installation

At each terminal, all of the carrier equipment and the antinoise sets and composites are mounted on the two sides of a standard rack. Figure 8 shows the Havana installation.

Test and Performance Data

In Cuba, the submarine cables land at Cojimar and are extended to Havana in underground cable, a distance of 4.44 nautical miles, see Table I. The receiving earths are carried back to Cojimar, paired with the corresponding cable conductors. In this situation, satisfactory duplex balances for both the physical circuit and carrier frequencies could not be obtained with any normal adjustment of the Havana artificial lines. The difficulty was solved by inserting in the earth-return conductor at Cojimar a simple resistance-capacitance network which partially matches the impedance of the submarine cable section. Identical networks were installed for each cable. Under this condition, normal adjustments of the Havana artificial lines produce adequate balances at all significant frequencies. An additional advantage of the networks is that the cable and earth conductors of the underground section are more nearly balanced against extraneous interference. At Key West, where the undergrounds are short, no duplex balance problem was encountered.

With metallic circuit connections, the noise level from all sources at the input to the receiving side of the transceiver is 35 to 40 decibels below the received signal at Havana, and 40 to 45 decibels below the received signal at Key West, depending upon the combinations of cables used. With the carrier superposed on any two of the three cables, excellent margins are provided for teleprinter, 33-cycle polar ticker and 3-channel multiplex operation. With 50-cycle 3-channel multiplexes on both channels, the margins are better than those obtained on the physical circuits of the cables.

Set up as a ground-return circuit, the carrier noise level ranges from 30 to 40 decibels below the received signal at Havana, and 20 to 30 decibels below the received signal at Key West. Compared with Havana, the received signal level is low at Key West, since the northbound channels utilize the top frequencies and are more heavily attenuated; also noise from extraneous sources is higher because the cables are in shallow water for a greater distance at the Key West end of the route. The noise measurements were made during the month of February; somewhat higher levels of natural disturbances, such as lightning, may be ex-

pected during the summer months.

For the greater part of the year, ground-return operation on *3KZ-HVA* and *4KZ-HVA* provides excellent transmission quality on both carrier channels for teleprinter, ticker or 3-channel multiplex. Under similar conditions, *2 KZ-HVA* is less effective by reason of its higher attenuation. Some deterioration of ground-return operation during the summer months is caused by the lightning disturbances.

The performance of the new system in traffic service has amply confirmed the excellent test results. Since completion of the installation, there have been several cable interruptions. During one period, two of the cables were out of service.

Through use of the new carrier, all essential services to Cuba were maintained on the single remaining cable. On another occasion with one cable interrupted, the new system was superposed on one cable while an old-type 300-cycle channel was operated southbound on the second cable, with excellent performance of all facilities.

Traffic experience with ground-return operation of the new system has developed a special circuit arrangement of some practical importance. When a cable is out of service because of an interruption or fault, that cable, under favorable conditions, may be utilized with an operating cable to provide a regular metallic circuit connection for the carrier, thus retaining the low interference levels normal with metallic operation. The nature and location of the fault and its effect on the duplex balance of the faulty cable determine the suitability of this arrangement in specific situations. If the fault is so near to one terminal that the carrier duplex balance cannot be restored readily, the ground-return connection would be used for the carrier at that terminal while the metallic connection could be used at the distant terminal. If the fault is in the midsection of the cable the metallic connection can be utilized at both terminals.

Operation of the polar differential duplex physical circuits is not affected appreciably by the new carrier equipment The field tests indicate that 4-channel 66-cycle multiplex operation will be feasible as a resistance-bridge duplex with signal-shaping amplifiers.

The Key West—Havanac ables utilize core types, Table I, typical in general of short submarine telegraph cables. Although the *C-3* carrier system was developed for specific conditions it is applicable to similar cables for distances not exceeding about 100 nautical miles or attenuations not greater than 80 decibels at 1,000 cycles per second. Modified systems, such as one 2-way channel or one to four 1-way channels, would be suitable for cables of somewhat greater attenuation.

Reference

1. A Frequency Modulation Telegraph Terminal Without Relays, F. H. Cusack, A. E. Michon. *AIEE Transactions*, volume 66, 1947, pages 1165–71.

No Discussion

Control System Synthesis by Root Locus Method

WALTER R. EVANS
MEMBER AIEE

Synopsis: The root locus method determines all of the roots of the differential equation of a control system by a graphical plot which readily permits synthesis for desired transient response or frequency response. The base points for this plot on the complex plane are the zeros and poles of the open loop transfer function, which are readily available. The locus of roots is a plot of the values of s which make this transfer function equal to -1 as loop gain is increased from zero to infinity. The plot can be established in approximate form by inspection and the significant parts of the locus calculated accurately and quickly by use of a simple device. For multiple loop systems, one solves the innermost loop first, which then permits the next loop to be solved by another root locus plot. The resultant plot gives a complete picture of the system, which is particularly valuable for unusual systems or those which have wide variations in parameters.

THE root locus method is the result of an effort to determine the roots of the differential equation of a control system by using the concepts now associated with frequency response methods.[1] The roots are desired, of course, because they describe the natural response of the system. The simplifying feature of the control system problem is that the open loop transfer function is known as a product of terms. Each term, such as $1/(1+Ts)$, can be easily treated in the same manner as an admittance such as $1/(R+jx)$. It is treated as a vector in the sense used by electrical engineers in solving a-c circuits. The phase shift and attenuation of a signal of the form e^{st} being transmitted is represented by $1/(1+Ts)$ in which s in general is a complex number. The key idea in the root locus method is that the values of s which make transfer function around the loop equal to -1 are roots of the differential equation of the system.

The opening section in this paper, Background Theory, outlines the over-all pattern of analysis. The following section on Root Locus Plot points out the great usefulness of knowing factors of the open loop transfer function in finding the roots.

The graphical nature of the method requires that specific examples be used to demonstrate the method itself under the topics: Single Loop Example, Multiple Loop System, and Corrective Networks. The topic Correlation with Other Methods suggests methods by which experience in frequency methods can be extended to this method. The topic Other Applications includes the classic problem of solving an nth degree polynomial. Finally, the section on Graphical Calculations describes the key features of a plastic device called a "Spirule", which permits calculations to be made from direct measurement on the plot.

Background Theory

The over-all pattern of analysis can be outlined before explaining the technique of sketching a root locus plot. Thus consider the general single loop system shown in Figure 1.

Note that each transfer function is of the form $KG(s)$ in which K is a static gain constant and $G(s)$ is a function of the complex number. In general, $G(s)$ has both numerator and denominator known in factored form. The values of s which make the function zero or infinite can therefore be seen by inspection and are called zeros and poles respectively. The closed loop transfer function can be expressed directly from Figure 1 as given in equation 1

$$\frac{\theta_0}{\theta_i}(s)=\frac{K_\mu G_\mu(s)}{1+K_\mu G_\mu(s)K_\beta G_\beta(s)} \tag{1}$$

The problem of finding the roots of the differential equation here appears in the form of finding values of s which make the denominator zero. After these values are determined by the root locus method, the denominator can be expressed in factored form. The zeros of the function θ_0/θ_i can be seen from equation 1 to be the zeros of $G_\mu(s)$ and the poles of $G_\beta(s)$. The function can now be expressed as shown in equation 2

$$\frac{\theta_0}{\theta_i}(s)=K_c s^\gamma\frac{(1-s/q_1)(1-s/q_2)\ldots}{(1-s/r_1)(1-s/r_2)\ldots} \tag{2}$$

The constant K_c and the exponent γ depend upon the specific system but for control systems γ is often zero and K_c is often 1.

The full power of the Laplace Transform[2] or an equivalent method now can be used. The transient response of the output for a unit step input, for example, is given by equation 3

$$\theta_0(t)=1-\sum_{i=1}^{i=n}A_i e^{r_i t t} \tag{3}$$

The amplitude A_i is given by equation 4

$$A_i=\left[\frac{\theta_0}{\theta_i}(s)(1-s/r_i)\right]_{s=r_i} \tag{4}$$

The closed loop frequency response, on the other hand, can be obtained by substituting $s=j\omega$ into equation 2. Fortunately, the calculation in finding A_i or $\theta_0/\theta_i(j\omega)$ involves the same problem of multiplying vectors that arises in making a root locus plot, and can be calculated quickly from the resultant root locus plot.

Paper 50-11, recommended by the AIEE Feedback-Control Systems Committee and approved by the AIEE Technical Program Committee for presentation at the AIEE Winter General Meeting, New York, N. Y., January 30–February 3, 1950. Manuscript submitted November 15, 1948; made available for printing November 22, 1949.

WALTER R. EVANS is with North American Aviation, Inc., Downey, Calif.

The author wishes to express his appreciation for the assistance given by his fellow workers, K. R. Jackson and R. M. Osborn, in the preparation of this paper. In particular, Mr. Osborn contributed the circuit analysis example.

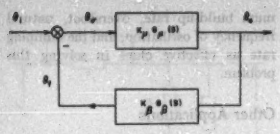

Figure 1 (left). General block diagram

Figure 3 (right). Single loop root locus

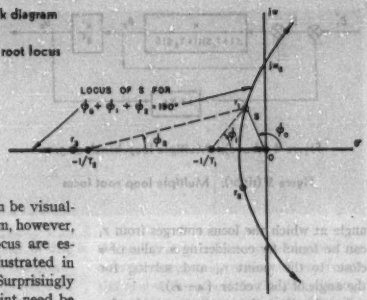

Root Locus Plot

The open loop transfer function is typically of the form given in equation 5.

$$K_\mu G_\mu(s) K_\beta G_\beta(s) = \frac{K(1+T_2 s)[\sigma_3^2+\omega_3^2]}{s(1+T_1 s)[(s+\sigma_1)^2+\omega_1^2]} \quad (5)$$

The parameters such as T_1 are constant for a given problem, whereas s assumes many values; therefore, it is convenient to convert equation 5 to the form of equation 6.

$$K_\mu G_\mu(s) K_\beta G_\beta(s) = \frac{K(1/T_1+s)T_2[\sigma_3^2+\omega_3^2]}{s(1/T_1+s)T_1[(s+\sigma_3+j\omega_3)(s+\sigma_3-j\omega_3)]} \quad (6)$$

The poles and zeros of the function are plotted and a general value of s is assumed as shown in Figure 2.

Note that poles are represented as dots, and zeros as crosses. All of the complex terms involved in equation 6 are represented by vectors with heads at the general point s and tails at the zeros or poles. The angle of each vector is measured with respect to a line parallel to the positive real axis. The magnitude of each vector is simply its length on the plot.

In seeking to find the values of s which make the open loop function equal to -1, the value -1 is considered as a vector whose angle is 180 degrees $\pm n$ 360 degrees, where n is an integer, and whose magnitude is unity. Then one can consider first the problem of finding the locus of values for which the angle condition alone is satisfied. In general, one pictures the exploratory s point at various positions on the plane, and imagines the lines from the poles and zeros to be constructed

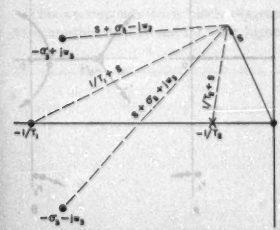

Figure 2. Root locus plot

so that the angles in turn can be visualized. For any specific problem, however, many special parts of the locus are established by inspection as illustrated in examples in later sections. Surprisingly few trial positions of the s point need be assumed to permit the complete locus to be sketched.

After the locus has been determined, one considers the second condition for a root, that is, that the magnitude of $K_\mu G_\mu(s) K_\beta G_\beta(s)$ be unity. In general, one selects a particular value of s along the locus, estimates the lengths of the vectors, and calculates the static gain $K_\mu K_\beta = 1/G_\mu(s) G_\beta(s)$. After acquiring some experience, one usually can select the desired position of a dominant root to determine the allowable loop gain. The position of roots along other parts of the locus usually can be determined with less than two trials each.

An interesting fact to note from equation 6 is that for very low gain, the roots are very close to the poles in order that corresponding vectors be very small. For very high gain, the roots approach infinity or terminate on a zero.

Single Loop Example

Consider a single loop system such as shown in Figure 1 in which the transfer functions are given in equation 7.

$$K_\mu G_\mu(s) = \frac{K}{(1+T_1 s)(1+T_2 s)s}; K_\beta G_\beta(s) = 1 \quad (7)$$

The poles of the open loop function are at 0, $-1/T_1$ and $-1/T_2$ as represented by dots in Figure 3.

The locus along the real axis is determined by inspection because all of the angles are either 0 degrees or 180 degrees. An odd number of angles must therefore be 180 degrees as shown by the intervals between 0 and $-1/T_1$, and from $-1/T_2$ to $-\infty$. Along the $j\omega$ axis, ϕ_0 is 90 degrees so that ϕ_2 must be the complement of ϕ_1, as estimated at $s=j\omega_c$. For very large values of s, all angles are essentially equal so the locus for the complex roots finally approaches radial lines at ± 60 degrees.

The point where the locus breaks away from the real axis is found by considering a value of s just above the real axis. The decrease in ϕ_0 from 180 degrees can be made equal to the sum of ϕ_1 and ϕ_2 if the reciprocal of the length from the trial point to the origin is equal to the sum of the reciprocals of lengths from the trial point to $-1/T_1$ and $-1/T_2$. If a damping ratio of 0.5 for the complex roots is desired, the roots r_1 and r_2 are fixed by the intersection with the locus of radial lines at ± 60 degrees with respect to negative real axis.

In calculating K for $s=r_1$, it is convenient to consider a term $(1+T_1 s)$ as a ratio of lengths from the pole $-1/T_1$ to the s point and from s to the origin respectively. After making gain $K=1/[G(s)]_{s=r_1}$ a good first trial for finding r_3 is to assume that it is near $-1/T_2$ and solve for $(1/T_2+s)$. After the roots are determined to the desired accuracy, the over-all transfer function can be expressed as given in equation 8.

$$\frac{\theta_o}{\theta_i} = \frac{1}{\left(1-\frac{s}{r_1}\right)\left(1-\frac{s}{r_2}\right)\left(1-\frac{s}{r_3}\right)} \quad (8)$$

The procedure in handling a multiple loop system now can be explained.

Multiple Loop System

Consider a multiple loop system in which the single loop system just solved is the forward path of another loop, as shown in Figure 4.

θ_o/θ_i is given in factored form by equation 8 so the roots of the inner loop now serve as base points for the new locus plot. For convenience, however, neglect the effect of the term $(1-s/r_3)$ so that the locus for the outer loop is shown in Figure 5.

The locus for the outer loop would be a circle about the $-1/T$ point as a center if the effect of θ_o/θ_i were completely neglected. Actually, the vectors from the points r_1 and r_2 introduce net angles so that the locus is modified as shown. The

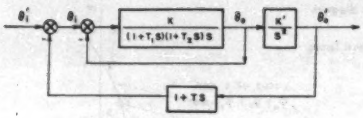

Figure 4 (above). Multiple loop block diagram

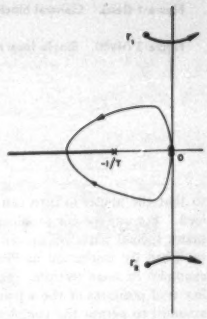

Figure 5 (right). Multiple loop root locus

angle at which the locus emerges from r_1 can be found by considering a value of s close to the point r_1, and solving for the angle of the vector $(s-r_1)$.

Assume that the static loop gain desired is higher than that allowed by the given system. The first modification suggested by the plot is to move the r_1 and r_2 points farther to the left by obtaining greater damping in the inner loop. If these points are moved far to the left, the loci from these points terminate in the negative real axis and the loci from the origin curve back and cross the $j\omega$ axis. Moving the $-1/T$ point closer to the origin would then be effective in permitting still higher loop gain. The next aspect of synthesis involves adding corrective networks.

Corrective Networks

Consider a somewhat unusual system which arises in instrument servos whose open loop transfer function is identified by the poles p_1 and p_2 in Figure 6(A). As loop gain is increased from zero, the roots which start from p_1 and p_2 move directly toward the unstable half plane. These roots could be made to move away from the $j\omega$ axis if 180 degrees phase shift were added. A simple network to add is three lag networks in series, each having a time constant T such that 60 degrees phase shift is introduced at p_1. The resultant locus plot is shown in Figure 6(B).

The gain now is limited only by the requirement that the new pair of roots do not cross the $j\omega$ axis. A value of gain is selected to obtain critical damping of these roots and the corresponding positions of all the roots are shown in Figures 6(A) and 6(B) as small circles.

Actually, greater damping could be achieved for roots which originate at p_1 and p_2 if a phase shifting bridge were used rather than the 3-lag networks. Its transfer function is $(3-Ts)/(1+Ts)$ and is of the "nonminimum phase" type of circuit.

Since these types of correction are somewhat unusual, it is perhaps well to point out that the analysis has been verified by actual test and application.

These examples serve to indicate the reasoning process in synthesizing a control system by root locus method. An engineer draws upon all of his experience, however, in seeking to improve a given system; therefore, it is well to indicate the correlation between this method and other methods.

Correlation with Other Methods

The valuable concepts of frequency response methods[1] are in a sense merely extended by the root locus system. Thus a transfer function with s having a complex value rather than just a pure imaginary value corresponds to a damped sinusoid being transmitted rather than an undamped one. The frequency and gain for which the Nyquist plot passes through the -1 point are exactly the same values for which the root locus crosses the $j\omega$ axis. Many other correlations appear in solving a single problem by both methods.

The results of root locus analysis can be easily converted to frequency response data. Thus one merely assumes values of s along the $j\omega$ axis, estimates the phase angles and vector lengths to the zeros and poles, and calculates the sum of the angles for total phase shift and the product of lengths for attenuation. The inverse problem of determining zeros and poles from experimental data is the more difficult one. Many techniques are already available, however, such as drawing asymptotes to the logarithmic attenuation curve. For unusual cases, particularly those in which resonant peaks are involved, the conformal mapping technique originated by Dr. Profos of Switzerland is recommended.[3]

The transient response is described by the poles of the transfer function. The inverse problem in this case is to locate the poles from an experimental transient response. One might use dead time, maximum build-up rate, overshoot, natural frequency of oscillation, and the damping rate as effective clues in solving this problem.

Other Applications

Many systems require a set of simultaneous equations to describe them and are said to be multicoupled. The corresponding block diagrams have several inputs to each loop so that the root locus method cannot be applied immediately. One should first lay out the diagram so that the main line of action of the signals forms the main loop with incidental coupling effects appearing as feedbacks and feed forwards. One then proceeds to isolate loops by replacing a signal which comes from within a loop by an equivalent signal at the output, replacing a signal entering a loop by an equivalent signal at the input. One can and should keep the physical picture of the equivalent system in mind as these manipulations are carried out.

The techniques of the root locus method can be used effectively in analyzing electric circuits. As a simple example, consider the lead-lag network of Figure 7(A).

It can be shown that the transfer function of this network is as given in equation 9

$$\frac{V_0}{V_i}=\frac{(1+R_1C_1s)(1+R_3C_3s)R_3}{(1+R_1C_1s)(1+R_3C_3s)R_3+R_1[1+(R_3+R_3)C_3s]} \tag{9}$$

The denominator can be factored algebraically by multiplying out and finding the zeros of the resulting quadratic. As an alternative, it will be noted that the zeros of the denominator must satisfy equation 10

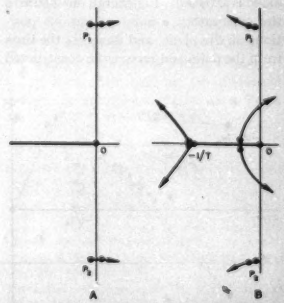

Figure 6. (A) Basic system. (B) Corrected system

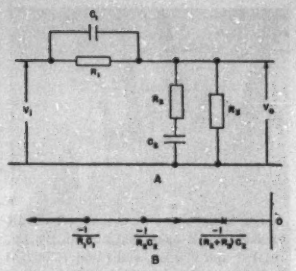

Figure 7 (left). (A) Circuit diagram. (B) Root locus

Figure 8 (right). Spirule

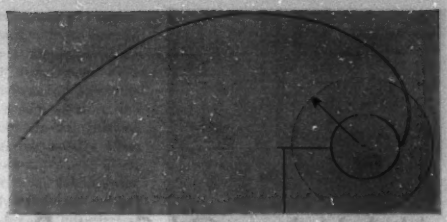

$$\frac{(1/R_1C_1+s)(1/R_2C_2+s)R_3(R_1C_1)(R_2C_2)}{[1/(R_2+R_3)C_2+s](R_2+R_3)C_2R_1} = -1 \quad (10)$$

The vectors in this expression are represented according to the root locus scheme in Figure 7(B). The two roots are thereby bounded as shown by the two dots and the cross. Their exact locations could be estimated or accurately determined by graphical methods.

The locus of roots now is simply intervals along the negative real axis between the open loop zeros and poles as shown in Figure 7 (B). The exact location of the roots along these intervals is determined in the usual way. Note that the constant in equation 10 is of the form $R'C_1$, in which R' is the effective value of R_2 and R_3 in parallel.

In more complicated networks, the advantages of the root locus concept over algebraic methods becomes greater; its particular advantage is in retaining at all times a clear picture of the relationships between the over-all network parameters and the parameters of individual circuit elements.

In the classical problem of finding roots, the differential equation is given in the form of a sum of terms of successively higher order. This can be converted to the form shown in equation 10

$$s^n+as^{n-1}+bs^{n-2}+\ldots+m = [(s+a)s+b]s+\ldots+m \quad (11)$$

This corresponds to a block diagram with another loop closed for each higher order term. Solve for the roots of the first loop which corresponds to the quantities in brackets above and proceed as before for the multiple loop system. If the roots close to the origin are of most interest, substitute $s=1/x$ first and solve for root values of x. Other combinations are, of course, possible because a single root locus basically determines the factors of the sum of two terms.

The root locus method is thus an analytical tool which can be applied to other problems than control system synthesis for which it was developed. But in attacking a new problem one would probably do well to try first to develop a method of analysis which is natural for that problem rather than seek to apply any existing methods.

Graphical Calculations

The root locus plot is first established in approximate form by inspection. Any significant point on the locus then can be checked by using the techniques indicated in this section. Note that only two calculations are involved, adding angles and multiplying lengths. Fortunately, all of these angles and lengths can be measured at the s point. Thus angles previously pictured at the zeros and poles also appear at the s point but between a horizontal line to the left and lines to the zeros and poles. A piece of transparent paper or plastic pivoted at the s point can be rotated successively through each of these angles to obtain their sum.

The reader can duplicate the "spirule" with two pieces of transparent paper, one for the disk and the other for the arm. Several procedures are possible, but the over-all purpose is to successively rotate the arm with respect to the disk through each of the angles of interest. Thus for adding phase angles, the disk is held fixed while the arm is rotated from a pole to the horizontal, whereas the two move together in getting aligned on the next pole. For multiplying lengths, the disk is held fixed while the arm is rotated from the position where a pole is on the straight line to the position where the pole is on the logarithmic curve. Rotations are made in the opposite directions for zeros than they are for poles.

Conclusions

The definite opinion of engineers using this method is that its prime advantage is the complete picture of a system which the root locus plot presents. Changing an open loop parameter merely shifts a point and modifies the locus. By means of the root locus method, all of the zeros and poles of the over-all function can be determined.

Any linear system is completely defined by this determination, and its response to any particular input function can be determined readily by standard mathematical or graphical methods.

References

1. Principles of Servomechanisms (book), G. S. Brown, D. P. Campbell. John Wiley and Sons, New York, N. Y., 1948.

2. Transients in Linear Systems (book), M. F. Gardner, J. L. Barnes. John Wiley and Sons, New York, N. Y., 1942.

3. Graphical Analysis of Control Systems, W. R. Evans. *AIEE Transactions*, volume 67, 1948, pages 547–51.

No Discussion

High-Voltage Oil Circuit Breakers for 5,000,000- to 10,000,000-Kva Interrupting Capacity

W. M. LEEDS
FELLOW AIEE

R. E. FRIEDRICH
ASSOCIATE AIEE

ONLY a few years ago, 3,500,000 kva was the maximum standard rated interrupting capacity for high-voltage circuit breakers, and the interrupting time ratings were mostly five and eight cycles. This paper describes recent developments in interrupting devices that have made available standard circuit breakers for 5,000,000-kva interrupting capacity and 3-cycle interrupting time for 138-, 161-, and 230-kv voltage classes. Particular attention is directed to the circuit breakers recently shipped to the 230-kv switchyard at Grand Coulee Dam which carry a 10,000,000-kva interrupting capacity rating on a 20-cycle reclosing duty cycle.

At the 1945 AIEE Winter Meeting, a paper was presented entitled The Next Step in Interrupting Capacity—5,000,000 Kva by A. W. Hill and W. M. Leeds,[1] which predicted that the growing needs of the electrical industry would soon require high-voltage circuit breakers having interrupting capacity in excess of the then maximum available rating of 3,500,000 kva. The development work by one manufacturer along this line was described, and test data were submitted to demonstrate the feasibility of designing higher capacity circuit breakers when required. Furthermore, the possibility of providing circuit breakers capable of operating on rapid reclosing duty with time intervals substantially shorter than 20 cycles was indicated.

The predictions of 1945 as to the future demand for high-voltage circuit breakers have been more than fulfilled, with circuit breakers now being built for not only 5,000,000 kva but as high as 10,000,000 kva, and even higher capacity being given consideration. Recognition of these growing demands for higher interrupting capacity is indicated by the American Standards Association (ASA) Preferred Ratings for Power Circuit Breakers,[2] which lists 5,000,000-kva ratings for 3-cycle oil circuit breakers in the 138-, 161-, and 230-kv voltage classes. Further evidence that this demand is not confined to one or two specific locations can be gained by considering the various places where high-power circuit breakers having 5,000,000-kva interrupting capacity or higher are actually being installed: 230-kv 10,000,000-kva circuit breakers for both Grand Coulee Dam and Hoover Dam; 230 kv 5,000,000 kva at 25-cycle frequency for the Hydro Electric Commission of Ontario; 230 kv, 5,000,000 kva at 50-cycle frequency for Electricité de France; 161 kv, 5,000,000 kva for the Aluminum Company of America in Tennessee; and 138 kv, 5,000,000 kva for the Ohio Power Company and Consolidated Edison Company of New York. These installations comprise 76 complete 3-pole circuit breakers from one manufacturer and its Canadian affiliate alone, representing an investment of between $4,000,000 and $5,000,000, with an appreciable number of additional high-power circuit breakers being built by other manufacturers for these and other power systems such as the Pacific Gas and Electric Company and the Bonneville Power Administration. The specifications for many of these circuit breakers provide that they shall be capable of performing on rapid reclosing duty.

The paper describes some of the special design features for steel-tank oil circuit breakers rated 5,000,000 kva at 138 kv, 161 kv, and 230 kv, and rated 7,500,000 or 10,000,000 kva at 230 kv. The method of verifying these interrupting capacities both in the manufacturers' high-power laboratory and by field tests on a customer's property is outlined, with special consideration given to the problems of switching line-charging currents and of interrupting high power repeatedly, under both standard duty and rapid reclosing duty cycles.

Types of High-Power Circuit Breakers

High-power circuit breakers for use at transmission voltages can be designed along at least three different lines. These three types may be classified as compressed air (air-insulated porcelain columns with air-blast arc interruption), low-oil-content (oil-insulated porcelain columns with oil-flow arc interruption), and steel-tank circuit breakers (oil insulation and oil-flow arc interruption). Compressed-air circuit breakers have found wide acceptance in European countries, although interrupting capacities do not approach 5,000,000 kva, and few, if any, circuit breakers have interrupting time ratings as short as the present American standard of 3 cycles or 0.05 second. A number of 138-kv and 230-kv air-blast circuit breakers are in operation in Canada, and there are two limited installations of 138-kv compressed-air circuit breakers in the United States.[3,4] A series of interrupting tests was made two years ago on the Bonneville Power Administration 230-kv system with a compressed-air circuit breaker manufactured before 1939 in Germany, rated 2,500,000 kva at 220 kv.[5] The tests indicated excellent fault-interrupting ability but unsatisfactory

Paper 50-12, recommended by the AIEE Switchgear Committee and approved by the AIEE Technical Program Committee for presentation at the AIEE Winter General Meeting, New York, N. Y., January 30–February 3, 1950. Manuscript submitted November 1, 1949; made available for printing November 22, 1949.

W. M. Leeds and R. E. Friedrich are both with the Westinghouse Electric Corporation, East Pittsburgh, Pa.

Figure 1. 230-kv 3-cycle oil circuit breakers at Columbia substation on the Bonneville Power Administration System

operation when clearing line-charging current. Still more effective air-blast circuit breakers have been designed and built for 230-kv and others are in process of development. However, the high-power compressed-air circuit breaker capable of a 3-cycle interrupting time rating in an adequately insulated structure for outdoor service, when considered together with necessary auxiliaries, does not appear at the present time to be competitive in cost with the most modern oil circuit breaker types.

The low-oil-content, or porcelain-clad type of circuit breaker designed for minimum oil volume, also has had considerable success in Europe, where interrupting time and arc-rupturing capacity requirements are not as severe as in this country. In the United States the most successful type of high-speed heavy-duty porcelain-clad circuit breaker is the so-called "impulse circuit breaker." The design and performance of this circuit breaker has been described several times before the institute.[6] While the interrupting performance on both line-charging currents and heavy faults leaves little to be desired, the need for separate current transformers, either porcelain-clad wound-type or the conventional through-type mounted on separate bushings independent of the circuit breakers, plus the extremely powerful operating mechanism required, in comparison with that used on conventional steel-tank circuit breakers, tend to make the impulse circuit breaker a rather costly device.

The steel-tank circuit breaker, Figure 1, has undergone continuous development during the past 30 years, taking in its stride a reduction in interrupting time from 25 cycles to 3 cycles, and an increase in interrupting capacity from one to 10,000,000 kva with a simultaneous reduction in physical dimensions. The availability of high-power laboratories has accelerated the design of more and more effective types of arc-extinguishing devices. Field tests, particularly those which provide short-circuit power in excess of that available in the laboratories, have been particularly helpful in verifying extensions of circuit breaker interrupting capacity into the higher ratings beyond 3,500,000 kva.

A group of three papers was presented at the 1948 AIEE Winter Meeting in Pittsburgh,[7,8,9] describing the design features, laboratory, and field performance of extra-heavy interrupting capacity circuit breakers being developed for 230-kv 3-cycle performance. It was concluded, at that time, that circuit breakers for use at Grand Coulee Dam, up to 10,000,000 kva, were entirely feasible. In the paper by Leeds and Cushing,[7] the elements of a steel-tank circuit breaker for heavy-duty interruption at high speed were outlined. Because of the relatively small amount of gas associated with the interruption of high-power arcs using modern interrupting devices, the tank diameter and clearances between live parts and ground are dictated almost entirely by the requirements of the standard 1-minute insulation test. At the present time, the minimum tank diameters appear to be in the neighborhood of 54 inches for 138 kv, 62 inches for 161 kv and 78 inches for 230/196 kv. The dimensions of the highest power interrupter assemblies make it necessary, in some cases, to increase these minimum diameters slightly.

Since the more conventional features of a heavy-duty high-speed steel-tank circuit breaker, such as oil-impregnated bushings and pneumatic operating mechanism, were adequately described in the earlier paper, this discussion will emphasize primarily the special design improvements, particularly in the interrupter assemblies, which have been developed recently to increase the speed of operation and maximum rupturing capacity on both standard and high-speed reclosing duty.

Design Features of a Heavy-Duty Multiflow Interrupter

The view in Figure 2, through the manhole of a 230-kv 10,000,000-kva circuit breaker, shows the location of a pair of heavy-duty multiflow "De-ion" grid contact assemblies for one circuit breaker pole. Only one interrupting unit per terminal is required, even for a 3-cycle interrupting time, because of the exceptional effectiveness of the arc-extinguishing elements. The aluminum moving contact bridges the two contact assemblies when raised to the closed position by the insulated lift rod.

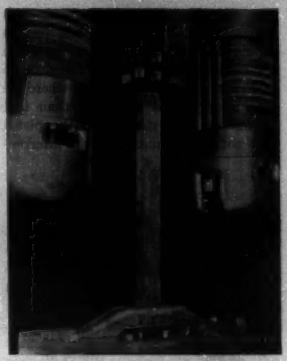

Figure 2. View of the multiflow grid interrupters inside one pole of a 230-kv 3-cycle circuit breaker rated 10,000,000 kva

The relative size of three different contact assemblies for 5,000,000 kva at 138, 161, and 230 kv as well as the 10,000,000-kva 230-kv assembly, is shown in Figure 3. It should be noted that these interrupters differ primarily only in physical dimensions, since the functioning is substantially the same for each rating. Figure 4 shows the 230-kv 10,000,000-kva interrupter in schematic cross section, and illustrates the essential functions of the several assemblies. The 3-cycle grid resembles the 5-cycle type of multiflow De-ion grid in operation, but has the additional feature of an oil-driving pump which augments the flow from the pressure-generating break at low magnetizing

Figure 3. Heavy-duty 3-cycle multiflow grids rated 138, 161, and 230 kv at 5,000,000 kva, and 230 kv at 10,000,000 kva

and line-charging currents. By this means, flat 3-cycle interrupting time is obtained for all values of current which the circuit breaker may be called on to interrupt. At higher currents, where the pressure produced is greater than that obtainable from the piston, the piston does not operate until after arc interruption occurs, and then serves to flush residue arc products from the grid. This function is of particular value on high-speed reclosing where it is desirable to clean out the gases remaining from the first interruption before the circuit breaker may be called on to open the circuit a second time within 20 cycles or less. For the interruption of line-charging currents where it is desirable to avoid arc restrikes that develop over-voltage surges, the oil-piston action is purposely delayed so that interruption will be attempted only after the contacts have parted sufficiently to be able to support the double voltage that appears one-half cycle later.

An important new feature is the arrangement by which the intermediate contact is spring-biased upwards and is free to move for one-half inch from the closed position. During an opening operation, the intermediate contact moves upwards for this distance, together with the tip on the rocker contact. At the same time, the lower contact is accelerated downward so that the interrupting gap is formed at a speed nearly three times that of the moving cross-member during the first quarter-inch of circuit breaker lift-rod travel. This feature makes it possible to eliminate multiplying levers between the lower contact and cross arm, and with only a slight increase in lift-rod speed the desired high-speed interrupting time and no-restrike performance on line-charging currents is obtained. The fact that the formation of the upper pressure-generating gap is delayed by this arrangement makes it possible to interrupt

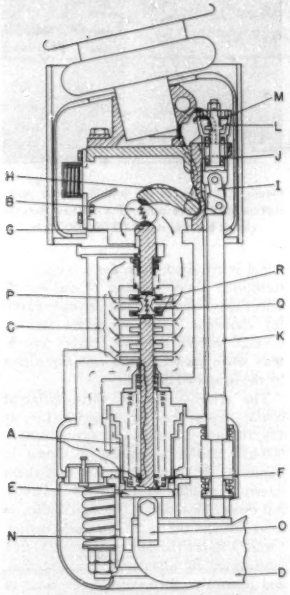

Figure 4. Cross section of 230-kv 10,000,000-kva multiflow grid

Light arrows indicate path of oil flow from piston *A*, augmenting flow (heavy arrows) from pressure-generating arc *B* to interrupting section *C*. When circuit breaker is tripped, cross member *D* moves down, followed by contact *E* and collar *F*, which collar picks up piston after short delay to provide time for adequate contact separation for charging current interruption without restriking. Intermediate contact *G* is biased upward, following rocker contact *H* for short distance. Contact *H* is rotated to open position through links *I* and contact loading spring *J* by means of operating rod *K*. Oil dashpot *L* opposes extension of spring *J*, speeding opening of contact *H*, but closing action is free due to check valve *M*. Lower contact *E* is stopped on shoulder *N*, allowing crossarm *D* to pull out of fingers *O* to form isolating gap after arc extinction. Vents *R* from interrupting section *C* are separated from oil channels by orifice plates *Q*

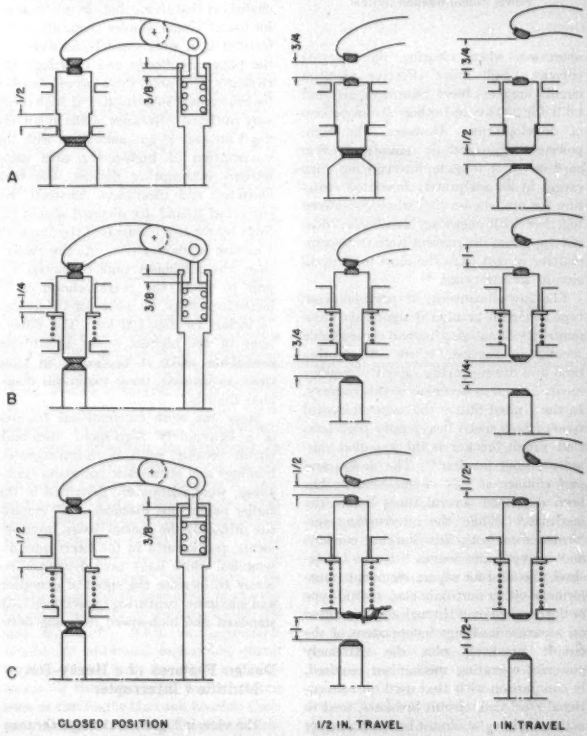

Figure 5. Comparative speed of contact gap opening in different types of interrupters

A—230-kv 5-cycle 2,500,000-kva multiflow grid
B—230-kv 3-cycle 5,000,000-kva multiflow grid
C—230-kv 3-cycle 10,000,000-kva multiflow grid

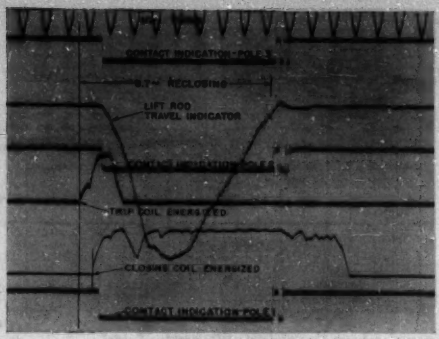

Figure 6. Timing test showing 8.7-cycle reclosing time on 3-pole oil circuit breaker rated 230 kv 10,000,000 kva

higher power, since excessive pressure is not built up waiting for a sufficient contact separation for arc interruption in the main contact gap.

An oil dashpot arrangement is incorporated into the upper end of the grid operating rod and is designed so as to delay relative motion between the rod and links attached to the rocker contact. This is made operative during an opening operation only, using a spring-biased check valve. Thus, during normal rapid opening of the contacts, the rocker contact begins to rotate upwards, allowing the intermediate contact to lift as soon as the moving cross-member moves downward, thus affording further savings in interrupting time.

A comparison of the relative positions of the pressure-generating and interrupting breaks is shown in the diagram of Figure 5 for (A) the older 5-cycle type of grid without piston, (B) the new grid with piston for applications up to 230 kv 5,000,000 kva, and (C) the 230 kv 10,000,000 kva with the dashpot arrangement on the operating rod. Successive contact positions are shown for (1) the circuit breaker closed, and (2) (3) after one-half and one-inch travel of the main moving cross-member attached to the circuit breaker lift rod. The greatest gap length for a given circuit breaker travel is obtained by the upward lifting intermediate contact and operating-rod dashpot combination in Figure 5(C).

After the lower grid contact is spring-driven to its open position against a stop, further travel of the moving cross-member forms a disconnect gap below the interrupter. This gap serves to remove voltage from the grid assembly while the circuit breaker stands in the open position, and also interrupts the small fraction of an ampere drawn by the voltage-dividing resistors which are provided to make sure that each interrupter handles its proper share of the recovery voltage.

The use of butt-type contacts with silver-tungsten arcing tips is retained because of the inherent high-speed opening obtained in comparison with finger-type contacts. Since the momentary current-carrying capacity of the contacts for these heavy-duty circuit breakers must be as high as 40,000 amperes, tests have been made to determine the amount of spring-loading required to assure the ability to handle this large amount of current without welding or excessive pitting of the contacts. Adequate heat conduction away from the sources of heat generation is provided to pass a 25,000 ampere current-carrying test for the rated 4-second period, and to carry continuously loads as high as 1,200 amperes without excessive temperature rise. An undesirable additional heat source from the helical springs surrounding the grid contacts is avoided by using nonmagnetic stainless steel for these items.

Circuit Breaker Operating Speeds

The interrupting time of a circuit breaker includes three steps: (1) the time from energizing the trip coil until the circuit breaker mechanism is unlatched; (2) the mechanical time required to separate the circuit breaker contacts;

Figure 7. High-power laboratory tests on 230-kv 10,000,000-kva circuit breaker

A—132 kv 12,200 amperes single pole—equivalent to 3-phase 230 kv 4,870 megavolt-amperes
B—66 kv 24,500 amperes half pole—equivalent to 3-phase 230 kv 9,760 megavolt-amperes
C—44 kv 36,200 amperes half pole—equivalent to 3-phase 230 kv 14,500 megavolt-amperes

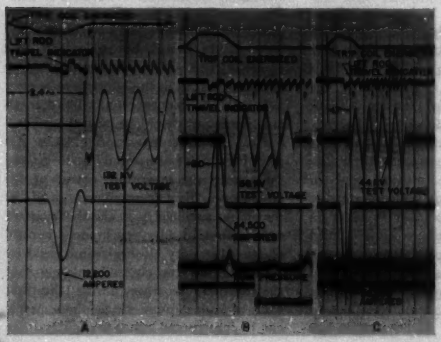

Figure 8. Comparison of high-power laboratory and field recovery voltage transients across single interrupter

A—44-kv 10,000-cycle undamped laboratory circuit with symmetrical short-circuit current of 20,700 amperes
B—66-kv damped transient on Grand Coulee circuit with symmetrical short-circuit current of 10,000 amperes
C—66-kv damped transient on Grand Coulee circuit with asymmetrical short-circuit current of 18,200 amperes

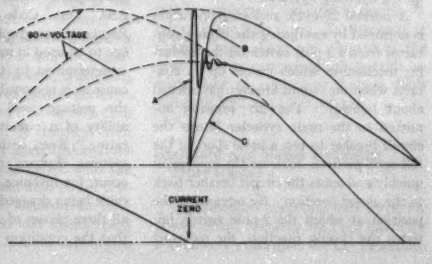

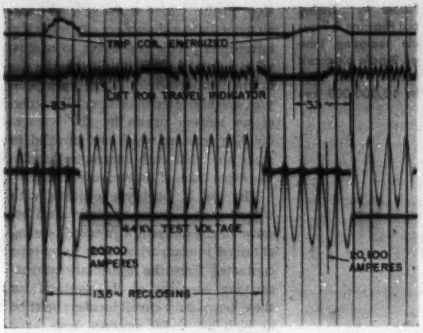

Figure 9. Oscillogram of 13.5-cycle reclosing duty test on 230-kv 10,000,000-kva circuit breaker opening 20,700 amperes at 44 kv across a half-pole unit equivalent to a 3-phase fault of 8,250,000 kva at 230 kv

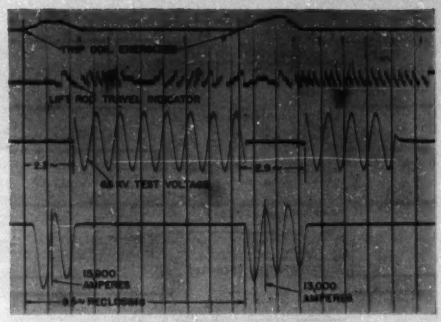

Figure 10. Oscillogram of 9.5-cycle reclosing duty test on 230-kv 10,000,000-kva circuit breaker opening 15,900 amperes at 66 kv across a half-pole unit equivalent to a 3-phase fault of 6,330,000 kva at 230 kv

and (3) the arcing time. While the first two steps take a fairly constant time interval, the arcing period is affected by the random occurrence of current zero with respect to the parting of the contacts so that a variation of at least one-half cycle in the arcing time, and therefore, in the total interrupting time, is inevitable. A typical timing test on a tripping operation of the 230-kv 10,000,000-kva 3-cycle circuit breaker shows 0.6 cycle to unlatch, 0.6 cycle to part contacts after unlatching, and an arcing time of 0.8 to 1.3 on fault interruptions, giving a total interrupting time of 2.0 to 2.5 cycles.

The closing time from energizing the electrically-operated air valve until the contacts touch requires only about 18 cycles, of which one and one-half cycles represents the time to get the inlet valve open and high pressure air on the piston of the pneumatic operating mechanism. A specially designed large-size air inlet valve with a 2-inch diameter port, together with a 2-inch flexible hose connection, is provided for the 10,000,000-kva circuit breaker to keep the cylinder pressure close to that in the air reservoir during a closing operation.

A normal 20-cycle reclosing operation is obtained by energizing the closing contactor from a 2-pole switch on the operating mechanism which makes up its contacts when the circuit breaker has opened about halfway. The air pressure admitted to the main cylinder brings the circuit breaker to rest a little short of the full open position, reverses the movement quickly and sends the circuit breaker back to the closed position. By advancing the position at which the 2-pole switch initiates the closing function, the reclosing time interval, measured from energizing the trip coil to the instant when the contacts touch on reclosure, may be reduced to as short as 12 cycles. By a reconnection of the control circuit so that the closing valve is energized directly by the 2-pole switch, reclosing times as short as 9 cycles, Figure 6, have been obtained on the 230-kv 3-pole circuit breaker operated by a single pneumatic mechanism. Insulator flashover deionization has been found to take from 10 to 16 cycles after fault interruption in the 3,500,000- to 10,000,000-kva range at 230 kv,[10,11] so that practical reclosing time intervals for 3-cycle circuit breakers at this voltage appear to be limited to not less than 15 cycles. However, it is evident that faster reclosing can be made available if the need should arise.

Demonstration of High-Power Interrupting Capacity

The limitations of high-power laboratory test power usually make it necessary to do most of the testing on a single-pole unit instead of making full 3-phase fault interrupting tests. Quoting from the ASA Test Code for Power Circuit Breakers, paragraph 9-1.2.4,[12] "the voltage to be used in making single-pole tests is determined by the manufacturer, because he is responsible for the adequacy of the voltage used to demonstrate the ability of a circuit breaker to meet its rating." Even with effectively-grounded systems, 3-phase ungrounded faults can occur, for instance, as a result of a steel cable being dragged by an airplane across all three phases of a transmission line, so that the condition of 87 per cent of line voltage across the first pole to clear must be considered as a possibility.

Another abnormal voltage condition may occur during transient instability when two parts of a system swing out of synchronism so that a tie circuit breaker could be called upon to interrupt practically double normal line-to-ground voltage across terminals, equivalent to approximately 115 per cent of line-to-line voltage across a single pole. For these reasons, it is considered desirable to demonstrate adequate voltage-interrupting ability of a high-voltage circuit breaker by including single-phase interrupting tests opening reasonable amounts of power, up to perhaps 25 per cent of the current interrupting capacity, with voltages as high as twice normal line-to-ground potential. As indicated by the test data in Table I, all of the 5,000,000-kva circuit breakers have been subjected to such factor-of-safety tests to be sure that the voltage-interrupting ability is adequate for any reasonable abnormal voltage condition to which it may be subjected in service. It should be recognized that some of this safety factor necessarily would be lost if, in the effort to save cost, proposals to reduce circuit breaker insulation levels should be pushed too far.

Heavier power-interrupting tests also have been made at normal line-to-ground voltage to the maximum power of the laboratory. By taking advantage of the maximum asymmetry in the short-circuit current, obtained by synchronous control of the laboratory closing switch, and by pretripping the test circuit breaker so that the contacts separate during the first cycle of fault current, single-phase power can be interrupted equal to slightly more

Table I. Factor of Safety High-Power Laboratory Interrupting Tests

Circuit Breaker Rating	Test No.	Single-Phase Voltage, Kv	Interrupting Current, Rms Amperes	Interrupting Time, Cycles	Equivalent 3-Phase Kva
138 kv, 5,000 mva, 3 cycles	1	160	160	2.4	77,000
	2	160	1,160	2.9	557,000
	3	160	3,500	2.8	1,680,000
	4	160	4,570	2.7	2,190,000
	5	160	6,030	2.8	2,900,000
161 kv, 5,000 mva, 3 cycles	1	198	160	2.8	95,000
	2	198	1,300	2.3	770,000
	3	198	2,150	2.5	1,280,000
	4	198	3,000	2.7	1,780,000
	5	198	4,950	2.7	2,950,000
230 kv, 5,000 mva, 3 cycles	1	264	120	2.2	95,000
	2	264	1,000	2.7	790,000
	3	264	2,100	2.4	1,660,000
	4	264	3,200	2.4	2,530,000
	5	264	3,750	2.8	2,960,000

Table II. Heavy-Duty High-Power Laboratory Interrupting Tests

Circuit Breaker Rating	Test	Single-Phase Voltage, Kv	Interrupting Current, Rms Amperes	Interrupting Time, Cycles	Equivalent 3-Phase Kva
138 kv 5,000 mva 3 cycles	Full pole—O	88	9,100	2.4	2,170,000
	Full pole—O	66	23,200	2.2	5,530,000
	Half pole—O	44	28,400	2.9	6,780,000
	20 cycle—OCO	44	19,500	2.6	4,650,000
			17,850	2.9	4,250,000
161 kv 5,000 mva 3 cycles	Full pole—O	88	14,800	2.5	4,120,000
	Half pole—O	44	20,600	2.7	5,720,000
	20 cycle—OCO	44	17,100	2.7	4,760,000
			14,700	2.9	4,100,000
230 kv 5,000 mva 3 cycles	Full pole—O	132	9,400	2.5	3,750,000
	Half pole—CO	66	13,600	2.3	5,410,000
	20 cycle—OCO	66	13,000	2.4	5,180,000
			12,500	2.8	4,980,000
230 kv 10,000 mva 3 cycles	Full pole—O	132	12,300	2.3	4,850,000
	20 cycle—OCO	132	9,500	2.3	3,770,000
			6,200	2.7	2,460,000
	Half pole—O	66	24,500	2.0	9,700,000
	20 cycle—OCO	66	13,000	2.4	5,170,000
			12,500	2.8	4,960,000
	Half pole—O	44	36,200	1.7	14,400,000
	13.5 cycle—OCO	44	20,700	2.3	8,210,000
			20,100	3.3	8,000,000
	9.5 cycle—OCO	44	15,900	2.2	6,310,000
			13,000	2.9	5,170,000

O = open. CO = Close-Open. OCO = Open-Close-Open.

than 1,500,000 kva, equivalent to a 3-phase fault approximating 4,800,000 kva. The oscillogram of Figure 7(A) shows such a test in which 12,200 amperes is interrupted at 132,000 volts to ground in a time of 2.4 cycles. Still higher powers up to twice this value of 9,600,000 kva are made available by shunting out one of the interrupting units in the test pole, and applying the full power at the laboratory at approximately one-half normal line-to-ground voltage across the half-pole unit. Such a test is shown in Figure 7(B) opening 24,500 amperes at 66,000 volts in 2.0 cycles. In verifying the interrupting ability of the 230-kv 10,000,000-kva circuit breaker for Grand Coulee Dam, even the test program just outlined fell a little bit short of the necessary power to demonstrate the rupturing capacity with a reasonable factor of safety.

Accordingly, further tests were made on a half-pole unit with the 44-kv transformer connection instead of 66 kv. By this means the oscillogram of Figure 7(C) was obtained, showing a short-circuit current of 36,200 amperes, which at 230 kv 3-phase would be a fault of 14,400,000 kva. Since the 60-cycle recovery voltage now was only two-thirds of the appropriate value for a single interrupting unit, it might be considered that this test was not valid in terms of both voltage and current involved in the interruption. However, the high rate of recovery voltage in the laboratory and amount of overswing at the first transient voltage peak, compared to the damped recovery voltage of a high-power fault circuit in the field, makes this test one of equal or even greater severity. In Figure 8 is replotted to a suitable time scale the recovery voltage transient from a symmetrical current interruption at 44 kv in the laboratory compared with the recovery transients from high-power 230-kv field tests at Grand Coulee Dam having both asymmetrical and symmetrical fault current. Not only is the rate-of-rise of recovery voltage highest on the laboratory test, but the amplitude of the first voltage peak is equal to or greater than both of the field test voltage transients. On this basis the 15-cycle reclosing test of Figure 9, opening a current a little more than the 25,000-ampere rating of the 10,000,000-kva circuit breaker, may be considered as imposing recovery voltage conditions on the interrupting unit at least as severe as would be encountered on a 230-kv system without pretripping and with only moderate current asymmetry.

Considering the wide range of voltage and current to which a circuit breaker is subjected during verification, it is remarkable how little variation there is in the interrupting time. The effectiveness of the multiflow principle of interruption, supplemented by a spring-driven oil piston to assist the interruption of low current, is indicated by the fact that currents from 0 to 100 per cent of the current interrupting capacity are all interrupted within the 3-cycle interrupting time. Interruption even at voltages approximating twice normal line-to-ground voltage only occasionally exceeds the rated time of three cycles. When considering piston-driven oil flow for the interruption of line-charging current with minimum arc restriking in comparison with self-generated oil flow alone or with parallel voltage-damping resistors, the ability to meet a flat 3-cycle interrupting time characteristic over the entire current range using the oil piston is a considerable advantage in its favor, as well as the interrupter-flushing action obtained during each operation.

The Leeds-Cushing paper[7] presented comparative results of heavy fault interruptions both in the Westinghouse High Power Laboratory and at Grand Coulee Dam on a 230-kv circuit breaker. These tests demonstrated that voltage conditions in the laboratory test imposed equal or greater severity as compared to the field tests. However, it is extremely valuable to have the opportunity of testing ultrahigh interrupting capacity circuit breakers directly on a power system to supplement and confirm results obtained in the laboratory. Further tests at Grand Coulee Dam are planned in the near future to carry single-phase fault interruptions to equivalent 3-phase fault values as high as 12,000,000 kva.

Standard and Rapid Reclosing Duty Cycles

The standard operating duty cycle for power circuit breakers has been based for a number of years upon the CO-15 second-

CO duty. The ASA Standard for Alternating-Current Power Circuit Breakers, paragraph 4-6.20.3b[13] says: "After a performance at or near its interrupting rating, it is not to be inferred that the breaker can meet its interrupting rating without inspecting and, if necessary, making repairs." The improvement in circuit interruption, particularly in the higher power 3-cycle circuit breakers described in this paper, has resulted in circuit breaker designs which are capable of performing their interrupting rating several times on the standard duty cycle without the necessity of inspection or maintenance. The rating factors given in Table I of NEMA Standard SG6-90[14] for repeated numbers of unit operations and for reclosing operations have been considered by operating people as unnecessarily drastic when applied to the most modern circuit breaker designs. Some liberalization of these factors is being made in a revision now in progress, but of necessity they must be standardized at values which can be met by a wide variety of circuit breakers. While some reduction in interrupting capacity is indicated by rapid reclosing tests on circuit breakers of the self-generated oil-flow type, the actual loss of interrupting ability on the second operation is not very great on 3-cycle high power circuit breakers which have been designed with an appreciable factor of safety in arc-rupturing capacity.

The data submitted in Table II is selected from the large number of interrupting tests made in the High Power Laboratory during the development and verification of the 3-cycle circuit breakers rated 5,000,000 kva at 138, 161, and 230 kv, and the 10,000,000-kva circuit breaker for 230 kv. Standard duty and rapid reclosing tests are included, with the fault power applied to a single-pole unit or only a half-pole as found necessary to demonstrate adequate interrupting ability.

Of particular interest is the 9-cycle reclosing test at 16,000 amperes, the oscillogram for which is shown in Figure 10. This represents voltage and current conditions applied to a single interrupting unit equivalent to a 3-phase fault of 6,650,000 kva at 230 kv.

Conclusion

From both theoretical considerations and the results of actual tests there does not seem to be any serious limitation on the maximum interrupting capacity of steel-tank oil circuit breakers equipped with heavy duty multiflow De-ion grid interrupters. Although 25,000-amperes interrupting capacity and 40,000-amperes momentary rating is close to the limitation of the butt-type contacts with silver-tungsten arcing tips, interrupters using finger-type contacts, with a slight increase in over-all interrupting time, can be made available if, in spite of more conventional practices limiting maximum fault power, still higher rupturing capacities seem justified.

By taking advantage of the inherently higher rate of rise of recovery voltage in undamped laboratory test circuits as compared to the overdamped transients under heavy fault conditions in the field, the test voltage in the laboratory may be lowered by as much as a third, thus expanding the available rupturing capacity by 50 per cent without serious loss in validity of the results.

High-speed reclosing, even at intervals as short as nine cycles, has been demonstrated satisfactorily, indicating that the circuit breaker need not be the limiting factor in establishing the shortest practical reclosing interval.

References

1. The Next Step in Interrupting Capacity—5,000,000 Kva, **A. W. Hill, W. M. Leeds.** *Electrical Engineering (AIEE Transactions)*, volume 64, June 1945, pages 317–23.

2. Preferred Ratings for Power Circuit Breakers. *C37.6-1949.* American Standards Association (New York, N. Y.), 1949.

3. A Vertical-Flow Compressed-Air Circuit Breaker and Its Application on a 132-Kv Power System, **H. A. P. Langstaff, B. P. Baker.** *Electrical Engineering (AIEE Transactions)*, volume 62, April 1943, pages 188–92.

4. A 3-Cycle 3,500-Megavolt-Ampere Air-Blast Circuit Breaker for 138,000-Volt Service, **H. L. Byrd, Ben S. Beall, III.** *Electrical Engineering (AIEE Transactions)*, volume 64, May 1945, pages 229–32.

5. Performance Test of the Allgemeine Elektricitats Gesellschaft Free-Jet Air-Blast 220-Kv 25,000-Megavolt-Ampere Reclosing Circuit Breaker, **Alexander Dovjikov, Clifford C. Diemond.** *AIEE Transactions*, volume 67, part I, 1948, pages 295–306.

6. Switchgear Equipment for Tidd High-Voltage Test Lines, **F. A. Lane, B. W. Wyman.** *AIEE Transactions*, volume 66, 1947, pages 1619–23.

7. A 230-Kv 3-Cycle Oil Circuit Breaker for Extra-Heavy Arc Rupturing Duty, **W. M. Leeds, G. B. Cushing.** *AIEE Transactions*, volume 67, part I, 1948, pages 236–42.

8. Unusual Performance of Standard 230-Kv Impulse and Tank-Type Oil Circuit Breakers on Field Tests, **E. B. Rietz.** *AIEE Transactions*, volume 67, part I, 1948, pages 267–70.

9. Field Tests for Development of 10,000,000-Kva 230-Kv Oil Circuit Breakers for Grand Coulee Power Plant, **C. L. Kilgore, W. H. Clagett.** *AIEE Transactions*, volume 67, part I, 1948, pages 271–87.

10. Insulator Flashover Deionization Times as a Factor in Applying High-Speed Reclosing Circuit Breakers, **A. C. Boisseau, B. W. Wyman, W. F. Skeats.** *AIEE Transactions*, volume 68, part II, 1949, pages 1058–67.

11. Deionization Time of High-Voltage Fault-Arc Paths, **Everett J. Harrington, E. C. Starr.** *AIEE Transactions*, volume 68, part II, 1949, pages 997–1004.

12. Test Code for Power Circuit Breakers. *C37.9-1945*, American Standards Association (New York, N. Y.), 1945.

13. Alternating-Current Power Circuit Breakers. *C37.4-1945*, American Standards Association (New York, N. Y.), 1945.

14. Operating Duty (Duty Cycle) for Standard and Reclosing Service. *SG6-90*, National Electrical Manufacturers Association (New York, N. Y.), July 1946.

Discussion

Robert H. Nau (University of Illinois, Urbana, Ill.): The paper possesses two characteristics which are most desirable for a technical paper: it is well written and presents a new contribution to the technical field.

Two years ago Leeds and Cushing presented a technical paper before the Institute,[1] which described the advantages of a dead-tank circuit breaker. Too, it was shown that by correlating studies of oil-flow, orifice sizes, inertia-impeded levers, and of scavenging that a 7,500,000-kva 230-kv oil circuit breaker was designed. The laboratory and field tests indicated a sound basis for extending the controlled design to 10,000,000 kva.[2]

It is evident that the extension of the principles of controlled design has led to the notable contribution of an ultra-high-power high-speed supervoltage oil circuit breaker. In the new multiflow deion grid the relationship of the two contact breaks, the oil flow through the orifices, the superspeed of contact opening, and the supplementary action of the oil piston all function to quench the arc as expeditiously as possible without producing excessive gas pressures in the interrupters before the interrupting contacts have sufficiently parted to withstand a high-voltage recovery rate following the interruption of superpower short circuits. Also, the action positively assures interruption of low power-factor charging currents in the required 3-cycle time. The operation is evolved as expressed by the paraphrased adage, "It is easy to keep the multiflow orifices clean, if they are not permitted to become fouled."

It is, indeed, commendable that the 10,000,000-kva 230-multiorifice oil circuit breaker has an appreciable factor of safety above the required interrupting rating. The recorded test data and oscillograms indicate superior performance.

References

1. See reference 7 of the paper.
2. See reference 9 of the paper.

Philip Sporn (American Gas and Electric Service Corporation, New York, N. Y.): The resourcefulness and inventiveness of the authors and the enterprise of the company with which they are associated in

proceeding with and in bringing into fruition the development of high-voltage circuit breakers from 5,000,000- to 10,000,000-kva rupturing capacity cannot be too highly commended. Certainly those who are charged with the responsibility of planning and projecting the growth of modern power systems fully appreciate the importance of having circuit breaker development and extension in capability of rupturing duty of high-voltage circuit breakers march, not hand in hand with system growth, but actually in advance somewhat of system growth, if that growth is to be projected and take place on most economical lines.

Yet, recognizing in full the ingenuity of the designs developed, one cannot help speculating, upon looking at and analyzing the heart of the design as shown by Figure 4 of the paper, for example, whether ingenuity has not been carried too far. Anyone who has had some experience in the operation of equipment embodying that design cannot, it seems to me, help but wonder whether that much ought to be put together in a construction in which so much mechanism is hung in cantilever from the end of a bushing and made dependent for its successful operation by an assembly subject to as much mechanical misalignment, and therefore potential difficulty, as the operating head assembly shown in Figure 2 of the paper. What this gets down to, therefore, is the question of whether after all the same principle of action could not be made to function in a totally different assembly, possibly an oil-poor assembly where the basic or inherent mechanical weaknesses would be eliminated because they would be taken care of by positive design features.

H. P. St. Clair (American Gas and Electric Service Corporation, New York, N. Y.): I would like to request clarification of the oil dashpot feature described in the fourth paragraph of the section on Design Features of a Heavy-Duty Multiflow Interrupter. It is not clear to me either from the description in the text or the explanation of the drawing of Figure 4 of the paper, just how the dashpot incorporated into the other end of the grid-operating rod brings about an increase in the speed of opening the rocker-arm contact.

In testing and demonstrating the interrupting capability of the new circuit breaker in the laboratory, the authors have unquestionably made the best possible use of the available test capacity and these tests, including reduced voltage tests on a single interrupter or one-half of a complete pole unit, certainly go a long way toward proving that the circuit breaker will be able to meet its rating. In this connection it is comparatively easy to take the first step of using one-half voltage across the half-pole unit, relying upon the resistor voltage divider to insure equitable voltage distribution in normal operation. In taking a further reduction from 66,000 volts to 44,000 volts across the half-pole unit, however, the authors have made an interesting comparison of the greater severity of transient recovery voltage obtained in the laboratory with that obtained under field circuit conditions, and have used this comparison to justify the validity of regarding such a test as something at least roughly equivalent to a 3-phase 230-kv test at 14,400,000 kva. Even though I assume there was no serious intention of claiming a fully equivalent test of this magnitude, I believe it would be well to point out that the severe recovery voltage transient shown in Figure 8 of the paper was based upon a symmetrical short-circuit test at 20,700 amperes and 44,000 volts, whereas the 36,200-ampere test shown in Figure 7(C) of the paper was a totally offset wave. It is well known, of course, that when the current wave is completely offset, the current zero and voltage zero practically coincide and there is no recovery voltage transient at all. In other words, the use of the greater severity of laboratory circuits as an offset to the reduced voltage associated with higher current tests should be confined to more or less symmetrical short-circuit tests, of which the 20,700-ampere test shown in Figure 8(A) of the paper is an example.

This again points up the discrepancy between our American method of rating circuit breaker duties on the total rms value of current, including both d-c and a-c components, as compared with the European method of rating circuit breakers on the symmetrical current only. There is a growing conviction in this country, I believe, that the symmetrical basis for rating circuit breakers is a sounder method and should be adopted. At the same time, of course, the mechanical forces resulting from offset current waves must be taken into account both in design and testing.

Finally, it is gratifying to know that the authors find in their tests and development of this circuit breaker a further substantiation of the idea that some of us have been advancing for a number of years that derating factors for high-voltage high-capacity circuit breakers are entirely too severe. It is gratifying that these are being somewhat liberalized in present revisions, but it is hoped that it will not be long before the values called for in standards can go all the way in accepting the realities of modern circuit breaker designs.

A. M. deBellis (Consolidated Edison Company of New York, Inc., New York, N. Y.): This paper, describing the development of higher steps of interruption capacity in high-voltage outdoor oil circuit breakers, is most interesting to us. We now are installing a number of 5,000,000-kva circuit breakers on our 138-kv tie-feeder system. This is the largest interrupting capacity available at this voltage.

Even with this size of circuit breaker we find it will be necessary to install four sets of 138-kv reactors a few years hence, in order to maintain interrupting duties within the 5,000,000-kva rating. This naturally leads one to think of the possibilities of using higher interrupting capacities at this voltage.

The authors state that 25,000-ampere interrupting capacity is close to the limitation of butt-type contacts with silver-tungsten arcing tips. At 138 kv this limits interrupting capacity, with this type of contact, to about 6,000,000 kva. It would be interesting to know what may be involved to obtain 7,500,000 or 10,000,000 kva which, at 138 kv, would require an interrupting rating of about 44,000 amperes with a momentary capacity of 70,000 amperes.

It is gratifying to know that careful attention was given to the problem of interrupting line-charging currents with a minimum of arc restrikes. We operate an underground cable system only within New York City, at 138 kv. We are naturally interested in avoiding severe overvoltages on these circuits. Interruption of low currents without restrikes is not only desirable but practically essential on a system of this type.

I also want to compliment the authors on the attention given to the possibility of interrupting high current with a higher-than-normal recovery voltage across the contacts of the circuit breaker. The possibility of out-of-phase switching is always present.

G. D. Floyd (The Hydro-Electric Power Commission of Ontario, Toronto, Ontario, Canada): An AIEE Joint Subcommittee has been studying the matter of out-of-phase high-voltage switching. It is of interest to note that in the paper by Mr. Leeds and Mr. Friedrich, this matter was considered of sufficient importance to justify tests on a high-capacity high-voltage circuit breaker, and a reference to these tests and discussion of their significance is made in the section on Demonstration of High-Power Interrupting Capacity of their paper. I believe out-of-phase switching may become of more importance than it has been in the past because of more widespread interconnection of systems, and the desire to rapidly reclose tie lines or to reconnect generating sources that may be connected to a system by a single high-voltage line. It usually is not difficult to determine the amount of current the circuit breaker would be required to interrupt in attempting to re-establish the system tie. Therefore, if it can be demonstrated by a test on the circuit breaker before purchase that it can interrupt a specified fraction of its current interrupting capacity under voltage conditions equal to twice normal line-to-ground voltage, the purchaser would feel more confident that he had made a sound application.

W. M. Leeds: The authors appreciate very much the comments regarding the design and performance of the high-power oil circuit breakers described in this paper. Mr. Sporn expressed some concern regarding possible difficulty in maintaining alignment between relatively heavy stationary contact assemblies, mounted at the ends of slanted terminals, and a bridging contact assembly moved rapidly by a long lift rod. However, over 20 years of successful experience with this type of circuit breaker construction, including the 287-kv Hoover Dam circuit breakers with multiple grid assemblies twice as heavy as modern interrupters, has developed confidence in the mechanical adequacy of this steel tank circuit breaker design. Over 3,000 mechanical operations on the first 230-kv 10,000,000-kva circuit breaker as well as hundreds of short-circuit interrupting tests have been made without any difficulty due to contact alignment. Furthermore many high-power short circuits have been interrupted with one grid by-passed, resulting in unsymmetrical

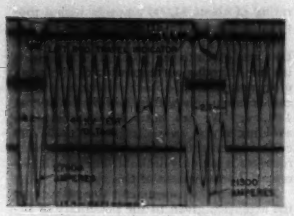

Figure 1. 11,000,000-kva 13.3-cycle reclosing duty test

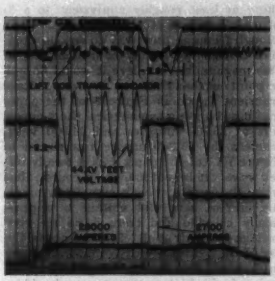

Figure 2. 11,200,000-kva 7.7-cycle reclosing duty test

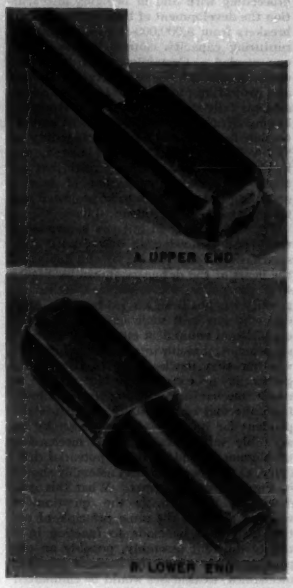

Figure 3 (right). 230-kv 10,000,000-kva interrupter intermediate contact after nine tests 10,000,000 to 12,000,000 kva

transient forces, and yet no guiding difficulties were experienced.

Mr. St. Clair has asked for a clarification of the function of the oil dashpot feature on the contact operating rod of the interrupter assembly shown in the contact assembly of Figure 4 of the paper. The opening motion of contact, Figure 5 (B) of the paper, with a resilient connection but no dashpot action in the connection from the operating rod to the rocker contact is compared with Figure 5(C) having dashpot action. During the first inch of downward movement of both the lower contact and the side operating rod, the sum of the two contact gaps is three inches in Figure 5(C), rocker ratio 2:1, where the dashpot maintains the 3/8-inch compression of the contact spring during this time. In Figure 5(B) the spring is extended three-eighths of an inch almost immediately so that twice this dimension or three-quarters of an inch is subtracted from the pressure gap, the sum of the upper and lower gaps thus equalling only $2^1/_4$ inches after one inch of circuit breaker cross arm travel.

The criticism of the highly asymmetrical fault current tests shown in Figure 7 of the paper has been based on the assumed approximate coincidence of the normal frequency voltage zero with the final current zero. As a matter of fact, the cathode ray oscillogram for the test of Figure 7(C) shows nearly 70 per cent of the normal-frequency recovery voltage at current zero with a superimposed high-frequency recovery-voltage transient oscillation reaching a peak 25 per cent above the normal 60-cycle crest value. It is recognized, of course, that symmetrical current testing must be included in any circuit breaker verification, and it is for just this reason that lower 60-cycle transformer test voltages with overshooting recovery-voltage transients are employed to make available higher amplitude symmetrical short-circuit currents.

In the rapid reclosing test of Figure 9 of the paper, the second interruption required 3.3 cycles or slightly more than the rated interrupting time. However, it should be observed that this was not due to excessive arcing but included at least one-half cycle delay in the second trip operation on account of inadequate ampere turns in the trip coil. The oscillogram of Figure 1 of this discussion was taken after this condition was corrected, interruptions of 27,500 and 21,300 amperes being cleared in 2.2 and 2.6 cycles with a reclosing interval of 13.3 cycles. Figure 2 of the discussion shows a reclosing test with both interrupted currents above the 25,000-ampere rating and with the reclosing interval reduced to the remarkably short time of only 7.7 cycles. This emphasizes the fact that the circuit breaker need not be the limiting element in determining the minimum permissible reclosing time interval even for circuit breakers rated as high as 10,000,000 kva at 230 kv. As further evidence of the ability of these high-power circuit breakers to interrupt heavy faults repeatedly without maintenance, Figure 3 of this discussion shows one of the butt-type intermediate contacts after nine successive short-circuit interruptions of 25,000 to 30,000 amperes, all above the current interrupting capacity of the 10,000,000-kva circuit breaker.

Mr. deBellis believes that there soon may be a need for 138-kv circuit breakers rated 7,500,000 kva or even 10,000,000 kva. The interruption of currents as high as 44,000 amperes is considered to be a practical possibility, but the provision of 70,000-ampere momentary rating would undoubtedly require finger contacts, and a consequent increase of approximately one-quarter to one-half cycle in the time to part contacts as compared to the present butt-contact design. The circuit breaker interrupting time under these conditions would still be entirely satisfactory for most applications.

Both Mr. deBellis and Mr. Floyd have noted with approval the demonstration of interrupting ability up to double normal operating voltage, simulating out-of-step conditions on a tie-line circuit breaker. While there are no standard specifications in this regard, the company with which the authors are associated believes it to be desirable to check all new high-voltage circuit breaker designs up to approximately one-quarter of rated current interrupting capacity under these extreme conditions.

A Printing Telegraph Tape-to-Page Translator

A. E. FROST
ASSOCIATE AIEE

Synopsis: The tape-to-page translator is a device employed in a reperforator switching telegraph system to permit the delivery of telegrams, handled throughout the system as "tape" printer messages, to patrons' offices equipped with page teleprinters. This paper describes the means employed for inserting the additional characters and the necessary conversions in the transmission of a message to produce the traditional format of the copy received on a page teleprinter.

THE Western Union Telegraph Company has recently extended reperforator switching methods to the delivery of telegrams to tie-line patrons. Some of these customers have tape teleprinters in their offices, while others prefer page machines. Out of the fundamental differences in operating requirements of the two types of teleprinters arises the need for a translator.

Tape printers type characters on a narrow gummed tape which is affixed to a telegraph blank by the receiving operator. A hand-tape moistener and a thimble having a tape-cutting edge facilitate this operation. It is a simple matter for the operator to arrange lines of printing in a prescribed manner to produce the familiar telegram. One type of tape teleprinter operating position is shown in Figure 1.

Page printers type directly on a paper page of message blank width. The blank is usually in roll form and messages are separated by cutting the blank along a knife edge. Figure 2 shows a page teleprinter mounted in a console. This instrument can be used for both sending and receiving. It differs from the tape teleprinter in several respects, including the need for transmitting signals to effect carriage return and line feed functions.

By far the greater proportion of telegrams handled by the telegraph company are recorded on tape printers, and all business allowed to enter the reperforator switching system is in the form of tape printer copy. To permit messages flowing through the reperforator switching system to be switched automatically to page tie-lines, the differences between tape and page signaling requirements must be reconciled automatically. This is the purpose of the tape-to-page translator.

Figure 3 shows tape and page teleprinter character assignments. Only the differences between them are shown in the page columns. The abbreviations *UC* and *LC* refer to upper case and lower case respectively. The page printer has two of the 32 possible combinations of the 5-unit code assigned to carriage return and line feed. The tape printer has four characters assigned to these code combinations, which means that the tape printer has four character assignments that do not appear on the page printer. The omitted characters are: paragraph sign, equal sign, English pound sign, and the per cent sign. The equal sign is not required; neither, obviously, is the paragraph sign, since it is used only as an indication to the tape printer receiving operator that a new line should be started. The English pound and the per cent must be spelled out in page printer operation. The translator performs a conversion for the per cent sign but the pound sign occurs so infrequently that tape printer routine now requires it to be spelled.

Translator Requirements

The following is a summary of the functions to be performed by the tape-to-page translator:

1. Count a certain minimum number of characters for a line and insert a carriage return and line feed on the following word space.
2. Convert the equal sign into carriage return and line feed.
3. Convert the number sign (upper case equal sign) into upper case *H*.
4. Convert the apostrophe (upper case *N*) into upper case *S*.
5. Convert the per cent sign (upper case *M*) into letter shift, *PCT*, figure shift.
6. Convert the paragraph sign (upper case *S*) into carriage return, line feed, and five word spaces to give a proper paragraph indentation on the page printer copy.
7. Convert the comma (upper case period) into upper case *N*.
8. Convert the period into figure shift, *M*, letter shift.
9. On double period (end of message) transmit a carriage return and line feed; initiate a request for the time and date; and, upon completion of the transmission of the time and date, end the message by transmitting a carriage return and eight line feeds.

Translator Plan

Figure 4 shows a block diagram of the translator components and illustrates the plan chosen to effect translation. Tape teleprinter signals are received and perforated by the reperforator. The perforated tape passes through the tape transmitter, which sets up the code combinations punched in the tape, character by character, on five reading relays. The reading relays carry several sets of contacts for reading the character and an additional set of contacts from which the selection may be transferred to the storing relays should no translation be required. Associated with the storing relays is a sending distributor for transmitting the signals to a page teleprinter circuit.

Should a character requiring translation

Paper 50-13, recommended by the AIEE Telegraph Systems Committee and approved by the AIEE Technical Program Committee for presentation at the AIEE Winter General Meeting, New York, N. Y., January 30–February 3, 1950. Manuscript submitted November 15, 1948; made available for printing November 22, 1949.

A. E. Frost is with the Western Union Telegraph Company, New York, N. Y.

Figure 1 (left). Tape teleprinter operating position

Figure 2 (right). Page teleprinter console

be set up on the reading relays, a circuit is established to energize one of the translator relays. One translator relay is required for each of the nine functions and, when operated, it sets up the conditions required for the particular translation. Since most of the conversions require that more characters be transmitted than are received, it is necessary to establish a condition whereby a succession of conversion characters may be transferred, one at a time, to the storing relays. This is the purpose of the transfer relays. Operation of a translator relay immediately causes the operation of an appropriate transfer relay which carries contacts for the transfer of the first conversion character to the storing relays. Provision is made that this transfer shall take place from the transfer relays and not from the reading relays; that is, the first conversion character is transferred to the storing relays in place of the character requiring translation. Then a second transfer relay is operated and the first one released to effect the transfer of the second character to the storing relays. This process is repeated as many times as is required. The operation of the last transfer relay establishes circuits for the restoration of normal transmission.

It is fundamental that transmission to the translator must be stopped during the transmission of additional conversion characters. The perforated tape furnishes the necessary loose coupling between the originating transmission and the translator. The tape transmitter is stopped and started again by the translator as required.

The translator is provided with two items not shown in this diagram. One is a counter to count the number of characters in each line of page copy to indicate that a carriage return and line feed should be inserted upon the reception of the following word space: the other is a rotary switch used to effect the transfer of the conversion characters for the paragraph sign and also the carriage return and eight line feeds at the end of a message.

Transfer and Storing Relay Circuits

All of the events required by translation are timed from local rings on the sending distributor shown in Figure 5. The distributor brushes are continuously rotating.

Local segments are shown in proper relation to the sending segments. Stepping of the transmitter takes place during the transmission of the start impulse. An auto-stop relay, differentially wound, is included in the circuit to stop the transmitter and hold its contacts to spacing when the auto-stop circuit is opened due to tight tape or because additional characters need be inserted for a translation. The count pulse steps the counter, resets it and releases certain transfer relays. The following segment is used to operate and release relays. The read pulse seeks a path through contacts of the reading relays to operate translator relays. The switch step segment steps the rotary switch for the conversion of the paragraph sign and for the message-ending characters. Timing of the transfer of a character to storing relays is done by the transfer segments.

Because of the number of conversions required in translation, the transfer of the desired selection to the storing relays was kept as simple as possible. The storing relays must be capable of responding to any one of 13 transfer relays and to 16 positions of the rotary switch in addition to the reading relays. The circuit is arranged so that a closed circuit to battery from any of the transfer points will prepare for the transfer of a marking signal to a storing relay and that an open circuit at all of the transfer points will effect the transfer of a spacing signal. This allows all of the transfer points to be paralleled. It is merely necessary, at the time of transfer, to insure that only the desired circuits are closed.

The operating circuit of the fifth storing relay is shown. When any one of the fifth pulse transfer points is closed, the relay is

CHARACTERS				CODE SIGNALS				
PAGE		TAPE						
UC	LC	UC	LC	1	2	3	4	5
		-	A					
		?	B					
		:	C					
		$	D					
		3	E					
			F					
		&	G					
#		£	H					
		8	I					
		BELL	J					
		(	K					
		)	L					
,		%	M					
,		!	N					
		9	O					
		0	P					
		1	Q					
		4	R					
'		¶	S					
		5	T					
		7	U					
		;	V					
		2	W					
		/	X					
		6	Y					
		"	Z					
		SPACE						
CAR. RET.		,	.					
LINE FEED		#	=					
		FIGURES						
		LETTERS						
		BLANK						

Figure 3 (left). Tape and page printer character assignments showing only the differences between page and tape in the page columns

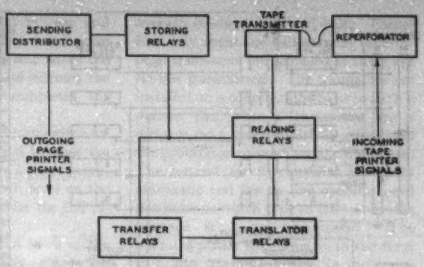

Figure 4 (right). Block diagram of translator

energized as the local brushes pass over the fifth transfer segment. The relay locks up to negative battery, and during the following revolution of the distributor a marking fifth pulse signal is transmitted to line. Should the next fifth pulse signal be spacing, all of the transfer points would be open as the brushes pass over the transfer segment in this revolution. Positive battery, through the transfer segment, is applied to the locking circuit in opposition to the negative locking battery, and the relay releases. On the following revolution of the distributor a spacing signal is transmitted to line. The location of the transfer segments is such that a storing relay will not be disturbed during transmission from its contacts.

Since the distributor brushes are continuously rotating, it is desirable to short-circuit the distributor when no intelligence is being transmitted. This, and to prevent the counter from stepping on blank characters, are two of the reasons for providing the cut-off relay. The cut-off pulse occurs during the transmission of the rest pulse, an essential requirement to avoid mutilating a character. Blank reading contacts determine the position of the cut-off relay.

Two of the more simple conversions have been chosen to describe in some detail. They are representative of the translator functions.

Equal Sign Conversion

Figure 6 shows the circuits involved in converting the equal sign to carriage return and line feed. When an equal sign is stepped into the transmitter, a marking second pulse is set up on the reading relays.

This occurs at the beginning of the transmission of the previous character to the page tie-line. The second pulse is read through contacts of the reading relays, operating the equal sign relay, which locks.

The carriage return transfer relay is immediately operated from contacts of the equal sign relay through contacts of the upper case relay. When the transfer takes place, the fourth storing relay is operated from contacts on the carriage return transfer relay. It will be noted that the second pulse set up on the reading relays is open at contacts of the equal sign relay. On the following revolution of the distributor, a fourth pulse for carriage return will be transmitted to the page tie-line. While the carriage return character is being transmitted, the auto-stop relay is operated by the transmitter step pulse because the auto-stop circuit is open at the equal sign relay. The transmitter magnet is energized, holding the transmitter contacts to spacing. The operate pulse operates the line feed relay which locks and releases the carriage return relay. When the local brushes pass over the transfer segments the second storing relay is operated and the fourth is released. On the next revolution of the distributor a second pulse for line feed is transmitted. During this revolution it is desired to reset the counter and restore

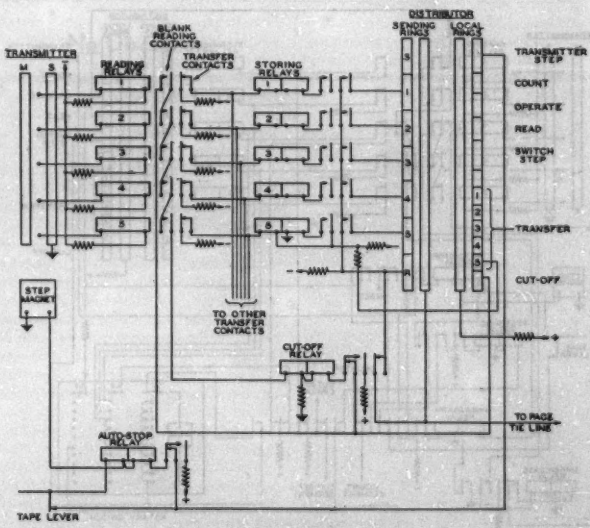

Figure 5. Transfer auto-stop, and cut-off circuits

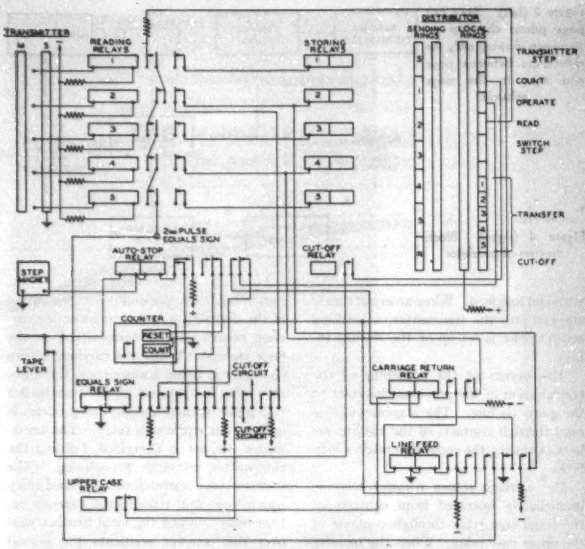

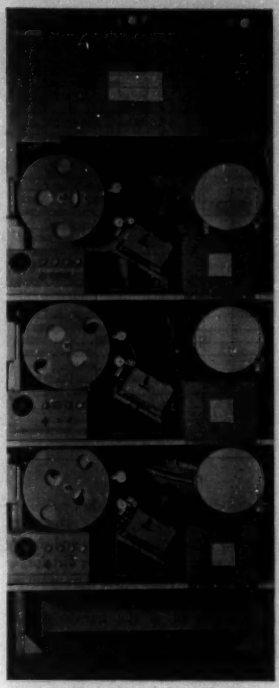

Figure 6 (above). Conversion of equal sign to carriage return and line feed

Figure 7 (below). Conversion of paragraph sign to carriage return, line feed, and five space characters

Figure 8 (right). Tape-to-page translator rack for three translators

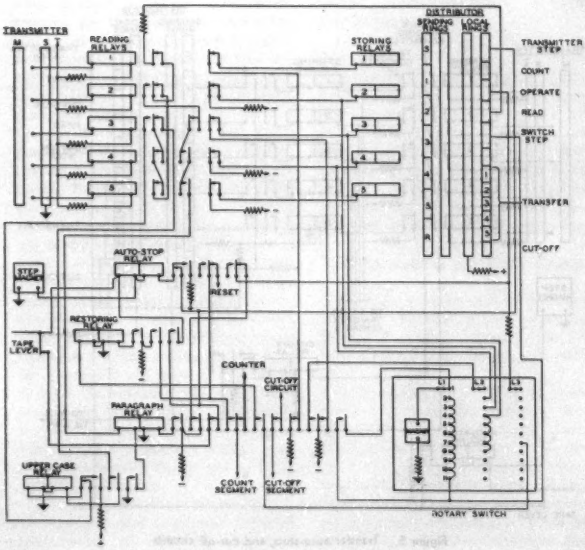

the circuits to normal. Operation of the line feed relay closed the auto-stop circuit which was opened by the equal sign relay. The transmitter pulse now releases the auto-stop relay and the transmitter steps the tape to the following character and sets it up on the reading relays. The count pulse resets the counter and also releases the line feed transfer relay. The operate pulse releases the equal sign relay, thus completing the conversion and the restoration of the circuits to normal.

For the natural end-of-line conversion, when the counter contacts close and the following word space is read, the same carriage return and line feed transfer relays are used.

Whenever a second pulse is read, whether upper or lower case, the equal sign relay responds. In the lower case the conversion of equal sign to carriage return and line feed takes place as described. In the upper case, however, the upper case relay is operated and, instead of operating the carriage return relay, the circuit is directed to another transfer relay for the conversion of the number sign.

Paragraph Sign Conversion

Figure 7 covers the conversion of the paragraph sign into carriage return, line feed, and five word spaces. The paragraph sign is upper case *S*. Therefore an upper case signal must have been received and read and the upper case relay operated and locked up. This completes the circuit for the operation of the paragraph relay when a 1, 3, marking combination is read. When the paragraph relay is operated the 1 and 3 transfer circuits from the reading relays are opened. The rotary switch step circuit is closed; the switch is stepped from the switch step segment, and through level 2 a fourth pulse for carriage return is transferred to storing relay number 4 in the same revolution in which the paragraph sign is read. On the following revolution the transmitter is auto-stopped; the switch steps again and then a second pulse for line feed is transferred to storing relay number 2. On each of the following five revolutions a third pulse for "space" is transferred to storing relay number 3. On the next to the last of these steps, a circuit is established through level 3 of the switch to prepare for the resumption of normal transmission. The restoring relay is operated by the operate pulse on the next revolution. This closes the auto-stop circuit so that on the following revolution the auto-stop relay re'eases and the transmitter stops. The count pulse releases the restoring relay and resets the counter. The operate pulse releases the paragraph relay, which completes the translation.

The application of the rotary switch for this translation is simplified because the conversion characters have a single marking impulse code. A fourth level on the same rotary switch is used for the end-of-message translation.

Figure 8 shows the front view of the tape-to-page translator rack. Each rack accommodates three translators. Each of the three shelves shown carries a reperforator, a transmitter, and a monitor unit.

The monitor unit houses the counter for indicating the end of line, signal lamps, and a monitor jack. The relay banks, distributors, and rotary switches are mounted on the rear of the rack.

Application

In practice a tie-line sending installation may involve as many as 20 or 25 tie-line transmitters, any one of which can transmit to any one of a maximum of 600 tie-lines served by a central office. The division of the tie-line traffic load between tape teleprinters and page teleprinters varies in different localities. The average is about half and half. Therefore, only about one-half as many tape-to-page translators are required as there are tie-line transmitters. The translators are installed on a concentrator basis in such a manner that when a transmitter has a message for a page tie-line it will obtain the connection through an idle translator. The request for a translator is wholly automatic and the tie-line operator need not know to which type of teleprinter the message is being transmitted. The operator places the message, in the form of printer perforated tape, in the transmitter. After noting the address, she cords the transmitter into the tie-line jack corresponding to the address. Should the patron have a page teleprinter, the circuits established will request a translator, and when the connection is obtained the transmitter will start. This transmitter at the sending position sends to the reperforator on the translator rack. The output of the translator transmits directly to the page tie-line.

The first application of the tape-to-page translator is with the new tie-line sending installations, beginning with those in the Boston office of the Western Union Telegraph Company. It is found to be very effective in improving the speed of service and efficiency in the delivery of telegrams to patrons' offices equipped with page teleprinters.

No Discussion

Lightning Arresters as a Criterion for Insulation Levels

HAROLD L. RORDEN
MEMBER AIEE

THE cost of high-voltage transmission equipment, particularly transformers and circuit breakers, is so heavily influenced by insulation that insulation levels should be chosen which are as low as are safely possible. Recent estimating data received from large manufacturers indicate that, within practical limits, the cost of average large power transformers, when purchased at recognized levels, is directly proportional to the basic impulse insulation level. The ratio of cost to the basic insulation level is greater than unity for smaller transformers, and less than unity for the larger ones. In a recent purchase of 230-kv oil circuit breakers, the ratio of reduction in cost to corresponding basic insulation level was greater than 1.5 to 1 and involved levels not recognized as standard.

Present generation and transmission facilities are far behind load requirements in the Northwest. On the basis of volume of new equipment contracted for by the Bonneville Power Administration within the past year for transmission voltages of 115 kv and above, a difference of 5 per cent in the basic insulation level could involve a difference in cost of a $250,000 annually. Somewhat greater reductions in basic insulation level than this seem feasible.

Basic Insulation Levels

Analyses and practice show that the presently-recognized basic impulse insulation levels are too conservative for the higher voltage systems, particularly since these systems are predominantly of the grounded-neutral type. This question is being considered by AIEE Standards Coordinating Committee Number 8. These basic insulation levels are substantially in linear relation to their respective operating voltages, and while they are not adopted standards, they have been accepted by the industry as defining the full-rated insulation level for the respective voltage classes regardless of the degree of grounding of the equipment. Many departures have been made from recommended levels, usually in terms of full steps because these steps only have been recognized as standard practice.

It would seem that available basic insulation levels should be such that the user can select a level that he decides is practical and economical for his system. If wide gaps exist between available insulation levels, the user may find it to his economic advantage to depart from standards; whereupon the standards cease to serve their intended purpose.

System Transients

Of the four types of transient voltages that commonly occur on modern high-voltage systems, lightning and switching surges are the most severe. They are the only ones which approach being dangerous to insulation, and of these, switching surges are not usually serious. By test, as well as from operating records, switching surges on the 230-kv Bonneville system only occasionally exceed twice normal voltage and are not known to have exceeded three times normal. These test potentials occurred on the line side of the circuit breaker during de-energizing an unloaded circuit, and were considerably lower on the bus.

The two dynamic transients produced by load rejection with accompanying overspeed, and unbalance due to faults can reach more or less the same overvoltage which is not high enough to endanger insulation. Voltages resulting from load rejection and subsequent instability have reached 40 per cent above normal on the Bonneville system. Calculations with the circuit impedances of the system (X_0/X_1 and R_0/X_1) indicate that under the worst fault conditions voltages can reach a maximum of 30 per cent above normal on the 115-kv system and 7 per cent above normal at any present 230-kv station containing transformation.

About Lightning Arresters

It seems logical to base impulse insulation levels on the levels to which a protective device such as lightning arresters can limit lightning surges. The minimum insulation level to which station equipment can be designed, using lightning arrester protection, includes:

1. A margin between the voltage rating of the system (line to ground for grounded-neutral equipment) and the voltage rating of the lightning arrester.

2. The voltage difference between the lightning arrester rating (converted to crest kilovolts) and its surge discharge voltage (protective level).

3. A margin between the protective level of the lightning arrester and the insulation level of the equipment.

With reference to the first item, if the system designer selects a lightning arrester rating below the dynamic transient voltage levels of his system, he is taking a risk, not on transmission equipment failure, but on lightning arrester failure. However, other factors might reduce the risk to the point where such a selection could be considered good practice. The

Paper 50-14, recommended by the AIEE Protective Devices Committee and approved by the AIEE Technical Program Committee for presentation at the AIEE Winter General Meeting, New York, N. Y., January 30–February 3, 1950. Manuscript submitted October 20, 1949; made available for printing November 22, 1949.

HAROLD L. RORDEN is Protection Engineer with the Bonneville Power Administration, Portland, Oreg.

Credit is due to the personnel of the Ohio Brass Company, particularly P. M. Ross and V. L. Crabb, for contriving the test line which made the lightning arrester tests possible, and for the efficiency and precision with which the tests were conducted; and to Ralph S. Gens of the Bonneville Power Administration for assembling and analyzing the data.

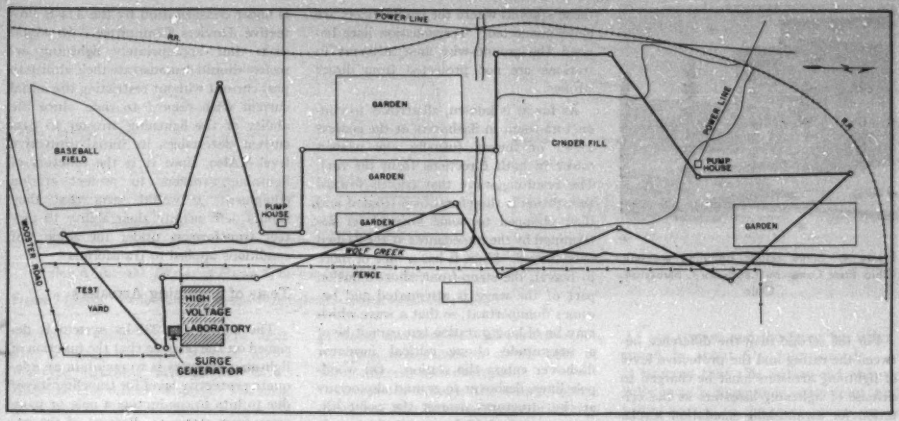

Figure 1. One-mile test line—the Ohio Brass Company High Voltage Laboratory

lightning arrester requires an initial transient voltage considerably in excess of any dynamic transient likely to be sustained in order to initiate lightning arrester discharge. This initial breakdown voltage is above most switching surges at the bus, so that it commonly requires lightning to set off the lightning arresters on unfaulted conductors at the instant the excessive dynamic voltage is impressed on the lightning arrester; otherwise no failure occurs. This may be possible, but the lightning voltage waves are usually on faulted conductors, and the unfaulted ones do not reach potentials that start lightning arrester discharge. In load rejection, surges caused by lightning have terminated before system swing and overspeed result in voltages that could destroy lightning arresters. No lightning arrester failure has occurred from load rejection on the Bonneville system. Two such cases are known by records to have resulted in dynamic voltages above the lightning arrester ratings on the 230-kv system.

Figure 2. Test line with lightning arresters 200 feet from station

If the system designer wants full assurance that his lightning arresters cannot fail from dynamic overvoltages, he must weigh the cost. A 3-pole 230-kv 80-per cent station-type lightning arrester, including labor of installation and fence enclosure, costs about $9,000 according to recent figures. Replacement of a single pole costs about $2,500. A reduction in basic insulation level of 5 per cent for a large 230-kv transformer bank and circuit breaker could save the user $30,000 to $50,000. A 42 per cent margin of lightning arrester rating over normal voltage is generally recommended for grounded-neutral systems. Normal line-to-ground voltage is 59 per cent of the line-to-line value, and recommended lightning arrester levels are 84 per cent (80 per cent with 5 per cent tolerance) for grounded-neutral service. This margin seems more than is necessary to protect lightning arresters from dynamic transients for many applications. What degree of risk might the user take, balancing the first cost versus the possibility of a lightning arrester (not transformer or circuit breaker) failure, involving an interruption to service and replacement of the lightning arrester (probably one or two poles); or is he taking much chance? If he has been using full-rated basic insulation level and can satisfy himself that it can be reduced from 10 to 25 per cent without taking much risk, it should be worthy of consideration.

Figure 3. 97-kv station-type lightning arrester with discharge counter and 90-kv line-type lightning arrester mounted for test

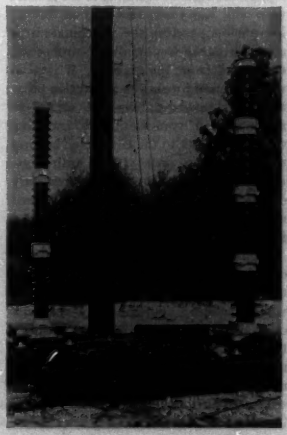

Figure 4. Surge testing lightning arresters, Ohio Brass Company Laboratory, Barberton, Ohio

For the second item the difference between the rating and the protective level of lightning arresters must be charged to defense of lightning arresters as the criterion for establishing insulation levels. Other forms of protection such as gaps may permit lower levels, but since they involve interruptions to service, they cannot usually be tolerated in large high-voltage stations. The combination of gap protection with high-speed reclosing circuit breakers offers possibilities for low basic insulation levels and an acceptable standard of service, including possible elimination of ground wires for other than station protection. The third item involves tolerances in lightning arrester performance and a factor of insurance against unknowns colloquially termed the "ignorance factor."

About Lightning Waves

The first line of defense for station equipment against lightning is the ground wire with low tower and station footing impedances, and if the combination is adequate, steep-fronted direct strokes are eliminated from the station. If ground wires are used for station protection only, the most severe anticipated surges to reach station equipment are traveling waves from hits to the conductor beyond the ground-wire area. If the entire system is protected with ground wires, only occasionally do voltages occur of sufficient magnitude to flash over insulation and invoke the use of additional protection.

Lightning protection of 230-kv stations on the Bonneville system containing transformers consists of overhead ground wires extending approximately one mile over all lines from the stations, station-type lightning arresters for grounded-neutral service, and low-resistance ground mats. The 115-kv stations are protected with one-half mile of ground wire over all lines, and full-rated lightning arresters at those stations where the transformers are delta connected. Transmission lines beyond the ground-wire area adjacent to stations are not protected from direct strokes.

As far as is known, all strokes to conductors result in flashovers at the nearest tower or towers (usually the nearest tower in both directions from the hit). The resulting wave that travels toward the station is therefore steep fronted and then chopped to some lower level determined by the impedances at the flashed over towers. Since it has a mile or more to travel, the steep-front, short-duration part of the wave is attenuated and becomes unimportant, so that a wave which may be of long duration but cannot be of a magnitude above critical insulator flashover enters the station. On wood-pole lines, flashover to ground also occurs at the structures nearest the point hit, and a wave of high magnitude travels down the line. This wave is chopped as it enters the protective ground-wire area to the level of the insulation at that point unless the potential is already below critical flashover. Flashovers also may have occurred at guyed structures or others with grounds brought near the pole top some distance from the hit.[1]

Traveling waves that enter the station are therefore limited in magnitude. The free wave that approaches the station may be considerably distorted in form, but any instantaneous value thereof obeys the relation $e=iZ$, where $Z=\sqrt{L/C}$ is the surge impedance of the line. With usual 230-kv insulation levels the critical flashover is 1,600 kv or less, the surge impedance is about 450 ohms, and so the current of approaching waves within the ground-wire area cannot exceed about 3,500 amperes and is less on lines with lower insulation levels. Since the ratio of voltage to current of the free wave is a constant, the voltage and current waves entering the station are of the same shape and cannot be displaced in time relation to each other.

Where surges of this nature and magnitude occur, they must be relieved by supplemental protective devices such as lightning arresters, since building equipment to withstand these voltages is impractical and uneconomical. In past practice, where a high margin was maintained between lightning arrester protection and basic insulation levels, standard 10/20 lightning arrester tests have been adequate. With reduced basic insulation levels, lightning arresters should be tested under conditions more nearly approximating service, particularly with respect to rates of rise of currents. This question is under consideration by the AIEE Protective Devices Committee. It would seem that appropriately lightning arresters should demonstrate their ability to pass current without restricting the initial current with respect to time, since the ability of the lightning arrester to pass current determines its initial protective level. Also, since it is the function of lightning arresters to protect station equipment, it would seem that they should demonstrate their ability to protect transformers under the same test conditions applied to transformers.

Tests of Lightning Arresters

The Bonneville 230-kv system is designed on the premise that the function of lightning arresters is to maintain an adequate protective level for traveling waves due to hits to conductors a mile or more away from stations. Because of the importance of maintaining adequate protective levels for reduced insulation of station equipment, a series of lightning arrester tests was conducted under conditions considered representative of the service to which lightning arresters are subjected on the system.

Facilities of the Ohio Brass Company were leased for these tests, and a mile of test line using number 4/0 aluminum-cable steel-reinforced conductor was constructed in the vicinity of the laboratory. The location of this line is shown in Figure 1, and the type of construction is illustrated in Figure 2. Both ends of the line terminated in the test area, so that records could be readily obtained at both ends. Average height of the line was 30 feet, and it was insulated with 15 $5^3/_4$-inch

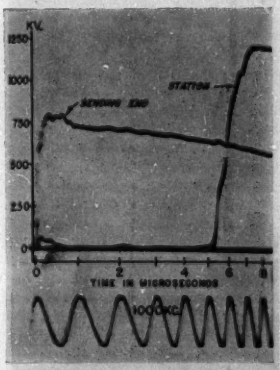

Figure 5. Voltage waves at the sending and station ends of the 1-mile test line

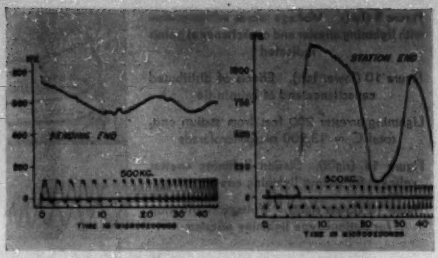

Figure 6 (above). Waves of Figure 5, on condensed time scale

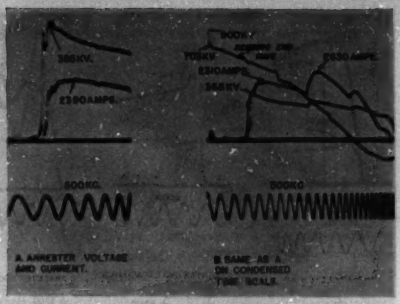

Figure 7 (right). Performance of station-type lightning arrester to traveling wave

suspension units. A station-type lightning arrester with surge counter, and a line-type lightning arrester are shown assembled for test in Figure 3. The surge generator and test platform are shown in Figure 4.

The surge generator was connected to have capacitance of 0.0716 microfarad, and to have a nominal voltage of 1,050 kv. Potentials at the sending end of the line reached about 800 kv which was considered sufficient to test lightning arresters for 115-kv grounded-neutral service. Connecting the generator to obtain sufficient potential to test 230-kv lightning arresters appeared impractical due to the short wave length of the resulting surge sent over the line. The surge impedance of the test line was measured to be about 445 ohms, the inherent inductance of the surge generator 40 microhenries, and its inherent resistance less than 2 ohms. Negative polarity was used throughout the tests except for a few at positive polarity for comparative purposes. Voltage records were obtained with the usual type resistance divider and currents by means of a twisted-pair shunt.

Tests were conducted on four station-type lightning arresters, each stacked to 97-kv rating and on three line-type lightning arresters, each consisting of three 30-kv units stacked so as to obtain a nominal voltage rating of 90 kv. This line-type arrester is beyond rated limits, but it was desired to determine whether its use on 115-kv systems appears feasible for traveling waves. The station-type lightning arresters consisted of two stacks each of the types made by two different manufacturers, denoted by *A* and *B*. One stack of each manufacturer, denoted by subscript 1, was taken from Bonneville stock, but which had never been in service. The other stack of each of the manufacturers, subscript 2, was removed from service for the tests. Line-type lightning arresters were all purchased for the tests and consisted of one each of three different manufacturers.

Except for voltage and current levels given in Table I, the oscillograms are representative of all similar lightning arresters tested, unless otherwise stated. Oscillograms showing a plurality of traces of similar characteristics, such as volt-time, were obtained by successive tests, and deflections on the records are directly comparable. Figure 5 illustrates the volt-time surge waves used in the lightning arrester tests. The wave at the sending end is equivalent to 0.4 by 22 microseconds and was impressed on the line directly from the surge generator without any extraneous impedances in the circuit. At the far end, hereinafter denoted as the station end of the line, the voltage has doubled due to reflection from an open end.

One-half of the recorded crest potential equals 85 per cent of the sending-end voltage, the difference accounting for the losses in the wave traveling one mile. At the station end the front has attenuated to about $2^1/_4$ microseconds. It is believed that this station-end wave is fully equal in magnitude, wave front, and initial energy to the more severe waves that reach stations protected with a mile of ground wire and entering over a line having the insulation level used in these tests. In fact, during preliminary tests the bus insulator stack supporting the test line at the station end flashed over. This insulation level is 40 per cent higher than is used on the Bonneville 230-kv system.

In Figure 5 the time interval between the wave fronts at the sending end and the station end is an accurate measure of the length of the test line, the oscillograph being synchronized to start recording from initiation of the surge generator for both records. In Figure 6 these same waves on a condensed scale show the wave shape after reflections occur. The steep but short overvoltage "kick" at the crest of the sending-end wave does not appear at the station end.

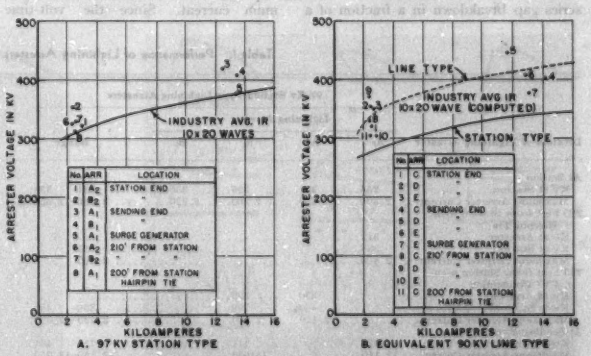

Figure 8. Performance characteristics of lightning arresters—tests compared with industry standards

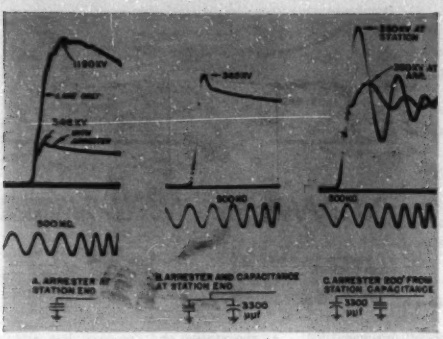

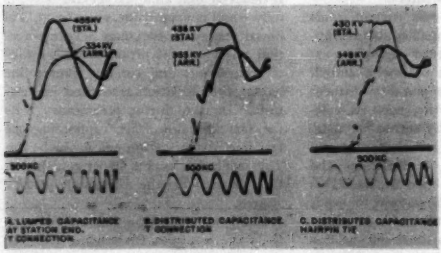

Figure 9 (left). Voltage waves within station with lightning arrester and capacitance at points indicated

Figure 10 (lower left). Effects of distributed capacitance and of hairpin tie

Lightning arrester 200 feet from station end, total C = 13,200 micromicrofarads

Figure 11 (right). Station lightning arrester voltages for various lightning arrester ratings

Figure 12 (lower right). Voltage distribution for station- type lightning arresters

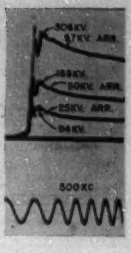

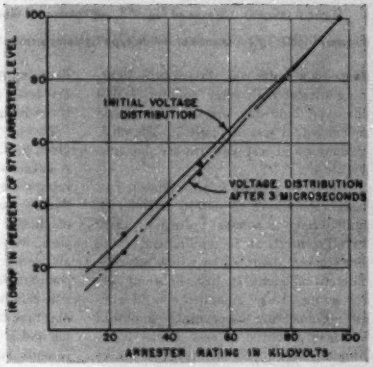

Station Lightning Arrester Tests

Figure 7(A) compares the lightning arrester voltage at the station end with the lightning arrester current, and illustrates the ability of the lightning arrester to pass current commensurate with the traveling wave voltage impressed upon it. The voltage wave reaches its crest after series gap breakdown in a fraction of a microsecond. The lightning arrester passes about 70 per cent of its maximum current almost instantaneously after gap flashover as is shown by the steep-fronted current wave, and in about 2 microseconds it passes maximum current. The initial voltage rises above the level of gap flashover, but falls to a flatter slope as the lightning arrester reaches its maximum current. Since the volt-time characteristic of major insulation also curves upward at the short time intervals, this initial rise is probably not serious. It is believed that the lightning arrester currents shown in this test are comparable to modern service conditions. The equivalent of this type of test was suggested some time ago.[2]

Figure 7(B) illustrates the same test as Figure 7(A) on a condensed-time scale.

Table I. Performance of Lightning Arresters

	97-Kv Station-Type Lightning Arresters					90-Kv Line-Type Lightning Arresters			
	Lightning Arrester						Lightning Arrester		
Location of Lightning Arrester	A_1	A_2	B_1	B_2	Range	Range	C	D	E
At Station									
Kv at Station	355	321	326	356	321– 356	331– 358	331	356	358
Maximum Arrester Current	2,390	2,500	2,500	2,320	2,390– 2,500	2,390– 2,470	2,390	2,340	2,470
200 Feet from Station with Hairpin Tie									
Kv at Arrester	312						306		
Kv at Station	395				395	346	346		
Maximum Arrester Current	2,400				2,400	2,440	2,440		
210 Feet from Station with "T" Connection									
Kv at Arrester		330	326				332	371	306
Kv at Station		405	390		390– 405	395– 494	395	440	494
Maximum Arrester Current		2,420	2,500		2,420– 2,500	2,370– 2,760	2,370	2,370	2,760
At Sending End									
Kv at Arrester	434		411		411– 434	405– 445	405	445	409
Maximum Arrester Current	12,150		13,650		12,150–13,650	11,600–14,100	14,100	11,600	12,700
On Surge Generator									
Kv at Arrester	375				375	376			376
Maximum Arrester Current	13,400				13,400	12,900			12,900

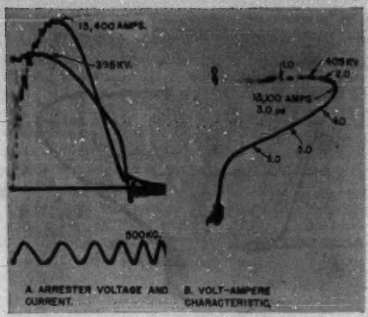

Figure 13. Performance of station-type lightning arrester with high current, no test line

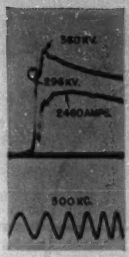

Figure 15. Performance of line-type lightning arrester at the station end

After return of the first reflected wave, the lightning arrester voltage response to the current wave is commensurate with published data for the 10/20 waves.

The first four columns of Table I list the voltages and currents of all station-type lightning arresters tested as in Figure 7. The test voltage levels are compared with standard 10/20 waves in Figure 8(A). Where repeat tests were made, the highest only is shown in the table and in Figure 8(A), since any lower values could not be depended upon as protective levels. Tolerances ranged from ±1 per cent to ±7.5 per cent from average for the four lightning arresters. The lowest level in Table I is about 4 per cent above industry average for the same current with the 10/20 wave, and the highest is about 15 per cent above that level. From these limited tests it would appear that modern lightning arresters can maintain a crest protective level for steep-fronted surges that is about 15 per cent above those of the 10/20 wave test.[4] There appears to be no uniformity or general trend in the performance of new versus used lightning arresters of the types tested.

Figure 9(A) compares the voltage at the station end (transformer location) with and without a lightning arrester. Without the lightning arrester the potential reached over twice the level of the full-rated basic insulation level for 115-kv equipment (basic insulation level–550 kv). The lightning arrester limited the surge crest to about 350 kv, reducing the potential to less than 30 per cent and providing a protective margin which appears somewhat greater than is necessary. Although the surge wave without the lightning arrester reaches its crest in more than two microseconds, the crest maintained by the lightning arrester resulted from a steep fronted wave and reached its maximum voltage level in about one microsecond. It would seem that this 80 per cent lightning arrester could adequately protect an 80 per cent basic insulation level (440 kv) even if the insulation curve were flat, and if the lightning arrester rating can be reduced proportionately.

Figure 9(B) shows the voltage when the lightning arrester at the station end was paralleled with a capacitance of 3,300 micromicrofarads (approximating an average small substation with one transformer bank). For Figure 9(C) the arrester was placed 200 feet from the station end, but the 3,300 micromicrofarads remained at the end of the line. Comparison of the several records of Figure 9 led to the conclusion that station capacitance and the location of the arrester play important parts in station protection. The addition of capacitance in the test circuit results in a resistance-inductance-capacitance-loop which, because the effective resistance of the combination of the lightning arrester and the line surge impedance is below critical damping, becomes oscillatory. Although the crest level obtained in Figure 9(C) at the capacitor would still protect 115-kv transformers with full-rated basic insulation level it probably would not afford protection at levels reduced by any appreciable degree. The nature of the circuit, as revealed by Figure 9(C), leads to the conclusion that the size of stations, location of the equipment contained therein, and the number of lines terminating at the bus

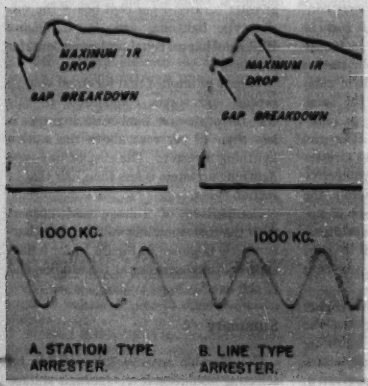

Figure 14. Initial breakdown and protective level of lightning arresters at the station end

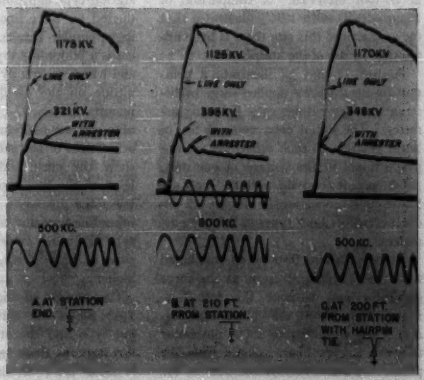

Figure 16. Voltage waves at the station end with and without line-type lightning arrester at points indicated

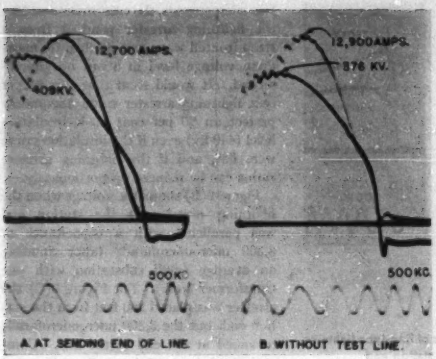

Figure 17. Performance of line-type lightning arrester to high current surges

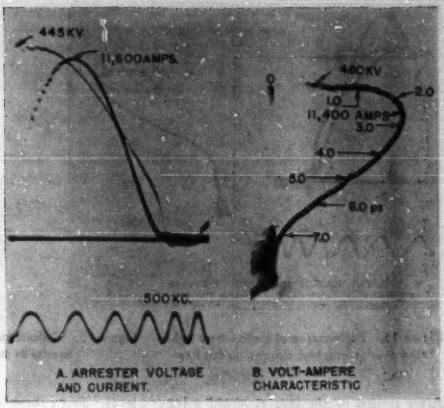

Figure 18. Performance of line-type lightning arrester to steep front, high current surge

are all of major importance in the protective level than can be provided by lightning arresters.

Figure 10 compares the voltages at the station end and at the lightning arrester with the lightning arrester 200 feet from the station end, for lumped capacitance versus distributed capacitance, and for the arrester connected with a "T" tap versus "V" or hairpin tie. For these tests the total station capacitance of 13,200 micromicrofarads approximates that of a large substation. Comparison of Figures 10(A) and 10(B) shows that the effect of assuming lumped versus distributed capacitance within the station has an appreciable effect upon the protective levels maintained by an arrester some distance from the protected equipment. The capacitances of Figure 10(B) consist of four 3,300-micromicrofarad units spaced at 50-foot intervals. A comparison of Figure 10(B) with 10(C) illustrates that for a station of this size there is little advantage by use of the hairpin tie.

Figures 11 and 12 illustrate a comparison for the same applied surge to different voltage ratings of a lightning arrester. The initial crest voltages are in linear relation to each other but are not proportional to the voltage of one unit. After current crest the voltage levels are linear and proportional. Figure 12 includes data for both types of lightning arresters.

Higher current tests were conducted with the lightning arresters at the surge generator and without the test line. Figure 13(A) shows the voltage and current levels while Figure 13(B) illustrates the volt-ampere characteristic with the parameter microseconds marked on the trace. At these currents of over 12,000 amperes, all lightning arresters reached their lowest resistance in $2^1/_2$ to 3 microseconds. The initial current shown by the steep rate of rise appears to be of the same order as for the lower current tests of Figure 7. The fall in voltage that occurs before current has reached its crest may be due in part to the limit of energy of the surge generator.

The initial flashover and voltage protective level for the station-type lightning arresters at the station end are shown in Figure 14(A) on an enlarged scale. The initial steep wave front, the point of gap flashover, and the voltage protective level are well defined.

Line-Type Lightning Arresters

Similar tests to those conducted on station-type lightning arresters were conducted on three line types with surprisingly similar results. Figure 14(B) records a 90-kv line type test at the station end which is directly comparable in magnitude on the oscillogram to the same manufacturer's 97-kv station-type lightning arrester of Figure 14(A). This and other tests of the same lightning arrester show the crest and voltage protective level of the line type to be slightly the lower for this wave. Comparison of another line type and corresponding station-type lightning arrester showed the line type to have a level 9 to 16 per cent higher.

Comparison of Figure 15 with Figure 7(A) shows the similarity between the line-type and the station-type lightning arresters for these tests. The protective levels of the 90-kv line types are given in columns 7 to 9 of Table I and are compared with extrapolated 10/20 levels in Figure 8(B). Figures 8(A) and 8(B) and columns 5 and 6 of Table I compare line and station-type protective levels.

The records of Figure 16 appear to indicate adequate protection with the lightning arrester 200 feet from the station end and show some advantage in reducing the oscillations by the hairpin tie.[4,5] These tests, unlike those of Figures 9 and 10, were conducted without added capacitance, and so they are not considered comparable to usual conditions in service.

Figure 17 shows the performance of a line-type lightning arrester without the test line. This 90-kv line-type lightning arrester is rated 7 per cent below the station-type lightning arresters of Figure 13(A) and has an equal protective level for this test.

It may be implied that for equal voltage ratings and surges comparable to this test, the protective level of the line type is less than 10 per cent above the station lightning arrester. The cost of line-type lightning arresters is less than half that of station types.

Comparison of voltage and current with the corresponding volt-ampere characteristic is shown in Figure 18 for a line-type lightning arrester at the sending end of the line.

Summary

Considerable savings are possible by selecting insulation levels for high-voltage

equipment that are as low as are feasible. This involves study of the cost and standard of service versus the degree of risk that can be assumed for the possibility of failure of the protective devices.

It seems desirable to use lightning arresters as a basis for determining basic impulse insulation levels for which lightning arrester characteristics must be known for conditions in service. The following conclusions are drawn from lightning arrester tests conducted under conditions believed comparable to those of the Bonneville Power Administration system:

1. The surges to which lightning arresters may be subjected in service have steeper fronts than the 10/20 wave.

2. On the basis of limited tests the protective level of station lightning arresters for traveling waves entering stations protected with a mile of ground wire should be about 15 per cent above industry standard 10/20 wave levels.

3. For tests with currents unrestrained with respect to time, after the lightning arrester current reaches maximum the protective level of a number of lightning arrester units stacked is proportional to the number of units in the stack.

4. An 80 per cent lightning arrester can protect an 80 per cent basic insulation level in terms of presently recognized ratings. If the lightning arrester level can be reduced further, the basic insulation level can be reduced in proportion.

5. Characteristics of line-type lightning arresters are similar to corresponding station types. For traveling waves of the nature used in the tests, line-type lightning arresters can provide protection for grounded station equipment at least up to 115 kv at a level only slightly above that of station-type lightning arresters.

6. Best protection for transformers is obtained by placing lightning arresters close to their terminals.

References

1. Wood-Pole Line Protection Without Ground Wires, H. L. Rorden. *Electrical World* (New York, N. Y.), December 9, 1944.

2. Report of the Lightning Arrester Subcommittee, J. R. North. *Electrical Engineering*, March 1938, page 183.

3. Characteristics of the New Station-Type Autovalve Lightning Arrester, W. G. Roman. *Electrical Engineering (AIEE Transactions)*, volume 56, July 1937, pages 819–22.

4. Field Tests on Thyrite Lightning Arresters Using Artificial Lightning of 1,500,000 Volts, B. K. McEachron, E. J. Wade. *AIEE Transactions*, volume 50, June 1931, pages 479–89.

5. The Hairpin Dip, Edward Beck. *Electric Journal* (East Pittsburgh, Pa.), August 1932.

Discussion

E. C. Starr (Oregon State College, Corvallis, Oreg.): The results of the tests reported in this paper are particularly gratifying to transmission engineers, in that they demonstrate the ability of modern lightning arresters to provide excellent protection against traveling-wave surges, even though they may be of extremely steep-front character, including the steep-front currents that may actually be encountered in practice. It is indicated that on the basis of the standard 10x20-microsecond current-wave test the momentary initial over-voltage across the lightning arrester, when discharging the same currents with a 2- to 3-microsecond front, may be of the order of 15 to 20 per cent. It is shown further, however that the duration of this momentary overvoltage is very brief, lying within the short-time high-strength region of transformer insulation. If the relative disruptive value of these voltage waves and the standard $1^1/_2$x40-microsecond wave when applied to transformer insulation were determined and presented, a further important step in clarifying the protection problem would be made.

Tests made during the program described by Mr. Rorden indicate the influence of length of circuit between transformer and lightning arrester, and of the surge capacitance of the transformer and its bushing. A traveling wave of sufficient magnitude to discharge the lightning arrester sets up a relatively simple resistance-inductance-capacitance oscillation between the lightning arrester and transformer that may result in higher crest voltages at the transformer than at the lightning arrester. The highest voltages for a given length of lead between lightning arrester and transformer were obtained with relatively low values of capacitance, while high values of capacitance both decrease the steepness of front and the magnitude of voltage impressed upon the transformer.

Figure 1 of this discussion presents a number of curves obtained from these data. The impinging traveling wave of current and voltage was much in excess of the lightning-arrester gap voltage and had a front of approximately 2.5 microseconds. The curves of voltage at the transformer as a function of time are actually envelopes of the crest values obtained when the equivalent transformer capacitance was varied from zero to a value so high that the initial wave front was slowed down considerably and the amplitude reduced as shown. The bottom curve indicates that for lightning arresters located immediately adjacent to transformers, the margin between transformer-insulation withstand voltage and lightning-arrester block voltage at the 8-microsecond point is actually increased for the shorter-time crests. For a 50-foot separation between lightning arrester and transformer, the 30-per cent margin at eight microseconds is reduced to approximately 16 per cent at 1.5 microseconds, and a 20-per cent margin at eight microseconds is reduced to approximately 6 per cent at 1.5 microseconds. For a 200-foot separation between lightning arrester and transformer certain values of transformer capacitance reduce the indicated margin from 30 per cent at 8 microseconds to slightly less than zero in the 2- to 4-microsecond region. While the data on transformer withstand strength and momentary overvoltage produced by lightning-arrester separation distance and transformer capacitance are not directly comparable, because of different wave shapes involved in the transformer withstand test, the results are indicative of the order of the margins to be obtained. It seems apparent that for separation distances of 50 feet or less, a margin of 25 per cent between transformer-insulation withstand value and the lightning arrester 10x20-microsecond standard block voltage, with due allowances for lightning arrester positive tolerances, should be adequate. Based upon these conclusions the following formula is suggested for determining the required insulation level of equipment to be protected by a given station-type lightning arrester located in relatively close proximity to the protected equipment in well-shielded stations:

$$\text{BIL} = (E_{avg} \text{ at } 5{,}000 \text{ amperes}) \times 1.067 \times 1.25 \text{ kv}$$

The first term is the industry average station-type lightning arrester 10x20-microsecond current-wave block voltage; the second factor allows for 6.7 per cent positive manufacturing tolerance in the lightning arrester, and the last factor allows the 25 per cent protective margin.

The lightning-arrester block voltage is, of course, dependent upon the maximum dynamic voltage rating of the lightning arrester.

This rating must be determined for the particular application by a careful analysis of the dynamic overvoltages to be expected due to unbalanced system faults and load rejection, including possible generator overspeed effects. If this formula and reasoning are applied to a 230-kv solidly-grounded system in which maximum dynamic overvoltages including harmonics are limited to 30 per cent above system maximum operating voltage to neutral, the indicated lightning-arrester rating is 182 kv, and the basic insulation level (BIL) required is 800 kv. This is just over 75 per cent of the present full-level BIL of 230-kv equipment

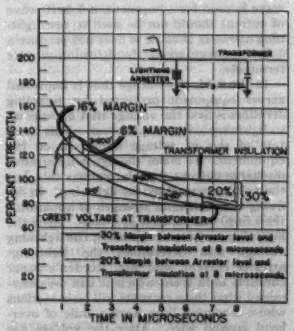

Figure 1. Transformer insulation and lightning arrester volt-time curves

and appears adequate for many important applications.

Because of the generally shorter times-to-crest of lower-magnitude traveling waves together with larger stacking factors when fewer lightning-arrester units are used, somewhat larger protective margins are probably desirable at the lower voltages. The following modification of the above equation may therefore be desirable:

$$\text{BIL} = (E_{avg} \text{ at } 5{,}000 \text{ amperes}) \times 1.067 \times 1.20 + 35 \text{ kv}$$

This equation allows a proportionally higher BIL at the lower voltages where the steep-front wave effects are more important, although generally largely offset by closer separation between lightning arrester and transformer.

A. M. Opsahl and E. Beck (Westinghouse Electric Corporation, East Pittsburgh, Pa.): In our opinion, the industry as a whole is indebted to both Mr. Rorden and the laboratories of the Ohio Brass Company, for the material published in Mr. Rorden's paper. The lightning arrester will be the foundation stone of the basic insulation levels finally to be agreed upon by the triple joint committee on insulation co-ordination. Therefore the performance data relating to high voltage lines is of much interest.

Mr. Rorden's data on lightning arrester voltage characteristics as related to discharge currents agree well with results obtained in our impulse laboratories without transmission lines. This should be reassuring as to the use of laboratory data in the determination of the protected levels provided by lightning arresters.

In correlating lightning arrester voltages with apparatus withstand levels, it seems to us that the discharge conditions used to determine the lightning arrester voltage should be such that the voltage developed across the lightning arrester has about the same shape, as nearly as practical, as the voltage in terms of which the withstand strength of equipment is stated, so that the two are comparable. We suggest that the 1.5x40 voltage wave is a good basis for comparison because it has some duration and because it is a standard for equipment. We would like to point out that because a 1.5x40 voltage wave is used for equipment, a 1.5x40 wave of current should not be used to test lightning arresters because it does not produce a 1.5x40 voltage across the lightning-arrester terminals.

In the field, the voltage that is impressed across equipment protected by lightning arresters is first the voltage that appears up to lightning-arrester sparkover. This is the rate of rise of voltage impressed on the equipment. It is not the lightning-arrester discharge current that determines this, but the voltage caused by the lightning. In defining the withstand strength of apparatus, the 1.5x40 wave is used as a basis. After the lightning arrester has sparked, the lightning voltage also determines the lightning-arrester current, and Mr. Rorden's paper contains data from which it can be determined what these currents will be in stations whose incoming lines have a mile of overhead ground wire. After the voltage has risen to lightning-arrester sparkover, the voltage at the lightning-arrester terminals depends on the discharge current and the lightning-arrester characteristics. The 10x20 wave that now is used for lightning-arrester discharge characteristic tests produces a voltage wave across the lightning arrester that has a tail closely approximating the tail of the 1.5x40 wave. As Mr. Rorden points out, the crest of the lightning-arrester discharge voltage at a given current is higher with rates of rise of discharge current higher than that of the 10x20 current wave.

We are not at this time making a brief for a particular shape of lightning arrester test current or voltage, as we feel that this may well be a subject of considerable discussion. We do advocate that the approach to the discussion be realistic, giving due weight to the manner in which apparatus withstand strengths are stated and to the lightning-arrester duty expected in the field, on which the Rorden paper sheds light.

In the case of the high-current tests described by Mr. Rorden, made with a lightning arrester at the surge generator, the voltages and currents are quite steep and the lightning-arrester voltages shown for example in Figures 12 and 13 of the paper are steeper and rise higher than those in Figures 7 and 9, the latter being the field conditions, and Figures 12 and 13 being a test condition that does not find its counterpart in the stations described in the paper. Figure 9, for example, shows that the voltage at the lightning arrester does not rise faster than the voltage produced by the incoming voltage wave.

At all rates of rise of current, the crest of the lightning-arrester discharge voltage appears before the crest of the discharge current, and at the crest of the current the voltage has dropped, as shown in the volt-ampere curve of Figure 12. The opinion has sometimes been held by some that the lightning-arrester voltage stays at crest for a long time. That is not the case in the lightning-arrester discharge voltage nor in the 1.5x40 test wave, as has been evident for a long time from laboratory tests.

In considering the selection of a wave shape of discharge current for lightning-arrester testing, some thought also should be given to test facilities. It is practical to produce lightning-arrester discharge currents of reasonably high crests and some duration, enough to cause a discharge voltage approximating closely to a 1.5x40 wave. It also is practical to produce steep high currents of short duration. It is not practical to produce a current that is steep and high and also long. The difference between a 5,000-ampere current with a 5-microsecond front and a 5,000-ampere current with a 2-microsecond front is serious in high energy surge generators.

In conclusion we wish to say that we have no criticism of the Rorden paper, which we consider a concise and useful contribution. Our discussion is merely a commentary on the general subject treated in the paper.

P. L. Bellaschi (Consulting Engineer, Portland, Oreg.): One of the factors to consider in the protection of station equipment is the lead effect between the protective device and the apparatus protected. As indicated in (A) and (B) of Figure 2 of this discussion, leads and busses of the usual lengths encountered in stations can well be represented by a lumped inductance (L_1) and for the short times involved the transformer in effect is a capacitance (C_T). The problem is conducive to calculation. A 60-foot bus corresponds to about 20 microhenries and a large power transformer in the order of 1,500 to 2,000 micromicrofarads. For an incoming surge on the line appearing at the lightning arrester, rising to lightning arrester crest voltage E in 1 microsecond and limited to that voltage by the lightning arrester, the surge voltage e_T at the transformer is (for L_1 = 20 microhenries and C_T = 2,000 micromicrofarads)

$$e_T = \left(t - 0.2 \sin \frac{2\pi}{1.26} t\right) E, \text{ for } 0 < t < 1 \text{ microsecond}$$

$$e_T = \left(1 + 0.192 \cos \frac{2\pi}{1.26} t - 0.145 \sin \frac{2\pi}{1.26} t\right) E \quad \text{for } t > 1 \text{ microsecond}$$

Thus as shown in Figure 2(C), of this discussion, for an incoming surge rising to lightning-arrester crest voltage E in 1 microsecond and maintained by the lightning arrester at that voltage and for a 60-foot bus between lightning arrester and transformer terminating at the transformer, the surge voltage the transformer (e_T) is the lightning-arrester voltage (e_A) plus a superimposed oscillation 24 per cent above the lightning-arrester crest voltage (E), of a period T_1 = 1.26 microseconds. For a 120-foot bus, the voltage attained at the transformer would be 55 per cent above the lightning-arrester crest voltage, of a somewhat longer duration because of the greater inductance of the bus.

The voltage at the transformer depends on the ratio of the front duration to the period of oscillation of the bus inductance and transformer capacitance (T_3/T_1). The dissipative characteristics of the lightning arrester, the resistance of the bus and other circuit elements as well as the surge impedance of the line all contribute to reduce the crest voltage developed at the transformer. The oscillations superimposed in most cases will decay practically to zero in a matter of several oscillations.

Present-day knowledge of lead effects, lightning arresters, and station apparatus is reasonably comprehensive and quantitative. It has been applied effectively to station design. For example, to quote briefly from Report 317 of the International Conference on High-Voltage Electric Systems[1] presented in 1939:

"It is apparent that for effective protection and co-ordination of station apparatus against very steep impulses, consideration must be given to the circuit feet of leads connecting the various station parts and to the proper location of the protective devices. The most effective method is to mount the arresters on the transformers. Conditions in the station layout or due to the apparatus may not always permit this arrangement. In such cases, the lead voltage can be minimized by locating the arrester as close as possible to the transformer or apparatus it is intended to protect. A protector tube or suitable rod gap located at the line end of the station, will afford additional protection to the station apparatus against steep-wave-front impulses that may enter the station. The problems arising in protecting a large station against very steep

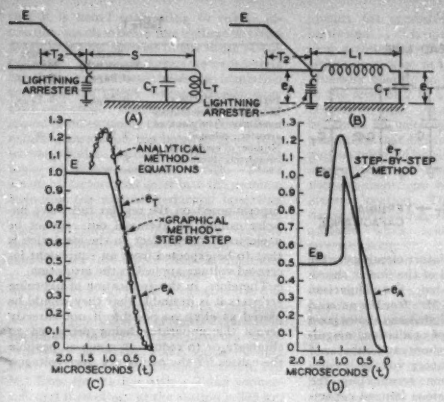

Figure 2 (above)

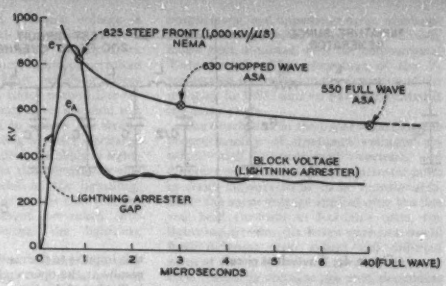

Figure 3. Impulse tests applied to transformer, full wave, chopped wave, and front of wave, and combination transformer-lightning arrester tests

Lightning arrester connecting to transformer through 40-foot lead (transformer withstand tests ASA and NEMA standards, 115-kv class)
e_A = voltage at lightning arrester;
e_T = voltage at transformer

voltages can be overcome by increasing the effectiveness of the overhead ground wire and the grounding (counterpoise) to the extent that the only possible voltages entering the station would be in effect impulse voltages of duration greater than 2 or 3 microseconds. It should be recognized that the presence of multiple lines, as well as the station capacitance, contribute beneficially and in no small measure to protection."

Another factor in protection at the shorter times arises due apparently to an inherent "delayed ionization effect" to rapid surge current discharge present in lightning arrester. It has the effect of accentuating the short time crest voltage developed at the transformer, as indicated in (D) of Figure 2 of this discussion. This effect has been apparent from the many impulse tests, commercial and experimental, that have been conducted since the middle 1930's in the various laboratories applied to transformers in combination with lightning arresters, such as illustrated in Figure 3 of this discussion. In this case, the voltage applied to the lightning arrester rises at the rate of 2,000 kv per microsecond, a value well in excess of what has ever been recorded in stations protected with overhead ground wire. The operation of the lightning-arrester gap is definite. Then follows a current inrush attaining 8,000 amperes approximately in less than 1 microsecond. As the result, the lightning-arrester voltage rises to 580-kv crest, then recedes in 1 microsecond to "normal" block voltage. Under these conditions the voltage at the transformer is a superimposed effect, due to the lead and lightning arrester, reaching well up to 850 kv, sustained for about 1 microsecond dropping to sustained or "normal" block voltage of the lightning arrester.

Because of their inherent strength at the shorter impulses,[1] transformers designed and tested in accordance with American Standards Association (ASA) (full and chopped waves) and National Electrical Manufacturers Association (NEMA) (front-of-wave) standards have been found well capable of withstanding combination tests of the character indicated. The lead and other short-time effects in relation to the volt-time characteristic of station insulation and to the over-all problem of station protection and co-ordination have been recognized and taken into account in station design, at least in certain quarters. However it is well that these problems be called attention to once again especially at this time and be re-examined particularly where reduced basic insulation levels are being applied. In the larger stations because of their extent and circuits involved, lead effects can become quite complex, requiring individual attention in each case. A certain amount of lead or bus between lightning arrester and transformer and between lightning arrester and other station equipment (circuit breakers) is permissible, the amount depending on the method of protection such as the use of overhead ground wire, the protective level and characteristics of the lightning arrester at short and long time, permissible lightning arrester tolerances, margins of protection, and volt-time characteristics and basic insulation level of the transformer and other station equipment.

The inherent "delayed ionization effect" due to rapid current discharge of the lightning arrester is clearly brought out in the tests reported by Mr. Rorden. This contribution sets forth and further emphasizes other important considerations that need be given attention in the application of arresters.

There remains a number of questions of fundamental character relating to station protection and co-ordination that require clarifying and rationalizing. Looking to the future here are a few suggestions on what need and can be done:

1. Present transformer levels are withstand and have no negative tolerance. Correspondingly, lightning-arrester protective levels should have no positive tolerances. Lately some progress has been made in this direction in an effort to reduce lightning-arrester tolerances to reasonable limits.

2. A closer correlation between lightning arrester and transformer impulse tests are very much needed. As they stand the two remain poorly co-ordinated. The transformer tests are hinged to the rod gap whereas protection is based more and more on the lightning arrester.

3. In connection with item (2), lightning-arrester voltage characteristics to a 3 or 2x20 microsecond current wave would be a logical addition or supplement to the present standards, inasmuch as a wave of this order has practical significance in protection and co-ordination.

4. The time has come for standardizing groups to consider basic insulation levels with reference to both the short and long duration impulses and to the wave forms of actual interest in protection, and not merely to the $1^1/_2$x40 microsecond voltage wave alone. Some progress has been made in this direction but more need be done to co-ordinate lightning arrester and equipment volt-time characteristics.

5. Additional improvement in the lightning-arrester 60-cycle dynamic and impulse characteristics coupled with effective methods of protection would pave the way to further rationalization in basic insulation levels and reduced levels, especially for applications to solidly grounded systems and at the higher voltages where economy is great.

6. The economics of protection in general need critical re-examining. For instance there seems to be little good justification in limiting line-type lightning arresters to voltages 73 kv and below. Because of their economic advantage this type of lightning arrester definitely has a place in the field of application to medium and even large power stations up to 115-kv to start with, and possibly even higher voltages eventually if such is found feasible.

7. To attain maximum economies in keeping with good engineering, we must avoid in planning and design pyramiding of conditions unlikely of simultaneous occurrence, which almost invariably will lead to unnecessarily higher costs. A more realistic approach to the problem of protection with a keen appreciation of probabilities is necessary.

References

1. Coordination and Protection of Station Insulation Against Lightning, P. L. Bellaschi.

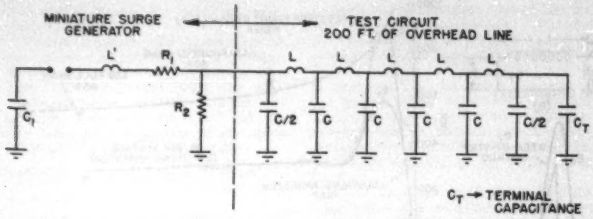

Figure 4. Equivalent circuit

Table I

	From Figure 9(B) of Paper	From Miniature System
Period of oscillations	0.78 μs	0.72 μs
Magnitude of oscillatory overshoot (per cent of arrester voltage)	1.27	1.3
Number of cycles before completely damped	8	9

Report Number 317, International Conference on Large High-Voltage Electric Systems (Paris, France) 1939.

2. Progress in Power-Transformer Insulation and Protection, P. L. Bellaschi. *Report Number 115*, International Conference on Large High-Voltage Electric Systems (Paris, France) 1946.

I. B. Johnson and **L. E. Saline** (General Electric Company, Schenectady, N. Y.): Mr. Rorden has added interesting experimental data on the performance of lightning arresters to traveling waves.

There are two statements made in the paper which we would like to amplify and comment upon:

1. "As the results of these tests were revealed, it appeared desirable to terminate the station end of the line with a capacitance comparable to that of a moderate-size station. Such capacitors were not available, but it is believed that their effect would be to increase the oscillatory nature of the voltage at the station in Figure 9(B)."

To determine the nature and magnitude of these oscillations as a function of terminal capacitance, an analysis (based on an extensive study to be reported subsequently) was made of Mr. Rorden's test circuit. This analysis was verified and extended on the transients analyzer by setting up in miniature the equivalent of Mr. Rorden's test circuit (a lightning arrester located 200 feet from the end of a line) as shown in Figure 4 of the discussion. The wave shape applied to this miniature circuit is shown on Figure 5 of this discussion, and is compared with the voltage across the lightning arrester at the station end as shown in Figure 7(A) of Mr. Rorden's paper. The application of this impulse to the miniature circuit gave the results at the open end of the line as shown in Table I of the discussion. For comparison the data obtained by Mr. Rorden as read from Figure 9(B) is included and shows good agreement for period of oscillation, magnitude of oscillatory overshoot, and number of cycles before the oscillatory voltage is completely damped. Upon terminating the miniature line with various lumped capacitances up to 5,000 micromicrofarads, the voltage at the capacitor increased to a maximum of 183 per cent of the voltage across the lightning arrester (for $C_T = 3{,}500$ micromicrofarads) as shown in Figure 6 of this discussion. Thus the transient analyzer studies of the miniature circuit show agreement with the results obtained in Mr. Rorden's staged tests for the open terminal case and have extended Mr. Rorden's study to show that the voltage at the line terminal is a function of the terminating capacitance and can increase considerably above the level held by the lightning arrester. Furthermore, the magnitude of the oscillatory over-voltage also is a function of the voltage wave shape at the lightning arrester and the separation between the lightning arrester and the protected apparatus.

Although the oscillatory voltages reported in Figure 6 of this discussion can be obtained for pure capacitance, somewhat lower values can be expected due to the inherent damping present in terminal apparatus represented by the lumped capacitance or due to surge impedance where relatively long lines (1,000 feet or more) are concerned.

For a lightning arrester located on the line 200 feet away, Mr. Rorden comments as follows:

2. "The crest of the first oscillation is higher than the level when the lightning arrester is located at the station end, but the average level is approximately the same."

Laboratory tests indicate that oscillations superimposed on the regular full wave impulse cannot be averaged out—cannot be neglected. Their effect on the insulation is that to be expected from an equivalent increased voltage applied to the insulation.

Therefore, in the application of lightning arresters it is desirable that they should be placed as close as possible if not directly across the apparatus being protected to eliminate or to reduce as much as possible the causes for the oscillatory over-voltages.

William L. Teague (Westinghouse Electric Corporation, Sharon, Pa.): In recent months the established basic insulation levels have been studied by several groups for the purpose of improving them and providing better standards for the industry. In his paper, Mr. Rorden has presented test data on lightning arresters under simulated service conditions, and an analysis of insulation levels from the user's viewpoint based on lightning-arrester performance. These are valuable contributions to the solution of the problem. There are two considerations that I would like to mention.

The first is the importance to the industry from both the manufacturer's and the user's viewpoint, of having and using standardized insulation levels. Even though most large transformers are specially designed, with the insulation levels standardized in steps, definite methods of constructions with particular interleavings of insulation and even standard drawings can be used. These can be developed and improved so that the end results are economy and quality. Both of these advantages should appeal to the user as well as the manufacturer. To reap the greatest benefit, the voltage steps must be large enough so as not to overburden the manufacturers with too many classes and yet small enough that a large majority of the users can and will conform to the standard classes.

The second thing I would like to say is to sound a warning against setting the insulation levels too low. Experience has shown

Figure 5. Voltage wave shape across lightning arrester

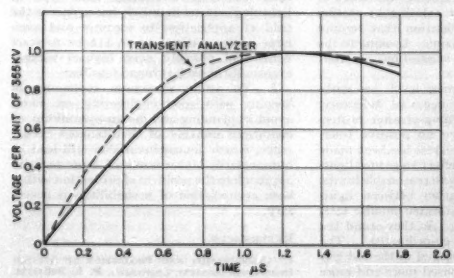

Figure 6. Capacitor voltage versus terminal capacitance as obtained on transient analyzer

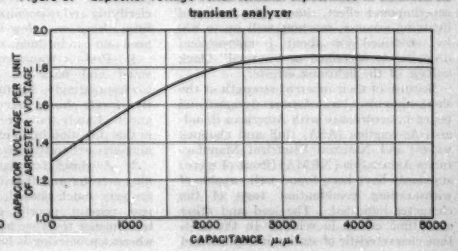

that it is sound engineering to reduce insulation one class below line voltage on effectively grounded systems in the range of 138 to 230 kv. As manufacturers we were among the first to advocate reducing insulation levels for the higher voltage classes more than one class. During the past year the appeal of the economy that might result from reducing insulation has been so great that we have had to rigidly set minimum levels below which we would not design. There are many factors that enter into the problem including the normal frequency operating voltage. Some of these cannot be evaluated except by experience. Also many variables that are difficult to control should be considered. In the application of lightning arresters alone small variations in installation practices may result in considerable differences in the voltage level at the equipment. A good example of this is Figure 16 in the paper. "A" shows the lightning arrester located at the station and a voltage of 321 kv. "B" shows the lightning arrester 210 feet from the station with a T-tap connection and the voltage at the station is 395 kv, or 23 per cent greater. "C" shows the lightning arrester 210 feet from the station with hairpin tie and a voltage at the station of 346 kv. Just the difference of a T-tap and a hairpin tie makes 14 per cent difference. Such variations that may result from differences in practices of various users of equipment must be considered in setting up insulation levels. All of the factors that enter into the problem should be considered, and total risk to equipment and to service balanced against the saving in cost. It would be poor economy indeed to permit the pendulum to swing too far in the reduction of insulation levels with an ever increasing demand for more reliable and dependable service.

W. A. McMorris, S. B. Howard and J. R. Meador (General Electric Company, Pittsfield, Mass.): Mr. Rorden is to be complimented on the test program reported in the paper. We agree with the viewpoint that equipment impulse insulation levels should be based on the protective levels afforded by lightning arresters, and agree with the three generalized factors for establishment of those levels which Rorden has enunciated in the section headed "About Lightning Arresters."

Regarding the selection of lightning-arrester voltage rating, it is fundamental that this rating be at least equal to the maximum line-to-ground dynamic voltage expected at the lightning-arrester location under any condition of operation, including load rejection and line-to-ground faults. Any compromise with that principle not only jeopardizes the lightning arrester, as Rorden points out, but, even more important, jeopardizes the equipment to be protected by introducing the possibility that overvoltage failure of the lightning arrester will remove protection from the equipment at the very time it is most needed—during the critical period when there is lightning on the system and the chance of getting additional strokes is prevalent. The statement in the paper: "This (lightning arrester) initial breakdown voltage is above most switching surges at the bus, so that it commonly requires lightning to set off the lightning arresters. . . . at the instant the excessive dynamic voltage is impressed. . . ." is open to question. Lightning arresters do frequently operate from switching surges; in fact, lightning arresters generally operate to limit switching surges to the level of 2 to 3 times normal line-to-neutral voltage. At any rate, it would not be sound engineering to ignore the strong possibility that lightning arrester discharge may be initiated by either switching or lightning at the same time that dynamic overvoltage conditions exist at the lightning-arrester location. This means that the dynamic overvoltage must be taken into account when selecting the lightning arrester rating.

In the section headed "About Lightning Waves," Rorden states, ". . . . if the (ground wire and low station-and-tower-footing impedance) combination is adequate, steep fronted direct strokes are eliminated from the station." He then goes on to calculate the traveling-wave voltages and currents which must be taken care of by the station lightning arresters in protecting the station apparatus. It appears to us to be more logical to base protection on the discharge currents measured in service through lightning arresters in stations, regardless of how these discharge currents are produced, that is, whether by direct strokes or by traveling waves. Some groups have questioned whether or not the 10x20 microsecond current wave, which appears in the present lightning arrester standards and which has been used for comparing lightning-arrester performance characteristics, is representative of the more severe discharges encountered in service. To answer this question, the Lightning Protective Devices Subcommittee is at present studying all available information on discharge currents through lightning arresters in service, with the object of evaluating the currents and wave shapes on which insulation co-ordination may most reasonably be based.

With regard to the section headed "Tests of Lightning Arresters," the lightning-arrester discharge voltage, for a current of given crest value and wave shape, is the same whether or not the discharge current arrives at the lightning arrester over a line impedance. The lightning-arrester discharge voltages obtained in Rorden's tests are in close agreement with results of our laboratory investigations, using currents of the same crest value and wave shape.

Rorden's test results on the effect of line inductance between lightning arrester and protected apparatus, in producing oscillatory voltages in excess of the lightning-arrester discharge voltage level, are comparable to the test results reported by K. B. McEachron in 1929.[1] Reference to that work shows that the voltage held at the apparatus terminals is increased to almost twice lightning arrester discharge voltage by the introduction of an inductance equivalent to 100 feet of overhead line between lightning arrester and apparatus terminals, with steep front surges applied. Both series of tests point to the necessity for installing lightning arresters in close shunt relationship to the apparatus they are intended to protect, if full advantage is to be gained of the protective levels available at the lightning arrester terminals.

With regard to the physical connection between line and lightning arrester, the "hairpin" or V-connection reduces the lightning arrester lead impedance drop, which appears at the protected apparatus terminals, below that obtained with the conventional T-connection. The advantage of the V-connection was called to the attention of the industry in 1931[2] and we have advocated it for many years.

The conclusion in the paper regarding the proportionality of discharge voltages obtained with "unrestrained" currents and different numbers of lightning-arrester units in series appears to us to be questionable. Since the surge voltage applied over the line was held constant in Rorden's tests, the lightning-arrester discharge currents would have different crest values and different rates of rise, which would result in different crest discharge voltages per unit, depending on the number of lightning-arrester units in the stack. With the surge current held constant, the lightning-arrester discharge voltage would have been proportional to the number of units in the stack.

Under "Line-Type Lightning Arresters," the statement is made that ". . . . the protective level of the line type is less than 10 per cent above the station lightning arrester (of equal rating)." This statement does not agree with the lightning-arrester performance values given in the Lightning Protective Devices Subcommittee report, Performance Characteristics of Lightning Protective Devices[3] which shows that line-type lightning arresters have discharge voltage 20 per cent above that of station-type lightning arresters at 5,000 amperes (10x20 microseconds) and even higher differentials at higher currents.

The thought expressed in Rorden's paper, that there should be a large number of small steps in the basic impulse insulation levels, should be taken with caution. Even though large high-voltage power transformers are not built on a production line, a considerable amount of standardization in design and manufacture has been achieved. For that reason, each element of the insulation structure must be carefully evaluated as to its effect on the whole. The number of insulating barriers, for example, cannot normally be changed in less than 10 to 20 per cent steps. The same is true to a lesser degree of turn insulation and oil-duct sizes. These "building blocks" can be and are standardized with resultant improvement in quality and reduction in cost. If the basic insulation levels are selected to fill the needs of the majority of users, the ultimate benefits of standardization will accrue to these users. Minor variations from the standard levels will not result in proportionate cost savings.

REFERENCES

1. CATHODE RAY OSCILLOGRAPHIC STUDY OF THE OPERATION OF CHOKE COILS ON TRANSMISSION LINES, K. B. McEachron. *General Electric Review* (Schenectady, N.Y.), Figures 14 and 16, December 1929, pages 663–73.

2. FIELD TESTS ON THYRITE LIGHTNING ARRESTERS, K. B. McEachron, E. J. Wade. *AIEE Transactions*, volume 50, June 1931, pages 479–80.

3. PERFORMANCE CHARACTERISTICS OF LIGHTNING PROTECTIVE DEVICES, Lightning Protective Devices Subcommittee. *AIEE Transactions*, volume 68, part II, 1949, pages 1330–33.

Harold L. Rorden: The question of location of lightning arresters with respect to protected equipment apparently is one of uppermost concern. In these tests the

lightning arresters have demonstrated their ability to maintain adequate protective levels at their terminals. When the lightning arrester is placed some distance from the protected equipment, the resulting loop circuit contains a combination of impedances which is likely to result in oscillatory voltages because the resistance of the lightning arrester falls below critical damping. The resultant voltage at transformer terminals will therefore probably be somewhat higher than that at the lightning-arrester terminals during the crest of the first half cycle of a highly-damped high-frequency wave. Analytically this potential might reach twice that at the lightning-arrester terminals, but other factors reduce the probability of obtaining such potentials to a rather remote possibility.

The oscillograms of Figures 9 and 10 of the paper illustrate the oscillatory nature and the magnitudes of voltages that might be impressed on a transformer as were obtained during the test. Figure 7 of this discussion compares the worst oscillatory voltage obtained by test at the station end (transformer terminals), with the protective level provided by the lightning arrester at the end of the line without added capacitance. A curve of transformer insulation having a strength of about 165 per cent of the minimum level at 1/2 microsecond also is given for comparison. This curve is plotted from commonly accepted data for a basic insulation level of 450 kv, which is one step reduced from presently recognized practice for 115-kv service and is about 82 per cent of the full-rated basic insulation level (550 kv). With the lightning arrester 200 feet away, the margin of protection at the first crest of the oscillatory voltage with 1,600-micromicrofarad capacitance at the station end is approximately 22 per cent. The margin of protection afforded by the lightning arrester without added capacitance at the station end is much greater at the short times, but more nearly parallels that of the transformer insulation for times beyond 4 microseconds. In this longer time area the margin of protection, even with the insulation reduced one step, is about 65 per cent. An ideal protective curve would be one that parallels the transformer insulation providing a uniform margin throughout. A protective curve plotted through the crests of the oscillatory voltage at the station with the lightning arrester 200 feet away, and with one step reduced basic insulation levels indicates a fair margin at any point in the curve. The curve of voltage at the lightning arrester terminals might well be said to provide more than necessary margin at the short times. Mr. Starr's data indicate that the protective curve with the lightning arrester at 50 feet is a fair parallel of the insulation strength, and that greater distances are tolerable if adequate margin is provided.

It appears therefore that although the greatest margin is unquestionably obtained by placing the lightning arrester close to the protected equipment, it is not of extreme importance to do so because of the nature of insulation strength in the short time range. When lightning arresters are mounted directly at the transformer, circuit breakers, particularly in large stations, may be a considerable distance away from the lightning arrester and therefore subject to rather severe surges. Circuit breakers also add capacitance to the station and can contribute to causing surges to become oscillatory at their terminals. In service, conditions, as mentioned by Mr. Bellaschi, are probably somewhat better with respect to limiting the oscillatory nature of overvoltages due to the distributed nature of station capacitance. Also where more than one line terminates at the bus, voltages are not doubled by reflection and will, in fact, be reduced below the level of the incoming surge at stations having three or more lines terminating at the bus. In two Bonneville 230-kv stations in the lightning area lightning arresters have not operated since the stations have been completed. One of these stations contains four transformer banks and two lines terminating on the bus. The other contains two transformer banks with seven lines terminating on the bus. Lightning hits have occurred to conductors close to these stations, but to date these hits have not resulted in lightning-arrester operations. The lightning arresters are equipped with counters one of which was checked during the Barberton tests and found to be in perfect working order.

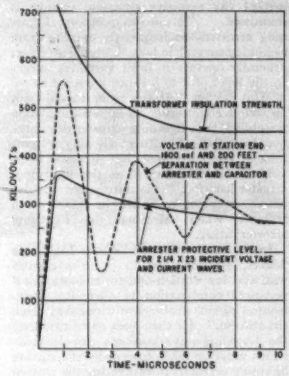

Figure 7. Voltages at station end and transformer insulation strength

97-kv station-type lightning arrester, 450-kv insulation class

Figure 7 of this discussion replies to Messrs. Johnson and Saline's statement that the oscillatory voltages cannot be averaged. The average level determines adequacy of protection at the longer times.

The agreement with laboratory tests reported by Messrs. McMorris-Howard-Meador, Opsahl-Beck, and Johnson-Saline is of particular interest in lending confidence to laboratory tests that attempt to duplicate service conditions. The tests at Barberton were conducted with a transmission line in order to minimize doubts that otherwise arise when service conditions are simulated. Once such tests have been conducted and duplicated by laboratory equivalents, further laboratory studies can be carried on with complete confidence. It is well known that traveling-wave phenomena can be accurately translated in terms of circuit constants and that transmission lines can be simulated in the laboratory.

Complete agreement is given with Messrs. Opsahl and Beck that realistic test waves should be adopted that are not difficult to obtain in the laboratory and that will provide the user with information that applies to conditions in service. It seems probable that one such test wave is inadequate because of extreme differences that may exist in transmission systems, such as use or absence of overhead ground wires for station protection.

We also agree with Mr. Teague that all factors affecting basic insulation levels must be considered in establishing insulation levels and that steps should be so chosen that they are large enough for economic design, yet small enough so that the user will not be tempted to go off standard in the interests of economy.

Mr. Starr's suggestion of an 800-kv basic insulation level for 230-kv operation represents an insulation level equal to 75 per cent of presently recognized practice. The tests have shown that a 75-per cent lightning arrester can adequately protect a 75-per cent basic insulation level, and recent NEMA recommendations suggest 75-per cent lightning arresters as the basis for selecting insulation levels for 230 kv. An 800-kv basic insulation level for 230-kv operation would effect substantial economies and appears satisfactory for many solidly-grounded systems.

Mr. Bellaschi's comment relative to delayed ionization is significant, since it indicates that some variable besides current is present in determining the resistance characteristic of lightning arresters. Mr. Bellaschi's summary of needs for further study of this subject is very complete and appropriate.

Messrs. McMorris, Howard, and Meador's statement that the number of lightning arrester units would be proportional to voltage if the current were kept constant is questionable, and published catalog data of lightning arresters do not so indicate. On the basis of lightning-arrester catalog data, the increase of discharge voltage per unit during the tests corresponds to 100 per cent increase in current. The actual current increase was about 25 per cent.

Analogue Computer for Multicomponent Fractionation Calculations

G. W. GOELZ
ASSOCIATE AIEE

J. F. CALVERT
FELLOW AIEE

IN THE petroleum and natural gas industries rather tedious trial-and-error computations have been employed in designing and predetermining the performance of multicomponent fractionating columns. The purpose of this paper is to describe an analogue computing machine, Figure 1, with the aid of which these calculations are carried out in approximately one-tenth the man-hours required for the more usual methods. A description of the physical operation of a fractionating column and a development of the equations applying to this operation will be presented. Following this, a description will be given of the computing machine and its principle of operation.

The Problem

A fractionating column, or tower, is a type of equipment which permits a liquid stream to cascade down over a series of trays or plates, Figure 2, and allows a vapor stream to bubble up through the plates countercurrent to the liquid stream. The feed stream (containing several components, such as ethane, propane, butane, and so forth) enters the column somewhere between the top and bottom plates. Often this stream is introduced about halfway up the tower. Each of the components of the feed is present in varying amounts in the liquid stream falling from a given plate and the vapor stream rising from a given plate. The relative amounts of the several components in a given stream leaving a specified plate within the column depend upon several factors including the temperature and pressure of that stream and the relative amounts of liquid and vapor components in the streams approaching and leaving the plate. In general the liquid stream as it cascades down the column from top to bottom contains increasing amounts of the less volatile components and decreasing amounts of the more volatile components. Conversely, the vapor stream in passing up the column becomes poorer in the less volatile components and richer in the more volatile ones. In this manner the feed, which contains substantial quantities of each of the components, is separated into a vapor product, which primarily consists of the more volatile components, and a liquid product which predominately contains the less volatile components. The vapor product leaves the top plate and the liquid product is withdrawn from the bottom one. In order to effect this separation it is necessary to maintain substantial liquid and vapor flows within the column. This is achieved by utilizing a heater to introduce heat into the bottom chamber, and using a cooler or condenser to remove heat at the top of the column (through which part of the vapor product is passed to produce a liquid stream which is recycled to the top of the tower).

The quantitative relationships between the compositions, quantities, temperatures, and pressures of the various liquid and vapor streams include material balances, enthalpy (or heat) balances, and equilibrium conditions. These relationships represent the performance of a fractionating column operating under steady state conditions as indicated in Figure 2. Consider that section of the column within the dashed line. Applying the foregoing relationships to this section:

1. The total mass of material entering the section is equal to the total mass of material leaving.
2. The mass of any one component entering the section is equal to the mass of that component leaving.
3. The enthalpy of entering streams plus any enthalpy added (as in the heater) is equal to the enthalpy of the leaving streams.
4. The composition of any vapor stream rising from a plate is in equilibrium with and at the same temperature as the liquid falling down from that plate.
5. The temperatures and stream quantities vary throughout the fractionating column in such a manner that the above conditions are met. In general, the pressure is fairly constant from plate to plate.

The detailed calculations may be made as follows:

1. Obtain the rate of flow and composition of the liquid bottom plate product.
2. Obtain the rate of heat input from the heater.
3. Obtain the column operating pressure.
4. Determine by trial and error the bottom plate temperature.
5. Calculate the composition of the vapor stream leaving the bottom plate.
6. Calculate the net enthalpy input to the bottom of the column (heater input less enthalpy of liquid bottom product).
7. Consider an envelope (similar to that represented by the dashed line in Figure 2) enclosing the bottom plate and the heater.

Figure 1. The computer

Paper 50-15, recommended by the AIEE Computing Devices Committee and approved by the AIEE Technical Program Committee for presentation at the AIEE Winter General Meeting, New York, N. Y., January 30–February 3, 1950. Manuscript submitted October 31, 1949; made available for printing November 22, 1949.

G. W. Goelz and J. F. Calvert are with Northwestern University, Evanston, Ill.

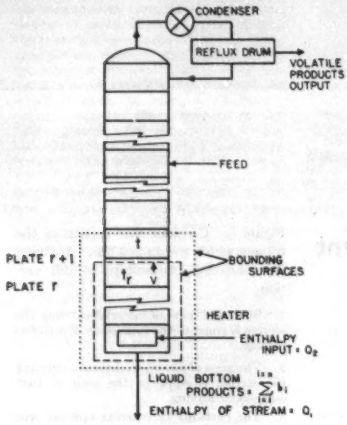

Figure 2 (left). Schematic diagram of a multicomponent fractionating column

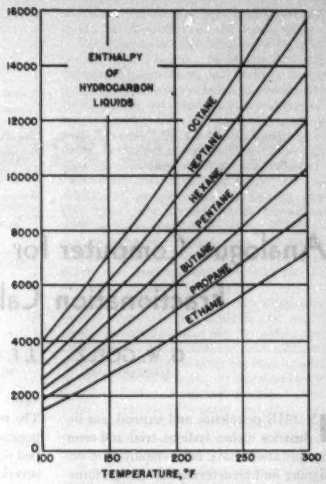

Figure 3(A) (right). Curves of $h_i(t)$ and $H_i(t_r)$

8. Using enthalpy balances, material balances, and equilibrium relationships, together with the data obtained in steps 4, 5, and 6, determine by trial and error the temperature, composition, and rate at which liquid leaves the second plate and the rate at which vapor rises from the bottom plate.

9. Calculate the composition of the vapor stream leaving the second plate.

10. Repeat steps 7, 8, and 9 for each plate between the bottom of the column and the feed plate.

11. Follow a similar procedure for the top section of the column by calculating down from the vapor product.

The calculations which are made upward and those which are made downward along the column are very similar in character, and the computing machine to be described may be employed for both. Therefore, for the sake of brevity, only upward computational procedures will be described here.

At this point reference should be made to the glossary. Consider plate r in Figure 2 and the volume enclosed by the

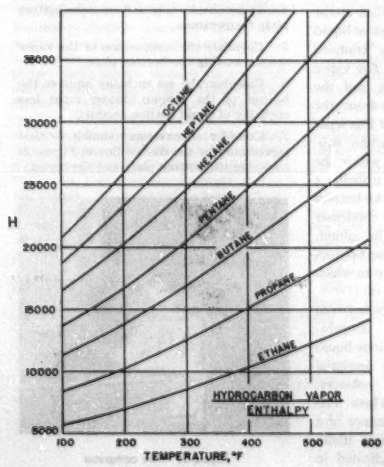

Figure 3 (left). Functions represented by the computer

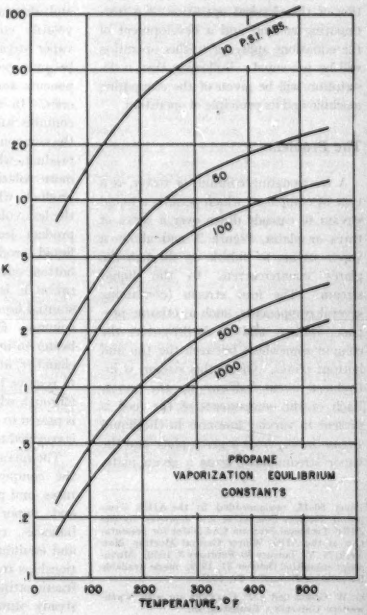

Figure 3(B) (right). A typical $K_i(t)$ curve

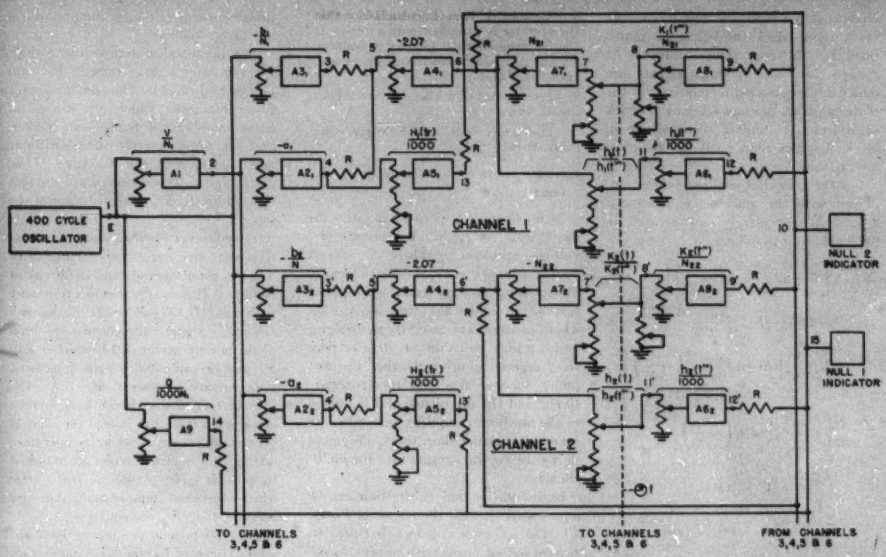

Figure 4. Computer block diagram

dashed line. For computations made upward, the equations to be solved when a problem involves n significant components are:

For equilibrium between the liquid and vapor streams leaving a plate

$$\sum_{i=1}^{i=n} [a_i V + b_i] K_i(t) - \sum_{i=1}^{i=n} [a_i V + b_i] = 0 \qquad (1)$$

For enthalpy balance,

$$\sum_{i=1}^{i=n} [a_i V + b_i] h_i(t) - \sum_{i=1}^{i=n} a_i V H_i(t_r) + Q = 0 \qquad (2)$$

The usual procedure is to assume a pair of values of V and t, and substitute in equations 1 and 2 to see if the equations are satisfied. If they are not, the procedure is repeated until the equations balance. In this process the functions, $K_i(t)$, $h_i(t)$, and $H_i(t_r)$, are obtained from graphs, see Figure 3. When those values of V and t have been found which simultaneously satisfy equations 1 and 2, new values of the coefficients, here called a_i', are obtained for the calculations to follow.

$$a_i' = \frac{[a_i V + b_i] K_i(t)}{\sum_{i=1}^{i=n} [a_i V + b_i] K_i(t)} \qquad (3)$$

The terms on the right side of equation 3 are taken from the preceding data. In order to proceed one more plate up the column, a new bounding surface, represented by the dotted line in Figure 2, is assumed which encloses the preceding volume and also the next plate above. To solve for the conditions associated with this next plate, equations 1, 2, and 3 are solved again. This time t_r is the temperature determined as t from the previous solution of the equations and the a_i values are those previously calculated as a_i' from equation 3. Calculations are made upward along the column in this fashion.

It is from this sequential procedure that the descriptive term plate-to-plate calculation is taken. The methods are described more fully in chemical engineering publications.[1]

The Analogue Computing Machine

Primarily, the computing machine is composed of resistors, potentiometers, and amplifiers, suitably chosen and connected to yield the electrical representation of the preceding equations, though in slightly modified forms. A 400-cycle carrier voltage is applied to a number of channels. One channel is required for each chemical component to be represented; and while six are provided in the present machine, this is not a basic design restriction. Each

Figure 5 (below). Multiplication circuits

Figure 6 (right). Addition circuit

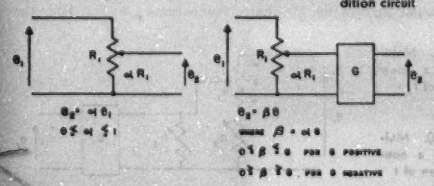

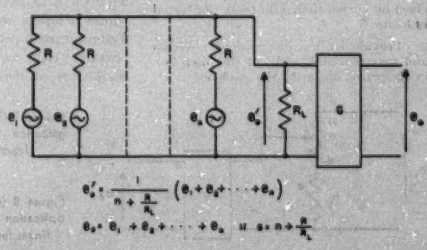

channel is composed of a number of circuits, along which the voltage is multiplied by the appropriate factors. At various locations, voltage signals are added and subtracted as required by the plate-to-plate equations. Figure 4, which illustrates a section of the machine in block diagram form, will be discussed later in some detail.

For the computational procedures employed with the machine, equations 1, 2, and 3, respectively, are treated in modified forms as follows

$$\sum_{i=1}^{i=n} \frac{1}{2.07}\left[E(-a_i)\frac{V}{N_1}+E\left(-\frac{b_i}{N_1}\right)\right]\times (-2.07)(-N_{2i})\frac{K_i(t)}{K_i(t''')}\frac{K_1(t''')}{N_{3i}}+ \sum_{i=1}^{i=n}\frac{1}{2.07}\left[E(-a_i)\frac{V}{N_1}+E\left(-\frac{b_i}{N_1}\right)\right]\times (-2.07)=0 \quad (1A)$$

$$\sum_{i=1}^{i=n}\frac{1}{2.07}\left[E(-a_i)\frac{V}{N_1}+E\left(-\frac{b_i}{N_1}\right)\right]\times (-2.07)\frac{h_i(t)}{h_i(t''')}\frac{h_1(t''')}{1{,}000}+ \sum_{i=1}^{i=n}E(-a_i)\frac{V}{N_1}\frac{H_i(t_r)}{1{,}000}+E\frac{Q}{1{,}000}=0 \quad (2A)$$

$$a_i'=\frac{\frac{1}{2.07}\left[E(-a_i)\frac{V}{N_1}+E\left(-\frac{b_i}{N_1}\right)\right]\times (-2.07)\times(-N_{2i})\frac{K_i(t)}{K_i(t''')}\frac{K_1(t''')}{N_{3i}}}{\sum_{i=1}^{i=n}\frac{1}{2.07}\left[E(-a_i)\frac{V}{N}+E\left(-\frac{b_i}{N_1}\right)\right]\times (-2.07)(-N_{2i})\frac{K_i(t)}{K_i(t''')}\frac{K_1(t''')}{N_{3i}}} \quad (3A)$$

Here, E is the magnitude of the input voltage carrier, the term $1/2.07$ is introduced by the circuit procedures employed for addition and subtraction, and terms such as N_1, N_{2i}, and $1/1{,}000$ permit certain design and constructional simplifications.

It is required for the satisfactory solution of equations 1A through 3A that the machine:

1. Represent the algebraic operations of addition, subtraction, and multiplication.
2. Represent, at least piece-wise, the data given on curves similar to those illustrated in Figure 3.
3. Provide for the independent insertion and variation of V and t at the discretion of the person operating the machine.
4. Combine all terms in such a fashion that the operator is presented with a measure of the balance or lack of balance in equations 1A and 2A, which result from his assumed values of V and t.
5. Provide data for the determination of the a_i' terms.
6. Place reasonable bounds on the equipment errors.

Representation of Algebraic Operations

Multiplication is performed either by means of a voltage divider network or a voltage amplifier. Where a voltage divider network is employed, the multiplying factor (voltage gain), α, is limited to positive values less than unity; but where an amplifier is used the multiplying factor β may be either negative or positive, depending upon whether the amplifier does or does not invert respectively, and the magnitude of β is limited to the maximum amplifier gain, which in general, is greater than unity. Figure 5 shows the typical circuits used for multiplication.

Both addition and subtraction can be represented through the circuit of Figure 6.[2] The 400-cycle voltages that are 180 degrees out of phase with respect to the positive reference voltage subtract, effectively, from the voltages in phase with the reference. In some cases, a voltage proportional to, but not necessarily equal to, the sum of the input voltages may be required. For these cases, the amplifier of gain G, see Figure 6, can be eliminated.

Piece-Wise Representation of Curve Data

A number of terms in the plate-to-plate equations are functions of either the known temperature, t_r, or the unknown temperature, t. The machine represents each of these by the over-all voltage gain of a voltage divider and amplifier arranged in cascade. The particular temperature at which a function is evaluated is represented by the angular position of a potentiometer located within the voltage divider. Each of the voltage divider-amplifier circuits is employed to represent a section of a given curve bounded by two chosen temperature limits, t' and t'''. Temperature bounds are selected by the operator with due regard given to the limitations of the machine and to the probable range of temperature needed in any given solution.

The functions of temperature, which the computer must represent, fall into two general classes. They are the almost linear functions, which are treated as linear over limited temperature ranges, and the approximately semilogarithmic and, hence, nonlinear functions. The $H_i(t_r)$ and $h_i(t)$ functions are of the first type while the $K_i(t)$ functions are of the second.

The circuit of Figure 7 could be used to represent the curves of Figure 3(A). The potentiometer indicated in the circuit is linear. If R_3 is adjusted to a resistance such that $R_3G/(R_1+R_3)=h_i(t')/1{,}000$ with $G=h_i(t''')/1{,}000$, the angular position of the potentiometer dial between θ' and θ''' can be calibrated linearly in terms of temperatures between t' and t'''. The over-all gain of the circuit, e_3/e_1, is then equal to $h_i(t_r)/1000$, when the dial is positioned at any specific temperature setting, t_r. Similar circuits are required to provide gains equal to $H_i(t_r)/1000$ when individual temperature dials are adjusted to read t_r, see equation 2A.

The 100 pounds per square inch absolute curve of Figure 3(B) can be approximated by the circuit of Figure 8.[2] Except that resistor R_3 has been added, the circuit of Figure 8 is identical to that of Figure 7. When the dial of the linear potentiometer R_1 is linearly calibrated, G, R_2, and R_3 can be adjusted such that the circuit will provide a function which, within a selected temperature range, closely approximates and at three points coincides with the desired curve. It is possible to draw two sets of curves of $K_i(t')/K_i(t''')$ versus $K_i(t'')/K_i(t''')$ with R_2 and R_3 as parameters. These curves may be referred to in choosing the approximate values of R_2 and R_3. A bridge type calibration circuit, to be described later, allows the operator to establish R_2 and R_3 exactly. The over-all gain of the voltage divider is made equal to $K_i(t')/K_i(t''')$ by adjusting R_2 with the potentiometer set to θ'. In like manner the over-all voltage divider gain is set equal to $K_i(t'')/K_i(t''')$ by varying R_3 with the potentiometer wiper positioned at θ''.

In the actual circuit, Figure 4, the voltage divider of Figure 8 is preceded by an inverting amplifier of gain N_{3i}. Thus, the

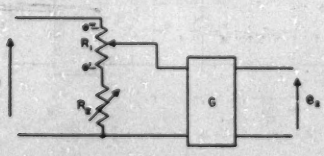

Figure 7 (left). Multiplication by a linear function of t

Figure 8 (right). Multiplication by a nonlinear function of t

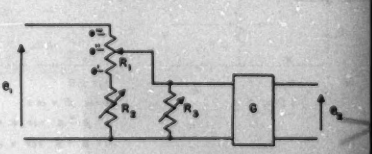

gain of the amplifier following the voltage divider is set to $K_4(t'')/N_{21}$. This design arrangement permits the machine to accommodate a wide range of values of $K_4(t'')$, and at the same time leads to a standardization of parts.

The closeness with which the curve is approximated depends upon the magnitude of the ratio $K_4(t')/K_4(t'')$. The error in fitting a curve can become rather large for small values of this ratio. However, the operator may easily keep the error involved in representing the K functions to within three per cent by proper choices of the pair of temperatures t' and t''. For flat K curves, a 100 degree Fahrenheit temperature range can be chosen, while for very steep K curves a 50 degree range may be required.

Independent Insertion of V and T

The computer represents V/N_1 as the over-all gain of a single potentiometer. Once a problem is put into the machine, the variable t is represented by the angular position of a ganged potentiometer shaft. Thus, by merely varying two knobs, the operator inserts successive, independent trial values of V and t until the machine indicates that a particular pair of settings satisfies the two plate-to-plate equations.

For a 6-component machine, a trial setting of the ganged potentiometer shaft must cause the insertion of 12 functions of t evaluated at the trial temperature setting. Six of the functions are of the linear class shown in Figure 3(A) and six are of the nonlinear class indicated in Figure 3(B). The first six functions are traced out by six circuits similar to that of Figure 7, and the second six are represented by six circuits similar to that of Figure 8. Thus, for a 6-component machine, the ganged potentiometer shaft mounts 12 linear potentiometers.

Combination of Terms and Representation of Equations

The line diagram of Figure 4 indicates how the machine is employed to represent the plate-to-plate calculations. The voltage gains existing throughout the circuit, when a solution has been obtained, are shown on the diagram. The voltage magnitudes that exist at the marked points indicated on Figure 4 are given in the following terms (an asterisk indicates that a voltage does not have the magnitude specified unless a solution has been obtained).

Point 1. E

Point 2. $E\,\dfrac{V^*}{N_1}$

Figure 9. Bridge-type calibration circuit

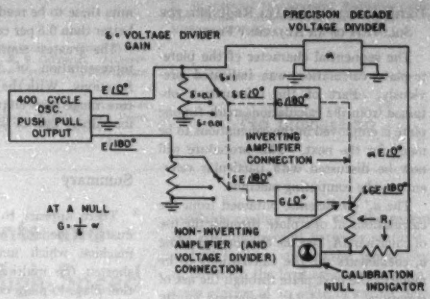

Point 3. $E\left(-\dfrac{b_1}{N_1}\right)$

Point 4. $E\dfrac{V}{N_1}(-a_1)^*$

Point 5. $\dfrac{1}{2.07}\left[E\dfrac{V}{N_1}(-a_1)+E\left(-\dfrac{b_1}{N_1}\right)\right]^*$

Point 6. $\dfrac{-2.07}{2.07}\left[E\dfrac{V}{N_1}(-a_1)+E\left(-\dfrac{b_1}{N_1}\right)\right]^*$

Point 7. $\dfrac{-2.07}{2.07}\left[E\dfrac{V}{N_1}(-a_1)+E\left(-\dfrac{b_1}{N_1}\right)\right]\times(-N_{21})^*$

Point 8. $\dfrac{-2.07}{2.07}\left[E\dfrac{V}{N_1}(-a_1)+E\left(-\dfrac{b_1}{N_1}\right)\right]\times(-N_{21})\dfrac{K_1(t)^*}{K_1(t''')}$

Point 9. $\dfrac{-2.07}{2.07}\left[E\dfrac{V}{N_1}(-a_1)+E\left(-\dfrac{b_1}{N_1}\right)\right]\times(-N_{21})\dfrac{K_1(t)}{K_1(t''')}\dfrac{K_1(t''')^*}{N_{21}}$

Point 10. Zero*

Point 11. $\dfrac{-2.07}{2.07}\left[E\dfrac{V}{N_1}(-a_1)+E\left(-\dfrac{b_1}{N_1}\right)\right]\times\dfrac{h_1(t)^*}{h_1(t''')}$

Point 12. $\dfrac{-2.07}{2.07}\left[E\dfrac{V}{N_1}(-a_1)+E\left(-\dfrac{b_1}{N_1}\right)\right]\times\dfrac{h_1(t)}{h_1(t''')}\dfrac{h_1(t''')^*}{1{,}000}$

Point 13. $E\dfrac{V}{N_1}(-a_1)\dfrac{H_1(t_r)^*}{1{,}000}$

Point 14. $E\dfrac{Q}{1{,}000N_1}$

Point 15. Zero*

Point 3′. $E\left(-\dfrac{b_2}{N_1}\right)$

Point 4′. $E\dfrac{V}{N_1}(-a_2)^*$

Point 5′. $\dfrac{1}{2.07}\left[E\dfrac{V}{N_1}(-a_2)+E\left(-\dfrac{b_2}{N_1}\right)\right]^*$

Point 6′. $\dfrac{-2.07}{2.07}\left[E\dfrac{V}{N_1}(-a_2)+E\left(-\dfrac{b_2}{N_1}\right)\right]^*$

Point 7′. $\dfrac{-2.07}{2.07}\left[E\dfrac{V}{N_1}(-a_2)+E\left(-\dfrac{b_2}{N_1}\right)\right]\times(-N_{22})^*$

Point 8′. $\dfrac{-2.07}{2.07}\left[E\dfrac{V}{N_1}(-a_2)+E\left(-\dfrac{b_2}{N_1}\right)\right]\times(-N_{22})\dfrac{K_2(t)^*}{K_2(t''')}$

Point 9′. $\dfrac{-2.07}{2.07}\left[E\dfrac{V}{N_1}(-a_2)+E\left(-\dfrac{b_2}{N_1}\right)\right]\times(-N_{22})\dfrac{K_2(t)}{K_2(t''')}\dfrac{K_2(t''')^*}{N_{22}}$

Point 11′. $\dfrac{-2.07}{2.07}\left[E\dfrac{V}{N_1}(-a_2)+E\left(-\dfrac{b_2}{N_1}\right)\right]\times\dfrac{h_2(t)^*}{h_2(t''')}$

Point 12′. $\dfrac{-2.07}{2.07}\left[E\dfrac{V}{N_1}(-a_2)+E\left(-\dfrac{b_2}{N_1}\right)\right]\times\dfrac{h_2(t)}{h_2(t''')}\dfrac{h_2(t''')^*}{1{,}000}$

Point 13′. $E\dfrac{V}{N_1}(-a_2)\dfrac{H_2(t_r)}{1{,}000}$

As indicated earlier, a 400-cycle voltage of magnitude E is applied to the signal circuit input. Since E appears in each term of equations 1A and 2A, the oscillator voltage control can be used to vary the voltage level throughout the computer signal circuits. The best signal to noise level is obtained when the voltage level is just below the point at which any one of the amplifiers is overdriven. In the interest of maximum accuracy, the optimum voltage level must be established prior to every solution on the machine. Beyond the input, amplifiers and voltage dividers are placed in the circuits at locations where the voltage signal is to be multiplied by a new factor. Where addition or subtraction must take place, a circuit similar to that of Figure 6 is used. Minus signs are taken care of by inverting amplifiers. A pair of null indicators provide the operator with a measure of the unbalance of the plate-to-plate equations.

Determination of Data Required for Solution of an Adjacent Plate

The sequential character of the plate-to-plate calculation was indicated previously. Part of the information obtained from the calculations made for one plate is employed in the calculations to be made for the next. This procedure will now be discussed with particular reference to the computing machine.

The a_i' coefficients, obtained from the calculations at one plate through the use of equation 3A, become the corresponding a_i coefficients for the calculations to be made at the next plate through the use of equations 1A and 2A. Referring jointly to equation 3A and to the preceding formulas for calculating voltage magnitudes, it will be found that the numerator of the equation appears in the appropriate computer channel as the magnitude of the voltage output of an *A8* amplifier. This voltage may be measured. The denominator of equation 3A is equal to the sum of the output voltages of all the *A8* amplifiers. When all the *R* resistors, Figure 4, which connect the *A4* amplifiers to the input of the Null 2 Indicator, have been disconnected, a voltage may be measured at this input location which is proportional to the sum of the output voltages of all the *A8* amplifiers.

The temperature, t, obtained from the calculations at one plate becomes the temperature, t_r, to be employed in equation 2B for the calculations at the next. The temperature, t, can be read for the appropriate plate from the t dial setting on the computing machine, see Figure 4.

Discussion of Potential Errors

To a large extent, the precision with which the operator can set the voltage gains (amplifiers and voltage dividers) controls the accuracy of the algebraic operations performed by the computer. The percentage error introduced in setting the voltage gain of a linear potentiometer by means of a calibrated dial would vary inversely with the voltage gain to be set. Because of this fact, calibrated dials are not employed for this purpose. Instead, all computer gains are established with the aid of a bridge circuit, see Figure 8 for a block diagram. The error signal is displayed simultaneously on ten dual *6AF6-G* tuning eyes so placed on the front of the panel that one is always in view for the operator. Each of the dual eyes simultaneously displays a high and a low sensitivity range. By means of these, voltage gains can be set to within 0.5 per cent.

Certain answers appear on the machine as voltage magnitudes. A voltmeter permits these to be read with an accuracy of better than 0.5 per cent.

The greatest source of error is in the representation of the semilogarithmic functions. With the selection of temperature range now employed, this potential inaccuracy can be kept below three per cent.

Summary

There appears to exist in the oil industry a definite use for a computing machine which may be employed to shorten the multi-component fractionation plate-to-plate calculations.

A machine believed to be of satisfactory accuracy and reliability has been designed and is in operation. It is estimated that it reduces the computing man hours to about ten per cent of that of the former procedures.

The machine can be employed not only on the design of new equipment, but also on the study of possible design and feed variations which might be made in existing fractionation columns.

Glossary

In equations 1, 1A, 2, and 2A it is assumed that: the desired flows of the components in liquid form through the bottom plate of the column are known; the desired net heat flow into the lowest chamber is known; and calculations have been carried upward through the rth plate and the chamber immediately above it. Therefore, from these conditions data are to be computed for plate $(r+1)$ and for the chamber immediately above the latter.

Equations 1 and 2 represent the material and the enthalpy balance established, under steady-state conditions, between the volume enclosed by the bounding surface represented by the dashed line in Figure 2 and the region outside of that volume.

Liquid Flows Per Unit of Time

L = total number of moles of liquid for all of the i components descending from the reference plate, r.

l_i = number of moles of liquid in the ith component of L.

b_i = number of moles of liquid in the ith component which is being withdrawn through the bottom plate of the column.

Vapor Flows Per Unit of Time

V = total number of moles of vapor for all of the i components rising through plate $(r+1)$.

v_i = number of moles of vapor in the ith component of V.

Steady-State Temperatures

t_r = temperature of the components (in both liquid and vapor form) on and immediately above plate r.

t = temperature of the components (in both liquid and vapor form) on and immediately above plate $(r+1)$.

t' = lower limit of the temperature range for a specific operating arrangement of the machine.

t''' = upper limit of the same temperature range (see t').

$t'' = (t'+t''')/2$.

t_g = a general term = a dial setting representing temperature.

Enthalpies

$h_i(t)$ = enthalpy per unit mass of l_i at temperature, t.

$H_i(t_r)$ = enthalpy per unit mass of v_i at temperature, t_r.

Q_1 = enthalpy input to bottom plate of column from heater.

Q_2 = enthalpy of the liquid stream leaving the bottom plate.

$Q = Q_1 - Q_2$.

Ratios

a_i = moles of vapor in the ith component of vapor rising through plate $(r+1)$ divided by V.

a_i' = defined similarly to a_i except with respect to plate $(r+2)$.

$K_i(t) = \dfrac{v_i/V}{l_i/L}$ and is a function of temperature, t, and of the pressure.

Voltage

E = magnitude of the 400-cycle signal voltage applied to the input of the computing machine.

Resistances

R = ohmic resistances (all equal in magnitude) used in the addition circuit.

R_1, R_3, etc. are ohmic resistances defined where used.

Amplifiers and Potentiometers

A_1 through A_9 represent negative feed-back low-output-impedance 400-cycle amplifiers.

θ' = angular position of potentiometer wiper which corresponds to the minimum gain on the voltage divider.

θ''' = angular position of wiper corresponding to unity gain on the voltage divider.

$\theta'' = (\theta'+\theta''')/2$.

α = voltage gain of a voltage divider $(\alpha \leqq 1)$.

β = over-all voltage gain of a voltage divider and an amplifier in cascade.

δ = voltage gain of a three-position voltage divider used in the calibration circuit.

G = voltage gain of an amplifier.

Constants

N_1 = a real number, chosen to be slightly greater than the largest value of b_i. It reduces the gains which would otherwise be required of amplifiers *A1*, *A2*, and *A3*, and permits the maximum gain of *A1* and *A3* to be made equal to unity.

N_{11} = A real number equal to the gain of

amplifier $A7$ in the ith channel. Through the use of this class of constants, problems may be solved on the machine involving a wide range of values for the function $K_i(t'''')$ and, in the process, the $A8$ amplifiers can be made identical to the $A6$ amplifiers if the $A7$ amplifiers are made identical to the $A4$ amplifiers.

References

1. Elements of Fractional Distillation (book), C. S. Robinson, E. R. Gilliland. McGraw-Hill Book Company, New York, N. Y., 1939, pages 81–84, 137–85.

2. The Theory of Mathematical Machines (book), Francis J. Murray. King's Crown Press, Morningside Heights, N. Y., 1947, page 17.

3. Electronic Instruments, Radiation Laboratory Series. McGraw-Hill, New York, N. Y., 1948, pages 97–98.

No Discussion

Consideration of Requirements and Limitations of Relaying and High-Speed Reclosing on Long and Heavily-Loaded Transmission Lines

C. E. PARKS
MEMBER AIEE

W. R. BROWNLEE
MEMBER AIEE

Synopsis: Present-day large interconnected power systems have many problems in common with regard to economical line loading, optimum placement of generating capacity, and satisfactory solution of protective relaying and line-reclosing requirements to provide the best over-all system performance. This paper suggests some of the engineering considerations which necessarily must be given incident to the planning and specification of the protective relaying and high-speed reclosing to be applied to transmission lines of considerable length which may serve as stabilizing ties between generating stations of an extensive system. For purposes of discussion, a hypothetical transmission system is analyzed. Companion papers[1,2] deal with the problems in the selection of relaying of the short and medium-length transmission lines of the same typical system.

ECONOMIES in generating costs have dictated the location of generating plants. These chosen locations are, in many cases, remote from the points of large load concentrations. This fact has led to close study of the economics of transmission and invariably included in these studies is the subject of adequate relaying facilities to be applied which will best satisfy the increasingly stringent line-loading requirements. It is well recognized that there is a continuing trend toward higher normal and emergency loading of transmission lines in order to take full advantage of their capability.[3] Higher standards of service at reasonable investment costs necessitate the consideration of a minimum number of transmission paths between load and generating areas. This dictates the operation of lines under short-time emergency loadings up to twice normal. These lines also must operate satisfactorily for very short intervals following system faults at even higher load or swing currents until normal system operation is restored.

Consideration must be given to equipment and methods to develop the full emergency (swing) capability of the transmission system. In the past, system separations have been attributed to out-of-step or simultaneous fault conditions when actually such conditions may not have been present or else could have been prevented easily by proper study and application of adequate protective relay systems. Use of the automatic oscillograph has done much to disprove complicated theories with regard to unexplainable system operations, making it evident that further study of the problem would have produced solutions.

System Studied

The purpose of this paper is to outline the relaying requirements of the two 70-mile 138-kv lines connecting station A, a base load economical generating plant, with a net load interconnected area, substations H and J, see Figure 1.

The two 70-mile transmission lines under discussion are required to serve primarily as the major power supply to the load areas at stations H and J. The generating capability of the local station D is assumed to be limited by lack of available cooling water, and the generating cost differential between stations A and D justifies substantial transmission of power to the load area near station D from station A in spite of rather heavy transmission line losses. Maintenance outages at station D may require heavier transmission line loading for periods totaling perhaps three months of the year than would be economical for year-round operation. A typical resultant heavy loading condition may be taken as 90 to 95 megawatts for each of the two 70-mile lines. While lines of this length are not ordinarily considered as long lines, the heavy concentration of generating capacity at each terminal and the high normal line loading result in relaying characteristics of the long line variety.

Relaying Requirements

Relaying requirements for phase-to-ground faults on the two lines are not too severe. The 138-kv transformer bank neutrals are solidly grounded at each terminal station of the lines, thus providing adequate zero sequence currents under practically any system operating condition. The mutual coupling between the lines must receive close scrutiny, however, to ascertain that positive and selective operation occurs for ground faults at any point on the lines near stations H and J, particular attention being paid to the back-up ground relays on the line between stations H and J.

Phase-relaying requirements are more complex and the solution to proper application in this regard must receive care-

Paper 50-16, recommended by the AIEE Relay Committee and approved by the AIEE Technical Program Committee for presentation at the AIEE Winter General Meeting, New York, N. Y., January 30–February 3, 1950. Manuscript submitted October 5, 1949; made available for printing November 22, 1949.

C. E. Parks is with the Public Service Company of Indiana, Inc., Indianapolis, Ind., and W. R. Brownlee is with the Commonwealth Services, Inc., Jackson, Mich.

The authors wish to acknowledge the assistance of Dr. E. L. Harder and Mr. A. J. McConnell who made a-c network analyzer and d-c calculating board studies on the system analyzed by this paper. The help of other members of a Project Committee of the Relay Committee in the final formulation of this paper also is gratefully acknowledged.

Figure 1. Typical transmission system

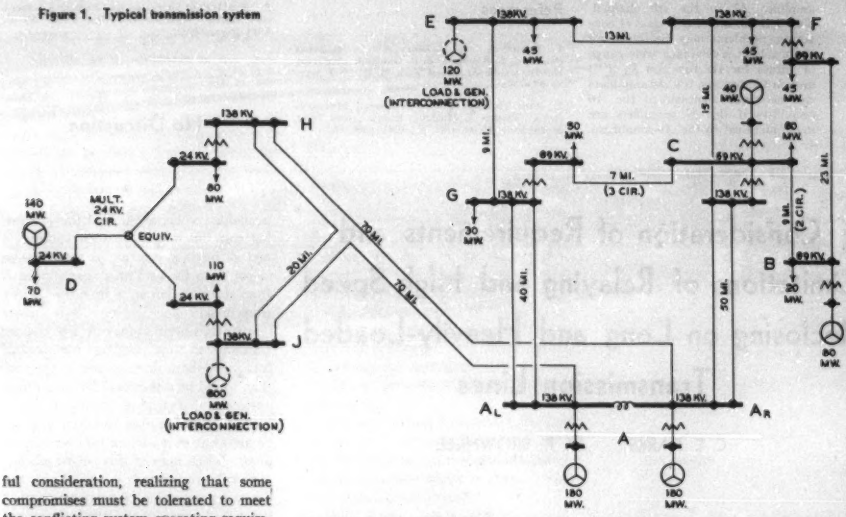

ful consideration, realizing that some compromises must be tolerated to meet the conflicting system operating requirements. The conditions which are to be met are summarized as follows:

1. Positive and complete fault protection for all generating and system operating conditions.

2. Adequate allowance for conditions presented by fault-arc impedance.

3. Some measure of backup protection, should the proper circuit breaker fail to operate on fault.

4. Operating reliability with approximately double normal load plus the addition of current caused by system oscillations.

5. Characteristics suitable for high-speed simultaneous tripping and reclosing.

It is of further importance to recognize that certain combinations of circumstances may cause actual out-of-step conditions to exist between systems across one or both of the 70-mile lines. In this case, it is imperative that the two systems be separated on the first complete swing in order to prevent serious disruption of the power system. This consideration obviates the use of any time-delay impedance sequence interlocking arrangement applied to prevent out-of-step tripping on swing currents.

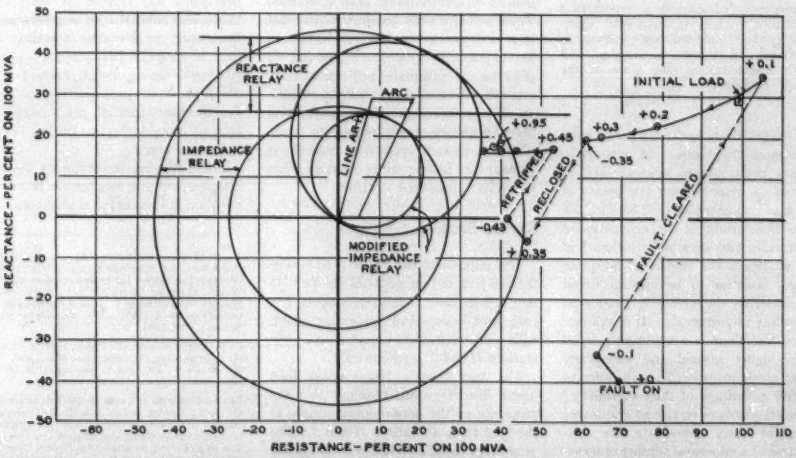

Figure 2. Impedance presented to relays at *AR*, circuit *H* with a 3-phase fault at *AL*, circuit *J*

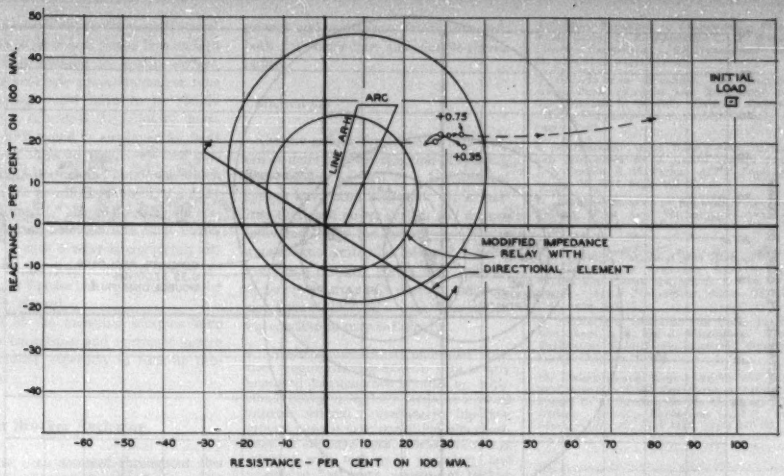

Figure 3. Impedance presented to relays at *AR*, circuit *H* following successful reclosing of lines *AR-H* and *AL-J*

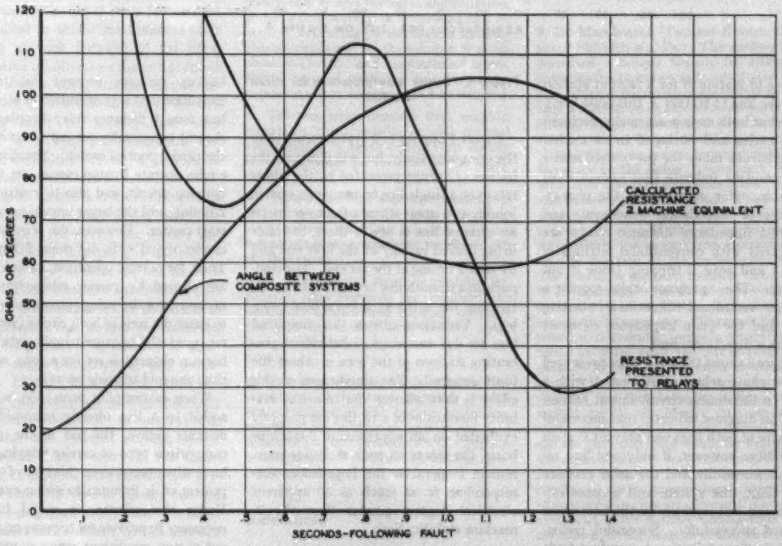

Figure 4. Variation of impedance at relays with external fault cleared sequentially

Network Analyzer Study

In order to provide information on phase relaying for the hypothetical system under consideration, an a-c network analyzer study was made, based on 3-phase faults with 1-cycle relaying and 5-cycle circuit breaker tripping. Three-phase faults only were studied for simplicity. These are only slightly more severe to the over-all system than those involving two phases and ground, which are reasonably common.

Figure 2 shows the impedance presented to the phase relays at station *A* on

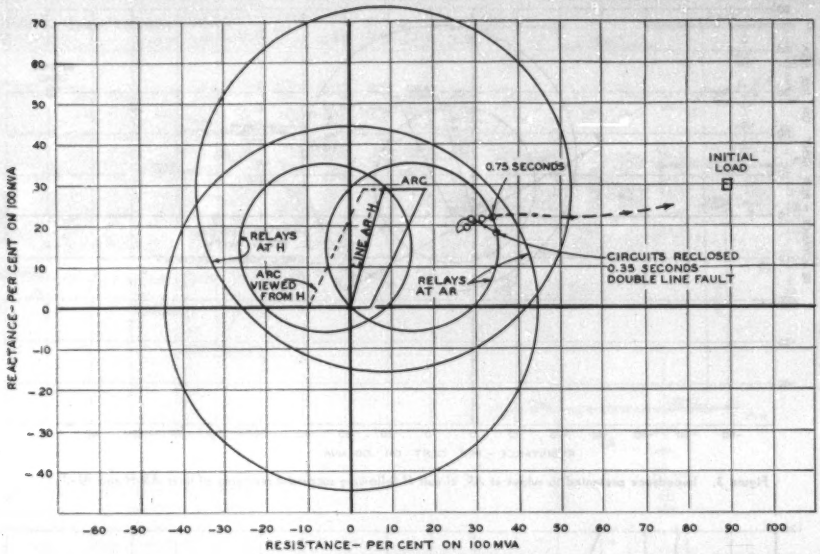

Figure 5. Carrier relay protection for circuit *AR-H*

the line to station H for a fault at station A on the line to station J, this fault being cleared at both ends in six cycles, reclosed in 20 cycles and retripped in six cycles. Swing curves taken for the system under this condition indicate that system itself is stable. For comparison, the characteristics of impedance, reactance, and modified impedance distance relays are illustrated with conventional settings of zone 1 and zone 2 tripping (zone 3 not shown). The reactance units require a voltage restrained directional starting unit, and the plain impedance elements require a directional unit.

Figure 3 shows the impedance presented to the phase relays at station A with a fault on the double-circuit line at station A. This diagram indicates that successful reclosure of both lines will prevent system instability; however, if only one line recloses successfully and the other recloses on a fault, the system will become unstable and will separate on the line which reclosed successfully. Successful reclosing of the lines following a transient fault requires that the phase relays should not trip on the resulting swing currents. For comparison, zones 1 and 2 settings of another form of modified impedance relay (with directional unit) are shown, indicating that the swing current is within the zone 2 setting for at least one-half second.

Figure 4 applies to a system other than the one under study, but will illustrate the nature of swings presented to the phase relays on a single-line transmission system joining two areas when a fault occurs on an external line of one of them, the fault being cleared rapidly at the near end and by zone 2 timing at the far end. For comparison a smooth line is plotted, based on treating the areas as a 2-machine problem. Variations about this simplified line are due to swings of individual generating stations of the area in which the fault occurred. The significance of this effect is that whereas the transient stability limitations of a tie line are properly evaluated on an approximate 2-machine basis, the relays on such a tie line must remain inoperative for impedances corresponding to as much as 30 apparent electrical degrees greater than the 2-machine stability limit.

Solution to Relaying Installations

Two possible solutions may be considered for the 70-mile problem under consideration. One of these might be a carrier-pilot scheme using a modified impedance or mho element, shown in Figure 5. In this scheme, a long time backup distance element (omitted for simplification) is in operation at all times, but zone 1 distance relay tripping (not shown) is normally cut out of service by the carrier control switch. The displaced circles operate to stop carrier, set up the tripping circuit, and also to control zone 2 timing, and the larger impedance circles start carrier. However, the presence of a carrier signal cuts out zone 2 tripping. Thus, for normal operation, all line faults are cleared by carrier relays but it is necessary for the swing current impedance to enter the zone of both circles (near and far terminals) to cause tripping where the backup element is set for a long enough time to avoid tripping on swings.

When carrier-pilot protection is to be added to a line already equipped with distance relays, the use of the phase-comparison type of carrier relaying may have advantages, since this type of carrier protection is immune to swing currents. Under this scheme, it would become necessary to provide for tripping on actual out-of-step conditions using a modified setting of the distance relay elements. The reach of the zone 1 elements of the distance relays may be shortened so as to just overlap, thus insuring that at least one end of the line will trip on actual out-of-step conditions, but minimizing the likelihood of undesired tripping. It would become necessary to make zone 2

tripping nonautomatic for normal operation and to set zone 3 timing long enough to prevent tripping on system swings. Application of the phase-comparison type of relaying would have to be closely studied to determine the sequence quantities which would be employed for fault detection. Due to the heavy load currents, both normal and abnormal, which flow on the two lines involved, the relay applied must be able to discriminate correctly between normal and fault conditions. If such a relay is completely desensitized for load currents, faults beginning as 3-phase line faults would not be correctly cleared.

Each of the foregoing schemes have serious limitations and represent severe compromises, especially in back-up protection.

Circuit Breaker Reclosing

It has been assumed throughout this discussion that high-speed reclosing would be applied on the two tie lines under consideration. This of course requires that carrier-pilot relaying of some form would be installed to obtain simultaneous fault clearing at each terminal of the lines. Generating conditions on the two portions of the system being studied further require that the resynchronizing of the two systems must be accomplished very rapidly if serious load-generation unbalance difficulties are to be avoided in the vicinity of stations *D* and *J*.

The most simple and inexpensive form of high-speed reclosing would be of the 3-pole type.[4] However, the serious stability problems that present themselves under any type of fault on one or both lines, whether complete successful 3-pole reclosure is accomplished or not, leads to the conclusion that serious consideration should be given the application of selective or single-pole tripping and reclosing.[5,6] In case of transient faults involving only one phase and ground, only the faulted phase would be tripped at time of trouble and reclosed at high speed. This would usually result in the maintenance of some tie between the two systems, even with certain phases of both circuits being open at the time of a fault. The phases which remain as ties between the two systems would carry synchronizing and some load current, thus retarding the angular drift between the systems during the dead time the faulted phases are being restored to service by high-speed reclosing action. Determination of the type of reclosing to be employed will depend on further stability analyses and on the relative number of single phase-to-ground and multiphase faults expected, both for single-line and double-circuit faults.

Conclusions

Certain salient points which may govern or determine the selection of relaying and reclosing applied to a hypothetical system have been discussed. It is realized that each power system will require individual study for the selection of the appropriate protective scheme. However, it is believed that a large number of power systems will contain transmission links of the type to which the following conclusions may well apply:

1. Modern transmission line-loading practices require relaying systems with greatly improved discrimination in order to: withstand heavy emergency loads and swing current without unnecessary trip-outs; provide positive fault protection with allowance for arc impedance; withstand swings inherent with high-speed reclosing; and provide at least some measure of backup protection.

2. High-speed reclosing of important tie lines should receive favorable consideration. Either 3-pole or single-pole reclosing may be applied, depending on the system stability characteristics and on the number of single phase-to-ground and multiphase faults. Either type of reclosing imposes severe requirements on transmission line relaying.

3. Distance relay elements with modified impedance characteristics provide reduced susceptibility to swing current, but usually are not sufficient for the more severe applications.

4. Time-impedance sequence blocking is seldom applicable to the longer tie lines, since system reliability requires that an actual out-of-step condition be cleared on the first swing.

5. Carrier relaying based on modified impedance relay elements can minimize the possibility of undesired tripping, provided the first and second zone distance relay backup elements are normally out of service.

6. Relaying schemes which minimize the possibility of incorrect tripping involve severe compromise with backup protection, especially the protection against the rare failure of a circuit breaker to trip. Further investigation of methods of backup protection is indicated.

References

1. Transmission Line Protection of Short Lines of the Metropolitan Area of a Typical System, W. E. Marter. *AIEE Transactions*, volume 69, part I, 1950, pages 468–72.

2. Relay Protection for Medium-Length High-Voltage Transmission Lines, J. H. Kinghorn. *AIEE Transactions*, volume 69, part I, 1950, pages 461–67.

3. Economics of Long-Distance A-C Power Transmission, S. B. Crary, I. B. Johnson. *AIEE Transactions*, volume 66, 1947, pages 1092–1102.

4. Analysis of the Application of High-Speed Reclosing Breakers to Transmission Systems, S. B. Crary, L. F. Kennedy, C. A. Woodrow. *Electrical Engineering* (*AIEE Transactions*), volume 61, June 1942, pages 339–48.

5. Relays and Breakers for High-Speed Single-Pole Tripping and Reclosing, S. L. Goldsborough, A. W. Hill. *Electrical Engineering* (*AIEE Transactions*), volume 61, February 1942, pages 77–81.

6. Experience with Single-Pole Relaying and Reclosing on a Large 132-Kv System, J. J. Trainor, C. E. Parks. *AIEE Transactions*, volume 66, 1947, pages 405–13.

7. Impedances Seen by Relays During Power Swings With and Without Faults, Edith Clarke. *AIEE Transactions*, volume 64, 1945, pages 372–84.

8. Graphical Method for Estimating the Performance of Distance Relays During Faults and Power Swings, A. R. van C. Warrington. *AIEE Transactions*, volume 68, part I, 1949, pages 608–21.

9. Protective Relaying for Long Transmission Lines, A. R. van C. Warrington. *Electrical Engineering* (*AIEE Transactions*), volume 62, June 1943, pages 261–68.

10. Performance Requirements for Relays on Unusually Long Transmission Lines, F. C. Poage, C. A. Streifus, D. M. MacGregor, E. E. George. *Electrical Engineering* (*AIEE Transactions*), volume 62, June 1943, pages 275–83.

Discussion

R. H. Macpherson (General Electric Company, Philadelphia, Pa.): The authors have described a unique system for obtaining power-swing blocking and out-of-step tripping which is particularly applicable to long lines which serve as ties between parts of a system. Relay characteristics are such that blocking during swings is effected by means of carrier from the remote terminal making it necessary for the swing impedance to enter the carrier-stop characteristics of both terminals before tripping can occur. The second-zone distance trip is also carrier blocked to prevent tripping if the swing impedance stays within the second-zone characteristic for the duration of the second-zone time. The scheme is designed to cause the system to be separated on an out-of-step condition at the section through which the power-swing impedance locus passes. There are systems where it is desirable to cause separation to occur at other than the power-swing impedance locus section in order to keep particular loads with particular generation sources. For such cases the equipment described by W. C. Morris[1] has particular application. Figure 1 of the discussion indicates that the relay would be located at the desired point of separation and all other terminals would be blocked on out-of-step conditions by a conventional time-delay impedance sequence arrangement. The characteristics of the authors' arrangement also are shown for the purpose of comparison.

If the line in question is of lesser importance so as not to warrant the special out-of-step tripping protection or carrier, then straight 3-zone distance relaying could be used.

For very long and heavily-loaded lines subject to frequent swings where carrier is used for functions other than relaying, the additional use of carrier for the power-swing blocking function may be somewhat inconvenient since the reach of the im-

pedance carrier-starting characteristic must be great. The use of the conventional time-delay impedance sequence arrangement for out-of-step blocking and reversed third zone for the carrier-start function would make for fewer interruptions to those carrier functions other than relaying, since the reversed third-zone impedance area can be made small compared to the area of the impedance characteristic described by the authors. See the dashed characteristic of Figure 1 of the discussion for reversed third-zone area, which provides backup protection for faults occurring in the reverse direction.

REFERENCE

1. ONE SLIP CYCLE OUT-OF-STEP RELAY EQUIPMENT, W. C. Morris. *AIEE Transactions*, volume 68, part II, 1949, pages 1246–48.

P. A. Jeanne (Bell Telephone Laboratories, Inc., New York, N. Y.): We, in the inductive co-ordination field, are somewhat concerned regarding the possibility of increased use of single-phase switching. There has been much benefit, of course, from the inductive co-ordination standpoint in the improved speed of clearance of transmission-line faults in recent years, and it is hoped that these advantages may not be offset by single-phase switching procedures which might increase materially the duration of induction. The induction I have in mind is that resulting from the unbalanced load currents that might flow during the period one phase conductor is open on a power system which is grounded at two or more points. While the induction under such conditions would usually be much less than under the fault condition, it might result in serious communication disturbance due to both low frequency and noise induction if it persisted for a considerable period such as might be the case if a fault did not clear on the first reclosure and the other two phases were not tripped out. I feel sure that most relay engineers will appreciate the importance of this matter and will take it into consideration in their power-system protection planning.

Cort Lowerison (Southern California Edison Company, Los Angeles, Calif.): The paper by Mr. Parks and Mr. Brownlee has been read by several people in our company who are interested in the solution to problems of this nature.

We wish to compliment the author on their skill in reducing a highly technical subject into a thoroughly interesting and readable paper, even for those of us who are not immediately confronted by such a problem.

We have had very little experience with the type of carrier-current relaying described and no experience at all with automatic high-speed reclosing. Therefore, we do not feel that we are in a position to discuss these phases of the subject. The paper indicates that the problem has been very thoroughly investigated, and everything has been done in so far as is possible with protective relaying equipment.

The subject of high-speed reclosing, however, is worthy of considerable discussion. We realize that the trend of modern engineering is in that direction. The development of very high-speed relaying equipment and modern high-speed oil circuit breakers has made reclosing possible. Whether it should or should not be applied should always remain a separate decision for each special case.

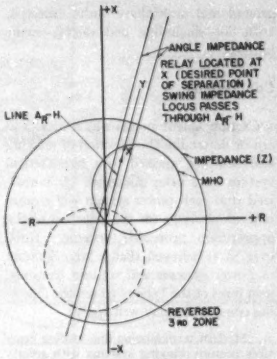

Figure 1. Impedance characteristics of one terminal of a power-swing blocking and out-of-step tripping relay scheme, a 1-slip-cycle out-of-step relay and reversed third zone

The paper will serve as an excellent guide in those cases where the economics of the problem dictate the use of this type of equipment. We realize that the paper is being presented as the solution to a hypothetical problem; however, it is difficult to refrain from suggesting that in real practice it would not be a completely satisfactory solution from our point of view.

The values of load and generating capacity shown in Figure 1 of the paper make it difficult for us to appreciate why a third line or an intermediate switching station would not be economically feasible.

W. A. Morgan (Bureau of Reclamation, Denver, Colo.): The Bureau of Reclamation has had in operation for three years an installation of mho-carrier relaying on two 140-mile 161-kv lines between Parker Dam and Phoenix in Arizona. This installation is one of the most critical that may be found either from the standpoint of length of lines or heavy loading, because of the low magnitude of the fault currents. The comments in this discussion are made with this background.

It is interesting to note that one of the relaying requirements in the paper under discussion is that the two systems be separated on the first complete power swing. This obviates the use of any time-delay impedance sequence interlocking arrangement applied to prevent out-of-step tripping on swing currents. The Bureau came to this same conclusion as described in reference 1 of this discussion. This reference paper has impedance characteristic diagrams for fault conditions quite similar to those presented in the authors' paper.

In subsequent specifications, the Bureau has taken care of the out-of-step tripping requirement in a manner such as to provide better backup protection. The need for backup protection was demonstrated by the staged fault test described in reference 1. The out-of-step blocking relays are specified to accomplish the following:

1. Provide backup protection for the zone 2 units of the distance relays.
2. Block tripping by carrier and by the first- and second-zone elements for out-of-step conditions.
3. Block high-speed reclosing after out-of-step tripping.
4. Permit tripping for line faults occurring after out-of-step blocking is initiated but prevent reclosing after such tripping.

These requirements of the out-of-step blocking relays are offered as an adjunct to the section on Solution to Relaying Installations in the paper by Mr. Parks and Mr. Brownlee in line with the last sentence of that section which states: "Each of the foregoing schemes have serious limitations and represent severe compromises, especially in backup protection."

With regard to single-pole reclosing, I would like to offer the following comments. I believe the complication of relaying and circuit breaker mechanism to accomplish single-pole reclosing makes it a marginal benefit difficult to justify for the following reasons:

Mutual coupling from the unfaulted phases maintains the arc of the faulted phase so that the minimum time for single-pole reclosing must be up to about eight cycles longer than for 3-pole reclosing. This has been established by French engineers, and recently by the Bonneville Power Administration in staged tests. The increased reclosing time required for single-pole reclosing leaves little benefit to be gained for transient stability conditions over the faster 3-pole reclosing where there is more than one line connecting the two systems.

The percentage of single-line-to-ground faults on steel tower transmission lines with overhead ground wires now is found to be closer to 40 per cent by automatic oscillographs, whereas it was thought to be close to 90 per cent when relay targets were used as the basis for data. In the same manner, 3-phase faults are found to represent about 30 per cent instead of 1 to 3 per cent. This is true because the relay-target circuits reduce the current through the remaining unoperated targets after one has operated. The basis for the more accurate percentages of one-line-to-ground and 3-phase faults is reference 2 of this discussion. Theoretical analysis of lightning-stroke phenomenon makes it logical to expect a larger percentage of 3-phase faults on steel tower lines with overhead ground wires than we previously designed for on rules of thumb based upon relay-target data. Accordingly, single-pole reclosing would be expected to operate for only about 40 per cent of lightning faults.

The use of a blinder relay element[1] would allow fast backup protection and avoid tripping on swings. This might overcome the point of weakness in Conclusion 3 of the paper. There is some objection to the use of a blinder relay element, however, in that it adds another gadget to the relaying which it is usually desirable to avoid.

It may be of interest to report to the credit of the mho-carrier relays, including the blinder elements, that the phase relays have operated correctly to prevent tripping on the unfaulted line during these three years of operation. During this time there have been four faults that have occurred on the two Parker-Phoenix 161-kv lines at different

times, after the modifications, as described in the Morgan and Evans paper,[1] were made. The modification of the carrier ground relay to prevent tripping on line-charging harmonic currents allowed false tripping in one instance of a ground fault outside the protected zone, however, and the relays are undergoing a change in connections, which it now appears will correct the error in the directional characteristic.

I believe that the value of a paper may be brought out by a healthy discussion both pro and con. Thus, I trust that the authors appreciate that my comments are offered for the purpose of stimulating thought in a subject in which I am greatly interested.

References

1. Relaying Difficulties Disclosed by Staged-Fault Tests, W. A. Morgan, Byron Evans. *AIEE Transactions*, volume 67, part 1, 1948, pages 73–82.

2. Performance of 161-Kv and 115-Kv Transmission Lines, K. E. Happgood, C. P. Almon, Jr. *AIEE Transactions*, volume 66, 1947, pages 863–71.

C. E. Parks and W. R. Brownlee: The amount of agreement expressed by the various discussers is most gratifying, especially in view of the recognized compromises which have been made between the conflicting relaying requirements imposed by the hypothetical power system

Mr. McPherson describes an alternative scheme in which a conventional time-delay impedance sequence arrangement is used to block tripping. The indicated use of the 1-slip-cycle relay does much to remove objections to earlier blocking schemes in which separation of out-of-step portions of the system was delayed. Where important loads are supplied from a major tie line, the preselection of the point of separation may be of value. However, it is important to provide rapid emergency separation (on the first swing) at some point on each major transmission linkage across which an out-of-step condition may occur.

We agree with Mr. McPherson that there is a definite field for distance relays on lines for which the more expensive carrier-current relaying cannot be justified.

Mr. Jeanne very properly places a high valuation on the co-operative work of communication company and power company engineers in the economic solution of inductive influence problems. The single-pole reclosing system with which the authors are familiar is associated with high-speed carrier-current relaying, so that the total time of fault current plus phase-to-neutral load current is of the same order as the total fault time with more common types of relaying systems. Also, if instantaneous reclosing is unsuccessful, all three poles of the circuit breakers are tripped together. The authors know of no scheme in the United States in which it is proposed to operate a high-voltage transmission line for longer than a fraction of a second with one pole of the circuit breaker open and the other two closed. Such a scheme might involve severe inductive influence problems.

The tests reported by Mr. Morgan have indicated that single-pole reclosing may require some eight cycles longer open time than 3-pole reclosing because of the mutual coupling from the unfaulted phases. On many 138-kv systems, the usual 3-pole reclosing time is about 20 cycles and the corresponding single-pole reclosing time some 35 cycles. Accordingly, it is not surprising that the limitations described by the discusser have not been encountered.

Individual study will determine the relative applicability of single-pole and 3-pole reclosing in specific instances. In the case of lines having only 40 per cent of single-phase-to-ground faults, the use of single-pole reclosing would be of limited value. However, it must not be inferred that the relatively high percentage of single-phase-to-ground faults (70 to 90 per cent) found on many 138-kv lines is based on relay targets. On the contrary, oscillographic records covering periods of over 20 years have established these ratios.

Mr. Lowerison questions whether a third 138-kv line is justifiable on an economic basis, recognizing that the hypothetical system described was chosen to illustrate certain relaying problems. The heavy loading which sets the relaying requirements may occur for only a short period each year, during times when a generator at Station *D* is out of service for maintenance. See Figure 1 of the paper. Accordingly, it might be difficult to justify a third line from Station *A* to the west on a loss evaluation basis. The possible justification of a third line from the standpoint of service reliability to Area *D-H-J* will depend on the probability of outages on Lines *A-H* and *A-J*, and especially on the probability of a 2-circuit outage along with a sustained fault on one of the lines. Regardless of the appropriate factors applied to any particular situation, it appears certain that improved relaying and reclosing schemes will make it possible to provide for adequate service at relatively lower transmission system investment.

Margins Between Lightning Arrester Protective Levels and Transformer Insulation

F. J. VOGEL
FELLOW AIEE

CURVES showing the relations between lightning arrester discharge voltages and transformer impulse strength are often published, to show the margin between the two and to illustrate how securely protection is obtained. As published, they always show a considerable margin, and further, they reflect the values set up as commercial standards.

Some engineers, particularly transformer engineers, are interested in the conditions possible in service to see if the apparatus they design is adequate for service.

Some operators, too, are interested, since they buy both lightning arresters and transformers, and the establishment of "basic insulation levels" depends on these relations.

Impulse tests have been made by transformer engineers in the past, using lightning arresters and transformers, for this purpose, but the results were never published. One such test is reported here, which does not conform to the usual impression of the relations between lightning arresters and transformers, but does indicate that a high degree of protection is obtained.

General

The standards of lightning arrester performance have recently been presented.[1] They are extremely valuable in standardizing the method by which lightning arresters can be tested to determine compliance with commercial standards and to give an idea as to the limiting voltages under these conditions.

Using such data, curves showing the degree of protection to apparatus can be drawn. The curves shown in Figure 1 are illustrative of the relations usually given, to show the minimum values of transformer insulation and the average lightning arrester performance. However, there are some other considerations to be taken care of to obtain the real picture. One of these is the fact that the lightning arrester performance is average and may exceed the values shown by 10 or 15 per cent. Actually, it is very likely that this is a pessimistic viewpoint. But there are some matters which make conditions worse. Such conditions are separation of the lightning arrester from the apparatus, and the possibility of high rates-of-current discharge, or high rates-of-rise of such discharges.

One method of allowing for them has been a fixed percentage, or a fixed quantity, or both. However, to the writer's belief, little experimental data as to the correspondence of this allowance and possible actual field conditions have been presented. Experience showing that the use of the allowance has given good service has been given as justification.

The transformer standards establish minimum values of transformer insulation. These values are exceeded for two reasons: first, there must be some margin allowed for testing. For example, if a chopped wave of 230 kv is required, the tester calibrates the surge generator at some lower voltage and determines the charging voltage for 230 kv by extrapolation. Depending on a number of variables, the actual voltage and specified time may be exceeded by 10 to 15 kv or one or more microseconds. Second, the designer will attempt to provide a margin to prevent failures on test and damage. On the other hand, the conditions used for test on the lightning arresters are not as severe as they might be, since a 10/20 current wave is the basis of test. Hence the commercial tests do not put the transformer in a particularly favorable light, and, on the contrary, they put the lightning arrester in a favorable one. A more logical method of procedure would be to use minimum strengths for the transformers, as is now done, and maximum (not average) which limiting voltages for lightning arresters should be at least one of the test or guarantee values. Perhaps also they should include the most severe current condition to be expected in service.

In order to illustrate this point of view, some tests were recently made on some 34.5-kv transformer coils and insulation, both with and without lightning arresters. The point was to illustrate the effect of steep rates-of-current rise and separation of the lightning arrester from the transformer. The tests are not beyond question so far as some technicalities are concerned, but they certainly are illustrative of possible field conditions.

Test Procedure and Results

The coils and insulation used were typical for 34.5-kv class, which should stand the following tests: full wave, 200 kv; chopped wave, 230 kv; steep-front wave, 345 kv in 0.5 microsecond.

The transformer coils and bushing were set up with a 9-inch rod gap as near as possible. The surge generator was adjusted to give a rate-of-voltage rise of

Paper 50-17, recommended by the AIEE Transformers Committee and approved by the AIEE Technical Program Committee for presentation at the AIEE Winter General Meeting, New York, N. Y., January 30–February 3, 1950. Manuscript submitted October 28, 1949; made available for printing November 22, 1949.

F. J. Vogel is with the Illinois Institute of Technology, Chicago, Ill.

The data presented in this paper were obtained during the development of a possible new line of transformers at the Pittsburgh works of the Allis-Chalmers Manufacturing Company.

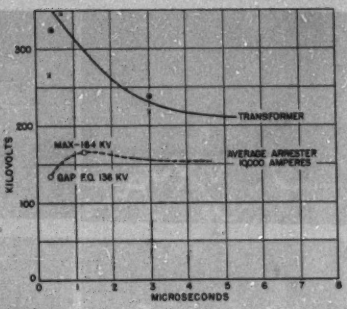

Figure 1. Relations between lightning arrester performance and test data

Average data for 37-kv-line-type lightning arrester shown on dash line. Curve is estimated but is assumed for 10/20 current wave to give a $1^1/_2/40$ voltage wave.

Solid line represents minimum values for transformers demonstrated by test.

Crosses (x) represent voltages at lightning arrester and transformer, with both as near together as possible. The crest of the wave was at less than one-half microsecond, and the average value was over 220 kv for the equivalent, approximately, of at least 3 microseconds, Figure 3(B). It is recognized that these do not form points on a time lag curve, but show comparative strengths only.

Circled crosses represent the lightning arrester and transformer voltages with 50 feet separation. The 326 kv at the transformer had very short duration, shown as less than one-half microsecond, Figure 3(E). The lightning arrester voltage is shown as 235 kv for the equivalent of 3 microseconds, Figure 3(F).

This comparison shows how the separation between the lightning arrester and transformer, leading to high frequency oscillations, requires steep wave front strength

about 1,500-kv per microsecond. The result of the test is shown in Figure 2(A). The voltage was 513 kv, reached in about 0.33 microsecond.

Next a 37-kv lightning arrester, of good manufacture and rated as a line-type arrester, was set up as close as possible to the transformer model. It will be noted that the voltage is greatly reduced as shown in Figure 2(B), to be a relatively long wave but to be only 176 kv.

Further tests were made with the lightning arrester between the transformer and generator. The generator setting was unchanged. On one such test, the voltage at the lightning arrester is shown in Figure 2(D), and was 176 kv. The voltage at the transformer was shown in Figure 2(E). The peak was 214 kv.

The distance between the lightning arrester and the transformer was 50 feet of line. It would seem that this might be a possible condition in the field. Although the voltage at the transformer was 214 kv, it existed for a small fraction of a microsecond.

Since voltage rises of lightning of 1,000 kv per microsecond have been cited, this might be considered to prove that, at least so far as ordinary rates-of-voltage rise are concerned, the lightning arrester has done a very good job, preventing flashover and limiting the voltage on the apparatus. In these tests about 500 ohms of resistance were in series within the generator.

Another series of tests were made without internal resistance in the generator. The model and 9-inch rod gap were close together. Figure 3(A) shows a flashover on the front of the wave of 556 kv, reached in one-fourth microsecond, giving a rate-of-rise of over 2,200 kv per microsecond. With the lightning arrester immediately adjacent, the maximum voltage was 262 kv and the average of the curve was 220 kv. It decreased rapidly in a microsecond or so. This is shown in Figure 3(B).

Similar tests were made with various separations between the lightning arrester and transformer. One such test was made with 25 feet separation. In that case the voltage at the lightning arrester was 246 kv and is shown in Figure 3(D). The voltage at the transformer was 310 kv and is shown in Figure 3(C).

It is easy to see that the duration of this voltage is only a fraction of a microsecond.

Results with 50 feet separation are shown in Figures 3(F) and (E), where voltages at the lightning arrester and transformer are shown in respective order. The highest voltages were 235 and 326 kv respectively. The 9-inch gap was in parallel with the transformer for all tests.

There were no gap flashovers during the tests described.

After these tests and many even more severe, investigation showed that no damage was done to the transformer insulation.

No measurements of discharge currents were taken, to simplify the tests. Such measurements would be desirable by those interested primarily in lightning arrester performance.

Discussion of Test Results

Although these tests make no pretense of being a complete study of the subject,

Figure 2. Oscillograms with 1,500 kv per microsecond wave

(A) Nine-inch rod-gap flashover on front of wave

(B) Lightning arrester voltage, same surge generator setting as (A)

(C) Transformer voltage 50 feet from lightning arrester

(D) Lightning arrester voltage corresponding to (C)

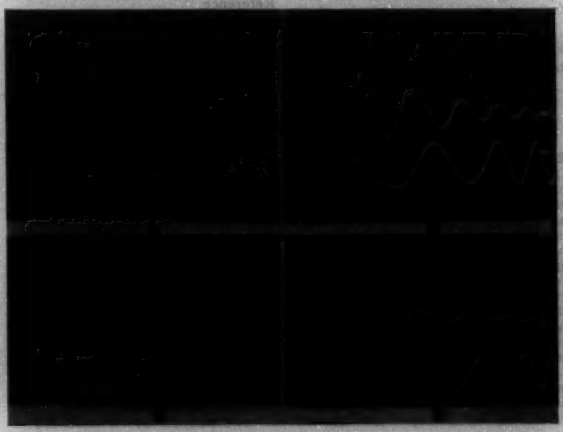

it is believed that they do permit drawing some conclusions, some not new.

For example, the conditions illustrated here, even in the worst case, are probably not as severe as they could be in service. Under these conditions, protection was actually obtained both to service and the apparatus with the lightning arrester. Protection to the apparatus was obtained only with gaps. The limits of assumed lightning severity perhaps should be further explored, since no general agreement as to lightning arrester current limits for given voltage classes and applications has been reached. Since the effect of separation of the lightning arrester and apparatus results in short steep-front oscillations, it would seem that steep-front strength in transformers is desirable. Unless conditions much worse than in these tests exist, normal transformer levels would seem to be sufficient. In other words, high-voltage oscillations due to reflections are not too greatly to be feared if steep-front strength is built into the apparatus.

The relatively longer steady voltage durations, with high lightning arrester currents, and with the arrester at the transformer, seem to be close to or exceed the present transformer levels. Actually they did not exceed the strength as actually built in, even in the worst case. If the transformer barely had the American Standards Association level of full wave strength, more failures might result in service. The usual relations shown for lightning arresters and transformers do not seem entirely correct. They are indicated in Figure 1. However, I do not believe margins should be added on to other margins. Present levels seem satisfactory to me.

The relations here given apply to the lower voltage classes. Conditions might be much different for higher voltage classes. Tests under these conditions have been made before, and it might be well if more comprehensive tests were made and reported. Due to overhead ground protection, surge currents are often small, and if so, transformer insulation might even be reduced.

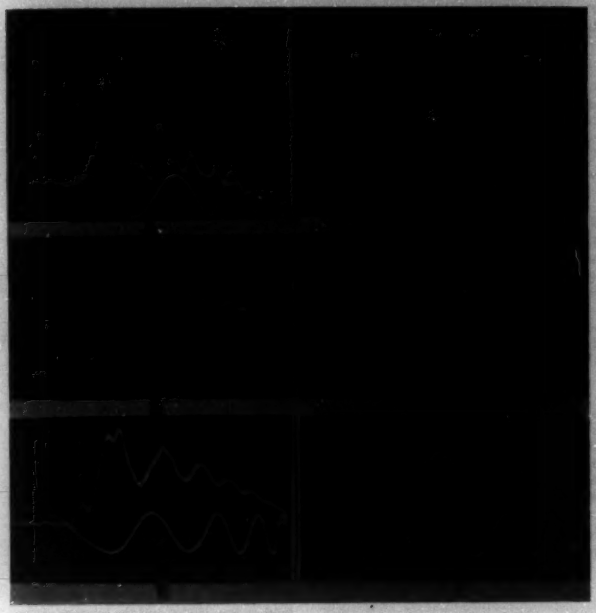

Figure 3. Oscillograms with 2,200 kv per microsecond wave

(A) Nine-inch rod-gap flashover on front of wave
(B) Lightning arrester voltage
(C) Transformer voltage 25 feet from lightning arrester
(D) Lightning arrester voltage corresponding to Figure 2(C)
(E) Transformer voltage 50 feet from lightning arrester
(F) Lightning arrester voltage corresponding to (E)

Reference

1. Performance Characteristics of Lightning Protective Devices, AIEE Committee Report. *AIEE Transactions*, volume 68, part II, 1949, pages 1330–33.

Discussion

E. C. Starr (Oregon State College, Corvallis, Oreg.): The information presented in this paper, together with that in the paper by Mr. Rorden,[1] will be of great value to engineers whose duty it is to design the insulation protective systems of high-voltage substation equipment. The performance of lightning arresters subjected to steep-front voltage and current waves has not previously been made available, generally, to utility engineers, and a seemingly unnecessarily large margin between lightning arrestor block voltage and transformer-withstand capacity has been recommended.

Mr. Vogel's oscillograms point out the necessity for a substantial margin, but they also indicate that for travelling-wave discharge duty, the lightning arrester momentary initial overvoltage, together with the overvoltage occasioned by modest lead lengths between the lightning arrester and transformer, is of such short duration as to fall within the short-time high-strength region of modern transformer insulation, and therefore not materially to reduce the margin indicated by the standard 10 by 20-microsecond current-wave tests on lightning arresters. For station-type lightning arresters located in close proximity to the protected equipment, that is of the order of 50 feet or less, it seems that a margin of 25 or 30 per cent between the average block voltage of the lightning arrester at 5,000 amperes and the transformer withstand value should be adequate when the station is so protected that surges of a traveling-wave character only, limited by line and station insulation flashover, are permitted to impinge upon the apparatus. The lightning arrester block voltage referred to is that obtained in the standard 10 by 20-microsecond current-wave test, and the transformer withstand value is that indicated by the 1.5 by 40-microsecond full-wave surge test.

The design factors now are rather clearly indicated.

Reference

1. Lightning Arresters as a Criterion for Insulation Levels, Harold L. Rorden. *AIEE Transactions*, volume 69, part I, 1950, pages 84–96.

P. L. Bellaschi (Consulting Engineer, Portland, Oreg.): In view of the renewed activities in rationalizing of basic insulation levels, the contribution by Mr. Vogel is pertinent in that it draws attention once again to some of the problems of protection

and co-ordination of station insulation. One of the factors to consider in the protection of station equipment is the lead effect between the protective device and the apparatus protected. Leads and busses of the usual lengths encountered in stations can well be represented by a lumped inductance (L_1) and for the short time involved the transformer in effect is a capacitance (C_T). A 60-foot bus corresponds to about 20 microhenries and a large power transformer in the order of 1,500 to 2,000 micromicrofarads. The problem is conducive to calculation. For an incoming surge on the line, appearing at the lightning arrester rising to lightning arrester crest voltage E in one microsecond and limited to that voltage by the lightning arrester, the surge voltage e_T at the transformer is

$L_1 = 20$ microhenries

$C_T = 2{,}000$ micromicrofarads

$$e_T = \left(t - 0.2 \sin \frac{2\pi}{1.26} t\right) E, \text{ for } 0 < t < 1 \text{ microsecond}$$

$$e_T = \left(1 + 0.192 \cos \frac{2\pi}{1.26} t - 0.145 \sin \frac{2\pi}{1.26} t\right) E, \text{ for } t > 1 \text{ microsecond}$$

Thus for an incoming surge rising to lightning arrester crest voltage E in 1 microsecond and maintained to that voltage at the lightning arrester, a 60-foot bus between lightning arrester and transformer and terminating at the transformer, the surge voltage at the transformer (e_T) is the lightning arrester voltage (e_A) plus a superimposed oscillation 24 per cent above the lightning arrester crest voltage (E), of a period $T = 1.26$ microseconds and decaying after several oscillations down to practically zero. For a 120-foot bus, the overvoltage attained would be 55 per cent above lightning arrester crest voltage, of a somewhat longer duration (period) because of the higher lead inductance.

The overvoltage at the transformer depends on the ratio of the duration of the front to the period of oscillation of lead (bus) inductance and transformer capacitance. The dissipative characteristics of lightning arrester, leads and other circuit elements naturally reduce the overvoltage developed. Another factor in the protection problem at the shorter times is due to an inherent "delayed ionization effect" in the lightning arrester proper when subject to rapid surge current discharges. This effect can accentuate the over-voltage at short times by an appreciable amount. The oscillations of the voltage appearing at the transformer shown in Mr. Vogel's paper are of the character indicated in the foregoing analysis. It would have given greater significance to the results presented in the paper had the author recorded the corresponding surge currents through the arrester.

Because of their inherent strength to the shorter impulses, transformers designed and tested in accord to current standards are well capable of withstanding voltages of the character indicated in this discussion and in the paper. A certain length of lead or bus between lightning arrester and transformer is permissible, the amount depending on the rate of rise of voltage at the lightning arrester, the surge current discharged (rate of rise and magnitude) through the lightning arrester, protective characteristics of the lightning arrester, volt-time characteristics of the transformer and its basic insulation level.

Present-day knowledge of lead effect, lightning arresters, and station apparatus is reasonably comprehensive and quantitative. It has been applied effectively to station design. For example, to quote briefly from Report 317 of the International Conference on High-Voltage Electric Systems[1] presented in 1939:

"It is apparent that for effective protection and co-ordination of station apparatus against very steep impulses, consideration must be given to the circuit feet of leads connecting the various station parts and to the proper location of the protective devices. The most effective method is to mount the lightning arresters on the transformers. Conditions in the station layout or due to the apparatus may not always permit this arrangement. In such cases, the lead voltage can be minimized by locating the lightning arrester as close as possible to the transformer or apparatus it is intended to protect. A protector tube or suitable rod gap located at the line end of the station, will afford additional protection to the station apparatus against steep-wave-front impulses that may enter the station. The problems arising in protecting a large station against very steep voltages can be overcome by increasing the effectiveness of the overhead ground wire and the grounding (counterpoise) to the extent that the only possible voltages entering the station would be in effect impulse voltages of duration greater than 2 or 3 microseconds. It should be recognized that the presence of multiple lines, as well as the station capacitance, contribute beneficially and in no small measure to protection."

During the past 15 years many impulse tests have been conducted in the various laboratories on transformers in combination with lightning arresters as well as other protective devices, and the findings in large part have been incorporated in station insulation design. The lead and other short-time effects in relation to the strength of station insulation at the short- and long-impulse times and to the over-all problem of protection and co-ordination have been recognized and taken into account, in certain quarters at least. However, it is well that attention is called to these problems and re-examined.

References

1. Coordination and Protection of Station Insulation Against Lightning, P. L. Bellaschi. *Report Number 317*, International Conference on Large High-Voltage Electric Systems (Paris, France), 1939.

2. Progress in Power-Transformer Insulation and Protection, P. L. Bellaschi. *Report Number 116*, International Conference on Large High-Voltage Electric Systems (Paris, France), 1946.

E. Beck (Westinghouse Electric Corporation, East Pittsburgh, Pa.): The paper touches on a subject of present importance because of the work that is being done on insulation co-ordination by the Triple Joint Committee. In the tests involving lightning arresters, it is regretable that records of the discharge currents were not made to correlate with the voltages recorded at the lightning arresters. As indicated in the paper, co-ordination demands that some conclusions must be reached on the lightning arrester discharge current which is to be used as a basis for determining a protected level maintained by the lightning arresters. In my opinion the performance data for lightning arresters should be chosen so that the voltage which appears across lightning arresters co-ordinates with the type of voltage on which transformer withstand strengths are based, for it does not seem logical to me to compare two sets of data of different nature. It should be noted that the lightning arrester used by Mr. Vogel was a line-type lightning arrester. In the discussion of basic insulation levels and so forth, it seems to me that the protective level on which the basic insulation levels are based, should be that afforded by station lightning arresters if full advantage is to be taken of available levels.

Although Mr. Vogel's paper contains no information on the magnitude or wave shape of the lightning arrester discharge current, there appears to be some disagreement between Mr. Vogel's paper and the data presented in Mr. Rorden's paper, as to the performance data, if the ratio is the same as the ratings of the lightning arresters tested by Mr. Vogel and Mr. Rorden. Tests made in our laboratories do not check with some of Mr. Vogel's results.

I am in agreement with Mr. Vogel's suggestion that lightning arrester performance be stated on the basis of the maximum value expected rather than the average, or possibly, subject to further discussion and debate, on some probable value which is higher than the average but lower than the maximum industry value, as has been suggested by the National Electrical Manufacturers Association.

A. M. Opsahl (Westinghouse Electric Corporation, East Pittsburgh, Pa.): In Mr. Vogel's tests there were no measurements made of the lightning arrester discharge currents so no direct comparison can be made with other measurements. The high test currents are very short in duration, about 4 microseconds for the first half cycle. The lightning arrester discharge voltage characteristic is a function of the rate of rise of the discharge current as well as the magnitude of the current. However, the measured lightning arrester discharge voltages in Figure 3 seem to be too high. Also in this figure the shape of the lightning arrester discharge voltage is not normal. Figure 3(A) is the sparkover of the 9-inch air gap. The voltage after sparkover does not fall immediately to zero as it should. The voltage passes through zero and reverses at crest current, 2 microseconds after the beginning of the surge. This excess voltage measured across the 9-inch rod gap can best be explained by inductive drop in the line and ground leads to the gap. The voltage across the gap leads is high, about 100 kv as the trace leaves the edge of Figure 3 (A) and still higher just after gap sparkover.

If such line and ground leads, or parts of the same leads are included in the arrester voltage measurement, Figure 3 (B), the shape of the arrester voltage can be understood. The inductive drop in the lightning arrester leads is directly additive to the discharge voltage. A correction for the voltage drop across the leads would bring the lightning arrester discharge voltage characteristic to the same level as in Figure 2. The lightning arrester characteristics in

Figure 2 are about normal for high rates of rise of current.

Effective protection of transformers under the rapidly rising surge voltages and currents used in these tests, requires that voltage drop due to line and ground leads to the lightning arrester be reduced to the minimum. Mr. Vogel's tests in the laboratory with very moderate length leads showed about 50 per cent overvoltage. In service, the optimum lightning protection would be obtained by mounting the lightning arrester on the transformer tank which can place it directly in parallel with the transformer bushings with a minimum of lead to reduce the effectiveness of the lightning arrester.

F. J. Vogel: I wish to thank Professor Starr for his discussion.

Referring to the mathematical part of Mr. Bellaschi's discussion, it is indeed old. However, the performance of the lightning arrester with steep rates of current rise has not been generally recognized, nor has its performance been compared directly with transformer characteristics publicly. Also, as Mr. Bellaschi stated, combination tests have been made, but to my knowledge, they have not been reported. The purpose of my paper was to call attention to the lower voltage class of transformers, up to 69 kv, where overhead protection from steep front waves might not be economical, and to show that they would be protected with even line-type lightning arresters, against very severe lightning surges.

The discussers generally called attention to the lack of discharge current information. One reason it was not obtained was because a study of lightning arrester performance was not within the scope of the project. It was desired to show that steep front strength of transformer insulation was desirable, that a new design of transformer would be protected against a very severe surge, and that it would give good service in use. The test was made with only one type and make of lightning arrester. Incidentally, it pointed out that the present lightning arrester standards did not tell that higher voltages occurred with steep front waves. Mr. Beck clearly appreciated this point of view, when he said that "co-ordination demands that some conclusions must be reached on the lightning arrester discharge current which is to be used as a basis for determining a protective level maintained by the lightning arresters." Some may claim they do this by using present standards and making allowances for these other effects. However, tests such as mine can be made easily, and if current measurements are necessary could be included. Station-type lightning arresters should not be the sole type studied in my opinion.

I am not much surprised that my data and Mr. Rorden's do not entirely agree. I am sure that the currents and the rates of current rise are much higher in my tests. There was no great length of line between the surge generator and the lightning arrester. Measurements were made as nearly as possible at the transformer.

I was very much interested in Mr. Opsahl's discussion, because in it he brings out a difference in point of view, and because he is technically correct in his reasoning as to Figure 3(A).

The circuits used for both Figures 2(A) and 3(A) were reported to be the same, except that a minimum of resistance and inductance were in the generator circuit for Figure 3(A). Nevertheless, a part of the inductance drop due to current in the main generator circuit is undoubtedly present. Personally, I doubt if it affected the magnitude of the voltage very greatly in the case of Figure 3(A), or for that matter the crest values of the other oscillograms. Other data for the 9-inch gap about checks that for Figure 3(A).

Insofar as the point of view is concerned, I am not so interested in what the lightning arrester does without leads as I am with them.

In Figure 3(B), a minimum of leads was present. The voltage measured was at the transformer. This is the value that interested me. Further, the lightning arrester I used might not have been representative of other lightning arresters made by Mr. Opsahl's company, or it might not even have been made by his company. And finally, the purpose of my paper, to show that some separation between lightning arrester and transformer still gave optimum protection, was entirely misconstrued, since I thought the paper showed that effective protection with line-type lightning arresters was obtained.

I would like to take exception to the lightning arrester standards if the proposal to use an average +2/3 of a possible maximum is adopted. I do not think that it will actually mean much since transformer insulation is not designed within 5 per cent, and this allowance would be in that order. But if some lightning arresters, on test at assembly, might be at the maximum value, I think it would be better to say so, and make provision for a test of a complete lightning arrester, if specially required, to demonstrate it was below this value. People seem to expect transformers to meet the tests, rather than the 5 per cent lower values.

Harmonic Index—A Tool for Transformer Audio Noise Investigation

W. H. MUTSCHLER, JR.
ASSOCIATE AIEE

T. F. MADDEN
ASSOCIATE AIEE

Synopsis: The harmonic index is the decibel difference between the noise level obtained with the flat weighting and the noise level obtained with the 40-decibel weighting. It is a qualitative measure of the harmonic content of the noise measured at a given point. The harmonic index was introduced several years ago,[1] but it has not realized the consideration which it merits. It is the purpose of this paper to demonstrate the value of the harmonic index when used in conjunction with the flat weighting measurements as a simple approach to the problem of evaluating the complex structures of the transformer.

TRANSFORMER audio noise is a problem which has confronted both the users and the manufacturers of transformers for many years. The rapid growth of transmission and distribution systems within recent years has necessitated the location of power transformers within residential districts and, at times, within buildings. As a result, power companies employing such installations have become even more noise conscious.

During the same interval a new electric core steel has been developed which operates at a much higher flux density to produce a smaller, more economical transformer. The magnetostrictive effect of these new highly oriented cold rolled steels is less for a given density; however, this advantage is offset by operating at higher densities. In order to utilize the economic advantage of these newer steels and to reduce the transformer noise at the same time, it becomes necessary to eliminate, as completely as possible, the sources of resonance in the transformer structure and to find methods for the attenuation of the noise energy within the transformer.

Means, such as sound absorbing enclosures, for the attenuation of the noise external to the transformer have been developed, but such devices are costly. Since, in most cases, the transformer noise must be decreased because of complaints, either a quieter transformer must be obtained for the location or these costly devices must be employed.

In order to eliminate the source of resonance and to find the attenuating effects of changes made in the transformer structure, it becomes necessary to evolve a simple method for the evaluation of the effects of these changes. The harmonic index and the physical noise level of the transformer are the tools which can be employed for this evaluation.

Magnetostriction

Magnetostriction, the minute dimensional variations in ferro-magnetic materials during magnetization, has long been recognized as the main source of transformer noise.[1,2,3] Magnetostriction is present in electrical sheet steel in the order of several micro inches per inch and varies with flux density as shown in Figure 1(A) for cold rolled steel and in Figure 1(C) for hot rolled steel. Although the magnetostriction in cold rolled steel is less than that of hot rolled steel at the same value of flux density (in Figures 1(A), 1(B) and 1(C) a flux density of 12 kilogausses was used) the higher flux density dictated by the economical operation of cold rolled steel more than offsets the reduction of magnetostriction accomplished by orientation in the steel. In either case, the minute vibrations set up by the alternating flux in the core constitute an appreciable source of sound energy. The predominance of the higher harmonics in cold rolled steel makes the noise generated by it more objectionable than that produced by hot rolled steel.

From the viewpoint of noise generation, cold rolled steel has one further disadvantage—it is sensitive to cold working which may result from rough handling during the manufacturing process. Figure 1(B) shows the effect of mishandling cold rolled steel. Cold working of this steel disturbs the orientation and the magnetostrictive characteristic becomes similar to the magnetostrictive characteristic of hot rolled steel.

In the economical application of these steels, the optimum in noise performance is dictated by the maximum amplitude of magnetostriction, the maximum operating flux density and the physical characteristics of the core. Since magnetostriction is a physical property of the steel, it is difficult to control internally the sound energy which the steel is capable of producing at a given flux density. By increasing the silicon content to approximately $6^1/_4$ per cent, the magnetostriction is reduced to a negligible amount but mechanical requirements prohibit the use of this high value of silicon content.[4,1] In all cases known to date, either mechanical or economical considerations prohibit the manufacture of a "zero-magnetostriction" electrical sheet steel. The only means available to the transformer manufacturer of curbing the noise generated is through the attenuation of the more objectionable frequencies in the noise spectrum.

Mechanical forces due to load currents in the coils will give rise to 120-cycle noise. The magnitude of the noise thus produced is in general sufficiently below the magnitude of the 120-cycle component produced by the core so that it will not contribute to the over-all noise picture.[1,2,3]

Paper 50-18, recommended by the AIEE Transformers Committee and approved by the AIEE Technical Program Committee for presentation at the AIEE Winter General Meeting, January 30–February 3, 1950. Manuscript submitted November 2, 1949; made available for printing November 29, 1949.

W. H. MUTSCHLER, JR. and T. F. MADDEN are with the Allis-Chalmers Manufacturing Company, Pittsburgh, Pa.

The authors wish to extend their appreciation to J. B. Hodtum for his helpful assistance throughout the preparation of this paper.

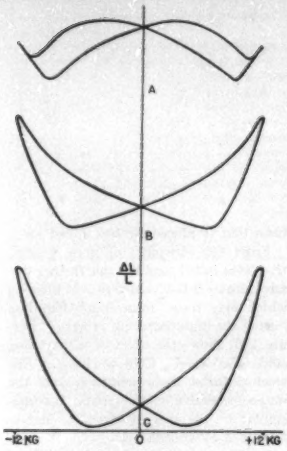

Figure 1. Magnetostriction characteristics of electrical sheet steel operating at a maximum flux density of 12 kilogausses

A. Cold-rolled steel
B. Cold-rolled steel after mechanical working
C. Hot-rolled steel

Resonance

The secondary source of audio noise in a transformer is resonance of the mechanical structure. Resonance and the extent of its influence on the noise level of a transformer may vary considerably depending upon the number of members in the structure that resonate, the resonant frequency of each member and the magnitude of the driving force of this frequency in the core.

If the vibrational amplitude of a given frequency is doubled by resonance, the noise level will be increased six decibels for this frequency. Resonance is capable of increasing the vibrational amplitude four or five times, which will cause an increase in noise level of 12 or 14 decibels. Fortunately, the distributed characteristic of the transformer noise plus the fact that resonance does not normally exist at more than two or three frequencies prevents the realization of such large increases in noise level; however, resonance may account for increases in noise level up to six decibels, which is often the difference between a noisy transformer and a quiet one.

For core-type transformers, as well as shell-type transformers, it has been found that the resonant frequency of the core can be determined analytically. In the core-type transformer, the resonant frequency is a function of the free length of the leg and the width of the laminations. By proper selection of these dimensions by the design engineer, resonance can be eliminated in the core and thereby the noise of the core can be reduced to a minimum. With the addition of side frames and the winding assembly, some resonance may be introduced into the transformer. What effect these additions will have can best be determined experimentally.

After the core and coil assembly is immersed in oil, the vibrations of the core are reduced by the damping force of the liquid.

This damping force is proportional to the density of the oil and of the frequency of the vibrations. The damping force, therefore, which acts on the higher frequencies is greater than the damping force which acts on the lower frequencies. It can then be expected that, after tanking, the physical noise as well as the harmonic content of the noise will be decreased.

Since the oil is an incompressible fluid, the vibrational amplitudes, decreased by the damping action, are then transmitted to the tank wall. Some of the vibrations are also transmitted to the tank wall by the supports of the core and coil assembly. The damping force of these supports depends upon the method of supporting. In general the damping forces of the supports are small, and the vibrations are transmitted to the tank with little damping.

When the vibrations reach the tank they are either attenuated by the mass and stiffness of the tank walls or accentuated by resonance in the tank structure. The tank surface is broken up into many small areas by radiators and other members which are welded to the tank wall. As a result, the tank will have numerous resonant frequencies and, as in the core and coil assembly, resonance cannot be treated analytically but can be determined experimentally.

Since some frequencies may be attenuated while others are accentuated, the noise spectrum of the transformer after tanking will be somewhat different from the noise spectrum before tanking. The noise spectrum is the distribution of harmonics determined by the harmonic analysis of the noise. Resonance therefore can be determined by obtaining the noise spectrum before tanking and comparing it to the noise spectrum after tanking to locate the frequencies at which resonance occurs.

Harmonic Analysis

The noise spectrum obtained for the core and coil assembly of a transformer to be used as a basis for comparison with the completed transformer is shown in Figure 2. After the transformer is tanked, the noise spectrum is again obtained, Figure 3.

By comparing these spectrums it can be seen that in the example chosen the 600-cycle as well as the 1,080-cycle noise level is higher after tanking which indicates that there is predominant resonance at these two frequencies. Steps were taken to eliminate resonance at these frequencies and the noise spectrum was again determined. Figure 4. Here the 600-cycle and the 1,080-cycle noise levels are reduced to values comparable to those obtained on the core and coil assembly alone. The noise level of the transformer before any changes were made was 55.8 decibels; and, after the changes were made, the noise level was 53.0 decibels. The elimination of resonance in this particular case caused a decrease in noise level of 2.8 decibels.

The noise spectrum provides an excellent method for obtaining the frequencies at which resonance occurs. In order to obtain the noise spectrum, however, numerous readings must be taken and analyzed. Since there are variations in magnetostriction from one lot of steel to the next, the refinements obtained by using the noise spectrum prevent the use of a typical noise spectrum. These two factors combine to make the harmonic

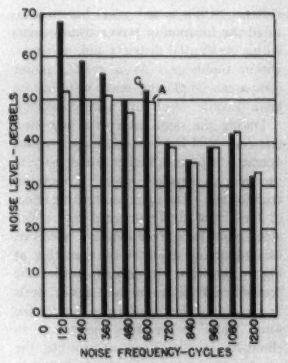

Figure 2. Noise spectrum of the core and coil assembly with 60-cycle excitation

C. Noise level—68.9 decibels
A. Weighted noise level —57.5 decibels

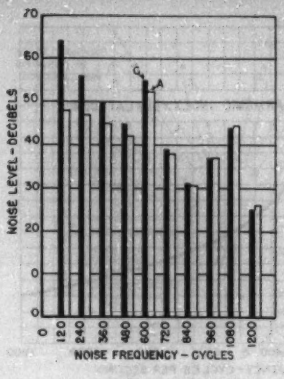

Figure 3. Initial noise spectrum of the transformer with 60-cycle excitation

C. Noise level—65.3 decibels
A. Weighted noise level—55.8 decibels

analysis impractical. A practical method of analysis then is one in which the data obtained is not quite so sensitive to variations in magnetostriction and one which requires only a very few readings.

Harmonic Index

The harmonic index, *hi*, is defined as the difference between the noise level measured by the "flat" response and the noise level measured by the 40-decibel response curve.

$$hi = db_{(flat)} - db_{40}$$

Since the noise level measured by the "flat" response is equal to the physical noise present and the noise level measured by the 40-decibel response is equal to the noise as determined by the ear, the harmonic index is actually a measure of the attenuation of the physical noise by the ear. Attenuation of the ear is a function of the frequency at which the noise is generated. This is best exemplified by considering two pure tones, one of 120 cycles and one of 480 cycles, both having a physical noise intensity of 55 decibels. The sensation experienced by the ear for the 120-cycle pure tone is approximately 39 decibels, and the harmonic index for this tone is

$$hi = 55 - 39 = 16db$$

With a pure tone of 480 cycles, the attenuation of the ear is less and the ear would experience a sensation equivalent to 51.5 decibels. The harmonic index for this particular tone is

$$hi = 55 - 51.5 = 3.5db$$

Obviously the energy, as observed by the ear, equivalent to a physical noise level of 55 decibels is less objectionable when generated at 120 cycles than it would be at 480 cycles. The importance of this principle is that it may be used to give an indication of the quality of a complex sound such as is generated in a transformer. Noise having a high harmonic index indicates a predominance of low harmonics while noise having a low harmonic index indicates a predominance of high harmonics. Extreme variations in the harmonic index as exhibited by the pure tones above do not take place in a transformer because of its complex nature; however, the significant factor in the application of the harmonic index is the manner in which it changes.

For a given size transformer core the sound energy will be a function of the harmonic content and the maximum amplitude of the magnetostriction in the steel used. Using the amplitude of each frequency obtained from a harmonic analysis of the magnetostriction versus time characteristic, it is possible to determine the average harmonic index and the physical noise level for the core.

If the core has been designed to avoid resonance, the harmonic index and physical noise level of the transformer should be equal to the calculated values. Factors, such as damping pressure, core impregnation, size, and weight of side frames and the windings may influence the noise level of the core. Here the harmonic index can be used to study the effects of each of these factors. If the physical noise level is increased above the calculated value, the range of resonant frequencies can be determined. Thus it is possible to determine what structural changes can be made in the core assembly for maximum noise attenuation.

Table I. Variation of Physical Noise Level and Harmonic Index Between Untanked Transformer and Tanked Transformer

	Variation of		Cause of Variation		
Item	Physical Noise	Harmonic Index	High-Frequency Resonance	Low-Frequency Resonance	Poor Damping
1	+	+		××	
2	+	O	×	×	××
3	+	−	××		
4	O	+		×	
5	O	O			×
6	O	−	×		
7	−	+		×	
8	−	O			
9	−	−	×		

+—Increase
−—Decrease
O—No change
×—Probable cause
××—Most probable cause

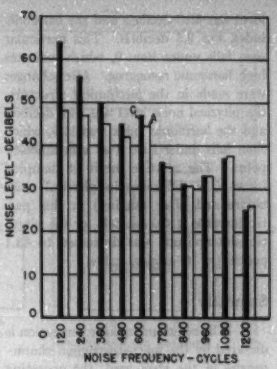

Figure 4. Noise spectrum of the transformer with 60-cycle excitation after the elimination of resonance

C. Noise level—64.9 decibels
A. Weighted noise level—53.0 decibels

When the transformer is tanked, most of the vibrations are transmitted from the core and coil assembly through the oil. The magnitude of these vibrations are decreased by the damping forces in the oil. Other vibrations are transmitted directly to the tank wall by the structural members which support the core and coils in the tank with very little damping.

By comparing both the physical noise level and the harmonic index before and after tanking, the extent of resonance can be determined. If the harmonic index has decreased, it indicates that high harmonic resonance may exist, and the change in the physical noise level will show to what extent it exists. Table I has been prepared to show the several different changes that can take place and their most probable cause. Item 8 represents the ideal case in which the physical noise level is decreased, while the harmonic index remains practically constant.

After resonance has been eliminated and the harmonic index remains practically constant before and after tanking, the change in the physical noise level is an indication of the damping merits of the oil and the core and coil assembly supports.

For the example in which the harmonic analysis was used, the physical noise level of the core was 68.9 decibels and the harmonic index was 11.4. For the finished transformer, the physical noise

level was 65.3 decibels and the harmonic index was 9.5 decibels. This particular case falls under item 9, which indicates high harmonic resonance. After changes were made in the mechanical structure, the physical noise level was 64.9 decibels and the harmonic index was 11.9, which then falls under item 8 as a satisfactory point. The relative merit of damping forces (the difference in physical noise before and after tanking) in this particular case is 4.0 decibels, or the vibrational amplitude was decreased to 63.1 per cent of its original value.

Summary

1. The optimum in noise generation is dictated by the magnetostriction characteristic of the steel used, the operating flux density and the physical characteristics of the core structure.

2. The harmonic index and the physical noise level provide a simple method for the practical investigation of resonance in transformers.

3. The elimination of resonance in transformers through the use of these methods will lead to a quieter transformer.

4. This method also provides a means for evaluating the attenuation effect of damping forces applied to transformers.

References

1. A Study of Sound Levels of Transformers, **H. Fahnoe.** *Electrical Engineering (AIEE Transactions)*, volume 60, June 1941, pages 277–83.

2. The Limitations of Transformer Noise, **B. G. Churcher, A. J. King.** *Metropolitan-Vickers Gazette* (Manchester, England), May 1940.

3. Causes and Characteristics of Transformer Noise, **J. Swaffield.** *Journal*, Institution of Electrical Engineers (London, England), volume 89, 1942.

4. Standard Handbook for Electrical Engineers (book), **A. E. Knowlton.** McGraw-Hill Book Company, Inc., New York, N. Y., 1949.

5. Magnetostriction in Electrical Sheet Steels, **F. Brailsford, R. G. Martingdale.** *Journal*, Institution of Electrical Engineers (London, England), volume 89, 1942.

6. Acoustical Terminology, Z24.1. American Standards Association (New York, N. Y.), 1942.

7. Noise Measurement, Z24.2. American Standards Association (New York, N. Y.), 1942.

8. Sound Level Meters for Measurement of Noise and Other Sounds, Z24.3. American Standards Association (New York, N. Y.), 1944.

Discussion

C. S. Murray (Consolidated Edison Company of New York, Inc., New York, N. Y.): The authors have demonstrated how the harmonic index can be used as a tool by the manufacturers for detecting resonance of the transformer structure.

Figure 1. Harmonic index of noise components

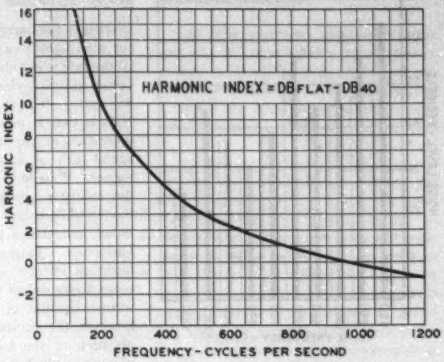

There is a possibility that the harmonic index also may be used as a tool by the user for obtaining an idea of the harmonic content of the noise emitted by his transformer.

In order to evaluate any noise, its harmonic content should be obtained, and the harmonic analyzer is considered as the best means for doing this. In many cases, however, a harmonic analyzer is not available and in other cases time does not permit the analysis of the noise at several positions around the transformer.

Most sound level meters are equipped with both the "flat" and the 40-decibel weighting networks wherein the value for either scale may be obtained by the mere operation of a switch. The extra time consumed by obtaining the sound level for the "flat" scale in addition to the value for the 40-decibel scale, when determining the average sound level of the transformer, is small. Furthermore, no additional training of the tester is required.

For convenience, the harmonic index as a function of pure tones is given in curve form in Figure 1 of this discussion. This curve is derived from the response characteristics of the sound level meter. The value of the harmonic index at the different frequencies is the same as used by the authors in their paper.

Figure 2 of the discussion shows the value of the harmonic index at various positions around a 60-megavolt-ampere transformer obtained by taking the difference in the indications of the "flat" and 40-decibel scales. It will be noted that the average value of the harmonic index is 6.5 and by referring to Figure 1 this indicates a transformer noise frequency of 360 cycles. An actual analysis of the transformer noise at various distances from it showed that the outstanding component was 360 cycles. The average value of the index obtained with the cooling fans in operation is practically the same as the case without fans indicating that the transformer noise is still the outstanding noise. An analysis of the noise at various distances from the transformer substantiated this conclusion.

Figure 3 of this discussion shows the value of harmonic index obtained for a 50-megavolt-ampere transformer installation. These results also show the possibilities of using the harmonic index.

It is recognized that sufficient data has not been presented here to determine the limitations or other possible interpretations of the results that may be arrived at by further use. Its possibilities should not be overlooked by those who do not have harmonic analyzers.

The authors make a statement that "the noise level measured by the 40-decibel response is equal to the noise as determined by the ear." We have not reached the stage where a single weighting network of an instrument is capable of following the characteristics of the human ear. The only time that the 40-decibel weighting network does accomplish this is when measuring a pure tone having an equivalent loudness level of 40 phons and with no other sounds present that may mask it. There is a large difference in the harmonic index value obtained if the value determined by the ear were used in place of the 40-decibel response network. For example, the noise spectrum for the transformer core and coil assembly given in Figure 2 of the paper, shows a harmonic index for the 120-cycle component of 16. If we use the published equal loudness contours of the ear,[2] and also realize that this particular component is not masked by the other harmonic tones present, we would arrive at a value of about nine for the harmonic index.

The harmonic index is simply the difference between the values given on two different scales of the sound level meter. Its value has been demonstrated by the authors and it is not felt that any other interpretation of the harmonic index is warranted.

References

1. See reference 8 of the paper.
2. See reference 7 of the paper.

S. Bennon (Westinghouse Electric Corp., Sharon, Pa.): The authors are to be commended for calling attention to the value of the "harmonic index," introduced by Mr. H. Fahnoe in his Institute paper[1] several years ago. In that paper the usefulness of the harmonic index, both as a parameter in the calculation of transformer levels as well as an indicator of resonance was outlined. Those of us who were associated with Mr. Fahnoe at Sharon have been using the

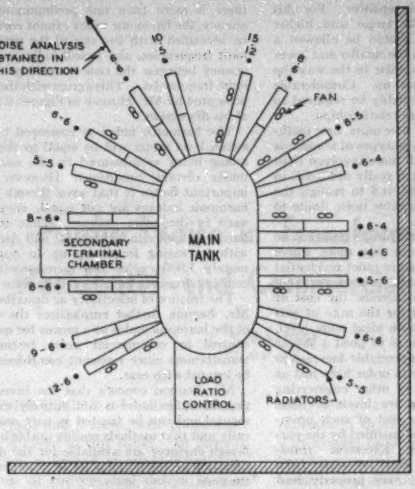

NOTE - NUMBERS IN ABOVE DIAGRAM ARE VALUES OF THE HARMONIC INDEX OF TOTAL NOISE OBTAINED WITHOUT FANS IN OPERATION, THOSE NEAREST APPARATUS ARE FOR 1/3RD TRANSF. HEIGHT AND THE REMAINING ARE FOR 2/3RD TRANSF. HEIGHT.

AVG H. I. WITHOUT FANS IN OPERATION = 6.5
WITH FANS IN OPERATION = 5.5

PREDOMINATING FREQUENCY OF NOISE EMITTED (WITH OR WITHOUT FANS) AT VARIOUS DISTANCES FROM TRANSFORMER = 360 CYCLE / SEC.

Figure 2. Harmonic index values for a 60-megavolt-ampere transformer in service

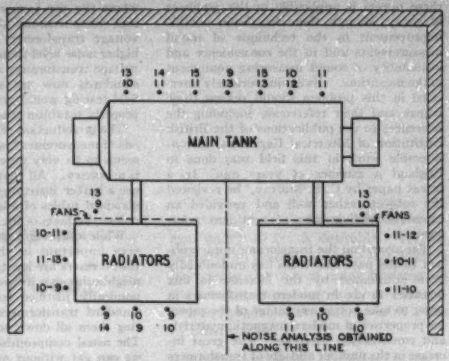

NOTE - NUMBERS IN ABOVE DIAGRAM ARE VALUES OF THE HARMONIC INDEX OF TOTAL NOISE OBTAINED WITHOUT FANS IN OPERATION, THOSE NEAREST APPARATUS ARE FOR 1/3RD TRANSF. HEIGHT AND THE REMAINING ARE FOR 2/3RD TRANSF. HEIGHT.

AVG. H. I. WITHOUT FANS IN OPERATION = 11
WITH FANS IN OPERATION = 6

DISTANCE FROM MAIN TANK FT.	PREDOMINATING FREQUENCIES OF NOISE EMITTED	
	WITHOUT FAN	WITH FANS
13	240	360 AND 480
37	240	360 AND 480
85	240	240 AND 480

Figure 3. Harmonic index values for a 50-megavolt-ampere transformer in service

harmonic index in a manner similar to that suggested by the authors. It is gratifying that the significance of this quantity now is attaining more general recognition.

One valuable feature of the harmonic index which is worth stressing, is its ability to detect important resonances and to ignore those which are unimportant. In commercial sound level testing, resonances are of importance when they raise the overall level of the transformer. A resonance which amplifies a relatively weak harmonic, and, therefore, adds very little to the sound energy, would not be of practical importance, as its effect on the ear also will usually be slight. Since the harmonic index is the difference between the sound levels using "flat" and "40" weighting, the resonances must change either one or both of these levels to produce a change in harmonic index. This selective response of the harmonic index, coupled with its ease in measurement using commercially available sound level meters, make it a valuable tool in practical sound level studies. Inasmuch as a complete harmonic analysis is involved and time consuming, the harmonic index provides the necessary criterion by which those units with important resonances can be weeded out for more thorough investigation.

Some mechanical resonances which occur in transformers are susceptible to calculation with engineering accuracy. One of these is the natural frequency of the transformer core as a closed-frame type structure. Although the frequency of a structure of this type is a function of the width of leg divided by the length squared, as stated by the authors, it is well to keep in mind that it is a function of other factors as well. The natural frequency of a rectangular frame with legs of length l_1 and l_2 can be expressed as[3]

$$f=\frac{(K_2)^2}{2\pi l_2^2}\sqrt{\frac{E_2 I_2}{m_2}} \qquad (1)$$

where E_2, I_2, and m_2 are the modulus of elasticity, moment of inertia of the cross-section and mass per unit length, respectively, of the leg of length l_2. For the usual case where the distributed parameters (E, I, and m) of the two legs are equal or bear a constant ratio, K_2 is a function of the ratio of the two leg lengths which we can designate as r. If we assume that the legs are of rectangular section (shell form) or of approximately circular section (core form) equation 1 reduces to

$$f=CF(r)\frac{W_2}{l_2^2}\sqrt{\frac{E_2}{D_2}} \qquad (2)$$

where C is a constant having a different value for core or shell form, $F(r)$ represents a function of the ratio of leg lengths, and W_2 and D_2 are the width and density respectively of leg l_2. Equation 2 indicates that even for a specific type of core and a fixed core material, the natural frequency will still be a function of the ratio of leg lengths as well as the ratio of leg width to the length squared. By choosing the subscript 2 to identify the longer of the two legs, the variation of $F(r)$ with r can be considerably reduced. This may sometimes tend to obscure the dependence of the frequency on the ratio of leg lengths when a limited range of r is considered.

References

1. A Study of Sound Levels of Transformers, H. Fahnoe. *AIEE Transactions*, volume 60, 1941, pages 277–83.

2. Natural Modes of Vibration of Simple Frames, S. Bembo. *Journal*, Franklin Institute (Philadelphia, Pa.), volume 243, January 1947, pages 13–39.

F. Von Voigtlander (Commonwealth Service Inc., Jackson, Mich.): The matter of audible noise from power transformers has been of recurrent interest during the past 20 years. R. H. George's paper given in 1931,[1] outlined many of the factors influencing noise in transformers and methods for noise mitigation in the transformers and in substation installations. A. P. Fugill's paper given in 1934,[2] and E. J. Abbott's paper given in 1935[3] outlined in some detail the successful mitigation of transformer and regulator noises in the equipment itself and in the substation installations.

Much of the work done and reported in

these papers is applicable to the problems of today, though there has been notable improvement in the technique of sound measurements and in the convenience and availability of sound measuring equipment in the meantime. Everyone seriously interested in this problem should review these papers and their references, including the references to the publications of the British Institution of Electrical Engineers, as considerable work in this field was done in England a number of years ago. In a recent paper by C. S. Murray,[4] he reviewed the subject rather well and provided an extensive bibliography of pertinent references.

The accent on the transformer noise problem in the past two years has undoubtedly been stimulated by the increase in flux densities in use in modern transformers in order to take better advantage of the superior properties of modern magnetic materials and construction methods. The great increase in the number and size of transformers being located in residential areas also is a very important factor in the problem.

Various writers have noted that noise level differences as little as 5 decibels have been sufficient to change customer complaint to customer satisfaction. One of the more widely used sound level meters is inherently limited in accuracy and its readings cannot be relied upon for values closer than ±2 decibels. This instrument does not integrate the effects of complex sounds accurately, particularly at the higher levels. There have been a number of references made that the use of the 40-decibel network gives values of noise that are much too low in practice and as a result Mr. Mutschler and Mr. Madden propose the "harmonic index." This approach has interesting possibilities, but it does not surmount the inherent limitations of some sound level meters and it therefore seems of less promise than the authors hoped for.

The writer believes that as a first step a better sound level meter should be used particularly as much better instruments are now available commercially at prices that come within the scope of the usual laboratory budget. Having a better instrument, the use of a flat response network should give consistent and adequate accuracy within the range of frequencies and levels that are of interest in transformer noise measurements. It should then only be necessary to revise the tabulations in the NEMA Standards to reflect more adequately the response characteristics of the human ear, the noise producing characteristics of transformers of various types and sizes, and the measurements made with a better quality flat response instrument.

Relating allowable noise levels to the kilovolt-ampere rating of transformers of a given type and voltage range seems reasonable as size would be proportional to kilovolt-ampere rating, and noise frequency characteristics would have a tangible relationship to size. The larger transformers would be expected to produce a greater proportion of noise in the lower frequency brackets, where the human ear is less sensitive, while the smaller transformers would be expected to produce a greater proportion of noise in the higher frequency brackets where the ear is more sensitive. For this and other reasons the larger and higher voltage transformers should be allowed a higher noise level than the smaller and lower voltage transformers similar to the way the standards now are set up. Considerable field testing would probably be required to properly establish these relationships.

The introduction of new units, new methods of measurement, and types of standards seems to be very much more involved than is necessary. All that is really needed is to use a better instrument and to realign the standard tables of allowable noise limits to reflect the facts of life.

While low level of transformer noise can be very important in those few cases where transformers are located in quiet residential neighborhoods, it would not seem economically justified to increase the cost of standard transformers for the sake of getting them all down to an ideal noise level. The usual compromise of as good a job as we can get without appreciable increase in cost would seem to be in order here just as it has been in so many other engineering matters. Where very low levels of noise are required the extra cost of such provisions would have to be justified by the particular circumstances. Excessive transformer noise just as excessive noise from any other equipment, may properly lead one to question the adequacy of the design or construction, so that reasonable noise levels may well be taken as one of the attributes of product quality.

References

1. Power Transformer Noise—Its Characteristics and Reduction, **Robert B. George.** *AIEE Transactions*, volume 50, March 1931, pages 347–53.

2. Measurement of Noise from Power Transformers, **A. P. Fugill.** *Electrical Engineering* (*AIEE Transactions*), volume 53, December 1934, pages 1603–08.

3. Quieting Substation Equipment, **E. J. Abbott.** *Electrical Engineering* (*AIEE Transactions*), volume 54, January 1935, pages 20–26.

4. Transformer Audio Noise Problems on an Electric Power System, **C. S. Murray.** *AIEE Transactions*, volume 68, part 1, 1949, pages 740–52.

W. H. Mutschler, Jr. and **T. F. Madden:** Mr. Murray demonstrates that the harmonic index also can be utilized by the user as a tool for the investigation of audio noise. Both Mr. Murray and Mr. Bennon agree that the harmonic index can be obtained in a comparatively short time requiring only a simple operation by the tester, and that it should not be overlooked as a tool when noise investigations are to be made.

It should be noted that the harmonic index versus frequency characteristic depends upon the weighting network of the particular sound level meter used. From the standard tolerances of the *A* and *C* weighting networks, it can be seen that a typical harmonic index versus frequency curve should be used with caution. The harmonic index will indicate the predominant frequency in a noise spectrum providing that the noise levels of all other frequencies are somewhat less than the noise level of the predominant frequency. If there is more than one predominant frequency, the harmonic index cannot correctly be identified with any one of the predominant frequencies, and it will indicate a frequency between the two extreme predominant frequencies. This agrees with the data presented by Mr. Murray in Figures 2 and 3 of his discussion.

The harmonic index as measured by the sound level meter will be equal to the harmonic index as measured by the ear only under certain conditions. However, the important factor is that even though these harmonic indexes are not equal, they will vary in the same manner. That is, the harmonic index in either case will decrease with increasing frequency up to approximately 1,000 cycles and increase with increasing frequencies above this value.

The feature of selectivity as described by Mr. Bennon further emphasizes the value of the harmonic index as a means for quality control in commercial noise testing of transformers since resonant conditions can be located with ease.

Mr. Bennon concurs that the investigation of audio noise is not entirely experimental and can be treated in part analytically and that methods readily usable by the design engineer are available for the determination of the frequencies of resonance of the core.

In the past, various compromises have been suggested for transformer noise measurement. As Mr. Von Voigtlander indicates, the basis for these proposals has been that the *A*-weighting curve does not exemplify the ear response for all intensities. The harmonic index was not proposed as a compromise method of measurement but rather as a means for investigating transformer noise and its elimination. One might conceivably use the harmonic index as a basis for determining a correction factor to be applied to the flat response to determine a sound level which would be nearer to the response of the ear. However, the determination of this correction factor might be rather involved.

Although the use of the flat response has been suggested, it will not overcome all of the inadequacies of the 40-decibel response. For example, consider two transformers; one having a predominant 120-cycle noise and one having a predominant 360-cycle noise, both transformers having a physical noise level of 70 decibels. By studying the equal loudness contours[1] it can be seen that the first transformer will have a loudness level of 60 phons and the second transformer will have a loudness level of 69 phons. Obviously, the second transformer might result in noise complaints when installed in a residential district.

It is to be noted that the method of noise investigation set forth in the paper is based upon using the same sound level meter for all the tests. The inherent inaccuracies of the instrument used will therefore be either completely eliminated or at least their effect will be reduced to a point well within the acceptable limits of engineering accuracy.

Reference

1. See references 6, 7, and 8 of the paper.

Audio Noise in Transformers in Residential and Commercial Areas

C. E. BAUGH
FELLOW AIEE

A DISCUSSION of utility problems, past and present, with transformer noise is given in this paper. In general, its scope is limited to outdoor unit substations of conventional design in sizes ranging from 2,000 to 4,000 kva with primary voltage ratings of 12,000 or 23,000 volts. Sound level data from installations on the Pacific Gas and Electric Company system and corrective measures applied to units having objectionable levels are discussed. Steps which manufacturers might take to minimize users' troubles are suggested.

Transformer Noise and Utility Operations

The Pacific Gas and Electric Company has in operation in the suburban and metropolitan areas adjoining San Francisco Bay about 70 unit substations, 2,000 to 4,000 kva, with primary voltages of 12,000 or 23,000 volts and secondary voltages of 4,160 or 4,330 volts. It operates about ten similar units in smaller communities and in addition has in operation 25 3,000- and 5,000-kva units in rural areas or on the outskirts of smaller cities with a primary voltage of 60,000 volts and secondary voltages of 4,330 or 12,470 volts.

Studies made some years ago indicated the economic desirability of handling load growth in urban and suburban residential or light commercial areas, already served at 4 kv, by installing unit substations to increase the input to the 4-kv system as an alternative to increasing the capacity of existing stations and constructing additional 4-kv feeders. To date this program has met the problems imposed by a tremendous postwar growth in load in such areas with respect to an economic utilization of time, manpower and capital.

The first 2,000-kva 12/4-kv unit substation was placed in operation in 1939 and a few units were installed in the ensuing years prior to the war, but the bulk of the units now in service have been installed since 1945.

If full advantage is to be taken of the various economies of the unit substation type of construction it will be necessary to install many units in areas zoned for residential or commercial occupancy.

In fact, many commercial zones outside of congested downtown areas extend only a half a block either side of a business thoroughfare, the remaining half blocks being zoned for residential use. As a result, transformer sound level is a matter of concern in the majority of the cases where the use of unit substation construction, particularly at primary voltages under 40 kv, is desirable. The alternative to holding sound levels down is to increase the cost of doing business by the amounts necessary to house substation equipment or attenuate sound levels by other means.

Sound Level Data from Pacific Gas and Electric System

The first complaint occasioned by noise from a 2,000-kva unit substation was in 1941. This unit was installed on the rear end of a 30 foot by 73 foot lot between two 2-story apartment buildings, the only complaint registered being from the occupant of a second floor apartment. Sound level measurements made with a General Radio sound level indicator in the manner specified by National Electrical Manufacturers Association rules showed an average sound level of 58.3 decibels, with an average ambient of 42.6 decibels. Figure 1 shows the lot on which the unit was located and shows the adjoining buildings. The original unit has been replaced with the 4,000-kva unit pictured, and no illustrations of the original installation are available. Figure 2 is a plot of the buildings adjacent to the lot and includes sound level measurements with and without the unit energized.

Except for a few other complaints, only one of which was serious enough to require corrective measures, see Figure 3, no particular trouble was experienced until 1948 when we installed the first of a

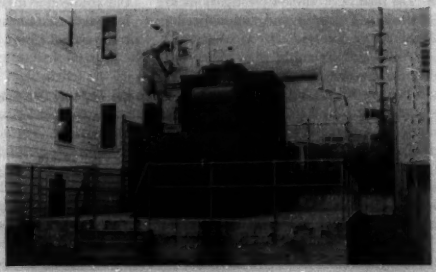

Figure 1. Site on which a 2,000-kva unit substation occasioned noise complaints—now occupied by a 4,000-kva unit

Paper 50-19, recommended by the AIEE Transformers Committee and approved by the AIEE Technical Program Committee for presentation at the AIEE Winter General Meeting, New York, N. Y., January 30-February 3, 1950. Manuscript submitted November 4, 1949; made available for printing December 6, 1949.

C. E. Baugh is with the Pacific Gas and Electric Company, San Francisco, Calif.

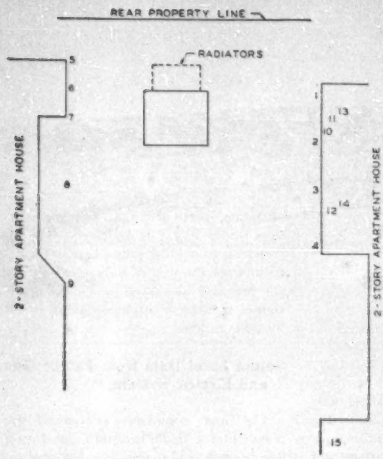

Figure 2 (left). Sound levels adjacent to buildings, Figure 1, with 2,000-kva unit—58.3 decibels—installed

Location	Sound Level-decibel Transformer Energized	Ambient	Remarks
1	56	40	42 inch elevation
2	55	42	42 inch elevation
3	54	41	42 inch elevation
4	47	42	42 inch elevation
5	52	42	42 inch elevation
6	56	43	42 inch elevation
7	53	45	42 inch elevation
8	53	42	42 inch elevation
9	44	41	42 inch elevation
10	56	44	7 inch elevation
11	38	28	Downstairs window
12	33	28	7 inch elevation
12		40	Automobile
13	29	28	18 foot elevation
14	30	29	18 foot elevation
15	62		Trolley bus
15	68		Trolley bus horn
15	29		Minimum street noise

group of 2,000-kva units built to the same general specifications as previous units but with high permeability cold-rolled steel cores.

Two of these units, installed in commercial zones but with residences on adjoining lots, immediately gave rise to complaints and prompted a general investigation of sound levels of a representative group of similar units. A General Radio sound level indicator was used and all measurements were made in strict accordance with the methods outlined in National Electrical Manufacturers Association Standards for Transformers.[1] No readings in locations where the ambient sound level was less than 7 decibels below the level of the ambient plus transformers have been included in the following data and very few of the readings have been adjusted for ambients between 7 and 10 decibels lower.

All measurements were made without fans or tap-changing equipment in operation.

The results of these investigations are plotted in Figure 4 and summarized in Table I.

All of these units have met the manufacturer's guaranteed values of 64 decibels for delta-Y connected transformers and 65 decibels for delta-zigzag connected transformers, but the only units known to have high permeability cold-rolled steel cores (those built by manufacturer *A* in 1948) show considerably higher sound levels than earlier units from the same manufacturer.

Measurements on one 4,000-kva 12/4-kv unit substation built by manufacturer *A* in 1948 to the same general specification as the four 2,000-kv units built in 1948 show a sound level of 49 decibels at an ambient of 34 decibels. Sound levels 19 feet from this unit with no shielding average 37 decibels. We are informed that the core in this unit is of ordinary silicon steel.

The data in Figure 4 and the summary, Table I, indicate a significant increase in noise level in units which have cores operating at flux densities higher than the earlier silicon steel cores. In this connection it is of interest to note the following statement from what appears to be a final report to the members of the Electric Equipment Committee of the Edison Electric Institute in March 1938. The statement reads in part:

"Apparatus noise levels will be dropped from our program as an active subject. The following observations indicate the reasons for this action: "..... We are therefore primarily concerned with the noise emanating from transformers located in network vaults and indoor and outdoor substations, the latter especially in residential areas.

"As previously stated, the noise produced by such installations is generally tolerable with transformers of the more modern (quiet) design....."

Undoubtedly this was a correct conclusion in 1938, but the development of new core steels which have permitted the use of higher flux densities without a corresponding increase in losses points toward the necessity for reopening the subject.

The sound level of one of the 1948 units occasioning a complaint is 61 decibels, and of the other 57 decibels. Other units that have been the cause of complaints show levels of 58.3, 55.5 and 54 decibels. No complaints have been oc-

Table I. Sound Levels of 2,000 Kva 12/4-Kv Unit Substations

	Sound Level of Units-Decibels		Ambient Sound Level-Decibels	
	Average	Range	Average	Range
Manufacturer A				
7 units manufactured in 1946 or earlier	51	46.5–53.5	40	35–48
4 units manufactured in 1948	58.5	57–61	37	32–42
Manufacturer B				
12 units manufactured in 1946 or earlier	54	47–59	38.5	31–47

Figure 3. Two 2,000-kva unit substations in enclosure of hollow concrete blocks

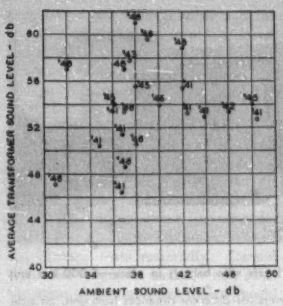

Figure 4 (left). Sound levels of 2,000-kva unit substations. Numerals indicate year of manufacture

● Manufacturer A
○ Manufacturer B

Figure 5(right). 2,000-kva unit substation with 2-sided sound barrier

Complaint from occupant of building at left. Sound level, 61 decibels

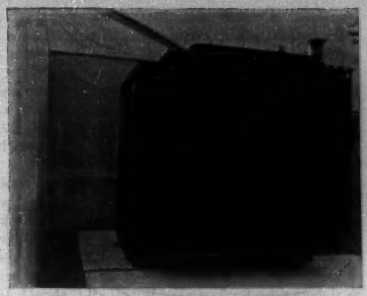

casioned by units having sound levels below 54 decibels although many of them are as close to residences as ones that have caused complaints. Other units are situated in areas not yet built up and it is possible that we will receive additional complaints when adjoining lots have been occupied.

Tentatively the conclusion has been reached that units with sound levels of 52 decibels or lower should be satisfactory for installation in residential areas unless reflection from adjoining buildings or walls serves to increase the intensity in a given direction to an undesirable value. Another tentative conclusion has been reached to the effect that complaints will not be serious if the operation of transformers in residential areas does not increase the sound level at points adjacent to adjoining buildings to values in excess of about 36 decibels.

As a matter of fact the sound levels specified in National Electrical Manufacturers Association standards are not realistic for unit substations of ratings suitable for outdoor installation in residential areas. These levels are so high that trouble can be expected from any unit whose level approaches the permissible value.

At this point it is not out of order to reiterate certain comments on the matter of taking sound level measurements. Considerable trouble has been experienced in collecting data and care is necessary if they are to be reasonably accurate. To avoid ambient sound levels that are higher than those prescribed in National Electrical Manufacturers Association rules, measurements frequently must be made at night, and reliable readings cannot be taken, even then, during periods when there is traffic on the street in front of a station. Children at play, dogs, birds, and traffic interfere with daytime measurements; crickets, other night life and traffic interfere with night measurements. Reliable data cannot be secured in a high wind or when it is raining. Instruction and some experimentation is required before the average observer can produce dependable and reasonably consistent readings.

Corrective Measures

Barriers and Housings

It has been necessary to apply corrective measures to three installations on the Pacific Gas and Electric system and studies are still under way to determine the best and most economical method of affording relief in other cases where conditions are severe enough to warrant correction.

As an emergency measure the 2,000-kva unit originally installed in the location shown in Figure 1 was enclosed by a structure about 12 feet high with adobe walls but no roof. This reduced the sound level to an acceptable value although the complainant, apparently very sensitive to noise, was not entirely satisfied. Subsequently she moved away and no complaints have been received from the new occupant of her apartment or from any other resident in either of the adjoining buildings. The 2,000-kva unit recently has been replaced with the 4,000-kva unit shown in Figure 1 with a sound level of about 49 decibels; no complaints have been received since the change.

Figure 3 shows two 2,000-kva unit substations in an enclosure consisting of walls about 12 feet high of hollow concrete blocks filled with sand and a concrete slab roof with an 8-foot square opening over each transformer. This housing eliminated all complaints from occupants of the two adjoining apartment houses. No records of sound level measurements at this location are available.

Figure 5 shows a unit substation manufactured in 1948 with a sound level of 61 decibels, installed on a narrow lot in a commercial zone, the other half of the block being zoned for residential occupancy. Complaints of undue noise were made by the occupant of sleeping quarters in the rear of the small store on the left. Occupants of single family dwellings on lots facing the next street did not find the noise objectionable.

Due to difficulties encountered in ventilating units completely surrounded by walls, experiments with a movable barrier were conducted to determine the effectiveness of partial barriers and the location of such barriers with respect to a unit for optimum results. Use of a sound-absorbing material for the barrier was considered but, to date, no material suitable for outdoor installation has been found. The objections to a hard-surfaced barrier are: the build-up of sound level on the transformer side of the wall which results in a less efficient attenuation; and the increase in intensity on the side of the unit opposite the barrier.

A portable barrier of plywood was located at distances of 30, 42, 53, and 63 inches from the side of the unit which is not equipped with radiators and Figure 6 shows the results of sound measurements made with this barrier in place. Levels adjacent to the barrier were naturally higher than measurements at the same point without the barrier. A distance of 45 inches from the sides of unit, on which no radiators are mounted, proved to be the best location for this particular unit, although this dimension is not critical. Other measurements were made on the radiator side of the unit but the sound pattern is so distorted by the radiators that it is impossible to secure results as definite as on the other side. In this particular case, distances of 6 feet–4 inches and 9 feet–3 inches gave equally good results, but more experiments with other units are necessary before positive conclusions can be drawn.

Figure 6 shows the permanent 2-sided

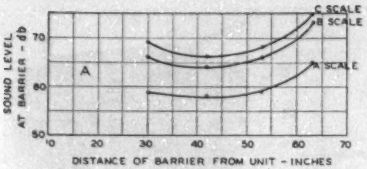

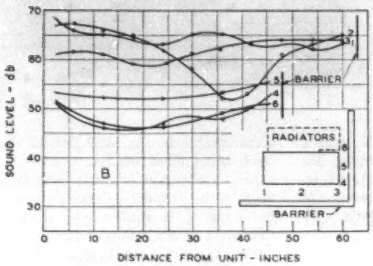

Figure 6 (left). Sound levels with barriers in place—2,000-kva unit

A. Sound levels at barriers for different distances from unit, on side opposite radiators. The A, B, and C curves refer to the "40", "70" and flat network scales of a standard sound level indicator

B. Sound level patterns between unit and permanent barrier

Figure 7 (above). 2,000-kva unit substation—complaint from neighbor in rear

Sound level, 57 decibels

barrier which consists of a wood frame faced with flat transite sheets and filled with rock wool. Figure 6 shows sound patterns between the unit and the permanent barrier. This construction was effective in reducing the sound level in the vicinity of the complainant's quarters to an unobjectionable value, and build-up in the opposite direction due to reflection was not noticeable except close to the unit. The cost of such a barrier 12 feet high will be on the order of $18.00 per lineal foot. It is estimated that a 4-walled, roofless cubicle of hollow building blocks can be built for about the same total cost if the length of the partial barrier is much in excess of 30 feet. Ventilation problems make a 4-walled cubicle undesirable and increase costs unduly. If ventilation is not provided, transformer loading must be held down; if ventilation is provided other noise problems arise.

Resilient Foundation Pads

Tests were conducted on a similar unit to determine the attenuating effect of a resilient pad between the unit and concrete foundation. Redwood planking was used on one unit, a $^3/_8$-inch thick sheet of a patented synthetic resilient material on another. Measurement of attenuation from the I-beam base of the units to the concrete foundations showed no significant improvement, as values were of the same order of magnitude as similar measurements on a unit installed on an identical foundation without pads. Sound level measurements made at property lines indicated a possible maximum decrease of about 3 decibels in the sound level of the unit installed on a synthetic resilient pad, although there was no perceptible reduction in audible noise. Apparently other utilities have had better success with resilient pads and further experiments are proposed.

Interior Linings

The inside surfaces of the walls of cable terminal compartments, circuit breaker compartment, and tap changer control compartment of one unit were lined with "acoustic" sheets chosen for fire-resistant qualities and mechanical suitability for this application. Sound level measurements indicated a reduction in sound level of about 3 decibels on the *A* scale and 1 decibel on the *B* scale in front of the treated surfaces. From the standpoint of auditory sensation the improvement was more noticeable than when resilient pads under units were used.

Equipment Construction

Radiators, doors, thin side panels on compartments and other mechanical details tend to contribute to over-all sound output. The sound level of several units has been reduced materially by tightening loose parts, improving the fit of doors, rebracing radiators, and so forth, but it should not be necessary for the user to apply remedies of this character.

Manufacturing Problems

Measures to reduce sound level available to the user are relatively few in number and are of the nature of "locking the barn door after the horse is stolen". The most effective measures applicable to unit substations are expensive, tend to be unsightly unless excessive expenditures are made, are liable to interfere with the use of equipment at its maximum output on a temperature-rise basis and complicate the performance of major maintenance and repair operations. There is much to be said for the unit substation as an answer to many distribution problems, but sound level will become an increasingly important factor if utilities are to take full advantage of the good qualities of this form of construction.

Evidence so far indicates that transformers with cores operating at high flux densities will be significantly noisier than earlier units. The efforts of manufacturers to reduce costs by this attack are appreciated but associated noise problems will require the attention of our most capable transformer designers and continued co-operation by the manufacturers and users if the maximum benefit from these cost reductions is to be obtained.

The fundamental cause or causes of transformer core noise need further study. While magnetostriction has been accepted generally as responsible, it is understood that recent experiments indicate that this quality is not the sole source of core noise. The development of quieter cores must depend on a more complete knowledge of the mechanics of noise generation in transformer steels.

Many publications, particularly some of European origin, point to the possibility of introducing features such as internal baffles, sound absorbent internal

tank linings and resilient mountings for core and coil assemblies to reduce sound transmission from core to tank walls. Vibration dampers have been suggested as a possible method of attack on core noise at its source. Tank designs should be watched to be sure that walls will not resonate at the frequency generated by the core. Radiators, doors, and other accessory parts, compartment walls, and so forth, should be so designed and assembled that they will not increase noise output. Attention to these details should not increase costs materially. Careful control of assembly methods and some attention to core and coil design should eliminate clamping structures as an incidental source of noise without causing an appreciable increase in costs. As an indication that sound level can be reduced by attention to detail, we have observed a variation of sound level in units furnished by the same manufacturer to the same specification and in the same year of as much as 12.5 decibels.

A joint study of presently specified standard sound levels, especially as applied to unit substations of ratings suitable for installation in residential and commercial areas should be undertaken. A maximum level on the order of 65 decibels is not realistic under these circumstances. Of all the 2,000-kva units we have purchased, one unit measured 61 decibels, the remainder under 60 decibels. A 60-decibel guarantee would have increased the cost of the transformer part of these substations by 10 per cent, a 55-decibel guarantee by 25 per cent. At the moment we see no advantage commensurate with the increased costs in specifying a lower sound level than standard, but this does not mean that we are complacent with respect to the increase in measured levels of recent units.

Attempts have been made to check some of our field measurements by comparison with factory test results. One manufacturer had not made a factory measurement of sound level on any units furnished us since 1945, and a second manufacturer had made such measurements on one unit only. As levels approach the guaranteed maximum and in view of the variation in level of units of the same design, it appears that more routine factory checks of sound level will be necessary.

Presently available sound level indicators are not entirely satisfactory as indicators of the noise level of transformers insofar as the effect on the average human ear is concerned. Standard sound level indicators are provided with three weighting networks, a "40" network, *A* scale, for sounds up to 60 decibels, a "70" network, *B* scale, for sounds from 50 to 90 decibels and a flat network, *C* scale, for sounds from 80 decibels up. A choice of networks is made on the basis of the level expected at the ear of the nearest observer and on this basis the "40" network is specified by National Electrical Manufacturers Association rules for use in measuring transformer sound levels. However, the same rules specify that measurements are to be made 12 inches from the surfaces of sound-producing equipment, and the "40" network cannot be expected to represent the effect on the ear of an observer some distance away of sounds which can reach the 83-decibel level at 12 inches in large high-voltage transformers. Measurements of the same sound will, in general, be higher using the "70" and flat networks than when the "40" network is used.

So many frequencies are present in transformer sound that observations of various units made by ear do not always check with measurements. One unit substation on our system that was rated as quiet by a group of observers had a higher measured sound level than another unit rated as noisy by the same observers.

Further consideration of the prescribed sound levels of transformers and methods of measurement to be certain that they represent the best possible correlation between measured quantities and the effect on the average human ear might result in considerable improvement insofar as consistency of end results is concerned. The development of a sound level meter that will permit a more realistic approach to the problem of transformer noise might be impractical, but certainly merits some thought on the part of acoustic engineers.

Conclusions

Widespread use of unit substations in or adjoining residential areas has focused attention on the noise generated by the transformer portion of these units. The problem, apparently, has been aggravated by the use of higher flux densities made possible by the development of new core steels. Smaller core and coil structures tend to reduce the cost of transformers, but part of this saving will be lost if higher sound levels in unit substations interfere with their use in residential areas.

Following complaints of objectionable noise, an investigation of sound levels of unit substations on the Pacific Gas and Electric Company system resulted in the following tentative determinations:

1. Units of the same design show a wide variation, as high as 12.5 decibels, in sound level.

2. Units with cold-rolled steel cores have an average sound level about 7.5 decibels higher than that of earlier units built to the same specifications.

3. If unit substations have an average sound level of 52 decibels or lower or if their operation does not result in a sound level higher than 36 decibels at points adjacent to nearby residences, the noise should not be objectionable.

The most effective corrective measures are 4-walled enclosures with or without complete or partial roofs. Sound bar-

Figure 8. 2,000-kva unit substation—complaints from neighbors
Second unit to be installed soon

Figure 9. 4,000-kva unit substation—no complaints
Sound level, 49 decibels

riers are effective if complaints are from one or two directions only. Enclosures interfere with air circulation and are unsightly unless unreasonable expenditures to improve appearance are made. The housing of unit substations is contrary to the philosophy under which this type of apparatus was developed.

Unreasonably wide variations in the sound levels of unit substations built to the same specifications in the same year by the same manufacturer suggest that more attention to design details and assembly methods is necessary, particularly if higher flux densities are used. Continued investigation of the fundamental nature of transformer noise is suggested, also the investigation of methods of reducing external sound levels by the use of internal baffles, tank linings, resilient core and coil mountings, vibration dampers, and so forth.

A review of prescribed standard sound levels of unit substations having ratings suitable for installation in residential areas and of the prescribed methods of determining sound levels might be in order.

Reference

1. Standards for Transformers. *Publication 48-132*, National Electrical Manufacturers Association (New York, N. Y.).

Discussion

T. D. Gordy (General Electric Company, Pittsfield, Mass.): The data presented by Mr. Baugh show the importance of low noise level of transformers located in residential and commercial areas. The introduction of cold-rolled steel as a cost reduction measure has increased transformer noise levels. As Mr. Baugh points out, the manufacturer is being challenged with continuing the use of cold-rolled steel and reducing noise levels simultaneously without seriously decreasing cost reductions obtained. Manufacturers must accept this challenge even though modifications necessary to reduce noise are reflected throughout most of the transformer design. This is a serious problem facing the manufacturer.

Mr. Baugh has arrived at an average sound level of 52 decibels or lower for substations not causing noise complaints. Due to construction arrangement of component parts, in some installations transformer noise level and substation noise level may be the same figure; for other installations, transformer noise levels would be different from substation noise levels. It would be worthwhile to know if the 52-decibel level applies to the substation as a whole or specifically to the transformer as measured under present NEMA specifications.

In the paper, installations are described to which noise barrier walls were added. Measurements taken between the transformer and the wall are given. If data are available, it would be interesting to know if noise reduction at the complaint has been correlated with the dimensions of the wall and the spacing of the wall relative to the transformer installation.

Noise requirements of the operator and utilization of improved materials of transformer construction appear to conflict. An economical solution satisfactory to both operator and manufacturer will have to be reached. A logical method of obtaining this solution is by close co-operation of manufacturers, operators, and national working committees. Presentation of data such as Mr. Baugh has presented is necessary for the successful operation of such committees.

E. G. Fischer (Westinghouse Research Laboratories, East Pittsburgh, Pa.): The paper by Mr. Baugh is important because it mentions something about all of the important factors in the transformer noise problem. It is gratifying to note that while the author is presenting the problems of the user, he also acknowledges the achievements of the manufacturers in keeping down unit costs and in supplying him with many units substantially below NEMA levels. The author's contributions made in the form of sound level data on practical noise-corrective transformer enclosures are of general value and much appreciated.

The author properly suggests "steps which the manufacturers might take to minimize users' troubles."

The writer is encouraged by Mr. Baugh's fair-minded criticisms; his acknowledgment of the possible savings to him introduced by the use of cold-rolled steel cores is a reasonable approach. The point is that manufacturers have developed new and better magnetic materials, but the users should decide what part of the resulting cost saving should be turned back to reduce noise level, and what part should be reflected as reduced cost to the user.

The author reports an upward noise level trend over the past few years from 51 to 59 decibels, which he feels requires housing of unit substations in residential areas, and yet all of the transformers under discussion have met the NEMA level of 64 to 66 decibels. Unless otherwise specified, the manufacturer designs all recently constructed units to meet the NEMA sound levels which are very realistic to him since he must meet them on highly competitive equipment. To establish industry noise levels such that all transformers are suitable for installations in quiet residential areas would mean increased cost for users, including many to whom the higher cost will be much more objectionable than the higher sound level. It is certainly fair to suggest that the increase in noise level reported may not be the fault of cold-rolled steel, rather it may well be a matter of economics; that is, with the ever-increasing cost of labor and materials and with the desire to keep down the sales price, the manufacturer may have been impelled to permit the noise level to approach NEMA levels. It is interesting to note that Mr. Baugh questions if a 3-decibel reduction is worth a 10 per cent increase in cost, or if a decrease from 64 to 55 decibels is worth a 25 per cent increase in cost. It is my understanding that these cost increases are much too low in many instances. This of course supposes the reduction to be achieved by reducing induction, after such factors as loose rattling parts or resonances have been eliminated. Since the cost of noise reduction is becoming more of a general problem, then as Mr. Baugh has suggested, close co-operation between manufacturer and user would be helpful in order to get a realistic solution to this problem. Such a solution could relate permissible levels to various applications and would of necessity consider transformer cost versus sound barrier cost.

In a general sense, noise problems are not new to the manufacturers of competitive electric equipment. It is a common research experience that noise problems are never solved completely where an industry is striving so hard, as the transformer industry, to keep down the cost of its product. With more knowledge about how to reduce noise, the manufacturer has the problem as to whether he will keep down the costs with the same noise level and satisfy one part of the industry or reduce noise level to satisfy another part. It is obvious no single solution will please everyone. The situation with regard to transformers is particularly difficult because the designs have been worked over by experts for a long time. The writer was once so rash as to suggest using a more viscous transformer oil to attenuate the noise transmission from core to tank. As most of you know, there are probably a dozen reasons, all of them good ones, why you cannot change the oil. Similar restrictions apply to all the other important features of transformer designs. In spite of the great amount of effort expended on the problem, at present there does not appear to be a radical solution to transformer noise in sight.

I would like to assure Mr. Baugh that all of his constructive suggestions to the manufacturers will receive careful consideration. The writer personally feels that further investigations of the use of external enclosures is desirable. This is a new field where the designer has lots of freedom, and its potentialities should certainly be examined in the light of the cost reductions possible by the full utilization of better magnetic materials. We believe Mr. Baugh infers a joint supplier-customer responsibility when he suggests a co-operative approach to the problem between manufacturers and users. Such a proposal will be helpful to the industry as a whole, for there is much in the noise problem that requires mutual consideration and evaluation.

E. A. Blomqvist (Consolidated Edison Company of New York Inc., New York, N. Y.): Mr. Baugh indicates that a transformer that produces a sound level of 36 decibels at a residence should not be objectionable. Our

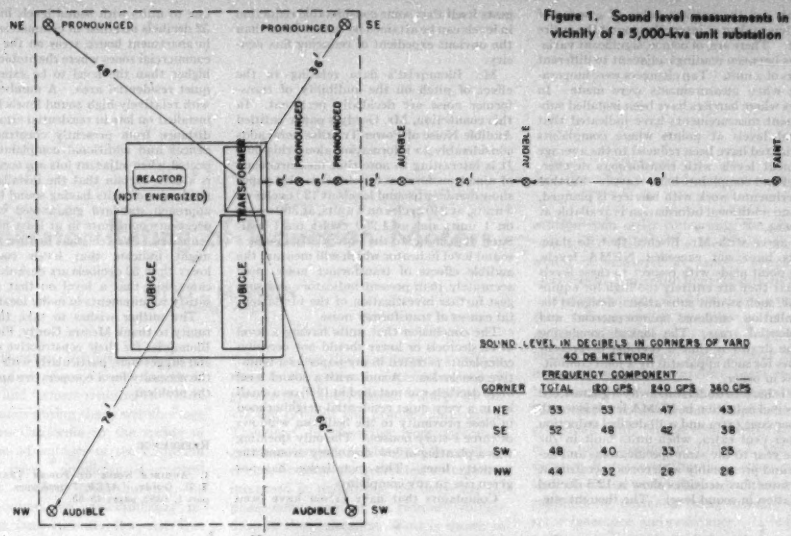

Figure 1. Sound level measurements in vicinity of a 5,000-kva unit substation

SOUND LEVEL IN DECIBELS IN CORNERS OF YARD
40 DB NETWORK

CORNER	FREQUENCY COMPONENT TOTAL	120 CPS	240 CPS	360 CPS
NE	53	53	47	43
SE	52	48	42	38
SW	48	40	33	25
NW	44	32	26	26

TRANSFORMER
5000 KVA 26400/4560 VOLT
OIL FILLED, SELF COOLED
NEMA SPECIFIED SOUND LEVEL-67 DB
NEMA MEASURED SOUND LEVEL-65 DB

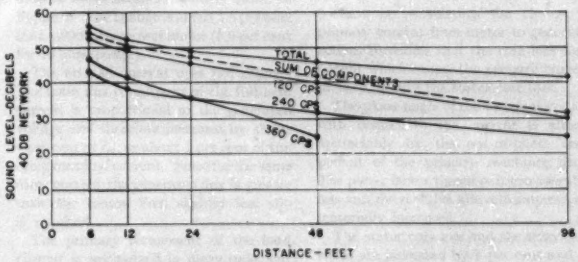

experience indicates that even lower values are necessary to insure freedom from complaints.

It has been our experience that it is the pitched note emitted by a transformer that causes complaints, even though the level of this note is far below the ambient sound level. For this reason, we have found it necessary to use an analyzer in our sound level measurements, since the pitched note does not add measurably to the ambient level.

A few examples of transformer noise that have caused complaints are listed in Table I of the discussion.

These may be considered borderline cases, but each one of them resulted in a vigorous complaint. It will be noted that all these locations are relatively quiet, and any appreciable increase in the ambient level would have masked out the objectionable pitched note. We have found that a pitched sound that is 20 to 25 decibels below the ambient level can be distinguished by the ear.

From these data, it appears that, to insure complete freedom of complaints, the pitched sound must be kept 20 to 25 decibels below the ambient level, except in quiet locations, where it should be kept below the threshold of hearing, or an absolute level of about 20 decibels. These values are in terms of the 40-decibel network.

Figure 1 of the discussion shows measured sound levels in the vicinity of a unit substation with a 5,000 kva 26,400/4,560-volt oil-filled self-cooled transformer. This transformer has an NEMA specified level of 67 decibels and a measured value of 65 decibels. The sound levels of the various frequency components, as well as the total noise, have been plotted as a function of distance from the transformer. The sum of the various components was calculated and also is plotted.

Table I. Sound Levels Measured in Connection with Complaints of Transformer Noise

Type of Location	Sound Level-Db (40-Db Network) Ambient	Pitched Noise	Frequency of Pitched Noise	Aural Observation
Sound studio	38	24	120	Faint
Bedroom of a residence	36	30	120	Faint
Bedroom of a residence	33	26	120	Clearly audible
Bedroom of a residence	33	20	360	Faint
Quiet office	43	34	120	Pronounced

It will be seen that, at a distance of 96 feet, the transformer noise is 32 decibels, which is only 10 decibels below the ambient level, and consequently can be heard.

These tests show that transformers of this type, having NEMA specified sound levels, must be located on a plot of considerable size so that 150- to 200-foot clearance is provided to the nearest residence, or else a costly barrier or housing must be provided.

C. E. Baugh: The apparent revival of interest in the subject of transformer sound levels, as evidenced by papers and discussions on this subject, is very gratifying, and continued co-operation and exchange of information between manufacturers and users should produce results beneficial to the entire industry.

The sound level data and conclusions presented in the paper deal primarily with unit substations of single-feeder construction in which the transformer, tap changer, and switchgear comprise a unit with a projected floor area, including radiators, which approximates a square. Sound level measure-

ments are the average value of a series of readings taken at intervals around the entire unit. There are, of course, significant variations between readings adjacent to different parts of a unit. Tap changers were inoperative when measurements were made. In cases where barriers have been installed subsequent measurements have indicated that sound levels at points where complaints originated have been reduced to the average ambient levels with transformers de-energized and complaints have ceased. Further experimental work with barriers is planned, but no additional information is available at present.

I agree with Mr. Fischer that, to date, units have not exceeded NEMA levels. The point made with respect to these levels is that they are entirely too high for equipment, such as unit substations, designed for installation outdoors in commercial and residential areas. The logical conclusion to be drawn is that a revision of present values for such apparatus by a joint committee is in order.

It is hard to understand why a guaranteed 5-decibel reduction in NEMA levels is worth 10 per cent extra and a 10-decibel reduction 25 per cent extra, when units built in the same year to the same specifications and design and presumably with cores operating at the same flux densities show a 12.5-decibel variation in sound level. The thought suggests itself that some considerable reduction in levels can be attained by means other than the obvious expedient of reducing flux density.

Mr. Blomqvist's data relating to the effect of pitch on the audibility of transformer noise are decidedly pertinent. In this connection, Mr. Gordy's paper entitled Audible Noise of Power Transformers[1] adds considerably to information along this line. It is interesting to note that measurements of nine transformers tabulated in this paper show dominant sound levels at 120 cycles on 3 units, at 240 cycles on 4 units, at 360 cycles on 1 unit, and at 1,200 cycles on 1 unit. Such data indicate the potential value of a sound level indicator which will measure the audible effects of transformer noise more accurately than present indicators and suggest further investigation of the fundamental causes of transformer noise.

The conclusion that units having a level of 52 decibels or lower should not occasion complaints is stated in my paper as a tentative conclusion. A unit with a sound level of 46 decibels was installed in 1946 on a small lot in a very quiet residential neighborhood in close proximity to the bedroom windows of three 1-story houses. The only shielding was a planting of low shrubbery around the property lines. This installation has not given rise to any complaints.

Complaints that have arisen have been due to units with sound levels higher than 52 decibels installed in commercial zones or in apartment house areas on the fringes of commercial zones where the ambient level is higher than the level to be expected in a quiet residential area. A number of units with relatively high sound levels have been installed on lots in residential areas at some distance from presently constructed residences and additional complaints are expected when adjacent lots are occupied. It is almost certain that the installation near residences of units having sound levels that approach standard guaranteed values will occasion complaints in at least nine out of ten cases. We feel that further experience might indicate that levels considerably lower than 52 decibels are desirable in some cases, but that a level on that order will satisfy requirements in many locations.

The author wishes to take this opportunity to thank Messrs. Gordy, Fischer, and Blomqvist for their constructive comments and suggestions, particularly with respect to the necessity for a co-operative approach to the problem.

Reference

1. Audible Noise of Power Transformers, T. D. Gordy. *AIEE Transactions*, volume 69, part I, 1950, pages 45–53.

Generator Rating of Induction Motors

OTTO J. M. SMITH
MEMBER AIEE

ENGINE-driven induction generators were ideal power sources for those industries and farmers required to curtail their demands during the power shortage in northern California in the spring of 1948. The advantages of the induction generator were: simplicity of control apparatus, freedom from hunting, no exciter required, no synchronizing required, low fault currents, low cost, and subsequent general usefulness in later motor applications.

The nameplate data on most induction machines would be motor ratings, and it is desirable to consider what changes must be made, if any, in order that the machine operate satisfactorily as a generator. If the speed is driven above synchronism by the same revolutions per minute that the machine normally operates below synchronism, the generator will deliver approximately rated current at rated voltage and rated efficiency. The electric power out will be approximately equal to the rated shaft motor power. The generator power factor will be much worse, being approximately equal to the motor power factor times the motor efficiency.

Typical Generator Rating

The approximate gross changes when using a 1,000-horsepower class A induction motor as a generator can be followed with the aid of the equivalent circuit shown in Figure 1, and the approximate vector diagram in Figure 2. The primed symbols refer to full load motor operation, and the double-primed symbols to full load generator operation. The terminal voltages, V_t' and V_t'', are equal in magnitude, but are shifted in phase with reference to the internal generated voltage. Figure 2 is drawn for equal rotor currents, so that I_2' and I_2'' are equal in magnitude, and θ_2'' is equal to θ_2'.

It can be seen that the motor generated voltage is less than the terminal voltage, whereas the generator internal voltage is greater than the terminal voltage by the voltage drop in the primary impedance. Therefore, in changing from motor to generator action, the internal flux will increase, because the generated voltage has increased in magnitude by twice the in-phase component of the primary voltage drop in the resistance. This is shown in Figure 2. The change is about 3.5 per cent for a 1,000-horsepower motor (5.6 per cent for 10 horsepower).

The no-load current does not change. The main flux component of the full-load current is proportional to the generated voltage and therefore increases by about 4 per cent of I_m, or about 1 per cent of the rated terminal current. Since for the same rotor current the generator flux is greater than the motor flux, slightly less slip is required.

The primary component of the load current is unchanged in magnitude, but its in-phase component is reversed in direction when the machine is operated as a generator. The load component of current is added to the magnetizing current to give the total primary current. This is shown in Figure 2 for both motor and generator action. The magnetizing component is increased because of the increased flux, but this does not change the total magnitude appreciably. The generator primary current is slightly less than for motor action because it is reduced vectorially by two times the stator core loss current, or is reduced in magnitude by about two times the no-load stator core loss expressed as a per cent of the motor full load input power. Because of small voltage angle shifts not considered in this approximate analysis, the actual current change is one-half of the approximate value. This is less than 1 per cent for a 1,000-horsepower motor (3 per cent for 10 horsepower). A word of caution is in order concerning the stator core loss. This is the core loss which would be measured at exactly synchronous speed. Under full load conditions the total core and stray load loss may be more than twice as much because of the additional tooth frequency losses which are usually large.[1] These losses appear as a magnetic drag and therefore there must be a component of torque proportional to them and a rotor current component to give this torque. In the equivalent circuit of the induction motor, Figure 1, the resistance R_s representing these stray core losses is placed across the load so that it is supplied by current flowing through the rotor reactance and resistance. It is important in considering the change in primary current from motor to generator action, to realize that the core loss component which causes the primary current to vary, is only the stator core loss.

The phase angle of the terminal voltage with respect to the current is altered appreciably by the out-of-phase component of the primary reactance drop. The power factor therefore is considerably less and the reactive kilovolt-amperes are materially increased.

The stator core loss and the stray load losses are increased by 7 per cent and 14 per cent respectively for a 1,000-horsepower motor (11 per cent and 23 per cent for 10 horsepower), due to the increased flux. The rotor copper loss is unchanged. The stator copper loss is decreased by about 2 per cent for 1,000 horsepower (7 per cent for 10 horsepower). The friction loss is proportional to the 3/2 power of the speed, and therefore increases about 5 per cent for 1,000 horsepower (10 per cent for 10 horsepower). The windage loss is proportional to the square of the speed

Paper 50-20, recommended by the AIEE Rotating Machinery Committee and approved by the AIEE Technical Program Committee for presentation at the AIEE Winter General Meeting, New York, N. Y., January 30–February 3, 1950. Manuscript submitted May 28, 1948; made available for printing November 29, 1949.

Otto J. M. Smith is an Associate Professor in Electrical Engineering at the University of California, Berkeley, Calif.

The author wishes to express his sincere appreciation to Professor T. G. Tarboux, author of Alternating Current Machinery,[2] for permission to quote the test figures given in Table I.

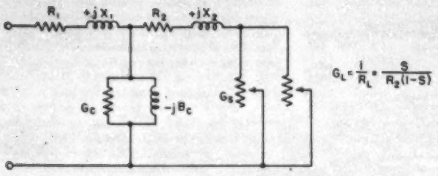

Figure 1. Exact equivalent circuit of induction machine

G_c is stator core loss conductance only
R_1 is rotor resistance at slip frequency referred to stator
$R_1 = R_{dc}(0.878 + 0.122e^{0.95f})$
$R_2 = R_{dc}(1 + |s|/9)$ at low slip
G_s is stray load loss conductance
$G_s = G_s s^2 + G_s$ at low slip
$G_s = kG_c/(s')^2$, approximately
$G_s = G_s Y_c^2 R_1^2$
k is 0.9 to 1.3
s' is slip at full load motor operation

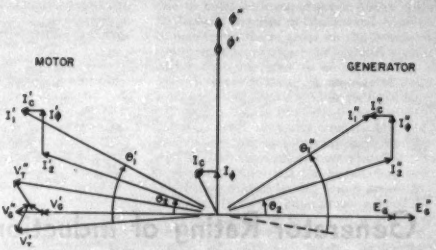

Figure 2. Approximate vector diagram for induction machine

Small detail is greatly exaggerated. Primed letters refer to full-load motor action. Double-primed letters refer to full-load generator action. The rotor current is the same in each case

but since it is usually smaller than the friction loss, it can be lumped with it and the 3/2-power variation applied to both without serious error.

The effect of all these changes is to give a net increase in the magnitude of the losses when shifting from motor to generator action of only 2 per cent of the losses for 1,000 horsepower (5 per cent of the losses for 10 horsepower). The cooling, however, due to the increased speed, is approximately 3 per cent greater (6 per cent for 10 horsepower), and therefore the temperature rise is essentially the same or slightly less.

The shaft torque is proportional to the square of the rotor current, and inversely proportional to the slip. If the generator is operated at the same rotor current as rated full-load motor conditions, the 1,000-horsepower machine, whose slip is reduced about 2 per cent, will have about 2 per cent more shaft torque (4 per cent for 10 horsepower). The speed increase due to the change in action is twice the slip or 3 per cent for 1,000 horsepower (8 per cent for 10 horsepower). The generator power input is the product of the shaft speed and torque and is therefore about 5 per cent greater than the 1,000-horsepower motor shaft output (12 per cent for 10 horsepower).

For these examples the total motor loss exclusive of friction as a percentage of shaft power output was 5 per cent for the 1,000-horsepower and 10 per cent for the 10-horsepower motor, the latter being more efficient than usual designs. Therefore the electrical output of the generator is essentially the same as the shaft output as a motor. Using this approximation

$$V'' I'' \cos\theta'' = V' I' \cos\theta' \text{ (eff)}' \quad (1)$$

$$\cos\theta'' = \cos\theta' \text{ (eff)}' \quad (2)$$

Primed symbols refer to rated motor conditions. Double-primed symbols refer to generator operation at the same rotor current.

If operated at nameplate terminal current, the generator rotor current would increase by 1 per cent (3 per cent for 10 horsepower), the total losses would increase by 2 per cent (6 per cent for 10 horsepower), but the cooling would only increase by 0.02 per cent (0.1 per cent for 10 horsepower). The temperature rise would go up quickly so it is important to know the correct operating current.

The previous discussion of approximate relationships is applicable only to class *A* motors. It has been shown that a squirrel-cage-rotor, low-slip induction motor designed for reduced-voltage starting can be operated as an induction generator at approximately rated terminal current. This may not be true for high-slip motors, or ones of unconventional construction. For motors over 1,000 horsepower, the exact conditions should be computed. The common types of motors are:

Class *A*—Normal torque, normal starting current.

Class *B*—Normal torque, low starting current (5 × full load *I*).

Class *C*—High torque, low starting current (loaded reciprocating compressors.)

Class *D*—High slip motors (used with flywheels).

Re-rating Equations

Generator characteristics computed on the basis of an equivalent circuit in which the stray load loss was lumped with the core loss, or was neglected, were considerably in error. It was necessary, therefore, to develop the equivalent circuit shown in Figure 1, in which the stray load branch is correctly represented for slips less than one-fifth the synchronous speed.

The important generator computations are current, slip, and temperature rise. Computations have shown that if the generator is operated at the same value of rotor current for which it was designed as a motor, the temperature rise is very near the rated value. Consequently, all subsequent formulas in this paper will be given for rated rotor current, and if their solution indicates that it is necessary to make a slight change in the operating condition, the new values can be computed by incremental methods.

The ratio of the generator to motor terminal current, for $I_2'' = I_2'$, is

$$I_1''/I_1' = 1 - 2(P_c \cos\theta_1'' - I_{oa}^2 R_1)/(VA) \quad (3)$$

where

P_c = no-load primary core loss per phase
I_{oa} = no-load current
R_1 = 60-cycle resistance of the primary
$\cos\theta_1'$ = full-load motor power factor
VA = volt-ampere rating per phase

The motor power factor is the only quantity above which requires a load for its measurement. Fortunately, it is not necessary that any of these quantities be known accurately. If each is within 5 per cent of its correct value, the current-ratio expression will be accurate to 1 per cent. It is necessary, however, to know the exact rated current. This can be obtained from the nameplate, which also will probably state the rated voltage, horsepower, and full-load speed. The total motor losses are

$$\text{Losses} = P_h' = 100\left[1 + \left(\frac{252}{\text{rpm}}\right)^2\right] \times \left[0.045 + 0.01\sqrt{\frac{1{,}000}{\text{hp}}}\right] \text{ per cent} \quad (4)$$

$$(\text{eff})' = 1 - \left[1 + \left(\frac{252}{\text{rpm}}\right)^3\right] \times \left[0.045 + 0.01\sqrt{\frac{1{,}000}{\text{hp}}}\right] \text{ per unit} \quad (5)$$

This empirical efficiency equation is within 2 per cent for the usual class A and B motors from 10 to 1,000 horsepower. This was derived to fit the typical efficiency curves given in reference 6. Wound-rotor and class C motors have efficiencies a few per cent lower, and high-slip class D motors about 5 per cent lower.[6] The motor power factor can be computed from the rated terminal current and the approximate efficiency.

$$\cos\theta_1' = P'/(\sqrt{3}\ V'\ I'\ \text{eff}') \quad (6)$$

Rerating the slip and temperature rise requires a separation of the losses. Typical values of primary core loss are 1 to 3 per cent; of primary resistance, 2 to 4 per cent; and of no-load current, 25 to 40 per cent.

The ratio of the generator to motor slip is

$$-s''/s' = 1 - s'(2 + 9P_s'/P_L' - 6s') \quad (7)$$

P_s'/P_L' is the per-unit stray load loss, and at full load it is approximately equal to the no-load core loss. In high-slip machines, it may be a larger percentage of the total losses. s' is the full-load motor slip. It is the most important constant in rerating a machine, and should be measured carefully if possible. Typical values are 1 per cent for 1,000-horsepower high speed, 2.3 per cent for 400-horsepower medium speed, 3.5 per cent for 15 horsepower, 1,800 rpm; 5 per cent for 5 horsepower, 900 rpm; and 9 per cent for class D, high slip motors.

The ratio of the temperature rises is

$$T''/T' = (1 - 2s')P_h''/P_h' \quad (8)$$

$$P_h' = P_f' + P_s' + P_c' + P_2' + P_1'$$

$$P_h'' = (1 + 3s')P_f' + (1 + 4s')P_s' + P_c' + p_2' + (1 + 80s'^2)P_1' \quad (9)$$

P_h' is the sum of the motor losses contributing to heating. The components, listed in order are: friction and windage, stray load, primary core loss, rotor copper loss, and stator copper loss. The reason the core loss does not appear to vary between P_h' and P_h'' is because the terms accounting for its increase cancelled some equal negative values in the other losses. The copper loss change is an approximation.

The correct expression is given in a tabulation at the end of this paper, called equation 58.

The air-gap torque in synchronous-watts is

$$-T_L''/T_L' = 1 + 2s' + 4P_s'/P_L' \quad (10)$$

The shaft torque differs from the air-gap torque above by the friction loss.

$$T_{\text{out}}' = T_L' - T_f'$$

$$T_{\text{in}}'' = T_L'' + T_f'$$

$$P_f''/P_f' = 1 + 3s' - 3s'^2/2 \quad (11)$$

$$T_f''/T_f' = 1 + s' \quad (12)$$

$$-T_{\text{in}}''/T_{\text{out}}' = -T_L''/T_L' + 2P_s'/P_L' \quad (13)$$

approximately, where P_f'/P_L' is the motor per unit friction loss.

The ratio of the power factors is

$$\cos\theta_1''/\cos\theta_1' = 1 + 2\tan\theta_1' \sin\theta_1' \times (n - \cos\theta_0)\ (1 + 6n)\ (I_{o0}/I_1') - 4n\tan\theta_1' \quad (14)$$

$$n = \tan\eta = 0.9\ R_1/X_c, \text{ approximately} \quad (15)$$

θ_0 is the angle of lag of the magnetizing current when the machine is being driven synchronously. It can be computed from the no-load current and the core loss in the primary only (synchronous core loss).

$$\cos\theta_0 = P_c/\sqrt{3}\ V\ I_m \quad (16)$$

The efficiency is essentially unchanged.

$$(\text{eff}'') - (\text{eff}') = (1 - \text{eff}')(\text{eff}')4s' - (1 - \text{eff}') \times P_2''/P_{\text{in}}' - (1 - \text{eff}' - 4\cos^2\theta_1' P_s'/P_{\text{in}}' - 12I_{o0}^2R_1\cos\theta_1''/P_{\text{in}}')P_1'/P_{\text{in}}' + (1 - \text{eff}')(3 + 4P_s'/P_L' - 4s')P_s'/P_{\text{in}}' \quad (17)$$

The generator output is slightly greater than the motor output.

$$P_{\text{out}}'' = (1 + 4s')P_{\text{out}}' - 0.35(1 + 2s)P_h', \text{ approximately} \quad (18)$$

Equivalent Circuit Constants

The constants of the exact equivalent circuit in Figure 1 can be obtained from several tests. The first is the conventional blocked rotor test. The equivalent 60-cycle resistance is the slope of the power versus current squared curve. P_e is the input power per phase corrected for the core loss at the reduced voltage.

$$(R_1 + R_2)_{(60\ \text{eqs})} = R_e = P_e/I_e^2$$

$$R_{1(60)} = 1.18R_{1(\text{dc})} \quad (19)$$

$$R_{2(\text{dc})} = P_e/1.18\ I_e^2 - R_{1(\text{dc})} \quad (20)$$

The circuit in Figure 1 has the same circle diagram of current that it would have if the stray load branch were omitted. The only difference is that the actual slip scale is not linear, and the torque and output power are reduced. The winding impedance should be taken for the value of current which makes the circle diagram best fit full load conditions, as is usually done. The total winding impedance is the slope of the voltage versus current curve. The winding impedance diminishes for higher currents. A good compromise is the extrapolated short circuit impedance for 70 per cent voltage.

$$jX_1 = jX_2 = (\mathbf{Z}_e - R_e)/2, \text{ vectorially}$$

The second test is the measurement of primary core loss at synchronous speed, while the friction and windage is supplied by a small d-c motor on the shaft. The measured values will be V_T, I_{o0}, and $P_c + I_{o0}^2R_1$. From these can be calculated the middle branch constants.

$$V_0 = V_T - I_{o0}\mathbf{Z}_1, \text{ vectorially}$$

$$G_c = P_c/V_0^2$$

$$Y_c = G_c + jB_c = I_{o0}/V_0$$

If it is not possible to measure the losses at synchronous speed, the conventional no-load test at variable voltage can be used. A plot of power input minus the primary copper loss versus the square of the voltage will give the friction and windage loss when extrapolated to zero voltage. The stray load loss is negligible and the increase in primary current magnitude due to the load component is small. However, the angle of the primary current has been changed, and G_c must be computed from $P_c = P_{\text{in}} - P_f - I_{o0}^2R_1$ and not from vector values of the voltage and current.

The stray load loss is due almost entirely to tooth-speed losses, which are proportional to the motor speed squared, and the stator current squared.[3]

$$P_s = R_s(1 - s)^2I_1^2$$

$$P_s \cong R_s(1 - s)^2V_g^2[1/(R_2/s)^2 + X_2^2) + (G_e^2 + B_e^2))] \quad (21)$$

It would at first appear that a stray load conductance G_{sm} could be connected across the magnetizing branch in the equivalent circuit. This would have the value

$$G_{sm} = R_s(1 - s)^2[(G_e^2 + B_e^2) + 1/((R_2/s)^2 + X_2^2)$$

or

$$G_{sm} = R_s(G_e^2 + B_e^2 + s^2/R_2^2)(1 - s)^2$$

approximately at small values of slip.

The stray load power is actually absorbed in the rotor, and there should be a component of rotor current to supply it. In the equivalent circuit, therefore, this branch should appear in parallel with the load, as in Figure 1. The current in equation 21 can be divided into load current and magnetizing current components.

$$P_s = R_s(1 - s)^2(\overrightarrow{V_L(G_L + G_S)} + \overrightarrow{V_g Y_e})^2 \quad (22)$$

On reverse rotation tests, these current vectors are nearly in phase, and can be added arithmetically. From light to full-load, the two current vectors are practically at right angles to each other. The current through G_s is only a few per cent of that through G_L at full-load, and is only a few per cent of that through Y_e at light load, so it can be neglected.

$$P_s \cong R_s(1 - s)^2V_L^2[(s/R_2(1 - s))^2 + Y_e^2], \text{ for small slips} \quad (23)$$

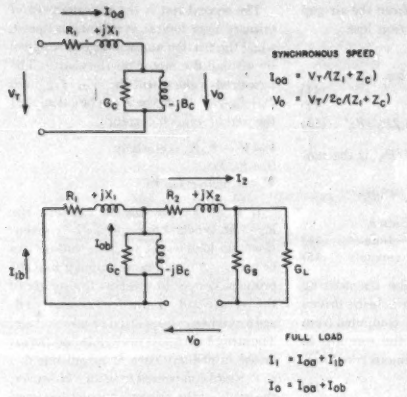

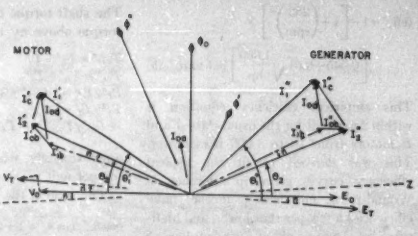

Figure 3 (left). Circuits to use for a superposition solution for the currents in figure 1

Figure 5 (right). Vector diagram of the load-current components

Small detail has been greatly exaggerated. Primed letters are for full-load motor action. Double-primed letters are for full-load generator action. The vector designations are the same as in Figure 3. I_1 is the line current and θ_1 is terminal power-factor angle

If this loss is represented by a conductance in parallel with the load, it would have the value

$$G_s = R_s(1-s)^2[(s/R_s(1-s))^2 + Y_c^2] \qquad (42)$$

Define a new constant, $G_4 = R_s Y_c^2$, then $G_s = G_4((1-s)^2 + s^2/Y_c^2R_s^2)$.

For a motor with 25 per cent no-load current and 2 per cent rotor loss, the last term at full-load might have a value around 36, which is large compared to one. It would be more convenient to lump this term with the constant, so that the second factor is only a correction term for changes in speed. If

$$G_3 = G_4/Y_c^2R_s^2 = R_4/R_s^2$$

then

$$G_s \cong G_3s^2 + G_4 = G_3s^2(1+Y_c^2R_s^2/s^2) \qquad (25)$$

$$G_s = G_3s^2, \text{ near full-load} \qquad (26)$$

Reverse Rotation Test

The stray load loss can be determined from a full-speed reverse rotation test.[3] The measured values would be the terminal voltage and current, V_d and I_d, and the electrical and mechanical power inputs, P_d and P_m. I_{oa} from the no-load test is needed corresponding to the voltage V_d.

$$I_{1b} = I_d - I_{oa}$$

$$I_{ob} = I_{1b}Z_1Y_c$$

$$I_2 = I_{1b}(1+Z_1/Y_c)$$

$$V_L = V_d - I_dZ_1 - I_2Z_2$$

This test gives an independent value for the rotor resistance at 120 cycles.

$$G_L = -2G_3 = -2/R_2 = -P_L/V_L^2$$

This value of R_2 with the 60-cycle value can be used to plot a curve from which the d-c rotor resistance may be read. These two values also can be used to determine the increase in resistance with frequency for the test machine.

The stray load loss is equal to the sum of the input powers minus the known losses. The stray load is large, and therefore, easily computed without error. The electric power component of the stray load loss is

$$P_g = P_d - I_d^2R_1 - (V_d - I_dZ_1)^2\,G_c - I_2^2R_2$$

The mechanical power component of the stray load loss is $P_L = P_M - P_{friction}$. The sum is

$$P_g + P_L = (I_{ob}+I_{1b})^2\,R_s = (I_{ob}+I_{1b})^2\,G_3R_s^2$$

Solve for (G_3) using R_2 measured at 120 cycles.

The construction of circle diagrams and computations based on the circuit of Figure 1 can be simplified by a transformation to the two circuits of Figure 3.[5] The load currents can then be obtained by the superposition of the equivalent currents.

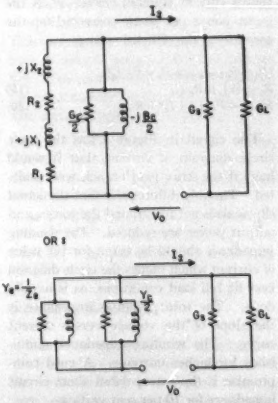

Figure 4. Simplifications of the load-component circuit in Figure 3

Induction Motor Calculations

The induction motor current calculation could be simplified by a transformation of the second circuit in Figure 3 to the circuit shown in Figure 4. This does not introduce any significant error because I_{ob} is only a few per cent of rated current, and the error is only a small fraction of this. For a slip s

$$I_2 = V_o/(1/(Y_c+Y_c/2)+(1/(G_s+G_L)) \quad \text{approximately}$$

If the exact circuit of Figure 3 is used

$$I_2 = V_o/(1/(Y_1+Y_c)+1/(G_s+G_L)+Z_1) \quad \text{exactly} \qquad (27)$$

$$I_1 = I_{oa} + I_2Z_s/(Z_c+Z_1) \qquad (28)$$

$$I_s = I_{oa} - I_2Z_1/(Z_c+Z_1) \qquad (29)$$

$$P_{1_{input}} = V_T.I_1 \qquad (30)$$

$$P_1 = I_1^2R_1$$

$$P_2 = I_2^2R_2$$

$$P_c = I_s^2G_c/Y_c^2 \qquad (31)$$

$$P_s = I_2^2G_s/((G_s+G_L)^2 \qquad (32)$$

$$P_{output} = I_2^2G_L/(G_s+G_L)^2 - T_{friction}(1-s) \qquad (33)$$

$$T_{output} = I_2^2G_L/(G_s+G_L)^2(1-s) - T_{friction} \qquad (34)$$

The air gap torque can be separated into two components

$$T = P_sG_L/(G_s+G_L)s - P_s/(1-s) \qquad (35)$$

The first is the slip-frequency torque produced by the rotor resistance loss. It is reduced slightly by the ratio of the useful G_L to the total rotor G. The second term is the stray-load torque, which is associated with the actual rotor speed,

and not with the slip speed. It is negative because it acts as a magnetic drag on the rotor, and therefore it is similar to a friction torque.

Induction Generator Calculations

Complete induction generator characteristics can be computed from the above motor formulas for negative slips. The factors for rerating a motor as a generator also can be obtained in the same manner. In the derivations which follow, primed figures will refer to motor values, and double-primed figures to the equivalent generator values for the same rated rotor current.

$$I_2'' = I_2'$$
$$I_{1b}'' = I_{1b}'$$
$$I_{0b}'' = I_{0b}'$$

The change in slip can be computed from the rotor impedance.

$$V_0 = I_2'(Z_2 + 1/(Y_1 + Y_c) + 1/(G_s' + G_L'))$$

The real part of this impedance must have the same magnitude but reversed sign, when the machine is operating as a generator.

$$R = (G_c + R_1/Z_1^2)/((G_c + R_1/Z_1^2)^2 + (B_c - X_1/(Z_1^2))^2) + R_2 + 1/G'$$

The sum of the first two terms can be called R_c. This may be simplified by assuming typical values for R_1, X_1, G_c, and B_c, and eliminating all but the significant ratios.

$$R_c = R_1(1 - X_1/X_c) + R_2, \text{ approximately}$$
$$R = R_c + R_2 + 1/G'$$
$$R = R_c + 1/(G_2 s^2 + G_2 s'), \text{ as a motor}$$
$$-R = R_c + 1/(G_2 s''^2 + G_2 s''), \text{ as a generator}$$

It is desired to solve for the ratio of the slips from these two equations by eliminating the unknown R. To facilitate it, let $-s''/s' = k$, and solve for an approximation for $R_c G_L$, from the sum of the two equations.

$$2R_c G_L = (1 + R_1(1 - X_1/X_c)/R_c)s'(1 + k)/(1 - s')$$

$$2R_c G_L = 2s'(1 + k) \text{ approximately}$$

Eliminating R, and substituting the ratio of powers for conductances

$$k(1 - s'(1 + k) + (1 + 3s'(1 + k))P_s'/P_L' = (1 + P_s'/P_L')(1 - 2R_c G_L(1 + P_s'/P_L')) \quad (36)$$

This can be simplified by solving for k by dividing the right side by the left side

$$-s''/s' = k = 1 - s'(1 + k)(1 - 4s' + 4P_s'/P_L') - (P_s'/P_L')^2$$

For low slip motors, $(1 + k)$ is almost 2, so that

$$-s''/s' = 1 - 2s', \text{ approximately.}$$

Substituting $(1 + k) = 2(1 - s')$, which is true for motors with rotor resistance equal to stator plus line resistance, and discarding high order terms

$$-s''/s' = 1 - 2s'(1 - 5s' - 4s'^2 + 4(P_s'/P_L')) - (P_s'/P_L')^2 \quad (37)$$

$$-s''/s' = 1 - 2s'(1 + 4P_s'/P_L' - 5s'), \text{ approximately} \quad (38)$$

Equation 37 holds for large low slip motors with equal equivalent stator and rotor resistances. A more exact expression is given in equation 64. It shows that the approximate equation 38 above gives values of generator slip which are too high. A much better approximation is

$$-s''/s' = 1 - s'(2 + 9P_s'/P_L - 6s') \quad (7)$$

The ratio of the speeds is

$$(1 - s'')/(1 - s') = 1 + 2s' - 2s'^2$$

Figure 5 shows the vector relationships of the load current components. I_2' and I_2'' are each at an angle θ_2 with the voltage V_b. I_{1b}' and I_{1b}'' are equal in magnitude, but their phase angles are $(\theta_2 - n)$ and $(\theta_2 + n)$. The angle n also is the angle of lead of V_0 ahead of V_T.

$$V_0/V_T = Z_c/(Z_1 + Z_c) = M/n$$
$$I_{1b}/I_2 = Z_c/(Z_1 + Z_c) = 1/(1 + Z_1 Y_c) = M/n$$

M is approximately equal to one minus the no-load per unit primary reactance drop.

$$I_1'/\theta_1' = I_{1b}'/-\theta_2 + n + I_{0a}/-\theta_0$$
$$I_1''/\theta_1'' = I_{1b}''/180 + \theta_2 + n + I_{0a}/-\theta_0$$

If all the current vectors are rotated n degrees clockwise I_{1b}' and I_{1b}'' will occupy symmetrical positions and the cosines of their angles will be the same. The out-of-phase component of I_{0a} will be essentially unchanged. Therefore, the projections of I_1' and I_1'' on a perpendicular to yz will be equal. The difference between I_1' and I_1'' will be cos θ times the in-phase differences. The projections on yz will be

$$I_1' \cos(\theta_1' + 2n) = I_{1b}' \cos(\theta_2) + I_{0a} \cos(\theta_0 + n) \quad (39)$$

$$I_1'' \cos(\theta_1'' - 2n) = I_{1b}'' \cos\theta_2 - I_{0a} \cos(\theta_1 + n) \quad (40)$$

$$I_1' - I_1'' = 2I_{0a} \cos(\theta_0 + n) \cos(\theta_1' + 2n) \quad (41)$$

This formula gives the reduction in line current for shifting from motor to generator full load. It is fairly accurate even for small machines. It is not important for the value of n to be known precisely.

$$n = \tan^{-1} X_c/R_c - \tan^{-1}(X_1 + X_c)/R_1 + R_c)$$

$$\tan n = \frac{X_c/R_c - (X_1 + X_c)/(R_1 + R_c)}{1 + X_c(X_1 + X_c)/R_c(R_1 + R_c)}$$

$$n = \tan n = \sin n = 0.87\ R_1/X_c \text{ radians, approximately} \quad (15)$$

$$I_1''/I_1' = 1 - 2I_{0a} \cos(\theta_0 + n) \cos(\theta_1' + 2n)/I_1'$$

This equation also is exact and contains no approximations. However, for many cases, an equation in different form is preferable

$$I_1''/I_1' = 1 - 2I_{0a}(\cos\theta_0 \cos\theta_1' - \sin n (\cos\theta_1' + 2\cos\theta_0))/I_1'$$

If sin n were about equal to cos θ_0, there would be no change in the primary current.

$$\cos\theta_1 = G_c/Z_c$$

$$I_1''/I_1' = 1 - 2\left(\frac{V_0 I_{0a} \cos\theta_0 \cos\theta_1'}{I_1' V_0} - \frac{I_{0a} R_1}{I_1' X_c}\right)$$

$$I_1''/I_1' = 1 - 2(P_c \cos\theta_1' - 3I_{0a}^2 R_1)/VA, \text{ approximately} \quad (3)$$

The per-unit generator terminal current is less than the motor current by twice the ratio of the difference between the no-load primary core loss times the full-load power factor minus the no-load primary copper loss to the machine volt-ampere rating. This value is less than the percentage core loss, and can even be zero if the primary resistance is quite large.

There is no simple equation for the ratio of the power factors. In Figure 5, V_T is the terminal voltage for both motor and generator action, and V_0 is the no-load internal voltage. The internal voltage with load is shifted in phase considerably. The actual magnetizing current with load is

$$I_m' = I_{0a} - I_{0b}' \quad (42)$$

The generated voltage is

$$V_g' = (I_{0a} - I_{0b}')Z_c \quad (43)$$

The difference between $(\theta_1' + 2n)$ and $(\theta_1'' - 2n)$ is very small.

$$d\alpha = -\sin^2\alpha d \cot\alpha$$

$$\theta_1'' - 4n - \theta_1' = \sin^2(\theta_1' + 2n) 2I_{0a} \cos((\theta_0 + n)/I_1' \sin(\theta_1' + 2n)$$

$$\theta_1'' - \theta_1' = 4n + 2(\sin\theta_1' + 2n \cos\theta_1')I_{0a}/I_1' \quad (44)$$

The above is the difference in power factor angle.

$$\cos\theta_1'' = \cos\theta_1' \cos(\theta_1'' - \theta_1') - \sin\theta_1' \times \sin(\theta_1'' - \theta_1')$$

$$\cos\theta_1''/\cos\theta_1' = 1 - 4n \tan(2I_{0a} \sin\theta'/I_1') - \tan\theta_1' \tan(2I_{0a} \sin\theta'/I_1')$$

$$\cos\theta_1''/\cos\theta_1' = 1 - (4n + \tan\theta_1') \tan(2I_{0a} \times \sin\theta_1'/I_1') \quad (45)$$

In actual computations, this equation appears to be quite inaccurate.

There is another method of obtaining the ratio of the power factors from equations 39 and 40.

$$\frac{\cos(\theta_1'' - 2n)}{\cos(\theta_1' + 2n)} = \frac{1 - 2I_{0a} \cos(\theta_0 + n)/I_{1b}'' \cos\theta_2}{1 - 2I_{0a} \cos(\theta_0 + n) \cos \times (\theta_1' + 2n)/I_1'}$$

Substituting $I_{1b} \cos\theta_2$ for $I_1' \cos(\theta_1' + 2n)$, and simplifying,

$$\cos\theta_1''/\cos\theta_1'' = 1-4s\tan\theta_1' - 2(I_{0a}/I_1')\times(\cos\theta_0 - n)(1+6n)\sin\theta_1'\tan\theta_1' \quad (14)$$

This equation is accurate to better than 20 per cent even for nonconventional motors.

The change in the magnetizing current is important in considering the core loss.

$$\mathbf{I}_{0b}/\mathbf{I}_1 = \mathbf{Z}_1/(\mathbf{Z}_1+\mathbf{Z}_2) = Z_1M/\underline{n}/Z_c = K/\underline{\beta}$$

$$\mathbf{I}_{0b}/\mathbf{I}_2 = 1.01X_1/X_2 - j.88R_1/X_2 = K/\underline{\beta},$$

approximately

$$\beta = \tan^{-1}(-0.87R_1/X_1) \quad (46)$$

$$K = Z_1/X_c \quad (47)$$

From Figure 5

$$I_c' = I_{0a} - (I_2Z_1/X_c)\sin(\theta_2+\beta) \quad (48)$$

$$\frac{I_c''}{I_c'} = \frac{1+(I_2Z_1/I_{0a}X_c)\sin(\beta-\theta_1)}{1-(I_2Z_1/I_{0a}X_c)\sin(\theta_2+\beta)}$$

$$I_e''/I_c'' = 1+2I_1'R_1\cos\theta_1'/V_0 \quad (49)$$

This says that when changing from motor to generator action, the magnetizing current increases in per unit values two times the power factor times the per-unit primary resistance. The actual generated voltage is proportional to the magnetizing current.

$$V_g''/V_g' = 1+2I_1'R_1\cos\theta_1'/V_0 \quad (50)$$

The primary core loss is proportional to the square of the generated voltage.

$$P_c''/P_c' = 1+4I_1'R_1\cos\theta_1'/V_0 \quad (51)$$

The primary copper loss is proportional to the square of the terminal current. Using equation 3,

$$P_1''/P_1' = 1-4(P_c\cos\theta_1 - 3I_{0a}^2R_1)/VA \quad (52)$$

If greater accuracy is required, equation 41 could be used, but its form is not as convenient.

The secondary copper loss is constant.

$$P_2''/P_2' = 1$$

The stray load loss is proportional to the speed squared and to the stator current squared

$$P_s''/P_s' = (1+2s')^2(1-4(P_c\cos\theta_1 - 3I_{0a}^2R_1)/VA)$$

$$P_s''/P_s' = 1+4s'-4(P_c\cos\theta_1 - 3I_{0a}^2R_1)/VA \quad (53)$$

This last equation is easy to visualize. The per-unit change in loss is $4s$ due to a speed change of $2s$. The last term is due to the change in primary current, which is mainly influenced by the core loss.

The variation in friction loss is

$$P_f''/P_f' = (1-s'')^{3/2}/(1-s')^{3/2} = 1+3s' - 3s'^2/2 \quad (11)$$

The power associated with G_L is the mechanical power input in excess of friction losses

$$P_L'' = I_2^2G_L''/(G_L''+G_s'')^2$$

Setting up the ratio of the powers

$$\frac{-P_L''}{P_L'} = \frac{G_L'(1+G_s'/G_L')^2}{G_L''(1+G_s''/G_L'')^2}$$

Substituting the values of G_L and G_s and eliminating the ratio of the slips between this equation and equation 36 will give

$$-P_L''/P_L' = (2-k)[1+s'(1+k)\{1+[1+k(1-3s'(1+k))]P_s'/P_L'\}^2]$$

$$-P_L''/P_L' = 1+2s'(2+s'+24(P_s'/P_L')^2)+4(1+(P_s'/P_L')-2(P_s'/P_L')^2-14s'^2)P_s'/P_L' \quad (55)$$

$$-P_L''/P_L' = 1+4s'+4P_s'/P_L', \text{ approximately} \quad (56)$$

Equation 55 has no approximations. It gives values of P_L'' which are too high, however. Equation 56 neglects the higher order terms, and is sufficient for high-efficiency low-slip machines. It gives values of P_L'' which are too low.

The machine handles more power as a generator than as a motor. Even if the rotor current is the rated value, the air-gap power will be increased due to the higher voltage, and the input power is even greater than this by the rotor losses. The internal torque in synchronous watts is

$$T = P_L/(1-s)$$

Substituting equations 55 and 7 in the above, and discarding third order terms

$$-T''/T' = 1+2s'(1+4s')+4(1+P_s'/P_L')P_s'/P_L' \quad (57)$$

$$-T''/T' = 1+2s'+4P_s'/P_L', \text{ approximately} \quad (10)$$

This gives generator values which are low.

The losses now may be tabulated.

Motor Losses	Generator Losses	From Equation
P_f'	$(1+3s')P_f'$	(11)
P_s'	$(1+4s'-4(P_c\cos\theta_1 - 3I_{0a}^2R_1)/VA)$	(53)
P_2'	P_2'	
P_1'	$(1+4I_{0a}^2R_1/VA - 4P_c\cos\theta_1'/VA)P_1'$	(52)
P_c'	$(1+4P_1'\cos\theta_1'/VA)P_c$	(51)
Sum $= P_h'$	Sum $= P_h''$	(58)

The sum of the losses can be simplified by assuming that typical design values of per unit R_1, $\cos\theta'$, and I_{0a} are functions of the slip, so that roughly

$$P_h'' = (1+3s')P_f'+(1+4s')P_s'+P_2'+(1+80s'^2)P_1'+P_c' \quad (9)$$

To illustrate the significance of these figures, the temperature rise can be computed. It is sufficiently accurate at this point to assume for a class A motor the following distribution of losses: 40 per cent of the total losses for P_1, 30 per cent for P_2, 10 per cent for P_s, 12 per cent for P_2, and 8 per cent for P_f.

The ratio of the total losses and therefore the heating as computed by equation 9 is $H''/H' = (1+1.7s')$. The temperature rise is $T''/T' = (1+1.7s')/(1+2s') = (1-0.3s')$. The difference of $0.3s'$ is less than a degree. Therefore a class A motor can be operated as a generator at rated rotor current and a terminal current of $1-2(P_c\cos\theta_1'-I_{0a}^2R_1)/VA$ times the rated stator motor current.

The generator output will be greater than the motor output.

$$P_{out}' = P_L' - P_f'$$

$$P_{in}'' = P_L'' + P_f''$$

$$P_{out}'' = P_{in}'' - P_h'' = P_L'' + P_f'' - P_h''$$

$$P_L'' = (1+4s'4s'+2s'^2)P_L'+(1+P_s'/P_L')4P_s' \text{ (From equations 11, 55, and 9)}$$

$$P_{in}'' = (1+4s'+2s'^2)P_{out}'+(2+7s')P_f'+(1+P_s'/P_L')4P_s'$$

$$P_{in}'' = P_{in}'+(2+s')2s'P_{out}'+(1+7s')P_f'+(3+4P_s'/P_L')P_s'-P_c'-P_1'-P_2' \quad (59)$$

$$P_{out}'' = (1+4s'+2s'^2)P_{out}'+(1+4s')P_f'+(3+4P_s'/P_L'-4s')P_s'-P_c'-P_2'-(1+80s'^2)P_1' \quad (60)$$

Assuming the same distribution of losses as before, the approximate new power rating is

$$P_{out}'' = (1+4.04s')P_{out}'-0.35(1+2s')P_2' \quad (18)$$

A motor with 94 per cent efficiency at 2 per cent slip would deliver about 6 per cent more power as a generator than its motor rating. A motor with 70 per cent efficiency at 10 per cent slip would deliver 22 per cent more power as a generator.

The ratio of the per-unit losses is

$$(1-\text{eff}'')/(1-\text{eff}') = P_h''P_{in}'/P_{in}''P_h'$$

$$P_h'' = P_h'+3s'P_f'+4s'P_s'+(80s'^2)P_1' \quad (61)$$

$$(\text{eff}'')-(\text{eff}') = (1-\text{eff}')(\text{eff}')4s+(1-\text{eff}'-s')P_f'/P_{in}'+(1-\text{eff}')(3+4P_s'/P_L'-4s')P_s'/P_{in}'-(1-\text{eff}')P_c'/P_{in}'-(1-\text{eff}')P_2'/P_{in}'-P_c'-P_2'-(1+80s'^2)P_1' \quad (62)$$

The relative magnitudes of these terms and the change in efficiency can be computed for the previously assumed distribution of losses, 85 per cent efficiency, and 3 per cent slip.

$$(\text{eff}'')-(\text{eff}') = (1-\text{eff}')(0.12\times0.85+0.08\times0.12+0.12\times0.468-0.1\times0.15$$
$$= 0.15(0.102+0.010+0.0561-0.015-0.045-0.032) = +0.011$$

This increase in efficiency of 1 per cent is a little more than the computed increase in temperature rise. Not only is it quite

Table I

	Test Motor	Test Generator	Exact	Calculated Generator Equation	Approximate	Equation
I_1	30 amperes	28.7 amperes	28.55 amperes	41	27.7 amperes	3
V_1	113 volts	118 volts	118 volts assumed			
P_{in}	5,000 watts	6,590 watts	6,710 watts	53	6,460 watts	56
			6,821 watts	59		
P_h	1,900 watts	2,180 watts	2,300 watts	58	2,213 watts	61
P_{out}	3,100	4,410	4,410 watts	55–58	4,607 watts	60
			4,521	59–58	4,247 watts	56–61
eff	0.62	0.67	0.658	55–58	0.75	63
					0.756	17
Slip	0.0666	0.0433	0.0425	64	0.0425	7
			0.0553	37	0.0563	38
Speed	1,120 rpm	1,252 rpm	1,251 rpm	64	1,251	7
			1,266.5 rpm	37	1,267.5 rpm	38
$\cos\theta$ = p.f.	0.84	0.752	0.758	41–55–59	0.621	2
			0.768	14	0.494	45

small, but it is due to the differences between several second-order effects. Third-order terms have been neglected, when they were not significantly large, so that the accuracy of this efficiency difference is poor. An examination of the relative magnitudes in the preceding equation shows that the first term is the most significant and that the sum of the second and fourth terms is essentially zero. It also should be noted that the last term, which is fairly large, is derived from equation 9 in which $80s'^2$ was substituted as an approximation for $4\cos\theta_1' P_s'/VA + 12\, I_{0a}^2 R_L/VA$. Replacing the exact value in equation 62

$$(\text{eff}'') - (\text{eff}') = (1-\text{eff}')(\text{eff}')4s'^2 + (1-\text{eff}'-s')P_f'/P_{in}' + (1-\text{eff}')(3+4P_s'/P_L'-4s')P_s'/P_{in}' - (1-\text{eff}')P_c'/P_{in}' - (1-\text{eff}')P_s'/P_{in}' - (1-\text{eff}' - 4\cos^2\theta_1' P_s'/P_{in}' - 12 I_{0a}^2 R_1 \cos\times \theta_1'/P_{in}')P_1'/P_{in}' \quad (63)$$

If the terms with friction and core loss are omitted this becomes equation 17 which has been previously stated. Both equations 63 and 17 give values for the change in efficiency for small machines which are much too large.

The increase in efficiency is usually small and will be greatest in machines with a high ratio of slip to per-unit rotor loss (high percentage stray load loss).

The best over-all test of this method and these formulas is a comparison between calculated generator characteristics and actuality.[7] For a small low-efficiency high-slip motor, the discrepancies should be large when the approximate formulas are used. Since many of the approximations are not valid for these conditions, this should make a good test to determine the limits of the extent of the applicability of these formulas. Table I shows these results quite strikingly. The more exact expressions for power and efficiency were fairly reliable, while the approximate expressions for power factor were quite poor. The computed speed using equation 37 was in error by 15 rpm, or over 1 per cent. This was due to the fact that in equation 37, the substitution $2R_sG_L = 4s$ was used.

For this machine, $2R_sG_L = 4.95s'$. Making this substitution in equation 36, one can derive a slip equation accurate for machines with rotor resistance different than stator plus line resistance.

$$-s''/s' = 1 - 2s'(1 + 2P_s'/P_L' - s' + (P_s'/P_L' - 2s')(1 + 0.95R_1/R_2)) - (P_s'/P_L')^2 \quad (64)$$

A simplification of this is

$$-s''/s' = 1 - s'(2 + 9P_s'/P_L' - 6s') \quad (7)$$

This equation was given previously without derivation. If it is used to compute the slip for the test machine, it yields

$s'' = 0.0426$, and $N'' = 1251$ rpm, only one rpm in error

The terminal voltage of the machine was a variable due to the regulation of the power supply. This was represented in the computations by a line resistance of 0.074 ohm per phase added to the primary resistance of 0.126 ohm per phase. The no-load voltage was 116 volts, and this was used to compute the V_0 in equations 3, 51, 52, and 53. The motor losses were 400 watts each for friction and core, 340 watts each for stator and copper losses, and 420 watts stray load loss.

References

1. Design of Electrical Apparatus (book), John H. Kuhlmann. John Wiley and Sons, New York, N. Y., 1940.

2. Induction Motor Characteristics at High Slip, T. H. Morgan, W. E. Brown, A. J. Schumer. *Electrical Engineering (AIEE Transactions)*, volume 59, August 1940, pages 464–68.

3. Reverse-Rotation Test for the Determination of Stray Load Loss in Induction Machines, T. H. Morgan, W. E. Brown, A. J. Schumer. *Electrical Engineering (AIEE Transactions)*, volume 58, July 1939, pages 319–24.

4. Stray-Load Loss Test on Induction Machines, II, T. H. Morgan, Victor Siegfried. *Electrical Engineering (AIEE Transactions)*, volume 55, May 1936, pages 493–97.

5. Experimental Electrical Engineering (book), V. Karapetoff. John Wiley and Sons, New York, N. Y., volume 2, 3rd edition, 1927, chapters 53 and 54.

6. Standard Handbook for Electrical Engineers (book), A. E. Knowlton. McGraw-Hill Book Company, New York, N. Y., 7th edition, section 7, 1941, pages 694–740.

7. Alternating Current Machinery (book), J. G. Tarboux. International Textbook Company, Scranton, Pa., 1947, chapter 23.

No Discussion

Quick and Accurate Production Testing on Large D-C Apparatus

M. J. BALDWIN
MEMBER AIEE

H. D. BARNHART
ASSOCIATE AIEE

THE testing method described was devised for the purpose of shortening the time and avoiding some of the inaccuracies of the customary methods of making routine production tests on large d-c machines. It is based on the use of the reluctance of the flux paths of the machine to indicate their uniformity, and involves a procedure in which the machine under test is driven as a generator without load. Results obtained during many months of factory use have amply demonstrated the superiority of this method, as a quick check on standard production machines.

Developmental Versus Commercial Tests

After a new type of machine is tested and all adjustments have been made from a design standpoint, the problem is then one of making all succeeding machines like the one just tested.

Load tests provide an adequate means of determining that no parts are rubbing, that the commutator is reasonably smooth, and that the bearings are free and properly lubricated. Readings of speed and commutation are customary and serve to indicate, in a rough way, whether a machine is working as it should. Frequently the service application of the machine is such that this is an adequate check. As the specific output of motors and generators is increased, more accurate gauges of speed and commutation adjustment are needed. With ordinary load testing, a good test on either of these points involves the use of a controlled condition of brush fit that is generally known as a full face load fit.

A full face load fit is difficult to obtain. The brushes must first be sanded and seated to what is known as a seater fit. With a fit of this kind, the brush is approximately, but not accurately, fitted to the commutator. The process of applying the seater changes the friction between the brush and commutator. This friction also varies with the amount of oxide film and brush deposit on the commutator. As the friction varies, the brush position varies microscopically; and with each brush position there is a change in commutation. It is difficult to obtain consistent test results even during developmental testing. To carry out the same tests for production machines would involve so much testing time that it is not practical.

The method of testing here described is intended to indicate the accuracy of speed and commutation adjustment without the use of carefully fitted brushes.

Development of the Method

A method used in testing some 300 machines during the war pointed the way to the development of a short commercial test for production machines. It is well known that the uniformity of the magnetic circuit in a given machine may be determined by checking its reluctance. This method has had wide commercial application for indicating the uniformity of the exciting flux paths variables within acceptable limits. In the case of the 300 machines, it also was used with great success to indicate the uniformity of the commutating flux path.

The experience gained in these first tests made it possible to build special equipment for the development of this method of indicating the commutation to be expected so that it could be applied to the commercial testing of traction motors on a high production basis. This application has made possible a complete revamping of the commercial test routine with numerous beneficial results.

Test Schedule

Fundamentally the schedule followed consists of four simple tests plus the customary overspeed, high-potential, and hot impedance tests.

1. A no-load saturation curve is taken with the main poles excited and the armature driven at a fixed speed. This curve is used to indicate uniformity of main flux circuit reluctance including the accuracy of the main pole air gaps. This, in turn, gives an indication of the full load speed.

2. A no-load saturation curve is taken with only the commutating poles excited and the armature driven at a fixed speed. This curve is used to indicate uniformity of commutating flux circuit reluctance including the accuracy of the commutating pole air gap. This, in turn, gives an indication of the grade of commutation to be expected.

3. The machine is operated for heating up and bearing test, at load speed with load current in the armature and commutating field, but with no main field excitation. Incidentally, variations in the power necessary to drive the machine in this test have been found to be an indication of the symmetry of the brush holders, the commutating poles, and the main poles.

4. High-voltage run (45 volts per bar) is made driving the hot armature at about 10 per cent overspeed.

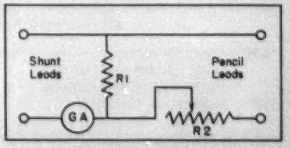

Figure 1. Simplified schematic diagram of compensation bridge circuit

Paper 50-21, recommended by the AIEE Rotating Machinery Committee and approved by the AIEE Technical Program Committee for presentation at the AIEE Winter General Meeting, New York, N. Y., January 30–February 3, 1950. Manuscript submitted October 31, 1949; made available for printing December 6, 1949.

M. J. Baldwin and H. D. Barnhart are with the Motor Engineering Division of the General Electric Company, Erie, Pa.

Figure 2. Pneumatic pencils and fixture used with compensation bridge

The test described is in no way a substitute for conventional developmental load testing which, as ever, is required in making adjustments on the first machine built. Neither does it eliminate the periodic load test as a check on machine quality. The new method, however, serves to indicate that the succeeding machines are like the first one, not only in that they will run, but also in that the speed and commutation will be like the first one tested. This is the factor upon which an accurate check must be made in the machines where close commutation adjustment is essential to successful operation.

Use of the Compensation Bridge

Certain refinements have been made in the method to read volts and amperes when checking commutation in test 2 previously mentioned.

The compensation bridge circuit shown in Figure 1 was developed for reading a ratio of volts per ampere directly. The circuits of this bridge (known generally as the *CP* bridge) are arranged so that the potential induced in the armature is picked up by special pencils bearing on the commutator and impressed across the resistance R_1 and R_2. The potential drop across a current shunt in the commutating field circuit is impressed on the terminals marked "shunt". By adjusting the value of R_2 until the voltage drop across R_1 is equal to that across the shunt, the flow of current in the galvanometer can be brought to zero. In this way the *CP* bridge can be used to indicate volts per ampere in terms of the value of the adjustment of R_2. The bridge offers a special advantage over the alternative method of taking simultaneous readings of pencil volts and commutating field amperes. In the normal operating range of a properly designed commutating pole flux circuit, the reluctance is essentially constant. With this constant reluctance, the bridge readings will be constant, even with small error in the setting of the commutating field current.

From these considerations it is evident that the bridge can be used to indicate the reluctance of the commutating flux path. It is only necessary to calibrate the resistance dial with a properly compensated machine in order to use the bridge to indicate the proper adjustment of the commutating poles. In the case of an overcompensated machine (too much commutating pole flux) the pencil voltage will be greater and, therefore, a higher resistance setting will be required to balance the bridge. For an undercompensated machine a lower setting will be required. The bridge circuit as now used for commercial tests is essentially the same as Figure 1, except that two protective resistors have been added, and a self-balancing bridge has been substituted for the galvanometer.

A special pneumatic pencil fixture, shown in Figure 2, has been developed for use in this application. Pencil lead operating under approximately 90 pounds per square inch pressure has been found best for the purpose. The lead should be at least 0.020 inch larger in diameter than the width of the undercut mica groove between segments. If the pencils are spaced far enough apart to include all the segments between which any appreciable amount of voltage is generated by commutating pole flux, it will not be necessary to provide any high degree of accuracy in the supporting fixture either as to spacing or location.

Speed Control

As pointed out previously, the setting of the commutating field current is not of critical importance. This then leaves only the accurate measurement of speed as the major consideration in the *CP* bridge readings.

The method used to indicate speed employs an oscilloscope to compare the frequency of an a-c tachometer with the frequency of a standard 250-cycle tuning fork. A phase-shifting network is used to obtain a second 250-cycle frequency with a 90-degree voltage lag with respect to the original. These two are then used for

Figure 3. View of test area showing test table, motors in test stands, and tracks and turntable for motor conveying dolly

Figure 4. Test table showing controls, oscillograph, bridge, and selector switches

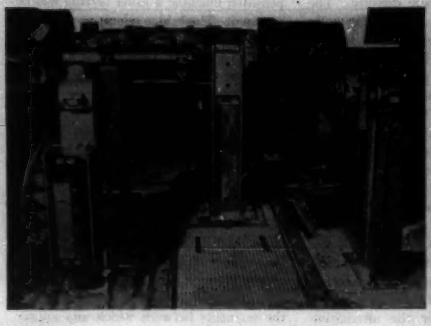

Figure 5. Test stand empty, showing pedestals, elevator for positioning motor, also nose support in background

Figure 7. Test motor on dolly ready for positioning in stand, showing adjustable nose support in foreground

vertical and horizontal input to obtain a circle trace on the oscilloscope. The tachometer frequency is applied to the Z-axis of the oscilloscope to modulate the circle trace, blanking out a small segment of the circle. When the two frequencies are different, the blanked portion will revolve, but when properly synchronized the blanked out portion will appear to stand.

The tuning fork itself is of bimetallic construction, making a close approach to a zero temperature coefficient possible. The accuracy of the fork is one part in 100,000 or 0.001 per cent with a temperature coefficient of one part in 1,000,000 per centigrade degree from 0 to 60 degrees centigrade.

One tuning fork was set up in the General Electric Company Laboratory with circuit provided for comparing directly with the time check broadcast by radio station, WWV. A signal from this fork was transmitted to the test floor over the company's telephone circuits. Two other forks were made up in oscilloscope cases to form portable speed-fixed frequency standards.

With normal control of speed it requires no special skill to hold the tachometer frequency almost the same as the standard 250-cycle frequency. This constant speed is required only long enough to obtain one *CP* bridge or saturation reading at a time. The ratio of 16 cycles per revolution makes the visual indication of speed very accurate. In terms of speed 1 rpm of oscilloscope indication represents only 1/16 of an rpm of the test motor.

Figure 6. Double universal drive for test motors. Coupling guard shown with cover open

Conclusions

The method described permits the use of a much simpler mechanical set-up on the test stand. See Figures 3, 4, and 5. In the case of testing a traction motor with axle and nose suspension, a 3-point suspension type of support is used as shown in Figures 5 and 7. The driving power is transmitted by a long, double-universal, drive shaft, see Figure 6, in order to adapt the set-up to all sizes of motors. Development installation now has been in operation for about two years. In that time, it has demonstrated many advantages, both from the standpoint of quality of the results and economy of time, as indicated below:

1. The *CP* bridge substitutes for the usual time-consuming and uncertain method of observing commutation during the load run an accurate method of indicating commutation which eliminates the inaccuracies caused by a poor brush fit, commutator film, commutator roughness, or instability of the brushes in the brush holders.

2. In addition to the indication of full-load speed normally obtained, it now is possible to obtain data indicating the accuracy of the air gap and the quality of the metal portion of the main exciting flux path.

3. The power requirements are small and are independent of machine rating for a given type of machine.

4. The same meters can be used for testing a large number of machines of the similar type with the single exception of the voltmeter to read terminal voltage.

No Discussion

Transient Response of Direct-Current Dynamos

H. E. KOENIG
ASSOCIATE AIEE

Synopsis: Equations for the transient current of both the armature and field of a d-c shunt-wound machine are developed. The equations are derived from the theorem of constant flux linkages and in terms of the mutual inductance between the armature and shunt field. Methods for measuring this mutual inductance as well as other constants of the machine are developed. It is believed that the analysis can be extended to include almost any type of d-c dynamo, including the amplidyne. The results obtained from the theoretical analysis are in agreement with experimental data.

THE problem of transient analysis of both a-c and d-c machines has been of great interest to electrical engineers for several decades. During the period from 1928 to 1930 many of the problems of transient short circuits on synchronous machines were solved by R. H. Park,[1,2] R. E. Doherty and C. A. Nickle,[3,4] and others. Most of this work had been directed toward the special problem of short circuits, since it was then the problem of major importance in the field of a-c machines. Much of R. H. Park's work, however, included a general solution that could be extended to practically any type of a-c machine problem involving transient conditions.

In recent years the increased use of d-c distribution systems on ships and the use of d-c dynamos in servo systems has made necessary a more complete understanding of d-c machine transient phenomena. One of the special problems was that of finding the transient short-circuit current of d-c generators for relay co-ordination. Since 1946 considerable work has been done on this special problem by T. M. Linville and H. C. Ward, Jr.,[5,6] and G. E. Frost.[7] Briefly their analyses consist of finding a transient and a subtransient impedance similar to the transient and subtransient reactances of synchronous machines. In general, the formulas are quite similar to the well-known formulas for synchronous machines.

For the particular problems concerning short-circuit currents and torques, the analyses available give reasonably good results. However, to the author's knowledge, no general analysis is available which is applicable to the type of transient problem met in servo control systems.

In the transient analysis of d-c machines it has been found convenient to use the 2-reaction theory similar to that used in synchronous machine studies.[1] The general method of attack consists of dividing the armature current, voltage and flux linkages into the direct- and quadrature-axis components. Expressions for the direct- and quadrature-axis flux linkages of the armature and field then are derived in terms of measurable quantities of the machine. Since the armature terminal voltage is a function of the rate of change of flux linkages, a differential equation finally is obtained for the terminal voltage of the machine in terms of the field voltage and constants of the machine. The analysis that follows is for the particular case of a shunt machine with commutating poles and zero brush shift. The same approach could be extended quite conveniently, however, to the analysis of compound machines and amplidynes.

Assumptions

In practically all machine analyses it is necessary to make certain simplifying assumptions. In this analysis the following assumptions are made:

1. The machine is symmetrical about both axes.
2. The eddy current and hysteresis losses are neglected in the development of the equations, but not in the evaluation of the constants of the machine.
3. The brush axis does not shift with load.
4. The magnetomotive force of the short-circuited winding undergoing commutation is negligible.
5. The coefficients of the equations are considered as constants over a limited range of operation.

Generalized Analysis

The direct and quadrature axes are chosen as shown in Figure 1. The direct-axis current is that component of armature current which produces armature reaction along the direct axis. Likewise, the quadrature component of armature current is that component which produces armature reaction along the quadrature axis.

For zero brush shift the brush axis is in line with the quadrature axis. Under this condition almost all of the armature reaction is in quadrature with the main field or direct axis. With zero brush shift a decrease in the direct-axis flux caused by an increase in armature current is a result of saturation of the shunt-field pole tips. The saturation of the pole tips which decreases the shunt-field flux causes a voltage to be induced in the field under transient conditions. Therefore the effect of this saturation must be included in the analysis. Since this voltage induced in the field is proportional to the quadra-

Paper 50-22, recommended by the AIEE Rotating Machinery Committee and approved by the AIEE Technical Program Committee for presentation at the AIEE Winter General Meeting, New York, N. Y., January 30–February 3, 1950. Manuscript submitted October 24, 1949; made available for printing December 9, 1949.

H. E. Koenig is with the University of Illinois, Urbana, Ill.

The author wishes to express his gratitude to Dr. G. H. Fett of the Electrical Engineering Department, University of Illinois, who suggested the study of this problem, for his suggestions and guidance in the preparation of this manuscript, and to Professors C. A. Keener, H. N. Hayward, and J. E. Williams, also of the Electrical Engineering Department, for their suggestions and comments.

The author also acknowledges the permission granted by the Graduate College of the University of Illinois to utilize material included in a thesis submitted under the same title in partial fulfillment of the requirements for the degree of Master of Science.

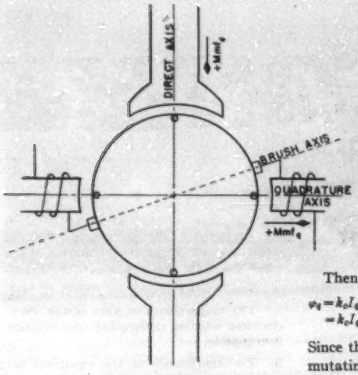

Figure 1 (left). Schematic diagram of dynamo showing reference axes

Figure 4 (right). Bridge circuit for measuring the mutual inductance between the armature and shunt field. Under balanced conditions $m_2/m_1 = R_2/R_1 = \beta_2/r$

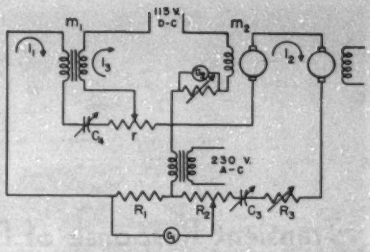

ture component of armature current, it can be represented by the product of a mutual inductance term, M_{af}', and Pi_q.

Let positive armature current in the direct axis be defined as that which produces positive armature flux linkages in the direct axis. If saturation except for that of the shunt-field pole tips is neglected, the general expression for the direct-axis armature flux linkages becomes

$$\begin{aligned}\varphi_d &= k_f I_d - (x_1 + x_d')i_d - x_d'' i_q \\ &= k_f I_d - X_d i_d - x_d'' i_q\end{aligned} \tag{1}$$

where x_d'' is an inductance term to account for the decrease in φ_d caused by the saturation of the shunt-field pole tips.

Similarly let positive armature current in the quadrature axis produce positive armature flux linkages in the quadrature axis.

Then

$$\begin{aligned}\varphi_q &= k_c I_q - (x_1 + x_q')i_q \\ &= k_c I_q - X_q i_q\end{aligned} \tag{2}$$

Since the effect of saturation of the commutating pole tips is very small, it is neglected in this expression.

The flux linkages with the field in the direct and quadrature axis are respectively

$$\gamma_d = L_f I_d + M_{af} i_d - M_{af}' i_q + M_{cf} I_q \tag{3}$$

$$\gamma_f = L_c I_q - M_{ac} i_q + M_{cf} I_d \tag{4}$$

For the special case of zero brush shift, $i_q = I_q$ = total armature current, and i_d is the short-circuit current of the coil undergoing commutation. Under this condition $M_{af} i_q$ and $X_d i_d$ are both negligible since the number of turns in the direct axis of the armature is very small.

If P is defined as the operator, d/dt, the expressions for the direct and quadrature components of armature voltage become

$$e_q = \varphi_d P\delta + P\varphi_q - P\gamma_q - i_q r_q \tag{5}$$

$$e_d = \varphi_q P\delta + P\varphi_d - i_d r_d \tag{6}$$

where $P\delta$ represents the speed of rotation of the armature. The voltage e_q is the voltage which produces i_q. In the particular case of zero brush shift, e_q is the terminal voltage of the machine.

By the proper choice of units, some of the constants of equations 1 thru 4 can be eliminated. Let the unit quantities be defined as shown in Appendix I. Equations 1 through 4 then reduce to the following

$$\varphi_d = I_d - x_d'' i_q \tag{7}$$

$$\varphi_q = k_c' i_q \tag{8}$$

$$\gamma_d = I_d - M_{(a+c)f} i_q \tag{9}$$

$$\gamma_q = L_c' i_q + M_{cf} I_d \tag{10}$$

where $k_c' = k_c - X_q$, $M_{(a+c)f} = M_{af}' - M_{af}$ and $L_c' = L_c - M_{ac}$.

Since the commutating field is connected in series with the armature it becomes convenient to choose the unit of γ_q equal to the unit of φ_d and φ_q. Equations 5 and 6 can then be written as

$$e_q = \varphi_d + P\varphi_q - P\gamma_q - i_q r_q \tag{11}$$

$$e_d = \varphi_q + P\varphi_d - i_d r_d \tag{12}$$

It now is possible to express all flux linkages in equation 11 in terms of E_d and i_q. As derived in Appendix II, the expression for the terminal voltage of the machine then becomes

$$\begin{aligned}e_q = Pk_c' i_q - P\Bigg[& L_c' i_q + \\ & \frac{M_{cf}(E_d + M_{(a+c)f} T_e P i_q)}{1 + T_e P}\Bigg] - r_q i_q + \\ & \frac{E_d + [(M_{(a+c)f} - x_d'')T_e P - x_d'']i_q}{1 + T_e P}\end{aligned} \tag{13}$$

This gives one equation with two unknowns, namely e_q and E_d. However, for any particular case one or the other would be known. For instance, in the case of a generator e_q would be known as a function of i_q.

To obtain an expression for the field current, equation 9 is substituted in equation 23 to give

$$I_d = \frac{E_d}{1 + T_e P} + \frac{M_{(a+c)f} T_e P i_q}{1 + T_e P} \tag{14}$$

It should be noted that if the armature current is zero, the first term of equation 14 represents the differential equation of the field circuit. If E_d is held constant the first term becomes E_d and the transient is given by the last term.

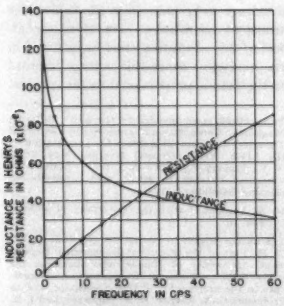

Figure 2. Apparent resistance and inductance of the shunt field as a function of frequency

Rms alternating current of 0.006 ampere. Direct component of current of 0.32 ampere

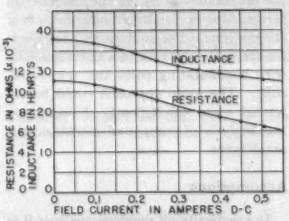

Figure 3. Apparent resistance and inductance of the shunt field as a function of direct component of field current

Rms alternating current of 0.006 ampere. Frequency of 60 cycles per second

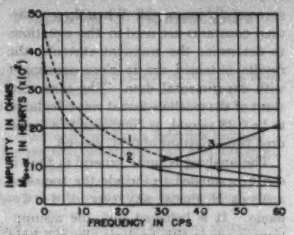

Figure 5. Combined mutual inductance of armature and commutating field with respect to the shunt field, as a function of frequency. Field current of 0.32 ampere of direct current

1. $M_{(a+c)f}$ for armature current of 7 amperes rms alternating current
2. $M_{(a+c)f}$ for armature current of 5 amperes rms alternating current
3. β_s for armature current of 7 amperes rms alternating current

Prediction of Transient

For the purpose of checking the foregoing analysis, consider the problem of a sudden increase in the shunt-field voltage of a separately excited generator. The generator is driven at constant speed and is delivering power to a pure resistance load.

The transient current of the armature and field are to be found. If r_L is the load resistance, then $e_q = i_q r_L$. Substitution of $i_q r_L$ for e_q in equation 13 gives

$$i_q = \frac{E_d(1 - M_{cf}P)}{(M_{cf}M_{(a+c)f} - k_c' + L_c')T_oP^2 + [L_a' - k_c' + (r_L + r_q + x_d'' - M_{(a+c)f})T_o]P + r_L + x_d'' + r_q} \tag{15}$$

The quantity $r_q + x_d''$ is sometimes referred to as the "synchronous resistance" of the armature,[7] since it is analogous to the synchronous reactance of a synchronous machine. It represents the steady-state resistance drop of the armature plus the demagnetizing effect of armature reaction.

The quantities $(k_c' - L_c')$, $E_d M_{cf} P$, and $M_{cf} M_{(a+c)f}$ have been found to be negligible in this particular case. However, if necessary, they could be determined from relatively simple measurements on the machine. Neglecting these terms equation 15 reduces to

$$i_q = \frac{E_d}{(r_L + r_s - M_{(a+c)f})T_oP + r_L + r_s} \tag{16}$$

where $r_s = r_q + x_d''$, the synchronous resistance of the machine.

Substitution of equation 16 in equation 14 gives

$$I_d = \frac{E_d(r_L + r_s)}{(r_L + r_s - M_{(a+c)f})T_oP + r_L + r_s} \tag{17}$$

If E_d is a step function of time, then equations 16 and 17 have the solution[8]

$$i_q = \frac{E}{r_L + r_s}(1 - e^{-t/T}) \tag{18}$$

$$I_d = E_d(1 - e^{-t/T}) \tag{19}$$

where

$$T = \frac{(r_L + r_s - M_{(a+c)f})T_o}{r_L + r_s}$$

Hence, both armature and field current change exponentially to the new values when the field voltage is suddenly changed on a separately excited d-c generator.

The coefficients of equation 18 must be expressed in terms of per unit values of the armature circuit, whereas the coefficients of equation 19 are expressed in terms of per unit values of the field circuit. The value of T can be expressed in terms of per unit values of either the armature or field. If L_f is in henrys and R_d is in ohms, then T_o and t are in seconds.

To determine the correctness of the theoretical analysis given above, the constants of the machine are used in equations 18 and 19 to predict the transient currents of the generator operating under the conditions as previously stated. The equations for i_q and I_d, as determined in Appendix III, are respectively

$$i_q = 0.862(1 - e^{-t/0.38}) \text{ units}$$

$$_d = 0.862(1 - e^{-t/0.38}) \text{ units}$$

From the oscillograms shown in Figure 10, the armature current is found to rise exponentially from 16.5 to 25 amperes, the time constant, T, being 0.367 second. The shunt-field current rises in the same manner and has exactly the same time

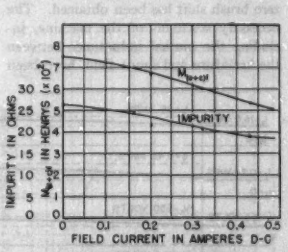

Figure 6. Combined mutual inductance of the armature and commutating field with respect to the shunt field, as a function of the direct component of field current

Armature current of 5 amperes rms alternating current
Frequency of 60 cycles per second

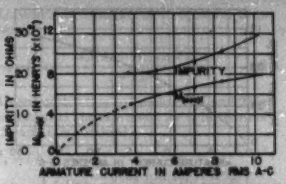

Figure 7. Combined mutual inductance of the armature and commutating field with respect to the shunt field, as a function of the rms alternating component of armature current

Field current of 0.32 ampere of direct current.
Frequency of 60 cycles per second

constant. This agreement is much better than one has a right to expect, but indicates very well the accuracy of the assumptions and shows that the method of measurement is satisfactory.

Measurement of Machine Constants

Shunt-Field Inductance

The inductance of the shunt field must be determined accurately. Because of the large eddy current losses in the magnetic circuit, it is necessary to use a Hayes bridge when measuring the inductance of the shunt field. The inductance is measured as a function of frequency down to about 5 cycles per second. The data then are plotted on log-log paper and the curve is extrapolated to the very low frequencies. The d-c inductance also can be determined from the open-circuit time constant of the machine. The data for the inductance of the shunt field as a function of frequency and direct component of current are shown in Figures 2 and 3. The curves indicate that the operating conditions must be known if satisfactory values of inductances are to be used in the equations.

Mutual Inductance, $M_{(a+c)f}$

The mutual inductance, $M_{(a+c)f}$ is the most difficult of the coefficients to evaluate. To the author's knowledge, this quantity has never been measured before. This inductance is a "combined mutual" of the armature and commutating field with respect to the shunt field. Since for zero brush shift the armature reaction is in space quadrature with the shunt field, any change in the shunt-field flux linkages must be caused by the saturation of the pole tips. That is, as the main field flux is shifted toward one pole tip, due to saturation the decrease in flux on one side of the pole is greater than the increase on the other side. The mutual coupling is

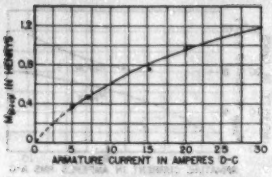

Figure 8. Combined mutual inductance of the armature and commutating field with respect to the shunt field, as determined from the oscillograms of the transients

therefore a peculiar type of coupling and not a true mutual inductance in the ordinary sense of the word. However, the change in the shunt-field flux linkages is proportional to the armature current; therefore its effect upon the field circuit can be represented by an equivalent mutual inductance.

It was possible to measure this mutual inductance $M_{(a+c)f}$ by means of the bridge circuit shown in Figure 4. Fundamentally the circuit is the Hartshorn Method[11] of measuring impure mutual inductances. By an impure mutual inductance is meant one in which the voltage induced in the secondary is not in exact quadrature with the primary current. The adaptation of the Hartshorn Method to this problem is believed to be original. The data for the mutual inductance, $M_{(a+c)f}$ are shown in Figures 5 through 8. Because of excessive oscillations of the armature, it was not possible to obtain readings below 30 cycles per second by use of the bridge circuit. It also is impossible to extrapolate accurately the curve to zero even after plotting the data on semilog paper. Therefore, a second method was used to obtain the mutual inductance at zero frequency.

Solution of equation 14 gives

$$I_d = \frac{E_d + M_{(a+c)f} T_e P i_f}{1 + T_e P}$$

If the field voltage is held constant then

$$I_d = E_d + \frac{M_{(a+c)f} T_e P i_f}{1 + T_e P} \tag{20}$$

Furthermore, if the armature current is a step function of time, then equation 20 has the solution

$$I_d = E_d + M_{(a+c)f} i_f e^{-t/T_0} \tag{21}$$

From the oscillograms which were taken when a load was suddenly applied to the generator operating at constant speed, Figure 9, it is seen that the armature current does approach a step function of time. Only a small error will be introduced when it is considered as such. If $t=0$ in equation 21, then

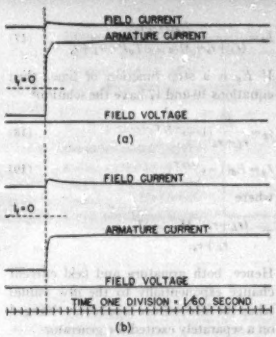

Figure 9. Oscillograms of transients for sudden application of resistance load to separately excited generator, armature speed maintained

	I_f	I_a	V_f	V_a
	Initial Conditions			
(a)	0.37	0	109.0	258
(b)	0.44	0	124.0	280
	Final Steady-State Conditions			
(a)	0.37	15.3	109.0	230
(b)	0.44	30.0	124.0	230

$$M_{(a+c)f} = \frac{I_d - E_d}{i_f} \tag{22}$$

From equation 22 and the data taken from the oscillograms of the suddenly applied loads of 5, 7, 15, 20, and 30 amperes, the curve shown in Figure 8 was obtained. The importance of knowing the operating conditions to select the constants is again emphasized.

Conclusions

The general solution to the problem of transient current of a shunt-wound d-c dynamo having commutating poles and zero brush shift has been obtained. The necessary constants of the machine, including the mutual inductance between the armature and shunt field, have been successfully measured. When these measured constants are used in the equations to determine the transient currents, the results obtained are in close agreement with experimental data. The time constant of the machine tested was calculated to be 0.38 second, as compared to a measured time constant of 0.367 second.

The analysis is quite general in that it can be extended to include the transient analysis of almost any type of d-c dynamo. It is believed that the assumptions made in this analysis also will hold in most d-c dynamo transient problems without introducing excessive error.

As stated in the section on Assumptions, any shift in brush axis due to change in load is neglected. This means that any sparking at the brushes produced by rapid change in armature current is neglected. Furthermore, it has been assumed that the armature magnetomotive force and flux are in time phase, and the effect of eddy currents and hysteresis in the poles and yoke can be neglected. For machines with laminated poles these assumptions are reasonable.

The analysis given through equation 15 includes the effect of armature leakage inductance and is quite general. It is seen that equation 15 is of the second order in P and therefore a sine or hyperbolic sine term is expected in the solution. In going to equation 18 the coefficient of P^2 was neglected. This was a reasonable assumption to make for the machine under consideration because of the magnitude of the coefficient of P^2. Also, the fact that the oscillograms of the transients show no presence of a sine or hyperbolic sine term verifies the assumption. The fact that these additional transient terms are sometimes observed in practice simply indicates that for that particular machine the P^2 term is not negligible.

Although this first analysis has assumed constant armature speed, the analysis can be extended to problems in which constant armature speed is not maintained.

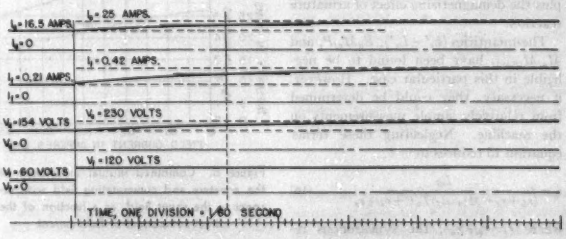

Figure 10. Oscillograms of transients for sudden increase in field voltage

Generator separately excited, resistance load, no external field resistance, speed constant

Appendix I. Nomenclature

φ_d = per unit flux linkages in the direct axis of armature
φ_q = per unit flux linkages in the quadrature axis of armature
γ_d = per unit direct-axis field flux linkages
γ_q = per unit quadrature-axis field flux linkages
i_d = per unit direct-axis armature current
i_q = per unit quadrature-axis armature current
e_d = per unit direct-axis armature voltage
e_q = per unit quadrature-axis armature voltage
r_d = per unit direct-axis armature resistance
r_q = per unit quadrature-axis armature resistance
I_d = per unit direct-axis field current
I_q = per unit quadrature-axis field current
E_d = per unit direct-axis field voltage
R_d = per unit direct-axis field resistance
x_1 = per unit leakage inductance of armature
x_d' = per unit fictitious inductance to account for armature reaction in the direct axis
x_q' = per unit fictitious inductance to account for armature reaction in the quadrature axis
x_d'' = per unit fictitious inductance of armature to account for saturation effect of i_q on the direct-axis field pole tips
$x_d = x_1 - x_d'$
$x_q = x_1 - x_q'$
L_q = per unit inductance of quadrature-axis field (commutating field)
L_f = per unit inductance of direct-axis field (shunt field)
$L_a' = L_q - M_{ac}$
M_{af} = per unit mutual inductance between armature and direct-axis field
M_{ac} = per unit mutual inductance between armature and quadrature-axis field
M_{af}' = per unit mutual coupling between quadrature-axis armature current and direct-axis field. This quantity accounts for the decrease in direct-axis flux as a result of the saturation of the direct-axis pole tips.
M_{cf} = per unit mutual inductance between direct- and quadrature-axis fields
$M_{(a+c)f}$ = per unit mutual inductance of armature and commutating field with respect to the shunt field = $M_{af}' - M_{cf}$
k_f = proportionality factor between direct-axis field current and the direct-axis flux linkages it produces with the armature at no load
k_c = proportionality factor between quadrature-axis field current and the quadrature-axis armature flux linkages it would produce if there were no armature current
$k_c' = k_q - X_q$ = proportionality factor between commutating field current and the quadrature-axis armature flux linkages it produces when $i_q = I_q$
T_o = open-circuit time constant of direct-axis field = L_f/R_d
P = operator, $\frac{d}{dt}$
unit e_d and e_q = rated terminal voltage at no load
unit φ_d and φ_q = flux linkages necessary to produce rated voltage at no load
unit i_d and i_q = rated armature current
unit I_d = field current necessary to produce unit φ_d at no load
unit γ_d = field flux linkages produced by unit I_d
unit P_o = rated armature speed
unit time = one second

Appendix II. Derivation of Armature- and Field-Voltage Equations

Field Voltage

If unit field voltage, E_d, is defined as that voltage necessary to produce unit I_d under steady-state conditions, then

$$E_d = CP\gamma_d + I_d$$

where C is a constant of proportionality between the voltage and flux linkages. Since unit E_d and γ_d were chosen independently of each other, C cannot be unity and therefore must be determined. Consider the condition when the field is shorted and the armature open-circuited. Under this condition $\gamma_d = I_d$, and

$$CP\gamma_d + I_d = 0$$

Also in conventional terms $PL_fI_d + I_dR_d = 0$

or

$$(T_oP+1)I_d = 0$$

Therefore

$$C = T_o \text{ and } E_d = T_oP\gamma_d + I_d \tag{23}$$

Armature Voltage

It is possible to express all flux linkages in equation 11 in terms of E_d and i_q. From equation 23 and equation 9

$$I_d = E_d - (I_d - M_{(a+c)f}i_q)T_oP \tag{24}$$

A substitution of equation 24 in equation 7 gives

$$\varphi_d = \frac{E_d}{1+T_oP} - \frac{[(M_{(a+c)f} - x_d'')T_oP - x_d'']i_q}{1+T_oP} \tag{25}$$

To determine γ_q as a function of E_d and i_d, substitute equation 24 in equation 10 to obtain

$$\gamma_q = L_a'i_q + \frac{M_{cf}(E_d + M_{(a+c)f}T_oPi_q)}{1+T_oP} \tag{26}$$

Upon substituting equations 8, 25, and 26 in equation 11 the expression for e_q in terms of E_d and i_q is obtained

$$e_q = Pk_c'i_q - P\left[L_a'i_q + \frac{M_{cf}(E_d + M_{(a+c)f}T_oPi_q)}{1+T_oP}\right] - r_qi_q + \frac{E_d + [(M_{(a+c)f} - x_d'')T_oP - x_d'']i_q}{1+T_oP} \tag{13}$$

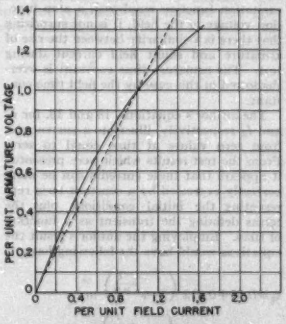

Figure 11. No-load saturation curve of d-c machine used in checking analysis

Appendix III. Prediction of Transient Currents

The machine used for all the following experimental work was a $7^1/_2$-horsepower 230-volt 1,200-rpm shunt-wound dynamo. The machine was equipped with commutating poles and had zero brush shift. The frame was solid cast steel. The poles, pole shoes, and armature were about 50-mil laminated steel. Per unit values of the armature and field circuit are as follows:

PER UNIT VALUES OF FIELD CIRCUIT

$E_d = 90$ volts
$I_d = 0.314$ ampere
$R_d = 287$ ohms
$L_f/t = 287$ ohms
$t = 1$ second
$L_f = 287$ henrys

PER UNIT VALUES OF ARMATURE CIRCUIT

$e_q = 230$ volts
$i_q = 30$ amperes
$r_q = 7.67$ ohms
$L_a/t = 7.67$ ohms
$t = 1$ second
$L_a = 7.67$ henrys

Suppose the generator is operating under the following initial conditions: $E_d = I_d = 0.67$ unit, $i_q = 0.55$ unit, $e_q = 0.67$ unit. A step voltage of 0.67 unit then is applied to the field. The increase in armature current, i_q, is given by equation 18. From the initial conditions $r_L = 0.67/0.55 = 1.22$ units. From Figure 11, considering the load line to be a straight line over the range of operation from about 16 to 30 amperes, $rs = 1.67$ ohms $= 0.218$ unit. The analysis is based upon the assumption that the magnetization curve of the field is a straight line. From Figure 11 it is seen that this assumption may not be valid. Therefore, it is necessary to take the saturation effects of the field into consideration. This can best be done by drawing a straight line through the no-load point as shown in Figure 11. An equivalent value for E_d is then found by projecting horizontally from the no-load saturation curve to the straight line. The initial value of E_d, therefore, has an equivalent value, $E_d' = 0.75$ unit. After taking saturation into consideration, a step voltage of 0.67 unit is equivalent to 0.45 unit. Because of the wide variation in $M_{(a+c)f}$, it is necessary to use an average value between the operating points.

From equation 18 the increase in armature current is

$$i_q = \frac{0.450}{1.44} = 0.312 \text{ unit}$$

giving a final steady-state value of armature current

$$i_q = 0.55 + 0.312 = 0.862 \text{ unit}$$

For a shunt field current of about 0.32 ampere and an armature current between 16 and 25 amperes, the average value of $M_{(a+c)f} = 1.0$ henry or 0.130 unit as determined from Figure 8. The time constant is given by

$$T = \frac{(r_L + r_s - M(a^+c)f)}{r_L + r_s} \qquad T_s = 0.91 T_o$$

From Figure 2, $L_f = 122$ henrys and $R_d = 287$ ohms, from which $T_o = 0.42$ second, and $T = 0.33$ second.

The equations for the armature current and field current then become

$$i_q = 0.862(1 - \epsilon^{-t/0.33}) \text{ unit}$$

$$I_d = 0.862(1 - \epsilon^{-t/0.33}) \text{ unit}$$

References

1. Two-Reaction Theory of Synchronous Machines, Generalized Method of Analysis—Part I, R. H. Park. *AIEE Transactions*, volume 48, July 1929, pages 716–30.

2. The Reactances of Synchronous Machines, R. H. Park, B. L. Robertson. *AIEE Transactions*, volume 47, April 1928, pages 514–36.

3. Three-Phase Short Circuit Synchronous Machines—V, R. E. Doherty, C. A. Nickle. *AIEE Transactions*, volume 49, April 1930, pages 700–14.

4. Synchronous Machines—IV, R. E. Doherty C. A. Nickle. *AIEE Transactions*, volume 47, April 1928, pages 457–92.

5. Solid Short Circuit of D-C Motors and Generators, T. M. Linville, H. C. Ward, Jr. *AIEE Transactions*, volume 68, part I, 1949, pages 119–24.

6. Current and Torque of D-C Machines on Short Circuit, T. M. Linville. *AIEE Transactions*, volume 65, 1946, pages 956–65.

7. The Short-Circuit Characteristics of D-C Generators, G. E. Frost. *Electrical Engineering* (*AIEE Transactions*), volume 65, June 1946, pages 394–402.

8. Operational Circuit Analysis (book), Vannevar Bush. John Wiley and Sons, New York, N. Y., 1946.

9. Transient Analysis of A-C Machinery, Yu H. Ku. *AIEE Transactions*, volume 48, July 1929, pages 707–15.

10. Definition of an Ideal Synchronous Machine and Formula for the Armature Flux Linkages, R. H. Park. *General Electric Review* (Schenectady, N. Y.), volume 31, June 1928, pages 332–34.

11. A Simplified Method of Analyzing Short-Circuit Problems, R. E. Doherty. *AIEE Transactions*, volume 42, June 1923, pages 841–49.

12. Electrical Measurement (book), Frank A. Laws. McGraw-Hill Book Company, New York, N. Y., second edition, 1938, page 447.

Discussion

E. L. Brancato and **J. Cybulski** (Naval Research Laboratory, Washington, D. C.): The author has made a good start by describing the flux linkages in d-c machinery not as a whole but in two parts; one for those composing the armature flux linkages and the other for the fields. By similarly extending the derivations for synchronous machines of R. H. Parks[1] the author also has subdivided flux linkages in each group into those in the direct and quadrature axes.

Up to this point the author has been quite general and explicit. The assumption neglecting saturation of commutating pole tips is allowable if the load transients do not overly exceed rated load on the applicable machines.

However, the paper is not clear on certain points and the following comments are made in the hope that they can be clarified:

1. Is it correct to gather that the term $M_{af}\, i_d$ in equation 3 was neglected and not as was stated $M_{af}\, i_q$?

2. It seems that equation 6 is not complete if the term Pr_d is omitted.

3. Equation 9 is to follow from equation 3 when $M(a+c)f$ is defined equal to $M_{af} + M_{cf}$. How is such a substitution to occur if equation 3 does not now contain the term $M_{af}\, i_q$? An explanation is desirable for the assimilation of the term $Maf'\, i_q$ in equation 9.

4. How have the eddy current and hysteresis losses been taken into account in the evaluation of the constants of the machine?

The equations which have been developed, 18 and 19, are not very general in the true sense of the word for the following reasons: In the development of equation 15, the author has neglected or omitted several terms which were termed negligible. Subsequently he then neglected two other terms which form the coefficient of the operator of the second order and in effect reduces the denominator from a quadratic to a linear term to form equation 16. For the solution of armature current as a function of time from equation 16, the particular excitation function employed consisted of an incremental increase in the field voltage, a step function of time in the field. A complete solution of the more general equation, 15, results in a time function composed of a constant plus two exponentials with different time constants. Depending on circuit parameters and initial conditions the armature and field currents may then rise to a peak and then decay to a steady-state value or rise essentially in some exponential form to a steady-state value. For the type of excitation function employed, a step function voltage in the field, it is not surprising that there is a similarity between the rise of armature and shunt field current during test. The armature time constant is overshadowed in this case by the field time constant.

The author's equations, 18 and 19, for i_q and I_d respectively, illustrate a current rise from zero values at time equal to zero. From the test results which were presented it appears that these currents can be more correctly expressed by a constant term representing the initial conditions plus the terms defining the transient as a function of time. Employing the author's result the equations would have the following form

$$i_q = 0.55 + 0.312\left(1 - \epsilon^{-\frac{t}{0.33}}\right) \text{ units}$$

$$I_d = 0.55 + 0.312\left(1 - \epsilon^{-\frac{t}{0.33}}\right) \text{ units}$$

The author is commended for the original manner of measuring the term $M(a+c)f$. However, it should be noted that d-c tests were resorted to for calculating $M(a+c)f$ after the bridge circuit method was found to be unsuccessful. In those tests armature currents of approximately equal to the expected armature transients must be used. This restricts the application to low level transients. If it is expected that this approach may be extended to calculations of short-circuit currents it becomes necessary that the various quantities be calculated from machine constants. It is felt that such an extension would require modification of assumptions two and three, and a consideration of reactance voltage.[2]

References

1. Two Reaction Theory of Synchronous Machines, R. H. Parks. *AIEE Transactions*, volume 58, part I, July 1929, pages 716–30.

2. Current and Torque of D-C Machines on Short Circuit, T. M. Linville. *AIEE Transactions*, volume 65, 1946, pages 956–65.

G. H. Fett (University of Illinois, Urbana, Ill.): Mr. Koenig has indicated a method of predicting the transient response of a d-c dynamo by the use of parameters which can be measured. The test which he made on the generator shows that the method is accurate when the parameters can be evaluated carefully. There is at least an equal interest in the transient speed and torque characteristics of the d-c motor which also should be investigated.

Suppose that a d-c motor is controlled by varying the voltage across the armature with the field supplied from a constant voltage source. The equations which apply in this case are

$$(Jp + f)p\delta = M \tag{1}$$

$$M = K(-i_q x_d - i_d x_q) \tag{2}$$

$$e_q = (I_d - x''_d i_q)p\delta + pK'_c i_q - pL_c' i_q - M_{cf} p I_d - i_q r_q \tag{3}$$

$$I_d = \frac{E_d + T_o p M_{(a+c)f} i_q}{1 + T_o p} \tag{4}$$

where equations 3 and 4 can be derived from the author's equations 11 and 23 together with equations 7 to 10, and the symbols are those of the author with the addition of

J = moment of inertia of motor and load
f = viscous friction parameter
M = torque of load (used to avoid confusion with other symbols used by the author) and
K = a constant relating torque and motor current and flux

Let the second term in equation 2 be neglected and let E_d of the field be assumed constant. Then an expression relating i_q and the mechanical constants can be written by combining equations 1 and 2. Thus

$$i_q = -(Jp + f)p\delta / Kx_d \tag{5}$$

and from equation 9 of the paper

$$i_q = -(Jp + f)p\delta / K(I_d - M_{(a+c)f} i_q) \tag{6}$$

Equation 6 shows that the differential equation of speed as a function of i_q is nonlinear.

The nonlinearity results from the inclusion of the coupling term $M(a+c)f$ between armature and shunt field because of saturation of the main field pole tips. The analogy

is the steady-state analysis of a series motor, wherein the current-speed characteristics are nonlinear. If this coupling can be neglected, and Koenig's analysis shows that it cannot, then $M_{(a+c)f}$ and also x_d'' vanish. Use of this simplification gives

$$i_q = -(Jp+f)p\delta/K\ I_d \tag{7}$$

and

$$I_d = \frac{E_d}{1+T_d p} = E_d \tag{8}$$

so that

$$i_q = -(Jp+f)p\delta/K\ E_d \tag{9}$$

Now from equation 3

$$i_q = (e_q - E_d p\delta)/(pK_c' - pL_a' - r_q) \tag{10}$$

Hence

$$(Jp+f)p\delta/K\ E_d = (e_q - E_d p\delta)/(-pK_c' + pL_a' + r_q) \tag{11}$$

and

$$p\delta = e_q K E_d / [(Jp+f)(r_q + pL_a' - pK_c') + E_d^2 K] \tag{12}$$

The latter equation is the usual relationship which is given between speed and parameters of the motor system when the demagnetizing effect of armature reaction is neglected.

The method of attack which results in equation 12 of the discussion is not valid yet it is equation 12 which is commonly used to represent the d-c motor in the type of control described. It is to be hoped that the method developed by Mr. Koenig will be extended to the study of the solution resulting when equation 6 of the discussion is used for the armature current.

Attention should be drawn to the unusual method developed by Mr. Koenig to measure the mutual coupling between armature and field. To the discusser's knowledge this is the first time that the coupling is considered as an inductance and measured and handled as a simple circuit element. It also is important to note that this coupling is not a constant and that a value must be used consonant with circuit conditions. This is indicated in the author's Figures 5 to 8. It is seen that, depending upon the armature current, this mutual inductance varied from 0.4 to 1.2 henrys. Had an incorrect value of $M_{(a+c)f}$ been chosen, such as 0.4 henry, the value of the time constant T would have been approximately $0.964T_0$. Had $M_{(a+c)f}$ been neglected entirely, a 9 per cent error in time constant of the armature circuit would have resulted.

H. E. Koenig: With reference to Messrs. Brancato and Cybulski's question concerning the M_{af} term in equation 3, and $M_{(a+c)f}$ in equation 9, in the preprint of the paper an error was made in the definition of $M_{(a+c)f}$. In the final printing it is correctly defined as: $M_{(a+c)f} = M_{af}' - M_{cf}$. With this definition of $M_{(a+c)f}$, equation 9 follows from equation 3.

In connection with the question concerning the omission of the $P\gamma_d$ term in equation 6, the nomenclature in Appendix I reveals that γ_d is the per unit direct axis field flux linkages. Hence $P\gamma_d$ would represent the voltage induced in the direct axis or shunt field under transient conditions. The shunt or direct-axis field is certainly not connected in series with the direct axis armature winding. Therefore, the $P\gamma_d$ term should not be included in the expression for e_d in equation 6.

In equation 5, $P\gamma_q$ appears because the commutating field is normally connected in series with the armature and any voltage induced in this field must be included in the expression for the quadrature armature voltage e_q.

To answer the question as to how the eddy current and hysteresis losses are taken into consideration in the evaluation of the constants of the machine, the following will be helpful. Due to the eddy-current and hysteresis losses in a magnetic circuit, the flux cannot be in time phase with the magnetizing current. Since the voltage induced in any winding about the core is proportional to the time rate of change of flux, the voltage cannot be in time quadrature with the magnetizing current. Therefore the effect of eddy currents and hysteresis losses is to decrease the quadrature component and increase the in-phase component of magnetizing current. If a Hayes inductance bridge is used to measure the inductance, both components of current must be balanced before the bridge is completely balanced. Thus the effect of the eddy-current and hysteresis losses is to increase the apparent resistance and decrease the apparent inductance.

Likewise in measuring the mutual coupling, $M_{(a+c)f}$, the eddy-current and hysteresis losses appear in the form of an equivalent resistance and is often referred to as the impurity. From Figure 5, it is seen that the impurity decreases very rapidly with frequency so that at one or two cycles per second the effect of eddy-current and hysteresis losses on the mutual inductance is negligible.

A question has arisen as to the generality of equations developed. The author considers the equations up to and including equations 13 and 14 quite general. From that point on beginning with the section on Prediction of Transient, a special problem of a separately excited d-c dynamo having zero brush shift and equipped with commutating poles was considered to verify the analysis. Equations 13 and 14 then were simplified as permitted by the special problem under consideration.

The author wishes to thank Messrs. Brancato and Cybulski for pointing out the correction in equations 18 and 19. The equations as they stand give the increase in armature and field current respectively under transient conditions. The complete expression for the armature and field current is then the sum of a constant term and the transient term as they have indicated.

With reference to the discussion concerning the measurement of $M_{(a+c)f}$, it must be kept in mind that it is necessary to measure $M_{(a+c)f}$ at or near expected values of armature and field current only because of the saturation of the shunt field pole tips. Since the mutual coupling, $M_{(a+c)f}$, is due chiefly to saturation of the pole tips, there seems to be no other way of obtaining a satisfactory value. However, this does not limit the application of this analysis to low level transients. The d-c value of $M_{(a+c)f}$ can be determined for value of armature current near short-circuit values in the same way it was determined for the values of armature current in Figure 8. Thus, it seems possible to extend the armature current scale shown in Figure 8 to about short-circuit value.

When the constants of the machine are actually measured in this manner and used in the equations developed, some of the effects of hysteresis and eddy-currents are taken into consideration.

Reactance voltage does appear in the equations which have been developed since all flux linkages have been considered.

Maximum Short-Circuit Current of D-C Motors and Generators

AN AIEE COMMITTEE REPORT

THE transient characteristics of d-c generators and motors are matters of considerable interest to those who must know how these machines perform in other than steady-state conditions.

The response of the machine within normal loading is important to the engineer responsible for its utilization. What the time-current characteristics will be under short circuit conditions determines the degree of protection needed and the structure of the machine connections.

The D-C Machinery Subcommittee of the AIEE Rotating Machine Committee have individually and collectively devoted their time and thought to the theories which permit the calculation of transient characteristics.

Paper 50-23, recommended by the AIEE Rotating Machinery Committee and approved by the AIEE Technical Program Committee for presentation at the AIEE Winter General Meeting, January 30-February 3, 1950. Manuscript submitted November 1, 1949; made available for printing November 29, 1949.

This report was prepared by A. G. Darling of the AIEE Subcommittee on D-C Machinery of the AIEE Committee on Rotating Machinery.

Acknowledgment is made of the assistance given by R. G. Rhudy of the General Electric Company, Schenectady, N. Y., in the preparation of this material, and also to the various manufacturers of machine characteristics furnished by Allis-Chalmers Manufacturing Company, General Electric Company, and Westinghouse Electric Corporation.

Individual investigators have advanced methods[1,2,3] for the determination of these characteristics. Where test data have been available, they have been compared with calculated results and modifications made accordingly.

As a first step in assigning parameters to the basic characteristics

r_d' per unit equivalent resistance
l_a' per unit inductance
l_{as}' per unit saturated inductance

several manufacturers have applied the selected theories[2,3] to typical machine constants and have obtained values of r_d' as a first step in the ultimate program.

As progress is made in the determination of inductances, it is expected that similar analysis and confirmation by test will be forthcoming.

While a number of references were tried by which to relate the value of r_d' to the particular machine, those that appeared to have the most usable and sound basis are the product of rated output in kilowatts or horsepower, depending on the machine being a generator or a motor, by its rated speed in, N, revolutions per minute.

Refinement of design, such as types of field windings, appear to have an effect on the r_d'. The principal differentiation, however, seems to be between machines with and without pole face windings.

In order not to confuse the investigator too greatly, it has been felt that for the present, at least, no sharper classifications should be attempted in respect to field windings.

Considerable differences appear in the various voltage, temperature rise, and utilization classes of machines. By utilization is meant such classes as general purpose, National Electrical Manufacturers Association (NEMA) ratings and traction or mill motors.

Figures 1 to 9 inclusive, showing the relation between r_d' and the product of the output (kilowatts or horsepower) and rated speed N, were, accordingly, made to include as broad classifications of design as would preclude an unacceptably wide dissimilarity of r_d'.

In each instance a median line following the trend of the points was drawn. Beside this, guide lines, showing practically the outside limits of r_d', were added.

From these, it is expected that the investigator can be as optimistic or pessimistic as he wishes to be but still stay within the realm of reality. Obviously, if the case warrants it, specific data for specific machines should be obtained from the machine designer.

All values of r_d' assume base (minimum rated) speed and voltage and no load on the machine.

References

1. Transient Characteristics of D-C Motors and Generators, A. T. McClinton, R. Panoff. *AIEE Transactions*, volume 68, part II, 1949, pages 1100–06.

2. Solid Short Circuit of D-C Motors and Generators, T. M. Linville, H. C. Ward, Jr. *AIEE Transactions*, volume 68, part I, 1949, pages 119–24.

3. Current and Torque of D-C Machines on Short Circuit, T. M. Linville. *AIEE Transactions*, volume 65, 1946, pages 956–65.

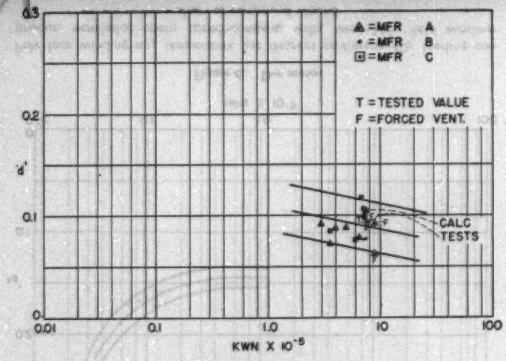

Figure 1. D-c generator

Pole face winding—yes; temperature rise degrees centigrade—40; loading—continuous; ventilation—forced and open; speed—constant; volts, rated—250; field winding—shunt or compound wound

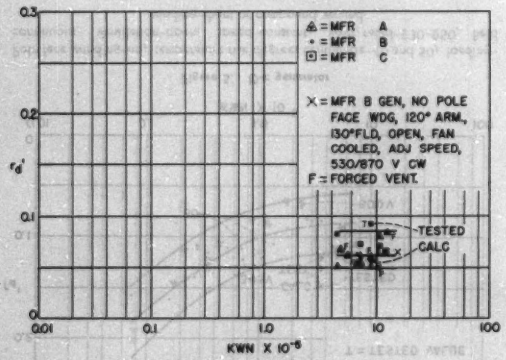

Figure 2. D-c generator

Pole face winding—yes; temperature rise degrees centigrade—40; loading—continuous; ventilation—forced and open; speed—constant; volts, rated—600, 750; field winding—shunt or compound wound

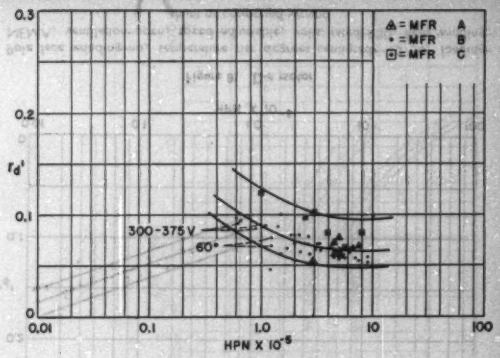

Figure 3. D-c motor

Pole face winding—yes; temperature rise degrees centigrade—40 and 60; loading—continuous; ventilation—forced and open; speed—adjustable; volts, rated—250, 300, 375, 500, 600, 750; field winding—shunt or compound wound

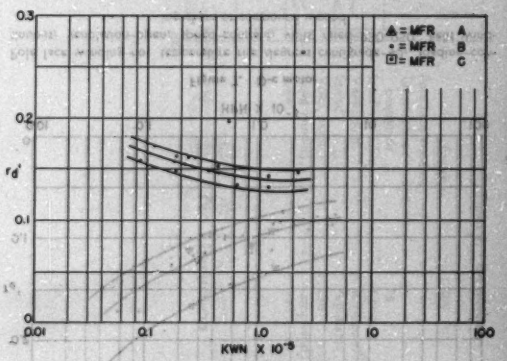

Figure 4. D-c generator

Pole face winding—no; temperature rise degrees centigrade—40; loading—continuous; ventilation—open; speed—constant; volts, rated 120, 125; field winding—shunt or compound wound

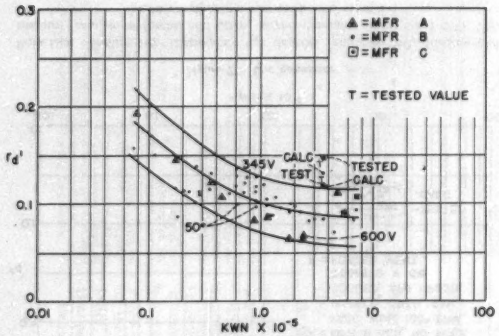

Figure 5. D-c generator

Pole face winding–no; temperature rise degrees centigrade–40 and 50; loading–continuous; ventilation–open; speed–constant; volts, rated–230–250; field winding–shunt or compound wound

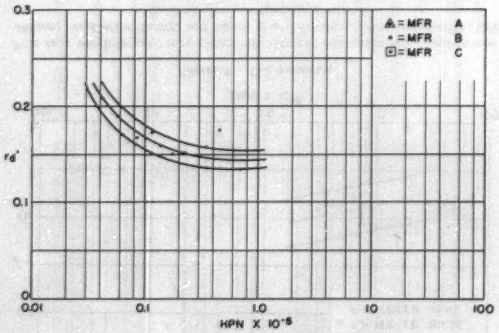

Figure 6. D-c motor

Pole face winding–no; temperature rise degrees centigrade–40; loading–continuous; ventilation–open; speed–constant; volts, rated–115; field winding–shunt or compound wound

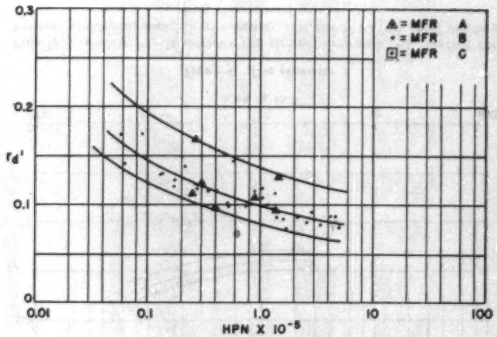

Figure 7. D-c motor

Pole face winding–no; temperature rise degrees centigrade–40; loading–continuous; ventilation–open; speed–constant; volts, rated–230–250; field winding–shunt or compound wound

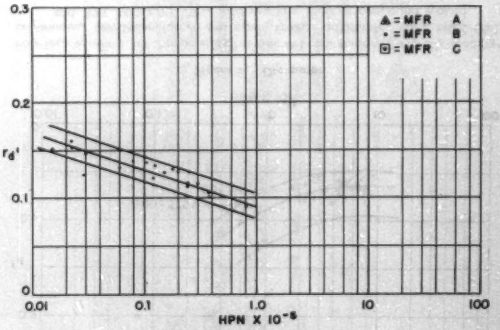

Figure 8. D-c motor

Pole face winding–no; temperature rise degrees centigrade–40/50; loading–NEMA; ventilation–open; speed–adjustable; volts, rated–230; field winding–shunt or compound wound

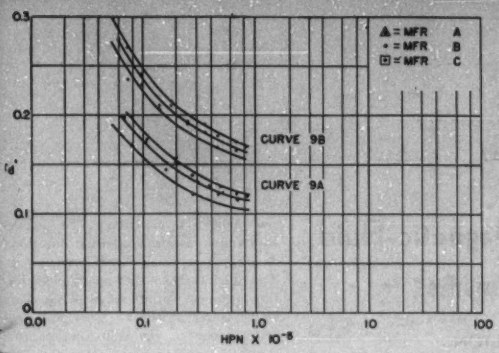

Figure 9. D-c motors

Curve	9A	9B
Pole face winding	No	No
Temperature rise degrees centigrade	75	75
Loading	1 hour	1 hour
Ventilation	Self-closed	Self-closed
Speed	Adjustable	Adjustable
Volts, rated	230	230
Field winding	Compound	Series
Type	Mill	Mill

No Discussion

Characteristics of Some Magnetic-Fluid Clutch Servomechanisms

A. J. PARZIALE
ASSOCIATE AIEE

P. D. TILTON
ASSOCIATE AIEE

A MAGNETIC-FLUID clutch transmits torque through the shear resistance of a mixture of iron powder and fluid. This "magnetic fluid" fills the gap between the faces of the clutch, which also are magnetic poles, and it "freezes" or solidifies when the small particles of powder cling together in the presence of magnetic flux. Torque is controlled smoothly by changing the magnetic field strength to vary the consistency ot the mixture and therefore its mechanical resistance.

In 1948, Jacob Rabinow at the National Bureau of Standards first reported such a clutch.[1] Its advantages for use in servomechanisms are its small size, simplicity, fast action, freedom from wear, smoothness, and a large ratio of output power to control signal power.[1,7,8]

The experimental work described herein is part of a preliminary investigation of magnetic-fluid clutches conducted by the Servomechanisms Laboratory, Massachusetts Institute of Technology under the sponsorship of the United States Air Force, Air Material Command, Wright Field. It is not related to the development of any specific application or apparatus, but seeks only to indicate the basic nature of the clutches and to evaluate their characteristics as servomechanisms components.

Description of Clutches

Figure 1 is an experimental magnetic-fluid clutch designed by the authors from early information published by the National Bureau of Standards.[1] The disk-type design was chosen to provide a means for adjusting the clutch gap clearance and to avoid seals or slip rings. The shafts are vertical, the clutch chamber is an enclosed cavity in the rotor, and the coil to energize the magnetic circuit is contained in a concentric stator out of which the flux passes radially to and from the rotor through annular air gaps. The clutch gap is adjusted by the rotor spacing screws which determine the space between the two parts of the rotor; the centering nuts on the disk shaft are used to equalize the gaps between the disk and the rotor. This experimental clutch is considerably larger, more complex and less efficient than is necessary to develop the same amount of torque.

Figure 2 is a cross-section of a clutch made by the Raymond Engineering Laboratory, model *731*. Although designed for laboratory use and investigation, it illustrates the simplification which is possible in clutches for commercial use, when experimental flexibility is not the objective. This clutch was intended to produce rapid response and, therefore, is a disk type with low output shaft inertia Its coils are wound for high impedance and dissipate about ten watts. A small field time constant can still be achieved by use of appropriate electronic amplifier output stages.

Table I is a comparative summary of important design data for the two clutches. Except where noted, the experimental clutch was used with a 0.032-inch clearance gap. The Raymond clutch had a gap of 0.015 inch for all studies.

A single clutch can exert torque only in the direction of its drive motor. One convenient method of obtaining a reversible servomotor is the arrangement shown in Figure 3. The continuously-rotating prime mover drives two clutches in opposite directions so that the net torque on the output shaft is equal to the difference of the opposing torques of the two individual clutches. The double clutch unit can drive in either direction, depending on which clutch is energized. The clutch coils are the balanced load for the push-pull output stage of an electronic power amplifier. This push-pull arrangement of the coils and of the clutches improves the linearity of the torque-current characteristic, as shown in Figure 4. When the bias current in each coil is properly adjusted, the output torque of the 2-clutch servomotor is proportional in the steady-state, to the differential current in the field coil circuit, and the region of very low gain (small slope) near the origin is eliminated. Improved linearity is obtained by sacrificing considerable energy, because the quiescent coil current results in opposing clutch torques at zero signal (differential coil current) that are from three to five times as large as the residual drag.

Steady-State Clutch Characteristics

The static torque-current curves for single clutches are shown in Figure 5. These curves show complete hysteresis loops, and indicate that the maximum torque deviations attributable to hysteresis amount to about 150 inch-ounces or approximately 12 per cent of rated torque for the experimental model, and almost 200 inch-ounces or 16 per cent of rated torque in the case of the Raymond model *731*. The clutch torque as a function of the coil current depends upon the reluctance of the magnetic circuit. The total reluctance is composed of the reluctance of the iron-oil gap and the re-

Paper 50-24, recommended by the AIEE Feedback-Control Systems Committee for presentation at the AIEE Winter General Meeting, New York, N. Y., January 30-February 3, 1950. Manuscript submitted May 25, 1949; made available for printing December 6, 1949.

A. J. PARZIALE is with the United States Air Force Cambridge Research Laboratory, Cambridge, Mass., and P. D. TILTON is with the Vickers Electric Division Vickers, Inc., St. Louis, Mo.

Acknowledgment is given for material taken from the thesis[9] of A. J. Parziale, submitted in partial fulfillment of the degree of Master of Science, Massachusetts Institute of Technology 1949, and for valuable stimulation from the parallel thesis[9] of C. A. Cibelius, and from the staff of the Raymond Engineering Laboratory, Middletown, Conn.

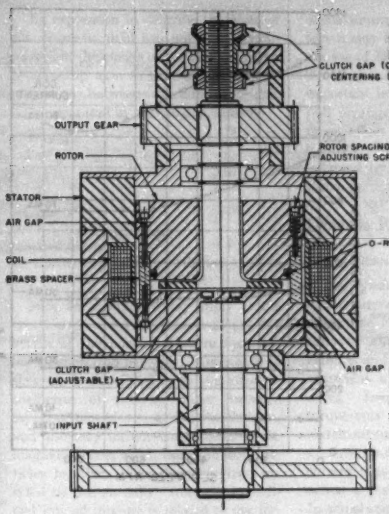

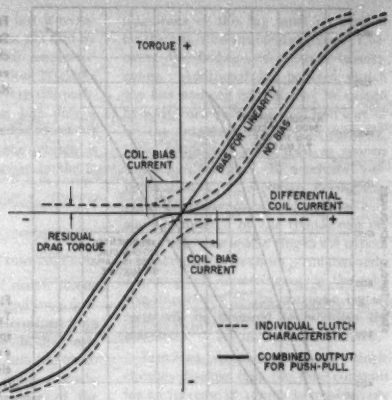

Figure 1 (left). Cross-section of experimental magnetic-fluid clutch

Figure 4 (above). Torque characteristics of 2-clutch servomotor

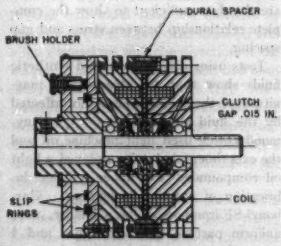

Figure 2. Cross-section of Raymond Engineering Laboratory model 731 magnetic-fluid clutch

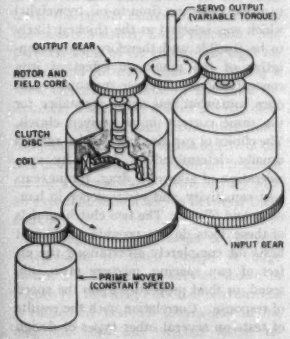

Figure 3. Schematic of push-pull arrangement for 2-clutch servomotor

luctance of the field core as determined by the material, length, and relative flux densities of the various core sections. If, as presently believed, the magnetic fluid has almost constant permeability,[1] a clutch with a large gap and a short iron core will tend to have flux density more nearly proportional to the magnetomotive force and over a wider range than if there is more iron and less gap. The shape of the magnetization curve for a magnetic-fluid clutch will be characterized by the magnetization curve for the iron core, but it is more linear when the gap contributes a larger portion of total reluctance. Although data of flux density versus magnetomotive force for the iron-oil mixture are difficult to obtain, the average per-

Table I. Clutch Design Data

	Experimental		Raymond 731
Dimensional			
Over-all length, inches	9 (approx.)	.....	3 3/4
Over-all diameter, inches	3 1/2	.....	3 3/4
Disk diameter, inches	2 1/2	.....	2 19/32
Disk thickness, inches	1/8	.....	1/16
Clutch gap clearance, inches	0.012 to 0.100	.....	0.015
Clutch gap effective area, square inches	8.24	.....	6.70
Clutch gap mean radius, inches	.928	.....	.935
Inertia, ounce inches squared (single clutch)	3.5	.....	1.3
Magnetic			
Core material	cold rolled steel	.....	SAE 1112
Disk material	cold rolled steel	.....	cold rolled steel
Magnetic fluid	Carbonyl E and special oil, 9/1 by weight	.....	Carbonyl E and light machine oil, 7/1 plus 1 per cent Antarox B-100 wetting agent
Air gap, inches	0.012 (radial)	.....	none
Coil, American wire gauge wire size	Number 32	.....	Number 41
Coil, number of turns	4,650	.....	4,800 (approx.)
Coil, resistance, ohms	570	.....	9,400
Coil, inductance, henries	122	.....	(no data)
Rating			
Torque, continuous, inch-pound	78(0.032-inch gap)	.....	35
Torque, maximum, inch-pound	145(0.020-inch gap)	.....	75
Coil current, ma., cont. torque	90	.....	17
Coil current, ma., max. torque	130	.....	30
Speed, rpm	1,000	.....	1,000
Power, hp (at 1,000 rpm)			
continuous	1.2	.....	.36
maximum	2.3	.....	1.2
Constants			
Torque/shear-stress factor in-oz/lb/sq. in.	122.4	.....	102.5
Torque/current sensitivity in-oz/ma	18	.....	41
Torque/inertia ratio (max.) second^{-2}	2.5×10^4	.....	3.5×10^4
Torque^2/inertia ratio (max.) in-lb-second^{-2}	3.7×10^7	.....	2.7×10^7
Power amplification (nominal, for continuous rating at 1,000 rpm)	132	.....	430

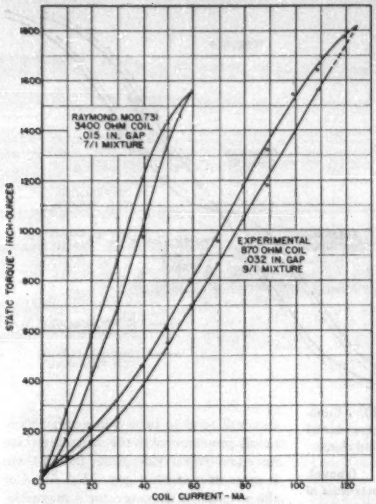

Figure 5 (left). Static torque characteristics of experimental and Raymond 731 clutches

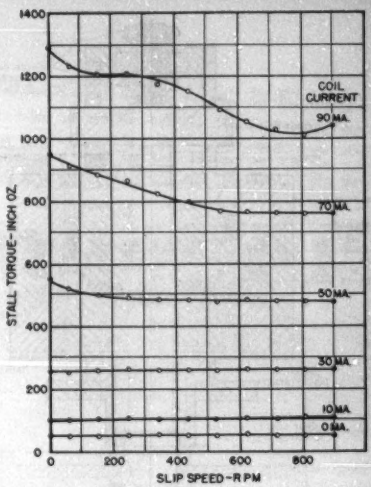

Figure 7 (right). Typical torque-speed curves, experimental clutch with 0.032-inch gap and 9/1 mixture (by weight) of Carbonyl E iron powder in special oil

meability of thick mixtures (9/1 by weight) has been reported as ranging from four to eight times that of air.[1,9]

The shear resistance of the iron-oil mixture as a function of magnetic field strength is the fundamental property of importance in the design of controllable clutches. Clutch torque is the product of the average shear stress in the fluid and a geometric factor that is equal to the active area of the clutch face times its mean effective radius. The magnetic field strength is determined by the design and excitation of the iron core, as noted previously. Its variation to control the clutch is obtained usually by varying the core magnetomotive force due to the coil current, although mechanical motion to alter gap spacing or the position of a permanent magnet might be used. The basic relationship of the magnetic fluid is obtained easily from torque versus current curves if the geometric factor can be evaluated for the design and the magnetization curve, flux density versus current, of the clutch is known.

Figure 6 gives curves of shear stress versus flux density for several different clutch gaps. The data were taken in the experimental clutch model for which the flux densities at several values of coil current and different gap spacings had been measured by means of a ballistic galvanometer connected to a search coil which was placed around the periphery of the disk to link the flux. For these curves, the shear stress varies as a power of flux density. The exponent ranges from 1.3 for 0.060-inch gap to 2.0 for a 0.045-inch gap. The other exponents are: 1.5 for a 0.020-inch gap and 1.7 for a 0.032-inch gap. Almost any exponent from about 1.4 to 1.7 can be used to fit all curves with an accuracy of about ten per cent if the scale factor used to match experimental data is based on a point above 6,000 gauss. Within the range of flux densities covered by Figure 6, the shear stress, and hence clutch torque, were apparently still increasing as the flux density increased. The reasons for shear stress variation with different gaps and the same flux density are not clear, nor are the data sufficient to show the complete relationship between stress and gap spacing.

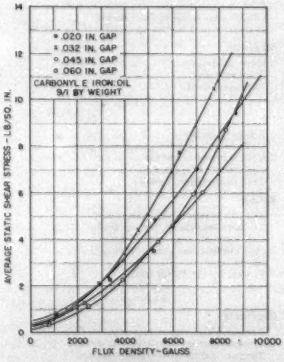

Figure 6. Static shear properties of magnetic fluid

Tests using different oils and synthetic fluids show that the steady-state magnitude of the shear stress is not affected by the fluid characteristics. The Raymond clutch used light machine oil and the experimental clutch employed a light oil compounded for upper-cylinder lubrication of automobile engines. Carbonyl SF iron powder has a smaller, more uniform particle size (between 1 and 4 microns) and gave slightly less shear resistance than the Carbonyl E, which has a wider range of particle size (3 to 12 microns). The data of Figure 6 apply only to a 9-to-1 mixture (iron-to-oil, by weight) which was selected as the thickest likely to be feasible and therefore is representative of the maximum effect of iron concentration. Thinner mixtures produce somewhat less shear resistance for the same current in any given clutch. The choice of gap size and iron/oil ratio is usually determined in design by consideration of allowable drag, torque/current sensitivity and convenience in handling and filling. The two clutch models of these tests do not provide a sufficient basis for completely ascertaining the effect of gap spacing, mixture ratio, slip speed, or fluid properties upon the speed of response. Correlation with the results of tests on several other types of design will be required before general design data can be established.

An expression to describe the state of the magnetic fluid has not been formulated, but the curves of Figure 6 suggest a relationship akin to that of the force of attraction between extended magnetic poles separated by a small gap, namely

$$F = c\frac{B^2A}{\mu} \tag{1}$$

where

F = force
B = flux density in the gap
A = area of the gap
μ = relative permeability of the gap medium
c = a constant of proportionality

Such an expression may apply to the creation of transverse shear stresses by the action of the normal pressure force, F, on the solid iron particles. Resistance to shearing is developed from the effective coefficient of friction, either between layers of particles or at the clutch faces, and also may include components of the magnetic forces which bind the iron particles together. The shearing stress exerted by the partially "frozen" or solidified iron-oil mixture is related to the formation of linear chains, each consisting of several individual spherical particles of the iron powder, which cling together and align themselves with the direction of the magnetic field. This formation has been observed microscopically with very "wet" mixtures in fairly weak fields and without relative motion between pole faces, but these observations alone cannot produce a sufficiently definite understanding of the phenomenon.

The observed variation of shear stress as the flux density raised to some power between the first and second indicates that the square-law expression suggested before is not adequate even if allowances are made for extremes in the variability of the friction coefficient. At the same time, the results cannot be explained on the basis of a strictly linear function. Apparently some of the chains pull tight together and saturate, each one adding a fixed incremental force to the shear resistance, while other chains are not completely saturated and contribute force components that vary as the square of the flux density. Thus, the resultant function for the total resistance seems to vary with an exponent somewhere in between these extremes.

For single clutches, torque is virtually independent of speed except at large values of exciting current, as shown in Figure 7. The drag torque at zero current is caused by residual magnetism in the magnetic core and viscous shear resistance of the fluid mixture. It is normally of the order of three to five per cent of maximum clutch torque, but if necessary it may be held below one per cent by the use of large gaps and thin mixtures.[1] The exact magnitude of the drag is seldom important in servos employing the push-pull arrangement, since it has only a minor effect on the bias adjustment for linearity. The drag of one clutch is balanced by that of the other in the 2-clutch servomotor.

Dynamic Response

Shear Phenomenon of Magnetic Fluid

The dynamic relation of clutch torque to coil current is characterized by a first-order time lag. This is determined from tests of the response of both single clutches and the push-pull servomotor to sinusoidal and transient input disturbances. Instantaneous measure of the torque was obtained by restraining the clutch output shaft in a fixture containing a conventional strain gage bridge. Coil current was measured by the voltage across a resistor in series with the coil. In actual application, where the time constant which relates torque to voltage is relevant, the voltage-to-current time constant also must be considered. It has been stated in reference 2, page 328, that the actual field time constant for a small generator excited by a vacuum tube may be in error by as much as a factor of six if effects of eddy currents, shorted turns, and so forth are ignored.

Figure 8 shows the attenuation and phase response of stall torque as a function of coil current. This figure applies to two experimental clutches in push-pull, with a sinusoidal input signal of constant amplitude and variable frequency. The shape of the curve indicates that the transfer function of the double clutch actuator may be given as

$$\frac{T(s)}{I(s)} = \frac{K_c}{T_c s+1} \tag{2}$$

where $T(s)/I(s)$ is the Laplace notation[4] for the torque-to-current transfer function in terms of the complex variable, s, K_c is the steady-state torque-current sensitivity of the clutches and T_c is the time constant of response. From Figure 8 the break frequency of the curve's asymptotes at about two cycles per second indicates a clutch time constant, T_c, of 70 to 80 milliseconds for the experimental clutch model.

The time constant for the torque-to-current response of a magnetic-fluid clutch may possibly be due to several effects other than a lag in the magnetic fluid itself due to the finite time required for the particles to form into chains. The magnitude of this lag must be verified for there is considerable disagreement between the findings of different investigators. Additional lag between clutch gap flux and coil current may be caused by eddy currents in the solid iron core or by the transformer action of nonmagnetic, conducting rings used as spacers which link the flux. In a private communication, C. K. Stedman, Boeing Airplane Company, calculated the time constant introduced by the transformer action of the brass spacer ring in the experimental clutch to be about 80 milliseconds. Experimental determination of the relative importance of the magnetic lag effects will be required to establish the magnitude of lag in the mixture itself.

Transient response tests on single clutches disclose that the time constant for an increase of torque is considerably longer than that for a decrease. With the experimental clutch, the time constant for torque release was about 80 milliseconds and that of build-up about 120 milliseconds. The discrepancy between these values and that obtained from sinusoidal tests of the push-pull arrangement cannot be fully explained. The Raymond model *731* clutch also showed a difference between build-up and release time constants, with values of about 20 milliseconds for release and about 40 milliseconds for build-up, but no comparison was attempted with this type of clutch in the push-pull arrangement.

An explanation of the difference between the time constants for build-up and release of torque in response to step-functions of current lies in the difference in the creation and release of shear resistance in the magnetic fluid. The physical forces acting on the particles are those of: attraction due to the presence of a magnetic field, which forms chains to give minimum reluctance flux paths; a variety of forces tending to disrupt or disturb the chains, among which may be included centrifugal forces, frictional, or other forces of mechanical contact due to particle density and relative motion between the clutch, faces, and fluid forces due to film strength, surface tension, and viscosity. Torque is developed at a rate depending on the speed with which the particles form into chains, but the release time is governed by the magnitude and speed of action of the various disruptive forces. There is no reason to suppose that both actions will take place with equal rapidity. The build-up time of the magnetic flux is equal to the release time, so this factor is insignificant when considering the difference between build-up and release times of the torque.

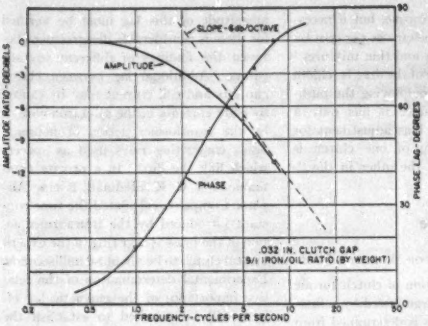

Figure 8. Torque/current frequency response of experimental 2-clutch servomotor

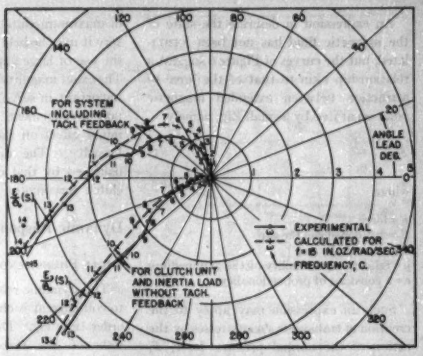

Figure 10. Inverse transfer function loci used to determine damping coefficient of 2-clutch servomotor

The faster response of the Raymond clutch may be attributed to: a smaller magnetic core; the use of a smaller gap clearance; a somewhat thinner mixture; and the addition of a wetting agent. The small core of the model *731* reduces eddy current lags. The smaller gap and more fluid mixture cause a faster action because of better mixing and fluid film conditions for quick motion of the iron particles in forming chains. Further investigation will be required to verify the causes of the time lag and to discover how the design factors influence it.

Double-Clutch Servomotor

The shear torque of a single magnetic-fluid clutch is independent of speed of rotation of the output, except at high values of current, as shown in Figure 6. This torque-speed characteristic is similar to that of other servomotors such as 2-phase a-c torque motors, which, when idealized, have no damping (decrease in torque output with increase in speed). With pure inertia loads such devices produce accelerations proportional to the applied signal. The servomotor characteristic is then described as a double integration, since the instantaneous position of the inertia shaft θ_o, is nearly proportional to a double integration with respect to time of the input signal.

By using equation 2, and equating applied and load torques, the transfer function for the output position of a single clutch and inertia load, J, may be expressed as

$$\frac{\theta_o(s)}{I(s)} = \frac{K_c}{Js^2(T_c s+1)} \tag{3}$$

Since the magnetic-fluid clutch never has less than 180 degrees of phase shift (a torque source), its use in a closed-loop position system will result in an unstable system unless some form or compensation is used.

The clutch servomotor using two experimental clutches in push-pull exhibits a small amount of damping in its performance.

This damping was found insignificant in stabilizing the closed-loop system, but it leads to a revised transfer function for a double clutch actuator, which is contrasted with that for a single clutch.

$$\frac{\theta_o(s)}{I(s)} = \frac{K_c/f}{s(J/fs+1)(T_c s+1)} \tag{4}$$

where f is the effective coefficient of damping. For ease in making analytical comparisons, it is convenient to treat the damping as viscous, although its source lies in many effects, some of which are more coulomb than viscous. Equation 4 differs from equation 2 which is applicable in the case of the 2-clutch actuator only when the output shaft is restrained, that is, no damping because of no output motion.

System Performance

The effective damping which the push-pull clutch unit introduces into the system was not measured directly. The effective value for the coefficient of damping, f, in a servomechanism system was determined from a comparison of calculated and measured data for a closed-loop positional response to sinusoidal inputs.

The basic servomechanism system was comprised of a standard synchro data system, a-c amplifier, full-wave demodulator, push-pull d-c power amplifier, the tachometer feed-back channel, and the clutch actuator, as shown in the block diagram of Figure 9. In this system, the time constant for the demodulator, T_d, was less than one millisecond and that for the power amplifier and clutch coil circuit, T_a, was about four milliseconds. These two time constants were small enough in comparison with the others to be neglected. The linear equations describing the system are given in the Appendix. Table II gives numerical values for the different system constants used in the various tests to be described.

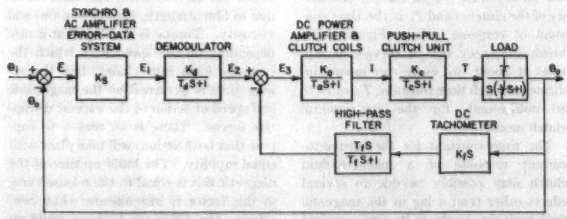

Figure 9. Block diagram of servomechanism system for testing magnetic-fluid clutches

Table II. Summary of Numerical Data for Closed-Loop System Response

	Linear		Optimum Conditions			
	Experimental Model (Curves, Figure 10)		Experimental Model (Curves, Figure 11)		Raymond 731 (Curves, Figure 12)	
	Calculated	Measured	Without Filter	With Filter	Without Filter	With Filter
Performance Data						
Torque constant, K_T, in-oz/rad	1,225.	1,230.	4,000.	4,000.	6,350.	3,770
Velocity constant, K_v, rad/sec/rad	21.	18.	37.	866.	81.	1,375
Peak amplitude ratio, M_p, dimensionless	0.8	1.0	1.1	1.3	1.8	1.7
Frequency of last peak (before cut-off) ω_r, cycles per second	10.	9.5	13.	12.	37.	32.
Lumped Gain Values						
Direct, K_a K_v/f, rad/sec/volt	*	12.1	22.	22.	**	**
Feedback, K_f, volts/rad/sec	*	0.63.	1.05	1.05	0.36	0.36
Open system, $K_v K_a$, volts/rad	*	13.	28.	28.	28.	24.

*Not calculated, use measured values.

**Indeterminate, since no value obtained for f.

The experimental data to evaluate damping were taken with the experimental clutch servomotor and direct tachometer feedback for stabilization. The gain constants and coil bias current were adjusted for linear, stable operation to provide valid comparison with curves based on linear theory and calculated from equations 14 and 15 of the Appendix. Response data were calculated for a system inertia of 98 ounce-inches-squared for the experimental clutch, a value for the clutch time constant, T_c, of 0.08 second, and measured gain settings as given in Table II. Several values of the damping, f, were tried in the calculations, of which 15 inch-ounces per radian per second matches the experimental data well, as shown in Figure 10. No evaluation of the damping in the Raymond clutch system was attempted.

One set of the curves of Figure 10 applies to the output/error transfer function of the system and includes tachometer feedback but without the high-pass filter shown in Figure 9. The other set of curves in Figure 10 has been modified to exclude the tachometer effect, and therefore represents the inverse transfer function for the direct-path elements, of which only the clutch actuator and the load contribute dynamic effects in the range of frequencies considered. The J/f time constant for the clutch and load is about 0.017 second and its effect upon the system response is negligible below 10 cycles per second. The damping value of 15 inch-ounces per radian per second is less than one-tenth the effective feed-back damping from the tachometer.

Adjustment of the gain factors of the experimental system with tachometer feedback for optimum servo performance gave a greatly improved closed-loop positional response, shown in Figure 11. The optimum conditions were taken to be those permitting the highest cut-off frequency, ω_r, and the largest amount of system gain with a peak amplitude ratio, M_p, of between one and two. The output/input response is only slightly attenuated at about 13 cycles per second where cut-off occurs with a slope of 18 decibels per octave that is characteristic of a third-order system. For the optimum system gain adjustment, the torque constant, K_T, is 4,000 inch-ounces per radian and the velocity constant, K_v, is 37 radians per second per radian. The former constant is an index of the system position stiffness. The latter is a figure of merit defined as the steady-state velocity per unit of displacement error, ϵ, required to follow that velocity. Both relations are derived in the Appendix.

The velocity constant, K_v, may be increased considerably by the addition of a conventional high-pass filter in the feed-back loop.[8] The effect of the high-pass filter is apparent from a comparison of the expressions defining the velocity constant with and without the filter, equations 17 and 19 in the Appendix. These indicate a factor of increase of about 20 for the clutch system with the numerical gain values for optimum response in Table II. Experimentally, the addition of the filter increased K_v by a factor of 23.4 for the experimental clutch and 17.1 for the Raymond 731 clutch.

The addition of the high-pass filter causes a higher system gain factor in the case of a steady-velocity input. Ordinarily, the voltage to the power amplifier,

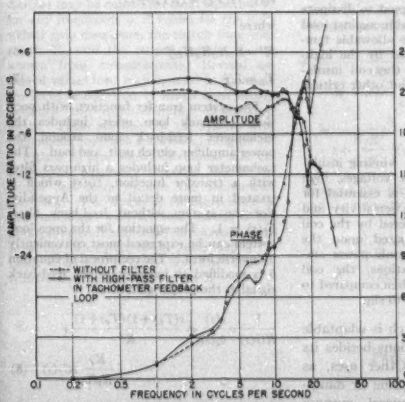

Figure 11. Closed-loop position response of servomechanism system with experimental 2-clutch servomotor

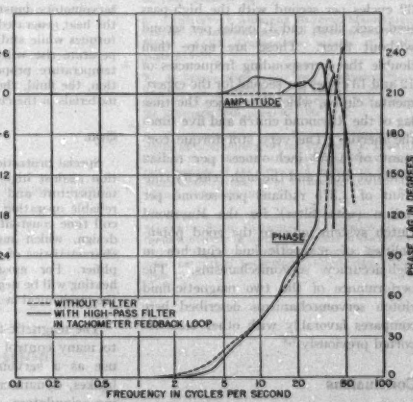

Figure 12. Closed-loop position response of system using Raymond 731 clutches

E_a in Figure 9, is smaller than the error voltage (E_e) by the amount of the tachometer feed-back voltage. Reduction of the latter enables a smaller system displacement error, ϵ, to generate the same amount of torque required at the output. The high-pass filter is capacitor-coupled, and at low frequencies it greatly attenuates the steady d-c voltage from the tachometer at the constant velocity of the system. In the case of a steady-state velocity, then, the torque per unit error (gain) is greater with the filter, than without it, and K_v is increased. The filter still permits the stabilizing feed-back signal to be introduced into the loop under transient or oscillatory conditions when damping is important.

The frequency response is not affected greatly by inclusion of the filter, as shown in Figure 11, although there is some augmentation of the amplitude ratio at low frequencies. For both clutch systems the time constant of the filter, T_f, was about 120 milliseconds to give a fairly low break frequency of 1.33 cycles per second. Above this frequency, virtually all of the stabilizing influence of the tachometer feed-back signal is retained.

The closed-loop response of the system using Raymond *731* clutches is given in Figure 12. These response curves reflect the smaller time constant noted previously for this clutch. The velocity and stiffness constants are considerably larger because the lower system inertia of about 20 ounce inches-squared with this model permitted more direct gain and less tachometer feed-back gain for the same relative stability. The frequencies of the last amplitude peak before cut-off are about 32 cycles per second with the high-pass feed-back filter, and 37 cycles per second without filter. These are more than double the corresponding frequencies of 12 and 13 cycles per second for the experimental clutch, which has twice the time lag of the Raymond clutch and five times the inertia. The very stiff torque constant of 6,350 inch-ounces per radian (without filter) and the high velocity constant of 1,375 radians per second per radian (with filter) for the Raymond clutch system indicate the good potentialities of magnetic-fluid clutches in high-accuracy servomechanisms. The performance of the two magnetic-fluid clutch servomechanisms described here compares favorably with other tests reported previously.[7,8]

Conclusions

Normal servomechanism design practice and familiar compensation techniques are applicable to systems using magnetic-fluid clutch servomotors. Optimum clutch design depends upon the nature of the system in which it is to be used. The speed of response of any particular clutch depends upon the clutch's size and design. It can be determined best by construction and test, although rough estimates from similar clutches may be made. Continued investigation with clutches of different sizes and configurations will establish the influence of design variables upon dynamic performance.

Among the several service limitations which must be overcome by further development, the following have been noted in these tests:

Magnetic Fluid

The iron-oil mixture must be able to withstand operation at temperatures as high as several hundred degrees Fahrenheit for long periods of time. The fluid propreties must prevent packing or settling of the iron powder into a dense, hard-packed mass during periods of storage or inactivity. This condition may be alleviated by the use of a wetting agent and a "warm-up" period of operation to stir the mixture.

Seals

Seals or labyrinth design to prevent loss of fluid must have long-life and be able to withstand the high temperatures encountered and abrasion from the iron powder. Face-type seals with hard graphite elements will probably surpass the conventional shaft or bearing seals under the severe service conditions usually imposed by magnetic-fluid clutches.

Heat Dissipation

Magnetic-fluid clutches, like some other servomotors, must be designed to dissipate the heat generated by working against load torques while stalled. The allowable temperature rise will be limited by the high-temperature properties of the coil insulation, the fluid, the seals, and other critical materials in the clutch.

Coil

Special protection of the winding insulation against high transient voltages, high temperature and abrasion is essential for reliable operation. Clutch sensitivity and coil time constant are affected by the coil design, which must be based upon the characteristics of the electronic power amplifier. For most applications, the coil heating will be negligible when compared to the mechanical heating due to slip.

The magnetic-fluid clutch is adaptable to many control applications besides its use as a servomotor. Other uses, as brakes, dynamometers, spring or damping simulators, and general purpose torque-loading devices for electromechanical mock-ups,[6] suggest themselves.

Appendix

The following equations which describe a servomechanism employing magnetic-fluid clutches are derived in terms of Laplace notation. A complete treatment of this method is given in references 2, 3, and 4.

General Transfer Function for the Complete System Employing Two Clutches in Push-Pull

The system transfer function is developed from the transfer functions of the individual components of the block diagram. An experimental determination of the dynamic response of a magnetic-fluid clutch indicates the transfer function given in equation 2

$$\frac{T(s)}{I(s)} = \frac{K_c}{T_c s+1} \tag{2}$$

where $T(s)$ is the Laplace transform of the clutch output torque, $I(s)$ is the transform of coil current, s is the Laplace complex variable, K_c is the steady-state torque-current sensitivity, and T_c is a characteristic time constant of the clutch response.

The load dynamics for the 2-clutch servomotor are taken into account by using equation 2 to equate the applied torque to the inertia and damping load torques, which gives

$$\frac{\theta_o(s)}{I(s)} = \frac{K_c/f}{s(T_c s+1)(J/f\, s+1)} \tag{4}$$

where J is the load inertia and f is the coefficient of the equivalent damping which is characteristic of the push-pull clutch arrangement, but is not noticeable in single clutches. The inductance-reactance time constant is considered negligible.

Incorporating the amplifier and demodulator gain factors, K_a and K_d respectively, in equation 4 gives the transfer function of the direct path, which omits tachometer and position feedback.

$$\frac{\theta_o(s)}{\epsilon(s)} = \frac{K'}{s(T_L s+1)(T_c s+1)} \tag{5}$$

where

$$K' = K_c K_a K_d K_s/f \tag{6}$$

$$T_L = J/f \tag{7}$$

The system transfer function, with position feed-back loop open, includes the tachometer feed-back loop around the power amplifier, clutch unit, and load. The tachometer loop includes a high-pass filter with a transfer function, $G_f(s)$ which is treated in more detail in the Appendix. For the system without feed-back filter, $G_f(s) = 1$. The equation for the open loop system can be expressed most conveniently in inverse form. The reciprocal of equation 5 is modified to incorporate the feed-back signal at the proper gain level.

$$\frac{1}{KG(s)} = \frac{\epsilon(s)}{\theta_o(s)} = \frac{s(T_L s+1)(T_c s+1)}{K'} + \frac{K_f}{K_a K_d} sG_f(s) \tag{8}$$

The closed loop response equation for the system described by the block diagram, Figure 9, may be found from the relation

$$\frac{\theta_o(s)}{\theta_i(s)}=\frac{KG(s)}{1+KG(s)}=\frac{1}{\dfrac{\epsilon(s)}{\theta_o(s)}+1} \tag{9}$$

$$\frac{\theta_o(s)}{\theta_i(s)}=\frac{1}{\dfrac{1}{K'}s(T_Ls+1)(T_es+1)+\dfrac{K_f}{K_sK_d}sG_f(s)+1} \tag{10}$$

Inverse Transfer Functions Used for Evaluating System Damping by Comparison with Experimental Result

The effective damping of the 2-clutch servomotor was evaluated by a comparison of experimental results with theoretical dynamic behavior of the system. This damping is associated with elements in the inner loop of the block diagram of Figure 9. For convenience, all of the damping is postulated as being associated with the load. This permits the concept of an idealized clutch and a single, lumped value for the coefficient, f, which is included in the load time constant, T_L, and the gain factor, K', in equations 6 and 7.

The experimental data were taken with the tachometer loop closed but without the filter, and the position loop open. This configuration is represented by equation 8 with $G_f(s)$ equal to unity. For response to a sinusoidally varying signal of constant amplitude and variable frequency the transform equation can be restated in terms of the real time frequency, ω. This transformation of variable in the Laplace method consists of replacing the complex variable s, by the complex frequency $j\omega$. Equation 8, letting $s \rightarrow j\omega$ and $G_f(s)=1$, then represents the system for the test conditions.

$$\frac{1}{KG(j\omega)}=\frac{(j\omega)[1+j\omega T_L][1+j\omega T_e]}{K_cK_aK_dK_s/f}+(j\omega)\frac{K_f}{K_sK_d} \tag{11}$$

The inverse transfer function vector, $1/KG(j\omega)$ may be calculated from equation 11 for any frequency, ω, if values for the individual gain constants, the clutch time constant, T_c, and the output inertia, J, are known from measurements. Several assumed values for f may be tried to calculate the locus of equation 11 which most nearly matches the experimentally determined locus. These two loci for the system with tachometer feedback are shown in Figure 10.

Figure 10 also shows calculated and experimental frequency response loci of the clutch and load without the tachometer feedback. The dynamic characteristics of the clutch and load are components of the greatest interest and these components comprise the direct path of the inner loop of the block diagram, Figure 9. The inverse transfer function for this path is

$$\frac{E_a(j\omega)}{\theta_o(j\omega)}=\frac{(j\omega)[1+j\omega T_L][1+j\omega T_e]}{K_cK_a/f} \tag{12}$$

Equation 12 is derived from equation 11 by a scale change to compensate for removal of the gain factor, K_sK_d, and a vector subtraction of the tachometer feedback term, $(j\omega)K_f$. Values for these changes can be evaluated readily from the experimental conditions. Calculation of the locus of equation 12 and revision of the experimental data for the same gain change and subtraction of tachometer feedback give the curves of Figure 10 for the clutch and load.

System Torque, or Stiffness Constant K_T

The stiffness constant, K_T, is the torque required in the steady state at the output for one radian of output angular displacement (error). It is the product of the sensitivities of all the feedforward components, that is, total direct gain contributing to torque.

$$K_T=K_sK_dK_aK_c\ \frac{\text{inch-ounce}}{\text{radians}} \tag{13}$$

Velocity Figure of Merit K_v, and Effect of High-Pass Filter in Tachometer Loop

A convenient criterion of the ability of positional servomechanisms to follow a steady velocity with minimum error is the velocity constant, K_v. This figure of merit is defined as the steady-state velocity per unit of displacement error. It is specified mathematically from the system transfer function, $KG(s)$.

$$K_v=\text{Lim}_{s\rightarrow 0}[sKG(s)]=\text{Lim}_{s\rightarrow 0}\left[\frac{s\theta_o(s)}{\epsilon(s)}\right] \tag{14}$$

From the inverse transfer function of equation 8

$$\frac{1}{K_v}=\left[\frac{(T_Ls+1)(T_es+1)}{K'}+\frac{K_f}{K_sK_d}\,G_f(s)\right]_{s\rightarrow 0} \tag{15}$$

where $G_f(s)$ denotes the transfer function of the high-pass filter.

$$K_v=\frac{1}{\dfrac{1}{K'}+\dfrac{K_f}{K_sK_d}\,[G_f(s)]_{s\rightarrow 0}}=\frac{K'}{1+\dfrac{K_fK'}{K_sK_d}\,[G_f(s)]_{s\rightarrow 0}} \tag{16}$$

Without the filter, $G_f(s)$ is equal to unity, and the velocity constant is

$$K_v=\frac{1}{\dfrac{1}{K'}+\dfrac{K_f}{K_sK_d}}=\frac{K_T}{f+\dfrac{K_fK_T}{K_sK_d}} \tag{17}$$

The effect of the filter function $G_f(s)$ or $G_f(j\omega)$ upon K_v is evident if it is considered in equation 16.

For a high-pass filter

$$G_f(j\omega)=\frac{j\omega T_f}{1+j\omega T_f} \tag{18}$$

T_f is the resistance-capacitance time constant of the filter circuit. The limit $s \rightarrow 0$ in equation 16 corresponds to $\omega \rightarrow 0$ in equation 18, for which $G_f(\omega) \rightarrow 0$.

The value of K_v in the limit of equation 16 is

$$K_v=K'=\frac{K_T}{f} \tag{19}$$

The increase in K_v at low frequencies (where $\omega << 1/T_f$) may be noted by comparing equations 17 and 19. At high frequencies, where $\omega >> 1/T_f$, the function $G_f(j\omega) \rightarrow 1$, and the full effect of the tachometer stabilizing signal is retained. The filter does not affect the stiffness, K_T, nor does it greatly alter the system transfer function.

References

1. The Magnetic-Fluid Clutch, *Report Number 1213*, United States Department of Commerce, National Bureau of Standards (Washington, D. C.), April 1948. Also, *Technical News Bulletin*, United States Department of Commerce, National Bureau of Standards (Washington, D. C.), volume 32, May 1948, page 54.

2. Principles of Servomechanisms, G. S. Brown, D. P. Campbell. John Wiley and Sons, New York, N. Y., 1948.

3. Analysis and Synthesis of Linear Servomechanisms, A. C. Hall. Technology Press, Massachusetts Institute of Technology (Cambridge, Mass.), 1943.

4. Transients in Linear Systems, M. F. Gardner, J. L. Barnes. John Wiley and Sons, New York, N. Y., 1942.

5. Comparison of Two Basic Servomechanism Types, H. Harris. *AIEE Transactions*, volume 66, 1947, pages 83–92.

6. Laboratory Aids for Electro-Mechanical System Development, G. C. Newton, Jr., W. T. White. *AIEE Transactions*, volume 66, 1947, pages 315–21.

7. A Servo Employing the Magnetic-Fluid Clutch, E. S. Bettis, E. R. Mann. *Review of Scientific Instruments* (New York, N. Y.), volume 20, February 1949, pages 97–100.

8. Determination of Dynamic Characteristics of a Magnetic-Fluid Clutch, A. J. Parziale. A thesis submitted in partial fulfillment of the requirements of the degree of Master of Science, Massachusetts Institute of Technology (Cambridge, Mass.), February 1949.

9. The Properties and Performance of the Magnetic-Fluid Clutch, C. A. Cibelius, Jr. A thesis submitted in partial fulfillment of the requirements of the degree of Master of Science, Massachusetts Institute of Technology, (Cambridge, Mass.), June 1949.

No Discussion

Application and Handling of Very Large Power Transformers on the System of the Bonneville Power Administration

RICHARD F. STEVENS
MEMBER AIEE

IN April 1938, the first power from a Federal dam on the Columbia River was marketed when the street lights of the little town of Cascade Locks, Oreg., were lighted with power brought over a 13-kv line from Bonneville. At the same time, design was starting on the 230-kv grid which was to become the power backbone of the Pacific Northwest. The first large power bank was energized at 230 kv in December 1940.

Only nine years have elapsed since then, yet the Bonneville Power Administration (BPA) now has 18 230-kv banks on its system with a total maximum continuous capacity of over 2,000,000 kva. In the nine years to follow, as other Federal power plants are put in service, this is expected to increase to 46 banks with a capacity of over 7,500,000 kva.

BPA has thus become one of the most important users of large, high-voltage transformers, and as such, its transformer practices may be of interest.

These practices have undergone an interesting evolution. Changes have been in the direction of decreasing costs, wherever operating experience and engineering studies have shown this possible without loss of reliability. In this case, there existed, beyond the normal responsibility for keeping down costs, a strong desire to offset the rising trend of labor and material prices by savings which would make possible a continuance of the low wholesale rates for which the Administration was noted. How successfully this was done, so far as transformation costs are concerned, is shown in Figure 14.

Rising price trends have been countered in the following ways:

1. Standardization and quantity purchases.
2. Use of larger units.
3. Use of lower basic insulation levels.
4. Use of autotransformation.
5. Use of forced oil cooling.
6. Use of modern compact designs to simplify erection and maintenance problems.
7. Use of mobile spares as stand-by for banks at many stations.

Standardization and Quantity Purchases

A rapid rate of growth has made possible quantity purchases of large transformers. Together with standardization of requirements, this has enabled manufacturers to spread design costs over a number of banks. The resulting interchangeability between stations has facilitated changes in plans, where required, to meet changes in the pattern of load growth. It also has made possible the use of one portable spare to serve several stations.

Most of the power generated at the Federal plants is transmitted to load centers at 230 kv and transformed to 115 kv by transformers designed to the following standards:

High Voltage—220 kv with two $1^1/_4$ per cent taps above and six $1^1/_4$ per cent taps below; nonautomatic load ratio control.

Intermediate Voltage—115.5 kv with taps at 117.88, 112.75, 109.75, 106.85, and 104.30; no load ratio adjuster.

Low Voltage—13.8 kv with reduced capacity taps at 11.5 kv; also at 4.02 and 9.78 for synchronous condenser starting.

Reactances are specified as follows:

For Transformers

High-low—16.5 per cent
High-intermediate—9.0 per cent
Intermediate-low—7.5 per cent

For Autotransformers

High-low—11.5 per cent
High-intermediate—4.0 per cent
Intermediate-low—6.5 per cent

Specified reactances are subject to a minus tolerance of 10 per cent. In the interest of system stability, they are

Figure 1. 230-kv transformers at Spokane Substation

Bank at right is a 150,000-kva 220-to-115 kv autotransformer bank with 13.8-kv secondary winding. Next two banks are 220-to-13.8 kv 2-winding, 75,000 kva each (100,000 kva forced oil cooled). The bank on far left is 220-to-13.8 kv 2-winding 100,000-kva forced oil cooled

Paper 50-26, recommended by the AIEE Transformers Committee and approved by the AIEE Technical Program Committee for presentation at the AIEE Winter General Meeting, New York, N. Y., January 30-February 3, 1950. Manuscript submitted October 31, 1949; made available for printing December 27, 1949.

RICHARD F. STEVENS is Head Design Engineer with the Bonneville Power Administration, Portland, Oreg.

Figure 2 (left). Removing core and coils of a 25,000/33,333-kva forced air cooled transformer at J. D. Ross Substation for inspection

This was formerly considered a necessary step in erection of all large transformers after transcontinental shipment

Figure 4. Standard untanking tower showing railroad spur entrance

chosen to be as low as possible consistent with economical transformer design.

Standard bank capacities are:

75,000-kva self cooled; 100,000-kva forced air cooled

150,000-kva self cooled; 250,000-kva forced oil cooled

Future 75,000-kva banks also will be provided with forced oil cooling, giving them a maximum rating of 125,000 kva.

Two smaller banks, conforming generally to the foregoing standards, but with a self-cooled rating of only 50,000 kva each also have been installed. A few more smaller 230-kv banks also may be added in the future.

Five banks of 100,000-kva maximum rating have been installed to step down power from 230 kv to 13.8 kv to serve concentrated electrochemical loads.

Banks with capacities up to 37,500 self-cooled/50,000 forced air cooled are used for stepping down from 115 kv. Voltages higher than 230 kv also are under study for some lines. Both higher and lower voltage transformers, however, are beyond the scope of this paper, since present problems of very large transformers on the BPA system concern only 230-kv banks.

Figure 3. Standard untanking tower (front)

Size of Units

The use of larger capacity transformers, where feasible, will obviously decrease the transformation cost per kilovolt-ampere. This advantage becomes even more apparent when the cost of associated switching is considered.

BPA originally selected as a standard bank size 75,000 kva self-cooled (100,000 kva with fans). Six banks of this size, which were considered quite large at the time, were purchased during the first few years of operation. In physical weight and dimensions, the single-phase units of these banks approached the largest sizes which could then be handled easily by rail. In kilovolt-ampere rating, the banks matched roughly what was then considered to be a normal loading for a 230-kv circuit.

As loads and generation increased by leaps and bounds in the years that followed, it became apparent that it would be better to provide transformation in larger units. This had become feasible electrically because increased loads and generations put everything on a larger scale. It had become feasible from the standpoint of physical handling because improvements in transformer design had provided enormously greater capacities with little increase in size or weight. It was therefore decided to buy banks of double the old standard self-cooled rating—that is, 150,000 kva per bank. All 230-kv banks bought since 1944 have been of this rating. In the meantime, the practice of quoting a supplementary rating increase of $66^2/_3$ per cent of the self-cooled rating for forced oil cooling has been adopted by manufacturers. Transformers purchased in the last few years have been equipped with oil circulating pumps and can therefore carry 250,000 kva with these pumps running. In the meantime, necessity had forced the Administration to carry, and it had carried successfully, loads of this magnitude on its 230-kv transmission lines.

Thus the new standard bank size is relatively well matched to normal 230-kv line capacity on the basis of the new concepts of line loading.

Use of Lower Basic Insulation Levels

When design of the Bonneville system first got under way in 1938 and 1939, a decision was made to use 196 kv in preference to 230 kv as a switch and bus insulation level for 230-kv circuits. This resulted in considerable saving and has proved entirely sound in practice. In keeping with this decision, 196-kv bushings also were specified for all 230-kv transformer line terminals.

Serious consideration was given at the same time to use of this insulation level for the winding itself, but, because of lack of operating experience, a conservative viewpoint prevailed, and transformer windings for many years were required to be designed on the basis of full 230-kv insulation (1,050-kv impulse test). Subsequent experience and studies in our organization and in the industry at large have convinced the Administration that

Figure 5. Standard untanking tower showing transfer track door

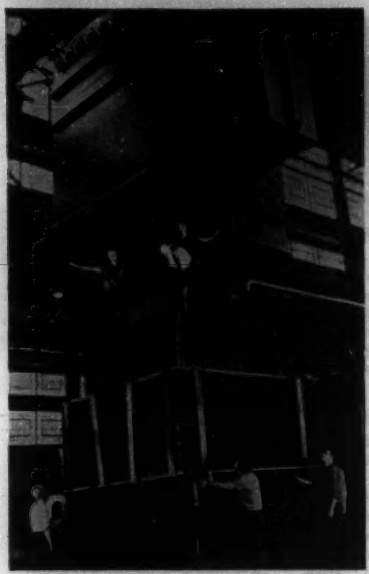

Figure 6 (left). Transformer for Snohomish Substation

Unit of first 150,000/250,000-kva forced oil cooled 220-115-13.8-kv bank purchased by BPA. Is of form-fit type

Figure 8 (right). First step in uprighting Snohomish transformers, using jacks

this was much too conservative. In 1948, therefore, specifications were issued which permitted alternate bids on high-voltage winding insulation of the 196-kv class (900-kv impulse test). These alternate bids showed substantial savings and were accepted.

BPA, however, was not completely satisfied. It is common knowledge that existing voltage levels were set up for ungrounded systems, though such systems are virtually nonexistent in the higher voltages. Many utilities, like BPA, have taken advantage of the lower maximum voltage stress on their grounded neutral systems and have selected the next lower standard voltage level. However, because the steps between voltage levels are not uniform, the resulting factors of safety are largely hit or miss. It is felt that it would be more logical to determine insulation levels in a rational way for the far more common grounded systems. For instance, BPA feels that an impulse level of about 800 kv would be adequate for its 230-kv equipment, assuming proper application of lightning arrester protection, and intends to specify this level in the future specifications. The Administration is investigating the possibility of reducing the required level still further for some applications.

It is believed that this lower insulation requirement may bring substantial cost savings as compared to the 900-kv impulse level associated with the 196-kv class, even if no change is made in industry standards. It is felt that 230-kv transformers purchased by BPA are too large to be production line items, and yet are purchased in sufficient quantities so that design costs may be spread over many units. Obviously, still greater savings would be possible to BPA and other users if industry standards could be rationalized along some such line as this. The Administration, therefore, has lately taken an active part in discussions looking toward this goal.[1] This matter is discussed in more detail in another AIEE paper.[2]

Use of Autotransformers

For the capacities and insulation levels originally specified, cost comparisons showed little saving in favor of autotransformers as compared with the transformers actually purchased.

On the other hand, the autotransformers offered a little more difficulty in regard to protection and in application of tap changing equipment. Moreover, they did not provide any possibility for connecting the 115-kv winding in delta in-

Figure 7 (left). Transformer of Figure 6 mounted on side on low bed car for shipment

Figure 9 (right). Second step in uprighting Snohomish transformers, using cables

Figure 10. Snohomish transformer upright, ready for mounting wheels

stead of star to serve possible 69-kv loads.

When prices were taken in 1947, however, on much larger transformers designed for a lower (196 kv) insulation level, it was found that the savings were sufficiently large to outweigh any of the disadvantages. Autotransformers have since been standard for 220- to 115-kv transformation.

In addition to direct cost saving, the smaller weight and dimensions are a big factor in making it possible to handle units of greater kilovolt-ampere capacity with less elaborate facilities.

Use of Forced Oil Cooling

In common with most other utilities, BPA standardized at the start on self-cooled transformers for its substations with provision for $33^1/_3$ per cent increase in capacity by the use of fans.

During the war, when faced by the necessity of providing the most capacity with the least material, BPA purchased transformers with forced oil circulation. The first BPA bank with this type of cooling was installed during the war at Spokane, Figure 1.

Forced oil cooling now is standard on all new 230-kv transformers. In general, the basic rating is specified on a self-cooled basis, with neither fans nor oil circulating pumps operating. A supplementary rating $33^1/_3$ per cent higher than the basic rating is specified with fans in operation. Where forced oil cooling is specified, a rating $66^2/_3$ per cent higher than the basic rating is specified, in addition to the other two ratings.

An exception was made in the case of the rail-mounted spare which will be described later. To make possible a design meeting difficult space and weight limitations, this transformer was not required to operate with oil circulating pumps shut down. However, two oil pumps are provided and the transformer must be able to carry 70 per cent of its rating with one pump out of service.

Use of Simpler Handling Facilities

Recent improvements by manufacturers in transformer design have made possible a great saving in the cost of handling facilities.

Until recently it was the universal BPA practice to untank the core and coils from each transformer after it was delivered and before it was put into service. Transformers shipped from eastern factories to the west coast over the long rail routes apparently take tremendous punishment en route. At times it has seemed that the transformer which arrived completely undamaged was the exception, not the rule. Untanking has often disclosed serious damage that would otherwise have gone undetected. Thus some heavy lifting device was formerly considered essential for this purpose, Figure 2.

Some type of lifting device also was necessary to remove the shipping covers commonly placed on the large power transformers for rail shipment, and substitute the permanent top sections. A means of installing the heavy bushings also was required. Some shelter from the weather was desirable and essential where work could not be scheduled for favorable weather. With rains common through the fall, winter, and spring in the western part of the BPA area, and dust storms common in the desert sections, favorable weather could seldom be assured.

A standard building, Figures 3 to 5 inclusive, was therefore designed to handle such work at our larger stations. The main crane aisle is 35 feet 8 inches wide, 70 feet 8 inches long, and 45 feet high to top of crane rail. A 100-ton travelling bridge crane, electrically operated, is provided.

This aisle is served by a spur from the nearest railroad, and by an extension of the transformer transfer track which generally enter from doors on opposite sides. This provides a convenient means for unloading from railroad cars, for untanking transformers for inspection or repair, and for assembly and loading of the transformers on the transformer transfer truck for the final trip to the permanent position in the switchyard. The aisle provides good repair facilities in case of damage in service, and also convenient means for unloading and working on other heavy equipment.

Combined in the same building are an oil pump room, small shops, a storage area, loading dock, and offices.

Convenient as this building is for construction and maintenance, it represents a rather heavy investment which is idle much of the time. Until recently, however, this investment was felt to be almost unavoidable.

Considerable thought was given to simplifying the facilities, substituting perhaps a square tower with fixed hoist, or hoist with travel in one direction only. Unfortunately, studies of these alternate

Figure 11. 100-ton trailer, "the Jeep", used by BPA in moving transformers to substations not equipped with rail spurs

Figure 12. Spare transformer bus

Where single-phase spares of the ordinary type are installed, special busses are mounted and connecting parts are made ready to facilitate quick electric connection of the spare if required, without moving it

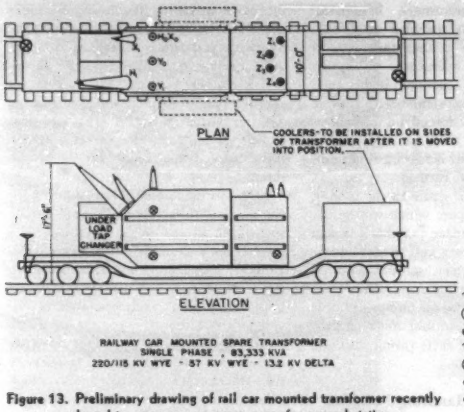

Figure 13. Preliminary drawing of rail car mounted transformer recently purchased to serve as a common spare for several stations

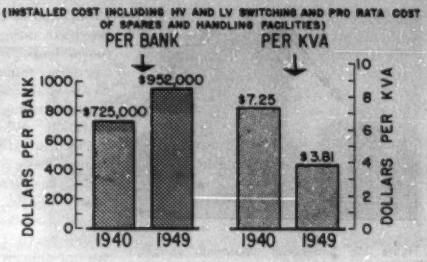

Figure 14. BPA transformation costs, 1940 and 1949

1940 costs based on transformer banks rated 100 megavolt-amperes (forced air cooled); 230-kv insulation level; one spare transformer for each two banks and an untanking tower for each three banks. 1949 costs based on autotransformer banks rated 250 megavolt-amperes (forced oil cooled); insulation level reduced from 230 kv to 196 kv; one rail car mounted spare transformer and one untanking tower for each eight banks. Weighted cost of untanking towers and standard 1940 transformers has increased approximately 100 per cent

schemes seemed to show that the cost savings would not have been commensurate with the conveniences sacrificed, as compared with the design adopted.

Buildings essentially identical with the one shown in Figure 3 have been built at Chehalis, Midway, and Covington Substations. The crane aisle section is essentially a duplicate of the crane aisle that forms part of the much larger building at J. D. Ross, and also of the crane aisle that was designed as part of the control house at Longview.

Restrictions on building construction imposed during and immediately following the war discouraged building of untanking towers at some of the later stations, such as the one at Spokane. At Snohomish, funds were not available in time to complete a building before the delivery there of the first large 230-kv transformer.

Fortunately, advances in transformer design had by then made it possible to ship even very large transformers completely assembled, except for bushings. The first such transformers purchased by BPA for Snohomish were of the so-called form-fit type, and were shipped lying on their sides. Our riggers had no particular difficulty in upending these on arrival, using the method illustrated in Figures 8, 9, and 10.

Some concern was felt about putting a transformer into service without direct inspection of the condition of core and coils after arrival. The manufacturer assured us, however, that this was unnecessary and results so far have confirmed this opinion.

A transformer bank of the same electrical capacity, make and type, has been ordered for the new 230-kv substation at Olympia, Wash. It is somewhat smaller in physical size, since the 115 kv is obtained from an autotransformer tap instead of a separate winding. It is proposed to install this bank in the same manner as the Snohomish bank, and the untanking tower originally intended for Olympia has been indefinitely deferred, with a resulting substantial cost saving.

Four other 150,000/250,000 kva autotransformer banks, electrically identical with the Olympia bank, also have been ordered. The first of these will be installed in the new 230-kv Goshen Substation near Eugene, Oreg. It will be of a different make and of the core type. It will be relatively wide and long in plan view and short in height, so that it will be possible to ship it mounted erect on a low-bed car. The manufacturer of this transformer bank claims that it also will be built and braced to avoid the necessity of untanking for inspection after delivery. The construction of an untanking tower at Goshen, therefore, also can be avoided or deferred.

Three other autotransformer banks of this size have been ordered which will be of a still different make. Although exact size and shape of these are not yet determined, they too will be suitable for erection without untanking.

Because of the size and weight of equipment involved, considerable effort has been taken to locate 230-kv stations where they could readily be served by spurs from existing railroad lines. Of 11 230-kv transformation stations in operation or under construction, only two are not so served. A 100-ton trailer, nicknamed "the jeep", Figure 11, was purchased for transporting transformers from the nearest railroad spurs to the 230-kv substations which have no spurs of their own.

Where indoor handling facilities are provided, the spur track enters one side of the building or the end, while a transfer track leaves the building from the other side and extends into the substation yard.

The transfer tracks are laid with the rails at the approximate level of the general yard grade. The transfer track rail gauge at all stations is 9 feet $7^{3}/_{8}$ inches. At some stations the railroad spur is centered on the same line as the transfer track, and the standard gauge rails are extended into the yard between the wide gauge transfer track rails, on the same ties. This permits flat cars and low bed cars with equipment to be unloaded as near as possible to the footings where the equipment will be installed.

Because of the plan to use a rail car mounted spare, this arrangement will be necessary at all 230-kv stations in the future in order that the spare can be moved into place quickly. Extensions and changes in spur tracks at existing stations will be made when and if feasible to provide this feature.

For the ordinary moving of transformers within the station, a standard transfer car is provided. This is designed with wheels set for our standard transfer track gauge of 9 feet $7^{3}/_{8}$ inches, and supports rails at right angles with a rail gauge of 6 feet 8 inches to suit the standard wheel gauge. These rails are 2 feet $2^{3}/_{8}$ inches

higher than the top of the transfer track rail, to match the standard elevation of the rails which support the transformers on their concrete footings.

It is planned to build in the future only such additional untanking towers and associated shops as are needed to make such facilities available at strategic centers in the region. They are no longer considered to be necessary at all major 230-kv stations.

Economical Application of Spare Transformers

Until recently, the Administration has sought to provide spare transformers at all major stations where the supply of the load is dependent on a single bank, and at some stations with more banks if the load is such that a prolonged outage of one bank would be disastrous. Often, however, this insurance could not be provided, either from lack of funds, or (as during the war) because of material shortages. In fact, it was necessary during the war to combine the station spares from Chehalis, Ross, and Covington to make up a much needed second bank at Covington.

Where spares have been used, it has been standard BPA practice to install bus work to permit rapid connection of the spare, in place of a faulted transformer in any phase, without physically moving either, in order to decrease the outage time, Figure 12.

Permanently mounted bus work for 230, 115, and 13.8-kv connections is installed to the extent which is feasible without interference with the regular bank wiring. Pre-cut cable and pipe bus connections are made up and stored against the day when they may be needed for connecting the spare transformer.

The cost of the insurance premium which spare transformers represent is high. In the case of BPA, the justification must rest entirely on judgment, since no accurate data exist on transformer life expectancy. There have been no failures whatsoever on BPA power transformers in service. A 40,000-kva transformer was recently untanked after about nine years of service, during much of which time it carried overloads exceeding 100 per cent. No signs of insulation deterioration could be detected. However, unlikely as a service failure of a transformer may be, the consequence of a prolonged outage, if it should occur with no spare available, might be very serious indeed.

A new approach to this difficult problem was taken in 1949 with the purchase of a rail car mounted spare, which is to be delivered in 1951.

This is to be a single-phase 83,333-kva 220-to-115 kv autotransformer, with standard electrical characteristics and load ratio control equipment, so that it can be substituted for a single-phase unit of any of the large 220-to-115 kv banks recently purchased. A special separate 57.1-kv winding also is provided so that it also can serve as a spare for the 220 to 57.1 kv bank at Troutdale substation.

Figure 13 shows the general design and approximate dimensions of the unit. Weight and dimensions are such as to insure that it can be shipped from eastern points to the Bonneville area over any of the main transcontinental lines or readily shifted between points within the area.

Forced oil circulation, with two pumps, is provided. To permit saving of size and weight, no self cooled or forced air cooled rating was specified, but the unit must be able to carry 70 per cent of its full rating with one pump shut down.

The spare can be removed from the car, if desired. BPA has often encountered troubles and delay in moving transformers from one station to another, due to the inability of the railroad lines to supply low bed cars promptly. It has frequently been necessary to pay demurrage charges for holding cars which had been used in shipping transformers from the East, until they could be used for some transformer move on the BPA system. In the future, it will be possible in such cases to unload the spare and use its low bed car for shipping a transformer between stations or to the factory for repairs.

The first rail car mounted spare will be kept normally at some central point on the BPA system, probably at Vancouver, Wash. It will serve as a spare for eight transformer banks existing or on order.

It is expected that as other banks are installed, additional rail car mounted spares will be added so the ratio of one spare to about eight banks will be roughly maintained. With the purchase of more spares, the average length of rail haul will be decreased. It seems likely that there may be three of these on the system by 1958, located at strategic points to serve the northwestern, southwestern, and eastern portions of the system, respectively.

The railroads have assured the Administration that a special train can be made available on two hours' notice in case of an emergency. While the transformer is being shipped to the station involved in the trouble, crews at the station can be disconnecting the faulted transformer and connecting the spare transformer busses to the phase affected. When the spare arrives, the transformer and car will be spotted in front of a specially equipped spare position with facilities for making connections quickly to the spare transformer busses. The transformer will then be rotated 90 degrees on the flat car, moved into position on the footing, and connected.

Actually, the complete lack of failures in service of any of the BPA power banks makes us hope that actual use of the rail car mounted spares, and of other spares now on the system, will be limited to scheduled maintenance. They will, however, be ready for use if required, at an investment cost less than one quarter of the amount which would have been required to provide separate spares for each station.

References

1. Basic Insulation Level Principles Adopted by Committee. *Electrical Engineering*, volume 68, number 5, May 1949, pages 453–54.

2. Lightning Arresters as a Criterion for Insulation Levels, Harold L. Rorden. *AIEE Transactions*, volume 69, part I, 1950, pages 84–96

Discussion

P. L. Bellaschi, Consulting Engineer, Portland, Oreg.: The strides in the application of 230-kv power transformers, related in the paper, were made possible through engineering of a high order combined with a well-co-ordinated and progressive approach to the over-all problem. Reduced insulation proportioned to the requirements of grounded-neutral operation, the advent and application of forced-cooling, utilization of autotransformers, in addition to advances in constructional features and in the basic materials used, all have contributed their part to a more effective equipment and to reduced size and weights. These advances combined have facilitated the design and shipment of complete units for 250,000-kva banks required to match present-day capability of 230-kv transmission lines, another advance in the art realized concurrently in the course of these developments. Finally full advantage has been taken of the increased reliability of the equipment and diversification made possible through system development, to reduce field installation equipment and transformer spares down to a new acceptable minimum.

The economical gains achieved are eloquently in evidence in Figure 14 of the paper. The question might then be raised as to

whether similar advances can be anticipated in the years to come in view of the extent of rationalization hereto achieved. Without speculating on the future, fundamentally certain facts stand out and are well to consider. For instance it is a fact that about one-half of the cost in present-day high-voltage transformer apparatus is accounted for by the insulation alone. Therefore this would appear as a fertile field for future investigation and study both in the design and application of the equipment. Again to consider another possibility, it is a fact that thermally insulation is the limiting factor which determines rating, permissible overload, and useful life of transformers. Advances that would permit higher operating winding temperatures would be a contributing factor towards more economical transformation costs. One could speculate further on possibilities, but one point is clear.

It is a foregone conclusion that continued progress in this field will call for sustained and co-ordinated effort in the years to come directed both to the development of the design proper and to further rationalization regarding the application of the apparatus in the field.

W. Gordon James (Westinghouse Electric Corporation, Sharon, Pa.): The author of this paper is to be complimented for his very timely and interesting treatment of the application and handling of very large power transformers on the system of the BPA.

Obviously the key note of the information presented in this paper is "economy."

Since I am a tax payer and also a designer of large power transformers such a key note certainly strikes a responsive chord.

Truly, "economic engineering is good engineering" and conversely, "good engineering is economic engineering" and surely the larger the kilovolt-ampere ratings and the higher the dynamic operating voltages become the greater the need for over-all economics such as specifically outlined in this paper.

The engineers of the BPA have contributed greatly to the over-all advancement of the art of large, high-voltage power transformer design and application by virtue of their knowledge and understanding of the problems confronting designers of such equipment as evidenced by their cooperativeness as regards design and application limitations as well as the constructive assistance they render to standardizing bodies whose objectives are to utilize to a maximum degree all developments of the art, consistent with over-all economics, and best engineering, to the end that long trouble-free service will be a natural result.

It also might be observed, without detracting from or minimizing this paper or the accomplishment of the BPA, that large power transformer manufacturers also have contributed heavily in making such economics possible through years of intensive research, at no little cost, to improve materials, methods, and processes whereby such application economics, as described in this paper, are possible.

Speaking for at least one manufacturer I believe, from many years of experience with the design and application of large high-voltage transformers, that the confidence placed in current power transformer design practice is very sound and well placed. Certainly the use of greater standardization, larger units, lower basic insulation levels, autotransformers, forced-oil cooling, more compact designs, and the reduction of capital investment in separate bank spares by the use of a mobile spare are, in general, sound practices and will result in great savings economically, provided, of course, that all these factors are properly co-ordinated with the requirements of the system.

Since, from an application and handling standpoint each of these items have been very adequately discussed in this paper I will not, in conclusion, comment further except as regards the use of lower basic insulation levels.

Although great strides have been made in recent years as regards insulation structures and protective equipment, making it possible to realize appreciable economics by using reduced basic insulation levels, further reductions should be approached with caution and only after a complete system study fully co-ordinated with the protective ability of protective equipment.

Richard F. Stevens: I agree heartily with Mr. James that great credit is due to the manufacturer for advances made in transformer design. I join Mr. Bellaschi in the hope and belief that still further advances may be expected. It is on these that we must depend, to a large degree, in keeping down our transformation costs.

Side by side with this goes the work of the utility application engineer. He must study his own system, consider all hazards, evaluate the effectiveness of protective equipment, and avoid unjustified risks on the one hand, and unjustified expenses on the other.

In passing, it might be pointed out that Mr. James is not strictly correct in inferring that he is directly affected as a taxpayer by what we pay for equipment, since all such costs must be returned from the sale of power.

The responsibility still exists, however, for economy as a means of maintaining the lowest possible electric rates. I believe that my paper shows, and the two discussions recognize, that this responsibility is being taken very seriously by the BPA engineering staff.

Liquid Cooling of A-C Turbine Generators—Part II

CARL J. FECHHEIMER
FELLOW AIEE

IN A previous paper[1] presented before the AIEE in 1947, a combination of three cooling media was advocated for large turbine generators: oil (or equivalent synthetic liquid) for the stator, water for the rotor, and hydrogen for the internal surroundings of the stator and rotor. From the thermal standpoint, this combination is believed to be superior to any other.

The opinion has been expressed, however, that complications are involved.

For simplification, the following now are proposed:

1. For small and medium-rated generators, the coolant in the ducts to be water for stator and rotor, with air in the internal surroundings. For the large machines, the coolant in the ducts to be water for stator and rotor, with hydrogen in the internal surroundings. The complications associated with oil for the stator are eliminated, as are also the complications associated with hydrogen for small and medium-size machines. The coil ends for both stator and rotor would be cooled by the internal gas, suitable small internal heat exchangers being provided.

2. All internal water systems could be hydraulically paralleled externally, and one external heat exchanger, circulating pump, and so forth, could be used for all, operation being in closed systems for each internal branch.

3. The external deaerator is to be omitted, as it was found by tests on the hydraulic model of the turborotor, to be unnecessary, as described in this paper.

4. The small ducts below the main slots in the rotor are to be omitted, as further calculations indicate that the water in the teeth ducts provides ample cooling, and the temperature drop in the steel is still reasonably low.

Other simplifications, most of which were brought out in the earlier paper mentioned above, are:

5. Omission of internal fans.

6. Omission of the large internal heat exchangers. Small internal heat exchangers would be needed for the gas for the coil ends. One external heat exchanger would be used for most of the losses.

7. Omission of vent ducts for the stator and rotor. Water cooling ducts are to be substituted for them.

8. Omission of ducts for coolant flow to and from the internal heat exchanger.

Commenting on item number 6, the heat flow in the external heat exchanger is from water to water, instead of from hydrogen (or air) to water. Therefore heat exchanger size will be considerably reduced. The frame diameters of hydrogen-cooled machines are much larger than they would be with liquid cooling because the gas to water heat exchangers must be placed internally, and the external diameters of the stator cores are appreciably larger. As the frame and end bells of a hydrogen-cooled machine are made to withstand an explosion, a large frame diameter is costly. Also, the external heat exchanger tubes need not be provided with rather costly fins, as needed with hydrogen or air.

This paper is divided into four parts: construction of the stator for water cooling; calculations of relative ratings as affected by the cooling media; hydraulic model of a liquid-cooled turboalternator rotor; and mitigation of Coriolis' forces.

Water-Cooled Stator

A longitudinal section of a water-cooled stator and rotor is shown in Figure 1. Two alternative schemes for the stator are shown in transverse section in Figures 2(A) and (B). Square or rectangular metal tubes are used, through which water (treated with a corrosion inhibitor) flows, instead of the usual vent duct spacers, but now the cooling is effected only through the water in the tubes. These tubes serve the dual purpose of cooling and of supporting the longitudinal pressure of the laminations. In Figure 2(A) additional supports are provided, but in Figure 2(B) the spiralled tubes in the core portion afford ample cooling surface and may be made to provide adequate support. The arrangements indicated in Figures 2(A) and (B) afford effective means for transferring the generated heat in the tooth-slot and core zones in accordance with the loss density therein. The designer can readily determine the number of tooth-zone tubes to connect in series, the losses having been calculated.

For the rotor and stator coil-ends, gas streams pass between consecutive coils. The high centrifugal forces are ample to secure adequate volumes of flow. High velocities at the coil surfaces are insured by suitable blocking for both the rotor and stator coil ends. Although such high velocities reduce the volume of flow slightly, the gain in velocities insures the relatively high heat transfer rate needed.[2] Calculations indicate that it is then possible to secure about the same temperatures as for the embedded copper, with water in the rotor ducts. It has been claimed for the present-day hydrogen-cooled rotors that lower coil-end temperatures are obtainable with the rotor blocking than for the ventilated embedded parts.[3] For the stator coil ends, with their thick walls of insulation, the external surface heat densities are much lower than for the rotor, and sufficiently low temperatures should be obtainable.

Paper 50-28, recommended by the AIEE Rotating Machinery Committee for presentation at the AIEE Winter General Meeting, New York, N. Y., January 30–February 3, 1950. Manuscript submitted November 20, 1948; made available for printing December 12, 1949.

CARL J. FECHHEIMER is a Consulting Engineer in Milwaukee, Wis.

The author acknowledges the helpful suggestions of K. L. Hansen, E. F. Vilter, Dr. J. F. H. Douglas and several Allis-Chalmers engineers. He also thanks the Milwaukee School of Engineering for facilities and aid in testing, in particular Fred Wutschel of the school's faculty.

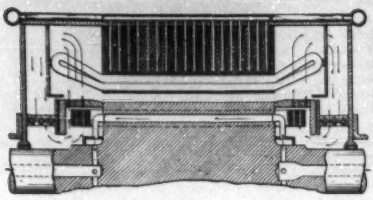

Figure 1 (left). Water - cooled stator and rotor. Longitudinal section

Figures 2 (A) and (B) (right). Water - cooled stator. Transverse section

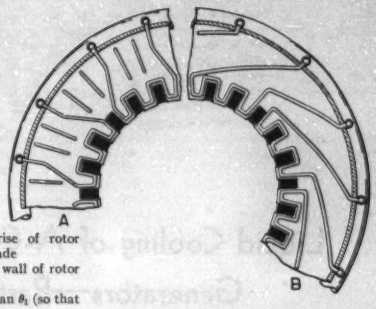

As shown in Figure 1, the coil-end gas streams pass through suitable internal stationary heat exchangers. A stationary disk (attached for convenience to the exchanger's inner side) prevents the pressure generated by the rotating rotor end disk from interfering with the radially inward gas flow.

Relative Ratings

All large turboalternators, supplying loads for which the current lags the voltage, are limited by rotor copper heating. In this study the rotor ampere turns, for a given temperature rise, are compared, for various cooling media.

The following are considered to be the same for any two rotors that are to be compared:

(1) Number of poles and frequency.
(2) Thickness of, and materials in, insulation wall.
(3) Slot dimensions, their number and spacing.
(4) Rotor diameter.
(5) The steady-state average copper temperature.
(6) Space factor of copper in a slot.
(7) Specific resistance of the rotor copper.

These seven items are the same, but the cooling media are changed. In general, the cooling ducts for liquids are narrower than for gas, but that does not affect the derivation and conclusions.

List of Symbols

A = cross section of one rotor conductor, square inches
C = number of rotor conductors per slot
d = depth of rotor slot below wedge, inches
D = rotor external diameter, inches
I = rotor amperes per conductor
K_1 = coefficient for temperature drop through wall of slot insulation
= approximately thermal conductivity of wall, watts/inch times degrees centigrade
K_2 = coefficient for all other rotor temperature drops, watts/square inch times degrees centigrade
K_3 = space factor in rotor slots = $(CA)/(Sd)$
n = number of rotor slots per group
p = number of poles
S = width of rotor slot, inches
t = thickness of single wall of rotor insulation, inches
θ = total mean temperature rise of rotor copper, degrees centigrade
θ_1 = temperature drop through wall of rotor insulation
θ_2 = temperature drops other than θ_1 (so that $\theta = \theta_1 + \theta_2$)
ρ = specific resistance of rotor copper, ohms per inch cube
τ = pole pitch on rotor periphery, inches

The total temperature rise of the copper is

$$\theta = \theta_1 + \theta_2 = \left(\frac{\rho CI^2}{A}\right)\left(\frac{t}{2(s+d)K_1} + \frac{pn}{\pi D K_2}\right) \quad (1)$$

Substituting for $A = K_3 Sd/c$ and $\pi D = \tau p$ and solving,

$$CI = \sqrt{\frac{\theta K_3 sd}{\rho}}\sqrt{\frac{1}{\dfrac{t}{2(s+d)K_1} + \dfrac{n}{\tau K_2}}} \quad (2)$$

The rating is evidently proportional to the ampere conductors per slot, CI. Suppose that, in one combination of coolants, the rotor is operated in certain gaseous surroundings, the coolant in the ducts being separately defined, which combination is referred by subscript I. These ampere conductors are to be compared with those of another combination for which subscript II applies. All quantities under the first radical in equation 2 are the same for the two combinations, and it therefore drops out in the comparison ratios

$$\frac{(CI)_I}{(CI)_{II}} = \sqrt{\frac{t\tau(K_2)_{II} + 2n(s+d)(K_1)_{II}}{t\tau(K_2)_I + 2n(s+d)(K_1)_I} \times \frac{(K_1)_I(K_2)_I}{(K_1)_{II}(K_2)_{II}}} \quad (3)$$

Generally, with liquids, the ingoing temperature is lower than for gases, and as the maximum temperature is the limitation, the allowable temperature rise, θ, with liquids should be greater than with gases, thereby making the rating ratio even more favorable for liquids than given by equation 3.

The ratio of ratings is then dependent upon the coefficients K_1 and K_2, and somewhat upon the choice of slot proportions. The determination of the coefficients now will be given.

From laboratory tests on transverse thermal conductivity of mica plate in air, the composite's thermal conductivity was found to be about 0.003 watt/inch times degrees centigrade. To arrive at numerical values for the ratio in equation 3, the slot lining in a turborotor is taken as 0.0625-inch thick, and the area per inch axially through which the heat flows is the arithmetical mean between the slot surface, 2 $(S+d)$, and the copper surface. For simplicity, in the above, the surface per inch axially is taken as $2(S+d)$, and as such surface is about seven per cent more than the mean, the equivalent transverse conductivity becomes $K_1 = 0.003/1.07 = 0.0028$.

In an atmosphere of hydrogen most of the air particles in the slot liner are supplanted by hydrogen, the thermal conductivity of which is about seven times that of air. Experiments indicate that the composite's conductivity is thereby approximately doubled, and consequently has been taken as 0.0056.

From a large number of tests on ventilated turborotors in air, the average value of K_2 was found to be about 0.083 watt/square inch times degrees centigrade. Comparisons with data from Luke's paper[4] on a revolving cylinder (plotted on log-log paper) show somewhat greater values. (At such high peripheral velocities the heat transfer rate does not change much with the speed.) The difference between the two probably is because the air windage loss augmented the temperature of the actual rotor more than for Luke's model; the internal drop in the steel in the actual rotor increased the copper temperature and such drop was zero in the model; and also because of heating of the air and inequalities in distribution of air in the radial vents which produce inequalities in copper temperatures. K_2 will be taken as 0.083 for air.

The heat transfer rate with hydrogen at one atmosphere is about 1.46 times that

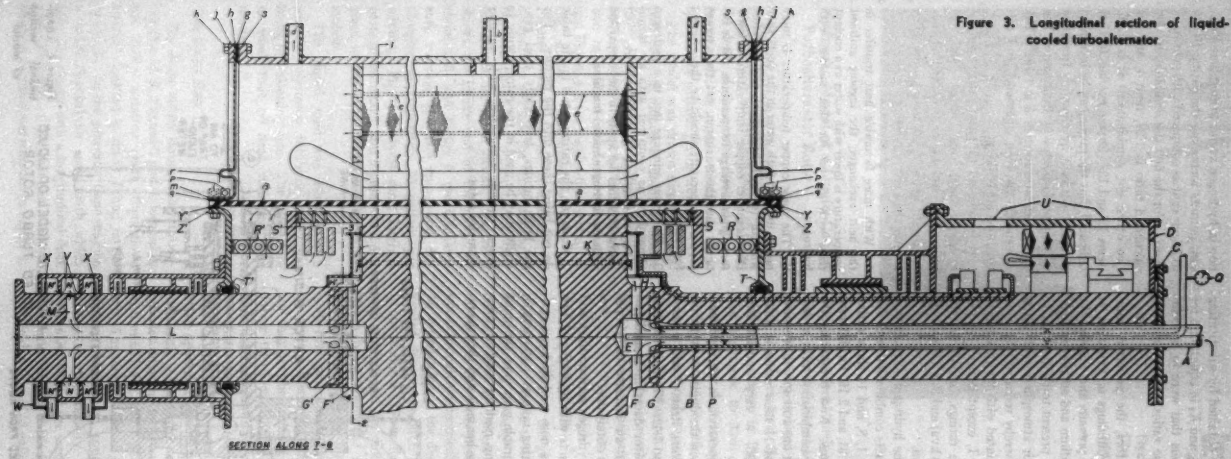

Figure 3. Longitudinal section of liquid-cooled turboalternator

Table I. Comparison of Ratings of Turborotors with Various Cooling Media

Col. No.	1	2	3	4	5	6	7	8	9	10	11	12	13	14	15	16	17
	Combination I			Combination II				Coefficients				Rotor and Proportions					
	Surroundings			Surroundings				Comb. I		Comb. II							
Item No.	Fluid	No. Atmos. Press.	Duct Fluid	Fluid	No. Atmos. Press.	Duct Fluid	Rating Ratio = (Amp. T.)I / (Amp. T.)II	$(K_1)_I$ (Insulation)	$(K_2)_I$ (Other)	$(K_1)_{II}$ (Insulation)	$(K_2)_{II}$ (Other)	No. of Poles	Frequency	Rotor Ext. Dia., (Inches) = D	Number of Slots Per Group = n	Slot Width (Inches) = s	Slot Depth Below Wedge (Inches) = d
1	H_2	1	H_2O	Air	1	Air	2.06	0.0056	1.00	0.0028	0.083	2	60	34	14	1.00	5.20
2	H_2	1	H_2O	H_2	1	H_2	1.62	0.0056	1.00	0.0056	0.121	2	60	34	14	1.00	5.20
3	H_2	1	H_2O	H_2	2	H_2	1.39	0.0056	1.00	0.0056	0.193	2	60	34	14	1.00	5.20
4	H_2	1	H_2	Air	1	Air	1.27	0.0056	0.121	0.0028	0.083	2	60	34	14	1.00	5.20
5	H_2	2	H_2	H_2	1	H_2	1.164	0.0056	0.193	0.0056	0.121	2	60	34	14	1.00	5.20
6	H_2	2	H_2	Air	1	Air	1.48	0.0056	0.193	0.0028	0.083	2	60	34	14	1.00	5.20
7	Air	1	H_2O	Air	1	Air	1.54	0.0028	1.00	0.0028	0.083	2	60	34	14	1.00	5.20
8	H_2	1	H_2O	Air	1	Air	1.91	0.0056	0.85	0.0028	0.083	2	60	20	8	1.00	3.60
9	Air	1	H_2O	Air	1	Air	1.42	0.0028	0.85	0.0028	0.083	2	60	20	8	1.00	3.60
10	H_2	1	H_2O	H_2	1	H_2	1.74	0.0056	1.00	0.0056	0.121	4	60	55	10	1.25	8.10
11	H_2	1	H_2O	H_2	1	H_2	1.695	0.0056	1.00	0.0056	0.121	4	60	50	8	1.375	8.32
12	H_2	1	H_2	Air	1	Air	1.260	0.0056	0.121	0.0028	0.083	4	60	55	10	1.25	8.10
13	H_2	1	H_2	Air	1	Air	1.260	0.0056	0.121	0.0028	0.083	4	60	50	8	1.375	8.32
14	H_2	1	H_2O	Air	1	Air	2.19	0.0056	1.00	0.0028	0.083	4	60	55	10	1.25	8.10

of air at one atmosphere. With hydrogen, the windage loss does not augment the temperature appreciably, but the internal drop in the steel would be the same as for air for the same flow of heat; in hydrogen, with larger heat flow, this drop is greater. One of these would have the effect of increasing the coefficient K_1, and the other of decreasing it. It is believed that very little error is introduced by taking K_2 for hydrogen (at one atmosphere pressure) to be 1.46 times that for air, that is, 0.121.

For hydrogen at two atmospheres pressure, the heat transfer rate from the surface is approximately $(2)^{0.8} = 1.74$ times that for one atmosphere. However, with the larger heat flow in the steel, there would be lower cylindrical surface temperature for a given internal copper temperature, which means less heat transferred for a given internal temperature. Again, for simplicity, take it to be $(1.8)^{0.8} = 1.6$ times that at one atmosphere, or 0.193 watt/square inch times degrees centigrade.

Several rotors were calculated with water in rectangular ducts. In such cases, when the I^2R loss is referred to the rotor's cylindrical surface, the total drop beyond the wall of insulation gave an equivalent K_2 of approximately 1.0 watt/square inch times degrees centigrade, or more, for the larger rotors, and 0.85 for the smaller. This took account of the water's mean temperature rise, the drop in the teeth, and the drop at the surface of the ducts.

In Table I, a combination is defined by the surrounding fluid; the pressure of that fluid; and the fluid in the ducts. The ratios were obtained by substituting the values of K_1 and K_2 in equation 3 for two combinations that were to be compared, and these ratios will be found in column 7.

For large rotors, the preferred combination is surroundings of hydrogen at one atmosphere pressure and water in the ducts. For medium and smaller ratings, it is believed at present to be desirable to operate in an air atmosphere with water in the ducts, thereby reducing the complications associated with hydrogen. All items in Table I, except items 8 and 9, pertain to large ratings, (usually of the order of 100,000 kva) and 8 and 9 apply to about 10,000 kva.

Comparing the hydrogen surroundings and water in ducts combination with air, for both, items 1, 8, and 14 show rating ratios of 2.06, 1.91, and 2.19, for different slot combinations. Now comparing the hydrogen-water combination with hydrogen-hydrogen at one atmosphere pressure, items 2, 10, and 11 show ratios of 1.62, 1.74, and 1.695, a very considerable gain.

Comparing operation in air surroundings and water in the ducts, with air for both combinations, items 7 and 9 show ratios of 1.54 and 1.42. Thus, by running water in the rotor ducts in a medium-rated generator an increase of 42 per cent in rating is obtainable.

Comparing hydrogen surroundings and water in the ducts with hydrogen at two atmospheres, as now used in large generators, the rating ratio is 1.39, item 3, again a considerable gain over the most favorable cooling medium used at present. Experience has indicated that operation in hydrogen at one atmosphere pressure permits increasing the rating by 25 to 30 per cent as compared with operation in air. For the first slot combination, the calculated ratio is 1.27, item 4, and for two other slot combinations it is 1.26, items 12 and 13. Experience has further indicated that the rating can be increased about 17 per cent by changing from one to two atmospheres of hydrogen. The calculated ratio in item 5 is 1.164. The agreements between experience and calculations are striking.

It is believed that the rating ratio of hydrogen-water over air-air, such as items 1, 8, and 14, or over hydrogen-1-hydrogen, items 2, 10, and 11, are even greater than given, because:

1. With more favorable heat transfer in the heat exchanger, the ingoing ambient temperature is lower with water as a coolant than with air (or for that matter, with hydrogen).

2. The rotor copper temperature is more nearly uniform with water in the ducts than with air (or with hydrogen), and therefore the maximum copper temperature is lower for a given average temperature. It is believed that the maximum, not the average copper temperature should be the criterion for rating.

3. The lower windage loss in a hydrogen atmosphere as compared with air means lower surrounding gas temperature. (Of course this does not apply to the comparison with the hydrogen-cooled machine.)

However, the rating ratios in the table do not bring these into the picture. For the large ratings, less costly steel generally may be used in the rotor, owing to lower stresses associated with smaller diameter rotor.

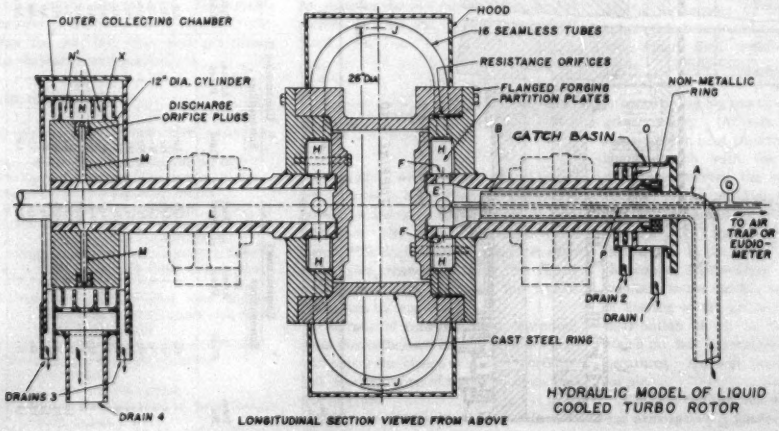

HYDRAULIC MODEL OF LIQUID COOLED TURBO ROTOR

Figure 4. Longitudinal section of model

Figure 5 (left). Intake end of stationary model

Figure 6 (right). Discharge end, running at 3,560 rpm

Hydraulic Model of a Liquid-Cooled Turboalternator Rotor

The construction and tests of a hydraulic model were undertaken chiefly to dispel the fears of those who doubted that a liquid could be passed through a high-speed rotor without giving trouble.

The model was driven direct by a 2-pole 60-cycle induction motor at nearly 3,600 rpm. Figure 3, reproduced from part I of this paper,[1] is a longitudinal section of a liquid-cooled turboalternator, and Figure 4 is the longitudinal section of the model. Corresponding parts in Figures 3 and 4 carry the same letters. A comparison reveals the close similarity between model and prototype. A few departures are given herein. Figure 5 shows the intake end of the model at stand still, and Figure 6 the discharge end, running at 3,560 rpm., and discharging approximately 55 gallons per minute. Figure 7 shows some internal parts of the model, and Figure 8 is a diagram of the model's external hydraulic system.

The liquid used was water plus a suitable corrosion inhibitor, operation being in a closed system. The losses were so small that no heat exchanger was needed.

The Inlet End

The water enters through the stationary pipe *A-B*, Figures 3 and 4, located in the hollow rotating shaft, then flows radially outward in ducts *F* and in the casing *H*. In the generator there may be a radial channel for each tooth which joins the casing with a longitudinal duct *J* in the teeth. (The junction is shown sharp in Figure 3 and rounded in Figure 1. This is considered further under mitigation of Coriolis' Forces.) In the model these ducts are replaced by 16 seamless tubes, 1-inch external diameter bent to semicircles, shown in Figures 4 and 7. The resistance to flow offered by the long generator duct was simulated in the model by resistance orifices, one for each tube. The hood surrounding the 16 seamless tubes was put on solely to reduce the windage loss, which was found, from wattmeter measurements, to be low.

The Discharge End

The left end of the generator's rotor body is nearly similar to the right end, the liquid flowing radially inward to the hollow shaft *L*. After flowing axially through *L*, the water flows radially outward through symmetrically spaced holes *M*, terminating in the discharge orifices, located close to the outer shaft diameter. In the model, a 12-inch diameter cylinder was pressed on the hollow shaft, 12 inches being about the shaft diameter needed to transmit the torque for a large 3,600-rpm generator. Four holes, *M* in the model, constitute a centrifugal pump, and they are the principal means for producing the flow of liquid. In Figure 3 these holes are shown curved adjacent to the shaft bore, but to simplify manufacture they were tapered in the model, which apparently reduced the shock loss sufficiently. Plugs were screwed into the cylinder adjacent to its outer periphery, with small holes, only 7/32-inch diameter, or 0.15 square inch for all four. Without allowing for stream contraction (vena contracta), the velocity through these orifices is 118 feet per second at cylinder peripheral velocity of 185 feet per second, and yields a flow of 55 gallons per minute.

The Discharge-Collecting Chamber

After discharge from the orifices into the stationary inner collecting chamber *N*, some liquid passes through holes in the cylinder separating the two collecting chambers.* The remaining liquid passes between stationary ribs and the shaft (or the model's 12-inch cylinder), into another inner collecting chamber *N'*, where under the action of the centrifugal forces from the rings *X*, most of this remainder is discharged through holes into the outer collecting chamber. The liquid is drained from the outer collecting chamber to the sump through drain 4, Figures 4 and 8. What little liquid is left should be carried to the sump through small drain 3 from which there was a trickle in operation. There are no rubbing seals. In the model, the side plates are slightly smaller at their inner diameters than the 12-inch cylinder. It is suggested that, in a generator, the part of the shaft enclosed by the collecting chamber be slightly larger in diameter than the adjacent parts, to compensate for the weakening due to the holes *M* and the holes for the orifice plugs.

During the passage of the liquid through the rotor, the centrifugal action thereon between the hollow shaft and the rotor ducts at the right end is balanced substantially by that at the left end. However, the head generated in the discharge holes *M*, functioning as a centrif-

*The outer collecting chamber is not shown in Figure 3 but is shown in Figure 4. In an actual machine the construction should be either like the model or should have additional sets of stationary and rotating ribs to insure against leakage. The parts should be machined and the two halves doweled; it then may be possible to secure leakless operation without more ribs. Figure 7 shows the collecting chamber with the upper part raised.

Figure 7. View of some exposed parts of model

ugal pump, is not balanced. Such head is considerable and appears largely as static pressure just below the discharge orifices, where it is converted into velocity head.

The Catch Basin at the Inlet End

This also is a departure from the construction in Figure 3. A nonmetallic ring is of such internal diameter that it clears the pipe *A-B*. This decreased the leakage, and most of the water that got past the ring escaped from the catch basin through drain *1*. The rotating ring between the two stationary disks serves to throw off the water, which is drained to the sump through drain *2*. There was no external leakage, and there are no rubbing seals. No doubt the resistance offered by the outside of the stationary pipe *A-B* and the inside of the rotating hollow shaft, causing the water to move in a spiral, also reduced the amount of liquid drained off.

Operation of the Hydraulic System

The setup is shown schematically in Figure 8. The water level in the elevated tank is only seven feet above the model's horizontal center line, and produced a pressure of about three pounds per square inch at standstill of the model and two pounds per square inch when running. The purpose of the elevated tank and sump is to secure two separately functioning systems which operate together in series in a closed system. Otherwise, with two centrifugal pumps in series, there would be likelihood of surging.

When starting, valves *1* and *3* are closed and *2* is opened to prime the pump. Then *2* is closed, the pump is started, and valve *3* is partly opened to fill the tank, the overflow assisting in maintaining the water levels. Then the model is turned over slowly by hand and valve *1* is opened. The model then is brought up to full speed, valve *3* being opened sufficiently to keep the tank full.

At full speed the volume of flow is determined largely by the centrifugal head generated in the holes *M*. With the small inlet head and with loss of head between *E* and *L*, the pressure in the hollow shaft near discharge is probably below atmospheric pressure. It is conceivable that this reduced pressure might affect the volume of flow. The drops in pressure between entrance and the shaft bore *L* can be reduced by beveling or rounding the various ducts when the liquid enters them; also by making the liquid rotate just before it leaves the enlargement *E*, at an angular velocity approaching that of the shaft. One way of accomplishing this is to rifle the bore of the hollow shaft. Raising the tank level also would raise the absolute pressure in the shaft bore *L*.

Some air was absorbed by the water as it discharged from drain *4*. The partition was included in the sump to prevent air entering the small pump and causing it to lose its priming. In a generator the drain pipes should be submerged; no partition then would be needed in the sump. Bubbles rose at times in the eudiometer, showing that the pipe *P* served a useful purpose. Descriptions of other interesting phenomena are omitted for brevity.

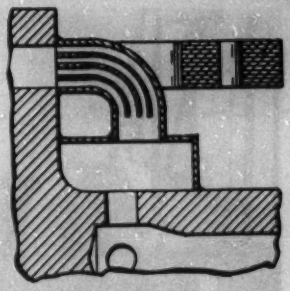

Figure 9. Section of rotor intake duct with guide vanes

Generator Rotor Losses and Water Temperature Rise

According to design calculations of a liquid-cooled generator, rated 100,000 kva., 85 per cent power factor, 3-phase, 3,600 rpm, with 0.81 short-circuit ratio, the total rotor I^2R loss is about 334 kw, with 254 kw loss in the embedded parts. If 55 gallons of water per minute are to absorb these 254 kw, the water temperature rise would be 17.6 degrees centigrade. The 80-kw loss in the coil ends

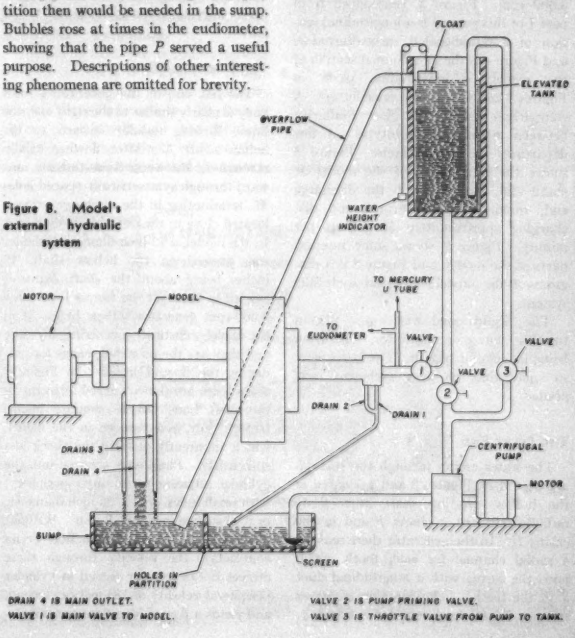

Figure 8. Model's external hydraulic system

would be taken up by the circulation of hydrogen, as described elsewhere. The hydraulic losses, most of which are in the internal centrifugal pump M, were found from measurements with a polyphase wattmeter in the driving motor circuit of the model to be 11.7 kw, which would cause the water temperature to rise 0.8 degree centigrade more. These losses appear mostly after the water has absorbed the rotor loss.

It may be desirable, to secure somewhat uniform temperatures longitudinally in the rotor copper in such a large generator, to reduce the water temperature rise by increasing the rate of flow. To secure a short-circuit ratio of about 0.81, with the large number of ampere-turns, a long air gap is necessary. The loss in the rotor surface due to tufting of flux from the stator teeth is very small. With a long air gap those stray losses (with balanced stator currents) appearing in the rotor surface are of little consequence. Also, when operated in a hydrogen atmosphere, the windage is small, and much of that loss is taken care of by the circulating hydrogen. Therefore, the only losses considered as affecting the rotor temperature rise have been the rotor I^2R. With the smaller ratings, for which an air atmosphere is proposed, the conditions are similar to the large machines with hydrogen.

In the discussion of the previous paper[1] it was stated that water cooling had been tried (the Parson's scheme) in 1915. One trouble was that air got into some ducts and caused bad mechanical unbalance. After the model had been balanced without water, there was no trouble with unbalance after water was admitted.

Mitigation of Coriolis' Forces

As may be found in various publications, the Coriolis' acceleration is given by the vector: $2\ (dr/dt)\times\omega$. For the liquid cooled rotor, (dr/dt) is the radial velocity of the liquid with respect to the rotor, and ω is the angular velocity. Multiplied by the mass density, this acceleration then gives the force per unit volume of liquid. With the relative flow in a radial direction, these forces are tangential.

At the entrance to the longitudinal ducts J, with sharp corners, suppose that a small volume of liquid turns the corner, and then flows axially. The velocity in the radial supply duct diminishes from the position at the bottom of the longitudinal duct J to the top thereof. Unequal tangential Coriolis' forces are produced which would cause the liquid to whirl just before entrance to J. At the exit end the phenomenon would be similar, but the sense of rotation of the whirl would be opposite. Such whirls would seriously obstruct the liquid flow.

In the model with the 16 curved tubes J, apparently the flow was not impeded by such whirls, as the flow was large. Evidently, if each tube had a straight portion longitudinally between two curved ends, there would not be any diminution in flow due to Coriolis' acceleration. Consequently, in an actual machine, if suitably curved tubes were used at each end, the harmful effects of the whirls would be eliminated. As such tubes would probably be of rectangular section (instead of circular, as in the model), and generally of unfavorable aspect ratios, they can conveniently be provided with curved guide vanes, as has been found very beneficial for stationary elbows. (An excellent article on reduction of losses by means of guide vanes is by Loring Wirt[5].) One of several suitable constructions is indicated in Figure 9.

Considering the casings H, on the side in which the liquid flows outward, as it leaves the holes F, it is moving in space at the tangential velocity corresponding to the outer diameter of the holes F. As the liquid moves outward in H, its tangential velocity would have to increase if it is to flow in radial paths (with respect to the rotor). The inertia (Coriolis) forces then would cause the liquid to fall back, with respect to the rotor, and thereby to flow in circumferential paths in opposition to the direction of rotation. With respect to outside space, it would move in the same direction as the rotor, but with reduced angular velocity. As this circumferential flow would interfere seriously with the desired radial flow, it is prevented by means of radial partition plates so that the liquid flows in radial paths (with respect to the rotor) as if there were radial ducts throughout.

On the return side the liquid flows radially inward, and the circumferential velocity tends to be in excess of that of the adjacent parts; that is, it moves at greater angular velocity in space than the rotor. Again partition plates are needed to prevent harmful circumferential flow.

When constraints cause the liquid to flow in prescribed paths, the Coriolis' forces produce pressure against the walls, all the way from the bore of the hollow shaft to the outermost radius of the radial ducts. On the outgoing side they act against rotation, and on the ingoing side with rotation; thereby torques are produced which substantially balance each other.

The possibility of resistance to flow at the entrance to, and the exit from, the rotor longitudinal cooling ducts J, shown in Figure 3, was brought to the writer's attention by Mr. C. M. Laffoon and Mr. R. A. Baudry of Westinghouse Electric Corporation. The further study of Coriolis' acceleration which was prompted by Laffoon and Baudry's warning led to a study of various means for mitigating the whirls arising from Coriolis' forces.

References

1. Liquid Cooling of A-C Turbine Generators—Part I, Carl J. Fechheimer. *AIEE Transactions*, volume 66, 1947, pages 553–64.

2. United States Patent 1,927,890. September 26, 1933.

3. Discussion by D. S. Snell of Vaporization Cooling of Large Electrical Machines, De Koning. *Power Generation* (Chicago, Ill.), September 1949, Figure 2, page 83.

4. The Cooling of Electric Machines, George E. Luke. *AIEE Transactions*, volume 42, June 1923, pages 636–52.

5. New Data for the Design of Elbows in Duct Systems, Loring Wirt. *General Electric Review* (Schenectady, N. Y.), June 1927, pages 286–96.

Discussion

D. S. Snell and C. E. Kilbourne (General Electric Company, Schenectady, N. Y.): The advantages of liquid cooling for rotating electric machines have long been recognized, and much time and effort have been expended by various manufacturers in the endeavor to make the application of liquid cooling to such machines a practical possibility. From a thermal standpoint, water is the ideal cooling agent for rotating electric machines and Mr. Fechheimer's analysis of the gains in output for turbine generators obtainable through a combination of water and hydrogen cooling in place of direct-hydrogen cooling appears to be entirely sound. In fact the gains he has shown are substantially confirmed by an analysis of stator and rotor heating for hydrogen-cooled generators given in a paper by D. S. Snell on Loading of Hydrogen-Cooled Generators at Elevated Gas Pressures[1] presented recently.

In Figures 6 and 16 of the Snell paper the temperature rises of the stator and rotor windings respectively, of a hydrogen-cooled generator, are shown to be made up of several components, some of which are influenced by the hydrogen pressure, others are independent of it. It can be shown readily that the components of temperature rise which are influenced by the hydrogen pressure would be nearly eliminated by the use of water cooling in place of direct hydrogen cooling; and since these components com-

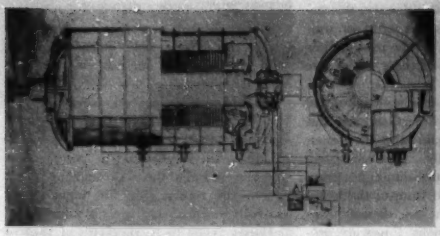

Figure 1. Horizontal hydrogen-cooled a-c generator with cooling pads in stationary-armature core

Figure 2. Unwound stationary armature for hydrogen-cooled a-c turbine generator rated at 50,000 kva, 3,600 rpm, 11,000 volts, 60 cycles, type ATB, 2 pole

prise, at 1/2-pound hydrogen pressure, approximately one-half of the total temperature rises of the windings, the use of water cooling in place of direct hydrogen cooling would reduce the temperature rise at a given load by nearly one-half; hence a large gain in output for the same temperature rises would be obtained.

It also is shown in the Snell paper,[1] that the temperature rise components which are influenced by hydrogen pressure become very small at high hydrogen pressures, so that at some pressure, possibly 50 pounds per square inch or higher, hydrogen cooling would become, from a thermal standpoint, nearly as efficient as water cooling. However, due to the increased windage losses at elevated hydrogen pressures, the operating efficiency of a generator at very high hydrogen pressures would not be as good as that of the generator proposed by Mr. Fechheimer, in which the stator and rotor cores are cooled with water and the end windings of both stator and rotor are cooled with hydrogen at 1/2 or 15 pounds per square inch pressure.

The General Electric Company has had considerable experience in the construction of rotating machines in which the stator is water cooled, and in most cases the cost of the added complications due to water cooling have more than offset the gains derived through increased cooling efficiency. Figures 1 and 2 of the discussion show the construction of the water-cooled stator for a 50,000-kva 3,600-rpm generator which the General Electric Company built for the Logan, W. Va., plant of the Appalachian Power Company, and which has been in successful operation for the past 13 years. The cooling of the stator core and embedded windings is accomplished by the use of hollow cooling pads sandwiched between the lamination packages, through which treated water is circulated. A heat exchanger outside the generator is provided for cooling the treated water. As shown in Figures 1 and 2, two types of cooling pads are used, one type being provided on one side with fins, the other type being plain. The finned pads are used in the center of the stator and serve to cool the hydrogen which is circulated for cooling the stator end windings and the rotor, as well as the core and embedded windings of the stator. The plain pads are used in the end portions of the core and cool only the core and embedded windings.

Although the performance of this generator has been entirely satisfactory and very little trouble with the cooling system has been experienced, this type of stator construction proved to be considerably more costly than the conventional type, using direct-hydrogen cooling and gas coolers, hence no other generators of this type have since been built.

In 1915 the General Electric Company built for test purposes, a 6,250-kva 1,800-rpm generator having a water cooled rotor, the operation of which was described in a discussion of Mr. Fechheimer's earlier paper.[2] This generator was successful from a thermal standpoint but gave considerable trouble mechanically. Mr. Fechheimer has demonstrated, by means of a model, that the mechanical problems inherent in the construction and operation of a water-cooled rotor can be successfully overcome. Whether the resultant complications in the rotor construction and in the auxiliary equipment will prove objectionable is another question, however, and this will require further study.

In the past several years hydrogen cooling has almost completely superseded air cooling for generators in sizes from 25,000 kw up, and now is being regularly applied to generators as small as 15,000 kw. Whether the additional expense of the hydrogen features can be justified for generators in these small sizes is debatable. Should water cooling be seriously considered as a successor to hydrogen cooling for generators, the lower limit of capacities in which water cooling would be economical would doubtless be considerably greater than with hydrogen cooling. It is quite possible, however, that for generators larger than about 60,000 kw, the additional cost and complication of water cooling would be more than offset by the savings due to the reduction in the amount of active material in the generator effected through water cooling. Also, for generators in sizes appreciably larger than those now being built with hydrogen cooling, it is probable that either a combination of water and hydrogen cooling as proposed by Mr. Fechheimer, or the use of direct-hydrogen cooling at very high pressures, would be necessary in order to make the construction of generators in these sizes a possibility.

We consider that Mr. Fechheimer deserves much credit for the design he has proposed, and for his persistence in promoting a system of generator cooling which offers as much promise as does liquid cooling.

References

1. Loading of Hydrogen-Cooled Generators at Elevated Gas Pressures, D. S. Snell. *AIEE Transactions*, volume 69, part I, 1950, pages 186–204.
2. See reference 1 of the paper.

Th. de Koning (Consulting Engineer, Philadelphia, Pa.): It is a pleasure to compliment Mr. Fechheimer on his paper. Why liquid cooling has been neglected for so long was a puzzle to me until I came to the conclusion that hydrogen cooling was so similar to air cooling that at first glance it looks as if the changes needed in the construction, and the development cost, would be small.

As is practically always the case when one takes half-measures, this one backfired. I have been told that hydrogen-cooling development costs were, and still are, outrageously high. This may be the reason why, when one dares suggest a better method of cooling, million dollar development cost-estimates regularly fly through the air. Perhaps Mr. Fechheimer will give us an idea of his development costs up to now?

We will all agree, according to the paper, the rotor design has been considerably improved. However the danger of the water circuits springing a leak, at a welded joint for instance, are not entirely eliminated. Should this happen, the end windings with the new construction of the stator, will get doused by part of the water-content of the rotor circuit. This calls for further improvement. I was glad to hear that the danger of air disturbing the rotor balance is eliminated. Did Mr. Fechheimer make tests of very long duration?

I regret that relatively so little space was given in the paper to liquid cooling of the stator. Liquid-cooled machines are small in size and weight, the stator core does not need air vents, and the insulation is more favorably stressed. A life time with air- and hydrogen-cooled machines must have left its mark. In the new design we get the air vents back in another form. The multitude of intricately bent small diameter water tubes now used is much more vulnerable and cools less evenly than the longitudinal channels in the solid stator core used in Mr. Fechheimer's earlier paper. See Figure 4 of the present paper.

A feature of liquid cooling in general, and of cooling the stator core in special, is that worked-out liquids used in the hydrogen coolers or vapor condensers are suitable. This cuts down on the amount of circulation liquid needed, and if boiler feedwater is used, the losses improve the thermal efficiency of the steam cycle. As the air gap is in the center of the heat losses, I do not consider it sound to attempt to ignore air

gap cooling since it has to be used for the end windings. Let each do its proper share, and with increasing load, the percentage of the stator iron and copper losses to be removed by liquid cooling can be increased very effectively.

My main objection is that when hydrogen is used for the air-gap all the difficulties with explosion proofing, shaft sealing, and hydrogen purity, and their auxiliary equipment remain. This reduces the attractiveness of this method of cooling very much. With air, hydrogen and vaporization cooling, all the heat is gathered by one medium. We cannot remove the hydrogen coolers, as about 3/10th of the rotor and stator copper losses remain to be removed by these coolers.

I think it reflects great credit on Mr. Fechheimer that, though he was instrumental in bringing hydrogen cooling to where it is today, he realizes that a better method of cooling is badly needed.

Carl J. Fechheimer: The commendatory statements of the discussers are very gratifying. I am pleased that Messrs. Snell and Kilbourne agree substantially with the gains given in Table I. In my opinion those rating ratios are conservative, and future experience will probably indicate that the water-cooled machine could be rated even higher.

The highest hydrogen pressure listed in that table is two atmospheres. With the same proportions as in the first seven items, a rotor with water in the ducts and with surroundings of one atmosphere of hydrogen, as compared with 30 pounds per square inch gauge of hydrogen in ducts and surroundings, gives a rating ratio of 1.27. Even if the hydrogen pressure is elevated to 50 pounds per square inch gauge, the rating is appreciably less than for the same water-cooled rotor. As stated by the discussers, the windage with the higher pressures affects the efficiency, and to a minor extent, the temperatures. Mr. Snell showed in his paper on elevated pressures that the rate of rating increase diminishes fairly rapidly as the pressures are raised; it is questionable whether it will pay to operate a hydrogen-cooled generator at pressures appreciably higher than 30 pounds per square inch gauge.

It is regrettable that the generator with a water-cooled stator built by General Electric Company some years ago was expensive. Recognition should be given to the following:

1. The first machine built in which the construction departs from previous machines, is always considerably more costly than succeeding ones with the new construction.

2. That the generator was probably limited by rotor heating; consequently, the stator's reduced temperature could not show advantageously from the cost standpoint. With the proportions obtainable with water cooling for rotor and stator, the over-all dimensions would be reduced and the cost would be lowered greatly.

3. The construction of the cooling pads is such as to make them expensive in comparison with the construction that I propose. Also, I am quite certain that a considerably larger number of pads were used than would be needed to obtain the usual guaranteed temperature. That is easily understandable, as it was the first of its kind. It is gratifying that the generator has been operating satisfactorily for 13 years; that should help to answer those who fear that a weld might leak.

As stated by the discussers, there is little doubt that the smaller and medium-sized generators can be made with considerable savings, with air for the surrounding internal gas. It is my belief that the reduction in D^2L obtainable with water cooling will reduce the costs so much that they can be water-cooled to advantage for sizes much smaller than 15,000 kw. Note that in Table I the 20-inch diameter is for a 10,000-kva rotor.

I am confident that large savings can be effected with generators larger than 60,000 kw also. Thus, the diameters and the length can be considerably reduced. The rotor diameter for 100,000 kva need only be 34 inches for 3,600 rpm, and then the stresses are sufficiently low to admit of standard carbon steel forging. It is my understanding that for an equal rating with hydrogen cooling the rotor diameter is such as to necessitate expensive alloy steel.

I suggest that comparisons be made by the estimating department of one or more manufacturers, of the cost of a large hydrogen-cooled generator, and one of equal rating that is water cooled. I would be pleased to co-operate in every way that I can. I believe that the engineers will then be surprised when they learn how large the savings will be. It is well that Messrs. Snell and Kilbourne consider water cooling favorably for generators for outputs greater than have been built so far.

In Figure 13 in the paper by Mr. Snell on elevated pressures, two ducts are shown for each rotor slot. Their combined sections are considerably greater than for water cooling. (Thus, for 100,000-kva rotor, the water duct dimensions are 0.188×2.4 inches.) Milling of two sets of ducts plus the extra milling for the small wedges for the tooth tunnels increases the cost of manufacture. Mr. de Koning's fears of the possibility of a water circuit springing a leak requires serious consideration. It is important that the duct systems be checked for leaks after completing the welds. In the model, after checking and welding leaks, before any water was admitted, there was no further trouble from that source. High-pressure high-temperature gasoline-cracking stills are welded, and it would be very serious if one of them were to spring a leak. High-pressure high-temperature boilers and piping are welded. The pressures and temperatures are low in the water-cooled stator. For the rotor, the temperatures are low, but the pressure in the cooling ducts may be of the order of 1,500 pounds per square inch in a 100,000-kva rotor. For both stator and rotor conditions are far more favorable than for the cracking-still or boiler. Skilled workmanship is required for the present hydrogen-cooled turbogenerator, and high-grade workmanship is needed for the water-cooled turbogenerator also.

As regards water cooling for the stator, the heat absorption and heat transfer rates with turbulent flow are so favorable that the heat can be transferred readily from the steel laminations to the water in the square tubes, even with the small surfaces. As stated in the paper, an insulating liquid is preferable from the thermal standpoint, particularly for high stator voltages.

The smaller D^2L obtainable with liquid cooling is advantageous to a utility company. For a given rating the ratio of D^2Ls is substantially the reciprocal of the ratio of ratings as given in Table I in the paper. Both the diameters and the length would be reduced, and consequently the weight would be less. This would then lower the cost of the generator's foundation. Also, the shorter length would mean lower building costs. These cost gains are in addition to the lower first cost of the generator itself.

Surface Heat-Transfer Coefficients for Hydrogen-Cooled Rotating Electric Machines

D. S. SNELL
MEMBER AIEE

R. H. NORRIS
NONMEMBER AIEE

MRS. B. O. BUCKLAND
MEMBER AIEE

Synopsis: A method is given for calculating the surface heat-transfer coefficients for hydrogen-cooled rotating electric machinery from the values of these coefficients as determined from tests in air. The influence of hydrogen purity and of the velocity exponent on the ratio of heat transfer in hydrogen to heat transfer in air is evaluated; also, for gas flowing in ducts, the effect of the type of flow on this ratio is discussed. A method is also given for calculating the heat-transfer coefficients for ventilating ducts, in either air or hydrogen, on an inlet temperature basis, as an aid to simplifying the calculation of the surface temperature rise.

IN THE calculation of the heating characteristics of rotating electric machinery, a knowledge of the heat-transfer coefficients which apply for the various cooling surfaces is essential. While values of these coefficients have been fairly well established for air-cooled machinery, relatively little has been published regarding the corresponding coefficients in hydrogen; and the few data which have been published appear to be inconsistent among themselves. (For example, in 1924, C. W. Rice[1] stated "the forced convection for high velocities over plane surfaces will be approximately equal in air and pure hydrogen and approximately 13 per cent greater in commercial hydrogen." In 1936, G. W. Penney[2] showed that for flat ducts a ratio of heat transfer in hydrogen to heat transfer in air of between 1.45- and 1.25-to-1 may be obtained in turbulent gas flow, while for velocities giving laminar flow in hydrogen the ratio may be considerably greater. Other authorities have given the hydrogen-air heat-transfer ratio as between 1.5- and 1.35-to-1.) In this paper an attempt has been made to reconcile these inconsistencies and to arrive at a basis for evaluating the heat-transfer coefficients in hydrogen from the values of these coefficients as determined from tests in air.

In the first section of the paper the various cooling surfaces in an electric rotating machine have been classified from a heat-transfer standpoint; then by the use of a convenient form of correlation which can be used for experimental data for any of these different surfaces, a general equation is derived. This equation gives the ratio of heat transfer in hydrogen to heat transfer in air (hereinafter often called merely the "hydrogen-air ratio") as a function of the ratios of the various gas properties and as a function of the exponent of the velocity in the correlation chosen to represent the heat-transfer coefficient for air.

Next, the available experimental data on heat transfer in hydrogen have been reviewed in an endeavor to confirm the accuracy of the derived equation for the hydrogen-air ratio. Satisfactory confirmation is obtained except for experiments wherein the hydrogen flow was not fully turbulent, so that comparison with fully turbulent air flow was not justified. Attention is thereby directed to the influence of the character of the gas flow on the hydrogen-air ratio for ventilating ducts.

For an ideal duct, having both smooth surface and rounded entrance, the minimum velocity limit for fully turbulent flow is much higher for hydrogen than for air. The hydrogen-air ratio for smooth ducts therefore may be considerably affected by a decrease in velocity below the limit of the turbulent range. The lower part of the range of gas velocities encountered in an idealized ventilating duct of a hydrogen-cooled machine is below this limit and therefore corresponds to flow with little or no turbulence.

For a duct having inlet conditions more closely simulating an actual ventilating duct in an electric machine, however, tests made by one of the authors indicate that the gas flow in such a duct may be fully turbulent, even though calculations indicate that laminar flow would be expected if the duct entrance were rounded; consequently the hydrogen-air ratio for turbulent flow seems likely to be applicable to lower velocities in such ducts than had been expected, and perhaps will apply to all of the ducts encountered in practical design work on rotating electric machines.

An example then is given, showing how the equation for the hydrogen-air ratio may be applied for determining the heat-transfer coefficients in hydrogen for a typical cooling surface in a hydrogen-cooled machine, from values of the coefficients determined from tests in air.

Finally, a method is described by which the heat-transfer coefficients for ventilating ducts, for either air or hydrogen, may be calculated on an inlet-temperature basis; which, for ducts of appreciable length, is frequently more convenient than the average-temperature basis commonly used.

Hydrogen-Air Heat-Transfer Ratio in Turbulent Flow for the Cooling Surfaces in Rotating Electric Machines

The principal cooling surfaces in hydrogen-cooled rotating electric machines from

Paper 50-29, recommended by the AIEE Rotating Machinery Committee and approved by the AIEE Technical Program Committee for presentation at the AIEE Winter General Meeting, New York, N. Y., January 30–February 3, 1950. Manuscript submitted November 1, 1949; made available for printing December 23, 1949.

D. S. Snell, R. H. Norris, and Mrs. B. O. Buckland are all with the General Electric Company, Schenectady, N. Y.

which heat is dissipated through forced convection are the following:

1. Radial ventilating ducts between stator laminations.
2. Axial and radial ventilating ducts in rotors (for turbine generators).
3. Outside surface of stator core.
4. Inside bore surface of stator.
5. Outside peripheral surface of rotor.
6. Sides of salient pole.
7. Rotor end windings (for turbine generators).
8. Stator end windings.
9. Finned tubes of surface gas cooler.

In the literature on heat transfer, theoretical and empirical relations have been derived for heat transfer from various types of surfaces by forced convection. These relations have been derived by the use of dimensional analysis for the form of the equations, and by tests to determine various numerical constants appearing in the equations.

Evaluation of the numerical constants depends upon the properties of the gas and hence upon the temperature for which the properties are evaluated. It is therefore essential, in employing any one of the various empirical correlations, to evaluate the gas properties for the temperature on which that particular correlation is based. This basis may be wall temperature, film temperature, inlet temperature, or average of inlet and outlet temperatures; but whichever it is, it should be recognized and used.

Most of the cooling surfaces, listed previously in an electric machine, may be classified as belonging to one or the other of these three types of configuration:

1. Internal surface of a duct, not necessarily round, but of a length which is much larger (by, say, 20 times) than the equivalent diameter. The diameter and not the length is here found to be the significant dimension for evaluating both the heat-transfer coefficient and also the Reynolds Number (the significance of which will be discussed later).

2. External surface of a body exposed to gas flow which is either parallel to the surface, starting at a leading edge, as for a flat plate, or perpendicular to the axis of the surface, as for flow across a cylinder, or across a salient pole, or across the conductors of an end winding. The dimension along the surface, more or less parallel to the flow, is here the significant dimension for evaluation of the heat-transfer coefficient and of Reynolds Number; for a flat plate it is length of the plate; for flow across a cylinder the cylinder diameter is commonly used.

3. Peripheral surface of rotor, and the stator surface immediately adjacent thereto. The clearance distance between rotor and stator here is believed to be the significant dimension.

For such surfaces in forced convection, it is convenient and customary in chemical and mechanical engineering to evaluate the heat-transfer coefficient as a product of several factors, in a form suggested by Colburn,[3] namely

$$h = jcG(c\mu/k)^{-2/3} \qquad (1)$$

This equation gives the value of the heat-transfer coefficient h in terms of mass velocity G, the gas properties c, μ, and k, and the dimensionless heat-transfer factor j. The factor j provides a useful means for correlating heat-transfer data on surfaces of different shapes; numerically, for many common shapes, it is approximately equal (within ±20 per cent) to the half-friction factor $f/2$, where f is the friction factor in the Fanning equation in hydraulics.

Using values of j determined by experiment equation 1 will be utilized in the following to determine the hydrogen-air ratio in turbulent flow for examples of two of the three classifications of surface mentioned previously. Treatment of the third could be made similarly.

A. Inside Surface of Smooth Straight Ducts

For this type of surface, which is the simplest example of ducts in general, the empirical relation for j in terms of Reynolds Number D_eG/μ and of length-to-diameter ratio L/D is plotted* in Figure 1. Only for Reynolds Numbers less than 8,000 does the ratio L/D have a controlling effect on the heat transfer, but then the curves here shown are restricted to round ducts; Norris and Streid[4] give

* The curves in Figure 1 are taken from reference 4 except that the values in the turbulent range have been reduced by 10 per cent to agree better with the consistent trend of more recent test results, including those of reference 5.

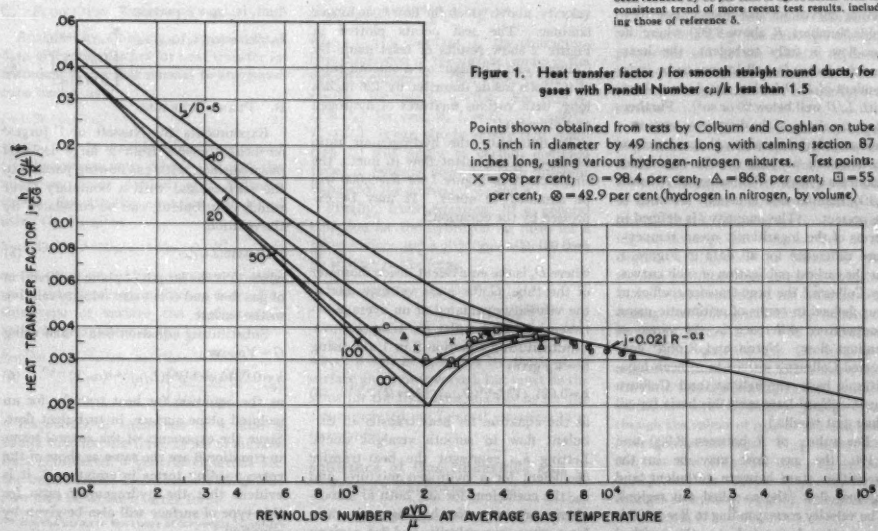

Figure 1. Heat transfer factor j for smooth straight round ducts, for gases with Prandtl Number $c\mu/k$ less than 1.5

Points shown obtained from tests by Colburn and Coghlan on tube 0.5 inch in diameter by 49 inches long with calming section 87 inches long, using various hydrogen-nitrogen mixtures. Test points: × = 98 per cent; ⊙ = 98.4 per cent; △ = 86.8 per cent; ⊡ = 55 per cent; ⊗ = 42.9 per cent (hydrogen in nitrogen, by volume)

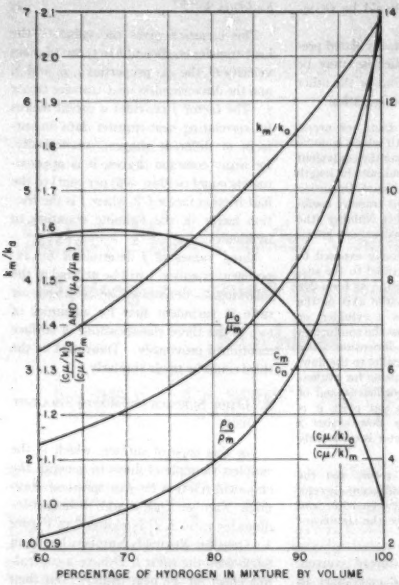

Figure 2. Ratios of properties of hydrogen-air mixtures to properties of air at 50 degrees centigrade

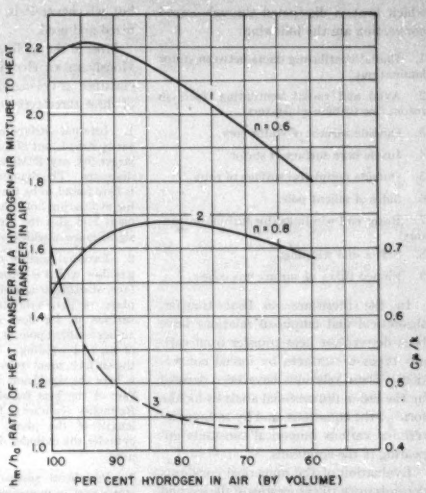

Figure 3. Calculated hydrogen-air heat-transfer ratio versus hydrogen purity for three types of surface. Also Prandtl Number versus hydrogen purity

Curves: 1—Heat-transfer ratio for gas flowing over staggered banks of cylindrical tubes. Velocity exponent $n=0.6$. 2—Heat-transfer ratio for gas flowing in smooth straight ducts or over plane surfaces. Velocity exponent $n=0.8$. 3—Prandtl Number $c\mu/k$

similar curves for flat ducts. For Reynolds Numbers, R, above 8,000, where the gas flow is fully turbulent, the heat-transfer factor is well known to be independent of L/D (unless the duct is short, with L/D well below 20 or so[4]). Furthermore the shape of the duct cross-section is immaterial (for common shapes, such as rectangular) as long as the equivalent diameter is used. For values of R below 2,100, laminar flow is usually assumed to be present. (The quantity j is defined in terms of the logarithmic mean temperature difference for all data in Figure 1. In the earliest publication of such curves, by Colburn,[3] the heat-transfer coefficient was defined in terms of arithmetic-mean temperature difference in the range of laminar flow. Norris and Streid[4] converted Colburn's curves to a mean logarithmic basis throughout, and Colburn and Coghlan[5] later used this basis for all their test results.)

For values of R between 8,000 and 2,100, the gas flow may be in the transition state between turbulent and laminar flow (the so-called dip region). The velocity corresponding to $R=2{,}100$ is commonly designated as the critical velocity, above which the flow is no longer laminar. The test points plotted in Figure 1 show results of tests made by Colburn and Coghlan[5] on a smooth tube of 0.5-inch inside diameter by 126 inches long, with various mixtures of hydrogen and nitrogen.

To determine the hydrogen-air ratio for gases in turbulent flow in ducts, the single curve in Figure 1 for $R>8{,}000$ will be assumed to apply. It may be expressed by the equation[8]

$$j=0.021\ (D_eG/\mu)^{-0.2} \tag{2}$$

where D_e is the equivalent inside diameter of the tube, G the mass velocity, and μ the viscosity evaluated at an average between inlet and outlet gas temperatures.

Substituting equation 2 in 1 and using $G=V\rho$ gives

$$h=0.021\ cV^{0.8}\rho^{0.8}(D_e/\mu)^{-0.2}(c\mu/k)^{-2/3} \tag{3}$$

as the equation for heat transfer in turbulent flow in smooth straight ducts. Letting h_{m1} represent the heat-transfer coefficient for a hydrogen mixture, and h_{a1} the coefficient for air, both at atmospheric pressure, the hydrogen-air ratio for a given gas velocity and for a given duct, is, from equation 3

$$h_{m1}/h_{a1}=(c_m/c_a)(\mu_m/\mu_a)^{0.2}(\rho_m/\rho_a)^{0.8}\times\left[\frac{(c\mu/k)_a}{(c\mu/k)_m}\right]^{2/3} \tag{4}$$

B. Plane Surfaces

Experiments by Nusselt and Jurges[6] on heat transfer from a large isolated plane surface, with gas flowing parallel to the surface and with a boundary layer which is turbulent, can be correlated by the relation

$$j=0.0346(LG/\mu)^{-0.2} \tag{5}$$

where L is the length of plane in direction of gas flow and G is mass velocity relative to the surface.

Substituting equation 5 in 1 and using $G=V\rho$ gives

$$h=0.0346\ cV^{0.8}\rho^{0.8}(L/\mu)^{-0.2}(c\mu/k)^{-2/3} \tag{6}$$

as the equation for heat transfer for an isolated plane surface, in turbulent flow. Since the exponents of the several terms in equation 6 are the same as those of the corresponding terms in equation 3, it is evident that the hydrogen-air ratio for this type of surface will also be given by equation 4.

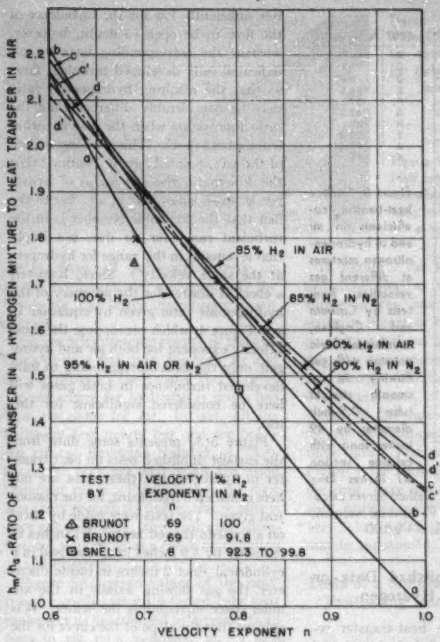

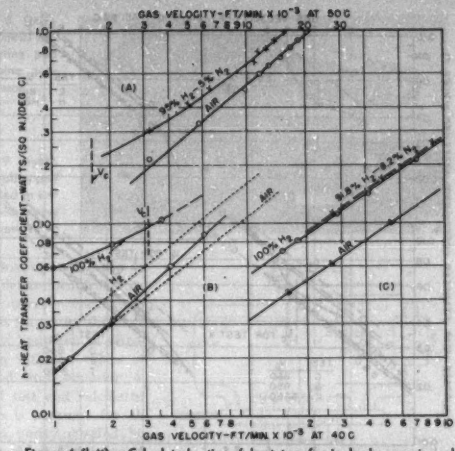

Figure 4 (left). Calculated ratio of heat transfer in hydrogen-air and hydrogen-nitrogen mixtures to heat transfer in air versus velocity exponent (equation 11). Test values shown for comparison

Figure 5 (above). Surface heat-transfer coefficients in air and hydrogen at different gas velocities from tests near atmospheric pressure

Curves: A—Tests by Rice on torpedo-shaped heater of 1.1-inch diameter by 5.9 inches long enclosed in cylinder of 2 inches inside diameter with axial gas flow. B—Tests by Penney on flat duct 3/8-inch wide. Dotted curves calculated from equation 3 for duct of 0.75-inch diameter. C—Tests by Brunot on finned-tube heat exchanger. V_c = critical velocity, corresponding to $R = 2{,}100$

C. Flow Over Banks of Tubes

Analysis by Colburn of experimental data gives the relation for heat transfer in turbulent** gas flow normal to staggered tube banks, as

$$j = 0.33\ (D_oG/\mu)^{-0.4} \tag{7}$$

where D_o is the outside tube diameter and G is the average mass velocity through the minimum cross section area between tubes. Substituting equation 7 in 1 and using $G = V\rho$ gives

$$h = 0.33c\ V^{0.6}\rho^{0.6}(D_o/\mu)^{-0.4}(c\mu/k)^{-2/3} \tag{8}$$

as the equation for heat transfer for staggered tube banks in turbulent flow. For this type of surface the hydrogen-air ratio, from equation 8, is

$$h_{m1}/h_{a1} = (c_m/c_a)(\mu_m/\mu_a)^{0.4}(\rho_m/\rho_a)^{0.6}\times\left[\frac{(c\mu/k)_a}{(c\mu/k)_m}\right]^{2/3} \tag{9}$$

Inspection of equations 3, 6, and 8 shows that for the three types of surface here considered, a general equation for the heat-transfer coefficient for turbulent flow may be written, of the form

$$h = C_1c(\mu/L')^{1-n}V^n\rho^n(c\mu/k)^{-2/3} \tag{10}$$

where C_1 is a constant, L' the characteristic dimension of the surface, and n is the velocity exponent. (For cases A and B, $n = 0.8$; for case C, $n = 0.6$. For case A, $L' = D_o$; for case B, $L' = L$; for case C, $L' = D_o$) It can also be shown that equation 10 will apply to certain common types of laminar flow, but with different values for the constants C_1 and n.

Finally, from equation 10 a general equation for the hydrogen-air ratio for a given surface and a given gas velocity may be written in the form

$$h_{m1}/h_{a1} = (c_m/c_a)(\mu_m/\mu_a)^{1-n}(\rho_m/\rho_a)^n\times\left[\frac{(c\mu/k)_a}{(c\mu/k)_m}\right]^{2/3} \tag{11}$$

where n will be specified by the type of surface and flow involved, but must be the same for the hydrogen mixture as for the air, as pointed out later, if equation 11 is to be valid.

Influence of Gas Impurities and of Velocity Exponent

The general equation 11 for the hydrogen-air ratio in turbulent flow derived in the foregoing section shows this ratio to be determined by the ratios of the gas properties and by the velocity exponent in the heat-transfer equation; the latter, in turn, being determined by the type of surface.

To illustrate the influence of hydrogen impurities on the hydrogen-air ratio, the latter will be calculated for values of $n = 0.8$, corresponding to surfaces of cases A and B; and 0.6, corresponding to case C, in the foregoing section. Assuming an average gas temperature of 50 degrees centigrade, the ratios of the various gas properties given by equation 11 have been calculated for different percentages of hydrogen in air, by volume, as shown in Figure 2. It will be observed that $c_m/c_a = \rho_{a1}/\rho m_1$ for the hydrogen mixtures considered. It also is noted that the ratio $(c\mu/k)_a/(c\mu/k)_m$ shows a marked variation with hydrogen purity, even though the values of $c\mu/k$ for air and pure hydrogen are the same. This follows from the fact that the ratios c_m/c_a, μ_m/μ_a, and h_m/h_a vary in different manner with changes in hydrogen purity, as explained in reference 7.

The values of the various ratios given

** For the limits to the range of Reynolds Numbers over which equation 7 is valid, see reference 8.

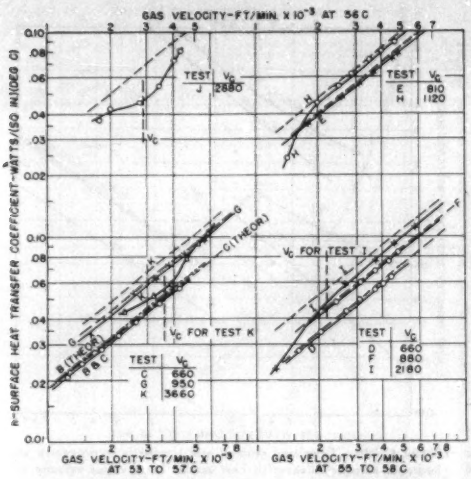

TEST	% H_2 IN N_2
B	(AIR)
C	(N_2)
D	8.8
E	28.5
F	37
G	42.9
H	55
I	86.8
J	94.4
K	98

Figure 6. Surface heat-transfer coefficients in air and in hydrogen-nitrogen mixtures at different gas velocities, from tests by Colburn and Coghlan, near atmospheric pressure with gas flowing in a smooth straight tube 0.5-inch diameter by 49 inches long with calming section 87 inches long

Solid curves from tests. Dashed curves calculated from equation 3. V_c = critical velocity, corresponding to $R = 2{,}100$

by Figure 2 have been applied in equation 11 to calculate the hydrogen-air ratio for the various types of surfaces at different values of hydrogen purity, as shown in Figure 3. It will be observed that for gas flow in smooth ducts or over plane surfaces, where $n = 0.8$, the hydrogen-air ratio has a value for pure hydrogen of 1.47; with decreasing purity the ratio at first increases, reaching a value of 1.68 for 82 per cent hydrogen in air, and then decreases. (For pure hydrogen the above value of the ratio is the same as was found by Pohl[8] for heat transfer in smooth tubes, by the use of the Nusselt equation for heat transfer, in which $n = 0.786$.) For gas flow over staggered tube banks, where $n = 0.6$, Figure 3 indicates that the ratio is 2.16 for pure hydrogen and rises to a maximum of 2.21 for a 94 per cent hydrogen-air mixture.

To show the effect of the velocity exponent n on the heat-transfer ratio, the latter has been calculated from equation 11 for several values of n from 0.6 to 1.0, and for four different values of hydrogen purity, using both air and nitrogen as the contaminating gas, with the results shown in Figure 4. The ratio is shown to increase sharply with decreasing n, while the influence of hydrogen purity on the ratio is shown to be the greatest for the highest values of n, and vice versa. For $n = 1.0$, which corresponds approximately to the type of flow in rough-walled ducts (as in axial ducts through iron laminations), the ratio is less than unity for pure hydrogen, but is 1.32 for 85 per cent hydrogen purity.

Correlation of Published Data on Heat Transfer in Hydrogen

Figures 5 and 6 give heat-transfer coefficients in hydrogen and air for several types of surfaces as determined from tests by various investigators. Many of the data in hydrogen were obtained at velocities sufficiently low for the turbulence of the flow to be open to doubt, however, whereas the corresponding tests for air indicated fully developed turbulent flow; so that the resulting hydrogen-air ratio may be considerably different than the ratio appropriate when the flow is turbulent for both gases. (This is a consequence of the fact, pointed out by Penney,[3] that the kinematic viscocity (μ/ρ) of hydrogen is seven times that of air; hence the fact that the Reynolds Number is in the turbulent range for air does not imply that it remains in this range for hydrogen, at the same velocity.) Since, however, a check is desired for the accuracy of the hydrogen-air ratio given by equation 11 and Figure 4, which presuppose the same velocity exponent for both air and hydrogen, only the data corresponding to fully developed turbulence in both gases will here be considered significant for this use.

Figure 5(A) presents some data from the earliest published tests on heat transfer in hydrogen, but these data are not here considered significant, for the reasons just given. The tests were made by Rice[9] on a torpedo-shaped heater, 1.1 inches in diameter by 5.9 inches long, enclosed in a cylindrical duct 2 inches in inside diameter, the gas flowing axially in the annular space surrounding the heater. It is evident that the slope of the curve for the hydrogen-nitrogen mixture is lower than that for air. Furthermore, the general magnitude of all the data in Figure 5(A) are much above the magnitude to be ex-

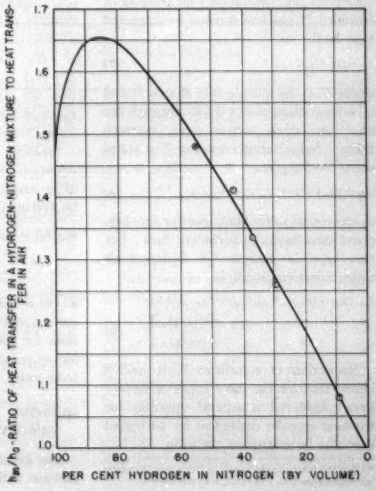

Figure 7. Calculated ratio of heat transfer in hydrogen-nitrogen mixtures to heat transfer in air for gas at 56 degrees centigrade and approximately atmospheric pressure, flowing in a smooth straight duct of 0.5-inch diameter, in fully developed turbulence. Test values by Colburn and Coghlan shown for comparison

Figure 8 (left). Monel-metal stator cooling pad for turbine generator

Figure 9 (right). Half cooling pad assembled in test box, with cover removed

pected from all subsequent tests on similar configurations; unfortunately the reason for this latter discrepancy is not evident.

Figure 5(B) presents results of tests by Penney[5] on a flat duct, for both air and pure hydrogen. Here again the slope of the test curve for hydrogen is much less than the slope for air; in fact, all the hydrogen test points but one are below the critical Reynolds Number of 2,100, hence the tests are well below the usual turbulent range. Furthermore, the duct was short enough so that entrance effects were not negligible; the results are therefore not applicable as a check on equation 11 and Figure 4.

Figure 5(C) gives values of the heat-transfer coefficient for a finned-tube heat exchanger as determined by Brunot[7] from tests in air, pure hydrogen, and a 91.8 per cent hydrogen-nitrogen mixture. The degree of turbulence was apparently the same for the air tests and the tests in the other gases, since the slopes of the curves are alike, yielding a velocity exponent of 0.69 and heat-transfer ratios of 1.75 for pure hydrogen and 1.8 for the hydrogen-nitrogen mixture. Referring to Figure 4, these two ratios are observed to be only 4 and 6 per cent respectively below the calculated values of the ratio for $n=0.69$, which may be considered a reasonably good check.

Figure 6 gives the results of several tests made by Colburn and Coghlan[8] for determining the heat-transfer coefficients in a smooth straight tube 0.5 inch in diameter by 49 inches long, with an 87-inch long calming section upstream, using air, nitrogen, and various hydrogen-nitrogen mixtures. These same results have also been included in Figure 1, in the alternative form of j-factor versus Reynolds Number. Values calculated from equation 3 are also shown in Figure 6 and are observed to agree closely with the test values whenever the velocity is well above the critical; furthermore, the velocity exponent, for turbulent flow, was 0.8 for all tests where the velocity was well above the critical.

In Figure 7 the hydrogen-air ratio in turbulent flow, as determined from the values of the heat-transfer coefficients given in Figure 6, is shown for different percentage values of hydrogen in nitrogen, for comparison with the values of this ratio calculated from equation 4. Close agreement of test and calculated values of the ratio is obtained for all values of hydrogen purity covered by these data. Test data are not shown in Figure 7 for hydrogen purities above 55 per cent, since all of the test results for such purities were for Reynolds Numbers below 6,000; hence, the turbulence may be questioned.

Tests of a Simulated Stator Ventilating Duct Using Hydrogen

In 1936, in connection with the design of a hydrogen-cooled generator provided with a system of water cooling for the stator core,[10] tests were made by one of the authors, on one of the finned cooling pads which were used in the stator, which furnished information on the relative heat-transfer coefficients and friction factors in hydrogen and air in long, narrow ducts. These tests are described in Appendix II. In the following, the principal results of these tests are given.

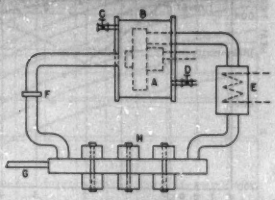

Figure 10. Schematic arrangement of test apparatus

A—Blower. B—Enclosure for A. C—Vent valve. D—Connection to hydrogen supply. E—Heater. F—Flow nozzle. G—Water supply and discharge lines from cooling pad. H—Cooling pad assembly

Heat-Transfer Tests

The construction of the cooling pads for the water-cooled stator is illustrated in Figure 8. For the tests, one of the finned pads was cut in two between the

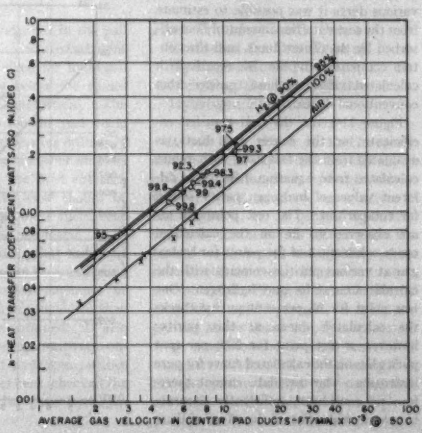

Figure 11. Estimated heat-transfer coefficients for center ducts of cooling pad from tests in air and hydrogen-nitrogen mixtures near atmospheric pressure, with values calculated from equation 3 shown for comparison

Numbers on test points give hydrogen purity at which tests were made. Points X = tests in air, ⊙ = tests in hydrogen

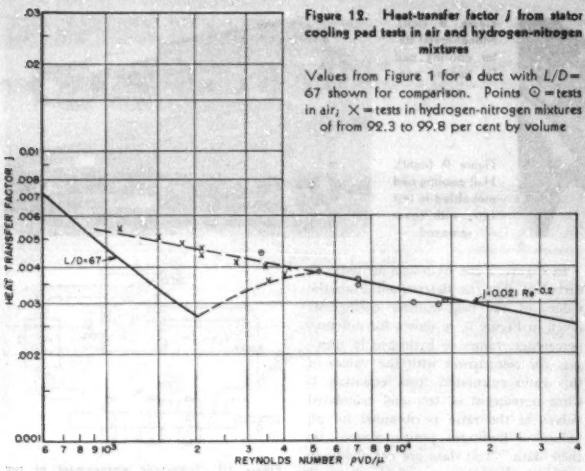

Figure 12. Heat-transfer factor j from stator cooling pad tests in air and hydrogen-nitrogen mixtures

Values from Figure 1 for a duct with $L/D=67$ shown for comparison. Points ⊙ = tests in air; × = tests in hydrogen-nitrogen mixtures of from 92.3 to 99.8 per cent by volume

padteeth, the opening thus made was brazed shut and a water connection added. The half-pad was assembled in a flat wooden box, with openings at either end for the circulation of gas through the ducts formed by the fins on the outer surface of one side of the pad, Figure 9. Water was circulated through the inside of the pad. The test arrangement is illustrated in Figure 10. The ducts formed by the pad fins were of various lengths and widths; however, about 75 per cent of the total pad and fin surface area was covered by ducts which were of fairly uniform length and cross section. By consideration of the cross section and surface areas of the various ducts it was possible to estimate from the test data the amount of heat absorbed by the center ducts, and thus obtain comparison of the test results with calculated values of heat transfer from conventional ducts.

Figure 11 gives the heat-transfer coefficients for the center pad ducts, as evaluated from the test data, with values calculated from equation 3 for three different values of hydrogen purity shown for comparison. The test points in air are observed to lie on the calculated curve, while most of the points for hydrogen at various purities coincide with the calculated curve for pure hydrogen. One test point for 95 per cent purity checks the calculated curve at this purity; however, a test point for 92.3 per cent purity lies on the calculated curve for pure hydrogen. The test data cannot therefore be considered sufficiently accurate to permit evaluation of the effect of these small variations in hydrogen purity on the heat transfer. The slope of the test curves for both air and hydrogen indicate a velocity exponent of 0.8 and a hydrogen-air ratio of 1.47, checking the value given by the curve in Figure 4 for pure hydrogen for $n=0.8$.

In order to consider how near to the laminar range these test data extend, the data have been expressed in the form of the heat-transfer factor j and plotted versus Reynolds Number as shown in Figure 12.

The j—R curve from Figure 1 for the L/D value pertinent to the center pad ducts also is shown. It will be observed that, except for two test points which lie below the trend of all the rest, all of the test points, for both hydrogen and air, agree closely with the curve calculated from equation 2 even for values of R well below the critical. This indicates that completely developed turbulence was present in the ducts down to Reynolds Numbers much lower than would be expected from experience with ducts with calming sections or rounded inlets.

Friction-Loss Tests

Following the heat-transfer tests, tests were made to determine the pressure loss in the pad at various gas velocities in both air and hydrogen. From the measured total pressure drop across the pad assembly, the friction loss in the pad ducts was estimated by deducting the calculated losses in the pad enclosure plus an estimated duct entrance loss calculated for two different assumed values for the entrance-loss coefficient, K_e, namely: 0.3 and 0.5. From the friction losses thus determined, the half-friction factor was calculated from the equations given in Ap-

Figure 13. Half-friction factor $f/2$ from stator cooling pad tests in air and hydrogen-nitrogen mixtures

Values shown are calculated by deducting from measured total losses the calculated external losses and the duct entrance losses as estimated for loss coefficient K_e assumed = 0.3 and 0.5. Theoretical values of $f/2$ for duct having $L/D_e=67$ shown for comparison. ⊙ and △ = tests in air; × and ⊡ = tests in hydrogen-nitrogen mixtures of from 95.3 to 98.6 per cent by volume

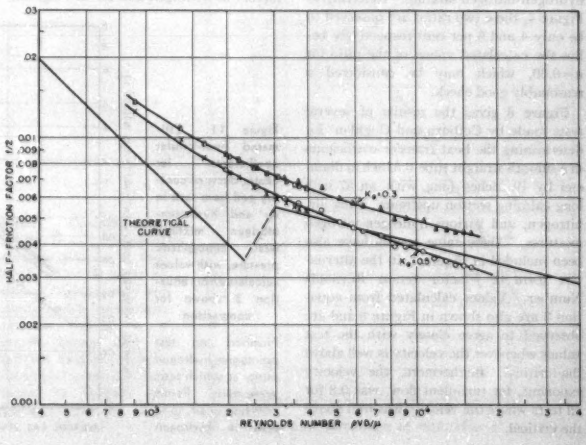

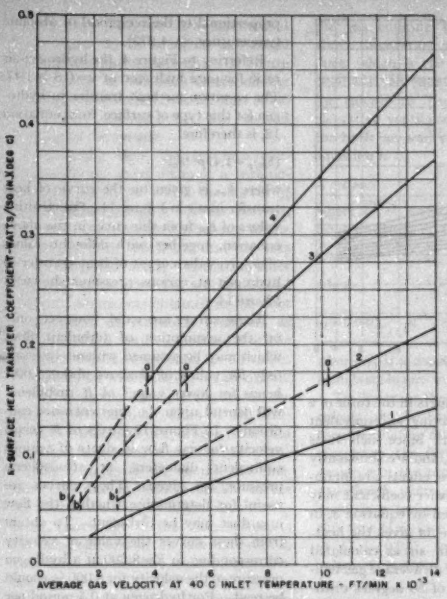

Figure 14. Surface heat-transfer coefficients for axial ventilating duct of turbine generator rotor in air and hydrogen, calculated with reference to average gas temperature in duct

Air curve from equation 3. Hydrogen curves from equation 13. For duct with equivalent diameter $D_e = 0.75$ inch. Average gas temperature 50 degrees centigrade. Velocities at points *a* and *b* correspond to Reynolds Numbers of 8,000 and 2,100, respectively. Curves: 1—Air at atmospheric pressure. 2—Hydrogen at 0.5 pound per square inch gauge. 3—Hydrogen at 15 pounds per square inch gauge. 4—Hydrogen at 25 pounds per square inch gauge

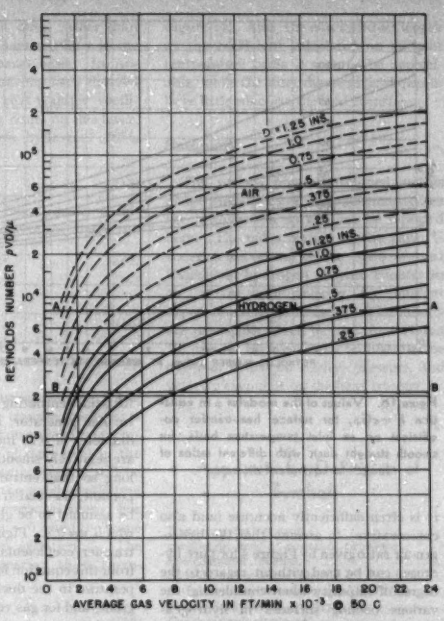

Figure 15. Values of Reynolds Number *R* at different gas velocities in ducts of various equivalent diameters, for air and pure hydrogen at 50 degrees centigrade and atmospheric pressure

Dashed curves for air. Solid curves for hydrogen. Lines A–A and B–B give upper and lower critical Reynolds Numbers, respectively. To obtain values of *R* at any gas pressure *p*, multiply values from curves by *p* (pressure in atmospheres)

pendix II, the calculated values being shown in Figure 13 for the different values of Reynolds Number. Figure 13 also gives the theoretical values of $f/2$ as presented by Colburn.[3]

It will be observed that the values of $f/2$ calculated from the pad tests for the assumption of $K_e = 0.5$ agree reasonably well with the theoretical values for fully developed turbulence, and that all values lie on a smooth curve which extends far into the transition and laminar regions of flow.

Since the half-friction factor should bear a nearly constant relation to the heat-transfer factor j, the similarity of the test curves of j and $f/2$ as shown in Figures 12 and 13 respectively tends to support the conclusions obtained from the heat-transfer tests.

It may be concluded from both the heat-transfer and friction-loss tests, therefore, that entrance conditions in the pad enclosure were such as to induce turbulent gas flow in the ducts even for hydrogen velocities considerably below the values customarily regarded as critical. The length/diameter ratio for the pad ducts was many times greater than is ordinarily used in the ventilating ducts of an electric machine, so that the duct entrance conditions in the latter case should be even more certain to promote turbulence than was the case in the pad tests.

It therefore seems likely that turbulent gas flow will be obtained in the ventilating ducts of hydrogen-cooled machines at velocities below which nonturbulent flow could theoretically be obtained. It also was shown that the hydrogen-air ratio obtained in the tests, at hydrogen purities between 92 and 99.8 per cent, checked the values of this ratio for pure hydrogen given by Figure 4.

Heat-Transfer Coefficients as Evaluated for One Type of Hydrogen-Cooled Surface, Including the Effect of the Hydrogen Pressure

It has been shown in the foregoing sections of the paper that the calculated ratios of heat transfer in hydrogen to heat transfer in air, as given by equation 11 and Figure 4, are in general agreement with available test data except where the turbulence is less in the hydrogen tests than in the air tests. It is evident, furthermore, from Figure 4, that the effect of impurities in the hydrogen, for hydrogen purities above about 95 per cent, is relatively small for the common range of n-values from 0.6 to 1.0. Considering that the gas purity in hydrogen-cooled machines is usually maintained as high as practicable (between 95 and 99 per cent),

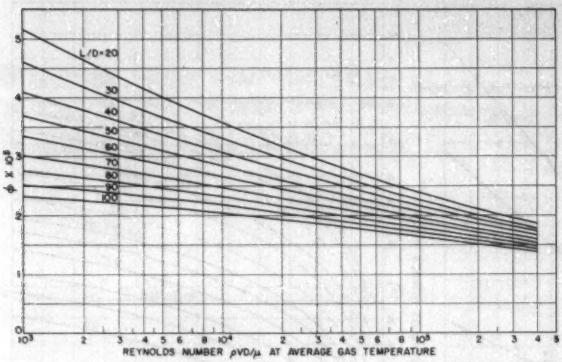

Figure 16. Values of the modulus ϕ in equation $h' = cG\phi$, for surface heat-transfer coefficient on an inlet temperature basis, for smooth straight ducts with different ratios of length to equivalent diameter

it is often sufficiently accurate (and also conservative) to assume that the hydrogen-air ratio given by Figure 4 for pure hydrogen can be used without regard to the degree of impurity when considering the various cooling surfaces in hydrogen-cooled machines. The heat-transfer coefficients in hydrogen at atmospheric pressure therefore may be obtained from the coefficients determined for these surfaces in air, merely by multiplying the latter by the value of $h_{m1}/_{a1}$, for pure hydrogen from Figure 4 corresponding to the velocity exponent n determined from the air tests.

Since the pressure of the hydrogen is, however, always above atmospheric in practice, an additional factor must be used to show the effect of pressure on the heat transfer. From equation 10, which shows the heat transfer to be proportional to the nth power of the gas density, the heat transfer for a given gas velocity at a given temperature must be proportional to p^n, where p is the hydrogen pressure in atmospheres. The gas properties other than density in equation 10 have been shown by Nusselt to be independent of pressure, for pressures at least up to 190 pounds per square inch gauge. Hence for a given gas velocity and temperature, the heat-transfer coefficient in hydrogen at any pressure is

$$(h_m)_p = (h_{m1}/h_{a1})p^n h_{a1} \qquad (12)$$

To illustrate the use of equation 12 in calculating the heat-transfer coefficients in hydrogen for rotating electric machines, these coefficients will be calculated for axial ventilating ducts in the rotor of a turbine generator, having an equivalent diameter of 0.75 inch. Since such ducts are relatively smooth, and are sufficiently long so that entrance effects are unimportant, the heat-transfer coefficient may be assumed to be given by equation 3, in which $n = 0.8$. Figure 14 gives the heat-transfer coefficients in air as calculated from this equation for an average gas temperature in the duct of 50 degrees centigrade, and for gas velocities calculated for an inlet temperature of 40 degrees centigrade. To correct the coefficients for any other temperature t_C, the coefficients should be multiplied by the correction factor

$$K_{t40} = \left[\frac{273+40}{273+t_C}\right]^n$$

since density, for a given pressure, is proportional to the reciprocal of absolute temperature, $(t_C + 273)$.

Referring to Figure 4, the hydrogen-air ratio for pure hydrogen at $n = 0.8$ is 1.47. The equation for heat transfer in hydrogen for this type of surface, from equation 12, is therefore

$$(h_m)_p = 1.47p^{0.8}h_{a1}$$

where h_{a1} is given by the curve of heat transfer in air in Figure 14. Substituting values of h_{a1} from this curve in the above equation, together with different values of p, gives the curves of heat transfer in hydrogen at various pressures shown in Figure 14.

These curves are valid, however, only on the assumption of turbulent flow, which may be assumed without question only for values of R above about 8,000; hence for lower values of R turbulence will depend upon the duct entrance conditions. In Figure 15 curves of R versus velocity for gas flow in ducts of various equivalent diameters, at atmospheric pressure, are given. These curves are useful for determining whether the flow in a duct may be turbulent. To obtain from these curves the value of velocity corresponding to $R = 8{,}000$ at a hydrogen pressure p, the velocity for $8{,}000/p$ should be read. For hydrogen at 0.5 pound per square inch gauge flowing in a duct of 0.75-inch equivalent diameter, reference to Figure 15 for $R = 8{,}000/1.03 = 7{,}750$ indicates a velocity of 10,200 feet per minute. For the critical value of $R = 2{,}100$, the corresponding velocity is 2,700 feet per minute. For hydrogen at pressures of 15 and 25 pounds per square inch gauge, respectively, the duct ve-

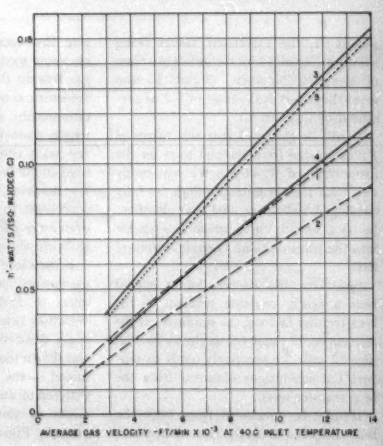

Figure 17. Surface heat-transfer coefficients for axial ventilating ducts of turbine-generator rotor in air at atmospheric pressure and in hydrogen at 0.5 pound per square inch gauge pressure, calculated with reference to inlet gas temperature. Average gas temperature 50 degrees centigrade

Curves: 1—Air, $D_e = 0.75$ inch; $L/D_e = 40$. 2—Air, $D_e = 0.75$ inch; $L/D_e = 80$. 3—Hydrogen, $D_e = 0.75$ inch; $L/D_e = 40$. 4—Hydrogen, $D_e = 0.75$ inch; $L/D_e = 80$. 5—Hydrogen, $D_e = 1.0$ inch; $L/D_e = 40$

locities for $R=8{,}000$ are determined from Figure 15 to be 5,200 and 3,800 feet per minute respectively. In Figure 14 the range of velocities corresponding to a range of R-values from 2,100 to 8,000 have been indicated by the dashed portions of the curves.

Considering that the entrance conditions for the axial ducts of a turbine-generator rotor, for which the curves of heat transfer in Figure 14 were derived, are such as to promote turbulence in the gas stream in the duct, and that the tests on a simulated stator ventilating duct described in the preceding section showed that turbulence was obtained in the duct in hydrogen at Reynolds Numbers as low as 1,100, it may be assumed that the curves in Figure 14 are valid for all values of velocity for which the curves are drawn.

The foregoing example illustrates the method of obtaining values of the heat-transfer coefficients in hydrogen from data obtained from tests in air, for one of the cooling surfaces in an electric machine. For other cooling surfaces, similar curves for heat transfer in hydrogen may be derived, providing: 1. that the coefficients for these surfaces in air are known; 2. that these coefficients, when plotted versus velocity on log-log scales, give a straight line; and 3. that the lowest Reynolds Number for the hydrogen curve is not lower than the lowest Reynolds Number obtained in the air test, unless there is reason to expect that the air curve, on log-log scales, if extended, still would give a straight line. The slope of such a line represents the velocity exponent n. Reference to the curve for pure hydrogen in Figure 4 gives the corresponding value of h_{m1}/h_{a1}, which then is substituted in equation 12, giving the equation from which the heat-transfer coefficients in hydrogen at various pressures may be determined.

If condition 2 given in the preceding paragraph should not be met, it still would be possible to obtain curves of heat transfer in hydrogen by plotting the j-factor versus Reynolds Number from the air test. This curve should be the same in hydrogen as in air.

Calculation of Heat-Transfer Coefficients for Ventilating Ducts on an Inlet Temperature Basis

In calculating the temperature rise of the surfaces of ventilating ducts having appreciable length (such as the axial ventilating ducts in a turbine-generator rotor) it is often convenient to use heat-transfer coefficients based on the temperature rise of the surface above the temperature of the gas entering the duct, rather than above the average gas temperature in the duct, which is the usual basis. In Appendix II an equation has been derived for calculating the heat-transfer coefficients for ventilating ducts on this basis, for both air and pure hydrogen. This equation is

$$h' = cG\phi \tag{13}$$

where h' = surface heat transfer coefficient on an inlet temperature basis and

$$\phi = (1-e^{-m})D_e/4L \tag{14}$$

where

$$m = 5.08C_1\frac{L}{D_e}R^{n-1} \tag{15}$$

where C_1 is a constant, to be determined from tests in air.

To illustrate the use of equation 13 in calculating the heat transfer coefficients for a ventilating duct on an inlet temperature basis, the type of duct used in the example in the preceding section will be considered, namely the axial ventilating ducts in a turbine-generator rotor. For this type of surface, $n = 0.8$ and the value of C_1 is 0.021, from equation 3. The value of m, from equation 15, is therefore

$$m = 0.107\frac{L}{D_e}R^{-0.2} \tag{16}$$

Using values of m from equation 16, values of ϕ have been calculated from equation 14 for different values of R and of the ratio L/D_e, and are shown in curve form in Figure 16. These curves permit a convenient evaluation of the factor ϕ at different gas velocities, for ducts of various lengths and equivalent diameters, of the type for which $n = 0.8$.

Assuming an average gas temperature in the duct of 50 degrees centigrade, and an inlet gas temperature of 40 degrees centigrade, and using $G = V\rho$, equation 13 becomes, for either air or pure hydrogen

$$h' = 0.0036\,\rho V\phi$$

Using this equation, curves of heat-transfer coefficients on an inlet temperature basis, versus duct velocity, have been calculated, and are shown in Figure 17, for straight smooth ducts of 0.75- and 1.0-inch equivalent diameter, respectively, for L/D_e = 40 and 80, respectively, and for air at atmospheric pressure and hydrogen at 0.5 pound per square inch gauge pressure. It will be observed that these curves give significantly lower values of heat transfer than the curves for the same type of duct calculated on an average gas temperature basis shown in Figure 14. Also, the effect of duct length on the coefficient calculated on an inlet temperature basis is seen to be appreciable, while the duct diameter is shown to have little effect on the heat transfer.

Summary

The various points developed in this paper already have been summarized in the introduction so will not be repeated here. The main feature of the paper is the determination of the ratio of heat transfer in hydrogen to heat transfer in air, at the same velocity, for different types of cooling surfaces. The results are principally given by equations 11 and 12, and by Figure 4, which illustrate the effect of hydrogen purity, pressure, and velocity exponent on the heat transfer.

Appendix I. Definition of Symbols

A = cross section area
c = specific heat at constant pressure
D = diameter, actual
D_e = diameter, equivalent = $4A/s$
f = friction factor = $(gD_e\Delta p)/(2\rho V^2L)$
g = acceleration of gravity
G = mass velocity = ρV
h = surface heat-transfer coefficient on basis of logarithm of the mean temperature difference between gas and surface
h' = surface heat-transfer coefficient on basis of inlet temperature difference between gas and surface
j = heat-transfer factor, defined by equation 1
k = thermal conductivity
L = length
m = a parameter defined in Appendix III, equation 25
n = exponent of velocity in heat-transfer equation
p = gas pressure, atmospheres
R = Reynolds Number
s = perimeter of duct cross section
t_c = temperature, degrees centigrade
V = velocity
V_c = critical velocity, corresponding to $R=2{,}100$
ρ = density
μ = viscosity
$c\mu/k$ = Prandtl Number

Subscripts

a = air
m = mixture of hydrogen and any impurity (air or nitrogen)
1 = value at a pressure of 1.0 atmosphere

Unless otherwise stated, the above quantities are expressed in the pound, hour, foot, Btu, degree Fahrenheit system. To convert heat-transfer coefficient given in Btu/hour (square feet) (degrees Fahrenheit) to watts/(square inches) (degrees centigrade), divide the former by 273.

Appendix II. Tests on Stator Cooling Pad

Test Arrangement

The cooling pad, on which the heat-transfer and friction-loss tests were made, was designed for the cooling system of a generator stator, and was made from two thin plates of Monel metal having the shape of a single segment of stator laminations, including two teeth. These plates were brazed together at the edges to form a hollow pad through which cooling water could be circulated, see Figure 8. Space blocks within the pad provided the strength to withstand compression and formed passages for the flow of the cooling water. Fins, 0.063 inch by 0.25 inch, brazed to one side of the pad, provided passages between the pad and the adjacent stator lamination for the flow of hydrogen. This same hydrogen also was used for cooling the stator end-windings and the rotor.

The half-pad used in the tests was encased in a flat wooden box, as shown in Figure 9. Gas-tightness was obtained by sealing the joints in the assembly with melted paraffin. A steel lamination 0.025-inch thick was attached by clamps to the underside of the box cover to make contact with the edges of the pad fins. This contact, although not brazed, was nevertheless under enough pressure to allow considerable heat flow from lamination to fins. Between the lamination and the cover an electric heating element was provided, through which the lamination was maintained much closer to the gas temperature than the pad so that the lamination absorbed from the gas only 15 to 20 per cent of the total heat given up by the gas. Temperatures of the pad and lamination were measured by thermocouples located at various points on their surfaces. Gas temperatures at inlet and outlet to the pad ducts were measured by several thermocouples located in the gas stream.

The test arrangement is shown in Figure 10. Two blowers arranged in series, which were housed in a section of 16-inch pipe, circulated the gas through the pad assembly. An electric heater enclosed in a section of 6-inch pipe supplied the heat input to the gas, while water circulating through the cooling pad removed the heat absorbed. A flow nozzle on the discharge side of the pad measured the gas flow. In the hydrogen tests a pressure of about three inches of water was maintained in the system with a gasometer. In the air tests the pipe enclosing the blowers was vented to atmosphere. Before filling the system with hydrogen, the air first was removed with nitrogen; hence this gas was assumed to be the contaminant in the hydrogen in the tests. The hydrogen purity was measured continuously with an Englehard Gas Analyzer, and checked periodically by chemical analysis.

Determination of Heat-Transfer Coefficients From Tests

From the measured total gas flows and the section areas of the various ducts in the pad, the average gas velocities in the various sections of the pad were calculated; the velocities were then corrected to 50 degrees centigrade by multiplying by $323/(273+t_d)$, where t_d is the average temperature in the ducts, degrees centigrade. In estimating the division of heat obtained between pad and lamination, the same heat-transfer coefficients were assumed to apply to both; however, since the pad temperature was very uniform, while that of the lamination showed several degrees variation between different points, the logarithmic mean temperature difference was used between gas and pad, $(\Delta T_m)_p$, and the arithmetic mean temperature difference between gas and lamination $(\Delta T_a)_l$. The combined surface area of pad and fins (assuming fins 100 per cent effective) was 204 square inches, and the area of lamination 84 square inches. Letting q_p and q_l represent the losses to pad and lamination respectively, we can write

$$E=q_p/q_l=\frac{204}{84}\frac{(\Delta T_m)_p}{(\Delta T_a)_l}=2.42\frac{(\Delta T_m)_p}{(\Delta T_a)_l} \quad (17)$$

and for a total loss of q_o watts given up by the gas in passing through the pad ducts

$$q_l=q_o/(1+E) \quad \text{and} \quad q_p=Eq_o/(1+E) \quad (18)$$

From the total losses given up by the gas in the tests, the losses absorbed by the pad and fins were calculated from the above equations, and the average heat-transfer coefficient for the entire pad determined. From this, together with the surface areas of the different sections of the pad and the velocities estimated for the different sections, it was estimated that 75 per cent of the total losses absorbed by the pad and fins was from the center ducts, which were of fairly uniform cross section. (The divergence of fins was under 1 degree.) Using this relation, the heat-transfer coefficients for the center pad ducts were calculated, as shown in Figure 11.

Friction-Loss Tests

From the friction losses in the center ducts of the cooling pad estimated from the test data, as outlined in the text, the half-friction factor $f/2$ was calculated from the equation

$$f/2=\frac{\Delta p_o g D_e}{G^2\,4L} \quad (19)$$

where p = friction loss in ducts, g = acceleration of gravity, D_e = equivalent duct diameter, L = duct length, and the other terms are as defined in the nomenclature. Letting $L=1.56$ and $D_e=0.0235$ for the center ducts, and expressing the pressure drop in inches of water, equation 19 becomes

$$f/2=0.63\,\Delta p''/G^2 \quad (20)$$

where $\Delta p''$ is the estimated friction pressure drop in inches of water.

The values of $f/2$ as calculated from the test data using equation 20 are shown in Figure 13 for comparison with the theoretical values for straight smooth ducts. The latter values were calculated from the equations given by Colburn[3]

$$f/2=14.2/R \quad (21)$$

for the region of laminar flow, and

$$f/2=0.007+0.0625R^{-0.25} \quad (22)$$

for the region of turbulent flow.

Appendix III. Calculation of Heat-Transfer Coefficients for Ducts on an Inlet Temperature Basis

In reference 11 a method is developed for calculating the average heat-transfer coefficient in a ventilating duct referred to the temperature of the gas entering the duct. In the following discussion this method will be utilized in conjunction with equation 10 of the first section of the paper, to determine the heat transfer coefficients for ventilating ducts on an inlet temperature basis, for either air or hydrogen.

Assuming the duct wall to have a constant temperature throughout its length, the heat-balance equation for the mean gas temperature in the duct at a distance x from the entrance is

$$hsdx(t_w-t)=c_pVAdt \quad (23)$$

where t = mean gas temperature at point x; t_w = wall temperature; and the other symbols are defined in Appendix I.

Equation 23 may be written

$$d(t_w-t)/dx=-m(t_w-t)/L \quad (24)$$

where

$$m=sLh/Ac_pV \quad (25)$$

L being the duct length in direction of flow.

Integrating equation 24 gives

$$t_w-t=Ce^{-mx}/L \quad (26)$$

Letting t_o = gas temperature at duct entrance $x=0$, C is determined from equation 26

$$C=t_w-t_o$$

and letting t_L = gas temperature at duct exit, $x=L$

$$t_w-t_L=(t_w-t_o)e^{-m} \quad (27)$$

whence

$$\frac{t_L-t_o}{t_w-t_o}=1-e^{-m} \quad (28)$$

Letting h' represent the average heat-transfer coefficient for the entire duct with respect to the temperature of the gas entering the duct, and q the total loss dissipated to the gas, we may write

$$h'=q/sL(t_w-t_o) \quad (29)$$

To evaluate m of equation 25, use equation 10 for heat transfer in ducts on an average temperature basis, wherein the characteristic dimension is the duct diameter

$$h=C_1cV^n\rho^n(D_e/\mu)^{n-1}(c\mu/k)^{-2/3} \quad (10)$$

and

$$s/A=4/D_e.$$

Then

$$m=4C_1\frac{L}{D_e}R^{n-1}(c\mu/k)^{-2/3} \quad (30)$$

in which C_1 is a constant, to be determined from tests in air.

Assuming an average gas temperature in the duct of 50 degrees centigrade, for which $c_p/k = 0.7$ for either air or pure hydrogen, the expression for m for either of these gases is, from equation 30

$$m = 5.08 C_1 R^{n-1}(L/D_e) \tag{31}$$

which appears as equation 15 in the main text.

Substituting $q = c_p V A(t_L - t_0)$ and equation 28 in 29 gives

$$h' = c_p V A(1 - e^{-m})/sL \tag{32}$$

Using $A/s = D_e/4$ in equation 32 gives equation 13 of the main text

$$h' = c_p V \phi = cG\phi \tag{33}$$

where

$$\phi = (1 - e^{-m}) D_e/4L \tag{34}$$

as the equation for the surface heat-transfer coefficient on an inlet temperature basis.

References

1. Forced Convection of Heat in Gases and Liquids, Chester W. Rice. *Industrial and Engineering Chemistry* (Easton, Pa.), volume 16, number 5, 1924, pages 460–77.

2. Hydrogen Cooling—With Near-Critical Velocities, G. W. Penney. *Electrical Engineering* (*AIEE Transactions*), volume 55, May 1936, pages 530–34.

3. A Method of Correlating Forced Heat-Transfer Data, A. P. Colburn. *Transactions*, American Institute of Chemical Engineers (New York, N. Y.), volume 29, 1933, pages 174–209.

4. Laminar-Flow Heat-Transfer Coefficients for Ducts, R. H. Norris, D. D. Streid. *Transactions*, American Society of Mechanical Engineers (New York, N. Y.), volume 62, 1940, pages 525–33.

5. Heat Transfer to Hydrogen-Nitrogen Mixtures Inside Tubes, A. P. Colburn, C. A. Coghlan. *Transactions*, American Society of Mechanical Engineers (New York, N. Y.), volume 63, 1941, pages 561–66.

6. Die Kuhlung eines erhitzten Wand durch eines Luftstrom, W. Russelt, W. Jurges. *Gesundheits-Ingenieur* (Berlin, Germany), volume 52.

7. Properties of Hydrogen Mixtures, A. W. Brunot. *Transactions*, American Society of Mechanical Engineers (New York, N. Y.), volume 63, October 1940, pages 613–16.

8. Grundsatzliches zur Warmeberechnung Elektrischer Maschinen, insbesondere des im Kreislaufes gekuehlten Turbogenerators, R. Pohl. *Archiv fuer Elektrotechnik* (Berlin, Germany), volume 12, 1923, page 361.

9. Free and Forced Convection of Heat in Gases and Liquids, Chester W. Rice. *AIEE Transactions*, volume 42, June 1923, pages 653–706.

10. The Hydrogen-Cooled Turbine Generator, D. S. Snell. *Electrical Engineering* (*AIEE Transactions*), volume 59, January 1940, pages 35–50.

11. Elektrische Maschinen (book), R. Richter. J. Springer, Berlin, Germany, 1924.

Discussion

Carl J. Fechheimer (Milwaukee, Wis.): Heat transfer with turbulent flow is associated with the higher values of Reynolds numbers. Then the velocity is usually taken as the volume per unit of time divided by the cross-sectional area. In electric machines, that comparatively simple picture is frequently not applicable. Thus, an obstruction in the fluid's path produces disturbances having characteristics which are entirely different from the simple symmetrical systems of vortices that obtain when the velocity in a smooth duct is raised above the critical value. For example, in the stator radial vent ducts, the gas must pass the coil portions in the vent ducts, which cause severe upsets comparable to disturbances in the Niagara Rapids.

These disturbances generally increase the heat transfer rate and also the pressure drop. Some moving pictures showed the character of flow in the wake of an obstruction to be periodic, changing from one instant to the next, the phenomenon being repeated in regular cycles.

Evidently, with such disturbances, the heat transfer rate changes from one position to the next; it is not a constant, but is a function of location. The total heat transferred (during the steady state), from a surface S is then

$$\int_S h_s \theta ds$$

where h_s is the variable heat transfer coefficient, θ is the difference in temperature between ds and the adjacent fluid, and the integral is taken over the entire surface S.

Might not the turbulent state which was obtained by the authors with hydrogen in a stator with Reynolds number as low as 1,100 be explained by disturbances in the fluid path?

It will be interesting for the authors to tell us under what conditions it is necessary for the Reynolds number to be as high as 8,000 for the flow to become turbulent. It has been my understanding that with smooth straight ducts the transition takes place with Reynolds numbers between 2,000 and 3,500.

The paper is a valuable contribution, but it is well to recognize that there are complexities for which solutions have not yet been obtained.

Sterling Beckwith (Allis-Chalmers Manufacturing Company, Milwaukee, Wis.): This paper gives a very useful analysis of heat-transfer rates for hydrogen and air mixtures. One of its main features, and one on which I should like to commend the authors, is the very fundamental and thorough nature of the analysis.

In the course of our studies on hydrogen-cooled machines we have also made tests which check very well the results given for friction factor and for heat transfer. Our tests included much longer ducts (length/width = 300), however, thus reducing end effects, and gave results slightly above those shown for $K_s = 0.3$ in the authors' Figure 13.

I would like to suggest one additional curve which may give a better physical picture of the proportions of a surface heat transfer circuit. This is to plot gas temperature vertically and duct length over duct width horizontally. Then for a parallel-sided duct with fixed wall temperature, the gas temperature will rise exponentially towards the wall temperature and the time constant of the exponential curve will be proportional to the per unit heat transfer coefficient j. For the complete range of the

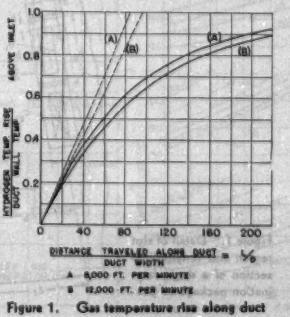

Figure 1. Gas temperature rise along duct

hydrogen test-data points shown in Figure 11, the suggested curves would be shown in Figure 1 of this discussion. This range of velocities, incidentally, covers reasonably well the normal velocities in the significant portions of almost all hydrogen-cooled generator vent ducts between laminations. For 3/8-inch ducts the "time constant" length is 31 to 36 inches, and for 1/4-inch ducts the "time constant" length is 20 to 24 inches.

D. S. Snell, R. H. Norris, and Mrs. B. O. Buckland: Professor Fechheimer's conclusion about the occurrence of turbulent flow in stator cooling ducts with Reynolds numbers as low as 1,100 being due to disturbances in the fluid path is undoubtedly true. The value of a long calming section or a rounded entrance in securing a conventional laminar-type velocity profile at low Reynolds numbers also is of significance. The upper limit of 8,000 for Reynolds number for transition to turbulent flow comes directly from Colburn and Coghlan's work on hydrogen-nitrogen mixtures, see reference 6 of the paper. In reference to the method of evaluating the total heat transfer coefficient, the test coefficients reported give an integrated average over the whole surface, and no attempt was made to evaluate local heat transfer coefficients.

Mr. Beckwith's confirmation of test results on friction factor and heat transfer is welcomed by the authors, since available data are all too scarce. His method for creating a better physical picture by showing the relation between ultimate hydrogen temperature rise and the length-to-diameter ratio gives a useful concept. For clarity his "time constant" might be defined as the length-to-diameter ratio at which the temperature rise of the hydrogen above inlet gas reaches 63.2 per cent of the rise it would attain in a duct of infinite length and uniform surface temperature. Designation of the heat-transfer factor f as a per-unit quantity is an interesting way of bridging the gap between the per-unit conception of the electrical engineer and the dimensionless-modulus conception of the heat transfer engineer.

Loading of Hydrogen-Cooled Generators at Elevated Gas Pressures

D. S. SNELL
MEMBER AIEE

Synopsis: This paper presents a study, based on calculations and tests, of the heating characteristics of hydrogen-cooled generators at elevated gas pressures, and discusses various criteria for determining the capability of generators at elevated pressures. It is shown that the assumption of constant temperature rise of the windings above cold gas temperature, as a basis for limiting the output at elevated hydrogen pressures (particularly the rise of the armature winding by embedded detector) is misleading, and that a more realistic basis of rating is the assumption of constant total temperature of the winding copper, for constant temperature of ingoing cooling water at different loads and hydrogen pressures.

OF THE many advantages obtained through the use of hydrogen as the cooling agent for electric rotating machinery, one of the most important is the ability to secure additional kilovolt-ampere output through an increase in the operating hydrogen pressure. Increasing the hydrogen pressure increases the hydrogen density, thereby increasing its capacity to absorb and remove heat so that increased kilovolt-ampere output may be obtained for the same temperatures of the windings. For most generators in service, the normal rating is specified at an operating hydrogen pressure of 0.5 pound per square inch gauge, while an increase of 15 per cent in kilovolt-ampere rating is given at 15-pound hydrogen pressure, and increases of from 20 to 25 per cent at hydrogen pressures of 25 or 30 pounds per square inch gauge are specified.

Although operation of generators at elevated hydrogen pressures now has become quite general, relatively little information on the operating characteristics of generators at elevated pressures has been published. Also, there does not as yet seem to be complete agreement among the various manufacturers of electric equipment as to the correct basis for estimating the capacity of a generator at elevated pressures. This paper represents an attempt to supply information of this type, and to offer data that may serve as a basis for estimating the gains in rating to be obtained from operation at elevated pressures. The practical limits to which the hydrogen pressure may be increased are indicated, and the use of elevated pressures to compensate for an increase in cooling water temperature, is discussed.

Since the output of a generator is limited mainly by the heating of its windings, this study begins with an analysis of the temperature rise of the windings of a typical generator at various loads and hydrogen pressures, confirmed by extensive tests. The maximum temperature rise of the armature winding copper is first calculated, from which the armature temperature rise as would be measured by an embedded temperature detector is estimated. It is shown by tests and calculation that the standard allowance for the temperature difference between armature copper and embedded detector, specified as 10 per cent of the observed temperature rise, may be considerably in error as applied to hydrogen-cooled generators operating at elevated loads and hydrogen pressures.

From these calculations, supported by test data, the output of a generator at elevated hydrogen pressures, as limited by the temperature rise of the armature winding, has been calculated. A similar analysis is then made with respect to the rotor winding. It is shown, however, that the assumption of constant temperature rise of the windings as a basis for determining the output of a generator at elevated pressures, is unrealistic, since the temperature of the cold gas does not

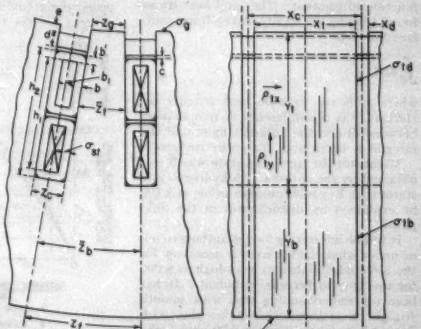

Figure 1. Detail of slot region and longitudinal section of a single lamination package in generator stator

Paper 50-30, recommended by the AIEE Rotating Machinery Committee and approved by the AIEE Technical Program Committee for presentation at the AIEE Winter General Meeting, New York, N. Y., January 30–February 3, 1950. Manuscript submitted October 27, 1949; made available for printing December 22, 1949.

D. S. SNELL is with the General Electric Company, Schenectady, N. Y.

The author wishes to express his thanks to H. D Taylor, C. E. Kilbourne, and B. M. Cain for their interest in the preparation of the paper and for their many constructive suggestions; and to W. J. Gilson, J. H. Carter, C. H. Holley, and J. L. Bialous for their careful work in conducting the tests and analyzing the test data, on which many of the conclusions in the paper are based.

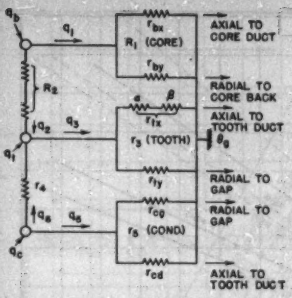

Figure 2. Thermal circuit of unit section of generator stator

Arrows show paths of heat flow

remain constant but increases appreciably, as the load and hydrogen pressure are increased.

It is suggested, therefore, that a better basis for determining the output of a generator at elevated pressures is the stipulation of constant total temperature of the winding, with constant temperature of the ingoing cooling water maintained. On this basis, curves are prepared showing the output of a generator at elevated hydrogen pressures as limited by the total temperatures of the armature and field winding copper. It is shown that in most cases the output of a generator will be limited by the heating of the armature copper, rather than by the heating of the rotor winding.

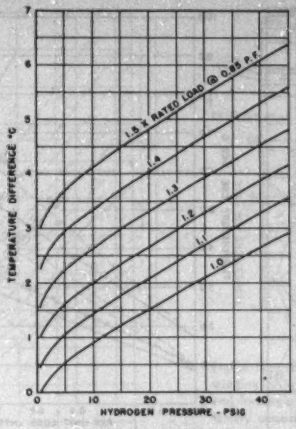

Figure 4. Calculated increase in cold gas temperature with increasing load and hydrogen pressure for 83,000-kw 3,600-rpm generator

For constant water temperature (95 degrees Fahrenheit) and rate of flow of water to gas coolers

Armature Heating Characteristics of Generators at Various Hydrogen Pressures

Calculation of Maximum Temperature Rise of Armature Winding Copper

In this section the maximum temperature rise of the armature winding copper of an 83,000-kw 3,600-rpm generator (rating at 1/2 pound* hydrogen pressure) has been calculated, for various generator loads at 0.85 power factor and at different hydrogen pressures. The method of temperature analysis developed by Soderberg[1] has been used for this calculation, considering a unit section of the armature conductor located in a discharge section of the core near the center of the generator. The influence of axial heat flow on the temperature rise of the conductor has been neglected, owing to the considerable length of the core, and the uniform cooling along its length obtained with the multi-

* Throughout paper, "pounds of pressure" indicates pounds per square inch gauge.

Figure 3 (below). A. Ventilation diagram for an 83,000-kw 3,600-rpm turbine generator. Arrows show direction of gas flow. Rotor shown divided axially into several sections for calculating temperature rise of winding

B. Calculated temperature rise of hydrogen in gap between stator and rotor for generator operating at rated load at 0.5 pound per square inch gauge hydrogen pressure

Figure 5 (right). Calculated maximum temperature rise and maximum total temperature of armature winding of an 83,000-kw 3,600-rpm generator at various loads and hydrogen pressures

Curves (a): maximum temperature rise of armature winding copper above 40-degree centigrade inlet gas. (b): temperature rise of hottest temperature detector above 40-degree centigrade inlet gas. (c): maximum total temperature of armature winding copper (includes increase in cold gas temperature with increasing load and hydrogen pressure). (d): total temperature of hottest temperature detector (includes increase in cold gas temperature)

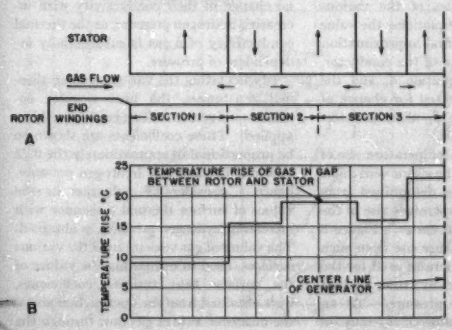

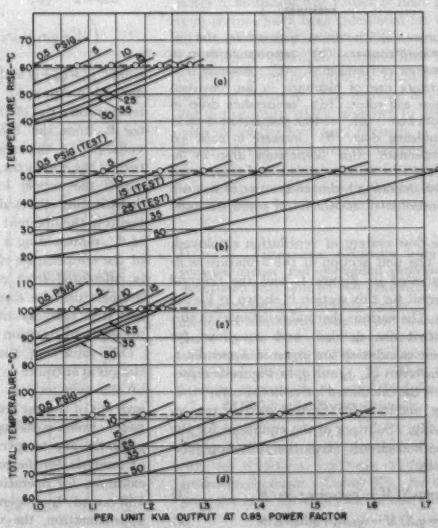

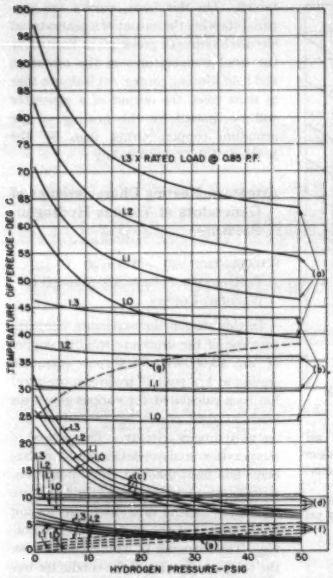

Figure 6. Calculated maximum temperature rise of armature winding copper and the components of this rise, also increase in cold gas temperature, for an 83,000-kw 3,600-rpm generator at various loads and hydrogen pressures

Curves (a): maximum temperature rise of armature copper. (b): temperature drop in armature coil insulation. (c): maximum temperature rise of hydrogen in gap between stator and rotor. (d): temperature drop in tooth iron. (e): surface temperature drop in ventilating duct. (f): increase in cold gas temperature. (g): temperature drop in insulation for assumption that load is increased with increasing hydrogen pressure to maintain constant total temperature of armature copper

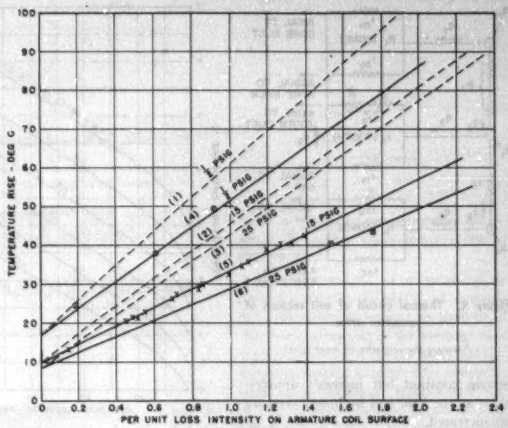

Figure 7. Temperature rise of armature winding by embedded detector as obtained by tests, also calculated temperature rise of armature winding copper at various loads and hydrogen pressures, for an 83,000-kw 3,600-rpm generator. Unit loss intensity corresponds to rated load at 0.85 power factor at 0.5 pound per square inch gauge hydrogen pressure

Curves (1), (2), (3): calculated maximum temperature rise of armature copper.
Curves (4), (5), (6): temperature rise of hottest temperature detector from tests

ple-flow system of ventilation employed.

The unit section of the armature is illustrated in Figure 1, and the thermal circuit for this section is shown in Figure 2. The various thermal resistances in this circuit are defined, and equations for their calculation are given in Appendix I. The terms q_b, q_c and q_t in Figure 2 represent the calculated losses in the core, winding, and tooth in the unit section, respectively. Solution of the equations for the thermal circuit gives the following relations

$$q_t = q_b N/M + (q_{bt} r_{tt} + q_c r_{ct}) r_t / M \qquad (1)$$

$$q_s = q_c S/M - (q_{bt} R_t + q_t R_t) r_t / M \qquad (2)$$

$$q_2 = q_{bt} + q_b - q_t \qquad (3)$$

$$\theta_s' = q_b r_4 + q_2 r_3 + \theta_g \qquad (4)$$

$$\theta_s = \frac{235 + T'}{235 + T' - q_b r_4} \times \left((\theta_g + q_b r_3 + q_b r_4 \quad \frac{(235 + T_a)}{(235 + T')} \right) \qquad (5)$$

where $q_{bt} = q_b + q_t$ and the other terms are defined in Appendix I. To calculate the temperature rise of the armature conductor θ_s from the foregoing equations, a value for T', the expected total temperature of the conductor, is first assumed, for which the copper loss q_c is calculated. Substituting the values of the various terms in the different equations, the value of θ_s', representing a first approximation of the temperature rise of the conductor, is calculated from equation 4, and the temperature rise corrected for change of loss with temperature, θ_s, then is determined from equation 5.

The value of θ_g, the temperature rise of the gas at entrance to the stator vent ducts of the unit section, is determined from analysis of the gas temperature rise in the gap between rotor and stator. Figure 3 gives the gap temperature rise from such an analysis, for the generator used for the example, for operation at rated load at 1/2-pound hydrogen pressure. As an approximation, the value of θ_g may in most cases be assumed equal to the total temperature rise of the gas through the generator, as determined from the losses and gas flow.

In calculating the thermal resistances of the thermal circuit of Figure 2, values of thermal conductivity of the various substances as determined from laboratory tests, have been used. The conductivity values are independent of the hydrogen pressure, since, although the presence of hydrogen in the insulation voids and between the stator laminations greatly improves the thermal conductivities of these materials over their values in air, there is no change in their conductivity with increasing hydrogen pressure, as the thermal conductivity of a gas is substantially independent of pressure.

In calculating the various surface thermal resistances, the heat transfer coefficients given in reference 2 have been applied. These coefficients are shown to be proportional to approximately the 0.75 power of the absolute hydrogen pressure, hence a considerable reduction in the values of surface thermal resistance with increasing hydrogen pressure, is obtained. The values of gas velocity over the various surfaces, used in estimating the values of the surface heat transfer coefficients, were obtained from the duct section areas, the measured rate of gas flow through the

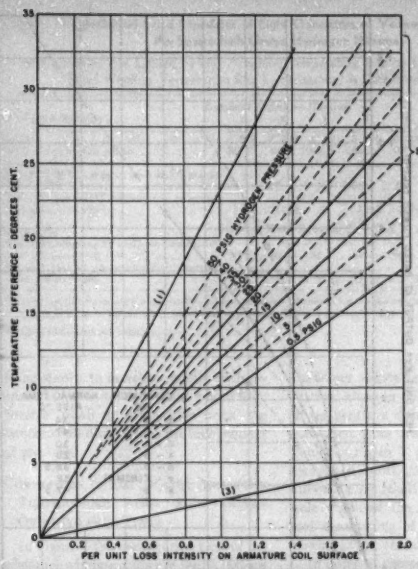

Figure 8 (left). Estimated temperature difference between armature winding copper and resistance-type embedded detector at different armature loads and at different hydrogen pressures, for an 83,000-kw 3,600-rpm generator. Also calculated temperature drop in armature coil insulation and theoretical temperature difference between copper and thermocouple-type embedded detector. Unit loss intensity corresponds to rated load at 0.85 power factor at 0.5 pound pressure

Curve (1): calculated temperature drop in insulation. Curve (2): estimated temperature difference between copper and embedded detector of resistance-type. Solid curves obtained from tests and calculations. Dashed curves obtained by cross-plotting solid curves. Curve (3): theoretical temperature difference between copper and embedded detector of thermocouple type

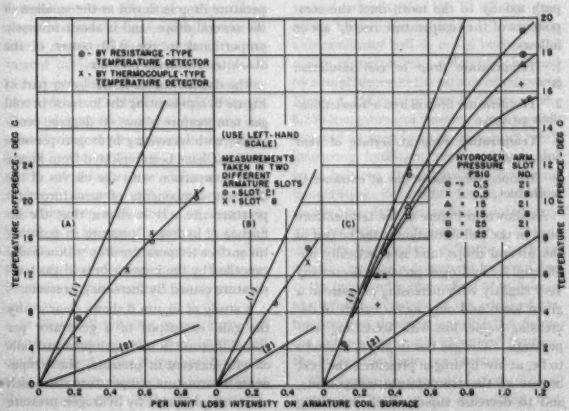

Figure 9. Temperature difference between armature copper and embedded detector as determined from tests on two generators having thermocouples on winding copper. Also calculated temperature drop in coil insulation (curve 1), and theoretical temperature difference between copper and thermocouple-type embedded detector (curve 2). Unit loss intensity corresponds to rated load for an 83,000-kw 3,600-rpm generator

Curves (A): for 35,300-kva 1,800-rpm 12,000-volt air-cooled generator. Curves (B): for 6,250-kva 3,600-rpm 13,200-volt air-cooled generator. Curves (C): for same generator as in curves (B) except operated in hydrogen

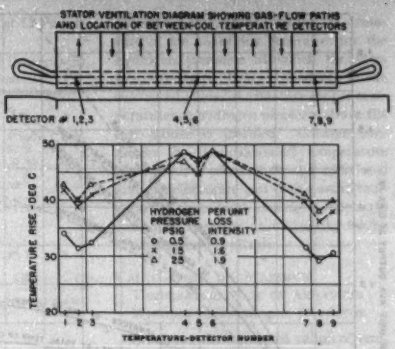

Figure 10. Temperature rises of the different detectors in stator winding of an 83,000-kw 3,600-rpm generator at various loads and hydrogen pressure as determined from tests. Unit loss intensity corresponds to rated load at 0.5 pound per square inch gauge hydrogen pressure

generator, and from the distribution of gas flow to the various ducts determined from model tests.

In calculating the values of copper temperature rise (θ_c) from equation 5, two different bases of calculation have been used; one, based on an assumed constant temperature of inlet gas at all loads and hydrogen pressures; the other, based on constant temperature of water to the gas cooler, and constant water flow, under all load and pressure conditions. For the latter assumption, the values of inlet gas temperature have been calculated for the 83,000-kw generator for different loads and different hydrogen pressures from the equations given in Appendix II, and are shown in Figure 4. The increase in cold gas temperature which is shown to occur with increasing hydrogen pressure is the result of the reduction in temperature rise of the gas through the generator with increasing pressure (due to the increased gas density), which tends to reduce the

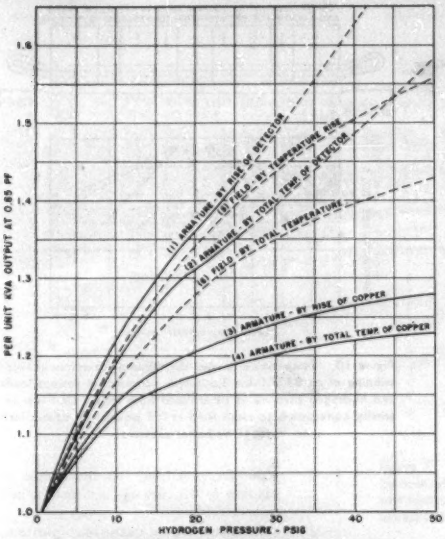

Figure 11. Estimated per-unit kilovolt-ampere output at 0.85 power factor at different hydrogen pressures for an 83,000-kw 3,600-rpm generator based on assumptions of constant temperature rise and constant total temperature of armature and field windings, from calculations

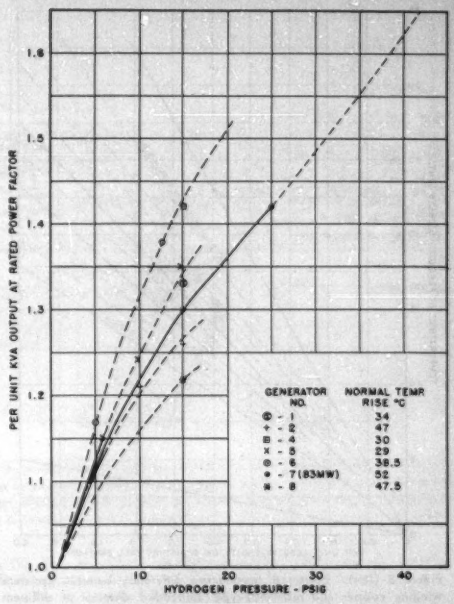

Figure 12. Estimated per-unit kilovolt-ampere output of several generators at rated power factor at different hydrogen pressures for assumption of constant temperature rise of armature winding by embedded detector, from tests

temperature difference from gas to water; so that an increase in cold gas temperature must occur in order to obtain sufficient temperature difference between average gas and average water temperatures to transmit the generator losses.

In Figure 5(A) are given the values of armature copper temperature rise above an inlet gas temperature assumed constant at 40 degrees centigrade, as calculated from equation 5 for the 83,000-kw generator operating at various loads from 1.0 to 1.4 times normal at 0.85 power factor and at hydrogen pressures from 1/2 to 50 pounds per square inch gauge.

Influence of Hydrogen Pressure on the Different Components of Armature Rise

In order to evaluate the influence of hydrogen pressure on the temperature rise of the armature winding copper, the different components of this temperature rise, calculated along a given heat flow path (together with the calculated total temperature rise above inlet gas temperature) are shown in Figure 6 for different generator loads, with hydrogen pressure as the independent variable.

For this analysis, the temperature rises of the armature winding copper have been calculated from equation 4, using assumed values for T', the total temperature of the copper, based on values for the temperature of inlet gas T_a as given by the curves of Figure 4. For the heat flow path axially to the tooth duct the components of the temperature rise θ_s' are as follows:

1. Temperature drop in coil insulation $q_b r_4$.
2. Temperature drop in iron across laminations $q_s r_{12} \alpha / r_{12}$.
3. Temperature drop at surface of vent duct, $q_s r_4 \beta / r_{12}$.
4. Temperature rise of gas at entrance to tooth duct, θ_g.

As shown in Figure 6, the temperature drop in the coil insulation is the largest of the several drops, and is practically unaffected by hydrogen pressure, decreasing very slightly with increasing pressure at a given load, and only as the result of decreasing copper loss with decreasing temperature. The gas rise in gap θ_g is shown to be, at low hydrogen pressures, the next largest of the temperature components, and to decrease rapidly with increasing pressure, being almost inversely proportional, at a given load, to the absolute hydrogen pressure. The temperature drop in the stator tooth is the next largest drop and is practically independent of hydrogen pressure. The surface temperature drop is shown as the smallest of the several drops, and is about inversely proportional to the 0.76 power of the absolute hydrogen pressure.

The dashed curves in the lower part of Figure 6, representing the increase in cold gas temperature above 40 degrees centigrade, with increasing hydrogen pressure and load, have been replotted from Figure 4 for comparison with the curves of the different components of armature temperature rise. It is shown that the influence of hydrogen pressure in reducing the surface temperature drop is practically cancelled by the increase in cold gas temperature caused by increasing pressure.

A study of Figure 6 shows clearly why the gain in output of a generator per pound increase in hydrogen pressure, falls off with increase in pressure, the components of armature temperature rise which are most influenced by hydrogen pressure

Table I. Hypothetical Load Capacities of Eight Generators of Various Ratings at 15 Pounds Per Square Inch Gauge Hydrogen Pressure

These Capacities Are Limited by (A) Armature, Temperature Rise by Embedded Detector; (B) Field Winding, Temperature Rise by Resistance, as Determined from Tests

Generator Number	1	2	3	4	5	6	7	8
Constant Armature Heating								
Rpm	3,600	3,600	1,800	3,600	3,600	1,800	3,600	1,800
Mva rating at 1/2 pound	35.7	43.8	43.8	62.5	62.5	75	97.2	111
Power factor	0.7	0.8	0.9	0.8	0.8	0.8	0.85	0.9
Rise max. RTD at rated load at 1/2 pound H_2 pres., °C	34	47	**	30	29	38.5	52	47.5
Per-unit kva at 15 pounds for constant temperature rise*	1.33	1.26	**	1.42	1.34	1.34	1.3	1.22
Constant Field Heating								
Rise field winding by resis. at rated load at 1/2 pound H_2 pres., °C	**	50	65	54	60	52	56.7	48.5
Per-unit kva at 15 pounds for constant temperature rise	**	1.3	1.31	1.26	1.29	1.29	1.28	1.27

* These output values are considerably higher than are obtained for constant temperature rise of armature copper and cannot therefore be considered as a proper basis of rating.

** Data obtained not reliable.

being shown to decrease rapidly with increase of pressure, to a point where they become small in comparison with the temperature drops which are independent of pressure.

Comparison of Calculated Armature Temperature Rises with Values Obtained from Tests

In Figure 7 the temperature rises of the armature winding copper of the 83,000-kw generator as calculated in a previous section for hydrogen pressures of 1/2, 15, and 25 pounds per square inch gauge are shown for different values of per-unit loss intensity on the armature coil surface, together with the temperature rises by embedded detector obtained from tests. (The shape of the calculated curves of temperature rise of armature winding copper was made to correspond with that of the curves of observed temperature rise, by using a value of thermal resistivity for the winding insulation 10 per cent above the value determined from laboratory tests which may be assumed as accounting for slot fit. Also, 1 degree was deducted from the calculated no-load temperature rises at 15 and 25 pounds pressure to obtain agreement with test values.) Deducting the observed temperature rises from the calculated rises of the armature copper, in Figure 7, at constant loss intensities, gives curves of temperature difference from copper to between-coil detector, at the above hydrogen pressures, as shown in Figure 8. Projecting and interpolating between the curves thus obtained, gives the curves shown for various hydrogen pressures up to 50 pounds per square inch gauge.

In Figure 8 are also shown curves of calculated temperature drop in the coil insulation and of the theoretical temperature difference between copper and a thermocouple-type embedded detector, the latter values being calculated by the method given in reference 3. The curves of temperature difference in Figure 8, as estimated from the calculated and test values of Figure 7, are observed to lie between the limits given by the above two curves. This result is due to the appreciable width of the temperature detector and the cooling of its edges by the gas flowing in the vent ducts.

In order to compare the values of temperature difference between calculated copper temperature and observed temperature, shown in Figure 8, with values of this difference obtained from actual tests made with thermocouples directly on the copper, Figure 9 has been prepared, giving values of this temperature difference as obtained from tests on a 35,300-kva air-cooled generator, and on a 6,250-kva experimental generator tested in both air and hydrogen,[4] the differences being shown, for convenience, for different values of per-unit loss intensity referred to normal intensity for the 83,000-kw generator used in the example. A considerable similarity will be noted between the curves of temperature difference obtained by actual tests and the estimated curves of Figure 8, the curves from the tests on the 6,250-kva generator showing a comparable increase in temperature difference with increasing hydrogen pressure, and also lying between the curves for theoretical temperature difference for a thermocouple-type detector, and calculated temperature drop in the insulation. The increase in temperature difference with increasing hydrogen pressure is believed due to the increased cooling effect of hydrogen at elevated pressures on the edges of the temperature detector, causing the detector to read lower, at a given coil loading, the higher the hydrogen pressure.

The foregoing analysis indicates good agreement between the calculated and observed temperature rises for the armature of the 83,000-kw generator, for the hydrogen pressures at which the tests were conducted; hence, confidence in the calculated values of armature copper temperatures at hydrogen pressures above the test values is justified. Greater confidence in the calculated temperature rises could, of course, be had if additional and more accurate test data on the temperature drop from armature copper to embedded detector at various hydrogen pressures were available.

Calculation of Maximum Temperature Rise of Armature Winding by Embedded Detector

Accepting the estimated values of temperature drop from armature copper to embedded detector as given by Figure 8 as reasonably accurate for the 83,000-kw generator, these values have been used in conjunction with the curves of calculated temperature rise of armature copper given in Figure 5(A) to obtain corresponding curves of temperature rise of embedded detector at various loads at 0.85 power factor and at various hydrogen pressures, as shown in Figure 5(B). The curves in this figure for 1/2, 15, and 25 pounds hydrogen pressure correspond with the test curves of Figure 8; the other curves are calculated.

Axial Temperature Distribution in Armature Conductor at Different Hydrogen Pressures

While the maximum temperature rise of the armature winding is of main importance in limiting the output of a generator at elevated hydrogen pressures, the axial temperature distribution along the conductor is of interest, especially since this distribution as obtained from tests on a number of generators at different hydrogen pressures, tends to confirm the accuracy of the analysis of the copper temperature rise given in the section on Calculation of Maximum Temperature Rise of Armature Winding Copper. In Figure 10 are shown the temperature rises of the various between-coil detectors located in the stator winding of the 83,000-kw generator as measured in tests at different loads and hydrogen pressures. It is shown that increasing the hydrogen pressure reduces the temperature differential between the detectors in the center of the stator and those near the ends, which may be explained by reference to Figures 3 and 6. In Figure 6 it is shown that at 1/2-pound hydrogen pressure, the gas temperature rise at center of gas gap is one of the largest components of the total temperature rise of armature copper. Re-

ferring to Figure 3, the gas rise in the gap for the end section of the generator is less than half of its value at the center, hence the temperature rise of the winding at the ends is correspondingly less. With increasing load and increasing hydrogen pressure, however, the temperature drop in the coil insulation becomes the predominating influence in the temperature rise of the winding. Since the rise in the gas gap becomes smaller at elevated pressures, there is less temperature difference in the gap axially, hence the temperature of the winding also, axially, is more uniform.

Calculation of Maximum Total Temperature of Armature Winding

In estimating the gain in output of a generator that may be obtained through increasing the hydrogen pressure, it is often assumed to be proper to limit the output at elevated pressures to values that will give the same temperature rises of the windings above inlet gas temperature as are obtained at rated load at 1/2-pound hydrogen pressure. This basis of rating, however, is somewhat fictitious, since the temperature of the inlet gas cannot usually be held constant, but increases with increasing load and hydrogen pressure. Since the actual winding temperatures, more than their temperature rises, determine the thermal deterioration of the insulation, a more realistic basis of rating would appear to be one which specifies the same total temperatures of the windings at all hydrogen pressures. In order to obtain an estimate of the gain in output of a generator to be obtained on the latter basis, the total armature copper temperatures of the 83,000-kw generator have been calculated for various loads at 0.85 power factor and at various hydrogen pressures, by adding to the values of T_a given by Figure 4 the values of copper temperature rise calculated from equation 5 for these values of T_a, giving the curves shown in Figure 5(C).

Similar curves for total temperature of the armature winding by embedded detector, at different loads and hydrogen pressures, have been derived from the curves of total maximum copper temperature given in Figure 5(C), by deducting therefrom the estimated temperature differences between copper and embedded detector given in Figure 8, giving the curves shown in Figure 5(D).

Estimated Generator Output at Elevated Hydrogen Pressures as Determined by Heating of the Armature Winding

In the foregoing section the maximum temperature rise and maximum total temperature of the armature winding, as would be measured by thermocouples on the winding copper and by temperature detectors between coils, have been calculated for an 83,000-kw generator for various loads and at various hydrogen pressures. These calculations are summarized in Figure 5. A horizontal line drawn through the resultant curves in each figure at the temperature or temperature rise for rated load at 1/2-pound hydrogen pressure, intersects the curves at points which give the loads which may be carried at various hydrogen pressures for constant armature temperature or temperature rise. Plotting these load points against hydrogen pressure gives the curves in Figure 11, showing the output at 0.85 power factor for 83,000-kw generator that may be obtained at different hydrogen pressures at constant temperature rise or constant total temperature of the armature winding. It will be observed that if criterion of constant temperature rise of hottest temperature detector be used, this gives higher permissible values of loading with increasing hydrogen pressure, than any of the other criteria; whereas the criterion of constant total temperature of the armature winding copper gives much lower permissible values of output. Also, whereas the curves of output calculated on the basis of constant temperature or temperature rise of the armature by embedded detector indicate no limit to the gains to be obtained by increasing the hydrogen pressure, the curves of output calculated for constant temperature or temperature rise of the armature copper tend to approach limiting values with increase in hydrogen pressure.

If it should be thought that the criterion of constant total temperature of the armature copper is too conservative a basis for determining the output of a generator at elevated pressures, one should note that no mention has been made of the increase in differential expansion between copper and iron which occurs at increased loads, as the result of the increased temperature drop in the insulation, and which may act to limit the life of the armature winding. If this item should be considered, the above criterion may be found to be actually not conservative enough. To indicate the magnitude of this item, the temperature drop in the armature insulation has been calculated for the 83,000-kw generator at the values of output given by curve 4 in Figure 11, and is shown as the single dashed curve in Figure 6. This curve shows an increase of 34% in the insulation temperature drop at 15 pounds pressure, and 43 per cent at 25 pounds.

While the curves given in Figure 11 have been calculated for a generator of modern design, and serve to illustrate the differences in output of a typical generator at elevated hydrogen pressures as specified by the various criteria presented, the actual values of per-unit output given by these curves will not necessarily apply to all generators, due to the variations in design that may exist. To evaluate the influence of differences in generator design on the gains in output at elevated hydrogen pressures, as specified by the several different criteria presented above, would be very laborious; however, an approximate evaluation of the influence of design differences may be obtained by comparison of the gains in output at elevated pressures for a number of representative generators on the basis of constant temperature rise of hottest armature temperature detector above inlet gas tem-

Figure 13. Detail of slot region for rotor of a turbine generator. Line A–A shows assumed location of surface of division of radial heat flow

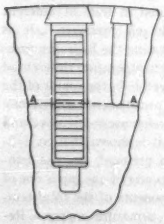

Figure 14. Equivalent thermal circuits for slot region of rotor of a turbine generator

Line A–A shows location of surface of division of radial heat flow

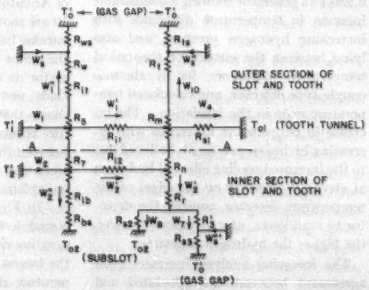

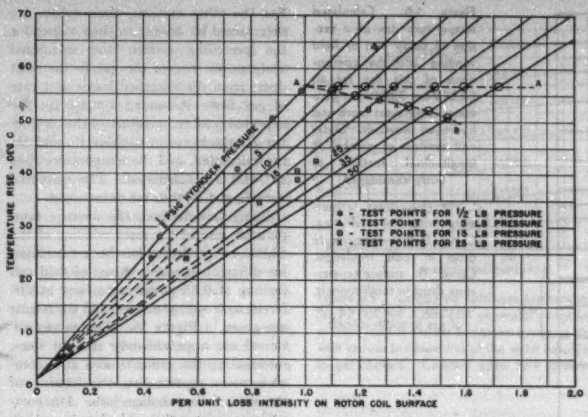

Figure 15. Calculated average temperature rise of field winding of an 83,000-kw 3,600-rpm turbine generator at different loss intensities on rotor coil surface and at different hydrogen pressures with values from tests shown for comparison

Unit loss intensity corresponds to rated load at 0.5 pound per square inch gauge pressure. Line A–A = locus of load points for constant temperature rise of winding. Line A–B = locus of load points for constant total temperature of winding

perature—admittedly an improper basis of rating, but a convenient, and fairly accurate basis of comparison. This has been done in Table I and Figure 12 in which the gains in output on this basis have been calculated from tests on eight generators of different ratings. It will be observed that for some of the generators, the outputs calculated on the basis of constant temperature rise of armature temperature detector are appreciably higher than for the 83,000-kw generator, while for others the outputs are less. These differences may be attributed partly to differences in the details of construction of the different generators, but must be considered as principally due to the differences in the normal temperature rise. For example, referring to Figure 7, if the normal 1/2-pound pressure rating of the 83,000-kw generator had been such as to give a temperature rise by hottest temperature detector of 40 degrees centigrade instead of 51.5 degrees centigrade, the per-unit loss intensity on the armature coil surface would have been 0.635 instead of unity, corresponding approximately to 80 per cent of normal rating. For the same temperature rise of the hottest detector in operation at 15-pound hydrogen pressure, the test curve in Figure 7 indicates that a loss intensity of 1.24 could be carried, corresponding approximately to 1.11 times normal rating. Hence the output at 15-pounds pressure, for 40 degrees centigrade rise of the hottest temperature detector, would be $1.11/0.8 = 1.39$ times normal, instead of 1.3, as estimated from the basis of a temperature rise of 51.5 degrees centigrade at 1/2-pound pressure at normal rating. Thus, the lower the temperature rise at 1/2-pound pressure and rated load, the greater is the output at elevated hydrogen pressures for constant temperature rise.

Rotor Heating Characteristics of Generators at Different Hydrogen Pressures

Calculation of Average Temperature Rise of the Rotor Winding

Depending on the design of a given generator, the heating of either the armature or the rotor winding may be the factor limiting the generator output at elevated hydrogen pressures. Having determined in the foregoing sections the output of generators as limited by the armature heating, a similar study will be made with respect to the heating of the rotor winding. In the present section an analysis of the average temperature rise of the rotor winding of the 83,000-kw 3,600-rpm generator used for an example above is made, for the generator operating at various loads and at different hydrogen pressures. In this analysis the rotor heating is assumed to be symmetrical about the transverse center line, and the half rotor is divided for calculation into several sections as shown in Figure 3. The temperature rises of the rotor end windings and of the three sections of the body are calculated separately and the average temperature rise of the entire winding then is calculated as the weighted mean temperature rise of the four sections.

The temperature rise of the rotor end windings, which are uninsulated, is calculated from conventional formulas. From the calculated losses in the end windings and the estimated rate of gas flow through the rotor body, the temperature rise of the gas entering the axial ventilating tunnels of the body is determined, which then is used in calculating the temperature rise of the body part of the winding.

The temperature rise of the body part of the rotor winding is calculated from equations given in Appendix III, which are based on the methods of analysis of Soderberg[1] and Peck.[5] A detail of a rotor slot of the 83,000-kw generator is shown in Figure 13, from which the thermal circuits shown in Figure 14 are derived. To simplify the calculation, it has been assumed that the losses generated in the slot for the section opposite the tooth tunnel pass to the tunnel and to the outside rotor surface, while the remainder of the slot loss passes to the subslot and to the pole center. The temperature rises of the outer and inner sections of the slot winding then are calculated independently and a weighted average rise for the two sections taken.

The method of calculating the temperature rise of the body part of the rotor winding from the equations in Appendix III is as follows. For a given section of the body the temperature rise in the gas gap T_g' is determined by analysis, see Figure 3. To this rise the surface temperature rises from pole face and friction loss are added, giving a fictitious gap rise, T_g. From the estimated gas velocities in the vent tunnels, heat transfer coefficients for these surfaces are calculated on the basis of inlet gas temperature, from equations given in reference 2. For the outer rotor surface the coefficients at different hydrogen pressures are determined by the method given in reference 2. From these coefficients the different surface thermal resistances of the thermal circuits of Figure 14 are calculated. The other thermal resistances are calculated from the slot and tooth dimensions and from values of thermal resistivity obtained from laboratory tests. For section 1 of the rotor body the gas rises T_{g1} and T_{g2} represent the rise of gas in passing through the rotor end windings.

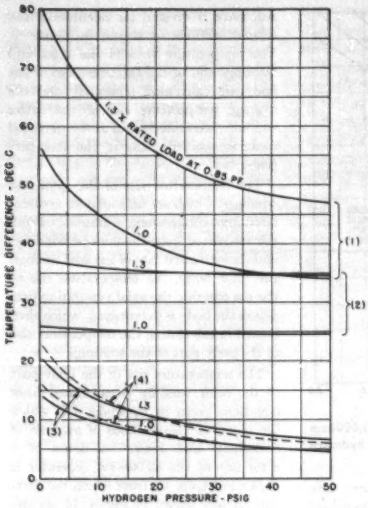

Figure 16. Calculated temperature rise of a section of body part of field winding and the components of this rise for an 83,000-kw 3,600-rpm generator at different loads and hydrogen pressures. Outer coil section of number 2 longitudinal section of body considered

Curve (1): total temperature rise of winding. Curve (2): temperature drop in coil insulation. Curve (3): surface temperature drop in tooth tunnels. Curve (4): temperature rise of gas in tooth tunnels

For the other sections, their values are determined by adding to their values for the preceding section the calculated temperature rise of the gas in the vent ducts from the absorbed losses and rate of gas flow. Assuming a value for the expected total temperature of the conductor T', the losses in the slot W_1 and W_2 are calculated, and the temperature rises T_1' and T_2' calculated. The corrected rises T_1 and T_2 then are determined.

Using this method, the average temperature rise of the rotor winding of the 83,000-kw generator has been calculated for different assumed values of field coil loading at 0.85 power factor and at different hydrogen pressures, and the results are given in Figure 15. The curves obtained are approximately straight lines, intersecting the ordinate axis at a common point representing the heating of the rotor from windage loss. For comparison with the calculated values, values determined from tests on this generator at various hydrogen pressures

Figure 17 (below). Estimated per-unit kilovolt-ampere output at 0.85 power factor at different hydrogen pressures for an 83,000-kw 3,600-rpm generator, based on assumptions of constant temperature rise and constant total temperature of field winding, from calculations; also estimated output at rated power factor at different hydrogen pressures, for several generators, on assumption of constant temperature rise of field winding, from tests

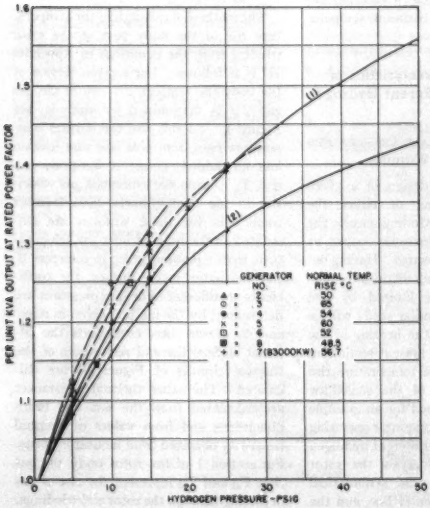

Figure 18. Estimated per-unit kilovolt-ampere output at different power factors (lagging) at different hydrogen pressures, for an 83,000-kw 3,600-rpm generator, based on assumptions of constant total average temperature of field winding and constant total maximum temperature of armature winding copper

Solid curves show output limited by field heating. Dashed curve shows output limited by armature heating

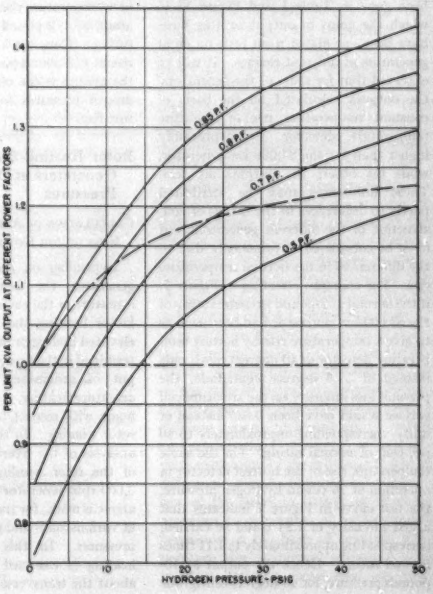

also are shown. It will be noted that close agreement between test and calculated temperature rises is obtained for 1/2-pound and 25-pound hydrogen pressure, while for 15-pound pressure the test points fall somewhat below the calculated values, especially at the lower values of field coil loading. This may indicate inaccuracies in the calculation method, in the values used for the various thermal resistivities or heat transfer coefficients, or both. Considering, however, that the thermal circuits on which the equations for temperature rise are based are necessarily approximate, and that the gas velocities in the ventilating tunnels, on which the surface thermal resistances were based, were estimated, and not measured, values, the agreement between test and calculated values may be regarded as sufficiently close to justify confidence in the values of temperature rise calculated for hydrogen pressures beyond the range of the test values.

Influence of Hydrogen Pressure on the Different Components of Temperature Rise of Rotor Winding

As in the case of the armature winding temperature rise, it is useful to consider the temperature rise of the rotor winding also as separated into its several components, so that the influence of hydrogen pressure on the different components may be evaluated. For the rotor winding the temperature rise of the outer section of the conductor, for section 2 of the rotor body, will be considered for separation into its components, and the heat flow path to the tooth tunnel considered. (This particular section of the rotor winding was chosen for this analysis, since its calculated temperature rise was in most cases most nearly equal to the calculated average temperature rise of the entire winding.) The components of temperature rise for this path are:

1. Temperature drop in coil insulation, $W_1'R_{i1}$.

2. Temperature drop at surface of tooth tunnel, W_4R_{t1}.

3. Temperature rise of gas in tooth tunnel, T_{g1}.

In Figure 16, these components and the total temperature rise T'_1 are shown for two different generator loads and for various hydrogen pressures. As with the armature winding, the largest component of the temperature rise of the rotor winding also is the temperature drop in the coil insulation, which is independent of the hydrogen pressure. The surface temperature drop and the gas rise in the tunnel are shown to be about equal, and

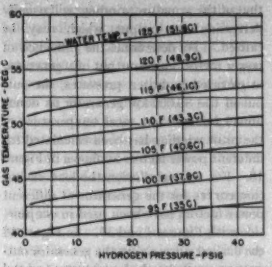

Figure 19. Calculated cold gas temperature for 83,000-kw 3,600-rpm generator operating at rated load at various hydrogen pressures and with various temperatures of the water supplied to gas coolers. Constant water flow assumed

to decrease at about the same rate with increasing hydrogen pressure. Since the components of temperature rise of the rotor winding which vary with hydrogen pressure comprise a greater part of the total rise than is the case for the armature winding, the curves of total temperature rise of the rotor winding, shown in Figure 16, do not approach a limit with increasing hydrogen pressure as rapidly as do the corresponding curves for the armature winding, shown in Figure 6; hence the heating of the armature, rather than of the field winding, will limit the output of the generator at elevated hydrogen pressures.

Estimated Generator Output at Elevated Hydrogen Pressures as Limited by Rotor Heating

Output Estimated at Rated Power Factor

In Figure 15 giving the calculated average temperature rise of the rotor winding at different hydrogen pressures, for different loss intensities on the rotor coil surface, a horizontal line drawn through the temperature rise at rated load at 1/2 pound hydrogen pressure intersects the temperature rise curves in points which define the coil loading at the different pressures to give normal temperature rise above 40 degrees centigrade. Taking the square roots of the values of loss intensity thus determined, and referring to the load excitation curve for this generator (not included) gives the generator output at 0.85 power factor at different hydrogen pressures for constant temperature rise of the rotor winding above 40 degrees centigrade. These values are shown in Figure 17 for the different hydrogen pressures. Next, to determine the output at elevated hydrogen pressures at constant total temperature of the rotor winding, for an assumed constant rate of water flow to the gas cooler at 95 degrees Fahrenheit, the values of cold gas temperature from Figure 4 are added to the temperature rises of the rotor winding given by Figure 15, to determine the loss intensities on the field coil at different hydrogen pressures at which the total winding temperature equals 96.7 degrees centigrade, the total temperature at rated load 1/2-pound hydrogen pressure. The locus of these load points is shown in Figure 15 as curve B. Taking the square roots of these loss intensities and referring to the load excitation curve gives the values of generator output for constant total temperature of the rotor winding, which are shown as the lower curve in Figure 17.

In order to compare the gains in output at elevated hydrogen pressures for constant rotor heating, as calculated for the 83,000-kw generator, with values determined from tests on generators of various designs, output values estimated from tests on six other generators, based on constant temperature rise of the rotor winding, are shown in Figure 17; in Table I the output gains at 15-pound hydrogen pressure for these generators are shown. It will be noted from Figure 17 that the output curve for the 83,000-kw generator for constant temperature rise of rotor winding represents approximately an average for all the other generators; hence it may be considered as fairly representative. It also will be observed that the generator output at elevated hydrogen pressures, as limited by the temperature rise of the rotor winding, is practically independent of the temperature rise at 1/2-pound pressure and rated load, which is not the case if the output is limited by the armature heating. This difference follows from the fact that the no-load temperature rise of the armature winding, being due to both windage and core losses, decreases with increasing hydrogen pressure; while the no-load temperature rise of the rotor winding, being due to windage loss alone, is independent of the hydrogen pressure.

In Figure 11 the curves of generator output at constant rotor heating for different hydrogen pressures, for the 83,000-kw generator, as given by Figure 17, are shown in dashed lines for comparison with the curves calculated for constant armature heating. It will be noted that the output values calculated for constant rotor temperature or temperature rise are considerably higher than those based on constant temperature or temperature rise

of the armature winding copper, indicating that the heating of the armature copper rather than of the rotor copper, determines the output of this generator at elevated hydrogen pressures. However, if the output should be based on constant observed temperature or temperature rise, for both rotor and stator, the curves show that the heating of the rotor winding would limit the output of the generator at elevated pressures.

Referring to Table I, showing estimated gains in output at 15-pound hydrogen pressure for generators of different capacities, based both on rotor temperature rise and also on observed temperature rise of the armature winding, it will be noted that on these two bases of rating the rotor heating would limit the output at elevated pressure in the majority of cases. However, comparing the outputs for the 83,000-kw generator as given by curves 1 and 4 and Figure 11, and assuming this relation would apply approximately to the generators listed in Table I, it is probable that on the basis of constant total temperature of the winding copper, the armature heating would in all cases limit the output at elevated pressures, rather than the rotor heating.

Output Estimated at Less than Rated Power Factor

In many cases, it is desirable to utilize increased hydrogen pressures to obtain additional reactive kilovolt-ampere capacity from the generator, which involves operation at less than the rated power factor. Under these conditions, the heating of the rotor winding rather than that of the armature winding, will usually determine the output which may be carried. To determine the influence of power factor on the output of a generator at elevated hydrogen pressures, the output of the 83,000-kw generator as determined for constant total temperature of the rotor winding has been calculated for different power factors as shown in Figure 18. For this calculation the load excitation curves for the generator at different power factors have been used in conjunction with Figures 4 and 15. In Figure 18 the dashed curve shows the generator output as calculated for constant total temperature of the armature winding copper, which has been replotted from Figure 11. Actually, the output as limited by armature heating will be reduced somewhat as the power factor is decreased, due to the increased temperature rise of the gas through the generator from the increased rotor I^2R loss, but this reduction is relatively small, and is here neglected.

Reference to Figure 18 shows that at 0.8 power factor, the generator output is limited by rotor heating at all hydrogen pressures below 11 pounds; above this pressure the output is limited by the armature heating. At 0.7 power factor, the rotor heating is shown to determine the generator output at all hydrogen pressure below 24 pounds; while at 0.5 power factor the rotor heating is shown to determine the output at all pressures below about 60 pounds.

The Use of Increased Hydrogen Pressure to Compensate for Increased Temperature of the Water Supplied to the Gas Cooler

In some localities, the temperature of the water supplied to the gas cooler of a generator may exceed its normal value during certain periods. With an air-cooled generator, such a condition would require a reduction in generator output in order to maintain normal total temperatures of the windings. With hydrogen cooling, however, an increase in water temperature can usually be compensated for by an increase in the hydrogen pressure, causing a sufficient reduction in the temperature rises of the windings to maintain constant total temperatures even though the cold gas temperature has increased. In order to determine the amount by which the hydrogen pressure in a generator must be increased to permit normal output to be carried with no increase in total temperatures of the windings, with the temperature of the cooling water increased above normal, calculations have been made for the 83,000-kw generator used as an example previously.

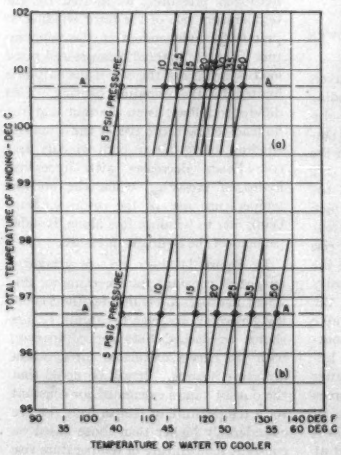

Figure 20 (left). Calculated maximum total temperature of armature winding copper and average total temperature of field winding at rated load at different hydrogen pressures and different temperatures of the water supplied to the gas coolers, for an 83,000-kw 3,600-rpm generator. Constant water flow assumed

Curve (a): maximum temperature of armature copper. Curve (b): average temperature of field winding. Lines A–A = loci of water temperature points giving winding temperatures obtained at 0.5 pound per square inch gauge hydrogen pressure with 95 degrees Fahrenheit cooling water

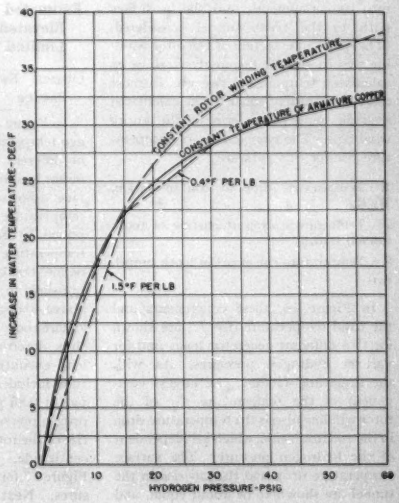

Figure 21. Calculated allowable increase in temperature of water to gas coolers above 95 degrees Fahrenheit (at constant water flow) with increasing hydrogen pressure, for an 83,000-kw 3,600-rpm generator operating at rated load, with total temperature of either armature or field winding copper held constant

In these calculations the temperature of the cold gas is first determined, from the equations in Appendix II, assuming normal rated load at various hydrogen pressures, and with various temperatures of the ingoing cooling water. The calculated temperatures for the generator are shown in Figure 19. Equation 5 is used for calculating the temperature rise of the armature copper θ_s at rated load and at different hydrogen pressures, using the values of T_a from Figure 19. The total temperatures of the armature copper determined from these calculations ($\theta_s + T_a$) then are plotted against temperature of ingoing cooling water, as in Figure 20(A) and a horizontal line drawn through the resulting curves corresponding to normal temperature at 1/2-pound pressure with 95 degrees Fahrenheit cooling water. The intersections of this line with the calculated curves gives the temperatures of the cooling water at the various pressures for constant total armature copper temperature. Deducting 95 from these temperatures gives the solid curve shown in Figure 21 representing the permissible increase in water temperature for different hydrogen pressures, at constant armature copper temperature.

A similar calculation is made for constant total temperature of the rotor winding, using the curves of rotor heating given in Figure 15. By a process of cut-and-trial, in which, for a given assumed value of inlet water temperature and a given hydrogen pressure, the value of loss intensity on rotor coil surface is determined from the foregoing figure, giving a temperature rise which, when added to the proper value of T_a from Figure 19, gives a total temperature of the rotor winding which, for normal field current, gives the loss intensity initially assumed—curves of total temperature of the rotor winding for different water temperatures and different hydrogen pressures are derived, as shown in Figure 20(B). A horizontal line drawn through these curves corresponding to normal total rotor winding temperature for 95 degrees Fahrenheit water, intersects the curves at points giving the temperatures of cooling water at different pressures for constant total rotor temperature. Deducting 95 from these values gives the dashed curve in Figure 21, representing the permissible increase in water temperature for different hydrogen pressures, for constant rotor winding temperature.

Figure 21 shows that for the 83,000-kw generator, operating at hydrogen pressures up to about 15 pounds, the calculated permissible increase in inlet water temperature at constant load, for constant total temperature of either armature or field winding copper, is about 1.5 degrees Fahrenheit per pound increase in hydrogen pressure. At pressures above about 15 pounds, however, the permissible increase in water temperature per pound increase in pressure steadily decreases, being somewhat less for the condition of constant armature temperature than for constant field temperature.

While the calculated value of permissible increase in water temperature with increasing hydrogen pressure given for the 83,000-kw generator in Figure 21 cannot be assumed to apply to all generators, they may, however, be assumed to be fairly representative, since the curves of output for different hydrogen pressures for this generator, as limited by stator and rotor heating respectively, given in Figures 12 and 17, appear to be fairly representative.

Conclusion

It has been shown here that the basis often used for estimating the output of a generator at elevated hydrogen pressures, by which the output is limited by the observed temperature rise of the armature and field windings above the temperature of the inlet gas, is misleading and may result in operation of a generator at elevated pressures with actual temperatures of the winding copper considerably in excess of those which are obtained at 1/2-pound hydrogen pressure. It is suggested, therefore, that the total temperatures of the windings, based on constant temperature and flow of water to the gas cooler, be used as the basis for determining the output of a generator at elevated hydrogen pressures. It also is suggested that the maximum temperature of the armature winding copper, as estimated from the temperature detector readings, rather than the temperatures as given by detectors alone, be used in estimating the generator output as limited by armature heating. This will involve obtaining information on the temperature drop from copper to embedded detector more accurate than is now available, and an investigation of this type is suggested.

The principal results of this investigation are summarized in Figures 4, 6, 11, and 21. If the criterion of constant total temperature of the winding copper is accepted for the determination of the output of a generator at elevated hydrogen pressures, and if it may be assumed, as seems likely, that in most cases the output will be limited by the armature heating rather than by the rotor heating, the calculated curve 4 in Figure 11 may be used as a general guide for determining the gain in output of a generator at elevated hydrogen pressures.

Appendix I. Equations for Thermal Resistances Used in Calculation of Temperature Rise of Armature Winding

Nomenclature

T_a = temperature of gas entering generator fans

T' = assumed temperature of armature copper, for use in calculating I^2r loss

θ_g = temperature rise of gas at center of gap between rotor and stator = total gas rise through generator

θ_s' = temperature rise of armature winding copper as determined for I^2r loss calculated at temperature T'

θ_s = temperature rise of armature copper, corrected for change of I^2r loss with temperature

δ_i = thermal resistivity of outside coil insulation

δ_{ci} = internal thermal resistivity of coil radially

δ_f and δw = thermal resistivities of driving strip and wedge, respectively

δ_{iz} and δiy = thermal resistivities of iron across and along lamination, respectively

$\sigma_g, \sigma_{td}, \sigma_{bd}, \sigma_{bf}$ = surface thermal resistivities for gap, tooth duct, core duct, and core back surfaces, respectively

q_0, q_c, q_t = core loss, copper loss, and tooth loss, respectively, per slot and package

q_1 to q_6 = losses flowing along paths shown in Figure 2

A_{bd}, A_{td}, A_{bf} = surface areas of core and tooth ducts including spacers, and core back, respectively

A_{cd}' = surface area of coil sides in duct

A_{tg} = surface area of tooth tip

A_{bz} and A_{by} = cross-section areas of core for axial and radial heat flow, respectively

A_{cd} and A_{ci} = cross-section areas of insulation in duct and slot, respectively

A_{tz} and A_{ty} = cross-section areas of tooth for axial and radial heat flow, respectively

A_{cy} = cross-section area of wedge for radial heat flow

Temperatures and temperature rises are given in degrees centigrade, thermal resistivities in degrees centigrade inches per watt, surface thermal resistivities in degree centigrade square inches per watt, areas in square inches, losses in watts. Surface resistivities are reciprocals of surface heat transfer coefficients. Refer to Figure 1 for dimensional symbols.

Equations:

$$r_{cd} = \frac{\sigma_{si}}{A_{cd}} + \frac{\sigma_{id}}{A_{cd}'}; \quad \sigma_{si} = b\delta_i$$

$$r_{cy} = \frac{b'\delta_i + C\delta_f + d\delta_w + \sigma_g}{A_{cy}} + \frac{h_1\delta_{ci}}{3_{21}X_c}$$

$$r_b = \frac{r_{cd}\sigma_{cy}}{r_{cd} + r_{cy}}; \quad r_{tz} = \alpha + \beta$$

$$\alpha_1=\frac{\delta_{1z}}{12A_{1z}},\ \beta=\frac{\sigma_{1d}}{A_{1d}};\ r_{1z}=\frac{\delta_{1y}Y_1}{3A_{1y}}+\frac{\sigma_y}{A_{1z}}$$

$$r_{2z}=\frac{r_{1z}r_{1y}}{r_{1z}+r_{1y}};\quad r_{b2}=\frac{\delta_{2z}Y_1}{12A_{b2}}+\frac{\sigma_{bd}}{A_{bd}}$$

$$r_{by}=\frac{\delta_{1y}Y_b}{3A_{by}}+\frac{\sigma_{bf}}{A_{bf}}\quad R_1=\frac{r_{b2}r_{by}}{r_{b2}+r_{by}}$$

$$r_4=\frac{\sigma_{st}}{A_{st}},\ R_3=\frac{\delta_{1y}}{9A_{1y}}+\frac{\delta_{1y}Y_b}{3A_{by}}$$

$$r_{s1}=r_4+r_3\quad r_{s43}=r_3+r_{s1}$$

$$R_{12}=R_1+R_3;\quad M=r_3r_{s1}+R_{12}r_{s43}$$

$$N=R_2r_{s43},\quad S=r_3(r_3+R_{12})$$

Appendix II. Calculation of Cold Gas Temperature for a Hydrogen-Cooled Generator

Nomenclature

A_o = over-all cooler heat transfer factor, kilowatts per degree centigrade log mean temperature difference gas to water

C = free cross-section area of cooler, square feet

d = density of pure hydrogen at temperature T_a' and atmospheric pressure, pounds per cubic foot

e = cooler efficiency, per cent (=100 for clean tubes)

G = hydrogen mass velocity through cooler, pounds per hour per square foot

G_o = water flow to cooler, gallons per minute

L_o = losses given to cooler, kilowatts

N = purity correction factor = (107.5-Z)/-7.5

P_a = hydrogen pressure, atmospheres

Q_o = gas flow through fans, cubic feet per minute

R = gas constant (degree centigrade per kilowatt at 1 cubic foot per minute) = 1,890 (273+T_a')/313 P_a

S = surface area of cooler, square feet

T_a' = average temperature of gas through fans, degree centigrade

T_1 = temperature of gas leaving cooler, degree centigrade

T_4 = temperature of gas entering cooler, degree centigrade

T_5 = temperature of water entering cooler, degree centigrade

T_6 = temperature of water leaving cooler, degree centigrade

U = over-all heat transfer coefficient for cooler tubes at 100 per cent efficiency, BTU per hour per square foot per degree Fahrenheit

Z = hydrogen purity per cent

Equations:

$$A_o=1.8e\ SU/341{,}500 \tag{6}$$

$$G=60Q_odNP_a/C \tag{7}$$

Let

$$T_1=T_4-T_6 \text{ and } T_2=T_1-T_5 \tag{8}$$

Then

$$T_1-T_2=T_4-T_5-(T_6-T_5) \tag{9}$$

Also

$$T_4-T_5=RL_o/Q_o \tag{10}$$

And

$$T_6-T_5=3.8\ L_o/G_o \tag{11}$$

Let

$$F_o=R/Q_o-3.8/G_o \tag{12}$$

Then from equation (9)

$$T_1-T_2=F_oL_o \tag{13}$$

Also

$$L_o/A_o=\frac{T_1-T_2}{2.3\log_{10}T_1/T_2} \tag{14}$$

Hence

$$\log_{10}T_1/T_2=F_oA_o/2.3 \tag{15}$$

Let

$$T_2=\frac{T_1-T_2}{T_1/T_2-1}\quad\text{and}\quad T_3=T_5+T_2$$

Then

$$T_3=T_5+\frac{F_oL_o}{T_1/T_2-1} \tag{16}$$

In order to calculate the cold gas temperature for a hydrogen-cooled generator from equation (16) for a given load and hydrogen pressure, the value of G is first determined from equation (7) and by reference to curves of over-all heat transfer coefficient U for different values of G at different water velocities in the cooler tubes, the correct value of U is determined. Assuming a value of efficiency e to take account of fouling of inside tube surfaces, the value of A_o is calculated from equation (6). Calculating the value of F_o from equation (12), the value of T_1/T_2 may be determined from equation (15) and the cold gas temperature T_3 may then be calculated from equation (16).

Appendix III. Equations for Temperature Rise of Body Part of Rotor Winding

Nomenclature

R_{i1} and R_{i2} = thermal resistances of side slot insulation, outer and inner sections of slot

R_m and R_n = radial thermal resistances of outer and inner sections of tooth

R_r = thermal resistance of tooth root

R_w and R_t = thermal resistances of coil wedge and tooth tip, respectively

R_3' = thermal resistance of iron path to pole center surface

R_{w2} and R_{t2} = surface thermal resistances of coil wedge and tooth tip, respectively

R_{i3} and R_{i4} = thermal resistances of insulation at top and bottom of slot, respectively

R_5 and R_7 = internal radial thermal resistances of conductor for outer and inner sections

R_{b3}, R_{s1}, R_{s2} = surface thermal resistances for underside of slot filler, tooth tunnel, and sub-slot, respectively, calculated on inlet temperature basis

R_{s3} = surface thermal resistance for pole center surface

S = resistivity constant of winding = 235 for copper, 225 for aluminum

T_a = temperature of gas entering fans

T' = assumed temperature of conductor for calculation of losses

T_1' and T_2' = temperature rise of outer and inner sections of conductor, calculated for losses W_1 and W_2

T_1 and T_2 = temperature rises T_1' and T_2' corrected for change in loss with temperature

T_f = temperature rise of rotor surface from friction loss

T_p = temperature rise of rotor surface from pole face loss

T_g' = temperature rise of gas in gap between rotor and stator

T_e = equivalent temperature rise of gas in gap = $T_g'+Tf+Tp$

T_{e1} = temperature rise of gas at entrance to tooth tunnel

T_{e2} = temperature rise of gas at entrance to subslot

W_2', W_2'', W_2''' = surface losses (friction and pole face losses) apportioned to wedge, tooth tip and pole face surfaces, respectively

W_1 and W_2 = losses in outer and inner section of coil, respectively, calculated at temperature T'

W_1'', W_2'' and so forth = components of W_1 and W_2 flowing along paths shown in Figure 14

Temperatures and temperature rises are given in degree centigrade, thermal resistances in degrees per watt, and heat flow in watts. One-inch axial length of rotor body is considered.

Equations:

$$R_3=R_3'+R_{s3},\quad R_4=R_w+R_{w2}+R_{i1}$$

$$R_{34}=R_3+R_4,\quad R_{10}=R_m+R_r+R_{i4}$$

$$R_{20}=R_{i3}+R_n+R_r,\quad R_{70}=R_7+R_{i3}+R_{b2}$$

$$R_{720}=R_{70}+R_{20},\quad A=T_o-T_{e1}$$

$$B=T_o-T_{e2},\quad C=R_{720}+R_{i2}$$

$$D=R_3+R_{s2},\quad E=R_{34}+R_{i1}$$

$$F=R_{10}+R_{s1},\quad G=A+R_{34}W_1$$

$$H=W_2T_{70},\quad J=EF+R_{10}R_{s1}$$

$$K=CD-R_{s2}^2$$

$$W_1'=(FG-AR_{s1})/J;\quad W_2'=(HD-BR_{s2})/K$$

$$W_4=(AE+GR_{10})/J;\quad W_7=(HR_{s2}-BC)/K$$

$$W_3=W_2'-W_7$$

$$T_1'=W_1'R_{i1}+W_4R_{s1}+T_{e1}=W_1''R_{i4}+T_o$$

$$T_2'=W_2'R_{20}+W_3R_{s2}+T_{e2}=W_2''R_{70}+T_{e1}$$

$$T_1=\frac{S+T'}{S+T'-(T_1'-T_{e1})}\times\left[T_{e1}+(T_1'-T_{e1})\frac{(S+T_a)}{(S+T')}\right]$$

$$T_2=\frac{S+T'}{S+T'-(T_2'-T_{e2})}\times\left[T_{e2}+(T_2'-T_{e2})\frac{(S+T_a)}{(S+T')}\right]$$

References

1. Steady Flow of Heat in Large Turbine-Generators, C. Richard Soderberg. *AIEE Transactions*, volume 50, June 1931, pages 782–98.

2. Surface Heat-Transfer Coefficients for

Hydrogen-Cooled Rotating Electric Machines, D. S. Snell, R. H. Norris, Mrs. B. O. Buckland. *AIEE Transactions* volume 69, part I, 1950, pages 174–85.

3. The Measurement of Temperatures by Thermocouples, H. Lundkvist. *ASEA Journal* (Vasteras, Sweden), volume 6, 1929, pages 90–93.

4. The Hydrogen-Cooled Turbine Generator, D. S. Snell. *Electrical Engineering (AIEE Transactions)*, volume 59, January 1940, pages 35–50.

5. Heat Flow in Turbine Generator Rotors, C. E. Peck. *Electrical Engineering (AIEE Transactions)*, volume 53, October 1934, pages 1359–65.

6. Application of and Operating Experience with Hydrogen-Cooled Synchronous Condensers and Alternators, Philip Spora, F. M. Porter. *AIEE Transactions*, volume 59, 1940, pages 890–907.

Discussion

V. V. Mason (The Hydro-Electric Power Commission of Ontario, Toronto, Ontario, Canada): The author goes through involved calculations based on a very much simplified equivalent thermal circuit of the windings and comes out with curves of the kilovolt-ampere output at various hydrogen pressures estimated on various criteria, Figure 11 of the paper. This figure indicates that the use of an embedded resistance-type temperature detector to control the loading of machines at elevated pressures will result in excessively high copper temperatures as calculated by the author's method. To support his calculations, the author gives his Figure 9, which shows excellent agreement between calculated and observed values for armature-coil surface losses of 0.5 per unit, but considerably poorer agreement (differences of the order of 50 per cent) at surface losses of 1.1 per unit. A surface loss of 1.1 per unit corresponds to a kilovolt-ampere output of $\sqrt{1.1}$ or approximately 1.05 per unit. Reference to Figure 11 shows that at a kilovolt-ampere output of 1.05 per unit, all methods of estimating the overload capabilities give very nearly the same results.

Even if the agreement between calculated and test values as shown in Figure 9 were exact, this would verify the curves of Figure 11 only at the 1.05 per unit kilovolt-ampere points. The lack of agreement between experiment and theory shown in Figure 9 makes even these points open to serious doubt. In effect then, it appears that the author has not been able to offer any convincing experimental confirmation of his calculations. Hence, it is suggested that his results be regarded as very pessimistic until such time as more complete experimental results are available.

I agree with the author that it is the total temperature of the windings which determines the permissible loading of the machine rather than the temperature rise. However, where there is a possibility of very low cooling-medium temperatures it may be wise to set a limit on the maximum allowable temperature rise to guard against excessive relative movement between copper and iron due to differential expansion.

Herman Halperin (Commonwealth Edison Company, Chicago, Ill.): The emphasis in this interesting paper on temperature of the copper conductors themselves in armature windings, in contrast to the usual reference to temperature of embedded armature detectors, seems to be a fundamental and necessary step in establishing load capabilities of generators. Of course, as the author indicates, this is particularly necessary for hydrogen-cooled generators when operating at the higher internal gas pressures. In general, however, the basic work on allowable temperatures, whether in regard to standard limits for various types of insulations or for various kinds of metal contacts, usually are (or should be, in my opinion) focused on the hottest temperature of the conductors involved. This applies, as is indicated by various AIEE articles and standards, particularly to insulated wires and cables, transformers, contacts of circuit breakers, bus-bar joints, and so forth.

In the third paragraph of the paper, the author refers to the "standard allowance for the temperature difference between armature copper and embedded detector" as being "specified as 10 per cent of the observed temperature rise." It would correspond at most to only 6 degrees centigrade (10 per cent of the standard limit of 60-degree rise by detector). However, the implication of the data in Figure 9 of the paper is that the temperature difference actually may be two or more times that amount for air-cooled machines and machines operating with hydrogen at 1/2 pound per square inch gauge. Comments on this point would be of interest.

Curve (*c*) of Figure 5 shows per-unit kilovolt-ampere output for various hydrogen pressures with a limit of about 101 degrees centigrade for armature copper. Is there an implication that this total temperature is satisfactory for safe operation throughout the life of generators? That temperature is materially less than allowed, in effect, by the usual limit of 60-degree centigrade rise by embedded detector, and is greatly less than permitted for class-*B* insulation when used in other apparatus; on the other hand, large modern machines generally have lower total temperatures at rated load than 101 degrees centigrade.

Loads on generators in service usually vary greatly each day. In connection with large machines, where the length of the armature coils may be, say, 22 to 25 feet it seems that the allowable daily temperature rise of the copper temperatures should be less than for relatively small generators. Otherwise the differential expansion between armature copper and iron may cause premature fatal weakening of the insulation.

The manufacturers apparently have recognized this point by designing very large machines for temperature rises measured by an embedded detector materially less than the standard limit of 60 degrees centigrade. The author mentions the point, but gives only a little discussion on it. Attention is drawn to it here because with hydrogen cooled machines operating at elevated gas pressures, that differential may be very large as compared to what has obtained for moderate-sized air-cooled machines which have operated without trouble for 25 to 30 years. For instance, according to Figure 6 of the paper, with a total armature-copper rise of 66 degrees centigrade at 20 pounds per square inch gauge hydrogen pressure for the given machine, the temperature drop in the armature coil insulation is about 40 degrees centigrade.

M. D. Ross and **R. A. Towne** (Westinghouse Electric Corporation, East Pittsburgh, Pa.): The calculations presented by Mr. Snell demonstrate qualitatively the reason hydrogen-cooled machines are rated and operated, at loads above the normal rating, on the basis of hydrogen pressure rather than temperature rise.

The calculation of the thermal circuit of an electric machine requires a complete analysis of the thermal circuit, an accurate knowledge of the thermal constants involved, and a precise segregation of all load losses.

The segregation of losses is a particularly knotty problem. Improper loss segregation can lead to appreciable errors in the temperatures calculated. Because of the difficulties involved in a temperature calculation of this nature, we believe that extensive copper temperature measurements should be secured to calibrate the calculations.

The behavior of temperature detectors in air has been studied,[1] but the effect of hydrogen on detectors has not been determined precisely, although the low temperature rises obtained during operation at elevated gas pressures indicate an obvious discrepancy.

Among the factors involving detector accuracy are:

1. Variation in eddy loss between top and bottom strands in the slot.

2. The effect of slot geometry and slot insulation thermal characteristics on the heat-flow path in the vicinity of the detector. The ratio of insulation thickness to slot width and the ratio of lateral to transverse thermal conductivity of the stator winding insulation are principal factors determining the heat-flow path.

3. The effect of the ventilating gas on the detector. The ventilating gas can cool the detector in two ways.

a. The radial flow of gas cools the edges of the detectors exposed in the vent spaces between packs of punchings.

b. An axial flow of gas along the clearance space between the edge of the detector, the rounded corner of the stator coils, and the slot side cools the edge of the detector along its length normally considered to be blanked off by the punchings. Since the lateral thermal conductivity of the detector material may be several times higher than the transverse conductivity, this cooling effect is considerable.

These cooling mechanisms are functions of the gas temperature in the immediate vicinity, the radial velocity, the gas pressure, the differential pressure across the punching packs, and the ratio of the vent width to the pack thickness.

Although the effect of many of the previously mentioned factors is known, the quantitative effect of others, especially those involving the ventilating gas, is obscure at present.

Model tests made some time ago indicated, in general, the effects on the detector which have just been mentioned. We propose to make factory tests on several large machines with thermocouples built into the neutral coils in order to measure the copper temperatures and compare them with adja-

cent temperature detectors. With so many factors influencing the detector error, we do not believe that it is worth while attempting to calculate this factor.

We have realized for some time that hydrogen-cooled machines, when operated at elevated gas pressures, cannot be loaded safely on the basis of embedded-temperature-detector readings, as internal temperatures in the stator coils may be excessively high at the high gas pressures. We have advocated that such machines be loaded in accordance with the nameplate rating. Most of our machines are rated relatively 100 per cent at 0.5 pound per square inch gauge gas pressure, 115 per cent at 15 pounds per square inch gauge and, in some cases, 125 per cent at 30 pounds per square inch gauge. We are satisfied that copper temperatures of any of our machines, designed for higher gas pressures, when loaded according to this schedule will be satisfactory.

The subject of hot-spot allowances in hydrogen-cooled machines could well be investigated further by the interested AIEE committees so that uniform methods of approximating the copper temperatures can be standardized. If a suitable temperature detector, shielded from the cooling action of the gas, can be developed, it may be possible to approximate more nearly the copper temperature.

It would seem that Mr. Snell's conclusion that all hydrogen-cooled machines should be loaded according to some such schedule as shown in curve 4 of Figure 11 of the paper is somewhat premature in the light of present data.

Ever since hydrogen-cooled machines have been operated at pressures above atmospheric, it has been recognized that a cooler designed for 40-degree centigrade outlet gas temperature at 0.5 pound per square inch gauge will have an outlet temperature of 42 to 43-degree centigrade at 115 per cent load and 15 pounds per square inch gauge gas pressure. To obtain 40-degree centigrade outlet temperature at 15 pounds per square inch gauge would involve as much as 40 per cent more surface and a considerably larger generator frame. This matter was recognized in making up AIEE Standard Number 602[2] for hydrogen-cooled generators where the outlet gas temperature is specified as 40 degrees centigrade at 0.5 pound per square inch gauge and the ambient is allowed to go up at the higher pressures. We would agree with Mr. Snell that the ambient gas temperature be left out of the temperature guarantee for hydrogen-cooled turbine generators and that the temperature rise be established above cooling-water temperature.

Mr. Snell is to be congratulated on a very fine discussion of the factors involved in loading hydrogen-cooled machines. The paper is an important contribution to the literature on this subject.

References

1. Embedded Temperature Detectors in Large Generators, F. D. Newbury, C. J. Fechheimer. *The Electric Journal* (East Pittsburgh, Pa.), volume 17, number 9, September 1920, pages 410–18.

2. Preferred Standards and Standard Specification Data for Large 3,600-rpm, 3-Phase, 60-Cycle Condensing Steam Turbine Generator. AIEE Standard Number 602, May 1949.

Carl J. Fechheimer (Consulting Engineer, Milwaukee, Wis.): The explosion pressure increases with the density of hydrogen for an optimum mixture with air. If generators are designed to withstand such explosive pressure, is not the increased cost to be given serious consideration, particularly with large diameters intended for the higher ratings?

The statement that the heating of the stator, rather than the rotor, may be the limit, is surprising. Would that be the case for a generator that had been intended previously to operate at 1/2 pound per square inch gauge and later was operated at elevated pressure? Or one for which the tools had been made and could not readily be altered? If the designer can start with a clean slate and select new proportions throughout, would not the rotor be the limit, assuming that the generator is to operate at about 85 per cent power factor, and not less than 0.8 short-circuit ratio? Is there any reason why the stator slots cannot then be made of sufficient depth to accommodate enough copper to secure the desired temperature?

Mr. Snell's statement that the temperature determined by a detector in the armature read low recalls a paper of 30 years ago.[1] Reasons for the detector's low reading are brought out; a map of heat flow and isothermal lines explains most of it. The derivation by Wilhelm Peters[3] enables the engineer to determine what differences to expect. Peters gives a plot in a family of curves, from which the ratio of the temperature drop by detector to the total drop can be read.

Mr. Snell has done much valuable work in calculating temperatures and ratings. I spent considerable time some years ago in a study of Soderberg's paper[4] and in its applications. The method is tedious, even when the equivalent electric circuit is sub-

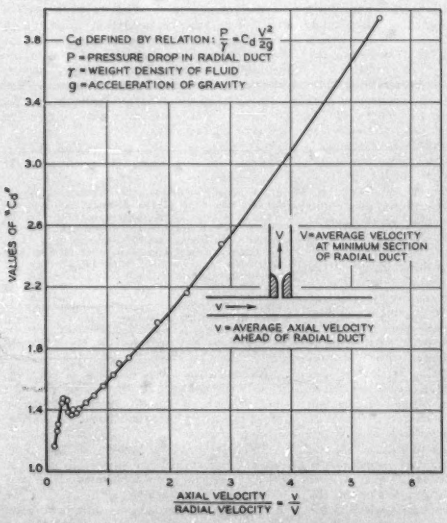

Figure 1. Coefficients of discharge in a turbine generator rotor vent duct

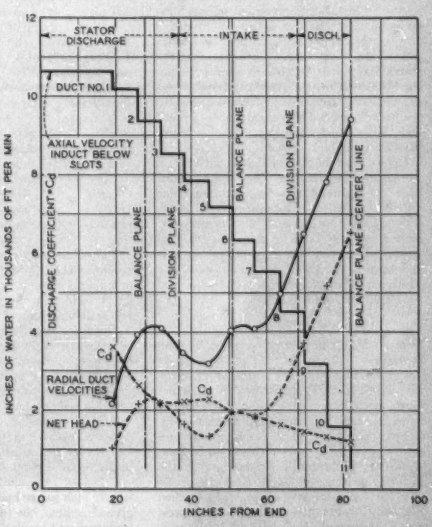

Figure 2. Calculated gas flow in a turborotor

stituted for the solution of the partial differential equations. In discussing the solution with Mr. Soderberg in 1931, he told me that one point that disturbed him was the location of the Surface of Division. Mr. Snell has located it in the rotor about halfway down in the slotted part. Then he calculated the temperature for each part and took a weighted mean. It would be interesting to learn about what percentage of error had been introduced by an inaccurate selection of the Surface of Division.

Another questionable point is the value of the surface heat-transfer coefficient where there are obstructions or sharp 90-degree turns in the fluid path. Studies that were made on enclosed ventilated motors, using an equivalent electric circuit, caused me to question results because there were uncertainties in some parts where obstructions entered and the flow was very complex.

Figure 1 of the discussion shows plotted data taken on a stationary model in which axial and radial rotor ducts of a turbine generator were simulated. The curve shows how the discharge coefficient varied with the ratio of axial to radial velocities.

Figure 2 of the discussion shows the calculated gas flow in a turborotor, for which data from Figure 1 were used. The calculations are rather long and tedious.

References

1. Some Practical Experiences with Embedded Temperature Detectors, F. D. Newbury, C. J. Fechheimer. *AIEE Transactions*, volume 39, part 1, 1920, pages 977-91.

2. Temperature Distribution with Two-Layer Windings, Wilhelm Peters. *Wissenschaftliche Veroffentlichungen aus den Siemens-Werken* (Berlin, Germany), volume 4, number 1, 1925.

3. See reference 1 of the paper.

T. de Koning (Consulting Engineer, Philadelphia, Pa.): Mr. Snell has favored us with an excellent paper. He emphasizes that a constant total temperature of the winding copper, which, however, cannot be measured readily, forms a realistic basis for a proper determination of the load that can be carried. Furthermore, he brings out that the embedded temperature detectors of the windings give misleading information. It is shown that the output of a generator is limited by the heating of the rotor copper or by the armature copper, but mostly by the latter. It is brought out that every machine reacts differently to hydrogen-pressure increases in regard to per-unit kilovolt-ampere output, and it looks as if the hydrogen-pressure distribution over the length of the machine is of influence, too. We have seen from the many illustrations how the power factor, the water temperature, and the hydrogen temperature influence the permissible load.

The obvious conclusion is, either we have to be very conservative about loading machines working with elevated hydrogen pressures, or we need some kind of complicated device which takes care of the permissible load determination. The simple way out would be to run the machine continuously with maximum hydrogen pressure, but most public-utility engineers do not like this idea. They claim it would decrease the efficiency of the machine and increase the hydrogen losses.

Adding one more gadget to the many a hydrogen-cooled machine needs most likely will not be considered objectionable. They seem to be well designed, and as long as they function well one forgets about the complications. However, from a development-cost standpoint the picture is less rosy. After spending large amounts of money on the shell, the coolers, the seals, hydrogen-sealing equipment, hydrogen-purity equipment, rotor copper alloys, and so on, we now will need some for a permissible load determination device. The question arises: was the choice of hydrogen cooling the right one, and might not another method have been better?

F. M. Porter (American Gas and Electric Service Corporation, New York, N. Y.): Mr. Snell is to be complimented on his thorough analysis of the factors affecting temperature rises in the various parts of generator stators and rotors when operating at gas pressures ranging up to 50 pounds per square inch gauge. A much clearer picture is now available of what to expect in the way of increased capacity, either in the form of kilowatts or reactive kilovolt-amperes, when utilizing higher gas pressures than 1/2 pound per square inch gauge.

We have in operation on the system of the American Gas and Electric Company 22 hydrogen-cooled generators. The first one of these units to be installed was at Logan, West Virginia, and this machine has been in service over 12 years. Some of the older machines have been operated either continuously or intermittently at gas pressures ranging from 5 to 15 pounds per square inch gauge, and in the case of the four most recent units, placed in service in the last six months, we are operating them satisfactorily at a gas pressure of 25 pounds per square inch gauge. With reference to the 18 older units, gas pressure up to 15 pounds per square inch gauge was utilized primarily to obtain greater kilowatt capacity, particularly during the war and postwar periods. We also have used it to keep down field temperatures when increased reactive kilovolt-amperes were required in emergency or otherwise. In a few cases, where cooling-water temperatures above 100 degrees Fahrenheit sometimes occur, we have resorted to increased gas pressure to keep the machine temperatures within proper limits.

The author suggests that the total temperature of the windings be used as a basis for determining generator output at elevated pressures, partly because of increase in cold gas temperature which, in turn, is based on constant temperature of water to the coolers and constant water flow through the coolers. As far as we are concerned, constant water flow is not a practical basis for determining rating, since all of our machines have coolers designed to provide sufficient water flow to remove losses resulting from increased loading at high gas-pressure operation and still maintain cold gas temperature at 40 degrees centigrade or below. In general, because of this adequacy of the coolers, we are able to maintain cold gas temperatures between 30 and 35 degrees centigrade although occasionally, on very hot summer days, this temperature may go as high as 40 degrees centigrade. Therefore, we believe this factor should be taken into consideration in determining the permissible increase in capacity at higher gas pressures. Furthermore, since the cold gas temperature may be as low as 30 degrees centigrade, it is our understanding that the manufacturers recommend a loading based on temperature rise above this cold gas temperature rather than total permissible temperature, which would be based on a cold gas temperature of 40 degrees centigrade. We believe that, in the case of machines with relatively low temperature rises for field and/or stator at rated load, one should consider taking advantage of this fact to obtain increased capacity from the machine, on a temperature basis, in the same manner that increased volt-amperage is permissible because of the increased cooling effect at higher gas pressures.

Referring to Figures 12 and 17 of the paper, which have to do with increase of unit kilovolt-ampere output of generators at various gas pressures, we have found, in the case of a 43,780-kva 0.9-power factor 1,800-rpm generator, that the following increases are indicated for the temperature rise obtained from stator temperature detectors:

Output, Per Unit Kilovolt-Amperes	Hydrogen Pressure Pounds per Square Inch Gauge
1.11	5
1.18	10
1.24	15

Similarly, for the field of this machine, unit kilovolt-ampere increases are indicated as follows:

Output, Per Unit Kilovolt-Amperes	Hydrogen Pressure, Pounds per Square Inch Gauge
1.11	5
1.23	10
1.32	15

These match some of the representative curves shown in the paper. We also have found, in the case of a 110,000-kva 0.9 power factor 1,800-rpm machine, that the corresponding unit kilovolt-amperes at 15 pounds per square inch gauge are 1.41 for the stator and 1.42 for the rotor, indicating that both field and stator limit the loading at about the same point in so far as observed readings are concerned. The values stated in this paragraph for generators of different capacities, together with data on those included in Mr. Snell's paper, indicate that wide variations are to be expected and that general conclusions cannot be drawn for all machines. Therefore, the size, speed, normal temperature rise of parts at low gas pressure, and other factors are going to affect the decision as to what increased capacity can be carried.

As a matter of interest, we are including similar unit kilovolt-ampere output data for a typical 18,750-kva 900-rpm hydrogen-cooled synchronous condenser which has been operating at gas pressures up to 25 pounds per square inch gauge for approximately 10 years. Temperature runs made in 1941 indicated that, for similar field and stator temperature rises, based on an initial 18,750-kva run at 1/2 pound per square inch gauge gas pressure, the following per-unit-kilovolt-amperes would apply:

		Gas Pressure, Pounds Per Square Inch Gauge		
		10	20	25
Unit kilovolt-ampere increase	Field	1.14	1.24	1.30
	Stator	1.16	1.31	1.39

Obviously, in this case the field temperature rise is the limiting feature. We have been carrying loads on this unit, as well as on five other similar machines, based on these increases in so far as the field heating is concerned.

To return to the general problem of generators, it is indicated that observable field temperature rise is a reasonably satisfactory means for determining maximum loading in so far as rotor heating is concerned. However, it is not permissible to use the stator temperature rise as obtained from the resistance temperature detector because of the variation in differential between this observed temperature and actual copper temperature at higher gas pressures. Since operation at elevated gas pressures is being employed continuously on many of the older units, and probably will be employed on practically all new units, it is essential that agreement on loading limitations be reached with the manufacturers as quickly as possible so that the operating companies may keep within the limits of any given unit while relying on temperatures which can be obtained and read continuously. We believe it is going to be necessary to determine these limitations for each individual unit because of the many variables involved. Obviously, the information presented by Mr. Snell has been a great step forward in clarifying this problem of generator operation at elevated gas pressures.

D. S. Snell: Mr. Mason's criticism of the accuracy of the temperature calculations given in the paper appears to be the result both of failure to read the paper carefully and of unfamiliarity with the method of temperature analysis given. The calculation of the armature and field-winding temperatures given in the paper, using the thermal circuits shown in Figures 2 and 14 of the paper, is based upon a method of temperature analysis developed by C. R. Soderberg[1] which, since its introduction in 1931, has been used widely and has been proved to be remarkably accurate whenever the values of the thermal resistances and unit loss intensity are known accurately. Mr. Mason has, apparently without adequate analysis, suggested that the calculations of the armature temperatures by this method are highly inaccurate, while overlooking the fact that the application of the same method to the calculation of the temperatures of the field winding gave results which checked the test results very closely. Since a check on the calculated armature copper temperatures was not possible, it was necessary in the paper to make an estimate of the temperature drop from copper to detector based on tests on other machines. Mr. Mason has assumed that the measured temperature drops given by Figure 9(C) of the paper for a 6,250-kva generator should apply for the 83,000-kw generator used in the example. This is incorrect since the theoretical temperature difference between copper and an ideal detector is considerably greater for the 6,250-kva generator than for the generator used in the example. By comparing Figure 9(C), curve 2, with Figure 8, curve 3, one can see that the temperature difference from copper to an actual detector also should be greater. If this difference in design between the two generators is taken into account, the estimated temperature differences from copper to detector shown by curves 2 in Figure 8 for the generator used in the example do not appear to be unreasonable. It appears, therefore, that Mr. Mason's suggestion that the results are to be regarded pessimistically is quite unwarranted.

Mr. Halperin's comments on the inconsistency of the present standards for hottest spot allowance with available test data are very pertinent. The present AIEE Standard[2] for hottest spot allowance of 10 degrees centigrade at rated load for class-*B* insulation is apparently based on the ten-per cent rule mentioned in the paper, which specified an allowance based on ten per cent of the observed temperature rise in degrees centigrade rounded off to the nearest multiple of five above the estimated value. Tests on both hydrogen-cooled and air-cooled generators indicate actual temperature differences considerably at variance with this rule. As shown in Figures 8 and 9 of the paper, the actual temperature differences between copper and embedded detector lie somewhere between the calculated temperature drops in the coil insulation and the theoretical temperature differences between copper and an ideal detector of the thermocouple type, having no heat loss, and hence will be different depending on the design of the armature coil. As suggested in the paper, an experimental determination of the temperature difference between copper and embedded detector, for hydrogen-cooled generators of modern design, is much to be desired.

For the generator used in the example, the measured temperature rise of armature winding at rated load and hydrogen pressure of 1/2 pound per square inch gauge was 52 degrees centigrade, and the calculated temperature rise of copper was 61 degrees centigrade. For 40-degree centigrade inlet gas, a hottest spot temperature of 101 degrees centigrade is thus indicated. Since it is considered good practice to limit the observed armature temperature rise of turbine generators to 60 degrees centigrade, and since AIEE Standards permit a hottest spot temperature of 130 degrees centigrade, it is evident that this generator is conservatively rated and should have a high life expectancy.

It is true, as Mr. Halperin suggests, that as the sizes of generators increase, the increased length of the armature bars makes a lower temperature gradient in the insulation desirable. The increased temperature drop in the insulation obtained at overloads when utilizing elevated gas pressures to secure increased output increases the differential expansion between copper and iron and therefore reduces somewhat the life expectancy of the generator. The extent of this reduction depends on the frequency and extent of the overloading; however, since operating experience at elevated pressures has been relatively limited, it is not possible at present to state the extent to which the life of a generator is impaired by such operation.

The author is indebted to Mr. Ross and Mr. Towne for amplifying and clarifying many of the points made in the paper. Calculation of the heating of the armature and field windings for the generator used in the example, to the degree of accuracy obtained, was made possible through a complete analysis of the various losses, confirmed by tests. These tests included laboratory tests to determine the thermal conductivities of the insulation and the stator laminations in hydrogen, model tests to determine the amount of gas flowing through the different stator vent ducts, and analysis and tests on a generator rotor operated in the open to determine the gas flow through the rotor vent ducts. However, as pointed out by the discussors, temperature calculation is a difficult and complicated matter, and the checks given in the paper on the calculated copper temperatures are not as conclusive as the author would desire. Tests to determine the actual armature copper temperatures of hydrogen-cooled generators are greatly needed, and it is gratifying to note that such tests now are being undertaken.

The analysis of the factors influencing the readings of embedded temperature detectors, given by Mr. Ross and Mr. Towne, is very useful. Efforts have been made by the General Electric Company to reduce the temperature differential between copper and embedded detector by packing the space between the rounded corners of the armature bars and the detector with asbestos putty, which tends to reduce the cooling effect of the ventilating gas on the edges of the detector. While this practice has reduced the temperature differential somewhat, the detectors still read appreciably below the theoretical values for an ideal detector having no heat loss. The development of a shielded type of detector which would read close to the theoretical temperature, as suggested by the discussors, would be a significant accomplishment.

The statement in the paper that curve 4 of Figure 11 might be used as a guide to determine the capabilities of generators at elevated gas pressures was not meant to be taken, as Mr. Ross and Mr. Towne have assumed, without some qualification; the statement presupposed a consideration of the other data given in the paper, particularly Figures 12 and 17, which show the variation in the calculated capabilities of different generators as determined for constant observed armature and field-temperature rises. It is evident from such consideration that curve 4, Figure 11, would be too conservative for some generators and not conservative enough for others. However, for large generators of modern design, this curve doubtless may be considered as fairly representative.

The points regarding cooler performance at elevated gas pressures, and the difficulty of obtaining constant cold gas temperatures at elevated pressures, are most pertinent. The author is gratified to find Mr. Ross and Mr. Towne in general agreement with the major conclusions of the paper and appreciates their generous estimate of the paper's value.

Mr. Fechheimer's discussion has covered several interesting phases of the problem of generator loading at elevated gas pressures. The increased explosion pressures at 25 or 30 pounds per square inch operating pressure can be protected against by a slight increase in the thickness of the generator wrapper plate, which does not increase the generator cost significantly. However, it should also be considered that the possibility of an explosion becomes increasingly remote as the hydrogen pressure is increased, due to the fact that the resultant increase in hydrogen

leakage maintains the hydrogen purity at a higher value.

It is quite possible to design a generator in which the output at elevated gas pressures would be limited by the rotor heating rather than by the armature heating. This would involve, however, operation at armature temperatures considerably below those for which generators are normally designed, which would be uneconomical. The reasons why the heating of the armature rather than of the field winding must limit the load at elevated gas pressures, for the generator used for the example, are given in the paper.

The references cited by Mr. Fechheimer dealing with temperature differences from copper to embedded detector are most pertinent. The article by Wilhelm Peters[3] gives a method for calculating this temperature difference which is more accurate than the method used by the present author in obtaining curve 3, Figure 8, and curve 2, Figure 9, in that it takes into account the difference in thermal conductivities of the armature insulation in the directions along and across the insulation layers, whereas the method used by the author based on H. Lundkvist's article[4] does not. Had Peters' method been used instead of the latter method, the above theoretical curves of temperature difference between copper and an ideal detector would have been appreciably closer to the curves of estimated and measured temperature difference between copper and conventional detector, given in Figures 8 and 9.

To answer Mr. Fechheimer's question on the location of the surface of division of radial heat flow in the rotor tooth, the construction of the rotor for the generator used in the example made it convenient to locate this surface at the bottom of the tooth ventilating duct. The justification for this location is the fact that the tests checked the calculations closely. For rotors having subslots only, the tooth ducts being omitted, the location of this surface will vary throughout the length of the rotor, as was shown in a discussion by the author of the paper by C. E. Peck.[5] However, Mr. Peck states that for rotors of such design little error is introduced in the final result by assuming the surface of division at the midpoint of the radial tooth height and taking a weighted means of the calculated winding temperatures on either side of the surface.

The presence of obstructions or sharp turns in the ventilation circuit of a generator has a significant influence on the heat transfer rate. This was demonstrated by G. E. Luke in his two papers[6,7] on surface heat transfer which showed the effect of change in air path in ducts and of the duct entrance conditions on the heat transfer. Also, R. Richter[8] evaluates an "eddy factor" for duct entrance. In the author's paper these elements of uncertainty were eliminated for the stator ducts through the use of experimentally derived data on heat transfer in ducts in air, corrected for hydrogen by the use of the device described by D. S. Snell, R. H. Norris, and Mrs. B. O. Buckland.[9] For the rotor ducts, their large length-to-diameter ratio made the use of data on straight smooth ducts seem permissible.

The data given by Mr. Fechheimer on duct discharge coefficients and gas flow for a turbine generator rotor are most interesting, and agree substantially with those obtained by the author and associates from similar tests on stationary models, and from the analysis made for the determination of the rotor duct velocities for use in calculating the duct surface heat transfer coefficients. Also, large-scale ventilation tests, using actual generator rotors, were made to confirm the analysis.

Mr. de Koning has suggested the need for an automatic device for determining the permissible loads at elevated gas pressures. The author believes, however, that if accurate data on the temperature difference between armature copper and embedded detector are made available, it should be possible to determine the permissible loads at elevated gas pressures quite simply, from tests at different hydrogen pressures, through plotting the test data as shown in Figures 7 and 15 of the paper.

Mr. de Koning questions whether, in view of the increased complications attendant on operation at elevated gas pressures, some method of cooling other than with hydrogen might not be more advantageous. He has himself proposed vaporization cooling[10] as one possible alternative; while Carl J. Fechheimer has proposed liquid cooling[11] as another. Both these alternatives undoubtedly have merit, but also introduce many complications which, for the present at least, make hydrogen cooling seem simple by comparison.

The increased explosion pressures at 25 or 30 pounds per square inch operating pressure, which Mr. de Koning has mentioned, were also mentioned by Mr. Fechheimer. The dimensions of the generator are determined primarily by its electrical characteristics, and the frame construction must be strong enough to support the stator core and the rotor, and must also be gas-tight. Fulfillment of these conditions as a rule automatically makes the frame strong enough to withstand safely the force of an explosion of the most explosive hydrogen-air mixture. Increasing the hydrogen pressure also increases the gas leakage; hence, it is more necessary than ever to provide adequate ventilation for all areas into which hydrogen leakage could conceivably occur.

Mr. Porter's discussion of the experience of the American Gas and Electric Company in the operation of their hydrogen-cooled generators and synchronous condensers at elevated gas pressures is of much interest and value. His company has pioneered both in the use of hydrogen-cooled equipment and in the utilization of elevated gas pressures, and many of the test data given in the paper were obtained on generators of this company's system.

Mr. Porter has questioned the author's use of an increasing cold gas temperature with increasing gas pressure in determining the capability of a generator at elevated pressures. This follows, however, from the assumption of a temperature of 95 degrees Fahrenheit for the cooling water, which is the temperature for which most coolers now are being designed, due to the increased use of condensate for cooling. With this temperature for the cooling water it is not practical to build coolers that will maintain a cold gas temperature of 40 degrees centigrade at elevated pressures; this point was also made in the discussion of Mr. Ross and Mr. Towne. However, for coolers designed for 90-degree Fahrenheit cooling water, as are the coolers for the generators mentioned by Mr. Porter, it is usually possible to maintain constant cold gas temperature with increasing gas pressure through an increase in the flow of cooling water. In this case, curve 3 instead of curve 4 in Figure 11 of the paper should be used as a basis of rating.

The author did not intend to suggest, as Mr. Porter has assumed, that constant total temperatures should be made the basis of operation at elevated gas pressures, but rather that the capability at elevated pressures be determined as the load giving the same total temperatures as are obtained at 1/2 pound per square inch gauge hydrogen pressure. To obtain the same total winding temperatures at increased output, as are obtained at rated load at a pressure of 1/2 pound per square inch gauge with a cold gas temperature of 40 degrees centigrade, either the hydrogen pressure may be increased or the cold gas temperature reduced. In either case, such operation must be regarded as an abnormal condition resulting in less favorable operating characteristics than are obtained at nameplate rating and causing increased temperature gradients in the winding insulation which may tend to reduce the life expectancy of the generator.

The 43,780-kva 1,800-rpm generator on which Mr. Porter has presented data from tests at elevated gas pressures is Generator Number 3 in Table I and Figure 17 of the paper. The gains in output for this generator at elevated gas pressures, as calculated by Mr. Porter on the basis of constant rotor heating, check the values given in the paper. The capability of this generator at elevated pressures on the basis of constant armature heating was not calculated in the paper, as the test data available to the author was not considered reliable. The 110,000-kva generator mentioned by Mr. Porter was a duplicate of Generator Number 8 in Table I and Figures 12 and 17 of the paper; however, the capability of this generator at 15 pounds per square inch gauge pressure, as calculated in the paper for constant armature and rotor heating, is considerably less than as calculated by Mr. Porter. We believe this discrepancy may be due to the fact that the test data from which Mr. Porter made his calculations were less complete than those available on Generator Number 8; also, the rotor heating data may be less accurate. Experience indicates that an accurate estimate of the capability of a generator at elevated gas pressures from tests requires that at least three or four test points at each pressure be obtained, and that the test data be plotted as illustrated in Figures 7 and 15 of the paper.

Mr. Porter's data on the capabilities of the 18,750-kva synchronous condenser at various gas pressures are interesting. His statement that the field temperature rise is the limiting factor is correct in this instance and applies in general to synchronous condensers.

The reason for this is that the field temperature rise is usually close to the guaranteed value, whereas the armature temperature rise is far below that value on machines designed for zero power-factor operation. If it is assumed that constant cold gas temperature can be maintained for a synchronous machine at elevated hydrogen pressures, so that its capability may be based on constant temperature rises of the windings rather than on constant total temperatures, reference to Figure 11 of the

paper shows that for the 83,000-kw generator at a pressure of 15 pounds per square inch gauge, the output for constant observed temperature rise of the armature winding would be 1.3 per unit kilovolt-amperes, for constant temperature rise of the field winding would be 1.28 per unit kilovolt-amperes, while the output based on constant temperature rise of the armature copper would be only 1.18 per unit kilovolt-amperes. Hence, although on the basis of constant observed temperature rises the field winding of this generator is the limiting feature, on the basis of constant temperature rise of the winding copper the armature is the limiting feature. It is probable that the same would be true for a synchronous condenser with a high armature copper loss where the observed temperature rise approached the guaranteed value.

We agree with Mr. Porter that prompt steps should be taken by the manufacturers to clarify their position relative to the permissible loading at elevated gas pressures. However, until the necessary studies can be made, the author believes that curve 4 in Figure 11 of the paper may be used as an approximate guide, using Figures 12 and 17 in conjunction with the several curves of Figure 11 to indicate the extent to which curve 4 of the latter figure should be corrected for a given generator.

References

1. See reference 1 of the paper.

2. Introduction to AIEE Standards—General Principles Upon Which Temperature Limits Are Based in the Rating of Electric Machines and Apparatus. AIEE Standard Number 1, June 1947, Sections 1–10, pages 8–9.

3. See reference 2 of C. J. Fechheimer's discussion.

4. See reference 3 of the paper.

5. See reference 5 of the paper.

6. The Cooling of Electric Machines, G. E. Luke. *AIEE Transactions*, volume 42, 1923, pages 636–52.

7. Surface Heat Transfer in Electric Machines with Forced Air Flow, G. E. Luke. *AIEE Transactions*, volume 45, 1926, pages 1036–47.

8. Elektrische Maschinen (book), R. Richter. J. Springer, Berlin, Germany, volume 1, page 327.

9. See reference 2 of the paper.

10. Vaporization Cooling of Electric Machines, T. de Koning. *Electrical Engineering*, volume 68, number 5, May 1949, pages 385–92.

11. Liquid Cooling of A-C Turbine Generators, C. J. Fechheimer. *AIEE Transactions*, volume 69, part I, 1950, pages 165–73.

Control of Large D-C Motors Supplied from Ignitron Rectifiers

O. W. LIVINGSTON
FELLOW AIEE

THE purpose of this paper is to explain the basic control methods that have been used in the control of large d-c motors supplied from ignitron rectifiers. Companion papers[1,2] describe the application requirements of this class of equipment, the functioning of the rectifier, and details of a specific application.

To successfully meet the requirements of most applications, a control must be able to start the motor and accelerate it to the desired speed either in the armature or field weakening range without distress or overload to the motor or connected load, to maintain the required speed within acceptable limits in spite of disturbing factors such as supply voltage or load torque fluctuations, and to decelerate or stop the motor without excessive overload or stress on the load. It is well known that a phase-controlled rectifier can be used as an adjustable voltage supply for either the armature or the field of a d-c shunt motor. A companion paper describes a phase controlled ignitron rectifier suitable for this service together with the method of affecting the phase shift. This equipment requires the application of current to the d-c windings of the phase shifting circuit to increase the average output voltage of the rectifier. To obtain full output voltage approximately 200 watts would be required of a typical equipment and the use of series resistance to improve the speed of response might bring the total power required up to 800 or 1,000 watts.

"Open Loop" Armature Control

Perhaps the simplest form of armature control for such a rectifier is shown in Figure 1. In this very simple circuit, a definite voltage derived either through closing of jog relay contacts *JR* or the run relay contacts *RR* is applied to the d-c coil of the phase shift circuit which causes a definite voltage to be impressed across the armature. The run potentiometer, might well be a motor driven device with suitable interlocks so that the run relay contacts may only be closed in the down position, and with an operating speed so adjusted to prevent overloading of the large motor or rectifier during acceleration. This type of system frequently referred to as an "open loop" system would not be particularly suitable for a number of reasons. Variation in supply voltage or variations in motor torque particularly in the low-voltage low-current range will be reflected in the rectifier output voltage and may cause undesirable fluctuations of the motor speed. In addition, variation in temperature, either due to ambient or self heating in the phase shifting circuit may cause uncompensated variations in the output.

Basic Closed Loop System[3]

To circumvent these difficulties a "closed loop" or negative feed-back system in which all or part of the output is compared with a reference or input and their difference, commonly called the error, is used to bring them into closer accord. Figure 2 shows a very simple system of this type showing the reference D, the actual motor voltage feed-back θ, and the error or difference ϵ. In normal operation D exceeds θ by only a small value of ϵ causing the current flow in the direction shown. If some disturbance, such as a line voltage drop causes θ to momentarily decrease 10 per cent, the value of ϵ will momentarily increase many fold which causes an increase in the control current in the phase shift circuit which tends to restore the output θ very close to its original value. However, since it has been necessary to increase ϵ slightly to take care of the increase phase advance necessitated by the low supply voltage the output voltage, θ will not be exactly restored to its original value. The larger D and θ with respect to ϵ required for full output, the smaller will be this percentage error. From this standpoint the higher the ratio of θ/ϵ or more precisely $\Delta\theta/\Delta\epsilon$ the less sustained output error will be experienced. This ratio $\Delta\theta/\Delta\epsilon$ is frequently referred to as the loop gain, just as though the phase-shift circuit and rectifier could be considered as an amplifier. It is evident that the higher this loop gain, the less the system output will be affected by disturbances. This elementary explanation can be supplemented with a mathematical analysis which shows that if the effect of a given disturbance on an unregulated system is known, the effect of the same disturbance on a regulated system with loop gain of K will be reduced by the factor $1/(1+K)$.

This desirability of high loop gain to minimize the effect of system disturbances makes the simple "closed loop" circuit of Figure 2 impractical, due to the large amounts of power required from the reference supply. To illustrate this let us assume that for full output 25 volts and 8 amperes or 200 watts are required by the phase shifting circuit. Let us further assume that the full output voltage is 500 volts supplied to the motor and this entire voltage is fed back to be compared with a reference which then must be 525 volts (500+25). Assuming that the output voltage is essentially proportional to the voltage applied to the phase shift circuit, the loop gain K may be shown to be

$$K = \Delta\theta/\Delta\epsilon = 500 \text{ volts}/25 \text{ volts} = 20$$

This value of loop gain, which is by no

Paper 50-32, recommended by the AIEE Electronic Power Converter Committee and approved by the AIEE Technical Program Committee for presentation at the AIEE Winter General Meeting, New York, N. Y., January–30February 3, 1950. Manuscript submitted November 2, 1949; made available for printing November 30, 1949.

O. W. Livingston is with the General Electric Company, Schenectady, N.Y.

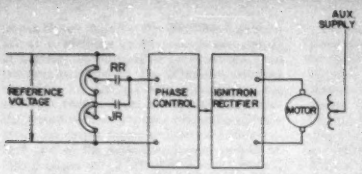

Figure 1 (left). Simple motor control without feedback

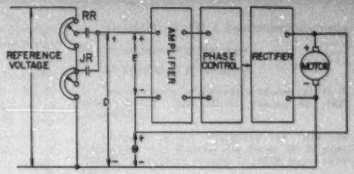

Figure 3 (right). Motor control with feedback and error amplifier

means excessive for high performance, requires a reference power supply of

525 volts × 8 amperes = 4,200 watts

Further consideration will show that for any loop gain K the wattage required from the reference supply is equal to the wattage taken by the input to the phase shift circuit multiplied by $(K+1)$. The actual wattage required will exceed even these figures because of the additional loss in the speed adjusting potentiometer which must be kept to a low ohmic value since any resistance it adds to the phase shifting circuit cuts down the loop gain. In the example illustrated, if the total resistance of the speed control and jog potentiometers are 12.5 ohms this will result in an effective resistance of $3^1/_8$ ohms added to the phase shifting circuit at the half speed setting. Since this equals the internal resistance of the phase shifting winding even this low value of resistance reduces the loop gain by one half to the rather low figure of 10. Even assuming such a low gain (and a variation in gain of two to one) is acceptable this results in a further demand on the reference power supply:

$$E^2/R = (550)^2/12.5 = 24{,}200 \text{ watts}$$

This gives a total demand of 28.4 kw on the reference supply which is rapidly assuming the proportions of the main unit and clearly impracticable.

The obvious solution to this situation is to insert an amplifier of some form ahead of the phase shift circuit to give a control system as shown in Figure 3. An amplifier would reduce the power requirements of the reference supply and control potentiometers in direct proportion to the power gain of the amplifier. Thus a gain of 1,000 or more in this amplifier, which is readily obtained, would require 30 watts or less from the reference standard for the same loop gain.

Amplidyne Amplifier[4]

Figure 4 shows an elementary circuit of an amplidyne amplifier suitable for such a control system. In this case the difference between the reference and the output voltage is applied to a control field of an amplidyne which is basically a two stage rotating amplifier which has been frequently described in the literature. A 1-kw 1,800-rpm machine operating over the linear portion of its range will have a power gain in the order of 8,000, which is more than enough to make the size of the reference power supply and adjusting potentiometers sufficiently small to be convenient. The low power level required (0.1 watt for 80 per cent voltage) also makes it convenient to add features which will be described later.

Electronic Amplifier[5]

Figure 5 shows a simple electronic amplifier for the control system being considered. It may be considered as two amplifiers in series, a high vacuum tube amplifier followed by a small phase controlled rectifier using hot cathode thyratron tubes. The error signal is impressed on the grid of the high vacuum tube *VT1* and the anode current is used to saturate the d-c winding of a small phase shifting saturable reactor. The phase shifting network in turn controls the output of the thyratrons *VT2* and *VT3* which are used in the phase controlled rectifier.

In such a system a change of about 2 volts on the grid of input tube is sufficient to control the output of the phase controlled rectifier from no load to full load which may be 1 kw or more depending upon the size of the thyratrons and the anode transformer. In this system if the full motor voltage of 500 were fed back as shown the resultant loop gain would be about 250

$$K = \Delta\theta/\Delta_4 = 500 \text{ volts}/2 \text{ volts} = 250$$

During the normal controlling range the grid current of a vacuum tube such as *VT1* is at least as low as 10^{-7} amperes and generally in the order of 10^{-9} amperes. During any period when the grid might be positive due to transient conditions the grid current that might flow may be limited by a grid resistor as shown. Thus the power input becomes so small and difficult to measure that the power required from the voltage reference source is practically limited by the adjusting potentiometers and that drawn by the anode of the amplifier tube which may for convenience use the same source.

It is interesting to note that such an amplifier requires a definite input voltage change for full output change. The amplidyne described previously requires only a definite power input and within reasonable limits by suitable change in the control field may be designed for full output for almost any input voltage. Thus the actual magnitude of D and θ determine the loop gain in the case of the simple electronic circuit, but not in the case of the amplidyne amplifier where the field winding may be controlled to give a required loop gain. Thus with the electronic amplifier shown, if the value of θ is cut down by a potentiometer across the output so that a more convenient reference in the order of 100 volts may be used, the loop gain will be cut down to about 50. The gain may be further lowered in the same manner if desired, or other simple circuit changes such as the insertion of a cathode resistor or input potentiometer may be employed. On the other hand, if it is desirable to increase the loop

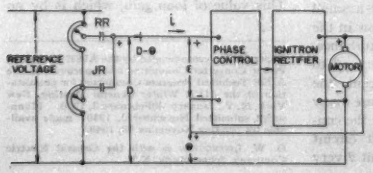

Figure 2 (left). Simple motor control with feedback

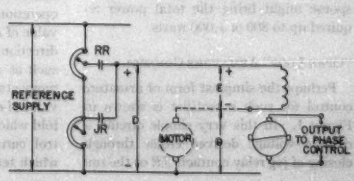

Figure 4 (right). Amplidyne used as error amplifier

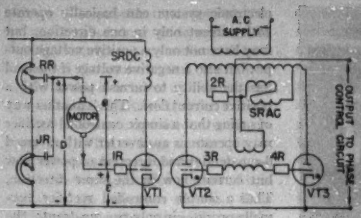

Figure 5 (left). Electronic error amplifier

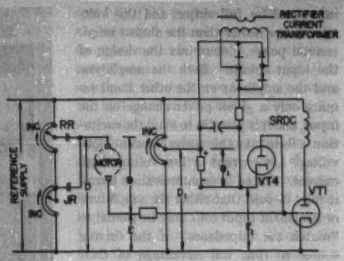

Figure 7 (right). Current limit added to electronic amplifier motor

gain it is possible to add additional vacuum-tube amplifier stages to obtain almost any gain necessary.

Amplistat[4]

Figure 6 shows an elementary circuit diagram of a magnetic amplifier of the self-saturating type frequently called an Amplistat, used in our control system in the same manner as either the amplidyne or electronic amplifier. It is possible within certain limits to consider this Amplistat a controlled rectifier similar to the output stage of the preceding electronic amplifier. In this case however, uncontrolled rectifier elements of the dry-disk type are used and two output windings of a saturable reactor are connected in series with two elements of a simple single-phase supply rectifier circuit of four elements known variously as "bridge" or "diametric double way." In normal operation the saturable reactor presents a high impedance for part of each half cycle resulting in almost zero voltage output for a portion of the time. Then the reactor becomes saturated and presents little impedance so that almost full output for the remainder of the half cycle is obtained. The point in the cycle when the reactor passes from an unsaturated to a saturated condition is controlled by the net magnetomotive force in the d-c windings. In this case three d-c windings are used. The speed reference voltage is applied to one winding to produce the reference magnetomotive force D, the output voltage to another winding to produce the opposing feed-back magnetomotive force θ, and the third winding is excited from a constant source to produce a bias magnetomotive force B, which merely sets the proper operating point. This differs from the two preceding circuits in that the basic subtraction of reference and feedback to produce the error signal is accomplished by subtracting magnetomotive forces. This has the advantage of isolating the control circuit from the output. It would appear superficially that this subtraction of magnetomotive forces could have been employed with the amplidyne as indeed it can for low loop gains. However we find that assuming the same space is available for the control windings the power dissipated in I^2R losses where magnetic subtraction is used is increased by the factor

$$2(K^2+(K+1)^2)\times\text{normal power}$$

Thus for a K (loop gain) of 20, the losses in the control windings would be 1,682 times as great as when electrical subtraction were employed. In the case of an amplidyne requiring an input of 0.1 watt on a single winding this would result in a copper loss of 168.2 watts, which would normally be excessive for a 1-kw output machine. In the case of the Amplistat, however, much higher power gains in the vicinity of 2.5×10^6 are readily attained which then requires an input power of only 4×10^{-5} watts for electrical subtraction for a 1-kw output. If magnetic subtraction is used with a loop gain of 20, this will result in a copper loss of about 6.75 watts which is not excessive for a saturable reactor having a size somewhat larger than 1 kva.

Comparison of the Three Methods

It is difficult to show that any one of these systems is to be preferred for all control problems of this type. Each of the systems have certain features which may make it most desirable for a given application and each of them have been successfully applied in actual installations. However we will try to compare the technical functions to illustrate some of the reasons for proper selection.

Input Considerations

At the present time the vacuum tube amplifier probably requires the lowest power input and gives the highest power gain per stage. This, however, is not the complete story since this type of amplifier requires a definite voltage change on the

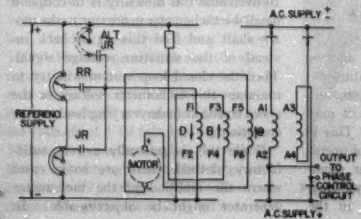

Figure 6 (left). Amplistat used as error amplifier

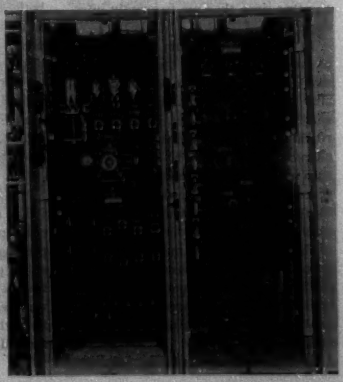

Figure 8 (right). Motor control using Amplistat

input grid for full output and this voltage change rather than the almost infinitesimal power, determines the design of the input circuit. Both the amplidyne and the amplistat on the other hand require only a given power change on the input, and it is possible to wind the excitation coils to take this power either at high-voltage low current or low voltage high current. Stated in communication terms, it may be said that either the amplidyne or Amplistat input coils may be wound to "match the impedance" of the driving source so that full advantage of their power gain may be utilized. On the other hand a vacuum tube amplifier operated from an error signal source capable of supplying considerable current but very little voltage change is incapable of taking advantage of the current supplying ability of the input. Under these conditions it gives no more output than if the input circuit were only capable of supplying microamperes. Thus the extremely high power gain of the tube amplifier is realized only with high impedance input circuits, such as from photoelectric tubes, but it is incapable of using with a similar efficiency the possible output of a millivolt shunt. The magnetic input to both the amplidyne and the Amplistat on the other hand can not only be designed to use the power available from low voltage input sources, but they have the property of electrically isolating the input from the output circuits which is not possible in a simple d-c electronic amplifier. They also permit, under certain conditions, the addition or subtraction of several electrical signals still maintaining electrical isolation.

Amplification and Speed of Response

These two characteristics are treated together since they are frequently interdependent.

In the d-c high vacuum amplifier such as we are considering, the voltage gain may be built up if necessary by successive stages with resultant control with smaller and smaller input, until the input reaches the level of random noise or tube characteristic drift. The time delay in such amplifiers are so small that they are generally of no consequence in most industrial power applications. The small saturable reactor used for phase control of the thyratron tubes in Figure 5 has a several cycles time constant which normally is of no consequence in most industrial controls. However, other methods of phase control may be used which have no time delay.

Both the amplidyne and the Amplistat

Figure 9. Motor control using electronic amplifier

have time delays due to the change of flux energy stored in the magnetic circuits in passing from one output condition to another. The "time constants" introduced by this are frequently reduced by such methods as adding series resistance to the signal coil circuits. Within certain limits the time constant of a single delay circuit is inversely proportional to the losses in the circuit. Thus if we add a resistor in series with the input winding of an amplidyne or Amplistat equal to the coil resistance, the power required to get the same output is doubled, but the time constant is reduced to one half. Thus, it is necessary to consider the time delays in both amplidyne and Amplistat control and many cases cut down the maximum power gain in order to get fast enough response. It is not uncommon to use two or more stages of amplistats to obtain both high gain and high speed. It is less common to employ two amplidynes to get high gain and speed although in a few cases this has been done.

Nature of Output

The output of the amplidyne may be either positive or negative in voltage depending upon the field excitation, and either positive or negative current may flow depending upon the load. This is very desirable in certain classes of operation where operation in all four quadrants of voltage and current are required.

The controlled rectifier used in the electronic system can basically operate with current only in one direction, but may have not only a positive voltage output but also a negative voltage if the load has the ability to furnish power with a positive current flow. This is another way of saying that a simple controlled rectifier may operate as an inverter with reversed d-c potential and direction of power flow but current flow in the same direction. Thus a simple controlled rectifier normally operates in only two quadrants; the positive voltage positive current quadrant, and the negative voltage positive current quadrant. Of course it is possible to arrange two opposing controlled rectifiers having opposite current directions to a common load but this requires additional equipment.

The simple amplistat is a somewhat restricted controlled rectifier in that it only works in the positive-voltage positive-current quadrant. It cannot be used to operate in the negative voltage, positive current, or invert quadrant. This property makes it difficult to use two reversely connected Amplistats on a common load without appreciable power loss.

Additional Functions

So far we have considered only the basic voltage regulator circuit. For successful control of d-c motors we must consider additional functions such as speed control, acceleration, deceleration current limit, and field weakening.

Speed Control and Voltage Drop Compensation

So far we have indicated the feed-back voltage simply taken from the ignitron rectifier output. While in some cases a constant armature voltage insures a sufficiently constant motor speed this is not always the case. When the load torque varies from zero to full value the motor speed for constant armature voltage may drop 5 per cent or 10 per cent of basic speed, depending upon the armature resistance, armature reaction effect, and series stabilizing fields if used. One way to overcome this difficulty is to couple a small d-c tachometer generator to the motor shaft and feed this signal back instead of the armature voltage signal. Then the closed loop system will try to maintain this tachometer voltage or the speed constant under varying load torque conditions.

While this is generally a very satisfactory method, there are some cases where the addition of the tachometer generator might be objectionable. In

this case it is possible to compensate for the motor speed drop by increasing the terminal voltage as a function of load drawn by the motor. One convenient way to do this is to insert a current transformer in the ignitron rectifier circuit, rectify the output and feed a small resistor load. The voltage across this resistor will then be proportional to the load current and an adjustable portion of it is added to the reference voltage. This voltage drop compensation, if properly adjusted, has the effect of raising the terminal voltage as the load torque is increased so that the motor continues to run at essentially the same speed as at no load.

Acceleration

Some method must be used to prevent applying full voltage to a large d-c motor at standstill or excessive currents will damage both the motor and the rectifier. One very simple method is time acceleration. The run potentiometers of Figures 4, 5, and 6 may be motor driven with suitable interlocks to prevent closing the run relay unless the run potentiometer has been returned to the bottom position. The speed of the motor-driven potentiometer is then made slow enough to permit the main motors to accelerate without damage to any of the equipment.

On those applications where varying load conditions prevail and maximum safe speeds of acceleration are desirable the control may be designed to accelerate the motor at a definite current limit. While a current limit "take over" function can be added to any of the three systems described earlier, Figure 7 shows the current limit function added to the front end of the electronic control shown in Figure 5. As in the case of voltage drop compensation, a signal is derived from a current transformer in the rectifier supply, rectified and impressed across a resistor giving us a voltage θ_1 proportional to rectifier or motor current. As long as the current signal is small compared to the permissible current limit signal D_1 the cathode of the diode *VT4* is positive with respect to its anode which is connected to the grid of *VT1* which is two or three volts negative with respect to the bottom bus. Under these conditions the diode *VT4* is like an open switch and the speed regulating function is undisturbed. However as the load current becomes greater θ_1 increases until it exceeds D_1 and soon the cathode of *VT4* falls below its anode. This causes a current to flow through the diode and through the rather large grid resistor in *VT1* circuit. This "take over" causes the grid potential of *VT1* to become more negative which then tends to decrease the current in *VT1* and ultimately the rectifier voltage in spite of ϵ becoming more positive. We see that under these current limit conditions a new closed-loop system is operative involving a current limit reference D_1, a current feed-back signal θ_1, and a current error ϵ_1.

Even if the run potentiometer were set at the top of its travel, such a circuit would maintain constant current during the acceleration period until the desired speed was obtained. At that point the speed error ϵ would make *VT1* grid more negative and since the current limit circuit cannot make the grid more positive, the speed error would "take back" the control and regulate the speed.

Field Weakening

In some cases where constant horsepower variable speed is required, it is necessary to run motors above basic speed by field weakening. This may be accomplished several ways. One of the simplest methods when a motor-driven potentiometer is available for acceleration is to have the resistance vary only during the first part of the travel. During the remainder of the shaft rotation, the slider travels on a conductive segment and the armature voltage does not change. Keyed to the same shaft is a second potentiometer for control of the field. During that period of travel when the armature voltage is increasing the slider of the field control potentiometer is running on a conductive segment. After the armature voltage ceases to rise the slider of the field potentiometer moves on the resistance section and reduces the field reference voltage. The field may be supplied by an amplidyne, controlled rectifier, or amplistat connected in a closed-loop control similar to that used for the armature circuit. Thus during acceleration to full armature voltage the field is maintained at full value and then is reduced by further shaft travel to the desired degree of weakening.

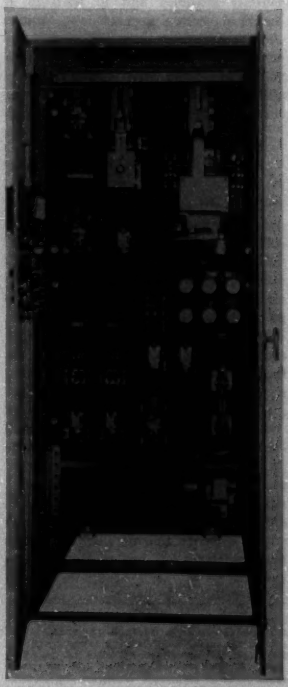

Figure 10. Motor control using amplidyne amplifier

While this paper has been primarily devoted to an explanation of the basic control methods that have been used with d-c motors supplied from ignitron rectifiers, Figure 8 may be of interest as an example of the class of control equipment being considered. Figure 8 shows the control equipment using an amplistat-type regulator for a printing press drive. The dynamic braking contractor is located in the upper left of the left-hand control, the motor driven rheostat in the center, and the d-c disconnecting switch in the lower left-hand side. No d-c loop contactor is required since the d-c circuit is effectively opened by removing the ignitor excitation for the rectifier. Many of the other relays are used in connection with a rather elaborate safety system which delays the initial start of the press while sufficient warning is given to the press operators to get clear.

The saturable reactor and selenium rectifier associated with the amplistat are situated in the rear of the rectifier cubicle located adjacent to the panel shown. The saturable reactor has the approximate physical size of a 1-kva transformer and the selenium rectifiers approximately that of a 1-kw selenium stack assembly.

This application differs from some others in that a variable number of motors may be run from one rectifier depending upon the number of presses to be run with a given folder. The right-hand panel is basically a motor transfer panel which permits connecting certain of the

press motors to either one or the other of two rectifiers depending upon the press set up for the particular edition.

Figure 9 shows similar equipment using an electronic amplifier. The central panel in the left-hand cubicle contains the high-vacuum tube amplifier with provisions for voltage drop compensation, current limit, and parallel operation of two rectifiers. The panel immediately below contains the thyratrons of a 6-phase controlled rectifier to saturate the phase shifting reactors of the ignitron rectifier. The panel below and slightly to the front of that contains the four thyratrons for the motor field supply.

Figure 10 shows the control panel using an amplidyne-type amplifier for affecting the phase shift of the ignitron rectifier. In this case a single 350-horsepower motor driving a flanging mill is involved.

Summary

From a consideration of the problems of the control of a d-c motor supplied from a phase controlled ignitron rectifier we have tried to show:

1. The closed loop or feed-back system is highly desirable.

2. Such a system requires the use of some form of amplifier between the reference and comparison circuit and the ignitron phase shift system.

3. Three different systems involving the use of amplidynes, electronic amplifiers, and amplistats have been successfully built to serve this function.

4. The choice of the best method for a particular application depends upon the particular requirements of that application.

References

1. Rectifier Equipment for Electronic D-C Motor Drives, M. J. Mulhern, S. H. Crawford. *AIEE Transactions*, volume 69, part I, 1950, pages 211–15.

2. Application of Electronic Motor Drives to Printing Presses, J. A. Johnson, E. M. Stacey. *AIEE Transactions*, volume 69, part I, 1950, pages 216–19.

3. Fundamental Theory of Servomechanisms (book), LeRoy A. MacCall. D. Van Nostrand Company, Inc., New York, N. Y., 1945.

4. Fundamental Principles of Amplidyne Applications, F. E. Crever. *Electrical Engineering* (*AIEE Transactions*), volume 62, September 1943, pages 603–06.

5. Electronic Control of D-C Motors, E. E. Moyer. *Electronics*, volume 16, May, June, July, September, and October 1943.

6. The Transductor (D-C Pre-Saturated Reactor) (book), Uno Lamm. *Esselte Aktiebolag*, Stockholm, Sweden, 1943.

No Discussion

Rectifier Equipment for Electronic D-C Motor Drives

M. J. MULHERN
ASSOCIATE AIEE

S. N. CRAWFORD
ASSOCIATE AIEE

RECTIFIERS have proved very reliable and successful in supplying d-c power to all types of application: street railway, mining, steel mills, electrochemical, and general industrial. The use of rectifiers for d-c motor control is a natural development due to their ease of control, high speed of response, and use of all static components. The study of economics made for d-c motor drives indicated that 550 volts of direct current gave the best return, and, accordingly, standards have been made at this voltage. A 3-phase double-way (full wave) rectifier will deliver 550 volts of direct current when supplied from a 460-volt 3-phase system. This is a standard distribution voltage and standard transformers are available, thus eliminating the added cost for special transformations.

The purpose of this paper is to give a description of the rectifier circuit, to show how voltage control is accomplished, to show how the "Amplistat" controls and regulates the output voltage, and to describe the physical layout of the rectifier.

The majority of d-c motor applications can be supplied from 150-, 300- or 500-kw power units, and rectifiers have been standardized in these ratings. The 300-kw rectifier is shown in all figures of this paper. The 150-kw size is identical except for tube size, but the 500-kw units are larger and use a larger size tube. The d-c motor drive unit is housed in four standard cubicles of dead front, totally-enclosed type, and each cubicle is assembled in line with the others. The first cubicle contains the low voltage a-c circuit breakers and the current limiting reactor. The second cubicle contains the sealed ignitron tubes, their excitation circuits and cooling system. The control cubicle is the next in line, followed by the cubicle containing the d-c motor switching circuits. The front view of this type of assembly is shown in Figures 5 and 6. A diagram of one complete rectifier equipment of this type is shown in Figure 7. A multiple arrangement of four similar rectifier units is shown by the diagram in Figure 8. Any number of similar combinations can be arranged in this manner to make a complete d-c unit substation.

Rectifier Circuit

The basic elements of a typical electronic d-c motor drive system are shown in the 1-line diagram of Figure 1. This diagram shows two identical rectifier units, an a-c tie circuit breaker and two sets of d-c motor switches. The a-c tie circuit breaker allows the equipment to be operated from either of the two secondary a-c feeders. The d-c motor switches permit selection of different motor and rectifier combinations. This affords a large degree of flexibility and reliability. A complete installation generally consists of one or more pairs of units connected in this manner.

The interrupting rating of the main a-c circuit breaker and the reactance of the current limiting reactor depend upon the maximum fault current capacity of the sealed ignitrons and the available short circuit kilovolt-amperes of the a-c system supply. The rectifiers may draw 10 to 20 times normal load current during a fault. The maximum fault current capacity of three types of sealed ignitrons is shown in Table I.

Table I. Maximum Fault Current Capacity of Three Types of Sealed Ignitrons

Ignitron	Rated Amperes	Maximum Fault Current, Amperes
A	100	3,500
B	200	12,000
C	400	25,000

The available primary 3-phase short-circuit kilovolt-amperes are usually 500,000 kva. The maximum rectifier fault current which can flow depends upon the kilovolt-ampere rating of the feeder transformer. If two 300-kw rectifier units are connected as shown in Figure 1, a current limiting reactor which has a value of 0.0163 ohms per phase will be sufficient to limit the fault current to a safe value. This reactance is obtained when either feeder transformer is assumed to be rated at 750 kva. The interrupting rating of the circuit breaker will be 25,000 amperes with such a transformer. Both the circuit breaker and the reactor will have a continuous current rating of 600 amperes. Rectifiers of ratings other than 300 kw will have corresponding values.

Power losses in the rectifier consist of two types. One is the kilowatt loss due to arc drop in the tubes and the resistance loss in the current limiting reactor. This loss varies with the load current being drawn from the rectifier. The resistance loss in the reactor is so small that it is usually included in the arc-drop value. The other type of loss is the power required by the rectifier excitation system and this is the no-load loss and is constant for all values of load. This is usually 1.7 kw for all ratings of the standard rectifiers. The over-all efficiency of the rectifier unit at full voltage ranges from 92.6 per cent at 25 per cent load to 93.4 per cent at 100 per cent load.

Paper 50-33, recommended by the AIEE Electronic Power Converters Committee and approved by the AIEE Technical Program Committee for presentation at the AIEE Winter General Meeting, New York, N. Y., January 30-February 3, 1950. Manuscript submitted November 2, 1949; made available for printing November 30, 1949.

M. J. MULHERN and S. N. CRAWFORD are both with the General Electric Company, Schenectady, N. Y.

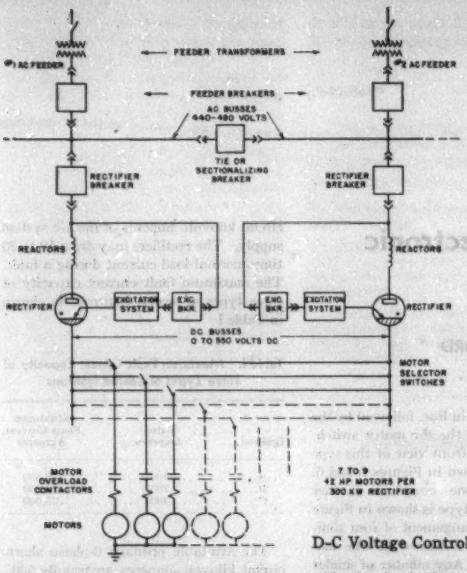

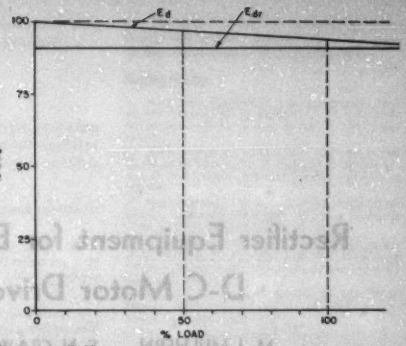

Figure 1 (left). One-line diagram of typical electronic d-c motor drive system

Figure 3 (above). Rectifier regulation characteristic

The circuit diagram of Figure 2 shows the complete power and excitation circuits for one rectifier unit. The tubes are connected in a 3-phase double-way circuit. At full output the waveform of the direct voltage has a 6-phase ripple. Standard d-c motors are not overheated when operated on a supply voltage with small percentage of ripple, and consequently do not have to be derated.

D-C Voltage Control

Conduction in the sealed ignitron tubes is initiated once during each cycle by the "firing" of the ignitor. The ignitor initiates emission, when it is fired, by establishing a "cathode spot" on the mercury pool. The ignitor is fired by the application of a high-voltage pulse of short duration. The tube will begin carrying current whenever the ignitor fires, if its anode voltage is positive. The conducting period of the tube will be reduced if the ignitor firing is delayed in time for an appreciable part of one-half cycle. The direct voltage output of the rectifier is correspondingly reduced, as shown in Figure 9. The direct voltage is, therefore, proportional to the angle of phase-retard of the ignitor pulse.

The effect of voltage regulation of the rectifier power supply is shown in Figure 3. The curve of E_d shows how the output voltage normally drops as load is increased from zero to full load. This would cause considerable change in motor speeds as load is applied to the motors. It would, therefore, be difficult to control accurately the speed of the motors if the load were being changed. This effect is greatly reduced when the armature voltage is regulated, as indicated by the curve of E_{dr}.

Figure 2. Rectifier circuit diagram

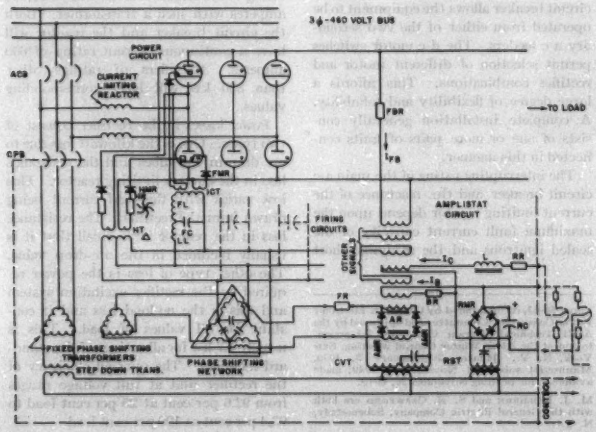

Excitation System

The excitation system consists of the circuits which control the conduction of the ignitron tubes. The principle requirements of a d-c motor drive are that: the armature voltage be continuously adjustable from zero to maximum voltage; that the armature voltage be regulated; and that the time of response in regulating be small compared to the inertia effects in the load.

These requirements are met by the various circuits in the excitation system. These circuits are shown in Figure 2. They may be broken down, for convenience, into four groups of circuits:

1. The ignitor and excitation anode circuits.
2. The variable phase-shifting network.
3. The fixed phase-shifting circuit.
4. The Amplistat and signal circuits.

The ignitor circuit consists of a static

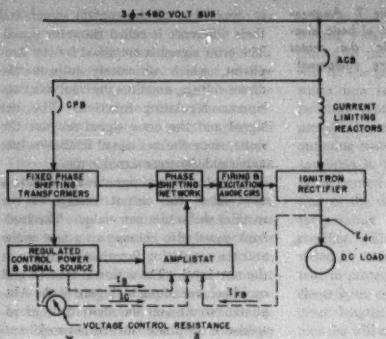

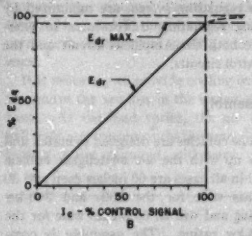

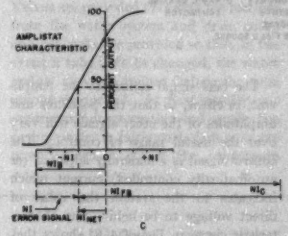

Figure 4. (A, B, and C). Functional diagram and characteristics of excitation system

magnetic firing circuit which provides a high-voltage firing pulse once each cycle for each ignitor. Each circuit is arranged to operate on both half-cycles of input voltage and thus produces two ignitor pulses 180 degrees apart. The excitation anode circuit energizes that element in the ignitron tube and maintains the cathode spot which is established by the ignitor. There are three ignitor firing circuits connected in 3-phase relation. There are also three excitation anode transformers and associated circuit elements connected in 6-phase relationship.

The phase-shifting network shifts the phase of the input voltages to the ignitor and excitation anode circuits. This network provides a constant voltage output over the full-phase shift range so that the performance of the firing circuits does not change. The time of response of this network is less than two cycles at 60 cycles.

The fixed phase-shift transformers are adjusted to bring the ignitor pulses into proper phase relation with their respective tube anode voltages. They consist of three multiple winding transformers which can be connected for fixed shifts of 5 to 355 degrees in ten-degree intervals.

The Amplistat and signal circuits combine and amplify all signals which are to modify the rectifier output voltage. The output of the Amplistat is a control current which varies the actual phase-shift angle in the phase-shifting network.

All of the excitation circuits provide continuous functions, and, therefore, continuous control of the rectifier voltage. This is illustrated by the functional diagram of Figure 4(B).

The Amplistat Circuit

This circuit is made up of a magnetic amplifier and its associated control signal circuits. The Amplistat circuit controls the amount of phase shift of the excitation voltages. The basic element is the magnetic amplifier reactor, a completely static device. The amplifier circuit has extremely high gain and over-all characteristics similar to an electronic amplifier or an amplidyne unit. The basic characteristics of these three types of amplifier are described in a companion paper. The Amplistat has been selected for this type of rectifier equipment because it has physical and electrical characteristics closely matching the firing-circuit and phase-shifting circuit components. It has no moving parts and no filament life. It is thus possible to build into all portions of the excitation system the same degree of reliability, freedom from frequent component replacement, and freedom from wear.

The Amplistat is a signal mixing device as well as an amplifier. The several con-

Figure 5. Front view of rectifier and control equipment for electronic d-c motor drive installation

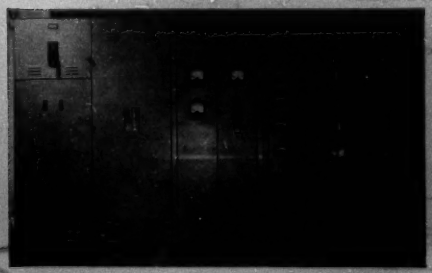

Figure 6. Front view of equipment of Figure 5 with doors open to show air circuit breaker, space for reactor, ignitron tubes, automatic control devices, and motor selector switches

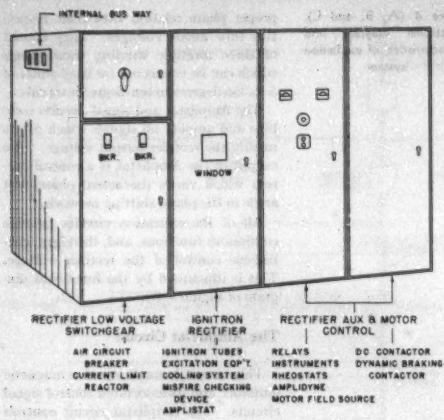

Figure 7. Arrangement of basic electronic d-c motor drive equipment

trol windings of the reactor all have ample insulation permitting connections to other circuits without the need for additional insulation. This results in greater simplicity and lower cost in the design of the control circuits by reducing the number of insulation levels required.

The characteristic of the Amplistat is shown in Figure 4(C). It has essentially a negative signal characteristic, that is, most of the control range is covered in the region of negative signal input.

The Amplistat differs from other amplifiers in that the actual input signal is ampere-turns (magnetomotive force) rather than voltage or current. This presents no practical problem because the signals are measured in terms of current in each circuit. When only one signal is applied to the Amplistat, its output is proportional to the amplitude of that signal. When more than one signal is applied, the Amplistat output is proportional to the algebraic sum of all of the signals. This sum is called the net signal. The output of the Amplistat is, therefore, determined by the instantaneous values of all the signals applied to it. In the d-c motor drive equipment, the minimum number of signals is three, as indicated in Figure 4(C). These signals are bias, control, and feed-back.

The bias signal calibrates the Amplistat, in effect, so that the polarities and amplitudes of the other signals will vary over the useful range of control. The control signal is a manually adjusted (or automatically controlled) current which indicates to the system the value of direct voltage to be held. The characteristic curve in Figure 4(B) shows that the output voltage of the rectifier is directly proportional to the magnitude of this signal current.

Voltage regulation also is a requirement of the system and the closed loop method is employed. The regulating loop is shown in Figure 4(A), and includes the Amplistat, phase-shifting network, firing circuits, and the rectifier. The loop is closed by the feed-back signal which is proportional to the instantaneous value of direct voltage. This signal is polarized in opposition to the control signal and their difference is called the error signal. The error signal is amplified by the Amplistat, which ultimately adjusts the direct voltage, and thus the result is a continuous regulating function. The net signal and the error signal are not the same, since the net signal is an absolute value and the error signal is not.

When the control signal is adjusted to a new value, the output voltage of the rectifier shifts to a new value. The feed-back signal also changes to a new value and the regulating function continues at the new level. The action is smooth and rapid because of the high gain of the Amplistat circuit and the short time of response of the phase-shifting network.

The effects of line-voltage changes on the regulating system are minimized by using regulating transformers to energize both the Amplistat circuit and the control circuits.

Assembly

The cubicles are designed to match and line up with the a-c switchgear cubicle and in all cases are 60 inches deep and 30 inches wide for the 150- and 300-kw rating and will be 60 inches wide for the 500-kw rating. The assembly is completely metal-enclosed, dead front, with doors both front and rear providing access to the ignitron tubes and excitation system. The sealed ignitron tubes are mounted in the front section on suitable insulators, and power connections are taken through the front panel to the rear, where factory assembled cables are brought out to the a-c and d-c connections respectively. The front of the equipment also mounts the cooling system for the ignitrons.

Figure 8 (below). Group arrangement of basic electronic d-c motor drives

Figure 9 (right). Rectifier voltage control

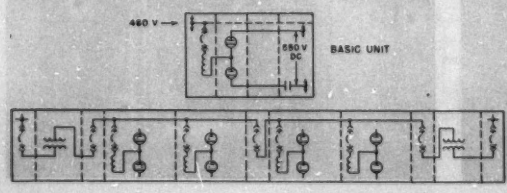

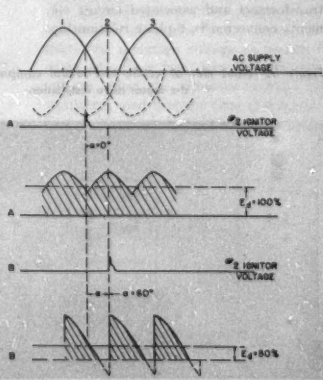

The cubicle assemblies are shown in Figures 5 and 6.

The rear door mounts the Amplistat which controls the d-c output of the rectifier by integrating signals from the magnetic control section. The Amplistat and its component parts employ all the available space on the rear door. The excitation systems are mounted in the interior of the equipment and all necessary components for two ignitors are mounted on one panel, therefore there are three excitation panels. The components for the excitation circuits are nested in together so as to use the least amount of space, but all component leads are brought to terminal boards which are readily accessible for testing. Should an emergency arise, components may be temporarily connected directly to these terminal boards. The operator may make permanent replacement at his convenience.

It is necessary to provide cooling water to remove the arc loss in the sealed ignitrons. As the load varies, the arc loss will vary and consequently the amount of cooling water required will vary. In order to protect the rectifier from loss of cooling water, a water flow relay is included in the outgoing water line which will de-energize the rectifier if sufficient water flow is not available. Overtemperature protection is provided by the use of a thermostat which is located in the outgoing water line so that if the water available is not sufficient for the load being carried but is sufficient for the setting of the water flow relay, the rise in temperature will also de-energize the rectifier. Electrolytic targets are provided at various points in the water system to protect the piping materials from electrolytic erosion. These are of sufficient lengths so that inspection at six months will enable the operator to know what future inspections are necessary. Valves are provided to isolate the rectifier from the water system and drain cocks and pet cocks are provided so that, in the event a tube is to be changed, the water system may be drained before the tube unions are opened. As most installations experience humid weather and usually the cooling water is fairly cool, drip pans are provided which collect the condensate from each tube and are of sufficient size so that natural evaporation will take care of the water collected.

Summary

This paper has endeavored to show a functional description of an adjustable voltage rectifier equipment which delivers moderate power and is suitable for the control of one or more d-c motors. These rectifiers incorporate high gain amplifier and excitation circuits which have a high degree of reliability and freedom from frequent maintenance. A well-regulated output voltage is obtained by the use of the Amplistat circuit. The output voltage may be continuously adjusted in response to several system conditions as required. The assembly is made compact and economical by full utilization of the cubicle space. These features make possible a packaged, unit type of rectifier equipment which meets all the service requirements of industrial applications requiring regulated variable voltage source.

No Discussion

Application of Electronic Motor Drives to Printing Presses

J. A. JOHNSON
NONMEMBER AIEE

E. M. STACEY
MEMBER AIEE

Synopsis: At least 50 years have passed since rotary web printing presses reached, essentially, their present form. As innumerable refinements gradually improved the quality of the product and increased speed of the presses, corresponding advances were made in electric motor drives. Press drives, as a result, are highly refined, specialized equipments designed to do a definite job. Application problems will be discussed, together with a comparison between conventional and electronic solutions.

The Printing Press

A modern high-speed metropolitan newspaper press is shown in Figure 1. Figure 2 shows schematically how a continuous web of paper is fed to each unit, is printed on both sides, and passes to the folder. It is delivered from the folder as a complete newspaper.

All rotational energy is imparted to the heavy newsprint feed rolls through the paper webs. With paper speeds of 1,500 feet per minute, or more, acceleration rates and torque peaks from the electric drive must be severely limited.

In preparing a press for printing, the paper webs are first threaded through at about 35 feet per minute. The electric drive must, therefore, provide a continuous threading speed of about $2^1/_2$ per cent of full speed.

Next, type plates are clamped to the plate cylinders. This requires jogging the press by fractions of an inch in order to position the slots into which the plates fit. The drive must provide crisp, accurate inching action for this service.

The press is then accelerated smoothly to approximately 20 per cent speed for registering the webs and other adjustments, after which it is gradually accelerated to its production speed. Production is normally at from 75 per cent to 100 per cent full speed. Thus, the drive must provide smooth acceleration and deceleration over a 5-to-1 speed range, and, preferably, high efficiency over the production range.

In event of a web break, or other mishap, the press must be stopped in about eight seconds from full speed. The electric drive normally furnishes a large part of the required braking torque.

Finally, and perhaps most important of all, a press drive must be reliable. Editions should not be late, and must not be missed.

Conventional Press Drive

A very serviceable answer to the press drive problem has been given in the past, and is still being given in many plants, by the a-c double-motor drive. The operating speed range is provided by a wound rotor main motor with secondary resistance control down to 20 per cent speed. A separate small threading motor is used

Paper 50-34, recommended by the AIEE Electronic Power Converters Committee and approved by the AIEE Technical Program Committee for presentation at the AIEE Winter General Meeting, New York, N. Y., January 30–February 3, 1950. Manuscript submitted November 3, 1949; made available for printing November 30, 1949.

J. A. Johnson is with the Times-Mirror Company, Los Angeles, Calif., and E. M. Stacey is with the General Electric Company, Schenectady, N. Y.

Figure 1 (below). A modern newspaper press

Figure 2 (right). Schematic view of press showing web runs

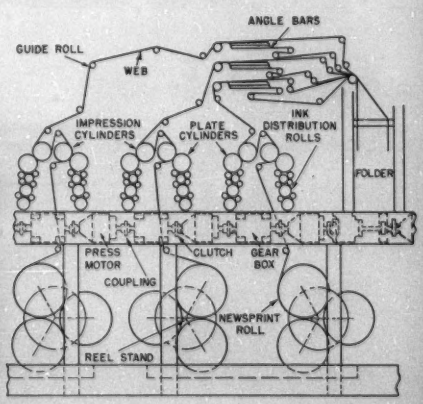

Figure 3. Electronic drive motor arrangement looking upward from reelroom floor

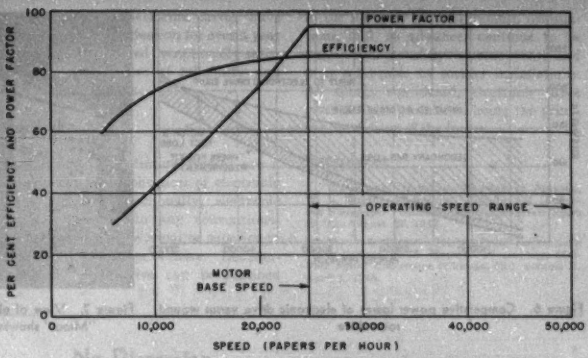

Figure 4. Efficiency and power factor characteristics of electronic press drive

for the jogging and low-speed threading functions.

The wound-rotor motor drive, however, suffers from certain inherent drawbacks. First of all, the extra threading motor, with necessary reduction gearing and over-running clutch, causes undesirable mechanical complications.

Secondly, efficiency of a wound rotor motor drops off directly with speed. This not only wastes energy, but, in large installations, makes necessary expensive provisions for getting rid of the secondary resistor heat. Production speed, counting various slowdowns, seldom averages more than 70 per cent of the full geared speed.

Thirdly, speed regulation gets progressively worse as speed is reduced. To compensate for different loads, as press units are added or subtracted to vary the number of pages in the newspaper, special adjustments must be made to the secondary resistors. Unless these are properly made, a web break may result from excessive acceleration when going from threading speed to minimum operating speed.

Electronic Drive

The electronic printing press drive[1] eliminates these drawbacks. Jogging and threading, as well as high-speed operations, are accomplished by the main motors. These are mounted on the side frame of the press, co-axially with the press shaft, in the simplest possible mechanical arrangement, Figure 3. Overall efficiency of the system stays at a high value over the full production range,

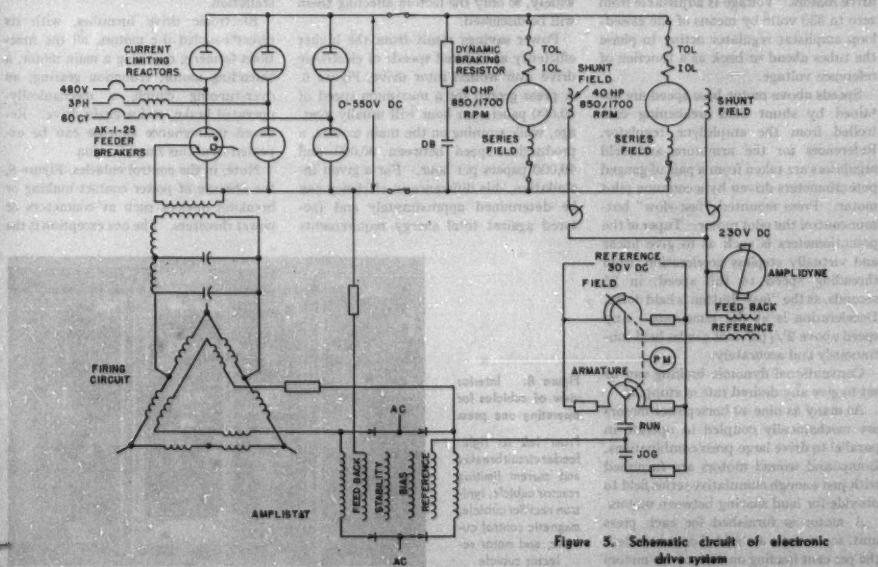

Figure 5. Schematic circuit of electronic drive system

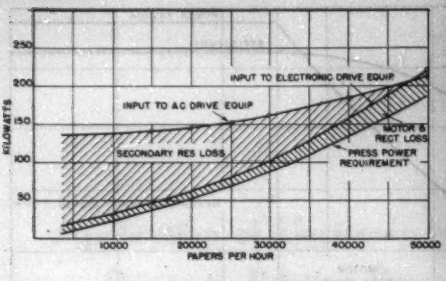

Figure 6. Comparative power losses of electronic drive versus wound rotor drive

Figure 7. View of electronic drive control room of the Los Angeles "Mirror" showing equipment for operation of three presses

Figure 4. Speed and acceleration rate are not materially affected by load changes.

The adjustable voltage rectifier[8] achieves all this by combining the advantages of a-c power distribution with the excellent speed control characteristics of d-c motors. At the same time, a high degree of reliability is maintained by use of dependable, time-proved components arranged in a basically simple system.

Figure 5 shows how 440-volt 3-phase power is rectified to direct current in a 3-phase double-way ignitron rectifier, and fed directly to the armatures of the press drive motors. Voltage is adjustable from zero to 550 volts by means of the closed-loop amplistat regulator acting to phase the tubes ahead or back as a function of reference voltage.

Speeds above motor base speed are obtained by shunt field weakening controlled from the amplidyne regulator. References for the armature and field regulators are taken from a pair of ganged potentiometers driven by a common pilot motor. Press mounted "fast-slow" buttons control the pilot motor. Taper of the potentiometers is such as to give linear and virtually stepless acceleration, from threading speed to full speed, in 35 seconds, as the "fast" button is held down. Deceleration is at the same rate. Any speed above $2^1/_2$ per cent can be held continuously and accurately.

Conventional dynamic braking can be set to give any desired rate of stopping.

As many as nine 40 horsepower motors are mechanically coupled to operate in parallel to drive large press combinations. Compound wound motors are furnished with just enough cumulative series field to provide for load sharing between motors.

A motor is furnished for each press unit, so, as units are added or subtracted, the per cent loading on each of the motors in use remains constant. Thus essentially shunt speed regulation characteristics are obtained regardless of press size.

Economic Considerations

The operational advantages just described can often be justified economically when all factors are considered. Although first cost of a complete electronic press drive is usually slightly higher than a-c wound rotor drive, the savings in power costs, maintenance costs, and installation costs tends to more than make up the difference. These savings vary widely, so only the factors affecting them will be discussed.

Power savings result from the higher efficiency at reduced speeds of electronic drive over wound rotor drive, Figure 6. A press geared for a maximum speed of 50,000 papers per hour will usually average, while running on the main motors, a production speed between 30,000 and 40,000 papers per hour. For a given installation, this difference in efficiency can be determined approximately and factored against total energy requirements and local power rates to find yearly savings. Often, a very material annual saving is indicated.

Electronic drive lends itself particularly well to treatment in the same manner as modern switchgear. Installation costs are reduced to a minimum by virtue of factory assembled and wired cubicles which need only be bolted down and interconnected, Figure 7. Since no major power is dissipated in the control room, special ventilation is not required. A saving of $15,000 on air conditioning equipment alone was estimated by the consulting engineers on a recent large installation.

Electronic drive furnishes, with its direct coupled d-c motors, all the functions formerly requiring a main motor, a threading motor, reduction gearing, an over-running clutch, a mechanically-operated brake, and a chain drive. Reduced maintenance expense can be expected from this simplification.

Note, in the control cubicles, Figure 8, the absence of power contact making or breaking devices such as contactors or power rheostats. The one exception is the

Figure 8. Interior view of cubicles for operating one press

From left to right: feeder circuit breaker and current limiting reactor cubicle, ignitron rectifier cubicle, magnetic control cubicle, and motor selector cubicle

dynamic braking contactor which operates infrequently. Otherwise power is turned on and off by the ignitron tubes which are noted for their reliability and long life.

At the present time large electronic press drive installations are operating in four metropolitan newspaper plants in this country. These total 28 ignitron rectifiers powering motors aggregating over 5,000 horsepower. Equipments for four more publishers, totalling ten rectifiers and approximately 2,000 horsepower in motors, now are in process of manufacture or installation.

A number of electronic drives have been on regular production for over a year now, and have proved exceptionally satisfactory on the score of reliability and general performance.

Conclusions

In conclusion, printing presses are a sound field for application of electronic motor drive. Functionally, electronic drive is superior to any conventional drive. Reliability is equal or superior to that of any other type of drive. Economically electronic drive can be justified in the majority of metropolitan installations, and, as advances continue to be made, will certainly become more and more adaptable to smaller installations. All things considered, electronic drive gives definite promise of being the printing press drive of the future.

References

1. Electronic Drive for Newspaper Presses, W. L. Wright. *Mechanical Bulletin 346*, American Newspaper Publishers Association (New York, N. Y.), August 29, 1947.

2. Electronically Controlled Adjustable Speed Drives, M. M. Morack. *Proceedings*, Midwest Power Conference (Chicago, Ill.), volume X. April 1, 1948.

No Discussion

Flame Detectors for Domestic Fuel Burner Safety Devices

JUSTIN A. DEUBEL
MEMBER AIEE

THE control of fully automatic domestic fuel burners has brought about diverse problems. Especially is this true where the fuel used is gas or oil, consequently entailing a certain degree of explosive hazard. Generally these burners are of the "on-off" variety under control of a room thermostat.

A typical domestic oil burning system is provided with means of feeding fuel to a combustion chamber and with means for electrically igniting the fuel. The electrical ignition system is usually turned off shortly after the start of each running period after the fuel is well enough lighted to self sustain ignition. The safety combustion control equipment for such a system, exclusive of other features, must be capable of accomplishing the following functions. It must:

1. Prevent starting until after a purge interval, if more than five seconds of unburned fuel, vapor or gas has accumulated in a hot combustion chamber.

2. Shut down to a manual reset safety position within two minutes in the event the fuel fails to ignite on a normal start.

3. Disconnect electric ignition means after fire is satisfactorily ignited.

4. Shut down to a manual reset safety position, or recycle after a safe scavenging period, in the event the fire fails after once having been successfully ignited.

In order to accomplish these functions, a detector must be used to enable the remainder of the control to know if flame is absent or present and to respond accordingly.

On an automatic domestic system burning gas, the safety equipment is less involved, since here intermittent electric ignition is not employed. A gas pilot is allowed to burn continuously. It is assumed that if the pilot is burning it is safe to admit fuel. The safety equipment for this application must permit the admission of fuel on demand for heat from the room thermostat if pilot flame is present, and must prevent admission if pilot flame is absent.

The purpose of this paper is to discuss various ways of detecting flame which are suitable to oil and gas applications. Devices for this purpose may be classified into four classes:

1. Those responding to the temperature of the products of combustion.

2. Those responding to the total radiant energy of the flame.

3. Those responding primarily to the luminous radiation of the flame.

4. Those responding to the electrical conduction of the flame.

The requirements for a flame detector for these applications are that the flame detector responds to actuate a switch as quickly as practicable, to the presence or absence of flame, in order to minimize hazards. The maximum response time actually permissible depends upon application and circuit arrangement but generally for oil the response to presence of flame should not exceed 30 seconds and response to absence of flame should not exceed 15 seconds. If this time can be held to less than five seconds circuit simplifications are possible. For gas the response should not exceed three minutes to either absence or presence of flame.

In order to meet speed requirements in both directions, it is often necessary to make detectors respond to *change* in condition rather than a fixed magnitude of condition. For example, if the detector is made to respond to the secondary property of the flame, temperature, it must operate as a function of the change of temperature. It must close on an increase of temperature of a prescribed amount and open on a decrease in temperature of a prescribed amount. It must not open and close at a fixed temperature as a conventional thermostat would do. In order to obtain these effects slip friction mechanisms are fre-

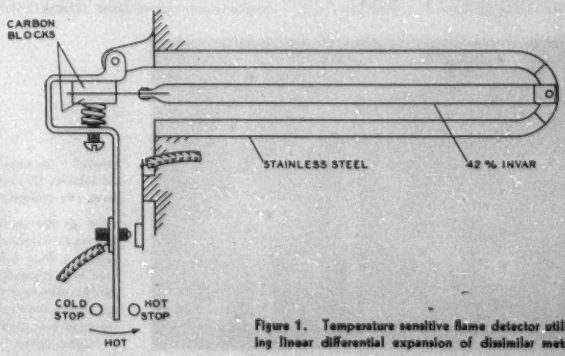

Figure 1. Temperature sensitive flame detector utilizing linear differential expansion of dissimilar metals

Paper 50-35, recommended by the AIEE Domestic and Commercial Applications Committee and approved by the AIEE Technical Program Committee for presentation at the AIEE Winter General Meeting, New York, N. Y., January 30-February 3, 1950. Manuscript submitted August 2, 1948; made available for printing December 6, 1949.

JUSTIN A. DEUBEL is with the Perfex Corporation, Milwaukee, Wis.

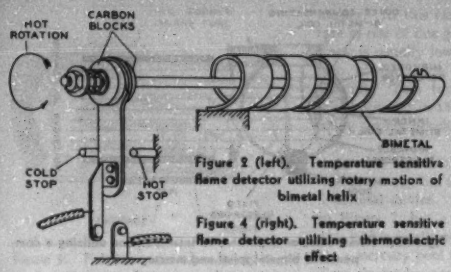

Figure 2 (left). Temperature sensitive flame detector utilizing rotary motion of bimetal helix

Figure 4 (right). Temperature sensitive flame detector utilizing thermoelectric effect

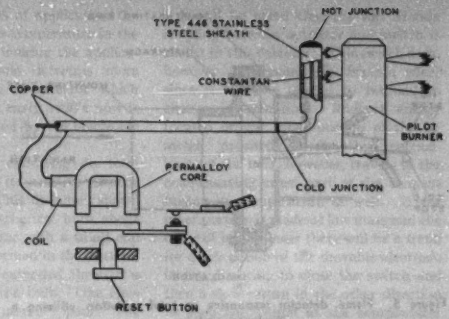

quently used as will be described here.

Also, flame detector switches must fail safe, or circuit arrangements be made to check the action of the switch so no more than 1-cycle sequence is completed if the switch is not functioning properly. This is often done by a "cold check" arrangement, a discussion of which is beyond the scope of this paper except to say that single-pole double-throw switch action with an over lap in one direction may be required. For simplicity the illustrations here show only single-pole single-throw switch action.

The life of switches for this purpose should be of the order of 100,000 operations. The switch load is usually nominal consisting of only control circuit components of about ten voltamperes.

Class 1. Detectors Responding to the Temperature of the Products of Combustion

By far the highest percentage of domestic oil and gas burner controls use the class one type of detector because of its simplicity and inexpensiveness. Elements of this nature are usually arranged to be mounted in the smoke stack of an oil burning furnace and adjacent to the pilot of a gas burner. They are constructed in several styles and in general use the differential thermal expansion of two dissimilar materials to actuate an electrical switch.

One form of such a device which made its appearance in commercial form about 1936 is shown in Figure 1. It comprises a relatively high-expansion U-shaped channel element of 18 mils thick, stainless steel secured at the open end and a relatively low expansion tube about 8 inches long of 18 mils thick, 42 per cent nickel invar secured to the bottom of the U-shaped element. Upon the application of heat, the legs of the U-shaped element lengthen, pulling the tube with them and providing a resultant motion of about 0.001 of an inch per 20 degrees Fahrenheit temperature change. This motion is coupled to the electrical switch through a "slip friction" transmission and a multiplying lever of approximately 20 to 1. The slip friction transmission consists of two carbon blocks secured to the switch actuator arm and arranged to have sandwiched between them a flexible blade secured to the inexpansive member of the thermal element. When there is a differential expansion of the thermal element, the inert member moves and the switch actuator arm follows due to force transmitted through the "sandwich" until the actuator arm engages either one of two mechanical limit stops.

Further motion of the thermal element results in slipping the flexible blade within the carbon block sandwich. A reversal in the temperature of the thermal element results in immediate reversal of the motion of the switch actuator. With this construction the switch is arranged to operate on temperature difference and is calibrated to close on a rise in temperature of about 25 degrees and open on a fall of temperature of about 75 degrees Fahrenheit. Total travel of the switch arm at the contacts between stops is approximately 0.1 inch. Such a device is suitable for use in locations where the maximum temperatures under continuous duty range from 350 to 1,000 degrees Fahrenheit.

Another form of the first class of detectors which made its first commercial appearance in the early 1920's is shown in Figure 2. Here a bimetal helix approximately 32 mils thick comprised of the same materials as the element described previously is arranged to rotate a shaft on temperature change. Rotation of the shaft is made to actuate a switch through a rotary slip friction transmission. Rotation of the switch arm is made to be approximately five mechanical degrees between stops. This motion corresponds to approximately 70 degrees Fahrenheit change in temperature.

Another form which commercially appeared about 1939 is shown in Figure 3. A group of bimetal elements is arranged to give linear motion. This motion through a slip friction transmission actuates the switch. In this case, motion from the thermal element proper is much greater than that shown in Figure 1 and does not need to be multiplied. The temperature motion relationships are otherwise approximately the same as for the first example. All three of the elements described are commonly built to mount in a smoke stack through a $1^1/_2$-

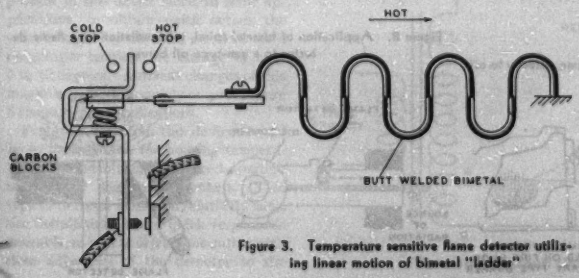

Figure 3. Temperature sensitive flame detector utilizing linear motion of bimetal "ladder"

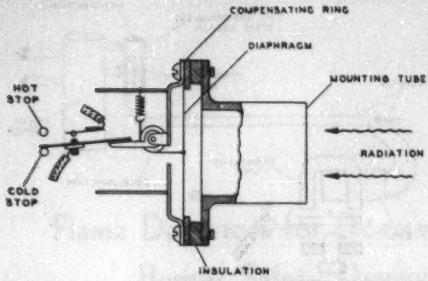

Figure 5. Flame detector responsive to total radiation utilizing a diaphragm and ring

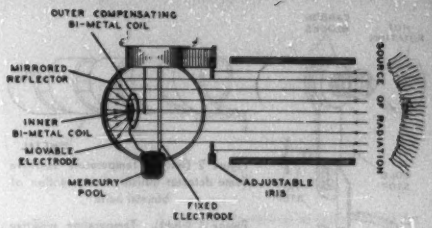

Figure 7. Flame detector responsive to total radiation utilizing a compensated bimetal spiral and mercury switch

inch diameter aperture and are from 4 to 8 inches long.

The three detectors just described are those most commonly used on conventional oil burner applications, and it is estimated that one of the three forms appear in 90 per cent of all current domestic installations. All three are reliable and function very satisfactorily although each type has its own proponent. All three, when installed in the stack of a conventionally designed furnace having ultimate stack temperatures of 400-700 degrees Fahrenheit, will respond in less than 30 seconds to the presence of, and in less than 15 seconds to the absence of, flame in the combustion chamber. The time constants of the detectors proper is of the order of 15 seconds. The additional time lag is caused by the furnace characteristics.

Shown in Figure 4 is another interesting form of flame detector used primarily to detect the absence or presence of a gas pilot flame using thermoelectric effect. A type *446* stainless steel and Constantan thermocouple is arranged adjacent to the pilot burner so a portion of the pilot flame impinges upon it. This thermocouple when heated excites a coil of an electromagnet producing about 16 ampere turns of magnetomotive force resulting in sufficient flux through a permalloy magnetic circuit to hold an armature in closed position, and thus keep an electrical switch closed. When the thermocouple is cooled the electromagnet is de-energized and the armature drops, opening the electrical switch.

The greater percentage of detectors of this sort are arranged so that the magnetic circuit must be closed manually but once closed will remain so, as long as the thermocouple temperature exceeds a certain set value. These devices may, however, be built as relays to both open and close circuit under the effect of temperature alone.

The portion of the thermocouple subjected to the pilot flame is cylindrical in shape about 1/4 inch in diameter and about 1 inch long. Normally one-half of this is bathed in the flame. The cold junction is located about $2^1/_2$ inches from the hot junction. Connections from the location of the cold junction to the electromagnet coil may be of copper, usually a copper wire within a copper tube.

The iron circuit may have a mean length of about $2^1/_4$ inches and a cross section of about 1/16 square inch. The temperature difference between the hot and cold junction must be of the nature of 600 degrees Fahrenheit in order to retain the armature in closed circuit position. This form of flame detector which appeared commercially about 1934, has found great favor in the gas field. It is estimated that 70 per cent of the currently installed flame detectors for gas pilots are of this type. This unit fails safe if the conductors fail either open or short circuited. It is both rugged and simple, has few moving parts and has proved to be very reliable. Ambient temperature of 900 degrees Fahrenheit may be tolerated with suitable design. The temperature of the hot junction under these conditions may approach 1,400 degrees.

Class 2. Detectors Responding to the Total Radiant Energy of the Flame

One form of detector operating on total radiation direct from the flame is shown in Figure 5. Here is a diaphragm of corrosive resistant material about 5 mils thick and $2^1/_2$ inches in diameter is welded at its circumference to a ring of the same kind of material, but thicker. This assembly is mounted to a housing which serves as a support and also a means of dissipating heat. Radiant energy from the flame under observation falls on the diaphragm heating it. Because of the configuration, the center of the diaphragm reaches a higher temperature than the circumference causing the diaphragm to "dish". A force in the left-hand direction is applied at the center of

Figure 6. Application of diaphragm and ring-type flame detector to oil flames

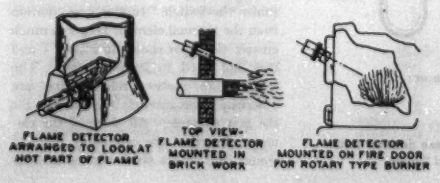

Figure 8. Application of bimetal spiral, total-radiation type flame detector to a gun-type oil burner

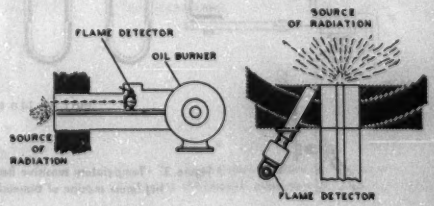

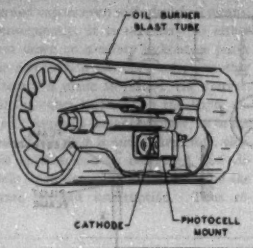

Figure 9. Flame detector responsive to luminous radiation utilizing a photoemissive photo tube

the diaphragm by means of a coil spring, through a metal ribbon which is secured at one of its ends to the coil spring, passes over a roller and is secured at the other of its ends to the center of the diaphragm. When the diaphragm dishes under heat there is clockwise motion of the roller and the arm secured to it, effecting closure of the switch contacts and somewhat later, engagement of the "hot stop". Further heating of the diaphragm results in slippage of the ribbon on the roller. Hence, here again the motion of the flame detector is coupled to the switch through a "slip friction element". Upon cooling of the diaphragm there is immediate counter-clockwise motion of the switch which continues until the "cold stop" is engaged. Further motion causes slippage of the slip friction element.

This device operates the switch on a change in temperature rather than at a fixed temperature, in the same manner as the switches described previously, but in addition has ambient compensation. Since the diaphragm and supporting ring are made of the same material there is no dishing of the diaphragm unless there is a difference of temperature between the center and circumference. This difference does not exist due to ambient changes except slightly during the transients. Ambient compensation is important in this device since, in some applications, to obtain quick action, the switch might be adjusted to close on a diaphragm temperature change of only 5 to 10 degrees. Ambient changes of this magnitude may commonly occur. Figure 6 shows typical applications.

For good operation this device should be so located that the housing temperature does not ultimately exceed approximately 300 degrees Fahrenheit. This type of detector is used in relatively large size installations where quick response is desirable, as well as is front mounting with close adjacency of the detector to the burner. In this class of application the rate of rise of flue gas temperature in the stack is usually low making the application of the class one detectors more difficult. This type of detector which first appeared in the early 1920's now is being largely obsoleted by the electronic type.

Another detector operating on total radiant energy has as its sensitive element a bimetal device. This detector, shown in Figure 7, has a spherical bulb about $1^1/_4$ inches in diameter with a small cup for a mercury pool formed in the bottom. Two electrodes are extended through a press at the top of the bulb. One electrode dips into the mercury pool. The other is a support for the bimetal element. The bimetal element is made up of a strip of bimetal about 1/16 inch wide and 10 mils thick wound in the shape of a spiral of Archimedes. The bimetal forming the inner portion of the spiral is reverse in action to the bimetal forming the outer portion of the spiral. The inner and outer portions are butt welded together to form one continuous element. Due to this reverse construction there is no resultant motion of the spiral on ambient temperature changes. One-half the inner surface of the bulb is mirrored and the bimetal element is placed in the bulb so that reflected radiation from the mirrored surface is focused only on the inner portion. When detector is subjected to radiation the inner portion of the bimetal heats while the outer portion remains relatively cool causing the spiral to have resultant motion. An electrode is secured to the free end of the spiral and is arranged to dip into the mercury pool when the difference in outer and inner portions of the spiral reach a predetermined amount. Immersion of this last electrode, due to bimetal action, causes completion of the electric circuit extending through the two electrodes and the mercury pool.

It will be noted that the slip friction coupling between actuator and switch is absent in this detector. This switch does, however, have some slip friction effect since it has the ability to respond to change in condition. Radiant energy focused on the inner portion of the bimetal, primarily heats this portion. Some of the heat, however, travels to the compensating outer part of the element raising its temperature as well. If the inner portion is made of low mass and the outer of higher mass there will be a trend for quick action of the movable electrode in one direction to close the switch and then a slow return in the other direction to open the switch as the compensator heats. Obviously if this effect is carried too far and the compensator allowed to reach almost the active bimetal temperature, the switch will be reopened. This must be guarded against. On a decrease in radiation the inner elements cool quickly to, or below, the compensator temperature and opens the switch. As the more massive compensator cools the trend is to reverse the switch action readying the switch for the next cycle. Figure 8 shows a typical application.

Detectors working on this principle first made their appearances in the early 1920's. A more modern version was developed in about 1938. Units of this nature having low mass and being radiant responsive have rather rapid response times. Also, since they are small in size, they may be frequently mounted within the blast tube of an oil burner eliminating the necessity of separate mounting and permitting factory assembly of a burner complete with integral safety combustion controls. It is estimated that about 4 per cent of domestic burners currently manufactured use this form of detector. Other detectors made to respond to total radiant energy and having no moving parts are presently under development by several

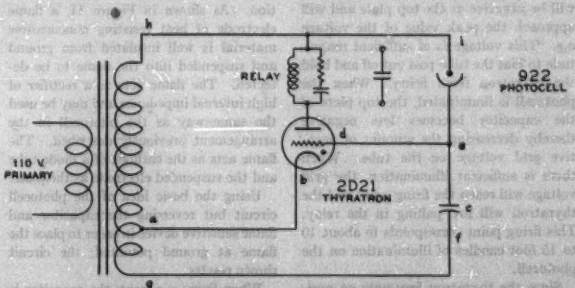

Figure 10. Electronic circuit for photoelectric flame detector

manufacturers and may become the subject matter of a future paper.

Class 3. Detectors Responding Primarily to the Luminous Radiation of the Flame

Perhaps the most recent distinctive type of flame detector to make its commercial appearance is the photoelectric type responding to the luminous radiation of flame. This appeared in about 1940. Photo cells frequently used for this service are the Radio Corporation of America type *922*. The photocell is mounted so that it will look into the combustion chamber at the flame. Often the cell is mounted inside the blast tube of a gun-type burner as shown in Figure 9. The cell is usually arranged to operate an electromagnetic relay through a suitable amplifier. This relay then performs the required functions in the remainder of the combustion control circuit.

An electronic circuit suitable for this application is shown in Figure 10. This circuit uses a type *2050* or *2D21* thyratron. The capacitor C is charged by grid current through the thyratron through the path *a,b,d,e,f,g*, during the portion of the a-c cycle when the bottom end of the transformer is positive. This charge is in a direction to make the top plate of the capacitor negative with respect to the bottom plate.

The capacitor also is charged by photocell current through the path *h,i,e,f,g*, during the portion of cycle when the top end of the transformer is positive. This current charges the capacitor in a direction to make the top plate positive with respect to the bottom plate. Since the two charging currents are in opposite directions, the resultant magnitude and direction of voltage appearing across the capacitor will depend upon the relative magnitude of the two charging currents. When the photocell is dark the capacitor will be negative at the top plate and will approach the peak value of the voltage *a,g*. This voltage is of sufficient magnitude to bias the tube past cut off and hold the thyratron from firing. When the photocell is illuminated, the top plate of the capacitor becomes less negative thereby decreasing the amount of negative grid voltage on the tube. When there is sufficient illumination, the grid voltage will reach the firing point and the thyratron will fire pulling in the relay. This firing point corresponds to about 10 to 15 foot candles of illumination on the photocell.

Since the thyratron fires only on positive alternations, a capacitor and current limiter are shunted around the relay coil to eliminate chatter. It should be noted that only d-c effects are utilized to obtain grid bias and signal. Symmetrical a-c effects over the course of a cycle cancel each other out. This makes the photocell circuit quite independent of lead capacity and resistance across the photocell mount, which is obviously highly desirable in dirty locations and under various mounting arrangements.

Since the photocell is small in size it too can be mounted directly within the blast tube of a burner, making for ease of installation and the possibility of locating the entire combustion control integral with the burner. Also, since the response is substantially instantaneous, the remainder of the combustion control may be simplified as explained later. It is estimated that about 2 per cent of currently installed burners are using this type of detector.

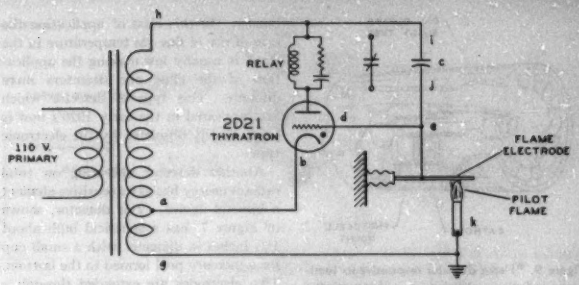

Figure 11. Electronic circuit for flame-conduction type flame detector

Class 4. Detectors Responding to the Electrical Conduction of the Flame

Still another form of flame detector works on the principle of flame conduction. As shown in Figure 11, a flame electrode of heat resisting noncorrosive material is well insulated from ground and suspended into the flame to be detected. The flame acts as a rectifier of high internal impedance and may be used the same way as the photocell in the arrangement previously described. The flame acts as the cathode of a diode tube and the suspended electrode as the plate.

Using the basic idea of the photocell circuit but reversing the capacitor and flame sensitive device in order to place the flame at ground potential, the circuit shown results.

When flame is absent, the capacitor is charged by grid current with the bottom plate negative to a value approaching the peak voltage *a,h*. This results in a grid cathode voltage around zero volts and causes the tube to fire. When flame is present, the capacitor is charged when the top end of transformer is plus along the path *h,i,j,e,k,g*, through the rectifying flame. The capacitor voltage then approaches the peak voltage *h,g* producing a negative grid to cathode voltage, cutting the tube off.

It will be noted that the relay action is opposite in this case to that of the photocell. Here, when flame is present, the relay drops while in the former case where flame was present the relay pulled in.

The flame conduction-type detector is not generally suited to oil flames because of the deleterious effect of the oil flame on the electrode and the failure of the flame rod insulator due to dirty products of combustion. This form of detector which first made its commercial appearance in about 1931 finds its primary application in checking gas pilot flames on large installations.

Both the photoelectric and the flame-conduction type detectors respond substantially instantaneously. For oil burning equipment this is quite advantageous in that it permits simplification of the combustion control as well as providing a greater margin of safety.

With the thermal responsive elements of the class 1 and 2 varieties, when flame failure occurs, some interval of time in the nature of 10 to 30 seconds is required for the flame detector to respond and make this fact known to the remainder of the combustion control. During this time, atomized fuel is being delivered to a hot combustion chamber. If this time is too long, there is danger of obtaining a rich enough mixture to ignite with violence from the hot combustion chamber and in any event after about five seconds, it is somewhat hazardous to ignite these un-

burned vapors even with electrical means. Consequently, it is necessary to either shut down on a safety lockout or purge the combustion passages before another attempt is made to restart the burner. On the other hand, when the flame detector responds instantaneously, as in the case of the class 3 and 4 detectors, electric ignition can be connected immediately upon flame failure, to re-ignite the flame without interruption. Thus recycling on flame failure may be obtained without complicating the control with a means for purging or scavenging burner.

It should be pointed out that electronic elements are presumed to fail either conductive or nonconductive and, therefore, in systems employing electronic circuits, means must be provided to make the system fail safe under either of these conditions. This may be accomplished with "cold check" devices, a discussion of which, as has been said, is beyond the scope of this paper.

The present deterent to wide applications of electronic domestic controls is the fact that the electronic components are expendable and that service personnel is not experienced in servicing electronic equipment. It appears that from the safety aspect, the high-speed response afforded by the electronic devices is not required on domestic size plants.

No Discussion

Spring and Damping Coefficients of Synchronous Machines and Their Application

LEE A. KILGORE
FELLOW AIEE

EUGENE C. WHITNEY
MEMBER AIEE

Synopsis: This paper develops simple formulas for spring and damping constants of synchronous machines. These formulas include the effects of induced currents in the damper winding and field. An approximation to the effect of primary resistance in producing a negative damping torque is given. An equivalent circuit is given which can represent accurately the mechanical system of several engine-driven generators or compressors operating in parallel. It is concluded that the conventional representation of synchronizing power as full-load power over full-load angle is sufficiently accurate for most cases, but that it is well to have a more accurate method for special cases.

IT HAS long been recognized that synchronous machines connected to each other or to a system exhibit electrical torques giving a spring action (torques proportional to angular displacement) and a damping action (torques proportional to velocity). The spring action together with the inertia results in a torsional natural frequency of the order of 1-to-4 cycles per second. In the application of synchronous motor-driven compressors and engine-driven generators, the compressor or engine torques may have components which could coincide with the natural frequency and give trouble from excessive current pulsation.

The conventional method of dealing with these problems is to use a synchronizing coefficient (spring constant) determined by full-load power over full-load electrical displacement angle. In generator practice, the spring constant is P_r which is the kilowatts per electrical radian, where

$$P_r = \frac{KVA \times PF}{\text{efficiency} \times \delta}$$

where the displacement angle in radians is

$$\delta = \tan^{-1} \frac{IX_q \cos \theta}{E_t + IX_q \sin \theta} \qquad (1)$$

For very low frequency oscillations (less than one cycle per second) it would be apparent that the slope of the power angle curve should be used for small angular oscillations which give in general a lower value than the above value. For higher frequencies of oscillation, currents are induced in the field and damper windings which tend to stiffen the spring action and may give values under load higher than the conventional method.

A more exact method is given here which should serve as a guide where the conventional methods may be safely used and as a tool for more accurate evaluation where needed. The usual assumption also treats each machine as if it were connected to an infinite system, whereas a method will be given here for using the constants determined for an infinite system to evaluate the effects of a limited number of other machines.

Neglecting primary resistance and assuming an infinite bus, the effects of induced rotor currents may be included as derived in Appendix I. This involves determining effective direct and quadrature resistances and reactances at the oscillation frequency (neglecting primary resistance). These are essentially the same constants used by the synchronous motor designer in calculating starting performance at a corresponding rotor frequency. The constants can be determined by locked test at low-primary frequency by measuring the low-frequency impedance and subtracting the primary resistance. The formula for per unit synchronizing torque per electrical radian is then

$$T_s = \left[\left(\frac{X_{qo}}{Z_{qo}^2} - \frac{1}{X_d} \right) E_t^2 \cos^2 \delta + \left(\frac{X_{do}}{Z_{do}^2} - \frac{1}{X_q} \right) E_t \sin^2 \delta + \frac{E_t E_d}{X_d} \cos \delta \right] \qquad (2)$$

In these formulas, unit torque is the torque corresponding to a power in kilowatts numerically equal to rated kilovolt-amperes; where

E_t = terminal voltage

E_d = internal voltage back of synchronous reactance and δ = internal or displacement angle

The damping coefficient is the ratio of per unit torque to per unit speed where speed is expressed as a fraction of rated speed and is equal to

$$T_d = E_t^2 \frac{\omega}{\omega_0} \left[\frac{r_{qo}}{Z_{qo}^2} \cos^2 \delta + \frac{r_{do}}{Z_{do}^2} \sin^2 \delta \right] \qquad (3)$$

The effect of line reactance between one machine and infinite system may be handled by adding the line reactance to the impedances used and using E_t as the system voltage.

The spring and damping constants are given in Figure 1 for typical generators with both the connected and nonconnected type dampers. The curves are based on $X_d = 1.22$; $X_q = 0.74$; and constants at 5 cycles of $X_{do} = 0.27$; $X_{qo} = 0.60$; $r_{do} = 0.20$; $r_{qo} = 0.27$, determined by locked line-to-line tests for a machine with nonconnected damper windings.

Figure 2 shows how these spring constants compare with the conventional

Paper 50-36, recommended by the AIEE Rotating Machinery Committee and approved by the AIEE Technical Program Committee for presentation at the AIEE Winter General Meeting, New York, N. Y., January 30–February 3, 1950. Manuscript submitted November 2, 1949; made available for printing November 30, 1949.

LEE A. KILGORE and EUGENE C. WHITNEY are both with Westinghouse Electric Corporation, East Pittsburgh, Pa.

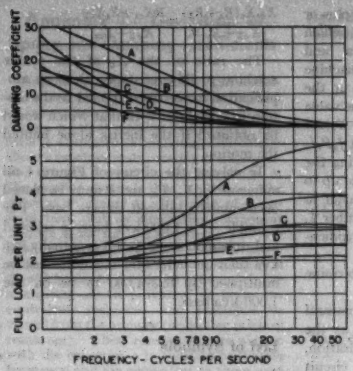

Figure 1 (left). Curves of synchronizing and damping coefficients

Figure 2 (right). Synchronizing coefficients as a fraction of the conventional value

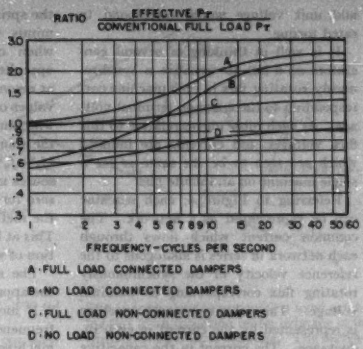

full load synchronizing power coefficient.

For synchronous motors, high-resistance damper windings of the connected type are used; and the synchronizing coefficients of Figure 2 for connected dampers may be used except the frequencies of the curve should be multiplied by about three in the typical case at full load. It should be observed that these curves are only typical, and individual machines may vary appreciably.

For the main-firing impulse of a diesel engine with a typical frequency of above 15 cycles per second, the error in the spring constant by conventional methods will be appreciable, but it is of little consequence since there is no chance of resonance with the machine natural frequency. In the range of 1.5 to 4 cycles, where there is a chance of resonance, the torque components in a diesel are those at revolutions per minute and half revolution-per-minute frequency due to irregularities in fuel injection. In this range the error in the conventional method is usually not great at full load, and at no load the approximate coefficient calculated as E_t^2/X_s is found to give fair results.

One or two cases are known where some trouble was encountered on older synchronous motors with low-resistance dampers where the spring constant was some 25 per cent higher than the conventional value.

In certain cases the damping coefficient given above must be reduced due to the negative damping effect of the primary resistance. The correction may be approximated as derived in Appendix II. Using the transient reactance of the machine and the voltage back of transient reactance, we can calculate a braking speed torque curve as if the primary were short circuited through line impedance and the primary resistance. The slope of this curve at full speed gives the change in torque per unit change in speed or the negative damping coefficient. This is equivalent to taking this "braking" torque at line frequency minus oscillation frequency, minus the value at line frequency, plus oscillation frequency, divided by the per unit difference in speed at these frequencies (or twice oscillation frequency divided by rated frequency). This coefficient can be shown to be approximately equal numerically to the braking torque calculated as before at full speed.

The approximate equation for this negative damping coefficient can be written as

$$T_{dn} \approx \frac{(E_d')^2}{(X_d')^2+r_1^2}\, r_1$$

A high value of primary resistance (such as might be encountered on a small machine or a large machine on a long line) $r_1=0.05$ would result in about 0.5 to 0.9 negative damping coefficient. Figure 1 curve "A" or "D" indicates values of 5 to 25 for the positive damping for typical generators. For synchronous compressor motors with high-resistance damper windings, the damping coefficient might be as low as 2, but here even with the high line resistance of 0.05 (assumed above) the negative damping would be about 0.3 or less due to the higher transient reactance.

In the compressor applications it has been customary to use a damping torque 10 per cent of the synchronizing torque. This is equivalent to using a resistance 0.1 of X_c in the equivalent circuit of Figure 3 or a damping coefficient of 0.1 of $2\pi f_c\,(2H)$. For typical values of H, this would give a damping coefficient of 4 which is higher than calculated here for motors with high-resistance dampers (as used in present-day practice to obtain low inrush). Fortunately in compressor applications the natural frequency is kept sufficiently removed from the torque impulse frequencies that the resistance effects are small and the conventional figure leads to little error.

In diesel engine practice some[1] have used an approximate damping coefficient 0.01 times the synchronizing torque in inch, pounds, radians. This is equivalent to a per unit damping coefficient of 3.77 times the per unit synchronizing coefficient or about eight in a typical case. Referring to Figure 1, this will be seen to be a generally conservative figure.

Parallel Operation of Engine Driven Generators

Particularly in diesel engine application it is desirable to have a means of considering the effect of one machine on another where there are a limited number of machines on the system. The method given here is based on representing each machine by an equivalent circuit, in which its inertia is represented by an inductance (L) its spring or synchronizing action by a condenser (C) and its damping by a resistance (R), see Figure 3. Unit current in this circuit would represent unit velocity (equal to rated velocity)

and unit voltage would correspond to rated torque.

It is well in thinking of several generators on a bus to visualize a synchronously rotating flux in each machine corresponding to the common terminal voltage. As each rotor moves relative to this flux, voltages, and currents are induced which are seen to be the same as for a single machine on an infinite bus.

Referring to Figure 4, each machine can be represented as a network. The common current which flows through each network in series is analogous to the reference velocity of the synchronously rotating flux corresponding to terminal voltage. The velocity of each machine is represented by the current in each inductance. The current in the capacitive branch then represents the relative velocity of the unit with respect to the reference.

The torque impulses of one engine at a time should be considered and the machine in which the impulse occurs will be referred to as the source machine. The torque impulse is represented as a voltage applied in the inductive branch, since the torque tries to change the velocity. This puts the series impedance of the other networks in parallel with the capacitive branch of the source machine. In mechanical terms, the torque developed between this machine and the others depends on its relative velocity and its spring and damping constants.

Examining the equivalent circuit, Figure 4, it is apparent that the resonant frequency will be affected by the other machines. In fact there will be as many natural frequencies as machines. All of these frequencies will be somewhat different from that of each machine alone on an infinite system.

The exact solution can be determined by solving the complete circuit for a series of frequencies. This can be done very readily on an a-c calculating board. We can, however, obtain certain information by simplifying the circuit by approximate relations.

The effect of the inertias is to cancel the spring constants leaving a net plus or minus value for each machine, which when combined would be equal and opposite to that of the source machine at resonance. Hence, we can add up the values of $X_eX_1/(X_1-X_e)$ to get the value which must be equal to $-X_eX_1/(X_1-X_e)$ for the source machine. We can plot $f_oP_r/(f_o^2-f_n^2)$ for each machine including the source machine, and these must add up to zero for resonance which is equivalent to the method given in reference number 1. This at least gives an approximate indication of where resonance will occur.

The next step would be to determine the approximate damping.

If any machine has the same natural frequency f_n (on an infinite bus) as the machine with source of torque pulsation, its impedance in the equivalent circuit will be very high compared with the others, and it will take most of the voltage which appears across the capacity and resistance of the source unit. Hence, the two machines will oscillate in angles approximately in inverse proportion to their inertia constants.

Even though the natural frequencies do not match, the impedance representing the combined machines may parallel with the capacity of the source machine so as to give resonance. Except where two natural frequencies are nearly coincident, the combined resonance frequency will differ sufficiently from the individual natural frequencies that we can use the above approximation for the effective spring constant (or X_e) and we can use $X_1^2R/(X_1-X_e)$ as an approximation to the damping of each unit in the series circuit. The limiting value of series resistance in resonance is X_1^2/R and if the value approaches this then the equation must be solved for the exact series impedance.

The combined resistance and reactance designated by R_Σ and $X_{e\Sigma}$ is then determined for the other machines and paralleled with the values of the source machine R_s and X_{es}.

Assuming R_Σ to be small (say not over 30 per cent of $X_{e\Sigma}$) then the resistance is

$$\frac{X_{es}X_s(R_s+R_\Sigma)}{(X_{e\Sigma}+X_{es})^2}+\frac{RX_{es}+R_sX_{e\Sigma}}{X_{e\Sigma}+X_{es}}$$

The ratio of the X_e of the source machine to this resistance gives an amplification factor to be applied to the motion as compared with that which would be obtained if the inertia alone limited the motion.

In solving the circuit of Figure 4 all values of X_1, X_e, T_d, and R must be placed on a common kilovolt-ampere base. For example, if a 1,000-kva base is selected and unit number 1, 2, or 3 is actually 625 kva then the values for this unit must be multiplied by 625/1,000 to be on the 1,000-kva base.

List of Symbols

E_e = see Figure 3
E_d = per unit excitation on the direct axis for an unsaturated machine
E_1 = see Figure 3
E_t = per unit terminal voltage of machine
H = inertia constant. See Figure 3
I = per unit machine line amperes based on rated amperes of the machine
i = unit current in the equivalent circuit corresponding to rated velocity
KVA = rated machine kilovolt-ampere
P_r = synchronizing coefficient in kilowatts per electrical radian
Per Unit = times normal rated value. 1 per unit = rated value
R = damping resistance in the equivalent circuit
r_d = per unit resistance direct axis
r_q = per unit resistance quadrature axis
Torque = 1.0 per unit torque corresponds to a kilowatt input equal to rated kilovolt-ampere at 1.0 power factor
WR^2 = weight times radius of gyration squared in pounds feet squared
X_e = capacitive reactance in the equivalent circuit
X_d = per unit direct axis synchronous reactance
X_1 = inductive reactance in the equivalent circuit
X_q = per unit quadrature axis synchronous reactance
Z_d = per unit direct axis impedance
Z_q = per unit quadrature axis impedance
δ = internal machine angle due to load in electrical radians $=\tan^{-1}\dfrac{IX_q\cos\theta}{E_d+IX_q\sin\theta}$
PF = power factor = $\cos\theta$
θ = power factor angle
$\omega_o=2\pi f_o$ = velocity in electrical radians per second at oscillation frequency
$\omega=2\pi f$ = velocity in electrical radians per second at rated machine frequency

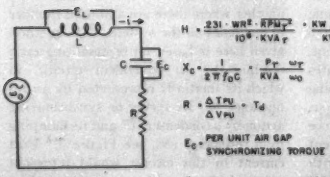

Figure 3 (left). Equivalent circuit representing the mechanical system of one machine

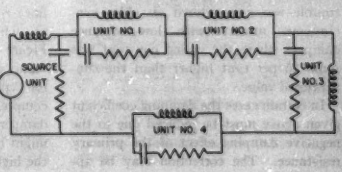

Figure 4 (right). Equivalent circuit of a number of generators on a system

Appendix I. Derivation of Spring and Damping Coefficients

Neglecting primary resistance and assuming a sinusoidally distributed winding and an infinite bus, the primary voltage E_1 produces a constant rotating field of flux. The rotor is visualized as oscillating sinusoidally about a synchronously rotating average position through a small angular amplitude Δ. The angular change is then $\Delta \sin \omega_o t$. The direct axis linkages ψ_d will consist of a constant term plus an alternating component $\Delta E_1 \sin \delta \sin \omega_o t$. The current also will have an average component I_d and an alternating component due to the pulsation in ψ_d which may be calculated as in any simple alternating circuit providing we know the equivalent resistance and reactance as viewed from the primary (neglecting primary resistance). These constants[a] are written with the subscript o to indicate oscillation frequency and are equivalent to those used in starting performance calculations at the same rotor frequency.

The instantaneous values of the direct and quadrature axis flux linkages and currents then are written as

$$\psi_d = E_d \cos \delta - E_1 \sin \delta \sin \omega_o t$$

$$\psi_q = E_1 \sin \delta + E_d \cos \delta \sin \omega_o t$$

$$i_d = I_d - \Delta E_1 \sin \delta \left(\frac{r_{do}}{Z_{do}^2}\right) \times \cos \omega_o t - \Delta E_1 \sin \delta \left(\frac{X_{do}}{Z_{do}^2}\right) \sin \omega_o t$$

$$i_q = I_q + \Delta E_d \cos \delta \left(\frac{r_{qo}}{Z_{qo}^2}\right) \times \cos \omega_o t + \Delta E_1 \cos \delta \left(\frac{X_{qo}}{Z_{qo}^2}\right) \sin \omega_o t$$

$$I_q = \frac{E_1 \sin \delta}{X_q}$$

and

$$I_d = \frac{E_1 \cos \delta - E_d}{X_d}$$

$$T = \psi_d I_q - \psi_q I_d{}^*$$

Oscillation frequency components of torque

$$\Delta E_1^2 \left[\cos^2 \delta \frac{r_{qo}}{Z_{qo}^2} + \sin^2 \delta \frac{r_{do}}{Z_{do}^2}\right] \cos \omega_o t +$$

$$\Delta E_1^2 \left[\cos^2 \delta \frac{X_{qo}}{Z_{qo}^2} + \sin^2 \delta \frac{X_{do}}{Z_{do}^2}\right] \sin \omega_o t +$$

$$\Delta E_1^2 \left[\frac{\sin^2 \delta}{X_q} - \frac{\cos^2 \delta}{X_d}\right] \sin \omega_o t +$$

$$E_1 E_d \frac{\sin \delta}{X_d} \cos \omega_o t$$

Damping constant = coefficient of $\cos \omega_o t + \Delta \omega_o$

$$T_d = \frac{\omega E_1^2}{\omega_o} \left[\cos^2 \delta \frac{r_{qo}}{Z_{qo}^2} + \sin^2 \delta \frac{r_{do}}{Z_{do}^2}\right]$$

Spring constant

$$T_s = \left[\left(\frac{X_{qo}}{Z_{qo}^2} - \frac{1}{X_d}\right) E_1^2 \cos^2 \delta + \left(\frac{X_{do}}{Z_{do}^2} - \frac{1}{X_q}\right) E_1^2 \sin^2 \delta + \frac{E_1 E_d \cos \delta}{X_d}\right]$$

* See reference 3.

Figure 5. Voltage vector diagram showing pulsating components

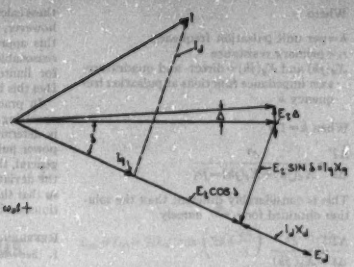

Appendix II. The Effect of Primary Resistance

The primary resistance is generally small, but it does produce a negative damping coefficient which in some cases can be appreciable. The major effect of the primary resistance may be evaluated by assuming the pulsating armature current to be the same as would be obtained if the field resistance to reactance ratio were negligible and the oscillation frequency currents in the damper windings are neglected. The currents are then the same as would be calculated using the assumption that the direct axis voltage back of transient reactance is constant.

The reaction of this voltage with the primary voltage gives the synchronizing torque, but feeding back through the system and the primary resistance it produces a torque in phase with the velocity. The assumption of constant flux linkage on the field is equivalent to assuming a fixed rotating flux in an induction motor primary or in the field of an electric coupling. The derivation for the torque reactions under these conditions was given in reference 5. It was shown there that the damping torque could be determined by the speed or slip torque curve assuming the winding short circuited through its resistance including in this case any line impedance. The difference in torque at the slip frequency plus oscillation frequency and at slip frequency minus oscillation frequency, divided by twice the per unit oscillation frequency gives the negative damping coefficient. This solution neglects some small effects due to the change of ψ_d and ψ_q due to line drop and the change of primary voltage drop due to secondary resistance.

References

1. Power Pulsations Between Synchronous Generators, Troels Warming. *Transactions*, American Society of Mechanical Engineers (New York, N. Y.), 1943, pages 165–176.

2. Starting Performance of Salient Pole Synchronous Motors, T. M. Linville. *AIEE Transactions*, volume 49, 1930, pages 531–47.

3. Two Reaction Theory of Synchronous Machines—Generalized Method of Analysis, Part I, R. H. Park. *AIEE Transactions*, volume 48, 1929, pages 716–29.

4. Calculation of Synchronous Machine Constants—Reactances and Time Constants Affecting Transient Characteristics, L. A. Kilgore. *AIEE Transactions*, volume 50, 1931, pages 1201–14.

5. Electric Couplings, M. R. Lory, L. A. Kilgore, R. A. Baudry. *Electrical Engineering* (*AIEE Transactions*), volume 59, August 1940, pages 423–28.

Discussion

R. V. Shepherd (General Electric Company, Schenectady, N. Y.): The correctiveness of the authors' novel approach to the determination of damping and synchronizing torques is confirmed by the fact that Mr. Park's general equation[1] for the electrical torque for small angular deviations from the average operating angle reduces to the authors' equations for the case where primary resistance is zero.

For usual values of load angle δ the contribution of the direct axis to damping is not great; in fact, for low pulsation frequencies the damping torque coefficient given in equation 3 of the paper is sensibly equal to equation 3 evaluated for $\delta = 0$, which, in turn, is equal to the per-unit quadrature-axis torque divided by the per-unit pulsation frequency.

It should be noted that the authors' derivations hold only for zero primary resistance and for small deviations from the average operating load angle. While zero primary resistance is never realized in practice, I have used the simplified formula with success for a number of years for the lower values of pulsation frequency usually encountered. However, I have not previously had occasion to consider pulsation frequencies approaching the machine rated frequency, but several checks which have been made indicate that the approximate equations diverge from the solution of Park's equation including resistance, at per-unit pulsation frequencies of the order of 0.5 and higher. That this might be expected can be inferred from the following:

At no-load unity-power-factor operation, Park's equation reduces to

$$\frac{\Delta T}{\Delta \delta} = \frac{e^2(1-h^2)X_d(jh) + jhe^2 r_1}{(1-h^2)X_d(jh)X_q(jh) + jhr_1[X_d(jh) + X_q(jh)] + r_1^2}$$

Where

h = per-unit pulsation frequency
r_1 = primary resistance
$X_d(jh)$ and $X_q(jh)$ = direct- and quadrature-axis impedance functions at pulsation frequency h

When $h = 1.0$

$$\frac{\Delta T}{\Delta \delta} = \frac{e^2}{X_d(jh) + X_q(jh) - jr_1}$$

This is considerably different than the solution obtained for $r_1 = 0$, namely

$$\frac{\Delta T}{\Delta \delta} = \frac{e^2}{X_q(jh)}$$

The solution of Park's equation requires laborious calculations; hence the authors' braking-torque coefficient correction to account for primary resistance simplifies these calculations considerably. Here again however, it seems reasonable to expect that this approximation will hold only over a reasonable range of pulsation frequency and for limited values of primary resistance. Has this been investigated?

In practice, deviation from the average operating angle on diesel-driven generators is determined by the allowable current or power pulsation, or angular deviation. In general, the values used are such as to make the deviations from the average angle small so that this assumption, on which the equations are based, does apply.

REFERENCE

1. See reference 3 of the paper

L. A. Kilgore and **E. C. Whitney:** We appreciate Mr. Shepherd's comment that he can confirm this derivation for small angles of oscillation starting with Park's equation[1] and neglecting primary resistance. These assumptions were stated in the paper. Mr. Shepherd seems to agree with the approximation using the braking-torque coefficient but questions the range of frequency and resistance over which this is valid.

Perhaps at some later date someone could start with the exact solution and show these limitations. We have no exact experimental proof but have made certain very important calculations on large machines using this approximation, which worked out well.

It is seldom required to determine the damping accurately at frequencies above the usual natural frequencies of several cycles per second.

REFERENCE

1. See reference 3 of the paper.

Per-Unit Inductances of Synchronous Machines

H. S. KIRSCHBAUM
ASSOCIATE AIEE

IN AN excellent series of papers[1,2] Mr. A. W. Rankin clarified and unified the situation regarding the meaning of the various per-unit impedances which have been used in synchronous machine theory. Heretofore, there had been confusion arising from the use of rotor base quantities which result in nonreciprocal mutual inductances between rotor and stator windings. The purpose of this paper is twofold. First, the synchronous machine equations will be developed from fundamental considerations using actual stator and rotor inductances rather than per-unit quantities. A critical examination will be made of the transformation from phase to direct and quadrature axis quantities with the physical implications of the transformation kept in mind. The transformation from phase to direct and quadrature axis currents is slightly different from that used by previous authors.[3] This was necessary in order to preserve the reciprocity of mutuals. Secondly, base rotor quantities will be chosen in such a manner that all the per-unit self-inductances on the direct axis are numerically equal to the direct axis synchronous inductance in per unit. The per-unit mutual inductances on the direct axis are then equal numerically to the coefficient of coupling between the two windings involved, times the direct axis synchronous inductance in per unit.

The Flux Linkage Equations

In writing the voltage equations of any or all the circuits on both sides of the air gap of a synchronous machine, it is usually most convenient to write them in terms of the time rate of change of the flux linkages with the various circuits. This necessitates a knowledge of all self and mutual inductances in the machine. The analysis which follows will be made for an ideal synchronous machine[4] as defined by Park.

When, in such a machine as illustrated in Figure 1, the direct axis of the rotor is coincident with the axis of phase a, the self-inductance of phase a is maximum since the permeance of the magnetic path of the phase also is a maximum. When the quadrature axis of the rotor is coincident with phase a its self-inductance is a minimum because the permeance of the magnetic path of phase a also is a minimum. Since each phase consists of N sinusoidally distributed turns, the self-inductance of phase a will vary as a cosine function of the angle 2θ in the following manner

$$L_{aa} = L_s + \Delta L_s \cos 2\theta \tag{1A}$$

In a similar manner the self-inductances of phase b and c can be written

$$L_{bb} = L_s + \Delta L_s \cos\left(2\theta + \frac{2\pi}{3}\right) \tag{1B}$$

$$L_{cc} = L_s + \Delta L_s \cos\left(2\theta - \frac{2\pi}{3}\right) \tag{1C}$$

When the direct axis of the rotor makes an angle of $-\pi/6$ radians with the axis of phase a as shown in Figure 2(A) the mutual inductance between phase a and phase b is a maximum. When the direct axis of the rotor makes an angle of $\pi/3$ radians with the axis of phase a the mutual inductance between phases a and b is a minimum. Thus the mutual inductance between phases a and b can be written

$$L_{ab} = L_m - \Delta L_m \cos\left(2\theta - \frac{2\pi}{3}\right) \tag{2A}$$

In a similar manner

$$L_{bc} = L_m - \Delta L_m \cos 2\theta \tag{2B}$$

$$L_{ca} = L_m - \Delta L_m \cos\left(2\theta + \frac{2\pi}{3}\right) \tag{2C}$$

Tests and calculations on synchronous machines show that the difference between the minimum and maximum self-inductance per phase is equal to the difference between minimum and maximum mutual inductance between phases. Or

$$\Delta L_s = \Delta L_m = \Delta L \tag{3}$$

In the ideal machine with sinusoidally distributed phase windings this is exactly true. Using these inductance coefficients the flux linkages with phases a, b, and c, resulting from the flow of armature currents alone are

$$\psi_{a1} = L_{aa}i_a - L_{ab}i_b - L_{ac}i_c \tag{4A}$$

$$\psi_{b1} = -L_{ba}i_a + L_{bb}i_b - L_{bc}i_c \tag{4B}$$

$$\psi_{c1} = -L_{ca}i_a - L_{cb}i_b + L_{cc}i_c \tag{4C}$$

These flux linkage equations can be written in terms of the direct axis, quadrature axis and zero sequence inductances per phase all of which are also directly measurable from the armature terminals. It is preferable to use these inductances since these are the ones most generally used and recognized by design and application engineers. Consequently, the flux linkages with phase a resulting from the flow of phase currents are as follows

$$\psi_{a1} = \frac{2}{3}\left[\frac{L_d + L_q}{2}\right]\left(i_a - \frac{i_b + i_c}{2}\right) + \frac{2}{3}\left[\frac{L_d - L_q}{2}\right]\left[i_a \cos 2\theta + i_b \cos\left(2\theta - \frac{2\pi}{3}\right) + i_c \cos\left(2\theta + \frac{2\pi}{3}\right)\right] + \frac{1}{3}L_0(i_a + i_b + i_c) \tag{5}$$

where

$$L_d = \left[L_s + L_m + \frac{3}{2}\Delta L\right] \tag{6}$$

$$L_q = \left[L_s + L_m - \frac{3}{2}\Delta L\right] \tag{7}$$

Paper 50-38, recommended by the AIEE Rotating Machinery Committee and approved by the AIEE Technical Program Committee for presentation at the AIEE Winter General Meeting, New York, N. Y., January 30-February 3, 1950. Manuscript submitted October 21, 1949; made available for printing November 30, 1949.

H. S. KIRSCHBAUM is Assistant Professor of Electrical Engineering with the Ohio State University, Columbus, Ohio.

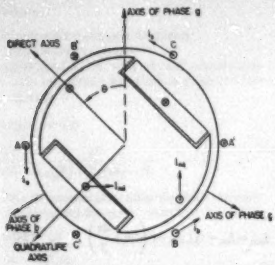

Figure 1. Ideal synchronous machine showing assumed positive directions of currents in the various windings

$$L_b = L_a - 2L_m \tag{8}$$

The flux linkages with phase b also can be written from equation 5 by advancing the subscripts of all currents by one phase letter and using for θ, the angle between the direct axis of the rotor and the axis of phase b. In a similar manner the flux linkages for phase c can be written.

In addition to the flux linkages with the stator phases resulting from the flow of stator currents, there are flux linkages with the stator phases because of the presence of rotor currents.

From Figure 1, it is obvious that these are, for phase a

$$\psi_{ra} = [L_{afa}I_{fa} + L_{a1d}I_{1d} + \ldots + L_{and}I_{nd} + \ldots] \cos\theta - [L_{a1q}I_{1q} + L_{anq}I_{nq} + \ldots] \sin\theta \tag{9}$$

Those for phases b and c are readily derivable. Since the maximum mutual inductances between a given rotor circuit and any of the stator phases are numerically equal, the flux linkages with phase b due to the presence of rotor currents can be written from equation 9 by using for θ, the angle between phase b and the direct axis of the rotor. Similarly for phase c. The total flux linkages with phase a due to both rotor and stator currents will be given by the sum of equations 5 and 9.

The flux linkages with the rotor windings on the direct and quadrature axes are as follows

$$\Psi_{fd} = L_{ffd}I_{fd} + L_{f1d}I_{1d} + \ldots + L_{fnd}I_{nd} + \ldots + L_{fad}\left[i_a \cos\theta + i_b \cos\left(\theta - \frac{2\pi}{3}\right) + i_c \cos\left(\theta + \frac{2\pi}{3}\right)\right] \tag{10}$$

$$\Psi_{nd} = L_{nfd}I_{fd} + L_{n1d}I_{1d} + \ldots + L_{nnd}I_{nd} + \ldots + L_{nad}\left[i_a \cos\theta + i_b \cos\left(\theta - \frac{2\pi}{3}\right) + i_c \cos\left(\theta + \frac{2\pi}{3}\right)\right] \tag{11}$$

$$\Psi_{nq} = L_{n1q}I_{1q} + L_{n2q}I_{2q} + \ldots + L_{nnq}I_{nq} + \ldots - L_{naq}\left[i_a \sin\theta + i_b \sin\left(\theta - \frac{2\pi}{3}\right) + i_c \sin\left(\theta + \frac{2\pi}{3}\right)\right] \tag{12}$$

Transformation to Direct and Quadrature Axis Quantities

It is possible by means of a suitable transformation to replace the actual system of stator currents and flux linkages by an equivalent system which when viewed from the rotor appears identical to the actual system. This transformation, which is well known, will be written as follows

$$\psi_d = A\left[\psi_a \cos\theta + \psi_b \cos\left(\theta - \frac{2\pi}{3}\right) + \psi_c \cos\left(\theta + \frac{2\pi}{3}\right)\right] \tag{13}$$

$$\psi_q = -A\left[\psi_a \sin\theta + \psi_b \sin\left(\theta - \frac{2\pi}{3}\right) + \psi_c \sin\left(\theta + \frac{2\pi}{3}\right)\right] \tag{14}$$

$$i_d = B\left[i_a \cos\theta + i_b \cos\left(\theta - \frac{2\pi}{3}\right) + i_c \cos\left(\theta + \frac{2\pi}{3}\right)\right] \tag{15}$$

$$i_q = -B\left[i_a \sin\theta + i_b \sin\left(\theta - \frac{2\pi}{3}\right) + i_c \sin\left(\theta + \frac{2\pi}{3}\right)\right] \tag{16}$$

Using this transformation in conjunction with the equations for stator and rotor flux linkages, it is possible to write the linkage equations for the direct and quadrature axis circuits. They will be written for only the direct axis since those for the quadrature axis are similar.

$$\Psi_{fd} = [L_{ffd}I_{fd} + L_{f1d}I_{1d} + \ldots + L_{fnd}I_{nd} + \ldots] + \frac{1}{B} L_{fad} i_d \tag{17}$$

$$_{nd} = [L_{nfd}I_{fd} + L_{n1d}I_{1d} + \ldots + L_{nnd}I_{nd} + \ldots] + \frac{1}{B} L_{nad} i_d \tag{18}$$

$$\psi_d = \frac{3}{2} A\,[L_{afd}I_{fd} + L_{a1d}I_{1d} + \ldots + L_{and}I_{nd} + \ldots] + \frac{A}{B} L_a i_d \tag{19}$$

Examination of equations 17 to 19 will show that the product of A and B must equal two-thirds in order that the reciprocity of mutuals be maintained. This follows from the fact that L_{nad} equals L_{nad}.

If A is set equal to two-thirds, then B must equal unity. Physically this may be interpreted with the aid of Figure 3. From the point of view of an observer on the rotor, the current distribution along the periphery of the stator, resulting from the flow of i_a, i_b, and i_c in phases a, b, and c respectively, has been replaced by an identical current distribution resulting from the flow of i_d and i_q in two sinusoidally distributed windings having N turns each. The winding carrying i_d has its axis coincident with the direct axis of the rotor and the winding carrying i_q has its axis coincident with the quadrature axis of the rotor. As each of these equivalent coils has the same number of turns as any of the actual stator phases, the mutual inductance between any rotor circuit on the direct axis and the equivalent direct axis stator circuit will be equal to the maximum mutual inductance between said rotor circuit and a stator phase. This also holds true for the quadrature axis.

With A and B equal to two-thirds and unity respectively the stator and rotor linkages on the direct axis are

$$\Psi_{fd} = L_{ffd}I_{fd} + L_{f1d}I_{1d} + \ldots + L_{fnd}I_{nd} + \ldots + L_{fad}i_d \tag{20}$$

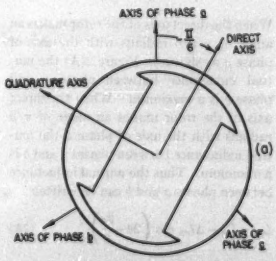

Figure 2(A). Position of rotor for maximum mutual inductance between phases a and b

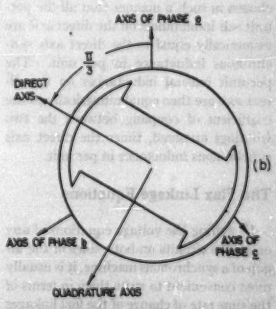

Figure 2(B). Position of rotor for minimum mutual inductance between phases a and b

$$\Psi_{nd}=L_{nfd}I_{fd}+L_{n1d}I_{1d}+\ldots+L_{nnd}I_{nd}+\ldots+L_{nsd}i_d \quad (21)$$

$$\psi_d=L_{afd}I_{fd}+L_{a1d}I_{1d}+\ldots+L_{and}I_{nd}+\ldots+\frac{2}{3}L_d i_d \quad (22)$$

All mutuals are thus reciprocal and the quantity $(2/3)L_d$ is the self-inductance of the equivalent direct axis coil. It can be shown that the average self-inductance per phase, L_s is equal to twice the average mutual between phases plus the slot leakage inductance per phase, or

$$L_s=2L_m+L_l \quad (23)$$

Consequently

$$\frac{2}{3}L_d=(L_s+\Delta L)-\frac{1}{3}L_l \quad (24)$$

The self-inductance of the equivalent direct axis stator coil is less than the maximum self-inductance per phase by one-third the slot leakage per phase. This is as it should be since the equivalent windings would be wound 2/3 as many slots each having 3/2 the width of the old ones.

By means of the transformation embodied in equations 13 to 16 the synchronous machine has been replaced by two n-winding transformers, one on the direct axis and one on the quadrature axis. Equations 20 to 22 are independent of θ.

Per-Unit Linkage Equations

Equations 20 to 22 express the linkages per circuit in terms of actual currents and inductance coefficients. This section will describe a transformation to per-unit linkages in terms of per-unit currents and inductances which preserves the reciprocity of the mutual inductances. For all direct axis circuits this transformation results in per-unit self-inductances which are equal to L_d in per unit and in per-unit mutuals which are equal to the coefficient of coupling between the two circuits concerned times L_d in per unit. Similar results can be obtained for the quadrature axis.

Let unit stator phase current and phase voltage be denoted as follows

$$i_{ao}=\sqrt{2}I_{\text{(rated per phase)}} \quad (25)$$

$$e_{ao}=\sqrt{2}E_{\text{(rated per phase)}} \quad (26)$$

Then unit current and voltage for the equivalent direct axis stator coil will be

$$i_{do}=\frac{3}{2}i_{ao} \quad (27)$$

$$e_{do}=e_{ao} \quad (28)$$

One unit of phase reactance will be equal to the ratio of unit phase voltage to phase current

$$x_{ao}=\frac{e_{ao}}{i_{ao}}\omega_o L_{ao} \quad (29)$$

This defines unit phase inductance as the ratio of unit phase reactance to unit stator angular frequency (rated angular frequency).

As a consequence unit phase and equivalent direct axis stator flux linkages are as follows

$$\psi_{ao}=i_{ao}L_{ao} \quad (30)$$

$$\psi_{do}=\psi_{ao}=i_{do}L_{do} \quad (31)$$

Unit inductance for the equivalent direct axis coil then will be

$$L_{do}=\frac{2}{3}L_{ao} \quad (32)$$

These unit quantities are fixed entirely by the machine kilovolt-amperes, voltage and frequency rating. They are not subject to arbitrary choice. However, this does not apply to the rotor circuits. As these circuits generally have no ratings affixed to them (if they do the ratings are fixed by circumstances other than those being considered here), it has been customary to arbitrarily assign unit quantities for rotor currents and flux linkages. In many cases the arbitrary choice results in nonreciprocal mutual inductances. By choosing the following rotor unit quantities, the per-unit mutual inductances will be reciprocal

$$I_{fdo}=\sqrt{\frac{\frac{2}{3}L_d}{L_{ffd}}}\,i_{do} \text{ or } i_{do}=I_{fdo}\sqrt{\frac{L_{ffd}}{\frac{2}{3}L_d}} \quad (33)$$

$$I_{ndo}=\sqrt{\frac{\frac{2}{3}L_d}{L_{nnd}}}\,i_{do} \text{ or } i_{do}=I_{ndo}\sqrt{\frac{L_{nnd}}{\frac{3}{2}L_d}} \quad (34)$$

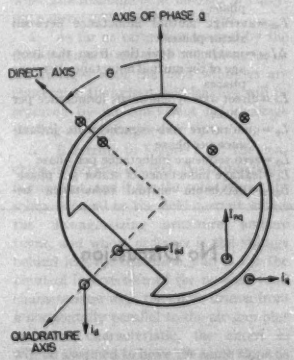

Figure 3. Equivalent synchronous machine showing assumed positive directions of currents in the various windings

$$\Psi_{fdo}=\sqrt{\frac{L_{ffd}}{\frac{2}{3}L_d}} \quad \psi_{do}=\left[i_{do}\sqrt{\frac{L_{ffd}}{\frac{2}{3}L_d}}\right]i_{do} \quad (35)$$

$$\Psi_{ndo}=\sqrt{\frac{L_{nnd}}{\frac{2}{3}L_d}} \quad \psi_{do}=\left[L_{do}\sqrt{\frac{L_{nnd}}{\frac{2}{3}L_d}}\right]i_{do} \quad (36)$$

Unit flux linkages with all direct axis circuits then can be written in terms of unit current in any of the direct axis circuits.

$$\Psi_{fdo}=\left[L_{do}\frac{\sqrt{L_{ffd}\frac{2}{3}L_d}}{\frac{2}{3}L_d}\right]i_{do}=\left[L_{do}\frac{L_{ffd}}{\frac{2}{3}L_d}\right]I_{fdo}=\ldots=\left[L_{do}\frac{\sqrt{L_{ffd}L_{nnd}}}{\frac{2}{3}L_d}\right]I_{nnd} \quad (37)$$

$$\Psi_{ndo}=\left[L_{do}\frac{\sqrt{L_{nnd}\frac{2}{3}L_d}}{\frac{2}{3}L_d}\right]i_{do}=\left[L_{do}\frac{\sqrt{L_{nnd}L_{ffd}}}{\frac{3}{2}L_d}\right]I_{fdo}=\ldots=\left[L_{do}\frac{L_{nnd}}{\frac{3}{2}L_d}\right]I_{ndo} \quad (38)$$

$$\psi_{do}=L_{do}i_{do}=\left[L_{do}\frac{\sqrt{L_{ffd}\frac{2}{3}L_d}}{\frac{2}{3}L_d}\right]I_{fdo}=\ldots=\left[L_{do}\frac{\sqrt{L_{nnd}\frac{2}{3}L_d}}{\frac{2}{3}L_d}\right]I_{ndo} \quad (39)$$

If equations 20 to 22 are divided by equations 37 to 39 the resulting equations will be per-unit flux linkage equations for the direct axis circuits.

A prime ′ will be used to denote quantities representing per-unit quantities.

$$\Psi_{fd}'=\left[\frac{\frac{2}{3}L_d}{L_{do}}\right]I_{fd}'+\left[\frac{\frac{2}{3}L_aL_{fnd}}{L_{do}\sqrt{L_{ffd}L_{nnd}}}\right]\times I_{1d}'+\ldots+\left[\frac{\frac{2}{3}L_aL_{fnd}}{L_{do}\sqrt{L_{ffd}L_{nnd}}}\right]I_{nd}'+\ldots+\left[\frac{\frac{2}{3}L_aL_{fnd}}{L_{do}\sqrt{L_{ffd}\frac{2}{3}L_d}}\right]i_d' \quad (40)$$

$$\Psi_{nd}' = \left[\frac{\frac{2}{3} L_d L_{afd}}{L_{do}\sqrt{L_{nnd} L_{ffd}}}\right] I_{fd}' + \left[\frac{\frac{2}{3} L_d L_{nid}}{L_{do}\sqrt{L_{nnd} L_{iid}}}\right] I_{id}' + \ldots + \left[\frac{\frac{2}{3} L_d}{L_{do}}\right] I_{nd}' \ldots + \left[\frac{\frac{2}{3} L_d L_{aod}}{L_{do}\sqrt{L_{nnd}\frac{2}{3} L_d}}\right] i_a' \quad (41)$$

$$\Psi_d' = \left[\frac{\frac{2}{3} L_d L_{afd}}{L_{do}\sqrt{L_{ffd}\frac{2}{3} L_d}}\right] I_{fd}' + \left[\frac{\frac{2}{3} L_d L_{aid}}{L_{do}\sqrt{L_{iid}\frac{2}{3} L_d}}\right] I_{id}' + \ldots + \left[\frac{\frac{2}{3} L_d L_{and}}{L_{do}\sqrt{L_{nnd}\frac{2}{3} L_d}}\right] I_{nd}' \ldots + \left[\frac{\frac{2}{3} L_d}{L_{do}}\right] i_d' \quad (42)$$

These equations for the per-unit direct axis flux linkages can be rewritten making use of the following identities

$$\left[\frac{\frac{2}{3} L_d}{L_{do}}\right] = L_d' \quad (43)$$

$$\left[\frac{L_{fnd}}{\sqrt{L_{ffd} L_{nnd}}}\right] = k_{fnd} \quad (44)$$

Equation 43 is recognizable as the definition of the per-unit direct axis synchronous inductance per phase, while equation 44 is the definition of the coefficient of coupling between two of the circuits on the direct axis of the machine.

$$\Psi_{fd}' = L_d' I_{fd}' + k_{fnd} L_d' I_{nd}' + \ldots + k_{fid} L_d' i_d' \quad (45)$$

$$\Psi_{nd}' = k_{nfd} L_d' I_{fd}' + k_{nid} L_d' I_{id}' + \ldots + L_d' I_{nd}' + \ldots + k_{and} L_d' i_d' \quad (46)$$

$$\psi_d' = k_{afd} L_d' I_{fd}' + k_{aid} L_d' I_{id}' + \ldots + k_{and} L_d' I_{nd}' + \ldots + L_d' i_d' \quad (47)$$

Similar expressions for the quadrature axis can be obtained by replacing the subscript d in equations 46 and 47 by the subscript q.

Conclusions

This paper has presented a consistent treatment of per-unit inductance coefficients for synchronous machines. These expressions are derived from similar expressions employing actual units. By choosing base rotor current and flux linkages for any rotor circuit in such a manner that base stored energy for all circuits on the direct axis is the same, the resulting per unit inductances are mutually reciprocal. In particular the choices embodied in equations 33 to 36 result in the very simple expressions of equations 45 to 47. In spite of their simplicity there are still considerable calculations involved in arriving at the coefficients of coupling.

Therefore this is not to be interpreted as a proposal to adopt the aforementioned system, since its implications will have to be explored further in its application to machine transients.

Appendix I. Nomenclature

All quantities in the paper are in actual amperes, henrys, weber turns, and so forth. A prime ′ is used to denote per-unit quantities.

L_{aa}, L_{bb}, L_{cc} = self-inductances of the stator phase circuits

L_{ab}, L_{bc}, L_{ca} = mutual inductances between stator phases

L_s = average stator phase self-inductance

ΔL_s = maximum deviation from the average of the self-inductance of a stator phase

L_m = average mutual inductance between stator phases

ΔL_m = maximum deviation from the average of the mutual inductance between phases

L_d = direct axis synchronous inductance per phase

L_q = quadrature axis synchronous inductance per phase

L_0 = zero sequence inductance per phase

L_l = leakage inductance of stator per phase

L_{and} = maximum mutual inductance between a stator phase and any rotor circuit on the direct axis

L_{anq} = maximum mutual inductance between a stator phase and any rotor circuit on the quadrature axis

L_{nnd}, L_{nnq} = self-inductances of any direct and quadrature axis rotor circuits respectively

L_{nmd}, L_{nmq} = mutual inductances between any two direct or quadrature axis rotor circuits respectively

L_{ao} = unit stator inductance per phase

L_{do} = unit stator inductance of direct axis circuit

k_{and} = coefficient of coupling between any direct axis rotor circuit and the equivalent direct axis stator circuit

k_{nmd} = coefficient of coupling between any two direct axis rotor circuits

i_a, i_b, i_c = stator phase currents

i_d, i_q = stator direct and quadrature axis currents respectively

L_{ffd}, L_{fad} = self inductance of field, mutual inductance between field and armature

I_{nd}, I_{nq} = rotor currents in any direct or quadrature axis rotor circuits respectively

i_{ao} = unit stator phase current

e_{ao} = unit stator phase voltage

i_{do} = unit stator direct axis current

e_{do} = unit stator direct axis voltage

I_{ndo} = unit rotor circuit current on the direct axis

ψ_{a1} = phase flux linkages due to stator currents alone

ψ_{a2} = phase flux linkages due to rotor currents alone

Ψ_{nd}, Ψ_{nq} = rotor flux linkages with any direct or quadrature axis rotor circuit respectively

ψ_d, ψ_q = stator flux linkages with equivalent direct and quadrature axis coils respectively

ψ_{ao} = unit phase flux linkages

ψ_{do} = unit direct axis stator flux linkages

Ψ_{ndo} = unit flux linkages for any rotor circuit on the direct axis

References

1. Per-Unit Impedances of Synchronous Machines, **A. W. Rankin.** *Electrical Engineering* (*AIEE Transactions*), volume 64, August 1945, pages 569–73.

2. Per-Unit Impedances of Synchronous Machines, Part II, **A. W. Rankin.** *Electrical Engineering* (*AIEE Transactions*), volume 64, December 1945, pages 839–41.

3. Two Reaction Theory of Synchronous Machines, **R. H. Park.** *AIEE Transactions*, volume 48, July section, 1929, pages 716–30.

4. Definition of an Ideal Synchronous Machine, **R. H. Park.** *General Electric Review* (Schenectady, N. Y.), volume 31, 1928, page 332.

No Discussion

Potier Reactance for Salient-Pole Synchronous Machines

SAAD L. MIKHAIL
ASSOCIATE AIEE

IN 1900, Potier presented an interesting paper,[1] in which he explained that the zero power-factor characteristic is displaced from the no-load characteristic vertically by an amount equal to λi and horizontally by an amount equal to αi, where i is the armature current, α is a coefficient of equivalence between the armature and field ampere turns, and where λ is a coefficient dependent on magnetic leakages. It is this λ that is known as Potier reactance and is determined by using the no-load magnetization curve and the zero power-factor (over-excited) magnetization curve.[2,3,4]

Potier reactance is easy to determine experimentally, it is useful in calculating the excitation required under load, and a thorough understanding of its nature is helpful in the analysis of the saturated synchronous machine, not only under steady-state conditions,[5,10] but also under transient conditions.[6,7]

Although Potier only said that the coefficient λ is dependent on magnetic leakages, it was recognized that Potier reactance is greater than the armature leakage reactance by an amount due to the change of field-leakage under direct-axis steady-state conditions. The change of field-leakage under direct-axis loading has been treated in previous articles.[3,4,6,9,10] Since it also is known that the direct-axis transient reactance is greater than the armature leakage reactance by an amount dependent upon the field-leakage,[11,12] it was natural to try to correlate Potier reactance, direct-axis transient reactance, and armature leakage reactance. Only empirical formulas for this correlation exist.[5,8] It is the object of this paper, to present a systematic treatment of the change of field-leakage under a direct-axis steady-state load, and to derive an expression for Potier reactance which is valid under certain assumptions and which can be obtained from design data. Since field-leakage in nonsalient-pole machines is generally small, the treatment is confined to salient-pole machines.

The per-unit system will be used and the following assumptions will be made:

Assumptions

1. The effect of the change of waveform of the flux due to a direct-axis load on the excitation requirement will be neglected.
2. The flux in the air-gap will be assumed the same as that effective in producing saturation in the armature.
3. The effect of saturation of the pole tips on the field-leakage will be neglected when the machine is at no-load or carrying a direct-axis steady-state load.
4. As far as saturation caused by the field-leakage in the pole body or as far as its linkages with the field windings are concerned, the actual field-leakage will be replaced by an equivalent field-leakage passing only between pole tips.
5. Referring to Figure 5, if the machine is carrying a direct-axis demagnetizing current, and if k is the point whose abscissa is equal to the field current minus the demagnetizing armature ampere turns, and whose ordinate is the voltage behind leakage reactance, and if s is the point of intersection of the no-load total characteristic with the curve drawn from k horizontally parallel to the air-gap plus armature characteristic, the chord ks will be assumed to have the same slope as the air-gap plus armature characteristic at the voltage behind Potier reactance. Also the no-load total characteristic will be assumed a straight line between s and the voltage behind Potier reactance.

The Magnetic Circuit of the Machine At No-Load

According to assumptions 2, 3, and 4, the magnetic circuit of the machine at no-load can be represented by the circuit of Figure 1, where:

ϕ_a = flux in the air-gap and the armature
R_a = reluctance of the air-gap and armature; its value varies with saturation
ϕ_l = equivalent leakage flux between pole tips
R_l = equivalent reluctance between pole tips and its value is assumed to be constant
ϕ_p = sum of the armature flux and the equivalent field-leakage flux, and will be called the equivalent pole flux or simply the pole flux
R_p = reluctance of the pole and its value varies with saturation

Equivalent Circuit Under Transient Conditions

For an unsaturated synchronous machine under direct-axis transient conditions, it has been shown[11,12] that the circuit of Figure 2, is a possible equivalent circuit where:

X_l = armature leakage reactance
X_{ad} = unsaturated direct-axis armature reaction reactance
X_f = field leakage reactance
X_f = field leakage when a current equal to $1X_{ad}$ flows in the field

Hence

$$X_f = \frac{X_{ad}}{R_l} \tag{1}$$

The unsaturated direct-axis synchronous reactance X_d' is the reactance between the two terminals a and b, when terminals c and d are short circuited, that is

Paper 50-39, recommended by the AIEE Rotating Machinery Committee and approved by the AIEE Technical Program Committee for presentation at the AIEE Winter General Meeting, New York, N. Y., January 30-February 3, 1950. Manuscript submitted October 20, 1949; made available for printing December 7, 1949.

SAAD L. MIKHAIL is Assistant Lecturer with Farouk 1 University, Alexandria, Egypt, and now is doing postgraduate work at Harvard University, Cambridge, Mass.

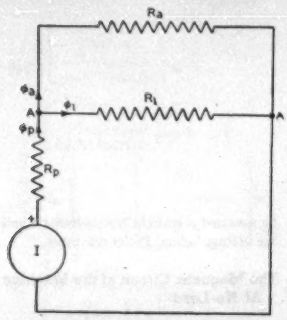

Figure 1. Representation of the magnetic circuit of the synchronous machine at no-load

$$X_d' = X_l + \frac{X_{ad}X_f}{X_{ad}+X_f} \tag{2}$$

or

$$X_f = \frac{X_{ad}(X_d'-X_l)}{X_{ad}-(X_d'-X_l)} \tag{3}$$

No-Load Relations

If M_{AA} is the magnetic potential across the air-gap and the armature, and if the subscript "o" indicates no-load conditions corresponding to a flux ϕ_a in the armature, the following relations become evident from Figure 1

$$M_{AA_o} = \phi_a R_a \tag{4}$$

Hence the no-load field-leakage is given by

$$\phi_{l_o} = \frac{M_{AA_o}}{R_l} = \frac{\phi_a R_a}{R_l} \tag{5}$$

And the pole flux is given by

$$\phi_{p_o} = \phi_a + \phi_{l_o} \tag{6}$$

And the no-load field current is given by

$$I_o = \phi_a R_a + \phi_{p_o} R_p \tag{7}$$

Direct-Axis Demagnetizing Load

When the armature is carrying a steady-state direct-axis demagnetizing current i, and when the armature flux is the same as at no-load, equal to ϕ_a, the main magnetic circuit of the machine can be represented by the circuit of Figure 3, where iX_{ad} is the counter ampere-turns of the armature.

From Figure 3, the following relations can be derived

$$M_{AA} = iX_{ad} + \phi_a R_a \tag{8}$$

The field-leakage is thus given by

$$\phi_l = \frac{M_{AA}}{R_l} = \frac{iX_{ad}}{R_l} + \frac{\phi_a R_a}{R_l} \tag{9}$$

Substituting equations 1 and 5 in equation 9, there is

$$\phi_l = iX_f + \phi_{l_o} \tag{10}$$

Also the pole flux is given by

$$\phi_p = \phi_a + \phi_l = \phi_a + \phi_{l_o} + iX_f \tag{11}$$

Substituting equation 6 in equation 11, there is

$$\phi_p = \phi_{p_o} + iX_f \tag{12}$$

Applying Kirchoff's second law to the outer circuit of Figure 3, there is

$$I - iX_{ad} = \phi_a R_a + \phi_p R_p \tag{13}$$

where I is the field current under load.

Substituting equation 12 in equation 13, there is

$$\begin{aligned} I - iX_{ad} &= \phi_a R_a + (\phi_{p_o} + iX_f)R_p \\ &= (\phi_a R_a + \phi_{p_o} R_p) + iX_f R_p \end{aligned} \tag{14}$$

Substituting equation 7 in equation 14, there is

$$I - iX_{ad} = I_o + iX_f R_p \tag{15}$$

Referring to Figure 4(A), e_t is the terminal voltage, $e_i = \phi_a$ is the flux in the armature or the voltage behind leakage reactance, $hj = I_o$. If to hj is added $iX_f R_p$ and iX_{ad}, the result will be equal to the necessary excitation under load. In Figure 4(B) is shown the magnetization curve of the poles alone, $0_1m = \phi_a$, ml is taken equal to ϕ_{l_o}, thus n represents the no-load saturation of the poles corresponding to an armature flux of ϕ_a. If lq is taken equal to iX_f, then np' represents $iX_f R_p$. Hence, taking $jk = np'$, then $kr = iX_{ad}$ thus $hr = 0r_1$ will represent the field current under the considered load, and r_2 whose abscissa is equal to $0r_1$ and whose ordinate is equal to e_t, will represent a point on the zero power-factor (over-excited) characteristic. $0ut$ is the magnetization curve of air-gap plus armature, the curve ks is drawn from k horizontally parallel to $0ut$, till it intersects the no-load characteristic in s. s has an ordinate $= e_i + ss'$ where

$$ss' = iX_{f_1} \tag{16}$$

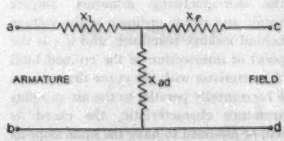

Figure 2. An equivalent circuit of the unsaturated synchronous machine under direct-axis transient conditions

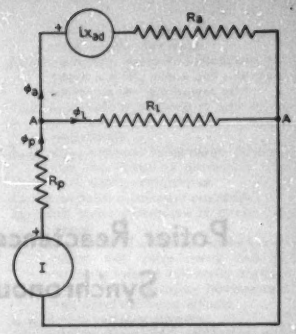

Figure 3. Representation of the main magnetic circuit of the synchronous machine under direct-axis demagnetizing steady-state load

The foregoing equation is the defining relation for X_{f_1}, which now will be evaluated

$uj = ls$ and $np' = jk$

Hence

$uk = ts = qp$

Since $st = qp$, hence when the machine is operating at no-load, s must represent a point where the flux in the poles is equal to

$$\phi_a + \phi_{l_o} + iX_f \tag{17}$$

The flux in the armature at point s is equal to

$$0f = \phi_a + iX_{f_1} \tag{18}$$

And the equivalent field-leakage is equal to

$$\begin{aligned} \frac{tf}{R_l} &= \frac{uk + s'k}{R_l} \\ &= \phi_{l_o} + \frac{\alpha}{R_l} iX_{f_1} \end{aligned} \tag{19}$$

Where α is the reciprocal of the slope of the air-gap plus armature characteristic at the voltage behind Potier reactance, which is taken equal to the reciprocal of the slope of the chord ks by assumption 5.

Substituting equation 1 in equation 19, the equivalent field-leakage at point s is equal to

$$\phi_{l_o} + \frac{\alpha}{X_{ad}} X_f iX_{f_1} \tag{20}$$

Adding equations 18 and 20, the pole flux at point s is equal to

$$\phi_a + \phi_{l_o} + \left(1 + \frac{\alpha X_f}{X_{ad}}\right) iX_{f_1} \tag{21}$$

Equating equations 17 and 21, there is

$$X_{f_1} = \frac{X_f}{1+\alpha X_f/X_{ad}} \tag{22}$$

or

$$\frac{1}{X_{f_1}} = \frac{1}{X_f} + \frac{1}{X_{ad}/\alpha} \tag{23}$$

Potier Reactance

Referring to Figure 5, Potier reactance is determined[2,3,4] by taking $r_2a = iX_d$, where X_d is the unsaturated direct-axis synchronous reactance, then drawing ac parallel to the air-gap line, till it intersects the no-load characteristic in c, then if X_p is the Potier reactance, there is

$$cc_1 = iX_p \tag{24}$$

It is obvious that ac passes by k and that

$$c_1c_2 = iX_l \tag{25}$$

It remains then to determine

$$cc_1 = iX_{fp} \tag{26}$$

Referring to assumption 5, and letting β be the reciprocal of the slope of the no-load total characteristic at the voltage behind Potier reactance, there is

$$ks' = kc_1 + c_1s' \tag{27}$$

or

$$\alpha i X_{f_1} = iX_{fp} + \beta(X_{f_1} - X_{fp})i \tag{28}$$

Thus

$$X_{fp} = \frac{\alpha-\beta}{1-\beta} X_{f_1} \tag{29}$$

From equations 22 and 29, there is

$$X_{fp} = \frac{\alpha-\beta}{1-\beta}\frac{X_f}{1+\alpha X_f/X_{ad}} \tag{30}$$

Substituting equation 3 in equation 30, there is

$$X_{fp} = \frac{\alpha-\beta}{1-\beta} \times \frac{X_{ad}(X_d'-X_l)/[X_{ad}-(X_d'-X_l)]}{1+\alpha(X_d'-X_l)/[X_{ad}-(X_d'-X_l)]} \tag{31}$$

Potier reactance is given by

$$X_p = X_l + X_{fp} \tag{32}$$

Substituting equation 31 in equation 32, there is

$$X_p = X_l + \frac{\alpha-\beta}{1-\beta} \times \frac{X_{ad}(X_d'-X_l)/[X_{ad}-(X_d'-X_l)]}{1+\alpha(X_d'-X_l)/[X_{ad}-(X_d'-X_l)]} \tag{33}$$

Equation 33 gives an expression that enables the calculation of Potier reactance from design data. All the quantities involved can be determined from design data.[13]

If all the saturation is in the poles, $\alpha = 1$ and thus $X_p = X_d'$. If all the saturation is in the armature, $\alpha = \beta$ and thus $X_p = X_l$.

It is obvious that the above equation, gives the variation of Potier reactance with the voltage behind Potier reactance. If its variation with the terminal voltage is required, it can be obtained afterwards by reducing the voltage co-ordinate of every point by an amount equal to iX_p, where X_p is the value of Potier reactance at the point considered.

Nomenclature

All quantities are in per-unit

X_d = unsaturated direct-axis synchronous reactance
X_{ad} = unsaturated direct-axis armature reaction reactance
X_l = armature leakage reactance
X_d' = unsaturated direct-axis transient reactance
X_f = field leakage reactance
X_{fp} = excess of Potier reactance over armature leakage reactance
X_p = potier reactance
X_{f_1} = defined by equation 16 and Figure 4
ϕ_a = flux in the air-gap and armature
ϕ_l = equivalent field-leakage flux
ϕ_p = equivalent pole flux
R_a = reluctance of air-gap and armature
R_l = equivalent reluctance of field leakage path between pole tips
R_p = reluctance of pole body
M_{AA} = magnetic potential across air-gap and armature
I = field current
i = armature current
e_t = terminal voltage
e_l = voltage behind leakage reactance
e_p = voltage behind Potier reactance
α = reciprocal of the slope of the air-gap plus armature magnetization curve at the voltage behind Potier reactance
β = reciprocal of the slope of the no-load total magnetization curve at the voltage behind Potier reactance
o = as a subscript indicates no-load conditions corresponding to a flux of ϕ_a in the armature

References

1. Armature Reaction of Alternators, A. Potier. *L'Eclairage Electrique* (Paris, France), volume 24, 1900, pages 139–41.

2. Test Code of Synchronous Machines. AIEE Standard Number 503, June 1945.

3. Approximating Potier Reactance, Sterling Beckwith. *Electrical Engineering* (*AIEE Transactions*), volume 56, July 1937, pages 813–18.

4. Armature Leakage Reactance of Synchronous Machines, L. A. March, S. B. Crary. *Electrical Engineering* (*AIEE Transactions*), volume 54, April 1935, pages 378–81.

5. Discussion of reference 4, L. A. Kilgore. *AIEE Transactions*, volume 54, 1935, pages 1117–18.

6. Saturated Synchronous Machines Under Transient Conditions in the Pole Axis, Reinhold Rüdenberg. *Electrical Engineering* (*AIEE Transactions*), volume 61, June 1942, pages 297–306.

7. Damper Circuits and Rotor Leakage in the Transient Performance of Saturated Synchronous Machines, R. Rüdenberg. *Journal*, Franklin Institute (Philadelphia, Pa.), volume 234, 1942, pages 40–61.

8. Voltage Drop in Polyphase Generators, J. Sumec. *Elektrotechnische Zeitschrift* (Berlin, Germany), volume 32, 1911, pages 77–80.

9. The Saturated Synchronous Machine, B. L. Robertson, T. A. Rogers, C. F. Dalziel

Figure 4 (below). Magnetomotive force and flux relations under direct-axis demagnetizing steady-state load

Figure 5 (right). Derivation of Potier reactance

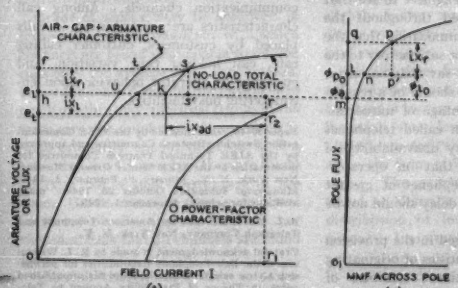

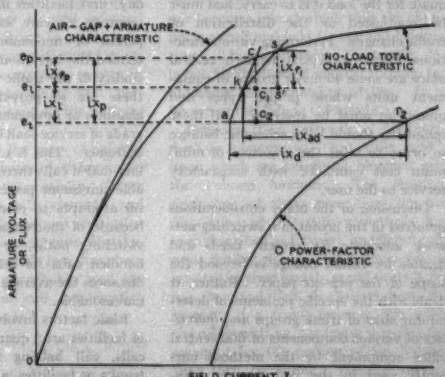

Electrical Engineering (*AIEE Transactions*), volume 56, July 1937, pages 858–63.

10. Correction for Saturation, **Thomas C. McFarland.** *Electrical Engineering* (*AIEE Transactions*), volume 61, May 1942, pages 233–35.

11. Reactances of Synchronous Machines, **R. H. Park, B. L. Robertson.** *AIEE Transactions*, volume 47, 1928, pages 514–35.

12. Synchronous Machines, Part III, Torque Angle Characteristics under Transient Conditions, **R. E. Doherty, C. A. Nickle.** *AIEE Transactions*, volume 46, 1927, pages 1–4.

13. Calculation of Synchronous Machine Constants, **L. A. Kilgore.** *AIEE Transactions*, volume 50, 1931, pages 1201–13.

No Discussion

Basic Theory Underlying Bell System Facilities Capacity Tables

A. L. GRACEY
NONMEMBER AIEE

ONE OF the principal tasks of the telephone traffic engineer is to determine the quantities of telephone equipment required for adequately and economically handling the traffic offered by telephone users. It is a complex problem, involving forecasts of the volumes and distribution of traffic originating and terminating in each central office of an exchange area, and detailed consideration of each of the components of the various switching systems used in the central offices. For example, the 1,750,000 telephones in the combined Manhattan and Bronx Boroughs in New York are served by 125 central offices; these are interconnected, directly or via intermediate switching centers, by upwards of 9,000 groups of trunks, varying in size from one or two up to a hundred or more, and totaling nearly a quarter-million. Each group must be made adequate for the load it is to carry, and must be readjusted as the distribution of traffic changes. Performing various functions within a typical modern central office are some 40 major groups of equipment units whose proper types and quantities must be specified. All these quantities should be in economic balance in order to meet the objective of minimum cost combined with satisfactory service to the user.

Discussion of the many considerations involved in the layout of a switching network adequate for present needs and flexible for future change is beyond the scope of the present paper. Rather, it deals with the specific problems of determining sizes of trunk groups and quantities of various components of dial central office equipment by the methods currently used in the Bell System. Examples are given, with illustrative tables. Enough of the probability theory underlying the tables is given to bring out the assumptions made to fit or approximate the various service conditions.

Among the basic formulas used are: the binomial, Poisson, Erlang B and C, and Pollaczek-Crommelin. Their application to the principal types of facilities capacity tables in the Bell System is discussed in this paper.

Basic Factors of Telephone Traffic

The commodity with which the telephone business principally is concerned is the telephone call. Calls are made by individual customers as they fit into the living habits or into the conduct of the business of each. In a unit such as the central office, the aggregate of customers' calls follows a varying pattern throughout the day, and facilities must be sufficient in quantity to care satisfactorily for the period of maximum demand, usually termed the busy hour. It is the responsibility of the traffic engineer to see that these are so provided throughout the channels of intercommunication that the grade of service shall be satisfactory to the customer. This is to say that on customer-dialed calls there should be a reasonable minimum percentage of unsuccessful attempts to reach called telephones because of momentary unavailability of switching paths, or that on operator-handled calls for telephones at greater distances the average delay should not be unreasonable.

Basic factors involved in the provision of facilities are: quantities of originating calls, call holding times, numbers of trunks or facilities, and grade of service.

The product of the first two factors is "offered load." It denotes the amount of time that a quantity of calls desires the use of facilities and usually is expressed in terms of hundred call-seconds per hour (ccs) or call-minutes per hour (min.). In European practice a load which engages one trunk completely for an hour is known as an erlang. Since there are 36 hundred call-seconds in an hour, an erlang is equal to 36 ccs or 60 min. Load in erlangs, or average simultaneous offered calls, divided by the number of trunks provided is the trunk efficiency; this value multiplied by 100 is the per cent occupancy. For a predicted load submitted to a group of trunks an appropriate grade of service is selected, and from the proper capacity table the required number of trunks is found. Capacity tables relate the three variable factors of offered load, numbers of facilities, and grade of service; they represent, for a specified number of facilities and grade of service, the load in ccs that can be handled in the busy hour.

It has been found that the laws of probability can be adapted to express conveniently the relationship among the three factors. Based on these laws, there have been developed over the years, by many people, formulas which have proved satisfactory for the derivation of suitable capacity tables.

Formulas used comprehend the characteristics of telephone calls as well as the physical relationship of call sources and communication channels. Among call characteristics are: distribution of calls placed by customers, customer calling rate, call holding time variation, and customer or operator behavior upon encountering busy facilities.

Paper 50-40, recommended by the AIEE Communication Switching Systems Committee and approved by the AIEE Technical Program Committee for presentation at the AIEE Winter General Meeting, New York, N. Y., January 30–February 3, 1950. Manuscript submitted October 26, 1949; made available for printing December 1, 1949.

A. L. Gracey is with the American Telephone and Telegraph Company, New York, N. Y.

Grateful acknowledgment is made to R. I. Wilkinson of the Bell Telephone Laboratories for permission to use selected material from his unpublished notes on Theory of Probability Applied to Telephone Traffic Problems.

Basic Factor Characteristics

Quantities of calls are estimated from prediction of future customer station growth and calling rates. These predictions are influenced by historical data, by knowledge of changing character of the community, by planned changes in office boundaries, by assignment practices among the equipment units in a wire center, or by proposed rate changes.

Elapsed time during which a call occupies facilities is called the holding time. On a call between customers this consists principally of the conversation time plus relatively small intervals required by the equipment to make completion and for the called customer to answer. Holding times for local calls, those within a base rate exchange area, are found to vary according to an exponential law. This is discussed later under formulas. Intertoll calls, those over much longer distances and bearing toll charges, are influenced by other factors such as the length of connection, charge per call, and overtime rate. Their holding times do not appear to follow a simple exponential law.

Holding time of a sender (which stores customers' dial pulses), required only long enough to perform its function in advancing a call, is much shorter than for trunks. While the holding time varies somewhat between calls, the behavior is such that it often is considered constant in nature.

Numbers of trunks in the fixed relationship among the three basic factors of a capacity table vary depending upon the accessibility of trunks to call sources. Ideally, every call source would have complete access to every channel available for completing a call. Economic and physical considerations in the design of dial equipment are such that this is not always true. Any limitation of access adversely affects the relationship of the basic factors. Variations in this condition are illustrated later.

Grade of service may be described in terms either of the frequency with which channels are found unavailable to offered calls or of the average delay encountered. When the call is dialed by one customer to reach another over interlocal trunks in the same city, the trunks or other connecting links ordinarily are provided on such a basis that, on the average, they are found all busy but a small percentage of the time. Grade of service then is expressed in terms of the number of times per thousand calls that all channels are found busy.

Intertoll trunks, since they interconnect cities often widely separated, are more expensive than interlocal trunks and hence usually are provided on a less liberal basis. Grade of service therefore is expressed in terms of the average delay on all calls. This criterion implies that the call is operator-handled. If there is a short delay, the customer may be held at the telephone; if it proves too great, he may be allowed to hang up whereupon the operator follows the situation and secures a trunk as soon as one is available.

Principal Formulas and Illustrative Capacity Tables

General Assumptions in Regard to Offered Traffic

Obviously the distribution of calls placed by customers has an important bearing on the number of channels required for completion; that is, they might be placed at uniform intervals, spasmodically, or at random. It is customary to assume that each customer originates his calls quite at random during his idle time and independently of all other customers. Although this latter assumption is not strictly true, for example, when two customers are talking there is clearly a restriction on their ability to originate calls independently, in general the correlation appears to be neglectible. For periods as long as the busy hour the random placement of calls usually seems to be quite well realized.

Each customer over a long period of time originates the same total call-seconds of load as every other customer; in other words, p, the probability that at any random moment any particular customer will be using his telephone, is assumed constant. This, of course, decidedly is not the case. Customer calling rates vary widely although the average calling rate of all customers is used in engineering. It can be shown in most cases, however, that the nonuniformity in offered load among customers results in slightly better service than that predicted by formulas based on the uniform load assumption.

Holding times for the cases of delayed call situations are assumed either to be constant or to vary exponentially. (Other formulas, for "lost calls cleared" and "held", are derivable without restriction as to the form of holding time distribution.) The exponential law has been found to describe remarkably well the distribution of local call conversation times.[1,2] Its formula is

$$P(\geq t) = \epsilon^{-t/t(\text{avg})} \qquad (1)$$

where

$P(\geq t)$ = the probability that any randomly selected holding time will equal or exceed a length t,
ϵ = the Naperian logarithmic base, 2.718,
$t(\text{avg})$ = the average holding time of all customers' calls.

Disposition of calls which do not find a trunk immediately available depends on a number of things. When such a call is dialed by a customer, the selecting mechanism ordinarily indicates to him that no path is available. The call then is lost from the system. However, in the majority of cases it is known that subsequent attempts are made to complete the call.[3] These attempts are not made in a random manner.

If, when a customer first lifts his receiver to make a call, a channel in the first step of the train of connection is not available, he usually waits until one becomes so. When calls are handled by operators and trunks are selected by them, the disposition of a call depends on the operating practice or upon the customer's instructions; he may be held at the telephone while repeated attempts are made to find an idle trunk or he may be given an immediate busy report.

From the foregoing it is seen that behavior varies when channels are not immediately available to receive a call.

In fact, it varies between two extremes. On the one hand, some calls, upon not finding a path immediately, disappear from the system not to return again in the same period, say the busy hour. This assumption, lost calls cleared, is the basis of a formula for obtaining the probability of loss known as the Erlang B formula which is discussed later. A lost call is one which, when offered to a group of trunks, finds all trunks busy regardless of what happens to it thereafter. On the other hand, some calls, upon finding no channel available, wait in suspense until one becomes idle at which time the channel is seized and held for the full holding time. This assumption, "lost calls delayed," is the basis of another formula for obtaining the probability of loss. It is known as the Erlang C formula.

Between these extremes is an intermediate assumption, "lost calls held", upon which are based the binomial and the Poisson formulas. The physical equivalent of these expressions for the disposition of lost calls sometimes has been described as follows: an offered call, upon finding no idle trunk, waits for an interval of time exactly equal to its holding time and then disappears from the system; if a trunk becomes idle while the call is waiting, the trunk is seized and occupied for the portion of the holding time then remaining. This behavior is

known as the lost-calls-held assumption to distinguish it from other assumptions used in other formulas.

Regarding what happens to lost calls, it readily is seen that the three assumptions (lost calls cleared, held, and delayed) have differing influences on the theoretical probability in each case of calls being lost. Where lost calls are cleared from the system, they do not occupy trunk time. For a given offered load this probability of lost calls is therefore lowest among the three assumptions. Where lost calls are held, they occupy some trunk time; if the probability of loss is low, they occupy nearly the full holding time. Probability of loss under this assumption is higher than for lost calls cleared. Where lost calls are delayed, they occupy trunks for the full holding time, and the probability of loss is thus highest of the three assumptions.

As stated earlier, telephone traffic is varied in its characteristics and does not behave in ways which are in all respects precisely like the basic assumptions underlying any of the various probability formulas; very often a system actually operates somewhere between the limiting cases. Although no systems present or contemplated perform the peculiar transfer of calls waiting to calls talking that is comprehended by the lost-calls-held assumption, the net result appears to be reasonably descriptive of customers' performance generally. Some, upon meeting an all-paths-busy signal, hang up and do not return; others wait a considerable interval and try again; and still others make repeated attempts at very short intervals. In the Bell System, therefore, formulas based on the lost-calls-held assumption have been adopted as the foundation for many of its engineering tables where spheres of use require that criterion of measurement.

Binomial Formula

The basic formula, or some variation of it, which underlies the greatest number of capacity tables used in the Bell System, is the binomial. As applied to a group of trunks, all of which are accessible to all sources, it expresses the probability of loss where calls are offered to the group with number of customers, probability of customers talking and wishing to talk, and number of available trunks known. Probability of loss is a term used to denote the probability of finding all trunks busy. The formula follows

$$P(c,n,p)=\sum_{x=c}^{x=n}\binom{n}{x}p^x(1-p)^{n-x} \qquad (2)$$

where

P = the probability that over some period, say an hour, any customer when placing his call will find all trunks busy.

c = the number of trunks available to receive calls.

$n+1$ = the total number of customers who have access to all trunks in the group.

p = the probability that at a random instant during the hour any particular customer is talking or wishes to talk. (The per cent occupied time of each customer or source is $100p$.)

Σ = the instruction to add together all solutions for the expression following it for values of x ranging from c to n in steps of one.

$\binom{n}{x}$ = a conventional way of indicating the number of combinations of n things taken x at a time and equals $n!/x!(n-x)!$

Illustrative Table

It is noted in the binomial formula that the number of sources which originate calls influences the probability of loss. In the case of switches in the step-by-step dial system, the relation between the number of traffic sources and trunk paths is such that the influence of number of traffic sources on probability of loss is recognized in the content of capacity tables. Here, the binomial formula is employed as a basis for relating loads and service. Capacity Table I illustrates load values selected from a typical step-by-step trunk table.

Table I. Capacity Table

Step-by-Step Graded Multiple Trunks; Hundred Call-Seconds (ccs); 10 Terminal Assignment; Table 10 Service

Trunks	Selectors Per Subgroup 320	240	160	120	80
11	166	168	170	172	176
15	240	245	246	249	254
25	426	430	434	444	465
35	602	614	626	650	692

Capacities in this as in subsequent table illustrations are, unless otherwise noted, in ccs. Table I is for step-by-step graded multiple groups where a given call has access to ten trunks only (10-terminal assignment). Values are such that when groups are loaded to the indicated capacity, ten calls in a thousand find all trunks busy (Table 10 service). Table numbers similarly used in later illustrations have the same significance; that is, the number indicates the number of calls per thousand offered which can be expected to find all trunks busy. Numbers of selectors per subgroup constitute the numbers of traffic sources from which calls are offered to the group. Figure 1 illustrates the equipment arrangement for 80 selectors and 15 trunks.

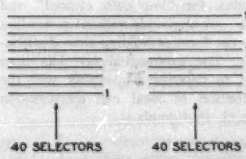

Figure 1. Graded multiple arrangement

With the graded multiple arrangement of trunks, all traffic sources do not have access to all trunks. Load values in Table I are modified to reflect the effect of this limitation. The arrangement is discussed later under Miscellaneous Modifications.

Poisson Formula

In the binomial formula, as the number of sources $(n+1)$ which supplies a given traffic load $[(n+1)p=a]$ increases, the probability of loss on c trunks also increases and approaches a limiting value as n becomes very large and p becomes correspondingly small. Under this condition, the formula can be expressed in different form. It is known as Poisson's Exponential Binomial Limit but usually is referred to simply as the Poisson.[4,5] The formula follows

$$P(c,a)=\sum_{x=c}^{\infty}\frac{a^x e^{-a}}{x!} \qquad (3)$$

where

P and c have the same significance as in the binomial formula.

a = the average simultaneous calls offered during the hour. It is equal in value to the product of the quantities n and p in the binomial. This average multiplied by 36 is the offered load in ccs.

The following statement serves to indicate roughly the field of application for the Poisson as compared with the binomial formula: when the number of sources is greater than eight times the number of trunks serving them, for commonly used grades of service ($P=0.02$ and smaller), the Poisson specifies fewer than five per cent excess trunks over the binomial formula.

With the exception of the step-by-step groups previously cited, the Poisson generally is used as the basis of capacity tables for most other types of facilities where the service criterion is in terms of probability of loss. This can be done because the number of traffic sources with respect to the number of trunks is such that the Poisson gives a reasonable approximation of the true binomial values.

Illustrative Table

Capacity Table II illustrates load values selected from tables for trunk groups in which all sources have access to all trunks. They are calculated directly from the Poisson formula. It is noted

Table II. Capacity Table

Ungraded Multiple Trunks, Hundred Call-Seconds (ccs)

Trunks	Service Table 1	Service Table 10	Service Table 20
40	837	964	1,012
50	1,115	1,261	1,317
60	1,400	1,565	1,627
80	1,986	2,184	2,258

that the capacity of an 80-trunk group is more than double that of a 40-trunk group for the same grade of service, which is to say that the larger group is more efficient. This increase in efficiency with increase in number of trunks per group is more marked in the lower ranges of group size.

Figure 2 demonstrates this characteristic in group sizes from 1 to 100 for Poisson probabilities of loss of 0.001 and 0.01 (Tables 1 and 10 service respectively). Trunk efficiency is the term a/c from Poisson formula values. As stated earlier, when multiplied by 100 it also is the per cent occupancy.

Erlang B Formula

When the probability of lost calls is low, there is little difference in trunk requirement among the several assumptions regarding lost call behavior. Although the Poisson generally is the basis for most Bell System capacity tables, there are types of problems for which it is not suited. Typical are those involving amount of switch hunt, amount of wear on terminals, and distribution of load over terminals. For these the Erlang B formula,[5,6] based on the lost-calls-cleared assumption, has been found suitable. It follows

$$B(c,a) = \frac{a^c/c!}{1+a+a^2/2!+a^3/3!+\ldots\ldots+a^c/c!} \qquad (4)$$

where

B = the probability that all trunks will be found busy. In this formula, B implies the lost-calls-cleared assumption as P in the binomial and Poisson implies the lost calls held.

c = the number of trunks available.

a = the average simultaneous calls offered during the hour.

This formula also is used widely in the determination of trunk requirements for

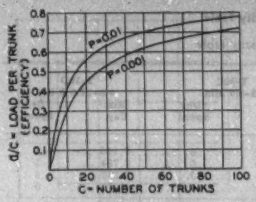

Figure 2. Load carried per trunk at a constant probability of loss

alternate routing. An alternate route arrangement of trunks from a central office is simply a variation of graded multiple, the principles of which are described later.

Alternate routing is a device, used at present only in crossbar-type dial offices, for improving interoffice trunk efficiency. Direct trunk groups between central offices are strongly cut back leaving the earlier choice, and hence more heavily loaded, trunks in service. The average efficiency of these direct trunks thus is increased materially over the former average for all interoffice trunks. The overflow calls from two or more such direct routes then are combined and sent via an alternate route to a tandem or intermediate switching center. Here similar alternate routed calls from other originating offices are sorted out and those to a specific terminating point recombined and sent over tandem completing trunks groups to the various destinations. By combining in this way the overflow traffic from a considerable number of direct routes, a sufficient load to (and from) tandem may be accumulated so that as suggested by Figure 2, a relatively efficient trunk group size can be attained for all alternate routes. Thus the over-all efficiency of the general trunk system is raised considerably above that obtainable with only direct interoffice trunking.

Illustrative Table

Table III is a portion of a table derived directly from the Erlang B formula, which

Table III. Alternate Routing Trunk Tables

CCS Carried by and Overflowing From Each Trunk Shown in Column Headings

CCS Offered	Trunk Number 10 Carried	10 Overflowing	11 Carried	11 Overflowing	12 Carried	12 Overflowing
300	16	41	13	28	10	18
305	16	44	14	30	10	20
310	17	46	14	32	10	22
315	18	49	14	35	11	24

is used in calculating alternate route trunk requirements. The significance of this table is explained by the following example:

If 300 ccs per hour are offered to ten trunks, the tenth trunk carries 16 ccs and 41 ccs overflow beyond it. This assumes that load always is offered to the trunks of a group in turn, beginning with the lowest numbered. Where this is not so, the significance of 16 in the example is expressed differently: the addition of a tenth trunk to a 9-trunk group results in the addition of 16 ccs to the load carried on the group.

Finding the proper combination of direct and alternate route trunks consists of determining for each outgoing traffic item the most economical number of direct trunks based on the cost ratios of alternate to direct channels. The efficiency of the alternate channel in ccs per trunk per hour, divided by the above ratio, is the load in ccs which should be equaled or exceeded by all trunks in the direct group. Alternate route group size is determined for the composite of the overflow from direct trunks. Although not rigorously correct, it is the usual practice to use the composite load to enter a Poisson table to determine the number of common paths required.

Pollaczek-Crommelin Formula

Where the probability of lost calls is not small and where operators handle the calls for customers, such as in the case of intertoll calls, the more significant measure of grade of service is average delay on all calls. The Pollaczek-Crommelin formula[4] best expresses the relation between load and grade of service for this class of traffic. It is based on assumptions of constant holding time and lost calls delayed.

Illustrative Table

Capacity Table IV is a portion of a table derived directly from the foregoing formula.[7] In this table the number 30 in column headings signifies that during the busy hour the average delay for service on all calls is 30 seconds. The capacity of 40 trunks, for example, when trunk holding times range from 5.8 to 7.2 minutes, is 2,246 call minutes per hour. Average delay on all calls offered throughout a day is six seconds. Capacity could be expressed in ccs by multiplying by 0.6.

Miscellaneous Modifications and Illustrative Capacity Tables

Graded Multiple

Graded multiple is an arrangement of trunks wherein subdivisions of the total number of calls offered to a group are pre-

Table IV. Capacity Table

Intertoll Trunk Capacity Table

Holding Times	T-30B 5.8–7.2 Min.		T-30C 7.3–8.9 Min.		T-30D 9.0–11.5 Min.	
Trunks	Min. Cap.	*Day Speed	Min. Cap.	*Day Speed	Min. Cap.	*Day Speed
40	2,246	6	2,222	6	2,196	6
50	2,841	5	2,813	5	2,784	5
60	3,434	5	3,407	5	3,377	5
80	4,632	5	4,600	5	4,571	5

* Average delay in seconds.

Table V. Capacity Table

Panel Graded Multiple Trunks; 20 Terminal Assignment; Table 10 Service

Trunks	CCS
40	860
50	1,090
60	1,310
80	1,750

Table VI. Capacity Table

Panel Customer Senders; Table 10 Service

Senders	CCS
40	785
50	1,026
60	1,271
80	1,775

sented first to subgroups of trunks individual to them; upon failure to find an idle trunk, the calls are next presented to one or more subgroups of trunks which are accessible to some or all of the other subdivisions of calls. A simple, symmetrical graded arrangement such as may be found in a step-by-step type dial office is illustrated in Figure 1.

In this group of 15 trunks, each subgroup of 40 selectors has access first to five trunks individual to it and thence to five common trunks accessible to the entire 80 selectors. Where it is not possible to use such an arrangement it would be necessary to provide individual subgroups, each not greater than ten trunks. The graded group is more efficient than an individual subgroup of ten trunks because the common trunks can team in giving access to calls that overflow the individual trunks thereby making them more efficient than tail-end trunks in an individual group. This subject is covered at length in an article by R. I. Wilkinson.[8]

Capacity of a graded arrangement is calculated by increasing the efficiency per trunk of a simple group equal in size to the access, by the theoretical percentage of gain (graded multiple gain) for that arrangement and multiplying by the number of trunks in the graded multiple group. This type of arrangement is used in dial offices where economic design considerations and a standard fixed switch size limit the access.

Illustrative Table

Capacity Table V shows selected values from a table for graded multiple groups in a panel-type dial office. Traffic sources here are sufficiently great in number so the table is based on the Poisson formula and values are increased by the graded multiple gain for each group size. Access for any one call is 20 trunks.

Call Count Correction

Occasionally, the count of dialed calls as used in engineering dial facilities does not include all uses of each facility, such as in the case of a customer sender in a panel or Number 1 type crossbar office. Here, the count of calls ordinarily includes only those where at least a central office code is dialed by the customer. However, customer senders function also when a code is not completely dialed or even when a receiver is lifted and replaced without any dialing.

In order to simplify engineering it is found expedient to base customer sender usage on the usual count of dialed calls and appropriate holding times. The senders required for the calculated load then are secured from a capacity table into which is incorporated an empirical allowance for sender usage not included in the count of calls. This allowance is based on average customer behavior in all dial offices.

Illustrative Table

Selected values from a table for panel-dial customer senders are shown in Capacity Table VI. They contain an allowance of 23 per cent for calls not included in the regular count; as actually derived they are based on Poisson formula values divided by 1.23. There is full accessibility between call sources and senders.

Primary-Secondary Arrangements

In dial practice there frequently are situations where some variety of primary-secondary arrangement is used in order to associate traffic sources with trunk paths. Such an arrangement is less efficient than one wherein all sources have complete access to all paths. It usually is very much less expensive, however. It has been found empirically in numerous cases of practical interest that the efficiency is about 5 per cent less than where there is full access. This is to say, that with full access and a requirement of 38 trunks, for example, there would be required with a primary-secondary arrangement 40 trunks for the same load and grade of service.

Figure 3 is a schematic drawing of a set of crossbar switches showing the method of interconnecting 100 sources with 100 paths. Ten primary and ten secondary switches, each set numbered zero to nine, have ten vertical and ten horizontal terminals. Figure 3 indicates the pattern for connecting the horizontals. Switches and horizontal terminals one to eight inclusive are not shown.

Illustrative Table

Capacity Table VII is a portion of a crossbar customer sender table. Values are based on the Poisson formula, modified for a call count correction of 23 per cent as in Table VI and also by a 5 per cent correction for reduction in efficiency due to the use of a primary-secondary arrangement. Senders are accessible to all calls.

Random Slip Multiple

Where design limitations are such that it is not feasible to give all traffic sources access to all trunk paths, another arrange-

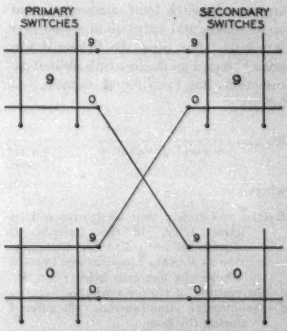

Figure 3. Crossbar primary-secondary arrangement

Table VII. Capacity Table

No. 1 Type Crossbar Customer Senders; Table 10 Service

Senders	CCS
40	745
50	970
60	1,200
80	1,670

ment is used where the equipment lends itself to such treatment. This is known as a random slip multiple distribution of load to trunks. It is a limited access arrangement wherein, if applied to senders, for example, the choice of the particular t senders to be available to one of a number of equal volumes of offered load is made in a random fashion such that, as far as possible, when x calls are in progress they will be as likely to be connected with any x senders as any other x senders out of a total of T.

Figure 4 illustrates a simple random slip multiple arrangement. Five equally loaded subgroups are served by five senders with but four available to any one subgroup.

The formula for probability of loss[9] with this arrangement is

$$P_t = \frac{a^t(T-t)!}{T!}[1-P(T-t,a)]+P(T,a) \qquad (5)$$

where

P_t = the probability of loss
a = the load in average simultaneous calls submitted to T
T = the total number of trunks
t = the number of trunks available to any one call

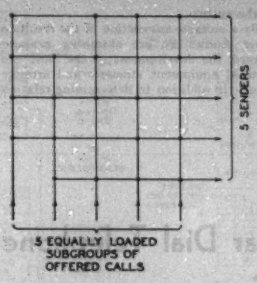

Figure 4. Random slip multiple arrangement

$P(T-t,a)$ and $P(T,a)$ are the Poisson expressions of loss for load a and for $(T-t)$ and T trunks respectively.

Illustrative Table

Table VIII. Capacity Table

No. 4 Type Crossbar Senders; 40 Sender Access; Table 10 Service

Senders	CCS
40	907
50	1,176
60	1,440
80	2,012

Capacity Table VIII contains selected values from a table for Number 4 type crossbar senders. Values are based on the probability of loss according to the random slip multiple formula. Maximum sender access for any subgroup of load is 40. Table values also have been modified for the effect of the primary-secondary arrangement of crossbar switches previously described.

Conclusion

Capacity tables illustrated by no means include all that are used in the Bell System. They do, however, cover the principal types and exemplify applications of the most used probability formulas, to the engineering of conversation channels and facilities.

References

1. Application of the Theory of Probability to Telephone Trunking Problems, **E. C. Molina.** *Bell System Technical Journal* (New York, N. Y.), Volume VI, July 1927, pages 461–94.

2. Solution of Some Problems in the Theory of Probabilities of Significance in Automatic Telephone Exchanges, **A. K. Erlang.** *Post Office Electrical Engineers' Journal* (London, England), Volume X, January 1918, pages 189–97.

3. An Aspect of the Dialing Behavior of Subscribers and Its Effect on the Trunk Plant, **Charles Clos.** *Bell System Technical Journal* (New York, N. Y.), Volume XXVII, July 1948, pages 424–45.

4. The Theory of Probabilities Applied to Telephone Trunking Problems, **E. C. Molina.** *Bell System Technical Journal* (New York, N. Y.), Volume I, November 1922, pages 69–81.

5. Probability and Its Engineering Uses (book), **T. C. Fry.** D. Van Nostrand Company, Inc., New York, N. Y., 1928.

6. Delay Probability Formulas, **C. D. Crommelin.** *Post Office Electrical Engineers' Journal* (London, England), Volume XXVI, January 1934, pages 266–74.

7. A Study of the Delays Encountered by Toll Operators in Obtaining an Idle Trunk, **S. C. Rappleye.** *Bell System Technical Journal* (New York, N. Y.), Volume XXV, October 1946, pages 539–62.

8. The Interconnection of Telephone Systems—Graded Multiples, **R. I. Wilkinson.** *Bell System Technical Journal* (New York, N. Y.), Volume X, October 1931, pages 531–64.

9. Trunking System, **E. C. Molina.** United States Patent 1,528,982.

Discussion

R. I. Wilkinson (Bell Telephone Laboratories, Inc., New York, N. Y.): In his excellent paper on Bell System facilities capacity tables, Mr. Gracey has suggested that much more work on the traffic carrying capacities of switching systems has been, and is being, done than he has described. This is quite the case. Since the fall of 1905 when E. C. Molina first used the binomial formula as proposed in an historic memorandum of October 22, 1903, by M. C. Rorty (then both with the American Telephone and Telegraph Company), the applications of probability to trunking theory in the Bell System have been many and varied.

Mr. Gracey presented formulas for relating load, size of group, and grade of service for three rather special, though widely-used assumptions as to the disposition of calls failing to obtain immediate service. It may be mentioned that in 1930 we at Bell Laboratories developed what has come to be called the "infinite source generalized trunking formula" which by the insertion of an added parameter, j, permits the calculation of the congestion corresponding to any desired lost calls assumption between the two extremes of "cleared" and "delayed."*

For the most general case of $n+1$ sources each originating on the average m calls per idle time h, where h is the average holding time, the loss expected on a full access group of c paths, will be

$$P = \sum_{x=c}^{n} f(x) = \frac{\displaystyle\sum_{x=c}^{n} \frac{n!}{(n-x)!c!} m^x \frac{(c/j)!}{j^{x-c}(c/j+x-c)!}}{\displaystyle\sum_{x=0}^{c-1} \frac{n!}{(n-x)!x!} m^x + \sum_{x=c}^{n} \frac{n!}{(n-x)!c!} \times \frac{(c/j)!}{m^x j^{x-c}(c/j+x-c)!}}$$

The disposition of delayed calls is regulated by j, and it may readily be shown that

$j=\infty$ corresponds to lost calls cleared
$j=1$ corresponds to lost calls held
$j=0$ corresponds to lost calls delayed

When $n \to \infty$ the congestion equations reduce to the Erlang B, Poisson, and Erlang C, respectively.

Until recently our detailed knowledge of subscriber telephone behavior has been insufficient to warrant more than meager use of j's other than those producing the formulas described by Mr. Gracey. However, we now are engaged in a series of field studies which promise ultimately to allow us to select j-factors more exactly suited to some of the important subscriber-central office situations. These field studies are a part of a considerably more comprehensive program of investigation of subscribers telephone performance.

We also are giving close attention to the operating characteristics of the various types of central offices in use by Bell System Companies. This involves a determination

*The equivalent formula for infinite sources (and using $\delta = h/j$) was derived independently by Dr. Conny Palm.[1] He also gave the formulas for the corresponding distribution of call delays.

of the over-all response of trains of equipment, often with complex interdependencies, to normal traffic loads and to specified degrees of overload. This is being done by means of theoretical analyses, by simulated traffic tests, and through field studies of the system.

By a suitable association of the results of these studies we are obtaining guidance toward the development of the most economical equipment amounts and arrangements, in addition to determining relationships useful for engineering and administrative purposes.

REFERENCE

1. ETUDE DES DELAIS D'ATTENTE, Conny Palm. *Ericsson Technics* (Stockholm, Sweden), number 3, 1937, pages 39–56.

The Number 5 Crossbar Dial Telephone Switching System

F. A. KORN
MEMBER AIEE

JAMES G. FERGUSON
ASSOCIATE AIEE

IN January 1939 a paper was presented to the Institute[1] by F. J. Scudder and J. N. Reynolds of Bell Telephone Laboratories which described a crossbar dial telephone switching system which was just being introduced in the Bell System. Known as the Number 1 Crossbar System, it was designed for large cities where the panel system had been used for almost 20 years. Since then approximately 350 crossbar dial offices of this type, serving nearly 5,500,000 subscriber stations, have been installed in the larger cities throughout the country. During these years improvements have been made in the Number 1 crossbar system to make it more serviceable to the telephone user and to meet the new problems which have arisen.

Bell Telephone Laboratories' engineers have continued their searches for new and better telephone switching systems. One such search was for a dial system which would better meet the telephone switching requirements for areas on the outskirts of metropolitan cities and at the same time care for medium-to-large sized offices in other areas. Work on this problem culminated in the development of the new Number 5 crossbar system, and on July 11, 1948 the first office of this type was placed in service at Media, Pa., a suburb of Philadelphia.

The field of application of this new switching system is more extensive than that of any developed previously. The Number 5 system is capable of operating with all present local, tandem, and toll switching systems of the Bell System and of the independent companies which connect with it. In addition, it can serve as a tandem or toll center switching office where this is advantageous. It can be readily equipped with features for operation as required at toll centers for nationwide operator toll dialing and also for automatic message accounting[2] which permits subscriber dialing to be extended to considerable distances. Number 5 crossbar is designed for operation with as few as four digits in a subscriber number or it can complete calls which require as many as 11 digits, (dialed by operators) three for the national area code,[3] three for the office code, four for the numericals and the last for the station letter of the called number on certain types of party line service.

General Description

The Number 5 crossbar system is like the Number 1 system in that:

1. It is essentially a relay system employing simple forms of relays and relay-type structures for all switching operations. The apparatus consists largely of crossbar switches, multicontact relays, and smaller relays similar to those generally employed in all telephone switching systems. Practically all have double contacts of precious metal to lessen the likelihood of contact failure and to improve transmission. The crossbar switch, multicontact relays, and general purpose relays were described in considerable detail by Scudder and Reynolds.

2. Primary-secondary arrangements of crossbar switches funnel the traffic from lines to trunks and from trunks to lines. Each group of trunks to a connecting office may have from two to several hundred circuits and the switches serve trunk groups economically whether they are large or small.

3. Utmost freedom of action in routing each call is provided by components which transfer all control over switching sequences from the subscriber's dial to circuit elements in the office. The digits dialed are stored in registers and can then be translated into other codes employing one or another pulsing means, not necessarily decimal. This translated information is then sent to the switches selected to give them whatever directions they need in the most suitable forms and at the time they need them.

4. The register, sender, and translator elements are employed for only a short time in each connection, thus small groups of them serve large groups of lines. Each element is brought into a connection for only the interval required to perform its function.

5. Control over practically all switching and pulsing operations is centered in groups of circuit elements called markers. They perform so quickly that a few of them will handle all calls in an office. The crossbar switch lends itself to this fast operation because its contacts stand ready to close in an instant and no time is lost in switch action to hunt for a connection. Since relatively small groups of these control circuits (markers, registers, senders, and so forth) are used over and over again by many other connecting circuits they constitute what is called common control operation.

6. Advantage is taken of secondary benefits from common control including the following:

(a). If all trunks are found busy in the preferred group first selected, the marker may choose an idle trunk in an alternate route.

(b). Each element in the connection tentatively selected for a call is tested, and if a trouble is encountered in the path, the marker makes a second trial and brings into the connection a different group of elements. Usually a different marker is called upon to make the second trial and this serves to minimize the reaction from trouble in the marker itself.

Paper 50-41, recommended by the AIEE Communication Switching Systems Committee and approved by the AIEE Technical Program Committee for presentation at the AIEE Winter General Meeting, January 30–February 3, 1950. Manuscript submitted November 1, 1949; made available for printing December 1, 1949.

F. A. KORN and JAMES G. FERGUSON are both with the Bell Telephone Laboratories, Inc., New York, N. Y.

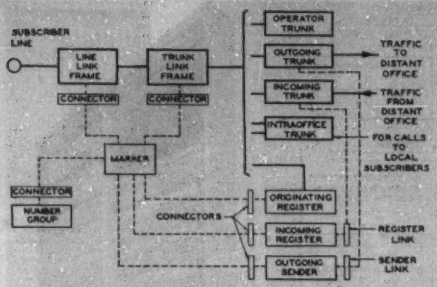

Figure 1. Basic arrangement of switching plan

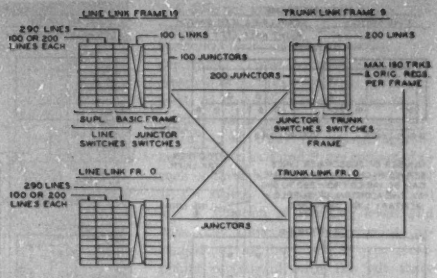

Figure 3. Line link and trunk link frames—simplified trunking plan

(c). Since the marker has access to most of the elements in an office it is endowed with the ability to gather information from many sources on the performance of the different parts. It is therefore able automatically to refer to the maintenance force incipient troubles (and their locations) before they react on service.

Number 5 crossbar differs materially from Number 1 in the following:

1. Switching plan.
2. Trunking arrangements.
3. Utilization of new items of apparatus.
4. Equipment design.
5. Circuit operation.
6. Maintenance provisions.

These are described briefly in this order in the sections which follow. The unusual combination of versatility with standardization, the extended use of the common control principle, and the introduction of new maintenance concepts described in these sections endows Number 5 crossbar with important features which are summarized in a concluding section.

Switching Plan

The Number 5 system differs from Number 1 primarily in its switching plan, a simple block diagram of which is shown in Figure 1. Each subscriber line appears on one of the line link frames and all trunk and originating register circuits on trunk link frames. It should be noted that, as in the case of Number 1, the line has but a single appearance on the line link frame and this serves for both originating and terminating calls. Every connection is set up from a trunk or a register to a calling or a called line through crossbar switches on trunk link and on line link frames. The common control equipment which is used to set up the various connections includes the markers, the connectors, the number groups, the senders and registers, and the sender and register links. Once a talking path is established, all control elements are released and only the line link, trunk link, and trunk circuit elements remain in the connection.

Before any talking path is set up, all needed information on calling and called parties is registered in a way which enables a marker in a uniform and flexible manner to call into the connection only those switching, signalling, transmission and supervisory features required for the particular call. On every subscriber call, the calling line, through a connector, engages a marker to connect the calling line temporarily to an originating register through crossbar switches of the line link and trunk link frames after which the connector and marker are released. When all of the needed information on calling and called parties is stored in the originating register, a marker is again engaged for a fraction of a second to establish the talking connection. Knowing both ends of the connection required and with no switching equipment committed, the marker is free to set up any kind of a call with the best combination of elements. If the call is to another subscriber in the same office, the marker connects an idle intraoffice trunk circuit to the calling and called lines.

If the call is to a destination outside the office, the marker recognizes this from the information dialed and proceeds to connect the calling line to a trunk circuit in the proper group. If a sender is needed, the marker connects one of the appropriate type to the trunk circuit through a sender link. Senders receive information from the marker and transmit it in the form of pulses to registers, other senders or directly to switches as required in the systems of the connecting offices. This information may be the called subscriber's numerical digits or it may include office code digits as well. Since senders must be capable of operating with the standard kinds of signaling, four types are available for "dial pulse," "revertive pulse," "multifrequency pulse" and "panel call indicator" operation. Multifrequency pulsing is generally used for signalling between Number 5 offices, to and from Number 4 toll crossbar offices, to Number 1 crossbar and to crossbar tandem offices.[4,5]

If the call is incoming from another office, the incoming trunk circuit associates itself with an incoming register through an incoming register link. The incoming registers receive information from senders, dials, or keysets in the distant offices and pass this information to the markers for establishing the switch-

Figure 2. Crossbar switch

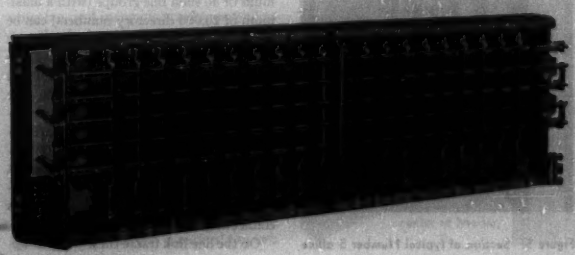

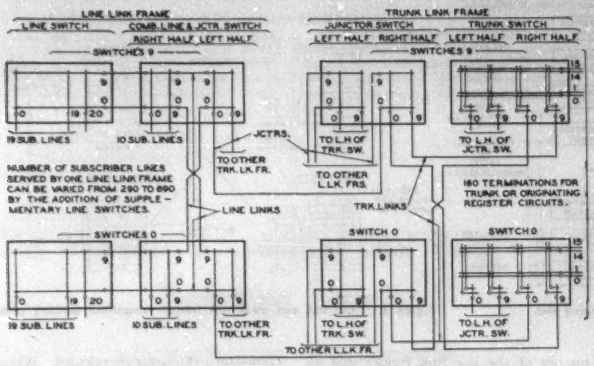

Figure 4. Simplified typical office trunking plan

ing connection either to a called subscriber line in the same office, or to a distant office when through switching of toll or tandem traffic is involved. Incoming registers, like senders, must be capable of operating with the standard kinds of signaling, hence there are "dial pulse," "revertive pulse," "multifrequency pulse" and "B switchboard" registers.

The flexibility afforded by this switching plan can be illustrated by a simple manual switchboard analogy. Imagine a manual operator who has direct access to lines and trunks of every variety in the quantities needed. Over a preliminary connection she is quickly given complete information regarding the nature of each call. Then, knowing all she needs to about both calling and called parties, she dismisses the preliminary connection and establishes the talking path by assembling the proper combination of transmission, signaling, supervisory, and charging circuits required for that connection and connecting that combination between the jack of the calling line or trunk and the jack of the called line or trunk.

Trunking Arrangement

The crossbar switch from which the system derives its name is shown in Figure 2. Since it has been described in detail by Scudder and Reynolds, it will be sufficient to describe it as a co-ordinate arrangement of contacts, giving 10 or 20 sets of contacts on one ordinate access to ten sets on the other. Thus 10 or 20 circuits may have access to ten circuits of a different type. The first 10 or 20 circuits referred to might be trunk circuits and the second ten, registers. The number of trunk circuits which can be given access to the same ten registers may be increased to 40 by adding a second switch with 20 additional trunk circuits connected to its verticals and by interconnecting the horizontal contact multiples of the two switches. By adding switches in this manner, any number of trunk circuits may be given access to the ten registers on the horizontals. This is known as the direct access form of trunking and is used in the Number 5 system for the sender and register link circuits.

To obtain access to a larger number of circuits, two groups of ten switches, known as "primary" and "secondary" are used and these are interconnected in a manner so that any particular line can be connected to any of a total of 100 or 200 outlets by closing contacts on two

Figure 5. Section of typical Number 5 office

Figure 6. Trunk link frame

switches. This type of trunking is used on both the line link and trunk link frames of the Number 5 system. The arrangement of switches on these frames and the junctor interconnections are shown in Figure 3. In the Number 5 system the "line" and "trunk" switches are the primaries and the "junctor" switches are the secondaries.

The basic line link frame of the Number 5 system has a capacity of 290 lines and by the use of 100- and 200-line supplementary bays as many as 690 lines may be assigned to form a line group. A maximum of 40 such line groups (with a maximum of 20,000 directory numbers) can be accommodated by one group of markers not exceeding 12 in number. These numbers are arbitrary design limits and can be increased without changing the system fundamentally if experience indicates a larger capacity to be more desirable. Each line link frame has 100 outlets, known as "junctors," which connect this frame to all trunk link frames—approximately an equal number of junctors connecting to each trunk link frame.

On the line link frame these junctors ap-

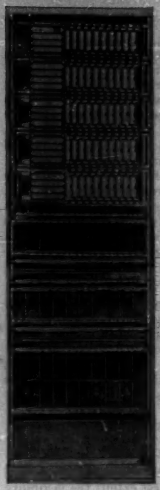

Figure 7 (above). Number group frame

Figure 8 (right). Marker

pear on the verticals of the combined line and junctor switches. These are 20-vertical switches on which the horizontal paths are separated between the 10th and 11th verticals so as to provide the equivalent of two 10-vertical switches each having ten horizontal paths. The horizontal paths of one section are directly connected to those of a line switch, thereby providing what is effectively a 30-vertical line switch. Each line on each of these extended line switches has access to the ten "line links" appearing on the horizontals. These ten links are distributed over the ten junctor switches so that each line has access to each of the 100 junctors.

The trunk link frames provide means for connecting the line link frames via their junctors to all of the intraoffice, outgoing, and incoming trunks, as well as to all of the originating registers required for dial tone service. This frame, in addition to having a capacity of 200 junctors to all of the line link frames, has 160 outlets to which trunks and originating registers may be connected. On this frame the junctor switches have their horizontal multiples divided to provide 200 horizontal paths for connecting junctors from all of the line link frames. Each junctor switch provides access between the ten junctors on each of the two half-sections and the ten "trunk links" on the verticals of each section. These 20 links are distributed over the ten trunk switches on the frame, two to each switch. Thus, each junctor has access to any trunk or register.

Figure 9 (left). Typical connector frame

Figure 10 (right). Maintenance center at Media, Pa.

A different arrangement is used at the trunk switches to obtain access to 16 horizontal terminations per switch or 160 per frame. These switches have 6-wire crosspoints on the upper eight horizontal levels so that two 3-wire circuits of the trunks and registers can be accommodated. Two trunk or register appearances, known as *A* and *B*, are connected to each of these levels to provide a total of 16 per switch. The lower two levels, 0 and 1, function as selecting levels and have only three sets of crosspoints arranged so that on level "0" the crosspoints correspond with the left three springs of the crosspoints on the upper levels and on level "1" with the right three springs. In this manner level "0" is used for *A* appearance trunks or registers, and level "1" for the *B* of the 16 that might appear on the switch. In this case the trunk links are not wired to the vertical multiple of these switches, but instead are wired to the individual contact points of both levels 0 and 1. Connection of a trunk link to a trunk or register is made by operating two selecting magnets; one, the selecting magnet corresponding to the trunk or register appearance and the other, either 0 or 1, depending upon whether the trunk or register is associated with the left or right half of the vertical multiple.

Since each trunk link frame provides 200 junctors and each line link frame only 100, there are usually twice as many line link as trunk link frames. The 100 junctors from a line link frame are distributed

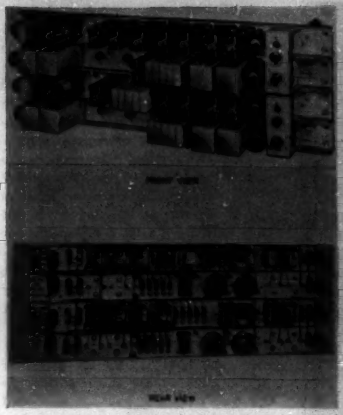

Figure 11 (left). Typical functional unit

Figure 13 (right). Section of frame showing method of opening or removing front cover

over the junctor switches of all the trunk link frames in an office. The number of junctors between these frames will vary depending upon the actual number of trunk link frames. There will be at least one junctor, as shown, from each junctor switch on a line link frame to a junctor switch on each trunk link frame, or a minimum of 10 junctor paths between any of these two types of frames. There will be at least 10 junctors between frames, which is the minimum to insure satisfactory call-carrying capacity. When there are more than ten trunk link frames or more than 20 line link frames, a supplementary bay of junctor switches is added to each trunk link frame to increase the number of junctor terminations from 200 to 400. In this case each junctor from a line link frame is connected to two trunk link frames. In order to connect a particular line to a particular trunk, an idle channel consisting of a line link, a junctor, and a trunk link is selected through the switches of these two types of frames. These three elements connect in series as shown in Figure 3.

The arrangement of links and junctors for a line link frame and trunk link frame is shown in Figure 3. Extension of this method of interconnecting for a typical office is shown in simplified form in Figure 4.

New Items of Apparatus

The Number 5 system takes advantage of some ten years of operating experience with the original Number 1 crossbar system and many advances in theory and technique that have resulted from continuous research in telephone switching. As one result, new or improved types of apparatus are used widely. The following are some examples:

1. Relays and switch designs have been improved. These also will have application in other systems.

2. Cold cathode tubes have found a number of new uses, particularly for time delay circuits.

3. Mercury contact relays are used in substantial quantities in some of the critical circuits of the marker. This relay consists of a sealed-in-glass mercury contact switch inserted in an operating coil, the assembly being mounted on a small wafer octal base and housed in a metal-vacuum-tube type of covering. All contact surfaces are covered with a thin film of mercury maintained by capillary action from a base pool. These relays are designed to provide long life with high stability of operation, freedom from open contacts due to dirt, fast operating, and releasing times and permit the switching of high current load when provided with adequate contact protection.

4. A new device known as a "trouble recorder" has been developed for this system. It is engaged when trouble is encountered by the control circuits and automatically records, by perforating a card, essential information which will aid the maintenance forces in locating such troubles.

Figure 12. Originating register

Equipment Design

The primary objective in equipment design for the Number 5 system was to exploit to the fullest extent the flexibility inherent in the switching plan. The second objective was to standardize the arrangements in the fewest patterns with the fewest parts and assemblies for most economical production. In spite of the fact that the two objectives are frequently incompatible, flexibility has been combined with standardization to an unusual degree.

Figure 5 shows a section of a typical Number 5 crossbar central office. As this picture suggests, the equipment arrangements in the new office are generally similar to those in other large crossbar offices. Lines of switch frames 11 feet 6 inches high and about 40 feet long are arranged on one or more floors of the building. Dimensions for ceiling heights, column spacings, and maintenance aisles are those standardized for universal use in various types of offices some years ago as most economical, taking into account both the initial and maintenance costs of the building and equipment.

The power plant consisting of storage batteries, regular and stand-by charging equipment, regulators, ringing machines and associated control equipment is usually in the basement. It serves switching equipment for one or more central offices on the floors above.

All of the switching components are arranged on the various frames in ways which were calculated to provide the best association for production, service, and maintenance and at the same time facilitate additions for central office growth. Since it is desirable from a cost standpoint to have as much work as possible done

in the factory, the equipment frames carry the largest possible groups of associated apparatus completely assembled, interconnected and tested in the shop. Field installation is in this way reduced to setting up the frames on the office floor, interconnecting them with the interframe cables, and testing the components and the system as a whole before turning it over to the telephone company.

The line link frame is quite similar in appearance to the trunk link frame shown in Figure 6. A number group frame is shown in Figure 7. The frames of the marker are shown in Figure 8 and a typical connector frame in Figure 9. The maintenance equipment in the maintenance center at Media, Pa. is shown in Figure 10.

It is unlikely that two central offices will be identical in numbers of switch frames of the various types or in the equipment provided on them. Some of the things which combine to make each office different are the number of subscribers it serves, the kinds of service they require, the number of times they call, the durations and destinations of their calls; the number of central offices in the same building and in the community; the nature, variety, and number of interconnecting circuits required to provide for the flow of traffic between the office and all other connecting offices. Because the Number 5 system provides so many services and is arranged to connect to so many existing kinds of offices whether in a large or small city, the deviations from office to office are more pronounced than ever before. Custom building is expensive and it was very important in the equipment design to develop the switching frames in a way which would not only provide innumerable necessary combinations of services initially, but also enable facilities to be added and traffic distribution patterns to be rearranged to care for growth, change, and the introduction of new features with the least amount of custom building and the lowest over-all engineering, manufacturing, and installing costs.

While no two offices are expected to be exactly alike, there are features within each that will be the same. Some are required in varying numbers in all offices, others are optional and specified more or less frequently. To meet this situation, a standard package was designed for each basic combination of features and these packages are used as the building blocks for all frame equipments. These standard basic units, which are generally not larger than one or two square feet in area, are reused wherever practicable to concentrate demands on the smallest number of items.

Figure 14. Method of removing rear cover

All Number 5 equipment is arranged in this way in small subassemblies, which are called functional units. Frequently an auxiliary service not required in every office employs one or two relays which cannot be economically packaged apart from a related functional unit. Each such option is coded separately for engineering and administration reasons. It may be furnished always or only as required depending on which arrangement is more economical. All functional units can be bench assembled, wired and tested and, where justified, straight line assembly methods can be employed. Interconnecting wires, precut to length and preskinned, are run along the surface of the mounting plates which support the components and are connected as run. A new wire with plastic insulation was developed for this purpose which reduces wiring congestion, fire hazard, and contact troubles from lint. The elimination of the wire cutting operation at the bench avoids wire clippings in the units. A typical functional unit is shown in Figure 11.

Frame equipment arrangements were similarly standardized to accommodate all needed groupings of functional units completely interconnected and tested in the factory. In order to make each frame as self-sufficient as possible, it is equipped not only with its particular complement of functional units but with fuse panels and all other items which serve it. Every frame arrangement permits the frame and its common equipment and wiring to be manufactured apart from its functional units. Then, at a later stage in the assembly, units and frames can be brought together in a flexible manner as required. Many combinations can thus be assembled from a few standard frames and a relatively few functional units. Each office can be engineered and manufactured with just the features it needs and with as little custom building as practicable. Patterns were developed for frameworks, fuse panels, testing facilities and all other frame equipment and wiring to enable a few parts and assemblies of each type to be brought together in different ways to constitute each standard frame and to permit it to serve any combination of functional units to be mounted on it. Parts, assemblies and patterns were reduced in number by organizing the frame equipments of all types into a few families with strong family resemblances.

Where at all practicable, one frame unit combination was standardized for use on all jobs. The line link, trunk link, and number group frames are in this category. For other frames, except one type which mounts assortments of trunk and miscellaneous units, ways were found to standardize the frame equipment and wiring apart from its units and to provide full flexibility to care for its various complements of units without too great reaction on production. Even in the one exception where the frame equipment and wiring as well as the unit complements vary widely from job to job, a pattern was developed which reduced the custom building and made it relatively easy to administer. As a result, a large proportion of Number 5 frames are fully equipped, wired, and tested in the shop. Space does not permit treatment of each of the patterns developed, but the arrangement for the family of sender and register frames is typical and a description of it will indicate the approach to the problem.

There are nine types of registers and senders in the Number 5 system. In a typical one of these basic types, the originating register for example, Figure 12, the things that vary from office to office include the number of digits which may be received (4 to 9), the number of line link frames in the office, the number of classes of service, the method of translation of digits, and the provision or omission of certain service features. Of the 14 func-

tional units available for originating register services, there are three which are always required with one or another combination of internal variables. These three are for register control, dial pulse counting, and class registration functions. In addition each register will require dial pulse register units in varying quantities depending upon the number of digits to be registered. The units not always required are those for coin service, 2-party test, digit timing, pretranslation and service code functions. Each of the functional units has a standard location in the register and two units are assigned the same location where one or the other, but not both, may be required in any office. Other senders and registers have similar functional units arranged in a similar manner.

By careful organization it was possible to standardize just three frames to care for all nine senders and registers. One of these frames accommodates five originating registers and the line-up of these frames in Figure 5 is typical for all senders and registers. The second frame cares for the four kinds of outgoing senders and the third is for the four kinds of incoming registers. Outgoing senders and incoming registers of the different types may be mixed in any desired combination on their respective frames to minimize frame and floor space requirements. With the frame and unit equipments thus standardized, the senders and registers can be tailored to the needs of each office in the later stages of assembly. For each sender or register frame equipment, one of the three standard frames is selected and on it are mounted the standard units which provide all needed services. Interconnections between the units of any sender or register will usually involve not more than 120 wires which are run loose in a channel provided for them on the rear of the frame. A pattern has been established which enables the shop to interconnect any desired combination of units with just the leads required and without specific job drawings.

A new line of frames and covers was developed for the Number 5 system, also to gain specific advantages in flexibility and in uniformity; flexibility so that the service capabilities of the system could be fully developed with the least restraint from equipment arrangements, and uniformity so that the parts and assemblies would be as few and as alike as practicable in spite of the wide variety of services foreseen. Formed sheet metal sections are used throughout the structure, and front and rear covers of a new design are incorporated, when needed, as part of the frame. In this way any area requiring covering for dust or mechanical protection can be enclosed to the extent desired in a consistent manner. Where maintenance advantages justify the extra cost, transparent plastic covers are substituted for metal.

Figure 13 illustrates the frame construction and the manner in which a front cover can be opened or removed from a frame. Figure 14 shows a rear cover being removed. Horizontal baffles separate the equipment on a frame into compartments of any desired size as shown in Figure 15.

Built into the structural portion of the frame are accommodations for fuse panels, battery filters, appliance outlets, testing and miscellaneous equipment of all varieties required. Each of these items has been reduced to a few standardized designs and all are assigned uniform locations about the base and side uprights of each frame to leave the entire central area free for the unrestricted arrangement of functional units in any combination.

Locations of frames on floors and their interconnections are likewise unified wherever possible. Frame terminations have been reduced to patterns which repeat from office to office. Each frame has power feeders terminated in solderless connectors which the installer can quickly patch to supply grids in the office for battery and commercial power. Cable rack of a new design enables the installer to run cable without sewing or clipping and with little planning; one rack over each wiring aisle serves two lines of frames.

Brief Description of Circuit Operation

Before describing the circuit operation, it may be desirable first to review the principal functions of a dial central office. Such an office is capable of serving about 10,000 subscriber line numbers and is provided with a sufficient number of connecting switches, trunks, and associated circuits to enable calls to be completed promptly under busy hour loads of traffic.

The central office circuits, in response to the lifting of the receiver by the calling subscriber, connect the subscriber line to the switching equipment at which time the dial tone is heard. After dialing, the equipment extends the calling line through several switching stages to the called line as determined by the called office code and line number dialed. When the connection has been established to the called line, the subscriber's bell is rung and, when the subscriber answers, the talking connection is completed. During the conversational period, the connection is held under control of the calling line, and when the telephone receivers are replaced, the central office equipment and

Figure 15 (left). Removal of horizontal baffle

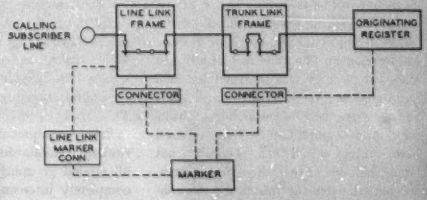

Figure 16 (right). Dialtone connection

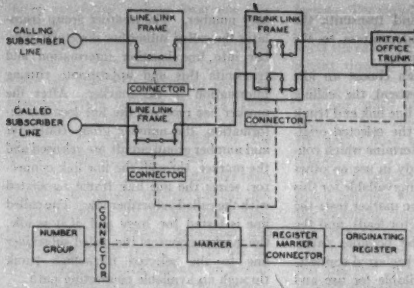

Figure 17. Intraoffice call

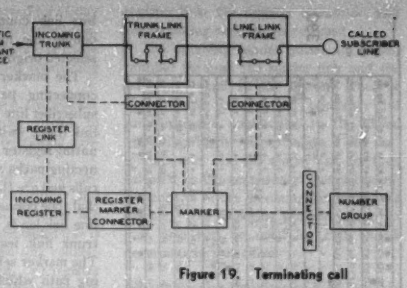

Figure 19. Terminating call

the telephones are released for use on other calls. The equipment, of course, transmits the busy tone signal to the calling subscriber if the called line is found busy. A call to a discontinued or an unassigned line is automatically routed to an operator who informs the subscriber of the status of such a line.

Operators and associated switchboards are provided in the dial systems to handle certain classes of calls and to render assistance to subscribers when required. Calls to these operators are established in response to the dialing of operator codes in a manner similar to the establishment of calls to other subscribers.

Operators are sometimes provided in dial offices to assist in terminating calls from manual offices. Where this method of operation is employed, the desired number is passed verbally from the operator serving the manual subscriber to the operator associated with the dial terminating equipment (called a *B* operator), and the *B* operator depresses push-button-type keys at the switchboard position which cause dial system equipment to establish connection with the called line. However, with the availability of operator-key-pulsing type equipment, the operators at manual switchboards can transmit signals directly to dial office equipment which then functions to establish connection to the called line in the dial office without need for a *B* operator.

The operation of the Number 5 crossbar system now will be described by tracing the progress of some typical calls through the system with the aid of the simplified block diagrams shown in Figures 16, 17, 18, 19, and 20. The following types of connections will be dealt with in this order:

1. The calling subscriber is connected to an originating register for the purpose of registering the called number which is dialed. This is commonly referred to as a "dial-tone" type of connection.

2. The calling subscriber dials the number of a subscriber who is associated with the same office. This is known as an "intra-office" call.

3. The calling subscriber dials the number of a subscriber who is associated with a distant office. This is known as an "outgoing" call.

4. A subscriber in a distant office dials the number of a subscriber who is associated with this Number 5 crossbar office. This is known as an "incoming" or "terminating" call.

5. A call from a distant office is switched through this Number 5 office to reach a called subscriber in still another distant office. In this case the office is used as a tandem switching point and the call is known as a "tandem" call.

There are, of course, many other kinds of switching connections which this office is capable of handling; however, the above are basic and should give an understanding of the general circuit operation of the system.

Dial-Tone Connection (Figure 16)

A subscriber originates a call by removing the receiver from the switchhook which operates a relay associated with the subscriber's line. The operation of this relay causes the line link frame, through the line link marker connector, to seize one of the idle marker circuits and to inform this marker that a dialing connection is to be established.

The marker determines the identification and location of the calling line. If more than one subscriber line on this line link frame is awaiting service, the marker singles one out for first attention.

At the same time as the marker is determining the identity of the calling line, it also is selecting an idle originating register circuit to serve this call. Several originating registers are associated with each trunk link frame and the marker determines which of the idle trunk link frames has one or more idle originating registers, selects one and connects to this trunk link frame through its trunk link connector. The marker then selects one

Figure 18. Outgoing call

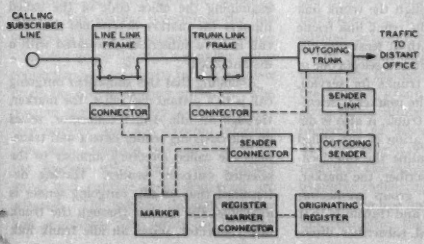

Figure 20. Tandem call

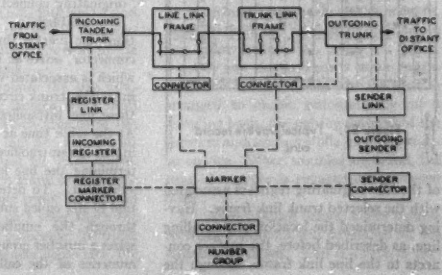

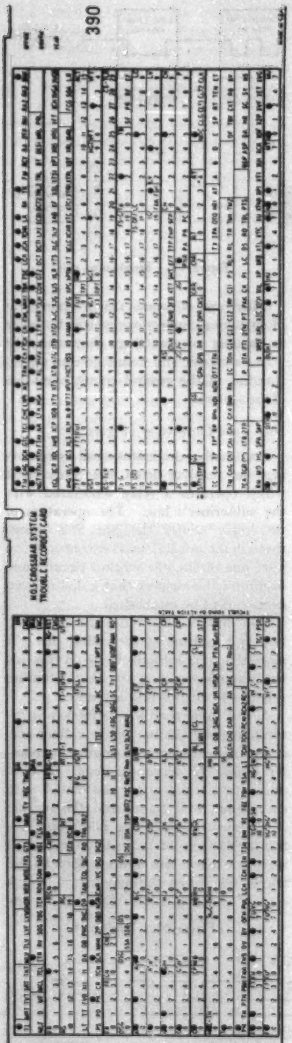

Figure 21. Typical trouble record card

of the idle originating registers associated with the selected trunk link frame. Having determined the location of the calling line, as described before, the marker connects to the line link frame, through the line link connector, and transmits the calling line location information to the selected originating register.

The marker will then choose an idle connecting path to extend the calling subscriber line through line link and trunk link frame switches to the selected originating register. To determine which connecting paths are already in use on other calls and are therefore unavailable for this dial tone connection, the marker tests the line link leads, the junctor leads, and the trunk link leads of the possible paths. The marker selects the preferred connecting path which is available for use and operates the magnets on the crossbar switches to establish this path.

After the connecting path has been established, the marker, the trunk link connector, the line link connector, and the line link marker connector are released and the originating register transmits dial tone to the calling subscriber as an indication that dialing of the called subscriber may be initiated. As the subscriber dials the called subscriber directory number, it is recorded in the originating register for later use in completing either an intraoffice or an outgoing call.

Intraoffice Call (Figure 17)

After the calling subscriber has dialed the complete called subscriber directory number, the originating register, through the register marker connector, seizes an available marker. The originating register transmits to the marker the called directory number and the calling subscriber line location. By examining the office code of the called subscriber number the marker determines that this call is for a subscriber associated with this office. As described in the following paragraphs, the marker then proceeds to establish a connecting path between the called subscriber line and an intraoffice trunk circuit which will be called a "terminating connection", and a connecting path between the calling subscriber and the same intraoffice trunk circuit which will be called an "originating connection".

To establish a "terminating connection" the marker through the trunk link connector, seizes an idle trunk link frame which is associated with at least one idle intraoffice trunk circuit and selects one of these idle intraoffice trunks for service. At the same time as the marker is selecting an idle intraoffice trunk, it also is determining the line location of the called subscriber. To determine the line location of the called subscriber, the marker, through the number group connector, seizes a number group and transmits to it numerics of the called subscriber directory number. The number group translates the called subscriber directory number into line location information and transmits this and appropriate ringing information to the marker. After the marker has received the line location information, the number group connector and number group circuit are released and the marker, through the line link connector, seizes the line link frame associated with the called subscriber line. The called line is tested for busy and, if it is idle, the marker connects the called subscriber line to the selected intraoffice trunk through an available connecting path.

After the marker has thus established the "terminating connection," the line link connector is released and the marker then proceeds to establish the "originating connection." However, if the called line is busy, the calling subscriber is connected through a connecting path to a trunk circuit which transmits a busy tone to the calling subscriber.

To establish an "originating connection" either to the called line or to the busy tone trunk circuit, the marker, through the line link connector, seizes the line link frame associated with the calling subscriber line and connects the calling subscriber line to the selected intraoffice or busy tone trunk circuit, through an available connecting path.

After a talking path has been established from the called subscriber through the intraoffice trunk to the calling subscriber, the marker, the line link connector, the trunk link connector, the register connector, and the originating register are released and the switches are held under control of relays of the intraoffice trunk circuit.

Subscriber Outgoing Call (Figure 18)

After the calling subscriber has dialed the complete called subscriber directory number, the originating register, through the register marker connector, seizes one of the idle marker circuits. The originating register transmits to the marker the called subscriber directory number and the calling subscriber line location. By examining the office code of the called number the marker determines that this call is for a subscriber associated with a distant office.

Assuming that this subscriber outgoing call is to a distant dial office, the marker, through an idle sender connector, seizes an idle outgoing sender circuit and transmits the called directory number to the selected outgoing sender. Having determined that an idle outgoing sender is available, the marker through the trunk link connector, seizes an idle trunk link

frame associated with at least one idle outgoing trunk circuit which connects to the required distant office and selects one of these idle outgoing trunks for service. After the marker has selected both the outgoing sender and the outgoing trunk circuit, the sender link circuit connects the selected outgoing sender to the selected outgoing trunk circuit.

When an idle outgoing trunk has been selected, the marker, through the line link connector, seizes the line link frame associated with the calling subscriber line and connects the calling line to the selected outgoing trunk through an available connecting path. After the connecting path has been established, the marker, the line link connector, the trunk link connector, the sender connector, the register connector, and the originating register are released.

The outgoing sender transmits, by the appropriate pulsing, the called directory number through the sender link and the outgoing trunk to the distant office to provide the information necessary for establishing a connection in the distant office to the called subscriber. The outgoing sender and the sender link are then released and supervision of the call is under control of the outgoing trunk.

Terminating Call (Figure 19)

A call from a distant office is extended to an incoming trunk circuit in the called office. The incoming trunk circuit, through a register link circuit, seizes an idle incoming register circuit. The distant office transmits the called number to the incoming register where it is recorded. Information to identify the trunk link frame which is associated with this incoming trunk is obtained from the register link. The register, through the register marker connector, then seizes an idle marker and transmits to it the called number and the identity of the trunk link frame associated with the incoming trunk.

The call is identified as a terminating call since it is associated with an incoming trunk circuit. The marker, through the trunk link connector, seizes the trunk link frame associated with the incoming trunk. The marker determines the line location of the called subscriber by seizing a number group through a number group connector and transmits to this number group the called directory numerics. The number group translates the called directory number into line location information, and transmits this information to the marker after which the number group and number group connector are released. The marker, through the line link connector, then seizes the line link frame. The called line is tested for a busy condition and, if it is idle, the marker connects the called line to the incoming trunk circuit through an available connecting path.

If the called line is busy, the marker informs the incoming trunk circuit to transmit a busy tone to the calling subscriber.

After a talking path has been established between the called subscriber and the incoming trunk circuit, or after the marker has indicated that the called line is busy, the marker, the trunk link connector, the line link connector, the register marker connector, the incoming register, and the register link are released and supervision of the call is under control of the incoming trunk.

Tandem Call (Figure 20)

A tandem call from a distant office is extended to an incoming tandem trunk circuit in the local office. Each incoming tandem trunk circuit has an appearance on a line link frame similar to a subscriber line as shown in Figure 20. The incoming tandem trunk seizes an idle incoming register circuit. The distant office transmits the called number to the incoming register where it is recorded along with the trunk number obtained from the link to identify the incoming tandem trunk. The incoming register then seizes an idle marker and transmits to it the called number and the identity of the incoming tandem trunk.

By examining the office code of the called number, the marker determines that this is a tandem call and is for a subscriber associated with a distant office. Assuming that this tandem call is to a distant dial office, the marker seizes an idle outgoing sender and transmits to it the called directory number. Having determined that an idle outgoing sender is available, the marker seizes an idle trunk link frame associated with at least one idle outgoing trunk which connects to the desired distant office and selects one of the idle outgoing trunks. After the marker has selected both the outgoing sender and the outgoing trunk, the sender link connects the selected outgoing sender to the selected outgoing trunk.

The marker determines the line location of the incoming tandem trunk from the number group which translates the given trunk number into line location information as described for calls above. The incoming tandem trunk is then connected to the outgoing trunk through an available connecting path after which the marker, the line link connector, the trunk link connector, the sender connector, the register link, the register connector, and the incoming register are released.

The outgoing sender pulses the called number through the sender link and the outgoing trunk to the distant office to provide the information necessary for establishing a connection to the called subscriber in the distant office. The outgoing sender and the sender link are then released and supervision of the call is under control of the incoming tandem trunk circuit. The incoming tandem trunk circuit also can be used for calls which terminate in this office.

Maintenance Provisions

In the development of the Number 5 system, it was a major design objective to produce a system which would be more nearly trouble-free than any system produced heretofore. In addition, if troubles could be made sufficiently infrequent, an office could be unattended for long periods of time with a resulting reduction in maintenance effort, testing facilities and maintenance costs.

Steps which have been taken toward these maintenance objectives include the following:

1. In designing circuits there was an endeavor to employ relays and switches in arrangements which would enable these devices to perform their required functions with maximum ease and allow maximum tolerance of maladjustment. This provides margin to allow for changes in operating characteristics which are inevitable as a result of apparatus wear, aging, and other factors.

2. Contact locking and contact erosion has been minimized by extensive use of contact protection networks.

3. Many self-checking and trouble detecting features are included in the common control circuits, particularly the marker. When a trouble is detected, a card record, Figure 21, is made by the trouble recorder. Meanwhile, wherever possible, a second trial is made to establish the connection for the subscriber. Because of the extensive use of the marker for switching operations in this system, these features are more effective than in any earlier system.

4. A new device known as an "automatic monitor" has been provided and is arranged to check, automatically on a sampling basis, the pulsing features of the registers and senders while handling regular service. When troubles are found, the trouble recorder is engaged and a record made.

5. As mentioned before, a new trouble recorder, Figure 22, was developed for the Number 5 system. This is a type of per-

forator which is engaged by a common control circuit when trouble is encountered and makes a card record of essential information which can be used by the maintenance force as an aid in locating the trouble. It will automatically record a succession of trouble indications and is sufficiently fast in its operation to record a large volume of indications within a short period of time and to minimize delays to the circuits which encounter troubles. The Number 5 system also makes extensive use of the trouble recorder to indicate test results.

6. Portable test boxes and frame mounted test circuits are made available for testing and maintaining circuits such as senders, registers, trunks and markers, and other circuit elements.

7. A simplified form of central office audible and visual alarms has been provided to direct attention to the presence of trouble conditions. The alarms are arranged to be transmitted to the maintenance force at another location when the office is unattended and under these conditions, an indication as to the nature or degree of trouble is given.

Maintenance activity in crossbar offices is controlled from a "maintenance center." This is the area in which all of the principal frames used in testing and trouble recording operations are located. In Number 5 crossbar this activity is controlled from the "master test frame." This is actually a group of frames and includes the trouble recorder, the automatic monitor, register and sender test, trunk test, and the associated circuits, including the master test frame connector which provides access to the various circuits for testing. Located here also are facilities which quickly permit taking any of the major circuits out of service to minimize trouble reactions. It is possible to obtain access to and test any of the individual major circuits in the office from the master test frame.

Summary of Number 5 Crossbar's More Important Features

1. The Number 5 system permits direct interconnection with all existing types of crossbar, panel, step-by-step, and manual offices. It can be used for a variety of sizes of offices with heavy or light traffic and can operate with few or many interconnecting offices of the various kinds. It also can operate with various types and combinations of numbering plans involving anywhere from 4 to 11 digits.

2. The Number 5 system has the ability to operate as a toll or tandem switching center for a moderate amount of toll

Figure 22. Trouble recorder

or of tandem traffic. In this respect, it includes arrangements which conform to plans for future nation-wide toll dialing.

3. The system is designed for long service life with a minimum of maintenance attention and prolonged periods of unattended operation. In the event of certain trouble conditions within the system, the second trial feature serves to maintain unimpaired service to the subscriber. Ample margins of circuit operation are included in the design to take care of changes in apparatus operating characteristics over the years. To a much greater extent than ever before, protective means have been applied to prevent destructive erosion of apparatus contacts.

4. The Number 5 system exploits the common control principle to a greater extent than any previous system. The common controls are concentrated in a small group of markers. Depending on its size, from 3 to 12 of these will serve any Number 5 office.

5. The equipment arrangements utilize the flexibility inherent in the switching plan and in the circuit arrangements and at the same time provide standardization which tends toward efficient manufacture, job engineering, installation, and maintenance.

6. As many as 30 classes of service for lines (individual or party with flat rate, message rate, coin or extended scope service) can be served through just one design of line link frame and one design of trunk link frame. Lines and trunks in any combinations are cared for by these two basic switch frames.

7. Every intraoffice and incoming trunk circuit in the Number 5 system can complete universally to any line and any party on it regardless of variations in ringing signals. This is so since each of these trunk circuits is represented by one vertical on a ringing switch which, when properly primed by the marker, sends out the correct ringing code on either tip or ring side of the called line.

8. Trunk circuits of each group are distributed as uniformly as possible over all trunk link frames, yet each type comprises a single efficient group and a marker can find any idle trunk of a group on any trunk link frame.

9. The addition of new features is facilitated as shown by the following:

(*a*). In the event that a new device to replace the dial as a calling instrument is developed in the future, the Number 5 system is adapted to accommodate such an arrangement and will do it economically. A new group of originating registers to respond to the signals from such a device would be provided in quantity as needed to serve the originating traffic offered by the subscribers provided with such devices. Both the present dial-pulse type and the new type of originating registers could be used in the same office and both would be associated in the same way with the trunk link frames, but an appropriate line link frame signal would cause the marker to associate the line with the proper type of register. Lines of the new type could be added in large or small quantities without disturbing the normal operation of a working office.

(*b*). In the Number 5 system, the method of associating a sender directly with the outgoing trunk circuit on calls to dial offices, (and manual *PCI*), and the availability of the various kinds of senders mentioned previously, provides a maximum degree of flexibility for inter-office pulsing signals. The senders of each type are relatively simple. They are furnished only when their specific services are required and then in only the quantities needed to handle the traffic in the particular office. If new inter-office pulsing systems are developed in the future, new groups of senders can likewise be provided economically for use with only those trunk circuits which are associated with the new facilities.

References

1. Crossbar Dial Telephone Switching System, F. J. Scudder, J. N. Reynolds. *Electrical Engineering* (*AIEE Transactions*), volume 58, May 1939, pages 179–92.

2. Fundamentals of the Automatic Telephone Message Accounting System, J. Meszar. *AIEE Transactions*, volume 69, part 1, 1950, pages 253–69.

3. Operator Toll Dialing, J. J. Pilliod, H. L. Ryan. *Bell Telephone Magazine*, volume XXIV, 1945, summer section, pages 101–18.

4. Multi-Frequency Pulsing in Switching, C. A. Dahlbom, A. W. Horton, Jr., D. L. Moody. *AIEE Transactions*, volume 68, part I, 1949, pages 392–96, and *Electrical Engineering*, June 1949, pages 505–10.

5. Crossbar Toll Switching System, L. G. Abraham, A. J. Busch, F. F. Shipley. *Electrical Engineering* (*AIEE Transactions*), volume 63, June 1944, pages 302–09.

No Discussion

Fundamentals of the Automatic Telephone Message Accounting System

JOHN MESZAR
MEMBER AIEE

RECENTLY, automatic message accounting (AMA) systems have been placed in commercial service by the Bell System in the Philadelphia and Detroit areas. These systems record in the central offices all the data required to charge for subscriber dialed telephone messages, both local and toll, and process this record in accounting centers through computing, sorting, summarizing, and printing machinery. Both the recording and processing arrangements have many unique technical aspects.

The AMA system is a major contribution to telephony. Its use will permit wide expansion of direct subscriber dialing to nearby and more remote points, with resultant increased economy, speed, and convenience to telephone service customers.

This paper discusses the economic background of the AMA system, explains its fundamental coding technique, describes its unique apparatus elements, and presents the basic features of both the recording and processing machinery.

Economic Background of AMA

It will be readily admitted by everyone that collection of earned revenue is essential for successful business. Before revenue can be collected, however, most business firms have to prepare and present bills to their customers.

Telephone companies have unique problems in preparing bills. They sell tailor-made service items to millions of customers. Each service item consists of putting temporarily at the customer's disposal an impressive physical plant, and a skilled human organization, to enable him to communicate at will with his family, friends, business associates, around the corner or thousands of miles away. A very large proportion of these service items is of truly low price. Although the Bell System, for example, is a multibillion dollar concern, its revenue is derived primarily from service items, a great many of which bring into the kitty only 5 cents or even less. There are, of course, items that bring in 10 cents, 15 cents, 20 cents, or higher, but even these can be honestly classified as low priced service items. What runs up the system's total annual revenue into hundreds of millions of dollars is the enormous volume of these low priced service items. In 1948, the Bell System handled, on the average, every minute of the year approximately 100,000 telephone conversations for customers who number upwards of 25,000,000.

It does not require much imagination to appreciate that the accounting and billing problems of such a business must indeed be great. These problems are, of course, eased by the fact that much of the Bell System's local telephone service is rendered on a "flat rate" basis, meaning that the payment by the customer of a fixed monthly sum entitles him to make an unlimited number of telephone calls within a specified local area. In great metropolitan centers, however, such as in the New York area, and under other conditions as well, local telephone service is metered. Metered service is rendered on a "message rate" basis, meaning that each completed call, even though within the local area, is individually charged for in terms of "message units." A local call may be worth one or more message units, and the telephone service rate structure uses four parameters for determining its value: that is, (a) variable intervals are allowed as initial conversation periods; (b) variable message unit values are assigned to these initial periods; (c) variable intervals are allowed as overtime periods; and (d) variable message unit values are assigned to these overtime periods. A particular combination of these four variable parameters is designated by an arbitrary number and referred to as the "billing index" of the call. Table I illustrates a message unit rate plan.

Message-unit type calls are referred to as "bulk-billed" calls because individually they are not listed on the customer's bill. Only the aggregate charges for all such calls in a billing month are shown. These charges are determined by converting the total message units of a billing month into dollars and cents prior to billing. The conversion factor may be, for instance, four cents per message unit or some other higher or lower value. (Metered service is, in general, offered on the basis of the customer paying a fixed minimum monthly sum, for which he is allowed a stated number of message units during the month. Message units used above this allowance are then charged for at the prevailing rate.)

Irrespective of whether local service is on the flat rate or message rate basis, calls to points outside the specified area are "toll" calls. The significant thing about toll calls from the accounting and

Table I. Message Unit Rate Plan

	Initial Period		Overtime Period	
Billing Index	Minutes	Message Units	Minutes	Message Units
1	Unlimited	1		
2	5	1	5	1
3	4	2	2	1
4	3	2	1	2

Paper 50-42, recommended by the AIEE Communication Switching Systems Committee and approved by the AIEE Technical Program Committee for presentation at the AIEE Winter General Meeting, New York, N. Y., January 30–February 3, 1950. Manuscript submitted November 1, 1949; made available for printing December 1, 1949.

JOHN MESZAR is with the Bell Telephone Laboratories, Inc., New York, N. Y.

billing standpoint is that they are listed individually and chronologically on each customer's "Toll Service Statement", which accompanies the bill. Furthermore, on this service statement, pertinent details of each toll message are shown, such as the date of the message, its destination, and its price. The determination of the price of the message has to take into account such factors as distance between calling and called areas, duration of conversation, the date and time of the call, and so forth.

One would think that only relatively high priced calls have to be identified in detail on customer's service statements. This is not so. Existing telephone rate structures, which are subject to state and federal government regulation, are such that a sizeable volume of even 5 cent or 10 cent calls are detail-billed toll calls. Table II gives some interesting Bell System figures.

As this table shows, there were in 1948 about 1.2 billion annual toll messages of 35 cents or less. Of the 1.2 billion about 50 per cent were 5 and 10 cent calls. The 450 million messages over 35 cents are the ones generally classed as long distance toll.

Two closely related factors should be emphasized at this point. The first is that most toll messages, even those priced at only 5 cents, are handled by operators at switchboards, in order to record on individual tickets the details required by the billing technique. Second, the billing technique itself is, in turn, greatly complicated by the necessity of carrying the originally recorded details of each toll call through the complete process.

In view of the foregoing, there is obviously an intense need to handle ever more efficiently the great volume of low revenue telephone service items. The urge is two fold: to improve the economy of establishing telephone connections; and to improve the economy of billing for the service. In the first area, one answer is the ever wider extension of automatic connecting methods, which permit both customers and operators to dial over greater and greater distances. In the second area, a most promising answer is the recently developed AMA system.

Existing Telephone Message Accounting Methods

While telephone message accounting today is mostly manual work, it makes full use of such modern office equipment as bill printing and addressing machines, inserting and mailing machines, and so forth. Furthermore, the bulk-billed messages are mostly automatically metered by individual subscriber message-registers. These registers score one or more counts for each chargeable message and indicate the total of such registrations. Manual work is, of course, involved in reading these registers, in subtracting the preceding month's registration from the current month's registration, and in arranging the net usage figures in telephone number order, to match the order in which subscribers' records are kept.

Table II. Bell System Toll Messages—Estimated for 1948

Charging Rate	Number of Messages, in Millions
5¢	140
10¢	450
15¢	260
20¢	140
25¢	90
30¢	70
35¢	50
Total 5¢–35¢	1,200
Over 35¢	450
Total	1,650

Another partial exception to manual accounting in the Bell System is used in the Los Angeles and San Francisco areas. Here, in certain step-by-step type dial telephone offices, multimessage-unit traffic is recorded automatically on slips of paper by a system called "automatic ticketing."[1]

It is not the bulk-billed message-unit type calls, however, but the detail-billed toll calls that offer the best opportunities for more economical operating and accounting techniques than have been used in the past. As stated previously, most of these calls today are established by operators in order to record on individual tickets the necessary billing details. The operator tickets are forwarded daily in packages from the operating telephone offices to an accounting center, where the accounting work is done for a group of offices. The staff of a typical accounting center may handle over a million operator tickets a month for, say, a quarter of a million customers. These tickets have to be timed, rated in dollars and cents, sorted into calling telephone number order, transcribed (by typing) onto customers' toll service statements, totalled, taxed, and finally posted on the customers monthly bills. This is a bare outline of what an accounting center has to do with over a million pieces of paper every month. Extra steps are superimposed for intercompany revenue settlements, for collecting essential statistics, for checking accuracy, and so forth.

In spite of the fact that this telephone message accounting is essentially manual work, through many years of intense effort it has been brought to very high efficiency. The ultimate objective of automatic techniques, such as the AMA system, is, of course, to make it even more efficient and economical by mechanizing the whole process, beginning with the initial recording of the required data, and ending with the printed monthly bill mailed to the customer. This is a major objective, and it was decided in the early stages of the AMA development not to try to accomplish it all at once. A more modest initial goal had been set instead, which called for the full development of the automatic recording technique in certain types of dial central offices, but assumed only partial mechanization of the accounting center processing.

Fundamental AMA Coding Technique

For each telephone message, the essential billing data are: (a) the identity of the calling customer who will foot the bill; (b) the identity of the called telephone; (c) the exact time that conversation starts, generally referred to as the "answer time"; (d) the exact time that conversation ends, generally called the "disconnect time." For bulk-billed calls it is not necessary to record the called telephone number. Instead, the arbitrary one digit billing index may be recorded to represent the charging treatment applicable to the call.

In addition to the data individual to each telephone message, there are certain items of information which are common to large groups of calls, and hence need be recorded but once. In this category are such data as the month and date of the calls, the identity of the recording central office, and so forth.

All of this information can be conveniently expressed in numbers. The calling customer is identified in terms of his telephone number. The called telephone is dialed of course as a number. The date of the call is one of 12 months and one of 31 days. The time at the beginning and end of the conversation is stated in hours, minutes, and tenths of minutes. Billing indices and all other incidental information also can be expressed in terms of numbers.

Thus, in the central office, the AMA system needs to record only appropriate numbers. This record of the original billing data has to be semipermanent for use subsequently in the accounting center. In fact, most telephone companies pre-

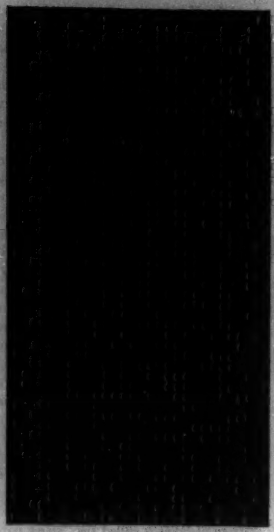

Figure 1. Section of central office AMA tape showing pattern of perforated holes

serve the central office record for several months. The AMA recording is done, therefore, in the form of patterns of holes on a 3-inch wide paper tape. The tape is supplied in 3,000-foot sections, and by splicing sections, the equivalent of a continuous supply is available. Figure 1 shows a piece of central office AMA tape. Across this AMA tape there are 28 hole-positions, divided into one group of three (referred to as the *A* digit), and five groups of five (referred to as the *B*, *C*, *D*, *E*, *F* digits). The *B*, *C*, *D*, *E*, *F* digits are each used to record a decimal (0 to 9) digit. This is done by perforating in each digit two out of five possible holes. There are exactly ten combinations of two out of five holes, or just enough to represent the ten values of a decimal digit. Rather than using arbitrary pairs of holes to represent the ten values, the five hole positions are designated

0, 1, 2, 4, 7,

and a digit is represented by punching the two holes whose designations add up to its value. Thus "1" is represented by punching holes designated 0 and 1; "2" is represented by punching holes designated 0 and 2; and so forth. There is a single exception to this additive arrangement. The digit "0" is represented by punching holes designated 4 and 7. Since this is the only exception to the additive rule, it can be easily remembered.

This so-called "2-out-of-5 additive code" is of fundamental importance in the AMA system. It is used not only in recording information on the central office paper tape, but is woven into the relay circuitry throughout the system. It requires only five elements, holes or relays, to represent any one of ten values and, even more important, its rigid pattern of two and only two elements out of five permits a constant, precise automatic check for correctness.

Since the *B*, *C*, *D*, *E*, *F* digits of the AMA tape can represent decimal digits, any 5-digit number can be recorded in one row of holes across the tape. The *A* digit has room for only three holes. To preserve the AMA system's rigid checking technique for valid combination of elements, these three hole positions are used to represent only one of four values by punching any one, or all three, of the holes, but never two holes. Thus a complete row of the 28-hole positions, *A* to *F* digits inclusive, is good for any one of 400,000 valid combinations of holes, representing any number from 000000 to 399,999. Figure 2 is a representation of a typical line of tape record. The black circles stand for perforated holes, the white ones are unperforated hole positions. The staggering into upper and lower rows is done only for physical spacing reasons in perforating mechanism.

AMA 6-Digit Number Language

Elaborations of the fundamental numerical representation just described are used to express all information the AMA system has to deal with. The information is always stated in terms of six digit numbers. Of these six digits, one or more are used as a code to specify the nature of the associated information. Thus, "282" in the *A*, *B*, *C* digits of the central office tape, for example, is the code which specifies that: "The associated *E* and *F* digits represent the date on which the recorded telephone calls were made." The verbal statement: "These telephone calls were made on the fifteenth day of the month" would, therefore, be stated in AMA language as

282015

The 0 in the *D* digit is simply a filler-in to satisfy the six digit requirement.

In the same manner, "283" in the *A*, *B*, *C* digits is the code which specifies that: "The associated *E* and *F* digits represent the month in which the telephone calls were made". The verbal statement: "These telephone calls were made during the month of December" would, therefore, be stated in AMA language as

283012

Not all codes specifying the nature of information are of three digits. For example, the number "1" alone in the *A* digit of the central office tape is used to specify that: "The associated *B*, *C*, *D* digits represent the time when a particular conversation started, and the *E*, *F* digits contain a number which identifies this conversation." (The significance of this identity number will be brought out later.) The AMA statement

148632

means that conversation number 32 started 48.6 minutes after the last recorded hour.

As one more example, the 2-digit code "23" in the *A*, *B* digits of the central office tape defines the significance of information contained in the associated *C* to *F* digits, as well as in the immediately succeeding three lines of digits. These four lines represent the full initial information available on a detail-billed call at the completion of subscriber dialing. A typical pattern specified by the code 23 is as follows:

239011
045665
081677
032356

In this pattern the 0 in the *D* digit of the first line is again a filler-in. The O's in the *A* digits denote supplementary lines of information.

The verbal equivalent of this AMA statement is: "A call has been initiated which will have to be detail-billed (23); the call is to be charged for in accordance with toll rate structure (9); the call is labelled number 11; the calling central office is designated number 4; the telephone number of the calling subscriber is 5665; the geographic area of the called place is designated number 8; the called

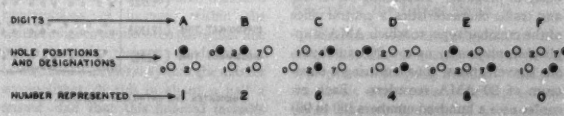

Figure 2. Representation of a line of AMA tape record

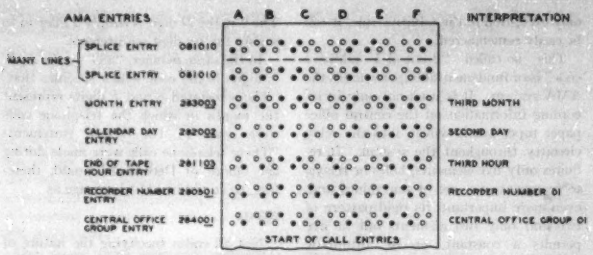

Figure 3. Representation of starting pattern of central office AMA tape

telephone number may contain a party letter (this information is conveyed by value 1 in the *C* digit of the third line); the called telephone office is 677 (this might be, for example, ORange 7); the called number is 32356 (since the last digit of this number corresponds to a party letter, the system will deliver it at its output as 3235M).

Enough examples now have been given to illustrate the AMA number language. In this language each statement is called an "entry." An entry consists of one or more 6-digit-numbers whose digits have a precise significance.

Central Office AMA Recording—General

The information required for billing for dialed telephone message service can only be collected within the central offices. It is the switching mechanism in the central office into which the calling subscriber dials his request for a telephone connection. It is the switching mechanism of the central office that determines his identity, establishes the requested connection, and times the conversation.

As stated before, the basic information per call required for billing purposes is: the calling telephone number, the called telephone number, the time conversation starts, and the time conversation ends. Each of these bits of information can be recorded automatically in a fraction of a second. Therefore, the tying up of a recorder with an individual call of minutes duration is unnecessary. In the AMA system one recorder is used for as many as a hundred calls that may be simultaneously in progress. Depending on its size and traffic characteristics, a central office of the crossbar type, to which AMA is applicable, may carry up to 2,000 simultaneous conversations, thus requiring a maximum of 20 AMA recorders. Each recorder uses a hundred numbers (00 to 99) to label its simultaneous calls. Physically, these 2-digit labels are assigned to the transmission channels (trunks), one of which is allotted to a calling subscriber by the dial switching mechanism for the duration of his call. An AMA recorder works with a particular group of 100 trunks, and is automatically connected to one of them only when billing information need be recorded for a call established over that particular trunk. Normally, per call, there are three such instances of association. First, the "initial entry" (calling and called telephone numbers) is recorded when the dialing has been completed by the calling subscriber. Second, the "answer time entry" is recorded when the conversation starts. Third, the "disconnect time entry" is recorded when the conversation ends. These entries are recorded by the common recorder in a chronological order as they occur on the various trunks. The central office tape from a recorder is in effect a log book of the billing events that occurred on a group of 100 trunks. Obviously, this recording technique results in the entries of the various calls getting interleaved. However, each entry of a particular call is identified by the same label, which is the two digit number of the trunk assigned to transmit the conversation. This is an important point to which reference will be made later in describing how the AMA accounting center processes the central office tape.

In addition to the individual call entries, the over-all accounting and billing job requires the recording of certain incidental information. For instance, information common to all calls, such as the month, day, recorder number, and so forth, is recorded right at the beginning as well as at the end of each tape. Also, the hour of the day is recorded every hour on the hour. Furthermore, since the central office tape has to be sent every day or every few days to the accounting center, it must be periodically cut. To mark the most convenient cutting spot, a distinct pattern of holes is automatically perforated at the right spot of the tape. The code for this pattern is 081010, and enough consecutive lines of this code are recorded to permit convenient cutting and subsequent handling. The 081010 pattern of holes is called the "splice pattern," because it also permits splicing tapes end-to-end without mutilating any of the useful information on the tapes.

A starting pattern of a central office AMA record is therefore as indicated on Figure 3. Figure 4 in turn represents a section of the central office AMA tape.

AMA Recording Apparatus

The unit that actually makes the pattern of holes in the AMA tape is called the perforator. Figures 5 and 6 present two different views of this perforator, and its

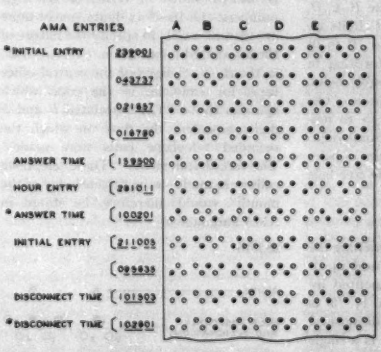

Figure 4. Representation of a section of central office AMA tape

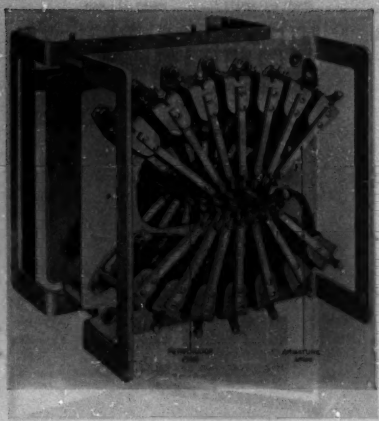

Figure 5 (left). Top view of AMA perforator

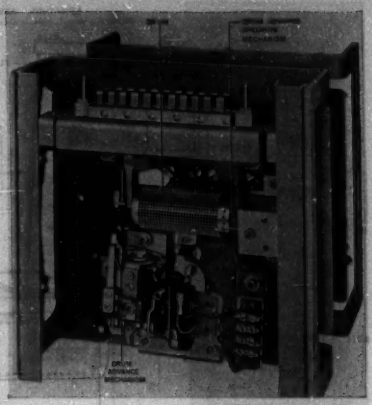

Figure 6 (right). Bottom view of AMA perforator

basic features are shown on Figure 7.

The perforator has 28 electromagnets, any valid combination of which can be energized by control circuits. When energized, each magnet pushes a mechanically coupled steel pin through the paper tape. The points of the 28 steel pins are physically concentrated into a row across the tape, with alternate pins slightly offset into an upper and lower row. The tape lies on the circumference of a cylindrical drum which has a countersunk hole opposite each steel pin. All the required holes for a 6-digit number are perforated at once. In most cases this means perforating 11 out of the possible 28 holes, 2 out of 5 for the *B*, *C*, *D*, *E*, and *F* digits and 1 out of 3 in the *A* digit. Occasionally the *A* digit requires three holes, and in this case a total of 13 out of the possible 28 holes is perforated all at once. As soon as the holes have been perforated, the electromagnets are de-energized, resulting in the withdrawal of the associated steel pins from the tape. Then the drum turns 1/10 of an inch, moving the tape with it. The tape is now ready for the next row of perforations. The perforated tape and the drum constitute a self-gearing arrangement without the necessity for any sprocket holes.

Blank tape is pulled by the perforator out of a bin which is replenished in such a manner as to give the equivalent of an endless supply. The perforated tape is reeled up automatically as it develops slack. Figure 8 shows a complete perforator cabinet with two perforators.

Central Office AMA Circuits

The relay circuits controlling the central office AMA perforators are not simple. Some of this circuitry is intimately integrated into the dial switching mechanism of the central office, but there are major units that are used exclusively for AMA. None of the circuits will be discussed here in detail. It is appropriate to say, however, that, like their companion switching circuits which automatically establish the telephone connections, these AMA circuits represent some of the most intricate creative accomplishments of the human mind. The jobs these circuits perform, and the precision and speed with which they work, are truly remarkable. To gain a general idea of what is involved, a functional block diagram of the AMA circuits in the Number 5 crossbar dial switching system[3] is shown in Figure 9, and Figure 10 shows one of the functional units. The following brief description of the basic AMA recording features is based on this diagram.

When a subscriber initiates a call, one of the "markers" which are the brainiest, costliest, and hardest working circuit units of the number 5 switching system, connects his line automatically to an "originating register" circuit unit, from which dial tone is received. This simple statement covers the job of spotting and identifying the calling subscriber amongst perhaps 20,000, of determining the class of service he is paying for, of searching and locating an available register from amongst dozens, and of choosing an appropriate one of several hundred thousand combinations of linkages within the central office to connect the particular line to the particular register. It also should be mentioned incidentally that the marker accomplishes all this in about a half a second, and that this interval includes passing the calling subscriber's identity and class of service into the register. Figure 9 shows the subscriber-to-register dialing connection in dotted, since it is part of the regular switching operation and precedes the AMA functions.

The subscriber now dials the desired telephone number into the register, which stores this information. During this dialing time the marker is attending to the needs of other subscribers.

Once the register has received the complete wanted number from the subscriber, it connects itself to an available marker, and requests this marker to set up the connection between the calling and called numbers. The marker first determines, from the relationship of the calling subscriber's class of service and the called number, that the call is a chargeable call, that a certain rate treatment is applicable to it, and that the called party has to be reached, say, via another central office. The marker then proceeds to select an available AMA type "outgoing trunk" to the desired central office and starts the job of establishing the connection between the calling subscriber and this chosen outgoing trunk. The job of establishing this connection is of the same nature as was that of establishing the connection between the calling subscriber and the register. This job also is an integral part of switching. The sole contribution to AMA is the choice of the proper type of outgoing trunk.

Recording the Initial Entry

Coincident with the selection of the outgoing trunk, the marker also selects an appropriate "outgoing sender." This is the circuit unit in the switching system whose primary function is to send the called number to the completing central

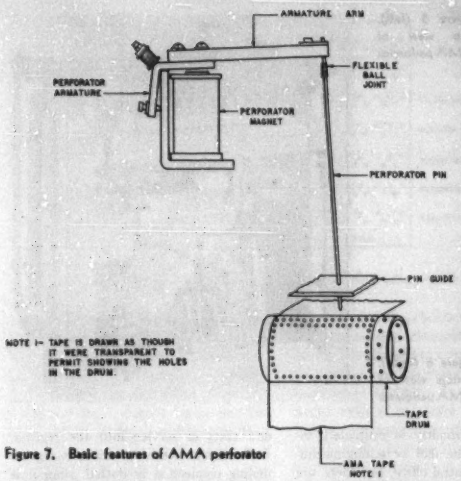

Figure 7. Basic features of AMA perforator

Figure 8. Perforator cabinet showing tape supply bins, perforators, and take-up reels

office at a time and in a form acceptable to that office. AMA superimposes another major function on this unit, which is to store temporarily certain billing data that the marker has determined, and which will eventually be recorded on the AMA tape. This is done, of course, to permit the marker to release from the call at the earliest possible moment to serve other calls. Typical AMA data stored in the sender by the marker are: (a) the identity of the calling subscriber; (b) the called number; (c) the message billing index for the call; and (d) the identity of the recorder which serves the selected trunk.

When the marker is almost finished with its work of establishing the connection from the calling subscriber to the outgoing trunk, it notifies the sender to connect itself to the "transverter." The transverter is exclusively an AMA circuit unit of some complexity. Its over-all function is to convert the initial information for the call into the 6-digit numerical AMA language, and to control the recording of this entry.

As soon as the sender connects to the transverter, it sends enough information into the transverter regarding the identity of the calling subscriber to enable the transverter to connect itself, in turn, to an appropriate "translator." The translator is also exclusively an AMA circuit unit of intriguing performance. Its over-all function is to translate the calling subscriber's identity into his telephone number. This function makes sense only when it is realized that the subscriber's identity is determined originally by the marker in terms of the central office equipment number to which his line is wired. To care for changes in traffic requirements, connection of new subscribers, and so forth, the relationship between subscriber line equipments and telephone numbers is made flexible, and the translator is, in effect, an ingenious electromagnetic card file system, which is "consulted" by the transverter to obtain up-to-the-minute information on this relationship. One unit of the translator corresponds to one of 20 drawers of the card file, each having a 1,000-card capacity. Once the appropriate translator unit is seized by the transverter, the complete central office line equipment number of the calling subscriber is transmitted to it partly by the transverter and partly by the outgoing sender via the transverter. In an instant, the translator returns the correct telephone number of the calling subscriber. The transverter memorizes this telephone number and dismisses the translator unit to serve other calls.

The transverter and sender, between them, now have most of the information necessary to record the initial entry of the call. The only missing item is the number of the selected outgoing trunk, which is required as a call-identifying label. On the basis of the recorder number given earlier to the sender by the marker, the transverter now connects itself to the "recorder." The recorder also is exclusively an AMA circuit unit containing the perforator and the paper tape supply. Through the transverter, the complete AMA statement for the initial entry is then furnished to the recorder and is perforated on the tape one line at a time. When it is time to perforate the line which requires the call-identity label, the transverter requests this information from the trunk via the "sender link" path. The trunk, with the aid of the "trunk identifier," another exclusively AMA circuit unit, furnishes the 2-digit call label in AMA form direct to the recorder. When the perforating of the initial entry is finished, the transverter and recorder release. The sender also restores to normal, provided that it had already finished its switching job of transmitting information to the completing central office.

The recording of the complete initial entry takes but a fraction of a second.

Recording the Answer Time Entry

If a call encounters a "line busy" or "don't answer" condition, obviously no time-entries are recorded for it. When a call is answered, the supervisory function of the outgoing trunk comes into play to signal the appropriate recorder through the trunk identifier. As a result, the recorder perforates the call identity label, and the time of day at that moment in terms of minutes and tenths of minutes. The recorder keeps track of time within itself under control of a common "master timer." The master timer is one more exclusively AMA unit. It is a circuit comprising a complete electrical calendar and clock.

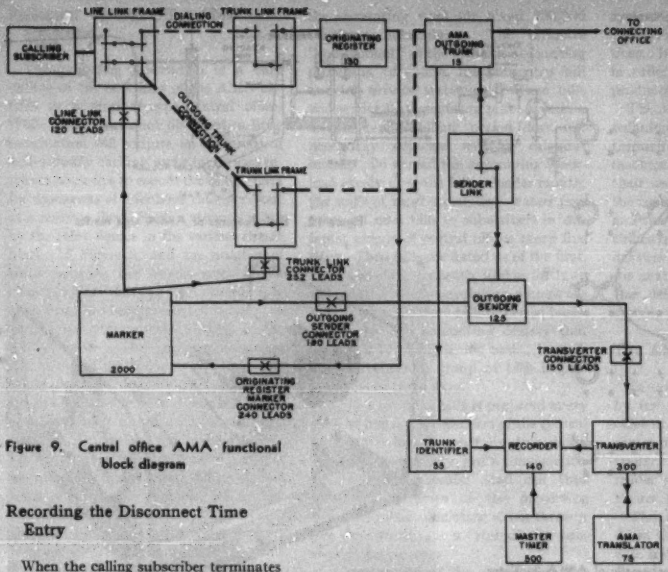

Figure 9. Central office AMA functional block diagram

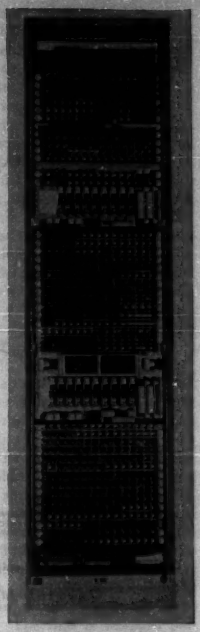

Figure 10. Front view of AMA master timer frame

Recording the Disconnect Time Entry

When the calling subscriber terminates the connection, the trunk via the trunk identifier again requests the recorder to perforate the time of day and the call identity label in the same manner as for the answer time.

Recording of Entries Common to Groups of Calls

It was already mentioned that there are certain entries recorded infrequently on the AMA tape, because such entries are common to groups of calls. Common entries are perforated by the recorder under direct control of the master timer. Thus, every hour on the hour the master timer connects itself to the recorder to perforate the hour information. The code for the hour is

2810XX

where XX is from 00 to 23. Midnight is the 00 hour.

Also, at 3 a.m., the master timer controls the perforation of the cutting or "end-of-tape" pattern which includes the month, day, recorder number, central office identity number, and so forth, followed by splice pattern. (3 a.m. was chosen because at that time the least number of telephone calls are in progress in the central office.) After the splice pattern is perforated, another set of the month, day, and so forth, entries are recorded to serve as the beginning pattern for the next day's business. The tape may be cut at the 3 a.m. splice pattern any time after 3 a.m. and transported to the accounting center.

Principles of the Translator

Earlier the statement was made that none of the circuit units of the central office will be described in detail. An exception will be made to this statement by introducing at this point a brief presentation of the principles of one unit, the translator. The translator is singled out both because its use illustrates an important practical problem AMA has to deal with, and also because of the ingenuity of its technical features.

The practical problem referred to comes about this way. The two wires of a subscriber's line terminate within the central office in an appropriate type of individual "line equipment". These line equipments are the subscribers' entrance points into the switching system. Line equipments are, of course, physical entities. For example, in a crossbar-type central office a line equipment consists of a line-relay and a crossbar switch vertical unit. These line equipments are designated by numbers which specify their location in the central office. It is in terms of this "line equipment number" that the marker in the Number 5 crossbar system originally identifies the calling subscriber. But, a telephone subscriber's ultimate identity is in terms of his telephone number, and these two numbers, that is, the line equipment and telephone numbers, are not at all identical. The problem of translation from one into the other would, however, not be troublesome if it were not for the fact that, for many reasons, the association between a subscriber and a particular line equipment does not stay put. Subscribers may change their class of service, requiring a new type of line equipment. Growth in the size of central office results in periodic rearrangement. Also, call congestion may develop in certain portions of the central office switching system, requiring subscriber line redistribution. Furthermore, a party-line equipment is used by several subscribers, with different telephone numbers. For these and other reasons, the problem of determining the exact relationship at any one time between telephone numbers and line equipment numbers is a troublesome

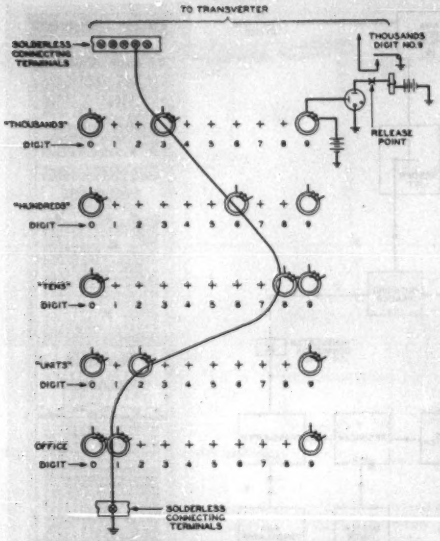

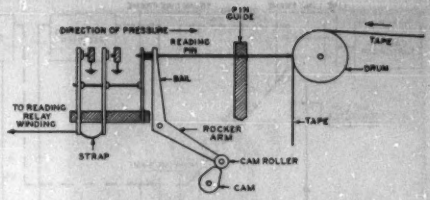

Figure 12. Basic features of AMA tape reader

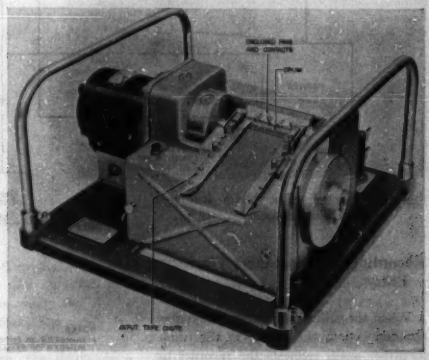

Figure 11 (above). Simplified schematic of AMA translator

Figure 13 (right). AMA tape reader

one. Figure 11 is a much simplified illustration of the AMA translator which is an ingenious solution of this problem.

Physically, the unit consists first of a row of terminals at its top, each of which represents a subscriber line equipment number. Below this row of terminals are five shelves, on which rest doughnut-shaped transformers with secondary windings only. The ten transformers on the first shelf are used to obtain the "thousands" digit of telephone numbers; the ten transformers on the second shelf are used to obtain the "hundreds" digit; the ten transformers on the third shelf are used to obtain the "tens" digit; and the ten transformers on the fourth shelf are used to obtain the "units" digit of telephone numbers. On each of these shelves the ten transformers are designated 0 to 9. There is a fifth shelf for use where the switching system is of the multioffice type. The transformers on this shelf are used to determine the office of a calling subscriber.

The terminals at the top are so designed that the bare end of a piece of insulation covered wire can be connected quickly to any one of them by solderless connection.

This piece of wire then represents a subscriber line equipment number. If the telephone number of the subscriber using the particular line equipment is, say, 3682, the wire is snaked through the doughnut hole in transformer number 3 on the "thousands" shelf, then through transformer number 6 on the "hundreds" shelf, transformer number 8 on the "tens" shelf, and transformer number 2 on the "units" shelf. In a multi-office switching system the wire is also snaked through one of the transformers on the last shelf, to obtain the office of the calling subscriber. The leading end of the wire is then connected, also by solderless connection, to an individual terminal at the bottom. The location of this bottom terminal is symmetrical with that of the top terminal.

The wire thus snaked through the holes of the particular transformers becomes in effect a single turn primary winding for these transformers. The secondary windings on the doughnut-shaped cores are coupled to this single turn primary through air, but they have many turns and are connected into voltage sensitive cold-cathode gas tube circuits, as is shown on Figure 11.

With this physical picture in mind, the operation of the translator is simple to understand. When it is called upon by the transverter to furnish the telephone number corresponding to a particular calling line equipment number, the transverter sends a heavy momentary surge of current through the wire representing the line equipment number. Due to the large turns-ratio, this primary current induces enough secondary voltage in the transformers involved to fire the associated gas tubes, which in turn operate their companion relays. The output, representing the thousands, hundreds, tens and units digit of the subscriber's telephone number, as well as his central office, is taken from the contacts of these relays.

In offices having party lines, separate translators are used for each corresponding group of parties. The originating register determines which party is calling, and the transverter is thus enabled to choose the appropriate translator.

It is obvious from the foregoing description that when a particular subscriber line equipment is reassigned to a new telephone number, only one wire need be pulled out and re-snaked through the appropriate transformers. This is a simple and quick operation, and thus the recurrent rearrangements in the central office between subscriber line equipments and telephone number assignments constitute but a reasonable burden on the AMA system.

Epilogue: Central Office AMA Facilities

The preceding description is a bare outline of the functions of the AMA circuits in a crossbar-type central office. While details were not discussed, a little imagination will conjure up hundreds of relays busily clicking away in various intricate hook-ups to record the billing data for thousands of telephone calls per hour in a central office. Such a vision is aided by the relay figures in the various circuit blocks of Figure 9, and the number of leads between the blocks over which these circuits "talk" to each other. Further, what has been presented is only the simple, straightforward AMA job in the central office. The commercial design has to guard the accuracy and integrity of the recorded data in spite of possible irregularities and malfunctionings. Thus, provisions have to be made for substitution of an emergency recorder for any of the regular recorders in case of trouble; for detecting falsely grounded or crossed leads, or open relay contacts, before they can cause wrong charging; for checking that the basic 2-out-of-5 AMA pattern is never violated; for insuring that the paper tape is moved after each perforation; for guaranteeing that the relay calendar and clock is precise; and so on.

The AMA Accounting Center—General

The accounting center is the place where the message accounting work is done for a number of telephone offices. An average accounting center may handle the accounting work for about 250,000 telephone subscribers. The ultimate "end-product" of the message accounting process is, of course, the subscriber bill and toll service statement. These bills and service statements are sent out once a month, but a billing period does not necessarily coincide with a calendar month. To spread the accounting workload evenly over the full calendar month, the staffs of most accounting centers prepare and mail bills to subscribers in different groups of central offices every five days. Thus bills are dated as of the first, sixth, eleventh, sixteenth, and so forth, of the month. Such accounting centers are said to work on the 6-billing period basis. There are also accounting centers that work on a 10-billing period basis. In such offices a different group of bills is prepared every three days.

While a group of bills is prepared every three or five days, collection of the central office AMA tape is generally done daily. This is not a necessity, but a convenience. The accounting center staff can thus finish certain steps of the processing daily, before accumulating either three or five days work into a "round" for subsequent processing.

It was stated at the outset that the scope of the initial AMA development included the complete central office recording technique, but visualized only a partial mechanization of the accounting center processing technique. This decision required setting a suitable cut-off point, where the output of the AMA system would conveniently merge into present manual message accounting practices. It is well to keep this point in mind, in order to appreciate the present end-products of the AMA system.

The AMA accounting center processing technique puts the central office data through a series of machines. These machines are designated in the order of their sequential use as: the assembler, the computer, the sorter, the summarizer, and the printer. The first of these machines receives the central office tape and delivers its output on fresh tape for use by the next machine, and so on until the last one delivers the end-products of the system.

The AMA Tape Reader

In order to "read" the data conveyed by the patterns of holes on the central office or other AMA tapes, the accounting center machinery needs first of all a "tape reader." The basic features of this reader are illustrated on Figure 12, and Figure 13 is an illustration of the device.

The reader has the same cylindrical drum as the perforator, with the lengthwise rows of 28 holes and the 0.1-inch circumferential separation between these rows of holes. There is thus a hole in the drum for every possible perforation in the AMA tape. The tape is wrapped partially around the drum for reading, and is "self-geared" with the drum by the spikes of the tape perforations. The drum can therefore move the tape forward step by step, bringing each row of tape holes into the reading position. The reading of the tape means, of course, a determination of which holes are per-

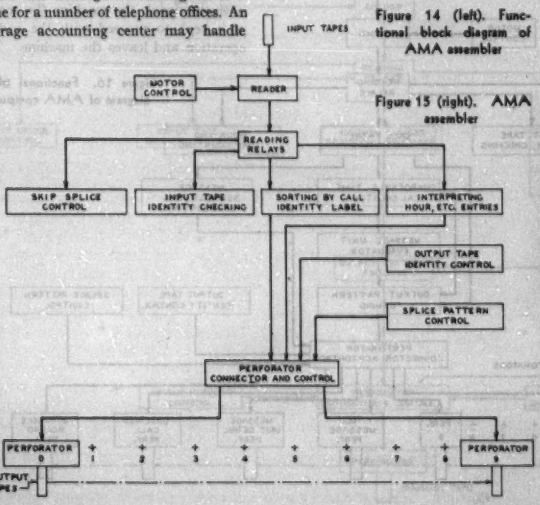

Figure 14 (left). Functional block diagram of AMA assembler

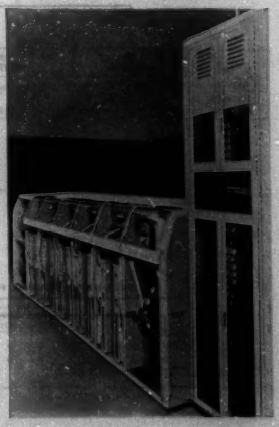

Figure 15 (right). AMA assembler

forated in each of the six digit-positions of a row. For this purpose the reader has a set of 28 thin blunt steel fingers mounted mechanically so as to form 28 feelers for holes. A tensioned spring pushes each of these steel fingers toward the drum. However, the fingers can only travel toward the drum as permitted by the contour of a restraining cam on a motor shaft. As this cam turns, and the steel fingers move toward the drum, those fingers finding a hole in the paper go through into the drum, while the other fingers are stopped in their motion by the paper. Each steel finger is mechanically coupled to a contact carrying detail, and the extra travel of the hole-finding fingers permits their respective contacts to close an electric circuit. The circuit closures in turn result in the operation of individual "reading relays." As the motor continues turning, the contour of the cam on its shaft soon forces all 28 steel fingers away from the drum, opening all contacts. Then the drum turns a tenth of an inch and a new row of tape holes is in position to be read. The motor driven cam now again permits the steel fingers to move toward the drum, and the reading cycle repeats. The reader is capable of going through this cyclic operation 16 times a second.

The AMA Assembler

A reel of central office AMA tape, 18 inches in diameter, contains the billing data for about 25,000 telephone calls. As brought out earlier, the call data are recorded as initial entries and conversation time-entries, each entry of a particular call being suitably labelled but sandwiched among entries of other calls. To permit computation of charges, the first step in the accounting center has to be used, therefore, to pick out and bring together the entries of each call. This is done by the assembler, a machine consisting basically of an input tape reader, a relay circuit of about 350 relays, and ten output recording perforators. Figure 14 is a functional block diagram of this machine and Figure 15 is an illustration of it.

The design of the assembler is based on the fact that the labelled entries of each call are recorded on the central office tape in chronological order. This order insures that, if there is on the central office tape an initial entry labelled, say, 32, the next time-entry on the tape with the label of 32 must be the answer-time entry of the same call, irrespective of the number of entries with other labels sandwiched in-between. It further follows that another succeeding time-entry with the label of 32 is the disconnect-time entry of the same call, no matter how far along the tape it was recorded. The label 32 is used, of course, subsequently for entries of other calls. However, as long as the sequence of the over-all record is not at all disturbed, (and this is a natural result of the tape recording technique) each initial entry serves as a new starting point for associating the next set of identically labelled time-entries.

Thus, the assembler's job is basically to sort the call entries according to their labels, without disturbing in any way their chronological order. Since the labels are two digit numbers, from 00 to 99, the sorting is done in two stages. First, the entries are sorted by the "units" digit of their label. If this digit is, say, 0, the entry is copied on the output tape of the 0 perforator. If the unit digit of the label is, say, 1, the entry is copied on the output tape of the number 1 perforator; and so on. The 0 to 9 output tapes gradually accumulate in their respective receiving bins. When the machine's operation is finished, these tapes are collected, spliced end to end, and reintroduced into the machine for sorting by the "tens" digit of the entry labels. As a result of this second sorting operation, the initial entry, answer time entry, and disconnect time entry of a particular call appear adjacent to one another on the appropriate one of the ten output tapes.

The physical operation of the assembler is, very briefly, as follows: First, by means of manually-controlled multi-position switches, the operator sets the machine to process the dated tape of a given central office recorder group. Then the machine is started and a few inches of splice pattern is perforated at the beginning of all ten output tapes. While the machine is doing this line by line, the operator inserts into the reader the beginning of the central office reel of tape made by the first recorder, using the splice pattern of this tape to engage the tape with the reader's drum. Then the operator signals the machine (by means of a key) to proceed with the sorting operation and leaves the machine. The

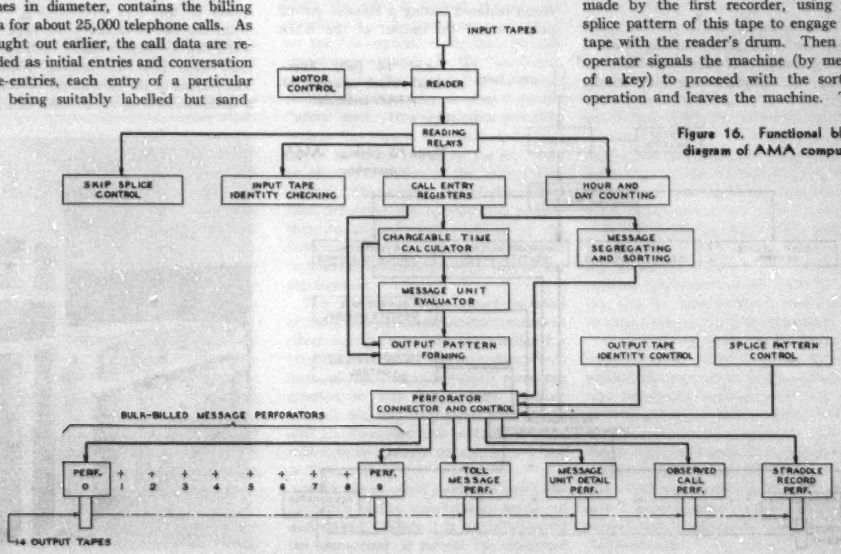

Figure 16. Functional block diagram of AMA computer

machine skips over the remaining splice pattern of the central office tape, until it comes to the tape identification rows of holes, containing the central office identity, the month and date of the tape, the recorder number, and so forth. The assembler matches the information in these rows of holes against its switch settings. If there is full agreement, indicating that the correct tape has been inserted, the machine proceeds to perforate identification information on its own output tapes. Then the machine sorts the individual call entries, pulling the input tape off the reel.

When the last call-entry has been reperforated on the appropriate output tape, and the end of the first recorder's tape runs out of the reader, the machine stops and signals the operator by sounding a chime signal. The operator now restarts the machine with the second recorder's tape. The machine checks the identity of this tape and then continues with its assembling operation. When the machine stops at the end of the last recorder tape, the operator signals it to perforate end-of-tape pattern on all its output tapes. Then, by pushing a key, the operator automatically cuts the ten output tapes, for removal to the splicing table.

What has been described is the simple, straight-forward working of the assembler performed at the rate of approximately 1,000 input tape lines per minute. The commercial version of the assembler has various complications superimposed on its basic functions. For example, the central office record of "every hour on the hour" has to be recognized by the assembler and appropriately associated with the call-entries; various erasure or skip orders received on the central office tape have to be recognized and obeyed; all central office recorders have to be serially accounted for; nonbillable test calls need be spotted and eliminated; central office trouble codes have to be interpreted and associated with calls affected; and so on. These features are, of course, in addition to the regular checking features woven throughout the AMA system.

The Computer

The ten output tapes of the second assembling stage—spliced together end to end and reeled—are fed daily into the reader of the next accounting center processing machine, which is the computer. This machine has, in addition to its input tape reader, a complex circuit of about 1,200 relays, and a number of perforators for recording the machine's output. Figure 16 is a functional block diagram of this machine.

The computer has several major functions. As its name suggests, its most basic function is to make computations. First, it calculates the conversation time of each completed call by subtracting the answer time from the disconnect time. Then it deducts a small fixed allowance to compensate for central office recording variations. The net conversation time is next rounded out to whole minutes, because telephone messages are charged for on the basis of minutes. This value of chargeable time is perforated on the output tapes of the computer for toll messages.

On bulk-billed messages, the computer makes additional calculations. It determines the message unit value of each such call, taking into account the chargeable time and the four parameters of the rate treatment applicable to the call. The message value is perforated by the computer on its output tapes of bulk-billed calls.

A second major function of the computer is to segregate the calls into different categories for facilitating subsequent processing. For example, as implied before, toll calls are segregated from local calls and both are perforated on separate output tapes. Another separate category is incompleted calls (calls that were not answered, and those that encountered a "line busy" condition). Such calls are simply discarded by the computer. Still another category is the message unit detail type calls. These are calls which are bulk-billed, but on which certain billing details are recorded and preserved for use by the business office

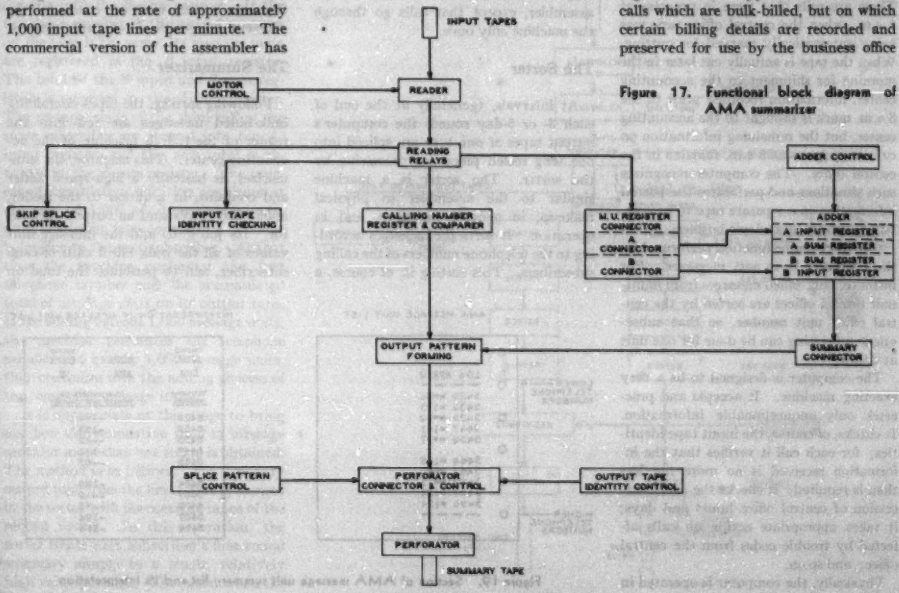

Figure 17. Functional block diagram of AMA summarizer

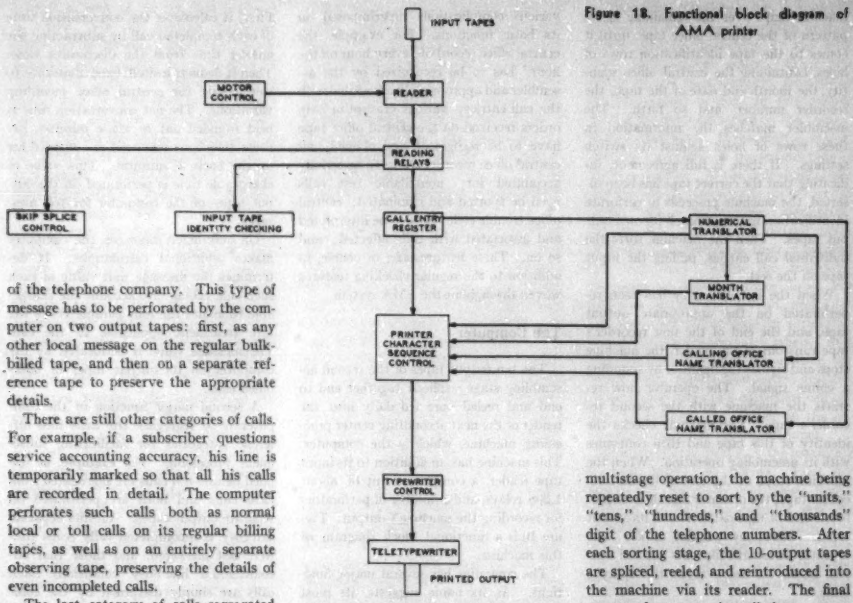

Figure 18. Functional block diagram of AMA printer

of the telephone company. This type of message has to be perforated by the computer on two output tapes: first, as any other local message on the regular bulk-billed tape, and then on a separate reference tape to preserve the appropriate details.

There are still other categories of calls. For example, if a subscriber questions service accounting accuracy, his line is temporarily marked so that all his calls are recorded in detail. The computer perforates such calls both as normal local or toll calls on its regular billing tapes, as well as on an entirely separate observing tape, preserving the details of even incompleted calls.

The last category of calls segregated by the computer is the "straddle" calls. These are calls that were in progress at 3 a.m., when the central office tape was being automatically marked for cutting. When the tape is actually cut later in the morning for shipment to the accounting center, information recorded prior to the 3 a.m. mark is brought to the accounting center, but the remaining information on calls in progress at 3 a.m. remains in the central office. The computer recognizes such situations and perforates the partial information on a separate tape to be combined with the next day's business.

One more major function performed by the computer is to sort messages. For instance, bulk-billed messages from multi-unit central offices are sorted by the central office unit number, so that subsequent processing can be done for one unit at a time.

The computer is designed to be a very exacting machine. It accepts and processes only unquestionable information. It checks, of course, the input tape identities; for each call it verifies that the information received is no more nor less than is required; it checks the exact succession of central office hours and days; it takes appropriate action on calls affected by trouble codes from the central office; and so on.

Physically, the computer is operated in a manner similar to that described for the assembler, except that calls go through the machine only once.

The Sorter

At intervals, (generally at the end of each 3- or 5-day round) the computer's output tapes of one type are spliced into one long reeled piece, for processing by the sorter. The sorter is a machine similar to the assembler in physical makeup, in general functions, and in operation. It sorts the messages according to the telephone numbers of the calling subscribers. This sorting is, of course, a multistage operation, the machine being repeatedly reset to sort by the "units," "tens," "hundreds," and "thousands" digit of the telephone numbers. After each sorting stage, the 10-output tapes are spliced, reeled, and reintroduced into the machine via its reader. The final output of ten tapes has all the messages in ascending telephone number order. Separate sorting runs are made for the different categories of computer outputs.

The Summarizer

Following sorting, the tapes containing bulk-billed messages are fed into the reader of the fourth machine of the accounting center. This machine, the summarizer, is basically a high-speed adder and contains, in addition to the reader, about 600 relays and an output perforator. Its job is to add the message unit values of all the bulk-billed calls of each subscriber, and to perforate the total on

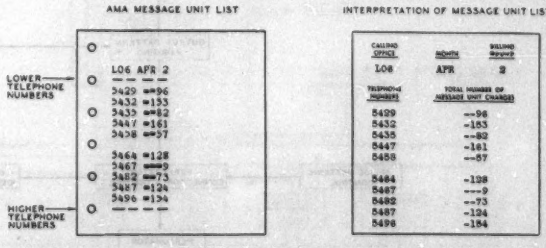

Figure 19. Section of AMA message unit summary list and its interpretation

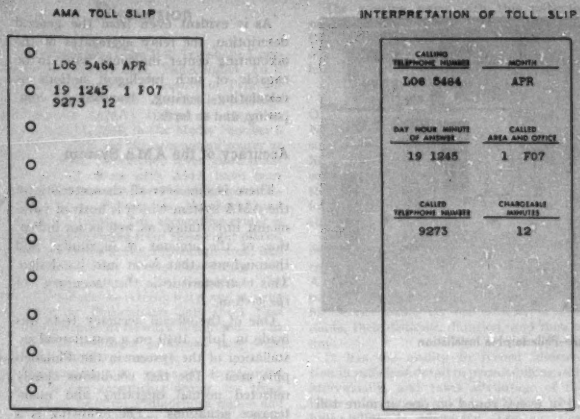

Figure 20. AMA toll slip and its interpretation

its output tape. Figure 17 is a functional block diagram of this machine.

The summarizer memorizes the calling telephone number of the first message on the input tape, and puts the message units into its A input register. Since this is the first message, the A-sum register has no sum in it. The message units in the A input register are therefore transferred directly into the B-sum register. If the telephone number of the second message on the tape is the same, its message units are registered in the B input register. The total of the B input and B-sum registers is recorded in the A-sum register. The message units of the third call of the same subscriber are steered into the A-input register, and the new total is recorded in the B-sum register. The process of cumulative addition continues at the rate of 1,000 additions per minute, until the input tape comes to a message belonging to the next subscriber. At that time the machine perforates the first telephone number and the accumulated total of message units on its output tape. If the adding exceeds 1,000 message units, the machine perforates the telephone number and exactly 1,000 message units, then continues with the adding process of the remaining message units.

It is appropriate at this stage to bring out how the cumulative total of message units for more than one round is obtained. The method is as follows. The summary output tape from the first round is merged in the sorter with the message tapes of the second round. In this operation, the sorter treats each subscriber's first round summary simply as a single, relatively high value message. Therefore, when the sorted tapes of this second round are put through the summarizer, the new message unit total includes the first round summary with the messages of the second round. In the same manner, the summary of the first two rounds is merged with the individual messages of the third round, and so on, until the final round of the billing period is included.

The Printer

This is the last accounting center machine, and its output is the output of the present AMA system. The machine comprises a tape reader, a relay circuit of about 800 relays, and a teletypewriter. Figure 18 is a functional block diagram of this machine.

The printer's main functions are to read an input tape, translate its patterns of holes into letters and numbers, arrange these letters and numbers in meaningful groups, and type the information, one character at a time, with appropriate headings and spacings. The typing is done at the rate of 600 characters per minute.

The basic translation done by the printer is, of course, from the 2-out-of-5 hole patterns into equivalent decimal numbers. Supplementary translations

Figure 21. Flow chart of AMA accounting center processing

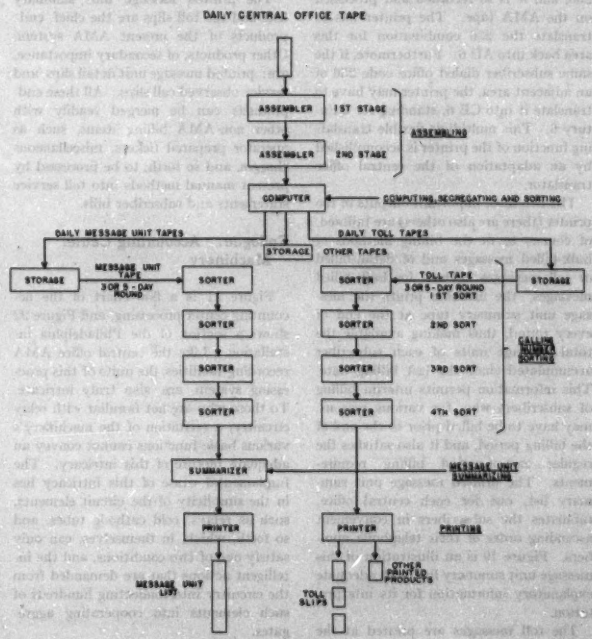

Figure 22. AMA accounting center—Philadelphia installation

from numbers into alphabetical characters are performed, for example, for month designations; that is, month number 12 is translated into DEC. The most flexible translation job in the printer is, however, used to obtain the called central office name for each detail billed message. A calling subscriber, for instance, dials the ADam 6 office in his home area as AD 6. Actually his dial pulses this office code as 236, and it is so recorded and processed on the AMA tape. The printer has to translate the 236 combination for this area back into AD 6. Furthermore, if the same subscriber dialed office code 236 of an adjacent area, the printer may have to translate it into CE 6, standing for CEntury 6. This multidigit flexible translating function of the printer is accomplished by an adaptation of the central office translator.

The two most important outputs of the printer (there are also others) are tailored, of course, to fit the billing methods of bulk-billed messages and of detail-billed or toll messages. Thus, for bulk-billed messages, the machine prints the message unit summary tape at the end of every round, thus making available the total message units of each subscriber accumulated since the last billing date. This information permits interim billing of subscribers who, for various reasons, may have to be billed prior to the end of the billing period, and it also satisfies the regular end-of-period billing requirements. The printed message unit summary list, one for each central office, tabulates the subscribers in convenient ascending order of their telephone numbers. Figure 19 is an illustration of this message unit summary list, with adequate explanatory information for its interpretation.

The toll messages are printed at the end of every round on one or more toll slips per subscriber. These slips show the required billing details of the subscriber's toll messages. One slip is sufficient for nine messages. These slips are automatically cut and stacked in the order of the calling telephone numbers. Figure 20 is an illustration of a single-message toll slip, with adequate explanatory information for its interpretation.

The printed message unit summary lists and the toll slips are the chief end-products of the present AMA system. Other products, of secondary importance, are: printed message unit detail slips, and service-observed call slips. All these end-products can be merged readily with other non-AMA billing items, such as operator prepared tickets, miscellaneous charges, and so forth, to be processed by present manual methods into toll service statements and subscriber bills.

Epilogue: Accounting Center Machinery

Figure 21 is a flow-chart of the accounting center processing, and Figure 22 shows a section of the Philadelphia installation. Like the central office AMA recording facilities, the units of this processing system are also truly intricate. To those who are not familiar with relay circuitry, a recitation of the machinery's various basic functions cannot convey an adequate picture of this intricacy. The fundamental cause of this intricacy lies in the simplicity of the circuit elements, such as relays, cold cathode tubes, and so forth, which, in themselves, can only satisfy one of two conditions, and the intelligent actions that are demanded from the circuitry interconnecting hundreds of such elements into cooperating aggregates.

As is evident even from the general description, the relay aggregates of the accounting center machines have to be capable of such intelligent actions as calculating, sorting, translating, comparing, and so forth.

Accuracy of the AMA System

There is one over-all characteristic of the AMA system which is both of paramount importance, as well as an indication of the amount of ingenuity, and thoroughness that went into its design. This characteristic is the "accuracy" of the system.

One of the official accuracy tests was made in July, 1949 on a commercial installation of the system in the Philadelphia area. The test conditions closely reflected normal operating and maintenance situations. The following is a quotation from the final report of the Committee in charge of the tests.

"The objectives of the tests were fully met. Six test runs were made from July 21 to July 26, inclusive, with a total of 38,198 AMA calls completed. There were no overcharges of any kind. The charges on three calls were lost, that is, undercharges occurred amounting to 0.78 per 10,000 messages or 0.0078 per cent. Two of these charge irregularities were on message unit messages and were introduced by circuit failures in the central office. Defective paper in the accounting center caused the loss of charges on one toll call . . . . ."

Future Development

The AMA system is a recent offshoot of control circuit technology, a technology which the Bell System has developed to an impressive extent for automatic telephone switching applications. Relay digital computing machines[3] form another relatively recent and related branch of the same technology. It is a technology with fundamental economic and philosophical implications, in that it mechanizes actions normally associated with logical thinking and intelligence. Great advances will be made in this field in the future, and the AMA system, as a specific branch, will both benefit by and contribute to that progress.

References

1. Automatic Ticketing of Telephone Calls, O. A. Friend. *Electrical Engineering* (*AIEE Transactions*), volume 63, March 1944, pages 81–88.

2. The Number 5 Crossbar Dial Telephone Switching System, F. A. Korn, James G. Ferguson. *AIEE Transactions*, volume 69, part I, 1950, pages 244–54.

3. The Bell Computer, Model VI, E. G. Andrews. *Electrical Engineering*, volume 68, September 1949, pages 751–56.

Discussion

C. M. Tomlinson (The Bell Telephone Company of Pennsylvania, Philadelphia, Pa.): The Bell Telephone Company of Pennsylvania has had the Automatic Message Accounting (AMA) system in operation since July 11, 1948, in the Media Number 5 crossbar office and the accounting center at Philadelphia. Since then seven more crossbar central offices with AMA have been placed in service in the Philadelphia metropolitan area, of both the Number 5 and Number 1 types. The accounting center is processing the tapes from these eight offices, from one office in the Pittsburgh area, and from three offices of the New Jersey Bell Telephone Company in Camden. The last-named service is temporary, and is being handled in Philadelphia only until New Jersey's center in Newark is finished. The completed messages processed now total about 1,250,000 per month.

The central office tapes are transported daily to the accounting center, by truck messenger from the Philadelphia region and by first-class mail from Pittsburgh. Processing is done on a 2-shift basis with four machine attendants, one supervisor, and a maintenance man for each shift.

The growing pains with this radically new system have been remarkably few. Our experience of over $1^1/_2$ years fully bears out the high accuracy of the system which had been indicated by the pre-cutover tests.

O. A. Friend (Bell Telephone Laboratories, New York, N. Y.): I would like to offer some observations on the Automatic Message Accounting (AMA) development so ably described by Mr. Meszar from the standpoint of how it fits into the pattern of forward-looking switching development in the Bell System.

Like the earlier developments of zone registration and automatic ticketing, intended for different fields of application, AMA is a tool for service measurement. It provides the means for billing subscribers for service based on the number of calls made, their distance, duration, and time of day.

It has the ability to record information in sufficient detail to permit billing calls individually, and takes advantage of the lesser information which is sufficient where bulk billing is adequate. The electrical methods used for the rapid and accurate transfer of information in the central office and in the accounting center machines are drawn largely from the techniques developed over the years in common-control switching systems and in the wartime developments of relay computers, which have earned an enviable reputation for reliability and accuracy.

AMA provides the recording means needed for extension of dialing. The conversion of local central offices to dial operation has gained pace since the war, and some 73 per cent of the Bell System telephones are now dial. Plans which have been widely discussed are being carried out for mechanizing the handling of long-distance calls in the form of operator toll dialing. The ability to record billing information paves the way for increasing the range of mechanized handling of calls to limits determined by commercial and engineering considerations.

The form of record is compact and flexible. It lends itself to mechanized accounting processes to the extent and in the forms that these prove advantageous.

The AMA system, like automatic ticketing, permits wide flexibility in rate treatment and billing practices. By broadening the field for operator and subscriber dialing beyond present limits, it will contribute substantially to improved speed and convenience of service.

A Frequency Response Method for Analyzing and Synthesizing Contactor Servomechanisms

RALPH J. KOCHENBURGER
ASSOCIATE AIEE

THIS paper introduces a procedure for synthesizing contactor servomechanisms in which the frequency response of the system is employed. In this respect it represents a radical departure from the techniques used previously to handle the analysis and synthesis of such discontinuous servomechanisms. While these earlier methods all involve step-by-step procedures based upon the transient response, the method proposed here permits the analysis and synthesis procedure to be determined from a knowledge of the response of the components to sinusoidal signals of various amplitudes and frequencies.

The successful application of the proposed method is based upon an approximation which is valid for most of the physical systems encountered in practice. This approximation permits the discontinuous contactor to be represented in terms of a linear describing function. The limitations imposed upon the use of this approximation are discussed in the paper.

Although the proposed method can be profitably applied to both the analysis and synthesis of contactor servomechanisms, it is the synthesis problem which is particularly facilitated by this approach. Instances are described in the paper where a synthesis procedure based on this method resulted in a selection of design constants which greatly enhanced the performance of a representative contactor servomechanism.

Servomechanisms and feed-back control systems in general, may be classified as either continuous types or discontinuous types. Most of the existing literature concerning feed-back systems deals only with the types in which control is continuous, particularly when problems of analysis and synthesis are discussed. The scarcity of published treatments dealing with systems in which control is discontinuous is due, in some part, to the difficulties encountered when such systems are subjected to a rigorous mathematical treatment. On the other hand, discontinuous controls represent a substantial number of the systems used in practice, and methods for analyzing and, still more important, synthesizing them would be of decided practical interest.

Figure 1 is a block diagram representing a simple feed-back control system. Such a system may be subdivided into the error-detecting means, the controller, and the servomotor and output-load combination as shown. It is assumed that a direct feed-back path is employed, and that no additional component need be introduced to represent dynamic factors which modify the feed-back signal. The case when such an additional component need be considered in the feedback can, however, be handled as well by the general method described here. The symbolism used to describe the input and output signals of the various components is indicated in Figure 1.

In the more familiar linear continuous systems, the relationship between the correction and error signals may be expressed as a continuous function. If the controller characteristic is plotted in terms of the quiescent response, or steady-state response to various nonvarying error signals, the relation between the correction signal D and the quiescent value of the error δ, called δ_q, may be plotted as in Figure 2(A). In discontinuous systems, this relationship cannot be expressed by such a continuous curve. In the discontinuous type of system discussed here, and specifically the contactor type of servomechanism, the D versus δ_q relationship is itself discontinuous, as shown in Figure 2(B). In other words, as the error of the system varies in some continuous manner, the correction signal applied to the servomotor varies in discrete jumps.

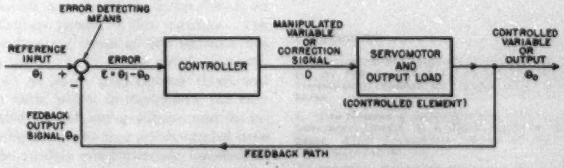

Figure 1. General form of single-loop servomechanism

Paper 50-44, recommended by the AIEE Committee on Feedback-Control Systems and approved by the AIEE Technical Program Committee for presentation at the AIEE Winter General Meeting, New York, N. Y., January 30-February 3, 1950. Manuscript submitted October 26, 1949; made available for printing December 1, 1949.

RALPH J. KOCHENBURGER is with the University of Connecticut, Storrs, Conn.

The material described in this paper represents some of the results obtained as part of a doctoral thesis research program conducted by the author at the Massachusetts Institute of Technology. The aid of various members of the Electrical Engineering Department and Servomechanisms Laboratory staffs and of H. K. Weiss of the Aberdeen Proving Grounds is gratefully acknowledged. The suggestions and criticisms furnished by Dr. Gordon S. Brown, Director of the Servomechanisms Laboratory, in his capacity as thesis supervisor were particularly helpful. Acknowledgment is due to the United States Air Forces, Air Materiel Command, Armament Laboratory, Wright Field, who sponsored the project under which this work was done.

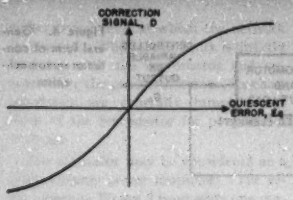

(a) CONTINUOUS SERVOMECHANISM

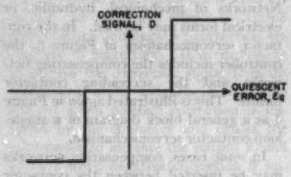

(b) CONTACTOR SERVOMECHANISM

Figure 2. Typical controller relations

The type of controller characteristic shown in Figure 2(B) is found in those systems which employ mechanically or hydraulically actuated electrical contactors, electromagnetic relays, electronic-control circuits of the trigger or flip-flop type, certain types of mechanical clutches, and some hydraulic and pneumatic valves. These devices are distinguished by an all-or-nothing characteristic. Their actual characteristics may be more complicated than shown, but will still possess the distinguishing feature of producing sudden jumps in the value of correction signal D. Because one of the most frequent applications of contactor servomechanisms involves electromagnetic relays, this general class is sometimes described as relay servomechanisms. Contactor servomechanisms have found widespread employment in both military and industrial fields. They frequently possess advantages over continuous types in economy of weight, bulk, complexity, and cost of control equipment. One of the major practical objections to their use has been the nonlinearity of the response relationship. Only the simplest versions have been amenable to analysis. It has been difficult to analyze their performance characteristics and to synthesize design constants and compensating networks which will provide a specified performance.

One of the earliest analyses of contactor-type servomechanisms was published by Hazen[1] in 1934. He employed the direct differential-equation method for analyzing performance and a number of characteristics peculiar to contactor types were demonstrated. This method becomes cumbersome when the system is at all complicated because a new equation must be established and solved for each switching cycle or correction interval initiated by the contactor.

The phase-plane method of analysis provided a simple graphical approach. This method has been employed by various authors[2,3] in connection with other forms of nonlinear systems. It was applied to contactor servomechanisms by Weiss[4] and MacColl[5] and the analyses of certain types of such servomechanisms were shown to be greatly facilitated. Unfortunately, the method is limited to systems possessing relatively few energy-storage elements. A recent AIEE paper by Kahn,[6] based on the differential-equation approach, proposes relatively simple graphical constructions to eliminate some of the computational labor associated with the analysis of such systems.

There are two basic disadvantages to these methods of treatment, which might be characterized as solutions in the time domain. One disadvantage is the great difficulty of treating systems of apparently elementary physical configuration which have only a few energy-storage elements. The second and more significant disadvantage from the standpoint

Figure 3. Typical contactor servomechanism for positional control

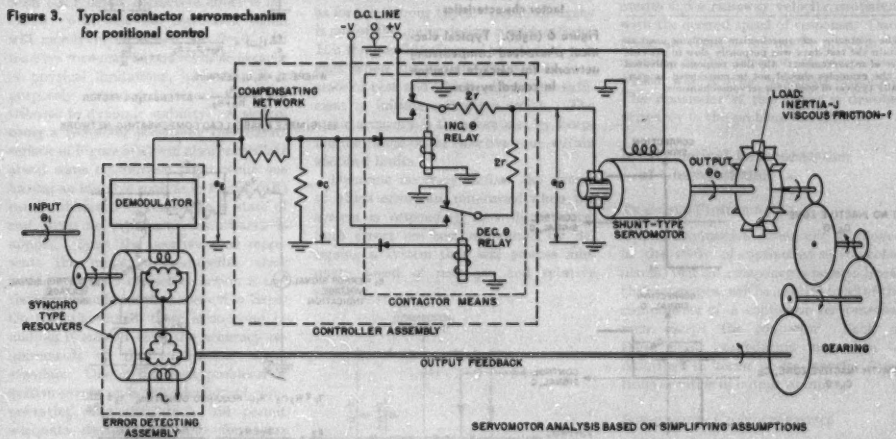

r_a = ARMATURE RESISTANCE – OHMS

K = MOTOR CONVERSION CONSTANT – $\frac{\text{GENERATED VOLTS}}{\text{RADIAN/SEC.}}$

J = LOAD & MOTOR MOMENT OF INERTIA

f = LOAD & MOTOR VISCOUS FRICTION COEFFICIENT

D = +1 UPPER (INC) RELAY CLOSED
= 0 NEITHER RELAY CLOSED
= −1 LOWER (DEC.) RELAY CLOSED

SERVOMOTOR ANALYSIS BASED ON SIMPLIFYING ASSUMPTIONS

$$\theta_o(s) = \frac{R}{s(T_s+1)}\,D(s); \qquad \theta_o(j\omega) = \frac{R}{j\omega(1+j\omega T)}\,D(j\omega)$$

WHERE: $R = \frac{KV}{K^2+f(r_a+r)}\ \frac{\text{RADIANS}}{\text{SECOND}}$ = "RUNAWAY VELOCITY"

$T = \frac{J}{f+\frac{K^2}{r_a+r}}$ SECONDS = "TIME CONSTANT"

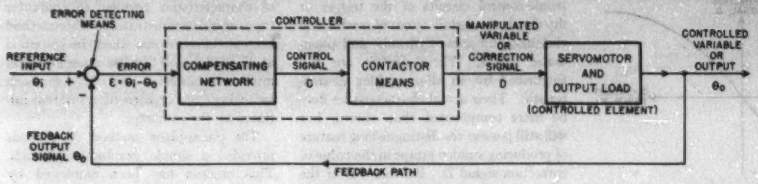

Figure 4. General form of contactor servomechanism

of usefulness is the fact that the methods are not directly adaptable to system synthesis.

It is the purpose of this paper to present an analysis and synthesis procedure in which the frequency response of the system is employed in a manner[7] analogous to its use with continuous servomechanisms. Results obtained by the method have been compared with those obtained by more cumbersome exact methods and with test data* and the agreement has been found sufficient for most engineering applications. The method is not limited by any inherent dynamic complexity, provided the system can be described by a control loop as shown in Figure 1. Furthermore, the proposed method is particularly adapted to synthesis and permits the selection of compensating networks suitable for the attainment of given performance requirements.

*The contactor servomechanism simulator used to obtain the test data was purposely slow to provide ease of measurement: the slow response indicated in the examples should not be considered as generally typical of contactor servomechanisms.

General Configuration of a Contactor Servomechanism

Figure 3 illustrates a typical contactor servomechanism for controlling angular position. In this example, the various signals are represented as voltage equivalents; that is, the voltage e_ε is an indication of the angular error ε. A simple lead-type compensating network is shown in this example.

The compensating network converts the error signal to a new form, here called the *control signal*, before application to the contactor means. When no compensating networks are employed, ε and C are identical. In almost all cases, the introduction of a suitable compensating network results in improved performance. Networks of mechanical, hydraulic, or electrical forms may be used. In the contactor servomechanism of Figure 3, the controller includes the compensating networks and the succeeding contactor means. This is illustrated again in Figure 4 as a general block diagram of a single-loop contactor servomechanism.

In some cases, compensating networks may be inserted between the contactor means and the servomotor. This is usually less practical than the arrangement shown in Figure 4 because of the

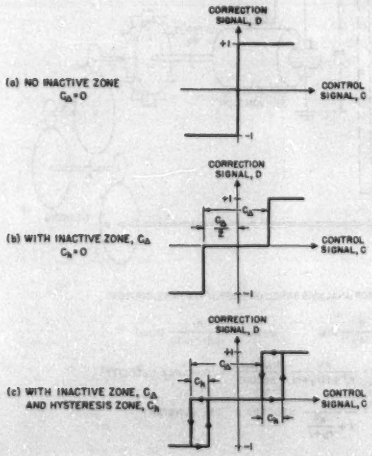

Figure 5 (below). Typical contactor characteristics

Figure 6 (right). Typical electrical phase-lead compensating networks for cascade insertion in control system

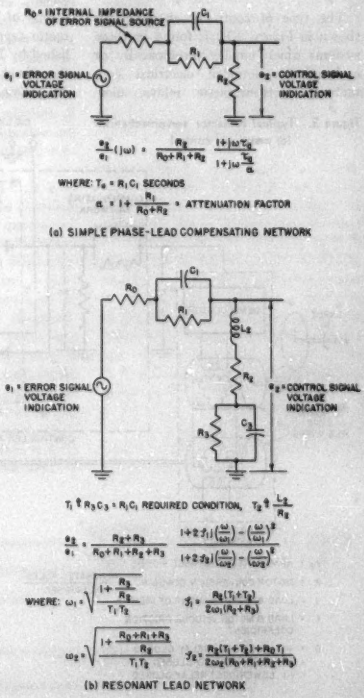

higher power level at which the network is operated. When the network is directly cascaded with the servomotor and appears after the contactor means, its characteristics are generally lumped with those of the servomotor for purposes of analysis.

The contactor may be considered as a discontinuous power amplifier. The relay shown in Figure 3 represents one particular type. The relationship between C and D might follow one of the characteristics shown in Figure 5. In these diagrams, symmetrical operation is assumed in that the corrective efforts associated with positive and negative correction are identical in magnitude. It is convenient to express the correction signal D in dimensionless units, assigning it the value $D=+1$ when positive correction is initiated by the contactor and causes the servomotor to increase the output θ_o and $D=-1$ when negative correction is initiated.

In Figure 5(A), a relationship is shown where the contactor will initiate either positive or negative correction, depending on the algebraic sign of the control signal C. In this case, the *inactive zone* or range of error within which no corrective effort arises is zero. In Figure 5(B) an inactive zone, C_Δ, is introduced and the control signal must have a magnitude greater than $C_\Delta/2$ before corrective effort is initiated; otherwise the correction signal will merely be expressed by $D=0$. An inactive zone may be unavoidable because of physical limitations, but often it is purposely introduced because it contributes to dynamic stability. A system using a contactor possessing the characteristic of Figure 5(A) will always oscillate about some equilibrium point while one having an inactive zone as in Figure 5(B) can be designed to remain in a state of rest when no significant disturbance is applied. Since the inactive zone represents the range of permissible error within which no corrective action is initiated, it should not be excessively large. On the other hand, there is no point in making it smaller than the accuracy requirements of the application might stipulate. One of the basic problems of system synthesis is the selection of compensating networks which will permit adequate dynamic stability for some specified range of inactive zone. This problem becomes more difficult as the specified range of inactive zone becomes smaller.

Many contactors possess a hysteresis effect. This means that the control signal necessary to initiate correction is greater than that necessary to cease correction. In the case of electromagnetic relays, for example, the coil current of an already-closed relay must usually be reduced to some value lower than that which originally caused the relay to close before the relay will reopen. Figure 5(C) illustrates the effect as designated by the symbol C_h.

It can be shown that a hysteresis effect generally adversely affects the dynamic stability.

More complicated types of contactor characteristics are met in practice; for example, nonsymmetrical corrective action, or multistep contactors. These will not be discussed in detail but the general method of treatment to be introduced is applicable to them as well.

The other components of the contactor servomechanism, as shown in Figures 3 and 4, are the servomotor and the error-detecting means. Both of these usually exist in essentially the same form as in continuous systems. In a contactor servomechanism, however, it is rarely necessary to design for continuously variable control of speed. This greatly simplifies the equipment.

Performance Criteria of a Contactor Servomechanism

The performance criteria of contactor servomechanisms are basically the same as for continuous types. Static accuracy is one of the major design considerations. It is the possible range of error which can exist when the servomechanism is in a state of rest and which will not be sufficient to initiate corrective action. The static accuracy is therefore met by keeping the range of the inactive zone within specified limits.

Dynamic accuracy defines the extent to which errors are minimized when the system is responding to a disturbance. Such errors are best minimized by designing a system that will possess adequate speed of response and relative stability.

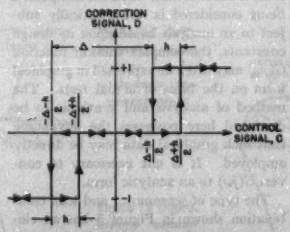

Figure 7. Dimensionless representation of contactor characteristics (case involving both inactive zone and hysteresis)

Speed of response deals with the rapidity by which errors are reduced to a tolerable level following some disturbance. The fastest response may be obtained by:

1. Using a runaway velocity that is as large as the stability limitations and servomotor capabilities permit.
2. Having the frequencies associated with any damped transient oscillation as high as possible.
3. Having adequate degree of stability for transient oscillations of amplitude greater than the region of error tolerance.

Stability is the tendency of a system to approach an equilibrium condition without excessive oscillation. Absolute stability is descriptive of a system incapable of self-sustained oscillations. Degree of stability refers to the rate with which transient oscillations disappear after a disturbance. A distinction must be made between the stability requirements imposed on nonlinear systems and those imposed on linear types. For the former, continuous self-sustained oscillations of a small amplitude may be permissible. For the latter, the amplitude of any self-sustained oscillations would tend to increase to an undesirably high value.

For contactor servomechanisms, performance requirements may be met by specifying a range of inactive zone consistent with the static accuracy requirements and a runaway velocity consistent with the desired speed of response. Once these are chosen, the major problem remaining is the selection of components which will provide adequate stability. The remainder of this paper is devoted primarily to the problem of stability.

Mathematical Representation of Characteristics

Transfer Functions

The assumption commonly employed in the study of continuous servomechanisms, that all components possess linear characteristics, will be applied to all of the components of a contactor servomechanism except the contactor. Each of these linear components may then be described in terms of its transfer functions or ratios of output to input.

Servomotor Characteristics

The transfer function of the servomotor, designated as $G_s(s)$, is defined by the ratio

$$G_s(s)=\frac{\theta_o(s)}{D(s)} \tag{1}$$

where $\theta_o(s)$ and $D(s)$ are the Laplace transforms of the output $\theta_o(t)$ and the

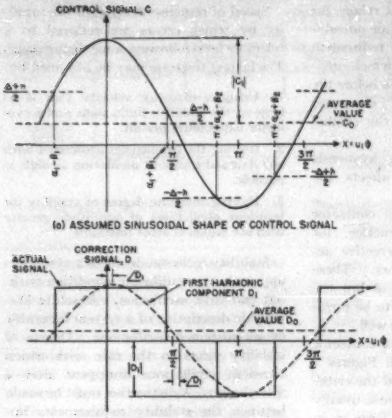

Figure 8 (left). Relation of correction signal to control signal for a simple contactor with hysteresis

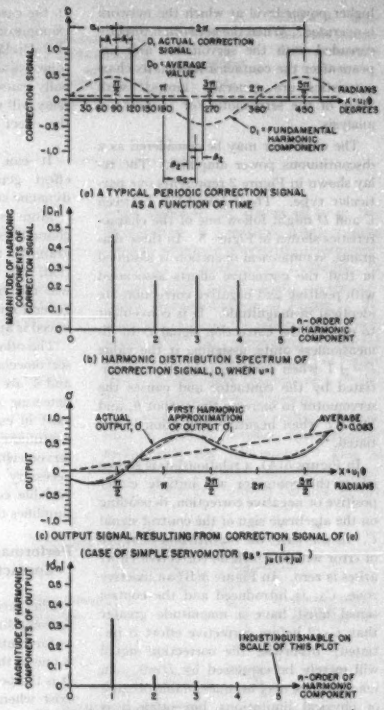

Figure 9 (right). Comparison—exact response of servomotor with that obtained from fundamental harmonic approximation

correction signal $D(t)$, subject to zero initial conditions. When the polynomials of the transfer function are factored, it will appear as

$$G_s(s)=\frac{\theta_o(s)}{D(s)}$$
$$=\frac{R(1+\tau_1 s)(1+\tau_2 s)\ldots}{s(1+T_1 s)(1+T_2 s)(1+T_3 s)\ldots}$$
units of output quantity (2)

The τ's and T's are time constants which may be either real or complex. Equation 2 applies to the most common form of servomotor which approaches the condition of a constant output rate of R output units per second. The quantity R is the runaway velocity for a given correction signal applied for a sufficiently long time. The linear factor s in the denominator of the transfer function represents a single-order pole at the origin of the complex s plane and identifies a system having a sustained rate for a constant input signal. The servomotor or equivalent may have other forms of transfer function; for example, in regulator applications, there may be no pole at the origin while, in other applications a higher-order pole may exist. Only transfer functions of the form given in equation 2 are treated herein although the method is generally applicable to any form.

The transfer function also might be described in terms of its steady-state response to various real frequencies by substituting the imaginary quantity $j\omega$ for the operator s ($\omega=2\pi f$=angular frequency).

Equation 2 then assumes the form

$$G_s(j\omega)=\frac{\theta_o(j\omega)}{D(j\omega)}$$
$$=\frac{R(1+j\omega\tau_1)(1+j\omega\tau_2)\ldots}{j\omega(1+j\omega T_1)(1+j\omega T_2)(1+j\omega T_3)\ldots} \quad (3)$$

One advantage of the frequency-function form is the fact that, when the component being considered is not practically subject to an analysis based upon its design constants, the complex transfer function $G(j\omega)$ may often be expressed in graphical form on the basis of actual tests. The method of analysis and synthesis to be described here possesses the advantage that such graphical data may be directly employed. It is not necessary to convert $G(j\omega)$ to an analytic form.

The type of servomotor and load combination shown in Figure 3 has an elementary transfer function if, for example, coulomb friction, armature reaction and armature inductance are neglected. In this case, $G_s(j\omega)$ becomes

$$G_s(j\omega)=\frac{R}{j\omega(1+j\omega T)} \quad (4)$$

where the relations for determining the runaway velocity R and the time constant T are given in Figure 3. For many engineering purposes, this simplified form of relationship is adequate for analysis and synthesis. Similar transfer functions arise in many other servomotors.

Compensating Networks

The characteristics of the compensating network may similarly be expressed in terms of a transfer function $G_c(j\omega)$ as

$$G_c(j\omega)=\frac{(1+j\omega\tau_a)(1+j\omega\tau_b)\ldots}{(1+j\omega T_a)(1+j\omega T_b)\ldots}=\frac{C(j\omega)}{\delta(j\omega)} \quad (5)$$

It will be noted that at zero frequency $G_c(j\omega)$ is unity. This is because both C and δ are expressed in units of the output quanity; C being described in terms of the equivalent value of δ under quiescent

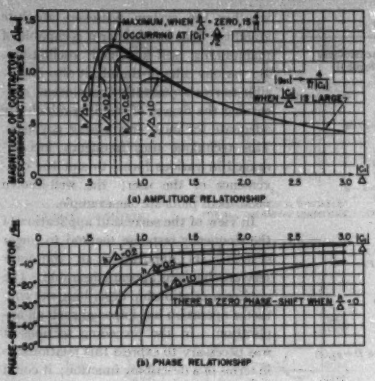

Figure 10 (left). Plot of the fundamental harmonic transfer function g_D—simple contactor with hysteresis ratio h/Δ, for case of zero input velocity ($d\bar{s}/dt=0$) and zero load torque ($\theta_L=0$)

conditions. Any attenuation or amplification occurring within the controller is described in terms of its effect on the range of inactive zone. This range is the sole measure of the zero-frequency gain of the system.

Figure 6 shows two common forms of compensating network for producing a phase-lead effect. For these networks, the transfer functions are given by

$$G_e(j\omega)=\frac{1+j\omega\tau_2}{1+j\omega\frac{\tau_2}{\alpha}} \text{ network of Figure 6(A)} \quad (6)$$

and

$$G_e(j\omega)=\frac{1+2\zeta_1 j\left(\frac{\omega}{\omega_1}\right)-\left(\frac{\omega}{\omega_1}\right)^2}{1+2\zeta_2 j\left(\frac{\omega}{\omega_2}\right)-\left(\frac{\omega}{\omega_2}\right)^2}$$

network of Figure 6(B) (7)

where

ζ_1, ζ_2 = numerator and denominator damping ratios, respectively

ω_1, ω_2 = numerator and denominator resonant frequencies, respectively

In the network of Figure 6(A), called a simple phase-lead network, the transfer function given in equation 6 includes the attenuation factor α, computed as shown in the diagram. The higher the value of α the more effective phase-lead effect is obtained. However, a high value of α results in a relative increase in the transmission of high-frequency noise. Some engineering compromise concerning its value is therefore required in practice.

Since the phase-lead effect of the circuit shown in Figure 6(A) cannot exceed 90 degrees, it may be inadequate for some applications. The resonant lead network shown in Figure 6(B) may then be employed. Equation 7 represents the transfer function of this latter network. Examples will be given where the use of these compensating networks materially improve system performance.

The Over-all Loop Transfer Function

Since the components represented by G_s and G_e are essentially linear and have transfer functions which depend only upon the applied frequency, they are called the frequency-variant portions of the system. On the other hand, the contactor, considered as having no dynamic lag but having a discontinuous characteristic, is nonlinear and therefore dependent on signal amplitude. Any dynamic lag action occurring in a physical contactor is conveniently lumped with either the servomotor or compensating network. The contactor represents the amplitude-variant portion of the system, and its describing function G_D, although independent of frequency, is dependent upon the control signal C. Other nonlinear effects such as backlash may be treated similarly in terms of amplitude-variant describing functions.

The over-all loop transfer function $G(j\omega)$ or combined transfer function of all linear and frequency-variant components is particularly significant. With the arrangement shown in Figure 4, this would merely be

$$G(j\omega)=G_s(j\omega)G_e(j\omega)=\frac{C(j\omega)}{D(j\omega)}\,\theta_1=\text{constant}$$

$$=\text{loop transfer function} \quad (8)$$

It will be shown how the loop transfer function and the contactor describing function may be used together to determine the performance characteristics of the control system.

Dimensionless Notation

The mechanics of analyzing and synthesizing contactor servomechanisms are simplified and the results obtained acquire more general utility if a dimensionless form of notation is used. This procedure is employed in many engineering fields and the system of notation proposed here is an expansion and modification of that introduced by Weiss.[4]

As a first step select a convenient time base t_b seconds. Then divide all variables and constants having the dimensions of time by t_b in order to obtain the corresponding dimensionless value; for example, $\phi=t/t_b$ = elapsed time. A convenient time base is frequently obtained

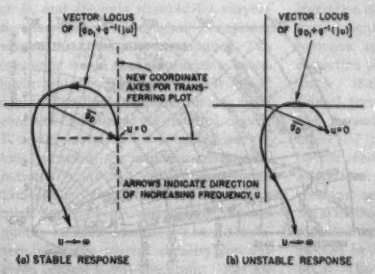

Figure 11 (left). Inverse response-function loci for single-loop servomechanisms

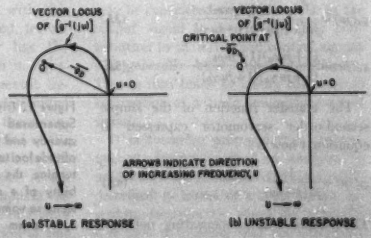

Figure 12 (right). Inverse transfer-function loci for single-loop servomechanisms

Table I. Dimensional and Dimensionless Symbols Used

	Quantity	Dimensional Symbol	Units	Dimensionless Symbol
Time Units	Time base	t_b	Seconds	
	Elapsed time	t	Seconds	$\phi = t/t_b$
	Time derivative operator	$p = d/dt$	Seconds^{-1}	$\lambda = t_b p = d/d\phi$
	Applied angular frequency	ω	Seconds^{-1}	$u = \omega t_b$
Signals in Control System	Signal base	$B = Rt_b$	Output-Units	
	Output	θ_o	Output-Units	$\sigma = \theta_o/B$
	Input	θ_i	Output-Units	$\delta = \theta_i/B$
	Error	$\varepsilon = \theta_i - \theta_o$	Output-Units	$\varepsilon = \varepsilon/B = \delta - \sigma$
	Control signal	C	Output-Units	$c = C/B$
	Correction signal	D	Dimensionless	D (same)
System Properties	Runaway velocity	R	Output-Units / Seconds	Unity
	Inactive zone	C_Δ	Output-Units	$\Delta = C\Delta/B$
	Hysteresis range	C_h	Output-Units	$h = C_h/B$
	Transfer functions:			
	Of servomotor	$G_s = \frac{\theta_o}{D}$	Output-Units	$g_s = \frac{\sigma}{D}$
	Of compensating network	$G_c = \frac{C}{\varepsilon}$	Dimensionless	$g_c = \frac{c}{\varepsilon}$
	Over-all loop	$G = G_s G_c$	Output-Units	$g = g_s g_c$
	Describing function of contactor	G_D where $D = G_D(C)$		g_D where $D = g_D(c)$
	Transfer function properties:			
	Time constant			
	In numerator	τ	Seconds	$\rho = \frac{\tau}{t_b}$
	In denominator	T	Seconds	$\gamma = \frac{T}{t_b}$
	Natural frequency	$\omega_1, \omega_2, \ldots$	Seconds^{-1}	$u_1 = \omega_1 t_b,\ u_2 = \omega_2 t_b \ldots$
	Damping ratio associated with a natural frequency	$\zeta_1, \zeta_2, \ldots$	Dimensionless	$\zeta_1, \zeta_2 \ldots$ (same)
	Attentuation factor of a compensating network	α	Dimensionless	α (same)

by setting $t_b = |T_1|$, where T_1 is the smallest time constant of the servomotor. In equation 4, for example, the only time constant T is naturally the lowest and $t_b = T$.

The next step is to select an output signal base B. All signals, such as the output θ_o, are divided by B in order to obtain the dimensionless equivalents, for example, the dimensionless output is expressed as $\sigma = \theta_o/B$. The inactive zone and hysteresis ranges, C_Δ and C_h, are dimensionlessly expressed as: $\Delta = C_\Delta/B$, $h = C_h/B$. The most convenient signal base B is the product of the runaway velocity and the time base, namely Rt_b. Table I summarizes the dimensional and dimensionless notation used.

In dimensionless form, the transfer functions of the servomotor and compensating network given in equations 3 and 5 become

$$g_s(ju) = \frac{(1+ju\rho_1)(1+ju\rho_2)\ldots\ldots}{ju(1+ju\gamma_1)(1+ju\gamma_2)\ldots} \tag{3A}$$

$$g_c(ju) = \frac{(1+ju\rho_a)(1+ju\rho_b)\ldots\ldots}{(1+ju\gamma_a)(1+ju\gamma_b)\ldots\ldots} \tag{5A}$$

The transfer function of the simple second-order servomotor expressed in equation 4 now is

$$g_s(ju) = \frac{1}{ju(1+ju)} \tag{4A}$$

The simple lead-compensating network and the resonant lead-controller network shown in Figures 6(A) and 6(B) now have the following dimensionless forms

$$g_c(ju) = \frac{1+ju\rho_a}{1+ju\frac{\rho_a}{\alpha}} \tag{6A}$$

$$g_c(ju) = \frac{1+2\zeta_1 j\left(\frac{u}{u_1}\right)-\left(\frac{u}{u_1}\right)^2}{1+2\zeta_2 j\left(\frac{u}{u_2}\right)-\left(\frac{u}{u_2}\right)^2} \tag{7A}$$

The Frequency-Response Method of Analysis and Synthesis

The frequency-response method of analysis and synthesis has been found to be a practical means for treating essentially linear servomechanisms.[7,8,9] By this method it is possible to determine whether the system possesses absolute stability; that is, whether it is capable of maintaining self-sustained oscillations. By various rules-of-thumb, it also is possible to reach qualitative conclusions concerning the degree of stability which are adequate for most engineering purposes. This technique uses frequency loci arranged in various forms to suit the convenience of the user; the well-known polar-locus plots are one example.

In view of the successful application of the frequency-response method to linear systems, its application to contactor servomechanisms appears desirable. The nonlinear relationship describing the contactor operation has impeded such an application. In the preceding sections it was necessary to express this relationship in terms of a describing function; it could not be expressed in terms of a linear transfer function. The frequency-response method is therefore not applicable unless certain assumptions are made.

In order to determine whether an adaptation of the frequency-response method might not be applied, let it be assumed that a sinusoidal control signal is applied to a typical contactor. Suppose that the contactor has the more general characteristic shown in Figure 7. If the control signal c is of the form

$$c = c_0 + |c_1| \cos u\phi \tag{9}$$

the contactor will initiate a positive correction when $c = \Delta/2 + h/2$, cease correction when $c = \Delta/2 - h/2$, initiate negative correction when $c = -\Delta/2 - h/2$, and cease correction when $c = -\Delta/2 + h/2$. These instants of time are designated by the angles, $u\phi = \alpha_1 - \beta_1$, $= \alpha_1 + \beta_1$, $= \pi + \alpha_2 - \beta_2$, and $= \pi + \alpha_2 + \beta_2$, respectively. This is shown in Figure 8(A). The angles $2\beta_1$ and $2\beta_2$ represent the duration of the positive and negative pulses, respectively; the angles α_1 and α_2 represent the phase lags associated with the respective pulses.

Figure 8(B) shows the rectangular form of the resultant periodic correction signal

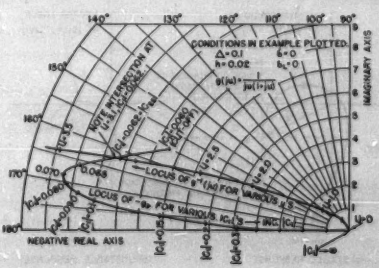

Figure 13 (right). Superposed frequency and amplitude loci to determine the stability of a contactor servomechanism

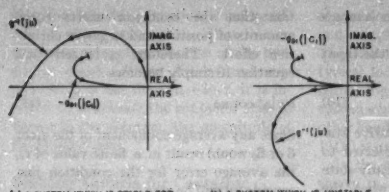

(a) A SYSTEM WHICH IS STABLE FOR ALL OPERATING CONDITIONS.

(b) A SYSTEM WHICH IS UNSTABLE FOR ALL OPERATING CONDITIONS.

Figure 14 (left). Significance of various relative configurations of the loci

Figure 15 (right). Vector relationships in loci diagram (used to determine relative stability)

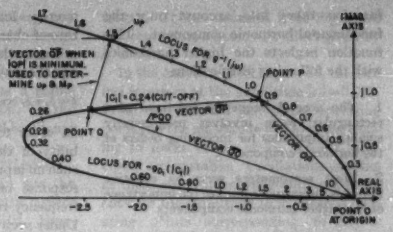

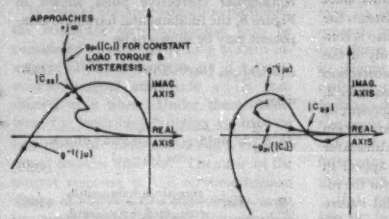

(c) A SYSTEM WITH A CONVERGENT EQUILIBRIUM POINT; WILL ALWAYS OSCILLATE.

(d) A SYSTEM WITH A DIVERGENT EQUILIBRIUM POINT; IS CONDITIONALLY STABLE (FOR SMALL DISTURBANCES)

Figure 16 (right). Values of M_p and ω_p (used in determining relative stability and speed of response)

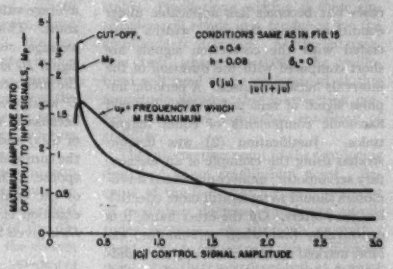

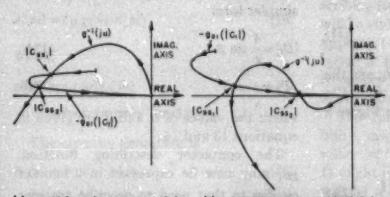

(e) A SYSTEM WITH A DIVERGENT & CONVERGENT EQUILIBRIUM; WILL OSCILLATE CONTINUOUSLY FOLLOWING DISTURBANCES OF SUFFICIENT AMPLITUDE.

(f) A SYSTEM WITH A DIVERGENT & CONVERGENT EQUILIBRIUM; WILL OSCILLATE CONTINUOUSLY AT FINITE AMPLITUDE UNLESS DISTURBANCES ARE EXCESSIVE.

D. The broken-line relation plotted in Figure 8(B) shows the average or zero-frequency component D_0 and fundamental harmonic component D_1 of this rectangularly shaped signal. Higher harmonic components which contribute to the corners of the rectangular shape are not shown.

If the correction signal consisted only of D_0 and D_1, only sinusoidally varying signals would exist throughout the system when sinusoidal inputs were applied. The contactor would then appear as a quasi-linear transfer device in that it would operate as a linear amplifier for any given constant amplitude of control signal. It would not operate as a truly linear device because of the nonlinear relationship between input and output amplitudes. Considering the contactor as such a quasi-linear device will permit the frequency-response method to be used in determining the system stability for any given control signal amplitude. The approximation which permits the higher harmonic components to be neglected so that the quasi-linear representation of the contactor may be employed must now be justified.

Figure 9 shows the relative importance of the harmonic components of the signals in a typical contactor servomechanism. Figure 9(A) shows a typical rectangular correction signal resulting from a periodic control signal. Figure 9(B) represents the harmonic spectrum associated with this correction signal. It is assumed, for example, that the servomotor has the typical transfer function given in equation 4, and that the fundamental frequency of the control signal is designated by the relation $u=1$. Under these considerations, an exact determination of the resultant servomotor output σ obtained by a mathematical determination of the repeated transients, would appear as plotted by the solid-line curve of Figure 9(C). The harmonic distribution of this output signal is shown plotted in Figure 9(D). It may be seen that, while the original correction signal D possessed higher harmonic components of significant amplitudes (referring back to Figure 9(B), these higher harmonic components have relatively small amplitudes, compared with the fundamental, when measured as part of the output signal.

The minor importance of the role played by the higher harmonic components also is demonstrated by the broken-line curve of the output response in Figure 9(C). This curve, designated as σ_1, represents the output response which would have been obtained if only the average and fundamental components of the correction signal had been present. It may be seen that this latter response curve is a fairly good approximation of the exact response represented by the solid-line curve.

If the higher-harmonic components may be considered negligible as far as the output signal is concerned, their contribution to the error and control signals will generally have minor significance. This in turn tends to justify the original assumption of a truly sinusoidal control signal.

It is therefore proposed that the frequency-response method of analysis be used where the contactor characteristic is described in terms of a quasi-linear describing-function $\mathfrak{L}_D$ where the subscript *1* is used to indicate that the describing

function takes into account only the fundamental harmonic component. This function neglects the higher harmonics with the following justifications:

1. The normal frequency spectrum of a rectangular wave involves progressively smaller amplitudes for increasing orders of the harmonic components.

2. Most servomotors serve as effective low-pass filters and minimize the importance of the higher-harmonic components.

Justification (1) above is valid for most cases but becomes less applicable under conditions where the pulse widths associated with the correction signals are short compared with the duration of the intervals between pulses. A periodic impulse signal of zero pulse width has odd harmonic components of equal magnitudes. Justification (2) was demonstrated using the example of an elementary servomotor; more complicated servomotors should serve as still more effective low-pass filters. On the other hand, it is conceivable that when servomotors exhibit marked resonance effects, the validity of the approximation may suffer under certain conditions where one of the neglected harmonic components might have a frequency near resonance and its effect on performance might therefore be particularly prominent.

At any rate, the previously-mentioned approximation is proposed so that the frequency-response method can be employed. Some conclusions concerning the general accuracy of the method may be reached by the comparisons given herein between the results thus obtained with those obtained by more exact methods of computation or by actual test. It should be kept in mind that the method proposed is an engineering approximation and that, even in the case of the better-understood continuous linear servomechanisms, conclusions regarding stability that are accurate to within 10-20 per cent are frequently satisfactory.

The Quasi-Linear Representation of the Contactor Describing-Function

The contactor may be approximately represented in the manner just described and cases involving the application of constant rates of input change or constant load disturbances may be taken into account. This entails additional mathematical complication because the duration of positive and negative corrective pulses will differ ($\beta_1 \neq \beta_2$). For brevity, only the case where symmetrical corrective operation occurs ($\beta_1 = \beta_2$) will be discussed. This implies the condition of zero average load torque and zero average rate-of-change of input.

Under this latter condition, the input signal δ may be of the form

$$\delta = \delta_0 + \delta_1 \cos u\phi \tag{10}$$

In order to determine the relative stability of the system when subjected to such an input signal, only the steady-state response need be considered when the frequency-response method is employed. Under such steady-state conditions, since the average value of input is constant, the average value of the output σ_0 also is constant. This can be the case only if the average component of the correction signal D_0 is zero, since from equation 2, the presence of an average component of D would result in an integrating action because of the s factor in the numerator of $G_y(s)$ and a $D_0\phi$ term would appear in the corresponding time solution for the response. The assumed sinusoidal nature of the control signal was expressed by equation 9. The average value of D or D_0 is given by

$$D_0 = \frac{\beta_1 - \beta_2}{2\pi} \tag{11}$$

Since, for this case $D_0 = 0_0$, $\beta_1 = \beta_2$, and the operation is symmetrical. But, from the trigonometric relations shown in Figure 8

$$\beta_1 = \frac{1}{2}\left\{\cos^{-1}\left[\frac{\Delta - h - 2c_0}{2|c_1|}\right] + \cos^{-1}\left[\frac{\Delta + h - 2c_0}{2|c_1|}\right]\right\} \tag{12A}$$

$$\beta_2 = \frac{1}{2}\left\{\cos^{-1}\left[\frac{\Delta - h + 2c_0}{2|c_1|}\right] + \cos^{-1} \times \left[\frac{\Delta + h + 2c_0}{2|c_1|}\right]\right\} \tag{12B}$$

Since $\beta_1 = \beta_2$ the average value of control signal c_0 must be zero, in which case

$$\beta = \beta_1 = \beta_2 = \frac{1}{2}\left\{\cos^{-1}\left(\frac{\Delta - h}{2|c_1|}\right) + \cos^{-1}\left(\frac{\Delta + h}{2|c_1|}\right)\right\} \tag{13}$$

Similarly, the phase-lag angles α_1 and α_2 shown in Figure 8 will be equal and will be

$$\alpha = \alpha_1 = \alpha_2 = \frac{1}{2}\left\{\cos^{-1}\left(\frac{\Delta - h}{2|c_1|}\right) - \cos^{-1}\left(\frac{\Delta + h}{2|c_1|}\right)\right\} \tag{14}$$

The foregoing results indicate that, for the case of an input disturbance represented by equation 9 and with zero average load torque, there will be zero average component of control signal. This also is based on the original assumption that the contactor exerts equal amounts of positive and negative corrective effort. Therefore, c_0 is zero and equation 10 simply becomes

$$c = |c_1| \cos u\phi \tag{15}$$

Since any average component of the error δ or δ_e would result in a finite value of c_0, the average error for the condition just considered will be zero.

By means of a Fourier analysis of the rectangular corrective pulse shown in Figure 8, the fundamental harmonic component may be shown to be

$$D_1 = |D_1| \cos\left(u\phi + \underline{/D_1}\right) \tag{16A}$$

where

$$|D_1| = \frac{2}{\pi}\sqrt{\sin^2\beta_1 + \sin^2\beta_2 + 2\sin\beta_1\sin\beta_2 \times \cos(\alpha_1 - \alpha_2)} \tag{16B}$$

$$\underline{/D_1} = -\tan^{-1}\frac{\sin\alpha_1\sin\beta_1 + \sin\alpha_2\sin\beta_2}{\cos\alpha_1\sin\beta_1 + \cos\alpha_2\sin\beta_2} \tag{16C}$$

If the fact that $\alpha = \alpha_1 = \alpha_2$ and $\beta = \beta_1 = \beta_2$ is considered, these equations acquire the simpler form

$$|D_1| = \frac{4}{\pi}\sin\beta \tag{17A}$$

$$\underline{/D_1} = -\alpha \tag{17B}$$

where the values of α and β are given in equations 13 and 14.

The contactor describing function, g_{D_1} may now be expressed in a manner similar to that used to describe transfer functions of linear components, that is, as the mathematical ratio of the output and input quantities, or

$$g_{D_1} = \frac{D_1}{c_1} \tag{18A}$$

which is written in vector form as

$$g_{D_1} = \frac{|D_1|}{|c_1|}\,\underline{/D_1} = \frac{4}{\pi}\frac{\sin\beta}{|c_1|}\,\underline{/-\alpha} \tag{18B}$$

The above expression represents the describing function for the quasi-linear approximate equivalent of the contactor. The angles α and β given in equations 13 and 14 are functions of the inactive-zone range Δ, the hysteresis range h, and the control-signal amplitude $|c_1|$. The amplitude and phase angle associated with the function g_{D_1} may be conveniently plotted as a function of the ratio $|c_1|/\Delta$ for various ratios of the quantity h/Δ representing the hysteresis effect. This has been done in Figure 10.

Figure 10 shows the amplitude and phase angle associated with the contactor describing-function for various control-signal amplitudes and various conditions of contactor hysteresis. It may be noted

that the describing function is independent of the frequency u. However, a phase lag is involved because of the hysteresis effect. When the control amplitude $|c_1|$ is less than $(\Delta+h)/2$, it is insufficient to actuate the contactor and, as shown in the diagram, the magnitude of g_{D_1} remains zero.

Stability Criteria for Contactor Servomechanisms

In view of the approximation proposed, the contactor servomechanism may be considered as equivalent to a system involving all linear components if a single constant signal amplitude $|c_1|$ is considered at a time. Under these conditions the describing function g_{D_1} may be treated in the same manner as a conventional transfer function. The ratio of the output response of the servomechanism shown in Figure 4 to a sinusoidally varying control signal of some dimensionless frequency u and of fixed amplitude $|c_1|$ would then be given by

$$\sigma(ju)=g_{D_1}g(ju)\mathcal{E}(ju) \tag{19}$$

where

$$g(ju)=g_c(ju)g_e(ju)$$

$$=\text{loop transfer function}$$

The error by definition is

$$\mathcal{E}(ju)=\delta(ju)-\sigma(ju) \tag{20}$$

If equations 19 and 20 are combined, the response ratio is conveniently given in inverse form as

$$\frac{\delta}{\sigma}(ju)=\frac{g^{-1}(ju)+g_{D_1}}{g_D} \tag{21}$$

where

$$g^{-1}(ju)=\frac{1}{g(ju)}$$

A system having an inverse response ratio as in equation 21 will be stable if, for a polar locus of $\delta/\sigma(ju)$ drawn for the complete range of frequencies, $-\infty<u<+\infty$, the origin of the plot always appears to the left of this locus as the locus is traversed in the direction of increasing frequency. This criterion is merely a simplified version of the well-known Nyquist criteria for stability. It applies only to single-loop systems.

Since only the orientation of the locus with respect to the origin is of interest, the criterion given could be applied as well to a locus representing merely the numerator of equation 21. Therefore only the locus of $g^{-1}(ju)+g_{D_1}$ need be plotted, since the quantity g_{D_1} appearing in the denominator of equation 21 is independent of frequency and simply represents a scale factor. This has been done in constructing the typical locus of Figure 11. In this example Figure 11(A) represents a stable system which fulfills the criterion. On the other hand the case represented by Figure 11(B) is unstable.

In the case of the loci of $g^{-1}(ju)+g_{D_1}$ shown in Figure 11, the origin was the critical point whose location with respect to the locus determined stability. However, it is convenient to shift the coordinate axes along the vector g_{D_1}. These translated axes are shown as broken lines in Figure 11. In Figure 12, the coordinate axes have been translated in this fashion and the point which was formerly the origin is now the point Q located at the tip of the vector $-g_{D_1}$. If such translated axes are used, the stability criterion given may be revised as follows:

If a polar locus of the inverse-loop transfer function $g^{-1}(ju)$ is drawn over the range of frequencies, u, and if a critical point Q is located at the tip of the describing-function vector $-g_{D_1}$ the system will be stable provided the point Q always appears to the left of the locus as the latter is traversed from zero to infinite frequency. Figure 12 demonstrates the application of the above criterion.

The foregoing test for absolute stability may be made for any specified value of control-signal amplitude $|c_1|$. It might in fact be found that the system will be stable for some amplitudes and unstable for others. The location of the point Q is dependent on the value of $|c_1|$. In order to obtain a complete picture of the stability, it is necessary that a second locus be drawn connecting the points Q over the complete amplitude range being considered. This curve will be referred to as the amplitude locus to distinguish it from the frequency locus plotted for the function $g^{-1}(ju)$.

The amplitude locus is drawn by plotting the tips of the vector values of the function $-g_{D_1}$ and connecting them by a curve. The two loci are superposed on the same graph and their relative orientation determines the stability characteristics of the system.

Figure 13 is an example of the superposed loci. The frequency locus shown is that representing the simple-loop transfer function given by the equation

$$g(ju)=\frac{1}{ju(1+ju)} \text{ or } g^{-1}(ju)=ju(1+ju) \tag{22}$$

The amplitude locus of Figure 13 represents the contactor describing function under conditions of a zero-average input velocity ($\delta=0$) and zero-average load torque. It was obtained from Figure 10 and represents a hysteresis effect given by $h/\Delta=0.2$.

In the case shown in Figure 13, the two loci intersect at the amplitude $|c_1|=0.062$. From the criterion just given, operating points on the amplitude locus corresponding to lower values of $|c_1|$, $0.060<|c_1|<0.062$, are unstable. Oscillations existing at these amplitudes will result in a tendency for the amplitude to increase. Operating points corresponding to higher values of $|c_1|$, that is, $|c_1|>0.062$, are stable. Oscillations existing at these amplitudes will result in a tendency for the amplitude to decrease. At the intersection itself, where $|c_1|=0.062$, the oscillations will tend to be maintained at this amplitude because this intersection corresponds to the borderline condition of stability.

The intersection point of the two loci is described as an equilibrium point. Because of the fact that higher amplitudes of oscillation decrease and lower amplitudes increase, the system's operating point tends to converge at this equilibrium point, it is therefore described as a point of convergent equilibrium.

The graphical construction shown in Figure 13 indicates that any initial disturbance sufficient to initiate the contactor, that is, $|c_1|>0.060$, will result in oscillations which will approach a self-sustained condition with an amplitude and frequency corresponding to the intersection point of the two loci. Disturbances less than sufficient to trip the contactor are beyond the cut-off point of the amplitude locus, where $g_{D_1}=0$, and naturally no oscillations result.

From Figure 13, the self-sustained oscillations will correspond to a dimensionless control-signal amplitude of $|c_1|=0.062$ (the error amplitude is the same since $g_e=1$) and a dimensionless frequency ratio given by $u=3.1$. The graphical construction which provides this result depends upon the basic approximation mentioned previously. It is therefore interesting to compare the predicted result with that actually observed or computed by more exact methods. Such calculations show that the actual conditions of steady-state self-sustained oscillations would be given by $|c_1|=0.066$ and $u=3.2$. The agreements concerning amplitude and frequency are within $6^1/_2$ per cent and 3 per cent respectively.

Convergent and Divergent Equilibrium

The preceding section illustrated an intersection of loci that indicated a con-

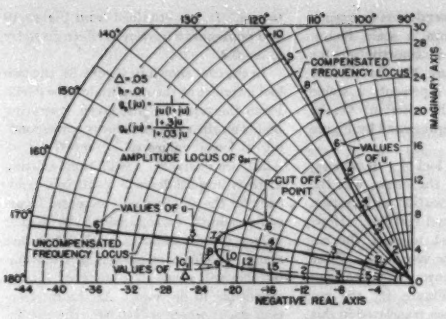

Figure 17. Loci diagrams illustrating stability improvement resulting from use of a phase-lead compensating network

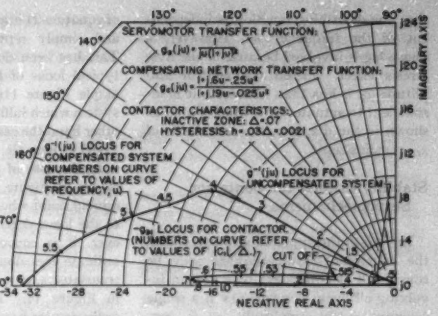

Figure 18. Loci plots for contactor servomechanism with critically damped servomotor

vergent condition of equilibrium. Figure 14 illustrates other possible configurations of the loci, some of which involve one or more intersections. In general, these intersections indicate convergent equilibrium if a slight increase in $|c_1|$ from its value at the intersection causes the locus of $-g_{D1}$ to enter the stable region and if a slight decrease causes it to enter the unstable region. In this event, self-sustained oscillations may result. If the intersections possess the converse properties, the equilibrium condition is divergent; it then does not correspond to a condition of self-sustained oscillation, but merely represents an amplitude boundary. The operating point will always tend to shift away from such a divergent equilibrium point. It may be noted from Figure 14 that the loci always intersect at the origin, corresponding to the condition that $|c_1| \to \infty$ and $u \to 0$. The origin equilibrium points are divergent in Figures 14(A), (C), and (E) and the amplitude of any oscillations which might arise will tend to decrease until either a convergent equilibrium point is reached or the contactor cut-off point, as marked by the abrupt termination of the amplitude locus is reached. The origin equilibrium points in Figures 14(B), (D), and (F) are convergent, indicating that if these systems are subjected to disturbances of sufficient magnitude, destructive oscillations will result.

It also might be noted that, in Figure 10, the amplitude of g_{D1} is plotted in terms of the quantity Δg_{D1}. This function is therefore inversely proportional to Δ for a given amplitude ratio $|c_1|/\Delta$. The inactive-zone range Δ appears as a reciprocal scale factor affecting the amplitude locus. The scale of this locus may be varied by changing the inactive-zone range, and the stability characteristics of the system may thus be altered. In the cases shown in Figures 13 and 14(A) and (E), the response can always be made stable for all conditions of operation by making the inactive-zone sufficiently large.

Degree of Stability

In many applications of contactor systems, a specification that requires merely a stable system is inadequate. The requirement that any transient oscillation following the correction of disturbance shall involve sufficient damping also is imposed. In other words the degree of stability is of importance.

In the case of linear servomechanisms, a rule-of-thumb procedure has been developed[7] which gives an indication of the degree of stability from the frequency-response loci. This procedure is to determine the peak value M_p of the output-input ratio $M = |\theta_o/\theta_i| = |\sigma|/|\delta|$. In general, it is found that satisfactory damping exists if $M_p < 1.3$, the exact limit imposed depending upon the application. This rule-of-thumb method must be used with caution. When it is backed up by the designer's past experience, successful system designs are obtained.

It is proposed that a similar rule-of-thumb criterion be used to determine the degree of stability of contactor servomechanisms. Figures 15 and 16 show how this might be done. Figure 15 contains the two loci shown previously in Figure 13. However, the inactive-zone range has been increased to a value of $\Delta = 0.4$. Under this condition, the system will possess absolute stability, as shown by the fact that the loci do not intersect.

The peak ratio of output-to-input amplitudes M_p may be determined for a given control-signal amplitude $|c_1|$ by graphical means now to be described. Equation 21 may be inverted and rewritten as

$$\frac{\sigma}{\delta}(ju) = \frac{g_{D1}}{g^{-1}(ju) + g_{D1}} = \frac{\text{output}}{\text{input}} \tag{23}$$

In Figure 15 the quantity g_{D1} is represented by the vector QO and the quantity $g^{-1}(ju)$ by the vector OP. The sum appearing in the denominator of 23 will therefore be represented by the vector sum $(QO + OP)$ or by the connecting vector QP. The output-input ratio is therefore expressed by the vector ratio

$$\frac{\sigma}{\delta}(ju) = \frac{QO}{QP} \tag{24}$$

The amplitude ratio or value of M is merely

$$M = \left|\frac{\sigma}{\delta}(ju)\right| = \frac{\text{length of } QO \text{ vector}}{\text{length of } QP \text{ vector}} \tag{25}$$

For a given value of $|c_1|$ the vector length $|QO|$ is constant. Therefore M_p or the peak value of M over the frequency range is given by

$$M_p = \left|\frac{QO}{QP}\right|_{\min} = \frac{\text{length of } QO \text{ vector}}{\text{minimum length of } QP \text{ vector}} \tag{26}$$

The minimum length of the QP vector is found by drawing an arc of shortest possible radius, tangent to the frequency-response locus from the point Q as a center. The frequency u at the point of tangency of the $QP_{\min}$ vector with the frequency-variant locus is designated as the peak frequency u_p.

The values of M_p and u_p determined over the entire range of control-signal amplitude $|c_1|$ provide a complete picture of degree of stability. This is shown in Figure 16. For the case considered in the examples, the values of M_p and u_p increase

with a decrease in control-signal amplitude. This indicates that during the beginning of a correction process involving high control-signal amplitudes, the system would act as though it possessed adequate response damping and had a relatively low natural frequency. On the other hand, as the correction process approached completion, the degree of stability would become poor and the frequency associated with the transient oscillations would increase. This is a common characteristic of uncompensated contactor servomechanisms. When an actual servomechanism having the properties represented by Figures 15 and 16 was subjected to a large disturbance, the initial correction process appeared well damped but slow with a moderate initial overshoot, but the final portion of the correction process appeared poorly damped but more rapid. Eight positive and eight negative corrective impulses were initiated by the contactor before the correction process ceased and the error finally remained within the inactive zone.

The foregoing example represents a servomechanism possessing a low degree of stability, as evidenced by the value of M_p approaching 4.5 before the cut-off point is reached. It has been found from experimental tests on various types of contactor systems that an M_p of 2.0 near the cut-off point and of 1.3 for higher control-signal amplitudes provides a satisfactory degree of relative stability for most applications.

In the example shown, the degree of stability was poor in spite of the large inactive zone. It is obvious that compensating networks are desirable to improve the response in even the most elementary types of contactor servomechanisms.

Application of a Simple Phase-Lead Type Compensating Network

The example in the preceding section involved a low degree of stability in spite of the large inactive zone employed ($\Delta=0.4$). In most practical applications, a smaller inactive zone would be specified because of accuracy considerations and a typical value might be given by: $\Delta=0.05$. In that case, the amplitude locus would appear as in Figure 17. The uncompensated frequency locus is the same as in the preceding example. Because of the decrease in Δ, the loci intersect and self-sustained oscillations occur. The point of intersection indicates that these oscillations involve a control-signal amplitude $|c_1|=0.74\Delta=0.35$, at a frequency $u=4.70$. Experimental tests indicate that the control-signal amplitude of oscillation (which also equals the error and output amplitudes since no compensation is assumed) is given by $|c_1|=0.040$ at a measured frequency $u=4.30$. The discrepancy between calculated values and test values is only 12 and 10 per cent, respectively.

A compensating network of the form shown in Figure 6(A) was employed to improve stability. An attenuation factor $\alpha=10$ was specified since this represents a practical compromise between the problem of obtaining a large phase lead and that of minimizing the amplification of noise signals. Plotting loci curves corresponding to various trial values of the time constant ratio ρ_a, given in equation 6A shows that the best stability characteristics are obtained when $\rho_a=0.3$. The dimensionless transfer function of the compensating network is then

$$g_c(ju)=\frac{1+0.3ju}{1+0.03ju} \tag{27}$$

The compensated frequency locus shown in Figure 17 is based on the network of equation 27. The frequency and amplitude loci no longer intersect and self-sustained oscillations will not occur. Furthermore, if the rule-of-thumb criterion for degree of stability is used as described previously, the value of M_p is a maximum when the control-signal amplitude $|c_1|$ is just at the cut-off point and is given by $M_{p\max}=1.76$. In view of the previous discussion on degree of stability, the compensated system should be adequately stable.

An experimental version of this servomechanism confirmed the results predicted above. The test equipment involved a runaway velocity R of 30 degrees per second and a time constant T of 2.3 seconds, giving a signal base of the dimensionless notation as $B=RT=69$ degrees. The actual inactive zone was 3.5 degrees (or $\Delta=C_\Delta/B=3.5/69=0.05$). The compensating network had a numerator time constant τ_a of equation 6 given by $\tau_a=\rho_a\rho_b=\rho_a T=0.3\times 2.30=0.69$ seconds. The electrical constants for the network of Figure 6(A) are $R_0=4{,}000$ ohms, $R_1=1.45$ megohms, $R_2=157{,}000$ ohms, and $C_1=1.0$ microfarad. When this compensating network was used, a sudden input change of 360 degrees resulted in an initial error overshoot of 15 degrees and then an undershoot of two degrees. The error then remained within the inactive-zone range. Such a response would be considered to have adequate degree of stability for most applications.

This experimental test not only confirmed the conclusions reached from the loci diagram, but also demonstrated that the addition of the compensating network resulted in a spectacular improvement in the transient response. It is interesting to note that the optimum value of the numerator time constant $\tau_a=0.69$ seconds selected on the basis of the loci diagram was also the optimum when experimentally selected by trial-and-error means.

Application of a Resonant Phase-Lead Type of Compensating Network

A contactor servomechanism possessing more complicated dynamic characteristics has also been investigated. The servomotor transfer function corresponding to equation 3 was

$$G_s(ju)=\frac{30}{ju(1+2.3ju)^2}\text{ degrees} \tag{28}$$

The runaway velocity was $R=30$ degrees per second as before. The basic time constant was again $T=2.30$ seconds. However, the transfer-function term involving the time constant is now second order and the servomotor response is critically damped. The dimensionless transfer function of the servomotor then is reduced to

$$g_s(ju)=\frac{1}{ju(1+ju)^2} \tag{29}$$

The uncompensated frequency locus in Figure 18 corresponds to the loop transfer function of the servomechanism without the compensating network. The amplitude loci curve of Figure 18 corresponds to a contactor inactive-zone range of $\Delta=0.07$ and a hysteresis effect given by $h=0.03\ \Delta=0.021$. This ratio of h to Δ represents a typical practical minimum for many applications. The two loci intersect at a value of control-signal amplitude $|c_1|=9.5\Delta=0.66$ which is relatively large. This would correspond to self-sustained oscillations with an error amplitude of 46 degrees. It would be necessary to increase the inactive-zone range to an impractically high value $\Delta=0.63$ or a static error range of $\pm B\Delta/2=\pm 69\times 0.63/2=\pm 22$ degrees in order to suppress these oscillations. The need for a compensating network is obvious.

Trial constructions of loci indicated that suitable compensation was not obtainable with a simple lead controller of the type shown in Figure 6(A). A resonant lead network similar to that shown in Figure 6(B) was therefore used.* The

*The actual compensating network possessed the same characteristics as that of Figure 6(B); however, a circuit arrangement employing electronic feedback was used. This was done in order to avoid the use of the impractically high values of inductance and capacitance which would otherwise have been required.

characteristics were selected by trial-and-error, graphical constructions of the frequency locus being employed. It was found that a resonant lead controller having a transfer function of the form stated in equations 7 and 7A provided the best response with the following constants

$$\zeta_1 = 0.6 \qquad \zeta_2 = 0.6$$

$$u_1 = 2 \qquad u_2 = 6.3$$

$$\omega_1 = \frac{u_1}{t_b} = 0.87 \frac{\text{radians}}{\text{second}} \qquad \omega_2 = \frac{u_2}{t_b} = 2.76 \frac{\text{radians}}{\text{second}}$$

$$\text{attenuation constant } \frac{\omega_2^2}{\omega_1^2} = 10$$

With a compensating network of this type the frequency-response curve is that described as the compensated-frequency locus in Figure 18. Since no intersections of the amplitude and frequency loci occur, the system is stable. The maximum value of M_p is determined graphically as $M_{pmax} = 2.5$. This value is somewhat higher than that specified previously but indicates that a reasonable degree of relative stability might be expected.

Experimental tests incorporating this compensating network with a critically damped servomotor having a transfer function of the form given in equation 29 were conducted. The transient response appeared satisfactory. A sudden input change of 360 degrees resulted in an initial error overshoot of 27 degrees, a subsequent undershoot of 13 degrees, an overshoot of seven degrees, and then an undershoot of two degrees before the correction process was completed. The total correction process described involved a time interval of 37 seconds; half of this time involved the initial correction process prior to the first overshoot when the speed of response is limited by the value of runaway velocity. In view of the inherently slow response of the servomotor (purposely made so to provide ease of measurement), the performance may be considered satisfactory.

The results described above corresponded to an inactive-zone range of 4.6 degrees ($\Delta = 0.07$). From Figure 18, a reduction in the inactive-zone range to a value given by $\delta_\Delta = 2.5$ degrees ($\Delta = 0.038$) would be just sufficient to cause the two loci curves to intersect and self-sustained oscillations to result. This change in inactive zone would be represented by a simple increase in the scale of the amplitude loci curve by the factor 0.07/0.038. The loci curves indicate that these oscillations would have a frequency given by $u = 5.9$ or $\omega = ut_b = 2.56$ radians per second or a period of $2\pi/\omega = 2.45$ seconds, and a control-signal amplitude given by $|\epsilon_1| = 0.027$. The corresponding dimensional error amplitude would be $|\delta| = B|\epsilon_1|/g_c(j5.9) = 0.76$ degrees.

Actual tests indicated that it was necessary to reduce the inactive-zone range to a value of $\delta_\Delta = 2.7$ degrees before self-sustained oscillations could occur. This is within 8 per cent of the predicted value of 2.5 degrees. The observed period of oscillation was 2.7 seconds, or 10 per cent longer than the predicted value of 2.45 seconds, and the error amplitude was 3/4 degree or equal to the predicted value of 0.76 degrees as closely as could be determined in view of the accuracy of measurement.

The condition of self-sustained oscillations obtained with the smaller inactive zone might be acceptable for some applications of contactor servomechanisms. On the other hand if the application's specifications prohibit such oscillations, an 80 per cent increase in inactive-zone range would provide the reasonably well-damped transient response described previously. It is to be noted that the error amplitude associated with self-sustained oscillations can be considerably smaller than the inactive-zone range when a phase-lead type compensating network is employed.

The effectiveness of the compensating network is best demonstrated by the fact that, in the case of the uncompensated system, an inactive-zone range given by $\Delta = 0.63$ was required to prevent the occurrence of excessive self-sustained oscillations. With the addition of the compensating network an inactive-zone range of $\Delta = 0.038$ was sufficient to prevent oscillation. This is a permissible improvement in static accuracy by a factor of seventeen.

Experimental Verification of the Theory

The examples previously mentioned represented several cases where the predicted performance was compared with that obtained by actual experimental tests. These tests were performed on a model of a contactor servomechanism designed to simulate actual systems. This simulator employed a shunt-type d-c motor as the servomotor and operated essentially as shown by Figure 3. The actual circuit details were, however, considerably more complicated than shown in that diagram. Various adjustable dynamic characteristics and contactor characteristics were provided and extraneous factors which might lead to incorrect results were minimized by suitable design. The simulator was designed so that the inactive-zone range and hysteresis range could be adjusted, so that the servomotor transfer function could assume varied forms including those involving finite time delays, and so that various compensating networks could be introduced. The details of construction of this device and that of the electronic-feedback type resonant-lead controller mentioned in the preceding section are not discussed here since they are not directly pertinent to the subject matter.

The instances given where the results predicted by the theory were compared with experimentally observed data represent only several examples of a large number of such tests made for various types of contactor servomechanism problems. In general, the percentage agreement was the same as shown in these examples. It was considered desirable that the results obtained by the simulator be of a form which could be visually recorded so that electrical recording instruments would not generally be required. For this reason, the relatively slow runaway velocity of 30 degrees per second and the basic time constant of 2.30 seconds were chosen. By employing proper scale factors, faster servomechanisms may still be represented by the simulator. The purposely slow response of the simulator should be kept in mind when evaluating the results described in the preceding sections; the dimensional performance figures given are not necessarily typical.

Conclusions

The investigation described in this paper leads to the following basic conclusions:

A frequency-response method of analysis and synthesis may be adapted to contactor servomechanisms by employing a simple approximation. This method is usually capable of providing sufficiently accurate results for most engineering applications.

The performance of contactor servomechanisms can be materially improved, in even the simplest cases, by the introduction of suitable compensating networks. The proposed frequency-response method of treatment is particularly adaptable to the selection of such networks.

The approximate method of treatment used here in application to contactor servomechanisms also is generally applicable to the analysis and synthesis of other nonlinear systems. It might prove of particular value if the nonlinear effects, such as backlash, coulomb friction, saturation, and so forth, appearing in essentially linear servomechanisms were treated by this means. It is hoped that the technique introduced here will contribute to the more effective employment of contactor servomechanisms in control applications.

References

1. Theory of Servomechanisms, H. L. Hazen. *Journal*, Franklin Institute (Philadelphia, Pa.), volume 218, number 3, September 1934, pages 279–330.

2. Theory of Oscillation (book), A. A. Andronow, C. E. Chaikin. Moscow, 1937. English Edition edited by Solomon Lefschetz. Princeton University Press, Princeton, N. J., 1949.

3. Introduction to Non-Linear Mechanics (book), Nicholas Minorsky. J. W. Edwards Brothers, Ann Arbor, Mich.

4. Analysis of Relay Servomechanisms, H. K. Weiss. *Journal of the Aeronautical Sciences* (New York, N. Y.), volume 13, July 1946.

5. Fundamental Theory of Servomechanisms (book), L. A. MacColl. D. Van Nostrand Company, New York, N. Y., appendix—Study of a Simple On-Off Servomechanism, 1945.

6. An Analysis of Relay Servomechanisms, D. A. Kahn. *AIEE Transactions*, volume 68, part II, 1949, pages 1079–88.

7. Principles of Servomechanisms (book), G. S. Brown, D. P. Campbell. John Wiley and Sons, New York, N. Y., 1948.

8. Fundamental Theory of Servomechanisms (book), L. A. MacColl. D. Van Nostrand Company, New York, N. Y., chapter I-VII, 1945.

9. Analysis and Synthesis of Linear Servomechanisms (book), A. C. Hall. Technology Press, Cambridge, Mass., 1943.

Discussion

George A. Philbrick (George A. Philbrick Researches, Boston, Mass.): Since many readers of this able and intelligent paper will not previously have come across its author, it is appropriate to mention an earlier, and unpublished, contribution by him. While working with the Propeller Division of Curtiss-Wright Corporation prior to 1946, Kochenburger prepared a skillful analysis of a compound automatic control problem in turbo-prop regulation. This analysis was happily received and applied in a related project by the present writer

The paper under discussion treats a fundamentally nonlinear servomechanism, which it appears to handle successfully by a harmonic method. It will thus give great comfort to frequency enthusiasts. If some of the comments which follow are at best dispassionate, attribute them to the fact that this writer is an enthusiast from another camp altogether.

Items which it is felt belong in the list of references include a paper by A. Ivanoff;[1] and the recently translated book, Dynamics of Automatic Control, by Oldenbourg and Sartorius.[2] Ivanoff studied the combined influences of inertness and static friction, under sinusoidal performance, in a manner related to the Kochenburger approach; the compensatory effects of inertness, for example, were clearly shown by him. In the Oldenbourg book, which contains many pioneering elements, similar nonlinear phenomena also are introduced into otherwise linear control loops, and the stability and performance evaluated through consideration of the behavior of the fundamental frequency, as is done in the present paper. A recent noteworthy paper in this same field was prepared by T. A. Rogers of the University of California.[3]

A more serious omission, from the writer's point of view, is the absence of any reference to the method of analogy as a tool of analysis and synthesis in the study of systems of this general type. The current availability of analogue computing components, as a concrete fact, requires the qualification, even the revision, of many of the statements in the paper. Such components are regularly employed in our laboratory, and elsewhere, to represent regulatory systems of which those described in this paper form a special case. In a few minutes after receipt of this paper the first example described was set up, operated, and the conclusions corroborated quantitatively through oscilloscope displays. The computing assemblage is shown in Figure 1 of the discussion. Straightforward additions lead to the second and slightly more involved example. All the components exhibited are perfectly standard catalog items.

An interesting outcome of our brief experience with the analog representation of this problem was the observation that substantially the same compensating characteristic is optimum when the nonlinear contactor-unit is replaced by the simplest linear approximation. As to the form of the time responses themselves, which are important for many applications, all will agree that these do not come readily from any frequency method. The analog of course, on the other hand, gives time responses directly for either discrete or random stimuli, and frequency responses as well for those who want them. In a more intricate nonlinear control or servo system, of which perhaps the mechanism discussed is a minor component, the applicability of the author's approach may be open to some additional doubt, whereas the abilities of the analog are inherently unaffected by the extent or complexity of the primary structure under study.

References

1. Theoretical Foundations of the Automatic Regulation of Temperature, A. Ivanoff. *Journal*, Institute of Fuel (London, England), February 1934.

2. Dynamics of Automatic Control (book), Oldenbourg, Sartorius. Translated by Dr. H. L. Mason. *American Society of Mechanical Engineers* (New York, N. Y.), February 1948.

3. Relay Servomechanisms, T. A. Rogers. *Paper 50-S-13, American Society of Mechanical Engineers* (New York, N. Y.), 1950.

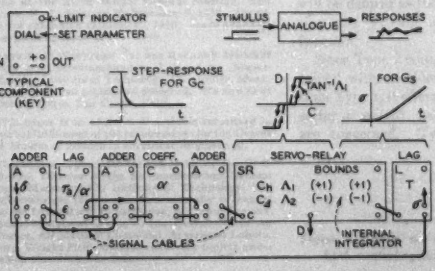

Figure 1. Analog computing assembly for the contactor servomechanism

Ralph J. Kochenburger: The author appreciates the constructive comments made by Mr. Philbrick in his discussion of this paper and wishes to thank him for calling attention to an earlier unpublished work in the field of feedback control systems. Several interesting points were raised in his discussion which warrant further clarification.

Mr. Philbrick classifies this paper as belonging to the "camp of frequency-response enthusiasts." There has been an unfortunate tendency to group engineers studying feedback control systems into two groups those interested in the transient response of such systems and those interested in the frequency response. Such a distinction is fallacious since all of these engineers are interested in the transient response of the system they are studying. It however happens that, in complicated feedback control systems, the operational calculus necessary for a direct approach involves computations which become unduly cumbersome and the seemingly "round-about" method of first studying the response of the system to sinusoidal disturbances and then predicting the transient response from these results represents a more practical approach. This is particularly the case when the system contains components whose input-output relationships are not readily subject to analytic representations but which can be described in terms of experimentally derived data.

It might be kept in mind that the Nyquist criteria, upon which the frequency response method is based, are no more than means for determining whether any objectionable terms exist in the transient response relationship. In its most frequently applied form, the locus of the transfer function is plotted for various values of "real frequency," that is, the substitution is made that $s = j\omega$ where s is the Laplace transformation operator. This form permits the question to be answered—is the system stable? It is however possible to use this general method to determine how stable the system is as well. If it is not only specified that it be stable but that its response involve no oscillatory components with damping ratios less than some specified value, ζ, it is merely necessary to draw a new transfer locus using the substitution, $s = \zeta\omega_n + j\sqrt{1-\zeta^2}\omega_n$ over the complete range of frequencies, ω_n, and then to apply the same graphical test as before. If the criteria are fulfilled for such a complex frequency locus, then all damping ratios involved in the response function will be greater than the

specified value ζ. Sometimes this second procedure is tedious and for this reason the engineer frequently determines the response function for the range of real frequencies only and then employs various well known rules-of-thumb to make approximate predictions covering the nature of the transient response.

Mr. Philbrick mentions two earlier contributions where other problems in nonlinear dynamics employ a similar approximation by which all but the average and fundamental frequency components of a nonsinusoidal periodic function are ignored. Such an approximation method has been used frequently and is generally well-known. The author consequently did not cite all of the contributions where such a procedure is employed. The paper under discussion merely suggests a combination of this procedure and of the Nyquist method which is particularly applicable to nonlinear servomechanisms. The reference given in the discussion to a recent paper by T. A. Rogers is of particular interest. The author has not yet had the opportunity to examine this contribution.

The discussion points out the omission of the analogue method for studying feedback control systems. The author agrees that this method should have been accorded more emphasis since it constitutes a practical means of attack in many instances. As a matter of fact, mention was made in the paper of a simulator or analogue device employed by the author to check the validity of the proposed method in the case of several specific problems. It is felt that the analytic and analogue approaches complement each other and that there is need for both in control system design. The analytic approach has an advantage in that it not only determines the nature of the response itself, but also shows which design factors are the cause of its various features. It consequently gives direct information leading to the synthesis of an improved system.

Analogue methods show the nature of the system response but the synthesis problem still involves a trial-and-error variation of design constants. Furthermore, the experimental facilities involved in such an approach may be expensive. Their use may well be justified in a laboratory dealing with a number of related control problems. In the case of industrial concerns which encounter problems in feedback control systems at only infrequent intervals, there is some question regarding their economic justification.

It is appreciated that Mr. Philbrick used his analogue computor to check some of the results presented in the paper. More quantitative information concerning the correlation of the two methods would have been of interest.

The discussion mentions that a prediction of the time response does not come readily from a frequency response method. Methods by which the general nature of the time response can be predicted from a knowledge of the frequency response have been mentioned. If an actual picture of the time response is desired, this too may be obtained by a method developed by Dr. George W. Floyd and described in Chapter 11 of reference 1 of the paper. In regard to elements of doubt regarding the applicability of the proposed method to more involved systems, it is true that, in view of space limitation, the paper discussed only the application to a basic single loop system. An extension of this method applicable to a multiloop system should follow directly and also should be valid provided the Nyquist criteria are correctly applied. The simple form of these criteria given in the paper holds only for single-loop systems with stable components. In any case, some check should be made in any given problem concerning the validity of the approximation upon which this method is based.

In conclusion, the author wishes to thank Mr. Philbrick for his discussion and for the number of interesting suggestions he has made.

Phase Lead for A-C Servo Systems with Compensation for Carrier Frequency Changes

ARTHUR P. NOTTHOFF, JR.
STUDENT MEMBER AIEE

THE basis for operation of a feedback-control system lies in the comparison of the output quantity with the input quantity. The equipment used to compare information contained in these two quantities comprises the data-transmission and error-measuring system. It is frequently convenient to transmit this information by means of an a-c signal whose envelope is at all times proportional to the error, and whose phase is determined by the sign (or sense) of the data signal, that is, data are transmitted as a suppressed carrier modulated signal. If, in addition, the signal which controls the system output member is an a-c signal, the system will be defined as an a-c system, as illustrated in Figure 1.

It has been demonstrated elsewhere[1] that networks which impart a phase lead to the error-data signal may be used to improve static and/or dynamic system performance. Phase lead for an a-c system may be introduced by either of the following basic techniques:

1. The modulated error signal, V_4, is demodulated, phase lead is introduced at a d-c level, and the resultant signal is remodulated to produce the control signal, V_1.
2. V_4 is impressed upon a network which operates upon the carrier frequency and its sidebands to give the modulation (or data signal) on V_1 a phase lead relative to V_4.

The former technique has been called[2] Type 1 compensation and the latter Type 2. Type 1 compensation is illustrated in Figure 2 and Type 2 in Figure 3; note that primed symbols represent the data signal which appears as modulation on the a-c signal represented by the corresponding unprimed symbol.

In the following discussion frequencies which are involved in the information carried by the data-transmission system will be referred to as data frequencies; those frequencies involved in the modulated a-c signal which carries this information will be called signal frequencies. For a Type 1 network the ratio V_1/V_4 will be defined as the signal transfer function and V_1'/V_4' as the data transfer function.

Since Type 2 compensation may be obtained with considerably less equipment than Type 1, it offers a decided advantage as far as weight, space, and maintenance are concerned. Type 2 compensation, however, possesses the following disadvantages:

1. There is a lower limit upon the data frequency at which useful phase lead may be obtained.
2. The compensation afforded by Type 2 networks varies with changes in the a-c carrier frequency.

The stated advantages of Type 2 compensation make this scheme extremely attractive if the attendant disadvantages may be overcome or tolerated. The first-mentioned disadvantage appears to be a basic one which restricts the use of Type 2 compensation to relatively "high-performance" servomechanisms. The purpose of this paper is to relax limitations resulting from the second-mentioned disadvantage by introducing techniques for minimizing the sensitivity of Type 2 networks to changes in carrier frequency.

Basic Action of Type 2 Lead Networks

Consider now the requirements on a network which is to impart phase lead to the modulation (or data signal) on a suppressed carrier modulated signal. If the network input voltage, V_4, consists of such a signal, as given in equation 1, the introduction of pure data phase lead will yield an output voltage, V_1, as given in equation 3.

$$V_4 = E \cos \omega_d t \cos \omega_c t, \tag{1}$$

$$= \frac{E}{2}\{\cos[(\omega_c+\omega_d)t] + \cos[(\omega_c-\omega_d)t]\} \tag{2}$$

$$V_1 = E \cos(\omega_d t + \theta_d) \cos \omega_c t \tag{3}$$

$$= \frac{E}{2}\{\cos[(\omega_c+\omega_d)t+\theta_d] + \cos[(\omega_c-\omega_d)t-\theta_d]\} \tag{4}$$

where

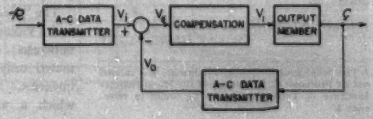

Figure 1. Basic a-c feedback-control system

Paper 50-45, recommended by the AIEE Feedback-Control Systems Committee and approved by the AIEE Technical Program Committee for presentation at the AIEE Winter General Meeting, New York, N. Y., January 30–February 3, 1950. Manuscript submitted October 10, 1949; made available for printing December 1, 1949.

ARTHUR P. NOTTHOFF, JR. was Research Assistant with the Servomechanisms Laboratory, Massachusetts Institute of Technology, Cambridge, Mass., at the time this paper was prepared. He now is at Dalmo Victor, San Carlos, Calif.

This paper is an abstract of a thesis submitted in partial fulfillment of the requirements for the Degree of Master of Science in Electrical Engineering.

The author appreciates the aid given by Dr. G. S. Brown, Director of the Servomechanisms Laboratory, Massachusetts Institute of Technology, and acknowledges the co-operation of many colleagues at the Laboratory, in particular, Mr. Paul Travers. Acknowledgment is due to the United States Air Forces, Air Materiel Command, Armament Laboratory, Wright Field, who sponsored the project under which this work was done.

Figure 2. Type 1 compensation

V_s = network input voltage
V_1 = network output voltage
ω_d = data frequency
ω_c = carrier frequency
θ_d = angle of data phase lead

Examination of equations 2 and 4 reveals that the network must impart a phase lead to the upper sideband of the carrier frequency and a phase lag to the lower sideband.

Type 2 Compensation Independent of Carrier Frequency

A more exact approach to the problem of design of Type 2 networks may be made if one seeks the relations between the signal transfer function and the data transfer function of a network which operates upon a modulated signal. It is desirable to construct the network signal transfer function so that no quadrature carrier components appear at the output of the network since most a-c output members are sensitive only to carrier components which are in phase with a fixed phase reference, ψ_R and are apt to be adversely affected by quadrature carrier-components. It has been shown* that the following constitutes a sufficient (although not necessary) set of conditions which guarantee that a network with signal transfer function $H(j\omega)$ will have a data transfer function $G(j\omega_d)$ and that no quadrature carrier components will be produced.

$$|H_e(\omega_d)| = |G(j\omega_d)| \tag{5}$$

$$\phi_0(\omega_d) = \angle G(j\omega_d) \tag{6}$$

$$|H_o(\omega_d)| = 0 \tag{7}$$

$$\phi_e(\omega_d) = \psi_R - \psi_c \tag{8}$$

where

ω = signal frequency
ω_d = data frequency
ω_c = carrier frequency
ψ_R = carrier reference phase angle
ψ_c = phase angle of carrier at network input

and the even component of $|H(j\omega)|$ taken about ω_c

$$|H_e(\omega_d)| = 1/2\{|H[j(\omega_c+\omega_d)]| + |H[j(\omega_c-\omega_d)]|\}$$

and the odd component of $|H(j\omega)|$ taken about ω_c

$$|H_o(\omega_d)| = 1/2\{|H[j(\omega_c+\omega_d)]| - |H[j(\omega_c-\omega_d)]|\}$$

* The development of these conditions, first carried out by Professor G. C. Newton of the Massachusetts Institute of Technology may be found in reference 3.

The even component of $\angle H(j\omega)$ taken about ω_c

$$\phi_e(\omega_d) = 1/2\{\angle H[j(\omega_c+\omega_d)] + \angle H[j(\omega_c-\omega_d)]\}$$

The odd component of $\angle H(j\omega)$ taken about ω_c

$$\phi_o(\omega_d) = 1/2\{\angle H[j(\omega_c+\omega_d)] - \angle H[(j\omega_c-\omega_d)]$$

These conditions require that $H(j\omega)$ have magnitude symmetry and phase assymetry about ω_c.

If the network data transfer function, $G(j\omega_d)$, is to be independent of ω_c, it may be seen from equations 5 through 8 that the following constitutes a set of sufficient conditions to be imposed on the signal transfer function, $H(j\omega)$

$|H_e(\omega_d)|$ must be invariant with ω_c (9)

$\phi_0(\omega_d)$ must be invariant with ω_c (10)

$|H_o(\omega_d)| = 0$ for all ω_c (11)

$\phi_e(\omega_d) = \psi_R - \psi_c$ for all ω_c (12)

A signal transfer function which is sufficient (although not necessary) to satisfy equations 9, 10, and 11, and which will introduce data phase lead, is offered by the $H(j\omega)$ illustrated in Figure 4. To satisfy equation 12, it will be necessary to introduce a second network to vary the phase of the carrier at the input terminals of the first network. If $H_c(j\omega)$ is defined such that

$$\psi_c = \angle H_c(j\omega) \tag{13}$$

the transfer function $H_c(j\omega)$ illustrated in Figure 5 will satisfy equation 12 provided the network which possesses this transfer function is placed at such a position in the system that it operates on the unmodulated carrier so as to vary ψ_c.

Reference to equations 1 through 4 reveals that the data transfer function associated with these "ideal" characteristics has a linearly increasing phase lead characteristic and a constant amplitude characteristic. Such a function, although different from conventional lead network data transfer functions, may be used to good advantage in many applications.

The "ideal" characteristics of Figures 4 and 5 violate the laws of minimum phase networks; hence, they may be approximated only over a small range of frequencies. The frequency range over which a valid approximation may be made is a function of the order of the transfer functions used to approximate $H(j\omega)$ and $H_c(j\omega)$.

Approximation of Ideal $H(j\omega)$

A preliminary investigation revealed that approximation of the ideal $H(j\omega)$ by means of a transfer function involving quadratic factors yielded, in most practical cases, networks which were insensitive of ω_c over a frequency range which was too narrow for most practical applications. Thus it was decided that a transfer function of fourth order (two quadratic factors) was the least complex one which would give a good approximation to the ideal characteristics over a sufficiently wide frequency range. It also was found that the large rate of change of phase of $H(j\omega)$ which is necessary to obtain useful phase lead for data frequencies involved in most practical cases could be obtained only by employing underdamped quadratic factors in the numerator of $H(j\omega)$.

A transfer function which meets the above-stated requirements, and which may be used to approximate the ideal $H(j\omega)$ over a reasonable frequency range, is as follows

$$H(ju) = \frac{[1-(u^2/m^2)+j2\zeta_m u/m]\,[1-m^2u^2+j2\zeta_m mu]}{[1-(u^2/r^2)+j2\zeta_d u/r]\,[1-r^2u^2+j2\zeta_d ru]} \tag{14}$$

where

$u = \omega/\omega_c$ = nondimensional frequency ratio
ζ_m, ζ_d = damping coefficients
m, r = coefficients which determine the undamped natural frequencies of the quadratic terms

This function will have amplitude and phase characteristics of the form illustrated in Figure 6.

Study of this function revealed that the best approximation to the ideal characteristics of Figure 4 may be obtained by constructing $H(ju)$ to have linear phase shift over as large a frequency range as possible. This approach is possible because the amplitude characteristic associated with the phase characteristic just described will, in all cases, vary only a few decibels for excursions of the carrier frequency which give a large change (over 90 degrees) in the phase characteristics.

Define

Figure 3. Type 2 compensation

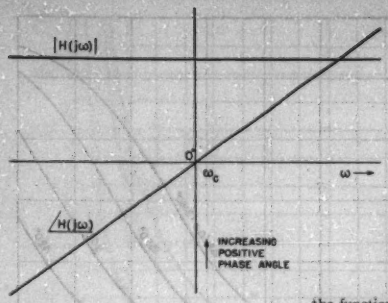

Figure 4 (left). Form of ideal $H(j\omega)$

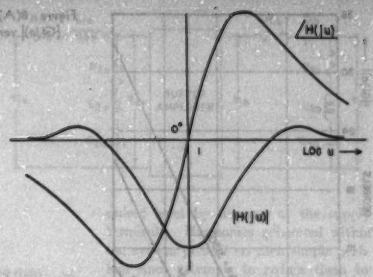

Figure 6 (right). Form of fourth order $H(ju)$

$\phi = /H(j\omega)$

$a = \omega_d/\omega_c$ = nondimensional data frequency ratio

$\Delta\phi/\Delta a$, the slope of the network phase characteristic for frequencies near $u=1$, is a basic quantity since it determines the amount of phase lead which will be introduced at any data frequency. This quantity must be chosen so that the compensation afforded will best meet the requirements of the particular system under consideration.

For a network whose transfer function is as given in equation 14, optimum insensitivity to ω_c may be attained by choosing ζ_n, ζ_d, m, and r to give the maximum range of linear phase shift for a specified phase slope. The choice of these coefficients must, however, be tempered by the fact that noise considerations make it desirable to have network attenuation at $\omega = \omega_c$ a minimum. These two specifications are in conflict, and a compromise must be made. It was decided that transmission at $\omega = \omega_c$ of 20 decibels below network transmission at low and high frequencies is a value which is acceptable for many applications.

Graphical constructions which utilize plots of phase slope versus frequency for the function $1-u^2+j^2\zeta u$ have been used[3] to determine the relations between ζ_n, ζ_d, m, and r which yield the maximum range of linear phase shift along with network attenuation of approximately 20 decibels for a specified phase slope, $\Delta\phi/\Delta a$. These relations are contained in Figure 7 along with the stipulation that

$$\zeta_d = \zeta_n \tag{15}$$

For specified phase slope, $\Delta\phi/\Delta a$, an $H(ju)$ constructed with the coefficients obtained from these relations will have linear phase shift for u between $1/m$ and m. Thus Figure 7 reveals that the extent of the range of linear phase shift varies inversely as phase slope, and the tolerance on ω_c must be made more strict for large values of phase slope than for small ones.

Approximation of Ideal $H_c(j\omega)$

The form of $H_c(j\omega)$ is dependent upon the value of ψ_R called for by a specific application. As an example $\psi_R = -90$ degrees will be considered. This value is applicable to the case of a 2-phase a-c motor servomechanism. In general, a second-order transfer function may be used to approximately $H_c(j\omega)$ since:

1. Failure to meet exactly equation 12 results in second-order effects.

2. The phase characteristic of $H_c(j\omega)$ must be linear only over the frequency range covered by a varying carrier frequency, while that of $H(j\omega)$ must be linear over the range covered by the varying carrier frequency and its sidebands.

A function which will satisfy equation 12 over a limited frequency range is

$$H_c(ju) = \frac{1}{1-u^2+j2\zeta_c u} \tag{16}$$

If $H(ju)$ is constructed with the coefficients of Figure 7, the phase slope of $H_c(ju)$ will be the negative of that of $H(ju)$ for u between $1/m$ and m providing

$$\zeta_c = \frac{m^2-1}{2m}\cot^{-1}\left[\left(\frac{m^2-1}{2m}\right)\frac{\Delta\phi}{\Delta a}\right] \tag{17}$$

is used in equation 16.

Choice of Phase Slope

For a specified phase slope of $H(ju)$, $\Delta\phi/\Delta a$, the restriction to fourth-order $H(ju)$ with optimum linear phase shift characteristic fixes $H(ju)$ and hence $G(ja)$, the data transfer function. It remains to integrate the choice of $\Delta\phi/\Delta a$ with the requirements of the particular servomechanism under consideration. Figures 8(A) and 8(B) show the amplitude and phase characteristics of the data transfer functions which result from networks constructed to give the fourth-order $H(ju)$ of equation 14 with coefficients obtained from Figure 7. Curves are shown for several values of $\Delta\phi/\Delta a$.

Define

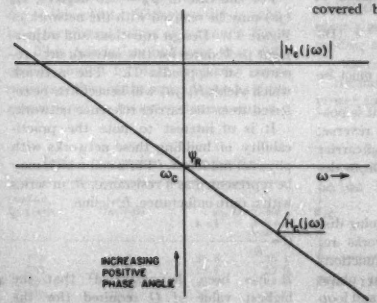

Figure 5 (left). Form of ideal $H_c(j\omega)$

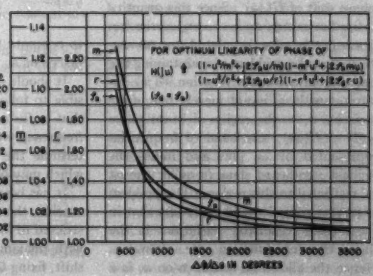

Figure 7 (right). ζ_n, m, and r versus $\Delta\phi/\Delta a$

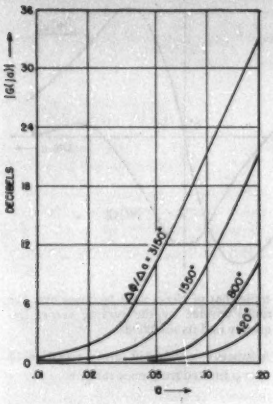

Figure 8(A) (left). $|G(j\alpha)|$ versus α

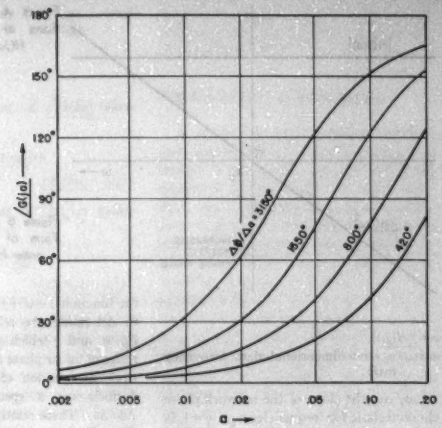

Figure 8(B) (right). $G(j\alpha)$ versus α

$\mathfrak{A}$ = system input

$\mathfrak{C}$ = system output, the controlled variable

M_p = peak value of $\left|\dfrac{\mathfrak{A}(j\omega_d)}{\mathfrak{C}(j\omega_d)}\right|$

ω_{dr} = value of ω_d at which M_p occurs

If the amplitude-phase plot of the uncompensated transfer function of the servomechanisms under consideration is available, the designer may use the characteristics of $G(j\alpha)$ in the usual trial-and-error synthesis to determine the values of $\Delta\phi/\Delta\alpha$ and loop gain which give the desired M_p and ω_{dr}.

A less precise, but very rapid, method of determining $\Delta\phi/\Delta\alpha$ may be used if one is satisfied to specify that $G(j\alpha)$ shall introduce a specified data phase shift, θ_{ds}, at one specified data frequency, ω_{ds}. On the assumption that phase of $G(j\alpha)$ increases linearly with "α" (a valid approximation since $H(ju)$ was designed to have a linear phase characteristic)

$$\frac{\Delta\phi}{\Delta\alpha} = \theta_{ds}\frac{\omega_c}{\omega_{ds}} \tag{18}$$

The allowable tolerance on ω_c is related to the extent of the region of linear phase shift of $H(j\omega)$. Since this quantity is fixed once $\Delta\phi/\Delta\alpha$ is chosen, carrier frequency tolerance is related to $\Delta\phi/\Delta\alpha$. Note that the problem of maintaining the network data transfer function, $G(j\alpha)$, invariant with ω_c is not merely one of restricting ω_c to the region of linear phase shift of $H(j\omega)$; the band of frequencies represented by ω_c plus and minus the highest significant data frequency must be restricted to this region. The problem is further complicated by the fact that in most cases reasonable variations in the data transfer function are allowable. Hence the allowable tolerance on ω_c is a function of $\Delta\phi/\Delta\alpha$, the bandwidth of significant data frequencies, and the allowable variation in $G(j\alpha)$.

Assume that the highest data frequency of interest is the system resonant frequency, ω_{dr}, and that the shift in $G(j\alpha)$ may be represented by $\Delta\theta_{dr}$, the change in $\underline{/G(j\alpha)}$ at $\omega_d = \omega_{dr}$.

Define

n = allowable fractional deviation of ω_c from normal

$b = n + \dfrac{\omega_{dr}}{\omega_c}$

$\Delta\theta_{dr,\max}$ = maximum allowable change in $\underline{/G(j\alpha)}$ at $\omega_d = \omega_{dr}$

A graphical construction based on the deviation of $\underline{/H(ju)}$ from linearity results in the curves of Figure 9, which give b as a function of $\Delta\phi/\Delta\alpha$ for several values of $\Delta\theta_{dr|\max}$. Thus once $\Delta\phi/\Delta\alpha$ has been established, it is only necessary to estimate $\Delta\theta_{dr|\max}$ refer to Figure 9, and utilize the relation

$$n = b - \frac{\omega_{dr}}{\omega_c} \tag{19}$$

to compute the tolerance which must be placed on ω_c.

It should be pointed out that it is possible to follow this procedure in reverse; that is, for a given specification of carrier frequency tolerance, it is possible to determine the maximum value of $\Delta\phi/\Delta\alpha$ which may be used.

It has been shown in the foregoing discussion that for Type 2 networks restricted to fourth-order transfer functions with maximum range of linear phase shift, fixing the values of $\Delta\phi/\Delta\alpha$ and loop gain fixes ω_{dr}, M_p, and n for any given system. Hence one may specify only two of the variables ω_{dr}, M_p, and n since in so doing he fixes the third.

Network Realization

$H(ju)$ has been realized as two networks separated by a buffer amplifier, rather than as a single network. The reasons for this decision are as follows:

1. The design procedure is simplified.
2. Such a configuration allows one to tune the networks for proper operation, thus eliminating the necessity for maintenance of strict element tolerances.

$H(ju)$ may be realized with the network of Figure 10. Detailed design equations and adjustment procedures for this network are presented in Appendix II. The network which produces $H(ju)$ will henceforth be referred to as the main compensating network.

For the case of $\psi_R = -90$ degrees, $H_c(ju)$ may be realized with the network of Figure 11. Design equations and adjustment procedures for this network are presented in Appendix II. The network which yields $H_c(ju)$ will henceforth be referred to as the carrier reference network.

It is of interest to note the practicability of building these networks with physical inductors. For a coil which may be represented as a resistance, R, in series with a pure inductance, L, define

$$Q = \frac{\omega_c L}{R}$$

It has been demonstrated[3] that the highest value of Q required (for the

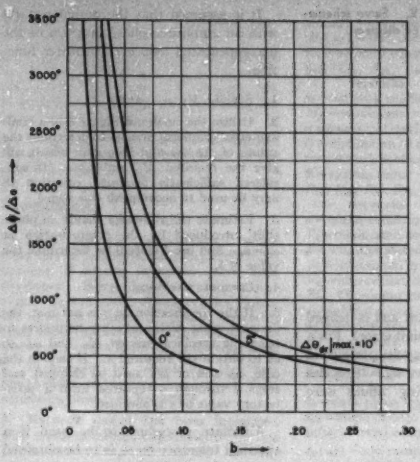

Figure 9 (left). $\Delta\phi/\Delta a$ versus b

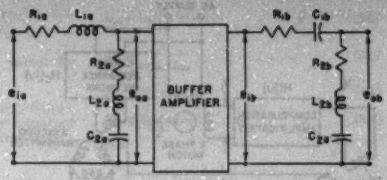

Figure 10 (above). Network for realization of $H(ju)$

greatest $\Delta\phi/\Delta a$ which falls on Figure 7) is approximately 50. Since such a value may be attained at frequencies near 60 or 400 cycles per second (the most commonly encountered values of ω_c), there should be no difficulty in building any networks called for.

System Noise

In general one may expect trouble from the usual sources of data frequency noise (such as backlash in gears, and variations in amplifier d-c supply voltages) as well as from harmonic components of the carrier frequency which are either present in the a-c supply or generated within the system.

As for all lead networks, data noise frequencies which lie in the high-frequency range are accentuated by the compensating network. α_d, the ratio of $|G(ja)|$ at very high frequencies to $|G(ja)|$ at very low frequencies, may be taken as a measure of this effect. This quantity is tabulated for several values of $\Delta\phi/\Delta a$ in Table I. This tabulation indicates that difficulties caused by data frequency noise sources will be of the same degree as those encountered in many systems using d-c lead compensation since $\alpha_d = 20$ decibels is a figure which is frequently used in the design of d-c lead networks.

The presence of harmonic components of ω_c in the carrier signal is undesirable for the following two reasons:

1. Such components result in heating of the output member.

2. If present is sufficient magnitude, harmonics may cause saturation of one or more components of the system.

A measure of the amplification given the kth harmonic of ω_c by the main compensating network is given by α_k, where

$$\alpha_k = \frac{|H(ju)|_{u=k}}{|H(ju)|_{u=1}} \tag{20}$$

and $k = 2, 3, 4, \ldots$.

Table I lists values of α_k for several values of $\Delta\phi/\Delta a$. (For k greater than 3, α_k may be taken as approximately equal to α_d.) Reference to this table will allow the designer to estimate the level below which the harmonic content of V_4, the error signal, must be held to avoid exceeding a prescribed harmonic content of V_1, the control signal.

Harmonics which are present in the a-c power source may be reduced to the required level by filtering at the supply terminals. Harmonics generated within the system present no such simple problem since attempts to reduce them by means of filters will, unless special care is taken, result in an alteration of $H(ju)$. It is best to hold such harmonics to the desired level by careful choice and design of system components.

Table I. α_d and α_k Versus $\Delta\phi/\Delta a$

$\Delta\phi/\Delta a$, Degrees	α_d Decibels	α_k, Decibels $k=1$	$k=2$
378	22.8	25.5	26.1
705	21.3	23.9	22.0
1,420	19.8	20.3	19.9
2,750	20.5	20.6	20.5

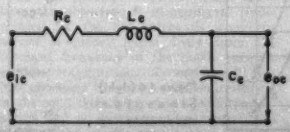

Figure 11. Network for realization of $H_c(ju)$, $\psi_R = -90$ degrees

Experimental Studies

The system illustrated in Figure 12 was constructed to provide a basis for experimental verification of the theoretical results as well as to provide some insight into the practical problems involved in the use of the carrier compensation scheme presented in this paper.

Since the uncompensated error transfer function of this system is a second-order function, it is theoretically possible to design compensation to yield any specified system resonant frequency. The following basic specifications were assigned as being typical values which might be encountered in practice:

$\omega_{dr} = 20$ cycles per second
$M_p = 1.5$
$n = \pm 5$ per cent

The components used include the following:

1. Output member: Kearfott *R-103-1A* 2-phase motor, 400 cycles per second, fixed phase—115 volts, control phase—26 volts.

2. Data transmitters: two Bendix *AY-101D* autosyns.

Detailed design of the compensation networks is carried out in reference 3. It is therein shown that for this servo system design of compensation to yield $\omega_{dr} = 20$ cycles per second and $M_p = 1.5$ gives $n = \pm 8$ per cent (approximately); hence the specification on carrier-frequency tolerance will surely be met.

With a carrier frequency of 400 cycles per second it was desired that the loop gain be adjusted for $\omega_{dr} = 20$ cycles per second. The extreme complexity of the frequency-response measurement, however, made this adjustment a very difficult trial-and-error process. Hence, when a condition of $\omega_{dr} = 18$ cycles per second was reached, it was decided that this con-

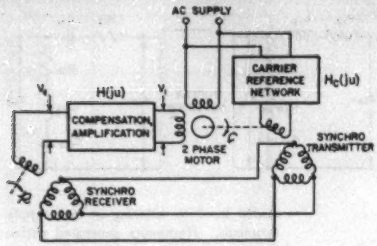

Figure 12. Servo schematic diagram

dition was sufficiently close to the design specifications. Correspondence between theoretical and actual performance may be determined for this setting as readily as for $\omega_{dr} = 20$ cycles per second.

With loop gain thus set the system frequency-response characteristics were experimentally determined for carrier frequencies of 380, 400, and 420 cycles per second. The results are plotted in Figures 13 and 14. From these curves it may be seen that if carrier frequency is kept within the specified range of 400 cycles per second ± 5 per cent, the variation in ω_{dr} will not be greater than 2 cycles per second and M_p will not change by more than 1.4 decibels. By visual inspection of the servo response to various types of inputs it was determined that system performance was still acceptable when the carrier frequency varied by ± 40 cycles per second. Instability did not occur until the carrier frequency was varied 50 cycles per second from its normal value.

For $\omega_{dr} = 18$ cycles per second the following values were predicted by theoretical considerations:

$M_p = 4.3$ decibels
$K_v = 1{,}800 \text{ sec}^{-1}$

K_v is the velocity constant and is defined as the output speed per unit error. For a carrier frequency of 400 cycles per second and loop gain set to give $\omega_{dr} = 18$ cycles per second, the following values were measured experimentally:

$M_p = 3.8$ decibels
$K_v = 1{,}020 \text{ sec}^{-1}$

Thus the measured value of M_p checks within 0.5 decibel of the theoretical value, and the measured velocity constant is within 5 decibels of the analytically obtained value. Thus it may be said that the experimental results satisfactorily corroborate the theory.

Design Procedure

The following summary of network design procedure may help the reader to obtain a clearer picture of the relations between the three basic quantities, M_p, ω_{dr}, and n which are imposed by the networks introduced in this paper.

It is assumed that the designer starts with an amplitude-phase diagram of the uncompensated loop error transfer function.

1. Specify M_p, ω_{dr}, and n.
2. Utilize the curves of Figure 8 in a trial-and-error graphical process to determine the values of $\Delta\phi/\Delta a$ and loop gain which will give the required M_p and ω_{dr}. (If considered sufficiently accurate, equation 18 may be used to accomplish this step.)
3. Estimate the allowable change in phase shift introduced by the compensation at $\omega_d = \omega_{dr}$, and use Figure 9 to determine the value of b.
4. Compute $n = b - \omega_{dr}/\omega_c$.
5. If the specification on n is not met, the designer must decide whether he desires to relax the specifications on M_p and ω_{dr} so as to obtain the required n. If such is the case, ω_{dr} and/or M_p must be changed and steps 2 through 4 repeated until a satisfactory value of n is obtained.

Alternate procedure to be used if a specified tolerance on ω_c is to be obtained at all costs:

1. Specify n and ω_{dr}.
2. Compute $b = n + \omega_{dr}/\omega_c$.
3. Use Figure 9 to determine $\Delta\phi/\Delta a$.
4. Use Figure 8 to determine M_p and loop gain.
5. If the value of M_p thus obtained is not tolerable, ω_{dr} must be changed, and steps 2 through 4 repeated until a satisfactory value is obtained.

Once the value of $\Delta\phi/\Delta a$ has been established proceed as follows:

6. Pick m, r, and ζ_n from the curves of Figure 7.
7. Use equations 1A through 10A of

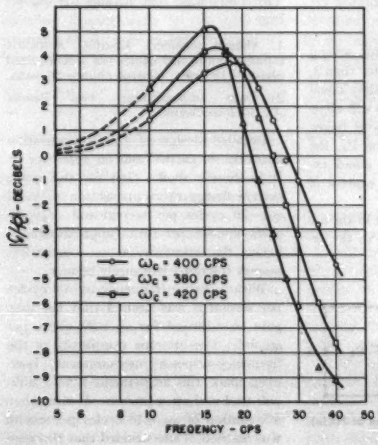

Figure 13 (left.) Sinusoidal steady-state response $|C/R|$ versus frequency

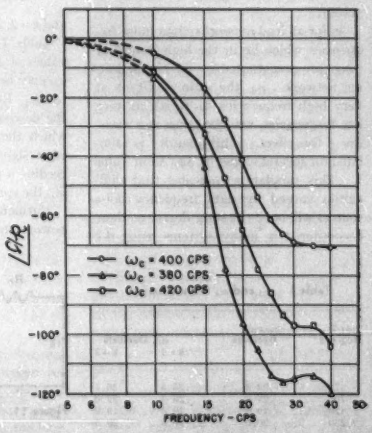

Figure 14 (right) Sinusoidal steady-state response $\angle C/R$ versus frequency

Appendix II to design the main compensation network.

8. If $\psi_R = -90$ degrees is to be used (as in the case of a 2-phase a-c motor servomechanism), equations 11A through 13A of Appendix II may be used to design the carrier reference network.

9. If ψ_R is to be other than -90 degrees, the carrier reference network must be designed to satisfy equation 12.

Conclusions

1. Ideal network characteristics which yield carrier compensation completely independent of carrier frequency have been developed. Since, however, the specified amplitude and phase characteristics violate the laws of minimum phase networks, these ideal characteristics may be approximated only over a finite range of frequencies.

2. Techniques for obtaining the best fourth-order approximation to these characteristics have been presented.

3. Network design has been integrated with servomechanism requirements; in this process carrier-frequency tolerance has been placed on a quantitative basis.

4. Practical difficulties imposed by nonideal inductors and system noise have been considered. In no case covered by the design curves presented will these effects impose insurmountable limitations.

5. Experimental studies have corroborated the theoretical prediction that it is practical to employ the networks discussed in this paper to meet the requirements of many a-c systems, which, because of frequency instability in the a-c supply, would not receive adequate compensation from previously developed carrier compensation schemes.

Appendix I

Symbols

a = nondimensional frequency ratio, ω_d/ω_c
δ = design parameter, $n+(\omega_{dr}/\omega_c)$
$C(j\omega_d)$ = system output, controlled variable
C_{1a}, C_{2a}, C_{3a}, C_e = capacitance values for networks
$G(j\omega_d)$ = data transfer function of main network
$H(j\omega)$ = signal transfer function of main network
$H_e(j\omega)$ = signal transfer function of auxiliary network
$|H_e(\omega_d)|$ = even component of $|H(j\omega)|$
$|H_o(\omega_d)|$ = odd component of $|H(j\omega)|$
K_v = velocity constant
L_{1a}, L_{2a}, L_{3a}, L_e = inductance values for networks
m = network coefficient
M_p = maximum value of $|C(j\omega_d)|/|R(j\omega_d)|$
n = fractional deviation of carrier frequency
Q = dissipation of coil at carrier frequency
r = network coefficient
$\mathfrak{R}$ = system input
R_{1a}, R_{2a}, R_{3b}, R_{3b}, R_e = resistance values for networks
u = nondimensional frequency ratio, ω/ω_c
V_1 = modulated control signal
V_1' = unmodulated control signal
V_e = modulated error signal
V_e' = unmodulated error signal
Z_{1a}, Z_{1b} = input impedances of networks
α_d = attentuation ratio of main network
α_k = amplification of kth harmonic in main network
ζ_c = nondimensional damping ratio of $H_e(j\omega)$
ζ_d, ζ_n = nondimensional damping ratios in $H(j\omega)$
θ_d = data phase lead angle
θ_{dt} = angle of $G(j\omega)$ at ω_{dt}
$\phi_e(\omega_d)$ = even component of $\angle H(j\omega)$
$\phi_o(\omega_d)$ = odd component of $\angle H(j\omega)$
ψ_c = phase angle of carrier at input to main network
ψ_R = carrier reference phase angle
ω_c = carrier frequency (a constant)
ω_d = data frequency (a variable)
ω_{dr} = data frequency corresponding to M_p
ω_{dt} = specific data frequency

Appendix II

Network Design Equations

Define Z_i = network input impedance for $\omega = \omega_c$. For the main compensation network

$$L_{2a} = \frac{|Z_{1a}|}{m^2\omega_c\sqrt{(2\zeta_n r)^2+(r^2-1)^2}} \tag{1A}$$

Table II. Network Adjustment Procedure

Adjust the Series Combination	For Resonance at the Frequency
1 ..... L_{2a}, C_{3a}	$m\omega_c$
2 ..... L_{2a}, L_{1a}, C_{1a}	ω_c/r
3 ..... L_{2b}, C_{3b}	ω_c/m
4 ..... L_{2b}, C_{3b}, C_{1b}	$r\omega_c$
5 ..... L_e, C_e	ω_c

$$L_{1a} = L_{2a}(m^2r^2-1) \tag{2A}$$

$$C_{3a} = \frac{1}{m^2\omega_c^2 L_{2a}} \tag{3A}$$

$$R_{2a} = 2\zeta_n m\omega_c L_{2a} \tag{4A}$$

$$R_{1a} = R_{2a}(mr-1) \tag{5A}$$

and

$$L_{2b} = \frac{|Z_{1b}|}{\omega_c\sqrt{(2\zeta_n r)^2+(r^2-1)^2}} \tag{6A}$$

$$C_{3b} = \frac{m^2}{\omega_c^2 L_{2b}} \tag{7A}$$

$$C_{1b} = \frac{C_{2b}}{(m^2r^2-1)} \tag{8A}$$

$$R_{2b} = \frac{2\zeta_n\omega_c L_{2b}}{m} \tag{9A}$$

$$R_{1b} = R_{2b}(mr-1) \tag{10A}$$

Construction of the network of Figure 10 as called for by these equations yields a transfer function equal to $1/m^2r^2$ times the $H(j\omega)$ of equation 14.

For the carrier reference network with $\psi_R = -90$ degrees

$$R_c = Z_{1c} \tag{11A}$$

$$L_c = \frac{R_c}{2\zeta_c\omega_c} \tag{12A}$$

$$C_c = \frac{1}{\omega_c^2 L_c} \tag{13A}$$

Network Adjustment

The adjustments shown in Table II, carried out in the order given, will yield proper network operation. Resonance is defined as the condition for which current and voltage are in phase.

References

1. Principles of Servomechanisms, G. S. Brown, D. P. Campbell. John Wiley and Sons, Inc., New York, N. Y., 1948.

2. Improvement in the Characteristics of A-C Lead Networks for Servomechanisms, D. McDonald. *Report Number 25*, Aeronautical Research Center, Engineering Research Institute, University of Michigan, Ypsilanti, Mich., 1948.

3. Phase Lead for A-C Servo Systems with Unregulated Carrier, A. P. Notthoff, Jr. Master of Science Thesis, Massachusetts Institute of Technology, Cambridge, Mass., 1949.

Discussion

George M. Attura (Industrial Control Company, Bronx, N. Y.): The problem of carrier frequency shifts in a-c servos has been under consideration by our group. It has been extremely interesting to hear of Mr. Notthoff's work, since our own efforts at analysis have led us to an approach somewhat different from that discussed in his paper.

It can be said that the basic theme of Mr. Notthoff's work is to eliminate by network design the envelope distortion which arises from the departure from conjugate transmission for the two sidebands when the carrier frequency shifts away from the resonant frequency of the notch network used for stabilization. To understand this it is necessary to understand the derivation of the conditions referred to as sufficient to assure that no quadrature components will be produced at the output of a network (equations 5, 6, 7, and 8).

It can be shown[1] that if a suppressed carrier sinusoidal modulation (V_e, equation 1) is impressed upon some network with signal transfer function $H(j\omega)$, the output signal can be resolved into two distinct sinusoidal suppressed carrier envelopes, whose carrier and modulation phases are in exact quadrature one with the other, for example

$$V_1 = E\frac{A_l+A_u}{2}\cos(\omega_d t+\phi_d)$$

$$\cos(\omega_c t+\phi_c)(\text{signal envelope})$$

$$+E\frac{A_l-A_u}{2}\sin(\omega_c t+\phi_c)$$

$$\sin(\omega_c t+\phi_c)\text{(quadrature envelope)}$$

where

$\omega_u=\omega_c+\omega_d$ = upper sideband frequency
$\omega_l=\omega_c-\omega_d$ = lower sideband frequency
A_u = network transmission at upper sideband
A_l = network transmission at lower sideband
ϕ_u = phase angle of upper sideband
ϕ_l = phase angle of lower sideband

and the rest of the symbols are the same as those used in the paper under discussion.

Now it is assumed that the presence of the quadrature envelope causes the reduction in damping observed experimentally in carrier frequency servos with unregulated carriers. Mr. Notthoff suggests that the $H(j\omega)$ be so shaped that its amplitude transmission is invariant about the carrier frequency. This suppresses the carrier of the quadrature envelope, for its amplitude is the difference between the transmissions of $H(j\omega)$ at the lower and upper sidebands. This seems to be accomplished by two cascaded resonant networks, tuned to different frequencies, whose over-all transmission is that of Figure 6.

Thus equation 11 gives a condition which makes it necessary that the amplitude of the quadrature envelope be zero throughout the range of carrier frequencies encountered. The type of stabilization which this type of network gives is pure phase lead, without the attendant rise in the amplitude transmission for the sidebands that is characteristic of the more commonly used quasi-derivative networks (parallel-T, bridged-T, and so forth).

While the results of this approach are certainly interesting and valid, it is questionable whether the best engineering compromise results in forcing the burden of quadrature envelope suppression on the stabilizing network itself. In our own work we have seen carrier frequency servos, stabilized by a conventional parallel-T, exhibit good stability margins over carrier frequency shifts greater than 50 cycles away from the center frequency of 400 cycles.

This observation suggested a study into the basic effects of the amplitude and phase asymmetry resulting from either the network configuration itself, or an otherwise symmetrical $H(j\omega)$ with a carrier frequency shifted from its resonant point.

In an unpublished thesis entitled Envelope Transfer Functions in Carrier Frequency Servomechanisms which I wrote, it was shown that the burden of quadrature envelope suppression could often be assumed by the load actuator itself.

These carrier frequency actuators, whether they be 2-phase induction motors, a-c torque motors, or phase-sensitive detectors, all have the characteristic of suppressing entirely any carrier frequency signal whose phase is in quadrature to some preferred phase ψ_R. Thus if the carrier phase of the signal envelope of equation 1 of the discussion is adjusted to be in phase with ψ_R, the carrier phase of the quadrature envelope will always be in quadrature to ψ_R, and no component due to this quadrature envelope will be present in the output of the actuator. It should be noted that a considerable simplification results since the networks necessary to generate $H_c(j\omega)$ are not required, and the damping circuits themselves are the relatively simple parallel-T, bridged-T, and so forth.

The analysis by which this may be proved rigorously is too detailed and lengthy to allow presentation here. It is hoped that the opportunity shall arise in the near future for publication of all the material. The major conclusions can be given here:

1. A carrier frequency shift will not destroy the damping introduced by a notch network provided the sidebands still fall on a portion of the $H(j\omega)$ which closely approximates that of an ideal derivative device.

2. Assuming a damping network configuration chosen to introduce the maximum data phase lead in the vicinity of the load's corner frequency, then no reduction in the stability margins of the servo-loop will be observed for carrier shifts smaller than the load corner frequency.

It can be seen that the higher the performance of the servo with centered carrier frequency, the greater the allowable carrier frequency shift. Or putting it another way, insensitivity to the carrier frequency shifts encountered in inverters for airborne equipment can be achieved by choosing servo loops that have extended frequency response.

Where the load time constant is great, then the allowable carrier frequency shift is too small to be of practical use. Here the method of Mr. Notthoff should find fruitful application since it is theoretically applicable to any servo regardless of load time constant. There does seem to be a limitation on this, and Mr. Notthoff himself mentions it when he states that there is a "lower limit upon the data frequency at which useful phase lead may be obtained." This limitation is caused by the impracticality of designing networks which give very high, phase slopes about the center frequency and hence significant data frequency phase lead for small values of ω_d. These networks are impractical because of the great amount of carrier attenuation necessary, with its attendant harmonic and noise frequency accentuation, and the requirements of very high inductance Q's.

In conclusion, we can attempt to tabulate the different methods of carrier frequency stabilization, insofar as the carrier frequency shift problem is concerned.

1. Load tachometric feedback from 2-phase induction generators will function well regardless of load time constant over a very broad range of carrier frequency shifts.

2. Where the load time constant is quite large, aside from 1 above, Type I compensation must be employed.

3. Where the load time constant is such that the first corner frequency of the load is beyond the region of 2 above, but still lower than the carrier shift required, then the technique of Mr. Notthoff is applicable.

4. Where the first corner frequency of the load is greater than the carrier frequency shift required, then the techniques suggested by Mr. Notthoff, though applicable, are not required, and the conventional notch networks can be used, with the attendant simplification of the accessory equipment and circuitry.

REFERENCE

1. STABILIZATION OF CARRIER FREQUENCY SERVOMECHANISMS—GAIN PHASE MARGIN DIAGRAMS OF CONTROLLER CHARACTERISTICS, A. SOBZYK. *Journal* (Franklin Institute, Philadelphia, Pa.), volume 246, July 1948, pages 21–43.

Arthur P. Notthoff, Jr.: Mr. Attura's discussion is, in general, quite applicable. His presentation of the possible applications for the networks presented in this paper as contrasted with more familiar compensating schemes should be of particular interest to the reader.

Mr. Attura suggests that the reduction in damping afforded by Type II networks which accompanies a carrier frequency shift is caused by the presence of a quadrature envelope at the output member. Such cannot be the case since, as he points out, virtually all a-c output members act so as to reject any quadrature signal. The reduction in damping (or data phase lead) results from the alteration in network data transfer function caused by carrier shifts. The networks presented in this paper were designed to give an invariant data transfer function over a wide range of carrier frequencies; the attendant suppression of quadrature components is of secondary interest.

It may be shown that a reduction in data phase lead must accompany a carrier shift for any single cascaded Type II network (such as a parallel-T). The importance of a given carrier shift is dependent upon the servo bandwidth and stability margin (a criterion of which is given by $M\phi$). The frequency shift which may be tolerated by a parallel-T network in any given application may certainly be placed on a rapidly ascertainable quantitative basis as has been done for the networks of this paper. The author eagerly looks forward to publication of such work.

Improvements in the Characteristics of A-C Lead Networks for Servomechanisms

DONALD McDONALD
MEMBER AIEE

ELECTRIC lead networks are used quite extensively to improve the response of servomechanisms.[1] Such lead networks may be required to operate on the servo error voltage, on the input or output signal voltages separately, on the feedback voltage from an output tachometer, on various internal loop voltages, and on other signals. In many cases, the input voltage to the lead network is a modulated suppressed-carrier voltage, and it is necessary that the output voltage of the lead network also be a modulated suppressed-carrier voltage of the same carrier frequency. Consequently, the basic d-c lead network of Figure 1(B), which is normally used where the output signal may be direct current, is not applicable by itself to these problems, and an a-c lead network must be used.

The conventional a-c lead networks do not operate on their input signals so effectively as does the network of Figure 1(B) in a d-c servomechanism. It is the purpose of this paper to suggest modifications in design and in the components used which will improve the characteristics of a-c lead networks.

Conventional A-C Lead Networks

Before considering improvements in the characteristics of a-c lead networks, it is desirable to summarize the general characteristics of these conventional a-c lead networks.

When the input and output voltages of a lead network must be modulated suppressed-carrier voltages, two general classes of a-c lead networks are normally used. In the first class, illustrated by Figure 1(A) the a-c signal is demodulated, then the demodulated signal is passed through a d-c lead network, like the one of Figure 1(B), and lastly, the carrier is modulated with the output voltage of the d-c lead network. This class of a-c lead networks will be called a class-I network.

As noted before, regardless of the type of lead network, it may be stated that the essential characteristic of an a-c lead network is that it produce a pronounced, positive phase shift of the modulating envelope over specific portions of the modulating frequency band. The analytical equations[2] 5, 6, and 7 show that the class-I lead network of Figure 1(A) and Figure 1(B) does have a pronounced positive phase shift ϕ which reaches a maximum value of ϕ_m at a signal frequency of w_m. Figure 11 is a plot of the phase shift and magnitude characteristics of this lead network.

The demodulator and modulator circuits of the first class of a-c lead networks produce noise or ripple. Filter circuits added to the demodulator and modulator tend to reduce the magnitude of this noise. Unfortunately, the reduction in noise by this method is accompanied by a time delay or an effective negative phase shift of the modulating envelope. Such a negative phase shift may be partially compensated for by an increase in the attenuation of the d-c lead network. This increase in the attentuation will result in an increase of the over-all noise-to-signal ratio. Hence, in the class-I a-c lead network, an engineering compromise must be reached between the amount of noise suppressed by filters in the demodulator and modulator, and the increase in noise-to-signal ratio resulting from the increase in attenuation required to offset the effect of the filters. These several factors cause this class-I network to produce a smaller maximum positive phase shift than the d-c lead network can produce by itself.

An example of the second class of a-c lead networks is shown in Figure 2(A), and this class will be referred to as class-II networks. The parallel-T network of Figure 3 is another simple a-c lead network of class II.[3] The networks of Figures 2(A), 2(B), and 3 are only a few of the several types of networks belonging to this class. Equations 10 through 12 and equations 20 through 23 of Figures 2 and 3, respectively, show that these networks modify the envelope of the modulated signal in approximately the same fashion as does the circuit of Figure 1.[4] (The equations of Figures 2 and 3 and similar equations of following figures are written in terms of the modulating envelope. This is justified only when the upper and lower side bands have symmetrical attenuation and asymmetrical phase characteristics with respect to w_c. These requirements are satisfactorily met for these networks over the range of modulating frequencies specified.)

The application of these class-II networks is restricted by the following two factors:

1. Most a-c lead networks of the second class are quite sensitive to changes in the carrier frequency because a change in carrier frequency can reduce the effective lead developed by these networks and can, in some cases, produce lag instead of lead. This effect is more noticeable at 400 cycles per

Paper 50-46, recommended by the AIEE Feedback-Control Systems Committee and approved by the AIEE Technical Program Committee for presentation at the AIEE Winter General Meeting, New York, N. Y., January 30–February 3, 1950. Manuscript submitted November 5, 1948; made available for printing December 1, 1949.

Donald McDonald is with the Research Laboratories Division of the Cook Electric Company, Chicago, Ill.

Acknowledgement is made of the assistance of K. C. Mathews and F. E. Theobald, University of Michigan, Aeronautical Research Center, in the mechanical design of the system of Figure 9, and to E. B. Therkelsen, University of Michigan, Aeronautical Research Center, in the preparation of some of the data and graphs, as well as for his helpful criticism.

Figure 1(A). Basic class-I a-c lead network

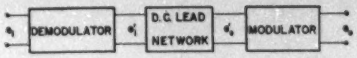

If

$$e_i = e \sin w_m t \sin w_c t \tag{1}$$

then

$$e_i' = e \sin w_m t \tag{2}$$

$$e_o = e_o' \sin w_c t \tag{3}$$

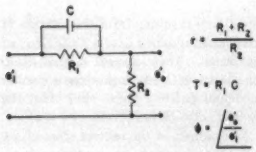

Figure 1(B). Basic d-c lead network

$$r = \frac{R_1 + R_2}{R_2}$$

$$T = R_1 C$$

$$\phi = \angle \frac{e_o'}{e_i'}$$

If

$$e_i' = e \sin w_m t \tag{4}$$

$$\frac{e_o'}{e_i'} = \frac{1}{r} \frac{1 + jw_m T}{1 + jw_m \frac{T}{r}} \tag{5}$$

Where maximum phase shift

$$\phi_{2m} = \sin^{-1}\left[\frac{r-1}{r+1}\right] \tag{6}$$

and occurs at

$$w_{2m} = \frac{\sqrt{r}}{T} \tag{7}$$

$$\left.\frac{e_o'}{e_i'}\right]_{w_m = \infty} \Big/ \left.\frac{e_o'}{e_i'}\right]_{w_m = 0} = r = \text{attenuation} \tag{8}$$

second than at 60 cycles per second, because it is the absolute change in carrier frequency which affects the network and, in general, 60-cycles-per-second sources are better frequency-regulated on an absolute basis than 400-cycles-per-second sources.

2. The maximum value of the lead time constant T of the second class of a-c lead networks is limited and this limits the minimum value of w_{2m}, the frequency at which the maximum positive phase shift of the modulating envelope occurs. (For the network of Figure 2(A), the maximum value of $T = 2L/R_3$ and for the network of Figure 3, the maximum value of $T' = 1/w_c$.) In some cases when the minimum value of w_{2m} is too large, it is possible to increase the phase shift at lower frequencies by increasing the attenuation. Unfortunately this increase in attenuation may increase the noise-to-signal ratio of the lead network sufficiently to offset any improvement derived from an increase in positive phase shift at lower frequencies.

Figure 2(B)[5] shows a modified form of the basic class-II a-c lead network. As will be noted from equations 16, 17, and 18, when the maximum phase shift ϕ_{2m} is the same for both the circuits of Figures 2(A) and 2(B), the minimum value of w_{2m} is smaller for Figure 2(B) than for Figure 2(A) by a factor of c. Inasmuch as the minimum value of r' is 1, the maximum value of c under the condition of equation 16 is r.

Modifications of the Class-I A-C Lead Network

As was mentioned before, the demodulator and modulator filters of Figure 1 (A) produce time delays or effective negative phase shifts of the modulating envelope. Figure 4(A) shows a circuit where the demodulator and modulator filters are used to an advantage. The arrangement of the components of Figure 4(A) shall be referred to as a feedback-type modification of class I. To simplify the consideration of this circuit, the time delays or phase shifts created by the filters of the demodulator and modulator have been lumped in the single resistance-capacitance time-lag network of Figure 4(A). Thus the minimum value of the time constant of the resistance-capacitance network of Figure 4(A) will be determined by the filters in the demodulator and modulator, but if required, additional filtering or delays may be added to increase this equivalent time constant.

The analytical expressions 33, 34, and 35 of Figure 4(A) show that the characteristics of this system are the same as for the basic class-I network. The attenuation r may be adjusted by adjusting the gains of the amplifier, demodulator, or modulator. The lead time constant T may be made as large as desired but does have a minimum value determined by the equivalent time constant of the demodulator and modulator filters which produce an acceptable noise level.

Figure 4(B) shows another arrangement of the components of the basic class-I a-c lead network and will be referred to as a parallel-type modification of class-I a-c lead network. The assumptions made in representing the circuit of Figure 4(A) are carried over into the circuit of Figure 4(B).

The analytical expressions 44, 45, and 46 show that the response of this network is similar to that of Figure 4(A). The parallel type has the limitation that,

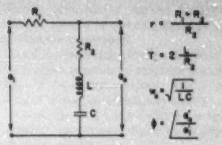

Figure 2(A). Basic class-II a-c lead network

If

$$e_i = e \sin w_m t \sin w_c t \tag{9}$$

then

$$\frac{e_o'}{e_i'} \cong \frac{1}{r} \frac{1 + jw_m T}{1 + jw_m \frac{T}{r}} \text{ for } w_m << w_c \tag{10}$$

The maximum phase lead (of the signal)

$$\phi_{2m} = \sin^{-1}\left[\frac{r-1}{r+1}\right] \tag{11}$$

and occurs at

$$w_{2m} = \frac{\sqrt{r}}{T} \tag{12}$$

In general a primed variable denotes the envelope of the variable (this statement applies also to Figures 2(B), 3, 4(A), 4(B), 5, 6, 7, and 8).

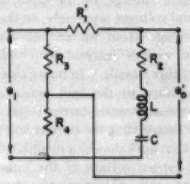

Figure 2(B). Modification of the basic class-II a-c lead network

$$r' = \frac{R_1' + R_3}{R_3} \qquad T = 2\frac{L}{R_3} \qquad w_c = \sqrt{\frac{1}{LC}}$$

$$b = \frac{R_3 + R_4}{R_4} \qquad c = \frac{b-1}{b-r'} \qquad \phi' = \angle \frac{e_o'}{e_i}$$

$$\frac{e_o'}{e_i'} \cong \frac{b-r'}{br'} \frac{1 + jw_m cT}{1 + jw_m \frac{T}{r'}} w_m << w_c \tag{13}$$

Where

$$\phi_{2m}' = \sin^{-1}\left[\frac{cr'-1}{cr'+1}\right] \tag{14}$$

$$w_{2m}' = \sqrt{\frac{r'}{c}} \frac{1}{T} \tag{15}$$

If

$$cr' = r \tag{16}$$

then

$$\phi_{2m}' = \phi_{2m} \tag{17}$$

$$w_{2m}' = \frac{\sqrt{r'}}{T} \frac{1}{c} = \frac{w_{2m}}{c} \tag{18}$$

where r, ϕ_{2m}, and w_{2m} refer to Figure 2(A)

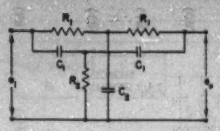

Figure 3. Parallel-T class-II a-c lead network

$$R_1C_1=\frac{1}{w_c}$$

Then if

$$e_1=e\sin w_s t\sin w_c t \tag{19}$$

$$\frac{e_2'}{e_1'}\cong\frac{1}{r}\,\frac{1+jw_sr T'}{1+jw_sT'}\qquad w_s\ll w_c \tag{20}$$

$$\phi=\angle\frac{e_2'}{e_1'} \tag{21}$$

$$\phi_{zm}=\sin^{-1}\left[\frac{r-1}{r+1}\right] \tag{22}$$

$$w_{zm}=\frac{1}{\sqrt{rT'}} \tag{23}$$

as noted from equation 43, the minimum value of the lead time constant is equal to r times the minimum value of the equivalent time constant of the demodulator and modulator filters. Inasmuch as this value may be too large for some servomechanism applications, the parallel type may not always be so useful as the feedback type.

The effectiveness of the demodulator and modulator filters or the complexities of the demodulator and modulator plus filters may be such as to limit the degree of suppression of noise generated. Such a limitation will establish the noise-to-signal ratio and determine the applicability of these circuits.

By a change in the type of components as well as the arrangement used in the basic class-I network, a system can be evolved having demodulators and modulators with excellent noise-to-signal ratios. Such a system will be referred to as an electromechanical a-c lead network—class I.

Electromechanical A-C Lead Networks—Class I

Figure 5 is an example of such a modified class-I network.[6,7] In its most general form, this network is equally applicable for d-c and a-c operation, but in this paper only its a-c form is discussed. In this system the motor functions as a demodulator and the generator as a modulator. Both of these functions are approximate with the limitations that w_s and the motor-generator speed be small compared to the carrier frequency and synchronous speeds, respectively. The analytical expressions of 57, 58, and 59 of Figure 5 show that the characteristics of this system are the same as for the basic class-I a-c lead network.* By proper ad-

* In the derivation of the equations of Figure 5 and following figures, it has been assumed that the torque developed by the motor is directly proportional to the excitation voltage. Actually, with increasing signal frequency the torque is no longer directly proportional to the excitation voltage but lags behind it in phase and is reduced in amplitude. This effect produces the equivalent of additional phase lags in the feedback path which increase the phase lead of the over-all system at higher frequencies.

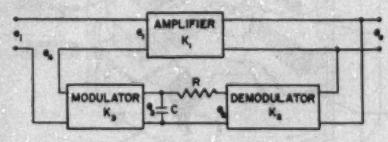

Figure 4(A). Feedback-type modification of class-I a-c lead network

$$e_1=e\sin w_s t\sin w_c t \tag{24}$$

$$e_3=K_1e_1,\quad e_2'=K_1e_1' \tag{25}$$

$$e_1=e_1-e_4,\quad e_1'=e_1'-e_4' \tag{26}$$

$$e_4'=K_3e_3 \tag{27}$$

$$e_3=\frac{e_2}{1+jw_sRC}\qquad w_s\ll w_c \tag{28}$$

$$e_2=K_2e_2' \tag{29}$$

$$\frac{e_2'}{e_1'}\cong\frac{K_1}{1+K_1K_2K_3}\;\frac{1+jw_sRC}{1+jw_s\dfrac{RC}{1+K_1K_2K_3}} \tag{30}$$

Let

$$r=1+K_1K_2K_3 \tag{31}$$

$$T=RC \tag{32}$$

Then

$$\frac{e_2'}{e_1'}\cong\frac{K_1}{r}\;\frac{1+jw_sT}{1+jw_s\dfrac{T}{r}} \tag{33}$$

$$\phi_{zm}=\sin^{-1}\left[\frac{r-1}{r+1}\right] \tag{34}$$

$$w_{zm}=\frac{\sqrt{r}}{T} \tag{35}$$

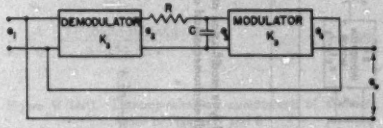

Figure 4(B). Parallel-type modification of class-I a-c lead network

$$e_1=e\sin w_s t\sin w_c t \tag{36}$$

$$e_3=e_1-e_4,\quad e_2'=e_1'-e_4' \tag{37}$$

$$e_4'=K_3e_3 \tag{38}$$

$$e_3=\frac{e_2}{1+jw_sT}\qquad T'=RC\qquad w_s\ll w_c \tag{39}$$

$$e_2=K_2e_2' \tag{40}$$

$$\frac{e_2'}{e_1'}\cong(1-K_2K_3)\frac{1+jw_s\dfrac{T'}{1-K_2K_3}}{1+jwT'} \tag{41}$$

Let

$$r=\frac{1}{1-K_2K_3} \tag{42}$$

$$T=rT'=rRC \tag{43}$$

$$\frac{e_2'}{e_1'}\cong\frac{1}{r}\;\frac{1+jw_sT}{1+jw_s\dfrac{T}{r}} \tag{44}$$

$$\phi_{zm}=\sin^{-1}\left[\frac{r-1}{r+1}\right] \tag{45}$$

$$w_{zm}=\frac{\sqrt{r}}{T} \tag{46}$$

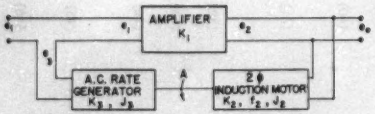

Figure 5. Feedback-type modification of class-I a-c lead network with electromechanical components

$$e_o = e_2 \tag{47}$$

$$e_1 = e_i - e_3 \tag{48}$$

$$e_3 = K_1 e_1 \tag{49}$$

$$K_2 e_2' \cong [(J_2 + J_3)p^2 + f_2 p]\ A$$

where

$$p = \frac{d}{dt} \tag{50}$$

$$e_2 = K_2 p A \tag{51}$$

$$J = J_2 + J_3,\ f = f_2 \quad w_s \ll w_c \tag{52}$$

$$\frac{e_o'}{e_i'} \cong \frac{K_1 f}{f + K_1 K_2 K_3} \times \frac{1 + p\frac{J}{f}}{1 + p\frac{J}{f + K_1 K_2 K_3}} \tag{53}$$

Let

$$\frac{f + K_1 K_2 K_3}{f} = r \quad T = \frac{J}{f} \tag{54}$$

$$\frac{e_o'}{e_i'} \cong \frac{K_1}{r}\ \frac{1 + pT}{1 + p\frac{T}{r}} \tag{55}$$

If

$$e_i = e \sin w_s t \sin w_c t \tag{56}$$

$$\frac{e_o'}{e_i'} \cong \frac{K_1}{r}\ \frac{1 + jw_s T}{1 + jw_s \frac{T}{r}} \tag{57}$$

$$\phi_{zm} = \sin^{-1}\left[\frac{r-1}{r+1}\right] \tag{58}$$

$$w_{zm} = \frac{\sqrt{r}}{T} \tag{59}$$

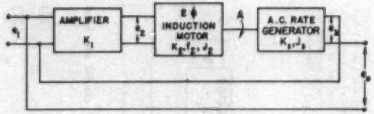

Figure 6. Parallel-type modification of class-I a-c lead network with electromechanical components

$$e_3 = K_1 e_1 \tag{60}$$

$$K_2 e_2' \cong [(J_2 + J_3)p^2 + f_2 p]\ A$$

where

$$p = \frac{d}{dt} \tag{61}$$

$$e_2 = K_2 p A \tag{62}$$

$$e_o = e_i - e_3 \quad w_s \ll w_c \tag{63}$$

$$J = J_2 + J_3,\ f = f_2 \tag{64}$$

$$\frac{e_o'}{e_i'} \cong \frac{f - K_2 K_3 K_1}{f}\ \frac{1 + p\left(\frac{J}{f - K_1 K_2 K_3}\right)}{1 + p\frac{J}{f}} \tag{65}$$

Let

$$\frac{f}{f - K_1 K_2 K_3} = r \quad T' = \frac{J}{f} \tag{66}$$

$$\frac{e_o'}{e_i'} \cong \frac{1}{r}\ \frac{1 + prT'}{1 + pT'} \tag{67}$$

or

$$\frac{e_o'}{e_i'} \cong \frac{1}{r}\ \frac{1 + w_s rT'}{1 + jw_s T'} = \frac{1}{r}\ \frac{1 + jw_s T}{1 + jw_s \frac{T}{r}} \tag{68}$$

Where

$$rT' = T \tag{69}$$

$$\phi_{zm} = \sin^{-1}\left[\frac{r-1}{r+1}\right] \tag{70}$$

$$w_{zm} = \frac{\sqrt{r}}{T} \tag{71}$$

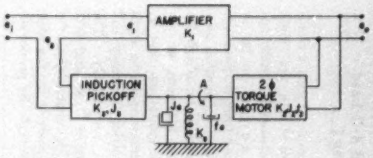

Figure 7. Feedback-type modification of class-I a-c lead network with electromechanical components—resonant lead controller characteristics

$$e_o = K_1 e_1 \tag{72}$$

$$e_1 = e_i - e_3 \tag{73}$$

$$e_3 = K_3 A \tag{74}$$

$$K_2 e_o' \cong [(J_2 + J_3 + J_a)p^2 + (f_2 + f_a)p + K_a]\ A,$$

where

$$p = \frac{d}{dt} \tag{75}$$

$$J = J_2 + J_3 + J_a,\ f = f_2 + f_a \tag{76}$$

$$\frac{e_o'}{e_i'} \cong K_1\ \frac{Jp^2 + fp + K_a}{Jp^2 + fp + (K_a + K_1 K_2 K_3)} \quad w_s \ll w_c \tag{77}$$

Let

$$e_i = e \sin w_s t \sin w_c t \tag{78}$$

$$w_n^2 = \frac{K_a}{J} \tag{79}$$

$$c = \frac{f}{2\sqrt{K_a J}} \tag{80}$$

$$h^2 = \frac{K_a + K_1 K_2 K_3}{K_a} \tag{81}$$

$$u = \frac{w_s}{w_n} \tag{82}$$

then

$$\frac{e_o'}{e_i'} \cong \frac{K_1}{h^2}\ \frac{1 - u^2 + j2cu}{1 - \left(\frac{u}{h}\right)^2 + j2\left(\frac{c}{h}\right)\left(\frac{u}{h}\right)} = K_L G_L(ju) \tag{83}$$

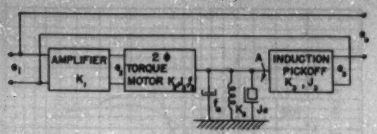

Figure 8 (top left). Parallel-type modification of class-I a-c lead network with electromechanical components—resonant lead controller characteristics

$$e_2 = e_1 - e_3 \tag{84}$$

$$e_3 = K_2 A \tag{85}$$

$$K_2 e_2' \cong [(J_2 + J_3 + J_4)p^2 + (f_2 + f_4)p + K_2]\, A,$$

where

$$p = \frac{d}{dt} \tag{86}$$

$$e_2 = K_1 e_1 \tag{87}$$

$$J = (J_2 + J_3 + J_4),\ f = f_2 + f_4 \quad w_2 \ll w_0 \tag{88}$$

$$\frac{e_2'}{e_1'} \cong \frac{Jp^2 + fp + (K_2 - K_1K_2K_3)}{Jp^2 + fp + K_2} \tag{89}$$

Let

$$e_2 = e \sin w_2 t \sin w_0 t \tag{90}$$

$$w_n^2 = \frac{K_2}{J} \tag{91}$$

$$c = \frac{f}{2\sqrt{K_2 J}} \tag{92}$$

$$q^2 = \frac{K_2}{K_2 - K_1K_2K_3} \tag{93}$$

$$u = \frac{w_2}{w_n} \tag{94}$$

$$\frac{e_2'}{e_1'} \cong \frac{1}{q^2}\ \frac{1-(qu)^2 + j2(qc)(qu)}{1-u^2 + j2cu} \tag{95}$$

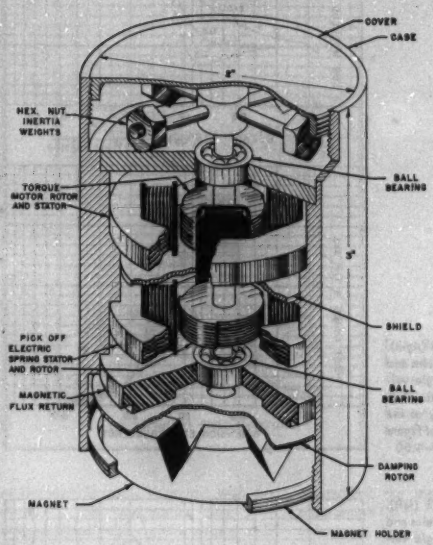

Figure 9 (left). Electromechanical components of the network of Figures 7 and 8

justment of K_1, K_2, and K_3, it is possible to establish any value of attenuation r. The lead time constant T can be made as large as desired by the addition of inertia to the common motor-generator shaft. Unfortunately the minimum value of T is $(J_2+J_3)/f_2$ and this value may be too high for some servo applications.

The arrangement of the components of the circuit of Figure 5 is such that this type of electromechanical network will be referred to as a feed-back type. Another arrangement of the components of Figure 5 is shown in Figure 6 and will be referred to as an electromechanical a-c lead network of the parallel type. This parallel type of electromechanical network has characteristics similar to those of the feed-back type except that its lead time constant T is greater by a factor equal to the attenuation r. Consequently, in many cases the parallel type is not so useful as the feed-back type of electromechanical a-c lead network. It is of interest to note that the amplifier K_1 can be omitted in the parallel type.

Figure 7 is a schematic of another electromechanical a-c lead network—class I. It is of the feed-back type but, as indicated by equation 83, does not have the phase and amplitude characteristics of the basic class-I a-c network. This network is a resonant lead controller of class I. Figures 12, 13, 14, 15, and 16 show the phase and amplitude characteristics of this electromechanical system.

Figure 8 shows the parallel-type counterpart of the electromechanical a-c lead network of Figure 7. Its characteristics are similar to those of the feed-back type.

Of the several types of electromechanical a-c lead networks discussed, that of Figure 7 appears to have the most desirable characteristics and also to be the simplest to manufacture. Figure 9 is a cut-away view of a pilot design of this electromechanical system. The main components of the system are (1) an induction torque motor, (2) a combination induction pickoff and electric spring, (3) an eddy-current damper, and (4) inertia weights. The induction torque motor and the combination induction pickoff and electric spring are made of simple, punched laminations and bobbin-wound coils and are called Microsyn elements.[8]

The induction torque motor is excited by a fixed a-c reference voltage and by the signal voltage. It develops a torque proportional to the signal voltage which is virtually independent of the angular displacement of its rotor. The coils of the combination induction pickoff and electric spring are arranged so that there is a separate circuit for both the pickoff and electric spring. The pickoff circuit is excited with a-c voltage, and the circuit

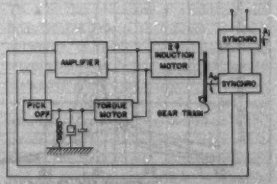

Figure 10. Two-phase servomechanism stabilized by the network of Figure 7

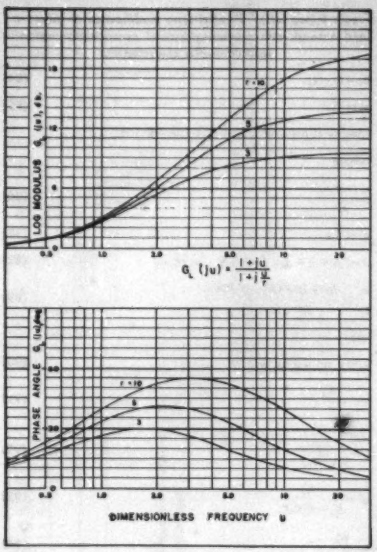

Figure 11 (left). Log modulus and phase angle versus dimensionless frequency of the d-c lead network of Figure 1(A)

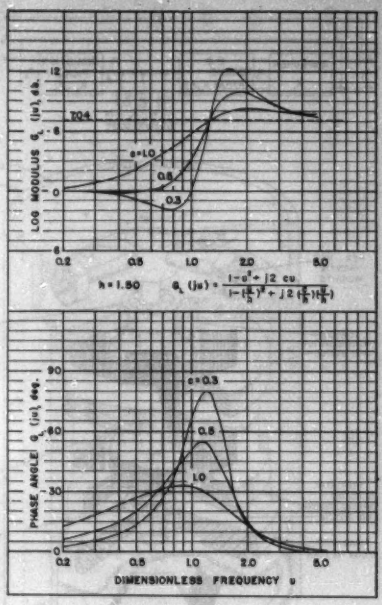

Figure 13 (right). Log modulus and phase angle versus dimensionless frequency of the network of Figure 7 for $h = 1.50$

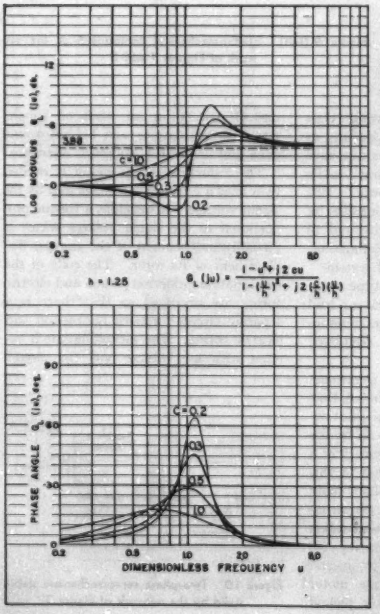

Figure 12 (left). Log modulus and phase angle versus dimensionless frequency of the network of Figure 7 for $h = 1.25$

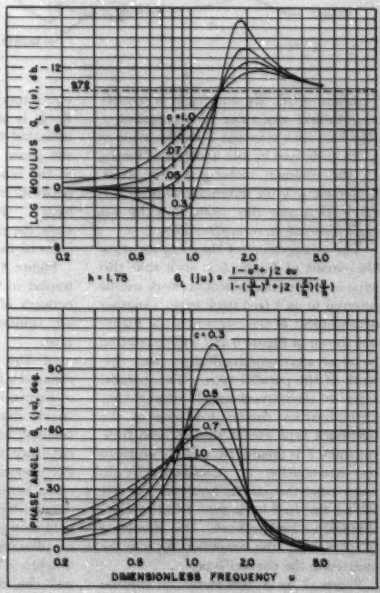

Figure 14 (right). Log modulus and phase angle versus dimensionless frequency of the network of Figure 7 for $h = 1.75$

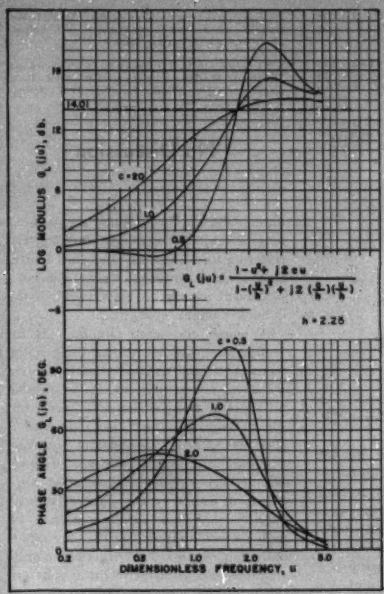

Figure 15 (left). Log modulus and phase angle versus dimensionless frequency of the network of Figure 7 for $h=2.25$

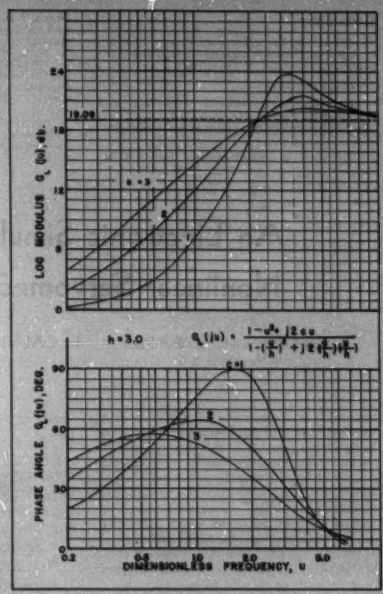

Figure 16 (right). Log modulus and phase angle versus dimensionless frequency of the network of Figure 7 for $h=3.0$

of the electric spring is excited with d-c voltage. This combination then produces a signal voltage and a torque, both of which are proportional to the angular displacement of the rotor from neutral. By changing the d-c excitation of the electric spring circuit, the torque gradient of the electric spring may be adjusted.

The eddy-current damper is made up of an aluminum damping disc and a multipole Alnico permanent magnet with its poles parallel to the axis of rotation. This magnet is threaded axially into the housing; therefore, it is possible to adjust the spacing between the magnet and damping disc, thus changing the damping coefficient f.

The total moment of inertia of the system may be changed by adjusting the position of the inertia weights.

Thus as there are three continuously adjustable parameters—the spring constant, the damping, and the moment of inertia—it is possible to adjust the two variables w_n and c independently. The attenuation factor h^2 also can be adjusted independently by changing the pickoff sensitivity or the amplifier gain.

As planned in a typical design, w_n and c are to be continuously adjustable from 1 to 6 cycles per second and 0.5 to 1 respectively. Over these ranges of network parameters, the maximum power consumption of the torque motor should not exceed one-third of a watt.

Changes in carrier frequency which will not prevent proper operation of any electromechanical components in the complete servo loop (such as motors and indicators) will not appreciably affect the operation of the electromechanical a-c lead networks described. Figures 12, 13, 14, 15, and 16 show that w_{pm} occurs near w_n, and, as noted before, w_n and hence w_{pm} may be adjusted to cover the region of frequencies 1 to 6 cycles per second. Also, as the network of Figure 7 is a resonant lead network, the maximum value of phase shift ϕ_{pm} produced by it may be made larger than for a simple lead network having the same attenuation or noise-to-signal ratio.

An example of the application of the electromechanical lead network of Figure 7 is shown in Figure 10. Here a 2-phase induction servo is being stabilized by the use of this electromechanical a-c lead network. As will be noted, the amplifier driving the servo motor is also used to drive the torque motor of the lead network. This is possible because of the very low power consumption of the torque motor.

In closing, if the feed-back paths of Figures 4(A), 5, and 7 are connected regeneratively, instead of degeneratively, and the parallel paths of Figures 4(B), 6, and 8 are connected so as to add, instead of subtract, these systems will become lag or integral networks instead of lead networks.

In general, it may be stated that the modifications in the circuit arrangements and the change in the type of components of the basic class-I lead network produces an a-c lead network which has all of the advantages of the class-I lead network with its disadvantages kept to a minimum. The general approach used in modifying the basic class-I a-c lead network has been to place all of the elements with negative phase shifts in a parallel or feed-back branch where they will effectively produce a lead instead of a lag. Thus by this procedure, the inherent and unavoidable delays that occur in many networks, such as in demodulators and modulators, can be put to an advantage instead of being a handicap.

The characteristics of the class-II a-c lead networks have been described in this paper in order to contrast more effectively the two classes, but no attempt will be made in this article to describe methods of improving the characteristics of the class-II a-c lead networks.

References

1. Principles of Servomechanisms (book), G. S. Brown, Donald P. Campbell. John Wiley and Sons, Inc., New York, N. Y., 1948.

2. *Ibid*, pages 202–04.

3. Parallel "T" Stabilizing Networks for A-C Servos. *Report 811*, Radiation Laboratory, Massachusetts Institute of Technology, Cambridge, Mass.

4. Theory of Servomechanisms (book), H. M. James, N. B. Nichols, R. S. Phillips. McGraw-Hill Book Company, Inc., New York, N. Y., 1947, page 117.

5. Differentiating Networks and Lead Networks, G. T. Coate. Department of Electrical Engineering, Massachusetts Institute of Technology, Cambridge, Mass.

6. A New Servomechanisms Technique, D. McDonald. *Report UMM-24*, Aeronautical Research Center, University of Michigan, Ypsilanti, Mich.

7. Stabilizing Servomechanisms, Donald McDonald. *Electronics* (New York, N. Y.), volume 21, November 1948, page 112.

8. Electronic Instruments (book), Greenwood, Holdman, MacRae. McGraw-Hill Book Company, Inc., New York, N. Y., (MIT Series), 1948, pages 365–66.

No Discussion

An Electronic Simulator for Nonlinear Servomechanisms

CHARLES M. EDWARDS
NONMEMBER AIEE

E. CALVIN JOHNSON, JR.
STUDENT MEMBER AIEE

Synopsis: An electronic computer for the simulation of autopilot servomechanisms is being developed as a small-scale flexible analog computer capable of reproducing electrically the dynamic behavior of systems in which certain of the dependent variables or their derivatives may be limited in magnitude but which otherwise can be characterized by linear differential equations having constant coefficients. Specifically, the simulator is being designed to represent on a one-to-one time scale several types of closed-cycle systems or servomechanisms which are linear except for possible limitations of such quantities as motor torque, output velocity, and output displacement.

THE Dynamic Analysis and Control Laboratory at the Massachusetts Institute of Technology has been constructing a large-scale analog computer, capable of solving the general equations of motion of an aircraft, which will be used primarily in the development of aircraft control systems. The "servo simulator" described in this paper is included as a portion of the computer to represent on a one-to-one time scale the dynamic characteristics of the control-surface servos. These servos usually are designed to operate linearly as proportional devices. However, a servo occasionally will be required to operate at the extreme limits of its physical capacity, beyond its linear range.

Some of these servos exhibit marked nonlinear effects which easily may be the most significant factors in determining the motion of the aircraft which they control. Systems, otherwise perfectly satisfactory, may even become unstable in the presence of certain types of nonlinearities. It is evident, therefore, that if simulation of the flight of an aircraft controlled by such servos is to be accurate, the nonlinearities in these servos must be represented. Moreover, if provision is made to simulate nonlinear servos, investigations can be made as to the extent to which nonlinearities in the control-surface servos can be tolerated, still maintaining satisfactory control characteristics and, above all, absolute stability. Information of this nature would aid in effecting the best compromise between size of the servo and its region of linear operation.

The exact nature of the nonlinearities to be expected depends upon the particular servo employed. Certain types of nonlinearities are fairly common. For example, the control-surface deflection usually is limited either by external limit stops or by the limited stroke of the power-output device itself, as in a hydraulic ram. In the case of a clutch-powered servo, the control-surface velocity is limited to the velocity corresponding to the speed at which the clutch is driven. Other frequent causes of nonlinear behavior are amplifier overloading and magnetic saturation in electric motors. In general it is true that these systems behave in a manner essentially linear except that certain quantities such as motor torque, output velocity, and output displacement may be restricted, inherently or otherwise, to definite maximum values. To be sure, the systems may be subject to nonlinear damping and restoring forces as well; but such limitations as those on torque, velocity and displacement usually are responsible for the dominant nonlinear effects.

Although the servo simulator is intended primarily to serve as a link in the main Dynamic Analysis and Control Laboratory computer, it also is suitable for investigations of a more general nature pertaining to the design and performance of closed-cycle control systems. The simulator, in fact, is capable of representing any system of reasonable complexity in which certain of the dependent variables or their derivatives may be limited in magnitude, abruptly or gradually, but which system otherwise can be characterized by a set of linear differential equations with constant coefficients.

Derivation of the Analog of a Nonlinear Servomechanism

Any two systems, whether electrical, mechanical, hydraulic, or thermal, may be said to be analogous when there exists a definite parallelism in the form of the mathematical relations which represent them. Hence, for each quantity in a given system there may always be found a corresponding quantity in an analogous system which behaves identically. The first system, then, is represented or simulated by its analog. Electronic simulation of a system involves the identification of an analogous electronic element with each portion of the given system to be represented explicitly. Logically, then, the simulation of a specific system should begin with a careful analysis of the system in mathematical terms and proceed through the medium of mathematics

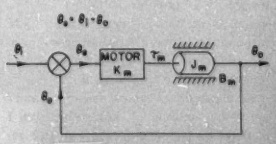

Figure 1. A simple servomechanism

Paper 50-47, recommended by the AIEE Computing Devices Committee and approved by the AIEE Technical Program Committee for presentation at the AIEE Winter General Meeting, New York, N. Y., January 30-February 3, 1950. Manuscript submitted November 3, 1949; made available for printing December 7, 1949.

Charles M. Edwards and E. Calvin Johnson, Jr. are both with the Dynamic Analysis and Control Laboratory, Massachusetts Institute of Technology, Cambridge, Mass.

The authors wish to express their gratitude to Dr. A. C. Hall for his active support in the development of this simulator and to thank F. C. McCoy for his assistance in construction of the equipment.

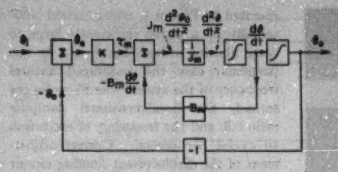

Figure 2 (left). Symbolic representation of the servomechanism of Figure 1

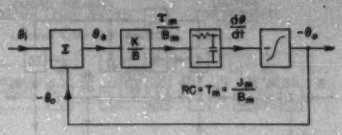

Figure 4 (right). Simplified analog of the servo of Figure 1

to the synthesis of a suitable analog.

As an illustration of the principles involved in such a synthesis, consider the simple servo shown schematically in Figure 1. The error quantity, θ_s, defined as the difference between the desired position, θ_i, and the actual position of the output shaft, θ_o, is converted to an appropriate signal which then drives the motor. The torque, τ_m, developed by the motor, assumed to be related to θ_s by the proportionality factor K_m, is utilized in accelerating the combined motor and load inertia, J_m, and in overcoming the equivalent viscous damping, B_m. The following equations describe the system mathematically

$$\theta_s = \theta_i - \theta_o \tag{1}$$

$$\tau_m = K_m \theta_s \tag{2}$$

and

$$J_m \frac{d^2\theta_o}{dt^2} + B_m \frac{d\theta_o}{dt} = \tau_m$$

or

$$J_m \frac{d^2\theta_o}{dt} + B_m \frac{d^2\theta_o}{dt} = \tau_m \tag{3}$$

These relations may be represented symbolically by the block diagram of Figure 2. If electronic elements are available which are capable of carrying out the operations of addition, constant multiplication or amplification, and integration as indicated in the diagram, the analog can be synthesized in exactly this form. For most purposes, however, this arrangement can be simplified considerably. For example, an amplifier and a series resistance-capacitance network may be substituted for the combination of adder, multipliers, and integrator which is required in Figure 2 to produce θ_o from τ_m. The analogy involved in this substitution is explained in Figure 3 by association of the differential equation which represents the amplifier and network

$$\frac{RC}{A}\frac{de_o}{dt} + \frac{1}{A}e_o = e_i \tag{4}$$

with equation 3, which relates, ν_m to $\frac{d^2\theta_o}{dt}$. The time constant, T_m, of the mechanical system is J_m/B_m, whereas in the electric circuit, T equals RC.

With the aid of this substitution and other minor simplifications, the electric analog shown in Figure 4 is obtained. Although the variable quantities are labeled exactly as they were in the original system, it should be understood that the diagram is meant to represent an electric system. This nomenclature has been adopted for the sake of simplicity and directness in emphasizing the relationships existing between the voltages in the analog and the quantities in the actual system.

Suppose, now, that it is desired to simulate the operation of such a system when there is added an external limit stop at the position θ_s. If the limit stop is to serve its purpose effectively, it must prevent the output, θ_o, from moving significantly beyond θ_s. Consequently, when the output strikes the limit, its velocity, and likewise the kinetic energy stored in the moving elements, must be reduced quickly to zero. In the electric analog of the simple servo, Figure 4, the output velocity is represented by the voltage across the network capacitor; the kinetic energy is represented by the energy stored in the capacitor, this energy being proportional to the square of the voltage across the capacitor. Evidently, then, when the output voltage attempts to rise beyond that voltage which represents the maximum allowable displacement, the voltage across the network capacitor must be reduced to zero. By this reasoning it is recognized that the method of simulation which limits the voltage at the output of the integrator does not provide a correct representation of the system. Because of the unilateral nature of electronic amplifiers and integrators, such a limiting could not affect the voltage across the capacitor. In fact, because of the increased error signal, the effect actually would be opposite to the one desired.

Consequently, it is necessary to examine the occurrence of displacement limiting from a more fundamental viewpoint.

As pictured in Figure 5, a stiffness, K_s, and a viscous damping, B_s, may be assigned to the stop. When θ_o is less than θ_s, the stop has no effect upon the behavior of the system. After the output strikes the limit stop, however, an additional torque, τ_s, is created which acts in opposition to the motor torque. Thus,

$$\tau_s = B_s \frac{d\phi}{dt} + K_s\phi \tag{5}$$

in which ϕ is defined as follows

$$\phi = \begin{cases} 0 & ; \theta_o < \theta_s \\ \theta_o - \theta_s & ; \theta_o \geq \theta_s \end{cases} \tag{6}$$

Equation 3, written for the system without limiting, now may be modified to include the effects of the limit stop

$$J_m \frac{d^2\theta_o}{dt^2} + B_m \frac{d\theta_o}{dt} = \tau_m - \tau_s \tag{7}$$

Figure 6 shows the symbolic representation of equations, 1, 2, and 7. The block labeled T.C. (so-called because of its electrical equivalent, the "threshold circuit") forms the quantity ϕ from θ_o and θ_s

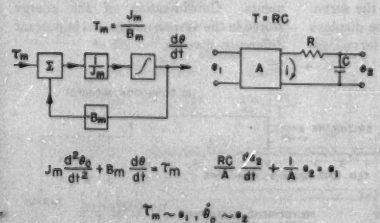

Figure 3 (left). Analogous systems

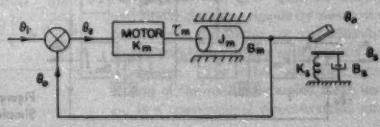

Figure 5 (right). A simple servo with displacement limiting

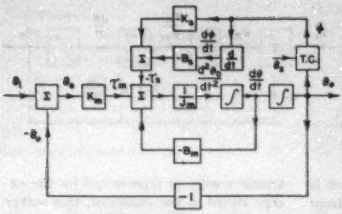

Figure 6. Symbolic representation of the system of Figure 5

in accordance with equation 6.

If the electric analog were to be realized with the arrangement given in Figure 6, an ideal electronic differentiator would be required. Actually, duplication of equation 5 as it stands is found to be easier. Equation 5 may be written in terms of the differential operator p as

$$\frac{\tau_s}{\phi} = K_s(T_s p + 1) \equiv K_s G_s \qquad (8)$$

in which

$$T_s = \frac{B_s}{K_s}$$

The displacement-limiting unit to be discussed later contains both the threshold circuit and an electronic circuit with approximately the characteristic expressed in operational language by equation 8. The simplified electric analog, Figure 7, which makes use of this operational notation, now can be constructed.

The simulation of displacement limiting by the method just described, which is applicable to any system in which the required torque summation can be performed, involves two parameters of the limit stop, the stiffness and the damping. In most instances, these parameters are unknown. Usually it is known only that the limit stop functions in a positive manner to halt the output motion and that any additional effects which may be introduced by the dynamics of the limit stop are neither apparent nor significant in the normal operation of the system. Consequently, in simulating such systems it is necessary only so to adjust the displacement-limiting circuit that its effects, other than the desired positive limiting, are far removed in both magnitude and frequency from those caused by the principle characteristics of the servo. Figure 8 shows cathode-ray-tube displays of the output of a second-order servo, represented by Figure 7, when excited sinusoidally by a signal sufficiently large to cause limiting in both directions. In this particular case the undamped natural frequency of the system was 25 cycles per second, the nondimensional damping ratio 0.3, and the frequency of excitation 10 cycles per second. Correct adjustment of the displacement-limiting circuit is illustrated by Figure 8(A); Figures 8(B) and 8(C) respectively, show the results when the gain K_s is too low and when the time constant T_s is too small. The maladjustments in these latter two cases are greatly exaggerated; actually, the adjustments for good limiting are not critical.

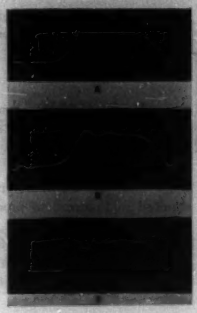

Figure 8. Displacement limiting of a second-order system when excited sinusoidally

A. Correct limiting
B. Gain K_s too low
C. Time constant T_s too small

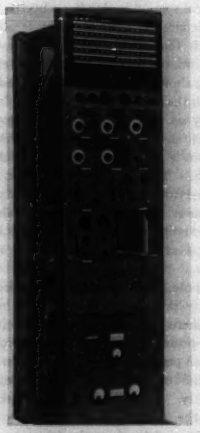

Figure 9. Autopilot simulator

Development of the electric analog in the manner just outlined has led to a system in which most of the variables of interest in the original servo, such as input, torque, velocity, and output, are represented by the voltage of some point with respect to a common terminal. Consequently, the analog is in general considerably more complicated than would be required to represent only the output-input relation of a system. Indeed, the behavior with respect to the input and output of the simple servo of Figure 1 can be simulated by a single-series resistance-inductance-capacitance network. The form of the analog shown in Figure 7, however, is convenient when it is necessary to study in detail quantities in the system other than the output. Moreover, the simulation of nonlinear effects often is greatly facilitated by the explicit appearance of the variables involved. For example, torque saturation and velocity limiting in the simple servo of Figure 1 can be represented by limiting the voltages in the analog which correspond to torque and velocity. In Figure 7 voltage limiters are shown at the appropriate places to accomplish this limiting. It should be emphasized that the voltage actually appearing across the network capacitor is the voltage proportional to the velocity. Hence it is this voltage which must be limited, not merely the voltage transmitted to the following elements. Consideration of the energy stored in the system makes this important difference obvious.

Figure 7. Simplified electric analog of the system of Figure 5

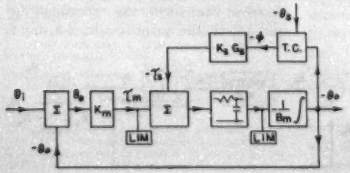

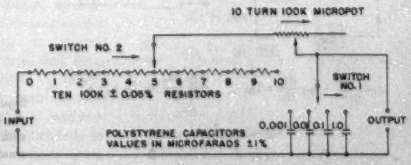

Figure 10 (right). Simple-lag network

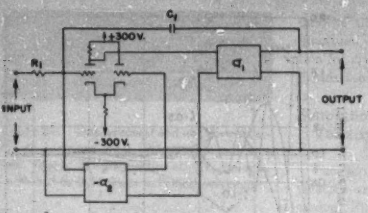

Figure 11. Drift-stabilized integrator

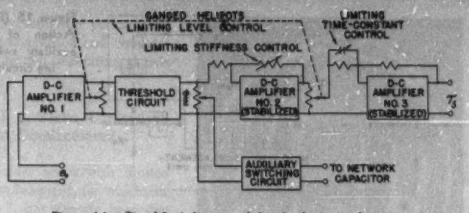

Figure 14. Simplified diagram of the displacement-limiting unit

Description of the Simulator Components

Synthesis procedures such as those described lead to analogs which require, for representing the linear behavior of a system, the following electric computing elements: summing circuits, voltage amplifiers, integrators, and passive networks composed of resistance, capacitance and inductance. A study of several basic servos,[1] including those having types of power-output devices such as induction motors, d-c generators and motors, field-controlled d-c motors, magnetic clutches, hydraulic transmissions, and valve-controlled hydraulic motors indicates, moreover, that the most important nonlinearities in these systems can be represented with reasonable accuracy by the addition of voltage limiters and the special displacement limiting circuit. In view of the fact that a large number of components would be required to simulate control about three axes of an aircraft, it seemed advisable to arrange the computing components in such a fashion that the equipment could be used not only to simulate autopilot servos but also as a general mathematical tool to solve certain types of nonlinear differential equations. Consequently, a series of standard simulator units were built, incorporating the above-mentioned computing elements. Figure 9 shows a portion of the simulator which now is in use at the Dynamic Analysis and Control Laboratory. The final installation will consist of three racks of equipment containing the following units: 8 *RC* simple-lag networks; 2 *RLC* quadratic-lag networks; 9 integrator units; 12 limiter-amplifier units; 4 displacement-limiting units; 4 input units; and 4 output units. Summing circuits, coefficient potentiometers, and initial-conditions generators will be included also, together with the necessary power controls and means to zero set and calibrate the various units. Input and output terminals of all units will be available at a single patch board for flexible interconnection.

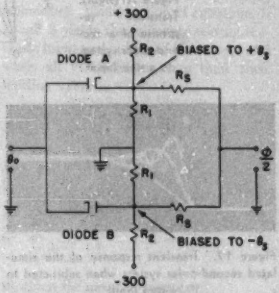

Figure 13. The threshold circuit

The simple-lag network, Figure 10, provides a continuously variable time constant ranging up to one second. The desired accuracy is obtained through the use of precision wire-wound resistors, a 10-turn micropot for fine control, and polystyrene capacitors accurate to within 1 per cent. Similar resistors and capacitors, together with a precision inductor, are used in the quadratic-lag network, the natural frequency and damping ratio of which may be varied in steps from 31.6 to 200 cycles per second and from 0.1 to 1.0, respectively.

Figure 11 shows the basic elements of the circuit employed in the integrator unit. The characteristic of integration is obtained by capacitive feedback around a high-gain direct-coupled amplifier. The amplifier in this unit is of a special form, similar to that developed by the Radio Corporation of America and others to provide stabilization against steady drifts.[2] It consists essentially of two amplifiers, Figure 11. One, denoted by α_2, provides "driftless" gain for steady and slowly changing signals by means of a mechanical modulator, a capacitively-coupled amplifier, and a synchronous demodulator. The other amplifier, consisting of the cathode-coupled stage and α_1, is a conventional direct-coupled am-

Figure 12. Servo-simulator limiter-amplifier unit

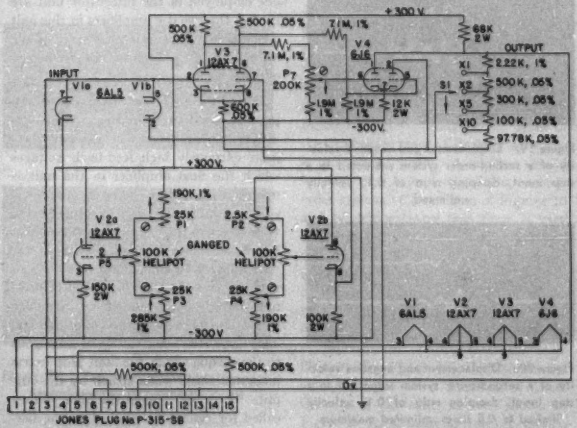

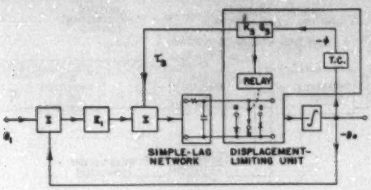

Figure 13 (left). Action of the auxiliary switching circuit

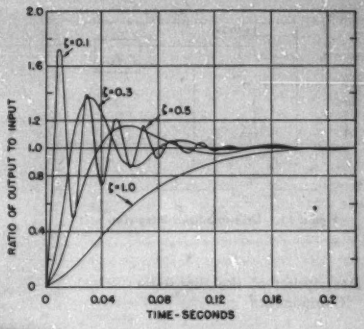

Figure 16 (right). Transient response of a second-order system to a step input

plifier. The two sections are so combined that drifts in the cathode-coupled stage and in α_1 are reduced in their effect on the output by the factor α_2.

If the feed-back capacitor in Figure 11 is replaced by a resistor, the circuit becomes a sign-changing voltage amplifier. In the integrator unit a switch permits the selection of input resistors and feed-back elements in such a way that the unit can be used either as an integrator with scale factors ranging from 1 to 100 or as an amplifier with gains of from 10 to 100.

The limiter-amplifier unit, Figure 12, contains both a voltage limiter and a direct-coupled feed-back amplifier. The amplifier consists of two cathode-coupled stages, utilizing the two twin-triode tubes, V_3 and V_4. Feedback is accomplished by virtue of the differencing property of the first cathode-coupled stage. This method of feedback, essentially cathode feedback, results in a non-sign-changing amplifier.

The voltage limiter, which precedes the amplifier, consists of two diodes, V_{1a} and V_{1b}, biased positively and negatively, respectively, by two cathode followers. The amplifier input, therefore, is limited in both positive and negative polarity to approximately the voltages applied to the grids of the cathode followers. The method of biasing by cathode followers provides low source impedance without excessive drain from the power supplies and, at the same time, permits easy and continuous adjustment of the limiting level by variation of the grid potential. In this unit the grids are so driven as to cause symmetrical positive and negative limiting at a level varying from 0 to 100 volts.

In discussing displacement limiting in the preceding section, consideration was given to limiting in one direction only. Actually, however, the limiting in many systems occurs symmetrically, that is, for outputs both greater than $+\theta_s$ and less than $-\theta_s$. Consequently, in general, the quantity ϕ has the following form

$$\phi = \begin{cases} 0 & ; \ -\theta_s < \theta_o < +\theta_s \\ \theta_o - \theta_s; & \theta_o \geq +\theta_s \\ \theta_o + \theta_s; & \theta_o \leq -\theta_s \end{cases} \qquad (9)$$

Figure 17. Transient response of the simulated second-order system when subjected to a step input

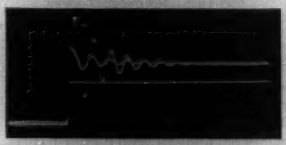

Figure 18. Transient response of a displacement-limited servo

Figure 19. Displacement and negative velocity of a second-order system subjected to a step input, damping ratio of 0.1, velocity unlimited

Figure 20. Displacement and negative velocity of a second-order system subjected to a step input, damping ratio of 0.1, velocity limited to 0.5 times unlimited maximum

The essential features of the threshold circuit, which generates ϕ, appear in Figure 13. Diodes A and B of this circuit are biased as indicated so that unless θ_o is greater than $+\theta_s$ or less than $-\theta_s$ the output of the circuit is zero. However, if θ_o should become greater than $+\theta_s$, diode A will conduct, and because its plate resistance is very low compared to R_1 and R_2, its cathode will rise by the excess of θ_o over $+\theta_s$. The output in this case is $(1/2)\ (\theta_o - \theta_s)$. Similarly, if θ_o is less than $-\theta_s$, the output is $(1/2)\ (\theta_o + \theta_s)$.

In the displacement-limiting unit shown in block-diagram form in Figure 14, the effective limiting level is varied by changing the gain of that portion of the circuit between the input and the threshold circuit. The characteristic $(T_s p + 1)$ which equation 8 indicates is necessary for the formation of τ_s is produced by a feed-back amplifier having suitable feed-back networks. Stabilizing circuits similar to the one employed in the integrator unit are used in the two d-c amplifiers in this unit which provide the gain necessary for the simulation of the high natural frequency of the limit stop.

In most cases, the circuits described produce the desired limiting. Some conditions, nevertheless, momentarily require extremely high feed-back voltages which the final amplifier in the unit is unable to generate because of power-supply limitations. For example, if the voltage across the capacitor in the simple-lag network (see Figure 7) is large, corresponding to a high output velocity, a very large voltage of opposite polarity must be fed back to the network to reduce the capacitor voltage to zero quickly. This large feed-back voltage is analogous to the torque which the limit stop exerts instantaneously when struck by the output. If for any reason the high voltage called for cannot be applied to the net-

Figure 21. Displacement and negative velocity of a second-order system subjected to a step input, damping ratio of 0.1, velocity limited to 0.15 times unlimited maximum

work, a longer time is required to discharge the capacitor. Since the output cannot stop increasing until the capacitor voltage is zero, the limiting is not sharp and appreciable overshoot usually results.

As illustrated in Figure 15, an auxiliary switching circuit in the displacement-limiting unit alleviates this situation by placing a short circuit across the capacitor when the required feed-back voltage is higher than the final amplifier can produce. Position b is the normal position of the switch. However, when ϕ becomes sufficiently large, the switch is caused to move to either position a or position c, depending upon the polarity of ϕ. The diode thus connected across the network immediately discharges the capacitor; but because the short circuit is unilateral, the capacitor is free to charge in the other direction to permit the output to "back off" from the limit stop. The switch then moves back to position b and normal operation is resumed.

Information is transmitted within the main Dynamic Analysis and Control Laboratory computer almost entirely by means of 400-cycles-per-second amplitude-modulated suppressed-carrier voltages. Therefore the input and output units of the servo simulator perform the functions of demodulation and modulation for accepting and generating signals in this form.

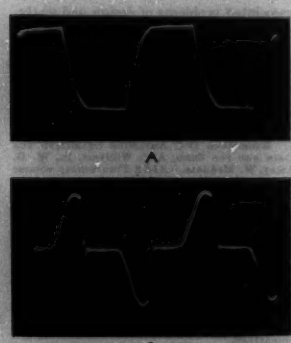

Figure 22. Response of the displacement-limited servo to sinusoidal excitation

A. Displacement B. Velocity

Simulation of a Servo Limited in Velocity and Displacement

The second-order servo with limited velocity and displacement, for which the analog, Figure 7, has already been discussed, can be used as a simple example to illustrate the results obtainable by analog techniques. Combination of equations 1, 2, and 3 yields the following relation between input and output of the servo, valid when all variables are less than their limiting values

$$J_m \frac{d^2\theta_o}{dt^2} + B_m \frac{d\theta_o}{dt} + K_m\theta_o = K\theta_i \tag{10}$$

In operational notation this equation can be written

$$\frac{\theta_o}{\theta_i} = \frac{1}{\frac{p^2}{\omega_n^2} + \frac{2\eta p}{\omega_n} + 1} \tag{11}$$

in which the natural frequency

$$\omega_n = 2\pi f_n = \sqrt{\frac{K_m}{J_m}} \tag{12}$$

and the damping ratio

$$\eta = \frac{B_m}{2\sqrt{K_m J_m}} \tag{13}$$

Figure 16 shows the theoretical response, computed from equation 11, of such a system when subjected to a suddenly applied input of fixed displacement. Curves are shown for several values of ω_n and ζ, all obtained by holding fixed the time constant, $T_m = J_m/B_m$. An electric analog was constructed from the simulator components described previously according to the arrangement shown in Figure 7. The response of this analog under conditions corresponding to those used in calculating Figure 16 is given in Figure 17. None of the quantities reached its limiting value in these tests; hence the response should be that of a completely linear second-order system. Comparison of Figures 16 and 17 demonstrates that there is very close agreement between the response of the analog and the theoretical behavior. (The minor ripples superimposed on the curves of Figure 17 are due to malfunctioning of the cathode-ray oscilloscope from which the photograph was taken.)

Displacement limiting of the servo is illustrated in Figure 18, which shows the analog output as a function of time. Curve a is the same as that shown in Figure 17 for a damping ratio, ζ, of 0.1.

Figure 23. Velocity versus displacement when the displacement is unlimited and when it is limited to 0.75, 0.5, and 0.25 times its unlimited value

Curves b and c represent the behavior of the same system when the displacement is limited to slightly greater and slightly less, respectively, than the magnitude of the displacement called for by the input. Both curves indicate that the output comes to an abrupt halt upon striking the displacement limit. At that point, when the input is less than the limit, as in curve b, the error signal is in the direction to cause the output to decrease. Therefore, since the velocity has been reduced to zero, the motion of the output immediately reverses. The remainder of the curve is the response of the linear system when subjected to a negative step input equal in magnitude to the difference between the limit and the displacement originally required. When the displacement is limited to less than that demanded

Figure 24. Velocity versus displacement when the velocity is unlimited and when it is limited to 0.75, 0.5, and 0.25 times its unlimited maximum

by the input, as in curve *c*, the error is such as to maintain the output against the limit continually.

Figures 19, 20, and 21 show simultaneously the output position and the negative of the velocity of this system. Figure 19 is again the response of a linear second-order system with a damping ratio of 0.1; in Figures 20 and 21, respectively, the velocity is limited to approximately 0.5 and 0.15 times the maximum velocity attained by the unlimited servo. In the latter two cases the response is exactly the same as that of the linear servo until the maximum permitted velocity is reached. The output displacement then increases at a constant rate until the error signal is less than that required to maintain the maximum velocity. From that point on, the response, again that of a linear second-order servo, may be calculated from equation 9 with the proper initial conditions.

The response of the displacement-limited servo to sinusoidal excitation is shown in Figure 22 (A). In this particular case, the displacement is limited to half of the maximum value which would be produced by an unlimited servo having the same input. The corresponding velocity is plotted in Figure 22(B). These illustrations show clearly that the velocity is reduced almost immediately to zero when the output reaches the limit. During the time that the error signal is sufficient to maintain the output against the limit, the velocity remains zero; then, when the sign of the error reverses, the velocity begins to build up in the opposite direction causing the output to leave the limit.

An interesting and useful means for presenting the information contained in Figure 22 is the so-called "phase-plane" diagram, in which velocity and displacement are plotted against each other. Such a presentation is shown in Figure 23, vertical distances representing velocity and horizontal distances, displacement. The circular trace, *a*, represents the system under sinusoidal excitation with no limit on the displacement, that is, when the system is operating linearly. Consequently, both displacement and velocity are sinusoidal; and since velocity is the first time derivative of displacement, the two quantities differ in phase by 90 degrees. The resulting graph, which can be made to appear circular by proper choice of horizontal and vertical scales, is traced in a clockwise direction, once for each cycle of the excitation.

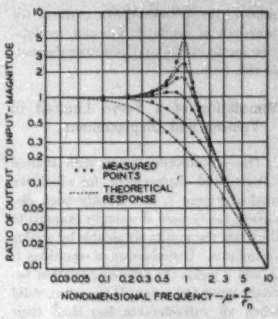

Figure 25. Frequency response of the simulated second-order servo

The other traces of Figure 23 are obtained by plotting similarly the velocity and displacement of a displacement-limited servo. The velocity and displacement of Figure 22, for example, when plotted along the vertical and horizontal axes, respectively, produce trace *c*. Figure 24 is a similar representation of a velocity-limited servo. All the trajectories in both of these figures are traced in a clockwise direction; in each diagram the scales are exactly the same for all traces.

Accuracy of the Simulator

When compared with the theoretical responses given in Figure 16, the measured linear transient responses, shown in Figure 17, indicate that the accuracy of simulation is good. A better measure of the accuracy of simulation over the linear range is obtained from steady-state frequency-response tests with the simulator components arranged to represent a second-order system as in Figure 4. The test results shown in Figure 25 indicate that the measured responses agree with the theoretical responses with an error of less than 1 per cent at the natural frequency. When the input and output units are added to the system, the tests made on a carrier basis give results comparable to those shown in Figure 25, except at frequencies above 25 cycles per second where the measured phase angles are larger than the theoretical values principally because of the filter used in the output unit.

The stability of the gain-determining resistance and capacitance components in the units is high so that more accurate results are obtainable from the equipment by calibrating each unit in comparison with a higher accuracy standard. Noise and drift in the units have been held to less than 0.1 per cent of full scale.

In simulating nonlinear effects, the errors in limiting levels are in general not more than 1 per cent of the maximum levels of the circuits employed. Operation at high levels, therefore, minimizes these errors.

The system chosen for illustration purposes was made simple intentionally to facilitate comparison of its theoretical linear behavior with the simulator response. Aside from its use in conjunction with the principal Dynamic Analysis and Control Laboratory computer, the servo simulator will be of greatest use in studies of more complex systems, particularly those containing nonlinearities, for which analytical treatment is impractical. For these systems, analog techniques such as are described in this paper represent a simple and direct means for obtaining solutions to the associated problems of design and analysis.

References

1. An Electronic Simulator for Nonlinear Servomechanisms, E. C. Johnson, Jr. *Thesis*, Electrical Engineering Department, Massachusetts Institute of Technology (Cambridge, Mass.), 1949.

2. Wide-Band D-C Amplifier Stabilized for Gain and for Zero, A. J. Williams, Jr., W. G. Amey, W. McAdam. *AIEE Transactions*, volume 68, part II, 1949, pages 811–15.

Discussion

Gerald Landsman (National Bureau of Standards, Washington, D. C.): The use of a flight simulator as a tool in the design and engineering of an aircraft control system, as contrasted to its use as a research and development tool, should be strongly emphasized. System and component engineering in an aircraft control system is facilitated to a surprising degree, if the control system is employed directly with its simulated airframe at every possible phase of engineering. Extensive use of this technique by the National Bureau of Standards has shown it to be an extremely useful tool.

In such a program of design and engineering, it is often found that the limiting features of the control system design are in the nonlinearities associated with the control system "hardware." Two major lines of attack may be followed in designing a control system in the presence of these nonlinearities.

The first involves the direct testing of the control system on the flight simulator with observations being made of the over-all airframe plus control system performance. These observations are then compared with

the results of system simulation with the autpoilot being considered a linear device to determine the acceptability of the control system design and engineering. However, in many cases, control systems are characterized by a large number of nonlinear elements. In such cases, the first line of attack is rendered extremely difficult and recourse must be made to a second line of attack. This involves the step-by-step simulation of control system nonlinearities. This nonlinearity simulation is accomplished by the methods so effectively developed in this paper.

An alternate method for the simulation of "dead space" to that indicated in Figure 13 of the paper is shown in Figure 1 of the discussion. It is possible with this method to avoid building extra units of the type indicated in Figure 13 and to use instead already

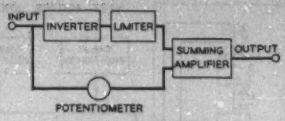

Figure 1. Threshold Circuit

available summing, inverting, and limiting amplifiers. Use of limiting amplifiers, as indicated in Figure 12, or by equivalent sharp cut-off circuits, has the advantages of sharper limiting characteristics plus the easy and continuous adjustment of the limit level mentioned in the paper. This method of threshold simulation may be easily employed by laboratories using many of the commercially available analogue computers.

C. M. Edwards and E. C. Johnson, Jr.: Mr. Landsman's alternative threshold circuit is a good suggestion for a way to obtain the characteristics of a dead space using standard analogue computing elements. Furthermore, it indicates the flexibility of analogue techniques by which a large variety of physical phenomenon can be simulated with different arrangements of a few basic units.

In some cases it may be more economical of space and expense to construct special units for a particular simulation problem rather than to use the existing standard units.

Limit stop simulation is almost always required in servo problems, therefore development of the special displacement limiting unit was carried out using the threshold circuit shown in Figure 13.

A Generalized Analogue Computer for Flight Simulation

ALBERT C. HALL
MEMBER AIEE

THE effort devoted to the development of aircraft up to the present has been directed largely toward the improvement of performance factors such as range, cruising speed, economy, operating altitude, and so forth. These factors in a particular case are determined primarily by the steady-state operating characteristics of the aircraft. On the other hand, factors such as maneuverability, speed of response, ease and accuracy of control, involve the dynamic properties of the aircraft and have received relatively little consideration. However, with the advent of higher flight speeds and increasing interest in automatically-controlled aircraft, dynamic problems are becoming of much greater importance, and in some applications are predominant in significance.

The mathematical solution of aircraft dynamic problems is characterized by considerable complexity due partly to the high order of the differential equations involved and particularly to the nonlinear nature of the equations. Nonlinear effects are introduced by the kinematics of rigid bodies with several degrees of freedom, the physical nature of the aerodynamic forces, and peculiarities of equipment provided to control the flight. The complexity is such that general solutions are not known and few specific cases have been solved without drastic assumptions.

Most of the mathematical analysis of aircraft dynamics has been devoted to the study of the so-called "linearized" equations. Here assumptions are made that eliminate the nonlinear effects and permit the problem to be represented by linear differential equations. Physically, these assumptions require that the motion of the aircraft be limited to infinitesimal departures from the steady-state condition, that a number of aerodynamic effects be neglected, and that the operation of any control system involved be restricted to the linear range. Even in cases where these drastic assumptions are permissible, however, the analysis is complex because of the high order of the differential equation and consequently most of the work has been limited to specific cases. While the study of the linearized equations has been of great value, the solutions are of limited usefulness because of the restrictive nature of the underlying assumptions.

The high order of the equations and the existing state of knowledge of nonlinear differential equations lead to the conclusion that the only practical method of solution of most aircraft dynamic problems is by means of computing machines. Unfortunately, the complexity of the problems is such that no existing computing machine was well suited to the solution of many urgent problems. Because of this need the Dynamic Analysis and Control Laboratory at the Massachusetts Institute of Technology undertook the development of a generalized analogue computer to contribute specifically to the solution of aircraft dynamic problems. The development was sponsored by the Bureau of Ordnance, Department of the Navy. The principal development problems and the salient characteristics of the analogue computer, which is presently in operation, are the subject of this paper.

While the design of the computer was generalized as much as possible in order not to restrict unduly its application to the broad field of computation, most of the machine specifications were determined by the requirements of aircraft dynamic problems, and for this reason the computer is called a flight simulator. The general characteristics desired in the computer are: reasonably high accuracy; considerable capacity for ordinary mathematical operations such as addition, multiplication and integration; special faculty to represent a sizable number of nonlinear effects, particularly of the trigonometric type; and high speed of computation. Means of securing these characteristics are discussed in this paper. The analogue computer also was planned for the dynamic testing of control systems employed in the automatic operation of aircraft. It is in this application of the flight simulator that high speed of computation is particularly important. In such applications the machine must compute on a 1-to-1 time scale, that is, it must compute the solution to an aircraft problem in exactly the time required for the process to occur in the physical situation. If such speed is achieved and proper auxiliary equipment made available, it is possible to simulate a flight problem by setting up the computer to represent

Paper 50-48, recommended by the AIEE Computing Devices Committee and approved by the AIEE Technical Program Committee for presentation at the AIEE Winter General Meeting, New York, N. Y., January 30–February 3, 1950. Manuscript submitted November 3, 1949; made available for printing November 30, 1949.

ALBERT C. HALL is with the Massachusetts Institute of Technology, Cambridge, Mass.

The author wishes to acknowledge the many helpful contributions from a number of engineers. The mechanical design of the flight table was carried out by Jackson and Moreland, Boston, and its fabrication was the responsibility of the Palmer-Bee Company, Detroit. The systems engineering of the computer was under the supervision of C. M. Edwards, and his contributions in this respect as well as those of L. C. Dozier, H. Jacobs, and G. H. Hart should be noted. Component development in general was directed by E. St. George and in this category the contributions of W. W. Seifert and M. T. Weiss on the repeater amplifier and summing network, W. J. Deerhake and A. Fuchs on the integrator, C. H. Woods on the multiplier, and B. B. Crocker on the arbitrary function generator, are particularly noteworthy. The hydraulic servo development is to the credit of J. F. Blackburn (also responsible for much of the flight table development) with effective contributions from I. Kotlier. The work of R. W. Bond, H. E. Blanton, and S. B. Williams on the flight-table servomechanisms must be mentioned and effective contributions in the development of the flight-table instrumentation were made by R. D. Atchley on the angular accelerometer, and W. G. Andrew, E. St. George and E. P. Blanchard on the rate gyroscope. Important detailed contributions, too numerous to list, were made by T. F. Jones, R. E. Kimball, F. C. McCoy, J. McHoul, and H. Price.

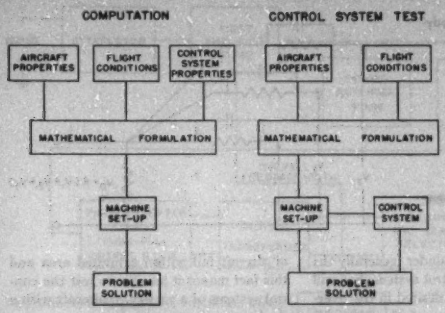

Figure 1. Comparison between the purely computational and the testing functions of the flight simulator

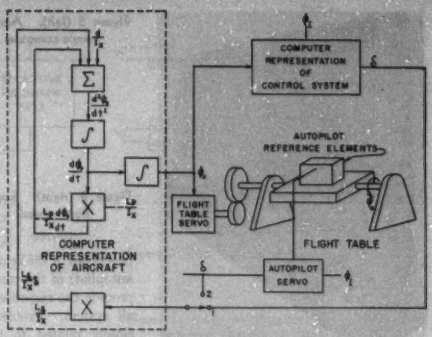

Figure 3. Simulator diagram for computer solution and component testing for a roll stabilized aircraft

the aircraft dynamics, employing the aircraft control equipment in a fashion analogous to that in which it is used to control the actual aircraft, and making use of auxiliary equipment to link the control equipment and the computer. This method of operation permits the dynamic performance of the aircraft control equipment to be tested under conditions closely similar to actual flight.

Topics in Aircraft Dynamics

While by no means restricted to such problems, the analogue computer was designed specifically to solve problems in the field of aircraft dynamics. Certain features of the machine, therefore, such as the auxiliary equipment required for the testing of aircraft control systems, are of limited application. In general, however, problems in aircraft dynamics are sufficiently varied that little compromise in versatility need or can be made. A few of the principal topics in aircraft dynamics are described and it may be seen that the problems contain elements common to dynamic problems in a variety of fields.

Stability and Transient Properties of Aircraft

An important consideration in the operation of aircraft is the stability characterizing its motion. The aircraft in general should be stable; that is, transient motions caused by gusts or motion of the control surfaces should decay rather than continue or build up. Moreover, most applications require that these transients decay at prescribed rates. Under some conditions these questions can be answered by analytical means alone. More often analytical procedures become cumbersome and the use of mechanical computation is advisable. Frequently the size of the disturbances is sufficiently large and the inherent nonlinearities so important that the use of a computer to solve for the transient motions of the aircraft is mandatory.

Design of Aircraft with Prescribed Dynamic Characteristics

While relatively little effort has been devoted in the past to designing aircraft with carefully specified dynamic properties, applications are arising which require close control of the dynamic performance. An analogue computer is of great use in such an undertaking if it permits ready variation of the design parameters since a rapid study can then be

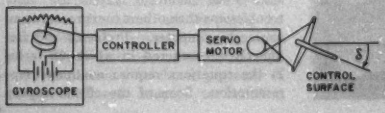

Figure 2 (left). Stabilization of an aircraft in roll

Figure 4 (right). Floor plan of the flight simulator

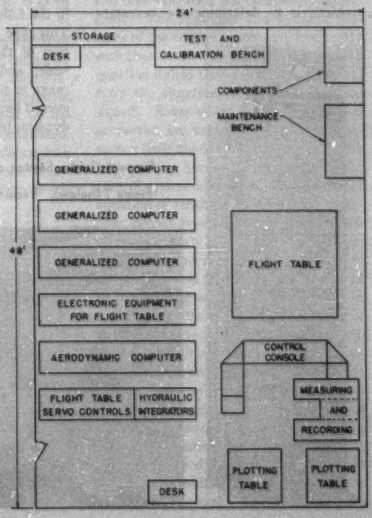

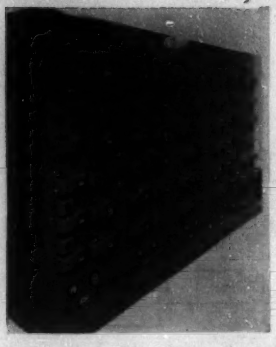

Figure 5 (left). Aerodynamic computer

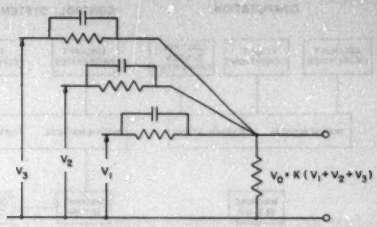

Figure 8 (right). Summation network

made of the dynamic properties of a variety of aircraft configurations. The computer should be of considerable range in order to represent the so-called second order effects. These effects are generally omitted in analytical studies but must be considered if good correlation is to be obtained between the predicted characteristics and those determined from flight tests.

Control System Synthesis

An important topic in aircraft dynamics is the synthesis of automatic pilots to obtain prescribed over-all response characteristics in the controlled aircraft. In applications of this sort a portion (generally the aircraft characteristics) of the control system is specified. The problem is to determine the necessary properties of the remainder (generally the autopilot) of the control system that will provide the response desired in the over-all system. Problems of this sort are closely related to the topics discussed above, except for the emphasis on the control system rather than the aircraft. In complex problems, synthesis procedures are developed by solving sufficiently numerous and diverse problems that patterns in the solutions can be recognized. Synthesis problems require speed and flexibility in the operation of the computer in order to solve quickly the required large number of specific cases.

Control System Test

Peculiarities in autopilot equipment make it desirable to test thoroughly the performance of the control system prior to installation in the aircraft. Simulation of the flight conditions by means of the analogue computer makes it possible to test the control components in the laboratory if auxiliary equipment described in the following paragraphs is employed. This type of operation requires the solution of the problems on a 1-to-1 time scale, and therefore only a restricted range of problems can be solved. However, it has been found that the important dynamic properties of a wide range of sizes of aircraft fall within a limited area and this fact makes it feasible to test the control systems of a variety of aircraft with a single type of computer.

Figure 6 (left). Section of the generalized computer

Figure 7 (below). Recording section of the simulator

Mathematical Characteristics of Problems in Aircraft Dynamics

The type of equation that is encountered widely in problems in aircraft dynamics is the nonlinear ordinary differential equation with varying coefficients with time as the independent variable. Partial differential equations are encountered less often and frequently can be approximated adequately by ordinary differential equations. The scope of the equations generally required is discussed in the following.

Order of the Equation

The highest order differential occurring in the general equation of motion can be between 20 and 30 (or higher) depending upon the complexity of the control system and the number of second order effects considered. If the motion being studied is that of a rigid body in space with unrestricted motion the system has six degrees of freedom and the order of the differential equation is 12 even though no aerodynamic forces act upon the body. If the aircraft is automatically controlled in the conventional manner by regulating the roll, pitch, and yaw orientation angles of the aircraft, the many dynamic effects introduced by the control system require a very high order of differential equation to represent the situation.

Nonlinear Terms

The number of nonlinear terms which require representation in aircraft dynamic problems is difficult to specify, and such a number is not particularly meaningful since some nonlinear effects are more troublesome than others to represent in an analogue computer. Problems are frequently encountered in which 20 terms in the equations require nonlinear representation. Some of the effects appear

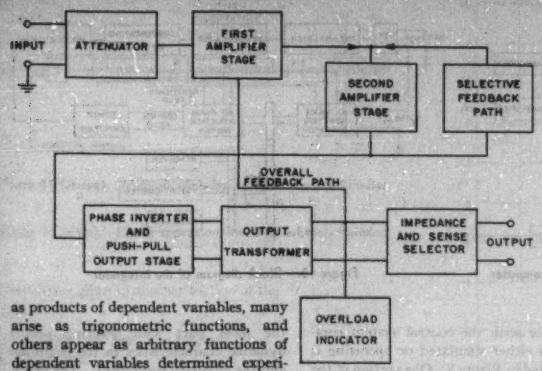

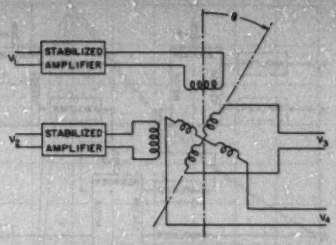

Figure 9 (left). Functional diagram of the repeater amplifier

Figure 11 (above). Application of the variable induction principle to vector resolution

as products of dependent variables, many arise as trigonometric functions, and others appear as arbitrary functions of dependent variables determined experimentally. The principal nonlinear effects are produced by the basic dynamic phenomena of a rigid body with six degrees of freedom, by the nonlinear nature of most aerodynamic effects, and by saturation and dead space peculiarities of the autopilot. Some of the effects can be represented in the computer by forming products of variables or by trigonometric functions. However, many cannot be analytically expressed in closed form and must be approximated by suitable means in the computer. Many of these nonlinear effects are known to be important to represent and to study. In other cases their importance is unknown but must be determined by computing-machine study.

Trigonometric Functions of Dependent Variables

An important source of complexity in aircraft dynamics is the large number of trigonometric functions present in most problems. Although trigonometric functions are nonlinear effects and as such have been mentioned before, their importance warrants special consideration. Trigonometric functions are introduced principally by the fact that the aerodynamic forces and moments acting upon an aircraft are best expressed relative to a coordinate system fixed in the aircraft while other effects, such as those produced by gravity and those initiated by reference elements such as unrestrained gyroscopes, operate in a co-ordinate system fixed in space. This difference in basic co-ordinate systems requires several transformations of vectors between sets of axes and consequently a number of trigonometric functions are required for mathematical representation. The complications thus introduced are substantial and it is necessary to choose processes of computation well adapted to handling these effects. A study of problems encountered in aircraft dynamics indicates that it is frequently necessary to transform as many as nine vectors between sets of three dimensional co-ordinates.

Dynamic Testing of Control Components

As indicated before, the flight simulator is designed to be employed in two general ways. In the first method of operation, the problem is defined completely in equation form and the computer is set up to solve the equations. In the second method of operation, the flight control components are employed with the computer in a fashion analogous to that in which they are used in flight.

Figure 1 compares the two methods of operation. When the analogue computer is used to represent completely the problem, the aircraft properties and the control system characteristics both must be determined and mathematically formulated. The computer is set up in accordance with the formulation, and the solution determined. However, if the flight simulator is used to test the control components, only the aircraft properties and the flight conditions need be formulated mathematically. The analogue computer is set up in accordance with this formulation as in the first method of operation. The properties of the control components do not have to be represented by the computer since the actual components are employed in obtaining the problem solution. The combination of the computer and the flight control system comprises the analogue of the problem. The advantage of using the flight simulator in the latter fashion lies in the fact that the machine representation of the control system is unnecessary. Many of the control systems in use and envisioned are complex and their operation not completely understood. The nonlinear and dynamic features of the control system are frequently such that the results of any test is open to question unless the system is used in exactly the situation for which it was designed. Even when the control system properties are known with sufficient accuracy their machine representation often is not easy. Accurate formulation of the control system may require a differential equation of tenth or higher order; moreover, certain types of nonlinearities which occur frequently are difficult to represent accurately in an analogue computer.

Figure 10. Repeater amplifier

The principal technical problem raised by the testing of control components in the flight simulator is the high speed of computation required of the computer. It is not feasible to make a time transformation in order to "slow down" the problem because the computational process must take place at the same rate as the physical process in order to subject the control components to the proper test. Therefore the dynamics of computation must be considered carefully, and the various extraneous time-lags always as-

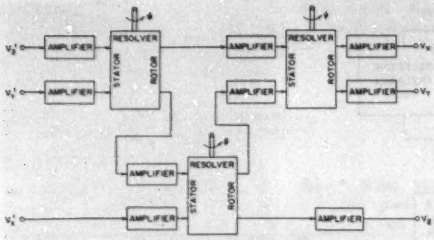

Figure 12. Resolution of a vector in the analogue computer

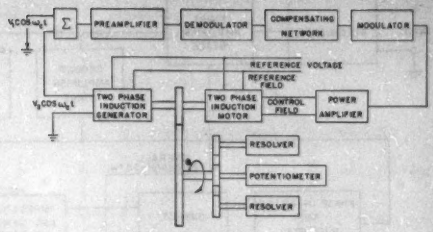

Figure 13. Block diagram of the integrator

sociated with computation must be reduced to a point at which they are insignificant relative to the dynamic effects of the problem if accurate results are to be secured.

The use of the analogue computer as either a computational device alone or alternatively as a testing device is illustrated by a simple example. Suppose the problem at hand is a common one, namely, the study of the stabilization of an aircraft in roll. The physical situation is illustrated by Figure 2. The orientation of the aircraft relative to axes fixed in space is denoted by ϕ_o. A correcting moment is applied to the aircraft by means of a pair of ailerons the angular deflection of which, relative to the neutral position, is denoted by δ. The ailerons are operated by a control system employing a vertical gyroscope as the reference element.

If a number of assumptions are made, such as that of no coupling between the other motions of the aircraft and its roll motion, the dynamic equations can be written as follows

$$L_\delta \delta + d = I_x \frac{d^2\phi_o}{dt^2} + L_p \frac{d\phi_o}{dt}$$

$$\delta = f(\phi_I - \phi_o)$$

In these equations

I_x = moment of inertia of the aircraft about the roll axis
L_p = damping coefficient
L_δ = coefficient of the control surface moment
ϕ_I = desired orientation of the aircraft

The first of the foregoing equations is the equation determining the aircraft roll motion and the second is the equation for the operation of the control system. The control system measures the roll angle ϕ_o, compares it with the desired orientation, and if required, produces a correcting motion of the control surfaces.

The study of this problem on the flight simulator with the control system components either simulated or operating is illustrated in Figure 3. One portion of the illustration shows how the aerodynamic equation is represented in the computer. Machine operations of summation, integration, and multiplication are indicated by the corresponding mathematical signs. If the analogue computer is to simulate the control system a second part of the computer must be set up and in Figure 3 this is indicated in block form only, since the control equation has not been specified. If the selector is in position one and the appropriate initial conditions are imposed, the computer is ready to solve the problem. An example of a typical problem is the determination of the roll angle ϕ_o as a function of time when a disturbance d, such as might be caused by a gust, is applied.

The second use of the simulator illustrated in Figure 3 is the test of the actual flight control unit. Auxiliary equipment, comprising a flight table and controlling servomechanism, is required in order to orient any reference element of the control unit, such as a gyroscope, in a manner corresponding to that occurring in flight. The reference element and the remainder of the flight control unit are interconnected in the way normally employed in flight, and the shaft or other type of mechanical output connecting the control unit to the ailerons may be loaded mechanically to simulate the effect of bearing friction, the mass of control surfaces, and the wind loading encountered in flight. The displacement of the output is measured by suitable means, such as a potentiometer, and the electrical signal supplied to the computer through the selector which is set in position 2. This method of operation provides as realistic a test of the control unit as may be had without actual flight.

The technical problems introduced by operation of the analogue computer to test flight components are associated for the most part with securing proper dynamic characteristics in the computer and the auxiliary equipment. The necessity of computing rapidly in order that the problem may be run on a 1-to-1 time scale has been pointed out. Dynamic effects in the flight table and its servos are equally important and are even more troublesome to control because of the dimensions and weight of the physical equipment required to carry and orient the flight components.

System Considerations

Computer Elements

The analogue computer consists of an array of computing elements, each of which carries out a particular mathematical operation, and associated equipment for so interconnecting the elements that the combination provides a representation or analogue of the problem being studied. Computing elements are provided for carrying out such mathematical operations as addition or subtraction, multiplication, integration, and trigonometric transformation. The operation of differentiation is not performed as a transformation of the equations characterizing the problem always make this operation unnecessary.

A description of each of the computer

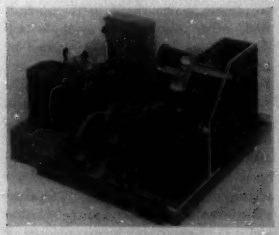

Figure 14. Integrator

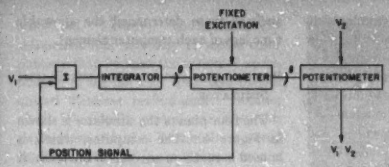

Figure 15 (above). Multiplication by means of a potentiometer

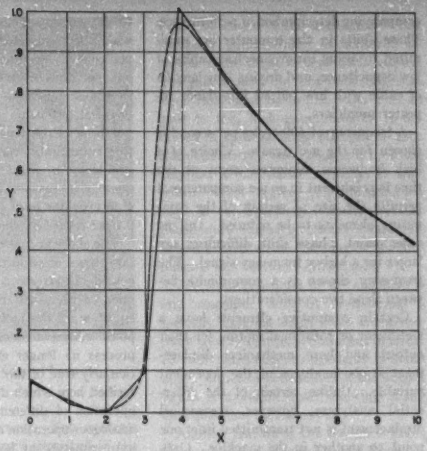

Figure 17 (right). Linear approximation to an arbitrary function

elements is given in another section of the paper.

Analogue of the Dependent Variable

A basic consideration in the design of an analogue computer is the means of representing in the machine the dependent variables of the problem. In general the machine analogue of the dependent variable can be an electrical signal or mechanical motion and frequently is the former in one portion of the computer and the latter in another portion. While analogue computers have been built in which the analogue quantity is a mechanical rotation or displacement throughout, such machines are less flexible than ones in which electrical signals alone, or both electrical signals and mechanical motions, are employed to represent variables.

If the machine variable is an electrical quantity, it may be a direct voltage proportional in magnitude and sign to the magnitude and sense of the corresponding dependent variable of the problem. The electrical signal also may be an alternating voltage of fixed frequency, the magnitude of which is proportional to the magnitude of the dependent variable and the phase of which is either zero or 180 degrees for positive or negative senses respectively of the dependent variable. The latter or a-c method was chosen for the computer described here, and the computer, therefore, is frequently called an a-c computer.

Among the advantages of the a-c type of computer are feasibility of employing a-c amplification and the corresponding freedom from drift and grounding problems encountered when d-c amplification is required; and simplicity with which trigonometric resolution is performed. The principal disadvantage of an a-c type analogue computer is the meticulous attention that is required to prevent phase shift difficulties. In this computer it was necessary to limit the phase shift occurring in each computation such as multiplication by a constant, addition, and so forth, to 0.05 degree, and to employ so-called quadrature rejection circuits in the integrators to render them insensitive to small phase shifts. The accuracy of computation is not affected directly by small phase shifts in the a-c signals, but overloading in amplifiers may occur with ac-

Figure 16 (below). Electromechanical strain-gauge multiplier

Figure 18 (right). Arbitrary-function generator

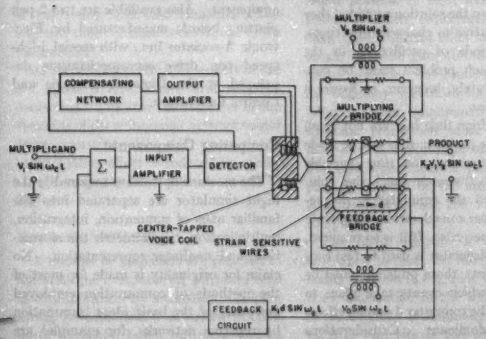

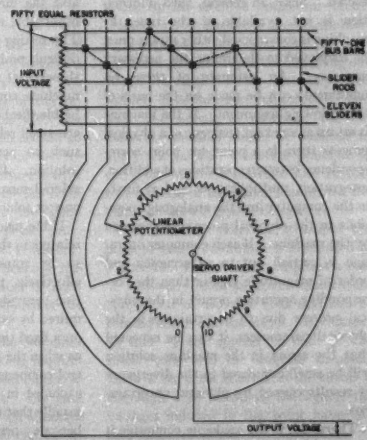

companying deterioration of performance. Phase shifts in the computer are minimized by using interconnecting cables of low capacitance, and driving long lengths of cable with low output impedance repeater amplifiers.

A frequency of 400 cycles per second is chosen for the a-c signals. Choice of a high frequency minimizes many of the time lags inherent in an a-c computer and permits the size of certain of the computing elements to be reduced. On the other hand, phase shift difficulties are larger for a higher frequency signal. The frequency chosen is a compromise between these two considerations.

Certain computing elements have a rectilinear or rotational motion for their output and here mechanical displacement is the analogue of the dependent variable. Unlike certain of the differential analyzers, however, mechanical displacement is not transmitted from one point to another in the machine. Only electrical signals are transmitted over appreciable distances.

Specifications on Computation Accuracy

An important problem in the development of a large scale analogue computer is the determination of the accuracy with which individual machine operations must be carried out. It is convenient to use the term "accuracy" to refer to the static or steady-state condition. Dynamic effects, which are equally important, are considered separately. Exact determination of the required accuracy does not seem to be feasible without detailed knowledge of the specific problems to be solved. Since, in general, such information is not available at the time the machine is constructed, other means must be employed to determine the necessary accuracy. An estimate of these requirements can be made on the basis of the following argument. If the machine is set up as an exact analogue of a physical process there is a point by point correspondence between operations of addition, integration, multiplication, and so forth, in the computer and the analogous operations in the physical process represented by the machine. If each computer operation is carried out to an accuracy and order of magnitude greater than the corresponding operation occurs in the physical process due to uncertainties in the physical parameters, it can be expected that the errors in the machine solution will be small compared to the divergence of results caused by physical uncertainties.

Therefore, if the analogue computer is to be employed to solve problems in which the parameters are known to a few per cent, an accuracy of a few tenths of one per cent in each machine operation should be sufficient. In a vast number of physical problems the parameters are not known to better than one per cent and this is certainly true for the majority of problems in flight dynamics. Consequently it was decided to set the allowable error for each computer element at 0.1 per cent of maximum.

The above argument should not create a false sense of security as far as accuracy considerations are concerned. It is frequently necessary to so transform the equations of the problem that a point by point correspondence with the physical process no longer exists. This is particularly true of the type of machine described here which does not perform the operation of differentiation although an analogous operation can occur physically, approximately at least. For these and other reasons each individual problem must be considered carefully when it is studied with the machine in order to obtain an estimate of the solution accuracy.

Dynamic Effects

The dynamic effects associated with each computer-element operation are equal in importance to steady-state accuracy considerations in affecting the correctness of the solution. No physical device will carry out such ideal operations as addition, integration, and so forth, with no associated time delay. If these time delays are too large the machine no longer can be considered as an analogue of the problem being studied and the machine solution will bear no observable relation to the true solution. The setting of allowable time delays is a difficult problem, but in general it can be shown that the time delays occurring in machine computation will have a negligible effect on the solution provided they are small relative to characteristic times, such as periods of oscillation, in the solution. Each problem must be considered separately, however, to assure a correct solution.

If the machine time lags are not small relative to the problem, they can be made so by transforming the time variable effectively to "stretch out" the solution, provided the computer is not required by other considerations to operate on a fixed time scale. If it is so required, as when the simulator is used to test control components, those problems must be excluded in which events take place so rapidly that the computer dynamic effects become predominant. Considerations such as these determined the allowable time lags of each computer element.

Physical Arrangement of the Flight Simulator

The floor plan of the simulator is shown in Figure 4. The computer, which is housed in racks on one side of the room, is separated into two portions. One portion, called the aerodynamic computer, is set up in a relatively invariable form to solve the set of aerodynamic equations that represents the usually considered effects. Figure 5 shows the major portion of this section of the computer. The remainder and larger part of the computer, called the generalized computer, is set up in flexible form to solve general equations of the type discussed early in this paper and is not limited to aerodynamic problems. However, the generalized computer is used for representing the less ordinary types of aircraft dynamic phenomena and in such problems it is interconnected with the aerodynamic computer.

Interconnections in the generalized computer are made by plug board arrangements. In both computers all components are of the plug-in type to obtain the maximum flexibility both in operation and maintenance. A rack of the generalized computer is shown in Figure 6. This rack contains an integrator and other computing elements normally associated with it. Interconnections among equipment in the rack are made at the top. The rack also contains calibration equipment, and, located at the bottom, the regulator for the direct current power required. Each rack has its own regulator in order to eliminate difficulties caused by common ground returns.

Recording and control equipment are located adjacent to the flight table which is described in another section of the paper. Figure 7 shows this section of the equipment. Also available are two 2-pen plotting boards manufactured by Electronic Associates Inc., with special high-speed pen drive servomechanisms developed at the Dynamic Analysis and Control Laboratory.

Computing Components

The machine operations required in the flight simulator are separated into the familiar ones of summation, integration, multiplication, trigonometric transformation, and nonlinear representation. No claim for originality is made for most of the methods of computation employed and some of the basic ideas (summation by resistive networks, for example) are

quite old. However, considerable development was necessary to secure components that realized the accuracy specification of 0.1-per cent error and the required dynamic performance. Because of the necessarily general nature of this paper it was felt that its usefulness would be little enhanced by references to the somewhat extensive literature. Other papers in preparation will discuss the more important components in detail and provide references to prior work. The salient features of each type of computing component is discussed below.

Summation Network

Operations of addition and subtraction are carried out in the computer by means of resistive networks illustrated in principle by Figure 8. When the problem requires that variables be added they are represented by electrical voltages and applied to the input of the network illustrated. The output voltage is proportional to the sum of the inputs multiplied by an attenuation factor which is a function of the magnitude of the resistors and the number of voltages being summed. The attenuation factor is constant for a particular network and is considered as a calibration constant. Networks are provided in the computer for adding up to eight signals, and additional signals can be summed by cascading summation networks properly separated by buffer amplifiers.

The accuracy of summation is a function of the accuracy and stability of the resistors in the network, as well as any variations in the source and load resistances of elements preceding and following the summation network. Over long periods of time the accuracy is a little better than ±0.1 per cent. The time lag associated with summation operations is determined by the reactive parameters of the network as well as those of the source and load elements. The effective time constant is below one-tenth millisecond.

As mentioned before, phase-shift in the a-c signal is troublesome and must be controlled. The stray inductances of the elements of the summation network would cause excessive phase-shift were not a compensating effect introduced by means of the trimming capacitances shown in Figure 8.

Repeater Amplifier

A number of amplifiers are required in the analogue computer for purposes such as multiplication by a constant, compensating for attenuation occurring in computer elements, buffer purposes, and as

Figure 19. Gimbal frame

low impedance sources. For example the summation network described in the preceding section should be followed by an element with high input resistance. Such networks, therefore, are usually followed by a repeater amplifier that not only serves as a high resistance load, but also makes up for the attenuation that occurs in the network. If the repeater amplifier is designed to have a low output resistance, long lengths of signal transmission cable can be connected to its output terminals without introducing excessive phase-shift. Indeed, the importance of minimizing phase shift makes it desirable to provide an impedance changing amplifier following any high resistance circuit if more than a few feet of cable are required to connect the circuit to the next element in the computer.

A repeater amplifier was developed to meet these and other needs of the computer. It was desirable that the number of types of amplifiers be kept small to minimize servicing difficulties and it was found possible to meet most of the repeater amplifier requirements with one basic type. Special effort was needed to insure that the gain stability of the repeater amplifier was commensurate with the accuracy specifications of the computer. Other requirements are good dynamic properties, small phase shift, flexibility of application, and reliability. The last requirement is particularly important because of the number of such amplifiers (more than 200) required in the computer.

The block diagram of the amplifier developed to meet the foregoing requirements is shown in Figure 9, and Figure 10 is an illustration of the unit. The gain of the amplifier is nominally ten although gains of one, two or five also can be selected by means of the attenuator. The necessary gain stability is achieved by means of the negative feed-back feature. The gain around the feed-back loop is at least 1,000 and by limiting the over-all gain to ten, high gain stability is obtained in spite of large changes in tube characteristics. The phase shift of the amplifier at the signal frequency is kept within ±0.05 degree. In addition, the slope at the operating frequency of the phase shift versus frequency characteristic is such that the time lag of the amplifier is well below 0.1 millisecond.

The input resistance of the amplifier is one megohm, and by employing a specially designed transformer in the output a choice of output resistances of either 75 or 10 ohms output impedance is available. Either or both senses of the output signal is available thus allowing ready multiplication by minus one.

Another feature of the amplifier is the overload indicator indicated in Figure 9. The linear range of the amplifier is better than 100,000 to 1, but overloads can occur if the problem set-up is incorrect. If overload occurs in the process of a problem solution, an erroneous answer is almost certain to result. By triggering a gas triode if the amplifier signal exceeds a predetermined level the overload indicator provides the operator with a warning that the linear range of the amplifier may have been exceeded.

Vector Resolver

The number of trigonometric functions appearing in problems of the dynamics of rigid bodies has been mentioned. These functions for the most part are introduced by the need to transform vector quantities from one set of axes to another. It is important, therefore, that the analogue computer be capable of carrying out vector resolution with accuracy and facility. The fact that the computer employs a-c signals to represent the dependent variables makes it possible to apply the variable induction principle to carry out vector resolution, and in fact this was one of the major reasons for deciding on the a-c type of computer.

The variable induction principle applied to vector resolution is illustrated in Figure 11. The resolver comprises a pair of stationary coils in space quadrature and a pair of movable coils that can be rotated relative to the stator. If voltages V_1 and V_2 are applied to each of the stator coils and the angular displacement of the rotor relative to the stator is the angle θ as shown in the figure, the voltages induced in the rotor have the following expressions

$$V_3 = K(V_1 \sin\theta + V_2 \cos\theta)$$
$$V_4 = K(V_1 \cos\theta - V_2 \sin\theta)$$

In these equations V_1, V_2, V_3, and V_4 are the amplitudes of sinusoids, and the coefficient K is a constant calibration factor.

The device illustrated in Figure 11 is called a resolver, and the availability of such a computing element makes it feasible to carry out relatively complex trigonometric resolutions. Consider the common problem in which it is necessary to determine the components of a vector with respect to one set of three orthogonal axes when the components are known with respect to an independent set of axes. This problem is frequently encountered in aircraft dynamics, where, for example, the velocity of the aircraft may be known with respect to axes fixed in the aircraft, but must be resolved into components measured relative to earth axes. If the components of the vector, V_x', V_y', and V_z', measured with respect to axes X', and Y', and Z', are known and the vector components V_x, V_y, and V_z, relative to axes X, Y, and Z, are to be determined the following are the transformation equations

$$\begin{aligned}
V_x = {} & V_x'(\cos\psi \cos\theta) + V_y'(\cos\psi \times \\
& \sin\theta \sin\phi - \sin\psi \cos\phi) + \\
& V_z'(\cos\psi \sin\theta \cos\phi + \sin\psi \sin\phi) \\
V_y = {} & V_x'(\cos\theta \sin\psi) + V_y'(\sin\phi \sin\theta \times \\
& \sin\psi + \cos\phi \cos\psi) + \\
& V_z'(\sin\theta \cos\phi \sin\psi - \sin\phi \cos\psi) \\
V_z = {} & V_x'(-\sin\theta) + V_y'(\cos\theta \sin\phi) + \\
& V_z'(\cos\theta \cos\phi)
\end{aligned}$$

The angles θ, ϕ, and ψ are the Euler angles that locate the axes X', Y', and Z' relative to X, Y, and Z. Figure 12 is a diagram of one means of carrying out this resolution in the computer. It is frequently necessary to resolve several vectors from one set of axes to another, and this figure is illustrative of the complexity involved.

The resolver employed in the analogue computer is one developed by the Arma Corporation. The accuracy of resolution is approximately 0.1 per cent, and while the time constant has not been measured directly it is expected to be below 0.1 millisecond. Each of the stator coils must be excited from a low impedance source and a version of the repeater amplifier described earlier is employed for this purpose. The resolver is shown among the instruments in Figure 20.

Integrators

Perhaps the most important single element in the analogue computer is the integrator. The type of unit employed most widely in the flight simulator in principle is essentially a velocity servomechanism and is shown in block diagram in Figure 13. In order to describe the method of operation suppose the integral with respect to time of a variable V_1 is desired. The computer signal $V_1 \cos \omega_c t$ is applied through a summing network and an amplifier to the control field of a 2-phase induction motor, the second or reference field of which is excited with a sinusoidal voltage of angular frequency ω_c and of constant amplitude. The motor revolves in response to the voltage on its control field and turns the rotor of an induction generator to which it is coupled mechanically. The induction generator is in principle a 2-phase induction motor with only one field excited. A voltage, $V_2 \cos \omega_c t$, appears at the terminals of the second field if the rotor of the induction generator is revolved, and with careful design of the generator characteristics, and constant generator excitation, the amplitude V_2 can be made accurately proportional to the speed of rotation of the rotor.

The output of the induction generator is returned to the input summing network in such phase that it tends to cancel the applied voltage $V_1 \cos \omega_c t$. Ideally, the two voltages would cancel and V_1 and V_2 would be equal. Practically, some difference always exists between V_1 and V_2 but if the gain around the loop is large (that is, if only a very small signal at the output of the summing network is required to produce a large amplitude V_2) the difference between V_1 and V_2 is very small. In such a case the motor speed is closely proportional to the amplitude V_1, and consequently the angular displacement, θ, of the motor shaft is accurately proportional to the integral of V_1 with respect to time.

Although the principle of the integrator is simple the performance of each of its components must be high to secure the desired static and dynamic accuracy. Particular attention must be given to the induction generator since it is the feedback element in the integrator. A generator developed by the Arma Corporation is employed in the computer with characteristics such that the output voltage is proportional to the rotor speed within 0.1 per cent of maximum. With this unit available the principal problem in the development of the integrator was that of obtaining a high-loop gain in order that the accuracy of the integrator would correspond to that of the induction generator. High-loop gain minimizes the effect of variations in the mechanical load on the accuracy of integration. High-loop gain also is important from the standpoint of minimizing the effective time constant associated with the operation of the integrator. By the use of a compensating network as indicated in Figure 13 and by giving careful consideration to the dynamic properties of the elements in the loop, it was possible to reduce the integrator time constant to approximately $1^1/_2$ millisecond.

Considerable difficulty with overload in the amplifier was encountered due to phase shift between the input V_1, to the integrator and the output V_2 of the induction generator. If instead of $V_2 \cos \omega_c t$ the output of the generator is $V_2 \cos (\omega_c t + \phi)$, complete cancellation of the input signal $V_1 \cos \omega_c t$ is not possible, and, due to its high gain, overload may occur in the amplifier even for small values of ψ. As shown in Figure 13, the difficulty is remedied by demodulating the amplifier signal and remodulating to drive the 2-phase motor. Demodulation also permits the use of compensating networks insensitive to changes in frequency of the a-c signal. An important advantage of the integrator lies in the fact that a number of instruments can be driven by the servomotor without impairing the accuracy of integration. In the unit employed in the computer as many as five instruments in addition to the induction generator, are driven by the motor. In most cases these instruments are either resolvers or potentiometers and to increase the flexibility, the mechanical design is such that these instruments can be used interchangeably. The fact that several instruments can be carried on the integrator output permits a sizable reduction in the number of computing components and consequently an important reduction in computing error and time lag.

For example, suppose the quantity $V_1 \int V_2 dt$ is to be computed. The variable V_2 is integrated and one of the potentiometers coupled to the integrator output is excited with a voltage proportional to V_1. The potentiometer output voltage is then the required function. Similarly, a function such as $V_1 \sin \int V_2 dt$ is readily computed by making use of a vector resolver coupled to the output shaft of an integrator. When a number of such operations are required a significant saving in equipment and improvement of performance is effected by use of this type of integrator.

The integrator is shown in Figure 14. In addition to the features already described, the unit includes indicator dials and means for setting initial conditions and starting integration properly at the initiation of the problem solution. The electrical and mechanical portions of the

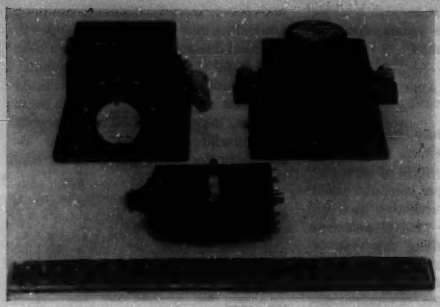

Figure 20 (above). Angular accelerometer, resolver, and rate gyroscope

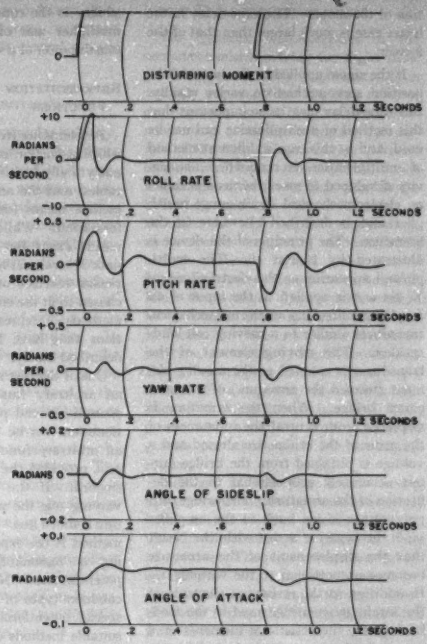

Figure 22 (right). Transients induced by disturbing moments about the roll and pitch axes of the aircraft

integrator together with the input and output amplifiers required by the potentiometers and resolvers driven by the integrator are housed in one rack. Reference has been made already to Figure 6 which shows the general arrangement.

Multiplication

Frequently the computer must carry out the multiplication operation in cases in which either the multiplier or multiplicand occurs as the integral of a variable. In such instances multiplication is performed by the means indicated in the example of the preceding section. That is, a voltage proportional to one of the factors of the desired product is used as the excitation of a potentiometer, the shaft rotation of which is proportional to the factor that occurs as an integral. The output signal of the potentiometer then is the product to be computed.

In other cases, however, neither of the factors appears as a mechanical motion, both occurring in the computer as electrical signals only. In such instances multiplication may be carried out in one of two ways. The first is to transform one of the factors to a mechanical rotation and carry out the multiplication by means of a potentiometer in the manner just described. In this method of multiplication, illustrated by Figure 15, the integrator is made to behave as a position servomechanism and provides a means of transforming an electrical signal into an angular motion. This is achieved by exciting one of the potentiometers coupled to the integrator output with a constant voltage and feeding the signal from the potentiometer, in negative sense, back into the integrator input. Operated in this way, the displacement θ (see Figure 15) of the integrator output is proportional to the electrical signal V_1, which is one of the factors of the desired product. If the voltage applied to another potentiometer is proportional to the second factor, the output of that potentiometer will be the desired product.

However, an important time delay can be introduced by this method of multiplication due to the time required for the integrator motor to rotate the shaft of the potentiometer through the several revolutions often required. A similar type of lag occurs in the operation of the equipment as an integrator, but is not nearly as important since in this case the time delay is proportional to the interval between the moment at which the input signal is applied and that at which the motor reaches its proper rate of rotation. When the unit is employed as a position servomechanism, however, the time delay is proportional to the interval between the application of the input signal and the attainment of the proper angular posi-

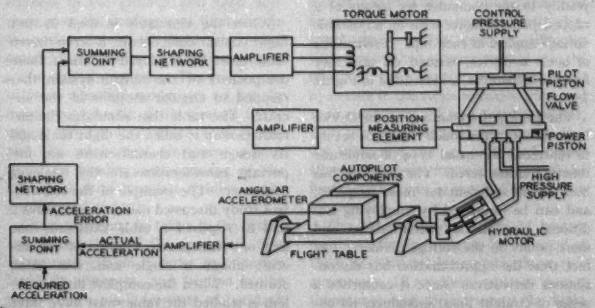

Figure 21. Block diagram of flight table servomechanism

tion of the motor. The time delay in the latter case is much larger than that of the former.

If the signal applied to the input of the position servomechanism varies rapidly, this time delay may be so important that this method of multiplication can not be used, and in this case a different method of multiplication is required. The device developed to meet the need is called an electromechanical strain-gauge multiplier and is described elsewhere in the literature. The principle of the device is illustrated by Figure 16. The multiplicand appearing as the electrical signal $V_1 \sin \omega_o t$, is applied to the input of an amplifier controlling an electromechanical transducer similar to a moving coil loudspeaker. The moving element of the transducer is coupled to the moving element (termed the armature) of a strain-gauge bridge. When the armature is displaced from neutral the resistances of the arms of the bridge are altered and a voltage is obtained from the bridge output accurately proportional to the deflection of the armature. The bridge output voltage is fed back to the amplifier input in negative sense with the result that the displacement of the armature becomes proportional to the variable V_1. In addition to the resistance elements of the strain-gauge bridge used in the feed-back path, the resistance elements of a second bridge are attached similarly to the armature, and the mechanical design is such that the unbalance in the second bridge is accurately proportional to that of the feed-back bridge. The excitation of the second bridge, however, is not fixed but is made proportional to the multiplier variable, V_2. Therefore the voltage output of the multiplying bridge is proportional to the product $V_1V_2 \sin \omega_o t$.

It has been possible to achieve an accuracy of 0.1 per cent and an effective time constant of one millisecond by careful design of the electrical and mechanical components of this multiplier. The small time constant is principally attributable to the fact that the maximum excursion of the strain-gauge armature is less than ± 0.002 inch. In practice four strain-gauge bridges are attached to the armature. The unbalance of each bridge is proportional, of course, to the multiplicand V_1. The feed-back bridge is constantly excited but each of the other three bridges can be separately excited, thus making it possible to form three products, V_1V_2, V_1V_3, and V_1V_4. This feature is found useful since in many problems several products must be formed which have a common multiplier. Another possibility is the computation with a single multiplier unit of the square, cube, or fourth power of a variable.

Representation of Arbitrary Functions

Problems are frequently encountered in which a portion of the data is not given analytically but in the form of curves or tables, and the analogue computer must include means for representing such information. While no general analogue means exists for handling this type of data several methods are useful and particular schemes or combinations can be chosen to fit the situation. Certain of the methods of representing arbitrary functions that have been found useful are described briefly.

One of the best methods of representing an arbitrary function is by means of specially wound potentiometers. Potentiometers can be wound to approximate an arbitrary function to within 0.1 per cent provided the function is reasonably smooth. If the function is a rapidly varying one the accuracy of representation is much less. The difficulty with this method is the expense involved in securing a reasonably accurate nonlinear potentiometer. Nevertheless, for several common types of nonlinear function the special potentiometer is one of the most suitable methods of analogue representation. Functions of the type $Y=X^2$, $Y=\tan X$, and $Y=1/X$ are readily handled over a range by this means.

Sometimes the function can be approximated to a sufficient degree of accuracy by a combination of linear and nonlinear functions. One of the simplest methods uses a series of linear functions to represent the desired function. This is illustrated graphically by Figure 17 in which a nonlinear function is approximated by several straight lines. This method of approximation is represented readily in the computer by means of a tapped potentiometer with an adjustable voltage applied at each tap. A schematic of such a device, termed an arbitrary function generator, is illustrated in Figure 18.

The principal advantage of the device is the facility with which it may be set up to represent the usual type of nonlinear function encountered. The accuracy has been found sufficient for most purposes, and can be improved by employing additional taps on the potentiometer and more points on the voltage divider. The fact that the approximation has discontinuous derivatives (since it comprises a series of straight lines) introduces no obvious difficulty since differentiation does not occur in the analogue computer. Difficulties may still be introduced by the fact that a time interval is required to establish in the computer the condition corresponding to a particular linear range. This time interval may or may not be important, depending upon the computer configuration, the magnitude of the change in slope, and the speed at which the problem is solved.

Another method of approximating an arbitrary function is by a combination of linear and nonlinear terms. Taylor's expansion, for example, is a well-known one in which the function $Y=f(X)$ is represented in the neighborhood of point a by the series

$$Y=f(a)+(X-a)f'(a)+\frac{1}{2}(X-a)^2f''(a)$$

where $f(a), f'(a), f''(a)$ and so forth are the value of the function and its derivatives at the point a. The analogue representation of such an expansion is straightforward although complex if many terms in the series are required. The square, cube, and higher order powers of the variable can be represented either by a series of potentiometers wound to represent the various power functions, or by use of multiplier units. Frequently a real saving in equipment and an improvement in accuracy is obtained by departing from a particular type of mathematical expansion. Combinations of trigonometric functions, power functions, and linear terms have been found useful.

The analogue problem becomes much more difficult when the arbitrary function has more than one dependent variable, such as $Z=f(X,Y)$. Series expansions are still useful but even more is accomplished by a judicious cut-and-try procedure involving both experience and intuition.

Flight Table

When the simulator is used to test flight control components, a servo-driven table must be employed to orient those components of the control system that respond to angular motions of the aircraft. The table that simulates the aircraft motion is called the flight table and its design and characteristics are important considerations in the analogue computer. The example of the roll control study discussed earlier (see Figures 2 and 3) required a table with only one axis of rotation since motion of the aircraft about a single axis was being studied. When the complete flight problem is studied the table must have three degrees of freedom in order to simulate

the pitch and yaw as well as the roll motion of the aircraft. The several degrees of freedom of the table, together with the severe requirements on the accuracy and dynamics of its control raised major development problems. These are discussed below.

Mechanical Features

The mechanical structure of the table, which is shown in Figure 19, consists of a platform for carrying the components to be tested, gimbal frames for obtaining the required angular motion, and gearing necessary to move each gimbal. Means are provided for moving the platform about four axes. Motion of the platform about the innermost axis simulates aircraft roll; the gimbal that carries the roll drive mechanism is moved in pitch; and the gimbal carrying the pitch drive mechanism is moved in yaw. Some problems study large motions of the aircraft in pitch and if only three gimbals were provided a condition could be encountered when the pitch gimbal moved through 90 degrees in which the table would have only two degrees of freedom. In order to avoid this situation, called gimbal lock, a fourth gimbal is provided. This gimbal moves in pitch in such a way as to maintain approximately an orthogonal configuration among the three innermost gimbals. Although such situations occur infrequently it is still possible to set up an aircraft maneuver that will produce gimbal lock. When gimbal lock is imminent it is necessary to stop the problem and reorient the gimbals. The problem can then be concluded.

The size of the gimbal frames is determined primarily by the size of the innermost platform, approximately 18 by 24 inches, which in turn is set by the dimensions and weight of the control components that are to be tested. Considerable care must be taken to insure maximum stiffness in the gimbals and their supports since the predominant limitation in the performance of the flight table is imposed by the modes of vibration present in the gimbal structure. The frequencies of these vibration modes are set by the moments of inertia of the gimbals themselves and the load which each carries and the mechanical elastances arising from the bending and twisting of the gimbals, lack of complete rigidity in the gearing, and so forth.

Great care must be taken in the design and construction of the gear train that drives each gimbal in order to minimize backlash, elastance, and friction in the train. Even small amounts of backlash or elastance can cause an oscillation in the flight table when it is servo driven that, although small, may obscure important difficulties in the aircraft control system under study.

Flight Table Instrumentation

The angular position, angular velocity, and angular acceleration of the flight table are measured and used in its control. Angular position measuring elements with the proper characteristics, such as resolvers and potentiometers, already were in existence and further development was unnecessary. However, it was found necessary to carry through a program of development to secure instruments with the desired properties to measure the other two quantities. In both cases it is desirable to measure the angular velocity and acceleration of the platform with respect to axes fixed in the platform in order to minimize problems of vector resolution. The measurement of angular velocity relative to space was obtained by means of a rate gyroscope. The measurement of angular acceleration is made by suspending a mass on frictionless pivots in such a way that it is relatively free to rotate but restrained from moving laterally. If the mass is then restrained in rotation by a spring, the rotation of the mass from its force-free position is proportional to the angular acceleration about the axis of rotation.

Both the angular accelerometer and the rate gyroscope are important links in the servomechanism controlling the flight table and it was necessary therefore that the resolution of both instruments be particularly good. Thus, while an error of about one part in 1000 is considered satisfactory, the resolution of both instruments should be better than this figure by about one order of magnitude. Principally because of the high resolution requirements it was decided to employ strain sensitive resistance gauges as the means of translating the small mechanical motions of each instrument into electrical signals. The primary difficulty with this method of measurement was the relatively large error due to mechanical hysteresis in the strain sensitive wires and their suspension. It was found, however, that the proper technique of suspending the wires and the use of a hard drawn alloy for the wire material permitted the hysteresis error to be reduced to less than 0.1 per cent.

The three principal types of instruments are shown in Figure 20. A total of three angular accelerometers, three rate gyroscopes, 15 resolvers, and one potentiometer is used to instrument the flight table.

Flight Table Servomechanisms

The dynamic characteristics of the servomechanisms driving the flight table gimbals are especially important. It is not only necessary that the time delay of each servo be small but that the servomechanism compensate in part for certain of the time delays of other portions of the control loop. Also important is the magnitude of the power that must be delivered by each servomotor in order to simulate the high angular accelerations and velocities frequently encountered in aircraft motion. It was found that a hydraulic-type servomechanism best fulfilled the various requirements and a block diagram of the system is illustrated in Figure 21. The servomotor is a rotating type, reversible hydraulic motor capable of developing ten horsepower and controlled by a power valve which supplies oil to either line of the motor. The power valve is supplied with oil at 3,000 pounds per square inch from a central source.

Because of the flow forces acting upon the valve and the requirement that it be positioned with a precision of better than 20 microinches, it is controlled by a pilot valve. The pilot valve is moved by an electrical torque motor, so named because of the limited angle through which the rotor turns, which in turn is excited from an amplifier.

Several types of feedback are employed to secure the desired characteristics in the servomechanism. In order to obtain precision of control the position of the power valve is fed back into the controlling amplifier through a compensating network. The angular acceleration of the flight table is measured by means of the angular accelerometer described above and the return of this signal into the controlling amplifier closes the dominant loop of the servomechanism. Because of the fact that an angular acceleration is set up in response to an electrical input signal, the control system is called an acceleration servomechanism. This is in contrast to a positional servomechanism in which the principal feed-back signal is proportional to the *position* of the output. In fact, however, both angular position and velocity signals are measured and fed back in the process of representing the aerodynamic and autopilot control functions of the aircraft.

The dynamic characteristics of the flight table servomechanism, including its load is determined by specifying the response of the acceleration servomechanism.

The effective time delay between the development of the required angular

acceleration and the application of the electrical signal is about two milliseconds.

Solution of a Typical Problem

One of the initial problems studied with the flight simulator was the determination of the stability characteristics of aircraft subjected to large disturbances. Under such conditions the linearity assumptions are not valid and several nonlinear effects must be considered. The complete problem is very complex and requires a lengthy program of machine computation for its solution. Certain specific cases, however, can be considered in a limited time and for the purpose of illustration, a simple problem is discussed here. The physical situation is that of an aircraft stabilized in roll by an elementary control system, but not stabilized in pitch and yaw.

A disturbance, such as might be caused by a gust, is applied simultaneously in roll and pitch, and the transient in each mode of the aircraft motion is to be determined.

The two principal assumptions in the problem are that the forward velocity of the aircraft is constant and that the nonlinearities are limited to certain simple types.

The first assumption is not particularly important for the specific case considered because of the fact that the transient is essentially complete before the aircraft velocity can change appreciably. The second assumption is untenable in many important cases, but was felt to be valid in the situation under study.

The assumption of constant forward velocity reduces the problem to one of five degrees of freedom. Five basic equations may be written, therefore, and under the conditions assumed are the following

$$L_\delta\delta + L_d = IX\frac{dp}{dt} + L_p p \text{ (roll equation)}$$

$$M_d = I_Y\frac{dq}{dt} + (I_Z - I_X)rp + M_q q + M_w w_q \text{ (pitch)}$$

$$0 = I_Z\frac{dr}{dt} + (I_X - I_Y)pq + N_r r + N_v v \text{ (yaw)}$$

$$-W_Z = m\frac{dw}{dt} + mVq - mvp - Z_w w \text{ (normal)}$$

$$W_Y = m\frac{dv}{dt} - mVr + mwp + Y_v v \text{ (lateral)}$$

In the foregoing equations, the symbols have the following definitions:

p, q, r = roll, pitch, and yaw angular velocities measured about the longitudinal, lateral and normal axes of the aircraft, respectively

v, w = rectilinear velocities along the lateral and normal axes

V = forward velocity of the aircraft

I_X, I_Y, I_Z = moments of inertia of the aircraft about the longitudinal, lateral, and normal axes

m = aircraft mass

W_Y, W_Z = components of aircraft weight along the lateral and normal axes, respectively

Z_w = aerodynamic force along the normal axis due to a unit velocity w

Y_v = aerodynamic force along the lateral axis due to a unit velocity v

L_p, L_δ = rolling moments (about the longitudinal axis) due to unit values of p and δ, respectively

M_q, M_w = pitching moments (about the lateral axis) due to unit values of q and w

δ = deflection of the ailerons

L_d, M_d = rolling moment and pitching moment disturbances

The preceding equations are written in terms of a co-ordinate system fixed in the aircraft and the nonlinear terms appear as products of dependent variables. However, the expression for the operation of the roll stabilization system and the explicit expressions for the gravity force require the use of the Euler angles, θ, ϕ and ψ that relate the aircraft axes to axes fixed in space. These equations introduce a number of trigonometric nonlinearities. For the type of control considered in this problem the equation is

$$\delta = k(\sin\theta\cos\phi\sin\psi - \sin\phi\cos\psi)$$

The angles θ, ϕ, and ψ are defined in standard texts on dynamics.

The components of the weight of the aircraft can be written explicitly in terms of the Euler angles in the following equations in which W is the total aircraft weight

$$W_Y = W\cos\theta\sin\phi$$
$$W_Z = W\cos\theta\cos\phi$$

Finally, the angular velocities p, q, and r can be expressed in terms of the Euler angles as follows

$$p = \frac{d\phi}{dt} - \frac{d\psi}{dt}\sin\theta$$

$$q = \frac{d\theta}{dt}\cos\phi + \frac{d\psi}{dt}\sin\phi\cos\theta$$

$$r = \frac{d\psi}{dt}\cos\phi\cos\theta - \frac{d\theta}{dt}\sin\phi$$

A solution of this problem for a particular set of parameters is shown in Figure 22. The machine record was traced to improve reproduction. A very large disturbance was applied in pitch and roll in order to make evident the nonlinear nature of the transient, which is particularly apparent in the record of the yaw transient where the frequency of oscillation is clearly twice the predominant mode occurring in pitch. The delay in the angle of sideslip transient also is interesting.

The angle of attack and angle of sideslip are the inverse sine functions of w/v and v/V respectively. This record was computed by the simulator in about 20 seconds. The speed of operation of the machine thus permits a few hundred of such records to be obtained in a day's time, with sufficient time allowed for parameter changes. The setup time of the machine of course is not included, and this will be more or less lengthy, depending upon the nature of the problem. Ample time must be allowed for this portion of the operation in order to verify carefully the accuracy of solution.

The foregoing example is illustrative of the type of problem encountered in aircraft dynamics. Approximately nine integrators, ten vector resolvers, 20 summing networks, 20 variable-potentiometer multipliers, 30 coefficient potentiometers, and 70 repeater amplifiers were used in the machine setup.

The generalized computer portion of the flight simulator has been in operation since the latter part of 1948 and the flight table has gone through its final tests and is being placed in operation at the present. Approximately 5,000 solutions, not including test solutions, have been computed by the machine since it began operation. The problems were such that each solution would require 100 to 1,000 hours to solve manually with a desk calculator. The operation thus far has been such to establish the merit of the design features and to prove the value of the simulator to aircraft dynamics and related problems.

No Discussion

Excitation System Performance with Motor-Driven Exciters

A. G. MELLOR
ASSOCIATE AIEE

M. TEMOSHOK
ASSOCIATE AIEE

THE performance of the motor-driven exciter as compared with the direct-connected exciter has been presented previously.[1] It has been demonstrated that a co-ordinated excitation system, consisting of an induction motor-driven exciter with added flywheel inertia, can meet satisfactorily the severe excitation requirements resulting from a 3-phase short circuit near the generator bus to which the motor-driven exciter set is connected.

The motor-driven exciter set may be one of a number of station auxiliaries on a bus which derives its power from either the main generator terminals through a transformer, from the external system through a transformer, or from a separate house generator. Under normal operating conditions or under emergency conditions resulting from the failure of an auxiliary power supply, it may be necessary to transfer the station auxiliaries from one bus to another. This study considers the case of the motor-driven exciter set which is transferred from an external power source to the terminals of the main generator. The electrical power input to the exciter motor is zero during the transfer period. The permissible time for this throw-over from one power source to another is determined by the ability of the generator to retain stability during the throw-over period.

A 3-phase fault at or near the terminals of the main generator results in a heavy load on the exciter as the main generator field current increases to several times normal during and following the fault period. The most critical operating condition for the exciter set during the short-circuit fault results when the motor driving the exciter is connected to the main generator terminals. In this case the power input to the exciter motor is zero during the fault period, and the voltage at the motor terminals after the fault is cleared is the recovery voltage of the generator.

The two main purposes of this study are: (1) to determine the length of time that can be taken to transfer the exciter motor from one power source to another and the effect of exciter set and system parameters on this transfer time, and (2) to determine the permissible clearing time of a 3-phase short circuit at the main generator terminals and the effect of exciter set and system parameters on this clearing time.

Scope of Study

The study was performed with the aid of the General Electric differential analyzer. For both the short-circuit and throw-over cases, the following variations of parameters were studied:

1. Effect of excitation methods:

(a). Hand control.
(b). Regulator control.

2. Effect of exciter-set inertia:

(a). $H=1.75$ (no added inertia).
(b). $H=5$.
(c). $H=10$.

3. Effect of main steam turbine generator size:

(a). 20,000 kilovolt-amperes ($H=6.0$, $T_{do}'=6.0$ seconds).

(b). 50,000 kilovolt-amperes ($H=4.5$, $T_{do}'=8.0$ seconds).

(c). 100,000 kilovolt-amperes ($H=3.5$, $T_{do}'=10.0$ seconds).

4. Effect of the size (equivalent reactance) of the system connected to main generator:

(a). Large system with reactance equal to 0.20 per unit (where base kilovolt-amperes equals generator kilovolt-amperes) including transformer.

(b). Small system with reactance equal to 0.40 per unit including transformer.

5. Effect of load power factor, with rated load on main generator:

(a). 0.8 power factor lagging (overexcited).
(b). 1.0 power factor.
(c). 0.8 power factor leading (underexcited).

6. Effect of load on main generator:

(a). Rated load.
(b). 125 per cent rated load.

Assumptions

1. Approximations of effect on exciter voltage of exciter set speed, exciter time constant, and regulator action are given by equation 8A of the Appendix.

2. The motor-driven exciter is unaffected by the other auxiliaries on the station bus.

3. The volt drop of the auxiliary power transformer has been neglected.

4. Regulators

(a). On throw-over, regulator action in holding the main generator terminal voltage constant holds exciter armature voltage constant as exciter speed decreases, until exciter ceiling voltage is reached, after which the exciter voltage is modified by exciter speed and field time constant.

(b). For a short circuit at the main generator terminals, regulator action is complete and instantaneous.

5. The system reactance as seen from the generator terminals remains the same before and after the 3-phase short circuit fault application.

6. Governor action is neglected.

7. The per-unit system of each case is

Paper 50-49, recommended by the AIEE Power Generation Committee and approved by the AIEE Technical Program Committee for presentation at the AIEE Winter General Meeting, New York, N. Y., January 30–February 3, 1950. Manuscript submitted March 23, 1949; made available for printing December 1, 1949.

A. G. Mellor and M. Temoshok are with the General Electric Company, Schenectady, N. Y.

Acknowledgment is given for the suggestions and constructive criticisms of C. Concordia, S. B. Crary, and J. B. McClure, and the aid in differential analyzer calculations of S. J. Jennings.

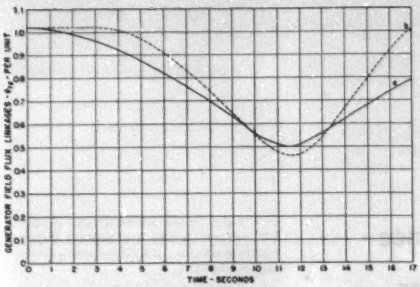

Figure 1(A). Effect of voltage regulator action on generator field flux linkages—throw-over case

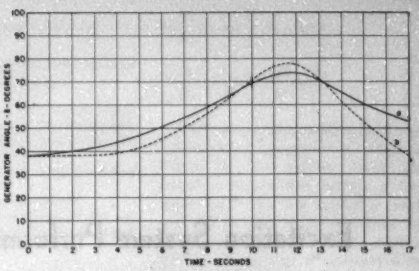

Figure 1(B). Effect of voltage regulator action on generator load angle—throw-over case

Curve *a*—with no regulator action. Curve *b*—with regulator action. Throw-over time = 10 seconds. System reactance = 0.2 per unit. Main generator: $H = 4.5$; $T_{do}' = 8.0$ seconds. Load = rated kilovolt-amperes, 0.8 power factor overexcited

based on the rating of the main generator of that case.

8. Damping torques are neglected.

Conclusions

THROW-OVER CASE (EXCITER MOTOR POWER SOURCE TRANSFER)

1. The maximum permissible throw-over time of a motor-driven exciter set with and without added inertia varies as follows, depending upon the initial operating conditions, the system parameters, and the type of main generator voltage regulator:

(*a*). Without added inertia (H of 1.75)—1.5 seconds to 6 seconds.

(*b*). With added inertia (total H of 5)—4 seconds to at least 10 seconds.

(*c*). With added inertia (total H of 10)—8 seconds to at least 10 seconds.

2. The ability of the excitation system to recover after the throw-over period is secondary to the ability of the system to sustain itself during the throw-over period.

3. (A). Favorable system operation for throw-over is appreciably affected by the following factors:

(*a*). Added exciter-set inertia; decreasing gain results with additional increases in inertia.

(*b*). Increase in the size of the system (lower system reactance) connected to the main generator.

(*c*). Increase in the size of the main generator with the resulting increase in open-circuit field time constant.

(*d*). A unity or leading power factor load on the main generator (generator underexcited), especially for short throw-over times.

(*e*). A high torque characteristic of the induction motor of the exciter set.

(*f*). Regulator action for short throw-over times and underexcited generator loads.

3. (B). Favorable system operation is slightly affected by:

(*a*). Regulator action for overexcited generator loads.

SHORT-CIRCUIT CASE

1. Short-circuit clearing times of one to two cycles less than the critical switching times based on constant generator field flux linkages are possible for all parameters studied.

2. The ability of the excitation system to recover after the short circuit is of equal importance with the ability of the system to sustain itself during the fault.

3. (A). Favorable system operation, during and after the short circuit on the main generator, is appreciably affected by the following factors:

(*a*). Increase in the size of the system connected to the main generator.

(*b*). Decrease in the size of the main generator with the resulting higher inertia factor.

3. (B). Favorable system operation is slightly affected by:

(*a*). Additional exciter inertia.
(*b*). Voltage regulator action.
(*c*). Smaller loads of lagging power factor.

4. Small main generators and generators connected to large systems can withstand longer switching times. Larger generators and generators connected to small systems require shorter switching times but for comparable switching times contribute to more stable system operation.

Discussion of Results

THROW-OVER CASE

The term throw-over implies a transfer of the exciter motor power from one source to another because of an emergency. This power transfer differs from a planned transfer where a synchronizing of the two power sources occurs, and at no time is the exciter motor without power. The minimum time for emergency throw-over is about one-half second and is determined by the ability of the mechanical switch in making the throw-over. This minimum time can impose a heavy, but safe, duty on the motor due to the trapped flux.[3]

If the throw-over is made from the main generator bus to the system or house generator bus, the actual voltage at re-energization due to the voltage drop through the auxiliary power transformer will approach that of the generator voltage used in the study.

If the throw-over is made from the system or house generator bus to the main generator bus, the voltage at the exciter motor terminals will be lower than that used in the study due to the voltage drop in the auxiliary power transformer. Analysis of the results to include the effect of this additional voltage drop indicates a sufficient margin of exciter motor power available for acceleration with no appreciable effect on the ability of the generator to recover and return to normal operation as indicated by conclusion 2 on the throw-over case.

The ultimate criterion in successful throw-over of the motor-driven exciter set from one power source to another is the stability of the main generator with re-

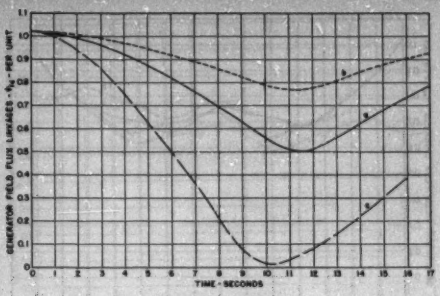

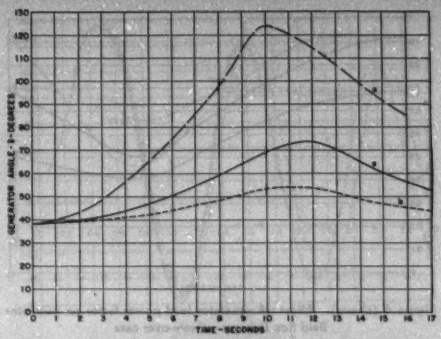

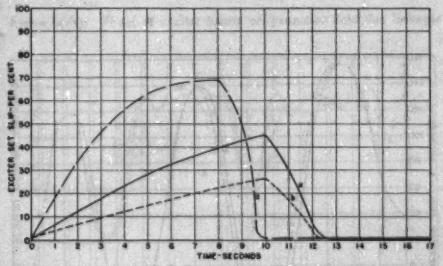

Figure 2(A) (top left). Effect of exciter inertia on generator field flux linkages—throw-over case

Figure 2(B) (above). Effect of exciter inertia on generator angle—throw-over case

Figure 2(C) (left). Effect of exciter-set inertia on exciter-set slip—throw over case

Throw-over times, curves *a* and *b*, 10 seconds; curve *c*, 8 seconds
Exciter set inertia constants: curve *a*, $H=5$; curve *b*, $H=10$; curve *c*, $H=1.75$
With no regulator action
System reactance = 0.2 per unit
Main generator: $H=4.5$; $T_{do}'=8.0$ seconds
Load = rated kilovolt-amperes, 0.8 power factor overexcited

spect to the system. The degree of stability determines the effectiveness of the parameters involved.

For any combination of system parameters, the variables determining the stability of the generator are the generator field flux linkages and the generator angle, as indicated by equation 16. In addition to serving as a criterion of stability, the variation in generator field flux linkages indicates fairly well the performance of other factors in the excitation system. These factors, exciter armature voltage and current, generator terminal voltage, and sometimes the exciter-set speed, vary in approximately the same manner as the generator field flux linkages, as these variables are generally interdependent.

For generators with hand control or normal regulator action and connected to a large system, throw-over times of ten seconds were possible if the motor-driven exciter set has added inertia of an amount resulting in a factor H of 5. The ten seconds time is not a limiting value of throw-over but contains a substantial margin of safety for most cases. It was not thought necessary to study throw-over times beyond ten seconds. The reduction of throw-over time from ten seconds to six seconds occurs with the use of exciter sets with no added inertia and with the generator connected to a small system. Curves *a* and *b* of Figures 1(A) and 1(B) indicate the variation of the generator field flux linkages and generator angle for a 10-second throw-over time. The limit of stability for this particular case results with the machine angle near 120 degrees, and because of reluctance torque the field flux linkages can decrease to about 0.1 per unit, indicating the stability margin available for the 10-second throw-over period.

Study of Figures 1(A) and 1(B) indicates the almost immediate recovery towards normal for both field flux linkages and machine angle after the throw-over was made, indicating very little improvement possible and that the major contribution to system stability would be in sustaining system variables at their normal values as long as possible.

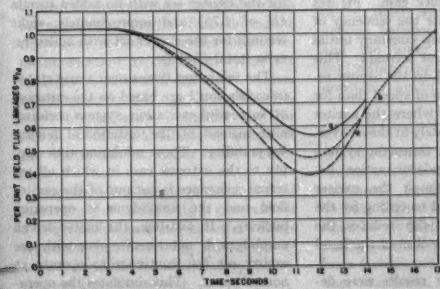

Figure 3. Effect of main generator size on generator field flux linkages—throw-over case

Curve *a*—$H=3.5$; $T_{do}'=10.0$ seconds
Curve *b*—$H=4.5$; $T_{do}'=8.0$ seconds
Curve *c*—$H=6.0$; $T_{do}'=6.0$ seconds
Throw-over time = 10 seconds
With regulator action
Exciter-set inertia, $H=5.0$
System reactance = 0.2 per unit
Generator load = rated kilovolt-amperes, 0.8 power factor overexcited

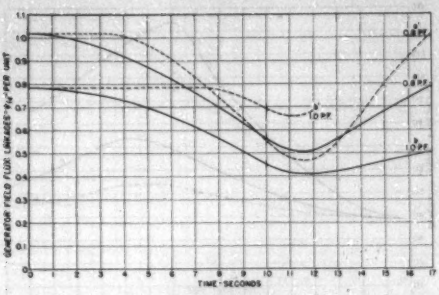

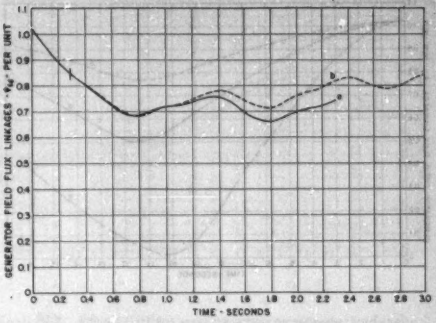

Figure 4 (above). Effect of generator load power factor on generator field flux linkages—throw-over case

Curves a and b—with no regulator action
Curves a' and b'—with regulator action
Throw-over time = 10 seconds
System reactance = 0.2 per unit
Main generator: $H = 4.5$; $T_{do}' = 8.0$ seconds
Load = rated kilovolt-amperes, 0.8 power factor overexcited, and 1.0 power factor
Exciter-set inertia, $H = 5.0$

Figure 5(A) (top right). Effect of voltage regulator action on generator field flux linkages—short-circuit case

Figure 5(B) (right). Effect of voltage regulator action of generator load angle—short-circuit case

Curve a—with no regulator action
Curve b—with regulator action
Switching time = 0.28 second
Exciter inertia constant, $H = 5.0$
System reactance = 0.2 per unit
Main generator: $H = 4.5$; $T_{do}' = 8$ seconds
Load = rated kilovolt-amperes, 0.8 power factor overexcited

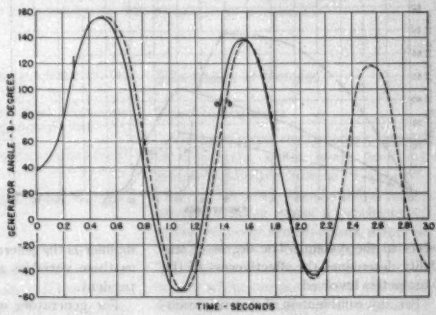

Effect of Exciter Set Inertia

The role played by added inertia to the exciter sets is significant as indicated by Figures 2(A) and 2(B). Instability of the generator resulted with a throw-over time of eight seconds with the use of the exciter set with no added inertia. Flywheel inertia aids in retaining stability but with a decreasing effect with additional increments of inertia. A very appreciable margin in generator stability results by increasing the inertia of the exciter set from the inertia factor H of 1.75 to H of 5. Much less gain in stability margin is experienced by increasing this inertia from an H of 5 to an H of 10, especially on throw-over times up to about five seconds.

Although the slip of the low inertia exciters may become two or three times as great as the slip for the large inertia exciters, the return to normal slip is made in less time as indicated by Figure 2(C).

Effect of System Reactance

Study of equation 16 of generator torque output against generator angle (or power output since the load angle change is small) shows the decrease in power resulting from an increase in system reactance. The change, from the large system with reactance of 0.2 per unit to the small system of 0.4 per unit, causes a decrease in maximum transient generator power of about 50 per cent which decreases the allowable time for throw-over.

Effect of Voltage Regulators

Use of voltage regulators results in little system performance gain. Figures 1(A) and 1(B) illustrate the tendency of regulator action to keep constant initial quantities up to several seconds. This imposes a heavier load on the exciter resulting in a greater loss of speed than for the hand control case where the exciter load decreases immediately at throw-over. For longer throw-over times the system performance with regulator action becomes inferior. Although the exciter voltage has been forced to ceiling by the regulator, the greater slip reduces the armature voltage below that of the hand control case.

Amplidyne regulator results were deduced by analysis of the results obtained with the study with other types of regulators.

Under normal operating conditions of the amplidyne, and assuming that the motor-driven amplidyne is thrown over with the motor-driven exciter, excitation system performance will approximate closely the performance with other types of regulators. Under these conditions the permissible throw-over times of the exciter set are approximately six seconds for the exciter set with no added inertia (H of 1.75) and approximately eight seconds for the exciter set with added inertia (total H of 5).

The minimum throw-over times stated in conclusion 1 are based on the criterion of successful excitation system performance instead of the criterion of generator stability. These minimum times apply to the extreme case in which all external resistance is cut out of the exciter field and the amplidyne is operating bucking. In addition, the motor-driven amplidyne is not thrown over with the exciter set but continues to operate at normal speed. This simulates the opera-

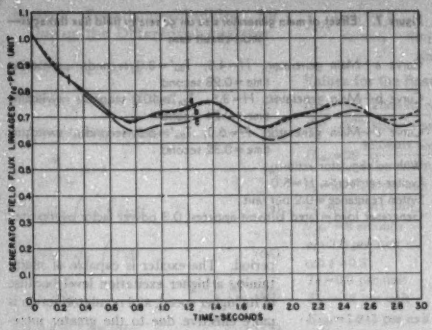

Figure 6(A). Effect of exciter inertia on generator field flux linkages

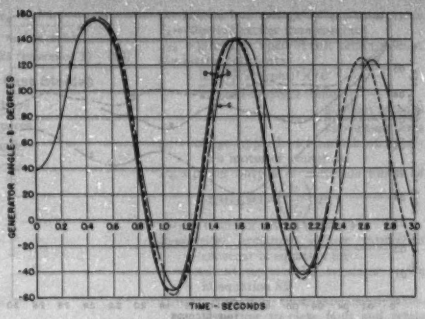

Figure 6(B). Effect of exciter inertia on generator load angle

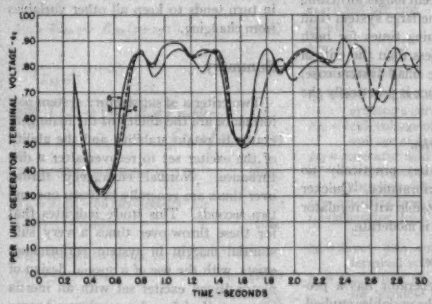

Figure 6(C). Effect of exciter inertia on generator terminal voltage

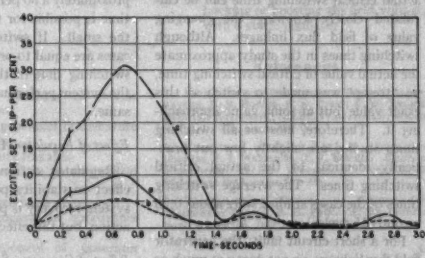

Figure 6(D). Effect of exciter inertia on exciter-set slip—short-circuit case

Switching time = 0.28 second. Exciter-set inertia constants: curve a—$H=5$; curve b—$H=10$; curve c—$H=1.75$. With no regulator action. System reactance = 0.2 per unit. Main generator: $H=4.5$; $T_{do}'=8.0$ seconds. Load = rated kilovolt-amperes, 0.8 power factor overexcited

tion of an amplidyne with very high inertia.

For this extreme case, to determine the absolute lower limit of throw-over times, the voltage at the exciter motor terminals after throw-over was taken as 70 per cent of rated generator voltage, a pessimistic value, instead of the actual voltage at the generator terminals which was considerably higher. Since during the throw-over period the exciter output remains constant at the initial value, the criterion of successful excitation system performance in this case is not the stability of the main generator but the margin of torque available to accelerate the motor-driven exciter after throw-over.

The addition of inertia to the amplidyne maintains the exciter output constant for a longer period, resulting in better voltage regulation but decreasing the margin of torque available for accelerating the exciter set after throw-over.

Effect of Power of the Generator Load

As the load power factor changes from lagging to unity to leading, performance of the system is improved as judged by generator stability. The improved performance is due to two factors as evidenced by a study of Figure 3: more effective regulator action exists because of the higher available incremental field voltage between exciter ceiling voltage and the lower steady-state generator field voltage; and the exciter set is slowed down less due to the smaller exciter load.

Effect of Generator Size

The generator inertia constant tends to decrease as the rating of the generator is increased. Small rating generators tend to have higher inertia factors and lower open-circuit field time constants and large rating generators tend to have lower inertia factors and higher open-circuit field time constants. The larger generators with their longer time constants possess the ability to sustain their field flux linkages as indicated by Figure 4, and therefore their electrical load for a longer period which tends toward greater stability.

Short-Circuit Case

There are two criteria of system performance during and after a 3-phase short circuit. One criterion of performance is the maximum time for clearing a 3-phase short circuit. A second criterion is system performance during and after the short circuit for various clearing times. For most cases studied a switching time of one cycle less than the critical switching time, based on constant generator field flux linkages, resulted in stable operation. For the worst cases a switching time of $2^1/_2$ cycles less than this critical switching time was necessary. But, as can be seen in Figure 5(A), the flux linkages decay appreciably during the fault period. The

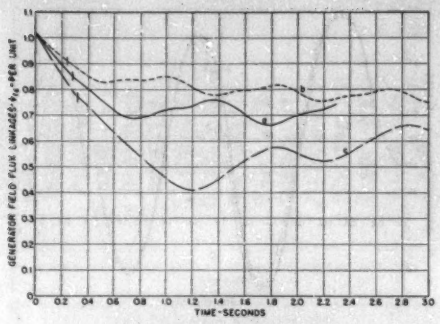

Figure 7. Effect of main generator size on generator field flux linkages—short-circuit case

Curve *a*—Main generator: $H=4.5$; $T_{do}'=8.0$ seconds; switching time = 0.28 second
Curve *b*—Main generator: $H=3.5$; $T_{do}'=10.0$ seconds; switching time = 0.24 second
Curve *c*—Main generator: $H=6.0$; $T_{do}'=6.0$ seconds; switching time = 0.32 second
With no regulator action
Exciter-set inertia, $H=5.0$
System reactance = 0.2 per unit
Generator load = rated kilovolt-amperes, 0.8 power factor overexcited

actual critical switching time can be calculated closely knowing the changing value of field flux linkages. Although switching times in the study approximate the actual value of critical switching time, no attempt was made to switch at this exact value, but at some value approaching it. Therefore, most or all switching times studied are slightly low but practically identical to the actual critical switching times. The average switching times of the cases studied were about 0.25 second (15 cycles).

For a short-circuit fault, the generator field flux linkages do not decay as much as for the throw-over case, and the generator can advance to about 160 degrees in most cases and still remain stable. The severe transients encountered during the fault make it as important for the excitation system to sustain itself during the fault as to recover after the fault is cleared. Figures 5(A) and 5(B) illustrate the almost equal increments of change in the generator field flux linkages and load angle during the fault and during the recovery period.

Effect of Exciter-Set Inertia

Study of Figures 6(A) and 6(B) demonstrates that practically no difference exists with exciters with inertia factors, H of 5 and 10 for the important variables, generator field flux linkages and generator load angle. The exciter-set slip, from time of short circuit to return to normal, varies inversely as the exciter-set inertia, as illustrated by Figure 6(C).

Effect of System Connected to the Main Generator

As for the throw-over case where the small system with its high reactance as seen from the generator terminals reduced the possible throw-over time, so for the short-circuit case the small system reduces the possible switching time. Approximately a 50 per cent longer switching time is possible for the large system than the small. If switching times for both cases are equal to or less than the critical switching time of the small system case, the system performance is practically the same.

Effect of Regulator Action

Regulator action has practically no effect on stability performance. Quicker system recovery is possible with regulator action, but this effect is moderate.

Effect of Generator Size

The size of the generator has a pronounced effect on all the variables studied. Since critical switching time varies as the inertia constant of the alternator, small machines having larger inertia constants would have the longest switching times. If switching times were equal to or less than the critical switching times of the largest generators, the latter have the better performance because of their longer field time constants, resulting in less change from normal for all variables. Figure 7, indicating the change in generator field flux linkages, is representative of changes in the other variables.

Effect of Main Generator Load and Power Factor

The effect of additional electrical load on the generator is to shorten the critical switching time. The actual system performance of generators carrying rated load and 125 per cent rated load is practically identical for the same switching times, for which both are stable.

Load power factor influences regulator action and exciter-set load. The excitation requirement for a leading power factor load is lower than for a lagging power factor load, and hence the exciter slows down much less during the short-circuit period. The exciter is capable of maintaining a higher excitation level because of its higher speed, and regulator action is more effective due to the greater increment between exciter ceiling and operating voltages. This sustained exciter output in turn tends to keep all other variables from changing.

Summary

Two criteria of satisfactory system performance are the ability of the main generator to retain stability and the ability of the exciter set to recover after a disturbance. Normal emergency throw-over times are generally between one and two seconds. This study indicates that for these throw-over times a very substantial margin in system performance exists, with the use of a special design of motor-driven exciter set with an inertia constant H of 5 and a maximum torque of about 325 per cent rated. This exciter set does not require a shorter throw-over time than any other essential station auxiliary. The high torque characteristic of the induction motor enables satisfactory system performance to be obtained with voltage at the motor terminals as low as 70 per cent of normal both on steady state and on re-energization after throw-over.

With this exciter, for a 3-phase short-circuit fault at or near the generator terminals, the maximum permissible switching time closely approaches the actual critical switching times which vary between approximately 11 and 20 cycles for the conditions studied. Practical switching times are generally below ten cycles. Additional special design considerations of the exciter set as presented in reference 1 further improve performance for the short-circuit fault operation.

Appendix

The system diagram is shown in Figure 8, and the vector diagram in Figure 9. The noureciprocal unit system of Park[3] was used for the generator equations.

System Equations—Modified for Use on the Differential Analyzer

$$I_{fd} = \psi_{fd} + (x_d - x_d')i_d \quad (1)$$

$$T_{do}'\psi_{fd} = \int E_{fd}dt - \int I_{fd}dt \quad (2)$$

$$(x_d' + x_e)i_d = \psi_{fd} - e_b \cos\delta \quad (3)$$

$$i_q = \frac{e_b}{x_q + x_e}\sin\delta \quad (4)$$

$$\int T_e dt = \int i_q d \int I_{fd}dt \quad (5)$$

$$\frac{2H}{2\pi f}p\delta = T_m t - \int T_e dt \quad (6A)$$

$$\delta = \int p\delta dt \quad (6B)$$

$$\cos\delta = -\int \sin\delta d\delta \quad (7A)$$

$$\sin\delta = \int \cos\delta d\delta \quad (7B)$$

$$E_{fd} - E_{fdo} = -E_{fdo}(s + k_T s') \quad (8A)$$

$$s' = \frac{1}{T_2 p + 1}(s + k_r) \quad (8B)$$

$$2H\left[\int s d_s - s\right] = \int P_m d \int e_m^2 dt - \int I_{fd}d \int E_{fd}dt \quad (9)$$

$$P_m = 659.4(s - 9s^2) \text{ for } s \leq 0.06 \quad (10A)$$

$$P_m = 21.91 - 65.89s + 68.82s^2 \text{ for } (0.06 \leq s \leq 0.40) \quad (10B)$$

P_m = induction motor curve for $(0.40 \leq s \leq 1.00)$ (10C)

$$e_{d1} = I_{fd} - x_d i_d \quad (11)$$

$$e_{q1} = x_q i_q \quad (12)$$

$$\frac{1}{2}e_{d1}^2 = \int e_{d1}de_{d1} \quad (13)$$

$$\frac{1}{2}e_{q1}^2 = \int e_{q1}de_{q1} \quad (14)$$

$$e_t^2 = e_{d1}^2 + e_{q1}^2 \quad (15)$$

$$T_e = \frac{\psi_{fd}e_b \sin\delta}{x_d' + x_e} - \frac{x_q - x_d'}{2(x_q + x_e)(x_d' + x_e)}e_b^2 \times \sin 2\delta \text{ (reference 1)} \quad (16)$$

Values for the Base Case Studied

$H_{gen} = 4.5$ kilowatt radians

$2\pi f$ 377 kilovolt-amperes

$H_{exc} = 29 \dfrac{\text{kilowatt seconds}}{\text{kilovolt-amperes}}$

$x_d = x_q = 1.1$ per unit

$x_d' = 0.15$ per unit

$T_{do}' = 8$ seconds

$e_t = 1.0$ per unit

$\cos\theta = 0.8$

$Te = 0.8$ per unit

$T_m = 0.8$ per unit

$E_{fdo} = 1.911$ per unit

$T_2 = 2.25$ seconds

$x_e = 0.20$ per unit

$e_b = 0.893$ per unit

$k_T = 0.5$

$k_r = -1.0$

Nomenclature

I_{fd} = field current of generator or exciter armature current

E_{fd} = field voltage of generator or armature voltage of exciter

ψ_{fd} = generator field flux linkages

e_d' = voltage proportional to generator field flux linkages

i_d = generator load current in direct axis

i_q = generator load current in quadrature axis

e_{d1} = direct axis component of generator terminal voltage

e_{q1} = quadrature axis component of generator terminal voltage

e_t = terminal voltage of main generator

x_d = generator direct axis synchronous reactance

x_q = generator quadrature axis synchronous reactance

x_d' = generator direct axis transient reactance

x_e = system reactance

δ = generator load angle between excitation axis and infinite bus voltage

θ = generator load power factor

T_e = electrical torque of main generator

T_m = mechanical torque input to generator rotor

e_d = infinite bus voltage in direct axis

e_q = infinite bus voltage in quadrature axis

T_2 = effective exciter time constant

T_{do}' = generator open circuit time constant

H = inertia constant = $\dfrac{0.231WR^2(\text{rpm})^2 \times 10^{-6}}{\text{kilovolt-amperes (base)}}$ kilowatt seconds / kilovolt-amperes

e_m = voltage applied to terminals of induction motor of exciter set

P_m = power output of induction motor of exciter set $= \left(\dfrac{V}{V_e}\right)^2 P_e$

s = slip of motor-driven exciter set

k_T = exciter armature voltage saturation constant in equation 8A

k_r = constant representing regulator action in equation 8B

Critical switching time—maximum allowable time to clear fault and retain generator stability

Buck-boost amplidyne regulator—rotating amplifier in exciter field circuit, bucking or boosting the field voltage, with a static regulator

References

1. Motor-Driven Exciters for Turbine Alternators, R. B. Bodine, S. B. Crary, A. W. Rankin. *Electrical Engineering* (*AIEE Transactions*), volume 65, May 1946, pages 290–97.

2. Transient Performance of Induction Motors, F. J. Magianiss, N. R. Schultz. *Electrical Engineering* (*AIEE Transactions*), volume 63, September 1944, pages 641–46.

3. Two-Reaction Theory of Synchronous Machines—Part I, R. H. Park. *AIEE Transactions*, volume 48, July 1929, pages 716–27.

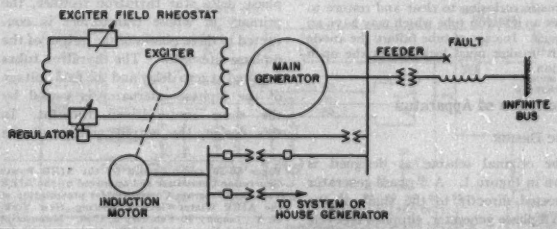

Figure 8. System line diagram

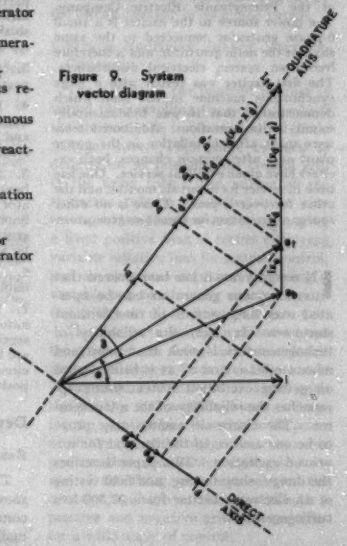

Figure 9. System vector diagram

No Discussion

Design and Test on Electronic Exciter Supplied from Common Shaft-Driven Generator

A. P. COLAIACO
ASSOCIATE AIEE

A. A. JOHNSON
MEMBER AIEE

J. E. REILLY
ASSOCIATE AIEE

Synopsis: Rectifier tubes have demonstrated their reliability over many years of service in industrial applications and to a limited extent on excitation systems. Thus in an effort to obtain more reliable and continuous excitation service, the decision was made to apply an electronic ignitron rectifier exciter to each of two new 37,500-kva 3,600-rpm turbogenerators in the Warren Plant of the Pennsylvania Electric Company. The power source to the exciter is a small 6-phase generator connected to the same shaft as the main generator, and is therefore free from system electrical disturbances. The first exciter was tested with a large synchronous machine in the shop which demonstrated that it was fundamentally sound in its operation. Additional tests were made after installation in the power plant and, after certain changes, both exciters have given excellent service. One has been in service for about six months, and the other for over a year. There is no other source of excitation for these two generators.

IN recent years it has been proved that synchronous generators can be operated over long periods of time without shutdown. In fact, the reliability of turbogenerators is such that more and more emphasis and effort is being placed on getting excitation system which approaches the reliability of the a-c generator. The electronic exciter may prove to be one answer to the demand for improved excitation. This paper describes the design, shop testing, and field testing of an electronic exciter for a 37,500 kva turbogenerator.

Requirements

To provide continuous service from a generator and fulfill other practical considerations, the electronic exciter should meet the following requirements:

1. It must be rugged, reliable, and capable of supplying continuous excitation over long periods of time. Ideally, it should never be the cause of a generator shutdown.

2. To give continuous service, component parts which require maintenance or replacement must be easily accessible and arranged so that a portion can be removed from service without affecting the generator load.

3. It should have a minimum of moving parts.

4. It must be capable of supplying the required excitation during system disturbances and have sufficient response to maintain stability.

5. It must be capable of operating over a broad range of d-c field current, from generator no load or less to maximum output. Short time values of field current much greater than full load requirements also must be available.

6. The supply to the exciter must be a reliable source free from system disturbances.

7. It must have anode circuit breakers with automatic reclosing to clear and restore to service an ignitron tube which may have an arc back. In case of tube failure the anode circuit breaker must lock out in the open position.

Description of Apparatus

Basic Design

The original scheme as designed is shown in Figure 1. A 6-phase generator connected directly to the shaft of the main 3-phase generator, supplied 60-cycle voltage to a 6-phase star ignitron tube rectifier, which supplied d-c power to the 250-volt field of the main generator. The field voltage of the main generator was regulated by an electronic regulator which controlled the firing point of the ignitron tubes and was set to maintain the 11.5-kv output voltage constant.

The 125-volt field of the 6-phase alternator also was supplied from the 6-phase rectifier. A motor-driven rheostat reduced the 250-volt output of the rectifier to the required 125 volts and also varied the field voltage to maintain a constant output voltage on the 6-phase generator, the action of the rheostat being controlled by a beam-type regulator. The unit is started up by energizing the field of the 6-phase generator from the station battery until the ignitron rectifier puts out the required voltage. After this the excitation for the 125-volt field is transferred from battery to rectifier and the unit continues self excited.

In service, it was found that the operation of the main generator required that the electronic regulator vary the output voltage of the ignitron rectifier frequently to maintain constant output voltage on the main generator. This also varied the voltage impressed on the field of the 6-phase alternator and required the motor-driven rheostat to operate just as frequently to keep the output voltage of this generator constant.

Since such frequent operation of a motor-driven rheostat is undesirable, the design was modified to that shown in Figure 2. This design is similar to that in Figure 1 except that the field of the 6-phase alternator is supplied by a 6-phase delta star thyratron rectifier, the primary of whose transformer is connected to three phases of the output of the 6-phase alternator. The thyratron tubes are fired at zero delay and the field voltage of the 6-phase alternator is varied by the same motor-driven rheostat. In this design, the output voltage of the

Paper 50-50, recommended by the AIEE Power Generation Committee and approved by the AIEE Technical Program Committee for presentation at the AIEE Winter General Meeting, New York, N. Y., January 30–February 3, 1950. Manuscript submitted November 2, 1949; made available for printing December 7, 1949.

A. P. Colaiaco and A. A. Johnson are with the Westinghouse Electric Corporation at East Pittsburgh, Pa., and J. E. Reilly is with the Westinghouse Electric Corporation, Pittsburgh, Pa.

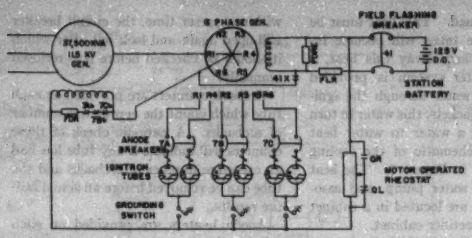

Figure 1 (above). Original design of electronic excitation system

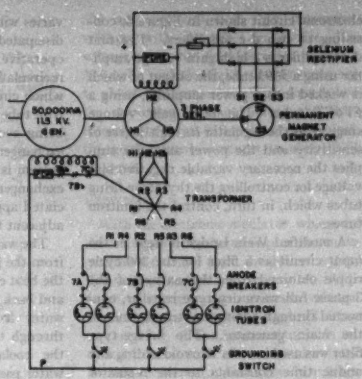

Figure 3 (right). Proposed design of electronic excitation system for future installation

thyratron rectifier is practically independent of the output of the ignitron rectifier. The motor-driven rheostat operates only when there are sudden large changes in the field current of the main generator, which are infrequent.

The ignitron tubes are divided into three groups of two tubes each, the two tubes of each group being connected to diametric phases of the 6-phase alternator through a 2-pole high-speed anode circuit breaker. Thus if a circuit breaker is opened, both tubes are de-energized. Each anode circuit breaker is provided with a field discharge switch in series with the field discharge resistor of the main generator so that if all three anode circuit breakers are opened, a discharge path is provided for the field of the main generator.

Each group of two tubes, its anode circuit breaker, grounding switch, firing tubes, and associated control circuit, are located in one of three individual compartments of the main rectifier cubicle. By opening the anode circuit breaker grounding switch, and firing tube circuit breaker, either of the ignitrons or associated firing tube can be replaced without disturbing the other four ignitron tubes which will continue to operate.

The six thyratron tubes supplying the field of the 6-phase generator are each provided with a disconnecting circuit breaker so that any one of these tubes may be replaced while the other five are in operation.

In Figure 3 is shown a scheme used in the Seward Plant of the Pennsylvania Electric Company. In this scheme, the 6-phase ignitron rectifier is supplied through a transformer by a standard 3-phase generator direct connected to the shaft of the main generator. The field excitation for this rectifier generator is in turn provided by a 3-phase bridge selenium rectifier supplied from a 3-phase permanent magnet generator which is direct connected to the shaft of the rectifier generator. No attempt is made to control the output voltage of the rectifier generator.

Ignitron Tube Firing Circuit

The firing circuit for each ignitron tube is of the anode firing type. A thyratron tube is connected in parallel with the ignitron through its ignitor. The thyratron is made conductive when its anode voltage is positive with respect to its cathode and its grid is released. It passes a current through the ignitor which initiates a cathode spot in the ignitron and fires it. When the ignitron fires, its low arc drop puts out the thyratron. The firing circuit is shown in Figure 4. Should the ignitron fail to conduct, the thyratron will try to carry the load current but will be tripped out by the circuit breaker in its anode circuit.

Ignitron Rectifier Direct Voltage Control

The output of the ignitron rectifier is varied by controlling the point at which the ignitron tube is released on its anode voltage wave. This point in turn is determined by releasing the control grid of the firing tube. The release of the thyratron tube is controlled by a sine wave grid transformer, a rectox supplying a fixed positive bias, a rectox supplying variable negative bias for manual control, and an electronic regulator supplying a variable negative bias for automatic control. The circuit is shown in Figure 4.

The sine wave voltage impressed upon the grids of the firing tubes is delayed almost 90 degrees from the tube anode voltage and is connected in series with the positive and negative biases. Varying the negative bias determines the point at which the grid voltage becomes more positive than the characteristic grid voltage of the firing tube and releases the tube for conduction. The use of both a positive and negative grid bias provides for a wide angle of control.

Electronic Voltage Regulator

The main generator voltage regulator employed with the electronic exciter is an

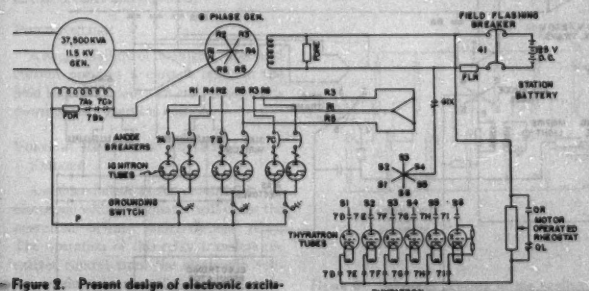

Figure 2. Present design of electronic excitation system as in operation

electronic circuit shown in Figure 5, consisting of two d-c amplifiers. The first d-c amplifier is a high gain voltage amplifier using a *5693* tube, the output of which is worked into a power amplifier, using a *6V6GT* tube. The high gain voltage stage gives the regulator its high degree of sensitivity and the power amplifier supplies the necessary variable negative bias voltage for controlling the thyratron firing tubes which, in turn, control the ignitron tubes.

A modified Wein bridge is used in the input circuit as a filter for the 360-cycle ripple obtained from the output of the 3-phase full-wave dry-type rectifier, connected through a potential transformer to the main generator. The bridge-type filter was used in order to avoid adding any undue time constants to the regulator circuit.

Ignitron Tube Auxiliary Anode

Auxiliary anodes are provided in the ignitron tubes to provide more positive pickup. The auxiliary anode is located close to the mercury pool and strikes an arc as soon as the ignitor is fired. The arc then transfers to the main anode as soon as it becomes sufficiently positive to pick up the arc. The auxiliary anode voltage usually is 30 degrees leading with respect to the main anode. The circuit is shown in Figure 4.

Ignitron Tube Cooler System

An arc drop of approximately 16 volts in the ignitron tubes, generates heat within these tubes, the magnitude of which varies with the load. This heat must be dissipated or the tubes will become inoperative. To carry away this heat, a recirculating water system is provided which circulates water through the ignitron tube water jackets, this water in turn being cooled by a water to water heat exchanger. A schematic of the cooling system is shown in Figure 6. The heat exchanger shell, water pump, and associated apparatus are located in a cabinet adjacent to the rectifier cabinet.

The water pump takes the heated water from the ignitron tubes, forces it through the heat exchanger shell where it is cooled and back again through the tubes. Raw water from an outside source passes through the heat exchanger and acts as the coolant. The temperature of the water passing through the ignitron tubes is controlled by a temperature regulating valve which regulates the quantity of raw water passing through the heat exchanger, and whose control bulb is located at the outlet to the ignitron tubes. A pressure regulator keeps a constant raw water pressure on the system. An expansion tank provides a reservoir of recirculating water and also maintains a positive pressure at the intake to the water pump to prevent air from entering the system.

Protection and Alarm Circuits

A number of devices are provided to warn of failures and impending troubles.

Arcbacks

In case of an arcback, the tube which arced-back and its companion tube are disconnected from the 6-phase generator by the anode circuit breaker which recloses immediately once the arcback is cleared. If the tube arcs-back again within a preset time, the circuit breaker will open again and lock out after which it should be checked before it is reclosed manually.

Arcback counters are provided on each tube which count the cumulative number of arcbacks. A periodic check of these counters will indicate if any tube has had an excessive number of arcbacks and the tube can be removed before an actual failure results.

Anode heaters are provided on each tube to keep the anode warm during light load periods and shutdowns to prevent mercury from condensing on the anode surface. Such condensation may cause arcbacks.

Misfires

In case the firing tube fails to fire the ignitor, a misfire light will indicate. The misfire lights are neon bulbs connected through a transformer across a resistor in series with the auxiliary anode as shown in Figure 4. When the auxiliary anode picks up, voltage appears across the resistor and lights the neon bulb. If the auxiliary anode does not pick up due to failure of the ignitor to fire, the bulb remains dark. If an ignitron tube should fail to conduct, the firing tube in parallel with it will try to carry all of the load current and the circuit breaker in its anode lead will trip it out giving an indication at the control desk.

Tube Over Temperature

If one of the ignitron tubes becomes overheated, an over temperature switch will operate and give warning. The tube can then be removed as stated previously and checked.

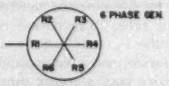

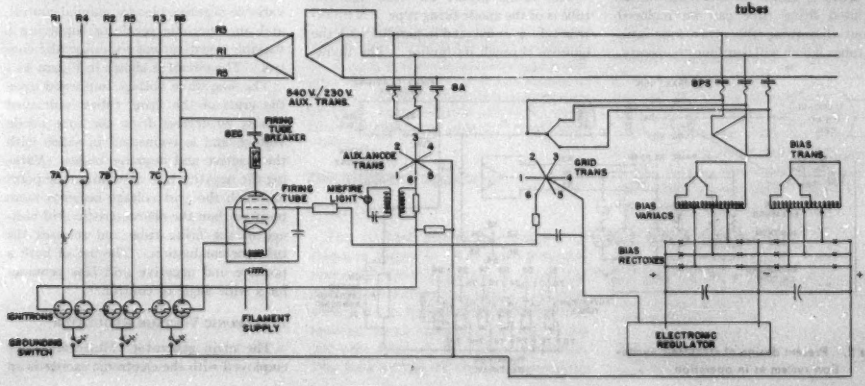

Figure 4. Firing control circuits for the ignitron tubes

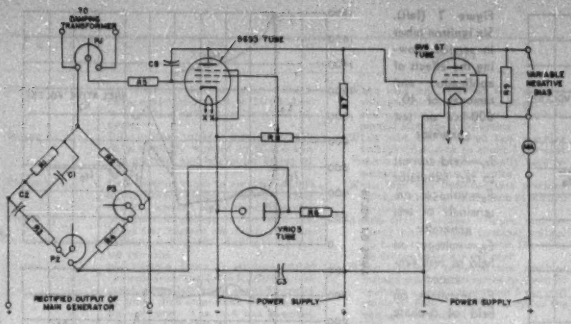

Figure 5. Schematic diagram of the electronic regulator for generator voltage

Failure of the Water Pump

If for some reason the water pump breaks down or fails to deliver the required pressure, a pressure relay operates and can be used to warn the operator and operate a motor-driven valve which will supply emergency water to the ignitron tubes. This emergency water is made to flow through the heat exchanger by a check valve in the exhaust of the water pump, through the ignitron tubes, the expansion tank, and out the overflow. The water pump can then be isolated by valves and serviced.

A bypass is provided around the pressure and temperature regulators in the raw water system so that they can be removed and serviced without interruption, the raw water being regulated manually.

Failure of Thyratron Rectifier Tubes

Failure of any of the thyratron rectifier tubes can be noted by visual inspection and the tube isolated by its respective circuit breaker and replaced.

Field Failure

A sudden failure of main generator field current operates a current relay in the field leads and causes an emergency shutdown of the generator unit.

Voltage Regulator Potential Failure

A sudden failure of the potential to the electronic voltage regulator will cause the operation of an under-voltage relay. The operation of this relay transfers the exciter control from the electronic voltage regulator to manual control and a preset value of excitation.

Exciter Characteristics

Current Output

Each of the six ignitron tubes in the exciter has a continuous current rating of 200 amperes. Thus with six tubes, which are normally in service, the exciter can supply a continuous direct current of 1,200 amperes as against the required full load excitation on the main generator of about 600 amperes. With four tubes a continuous current of 800 amperes can be supplied which also is in excess of the generator full load requirement. Since each tube has an overload capacity of 300 amperes for two hours, even two tubes can supply practically full load excitation for a short time.

The normal voltage across the main generator field is about 220 volts. The ceiling voltage at no load on the exciter with six tubes is about 375 volts, and with four tubes about 355 volts. With two tubes the ceiling voltage at no load on the exciter is about 265 volts.

The field winding of the main generator has a resistance of about 0.356 ohm at 75 degrees centigrade. Thus with a normal voltage of 214 volts, the required 600 amperes will flow. At maximum voltage, with six tubes in service, the voltage across the field increases to about 330 volts and the field current increases to about 920 amperes. With four tubes the maximum voltage across the field increases to about 310 volts, and therefore the field current increases to about 870 amperes.

Response

With the electronic regulator, whenever the voltage on the terminals of the main generator changes from the desired value, the voltage output of the exciter tends to go to maximum or minimum voltage. For a drop in voltage the angle of delay in the firing of the ignitron tubes is reduced to zero until the terminal voltage is back to normal. For a rise in voltage the angle of delay is a maximum. The exciter has a rate of response in excess of minimum speed of response ratio of 0.5 used on most power system excitation systems.

Recovery After Tube Arcback

As demonstrated by tests, a tube arcback has a relatively minor effect on the terminal voltage of the main generator. The voltage is affected for only a few cycles and the maximum deviation from normal is less than 5 per cent. Thus by the high-speed operation of the anode circuit breaker, the tube is removed from service long enough for elimination of the arcback and then reinserted into service.

Sensitivity to Normal System Voltage Regulation

In conjunction with the electronic regulator, the electronic exciter is very sensitive to changes in generator-terminal voltage and corrections are made very rapidly. Even small changes from normal voltage instantly affect the output of the exciter and therefore high speed of

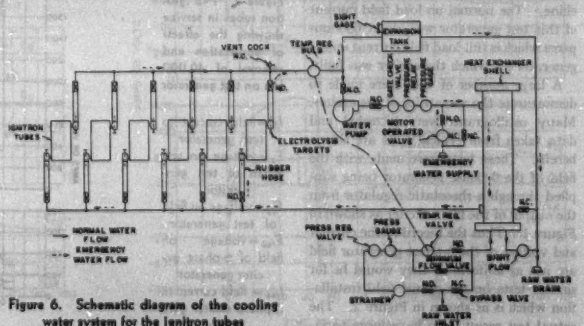

Figure 6. Schematic diagram of the cooling water system for the ignitron tubes

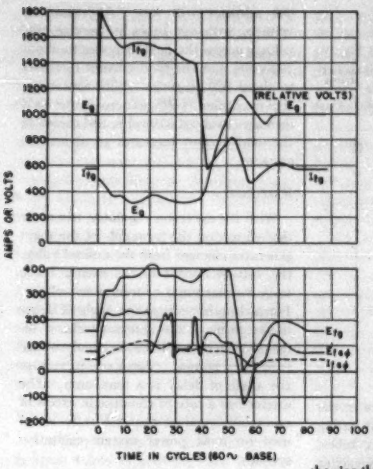

Figure 7 (left). Six ignitron tubes in service showing the effects of application and removal of 40,000-kva on test generator

I_{fg} = field current to test generator
E_g = voltage on terminals of test generator
E_{fg} = voltage on field of test generator
$E_{f6\phi}$ = voltage on field of 6-phase exciter generator
$I_{f6\phi}$ = field current in 6-phase exciter generator

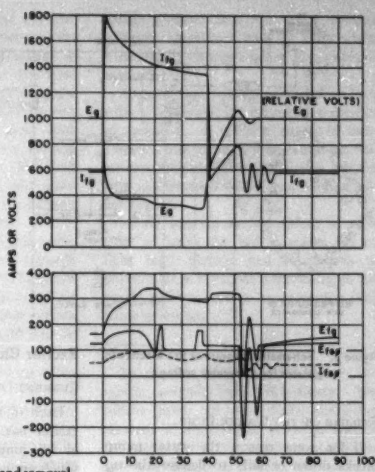

Figure 8 (right). Four ignitron tubes in service showing the effects of application and removal of 40,000 kva on test generator

response is obtained for minor variations in voltage.

Effects of System Frequency

The electronic regulator and the electronic exciter are not affected by variations in system frequency over a wide range. Even if the system frequency should drop to as low as 50 cycles, the exciter system will maintain substantially the same generator terminal voltage as normally exists for 60 cycles.

Laboratory Tests

The electronic exciter was tested before it was shipped. The 625-kva 6-phase 3,600-rpm generator was driven by a d-c motor at rated speed. The output of the rectifier was fed to the field of a 20,000-kva High Power Laboratory Test machine. The normal no-load field current of this test generator was about 600 amperes which is full-load field current on the generator for which the exciter was built.

A large number of tests were made to demonstrate the versatility of the exciter. Many oscillograms were recorded and data taken from typical tests are shown herein. These tests were made with the field of the 6-phase generator being supplied through a rheostatic regulator from the output of the main exciter as shown in Figure 1. Thus the record of the current and voltage of the 6-phase generator field are not as uniform as they would be for similar tests on the actual field installation which is as shown in Figure 2. The actual test results also have more variations in the main generator field current and voltage than would be the case for the final layout.

Typical results showing the variations in main field current (I_f), main field voltage (E_f), 6-phase generator field current ($I_{f6\phi}$), 6-phase generator field voltage ($E_{f6\phi}$) and the terminal voltage of the 20,000-kva test generator (E_g), plotted against time in cycles, are given in Table I.

In each of the tests when 40,000 reactive kilovolt-amperes of load was applied to the test machine the field current increased suddenly to about 1,800 amperes, induced from the machine armature. In every test the exciter operated properly. Tubes were switched out and in for all combinations and in each test the voltage was stabilized quickly.

Figure 12 is an oscillogram showing the various currents and voltages for one test where the excitation to the 6-phase generator was transferred from the battery source to the main rectifier. It will be noted that the field voltage is not what is regarded commonly as d-c voltage, but rather a whole series of half waves having an average value which is a d-c voltage. The field current, however, is very nearly a smooth direct current record.

When starting, the excitation for the 6-phase generator field was obtained from a separate d-c service. After voltage was built up on the output of the exciter, the

Figure 9. Two ignitron tubes in service showing the effects of application and removal of 40,000 kva on test generator

I_{fg} = field current to test generator
E_g = voltage on terminals of test generator
E_{fg} = voltage on field of test generator
$E_{f6\phi}$ = voltage on field of 6-phase exciter generator
$I_{f6\phi}$ = field current in 6-phase exciter generator

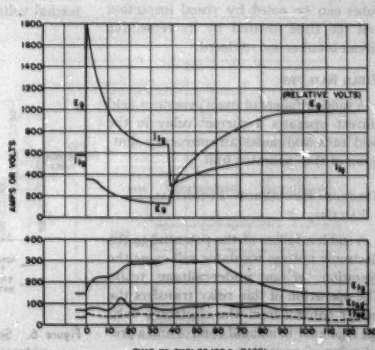

Table I

Tests		Results
Figure 7	six ignitron tubes in service—40,000 rkva suddenly applied to 20,000-kva test machine and left on for about 41 cycles	When load was removed test machine voltage (E_g) went to about 13 per cent above normal and was finally back to normal after about 30 cycles
Figure 8	four ignitron tubes in service—40,000 rkva suddenly applied to 20,000-kva test machine and left on for about 40 cycles	When load was removed test machine voltage (E_g) went to about 7 per cent above normal and was finally back to normal after about 35 cycles
Figure 9	two ignitron tubes in service—40,000 rkva suddenly applied to 20,000-kva test machine and left on for about 38 cycles	When load was removed test machine voltage gradually came back to normal in about 70 cycles
Figure 10	six ignitron tubes in service—610 amperes field current on 20,000-kva test machine at no load. Arcback imposed on one tube	Anode circuit breaker tripped and reclosed with machine terminal voltage E_g back to normal in about 15 cycles E_g dropped about 7 per cent
Figure 11	six ignitron tubes in service—40,000 rkva suddenly applied to 20,000-kva test machine and left on for about 38 cycles at which time an arcback was imposed on one tube. The load was removed after about 40 cycles	When load was removed test machine voltage gradually increased in about 25 cycles to a peak value about 6 per cent above normal. In about 35 cycles the voltage was normal

6-phase generator field was transferred automatically to the output of the exciter. This is the normal start-up procedure for the actual installation where the separate d-c source is the 125-volt station battery.

Field Tests

With the installation of the first of the two electronic exciters as described previously, field tests were planned to determine the best operating procedures and the extent of the capabilities of this form of excitation. The tests which were performed are discussed in the following. Figure 13 shows an electron exciter installation.

Stability Test Under Full Automatic Control

The first stability test was made on the original design of the exciter as shown in Figure 1 where excitation to the main generator and the 6-phase generator was obtained from one 6-phase ignitron rectifier. As stated previously, a voltage regulator controlled the output voltage of the 6-phase generator by means of a motor-operated rheostat in the field circuit.

When excitation to the main generator was varied by means of the electronic voltage regulator, the field voltage of the 6-phase generator also changed. This necessitated operation of the 6-phase generator voltage regulator and the motor-operated rheostat to attempt to maintain its terminal voltage, but it caused an excessive number of operations of the 6-phase generator voltage regulator and motor-operated rheostat.

The system was modified to use a small 6-phase thyratron rectifier operating from three phases of the 6-phase generator as a source of d-c excitation to the 6-phase generator. This eliminated the excessive number of operations of the 6-phase generator regulator and the apparent instability between the two voltage regulators. After the separation of the two regulator circuits, operation was satisfactory under fully automatic control. No antihunt devices were found necessary under no-load conditions on the main generator.

With the above changes in the excitation system, the exciter operated satisfactorily under adverse conditions with various numbers of tubes made inoperative, with the main generator carrying load.

Automatic Control Test

The first tests were performed on the main ignitron rectifier exciter with the generator under the control of the electronic voltage regulator, but with the generator disconnected from the system. The anode circuit breaker for one pair of ignitron tubes was opened and no effect was noted on the generator voltage. A second anode circuit breaker was opened, leaving only a single pair of ignitron tubes

Figure 10 (below). Six ignitron tubes in service showing effects of tube arc-back with 610 amperes exciter output

Figure 11 (right). Six ignitron tubes in service showing effects of application and removal of 40,000 kva on test generator plus a tube arc-back

I_{fg} = field current to test generator
E_g = voltage on terminals of test generator
E_{fg} = voltage on field of test generator
$E_{f6\phi}$ = voltage on field of 6-phase exciter generator
$I_{f6\phi}$ = field current in 6-phase exciter generator

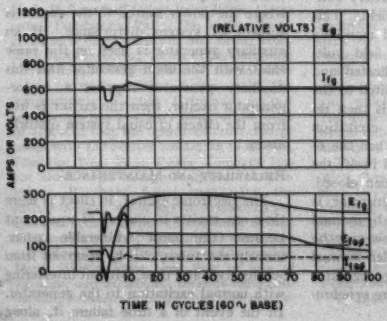

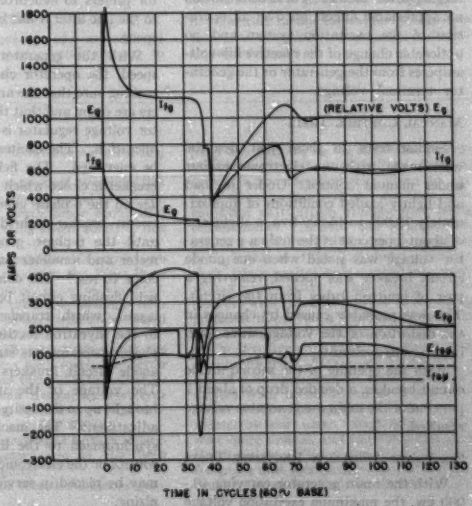

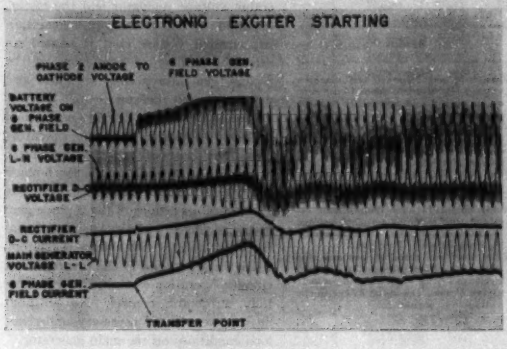

Figure 12. Oscillogram showing currents and voltages when excitation to 6-phase generator was transferred from battery source to the main rectifier

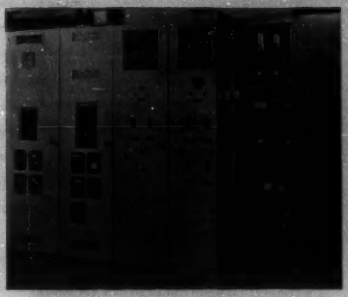

Figure 13. Electronic exciter in place showing the two switchgear compartments on the left, the heat exchanger compartment on the right, and the three tube compartments

in operation, and again no effect was noted on the generator voltage. During these tests of eliminating various pairs of ignitron tubes, a cathode-ray oscilloscope was connected across each of the three phases of the main generator by means of potential transformers to view the wave shape of the voltage and no harmonics or wave distortion was noted on the screen.

The same tests were again performed as described previously with the main generator operating in parallel with the rest of the system and carrying consecutive loads of 10,000-, 20,000-, and 30,000-kw at approximately 90 to 95 per cent lagging power factor. These tests showed no appreciable effects on over-all operation of the excitation system and no noticeable change of the reactive kilovolt-amperes from the generator or the generator terminal voltage.

Manual Control Tests

Similar tests to those just describe were made with the electronic exciter under manual control. Under no-load and lightly-loaded conditions of approximately 10,000 to 15,000 kva, a slight rise of about 3 per cent of the main a-c generator voltage was noted when one anode circuit breaker was opened, removing a pair of ignitron tubes from the circuit. This was probably caused by changes in the distortion of the voltage wave form in the control circuits.

With the opening of the second anode circuit breaker, a decided drop of about 7 per cent of the main a-c generator voltage resulted.

Six-Phase Auxiliary Rectifier Tests

With the main generator carrying 40,000 kw, the maximum excitation voltage required for the 6-phase generator to maintain its output voltage constant is 95 volts. The removal of two electrically adjacent thyratron tubes, an extreme condition, gives 97 volts of direct current. The difference between these two voltages is taken up in the drop across the rheostat in the field circuit.

Operating Technique

Normal Start-Up

The normal starting procedure can be covered in three to four steps, depending on the particular method which the operator prefers to synchronize the generator to the line after it has been brought up to speed.

With the generator at synchronous speed, the operator checks the controls, making sure that the anode circuit breakers are open, and that the 6-phase generator voltage regulator is set for automatic operation. The exciter is then ready to be energized. The field flashing circuit breaker is closed which puts battery voltage on the 6-phase generator field. This circuit breaker is held closed manually until the 6-phase generator field voltmeter and ammeter have indicated and come to rest. The control switch to the field flashing circuit breaker is then released, which transfers the excitation to the thyratron rectifier. When the 6-phase generator has stabilized itself, the anode circuit breakers are then closed. The voltage of the main generator is brought up to the desired value by manual adjustment. The machine now may be synchronized to the line under manual control or the electronic voltage regulator may be placed in service before synchronizing.

Normal Shutdown

For normal shutdown, the operator performs the usual operation of removing the generator from the line, then opens the three anode circuit breakers, thereby removing all excitation from the main generator. In order to remove voltage from the 6-phase generator, the voltage regulator is taken out of service and the motor-operated rheostat is run to the all-in position which causes the voltage to collapse.

Application

System Disturbances

This type of electronic exciter is a self-contained unit having its own source of power from the 6-phase generator which is entirely free from system disturbances. In this respect this electronic exciter is comparable to other exciter systems where direct-connected commutator exciters are used. It is better in this respect than a separate motor-generator set where the power source to the motor is subject to system disturbance. If an auxiliary generator is used on the same shaft with the main generator and this auxiliary generator supplies a motor-generator exciter, then the exciter is free from the effects of usual system disturbances.

Reliability and Maintenance

The electronic exciter, in effect is more than one exciter in one set of equipment because the most vulnerable parts, namely the tubes, can be removed from service, two at a time, without interfering with normal excitation to the generator. In the event of a tube failure it, along

with a companion tube, is removed automatically from service by an anode circuit breaker and can be replaced and restored to service. For other types of excitation systems, certain types of failures will cause an immediate generator outage. It is expected that this type of electronic exciter system will be relatively free from troubles which will cause generator outages; however, experience must supply the proof.

Required Space

The electronic exciter requires more space and volume than conventional-type direct-connected commutator exciters. However, it does not require more and probably not as much space and volume as a motor-generator type separate exciter. The electronic exciter does not necessarily require critical floor space because the exciter under discussion is mounted on a balcony adjacent to and on the same level with the generator terminal leads under the generator.

Voltage Regulation and System Faults

The output of the electronic exciter can be varied over a wide range by controlling the point on the voltage wave at which tube firing takes place. No generator rheostat is required to get the full operating range of field currents for the generator. Since the voltage regulator controls only the firing circuit, it can be and is a low energy device; in this case it is an electronic regulator. The electronic exciter also has the capacity to build up to its ceiling voltage practically instantaneously, making it well suited for high speed of response when increased excitation is required for system transient stability.

Due to the time constant of the generator field circuit, the time required for the regulator and exciter to take action is of little significance since all types of regulators take action in about three cycles or less. The speed with which ceiling voltage is reached, and the magnitude of the ceiling voltage, however, affect the speed at which generator field current is increased. The electronic exciter has high speed action, a fast change to ceiling voltage, and a high ceiling voltage.

Due also to the time constant of the generator and to high-speed relays and circuit breakers, the electronic exciter will not cause higher short-circuit currents on system faults. For faults which hang on for longer periods of time the currents may be affected slightly, but the reactance of the generator increases with time, thus introducing a limiting effect.

Cost

The electronic exciter costs between two and three times the cost of a conventional direct-connected exciter. The cost of a spare excitation source, however, should be considered when comparing the over-all cost of excitation facilities. No spare source of excitation is required with this type of electronic exciter. The over-all cost must therefore be evaluated for each application.

Advantages

1. Parts may be maintained or replaced with rest of unit in service.
2. It is a static device.
3. Has inherent qualities of a conventional direct-connected exciter with respect to freedom from system disturbances, high-speed excitation, range of excitation, and so forth.
4. Expected to prevent generator outages caused by failure of excitation.
5. Equivalent to more than one conventional exciter.

Disadvantages

1. High cost as compared with conventional types of exciters having d-c generators direct-connected or motor-driven may be, in some cases, a detrimental factor.
2. Requires more space and volume than a conventional direct-connected exciter although the space and volume taken by conventional spare exciters must be evaluated.
3. Has many more component parts, consisting of control transformers, tubes, control wiring, contacts, and so forth than are required by conventional excitation systems.

Conclusions

1. Laboratory and field tests under normal and abnormal conditions, indicated that the electronic exciter would perform in a manner which would provide dependable excitation.
2. The service record, of over one year, indicates that the electronic exciter is providing satisfactory excitation for normal operation and under system fault conditions.
3. The separate a-c generator provides a source of power for the exciter which is free from system disturbances. It is therefore a type of direct-connected exciter.
4. This exciter has a high speed of response and a high ceiling voltage.
5. This exciter is equivalent to more than one exciter since it is possible to provide continuous excitation while parts of the exciter are out of service for maintenance.
6. The cost of this excitation system is in excess of that for a conventional direct-connected exciter.

Discussion

H. A. P. Langstaff (West Penn Power Company, Pittsburgh, Pa.): The authors have given us a very interesting and rather complete story involving the use of the electronic exciter which should prove of considerable value to the industry. I note that the Pennsylvania Electric Company is not providing a spare exciter; therefore, it must be assumed that the operators must change tubes with the exciter remaining in service. This the West Penn Power Company has not done even though facilities are provided. We have found that when the exciter is taken out of service to make a tube change, we experience an epidemic of bad tubes and we end up by changing more than one before the exciter is returned to service. Most failures have been due to loss of vacuum, and we suspect there is some connection between a tube that has been in service for a while and allowed to cool, causing loss of vacuum.

If the manufacturers could overcome this vacuum-tube problem, it would prove the electronic exciter much more economical with each tube costing about $300.00, this becomes expensive.

The exciters discussed in this paper have several improvements over the West Penn unit which, of course, is to be expected. The duplication of the water cooling system would reduce the outages which are caused mostly by the pump.

The life of the Thyratron tubes with the West Penn unit has been somewhat better than $1^1/_2$ years, and this will be improved by changing to the new design, namely, type *WL-105*, replacing the old type *K U-676*, each costing approximately $30.00.

The following paragraphs pertain to electronic exciter performance at the West Penn Power Company.

In 1944 when the West Penn Power Company was planning for the 80,000-kw generator addition to its Springdale Power Station, extensive consideration was given to the type of excitation system. At that time generator shaft-driven exciters were being recommended. In 1937 the company installed a 50,000-kw, 3,600-rpm topping unit in Springdale and this included a generator shaft-driven exciter with a standard shunt-wound pilot exciter. This company's experience with this unit resulted in our being reluctant to provide a shaft-driven unit for the new Number 7 generator.

The first five units for this station varied in capacity from 25,000 to 50,000 kw over a period of six years, namely, 1920 to 1926—all excited from motor-driven or motor- and steam-driven overcapacity exciters supplemented by spare units. Excitation troubles were quite limited, and the difficulties with the direct-connected exciter on the Number 6 topping unit prompted considerable reluctance in repeating such an installation for

the proposed largest unit on the system. Various combinations were considered, resulting in the selection of the electronic exciter having a rating of 860 amperes at 250 volts. It was understood this would be an experimental installation; nevertheless, the background of experience with ignitron rectifiers and various types of application substantiated the decision. It was understood the unit would be designed and delivered about a year in advance of the generator. This period should have provided ample time to eliminate the possible growing pains. This schedule was not met, and the company finally decided to use the dual-driven 300-kw 250-volt exciter then being used for our Number 5 50,000-kw generator installed in 1926. This 23-year old combination is still in use, and there has been no excitation or electrical failure of any kind causing an outage to this 80,000-kw generator which went in service in December 1945.

The electronic exciter went through a series of factory tests and finally was delivered without the compensating transformers which were to have been installed in the generator leads. During installation it was decided to connect the rectifier transformer to the Number 5 section of the existing station auxiliary bus and to date it remains so connected. The new station auxiliary switching for the Number 7 unit included a control cubicle with circuit breaker, and so forth, for the electronic exciter transformer but it has never been used as such.

It also was decided that the electronic exciter would first be used with the smallest station unit, namely, 25,000 kw. The operating group was quite reluctant to take any chance on loss of station capacity in view of system load conditions.

The electronic exciter went in service on March 12, 1946, providing excitation for the 25,000-kw unit during off-peak periods. The exciter was out of service from March 27 until June 17 because of damage to the electrolytic arresters which provide surge protection to the generator field. This damage was caused by circulating current rectified by the lightning arrester at the rate of six impulses per cycle. On June 17 the exciter was returned to service and shortly thereafter the Number 1 generator-field-circuit resistance-to-ground was found lower than that of the other machines.

In order to inhibit some parts of the cooling system where iron was used, it was recommended that a 5 per cent solution of dichromate be added, and this accounts for the high conductivity. Considerable time was lost in eliminating this condition.

On August 13 the exciter was connected to the Number 2 station unit, a duplicate of Number 1, where it remained in service until January 3, 1947. During this period it was tested for operating, exciting both Number 1 and Number 2 generators simultaneously for a period of four hours. Considerable improvement was noted in the regulation of the 25-kv transmission voltage as compared with the Tirrell vibrating regulators.

On January 3, 1947, the electronic exciter was transferred to the Number 5 50,000-kw generator where it continues to provide dependable excitation.

During the three years that this exciter has been in use there have been a number of arc backs and misfires, but in no case have we ever lost a generator due to these or any other conditions. Numerous tests have been made to determine what might happen in case of loss of tubes and the like. On February 1, 1947, when supplying excitation for Number 5 generator, three ignitron tubes were removed from service, first with a load of 29,000 kw, then 40,000 kw, and finally with full load of 50,000 kw. The test was successful, and this materially improved the operator's confidence in the exciter. With two tubes out of service the main exciter voltage was 350 volts, with three tubes out it was 275 volts, and with four tubes out of service it was 200 volts. The generator required 210 volts across the field to supply the necessary excitation for 50,000 kw at 94 per cent power factor, with a terminal voltage of 11,750 volts. These tests prove that satisfactory excitation could be provided with three tubes out of service, but not quite satisfactory with four tubes out.

During the three years the exciter has been in service, several changes have been made. Fuses originally in the misfire circuits have been replaced with small deion circuit breakers, thus reducing the time a firing circuit is out of service following a misfire. Anode heaters have been added to prevent condensation of mercury vapor on anodes during periods that the equipment is out of service for maintenance, thus reducing the number of arc backs experienced immediately after placing the equipment back into service.

All arc backs have been properly cleared by the tripping of the proper anode circuit breakers and all tubes restored to service by their immediate reclosing. The outage period has proven of such short duration that no noticeable reactive swings were observed. Most arc backs have occurred while the exciter was under the control of the silverstat regulator. Even though the anode circuit breaker had not successfully closed, the regulators would have corrected the excitation, thus preventing violent swings in load and reactive kilovolt amperes.

The original power tubes supplied with the equipment have all been replaced. Three tubes lasted 26 months, one 25 months, and one had to be replaced within two months because it was defective. The life of the balance of the tubes has averaged somewhat better than one year. There has been a second replacement of three tubes. All of the first set of Thyratron tubes have been replaced, and of these there have been two second replacements.

Table I of the discussion gives the details of the ignitron tube record. Loss of vacuum has been the major cause of replacements. Any or all of these tubes can be replaced without removing the rectifier from service, but unfortunately the operators have not been so convinced; thus we have an unused facility.

The over-all efficiency of this exciter is approximately 82 per cent as determined by our own measurement of a-c input to the power supply transformer and the d-c voltage and current to the generator field. This includes power supply to the heat-exchanger unit.

This exciter was furnished by the manufacturer on an experimental basis with the understanding that if proven satisfactory, West Penn Power Company would have the right to accept or reject the unit. When the generator was installed, foundations were provided for the future installation of a direct-connected exciter. To date we have no intention of providing a direct-connected exciter. The application of the electronic exciter to the unit it was intended for is still in question. An additional expenditure for cable connections is required, and this has not as yet been justified. Existing operating conditions are quite satisfactory and may remain so as long as present load conditions continue. The 300-kw duel-driven exciter was equipped with a pilot exciter and this, along with a *BJ-90* regulator, continues to provide a very dependable excitation system. There are provided switching facilities whereby the Number 7 field may be excited from a spare exciter bus but this is very seldom, if ever, used. The West Penn Power Company, as well as the manufacturer, have gone to considerable expense in completing this experiment, and after considerable review of expenditures the West Penn Power Company and the manufacturer agreed upon a purchase price which, of course, was somewhat in excess of the omission price for the direct-connected exciter which was included in the contract for the generator.

Table 1. Ignitron Record

Tube Number	Position	Date Installed	Date Removed	Life, Months
*26317	1	3-12-46	5-20-48	26+7
26322	2	3-12-46	9-19-47	18
26290	3	3-12-46	Transferred to number 4—12-6-46	
26294	4	3-12-46	Transferred to number 3—12-6-46	
27239	5	3-12-48	5-20-48	26
26297	6	3-12-46	5-20-48	26
27945	1	5-20-48	In service	
27848	2	9-19-47	4-12-48	7
804077	2	4-12-48	In service	
26290	4	12-6-46	4-12-48	25
26294	3	12-6-46	12-28-46	(22 days)
28071	4	4-12-48	In service	
752033	5	5-20-48	6-1-48	(Faulty tube)
*26317	5	6-1-48	1-21-49	
843015	5	1-21-49	1-11-50	12
843088	5	1-11-50	In service	
59566	3	12-28-46	5-20-48	17
804011	3	5-20-48	In service	
804048	6	5-20-48	In service	

When purchasing the two 80,000-kw units for the new Mitchell station, it was decided to accept the direct-connected exciter and Rototrol pilot arrangement. A spare motor-driven exciter and Rototrol pilot have been provided for use with either generator. Twelve years' experience with the direct-connected exciter on Number 6 topping unit at Springdale and one year's experience with the first unit at Mitchell have not proven direct-connected exciters to be as dependable as the old motor-generator sets or the electronic exciter at Springdale.

The possible economies of the direct-connected exciters must be recognized; nevertheless, the service and the expense incurred by failures and the loss in generation may more than account for these economies.

The two 20,000-kw package-type 3,600-rpm generators for the new Milesburg station now being constructed include direct-connected exciters with standard shunt-type pilot exciters. A spare motor-generator set with shunt-type pilot is being installed.

A. P. Colaiaco, A. A. Johnson, and J. E. Reilly: The ignition tube life experienced on

the electronic exciter at the Springdale Station of the West Penn Power Company as related by Mr. Langstaff is considerably shorter than that experienced with similar ignitron tube electronic exciters and on many other industrial installations.*

In F. M. Porter's and J. H. Kinghorn's discussion of Excitation Improvement,[1] they point out that on the three electronic exciters operated by their organization, the actual operating life of the ignitron tubes has averaged 32,680 hours or almost 4 years. Similar ignitron tube life has been experienced on several hundred other industrial applications.

In one installation in particular, the New Carlisle Station of the Indiana and Michigan Electric Company, a Westinghouse electronic exciter using ignitron tubes has operated for the past $7^1/_2$ years with the same set of six ignitron tubes. A life of $7^1/_2$ years for a group of six tubes is unusual. However, it does emphasize that short tube life such as experienced by the Springdale electronic exciter* is also unusual and must have an underlying cause which can be remedied.

An investigation should be made of the Springdale electronic exciter to determine the cause or causes of these excessive tube failures and steps should be taken to correct them.

*Note that tube 26317 listed in Table 1 of the discussion as having been removed from position 1 on 5-20-48 with 26 months' life was later installed in position 5 on 6-1-48 where it operated for seven more months or a total life of 33 months.

Reference

1. Discussion by F. M. Porter and J. H. Kinghorn of Excitation Improvement—Electronic Excitation and Regulation of Electric Generators as Compared to Conventional Methods, A. H. Phillips, W. H. Lambert, D. R. Pattison. *AIEE Transactions*, volume 69, part 1, 1950, pages 340–41.

Excitation Improvement—Electronic Excitation and Regulation of Electric Generators as Compared to Conventional Methods

A. H. PHILLIPS
MEMBER AIEE

W. H. LAMBERT
ASSOCIATE AIEE

D. R. PATTISON
FELLOW AIEE

IN A period of four years in the early 1940's the writers gathered a background of exciter failure information, both on their own system and others, involving some 38 exciter failures. These failures caused shutdowns of generators having so-called conventional exciter units using both direct-connected and motor-driven commutating exciters, most with pilot exciter combinations driven from common shaft of main generator.

It was concluded that the entire exciter system was definitely not in accord with the ruggedness of design built into the turbogenerator. Whereas the turbogenerator could run for periods of two or three years without shutdown for service, the commutating-type exciter was not in this class and something should be done to improve this situation.

From these investigations it was determined that the weakest link in the excitation system was the pilot exciter as it is small and subject to vibration hazards. This was eliminated by the substitution of a permanent magnet pilot using stationary dry-type rectifiers or electronic rectifiers. Later two new machines, equipped with entirely new complete electronic systems, were put in service at the Warren Station of Pennsylvania Electric Company. A third unit with slightly revised layout now is being installed. This paper discusses the factors influencing the design and adaptation of this equipment and the field experience to date.

It is common knowledge that the rotating commutator and brush combination, to say nothing of the other components which go to make up an exciter system, is most vulnerable due to the fact that it could never be called upon to run long, continuous periods of time without shutdowns for servicing. Therefore it was the writers' intention in considering the designs for any improvement to be able to service vulnerable parts without shutdowns or affecting the generator output, and at the same time supply all spare exciter capacity necessary. It was firmly believed that the exciter and regulator performance could be improved by the use of electronic components, which had already proved themselves over long periods of time in other industrial applications.

Results of Investigation

As a result of investigation it was found that the frequency of exciter troubles, as well as the uncertainty of maintenance requirements, were due principally to the following causes:

1. Variation in brush structure and composition, even with so-called identical style brushes, and sometimes with brushes from the same batch.

2. The influence variation of current density on commutator performance.

3. Copper structure variation which led to commutator irregularities resulting in high bar and thermal instability.

4. Commutator bar slippage as affected by unusually high vibration causing brush skip due to high mica or commutator bar.

5. Commutator wear which required shutdown for proper correction.

6. Humidity variations.

7. Dust and dirt effect on brush wear and commutator cutting.

8. Banding failures due to overloading or mechanical failure.

9. Commutator riser failures.

10. Generator field circuit breaker failures due to contact corrosion when not operating over long periods of time.

11. Difficulties with parallel operation of exciters on common bus excitation system.

Although it was realized that steps have been taken to improve brush-type commutator machines, maintenance still cannot be completely accomplished while the unit is in operation. It was therefore felt that the electronic exciter offered the best possibility of eliminating most of the difficulties experienced.

Some of the other features considered favorable to the electronic exciter are the following:

1. Simplicity of the exciter alternator, its winding and installation, as compared to a d-c generator winding. Also the inherently smaller rotor and the total absence of banding, brush rig, risers, and commutator.

2. Electronic exciters could be a combination of all time tried equipment:

a. The alternator is generally acknowledged by everyone to be in this class.

b. The ignitron tubes have served for years and have replaced the rotating commutator generators in many places.

3. The complete freedom from system disturbances as would not be the case with separate excitation furnished by motor generator sets.

4. No spare excitation required.

5. Eliminates field circuit breakers and bussing with their inherent hazards.

6. No exciter paralleling problems.

Paper 50-51, recommended by the AIEE Power Generation Committee and approved by the AIEE Technical Program Committee for presentation at the AIEE Winter General Meeting, New York, N. Y., January 30-February 3, 1950. Manuscript submitted October 31, 1949; made available for printing December 16, 1949.

A. H. Phillips is with Gilbert Associates, Inc., Reading, Pa., and W. H. Lambert and D. R. Pattison are both with the Pennsylvania Electric Company, Johnstown, Pa.

Permanent Magnet Pilot Exciter

Our first step in eliminating exciter troubles was to improve the pilot exciter. Since the pilot on the end of the shaft was subjected to occasional vibration and by reason of its size was not as stable as the main exciter, it was decided to use a 4-pole permanent magnet rotor and 3-phase stator to deliver 120-cycles to a stationary dry-type or electronic rectifier. A unit of this type was manufactured and placed on test for a period of eight months. It was subjected to all known hazards of short circuits and load variations, and was found to be a very stable machine. Another unit was manufactured to coincide with the mounting conditions for a 40,000-kw unit at the Seward Station for Pennsylvania Electric Company. This unit went into service in August 1947. Thus we have had approximately $2^1/_2$ years of experience with this pilot exciter.

During a scheduled shutdown for inspection and maintenance of the turbine approximately 15 months after the unit was put in service, a complete change of rectifier tubes was made but no tube replacements were made during that period. Several tubes had loose bases but this condition has been corrected in the tubes as now produced. During the initial operation of the unit it was apparent that tube life could be extended by preheating the filaments, so equipment providing automatic change-over to the station power supply was ordered and the installation made after 15 months operation of the original unit. In addition to prolonging tube life the change-over to the separate power source provides field current for a longer period during shutdown of the generator, also supplies an emergency power source for the rectifier, and is simpler and more reliable than a hand-operated circuit breaker or time delay circuit in the anode supply of the rectifier.

Since it was recognized that the pilot exciter was responsible for a large number of unscheduled shutdowns, temporary action was taken on several machines by Pennsylvania Electric Company as well as a large number of other utilities waiting experience on the new magnetic pilot. This temporary action was in the form of using a storage battery in place of the pilot exciter source and providing shaft extension for the application of the permanent magnet pilot at a later date.

Warren All Electronic Excitation and Voltage Regulation

When the excitation for the two 37,500-kva turbine-generator units for the new Warren Station was under consideration in 1944 it was felt advisable to review the possibility of a complete elimination of commutator-type exciters from the shaft of these two units. Also the possible elimination of all rotating commutator d-c machinery in this plant was the general keynote. The final result is that the only equipment of the rotating commutator type installed in this plant consists of a few small, reversible, positioning, and valve operating motors.

It also was felt that the electronic exciter, in addition to the features cited previously, would be superior in its response and ability to take overloads as full electronic excitation provides the only ideal medium for the application of electronic regulation, which also was to be a part of this excitation system. In contrast to the brush-type commutation, the electronic would have a much wider operating range for the electronic exciter can operate at very light loads or severe overloads for long periods of time without damage. In further consideration, if parallel operation was ever required this could be accomplished with simplicity and without the danger of feedback.

At the time the original electronic excitation system was proposed, the permanent magnet pilot was to be an integral part of the system as outlined in Figure 2. However, when the Warren plant units were laid out as shown in Figure 1, it was not included due to lack of actual field experience. It was finally conceded as superior in many ways as stated in the paper on Design and Test on Electronic Exciter by Colaiaco, Johnson, and Reilly.[1] As pointed out by them, it would provide an entirely separate low-voltage excitation unit for the main exciter. It is included in the new generator about ready for service at Seward Station of Pennsylvania Electric Company.

With the possibility of realizing complete electronic excitation for the Warren generators, steps were taken to exploit all the necessary details with the manufacturer. These details have been described in the aforementioned paper. Several small defects were discovered and remedied when the number 1 machine was put in service. Otherwise the operation has proved very satisfactory. The difficulties experienced were all of minor consequence and were to be expected in the initial product. The time required to correct them was amplified by the fact that the main generator had to be up to full speed before any adjustments or checking could be done on any exciter units. In the more recent unit for the

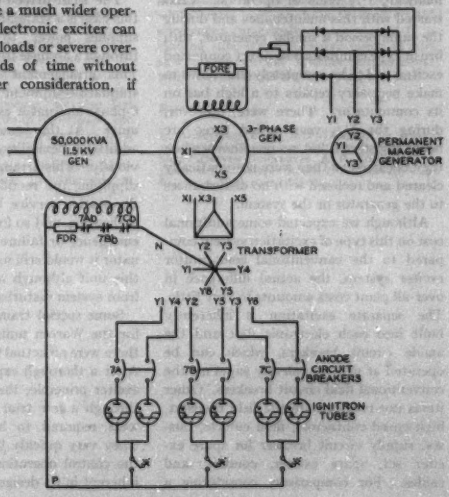

Figure 1 (below). Design and layout of first system installed at Warren Station

Figure 2 (right). Original design of electronic excitation system unit as being installed on Seward generator

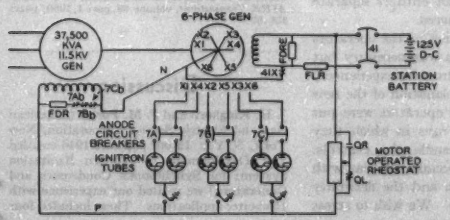

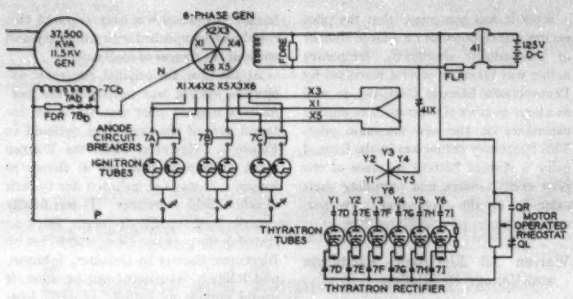

Figure 3. Final layout of electronic excitation at Warren Station

Seward Station, a separate 3-phase supply from the station service can be used for checking prior to the time that the turbo-generator unit is ready for service. Although a rather remote possibility, a failure of the exciter alternator would not be too serious since the electronic rectifier can be supplied from any 3-phase source.

It is of interest to note that during the first week of operation of the number 1 generator at Warren plant a gaseous ignitron tube was discovered. This condition was not previously detected because the tubes were not check tested after shipment. It is significant that this tube section was immediately isolated and the tube replaced while the generator was in full load operation. Due to the fact that the rectification is removed from the shaft, no shutdowns were required in the following $1^1/_2$ years of operation. Contrasted with this maintenance and during the same period a similar generator, with brush-type commutation direct connected exciter, had to be completely shut down to make necessary repairs to a high bar on its commutator. There were, however, during the $1^1/_2$ year period three arc backs registered, but no one knows when they occurred as they were automatically cleared and reclosed with no disturbances to the generator or the system.

Although we expected some additional cost on this type of excitation system compared to the conventional commutator exciter system, the actual difference in over-all plant costs amounts to very little. The separate excitation is inherently built into each electronic unit and the anode circuit breakers, which can be operated at will, completely supplant the conventional field circuit breakers. Other items not required are the field rheostat, high speed contactors, field cubicle, busses, supply circuit breaker for spare exciter set, spare exciter, conduit, and cables. For comparison, considering a similar two generator station equipped with two 40,000-kva units, the cost of the miscellaneous equipment necessary in conjunction with the conventional excitation and including a spare exciter shows less than ten per cent difference in actual over-all exciter cost.

As indicated previously, the electronic exciter for the new 50,000-kva unit at Seward is being installed as shown in Figure 2. In this arrangement the permanent-magnet type 3-phase pilot is to produce essentially a fixed field on the exciter alternator and through a selenium rectifier rather than the electronic rectifier. The change to the selenium rectifier was felt advisable due to its excellent record in similar low power applications and it is thought it eliminates possible tube troubles.

The shaft-driven exciter alternator in this case is a standard 3-phase unit which supplies power to the rectifier unit through a 3-phase to 6-phase transformer. This arrangement allows the use of standard equipment rather than a special 6-phase alternator as used in the Warren units. At the same time it introduces additional flexibility, as pointed out previously. This arrangement would permit supplying the rectifier transformer from the station service bus for prechecking, preheating, and so forth. In the event of emergency or failure to the exciter alternator it would still maintain excitation on this unit although not entirely separate from system disturbances.

Some special training of the operators for the Warren units was necessary but there were no actual troubles experienced. After a thorough explanation of the new exciter principle, the operators were put through a few trial runs in which they were required to handle the controls. They very quickly became familiar with the control operation and the flexibility inherent in its design. We wish to stress the point brought out in the paper by Colaiaco, Johnson, and Reilly[1] for they have shown a number of oscillograph tests conducted from data collected from the test floor, that is, the ability of these machines to ride out system disturbances. In actual service they seem far superior in their stability and much more readily adjust themselves to operating conditions than the older style excitation.

At the end of the 1-year period, the Warren generator was taken down on a prescheduled date for general inspection of turbine and auxiliaries. At this time no changes were made to the tubes or other electronic equipment except that the anode electrolysis targets in the main rectifier cooling system were replaced, having lost approximately one-half of their active material in the 1-year period. We do not expect to make any over-all tube replacements on a periodic basis in these exciter systems as there is inherently sufficient capacity to allow for tube failures without affecting generator output or performance.

Conclusions

1. Flexibility of operation and range of control are inherently a part of the electronic exciter voltage regulator combination.
2. Electronic regulation is most effective when coupled with electronic excitation system and provides high speed regulation.
3. Reserve capacity built in requiring no extra excitation source.
4. Excitation system entirely separated from system disturbances.
5. Ease of maintenance at comparatively low cost.
6. Comparable first costs compared to the over-all exciter application.
7. No feed-back problems.
8. No field circuit breaker maintenance troubles as any anode circuit breaker can be taken out of service for maintenance or inspection at any time.
9. Capable of long periods of operation without shutdown of main generator.

Reference

1. Design and Test on Electronic Exciter Supplied from Common Shaft Driven Generator, A. P. Colaiaco, A. A. Johnson, J. E. Reilly. *AIEE Transactions*, volume 69, part I, 1950, pages 328–37.

Discussion

J. H. Kinghorn and **F. M. Porter** (American Gas and Electric Service Corporation, New York, N. Y.): In our paper of 1946 entitled The Development of Modern Excitation Systems for Synchronous Condensers and Generators,[1] we related our experience with 15 exciter applications. These included four

direct-connected main exciters with electronic pilot exciters, three synchronous condensers with electronic main exciters, and six direct-connected exciters with amplidyne controls. All of these have electronic regulators.

We pointed out at that time that 47 machine years of operation with electronic pilot exciters and 29 machine years of operation with electronic main exciters had demonstrated the excellent performance and reliability of this type of excitation. Since then we have experienced four more years of satisfactory performance on all of these units, making the operation to date 63 machine years for electronic pilot exciters and 41 machine years for full electronic exciters.

Also, the 87 machine years of satisfactory electronic regulator performance on these units, experienced as of 1946, have increased to 143 machine years. Therefore, we have every reason to believe that very satisfactory results will be obtained from the electronic features of the new excitation arrangements described by Phillips, Lambert, and Pattison.

Further analysis of tube failures for the past four years has been made for the three electronic main exciters. It is found that thyratron tube life has shown slight improvement over this period, the average service hours per tube failure being 13,650. Ignitron tube life has doubled from the previous 16,340 hours per tube failure to 32,680 hours. Furthermore, one exciter has operated for the entire four years without an ignitron failure and all of its tubes now have been in service for $7^1/_2$ years. However, in general the foregoing figures indicate that expenditures for tube replacement still are an appreciable item in maintenance costs.

As pointed out in our 1946 paper, we also have found that the performance of the amplidyne control system with direct-connected exciters has been essentially equal to that obtained from the electronic main or electronic pilot exciter applications. The authors state that the installation of the electronic exciter is about 10 per cent more costly than a single direct-connected exciter plus a spare exciter. However, when several generators are involved, as is frequently the case, the cost of one spare exciter is spread over several machines and therefore the installed cost per generator is reduced. The additional cost of extra equipment in the electronic exciter such as ignitron tubes, power transformer, and heat exchanger, is readily apparent. Because the direct-connected exciter with amplidyne control results in a simpler and more economical arrangement, and, practically speaking, provides high speed and accurate voltage regulation equivalent to that of the electronic scheme, we are utilizing it on four large turbogenerators recently placed in service and on eight more generators to be installed in the next three years.

We cannot agree that the direct-connected exciter is the unreliable piece of equipment that has been stated. We would be interested in knowing the age of the generators and exciters involved in the 38 exciter failures as an aid in evaluating design improvements. Our own experience with direct-connected exciters over a period of approximately 30 years has been quite satisfactory. This includes 23 units in service for 25 years or longer, and 18 additional units installed since 1936. We have had the usual amount of brush and commutation troubles but these have not been too serious. Obviously exciters, the same as other equipment, require maintenance and repairs and eventually rewinding and replacement of some parts, particularly commutators. We have found it possible to take care of grinding commutators and other major repairs during shutdowns for turbine or generator maintenance. In most cases we have a motor-driven exciter set or sets which serve not only for emergency use in case of trouble with the direct-connected exciter but also in many cases for simultaneous starting of two generators involved in cross-compound units. The emergency shutdowns may be required for many reasons other than exciter trouble. This is particularly the case for power generation unit installations where there is one boiler, one turbogenerator with accessory equipment, all entirely independent of other units at the same plant. As far as the system of the American Gas and Electric Company is concerned, it is designed and operated so that any turbogenerator unit can be shut down for emergency repairs without affecting service from the system.

We conclude by stating that we believe the scheme described, utilizing direct-connected alternator with electronic excitation and regulation is another excellent and reliable arrangement for obtaining high-speed accurate voltage regulation and response for a turbogenerator. However, we also feel that based on many years of experience, the direct-connected exciter has proved to be a reliable piece of equipment, particularly with the design improvements that have been made in the last ten years. It is our opinion that the excitation scheme utilizing direct-connected exciter with amplidyne control is for all practical purposes just as good an arrangement, insofar as high-speed and accurate voltage regulation are concerned, and also that it results in a simpler and more economical installation.

Reference

1. The Development of Modern Excitation Systems for Synchronous Condensers and Generators, F. M. Porter, J. H. Kinghorn. *AIEE Transactions*, volume 65, 1946, pages 1020–28.

A. H. Phillips, W. H. Lambert and D. R. Pattison: I wish to thank Kinghorn and Porter for their discussion. They certainly have brought out revealing facts regarding the reliability of electronic excitation, together with their valuable experience in the operation of such equipment.

I would like to make one comment on the cost, that is, where they referred to the statement in our paper that the cost is 10 per cent more than the cost of a single exciter plus a spare, and so forth. This is not exactly the comparison we made, as our 10 per cent cost value is based on a 2-unit plant. My personal feeling is that there should not be any additional cost in new excitation as it is simply a matter of production and application. If anything, in the long run the electronic excitation should be cheaper than the so-called conventional types.

I cannot connect statement of Kinghorn and Porter that any type of amplidyne control can be simpler or more economical, nor can it compare in speed of regulation. It still uses a multiplicity of commutators and brushes and we are sure it could not be as reliable, nor would it have spare excitation built in.

Refer to Mr. Langstaff's discussion of a previous paper[1] on electronic excitation versus conventional types. In regard to the accessibility of the equipment for repairs while under load, we have worked on this equipment (practically every part of it including tube changes, water pump repairs, and anode circuit breaker adjustments) while the machine was carrying full load.

Reference

1. Discussion by H. A. P. Langstaff of Design and Test on Electronic Exciter From Common Shaft Driven Generator, A. F. Colaiace, A. A. Johnson, J. E. Reilly. *AIEE Transactions*, volume 69, part I, 1950, pages 335–36.

The Thermal Resistance Between Cables and a Surrounding Pipe or Duct Wall

F. H. BULLER
MEMBER AIEE

J. H. NEHER
MEMBER AIEE

ONE step in the calculation of underground cable temperatures involves the determination of the temperature rise of the cable surface above the immediately surrounding inclosure such as a duct structure or a gas- or oil-filled pipe. Since the intervening medium is a fluid, the mode of heat transfer simultaneously involves convection, conduction, and radiation.

The semiempirical methods now in use for this determination in the case of cables in duct are not entirely satisfactory, and with the advent of gas- or oil-filled pipe-type cables there has arisen a definite need for a method of evaluation for these cable types as well.

Because of the complex nature of the problem and the number of independent variables which are present, it is impractical to cover completely all possible combinations which may be met within practice solely by tests. By developing a theoretical relationship between the variables, however, it is possible to develop procedures by which the test data available may be analyzed in such a way that relatively simple working expressions may be derived which may be applied with sufficient accuracy over the entire working range.

The theoretical relationship for the case of cables in duct was recently presented in a paper by one of the authors.[1] In the present paper this relationship has been extended to cover oil and gas pipe systems as well, and from the test data presented the requisite working expressions for thermal resistance or surface resistivity factors have been obtained.

Theoretical Considerations

The theoretical relationships given in Appendix II of reference 1 for the case of cables in duct have been expressed more completely to account for the physical characteristics of the media involved in Appendix I of this paper. The resulting equations for the the thermal conductivity between cable and duct or pipe with air or gas as the intervening medium are

$$\frac{Q}{\Delta T}(\text{gas}) = \frac{0.092\ D_s'^{3/4}\Delta T^{1/4}P^{1/2}}{1.39+D_s'/D_d} + \frac{0.0213}{\log_{10}D_d/D_s'} + 0.102D_s'^4(1+0.0167T_m)$$

watts per degree centigrade foot (1)

and with oil as the medium

$$\frac{Q}{\Delta T}(\text{oil}) = \frac{0.053D_s'^{3/4}\Delta T^{1/4}T_m^{1/2}}{1.39+D_s'/D_d} + \frac{0.116}{\log_{10}D_d/D_s'}$$

watts per degree centigrade foot (2)

For a single cable $D_s' = D_s$, the diameter of the cable. For three cables in the pipe or duct it is customary to base D_s' on the circumscribing circle of the cables in triangular configuration, $D_s' = 2.15\ D_s$. For two cables the relationship $D_s' = 1.65\ D_s$ is satisfactory.

It will be noted that the primary variable in equation 1 is D_s'. As a result, subsequent analysis and development will be facilitated if this equation is written in the equivalent form

$$\frac{Q}{D_s'\Delta T} = \frac{0.092\,\Delta T^{1/4}P^{1/2}}{D_s'^{1/4}(1.39+D_s'/D_d)} + \frac{0.0213}{D_s'\log D_d/D_s'} + 0.102_s(1+0.0167T_m)$$

watts per degree centigrade foot inch (1A)

From the method of derivation which assumes a coaxial arrangement of the cable within the duct or pipe, the numerical constants of the first two terms of equations 1, 1(A), and 2 must be considered as being approximate only. They will serve, however, to evaluate the relative magnitudes of the terms, and the corresponding values finally employed will be based on test data.

As a practical matter, a high degree of accuracy is not required since the thermal resistivity between cable and duct or pipe represents a relatively small part of the total thermal circuit, and we are justified in materially simplifying these equations. From the standpoint of analysis of the test data and the subsequent development of working expressions, it is desirable to utilize the simple linear relationship

$$y = ax + b \qquad (3)$$

where y and x are variables and a and b are constants. Equations 1 and 2 are of this form provided that the second (conduction) and third (radiation) terms may be considered as constants within the desired accuracy of the final result. Considering equation 1A the conduction term constitutes about 14 per cent of the total in the case of a typical cable in duct installation, and about 8 per cent for a typical gas-filled pipe-type installation at 200 pounds per square inch. The corresponding values for the radiation term are 63 and 43 per cent.

Normal variations in D_s'/D_d may produce considerable variation in the conduction term, but the effect on the overall picture is small, because conduction is such a small part of the total heat flow. Variations of T_m can affect the radiation term by as much as 20 per cent over a sufficiently wide operating range; however, when calculating a cable rating, with a fixed copper temperature of the order of 70 degrees to 80 degrees centigrade, the range of this variable is very small, and an accuracy of the order of 3 per cent to 5 per cent may be expected.

In the case of equation 2, the conduc-

Paper 50-52, recommended by the AIEE Insulated Conductors Committee and approved by the AIEE Technical Program Committee for presentation at the AIEE Winter General Meeting, New York, N. Y., January 30-February 3, 1950. Manuscript submitted October 31, 1949; made available for printing December 7, 1949.

F. H. BULLER is with the General Electric Company, Schenectady, N. Y., and J. H. NEHER is with the Philadelphia Electric Company, Philadelphia, Pa.

Table I. Test Data on Gas-Filled Pipe-Type Cable Systems

Test Number	Source	D_s'	D_d	P	Q	ΔT	T_m	$\frac{Q}{D_s'\Delta T}$	$\frac{\Delta T^{1/4}P^{1/3}}{D_s'^{1/4}}$
1	Detroit Edison Company	3.42	6.07	1	23.4	20	32	0.34	1.56
				7.8	27.3	15.6	51	0.51	4.08
				14.6	28.6	13.1	51	0.64	5.34
					28.9	17.1	50	0.49	5.71
					28.9	14.4	51	0.59	5.48
					27.5	14.0	51	0.58	5.43
2	General Electric Company	3.92	6.07	1.7	7.3	6.2	39	0.30	1.64
					11.4	9.7	45	0.30	1.63
					15.2	12.4	50	0.31	1.73
				7.8	8.8	4.7	39	0.37	2.92
					11.5	7.0	43	0.42	3.22
					14.9	8.9	45	0.43	3.42
				14.6	6.8	3.7	35	0.46	3.77
					11.2	5.8	40	0.49	4.22
					15.9	8.0	45	0.51	4.55
3	General Cable Corporation	4.90	6.07	14.6	25.9	9.2	56	0.57	4.47
4	General Electric Company	4.90	6.07	14.6	23.1	11.8	44	0.40	4.77

Table II. Test Data on Cables in Fiber and Transite Ducts Encased in Concrete

Test Number	Source	Duct	D_s'	D_d	Q	ΔT	$\frac{Q}{D_s'\Delta T}$	$\frac{\Delta T^{1/4}P^{1/3}}{D_s'^{1/4}}$
5	Barenscher	Fiber	0.69	3.5	1.0	6.4	0.226	1.74
					1.7	11.8	0.203	2.03
					2.5	15.1	0.235	2.17
					4.4	24.6	0.257	2.44
					6.6	34.2	0.281	2.65
					8.1	39.7	0.296	2.76
					12.3	56.1	0.318	3.00
			1.13	3.5	1.0	4.5	0.204	1.41
					1.7	7.1	0.207	1.59
					4.5	16.3	0.246	1.95
					8.0	30.4	0.253	2.28
					11.0	32.6	0.300	2.32
					14.6	48.5	0.268	2.52
					16.8	52.4	0.285	2.61
					18.4	58.7	0.278	2.69
			3.13	3.5	0.9	1.6	0.194	0.84
					1.7	3.2	0.173	1.00
					2.4	3.8	0.203	1.05
					4.5	7.7	0.188	1.73
					8.1	12.1	0.213	1.40
					14.8	21.9	0.217	1.63
6	Johns-Manville	Fiber	3.88	3.88	12.5	16.8	0.220	1.50
					14.9	19.2	0.230	1.56
					17.5	21.7	0.238	1.59
7	Johns-Manville	Transite	3.88	3.88	16.7	16.9	0.292	1.50
					19.6	19.4	0.299	1.55
					23.3	22.0	0.314	1.60
					26.4	24.5	0.318	1.64

tion term constitutes about 24 per cent of the total for a typical oil pipe installation. Variation is more important than is the case with the gas-pipe cable, but is still within tolerable limits.

One peculiar phenomenon has been observed. The ratio of D_d/D_s', which appears in the conduction term also, appears in the first (convection) term of equations 1 and 2 but in such a way that a change in this ratio produces an opposite, though lesser, effect on the total value of these equations. A minimum error should, therefore, prevail when the conduction term is treated as a constant if the denominator of the convection term also is treated as a constant. This procedure will simplify the convection term but it will have the effect of approximately halving its numerical constant as compared with equations 1 and 2 since the numerical value of the denominator omitted is in the order of two. Actually the test data was analyzed both with and without this simplification, and no apparent change in consistency in the results was observed.

Analysis of Test Data

It follows from the preceding discussion that the test data for cables in duct and for gas-filled pipe-type installations may be analyzed by plotting the observed values of

$$y=\frac{Q}{D_s'\Delta T};\quad \text{against } x=\frac{\Delta T^{3/4}P^{1/3}}{D_s'^{1/4}} \qquad (4)$$

The data given in Table I were compiled from tests on gas-filled pipe-type cable systems by The Detroit Edison Company,[3] the General Electric Company, and the General Cable Corporation. These data are plotted in Figure 1 and the values of a and b in equation 3 are established as $a=0.070$; $b=0.20$.

Table II presents similar data for cables in single dry fiber and Transite ducts in concrete taken from the Barenscher[4] and Johns Manville tests discussed in reference 1. These data also are plotted in Figure 1 where it will be seen that the Transite duct points fall on the gas in pipe curve, but the fiber duct points result in a different curve having the same value of $a=0.07$ but $b=0.10$. This difference may be explained by the fact that the duct wall departs from an isothermal as a result of the relatively high thermal resistance of the materials used, that of the dry fiber being considerably higher than that of the transite.[1]

The test data for oil-filled pipe-type cable systems from tests by The Detroit Edison Company,[3] the General Electric Company, and the Okonite Company are presented in Table III and plotted in Figure 2. In this case, the analysis has been made by plotting the observed values of

$$y=\frac{Q}{\Delta T};\quad \text{against } x=D_s^{3/4}\Delta T^{3/4}T_m^{3/4} \qquad (5)$$

and results in the values of $a=0.025$ $b=0.60$ in equation 3.

It will be seen from the analysis of the test data that the agreement between theoretical and observed numerical constants of the simplified convection term is extremely good in the case of oil as the medium, but in the case of gas, the observed value of 0.07 is somewhat higher than the expected value of about 0.046. This is rather surprising since tests number 2 (with gas) and number 9 (with oil) which are consistently close to the established curves in Figures 1 and 2 were made with the same physical setup which remained unchanged throughout the tests except for the change in the media employed. Therefore, we should expect the ratio of values obtained to be the same as the ratio of the numerical constants of the convection terms in equations 1 and 2.

This discrepancy seems to be due to the fact that in the case of several cables within the pipe, a condition of the majority of test data, there is an additional circulation of the gas between the cables themselves which is not properly accounted for by the use of an equivalent diameter for the three cables, but which is apparently not effective when a more viscous medium such as oil is employed.

As indicated before, however, a high degree of accuracy is not required, and it is

Table III. Test Data on Oil-Filled Pipe-Type Cable Systems

Test Number	Source	D_s'	D_d	Q	ΔT	T_m	$\frac{Q}{\Delta T}$	$D_s^{3/4}\Delta T^{1/4}T_m^{3/4}$
8	Detroit	4.83	6.07	26.2	8.9	49	2.94	104
9	General Electric Company	3.92	6.07	6.6	3.0	37	2.19	55
				11.4	4.5	44	2.55	69
				16.5	5.8	48	2.88	79
10	Okonite Company	4.50	6.13	4.1	2.5	25	1.65	43
				9.4	4.4	31	2.14	58
				9.4	5.4	25	1.75	53.5
				1.1	7.5	38	2.81	79
				21.5	8.8	41	2.45	85.5
				35.2	11.4	50	3.00	106
				34.9	11.7	48	2.98	133

felt that a working expression based on the foregoing analysis will be sufficiently accurate.

Working Expressions

In formulating the thermal resistance between cable and duct, it is customary to express this resistance in terms of an equivalent surface resistivity factor, assuming that the entire resistance was concentrated at the cable surface, according to the expression

$$H_{sd}=0.00411\,\frac{\beta}{D_s'}\ \text{thermal ohm feet} \qquad (6)$$

in which β is expressed in degrees centigrade square centimeters per watt. Since $H_{sd}=\Delta T/Q$ it follows from equation 6 that

$$\beta=243\,\frac{D_s'\,\Delta T}{Q}\ \text{degree centigrade centimeter per watt} \qquad (7)$$

and

$$\Delta T^{1/4}=0.253\,\frac{\beta^{1/4}Q^{1/4}}{D_s'^{3/4}}\ (\text{degrees centigrade})^{1/4} \qquad (8)$$

It is thus possible to develop working expressions in terms of β in the case of cables in duct- or gas-filled pipe by substituting equations 7 and 8 in equations 3 and 4 with the appropriate values of a and b. In the case of oil-filled pipe a simpler expression is obtained in terms of H_{sd}.

For cables in single dry fiber ducts

$$\beta=\frac{13{,}700}{\beta^{1/4}\left(\frac{Q^{1/2}P}{D_s'}\right)^{1/2}+5.7}\ \text{degrees centigrade square centimeters per watt} \qquad (9)$$

For cables in other types of single dry ducts and in gas-filled pipe

$$\beta=\frac{13{,}700}{\beta^{1/4}\left(\frac{Q^{1/2}P}{D_s'}\right)^{1/2}+11.3}\ \text{degrees centigrade square centimeters per watt} \qquad (10)$$

For cables in oil-filled pipe

$$H_{sd}=\frac{40}{H_{sd}^{1/4}(QD_s'^2T_m^3)^{1/4}+24}\ \text{thermal ohm feet} \qquad (11)$$

The value of β from equations 9 and 10 is plotted in Figure 3 as a function of $(Q^{1/2}P/D_s')^{1/2}$ and the value of H_{sd} from equation 11 appears in Figure 4 as a function on $(QD_s'^2T_m^3)^{1/4}$. Also indicated on these figures are the values of these parameters for typical conditions.

In the case of cable in fiber duct, the thermal resistance of the duct wall is appreciable and should be accounted for. This is most readily accomplished by modifying equation 6 to include this resistance. Thus

$$H_{sd}'(\text{fiber})=0.00411\,\frac{\beta}{D_s'}+0.33\ \text{thermal ohm feet} \qquad (12)$$

in which the second term represents the difference in thermal resistance between a 4-inch fiber duct and the corresponding section of concrete which it replaces.

Discussion of Values for Cables in Duct

It will be seen that the method of determining the thermal resistance between cable and duct presented herein differs somewhat from the method given in reference 1, although the results are substantially the same for terra cotta and fibre ducts. For Transite ducts, the values of thermal resistance derived in a more fundamental manner in the present paper, are slightly lower than those appearing in the reference, being equal to those assumed for terra cotta.

It will be recalled that the reasoning used in developing algebraic expressions for these values assumes an isothermal duct wall. The test data presented in

Figure 1. Analysis of test data for cables in duct- and gas-filled pipes

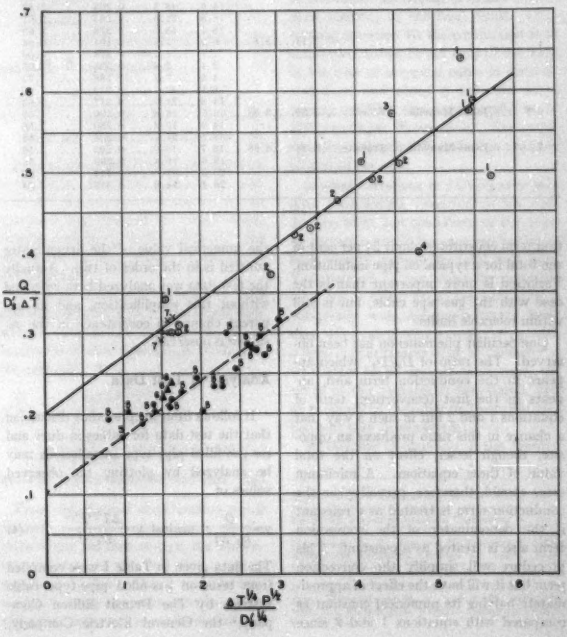

Table II and plotted in Figure 1, however, indicate a good correlation even where there is substantial deviation from the assumed isothermal as indicated by the basic data on which the table is based. Within the range covered by the data, increasing the departure from the isothermal changes the resulting constants somewhat but does not invalidate the method of analysis.

It follows therefore that a considerable variation in β for cables in single-fibre ducts may be expected depending upon the relative thermal resistivities of the duct wall and the surrounding medium, and other data which has come to the authors' attention confirms this. Thus the curve of Figure 3 for fibre duct should be considered as an upper limit.

Similarly, the application of the values given for single ducts to the case of cables in a multiduct structure, depends upon the effect which the total heat field has in further changing the temperature gradients around the individual duct walls. The data given by Smith in his discussion of reference 1 indicates a value of β for multiple-fiber ducts in concrete corresponding closely to the curve for cable in pipe.

As indicated in reference 1, additional test data taken on multiple-duct assemblies are desirable to definitely establish the limits under these conditions.

For reasons also indicated in reference 1 these values are not directly comparable to the values adopted by the Insulated Power Cable Engineers Association[6] and are not directly adaptable to their calculation procedure.

Conclusions

1. The theoretical relationships between the various quantities involved in the effective thermal resistance between cables and a surrounding single duct or pipe have been developed in a manner which properly accounts for the simultaneous modes of heat transfer by convection, conduction, and radiation.

2. By means of these relationships certain test data on cables in duct and in gas- and oil-filled pipes have been analyzed and working curves are presented for determining the thermal resistance for any particular case which may be encountered in practice.

3. Under typical conditions representative values of the equivalent surface resistivity factor β for use in equation 6 are 800 degree centigrade square centimeters per watt for cables in pipe, single dry terra cotta or transite ducts at atmospheric pressure, 450 for cables in gas-filled pipe-type installations at 200 pounds per square inch, and 350 for cables in oil-filled pipe-type installations. Representative values of β for cables in single dry fiber ducts will vary from 850 to 1,100.

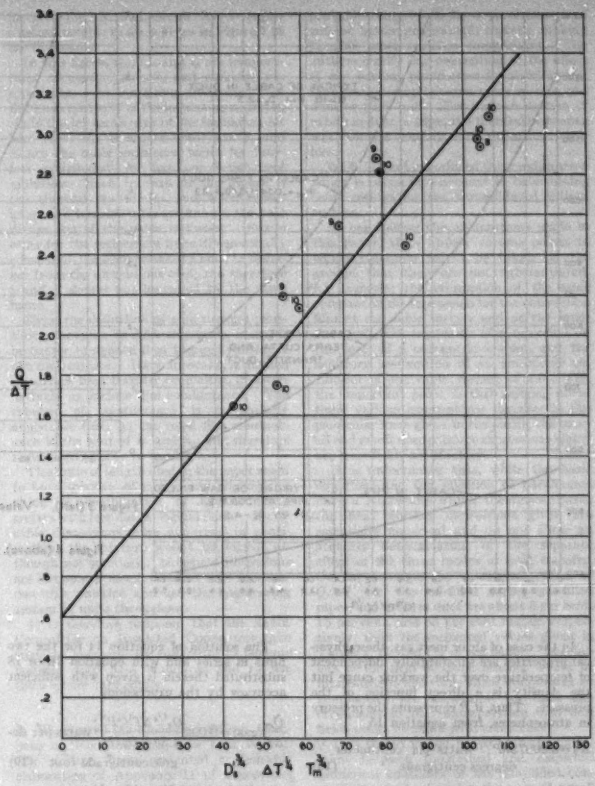

Figure 2. Analysis of test data for cables in oil-filled pipe

Appendix I. Theoretical Development of Thermal Conductivity between Concentric Isothermal Cyclinders with Gas or Oil as the Intervening Medium

The mechanism of heat transfer between a cylindrical radiator and an enveloping isothermal enclosure through an intervening fluid medium is such that a portion of the total heat flow Q is carried by convection Q_{cv}, a portion by conduction Q_{cd}, and the remainder by radiation Q_r. In formulating the components of the thermal circuit, therefore, it is more convenient to work in terms of thermal conductances rather than thermal resistances since the former quantities are directly additive. Thus, if ΔT is the temperature drop in degrees centigrade across the circuit

$$\frac{Q}{\Delta T}=\frac{Q_{cv}}{\Delta T}+\frac{Q_{cd}}{\Delta T}+\frac{Q_r}{\Delta T} \text{ watts per degree centigrade foot} \quad (13)$$

The phenomenon of convection involves the conception of the temperature drop being concentrated in two films, one at the surface of the cylindrical radiator of diameter substantially equal to the diameter of the radiator D_1 in inches, and one at the surface of the enclosing isothermal surface which will be considered also being cylindrical of diameter D_4. The following formula based on McAdams[3] (equation 42, page 251, 1st edition only) is applicable to either film.

$$Q_{cv}=122D_f^{5/4}\Delta T_f^{5/4}K \text{ watts per foot} \quad (14)$$

in which D_f is in inches, and

$$K=\left(\frac{\beta^2 C_p g\, e}{\mu\ \rho^2}\right)^{1/4} \text{ watts per centimeter}^{7/4} \text{ degrees centigrade}^{5/4} \quad (15)$$

The significance of the components of equation 15 and representative values for gas (air or nitrogen) and Suniso number 6 oil are given in Table IV.

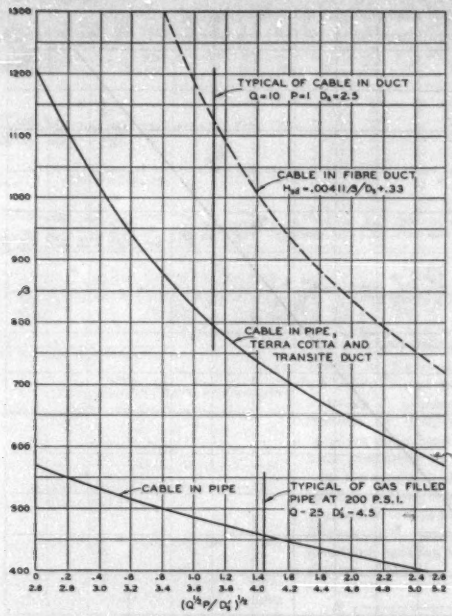

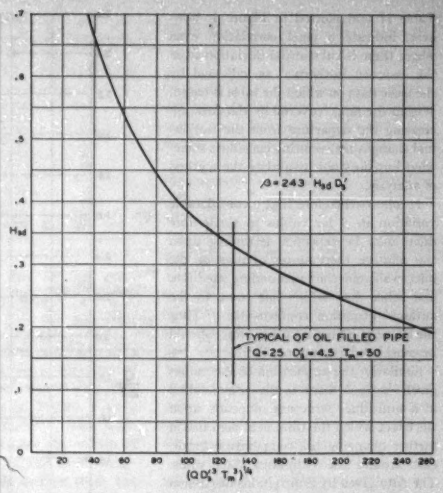

Figure 3 (left). Values of β for cables in dry single ducts and gas-filled pipe

Figure 4 (above). Values of H_{sd} for cables in oil-filled pipe

In the case of air or inert gas, these physical properties are substantially independent of temperature over the working range but the density is a direct function of the pressure. Thus, if P represents the pressure in atmospheres, from equation 15

$$K_g = 0.000755P^{1/2} \text{ watts per centimeter}^{7/4} \text{ degrees centigrade}^{5/4} \quad (16)$$

When oil is employed as the medium the physical constants are substantially independent of pressure and temperatures with the exception of the viscosity which for the type of oil commonly employed (Suniso number 6) may be taken as varying inversely as the cube of the temperature according to the relationship

$$\mu_0 = \frac{94{,}000}{T_m^3} \text{ grams per centimeter second} \quad (17)$$

The value of K for oil thus becomes

$$K_o = 0.000434T_m^{5/4} \text{ watts per centimeter}^{7/4} \text{ degrees centigrade}^{5/4} \quad (18)$$

The solution of equation 14 for the two films in series and with equation 16 or 18 substituted therein is given with sufficient accuracy by the expressions

$$\frac{Q_{cs}}{\Delta T}(\text{gas}) = 0.092\frac{D_s^{3/4}\Delta T^{1/4}p^{1/2}}{1.39+D_s/D_d} \text{ watts per degree centigrade foot} \quad (19)$$

$$\frac{Q_{cs}}{\Delta T}(\text{oil}) = 0.053\frac{D_s^{3/4}\Delta T^{1/4}T_m^{5/4}}{1.39+D_s/D_d} \text{ watts per degree centigrade foot} \quad (20)$$

From a theoretical standpoint the expression for the conduction component should take into account any eccentricity between the cylindrical radiator and the enveloping isothermal enclosure. In the practical case of cables in duct or pipe the cables will not rest uniformly on the bottom of the duct, and also in the case of a nonmetallic duct the duct wall is not strictly maintained as an isothermal. Since these effects cannot be evaluated, the familiar expression for the resistance between two concentric cylinders in terms of the dimensions of the cylinders and the thermal resistivity of the medium will be used. Thus

$$\frac{Q_{cd}}{\Delta T}(\text{gas}) = \frac{0.0213}{\log_{10} D_d/D_s} \text{ watts per degree centigrade foot} \quad (21)$$

$$\frac{Q_{cd}}{\Delta T}(\text{oil}) = \frac{0.116}{\log_{10} D_d/D_s} \text{ watts per degree centigrade foot} \quad (22)$$

The radiation component with gas as the medium is given with sufficient accuracy by the following expression based on McAdams[3] equation 5, page 61, first edition

$$\frac{Q_r}{\Delta T}(\text{gas}) = 0.102D_s\epsilon(1+0.0167T_m) \text{ watts per degree centigrade foot} \quad (23)$$

in which ϵ is the emissivity coefficient of the surface of the cable and T_m is the average temperature of the medium. The radiation term is ineffective when oil is the medium.

The over-all thermal conductivity is obtained by substituting equations 19, 21, and 23 or equations 20 and 22 in equation 13.

Table IV

Symbol	Quantity	Units	Gas at 50 C	Oil at 50 C
ρ	Thermal resistivity	C cm/watt	3,900	715
μ	Average absolute viscosity	grams/cm sec	0.000195	0.75
δ	Density	grams/cm³	0.00110 P	0.906
C_p	Specific heat at constant pressure	watt sec/C gram	0.995	3.10
g	Acceleration due to gravity	cm/sec²	980	980
ϵ	Thermal coefficient of expansion	1/C	0.00310	0.00068

Appendix II. List of Symbols

Q = total heat flow from equivalent sheath to duct wall or pipe in watts per foot
ΔT = temperature drop in degrees centigrade
P = pressure in atmospheres
D_s = diameter of the sheath in inches
D_s' = equivalent diameter of a group of cables in inches
D_d = inside diameter of the duct wall or pipe in inches

T_m = average temperature of the medium in degrees centigrade

ϵ = coefficient of emissivity of the cable surface

x and y = rectangular coordinates

a and b = experimentally determined constants

H_{td} = thermal resistance between equivalent sheath and duct wall or pipe in thermal ohm feet

H_{td}' = equivalent thermal resistance between equivalent sheath and fibre duct wall including the increased thermal resistivity of the duct wall over that of the surrounding medium in thermal ohm feet

β = equivalent surface resistivity factor in degrees centigrade square centimeters per watt

ρ = thermal resistivity in degrees centigrade centimeters per watt

μ = average absolute viscosity in grams per centimeters second

δ = density in grams per cubic centimeter

C_p = specific heat at constant pressure in watt seconds per degree centigrade gram

g = acceleration due to gravity in centimeters per second squared

e = thermal coefficient of expansion in centimeters per centimeter degree centigrade

K = a factor dependent upon the physical constants of the medium in watts per centimeter$^{1/4}$ degrees centigrade$^{5/4}$.

References

1. The Temperature Rise of Cables in a Duct Bank, J. H. Neher. *AIEE Transactions*, volume 68, part I, 1949, pages 540-49.

2. Heat Transmission (book) W. H. McAdams. McGraw-Hill Book Company, New York, N. Y., first edition, 1933.

3. Thermal Characteristics of a 120-Kv High-Pressure Gas-Filled Cable Installation, W. D. Sanderson, J. Sticher, M. H. McGrath. *AIEE Transactions*, volume 67, Part I, 1948, pages 487-98.

4. A Study of the Temperature Distribution in Electric Cables in Underground Ducts, P. J. Barenscher. *Thesis*, Department of Electrical Engineering, University of Wisconsin (Madison, Wis.), 1925.

5. Current Carrying Capacity of Impregnated Paper, Rubber and Varnished Cambric Insulated Cables. *Publication Number P-29-226*, Insulated Power Cable Engineers Association (New York, N. Y.), first edition, 1943.

Discussion

R. H. Norris and Mrs. B. O. Buckland (General Electric Company, Schenectady, N. Y.): Efficient work in the heat-transfer field on a variety of applications requires awareness of the definitions and units, in order to avoid confusion and misunderstanding. In this paper and other papers written by cable engineers, confusion arises as to the exact meaning of the expression "thermal resistivity." Resistivity as normally defined (by the American Standards Association (ASA) for example) is a property of a substance and is not affected by its geometry; for example, the resistivity of copper has a constant value at any specified temperature, while its resistance depends on its size and shape. Then the use of the word "resistivity" for surface phenomena is a misuse of the term.

To show how the distinction between resistance and resistivity enters into the picture, the thermal circuit for a single-conductor cable in air is given in Figure 1 of the discussion.

In this figure, t_{cu}, t_{sh}, and t_a are temperatures of copper, sheath, and ambient, respectively, δ is insulation thickness, ρ is thermal resistivity of the insulating material, A_L is the log mean area of the insulation for heat flow, A_{sh} is sheath area, and β_c and β_r are the cable engineers' terms for "surface resistivity" for free convection and radiation. Each fraction in the Figure is the thermal resistance; and when resistances and temperatures are known, the heat dissipation of the cable is known. But in order for the resistances to be dimensionally consistent, the dimensions of ρ must be different from the dimensions of β, and therefore ρ and β should not be called by the same name.

Since the definition of ρ as thermal resistivity conforms to ASA standards, it might be better to denote β as thermal resistance of a unit surface. Its reciprocal h, is defined as surface heat transfer coefficient, or alternatively as surface film conductance. The concept of conductance is particularly applicable here, as the total film conductance is the sum of h_r and h_c, and therefore numerically easier to handle.

The units of length used in the paper seem to be a mixture of metric and engineering units. A combination of square centimeters with feet has no logical basis. If any cable dimensions were expressed in centimeters, the mixture would be logical although not standard; but since dimensions are not so expressed, it seems time to abandon this practice and use the engineering system of units throughout.

It is therefore proposed that the AIEE Committee on Insulated Conductors take steps to persuade its adherents to become familiar with ASA standards and to use them where they apply.

R. W. Burrell (Consolidated Edison Company of New York, Inc., New York, N. Y.): The authors have presented a desirable elaboration of Appendix II of a previous paper by Mr. Neher.[1] Although the approach to the problem is not changed, the material presented in the Appendix referred to is of sufficient importance to justify a more detailed presentation.

It is apparent to those engaged in the field of cable heating that the Insulated Power Cable Engineers Association recommended value of β, while perhaps sufficiently conservative for general design, lacks the flexibility needed in comparing alternative constructions. Precise determinations of β for various types of installations may not be possible because of inherent variations in the physical constants involved; however, as additional test data are compiled, the

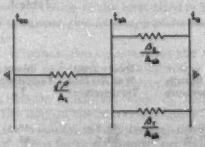

Figure 1. Thermal circuit for single conductor in air

probable range of β, for a particular case, will be better understood, thereby making possible more realistic comparisons. The authors clarify our conception of the effect of the various parameters involved in the temperature drop between cable surface and duct or pipe wall. For a given system of cables in duct or pipe, the thermal resistance will decrease sensibly with increasing watts loss.

W. B. Kirke[3] introduced this modification which is taken into account in determining cable ratings for the Consolidated Edison system.

As one follows the assumptions made in this paper, there appear various points to which exception might be taken on the ground that they are not substantiated, for example: the assumption of the same constant in the expression for the convection film at the cable surface and at the inner duct wall, the treatment of conduction on the basis of a concentric system, and the arbitrary assumption of an emissivity coefficient of the cable surface of 1.0. Yet, the important point is that putting all of these various assumptions together in the particular form given in the paper, the over-all end result does produce expressions which are reasonably satisfactory.

It is unfortunate that, while the basic equations and the selection of parameters have a reasonably sound theoretical basis, the final working expressions given are essentially empirical and do not allow an accurate determination of the separate effect of the three modes of heat transfer. On the average, the calculated values of $Q/\Delta T$ for the oil-filled pipes, gas-filled pipes, and cable in duct are about 5 per cent, 15 per cent, and 55 per cent higher, respectively, than the measured values given in Tables I, II, and III of the paper. Specialists in the field of cable heating would be interested in knowing which component or components are responsible for these discrepancies so that extrapolation into new fields could be made with confidence.

It is stated in the paper that the agreement between theoretical and empirical numerical constants of the simplified convection term is close for the case of an oil medium, but is off appreciably for the case of a gas medium. It also can be said that the conduction-radiation constant agrees with theory for the case of a gas medium; however, for the case of an oil medium, the constant theoretically appears to range from 0.60, as given in the paper, to nearly twice that value, depending upon the values of D_i' and D_d involved.

From the over-all standpoint, it nevertheless appears that the expressions for β and H_{td}, as given in equations 9, 10, and 11 of the paper are quite workable and agree with test data as well as could reasonably be expected. A high degree of accuracy in the calculation of allowable current ratings of cables is not yet to be expected but important work has been done in the past few years in clarifying our understanding of heat flow through duct structures and the earth, and this paper is an important contribution to such understanding.

References

1. See reference 1 of the paper.

2. The Calculation of Cable Temperatures in Subway Ducts, W. B. Kirke. *AIEE Journal*, volume 49, 1930, page 855.

R. J. Wiseman (The Okonite Company, Passaic, N. J.): I like the author's paper very much. It explains the three methods of heat flow from a cable to a surrounding medium, namely, conduction, convection, and radiation. Also, they give the various parameters which influence each factor namely, cable diameter, temperature, and temperature difference, and viscosity of the medium. The various formulas look quite formidable when we note terms raised to fractional powers. It is not easy to obtain the constants for each formula as they are dependent on conditions not easily calculable so it is necessary to get test data and work back to numerics which will give the desired results. It so happens that as all three modes of heat transfer are functioning at the same time, a change in dimensioning tends to work in opposite directions, reducing thereby the effect of diameter. Also the range in temperature is not great and as we take the one-fourth power of temperature difference and three-fourths power of temperature, the variation with temperature is not great.

About two years ago we decided to restudy the thermal constants we obtained when we originally set up the Oilostatic cable system. At that time we used the cylindrical log formula of ratio of internal pipe diameter to circumscribed circle over the assembled conductors, and also a constant which was a function of the temperature.

Our more recent tests showed that the thermal resistance was almost independent of temperature (a variation of about 10 per cent between 30 and 61 degrees centigrade) for an oil pressure zone and a very few per cent for a gas pressure zone at 200 pounds per square inch. We also noted that within the accuracy of testing we could safely assume the thermal resistance to vary as inversely as the diameter of the shielding tape over the insulation. As a result, we have set up two simple formulas for the determination of the thermal resistance of the pressure zone for three cables in a pipe, namely, for oil-pressure system $H=1.60/D$ thermal ohms per foot per conductor where, D is the diameter in inches over the shielding tape; and $H=2.58/D$ thermal ohms per foot per conductor for a gas pressure zone operating at 200 pounds per square inch. You will find these values of thermal resistance for the pressure zones amply accurate.

As the authors refer to the surface resistivity factor β, the values of β comparable to the above constants in $H=0.00411\ \beta/D$ are $\beta=390$ for an oil-pressure system as compared to 350 given by the authors and $\beta=627$ for a gas-pressure system at 200 pounds per square inch as compared to 450 given by the authors. We are quite confident in our values and have been using them for over a year.

Paul Greebler (Johns-Manville Corporation, Manville, N. J.): In this paper the authors have contributed immensely toward an understanding of the mechanisms of heat transfer from the cable to its surrounding pipe or duct wall. The theoretical analysis was necessarily based upon the simplifying assumption of a coaxial cable in duct arrangement. This does not, however, detract from the value of the analysis given in the paper, since this analysis gives the order of magnitude contributed by each of the three mechanisms of heat transfer.

The authors have assumed for cable in duct that the component of the thermal conductivity due to radiation can be treated as a constant in the range of normal operating temperatures. Only the component due to convection was considered as variable with changing cable diameter and heat flow. This assumption does not lead to a true picture of the variation in thermal resistivity with heat flow, or more fundamentally, with cable temperature. Mr. Barnett and I have stated in our paper[1] that the decrease in thermal resistivity with increasing sheath temperature is caused primarily by variation in the radiation component of heat transfer, and that the effect of temperature variations on convection are negligible over the normal operating range. This statement is verified by calculations based upon equation 1A of the Buller-Neher paper, which is repeated here:

$$\left(\frac{Q}{D_s'\Delta T}\right)=\underbrace{\frac{0.092\,\Delta T^{1/4}\rho^{1/3}}{D_s'^{1/4}(1.39+D_s'/Dd)}}_{\text{(convection)}}+\underbrace{\frac{0.0213}{D_s'\log D_d/D_s'}}_{\text{(conduction)}}+\underbrace{0.102\epsilon(1+0.0167T_m)}_{\text{(radiation)}} \qquad \text{(1A)}$$

in watts per degree centigrade foot inch. The emissivity factor, ϵ, is assumed to be unity at atmospheric pressure.

Table I of the discussion lists two representative sheath temperatures from our test data on fiber duct in concrete, and these temperatures might very well be representative of the operating range of a cable. The term $(Q/D_s'\Delta T)$ evaluated in equation 1A is inversely proportional to the surface resistivity factor, β.

The three terms in the equation give the thermal conductivity components due to convection, conduction, and radiation respectively. As we increase the sheath temperature over the range shown, the increase in the radiation term produced by substituting our experimental data in the Buller-Neher equation is five times greater than that of the convection term. This shows that the experimentally observed decrease in β over this range is due almost entirely to the increase in the radiation term. These calculations are based, of course, on the rather large cable size that we employed in our tests. A smaller cable size will increase the effect of the convection term only slightly, however, and not nearly enough to make its variation with temperature equal to that of the radiation term. Identical calculations with our data on Transite in concrete, Transite in air, and fiber in air, show similar relative variations in the radiation and convection terms.

The authors have neglected the variation in radiation component of conductivity with temperature, pointing out that these variations are quite small. This is justifiable from a practical standpoint. However, the variations in the convection component with temperature also should be neglected for practical considerations, since, as is shown in Table I of the discussion this factor is even smaller than the change in the radiation term. This would considerably simplify the Buller-Neher equations for the surface resistivity factor. In their equations 9 and 10, the surface resistivity factor, β, depends upon the fourth root of the heat flow. This does not have much significance since it is based upon the variation in the convection term, a second order effect compared with the radiation term. Similarly the dependence of β upon the square root of the sheath diameter is doubtful, since the change from a fourth root to a square root dependence in the convection term also was based on the very small change in convection conductivity with temperature.

The foregoing discussion was confined to cable in duct with air as the intervening fluid. Its applicability to cable in gas-filled pipe at high pressures, where convection becomes the principal mechanism of heat transfer, requires further study.

The authors have done an excellent job in helping to establish the theoretical groundwork necessary to both encourage and guide experimental workers in the duct heating problem.

Reference

1. Heat Transfer Study on Power Cable Ducts and Duct Assemblies, Paul Greebler, Guy F. Barnett. *AIEE Transactions*, volume 69, part I, 1950, pages 357–67.

A. H. Kidder (Philadelphia Electric Company, Philadelphia, Pa.): This paper by Buller and Neher, together with two previous papers by Mr. Neher,[1,2] completes presentation of the steady-state considerations involved in a project which was started about four years ago when Philadelphia Electric Company interested Mr. Neher in undertaking an investigation of fundamental relationships, as necessary to determine approximately what pipe-type cable circuit load ratings would be accurately comparable with the load ratings of conventional cable circuits in ducts.

The thermal resistance through the spaces between the cable sheaths and the pipe or duct wall inclosures is an important link in the thermal circuit. It had been hoped that a general relationship could be developed in such a form that all of the differences be-

Table I. Greebler-Barnett Data

Lead Sheath Temperature	Inside Duct Wall Surface Temperature*	Mean Temperature T_m	Temperature Drop ΔT	Buller-Neher Equation 1A: Convection Term	Buller-Neher Equation 1A: Radiation Term	Greebler-Barnett Data β in °C(cm)²/w
66.2	46.8	56.5	19.4	0.062	0.198	990
77.2	53.6	65.4	23.6	0.065	0.213	930
			increase →	0.003	0.015	60 ← decrease

*Temperatures are in degrees centigrade. The inside duct wall surface temperature is an average value.

tween cables in air in ducts and cables in high-pressure gas or oil-filled pipes could be explained in terms of the physical constants which characterize the respective fluids and the pertinent geometrical relationships.

The method presented by Buller and Neher has approximately achieved this result, at least to the extent of permitting the correlation of data obtained by various investigators at various times in various constructions. It does not disturb me particularly to find that there is some apparent difference between the effects of Transite and fiber duct walls, respectively, under the conditions which prevailed at the time the tests were made. I think we should hesitate to attach much significance to these apparent differences because there was no attempt to control the moisture content in the fiber or the Transite, or even to make the tests under conditions comparable to those to be expected in the usual exposures to natural but variable moisture conditions to be encountered in underground structures. The significant point is that Buller and Neher have obtained a correlation which now permits estimating the thermal resistance from cable to pipe or duct wall with sufficient accuracy, so that little, if any, practical improvement in cable load ratings can be gained by introducing further refinements in their analysis of this part of the thermal circuit.

REFERENCES

1. THE TEMPERATURE RISE OF BURIED CABLES AND PIPES, J. H. Neher. *AIEE Transactions*, volume 68, part I, 1949, pages 9–17.

2. See reference 1 of the paper.

F. H. Buller and J. H. Neher: Mr. Norris and Mrs. Buckland have taken us somewhat to task for our apparent inconsistency in expressing our physical units in one system and our geometric units in another. For better or worse it has long been the custom in cable rating procedure to express the physical units involved in the watt-second-centimeter-gram system, and to express lengths in feet and diameters in inches. In developing our equations it would have been more consistent to have expressed the latter quantities also in centimeters, and then to have converted the final expressions to the system of measurement used in practice. We chose to use the mixed system throughout, however, in order that the reader might be able to use any equation in the development, directly, without encountering the uncertainty which inevitably arises as to whether you multiply or divide by the transformation constants.

The use of the term "surface resistivity factor" is a slightly different matter, and as our mentors have pointed out, it has dimensions which are not those of true, or volumetric, "resistivity." Here again, this nomenclature has been hallowed by time and is thoroughly understood by cable engineers, for whom this paper was written. It should be stressed, however, that this "surface resistivity" is not a fundamental physical quantity, in the sense that volumetric resistivity is; but as pointed out, is the resistance of a unit surface of a film which, purely for purposes of convenience, is assumed arbitrarily to represent the entire thermal resistance of the composite heat transfer effects operating in the region between cable sheath and duct wall. It is unfortunate that we do not have a more distinctive name for it.

Mr. Burrell has presented a thoughtful discussion of the assumptions which we have made in developing the theory used for correlating the test data. In this respect, a book by Prof. McAdams[1] gives a constant for the convection film on the outside of a cylindrical surface in a free medium which is about 20 per cent lower than that for the inside of a pipe and which we have used for both films. We have not distinguished between the two constants because no information is given as to the values of these constants when the cylinder is placed within the pipe. While a formula for the conduction component in a non-concentric system is given by Whitehead and Hutchings[2] it is far too complicated to use in this analysis, and it reduces substantially to the concentric formula which we have employed except for extremely small separations between the cylinders at one point. Further there is considerable experimental evidence to support the assumption that the emissivity constant is substantially unity for the types of cable surfaces employed.

Discrepancies were expected, because of the assumptions which had to be made, and because the physical location of the cables within the pipe cannot be controlled. We have used assumptions and theory only to obtain a sensible understanding of the problem with which we have to deal and to determine what simplifications can justifiably be made in order to obtain practical working expressions. These working expressions were then developed directly from actual tests rather than from theory. We do not share Mr. Burrell's desire for working expressions of sufficient complexity to identify the separate effects of the three modes of heat transfer.

Dr. Wiseman's simplified formulas for calculating h_{sd} (on a per cable basis) for three cables in an oil-filled pipe or in a gas-filled pipe at 200 pounds per square inch are very interesting and similar formulas may be derived from Figures 3 and 4 of the paper assuming that Q, P, and T_m have fixed typical values. Unfortunately Dr. Wiseman's derivation of the equivalent β in his formulas gives values which are not comparable to β as defined in this paper. The corresponding relationship for β as defined in the paper is

$$\frac{h_{sd}}{3} = \frac{0.00411\beta}{2.15D_s}$$

and this yields $\beta = 290$ for the oil-pressure system and $\beta = 450$ for the gas-pressure system.

We cannot accept his formula for the oil system since its corresponding value on a total heat flow basis is $H_{sd} = 1.15/D_s'$ which is equivalent to $Q/\Delta T = 3.9$ for $D_s' = 4.5$. None of the tests cited in Table III of the paper give any support for so high a value.

Dr. Wiseman also assumes that the overall thermal resistance varies inversely with the diameter whereas we believe that a more representative variation may be deduced from the slope of the curves of Figures 3 and 4 in the vicinity of the typical operating points. Thus for $Q = 25$ watts per foot and $T_m = 50$ degrees centigrade, we derive the simplified expressions

$$H_{sd}\ (\text{oil}) = 0.70/D_s^{0/2}\ \text{thermal ohm feet} \quad (1)$$

$$H_{sd}\ (\text{gas at 200 psi}) = 1.20/(D_s')^{0.7}\ \text{thermal ohm feet} \quad (2)$$

The corresponding equations on a per cable basis and with three cables in the pipe are

$$h_{sd} = \frac{1.44}{\sqrt{D_s}} \text{ and } h_{sd} = \frac{2.07}{(D_s)^{0.7}} \text{ respectively}$$

Figures 3 and 4 are intended to give practical working values of β or H_{sd} over a wide range of operating conditions. Mr. Greebler is right in pointing out that the effect of temperature variations upon the radiation component is considerably greater than the effect of variations in the convection term which is the essential variant in Figure 3. The inclusion of the temperature of the medium in the working expressions would vastly complicate them, however, and as a practical matter this is unnecessary.

In all of the Greebler-Barnett data[3] it will be observed that β varies inversely as $Q^{1/4}$ within the accuracy of measurement. The dependence of β upon D_s cannot be evaluated from this data since only a single value of D_s was employed, but since the convection term theoretically varies directly as $Q^{1/4}/D^{1/4}$ we believe that the temperature variation in the radiation term which Greebler has mentioned will be accounted for with sufficient accuracy by expressing the Greebler-Barnett data for fiber and Transite ducts in the form

$$\beta(\text{fiber}) = 1120D_s^{1/4}/Q^{1/4}\ \text{degrees centigrade square centimeters per watt} \quad (3)$$

$$\beta(\text{Transite}) = 990D_s^{1/4}/Q^{1/4}\ \text{degrees centigrade square centimeters per watt} \quad (4)$$

This will have the effect of changing the slope of the curves when plotted in accordance with Figure 3.[4]

The corresponding values of H_{sd} assuming a working value of $Q = 10$ watts per foot are

$$H_{sd}\ (\text{fiber}) = (2.59/D_s^{1/2}) + 0.33\ \text{thermal ohm feet} \quad (5)$$

$$H_{sd}\ (\text{Transite}) = 2.29/D_s^{1/2}\ \text{thermal ohm feet} \quad (6)$$

While further theoretical and experimental work may well be undertaken in order to clear up some of the apparent discrepancies between theory and practice and to yield more factual data on the performance of cables in duct; we agree with Mr. Kidder that little of any practical improvement in cable load ratings will result. We do not wish to discourage further efforts in this direction, but we feel that it is sufficient to base cable ratings on Figures 3 and 4 of the paper or more simply on equations (1, 2, 5, and 6) just given.

REFERENCES

1. See reference 2 of the paper.

2. CURRENT RATING OF CABLES FOR TRANSMISSION AND DISTRIBUTION, S. Whitehead, E. E. Hutchings. *Journal*, Institution of Electrical Engineers (London, England), volume 83, 1938, equation 10.3, page 831.

3. HEAT TRANSFER STUDY ON POWER CABLE DUCTS AND DUCT ASSEMBLIES, Paul Greebler, Guy F. Barnett. *AIEE Transactions*, volume 69, part I, 1950, pages 587–97.

4. Discussion by J. H. Neher of reference 3 above, pages 365–66.

Development of Improved Luminous Sign Cable

L. F. ROEHMANN
MEMBER AIEE

E. W. GREENFIELD
MEMBER AIEE

TEN million feet of luminous sign cable were used last year, enough to be stretched along the entire Appalachian Trail (from Maine to Georgia). All of this cable is at high voltage, nominally rated at 5, 10, and predominantly, 15 kv. Nevertheless, installation techniques follow, by and large, accepted practice of low-voltage utilization wiring. Cables in outdoor installations are sometimes laid on roofs, in gutters, over cornices. They are exposed to sun and rain, dirt and salt deposits, notably near the sea coasts. Joints and terminals, integral components of power cables, are almost unknown to the luminous sign trade. Rubber and friction tape is applied for joints, and terminals are made by stripping the insulation. Furthermore, post-war business expanded not only in number of installations (nearly every roadside inn and many filling stations have neon signs) but equally important, the power rating of the individual installation was successively increased, first from 30 to 60, later from 60 to 120 milliamperes.

The Problem

This situation has been a challenge to the manufacturer of luminous sign cable. For various reasons there is little hope to elevate neon sign cable to the level of power cable and to ask for, and to expect, properly made joints and terminals. Rather, the problem presented to the designer is as follows:

1. Develop luminous sign cable which is safe in operation, unaffected by moisture, contamination, and salt deposits at the ends.
2. Design cable which requires no special knowledge and skill in handling but can be installed by any electrician familiar with utilization wiring.
3. Meet existing specifications,[1] notably for flame resistance.
4. Remain competitive.

To show how this challenge was met is the essence of this paper.

Previous Designs

Pre-war luminous sign cables were generally designed with a number 14 American Wire Gauge stranded copper conductor with rubber as insulation, and with saturated or lacquered textile braids as covering (sign cables have no shield). Comparatively large diameters provided the necessary dielectric strength, and flame-resistance was obtained by suitable impregnants. End failures due to contamination occurred on occasion, and necessitated replacements, notably in exposed locations.

During the last war, polyethylene was developed and used in ever-increasing quantities for the manufacture of high-frequency cables (type *RG-/U*). Its outstanding dielectric properties, coupled with the fact that the mills had acquired the "know-how" of its processing and extrusion, made it a natural choice for the insulation of post-war luminous sign cables. Unfortunately, plain polyethylene when ignited continues to burn and develops flaming drops. It is therefore unacceptable for luminous sign cable. As a consequence, the first post-war sign cables had an extruded plain polyethylene core over the conductor, and an over-all extruded, flame retardant, black polyvinyl-chloride jacket. Conservatively, the first cables of this type had a rather heavy wall of polyethylene (85 mils, for 15-kv cable). Soon afterwards, however, one manufacture reduced the polyethylene wall thickness to 55 mils, for 15-kv cable, and other manufacturers followed suit. Such *GTO-15* cable (Gas Tube and Oil-burner ignition cable, 15 kv) has an over-all diameter of approximately 1/4 inch, smaller than a pencil but operates satisfactorily, dielectrically, because of the high dielectric strength of polyethylene, and satisfactorily as to flame-resistance, because of the polyvinyl-chloride jacket. End failures due to contamination, however, and failures in splices continued to occur occasionally.

Laboratory Investigations

In fact, it were reports of certain end failures, notably in installations along the sea coasts, which accelerated our development program on this type of cable. As a first step, the operation of a complete installation with transformer, tubes, and cables was studied in the laboratory.

Operating Conditions—Electrical

Figure 1, top, shows schematically a luminous sign transformer: primary, 115 volts, 60 cycles; secondary, 15 kv, 60 milliamperes. This is a high-reactance transformer which inherently limits the current to the rated value.[2] The transformer is connected by means of *GTO* cables to a luminous sign (two sections, with the midpoint grounded). Figure 1, bottom, shows high-voltage rms; high-voltage, crest; and sign current as a function of primary voltage. Before the sign ignites, the voltage shape is approximately sinusoidal, and the ratio of crest to rms is approximately 1.4. Tube current is zero. Once the tube ignites, at some 60-volts primary, the transformer rms voltage value decreases but the crest reaches 10 to 12 kv to ground. Ratio between crest and rms then becomes 3.5, at rated primary voltage. The reason is evident from Figure 2 which shows oscillograms of the

Paper 50-53, recommended by the AIEE Insulated Conductors Committee and approved by the AIEE Technical Program Committee for presentation at the AIEE Winter General Meeting, New York, N. Y., January 30–February 3, 1950. Manuscript submitted October 3, 1949; made available for printing December 7, 1949.

L. F. Roehmann and E. W. Greenfield are both with the Anaconda Wire and Cable Company, Hastings-on-Hudson, N. Y.

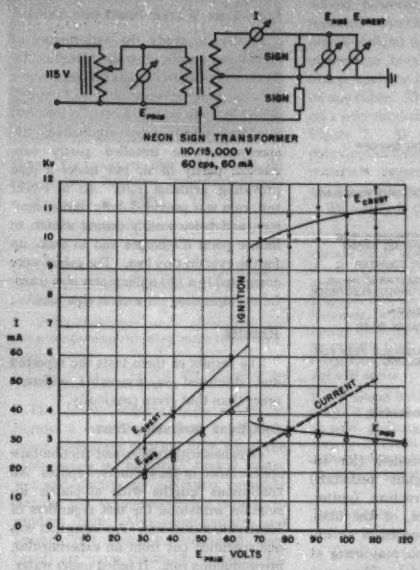

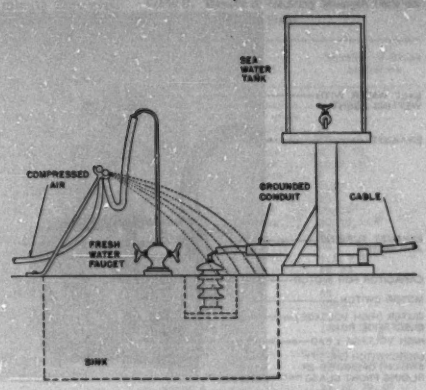

Figure 1 (left). Neon sign load characteristics before and after tube ignition

Figure 3 (above). Simulated service tests for terminal tracking strength investigation

high voltage before and after ignition of the tube. After ignition, the gas column breaks down, every half wave of 60 cycles, and the steady state is reached after a damped oscillatory discharge. Oscillation frequency depends on the circuit parameters. In the case shown it is in the order of 4 kilocycles per second. Small wonder then that these high crest voltages, in conjunction with an elevated frequency, necessitate an insulation of exceptionally high dielectric strength.

Operating Conditions—Physical

But this is only half of the story. Outdoor signs, where most of the failures occurred, have the cables installed, or supposedly installed, in grounded metallic conduit. Between conduit end and high-voltage sign electrode, the National Electrical Code[3] specifies a clearance of four inches for the commonly used *GTO-15* cables. It is in this clearance length that trouble due to intense surface discharges developed on occasion, particularly in locations near the sea-coast.

Simulated Surface Discharge Tests on Cables

Early in the course of the laboratory investigation, salt deposits were suspected as a contributory factor for such terminal discharge failures. A set-up was constructed therefore to simulate field conditions and to induce terminal "tracking" failures in the laboratory. Figure 3 shows the apparatus. A neon sign transformer operating on a neon sign load is connected to the cables under test which are installed in grounded conduits. The conductor is connected to a terminal block, and the 4-inch exposed length is alternately sprayed with sea-water and fresh water, with wind-drying (compressed air) and calm-drying periods in between. The cycle as arbitrarily established is given in Table I.

Table I. Spraying Cycle

Sea-water spray	5 minutes
Wind-drying	25 minutes
Calm-drying	1½ hours
Fresh-water spray	5 minutes
Wind-drying	25 minutes
Calm-drying	1½ hours
Total time, one cycle	4 hours

Figure 2. Oscillograms of high voltage

(Left) before tube ignition
(Right) after tube ignition

The main idea of the test procedure was to have first, a salt deposit dried on, and afterwards washed off by a rain.

In testing cables with this equipment, ten spray cycles were tentatively established as a satisfactory limit. It was found that a good insulation or covering which stands ten spray cycles will stand many more while a poor dielectric will fail before 10 cycles are completed. Furthermore, ten spray cycles were established for practical reasons because they are completed in a 5-day week (two 4-hour cycles per day).

Slab Cell Tests

In addition, for evaluating the surface discharge strength of compounds, a slab cell was built in the course of our development work. Such a cell dispensed with the necessity to manufacture luminous sign cables for the sole purpose of compound evaluation. The cell, Figure 4. is fashioned after one described some years ago by K. S. Wyatt[4] which, in turn, appears to have been based on a Swiss design. Basically, two concentric electrodes are placed on the test material in slab form, and salt water, containing some wetting agent, is dropped on the slab into the space between the electrodes. Dropping rate is approximately one drop every three seconds, and the number of drops to surface breakdown is then an index of the surface discharge strength. As we were interested in compound evaluation for luminous sign cables we energize the cell from a neon sign transformer operating on a sign load. Such high-voltage opera-

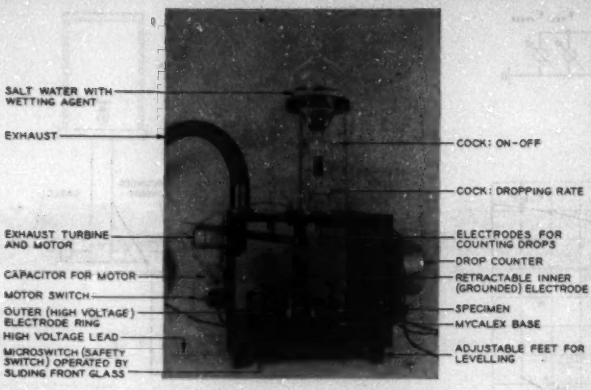

Figure 4. Slab cell for evaluating tracking strength of insulating materials

tion necessitated a safety interlock. In addition, a sensitive counter is provided for counting the number of drops to breakdown. A specimen fails when the neon sign permanently extinguishes, after which the number of drops is read on the counter. Similar tests have been described recently by Yarsely and Grant.[8]

In making tests with the slab cell, no number of drops was specified, even tentatively, as a criterion for good and poor dielectrics. The slab tests were exploratory, and intended to give an idea of classes of dielectrics and surface treatments, rather than of specific formulations or colorings. It appears that dielectrics which fail at less than 50 or 60 drops will be unsatisfactory with respect to tracking, and not worth investigating further for sign cable application.

Point Discharge Tests

Another set-up was devised for testing "wet-ground contacts" that is, point discharges which may occur when a wet cable, otherwise ungrounded (for instance, mounted on glass pedestals) touches a grounded structure (gutter, metal frame of the sign, or the like). Such surface point discharges of an unshielded high-voltage cable may occur at any point (not at the ends). They were considered as a possible source of occasional failures for instance well inside a grounded conduit in contradistinction to end discharge failures, which are relatively more common.

The test set-up is shown in Figure 5. The cables, connected to a neon sign load and with ends well protected, are draped over a grounded metal angle and intermittently sprayed with artificial rain. The illustration, a double exposure, shows point discharges at the two cables in the rear.

Figure 5. Point discharge test

Notice discharge on the two rear cables where they make contact with grounded angle

Figure 6. One-year immersion test

Installation of cables and splices in water tank

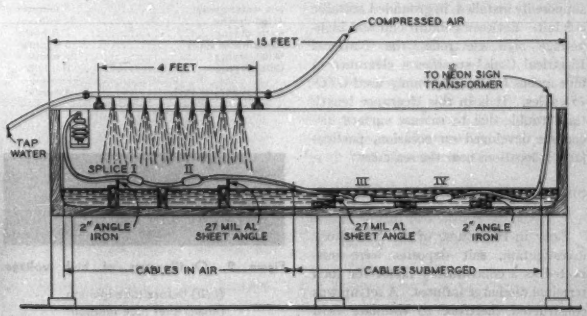

Long-Time Water Immersion Tests

Finally, to study the performance of splices and unspliced straight lengths, 20-foot specimens were installed in a water tank as shown schematically in Figure 6. With the ends well protected so that end discharge effects were eliminated, the specimens were installed partly submersed, partly in air but under a pipe providing artificial rain. In a 1-year test, rain was provided daily during summer, and twice weekly during winter, to induce point discharges and to make up for the evaporation loss. The cables were connected to a 120-milliampere sign transformer operating on a neon sign load.

Results

The results of these tests are reported and discussed in somewhat different order than that given previously.

One-Year Immersion Test

All cables with rubber-and-friction-tape splices failed in the submersed splices. All continuous lengths with all-plastic insulation withstood the test regardless of construction and size. An exception was one specimen cut from an experimental, preproduction run. It failed under water. No failures due to point discharge occurred though point discharges (sparks) were observed at the grounded angle supports, after wetting.

We conclude therefore as follows:

1. Rubber-and-friction-tape splices are not permissible in exposed sign cables. Plastic tapes, for instance polyethylene tape, may show better performance but have some practical disadvantages: they are fairly expensive, and one cannot expect that the electrician who installs a sign will have such tape at hand and use it. As sign cable runs are short as a rule, and sign cable is fairly inexpensive, only continuous lengths should be used, particularly in exposed, outdoor installations.

2. All-plastic insulated cables are adequate even under severe operating conditions pro-

Figure 7. Luminous sign cable GTO–15, polyethylene insulation, polyvinyl-chloride jacket

Jacket damage due to point discharge

vided the question of end-discharge is taken care of (ends either immune to tracking, or ends properly prepared or protected).

3. Point-discharges while observable are too weak to cause, at most, more than superficial damage.

Point Discharge Tests

The point-discharge tests shown in Figure 5 confirm the last conclusion. Point discharges develop only when the cable surface is "mottled," that is, partly wet and partly dry. Neither complete wetting nor complete drying is able to produce them. Also, some surfaces and finishes (for instance, lacquered glass braid) are more conducive to point discharges than others. The surface voltage is high, as measured with probe ring and electrostatic voltmeter. The energy involved, however, is so minute that even repeated "mottling" produces, at worst, but superficial damage. Despite patient efforts, no breakdown from point discharge could be induced in the laboratory on any cable. The small damage obtained on a polyvinyl-chloride jacket is shown in Figure 7. As will be discussed later, polyvinyl-chloride is among the poorest materials regarding resistance to discharges when exposed to water spray.

We conclude therefore as follows:

1. Point discharges of unshielded high-voltage cable inside a wet conduit, or at a metal support, are not conjectures but an actuality.[4,7] They can be seen and photographed, and the voltage can be measured. However, in luminous sign installations the energy involved in these brush discharges is so minute that, under the worst possible conditions, not more than superficial damage will occur.

2. It seems unlikely that the rare failures inside a grounded conduit can be ascribed to point discharges only, without contributory factors such as insulation damage from a sharp edge or burr or foreign matter, overstressing in pulling, or the like.

Resistance to Surface End-Discharges—Simulated Spray Tests

The results of these tests are particularly important, as they furnish the basis for improved luminous sign cables.

Table II. Results of Tracking Strength Tests on Slabs

Specimen Material	Number of Drops to Failure
Silicone varnished glass cloth	4, 3, 4
Silicone, varnished glass cloth plus silicone grease	9
Buna S, plus silicone grease	17
Polyvinyl-chloride white	9, 15, 16
beige	15, 9, 10
yellow	7
green	9, 17
red	10
blue	20, 24
black	20, 12, 15
Polybiend	37
VGA Bakelite	30
Neoprene A	1, 6, 1, 1
Neoprene B	29, 23
Varnished cloth	68
Varnished glass	62
Buna S	100+
Buna S plus silicone grease	17
Polyethylene pure	100+, 100+, 100+
Polyethylene 3 per cent reclaim	100+
Styraloy	100+, 100+
Experimental jacket compound A	38, 56, 29, 40
Experimental jacket compound B	75, 100+, 61, 63
Experimental insulation plus jacket compound	80, 73

First of all, the end failures obtained in the laboratory closely resembled those obtained in the field. Evidently, the test set-up reproduced the field conditions.

Secondly, all cables, regardless of size and specific construction, developed end failures in less than ten spray cycles. Representative cables tested are shown in Figure 8. Failures occurred on the commercially used rubber insulated cables. For instance, the all-rubber construction, without jacket or braid, failed in the third cycle. A rubber insulation, covered with an asphalt-saturated cotton braid showed particularly poor tracking re-

LUMINOUS SIGN CABLES GTO-15
RESULTS OF SIMULATED SERVICE TESTS

CABLE CONSTRUCTION	O.D. INCHES	PERFORMANCE
ALL RUBBER	0.417	FAILED 3RD CYCLE
RUBBER, 1 COTTON BRAID, ASPH. SAT.	0.395	FAILED 1ST CYCLE
RUBBER, 2 COTTON BR., LACQUER	0.439	FAILED 5TH CYCLE
RUBBER, 2 GLASS BR., LACQUER	0.315	FAILED 2ND CYCLE
RUBBER, P.V.C. JACKET	0.350	FAILED 3RD CYCLE
RUBBER, NEOPRENE JACKET	0.370	FAILED 2ND CYCLE
POLYETHYLENE, P.V.C. JACKET	0.245	FAILED 3RD CYCLE
POLYETHYLENE, P.V.C. JACKET	0.256	FAILED 3RD CYCLE
POLYETHYLENE, EXP. JACKET "A"	0.242	NO FAILURE IN 10 CYCLES
POLYETHYLENE, EXP. JACKET "B"	0.250	NO FAILURE IN 10 CYCLES
EXP. INSUL. PLUS JACKET COMP.	0.234	NO FAILURE IN 10 CYCLES

Figure 8 (left). Display board

(Left) cutback ends
(Right) tested ends

Figure 9 (below). Cable ends after tracking tests

Top—Rubber, two glass braids, lacquer: failed second cycle
Center—Polyethylene insulation, polyvinyl-chloride jacket: failed third cycle
Bottom—Flame-retardant polyethylene-derived compound: No failure in ten cycles

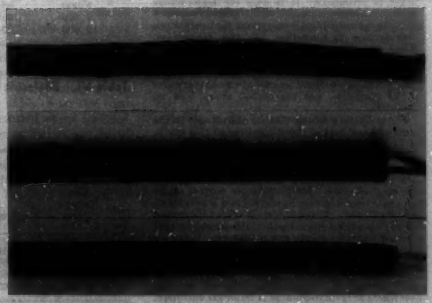

Table III. Physical Properties of Type *FR* Compound from GTO-15 Cables

Initial tensile strength, psi	1,730
Initial elongation, per cent	471
Cold bend limit, degrees centigrade	−68 Underwriters' test—Mandrel of 1 times cable O.D.
Specific gravity, g/cc	1.28
Softening temperature, degrees centigrade	+109

Accelerated Weathering in Weather-o-Meter

	After 500 Arc-Hours	After 1,000 Arc-Hours
Tensile strength, psi	1,448	1,360
Tensile strength, per cent of initial	83.6	78.6
Elongation, per cent	137	233
Elongation, per cent of initial	29.1	49.5
Cold bend limit, degrees centigrade	between −60 and −68	between −60 and −68

Table IV. Dielectric Properties of Type *FR* Compound

Slab Tests—Blue Stock

Frequency	Power Factor Per Cent 25 C	60 C	85 C	Dielectric Constant 25 C	60 C	58C	Insulation Resistivity Megmegohms—Cm 25 C	60 C	85 C
D-c							>300		197
60 cps	0.23	0.33	0.37	2.60	2.59	2.51			
1 megacycle	0.33	0.23		2.63	2.58				
25 megacycles	0.30	0.13		2.55	2.47				
70 megacycles	0.18	0.13		2.38	2.28				

sistance: it failed in the first cycle. A cable with Neoprene jacket failed in the second spray cycle. A cable with rubber insulation and two lacquered glass braids failed in the second cycle. This cable, together with two other constructions, is shown in Figure 9.

Of particular interest are the polyethylene-core, polyvinyl-chloride jacket constructions which failed in the second and third cycles, Figures 8 and 9. When the polyvinyl-chloride jacket was cut back four inches and removed from the end, thus exposing the polyethylene insulation, no failure occurred within ten spray cycles. Clearly, it is the polyvinyl-chloride which has the low resistance to tracking and which is responsible for the poor performance under high voltage.* Contrariwise, polyethylene has a very high resistance to tracking. It is therefore recommended that for such cables the jacket be stripped off at least four inches back from the tube terminal.

However, such procedure is an expediency. It is not an ultimate solution because the cutting back, unless done with proper tools and with proper care, may damage the insulation, thus doing more harm than good. Furthermore, it seems illogical to provide a flameproof protection within a metallic conduit but to remove it where the cable emerges from the protective enclosure.

For these reasons, development work proceeded towards the following objectives:

Develop a plastic insulation for high-voltage application which has: high dielectric strength; flame resistance; and high tracking resistance.

Such compound to be extruded as a one-wall insulation, without protective jacket. Alternatively, develop a jacket which is flame resistant and tracking resistant, and which is to be extruded over an insulating polyethylene core.

Slab Tests

With these objectives in mind, a number of existing compounds, and new experimental compounds, were evaluated regarding their tracking resistance. Representative results are summarized in Table II. Corroborating the spray tests, polyethylene was again found to be excellent, and polyvinyl-chloride comparatively poor along with siliconed surfaces, neoprene and a number of other commonly used materials.

Experimental compounds were developed by our Plastics Laboratory in June 1948 which achieved the desired objective. These compounds were, essentially, mixtures of polyethylene and chlorine compounds. The latter constituent imparted flame-resistance to the former without lowering the dielectric and tracking strength of plain polyethylene to

Table V. Dielectric Properties of GTO-15 Cable with Type *FR* Insulation—One Wall, No Jacket

Over-all Diameter 0.260 Inch—Black Stock

Test Voltage, Volts	Frequency	Average Stress, Volts Per Mil	Power Factor 25 C Per Cent	Capacitance 25 C, μμF/Ft	Dielectric Constant, 25 C	Insulation Resistance, 25 C Megmegohm, Cm
220	Dc					>10⁹
5,000	60 cps	54.6	0.81	36	3.75	
7,500	60 cps	80.7	0.86	36	2.75	
10,000	60 cps	112.0	0.92	36	2.75	

Table VI. Dielectric Properties of GTO-15 Cable Using Regular Polyethylene Insulation and a Type *FR* Compound Jacket

Over-all Diameter 0.238 Inch—Blue Stock

Test Voltage Volts	Frequency	Average Stress, Volts Per Mil	Power Factor 25 C, Per Cent	Capacitance 25 C, μμF/Ft	Dielectric Constant, 25 C	Insulation Resistance, 25 C Megmegohm, Cm
220	Dc					>10⁹
1,000	60 cps	12.2	0.42	35.6	2.58	
5,000	60 cps	60.8	0.66	35.6	2.58	
7,500	60 cps	91.0	1.38	35.6	2.58	

* The following remark about polyvinyl-chloride insulations and jackets seems in order. Any impression gained from this paper that polyvinyl-chloride is generally unsuitable as insulation or jacket is erroneous. It is only for high-voltage application where the question of tracking resistance under moist conditions is important that polyvinyl-chloride has its limitation. In this connection, Boyer and Woodland[9] ascribe the relatively low tracking resistance of polyvinyl-chloride and similar compounds to their conjugated double bond structure. *HCl* is produced as one of the by-products of the discharge, and the carbon atoms link up rapidly.

For utilization wiring that is, at voltages in the order of 1 per cent of those discussed in this study, polyvinyl-chloride has its outstanding merits. Building wire with polyvinyl-chloride insulation is rightfully used in ever-increasing amounts. There is no better insulation for machine tool wiring than polyvinyl-chloride. Multiconductor control cables have polyvinyl-chloride insulation and a polyvinyl-chloride jacket. Communication cables for carrier current operation have a polyvinyl-chloride jacket over polyethylene-insulated conductors. It is only in the field of higher voltages where surface tracking becomes a problem that polyvinyl-chloride jackets are objectionable. The new flame retardant polyethylene-base compounds, fortunately, take over where polyvinyl-chloride is no longer adequate.

Table VII. *GTO-15* Cable with Type *FR* Compound Insulation—One Wall, No Jacket

Over-all Diameter 0.271 Inch—Blue Stock—Long-Time Saline Water Absorption Test at Room Temperature

Immersion Time, Months	Power Factor, 60 cps, 400 V, 25 C Per Cent	Dielectric Constant, 400 V, 25 C	Insulation Resistance 25 C Megohm—1,000 Ft
Initial	0.35–0.40	2.35	>10,000
1	0.44–0.46	2.30	>10,000
2	0.45–0.46	2.40	>10,000
3	0.50–0.58	2.40	>10,000
4	0.51–0.55	2.38	>10,000
7	0.52–0.53	2.40	>10,000

such a degree that the material would not pass the specified tests. Experimental lengths of sign cable were manufactured with such compounds both as 1-wall insulation, and as jacket over plain polyethylene. In every case, ten spray cycles were sustained without failure, and without any visible damage to the ends.

Commercial Compounds

At this stage of development, one of the large chemical manufacturers offered us new, experimental, flame-retardant polyethylene-derived compounds for evaluation. This offer fitted accurately into our development program. All the routine physical and dielectric tests were undertaken. One compound, which we have tentatively designated as type *FR* (flame retardant) was selected. Some of its physical and dielectric properties are given in Tables III and IV. Significant physically are the extremely low cold bend limit on one end of the temperature scale, and the high softening temperature (over 100 degrees centigrade) on the other. Dielectrically, the compound has a very low power factor, comparable to oil-impregnated paper, and a dielectric constant of about half of that of rubber. The consequences are low dielectric loss at high voltage, and reduced capacity per unit length. The latter factor may have some future bearing on *Section 6031g* of the National Electrical Code which now limits cable runs of cable above 5 kv to ground to 20 feet, in metal raceways.

Experimental sign cables were manufactured from the new compound. Some of them had the type *FR* compound extruded in one wall (without a jacket), others had it extruded as a jacket over a core of plain polyethylene. These cables were subjected to the routine sign cable tests (mandrel test, flame-resistance test). In addition, they were subjected to the special tests described in this paper (spray test for tracking resistance, point discharge test, and long-time immersion test) and to the tests reported in Tables V, VI, and VII, namely dielectric properties as a function of voltage and of time. The test results indicated that the new cables met not only the requirements previously set up for this type of service, but also were highly tracking resistant. Both types of cable construction have been tested and approved by the Underwriters' Laboratories.

These cables maintain flexibility at very low temperatures, are resistant to heat, to moisture, and to the many solvents to which polyethylene can be exposed. Most important, they have the following features:

1. They are safe in operation—they withstand the ultra-conservative mandrel test for dielectric strength.

2. They are flame-retardant—they do not support combustion and develop no flaming drops.

3. They are the only sign cables with high tracking resistance—they will not develop end failures in moist and dirty locations. There is no need for special end preparation.

References

1. Standards for Gas-Tube Sign and Ignition Cables. Underwriters' Laboratories, Inc., (Chicago, Ill.), third edition, 1948.

2. High-Reactance Transformer Supply, J. A. Uttal. *Electrical World* (New York, N. Y.), January 31, 1948, pages 50–52.

3. National Electrical Code. National Fire Protection Association (Boston, Mass.), 1947.

4. The Trend of Power Cable Research in America, K. S. Wyatt. *Electrical Power Engineer* (London, England), March 1939, pages 191–200.

5. Tracking in Solid Insulating Materials—A Critical Résumé, V. E. Yarsley, W. J. Grant. *Technical Report L/T 177*. The British Electrical and Allied Industries Research Association (London, England), 1948, 16 pages.

6. Braid Discharge in Single Conductor Cable in Ducts, M. J. Lowenberg. *AIEE Journal*, volume 47, July 1928, pages 534–35.

7. Semiconducting Shielding for A-C Power Cables, Edwin J. Merrell. *Electrical Engineering* (*AIEE Transactions*), volume 65, August–September, 1946, pages 605–09.

8. Some Arc Resistance Studies on Plastics, R. F. Boyer, P. G. Woodland. Conference on Electrical Insulation, National Research Council (Washington, D. C.), 1947, page 18.

Discussion

G. S. Eager, Jr. (General Cable Corporation, Bayonne, N. J.): The authors have presented a great deal of useful information concerning the postwar *GTO-15* cables. Since these cables operate at a relatively high voltage and the terminals are generally not protected, surface tracking may develop under some conditions.

The authors have chosen to represent the conditions which cause surface deterioration by a special cycle of fresh- and salt-water spray, with intermediate drying periods. While this has contributed to their study, we believe that more realistic information can be obtained by the aid of a quite different cycle of testing. During the four-hour-long cycle, significant deterioration occurs during only a very small proportion of the time. No account is taken of the serious effect of soot deposits and of the fact that the deteriorating effect of a mist or fog is much longer lasting than that of a rain which soon washes away contaminants which have been accumulating in dry weather. Moreover, in our interior cities, the deteriorating conditions usually do not include salt spray.

In our accelerated tests, intended to simulate the damaging kinds of service conditions, we have represented these by soot accumulations which may be accompanied by an atomized spray of fresh water or of salt water. Our tests show that, under dry conditions and with natural soot contamination only, satisfactory life can be expected from cables made with (1) polyethylene core, polyvinyl-chloride jacket, (2) rubber core, glass braid, lacquer, (3) one wall of polyvinyl-chloride. These results are substantiated for the most part by field performance.

If, now, these soot-covered dry samples are sprayed with tap water by means of an atomizer, our tests show that a polyethylene surface is superior to a polyvinyl-chloride surface in resisting surface tracking. These simulate conditions inland from our coasts where soot or dust and rainwater are the contaminating agents.

Along the Atlantic and Pacific coasts, salt must be added to the soot and water in order to make a reasonably complete contaminant test. Such tests show that while natural and flame-resistant polyethylene can be made to fail by the formation of a semiconducting path on the surface with normal voltage and creepage distances, the two types appear to be not greatly different in ability to resist the formation of a semiconducting path on the surface with soot and salt-water contamination.

The fact that natural polyethylene with a suitable creepage distance is giving good field service indicates that field conditions

are generally less severe than the surface contamination conditions of our soot-salt-water tests.

S. J. Rosch (Anaconda Wire and Cable Company, Hastings-on-Hudson, N.Y.): The paper by Dr. Roehmann and Dr. Greenfield is a real contribution to a phase of electrical engineering, replete with a number of phenomena on which very little information has been available in the engineering literature.

During the past fifteen years, the present discusser has had the opportunity of personally examining numerous luminous-sign installations where failure of the high-voltage conductor had occurred. The defects examined were not confined to any one design but included every type available on the market. Many of these defects were of a type that readily disclosed the cause, particularly those which occurred due to flashover from the protruding end of the cable to the metallic conduit in which it was installed. However, there were numerous other instances where no defects appeared at the protruding ends but rather in that portion of the length included well within the conduit. These latter defects occasionally were accompanied by very visible signs of tracking along the surface of the outer covering; evidence of such tracking sometimes even was visible below the fibrous outer covering where some type of rubber compound was used as insulation.

The experimental laboratory investigations described in the paper very ably reproduced many of the different types of defects found to have occurred under actual service conditions, thereby throwing considerable light on the mechanism leading to these failures. Once these mechanisms were understood the way was opened to eliminate them, and this present paper offers one method for such approach, which has proven very effective. Others will undoubtedly be developed as soon as these failure mechanisms are thoroughly understood.

The implifications in this paper should go far beyond the question of improved luminous-sign cable. The solution for the development of the latter consisted in finding a thermoplastic material possessing excellent flame-retarding properties without dripping when exposed to flame, excellent resistance to a wide variety of liquid media, resistance to weathering and ozone, and, at the same time, possessing electrical properties comparable to some of the very best electrical insulating materials available to the industry to date. When it is further considered that this new material can be flexed during installations at subzero temperatures, that it readily can be applied with existing facilities, and that, coincident with these properties, it also possesses excellent resistance to high-voltage surface discharges, it becomes apparent to the cable designer and user that here is a material which offers a new approach to the solution of a number of vexing cable problems in the power, communication, and signalling fields.

L. F. Roehmann and **E. W. Greenfield:** Mr. Eager's discussion is much appreciated. There appears to be general agreement with regards to the superiority of polyethylene and polyethylene-derived materials in resisting surface discharges induced by electrolytic contaminations.

There are a few points to be clarified, however. Mr. Eager questions the severity of our aging cycle and indicates that an atomized spray is more severe than a watery downpour. We agree. In all of our tests, a finely divided spray has been used; this is evident from the paper. It is significant to note that only two or three spray cycles are sufficient in most cases to eliminate all but the best track-resistant materials.

With regard to the question of salt spray versus soot contaminations, we believe there may be some misunderstanding concerning the basic phenomena involved in tracking. Tracking is a surface discharge along an insulator in the presence of moisture and an electrolyte. A dry surface, even if contaminated with, for instance, soot, does not track; neither does a moist surface when an electrolyte is absent. On this basis, even soot plus water does not necessarily induce tracking because soot, in its narrow sense, is finely divided carbon. The soot particles are islands, conductive islands so to speak in a sea, but unless the sea is electrolyzed, either because the soot or the water is impure, no tracking will take place. On the other hand, sea water, with its known and reproducible composition, is a strong electrolyte, and readily induces tracking.

Use of a sea-water spray was predicated primarily because most of the field tracking failures came from the Eastern and Western seaboards. However, it was soon realized that the principle by which any dirt or other surface contamination induced tracking was by virtue of the ionizable salts present in the contaminants. Thus sulphates, carbonates, phosphates, and many others, both inorganic and organic, when present as inherent ingredients of surface contaminations, liberate free ions in the presence of moisture and initiate the surface discharges which prove so destructive to most cable materials. The dry dust itself is unimportant—the hydrolysis of the salts is of greatest importance. It is for these reasons that standard sea-water spray was adopted as contaminant; we believe it has answered the purpose admirably.

It gives us satisfaction that the tests made at General Cable Corporation confirm our findings of the superiority of polyethylene over polyvinyl-chloride regarding tracking. On the other hand, Mr. Eager states that "the two types appear to be not greatly different in ability to resist the formation of a semiconducting path on the surface with soot and salt-water contamination." This brings us back to the picture of the carbon islands in an electrolyzed sea. If the islands become so numerous, or so large as to form a semiconducting parallel path to the cable termination, the cable end may well be damaged by the heat generated in this parallel path. This, however, is not tracking. And while this differentiation may sound academic, it should be emphasized that no failures were reported to us on plain or flame-retardant polyethylene terminations.

Thus, it seems to be tracking one has to contend with in the field, and the new nontracking flame-retardant polyethylene-derived resin seems to be a distinct progress in the art.

The authors are appreciative of Mr. Rosch's kind words. As he has stated, the findings of our present paper are applicable to many other types of cable services. We hope to bring, in due time, such further developments to the attention of the engineering profession.

Heat Transfer Study on Power Cable Ducts and Duct Assemblies

PAUL GREEBLER
NONMEMBER AIEE

GUY F. BARNETT
ASSOCIATE AIEE

STUDIES of heat transfer on power cable in duct have indicated the need for more experimental data to establish thermal resistivity values for several components of the duct system, particularly that portion of the heat flow path from the cable sheath to the outer duct wall surface. Theoretical considerations of heat transfer from the cable to the outer duct wall surface have treated the duct wall as an isothermal surface; and, generally, no consideration has been given to the effect of the thermal resistivity of the duct material upon the heat flow from the cable. These approximations are made necessary in theoretical studies of cable systems by the complex geometry of the duct assembly, the cable sheath resting nonuniformly at the bottom of the duct. While such studies, supported by the experimental evidence available, yield reasonably accurate thermal resistivity values, the effects of a nonisothermal duct wall and of the thermal resistivity of the duct material can be taken into account by performing measurements on a duct assembly.

In 1938 a study of heat flow in duct systems was begun at the Johns-Manville Research Center to determine the thermal resistance of the components of the heat flow path in a duct assembly. Transite and fiber duct, the latter possessing the higher thermal resistance, were selected for the tests.* Preliminary experiments were performed with each type of duct encased in concrete and buried in earth, an iron pipe enclosing a heater resting on the bottom of each duct. The temperature of the iron pipe in the Transite was sufficiently different from that in the fiber duct, both measured under conditions of equal heater load, to justify further study of the effects of the thermal resistivity of the duct upon the thermal resistance from sheath to outer duct wall surface in a cable system.

After about two years, during which time tests and procedures were established, the control apparatus was designed and assembled; and work was started on the first stage of the 2-stage program, which was planned to include investigation of (1) ducts in air; (2) single duct encased in concrete. This paper contains a description of the tests covering this program, and the application of the test results is indicated to the solution of heat flow problems in duct banks.

Thermocouple Assembly

Eight-foot lengths of Transite and fiber duct were employed for the tests in air. The main components for this test are the duct, the lead sheath resting on the bottom of the duct and containing a Calrod heater along its axis, and the apparatus for regulating the power supply and measuring the thermocouple electromotive forces.

Since the geometry of the duct assembly is not radially symmetric, it was realized early in the study of this problem that, in order to obtain an accurate average temperature around a duct surface, it would be necessary to use a large number of thermocouples spaced circumferentially around the surface. Furthermore, it was recognized that the temperature distribution along the length of the duct would be nonuniform due to the irregular contact between the inner duct wall surface and the lead sheath; and so it was necessary to space the thermocouples along the duct length as well. A 2-foot length of duct, placed in the center of the 8-foot assembly, was employed for the measurements. Thus 3-foot sections of duct on each side of this test length served as guards, reducing end effects and thereby allowing the test area to more closely represent a small section of a long duct.

A preliminary survey of the temperature distribution around the duct surfaces showed that 48 thermocouples along the 2-foot length placed in a 3-turn helix of 16 couples per turn would provide enough temperature readings to yield a true

Paper 50-55, recommended by the AIEE Insulated Conductors Committee and approved by the AIEE Technical Program Committee for presentation at the AIEE Winter General Meeting, New York, N. Y., January 30–February 3, 1950. Manuscript submitted July 18, 1949; made available for printing December 8, 1949.

PAUL GREEBLER is a physicist with the Johns-Manville Research Center, Manville, N. J., and GUY F. BARNETT is Electronics Engineer with the National Bureau of Standards, Washington, D. C., formerly with Johns-Manville Research Center.

The authors wish to acknowledge the helpful suggestions and contributions to this paper by M. H. McGrath of the General Cable Corporation, C. B. Bradley of the Johns-Manville Corporation, and also to Mr. Dillon, Mr. O'Donnell, Mr. W. Gulick, and to members of the Physics Section.

Figure 1. Thermocouple assembly on outside duct surface

* The respective ducts referred to herein are type *I* fiber conduit covered in Federal Specification *W-C-581*, August 1, 1939; and asbestos cement conduit type *I* (J-M Korduct) covered in Federal Specification *W-C-571*, April 3, 1942. Both ducts are of 0.31-inch wall thickness.

Figure 2 (left). Front view of control board. Power and thermocouple circuit components are numbered as follows: (1) fuse boxes and transtats, (2) ammeter, (3) integrating wattmeters, (4) celectray temperature controller (5) pilot lights (6) type *K*-2 Leeds and Northrup potentiometer (7) galvanometer spot reference glass (8) type *R* Leeds and Northrup galvanometer and optical system, and (9) thermocouple selector switches

Figure 4. Ducts encased in concrete. The lead sheaths are seen protruding from the duct assemblies. The ducts are not clearly visible since their ends have been packed with rock wool. An experimental conduit is shown in test position in addition to the Transite and fiber duct assemblies

average surface temperature. Figure 1 shows the assembly of the temperature measuring thermocouples on a test length of fiber duct. The constantan wires are soldered to a narrow strip of thin copper foil, which is cemented to the outside surface of the duct. An identical thermocouple assembly is employed on the inside surface. As can be seen in Figure 1, the constantan wires on the outside surface helix are run about two inches along the surface and then inserted into holes taking them inside the duct.

All of the constantan leads were carried inside the duct to reduce the possibility of abrasion when set in concrete. Also, the leads were run along the duct surface for at least two inches to avoid change in the junction temperature by conduction along the wire. In order to permit the measurement of the average surface temperature of a duct by connecting the couples on that surface in parallel, the constantan leads were all cut to lengths of equal resistance. Consideration was given to the effect the mass of wires inside the duct might have on the surface temperature of the lead sheath and of the inner duct surface. Since the total cross-sectional area of the 96, number 30 Brown and Sharpe gauge constantan wires is equal to that of a single 10-gauge wire, it was concluded that this quantity of wire has negligible effect upon the heat flow.

The Transite and fiber ducts employed in the tests each had a 4-inch inside diameter and 0.31-inch wall thickness.

The Heating Unit

The lead sheath used in the duct assembly was cut from a lead pipe of $3^1/_2$-inch outside diameter and 1/8-inch wall thickness. The pipe was stored in the laboratory for over a year before the tests were begun, and so the lead surface had sufficient time to attain a high emissivity oxide coating. A 7.75-foot length Calrod heater, consisting of a coaxial nichrome wire and metallic shield separated by a refractory material, was placed along the axis of the lead sheath and held in place by thin Transite disk spacers. The shield was used as the return current lead to eliminate the possibility of inducing potentials in the thermocouple leads. The resistance of the Calrod heater was measured as approximately 3.4 ohms per foot with ten watts per foot heat flow in the assembled duct.

After some investigation, sand was found to be a suitable medium with which to surround the Calrod heater inside the lead sheath. Five copper-con-

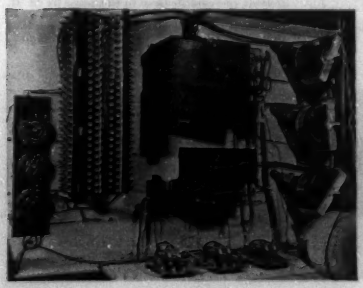

Figure 3 (left). Rear view of control board. Numbered elements are (1) the thermocouple terminal board (2) the survey couple selector switch assembly, and (3) the power circuit relays

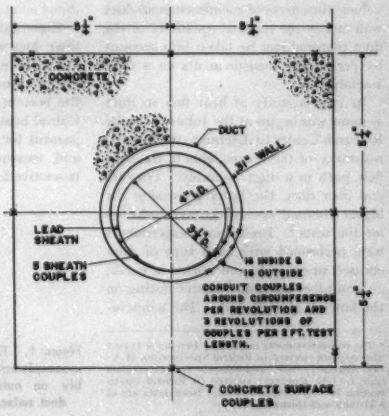

Figure 5 (right). Cross-section detail of duct encased in concrete for "Test Series 1." A 12-inch concrete casing was employed in "Test Series 2." The lead sheath encloses a centered Calrod heater

stantan thermocouples made from number 24 Brown and Sharpe gauge wire were placed in a helical arrangement along a 2-foot length in the middle of the lead pipe. The duct assembly was then completed by placing the sheath inside the duct, the lead pipe resting on the bottom and forming an air crescent with the inner wall surface.

Apparatus

Figures 2 and 3 show the front and rear respectively of the control board. The power circuit controls and the thermocouple circuit instruments are numbered to simplify their identification.

The lead sheath temperature was maintained constant during a test run by means of the Celectray temperatue controller, which surveyed the control couples of each duct assembly once a minute. The control couples were mounted on the lead sheath, and the controller functioned to reduce the current through the Calrod heater when the lead sheath temperature exceeded the set value and to increase it when the temperature fell below the setting. Pilot lights on the control board showed which duct assembly was being surveyed by the controller at any given time. Although the controller has a sensitivity of 0.1 degree centigrade, the temperature variations of the sheath exceeded this quantity because of the appreciable thermal capacity of the duct system. The deviation from the set value was held, however, within 1 per cent of the sheath temperature setting, varying periodically between high and low values.

Energy dissipation in a duct heater during a test interval was measured with integrating wattmeters, and the average power was computed from the time interval of the test run. Thermocouple electromotive forces were measured with a type *K-2* Leeds and Northrup potentiometer, and thermocouple switches were connected so that the electromotive forces of each couple could be measured separately or an average surface temperature reading be made by connecting in parallel the couples on that surface.

Method of Test

All temperature measurements were made under steady-state conditions of heat flow. Thermal equilibrium was generally attained about 72 hours after the initial setting of the controller and power transtats, minor power adjustments being made during the first 48 hours of this period. This steady-state condition was maintained throughout the test period of three to six hours by controlling the temperature of the lead sheath and that of ambient air.

The ends of the duct were packed with rock wool to cut down convection, contributing to the effectiveness of the guard sections in eliminating end effects. Temperature measurements along the test length of the lead sheath during the test period showed variations from the mean temperature of about one per cent. These temperature variations were random along the test length of the sheath, with no indication of a maximum temperature near the center, indicating that the guard sections were effective in eliminating end effects. Along the top of the duct, the temperature was nearly constant along the 2-foot test length. Appreciable temperature differences were measured along the length on the bottom of the duct, but these differences were random and can be attributed to the nonuniform contact between lead sheath and duct wall.

Three "points" each at four different sheath temperatures were obtained for each duct, Transite and fiber, after thermal equilibrium had been obtained. A point consisted of obtaining a record, by means of the integrating wattmeter, of the power dissipated in each duct throughout the test period, recording the surface temperatures of the sheath and duct wall at intervals during the test period, and noting the ambient air temperature. The tests were run in a constant temperature room (34 degrees centigrade) so that little change was noted in the ambient air temperature.

Test Assembly

The assembled ducts were suspended side by side in air, with a separation of one foot, behind the control board. Temperature measurements in the air space between the Transite and fiber ducts showed that their mutual heating effects were negligible. Thermocouple leads were carried through the inside of each duct and connected to the terminal board.

The second stage of the investigation, namely the study of single duct encased in a concrete envelope, was carried out employing the following concrete mix: 440 pounds cement; 1,295 pounds sand; and 2,100 pounds 3/4-inch stone.

This is approximately a 1:3:5 mix, based upon the following densities: sand 100 pounds per cubic foot, stone 100 pounds per cubic foot, and cement 94 pounds per cubic foot. No allowance was made for moisture content of the sand.

The concrete casings were aged before tests were started until the electrical resistance of wood blocks containing metal electrodes, which were cast in the concrete, reached an equilibrium condition. The aging period, as judged by this method, was approximately four months.

Seven thermocouples were placed around the surface of the concrete envelopes to obtain surface temperatures. With the additional observation of outside concrete surface temperature, the test method was identical with that described for ducts in air.

Figure 4 shows the concrete encased ducts in test position behind the panel board. The concrete envelopes are spaced ten inches apart, and the temperature in the air space midway between the encased ducts exceeded room temperature by less than 1 degree centigrade. A duct bank of experimental conduit is shown in addition to the Transite and fiber duct assemblies. Figure 5 shows a cross-section detail of ducts in concrete.

A second series of tests was conducted on Transite and fiber duct, using two additional samples, to add weight to the original data obtained. The test assembly in air was identical with that described before except that the length of the duct assembly was reduced to six feet and the number of lead sheath thermocouples was increased to seven. An additional change made for the tests on ducts in concrete was to increase the size of the concrete envelope so that the total cross-section of the duct bank was a 12-inch square. It is believed that this larger concrete envelope more closely represents a single-duct bank buried underground. The method of test employed in the second test series was identical with that of the first series except that "points" were taken at a larger number of lead sheath temperatures with only one "point" for each temperature. Also the tests were run in a lower ambient room temperature (about 26 degrees centigrade). Data pertaining to the first and second series of tests will be designated respectively as Series 1 and Series 2.

Results

Table I contains typical observations and calculations from the tests on ducts in air and in concrete. Although this table contains only a small number of the total test points employed in the investigation, it shows the method of calculation used to obtain the values of thermal resistance and resistivity employed in the illustrations.

Values of thermal resistance are plotted

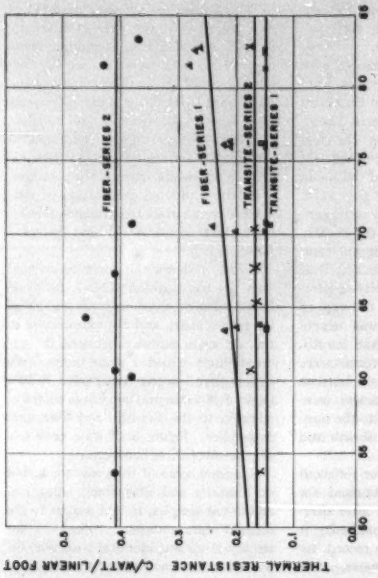

Figure 8. Thermal resistance of the duct wall versus lead sheath temperature for Transite and fiber ducts in air

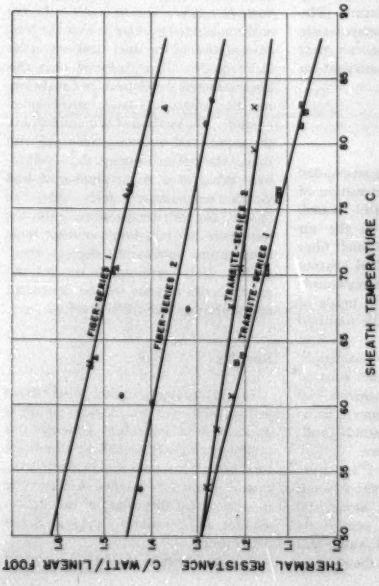

Figure 6. Thermal resistance from lead sheath to inside duct surface versus lead sheath temperature for Transite and fiber ducts in air

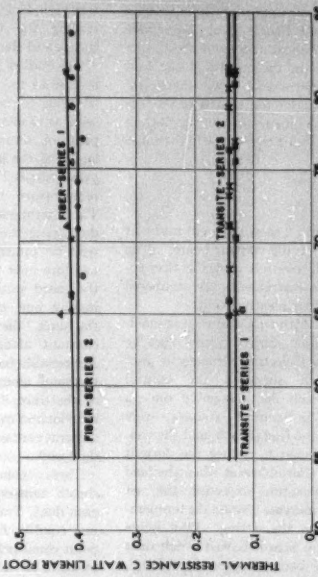

Figure 9. Thermal resistance of the duct wall versus lead sheath temperature for Transite and fiber ducts encased in concrete

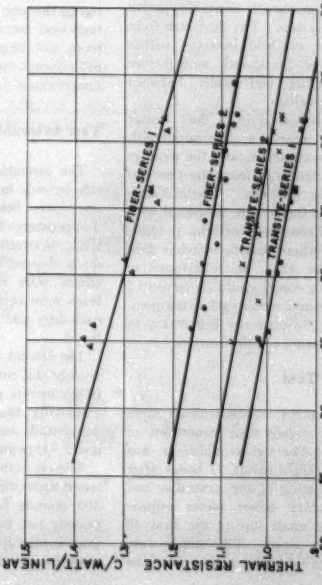

Figure 7. Thermal resistance from lead sheath to inside duct surface versus lead sheath temperature for Transite and fiber ducts encased in concrete

Table I. Typical Experimental Data

Duct Material*	Watts Per Ft	Temperature, °C: Sheath	Inside Duct Wall Surface	Outside Duct Wall Surface	Outside Concrete Surface	Ambient	Thermal Resistance, °C Per Watt Per Linear Ft: Sheath to Duct	Duct Wall	Duct to Air	Concrete Envelope	Thermal Resistivity**: Surface Resistivity C cm²/watt: β	β_d	β_c	Volume Resistivity C cm/watt: ρ_d	ρ_c
Ducts in Air															
Fiber (I)	10.5	63.4	47.4	45.1		33.9	1.53	0.22	1.07		1,300	1,200		300	
Fiber (I)	13.2	70.6	51.1	47.9		35.0	1.48	0.24	0.98		1,260	1,100		320	
Fiber (I)	18.3	82.7	57.4	52.6		34.4	1.35	0.26	0.99		1,170	1,110		350	
Fiber (II)	12.5	60.7	42.4	37.2		25.6	1.47	0.41	0.93		1,250	1,050		550	
Fiber (II)	13.5	64.3	43.9	37.7		25.0	1.51	0.46	0.94		1,280	1,060		620	
Fiber (II)	21.9	81.6	53.6	44.2		25.1	1.28	0.43	0.87		1,090	980		580	
Transite (I)	12.6	63.4	48.2	46.3		33.9	1.21	0.15	0.98		1,030	1,100		200	
Transite (I)	16.3	70.1	51.6	49.1		33.9	1.14	0.15	0.93		970	1,050		200	
Transite (I)	19.1	76.2	54.7	51.7		33.9	1.12	0.16	0.93		950	1,050		220	
Transite (II)	14.0	58.2	40.7	38.6		25.9	1.23	0.15	0.90		1,060	1,010		200	
Transite (II)	18.3	67.6	45.3	42.3		27.6	1.22	0.17	0.80		1,040	900		230	
Transite (II)	24.0	79.7	51.7	48.2		28.3	1.17	0.15	0.83		1,000	930		200	
Ducts in Concrete															
Fiber (I)	12.4	64.9	48.3	43.0	37.3	33.5	1.35	0.43		0.46	1,150		1,000	580	83
Fiber (I)	14.9	71.1	51.8	45.6	38.5	33.5	1.30	0.42		0.48	1,110		1,100	560	87
Fiber (I)	19.9	81.9	57.6	49.3	40.3	33.5	1.22	0.42		0.45	1,040		1,110	560	81
Fiber (II)	16.7	66.2	46.8	40.0	30.6	26.1	1.16	0.41		0.56	990		1,000	550	90
Fiber (II)	21.6	77.2	53.6	45.2	33.0	26.1	1.09	0.39		0.56	930		1,180	520	90
Fiber (II)	23.6	82.5	57.3	47.6	34.4	27.2	1.07	0.41		0.56	910		1,130	550	90
Transite (I)	16.7	65.3	48.2	46.1	39.7	33.5	1.02	0.12		0.39	870		1,210	160	71
Transite (I)	19.9	71.1	51.8	49.1	41.3	33.5	0.97	0.14		0.39	830		1,260	190	71
Transite (I)	26.3	81.7	57.3	53.7	43.5	33.5	0.93	0.14		0.39	790		1,340	190	71
Transite (II)	19.5	65.1	44.3	41.7	30.6	26.1	1.07	0.13		0.57	910		860	180	92
Transite (II)	25.2	77.0	51.5	48.1	33.8	26.1	1.01	0.13		0.57	860		1,130	180	92
Transite (II)	27.0	80.7	54.1	50.3	34.7	27.2	0.99	0.14		0.58	840		1,030	190	93

* Number in parentheses represents the test series from which the data was taken.

** β, β_d, and β_c are surface resistivity factors respectively from sheath to duct wall, from duct wall to ambient air, and from concrete to ambient air. ρ_d and ρ_c are volume resistivities of duct and concrete respectively. These thermal resistivity values are computed from the following equations

$$\beta = \frac{R_{ths} D_s}{0.00411}, \quad \beta_d = \frac{R_{thd}' D_d}{0.00411}, \quad \beta_c = \frac{R_{ths}' D_s}{0.00411}, \quad \rho_d = \frac{R_{thd}}{0.012 \log_{10} D_d/D_i}, \quad \rho_c = \frac{R_{ths}}{0.012 \log_{10} D_e/D_d}$$

where R_{ths}, R_{thd}, R_{ths}', R_{thd}', and R_{the} are the respective thermal resistance values shown above from sheath to duct wall, duct wall to air, concrete to air, of the duct wall, and the concrete envelope; and D_s, D_i, D_d, and D_e are in inches the respective diameters of sheath, inner duct wall surface, outer duct wall surface, and equivalent concrete diameter.

against lead sheath temperature for the components of the heat flow path in the ducts, Figures 6 through 9. Figures 6 and 7 show the variation with sheath temperature of the thermal resistance from sheath to inside duct wall for ducts in air and ducts in concrete respectively. Since radiation through the air crescent between sheath and inside duct surface is an important factor in the heat transfer between these surfaces, the thermal resistance values decrease with increasing lead sheath temperature. It was not expected that the heat transfer due to convection would increase so rapidly with increasing sheath temperature as that due to radiation, the former varying nearly linearly with the temperature difference of the two surfaces, the latter with the difference in the fourth powers of the surface temperatures.[1]

Two general conclusions can be drawn from these curves regarding the relative thermal resistance values from the lead sheath to the inside duct surface. For a given sheath temperature, the thermal resistance is consistently higher for ducts in air than in concrete. Also the fiber duct consistently gives a higher resistance from sheath to inside duct wall than does the Transite duct. The influence of the concrete casing can be attributed to its effectiveness in producing more uniformity of the heat flow lines in the entire duct assembly, since its thermal resistivity is relatively low. Differences between the fiber and Transite assemblies can be attributed to the heat transfer from sheath to duct by direct conduction. The lead sheath "snakes" throughout the bottom of the duct, making a nonuniform contact with it. The duct material of lower thermal resistivity more readily conducts heat away from the lead sheath.

The difference in the thermal resistance from lead sheath to inside duct wall as between the Transite and fiber ducts is considerably greater in Series 1 tests than in Series 2. The deviation in the two test values for the fiber duct assembly is about 15 per cent of the resistance from sheath to duct wall, and we attribute it to the variable factor of contact area between lead sheath and the duct containing

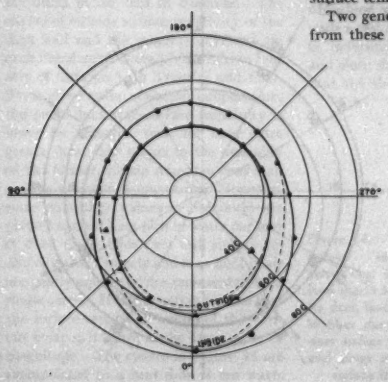

Figure 10 (left). Temperature distribution around the fiber duct surfaces at 82 degrees centigrade lead sheath temperature. The solid lines represent the duct encased in concrete, the dotted lines in air

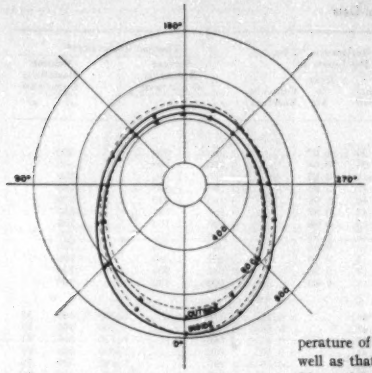

Figure 11 (left). Temperature distribution around the Transite duct surfaces at 82 degrees centigrade lead sheath temperature. The solid lines represent the duct encased in concrete, the dotted lines in air

it. This deviation is not unreasonably high, since considerations of the heat transfer from sheath to duct by Whitehead and Hutchings[3] indicate that variations in spacing between the sheath and the bottom of the duct produce considerable effect upon the thermal resistance of this component of the heat flow path.

Figures 8 and 9 show the thermal resistance of the duct itself as a function of lead sheath temperature for ducts in air and ducts in concrete respectively. This factor is small compared with the total resistance of the heat flow path from the sheath to ambient surroundings, but it serves to measure the effect of the thermal resistance of the duct upon the over-all heat flow through the duct assembly. The Transite duct possesses a lower resistance in concrete than in air, possibly due to the reduction in its outside surface resistance when in contact with the concrete envelope, Transite and concrete both being cement products. An anomalous curve in the set shown in Figures 8 and 9 is that for the Series 1 tests on fiber duct in air. Moisture content, among other factors, was considered as an explanation for this anomaly, but it was discounted since the Transite and fiber ducts were exposed to identical environments before and during the tests. Since the fiber duct samples employed in the two tests were identically assembled, no satisfactory explanation for the anomalous curve has been found.

The thermal circuit for ducts in air is completed with the outside duct wall surface resistance, typical values for which are shown in Table I. These values give the order of magnitude of the outside surface resistance of the duct wall, and in an actual installation, the exact value of this resistance will depend upon the temperature of the ambient surroundings as well as that of the outside duct surface. The resistance of the concrete envelope completes the thermal circuit for ducts in concrete in the laboratory installation, although the thermal resistance of the surrounding earth would also be considered in an underground duct bank. Table I also contains the thermal resistance values for the concrete envelopes, the values for the Series 2 tests being greater since the larger concrete envelope was employed for these tests.

Figures 10 and 11 are polar graphs showing the temperature distribution around the duct walls respectively for fiber and Transite ducts at a sheath temperature of 82 degrees centigrade. The solid lines represent ducts in concrete, dotted lines, ducts in air. The average temperature of the three thermocouples at each 22.5 degree radial position (corresponding to each turn of the three-turn helix of couples) was employed to obtain the points for these curves. The departure from uniform radial heat flow in the duct is shown by the large temperature difference between the top and bottom of the duct wall. Also since the lead sheath does not rest uniformly on the bottom of the duct, the heat flow is not entirely symmetrical about the vertical axis. The temperature distribution around the duct walls for ducts in air at the same sheath temperature is similar to that in concrete, except that a higher percentage of the total heat flow occurs near the bottom.

Figures 12 and 13 show reduced scale drawings of the fiber and Transite ducts with their lead sheaths. The temperatures on the duct walls at each 30 degree radial position were taken from the solid line polar graphs, Figures 10 and 11, representing ducts encased in concrete, and recorded on the drawings. The temperature falls off rapidly on the bottom half of the duct from the region of contact with the lead sheath, and it remains nearly constant on the top half. The direction of the temperature gradient through the duct is indicated by the arrows.

Calculations of thermal resistance for the heat flow components of a duct system are usually based upon accepted values of thermal surface or volume resistivity. Resistivity values are more useful to the cable engineer than are resistance values since the former are independent of the dimensions of the components of the duct system. The thermal resistance values obtained from the tests have been employed to calculate surface resistivity of the lead sheath, volume resistivity of the duct material and of the concrete, and surface resistivity of the outer duct wall in air. These values are shown in Table I, and since there is some interest in the surface resistivity of the outside of the concrete casing in air, these latter values are also given. Lead sheath surface resistivity values in fiber and

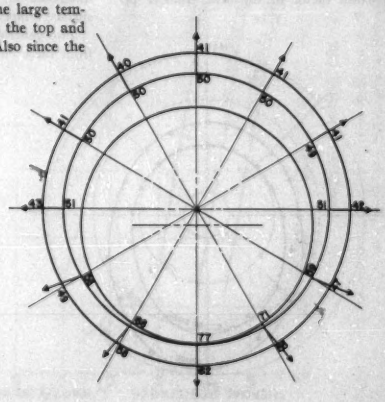

Figure 12 (right). Reduced scale diagram of sheath and duct showing the temperature distribution around the fiber duct encased in concrete at 82 degree centigrade sheath temperature. Arrows show the direction of the temperature gradient

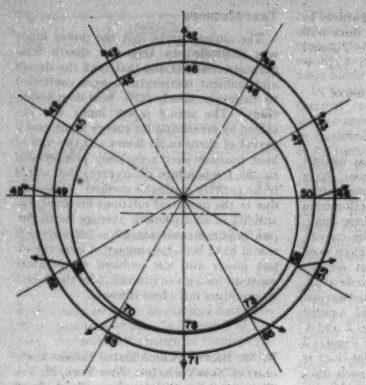

Figure 13 (left). Reduced scale diagram of sheath and duct showing the temperature distribution around the Transite duct encased in concrete at 82 degree centigrade sheath temperature. Arrows show the direction of the temperature gradient

Table II. Thermal Resistivity Factors—10 Watts Per Foot Heat Flow

Thermal Component	Symbol	Resistivity
Lead sheath in fiber duct, surface resistivity	β	1,200 C cm²/watt
Lead sheath in Transite duct, surface resistivity	β	1,020 C cm²/watt
Duct in air, surface resistivity	β_d	1,110 C cm²/watt
Concrete in air, surface resistivity	β_c	1,120 C cm²/watt
Fiber duct, volume resistivity	ρ_d	480 C cm/watt
Transite duct, volume resistivity	ρ_d	200 C cm/watt
Concrete, volume resistivity	ρ_c	84 C cm/watt

Transite ducts are computed, as is customary in cable calculations, by formulating the thermal resistance from sheath to inner duct wall in terms of the sheath surface resistivity. The surface resistivity of the concrete envelope in air, and also its volume resistivity, is calculated by employing a diameter of a circle whose perimeter is equal to that of the square concrete casing. The concrete surface resistivity values are computed from the least precise of all the temperature measurements made on the duct assemblies, and the data should be weighted accordingly.

Figure 14 shows thermal surface resistivity values for various duct assembly components versus heat flow in watts per foot of duct. Curves of lead sheath surface resistivity in fiber and Transite duct are based upon average values from the four sets of tests; that is, Series 1 and 2 for ducts in air and in concrete. The curves of outside surface resistivity of the duct wall and the concrete envelope are each based upon average values from four sets of tests on both Transite and fiber. For a given value of sheath temperature, the outer duct wall surface resistivity is lower for Transite than for fiber since greater heat flow occurs in the assembly of the former, giving its outer duct wall surface a higher temperature. However, since resistivity values in Figure 14 are plotted against heat flow in watts per foot of duct, the outside duct wall surface resistivities for Transite and fiber duct in air are nearly equal and are represented by a single curve. It is interesting to note that the surface resistivity values of the various components are of the same order of magnitude. The curves in Figure 14 are extrapolated to a heat flow of ten watts per foot, and the values thus obtained may be used conveniently as duct constants in cable calculations. These values, along with the volume resistivities of duct wall and concrete obtained from the tests, are contained in Table II.

The temperature rise of a cable in a duct in air is given by the equation

$$T_c = \left(R_{\beta d} + 0.00411\frac{\beta}{D_s} + 0.012\rho_d \times \log_{10}\frac{D_d}{D_i} + 0.00411\frac{\beta_d}{D_d}\right)Q$$

where the four terms in parentheses represent the thermal resistances respectively from copper to lead, lead sheath to inside duct wall, across the duct wall, and outer duct wall to ambient air; and Q is the heat flow in watts per foot of cable. The symbols employed in the last three terms in the parentheses are defined in Table I, and the resistivity values are contained in Table II. The equation assumes that the sheath to duct resistance is independent of the duct diameter; and since theoretical considerations show that the sheath diameter is the primary variable in the heat transfer from sheath to duct, this assumption probably does not introduce an appreciable error in cable calculations. In temperature measurements on a cable sheath and the inside of an enclosing fiber duct encased in concrete, Barenscher[3] obtained data indicating the correctness of the inverse relationship between sheath diameter and thermal resistance from sheath to duct wall. The temperature rise of a given cable in a buried duct bank above ambient earth is obtained by replacing the fourth term in the equation with the expression derived by Neher[4], the latter taking into consideration the thermal resistance of concrete and surrounding earth and the heating produced by the other loaded cables in the duct bank.

Further tests on various duct materials should be of great value to cable engineers in establishing duct constants for these materials, and should add weight to the data submitted here on Transite and fiber duct. A more complete investigation is needed of the thermal resistance of the heat flow path from the cable sheath to the outside of the duct wall, including experimental data on the effect of variations in lead sheath and duct diameters and in thermal resistivity of the duct wall material. Tests on groups of ducts in a duct bank would also be of considerable interest, although the heat flow path outside the duct wall can be treated, with

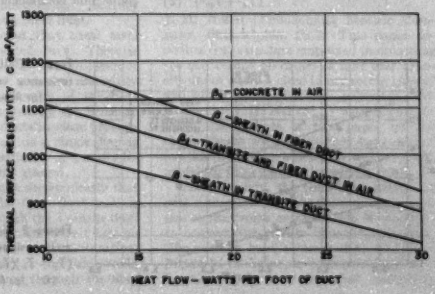

Figure 14. Thermal surface resistivity versus heat flow for lead sheath in Transite duct, lead sheath in fiber duct, outer duct surface in air, and outer concrete surface in air

considerable degree of accuracy, with conventional methods of heat flow calculations.

References

1. Heat Transmission (book), W. H. McAdams. McGraw-Hill Book Company, New York, N. Y., second edition, 1942.

2. Current Ratings of Cables for Transmission and Distribution, J. B. Whitehead. *Journal*, Institution of Electrical Engineers (London, England), volume 83, 1938, page 539.

3. A Study of the Temperature Distribution in Electric Cables in Underground Ducts, P. J. Barenscher. *Thesis*, University of Wisconsin (Madison, Wis.), 1925.

4. The Temperature Rise of Cables in a Duct Bank, J. H. Neher. *AIEE Transactions*, volume 68, part I, 1949, pages 540–49.

Discussion

V. V. Mason (The Hydro-Electric Power Commission of Ontario, Toronto, Ontario, Canada): This discussion deals with two points which may not bear greatly on the practical value of the results attained by Mr. Greebler and Mr. Barnett but which are of some importance as regards the experimental method and the presentation of the results.

Presentation of Results

The authors present their results for the sheath-to-duct thermal resistance, R_{1h_2}, as a graph with the sheath temperature as the independent variable, and express some concern over the lack of agreement of these curves for the Series I and Series II tests. To find a more suitable quantity against which to plot R_{1h_2} consider that the rate at which heat is transferred from sheath to duct, being partly by conduction, partly by convection, and partly by radiation, may be written thus

$$P = k_1 \Delta T + k_2 (\Delta T)^{1.25} + k_3 \Delta (T^4) \qquad (1)$$

where k_1, k_2, k_3 are constants, and T is the absolute temperature in degrees Kelvin. The exponent of the temperature difference for the convection term actually may vary from 1 to 1.5, but 1.25 is probably fairly near the true value.

The thermal resistance R_{1h_2}, then, is given by

$$\frac{1}{R_{1h_2}} = \frac{P}{\Delta T} = k_1 + k_2 (\Delta T)^{0.25} + k_3 (T_s + T_w) \times (T_s^2 + T_w^2) \qquad (2)$$

where T_s and T_w are the temperatures in degrees Kelvin of the sheath and duct wall respectively, so that $\Delta T = T_s - T_w$ and $\Delta(T^4) = (T_s - T_w)(T_s + T_w)(T_s^2 + T_w^2)$.

We see then that R_{1h_2} is a function of

$$(\Delta T)^{0.25} + k(T_s + T_w)(T_s^2 + T_w^2)$$

where $k = k_3/k_2$.

In plotting their values for R_{1h_2} against sheath temperature, the authors have assumed that the duct wall temperature T_w is constant and that the convection term is negligibly small. To see how these quantities affect the appearance of the curves, Figures 1 to 4 of the discussion have been prepared from the complete test records which Mr. Greebler very kindly made available for this purpose. R_{1h_2} is plotted against $(\Delta T)^{0.25}$ in Figures 1 and 3 and against $(T_s + T_w)(T_s^2 + T_w^2)$ in Figures 2 and 4. Figures 1 and 2 are for fiber while Figures 3 and 4 are for Transite. Curves for duct in air and in concrete are given in each illustration because, for the purpose of this discussion, it is of most interest to compare all the values for a given kind of duct. Figures 1 and 3, R_{1h_2} versus $(\Delta T)^{0.25}$, would hold if the heat transfer due to radiation were small compared to that by convection, while Figures 2 and 4 would hold for negligible convection. That is, these figures represent extremes; any practical case will be some combination of the two, obtained by assigning a suitable value to k.

Examination of these figures indicates that for fiber ducts, the agreement between Series I and II in both air and concrete is considerably better when plotted against $(\Delta T)^{0.25}$ than when plotted against T_s or $(T_s + T_w)(T_s^2 + T_w^2)$. Transite, on the other hand, exhibits the most reasonable behaviour when $(T_s + T_w)(T_s^2 + T_w^2)$ is used for the abscissa. This would seem to indicate that with the fiber duct a large part of the heat transfer is due to convection, while with Transite, radiation is the more important mechanism. This difference may be ascribed to the difference in the thermal emissivities of the Transite and fiber surfaces.

The agreement between the two series of runs is still far from perfect, but does appear to be considerably improved. Another possible point of difference between the various tests not considered by the authors is the presence of the thermocouple leads with regard to their effect on the convection currents. Small changes in their position could affect materially the magnitude of the convection component of heat transfer.

Test Methods

The authors state that the power input was controlled to keep the sheath temperature constant and that both the sheath and ambient temperatures were controlled to maintain steady-state heat-flow conditions. The actual power input was obtained by measuring the energy input over a period of three to six hours. If the rate of heat transfer were accurately proportional to the temperature differences, this would be an entirely justifiable method. However, due to the nonlinear relations involved, the validity of an arithmetic average for the input power is questionable. Moreover, it would have been far simpler to keep the input power and the ambient temperature constant for a given run and to let the sheath temperature fall where it would.

R. W. Burrell (Consolidated Edison Company of New York, Inc., New York, N. Y.): The data presented by the authors are of considerable interest to cable engineers, and the Johns-Manville Company and the authors are to be congratulated for the presentation of this data. The painstaking care used in making these tests is commendable. The results would have been of still greater value if the tests could have been carried out on more than one cable size or at least on a more representative combination than a $3^1/_2$-inch cable in 4-inch duct. The data presented contribute significantly to our understanding of the thermal drop from cable sheath to duct wall. Of particular interest are the polar graphs of Figures 10 to 11 of the paper showing the temperature distribution around loaded duct walls. A need for further exploration of this phenomenon is indicated when these data are compared with the values shown in Figure 1 of Mr. F. V. Smith's discussion of a paper by J. H. Neher[1] presented in 1949. It should be noted that the temperatures given in Mr. Smith's discussion are outside duct wall values, but these show little departure from an isothermal surface in contrast with the values for outside wall shown in Figures 10 and 11 of the paper by Mr. Greebler and Mr. Barnett. Unfortunately, in the case of Mr. Smith's data, the heat loss per foot of cable, 3.0 watts, is relatively low for an average cable of a diameter of 2.52 inches. The comparison is also obscured by the possible variations as between single and multiduct structures.

There are a number of effects indicated in the data presented by the authors which

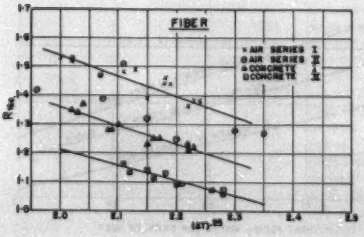

Figure 1 (left). Thermal resistance versus $\Delta T^{0.25}$ for fiber ducts

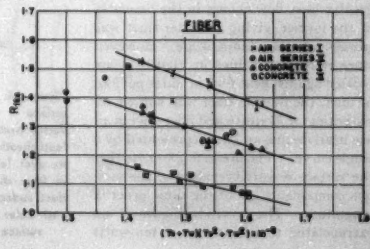

Figure 2 (right). Thermal resistance versus $(T_s + T_w)(T_s^2 + T_w^2) \times 10^{-9}$ for fiber ducts

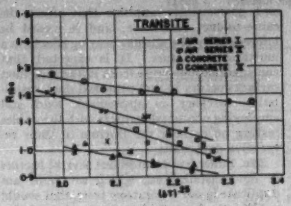

Figure 3. Thermal resistance versus $\Delta T^{0.25}$ for Transite ducts

possibly may be taken as random deviation rather than true effect. In Figure 6 of the paper, the indicated change in thermal resistance from sheath to duct wall, for the case of fiber ducts in air, as between Series I and Series II, indicates the need for tests on a representative number of samples before firm conclusions can be drawn, although there is no doubt that the thermal resistance is higher in the case of dry fiber ducts as against Transite ducts.

The data on the volume thermal resistivity of Transite and fiber material are of interest. The average value for Transite is less than that formerly used by the Consolidated Edison Company in rating calculations, and we have adopted the lower value since these data were first released by the Johns-Manville Company some few years ago. The value for fiber is higher than our normal standard, and it is to be noted that the values derived from these tests are for the dry condition and may be appreciably lower when wet.

Considering the various values of β presented so far from different sources, apparently for the present we must accept a possible 10- to 20-per cent plus or minus variation in β for a given installation. Additional test data of the detailed type presented by the authors, on single and multiduct structures, in air and especially in earth, with cables of representative size and loading, are required before positive conclusions can be drawn.

Reference

1. Discussion by **Frank V. Smith** of The Temperature Rise of Cables in a Duct Bank, J. H. Neher. *AIEE Transactions*, volume 68, part I, 1949, pages 547–48.

R. J. Wiseman (The Okonite Company, Passaic, N. J.): This paper is a welcome addition to the investigation which has been going on in recent years as to the thermal resistance of duct systems. It, along with Mr. J. H. Neher's paper,[1] can well be studied for more exact thermal constants for ducts. Today there is a desire to obtain every ampere possible out of a cable. As the physical structure of the duct bank is important in determining the total thermal resistance of the duct bank, better knowledge of the influence of the kind of duct is desirable. The paper by Mr. Greebler and Mr. Barnett furnishes this information to us.

I wish the authors had used a heating load which would have given a sheath temperature of 40 to 45 degrees centigrade, as this is the range of temperature actually obtained in practice, and not the 82 degrees centigrade reported in the paper. We then would have obtained thermal constants more likely to exist.

In Table II of the paper the authors give thermal resistivity values. The value of surface resistivity for the lead sheath should be qualified that it is for a sheath diameter of 3.5 inches. Past tests indicate that it is actually a function of diameter. In the Insulated Power Cable Engineers Association we take cognizance of this by assuming that it increases from $\beta = 660$ ohms per square centimeter for $D = 0$, to 1,200 ohms per square centimeter for $D = 1.75$ inches and constant thereafter. According to Table II, these values may apply to fiber duct.

For Transite duct perhaps we should have a reduction of 15 to 20 per cent. The volume resistivity values for fiber duct, Transite duct, and concrete are very welcome. We have been taking a value of 100 thermal ohms per centimeter for concrete, so were on the conservative side.

Reference

1. See reference 4 of the paper.

F. H. Buller (General Electric Company, Schenectady, N. Y.): There are two points in connection with this paper which are particularly worthy of notice. All tests were taken on ducts in air, or encased in a concrete envelope situated in air, and the ends of the ducts were plugged up to prevent longitudinal convection. These statements also apply to the Barenscher investigation.[1]

Let us examine the significance of these points. Mr. Greebler and Mr. Barnett have presented curves (Series 2 tests) which show the effect of increasing the mass of concrete around the duct with the thought that the heavier mass of material simulated somewhat more closely the effect of underground burial of the duct bank. In this thought they are probably correct, and it will be noted from Figure 2 of the paper that the surface thermal resistance of the cable falls off materially in the case of the fiber duct and increases slightly in the case of the Transite duct, thus bringing these two types of duct closer together in their thermal properties. Presumably, burial in earth would exaggerate this effect further; it is quite possible, however, that such burial might ultimately reduce the values of surface thermal resistance in both cases below those given here for ducts in air. Further research is needed along these lines.

Moreover, it is noted that these tests were made on an isolated duct. There is reason to believe that in a multiple-duct bank, the value of β may be materially affected by the modification of the heat field in the duct structure by the presence of additional loaded ducts in close proximity, so that a test in air on a single duct is not necessarily representative of a multiple-duct bank buried in the ground.

The authors also have shown clearly that the drop through the fiber duct wall is greater than that through the Transite duct wall. However, these tests were taken on dry ducts. Presumably water saturation, which frequently occurs in the field, would tend to reduce the drop through the fiber

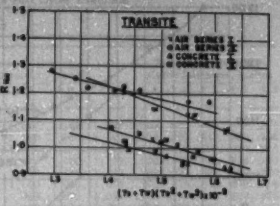

Figure 4. Thermal resistance versus $(T_s + T_w)(T_s^2 + T_w^2) \times 10^{-8}$ for Transite ducts

duct wall while affecting the Transite duct wall comparatively little.

Next, consider the question of plugging up the duct ends. The authors were undoubtedly justified in this procedure, since on such a short length of duct any appreciable longitudinal flow of air probably would have distorted observed results to a point where they became meaningless. However, it is not customary to seal up duct mouths in service, although it is sometimes done. Hence, in service, we may expect some longitudinal movement of air, which would tend to reduce the value of β below what was observed by the authors. Pipe cables, on the other hand, are necessarily sealed in service, since they operate under pressure.

These facts may explain, at least in part, the difference between the β values obtained by the authors and the lower ones observed in field tests on cable-installed underground in multiple-duct banks, notably those reported by Mr. Halperin.[2]

To sum the matter up, while it would appear that these tests were very carefully made, and while the technique used can probably be properly taken as a model for any future tests made on ducts in air, the results are not necessarily representative for the case of duct banks buried in the ground and operated under service conditions. They might possibly approximate more closely to the case of duct banks in air as sometimes used indoors in power stations and elsewhere.

References

1. See reference 3 of the paper.

2. Load Ratings of Cables, Herman Halperin. *Electrical Engineering* (*AIEE Transactions*), volume 58, October 1939, pages 535–58.

J. H. Neher (Philadelphia Electric Company, Philadelphia, Pa.): This paper describes the procedure employed in obtaining the test results on cables in fiber and Transite ducts which I cited in my recent paper,[1] and which also appears in a paper by F. H. Buller and J. H. Neher.[2] I wish to compliment the authors of this paper on the thoroughness with which they have worked out this procedure, which may well serve as a model for future work along these lines.

Unfortunately, the tests were conducted with a single, and larger than average, cable size so that some extrapolation is necessary to convert the results to normal practice. The authors have attempted to do this in Figure 14 of the paper by expressing β as a function of the heat flow, but completely

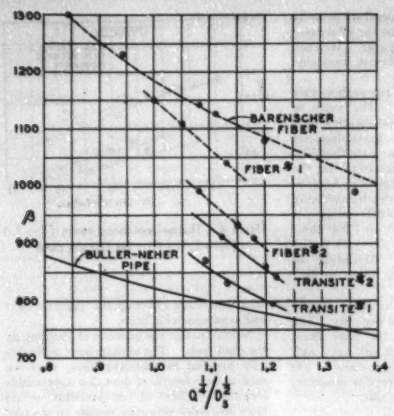

Figure 5. Comparison of test data on fiber and Transite ducts in concrete

disregarding the effect of the cable diameter upon β. Mr. Buller and I have shown in our paper[3] that as a best approximation β is dependent upon the fourth root of the heat flow and the square root of the cable diameter.

Figure 5 of the discussion shows the data of Mr. Greebler and Mr. Barnett plotted as a function of the parameter $Q^{1/4}/D_s^{1/2}$ (Q in watts per foot; D_s in inches) together with the Barenscher[1] data for fiber ducts and the curve for cable in pipe given in the Buller and Neher paper.[2]

It should be noted that the Buller and Neher curve for fiber duct is based on the Barenscher data with which the fiber Series 1 test data of Mr. Greebler and Mr. Barnett is in fairly good agreement. Similarly, the Greebler and Barnett Transite Series 1 test data is so close to the cable in pipe curve that a distinction between the two is scarcely warranted. Only the Series I Greebler and Barnett tests were available to Mr. Buller and myself when our paper was prepared.

The second set of tests by the authors, falling as they do between the first tests on Figure 5 of the discussion, would seem to indicate that in the case of both fiber and Transite duct, β is a not too definite quantity ranging from 900 to 1,100 degrees centigrade square centimeters per watt for a typical cable installation in fiber duct and from 750 to 850 with a Transite duct.

I heartily indorse the authors' concluding paragraph to the effect that further tests along these lines would be valuable.

References

1. See reference 4 of the paper.
2. The Thermal Resistance Between Cables and a Surrounding Pipe or Duct Wall, F. H. Buller, J. H. Neher. *AIEE Transactions*, volume 69, part I, 1950, pages 342–49.
3. See reference 3 of the paper.

Paul Greebler and Guy F. Barnett: Probably the most common criticism of the test procedure arises from the fact that the sheath diameter employed was somewhat large. This cable size was taken from an actual installation in the field, but it is larger than that commonly employed in a 4-inch duct. The earlier experimental work by P. J. Barenscher,[1] as well as the more recent theoretical study by F. H. Buller and J. H. Neher,[2] indicates that the inverse relationship between the sheath diameter and the thermal resistance from the sheath to the duct is valid, as a good approximation, over an appreciable range of cable diameters. Additional tests on Transite and fiber ducts, using several smaller cable diameters, would add greatly to the value of these experimental and theoretical investigations.

Mr. Mason has presented data in his plots of R_{ia_1} versus variables in the convection and radiation terms that are very helpful toward understanding the mechanisms of heat transfer from the cable to the duct. We have not assumed in our paper, however, that the duct wall temperature is constant nor that the convection term is negligibly small. It was stated in the paper that variations in the convection term were small compared with those in the radiation term. This statement is verified by calculations carried out by Mr. Greebler in his discussion of a paper by Buller and Neher.[3] Values for R_{ia_1} were plotted against sheath temperature since this temperature is the principal variable in the thermal resistance from the cable to the duct for a given cable in duct geometry. Mr. Mason is entirely correct in pointing out that the arithmetic average of a periodically varying power input does not necessarily give the same results as an equivalent constant-power input, since the relationship between thermal resistance from cable to duct and power input is not linear. In our tests, however, the periodic power fluctuations were very small compared with the average input power, justifying the use of the latter as a highly accurate first-order approximation.

Mr. Burrell has discussed the polar graphs of Figures 10 and 11 of the paper showing the temperature distribution around loaded duct walls, and has compared these with similar data presented by Mr. F. V. Smith in a discussion of a paper by Mr. Neher.[4] The temperature distribution around the duct wall depends upon all of the thermal and geometrical variables that affect the cable-to-duct resistance, and it would be influenced by the mutual heating effects in a multiduct structure. It is expected that considerable departure from isothermal-duct surfaces occurs in any practical duct installation carrying an appreciable load and employing nonmetallic ducts with the cables resting on or near the bottom of their respective duct walls.

Mr. Buller has pointed out several factors in field installations, which we could not duplicate in our laboratory tests, that would modify the heat field and, therefore, influence the value of the cable thermal surface resistivity β. These factors tend, in general, to lower the value of β, and so the values given in our paper are slightly on the conservative side when applied to current rating calculations in buried duct structures.

Both Mr. Burrell and Mr. Buller have discussed the influence of moisture on the thermal resistivity of the duct materials in the field. It is true that the presence of moisture would produce a decrease in the thermal resistivity of the duct wall. However, for design purposes it would appear advisable to base calculations on the limiting case of dry ducts because it is not uncommon to encounter such conditions in practice, particularly for extended periods during the summer months. For continuously submerged ducts, special experimental determinations may be justified and may be expected to show a significant reduction in the component from sheath to duct wall.

The tests described in our paper cover the range of cable sheath temperatures from 50 to 80 degrees centigrade for duct in air and 60 to 80 degrees centigrade for duct encased in concrete. Dr. Wiseman has pointed out that temperatures for cable sheaths obtained in practice are normally below the range of temperatures covered in our tests. It is pertinent to point out that more and more emphasis is being placed on emergency loading at allowable copper temperatures that, for example, may be as high as 96 degrees centigrade at 15 kv (Association of Edison Illuminating Companies). Under such conditions a sheath temperature of the order of 80 degrees centigrade would not appear to be unduly high. The thermal volume resistivity values given in Table II of the paper are essentially independent of temperature over the entire operating range, but the surface resistivities increase as the cable temperature is lowered. The surface resistivity values given in Table II of the paper were obtained by extrapolating the curves of Figure 14 of the paper to a heat flow of ten watts per foot. The β values thus obtained represent a sheath temperature near 70 degrees centigrade for ducts in air and below 50 degrees centigrade for ducts in concrete. Extrapolation of these values to lower sheath temperatures, assuming a linear relationship over the operating range, is justifiable as a good approximation. The departure from a linear relationship when extrapolating to a lower temperature should yield resistivity values slightly on the conservative side, since it is expected from theoretical considerations that the slope of a β versus sheath temperature curve would approach zero as the temperature is lowered.

Mr. Neher has pointed out that Figure

Table I. Thermal Resistivity Factor β As a Function of Sheath Temperature and Cable Diameter

β in Degrees Centigrade Square Centimeter Per Watt

Temperature, Degrees Centigrade	Fiber in Air; Cable Diameter, Inches					Transite in Air; Cable Diameter, Inches					Fiber in Concrete; Cable Diameter, Inches					Transite in Concrete; Cable Diameter, Inches				
	1.5	2.0	2.5	3.0	3.5	1.5	2.0	2.5	3.0	3.5	1.5	2.0	2.5	3.0	3.5	1.5	2.0	2.5	3.0	3.5
40	1.160	1.230	1.290	1.320	1.350	.970	1.030	1.070	1.110	1.130	1.090	1.090	1.140	1.180	1.200	.840	.890	.920	.950	.970
45	1.140	1.210	1.270	1.300	1.330	.960	1.010	1.060	1.090	1.110	1.020	1.070	1.120	1.160	1.180	.820	.860	.910	.930	.950
50	1.120	1.180	1.240	1.270	1.300	.950	1.000	1.050	1.080	1.100	990	1.040	1.090	1.130	1.150	.810	.850	.890	.920	.940
55	1.100	1.160	1.220	1.250	1.280	.930	980	1.030	1.060	1.080	960	1.020	1.070	1.100	1.120	.790	.840	.870	.900	.920
60	1.080	1.140	1.190	1.230	1.250	.910	960	1.010	1.040	1.060	940	990	1.040	1.070	1.090	.780	.830	.860	.880	.900
65	1.060	1.120	1.170	1.200	1.230	.900	950	990	1.020	1.040	920	970	1.020	1.050	1.070	.770	.810	.840	.870	.890
70	1.050	1.090	1.140	1.180	1.200	.870	920	960	990	1.010	900	950	990	1.020	1.040	.750	.790	.820	.850	.870
75	1.010	1.060	1.110	1.150	1.170	.850	900	940	970	990	880	930	970	1.000	1.020	.730	.770	.800	.820	.840
80	990	1.040	1.090	1.130	1.150	.830	870	910	940	960	850	900	940	970	990	.710	.750	.780	.800	.820

14 of the paper does not give a complete picture of the variation in β since the effect of the cable diameter is not included. It is unfortunately true that β varies in a rather complicated manner with sheath temperature, cable diameter, and the many other factors in the over-all heat flow path from conductor to ambient that affect the heat field and, therefore, determine the temperature drop from the sheath to the duct. On the fortunate side, however, all of these variables produce only small changes in β over normal operating ranges; and so β can be treated as a constant for a given duct material or pipe for most practical thermal calculations.

The authors of this paper do not agree with Mr. Neher that as a best approximation β is dependent upon the fourth root of the heat flow, and this divergence has been elaborated upon by Mr. Greebler in his discussion of a paper by Mr. Buller and Mr. Neher.[4] The value of β is determined by the temperature distribution in the air space between the cable and the duct, and in relationship to the duct variables, this is most intimately associated with the sheath temperature. The cable diameter is probably the second most important of the variables that affect the value of β. In order to take into consideration variations in β with sheath temperature and cable diameter, values of β are tabulated in Table I of the discussion for sheath temperatures ranging from 40 to 80 degrees centigrade and for cable diameter from 1.5 to 3.5 inches. Four cases are considered separately, namely, fiber duct in air, Transite duct in air, fiber duct in concrete, and Transite duct in concrete. Thermal surface resistivity values shown in the table for a 3.5-inch diameter cable are the averages of the two series of tests, with the assumption that linear extrapolation to 40 degrees centigrade is justifiable. Approximate values of β for cable diameters smaller than 3.5 inches were obtained by assuming that convection contributes 30 per cent of the total heat transfer from the cable to the duct and that variations in the cable diameter produce an appreciable effect only upon the convection component of the thermal conductivity of the air space from the cable to the duct. These calculations are based in principle upon an analysis given by Mr. Buller and Mr. Neher[3] in which the convection component of thermal conductivity is shown to vary inversely with the square root of the cable diameter. The thermal conductivity is just the reciprocal of the resistivity factor β, and the resistivity value for a cable diameter D_s is computed from that experimentally determined for a 3.5-inch diameter $\beta_{3.5}$ employing formula

$$\beta = \frac{\beta_{3.5}}{0.70 + 0.56 D_s^{-1/2}}$$

This formula is consistent with the assumption mentioned earlier in this paragraph, and the value of β thus obtained is associated with the same sheath temperature as the $\beta_{3.5}$ that is used in the formula. Table I of the discussion shows that a decrease in the sheath temperature of 20 degrees centigrade coupled with a 100 per cent increase in cable diameter produces an increase in β of the order of magnitude of 20 per cent for each of the four cases considered. These data substantiate the previous statement that for most practical calculations β may be considered as a constant for a given duct material in air or in concrete over the normal operating range of sheath temperatures. The values given in Table I of the discussion indicate, however, that averaging β values for duct in air and duct in concrete, as was done in Figure 14 and Table II of the paper, is not entirely justifiable.

The various discussions indicate that more experimental data are desired for a more complete investigation of the duct heating problem, and the authors heartily concur in this opinion. If our paper encourages additional experimental investigations and serves as a guide toward obtaining reliable data from such further work, it will have succeeded in its major objective.

References

1. See reference 3 of the paper.
2. The Thermal Resistance Between Cables and a Surrounding Pipe or Duct Wall, F. H. Buller, J. H. Neher. *AIEE Transactions*, volume 69, part I, 1950, pages 342–49.
3. Discussion by Paul Greebler of reference 2, page 348.
4. Discussion by Frank V. Smith of The Temperature Rise of Cables in a Duct Bank, J. H. Neher. *AIEE Transactions*, volume 68, part 1, 1949, pages 547–48.

Statistical Nature and Physical Concepts of Thyratron Deionization Time

H. A. ROMANOWITZ
MEMBER AIEE

W. G. DOW
FELLOW AIEE

THYRATRON tubes are often used in circuits in which the anode voltage is made positive a very short time after the tube has been extinguished. In such a circuit a thyratron may refire when the anode voltage is made positive, even though the grid potential is considerably more negative than the amount required to prevent firing in the static case with the same anode voltage present. In such an instance residual ions in the tube are responsible for the failure of grid control. These ions are present due to the fact that not enough time is allowed between tube extinction and the instant of reapplication of positive anode voltage for the ions to disappear from the interelectrode space.

The time required for the tube to deionize sufficiently to prevent breakdown upon reapplication of positive anode voltage, with normal operating grid bias voltage present, is called deionization time.

This critical time interval is a very important factor that places an upper limit on the operating frequency of apparatus employing thyratrons, such as inverters and frequency changers, and is a significant design factor in many timing circuits employing thyratrons.

Statement of the Problem

The objectives of the research reported herein have been:

1. To measure directly the time intervals, between thyratron extinction and recurring positive anode voltage, that are required to prevent loss of grid control under conditions in which variations of important parameters are concerned.

2. To observe directly, for each of many individual trials, the variation of a thyratron's anode voltage during extinction and subsequent reapplication of positive anode voltage, in order to investigate the statistical nature of the probability of refiring.

3. To study the data and results in the light of existing facts and theory with the purpose of attempting to explain new aspects of the problem.

The parameters affecting deionization time in a given thyratron are: grid potential, grid circuit resistance, amplitude of anode voltage in both positive and negative directions, anode current prior to extinction, and condensed-mercury temperature.

Experimental Procedure

The tube used was a Westinghouse type *KU-627* mercury-vapor thyratron. A dimensioned sketch of it is shown in Figure 1. The test circuit diagram is shown in Figure 2. By means of this circuit the anode potential of the thyratron under test, T_1, was suddenly driven negative while it was conducting. After a time delay that could be controlled, the circuit reapplied a positive potential to the anode.

T_2 and T_3 each represent four type *6L6* tubes in parallel; T_4 and T_5 are small control thyratrons, and T_6 is a *6L6*, the grid of which receives the actuating voltage of the circuit. The actuating voltage is the voltage that builds up across the 0.01-microfarad capacitor when the S_1 section of the multiple key switch is closed. The grid of T_6 is thus made increasingly negative; this causes a rapid reduction of plate current in the tube.

The effects of the reduction in plate current of T_6 are: the firing of T_4, which cuts off T_2 and thus reduces the plate current of T_1 to zero; and the firing of T_5, after a time delay controlled by VD_2, which brings T_2 well up above cut-off and thus provides a path for the current of T_1 if conditions are such that it refires. At the beginning of the test cycle T_1 and T_2 are conducting and T_5 is not.

If the deionization has progressed sufficiently during the time interval Δt between the firings of T_4 and T_5, T_1 will fail to refire when its plate is driven positive, and the plate to cathode voltage of T_1 will have the wave-form *A-B-C-D-E-F-H* as shown in Figure 3. If, however, deionization has not been sufficiently complete, T_1 will refire and its plate-to-cathode voltage will drop to the conduction value indicated at *G*. Refires usually occur, if at all, before the voltage reaches point *F*.

The voltage to which the plate is driven negative is controlled by power supply number 1. The value of recurring positive voltage that follows the removal of the negative plate voltage is adjusted by the resistors R_1 and R_3. The operating plate current of T_1 is controlled by R_5, and the voltage of the generator supplying the main bus.

In order that the screen pattern of the transient voltage could be seen and photographed, it was necessary to increase the beam current of the cathode-ray tube during its motion from left to right on the screen. This was accomplished by short-circuiting the intensity control potentiometer of the oscilloscope by means of contacts of a key switch. The contacts closed just before the plate of T_1 was driven negative and opened just after it was driven positive. Another contact started the single sweep of the scope at the proper instant.

Three relays in the circuit were energized by lifting the handle of the key switch after each test observation. They opened the plate circuits of T_4 and T_5, extinguishing them, and the grid circuit of

Paper 50-56, recommended by the AIEE Electronics Committee and approved by the AIEE Technical Program Committee for presentation at the AIEE Winter General Meeting, New York, N.Y., January 30–February 3, 1950. Manuscript submitted November 1, 1949; made available for printing December 27, 1949.

H. A. ROMANOWITZ is with the University of Kentucky, Lexington, Ky., and W. G. Dow is with the University of Michigan, Ann Arbor, Mich.

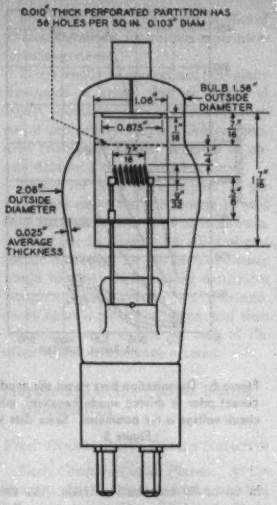

Figure 1. Dimensioned sketch of the Westinghouse type *KU627* mercury-vapor thyratron employed in the tests

T_1, allowing it to refire if it failed to do so during the test.

When photographs were made it was necessary to superimpose a timing wave upon the plate voltage pattern. In taking a picture of the plate voltage wave, the camera lens, mounted in an extension tube, was placed inside the small open end of a light-proof cone that covered the screen. The shutter was opened before the key switch was pressed and closed immediately afterward. Then the switch S_4 was turned to the oscillator side of the circuit and the key switch again pressed while the shutter was held open. The oscillator frequency and the oscilloscope gain and frequency control positions were the same for both exposures. Therefore, the sine wave gives correct values for time intervals.

The oscillogram in Figure 4(A) shows a typical condition in which the tube failed to refire. The elapsed time (about 270 microseconds) between extinction and the reapplication of positive anode voltage was at least long enough for deionization to take place sufficiently for the grid to regain control. It can be seen that after the plate voltage was changed from a negative to a positive value, with respect to the cathode, it stayed at that value for the remainder of the test cycle.

The oscillogram in Figure 4(B) was taken under the same conditions as Figure 4(A) except that the time interval allowed for deionization was shortened until the tube refired consistently when the positive voltage came back on the plate. The horizontal gain of the oscilloscope was increased somewhat in order that the pattern would not be so narrow on the screen. The same timing wave was used, and it is seen that the time interval was about 125 microseconds. Figure 4(C) is a print made of another negative on which was drawn a positive voltage peak, or "spike," to illustrate the visual appearance on the cathode ray tube screen. The rapid change in voltage when the peak occurs causes the brightness in that region of the screen pattern to be so low that, although it is clearly visible, it does not affect the film emulsion sufficiently to show more than an extremely weak trace which will not print. A great many of these patterns were observed as the time allowed for deionization was being changed through the critical range.

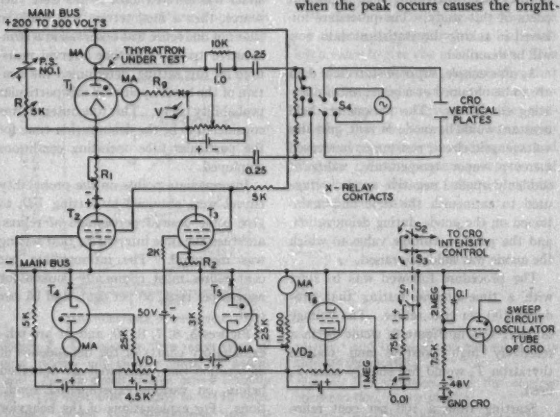

Figure 2. Diagram of circuit used for deionization time measurements

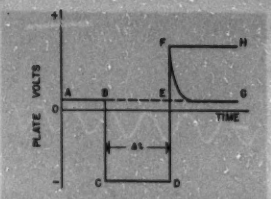

Figure 3. Types of plate voltage wave forms observed: At *B* the anode circuit voltage is driven negative to the *CD* value, extinguishing the tube. At *D* the anode circuit voltage is driven positive to the *FH* value. Consequently, if the grid retains control, the shape *DEFH* is followed; if the tube refires, but at a low probability of refiring, the shape *DEFG* is followed; if the tube refires, but at a moderately high probability of refiring, the form *DEG* is followed

With medium, and also with comparatively long, time interval settings the voltage wave is rectangular, and the horizontal segment, when the plate voltage is negative, may be used as the time interval indicator on the scale. When the interval is short the lower left hand corner of the wave pattern is rounded off as in Figure 4(C), because the time required for the plate voltage to go negative is an appreciable part of the total time interval.

Readings were taken mostly by observation of repeated wave forms. Many repetitions of screen patterns were made at each circuit setting when data were to be recorded. This was desirable because the positions on the scale at the beginning and at the end of the pattern had to be determined so that the number of timing wave cycles taken up by the deionizing period could be accurately determined. It was deemed necessary that at least four or five successive identical patterns be obtained before the scale readings were considered reliable. The key was pressed at time intervals of about two to three seconds. The error in these observations is estimated to be about 6 per cent.

The time interval value recorded as the deionization time was the time interval corresponding to zero per cent refires.

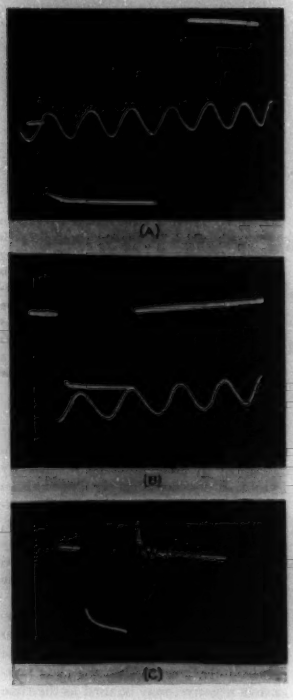

Figure 4. Oscillograms

(A) Nonrefiring plate voltage oscillogram, of the type *A-B-C-D-E-F-H*, Figure 3. Typical record for conditions producing zero refire probability. 10,000 cycles per second timing wave

(B) Refiring plate voltage oscillogram, of the type *A-B-C-D-E-G*, Figure 3. Typical for conditions producing just about 100 per cent refire probability. 10,000 cycles per second timing wave

(C) Barely refiring plate voltage oscillogram, of the type *A-B-C-D-E-F-G*, Figure 3. Typical refire record for conditions producing very small refire probability

From an engineering viewpoint that is the minimum time that must elapse before the plate is again made positive.

Statistical Nature of the Results

In the explanation of the method employed in measuring the time interval, it was pointed out that the time interval that resulted in zero per cent refires was

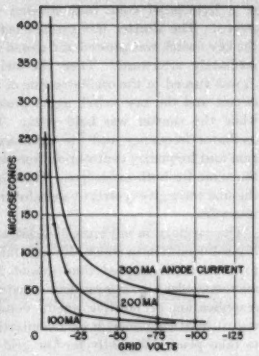

Figure 5. Deionization time versus grid circuit volts, Westinghouse *KU627* mercury-vapor thyratron, anode circuit voltage driven abruptly negative to −200 volts, then abruptly positive to +200 volts. Grid resistor 5,000 ohms, condensed-mercury temperature 52 degrees centigrade. Parameter is anode current prior to driving anode voltage negative

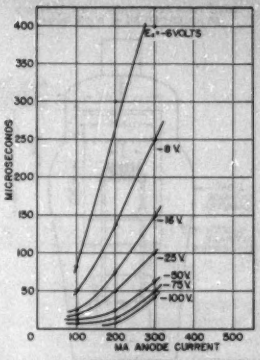

Figure 6. Deionization time versus the anode current prior to driving anode negative; grid circuit voltage is the parameter. Same data as Figure 5

selected as the deionization time for that set of operating conditions. However, it was found that when slightly shorter time intervals were allowed for the deionizing process the application of positive voltage to the plate resulted in some refires and some failures. The percentages of these two kinds of behavior in a given series of test trials could be varied at will by varying the time interval. A study of the statistical nature of tube refires forms one of the most interesting and important parts of this study. The procedure followed in taking the statistical data now will be described.

As an example, suppose statistical data are to be obtained at a given set of operating conditions. The parameters held constant would be anode current, grid bias voltage, grid circuit resistance, condensed mercury vapor temperature, value of suddenly applied negative anode voltage used to extinguish the tube and maintained on the anode during deionization, and the positive voltage value to which the anode was suddenly raised.

The procedure followed was to start with a time-interval setting that produced 100 per cent refires. The voltage divider, VD_2 in Figure 2, would be in a relatively high position and control thyratron T_2 would fire shortly after T_1 fired.

Starting from a 100 per cent refire condition, the slider was lowered a little at a time until a refire or two was observed in 25 or 30 consecutive trials. At this point increments of upward movement of the sliding contact on VD_2 were employed until not a single failure to refire was observed in a series of 50 consecutive trials. The time interval for this setting of VD_2 was then measured, and was taken as the longest time that would result in 100 per cent refires. This was the value used to locate the topmost point on this particular probability curve, as for example any one of the curves in Figure 9.

To determine the shortest time that would result in 0 per cent refires, the VD_2 slider was lowered until refires were very scarce, then a final setting was made so that not one refire was observed in 50 consecutive trials. The time interval measured for this setting determined the location of the lowest point for this particular probability curve. This time interval was considered to be the deionization time for the particular tube operating conditions employed.

Intermediate points on the probability curves were obtained by setting VD_2 to give some desired percentage of refires, and then the time interval for that setting was measured. The intermediate per cent refires most commonly looked for were 5 per cent, 50 per cent, and 95 per cent.

Figures 5, 6, 7, 8, 20, and 21 are self-explanatory charts of the dependence of dionization time, measured as described before, on various experimental conditions. For explanations of the behavior displayed, see later discussions of happenings in the dying plasma.

Figures 9, 10, 11, and 12 are families of probability curves for various experimental arrangements.

It can readily be appreciated that many thousands of trials, that is, cycles of circuit operation, were required for each set of probability curves. Several hundred trials were usually required to obtain data for a single statistical curve.

Except for the 0 per cent and 100 per cent refire cases, the points were located from data taken with 40 to 50 trials each. A set of curves showing the effect of grid circuit resistance, for instance, obviously would be obtained by taking data for a complete curve, keeping the resistance constant at a particular value, and then repeating the procedure for each of the other values of resistance selected.

Happenings in the Plasma During Deionization

First Event—Plate Driven Negative

Early Conditions in the Plasma. At the moment that the plate is driven negative (dashed curve in Figure 13(A)), the input of energy tending to maintain the plasma electron temperature ceases. Also, the negative potentials on grid and plate make it impossible for plasma electrons to reach either grid or plate.

Therefore, immediately after the plate is driven negative, the plasma potential drops from its normal value (perhaps ten volts above the cathode) to approximate equality with the cathode; see the solid-line curve in Figure 13(A). O. E. Johnson and L. Malter, in a paper presented before the American Physical Society in Chicago, Ill., November 25, 1949, demonstrated that the electron temperature drops, with almost equal rapidity, to approximately the cathode temperature. The reason for this change is that a Boltzmann-relation electron exchange equilibrium is established at once between cathode and the dying plasma because the plasma cannot deliver electrons either to grid or plate. The equilibrium is not precise because the electron flow to the cathode must exceed that from the cathode by about the amount of the total ion current delivered by the plasma to grid and plate; however, this total ion current is a very small fraction of the equilibrium-condition electron exchange between cathode and dying plasma. The plasma existing during deionization will sometimes be called a rest-plasma.

Thickening of the Sheaths.[8,2] For purposes of discussion consider that the plasma drops to cathode potential, and the plasma electrons to cathode temperature, as soon as the anode goes negative. Ions are passing out of the rest-plasma to the grid and the plate, through the sheaths adjacent to those electrodes.

In a mercury-vapor thyratron of the type here employed, and under normal use conditions, the mean free paths of electrons and ions are several times the interelectrode distances. Therefore, the long-mean-free-path type of study is involved. Ambipolar diffusion considerations do not apply, because ambipolar diffusion is a characteristic feature of short-mean-free-path conditions.

In this plasma ion and gas temperatures will be equal, because the mechanism that raises plasma ion temperatures above gas particle temperatures is that of ion collisions; however, very few collisions occur, because free paths are long.

No new ions are being produced because the electron temperature has fallen to too low a value to give rise to ionization. It is not difficult to show analytically that under these conditions the ion concentration is uniform throughout the rest-plasma, that the rest-plasma is an equipotential region between the sheaths, and that the following equation expresses at any instant the ion current density through the sheaths

$$J_{ri} = \frac{N_i \alpha_g q_g}{2\sqrt{\pi}} \qquad (1)$$

Here

J_{ri} = random ion current density in the plasma,[3] and therefore ion current density through the sheaths;

N_i = ion concentration, also the electron concentration, in the plasma;

α_g = the particle velocity characteristic of the gas and ion temperature T_g, for particles of mass m_g, given by

$$\alpha_g = \sqrt{\frac{2kT_g}{m_g}} \qquad (2)$$

K = the Boltzmann gas constant, 1.372×10^{-23} joule per particle per degree Kelvin

All equations are in meter-kilogram-second units.

Under these conditions the sheath thickness will be given by s in the familiar 3/2 power equation[8]

$$J_{ri} = \frac{2.33 \times 10^{-6} E_s^{3/2}}{\sqrt{m_g/m_e}\, s^2} \qquad (3)$$

where

E_s = potential difference across the sheath.
s = sheath thickness.
m_g/m_e = ratio of gas-particle mass to electron mass; for mercury $\sqrt{m_g/m_e} = 610$.

Obviously as ions run out to the cathode, grid, and plate, N_i will become less and J_{ri} therefore smaller; thus from equation 3 the sheath thickness s must increase. Thus the condition of Figure 13(A) changes in due course to that of Figure 13(B).

In some measurable number of microseconds the sheath will become thick enough to fill the holes in the grid; immediately a new set of conditions appears.

Grid-Plate Plasma Drops Below Cathode Potential. The grid-cathode rest plasma remains at or near cathode potential indefinitely, as the cathode is the least negative adjacent electrode. As long as the sheath has not closed the holes in the grid, a conducting path exists between the

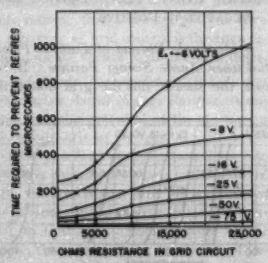

Figure 7. Deionization time versus value of grid resistor; grid circuit voltage the parameter. Anode circuit voltage driven abruptly to −150 volts, then abruptly to +150 volts. Anode current 200 milliamperes prior to driving anode voltage negative. Condensed-mercury temperature 58 degrees centigrade

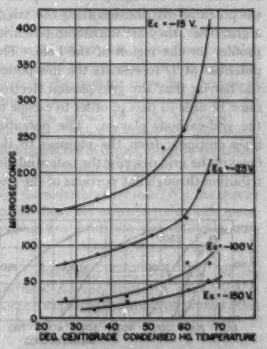

Figure 8. Deionization time versus condensed-mercury temperature; grid circuit voltage the parameter. Anode circuit voltage driven abruptly to −200 volts, then to +200 volts. Anode current 300 milliamperes prior to driving anode negative. Grid resistor 3,000 ohms

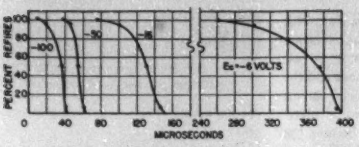

Figure 9. Experimentally observed probability of refire versus time allowed for deionization; grid circuit voltage the parameter. Anode circuit voltage driven abruptly to −200 volts, then to +200 volts. Anode current 300 milliamperes prior to driving anode negative. Grid resistor 5,000 ohms. Condensed-mercury temperature 55 degrees centigrade

Figure 11 (right). Same as Figure 10, except that grid circuit voltage is −50

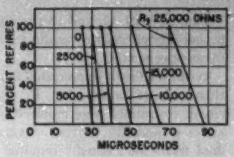

two plasma regions, and they remain at a common potential, about that of the cathode. As soon as the sheath does close the holes in the grid, the potential of the grid-anode plasma begins to drop; see Figure 14. The reason for this is that positive ions are continually running out, and if electrons cannot pass to the grid, the grid-anode plasma potential must drop because of the continuing removal of positive charge. The potential assumed by the grid-anode plasma at any instant will be such as to allow electrons to escape through or to the grid, or to the plate, just rapidly enough to balance the loss of ions.

The potential curves in Figure 14 are similar in nature to those familiar from a study of potential distributions in a high-vacuum parallel-plane triode. Thus the potential lines through points D represent the potential distribution along the axis of a grid hole; they are maximum-potential profiles for the region of the hole. The potential at D represents the low-potential barrier that any grid-plasma electron must be able to pass in order to escape to the grid-cathode plasma. The potential lines dropping from the plasmas to the faces of the grid describe the potential distribution through flat portions of the grid sheaths; these are minimum-potential profiles.

Qualitatively, in relation to Figure 14(B), one may think of the grid-cathode and grid-anode plasmas as establishing the plate and cathode potentials respectively (note the order) of a high-vacuum triode, whose grid potential E_g is just about that to produce cut-off, that is, limitation of leftward electron flow past D to a very minute amount.

In Figure 14(A) the sheath thickness s is barely more than enough to occlude the grid holes; by means of a drop of grid-anode plasma potential to a few volts below cathode potential, the electron-blocking potential minimum along the hole axis is almost eliminated. Thus just enough high-random-energy electrons to balance the ion loss from the grid-anode plasma are able to escape past this dip. In Figure 14(B) the sheath is thick enough so that a very substantial drop of grid-anode plasma potential is necessary in order to make the along-hole-axis potential dip E_d little enough to permit the escape of the necessary few electrons past it.

The grid-anode potential will never drop below its value in Figure 14(C), because to do so would cause a large electron flow to the grid, again raising its potential. Thus the grid-anode plasma potential cannot fall below that of the grid. Similarly it cannot fall below anode potential.

In principle then, after the grid holes are closed, the potential of the grid-anode potential falls, more or less abruptly, to a value differing very little from that of the least negative adjacent electrode. E. O. Johnson and L. Malter have demonstrated this experimentally. They have also shown, by a method of experimentation suggested by W. G. Dow, that the electron temperature in the grid-anode rest plasma drops to about room temperature as soon as the two rest plasmas become separated potential-wise.

Thus after grid-hole closure the potential distribution resembles one of the other of those in Figure 15(A), depending on whether or not the anode potential is below that of the grid. There are two important grid sheaths, one adjacent to the anode, the other adjacent to the face of the grid nearest the cathode.

In due time all of the electrons run out, leaving a distribution like that of Figure 15(B); the sheaths occupy the entire tube. Eventually all the ions run out leaving the typical space-charge-free distribution illustrated by Figure 15(C).

In summary, note that (1) for a time the grid holes are open, and the grid-anode and grid-cathode plasmas have a common potential; (2) after the sheaths fill the grid holes, the grid-anode plasma drops, approximately, either to grid or to anode potential; (3) after considerable time the sheaths fill both regions during transition to the space-charge-free condition ultimately existing if the anode remains negative indefinitely.

Second Event—Plate Driven from Negative to Positive

Gride-Anode Plasma at Cathode Potential when Anode Swings Positive. If, before the sheath fills the grid holes, the

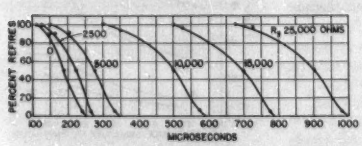

Figure 10. Experimentally observed probability of refire versus time allowed for deionization; grid resistor the parameter. Anode circuit voltage driven abruptly to −150 volts, then to +150 volts. Anode current 200 milliamperes prior to driving anode negative. Grid circuit potential −6 volts. Condensed-mercury temperature 58 degrees centigrade

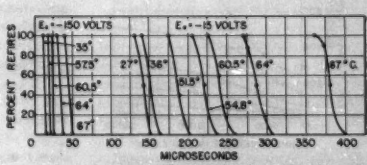

Figure 12. Experimentally observed probability of refire versus time allowed for deionization; condensed-mercury temperature the parameter. Anode circuit voltage driven abruptly to −200 volts, then to +200 volts. Anode current 300 milliamperes prior to driving anode voltage negative. One set for a grid circuit voltage of −150, another for a grid circuit voltage of −15 volts. Grid resistor 5,000 ohms

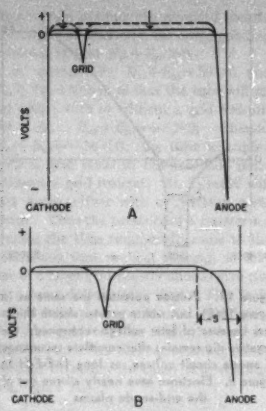

Figure 13. Potential distribution in the plasma

(A) At the moment the plate is driven negative, the plasma potential is unchanged; a sheath is established adjacent to the anode as in the dashed-line distribution. Immediately thereafter the plasma potential drops to a value such that its net loss of electrons to the cathode just equals its loss of ions to all electrodes; this potential is approximately that of the least negative adjacent electrode, in this case the cathode as shown in the solid-line distributions. The electron temperature quickly drops to thermal equilibrium with the cathode temperature

(B) Considerably later than (A); grid and anode sheaths have thickened substantially, but the plasma is still continuous through the holes in the grid

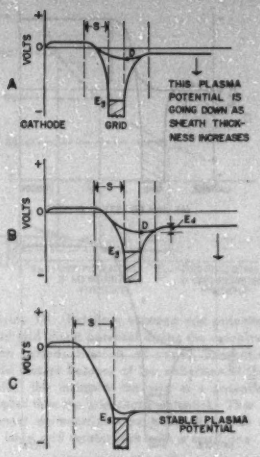

Figure 14. Decline of potential of grid-anode plasma following closure of grid holes by thickening of the grid sheath. The change from (A) to (B) to (C) is a consequence of the continuing thickening of the grid sheath. In each case the grid-anode plasma is low enough to make the grid-hole negative dip little enough so that the rate of electron escape to the cathode-grid plasma just equals the rate of ion loss from the grid-anode plasma to the grid and anode

(A) Shortly after sheath due to full grid potential is thick enough to fill grid holes

(B) Sheath somewhat thicker than for (A)

(C) Lowest potential reached by grid-anode plasma; this is the potential at which electron loss to an adjacent electrode just equals the ion loss. This potential is approximately that of the least negative adjacent electrode, which might be either grid or anode. As shown here it is the grid

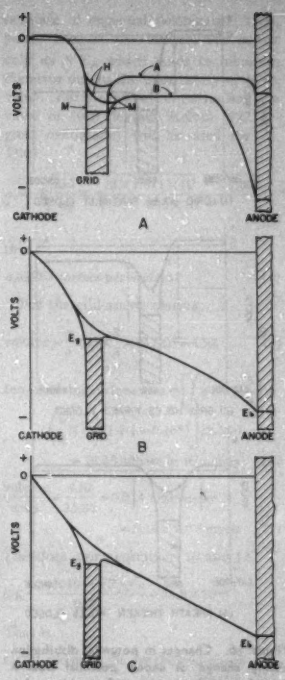

Figure 15. Potential distribution changes during the deionization process, as during CD in Figure 3

(A) Illustrative potential distributions after grid-anode plasma potential has stabilized at a potential about that of the least negative adjacent electrode, which is the anode for curve A, the grid for curve B. Arrows H point to potential distribution through the grid holes, arrows M show it through the grid metal. Along curve B the grid sheath has disappeared of course, because the plasma is at grid potential

(B) Considerably later than (A); the sheaths occupy almost the entire interelectrode space; all electrons have run out, either to the cathode or the grid

(C) Considerably later than (B); all the ions have run out, leaving a typical space-charge-free potential distribution, shown along paths through and between grid holes

anode is abruptly driven positive, there exists a direct path for electron flow from cathode to anode, and the tube immediately refires; thus the least possible time to recovery of grid control is the time required for the sheath to fill the grid holes.

Grid-Anode Plasma below Cathode Potential when Anode Swings Positive. Consider that the potential of the plasma on the anode side of the grid is well below cathode potential at the instant the anode suddenly swings positive; see Figure 16 (A). Electrons pour into the anode from the plasma raising the rest-plasma potential on that side. As shown in Figure 16(B), the sheath on the anode side of the grid is re-established. The electron flow through the grid holes stops. At the instant the plasma potential on the right reaches cathode potential, the holes are still firmly closed, Figure 16(C). A fraction of a microsecond later the plasma potential is well above cathode potential, but the holes are still closed by a negative dip, Figure 16(D). This is followed immediately by the situation shown in Figure 16(E), which results in refiring of the tube. The behavior just described corresponds to Figure 4(C), and to the pattern *A-B-C-D-E-F-G* on the Figure 3.

The operation just described can be thought of qualitatively as being similar to the action in a high-vacuum triode having as its cathode the plasma face of the sheath to the left of the grid, and as its anode the plasma face of the sheath to the right of the grid, in Figures 16(D) and 16(E) particularly. In Figure 16(D) this triode is still below cut-off; in Figure 16(E) its plate potential has risen above cut-off.

If the sheaths are thicker, as in Figure 17, there may still exist, for a high recurring anode voltage, a negative dip along the grid axis; the comparable triode does not rise above cut-off. In that case the tube does not refire; as time passes the

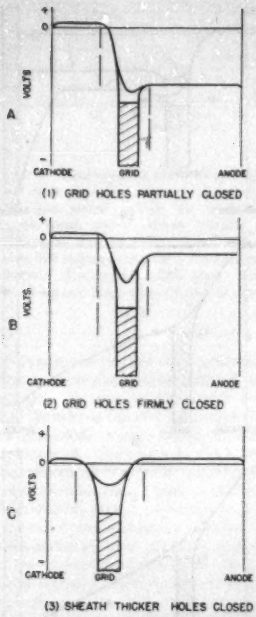

Figure 16. Changes in potential distribution during change of anode potential from a strongly negative to a strongly positive value causing refire, as at moment *D–F* along *D-E-F-G*, Figure 3

(A) Anode potential has just started up from its position as along curve B in Figure 15(A), re-establishing a small sheath on the anode side of the grid, so re-establishing a negative dip and preventing further electron drainage toward the cathode. Grid-anode potential is that of the least-negative adjacent electrode, in this case the anode

(B) A fraction of a microsecond later than (A); anode potential still rising. Note the pronounced negative dip through grid holes

(C) Rising anode potential becomes equal to cathode potential; electrons cannot move between the two plasmas because of the negative dip through the holes in the grid

(D) Rising anode potential has substantially lifted the bottom of the dip in grid holes, but not enough to permit electrons to flow to the right, past it

(E) Tube will fire immediately, as at *F* along *D-E-F-G* of Figure 3, because the anode potential has lifted the grid-anode plasma high enough to eliminate the dip

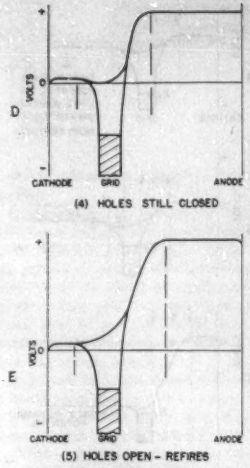

Figure 16 (continued)

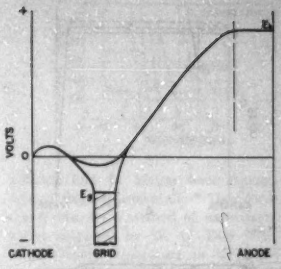

Figure 17. Anode potential the same as in Figure 16(E), but with a greater sheath thickness because of later voltage recurrence; the negative dip remains after complete recurrence of anode circuit voltage, as long *D-E-F-H* in Figure 3. Electrons have nearly all run out of the grid-anode plasma

electrons and ions run out, with eventual transition to the space-charge-free condition of Figure 18.

The Unique Time Interval. The points of view so far presented lead to certain indications, as follows:

1. There is a unique time interval, the time required for the sheaths to occlude the grid holes. If the anode voltage is driven positive before the elapse of this unique time interval, the tube will certainly refire at the moment the rising anode potential reaches a value a very little above the cathode potential. If more than the unique time interval has elapsed, refire will not occur until the anode has risen appreciably above cathode potential, and it may not occur at all, depending on the details of the cut-off action of the triode analogue to the grid-sheath combination. A high recurring anode voltage may cause refire to occur when a low recurring anode voltage will not; see Figure 21.

2. The unique time interval is independent of the potential to which the anode is driven negative in the first event, because the rate of loss of ions in either region is, to a first approximation, independent of the potential of the adjacent electrodes. Therefore, the deionization time should be independent of the potential of the anode during the dark period of the deionization test cycle. This agrees with experiment; see Figure 20.

3. The unique time interval is dependent on the grid potential, being less when the grid potential is low (that is, strongly negative). This is, of course, because a large sheath potential will produce a thick sheath even when the ion density is relatively large. This expectation is verified experimentally; see Figure 5.

4. Consider a circumstance in which the sheaths on the two sides of the grid are of unequal thickness due to unequal volume-to-surface ratios for the two regions. The question arises: which sheath thickness determines whether the holes are closed for the moment when the anode potential has risen just to equality with that of the cathode-grid region? Although no firm proof of the answer is presently available, the general concepts of space potential distribution, as in the analogous high-vacuum triode, suggest that with the two plasmas at a common potential there will exist a negative potential dip on the hole axis whenever the thicker of the two sheaths appreciably exceeds the half-diameter of the hole in thickness. This implies that the deionization time should depend on the rate of loss of ions in the most rapidly decaying of the two plasmas, in this case the grid-anode plasma. Figure 23 tends to support this conclusion.

Effect of the Grid Resistor. At the moment of anode voltage recurrence the grid current consists of ion current from both rest plasmas. Grid potential, relative to the cathode, is raised (made less negative) by the grid current voltage drop through the grid resistor. Thus the presence of a grid resistor makes the actual grid potential a function of time during the dark period, because the ion currents are declining during this period.

The following discussion, relative to Figure 19, illustrates the effect of a grid resistor on grid sheath thickness. Arbitrary voltage values are used. Curve E_{so}, Figure 19, shows the sheath potential required to prevent firing. Curve E_{gr} shows the approach of the actual grid voltage to the grid bias voltage E_{go}, as the ion-borne grid current declines during the dark period. If at a moment of anode voltage recurrence $E_{ao}+E_{gr}>0$ (of course, E_{gr} is negative) the tube will refire, as E_{gr}

then cannot produce the required sheath. Without a grid resistor, the corresponding criterion is that $E_{s0}+E_{g0}>0$.

At moment T_1, $E_{s0}+E_{g0}=50>0$, and $E_{s0}+E_{g0}=30>0$, so that the tube will refire either with or without a grid resistor. At T_2, $E_{s0}+E_{g0}=+5>0$, whereas $E_{s0}+E_{g0}=-10<0$; the tube will refire with a grid resistor, but will not refire without a grid resistor. At T_3 refire will not occur, either with or without a resistor. Thus the presence of a resistor increases the time required to come to the conditions that prevent refiring, so that use of a large grid resistor should give rise to a long deionization time. This is in accord with the experiments; see Figure 7. The grid resistor similarly has, indirectly, an effect on the recurring anode voltage necessary to cause late refiring; see Figure 21.

Analytical Determination of Deionization Time

The total ion content is volume V of the plasma multiplied by ion density N_i. The change of ion content in time dt is the electrode area presented to the plasma times

$-\frac{N_i\alpha_g}{2\sqrt{\pi}}dt$. The negative sign indicates a loss.

Note that

$$d(\text{volume}\times N_i)=-\text{area}\times\frac{N_i\alpha_g}{2\sqrt{\pi}}dt \tag{4}$$

Rewriting this

$$\frac{dN_i}{N_i}=-\frac{\text{area}}{\text{volume}}\times\frac{\alpha_g}{2\sqrt{\pi}}dt \tag{5}$$

Integrating

$$\log_e N_i=-\frac{\text{area}}{\text{volume}}\times\frac{\alpha_g}{2\sqrt{\pi}}t+\text{constant} \tag{6}$$

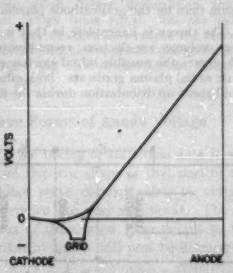

Figure 18. Many microseconds later than Figure 17, all electrons and ions have run out, leaving a space-charge-free potential distribution with a negative gradient adjacent to the cathode

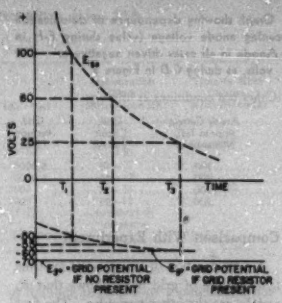

Figure 19. Relations between grid potential and grid circuit potential during the deionization period; there is, of course, substantial grid current because of ion collection at the grid; this maintains the grid at a potential higher than the grid circuit potential. Thus a longer deionization time is required with a large grid resistor than with a small one

When $t=0$, $N_i=N_{i0}$ (plasma ion concentration before extinction). Therefore the constant of integration is $\log_e N_{i0}$.

$$\log_e\frac{N_i}{N_{i0}}=-\frac{\text{area}}{\text{volume}}\times\frac{\alpha_g}{2\sqrt{\pi}}t \tag{7}$$

$$\frac{N_i}{N_{i0}}=\exp\left(-\frac{\text{area}}{\text{volume}}\times\frac{\alpha_g}{2\sqrt{\pi}}t\right) \tag{8}$$

that is

$$\frac{N_i}{N_{i0}}=\exp\left(-\frac{t}{t_0}\right) \tag{9}$$

where

$$t_0=\frac{\text{volume}}{\text{area}}\times\frac{2\sqrt{\pi}}{\alpha_g} \tag{10}$$

which may be called the ion decay time constant.

Computation of t_0

The ion decay time constant will be computed for the tube used in the tests, for the grid-anode rest plasma and for the grid-cathode rest plasma, employing dimensions as shown in Figure 22. The volume and area occupied by the cathode are comparatively small and will be neglected. The anode will be treated as a surface one inch in diameter. The holes occupy 46.7 per cent of the grid baffle area.

The gas-and-ion temperature T_g is not definitely known, nor is it easily measurable. It is certainly higher than the temperature of the glass envelope of the tube and probably lower than the cathode temperature. It is not necessary to know T_g accurately in order to obtain a reasonable estimate of expected deionization time, partly because the temperature occurs only as $\sqrt{T_g}$, which tends to minimize the error due to the uncertainty as to its value. For the purpose of estimating t_0, a value of 1000 degrees Kelvin (727 degrees centigrade) will be used for T_g. Thus

$$\alpha_g=\sqrt{\frac{2kT}{m_g}}\cong\sqrt{\frac{2\times1.371\times10^{-23}\times1{,}000}{333\times10^{-27}}} \tag{11}$$

that is,

$$\alpha_g\cong287 \text{ meters per second} \tag{12}$$

For the grid-anode plasma:

$$\text{volume}=\frac{\pi}{4}\times1^2\times\frac{3}{8}\times(2.54)^3=4.82 \tag{13}$$

$$\text{Ion-receiving surface area}=\left[\left(\pi\times1\times\frac{3}{8}\right)+\left(\frac{\pi}{4}\times1^2\right)(1+1-0.467)\right](2.54)^2$$
$$=15.35 \text{ square centimeters} \tag{14}$$

$$\frac{\text{volume}}{\text{area}}=\frac{4.82}{15.35}=0.314 \text{ centimeter}$$
$$=3.14\times10^{-3} \text{ meter} \tag{15}$$

Therefore, using equations 10 and 12

$$t_0\cong\frac{3.14\times10^{-3}\times2\sqrt{\pi}}{287}=38.8\times10^{-6}$$

That is

$$t_0\cong39 \text{ microseconds, for the grid-anode plasma} \tag{16}$$

For the grid-cathode plasma, a similar calculation leads to

$$t_0\cong\frac{12.9\times10^{-3}\times2\sqrt{\pi}}{22.9\times287}=69.2\times10^{-6} \tag{17}$$

That is

$$t_0\cong69 \text{ microseconds, for the grid-cathode plasma} \tag{18}$$

The shorter period (for the grid-anode

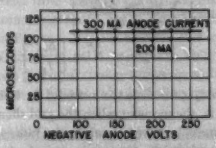

Figure 20. Graph showing that deionization time is independent of the magnitude of the suddenly applied negative anode voltage (value during C-D in Figure 3). The parameter is plate current prior to driving anode voltage negative. Grid circuit voltage, −16 volts; grid resistor, 5,000 ohms; recurring anode voltage, +200 volts (value of voltage during F-H in Figure 3)

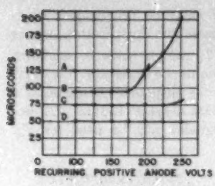

Figure 21. Graph showing dependence of deionization time on recurring anode voltage (value during F-H in Figure 3). Anode in all cases driven negative to −200 volts, as during C-D in Figure 3

Other test conditions as follows:

	Anode Current Prior to Test, Milliamperes	Grid Circuit Voltage	Grid Resistor, Ohms
Curve A	300	−16	5,000
Curve B	200	−16	5,000
Curve C	200	−16	0
Curve D	200	−25	0

plasma) may be expected to control the deionization time.

Computation of Deionization Time

The ion current density to the grid at the instant the first event occurs is

$$J_{io}=\frac{N_{io}\alpha_g q_g}{2\sqrt{\pi}}=\frac{I_{go}}{A_g} \tag{19}$$

where I_{go} is the easily measurable grid current just before the anode is driven negative, and A_g is the ion-collecting area of the grid, considering both plasmas. Equation 19 can be written

$$N_{go}=\frac{2\sqrt{\pi}I_{go}}{q_g\alpha_g A_g} \tag{20}$$

At any instant t seconds later, and before anode voltage recurrence

$$N_i=\frac{2\sqrt{\pi}I_{go}}{q_g\alpha_g A_g}\exp\left(-\frac{t}{t_0}\right) \tag{21}$$

Also, from equations 1 and 3

$$N_i=\frac{2\sqrt{\pi}\times 2.33\times 10^{-6}E_a^{3/2}}{s^2\alpha_g q_g\sqrt{m_g/m_e}} \tag{22}$$

Combining the last two equations

$$\exp\frac{t}{t_0}=\frac{\sqrt{m_g/m_e}}{2.33\times 10^{-6}}\,\frac{I_{go}s^2}{A_g E_a^{3/2}} \tag{23}$$

This can be solved for t; with the half-diameter $d/2$ of the grid holes used for s, it then becomes

$$t=t_0\log_e\left[\frac{\sqrt{m_g/m_e}}{2.33\times 10^{-6}}\,\frac{(d/2)^2}{A_g}\right]-t_0\log_e\left[\frac{E_a^{3/2}}{I_{go}}\right] \tag{24}$$

where t_c is the time to closure of the holes, that is, the moment when the grid sheath thickness becomes equal to the radius of the grid holes, for a plasma of about cathode potential.

The area A_g in the above equations is the grid area exposed to both plasmas before the first event, and is

$$A_g=\left[\left(\pi\times 1\times\frac{11}{8}\right)+2\left(\frac{\pi}{4}\times 1^2\right)(1-0.467)\right]\times(2.54)^2=33.3 \text{ square centimeters} \tag{25}$$

Comparison With Experiment

A consideration of equation 24 for time t_c to closure of grid holes shows that E_a and I_{go} are the other variables. The first term on the right-hand side is a constant and becomes

$$39\times 10^{-6}\log_e\left[\frac{610}{2.33\times 10^{-6}}\times\frac{\left(\frac{0.103\times 2.54}{2}\right)^2}{33.3}\right]=461\times 10^{-6} \tag{26}$$

Equation 24 becomes, for the grid-anode plasma

$$t_c=461\times 10^{-6}-39\times 10^{-6}\log_e\frac{E_a^{3/2}}{I_{go}} \tag{27}$$

The similar relation for the gride-cathode plasma is

$$t_c=815\times 10^{-6}-69\times 10^{-6}\log_e\left[\frac{E_g^{3/2}}{I_{go}}\right] \tag{28}$$

The relations described by equations 22 and 23 appear as straight lines in the coordinates of Figure 23.

The time to closure of grid holes in a plasma at about cathode potential should correspond approximately to the 100 per cent refire condition in the statistical curves. To understand why this is true, note that refire may occur if the anode voltage recurs well after hole closure, but it will always occur if voltage recurrence happens before hole closure. Deionization time as used in this paper corresponds to the 0 per cent refire condition, for obvious engineering reasons; therefore, the deionization time should always be somewhat longer than the time to hole closure. This difference is much greater proportionally with large than with small grid voltages, for reasons associated with the facts brought out later in the discussion of possible mechanisms causing the statistical behavior; see also Figure 21.

If no grid resistance is employed the grid sheath potential E_s may be reasonably well identified with grid potential E_g, so that data for which $R_g=0$ may be employed for comparison with theoretical considerations. Thus the curve of measured deionization time is obtained by using the $R_g=0$ points of Figure 7, using $E_s=-E_g$, and employing values of I_{go} based on measured grid currents. The useful grid-current-grid-voltage data, for conditions prior to the first event, R_g being zero, are plotted in Figure 23(B). This exhibits the usual nearly constant grid current for strongly negative grid voltages with a sharp upturn at about $E_g=-15$, due to the onset of electron penetration through the sheath. In accord with established practice in plasma probe studies, the value of I_{go} used for $E_g=-6$ and $E_g=-8$ is the ion current, obtained along the dashed extrapolation shown in Figure 23(B).

The line on Figure 23(A) indicating measured time to hole closure is based on (1) two firm points, taken from Figures 10 and 11, at $E_g=-6$ volts and $E_g=-50$ volts, together with (2) the general observation from the data as a whole that there is relatively little difference between hole closure (100 per cent refires) and deionization time (0 per cent refire) for short closure times, but a very great difference for long closure times. Table I gives further data.

The significant aspects of the comparison in Figure 23(A), between the theory and the experimental results, are as follows:

1. The time to hole closure, and the deionization time for strongly negative grid voltages, make straight-line plots when represented as a function of $\log_e(E_a^{3/2}/I_{go})$. This is in accord with the results of previous experimenters and with the theory presented above.

2. The theory gives the correct order of magnitude of time to hole closure except for the extremely short times observed for strongly negative grid potentials.

3. As is to be expected, the experimental data represent behavior closer to that computed for the rapidly decaying grid-anode plasma than for the grid-cathode plasma.

4. The theory is incomplete in that it ignores volume ion-electron recombination and ignores the possible initial existence of gentle radial plasma gradients; both effects would speed up deionization during the first

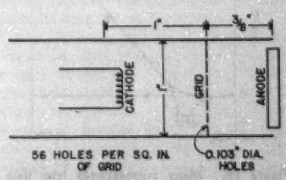

Figure 22. Diagram showing surface to volume proportions, in connection with theoretical computation of deionization time

Table I. Data For Experimental Plots, Figure 23A

From Figures 7, 10, 11; $R_g = 0$

E_g (volts) $= -E_g$	I_{pa} (Milliamperes Measured)	I_{pa} (Milliamperes Ion Current)	$\log_2 (E_g^2/I_{pa})$	Deionization Time (Microseconds)	Time to Hole Closure (Microseconds)
6	5.5	11.7	7.13	250	112
8	7.5	11.8	7.56	150	
16	12	12	8.58	75	
25	12.1	12.1	9.24	50	
50	12.4	12.4	10.3	33	30
75	12.8	12.8	10.9	12	
150	14.5	14.5	11.7	too short to measure	
158	14.8	14.8	11.81		

few microseconds after the first event. Significant volume recombination does not occur in an active plasma because of the high electron temperature, but it may occur in the rest plasma with its modest electron temperature. However, the rate of volume recombination ion loss varies inversely as the square of the ion density, so will decline much more rapidly than the density. Therefore, it will be important, if at all, only during the initial stages of deionization when the ion density is greatest. Over-all, it is seen that the difference between measured and computed time to hole closure is of the kind to be expected on the basis of known incompleteness of the standard theory presented above.

5. The zero-time-intercept, at $E_g = -158$ volts, of the computed hole closure curve, implies that at this grid voltage the grid sheath should be sufficient to fill the holes in the presence of an active plasma, thus interrupting the flow of plate current. This grid snuff-out is a familiar phenomenon in the type desirable, *2050* and *2051* thyratrons used for cathode-ray time axis circuits.

6. Note that the contributions of this paper to the theory are chiefly clarifications of concepts within a well-established framework. The theory consists basically of fairly obvious applications of well-known and relatively simple principles of plasma behavior. The extension to cover large-hole thyratrons, such as the *FG-57* and the *FG-95*, is straightforward in principle, but requires care in detail. Larger holes of course mean longer deionization times, other things being equal. On the other hand, any changes that reduce the current density in the active plasma, for given total current, will tend to shorten the deionization time.

Wave Forms of Anode Voltage

In the taking of statistical data it was found that the shape of that part of the voltage wave corresponding to voltage recurrence was very significant. The relation of these wave form details to the statistical curves will now be discussed.

The Spike

Each statistical curve, as for example in Figure 9, identifies a time interval which corresponds to the latter portion of the deionization period, during which the grid-anode plasma is at a potential lower than that of the cathode but not lower than that of the grid. Oscilloscope screen patterns for all refiring observations during this less-than-100-per-cent-refire probability period were characterized by a positive voltage peak, or spike, as shown in Figure 24(A) and in Figure 4(C). The spike had near-maximum height for the refire occurrences at the 5 per cent refire probability time setting. Refire observations at the 95 per cent refire setting exhibited a very small spike, as shown at *A* in Figure 24(B). The spike practically disappeared at the just 100 per cent refire setting (hole closure), and for still shorter time settings the pattern rounded off at *B* in Figure 24(B).

Figure 25 illustrates the nature of the variation of the anode voltage wave form for various positions along a statistical curve.

The Rounding Off of the Wave

The rounding off of the recurring voltage wave, as at *B* in Figure 24B, implies a certain behavior in the thyratron plate circuit. Figure 26(A) shows a simplified plate circuit diagram with a reversible supply voltage source. The supply voltage is initially +200 volts, as in Figure 26(A), changes abruptly to −200 volts, and after a few hundred microseconds reverts to +200 volts. The rounding-off shown in Figure 26(B) means that at the moment *TT'* the circuit potentials are as shown in Figure 26(C).

Note that at this moment the anode is 15 volts below cathode potential, yet there is a current $i = 215/R_L$ through the tube and R_L in the normal direction. The grid-anode rest plasma is momentarily acting as a generator delivering an electron current appreciably exceeding the normal load current against an opposing potential of 15 volts. This is the same type of behavior as occurs at the onset of electron current in the grid current characteristic, Figure 23(B). Note that this

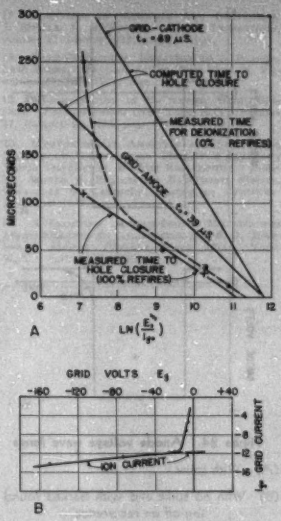

Figure 23. Experimental and computed data

(A) Curves of time to closure of grid holes and deionization time plotted relative to the significant logarithmic parameter. For the experimental data the anode was driven abruptly to −150 volts, returned to +150 volts, pre-test anode current 200 milliamperes, zero grid resistance, condensed-mercury temperature 58 degrees centigrade

(B) Pre-test grid currents, corresponding to the experimental data of (A)

occurs only for time settings prior to hole closure so that the grid holes are open and both rest plasmas are at about cathode potential and have an electron temperature about that of the cathode.

As rest-plasma properties change during deionization the available electron current from the grid-anode rest-plasma becomes markedly less. Thus for curve *A* in Figure 24(B) the electron current to the anode is little enough so that the anode potential change keeps up with the change of supply voltage during reversal.

Statistical Behavior Mechanisms

The occurrence of spikes on the voltage wave form, as in Figure 24(A), is correlated with the condition of a low percentage of refires. The occurrence of these comparatively few refires in a given number of trials always seemed random in nature. For instance, they were as likely to occur early as late, or to be bunched or

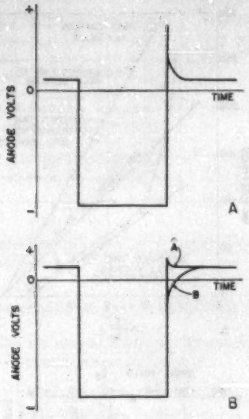

Figure 24. Anode voltage wave forms

(A) With spike

(B) With no spike and with marked rounding-off on recurrence

separated, in any set of forty successive observations. An examination of potential distribution diagrams will indicate an explanation of the correlation between the occurrence of spikes and the low-percentage refire condition.

The diagram in Figure 16(D) suggests the potential distribution in the tube at an instant near the end of deionization, when the anode voltage is about +100 volts and is rising rapidly. The tube has not refired. However, the potential within the grid holes dips below the cathode-to-grid plasma potential; the tube cannot refire as long as this dip is pronounced enough to prevent the electrons of higher random energies from getting through to the grid-anode region.

In Figure 16(E), the anode potential has risen high enough to eliminate the dip; within less than a microsecond the tube will fire due to electrons passing from left to right in substantial volume. This is the condition at the crest of a spike.

In Figure 17, for the same electrode voltages and grid sheath potentials as for Figures 16(D) and 16(E), and again at the instant the rapidly-rising anode voltage is at 100, the dip is so deep that its bottom is rising relatively slowly. This time the tube will not refire because a residual dip will still exist when the anode potential levels off at +200 volts.

However, if in this case the anode potential were to go on past +200 volts and in another half microsecond or so reach +300 volts, the dip would be eliminated and the tube would refire. This explains the reason for the sensitivity to recurring anode potential when the time allowed for deionization is almost long enough to reduce the per cent refires to zero (see curves *A* and *B* in Figure 21).

This suggests that the randomness in the deionization time interval may be attributable to variations, from trial to trial, in the potential at the bottom of the dip for a given rising anode potential. Such a variation could result from relatively small random variations in the ionic space charge content and distribution in the immediate neighborhood of the largest hole in the grid. It is to be expected that the potential distribution as illustrated in Figure 16(D) is subject to local rapid irregular fluttering as a result of space charge changes similar in origin to plasma ion oscillations. The firing or not in a particular trial will then depend on whether the moment of reapplication of voltage coincides with a moment of low or high potential at the bottom of the dip. The concept of the phase position of the moment of voltage return, relative to a plasma ion oscillation situation, may be helpful in picturing the cause of the randomness.

Conclusions

1. It has been shown that deionization time is a statistical concept (see Figures 8, 10, 11, and 14); the spread of the randomness increases more rapidly than the deionization time.

2. The statistical behavior has been correlated with changes in the wave form of the recurring anode voltage (see Figure 25) and with a reasonably rational mechanistic explanation as to the origin of the randomness.

3. Clarifying concepts have been introduced relative to the theory of the dependence of deionization time on tube geometry and potentials, and the theory has been shown to be in reasonably satisfactory agreement with the experiments here described.

4. The nature of the dependence or otherwise of deionization time on grid potential, grid circuit resistance, condensed-mercury temperature, and anode voltage has been shown experimentally and satisfactorily explained.

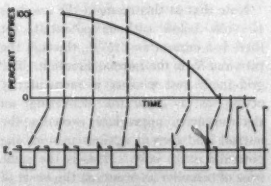

Figure 25. Correlation between per cent refires and voltage wave forms

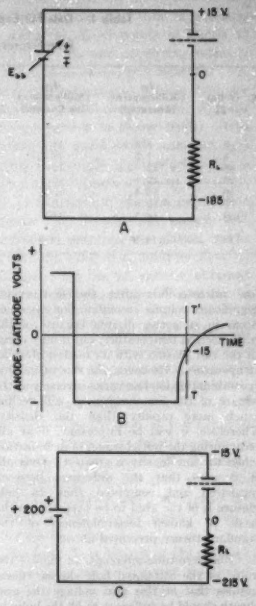

Figure 26. The rounding-off behavior

(A) Anode circuit conditions as expected during voltage recurrence on refire

(B) Actual wave form for high-probability refire

(C) Circuit conditions corresponding to (B), requiring electron collection from plasma

References

1. Gaseous Conductors (book), J. D. Cobine. McGraw-Hill Book Company, Inc., New York, N. Y., 1941.

2. Fundamentals of Engineering Electronics (book), W. G. Dow. John Wiley and Sons, Inc., New York, N. Y., 1937.

3. The Kinetic Theory of Gases (book), L. B. Loeb. McGraw-Hill Book Company, Inc., second edition, 1934.

4. Reignition Potential of Hot Cathode Grid-Glow Tubes, W. E. Berkey, C. E. Haller. *Electric Journal* (East Pittsburgh, Pa.), volume 31, 1934, page 483.

5. Equivalent Electrostatic Circuits for Vacuum Tubes, W. G. Dow. *Proceedings*, Institute of Radio Engineers (New York, N. Y.), volume 28, number 12, December 1940.

6. Disintegration of the Plasma of a Low-Pressure Electrical Discharge, V. L. Granovsky. *Journal of Physics*, Academy of Sciences of the USSR (Moscow, Russia), volume 8, number 2, 1944, pages 76–88.

7. Entionisierung und Wiederzundung in Gittergesteuerte Gasentladungsgefasse, P.

K. Herman. *Archiv fuer Elektrotechnik* (Berlin, Germany), volume 30, number 9, September 8, 1936, page 555.

8. Control of an Arc Discharge by Means of a Grid, A. W. Hull, I. Langmuir. *Proceedings*, National Academy of Science (Washington, D. C.), volume 15, 1929, pages 218–25.

9. On the Theory of Recombination of Ions in Gases, George Jaffe. *Physical Review* (New York, N. Y.), volume 58, December 1940, page 968.

10. Residual Ionization and Arc-Back in Thyratrons, K. H. Kingdon, E. J. Lawson. *General Electric Review* (Schenectady, N. Y.), volume 42, November 1939, page 474.

11. Carrier Diffusion Currents in Grid-Controlled Hot-Cathode Rectifiers, H. Kniepkamp. *Wissenschaftliche Veroeffentlichungen aus dem Siemens-Werken* (Berlin, Germany), volume 15, number 2, page 25, 1936.

12. Uber Sondenmessungen in Zeitlich Veranderlichen Entladungen, W. von Koch. *Zeitschrift fuer Technische Physik* (Leipzig, Germany), volume 16, number 11, 1935, page 461.

13. Experimenteller Nachweis der Ionenschichten um Electroden von Stromrichtern waehrend der Entionisierung, W. Von Koch. *Zeitschrift fuer Technische Physik* (Leipzig, Germany), volume 16, number 11, 1935, page 461.

14. Low Grid Current Vacuum Tubes, G. R. Metcalf, B. J. Thompson. *Physical Review* (New York, N. Y.), volume 36, 1935, pages 1489–94.

15. Entionisierungszeiten von Stromrichtern, Ostendorf. *Elektrotechnische Zeitschrift* (Berlin, Germany), volume 59, number 4, January 27, 1938, page 87.

16. Rate of Change of Electron Temperature in the Mercury Afterflow, Randall, Webb. *Physical Review* (New York, N. Y.), volume 48, number 6, September 15, 1935, page 544.

17. Backfires in Mercury Arc Rectifiers, J. Slepian, L. R. Ludwig. *AIEE Transactions*, volume 51, March 1932, pages 92–104.

18. High-Frequency Behavior in a Plasma, Lewi Tonks. *Physical Review* (New York, N. Y.), volume 37, June 1931, page 1458.

19. Recombination in Hg Vapor, Webb, Sinclair. *Physical Review* (New York, N. Y.), volume 37, January 15, 1931, page 183.

20. Measurements, Analysis, and Statistical Nature of Deionization Time in a Mercury Vapor Thyratron, H. Alex Romanowitz. *Bulletin Number 6*, Engineering Experiment Station, University of Kentucky, Lexington, Kentucky, December 1947.

21. A Floating Double-Probe Method for Measurements in Gas Discharges, E. O. Johnson, L. Malter. *Physical Review* (New York, N. Y.), volume 78, 1950.

No Discussion

Effect of Buck-Boost Voltage Regulator on Steady-State Power Limit

C. CONCORDIA
FELLOW AIEE

FOR a long time it has been known that use of a properly-designed generator voltage regulator can increase the steady-state power limit of a synchronous machine appreciably. A previous paper[1] showed how to calculate the magnitude of the possible gain in power limit and presented some data showing quantitatively the gain as affected by the characteristics of the voltage regulator used. From these data it would naturally be inferred that to obtain maximum benefit the alternator field exciter should be separately excited rather than self excited; that is, the alternator field exciter should derive its own field excitation from its voltage regulator and/or pilot exciter rather than from its own generated voltage. However, there have been developed voltage regulating systems that partake of most of the advantages of both kinds of excitation. A typical system is the buck-boost system, in which the exciter field is supplied in part from its own generated voltage and in part from a regulating machine, for example, an amplidyne, which bucks or boosts this voltage. Figure 1 shows such a system. The regulator output voltage is put in series with the exciter terminal voltage across the exciter field.

Interest in this case arises from the fact that the buck-boost regulator is coming into use in central station applications, and it is thus becoming more and more necessary to be acquainted with the possibilities of increasing power limits, still retaining the advantages of close voltage regulation, reliability, and small regulator power requirements possessed by the buck-boost system. The first applications of voltage regulators to improve power limits, made in connection with the previous study,[1] were to ship propulsion systems in which there was not nearly so much incentive to use a buck-boost system.

In this paper it is shown that by proper stabilizer design it is possible to increase the power limit practically as much with a buck-boost excitation system as with the previously-considered separately-excited system. In all the cases discussed here, the exciter field resistance and saturation lines have been assumed to be parallel, so that the over-all steady-state amplification factor is infinite, that is, the voltage regulation is zero.

Conclusions

1. For the power system considered, and with the addition of a proper stabilizer, the steady-state stability limit can be increased practically as much with a buck-boost regulator (having an infinite steady-state amplification) as with the separately-excited exciter considered in reference 1.

2. For best results with a stabilizer supplied only from exciter voltage, the stabilizer washout time constant should be at least of the same order of magnitude as the alternator field time constant (under load).

3. The stability limit may also be increased by the aid of a stabilizer supplied from alternator terminal voltage. In this case the stabilizer washout time constant need not be large. This conclusion does not necessarily imply that the terminal-voltage stabilizer is to be preferred, as there are additional obstacles to be overcome in the practical application of such a stabilizer.

4. The gain in power limit is not affected greatly by the magnitude of the stabilizing signal as long as it is sufficiently large.

5. Tests have confirmed that stable operation at powers greater than the unregulated steady-state limit is possible with a buck-boost voltage regulator.

Paper 50-57, recommended by the AIEE Power Generation Committee and approved by the AIEE Technical Program Committee for presentation at the AIEE Winter General Meeting, New York, N. Y., January 30–February 3, 1950. Manuscript submitted June 16, 1949; made available for printing December 1, 1949.

C. CONCORDIA is with the General Electric Company, Schenectady, N. Y.

The calculations upon which this paper is based were made by Mrs. S. Sutphen and Miss M. V. Barry.

Analysis

POWER SYSTEM

The electric power system studied here is the same as that considered in detail in parts A of the "Analysis" and "Application" sections of reference 1. This same system also has been used in reference 2, for a comparative study of an angle regulator. As the same notation and assumptions used in references 1 and 2 are used here, the derivation of the system equations will not be repeated. The system consists of a synchronous machine connected through a tie line to an infinite bus.

Under equilibrium conditions, unity power factor and voltage are maintained at the terminals of the machine. The power system parameters are as given in equations 30 and 31 of reference 1, and also are given in Tables I and II of this present paper.

It is evident from the derivation given in reference 1 that the characteristic equation of the coefficients of the system variables in the differential equations representing the power system is

$$p^{5}2MT_e(1+x_d')\cos^3\frac{\delta}{2}+p^{3}\,2M\times\left[2-g(p)\ \cos\frac{\delta}{2}\right]\cos^3\frac{\delta}{2}+p^{1}T_e\times[(1+x_d')\cos\delta+(1-x_d')\sin^2\delta]+p^{0}\left[2\cos\delta-g(p)\cos\frac{\delta}{2}\right]=0 \quad (1)$$

where

$$\Delta E=g(p)\,\Delta e_t \quad (2)$$

is the regulating system equation relating the change of alternator excitation voltage ΔE to the change of alternator terminal voltage Δe_t.

Equation 1 is essentially the same as equation 32 of reference 1 and equation 12 of reference 2. Only this characteristic

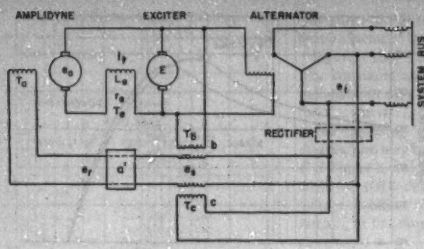

Figure 1. Voltage regulating system

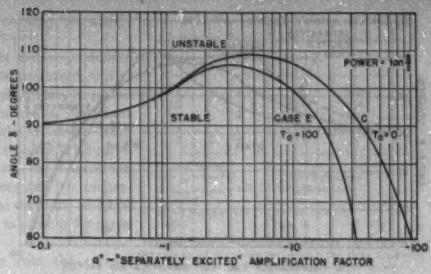

equation is necessary for the study of stability by Routh's criteria.[2]

Regulating System

The regulating system is shown in Figure 1. The alternator field is supplied by the exciter voltage E. The exciter field is in turn supplied by the exciter voltage E and the amplidyne voltage e_a. The field voltage equation is therefore

$$(T_e p+1) r_e i_f = E + e_a \tag{3}$$

where

$p = d/dt$ = the time-derivative operator
$T_e = L_e/r_e$ = exciter field time constant
L_e = exciter field inductance
r_e = total exciter field resistance
i_f = exciter field current

and the variables are considered to be small deviations from their equilibrium values in all of the regulating-system equations in this paper.

The slope of the exciter saturation curve is M_e, so that

$$E = M_e i_f, \text{ (or } i_f = E/M_e) \tag{4}$$

Substituting equation 4 in equation 3, and solving for E, we find

$$E = \frac{(M_e/r_e)e_a}{T_e p + 1 - (M_e/r_e)} \tag{5}$$

The amplidyne output voltage e_a is taken as equal to the regulator output voltage e_r with a single time lag T_a

$$e_a = \frac{e_r}{T_a p + 1} \tag{6}$$

The regulator output voltage e_r is proportional to the sum of the alternator terminal voltage deviation e_t and the stabilizer voltage e_s

$$e_r = a'(e_t + e_s) \tag{7}$$

There are two stabilizers, one supplied from the exciter voltage E and the other from the alternator terminal voltage e_t. The stabilizer output voltage e_s may be represented for the present purpose by the relation

$$e_s = -\frac{bT_b p}{T_b p + 1} E + \frac{cT_c p}{T_c p + 1} e_t \tag{8}$$

The stabilizers thus have the characteristic of transmitting a signal to the regulator during sudden changes or oscillations but no signal in the steady state.

Substituting equation 8 in equation 7, the regulator voltage e_r becomes

$$e_r = a'\left[\frac{(1+c)T_c p + 1}{T_c p + 1} e_t - \frac{bT_b p}{T_b p + 1} E\right] \tag{9}$$

From equation 6, the amplidyne voltage is

Figure 3. Effect of voltage regulator on steady-state stability limit. Effect of regulator time lag

$$e_a = \frac{a'}{T_a p + 1}\left[\frac{(1+c)T_c p + 1}{T_c p + 1} e_t - \frac{bT_b p}{T_b p + 1} E\right] \tag{10}$$

From equation 5, and with some rearrangement, the exciter voltage E is

$$E = \frac{a''(T_b p+1)[(1+c)T_c p+1]}{[(T_e p+1-R)(T_a p+1)(T_b p+1)+ a''bT_b p](T_c p+1)} e_t \tag{11}$$

where

$R = M_e/r_e$

and

$$a'' = (M_e/r_e)a' \tag{12}$$

The steady-state amplification factor of the regulating system is, from equation 11 with $p=0$,

$$\frac{E}{e_t} = \frac{a''}{1-R} \tag{13}$$

As stated before, in all cases considered, $M_e = r_e$ or $R = 1.0$, so the amplification factor is infinite. For this reason the maximum power limit has been plotted against a'', which is the amplification

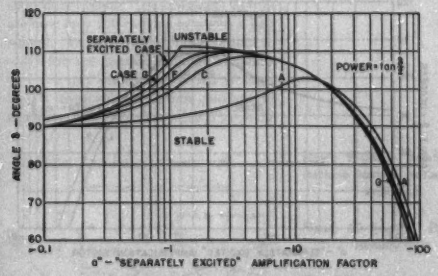

Figure 2. Effect of voltage regulator on steady-state stability limit

Effect of stabilizer washout time constant

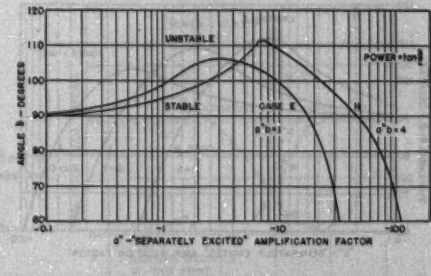

Figure 4. Effect of voltage regulator on steady-state stability limit

Effect of magnitude of stabilizer signal

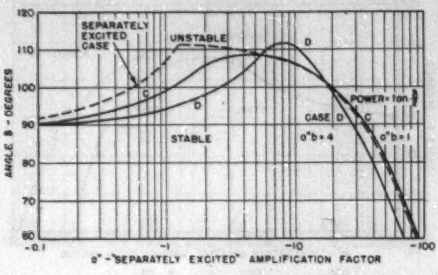

Figure 5. Effect of voltage regulator on steady-state stability limit

Effect of magnitude of stabilizer signal

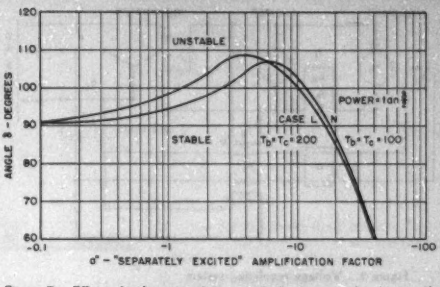

Figure 7. Effect of voltage regulator on steady-state stability limit with terminal-voltage stabilizer

Effect of stabilizer washout time constants

factor which the same regulating system would have with a separately-excited exciter.

Complete System

To obtain the characteristic equation for the complete system, we recognize equation 11 as identical to equation 2, so the coefficient of e_t in equation 11 is substituted for $g(p)$ in the power-system equation (equation 1). The stability of the system as represented by this final equation has been studied by Routh's criteria, and the results are discussed in the following section.

Cases Studied

Exciter-Voltage Stabilizer

The results obtained with the exciter-voltage stabilizer acting alone ($c=0$) are shown in Figures 2, 3, 4, and 5, in which the maximum stable operating angles δ are plotted against the voltage-regulating-system separately-excited amplification factors a''. For the power system considered, the power P corresponding to any given operating angle δ is given by the formula[1]

$$P = \tan\frac{\delta}{2}$$

The power corresponding to any particular angle can thus be very simply determined. The system parameters are given in Table I.

Figure 2 shows the effect of the stabilizer washout time constant T_b. It is seen that the larger the time constant, the greater the power limit, but on the other hand the gain is small for increases of T_b beyond the value of the alternator field time constant, which under the present system conditions is $T_a\ (x_d'+x)/(x_d+x) = 1{,}300$ radians or about 3.5 seconds. This is more or less in agreement with the similar conclusion presented in references 4, 5, and 6. Curve C of Figure 1 of reference 1 also is plotted in Figure 2 of this paper as the Separately-Excited Case. It is evident that as the stabilizer washout time is increased the buck-boost case approaches the separately-excited case. This may be seen mathematically if in equation 11 we let T_b be infinite (with $c=0$, $T_a=0$, and $a''b=1$). The regulator equation then becomes

$$E = \frac{a''}{T_e p+1}\, e_t = \frac{a''}{400p+1}\, e_t \tag{14}$$

which is exactly the same as the separately-excited case of reference 1.

Figure 3 shows the effect of including in the calculations the effect of an additional time lag T_a in the amplidyne. As was expected, the region of stable operation is diminished somewhat.

Figures 4 and 5 show the effect of varying the magnitude of the stabilizing signal ($a''b$). The maximum power limit is slightly improved by a four-fold increase of ($a''b$), and the effect on the permissible range of regulating-system amplification factor depends on the amplidyne time lag.

The effect of $a''b$ shown in Figure 5 may be correlated with that previously observed in the separately-excited case by

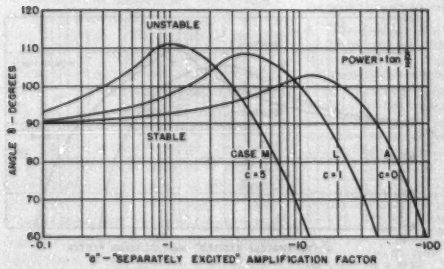

Figure 6. Effect of voltage regulator on steady-state stability limit with terminal-voltage stabilizer

Effect of magnitude of terminal-voltage stabilizer signal

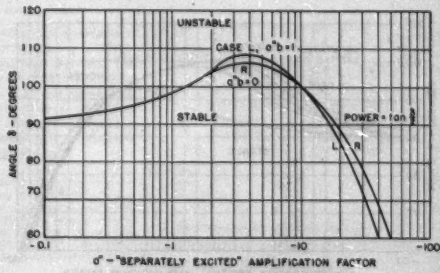

Figure 8. Effect of voltage regulator on steady-state stability limit with terminal-voltage stabilizer

Effect of removing exciter-voltage stabilizer

Table I. Exciter-Voltage Stabilizer

Case	Figure	T_b	T_a	$a''b$
A	2	200	0	1
C	2, 3, 5	1,000	0	1
F	2	2,000	0	1
G	2	4,000	0	1
E	3, 4	1,000	100	1
H	4	1,000	100	4
D	5	1,000	0	4

For all cases:
$x_d = x_q = x = 1.0$ $\quad r = 0$
$p.f._{norm} = e_{norm} = 1.0$ $\quad T_s = 2000$ radians
$x_d' = 0.3$ $\quad T_a = 400$ radians
$M = 4{,}000$ radians $\quad R = Me_s/\gamma = 1.0$

Note: As all values are in per unit, for a rated frequency of 60 cycles per second, the time constants in seconds are 1/377 times the numbers shown.

noting that with $a''b = 4$ and $T_b = \infty$ (with $c = 0$ and $T_a = 0$ as before), the regulator relation becomes

$$E = \frac{\frac{a''}{4}}{100p + 1} e_1$$

This means that the stability curve should lie between curves A and C of Figure 1, reference 1, except that the amplification factor a'' is multiplied by 4. Comparison of curve D of Figure 5 with curve A of Figure 1, reference 1 shows that this concept is a reasonable one.

Terminal-Voltage Stabilizer

The results obtained with the addition of the terminal voltage stabilizer are shown in Figures 6, 7, and 8. The system parameters are given in Table II.

Figure 6 shows the effect of the terminal-voltage stabilizer amplification factor c. The terminal-voltage stabilizer has been added to a system having already an exciter-voltage stabilizer with $a''b = 1.0$. The maximum power limit is increased considerably, but just as in the case of the exciter-voltage stabilizer, most of the increase is obtained by moderate values of the amplification factor c. Note that the stabilizer washout time constants $T_b = T_c$ are now only 200 radians or about a half second. In fact, we may observe that in order for the terminal-voltage stabilizer to have any stabilizing action it must have a reasonably small time constant, as equation 11 shows that with $T_c = \infty$ the only effect of c is to multiply the amplification factor a'' by $(1+c)$.

Figure 7 shows that the two stabilizer time constants can be decreased to 100 radians with only a slight loss in power limit. Curve L, having a maximum stable operating angle of about 108.5 degrees, also may be compared with curve C of Figure 2, which also has a maximum angle of 108.5 degrees and an exciter-voltage-stabilizer time constant of 1,000 radians, or five times as great as for curve C.

Figure 8 indicates that the exciter-voltage stabilizer can be eliminated and still an appreciable gain can be realized by use of the terminal-voltage stabilizer acting alone.

Correlation with Test Results

While no direct quantitative test check of the calculations presented in this paper has been made, the possibility of operation in the so-called dynamic-stability region (that is, operation at powers greater than the maximum possible with manual excitation control) with a buck-boost regulating system has been demonstrated by tests on an actual electric power system. These tests will be briefly described, since they show that operation beyond the normal steady-state stability limit can be demonstrated without exceeding tolerable limits of the test machine and without the necessity of involving long transmission lines.

In 1946, tests were made on a 20,800-kva hydrogenerator to obtain information regarding operation in the region of dynamic stability.

The procedure in making these tests was:

1. To arrange the station circuits so as to introduce maximum reactance between the system and the test machine.

Table II. Terminal-Voltage Stabilizer

Case	Figure	$T_b = T_c$	$a''b$	c
A	6	200	1.0	0
L	6, 7, 8	200	1.0	1.0
M	6	200	1.0	5.0
N	7	100	1.0	1.0
R	8	200	0	1.0

For all cases:
$x_d = x_q = x = 1.0$ $\quad T_s = 2000$ radians
$p.f._{norm} = e_{norm} = 1.0$ $\quad T_a = 400$ radians
$x_d' = 0.3$ $\quad T_a = 0$
$M = 4{,}000$ radians $\quad R = Me_s/\gamma = 1.0$
$r = 0$ $\quad T_b = T_c$

Note: As all values are in per unit, for a rated frequency of 60 cycles per second the time constants in seconds are 1/377 times the numbers shown.

2. To remove all compensation from the voltage regulator to be tested.

3. To put the other machines in the station on hand control.

4. To set the test machine load at about 50 per cent.

5. Finally, to reduce the terminal voltage level held by the regulator under test until the stability limit was reached.

This method of reaching the stability limit was followed since it appeared impractical to attempt to overload the test machine at its normal operating voltage. The power and reactive kilovolt-ampere limits of the machine would be greatly exceeded for pullout at normal terminal voltage. Even for pullout at half rated power the machine kilovolt-amperes and armature current ratings are exceeded to some extent.

As the voltage level at the machine terminals is reduced the field current decreases. This keeps up until the limit of stability with hand control is reached. If it is possible to operate in the dynamic stability region the field current will then increase as the voltage level is reduced further. The nature of this phenomenon is illustrated in Figure 9. In this figure, e_1 is the constant system voltage, and the

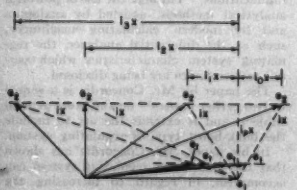

Figure 9 (left). Relations of machine terminal voltage and excitation

Figure 10 (right). Dynamic stability tests

Generator is in dynamic stability region for terminal voltage less than 10,000

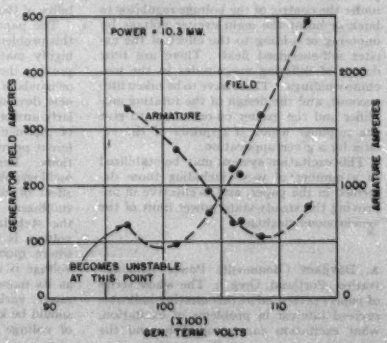

various values of e_t are the machine excitations corresponding to operation at the various terminal voltages e_t. We have taken the simple round-rotor case wherein the total reactance is 1.0 per unit; 0.8 in the machine, and 0.2 in the system.

It is seen that the voltage drop caused by the power component of current i_p (the component in phase w'th the system voltage) remains constant at 0.5, since the power remains constant at 0.5, and only the reactive components i_x i_1, i_2, i_3 vary as the terminal voltage e_t is reduced. The amount by which the field current e_3 can increase from the minimum value reached as the terminal voltage is continually reduced is evidently a measure of the amount by which the hand-control steady-state power limit may be exceeded.

The armature and field current obtained in the tests as the terminal voltage was reduced are plotted in Figure 10. The field current first decreased to about 90 amperes and then increased to about 130 amperes, thus showing that the machine could operate in the dynamic-stability region with the buck-boost voltage regulating system as set for normal operation.

In order to interpret this test increase in field current in terms of increased power limit under more usual operating conditions, the significant effect of the regulator has been assumed to be to reduce the effective direct-axis reactance x_d of the machine, as discussed in reference 2. For example, if the voltage regulator maintained constant field flux linkages instantaneously, it would effectively reduce the machine direct-axis reactance x_d to the transient value x_d'.

The interpretation procedure has, therefore, been to calculate field current versus effective direct-axis reactance at the stability limit, for the system and load conditions of the test, in order to determine the effective reduced x_d produced by regulator action as indicated by the allowable increase of excitation. Then using this effective x_d the power limits for normal operating conditions are calculated and compared to the limits obtained with the actual x_d and x_d'.

References

1. Steady-State Stability of Synchronous Machines as Affected by Voltage Regulator Characteristics, C. Concordia. *AIEE Transactions*, volume 63, 1944, pages 215–20.

2. Steady-State Stability of Synchronous Machines as Affected by Angle Regulator Characteristics, C. Concordia. *AIEE Transactions*, volume 67, part I, 1948, pages 687–90.

3. Advanced Rigid Dynamics, E. J. Routh. Macmillan and Co., Ltd., London, England, 1905.

4. Solution of the General Voltage Regulator Problem by Electrical Analogy, E. L. Harder. *AIEE Transactions*, volume 66, 1947, pages 815–24.

5. Discussion of reference 4, C. Concordia. *AIEE Transactions*, volume 66, 1947, page 824.

6. The Transient Behavior of the Two-Stage Rototrol Main Exciter Voltage Regulating System as Determined by Electrical Analogy, J. T. Carleton. *AIEE Transactions*, volume 68, part I, 1949, pages 59–63.

Discussion

C. E. Valentine (Westinghouse Electric Corporation, East Pittsburgh, Pa.): There are a number of regulating machines, or rotating amplifiers, any one of which may be used as part of a voltage-regulating and excitation system for a synchronous machine. The buck-boost action of the rotating amplifier may be obtained by connecting the output terminals of the amplifier in series with the shunt-field winding of a self-excited exciter as shown in the paper or by connecting the output of the amplifier to an independent field on the exciter. The Rototrol buck-boost exciter is being used in the latter manner although it is capable also of application as a main turboexciter, in which case there is no pilot or buck-boost exciter.

When the Rototrol works into an independent field on a main exciter, it operates under the control of the voltage regulator to buck or boost the main exciter voltage by opposing or adding to the effect of the exciter self-energized field. There are time delays of differing magnitudes in the machine windings. These have to be taken into account, and the design of the rotating amplifier and the exciter co-ordinated to give the response which is required of the exciter for a given application.

This excitation system may be stabilized in a number of ways including those described in the paper, and is effective in improving the steady-state power limit of the synchronous machine.

A. Dovjikov (Bonneville Power Administration, Portland, Oreg.): The whole series of papers presented at this meeting indicates revived interest in problems of excitation, what excitation can accomplish, and the means to accomplish it. All papers indicate that the conventional system of excitation, consisting of main exciter, its pilot exciter, and of an automatic voltage regulator with its moving contacts, could be advantageously replaced by other forms of exciters, either of the electronic type or of the rotating-machine type. The fundamental difference of both types as compared with the conventional system is that the amount of power handled by the automatic voltage regulator is much smaller and therefore much more sensitive and faster types of static automatic voltage regulators may be used.

In the first applications of this new type of excitation, the emphasis was put on close voltage regulation, but it is only natural that the advantageous features of this new type of excitation were thought of when the problems of the operating engineer required faster excitation, for example, for an increase of steady-state and dynamic stability of the system.

The paper is a welcome contribution to this problem, but, although admirable in its highly mathematical analysis, it does not provide the operating engineer with curves or bands of numerical characteristics of this new development. We would be particularly anxious to see the sample oscillograms of this new excitation which illustrate different points of Mr. Concordia's considerations. Particularly interesting would be oscillographs of the speed of action and the effect of elimination of the exciter-voltage stabilizer. We always wondered whether the stabilizer across the exciter terminal voltage is not rather detrimental in cases where quick response of exciter terminal voltage is desirable because this stabilizer, as its name implies, tends to prevent too rapid variation of exciter voltage. It should be kept in mind that rapid variation of voltage of the exciter is desirable, not only from the stability point of view, but because it is also necessary in cases of load rejection, particularly with one or more long, high-voltage lines hanging on the station bus. The overvoltage on the generating bus due to generators' acceleration is one of the main factors determining the sealoff voltage of lightning arresters connected to this bus, and through that it determines the rating of the arresters and the basic insulation level of generating stations.

John G. Noest. (Consolidated Edison Company of New York, Inc., New York, N. Y.): In these days, whenever increasing costs put heavy economic pressure on the fullest utilization of equipment, new and greater emphasis is placed on any device which promises a step in that direction.

Automatic voltage regulation for synchronous generators is a subject of consistent interest to the industry because, when properly designed, it permits an increase in the steady-state power limits, in addition to its other, well-recognized advantages.

In the past there have been presented before the Institute a large number of papers dealing with this subject and these papers have, with increasing clarity and with greater precision, attacked the problem on a broad front and in its narrower ramifications. Through the use of powerful analytical methods, assisted by analogues and by modern calculating machinery, such as the differential analyzer, the regulating system characteristics which permit proper design are being disclosed.

The paper by Mr. Concordia is a sequel to two earlier papers[1,2] on the same general subject, and it extends the art to include the buck-boost type of regulating system.

In his paper, Mr. Concordia has shown that the buck-boost regulating system can accomplish, in regard to increasing the

steady-state stability limit, practically the equivalent of that regulation obtainable with separately excited systems. The buck-boost system accomplishes this with greater fundamental simplicity and greater economy of means.

It seems to me that with proper modification of the parameters and of the excitation system transfer function, $g(p)$ of equation 2 of the paper, the methods employed in the 1944[1] and present papers become directly applicable to the electronic type of excitation system as well.

To all engineers, and particularly to the younger men, Mr. Concordia's methods of attacking the problem should give great inspiration. The use of the operational method, together with the application of Routh's[2] and Hurwitz'[4] criteria in the determination of stability, permit the treatment of the problem with simple clarity and economy of effort.

References

1. Steady-State Stability of Synchronous Machines as Affected by Voltage-Regulator Characteristics, C. Concordia. *Electrical Engineering* (*AIEE Transactions*), volume 63, May 1944, pages 215–20.

2. Steady-State Stability of Synchronous Machines as Affected by Angle-Regulator Characteristics, C. Concordia. *AIEE Transactions*, volume 67, part I, 1948, pages 687–90.

3. See reference 3 of the paper.

4. The Mathematics of Circuit Analysis (book), E. A. Guillemin. John Wiley and Sons, Inc., New York, N. Y., May 1949.

E. E. Cobb (Ebasco Services, Inc., New York, N. Y.): What is the expected performance of a buck-boost voltage regulator when operating generator at 95-per cent leading power factor and 100-per cent load? Also, what will be the effect on stability during transient fault conditions?

C. Concordia: Mr. Dovjikov has pointed out in his discussion an important point that was perhaps not sufficiently emphasized in the paper; namely, that we are concerned in this paper with continuously-acting voltage regulators, that is, regulators having essentially no dead band, as distinguished from motor-driven rheostatic-control voltage regulators having a definite dead band. The continuously-acting regulator is practically a necessity if advantage is to be taken of possible steady-state operation beyond the unregulated power limit. We should not infer that such dynamic-stability operation is necessarily made possible by high rates of response. On the contrary, the usual rheostatic regulator has incorporated in its design the so-called high-speed contacts, which will permit high rates of response if the voltage deviation exceeds a prescribed band width, and there is no reason why with proper design the response cannot be as fast as with the continuously-acting type under this condition. A further advantage of the no-dead-band type is, of course, the possibility of closer voltage regulation, as Mr. Dovjikov has remarked.

In regard to oscillograms of response we call attention to Figure 8 of the paper by F. M. Porter and J. H. Kinghorn,[1] which shows the response of an amplidyne buck-boost voltage regulating system to a sudden change of regulated voltage level. On load rejection, either the buck-boost amplidyne regulator, even with an exciter-voltage stabilizer, or the rheostatic type with high-speed contacts, should give comparable performance; in this case the time to maximum voltage is rather long, that is, at least a few seconds.

Mr. Valentine has very properly pointed out that other types of continuously-acting voltage regulators can be made to give an improvement in power limit if properly stabilized. We have preferred to consider the rotating-amplifier buck-boost voltage to be inserted in series with the exciter field rather than on a separate field winding, as described by Mr. Valentine, for the reason that he himself mentions, namely, that operation through a separate field involves additional time lags.

Mr. Cobb has asked what is the expected performance of a buck-boost voltage regulator when operating a generator at 95-per cent leading power factor and 100-per cent load. This, of course, depends on system conditions, but in general we should expect no difficulty on the usual system. Such operation is discussed in a paper by C. G. Adams and J. B. McClure.[2] It need not, and in general does not, involve operation in the dynamic-stability region so that no special regulating system is required, but it is desirable that the voltage be under automatic control.

A rather complete discussion of the problems involved in leading-power-factor operation was given in a series of unpublished conference papers presented at the AIEE 1950 Winter Meeting.

The effect on transient stability of any properly designed voltage regulator should be beneficial but is in general rather slight, as the times involved are usually so small as to permit little change in generator field flux.

Moreover other factors, not involved in the calculation of steady-state stability, become pertinent, in particular, the exciter ceiling.

Mr. Noest's comments are appreciated. We particularly agree with him that the methods of this paper are directly applicable to the electronic type of excitation system.

In conclusion, we wish to thank all of the discussers for their contributions to this important subject.

References

1. The Development of Modern Excitation Systems for Synchronous Condensers and Generators, F. M. Porter, J. H. Kinghorn. *AIEE Transactions*, volume 65, 1946, pages 1020–35.

2. Underexcited Operation of Turbogenerators, C. G. Adams, J. B. McClure. *AIEE Transactions*, volume 67, part I, 1948, pages 521–28.

Bus Transfer Tests on 2,300-Volt Station Auxiliary System

A. A. JOHNSON
MEMBER AIEE

H. A. THOMPSON
NONMEMBER AIEE

Synopsis: Transfer tests were made of one auxiliary bus section in a large power station from one source to another source. The two sources, one an auxiliary generator and the other a service transformer, were not paralleled during the transfer operation. The optimum open time interval was determined and inrush currents, voltage changes, and some power measurements were made on the combined bus load and on several individual motors. Successful transfers were made at time intervals up to about 150 cycles. The motors, the auxiliary generator, and the station boilers operated satisfactorily for all tests.

RELIABLE auxiliary power systems for steam power plants are indispensable, and at least two sources of power are usually available from which the auxiliaries may be supplied. In the event of failure of one source, the load can be transferred to the other. The manner in which a transfer is made affects the auxiliary feeder circuit breakers, feeder and bus protective relays, the motors, and other equipment in the station. Bus transfer tests made on the auxiliary power system of the Phillips Power Plant of the Duquesne Light Company give results which determine the optimum conditions for transfer. The relaying is not discussed in this paper.

Description of Test System

The Phillips Plant has one 75,000-kva turbogenerator with a 7,500-kva 2,300-volt, 3,600-rpm auxiliary generator on the same shaft with the main unit. The auxiliaries shown schematically in Figure 1 are divided into two major groups, and either group may be supplied from the auxiliary generator or from a 7,500-kva station service transformer. The auxiliary system includes all of the large motors for boiler and turbine service, the 440-volt power and station lighting. Normally one bus is connected to the station service transformer, and one to the auxiliary generator. Voltage transfer equipment is provided between these two main sources. If the power source feeding one of the busses fails, that source is disconnected automatically and the circuit breaker to the other source is closed automatically. At no time are the two sources of power paralleled because the air circuit breakers on the auxiliary system were not installed to handle simultaneously the short circuit kilovolt-amperes from both sources. In addition, the two sources may not be in phase and large circulating currents may be present if both are closed at the same time. During start-up of the station, both auxiliary busses, *1-A* and *1-B*, are supplied from the station service transformer. After the main unit is synchronized to the system, one of the auxiliary bus sections, usually *1-B*, is transferred by "open transition" to the auxiliary generator.

Test Objectives

The tests were to determine the optimum time interval between the opening of one circuit breaker and the closing of the other circuit breaker for a bus transfer. It is difficult to determine the optimum time interval except by actual test since an induction motor or a group of induction motors, when disconnected from their source, will continue to generate a voltage for some period of time. The period of time required for this voltage to decrease to substantially zero will vary depending upon the size, speed, and load on the motors. Figure 2 gives the typical open circuit time constants of typical motors. If the transition time is too short, the residual voltage on the motors which can be 180 degrees out of phase with the other source may cause excessive currents to flow in the motor windings when they are connected to the other source. (Squirrel-cage induction motors are designed to withstand mechanically a fully displaced locked rotor current from an infinite bus at the motor terminals.) If the transition time is long, other detrimental effects may be encountered in the station which will be discussed later.

Test records also were obtained on the operation of the automatic voltage regulator in the field circuit of the auxiliary generator when a bus was suddenly transferred to the generator. The recovery of the generator voltage depends on the action of the regulator which, in turn, is affected by the time for the various motors to come back to normal speed and power consumption.

Test Outline

The setup in the power plant is such that the speed at which a voltage transfer operation may be accomplished can be varied from a minimum of about 10 cycles up to several seconds. The longest transfer time is limited by the deceleration time of the circulating water pumps, whose discharge valves must be closed in the event voltage is removed for several seconds to prevent them from reversing. The circulating water pump may reverse if it is deenergized very long because the other circulating water pump will force water through the first one instead of through the condenser. To obtain test results for three time intervals, it was planned that transfers could be and would be made in about 10, 75, and 150 cycles.

It was desired to get as much informa-

Paper 50-59, recommended by the AIEE Power Generation Committee and approved by the AIEE Technical Program Committee for presentation at the AIEE Winter General Meeting, New York, N. Y., January 30—February 3, 1950. Manuscript submitted March 21, 1949; made available for printing December 1, 1949.

A. A. Johnson is with the Westinghouse Electric Corporation, East Pittsburgh, Pa., and H. A. Thompson is with the Duquesne Light Company, Pittsburgh, Pa.

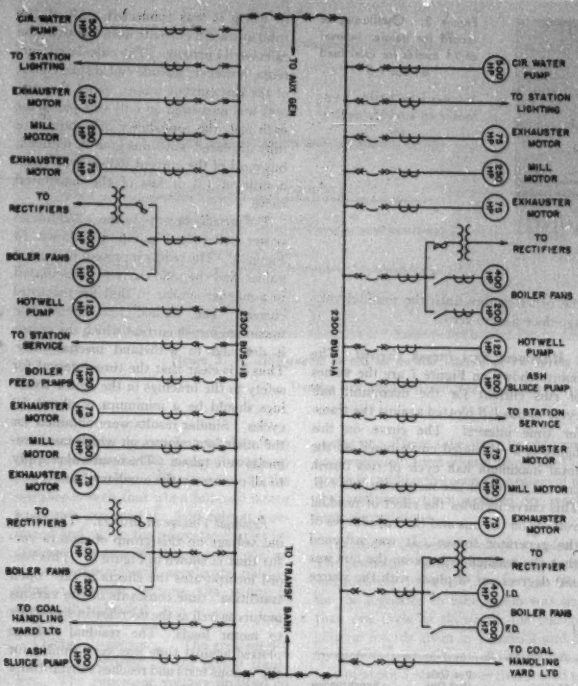

Figure 1. Schematic diagram of auxiliary system

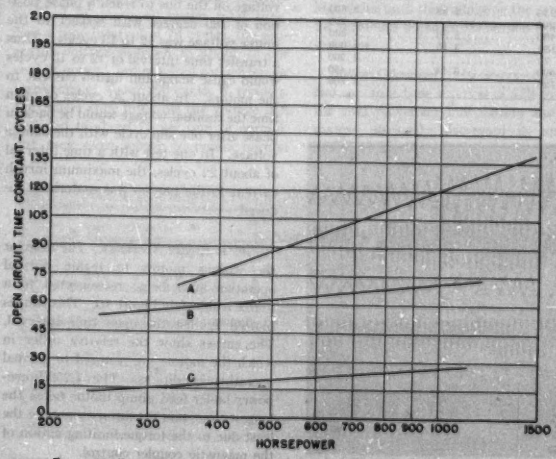

Figure 2. Typical time constants for 2,300-volt squirrel-cage induction motors

A—3,600 rpm; *B*—1,800 rpm; *C*—600 rpm

tion as could be obtained on three oscillographs operating simultaneously. In addition to obtaining current to the large motors and the total bus current, power measurements were made for more complete information. The following simultaneous oscillograph records were obtained:

Currents	Power
Total to bus *1-B*	Total to bus *1-B*
Boiler feed pump	Boiler feed pump
Circulating water pump	Circulating water pump
Mill motor	**Voltages**
Forced draft motor	
Induced draft motor	Generator
Generator field	Bus *1-B*

The total current to bus *1-B* was obtained by paralleling the secondaries of the current transformers from the auxiliary generator and the service transformer so that when the bus was transferred, the current changed from one source to the other on the same record.

The first part of the tests covered four transfers of bus *1-B* from the generator to the transformer and back to the generator. During these tests the load on bus *1-A* was supplied from the transformer. Measurements were also made on tests involving three transfers of bus *1-B* from the transformer to the generator with bus *1-A* being supplied from the generator.

Bus 1-B Motors

The load on bus *1-B* of this auxiliary system during the tests consisted of about 2,500 kw made up of the 2,300-volt motors shown in Table I.

Test Results

Typical Oscillograms. Figure 3 is an oscillographic record of generator voltage, bus *1-B* voltage, total current, and total power before, during and after an 11-cycle transfer from the transformer to the generator. The generator field current also is shown. It will be noted from this record that bus *1-B* voltage decreased during the time the source was disconnected. At the instant of closing the circuit breaker to the generator, the first half cycle of total bus current is more than double the maximum half cycle of the current which follows. This is due apparently to a readjustment of flux conditions in the motor, and after a few cycles the motors take the normal current for their speed and load conditions. Figure 3 also shows that the average field current to the generator about doubled in less than one cycle. Figure 4 is an oscillographic record of the current and power to the 1,250-horsepower boiler feed pump motor, and the

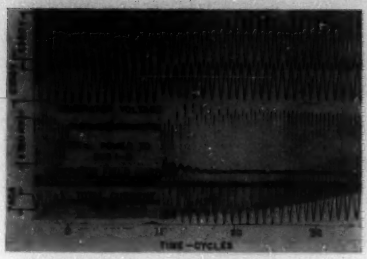

Figure 3. Oscillographic record for transfer interval of 11 cycles for total load on bus 1-B

Transfer from service transformer to auxiliary generator

500-horsepower circulating water pump motor for a similar transfer time. The boiler feed pump acts as a generator when the source is disconnected, and supplies power to other motors connected to the bus. The power record on these motors is not the true total power because the measurements were made using a line-to-line voltage and a single-phase current which lagged the voltage by 30 degrees plus the power factor angle. Figures 5 and 6 show the same results for a transfer time interval of about 75 cycles. For Figure 5 the generator was carrying bus *1-A* prior to picking up bus *1-B*. The boiler feed pump motor supplies power to the other motors until the residual voltage decreases to zero.

Maximum Rms Inrush Current. The points shown on Figure 7 are the values of rms current for the maximum half cycle to bus *1-B* plotted against the transfer time interval. The curve on this figure is a calculated curve based on the total maximum half cycle of rms inrush current for all of the motors on bus *1-B*. This curve includes the effect of residual voltage on the bus and the impedances of the generator source. It was assumed that the residual voltage on the bus was 180 degrees out of phase with the source to which it was connected. All of the total measured currents were less than the calculated currents. The calculated currents, however, include full displacement of the rms current wave. Since the current was measured on only one phase for each test, the probability of obtaining a fully displaced wave was greatly reduced, but most of the current values are within a ratio of 1.6 or less of the calculated curve.

The inrush currents to the 1,250-horsepower boiler feed pump are shown in Figure 8. The points represent measured values, and the solid curve was calculated in a manner similar to that for the total current. The dashed line shows the maximum inrush current which the motor is designed to withstand mechanically. Thus it is clear that the time interval for safety to the bracings in the motor windings should be a minimum of about 50 cycles. Similar results were obtained for the other four motors on which measurements were taken. The results also apply to all motors on the auxiliary bus.

Residual Voltage on Motors. The residual voltage on this group of motors versus time is shown in Figure 9. This record incorporates the effects of the "open transition" time constants of the various motors as well as the decrease in speed due to motor loads. The residual voltage plotted against time was very similar for the various tests and reaches substantially zero in about 60 cycles.

The time required for the residual voltage on the bus to reach a phase position of 180 degrees with respect to the source voltage was 12 to 13 cycles. Thus a transfer time interval of 12 to 13 cycles would cause maximum inrush current to the motors. In about 20 cycles of open time the residual voltage would be back in phase after one slip cycle with the source voltage. In one test with a time interval of about 22 cycles, the maximum inrush current to the motors was materially reduced.

Time to Regain Normalcy. The time for the various motors to regain normal operation after being reconnected to a source is shown in Figure 10. This time is plotted against the open time interval. The curves show the relative order in which the motors are restored to normal operating conditions. The 1,250-horsepower boiler feed pump motor takes the longest time, and the fan motors take the least due to the torque limiting action of the magnetic coupler control.

The fan motors are connected to the fans through magnetic couplers. The

Table I

Motors	No. Units	Motor, Horsepower	Per Unit Pull Out Torque	Synchronous Speed
Boiler Feed Pump	1	1,250	2.38	3,600
Forced draft fans	2	200		1,200
Induced draft fans	2	400	2.30	900
Pulverizer mills	9	250	3.15	900
Pulverizer exhausters	4	75		1,200
Circulating water pump	1	500	3.14	450
Hotwell pump	1	125		1,200

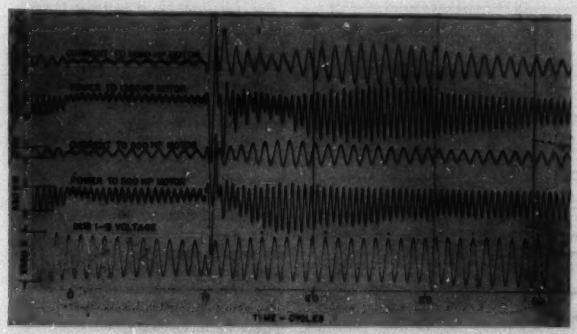

Figure 4. Oscillographic record for transfer interval of 11 cycles for boiler feed pump motor and circulating water pump motor

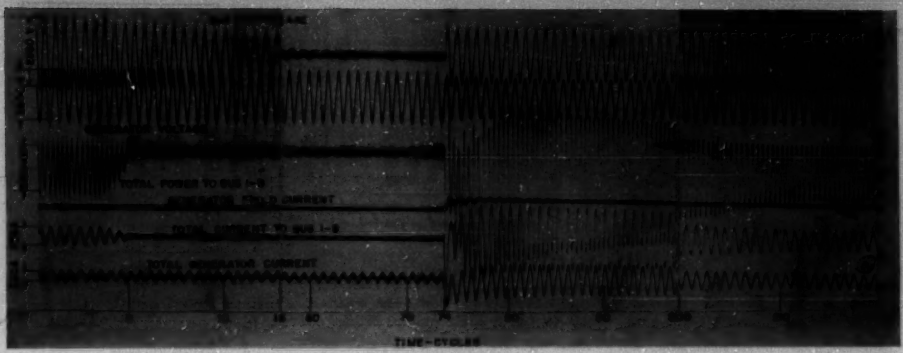

Figure 5. Oscillographic record for transfer interval of 75 cycles for total load on bus 1-B

Transfer from service transformer to auxiliary generator

field current to the couplers is taken from the supply to the fan motor through an electronic rectifier. The control on the rectifier is such that when full-load motor current is exceeded the field current is reduced and slip in the magnetic coupler increases. Thus with this type of control the fan motors will accelerate quickly after a transfer because the motor is essentially unloaded.

Voltage Disturbances. The greatest dip in voltage occurred for the fastest transfers. The generator voltage dropped to about 65 per cent of normal following an open time interval of 11 cycles, but recovered in about 60 cycles total time. For a time interval of 75 cycles, the generator voltage dropped to about 75 per cent of normal, but required a much longer total time of about 200 cycles to recover. For longer time intervals the voltage still dropped to about 75 per cent of normal, but took even longer to regain normal operation. These times may be obtained approximately from Figure 10 referred to above by adding the open time interval to the additional time required to reach normal conditions.

Auxiliary Generator Voltage Regulator. The generator voltage regulator operated satisfactorily for every test. The time for the regulator to take action was less than one cycle as shown on the oscillographic records given in Figures 3 and 5. In each case when bus *1-B*, which has a load of about 2,500 kw, was transferred to generator, the average field current increased about 100 per cent and stayed at a high value until the voltage on the generator terminals regained its normal operating value.

Boiler Operation. In every transfer test, up to a time interval of 150 cycles, the coal pulverizer mill motors and fan motors obviously decreased in speed; however, this decrease in speed had no noticeable effect on the fires in the boilers, nor was there any evidence of unsatisfactory operation of the boilers. The pulverizer mills were the ball mill Hardinge type and gave no evidence of stalling or unnecessarily increasing the duty on the motor when it was connected to the new source.

General Discussion

Tests which were limited to a maximum of 150 cycles had satisfactory motor transfers except that the circulating water pump was lost on one test. One period of time developed to be about 300 cycles, and many of the auxiliary motors were shut down by protective relays. Without question, this time of transfer is entirely too long, and in fact 150 cycles also is entirely too long. The preferred time interval should be when the residual voltage approaches zero, or for this system about 50 cycles.

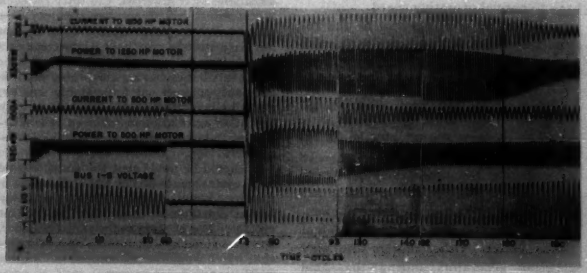

Figure 6. Oscillographic record for transfer interval of 75 cycles for boiler feed pump motor and circulating water pump motor

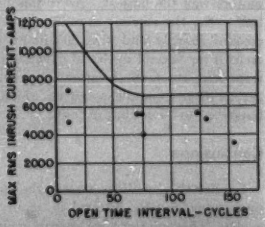

Figure 7. Maximum rms inrush current to bus 1-B versus open time interval in cycles

Points obtained from tests. Curve is theoretical maximum

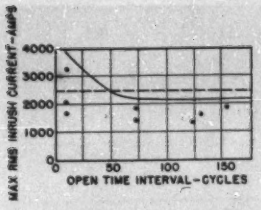

Figure 8. Maximum rms inrush current to boiler feed pump motor (1,250 horsepower)

Points obtained from tests. Solid curve is theoretical maximum. The dashed curve is the maximum current for which the motor is designed

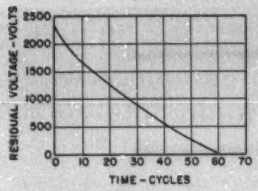

Figure 9. Residual voltage versus time for all motors connected to bus 1-B

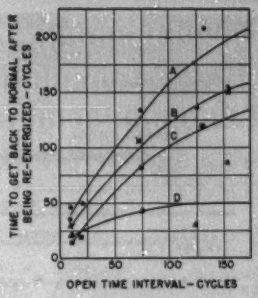

Figure 10. Time for motors to regain normalcy

A—Boiler feed pump motor
B—Pulverizer mill motor
C—Circulating water pump motor
D—Forced and induced fan motors

During the transfer tests the station lighting and the 440-volt power equipment were connected to another source so they would not be affected. The control room fluorescent lighting was placed on another source because if the voltage is removed, the lights will go out and require several seconds to relight. The flickering of these lights on return of voltage would have been disturbing during the test periods. Under normal operating conditions this factor may not loom large in the over-all considerations of how auxiliaries should be transferred, but should be considered and additional lighting made available from some other source.

With the generator supplying bus *1-A* and transferring bus *1-B* to the generator, the voltage regulator performance also was very satisfactory. In fact, the results were similar to the first group of tests in which the generator was carrying no load prior to picking up bus *1-B*. The inrush currents to the motors also were approximately the same whether the generator was operating with or without bus *1-A*.

In practically every transfer test the first half cycle of inrush current to the motors was the largest. After this first half cycle, the current in most cases decreased sharply and then gradually increased for several cycles to a value corresponding to normal current for motor acceleration from the speed at which it happened to be at that instant.

Conclusions

1. For this auxiliary system the optimum transfer time interval is about 50 cycles. This transfer time assures greater mechanical safety to the motor windings than if a shorter transfer interval were used.

2. For transfers made in approximately 10 to 15 cycles, abnormally high motor currents may flow. This is caused by the fact that the residual voltage on the bus is still about 75 per cent of normal and is about 180 degrees out of phase with the new source voltage. This condition may cause a current considerably in excess of that for which the motor was designed mechanically.

3. The transfer of auxiliary bus sections by "open transition" can be safely accomplished. For any auxiliary system the preferred open time interval is determined by the time required for the residual voltage to decay to approximately zero. The actual time should correspond to no less than that which gives an inrush current to the motors equal to or less than the fully offset current which each motor would take when starting across the line from an infinite source at its terminals.

4. Automatic "open transition" transfers should be controlled by devices which give an accurate fixed open time interval. Such a device would insure that the inrush currents were not excessive, and also that the reclosing would not be delayed unnecessarily.

5. After the residual voltage has decreased to zero, the maximum inrush current to each motor is substantially the same for any time interval. The longer the open time interval, however, the longer it takes the motors to accelerate back to normal operating speed.

6. Delaying the transfers to the required 50 cycles will probably extinguish fluorescent lighting, but emergency lighting should assure that no area will be in darkness. The fluorescent lighting reestablishes itself when the bus is connected to the new source, but the flicker may be somewhat disturbing.

7. During the time residual voltage exists on the bus, the boiler feed pump motor supplies power to other motors. This has the effect of reducing the residual voltage faster. Other motors also may serve as generators during the time residual voltage exists if they have enough stored energy in the rotating parts.

8. When the load is transferred to the auxiliary generator, the voltage regulator must function to limit the voltage drop and to restore the voltage to normal.

9. The coal pulverizers operated satisfactorily for all transfer time intervals up to 150 cycles.

10. For all tests of 150 cycles or less, there was no noticeable effect on the normal operation of the station boilers.

Discussion

A. G. Mellor and **M. Temoshok** (General Electric Company, Schenectady, N. Y.): Although the open-circuit time constants for a group of induction motors are known individually, their effective time constant as a group connected together on a bus can be determined expediently only by test. In the present case the effective time constant of the bus was about one-half second although individual units may have had open-circuit time constants up to two seconds. This factor indicates a conclusion that should be emphasized: when a group of auxiliaries is transferred, the duty on each motor will be less severe than the duty on a single unit being transferred. Some station auxiliary motors can have time constants approaching four seconds, and to throw over single auxiliaries having this value of time constant, or even one appreciably smaller, alone or in combination with only a very few other auxiliaries would need re-evaluation of the time for the bus voltage to decay.

It should be noted that the transfer time of 50 cycles mentioned by the authors is the time for a planned transfer from an auxiliary bus at unit voltage to another bus at unit voltage. For this type of planned transfer, the time given by the authors approximates that which would be recommended for most auxiliary bus arrangements.

An auxiliary power system using a separate house generator which is not paral-

leled with the station service transformer requires that station auxiliary motors be transferred from the system to the house generator each time the station is started up or shut down.

A more common type of auxiliary power system uses a station service transformer connected to the main generator terminals and a starting transformer connected to the system. In this case, the auxiliary motors are started on the supply from the system and, after the main generator is up to speed, the transformer that is connected to the generator terminals is temporarily paralleled with the starting transformer. The starting transformer then is disconnected. This is what can be called a synchronized transfer during which the auxiliaries are never de-energized. With this system the only time motors are de-energized during transfer is in the case of an emergency transfer. In general, an emergency transfer would be made either because of loss of voltage on the auxiliary bus or because of a short circuit in the equipment supplying power to the auxiliary bus.

For the loss-of-voltage case, the voltage on the auxiliary bus would be reduced before transfer was actually started, and so the bus residual voltage would decay to a low value in a very few cycles after the start of transfer. For the extreme case of a 3-phase short circuit in the auxiliary power source, the motors on the auxiliary bus may feed into the short circuit, and the equivalent time constant of the bus would approach the short-circuit time constants of the motors, a matter of a few cycles. However, most emergency transfers will be made under circumstances less severe than this extreme case, and thus in some cases the reduction in residual flux of the induction motors may be approximately that shown in the paper.

Under emergency conditions, such as a fault on the auxiliary power source, it is often desirable to transfer the auxiliaries as rapidly as possible. Since motors are capable of standing, on an occasional emergency basis, the currents associated with rapid transfers, and since many operators have had years of successful experience with immediate transfers, it is recommended that all emergency transfers be made as rapidly as possible.

John G. Noest (Consolidated Edison Company of New York, Inc., New York, N. Y.): For the supply of generating station auxiliary power, it has been for a long time common practice to provide at least two sources of supply with switching arrangements to permit the choice of either.

In some of these cases it has been found either expedient or necessary to prevent parallel operation of the two supplies. In such cases, provisions must be made for the transfer of the load from one source to the other without intermediate paralleling. It is this latter type of arrangement which is treated by the paper.

Although such transfer schemes have been used for many years, there have been no reports of difficulties until just recently. The subject was first brought to the attention of the industry by Mr. E. H. Snyder of the Public Service Electric and Gas Company of New Jersey at the February 1948 meeting of the Edison Electric Institute at Cincinnati, Ohio.

The current paper by Mr. Johnson and Mr. Thompson furnishes quantitative data which should prove to be of considerable value to anyone confronted with a similar problem.

In connection with the paper, there arises one big question: Why is it that there have been no difficulties with bus transfer schemes throughout the many years that such schemes have been in use?

The answer to this question seems to lie in circuit breaker development. Where older circuit breakers had closing times of 30 to 40 cycles, with opening times of 8 to 12 cycles, a bus transfer scheme, without the provision of definite time delay, required 50 to 60 cycles in any case. Modern circuit breakers, with mechanisms designed for rapid reclosing, are so much faster that without definite time delay the transfer operation might take only as little as 20 cycles, and therefore the problem.

Another point of interest is brought out in this paper. It is the observation that boiler operation was unaffected with transfer times even up to 150 cycles. With pulverized-fuel-fired boilers there has been some apprehension on this point.

R. L. Webb (Consolidated Edison Company of New York, Inc., New York, N. Y.): We are much interested in the test results presented by Mr. Johnson and Mr. Thompson in their paper concerning transfer of station auxiliary motor load from one supply source to another. This subject received considerable attention in the Edison Electric Institute about two years ago. At that time some oscillograph tests were made in our Hudson Avenue Station on a system similar to that described in the paper.

In our case, six main auxiliary motors are connected to a single 2300-volt bus which is switched to a house service supply transformer, while the generator is being started. After the machine is synchronized to the main bus, the auxiliary bus is automatically transferred from the house service transformer to a 2,300-volt tertiary winding of the main generator autotransformer.

This 2,300-volt bus supplies two 600-horsepower 1,200-rpm induced-draft fan motors, two 250-horsepower 900-rpm forced-draft fan motors, one 450-horsepower 300-rpm circulating water pump motor, and one 75-horsepower 720-rpm Hotwell pump motor, or a total of 2,225 horsepower.

The transfer time, from the opening of one supply circuit breaker to the closing of the other, is about 45 cycles. This time is consumed by the operating time of the transfer relays plus the time taken by the incoming circuit breaker to close.

Figure 1 of the discussion shows two oscillograph records; the upper shows the current wave for all the motors combined, while the lower record is that of one 600-horsepower induced-draft fan motor alone.

Following the tripping of the supply circuit breaker, the motor bus voltage decreases with a time constant of approximately 23 cycles to 33 per cent of normal when the incoming circuit breaker was closed. During the 45-cycle period, the motors lost $1^1/_4$ cycle, indicating a speed drop of approximately 3 per cent. It will be noted that the motor voltage is approximately 180 degrees out of phase with the supply voltage after about 25 cycles. At the time the incoming circuit breaker was closed, the motor voltage was leading the supply voltage by approximately 90 degrees.

The lower record shows the motor load current to be 90 amperes before the first supply circuit breaker was opened. After tripping, it dropped to 46 amperes but reversed approximately 180 degrees, which indicates the motor was supplying power toward the bus without much change in the current value, for approximately 30 cycles. When the incoming circuit breaker was closed, the inrush current to the motor was less than 45 per cent of the normal starting inrush for this unit.

These records indicate no undue stresses are being imposed on these motors when they are transferred from the one source of supply to the other. The inrush current would be at about the minimum, if the transfer were made when the motor and supply voltages are exactly in phase with each other, which would have been about eight cycles earlier. However, it is not felt justified to make any changes in the control to gain this small advantage.

In 90 cycles after the load was transferred, the total motor running current was normal.

J. A. Elzi and **W. R. Brownlee** (Commonwealth Services, Inc., Jackson, Mich.): The tests described in this paper apply to one type of auxiliary power system, namely, one which is supplied from a shaft generator and a station service transformer. Much of

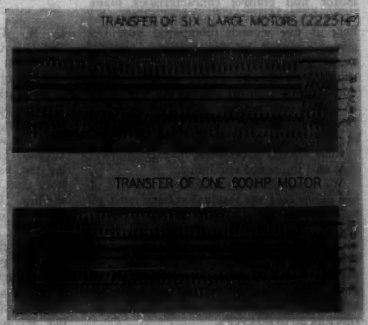

Figure 1. Upper oscillogram shows current wave for all motors combined; lower oscillogram shows one 600-horsepower induced-draft fan motor alone

A, B, C—Phase currents
D—Differential voltage between motor terminals and incoming supply source
E—Motor bus voltage
F—Voltage of incoming supply source

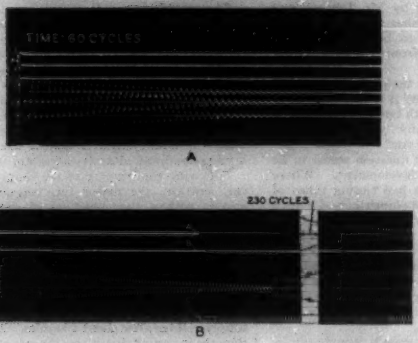

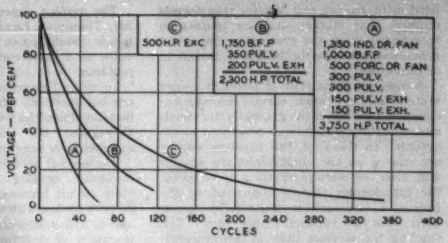

Figure 2 (left). Voltage decay of busses at generating stations

Figure 3 (right). Percentage voltage versus frequency

the test data is applicable to other types of auxiliary power systems and provides much useful information for the design and operation of such systems. It may be well to point out, however, that the method of transition and the conditions found to be optimum for this installation may not be found to be so for other systems. As the authors point out, even for a similar system the optimum conditions may be different depending on the number, speed, and size of the motors and the type of loads.

For this installation, open transition was used in order to avoid excessive duty on the circuit breakers and because of possible phase displacement. The circuit breaker duty could, of course, be taken care of by several methods, but the phase displacement might dictate open transition where an auxiliary generator is used. In station auxiliary systems supplied entirely from suitable transformers without the use of an auxiliary generator, the phase and voltage relations have been found to be such as to permit closed transition for normal operation, even for the most unfavorable conditions. This does not preclude the use of open transition during emergencies.

The system described by the authors uses a shaft house generator which avoids certain voltage dips, but it appears from the test data that the control may still be subject to such dips. Tests were reported in 1945 on a system using transformers to supply auxiliaries[1] where co-ordination of motor and control characteristics made operation immune to total interruptions as long as five seconds (compared with 150 cycles reported by the authors). Subsequent tests showed that this transformer supply system can operate on a sustained voltage reduction for several minutes down to 60-per cent voltage although the reduction in voltage due to open-circuit transition is only in the order of 10 per cent. This system affords substantial investment savings and improved reliability.

We disagree with conclusions 3 and 4 of the paper that the residual voltage must go to zero and that a fixed time interval is required for automatic open transition. Such an arrangement seems undesirable from a reliability standpoint, and appears to be unnecessary. For example, prevention of flame extinction with certain types of coal-pulverizer mills may require transfer time as short as 20 to 30 cycles.

Standard motors of some manufacturers will withstand such duty and if designs now contemplated do not allow for such operation, then these designs should be reviewed. This duty is very similar to that experienced with usual industrial applications where standard a-c contactors open and reclose motor circuits on external voltage dips lasting 10 to 30 cycles. Ordinary compensator starting provides a similar open interval using motors that may not have been braced for full voltage starting; also instantaneous reclosing on feeders supplying industrial loads is becoming the rule rather than the exception.

It is noted that high currents associated with short-time transfer are confined to one-half cycle. This would be expected and is consistent with other tests. We would like to ask the authors whether they feel that a one-half cycle current followed by normal starting current is likely to produce the mechanical stress expected with an offset wave having gradually decreasing peaks. It is recognized that the maximum station bus stresses are experienced a few cycles after the occurrence of a short circuit. It may be that the inertia of the motor conductors provides added margin for high currents during the first half-cycle.

Reference

1. Electric Drives for Steam-Electric Generating-Station Auxiliaries, W. R. Brownlee, J. A. Elzi. *AIEE Transactions*, volume 64, 1945, pages 741–45.

D. W. Taylor (Public Service Electric and Gas Company, Newark, N. J.): We have four 100,000-kw units in operation using practically the same throwover scheme of auxiliaries described in the paper by Mr. Johnson and Mr. Thompson. All essential auxiliaries, including a motor-driven exciter set, are thrown over to the shaft-end auxiliary generator shortly after synchronizing the main generator and are operated from that source until the unit is taken off the line. Only non-essential auxiliaries are normally operated from the station transformers. The automatic throwover therefore is needed only in one direction, from the auxiliary generator to the transformer feed. Two induction-type undervoltage relays are used to inaugurate the throwover on loss or lowering of the auxiliary generator voltage, one set for 70 per cent voltage and 12 seconds, to allow for a several-second dip in voltage occasioned by the starting of the 2,000-horsepower feedwater pump motors, and the other set for 50 per cent voltage, one-half second, to catch a more abrupt decline in voltage.

Tests we have conducted check well the results given in the paper. We find, however, quite a difference in time in the decay of the residual voltage, depending on the motors in service. Times from 50 to 100 or more cycles have been recorded. For this reason we use, instead of a fixed time delay, an undervoltage relay on each bus that delays the closing of the incoming circuit breaker until the residual voltage is reduced to about 20 to 25 per cent of the normal 2,400 volts. The closing time of the circuit breaker being added results in re-energizing the motors at about 400 volts residual. Inrush current can only be slightly greater than locked-rotor current, and tests show it is generally less. The fact that our boilers can be fired by either coal or oil, and some by gas, varies the motor load, as the mills and exhausters reduce the time of decay of the residual voltage. Thus it is possible to obtain a variation of the time to reach zero voltage on a given unit depending on the operating setup. We have found that the residual voltage slips 180 degrees out of phase in about 17 cycles with a decrement to zero of 70-80 cycles.

The operation of the four units now in service has been entirely satisfactory, and in several instances the automatic throwover has been tested by tripping the undervoltage relay and transferring the auxiliary load of 5,500 kw to 6,200 kw, including the motor-driven exciter set, with the main generator carrying from 80,000 to 100,000 kw.

F. W. Gay (Public Service Electric and Gas Company, Newark, N. J.): Figure 2 (A) of the discussion shows the voltage decay of number 14 bus at Burlington Generating Station. The voltage decays substantially to zero in about 50 cycles. This curve conforms very closely to the curve shown in Mr. Johnson's and Mr. Thompson's paper. The speed decays to approximately 90 per cent in 40 cycles.

Figure 2(B) of the discussion shows the voltage decay on bus Number 13 on Number 1 generator at Essex Generating Station. The two oscillograms are reduced so they show the same number of cycles per inch; therefore, the time of deceleration is propor-

tional to the physical length of the curves as shown on the two films.

In Figure 2(B) all of the auxiliaries connected with Number 1 generator at Essex Generating Station (100 megawatts) were thrown from the auxiliary power generator to the auxiliary power transformer simultaneously with the main unit carrying 85 megawatts; that is, the undervoltage relay that controls the automatic throwover was tripped. The curve shows that one of these circuit breakers delayed three or four cycles in opening, and it is believed that this was the Number 13 bus circuit breaker. Trace A, Figure 2(B) indicates the transformer current and shows the current taken by the transformer as the several busses were switched on. It appears that the Number 11 bus and the exciter switched on at approximately the same time. The Number 12 bus followed and the Number 13 bus was the last.

Trace *B*, Figure 2(B), gives the voltage on Number 13 bus. A study of this curve shows that the bus was de-energized for a little over 100 cycles. The speed fell to approximately 80 per cent and the voltage decayed to approximately 15 per cent in approximately 80 cycles. The break in the curve represents 230 cycles.

The transformer voltage as shown by Trace *C*, Figure 2(B), indicates approximately 1,220 volts at the time Number 13 bus was switched to the transformer; therefore, the transformer service voltage dropped from 2,400 to nearly 1,200 with a sustained current corresponding to a load at full voltage of approximately 20,000 kva. The large drop in voltage was produced by the transformer reactance and the protective reactors in the primary feed to the transformer.

Figure 3 of the discussion shows percentage voltage as ordinate and frequency as abscissa. Curve *A* shows the percentage voltage-time curve for the Burlington test; Curve *B* shows the percentage voltage-time curve for the Essex test shown in Figure 2; and Curve *C* shows the percentage voltage-time curve for a 500-horsepower motor driving the generator exciter.

It will be seen that it is rather dangerous to switch busses on the basis of time only when these curves show that there may be so great a discrepancy between the voltage decay curves under different conditions.

The designers of large motors tell us that large motors designed for across-the-line starting should not be re-energized until their residual voltage has fallen to about 20 per cent of normal. Accordingly we have equipped all busses with relays set to throw-over at approximately 500 volts. Since there is a time delay in the relay operation and circuit breaker closing, the actual voltages at the instant of re-energizing are considerably less than the 20 per cent specified by the designers. The 500-horsepower motor, Curve *C*, Figure 3, is designed especially for high-current starting, and the relays on this motor are set to throw-over at approximately 50 per cent residual voltage; but time delay due to circuit breaker closing, and so forth, after this voltage is reached gives a considerably lower voltage upon closing.

The tests on the 500-horsepower exciter motor were made at no load, and the speed during the 300 cycles diminished about one per cent.

A similar test was made on the same exciter at the Sewaren Station with a loaded generator and 850 amperes, or about 85 per cent of full-load field current, on the machine. At the end of 230 cycles after the opening of the circuit breaker the residual voltage was about 11 per cent and the speed about 77 per cent. The re-energizing was at 284 cycles, and the field current during this period fell from 850 to 600 amperes. The voltage regulator on this machine was cut out of service for this test.

A. A. Johnson and H. A. Thompson: The discussions by Mr. Taylor and Mr. Gay have added additional information on this problem which is very valuable. Their information adds appreciably to that which is contained in our paper. We agree that each auxiliary bus should be studied, or preferably tested, to determine its performance with respect to the residual voltage on motors. The use of an undervoltage relay, as employed by Mr. Taylor and Mr. Gay to delay the closing of the incoming circuit breaker until the residual voltage is reduced to about 20 to 25 per cent, is one way of insuring that the inrush current, when the auxiliary bus is reclosed, is limited. This method, however, in certain cases with motors or busses having long-time constants, may have to have the undervoltage relay set at a somewhat higher value than 20 per cent of rated voltage. In other words, this would be a compromise in order to protect critical loads in some applications. Consideration should be given in each case to the supply impedance in order to determine the inrush current to the motors when a bus is re-energized. The inrush current should be limited to a value equal to or less than the inrush current to each of the motors if they were started from an infinite bus at their terminals.

Mr. Brownlee and Mr. Elzi, in their discussion, point out that system tests have been made before and that interruptions having a time of five seconds could be tolerated. The 150 cycles or 2.5 seconds recommended in the paper was to some extent an arbitrary time because it was felt that this was very adequate even for making a test on the particular auxiliary system involved. We can see no reason for delaying the reclosure of the circuit breakers on to a new bus any longer than it takes for the residual voltage to decrease below the point where the inrush current to the motor will be limited. In connection with conclusions 3 and 4 of the paper, the only point involved here is that we are convinced that the motors should have the inrush current limited in order to be sure that they will give a satisfactory life. Whether this is done by a fixed time interval or by the use of an undervoltage relay as mentioned by Mr. Taylor and Mr. Gay seems immaterial as long as the motors are protected. Mr. Brownlee and Mr. Elzi also point out that to prevent flame extinction with certain types of coal-pulverizer mills requires transfer time as short as 20 to 30 cycles. The authors are not acquainted with any situation where such a short interval of time is necessary. Actually, we have no test results on this point except in a test where the Hardinge Mills were used, and there was apparently no effect on the flames for the time intervals used during this test. We have heard, however, of other abbreviated tests where the flame extinction was an important point when the time interval was about a minute or more.

Mr. Brownlee and Mr. Elzi also make the statement that standard motors should be capable of withstanding immediate reclosure when transferred by the open-transition method as discussed in the paper, and if the designs do not, then they should be reviewed. We do not know of any difficulties which have been experienced on motors from this cause, but it would appear that this is not necessarily a requirement of a standard motor and these special requirements should be discussed with the designer in advance of building such motors. It also was pointed out that reclosing on industrial feeders was frequently accomplished from 10 to 30 cycles and that industrial motors should be braced to withstand inrush currents from such service. It should be noted that the impedance in the feeder circuits will limit inrush currents to industrial motors to current values which are usually safe for the motors. Mr. Brown and Mr. Elzi mentioned that the inertia of the motor conductors on auxiliary systems may provide a margin of safety for the half-cycle of high-peak current. We have no specific data on this point, but we recognize that it well may be an important factor.

We appreciate the additional data provided by Mr. Webb in his discussion. In connection with transfering his group of motors eight cycles earlier in order for the two voltages to be in phase, it is quite likely that the variable load on the motors will cause the optimum time point to vary over a range of a number of cycles. It would appear that with the voltage reduced to the value shown in Figure 1 of the discussion the motor when re-energized will have the current limited to a safe value. Again the system reactance will help accomplish this.

Mr. Noest raised the question as to why it is that there have been no difficulties with bus-transfer schemes throughout the many years that such schemes have been in use, and very ably offered the answer. Most transfers in the past have had open-time intervals of sufficient duration to allow the residual voltage on the motors to reduce to a point where upon being re-energized the maximum inrush current has been limited. However, in recent years with higher speed circuit breakers and relaying the time interval may have to be controlled by probably introducing longer delays than that inherently offered by the circuit breakers. This is a primary reason for making the tests presented in the paper.

The discussion by Mr. Mellor and Mr. Temoshok gives a further review of some of the factors involved in open transition. We agree that the duty on each motor when transferred as a group will be less severe than the duty on a single motor being transferred. On the basis of the results in the paper, however, we disagree that the transfer time of 50 cycles is the time for a planned transfer. It is a time interval which should be used for all transfers to provide maximum safety to the motor. As to the closed transition where the supply to the auxiliary busses is provided from transformers, we feel that there is a definite hazard if it is left up to the operator to disconnect one of the power sources after the transfer has been accomplished. In one

case on the Duquesne Light Company's system where two transformers were used, the operator forgot to disconnect one source and the circulating current, because of too large a phase angle between the two sources, caused the current transformers in the common connection to heat up and fail. If closed transition is used, there should be some automatic arrangement provided so that after a short time interval one of the sources is automatically disconnected. We know of several cases where the transfer from one bus to another was made because the voltage on one source was reduced below normal value and remained at this point for an appreciable time interval. Therefore, we feel that the open-time interval should be either a fixed quantity which has been determined to be safe, or undervoltage relays which measure the residual voltage should dictate when the motors are closed in on the good source. There are too many possible combinations of situations which may arise to try to differentiate between when a source has a short circuit and when the voltage is reduced for some other reason. If it is safe to transfer on a planned basis with a time delay of, say, 50 cycles as in this case, then we feel that it is also safe to transfer in this time for any of the situations which might occur.

We appreciate the comments and the contributions given in the discussions. We would like to re-emphasize the point which has been made that there have been many auxiliary busses transferred on the open-transfer basis, but that inherently most of these have had time delays ranging from 30 to 60 cycles, depending upon the relay and circuit breaker times. With the more modern circuit breakers and relays operating at much faster times, this question of time interval assumes more importance, and we think should be given consideration when this scheme is used. The scheme has a very definite advantage in that the two sources are not paralleled, and, therefore, troubles from this are not in evidence. In addition lower short-circuit kilovolt-ampere circuit breakers can be used because on the closed transition, in order to protect for possible short circuits during the closed time interval, either higher short-circuit kilovolt-ampere circuit breakers are required, or current-limiting devices such as series reactors must be provided. In any event, if the closed transition scheme is used, some measure of limiting the short-circuit current should be built into the system.

As a matter of interest, the test results given in the paper were obtained in November 1948.

Regulation of A-C Generators with Suddenly Applied Loads—Part II

E. L. HARDER
FELLOW AIEE

R. C. CHEEK
MEMBER AIEE

J. M. CLAYTON
ASSOCIATE AIEE

THE determination of the voltage regulation of a-c generators with suddenly applied load has become a problem of considerable importance. When the load which may be added suddenly is appreciable compared with the connected generating capacity, consideration must be given to the effect of the voltage drop on other connected load as well as on that just added. Too great a drop may result in the dropping out of a-c contactors on other equipment, stalling of heavily loaded motors, malfunctioning of radar or other voltage-sensitive equipment, and in adverse effects upon the starting characteristics of motors thrown on the line. Relatively small power plants with large motor loads are particularly subject to this phenomenon since the starting load may be several times the running load. Examples are isolated coast-defense gun installations, naval ship-service generators, industrial power plants, and the auxiliary house generators of central-station power plants. In the latter case a heavy auxiliary motor load may be transferred suddenly to the house generator in the event the normal supply fails.

In a previous paper[1] the case of generators with self-excited exciters was treated. Curves were given showing the maximum voltage drop as a function of the added load, the exciter response, and the generator reactance and time constant. The exciter responses covered were 0.5, 1.0, and 3.0. Later problems arose making it desirable to extend the data to include response of 10.0 in order to permit interpolation for responses above 3.0 in special cases. The resulting curves are presented here without further explanation since their basis is thoroughly discussed in the earlier paper.

This paper deals primarily with generators having separately-excited exciters, Figure 1. This arrangement is used primarily for large central-station generators where the voltage-drop problem occurs less frequently, but also applies to house generators and to generators in large industrial plants, where voltage drop is of prime importance.

However, the curves presented are the mathematical solution of a basic regulating system whose performance may be expressed as follows: At time zero, Figure 2, a load, or an additional load, suddenly is thrown on the generator, causing a sudden drop in terminal voltage. A definite time, h, later a direct voltage, is suddenly impressed in the exciter field circuit and starts to build up the exciter field current. In the indirect-acting regulator this is accomplished by closure of the quick response contactor, Q, Figure 1. As the exciter builds up, the downward trend of generator voltage is halted at some time, t, and the voltage is started upward toward normal. Thus any regulating system which can be interpreted as impressing the same fixed voltage into the exciter field circuit a definite time, h, after the disturbance, can be treated by this data. It is the solution for a basic regulating system, taking into account exciter and generator characteristics.

The voltage-drop curves are presented with a statement of the basic assumptions, some examples of application and supplementary information for estimating machine constants when accurate design values are not known.

The theoretical analysis is given next, including the conversions to and from the electrical analog used on the Anacom.[2,3] All of the basic computations were carried out on the Anacom, an electric analog computer. An analytical solution, corresponding to that given in the previous paper,[1] is included for use with specific problems where the Anacom is not available.

Voltage-Drop Curves for A-C Generators with Separately-Excited Exciters

The voltage-drop curves for generators with separately-excited exciters are given in Figure 3. There are 12 graphs in all, covering four values of exciter response, R, from top to bottom, and three values of generator open-circuit time constant, T_{do}', from left to right. Each graph is a family of five curves for different values of generator transient reactance, x_d'. The maximum voltage drop is plotted as ordinate against the suddenly-applied load as abscissa. The applied load is treated as a fixed impedance of low power factor and is expressed, not as the current actually drawn, but in terms of that which would have been drawn with maintained voltage. This current is expressed in per cent of generator rating.

Example 1: The simplest problem is a direct one. Determine the voltage drop that would be caused by a 300-horsepower induction motor starting at reduced voltage of 60 per cent through a starting transformer on a 2,000-kva generator having an open-circuit time constant, T_{do}', of 3.0 second, and a transient reactance, x_d', of 20 per cent. R is 1.0, and an indirect-acting regulator with quick response contactors is used. The full-voltage starting current of the motor is given as 6.5 times normal and the rated kilovolt-amperes as 280.

Paper 50-58, recommended by the AIEE Power Generation, and Transmission and Distribution Committees and approved by the AIEE Technical Program Committee for presentation at the AIEE Winter General Meeting, New York, N. Y., January 30–February 3, 1950. Manuscript submitted November 1, 1949; made available for printing December 1, 1949.

E. L. Harder, R. C. Cheek, and J. M. Clayton are all with the Westinghouse Electric Corporation, East Pittsburgh, Pa.

The derivations of Appendixes II and III were taken from a thesis, "Suddenly-Applied Loads on Generators with Quick-Response Excitation," by R. C. Cheek, submitted to the University of Pittsburgh in partial fulfillment of the requirements for the degree of Master of Science, June 1943.

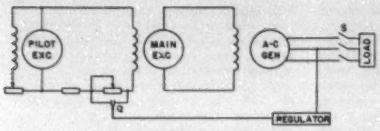

Figure 1. Essential components of excitation system with indirect-acting regulator and separately-excited exciter

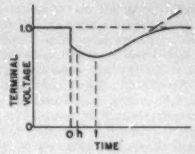

Figure 2. Terminal voltage versus time after a sudden load application

At the reduced voltage (assumed maintained) the motor inrush in per cent of generator rating would be

$$\text{Applied load} = \frac{280 \times 6.5 \times (0.60)^2}{2{,}000}$$

$$= \frac{656}{2{,}000} = 32.8 \text{ per cent}$$

In Figure 3, curves are available for a response of 1.0 but it will be necessary to interpolate between $T_{do}' = 2$ and 4. For $R = 1.0$, $T_{do}' = 2.0$, the voltage drop at 32.8 per cent load is 6.5 per cent as read on the curve for $x_d' = 20$ per cent. For $R = 1.0$ and $T_{do}' = 4.0$, the drop at 32.8 per cent load is 6.4 per cent. These values are the same within the accuracy of the curves. The voltage drop may be taken as 6.5 per cent.

Example 2: The indirect problem may occur in many forms. One might be to determine the size of the largest motor that can be started across the line on a 5,000-kva generator without exceeding 15 per cent drop under the following conditions:

Separately-excited exciter.

Indirect-acting regulator with quick-response contacts.

Generator open-circuit time constant, $T_{do}' = 2.0$ seconds.

Generator transient reactance, $x_d' = 20$ per cent.

Exciter response, $R = 0.5$.

Ratio, motor kilovolt-ampere per horsepower $= 0.9$.

Motor starting current $= 6$ times normal.

From the curve of Figure 3 for $R = 0.5$, $T_{do}' = 2.0$, $x_d' = 20$ per cent, the applied load to result in 15 per cent drop is found to be 52 per cent. The starting inrush therefore may be 52 per cent of $5{,}000 = 2{,}600$ kva, or the motor kilovolt amperes may be $2{,}600/6 = 433$. The largest motor permissible with the specified conditions is $433/0.9 = 480$ horsepower.

Use of Curves with Other Regulating Systems

A certain amount of information regarding voltage drop with other types of regulators can also be derived from the curves of Figure 3. Any regulating system which has the same field-circuit time constant and impresses the same voltage in the same time will result in identical voltage drop for a given added load.

In particular, if the variable field-circuit resistance in the system treated were eliminated and a regulating system which inserted a voltage directly in the field circuit were used, the same drop would be obtained upon application of load if the regulator inserted the same voltage as that which previously appeared across the variable field-circuit resistance at no load.

For example, suppose an exciter has a certain nominal response and is designed to have 82 volts across the variable resistance when operating at no generator load. Also, suppose that the fixed resistance in the circuit, including the field and any external resistance not short circuited is 40 ohms. The voltage impressed by a different regulating system as a result of the voltage drop would have to be 82 volts and the resistance of the field circuit into which it was impressed would have to be 40 ohms in order for the curves of Figure 3 to apply. If the voltage were less or the field-circuit resistance more, the voltage drop would be increased, and vice-versa.

Factors Influencing Voltage Regulation

The maximum voltage drops have been given as functions of the four principal parameters; namely, added load, generator transient reactance, generator time constant, and exciter response. There are a number of other factors entering into the equations for maximum voltage drop, but as has been shown previously[1] these are generally minor factors which justifiably can be represented by average values in determining voltage drops.

All the various factors that affect the terminal voltage of a generator during the starting of a large motor or other load were discussed in detail in the previous paper. In this paper, only a brief statement adequate to define the conditions for these curves is given in regard to each factor.

Typical values of the principal factors affecting voltage drop are given in Table I and Figure 4. In the Table the value above the line represents the average of a large number of machines considered and the values below the line give the range. The values of all the minor parameters held constant in the study are given in Table II.

Generator Transient Reactance, x_d'

The curves of Figure 3 are plotted in terms of the saturated or rated-voltage value of transient reactance, x_d' saturated, which is the value customarily supplied by the manufacturer as the transient reactance, x_d', of the machine.

Generator Synchronous Reactance, x_d, and Short-Circuit Ratio

The maximum voltage drop increases with an increase in synchronous reactance. With average generator and exciter characteristics, the change in maximum drop at 100 per cent applied load is about two parts in 25 as x_d is varied from 120 per cent down to 100 per cent or up to 140 per cent. With 20 per cent saturation at no load, the corresponding variation in short-circuit ratio is from 1.0 up to 1.2 or down to 0.86. These variations from the average x_d of 120 per cent are as large as are usually encountered among normal machines, and the curves of Figure 3 can be used directly for normal machines without serious error for most purposes.

An accurate figure for maximum voltage drop may be required in some cases where generator synchronous reactance differs greatly from 120 per cent. The curves of Figure 3 can be used for the precise determination of drop in such cases by first expressing generator reactances and the applied load on a new kilovolt-ampere base, such that x_d on the new base is 120 per cent, and then applying the curves. For example, suppose a low power-factor load of 1,500 kva (expressed at full voltage) is to be applied to a 3,000-kva generator having 30 per cent transient reactance and 150 per cent synchronous reactance. Suppose that the generator time constant is 4.0 seconds and the exciter has a nominal response of 1.0. To determine the drop, express the transient reactance and the applied load on the kilovolt-ampere base upon which x_d is 120 per cent. The base in this case will be 3,000 by $120/150 = 2{,}400$ kva. On this base the transient reactance x_d' is 30 by $2{,}400/3{,}000 = 24$ per cent, and the applied

load is 1,500/2,400 = 62.5 per cent. From the curves of Figure 3, the maximum voltage drop is 13 per cent for 62.5 per cent load applied to a generator having 24 per cent transient reactance, a time constant of 4.0 seconds, and an exciter of 1.0 nominal response. This same maximum drop would be obtained with the machine and load under consideration.

Generator Open-Circuit Time Constant, T_{do}'

This time constant is the ratio of inductance to resistance of the generator field circuit under unsaturated conditions. The resistance should include all resistance in the field circuit. Typical values for the machine alone are given in Figure 4.

Generator Quadrature-Axis Synchronous Reactance, x_q, and Saturation, s

The drop is almost independent of x_q over the practical range of its variation, the value 0.75 being a good average. Curves are based on 20 per cent saturation ($s = 0.20$) although s can be varied from 0 to 0.4 without materially altering the drop.

Exciter Response, R

The exciter response, R, is the nominal response as defined by the American Standards Association. It is the average rate of open-circuit exciter voltage increase from nominal voltage during the first half-second after the field resistance is short-circuited, expressed in per unit of nominal voltage. Nominal voltage is understood to be that required on the slip rings when the generator is operated at rated voltage, load and power factor. It is necessary that the response, R, used in estimating voltage drop be based on cutting out the same resistance as is cut out by the quick-response contactors in the actual application.

Regulator Operating Time, h

The regulator operating time has been taken as three cycles or 0.05 second. The quick-response contactors of indirect-acting regulators are frequently guaranteed to operate within this time for a voltage drop of ten per cent or more. If the transient-reactance voltage drop is insufficient to operate the quick-response contacts, the regulator action is comparatively slow and the curves do not apply in this region.

Initial Load

The curves are based on no initial load but also apply if initial load is present. It has been shown that the effect of initial load is to cause somewhat less drop if the load is static, somewhat more drop if the load is dynamic (running motors), and about the same drop if the load is about evenly divided. Thus the no-load case also is representative of an average mixed initial load.

Characteristics of Applied Load

The curves of Figure 3 are based on a constant-impedance applied load, which can be used to represent an induction motor during the starting period. In the curves, the power factor of applied load was taken as 35 per cent, a typical motor-starting power factor. The maximum voltage drop is practically the same for all power factors from zero to 40 per cent but decreases rapidly for power factors above this.

Solution on the Anacom

Preparation of the curves of Figure 3 required maximum voltage-drop calculations for some 300 conditions (3 time constants by 4 exciter responses by 5 reactances by 5 applied loads), and so it was decided to use the Anacom for the actual computation. There were several main steps to the solution.

THEORY DEVELOPMENT

1. Derivation of equations describing the phenomena.

2. Conversion from exciter response, R, to an equivalent ceiling voltage, e_g, and time constant.

3. Development of an analog and determination of the analogous relations.

COMPUTATIONS

4. Computation of e_c and T_c.

5. Determination of initial conditions and conversion of data to analog.

6. Analog computations of e and conversion to e_d.

7. Machine or slide rule computation of e_t from e_d.

These various steps now will be discussed.

1. *Derivation of Equations of the System*

The necessary equations for use in the analog method of solution are described in Appendix I, directly or by reference. Equations 3, 3A, and 6 give conversions from e_d' to e_t, e_t to e_d, and T_{do}' to T_d', required in the computations. Equations 11A and B give the differential equation in two regions, first from the time that load is added at $t = 0$ until the regulator acts at $t = h$.

2. *Conversion from Exciter Response to Ceiling Voltage and Time Constant*

Appendix II is a derivation of the relationship between the exciter nominal re-

Table I. Typical Values of Principal Factors Affecting Voltage Drop*

	x_d	x_d' saturated
Two-pole turbine generators	1.10	0.155
	0.95–1.45	0.12–0.21
Four-pole turbine generators	1.10	0.23
	1.00–1.45	0.20–0.28
Salient-pole generators	1.15	0.37
	0.60–1.45	0.20–0.80
Exciter response		1.0
		0.5–3.0

* Reactances are per unit. Values below the line give the range of values, while those above give an average value.

Table II. Summary of Basis of Curves of Figures 3 and 9

Description	Notation	Value
Direct-axis transient reactance	x_d'	1.07 x_d' saturated
Direct-axis synchronous reactance	x_d	1.20 per unit
Quadrature-axis synchronous reactance	x_q	0.75 per unit
Excitation for saturation at no load, normal voltage	s	0.20 per unit
Regulator equivalent operating time	h	0.05 second
Added load—constant impedance		0.35 power factor
Initial load		Zero
Regulating systems		As shown in Figures 1 and 8 for voltage-drop curves of Figures 3 and 9 respectively

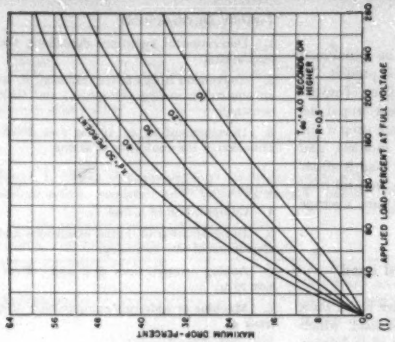
MAXIMUM DROP—PERCENT
APPLIED LOAD—PERCENT AT FULL VOLTAGE
T_{ge}=1.0 SECOND
R=0.5
X'd=30 PERCENT
40
50
60
70
80
0
0
8
16
24
32
40
48
56
64
0
40
80
120
160
200
240
280

(A)

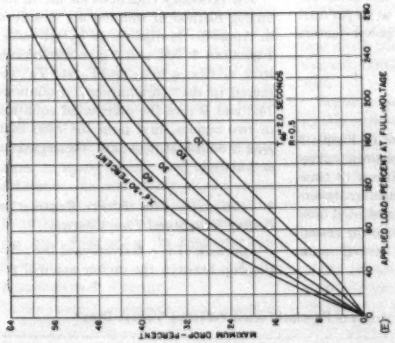
MAXIMUM DROP—PERCENT
APPLIED LOAD—PERCENT AT FULL-VOLTAGE
T_{ge}=2.0 SECONDS
R=0.5
X'd=30 PERCENT
40
50
60
70
80
0
0
8
16
24
32
40
48
56
64
0
40
80
120
160
200
240
280

(E)

MAXIMUM DROP—PERCENT
APPLIED LOAD—PERCENT AT FULL VOLTAGE
T_{ge}=4.0 SECONDS OR HIGHER
R=0.5
X'd=30 PERCENT
40
50
60
70
80
0
0
8
16
24
32
40
48
56
64
0
40
80
120
160
200
240
280

(I)

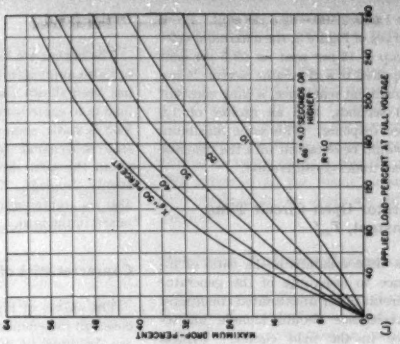
MAXIMUM DROP—PERCENT
APPLIED LOAD—PERCENT AT FULL VOLTAGE
T_{ge}=1.0 SECOND
R=1.0
X'd=30 PERCENT
40
50
60
70
80
0
0
8
16
24
32
40
48
56
64
0
40
80
120
160
200
240
280

(B)

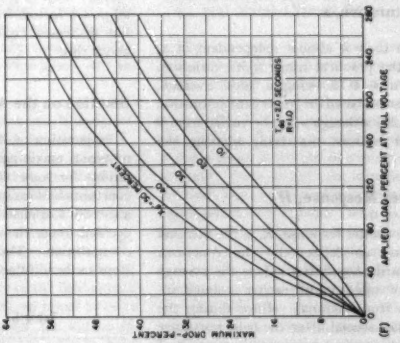
MAXIMUM DROP—PERCENT
APPLIED LOAD—PERCENT AT FULL VOLTAGE
T_{ge}=2.0 SECONDS
R=1.0
X'd=30 PERCENT
40
50
60
70
80
0
0
8
16
24
32
40
48
56
64
0
40
80
120
160
200
240
280

(F)

MAXIMUM DROP—PERCENT
APPLIED LOAD—PERCENT AT FULL VOLTAGE
T_{ge}=4.0 SECONDS OR HIGHER
R=1.0
X'd=30 PERCENT
40
50
60
70
80
0
0
8
16
24
32
40
48
56
64
0
40
80
120
160
200
240
280

(J)

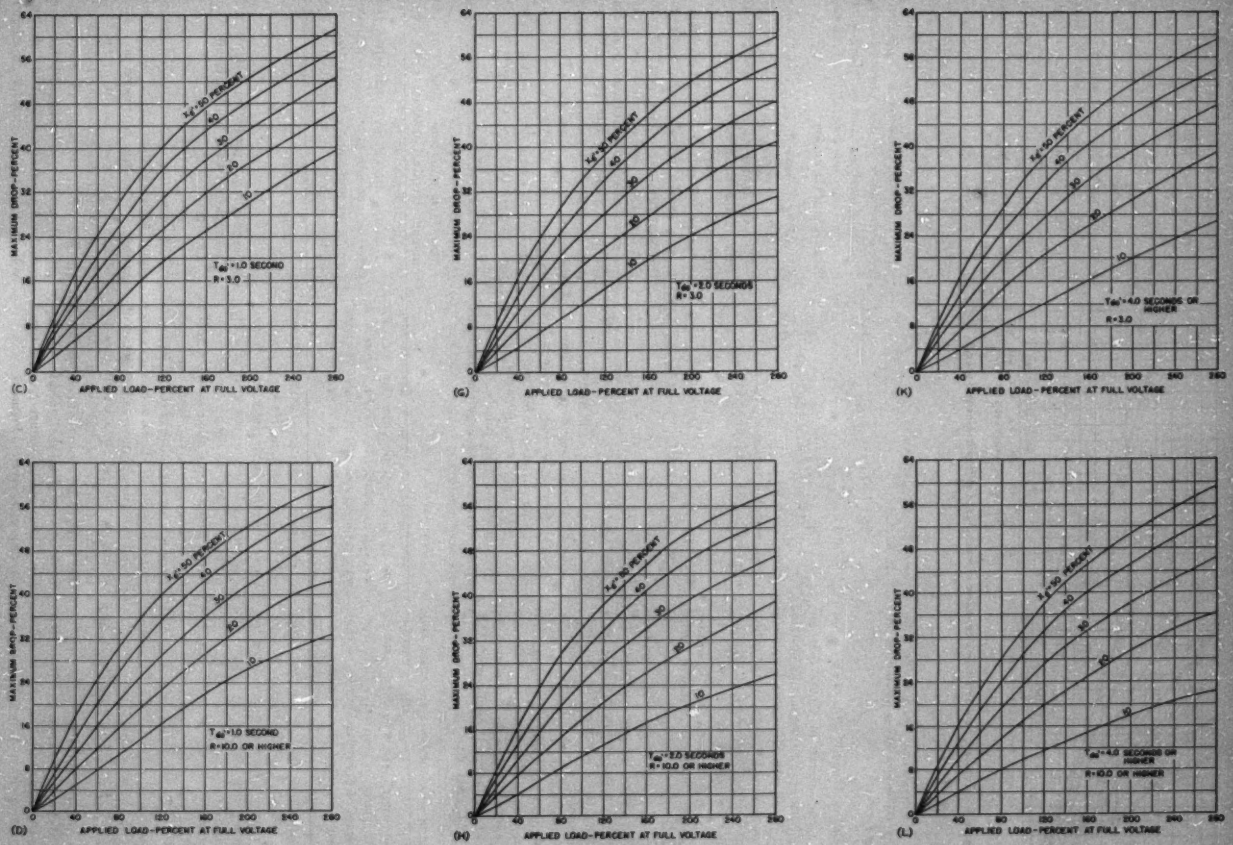

Figure 3. Voltage drop versus suddenly applied load for generators having separately-excited exciters and with various transient reactances, x_d', time constants, T_{do}', and nominal exciter responses, R

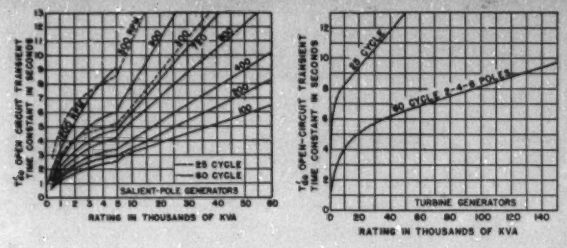

Figure 4. Typical open-circuit time constants of machines of different sizes and speeds

sponse and its ceiling voltage and time constant, the results being plotted graphically in Figure 6.

3. *Electrical Analog of Regulating System*

The circuit shown in Figure 5 is an electrical analog of the regulating system after the load has been added at $t=0$. This may be shown by comparing the differential equation for $(e+E_2)$ of Figure 5 with that for (e_d-1) of the actual generator. Note particularly that the analog does not give the initial transient-reactance drop, but only the variation of voltage after this drop has occurred. When S_2 is closed, the condition simulated is that of the actual system just *after* $t=0$. The analog gives, in effect, the variation of field current, which is proportional to e_d, from this instant on.

In Figure 5, S_2 closes at $t=0$ and E_2 starts to charge C_2 negatively. (This is equivalent to placing a positive charge on C_2 at $t=0$ and letting it discharge.) The circuit R_2C_2 has very high impedance compared with R_1C_1 so that the voltage of C_1 remains substantially zero during this interval. At $t=t_1=h$, the regulator-operating time, switch S_1 closes and E_1 starts to charge C_1 positively. The positive voltage of C_1 eventually rises so that the downward trend of e is halted and e starts upward. It may be noted that this action simulates that of the regulating system. Mathematically the performance of the circuit is expressed as follows, the equations being written by inspection from Figure 5.

If $0<t<t_1$

$$0=(e+E_2)(1+pT_2) \tag{1A}$$

If $t>t_1$

$$E\left(1-\epsilon^{-\frac{t-t_1}{T_1}}\right)=(e+E_2)(1+pT_2) \tag{1B}$$

E_2 is simply a convenient equivalent to an initial charge placed on C_2. Note that $pT_2E_2=0$. Equations 11A and B of the actual system from Appendix I are included here for reference.

If $0<t<h$

$$0=(e_d-1)(1+pT_d') \tag{11A}$$

If $t>h$

$$(e_c-1.2)\left(1-\epsilon^{-\frac{t-h}{T_e}}\right)=(e_d-1)(1+pT_d') \tag{11B}$$

Observe that equations 1A and B are identical to 11A and B provided that

$$e+E_2 \equiv e_d-1 \tag{2A}$$

$$T_2 \equiv T_d' \tag{2B}$$

$$t_1 \equiv h \tag{2C}$$

$$T_1 \equiv T_e \tag{2D}$$

$$E_1 \equiv e_c-1.2 \tag{2E}$$

Hence the circuit of Figure 5 is analogous to the regulating system, Figure 1. Suitable time-scale and voltage-magnitude transformations can be made to suit the requirements of the analog computer. The impedance base can be selected at will since it is not fixed by the analogous relations, equation 2.

4. *Determine e_c and T_e*

The exciter response, R, must be converted to an exciter time constant, T_e, and ceiling voltage, e_c. From Figure 6 it may be observed that the same response may be obtained with different ceiling voltages.

However, exciters with different ceilings and the same response produce about the same maximum voltage drop so that this solution is not critical. The ratios of ceiling to nominal voltages selected for the study all lie on the straight line drawn across the figure and vary from 1.5, for a response of 0.5, to 5.0 for a response of 10.0. These values all correspond to reasonable designs. Selection of ceiling to nominal voltage ratio fixes the time constant. Nominal exciter voltage was taken as 2.4 times that corresponding to rated voltage on the generator air-gap line. Thus ceiling voltage e_c is 2.4 times the ratio e_c/e_n given in Figure 6.

5. *Determine the Initial Value of e_d*

The direct-axis transient internal voltage, e_d', prior to $t=0$ can be calculated from equation 3, e_t being unity before load is added; e_d' is proportional to the flux linkages with the main field and does not change when the load is added. Thus it has the same value immediately after $t=0$. The initial value of e_d, after $t=0$, can be obtained from e_d' using equation 5. This provides the initial value of e_d and hence of the variable (e_d-1) used in equations 11A and B. Next determine T_d' from T_{do}' using equation 6. The parameters e_c, T_e, T_d', h, and the initial value of e_d now are known and can be converted to analog values, E_1, T_1, T_2, t_1, and E_2 respectively, using equation 2. Note here the convenience of the direct analog-computing method in that each parameter influences only one separately-adjustable parameter of the analog.

6. *Analog Computations of e and Conversion to e_d*

With the analog set at these or proportional values, the minimum value (greatest negative value) of e is read from the computer. Figure 7 shows the voltages E_1 and E_2 and a typical solution for e from the computer. It is of interest to note that the time as well as magnitude of the lowest voltage can be obtained using the computer although only the maximum drop was used in this study. Now having the most negative value of e, we have the minimum value of $e+E_2$, which is minimum (e_d-1), except for the voltage transformation selected from computer to system.

7. *Computation of e_t from e_d*

From the minimum value of e_d the minimum terminal voltage, e_t, is computed using equation 3A.

Thus the analog computer solves the differential equations of the system to determine the minimum e_d, whereas the computations represented by equations 3, 3A, 5, and 6 are done by slide rule or desk-calculating machine.

Voltage-Drop Curves for A-C Generators with Self-Excited Exciters

The regulating system studied previously,[1] for generators having self-excited exciters, is shown in Figure 8. The voltage-drop curves for this regulating system, which also have been published,[1] are included in this paper, Figure 9. Additional curves, not published before, are included for an exciter response of 10.0; voltage drops on systems having exciter

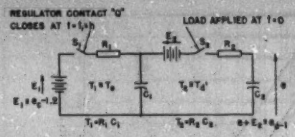

Figure 5 (above). Analog of regulating system during voltage drop caused by suddenly applied load on generator with separately-excited exciter

Figure 7 (right). Impressed voltages E_1 and E_2 and a typical solution of terminal voltage for a generator having separately-excited exciter with $R=1.0$, $T_{do}'=4.0$, $x_d'=10$ per cent and applied load=250 per cent

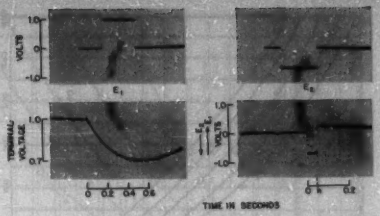

responses above 3.0 can be interpolated readily with these curves.

Analytical Solution for e_d' and Time of Maximum Drop

In the previous paper analytical expressions for e_d' and the time of maximum drop were derived for the case of self-excited exciters. A corresponding derivation is given in Appendix III for the separately-excited system. These expressions may be used in longhand calculations of specific problems where a computer such as the Anacom is not available. The voltage e_d' can be converted to e_t by use of equivalent relations given in Appendix I.

Verification of Voltage-Drop Curves

As the method of computation has been verified already[1] by experimental tests, it was only necessary in this case to spot check the 300 computer calculations. Seven strategically spaced points were checked by direct calculation from the formulas and all agreed with the computer results to well within ±1.0 per cent drop. This is within the expected computer accuracy.

Conclusions

As a result of the studies described in this paper and in reference 1, the following conclusions have been reached regarding the importance of various factors affecting voltage drop with suddenly applied low power-factor load:

1. The maximum voltage drop accompanying suddenly applied low power-factor load can be expressed in terms of four main parameters for generators with self-excited exciters and separately-excited exciters.

2. In the generator, the transient-reactance and the open circuit time constant are of prime importance. Reasonable variations in synchronous reactance have less effect. A method is presented for correcting for wide variations in synchronous reactance when using the voltage-drop curves; this method applies to generators with self-excited or separately-excited exciters. Variations in quadrature reactance and saturation have practically no effect on maximum voltage drops.

3. For self-excited and separately-excited exciters, the nominal response adequately expresses for practical cases the effect of exciter characteristics upon maximum voltage drops.

4. As has been shown before,[1] the regulator operating time, initial load, and variations in the power factor of the applied load from 0.0 to 40 per cent have negligible effect on the maximum voltage drop.

In general, greater voltage drops occur on generators having self-excited exciters with a given response than on generators having separately-excited exciters with the same response, assuming that all other factors affecting voltage drop are equal. For the range of parameters covered by the curves, the difference in the voltage drops for similar operating conditions may be as great as 14 per cent or may be less than 0.5 per cent depending upon the particular machine constants and applied load conditions. For a large number of cases the difference in the voltage drops for the two excitation systems will be within a range of 2 to 10 per cent. This gives some idea of the error involved if the voltage-drop curves presented in the previous paper are used to determine the voltage drop on generators with separately-excited exciters. Even though it is recognized that the voltage drop given by the previous curves is pessimistic for generators with separately-excited exciters, the magnitude of the error cannot be estimated readily, since it varies with machine and exciter constants and applied load conditions. Therefore, this separate treatment of systems with separately-excited exciters is considered necessary.

Appendix I. Equations for Terminal Voltage as a Function of Time for Generator with Separately-Excited Exciter and Suddenly Applied Load

As shown in Figure 1 for a sudden load which drops the terminal voltage enough to close the regulator quick-response contacts, a block of resistance is short-circuited in the exciter field circuit.

Neglecting subtransient effects, the generator terminal voltage suffers a sudden initial transient drop, followed by a gradual drop from transient toward the synchronous value. In the meantime regulator action raises the exciter voltage, halting further drop and restoring voltage to normal. As the voltage approaches normal, antihunt devices take effect, slowing the rise. However, these usually will have no effect on the minimum voltage reached during the dip.

If it is assumed that the build-up of exciter voltage follows an exponential law from its

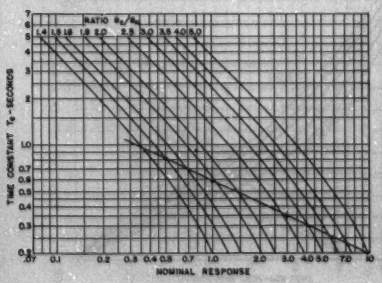

Figure 6 (left). Exciter time constant, T_{dx}, versus response for various ratios of ceiling voltage, e_{xc}, to nominal voltage, e_n

Figure 8 (right). Essential components of excitation system with direct-acting regulator and self-excited exciter

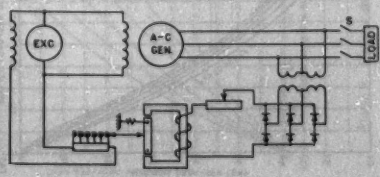

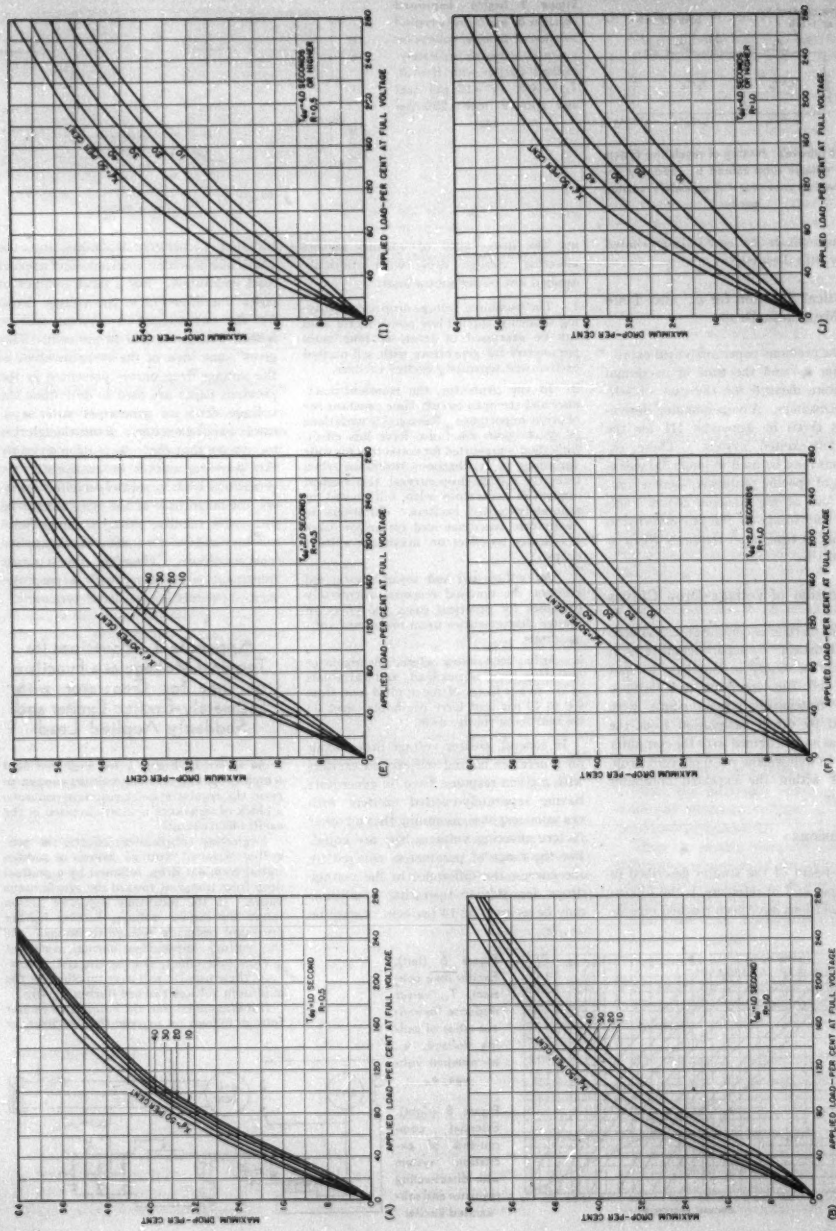
(A)
t_{av}=1.0 SECOND
R=0.05
(B)
t_{av}=1.0 SECOND
R=1.0
(E)
t_{av}=2.0 SECONDS
R=0.5
(F)
t_{av}=2.0 SECONDS
R=1.0
(I)
t_{av}=4.0 SECONDS
R=0.5
OR HIGHER
(J)
t_{av}=4.0 SECONDS
R=1.0
OR HIGHER
APPLIED LOAD—PER CENT AT FULL VOLTAGE
MAXIMUM DROP—PER CENT

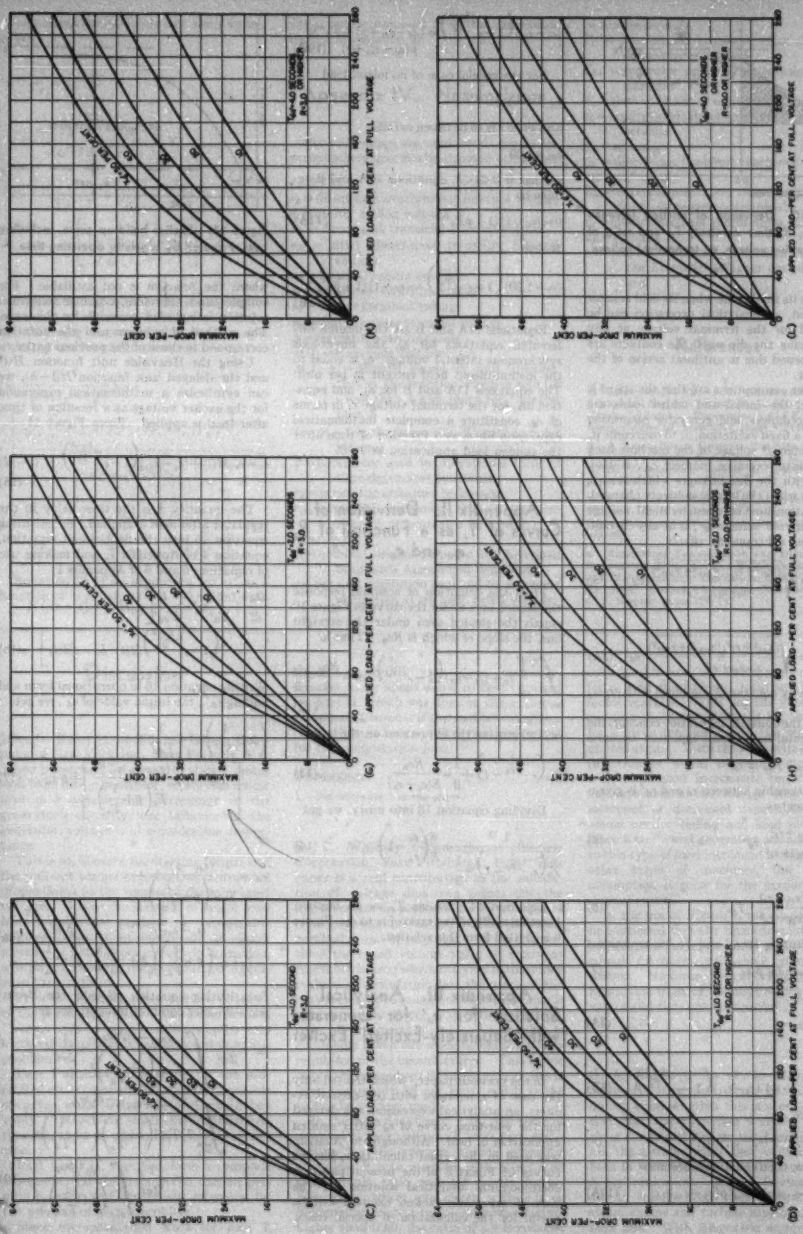

Figure 9. Voltage drop versus suddenly applied load for generators having self-excited exciters and with various transient reactances, x_d', time constants, T_{d0}', and nominal exciter response, R

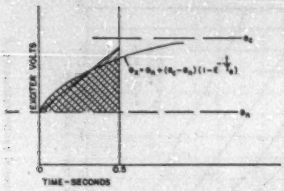

Figure 10. Derivation of relation between response, R, time constant, T_e, and ratio of exciter ceiling voltage, e_c, to nominal voltage, e_n

initial to its final value when its field resistor is cut out, an analytical expression can be obtained for the terminal voltage at any time during the dip until the contacts are again opened due to antihunt action of the regulator.

Further assumptions are that the speed is constant, the initial and added loads are pure impedances, and generator saturation requires a fixed excitation, s, to overcome it.

The internal voltage of the machine back of transient reactance, namely e_d', is associated with the flux linkages which remain constant when the load is suddenly changed. The relationship[4] between terminal voltage e_t and internal voltage e_d', is at any instant, neglecting subtransient effects

$$e_t=\sqrt{\frac{(x_{qt}^2+r_t^2)(x_{wxt}^2+r_{wxt}^2)}{x_{dt}'x_{qt}+r_t^2}}\;e_d' \qquad (3)$$

Also

$$e_t=\sqrt{\frac{(x_{qt}^2+r_t^2)(x_{wxt}^2+r_{wxt}^2)}{x_{dt}x_{qt}+r_t^2}}\;e_d \qquad (3A)$$

as shown by equation 5 combined with equation 3.

Using the constant saturation concept, the fundamental field-circuit equation becomes

$$e_x-s=e_d+T_{do}'\,p\,e_d' \qquad (4)$$

The relationship between e_d and e_d' is given by Wagner[4] as

$$e_d=\frac{x_{dt}x_{qt}+r_t^2}{x_{dt}'x_{qt}+r_t^2}\;e_d' \qquad (5)$$

Also[4]

$$T_d'=\frac{x_d'x_{qt}+r_t^2}{x_{dt}x_{qt}+r_t^2}\;T_{do}' \qquad (6)$$

Substituting for e_d' and T_{do}' in equation 4

$$e_x-s=e_d+T_d'p\,e_d \qquad (7)$$

If $0<t<h$

$$e_x-s=e_{x1}-s \qquad (8A)$$

If $t>h$

$$e_x-s=e_{x1}-s+(e_c-e_{x1})\left(1-\epsilon^{-\frac{t-h}{T_e}}\right) \qquad (8B)$$

And since

$$e_d=(e_{x1}-s)+(e_d-e_{x1}+s) \qquad (9)$$

If $0<t<h$, then equation 7 becomes

$$0=(e_d-e_{x1}+s)+T_d'p(e_d-e_{x1}+s) \qquad (10A)$$

If $t>h$

$$(e_c-e_{x1})\left(1-\epsilon^{-\frac{t-h}{T_e}}\right)=(e_d-e_{x1}+s)+T_d'\times p(e_d-e_{x1}+s) \qquad (10B)$$

For the special case of no initial load

$$e_{x1}-s=1.0$$

and since s is to be taken as 0.20

$$e_{x1}=1.20$$

so that if $0<t<h$, equations 10A and B reduce to

$$0=(e_d-1)(1+pT_d') \qquad (11A)$$

If $t>h$

$$(e_c-1.20)\left(1-\epsilon^{-\frac{t-h}{T_e}}\right)=(e_d-1)(1+pT_d'). \qquad (11B)$$

Equations 11A and B are the desired differential equations for e_d, the direct-axis synchronous internal voltage; e_d is equal to the instantaneous field current in per unit. The equations 11A and B for e_d, and equation 3A, for the terminal voltage e_t in terms of e_d, constitute a complete mathematical expression for e_t as a function of time after the sudden load application at $t=0$.

Appendix II. Derivation of Curves of T_e as a Function of R, e_c, and e_n

From the definition of nominal response the shaded area under the curve in Figure 10 equals the shaded area under the straight line, the slope of which is Re_n. That is

$$\int_0^{0.5}\left[e_n+(e_c-e_n)\left(1-\epsilon^{-\frac{t}{T_e}}\right)\right]dt=\frac{Re_n}{8}+\frac{e_n}{2} \qquad (12)$$

or, integrating the expression on the left

$$T_e\left(\epsilon^{-\frac{1}{2T_e}}-1\right)+\frac{1}{2}=\frac{Re_n}{8(e_c-e_n)} \qquad (13)$$

Dividing equation 13 into unity, we get

$$\frac{1}{T_e\left(\epsilon^{-\frac{1}{2T_e}}-1\right)+\frac{1}{2}}=\frac{8}{R}\left(\frac{e_c}{e_n}-1\right) \qquad (14)$$

Equation 14 contains T_e as an implicit function of R and the ratio of e_c to e_n. Figure 6 is plotted from this relation.

Appendix III. Analytical Solution for e_d' for Generator with Separately-Excited Exciter

In the previous paper,[1] which treated only the case of generators with self-excited exciters, an analytical expression was derived for the volt-time curve of e_d' after sudden application of load. Although the Anacom was used in the actual calculations for the curves of Figure 3 of the present paper, a corresponding analytical solution for the case of separately-excited exciters will be useful for the calculation of special cases,

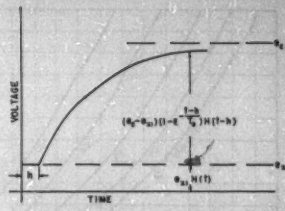

Figure 11. Exciter build-up curve, including delay caused by regulator operating time, h

where the Anacom is not available. For completeness, therefore, a similar analytical solution is included herewith for this case. The method of solution and the notation correspond to those of the previous paper.

Using the Heaviside unit function $H(t)$ and the delayed unit function $H(t-h)$, we can synthesize a mathematical expression for the exciter voltage as a function of time after load is applied. From Figure 11

$$e_x=e_{x1}H(t)+(e_c-e_{x1})\left(1-\epsilon^{-\frac{t-h}{T_e}}\right)H(t-H) \qquad (15)$$

The quantity h is the time delay in the regulator after load is applied. Substituting equation 15 into the field-circuit equation, equation 4 of Appendix I, and making use of equations 5 and 6 of Appendix I

$$\frac{de_d'}{dt}+\frac{1}{T_d'}e_d'=\frac{1}{T_{do}'}\left[e_{x1}H(t)+(e_c-e_{x1})\times\left(1-\epsilon^{-\frac{t-h}{T_e}}\right)H(t-h)-sH(t)\right] \qquad (16)$$

Writing equation 16 in operational form and adding $e_d'{}_1$, the initial value of e_d', we get

$$\left(p+\frac{1}{T_d'}\right)e_d'=\frac{1}{T_{do}'}\times\left[(e_{x1}-s)+\frac{(e_c-e_{x1})\epsilon^{-ph}}{T_e\left(p+\frac{1}{T_e}\right)}\right]+p\,e_d'{}_1 \qquad (17)$$

or

$$e_d'=\frac{(e_{x1}-s)}{T_{do}'\left(p+\frac{1}{T_d'}\right)}+\frac{(e_c-e_{x1})\epsilon^{-ph}}{T_eT_{do}'\left(p+\frac{1}{T_e}\right)\left(p+\frac{1}{T_d'}\right)}+\frac{p\,e_d'{}_1}{p+\frac{1}{T_d'}} \qquad (18)$$

Substituting equation 18 into the Bromwich-Wagner complex integral, we get

$$e_d'=\frac{1}{2\pi i}\int_{Br_1}\frac{(e_{x1}-s)\epsilon^{tz}dz}{T_{do}'\left(z+\frac{1}{T_d'}\right)z}+\frac{1}{2\pi i}\times\int_{Br_1}\frac{(e_c-e_{x1})\epsilon^{-zh}\epsilon^{tz}dz}{T_eT_{do}'\left(z+\frac{1}{T_e}\right)\left(z+\frac{1}{T_d'}\right)z}+\frac{1}{2\pi i}\int_{Br_1}\frac{e_d'{}_1\epsilon^{tz}dz}{\left(z+\frac{1}{T_d'}\right)z} \qquad (19)$$

Evaluating the integrals and simplifying, we get

$$e_d' = \frac{T_d'}{T_{do}'}(e_c - s) + \left[\frac{(e_c - e_{s1})T_d'^{2}\epsilon^{\frac{h}{T_d'}} - (e_{s1} - s)}{T_{do}'(T_s - T_d')} \times \frac{(T_s - T_d')T_d' + e_{d1}'T_{do}'(T_s - T_d')}{T_{do}'(T_s - T_d')}\right]\epsilon^{-\frac{t}{T_d'}} - \left[\frac{(e_c - e_{s1})T_d'T_s\epsilon^{\frac{h}{T_s}}}{T_{do}'(T_s - T_d')}\right]\epsilon^{-\frac{t}{T_s}} \quad (20)$$

Differentiating equation 20, setting the result equal to zero, and solving for t, we get the following expression for the time at which e_d' has its minimum value

$$t = \frac{T_d'T_s}{0.434(T_s - T_d')}\log_{10}\left[\frac{e_{d1}'\frac{T_{do}'}{T_d'}(T_s - T_d') + (e_c - e_{s1})T_d'\epsilon^{\frac{h}{T_d'}}}{(e_c - e_{s1})T_d'\epsilon^{\frac{h}{T_s}}} - \frac{(e_{s1} - s)(T_s - T_d')}{(e_c - e_{s1})Td'\epsilon^{\frac{h}{T_s}}}\right] \quad (21)$$

Equation 20 is an expression for e_d' as a function of time after $t = h$. Terminal voltage e_t can be obtained from this expression by use of equation 3.

Appendix IV. Nomenclature

Per-unit values are used for all quantities except where specifically denoted otherwise.

$\epsilon = 2.718$
e_d = direct-axis synchronous internal voltage
e_c = exciter ceiling voltage
e_d' = direct-axis transient internal voltage
e_{d1}' = initial direct-axis transient internal voltage
e_n = nominal exciter voltage
e_t = generator terminal voltage
e_s = exciter terminal voltage
e_{s1} = initial exciter terminal voltage
h = regulator operating time
$H(t)$ = Heaviside unit function
$H(t-h)$ = delayed Heaviside unit function, that is, the function which is zero for t less than h and unity for t greater than h
i = $\sqrt{-1}$ in the Bromwich-Wagner complex integral
p = parameter used in operational form of time-dependent functions
r_a = generator armature resistance
r_{ext} = external resistance, that is, load resistance at generator terminals
$r_t = r_a + r_{ext}$
R = nominal exciter response by American Standards Association definition
s = per unit excitation required to overcome saturation at no load, rated voltage
t = time in seconds
T_d' = short-circuit transient time constant defined by equation 6
T_{do}' = generator open-circuit transient time constant
T_s = time constant of exciter build-up
x_d = unsaturated direct-axis synchronous reactance
$x_{d1} = x_d + x_{ext}$
x_d' = direct-axis transient reactance
$x_{d1}' = x_d' + x_{ext}$
x_{ext} = external reactance, that is, load reactance at generator terminals
x_q = quadrature-axis synchronous reactance
$x_{q1} = x_q + x_{ext}$
z = complex variable parameter used in the Bromwich-Wagner complex integral

References

1. Regulation of A-C Generators with Suddenly Applied Loads, E. L. Harder, R. C. Cheek. *Electrical Engineering* (*AIEE Transactions*), volume 63, June 1944, pages 310–18.

2. A Large-Scale General-Purpose Electric Analog Computer, E. L. Harder, G. D. McCann. *AIEE Transactions*, volume 67, part I, 1948, pages 664–73.

3. Computer-Mathematical Merlin, G. D. McCann, E. L. Harder. *Westinghouse Engineer* (East Pittsburgh, Pa.), November 1948, pages 178–83.

4. Electrical Transmission and Distribution Reference Book (book). Westinghouse Electric and Manufacturing Corporation, East Pittsburgh, Pa., 1944. Chapter 7: Machine Characteristics by C. F. Wagner, pages 129–74.

Discussion

John G. Noest (Consolidated Edison Company of New York Inc., New York, N. Y.): When it becomes necessary to start a motor load from an a-c generator, where this motor load is a considerable percentage of the generator's capacity, the behavior of the generator voltage is of considerable importance.

This is so, because the starting torque and the pull-out torque of induction motors are proportional to the square of the impressed voltage. Where the starting of motor load from a generator produces a considerable voltage drop, it is important to know whether or not motors, already in operation, will pull out and in doing so further aggravate the condition.

Prior to the publication, in 1944, of part I of the present paper by Messrs. Harder and Cheek,[1] only a cumbersome step-by-step method was available for the solution of this problem.

Part I attacks the problem for the self-excited exciter case analytically and gives sets of curves, which are very helpful, where they apply. The present paper extends the investigation to the separately-excited exciter case.

Part I and II, together, form a complete treatment and the data given therein permits a ready and convenient reference for the solution of such a problem.

Since the calculation work for part I, which apparently was done manually, appears to be about equal to that required for part II, which was done on the analogue computer, I wonder if the authors can give a comparison in terms of time required or cost for the computation jobs.

Reference

1. See reference 1 of the paper.

E. C. Whitney (Westinghouse Electric Corporation, East Pittsburgh, Pa.): This paper is a real contribution to the calculation of voltage dips and points out the improvement in performance by the use of separately-excited exciters with the same nominal speed of response. In the calculations the rated voltage value of transient reactance is used which is a very satisfactory method of calculation but the users of the curves should be cautioned that this value is approximately 88 per cent of the rated current or unsaturated value X_{du}' which is commonly given out when reactance data is requested of the manufacturer. This factor may vary from about 80 to 98 per cent, but is most commonly 88 per cent, which is the value the authors used.

In the determination of e_c/e_n, the value of nominal exciter voltage of 2.4 is very satisfactory for the average turbine generator and diesel-driven machine with about 0.85 short-circuit ratio and 0.8 power factor. For water wheel generators with 1.0 or higher short-circuit ratio and power factors higher than 0.80, the ratio of 2.4 is reduced considerably and will be approximately 1.4 for a 1.50 short-circuit ratio unity power factor machine. This has the effect of increasing the drop calculated by the curves for a given reactance with the separately-excited exciter. With the self-excited exciter, performance would be improved slightly with small load increments but for large load increments, the voltage drop may be increased or decreased depending on the actual exciter ceiling and load increment. Since water wheel generators are not subject to this type of load increment as often as the other types of machines, the authors' assumption is good for the preparation of general curves.

In the use of Figure 4, the reader should be cautioned that the time constants shown are general tendencies only and a plot of actual machines will show considerable scatter. However, the curves do provide a reasonable basis of assumption for average values and thus are very useful.

G. A. Nagel (Office of the Comptroller, State of Connecticut, Hartford, Conn.): I do not know whether this is a proper question since the discussion seems to be more along the line of design, but I would like to ask the authors what their experience has been in connection with voltage control for X-ray equipment. We are having trouble due to voltage drop when using a Skinner steam engine and turbine supplying a common bus. With diagnostic equipment we

frequently lose pictures and in connection with deep therapy the condition is especially serious, as we are limited to a variation in radiation output of not over 15 per cent.

E. L. Harder, R. C. Cheek, and J. M. Clayton: The authors appreciate the additional contributions to this subject offered by Mr. Whitney. He brings up the point that the unsaturated value of transient reactance, x_{du}', is the value commonly given out as the transient reactance of water-wheel generators and salient-pole engine-driven generators when reactance data is requested of the manufacturer. For the calculation of critical cases, the user should request the manufacturer to supply the saturated or rated voltage value of transient reactance, since the curves are plotted on this basis. In all cases, however, results obtained by entering the curves with the unsaturated value will be pessimistic and hence the error will be on the safe side.

Differences in the ratio e_c/e_n may affect slightly the results obtained with a given response ratio, but the response ratio itself takes this factor into account by definition, and variations resulting from different ratios of e_c/e_n should have only a secondary effect upon the results.

With regard to Mr. Nagel's question, the curves do not take into account the effect of speed change of the prime mover, and a correction for this factor would have to be made separately in using the curves.

Mr. Noest asked for a comparison of the time required for the computation of the curves presented in this paper, as compared with the time required for the computation of the similar set of curves in the previous paper. The use of the analog computer made it possible to reduce the computation time to about one-fourth that required in the previous case, although the time required for manual calculation in this latter case would have been about equal if the Anacom had not been available.

A New Grounding and Testing Device for Metal-Clad Switchgear

H. KRIDA
ASSOCIATE AIEE

E. T. McCURRY
ASSOCIATE AIEE

THIS paper describes a new improved type of grounding and testing device for use in metal-clad switchgear of the type shown in Figure 1 in voltage ratings of 4,160 and 13,800 volts. With this device, checking and grounding functions incidental to the installation of the switchgear and operational maintenance of connected cables and other electric apparatus can be performed easily and safely.

It consists of a unit which is mechanically interchangeable with, and which uses the same vertical lift elevating mechanism as a corresponding type of power circuit breaker. The primary disconnecting contacts also are similar to those provided with the power circuit breaker, except that removable ball-type contacts are provided on the bushing studs to permit using the device in circuit breaker metal-clad compartments designed for 600-, 1,200-, or 2,000-ampere power circuit breakers.

Functional Requirements

In the course of placing into service or subsequently testing the power circuits and electric apparatus (busses, feeders, incoming and tie lines, power transformers, generators, and the like) connected to the two sides of the power circuit breaker, it is often desirable or necessary to perform functions of the following nature:

1. Check the presence or absence of voltage on either the bus or the line, preliminary to grounding or other testing operations.

2. Check either the relative phase sequence between both sides of the circuit or the actual phase sequence on each side.

3. Apply a test voltage to either the bus or to the line for the purpose of checking the insulation resistance of the circuits.

4. Connect a resistance measuring device to either the bus or line to measure the resistance of a fault on either circuit in order to determine its proximity to the station.

5. Solidly ground all the conductors on either the bus or the line to insure the safety of operating and maintenance personnel who may work on the grounded conductors.

Analysis of Design Requirements

For open-type switchgear it has generally been the accepted or common practice to make temporary and often hazardous bolted connections from the exposed conductors to the required external apparatus such as potential transformers with necessary instruments, kenetron test set, short circuiting connectors or circuit breakers, and so forth for accomplishing the necessary functions. This practice leaves much to be desired as regards safety to personnel, and ease and time of accomplishment.

Metal-clad switchgear used on voltages from 2,300 to 13,800 volts, due to its design for safety to operating personnel, and in order to confine a failure should this occur, is divided into several isolated compartments in which all of the main connections and busses are completely insulated. There are no exposed conductors accessible for making temporary connections to external apparatus as in open-type switchgear. Consequently, it is impracticable to follow the same procedure as is used with open-type switchgear and it is, therefore, necessary to provide other facilities for performing the necessary grounding and testing functions.

The stationary contacts in the metal-clad housing which are used for plugging in the ball contacts of the circuit breaker element are the points most readily available for making the necessary electrical connections. The logical approach, therefore, is to design a device which will utilize these contacts. Such a device should, in general, fulfill the following requirements:

1. The device should replace its corresponding type of power circuit breaker in the metal-clad compartment, while all of the required testing and grounding functions enumerated previously are being performed.

2. It should be designed so that all of the required functions can be performed with maximum safety to operating personnel. The device should have adequate mechanical and electrical interlocking, dead front features, and provision for remote control.

3. The device, including its external accessories, should be designed for maximum ease in operating and handling, and utilize all of the conveniences provided for handling the circuit breaker including the vertical-lift elevating mechanism in the metal-clad housing.

4. For the testing function, each of the individual bus and line conductors should be provided with a conveniently-accessible point of contact or receptacle for connecting an external source of test voltage to a recognized type of external testing device.

5. For the grounding function it should be possible to short circuit and ground either of the three bus or three line conductors. All parts should be designed to withstand full short-circuit current stresses without damage if the device should accidentally be applied to a live circuit.

6. All of the primary conductors required for the grounding function should be self-contained in the device, so that no external cable connections will be required and so that it will be possible to close and lock the door of the metal-clad compartment with the device in position.

7. The same device should be suitable for use with similar types of 600-, 1,200-, and 2,000-ampere circuit breakers.

8. The device should be capable of performing its grounding function even when control power is not available in the station. For safety reasons, it is desirable that this function be initiated from a remote point.

Paper 50-60, recommended by the AIEE Substations and Switchgear Committees and approved by the AIEE Technical Program Committee for presentation at the AIEE Winter General Meeting, New York, N. Y., January 30–February 3, 1950. Manuscript submitted November 2, 1949; made available for printing December 7, 1949.

H. KRIDA and E. T. McCURRY are both with the Switchgear Division of the General Electric Company, Philadelphia, Pa.

Figure 1. Typical installation of metal-clad switchgear equipped with vertical lift removable element magne-blast circuit breakers

Figure 3. Grounding and testing device showing view of selector switch and grounding contact through transparent barrier

Charging handle and selector switch handle in place

Past Practice

There have been previous steps in the development of devices for grounding and testing purposes, but no prior device has incorporated all of the functions in a single unit which would meet the foregoing requirements.

One design consisted of a box with metal-clad power circuit breaker bushings to the lower end of which copper bars were connected. These bars were extended to the front of the box to permit connection of the external testing or grounding apparatus. With this device, the grounding and testing functions were similar to those for open-type switchgear. It fulfilled the testing function requirements better than it did the grounding function requirements, for obviously a separate short-circuiting and grounding device, such as an external circuit breaker should preferably be used to complete the final circuit.

Since the grounding function is in many cases the important one, another design just for that purpose was evolved. It consisted of a power circuit breaker with one set of three specially-designed bushings shortened at the top and provided with a short-circuiting bar connected through a grounding shoe to the ground bus. No testing features were included in this design.

It now has been found possible to combine the functions of both of these devices into one new design, and in addition, incorporate into this new design extra features not heretofore available, making it meet substantially all of the requirements listed previously.

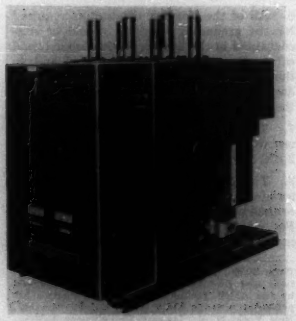

Figure 2. Grounding and testing device showing arrangement of front panel

Cover for test receptacles in place

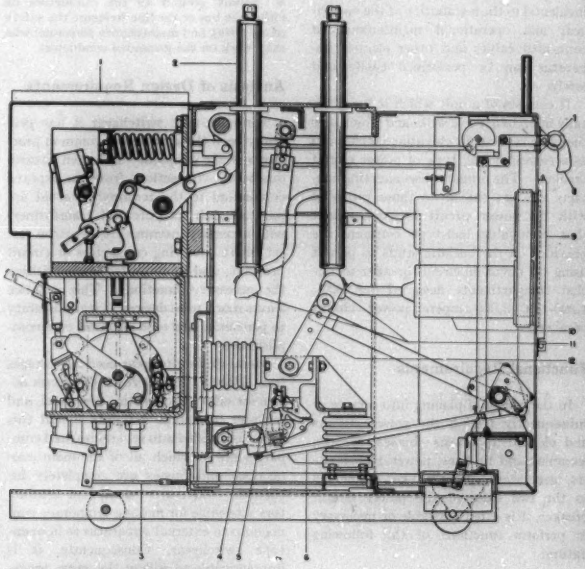

1. MANUALLY CHARGED SPRING OPERATED MECHANISM.
2. BUSHINGS WITH REMOVABLE BALL CONTACTS.
3. MANUAL RELEASE LINKAGE FOR CLOSING GROUNDING CONTACTS.
4. MOVABLE GROUNDING CONTACT BLADES.
5. STATIONARY MAIN CONTACT FINGERS FOR THREE POLE GROUNDING CONTACTS.
6. MECHANICAL CONNECTION FOR GROUNDING CONTACT INDICATOR.
7. MANUAL RELEASE LEVER FOR CLOSING GROUNDING CONTACTS.
8. REMOVABLE HANDLE OF THE CONTROL TRANSFER SWITCH.
9. REMOVABLE COVER FOR TEST RECEPTACLES.
10. TEST RECEPTACLES.
11. STATIONARY CONTACTS FOR THREE POLE DOUBLE THROW SELECTOR SWITCH.
12. CONTACT BLADE FOR THREE POLE DOUBLE THROW SELECTOR SWITCH.

Figure 4. Cross section of grounding and testing device

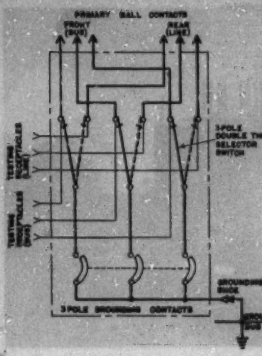

Figure 5. Power circuit diagram for grounding and testing device

Description

This new device, mounted on four wheels, two of which are swivelled, is shown in Figures 2 and 3. A cross-section is shown in Figure 4, and the primary circuit connection diagram in Figure 5. The ball contacts on top of the bushings are removable and provision is made to use 600-, 1,200-, or 2,000-ampere contacts as required by the metal-clad equipment.

Testing Functions

The testing functions are provided for by means of six receptacles on the front of the device which are connected to the six primary bushings. These receptacles provide a ready means of contacting the bus or line with voltage detectors, leads for insulation testing, or phase checking devices.

Figure 6. Grounding and testing device installed in metal-clad compartment with connections made to test receptacles by means of test plugs

Plugs

Suitably insulated plugs which fit into the receptacles on the front provide a means of connecting test cables to either the bus or line contacts as shown in Figure 6. These may be used in connection with high-voltage a-c or d-c equipment for testing the insulation of the cable or bus. The same plugs also can be used for making connections to resistance-measuring equipment to determine proximity of faults in cables or even to a testing or checking unit containing potential transformers with required secondary devices for checking voltage, phase sequence, and so forth as desired.

The plugs shown in Figure 7 are constructed so that they can be disassembled easily without the use of tools for attaching test cables to the terminals. Unscrewing the ball contact releases the stud to which is attached a bolt-type terminal for connecting the test cable. This terminal is suitable for any size wire up to Number 4 and could, if necessary, be changed readily to a larger-size terminal. The inside diameter of the insulating tube through which the test cable is taken is about two inches, and therefore will accommodate any test cable ordinarily used.

Glow Tube Voltage Detector

An electrostatic-type glow tube mounted in an insulated housing and supported on an insulated handle, commonly designated as a "hot stick" is shown in Figure 7. It has contact plugs suitably spaced to permit simultaneously contacting any two adjacent test receptacles on the grounding and testing device. One of the two contact plugs is threaded to the main support so that it can be turned to a position which will permit contacting a single conductor with one plug.

When both plugs are used, as shown in Figure 8, a means is provided for checking by voltage difference indication across corresponding phase conductors whether the relative phase sequence and the phasing of the two circuits are correct. If they are not correct, there will be a voltage difference across each of the three pairs of conductors and the tube will glow.

The single plug is used to determine the presence or absence of voltage on any conductors preliminary to grounding the circuit.

It will glow if voltage is present.

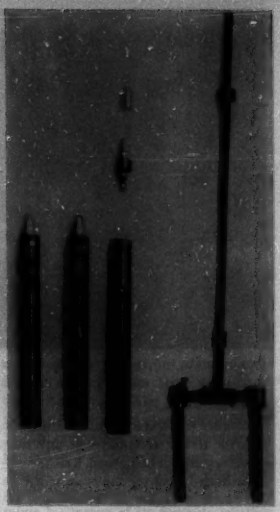

Figure 7. Test plugs for use in making connections with test receptacles

Double hot stick for use in testing for voltage and phasing on the test receptacles of the device

The usual procedure is to contact a known source of voltage with the plug to determine that the glow tube is operative preliminary to contacting the conductor which it is desired to test. If the tube fails to glow during test, the plug again is contacted with a known source of voltage to insure that the failure to glow during test was not due to tube failure.

Figure 8. Grounding and testing device installed in metal-clad compartment with hot stick in use

Figure 9 (left). Selector switch being manually operated prior to inserting the device into the metal clad compartment

Figure 10 (right). Electrical operation of the grounding and testing device with the control cable

Removable Cover

In order to prevent accidental contact with the testing receptacles at any time when they are not being used, a removable cover hinged from the top is provided, as illustrated in Figure 2. This cover, arranged for locking in position by padlock, blocks access to the receptacles except during the testing period.

Grounding Function

The grounding function is obtained with the following components of the device:

1. Manually-operated and interlocked 3-pole double-throw selector switch, using the lower end of the bushing studs for the stationary contacts.
2. Three-pole grounding contacts operated by a spring charged mechanism, with necessary electrical control and interlocking features.
3. Grounding shoe connection to ground bus inside of the metal-clad switchgear.

Three-Pole Double-Throw Selector Switch

This switch uses the lower ends of the two sets of primary bushing studs as the stationary contacts and transfers these by means of the blades to the stationary ends of the 3-pole grounding contacts.

The selector switch is manually operated by a removable handle, Figure 9, which is inserted at the side of the device. To insure that the switch contacts cannot be used to make or break the ground connection, the switch mechanism is so designed and interlocked that it cannot be operated after the device is inserted into the metal clad compartment.

This is accomplished by providing interference between the handle and stops in the metal-clad compartment so that the handle must be removed before the device can be rolled into position.

To insure that the switch is completely closed in one of the two operating positions before insertion into the metal clad compartment, the design is such that the handle cannot be removed with the switch in an intermediate position.

The position of the selector switch is indicated on the front of the device by means of a mechanically connected target reading either "bus" or "line." Transparent covers on the sides and barriers of the same material between poles (as shown in Figure 3) provide for visually checking the position of the selector switch prior to rolling the device into the metal-clad compartment.

Three-Pole Grounding Contacts and Operating Mechanism

Main and Arcing Contacts. The hinged side of these contacts connects to the grounding shoe on the device and the stationary contacts connect to the hinged contacts of the selector switch as shown in Figures 4 and 5. In closing, these contacts perform simultaneously both the grounding and short-circuiting functions.

Both main and arcing contacts are incorporated, the latter for decreasing the burning on the main contacts should they accidentally be closed on a line which has not been de-energized. The main contacts are surfaced with silver and the arcing contacts are surfaced with arc resistant material. Both sets of contacts and all other parts are designed to withstand the mechanical forces and to close and latch on the maximum available short-circuit currents associated with the rating of the equipment.

The contacts have not been designed for any interrupting duty and therefore no arc chutes are provided. In case the grounding contacts should be accidentally closed on a live line, other circuit breakers on the system must remove the fault.

The position of these contacts also is indicated on the front of the device by a mechanically-connected target reading either "open" or "closed." The transparent covers and barriers mentioned previously in connection with the selector switch also permit checking the condition and position of the grounding contacts prior to rolling the device into the metal-clad compartment.

Manually-Charged Spring-Operated Mechanism. The grounding contacts are operated by a manually-charged spring-operated mechanism. This mechanism has already been described, in a previous AIEE paper.[1] It is inherently well adapted for this application because it can be used independently of a control power source. It can be operated at any time, even when control power may not be present in the station.

The mechanism provides adequate power for closing the contacts and latching them closed against full rated momentary current corresponding to the circuit breaker rating which it replaces. An inherent feature in the mechanism is that the closing operation cannot be initiated until it has reached the fully-charged position preliminary to closing. This feature insures full power for all closing operations.

The mechanism is located at the rear of the device and must be charged before the device is inserted into the metal-clad compartment. Hence, it will supply only one closing operation after it has been inserted into position in the compartment. This arrangement is, of course, a result of available space limitation but it is not believed that from a practical stand-

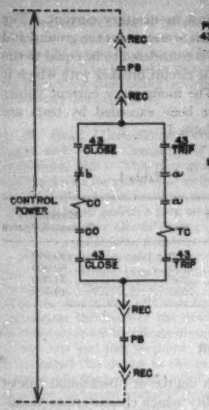

ABBREVIATIONS
PB-CONTROL PUSH BUTTON
43-TRIPPING & CLOSING CONTROL TRANSFER SWITCH
a-AUXILIARY SWITCH OPEN WHEN GROUNDING CONTACTS ARE OPEN
b-AUXILIARY SWITCH CLOSED WHEN GROUNDING CONTACTS ARE OPEN
CC-CLOSING OPERATING COIL
CO-CUT-OFF SWITCH CLOSED WHEN OPERATING MECHANISM IS FULLY CHARGED
REC-CONTROL CABLE RECEPTACLES
TC-TRIP OR OPENING COIL

Figure 11 (left). Control circuit diagram for the grounding and testing device

Figure 13 (right). Front view of 4.16 kv and 13.8 kv grounding and testing devices

point that this single-operation feature is objectionable. Grounding of a circuit is an infrequent and deliberate act, and this single-operation feature actually provides effective interlocking against accidental reclosure of the grounding contacts once they have been opened.

The mechanism can be operated to close the grounding contacts by pulling a release lever located on the front of the unit. This lever is in the shape of a ring, to which a cable or lanyard may be attached, thereby permitting its operation from some distance away from the switchgear. By this means, the same degree of safety is obtained as would be the case when operation is initiated electrically by the control push button connected to the control cable.

Electrical Control and Interlocking Features. The mechanism is provided with separate electrical release features and coils for the closing and opening operations, respectively. These coils can be wound for either a-c or d-c control power as required.

For remote electrical operation there is provided a control cable, Figure 10, with a push-button station, a plug for connecting to an electric outlet to supply the control power, and another plug for use on a receptacle in the front of the grounding and testing device for connecting to the release coils. The control connections are shown diagrammatically in Figure 11. A removable handle control transfer switch with three positions, namely, "close," "off," and "trip," and with mechanical interlocking features, determines by means of its contacts whether the remote push-button station is to perform the closing or opening operation. This feature insures that the remote operator can perform only the one operation

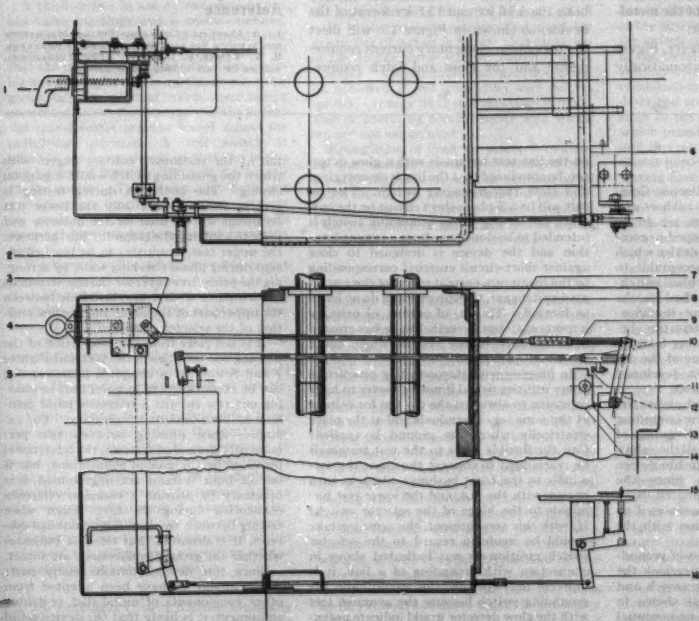

Figure 12. Interlocking scheme for the grounding and testing device

1. Control Switch Handle
2. Interlock Trip Lever
3. Interlock Cam
4. Manual Closing Lever
5. Manual Closing Linkage
6. Trip Latch Pin
7. Interlock Rod
8. Trip Interlock Rod
9. Spring
10. Interlock Coupler
11. Interlock Trip Bolt
12. Interlock Trunnion
13. Stop Bolt
14. Interlock Pawl
15. Closing Latch Release Rod
16. Manual Closing Linkage

that was intended, and cannot accidentally also perform the other. When this transfer switch is placed in the "close" or "off" positions, the mechanical interlocking through bevel gears and a stop, Figure 12, physically blocks the mechanism trip latch, so that the main contacts cannot trip free during the closing operation, and so that the mechanism will be blocked closed except when tripping is actually desired. When this transfer switch is placed in the "trip" or "off" position, mechanical interlocking is provided through the bevel gears and notched segment to prevent manual release of the mechanism to close the grounding contacts.

The handle of the transfer switch is removable only in the "off" position, and by this means any unauthorized electrical or manual closing or electrical opening of the grounding contacts can be prevented. As an added safeguard, padlock hasps are provided for the purpose of preventing unauthorized manual closing or opening operations regardless of the position of the transfer switch. When the device is padlocked to prevent manual opening of the grounding contacts, it also is locked so that the device cannot be lowered in the metal-clad compartment. Unauthorized operation also can be prevented by providing a key lock on the door of the metal-clad unit and locking the door.

Through the interlock trip lever, Figure 12, provision is made for automatically opening the grounding contacts should the device be raised into position in the metal-clad compartment with these contacts in the closed position. This same trip lever interlocks the device with the metal clad to prevent closing of the grounding contacts while the device is in an intermediate position in the metal-clad compartment.

Grounding Shoe Connection to Ground Bus

When the grounding and testing device is raised to the operating position in a unit of metal-clad switchgear, the grounding shoe which consists of a sliding contact on the device, engages a contact on the stationary structure which connects the hinged side of main grounding contacts to the ground bus in the switchgear. This eliminates the necessity for any external cable connections during the period that a circuit is grounded and permits closing the door to the compartment. Thus, there is no interference or hazard to attendants in operating the rest of the apparatus in the switchgear and station, and unauthorized or accidental removal of the grounding connection is prevented.

Tests

Tests have been made to assure that both the 4.16 kv and 13.8 kv forms of the device, as shown in Figure 13, will meet the maximum momentary current requirements and the close and latch requirements against momentary current. The required current values for the ground and test device is considered to be equal to the rating of the circuit breaker with which it is used. The momentary current values which have been exceeded by tests are shown in Table I.

Table I

Rated Voltage	Rated Mva	Momentary Current-Amperes
4.16	150	40,000
4.16	250	80,000
13.8	250	35,000
13.8	500	40,000

Conclusion

The high degree of operational safety and reliability which characterizes metal-clad switchgear has been extended to the recognized functions of circuit testing and maintenance by means of this improved grounding and testing device. Inconvenient and cumbersome makeshift methods of dubious safety need no longer be resorted to and grounding testing of circuits now can be quickly and safely affected.

Reference

1. A Manually-Operated Spring Mechanism for Medium Voltage Oilless Circuit Breakers, B. W. Wyman, E. J. Casey. *AIEE Transactions*, volume 68, part I, 1949, pages 357–63.

Discussion

O. B. Vikoren (Philadelphia Electric Company, Philadelphia, Pa.): The authors and the General Electric Company are to be congratulated on having developed a combination grounding and testing device which holds forth promise of being acceptable to the majority of users of metal-clad switchgear, either in the form described in the paper or with relatively minor modifications. The device is very interesting because it embraces important safety features which have been lacking in some of the devices which formerly have been developed for grounding and testing purposes.

The question may be raised, however, whether the designers of the new grounding and test device have taken full advantage of the opportunity to incorporate all the safety features which can be built into the device without adding extra parts. Since the human element cannot be eliminated, have they considered fully the consequences if an error is introduced in connection with the use of the device?

For example, if in the process of grounding a line, an operator should overlook the correct position of the selector switch and leave it in the bus position as shown in Figure 4, he may, by detecting no potential on the line test terminals with a glow detector, be convinced that the line is de-energized and close the grounding switch. The result will be a 3-phase short circuit on the bus. Since the closing of the grounding switch is intended to be done only from a remote location and the device is designed to close against short-circuit currents corresponding to the maximum current rating of the associated switchgear, the operator can do no harm to himself. This is, of course, of primary importance; but nevertheless he has created a disturbance to the system which could have been prevented.

In keeping with the operating practice of many utilities would it not be better to have provision to always make the test for voltage at the same set of terminals and at the place electrically where the ground is applied? Can the flexible leads to the test terminals be rearranged to connect the upper test terminals to the front bushings which in turn engage with the bus, and the lower test terminals to the hinge of the selector switch? If, with this arrangement, the same mistake should be made in regard to the selector switch position as was indicated above in connection with grounding of a line, it is unlikely that the operator would close the grounding switch because the assumed test with the glow detector would indicate potential at the stationary contact fingers with which the grounding switch would engage on closing. The confusion during testing is greatly reduced since only the lower test terminals will be used for the detector test prior to applying the ground. Furthermore, the upper test terminals can be blocked except during phase checking tests, by arranging the protective cover for the test terminals in two parts with a key interlock between the upper part of the cover and the line position of the selector switch.

It is not clear from the description of the phasing out facilities in the text and Figures 7 and 8 whether a complete phaseout test can be made, keeping in mind that in phasing out two circuits a reference point common to both circuits is necessary. For example, when phasing between two permanently grounded systems, the reference is provided by the ground connections, but if one or both systems are ungrounded, it is necessary to provide a common reference connection during the test. Even when testing between two normally grounded systems, it is essential that the test indicates whether the ground connections are intact.

Since this device contains many parts which appear to have been adopted from other components of metal-clad switching equipment, it is likely that the device could

be manufactured on a production basis, which in turn would mean that the user eventually should receive considerable benefit. This will be favorably received because the grounding and testing devices developed previously are expensive.

J. M. Graff (Consolidated Gas, Electric Light and Power Company of Baltimore, Baltimore, Md.): This new grounding and testing device for metal-clad switchgear contains many valuable features, such as means of phasing and positive grounding in case of grounding a live circuit through error, that were not available on previous devices.

The first device used on our system consists of a circuit breaker frame with six bushings. Copper straps are brought out from the lower end of these bushings to a point near the front of the device. Access to these straps is by means of separate doors to the bus and line sections. Our practice is to install this device in the compartment, make a test for potential and if no potential is shown, to fasten portable ground leads to the circuit to be grounded. For phasing, both doors are left open and our phasing device used.

The next device consists of a circuit breaker frame with only three bushings. These bushings can be moved as a unit to connect the device to either the bus or the line with an indicator in the front of the device to show the position of the bushings. A manually-operated disconnecting switch provides the grounding facilities. With this device, phasing out facilities are not available, but tests can be made for potential.

A third device in use on our system also has three bushings and a motor-operated disconnecting switch. It is equipped with three potential transformers and relays so that the motor can not close the disconnecting switch if potential is on the circuit to be grounded. In addition, three neon lamps connected across the secondary of the potential transformers provide visual means for indicating potential. A test switch is wired in the lamp circuit so that the lamps can be tested from the 125-volt d-c supply to the motor. This device also does not provide means for phasing out but tests can be made for potential. It is remotely operated by push-buttons on an extension cord.

We have purchased but have not as yet obtained one of the devices outlined in the author's paper but on future orders, we will probably request that two additional features be incorporated.

First, that an additional set of three test sockets connected to the centerpoint of the selector switch be provided so that a final check for potential can be made on the circuit to be grounded.

Second, that means be provided to charge the spring mechanism from the front of the device. On some jobs, it is necessary to remove the ground for low-voltage testing and then to restore it. With the device as described, it is necessary to remove it from the compartment, charge the closing mechanism and reinstall it in the switchgear. The two modifications just suggested should improve the safety and versatility of the grounding and testing device.

B. M. Carothers (Union Electric Company of Missouri, St. Louis, Mo.): That there is need for a grounding and testing device is well recognized by anyone who has had occasion to perform any of the various test operations or provide a substantial power circuit ground in metalclad switchgear. The various functional requirements are well set out. The design of a single unit to satisfy all these needs is an ambitious undertaking. The paper and illustrations are quite clear on all the various features.

One rather common operation will be somewhat inconvenienced due to the storage of energy for only one close-open operation of the grounding contacts. When a cable is to be swung to another circuit, or crotched, safety requires a ground at the terminus during cutting. Then, when the conductors are bared, it is necessary to apply low voltage from the station for phase identification by the splicer at the cut. When phases have been tagged, it is then necessary to re-establish a protective ground during completion of the splice. This will require that the station operator remove the device from the cell for recharging the closing mechanism after phase identification has been obtained.

As indicated in Figure 4, it is necessary that line side conductors be brought forward between bus side bushings to the front test couplers. This would appear to reduce the dielectric margin of the device as compared to the simpler box-type unit where these conductors were completely isolated. This was possible by dropping line leads down then across under those of the bus and reversed configuration of test couplers. Data is presented to indicate that momentary current capabilities are adequate. Does the same reserve in dielectric strength exist?

It is the writer's opinion that need for grounding of busses is so rare that inclusion of the double-throw selector switch is questionable. Considerable simplification could be achieved if bus grounding were not required. It may be that this feature is desirable in operating arrangements with which we are not acquainted.

Recognition of need for safety is evident in the various protective arrangements. Even so the operator must be cautious at all times due to the great number of possibilities of hazard. There is some likelihood that complexity of the device offsets a part of the safety designed into the unit.

B. I. Hayford (Westinghouse Electric Corporation, East Pittsburgh, Pa.): The authors describe a novel metal-clad accessory device which combines the functions of grounding through a power operated closing switch with phase out and testing features in the one device which is physically interchangeable with the metal-clad circuit breaker unit. Combining the functions of grounding either the bus or line with the testing functions seems to make the device unnecessarily complicated, particularly since it is not used in every day operation once the initial installation has been completed. During the installation period, while the device is in frequent use the operators will become familiar with it and proceed in a routine manner without loss of time, but when it is used infrequently, as will be the case when the station is in normal service the operator will need to take time to freshen up on the instructions to make the necessary setup.

Such operations are apt to be under emergency conditions when the system is in trouble and any lost time may be serious.

The use of the manually-charged spring mechanism is discussed in the paper. Because of its location in the rear, it must be charged before the device is placed in the housing and is then good for only one grounding operation. This feature is cited as an advantage as it automatically guards against accidental reclosure of the grounding device. However, it is not clear why accidental reclosure of the grounding device is any more of a hazard than the possibility of an accidental initial closure.

Consider the case of a cable circuit grounded for work. It may be desired to release the ground for preliminary testing and then reapply the ground to complete the job. With the method of operation described in the paper it would be necessary to remove the device from the housing to recharge the spring mechanism before the circuit could be regrounded. The 1-shot grounding feature of the manually-charged spring mechanism appears to defeat the original purpose of combining the test and grounding functions in the one device to eliminate the necessity of handling different devices in and out of the housing during the progress of checking, repairing, and testing the cable circuit. Electrical operation from the station battery would permit opening and restoring the ground as often as necessary during the progress of repairs and testing without removing the device from the housing.

The use of a double-throw selector switch to make the setup for grounding either the bus or line necessitates bringing both sides of the circuit into the same compartment at the switch contacts. Fundamental barriers in the metal-clad structure separate the bus and line compartments. In this respect the combination grounding and testing device described sacrifices the safety barriers possible in the simple device used in the past which permits complete isolation of the bus and line portions of the circuit. This isolation is particularly desirable when using the testing functions of the device for applying kenetron or similar over-potential tests to the cable circuit. This overvoltage test potential will appear in the same compartment as the exposed live bus contacts and only a few inches away at the selector switch contacts. This is an undesirable condition if not an actual hazard when it is considered that workmen will be in close proximity to the equipment during the testing procedure.

The problem of grounding and testing circuits is receiving more and more attention among both the purchasers and manufacturers of metal-clad switchgear. Devices have been built to meet various users requirements ranging from a simple 3- or 6-bushing device to some very elaborate power operated devices with complicated interlocking. The simplest is of course the 3-bushing device which merely brings the circuit live parts out into barriered compartments where they are accessible for checking and attaching ground connections in the same manner as used with previous open structures. At the other extreme, one very elaborate device consists of a motor-operated grounding switch with potential transformers, signal lights and interlocking relays which prevent closing the switch on a live

circuit. Another arrangement consists of an interposing device which placed in the housing ahead of the circuit breaker unit permits grounding through a standard circuit breaker. There is less uniformity in practice and opinion on circuit grounding than on almost any other operating requirements. Replies to committee questionnaires on switchgear practice show this. It is hoped that as this subject receives more study through Institute papers and those of operating engineer associations, that some standardization will develop to guide the users and manufacturers toward a solution of this problem which will be generally acceptable to the industry whether it may be along the lines discussed in this paper or by some other approach.

J. F. Chipman (Allis-Chalmers Manufacturing Company, Boston, Mass.): The authors should be complimented on a comprehensive description of this new grounding and testing device for metal-clad switchgear. The device appears to offer to the users of this class of equipment a much improved, safer, and more economical means of performing the various test functions necessary to efficiently install and maintain their switchgear.

While the paper leaves little to the imagination, I would like to offer the following comments.

First, would it not be desirable to have this device capable of more than a single grounding operation without racking it down and completely removing it from the cell, since in cases involving repairs, the work pattern frequently follows a sequence such as test, then ground for safety while making adjustments or repairs, then unground and test, and more often than not, reground while either taking further corrective measures or while equipment is made ready for re-energization. In case of an outage where two or more grounding operations are required, the single shot device may entail loss of valuable time for recharging. Possibly arrangement for power closure would offer a solution to this operating limitation. This would, of course, require that control power be available to operate the grounding device, but this latter could prove to be a form of insurance since it would prevent inadvertent short circuiting of a bus at a time when no control power is available to trip the bus-feeding circuit breaker or circuit breakers in the switchgear. Otherwise, to clear such a short circuit would require de-energizing external feeders which might involve an outage not restricted to the switchgear alone but including everything served by the back-up circuit breakers. Inadvertent tripping of such a grounding device as described by the authors under these circumstances could be very dangerous if the back-up protection included automatic reclosing.

It is recognized that for safety purposes the device must be provided with adequate interlocking to eliminate insofar as possible the element of human error. The paper states that with the transfer switch in the "off" position and the handle removed, unauthorized electrical opening or closing, and manual closing of the grounding device is prevented. It further indicates how the trip mechanism is blocked to prevent trip-free operation on closing and to prevent tripping unless actually desired, but it does not specify whether or not the grounding contacts can be manually tripped when the transfer switch handle is removed. If the removal of this handle is to serve every purpose, it should thereby prevent all operation with the possible exception of tripping by the vertical lift interlock. To be fully effective the trip interlock lever, which is actuated upon raising the grounding device in the gear, must be able to open the grounding contacts regardless of the position of the transfer switch, but when the grounding device is fully elevated into operating position, the trip lever of Figure 12 should be fully shielded to prevent tripping by manual actuation, deliberate or otherwise. Such provisions may exist although they are not specifically mentioned in the paper.

E. A. Bishop (Commonwealth Edison Company, Chicago, Ill.): The utility companies have accepted metal-clad switchgear for many of their switching substations. As the first units were designed for industrial use the procedures required for checking, testing, and grounding were not present in the metal-clad gear. Much thought has been given to protect the operators from gaining entrance to live parts and promoting safety by interlocks.

The utilities requirements are special because of the widespread distribution system which connects to the switching center and because of the several working divisions which are involved in the installation, operation, and repair of the switchgear or the distribution cables connected thereto. There are several procedures and requirements for safety and checking of the switchgear and cables, which most utilities require before any cables or feeders are made alive for service. Likewise, when any feeder is taken out of service for inspection, repairs, or other work there are definite safety provisions which must be followed. This also is true of the switchgear.

Some of the requirements which are necessary are set forth below:

1. Grounding of any feeder cable leaving the metal-clad switchgear.

2. Grounding of the busses for work on the switchgear.

3. Provision for applying voltage to either bus or feeder cable for phase checking, high potential testing, or cable fault location.

4. Means of checking safely either bus or feeder cable potential.

The new grounding and testing device for metal-clad switchgear fills a need which has existed since the first use of utilities of metal-clad switchgear in that it combines in one unit the facilities which formerly required the use of two separate devices. The result is one less piece of equipment to occupy valuable floor space.

The fact that the spring-operated mechanism is in the rear of the device makes it necessary to remove the device from a compartment each time it is required to close it to ground. This is particularly tedious in locations where the device must be cranked by hand to or from the operating position.

H. Krida and E. T. McCurry: The authors are very gratified with the widespread interest manifested in the new grounding and testing device. The discussions do not indicate a unanimity of opinion on some of the features of this device but are generally in agreement regarding the need for a device incorporating the functions for which it is designed.

Mr. Vikoren suggests that the upper test receptacles be connected to the bus, and the lower set to the hinge contact of the main selector switch. This change in connections could readily be made, but it is doubtful whether this slight advantage would offset some other disadvantage. If the main transfer switch were closed to the bus contacts at a time when it is desired to perform relative phase sequence checking operations, or similar test functions, the resulting indications would be misleading because both sets of test receptacles would be connected to the same electrical points. It would seem that there is less chance of confusion if all receptacles are permanently connected to known sources.

Mr. Graff suggests the addition of three separate test receptacles connected as suggested by Mr. Vikoren. This would add to the complexity of the device out of proportion to the advantage gained. Too many receptacles could become confusing to an operator and would increase rather than minimize the chances of checking the wrong conductors preliminary to closing the grounding contacts. Mr. Carothers suggests that the device is already too complicated.

Mr. Carothers and Mr. Hayford both question the omission of fundamental barriers between components of this device. The insulation between the line and bus conductors is consistent with the insulation level of the corresponding type of power circuit breaker and class of metal-clad switchgear. It is expected that any overvoltage tests applied to the cable or bus will be within these limits. In order to provide complete facilities for testing and checking phase relationship, both the bus and line must be made accessible.

Mr. Carothers states that need for grounding the bus is so rare that the main selector switch could be eliminated in the interest of simplicity. This view is evidently not shared by all users of this type of device, because the majority indicate that facilities for bus grounding are necessary.

Mr. Chipman suggests the addition of a shield over the trip interlock in order to prevent manual tripping when the device is in the raised or operating position. Provision has been made to padlock the mechanical trip to prevent accidental or unauthorized tripping of the ground contacts. If the trip mechanism were shielded in the operating position, it would be impossible to trip the ground contacts manually. Conceivably, it may be necessary to open these contacts even if no control power source was available for tripping electrically.

Mr. Bishop and several other discussion papers described the desirability of providing for more than one closing operation of the grounding contacts without the necessity of removing the device from its housing for recharging the mechanism. Charging the mechanism from the rear was considered desirable as an interlock, or added safety

feature, which would more than offset the inconvenience of removing the device from its housing for recharging in those cases where more than one grounding operation was required. An investigation will be made, however, to determine whether provision for more than one operation could be incorporated without sacrificing some safety features for this added convenience.

Mr. Vikoren brought out the fact that this device was largely made up of parts common to other equipment currently being manufactured, and therefore, it should be possible to produce it at a reasonable cost. From the start, this has been one of our objectives. This advantage, however, can be largely defeated if it becomes necessary to incorporate special features for individual users.

Cost, in a large measure, is determined by the possibility of repetitive manufacture of a single design. Conceivably, it would be possible to produce a single device incorporating all functions prescribed by several users at less cost than would be possible if some of these features were omitted when they are not required.

In designing this device, an attempt was made to incorporate the major requirements of a great many users, with their varying operating procedures. This necessarily resulted in some compromises. To us it seems that the same problems of grounding and testing would apply to all operating companies, and therefore, a single device should be capable of providing all the facilities necessary to perform the functions associated with testing, grounding, and so forth.

In those cases where a user's operating practice differs substantially from the majority, thereby requiring facilities not provided in the standard design, it will be necessary to consider a special design for that user, rather than to incorporate these features in all cases. It is hoped, however, that a single device will meet all essential requirements.

A New 69-Kv Oil-Blast Circuit Breaker

E. B. RIETZ
ASSOCIATE AIEE

C. J. BALENTINE
NONMEMBER AIEE

Synopsis: All recent circuit breaker developments in the higher voltage transmission field have included such features as faster fault clearing, faster reclosing after faults, reduced oil requirements, and reduced maintenance. This paper describes the development of an improved line of oil-blast circuit breakers incorporating these features at 69 kv. The new circuit breakers as compared with superseded designs are smaller, require less oil, have improved oil-blast interrupters, use sealed bushings without gaskets, have a simplified top frame and linkage design, and use air operators. Complete laboratory tests have been made to check the electrical and mechanical characteristics of these new circuit breakers. These tests then were supplemented by actual field tests at 66-kv interrupting staged short circuits over a wide range of currents as well as switching the capacitance current of long unloaded 66-kv lines.

TEN YEARS ago 8-cycle operating times were considered adequate for most oil circuit breakers at all voltages. Since that time, however, the advantages to be obtained from higher speed operation in the higher voltage transmission field (115 kv and above) have become widely recognized. Among these advantages are:

1. Improved system stability by faster fault clearing.

2. Reduction in damage to equipment at the point of fault.

3. Reduction in reclosing times to 20 cycles or less, thereby improving service continuity and further increasing system stability.

4. Reduction in oil requirements and tank sizes made possible by the shorter arcing times and more efficient interrupters which reduce oil carbonization.

5. Reduced contact deterioration.

To secure these advantages of higher speed operation, considerable development has taken place in the past ten years in higher voltage transmission circuit breakers (115 kv and above). In addition, the circuit breakers developed to obtain these faster operating times have included many mechanical and electrical improvements, such as completely sealed bushings, simplified operating mechanisms, greater interchangeability of parts between ratings, simplified assembly and alignment, and increased mechanical life.

A review of the advantages to be obtained from higher speed operation and the improved operating characteristics which have resulted indicate that most of these advantages are just as desirable at 66 kv and below as they are in the higher voltage field of 115 kv and above. A new 69-kv oil circuit breaker has been developed and is shown in Figure 1. The specifications set up for this new circuit breaker were:

1. General—Applicable American Standards Association, Association of Edison Illuminating Companies, and National Electrical Manufacturers Association specifications to be followed in order to meet the requirements of good practice and accepted standards.

2. Voltage—A basic insulation level of 160-kv 60-cycle withstand and 350-kv impulse-voltage withstand.

3. Interrupting Ratings—1,000-, 1,500-, 2,500-, and 3,500-megavolt-ampere interrupting ratings in accordance with new American Standards Association standards with the maximum number of interchangeable parts between ratings.

4. Continuous Current Rating—600 and 1,200 amperes with the circuit breaker to be designed for the maximum rating of 1,200 amperes.

5. Interrupting Time—Nominal 8-cycle rating, with the circuit breaker and interrupters to be designed for not more than five cycles, with appreciation of the fact that three cycles would be desirable.

6. Reclosing Time—Nominal 20-cycle rating, but as short a time as possible should be obtained.

7. Size—Minimum diameter tank consistent with required electrical performance in order to reduce volume of oil to be filtered to a minimum.

8. Maintenance Requirements—Minimum carbon generation to reduce oil maintenance. Insulation members to be designed so that they are not affected by operating conditions, that is, bushings to be sealed and other insulation material to be designed for minimum atmospheric deterioration. Internal insulation surfaces to be designed to retard carbon deposition. All parts to be designed for long mechanical life with constancy of adjustments. Parts requiring regular inspection to be designed for easy checking.

Features of the New Breaker

Development of New Dual-Flow Cross-Blast Interrupter

The interrupting ability of the original radial oil-blast contacts had been well demonstrated by laboratory tests and field operations through the years, but shorter interrupting times and improved interrupting performance required a substantial reduction in arc duration and energy. The inherent simplicity of the contact arrangement using two sequential arcs to secure the necessary oil-blast action was obvious, so the problem reduced itself to designing an interrupting structure which would give substantial reductions in the lengths of the two arcs.

Since the duration of the interrupting arc is dependent on the oil-blast action, it became necessary to provide for a more efficient utilization of the oil flow caused by the pressure generating arc. Recent developments had shown that cross-blast oil flow was more efficient than radial-blast in this respect. Therefore, an arrangement of baffles was added in the region of the interrupting arc to provide for

Paper 50-61, recommended by the AIEE Switchgear Committee and approved by the AIEE Technical Program Committee for presentation at the AIEE Winter General Meeting, New York, N. Y., January 30–February 3, 1950. Manuscript submitted August 13, 1948; made available for printing December 7, 1949.

E. B. Rietz and C. J. Balentine are both with the General Electric Company, Philadelphia, Pa.

We wish to express our appreciation to the Pennsylvania Power and Light Company for their cooperation in making available their system and facilities for this contribution to the industry, and to their engineers and operating personnel who materially assisted in the successful culmination of the field tests.

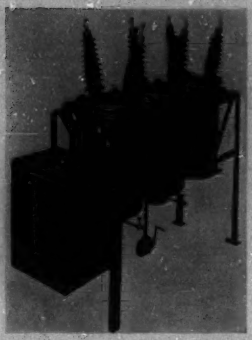

Figure 1. New 69-kv oil-blast circuit breaker, showing simplified design of top frame, solder-seal bushings, and portable tank lowering device

a movement of oil into the arc at right angles to it. Of the baffle arrangements that were tried, the most effective proved to be the dual-flow cross-blast arrangement shown schematically in Figure 2. The dual-flow converges simultaneously from both sides on the arc and sweeps the arc products out at right angles in both directions.

The pressure generated by the upper arc is a function of the current to be interrupted. This resulted in the problem of controlling the pressure generated at the higher currents. Therefore, a baffle structure was added which surrounds the pressure-generating arc and stabilizes it in a straight line between the two contacts. This limits the arc energy liberated for a given contact spacing to a minimum. It also eliminates magnetic looping of the arc which insures close duplication of pressure on each operation when interrupting the same current.

Figure 3 shows a cutaway view of the new interrupter. The upper and intermediate contacts are enclosed in a heavily walled insulation tube which is fastened readily to the metallic adapter mounted on the lower end of the bushing. This insulation-tube enclosure replaces a metallic chamber which had to be provided with external and internal insulation linings to prevent the arc striking over to it. All contacts are faced with arc-resisting material to increase their life and reduce maintenance.

The enclosing-tube assembly with the intermediate contact and the two sets of baffles can be removed from the adapter as a unit as shown in Figure 4. Four threaded studs hold it in place. After removal, all interrupter parts are visible for inspection. The contact alignment and compression are not disturbed, so it is not necessary to readjust for these points after reassembly. The moving contact rod is positively aligned by the method used to key its support into the crossbars. It can be adjusted easily to enter the chamber centrally for obtaining contact compression.

Design of Pole-Unit Structure

The best design of pole-unit structure includes a minimum of separate parts and exposed gasket surfaces. Figure 5 is a cross section through the new pole unit showing the top frame supporting the bushings, interrupters, mechanism linkage, and tank.

The improved interrupters permitted a reduction in the tank diameter from 42 inches to 36 inches. This reduced the over-all dimensions and the quantity of oil. As a result foundations can be smaller and there is less oil to handle during maintenance.

The pole-unit top frame consists of a formed-dome welded to a heavy base plate which carries the supports for the mechanism linkage and incorporates the recess for the tank gasket. On the dome are mounted the bushing supports and the standard accessories such as float-type oil gauge, fill valve, oil separator, and emergency vent. The bushing supports have a gasket arrangement which permits tilting the bushings to obtain proper alignment of the interrupters. The top frame provides a support and housing for the bushing-type current transformers. In the new circuit breaker, there are provisions for two transformers for each bushing. This makes possible additional relaying and metering transformers for special purposes. The pole-unit top frames are made up individually and are held in proper relationship to each other by being doweled to the supporting framework. They are so designed for greater ease in handling during fabrication and to

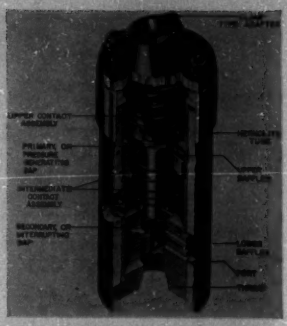

Figure 3. Cutaway view of the new dual-flow cross-blast interrupter, showing the insulation tube enclosure, contacts, the upper arc restraining baffles, and the lower oil-flow directing baffles

Figure 2. Schematic view of interruption taking place in new dual-flow cross-blast interrupter, showing the dual-flow blast action entering simultaneously on both sides of the arc and sweeping the arc products out at right angles in either direction

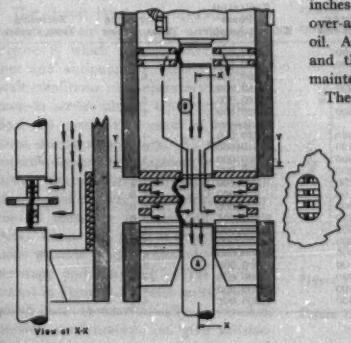

Figure 4 (right). View of interrupter after removal from adapter, showing ease of disassembly and inspection of contacts

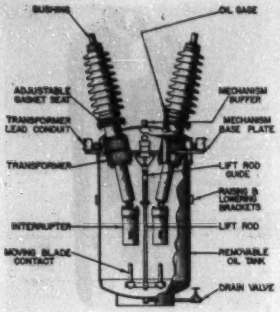

Figure 5 (left). Cross section view through a pole unit of the new 69-kv circuit breaker, showing the new solder-seal and easily adjustable bushings base-plated mounted type of linkage, provision for two current transformers per bushing, and the new interrupters in place

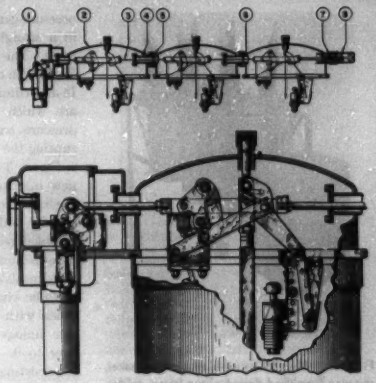

Figure 7 (right). Cutaway view of pole-unit mechanism linkage which is permanently fastened to the top frame base plate and which provides straight line contact motion. View also indicates both internal and external stop clearance settings

facilitate arrangements for single-pole reclosing which is sometimes required.

The bushings in Figure 6 are of an improved design utilizing the well-known liquid-filled type-*L* construction. The outer weatherproof porcelain shells are soldered to metal fittings at each end, thus eliminating gasketed joints. The terminal connections are silver-surfaced. The exposed insulation at the lower end of the bushing has a special coating to retard carbon deposition which also seals it against moisture absorption.

Each pole unit has its own mechanism linkage, see Figure 7, which provides straight-line contact motion and which is permanently fastened to the top-frame base plate. Reference points for adjustment are available in each pole-unit top frame, but a ready check can be made at the front crank housing without dropping the tanks. Travel recorder connections can be made on each pole unit. Interchange of gas and oil between pole units is prevented by adjustable seals through which interphase connecting rods slide.

Lightweight portable tank lifters which can be readily attached to the framework permit rapid and easy lowering of the tanks for contact inspection without removing the oil. The two tank-lifter units are self-contained, and their cables can be quickly attached to suitable lifting straps on the tank. Two-man operation is required, but this cancels the former laborious task of threading wire cables through pulley blocks and sheaves.

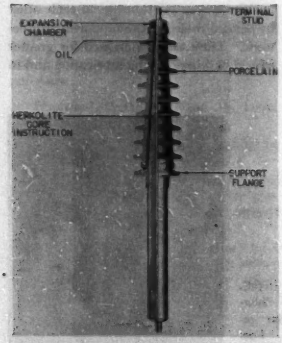

Figure 6. Cutaway view of improved design liquid filled type-L bushing, showing soldered metal to porcelain fittings and elimination of gasketed joints

Table I. Summary of Results of Siegfried Field Tests, November 1946

Type FK-439-1500 69-kv Oil-Blast Circuit Breaker

Line Dropping Tests

Test Number	Duty	Current, Amperes rms	Interrupting Time, Cycles	Length of Line Miles
1A	0*	4.2	2.4	24
1B	0	11	2.7	50
1C	0	14	3.4	70

Phase-to-Ground Fault Tests

Test Number	Duty	Arc Current, Amperes rms	Equivalent 3-Phase Kilovolt-Amperes	Interrupting Time, Cycles	Reclosing Time, Cycles
2A	O	1,400	160,000	4.6	
3A	O	2,900	330,000	3.6	
3B	CO**	2,900	330,000	4.7	
4A	O	5,600	640,000	3.7	
4B	CO+	5,600	640,000	5.0	
	2 Seconds+CO+	5,400	620,000	4.5	
	2 Seconds+CO+		No Record		
	11 Seconds+CO	5,400	620,000	4.7	
4C	O+	5,600	640,000	3.7	
	Instantaneous+CO	5,400	620,000	5.5	17
5A	O	7,300	830,000	3.2	
5A1	O	7,200	820,000	4.3	
5B	O+	7,100	810,000	4.0	
	Instantaneous+CO	6,900	790,000	6.0	21
6A	O	11,400	1,300,000	3.6	
6B	CO	11,500	1,300,000	4.5	
6C	O+	11,900	1,400,000	3.5	
	Instantaneous+CO	11,400	1,300,000	4.6	28
6D	O+	11,200	1,300,000	3.5	
	Instantaneous+CO+	11,200	1,300,000	4.6	21
	1 Minute+CO+	11,200	1,300,000	4.3	
	1 Minute +CO	11,400	1,300,000	4.1	

* O stands for Open.
** CO stands for Close-Open.

Figure 8. Right-side view of pneumatic trip-free compressed air mechanism, showing the mechanism linkage parts and compressed air-storage tanks

The new smaller circuit breaker permits shipment of a completely assembled breaker except for the lower end sections of the supporting framework which are removed to reduce the height. This makes installation easier because the circuit breaker is received with all factory adjustments and wiring completed. There is little to do in the field except locate the circuit breaker on its foundation and connect to it.

The circuit breaker is operated by a compressed-air mechanism as shown in Figure 8, which is pneumatically trip-free and antipumping when closing on fault conditions. Air operators now have been in service almost ten years and reflect the constant program of improvement during these years. All of the associated air-supply equipment is included within the weatherproof and dust-tight sheet-metal housing. Electrical and air-control units are mounted on a single panel where the front-of-board connections provide ready accessibility for observance and checking. This is illustrated in Figure 9. Heater units, some of which are thermostatically controlled, prevent condensation and give satisfactory cold weather operation down to −40 degrees Fahrenheit. High-speed reclosing of less than 20 cycles is obtained easily on all circuit breakers, and there is sufficient air storage to give at least eight circuit breaker closings without compressor operation.

Proof of Performance

Proof of performance can only be obtained by exhaustive design tests. The following tests demonstrated the adequacy of the design for protection of 69-kv backbone subtransmission systems.

1. Overvoltage tests were made at 60-cycle frequency and impulse voltages. Withstand tests were made at 60 cycles up to 10 per cent above rating or 176 kv to determine the margin of safety with the smaller tank. Impulse voltages up to 529 kv were held. Impulse flashover occurred at 625 kv.

2. Continuous current-carrying heat runs at 1,200 amperes were made indicating a comfortable margin of safety.

3. Operating tests were made to check closing, opening, and reclosing characteristics. Figures 10(A) and 10(B) show travel-time charts of actual no-load circuit breaker operations. Mechanical life tests totalling over 20,000 operations were made on both circuit breaker and mechanism parts without signs of appreciable wear.

4. Extensive laboratory interrupting tests were made on all types of duty previous to the field tests.

Field Tests

After the tests in the factory, arrangements were made to supplement them with field tests on a user's property.

These field tests were of interest because they represented, as far as known, the highest capacity 66-kv field tests ever made. The tests were made at the Siegfried Substation of the Pennsylvania Power and Light Company, which is the center of the 66-kv transmission network of that system. Short-circuit duties up to nearly 1,500 megavolt-amperes could be obtained at that location.

Figure 9. Left-side view of compressed air mechanism, showing electrical and air control units, front connected and mounted on a single panel for easy accessibility

Two series of tests were made, one on a sample circuit breaker of the proposed design for the 1,500 megavolt-ampere rating and the second on new 2,500-megavolt-ampere interrupters installed in a modernized circuit breaker. The new 69-kv circuit breaker was solidly bolted to I-beams which were in turn secured to the transformer track rails in a clear area between the 66-kv and 220-kv yards. All tests were made single-phase line-to-ground. The ground side of the circuit breaker was tied in to the overhead

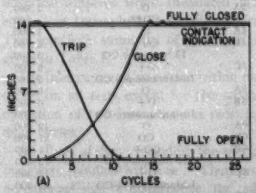

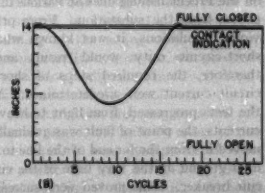

Figure 10(A). Closing and tripping curves of the new 69-kv circuit breaker, showing the high-speed operation of the air operator

Figure 10(B). Reclosing curve of the new 69-kv circuit breaker, showing a 16-cycle reclosing operation

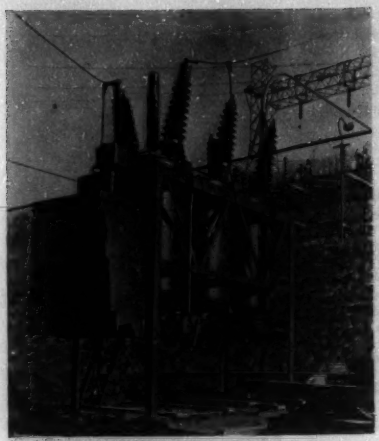

Figure 11 (left). View of the new 69-kv circuit breaker in position for a series of field tests at the Siegfried Substation of the Pennsylvania Power and Light Company

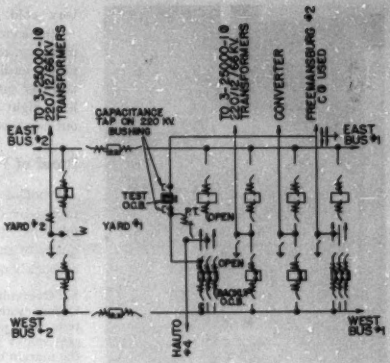

Figure 12 (right). Station bus setup for 69-kv circuit breaker field tests, showing test circuit breaker connected to Freemansburg Number 2 test line

ground wire on the 220-kv towers except at maximum capacity where the ground lead was connected directly into the station ground mat to the foot of the circuit breaker. Figure 11 shows the circuit breaker set up for test.

The breaker in which the 2,500-megavolt-ampere interrupters were installed was located in the lower 66-kv switchyard.

This circuit breaker had been modernized recently with 8-cycle oil-blast contacts, new pole-unit linkages, and an air operator. The new 2,500-megavolt-ampere interrupters replaced the 8-cycle interrupters, and very little additional work was required to prepare the circuit breaker for test. A similar arrangement of connecting the circuit breaker into the switchyard was used.

Siegfried Substation had been used on previous occasions for short-circuit tests, and the method of applying various fault duties had been worked out to give the least inconvenience and danger to the rest of the system. Faults were applied on the Freemansburg lines at various distances from the substation. From previous calculations, it was known what short-circuit duty would result and, therefore, the required steps of short-circuit current were predetermined. As the tests progressed, from light to heavy currents, the point of fault was gradually moved in from the far end of the line to a final ground at the very base of the circuit breaker. This proved very successful and involved no system or generator switching. Figure 12 shows the station bus setup for the tests.

Magnetic and cathode-ray oscillographs were used to obtain the records during the tests. The magnetic oscillographs measured the three bus voltages, fault current through the circuit breaker, voltage across the circuit breaker, circuit breaker travel, tank pressure, and trip current. A portable cathode-ray oscillograph was set up to measure the line and bus voltages on the line-switching tests and across the circuit breaker on the fault tests. Two capacitance-type 230-kv bushings were located on either side of the circuit breaker and acted as voltage dividers to give voltage indication for the oscillograph. For the tests on the 2,500-megavolt-ampere interrupters, a string of line insulators was used in place of the capacitance-type bushings.

Both the cathode-ray and the magnetic oscillographs were mounted in a truck located approximately 100 feet from the circuit breaker under test. This provided a very satisfactory portable oscillograph house. All leads running from the test location to the truck were properly shielded.

Table II. Summary of Results of Siegfried Field Tests, November 1946

69-kv 2,500-megavolt-ampere Oil-Blast Interrupters

Line-Dropping Tests

Test Number	Duty	Current, Amperes rms	Interrupting Time, Cycles	Length of Line, Miles
1A	O*	3.7	2.5	24
1B	O	5.9	2.6	50
1C	O	10.0	2.5	70

Phase-to-Ground Tests

Test Number	Duty	Arc Current, Amperes rms	Equivalent 3-Phase Kilovolt-Amperes	Interrupting Time, Cycles	Reclosing Time, Cycles
2A	O	1,340	150,000	4.3	
3A	O	2,800	320,000	4.0	
3B	CO**	2,100	240,000	5.0	
4A	O	4,900	560,000	4.1	
4B	CO+	5,100	580,000	4.5	
	15 Seconds+CO	5,100	580,000	4.6	
4C	O+	5,100	580,000	4.1	
	Instantaneous+CO	5,100	580,000	6.4	16.5
5A	O	6,200	710,000	3.6	
5B	O+	6,300	720,000	4.0	
	Instantaneous+CO	6,100	700,000	6.6	18
6A	O	12,500	1,400,000	3.8	
6B	CO	11,900	1,400,000	4.2	
6B	CO+	11,800	1,300,000	4.3	
	15 Seconds+CO	12,000	1,400,000	4.3	
6C	O+	12,300	1,400,000	3.7	
	Instantaneous+CO	12,200	1,400,000	5.6	19.5
6D	O+	12,300	1,400,000	3.7	
	Instantaneous+CO+	12,000	1,400,000	5.7	19
	1 Minute+CO+	11,200	1,300,000	4.3	
	1 Minute+CO	12 100	1,400 000	4.2	

* O stands for Open.
** CO stands for Close-Open.

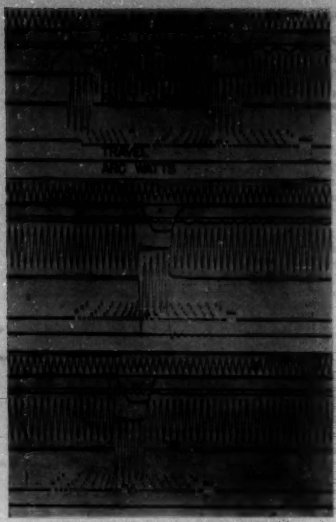

Figure 13 (top left). Oscillogram showing interrupting performance on open—instantaneous—close-open plus 1 minute close-open plus 1 minute close-open duty cycle for the 1,500-megavolt-ampere circuit breaker

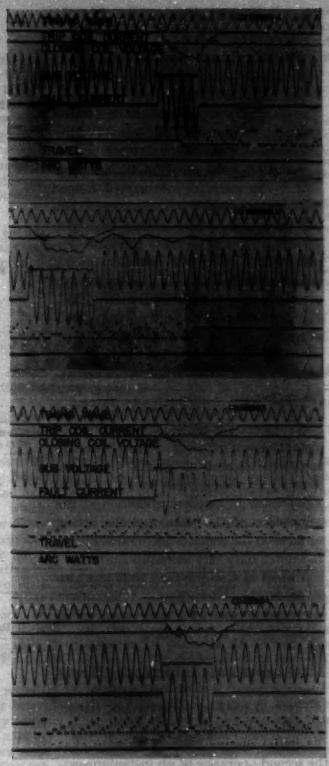

Figure 14 (lower left). Condition of the contacts on the 69-kv 1,500-megavolt-ampere circuit breaker after interrupting 21 fault currents, eight of which were at full rating. The slight burning indicates they would have been capable of many more operations without maintenance

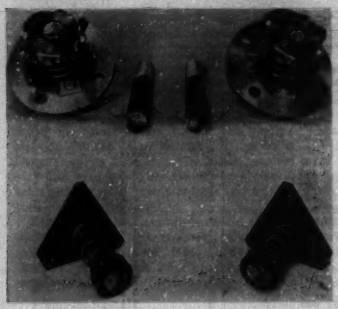

Figure 15 (right). Oscillogram showing interrupting performance on open—instantaneous—close-open plus 1 minute close-open plus 1 minute close-open duty cycle for the 2,500-megavolt-ampere interrupters

Results of Tests

New 1,500-Megavolt-Ampere Circuit Breaker

In all, 22 fault tests were made in a series, made of Open, Close-Open, Close-Open—15 Seconds—Close-Open, and Open—Instantaneous—Close-Open duty cycles. As part of the 22 interruptions, a special duty-cycle series was made which consisted of an Open—Instantaneous—Close-Open—1 Minute—Close-Open—1 Minute—Close-Open. This latter test was made at the maximum available short-circuit kilovolt-amperes of the station. Figure 13 is an oscillogram of the test.

The currents interrupted ranged from 1,400 amperes on the initial test to a value of 11,900 amperes on the final tests. This corresponds to a range of 160 to 1,400 megavolt-amperes when translated into equivalent three-phase megavolt-ampere. The complete summary of the tests is given in Table I.

The interrupting times were within five cycles on all tests except for the second operation of two instantaneous-reclosing duty cycles.

All types of duty, including the special one, were handled with ease. There was no external sign of disturbance, the only indication of circuit breaker operation being the movement of the circuit breaker position indicator.

Otherwise there was no means of telling that an operation actually had taken place.

Oil samples were taken throughout the tests, and although the oil became slightly discolored as the program progressed, the oil tests did not disclose any appreciable amount of carbon present even at the completion of the series.

Examination of the contacts, which are illustrated in Figure 14, showed some burning of the arcing surfaces. Their general condition, however, was good, and they undoubtedly could have withstood a similar additional series of tests.

A series of line-dropping tests was conducted on 24, 50, and 70 miles of line. Interruptions were prompt on all tests, the maximum time being 3.4 cycles to final clearing of the circuit. Although some restriking occurred on these tests, the maximum overvoltages in all cases were limited to less than twice the peak value of the test voltage.

New 2,500-Megavolt-Ampere Interrupters

The schedule of tests was essentially the same as that followed on the initial series. A total of 21 fault tests were made. The special Open—Instantaneous—Close-Open—1 Minute—Close-Open—1 Minute—Close-Open duty cycle was repeated. Figure 15 is an oscillogram of this operation. The currents interrupted ranged from 1,340 to 12,500 amperes corresponding to an equivalent 3-phase megavolt-amperage of 150 to 1,400 megavolt-amperes. The complete summary of results is given in Table II. This represents a coverage of from 6 to 56 per cent of rating. Together with the data from laboratory interrupting tests up to 28,000 amperes in the arc, this indicates the ability of the interrupter to handle its interrupting rating.

All interrupting times were within five cycles except for the second operation of instantaneous-reclosing tests. The interrupters cleared all faults with ease, showing no visible signs of disturbance. The oil was in excellent condition at the completion of the tests, and the arcing surfaces on the contacts pictured in Figure 16 showed only very moderate burning.

A series of line-dropping tests was also made on this interrupter. A maximum interrupting time of 2.6 cycles was needed to clear 24, 50, and 70 miles.

Final Laboratory Interrupting Tests

The field tests on both the new circuit breaker and new interrupters confirmed the initial factory tests in showing that the second operation of an instantaneous-reclosing duty cycle had slightly longer interrupting times. Further development in the laboratory after the field tests

Table III. Laboratory Interrupting Test Data

Type FK-439 69-kv Oil-Blast Circuit Breaker
1,500-megavolt-ampere Rating, 12,600 Amperes at Rated Voltage

Duty	Test Voltage,* Kilovolts	Arc Current, Amperes rms	Arc Duration, Cycles	Arc Length, Inches	Interrupting Time, Cycles
O**	66	190	3.5	4.3	5.5
		1,300	3.0	4.1	5.0
		2,200	2.5	3.9	4.5
		3,500	2.6	4.0	4.6
	44	240	4.0	5.3	6.0
		1,440	2.8	4.2	4.8
		2,800	2.4	3.5	4.4
		5,000	1.4	2.2	3.4
	22	8,500	1.1	1.6	3.1
		12,100	1.0	1.6	3.0
		18,400	1.4	2.4	3.4
O+	44	250	4.1	5.4	6.1
20 Cycles+CO†		250	4.2	5.0	6.5
		820	3.1	4.3	5.1
		970	2.9	4.2	5.2
		1,890	2.9	4.4	4.9
		2,100	2.9	4.4	5.2
		4,700	1.5	2.5	3.5
		4,300	2.6	4.0	4.9
	22	7,100	1.9	2.9	3.9
		6,900	2.5	3.5	4.8
		14,100	1.1	1.6	3.1
		9,000	1.6	2.4	3.9
	14.5	17,300	1.0	1.6	3.0
		18,300	1.7	2.5	4.0

* Test voltage across a single pole.
** O stands for Open.
† CO stands for Close-Open.

Table IV. Laboratory Interrupting Test Data

Type FK-439 69-kv Oil-Blast Circuit Breaker
2,500-megavolt-ampere Rating, 21,000 Amperes at Rated Voltage

Duty	Test Voltage,* Kilovolts	Arc Current, Amperes rms	Arc Duration, Cycles	Arc Length, Inches	Interrupting Time, Cycles
O**	66	200	3.4	4.2	5.4
		1,110	4.0	6.0	6.0
		2,600	2.8	4.0	4.8
		3,500	2.8	4.1	4.8
	44	470	4.0	5.4	6.0
		4,200	1.5	2.3	3.5
		8,800	1.3	2.3	3.3
		8,100	1.7	2.7	3.7
	22	10,300	1.3	2.1	3.3
	14.5	21,000	1.5	2.3	3.5
		28,000	1.2	2.3	3.2
O+	44	460	4.1	6.3	6.1
20 Cycles+CO†		450	3.9	4.8	6.2
		1,380	2.0	2.9	4.0
		1,540	2.4	3.5	4.7
		3,500	1.9	2.9	3.9
		3,700	2.5	3.5	4.8
	22	11,900	1.3	2.1	3.3
		8,500	2.5	3.5	4.8
	14.5	18,700	1.6	2.5	3.6
		24,500	2.2	3.5	4.5
		28,000	1.3	2.4	3.3
		23,000	0.8	1.6	3.1

* Test voltage across a single pole.
** O stands for Open.
† CO stands for Close-Open.

Figure 16. Condition of the contacts on the 69-kv 2,500-megavolt-ampere interrupters after interrupting 21 fault currents. The slight burning indicates they would have been capable of many more operations without maintenance

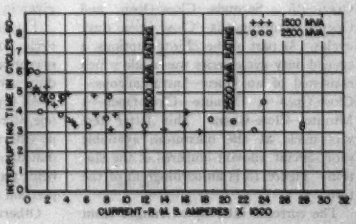

Figure 17 (right). Plot of representative laboratory tests on final 1,500- and 2,500-megavolt-ampere interrupters with voltages of 66, 44, 22 and 14.5 kv across a single pole unit. 20-cycle reclosing tests are included. 5-cycle circuit breaker performance is shown for all duty cycles

showed that the performance on the second operation of an instantaneous-reclosing duty cycle could be shortened by a simple rearrangement of the baffles in the vicinity of the interrupting arc. Tables III and IV are summaries of the interrupting test data on the final designs of the 1,500- and 2,500-megavolt-ampere circuit breakers. These data, plotted in Figure 17 for all types of duty cycles, show the improvement in performance over the original designs. It will be noted that the final circuit breaker interrupting times are less than five cycles from 25 to 100 per cent of rating and barely exceed five cycles even for very low currents.

Conclusions

1. All objectives outlined have been attained in the development of a new 69-kv oil circuit breaker, thereby providing higher speed fault clearing, higher speed reclosing, and reduced contact and oil deterioration in reduced dimensions. Also the greater interchangeability of parts simplifies stocking of maintenance parts when several ratings are required as well as simplifying changeover when system growth demands increased interrupting capacity.

2. The dependability of this new circuit breaker under all service conditions has been verified by exhaustive tests both under controlled laboratory conditions and under actual system conditions.

3. The value of field tests with the circuit breaker operating under actual service conditions in the development of dependable high capacity circuit breakers again has been demonstrated.

References

1. A New Line of High-Voltage Outdoor Tank-Type Oil Circuit Breakers, W. F. Skeats, E. B. Rietz. *Electrical Engineering (AIEE Transactions)*, volume 65, April 1946, pages 224–31.

2. Unusual Performance of Standard 230-Kv Impulse and Tank-Type Oil Circuit Breakers on Field Tests, E. B. Rietz. *AIEE Transactions*, volume 67, part I, 1948, pages 267–70.

3. A Pneumatic Mechanism for Outdoor Oil Circuit Breakers, L. J. Linde, E. B. Rietz. *Electrical Engineering (AIEE Transactions)*, volume 63, July 1944, pages 543–46.

Discussion

A. W. Hill (Westinghouse Electric Corporation, East Pittsburgh, Pa.): It might be inferred that the new 69-kv oil-blast circuit breaker described by the authors carries four ratings: 1,000, 1,500, 2,500, and 3,500 megavolt-amperes. The text is not clear as to the difference, if any, and since no test data are given for the 3,500-megavolt-ampere rating, the reader is prompted to inquire if it actually is contemplated in this particular structure and what interrupter would be used.

The familiar appearance of the interrupter shown in Figure 2 of the paper is embellished with arrows indicating the movement of the arc, gas, and oil, but, I believe, indicates a very inefficient use of oil since much of it flows off to one side without even coming close to the arc. Furthermore, if the arc is lengthened as indicated, by being pushed into the vent slots, an unnecessary rise in arc energy would result, which is contrary to usual design trends.

Figure 3 of the paper indicates a smooth bore for the contact adapter. This is an interesting departure from conventional threaded connections, offering closer adjustment, but possibly less security against misalignment.

In Figure 5 of the paper, it is apparent that the bushing-type current transformers are not entirely enclosed. Comments of the authors or users of this type of equipment would be appreciated, indicating to what extent this is found acceptable. This point is raised after recalling opinions of certain operators that enclosures are desirable protection.

The design of the bushing shown in Figure 6 of the paper seems to have changed without affecting the type designation and now includes solder-seal features which should add appreciably to its weather tightness. In the text of the paper, the authors say "the exposed insulation at the lower end of the bushing has a special coating to retard carbon deposition, which also seals it against moisture absorption." Some further discussion of this feature would be appreciated to bring out whether it is mechanical in action, like a glazed surface, or whether it repels carbon particles electrostatically.

At first glance, it appears that the records of field tests show somewhat longer interrupting time than do the laboratory tests, although that may be explained in part at least by the low voltage of laboratory tests at high current. The records do bring out rather forcibly that on instantaneous reclosure the second interruption is longer than the first, and they emphasize the justification for rating factors less than 100 per cent for this type of duty.

My experience with circuit breakers of this type and size, and interrupters of this general design which we have subjected to extensive laboratory and field tests, indicates that the authors have here a circuit breaker which will find quite general approval.

E. B. Rietz and C. J. Balentine: We recognize Mr. Hill's power circuit breaker experience and, therefore, are very appreciative of his conclusion that this new 69-kv circuit breaker will find quite general approval.

The circuit breakers described in this paper do not include the 3,500-megavolt-ampere rating. This higher rating would require a modification of the interrupter and larger diameter pole-unit tanks.

It would seem that practically all arrangements of baffles in the vicinity of an interrupting arc are intended to control the arc and at the same time to cool and deionize the arc as it is forced against the surface of the baffles by the oil movement. This design follows this pattern and, therefore, we cannot agree that there is inefficient use of the oil. Tests show the excellent results which are obtained.

The bushing current transformers are adequately protected against flashover within the tanks due to abnormal causes. For almost 20 years a similar arrangement has been used on 15- to 46-kv circuit breakers, and there seems to be no real justification for a complete enclosure to insure protection.

A New Line of Orthomagnetic Bushing-Type Current Transformers

JOHN W. FARR
ASSOCIATE AIEE

BUSHING-TYPE current transformers provide an ideal means of measuring current because they can be mounted around the high-voltage bushing in power circuit breakers and power transformers without taking up extra space and requiring installation work in the station. The space and installation details become increasingly important considerations in the higher voltage stations, where the usual "wound-type" current transformers are large and relatively expensive.

The use of the conventional bushing-type current transformer is considerably limited with respect to metering applications because the high potential winding consists of a single (1-turn) primary with consequent low accuracy, for the low line current designs. Therefore, practical means of providing compensation to improve the accuracy in these transformers will greatly broaden their field of application.

A method of accomplishing this was described by Boyajian and Camilli[1] in 1945. In their paper they presented data obtained from a laboratory sample. However, further refinements were required before the "orthomagnetic" current transformer could be placed in production and made available to the industry.

It is the purpose of this paper to present the general design and constructional details of a new and improved form of orthomagnetic current transformer for voltages as high as 230 kv and currents as low as 100 amperes, which now is suitable for manufacturing on a commercial basis and which are available to the industry.

A brief review of the basic principles is given, the features and some details of the new design are presented, together with an indication of the accuracy obtainable with 600-ampere multiratio designs.

With respect to the American Standards Association (ASA) accuracy classifications, the accuracy for metering applications ranges from an ASA-accuracy class rating of 0.6 B-0.5 on the 100-ampere tap and 0.6 B-2 on the 200- and 300-ampere taps, to an accuracy class rating of 0.3 B-2 on the 400- and 600-ampere taps. The ASA-accuracy for relaying application is 10L200, no different than for an uncompensated transformer.

This improved design makes it possible to obtain excellent accuracy when the lower tap of the bushing-type current transformer is used and also when it is necessary to design for a low primary current rating.

Current Transformer Error

The fundamental detail and mathematical solution of the current transformer circuit are well known. However, they will be briefly reviewed, in part, to clarify the operating principles and show how high accuracies have been obtained in the new "orthomagnetic" design through the effective reduction of its exciting current losses to low, substantially linear, quantities.

In the ideal or perfect transformer the ampere-turns of the primary winding and the secondary winding are identical, both as to magnitude and phase. On a 1-to-1 turn-ratio basis the secondary current would be equal to, and in phase with, the primary current and the transformer would have no error.

However, in the actual transformer a part of the primary current, which may be referred to as the "error-current" or more usually the "exciting-current," is required to supply its core losses and core magnetizing-current and there is a resultant error in the secondary current.

The phase position of the exciting-current also may result in a phase-position error, usually called "phase-angle" error, between the primary and secondary currents.

In the equivalent circuit and vector diagram of Figure 1, I_p is the primary current, I_s the secondary current and I_e is the error or exciting-current. The phase-angle error is indicated as θ.

The exciting-current quantity may be expressed in rms amperes and it is dependent on the secondary voltage (across the core), the number of secondary turns, also the dimensions and excitation characteristics of the transformer core.

The exciting-current may be resolved into two components: the in-phase or loss component; and the quadrature or magnetizing component. The loss component may, in turn, be resolved into two parts, the eddy current loss and the hysteresis loss. The exciting-current must be determined to calculate current transformer errors. Measurements for this purpose are more conveniently made from the secondary side because of the greater number of turns.

For the purpose of this paper the secondary voltage across the core, given as E in Figure 1(A), is the sum of the voltage drop across the external burden, the voltage drop in the leads and the voltage drop across the equivalent secondary impedance within the transformer. For a bushing-type current transformer the secondary leakage reactance is considered negligible and the resistance of the secondary

Paper 50-62, recommended by the AIEE Instruments and Measurements Committee and the Transformers Committee, and approved by the AIEE Technical Program Committee for presentation at the AIEE Winter General Meeting, New York, N. Y., January 30-February 3, 1950. Manuscript submitted October 31, 1949; made available for printing December 8, 1949.

JOHN W. FARR is with the Power Transformer Engineering Division of the General Electric Company, Pittsfield, Mass.

The author wishes to acknowledge the assistance given by J. E. Clem of the General Electric Company in the review of this paper.

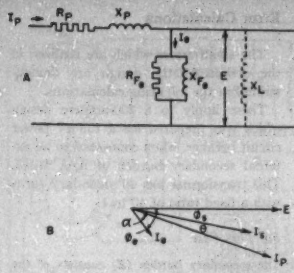

Figure 1(A). Equivalent circuit of bushing current transformer
(B). Equivalent circuit vector diagram

I_p = primary (line) amperes
I_s = secondary amperes
I_e = Transformer exciting amperes
E = voltage across core
$R_p + jX_p$ = primary circuit impedance (does not affect accuracy)
X_{Fe} and R_{Fe} = reactive and watt components of the core exciting current
X_B and R_B = reactive and watt components of the secondary burden (including leads and internal secondary circuit impedance)
X_C and X_L = capacitance and/or inductive that could be added to change exciting current power-factor (used in "orthomagnetic" design)
$\alpha = \phi_s - \phi_e$

where

ϕ_s = secondary burden power-factor angle
ϕ_e = transformer exciting current power-factor angle
θ = phase angle

winding is usually used as the equivalent internal secondary impedance.

For practical reasons the current transformer ratio error and phase-position (or phase-angle) error are considered in two steps and calculated separately. The ratio error is the arithmetical error current usually expressed in per cent of secondary current. The phase-angle error is the difference in phase position of the primary and secondary current, usually given in minutes.

With reference to Figure 1(B), the ratio and phase-angle errors are closely given by the following expressions when the power-factor of the secondary burden and of the transformer exciting-current are in the same order of magnitude. These are sufficiently accurate for the purpose of this paper.

$$\text{Per cent ratio error} = \frac{(I_e \cos \alpha)100}{I_s} \qquad (1)$$

$$\text{Phase angle (min)} = \frac{I_e \sin \alpha}{0.000291\, I_s} \qquad (2)$$

when α is small.

Irreducible Error in Conventional Bushing-Type Current Transformer

For a transformer with a fixed number of secondary turns and constant secondary burden impedance (Z)

$$E = I_s Z \qquad (3)$$

where

E and I_s = same as Figure 1
Z = total secondary burden impedance (internal and external, including leads)

and

$$B = \frac{22.5 \times 10^8 E}{fNCS} \qquad (4)$$

where

B = kilolines per square inch (in transformer core)
E = same as above
f = line frequency
N = transformer secondary turns
CS = square inch cross-section of core

When the primary (line) current varies the secondary current will vary, essentially, in a direct proportion because the secondary turns are fixed. Also, from equations 3 and 4, the voltage, E, and core density, B, will vary directly with the secondary current.

If the exciting current (I_e) varied in a linear relation (in direct proportion) to the core density and hence to the secondary current (I_s), it is evident from equations 1 and 2 that the errors would be constant. If this were the case, compensation could be provided in the form of turns adjustment to eliminate ratio error and exciting-current power-factor adjustment and to eliminate phase-angle error, (see Figure 1(A)—X_c and X_L).

However, in the conventional design, the exciting-current is a nonlinear function of the core density (see exciting-current curves Figure 2, curve A, for typical case) and, hence, it varies in a nonlinear relation to the secondary current. Then, in accordance with equations 1 and 2 the errors will be different for different values of secondary current.

The change in error cannot be corrected by usual means of compensation and is considered irreducible in the conventional design.

Bushing-type current transformers frequently contain taps to change the turn-ratio by changing the number of secondary turns so that rated secondary current can be obtained for different values of rated line current.

Assuming the secondary current, I_s, the total secondary burden impedance, Z, the line frequency, f, and the core cross-section, CS, to be constant, it is shown in equations 3 and 4 that the core density, B, will become greater as the secondary turns, N, becomes smaller.

Since the exciting-current, I_e, will increase as the core density becomes greater

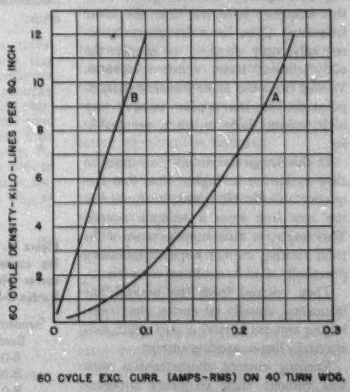

Figure 2 (right). Orthomagnetic bushing current transformer exciting current curves. For 200-ampere rating used in 138-kv power circuit breaker

(A) Without 180-cycle excitation
(B) With 180-cycle excitation

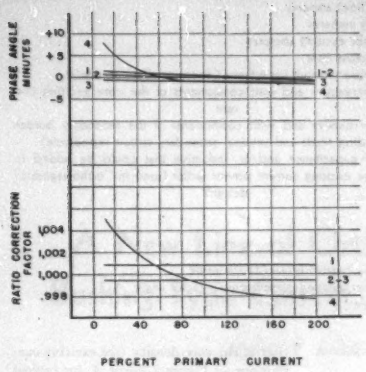

Figure 3. Orthomagnetic bushing current transformer accuracy curves with normal adjuster settings for each burden. For 200-ampere rating used in 138-kv power circuit breaker

Standard ASA Burden	Curve Number
B-0.1	1
B-0.2	2
B-0.5	3
B-2.0	4

and the number of secondary turns becomes smaller, it is obvious that the transformer errors will be greater as fewer secondary turns are used to obtain the standard secondary current of 5 amperes at the lower primary current ratings.

The error increase in the lower primary current designs makes the problem of error compensation increasingly difficult.

Orthomagnetic Design

The orthomagnetic current transformer makes use of the fact that when ferromagnetic material is simultaneously excited at more than one frequency, the higher frequency source of power will supply more than its proportional share of the total hysteresis losses and reactive volt-amperes required, in addition to the eddy current losses which it causes.

The proportion of loss supplied by the higher frequency becomes great when this frequency is several times the lower frequency. The lower frequency is, essentially, only required to supply the eddy current losses which it creates. Viewed from the lower frequency standpoint the core iron appears to have very high, substantially constant, permeability.

In this design the circuit is arranged so that excitation at higher than line frequency, usually 180 cycles, is supplied to the core iron from a separate source. This source, in turn, supplies most of the total exciting current required including practically all of its nonlinear components.

Then, viewed from the normal line frequency, usually 60 cycles, the transformer appears to have a very small, substantially linear, exciting current.

Exciting current characteristics with and without high frequency superimposed excitation are shown in Figure 2.

By reference to equations 1 and 2 the great advantage of this design in reducing errors is apparent.

1. The 60-cycle exciting current has been reduced to a low relative value, so that the ratio and phase-angle errors are small.

2. The remaining 60-cycle exciting current has been made, essentially, a linear function of density, so that the remaining error is nearly constant.

The small remaining error is further reduced by adjustment of the effective turn-ratio of the transformer, by use of a tapped autotransformer and the adjustment of the effective power-factor of the exciting-current, by use of a tapped capacitor and reactor combination. See Figures 1 and 5. Direct turn compensation cannot be used because in the usual design the change of a single turn would make too great a change in the transformer ratio to compensate for the small error.

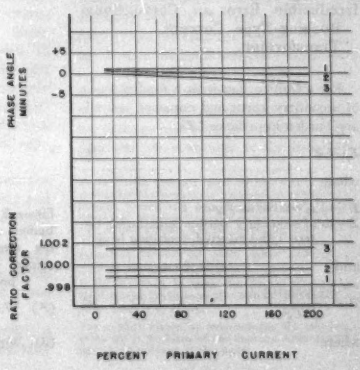

Figure 4. Orthomagnetic bushing current transformer accuracy curves with adjuster settings for burden B-0.2 and remaining fixed

Standard ASA Burden	Curve Number
B-0.1	1
B-0.2	2
B-0.5	3

Error Calculations

The small errors which are realized in the orthomagnetic design are demonstrated in the following calculations.

These apply to a 200-ampere design which was prepared for a 138-kv power circuit breaker, when connected to an external secondary burden of ASA B-0.5. This transformer has 40 secondary turns with a fixed ratio of 40 to 1.

For This Case

The secondary burden ($\mathbf{Z}$) consists of the components of ASA burden B-0.5 = (0.45 + j0.218 ohm), plus the internal winding resistance of 0.0376 ohm.

Then

$$\mathbf{Z} = (0.45 + 0.0376) + j0.218 = 0.534 \angle 24.3$$

also

$I_s = 5$ amperes at 100 per cent of rated current

$f = 60$ cycle, line frequency

$N = 40$ secondary turns

$CS = 13.1$ (square-inch cross-section of core)

and

$$E = 5 \times 0.534 = 2.670 \quad \text{(from equation 3)}$$

so that

$$B = \frac{22.5 \times 10^8 \times 2.670}{60 \times 40 \times 13.1} = 1.912 \quad \text{(at 100 per cent rated current)}$$

From the exciting-current curve, Figure 2(B), which applies to this case: 1.912 kilolines per square inch density corresponds to an exciting-current

$I_e = 0.01562$ ampere

The power-factor angle of the exciting current (ϕ_e) is assumed to be made equal to the

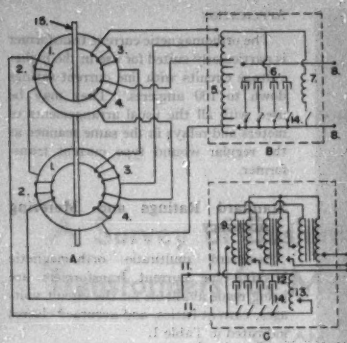

Figure 5. Orthomagnetic bushing current transformer schematic circuit diagram

(A). Bushing current transformer
(B). Adjuster unit
(C). Frequency converter

1. Bushing current transformer core (in two equal parts)
2. Exciting winding (180 cycles, 120 volts)
3. Test winding (60 cycles, 5 amperes)
4. Secondary winding (60 cycles, 5 amperes)
5. Autotransformer (ratio setting)
6. Phase angle capacitor for phase angle setting
7. Phase angle reactor for phase angle setting
8. Secondary terminals (60 cycles, 5 amperes)
9. (3) transformers (Y-broken delta)
10. Input terminals (3-phase, 60-cycle, 120/208Y)
11. Output terminals (1-phase, 180-cycles, 120 volts)
12. 180-cycle load power-factor adjustment
13. 180-cycle loading adjustment
14. Selector switches
15. Primary circuit

power-factor angle of the burden current (ϕ_2) so that

$$\phi_2 = \phi_4$$

and from Figure 1 the difference angle

$$\alpha = \phi_2 - \phi_4 = 0$$

Then from equation 1

$$\text{Per cent ratio error} = \frac{0.01562 \times 1 \times 100}{5} = 0.3125$$

Since the exciting-current curve is essentially a straight line (linear) the same ratio error will exist over the range from 5 per cent to 200 per cent rated current or more. It can be reduced to a value close to zero by the tapped autotransformer, see Figure 5.

If it were required to calculate the phase-angle error it would be necessary to know the power-factor angle of the exciting-current, ϕ_2, as well as the power-factor angle of the secondary burden current, ϕ_4, so that the difference angle, α, could be determined, see Figure 1, and used in equation 2. However, the difference angle may be made closely equal to zero by means of the exciting-current power-factor adjustment, see Figures 1 and 5, so that the resultant phase-angle is essentially zero.

For cases with higher ohm burdens with the resulting higher secondary voltage drop, E, and higher core density, B, the higher range of exciting-current, I_e, may not be entirely linear and the results are not quite as good.

Measured Accuracy

Figure 3 shows typical accuracy curves at the standard ASA metering burdens taken from actual tests on the same transformer design used in the foregoing calculations. The difference between the calculated and measured errors is too small to be significant.

Figure 4 shows the variation in accuracy on this transformer when the burden is changed from B-0.2 to B-0.1 and to B-0.5 without resetting the adjustment.

General Operating Characteristics

Effect of Variation in High-Frequency Exciting Voltage

Tests show that the transformer accuracy is not critical with respect to the high-frequency 180-cycle excitation. Variations of ±10 per cent in the 180-cycle exciting voltage does not noticeably affect the accuracy. This corresponds to a variation of approximately ±5 per cent in the 3-phase 60-cycle voltage supplied to the frequency converter and used to obtain the 180-cycle power source.

Self-demagnetization

The high-frequency 180-cycle excitation serves the further purpose of keeping the transformer core essentially demagnetized. The metering accuracy will not be affected by residual magnetism from surge currents.

Effect of High-Frequency Excitation on Relay Operation and Accuracy

The orthomagnetic bushing current transformer will have, essentially, the same relay accuracy class as a conventional transformer of the same size and rating. Relay accuracy is largely a function of the saturating characteristics of the current transformer core. The high-frequency excitation has little effect on this since the core density, B_1, caused by the rated line frequency adds to the density, B_2, caused by the higher frequency to give a resultant density, B_{res}, as follows

$$B_{res} = \sqrt{B_1^2 + B_2^2} \qquad (3)$$

where

B_{res} = resultant density
B_1 = 60-cycle density
B_2 = 180-cycle density

then if

$B_1 = 100$ (assumed start of 60-cycle saturation)

$B_2 = 35$ (180-cycle density used)

$B_{res} = \sqrt{100^2 + 35^2} = 106$

It is seen that the high-frequency excitation has only increased the effective density from 100 to 106 kilolines (6 per cent).

If, for any reason, high-frequency excitation is lost the accuracy is reduced to that of a conventional bushing current transformer and the operation of protective relays (when used) is not greatly affected.

Effect of High Frequency Excitation on Temperature Rise

The core loss resulting from the high-frequency excitation will cause some additional temperature rise in the current transformer. For the usual design, the temperature rise will amount to approximately 5 degrees centigrade when the transformer is mounted in oil or 25 degrees centigrade when it is mounted in air.

Construction

The complete orthomagnetic bushing current transformer consists of the transformer itself and the compensating equipment. This equipment uses a frequency converter (or tripler) to supply the high-frequency excitation to the current transformer cores and an Adjuster Unit to set the current transformer ratio and phase angle to unity and zero respectively. A cabinet is provided in which the compensating equipment is mounted.

Figure 6 shows the arrangement of the compensating equipment in an early model. A schematic circuit diagram is shown in Figure 5.

The circuit components are described in subsequent paragraphs.

Current Transformer

The current transformer is constructed in the same general manner and has the same size as a comparable conventional bushing current transformer. The core is divided in two symmetrical parts, Figure

5, with a half of the high-frequency winding wound, in opposition, on each part and connected in series. Each half of the high-frequency winding induces an equal and opposite voltage in the low-frequency windings where they cancel. This arrangement neutralizes the mutual coupling so that there is no transfer of energy between the high-frequency exciting circuit and the low (normal) frequency secondary circuit.

The secondary winding and test winding have the same number of turns and are wound around both parts of the core in the same direction. The test winding gives a true representation of the high-voltage line current and makes it possible to test the transformer on a 1-to-1 ratio basis. It is unnecessary to use a "standard" in making accuracy tests since the secondary current can be compared directly with the primary or test-winding current.

The transformers can be made multiratio by bringing out taps in the same manner as in the conventional design. They can be assembled around bushings in power circuit breakers and power transformers in the usual manner.

Frequency Converter

The frequency converter unit consists of three small 2-winding transformers with their primary (input) windings connected in Y and their secondary (output) windings connected in broken-delta. The transformer cores are operated at a suitable flux density to generate the desired value of third harmonic energy which is taken from the delta circuit to excite the current transformer cores.

The transformer windings are provided with taps which, together with a loading rheostat and tapped capacitor, are used for the high-frequency load power-factor and voltage adjustment.

This converter contains no moving parts such as rotors or commutators and is free from mechanical wear.

The converter components are mounted on a panel and provided with selector switches for adjustment. A single converter unit will supply sufficient energy to excite a complete 3-phase bank of current transformers.

Adjuster Unit

The adjuster unit consists of a tapped autotransformer for ratio adjustment and a tapped capacitor and reactor for phase angle adjustment. These components are mounted on a panel and provided with selector switches.

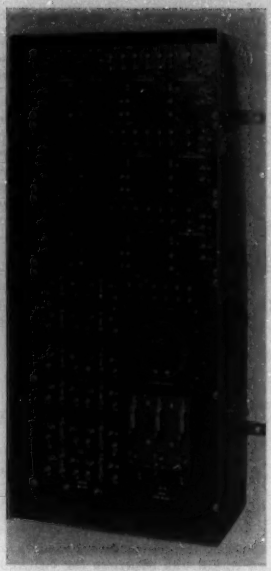

Figure 6. Compensating equipment for orthomagnetic bushing current transformer

Three adjuster panels in upper part, one frequency converter panel in lower part

Table I

Circuit Voltage	Maximum Primary Amperes
115 kv	600
138 kv	600
161 kv	600
230 kv	600

Tap Ratios, Amperes	Metering Accuracy Classes
100 to 5	0.6 B0.1, 0.6 B0.2, 0.6 B0.5
200 to 5	0.3 B0.1, 0.3 B0.2, 0.3 B0.5, 0.6B2
300 to 5	0.3 B0.1, 0.3 B0.2, 0.3 B0.5, 0.6B2
400 to 5	0.3 B0.1, 0.3 B0.2, 0.3 B0.5, 0.3B2
600 to 5	0.3 B0.1, 0.3 B0.2, 0.3 B0.5, 0.3B2

Cabinet

In the standard set of equipment a steel outdoor cabinet is provided with mounting space for one frequency converter unit and three adjuster units. This set of components will supply compensation for a bank of three current transformers.

Application

The orthomagnetic current transformer is particularly suited for use in the higher voltage circuits with line current ratings down to 100 amperes. They may be used with all the usual arrangements of meters and relays in the same manner as the regular wound type current transformer.

Standard Ratings and Metering Accuracy

Standard multiratio orthomagnetic bushing-type current transformers are being made available for the circuit voltages, current ratios, and accuracy classes indicated in Table I.

Relay Accuracy

These transformers will have a minimum relay accuracy of (ASA) 10L200 on the full winding (600-5 ampere tap).

Typical Input Power Requirements

Typical input power requirements for compensating equipment for bank of 3 138-kv bushing current transformers:

Input from supply circuit is 1.5 kva at 28 per cent power factor (420 watts) 3 phase, 60 cycles, 120/208Y.

Output to excite bushing current transformers cores is 250 volt-amperes at 80 per cent power factor (200 watts) 1 phase, 180 cycle, 120 volts.

Summary

The development of this new line of orthomagnetic bushing-type current transformers makes it possible to obtain the higher classes of metering accuracy, in the lower range of line current ratings, in high-voltage systems. At the same time it is possible to retain the advantage of minimum space, easy installation, dependable operation, and much of the economy of the usual bushing-type current transformer.

The multiratio feature incorporated in the design of these transformers will materially facilitate their application on circuits where load conditions may change.

References

1. Orthomagnetic Bushing Current Transformer for Metering, A. Boyajian, G. Camilli. *Electrical Engineering (AIEE Transactions)*, volume 64, March 1945, pages 137–40.

2. Electric Induction Apparatus, A. Boyajian, G. Camilli. United States Patent 2,467,807, April 10, 1949.

No Discussion

A Survey of Bushing-Type Current Transformers for Metering Purposes

G. CAMILLI
FELLOW AIEE

Synopsis: The great simplicity, reliability, and low cost of bushing-type current transformer has led inventors to devise various schemes to improve its accuracy to metering standards. This paper reviews these schemes, culminating in the orthomagnetic device described in detail in a paper by J. W. Farr.[10]

INVENTORS in the instrument transformer field have been intrigued for many years by the bushing-type current transformer, as may be gathered from the 160-item current transformer bibliography given at the end of this paper. The bushing-type current transformer is a device with exceptional simplicity, convenience, reliability, adaptability to the highest voltages (present and future) and economy, and yet it has been disappointing in not being so adaptable to the smaller line currents. For line currents under 1,000 amperes, its accuracy diminishes with diminishing current. The story of the development of this type of a current transformer is therefore that of attempts at improving its accuracy to make it suitable for metering at the smaller line currents.

Impressing voltage on a transformer brings into play an exciting current, and drawing current from the transformer brings into play an impedance voltage. In a current transformer, the impedance voltage may be ignored, but not the exciting current because it affects the current ratio. Operating at a reasonable flux density, a transformer requires a certain number of ampere-turns, so that the more the turns the less the current will be. As the bushing-type current transformer, built around the bushing conductor as its primary, has only one turn its exciting current has to be larger than that of units with many turns. If this were the only problem, the challenge of the bushing current transformer would not have been half as difficult as it actually has been.

The exciting current varies nonlinearly with the load and thus resists simple corrective measures such as compensation by modification of turn ratio.

The object of this paper is to review briefly the various schemes that have been proposed or used to overcome these difficulties. While most of these schemes are applicable to both the wound-type and the bushing-type current transformers, emphasis will be placed on the latter.

Analysis of the Problem

Before discussing the several different arrangements that have been used for increasing the accuracy of current transformers in general, and of bushing-type current transformers in particular, it is worthwhile reviewing the nature of the problem involved in this discussion. All current transformer performance characteristics are given by curves of ratio and phase angle since these vary in value as the primary current varies from full load to fractional loads. It may be appreciated on reflection that the magnitude of a ratio correction factor would be of little or no consequence if it were constant from full load to, say, 10 per cent of full load, since any multiplier would be easily applied to a watthour meter reading. But, if the correction factor is not the same at all loads, doubt can arise as to what multiplying factor is to be applied to the monthly total of the watthour meter.

The case of phase angle also is troublesome because even if the angle of phase shift were constant, the ultimate correction would differ for different power factors, and power factors are normally different at different loads.

The problem, therefore, is to make the ratio error at least constant (if not smaller) and the phase angle smaller (if not constant). The ratio and phase angle vary with load because the exciting current is not proportional to the load. If they were constant the current transformer would have a single ratio correction and single-phase angle correction at all currents.

Since current transformers are operated at low densities the deviation of the excitation curve from a straight line is not due to saturation but by just the opposite, that is, the increase in permeability with increasing density around the lower bend of the magnetization curve, see Figure 1.

The results of this nonlinearity are almost as objectionable as those of saturation with the difference that the errors are larger at the smaller loads instead of at the higher loads.

In the final analysis, however, the errors of a current transformer are dependent

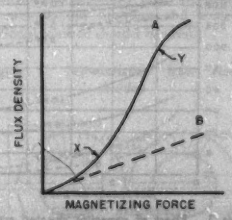

Figure 1. Characteristic shape of magnetization curve for iron

X—Region of increasing permeability
Y—Threshold of saturation

Paper 50-63, recommended by the AIEE Instruments and Measurements, and Transformers Committees and approved by the AIEE Technical Program Committee for presentation at the AIEE Winter General Meeting, New York, N. Y., January 30-February 3, 1950. Manuscript submitted October 31, 1949; made available for printing December 2, 1949.

G. Camilli is with the General Electric Company, Pittsfield, Mass.

The author wishes to express his appreciation for the assistance given him by W. F. Dripps and J. R. Harvey.

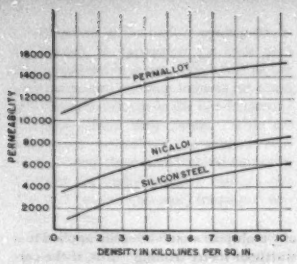

Figure 2. Permeability of core materials at low flux density

upon the phase angle and magnitude of its exciting current, and the smaller this current the smaller are the resultant errors.

Corrective Schemes

Various schemes proposed for improving the accuracy of current transformers can be grouped under the following classifications:

1. Direct reduction of the exciting current I_0.

2. Two-stage transformation. Without modification of the exciting current I_0, an attempt is made to modify the secondary current by a quantity equal to the exciting current.

3. Rotation of the exciting current vector. The phase angle is reduced by producing a rotation of the exciting current I_0 and subsequently the ratio error is modified by other schemes.

4. Straightening the exciting current curve.

5. Straightening of the exciting curve and simultaneous reduction of the exciting current.

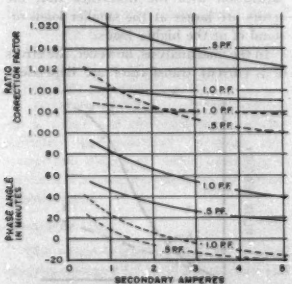

Figure 3. Effect of capacitor shunted across tertiary winding and of burden power factor

Solid lines: No compensation
Dashed lines: Capacitor across tertiary winding

Direct Reduction of the Exciting Current

A reduction of the exciting current can be accomplished by an increase in core weight as well as in the number of primary turns. The latter corrective measure, of course, does not apply to bushing-type current transformers where the primary ampere-turns equal the primary current. To produce a high-voltage current transformer with negligible errors, using ordinary silicon steel, the core would have to be increased to prohibitive dimensions.

Current transformers are operated at very low flux densities (100 to 5,000 lines per square inch) and, therefore, in order to reduce I_0 a material is desired which has low losses and high permeability at low inductions. Such materials are now available[47] and are known in the trade under such names as Nicaloi, Hypernik, Permalloy, and Mumetal. These nickel-iron alloys, especially the permalloys (78.5 per cent nickel, 21.5 per cent iron), have several times the permeability of the silicon steels (see Figure 2) and would be very useful in the construction of bushing-type current transformers except for some disadvantages which limit their use to special applications only.

The good qualities of these alloys depend on the purity of their ingredients and to a larger extent on the accuracy of manufacture. The cost of these materials is several times that of ordinary steel; their saturation densities are low and they have very poor resistance to mechanical shocks.

Mumetal (77 per cent nickel, 5 per cent copper, 16 per cent iron, 2 per cent manganese) is less sensitive to mechanical stresses and shocks than Permalloy. With such materials it is possible to obtain bushing-type current transformers having fairly good accuracy at a rated primary current 500 amperes and higher. For lower currents more complicated additional schemes must be used.

For the purpose of reducing the wattless component of the exciting current, the current transformer could be loaded with an additional capacitive burden.[121, 32, 49] For this purpose it would be sufficient to add a capacitor in parallel with the normal burden. An extremely large capacitor would be required to produce an appreciable effect because the voltage across the secondary of the current transformer is normally only a few volts. This difficulty can be overcome by providing the transformer with a tertiary winding with many turns to which is connected a relatively small size capacitor. For a constant useful burden, and a

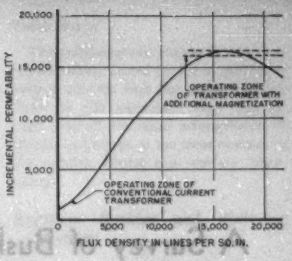

Figure 4. Incremental permeability of silicon steel

fixed primary current, the compensation of the wattless component of the exciting current can be complete. In general, by this scheme, it is possible to obtain similar errors at a primary current of 600 amperes as would be obtained at 1,000 amperes without the use of the capacitor (see Figure 3). This scheme has a very important drawback. Under overloads or during an accidental open-circuit condition the voltage induced in the tertiary winding will be extremely high which may result in the failure of the capacitor. This failure may or may not be detected. The capacitor could be protected by a gap but this is added complication. This type of compensation has received very little or no support by the industry.

Bushing-Type Current Transformers with Supplemental Constant Excitation at Normal Frequency

As has been stated before, current transformers, in general, are operated at very low alternating flux densities so as to reduce their exciting current, but a benefit proportional to the reduction in density is not realized because at such low densities the permeability of the core also is greatly reduced.

Referring to Figure 4 it will be seen that the permeability (incremental or instantaneous permeability) of a representative sample varies 10-to-1 in the range of

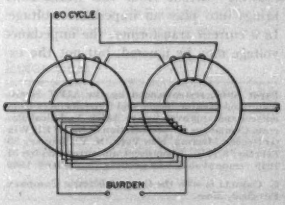

Figure 5. Auxiliary excitation scheme of Illovici

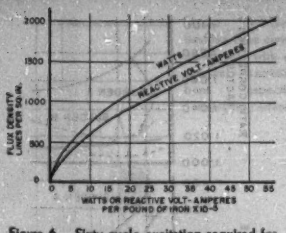

Figure 6. Sixty-cycle excitation required for silicon steel which is pre-excited at 60 cycles to 10 kilolines per square inch

densities from 0 to 16 kilolines per square inch.

Although the 60-cycle component of the exciting current is not a direct function of this permeability but a complicated function of the curve of permeability for the range of the a-c flux density, yet the incremental permeability is used here as a convenient magnifying lens or index.

A bushing-type current transformer is likely to operate at 500 lines per square inch, a zone in which the permeability is one-sixteenth of that at 16 kilolines per square inch. If a current transformer could be operated with a low alternating flux density (say, 500 lines per square inch as before) but at the highest permeability of iron, then some real benefit could be gained.

Figure 7. Characteristics of transformer of Figure 5 with constant voltage excitation for different line power factors

Connection: 200 amperes
Burden: 60 volt-amperes at 1.0 power factor
Differential excitation: 70 volts

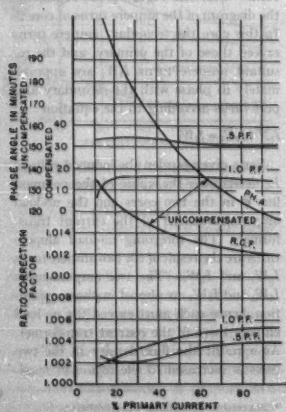

Ilovici[35,36,37] accomplished this by magnetizing the core to maximum permeability by an independent source of power.

In its simplest construction the core is split up into equal parts, half of the turns of the auxiliary exciting winding are wound around the first core part, the other half is wired in opposite direction around the second core part. The secondary winding is wired around the total core in the usual manner (see Figure 5). With this arrangement the mutual inductance between the auxiliary circuit and the other windings is eliminated.

The scheme requires a source of constant voltage. One of the advantages of the scheme is the facility with which the performance characteristics of the current transformer can be predetermined. This can be simply done with the help of data as shown in Figure 6. The disadvantages of the scheme are:

1. When the auxiliary voltage is obtained from the same power circuit to which the current transformer is connected, the performance of the current transformer is dependent upon the power factor of the load to be measured.

2. The performance of the current transformer is influenced by the voltage variations in the supplemental excitation.

The change in the characteristics brought about by the changes in the power factor of the circuit to which current transformer is connected, can be seen from the curves of Figure 7.

That the performance of this type of current transformer is affected by the variations in the voltage applied to the auxiliary exciting winding, can be seen from Figure 8.

Self-Excited Current Transformers

The excitation necessary to improve the accuracy of bushing-type current transformers can be provided by the following three methods:

Self-Excitation Through a Tertiary Winding Connected Across an Auxiliary Burden

This scheme is shown in Figure 9.

The core is divided in two equal portions; auxiliary windings are wound on each core section and are connected as shown in the diagram with the two free terminals connected across an auxiliary burden.

With this scheme good accuracy can be obtained for any one value of secondary current but not throughout the ordinary range of secondary currents, see Figure 10.

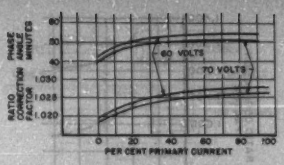

Figure 8. Effect of differential excitation voltage on transformer of Figure 5

Burden: 6.0 volt-amperes at 1.0 power factor
Load condition: 1.0 power factor
Connection: 100 amperes

Auxiliary Excitation Can be Obtained from an Auxiliary Core as Shown in Figure 11

The main core[14] is split into two portions, each portion being magnetized in the opposite direction by a winding energized from an auxiliary core.

The two portions of the core being magnetized in the opposite sense there is no resultant effect on the secondary winding if the two portions are equal, as the induced electromotive forces in any winding which embraces both portions will cancel out. Actually, however, it is sometimes convenient to arrange for the two portions to be slightly unequal as this then has the same effect as keeping proportions equal and retaining the ratio compensation by some of the secondary turns embracing the auxiliary core.

By this scheme the phase angle can be reduced to roughly one-half of the figures normally obtained by the use of silicon steel cores, Figure 12. Furthermore, the phase relationship which exists between the cross flux and the main flux is such that an improvement can be obtained when the secondary burden becomes reactive. This automatically compensates for the greater ratio error which otherwise exists when the burden becomes reactive.

From the test results shown in Figure 12 it is evident that while this scheme is beneficial it does not give the complete answer to our problem and some additional method should be used.

Figure 9. Self-excitation from auxiliary burden

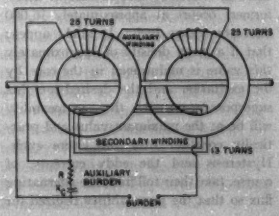

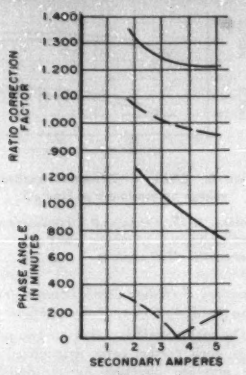

Figure 10. Characteristics of scheme of Figure 9

69-kv bushing-type current transformer
Primary amperes: 65
Burden: 16 volt-amperes at 1.0 power factor
Auxiliary burden: $R=0.040$ ohms
$X_c=14.75$ ohms
Solid line: no additional excitation
Dashed line: excitation from auxiliary burden

Excitation by Charging Current

Bushing-type current transformers can be improved by separate excitation with a current substantially in quadrature with the normal working current. The latter can be furnished by a capacitor-type bushing as shown in Figure 13.

Calculations and test results show that with certain limitations the scheme is feasible. Small changes in the phase of the compensating current do not seriously affect the phase angle and ratio but a large change greatly alters the characteristics. A change of burden entirely changes the amount of compensation required.

The Effect of D-C Excitation of the Core on the Characteristics of a Current Transformer

From Figure 4 it will be seen that the maximum incremental permeability of the iron ordinarily used in current transformers occurs at approximately 16,000 lines per square inch. It might appear that if a mean density of approximately this value is maintained in the core by d-c excitation and the desired a-c flux superposed on it, the permeability will be at the maximum value and practically constant over the entire cycle. Hysteresis and the eddy currents, of course, take their toll from the alternating flux so that the permeability realized for the alternating flux will not be as good as judged by a d-c magnetization curve, but still it may be expected that the permeability in the zone of high flux density would be far better than at the beginning of the saturation curve. If no further provision is made other than direct current, however, the hysteresis loss will be higher at the higher mean density than at the original, the eddy currents remaining unchanged. In general, the a-c excitation for a given alternating flux density is increased by superposed d-c excitation.[107] Thus, Figure 14 gives the core loss and exciting current obtained on annular ribbon wound core, while Figure 15 gives the results obtained on a current transformer when it was tested with and without additional d-c excitation.

The A.E.G.* Transformer[99,109,110]

Instead of using an auxiliary core to furnish a current for the premagnetization of the working core of the current transformer, the auxiliary magnetizing current can be derived directly from the secondary current of the current transformer, Figure 16(A).

The flux in each core is due to the result of the primary and secondary ampere turns. By the proper selection of the direction of winding and of the number of turns of the auxiliary windings in core 1, the ampere turns of the primary can be made to exceed those of the secondary, while in core 2 the secondary ampere turns can be made to exceed those of the primary. In other words, for core 1

$$NI_1=(N_s-M_2)I_2$$

and for core 2:

$$NI_1=(N_s+M_2)I_2$$

The connections shown in Figure 16(B) are equivalent to those of Figure 16(A), in which

$$N_s-M_2=N_1$$

$$N_s+M_2=N_2$$

Figure 17(A) shows the vector diagram of the ampere turns of a normal current transformer. Figure 17(B) shows the diagram of the ampere turns of core 1 of our premagnetized current transformer.

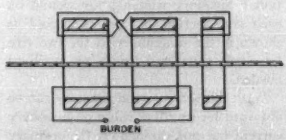

Figure 11. Additional excitation from auxiliary core

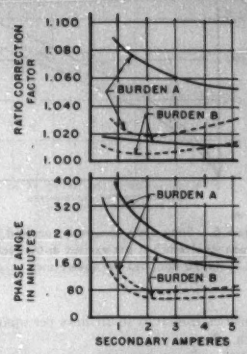

Figure 12. Characteristics obtained by excitation from auxiliary core

Main cores: 16 inches inside diameter by 21 inches outside diameter by $3^1/_8$ inches
Auxiliary core: 16 inches inside diameter by 21 inches outside diameter by $1^1/_4$ inches
Connection: 1-turn primary
40-turn secondary
4 compensating turns on each core
Burden A: 19 volt-amperes at 0.89 power factor
Burden B: 6 volt-amperes at 1.0 power factor
Solid lines: uncompensated
Dashed lines: compensated

In this core the primary ampere turns exceed those of the secondary, and the resultant ampere turns I_1W_1 are

$$I_1N+I_2N_1=I_1W_1$$

It should be noted that the resultant ampere turns in this core are approximately in phase with the primary ampere turns. Likewise Figure 17(C) represents the diagram of the ampere turns of core 2. In this core the secondary ampere turns exceed those of the primary, and the resultant ampere turns I_2W_2 are approximately in phase with the secondary ampere turns according to the equation

$$I_1N+I_2N_2=I_2W_2$$

For a given burden the induced voltage E_2 determines the value of the common flux ϕ in the two cores and the no-load ampere turns I_1N of the current transformer. The foregoing no-load ampere turns are the result of the two ampere turns I_1W_1 and I_2W_2. The two ampere turns I_1W_1 and I_2W_2 are almost in phase opposition, hence each must exceed the no-load ampere turns of the current transformer. As a result the flux density in the two cores is increased to the region of maxi-

* Allgemeine Elektrisitats Gesellschaft

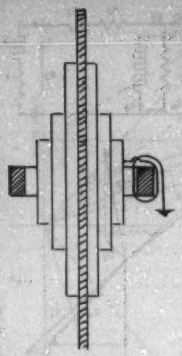

Figure 13 (left). Bushing-type current transformer with additional excitation from capacitor-charging current

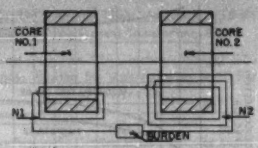

Figure 16(A). Schematic diagram of a current transformer with auxiliary excitation derived from the secondary side of the current transformer

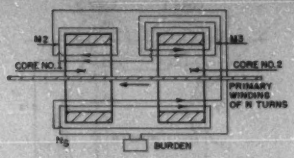

Figure 16(B). Simplified diagram of the connections of the current transformer shown in Figure 16(A)

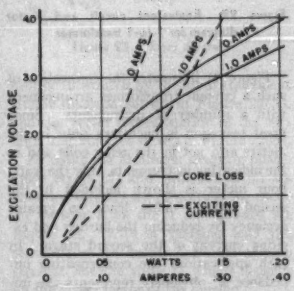

Figure 14. Effect of additional d-c magnetization on annular ribbon-wound core

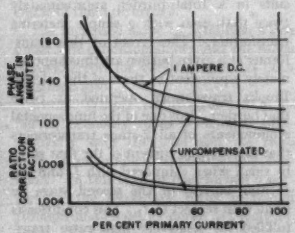

Figure 15. Effect of d-c excitation from battery on current transformer characteristics

Connection: 200 amperes
Burden: 6 volt-amperes at 1.0 power factor

mum permeability. It follows that the exciting current is greatly reduced because it is the resultant of two components which not only are fairly small in value but also are almost in phase opposition. Due to the fact that in one of the cores the magnetization is proportioned somewhat higher than that of maximum permeability, and in that of the second core somewhat lower than maximum permeability, it follows that satisfactory operation of the transformer is obtained throughout the working range of the current transformer.

These theoretical considerations have been limited to two cores. However, the wound-core construction permits the same results to be obtained with a single core by placing some of the turns between the layers of the core spiral.

Typical results obtainable from this type of compensation are shown in Figure 18.

Two-Stage Current Transformers[34]

The Brooks 2-stage transformer is one of the most fundamental and most effective means for the reduction of transformer errors. It automatically corrects ratio and phase-angle errors caused by changes in primary or secondary current.

This current transformer has two toroidal cores, Figure 19(A). The first core has an ordinary secondary winding and when taken by itself would yield a current with errors identical to those in the ordinary silicon iron transformer. Both primary and secondary current pass through respective windings of the second transformer, the ratio of turns is approximately equal to the desired ratio of the primary to secondary current. On the second core the secondary and primary ampere turns are in opposition. This core has another winding N_3 called the auxiliary or tertiary winding, having approximately the same number of turns as the secondary winding.

Referring to Figure 19(B) the primary current I_1 of the first stage will be equal to the secondary current I_2 plus the exciting current I_{e1}. I_{e1} also represents the primary current of the second stage transformer, and is thus equal to the vector sum of the tertiary current I_3 plus the exciting current I_{e2} of the second stage. If the exciting current I_{e2} is small compared to I_{e1} then the vector I_{1R} will very closely approximate I_1.

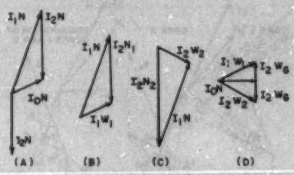

Figure 17. Ampere-turns diagrams for excitation scheme of Figure 16(B)

(A)—Normal current transformer
(B)—Core number 1
(C)—Core number 2
(D)—Resultant excitation

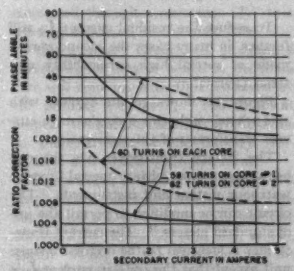

Figure 18. Characteristics of transformer of Figure 16(B)

Cores: Silicon steel 16¹/₄ inches inside diameter by 18¹/₂ inches outside diameter by 4 inches
Burden: 12.5 volt-amperes at 0.9 power factor
Connection: 300 amperes

The current I_3 circulating in the tertiary winding acts on an auxiliary current coil of a special wattmeter. If I_3 were equal (vectorially) to I_{e1} the correction would be perfect and the errors would always be zero. This would be true if the impedance of the tertiary circuit was zero. In practice, of course, the tertiary circuit has impedance which necessitates flux in the second core. This flux requires an exciting current I_{e2} which is the cause of the residual error.

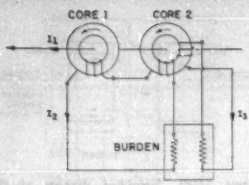

Figure 19(A). Diagram of 2-stage current transformer

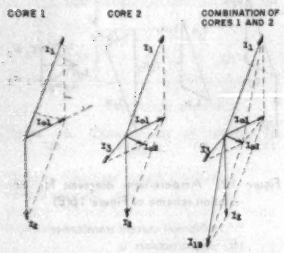

Figure 19(B). Vector relations of 2-stage current transformer

To reduce the residual current I_{e2} still further, in many cases the second core is made of special high permeability material (Permalloy).

Figure 20 shows results typical with this scheme and with a single stage current transformer of the same rating.

The 2-stage transformer has the disadvantage of requiring special 2-stage watthour meters and instruments. The circuit can be modified to permit the use of standard meters.[14] The current transformer is identical to the original 2-stage unit except that the tertiary current I_3 is brought to the terminals of the burden Z in such a manner that it adds (vectorially) to the current I_3.

Connecting directly to the tertiary winding would not accomplish this result. If we neglect, for the sake of simplicity, the impedance of the windings which we assume to be of equal turns, then the voltage ZI_3 produced by the current I_3 is equal to electromotive force E_3 due to the flux ϕ_e in the first core. The voltage existing at the terminals of the tertiary winding before it is connected to the burden Z also is equal to E_3 because the flux in the second core (when the tertiary winding is open) also is equal to ϕ_e. Therefore, the connection of the tertiary winding directly across the terminals of the main burden will not cause it to draw any current from the tertiary winding.

To draw a current from the tertiary

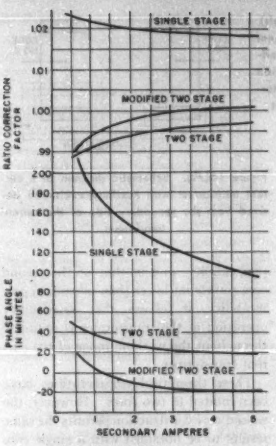

Figure 20. Characteristics of 2-stage current transformers of Figures 19(A) and 21

Burden: $Z = 40$ volt-amperes, 0.996 power factor
$Z' = 6.2$ volt-amperes, 0.80 power factor

winding it is necessary to produce a voltage drop in the tertiary circuit equal and opposite that produced across the burden by the secondary current I_3. This can be done by inserting an impedance Z' equal to the compensated burden in the tertiary circuit and by forcing through it a current equal and opposite to I_3. The latter is supplied by a 1-to-1 ratio transformer connected in the main circuit of the transformer. The complete scheme of connection is shown in Figure 21. The net mutual impedance between the secondary and tertiary winding is brought to zero and although the two circuits have a common connection (across the burden) they act as though they were completely independent and do not influence each other.

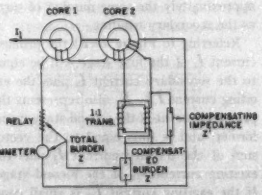

Figure 21. Scheme for using single element meter with 2-stage transformer

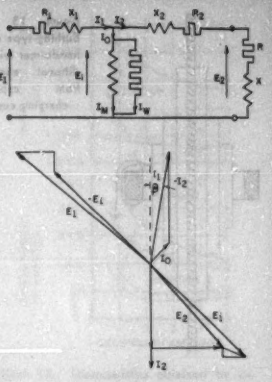

Figure 22. Equivalent circuit and vector diagram for 1-to-1 transformer

Figure 21 illustrates the connection of such a current transformer arrangement with a number of instruments. Since great precision is necessary only in the meters and not in the relay coils and in the indicating instruments, only the watthour meter is shown included in the second stage. This leads to greater accuracy by reducing the burden and exciting current of the second stage. In such applications the compensating impedance Z' obviously represents the impedance of only that portion of the total burden that must be corrected.

The addition of a dummy burden results in a total burden approximately twice that used with a simple metering transformer. The errors of this transformer at a given burden are thus approximately equivalent to those of the original Brooks transformer operated at twice that burden. It is one of the fundamental requirements of all 2-stage transformers that the exciting current of the first stage be small when compared with I_2 and the exciting current of the second stage be small with respect to I_3. This condition is fulfilled for relatively high ratio transformers as well as low ratio transformers with very low burdens. Very satisfactory results can be obtained for these cases, see Figure 20.

Systems Based on the Rotation of the Exciting Current Vector I_e

Before reviewing compensation methods based on rotation of the exciting current vector I_e, it is desirable to discuss the modified current diagram proposed by Mollinger.[21]

The theory of a current transformer can

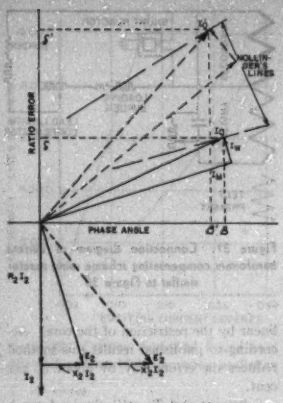

Figure 23. Error diagram

best be illustrated by the usual equivalent circuit diagram shown in Figure 22(A), and the vector representation of the currents and voltages shown in Figure 22(B).

By using the Mollinger diagram phase-angle errors (β) and ratio errors (δ) are obtained directly by projecting the exciting current I_e on the X and Y axes, see Figure 23. With a variable load the terminus of the vector I_e moves along a straight line the slope of which depends on the power factor of the burden.

Figure 23 shows that a rotation of the vector I_e (from I_e to I_e') would produce a reduction of the phase angle β and an increase of the ratio error δ.

The increased slope of Mollinger's line under this condition shows that the range of ratio errors for variable load has been increased also.

In the "Wilson" transformer[55] the number of secondary turns is changed automatically with the load and the ratio error is maintained approximately constant. In this type of transformer a portion of the secondary turns is wound through small holes as shown in Figure 24.

Figure 24. Wilson's transformer

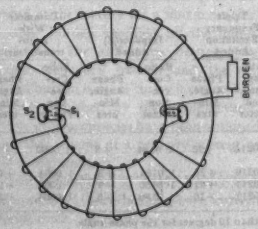

Table I. Data for High Accuracy 115-Kv Bushing-Type Current Transformer, 400-5

Internal Diameter 17¼ Inches; Weight 270 Pounds; Burden 50 Volt-Amperes at 50 Per Cent Power Factor

Secondary, Amperes	Ratio Correction Factor	Phase Angle, Minutes
0.5	1.0006	−11
1.0	1.0001	−7
2.0	1.0007	0
3.0	1.0004	+1
4.0	1.0000	0
5.0	0.9999	+1

Short-circuited turns also embrace a portion of the core S_1. The currents which circulate in the auxiliary turns and in short-circuited turns produce a decrease and a rotation of the flux which links the section S_1. This rotation reduces the phase angle error because the flux in S_1 induces an electromotive force in the auxiliary turns which lags the output electromotive force. Since the output electromotive force is fixed by the loading and by the burden it follows that the resultant flux and the exciting current are rotated in the direction of producing a reduction in the phase angle. The auxiliary windings also have the effect of increasing the flux density in S_2 and of decreasing the flux density in S_1 with the net result that the material will be working in two different regions of the magnetization curve. By the proper selection of the number of auxiliary turns and the relative cross sections of S_1 and S_2, it is possible to flatten the ratio error curve.

This scheme has been very successfully applied to wound-type current transformers and with limited results to bushing-type current transformers.

Wellings and Mayo Current Transformer[74]

This transformer consists of a main core "A" and an auxiliary core "B" which are assembled on the primary conductor, see Figure 25. The first core of relatively

Figure 25. Wellings and Mayo's current transformer

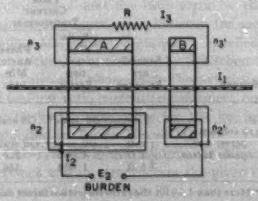

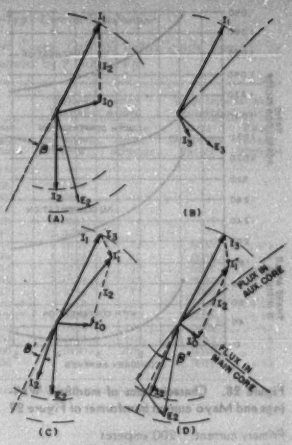

Figure 26. Vector diagrams of Wellings and Mayo's current transformer

large cross section has a secondary winding n_2. The second core "B" of small cross section has a winding n_3' which is connected through a resistance "R" to a winding n_3 wound on the main core "A." In this auxiliary circuit will circulate a current I_3 the flux of which in the main core will combine with that produced by the primary current I_1. The resultant ampere turns of the exciting current is due to vectorial sum of the primary, secondary, and auxiliary ampere turns.

Figure 26(A) is the vector diagram of a single core current transformer considered on a 1-to-1 basis. The exciting current I_e is the vector sum of I_1 and I_2. Figure 26(B) is the diagram for the auxiliary core. If the two diagrams are combined so that the common vectors I_1 of Figures 26(A) and 26(B) coincide, the vector diagram of the combination can be drawn. Figure 26(C) shows how vector I_3 combines with vector I_1 giving a net primary current I_1' with an exciting cur-

Figure 27. Modified Wellings and Mayo scheme. Additional magnetization from auxiliary core plus compensation by method of Wellings and Mayo

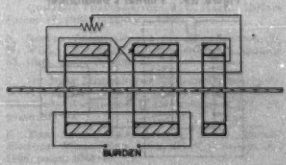

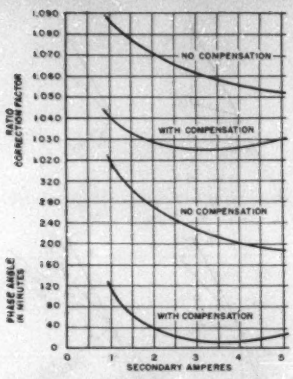

Figure 28. Characteristics of modified Wellings and Mayo current transformer of Figure 27

Primary current: 200 amperes
Burden: 19.2 volt-amperes, 0.89 power factor
Main cores: 16 inches inside diameter by 21 inches outside diameter by $3^1/_8$ inches
Auxiliary core: 16 inches inside diameter by 21 inches outside diameter by $1^1/_4$ inches

rent I_e' which is the vector sum of I_1' and I_2. The net result is a reduction in phase angle and increase in ratio I_1/I_2. A few turns of the secondary current are wound on the auxiliary core to compensate for the ratio error, see Figure 25. The effect is to rotate the exciting current vector to I_e'', Figure 26(D), which gives further reduction in phase angle as well as a reduction in ratio.

With this scheme reasonably good results have been obtained in bushing-type current transformers when the rated primary current is not lower than 600 amperes. This limiting value of course applies to high-voltage current transformers. Better results have been obtained with the scheme just described if it is combined with that shown in Figure 11. This combination is shown in Figure 27, and the comparative results with and without compensation are shown in Figure 28.

Figure 29. Pfiffner's transformer

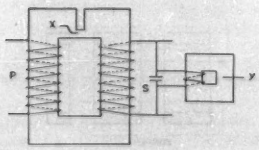

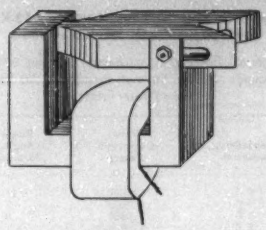

Figure 30. Reactor with adjustable core

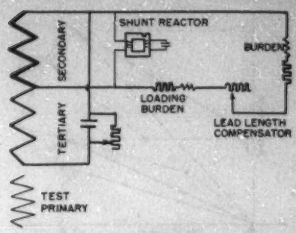

Figure 31. Connection diagram of current transformer compensating scheme using reactor similar to Figure 30

Straightening of the Exciting Current Curve

The exciting current is the source of both ratio and phase angle errors, and any scheme that makes exciting current linearly proportional to primary current will make both these errors constant. Once made constant their magnitude can be reduced by several different methods.

A general principle which has been used is to balance increasing and decreasing permeability against each other.

One method of accomplishing this is to combine the separate exciting currents of separate cores, one saturated, the other operated at low densities. This result may be obtained in a single unit if the core of the current transformer is so constructed that one section or length of the core operates saturated, another at very low density, resulting in a straight line volt-ampere curve for the whole core. The proper execution of this requires that the magnetic circuit does not have the same cross section along its entire length but be reduced in one or more places. E. Pfiffner[88] did this by slotting the main core to produce high saturation at section X, Figure 29. The capacitor and the reactor shown in the figure neutralize the exciting current which is rendered approximately linear by the restriction of the core. According to published results this method reduces the errors only by about 50 per cent.

Schwager and Treat[111] obtained much better accuracies by connecting a special reactor across the burden, see Figure 30. In this scheme the transformer core has uniform cross section and the shunt reactor has sections working at different degrees of saturation. After the straightening of the exciting current has been accomplished, the errors are compensated by the addition of capacitors and resistances as shown in Figure 31.

With this scheme the errors at all loads are equalized by increasing the errors at those points where they would otherwise be low. At best the magnetization curve can be straightened at the expense of increasing the actual value of the magnetizing current as is shown in curve "B" of Figure 1.

The capacitor is connected to a tertiary winding having a large number of turns to reduce its size. Under large overload conditions the voltage across the capacitor can assume large values which may result in its failure.

This type of transformer is very sensi-

Table II. 69-Kv Current Transformer

100:5 Amperes (20 Secondary Turns), Two Cores, Each $10^3/_8$ Inches Inside Diameter by $12^3/_8$ Inches Outside Diameter by $5^1/_4$ Inches High, Total Core Weight = 100 Pounds

Burden	Secondary Amperes	Plain Current Transformer: Ratio Correction Factor	Plain Current Transformer: Phase Angle, Minutes	Triple Frequency Excitation Added: Ratio Correction Factor	Triple Frequency Excitation Added: Phase Angle, Minutes	Impedor(Z) Added: Ratio Correction Factor	Impedor(Z) Added: Phase Angle, Minutes	Complete With Auto-transformer: Ratio Correction Factor	Complete With Auto-transformer: Phase Angle, Minutes
Y	0.5	Off scale*	Off scale*	1.0215	+25	1.0184	+3	1.0005	+5
(15 volt-amperes) 0.9 power factor	1.0	Off scale*	Off scale*	1.0216	+26	1.0184	+3	1.0004	+4
	3.0	1.082	216	1.0211	+21	1.0180	−1	1.0003	+1
	5.0	1.068	156	1.0212	+16	1.0180	−5	1.0004	−2

* More than 1.10 for the ratio correction factor and more than 10 degrees for the phase angle.

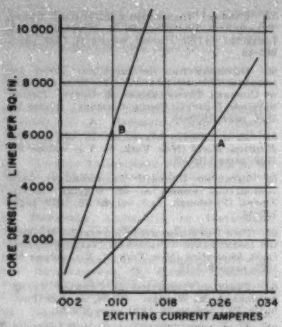

Figure 32. Exciting current of wound core with and without triple-frequency excitation

A—60 cycles
B—60 cycles plus 180 cycles (32,250 lines per square inch)

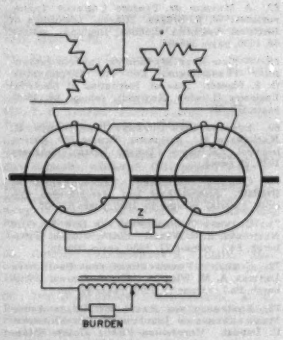

Figure 33. Diagram of connection of a bushing-type current transformer with auxiliary triple-frequency excitation

tive to changes in the secondary burden. A change in the burden would involve the readjustment of the secondary reactor. To avoid having to return the transformer to the factory when it is necessary to make changes in the burden, each individual transformer and its reactor are adjusted at the factory for a maximum permissible burden specified by the manufacturer. The difference between the actual secondary burden and the adjusted burden is made up by a replaceable burden furnished by the manufacturer. Fairly good accuracies have been obtained with this scheme at a primary current as low as 300 amperes.

The data shown in Table I refer to a 400-ampere 115-kv bushing-type current transformer.

Table III. 161-Kv Bushing-Type Current Transformer

Ratio 150/5 Amperes (30 Secondary Turns), Two Cores, Each 20 Inches Inside Diameter by 24¾ Inches Outside Diameter by 2 Inches High

Burden	Secondary Amperes	Plain Current Transformer: Ratio Correction Factor	Plain Current Transformer: Phase Angle, Minutes	High-Frequency Excitation Added: Correction Factor	High-Frequency Excitation Added: Phase Angle, Minutes	With Impedor and Autotransformer: Ratio Correction Factor	With Impedor and Autotransformer: Phase Angle, Minutes
X (2.5 volt-amperes, 0.9 power factor)	0.5	1.0174	103	1.0022	3		
	1.0	1.0154	81	1.0027	4		
	2.0	1.0138	64	1.0028	4		
	3.0	1.0130	59	1.0031	4		
	5.0	1.0119	43	1.0033	5		
Y (15 volt-amperes, 0.9 power factor)	0.5	1.0665	262	1.0149	12	1.0056	+4
	1.0	1.0591	196	1.0156	13	1.0050	+3
	2.0	1.0510	134	1.0157	13	1.0047	+2
	3.0	1.0463	103	1.0158	13	1.0045	1
	5.0	1.0400	72	1.0158	13	1.0043	0
Z (50 volt-amperes, 1.0 power factor)	0.5	Off scale*	Off scale*	1.0443	125	1.0020	+18
	1.0	Off scale*	Off scale*	1.0439	120	1.0014	+10
	2.0	Off scale*	Off scale*	1.0433	106	1.0008	+2
	3.0	1.086	350	1.0433	100	1.0112	−4
	4.0	1.081	300	1.0440	100	1.0018	−7
	5.0	1.077	250	1.0442	100	1.0019	−14

*More than 1.10 for the ratio correction factor and more than 10 degrees for the phase angle.

Straightening of the Exciting Curve and Simultaneous Reduction of the Exciting Current

The principle of operation of these transformers[57,158,153] is as follows:

If a core is excited from an a-c source and then a higher frequency excitation superimposed on it through a separate winding of suitable design, maintaining the original excitation unchanged, it will be observed that the volt-ampere input by the original (lower frequency) circuit is diminished by the superimposition although the total losses in the core may be considerably increased. To the lower-frequency source, the iron behaves as an improved material: reduction of the exciting current to less than 50 per cent of its original value, without high-frequency superimposition, has been obtained, see Figure 32. A much more important result of auxiliary high-frequency excitation is it makes the low-frequency exciting current proportional to the primary current. By the superimposition of the additional high-frequency excitation ratio errors are divided by more than ten, and phase angle errors by more than 60. With the errors rendered constant the phase-angle error is compensated for by an auxiliary impedance *Z* and the ratio error by the tapped autotransformer between the secondary and burden, Figure 33. Excellent accuracies can be obtained by this scheme. The ratio and phase-angle characteristics of two low ratio current transformers, one for 69 kv and the other for 161 kv, are exhibited in Tables II and III.

Other details in the performance characteristics and in construction are given in the paper by J. W. Farr.[149]

Conclusions

Much progress has been made in the design of bushing-type current transformers. In spite of this progress the wound-type transformer will maintain a limited field of application. It will fill the gap for the lowest ratios such as 5/5 to 100/5 and also will be used in all those cases where insensitivity to fairly large burden variation is imperative.

The latest bushing current transformers and in particular the orthomagnetic type could replace the wound-type current transformers of ratios 100/5 and higher. Compactness, convenience, facility of maintenance, and economy are the factors which will in many cases have decisive factors in favor of the bushing type.

Bibliography on Current Transformers

1. On Hysteresis in Presence of Alternating Currents, G. Finzi. *Electrician* (London, England), volume 26, 1891, pages 672–73.

2. On Hysteresis in Presence of Alternating Currents, G. Gorosa, G. Finzi. *Rendiconti*, Regio Instituto Lombardo (Milan, Italy), volume 24, 1891, number 10.

3. Magnetic Induction in Iron and Other Materials (book), J. A. Ewing. D. Van Nostrand Company, Inc., New York, N. Y., 1892, pages 93–117.

4. Electrical Measuring Instruments, Siemens Brothers and Company. British Patent 17263/1899, August 25, 1899.

5. Current Transformers, A. C. Hosp. British Patent 47/1903, January 1, 1903.

6. Series Transformers for Wattmeters, L. W. Wild. *Electrician* (London, England), volume 56, 1906, pages 705–06.

7. On Best Method for Demagnetizing Iron, C. W. Burrows. *Bulletin*, United States Bureau of Standards (Washington, D. C.), volume 4, 1907–08, pages 205–74.

8. The Series Transformer, E. S. Harrar. *Electrical World* (New York, N. Y.), volume 51, 1908, pages 1044–46.

9. Determination of Constants of Instrument Transformers, **P. G. Agnew, T. T. Fitch.** *Bulletin*, United States Bureau of Standards (Washington, D. C.), volume 6, 1909, pages 281–99.

10. Electrical Measurements on Circuits Requiring Current and Potential Transformers, **L. T. Robinson.** *AIEE Journal*, volume 28, 1909, pages 1005–39.

11. Magnetisch Korrespondierende Zustände, **R. Gans.** *Physikalische Zeitschrift* (Leipzig, Germany), volume 11, 1910, pages 988–91.

12. Notes on Instrument Transformers, **K. Edgcumbe.** *Electrical Review* (London, England), volume 67, 1910, pages 163–65.

13. Some Recent Developments in Exact Alternating Current Measurements, **C. H. S. Sharp, W. W. Crawford.** *AIEE Transactions*, volume 29, 1910, pages 1517–41.

14. Theory and Design of Current Transformers, **A. F. Young.** *Journal*, Institution of Electrical Engineers, (London, England), volume 45, 1910, pages 670–78.

15. A Study of Current Transformers with Particular Reference to Iron Loss, **P. G. Agnew.** *Bulletin*, United States Bureau of Standards (Washington, D. C.), volume 7, 1911, pages 423–74.

16. Current Ratio and Phase Angle Test of Series Transformers, **H. S. Baker.** *Electrical World* (New York, N. Y.), volume 57, 1911, pages 234–35.

17. Die Gleichung der Kurve der reversiblen Suscptibilitat, **R. Gans.** *Physikalische Zeitschrift* (Leipzig, Germany), volume 12, 1911, pages 1053–54.

18. Characteristics and Limitations of Series Transformers, **A. R. Anderson, H. R. Woodrow.** *Bulletin*, University of Illinois (Urbana, Ill.), October, 1912.

19. Measurement of Energy with Instrument Transformers, **A. Maxwell.** *AIEE Transactions*, volume 31, 1912, pages 1197–1202.

20. The Testing of Instrument Transformers, **P. G. Agnew, F. B. Silsbee.** *AIEE Transactions*, volume 31, 1912, pages 1635–38.

21. Zum Diagram des Stromwandlers, **J. Mollinger, H. Gewecke.** *Elektrotechnische Zeitschrift* (Berlin, Germany), volume 11, 1912, pages 270–71.

22. Accuracy of the Formulas for the Ratio, Regulation, and Phase Angle of Transformers, **P. G. Agnew, F. B. Silsbee.** *Bulletin*, United States Bureau of Standards (Washington, D. C.), volume 10, 1913, pages 279–93.

23. The Current Transformer, **A. G. L. McNaughton.** *Journal*, Institution of Electrical Engineers, (London, England), volume 53, 1914, pages 269–71.

24. The Milliampere Current Transformer, **E. Bennett.** *AIEE Transactions*, volume 33, 1914, pages 625–40.

25. The Calibration of Current Transformers by Means of Mutual Inductances, **C. L. Fortescue.** *AIEE Transactions*, volume 34, 1915, pages 1199–1215.

26. The Phase Angle of Current Transformers, **C. L. Dawes.** *AIEE Transactions*, volume 34, 1915, pages 1585–98.

27. The Unsymmetrical Hysteresis Loop, **J. D. Ball.** *AIEE Transactions*, volume 34, 1915, pages 2693–2715.

28. A Variable Self and Mutual Inductor, **H. B. Brooks, F. C. Weaver.** *Bulletin*, United States Bureau of Standards (Washington, D. C.), volume 13, 1917, pages 569–80.

29. A Method for Testing Current Transformers, **F. B. Silsbee.** *Bulletin*, United States Bureau of Standards (Washington, D. C.), volume 14, 1918, pages 317–29.

30. Current Transformer Ratio and Phase Error by Test Ring Method, **H. S. Baker.** *AIEE Transactions*, volume 37, 1918, pages 1173–83.

31. Electric Measuring and Calibrating Method, **O. Knopp.** United States Patent 1,372,821, 1921.

32. Minimizing the Errors of Current Transformers by Means of Shunts, **H. W. Price, C. K. Duff.** *Bulletin*, University of Toronto (Toronto, Ontario, Canada), 1921, pages 217–31.

33. Watthour Meter Method of Testing Current Transformers, **J. R. Craighead, C. T. Weller.** *General Electric Review* (Schenectady, N. Y.), volume 24, 1921, pages 642–51.

34. The Two-Stage Current Transformer, **H. B. Brooks, F. C. Holz.** *AIEE Transactions*, volume 41, 1922, pages 382–91.

35. Compounded Current Transformers, **A. Iliovici.** *Bulletin*, Societe Francaise des Electriciens (Paris, France), volume 3, 1923, pages 55–70.

36. Elementary Theory of the Current Transformer, **E. G. Reed.** *Electric Journal* (Pittsburgh, Pa.), volume 20, May 1923, pages 182–86.

37. Il Perfezionamento dei Riduttori di Corrente nei Riguardi della Precisione, **D. Garelli.** *Elettrotecnica* (Milan, Italy), volume 10, 1923, pages 539–45.

38. Lead Resistance for Current Transformers, **F. B. Silsbee.** *Electrical World* (New York, N. Y.), volume 81, May 12, 1923, pages 1082–83.

39. Electrical Measuring Instruments (book), **C. V. Drysdale, A. C. Jolley.** D. Van Nostrand Company, Inc., New York, N. Y., 1924, pages 262–311.

40. Iron Losses Due to Simultaneous Magnetization of Two Different Frequencies, **F. Schroeter.** *Archiv fur Elektrotechnik* (Berlin, Germany), volume 13, March 31, 1924, pages 30–34.

41. Methods for Testing Current Transformers, **F. B. Silsbee.** *AIEE Transactions*, volume 43, 1924, pages 282–94.

42. Resolution of Transformer Reactance, **A. Boyajian.** *AIEE Journal*, volume 44, 1925, pages 842–46.

43. The Phase Angle of the Current Transformer, **E. G. Reed.** *Electric Journal* (Pittsburgh, Pa.), volume 22, 1925, pages 594–96.

44. Transformers for Single and Multiphase Currents (book), **G. Kapp**, revised by R. O. Kapp. Sir Isaac Pitman and Sons, Ltd., London, England, 1925, pages 290–97.

45. Current Transformer Calculations, **E. G. Reed.** *Electric Journal* (Pittsburgh, Pa.), volume 23, 1926, pages 67–71.

46. Current Transformer Characteristics, **G. L. Metz.** *Electrician* (London, England), volume 97, 1926, pages 260–61.

47. Current Transformers with Nickel-Iron Cores, **T. Spooner.** *AIEE Journal*, volume 45, 1926, pages 540–45.

48. High Voltage Current Transformers Developed at Niagara, **L. C. Nicholson.** *Electrical World* (New York, N. Y.), volume 87, 1926, pages 868–69.

49. I Metodi di Costruzione dei Riduttori di Corrente, **G. Keinath.** *Energia Elettrica* (Milan, Italy), volume 3, 1926, pages 821–30.

50. The Testing of Current Transformers, **R. G. Isaacs.** *Review of Scientific Instruments* (New York, N. Y.), volume 4, 1926, pages 75–78.

51. Essentials of Transformer Practice (book), **E. G. Reed.** D. Van Nostrand Company, Inc., New York, N. Y., 1927, pages 193–229.

52. Some Recent Advances in Alternating Current Measuring Instruments, **K. Edgcumbe, F. E. J. Ockenden.** *Journal*, Institution of Electrical Engineers (London, England), volume 65, 1927, pages 553–99.

53. Die Messwandler (book), **J. I. Goldstein.** Julius Springer, Berlin, Germany, 1928, pages 1–165.

54. Two-Stage Current Transformer, **W. K. Dickinson, M. S. Wilson.** *General Electric Review* (Schenectady, N. Y.), volume 31, 1928, pages 556–59.

55. A New High-Accuracy Current Transformer, **M. S. Wilson.** *AIEE Journal*, volume 48, 1929, pages 179–82.

56. Bushing-Type Current Transformers for Metering, **A. Boyajian, W. F. Skeats.** *AIEE Journal*, volume 48, 1929, pages 308–10.

57. Current Transformer, **A. Boyajian, G. Camilli.** United States Patent 1,706,139, March 19, 1929.

58. Current Transformer, **Emil Pfiffner.** United States Patent 1,731,865, 1929.

59. Current Transformer Excitation Under Transient Conditions, **D. E. Marshall, P. O. Longguth.** *AIEE Journal*, volume 48, 1929, pages 884–88.

60. Determination of Secondary Stray Inductance Winding Error and No Load Current of Current Transformers, **K. Gocht.** *Elektrotechnische Zeitschrift* (Berlin, Germany), volume 50, 1929, pages 1653–55.

61. High Tension Metering, **H. M. Sanders.** *Electrical World* (New York, N. Y.), volume 94, 1929, pages 1168–69.

62. Improved Current Transformers with Nickel-Iron Cores, **A. M. Wiggins.** *Electric Journal* (Pittsburgh, Pa.), volume 26, 1929, pages 152–54.

63. New Developments in Electrical Measuring Instruments. *Proceedings*, National Electric Light Association (New York, N. Y.), volume 86, 1929, pages 813–18.

64. Parallel Operation of Current Transformers, **A. M. Wiggins.** *Electric Journal* (Pittsburgh, Pa.), volume 26, 1929, pages 379–81.

65. Some Applications of the A.C. Potentiometer, **C. V. Drysdale.** *Electrical Review* (London, England), volume 105, 1929, pages 1164–65. *Journal*, Institution of Electrical Engineers (London, England), volume 68, 1930, pages 339–60.

66. The Properties of Sheet Magnetic Materials, **B. G. Churcher.** *Electrician* (London, England), volume 103, 1929, pages 659–62.

67. A Method of Testing Current Transformers, **W. E. Bruges.** *Journal*, Institution of Electrical Engineers (London, England), volume 68, 1930, pages 305–07.

68. A New Null Method of Testing Instrument Transformers and Its Applications, **G. F. Shotter.** *Journal*, Institution of Electrical Engineers (London, England), volume 68, 1930, pages 873–88.

69. Bushing Type Current Transformer, **K. Maekawa et al.** *Researches Number 280, Electrotechnical Laboratory* (Tokyo, Japan), February 1930, 29 pages.

70. Cascade Instrument Transformers, **K. Grundig.** *Elektrotechnik und Maschinenbau* (Vienna, Austria), volume 48, 1930, pages 633–36.

71. Current Transformers for Low Voltage Networks, **E. C. Wentz.** *Electric Journal* (Pittsburgh, Pa.), volume 27, 1930, pages 509–10.

72. Current Transformers for Protective Devices, **A. M. Wiggins.** *Electric Journal* (Pittsburgh, Pa.), volume 27, 1930, pages 39–41.

73. Equipment for Ratio and Phase Angle Measurements of Instrument Transformers, **C. Dannat.** *Metropolitan-Vickers Gazette* (Manchester, England), volume 12, 1930, pages 45–48.

74. Factors in Connecting Secondaries of Current Transformers, **J. Auchincloss.** *Southern Power Journal* (Atlanta, Ga.), volume 48, November 1930, pages 51–53.

75. I piu Recenti Progressi nei Riduttori di Corrente, **G. Keinath.** *Energia Elettrica* (Milan, Italy), volume 7, 1930, pages 1033–46.

76. Instrument Transformers, **J. G. Wellings, C. G. Mayo.** *Journal*, Institution of Electrical Engineers (London, England), volume 68, 1930, pages 704–35.

77. Notes on the Design of Four-Terminal Resistance Standards for Alternating Currents, **F. B. Silsbee.** *Journal of Research*, United States Bureau of Standards (Washington, D. C.), volume 4, 1930, pages 73–107.

78. Precision Testing of Current Transformers, **A. H. M. Arnold.** *Journal*, Institution of Electrical Engineers (London, England), volume 68, 1930, pages 898–911.

79. Some Accessory Apparatus for Precise Measurements of Alternating Current, **R. S. J. Spilsbury, A. H. M. Arnold.** *Journal*, Institution of Electrical Engineers (London, England), volume 68, 1930, pages 889–97.

80. Tendencies in Construction and Utilization of Instrument Transformers, **A. Iliovici.** *Bulletin*, Societe Francaise des Electriciens (Paris, France), volume 10, 1930, pages 1191–1215.

81. The Accuracy of Current Transformers, **J. B. Gibbs.** *Electric Journal* (Pittsburgh, Pa.), volume 27, 1930, pages 204–06.

82. Transformation Ratio and Current Transformers in the Saturation Range, H. Buchholz, P. Meyer. *A.E.G. Mitteilungen* (Berlin, Germany), volume 39, 1930, pages 317–23.

83. Bushing Type Current Transformers, C. Bresson. *General Electric Review* (Schenectady, N. Y.), volume 29, 1931, pages 227–34.

84. Calculation of Instrument Transformer Burdens, T. A. Hammond. *General Electric Review* (Schenectady, N. Y.), volume 34, 1931, pages 115–26.

85. Current Transformer Summations, E. W. Hill, G. F. Shotter. *Journal*, Institution of Electrical Engineers (London, England), volume 69, 1931, pages 1251–64.

86. Desirable Accuracies in Instrument Transformers, E. C. Wentz. *Electrical Engineering*, volume 50, August 1931, pages 657–59.

87. Die Entwicklung der Messeinrichtungen fur Hochspannung, G. Keinath. *Elektrotechnische Zeitschrift* (Berlin, Germany), volume 52, 1931, pages 1596–1600.

88. Direct Method of Determining the Leakage Field of a Transformer, H. W. L. Bruckman, W. Engelenburg. *Elektrotechnische Zeitschrift* (Berlin, Germany), volume 52, 1931, pages 1171–72.

89. Ein einfaches Verfahren zur Ermittlung der Streuerraktanz, der Windungsabweichung und der Leerlaufcharacteristik von Stromwandlern, A. Berghahn. *Elektrotechnische Zeitschrift* (Berlin, Germany), volume 52, 1931, pages 605–07.

90. Messwandler fur Hochtsspannungen, R. Kuchler. *V.D.E. Fachberichte* (Berlin, Germany), 1931, pages 40–42.

91. Metering Transformers, E. Steinert. *Electric Journal* (Pittsburgh, Pa.), volume 28, 1931, pages 612–14.

92. Permeability of Hyperpik Reaches 167,000, T. D. Yensen. *Electric Journal* (Pittsburgh, Pa.), volume 28, 1931, pages 386–88.

93. The Testing of Protective Current Transformers, W. Wilson. *World Power* (London, England), volume 15, 1931, pages 371–74.

94. Through Type Current Transformer and Amplifier for Measuring Alternating Currents of a Few Milliamperes, W. B. Kouwenhoven. *Review of Scientific Instruments* (New York, N. Y.), volume 2, 1931, pages 541–48.

95. Current Transformers, E. V. Clark. *Electrician* (London, England), volume 109, 1932, pages 191–92.

96. Der Fehlerlose Stromwandler, A. C. Schwager. *Bulletin*, Association Suisse des Electriciens (Zürich, Switzerland), volume 23, 1932, pages 514–32.

97. Developments in the Construction and Standardization of Instrument Transformers, A. Ilovici. *Bulletin*, Societe Francaise des Electriciens (Paris, France), volume 12, 1932, pages 1117–31.

98. Die neuste Entwicklung im Stromwandlerbau, J. Goldstein. *Elektrotechnische Zeitschrift* (Berlin, Germany), volume 53, 1932, pages 377–80, 428–31, 503–05.

99. Die Verbesserung des Stabstromwandlers fur Kleine Primarstromme, W. Reiche. *Elektrotechnische Zeitschrift* (Berlin, Germany), volume 53, 1932, pages 961–65.

100. Energy Measurement at Very High Voltages, A. Moig. *Bulletin*, Societe Francaise des Electriciens (Paris, France), volume 2, 1932, pages 182–94.

101. Hyperpik—Its Uses and Limitations, E. C. Wentz. *Electric Journal* (Pittsburgh, Pa.), volume 29, 1932, pages 227–29.

102. Testing of Bushing Type Current Transformers, K. Rottsleper. *A.E.G. Mitteilungen* (Berlin, Germany), volume 8, August 1932, pages 289–91.

103. Transformer System and Apparatus, A. C. Schwager. United States Patent 1,863,936, 1932.

104. Compensated Cable-End Current Transformer, K. Rottsleper. *A.E.G. Mitteilungen* (Berlin, Germany), volume 2, March 1933, pages 38–40.

105. Current Transformers, D. Garelli. *L'Elettro* (Milan, Italy), volume 20, 1933, pages 539–45.

106. Equipment for Testing Current Transformers, F. B. Silsbee, R. L. Smith, N. L. Forman, J. H. Park. *Journal of Research*, United States Bureau of Standards (Washington, D. C.), volume 11, 1933, pages 93–122.

107. Loss Characteristics of Silicon Steel at 60 Cycles with D-C Excitation, R. F. Edgar. *AIEE Transactions*, volume 52, 1933, pages 721–25.

108. Magnetization of Current Transformers, G. Stein. *Physikalische Zeitschrift* (Leipzig, Germany), volume 14, 1933, pages 495–99.

109. Messwandler, Vierter Referat, J. Goldstein. *Bulletin*, Schweizerischer Elektrotechnischer Verein (Zurich, Switzerland), volume 24, 1933, pages 100–04.

110. Neue Wege im Stromwandlerbau, J. Goldstein. *Elektrotechnik und Maschinenbau* (Vienna, Austria), volume 51, 1933, pages 480–92.

111. Shaping of Magnetization Curves and the Zero Error Current Transformers, A. C. Schwager, V. A. Trest. *AIEE Transactions*, volume 52, 1933, pages 45–52.

112. A-C Premagnetization in Current Transformers, J. Goldstein. *Bulletin*, Association Suisse des Electriciens (Zurich, Switzerland), volume 25, 1934, pages 229–32.

113. Current Transformer, A. Boyajian, G. Camilli. United States Patent 1,971,207, August 21, 1934.

114. Current Transformer Testing, A. H. M. Arnold. *Journal*, Institution of Electrical Engineers (London, England), volume 74, 1934, pages 424–37.

115. Current Transformers with Composite Cores, E. Billig. *Elektrotechnik und Maschinenbau* (Vienna, Austria), volume 52, 1934, pages 199–203.

116. Iron Biased by A-C Magnetic Properties and Their Importance in the Development of Current Transformer Technique, G. Stein. *Electrician* (London, England), volume 112, 1934, pages 391–93.

117. Leakage Phenomena in Ring Type Current Transformers, A. H. M. Arnold. *Journal*, Institution of Electrical Engineers (London, England), volume 74, 1934, pages 413–23.

118. Magnetization of Current Transformers, H. Vahl. *V.D.E. Fachberichte* (Berlin, Germany), 1934, pages 38–40.

119. Accuracy of High-Range Current Transformers, J. H. Park. *Journal of Research*, United States Bureau of Standards (Washington, D. C.), volume 14, 1935, pages 367–92.

120. Current and Voltage Transformers, W. Reiche. *V.D.E. Fachberichte* (Berlin, Germany), 1935, pages 166–68.

121. Instrument Transformers (book), B. Hague. Sir Isaac Pitman and Sons, London, England, 1936, pages 1–209.

122. Some Applications of Instrument Transformers, Otto A. Knopp. *Electrical Engineering*, volume 55, May 1936, pages 380–89.

123. Commercial A-C Measurements (book), G. W. Stubbings. D. Van Nostrand Company, Inc., New York, N. Y., 1937.

124. Current Transformers with Regulated Pre-Magnetization, J. Goldstein. *Bulletin*, Association Suisse des Electriciens (Zürich, Switzerland), volume 28, 1937, pages 366–69.

125. Effect of Wave-Form Upon the Performance of Current Transformers, J. H. Park. *Journal of Research*, United States Bureau of Standards (Washington, D. C.), volume 19, 1937, pages 517–30.

126. Shunt Method of Testing Current Transformers, C. O. Werres, A. R. Hand, C. W. LaPierre. *General Electric Review* (Schenectady, N. Y.), volume 41, 1938, pages 370–74, 413–22.

127. Separately Excited Current Transformer as Universal Transformer for Oscillograph Records of A-C and D-C Components, W. Kraner. *Elektrotechnische Zeitschrift* (Berlin, Germany), volume 60, 1939, pages 593–98.

128. A Proposed Method for the Determination of Current-Transformer Errors, G. Camilli, R. L. Ten Broeck. *Electrical Engineering* (*AIEE Transactions*), volume 59, September 1940, pages 547–50.

129. Analysis of Bushing-Current-Transformer Performance, J. P. Gebelein, J. A. Eisl. *Electrical Engineering* (*AIEE Transactions*), volume 59, September 1940, pages 541–46.

130. Computation of Accuracy of Current Transformers, A. T. Sinks. *Electrical Engineering* (*AIEE Transactions*), volume 59, December 1940, pages 663–68. Discussion, pages 1252–53.

131. Electrical Metermen's Handbook (book). Edison Electric Institute, New York, N. Y., 1940.

132. New Developments in Current-Transformer Design, G. Camilli. *AIEE Transactions*, volume 59, 1940, pages 835–42.

133. Overcurrent Performance of Bushing-Type Current Transformers, C. A. Woods, Jr., S. A. Bottonari. *Electrical Engineering* (*AIEE Transactions*), volume 59, September 1940, pages 554–60.

134. A Simple Method for Determination of Ratio Error and Phase Angle in Current Transformers, E. C. Wentz. *Electrical Engineering* (*AIEE Transactions*), volume 60, October 1941, pages 949–54.

135. Instrument Transformers. *Bulletin 601-H*, General Electric Company (Schenectady, N. Y.), March 1941.

136. New Current Transformer for Bus Differential Protection, L. F. Kennedy, A. T. Sinks. *AIEE Transactions*, volume 60, 1941, pages 1180–87. Discussion, pages 1363–65.

137. Transformers, G. Camilli. United States Patent 2,244,386, June 3, 1941.

138. A Practical Discussion of Problems in Transformer Differential Protection, P. W. Shill. *Electrical Engineering* (*AIEE Transactions*), volume 61, December 1942, pages 854–58.

139. Current- and Potential-Transformer Standardization, AIEE Committee Report. *Electrical Engineering* (*AIEE Transactions*), volume 61, September 1942, pages 693–706.

140. Current-Transformer Performance Based on Admittance-Vector Locus, A. C. Schwager. *Electrical Engineering* (*AIEE Transactions*), volume 61, January 1942, pages 26–30.

141. Instrument Transformers, I. H. Slater, G. Camilli. *General Electric Review* (Schenectady, N. Y.), volume 45, 1942, pages 521–25.

142. Linear Couplers for Bus Protection, E. L. Harder, E. H. Klemmer, W. K. Sonnemann, E. C. Wentz. *Electrical Engineering* (*AIEE Transactions*), volume 61, May 1942, pages 241–48.

143. Transient Characteristics of Current Transformers During Faults, C. Concordia, C. N. Weygandt, H. S. Shott. *Electrical Engineering* (*AIEE Transactions*), volume 61, May 1942, pages 280–85.

144. A Simple Method for the Determination of Bushing-Current-Transformer Characteristics, S. D. Moreton. *Electrical Engineering* (*AIEE Transactions*), volume 62, September 1943, pages 581–85.

145. Current Transformer Testing, A. H. M. Arnold. *Journal*, Institution of Electrical Engineers (London, England), volume 74, 1943, pages 424–36.

146. Leakage Phenomena in Ring-Type Current Transformer, A. H. M. Arnold. *Journal*, Institution of Electrical Engineers (London, England), volume 74, 1943, pages 413–23.

147. The Effect of Current-Transformer Residual Magnetism on Balanced-Current or Differential Relays, H. T. Seeley. *Electrical Engineering* (*AIEE Transactions*), volume 62, April 1943, pages 164–69. Discussion, page 384.

148. Current-Transformer Output and Application Charts, R. Koller. *Electrical Engineering* (*AIEE Transactions*), volume 63, August 1944, pages 573–77.

149. Instrument Transformers, A. Hobson. *Journal*, Institution of Electrical Engineers (London, England), volume 91, 1944, pages 147–68.

150. The Evolution of Standard Lines of Current Transformers for High Overcurrent Capacity, E. C. Wentz. *Electrical Engineering* (*AIEE Transactions*), volume 63, September 1944, pages 658–62.

151. Biased-Core-Current-Transformer Design Method, Theodore Specht. *Electrical Engineering* (*AIEE Transactions*), volume 64, September 1945, pages 635–40.

152. Field Test Yields Ratio of Delta-Connected Bushing Current Transformers, C. E. Asbury. *Electrical World* (New York, N. Y.), volume 124, November 24, 1945, pages 72–75.

153. Orthomagnetic Bushing Current Transformer for Metering, A. Boyajian, G. Camilli. *Electrical Engineering* (*AIEE Transactions*), volume 64, March 1945, pages 137–40.

154. Progress in Design and New Principles for Instrument Transformers, J. Goldstein. *Bulletin*, Association Suisse des Electriciens (Zürich, Switzerland), volume 36, 1945, pages 245–51.

155. Protection of Current Transformer Secondaries, G. Camilli. *General Electric Distribution* (Schenectady, N. Y.), July 1945, pages 14–15.

156. Instrument Transformers. *Bulletin Series 45-000*, Westinghouse Electric Manufacturing Company (Pittsburgh, Pa.), 1946.

157. Instrument Transformer Standards. *C57.13*, American Standards Association (New York, N. Y.), 1948.

158. Electric Induction Apparatus, G. Camilli A. Boyajian. United States Patent 2,467,807, April 19, 1949.

159. Revolutionary Advance in Instrument Transformer Design, I. F. Kinnard. *General Electric Review* (Schenectady, N. Y.), volume 52 June 1949, pages 15–19.

160. A New Line of Orthomagnetic Bushing-Type Current Transformers, John W. Parr. *AIEE Transactions*, volume 69, part I, 1950, pages 424–28.

No Discussion

The Theory of the Current Transductor and Its Application in the Aluminum Industry

T. R. SPECHT
ASSOCIATE AIEE

R. N. WAGNER
ASSOCIATE AIEE

THE current transductor is one of the great family of apparatus known variously as magnetic amplifiers, saturable core reactors, or transductors. These devices are a-c inductors, whose effective inductance can be changed by superimposing a d-c magnetomotive force. The current transductor is a transductor specially designed and calibrated so that the alternating current flowing in the a-c circuit is a direct measure of the direct current flowing in the d-c circuit. It is meant to be used for the measurement of the direct current.

The current transductor in comparison with the conventional d-c ammeter shunt commonly used in d-c power circuits has two outstanding advantages:

1. Insulation of the secondary circuit from the measured source. With the d-c shunt, the voltage of the main circuit appears at the instruments on the switchboard. With the transductor, the secondary circuit is fully insulated and may be grounded. The importance of isolation of the main or primary circuit is well understood in a-c practice. Isolation prevents damage to the primary circuit from any possible grounds in the secondary circuit. Insulation prevents damage to any of the instruments or injury to any of the operating personnel. It permits instruments to be installed at any convenient location without regard to primary voltage. To realize the full benefit of this advantage, the secondary circuit of the transductor should of course be grounded.

2. Convenience and economy in use of any number of instruments. With the d-c shunt, the value of the lead resistance to the meters is critical, and in the lower current ratings the number of meters that can be connected to one shunt is limited. As the current transductor has characteristics similar to the regular a-c transformer, the resistance of the meter or leads is not critical. The current transductor can be designed to carry as many meters as is desired, even in the low current range. In addition to his freedom to add additional instruments, relays, or other current operated devices as he may desire, the operator has the choice of all the wide range of a-c devices to be used in the secondary a-c circuit of the current transductor.

Connections for Current Transductors

A current transductor resembles, physically, a double-secondary a-c transformer. For purposes of analysis, the current transductor may be visualized most easily by thinking of it as two conventional a-c transformers with their primaries connected in series. See Figure 1. The secondary windings may be connected in series or in parallel as is shown in the figure, but in both cases one of the secondary windings must be connected in reverse polarity to that of the other winding. The secondary windings are then excited from a source of alternating voltage and an ammeter or other burden is put in the a-c line. For purposes of this analysis, it is assumed that the voltage drop across this burden (the ammeter) is small compared to the source voltage.

Application in the Aluminum Industry

It is customary in aluminum reduction plants to operate several d-c machines in parallel on a common bus to produce the relatively large amounts of current required for aluminum production. The central switchboard from which these machines are operated usually contains for each machine a millivoltmeter operated from a shunt in the d-c leads and calibrated in machine amperes. The leads from these shunts are often long and may require special meter calibration. The leads operate at bus voltage and are difficult to protect satisfactorily by fuses or other devices. Therefore, they produce electrical hazard in the switchboard and some fires have resulted.

In the hope of eliminating some of theses disadvantages, a new aluminum reduction plant has been equipped recently with 120 transductors rated 2,000 amperes direct current to 1 ampere alternating current. These transductors were made with the a-c coils in series. This unit is shown in Figure 12. These are in the d-c machine leads and each operates two a-c ammeters in series. One is located near each machine and the other is located several hundred feet distant at a central control switchboard. At this switchboard is located a 110-volt 60-cycle source large enough in capacity to supply 40 transductors. One side of this source is common to all the instruments and the other is run as a bus the length of the station and connecting to each transductor. With this circuit arrangement, it can be seen that only one wire is required from each machine to the central board for load indication. This lead is only at 110 volts and can be adequately fused. Especially calibrated dials were used on the instruments which were made from test curves on the first transductor. All transductors and all instruments are alike. The transductor is constructed similar to a current transformer and should be stable over a number of years.

A second application in the aluminum

Paper 50-64, recommended by the AIEE Instruments and Measurements, and Transformers Committees and approved by the AIEE Technical Program Committee for presentation at the AIEE Winter General Meeting, New York, N. Y., January 30-February 3, 1950. Manuscript submitted November 1, 1949; made available for printing December 2, 1949.

T. R. Specht is with the Westinghouse Electric Corporation, Sharon, Pa., and R. N. Wagner is with the Aluminum Company of America, Pittsburgh, Pa.

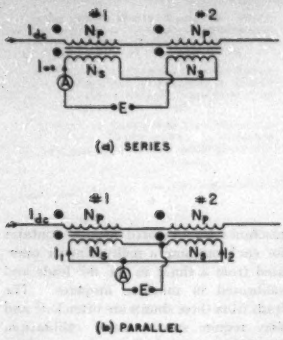

Figure 1. Connections for current transductors

industry is in the main d-c circuit to the cell lines. Here it is required to measure currents often as high as 50,000 amperes with the greatest possible accuracy. The shunts for these circuits are mammoth devices weighing several hundred pounds. Their resistance is so low that it requires very special equipment to calibrate them to the required accuracy. The millivolt output must be kept low or the power consumption and heating will be prohibitive. This latter objection makes it difficult to provide the necessary instruments at remote locations required by the operating personnel. In some cases it has been necessary to use shunt leads as large as 500,000 circular mils to operate meters at the distances required.

With these objections in mind, the cell line circuits in the plant are being equipped with transductors nominally rated 75,000 amperes direct current to 37.5 amperes alternating current. These units also had the a-c coils connected in series. This transductor as installed is shown in Figure 18, and during factory test in Figure 9. The switchboard instruments in this case are 5-ampere iron vane instruments specially calibrated and operated from a current transformer in the 37.5-ampere 440-volt exciting circuit. Several remote indicating and recording instruments are used which constitute a circuit some 3,000 feet long.

The ability to insulate instrument circuits is very important. The ease of installation of the transductor, the wide choice of instruments available, and the possibility of locating these instruments at any point without thought to lead length are further important advantages. The 16.5 kva of exciting power may be considered a disadvantage, however, the actual watts in excitation are below 1,000 and are less than in a large shunt.

Graphical Solution for Series Connection

The alternating current flowing in the secondary can be determined by the following graphical method. Referring to Figure 2, the change in the flux linkages linking the a-c secondary coil of unit Number 2 is plotted as a function of the secondary current for a particular value of direct current in the primary winding. It is assumed in this analysis and throughout this paper that there is no leakage flux from the cores; that is, that in a given core and a given instant of time, the flux density is the same throughout the core. The effect of the return conductor is discussed more fully later in this paper. Referring again to Figure 2, the zero point for the flux linkages is the value of flux linkages due only to the direct current with no alternating current flowing. In Figure 3, the curve from Figure 2 is replotted for unit Number 2, and also the similar curve for unit Number 1. Since the two units are supposed to have identical characteristics, these two curves will be symmetrical with respect to the origin. Also, plotted on Figure 3 is the sum of the curves for units 1 and 2. This curve then gives the total change in flux linkages in the secondary coils as a function of the alternating secondary current. It will be assumed the applied voltage is sinusoidal, and that the series voltage drop across the burden is negligible. It then can be shown that the necessary flux linkages in the secondary coils are sinusoidal.

$$e = \sqrt{2}E \sin \omega t; \quad \phi N = \frac{\sqrt{2}E10^8}{\omega} \cos \omega t$$

From Figure 3, the alternating current

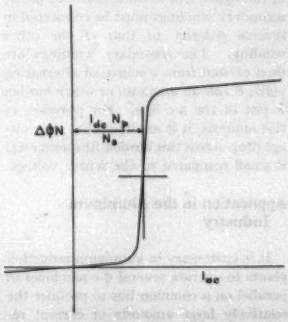

Figure 2. Change of a-c coil flux linkages as a function of the alternating current

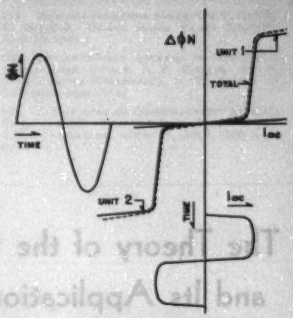

Figure 3. Required alternating current for sinusoidal applied alternating voltage and flux linkage

necessary for sinusoidal flux linkages developed in the units is shown. The alternating current that flows is essentially a series of positive and negative polarity rectangular pulses. The maximum value of the alternating current is nearly the direct current times the ratio of the d-c turns to a-c turns. If the slope of the saturation curve above the knee were zero, the alternating current would reverse instantly as it went through zero. As the slope is not zero, it takes the alternating current a definite length of time to reverse so the alternating current wave shape is trapezoidal rather than rectangular.

From Figure 3, the shape of the alternating voltage wave across each secondary can be determined. When the alternating current is positive, the core of unit Number 1 is almost completely saturated. There is very little flux change in unit Number 1, and consequently it develops very little voltage. Hence unit number 2 must develop most of the voltage when the alternating current is positive. As the flux change in number 2 is from zero to a maximum and back to zero, the voltage induced starts from a maximum to zero and to a minimum. During the half-cycle the alternating current is negative, the other unit will develop the induced voltage to oppose the applied alternating voltage.

The secondary alternating current is relatively insensitive to changes in alternating voltage. This is seen readily from Figure 3. If the alternating voltage and hence the a-c flux is decreased, it will take a little longer for the alternating current to reach its maximum value, but it will reach the same maximum value. The average alternating current will decrease some, but not nearly in proportion to the

voltage decreases. In a typical design, a 5 per cent change in voltage results in less than 1 per cent change in current. This is so slight that no precautions need be taken usually for voltage variations. The effect on the secondary current of changing the burden is about the same as that of changing the voltage. The secondary current does not decrease nearly as rapidly as the burden voltage drop increases.

The foregoing method is purely graphical. It is possible to make a mathematical analysis by assuming some certain formula for the saturation curve. In Appendix I a method is derived for simplifying the analysis using the actual saturation curve, and an approximate solution using a saturation curve of two straight lines. The latter approximation will give answers sufficiently close for practical purposes.

The analysis for the series case assumes a pure direct primary current. When the transductor is operating, alternating voltages appear across the d-c input coils. If the impedance of the d-c circuit is low, alternating currents will flow in the d-c circuit, and the foregoing analysis will not hold. Actually if the d-c impedance is very low, the analysis of the series connections is identical to that of the parallel connections. See reference 1. Ordinarily the d-c impedance will be very high.

Graphical Solution for Parallel Connections

Instinctively, one would not feel that the parallel connection, also shown in

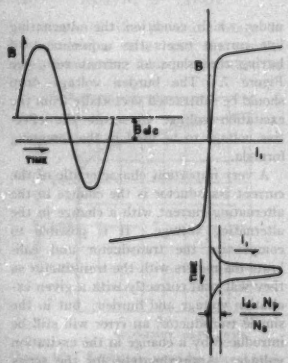

Figure 4. Parallel connection of current transductor

Flux density in one core and total amperes on a-c turns basis as functions of time

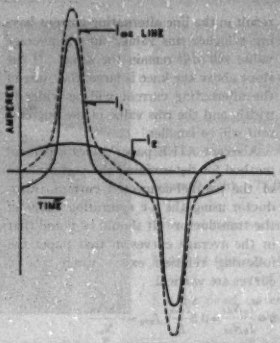

Figure 5. Parallel connection, alternating current in each secondary, and alternating line current

Figure 1, could be used for current measurement. One would think that one or the other core would be always saturated, and the current flow would be unlimited. Such is not the case, however; the current is definitely limited, as will be shown now.

Each of the units of the parallel connection of Figure 1 operates independently, as each is connected directly, except for the meter drop, to the alternating voltage; and each has a definite primary direct current. The problem resolves itself into finding the alternating current flowing in one winding of a transformer when there is a pure direct current flowing in another.

Figure 4 shows the excitation curve for one of the cores. The current is on the secondary turns basis. Since there is a d-c magnetomotive force on the core, there must be a d-c component in the flux density, although its magnitude cannot be directly determined. As the applied voltage is sinusoidal, the flux density in the core also must vary sinusoidally, neglecting the resistance of the a-c winding.

If the value of the d-c flux in Figure 4 were zero, the total current required for sinusoidal flux variation would have no d-c component. If the d-c flux is not zero there will be a d-c component in the total current. It is fundamental that there can be no direct current flowing in a circuit consisting of a constant resistance and a constant or variable reactance supplied from an a-c supply after the transient currents have subsided. This is almost self-evident, but is demonstrated in Appendix II. It follows that the d-c component of the current in the total current, when there is a d-c component in the flux, can be supplied only from the d-c winding.

The d-c component of flux adjusts itself until the d-c component in the total current is equal to the direct current, all referred to a-c turns basis. The process of analysis is indirect: a value of d-c flux must be found by trial which gives the known value of direct current. In Figure 4, the d-c component of the current is shown as the dot-dash line, and as marked on the figure must be equal to $I_{dc}N_p/N_s$. If the dot-dash line is considered the zero line, the current as shown in Figure 4 will be the alternating current flowing in one secondary, for the alternating current would be instantaneously the total current minus $I_{dc}N_p/N_s$.

In Figure 5 is shown the alternating current in each secondary, and then the line current, which is the sum of the two. This process for determining the secondary currents is general. If some approximations are made, though, some very revealing facts can be deduced regarding the basic operation of this circuit. Referring to Figure 6, the initial part of the saturation curve is assumed vertical up to a value of flux density equal to or greater than B_{dc}. This will result in the total amperes being zero for a half-cycle or more. As was explained previously, the average value of the total current required must be $I_{dc}N_p/N_s$, shown again as the dot-dash line on Figure 6. Referring to the areas shown on Figure 6, it must be true

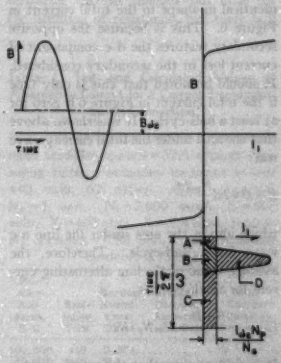

Figure 6. Parallel connection of current transductor

Flux density in one core and total amperes on a-c turns basis as functions of time. Same as Figure 4 except the initial part of the saturation curve is assumed vertical

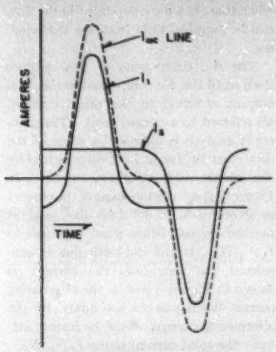

Figure 7. Parallel connection, alternating current in each secondary, and a-c line current for idealized curve of Figure 6

$$A+B+C=I_{dc}\frac{N_p}{N_s}\frac{2\pi}{\omega}$$

$$A+C=D$$

Therefore

$$B+D=I_{dc}\frac{N_p}{N_s}\frac{2\pi}{\omega}$$

Again the alternating current flowing in each secondary is the current shown in Figure 6 with the dot-dash line as the zero line.

In Figure 7 is shown the current flowing in each secondary winding, and the line current, the sum of the two. It will be noted that the line current is exactly identical in shape to the total current in Figure 6. This is because the opposite secondary restores the d-c component of current lost in the secondary considered. It should be noted that this is only true if the total current in Figure 6 is zero for at least a half-cycle. It was shown above that the area under the total current wave was

$$B+D=I_{dc}\frac{N_p}{N_s}\frac{2\pi}{\omega}$$

which also is the area under the line a-c wave for a half-cycle. Therefore, the average value of the line alternating current for a half-cycle is

$$I_{ac\text{-}avg}=\frac{B+D}{\pi/\omega}=2I_{dc}N_p/N_s$$

It is evident then that the average value of the alternating line current is directly related to the direct current, regardless of the slope of the saturation curve above the knee. If the slope is small, the pulse of alternating current will be small in width and high in peak value. This will result in the line alternating current having a higher rms value, but the average value will still remain the same. If the slope above the knee is large, the pulse of the alternating current will be wider in width, and the rms value of the line current will be smaller.

A recent AIEE paper[1] gives a general method for determining the performance of the parallel-connected current transductor using the a-c saturation curve of the transductor. It should be noted that in the average curves in that paper the following relation exists where the b curves are vertical

$$b=\frac{I_0N_{dc}}{I_bN_{ac}}=0.5\frac{I_{avg}}{I_b};\ I_{avg}=\frac{2I_0N_{dc}}{N_{ac}}$$

This is true for the reasons outlined previously. Note that the definition of N_{ac} per the reference paper and N_s per this paper are not the same, but they are equal for the parallel connection. In Appendix II, a mathematical analysis is made with a saturation curve consisting of two straight lines that give an approximate analytical answer to the problem. The principle value of this solution is that the effect of the various constants on the performance of the transductor can be directly seen.

Formulas for a Two Straight-Line Saturation Curve

The secondary a-c saturation curve for one core is as shown in Figure 8, where the current should be sinusoidal and the voltage measured with an average reading voltmeter. Effective values of initial slope, X_i, and saturated slope, X_s are chosen, as well as a value for E_s, the saturation voltage. These should be chosen so as to take into consideration the rounded knee of the actual saturation curve.

For the series connection, the average value of the alternating current will be (see Appendix I)

$$I_{avg}=\frac{N_pI_{dc}}{N_s}\left[1-0.45\frac{X_sN_pI_{dc}}{EN_s}\right]-\frac{\sqrt{2}E_s}{X_i}+0.9\frac{E}{X_i}$$

The rms value of the current for the series connection is

$$I_{rms}=\frac{N_pI_{dc}}{N_s}\left[1-0.6\frac{X_sN_pI_{dc}}{EN_s}\right]^{1/2}-\frac{\sqrt{2}E_s}{X_i}+0.9\frac{E}{X_i}$$

The above formulas are for zero secondary resistance and series burden. To take these into account, subtract the resistance

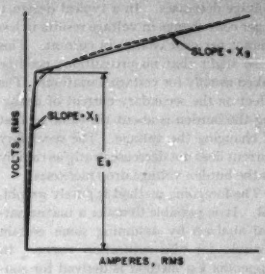

Figure 8. Excitation curve for one core

The dotted curve is the actual curve, and the solid lines the approximate two straight-line curve

drop vectorially from the secondary excitation voltage to secure an effective value for E; and add one-half of the burden reactance to X_s and one-half to X_i to take the reactance into account. These formulas will apply down to approximately the point where the calculated current is in the order of magnitude of the alternating exciting current at zero direct current.

For the parallel connection, the average alternating line current is (Append'x II)

$$I_{ac1}=\frac{2N_pI_{dc}}{N_s}-\frac{2}{X_i}\left[\sqrt{2}E_s-2.32E+2.5X_s^{2/3}\left(\frac{N_pI_{dc}}{N_s}\right)^{2/3}E^{1/3}\right]$$

This expression is valid only if

$$I_{dc}\leq 0.583\frac{N_sE}{N_pX_s}$$

under which condition the alternating line current meets the requirement of having zero slope at current zero, see Figure 7. The burden voltage drop should be subtracted vectorially from the excitation voltage to secure the effective voltage to be used in the foregoing formula.

A very important characteristic of the current transductor is the change in the alternating current with a change in the alternating voltage. It is possible to compensate the transductor and calibrate the meters with the transductor so they will read correctly with a given excitation voltage and burden; but in the simple transductor, an error will still be introduced by a change in the excitation voltage. Approximately, for the series connection the per-unit change in average current is

$$\frac{\Delta I_{avg}}{I_{avg}}=\left(0.45\frac{N_pI_{dc}/N_s}{E/X_s}+0.9\frac{E/X_i}{N_pI_{dc}/N_s}\right)\frac{\Delta E}{E}$$

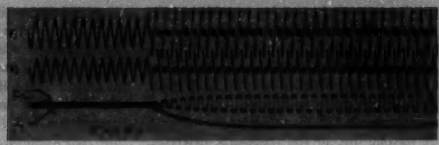

Figure 9 (left). 75,000-ampere d-c to 37.5-ampere a-c transductor. Series connected

The unit is shown on test with a special primary winding of 75 turns

Figure 11 (above). Oscillogram of tests made on 75,000-ampere current transductor at 50 per cent current

I_1 is the direct current, I_2 the alternating current. V_2 and V_3 are the voltages across the coils on each core

For most transductors, the latter part is negligible, and

$$\frac{\Delta I_{avg}}{I_{avg}} = 0.45 \frac{N_p I_{dc}/N_s}{E/X_s} \frac{\Delta E}{E}$$

For the rms current in the series connection

$$\frac{\Delta I_{rms}}{I_{rms}} = 0.3 \frac{N_p I_{dc}/N_s}{E/X_s} \frac{\Delta E}{E}$$

With the parallel connection, the per-unit change in the average line current is

$$\frac{\Delta I_{sol}}{I_{sol}} = \frac{E/X_f}{N_p I_{dc}/N_s}\left[2.32 - 0.83\left(\frac{N_p I_{dc}/N_s}{E/X_s}\right)^{2/3}\right]\frac{\Delta E}{E}$$

For most transductors, the quantity to the 2/3 power will be less than unity, and the expression becomes quite closely

$$\frac{\Delta I_{sol}}{I_{sol}} = 2.32 \frac{E/X_f}{N_p I_{dc}/N_s} \frac{\Delta E}{E}$$

In comparing the per-unit change in current in the series and the parallel cases, it should be kept in mind that the voltage E for the series connection will be about twice as much as for the parallel connection. Examples to be shown later indicate that the sensitivity to voltage change is about the same for the series or parallel connections.

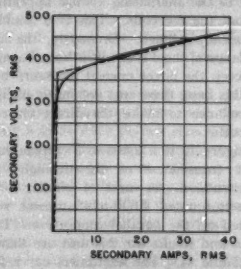

Figure 10. Excitation curve for current transductor

75,000 amperes direct current to 37.5 amperes alternating current; 60-cycle excitation curve for each core. $X_f = 400$ ohms, $X_s = 2.4$ ohms, $E_s = 365$ volts

Noting the equations for the change in average current for the series connection, it is seen that the change varies as the direct current squared, whereas in the parallel connection it is independent of the direct current. Sometimes a capacitor is put across the a-c terminals of the transductor to neutralize the change in alternating current with a change in alternating voltage. It is evident that with the series connection, it can only be made to neutralize at one value of direct current, whereas with the parallel connection, it would be balanced for all direct currents. With the series connection, though a value of capacitance could be chosen that would be a compromise, and would help to some extent.

It also would be desirable to determine the effect of the burden on the alternating current. For the series connection, adding the reactance of the burden can be simulated by increasing both X_f and X_s by one-half the burden reactance, X_b. The change in the current due to a change in X_f is negligible. The effect of a change in X_s on the average current is

$$\Delta I_{avg} = -0.45\left(\frac{N_p I_{dc}}{N_s}\right)^2 \frac{\Delta X_s}{E}$$

and approximately

$$\frac{\Delta I_{avg}}{I_{avg}} = -0.225 \frac{I_{avg}\,\Delta X_b}{E}$$

For example, if the burden per cent reactance drop were 10 per cent based on the secondary excitation voltage, the secondary current would decrease 2.25 per cent. To determine the change in alternating current for the series connection due to the burden and secondary resistance, use is made of the relation developed in Appendix I; the secondary resistance drop is subtracted vectorially from the applied voltage to secure the effective voltage applied to the transductor.

$$E_r = [E^2 - I_{avg}^2 R_b^2]^{1/2} \cong E - \frac{(I_{avg}R)^2}{2E}$$

The change in the voltage applied to the transductor from the voltage with zero resistance is

$$\frac{\Delta E_r}{E} = \frac{E_r - E}{E} = -\frac{1}{2}\left(\frac{I_{avg}\,\Delta R}{E}\right)^2$$

If the resistance drop is, for example, 20 per cent, the reduction in the voltage is 2 per cent. The reduction in the alternating current will be still less, as would be determined by the formulas for the change in current with a change in voltage. The net effect is that the alternating current changes but little for the addition of resistance, but there is a

Table I. Test and Calculated Values of Alternating Current for a Current Transductor, Series Connection

Primary current 75,000 amperes direct current; rated secondary current = 37.5 amperes alternating current; secondary excitation voltage 440 volts, 60 cycles; series connected, $N_p = 1$ turn; $N_s = 2{,}000$ turns; $E_s = 365$ volts; $X_f = 400$ ohms; $X_s = 2.4$ ohms; secondary resistance = 0.88 ohm; rated secondary burden: 0.75 ohm

Primary Amperes, D-C	Excitation Volts	Burden Resistance, Ohms	Average Current, Amperes Test	Average Current, Amperes Calc.	Rms Current Amperes Test	Rms Current Amperes Calc.
100,000	440	0.375			44.7	45.4
75,000	440	0			34.6	34.8
75,000	480	0.375			34.9	35.0
75,000	440	0.375	33.4	33.7	34.7	34.8
75,000	400	0.375			34.5	34.5
75,000	300	0.375			33.4	33.3
75,000	440	0.75			34.7	34.8
56,250	440	0.375	25.9	25.9	26.0	26.5
46,700	440	0.375			21.8	22.1
37,500	440	0.375	17.2	17.6	17.8	17.9
18,750	440	0.375	8.5	8.9	8.7	8.9
7,500	440	0.375	3.5	3.4	4.0	3.4

fair amount of change due to addition of reactance.

For the parallel connection, as was pointed out previously, the effect of the series resistance and reactance is to reduce the effective voltage applied to the transductor. The formula for the change in voltage due to the resistance derived above applies. For the addition of reactance

$$E_r = [E^2 - I^2R_b^2]^{1/2} - IX_b$$

$$\frac{\Delta E_r}{E} = -\frac{I\,\Delta X_b}{E}$$

For the parallel connection then, the same percentage increase in reactance drop and percentage decrease in applied voltage will result in the same change in the alternating current.

Construction of Some Current Transductors, and Comparison of Experimental and Calculated Results

As the current transductor has two sets of secondary coils and cores, the device is constructed very similarly to double-secondary current transformers. Figure 9 shows a 75,000-to-37.5 ampere current transductor that will be used for measuring current in an aluminum reduction line. Each core on the unit has 14 coils. The primary bus opening is 11 by 34 inches. It was necessary to build a primary winding of 75 turns around the unit for purposes of testing as current in the order of 75,000 amperes was not readily available. This unit is series connected, with lightning arresters connected across the coils on each core. With the series connection, if the primary current should change suddenly, while the primary current is small, a transient voltage is built up across each set of coils on the two cores. In the higher current ratings, it is difficult to provide enough insulation in the coils to stand this voltage, so lightning arresters are used. The secondary coils may seem to be spaced unnecessarily far from the primary bar, but the longer the length of the core, the thinner the coils will be. This will result in a smaller air-cored reactance, and hence saturated reactance X_s, and consequently better performance.

In Table I are given the data and test results for the 75,000-ampere current transductor. The excitation curve for both cores on this unit is shown in Figure 10. From this curve, values of X_t, X_s, and E_s can be determined.

In Table I are listed the test and calculated values of average and rms alternating current. The average current was read by a rectifier voltmeter reading the voltage across a known resistance. The rms current was read by a dynamometer ammeter. Sample calculations for this transductor follow for 75,000-ampere 440-volt excitation 0.375-ohm burden point

$$I_{avg} = \frac{N_pI_{dc}}{N_s}\left[1 - 0.45\frac{X_t}{E}\frac{N_pI_{dc}}{N_s}\right] - \frac{\sqrt{2}E_s}{X_t} + 0.9\frac{E}{X_t}$$

$$= \frac{(1)(75{,}000)}{2{,}000}\left[1 - \frac{(0.45)(2.4)(37.5)}{440}\right] - \frac{\sqrt{2}(365)}{400} + 0.9\frac{440}{400}$$

$$= 37.5[1 - 0.092] - 1.29 + 0.99 = 33.7$$

To take into account the secondary resistance which is 0.375 + 0.88 = 1.255 ohms

$$\frac{\Delta E_r}{E} = -\frac{1}{2}\left(\frac{I\,\Delta R}{E}\right)^2 = -\frac{1}{2}\left(\frac{33.7 \times 1.255}{440}\right)^2 = -0.0047$$

$$\frac{\Delta I_{avg}}{I_{avg}} = 0.45\frac{N_pI_{dc}/N_s}{E/X_s}\frac{\Delta E}{E} = \frac{(0.45)(37.5)}{440/2.4}(-0.0047) = -0.00043$$

The change due to the addition of the burden is negligible. From the test data it can be seen that addition of the burden causes hardly any change in the current. This value of 33.7 amperes calculated is 1 per cent higher than the test value of 33.4 amperes.

For the rms current, at 75,000-amperes, 440-volts' excitation, and 0.375 ohms' burden, the current calculates 34.8 amperes. A separate calculation can be made for the 480-volt point, or the change calculated as follows

$$\frac{\Delta I_{rms}}{I_{rms}} = 0.3\frac{N_pI_{dc}/N_s}{E/X_s}\frac{\Delta E}{E} = \frac{(0.3)(37.5)}{440/2.4}\frac{(480-440)}{440} = (0.062)(0.091) = 0.0057$$

The secondary current at 480 volts would be

$$(1.0057)(34.8) = 35$$

The measured values were 34.7 and 34.9 amperes respectively.

Figure 11 is an oscillogram of a test made on the 75,000-ampere transductor. This oscillogram shows the alternating voltage on each of the a-c coils, the direct current, and the alternating current. The test was made at about 50 per cent direct current. The oscillogram shows the transient response of the transductor with a suddenly applied direct voltage. The direct current rises to its steady-state value. The alternating current has the characteristic square wave shape of the series-connected transductor. It follows the direct current very closely; the transient response of the series-connected current transductor is very excellent. The top two curves show the alternating voltage on the two a-c coils. Before application of the direct current, the voltages on the coils are sinusoidal and are about equal. As soon as the direct current is applied, each core is saturated in turn for a half-cycle. The voltage must appear across the other coil. Hence the alternating voltage on each a-c coil is double its normal value for a half-cycle and zero the other half-cycle after the direct current is applied.

The ripple in the direct current was due to the alternating voltage appearing across the d-c coils. This is a double-frequency voltage. Ordinarily, the impedance of the d-c circuit is large enough to keep the direct current uniform; but in this case, there was not quite enough impedance to make the direct current smooth

Figure 12 is a 2,000-to-1 ampere current transductor of the through-type construction. A unit of similar construction rated 4,000-to-4 amperes was tested on the parallel connection. The data and results for this unit are shown in Table II. The excitation curve for each core is shown in Figure 13. Two sets of calculated figures are shown in Table II. One set is calculated according to the two straight-line saturation curve method outlined previously and the other set is calculated by the method

Table II. Test and Calculated Values of Alternating Current for a Current Transductor, Parallel Connection

Primary current 4,000 amperes direct current; rated secondary current: 4 amperes alternating current; secondary excitation voltage: 58 volts, 60 cycles; parallel connected, $N_p = 1$; $N_s = 1{,}930$ turns; $E_s = 110$ volts; $X_t = 1{,}100$ ohms; $X_s = 11.7$ ohms; secondary resistance: 1.35 ohms; rated secondary burden: 2.5 ohms

Primary Amperes, D-C	Excitation Volts	Burden Resistance, Ohms	Test	Average Current, Amperes Calculated 2 Straight-Line	Universal Curve
4,000	72	0.8	4.20	4.00	4.11
4,000	58	0.8	4.14	3.90	4.07
4,000	43	0.8	4.02	3.91	
3,000	58	0.8	3.14	2.96	3.05
2,000	72	0.8	2.15	1.99	2.05
2,000	58	0.8	2.08	1.95	2.03
2,000	43	0.8	2.01	1.89	1.97
1,000	58	0.8	1.10	0.95	1.00
400	58	0.8	0.45	0.35	0.40

Figure 12. A 2,000-to-1 ampere current transductor

outlined in reference 1. The latter figures are closer to the test results, about 2 per cent low, while the two straight-line approximation calculates about 6 per cent low. The excitation-curve data was taken with an iron vane voltmeter; if a rectifier-type voltmeter had been used, the curve would be closer to the d-c magnetization curve.

Series Versus Parallel Connection

The series connection of the a-c coils is the simpler circuit, but there may be cases in which the use of the parallel connection is more desirable. If the d-c circuit has very low impedance, appreciable alternating current may circulate if the series connection is used. This will throw off the calibration of the instrument, although the variation is not a major one. With the parallel connection there is practically no alternating voltage across the d-c coil, and a parallel-connected transductor would be unaffected by the impedance of the d-c circuit. In other circuits, it is possible that the circuit could not tolerate the alternating voltage developed across the d-c coil. With these, the parallel connection may be more desirable.

When the direct current is small, with the series connection, there are times during a cycle when neither core is saturated. If the direct current should change rapidly at these low values of direct current, high peak voltages may be induced across the a-c coils. This does not occur at higher values of direct current, as under this condition one of the cores is always saturated, and the peak voltage induced in the other coil is short-circuited through the saturated coil and the a-c supply. In the lower current ratings, it may be possible to design the coil to stand the voltage. In higher current ratings, and where the peaks do not occur too often, it is possible to protect the coils with lightning arresters. Where too much current passes through the lightning arrester, a limit may be reached where this method is not practical. The parallel connection can be used in these cases. With this connection, the a-c component circulates harmlessly around the a-c coils. Another solution would be to wind the a-c coils for a lower voltage, which would then directly decrease the number of a-c turns and the peaked voltages.

Another application that might dictate the use of the series-connected current transductor is one where it is desired that the transient response will be very rapid. With the series connection, a ripple frequency in the direct current up to six times the excitation frequency should be faithfully reproduced in the alternating current. When the direct current is suddenly applied, the alternating current will follow the direct current faithfully as is shown in Figure 11. With the parallel connection, a sudden change in the direct current causes an equal and opposite current to circulate between the a-c coils. Until this current decays, there is no increase in the effective d-c magnetomotive force on the cores. It will require one or two cycles on a 60-cycle basis for the circulating current through the a-c coils to decay. For use with indicating instruments, this is sufficiently rapid, but for relaying, it may not be.

Accuracy

If the ammeters are specially calibrated with the current transductors, the only errors that can arise in application are those due to changes in excitation voltage and burden impedance. The latter about amounts to the former, for either one has the effect of changing the excitation voltage at the terminals of the transductor. By designing for higher values of excitation voltamperes, the sensitivity of the series-connected transductor to voltage changes can be reduced from that of the standard design. To demonstrate this, if it is assumed that the following sequence takes place:

Turns remain constant.
Core area increases.
$E_a \propto$ core area.
$E \propto$ core area.
$X_t \propto$ core area.
Excitation $VA \propto$ core area.

Then E_a/X_t and $E/_tX$ remain constant. Although casually it would be assumed that X_s also is proportional to the core area, such is not the case, for in the usual design X_s includes much flux in the air. Increasing the core area will not result in

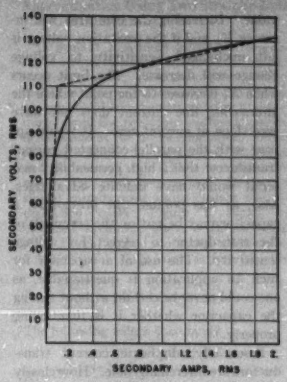

Figure 13. Excitation curve for current transductor

4,000 amperes direct current to 4 amperes alternating current; 60-cycle excitation curve for each core. $X_t = 1{,}100$ ohms, $X_s = 11.7$ ohms, and $E_a = 110$ volts

a proportionate increase in X_s. Consequently, the ratio of X_s/E will decrease as the core area increases. Referring to the equations for average and rms current for the series connections, it will be seen that this will result in decreased sensitivity to voltage changes. Another approach is possible where the alternating exciting current for the transductor at zero primary direct current is smaller than is necessary. In the lower current designs of around 2,000 amperes, this is not true, but around 10,000 to 20,000 amperes the current does become less than 1 per cent of rated current. If the mean length of the core is increased, X_t will decrease. X_s will decrease, as the thickness of the coil is decreased and the length increases. Increasing the length of the core is quite effective in reducing voltage sensitivity where the exciting current is not a limit. At the present time, a change of 2 per cent in current for a 10 per cent change in excitation voltage results in a unit that has reasonable dimensions and excitation-voltampere requirements. For this limit, 2,000 amperes direct current requires about 110 voltamperes excitation. The excitation increases more rapidly than the direct current so that at 20,000 amperes direct current, about 2,600 voltamperes are required.

With the parallel-connected transductor, apparently the major cause of sensitivity to voltage variations is due to X_t, the initial reactance, as long as the saturated reactance is less than a certain

value. Increasing the core area will increase X_t, and if the excitation voltage is left unchanged, sensitivity to voltage change will decrease. The limit occurs when X_t increases to the point where the alternating line current does not have zero slope at current zero. It would appear with the parallel-connected current transductor that a high permeability material would have definite advantages. Also, as was pointed out previously, a capacitor may be put on the terminals of the transductor to correct for voltage sensitivity. The use of a capacitor for such an application is questionable, as one could never be certain without testing the capacitor whether it is functioning properly.

Essentially, duplicate current transductors are interchangeable. How closely this is met can be demonstrated as follows. For the series-connected current transductor, the average current is

$$I_{avg} = \frac{N_p I_{do}}{N_s}\left[1 - 0.45\frac{X_t N_p I_{do}}{E\ N_s} - \frac{\sqrt{2}E_s/X_t}{N_p I_{do}/N_s} + \frac{0.9E/X_t}{N_p I_{do}/N_s}\right]$$

It is possible to adjust the iron stack on test so that the unit will have correct ratio at some particular value of current; for instance, 100 per cent current. At some other value of current, the ratio may not be the same as the reference unit though. For example, if the values in the foregoing equation at 100 per cent direct current are

$$I_{avg} = 1.118[1 - 0.10 - 0.02 + 0.015] = 1$$

At 50 per cent direct current, the value of I_{avg} will be

$$I_{avg} = 0.559[1 - 0.05 - 0.04 + 0.03] = 0.525$$

The dial of the meters would be calibrated to these values of currents, and would read properly. If another unit though, has other values of X_t, X_s, and E_s, the core stack would be adjusted so I_{avg} would be one at 100 per cent direct current. For instance, if another unit had these values at 100 per cent direct current.

$$I_{avg} = 1.118[1 - 0.095 - 0.04 + 0.03] = 1$$

But at 50 per cent direct current, I_{avg} now will be

$$I_{avg} = 0.559[1 - 0.0475 - 0.08 + 0.06] = 0.521$$

This is an error of 3/4 per cent based on the actual current, or 3/8 per cent based on rated current. These represent about the values for an average unit, and the variation that might be expected between units.

For the series-connected current transductor, the position of the return conductor may have some effect on the accuracy. Ideally, the a-c ampere turns should be distributed around each core so that for each element of length of the core, the a-c ampere turn can balance the d-c ampere turns. If this is not the case, there is danger of local saturation due to the return conductor principally. If the core is of sufficiently large size, the flux density in the core due to leakage flux caused by the return conductor may be small enough so that it will not produce local saturation of the core. The cores in current transductors are relatively small in area, so the ratio between the surface area and the cross-sectional area is large. These relative proportions tend to increase the leakage flux density in the core. Local saturation of the core due to the return conductor is almost always a problem in current transductors. It is best solved by winding the coils on each core so they can be connected in parallel. The alternating currents will then automatically divide between the various paths so that for the length of each coil the d-c and a-c ampere turns will be balanced. The number of parallel paths to use can best be determined by experience. Tests were made on a 2,000-ampere transductor at rated current with the following results. With two parallel circuits on each core, the secondary current was 100 per cent with the return conductor distant, and was 98.5 per cent with the return conductor close to the transductor. With all turns in series on each core and with the return conductor close to the transductor, the secondary current was 87 per cent. It is somewhat surprising that the secondary current decreases when the return conductor is brought closer to the transductor; instinctively, one would feel it should increase.

Conclusions

The current transductor, a device with many of the characteristics of the a-c transformer, is a practical piece of apparatus for metering direct currents. It has a secondary a-c output that is proportional to the input direct current and that is little affected by the burden in the metering circuit or the voltage or frequency of the excitation voltage. The secondary metering circuit is electrically isolated from the d-c circuit that is being metered.

The time of response is very rapid with the series-connected current transductor in the order of a fraction of a cycle. With the parallel-connected transductor, the time is in the order of one to two cycles, which is still sufficiently rapid for use with indicating instruments.

With meters specially calibrated with the transductors, and with voltage variations limited to 2 or 3 per cent, a maximum error in the order of 1/2 of 1 per cent plus the meter tolerance (about 1/2 of 1 per cent for the best meters) should be practical. For interchangeable manufacture of transductors and meters, and voltage variations of about 5 per cent, over-all accuracy of 2 per cent can be attained. It is possible to have better accuracy with larger excitation voltamperes, to a limit dependent on the characteristics of the core material.

The transductor will do some things the d-c shunt will not do. Some devices, such as thermal relays, would not operate too satisfactorily from a d-c shunt. The transductor provides insulation between the d-c circuit and the metering circuit. Transductors have been built for currents of 75,000 amperes and tested at 100,000 amperes direct current. This unit had 16.5-kva excitation at 75,000 amperes. The excitation can be reduced at the expense of accuracy. Transductors for higher currents than these should be feasible without any major difficulties. By proper design, the effect of the position of the return conductor can be made negligible, even at these high currents.

The transductor is not responsive to the direction of the direct current. The magnitude and phase position of the alternating current are unchanged with reversal of the direct current. There are various ways to overcome this difficulty by various auxiliary circuits or devices; but the inherent polarity indication of the d-c meter would be an advantage that would make it difficult to justify a transductor for these installations. Nevertheless, the transductor is a new device that will permit a new approach to an old problem. It should find a permanent place for itself in the field of instrumentation.

Appendix I. The Series-Connected Current Transductor

The centimeter-gram-second system of units is used in these appendixes. Based on the graphical method shown in Figure 3, it is possible, using the saturation curve and some approximations, to deduce some relations that will make the process of calculating performance somewhat simpler. Referring to Figure 14, top, the saturation curve for the core material is shown. This is really the effective curve as built into the unit. In the bottom part of the figure is shown the effective saturation curve from the secondary a-c terminals, which is the

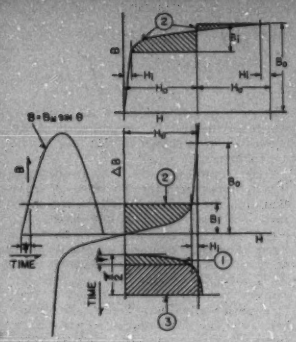

Figure 14 (left). Curves for series connection, for mathematical analysis

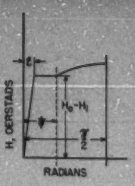

Figure 15 (right). Approximate curve for determining the rms current for series connection

sum of the ΔB curves for each of the cores for some value of d-c magnetomotive force, H_0. Also shown are the required flux density curve for sinusoidal applied secondary voltage and the resultant H curve as functions of time. A number of quantities are shown on the lower curve. H_0 is the magnetomotive force due to the primary direct current. B_0 is the sum of the flux changes in the two cores if an a-c magnetomotive force equal to H_0 is applied. The curve for ΔB is assumed to be a straight line above B_t, until the top knee is reached. It is evident by comparing the top and bottom curves that the values of B_0, B_t, and H_t can be read directly from the top excitation curve as shown.

The transductor is designed so that in virtually all cases the maximum total a-c flux density will be well in excess of B_t, so that referring to Figure 14, the relation between the a-c flux density and time will be virtually a straight line-up to a value of flux density change equal to B_t. Also, as we have pointed out, H is a linear function of ΔB above B_t.

To determine the average value of the a-c magnetomotive force, the areas 1 and 3 in Figure 14 must be determined. But the area 1 is equal to the area 2 times the ratio, ψ/B_t. This is true as long as the flux changes linearly with time to the angle ψ. The sum of the two areas indicated as 2 in the top excitation curve can be shown equal to the area 2 in the bottom curve. Then

$$B_m=\frac{\sqrt{2}E10^8}{\omega N_s A}\text{ gauss}$$

$$\psi=B_t/B_m=\frac{B_t\omega N_s A}{\sqrt{2}E10^8}\text{ radians}$$

$$\frac{\psi}{B_t}=\frac{1}{B_m}=\frac{\omega N_s A}{\sqrt{2}E10^8}$$

The relation between ΔB and H for ΔB larger than B_t is

$$\Delta B-B_0=\frac{B_0-B_t}{H_t}(H-H_0)$$

but

$$\Delta B=B_m\sin\theta$$

$$H=H_0+\frac{H_t}{B_0-B_t}(B_m\sin\theta-B_0)$$

$$H=H_0-\frac{H_tB_0}{B_0-B_t}+\frac{H_tB_m}{(B_0-B_t)}\sin\theta$$

The area 3 is

$$\text{Area 3}=\int_\psi^{\pi/2}H\,d\theta$$

$$=\left[H_0-\frac{H_tB_0}{B_0-B_t}\right]\left(\frac{\pi}{2}-\psi\right)+\frac{H_tB_m}{(B_0-B_t)}\cos\psi$$

The average a-c magnetomotive force then is

$$H_{ac\ avg}=\frac{(\text{area 1})+(\text{area 3})}{\pi/2}\text{ oerstads}$$

$$=\left\{(\text{area 2})(1/B_m)+\left[H_0-\frac{H_tB_0}{B_0-B_t}\right]\times\left(\frac{\pi}{2}-\psi\right)+\frac{H_tB_m}{(B_0-B_t)}\cos\psi\right\}\frac{2}{\pi}$$

where

$$\psi=B_t/B_m=\frac{B_t\omega N_s A}{\sqrt{2}E10^8}$$

The determination of the rms value of the a-c magnetomotive force can be approximated by the following method. Although the portion of the curve corresponding to area 1 is curved, it could be approximately replaced by a polygon as shown in Figure 15, which has the same area as area 1.

$$(\text{area 1})=(\text{area 2})\frac{1}{B_m}=\left(\psi-\frac{\epsilon}{2}\right)(H_0-H_t)$$

$$\epsilon=2\left[\psi-\frac{(\text{area 2})}{B_m(H_0-H_t)}\right]$$

Then

$\int_0^{\pi/2}H^2d\theta$ is

$$\int_0^\epsilon\left[\frac{H_0-H_t}{\epsilon}\theta\right]^2d\theta+\int_\epsilon^\psi(H_0-H_t)^2d\theta+\int_\psi^{\pi/2}\left[H_0-\frac{H_tB_0}{B_0-B_t}+\frac{H_tB_m}{B_0-B_t}\sin\theta\right]^2d\theta$$

$$=(H_0-H_t)\left(\psi-\frac{2\epsilon}{3}\right)+\left[H_0-\frac{H_tB_0}{B_0-B_t}\right]^2\times\left(\frac{\pi}{2}-\psi\right)+2\left(H_0-\frac{H_tB_0}{B_0-B_t}\right)\frac{H_tB_m}{B_0-B_t}\times\cos\psi+\left(\frac{H_tB_m}{B_0-B_t}\right)^2\frac{\pi}{4}$$

The rms value of H_{ac} then will be

$$H_{ac\text{-}rms}=\left[\frac{2}{\pi}\int_0^{\pi/2}H^2d\theta\right]^{1/2}\text{ oerstads}$$

Approximation Using Two Straight-Line A-C Excitation Curve

In general, it is more convenient to take the a-c saturation curve instead of the d-c saturation curve. The assumption will be made that the excitation current and voltage are sinusoidal and the permeability as determined from the peak flux and peak current is the same as the d-c permeability. If the exciting current is maintained sinusoidal and the voltage read with an average voltmeter, the peak current-peak flux curve should approximate quite closely the d-c excitation curve. Figure 8 shows an idealized excitation curve with an initial slope X_t and a final slope X_s. Saturation voltage is E_s. This curve is for one core.

$$B_m=\frac{\sqrt{2}E10^8}{\omega N_s A};\quad H=\frac{\sqrt{2}\,0.4\pi N_s I}{l}$$

The following values then apply

$$H_t=\frac{\sqrt{2}\,0.4\pi N_s E_s}{l\,X_t}$$

$$H_0=\frac{0.4\pi N_p I_{do}}{l}$$

$$B_t=\frac{\sqrt{2}\left[X_s2\left(\frac{I_{do}N_p}{\sqrt{2}N_s}-\frac{E_s}{X_t}\right)\right]10^8}{\omega N_s A}$$

$$B_0=\frac{\sqrt{2}\left[E_s+\frac{2X_sI_{do}N_p}{\sqrt{2}N_s}-\frac{X_sE_s}{X_t}\right]10^8}{\omega N_s A}$$

$$\text{Area 2}=\frac{1}{2}B_t(H_0-H_t)$$

$$=\frac{2X_s0.4\pi10^8}{\omega Al}\left(\frac{I_{do}N_p}{\sqrt{2}N_s}-\frac{E_s}{X_t}\right)^2$$

$$\psi=B_t/B_m=\frac{2X_s\left(\frac{I_{do}N_p}{\sqrt{2}N_s}-\frac{E_s}{X_t}\right)}{E}$$

Substituting these expressions in those for the average magnetomotive force above, and solving for the average line current, I_{avg}

$$I_{avg}=\frac{2}{\pi}\left\{\frac{X_s}{\sqrt{2}E}\left(\frac{I_{do}N_p}{N_s}-\sqrt{2}\frac{E_s}{X_t}\right)^2+\left[\frac{N_pI_{do}}{N_s}-\frac{\sqrt{2}E_s}{X_t}\right]\times\left(\frac{X_t-X_s+\frac{\sqrt{2}X_tX_sI_{do}N_p}{N_sE_s}}{X_t+X_s}\right)\times\left(\frac{\pi}{2}-\psi\right)+\frac{\sqrt{2}E}{X_t+X_s}\cos\psi\right\}$$

In this form the equation is rather difficult to use. A very useful and quite accurate approximation can be secured if X_t is large, as is usually the case, by letting $y=1/X_t$ in the expression for I_{avg}. Then expand I_{avg} as a function of y in a Maclaurin's series

$$I_{avg}=(I_{avg})_{y=0}+\left(\frac{dI_{avg}}{dy}\right)_{y=0}y$$

If this is done and X_t substituted back in, the resulting expression is

$$I_{avg}=\frac{N_pI_{dc}}{N_s}\left[1-\frac{\sqrt{2}}{\pi}\frac{X_s}{E}\frac{N_pI_{dc}}{N_s}\right]-\left[1-\frac{2\sqrt{2}X_sI_{dc}N_p}{\pi EN_s}\right]\left[1+\frac{\sqrt{2}X_sI_{dc}N_p}{N_sE_s}\right]\times\frac{\sqrt{2}E_s}{X_t}+\left(\cos\frac{\sqrt{2}X_sI_{dc}N_p}{EN_s}\right)\frac{\sqrt{2}\,2E}{\pi X_t}$$

In most cases

$$\frac{X_sI_{dc}N_p}{EN_s}\text{ and }\frac{X_sI_{dc}N_p}{E_sN_s}<{}^1/_4$$

and even if they are somewhat larger, the coefficients of $\sqrt{2}E_s/X_t$ and $2\sqrt{2}E/\pi Xi$ are such the coefficients will still be nearly unity. The expression reduces to

$$I_{avg}=\frac{N_pI_{dc}}{N_s}\left[1-\frac{\sqrt{2}}{\pi}\frac{X_s}{E}\frac{N_pI_{dc}}{N_s}\right]-\frac{\sqrt{2}E_s}{X_t}+\frac{2\sqrt{2}E}{\pi X_t}$$

A very similar process may be followed to find the value of the rms current. The expression for the rms current is

$$I_{rms}=\sqrt{\frac{2}{\pi}}\times\left\{\left(\frac{I_{dc}N_p}{N_s}-\frac{\sqrt{2}E_s}{X_t}\right)^2\frac{\psi}{3}+\left[\frac{I_{dc}N_p}{N_s}-\frac{\sqrt{2}\left(E_s+\frac{\sqrt{2}X_sI_{dc}N_p}{N_s}-\frac{X_s}{X_t}E_s\right)}{X_t+X_s}\right]^2\times\left(\frac{\pi}{2}-\psi\right)+2\left[\frac{I_{dc}N_p}{N_s}-\frac{\sqrt{2}\left(E_s+\frac{\sqrt{2}X_sI_{dc}N_p}{N_s}-\frac{X_s}{X_t}E_s\right)}{X_t+X_s}\right]\times\frac{\sqrt{2}E}{X_s+X_t}\cos\psi+\left(\frac{\sqrt{2}E}{X_s+X_t}\right)^2\frac{\pi}{4}\right\}^{1/2}$$

Expanding the part inside the brackets in a Maclaurin's series in y, where $y=1/Xi$, and then resubstituting in the expression $y=1/X_t$

$$I_{rms}=\sqrt{\frac{2}{\pi}}\times\left\{\left(\frac{I_{dc}N_p}{N_s}\right)^2\left(\frac{\pi}{2}-\frac{2\sqrt{2}X_sI_{dc}N_p}{3E\ N_s}\right)+\frac{1}{X_t}\left[\frac{2\sqrt{2}I_{dc}N_pE}{N_s}\times\cos\frac{\sqrt{2}X_sI_{dc}N_p}{E\ N_s}-2\sqrt{2}\frac{I_{dc}N_p}{N_s}\times\left(\frac{\pi}{2}-\frac{\sqrt{2}X_sI_{dc}N_p}{N_s\ E}\right)\left(E_s+\frac{\sqrt{2}X_sI_{dc}N_p}{N_s}\right)\right]\right\}^{1/2}$$

Neglecting the smaller parts of this expression

$$I_{rms}=\left\{\left(\frac{I_{dc}N_p}{N_s}\right)^2\left(1-\frac{4\sqrt{2}X_sI_{dc}N_p}{3\pi EN_s}\right)+\frac{1}{X_t}\left[\frac{4\sqrt{2}I_{dc}N_pE}{\pi N_s}-\frac{2\sqrt{2}I_{dc}N_pE_s}{N_s}\right]\right\}^{1/2}$$

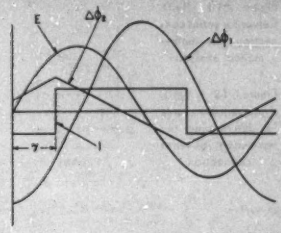

Figure 16. Phase angle at which alternating current is zero, with addition of resistance in series connection

which is very closely

$$I_{rms}=\frac{I_{dc}N_p}{N_s}\sqrt{1-\frac{4\sqrt{2}X_sI_{dc}N_p}{3\pi E\ N_s}}+\frac{2}{\pi}\frac{\sqrt{2}E}{X_t}-\frac{\sqrt{2}E_s}{X_t}$$

Addition of Series Burden in A-C Circuit

The addition of series reactance can be taken care of by adding to the values of X_s and X_t, a value equal to one-half of the series reactance. If this is done, it is seen from the foregoing analysis that at all points on a cycle the reactance is increased by twice one-half of the series reactance, which is what is desired. This makes it possible to use the same formula developed previously.

The addition of series resistance is more complicated. If there is no resistance in series with the a-c circuit, the phase angle at which the current goes through zero must lag the voltage zero by 90 degrees. Addition of resistance will reduce this phase angle. As a first approximation it will be assumed the current reverses instantaneously at current zero.

Then, referring to Figure 16, the following must be true

$$\int_0^{2\pi}ie\,d\theta=\frac{\sqrt{2}EI_{dc}N_p}{N_s}\left[\int_0^{\gamma}-\sin\theta\,d\theta+\int_{\gamma}^{\gamma+\pi}\sin\theta\,d\theta\int_{\gamma+\pi}^{2\pi}\sin\theta\,d\theta\right]=\frac{\sqrt{2}EI_{dc}N_p}{N_s}4\cos\gamma=\left(\frac{I_{dc}N_p}{N_s}\right)^2R2\pi$$

$$\cos\gamma=\frac{\pi}{2}\frac{I_{dc}N_p}{N_s}\frac{R}{\sqrt{2}E}$$

where R is the series resistance in ohms and includes the secondary resistance of the current transductor. This equality comes from the fact there can be no net energy storage in the inductance over a full cycle. The voltage induced in the transductor is

$$\sqrt{2}E\sin\omega t-iR$$

Again as a first approximation it is assumed the current reverses instantaneously at current zero.

The flux change in the core to develop this voltage is

$$\Delta\phi=\frac{10^8}{N_s}\int[\sqrt{2}E\sin\omega t-iR]dt=-\frac{\sqrt{2}\,E10^8}{\omega N_s}\cos\omega t-\frac{10^8}{N_s}\int iRdt+C$$

Also on Figure 16 are shown $\Delta\phi_1$, and $\Delta\phi_2$ which are the first and second parts of this equation. C is chosen so that $\Delta\phi_2$ has no d-c component.

Referring to Figure 14, if X_t is very large, it is apparent from the ΔB versus H curve that after the first knee at B_t the secondary current is constant and proportional to H_0, regardless of how the flux varies if the flux is larger than B_t. This will assume X_t is infinite, and that the change in current when X_t is not infinite is the same, whether R is zero or not, as long as the series drop through R is small compared to the applied voltage. The time required for the current to reverse is the same as the time for ΔB to change from $-B_t$ to $+B_t$. Referring to Figure 16, the current has been assumed rectangular, although it really is not. It is most likely the current is not even a straight line as it goes through zero, but it would not be too bad an approximation to say that the $\Delta\phi_2$ curve, which is essentially the integral of the "i" curve, is constant over the interval of the transient reversal of i. The time rate of change of $\Delta\phi$ is then the same as that of $\Delta\phi_1$. The time required for the current to reverse is then inversely proportional to the value of the time rate of change of $\Delta\phi_1$ at the angle γ. It is possible, though, to have a similar circuit with zero resistance and with a smaller alternating voltage that will cause the same rate of change of flux at current zero. This circuit should give the same current wave shape as our desired circuit, as the time required for the flux to reverse from $-B_t$ to $+B_t$ is the same. Call this effective voltage E_r

$$\Delta\phi_R=-\frac{\sqrt{2}E_r10^8}{\omega N_s}\cos\theta$$

$$\left(\frac{d\,\Delta\phi_r}{d\theta}\right)_{\theta=\pi/2}=+\frac{\sqrt{2}E_r10^8}{\omega N_s}$$

And for the actual voltage E

$$\Delta\phi=+\frac{\sqrt{2}E10^8}{\omega Ns}\cos\theta$$

$$\left(\frac{d\,\Delta\phi}{d\theta}\right)_{\theta=\gamma}=+\frac{\sqrt{2}E10^8}{\omega N_s}\sin\gamma=+\frac{\sqrt{2}E10^8}{\omega N_s}\sqrt{1-\left[\frac{\pi}{2}\frac{I_{dc}N_p}{N_s}\frac{R}{\sqrt{2}E}\right]^2}$$

Equating the two

$$E_r=\sqrt{E^2-\left[\frac{\pi}{2}\frac{I_{dc}N_p}{N_s}\frac{R}{\sqrt{2}}\right]^2}$$

The quantity $\pi/2\sqrt{2}=1.11$; so very closely, the effective voltage applied to the reactor is the *vector* difference between applied voltage and secondary resistance drop.

Appendix II. Solution for the Parallel Connection

In a series circuit consisting of constant resistance and constant or variable react-

ance which is supplied from an a-c supply, there cannot be any d-c component of current in the steady state.

$$E \sin(\omega t+\theta) = iR + \frac{d(N\phi)}{dt}10^{-8}$$

$$\int_0^\infty E \sin(\omega t+\theta)dt = \int_0^\infty \left[iR + \frac{d(N\phi)}{dt}10^{-8}\right]dt$$

$$\int_0^\infty E \sin(\omega t+\theta)dt = \int_0^\infty iRdt + 10^{-8}\left[N\phi\right]_0^\infty$$

As there is a definite resistance in the circuit, the current cannot be infinite. Also with all magnetic materials, the permeability is finite; therefore the flux linkages, the last term in the equation above, must be finite. The term to the left of the equal sign also is finite. Hence the term involving the current to the right of the equal sign must be finite, and therefore the d-c component of this current must approach zero as time approaches infinity. A variable reactance cannot produce rectification, a variable resistance can. With the series-connected current transductor, the alternating current that was determined had no d-c component, so the above principle did not need to be considered. With the parallel-connected current transductor, use was made of this principle.

A previous paper[1] gives a general method for calculating performance of the parallel-connected current transductor. The method is very good and has the desired accuracy for calculation purposes. As it is graphical, though, it is difficult to see how the various quantities affect the performance as a current transductor. It is possible to develop some approximate relations that will give the secondary current mathematically, and will give a different viewpoint to the problem.

It is assumed the circuit is as in Figure 1(B). The d-c saturation curve will be assumed to be two straight lines, as shown in Figure 17. The figure shows the characteristics for one core. This analysis will use the artifice of the previous paper[1] of the reduced saturation curve. Referring to Figure 17, the actual saturation curve is assumed to have an initial slope of μ_i, and a final slope of μ_s, with saturation at B_s. The equations for the two portions of the curve are shown on the figure. The artifice then is introduced of the reduced saturation curve, shown dotted in Figure 17, where the initial straight-line portion of the actual curve is subtracted out. Obviously then, H_r, the reduced magnetomotive force, is zero up to B_s, and above B_s is

$$H_r = \left[\frac{B}{\mu_s} + B_s\left(\frac{1}{\mu_i} - \frac{1}{\mu_s}\right)\right] - \frac{B}{\mu_i} = (B - B_s)\left(\frac{1}{\mu_s} - \frac{1}{\mu_i}\right)$$

It is now possible to quite simply find the d-c magnetomotive force for a particular value of B_0, the d-c flux in the core, for the H_r curve; as H_r is zero for values of flux less than B_s. This was explained in the main part of this paper. The actual value we desire, though, is

$$H = H_r + B/\mu_i = H_r + \frac{1}{\mu_i}(B_0 + B_m \cos\theta)$$

The added portion consists of a pure d-c component and a pure a-c component. The d-c component means there will be an increase in the required d-c excitation. The a-c component will mean there will be an increase in the alternating current. For the opposite core, exactly the same increase in d-c excitation will be required, and an added alternating current will flow in the secondary in exactly the same phase position and magnitude as the above core. The two currents then will add for the total secondary line current.

The principle quantity that is not known is the value of B_0, the d-c biasing flux. As the added direct current due to B_0 is small, it is not needed to know B_0 too accurately, so this approximation will be made

$$B = B_0 + B_m \cos\theta = B_0 + B_m - B_m\frac{\theta^2}{2}$$

This is a good approximation in the range over which θ will be used, from $-\pi/2$ to $+\pi/2$.

$$H_r = (B - B_s)\left(\frac{1}{\mu_s} - \frac{1}{\mu_i}\right) = \left(B_0 + B_m - B_m\frac{\theta^2}{2} - B_s\right)\frac{1}{\mu_s}$$

Let

$H_r = 0$ when $\theta = \phi$

then

$$B_0 = B_m\frac{\phi^2}{2} + B_s - B_m$$

$$H_r = \frac{B_m}{2\mu_s}(\phi^2 - \theta^2)$$

$$H_{dcr}2\pi = \int_{-\phi}^{+\phi} H_r d\theta = \frac{2B_m\phi^3}{3\mu_s}$$

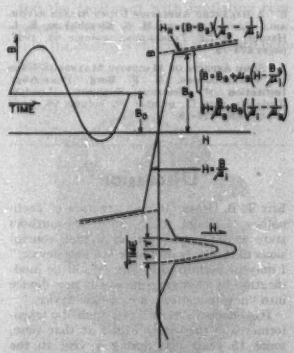

Figure 17. Two straight-line excitation curve and reduced excitation curve for parallel-connected current transductor

$$\phi = \left(\frac{3\mu_s H_{dcr}\pi}{B_m}\right)^{1/3}$$

$$B_0 = B_s - B_m + \left(\frac{3\pi}{2}\right)^{2/3}(\mu_s H_{dcr})^{2/3}B_m^{1/3}$$

$$= B_s - B_m + 2.33(\mu_s H_{dcr})^{2/3}B_m^{1/3}$$

as μ_s and μ_i are very nearly equal.

H_{dc}, the actual primary d-c mangetomotive force becomes

$$H_{dc} = H_{dcr} + \frac{B_0}{\mu_i}$$

$$H_{dcr} = H_{dc} - \frac{1}{\mu_i}\left[B_s - B_m + 2.23(\mu_s^2 H_{dcr}^2 B_m)^{1/3}\right]$$

For all practical purposes, H_{dcr} will be equal to H_{ds}, and H_{dc} can be used in place of H_{dcr} in the right-hand side of the foregoing expression.

The average value of the a-c magnetomotive force based on the line current is twice H_{acr}. To this must be added twice the average value of the added a-c magnetomotive force due to the initial slope of the saturation curve.

The total line magnetomotive force would be

$$H_{tot} = 2\left\{H_{dc} - \frac{1}{\mu_i}\left[B_s - B_m + 2.23(\mu_s^2 H_{dc}^2 B_m)^{1/3}\right]\right\} + 2\frac{2}{\pi}\frac{B_m}{\mu_i}$$

$$= 2\left\{H_{dc} - \frac{1}{\mu_i}\left[B_s - \left(1 + \frac{2}{\pi}\right)B_m + 2.23(\mu_s^2 H_{dc}^2 B_m)^{1/3}\right]\right\}$$

If it is assumed that the two straight-line a-c saturation curve shown in Figure 8 is the same as the d-c saturation curve, and that the same remarks made concerning this curve under the series analysis apply, the following would be true

$$\mu_i = \frac{X_i 10^8}{\omega 0.4\pi N_s^2 A}$$

$$\mu_s = \frac{X_s 10^8}{\omega 0.4\pi N_s^2 A}$$

$$B_m = \frac{\sqrt{2}E10^8}{\omega N_s A}$$

$$B_s = \frac{\sqrt{2}E_s 10^8}{\omega N_s A}$$

$$H_{dc} = \frac{0.4\pi N_p I_{dc}}{l}$$

$$H_{acl} = \frac{0.4\pi N_s I_{acl}}{l}$$

Substituting these in the expression for H_{acl}

$$I_{acl} = \frac{2N_p I_{dc}}{N_s} - \frac{2}{X_s}\left[\sqrt{2}E_s - 2.32E + 2.5X_s^{2/3}\left(\frac{N_p I_{dc}}{N_s}\right)^{2/3}E^{1/3}\right]$$

This is good only as long as the angle of current flow is less than π radians. Substituting the above quantities for μ_s, H_{dc}, and B_m in the equation for ϕ

Figure 18. The 75,000-ampere transductor as installed on the d-c bus

The transductor opening is 11 by 34 inches

$$\phi = 1.88\left(\frac{X_s N_p I_{dc}}{N_s E}\right)^{1/2}$$

$$\text{If } \phi = \pi/2;\ I_{dc} = 0.583\frac{N_s E}{N_p X_s}$$

The rms currents flowing vary considerably, depending on X_s, the slope of the saturation curve over the knee. Use of the rms currents for metering is impractical; but where it is desirable to know them, they can be calculated from the previous paper.[1] An approximate formula for a one straight-line saturation curve can be deduced and may be of use.

This assumes μ_l is infinite and μ_s is finite, and ϕ is less than $\pi/2$.

$$H = \frac{B_m}{2\mu_s}(\phi^2 - \theta^2)$$

$$\pi H^2{}_{(ac\,l\text{-}rms)} = \int_{-\phi}^{+\phi} H^2 d\theta = \frac{B_m{}^2 4\phi^5}{\mu_s{}^2 15} = \frac{4}{15}(3\pi)^{5/2}\left(\frac{B_m}{\mu_s}\right)^{1/2} H_{dc}{}^{5/2}$$

Substituting the value of B_m, μ_s, and H_{dc} in this, the line current is

$$I_{ac\,l\ rms} = 2\left[I_{dc}\frac{N_p}{N_s}\right]^{3/4}\left(E/X_s\right)^{1/4}$$

It also is possible to find the value of the winding rms alternating current. Referring to Figure 6, the total magnetomotive force for one core is the same as the line magnetomotive force, except the line magnetomotive force has positive and negative lobes, whereas the total magnetomotive force for one core has only one lobe. The rms value of the total magnetomotive force for one core then is equal to 0.707 times the line magnetomotive force. Since the actual a-c winding current has no d-c component, it follows

$$(0.707\ H_{ac\,l\ rms})^2 = H_{acw\ rms}{}^2 + H_{dc}{}^2$$

$$H_{acw\ rms} = \left[\frac{H_{ac\,l\ rms}{}^2}{2} - H_{dc}{}^2\right]^{1/2}$$

This formula applies as long as ϕ is equal to or less than 90 degrees.

This above equation, rewritten in terms of current is

$$I_{acw\ rms} = \left[\frac{I_{ac\,l\ rms}{}^2}{2} - \left(\frac{N_p I_{dc}}{N_s}\right)^2\right]^{1/2}$$

Effect of Series Resistance and Reactance

No attempt is made to develop formulas to take care of the series resistance and reactance. Reference 1 recommends that the series voltage drop be subtracted vectorially from the applied alternating voltage, and performance of the reactor calculated with this voltage. This assumes the current is sinusoidal, which is true if ϕ is 90 degrees. It is probably close enough even if ϕ is less than 90 degrees.

References

1. Universal Curves for D-C Controllable Reactors, **W. C. Johnson, B. C. Merrell, R. E. Alley, Jr.** *AIEE Transactions*, volume 68, part I, 1949, pages 31–39.

2. The Transductor with Special Reference to Transductor Control of Rectifiers (book), **Uno Lamm.** Esselte Aktiebolag, Stockholm, Sweden, 1943.

3. Effect of Direct Current in Transformer Windings, **E. L. Harder.** *The Electric Journal* (Pittsburgh, Pa.), volume 27, October 1930, pages 601–07.

4. Some Fundamentals of a Theory of the Transductor or Magnetic Amplifier, **Uno Lamm.** *AIEE Transactions*, volume 66, 1947, pages 1078–85.

5. Transductor Fundamentals, **Sven-Eric Hedstrom, Lennart F. Borg.** *Electronics* (New York, N. Y.), September 1948, pages 88–93.

6. A Balanced Amplifier Using Biased Saturable Core Reactors, **H. S. Kirschbaum, E. L. Harder.** *AIEE Transactions*, volume 66, 1947, pages 273–78.

7. Some Aspects of Magnetic Materials Used in Transductors, **L. F. Borg.** *Proceedings*, Institution of Electrical Engineers (London, England), part II, number 50, volume 96, April 1949, pages 310–18.

Discussion

Eric T. B. Gross (Illinois Institute of Technology, Chicago, Ill.): Since the authors state in the last paragraph of their conclusions that "the transductor is a new device," I may be permitted to suggest a little modification by changing the words new device into "new name for a not-so-new device."

It so happens that I saw such d-c transformers, as they were called at that time, some 15 years ago during a visit to the shops of the AEG Transformer Works in Berlin, where they were built for commercial applications similar to those described in the paper. W. Kraemer, who was mainly responsible for the first commercial design of these transductors, described this work in a number of papers, two of which are listed below.[5,2]

However, I should think that the new materials which we now have available brought about further improvements, though no changes of the principle of operation, which is still older than the commercial application, and I am wondering if the authors would care to indicate the differences between the transductors of today, and the d-c transformers of the past.

References

1. A Simple D-C Instrument Transformer with Real Current-Transformer Characteristics, **W. Kraemer.** *Elektrotechnische Zeitschrift* (Berlin, Germany), volume 58, 1937, pages 1309–13.

2. New D-C Current Transformer for Heavy Current Circuits, **W. Kraemer.** *A. E. G. Mitteilungen* (Berlin, Germany), March 1938, pages 113–16.

E. C. Wentz (Westinghouse Electric Corporation, Sharon, Pa.): This paper is particularly valuable on account of the complete and quantitative nature of the material given. Admittedly there is a great deal of mathematics in the paper, but the result of this mathematics is very real and practical; one can calculate the exact performance of the transductor from the data given.

Of particular interest is the discussion of the parallel-connected transductor and the demonstration that the output in average current as distinguished from rms is a relatively simple function and calculated very easily.

Of course, the rms current also can be calculated according to the paper, but the difficulty with rms current is that most standard ammeters do not actually read rms current if the wave form is distorted. Average reading ammeters are available in milliampere sizes and can be used with a current transformer. At the present time there are no standard current transformers with milliampere secondaries, and the exact measurement of ratio of such transformers cannot be accomplished on the conventional current transformer test sets; but there seems to be a good possibility that these gaps can be filled in. This would make possible the design, construction, and application of transductors on the same basis as conventional current transformers, and would eliminate the present necessity for calibration of ammeters with transductors.

T. R. Specht and **R. N. Wagner:** In reply to Mr. Gross' comments, relatively, the current transductor is new in this country. There has been little in American literature, and practically no current transductors have been built.

In the current transductor, the quality of the core material does not cause a major change in the characteristics of the device. There are applications, such as magnetic amplifiers and mechanical rectifiers, where the modern core materials with rectangular hysteresis loops are very desirable and have considerable effect on performance.

This is not the case with the current transductor.

A New Dry-Type Insulation for Instrument Transformers

R. A. PFUNTNER
ASSOCIATE AIEE

R. E. FRANCK
ASSOCIATE AIEE

F. R. D'ENTREMONT
ASSOCIATE AIEE

ONE OF the most important functions of instrument transformers is that of insulation. Whether it is a high voltage or a high current that is to be measured, the measurement can be made in a practical manner only if the end device is insulated from the normally high circuit voltage.

It has been considered good practice to use two types of instrument transformer insulation depending on the circuit voltage. In general, above 15,000 volts, liquid-filled designs have been used, while below this voltage the dry or compound-filled construction has been employed.

A new dry-type insulation, a molded butyl compound, has recently been developed. This new insulation possesses many outstanding advantages over former dry-type insulation. The use of molded butyl insulation on a 5,000-volt indoor current transformer is shown in Figure 1.

Present Types of Dry- or Compound-Filled Insulation

Dry Type

Present practice of producing dry-type instrument transformers differs somewhat in detail between various manufacturers, but the basic process is essentially the same for all. The coils are wrapped with a fibrous material in the form of tape or sheets so that a given number of layers of insulation cover the entire surface of the coil. This taping is usually applied to the high-voltage coil and is sometimes repeated to a lesser degree on the low-voltage coil. The coils are then assembled together and the core is placed in position. The complete assembly is dried out thoroughly and vacuum-impregnated with an insulating compound.

Some manufacturers use crepe paper for wrapping the coils and others use varnished cambric or other similar materials. Asphalt compound or varnish usually is used as the impregnating medium.

Compound Filled

Compound-filled transformers are insulated in much the same manner as dry types, except that a metal and porcelain casing is placed around the core and coils and the treatment with insulating compound is done in this casing. As a result, the casing is entirely filled with compound.

New Molded Butyl Insulation

The new butyl insulation is placed around the coils of the transformer by a molding process. The core and coils are assembled together without previously being wrapped with any insulating material. In the current transformer design shown in Figure 1, the low-voltage coils are mounted on the legs of the core. The high-voltage coils are assembled over the low-voltage coils and core with adequate clearance between parts to provide space for the butyl insulation. This complete assembly is given in Figure 2.

The assembly then is placed in the mold which has an internal cavity that will form the outside contour of the transformer. The proper relationship between parts is determined by the mold, which supports the components in such a manner as to provide continuous and homogeneous insulation throughout the transformer. Butyl compound is injected into the mold under controlled pressure and temperature conditions. After curing for the proper time and temperature, the completely insulated transformer is removed from the mold.

Both the new process for insulating instrument transformers, and the butyl compound used in the process, have distinct advantages over former types of hand-taped and impregnated forms of insulation.

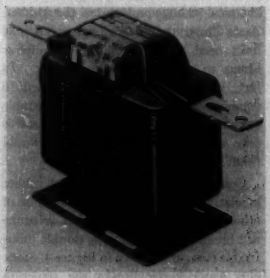

Figure 1. General Electric type JKM-3 butyl-molded instrument current transformer

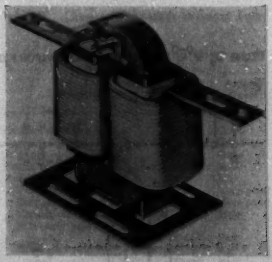

Figure 2. Assembled core, windings, and base of type JKM-3 instrument current transformer before molding with butyl

Paper 50-66, recommended by the AIEE Transformers Committee and approved by the AIEE Technical Program Committee for presentation at the AIEE Winter General Meeting, New York, N. Y., January 30-February 3, 1950. Manuscript submitted July 19, 1949; made available for printing December 2, 1949.

R. A. Pfuntner, R. E. Franck, and F. R. D'Entremont are all with the General Electric Company, West Lynn, Mass.

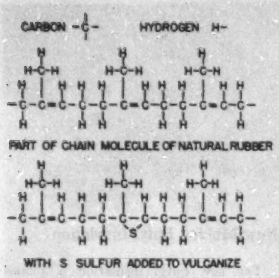

Figure 3. Structural representation of natural rubber molecule

The molding process assures machine precision of dimensions, as well as producing a 1-piece homogeneous insulation which completely surrounds the high-voltage winding, fills all the spaces between the windings and the core, and forms a protective coating over the outside of the transformer. Molding also provides a ready means of obtaining an attractive appearance in the finished product.

The special butyl compound used in the process has excellent dielectric properties over a wide range of temperature and humidity, and will withstand many abnormal operating conditions without serious deterioration. It is tough and resilient so that it will withstand the mechanical shocks of high overloads and accidental rough handling without damage to the transformer.

Description of Transformer Butyl Compound

Butyl is a synthetic rubber-like material developed just prior to, and during the war. One major application for this material at the present time is for automobile inner tubes, since butyl holds air extremely well. Another application is for cable insulation; a special compound with excellent electrical properties having been developed for this purpose. The basic gum used in cable butyl is compounded with slightly different fillers to make transformer insulation.

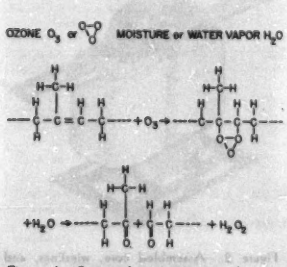

Figure 4. Structural representation of ozone and moisture attack on natural rubber

The basic gum is a co-polymer of polyisobutylene and isoprene, both derived from petroleum. Polyisobutylene is a gum-like material made up of carbon and hydrogen atoms so joined together as to be relatively inactive chemically. As such, it cannot be vulcanized with sulphur or other agents to change the soft gum into a rubber-like product. However, by the addition of 1 to 3 per cent of isoprene, which is vulcanizable, the entire mixture can be vulcanized to impart to it many of the excellent physical properties of natural rubber, without the relative chemical instability of this material.

To understand the chemistry of butyl, let us compare it with that of natural rubber. Natural rubber also is a gum-like material composed of carbon and hydrogen atoms. As represented in Figure 3, these are joined together chemically by valence bonds or links; hydrogen requiring one link to be chemically combined, and carbon requiring four. In natural rubber, the ratio of carbon to hydrogen atoms is five to eight, and these are arranged as shown, in long chains forming very large molecules.

As is illustrated, hydrogen is joined with single links while four links must radiate from each carbon atom. However, there are not enough hydrogen atoms in natural rubber, so two carbons are double linked together. This is a relatively unstable condition, and the addition of another element, such as sulphur, destroys the double link which for the purposes of this paper is shown in simplified schematic form in Figure 3. This chemical change vulcanizes the rubber. As is illustrated, not all of the double links need to be stabilized by sulphur atoms to get proper vulcanization. In fact, if enough sulphur were added to combine completely with all the unstable carbon atoms, hard rubber such as was once used on telephone receivers would result.

Consequently, even vulcanized rubber is relatively unstable, and the addition of other elements such as oxygen or ozone will break up the remaining double links. In this case, as is shown in Figure 4, ozone plus water vapor breaks the structure apart and destroys the rubber properties. Cracking and hardening, usually found in old rubber, are characteristic of this destruction.

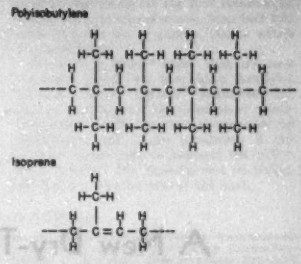

Figure 5. Structural representation butyl compound

Butyl gum, on the other hand, does not have this instability. Polyisobutylene, which comprises 97 to 99 per cent of the gum, has no double links, as is illustrated in Figure 5. The 1 to 3 per cent of isoprene, also illustrated in this figure, has the same double links as found in natural rubber. However, practically all of these extra valence bonds are used up in the vulcanization process, so that a remarkably stable material results.

To use butyl gum for insulation, it must be mixed or compounded with suitable fillers to give it increased hardness, and with a small amount of sulphur and other similar agents, to provide for vulcanization. This compounding changes the sticky translucent gum to the opaque vulcanizable material used in the molding of transformers. The vulcanizing process, which produces the tough, flexible insulation of the final product, occurs during the cure, after the butyl has been completely injected into the mold and around the other parts of the transformer.

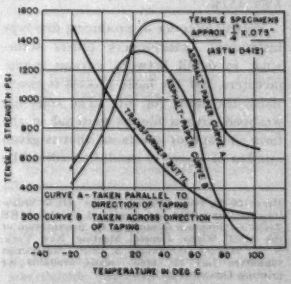

Figure 6. Tensile strength versus temperature transformer butyl and asphalt paper

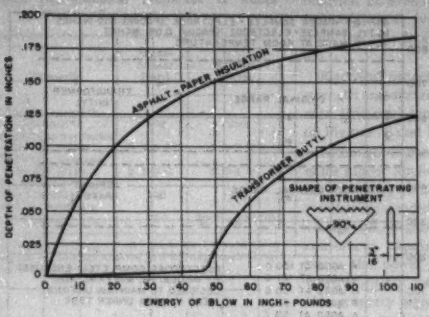

Figure 7 (left). Resistance to mechanical damage—transformer butyl and asphalt paper

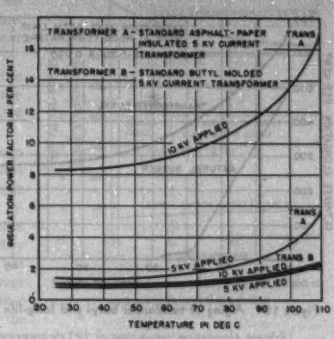

Figure 9 (right). Power factor versus temperature—transformer butyl and asphalt paper

Characteristics of Butyl Insulation

Before butyl insulation could be used for instrument transformers, its properties had to be evaluated in terms of all the various conditions such insulation is required to meet. These characteristics were determined primarily by laboratory test. Since the first instrument transformer placed in production using butyl insulation was the 5,000-volt indoor current transformer illustrated in Figure 1, the over-all performance of butyl was evaluated by tests on this design. Many individual properties also were evaluated by tests on other designs of current transformers, and on other, simpler test samples. For control purposes, samples of asphalt-impregnated paper insulation of the type presently used on dry-type transformers also were included in the tests.

Physical Properties

The physical properties of both the special transformer butyl compound and the present asphalt-paper insulation are shown in Table I. The tensile strength of both materials varies with temperature. As indicated in Figure 6, the direction of lamination affects the strength of asphalt-paper, while butyl has the same strength in all directions. At the normal top operating temperature of 85 to 95 degrees centigrade, butyl is stronger than the older insulation, although both are adequate for the application.

The elongation of butyl is much greater than that for asphalt-paper, which is a distinct advantage, since the thermal expansion of parts and severe distortion forces caused by high momentary overloads or accidental rough handling will not crack the butyl.

As shown in Figure 7, butyl is much more resistant to mechanical damage than the older style insulation. The depth of penetration listed in this curve is the permanent damage done to the insulation; the depth of the cut in the material after each blow.

Chemical Properties

Comparative chemical properties of transformer butyl and asphalt-paper are listed in Table II. Like most organic insulations, butyl compound is attacked by organic solvents, but its resistance to these materials is much greater than that of asphalt paper.

Toluene, for example, completely dissolved the asphalt from asphalt-paper insulation in six hours at room temperature. Butyl swelled to 65 per cent larger volume and its elongation was reduced from 680 per cent to 100 per cent in one day, and very little further change occurred in three weeks. Thus, while butyl is attacked by toluene, the rate of attack and severity of the result are much less than for the older insulation. Carbontetrachloride and various light oils also gave similar results as indicated in the table.

Acids do not affect butyl appreciably, but do attack asphalt-paper. A 30-per cent solution of sulphuric acid left no visible signs of attack on butyl after three weeks at room temperature. Asphalt-paper, during the same period, lost most of its tensile strength, probably because the paper was attacked by the acid.

Alkalis do not affect butyl but do attack asphalt paper. A 10-per cent solution of sodium hydroxide delaminated the

Table I. Physical Properties at Room Temperature

Property	Transformer Butyl	Asphalt-Paper
Tensile Strength (ASTM D412) (lb/sq. in.)	700	1300
Elongation (ASTM D412)	680%	10–30%
Hardness (Shore "A")	50	90
Elasticity (Shore)	38	
Abrasion resistance	Satisfactory	Satisfactory
Flexing resistance	Excellent	Poor
Cutting resistance	Satisfactory	Satisfactory
Tear resistance	Satisfactory	Satisfactory
Resistance to mechanical damage	Excellent	Good
Specific gravity	1.3	1.1
Water absorption*	7%	30%
Specific heat	0.36	0.30
Thermal conductivity (Cal/sec/cm²/deg C)	6.45×10^{-4}	5.02×10^{-4}

*Per cent weight increase after one week immersion in 70 degree centigrade water.

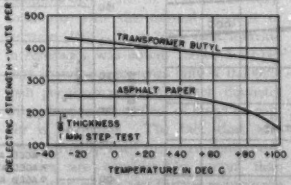

Figure 8. Dielectric strength (60 cycle) versus temperature

Transformer butyl and asphalt paper

Table II. Chemical Properties at Room Temperature

Property	Transformer Butyl	Asphalt-Paper
Corona resistance	Good	Good
Ozone resistance	Good	Good
Sunlight resistance	Good	Good
Flame resistance	Good	Poor
Resistance to attack by:		
Toluene	Poor	Very poor
Carbontetrachloride	Poor	Very poor
Transit oil	Fair	Poor
Sulphuric acid (30% solution)	Good	Fair
Sulphuric acid (3% solution)	Good	Fair
Sodium hydroxide (10% solution)	Good	Poor
Sodium hydroxide (1% solution)	Good	Fair

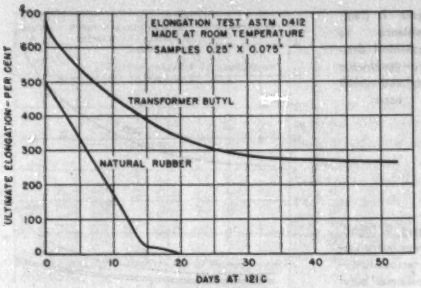

Figure 10. Aging of transformer butyl and long-life natural rubber

Ultimate elongation versus time at 121 degrees centigrade

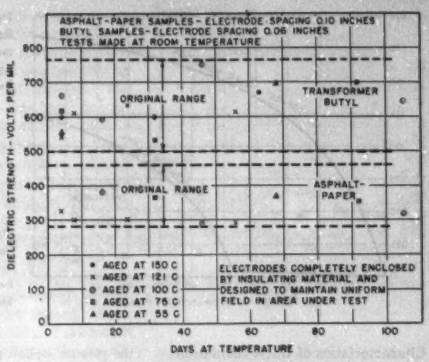

Figure 12. Aging of transformer butyl and asphalt paper

Dielectric strength versus time at temperature

asphalt-paper insulation in one day, but showed only a slight surface hardening on the butyl after three weeks.

Butyl also is more flame-resistant than asphalt-paper. Both will burn under the right circumstances, but butyl burns much less readily and much slower. A test used by one fire insurance company is to play the hottest part of a bunsen burner flame on the sample for 15 seconds, remove it for an equivalent time, and repeat until the sample continues burning during the entire interval between applications of the flame. Under this test, butyl averaged eight cycles while asphalt-paper continues burning after the first application of flame.

Electrical Properties

Comparative electrical properties of transformer butyl and asphalt-paper insulation are shown in Table III. As may be seen, the dielectric strength is much higher for the new material. However, such factors as the thickness of butyl tested, the thickness of the paper, and thus the number of layers, in the asphalt-paper sample, will affect the absolute value of the result. In general the relationship between both types of insulation will be maintained under all ordinary conditions. The effect of temperature on the dielectric strength of both materials is shown in Figure 8.

The insulation power factor is considerably lower for butyl than for asphalt-paper. Again, the specific design on which these insulations are used may cause the power-factor to vary somewhat from the range indicated which is for the materials above. The power factor of molded butyl is not appreciably changed by variations in temperature or voltage; a distinct advantage. The power factor of asphalt-paper insulation is affected much more as shown on Figure 9.

Stability of Properties with Time and Other Factors

In order to make as complete an evaluation as possible, the ability of butyl to retain its properties under various conditions was investigated.

The effect of time and temperature on the various properties of the special transformer butyl compound is shown in Figures 10 through 13. As shown on Figure 10, butyl at 121 degrees centigrade remains elastic for a much longer period than long-life natural rubber of the type used for cable insulation. Since the normal operating temperature is under 100 centigrade, this test represents an accelerated condition. The change in tensile strength, as shown on Figure 11, also

Figure 11. Aging of transformer butyl—tensile strength versus time at temperature

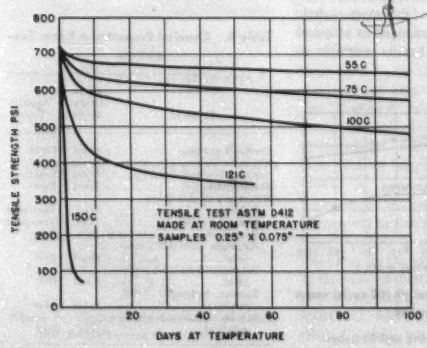

Figure 13. Aging of transformer butyl—arc tracking versus time at temperature

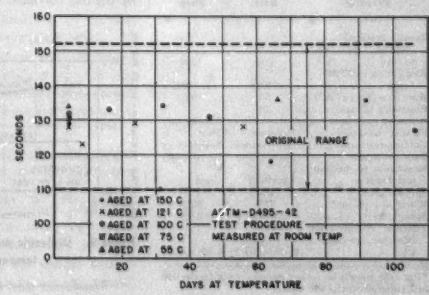

Table III. Electrical Properties at Room Temperature

Property	Transformer Butyl	Asphalt-Paper
Dielectric strength (volts/mil)*	400	250
60-cycle power factor (ASTM D150)	0.8–0.8%	1.0–3.0%
Dielectric constant (ASTM D150)	2.5–3.5	3.0–4.0
Arc tracking (seconds ASTM-D495-42)	130	130
Volume resistivity (ohms/cm³)	10^{15}	10^{14} to 5×10^{14}

*Dielectric strength tests made on 1/8-inch thick samples. Voltage applied in 5-kv steps each of one minute duration.

is very small in the operating temperature range. Other physical properties, such as elongation and elasticity, exhibited a similar change with time and temperature.

Because these tests were made on thin sheets of butyl there appears to be an aging effect. Additional tests have shown that the deterioration of the material is a surface effect, working from the outside in. Complete transformers, for example, exhibited signs of cracking and deterioration on the surface after 1,500 hours at 150 centigrade. However, dissection of the transformers after test showed that good solid butyl existed 1/16 to 1/8 inch beneath the surface, and thin sheets cut from these inner sections showed normal values of hardness and elongation, and a 30 to 50 per cent reduction in tensile strength from initial values. Thus, the changes in the sheets which

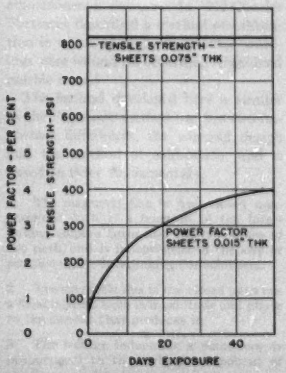

Figure 14. Transformer butyl sheets: effect of exposure to 90 per cent relative humidity at 35 degrees centigrade

occurred at even 150 centigrade are interesting data, but are not significant from the standpoint of the transformer life.

Electrical properties, such as dielectric strength and arc tracking, show no change with time and temperature as indicated on Figures 12 and 13.

Although the new transformer design is for indoor applications only, the effect of humidity and simulated outside weathering conditions on butyl was investigated. Figures 14 and 15 show that continuous exposure to high humidity raises the power factor somewhat, but weatherometer conditions do not change this property significantly. Again these tests were made on thin sheets where the surface effect greatly exaggerates the changes.

Since a small amount (approximately 0.5 per cent) of sulphur is needed to vulcanize the transformer butyl, the possibility of the molded insulation corroding the copper parts of the transformer was investigated. Figure 16 shows typical time versus resistance curves for very small wires molded in butyl and exposed to various temperature and humidity conditions. As indicated by the flattening of the curves, the corrosive effect becomes negligible after a short period of time, probably because all the sulphur compounds in the butyl adjacent to the copper are used up, and the rate of additional sulphur penetration to this area is extremely slow.

Corrosion data for various sizes of wire, temperatures, and amounts of sulphur in the butyl are shown in the Graeco-Latin squares of Figure 17 for tests in air and water vapor. The notation, 100% S, indicates the amount of sulphur (approximately 0.5 per cent) used in transformer butyl. Other amounts, varying as shown from this normal value, were milled into the butyl for the other samples.

The percentage figure shown in the center of each square (1%, 4%, 12%, and so forth) indicates the ultimate increase in resistance as shown for typical examples on Figure 16. Under the worst condition with the normal amount of sulphur (100% S), a 3 per cent increase in resistance was noted. Since a 10 per cent increase represents only a 0.00025-inch penetration in 0.010-inch diameter wire, the corrosive effect of butyl on copper is negligible. The fact that wire sizes normally used in instrument transformers are considerably larger than those used in this test further reduces the significance of corrosion as a factor in transformer life.

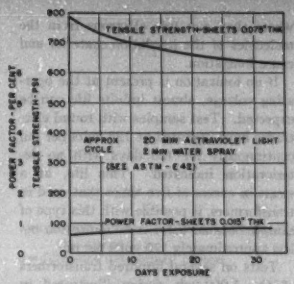

Figure 15. Transformer butyl sheets: effect of exposure in weatherometer

Ionization Characteristics of Butyl

The foregoing data indicates that butyl has very excellent properties as a transformer insulation, and that these properties may reasonably be expected to remain constant for long periods of time under the many conditions of use to which transformers might be exposed. However, any insulation material will fail in a relatively short time if it is operated continuously at too high a voltage stress, even though this stress is considerably below the short-time dielectric breakdown value. The importance of this phenomena has warranted the investigation of many types of material by various methods. In general, the most widely accepted method is that of determining the amount of ionization present at the operating voltage.

As applied to electrical insulation materials, ionization is commonly thought of as a phenomenon resulting from the bombardment of molecules by particles of atomic or even smaller dimensions. When the voltage stress is high enough these particles are accelerated to a point

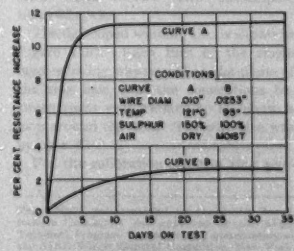

Figure 16. Corrosion of bare copper wire molded in transformer butyl

Typical time versus resistance curves

where they can free electrons from the molecules of the insulation material and cause ionization.

If no ionization is present at the operating voltage, almost infinite life can be expected. Test samples with round electrodes have operated at 125 volts per mil continuously for 120 days with no deterioration indicated. This life, at a stress in excess of five times that used in transformers, is possible with this type of sample because there is no ionization below approximately 175 volts per mil.

Tests on several hundred transformers of the 5,000-volt design illustrated in Figure 1 have shown that ionization does not start until a voltage well above 5,000 volts is reached, and stops above this value when the test voltage is reduced. Without ionization at the operating voltage, there is no cause for electrical deterioration. This fact, plus the chemical and physical stability of transformer butyl, makes it an ideal dry-type insulation.

Conclusion

1. A new solid insulation useful for voltages presently handled by instrument transformers made with dry-type insulation has been described. This insulation, molded butyl, has been applied to instrument transformers and represents a significant advance in the design and manufacture of these devices.

2. The properties of molded butyl compound are significantly better than those of older insulation, both in initial characteristics, and long time stability under adverse operating conditions.

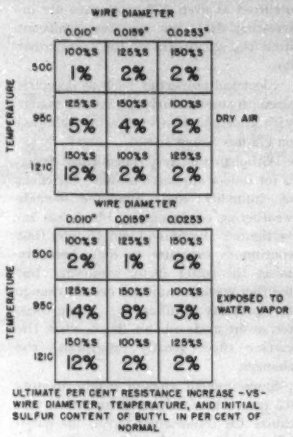

Figure 17. Corrosion of bare copper wire molded in transformer butyl

Ultimate resistance increase

References

1. Butyl Rubber, R. M. Thomas, I. E. Lightbown, W. J. Sparks, P. K. Frohlich, E. V. Murphree. *Industrial and Engineering Chemistry* (Easton, Pa.), volume 32, October 1940, page 1283.

2. Butyl Rubber Engineering Data, E. N. Cunningham, L. B. Turner. *Product Engineering* (New York, N. Y.), November 1945.

3. Buna and Butyl Rubbers, J. A. Britton. *Oil and Gas Journal* (Tulsa Okla.), November 26, 1942.

4. Structure of Copolymers of Isobutylene and Isoprene, John Rehner, Jr. *Industrial and Engineering Chemistry* (Easton, Pa.), volume 36, 1944, pages 46–51.

5. Effects of Molecular Structure on Physical Properties of Butyl Rubber, Paul J. Flory. *Industrial and Engineering Chemistry* (Easton, Pa.), volume 38, 1946, pages 417–36.

6. Development of Butyl Rubber, George Herrich. *Rubber Age and Synthetics* (London, England), volume 24, 1943, pages 129–30.

No Discussion

A Primary Method of Measuring the Ratio and Phase Angle of Current Transformers

ALLAN L. BROWNLEE
ASSOCIATE AIEE

A METHOD of measuring the ratio and phase angle of current transformers has been developed to extend the range of the present current transformer testing apparatus to higher current values.

Shunts with a top range of 2,500 amperes now are used. Since 2,500 amperes is about the top limit for an a-c shunt, either a multiturn primary transformer had to be used, or some other method employed.[1] Tests indicate that mutual inductors are practicable, inexpensive, and have an accuracy comparable to shunts for a direct calibration of current transformers in all current ranges.

The use of ring solenoids in the place of shunts for the calibration of current transformers is not new. In 1915 Charles Fortescue described a method of calibration in which carefully distributed windings were wound on accurately machined marble cores.[2]

The method developed here is similar to the Fortescue method but has two important differences, the solenoid design and the method of calibration, and is based on three fundamentals:

1. The magnetic flux in any closed nonmagnetic path is a function of the interlinking ampere turns and the reluctance of the path, and is independent of the size or position of the interlinking convolutions.

2. The magnetic flux in the closed path has a fixed relation both in magnitude and phase to the current that produces it.

3. The voltage induced in a plane loop is proportional to the vertical component of the flux threading it.

The flux induced in the core of the ring solenoid, Figure 1(A), by interlinking ampere turns, not shown in the figure, is independent of the size and position of the interlinking convolutions, but is dependent on the dimensions of the core (reluctance of the path).

The voltage induced in a loop around the core is proportional to the component of flux tangential to the axis of the solenoid if the loop is in the plane of the axis. The voltage generated in a series of such loops spaced on the core of the solenoid measures the tangential components at corresponding points on the core and approaches a true measure of the flux in the core as the loops are increased.[3]

The series connection of the loops must be so arranged that, as G. A. Campbell pointed out in his discussion of the Fortescue paper,[4] the connections do not form a loop around the axis of the ring. The connections used to eliminate this loop are shown in Figure 1(B). Two such solenoids can be compared by using a series current in the interlinking turns of each solenoid and then with an appropriate change in the interlinking turns again compared one in the primary and one in the secondary of a current transformer.

When so compared, the following relationship holds for small phase angles.

$$R = \frac{NcpNs}{NcsNp}(1 \doteq b \doteq a)$$

R = true transformer ratio
Ncp = interlinking turns, primary solenoid series comparisons
Ncs = interlinking turns secondary solenoid series comparison
Np = interlinking turns primary solenoid test
Ns = interlinking turns secondary solenoid test
b = constant difference determined by series comparison
a = difference determined by test

The phase angle is

$$\theta = \tan^{-1} \frac{r}{\omega M(1 \doteq b \doteq a)}$$

r = resistance introduced into the test to compensate for the phase angle of the current transformer
M = Mutual inductance of secondary solenoid (calculated)

The usual corrections can be made where the phase angle causes appreciable error.

Since mutual inductance does not appear in the ratio formula the only requisite is that, as affected by the ring solenoids, it remain constant between comparison and test.

The accuracy of the method was tested on a 1,500-to-5-ampere current transformer checked by the National Bureau of Standards. The results of this test are shown in Table 1; the ring solenoids in Figure 1; and the schematic diagram of connections in Figure 2.

The ring solenoids were built of laminated wood, turned on the face plate of a lathe in halves, with a semicircular core cross section, and doweled together to form the finished ring. With the dimensions and turns shown in Figure 1(A) the voltage induced in solenoid P is about 1.1 volts when excited by 1,500-ampere turns, and the voltage induced in S is the same when excited with 500-ampere turns 60 cycles.

The developed winding also is shown in Figure 1(B). Each turn of the single layer winding was wound in the plane of the ring axis, and the connections between turns were twisted to eliminate a loop around the axis. The wire size was number 30.

For the calibration the two ring sole-

Paper 50-67, recommended by the AIEE Transformers Committee and approved by the AIEE Technical Program Committee for presentation at the AIEE Winter General Committee, New York, N. Y., January 30–February 3, 1950. Manuscript submitted October 28, 1949; made available for printing December 13, 1949.

ALLAN L. BROWNLEE is with the Commonwealth Edison Company, Chicago, Ill.

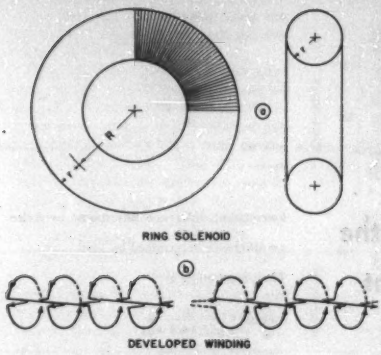

Figure 1. Primary solenoid (P) dimensions in inches $R=6$, $r=2$; winding 180 turns number 30 double-cotton covered. Secondary solenoid (S) dimensions in inches $R=4$, $r=1.96$; winding 360 turns number 30 double-cotton covered

Turns equally spaced on cores in plane of axis of solenoid. Only portion of turns shown

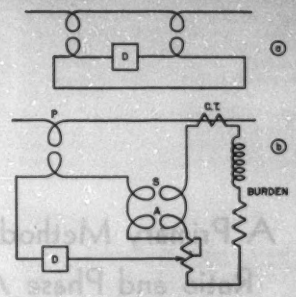

Figure 2. Connections for current transformer calibration

(a) Series comparison of two ring solenoids
(b) Test connections after solenoids have been calibrated by series comparison

noids were compared as shown in Figure 2(A). Solenoid P was interlinked with three turns, S with one turn. The current was 500 amperes. Exact balance was obtained by separating the appropriate core with equally spaced wedges. This adjustment reduced the constant b in the ratio equation to zero. Solenoid S then was compared with the inductometer A using 1-to-5 turns on S with 5-ampere series current and balancing the inductometer against S to calibrate the inductometer in terms of a in the ratio formula.

For the transformer calibration, connections shown in Figure 2(B) were used, with one turn on P and 100 turns on S, and balance was obtained for the various current values. Then

$$R=\frac{3.100}{1.1}\ (1 \doteq a)$$

$$\theta=\tan^{-1}\frac{r}{0.221(1 \doteq a)}$$

The balance was stable with a null detector sensitivity of about 0.0001 volt and an impedance of one megohm. No shielding was used, and no effort was made to reduce the size of external loops, but the interlinking convolutions were approximately the same size and in the same position on the solenoids for the series comparison and the test.

To determine the effect of size and position of interlinking convolutions, a ratio and phase angle balance was made with 1,500-amperes primary current, with the single turn through the solenoid P centered and the return loop about four feet distant from the solenoid. This loop then was closed to about six inches and balances obtained for eight positions around the ring; these data are shown in Table II.

The differences shown at the various locations of the small loop around the ring are due to variations in the core diameter and the resulting change in the area of the corresponding turns. A straight centered turn averages these differences. The differences do not enter as errors in the calibration if the size and position of the interlinking convolutions is the same for the series comparison and the test.

To determine the effect of external field the voltage induced in the solenoid P was measured when a 15-inch loop carrying 1,500 amperes, 60 cycles was placed at various locations with respect to the solenoid, but not interlinking with it. The maximum voltage measured was 0.0035 volt when the plane of the loop was perpendicular to the ring axis and symmetrical with it. For all other positions the induced voltage decreased and when parallel to the axis was less than 0.001 volt.

The work done is preliminary to the final design. Ring solenoids of a more suitable material than wood will be carefully machined to calculated dimensions and slots milled to position the detecting winding. Instead of changing dimensions with wedges to exactly balance in the series comparison the difference, factor b in the ratio formula will be determined. With stable material in the core of the ring the frequency of the series comparison tests should be comparable with the shunt calibrations in the present current test apparatus, about once a year, and the factor b comparable to the corrections applied to shunts.

A comparison of the data in Table I indicates that with carefully machined cores of suitable material accuracies of 0.01 per cent in ratio and one minute in phase angle can be obtained.

Table I. Ratio and Phase Angle; 1,500- to 5-Ampere Current Transformer; Secondary Burden 100 Volt-Amperes at 50 Per Cent Power Factor

Amperes	Ratio Per Cent: National Bureau of Standards	Ratio Per Cent: Commonwealth Edison Company	Phase Angle, Minutes: National Bureau of Standards	Phase Angle, Minutes: Commonwealth Edison Company
0.5	101.22	101.15	+17	+30
1.0	101.05	101.00	+13	+16
3.0	100.76	100.79	+ 6	+ 6
5.0	100.63	100.68	+ 3	+ 3

Table II. Change in Ratio With Size and Position of One Interlinking Convolution

No Change in Phase Angle

Position	Per Cent Change in Ratio
Center	0
1	+0.09
2	+0.13
3	+0.24
4	+0.26
5	+0.25
6	−0.16
7	−0.19
8	−0.21
Average	+0.03

References

1. Methods for Testing Current Transformers, Francis B. Silsbee. *AIEE Transactions*, volume 43, 1924, pages 282–297.

2. The Calibration of Current Transformers by Means of Mutual Inductances, Charles Fortescue. *AIEE Transactions*, volume 34, part 2, 1915, pages 1599–1626.

3. Electricity and Magnetism (book), James Clerk Maxwell. Clarendon Press (Oxford University Press, Oxford, England). Article 681—An Endless Solenoid, volume 2, third edition, 1904, page 313.

4. Discussion by George A. Campbell of The Calibration of Current Transformers by Means of Mutual Inductances, Charles Fortescue. *AIEE Transactions*, volume 34, part 2, 1915, pages 1616–18.

No Discussion

Relay Protection for Medium Length High-Voltage Transmission Lines

J. H. KINGHORN
MEMBER AIEE

PROTECTIVE relaying development over the years has produced a wide choice of equipment varying from simple instantaneous current types to more complicated directional and impedance types. The ingenuity of relay engineers has produced a still wider choice of methods of applying the various types of relays which are available. It is the purpose of this paper to discuss the various types of relay protection which are applicable to medium-length high-voltage lines and, using a typical system as an example, examine some of the advantages and disadvantages which are inherent in them. Companion papers[1,2] treat the protection problems for long and short lines. In order to limit the discussion to reasonable length it will be confined to types of relaying available as standard equipment, although the possibility of special schemes for special purposes must be recognized.

Description of Typical System

Figure 1 shows a hypothetical system selected to represent a range of conditions frequently encountered. It is assumed to be a predominantly steam-driven system where transmission line loading can vary considerably depending upon the location at which power can be generated economically or upon what generating units are out of service for either scheduled or emergency maintenance. The system is simplified to the extent that elements not essential to the problem of protective relaying have not been shown.

The lines from station A to stations G and C are respectively 40 and 50 miles long and are typical medium-length lines. They have to meet sufficiently similar conditions so that their required relay protection is identical. The discussion will therefore be confined to lines AL to G.

Figure 2 shows a typical heavy loading condition on these lines such as can be expected with generators at B and C out of service. It represents about as heavy power transfer as can be expected from station A to stations G and C for any except emergency conditions. Figure 3 shows 3-phase short-circuit values for the various station busses.

Transient as well as steady-state conditions must be considered. A permanent 3-phase fault on lines AL to G during which they are tripped, reclosed high speed and retripped would represent about as severe a condition as the relays on lines AR to C might be called on to handle. Figure 4 shows the power-angle-swing curves for this condition with the heavy initial loading of Figure 2. Figures 5 and 6 show the impedance seen by relays at the two ends of the line during the oscillations caused by such a fault. The circles represent suggested relay operating point loci as will be discussed in this paper.

General Objectives

The objective will be to provide the best type of relaying available with ability to meet all expected conditions being given first consideration and cost being taken into account after technical requirements have been met. This is considered justified by the importance of the four lines in question which under certain conditions are expected to carry a total of about 300,000 kw, Figure 2. This relaying must be reliable and fast in operation. It must be capable of clearing minimum fault currents expected and at the same time must be capable of carrying the heaviest load currents and transient swings without false tripping.

General Advantages Gained by Employing One-to-Two-Cycle Relaying

The advantages of obtaining the fastest possible tripping time for faults at any point on the protected lines are well known. Those most commonly mentioned are:

1. Reduction of short-circuit damage with consequent increased chance of re-energizing the line immediately.
2. Minimization of the objectionable effects of voltage dips on customer's motors.
3. The ability to carry higher loads without loss of synchronism because of short circuits.
4. The ability to employ ultrahigh-speed reclosing (20 cycle or less) and so increase the maximum loading which can be carried safely.

Pilot wire or carrier relaying schemes must be employed to obtain this speed for they are the only types of relaying currently available which do not require graded time settings to insure selectivity with relays on adjacent line sections. Without examining the problem in detail it is evident that the line lengths involved make pilot wire relaying uneconomical and it will therefore be disregarded.

Extent to Which One-to-Two-Cycle Relaying Advantages Are Realized on Typical System

For lines as heavily loaded as these the ability to re-energize immediately after a flashover is of considerable importance. The loss of one line produces heavier loading on the remaining three, and although these lines are capable of carrying this loading, the increased line losses and poorer voltage regulation at inter-

Paper 50-68, recommended by the AIEE Relay Committee and approved by the AIEE Technical Program Committee for presentation at the AIEE Winter General Meeting, New York, N. Y., January 30–February 3, 1950. Manuscript submitted October 31, 1949; made available for printing December 2, 1949.

J. H. Kinghorn is with the American Gas and Electric Service Corporation, New York, N. Y.

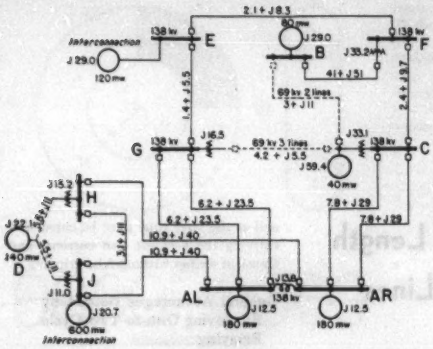

Figure 1. Typical system; positive sequence impedance per cent on 138,000-kva base

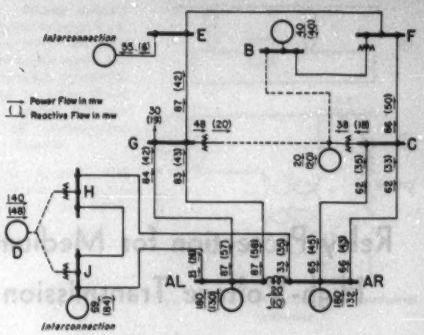

Figure 2. Heavy loading condition on lines *AL* to *G* and *AR* to *C*

mediate stations might be sufficiently objectionable to make necessary a reduction in the amount of power interchange. These objectionable conditions could be minimized still further if ultrahigh-speed reclosing were employed, because in about 90 per cent of the cases it would permit the line to be restored to normal before any objectionable voltage conditions could appear on the system. The advantages of reclosing at once are even more pronounced if one line is assumed out of service and a fault occurs on the second line.

Faults on an extensive high-voltage system of this sort are reflected usually in in voltage dips over a considerable geographical area which may affect service to a large number of industrial customers. While modern practice provides time delay undervoltage protection for industrial motors to prevent their loss during momentary voltage dips, there are sometimes heavily-loaded synchronous motors which can lose synchronism during relatively minor system disturbances. High-speed fault clearing helps to prevent this loss of synchronism. Data are not included for a detailed analysis of the system under consideration and generally such analyses are not worth while unless inspection discloses cases which may be critical. There usually are some such individual instances, but their extent and importance cannot be evaluated here.

A transient stability study of the system, Figure 4, shows that a double-line 3-phase fault at *AL* on the lines from *AL* to *G* can be tripped, reclosed into the fault in 20 cycles, and retripped without loss of synchronism over lines *C* to *AR*. This shows the system to be quite stable under heavy load and severe fault conditions, and demonstrates that from this standpoint 20-cycle reclosing is unnecessary. However, it further shows that 20-cycle reclosing will not be instrumental in causing loss of synchronism when reclosing into a permanent fault.

Carrier-Current Relaying

These considerations lead to the conclusion that carrier relaying is justified and should be installed on these lines for the increased chance it offers of avoiding prolonged line interruptions and therefore avoiding the poorer voltage regulation and increased transmission losses which such interruptions produce in the rest of the system. Furthermore, with carrier relaying installed, ultrahigh-speed reclosing can be employed at practically no additional cost and should be used for the same reasons. Further justification is found in the improvement of customer's service and in the increase in permissible loading limits which may be of value under possible emergencies or as loads grow in the future.

Carrier relaying, in common with any other type, must be capable of tripping under minimum short-circuit conditions. Furthermore if maximum speed of fault clearing is to be attained this minimum must be determined with both ends of the line closed to avoid sequential tripping. The fault detector relays should not pick up under maximum load conditions because this would cause continuous carrier transmission. This is considered objectionable because of possible interference with other carrier channels. Tripping relays must not pick up because, while incorrect tripping would not result as long as carrier transmission continued, there is always danger of it if any momentary interruption to transmission or reception should occur. Keeping these limitations in mind, phase comparison and directional comparison using impedance-type relays, which are the two types of carrier relaying in common use, will be considered.

Phase Comparison Carrier

Phase comparison is essentially a simple overcurrent type of relaying in that its tripping and carrier starting points are determined entirely by current measurement. Considering the lines from *AL* to *G* the maximum indicated load is about 430 amperes, and if one line were out it would probably be above 600 amperes. For a 3-phase short circuit at *AL* with the system normal, 990 amperes flows over each line from *G*, Figure 3. To insure that carrier not be transmitted continuously, the starting relay should have a pickup not lower than 600 times 1.5 = 900 amperes. If it is considered that this loading is of sufficiently infrequent occurrence as to be neglected then the starting relay can be set at 430 times 1.5 = 645 amperes. The tripping relay should be set at least 25 per cent above the starting relay to insure co-ordination which gives at least 806 amperes. This value is dangerously close to the minimum short-circuit value of 990 amperes and leaves no margin for the further reduction of this value which will occur when system conditions are abnormal. Furthermore, there is no chance of handling heavier loads, should they develop. If a negative phase-sequence network were employed, the setting would become independent of load current, but the relay would then be incapable of operation on 3-phase short circuits. For these reasons phase comparison carrier relaying does not appear adequate.

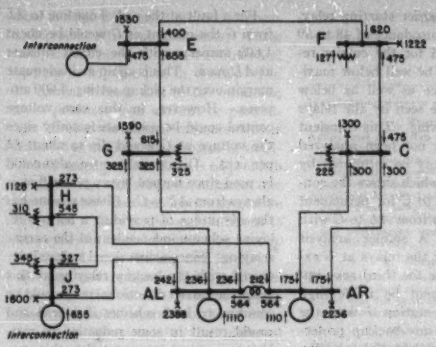

Figure 3. Three-phase fault distribution in megavolt-amperes

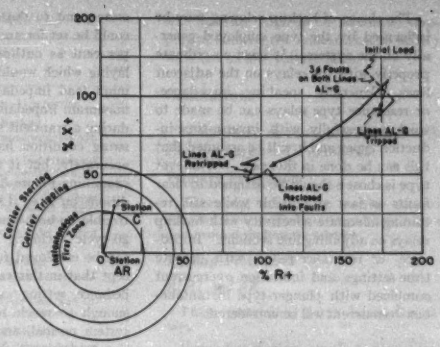

Figure 5. Impedance locus seen by relays on lines *AR* to *C* at *AR* for simultaneous 3-phase faults on lines *AL* to *G* near *AL*

Directional Comparison Carrier

Directional comparison carrier relaying using conventional reactance or impedance-type relays for carrier starting and tripping will avoid some of the objectionable features of a simple overcurrent scheme. For discussion purposes an impedance type relay will be considered. Line *AL-G* has an impedance of about 24 per cent. It is generally considered conservative practice if the carrier tripping relay impedance setting be made 50 per cent higher than the line impedance, which would be 36 per cent. The carrier starting relay impedance should be at least 25 per cent higher than the tripping relay, which would amount to about 45 per cent. This setting would correspond to about 1,280 amperes at normal voltage, which is an adequate margin over the maximum expected load current of 600 to 700 amperes. It therefore appears that directional comparison using impedance-type relays can adequately protect against minimum faults and still handle maximum loads without incurring continuous carrier transmission.

By a similar method of analysis it can be shown that reactance-type relays also will give satisfactory results. It is obvious, therefore, that the mho- and modified-impedance-types also would cover the conditions with probably an even greater safety margin.

The ground relaying for carrier should be provided with a separate ground directional relay, either current or potential polarized, and arranged in the conventional way to provide ground preference type of operation. This is necessary to avoid any possible incorrect operations which might be caused by the effect of load currents on the action of the phase directional relay during ground faults. As in the case of the phase relays, the ground-tripping relay should be sufficiently sensitive to insure tripping on minimum ground faults, and it is suggested that the pickup be not higher than one-third of the minimum calculated ground fault to provide a reasonable safety factor for possible impedance at the point of fault. Furthermore, it is desirable that at minimum calculated fault currents the relay operating time be at least as short as that of the phase relays under phase-to-phase faults, and that this time be about the same at both ends of the line even though the fault currents at the two ends differ materially, so that ultrahigh-speed reclosing can be successful. If ground-directional relays having an operating time which varies with torque are used it may be necessary to make the setting even more sensitive than the value suggested previously to insure that, at minimum fault currents, operation is on the flat part of the timing curve.

Phase-Backup Relaying

Although the primary carrier relaying can be expected to clear all faults in the protected line section under normal conditions, backup relaying is still required for a number of reasons. There are times when the carrier must be taken out of service for repair or calibration. Occasionally conditions arise, such as sleet formation on the conductors, when the carrier signal cannot be received. If an oil circuit breaker should fail to trip on a faulty line section, some means is needed for tripping adjacent sections. Tie lines between generating stations sometimes must be tripped under out-of-step conditions. Backup relaying must be provided to obtain as many of these features as possible.

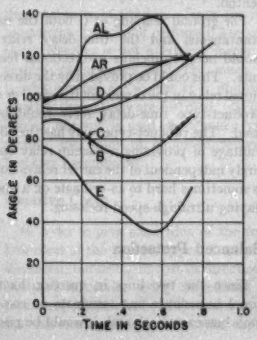

Figure 4 (left). Power-angle swing curves, simultaneous 3-phase faults on lines *AL* to *G*, both lines reclosed and retripped

Figure 6 (right). Impedance locus seen by relays on lines *AR* to *C* at *C* for simultaneous 3-phase faults on lines *AL* to *G* near *AL*

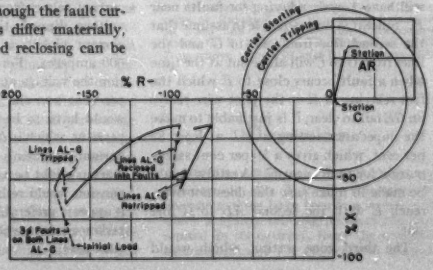

The choice of backup relaying may be influenced by the type employed generally on the system. It must co-ordinate properly with the relays on the adjacent lines. Generally speaking impedance- or reactance-type relays can be made to work successfully with inverse-time-induction types and it will be assumed that this can be done in this case. Whatever type is chosen should be designed to clear faults as fast as possible while still retaining adequate selectivity with backup relays on adjoining line sections. Impedance- or reactance-relays with definite time settings and induction overcurrent combined with plunger-type instantaneous overcurrent will be considered.

Three-Step Impedance Relaying

Impedance-type relays with the conventional 3-step arrangement for phase protection would be subject to the same limitations in sensitivity and load-carrying ability as those outlined for carrier relaying. For the lines from AL to G at AL the first, or instantaneous, tripping zone could be set to cover about 90 per cent of the line. The second zone must have a time setting selective with the protective relays on the other outgoing lines and with any time delay transformer or bus differential relays at G. The worst condition would probably be selectivity with the relays on the line from G to E. The total line impedance from AL to E is about 30 per cent, which is only about 25 per cent greater than the impedance of line AL to G. If the second zone setting is not to reach beyond E this would give an impedance setting with a rather narrow safety margin. However, with the system normal and a fault at E the apparent impedance seen by the relays at AL is much higher than 30 per cent. Even with one line out from AL to G this is true because of the effect of the lines from G to C. Furthermore, it is assumed that line GE will have carrier or pilot wire relaying for primary protection so that its relay time will normally be one to two cycles and that all lines out of E will have 1-cycle relaying for faults near E. Since it is unreasonable to assume that the second line from AL to G and the lines from G to C will all be out at the time when a fault occurs close to E which the fast relaying of E or the pilot wire relays on GE fail to clear, it is justifiable to make the impedance setting at AL at least 35 per cent, which gives a 50 per cent safety margin for faults near G. A study should be made to make sure this does not overreach E with the second AL to G line out.

The third zone setting, which would correspond to the carrier starting relay, could be set for an impedance of 48 to 50 per cent as outlined for the carrier relaying which would be well below maximum load impedance as well as below maximum impedance seen by the relays during a transient swing. This transient swing condition has not been analyzed accurately, but it may be estimated by examining Figure 5 which shows the conditions on lines AR to C for permanent trouble on both lines from AL to G with 20-cycle reclosing. A similar analysis can be employed for the relays at G except that in this case the third zone impedance setting cannot be made high enough to reach to station J with the system normal, and any backup protection to cover oil circuit breaker or relay failure of AL would have to be provided by some scheme installed at station AL.

Simple Overcurrent Relaying

If time-delay induction overcurrent combined with plunger-type instantaneous relays were employed on AL to G their limitations would be similar to those outlined for phase comparison carrier. The instantaneous relays at both ends could easily be set to cover 90 per cent of the line length. At G their tripping would have to be controlled by a directional relay. The time-delay relays at both ends would have to be set above 900 amperes to prevent operation on heavy load currents with one line out. However, it is not necessary that they operate on minimum fault conditions with all lines in but merely that they operate with a reasonable safety margin after the opposite end has opened.

For a fault at the end of one line to G the current from AL would be about 2,000 amperes after the circuit breaker at G has opened. Since this is based on maximum generating conditions and on all lines being normal except the one in trouble, it is a rather narrow safety margin over the 900-ampere pickup setting. A voltage control scheme might be introduced which would prevent the overcurrent relays from operating unless the voltage dipped, thereby permitting the current pickup to be reduced to about 600 amperes. For the same fault condition the voltage at AL would be about 80 per cent and the voltage control device would have to be set to drop out at 90 per cent, which is dangerously close to the normal operating point. This narrow margin might be tolerated but future expansion would reduce it still further and it appears preferable at AL to employ impedance relays where a satisfactory margin exists.

For a fault at the end of one line to AL from G the current at G would be about 1,600 amperes with the circuit breaker at AL open. This is again an inadequate margin over the pickup setting of 900 amperes. However, in this case voltage control could be used satisfactorily since the voltage at G would dip to about 65 per cent. Directional control also could be used since normal heavy power flow is always from AL to G. Either scheme has the advantage of providing a backup relaying scheme independent of the carrier relaying. Since a directional feature is required with the backup relaying at this point the carrier directional relay could be common to both schemes if desired and would result in some reduction in cost. Voltage control is suggested in this case primarily because the same voltage relays can be used for the other lines at the station and it therefore will be the more economical setup.

Ground-Backup Relaying

For ground relaying at AL an instantaneous, plunger-type relay can be employed set to pick up at about 105 to 110 per cent of the ground current in the line for a fault at G with the parallel line out. An induction overcurrent relay set to pick up at about one-third of this same short-circuit current can be used to cover faults below the pickup of the instantaneous relay. The pickup value of one-third of a solid fault at the far end of the line should be ample to cover any high-impedance grounds which might be encountered. A product-type relay polarized by zero sequence voltage or transformer neutral current might be used instead of a simple overcurrent relay. Since a directional feature is not required at AL it would have no advantage except to reduce somewhat the impedance in the bushing current transformer circuit, which is not essential.

For ground relaying at G both the instantaneous and the time-delay relays would need to include a directional feature. This could be provided by the directional relay in the carrier set if desired or a product-type time-delay relay could be used. The product-type relay has the advantage of providing a backup relay entirely independent of the carrier relays but is sometimes hard to co-ordinate on a line having ultrahigh-speed reclosing.

Balanced Protection

Since the two lines in question have equal impedance and terminate on common busses at each end, it would be pos-

sible to employ balanced protection phase and ground relays at both ends. These compare the currents in the two lines and operate to trip the line in trouble when its current exceeds that in the other line by a predetermined amount or percentage. Power directional measurement is included at stations not a source of short-circuit current. Since there is no problem of selectivity with relays on adjacent line sections they can be instantaneous in operation. They would operate in one to two cycles for single-circuit faults over 80 to 90 per cent of the line and for the remainder of the line would operate sequentially after the other end had tripped. They also would operate for some cases of simultaneous trouble on different phases of the two lines when the impedance relays might measure a false impedance. For single-line phase-to-phase faults beyond the instantaneous zone of the impedance relays they should shorten the total clearing time because, even with sequential tripping, the total time would probably be shorter than the time of the second zone of the impedance relays. For ground faults in a similar location sequential instantaneous tripping would probably occur from the instantaneous ground relays, because there is an increase in ground current after the near end has tripped which will permit the relay at the far end to pick up. Similarly for simultaneous faults on different phases of the two lines there is a good chance that the instantaneous ground relays will operate, even for the infrequent case when these faults do not involve ground.

It appears therefore that tripping time is shortened only for phase-to-phase faults in the last 10 per cent of the line which is 20 per cent of the faults not involving ground. If 90 per cent of the faults involve ground (this depends on line construction and other physical factors), then improvement is obtained in only 0.10 times 20 per cent = 2 per cent of the total cases of trouble. Since the improvement obtained of perhaps 0.3 second faster clearing is not a critical factor in system performance and the cases of trouble covered are so few, it is doubtful whether these relays are justified. When carrier relaying is used as primary protection the value of balanced relaying becomes insignificant.

Relative Costs

In order to give some idea of the relative costs of the various types of relaying discussed, the installed cost of directional comparison carrier using impedance or reactance relays has been assumed to be 100 per cent. This includes the capacitor, transmitter-receiver, line trap, relays, cable for transmitter-receiver, installation labor, and overhead. The relay setup available as standard equipment includes impedance backup and any type of ground backup required. On this basis the installed costs of other type would be approximately as shown in Table I.

Table I

	Per Cent
Modified-impedance or mho-type carrier	100
Phase Backup	
Added cost for 3-step impedance backup (phase only)	0
Added cost for time and instantaneous overcurrent with voltage control and using carrier phase directional relay	6
Added cost for directional controlled phase overcurrent using self-contained single-phase directional relays and instantaneous overcurrent controlled by carrier directional relay	8
Ground Backup	
Added cost for time and instantaneous overcurrent ground relay	0
Added cost for product type time and instantaneous overcurrent ground relay	0
Balanced Protection	
Added cost for high-speed current balance relays	11

These figures indicate that if a standard carrier relaying setup is purchased, a small additional premium must be paid to obtain a phase backup arrangement using relays separate from those employed for the carrier. However, it is possible to employ special relays for carrier which have only the features which are needed for the carrier functions at a considerably reduced cost. This can be combined with separate 3-step impedance backup at a total cost about 3 per cent higher than that of a standard setup. In any case the relaying is a small proportion of the total value of the line being protected, and is even a small proportion of the cost of the remaining terminal equipment such as circuit breakers and disconnect switches. Once carrier relaying has been decided on, the choice of backup protection on important lines can be based almost entirely on technical considerations. Further, the relatively small cost of carrier as compared with the equipment and service which it protects makes its selection likewise dependent primarily on the technical advantage which it offers on important lines. Since the dollar cost of carrier goes down only a small percentage on lower voltage lines and that of backup relays not at all, economic factors assume greater importance as the voltage and importance of the lines involved decreases. From this standpoint there is an important field of development open for relaying schemes including carrier, which will provide high-speed accurate tripping at sufficiently reduced cost to justify their use on low-voltage lines.

Conclusions

A summary of relay protection which has been suggested is as follows:

Primary Protection

Directional comparison carrier current relaying using impedance-type phase relays and ground preference scheme.

Backup Protection

At AL and AR

Phase protection, 3-step impedance relays.

Ground protection: simple instantaneous plunger relays and inverse time induction relays.

At G and C

Phase protection: simple instantaneous plunger-type relays, inverse time induction overcurrent relays with voltage control, using the carrier directional relay.

Ground protection: simple instantaneous plunger-type and inverse time overcurrent relays using the carrier directional relay.

The elements available for building up an adequate protective scheme have multiplied and improved as the needs have grown and we have every right to expect that this progress will continue. Advantage of special arrangements to cover special situations must always be taken by the relay engineer, but in making such applications the effect of changing conditions due to system expansion must always be kept in mind. These suggestions are based on standard equipment available from manufacturers which is suitable for the typical system involved and will accomplish the objectives of fast, reliable protection insensitive to maximum load currents and transient swings.

References

1. Transmission Line Protection of Short Lines of the Metropolitan Area of a Typical System, W. E. Marter. *AIEE Transactions*, volume 69, part I, 1950, pages 458–72.

2. Consideration of Requirements and Limitations of Relaying and High-Speed Reclosing on Long and Heavily Loaded Transmission Lines, C. E. Parks, W. R. Brownlee. *AIEE Transactions*, volume 69, part I, 1950, pages 103–09.

Discussion

A. J. McConnell (General Electric Company, Schenectady, N. Y.): In the technical literature, there have been few instances in which a system relaying problem has been treated in its entirety, from the complete determination of the problems to ultimate

solutions. For this reason, Mr. Kinghorn's paper, together with the Parks-Brownlee and Marter papers,[1] should prove valuable to other operating engineers.

It is interesting to note that Mr. Kinghorn and the others all chose some form of pilot relaying for the "typical" system studied. Though there can be little or no criticism of the conclusions reached, it should be noted that many systems, or portions of systems, do not yet require pilot relaying. In many instances, distance relaying, with its high-speed tripping for all faults except those near the remote line terminal, is quite adequate. Such relaying is particularly advantageous in that carrier relaying can be added easily when required.

Mr. Kinghorn rightly cautions that the second time zone of distance relays should incorporate sufficient time delay to be selective with any time delay transformer or bus differential relays. However, it is not presumed that Mr. Kinghorn is advocating the use of slow-speed bus or transformer relays since it is axiomatic that if high-speed line relaying is required, there is equal necessity for high-speed bus and transformer relays.

REFERENCE

1. See references 1 and 2 of the paper.

O. Ramsaur (Pennsylvania Power and Light Company, Allentown, Pa.): The example set by the author in putting down the requirements for the relaying on each line and comparing them with the accomplishments of the various types of relaying is one that relay engineers who are not already doing so will do well to follow. All too often it has been found that the obvious solution to a relay problem is not necessarily the best solution. With particular regard to carrier current relaying, it is evident in many cases that no other type will achieve the desired end; but once in a while it may be found that the slight additional advantage of carrier current relaying over conventional relaying is not worth the considerably greater cost and complexity.

One example pointing up this condition is a very recent case of a 132-kv tie line now being built, tying together two points in a 66-kv network. Because neither ultra high-speed tripping nor ultra high-speed reclosing is required, the line is to be tapped near the center by a 10,000-kva autotransformer, tying into the same 66-kv network, creating a 3-point line with feed-in at all three points and the condition that current flows out of the 132-kv line at the autotransformer for faults near the end of the 132-kv line. Careful analysis disclosed that to achieve instantaneous clearing of faults with carrier current relays would require remote trip and other complications that probably could never be worth either their cost or the hazard of faulty operation; and that the clearing times for a system of "zoned" instantaneous and definite time overcurrent relays we have developed for such cases is the same as that obtained by ordinary carrier current relays over almost the entire line and is fast enough for the remainder of the line. The use of conventional relays will save many thousands of dollars in first cost and will greatly reduce the hazard of incorrect operation, as they are simple, straightforward, and reliable. While this case is unusual, it does point up the injudiciousness of jumping to conclusions.

It appears that the use of the carrier current directional relays for backup purposes is contrary to the stated aim of providing back-up relays separate from those employed for carrier current. Since this is a moot question among relay engineers, it would be interesting to know why it is considered necessary to have completely separate backup relays as a matter of principle. If one would not provide separate phase backup for a straight 3-zone distance relay scheme without carrier control, it seems unnecessary to provide it with carrier current control. All the carrier current control does is by-pass the second zone timer; and shut-down of carrier removes only that feature, leaving the complete 3-zone relaying in service. Of course, backup ground relaying is required in most cases for the obvious reason that two different settings are necessary.

Also, it would be interesting to know what provision is made for out-of-step conditions.

C. E. Asbury (Commonwealth Services Inc., Jackson, Mich.): The author has no doubt found it difficult to cover this subject matter in a general way and include a variety of system conditions which are often encountered in practice. He chose to select a particular system and discuss application of relaying to certain lines in that system. Had a different line or a different system been chosen, the conclusions may have been entirely different. This should be kept well in mind when reading the paper. The author refers to this system as a typical system; however, it would perhaps be difficult to define what is required to constitute a typical system from a relaying view. Each system and line under consideration usually has certain peculiar requirements or special characteristics that set it apart from a number of other lines and systems. These individual lines and system characteristics influence the decisions of relay application. Some of the characteristics of this system which make it different from many other systems may be summarized as follows:

1. There is a heavy concentration of generation at one end of the system, busses AL and AR. If the system generation should be distributed differently or if the load was distributed differently, the relaying problem could be influenced greatly, especially as far as phase comparison carrier is concerned.

2. It appears from observing Figures 5 and 6 that there is no particular problem from the power angle swing since the impedances seen by relays do not impose any unusual conditions.

3. The lines considered on this particular application are part of a network. Had they been high-voltage radial lines to a load center (single end feed), the problem would be entirely different. Overcurrent relays with instantaneous attachments often are adequate in such applications.

4. Had the stability limits been more critical for this particular system, single pole relaying and reclosing may have been required.

One factor that influences relay application is the general philosophy and policies set forth by the particular group of engineers responsible for system operation and for protection. Some allow greater margins between relay pickup and loads or minimum short circuit current as well as impose more stringent system conditions for correct relay performance. In this particular paper the author has considered 3-phase double circuit faults and has applied relays on that basis. This is a rather severe condition; but if it can be accomplished within reasonable limits, it would perhaps be logical to do so.

However, with high-speed relaying it is rather difficult to see how a 3-phase fault could involve six conductors simultaneously (within 5 or 6 cycles) having wide spacing, such as used on 138 kv.

Considering further the margins allowed between relay pickup and minimum short circuit currents and load current, the author considered the phase comparison carrier relaying inadequate on the basis of a load of about 430 amperes and a minimum fault current of approximately 1000 amperes, a ratio of about 2.50. It should be kept in mind that as the fault location changes and moves from bus AL toward bus G, the fault current from G increases. Considering that for most high-voltage lines constructed within the past few years a performance of one or two faults per year on a line of this length (40 to 50 miles) may be expected and that experience shows that 75 or 80 per cent of these faults will be line to ground with a high percentage of the remaining 20 or 25 per cent of faults being phase to phase, it appears that a 3-phase fault may occur on an average perhaps once every six or eight years. The probability of such a 3-phase fault being in the critical section of the line, possibly 20 per cent of line near bus AL, is possibly still 5/1. Should a 3-phase fault occur near bus AL with phase comparison relaying being applied, there would be a good chance that it would clear by both ends of the line tripping simultaneously. However, if it did not, high-speed sequential tripping would occur, possibly locking the line out, which would probably be less severe on the system than the 3 phase double line fault considered.

Since the calculated risk is not very great for the application being considered, other factors such as economics might influence the decision as to the type of carrier relaying to be applied.

If the application was on an existing system where adequate backup relays existed which could not be used as part of a directional comparison carrier arrangement, an appreciable savings may be realized. Such savings would pay for an appreciable part of the phase comparison carrier arrangement.

The area described shows transmission lines supplying a total of 300 megavolt-ampere load. Mention is made in the paper of the loss of one line causing greater system losses.

Since I^2R and I^2X line losses are not normally considered in relay applications, it would be helpful if the author would clarify this problem. Apparently, this refers to persistent faults on a line which would take it out of service for an extended period of time. Is it expected that this might be caused by line burn downs caused by slow relaying? It is hardly likely that burn

downs would occur on a system such as this capable of carrying 600 to 700 amperes load current per line with fault currents in the order of 2,000 amperes for second zone tripping as mentioned in the paper, if the protection was provided by step-distance phase relays supplemented with directional ground relays and directional instantaneous ground relays at each line terminal.

The author's example emphasizes one limitation in the application of phase comparison type of carrier relaying. This limitation concerns the ratio of minimum fault current to maximum load current. It is important that the relays pick up for minimum fault conditions even when considering the fault current division from either end of the line under normal closed conditions. If complete protection for 3-phase faults is to be provided throughout the line section and if margins of about 1.5 times load current are allowed for carrier starting and minimum fault currents are to be at least 1.5 times fault detector (2) pickup, then a minimum ratio of about three is required between minimum fault current and maximum load current for the application of phase comparison carrier.

When considering backup relays, the author makes a comparison between overcurrent relays and phase comparison carrier. While there is some similarity between them there are two distinct differences in such a comparison, (1) overcurrent phase relays are susceptible to system swings, while phase comparison relays are immune to system swings, and (2) overcurrent backup relays will trip the circuit breakers when they pick up on overload. Phase comparison carrier will not produce tripping under severe load conditions, but will merely start carrier.

In this particular paper the author makes no mention of considering the application of step-distance ground relays. It would be interesting if some mention could be made of whether such relays were considered and what the conclusions were.

Mention is made of using balanced current phase and ground protection on the parallel lines. One problem that must not be overlooked in making such applications, especially for balanced current ground relays, is that of mutual coupling, which may exist between the parallel circuits and other circuits carrying ground current. This mutual coupling may disturb considerably the distribution of ground current and cause incorrect balanced current ground relay operations. Another point that must be considered rather thoroughly before applying balanced current protection, especially of the high-speed type, is the effect of current transformer residual magnetism.[1]

REFERENCE

1. THE EFFECT OF CURRENT-TRANSFORMER RESIDUAL MAGNETISM ON BALANCED-CURRENT OR DIFFERENTIAL RELAYS, H. T. Seeley. *Electrical Engineering* (*AIEE Transactions*), volume 62, April 1943, pages 164–69.

J. H. Kinghorn: In employing a specific system protection problem as a means of presenting the entire field of available tools, the final result must of necessity discard some of them for reasons which are based on judgment and experience rather than on any rigorous mathematical analysis. There is danger that the conclusions may be accepted as the only right kind in other cases where actually system requirements are less severe and a less expensive installation will give satisfactory results. It is very gratifying that the discussions have helped to bring out this point.

Mr. McConnell and Mr. Ramsauer are correct in pointing out that many systems do not yet require pilot relaying. It might even be added that there are a good many lines where simple time delay combined with instantaneous overcurrent is still giving good results. The progression from this to distance relaying and finally to pilot relaying is one which is usually dictated by increasing importance of the line because of heavier loading. Mr. Ramsauer's 3-terminal line is the well-known relay engineer's nightmare, the protection for which is sometimes difficult with distance relays, often requires special treatment with carrier current relaying, and becomes doubly difficult when the more rigid requirements of high-speed reclosing are added. Complications in relay schemes should be avoided wherever possible but they must be accepted in those cases where their use will provide definite improvement in system performance.

The extent to which backup protection should be independent of primary carrier protection is, like the choice of carrier itself, not always subject to rigorous analysis. Choice is often influenced by the engineer's experience and can lie anywhere between the one extreme of complete separation including separate current transformers, and the other of eliminating all duplicate elements and simply superposing the carrier function on the backup relaying. The modern trend appears to be in the latter direction. It was the intention to present the general problem including a possible middle ground compromise on common use of the directional relay without drawing conclusions as to how far backup duplication should go.

Out-of-step protection was not discussed because it does not present a problem in the system studied, as shown by the transient stability study. It would appear that under such circumstances its additional complications and compromises should not be employed.

Mr. Asbury rightly points out that different system requirements or a different setup could have produced different conclusions. However, as to the possibility of finding a solution to a stability problem through single-pole relaying and reclosing it should be pointed out that this requires very careful analysis, keeping in mind that single-pole reclosing usually requires relatively long reclosing time to permit fault arc deionization and that this can be disadvantageous when three pole operations are involved.

Three-phase double-circuit faults were considered only in determining system transient performance but not in determining relay applicability. Since stable operation was obtained under this severe condition there was no need for further study of other more probable but less severe faults. The relay application was based on a 3-phase fault on one line with the parallel line in service, which is the condition giving minimum current through the relays and is therefore the condition where simultaneous tripping at both ends is hardest to obtain.

In cases where phase comparison carrier relaying can show an appreciable saving in cost over directional comparison after taking backup relaying into account, the risk of an occasional high-speed reclosing failure and the small sacrifice in tripping speed may be justified. It is conceivable that in some cases a single such failure would result in expenses in excess of the amount saved and it is considerations of this sort which must determine the choice.

It is not expected that fault current in the order of 2,000 amperes would burn down a conductor even if it existed for the duration of the second zone timing. The total damage to the conductor would be caused by the combination of this current plus the total short-circuit current of 6,600 amperes which would exist until the near circuit breaker tripped. If we measure conductor damage by i^2t, we might estimate that the second zone timing increases the total damage by 50 per cent. The author does not know of any data available for determining conductor or insulator damage due to arcing which could lead to the selection of a maximum permissible arcing time, but accumulated experience with a considerable number of 132-kv transmission lines, both before and after adding carrier relaying, has shown that its addition almost completely eliminates conductor and insulator damage from this cause. Damage insufficient to produce immediate total failure of either insulator or conductor is usually considered a potential source of trouble and repairs are therefore made at the earliest opportunity. For this reason it is felt that every reasonable effort should be made to keep tripping time to a minimum.

Step-distance ground relays are a rather complicated and expensive type of relaying. They can offer the same advantage of reduced end zone time in some cases as is obtained by phase distance relays. In this case with the system solidly grounded at each station (this was not stated in the paper) instantaneous overcurrent relays give the same results as the first zone of the step-distance relay for 90 per cent of the line and for the remaining 10 per cent will trip sequentially after the remote oil circuit breaker has opened.

Transmission-Line Protection of Short Lines of the Metropolitan Area of a Typical System

W. E. MARTER
ASSOCIATE AIEE

AS A result of a study made by a Working Group of the AIEE, two companion papers[1,2] have been prepared on transmission-line protection. The papers are based on a study of a typical transmission system which is shown in Figure 1. A reactance diagram of the system is shown in Figure 2. The study was divided into three parts covering the short lines interconnecting the metropolitan area of the system, the medium length lines tying to nearby sources or interconnecting with other systems, and the long lines connecting to remote sources or systems.

This paper deals with protection which might be applied to the short lines connecting the generation and switching stations in the metropolitan area. These are the lines between station busses *B*, *C*, *E*, *F*, and *G* on Figure 1. These lines consist of three 138-kv lines of 9, 13, and 15 miles, and six 69-kv circuits consisting of three parallel circuits of seven miles each, two parallel circuits of nine miles each, and one circuit of 23 miles.

These circuits form a metropolitan network with a load of 395 megawatts and local generation of 140 megawatts. The remainder of the load in this area must be supplied from other sources which are comparatively remote from the load. The distribution of generation on the system and the fact that various sources might be shut down during light load periods indicated that difficulty would be encountered if an attempt was made to relay the short lines of the system on a time selection basis. Since the metropolitan network of the system forms the tie between various remote sources, it was felt that protection should be installed which would not be affected by through-fault or swing currents and would clear the faults as rapidly as possible. The rapid clearing requirement suggests the use of either carrier-current protection or, with the short lines involved, pilot-wire protection.

Comparison of Pilot Wire and Carrier-Current Protection

A choice between pilot-wire protection and carrier-current protection from the standpoint of speed of operation is difficult to make, as the operating time of either type is approximately one cycle.

With regard to the reliability of pilot-wire circuits, a few quotations from a report prepared by an AIEE Relay Subcommittee in 1942[3] indicates the excellent reliability of pilot-wire circuits. The introduction states: "This report is based on replies of 32 companies covering 436 circuits used for protective relaying. The information thus obtained covers 1,351 route miles of pilot-wire circuit and a period of 5,570 circuit years."

The summary, item 5, says: "The service continuity reported based on 5,570 circuit years indicates an average out-of-service time of less than 0.0335 per cent. It appears that the leased circuits have more frequent interruptions, but of shorter duration than the privately-owned circuits." An analysis of the figures in this report indicates 1.32 interruptions per circuit year with an average of 2.58 hours each for leased circuits, while the privately-owned circuits have 0.575 outages per year with an outage time of 5.08 hours per outage. The out-of-service time includes "planned interruptions" or "circuit rearrangements".

A similar report on performance of carrier channels would be of interest for comparative purposes, but no such summary is available as far as is known. It is expected that comparable information will be available.

The cost of pilot-wire protection cannot be fixed easily since the cost per terminal varies with the cost of the pilot-wire channel, assuming that one-half the cost of the pilot wire is charged to each terminal. If the cost of the terminal equipment for pilot wire is considered, the difference between that cost and the cost of a carrier-current terminal determines the maximum amount which can be spent for a pilot-wire channel.

The installed cost of a single-terminal carrier-current protection varies on the average from $6,500 to $7,500. This cost is broken down into approximately $4,500 for equipment and $2,000 to $3,000 installation costs. These are conservative figures, and in some cases, estimates as high as $15,000 per terminal have been made.

The installed cost of a single terminal equipment for pilot-wire protection is approximately $2,500 to $3,500, of which $1,200 is the approximate cost of equipment, including continuous supervision and neutralizing transformers. This allows an over-all cost of pilot-wire channel of approximately $8,000 at which figure the two schemes of protection are economically equal. If a pilot-wire channel costs more than $8,000, it is more economical to use carrier protection, and if it costs less than $8,000, it is more economical to use pilot-wire protection.

With either carrier-current protection or pilot-wire protection, it is sometimes

Paper 50-69, recommended by the AIEE Relay Committee and approved by the AIEE Technical Program Committee for presentation at the AIEE Winter General Meeting, New York, N. Y., January 30-February 3, 1950. Manuscript submitted October 20, 1949; made available for printing December 2, 1949.

W. E. MARTER is with the Duquesne Light Company, Pittsburgh, Pa.

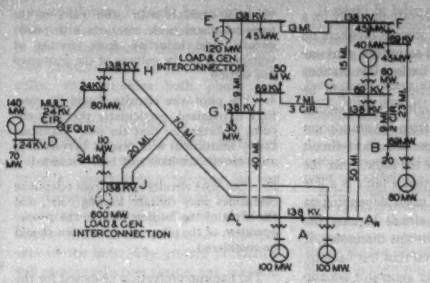

Figure 1. Typical transmission system showing generation, load, and line lengths

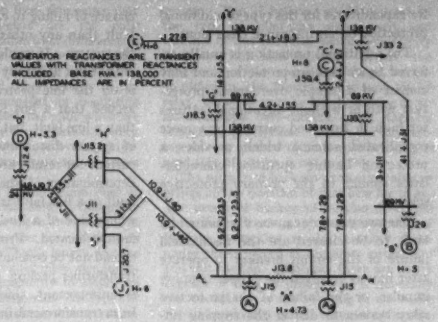

Figure 2. Positive sequence impedance diagram of a typical transmission system

necessary to remove the carrier transmitter or pilot-wire circuit from service for maintenance. Since this removal of equipment from service generally makes the relay protection inoperative, it is necessary to provide additional relay protection on the line if it is desired to keep the line in service. This additional protection provides primary protection for the line when the carrier or pilot-wire equipment is out of service, and frequently can be made to serve as back-up protection when pilot wire or carrier is in service.

Pilot-Wire Circuits

Pilot-wire circuits either may be leased from the local telephone company or owned by the power company. In some cases, power companies own telephone or other circuits which can be used for pilot-wire protection. It may be necessary to build pilot-wire circuits.

Leased Circuits

Conductors leased from telephone companies average $40 to $50 per year per loop mile of pilot-wire circuit, excluding taxes. If the $50 rental is capitalized at 12 per cent, the investment represented is $417 which would permit leasing a pilot-wire circuit 8,000/417 = 19 miles long. If an 18 per cent capitalization figure is used, the length of pilot-wire circuit which would be justified economically is increased by 50 per cent, so that the economically justified length of pilot-wire on a lease basis depends on the percentage on which the rental charge is capitalized.

Privately-Owned Circuits

If pilot-wire channels are to be built and the relay manufacturers' preference for lead-covered cable circuit is followed, the length of pilot-wire circuit is quite limited because of cost. There are in successful use several pilot-wire channels which are not in cable, which should be considered. Pilot-wire channels consisting of insulated copperweld wire closely spaced and mounted on distribution poles have been in operation for some time. In addition to low cost, this type of channel has two advantages over a telephone cable type of circuit. The resistance and capacitance of such a circuit are low and the insulation level is high.

Conductors used for such an installation are mounted on a single grooved spool and have a spacing of less than two inches. The conductors are number 10 copperweld-copper, 40 per cent conductivity with 3/64-inch performance-grade rubber insulation, American Society for Testing Materials designation *D-27*, containing 30 to 33 per cent crude rubber, and two asphalted braids slicked. Breakdown voltage of such insulation is 300 volts per mil, or slightly under 15,000 volts. Such a conductor will withstand a direct contact with a 4-kv or 6.9-kv distribution circuit without damage or any effect on the pilot-wire protection. Loop resistance is 13.5 ohms per mile of circuit. The cost of such a circuit is 4.5 cents per foot per conductor on existing poles, or slightly over $475 per loop mile. This figure is somewhat above the $50 rental figure capitalized at 12 per cent.

The use of "spiral-four" cable for pilot-wire circuits has been quite successful. This cable has four rubber-covered conductors enclosed in a foil shield and woven steel wires all enclosed in a rubber jacket. Since the war, this material has appeared on the market as war surplus material at a very reasonable cost.

Another expedient for reducing the cost of pilot-wire installations would be to use a phantom simplex circuit where several pilot wires follow the same route. No information on the use of such a scheme has appeared in any articles which have come to the attention of this author, but it seems that such a connection might have sufficient merit to be investigated, since circuits of this type have been used successfully by telephone companies for many years.

The major objection to such a scheme is that an outage on one pilot-wire pair will remove the pilot-wire protection from two lines, but usually pilot-wire outages are rare, and if adequate backup protection is provided, the double pilot-wire protection outage is not too objectionable. The simplex scheme will reduce the pilot-wire resistance, but where the simplex circuit is in, cable may raise the capacity of the pair to an objectionable value.

Backup Protection

With pilot-wire protection or any other type of protection which will not recognize a fault in the adjacent section, it is necessary to install some additional protection on the system, since a failure of the pilot-wire type of protection to clear a fault in its protected zone has no effect on the protection of this type on the remainder of the system, and therefore, a fault could remain uncleared. An uncleared fault on a system can result in serious and expensive damage to conductors and windings of equipment feeding the fault and may cause additional failures resulting in a complete system shutdown. Several cases of this type have occurred in various parts of the United States, and there is a definite justification

for expenditures for this type of additional protection on an insurance basis alone.

The additional protection is usually referred to as back-up protection and may consist of a simple overcurrent protection with or without directional features set high in time and current, or a more complicated scheme which provides a protection having operating characteristics similar to the primary protective scheme.

The two primary causes of a failure of a fault to be cleared are the mechanical failure of the circuit breaker to operate after having received the proper tripping impulse, or the failure of the protective relay system to deliver the tripping impulse.

Mechanical failure of circuit breakers to trip may be caused by a failure of any one of the many mechanical parts of a circuit breaker, such as bearing failures in any one of the many pin bearings, broken or bent trip plungers, or broken or distorted castings or other parts of the mechanism. Collection of moisture in circuit-breaker mechanism housings may freeze during low temperatures and prevent the operation of the circuit breaker.

Failure of the circuit breaker to receive a trip impulse may be caused by a failure of the instrument transformers feeding the relays, or may be in the wiring between the instrument transformers and relays. The failure may be due to open- or short-circuited windings in the coils of the relay or some foreign matter blocking the operation of the relay or to defective relay contacts. Failure may be due to failure of the tripping source or to any of the numerous contacts, coils, or wiring that comprise the trip circuit.

In order to furnish a complete backup for any or all of these failures, it is necessary to have an independent set of relays operating from separate instrument transformers and having a separate trip source tripping a separate circuit breaker or group of circuit breakers. Backup protection seldom, if ever, goes to the extent which has been described, but the condition is closely approached. The application of backup protection is influenced on any given system by past experience on the system and experiences which have been reported on other systems. Applications are made to cover failures which have had serious results in the past, or from on analysis of the system which shows that serious results could occur from a failure to clear a fault.

On any high-voltage system, the equipment which has the highest failure rate is the transmission line. Therefore, the line circuit breakers have a greater chance of failing to operate properly on a fault than any other circuit breakers on the system. It would seem then that one of the most necessary backup installations is on the line protection. It might be argued that a bus fault is more serious than a line fault, but from the standpoint of system disturbance and short-circuit current the results are the same, since the determination of whether a fault is a line fault or a bus fault is made depending on which side of a line circuit breaker the fault is located. From this discussion, it should not be concluded that bus backup, transformer backup, or generator backup is unimportant, since oil fires resulting from transformer failures and iron damage due to prolonged faults in generators can have serious effects on a system.

Protection Recommended for the Short Line

From the comparison of costs of carrier-current protection and pilot-wire protection, it can be seen that with 18 terminals involved and with a cost differential $4,000 per terminal installed, the two schemes would be economically equal if the pilot-wire circuit cost was $72,000. Since pilot-wire circuits could be built for the 99 miles of line involved for approximately $47,000, the saving in favor of pilot-wire circuit is $25,000.

An additional advantage of pilot-wire over carrier protection is the simplicity of the pilot-wire circuits and connections.

Pilot-wire protection therefore is chosen for the primary protection of these lines and provides instantaneous clearing of both phase and ground faults for the entire line.

The following items should be considered and, where necessary, included in the pilot-wire protection:

1. Rise in station ground potential and induction should be studied to determine whether neutralizing transformers are required.

2. Consideration should be given to the installation of continuous supervision on the pilot-wire circuit for the purpose of cutting out the pilot-wire protection when the pilot-wire circuit becomes defective and for the purpose of automatically switching the backup protection where simple backup is used; there also may be some question of the back-up operating unnecessarily under certain system conditions.

3. Use of instantaneous phase and ground overcurrent relays with their trip contacts in series with the pilot-wire relay trip contact should be considered. These relays have been found to be very successful in preventing unnecessary operation of the pilot-wire relays due to foreign voltage on the pilot-wire circuits from such causes as accidental application of telephone test voltages, contacts with other pairs in the same telephone cable, contacts with power circuits, and induction from circuits at voltages below the voltage of the protected line section.

4. The pilot-wire circuits should be carefully scrutinized, particularly the long circuits, to determine that the relay manufacturers' limitations with respect to resistance and capacitance have not been exceeded.

5. Pilot-wire circuits leased from telephone companies may contain loading coils, and the effect of the loading coils on the proper operation of the pilot-wire protection should be considered.

The backup protection proposed for the lines being discussed is step-distance protection with product-type ground protection. A consideration of directional overcurrent protection indicates that some difficulty might be encountered in obtaining proper time selection, since the location of power sources could vary widely with different generating sources shut down for maintenance purposes or during light load conditions on the systems.

The backup relays should be connected to auxiliary current transformers connected in the secondaries of the bushing current transformers on the line side of the circuit breaker. These current transformers normally feed bus differential, and the current transformers on the bus side of the line circuit breakers are used for the primary line protection. With this connection, the operation of the bus differential must be checked to see that it has not been adversely affected by the additional burden.

The backup relays should trip the line circuit breaker and at the same time energize a time-delay relay. The time-delay relay is set with sufficient time delay to allow the line circuit breaker to clear the fault. If the fault is not cleared, the contacts of the time-delay relay should be connected to an auxiliary relay which will clear the bus section to which the defective line is connected. The primary line protection should also operate the same time-delay relay. One time-delay relay per bus section is required for this back-up scheme.

The backup protection described provides independent relays fed from independent current transformers and provides backup for a mechanically sticking circuit breaker. It is assumed with this type of backup that failure of two pieces of equipment will not occur at the same time. As an example, if pilot-wire protection is defective, it is assumed that the current and potential transformers feeding the backup protection will not be defective at the same time.

In conclusion, it might be pointed out that on short lines requiring protection in the instantaneous classification, pilot-wire protection can be justified economically, and provides both phase and ground protection.

The backup protection chosen provides phase protection which, while not the equivalent of pilot-wire protection, provides instantaneous tripping for one circuit breaker of the line on all faults and instantaneous tripping of both ends of the line for faults in the middle 75- to 80-per cent of the line. The ground protection will require selective timing, the selection being determined from a ground fault study of the system.

With the back-up timer connected, as indicated, all possible line tripping failures are covered except a failure of the control battery.

References

1. Consideration of Requirements and Limitations of Relaying and High-Speed Reclosing on Long and Heavily-Loaded Transmission Lines, C. E. Parks, W. R. Brownlee. *AIEE Transactions*, volume 69, part 1, 1950, pages 103–09.

2. Relay Protection for Medium Length High-Voltage Transmission Lines, J. H. Kinghorn. *AIEE Transactions*, volume 69, part 1, 1950, pages 461–67.

3. Pilot-Wire Circuits for Protective Relaying—Experience and Practice, AIEE Committee Report. *Electrical Engineering* (*AIEE Transactions*), volume 62, May 1943, pages 210–14.

Discussion

C. A. Mathews (General Electric Company, Philadelphia, Pa.): The open-wire pilot channels described and recommended in this paper are attractive because their loop resistance is very much less than that of the ordinary telephone cable. However, open wires are more subject to induced voltage between pilot wires than are the twisted and shielded pairs, and individual applications require checking to insure that the 15-volt maximum under fault conditions is not exceeded. Frequent transpositions of the pilot channel might be necessary to reduce this voltage difference.

The spiral-four cable referred to should be as effective as the recommended twisted pairs in reducing the voltage difference between wires due to induction. The cable shield should be grounded at points distant from the terminal stations for lightning protection.

The simplex-phantom circuit can be used, with certain precautions, for those applications where three channels are required between any two given points and where the power company is providing its own channel. Both side circuits should be spiralled in the same cable to avoid voltage difference due to induction on the phantom loop. The two side circuits can be supervised separately with little difficulty.

It might be inferred from this paper that neutralizing transformers are the only means of avoiding trouble from difference in station ground potentials or longitudinally induced voltage on the pilot wires. For those cases where all other circuits in the same cable are terminated in insulating transformers, and where the pilot wires are not connected directly to the station battery or other control equipment lacking high-voltage insulation, insulating transformers alone are sufficient.

A cost comparison on individual lines of this typical system would indicate that pilot-wire equipment is less expensive on eight of the nine lines, while carrier equipment costs less on the one line of 23-mile length, yet the authors have recommended pilot-wire equipment for all lines, apparently to avoid the inconvenience of dealing with two types of relays. On actual systems where phase-comparison carrier equipments are used on the medium length lines, they can be applied to some of these so-called short lines with a saving in cost and with no inconvenience due to introducing a different type relay on the system.

The author suggests that consideration be given to the use of supervisory relays for cutting out the pilot-wire protection when the pilot channel becomes defective in order to prevent false tripping. It should be pointed out that this practice will not prevent all false tripping, because of the high speed of the pilot-wire relays. Unless the supervisory relays are faster than the pilot-wire relays, defective pilot channels may cause false tripping whenever the load current is greater than the pilot-wire relay pickup value, depending on whether the pilot wires are short- or open-circuited.

A refinement of the product-type ground protection suggested for backup would be a directional overcurrent relay with directional control of the instantaneous as well as the time unit.

L. L. Fountain (Westinghouse Electric Corporation, East Pittsburgh, Pa.): This paper gives a needed comparison between pilot-wire and carrier-current protection of transmission lines, both from the economic as well as the performance viewpoint.

The $8,000 limit set for the economical use of pilot-wire protection seems to be substantiated where just relaying is involved. In many cases, however, supervisory control, telemetering, and communication also require pilot wires that can be included in a multipair cable along with the relay pilot wires. This might alter the economic situation in many cases to where the limiting factor becomes one of electrical performance rather than cost. In other words, where supervisory control, communication, and so forth, require a pilot-wire cable, the addition of relaying will cost very little more, since it requires only a single pair out of a multipair cable.

In some cases pilot wires do not necessarily follow the transmission line right of way, but are run over a shorter route. This can be especially true in a metropolitan area. In such a case, of course, pilot-wire mileage would have to be considered and not the power transmission distance.

In several places in the paper mention is made of the loss of protection when the pilot wire is taken out of service by a planned outage. This, I believe, would depend on the type of pilot-wire relay used and whether or not the relay pickup sensitivity is below full load current. Where the scheme is of the opposing voltage, as exemplified by the Westinghouse-type *HCB* relay, the relay may be left in service as an instantaneous over-current relay, thereby still giving protection. Where the circulating current method of pilot-wire relaying is used this, of course, is not possible.

The subject of back-up protection always brings up the question of just how far to go. The extent of backup protection described in the paper in paragraph 6 of the section on Backup Protection would certainly come under the category of duplicate protection and not backup. Whereas there are many degrees of backup protection, it generally can be defined as the tripping of the same circuit breaker by other relays or other elements in the same relay. In case of a circuit breaker failure, the tripping of the next adjacent circuit breakers by means of their relays with the necessary time delay would constitute backup protection.

C. E. Asbury (Commonwealth Services Inc., Jackson, Mich.): The author has done an excellent job in preparing this paper. His approach to the problem of economics is useful and interesting and is perhaps a point too often overlooked by relay engineers. It is realized that the cost comparisons made are only typical and they will vary with individual installations depending upon local conditions. For instance, the cost of installation of carrier current is often affected appreciably by whether or not coupling capacitors may already be available on high-voltage lines as capacitor potential devices. In some installations step-distance relays may already be available for line protection which can easily be modified to control directional-comparison type of carrier.

Some of the factors which affect leasing pilot wires are: the type of circuit available, whether local loops or whether both line terminals are located in the same exchange area, whether toll circuits are involved, and the particular telephone company's tariff, which varies somewhat in different states.

When comparing the cost of carrier current versus pilot-wire relays, one must consider whether the cost of a set of distance relays should be charged to the carrier-current installation. When phase-comparison type carrier is used, backup relays are required; however, these relays do not control the carrier. When directional-comparison type of carrier is being installed on lines equipped with modern step-distance relays, the cost comparison should not include the step-distance relays.

It would be helpful if the author would indicate whether or not the $4,500 material cost for each carrier terminal includes a set of step-distance relays. If the cost of step-distance relays has been included and is subtracted from the figure of $4,500 material cost, this gives approximately $3,200 or an installed cost of about $5,000 per carrier terminal. If the 25 per cent federal tax is considered on the telephone channel, the annual rental for a pilot-wire channel would be about $62 per loop mile. If this $62 rental is capitalized at 12 per cent, the in-

vestment represented is approximately $512, which would permit leasing a pilot-wire circuit 5,000/512=approximately 10 miles long. The paper points out that the economics involved in justifying the length of pilot wires on a leased basis depends on the percentage on which the rental charge is capitalized. As pointed out in this paragraph, other factors affecting these comparisons are: the presence of existing equipment which may be utilized as part of the carrier installation, and whether or not federal taxes are considered as part of the telephone leased cost.

One other factor that often affects the application and cost of pilot-wire relaying is the ratio of emergency load current to minimum fault current. If the pilot-wire relays are set sensitive enough to trip for internal faults for minimum generating conditions, they may require fault detectors to avoid incorrect tripping during maximum load conditions should the pilot-wire channel be open for any reason. If the system is subject to considerable variation in generation, it is often desirable that the phase fault detectors be of the distance type. This situation is often aggravated further if the pilot-wire relays are required to trip for a minimum line-to-line fault when testing the line from one end. The cost of these fault-detector relays will affect the investment required for the pilot-wire installation and should be taken in consideration where such a pilot-wire application is being compared with carrier.

Another factor which often affects the application of both carrier and pilot-wire relays is protecting lines supplying tapped loads. While this problem affects both applications, any particular application may affect the two differently, depending on the location of the tapped load, the size of the load, and the size and relative impedance of the step-down transformer bank supplying the load.

W. E. Marter: The comments of Mr. Fountain and Mr. Asbury point out additional factors involved in the economic comparison of pilot-wire and carrier-current relay protection.

Mr. Fountain's comment in connection with reduction of cost of the pilot-wire circuit due to use of a single pair in a cable installed for several functions might also apply to reduce the cost of the carrier channel due to multiple functions.

In permitting pilot-wire relays of the opposing voltage type to remain in service for backup protection with the pilot wire out of service, the only problem is whether or not it is permissible to allow the line involved to trip on a through fault or not. In general, it is undesirable to lose two lines for a fault on one line if it can be avoided. Allowing pilot-wire relays to remain in service with the pilot wire out of service would result in losing all lines with the pilot wire out of service for a fault in an adjacent line section.

The definition of backup protection would seem to depend on what is being backed up, and if it is desired to back up the protection from the current transformers through the relays to the circuit breaker, duplicate protection is necessary.

In Mr. Asbury's comments he questioned what relays were included in the cost comparison of pilot wire and carrier current. In this comparison only the cost of the pilot-wire and carrier-current protection was considered and backup protection was not included.

The use of distance carrier relays for the backup protection, although it may provide satisfactory backup for a circuit-breaker tripping failure, does not provide a backup for relay or instrument transformer failure since the same instrument transformers and relays are used for both the carrier protection and the backup.

In the cost comparison, current interlock relays were included in the pilot-wire cost, but if exceptional conditions require the use of a distance-type interlock the cost would increase.

In general, it is usually possible to set the current interlock relays so that the effect of the increased pickup of the pilot-wire protection on single-end feed to a phase-to-phase fault is minimized by setting the pilot wire below maximum through load and controlling the trip current value of the pilot-wire protection by the setting of the current interlock relays. The pickup of the current interlock relays remains the same for all fault conditions. In general, on the short lines of a metropolitan transmission network the minimum fault current is enough greater than the maximum load current to obtain satisfactory protection using current interlock relays.

In Mr. Mathews' comments it is pointed out that the open-wire pilot-wire circuit described is subject to induced voltage. This is true, but in general the open-wire circuits are run on distribution poles and are not inductively coupled with the high-voltage line being protected. This fact, coupled with the recommended use of current interlock relays, means that sufficient high-voltage current must be flowing to pick up the interlock relays at the same time a fault on a distribution circuit occurs, which induces voltage on the pilot-wire circuit.

With interlock relays set above maximum load current the supervisory relays can cut out the pilot-wire protection in the event of a pilot-wire failure, without a line tripout, and will prevent an incorrect operation on through fault current to a fault on some other line on the system.

In the interest of brevity, perhaps too many details were omitted, such as a cost comparison of the individual lines suggested by Mr. Mathews. Since the merits of carrier protection were to be presented in companion papers,[1] the author felt justified in lumping the short lines in one group and discussing only the pilot-wire protection. An additional refinement in the ground backup protection would be the use of distance ground relays to match up with the phase-distance backup protection.

Reference

1. See references 1 and 2 of the paper.

Sensitive Ground Protection

AN AIEE COMMITTEE REPORT

THE Project Committee has collected information on available methods for sensitive ground relaying of 3-phase distribution and transmission systems. Several reliable methods for transmission circuits and unigrounded as well as ungrounded distribution systems have been reviewed. The limitations of presently known systems for the protection of 3-phase 4-wire multigrounded systems, as well as some results of investigations concerning "arc frequency relaying" which need further experimental study, are indicated.

In the fall of 1946, a working group was appointed to study present-day sensitive ground protection of 3-phase systems and to prepare a report on this subject. It was realized that the Project Committee would not be able to find new solutions to some of the problems, but it was felt that it would be helpful to summarize present-day practices and to give an indication where developments and improvements are necessary or desirable. A number of papers which concern certain phases of sensitive ground protection have been published during the last ten years, and they are given in the list of references, which describe in detail some of the fine points not repeated in this report.

Definition of Sensitive Ground Protection

Sensitive ground protection dealt with in this report comprises relaying of ground faults, (that is, either the indication of the faulted feeder of a system, or its automatic switching off) with fault currents to ground of a magnitude in the order of about 1 per cent of the normal or full load current of the feeder.

This will mean in general that the primary fault current will be between 1 and 10 amperes.

Objectives of Sensitive Ground Protection

1. Limitation of physical damage and reduction of number of sustained faults.

2. Facilitation of joint use with communication circuits. The degree of sensitivity proposed herein greatly exceeds the requirement of positive operation at 50 to 100 amperes in five seconds or less.[1,2]

3. Disconnection of broken conductors on the ground or on grounded objects. This is important on circuits along or crossing school yards, playgrounds, highways, and so forth.

4. Co-ordination of branch fuses, relaying and reclosing cycles of substation circuit breakers. This may be accomplished by temporarily locking out the sensitive ground relays rather than by settings above the minimum blowing of branch fuses.

Ground Relaying of Transmission Circuits

Analyses of transmission system faults have indicated a mode fault resistance of about 20 ohms with less than 5 per cent of all faults exceeding a resistance of 90 ohms. This analysis was made[3] on many systems ranging from 26 kv to 220 kv. As a general rule, adequate ground relaying of transmission circuits may be obtained with the more conventional methods and equipment.

Ground Relaying of Distribution and Subtransmission Systems

With few exceptions, only distribution or subtransmission systems will be so grounded that sensitive ground protection will become necessary. The fault current to ground is comparatively small in:

A. *Delta systems* (ungrounded systems) of small or moderate mileage. The fault current is small in such systems since it is the result of the capacity-to-ground of the system. The magnitude of the fault current to ground can be estimated for single-circuit overhead-line systems from the "rule of thumb" formula

$$I \text{ amperes} = \frac{\text{miles times kilovolts (line-to-line)}}{160}$$

B. *Systems unigrounded through high impedance.*

C. *Resonant grounded systems* (as defined in Standard AIEE number 32).[4]

D. *Effectively grounded systems* (as defined in Standard AIEE number 32) having high fault resistances, in particular in some multigrounded 4-wire systems. Small fault currents result in many cases from indirect grounds without a conductor on ground, that is, grounds with high fault resistance.

In systems as described in A, B, or C unbalances of the primary loads, and even more so their effects on the secondary side, are so small that the ground relay if connected in the common return of three identical, paralleled current transformers (four current transformers in case of 4-wire circuits) will measure correctly the ground fault current of the particular feeder. Greater accuracy may be achieved economically by cable-ring transformers.[5] Another solution are 3-phase[6] current transformers.

A. Delta Systems

Very satisfactory experiences have been gained with an installation of ground relays in ungrounded, radial delta systems of 13.8-kv operating voltage. These relays are of the directional type since they must operate only in the direction to

Paper 50-70, recommended by the AIEE Committee on Relays and approved by the AIEE Technical Program Committee for presentation at the AIEE Winter General Meeting, New York, N. Y., January 30–February 3, 1950. Manuscript submitted November 18, 1949; made available for printing December 2, 1949.

Prepared by the Project Committee of the AIEE Committee on Relays. Committee Personnel: Eric T. B. Gross, *Chairman*, C. J. Berghs, R. J. Cooper, T. R. Halman, F. A. Jeanne, Cort Lowerison, W. K. Sonnemann, and A. R. van C. Warrington.

the fault. The relay sensitivity is high enough to permit relay operation on ground faults of considerable contact resistance. In many cases the fault current to ground was so small that the fault on the feeder, which had been recognized by the relay, could be found only after temporary solid grounding of another phase and repeated switching in on the fault had produced sufficiently great damage to indicate the location of the fault.

B. Systems Unigrounded Through High Impedance

In order to make possible the positive indication of ground faults, extensive tests were made by the Southern California Edison Company and a relaying system developed where grounding of 3-or 4-wire systems could be limited to one station. This system was planned originally for radial systems[7] and later extended to mesh-systems by the use of carrier channels.[8] The fault current to ground is kept below approximately 4 amperes. The grounding reactance is designed to take into account the capacitive single-line-to-ground fault current of the systems, and is low enough to produce a residual fault current which is lagging (inductive). The whole grounding system is basically a greatly overcompensated resonant grounded system, with the ground relays acting under the influence of the quadrature component of the residual feeder current.

C. Resonant Grounded Systems

Sensitive directional ground relays[9] may be used in resonant grounded systems. With this type of protection, the relays operate on the in-phase component of the residual current.

The relays used in A, B, and C are very similar, the main difference being that a different component of the residual current is used in each case to produce maximum positive torque, namely the leading quadrature component of the residual current in A, the lagging quadrature component of the residual current in B, and the in-phase component of the residual current in C. To the relay terminals of the second (polarizing) coil of this directional-type relay is supplied the voltage from neutral to ground (zero sequence voltage of the system) in all three cases in the same manner, or sometimes the current in the neutral of the grounding device.

Many operators of delta and high impedance or resonant grounded systems feel that neither a circuit nor a major part of a circuit should be disconnected to remove a low-current ground fault. A sensitive relay scheme is desirable. If the ground persisted and if desired a source of ground current sufficient to blow branch fuses with low resistance faults could be connected to the system for a definite time and removed. In any event an alarm would be sent in and operating personnel dispatched to locate and correct the fault condition.

D. Effectively Grounded Systems Having High Fault Resistance

The greatest problem in 4-wire multigrounded systems[1] is that high resistance ground faults and load unbalances have similar current magnitudes so that grounds are difficult to recognize. In a small number of systems multigrounding has been eliminated and relay schemes are used quite satisfactorily[7] as described in B. In many cases, systems operate with multiground common primary and secondary neutrals where only ground relays with current settings that are considerably higher than "sensitive ground protection" prevent relay operation on load unbalances.[1] However, fault currents to ground may be too small for relay operation if, for example, they are on a dry roadway or in contact with trees, and it is this kind of fault which makes improvements and new developments desirable.

Since it is difficult to distinguish between load unbalances and high resistance grounds, in a multigrounded system, a relay scheme which uses other than 60-cycle currents may lead to a satisfactory solution of this problem. Though a successful method of securing selective ground indication has not yet been found, it should be mentioned that tests have been made with devices which utilize the fact that arcs to ground produce high frequencies which are not present, to the same extent at least, under conditions of load unbalances. Two different kinds of equipment were tested. The one consisted of a carrier frequency receiver with coupling capacitors and traps so that the arc frequencies would be recognized. With this arrangement, it was found that the equipment reacted also without grounds on the line when equal frequencies were produced by apparatus not connected to the line, as for example passing streetcars. The other kind of equipment utilized the high-frequency current supplied from the secondaries of current transformers and filters which would eliminate low frequencies. However, it was found that not only the arcs of ground faults, but also harmonics present in the ordinary load current actuated the relay. The relays used had to have broad frequency response, since different types of arcing faults did not produce the same frequencies, and tuned relays would not be satisfactory. It is evident that extensive development and study will be necessary to clarify further possibilities of "arc frequency relaying." It should be highly desirable to continue with these experiments and tests, since they may show the way to a solution.

Conclusions

1. A reasonable sensitivity in relay protection against ground faults is highly desirable to improve service through reduction of the number of sustained faults.

2. Fault resistances on transmission systems (at 26 kv and above) are such that desirable sensitivity of ground relaying usually may be obtained with conventional schemes.

3. Fault resistances of a grounded conductor may be very high on distribution systems requiring unusual equipment and methods to provide the desired sensitivity of ground relaying.

a. Ground relaying on delta systems, resonant grounded systems, and systems unigrounded through high impedance may be provided with sensitive directional product relays, giving proper attention to current characteristics. Residual voltage devices may be used in some cases.[10]

b. Grounded neutral systems, with 3-wire circuits, or 4-wire with the neutral grounded at the supply point only, may be relayed sensitively by a number of methods such as current polarized directional ground relays with means to prevent relay damage on heavy currents, cable-ring transformers, special 3-phase current transformers, and so forth.

4. Multigrounded 4-wire distribution circuits offer the most severe problem in securing sensitive ground relaying because of unavoidable unbalances in load current and residual transients when a circuit is reclosed.

5. Radical departures from conventional methods have been tried, such as devices responding to harmonics generated by arcs but no practical success with these has yet been reported. In the present state of the relaying art, it is believed that there is no practical method of securing sensitive ground relay protection for 4-wire multigrounded distribution circuits.

References

1. Positive Disconnection of Distribution Circuits During Faults to Ground. *Engineering Report Number 47*, Joint Subcommittee on

Development and Research, Edison Electric Institute and Bell Telephone System (New York, N. Y.) volume 5, 1942.

2. Performance of Ground-Relayed Distribution Circuits During Faults to Ground, C. L. Gilkeson, P. A. Jeanne, J. C. Davenport. *Electrical Engineering (AIEE Transactions)*, volume 61, January 1942, pages 40–48.

3. Characteristics of Power Systems Faults to Ground. *Engineering Report Number 39*, Subcommittee on Development and Research, Edison Electric Institute and Bell Telephone System (New York, N. Y.), volume 5, 1937.

4. Neutral Grounding Devices. *AIEE Standard Number 32*, May 1947.

5. Earth Leakage Relays, Eric T. B. Gross. *The Electrician* (London, England), volume 123, number 3191, 1939, page 93.

6. Zero-Sequence Current Transformer for Ground Protection, J. W. Graff. *Electrical World* (New York, N. Y.), volume 102, 1933, page 822.

7. Sensitive Ground Protection for Radial Distribution Feeders, L. F. Hunt, J. H. Vivian. *Electrical Engineering (AIEE Transactions)*, volume 59, February 1940, pages 84–90.

8. Sensitive Ground Relay Protection for Complex Distribution Circuits, L. F. Hunt. *Electrical Engineering (AIEE Transactions)*, volume 65, November 1946, pages 756–68.

9. Sensitive Ground Protection for Transmission Lines and Distribution Feeders, Eric T. B. Gross. *Electrical Engineering (AIEE Transactions)*, volume 60, November 1941, pages 963–71.

10. A New Method of Ground Fault Protection, F. M. Starr. *Electrical Engineering (AIEE Transactions)*, volume 53, November 1934, pages 1472–77.

Discussion

L. F. Kennedy (General Electric Company, Schenectady, N. Y.): The writer believes that the Project Committee has overlooked one item which should have been included in their report. From the general tone of the report, the reader would be justified in concluding that reliable sensitive ground relaying of ungrounded or neutralizer grounded systems could be obtained easily. Reference 9 of the paper was cited as an instance where satisfactory experience was obtained.

Unfortunately, the application of relays of adequate sensitivity will not of itself assure correct operation on fault currents of the general order of 1 per cent of load. There have been other attempts to relay both ungrounded and neutralizer-grounded systems which have not been successful. These experiences, of course, have not been made the subject of papers, so no references to them are readily available.

It should be perfectly obvious that in order to be able to have any chance for correct operation the residual unbalance of the system must be materially less than the expected magnitude of fault current. After the required system symmetry has been obtained, it is further necessary to supply the relays from current transformers of sufficient accuracy. However, a little thought about current transformer accuracies will show how difficult it may be to achieve reliable results.

The best current transformers commercially available carry an American Standards Association accuracy classification of 0.3, or, in other words, are permitted a net error including effects of ratio and phase angle of the equivalent of 0.3 per cent in ratio. With such current transformers, it is possible to have an error in the relay current great enough to cause improper performance.

The problem is not one involving basic relay sensitivity, since there are available suitable relays with sensitivity of less than one per cent. What is involved, but is not mentioned in the report, is the purely practical and economic problem of obtaining sufficient over-all accuracy to do the job. Since it is difficult to achieve system symmetry and since available current transformers may not be as good as the example cited above, it seems in order to suggest that the report should have included some statement along the following lines:

"Although relays are available with adequate sensitivity to provide sensitive ground protection for fault current of the order of one per cent of load, proper relay operation can be obtained only under conditions approaching the ideal. The ideal means the elimination of both system residual unbalances and current transformer errors."

Willard S. Wilder (Wisconsin Electric Power Company, Milwaukee, Wis.): This report is of considerable interest to us. We have an extensive rural 4,800-volt distribution system; the average substation serving an area of 38 square miles.

We would favor the indication of the faulted feeder, rather than its tripout, for the reason that we place considerable reliance for continuity of service on the ability of our 4,800-volt delta rural distribution lines to operate with one phase grounded. This is particularly important in wooded areas, where it is almost impossible to stay entirely clear of trees when the wind is blowing.

It will be realized that the system covers a lot of area, and we could hardly do business in any other manner as economically. The ungrounded operation of our rural system requires service free from interruptions, and we are able to operate quite well and economically in this manner, at least more so than by grounding and using numerous circuit reclosers.

R. W. World (Bureau of Reclamation, Denver, Colo.): As stated in the committee report, transmission systems rarely require ground-fault protection of the defined sensitivity. However, there are cases where sensitive protection might be applied even though the minimum total fault current greatly exceeded 1 per cent of normal load current:

1. If a transmission line is long and grounded-neutral transformers at the terminal stations are large, ground faults near one terminal may require sensitive relays at the other terminal for simultaneous tripping.

2. If either terminal clears line faults by opening a low-voltage circuit breaker, the other terminal may have to have sensitive relaying for sequential tripping.

3. In (1) and (2), greater relay sensitivity is required if load substation transformers tapped to the line have grounded high-voltage neutrals and either the substation is not tripped off for line faults or else a low-voltage circuit breaker is tripped. Since the critical fault locations are ones of heavy total fault current, fault resistance also accentuates the problem.

These conditions cause a disproportionate distribution of ground current among the several transformer neutrals. The need for extreme sensitivity possibly might be overcome by use of relays actuated by the positive- and negative-phase-sequence components of the current instead of the zero-sequence component commonly used in ground relays, and the application of distance ground relays is being investigated. It is expected that this relaying problem will arise in the design of some of our new transmission systems where 20-cycle reclosing circuit breakers with carrier relaying will be furnished at the main terminals of long tapped lines.

J. R. Linders (Cleveland Electric Illuminating Company, Cleveland, Ohio): This is an interesting and informative project committee report on sensitive ground protection. It will be noted that all of the methods discussed in this report rely on current-sensitive relays. We have been using a voltage-sensitive system for about 15 years with good results.

On 2,300- and 4,600-volt 3-wire ungrounded-delta radial distribution we connected a grounded-wye broken-delta potential transformer to the substation bus. A voltmeter connected across the open corner of the delta reads zero except when a ground exists on one of the feeders. Each feeder is equipped with three voltage regulators. When a ground occurs, the voltmeter will give a reading, its magnitude depending on the fault resistance and regulator position. Regardless of the actual reading on the voltmeter when the voltage regulator on the faulted phase of the faulted feeder is operated the voltmeter will change. Operation of other regulators in the station will have negligible effect on the voltmeter reading.

The only problem which we have had with this method of ground-fault location has been ferro-resonance causing the primary fuses of the potential transformers to blow. We have solved this by connecting a 40- to 150-ohm resistance in parallel with the voltmeter across the open corner of the delta-connected secondaries of the potential transformers.

Lloyd F. Hunt (Southern California Edison Company, Los Angeles, Calif.): The Southern California Edison Company has been using sensitive ground protection for may years with gratifying success.

The magnitude of sensitive ground protection is from 1- to about 6-amperes minimum trip on circuits of 2.3, 4.1, 7.2, 12, and 16.5 kv. With these low settings of ground fault tripping, unnecessary isolation very rarely occurs. Tree grounds, and the like, seem to give insufficient current to trip. In most cases, repetitive unknown trippings have been solved and in every case some de-

fect in the circuit was discovered and corrected.

The improvement in current transformers by using high-grade cold rolled steel cores have allowed the use of bushing current transformers with the very sensitive type of relaying. This is another saving in the first and installation costs of sensitive ground protection.

A great number of the circuits of the voltages listed above are now equipped with sensitive ground protection and many that require the feature are being equipped each year.

Eric T. B. Gross: The interest shown in this committee report through informal and formal discussions is greatly appreciated by the Committee. This report was presented last year, at the 1949 Winter Meeting, in preliminary form as a conference paper; it was circulated at that time among all members of the Relay Committee and also among approximately 100 other relay engineers in this country. All suggestions received were duly considered by the Project Committee and are incorporated in this report, therefore, it presents the present-day picture of sensitive ground protection in all phases of the problem.

Mr. Kennedy feels that "the Committee has overlooked one item which should have been included in this report." I believe that, had Mr. Kennedy looked more carefully at the text of the report, he would not have drawn this conclusion. It is clearly stated in the last paragraph of the section on "Ground Relaying of Distribution and Subtransmission System" that three "identical" current transformers will measure correctly the ground fault current of the particular feeder, and that this is all that is necessary, has been demonstrated in numerous practical applications. Mr. Kennedy overlooked the fact that even current transformers of very poor accuracy will not produce an error current in their secondary zero-sequence path, if current transformers are used that are practically identical as to errors in ratio and phase-angle. This fact has been known for at least 25 years to relay engineers who have been using sensitive ground relaying, and some early papers that were written on this subject[1] are mentioned in the papers which are included in the references given at the end of the report. I happen to know that a few thousand sensitive ground relays have been in successful operation abroad in resonant grounded systems where Petersen coils are designed for continuous operation, and many of these relays have a sensitivity of 0.01 ampere. Therefore, it must be concluded that the few unsuccessful attempts, referred to by Mr. Kennedy, are the very unusual cases. Furthermore, there is reason to assume that remedial measures were not tried by Mr. Kennedy. Such measures are described in the literature.[2]

As for the electrostatic unbalance of the system, mentioned by Mr. Kennedy, it should be perfectly obvious from a consideration of the equivalent circuit diagram that this unbalance with respect to ground changes the fault current by but a fraction, so that its influence is negligible. If we call E_0 the neutral displacement of the system without a ground fault, and E_ϕ any of the 3-phase voltages, the expressions for the ground-fault current will be $(E_\phi + E_0)\omega C_g$ with unbalance, and $E_\phi \omega C_g$ without unbalance. In a delta system, E_0 is always a small fraction of E_ϕ, so that this kind of unbalance is not worth mentioning. The experiences with sensitive ground protection in delta systems have been very satisfactory, as reported to our Committee. In the few cases that require balancing of resonant grounded systems, however, attempts are always made to reduce unbalances through transpositions which are desirable for other reasons. In such systems, the in-phase component of the residual current is influenced by unbalances to a somewhat larger degree; however, correct relay operation can always be secured easily by appropriate auxiliary means.

Mr. Hunt has had many years experience with sensitive ground protection; he has used current transformers of customary design in the past. It is very interesting to learn that bushing transformers also are being used now for sensitive ground relaying.

I agree with Mr. World that sensitive ground protection has its place in transmission systems. The examples cited by him are very interesting, especially his reference to distance ground relaying. It appears that distance ground relaying deserves more consideration than it has had in the past.

Mr. Wilder's viewpoint is shared by many who want to have continuity of service and prefer to operate with one phase grounded until the fault can be cleared without interruption to service. Sensitive ground relaying is of great help in such cases.

Mr. Linders' discussion is a valuable addition to the report. Since it is customary to use such feeder voltage regulators, this method seems an ideal way of locating the faulted feeder.

I know that I express the feeling of all the members of this Committee in giving thanks to all those who helped improving the report by constructive criticism, and informal or formal discussion.

References

1. Sensitivity of Sensitive Ground Relays in High Voltage Systems, **E. Gross, W. Weller.** *Electrotechnik und Maschinenbau* (Vienna, Austria), volume 50, part B 1932, pages 117–23.

2. Ground Faults in High Voltage Systems (book), **R. Willheim.** Julius Springer, Berlin, Germany, 1936.

3. Modern Earth Fault Relay Equipment for Use in Systems Protected by Petersen Coils, **L. B. S. Golds, C. L. Lipman.** *Journal*, Institution of Electrical Engineers (London, England), volume 91, 1944, part 2, pages 289, 377.

4. *Discussion* by **Eric T. B. Gross** of Report on Survey of Unbalanced Charging Currents on Transmission Lines as Affecting Ground-Fault Neutralizers, **AIEE Committee Report.** *AIEE Transactions*, volume 68, part II, 1949, pages 1328–29.

Clampers in Video Transmission

S. DOBA, JR.
NONMEMBER AIEE

J. W. RIEKE
ASSOCIATE AIEE

ONE of the major problems connected with the transmission of television signals is the exceptionally wide video band of frequencies involved. For the present black-and-white standards this amounts to about 4 megacycles. In the transmission of the television signal at video frequencies, that is, noncarrier transmission, the problem is further complicated because the lower limit of the frequency range extends literally to zero frequency.

It is fortunate that the d-c and other low-frequency components need not be transmitted. However, they must be reconstructed at the receiving end for a satisfactory picture. The possibility for this reconstruction exists because of the scanning and blanking process normally used in generating the television signal. The effect of these processes is illustrated in Figures 1(A) and 1(B). Figure 1(A) shows a video signal as it might be generated by a scanning process having zero retrace time. This signal has an average value which corresponds to the average brightness of the scene. Insofar as this average value will change, the signal contains low-frequency components which extend in frequency upwards from zero.

Figure 1(B) shows the same signal after the blanking process. Here it may be seen that the effect of blanking is to multiply the original signal by a blanking wave form which is unity at all times except in the blanking interval, when it is zero. This multiplication will be recognized as a modulation, where the blanking wave form, shown in Figure 1(C), plays the part of the carrier. By straightforward Fourier analysis it may be shown to consist of a d-c or average term plus the fundamental and harmonics of the line scanning frequency.

The result then of modulating the original signal with this nonsinusoidal carrier is to obtain new frequency components. These new components are the harmonics of the line scanning frequency modulated by the frequency components of the signal. In addition to these, the original components also are present as a result of the modulation of the average or d-c value of the carrier by the signal. Therefore the original low frequencies which are present in the blanked video signal are redundant, that is, they also exist as modulation products of the line frequency component and its harmonics. Hence they need not be transmitted as long as they are reconstructed (by a proper demodulation process) at the receiving end. In this case, the tips of the blanking pulses of the transmitted wave form will describe as their "envelope" those low frequencies which have been lost in transmission.

To the blanked video wave form, a synchronizing pulse is usually added. Since this is an additive process, it does not modify the discussion above.

To indicate how low frequencies are lost in transmission, consider the wave form due to a half-white half-black field with a horizontal line of demarcation as indicated in Figure 2(A). This is a video signal complete with horizontal synchronizing pulses, though for simplicity the vertical synchronizing pulses are not shown. If the average value of this signal is removed, due to lack of d-c transmission, the tips of the synchronizing pulses will extend below the zero voltage line, in a negative direction. If the average value of the signal changes, the extension of the synchronizing pulses in a negative direction also will change. This effect has been called the "zero wander."

It may be seen that any process which lines up the tips of the synchronizing pulses at the zero, or any other fixed, level reintroduces these low frequency components lost in transmission.

Moreover, it is evident that this reinsertion is nothing more than a sampling process, that is, the wave is sampled periodically and any deviation from zero is corrected. In common with all sampling processes the highest frequency component which may be regenerated by this means is limited to a frequency of one-half the sampling or line frequency. For practical reasons, the maximum frequency which may be regenerated is limited to a considerably lower value.

Low-Frequency Transmission Problems

In order to study the low-frequency transmission effects, the wave form of Figure 2(A) will be used, since it has the maximum field frequency (60-cycle) component. The analysis can be considerably clarified, however, if we separate this signal into two components as shown in Figures 2(B) and 2(C). The former of these contains the high frequency components and virtually none of the lows, while the latter contains the low-frequency components and virtually none of the highs. Since only 75 per cent of the video amplitude and 85 per cent of the time are used for picture information, the amplitude of the low-frequency signal of Figure 2(C) (in terms of a 1-volt video signal) is: $0.75 \times 0.85 = 0.64$.

By the separation of the high-and low-frequency components, the problem of investigating transmission deviations in the low-frequency region is considerably simplified. For this purpose it is sufficient to consider the wave of Figure 2(C) only, on the assumption that the wave of Figure 2(B) will be transmitted faithfully.

Consider the effect of a single low-frequency cut-off consisting of a series capacitor and shunt resistance, of time-constant T. For a value of T moderately

Paper 50-72, recommended by the AIEE Television Broadcasting Systems Committee and approved by the AIEE Technical Program Committee for presentation at the AIEE Winter General Meeting, New York, N. Y., January 30–February 3, 1950. Manuscript submitted November 16, 1948; made available for printing December 5, 1949.

S. Doba, Jr. and J. W. Rieke are both with the Bell Telephone Laboratories Inc., New York, N. Y.

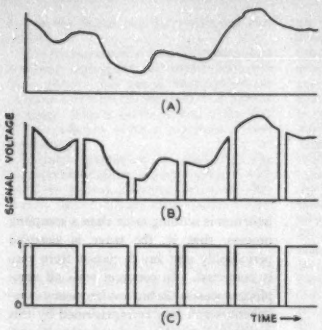

Figure 1 (left). The video blanking process

A. Unblanked signal
B. Blanked signal
C. Blanking signal

Figure 2 (right). Waveform for half-white, half-black field

A. The complete video waveform
B. The high-frequency component
C. The low-frequency component
D. Low-frequency cut-off distortion of the low-frequency component

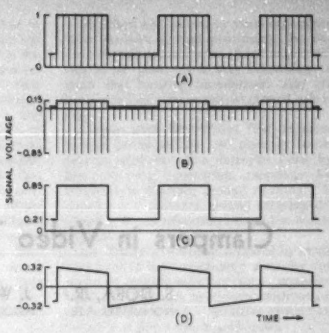

large compared to the field (60-cycle) frequency, the effect of applying the wave of Figure 2(C) will appear as shown in Figure 2(D), that is, the main characteristic of such distortion is to produce a slope, or tilt, in the wave form.

As the number of low-frequency cut-off circuits in the transmission system is increased, the resultant distortion remains essentially the same provided the time constant of each is increased in proportion to the number of circuits. When viewed on a picture monitor, this type of distortion results in a shading which is most noticeable in the darker portions of the picture. It is evidenced by a decrease in brightness in the region immediately following the white portion of the picture, which decrease in brightness shades to an increase in brightness in the region immediately preceding the white portion of the figure.

A change in brightness corresponding to a slope in the low-frequency wave, Figure 2(D), of 1 per cent, for example, would be produced by a single low-frequency cut-off element having a time constant of 0.4 second. In terms of the steady-state transmission characteristic, the 3-decibel loss point occurs at 0.4 cycle and the phase shift at 60 cycles amounts to 0.38 degree. For large numbers of cut-off circuits in tandem, the 60-cycle phase shift adequately describes the resulting wave form slope.

The extremely low frequencies which must be transmitted, as indicated before causes considerable difficulties particularly when coupled with the 4-megacycle band width required for the transmission of fine detail. This is a serious practical matter, since to obtain wide band widths and reasonable gain from vacuum tube interstage circuits the parasitic capacitances must be made small. To pass the low frequencies, however, requires large coupling capacitors with a resultant high parasitic capacitance.

Furthermore, under these conditions, the use of transformers as coupling elements has been impossible due to the difficulty of incorporating the extended low frequency cut-off and wide band width into one design.

One method of reducing the low-frequency range is to utilize a circuit which reduces phase shift at the field frequency. This is the well-known plate decoupling or low-frequency compensation circuit, which is shown in Figure 3. The effect of this circuit is to place a "bump" in the transmission characteristic, usually well below the field frequency. The phase shift at the field frequency is materially reduced. The net effect is that the "slope" or tilt of the low-frequency signal is eliminated. If the gain bump produced extends up to field frequency, a slight "bow" distortion may be produced.

With this artifice it is possible, at least theoretically, to reduce the size of the coupling capacitor in the interstages and compensate, by means of the plate decoupling circuits, for the distortion produced.

There are two difficulties attendant to this procedure. The first lies essentially in a balance of distortions. This may be seen most readily by considering the plate circuit as a predistorter and the grid circuit as a restorer. Obviously if the predistortion and restoration are considerable, a precise balance between the two is required to limit the net distortion to a threshold value. A further difficulty arises from the magnitude of the gain bump produced. This is serious only when a considerable number, ten or more, of coupling circuits are employed.

The effect of a high gain bump is most noticeable on switching transients such as are caused by switching from one circuit or camera to another and is seen as a low-frequency damped oscillation. For these reasons the benefits to be derived from low-frequency compensations are limited.

Regeneration of Low Frequencies

The analysis of distortion has so far neglected the distortion produced by the deletion of the d-c or average value of the video signal. For a still picture this distortion could be eliminated by a manual adjustment of the background brightness of the picture monitor.

When there is motion in the picture, however, an automatic means is required. This need is met by the so-called "d-c restorer," a schematic of which is shown in Figure 4. The operation of the d-c restorer is as follows. The diode is arranged so as to conduct on the synchronizing pulses. With the diode resistance low enough in the conducting direction, the coupling capacitor will be charged to such a value as to just reduce the diode current to zero. The voltage on the following grid at this instant will be zero, and hence the video signal will be positive for the picture time. If for any reason, such as zero wander, the synchronizing pulses tend to go more negative, the coupling capacitor is quickly charged by the diode so that the minimum signal at the grid is again zero. If on the other hand the synchronizing pulses tend to go more positive, the diode ceases to conduct. However, the shunt resistance across the diode discharges the coupling capacitor to such a value as to cause the diode to conduct again on the synchronizing pulses. Hence the line-up of synchronizing pulses is maintained. In effect, the d-c and those low frequencies lost in transmission have been regenerated by the d-c restorer.

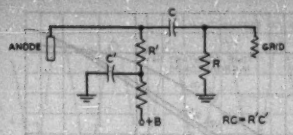

Figure 3. A low-frequency compensation circuit

A shortcoming of the d-c restorer lies in the finite resistance of the diode in the conducting direction. As a consequence of this the blocking capacitor never becomes charged to the full peak value of the synchronizing pulses, but a part of the synchronizing pulse at the grid extends in the negative direction. The amount of this extension depends upon the wave shape of the video signal. The net effect of this is that a certain amount of residual distortion is always present.

The d-c restorer, as an element in a system designed to maintain low-frequency cut-off distortion at threshold values, has a further disadvantage. For positive operation as a low-frequency restorer, the resistance-capacitance time constant of the restorer should be small compared to that of the system which precedes it. This means that the net system low-frequency distortion after restoration will be due mainly to the restorer instead of the multitude of system cut-off elements. Hence, it should be used only for the restoration of d-c and very low frequencies.

The shortcomings of the d-c restorer are overcome in a device called a clamper. A simplified schematic is shown in Figure 5, from which it may be seen that this form of clamper is merely the d-c restorer with a pulse-operated switch replacing the diode and resistance. In this form the clamper may be defined as a pulsed d-c restorer. The pulses used are normally the synchronizing pulses.

The clamper has over the d-c restorer the advantage that a low impedance to ground is obtained whenever the clamper switch is closed, that is, during the synchronizing pulse time. Hence the coupling capacitor may be rapidly charged or discharged to maintain line-up of synchronizing pulses. During the remainder of the time, the switch is open and no leakage path to ground need be provided. Hence the clamper does not of itself cause distortion of the signal.

If we consider the clamper as a demodulator, then the demodulated wave form is that which exists across the coupling capacitor. This wave form is a staircase or stepped wave and may be called the envelope since it is the negative of the envelope of the tips of the synchronizing pulses at the clamper input. The output of the clamper is the input wave minus its envelope.

For the case of a transmitted still picture, which lacks only its d-c value, the derived envelope will be this d-c value. Hence the clamper output will contain the original signal including the d-c component.

For the case of a transmitted moving picture from which the direct current and low frequencies have been removed, the derived envelope will contain the direct current and, to a varying approximation, the low frequencies up to half-line frequency. Above half-line frequency the derived envelope is no longer even an approximation to the deleted frequencies.

Although clamping has been referred only to the synchronizing pulses, any reference or datum value of the signal may be used. These also occur at the front and back "porches" of the standard video signal. For certain uses, such as in picture monitors, back porch clamping may be advantageous inasmuch as the black level is maintained more nearly independent of signal amplitude than if synchronizing pulse clamping is employed. For most purposes, however, the attendant difficulties of generating delayed pulses necessary for back porch clamping make its use less attractive.

Operation of Clampers

The low-frequency cut-off of a video transmission system produces a distorted video signal at the output which may be thought of as the sum of the undistorted video wave form and a low-frequency distortion wave. The low-frequency wave is the negative total of all the low frequencies lost in transmission. It is intended that the process of sampling at the line frequency synchronizing or blanking times will yield substantially this low-frequency distortion wave form. The sampled distortion envelope can then be subtracted from the distorted video wave form to yield substantially undistorted video. However, sampling at finite intervals can yield a wave form which is correct only at the time of sampling. Between intervals the envelope wave yielded by sampling remains constant while the low-frequency distortion wave form which is sampled is continuously changing so that when the derived wave is subtracted from the input wave, a residual distortion remains. This is illustrated in Figures 6(A), (B), (C). Figure 6(A) is a typical low-frequency distortion wave such as might be due to a single resistance-capacitance cut-off acting upon a video wave form which contains a square wave of low frequency. Figure 6(B) shows the wave which is derived by sampling the low-frequency wave at a finite rate. Figure 6(C) shows the wave form which remains when the sampler derived wave is subtracted from the low-frequency wave.

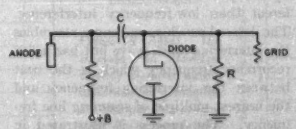

Figure 4. The d-c restorer circuit

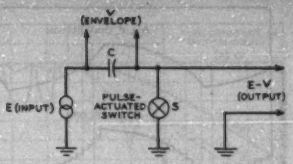

Figure 5. A simplified clamper circuit

The residual distortion wave form of Figure 6(C) produces a characteristic raster distortion pattern. The effects of low-frequency cut-off distortion when clamped are zero at the left side of the raster and increase toward the right so that the effects are first noticeable along the right edge of the raster. These effects are characterized by sudden changes in the background which occur whenever the low-frequency distortion wave suddenly changes slope. Such slope changes will occur wherever there are sudden vertical divisions in brightness as might be the case at the horizon in an outdoor scene. Figure 7 consists of raster photographs where the picture material is an artificially generated white square. Figure 7(A) is an undistorted case. Figure 7(B) shows the low-frequency cut-off distortion caused by a single resistance-capacitance coupling network when no clamping is employed. Figure 7(C) is the same raster after the cut-off distortion has been reduced by clamping. The time constant has been chosen small enough so that the distortion may still be seen in the clamped case. It appears as a dark streamer to the right of the square.

The peak-to-peak amplitude of the residual distortion establishes the low-frequency cut-off requirement of a system which employs a clamper. This amplitude is equal to the amount of slope in the

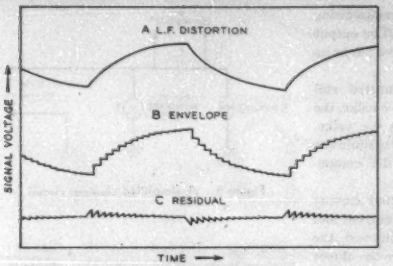

Figure 6 (left). The result of clamping low-frequency distortion

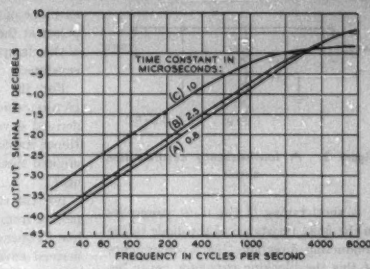

Figure 8 (right). Peak interference reduction by clamping

low-frequency wave form, Figure 2(D), which accumulates during the time of one scanning line. The amplitude in the nonclamper case is the slope which accumulates over one-half frame scanning time. For equal distortion amplitudes in the two cases, a possible reduction in the required low-frequency time constant due to the use of clampers is about 65 times. The lowered value of the cut-off time constant simplifies video interstage design and permits the use of transformers, with their attendant advantages, as video coupling elements.

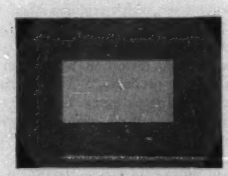

Figure 7(A). A white rectangle with a grey background. No low-frequency cut-off distortion

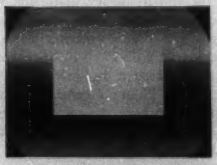

Figure 7(B). The effect of a large amount of low frequency cut-off distortion

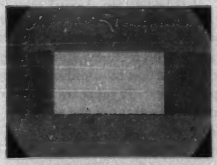

Figure 7(C). The effect of clamping applied to the signal of Figure 7(B)

The subtraction of the sampled envelope of the input wave from the input wave itself is as effective in reducing low-frequency interference as it is in reducing the distortion caused by the low-frequency cut-off of the transmission system. The low-frequency interference may be comprised of any number of low-frequency sine waves which are added to the video wave form during transmission. When this wave is sampled at a rate which is high compared to the interfering frequency, the derived envelope is similar in form to the interfering wave but progresses in the manner of a staircase. As the interfering frequency is lowered the sampled envelope becomes a better and better approximation to the input wave so that after substraction a smaller and smaller interference remains. The residual interference has a maximum value given by the maximum change of the input wave in the time of one scanning line. Where the time of one scanning line is T_0 and the interference is of the form; $\epsilon = \sin \omega t$, the remaining interference, R, is given by: $R = \sin \omega(t+T_0) - \sin \omega t$ and has a maximum value, (when $\omega t = -\omega T_0/2$), equal to $2 \sin \omega T_0/2$. This function is plotted in decibels in Figure 8(A) for values of interference frequency, (f), from 20 cycles to 15750/2 cycles. This curve represents the ratio of peak output distortion to peak input distortion achieved by ideal low-frequency clamping of this form. The suppression of 60-cycle power frequency interference by 33 decibels might alone justify the addition of a clamper in many situations.

High-frequency interference is affected by clampers in a manner altogether different than low-frequency interference. The derived envelope no longer resembles the interfering input wave but has a low recurrence frequency which is the beat between the interfering frequency and the nearest multiple of scanning line frequency. The process is illustrated in Figure 9 which shows an interference frequency nearly equal to scanning line frequency and the resulting low recurrence frequency of the derived envelope.

Reference to Figure 10 will serve to show how this generation of low beat frequencies may degrade intolerably a system which is otherwise acceptable. The signal-to-noise ratio which is required of an acceptable system falls off rapidly as the frequency of the "noise" is increased. If from a high-frequency interference having a low signal-to-noise requirement the clamper generates a beat frequency having a high signal-to-noise requirement, the effective requirement at the high interference frequency is determined by the requirement for the generated beat frequency and becomes severe at all frequencies.

When the interference is in the form of wide band random noise, the derived envelope has a random value from line to line which is unrelated to the noise during the picture time so that the envelope when added back into the video contributes an additional random interference. This interference has the appearance of streakiness in the picture. It might be well to point out that the clamper is not affected by the characteristic noise of the camera tube because this noise does not appear in the synchronizing region. Random noise added into the system beyond the blanking stage will presumably exist in the synchronizing region and will generate the streakiness in clamper output.

A possibility for reducing the amplitude of beat frequencies generated by the clamper exists in the finite duration of the synchronizing pulse during which time the envelope is derived by sampling. A process of averaging over this duration in the derivation of the envelope yields a beat frequency amplitude which is equal to the interference wave amplitude multiplied by the function, $\sin \pi f\tau / \pi f\tau$ where τ is the time duration of the synchronizing pulse and f is the frequency of interference, (see Appendix II). This function at high frequencies decreases as $1/f$.

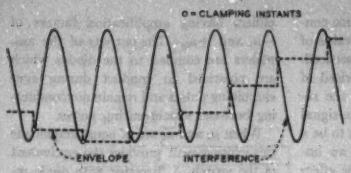

Figure 9 (left). The low-frequency beat which is generated by the clamping of a high-frequency interference waveform

Figure 11 (right). The reduction in amplitude of generated beat frequency as a function of clamper time constant

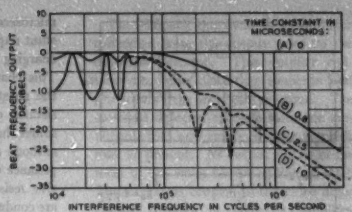

Averaging of this kind will reduce the beat frequency amplitudes to values such that they will no longer affect the interference requirement at high frequencies. At frequencies between 2.5 kc and 100 kc the function $\sin \pi f\tau / \pi f\tau$ has not yet become effective in reducing the generated beat frequency amplitude. In this region the signal-to-noise requirement is perhaps 6 decibels worse with clampers than without. This seems to be a minimum penalty to be paid for the use of the clamper.

The averaging of the values of the interference over the time duration of the synchronizing pulses is accomplished by means of a time constant in the envelope detector circuit. A resistance-capacitance circuit has been employed thus far and modifies the generation of the envelope as follows. The envelope follows the low-frequency wander of the video wave form abruptly at the beginning of the synchronizing pulse when there is no time constant. When a time constant is employed, however, the envelope voltage cannot change suddenly, but during each synchronizing pulse approaches exponentially the changed level of the video wave form. The instantaneous envelope detector follows a high-frequency interfering wave form without attenuation during the synchronizing pulse so that at the end of the synchronizing pulse the instantaneous value of the interfering wave remains as the envelope voltage. When a time constant is employed the interference is attenuated so that the envelope voltage at the end of the synchronizing pulse is less and less determined by the interference as the frequency of the interference is increased. The amplitude of this generated envelope beat frequency versus the interference frequency is plotted in Figure 11. The derivation of the curves is developed in Appendix I.

The addition of a time constant to reduce the generation of beats from high-frequency interference reduces somewhat the efficiency with which the clamper acts to suppress low-frequency distortion and interference. The increase in low-frequency clamper output distortion as a function of the clamper time constant is shown in Figure 12, for the standard wave form having a synchronizing pulse width equal to 5 microseconds (see Appendix II). The curves of low-frequency interference reduction, Figure 8, show the same effects of clamper time constant to reduce the effectiveness of the clamper as a low-frequency interference suppressor.

Reference to these curves and the curves of beat frequency amplitudes, Figure 11, show that great reductions in beat frequency amplitude at high interference frequency are possible with only a slight decrease in the low-frequency performance of the clamper. Evaluation of these data make it possible to choose a value for this time constant of about 2.5 microseconds as being close to an optimum value. With this choice, low-frequency performance is degraded about 1.5 decibels while the beat frequency output at 1 megacycle has been reduced 22 decibels. This value of time constant has been incorporated into the clamper circuits to be described. In the frequency region from 2.5 kc to 100 kc the maximum amplitude of the generated low-frequency beats is not much reduced by the time constant of the clamper so that in this region the transmission interference requirements are about 6 decibels worse when clampers are employed.

Clamper Circuits

The usual form of clamper, which we shall designate as the series capacitor clamper, is shown in Figure 5. In this case the envelope is obtained across capacitor C by the periodic closing of the switch, S. The closed period corresponds in time to the synchronizing pulse time of the video wave form so that the capacitor is charged to the value of the video wave at this time. The charge acquired during the closed period remains unaltered during the open period, and therefore represents an envelope of the peak voltage of the video wave form during the synchronizing pulse times. The output voltage is then obtained as the difference between the input voltage and the sampled envelope.

The rapidly closing switch is achieved electrically by a pair of diodes as shown in Figure 13(A). These diodes are caused to conduct during the synchronizing pulse intervals by driving pulses of the same form as the synchronizing pulses. The diodes and pulses taken together constitute a switch between the signal point and ground because periodically they present a low impedance to ground.

Figure 10 (left). The relative visibility of single-frequency interference. Viewing distance is five times the picture height

Figure 12 (right). The increase in low-frequency clamper output distortion as a function of clamper time constant (for a synchronizing pulse width equal to five microseconds)

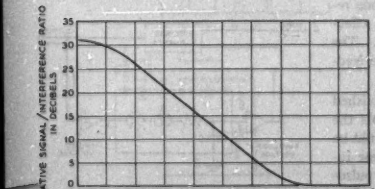

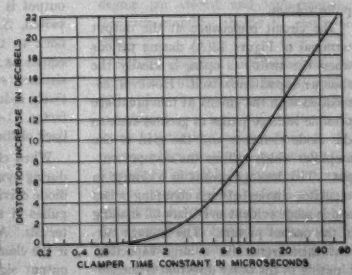

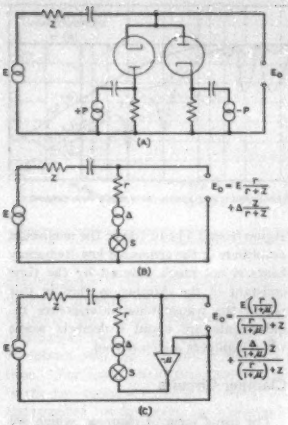

Figure 13. The series capacitor clamper circuit and its electrical equivalent

A. The diodes and driving pulses
B. The pulsed diode equivalent
C. Envelope feedback to reduce diode distortion and resistance

None of the driving pulse voltage, ideally, is transmitted to the signal path because the pulses are coupled to the signal path in equal magnitude and opposite polarity and generate only a loop current in the diode circuit. The capacitors and resistors associated with the circuit provide a biasing arrangement so that the diodes will conduct at the peaks of the driving pulses and be well cut off between conducting periods. The value of bias which is developed determines the maximum value of voltage that may be transmitted in the signal path of the circuit. Higher signal voltages will cause diode conduction during normally nonconducting periods. This consideration furnishes the requirement for the required driving pulse amplitude since the bias voltage is equal to the peak amplitude of the driving pulse voltage.

The circuit impedance at the output terminal of Figure 13(A) during periods when the switch is open, is ideally the clamper capacitance itself. However, associated with the circuit at this point are possible leakage paths to ground such as the diode elements and the grid of the amplifier which utilizes the clamper output. This leakage results in a change in capacitor charge between clamping pulses and is made evident as horizontal shading in the output picture. The leakage current then argues for a large capacitor. Limiting in the other direction is the 2.5-microsecond capacitor charging time constant required and the minimum value of charging resistance which can be secured. This charging resistance is comprised of the resistance of the diodes and the resistance of the signal source. The signal source, has, therefore, been chosen to be a cathode follower and may have an impedance of 100 to 200 ohms. The effective resistance of the diodes when they are conducting is of the same order so that a total charging resistance of 200 to 300 ohms is obtained in this form of circuit. Such a value yields 0.01 microfarad as about the maximum value for the charging capacitance. With this value of capacitance a leakage resistance of 10 megohms would yield the amount of horizontal shading equivalent to a 0.1 second time constant and is considered to be a tolerable value for the shading due to a single circuit element.

The combination of diodes and driving pulses departs from an ideal switch in two ways; it has resistance as mentioned before and it is subject to unbalance. The unbalance results in placing on the clamping capacitor a charge due to the driving pulses and as these pulses vary in form through the vertical synchronizing pulse region the amount of charge coupled to the clamping capacitor will likewise vary, producing in the clamped output a distorting envelope voltage. Schematically this distortion might be represented as a voltage source in series with the switch as in Figure 13(B) where it is labeled Δ. This figure shows conditions which exist when the diodes are conducting. Ideally the output at this time should be zero but due to the diode resistance r and the voltage source Δ a residual output is present.

This residual output during the conducting period can be reduced considerably if feedback is employed in the manner shown in Figure 13(C). The residual voltage appearing at the output terminals is amplified and reversed in polarity by the amplifier labeled, $-\mu$. The amplifier output is returned through the clamper switch, S, and the diode resistance, r, back to the output terminals. Circuit equations reveal that both the diode resistance, r, and distortion, Δ, are effectively reduced by a factor, $(1+\mu)$. The factor, $(1+\mu)$, is recognized as the feedback of the circuit.

When clamping is to be accomplished during synchronizing pulse intervals the diode driving pulses preferably should be pulses of the same duration as these intervals. A suitable source of such pulses is the clamped output signal itself. The output signal is amplified by two amplifiers having amplification factors of $-\mu_1$ and $+\mu_2$. The outputs of the amplifiers are coupled to the diodes which are polarized to conduct during synchronizing pulses and remain nonconducting between synchronizing pulses.

When μ_1 and μ_2 are of equal magnitude this arrangement provides the equivalent of the switch, S, together with diode resistance, r, and distortion, Δ, shown in Figure 13(B). If μ_1 is greater than μ_2 a negative feedback circuit exists. The magnitude of the net feedback $(1+\mu)$ is equal to $1+(\mu_1-\mu_2)/2$, and is useful in reducing the effects of the diode distortion and resistance as in Figure 13(C).

When the diode driving pulses are derived from the video wave form there is a requirement that the maximum envelope distortion from one line to the next must not exceed the amplitude of the synchronizing pulse since amplitude selection is the basis of pulse extraction. Envelopes greater in amplitude than synchronizing pulse result in video information being present at the pulse clipping amplitude level. Low-frequency interference or distortion having an amplitude greater than the synchronizing pulse amplitude is tolerable because it is progressively removed from line to line by the clamper. This restriction affects primarily the response of the clamper to sudden transients such as impulse noise or contact noise.

There is another approach to the clamping problem which is suggested by feedback amplifier techniques. Figure 14 illustrates the method. The switch and capacitor combination are rearranged so that its useful output is the envelope voltage rather than the difference between signal and envelope as in the case of the series capacitor clamper. This envelope detector is a β circuit element in a feedback circuit, arranged to reduce the overall forward gain to distortion and interference voltages without affecting gain to a video wave form which is free of such voltage. The result of such an arrangement is an improvement of signal-to-noise ratio by the amount of loop gain employed.

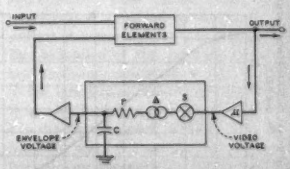

Figure 14. The envelope detector as a circuit element in a feedback clamper circuit

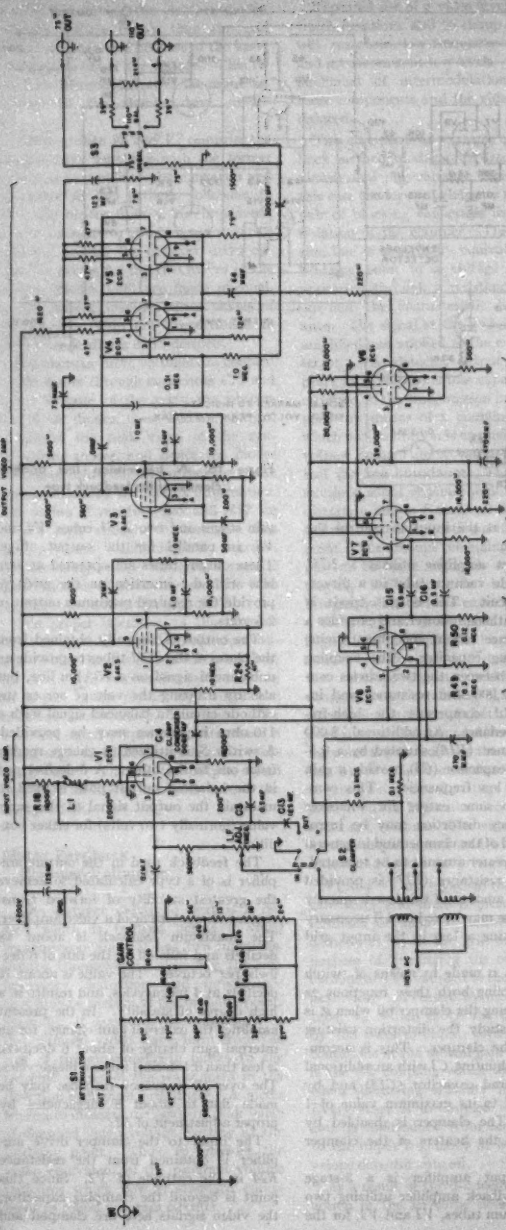

Figure 15. Series capacitor clamper (W.E. 1-B clamper-amplifier)

The feedback loop includes an amplifier connected from the output point to the envelope detector. This amplier contains no video distorting elements and provides all the loop gain required. The envelope detector extracts from the amplified video any envelope voltage which may be present. Its output will be of the form of the wave shown in Figure 6(B). This output is coupled to the video input circuit through a coupling amplifier which is usually necessary as an impedance transformer.

In the forward path of the feedback loop there may be transmission elements of a wide variety of forms. The envelope distortion which might normally be introduced by these elements is reduced by the feedback in the same way as input distortion. These elements might include nonvideo components such as amplitude-modulation or frequency-modulation components delivering an output carrier wave rather than a video wave. In such a case complementary elements would be included in the feedback path to restore the signal to a video wave form at the envelope detector input terminals. The carrier counterpart of the video distortion would then be suppressed.

The effective clamping time constant for the feedback connection is the time constant of the envelope detector divided by the feedback factor, $1+\mu$, (see Appendix III). In order, therefore, to secure an effective time constant of 2.5 microseconds, the envelope detector time constant is increased by increasing the capacitance or driving resistance or both. In terms of the $\mu\beta$ frequency characteristic the effective 2.5-microsecond time constant means that $\mu\beta$ is reduced to unity at a frequency of about 64 kc. The phase shift of $\mu\beta$ at this frequency will be 90 degrees plus whatever phase shift is contributed by the high-frequency cut-off of the remaining circuits. Since these circuits would normally extend to about four megacycles they contribute phase shift at 64 kc of the order of one degree per circuit and high-frequency feedback stability should be easily obtained.

Stability against oscillation at low frequencies will usually present greater difficulties. It is important that $\mu\beta$ be maintained at a large value beyond the lowest distortion or interference frequency which must be suppressed. Cutting off the loop gain in an orderly manner in the region below a few cycles per second is in most cases impracticable. An alternative to cutting off $\mu\beta$ at the low end is that of maintaining the feedback loop gain to zero frequency. This pro-

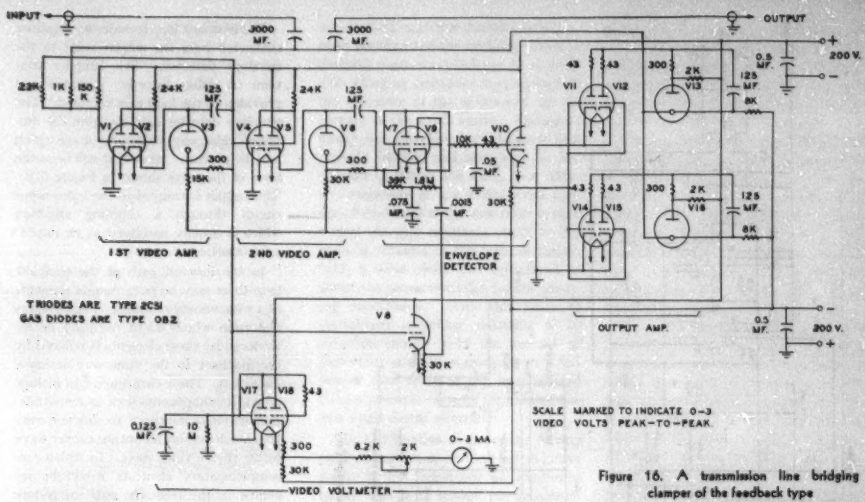

Figure 16. A transmission line bridging clamper of the feedback type

cedure avoids the cut-off problem and results in the additional advantage that those elements within the feedback circuit are d-c stabilized at the clamping pulse intervals. In this manner the value of carrier radiated by a television transmitter could be maintained at a constant value at synchronizing pulse times by including the transmitter as one of the forward path elements of such a clamper feedback loop.

Two examples of clampers will now be described in detail. The first is a series capacitor clamper-amplifier which has application as a video line terminating amplifier. The second clamper is of the feedback type and is a device which may be bridged across a video line to suppress video distortion and interference and which, incidentally, serves to measure the peak-to-peak video voltage existing at this point.

Series Capacitor Clamper Circuit

The Western Electric Company *1B* clamper-amplifier is shown schematically in Figure 15. It fulfills the 2-fold function of reducing low-frequency distortion and providing a maximum of 18 decibels gain. The amplifier proper is comprised of an input amplifier providing about 12 decibels gain, and an output amplifier with 6 decibels gain. The clamping capacitor (*C4*) is the coupling element between the two. A gain control consisting of a stepped potentiometer having nine two decibel steps and a 1-decibel attenuator is provided at the input to control the over-all gain.

The input amplifier utilizes a *2C51* double triode vacuum tube in a direct-coupled circuit. The output triode is used as a cathode follower and provides a low-impedance (about 250 ohms) facing the clamping capacitor. The coupling impedance between the two triodes consists of a 2,000-ohm resistance and inductance *L1* comprising the high-frequency impedance. An additional 18,000 ohm resistance (*R18*) shunted by a 0.5-microfarad capacitor (*C3*) provide a gain increase at low frequencies. This compensates to some extent for whatever low-frequency distortion may be introduced ahead of the clamper and in general permits a greater amount to be tolerated. A variable resistance (*R17*) is provided so that the amount of this low-frequency gain increase may be reduced if necessary by introducing a loss in the input grid circuit.

Provision is made by means of switch S_1 for disabling both these functions as well as turning the clamper off when it is desired to study the distortion existing ahead of the clamper. This is accomplished by shunting *C3* with an additional 125-microfarad capacitor (*C13*) and by raising *R17* to its maximum value of 1 megohm. The clamper is disabled by turning off the heaters of the clamper diodes (*V8*).

The output amplifier is a 3-stage cathode feedback amplifier utilizing two *6AK5* vacuum tubes, *V2* and *V3*, for the gain stages and two *2C51* tubes, *V4* and *V5*, in parallel for the output stage. These output tubes are operated at zero bias with d-c insertion on the grids to provide the required maximum output of 2.5 volts.

The output is normally obtained from the plates of the *2C51* tubes to provide an unbalanced signal on a 75-ohm line, but also by utilizing the voltage across the cathode circuit, a balanced signal with a 110-ohm impedance may be provided. A switch S_2 is utilized to change readily from one to the other. A 5-decibel pad in the balanced output path is used to maintain the output signal at the same value (normally two volts) for either condition.

The feedback used in the output amplifier is of a type calculated to achieve the greatest stability of forward transmission characteristic of a video amplifier. The maximum feedback is about 48 decibels and falls off at the rate of 6 decibels per octave. The value is about 15 decibels at 4 megacycles, and results in a high degree of stability. In the present amplifier the external gain change, for an internal gain change of about 6 decibels, is less than 0.1 decibel up to 4 megacycles. The over-all frequency response may be made flat to about 8 megacycles by proper adjustment of *L1*.

The input to the clamper drive amplifier is obtained from the resistance *R24* in the cathode of *V2*. Since this point is beyond the clamping capacitor, the video signals here are clamped and

suitable for driving the clamper diodes. Cathode voltage rather than the grid voltage of *V2* is used because of the lower impedance level of the former. This reduces the shunting effect of the input impedance of the clamper-drive amplifier.

Vacuum tubes *V6* and *V7* comprise the clamper-drive amplifier with the former serving as an amplifier-phase inverter and the latter as two cathode followers to drive the diodes from a low impedance point. In order to obtain a net negative feedback around the clamper drive circuit, the drives for the two halves of the clamper diodes (*V8*) are made unequal. In the present instance these values of driving pulse gain are proportioned to yield a net feedback of 15 decibels.

The clamper drive voltages are coupled to the diodes through capacitors *C15* and *C16*. Because of the rectifying properties of the diodes, these become charged to almost the peak value of the synchronizing pulses, and hence the diodes are biased below cut-off for the part of the signal containing the picture information. The values of resistors *R49* and *R50* are chosen high enough to maintain this charge almost undiminished between synchronizing pulses, while their ratio is made such as to maintain zero bias with respect to ground at the grid of *V2*.

The proper operation of the clamper depends upon the signal amplitude available to bias the diodes. If this is too low, the diodes will become conductive during all or part of the picture time and hence introduce considerable distortion. With a normal signal output of 2 volts, there is about a 10- to 12-decibels margin in operating value. That is, the output signal may fall to about 0.5 volt before the clamper fails.

Shunt Feedback Clamper-Voltmeter

The clamper described next is a device which is bridged across a video transmission line. It has two functions. Firstly, it removes, by clamping, the low-frequency distortion and interference that may be present at the bridging point. Secondly, it measures the amplitude of the clamped video wave form from the tips of the synchronizing pulses to the extreme values of the wave form in the direction of highest brightness. A meter is used to indicate the peak-to-peak value of clamped video voltage existing at the bridging point. Thus, it provides the video equivalent of the program volume indicator which now is standard equipment in sound program circuits.

Repeated use of a video level indicator which functions also to clamp the signal will maintain low-frequency distortion and interference at low levels. Thus, the likelihood of intermodulation between these components and the video signal is reduced.

This clamper is an example of the feedback method of clamping described previously and illustrated in Figure 14. In this case the forward elements reduce to a pair of blocking capacitors used for d-c isolation of the clamper. The transmission line is electrically equivalent at the bridging point to a voltage source, E, appearing through a resistance equal to one-half the characteristic line impedance. The signal at the bridging point is amplified and applied to the envelope detector. The detector output which appears as a voltage across capacitor, C, is returned to the transmission line bridging point by means of a coupling amplifier which for illustration is assumed to have a voltage gain of unity working into one-half the line impedance. This feedback envelope is out of phase with the original distortion due to E and therefore reduces the net distortion existing at the bridging point. The amount remaining in the output can be made negligibly small by employing sufficient gain between the bridging point and the envelope detector.

Referring to the schematic diagram, Figure 16, the feedback loop is seen to consist of two video gain stages ahead of the envelope detector and an output coupling stage consisting of two similar circuits in parallel to inject the envelope back into the bridging point. The bridging point is isolated from the transmission line by two 3,000-microfarad capacitors to remove any direct voltage that may be present on the line and which the clamper could not tolerate. The video distortion in the output occasioned by the 3,000-microfarad capacitors is negligible.

V_1 and V_2 are together the first video gain stage and there is present negative feedback of about 6 decibels from the cathode of V_2 to the grid of V_1 for the purpose of linearizing the output. The cathode of V_2 is coupled to the input of the next video gain stage by means of a gas tube, V_3, which drops the d-c potential by 105 volts to obtain correct d-c input conditions at the second gain stage. This is the d-c coupling which was spoken of when discussing stability requirements. Every stage is so coupled that the loop gain is maintained from zero frequency to the upper frequency at which the envelope detector cuts off.

As a result of the d-c feedback and the action of the envelope detector, the instantaneous potentials within the feedback loop are stabilized at fixed values at the synchronizing pulse times regardless of signal level or picture content. This assures that the optimum operating point obtains at synchronizing pulse times and that distortion will be minimized at this part of the signal wave form.

A by-product of great usefulness is due to this d-c stabilization of the synchronizing pulse value of the wave form. This means that, if a rectifier is connected to obtain the peak value of signal departure from the d-c level with no signal applied, then the rectified voltage is a measure of the peak-to-peak video input level and a peak-to-peak meter of good characteristics results. *V17* is such a peak rectifier diode and the rectified voltage is applied to a meter by means of the cathode follower *V18*. The zero setting of this circuit is sufficiently stable that the mechanical zero adjustment of the meter suffices to adjust zero. A scale factor adjustment, *R1*, compensates for variations in gain of the first video gain stage and variations of other elements. It is because the meter possibilities are exploited that linearizing feedback is applied to the first video gain stage. Figure 17 shows the peak factor characteristics of the metering circuit.

The second video stage is similar to the first. However, there is no feedback from the output to the input since there is no linearity requirement. In fact, for normal levels the video is completely stripped off the synchronizing pulses at the cathode of *V5*. However, since stabilization occurs at the tops of the synchronizing pulses, the amplifier stages are linear at these instants and there is no danger of clipping the distortion wave carried by the synchronizing pulses. The gas tube, *V6*, reduces the d-c potential to a value near zero for the envelope detector but couples without loss the variations due to input signals. Gas tubes have the characteristic whereby their resistance increases with frequency so that the resistance even at moderately low frequencies is substantially different from the d-c value. For this reason the gas tube must be effectively by-passed at all frequencies within the range of interest, otherwise envelope distortion will be produced in the video gain stages. It is found that a coupling time constant of about 0.25 second neglecting the gas tube will reduce envelope distortion in the gain stages to a negligible value.

V7 and *V9* are the two diodes which, together with r and C, constitute the envelope detector. The output of the second video gain stage is connected to

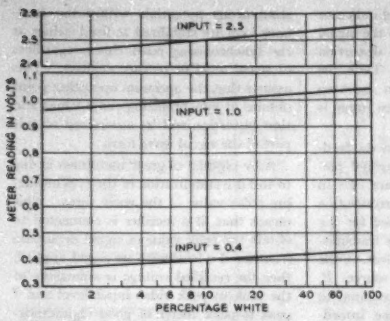

Figure 17. The video voltmeter peak factor characteristics

the cathode of *V7* while a smaller signal of opposite polarity is connected to the plate of *V9*. The signal of opposite polarity is conveniently obtained from the output of the first video gain stage. A cathode follower, *V8*, is used as the drive for *V9* so that the diode current will not produce distortion at the first video stage output point. The capacitance, across which the envelope voltage appears, is connected through a resistance to the junction of the anode of *V7* with the cathode of *V9*. The resistance-capacitance product of the two elements and the loop gain of the circuit determine the effective time constant of the clamping action.

V10 is a cathode follower to couple the envelope voltage to the grids of the output amplifiers. The output amplifiers are triodes which operate at high current and are coupled to the bridging point with gas tubes and large capacitors. Four tubes are required to handle the peak envelope expected from a 2.5-volt video signal. These tubes are split into two pairs so that tube aging will be more easily detected in maintenance.

The range of levels, which this clamper will handle is nominally 0.2 to 2.5 volts peak-to-peak. The passive elements which shunt the bridge point to ground produce a shunting loss of about 0.8 decibel which is constant over the video band of frequencies. If the impedance irregularity produced by this shunt is undesirable, a T-pad may be constructed by using series resistors in the input and output leads. These resistors of about 7 ohms will provide 75-ohms impedance in each direction and a loss of 1.6 decibels.

Some experiments have been carried out using 75-ohm to 110-ohm transformers at the clamper terminals. With this arrangement signals on balanced 110-ohm circuits may be clamped. Using *197A* repeating coils the clamped output appeared to be free of low frequency distortion. Since the clamper effectively drives the coils with an envelope source impedance approaching zero ohms the low-frequency cut-off of the coils is extended to the point where no video distortion is noticeable.

Conclusions

The effects which result from the use of clampers may be summarized as follows:

Low-frequency interference which adds to the video wave form may be suppressed by a factor inversely proportional to the frequency of the interference. The factor is large, over 30 decibels, at 60 cycles.

The effects of high-frequency interference in the frequency range from 2.5 kc to 100 kc are doubled in amplitude due to the generation of low frequency beats between the interfering frequency and multiples of the video line frequency, (15.75 kc). The amplitude requirement for interference in this range of frequencies is therefore 6 decibels worse with clampers than without. The low-frequency amplitude cut-off requirement of the video system using clampers may be raised in frequency by a factor of 10 to 65 times as compared with a nonclamper cut-off of one to five cycles depending upon the amount of low-frequency gain bump used for 60-cycle phase compensation. Savings are then made in the size of components required for low-frequency transmission.

Transformers as video coupling elements become practicable when clampers are used. The increase of the low-frequency cut-off frequency means that reasonably sized units may be constructed to cover the video transmission band.

Appendix I. Derivation of Envelope

Let the sampling frequency be f_0, and the duration of the sampling time infinitesimally short. Then for an input wave $E=E(n/f_0+t)$ where $0<t<1/f_0$, and n is an integer, the resultant derived wave may be designated by

$$V=E\frac{n}{f_0} \tag{1}$$

and is merely the amplitude of the input wave at the nth sampling interval.

If E is a cosine wave represented by

$$E=\epsilon^{j\omega\left(\frac{n}{f_0}+t\right)}$$

then

$$V=\epsilon^{j\omega\left(\frac{n}{f_0}\right)} \tag{2}$$

If $\omega=2\pi(mf_0+F)$ where m is an integer including zero and $|F|<f_0/2$, then

$$V=\epsilon^{j2\pi\left(m+\frac{F}{f_0}\right)n}=\epsilon^{j2\pi\frac{Fn}{f_0}} \tag{3}$$

since $\epsilon^{j2\pi mn}=1$.

From equation 3 it may be seen that the envelope frequency corresponds not to the input frequency but to the beat between the input frequency and the nearest multiple of sampling frequency including zero.

For the case where the duration of the sampling time is finite, say τ seconds long, let the value of the input wave during the nth sampling time be: $E=E(n/f_0-\tau+t)$ where $0<t<1/f_0$ and as before n is an integer. Further let the resistance-capacitance product of the clamping circuit be T. Then, the envelope after the nth sampling may be represented operationally by

$$V\frac{n}{f_0}=\frac{V\frac{n-1}{f_0}pT+E\left(\frac{n}{f_0}-\tau+t\right)}{1+pT} \tag{4}$$

where $V(n-1/f_0)$ is the value of the envelope derived at the preceding sampling interval, and p is the operator d/dt. The integral equation corresponding to equation 4 is

$$V\frac{n}{f_0}=V\frac{n-1}{f_0}\epsilon^{-\tau/T}+\frac{\epsilon^{-\tau/T}}{T}\times\int_0^\tau E\left(\frac{n}{f_0}-\tau+t\right)\epsilon^{t/T}dt \tag{5}$$

If again E is a cosine wave represented by

$$\epsilon^{j\omega\left(\frac{n}{f_0}-\tau+t\right)},\ 0<t<\frac{1}{f_0}$$

$$V\frac{n}{f_0}=V\frac{n-1}{f_0}\epsilon^{-\tau/T}+\epsilon^{j\omega\frac{n}{f_0}}\left(\frac{1-\epsilon^{-\frac{\tau}{T}(1+j\omega T)}}{1+j\omega T}\right) \tag{6}$$

Since the input is a periodic wave, in the steady state

$$V\frac{n-1}{f_0}=\epsilon^{-j\omega/f_0}V\frac{n}{f_0}$$

and hence, with this substitution in equation 6

$$V\frac{n}{f_0}=\frac{\epsilon^{j\omega n/f_0}\left(1-\epsilon^{-\frac{\tau}{T}(1+j\omega T)}\right)}{(1+j\omega T)\left(1-\epsilon^{-(\tau/T+j\omega/f_0)}\right)} \tag{7}$$

In this instance also, the envelope has the same period as the input wave only if the frequency is less than half the sampling frequency. In only this case is it proper to speak of a residual distortion as being equal to the difference between the input and the envelope. This is given by

$$E\left(\frac{n}{f_0}-\tau+t\right)-V\frac{n}{f_0}=\epsilon^{j\omega\left(\frac{n}{f_0}-\tau+T\right)}\times$$

$$\left[1-\frac{e^{-j\omega(1-\tau)}\left(1-e^{-\frac{\tau}{T}(1+j\omega T)}\right)}{(1+j\omega T)\left(1-e^{-(\tau/T+j\omega/f_0)}\right)}\right] \quad (8)$$

This, in general will have a maximum value at the time just preceding the sampling interval, that is, when $t=1/f_0$. The maximum value of the absolute amplitude of the residual then is defined as

$$R=1-\frac{e^{-j\omega\left(\frac{1}{f_0}-\tau\right)}\left(1-e^{-\frac{\tau}{T}(1+j\omega T)}\right)}{(1+j\omega T)\left(1-e^{(\tau/T+j\omega/f_0)}\right)} \quad (9)$$

When $\omega << f_0$ equation 9 reduces to

$$R=\left[\omega\left(\frac{1}{f_0}-\tau\right)\right]\left[\frac{1}{1-e^{-\tau/T}}+\frac{f_0T}{1-f_0\tau}\right] \quad (10)$$

The second factor of equation 10

$$\left[\frac{1}{1-e^{-\tau/T}}+\frac{f_0T}{1-f_0\tau}\right]$$

is a factor which shows how the clamper time constant reduces the effectiveness of the clamper in reducing low-frequency distortion. It has been plotted in decibels as a function of T in Figure 12. It is identical with an expression equation 16, for the effects of time constant upon the reduction of cut-off distortion.

Values of R against $f=\omega/2\pi$ have been plotted in Figure 8 for the following values of parameters

$f_0=15{,}750$ cycles
$\tau=5$ microseconds
$T=0.8,\ 2.5,\ 10$ microseconds

When $T\to 0$, equation 9 reduces to

$$R\doteq 2\sin\left(\frac{\omega}{2}\left(\frac{1}{f_0}-\tau\right)\right) \quad (11)$$

When $f>f_0/2$, the envelope generated is extraneous and it is proper to speak of it as a new source of interference. As before, let $\omega=2\pi(mf_0+F)$. The beat is then given from equation 7, by

$$V\frac{n}{f_0}=\frac{e^{j2\pi\frac{Fn}{f_0}}\left(1-e^{-\frac{\tau}{T}(1+j\omega T)}\right)}{(1+j\omega T)\left(1-e^{-\left(\frac{\tau}{T}+j\pi F/f_0\right)}\right)} \quad (12)$$

The absolute amplitude of equation 12 may be reduced to

$$A=\sqrt{\frac{(\sinh^2\tau/2T+\sin^2\pi f\tau)}{(1+\omega^2T^2)\left(\sinh^2\frac{\tau}{2T}+\sin^2\frac{\pi F}{f_0}\right)}} \quad (13)$$

Values of A against frequency have been plotted in Figure 11 for the same range in values of T.

Only the first few cyclic variations in A have been plotted. In the region from about 60 to 500 kc, only the values of A when $F=0$ have been indicated. Above 500 kc, only the extreme values obtained when $F=0$, and $\sin(\pi f\tau)=1$ have been shown.

Appendix II. Reduction of Low-Frequency Video Distortion

Where the video signal has been applied to several stages of capacity coupled amplifier stages, or several transformers have been used, the resulting wave form will be characterized by a slope or tilt. This may be analyzed by considering the clamper input as made up of an undistorted signal plus an additional saw-tooth voltage. Then since the clamper leaves the undistorted signal unmodified except for the addition of a d-c component which may be disregarded, the remaining saw-tooth term need only be considered.

It will be assumed for simplicity that this saw-tooth wave is of constant slope and of sufficiently long duration compared to the time of operation of the clamper as to be essentially infinite in duration.

We take as our point of departure equation 5 of Appendix I, and let $E=\alpha(n/f_0-\tau+t)$. Substituting this value of E in equation 5 we obtain after integration

$$V\frac{n}{f_0}=V\frac{n-1}{f_0}e^{-\tau/T}+\frac{\alpha n}{f_0}(1-e^{-\tau/T})+\alpha\tau e^{-\tau/T}-\alpha T(1-e^{-\tau/T}) \quad (14)$$

In the steady-state condition, the increase in envelope voltage in proceeding from one sampling interval to the next must be equal to the corresponding increase in input voltage. That is

$$V\frac{n}{f_0}-V\frac{n-1}{f_0}=E\frac{n}{f_0}-E\frac{n-1}{f_0}=\frac{\alpha}{f_0}$$

Equation 14 may then be reduced to

$$V\frac{n}{f_0}=\alpha\left(\frac{n}{f_0}-T\right)-\alpha\left(\frac{1}{f_0}-\tau\right)\frac{e^{-\tau/T}}{1-e^{-\tau/T}} \quad (15)$$

The maximum value of the residual distortion is then given by

$$R=E\left(\frac{n+1}{f_0}-\tau\right)-V\frac{n}{f_0}=\left[\alpha\left(\frac{1}{f_0}-\tau\right)\right]\times\left(\frac{1}{1-e^{-\tau/T}}+\frac{f_0T}{1-f_0\tau}\right) \quad (16)$$

The second factor in equation 16 indicates the dependence of the residual distortion on the time-constant T, and has been plotted in Figure 12.

Appendix III. Derivation of Envelope for Feedback Loop Clamper

Referring to Figure 14, let $rC=T$. During the nth clamping interval, the output voltage (neglecting Δ) may be represented operationally

$$E_o\left(\frac{n}{f_0}-\tau+t\right)=E\left(\frac{n}{f_0}-\tau+t\right)-\frac{\mu}{1+pT}E_e\left(\frac{n}{f_0}-\tau+t\right)-\frac{E_e\frac{n-1}{f_0}pT}{1+pT}$$

$$=\frac{E\left(\frac{n}{f_0}-\tau+t\right)-\frac{E_e\frac{n-1}{f_0}pT}{1+pT}}{1+\frac{\mu}{1+pT}} \quad (17)$$

Where E_e is the value of the derived envelope across the capacitor C. As in Appendix I, $E_e(n-1)/f_0$ is the value of the envelope for the preceding interval. Then since the difference between the input and output wave is the envelope, we have from equation 17, after the sampling interval

$$E_e\frac{n}{f_0}=\frac{\frac{E_e\frac{n-1}{f_0}p\frac{T}{1+\mu}}{1+p\frac{T}{1+\mu}}+\frac{\frac{\mu}{1+\mu}E\left(\frac{n}{f_0}-\tau+t\right)}{1+p\frac{T}{1+\mu}}}{} \quad (18)$$

Comparing equation 4 we see that it is entirely similar provided we recognize that the effective time-constant has been reduced by the factor $1+\mu$, and that the amplitude of the input is modified by the term $\mu/1+\mu$. Hence we conclude

$$E_e=\frac{\mu}{1+\mu}V \quad (19)$$

References

1. The Marconi-E.M.I. Television System, A. D. Blumlein, C. O. Brown, N. E. Davis, E. Green. *Journal*, Institution of Electrical Engineers (London, England), December 1938, pages 758–66.

2. The Clamp Circuit (part I and part II), C. L. Townsend. *The Broadcast Engineers' Journal* (New York, N. Y.), January 1947, pages 7–9, April 1947, pages 6–9.

3. Television D-C Component, K. R. Wendt. *RCA Review*, (New York, N. Y.), volume 9, March 1948, pages 85–111.

4. A TV Sync Stretcher, R. C. Palmer. *Communications* (New York, N. Y.), March 1948, pages 10–11.

No Discussion

Noncontacting Thickness Gauge Using Beta Rays

C. W. CLAPP
NONMEMBER AIEE

S. BERNSTEIN
NONMEMBER AIEE

An earlier paper[1] has described the use of X-rays to measure the thickness of steel as it is being rolled in a hot strip rolling mill. The great success of this method of measurement has stimulated study of the possibilities of using other types of radiation in a similar manner. Of these, beta rays appear to hold the greatest promise at the present time.

Beta rays are electrons emitted spontaneously by certain radioactive materials. Depending on the nature of the source material, these electrons are emitted with maximum energies varying from a few thousand electron volts up to several million electron volts. Those electrons emitted with high initial energy are able to pass through an appreciable thickness of solid material. For example, an electron with an initial energy of 1.3 million electron volts will lose only one half of its energy in passing through a sheet of aluminum 0.038 inch thick.

In principle, it is therefore possible to measure the thickness of a homogeneous sheet of material by placing a source of beta rays at a fixed position on one side of the sheet and measuring the number or the energy of the beta rays which pass through the sheet and reach a detector at a fixed position on the other side. Such a thickness gauge has the important advantage of not requiring physical contact with the sheet being measured. It can therefore be used to measure the thickness of soft uncured rubber or plastic, of textiles or paper coated with soft gummy substances, as well as harder materials such as glass, aluminum, steel and so forth.

Using an ionization chamber as detector, Figure 1 shows the detector current produced by a beam of beta rays after it has passed through different thicknesses of aluminum. The ionization chamber was filled with air at atmospheric pressure, and was provided with an aluminum window only 0.001 inch thick to allow the rays to enter with the minimum of fixed absorption. The thickness of the aluminum absorber is expressed both in inches and in ounces per square yard. Essentially the same curves are obtained for paper, plastic, or rubber, providing the thickness of the material is expressed in terms of its weight per unit area. Since the absorber thickness has been plotted on a logarithmic scale, the slope of the curve is a measure of the change of ionization current for a given small percentage change in the absorber thickness. The range of thickness over which a particular source can be used effectively is limited at each end by loss in sensitivity as evidenced by flattening of the absorption curve.

The source chosen for the gauge to be described consists of strontium 90*. This material gives off beta rays with a maximum energy of 0.65 million electron volts, and has a half-life of 25 years. (The intensity of any radioactive source, as measured by the number of particles emitted per second, falls off exponentially with time. The time required for the intensity of any source to fall to one-half of its initial value is called its "half-life.") With each emission of an electron, an atom of strontium 90 is converted to an atom of yttrium 90. This product material is in turn radioactive, emitting beta rays with maximum energy of 2.16 million electron volts, and has a half-life of 62 hours. Unlike most radioactive materials, no gamma rays accompany the dissociation of strontium 90 or its daughter yttrium 90. This simplifies measurements of the beta ray beam and reduces the amount of shielding needed to prevent stray radiation.

An ionization chamber was chosen as the means to measure the energy in the transmitted portion of the beta ray beam. This detecting means has good stability, does not require high voltages for its operation, and can operate satisfactorily over a wide range of beam intensities. The chamber is filled with air at atmospheric pressure and is sealed to prevent entrance of moisture or other vapors which might adversely affect its operation.

The components of a complete beta-ray thickness gauge are shown in block form in Figure 2. Between the source and the sheet to be measured is a motor-driven chopper or modulator which interrupts the beam 90 times per second. The signal from the ionization chamber is therefore a 90-cycle signal which can be amplified by stable a-c amplifiers, thus avoiding the usual drift problems associated with low-level d-c amplification. To provide an expanded easily-read thickness scale, a potentiometer-type measuring circuit is employed. In this circuit, the output voltage of the ionization chamber is compared with a second 90-cycle voltage of opposite phase which is adjusted in magnitude until the difference between the two voltages is zero. The comparison voltage is derived from a small permanent-magnet alternator driven from the chopper shaft. The attenuator used to adjust the magnitude of the comparison voltage may be calibrated in terms of the thickness or weight per unit area of the material in the beam.

Alternatively, the variable attenuator or gauge dial may be set at the position corresponding to the desired thickness of material to be gauged. The difference be-

* This radioactive material as well as others used in this investigation were procured from the United States Atomic Energy Commission at Oak Ridge, Tenn.

Paper 50-73, recommended by the AIEE Instruments and Measurements Committee and approved by the AIEE Technical Program Committee for presentation at the AIEE Winter General Meeting, New York, N. Y., January 30–February 3, 1950. Manuscript submitted September 9, 1949; made available for printing December 5, 1949.

C. W. Clapp and S. Bernstein are both with the General Electric Company, Schenectady, N. Y.

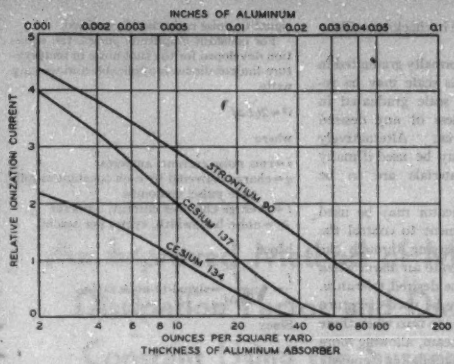

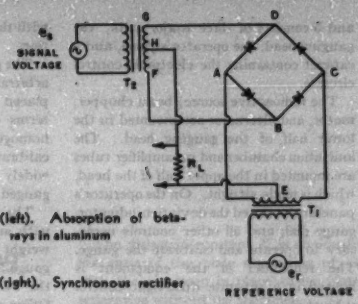

Figure 1 (left). Absorption of beta-rays in aluminum

Figure 3 (right). Synchronous rectifier

tween the comparison voltage and the ionization chamber voltage is then a measure of the deviation of the material from the desired thickness.

To read this deviation, the small 90-cycle difference voltage is first amplified by a conventional electrometer tube arrangement. The electrometer tube together with its grid leak and associated circuit components is contained within the sealed ionization chamber to minimize electrical pickup and leakage in the high impedance portions of the circuit. After further amplification, this voltage is then converted to a direct voltage in a synchronous-rectifier type of detector as shown in Figure 3.

Very briefly, its operation is as follows. A constant reference or switching voltage e_r, obtained from the alternator on the chopper shaft is applied through transformer T_1 to two opposite corners of a rectifier bridge. The amplified signal (deviation) voltage, e_s, is applied through transformer T_2 to the remaining two corners of the bridge. The reference voltage has an amplitude from two to three times that of the largest signal voltage, and therefore controls the operation of the rectifier bridge.

During the half cycle of e_r when point A is positive with respect to C, the path ABC is conducting and the path ADC is essentially nonconducting. During this half cycle therefore, the winding HF on transformer T_2 is connected across the load resistance R_L through the two parallel paths $FBAE$ and $FBCE$. Similarly, on the next half cycle of e_r the winding HG is connected across R_L through the parallel paths $GDAE$ and $GDCE$. If e_s contains any 90-cycle component, a direct voltage will be developed across R_L proportional to the component of e_s in phase with e_r.

The output voltage across R_L is applied to a single stage d-c amplifier and thence to a d-c milliammeter calibrated in per cent deviation. The output amplifier is capable of driving up to four such instruments for indicating or recording the thickness deviation.

Since the emission of beta particles from the source is a random phenomenon, the strength of the beam is constant only in a statistical sense. The current in the ionization chamber therefore contains a fluctuating noise component analogous to the "shot" noise current in vacuum tubes. To reduce this noise component and permit easier reading of the deviation indicator, a resistance-capacitance type low-pass filter is inserted in the output circuit. Under these conditions, the rms signal-to-fluctuation-noise ratio (for derivation, see appendix) is approximately equal to $\sqrt{2nT}$, where

n = number of primary beta particles entering ionization chamber per second

T = time constant of single-section low-pass output filter

To reduce the effect of random fluctuations in beam intensity it is apparent that the strength of the source should be as great as possible consistent with economy and safety of operation. Furthermore, the configuration or geometry of the gauge should be such that the radiation detector will intercept as many as possible of the emitted beta particles. When this has been done, the time constant of the output filter may be selected to give the best compromise between high speed of response and low random fluctuations of the deviation indicator.

The beta-ray gauge shown in Figures 4

Figure 2 (below). Block diagram of beta-ray thickness gauge

Figure 4 (right). Beta-ray thickness gauge

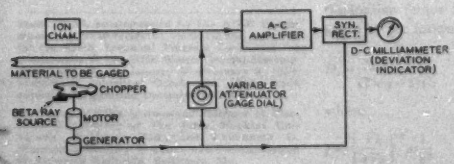

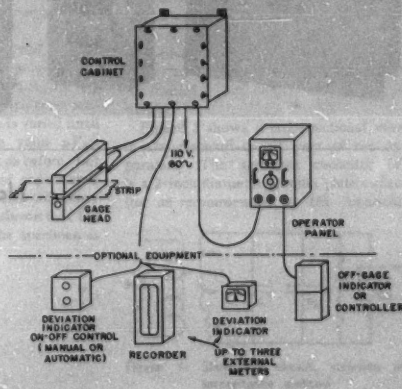

and 5 consists of three major units; the gauging head, the operator's panel, and a cabinet containing the electronic control circuits.

The radioactive source, beam chopper, motor, and alternator are mounted in the lower half of the gauging head. The ionization chamber and preamplifier tubes are mounted in the upper half of the head, which is made airtight. On the operator's panel are mounted the deviation indicator, gauge dial, and all other controls necessary to operate and calibrate the gauge. The remainder of the equipment is housed in a separate dust-tight control cabinet.

Over a period of several hours unavoidable drift in the ionization chamber characteristics and in tubes and circuit components may introduce reading errors which must be corrected by recalibration of the gauge. To maintain reading errors below 2 per cent over the normal thickness range of 5 to 150 ounces per square yard, a calibration check is specified at approximately 4-hour intervals.

To check the gauge, all material must first be removed from the throat of the gauge head. The head is normally mounted on a movable slide so that it may be removed easily from a process line for this purpose. A test plate is furnished with the gauge for use in checking calibration.

The gauge dial is normally graduated in arbitrary units. This scale may be replaced by a special scale graduated in terms of the thickness of any desired homogeneous material. Alternatively calibration charts may be used if many widely different materials are to be gauged.

The deviation indicator may be used with auxiliary equipment to control the weight of material passing through the gauge head, or to operate an alarm when the weight exceeds the desired tolerance. Other equipment may be used to return the deviation indicator to zero when there is no material in the beam, allowing more rapid gauging of sections or separate sheets.

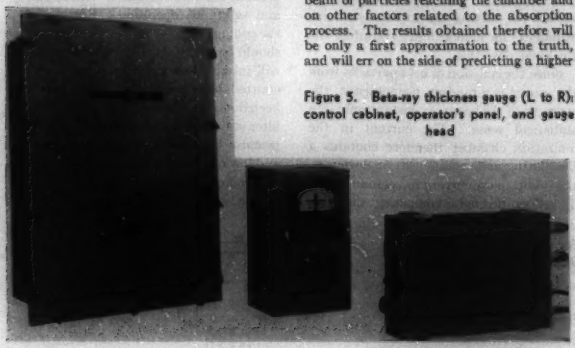

Figure 5. Beta-ray thickness gauge (L to R): control cabinet, operator's panel, and gauge head

Appendix. Calculation of Signal-To-Noise Ratio for Ionization Chamber Current

In the following, it is assumed that the current through the ionization chamber consists of a series of short discrete pulses of constant amplitude randomly distributed in time. Actually, of course, the pulse amplitudes vary through a considerable range depending on the energy distribution in the beam of particles reaching the chamber and on other factors related to the absorption process. The results obtained therefore will be only a first approximation to the truth, and will err on the side of predicting a higher signal-to-noise ratio than is justified.

For constant-amplitude pulses, the equation developed for the shot noise in temperature-limited diodes is applicable and we may write

$$i^2 = 2qI\,\Delta f$$

where

i = rms noise current, amperes
q = charge delivered by each constant amplitude pulse, coulombs
I = average chamber current, amperes
Δf = noise bandwidth, cycles per second

hence

$$\frac{I}{i} = \sqrt{\frac{I}{2q\,\Delta f}} = \text{signal-to-noise ratio}$$

Since

$$I = nq$$

where

n = number of primary beta particles entering chamber per second

we may write

$$\frac{I}{i} = \sqrt{\frac{n}{2\,\Delta f}}$$

The noise bandwidth Δf is determined by the transmission characteristic of the output low-pass filter. Let us assume this consists of a single resistance-capacitance section of time constant $T = RC$ seconds. The transmission of such a filter in terms of frequency may be written

$$A = \frac{1}{1 + j2\pi f T}$$

hence

$$\Delta f = \int_0^\infty |A|^2\,df = \int_0^\infty \frac{df}{1 + 4\pi^2 f^2 T^2} = \frac{1}{4T}$$

Therefore, the signal-to-noise ratio is given by

$$\frac{I}{i} = \sqrt{2nT}$$

Reference

1. An X-Ray Thickness Gauge for Hot-Strip Rolling Mills, C. W. Clapp, R. V. Pohl. *AIEE Transactions*, volume 67, part I, 1948, pages 820–8.

No Discussion

An Improved Method of Measuring Dissipation Factor and Dielectric Constant Using the Susceptance Variation Principle

C. FRANK MILLER
MEMBER AIEE

FREDERICK G. WHELAN
ASSOCIATE AIEE

THIS paper describes apparatus and techniques which greatly increase the speed and, under certain conditions, the accuracy of the susceptance variation method of measuring dielectric properties. With only slight modification the apparatus is capable of providing a continuous record of the data required to compute the dielectric constant and dissipation factor of solid insulation materials.

The variation of susceptance method of measuring dissipation factor has been described by Hartshorn and Ward.[1] The circuit in its simplest form, Figure 1, consists of an inductance coil and two calibrated standard air capacitors, C_1 which is the specimen capacitor, generally of the parallel-plate type, and C_2 a tuning capacitor, all connected in parallel. A high-impedance vacuum-tube voltmeter is connected so as to measure the voltage across the specimen, and an oscillator loosely coupled to the circuit supplies the voltage.

To measure the dissipation factor of a specimen, the specimen is placed between the plates of capacitor C_1 and the plate separation, d_1 is noted. The capacitor C_2 then is adjusted to give resonance as indicated by a maximum voltage across the specimen. Call the total capacitance at this point C_B, and the voltmeter reading V_B, see Figure 2. The capacitance C_2 then is varied until the specimen voltage drops to some value $V=aV_B$, where a is some number less than 1. Call the total capacitance at this point C_A. The capacitor C_2 then is tuned back through resonance until the specimen voltage again drops to the same value V, this time on the other side of resonance. Let the total capacitance at this setting be called C_B; let $C_A-C_B=\Delta C_1$ be the difference. Capacitor C_2 now is adjusted to the resonant point C_B, and the specimen is removed from capacitor C_1.

With the specimen removed, capacitor C_1 is varied until the voltage across it is again a maximum V_B'. Let this setting of C_1 be called C_0 and its plate separation be called d_2. Again, C_2 is varied until the voltage drops to the value aV_B', where a is the same fraction as before. Let the corresponding values of capacitance be called C_A' and C_B' and their difference $C_A'-C_B'=\Delta C_0$. It can be shown that the dissipation factor D_s of the specimen is given by the formula[1]

$$D_s=\frac{\Delta C_1-\Delta C_0}{(2\sqrt{q}-1)C_0} \qquad (1)$$

where

$$q=\left\{\frac{V_B}{aV_B}\right\}^2=\frac{1}{a^2}$$

The dielectric constant K is obviously the ratio of the plate separation of C_1 with the specimen in place to its plate separation without the specimen. That is

$$K=\frac{d_1}{d_2} \qquad (2)$$

It can be seen that a set of readings by this method not only takes considerable time, but also offers considerable opportunity for error, since five capacitor settings must be read and voltage must be accurately adjusted and read seven times. In order to overcome this difficulty it was decided to use a recording meter to obtain a trace of the resonance curve.

This is done by having a constant-speed motor-driven capacitor tune the circuit through resonance while a recording milliammeter operated from the vacuum-tube voltmeter traces the resonance curve. Limit switches operate relays which reverse the motor at each end of the travel of the micrometer tuning capacitor, so that the circuit is tuned automatically back and forth through resonance until the motor is stopped. During the test itself it is necessary to make only two readings, the settings of the specimen capacitor with and without the specimen in place, and to make only one accurate manual capacitor setting for resonance. The resonance curves can be examined at leisure and the computations can readily be made from them. A permanent record of the test thus is obtained.

Figure 3 shows a cross-sectional view of the resonant-circuit part of the apparatus. The specimen capacitor (4) is a 2-inch diameter parallel-plate capacitor as recommended by the American

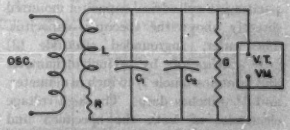

Figure 1. Simplified circuit, variation of susceptance method

Paper 50-74, recommended by the AIEE Instruments and Measurements Committee and approved by the AIEE Technical Program Committee for presentation at the AIEE Winter General Meeting, New York, N. Y., January 30–February 3, 1950. Manuscript submitted October 21, 1949; made available for printing December 28, 1949.

C. FRANK MILLER is Assistant Professor of Electrical Engineering at The Johns Hopkins University, Baltimore, Md., and FREDERICK G. WHELAN is Electrical Engineer with the Association of American Railroads, Baltimore, Md.

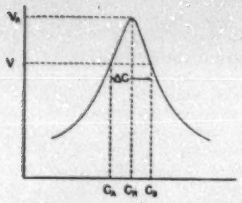

Figure 2. Resonance curve nomenclature

Society for Testing Materials,[3] the electrodes being of brass. The upper electrode, which is the ungrounded one, is suspended from the grounded frame by four ceramic cylinders (8) which are 2-inches long by 3/4 inch in diameter. The lower, grounded electrode of the specimen capacitor is mounted on a piece of ceramic tubing (5) which is 2 inches long by $1^1/_4$ inches outside diameter, having a wall thickness of 3/16 inch. The outside of this tube is painted with du Pont ceramic silver coating number *4545*, and copper plated. This method was adopted in order to get low electrical resistance and at the same time low thermal conductance so that heat would not be carried away from the specimen too rapidly at elevated temperatures. The brass electrode is soldered to this copper plating, the other end of the tube being soldered to an Invar rod (6) which is $1^1/_2$ inches in diameter and $2^3/_4$ inches long. This Invar rod is threaded with 40 threads per inch for a distance of $1^1/_2$ inches and threads through a hole in the grounded frame of the apparatus. "Oil dag" is used for lubricating the threads and at the same time, getting good electrical contact between the Invar rod and the frame of the apparatus. Invar was used for the threaded parts so that the material would not expand and jam the threads at elevated temperatures. A 3-inch diameter disk (7) accurately divided around its circumference into 100 divisions is attached to the bottom of the Invar rod beneath the grounded frame of the apparatus so that changes in the spacing of the specimen capacitor may be accurately made to 0.00025 inch.

The known variable (micrometer) capacitor is a cylindrical capacitor mounted directly above the specimen capacitor. The outer, ungrounded electrode (3) is $1^1/_2$ inches long by 5/8 inch in diameter and contains a hole 7/16 inch in diameter, and $1^9/_{16}$-inches deep. The high-voltage electrodes of both the specimen and micrometer capacitors are turned from a single piece of brass so as to eliminate the resistance and inductance of the leads between them. The lower $3^1/_2$ inches of the inner grounded electrode (2) is 3/8 of an inch in diameter, the remainder, except for the top one inch, being threaded with 5/16-40 threads. A 1/4-inch diameter hole approximately 1-inch deep is drilled up through the bottom of the grounded electrode to eliminate capacitance between the bottom of the grounded electrode and the ungrounded electrode, thereby obtaining a more nearly linear relationship between the position of the ungrounded electrode and the capacitance of the micrometer capacitor. A 1/8-horsepower 1,200-rpm motor drives the grounded electrode in or out of the high-voltage electrode by means of a set of reduction gears and a pair of helical gears. The electrode is driven at a rate of 1.6 seconds per revolution which gives a change in capacitance of 8.76 micromicrofarads per minute.

The same motor which drives the micrometer capacitor also drives a small worm gear. This worm gear has a pin driven into it which trips a limit switch just before the micrometer capacitor has reached the end of its travel in either direction. This limit switch operates a set of relays which: stops the motor; applies a brake (a 1/10-horsepower d-c motor operated as a separately-excited generator with a very low resistance load across its armature); removes the brake after the motor has slowed down sufficiently; and starts the motor in the opposite direction. The wiring diagram of this relay system is shown in Figure 4. Thus, if the midpoint of the micrometer capacitor travel is the resonant point, the circuit will automatically be tuned back and forth through resonance continuously.

The inductance consists of a coil of $9^1/_2$ turns of 1/4-inch copper tubing, the coil having an average diameter of $2^3/_4$ inches. One end of this coil is directly connected to the grounded frame. The tuning capacitor is an ordinary variable air capacitor having a maximum capacitance of 175 micromicrofarads. Figure 5 is a wiring diagram of the resonant circuit, oscillator, and voltmeter.

The micrometer and specimen capacitors are mounted within a frame, Figure 3, 6-inches wide and $5^3/_4$-inches high and 3-inches deep, the pieces being 7/16-inches thick, and made of Invar so that their lengths will not change with temperature.

A smaller cast iron framework fits on top of the main one so as to enclose the gear which drives the movable electrode of the micrometer capacitor. The threaded bushing on which this gear is mounted and keyed enables the electrode to be driven up and down without turning. In order to prevent turning of this electrode, a pin driven horizontally through the electrode at its top protrudes through a vertical slot cut in a brass tube fastened on top of the upper frame concentric with the movable electrode. A brass bushing $1^1/_2$-inches long mounted in the upper horizontal member of the main ground frame eliminates any possible wobble of the movable electrode of the micrometer capacitor as it travels up and down.

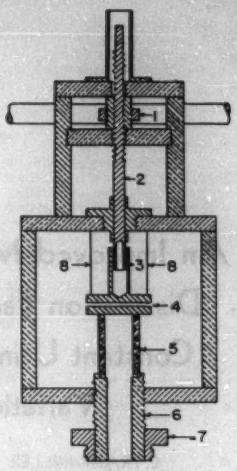

Figure 3. Sectional view of motor-driven micrometer capacitor assembly

Twenty-four ounce sheet copper is used throughout for shielding. One shield completely encloses the coil, while a second shield encloses the three air capacitors. The front of the shield is divided into three sections, the central one of which is hinged so as to allow specimens to be inserted and removed readily. The high-voltage lead from the generator also is shielded. The voltmeter terminals protrude through holes in the front shield. These terminals are of copper tubing, the ungrounded one being screwed into the upper (ungrounded) plate of the specimen capacitor while the ground terminal is screwed to the grounded frame.

The voltage across the specimen is measured with a General Radio type *726-A* vacuum-tube voltmeter. In order to record the voltage, the meter circuit of the vacuum-tube voltmeter was opened

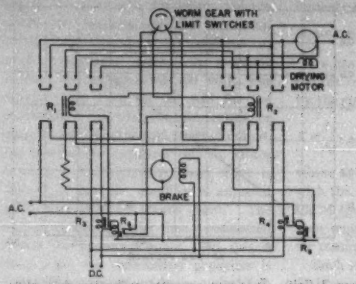

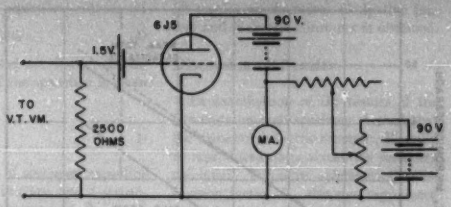

Figure 4 (left). Motor control circuit

Figure 6 (above). Schematic of amplifier

and a 2,500-ohm resistor was inserted. This was made the grid-leak resistor of a single-stage d-c amplifier, Figure 6, using a *6J5* tube biased at -1.5 volts with a plate supply of 90 volts. A 1-milliampere Esterline-Angus recording meter model *AW* is connected in the plate circuit and a compensating circuit is used to balance out the normal plate current so that the recorder reads zero when no voltage is applied to the vacuum-tube voltmeter. Although this amplifier is not perfectly stable, it is quite satisfactory since the zero point can be checked and adjusted readily at frequent intervals.

Voltage is supplied to the resonant circuit from a 1-kilowatt Westinghouse industrial high-frequency generator style *867692*. The oscillator is loosely coupled to the resonant circuit by means of capacitive coupling, so that the frequency of the oscillator remains constant during a test and so that the oscillator presents practically infinite impedance to the resonant circuit.

The chart speed used gives a curve width (for $V/V_r = 0.707$) of approximately 0.5 inch for air, and curve width of approximately 0.5 inch to 6.0 inches for various specimens tested. There appears to be a very slight lag in the response of the recorder at this speed, but it apparently does not affect the results, since several results were checked almost exactly by the familiar indicating voltmeter and hand-operated capacitor method.

Calibration of Apparatus

In order that the apparatus give an accurate measurement of dissipation factor and dielectric constant, it is necessary that the several components be calibrated.

The specimen capacitor was calibrated with a Bendix capacitor checker employing the beat-note principle. A plot of the calibration data is shown in Figure 7. Here the measured value of total capacitance has been plotted against $1/t$ where t is the spacing of the specimen capacitor in inches. The computed geometric capacitance (neglecting edge and stray effects) is plotted on the same set of axes. It can be seen that the measured total capacitance gives a straight line parallel to that of the computed geometric capacitance for values of t greater than 1/32 inch. This means that the sum of the stray capacitance and edge-effect capacitance is a constant for the working range of the apparatus and can be considered to be a part of the tuning capacitance and ignored. This calibration was made with the tuning capacitor and the micrometer capacitor both set at their minimum capacitance positions. The capacitance of these two elements is considered as part of the stray capacitance. If the tuning capacitor had been set near the middle of its range as it frequently is during the measurement of a specimen, then its constant capacitance would obscure the small variations in the edge effect capacitance even more completely.

The micrometer capacitor must be perfectly linear over its working range. Its calibration was accomplished by the procedure employed in the calibration of the specimen capacitor, using a type *222* General Radio precision air capacitor as a standard. In Figure 8 the capacitance of the standard capacitor is plotted against the position of the grounded electrode. Only the central portion of the capacitor range is used on any of the specimens reported on in this paper, and here the micrometer capacitor is seen to be almost perfectly linear. This calibration was checked several times with almost identical results. The average change in capacitance of the micrometer capacitor was found to be 9.35 micromicrofarads per inch of electrode travel. This is quite close to the computed value of 9.16 micromicrofarads per inch.

The micrometer capacitor is driven at a rate of 1.6 seconds per revolution of the driving gear; and since there are 40 threads per inch on the electrode shaft, the driving rate is 64 seconds per inch of electrode travel. This gives a rate of change of capacitance of 9.35/64 or 0.1461 micromicrofarads per second, or 8.76 microfarads per minute.

The chart of the Esterline-Angus recorder is driven at a rate of $6^1/_2$ inches per minute. Thus the rate of change of capacitance with respect to chart speed is found to be

$\Delta C = 1.43$ micromicrofarads per inch of chart travel

It was next necessary to check the recording voltmeter. In the susceptance-variation method, it is not necessary to read any actual voltages, but the ratio of two voltages must be known. This means that if the device used to indicate the specimen voltage does not actually

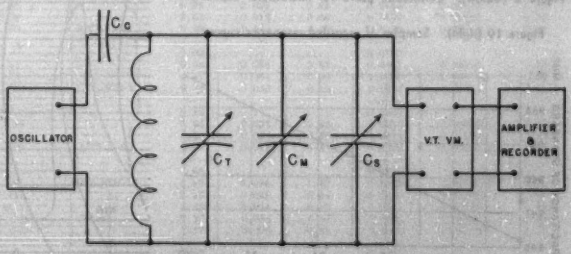

Figure 5. Wiring diagram of resonant circuit, oscillator, and voltmeter

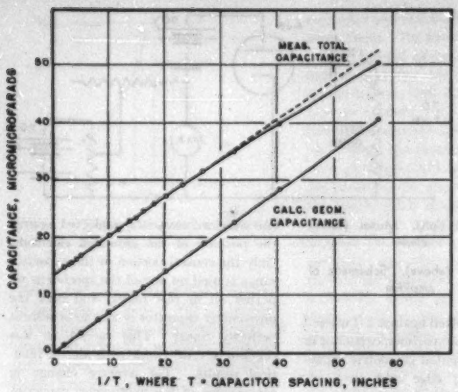

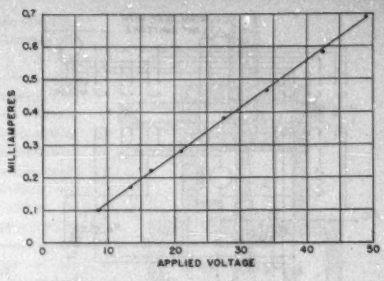

Figure 7 (left). Specimen capacitor calibration data plot

Figure 9 (above). Calibration curve for recording voltmeter and amplifier

measure this quantity in volts, it must at least have a constant characteristic, preferably linear or square-law, over its entire range.

In this apparatus the amplifier was so designed that the deflection of the recording meter is directly proportional to the specimen voltage. The results of the calibration of the recording meter are shown in Figure 9. The calibration was made with a second General Radio type *726A* vacuum-tube voltmeter, since the indicating meter of the vacuum-tube voltmeter used to drive the amplifier does not read quite correctly because of the additional 2,500-ohm resistor connected in series with it. Figure 9 shows that the recording meter gives a deflection directly proportional to the specimen voltage.

Description of Tests

A total of 35 specimens was used in the work reported in this paper. Of these, four were glass and the remainder were plastics. There were three specimens each of ten different plastics and a single specimen of an eleventh plastic. This single specimen was molded thermosetting material, two other materials were rigid thermoplastics and the remainder were laminated thermosetting materials. The specimens were all 2.000 ± 0.005 inch in diameter and the plastics ranged in thickness from 0.110 to 0.132 ± 0.002 inch, while the glass specimens were 0.246 to 0.248 ± 0.002 inch thick.

In preparing the specimens, the American Society for Testing Materials standards[3] were followed as closely as possible. Electrodes made of lead foil 0.003-inch thick were used. These electrodes were affixed with a very thin film of petrolatum and rolled down until no visible imprint could be made on the surface with the roller. Both electrodes were of the same diameter as the specimen.

All specimens were kept in desiccators containing a solution of NH_4NO_3. This kept the humidity within the desiccators at 63 per cent, which is approximately the average room humidity during the tests. The specimens were run at normal room temperatures which ranged from 76 to 81 degrees Fahrenheit.

Before starting a test, the oscillator, vacuum-tube voltmeter, and amplifier are warmed up for several minutes, and the micrometer capacitor is set at the center of its travel.

The first specimen then is removed from its desiccator and inserted in the specimen capacitor, the lower plate of this capacitor is screwed up tight against the specimen, and the capacitor spacing is noted. The copper shield is closed, and the vacuum-tube voltmeter is plugged in across the specimen.

The plate voltage of the oscillator then is turned on, the tuning capacitor is ad-

Figure 8 (below). Calibration curve for micrometer capacitor

Figure 10 (right). Samples of recorded resonance curves

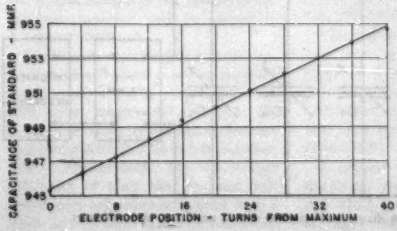

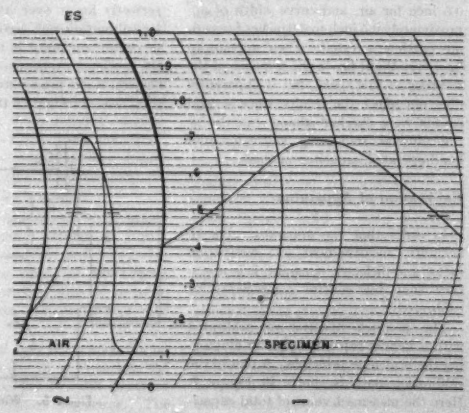

justed so as to get maximum voltage across the specimen, and this maximum voltage is adjusted at the oscillator to some convenient value. A resonant voltage of approximately 50 volts was always used, both for air and for the specimens. The vacuum-tube voltmeter then is disconnected and short-circuited, the micrometer capacitor driving motor is started, the recording chart drive is turned on, and the amplifier is adjusted until the recorder reads zero. The vacuum-tube voltmeter then is connected across the specimen again. All this is done while the micrometer capacitor is being driven from its midpoint to its all-in or maximum position. It is not necessary to check the zero point before each specimen is tested, but it should be done occasionally because the amplifier has a small drift.

When the micrometer capacitor reaches its all-in position the motor reverses, decreasing the capacitance of the micrometer capacitor. As the capacitor is driven to its all-out or minimum position, the circuit is tuned through resonance and the recorder traces out the resonance curve on its chart. Typical resonance curves for a specimen and for air are shown in Figure 10.

As soon as the micrometer capacitor reaches its all-out position the motor again is reversed, driving the capacitor back to resonance. When the resonant point is reached, the motor is stopped, the oscillator voltage is reduced, and the specimen is removed from the specimen capacitor. The specimen capacitor then is adjusted to give voltage resonance, the micrometer capacitor driving motor and chart are started, and the resonance curve for air is obtained.

After the specimens are all tested, the chart is removed from the recorder and examined. First the two points on each curve where the voltage dropped to 0.707 V_R are marked. (q was made equal to two throughout the tests so as to simplify the calculations.) The width of each curve at the 0.707 V_R marks then is measured to the nearest 0.01 inch. Knowing the width of the specimen curve, ΔC_t, the width of the air curve, ΔC_0, and the capacitance C_0 of the specimen capacitor after the specimen has been removed and the capacitor has been readjusted to resonance, the dissipation factor of the specimen, D_s, can be computed readily from equation 1. If we let W_t and W_0 be the widths of the specimen and air resonance curves, measured in inches, and d_2 be the spacing of the specimen capacitor, in revolutions (1 revolution = 1/40 inch) after the specimen has been removed, then the equation reduces to

$$D_s = 0.0253\,(W_t - W_0)d_2 \qquad (3)$$

As has been stated previously, the dielectric constant of the specimen is given by the equation

$$K = \frac{d_1}{d_2} \qquad (2)$$

where d_1 = spacing of specimen capacitor with the specimen in place, and d_2 = spacing of specimen capacitor with the specimen removed and the capacitor retuned for resonance.

Each specimen was tested five times at 24-hour intervals, in order to get an average value of the dissipation factor and dielectric constant. Since an attempt was made to take all of the measurements under identical conditions, an idea of the reproducibility of the results for specimens of various dissipation factors and dielectric constants is obtained.

Discussion of Results

An examination of the results of the five tests on each specimen showed that the values of dielectric constant, K, could be reproduced quite accurately for every specimen. For most specimens the dissipation factor, D_s, also was reproduced quite closely.

In order to get a better idea of how closely the results could be repeated, the averages of the five values of K and D_s for each specimen were calculated. The deviation of each of the five original results from this mean value was found, and the average of these five deviations from the mean was calculated for each specimen. Table I shows for each specimen

Table I. Compilation of Results

Spec. No.	Material	K	Average Deviation	Per Cent Average Deviation	D_s	Average Deviation	Per Cent Average Deviation
1	LTS-E-2	5.94	0.022	0.37	0.0539	0.00160	2.97
2		5.91	0.048	0.81	0.0521	0.00118	2.26
3		5.88	0.022	0.37	0.0523	0.00096	1.84
Av.		5.91			0.0528		
4	LTS-E-5	4.44	0.040	0.90	0.0363	0.00080	2.17
5		4.42	0.018	0.41	0.0368	0.00068	1.85
6		4.46	0.024	0.54	0.0372	0.00078	2.10
Av.		4.44			0.0369		
10	LTS-E-2	5.23	0.080	1.53	0.0531	0.00204	3.84
11		5.67	0.044	0.78	0.0551	0.00080	1.45
12		5.51	0.094	1.70	0.0535	0.00056	1.05
Av.		5.47			0.0539		
13	LTS-M-4	5.81	0.070	1.20	0.0651	0.00046	0.71
14		5.81	0.048	0.83	0.0666	0.00232	3.48
15		5.90	0.048	0.81	0.0648	0.00066	1.02
Av.		5.84			0.0655		
16	RTP-GH-1	4.16	0.034	0.82	0.0426	0.00030	0.70
17		4.18	0.014	0.34	0.0417	0.00074	1.77
18		4.14	0.034	0.82	0.0424	0.00154	3.64
Av.		4.16			0.0422		
19	LTS-E-4	5.65	0.038	0.67	0.0546	0.00092	1.68
20		5.64	0.052	0.92	0.0530	0.00142	2.68
21		5.61	0.028	0.50	0.0541	0.00106	1.96
Av.		5.63			0.0539		
22	LTS-E-5	4.13	0.036	0.87	0.0329	0.00122	3.71
23		4.14	0.028	0.68	0.0325	0.00076	2.34
24		4.15	0.024	0.58	0.0333	0.00088	2.64
Av.		4.14			0.0329		
28	RTP-OS-2	2.99	0.026	0.87	0.0135	0.00066	4.89
29		3.01	0.018	0.60	0.0132	0.00062	4.70
30		2.99	0.014	0.47	0.0128	0.00040	3.13
Av.		3.00			0.0132		
31	LTS-EM-1	6.38	0.054	0.85	0.0637	0.00086	1.35
32		6.47	0.064	0.99	0.0640	0.00082	1.28
33		6.36	0.046	0.72	0.0621	0.00194	3.12
Av.		6.40			0.0635		
34	LTS-E-5	3.95	0.038	0.96	0.0314	0.00068	2.16
35		3.99	0.024	0.60	0.0314	0.00036	1.15
36		3.95	0.032	0.81	0.0310	0.00060	1.94
Av.		3.96			0.0313		
37	MTS-MH-2	5.88	0.084	1.43	0.1448	0.00366	2.53
G1	Glass	7.26	0.032	0.44	0.0040	0.00048	9.80
G2		7.28	0.024	0.33	0.0043	0.00038	8.83
G3		7.27	0.034	0.47	0.0040	0.00040	10.00
G4		7.27	0.026	0.36	0.0043	0.00022	5.11
Av.		7.27			0.0043		

the average or mean value of K and D_s, and the average deviation from this mean value expressed first as a pure number and then as a percentage of the mean. The average of the mean values of K and D_s for the three specimens of each material was found, so as to get an average value of K and an average value of D_s for each material. These values are shown in Table I.

For all values of dielectric constant found, ranging from 3.0 to 7.3, the average deviation from the mean was always less than 0.1, and it was less than 0.05 in all but a few cases. The higher deviations from the mean occur where the capacitance of the specimen capacitor was highest. This can be seen from the fact that for 1/8-inch plastic specimens the deviation becomes large for values of K above 5, while for the 1/4-inch glass specimens excellent results are obtained even though the value of K is above 7. Comparatively large deviations in the value of K are believed to be due to the fact that the capacitance of the specimen capacitor changes rapidly with small changes in the electrode spacing when the spacing is small and therefore the capacitance cannot be read as accurately as it can be for larger spacings.

The values of dissipation factor could not be reproduced so well as those of dielectric constant. The results are still quite good, however. Only in the case of glass are the percentage errors large and here the average deviations are quite small, being less than 0.005 in every case. At the 0.707 point where the widths of the curves were measured, the curves for glass and the curves for air differed by only slightly more than 0.1 inch. Since the curves could be measured only to the nearest 0.01 inch, a percentage error of about 10 per cent is to be expected. In the case of specimens 28, 29, and 30, the per cent deviation also is rather high, but here again it is because the dissipation factor of that material is so low rather than because the deviations themselves are high. In most cases the per cent average deviation is about 2 per cent or less, which is quite good for all but the most precise work.

In general it appears that the higher the dissipation factor, the higher the average deviation is. It is believed that the variations are in the specimens rather than in the apparatus. It seems reasonable to suppose that if the loss component of current is quite small, variations in it will be smaller than in the case of a larger loss component. It is felt, with several exceptions, that one measurement is just as accurate as another for all of the specimens discussed here.

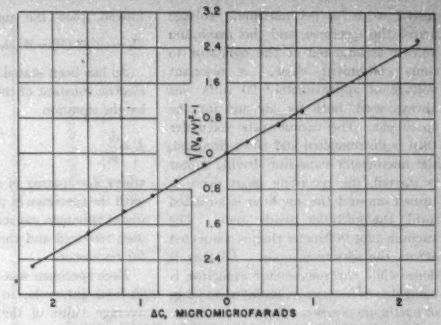

Figure 11. Plot of data required to check shape of recorded resonance curves

The results on specimen 37 are not so good as they might be because this material is really slightly out of range of the apparatus. Its dissipation factor is so high that its resonance curve did not drop to 0.707 times the maximum value. A q of 1.64 rather than 2 had to be used in calculating its dissipation factor.

In order to determine whether the resonance curves obtained conformed to the theoretical resonance curve, the method proposed by Sinclair[3] was tried. This consists of plotting $\sqrt{q-1}$ against the change in capacitance for a number of points on the resonance curve. The dissipation factor for the resonant combination is given by

$$D=\frac{\Delta C}{2C_s\sqrt{q-1}}$$

Here C_s is the total shunt capacitance at resonance and ΔC is the width of the resonance curve corresponding to the value of q used. Since D and C_s are constant for any one run, $\sqrt{(V_R/V)-1}$ must be proportional to ΔC. Hence, if we plot $\sqrt{q-1}$ against ΔC, we should get a straight line having a slope of $1/(2C_sD)$, or W/G.

This was tried for several resonance curves picked at random. Such a plot is shown in Figure 11, where the points lie almost exactly along a straight line. This shows that the curve traced out by the recording meter is a true resonance curve and that no appreciable error results from measuring the widths of the resonance curves only at the 0.707 point rather than at several points. Sinclair points out that for most accurate results all data should be plotted in this way and that the slope of the best straight line through all of the points be used in computing D. No doubt the accuracy of the results here presented could be increased somewhat by this method, but the improvement would apparently not warrant the additional time and work.

Modification to Permit Continuous Recording of Dielectric Constant and Dissipation Factor Data

This apparatus can be modified easily to obtain a continuous record of the data required to calculate the dissipation factor and dielectric constant. With constant chart speed, such data will be plotted against time as abscissa. If the corresponding temperature-time characteristic of the sample is obtained by a separate record, complete data for the "temperature versus dielectric constant" and "temperature versus dissipation factor" characteristics are obtained.

The only modification required in the apparatus is the addition of a means of providing a marker "pip" or "dent" in the voltage record to indicate a position of the micrometer capacitor at which its capacitance is known.

Conclusions

1. A recording device for measuring dissipation factor and dielectric constant by the susceptance-variation principle has been built. The performance of this apparatus has been investigated, and it has been found to be very satisfactory and reliable. Its use results in a great saving in time and care in making such measurements.

2. The dissipation factor and dielectric constant of a total of 31 specimens of 11 commercial plastics and four specimens of glass have been measured by this apparatus. These measurements were made at room temperature at a frequency of 10 megacycles per second, using a stress of the order of 0.2 to 0.4 volt per mil.

3. The results of these measurements

have been analyzed to determine the approximate accuracy of the apparatus. For 1/8-inch plastic specimens having dielectric constants ranging from 2.99 to 6.47, the maximum value of the average deviation from the mean of five measurements was 0.094, and 1.70 per cent. For dissipation factors ranging from 0.0128 to 0.0666, the maximum value of the average deviation was 0.00232, and 4.89 per cent. Most deviations were considerably smaller than these.

4. The effect of extensive screening of the apparatus on the accuracy of the results has been studied. The screening apparently added some losses to the system while eliminating others, and the width of the resonant curve was found to be essentially the same with and without screening. The screening was found to aid greatly in eliminating slight wiggles in the resonance curves, however, and thus increased the accuracy of the results.

5. The method presents many advantages for the routine measurement and control of large numbers of commercial and industrial samples.

References

1. The Measurement of the Permittivity and Power Factor of Dielectrics from 10^4 to 10^9 Cycles per Second, L. Hartshorn, W. H. Ward. *Journal*, Institution of Electrical Engineers (London, England), volume 79, 1936, pages 597–609.

2. Tentative Methods of Test for Power Factor and Dielectric Constant of Electrical Insulating Materials. *ASTM Designation D*, 150–45, American Society for Testing Materials (Philadelphia, Pa.), 1945.

3. Parallel Resonance Methods for Precise Measurements of High Impedances at Radio Frequencies and a Comparison with the Ordinary Series Resonance Methods, D. B. Sinclair. *Proceedings*, Institute of Radio Engineers (New York, N. Y.), volume 26, 1938, pages 1466–97.

No Discussion

An Analysis of Transients in Magnetic Amplifiers

D. W. VER PLANCK
MEMBER AIEE

L. A. FINZI
MEMBER AIEE

D. C. BEAUMARIAGE
STUDENT MEMBER AIEE

Synopsis: Analytical expressions are developed for the envelope of the transient output current of a magnetic amplifier when the control voltage is varied. The magnetization curve of the core material is expressed in a convenient analytical form and the differential equations of the system are integrated under certain simplifying assumptions. The analysis applies to transients lasting a few cycles of the supply frequency, or longer; and experimental checks show good agreement within the range of transients specified above. The results are given in the form of dimensionless curves expressing the average flux density, average magnetizing intensity, and output currents as functions of time. Thus the influence of the core material and of factors of design upon the transient response of the amplifier are determined.

THE steady-state theory of interlinked electric and saturable magnetic circuits (as they occur in magnetic amplifiers) has been given in a number of recent papers.[1,2,3,4] The transient response to a sudden change in control circuit conditions has been described qualitatively,[4,5] but no quantitative analysis has been published heretofore. The purpose of this paper is to give such a study, limited in the present work to configurations without feedback. To illustrate the method, it is assumed that the transient is initiated by suddenly closing the control circuit through a battery, the load impedance being zero.

Paper 50-76, recommended by the AIEE Electronics Committee and approved by the AIEE Technical Program Committee for presentation at the AIEE Winter General Meeting, New York, N. Y., January 30–February 3, 1950. Manuscript submitted July 8, 1949; made available for printing December 2, 1949.

D. W. VER PLANCK, L. A. FINZI, and D. C. BEAUMARIAGE are all with the Carnegie Institute of Technology, Pittsburgh, Pa.

This work was done in part by D. C. Beaumariage in partial fulfillment of the requirements for the degree of Doctor of Science at Carnegie Institute of Technology.

The authors gratefully acknowledge the support afforded by the Office of Naval Research during the initial stages of this work and the contributions of M. W. Green and G. W. Samson, graduate students engaged on the project.

Method and Assumptions

The method of analysis is an extension of that already given for the steady state.[1,3,4] Briefly it is to apply Kirchhoff's voltage law to the electric circuits, Ampere's line integral law to the magnetic circuits and to use the normal magnetization curve expressed in some convenient analytical form to relate currents and flux densities. In doing this it is assumed that sinusoidal voltage is impressed directly on the amplifier terminals and thus effects of load impedance are neglected. Other simplifications are to ignore leakage fluxes, hysteresis, and eddy currents. In the steady-state analysis all resistances are assumed small although not neglected entirely. In the transient analysis this necessarily is modified as will be seen by taking control circuit resistance more fully into account.

If one assumes that sinusoidal voltage is impressed on the a-c terminals of a magnetic amplifier and neglects the impedance of the control circuit to harmonic currents, one finds in the steady state that the flux density in each of the cores varies sinusoidally about an average or direct component of flux density B_0 which is the same for both cores. Moreover it is found that this "d-c flux density" is not a simple function of the direct control current alone, as one might think, but also depends on the magnitude of the superimposed alternating flux density which is required to sustain the impressed alternating voltage. In the steady state it is found that the magnetomotive force acting on each core is expressible as a Fourier series having a term of fundamental frequency, both odd and even harmonic terms, and a constant term referred to, in what follows, as the direct component. In the circuits studied it is found, as would be expected, that the current flowing in the load consists only of the fundamental and odd harmonics, and that only a direct component and even harmonics flow in the control circuit.[4]

For every steady state determined by a value of control current and a value of impressed a-c voltage there corresponds a value of B_0. If the control current or a-c voltage or both are changed, B_0 must in general change to a new value for the new steady state. Thus any study of transient behavior must be concerned primarily with the growth or decay of B_0 as also has been noted by others.[3]

The present treatment is limited to cases where a transient of appreciable magnitude persists for at least several cycles of the applied alternating current, as in fact is usually the case in practice. This makes it reasonable to focus attention on the transients in the direct components of the various quantities and to assume that the alternating components at any instant have the magnitude determined from steady-state relationships using the value of B_0 for the instant in question. The legitimacy of this approxi-

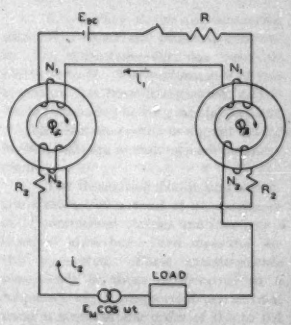

Figure 1. Series-connected magnetic amplifier ($i_L = i_2$)

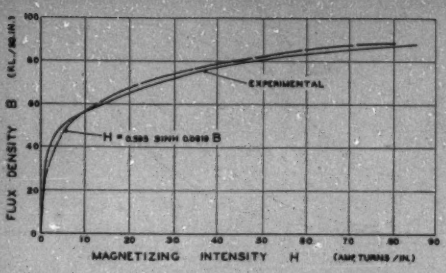

Figure 2. Normal magnetization curve and its analytical representation

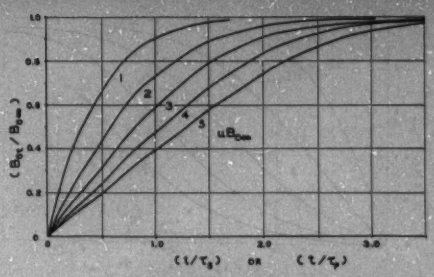

Figure 4. Transients of the direct component of flux density shown in dimensionless form for the circuits of Figures 1 and 3

mation has been checked by making several step-by-step integrations of the circuit equations for a number of configurations, and also it results in satisfactory over-all checks with experiments, as will be shown later on in the paper.

Series-Connected Magnetic Amplifier

As a first example, a transient analysis will be made of the magnetic amplifier with output coils connected in series, shown in Figure 1.

The analysis starts by assuming that one can express the instantaneous flux densities in the cores B_α and B_β respectively by

$$B_\alpha = B_m \sin \omega t + B_{0t} \tag{1}$$
$$B_\beta = -B_m \sin \omega t + B_{0t} \tag{2}$$

These expressions are exactly like those which have been developed for the steady state[1,3,4] except that here the direct component of flux density B_{0t} is not a constant but may vary in time, a fact denoted by the second subscript, t. As in the steady-state case and using meter-kilogram-second units, $B_m = E_m/2N_2A\omega$ where E_m and ω are respectively the crest value and angular frequency of the applied a-c voltage (assumed constant throughout the transient), A is the cross-sectional area of each core and N_2 is the number of turns in each output coil.

Application of Kirchhoff's voltage law to the control circuit gives

$$E_{dc} = 2R_1 i_1 + N_1 A \frac{d}{dt}(B_\alpha + B_\beta) \tag{3}$$

Here E_{dc} is the control battery voltage and $2R_1$ is the entire resistance of the circuit, represented by R in the figure. Then substituting equations 1 and 2 in equation 3, and considering only the direct components one obtains

$$E_{dc} = 2R_1 I_{1t} + 2N_1 A \frac{dB_{0t}}{dt} \tag{4}$$

where I_{1t} is the direct component of i_1. Upon separation of variables, the time t for the direct component of flux density to change from an initial value B_{00} to another value B_{0t} may be written as

$$t = \frac{N_1^2 A}{R_1} \int_{B_{00}}^{B_{0t}} \frac{dB_{0t}}{N_1 I_{1\infty} - N_1 I_{1t}} \tag{5}$$

Here use has been made of the fact that the final ($t = \infty$) value of control current $I_{1\infty}$ and the battery voltage E_{dc} are related by $E_{dc} = 2R_1 I_{1\infty}$.

To evaluate the integral in equation 5, one must have a relationship between B_{0t} and $N_1 I_{1t}$. This relationship for the steady state is dependent on B_m, the magnitude of the alternating flux density, and is obtainable from the normal magnetization curve as shown elsewhere.[1,4] It is assumed here that this steady-state relationship also holds in the transient case. Evaluation of equation 5 then can be carried out graphically by well known procedures.[7]

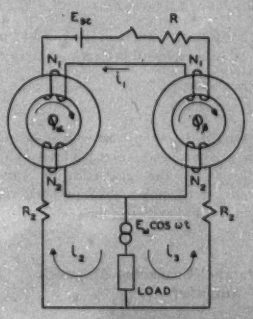

Figure 3. Parallel-connected magnetic amplifier ($I_L = i_2 + i_3$)

To carry out the integration analytically, the normal magnetization curve must be expressed in analytical form, and for this the relation

$$H = U \sinh uB \tag{6}$$

is used, which permits relatively simple integrations. Here H is the magnetic field intensity, B is the flux density and U and u are constants determined by the shape of the magnetization curve. This function fits well enough to yield satisfactory transient results for common core materials such as hypernik and silicon steel. The fitting for the hypernik used in the experimental checks is illustrated in Figure 2. Again, as in the steady-state treatment, use is made of Ampere's circuital law to relate currents and magnetic field intensities, thus

$$N_1 i_1 + N_2 i_2 = LH_\alpha \tag{7}$$
$$N_1 i_1 - N_2 i_3 = LH_\beta \tag{8}$$

where H_α and H_β are the magnetizing intensities in cores α and β respectively and L is the mean length of magnetic path per core. H_α and H_β are found by substitution of the flux densities as given by equations 1 and 2 into the function, equation 6, representing the B-H curve. The results are Fourier series each containing both odd and even harmonic terms and a constant, or direct component which is the same for both cores.[4] As already explained the direct component for purposes of this study is considered to vary during the transient. Substitution of the series for H_α and H_β into equations 7 and 8 yields the following relation between direct components

$$N_1 I_{1t} = LH_{0t} \tag{9}$$

where H_{0t} is the direct component of either H_α or H_β and is given by

$$H_{0t} = U\mathcal{J}_0(uB_m) \sinh uB_{0t} \tag{10}$$

where $\mathcal{J}_0(uB_m)$ is the modified Bessel

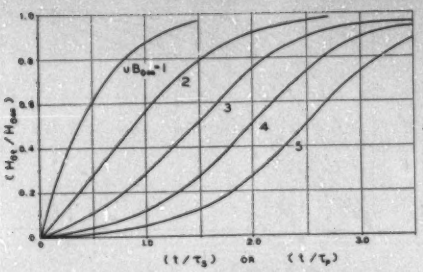

Figure 5. Transients of the direct component of magnetic intensity shown in dimensionless form for the circuits of Figures 1 and 3

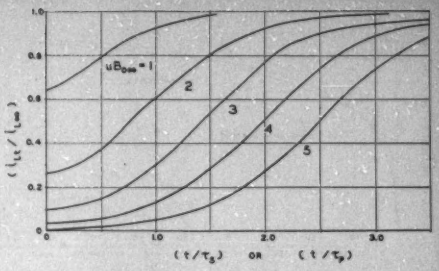

Figure 6. Envelopes of the output current i_L shown in dimensionless form for the circuits of Figures 1 and 3

function of the first kind of zero order.[6]

Substitution of equation 9 in equation 5 results in

$$t=\frac{N_1^2A}{R_1}\int_{B_{\theta 0}}^{B_{\theta t}}\frac{dB_{\theta t}}{N_1I_{1\infty}-LH_{\theta t}} \tag{11}$$

and further substitution of equation 10 permits evaluation of the integral.

For the case where $B_{\theta 0}$ is initially zero, that is, the control circuit is initially open (and there is no residual) and then suddenly closed at $t=0$, the result is

$$\frac{t}{\tau_s}=\tanh uB_{\theta\infty}\tanh^{-1}\left\{\frac{\tanh\dfrac{uB_{\theta t}}{2}}{\tanh uB_{\theta\infty}-\operatorname{sech} uB_{\theta\infty}\tanh\dfrac{uB_{\theta t}}{2}}\right\} \tag{12}$$

where τ_s, a quantity having the dimensions of time, is given by

$$\tau_s=\frac{4N_1A}{uE_1}=\frac{2N_1A}{uR_1I_{1\infty}}=\frac{2N_1^2A}{LR_1U_p u\mathfrak{J}_0(uB_m)\sinh uB_\theta} \tag{13}$$

and $B_{\theta\infty}$, the final ($t=\infty$) value of the direct component of flux density, is given by

$$uB_{\theta\infty}=\sinh^{-1}\left(\frac{N_1I_{1\infty}}{LU\mathfrak{J}_0(uB_m)}\right) \tag{14}$$

Equation 12 also may be solved explicitly for $B_{\theta t}$ as a function of time

$$uB_{\theta t}=2\operatorname{ctnh}^{-1}\left\{\operatorname{ctnh} uB_{\theta\infty}\operatorname{ctnh}\left[\frac{t}{\tau_s}\operatorname{ctnh} uB_{\theta\infty}\right]+\operatorname{csch} uB_{\theta\infty}\right\} \tag{15}$$

Equation 15 gives in dimensionless form the transient of the direct component of flux density and is valid for any core material which equation 6 can be made to fit.

Equation 10 gives the transient of the direct component of magnetizing intensity $H_{\theta t}$ upon substitution of the value for $B_{\theta t}$ from equation 15. This is conveniently expressed as a ratio of the transient value to final steady state value $H_{\theta\infty}$ by

$$\frac{H_{\theta t}}{H_{\theta\infty}}=\frac{\sinh uB_{\theta t}}{\sinh uB_{\theta\infty}} \tag{16}$$

By virtue of equation 9 the transient of the direct component of control current in the series-connected magnetic amplifier is also given in dimensionless form by equation 16.

To find the transient of the output current, equations 7 and 8 are solved simultaneously for the output circuit ampere-turns, giving

$$N_2i_2=\frac{L}{2}[H_\omega-H_\theta]=L[H_1\sin\omega t+H_3\sin 3\omega t+H_5\sin 5\omega t+\ldots] \tag{17}$$

where the harmonic coefficients[4,8] are

$$\begin{aligned}H_1&=2u\mathfrak{J}_1(uB_m)\cosh uB_{\theta t}\\ H_3&=-2u\mathfrak{J}_3(uB_m)\cosh uB_{\theta t}\\ H_5&=2u\mathfrak{J}_5(uB_m)\cosh uB_{\theta t}\end{aligned} \tag{18}$$

Therefore the transient of output current, also expressed in a ratio, is given by

$$\frac{i_{Lt}}{i_{L\infty}}=\frac{\cosh uB_{\theta t}}{\cosh uB_{\theta\infty}} \tag{19}$$

where i_L, the output current is equal to i_2. As a consequence of the representation chosen for the magnetization curve, equation 19 applies alike for peak, rms, and rectified average values.

Parallel-Connected Magnetic Amplifier

The second configuration considered is the magnetic amplifier with output coils connected in parallel as shown in Figure 3.

In the steady state, no direct current components can flow in the output windings, and the direct component of magnetizing intensity is wholly supplied by the control direct current. During a transient, however, if the control circuit is suddenly energized, direct components of current do flow in the outside series loop of the output windings in agreement with the requirements of the constant flux linkage theorem. Thus, upon closing the switch, the control current exhibits a jump while the current in the series path through the output coils jumps in the opposite direction, the magnitudes being determined by the relative resistances and turn ratios. Thus in the calculation of the transient, two paths for the flow of the direct com-

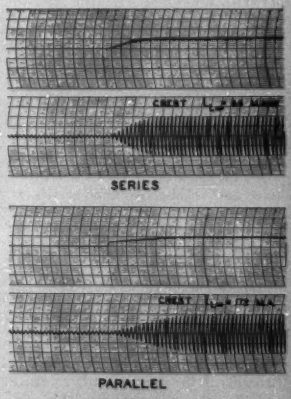

Figure 7. Oscillograms comparing transients for series and parallel connections

The upper trace is control current and the lower, output current

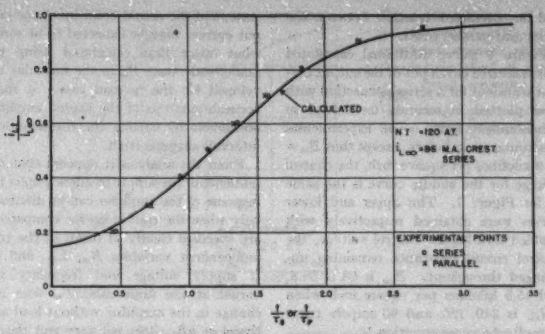

Figure 8. Calculated envelopes of output current in dimensionless form compared with points measured from the oscillograms of Figure 7

ponents of currents must be considered.

The flux density again is assumed to vary sinusoidally with time about a d-c value B_{0l} and consequently equations 1 and 2 also apply for this case except that here $B_m = E_m/N_2A\omega$.

Application of Kirchhoff's voltage law to the control circuit and to the circuit through the output coils in series, Figure 3, results in

$$E_{dc} = 2R_1i_1 + N_1A\frac{d}{dt}(B_\alpha + B_\beta) \tag{20}$$

$$0 = R_2(i_2 - i_3) + N_2A\frac{d}{dt}(B_\alpha + B_\beta) \tag{21}$$

where R_2 is one-half of the total series resistance of the outside loop and the other symbols are as before.

Substituting equations 1 and 2 in equations 20 and 21, replacing instantaneous values by their Fourier series components results in the following relations between the direct components

$$E_{dc} = 2R_1I_{1l} + 2N_1A\frac{dB_{0l}}{dt} \tag{22}$$

$$0 = R_2(I_{2l} - I_{3l}) + 2N_2A\frac{dB_{0l}}{dt} \tag{23}$$

where I_{2l} and I_{3l} are the direct components of i_2 and i_3 respectively.

From application of Ampere's line integral law one obtains the instantaneous relationships

$$N_1i_1 + N_2i_2 = LH_\alpha \tag{24}$$

$$N_1i_1 - N_2i_3 = LH_\beta \tag{25}$$

from which follow the corresponding relationships among the direct components

$$N_1I_{1l} + N_2I_{2l} = LH_{0l} \tag{26}$$

$$N_1I_{1l} - N_2I_{3l} = LH_{0l} \tag{27}$$

Simultaneous solution of equations 22, 23, 26, and 27 leads at once to

$$t = \left[1 + \left(\frac{N_2}{N_1}\right)^2\frac{R_1}{R_2}\right]\frac{N_1^2A}{R_1} \times \int_{B_{0l}}^{B_{0l}} \frac{dB_{0l}}{N_1I_{1\infty} - LH_{0l}} \tag{28}$$

which is identical with equation 11 except for the presence of the constant multiplying factor in square brackets. Since equation 10 applies here also, except that now $B_m = E_m/N_2A\omega$, the integration is carried out as in the series case and the result is the same except that the time scale factor τ_s is replaced by a new time scale factor given by

$$\tau_p = \left[1 + \left(\frac{N_2}{N_1}\right)^2\frac{R_1}{R_2}\right]\tau_s = \frac{2N_1A}{uI_{1\infty}} \times \left[\frac{1}{R_1} + \left(\frac{N_2}{N_1}\right)^2\frac{1}{R_2}\right] \tag{29}$$

Therefore equations 12 through 19 defining the transient behavior of the series magnetic amplifier apply also for the parallel case except for modification of the time scale factor in accordance with equation 29.

In the parallel case the output current i_L is $i_2 + i_3$.

In the parallel case the transient in the direct component of control current is different from that in the series case. As already pointed out, there now is an initial jump in the control current when the control circuit is suddenly energized and a corresponding jump in the direct component of current which circulates in the series circuit through the two output coils. These initial currents are found using equations 22 and 23 and the condition that the flux linkages of each of the two circuits in question cannot change instantaneously.

The results are

$$I_{10} = \frac{E_{dc}}{2R_1 + 2R_2\left(\frac{N_1}{N_2}\right)^2} \tag{30}$$

$$I_{20} = -I_{30} = -\frac{N_1}{N_2}I_{10} \tag{31}$$

The direct component of control current I_{1l} then increases gradually from I_{10} to $I_{1\infty}(=E_{dc}/2R_1)$ while I_{2l} and $_3I$ decay to zero.

Discussion of Analytical Results

From the foregoing analysis it is apparent that the transient variation of the direct component of flux density B_{0l} has great importance since it determines the transient behavior of the currents. B_{0l} is given by either of equations 12 or 15 and is plotted in dimensionless form in Figure 4 for different values of the parameter uB_{0m}. This parameter is, as shown by equation 14, a function of the final steady-state control current, $I_{1\infty}$, and of B_m, which is determined by the applied a-c voltage. Thus the curves given in Figure 4 are general and usable for series or parallel-connected amplifiers whose core materials have normal magnetization curves representable by equation 6. For the series case the time t to reach any specified value of B_{0l} depends on a factor τ_s which has the dimensions of time and is somewhat analogous to the time constant of a simple linear L-R circuit. However this time factor τ_s is not a constant as in the linear case since it depends, as shown by equation 13, not only on the design constants of the control winding and core but also on the magnitude of the driving voltage E_{dc}. τ_s is not dependent in any way on quantities associated with the a-c circuit; these quantities enter in the determination of B_m and therefore of uB_{0m} as shown in equation 14.

It is significant that Figure 4 also applies to the parallel case except for the replacement of τ_s by another time factor τ_p which depends in addition on the number of turns and resistance of the output coils as shown in equation 29. If a series-connected magnetic amplifier has its output coils reconnected in parallel and the a-c voltage reduced to half its former value, the steady-state performance will remain unchanged except for a doubling of the load current since B_m and B_0 will remain the same for equal control currents.[1] Such a change, however, will always slow down the transient response since, as may be seen from equation 29, the time scale factor will be reduced. For example, if $R_1 = R_2$ and $N_1 = N_2$, then $\tau_p = 2\tau_s$ and the transient response with

the parallel connection will be just twice as long as with the series connection.

Figure 5 shows dimensionless plots of the transient of the direct component of magnetic intensity plotted from equation 16. Of greater practical interest is Figure 6 in that it shows the transient in the output current, again in dimensionless form, as obtained from equation 19.

It is evident that the transient response curves for output current, shown in Figure 6, are not in general of exponential form. Therefore the practice, which has become rather common, of describing magnetic amplifier transients in terms of the time for the change to reach 63 per cent of completion, by analogy with a linear case, may not be justified.

Experimental Checks

The results of the analysis given here have been checked thoroughly by experiment. The experiments to be described were done with the hypernik cores used in earlier work[1,3,4] but extensive measurements also were made using a pair of conventional 1.5 kva single-phase power transformers connected as magnetic amplifiers in accordance with Figures 1 and 3, and the agreement with the analytical results was equally satisfactory.

Two typical oscillograms obtained with a direct-inking type instrument are shown in Figure 7. The upper trace in each case is the control current and the lower, the load current. Since it often was extremely difficult to determine the starting point of the transient, a small auxiliary circuit was used to give a pip on the control current trace at the instant of closing the switch.

The upper record of Figure 7 is for an amplifier with series-connected output coils, Figure 1, and the lower for one with the parallel connection, Figure 3. The core material is that for which Figure 2 is drawn.

In both cases $N_1I_{1_\infty} = 120$ ampere-turns, $R_1 = 98.5$ ohms, $R_2 = 109$ ohms, $N_1 = N_2 = 2{,}000$ turns, $B_m = 45.7$ kilolines per square inch and $B_0 = 43.2$ kilolines per square inch resulting in $uB_{0_\infty} = 2.66$. The factors τ_s and τ_p are calculated to be respectively 0.0715 and 0.137 second. The supply frequency is 60 cycles. The slower response of the parallel case as predicted, and the initial jump in control current in this case are evident. Figure 8, for the same cases as Figure 7, shows the transient envelope of output current plotted against time in dimensionless form as in Figure 6. It satisfactorily confirms both the predicted form of the transient and the predicted relation between the series and parallel cases.

Figure 9 shows additional calculated and measured envelopes of the output current transient for a series connection with time plotted in seconds instead of in dimensionless form. The experimental conditions are as before, except that $B_m = 22.9$ kilolines per square inch, the control voltage for the middle curve is the same as for Figure 7. The upper and lower curves were obtained respectively with doubled and halved control voltage, the control circuit resistance remaining unchanged throughout. B_{0_∞} is 68.1, 56.8, and 45.5 kilolines per square inch when $N_1I_{1_\infty}$ is 240, 120, and 60 ampere turns respectively as per equation 14.

Finally Figure 10 reproduces the middle curve of Figure 9 and an additional curve (calculated and experimental) obtained by doubling both the control circuit resistance and control voltage. Thus the influence of control resistance on the time scale for unchanged values of B_m and B_{0_∞} is evidenced.

Effects of Load and Frequency

The transient response curves of Figure 6 are derived for the case of zero load impedance. For loaded amplifiers in the steady state it is conventional, as has been noted,[4] to investigate the performance using for the voltage E_m across the amplifier the vector difference between the supply voltage and the load voltage drop ignoring harmonics. The same procedure can be applied in the transient case obtaining B_m from the value of E_m corresponding to the final steady state. Actually higher values of voltages than this will exist across the load coils before the output current reaches its steady state, and the actual build-up of the output current may be expected to be somewhat faster than calculated using the final steady state B_m in the formulas developed for the no-load case. A more accurate analysis of the loaded amplifier obtainable by cutting the transient into intervals suggests itself.

From the analysis it appears that the influence of the supply frequency upon the response of the amplifier can be discussed only when the conditions for comparison are specified clearly in terms of the true independent variables B_m, E_{dc}, and R_1. If supply voltage and frequency are varied at the same rate, B_m does not change in the amplifier without load and therefore uB_{0_∞} does not vary and the response time in seconds remains unchanged. A readjustment of voltage and frequency for a loaded amplifier will generally also involve rematching of the load. Suppose specifically that a-c supply voltage and frequency are doubled and that the load resistance also is doubled, then the transient response is not affected, while of course the gain resulting will be doubled.

It is conceivable then to increase R_1 and E_{dc} thus improving the transient response at the expense of gain. For instance, if R_1 and E_{dc} then also are doubled the gain will be brought back to the value at the original frequency while the factor τ_s will be cut to one-half and the build-up transient for the series-connected amplifier will be twice as fast. General statements to the effect that transient durations should be measured in cycles of the supply frequencies rather than in seconds probably imply that changes of frequency are actually accompanied by changes in load, supply voltage, control circuit voltage, and control circuit resistance, as indicated before, and that

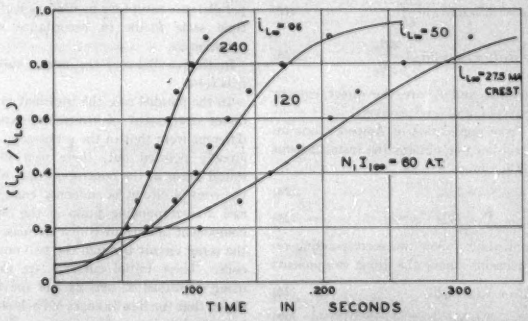

Figure 9. Envelopes of output current transients for a series-connected magnetic amplifier

The curves are calculated; the points are measured

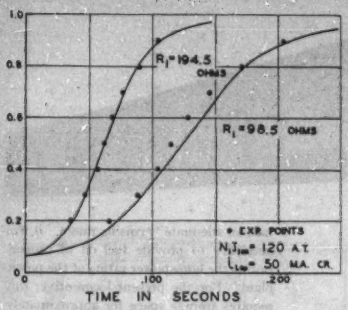

Figure 10. Envelopes of output current transients for a series-connected magnetic amplifier showing the effect of control circuit resistance

The curves are calculated; the points are measured

higher gains inherent to higher frequencies are being entirely sacrificed for higher speed of response. In any event these considerations apply, as stated initially, in the range of frequency in which eddy currents may be neglected.

Conclusions

The foregoing analysis is based on the approximation that during the transient, the values of the direct component of core flux density (B_{0i}) are obtained in terms of the crest of the a-c voltage across the amplifier and of the direct component of control current by use of the same expression which has been derived in reference 4 for steady-state operation. This approximation, suggested from the results of a number of step-by-step computations, allows development of a theory which yields results checking with experiments for materials whose normal magnetization curves can be reasonably fitted with a hyperbolic sine function and for transients which, as commonly happens, persist for at least several cycles of the applied alternating voltage.

Formulas and curves are obtained which express the build-up of the a-c envelopes for series-connected and parallel-connected 2-core amplifiers without feedback. Influence of core material, control voltage, and design data is embodied in a time factor. Effects of load and influence of supply frequency are discussed.

References

1. An Analysis of Interlinked Electric and Magnetic Networks with Application to Magnetic Amplifiers, D. W. VerPlanck, M. Fishman. *Proceedings*, Institute of Radio Engineers (New York, N. Y.), volume 37, 1939.

2. Universal Curves for D-C Controllable Reactors, B. C. Merrell, R. E. Alley, Jr. *AIEE Transactions*, volume 68, part I, 1949, pages 31–39

3. An Analysis of Magnetic Amplifiers with Feedback, D. W. VerPlanck, M. Fishman, D. C. Beaumariage. *Proceedings*, Institute of Radio Engineers (New York, N. Y.). volume 37.

4. Analytical Determination of Characteristics of Magnetic Amplifiers with Feedback, D. W. VerPlanck, L. A. Finzi, D. C. Beaumariage. *AIEE Transactions*, volume 68, part I, 1949, pages 365–70.

5. Some Fundamentals of D-C Controlled Reactors with Resistive Load, H. F. Storm. *AIEE Transactions*, volume 68, 1949, pages 188–94.

6. The Theory of Magnetic Amplifiers and Some Recent Developments, E. H. Frost, Smith. *Journal of Scientific Instruments* (London, England), volume 25, August 1948, page 271.

7. Mathematics of Modern Engineering (book), R. E. Doherty, E. G. Keller. John Wiley and Sons, New York, N. Y., volume 1, 1936, page 164.

8. A Five-Figure Table of Bessel Functions $I_n(x)$, H. B. Dwight. *Electrical Engineering (AIEE Transactions)*, volume 60, March 1941, pages 135–39.

No Discussion

The Alco-GE 4,500-Horsepower Gas-Turbine Electric Locomotive

A. H. MOREY
NONMEMBER AIEE

BASIC design features of this locomotive were dictated by current railroad needs. The keynote is simplicity, as far as this is compatible with the application of a new type of prime mover to railroad motive power. The result has been a unit with control and characteristics essentially the same as those of the modern diesel-electric locomotive, except where power-plant characteristics required or permitted advantageous differences.

General Design

The Alco-GE gas-turbine electric locomotive, shown in Figure 1, is designed for freight service. It is an 8-axle 8-motor B-B-B-B locomotive, weighing 253 tons (average) and rated at 4,500 horsepower for traction (at 80 degrees Fahrenheit and 1,500-feet elevation). The locomotive is 83-feet $7^1/_2$-inches long, and 14-feet 3-inches high over the roof sheets. It will negotiate curves of 288-feet radius.

This locomotive is designed to burn grade 6 fuel oil with some restrictions. Its specific fuel consumption is relatively high compared to diesel-electric locomotives, and low compared to oil-burning steam locomotives.

The general design, especially the power rating and weight of the locomotive, was developed from analyses of freight and passenger locomotives in use in this country in 1941 and 1946. These analyses indicated that about 75 per cent of the freight locomotives were in the 4,000- to 5,000-horsepower range and had approximately 500,000 pounds on drivers. The studies also showed that approximately 90 per cent of the total locomotives in use in road service handled freight. Consequently, it was decided to concentrate on designing a freight locomotive in this range of power and weight. To be attractive and profitable to the railroads, this locomotive must show a low initial investment, low fuel cost, and low maintenance cost.

Mechanical Construction

The mechanical construction of the locomotive is somewhat unconventional. Instead of the usual truss work in the sides of the locomotive cab, the equivalent mechanical structure is built into the cab underframe. The superstructure, including the roof, hatch covers, side walls, and so forth, is supported on vertical uprights from this main underframe in what we have called an "umbrella type" construction. This is illustrated in Figure 2. This design was developed because of the necessity for carrying relatively large amounts of fuel and for keeping this fuel below the level of the power plant and generating equipment. In order to obtain an adequate "cruising range," it was necessary to provide fuel oil in proportion to the horsepower rating of the power plant. For the present locomotive, this requires storage space for approximately 6,500 gallons of fuel. Such a quantity is much larger than can be carried in a conventional manner between the trucks. Consequently, the fuel storage tanks are built into the main underframe structure of the cab.

The trucks are of the conventional 2-axle swing-bolster type, as indicated in Figure 3. Each pair of trucks is connected by a span bolster which, in addition to spanning the two trucks and supporting the locomotive cab, also acts as a traction-motor air duct. This arrangement gives a high degree of flexibility on curves. It also has sufficient vertical flexibility to give satisfactory riding qualities even on comparatively rough track. Resonant vibration between the truck equalizers and the swing bolsters was encountered at low speeds. Damping means were provided in the spring system and no further trouble has been encountered.

Power Plant

The power plant, Figure 4, is the simplest type of gas-turbine power plant having the compressor and turbine rotors essentially on the same shaft. It is of the "straight-through" type of construction. Air entering the inlet at the left goes through the compressor, where the pressure is raised to approximately five atmospheres gauge. It then enters the combustion chambers where fuel is admitted and burned. The products of combustion pass through the two turbine stages where

Figure 1. Alco-GE gas-turbine electric locomotive ready for service tests on the Union Pacific Railroad

Paper 50-77, recommended by the AIEE Land Transportation Committee and approved by the AIEE Technical Program Committee for presentation at the AIEE Winter General Meeting, New York, N. Y., January 30–February 3, 1950. Manuscript submitted October 26, 1949; made available for printing December 5, 1949.

A. H. MOREY is Project Engineer in the Locomotive Engineering Division of the General Electric Company, Erie, Pa.

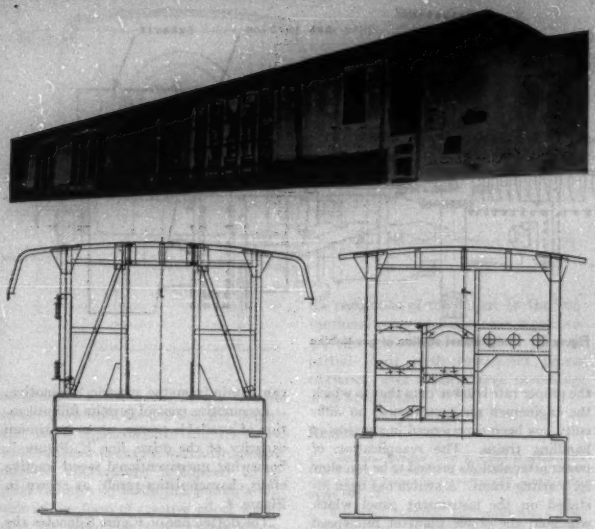

Figure 2. Side view and cross sections of locomotive cab showing "umbrella type" construction

the available energy is transformed into mechanical energy, and through the exhaust ducts to the roof discharge. No heat exchangers or intercoolers are used. The power-plant governor, fuel pumps, and so forth, are mechanically driven from the shaft extension on the inlet end. The power output is taken off through a shaft extension on the exhaust end of the machine.

Electric Equipment

The electric transmission consists of four d-c traction generators driven by the power plant through a reduction gear. This power is absorbed in eight traction motors, each pair of traction motors being connected to a single generator with no electrical interconnections. Auxiliary power is furnished by a d-c generator driven directly from one of the traction generators. This supplies the necessary power for the auxiliaries which are used in starting. The balance of the auxiliary power is furnished by an alternator direct connected to another of the traction generators. Such auxiliaries as traction-motor blowers, water circulating pumps, cooling fans, amplidyne exciters, and so forth, receive power from this source.

The power plant is started by a diesel engine-driven generator set. This generator is connected across one of the traction generators serving as a motor to crank the power plant up to the firing speed and to assist in further acceleration to a speed where the power plant is self-supporting.

Necessary fuel heating and cab heating is accomplished by a vapor car-heating boiler. The heating system and boiler are operated on a closed cycle so that storage space need be provided only for the necessary makeup water.

Apparatus Location

The relative location of various pieces of apparatus is shown in Figure 5. The nose compartments of the locomotive are taken up with train control and air brake equipment. The operating cabs are quite conventional and follow closely the pattern set by the diesel-electric locomotives. Necessary transmission and auxiliary control are located in the two control cabinets just back of the operating cab at each end. The diesel-engine with its generator and the heating boiler are shown adjacent to the right control cabinet. Following these, to the left, is the train air compressor and above it the radiators for cooling the lubricating oil. In the center is shown the gear unit with its four traction generators, the two auxiliary generators, and a connection through the alternator for driving the train air compressor. At the left in the equipment cab is the main power plant and the second control cabinet.

Figure 6 shows a typical cross section through the locomotive. It is of interest in that it shows the location of the main fuel tank, air inlet louvers and, particularly, the bus bars and control wiring above the aisles. All piping is located beneath the aisle floors or beneath the main fuel tank. This calls for a rather unusual treatment of the sand boxes since they must be below the bus bar and control wiring locations.

This location of the electric connections was designed to keep them dry. It has proved quite effective even though snow and water are drawn through the air inlet louvers into the cab. It also is quite effective in keeping cleaning compounds that may be used in the locomotive from coming into direct contact with the wiring and deteriorating the insulation.

Control

The control requirements on this locomotive are essentially the same as the requirements for any internally-powered locomotive. The control, at least from the engineman's point of view, must be simple. It must give adequate control of tractive effort for safe and satisfactory train handling. It also must provide the necessary safeguards against such things as: locomotive overspeed, low or high lubricating oil pressure, overspeed, or excessive temperature on equipment.

Automatic motor transition and field shunting, operating as a function of locomotive speed, are provided. The dynamic braking control is the same as that used on diesel-electric locomotives, with the energy dissipated in resistors. In short, since the diesel-electric locomotive has become the standard of com-

Figure 3. Running gear showing span bolster and two swivel trucks

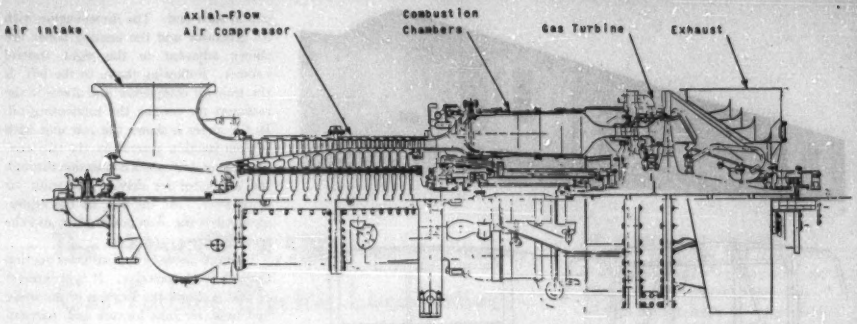

Figure 4. Longitudinal section of gas turbine

parison for new motive power, the same pattern of control was followed. Full details of the control will be covered by other papers.[1,2]

This locomotive is handled in essentially the same manner as the diesel-electric. It differs in only one feature, namely, the rate at which the controller can be advanced from notch to notch. This is lower than the rate on the diesel-electric locomotive. The power plant, with its connected load, has considerably more inertia than the diesel-electric power plants on present-day locomotives. Consequently, its rate of acceleration is lower.

A notching guide is provided on the instrument panel at the engineman's position to aid in advancing the controller on this locomotive at a proper rate. This guide will indicate, at a glance, whether the engineman is moving the controller handle too rapidly. Although the proper rate is lower than that to which the enginemen are accustomed, no difficulty has been experienced in starting or handling trains. The reapplication of power after shutoffs proved to be too slow for starting trains. A switch has been installed on the instrument panel which will hold the power plant at full speed under these conditions and permit rapid reapplication.

Locomotive Characteristics

The locomotive characteristics are, of course, the characteristics of any internally-powered electrically-propelled locomotive as far as speed and tractive effort are concerned. The capacity of this type of power plant varies with changes in ambient temperature and elevation.

The engineman, however, only sees a change in the power which he can obtain from the electric locomotive.

Locomotive control permits full utilization of available power, up to maximum capacity of the drive, line *E*, Figure 7. Somewhat unconventional speed-tractive effort characteristics result, as shown in Figure 8.

The dotted line of Figure 8 denotes the constant horsepower characteristic, line *D* of Figure 7, while the solid line of Figure 8 corresponds to maximum power conditions, line *E*, Figure 7. Speed-tractive effort characteristics in the cross-hatched area between the dotted and solid lines in Figure 8 will be realized when the locomotive is operating under the conditions corresponding to the cross-hatched section of Figure 7. These areas represent extra power available due to the particular characteristics of the gas turbine.

Installing power-plant capacity to fully utilize all of the capacity in the electric drive is entirely a question of

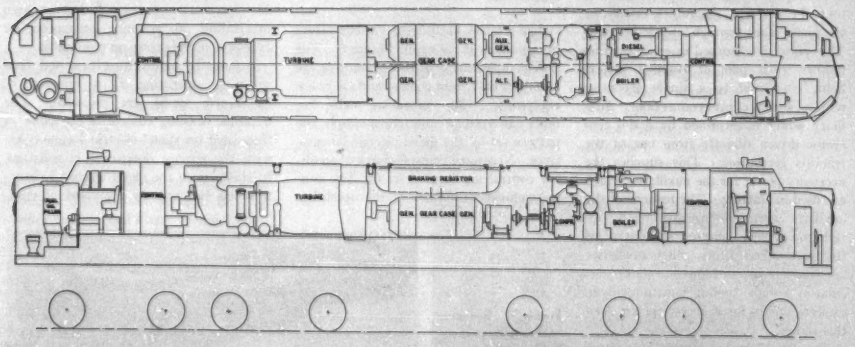

Figure 5. Layout of apparatus in locomotive cab

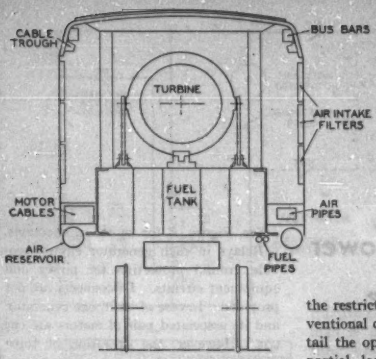

Figure 6 (left). Cross section of locomotive cab showing location of electric wiring and piping

Figure 7 (right). Chart of typical gas-turbine electric drive performance

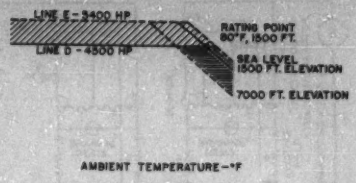

economics. In the case of the gas-turbine power plant with its low specific weight and space characteristics and its fairly wide variation in output with altitude and ambient temperature, it appears to be good business to make this power available in the form of tractive effort whenever the power plant is capable of developing it. This is especially true since the restriction of the output to the conventional constant horsepower would entail the operation of the power plant at partial loads, with consequent poorer efficiency, over a fairly large percentage of its normal life.

References

1. Control System for a 4,500-Horsepower Gas-Turbine Electric Locomotive, T. J. Warrick. *AIEE Transactions*, volume 69, part I, 1950, pages 508–13.

2. Rotating Electric Equipment for a Gas-Turbine Electric Locomotive, O. C. Cobo. *AIEE Transactions*, volume 69, part I, 1950, 514–18.

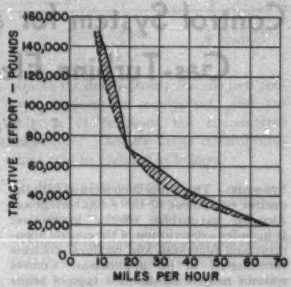

Figure 8. Locomotive speed-tractive effort curve

No Discussion

Control System for a 4,500-Horsepower Gas-Turbine Electric Locomotive

T. J. WARRICK
ASSOCIATE AIEE

Synopsis: This paper is concerned with the control equipment of the 4,500-horsepower Alco-GE gas-turbine electric locomotive. It includes a description of the control apparatus and functions, and outlines problems encountered in its application. Control systems relative to this new type of prime mover are dealt with in particular.

Basic Considerations

THE main objective of the gas-turbine electric locomotive development program is the evaluation of the gas-turbine power plant as a prime mover for locomotive use. On this basis, new developments were limited to those peculiar to this type of power plant application. Wherever possible, control equipment comparable to that employed on diesel-electric road locomotives was used.[1] When chosen, this equipment represented the best possible in design, and it has since proved reliable and successful. Further benefits derived from applying this standard equipment are lower first cost and simplification of the maintenance, servicing, and renewal parts problems.

Previous articles have been published on design and testing of the gas turbine power plant.[2,3] Two additional papers are being presented at this session.[4,5] One concerns the construction, design, and operation of the locomotive; while the other deals with the rotating electric apparatus.

Paper 50-78, recommended by the AIEE Land Transportation Committee and approved by the AIEE Technical Program Committee for presentation at the AIEE Winter General Meeting, New York, N. Y., January 30-February 3, 1950. Manuscript submitted October 26, 1949; made available for printing December 5, 1949.

T. J. Warrick is with the Control Engineering Division of the General Electric Company, Erie, Pa.

Propulsion Control

For maximum hauling power in freight service, all eight locomotive axles are driven by series-wound d-c traction motors. Two motors are powered from each of the four main generators and each system is electrically independent of the others during motoring. Conventional series and parallel connections are used with a single step of field shunting in the parallel connection. Referring to Figure 1, the "hole" in the speed tractive effort curve at the transition point from series to parallel connection of the motors is small enough that field shunting in the series connection is not warranted.

Automatic transition, operating as a function of locomotive speed, is provided from series to parallel, and from parallel full field to parallel shunted field. Referring again to Figure 1 and extending the series and parallel curves at their intersection, it can be seen that for optimum locomotive performance the transfer from series to parallel should occur at 19 miles per hour. The fact that the transfer is automatic relieves the engineman from the responsibility of initiating it at the proper speed, and assures that both forward and backward transitions will be correctly made. This results in less shock to the train and the electric equipment of the locomotive. Supervisory control is not provided. Smoother forward transition is obtained by transferring four motors at a time. The first four, after completing the cycle, transfer the remaining two generators and their motors. The controls are such that even though one generator is cut out, its associated generator and its motors will transfer. Backward transition is not staggered.

See Figure 2 for motor connections.

Relays in each generator circuit provide ground protection for power and equipment circuits. Disconnects are not provided. In case of fault, one generator and its associated pair of motors are cut out. However, the operation of three generators and their motors continues. These ground relays can be operated manually to cut out any generator, thereby eliminating the need for separate traction motor cutouts.

Controls identical to those on diesel-electric road locomotives are used for dynamic braking. On this locomotive, however, twice the equipment is necessary since eight motors are used instead of four. Two generators are used to excite the traction motor fields during dynamic braking. Four identical braking resistors are necessary to dissipate the power developed by the traction motors.

Figure 3 shows the power connection diagram for half of the locomotive during braking. The four traction motor exciting fields are tied in series across generator 2. Each pair of motors is connected to one braking resistor and, in effect, becomes a pair of separately excited generators. By varying the output of the exciting generator in much the same manner as during motoring, the amount of braking effort is controlled. Figure 4 illustrates the speed-braking effort curve.

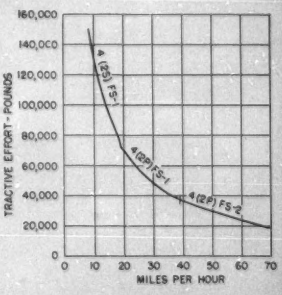

Figure 1. Speed tractive-effort curve for a 4,500-horsepower gas-turbine electric locomotive

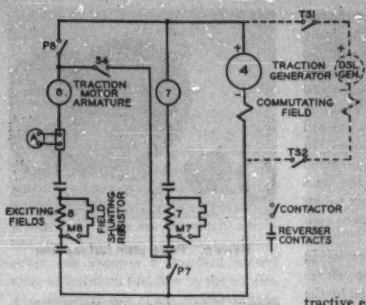

Figure 2 (left). Schematic diagram of motoring connections

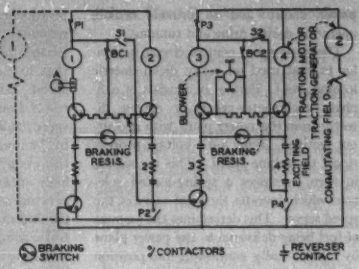

Figure 3 (right). Schematic diagram of braking connections

CONNECTION	S4	P7	P8	M7	M8
SERIES FS1	•				
PARALLEL FS1		•	•		
PARALLEL FS2		•	•	•	•

The excitation scheme is quite similar to that currently employed on diesel-electric road locomotives.[6] The main difference lies in the current limit portion of the control. On diesel-electrics the excitation system provides for limiting generator line and field currents to safe values at the high-current and high-voltage ends of the characteristic curve, respectively. Since a diesel engine is essentially a constant horsepower machine at any particular speed, the load control rheostat on the governor is depended upon to limit maximum generator output. This scheme is not suitable for a gas turbine since its power output varies, depending upon the altitude and ambient temperature at which it is operating. It is not practical to design generators and motors to absorb all the available power that the turbine is capable of delivering under ideal conditions. A field-current-biased line current scheme was developed to replace the straight line current feature of the diesel-electric scheme. This, in effect, limits the line current at the high-current end of the characteristic curve and also limits the power at the maximum power portion of the curve, as shown in Figure 5.

Control of power plant speed and generator power demand (locomotive power) is provided in 20 steps on the controller. This number of throttle notches was selected, instead of the customary eight, to give finer and better control of tractive effort as well as better locomotive performance when working near limiting adhesion. The throttle handle operates a potentiometer which feeds a d-c signal into the excitation system of all four generators. By the proper selection of taps on the potentiometer, equal increments of tractive effort are obtained. The engineman is prevented from advancing the throttle handle too fast (and consequently making too rapid an increase in power plant speed and output demand) by an "automotoneer." This feature is a mechanical lock on each throttle notch position which prevents the handle from being advanced more than one notch at a time. To advance another notch it is necessary to retard the throttle handle a half notch and then advance to the next position.

To obtain optimum locomotive performance and to have better control of tractive effort, a notching guide in the form of a voltmeter is installed beside the ammeter on the engineman's panel, see Figure 8. This meter is connected across the stabilizing potentiometer of the fuel regulator and, by the colored band scale markings, indicates the availability of power-plant output. The two main divisions of the meter show whether the power plant is operating in either fuel control or load control. When in fuel control, the power plant is capable of developing more output than the load is demanding; but when in load control any further called-for increase in load demand will be nullified by governor action. By watching the amount of generator load reduction, the engineman can govern the rate at which he advances the throttle handle to call for more tractive effort.

By means of a switch, located at the engineman's panel, the power plant can be accelerated to, or held at, full speed without power being delivered to the traction motors. With this arrangement, the throttle handle may be manipulated so as to secure the desired tractive effort more rapidly and with better control than if part of the power output of the turbine is diverted to accelerating the power plant.

New Control Problems

The application of a gas-turbine power plant as a locomotive prime mover necessitated the development of some new control systems and equipment, and the solution of problems not encountered heretofore. The new major control functions may be grouped as follows:

1. Power plant control.
2. Power plant cranking and cooldown.
3. Generator power limit.

Some of the new components developed for these applications were: a power plant regulator incorporating an electric positioning motor, a magnetic amplifier for controlling this positioning motor, a flame detector system, a voltage regulator for the 400-cycle power supply, an excitation system incorporating a power limit separate from that of the governor, and new control schemes for turbine cranking and cooldown.

Power Plant Regulator (Governor)

The power plant regulator is shown in Figure 6. The functions of the regulating system are: to control load and power plant speed; to protect the turbine from excessive exhaust temperatures and overloads; to recognize the ability of the

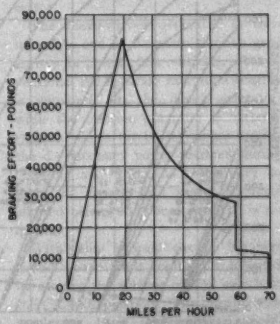

Figure 4. Speed braking-effort curve for a 4,500-horsepower gas-turbine electric locomotive

power plant; and to provide remote operation during firing and running.

The basic speed control circuit is similar to that used on many diesel-electric locomotives.[7] Part of it consists of a 3-phase tachometer-generator driven directly from the power plant with its output rectified, giving a d-c voltage proportional to turbine speed. This d-c signal, in turn, energizes a spring-loaded solenoid which operates the pilot valve of the speed servo. This determines the amount of fuel being delivered to the power plant by hydraulically controlling the position of the wobble plate which changes the effective stroke of a 6-port pump driven by the power plant. Power plant speed is determined by the circuit resistance and is proportional to it since a constant current of 0.475 ampere is required to balance the system.

In order to prevent undue thermal shock it is necessary to limit the rate of change of temperature in the turbine. For this reason temperature measuring equipment, consisting of a gas-filled bellows located in the exhaust chamber, forms an essential part of the governor system. The rate of temperature change is controlled by a rate piston which restricts the rise to 20 degrees per second after an initial instantaneous jump of 200 degrees Fahrenheit. A mechanical stop is used to limit the maximum temperature.

Further control of the rate of temperature change is obtained by an electric positioning motor, located within the fuel regulator. This motor is mechanically geared to the speed-setting rheostat, so that its position determines power plant speed. The thermal shock which would result from an instantaneous change in speed (and hence in fuel rate) is lessened by limiting the speed of this motor. In the event of too rapid a change or too high an exhaust temperature, the temperature measuring equipment can reduce the fuel rate called for by the speed control circuit.

During normal running, the positioning motor receives its signal from the voltage taken off a potentiometer operated by the throttle handle. During firing this signal is received from a master rheostat governed by the turbine control switch. Rectified 400-cycle power controlled by a magnetic amplifier is used to drive this motor. The voltage at the brush arm of the follow-up rheostat, which is gear-driven by the positioning motor, signals the position of the motor. This brush arm is electrically connected, through the windings of two saturable reactors, to the brush arm of whichever potentiometer is controlling speed. With both voltages equal no current flows and the reactors are balanced. When the called-for speed-voltage is different from that of the follow-up rheostat, current flows through the reactors causing an unbalance in the system. Depending on the direction of current flow, power is supplied to the proper field of a split-pole series d-c motor

Figure 6. Power plant fuel regulator

causing it to rotate until the system is again balanced.

Under certain conditions, it is necessary to further control the load demand of the traction generators. The feature of the governor which provides for this is similar to the one used on many diesel-electric road locomotives. With the power plant loaded and the fuel regulator allowing maximum fuel rate (permitted by the aforementioned limits) the speed control portions of the regulator can overtravel and regulate the speed by the control of the generators' output through a load control rheostat. When this overtravel takes place it, in effect, commutates resistance in the current-controlling reactor of the excitation system to reduce the field excitation and hence load demand of all four traction generators.

Power and Speed Scheduling

The large power required for acceleration, the characteristics of this type of power plant, and certain economic considerations made it desirable to incorporate a variable speed schedule into the power plant speed control circuit. A rheostat in the high side of the potentiometer circuit provides this variable speed program. The idle speed range is between 60 and 100 per cent of full speed (6,900 rpm).

When the power plant speed is below the called-for speed, the governor reduces the power demand of the generators through the medium of the aforementioned load control rheostat, making more power available for acceleration. Greater acceleration could be obtained by reducing the power plant output to zero, but then the locomotive would be subjected to sudden shocks of varying power. A compromise is reached by providing 40 per cent reduction in the generator power demand. It also is possible to vary the speed change per notch by the use of a nonlinear potentiometer. By having the lower notches produce greater speed

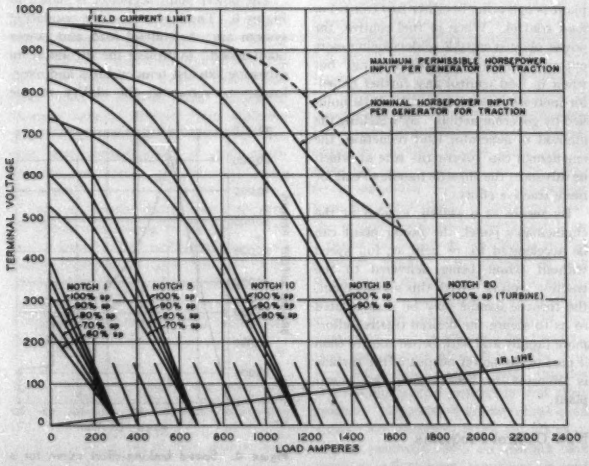

Figure 5. Traction generator characteristic curves for a 4,500-horsepower gas-turbine electric locomotive

changes, better locomotive performance is obtained.

Flame Detector

The function of the flame detector is to hold the fuel valve open as long as fire is sustained in the combustion chambers. The flame detector system includes two sets of thermopiles located in two of the combustion chambers. The d-c signals produced by them are separately amplified and, with their outputs paralleled, either can energize a standard control relay to maintain fuel flow to the nozzles. The amplifiers are of the magnetic type with two stages of amplification.

Several problems were encountered in the design of this system. It must be fast enough to detect the presence or absence of fire in the combustion chambers before an excessive amount of fuel can be injected, with consequent damage resulting from high temperature when ignition does take place. To meet these conditions a rugged, yet small-time-lag thermopile was built and so located in the combustion chamber that it is not directly in contact with the fire. Cooling air is directed so as to provide the cold junction within the element as well as the necessary general cooling.

In order to obtain satisfactory amplification, a constant a-c voltage supply was needed. Since 400-cycle power was already available, it was only necessary to provide better voltage regulation. A magnetic-type regulator was developed for this purpose which consists fundamentally of a single-stage amplifier and a reference and voltage build-up circuit.

Auxiliary System

There are two separate electric auxiliary power systems on this locomotive.

1. The d-c system comprises those auxiliaries which must function when the power plant is shut down. A 32-cell battery charged from either one of two identical auxiliary generators furnishes stand-by power. One generator is driven by the turbine and the other by a diesel engine which is not in use during normal turbine operation. The power plant starting fuel pump, fuel heat boiler, locomotive lighting, power plant cranking control, 400-cycle motor-alternator set, and the lubricating and water booster pump motors are all required previous to and during power plant starting, and hence are d-c powdered.

The high inertia of the power plant and its connected load, and the time required to crank it to self-sustaining speeds,

Figure 7. Turbine control panel

(above) with covers
(below) without covers

necessitate a large power supply. Weight and space limitations prohibited the use of batteries as the source of supply, hence an auxiliary diesel-driven generator set is employed. The diesel engine is rated 210 horsepower at 2,100 rpm and its generator is capable of delivering 140 kw at this speed. Both turbine-driven and diesel-driven generators are rated 50 kw for battery charging.

2. The a-c system comprises those auxiliaries which function only when the power plant is operating. A 3-phase 80-cycle 290-volt alternator, driven from the main power plant, provides for operating the following pieces of induction-motor-driven apparatus: four amplidyne exciters, four traction motor blowers, two radiator fans, and the coolant, lubricating, and fuel pumps. Most of these motors are permanently connected to the alternator through circuit breakers. The radiator fan and coolant pump motors are connected through separate contactors (with overloads) which are controlled as a function of lubricating oil temperature.

Power Plant Cranking and Cooldown

Power plant cranking and diesel control are practically automatic. A 3-position diesel control switch and a five-position turbine control switch are located on the turbine control panel, Figure 7. This, along with the d-c circuit breaker panel, is mounted at the side of the power plant. The positions of the diesel control switch are *OFF—RUN—CRANK*, and those of the turbine control switch are *OFF—CRANK OR COOLDOWN—FIRE AND IDLE—BUNKER "C"—RUN.*

Diesel Starting. Before starting the diesel engine, the water booster pump must be started by closing its circuit breaker and the diesel and turbine-start circuit breaker must be closed. The control switch is moved to the *RUN* position. This allows the throttle operator on the diesel to advance to idle speed setting. An electric positioning motor drives the speed adjusting shaft of a conventional hydraulic speed-droop governor at proper limited speed. Cam-operated contacts on the throttle operator are used to control the position of the motor. When ready to crank, the diesel control switch is moved to the *CRANK* position and held there. The generator, acting as a series motor powered from the battery, cranks the engine. As soon as the diesel fires, the switch is released and springs back to the *RUN* position. In this position the diesel-driven generator is automatically regulated at 75 volts and is connected to the d-c auxiliary bus for battery charging and supplying the auxiliary load.

Power Plant Cranking. Previous to starting the power plant the grade 6 fuel oil is heated to approximately 200 degrees Fahrenheit by the fuel-heating steam generator.

The diesel-driven generator is connected to one of the main traction generators for power plant cranking. A conventional self-separate excitation scheme is employed on the diesel generator, while the traction generator is battery-excited. Since the battery must furnish the d-c auxiliary power required during cranking and firing, it is necessary to limit the number and length of starts allowed before additional charging is required.

With the proper circuit breakers closed, power plant cranking is initiated by moving the turbine control switch to the *CRANK* position. The diesel engine accelerates to a predetermined speed, simultaneously accelerating the power plant. The control switch now may be moved to the *FIRE AND IDLE* position,

Figure 8. Engineman's position, showing controls and instruments

but fuel injection and ignition will not take place until the minimum speed relay operates at 10 per cent of power plant speed. This relay measures speed indirectly from the rectified output of the turbine-driven tachometer-generator. If the fuel does not ignite within 45 seconds, the fuel valve is automatically closed and ignition shut off.

A time-delay relay prevents repetition of the firing cycle for a period of four minutes to allow sufficient time for purging fuel from the combustion chambers. In case of a mis-fire it is necessary to move the turbine control switch to the *CRANK* position and, after the required time delay, back again for firing. When firing occurs, the flame-detector relay operates and causes the diesel engine to accelerate to full speed. After firing, a relay introduces a 90-second time delay before the fuel rate of the power plant is increased, thereby allowing the exhaust temperature bellows to become operative. As the power plant approaches idling speed a reverse-current relay automatically uncouples the diesel-driven generator from the main traction generator, and the diesel engine returns to idling speed for battery charging. The diesel engine may be shut down and the turbine-driven auxiliary generator used for battery charging by moving the diesel control switch to the *OFF* position. The same voltage regulator, overload relay, and reverse current relay control both the diesel- and the turbine-driven auxiliary generators.

Grade 3 fuel oil is used during firing. The transfer to grade 6 is, at present, a manual operation. As soon as the transfer is complete, the locomotive is ready for service.

Approximately four minutes are required to crank, fire, and accelerate the unit to idle speed. The control of the locomotion of the gas turbine-electric locomotive is quite similar to that of a diesel-electric road locomotive, as indicated by Figure 8.

Power Plant Cooldown. Normally, at shutdown the power plant is cranked at low speeds for 15 to 20 minutes. Low power is required for this cranking and hence the diesel engine is operated at idling speed. It also furnishes power for battery charging during this cooldown period.

Hostler Operation

A means has been provided for moving the light locomotive around yards and terminals without starting the main power plant, by a simple commutation of control circuits. For such movements the diesel engine is started in the normal fashion and the hostler control switch is turned to the *ON* position. This connects the diesel-engine driven generator to two of the traction motors in series. The same self-separate excitation arrangement is used for hostler operation as for power plant cranking. Since the diesel-driven generator cannot be used for battery charging during hostling, the length of time allowable for such movements depends on the condition of the battery and what d-c auxiliaries are being operated.

The hostler controls the tractive effort with the throttle lever indirectly by varying diesel engine speed. Notch 1 produces tractive effort with the diesel engine at idling speed; Notch 2 holds the speed at which the diesel engine is operated; Notches from 3 onward cause the diesel throttle operator to advance steadily to obtain diesel speeds between idle and full. On level track the locomotive will attain a speed of about 12 miles per hour.

Protective Equipment

Six emergency stop switches, one at each engineman's stand and the rest in the engine room, provide means of shutting down the turbine, fuel heat boiler, diesel engine, and starting fuel pump.

No fuses are used, but all electric circuits and equipment are fed through circuit breakers for protection. All the a-c, and most of the d-c circuit breakers are for protection only and are normally left closed. The d-c circuit breakers controlling the lubricating oil pump, the 400-cycle set, the water booster pump, the starting fuel pump, and the diesel and power plant start circuit breaker are used both for protection and as switches.

Both the power plant and the diesel engine are protected against overspeed. The overspeed switch on the diesel engine is part of the governor and mechanically trips the fuel valve. On the power plant, the contacts open to de-energize the turbine stop relay, thereby shutting off fuel and also by-passing the control oil so that the pump goes to zero stroke.

A manually reset, overload relay in the common negative circuit of the diesel and turbine-driven auxiliary generators provides overload protection for both machines. If the overload trips, field is removed from both generators and the line contactors are de-energized.

Temperature and pressure switches protect the power plant and main reduc-

tion-gear unit in case of low-lubricating oil pressure and high-lubricating oil temperature. The turbine is protected against too high an exhaust temperature by a bellows-operated shutdown switch.

The d-c lubricating oil pump motor is powdered through a contactor which operates as a function of lubricating oil pressure. In cranking the power plant the d-c pump furnishes lubricating oil. As the a-c pump increases in speed, their combined output increases until an oil pressure switch operates and shuts down the d-c pump. In case the a-c pump fails for any reason, and the oil pressure drops, the d-c pump will automatically start before any damage is done to the bearings.

Summary of Tests to Date

Preliminary testing of this locomotive has indicated that the control equipment is basically sound. There have been no troubles encountered to date with the well-seasoned standard equipment used. Little difficulty has been experienced with the new equipment developed specifically for this application. Future testing may result in minor alterations of control equipment; however, no basic changes in the over-all control structures are contemplated.

References

1. Developments in Control Systems for Diesel-Electric Locomotives, M. D. Henshaw. *AIEE Transactions*, volume 66, 1947, pages 233–41.

2. Design Features of a 4,800-Horsepower Gas-Turbine Power Plant, Alan Howard. *Mechanical Engineering*, volume 70, April 1948, pages 301–06.

3. Tests of a 4,800-Horsepower Gas-Turbine Power Plant, Alan Howard, B. O. Buckland. *Mechanical Engineering* (New York, N. Y.), January 1949, page 38.

4. The Alco-GE 4,500-Horsepower Gas-Turbine Electric Locomotive, A. H. Morey. *AIEE Transactions*, volume 69, part I, 1950, pages 504–07.

5. Rotating Electric Equipment for a Gas-Turbine Electric Locomotive, O. C. Cohe. *AIEE Transactions*, volume 69, part I, 1950, pages 514–18.

6. Developments in Diesel-Electric Traction-Generator Excitation Control Systems, C. A. Brancke, G. M. Adams. *AIEE Transactions*, volume 66, 1947, pages 223–28.

7. A Power Plant Regulating System for Diesel-Electric Locomotives, C. B. Lewis. *AIEE Transactions*, volume 66, 1947, pages 243–48.

No Discussion

Rotating Electric Equipment for a Gas-Turbine Electric Locomotive

O. C. COHO
ASSOCIATE AIEE

Synopsis: A new type of prime mover, in the form of a gas-turbine power plant, recently has been successfully applied in a locomotive. The problems encountered and the electric equipment employed are, in many respects, similar to those of diesel-electric locomotives. This presentation deals primarily with those features, as regards this locomotive application, that it is felt are sufficiently unique to be of general interest.

Electrical Drive

THE BASIC problem in the application of electrical drive is that of converting the prime-mover power available in the form of torque at high rotative speed to tractive effort at the driving wheels over the range of locomotive operating speed. It is desired to make the full prime-mover power available as tractive effort, from the minimum locomotive speed at which point the wheels will slip, to the maximum full-power speed. The latter is usually a high fraction of the maximum permissible locomotive speed as dictated by other considerations. At low locomotive speeds, the prime-mover power appears as high tractive effort whereas, at high speeds, the tractive effort decreases essentially in inverse proportion to the locomotive speed. The system is thus basically a torque converter of infinitely variable ratio within the rating capabilities of the equipment.

In the design of such an electrical drive system, cognizance is taken of the fact that below a certain locomotive speed, full-power application is generally of limited duration, such as in starting a train or ascending a grade. Advantage is taken of this fact to utilize the short-time torque overload capacity of electric apparatus, thus resulting in smaller, lighter equipment than would be required if continuous operation in the low-speed range were provided.

The foregoing is merely a brief review of the electrical drive in general. The remarks are equally applicable for any system with a constant-speed, constant-torque prime mover.

Gas-Turbine Prime Mover

The type of gas turbine selected for this application is essentially a constant-speed, constant-torque power plant at full power and, in this sense, is comparable to the diesel engine. Its nominal rating is 4,800 horsepower, of which 4,500 horsepower is allocated for traction and 300 horsepower for auxiliaries. This rating is stipulated at 80-degree Fahrenheit ambient and 1,500-foot elevation. However, the turbine power available is a function of both ambient air temperature and pressure (altitude). At low temperatures and elevations, the power capabilities of the turbine are somewhat higher than at high temperatures and/or altitudes.

Thus the first problem encountered in this application was that of selecting the rating point about which the design of the electric propulsion equipment should be centered. To provide equipment suitable for transmitting the maximum available power-plant output over the entire range of locomotive speed would mean carrying much extra and expensive equipment weight on the locomotive when ambient conditions were such that this peak power was not available. Accordingly, the electric transmission was chosen finally to handle 4,500 horsepower for traction over essentially the entire speed range.

Locomotive Performance

The full-power performance of the locomotive is illustrated in Figure 1, which shows the relationship of tractive effort and speed. One of the curves represents the locomotive characteristic at the nominal 4,500-horsepower rating, and the other the limiting characteristic permitted by the electrical drive when more than nominal power is available from the power plant. The equipment is designed for a maximum tractive effort of 150,000 pounds. This is dictated by wheel slip based on 30 per cent adhesion. The maximum speed, 69 miles per hour, is determined by the limiting speed of the traction motors. The tractive effort at the continuous rating of the traction motors is 77,800 pounds at 18 miles per hour.

This performance characteristic is obtained through the use of eight traction motors receiving their power from four traction generators geared to the gas-turbine power-plant shaft. Each generator independently furnishes power to two traction motors. From standstill to 19 miles per hour, the two traction motors are connected in series across the generators, and from 19 to 69 miles per hour, they are connected in parallel. At 38 miles per hour, the motor series fields are shunted to extend the speed range over which full power can be handled.

Traction Generators

Considerable thought was given to the arrangement and design of the traction-generating equipment. Inasmuch as the full power-plant speed is 6,700 rpm, gearing is necessary to reduce the speed to a value which can be handled by traction generators built within current design practice. Various studies were made as

Paper 50-79, recommended by the AIEE Land Transportation Committee and approved by the AIEE Technical Program Committee for presentation at the AIEE Winter General Meeting, New York, N. Y., January 30–February 3, 1950. Manuscript submitted October 24, 1949; made available for printing December 6, 1949.

O. C. Coho is with the General Electric Company, Erie, Pa.

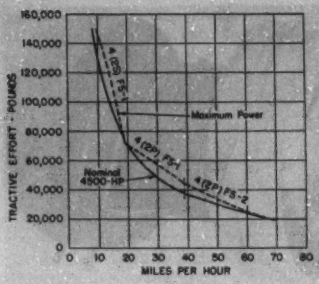

Figure 1 (left). Speed-tractive-effort curve showing full-power performance

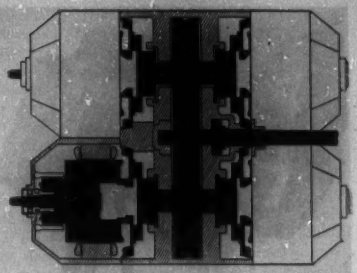

Figure 3 (right). Schematized section of generator gear-unit assembly

to the best arrangement of the equipment centered around such a reduction gear unit.

While the power is too great to be handled by a single commutator machine of a diameter that will readily fit in the locomotive, it is possible to design a generating unit having two armatures. Such a pair of generators, however, could not be assembled with the gear reduction set as a self-contained unit. This would involve individual installation of the components within the locomotive and connection through a parallel misalignment type of flexible coupling. Additional study showed that this solution had no advantage in weight and was possibly at a disadvantage from the cost and space standpoint. The 3-generator layout was eliminated for similar reasons plus the fact that it is quite awkward to match the output of three generators to eight traction motors. The design was ultimately resolved into a single self-contained generating unit consisting of a gear box with four overhung, close-coupled generators. The gearing consists of a single 6,700-rpm double helical pinion driving two low-speed gears at 1,600 rpm. The pinion is driven by a splined shaft, so designed as to be readily removable in the event of interchange of equipment. The gears and pinion are supported and aligned within the box by their own bearings. Forced lubrication of the gears and bearings is obtained from the main lubricating oil system which also handles the power-plant bearing lubrication.

The four single-bearing generators are end-bell supported from the walls of the gear case. Each of the two low-speed gears drives two generators, one on each side, through steel disk-type flexible couplings. The gear bearings are designed to sustain not only the gear loading itself, but also the thrust and radial loads due to the weight and coupling of the generators. The over-all design is such that the generators may be mounted on the gear box on the assembly floor, and the complete assembly installed in the locomotive as a unit. Line-up within the locomotive, between the generating unit and the power plant, is then a relatively simple problem. Individual generators may be readily removed and replaced at any time after complete unit installation without disturbing the line-up of any other equipment.

The complete 4-generator gear unit weighs 38,000 pounds.

Figure 2 illustrates the general assembly details of the generators and gear unit. The high-speed power-plant shaft coupling passes between the two generators slightly above their centers. Scallops in the generator magnet frames to provide clearance with the shaft are evident in the picture. All frames are thus cut out on each side to provide a maximum of standardization and interchangeability. The generator frame has an outside diameter of $43^1/_2$ inches and an over-all length from bearing cap over coupling of 40 inches.

Further assembly details are illustrated by the cutaway plan view, Figure 3, where the rotating components of couplings, gearing, and one generator are shown in silhouette.

Each generator is nominally rated at 1,125-horsepower input for traction, consistent with the nominal power-plant rating, and in accordance with the AIEE standards for this type of equipment.

The generators are of the noncompensated type without pole-face windings. Each machine has six exciting poles and six commutating poles. They are conservatively designed, based on proved practice as regards mechanical and dielectric stresses, heating and ventilation, commutation, and performance limits.

Figure 4 illustrates the generator volt-

Figure 2 (below). Traction generator gear-unit assembly

Figure 4 (right). Generator characteristic curve for a 4,500-horsepower gas-turbine electric locomotive

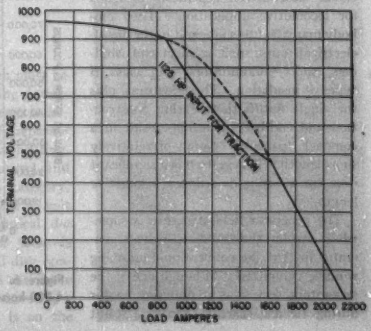

Figure 5 (left). GE-752 traction motor

Figure 7 (right). Braking - resistor blower unit

ampere characteristic curve. The continuous rating of the generator is 1,125 horsepower, 1,600 rpm, 535 volts, 1,450 amperes. This figure shows also the limiting power curve to which the generators may be loaded when excess power is available from the power plant.

The generators are self-ventilated, each one being equipped with its own radial-discharge type fan located at the back of the generator as part of the steel-disk coupling assembly. Ventilating air is drawn from within the cab after it has passed through filters located in the side walls of the locomotive. The air enters the generators at the commutator end and then divides, part passing through the commutator risers and the armature core, and part passing over the surface of the armature and between the field coils. The air is discharged in chambers within the gear box and subsequently directed vertically out of the roof of the locomotive.

Comparison with Diesel-Electric Traction Generators

The generators are quite similar in general design and appearance to conventional diesel-driven generators designed for locomotive application. They embody many features inherent in the diesel-electrical units, such as short end windings, short commutators, and class *B* types of insulation. These features, plus the single antifriction bearing construction and end-bell mounting, result in a compact "pancake" design of relatively short length. This in itself is a significant item contributing to reduced locomotive length.

The generator field structure is somewhat simpler than a diesel-driven generator in that the conventional cranking winding is omitted. Although one of the generators serves as a cranking motor during turbine starting, separate shunt excitation is provided in this case. A further difference is found in the magnetic path design. In order to maintain good commutation at higher than normal rated horsepower, but within normal field and armature current limits, the magnetic structure is relatively heavier than that in the usual diesel-driven generator. This allows for the simultaneous existence of large exciting and commutating fluxes associated with such high horsepower, without the adverse effect of saturation on commutation.

Traction Motors

General Electric model *GE-752* traction motors, Figure 5, are provided. The locomotive has a total of eight motors, one on each axle. The motors are of the conventional force-ventilated 4-pole axle-hung series-wound type geared to the axle with single-reduction spur gearing. They are designed for heavy duty railway service and are a currently standard model in wide use on diesel-electric locomotives with similar axle loadings (62,500 pounds per axle). These motors heretofore have been rated at 900 amperes continuous for application at 500 horsepower with forced ventilation of 2,300 cubic feet per minute air flow. For the gas-turbine electrical application at 562.5 horsepower per motor, the core losses become of greater relative significance so that the continuous rating has been reduced to 875 amperes. Based on 74/18 gearing with 42-inch diameter wheels, this corresponds to a continuous tractive effort of 9,725 pounds per motor or 77,800 pounds total at 18 miles per hour. The motors are applied to transmit the full available horsepower over the speed range from 30 per cent adhesion at 8 miles per hour to 95 per cent of full speed or 66 miles per hour.

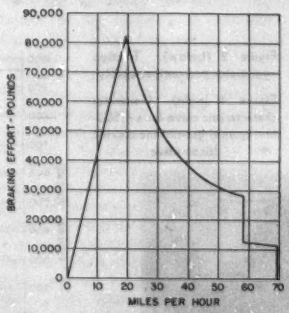

Figure 6. Speed-braking-effort curve for a 4,500-horsepower gas-turbine electric locomotive

Dynamic Braking

Since the locomotive has been designed particularly for use on freight applications, dynamic braking has been provided. This braking may be used independently or together with the train air brakes. The traction-motor armatures are loaded in pairs across fixed braking resistors while the separate excitation for the motor fields is furnished by two of the main generators. Braking control is obtained by varying the motor field excitation. The maximum braking rate is determined by motor armature and field heating as well as commutation limits. Between 19 and 58 miles per hour, 4,100 braking rail horsepower is available. Below 19 miles per hour, the available horsepower falls off essentially in proportion to speed, whereas above 58 miles per hour, the braking is restricted to 2,000 horsepower. Figure 6 shows the characteristic curve of available braking effort versus miles per hour.

The braking resistors are force ventilated by axial-flow blowers driven by a series motor which obtains its power

through a permanent connection across part of the resistor. Thus, maximum resistor ventilation is obtained automatically at the maximum braking rate. Figure 7 illustrates one of the blower units, a current standard General Electric model *GY-19*, showing the dual-fan contravane assembly integral with the driving motor. There are two such units on the locomotive.

A-C Auxiliary System

Entirely aside from such functions as cab heaters, train control, battery charging, and so forth, more than a dozen different auxiliary operations must be performed, powered by electric motors. In order to have the highest degree of reliability and a minimum of maintenance, as many of the auxiliaries as possible are driven by 3-phase induction motors; see Table I.

A 6-pole 3-phase alternator driven through a flexible steel-disk coupling from a shaft extension on one of the main traction generators furnishes power for the a-c system. Inasmuch as the power plant operates at variable speed, depending upon loading, the frequency of the system will vary between 80 and 48 cycles. The rated voltage of the system was chosen as 290 volts, 80 cycles so that normal motor flux conditions would prevail when checking or testing with standard 220-volt, 60-cycle power.

Class *B* insulation is applied on all this equipment. In order to reduce size and weight, the designs are such that the temperature rises are somewhat in excess of those encountered in normal industrial practice. However, in view of limited field experience with this line of apparatus, the temperatures were kept well below the AIEE standards for transportation equipment. In all cases where the motors may operate in dirty or oily atmospheres, the totally-enclosed fan-cooled construction has been used.

The motors are permanently connected across the alternator. One of the first steps in the procedure of starting the main power plant is to excite the alternator field. As the plant is started from rest and brought up to speed, each auxiliary motor, according to its break-away torque requirements, will begin turning at between 3 and 13 cycles of applied frequency, and from then on come up in speed along with the main power plant. There is no modulation of the alternator field. The unit is of the self-regulating type with sufficient capacity, in case of emergency, to start the largest motor at full frequency and rated excitation without the voltage dropping to the point where other loaded motors may stall. The alternator is nominally rated at 150 kva, 80 per cent power factor, 1,600 rpm, 290 volts, 3-phase 80 cycles.

The traction-motor blowers are perhaps the most unique of the a-c auxiliary equipment, involving special development for this locomotive. The basic locomotive design is such that the traction-motor ventilating air must be furnished through restricted duct work involving high pressure drops. Blower requirements indicated a fan rated 5,375 cubic feet per minute at 8.5 inches of water static pressure. This delivery is obtained by the use of a $16^1/_2$-inch diameter 24-blade single-stage axial-flow fan at 4,650 rpm. The fan, contravane, and 15-horsepower motor are assembled as a self-contained unit. The motor core and windings are totally enclosed. Cooling is obtained from the high-velocity air flow passing over the outside of the motor frame. Rotation is about the vertical axis. In order to insure satisfactory bearing lubrication at the high rotational speed, metered oil lubrication features were utilized for both bearings.

Figure 8 shows the assembled blower unit. Air inlet is through the top and sides of the expanded metal cover. As much inlet area as possible is provided in order to reduce entrance velocities, thus minimizing the tendency to accumulate dirt in the traction motors.

Table I

Function	Horsepower	Revolutions Per Minute
1 fuel sump pump	3	1,150
1 fuel booster pump	3	1,130
1 lubricating oil pump	8.5	1,525
1 coolant pump	5	2,335
2 coolant radiator fans	6 each	1,140
4 amplidyne exciters	8.5 each	2,340
4 traction-motor blowers	15 each	4,650

D-C Auxiliary System

The auxiliary functions which must be in operation prior to and during power-plant starting, before a-c power is available, are handled by an entirely separate d-c system. Such operations as lighting, locomotive and fuel heating, control, and turbine cranking are in this category. This system is centered about a 75-volt storage battery and two identical d-c auxiliary generators. One of these is driven through a flexible steel-disk coupling from a shaft extension on one of the main generators. The other is driven by a diesel engine and, normally, is on the system only when the main power plant is not in operation.

The battery is a 32-cell lead-acid type having 426 ampere-hour capacity. It must furnish the auxiliary power required during the period of power-plant cranking, and accordingly was chosen to have ample capacity to handle at least three successive starts without the necessity of recharging.

The auxiliary diesel-driven generator also furnishes power to one of the main generators operating as a motor. This occurs during power-plant cranking wherein approximately 140 kw is developed when driven by the 210-horsepower 2,100-rpm diesel engine. This cranking power is applied up to over 50 per cent speed until the power plant is self-sustaining by its own developed power. For this application, the generator is rated at 210-horsepower input, 310/180 volts, 460/700 amperes, 2,100 rpm. For battery-charging service, both the diesel-driven generator and the identical turbine-driven auxiliary generator are rated 50-kw output, 75 volts, 667 amperes, 800 to 1,600 rpm. The generators are designed to permit a conventional voltage regulator to operate with stability over an 800- to 1,600-rpm speed range.

Part of the power-plant shutdown sequence involves cranking at approximately 7 per cent speed to equalize various power-plant temperatures. This is done at 75 volts, thereby enabling the diesel-driven generator to charge the battery at the same time.

One significant function operated from the d-c auxiliary system is the stand-by lubricating oil pump. Prior to power-plant starting, the main lubricating oil is heated and circulated throughout the system by a pump driven by a 75-volt

Figure 8. Traction-motor blower unit

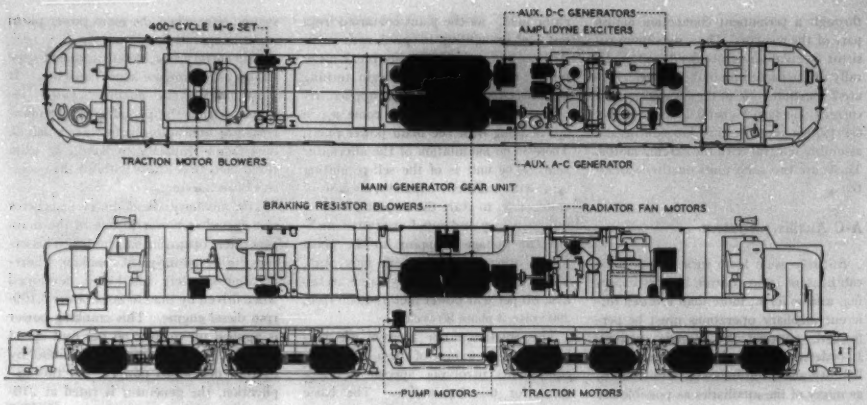

Figure 9. Layout of apparatus for a 4,500-horsepower gas-turbine electric locomotive

motor. This pump also serves as an automatic stand-by during locomotive operation in the event of failure of the a-c motor driven pump.

Table II is a general listing of the various motors and generators connected with the auxiliary d-c system.

Table II

Function	Power	RPM
1 diesel-driven generator	50 kw	800 to 1,600
1 turbine-driven generator	50 kw	800 to 1,600
1 stand-by lubricating pump motor	13 hp	1,550
1 400-cycle control motor-generator set	3 hp	3,600
1 water booster pump motor	3 hp	1,750

An additional 25 kw is furnished for various other auxiliary services including heating boiler, lights, cab heaters, defrosters, train control, battery charging, and field excitation.

Conclusions

As is to be expected, the advent of the gas-turbine power plant as a prime mover, with its accompanying light weight and small space per-unit horsepower, tends to focus more attention upon the electric rotating equipment, from the standpoint of the over-all locomotive design.

This is evidenced by its predominance in the locomotive as shown by layouts of Figure 9 where the electric rotating equipment is silhouetted. This apparatus makes up approximately 25 per cent of the weight of the locomotive; 22 per cent of which is for propulsion, and 3 per cent for auxiliary drives. It is of interest to point out that the propulsion equipment, including gear box, main generators, and traction motors weighs approximately 22 pounds per horsepower. This compares with the value of 25 pounds per horsepower for a typical diesel-electric freight locomotive of comparable axle loading.

Based on tests and locomotive operation to date, it is felt that all functions are being performed in a highly satisfactory manner. Fundamental difficulties have yet to appear in any of this equipment, either performance-wise or from a general maintenance standpoint. This is in spite of many exceptional overloads and abuses attending the various initial tests of a special nature which have been part of the performance evaluation of the power plant and locomotive to date.

No Discussion

Rectifier-Type Motive Power for Railroad Electrification

L. J. HIBBARD
MEMBER AIEE

C. C. WHITTAKER
NONMEMBER AIEE

E. W. AMES
ASSOCIATE AIEE

TESTS on rectifier motive power equipment which have been announced recently[1] constitute a very important development in the electrification of steam railroads. Not only does this development mark another important step of progress in the use of electric energy as motive power on railroads, but it forms another practical demonstration of the inherent flexibility of the single-phase a-c system for railroad electrification.

The chief advantage of present d-c electrifications lies in the use of d-c series traction motors on the motive power units.

The fundamental advantage of the single-phase a-c system is its ability to use a high-voltage trolley wire, thus making it possible to supply, economically, large blocks of power over long distances for heavy concentrations of traffic.

Three types of motive power units have been built to operate from an a-c system, namely, the a-c series-motor type, the split-phase type, and the motor-generator type.

The a-c series motor motive power unit is well adapted to any application. The best present-day examples of a-c series motor locomotives are the Pennsylvania Railroad class *GG1* and the New York, New Haven, and Hartford Railroad class *EF3*. Although these locomotives are officially rated at 4,620 continuous horsepower, each can deliver from 8,000 to 9,000 maximum horsepower if occasion arises. These ratings are outputs at the rail. Output in excess of the continuous rating can be delivered at the rail over the entire speed range of the locomotive.

Another important asset of the a-c series motor motive power unit lies in the simplicity and flexibility of the locomotive control system, that is, voltage control, which means a minimum of accelerating losses, a minimum peak power demand, and a large number of running speeds.

The motor-generator motive-power unit combines all the advantages of the flexible high-voltage single-phase a-c trolley system and the advantages of the d-c traction motor with the simplicity and flexibility of voltage control, but it does not have the ability to produce economically high short-time accelerating horsepowers at high speed since the best proportions of the motor-generator set produce a motive power unit with constant horsepower characteristics.

The rectifier motive power unit combines all the advantages of the high-voltage a-c trolley system with the simplicity and flexibility of voltage control plus the advantage of the d-c traction motor and it has the ability to develop high accelerating horsepowers at high speed even more economically than is possible with the a-c series motor motive power unit.

Thus the rectifier motive power unit furnishes an attractive means of utilizing the power which can be delivered to it by a flexible high-voltage single-phase a-c trolley.

Advantages

The advantages of rectifier motive power are summarized in the following:

Rectifier Motive Power versus Single-Phase Series-Motor Motive Power

The rectifier motive power unit has the following advantages on a 25-cycle trolley system. Some of these advantages will be increased if a 60-cycle trolley system is used.

1. Lower weight of equipment.
2. Less space required for equipment.
3. Higher running efficiencies and less standby losses.
4. Higher power factor.
5. Less maintenance. This point must be proved in service. However, the higher efficiency (which means less watt hours per ton mile) plus the reduced maintenance of the traction motor and gearing should easily overbalance the added maintenance of the rectifier equipment.
6. Superior tractive effort rating and tractive effort characteristics. Westinghouse standard diesel locomotive motor type *370-F* with 15/63 gearing on 42-inch wheels (65 miles per hour top speed) will develop 10,700 pounds tractive effort continuously up to 17.5 miles per hour. This is a much greater tractive effort and a higher speed than is possible with an a-c series motor. The speed-tractive effort characteristics of the rectifier motive power unit are similar to the speed-tractive effort characteristics of a motor-generator locomotive (that is, they are flat) and hence should have the same antislip features now enjoyed by the motor-generator locomotive. The rectifier motive power unit can be applied safely at higher adhesions than is permissible for a-c series-motor motive power. The net result of these tractive effort advantages means that fewer axles will be needed for a rectifier motive power unit to meet a given duty cycle than will be needed for the single-phase series-motor motive power unit.
7. Rectifier motive power will develop its continuous horsepower rating at approximately 30 per cent of its top speed, whereas most a-c series motor motive power units do not develop their continuous horsepower rating until they reach 50 to 60 per cent of top speed. This characteristic plus its ability to produce economically high accelerating horsepower at high speed makes rectifier motive power ideally suited for use either in freight or passenger service.

The rectifier motive power unit can be used under a 60-cycle trolley. The rectifier motive power unit can be used interchangeably between two trolley zones involving:

Paper 50-81, recommended by the AIEE Land Transportation Committee and approved by the AIEE Technical Program Committee for presentation at the AIEE Winter General Meeting, January 30–February 3, 1950. Manuscript submitted November 2, 1949; made available for printing December 6, 1949.

L. J. Hibbard, C. C. Whittaker, and E. W. Ames are with the Transportation Engineering Department of the Westinghouse Electric Corporation, East Pittsburgh, Pa.

1. Two frequencies, 25 cycles and 60 cycles.
2. Alternating current and direct current.

The rectifier motive power unit permits more horsepower capacity per cab than any other type.

Rectifier versus Motor Generator Motive Power

The rectifier locomotive has the following advantages:

1. Less weight of conversion equipment.
2. Less cost of conversion equipment.
3. Less space requirements for the conversion equipment.
4. More capacity per cab permitted.
5. Simpler and cheaper mechanical parts because of item 3.
6. Reduced standby losses and higher operating efficiencies.
7. High accelerating horsepowers at high speeds.

Rectifier versus Diesel-Electric Motive Power

The price of electric energy has been relatively stable, whereas the long term trend of liquid fuel prices has been upward. Where economic conditions justify the electrification of a dieselized railroad, the diesel electric locomotives can be transformed into rectifier locomotives by removing the diesel engines and their appurtenances and applying pantographs, transformers, auxiliaries, and rectifier equipment.

The rail horsepower rating of most diesel electric locomotives can be substantially increased when and if such a change is made.

History

The desirability of producing a system of electrification embodying the advantage of high-voltage a-c transmission with low-voltage d-c traction motors has been a dream of transportation engineers ever since Westinghouse, in the year 1914, first ran a rectifier car in revenue service on the New Caanan branch of the New York, New Haven, and Hartford Railroad. This car was equipped with a multianode pumped-type rectifier. Two fundamental limitations were encountered in the use of this car as a motive power unit.

It was limited by the requirement of pumping to maintain the vacuum in the rectifier. At that time, the technique of vacuum pumping and vacuum seals had not reached the present stage of perfection.

The car produced telephone interference and it was necessary to install

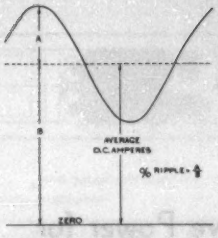

Figure 1. Explanation of ripple

track booster transformers in the test section to force all the trolley current to return through the rail.

Prior to 1937, all rectifiers were of the multianode pumped type, with as many as 18 anodes per tank. Subsequently, two developments, the sealed tube[2] and the ignitor, combined with a single anode made the application of sealed tube ignitrons to moving vehicles particularly attractive. With the great impetus which World War II gave to the production of aluminum and magnesium by the use of ignitrons, which supplied large amounts of d-c power, the ignitron was produced in quantity. Concurrently, the large demand for diesel electric locomotives has similarly put the low-voltage d-c traction motor into mass production. Hence rectifier-type motive power becomes a product which will be benefited greatly by these two high-production items.

In the past, three main problems have deterred the use of ignitrons and other forms of rectifiers on rectifier motive power units:

1. The effect of shock and vibration encountered on a moving vehicle with respect to the strength of ignitron tube parts, and with respect to the effect of a turbulent mercury pool on the performance of the ignitors.
2. The effect of the ripple in the rectified single-phase current wave form with respect to the heating and commutation of conventional d-c motors.
3. The effect of interference with communication circuits when operating from a single-phase trolley with ground return.

Table I. Effect of Power Supply on Commutation

Volts	Amperes	Commutation
		With a 5 Per Cent Ripple
315	500	Black
430	595	Black occasional pin point
430	638	Black
		With a 30 Per Cent Ripple
290	300	Black
335	400	Black
375	500	Few pin points on one brush
406	600	Few pin points on one brush
425	650	Few pin points on one brush
		With a 75 Per Cent Ripple
256	300	Almost black
290	400	Few pin points
320	500	Intermittent pin points on one brush
345	597	Black with intermittent pin points
358	670	Intermittent pin points

Laboratory Tests

Problem 1 was approached by determining the maximum values of acceleration forces expressed in terms of g (acceleration of gravity) observed on an electric locomotive classified as a satisfactory riding unit. These values were: maximum cab lateral observed, 0.66 g; usual cab lateral, 0.16 g. Both values were read on curved track at 95 miles per hour. Cycles of oscillation were 78 per minute.

Similar tests on another locomotive classified as an unsatisfactory riding unit indicated that the usual cab lateral was approximately 0.32 g while the frequency at 90 miles per hour was 114.

Based on the above, an oscillating test table was made on which the ignitrons were rigidly mounted. This table had an amplitude of vibration which could be varied from one to three inches and a frequency which could be varied up to 250 cycles per minute, giving values as high as 1.8 g acceleration, or well in excess of those observed on a rough-riding locomotive.

With this laboratory setup, two standard type *WL-653-B* ignitron tubes, mounted rigidly on the shaking table, delivered 200 to 800 amperes to a Westinghouse type *362* railway motor while shaking at a frequency of 120 cycles per minute and one-inch amplitude. This particular railway motor is standard on Westinghouse 660- and 1,000-horsepower diesel electric switcher locomotives. At this shaking frequency no misfires occurred during several hours of operation. By a misfire is meant failure of the ignition circuit to start an arc for one or more half-cycle waves. One or several misfires in traction service would not be more serious than a pantograph bounce of short duration. This test was continued for several months, and no weakness was apparent in the design of the tube when exposed to these severe tests.

Problem 2 deals with the effect of ripple on commutation and heating of the traction motors. By ripple is meant the amount of deviation from a straight line wave form of rectifier current. See Figure 1.

Tests on the type *362* motor were made at various loads and at various ripples in the power supply as affecting commutation. This motor is rated at 510 amperes, continuous on 310 volts.

With a d-c circuit reactor to limit the ripple, the results shown in Table I were obtained.

A temperature test was made on the type *362* motor using rectified current with a 30 per cent ripple. This test showed a temperature increase in the motor windings of from 1 to 2 per cent over the results obtained with generated d-c power.

Tests with rectified current also were conducted on two other traction motors, one a type *1447* used on the New York Board of Transportation subway cars and the other a type *559-DR3* used on the Long Island Railroad cars. Both of those motors showed equally as good commutation and stability as the type *362*.

Problem 3, pertaining to possible telephone interference, was studied in the laboratory. The type *362* motor was operated at 600 to 700 amperes with a single-phase ignitron. The harmonic content of the single-phase line current feeding the single-phase ignitron was measured by means of a harmonic analyzer.

In order to have a single-phase full-wave rectifier produce a square wave alternating current, the following theoretical conditions are required:

1. Infinite inductance in the d-c circuit.
2. Zero angle of overlap.

This means that each half a-c wave must be a square wave. The square a-c wave can be expressed mathematically by the Fourier series as follows:

$$e=\frac{4E}{\pi}\left(\sin\ \omega t+1/3\ \sin\ 3\ \omega t+1/5\ \sin\ 5\ \omega t \ldots\ldots+\frac{1}{n}\sin\ n\ \omega t\right)$$

Table II. Harmonic Currents for Various Values of *IT*

Harmonic	Frequency	Calculated Square Wave Current, Amperes	Test Amperes, Dec. 16, 1947	Test Amperes, Feb. 3, 1948
1	25	210	210	210
3	75	70	59.7	41.5
5	125	42	32.7	27.8
7	175	30	20.1	10
9	225	23.3	13.8	2.66
11	275	19.1	9.25	0.6
13	325	16.15	6.18	0.5
15	375	14	4.37	0.258
17	425	12.35	3.00	0.104
19	475	11.05	2.15	0.074
21	525	10.0	1.61	0.088
23	575	9.12	1.46	0.040
25	625	8.38	1.35	0.0142
27	675	7.77	1.21	0.0195
29	725	7.24	1.13	0.031
31	775	6.78	1.00	0.00565
33	825	6.37	0.84	0.0150
35	875	6.00	0.695	0.0126
37	925	5.68	0.58	0.0048
39	975	5.39	0.492	0.0043
41	1,025	5.12	0.457	
43	1,075	4.89	0.434	
45	1,125	4.67	0.428	
47	1,175	4.47	0.405	
49	1,225	4.28	0.350	
51	1,275	4.12	0.344	
53	1,325	3.97	0.299	
55	1,375	3.82	0.268	
57	1,425	3.69	0.248	
59	1,475	3.56	0.240	
61	1,525	3.45	0.224	
63	1,575	3.33	0.210	
65	1,625	3.23		
67	1,675	3.13		
69	1,725	3.04	0.188	
71	1,775	2.96		
73	1,825	2.87		
75	1,875	2.80		
IT		165,000	16,700	357

where

e = instantaneous value
E = crest value
$\omega = 2\pi f$
f = fundamental frequency
n = any odd integer
t = instantaneous value of time

The term *IT* is used to indicate the intensity of telephone interference. Briefly, it is the product of current by *T*, a weighting factor which is dependent upon the frequency, coupling, and sensitivity of instruments and of the human ear.

The calculated *IT* product of a 25-cycle square wave having 210-ampere fundamental is 165,000 based on the 1935 weighting. This is a very high value of *IT* and taken by itself would tend to discourage the use of rectifier motive power. However, it is not possible to obtain infinite inductance in the d-c circuit or zero angle of overlap in the a-c circuit.

In order to approach with practicable test equipment the theoretical square wave conditions, all the available suitable inductance in East Pittsburgh for the d-c circuit was utilized and the ignitrons were energized at a point where there was very little reactance in the power circuit. With this special setup, the maximum *IT* value obtained by test was approximately 10 per cent of the calculated *IT* value.

With the aid of practicable filtering means, the *IT* value for 210 amperes fundamental was reduced to 357.

Figure 2. Rectifier test car main circuit

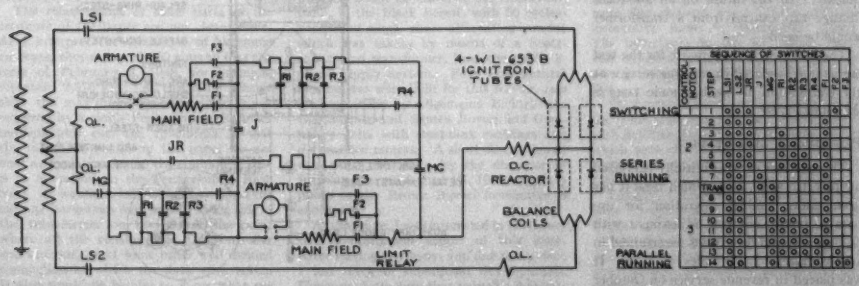

Table II gives a picture of the various harmonic currents involved for the conditions mentioned previously.

Tests on Pennsylvania Railroad

Laboratory tests were so favorable that it was decided to make tests in service under actual electrification operating conditions. Co-operation of the Pennsylvania Railroad was sought for the assembly of propulsion and control apparatus furnished by Westinghouse Electric Corporation and the multiple-unit car and its auxiliary apparatus by the Pennsylvania Railroad Company. This assembly has been in trial performances for adjustment and refinement of apparatus for some months. The car now is in revenue service.

In addition to this procedure, the Bell Telephone Laboratories and the American Telephone and Telegraph Company co-operated with Westinghouse and the Pennsylvania Railroad in conducting a series of tests to determine the telephone noise influence aspects of the rectifier car and existing single-phase a-c series motor equipment.

The results of telephone noise influence tests are still in preliminary form and are not contained herein.

Description of Car and Control

This car was a combination type, half its length being a baggage compartment. All test equipment requiring adjustment and observation, instruments, and oscilloscopes were mounted in this baggage compartment.

The electric equipment consisted of a specially-designed transformer, four type *WL-653-B* ignitron tubes for single-phase full-wave rectification, plus a variety of capacitors and reactors as variable test equipment. Two Long Island-type traction motors with control boxes and accelerating grids were used primarily because they could be secured quickly. In the future on an a-c road, voltage tap control from a transformer would be used.

The main circuit schematic for the test car as it was placed in revenue service at the completion of the harmonic tests is shown in Figure 2.

Preliminary Test Results

This rectifier car was initially energized on July 15, 1949, since which time it has been under limited operation for apparatus refinement and adjustment with no fundamental difficulties ascertained in approximately 2,500 miles of trial. It was placed in revenue service on October 26, 1949. Since then to April 15, 1950, the car has been trouble-free, has operated 26,000 miles, and is in the multiple unit car pool, going wherever dispatched.

Problem 1

Shock and vibration during normal operation has not affected operation in the least. The car has been operated most of the time during the tests pulling a second car as a trailer. It has been operated successfully for sustained periods of time with full-wave rectification from two tubes only, first one pair of tubes were used up to 60 miles per hour for 25 successive accelerations, then the other pair of tubes were used in the same manner. Normally all four tubes would be used. It has been operated intentionally for short periods of time on two tubes with half-wave rectification.

Problem 2

The motors have been operated most of the time with approximately 33 per cent ripple in the direct current. The commutation under these conditions has been black at all times and the commutators and brushes have an excellent appearance. Limited testing was done with a 5 per cent and a 55 per cent ripple.

The test car was operated for three round trips making all stops between Broad Street Suburban Station, Philadelphia and Paoli with approximately a 33 per cent ripple in the direct current. The three round trips were repeated the next day with a 5 per cent ripple in the direct current. Both tests resulted in an 86 degree centigrade rise (by thermocouple) in the interpole winding.

Problem 3

The telephone influence of such a rectifier is being investigated on a 25-cycle system. The results, though not complete, include field test data taken on the ignitron-equipped multiple-unit car. They indicate that practical filters can be produced which will permit the use of rectifiers as a power supply for individual traction units of an electrified railroad system paralleling associated and commercial communication circuits.

The authors are confident that practical filters can be built to permit the operation of rectifier motive power on 60-cycle trolleys in parallel with shielded communication circuits.

Summation

A great deal of engineering data has been collected during our laboratory tests and tests are still in progress. Also a great deal of engineering data was taken during our joint car tests with the Bell Telephone Company and Pennsylvania Railroad.

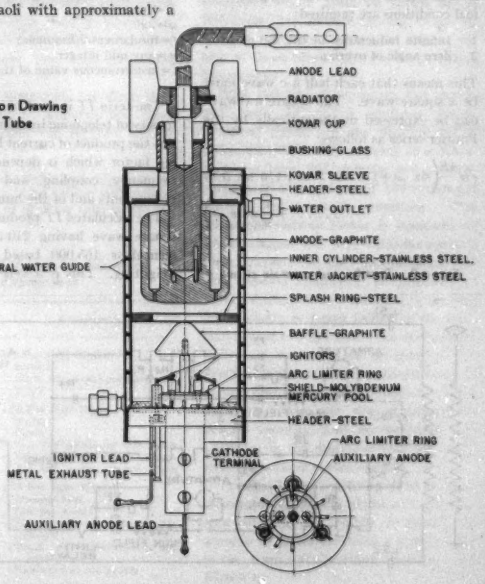

Figure 3. Section Drawing of Ignitron Tube

These data cover numerous tests on different filter combinations and constants and the effect of these constants on telephone interference compared with the interference generated by one of the cars equipped with single phase series motors.

The laboratory test data and the car test data are being correlated and analyzed but with only preliminary results available at this writing. It is hoped that the information can be presented jointly by the parties involved at some time in the future.

A full discussion of the problems involved cannot be made until the foregoing analysis has been completed.

It is confidently predicted that rectifier motive power units will find wide use on present electrified systems and will hasten the electrification of additional railroad mileage.

References

1. The Rectifier Railway Car—A-C Supplied—D-C Driven, Richard W. Dodge. *Westinghouse Engineer* (East Pittsburgh, Pa.), volume 9, number 6, November 1949, pages 179–180.

2. Mercury Arc Power Converters in North America, AIEE Committee Report. *AIEE Transactions*, volume 67, number 2, 1948, pages 1031–59.

Discussion

D. R. MacLeod (General Electric Company, Erie, Pa.): The important fact in this paper is that once again a single-phase rectifier multiple-unit car is in revenue service energized from a 11,000-volt 25-cycle trolley. This test will answer several questions which can be answered only by extended operation in revenue service. The test is in the competent hands of two engineers who have had long and varied experience in a-c traction development and is being conducted under the watchful eyes of the engineers of the railroad which has had more experience than any other in pioneering developments in a-c traction. We applaud this effort to advance the art and offer our congratulations to the men who by their faith, skill, and perseverance have made the test possible.

The relationships of some parts of the contents of the paper are not clear to me. As I interpret the tabulation of harmonic currents, they are at 11,000 volts so that the tests of February 3, 1948, for example, represent 2,376 kva. As this is far greater than the maximum kilovolt-ampere input required by a single Pennsylvania Railroad multiple-unit car, the conclusion is that the tabulated results in the paper do not bear any relationship to the equipment that is in operation on the Pennsylvania Railroad. It would be helpful to know what the current harmonics were on the 11-kv side of the transformer on the car at the point where all the resistance in the controller was cut out, or at some other well defined connection at which the data were taken. It also would be helpful to know what per cent ripple there was in the current supplied to the d-c motors corresponding to the harmonics measured in the 11-kv input current.

C. C. Herskind (General Electric Company, Schenectady, N. Y.): This paper is of interest as it represents an application of mercury arc rectifiers that has been dreamed about for many years. Not only did engineers consider the use of rectifiers on a railway car at a very early date, but the subject has been revived from time to time.

As recently as 1944 General Electric engineers made extensive tests on sealed ignitrons under shock and vibration conditions simulating those encountered in railway service. At the same time load tests were made on d-c traction motors supplied from a 2-tube rectifier. These tests were made to establish the basic factors that affect the operation of d-c traction motors on a single-phase rectifier circuit.

In addition to the motor heating and commutation problem, there remains the problem of wave shaping. The 2-tube rectifier delivers two sinusoidal pulses of voltage to the motor load every cycle. In order to obtain smooth direct current, a large inductance is placed in series with the load. The rectifier, therefore, delivers square waves of current to the load. But these square waves also appear in the a-c lines where they must be reshaped to sinusoidal form.

The necessity for shaping the waves, that is, filtering on both d-c and a-c sides presents a serious space, weight and cost obstacle. Perhaps satisfactory wave shapes can be readily obtained on a single-car equipment. However, when a large number of cars operate on a 25-cycle system so that their combined load is a substantial part of the system capacity, more perfect filtering will no doubt be required in order to avoid excessive wave deformation. It would appear that the wave distortion caused by the 2-tube rectifiers may result in trouble both from telephone interference, generator heating, and system over-voltages. We would appreciate the author's comments on this problem.

L. F. Roehmann (Anaconda Wire and Cable Company, Hastings-on-Hudson, N. Y.): In 1935 and 1936 the German Reichs Railroads embarked upon a rather interesting experiment. They electrified two sections, totalling about 35 miles, of the Hoellentalbahn, in the Black Forest, with 50 cycles-per-second single-phase alternating current which was taken, by means of a Scott-connected transformer, from the public 3-phase supply system. Four experimental locomotives were built for this service, two of them (built by Allgemeine Elektrizitats Gesellschaft and Brown Boveri and Company) units with steel-tank rectifiers and d-c traction motors. A short description of this work was given by the discussor in Railway Age of August 28, 1937,[1] where a photo of the Brown Boveri locomotive is shown.

At that time, I was interested in the inductive co-ordination aspect of this work. After leaving Germany, and due to the war, I lost track of subsequent developments. However, I am sure that valuable information of both the power and the inductive interference aspects can still be secured. I recommend that this be done and that the experience be used to good advantage for the work now in progress in this country. As to inductive interference, it should make no difference whether the direct current for the traction motors is obtained through ignitrons, or from a multianode rectifier.

References

1. Electrification at Commercial Frequencies, Ludwig F. Roehmann, *Railway Age* (New York, N. Y.), volume 103, number 9, August 28, 1937, page 273.

P. A. Jeanne (Bell Telephone Laboratories, Inc., New York, N. Y.): The Bell Telephone Laboratories appreciated the opportunity afforded by the Pennsylvania Railroad and the Westinghouse Company to take part in the tests of the rectifier motive-power unit described in the paper by Mr. Hibbard and his associates. Comprehensive noise influence measurements of the small rectifier powered unit used in the Pennsylvania Railroad tests were made together with comparative tests of the influence of the present conventional motive power.

From these data, it is hoped to reach a reasonably reliable estimate of what would be expected in the way of influence from a large rectifier powered passenger or freight locomotive operating at 25 cycles. Also, it is hoped that these estimates may be supplemented by actual tests of such a large locomotive. The authors feel that they also can successfully filter rectifier power equipment operating at 60 cycles.

This frequency of operation is naturally of more concern to communication engineers because the important harmonics produced in the a-c supply to the rectifier fall higher in the voice frequency range where the influence per ampere of current is more important, and because 60-cycle systems from which the railway would draw its power might also be involved in close exposures with communication lines. We are, therefore, somewhat less optimistic regarding the possibilities of successfully mitigating inductive interference from 60-cycle operation than we are concerning 25-cycle operation and will welcome any opportunity to check results in field tests.

L. J. Hibbard: In reply to D. R. MacLeod's discussion we wish to state the test amperes of February 3, 1948 represent the approximate line amperes for a 5,000-horsepower locomotive under a 24,000-volt trolley. The inductance in the d-c motor circuit was adjusted to give approximately a 30 per cent ripple in the direct current for this test.

The harmonic measurements made during the joint tests last summer were obtained with Bell Telephone Laboratory noise meters which gave the *IT* product due to all harmonics but did not give a measure of the individual harmonics.

Typical *IT* products obtained with these noise meters during our tests are given in Table I of the discussion.

With reference to C. C. Herskind's discussion, we do not expect all the harmonics from a large number of rectifier motive power units operating simultaneously on an

electrified railroad to add up arithmetically. The phase angle between the line voltage and the locomotive transformer line amperes on various rectifier motive-power units will vary a few degrees for each different trolley location.

If we assume that the fundamental amperes of one motive power unit lags 4 degrees 23 minutes behind the fundamental amperes of a second motive power unit, the phase difference between the two groups of harmonics associated with each of these fundamentals will rapidly increase as the frequency of the harmonic increases.

If the fundamentals are 4 degrees 23 minutes apart, the third harmonics will be approximately 13 degrees 9 minutes apart, the fifth harmonics will be approximately 21 degrees 55 minutes apart, the seventh will be approximately 30 degrees 41 minutes apart, the ninth will be approximately 39 degrees 27 minutes apart, and so forth, and the 41st harmonics will be approximately 180 degrees apart.

In the case of adjacent motive-power units, we can set up the motive-power unit circuit constants or angle of delay in firing to insure a few degrees difference in the phase position of their line ampere fundamentals.

Table I

Car and Status	Telephone Interference *IT* Product—1935 Weighting Measured on Test Train Maximum
412 motor car	2,500
Rectifier car—without filters	1,800
Rectifier car—with filters	280

Likewise in the case of independent rectifier units on a given motive-power unit, we also can set up a few degrees difference in the phase of their fundamental amperes received from a common transformer.

The author wishes to thank Mr. Roehmann for his discussion.

Westinghouse representatives from East Pittsburgh and England visited the Hoellentalbahn Black Forest 50-cycle electrification recently and report that the rectifier motive power units are performing successfully.

They also report that telephone conversation over the railroad's telephone system was perfectly satisfactory while the rectifier locomotives were drawing current from the line.

The writer has no knowledge of any noise measurements or harmonic analyzer measurements being made by the Germans on this rectifier locomotive application.

Mr. Jeanne's discussion was very interesting. We hope to obtain joint noise tests on a 25-cycle rectifier locomotive some time during 1951 and have hopes of obtaining tests on a 50-cycle or a 60-cycle rectifier motive power unit a few months thereafter.

Future 60-cycle railroad electrifications will almost surely involve higher trolley voltages and the writer expects to see the trolley voltage approach 50,000 volts.

A 5,000 horsepower 25-cycle locomotive will draw approximately 400 amperes at 12,000 volts, while a 5,000-horsepower 60-cycle locomotive will draw approximately 100 amperes at 48,000 volts.

Hence, an increase in trolley voltage from 12,000 volts to 48,000 volts will reduce the trolley current sufficiently to largely offset the increase in *IT* product caused by the fact that the important harmonics (for 60-cycle trolley) fall higher in the voice frequency range

New Lightning Arrester Standard

H. R. STEWART
FELLOW AIEE

F. M. DEFANDORF
FELLOW AIEE

FOR the past several years there have been three separate AIEE Standards bearing on the lightning protective devices field; namely, Report on Proposed Standard for Protector Tubes, American Standards for Lightning Arresters for Alternating Current Power Circuits, and Proposed Standard for Expulsion Type Distribution Lightning Arresters,[1,2,3] all prepared under the sponsorship of the AIEE Protective Devices Committee. By the time of the publication of the last Standard mentioned above, it was evident that there was much material in these various Standards which had a common application, and many of the definitions and test procedures were common. W. J. Rudge, then Chairman of the Lightning Protective Devices Subcommittee of the Protective Devices Committee, perceived the advantages of merging all three Standards, and set up a working group for such a project. It was believed that the combining of Standards on lightning protective devices should not only lead to improved nomenclature but would bring into sharper focus the inherent characteristics of the different species of lightning arresters, and at the same time would improve the accessibility of desirable information.

Early in the course of the undertaking, the Working Group* encountered a tendency to incorporate in the Standard material which was of considerable importance in the proper application of lightning arresters. After very careful consideration by the Lightning Protective Devices Subcommittee, it was the consensus of opinion that inasmuch as this material concerned primarily the nature of the associated circuits and lines, a separate project be set up to devise a suitable application guide for lightning arresters that would fulfill the needs of the user more completely than one could hope for by inclusion of a few precautionary suggestions in the Standard. Even with this desirable simplification, the working group of users' and manufacturers' engineers found a number of loose ends to tie together in their task of improving and combining, through nine drafts, earlier efforts into a single standard.

A perusal of the definitions in the new Lightning Arrester Standards for Valve and Expulsion Arresters,[4] will show several differences adopted primarily to improve clarity and definiteness of expression. These new definitions have been correlated with the current revision being made in American Standard Definitions of Electrical Terms.[5]

It will be noted that the term "protector tube" has been superseded by "expulsion arrester" so that all devices covered by the new Standard are referred to as "arresters" of one type or another. Classifications such as "station type," "line type," "distribution type," and "secondary type" are not defined in the Standard, and it is left to the maker to apply such designations. However, the Standard does state the appropriate tests to apply to lightning arresters of these various classifications.

In the matter of discharge current withstand tests (formerly called discharge capacity) of lightning arresters and prorated sections, the requirements have been altered to bring them in line with tests that can be performed in existing laboratories. The formerly-specified 5 by 10 wave (with stated tolerances) has been changed to "a surge current with wavefront duration between 5 and 10 microseconds and wave-tail between 10 and 20 microseconds" having crest ampere values of 100,000 for station....., 65,000 for line and distribution, and 10,000 for secondary-arresters, it being specified that tests shall be on complete lightning arresters up to 9 kv or prorated characteristic elements whose ratings are 3 kv or greater, but need not exceed 9 kv. This restatement is in better accord with laboratory tests that can actually be made with existing surge-testing equipment.

With respect to duty cycle tests on expulsion lightning arresters, it is recognized that the severity of the test is very dependent on the voltage recovery rate of the test circuit. However, with the past lack of knowledge of the range of recovery rates on the circuits on which these devices are used in service, particularly on distribution circuits, it has not been possible to include in the Standard any specified voltage recovery voltage rates for the duty cycle test circuit with any assurance that they would reflect conditions found in service. At the present time a Joint Working Group of the Transmission and Distribution Committee and of the Lightning Protective Devices Subcommittee appointed to study rates of rise of recovery voltage on distribution systems has made considerable progress on this matter, both by field and laboratory tests. It is expected that the results of this broad-scale study will be valuable not only in the future revision of lightning arrester Standards but also to standardizing groups interested in fuses and other distribution type interrupting devices.

Similarly, it has not been possible to

*Membership of this Working Group has included: E. Beck, R. H. Earle, H. N. Ekvall, I. W. Gross, E. H. Grosser, D. D. MacCarthy, J. R. McFarlin, W. A. McMorris, A. M. Opsahl, W. J. Rudge, W. E. Rushlow, A. H. Schirmer, H. R. Stewart, J. M. Towner, H. B. Wolf, E. H. Yonkers, and F. M. Defandorf, *chairman*.

Paper 50-82, recommended by the AIEE Protective Devices Committee and approved by the AIEE Technical Program Committee for presentation at the AIEE Winter General Meeting, New York, N. Y., January 30-February 3, 1950. Manuscript submitted July 28, 1949; made available for printing December 8, 1949.

H. R. STEWART is with the New England Power Service Company, Boston, Mass., and F. M. DEFANDORF is with the National Bureau of Standards, Washington, D. C.

The new Standard covered by this paper, Lightning Arrester Standards for Valve and Expulsion Arresters,[4] was prepared under the sponsorship of the AIEE Protective Devices Committee, G. B. Dodds, *chairman*, and its Lightning Protective Devices Subcommittee consisting of H. A. Cornelius, F. M. Defandorf, R. H. Earle, Milan Getting, I. W. Gross, E. H. Grosser, H. W. Hartzell, T. H. Mawson, T. I. Eldridge, W. A. McMorris, A. M. Opsahl, W. E. Rushlow, A. H. Schirmer, J. M. Towner, E. R. Whitehead, E. H. Yonkers, and H. R. Stewart, *chairman*.

include in the new Standard[4] any values for radio influence tests due to lack of knowledge of requirements and pending extensive work by various industry groups needed before Standards can be formulated.

It will be noted that for special lightning arresters used for the protection of rotating machinery, the acceptance tests as to the current magnitude at which the discharge voltage test is made and the rate of rise of voltage for the impulse sparkover test are lower than those respectively required for Standard lightning arresters. This is in recognition of the fact that these special lightning arresters are usually applied in conjunction with wave sloping capacitors which materially change the service conditions under which the lightning arresters are called upon to operate.

Table I of the Standard specifying withstand test values for the assembled insulation of lightning arresters represents a considerable change from the similar table in Standard Number 28. Whereas the earlier Standard stated that "Where application is to be made of an arrester having a lower voltage rating than the rated voltage of the circuit on which it is to be used, such as on grounded-neutral circuits, the insulation test shall be that specified for the insulation class one step lower than the rated circuit voltage," the new Standard includes these intermediate ratings in the listed lightning arrester voltage ratings and assigns to them withstand test values which are interpolated between withstand test voltages assigned to the formerly listed next higher and lower ratings, each of which corresponds to Standard Basic Insulation Levels. It will be noted that no insulation classifications are assigned to these intermediate lightning arrester ratings.

The inclusion of the intermediate lightning arrester ratings in Table I in this manner is a compromise solution of a very difficult problem on which widely diverging views were held. One view was that whereas grounded neutral circuits usually are built with full insulation, grounded neutral lightning arresters used on those circuits also should have full insulation rather than insulation conforming with one basic insulation level step lower. On the other hand, this might mean a redesign of some of the intermediate voltage rating lightning arresters if they should conform to the basic insulation level of the fully insulated circuit on which they are used. Since a general redesign of lightning arresters may be imminent if the present deliberations of the Joint AIEE-EEI-NEMA Committee on Insulation Co-ordination should result in a revision of present Basic Insulation Levels, it did not seem wise to call for insulation values in the new Standard which would necessitate a possible interim redesign. It will be noted in view of this activity by the Joint Committee on Insulation Co-ordination that all values in Table I are to be considered, as expressed in a footnote, as interim values subject to revision when the report of the Joint Committee is issued. Also, the addition of the intermediate lightning arrester values to Table I should not be considered as a precedent for adding Basic Insulation Levels to an existing Standard list on the part of groups standardizing tests on individual types of apparatus.

Like all other Standards, the "revised and combined" Lightning Arrester Standard is not presented as the last word but rather as a closer approximation to a desirable Standard. More information as to better tests for Lightning Arresters will always be needed and the Standard will continue to be improved as the result of improved tests.

References

1. Report on Proposed Standard for Protector Tubes. AIEE Standard Number 24, July 1940.

2. American Standards for Lightning Arresters for Alternating Current Power Circuits. AIEE Standard Number 28, May 1944.

3. Proposed Standard for Expulsion Type Distribution Lightning Arresters. AIEE Standard Number 47, December 1945.

4. Lightning Arrester Standards for Valve and Expulsion Arresters. AIEE Standard Number 28A, January 1950.

5. American Standard Definitions of Electrical Terms. *ASA C42–1941*, AIEE, 1941.

No Discussion

Surge Protection of Cable-Connected Equipment

R. L. WITZKE
MEMBER AIEE

T. J. BLISS
ASSOCIATE AIEE

THE adequate surge protection of electric equipment connected to overhead lines through cable has been a subject of discussion for many years. The usual question is "How long can a cable be without requiring lightning arresters at the equipment in addition to those at the junction between the cable and overhead circuits?" This question is taking on increasing importance because of the trend toward the use of cable connections in unit substations. This practice has the advantages of decreased congestion in the vicinity of substations and of improved appearance, the latter being particularly important in residential districts. The use of cable does, however, influence the surge protection problem because of the added complications incident to the installation of lightning arresters close to the equipment being protected. With overhead connections, the generally accepted practice is to install lightning arresters as close as possible to the equipment, whereas with cable the more common practice is to install lightning arresters only at the junction between the cable and overhead circuits. The purpose of this paper is to review the latter practice and show the degree of protection afforded.

The general data included in this paper are based on analogue computer studies. Tests made on 15-kv power cable in the Impulse Laboratory showed that very good results could be obtained on the analogue computer. This is fortunate because the use of the analogue computer permits a study of the wide range in conditions that must be considered to obtain a complete picture of this important surge protection problem. The general data included permit an evaluation of the influence of the magnitude and rate-of-rise of surge currents, lightning-arrester discharge-voltage characteristics, cable surge impedance, as well as other factors. Typical oscillograms are included to show the general wave shape of the surges across the equipment.

Tables of permissible cable lengths are included for switchgear assemblies and oil-insulated transformers in the voltage classes up to, and including, 34.5 kv. These tables are based on surge currents with a 10,000-ampere crest and a rate-of-rise of 4,000 amperes per microsecond. The cable lengths based on these assumptions, which were considered reasonable and not severe, appear to be short when viewed in the light of experience, especially with oil-insulated transformers. This would indicate that certain probability factors, which are normally neglected, are important in these applications. These might include probable lightning-arrester characteristics and possibly the probable margins in equipment insulation levels for the surges encountered. Available data do not permit a detailed consideration of each of these probabilities at this time. A survey of current practices and experiences may be required before any table of values, completely acceptable to the industry, can be formulated. The tables included in this paper for oil-insulated transformers are believed to be fairly conservative and subject to modification as more data and experience are obtained. The table of values for switchgear assemblies are probably not as conservative as the values for oil-insulated transformers.

Application Guides

The studies reported in this paper are limited to the case of a single overhead circuit connected to a single metallic-sheath cable terminated in a circuit breaker or transformer, see Figure 1. The results thus obtained will be conservative when applied to cases involving a cable terminated in a bus having a multiplicity of circuits. It is assumed that the cable has a continuous metallic sheath bonded to the transformer case, or to the circuit-breaker frame. At the junction end a lightning arrester is connected between a phase conductor and the metallic sheath with leads of the shortest possible length.

Lightning-arrester ground resistances can be neglected because they will not have any practical influence on the conductor-to-sheath voltages in lead-covered cable. The surge characteristics of the transformer are represented by a capacitance, which is permissible for surges of short duration, such as obtained in this investigation. The same representation would apply for cases involving a circuit breaker, the only difference being in the magnitude of the capacitance.

It is assumed that any surge arriving at the junction between the overhead and

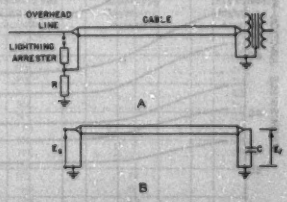

Figure 1. Circuit considered in general investigation and simplified circuits used in studies

Paper 50-83, recommended by the AIEE Protective Devices Committee and approved by the AIEE Technical Program Committee for presentation at the AIEE Winter General Meeting, New York, N. Y., January 30–February 3, 1950. Manuscript submitted November 2, 1949; made available for printing December 6, 1949.

R. L. Witzke and T. J. Bliss are both with the Westinghouse Electric Corporation, East Pittsburgh, Pa.

The authors acknowledge the helpful suggestions made by W. L. Teague, L. B. Rademacher, R. L. Harder, R. W. Beck, and A. M. Opsahl during the course of the investigations reported.

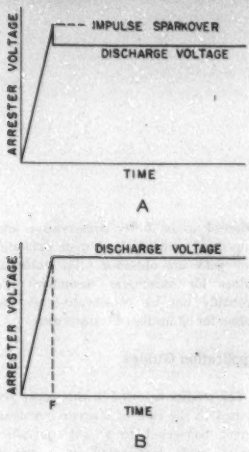

Figure 2 (left). Lightning arrester volt-time characteristics

A. Discharge voltage less than impulse sparkover voltage

B. Discharge voltage equal to impulse sparkover voltage

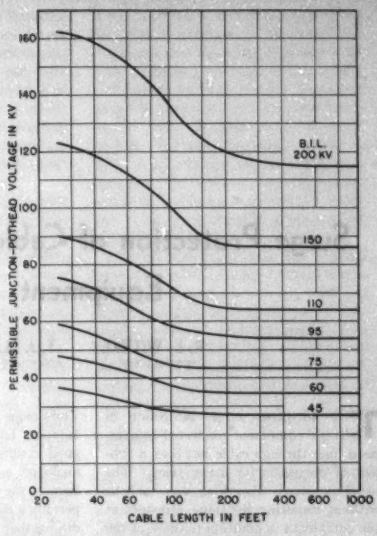

Figure 4 (right). Permissible junction-pothead voltage for Class II equipment

cable circuits has a uniform rate of rise. Based on this assumption, the voltage across the junction pothead will have a uniform rate of rise, except with short cables, where reflections from the equipment end may modify the junction-pothead voltage before the junction lightning arrester operates. With the longer cables, the lightning-arrester voltage will increase at a constant rate to the impulse sparkover value and then change to a discharge voltage drop determined by the current through the lightning arrester.

The lightning-arrester voltage will have the general shape shown in Figure 2(A) if the discharge voltage is less than the impulse sparkover voltage, or the shape in Figure 2(B) if the discharge voltage is equal to or greater than impulse sparkover voltage.

The voltage at the junction pothead will include lead drop as well as lightning-arrester voltage. The lightning-arrester leads will have an inductance of approximately 0.4 microhenry per foot, which gives a voltage of 0.4 kv per foot for each 1,000 amperes per microsecond rate-of-rise in the lightning-arrester current. The maximum lead drop will be present as long as the lightning-arrester current is changing at the assumed rate. As the lightning-arrester discharge voltage also is a maximum during the maximum rate-of-rise of current, it is permissible to add the lead drop directly to the lightning-arrester discharge voltage.

The studies are based on the assumption that excepting as modified by reflec-

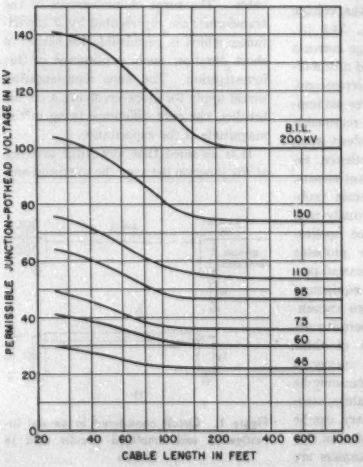

Figure 3 (left). Permissible junction - pothead voltage for Class I equipment

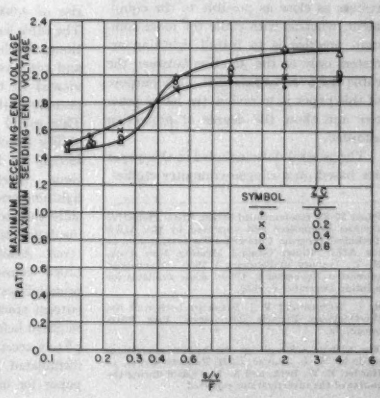

Figure 5 (right). Maximum receiving-end voltages expressed as a ratio to the maximum sending-end voltage. Data obtained from analogue computer studies

Table I. Assembled Switchgear Basic Insulation Levels

Rated Kilovolts	Basic Insulation Level, Kv
4.16	60 (45)*
7.2	95 (75)*
13.8	95 (75)*
14.4	110
34.5	150**
34.5	200

* Some circuit breakers have lower insulation levels in the open position as indicated by the values in parentheses. It is the intention of the industry to raise these values to the basic levels as soon as design improvements permit.
** The 150-kv basic insulation level may be used in applications where adequate surge protection is provided.

tions from the equipment end of the cable, the total voltage across the junction pothead rises at a uniform rate to a maximum value determined by the lightning-arrester discharge voltage plus lead drop, and that this maximum voltage is maintained for at least twice the cable propagation time. Based on this assumption the total voltage across the junction pothead has the general shape shown in Figure 2(B). The front F is obtained by dividing the maximum voltage across the junction pothead by the rate-of-rise of voltage across the pothead. A front of 0.4 microsecond was used in the analogue computer studies; however, the results are generalized to permit an evaluation of other fronts.

In the cases where the junction-pothead voltage is modified by reflections from the equipment end before the maximum voltage is reached, the front F is defined as the maximum junction-pothead voltage divided by the initial rate-of-rise of voltage. The reflections therefore do not enter into the definition of the front F.

Equipment Insulation Levels

For surge protection purposes it is necessary to differentiate between equipments having only a full-wave test level, and equipments having full-wave, chopped-wave, and front-of-wave levels. Conservative practices will require that the surge voltages be limited to the full-wave level whenever the standards do not specify chopped-wave or front-of-wave levels. In the case of apparatus having higher short-time levels, it should be possible to exceed the full-wave levels when the applied surge is of short duration. For these reasons the equipments normally encountered in cable-connected applications have been divided into two classifications, as follows:

Class I

Switchgear assemblies.
Dry-type distribution and power transformers.

Class II

Liquid-filled transformers.
Dry- and compound-filled instrument transformers.

The basic insulation levels for switchgear assemblies are given in Table I. The levels for dry-type distribution and power transformers are included in Table IV. Protection for Class I equipments should be based on limiting the surge voltages at the equipment to the basic insulation levels.

In the case of Class II apparatus it should be possible to exceed the basic insulation levels in cable-connected applications where the surge voltages are of short duration. The permissible overvoltage, however, should be associated with the wave shape of the applied surge. As these wave shapes vary over a wide range and differ considerably from standard test waves any exact determination of the permissible overvoltage is impossible at this stage of the art. The authors have derived an integration method for evaluating the disruptive effect of surges of nonstandard wave shape. However, the method is not proposed for general application purposes at this time. The authors have chosen to co-ordinate with the chopped-wave level of Class II apparatus, using the integration method as a guide in evaluating the adequacy of the protection provided.

Application Tables. Tables II and III give the maximum permissible cable lengths for Class I and Class II equipments for basic insulation levels between 45 and 200 kv. If these lengths are exceeded in any application, lightning arresters must be installed at the equipment, in addition to those at the junction pothead, or the application should be studied in detail, using procedures discussed in a later section. The tables are based on the following assumptions:

1. Protection is provided for lightning-arrester currents of 10,000 amperes.
2. Lightning-arrester discharge voltages as given in Table VII.
3. Lightning-arrester lead lengths and voltages as given in Table VIII.

Table II. Suggested Maximum Cable Lengths With Class I Equipment

Equipment Basic Insulation Levels, Kv	Lightning Arrester Rating,* Kv	Maximum Cable Length, Feet: Station-Type Lightning Arrester	Line-Type Lightning Arrester	Distribution Lightning Arrester
45	3	NL		70
60	3	NL		NL
	6	NL		25
75	3	NL		NL
	6	NL		56
	9	68		S
95	6	NL		NL
	9	NL		34
	12	76		S
	15	30		S
110	9	NL		76
	12	NL		32
	15	70		S
150	20	94	S	
	25	30	S	
200	30	74	S	
	37	S	S	

NL means no limit to cable length.
S means cable length too short to consider.
* Rating of arrester at junction between cable and overhead circuits.

Table III. Suggested Maximum Cable Lengths With Class II Equipment

Equipment Basic Insulation Level, Kv	Lightning Arrester Rating,* Kv	Maximum Cable Length, Feet: Station-Type Lightning Arrester	Line-Type Lightning Arrester	Distribution Lightning Arrester
60	3	NL		NL
	6	NL		83
75	3	NL		NL
	6	NL		NL
	9	NL		80
95	9	NL		75
	12	NL		32
	15	80		S
110	9	NL		NL
	12	NL		90
	15	NL		30
150	20	NL	77	
	25	90	S	
200	30	150	45	
	37	64	S	

NL means no limit to cable length.
S means cable length too short to consider.
* Rating of lightning arrester at junction between cable and overhead circuits.

Table IV. Maximum Receiving-End to Sending-End Voltage Ratios for Dry-Type Distribution and Power Transformers

Insulation Class, Kv	Basic Insulation Level, Kv	Lightning Arrester Rating,* Kv	Junction Pothead Voltage	E_r/E_s
1.2	10	3	15.0	0.67
2.5	20	3	15.0	1.33
5.0	25	3	15.0	1.67
3.66	35	6	28.0	1.25
15	50	12	52.0	0.96

* Rating of lightning arrester at junction between cable and overhead circuits.

4. The maximum rate-of-rise of the junction-pothead voltage results from a 4,000-ampere-per-microsecond current surge into the cable, and the cable surge impedances in Table IX.

5. Terminal equipment capacitances of zero or 3,200 micromicrofarads, depending upon which value results in the highest voltage across the equipment.

6. The maximum equipment voltage is limited to the full-wave level for Class I equipment, and to the chopped-wave level for Class II equipment.

In using these tables it is necessary to know the basic insulation level (BIL) of the equipment being protected, and the type and rating of the lightning arrester at the junction between the overhead and cable circuits. The lightning-arrester rating is determined by the system voltage and grounding conditions as in any other application. The cable lengths given in the tables will be shorter than necessary in many cases because of the conservative assumptions that had to be made to obtain a table of values independent of cable surge impedance, equipment capacitance, magnitude and shape of incoming surge, and so forth. Less conservative applications can be made only by a detailed consideration of all the factors involved.

Dry-Type Distribution and Power Transformers. The proposed insulation levels for dry-type distribution and power transformers are given in Table IV. These levels are such that adequate protection cannot be provided without lightning arresters at the transformers, whenever the equipment is connected to exposed overhead lines through cable. Even with station-type lightning arresters at the junction between the overhead and cable circuits, the junction pothead voltage is so high in terms of the transformer levels that adequate protection is not provided even with short cables, unless additional lightning arresters are installed at the transformers. Assuming station-type lightning arresters at the junction between the overhead and cable circuits, the junction pothead voltage based on the lightning-arrester and lead voltages in Tables VII and VIII will be as given in Table IV. Dividing these voltages by the transformer insulation levels gives the maximum permissible receiving-end to sending-end voltage ratios. Comparing these ratios in Table IV with the data in Figure 5 shows that lightning arresters are generally required at the transformers.

A more comprehensive discussion of the protection of these transformers is given in reference 1.

Application Curves. The curves in Figures 3 and 4 give the maximum permissible voltages across the junction pothead for cable lengths up to 1,000 feet. These curves are based on the same conditions as used in preparing the application tables, excepting that no assumptions are made relative to lightning arrester characteristics and lead lengths. These curves permit an evaluation of the influence of lightning arrester discharge voltages and lead lengths on the permissible cable lengths. In a particular application, where the cable length is known, the permissible junction-pothead voltage can be obtained from the curves. A study then is made to determine whether available lightning arresters and possible lead lengths will limit the voltage to this level.

Application of Basic Data

The data in Figure 5 should be used when an application is to be checked in detail. These data are expressed in terms of $(s/v)/F$ and ZC/F ratios, where

s = cable length in feet

v = velocity of surge propagation in feet per microsecond

Z = cable surge impedance

C = equivalent surge capacitance of terminating equipment in microfarads

F = front in microseconds of surge voltage across the junction pothead

Some discussion of these variables is required as a basis for using the data in Figure 5.

The velocity of propagation of surges in power cables depends only on the dielectric of the cable and never varies appreciably from 500 feet per microsecond for oil-impregnated paper-insulated cables. Little general data are available on the effective capacitance of equipment to surges of short duration. Typical values will range between several hundred micromicrofarads for circuit breakers and 1,000 to 3,000 micromicrofarads for transformers. The capacitance C appears in the problem as a product with the cable surge impedance Z, the resulting ZC product being the time constant of the circuit consisting of the cable and the terminal equipment. The maximum practical ZC/F ratio is estimated at 0.4, which is obtained with a 50-ohm cable, a capacitance of 3,200 micromicrofarads, and a front of 0.4 microsecond. The minimum ZC/F ratio will be very close to zero. A study of Figure 5 will show that the surge voltage at the equipment will not vary more than ±3 per cent as the ZC/F ratio varies between zero and 0.4, which indicates that it is not essential to have exact data on the terminating capacitance. It is suggested that protection practices be based on a capacitance of zero or 3,200 micromicrofarads, depending on which value gives the most severe voltage at the terminal equipment.

The cable surge impedance Z appears

Table V. Surge Impedance of Cables

Conductor Size, Thousand Circular Mils	Voltage Class, Kv 4–5	7–8	14–15	22–23	34–35
83.69	14.4	19.6	25.6	30.5	
133.1	12.0	16.6	21.8	26.3	32.8
250	9.0	12.8	17.0	21.0	26.6
500	6.8	9.7	13.0	16.2	20.8
1,000	5.1	7.2	9.8	12.1	16.0

Note: The above impedances are for single-conductor lead-covered cables. The effective impedances of 3-conductor belted cables may be estimated as $1^1/_3$ the values given.

Table VI. Influence of Line Insulation Level on Protection Provided

Line* Insulation Level, Kv	Stroke Current, Amperes	Protected Distance, Feet	Strokes** Per 100 Miles Per Year	Probable Protection Period, Years
250	10,000	125	50	80
	20,000	62.5	30	266
	40,000	31.25	10	1,600
500	10,000	250	50	40
	20,000	125	30	133
	40,000	62.5	10	800
1,000	10,000	500	50	20
	20,000	250	30	66.5
	40,000	125	10	400

* Insulation level to ground.
** Data from reference 2.

Table VII. Maximum Lightning Arrester Voltages For Co-ordination Purposes

Lightning Arrester Rating, Kv	Lightning Arrester Voltage, Kv: Station-Type Lightning Arrester[1]	Line-Type Lightning Arrester[2]	Distribution Lightning Arrester[2]
3	12		21
6	24		38
9	36		57
12	47		69
15	58		85
20	77	101	
25	97	122	
30	116	149	
37	142	181	

[1], [2] Average discharge voltage at 10,000 amperes, plus one-half of maximum positive tolerance.
[2] Average discharge voltage at 10,000 amperes, plus full positive tolerance.

in the ZC product, as discussed before, and also influences the magnitude of the front F. It will be recalled that the front F was defined as the ratio of the maximum voltage to the rate-of-rise of voltage at the junction pothead. Assuming a current surge having a rate-of-rise of K kiloamperes per microsecond coming in over the overhead circuit, the rate-of-rise of voltage at the junction pothead is $2Z_1ZK/(Z_1+Z)$. The overhead-circuit surge impedance Z_1 appears in both the numerator and denominator, and is large by comparison to the cable surge impedance, so practical variations in this impedance will have only a small influence on the rate-of-rise of voltage at the junction pothead. The use of a typical value of 500 ohms should, therefore, be satisfactory. The cable surge impedance, however, has considerable influence on the rate-of-rise of voltage at the pothead, and consequently on the front F, so should be retained as a variable. Typical values are included in Table V.

Surge Currents. The front F is a function of the maximum voltage and the maximum rate-of-rise of voltage across the junction pothead, and, therefore, depends on the magnitude and rate-of-rise of the surge currents reaching the junction between the overhead circuit and the cable. Surges originating at some distance will be limited in magnitude by the overhead-line insulation level and surge impedance. Assuming a line level of 1,000 kv, which is probably higher than used on low-voltage circuits, even with woodpole construction and no down leads, the maximum current in an incoming surge is limited to less than 2,000 amperes. Considering reflections, the lightning-arrester current might approach twice this value, or 4,000 amperes. If low-voltage circuits were protected with properly designed shielding, it would be considered adequate to base equipment protection on lightning-arrester currents of this order of magnitude. However, as shielding is not generally used over the lower voltage lines, consideration should be given to close-in strokes to the line conductors. For such strokes, the struck point may be protected from flashover by reflections from the cable, in which case the lightning-arrester current may approach the stroke current.

The distance over which these reflections can protect the line insulation depends on the rate-of-rise of stroke current and on the line insulation level. Assuming a rate-of-rise of current of 4,000 amperes per microsecond, which might correspond to a 10,000-ampere stroke with a $2^1/_2$ microsecond front, the voltage at the struck point will rise at 1,000 kv per microsecond, assuming a 500-ohm line. If the line insulation level to ground is 500 kv at this rate-of-rise, reflections must return from the cable in 0.5 microsecond to prevent flashover, which means the struck point must be within 250 feet of the cable junction. The probability of exceeding 10,000 amperes in a stroke is 50 strokes per 100 miles per year,[3] or one stroke in 40 years to a 250-foot line section. If protection were based on a 10,000-ampere stroke with a $2^1/_2$-microsecond front, the protection limit would be exceeded on an average of once in 40 years. This, however, does not mean that apparatus failures would result this often because probable lightning-arrester characteristics and equipment margins, which were not considered, enter into the overall probability picture.

The data in Table VI show the influence of line insulation level on the protection afforded if such protection is based on the stroke currents given in the table. These results are based on a stroke current having a $2^1/_2$-microsecond front, which is probably on the conservative side. It is evident that the line insulation level is a primary factor in the surge protection of cable-connected equipment. In any particular application, where the line insulation level is known, it is possible to select a lightning-arrester current for co-ordination purposes and estimate the probability of exceeding this current. However, for general application purposes it would be highly desirable to simplify procedures by basing all excepting special cases on the same lightning-arrester current. With this in mind, the authors have tentatively selected a current having a magnitude of 10,000 amperes and a rate-of-rise of 4,000 amperes per microsecond. The calculated results in Table VI indicate that this protection limit might be exceeded once in 40 years if the line insulation level is as high as 500 kv to ground. Field studies show that approximately 0.8 per cent of the current discharges in station lightning arresters might exceed 10,000 amperes.[3] By comparison to the 4,000 amperes per microsecond rate-of-rise, the highest rate ever recorded in an arrester was between 5,000 and 5,500 amperes per microsecond.[4]

Lightning Arrester Characteristics. The published information on valve-type lightning arresters includes average impulse sparkover and discharge voltages, and permissible tolerances. Only a small percentage of the lightning arresters manufactured will have positive tolerances exceeding one-half the permissible maximum values. For this reason the authors have chosen to base protection of cable-connected equipment on lightning-arrester characteristics equal to the average published values plus one-half the permissible positive tolerances. The only exception is the discharge voltage of distribution lightning arresters, in which case the maximum tolerance is used. This exception is made because all manufacturers do not design to the same average discharge voltage in these lightning arresters, and consequently a larger percentage of these lightning arresters may

Table VIII. Maximum Lead Drops Assumed in Tables II and III

Insulation Class, Kv	Lead Drop, Kv	Permissible Lead Length, Feet
5	3	1.88
8.66	4	2.50
15	5	3.12
25	6	3.75
34.5	8	5.00

Note: Lead length is based on inductance of 0.4 microhenry per foot and 4,000-amperes-per-microsecond rate-of-rise.

Table IX. Calculated Rate-of-Rise of Junction-Pothead Voltage

Cable Insulation Class, Kv	Cable Surge Impedance, Ohms	Rate-of-Rise,* Kilovolts Per Microsecond
4–5	19.2	77
7–8	26.1	104
14–15	34.1	138
22–23	40.6	163
34–35	43.7	175

* Based on 4,000 amperes per microsecond into cable.

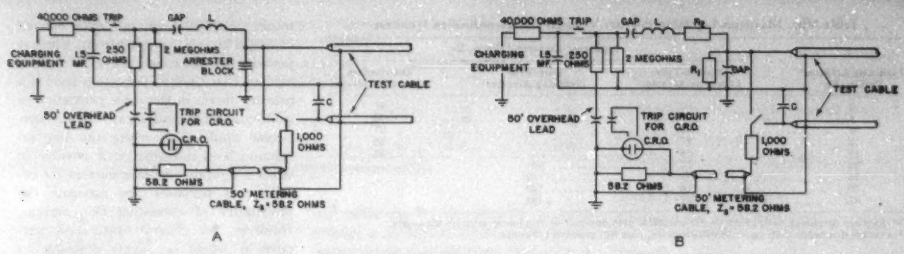

Figure 6. Impulse Laboratory test circuits

A. Sustained-tail surge applied
B. Chopped wave applied

have discharge characteristics exceeding those that would be obtained if only one-half the permissible tolerance were used. The maximum lightning-arrester voltages used for co-ordination purposes are given in Table VII for ratings up to 37 kv. These are based on the lightning-arrester discharge voltages at 10,000 amperes, including tolerances as discussed above.

Lightning Arrester Leads. Careful consideration should be given to the length of lightning arrester leads because approximately 1.6 kv will appear across each foot of lead at discharge currents of 4,000 amperes per microsecond. The voltages given in Table VIII have been assumed for general co-ordination purposes and are based on an inductance of 0.4 microhenry per foot of lead and a current rate-of-rise of 4,000 amperes per microsecond. The lead lengths required to produce these voltages also are included. The general data in this paper permit an evaluation of the protection afforded in those applications where the lead lengths differ from those in Table VIII.

Evaluating the Front F. Having established the maximum voltage across the junction pothead, which is the lightning-arrester voltage plus lead drop, it is next necessary to determine the maximum rate-of-rise of voltage across the pothead to evaluate the front F. As given in a previous section, the rate-of-rise of voltage is equal to $2Z_1ZK/(Z_1+Z)$, where Z_1 and Z are the overhead line and cable impedances, and K is the rate-of-rise, in kiloamperes per microsecond, of the incoming surge. The front F, in microseconds, is then obtained by dividing the total junction pothead voltage by the rate-of-rise of pothead voltage.

For general application purposes, the authors have assumed a current with a 4,000-ampere-per-microsecond front entering the cable. This rate-of-rise multiplied by the maximum cable surge impedance expected in any voltage class gives the rates of voltage rise in Table IX.

Illustrative Example. To illustrate the application of the basic data included in Figure V, a typical case will be reviewed in detail. In this example the following conditions are assumed:

200-foot 15-kv power cable with a surge impedance of 25 ohms.

Voltage at terminal equipment to be limited to 95 kv.

Terminal equipment capacitance = 1,000 micromicrofarads.

Lightning-arrester lead length = 3 feet.

Protection to be based on a surge current with 10,000 ampere-magnitude and 4,000-amperes-per-microsecond rate-of-rise.

The lowest voltage lightning arrester normally used with 95-kv equipment is the 12-kv unit. Assuming a 12-kv station-type lightning arrester, the maximum lightning-arrester voltage is 47 kv as given in Table VII. Based on 0.4 microhenry per foot, the lead drop is 4.8 kv, giving a total voltage of 51.8 kv across the junction pothead.

The maximum rate of rise of voltage across the junction pothead is equal to 100 kv per microsecond, which is based on a 4,000-ampere-per-microsecond surge into a 25-ohm cable.

$$\text{Front } F = \frac{51.8}{100} = 0.518 \text{ microsecond}$$

$s = 200$ feet

$s/v = 200/500 = 0.4$ microsecond

$$\frac{s/v}{F} = 0.4/0.518 = 0.771$$

$$\frac{ZC}{F} = \frac{25 \times 1{,}000}{0.518} \times 10^{-6} = 0.0483$$

From Figure 5

$E_r/E_a = 1.96$

$E_r = 1.96E_a = 1.96 \times 51.8 = 102$ kv

As this voltage exceeds the permissible voltage of 95 kv, the protection is inadequate. Protection cannot be provided for a 10,000-ampere 4,000-ampere-per-microsecond surge without additional lightning arresters at the equipment. If the terminal apparatus were in Class II, having a 95-kv full-wave level and a 110-kv chopped-wave level, the protection would be considered adequate without additional lightning arresters at the equipment.

General Studies

This part of the paper discusses in some detail the impulse laboratory and analogue computer studies made to obtain the basic data used in formulating the application guides in the first part of the paper. In general, the procedure consisted of making tests in the Impulse Laboratory on 15-kv power cable, and then using these data to show that satisfactory

Table X. Impulse Laboratory Test Results With Sustained Waves Applied

Test Number	Cable Length, Feet	Front, Microseconds	Terminating Capacitance, Micromicrofarads	Maximum Applied Voltage, Kv	E_r/E_a
61–62	1,000	1.1	0	10	1.93
63–64		1.1	0	9.8	1.92
65–67		1.1	500	10.0	1.84
68–70		1.1	2,000	9.9	1.90
71–73		1.1	6,300	9.7	1.91
74–75		0.5	0	12.2	1.83
76–80		0.5	0	12.0	1.87
81–83		0.5	0	12.4	1.93
84–86		0.5	2,000	11.5	1.92
87–89	200	0.5	0	12.0	1.91
90–92		0.5	500	11.6	1.87
95–97		0.5	2,000	11.6	1.92
98–100		0.5	6,300	11.2	1.98

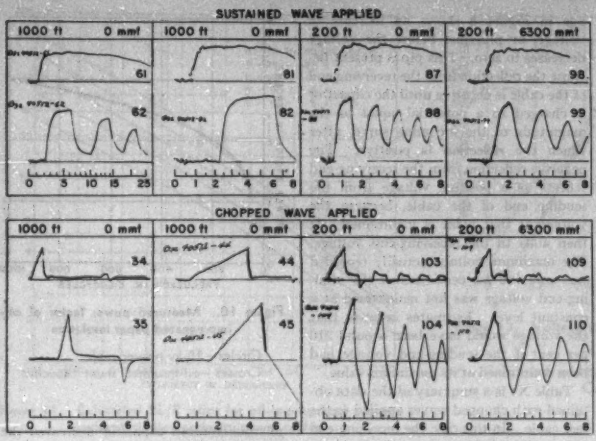

Figure 7. Typical oscillograms obtained in Impulse Laboratory tests

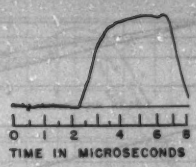

Figure 8. Surge voltage across a 14,300-micromicrofarad capacitor at the end of a 1,000-foot cable

results could be obtained by making the general studies on the analogue computer.

Impulse Laboratory Tests

In order to obtain fundamental data on the propagation of surge voltages through cables, a series of tests was conducted in the Impulse Laboratory on 200- and 1,000-foot lengths of 15-kv 2/0 single-conductor lead-covered cable. In making the tests the cable was removed from the reel and looped back and forth on the dry concrete floor in the laboratory. This precaution was taken to rule out the possibility of extraneous effects due to contact or capacitance between adjacent turns on a reel. The two ends of the cable were brought to a common point and the lead sheath bonded to the surge generator ground. Steps were taken to keep terminal lead lengths as short as physically possible. The general arrangement of the laboratory circuits is illustrated in Figure 6. Tests were made with an applied wave having a sustained tail and also with an applied wave, chopped on the front. The sustained-tail tests were made by discharging the surge generator into a 3-kv station-type lightning arrester block connected conductor-to-sheath at one end of the cable. The front was controlled by inductance in series with the surge generator. In making the chopped-wave tests, the lightning arrester block was replaced by a sphere gap, and the front controlled with resistance in parallel with the gap, and resistance and inductance in series with the generator.

Six records were taken at each end of the cable for each test condition, primarily to show that consistent records were being obtained.

Table X summarizes the results of the tests made with an applied voltage having a sustained tail. Terminating capacitance values up to 6,300 micromicrofarads were used with both cable lengths. The maximum value of the applied surge is given in kilovolts, and the crest receiving- or remote-end voltage is expressed as a ratio to the applied voltage. The receiving-end voltages generally fall between 1.83 and 1.93 times the applied voltage for the 1,000-foot cable, the results being substantially independent of the wave front and the terminating capacitance. The voltages recorded in the 200-foot-cable tests range between 1.87 and 1.98, the highest value being obtained with a 6,300-micromicrofarad terminating capacitance. The tests do show that the receiving-end voltages approach, within about 5 per cent, the theoretical figure of 2.0 for an open-end cable without loss, indicating that attenuation is not a primary factor in cable lengths up to 1,000 feet. It also is apparent that attenuation does not increase directly with cable length.

The oscillograms in Figure 7 are typical records obtained in the tests made with an applied surge having a sustained tail. Oscillogram 88 shows the receiving-end voltage for the case of a 0.5-microsecond-front wave applied to a 200-foot cable, open circuited at the receiving end. The maximum receiving-end voltage is approximately 191 per cent of the crest value of the applied voltage. Oscillogram 82 shows a receiving-end voltage of 193 per cent for the same surge applied to a 1,000-foot cable, open circuited at the receiving end. These data show that attenuation factors obtained from tests on one cable length cannot be used to calculate attenuation in other cable lengths. If attenuation were directly proportional to cable length, the over-voltage recorded on a 1,000-foot cable would have been considerably lower than on a 200-foot cable. The fact that the recorded voltage is higher on the longer cable is not

Table XI. Impulse Laboratory Test Results With Chopped Waves Applied

Test Number	Cable Length, Feet	Front Microseconds	Terminating Capacitance, Micromicrofarads	Maximum Applied Voltage, Kv	E_r/E_a
56–59	1,000	0.45	0	10.3	1.46
34–35		0.5	0	11.1	1.50
52–53		1.5	0	11.1	1.77
28–29		1.7	0	11.2	1.78
38–41		1.7	0	11.2	1.77
32–33		2.5	0	11.0	1.83
44–46		3.5	0	11.2	1.94
47–48		3.5	0	11.1	1.88
103–4	200	0.7	0	11.7	1.97
105–6		0.7	500	12.0	1.87
107–8		0.7	2,000	11.8	1.90
109–10		0.7	6,300	11.6	1.87
113–14		2.2	500	12.1	1.17
115–16		2.2	2,000	12.0	1.19
117–18		2.2	6,300	12.2	1.19
119–20		4.2	0	11.4	1.09
121–22		4.2	500	11.1	1.12
123–24		4.2	2,000	11.2	1.11
125–26		4.2	6,300	11.3	1.12

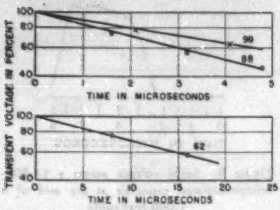

Figure 9. Plot of transient components of surge voltages from oscillograms 62, 88, and 99 of Figure 7

significant because the difference is less than the accuracy expected in reading the oscillograms.

An inspection of oscillogram 82, Figure 7, shows that attenuation is much larger on the front than on the tail of the wave. On the front, when the rate-of-change of current in the cable is high, the current penetration into the surface of the copper and lead is very small, resulting in a large effective resistance. The lower rate-of-change of current on the tail permits a deeper current penetration and a lower effective resistance. It will be noted, however, that there is no abrupt change in attenuation because time is required for the current to redistribute in the conductors. Shunt losses will also be higher on the front when the rate-of-change of voltage across the cable insulation is a maximum. These factors make the analytical determination of attenuation extremely difficult.

Oscillogram 62, Figure 7, was recorded on a 1,000-foot open-end cable with the front of the applied surge increased to 1.1 microseconds. Several cycles of the oscillation are included to show the general attenuation of the open-end voltage. The maximum receiving-end voltage is 193 per cent of the applied voltage, which is the same as recorded with a 0.5 microsecond-front applied surge. This shows that, within limits, the front has little influence on the maximum voltage. This condition should hold for fronts as long as twice the cable propagation time.

In obtaining oscillogram 99, Figure 7, the 200-foot cable was terminated in a 6,300-micromicrofarad capacitor. The receiving-end voltage was 198 per cent as compared with 191 per cent recorded without the capacitor termination, indicating that the maximum voltages are not obtained with open-end cables. In order to obtain a better picture of the influence of capacitance, a 1,000-foot cable was terminated in a 14,300 micromicrofarad capacitor. The receiving-end voltage in Figure 8 shows an increase in voltage, or pip, just before the voltage decreases to zero. This pip is present because the reflection from the receiving end of the cable is negative until the capacitor is charged to a potential equal to the magnitude of the incoming surge, after which the reflection is positive. The negative reflection from the receiving end reflects as a positive voltage from the sending end of the cable, because the voltage at that point is maintained. It then adds to the receiving-end voltage. The maximum voltage actually recorded was only 192 per cent because the sending-end voltage was not maintained at a constant level. Estimates indicate that the voltage would have been around 210 per cent if the sending-end voltage had been maintained at its maximum value.

Table XI is a summary of the data obtained with chopped waves applied to the test cable. In this case the receiving-end voltages are influenced considerably by the front of the applied voltage. With the 1,000-foot cable the voltages vary between 1.46 and 1.94 as the front is changed from 0.45 to 3.5 microseconds. The voltages recorded with the longer fronts do not differ significantly from the maximum voltages measured with an applied wave having a sustained tail. Adding capacitance at the receiving end definitely reduces the voltages. Tests 113-26 were made with an applied surge having a front considerably longer than twice the cable propagation time, which accounts for the low voltages recorded. In these cases the receiving-end voltage is chopped by reflections before the voltage has a chance to build up to twice the incoming surge. With chopped waves the attenuation is more nearly proportional to cable length, which was not the case with applied voltages having sustained tails.

The oscillograms in Figure 7 are typical of the ones obtained in the chopped-wave tests. Oscillogram 104 applies for the case of a 0.7-microsecond-front surge applied to a 200-foot open-end cable. The receiving-end voltage was equal to 1.97 times the crest of the applied voltage. Terminating the same cable with a 6,300-micromicrofarad capacitor decreased the voltage to 1.57 (see oscillogram 110). Oscillograms 35 and 45 show the voltage at the receiving end of a 1,000-foot cable with applied voltages having fronts of 0.5 and 3.5 microseconds, respectively.

Table XII. Comparison Between Measured and Calculated Resistance

Condition	Measured Resistance, Ohms*	Calculated Resistance, Ohms
200-foot open-end cable	3.72	2.06
200-foot cable terminated in 6,300-micromicrofarad capacitor	2.24	1.67
1,000-foot open-end cable	3.47	3.03

* Resistance obtained from decrement of surge voltage recorded in Impulse Laboratory cable tests.

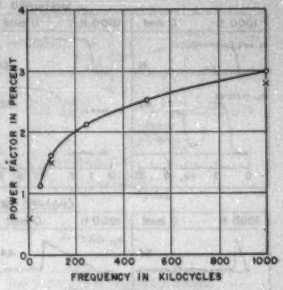

Figure 10. Measured power factor of oil-impregnated paper insulation

Circles—15-kv power cable
Crosses—oil-insulated shunt capacitor

Losses. The general shape of the voltage in oscillogram 88, Figure 7, indicates that the receiving-end voltage might be approximated by a steady-state component equal to the applied voltage, and a transient component that decays exponentially with time. This representation, although not strictly correct, furnishes a method of estimating attenuation analytically. Figure 9 is a plot of the transient components obtained from oscillograms 62, 88, and 99. In these plots the voltage is expressed in per cent of the magnitude of the transient component at the instant of the maximum receiving-end voltage. Time is measured from the instant of maximum receiving-end voltage. It will be noted that the plotted points fall very close to straight lines indicating that the decrement can be approximated by the use of the simple resistance-inductance-capacitance circuit damping factor $\epsilon^{-Rt/2L}$. The inductance of the test cable was estimated at 9.93 microhenries per 200 feet. Using this inductance and the data from oscillogram 88, Figure 7, the effective cable resistance is estimated at 3.72 ohms per 200 feet. An effective resistance of 2.24 ohms was estimated for the case involving the 6,300-micromicrofarad terminating capacitance, indicating that capacitance has some influence on loss. The estimated resistance for the 1,000-foot open-end cable is 3.47 ohms, which is actually less than the effective resistance of the 200-foot open-end cable.

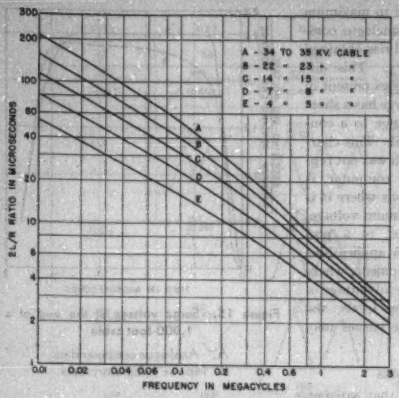

Figure 11. Calculated $2L/R$ ratios for oil-impregnated paper-insulated, single-conductor power cables

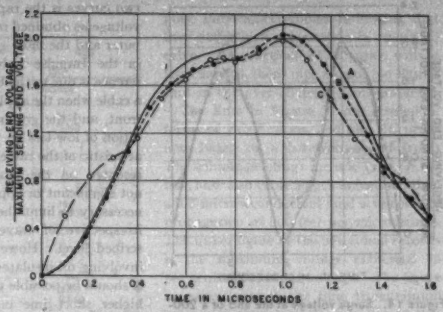

Figure 13. Voltage at the end of a 200-foot cable terminated in a capacitor

A. Calculated without attenuation. B. Analogue computer data
C. Impulse Laboratory data

As a basis for checking the effective resistances obtained from an analysis of the oscillographic data, a method was developed for estimating loss from the cable characteristics. The cable power factor was measured over a frequency range of 950 kc as shown in Figure 10. Also, included are test points obtained in measurements on an oil-insulated capacitor unit.[8] The close agreement between the cable and capacitor test data illustrates that the power factor is a function of the insulating materials only.

Knowing the cable capacitance and power factor, it is possible to determine the effective shunt resistance of the cable at any frequency. This shunt resistance can be converted to an equivalent series resistance, as follows:

$$\text{Loss} = i^2R(\text{series}) = \frac{e^2}{R(\text{shunt})}$$

$$R(\text{series}) = \frac{e^2}{i^2R(\text{shunt})} = \frac{Z^2}{R(\text{shunt})}$$

where

Z = cable surge impedance

This relation between shunt resistance and equivalent series resistance can be considered approximate only when dealing with traveling waves, because voltage and current are not always related by surge impedance at all times and locations in the cable. The relation has been retained, however, because no better practical method has been developed for introducing attenuation due to dielectric loss.

The series resistance of the conductor and lead sheath are calculated, at the desired frequencies and added to the equivalent series resistance, used to represent shunt loss. Following this method, the effective resistances given in Table XII were calculated for the cases discussed previously. The measured losses are higher than the calculated values, which is partially explained by the more rapid attenuation of the higher-frequency components in the measured voltages, and by reflection losses present because the applied voltage was not held exactly constant. Both the measured and calculated values show that the effective resistances are influenced by terminal capacitance and by cable length.

As a basis for estimating attenuation in single-conductor cables, the $2L/R$ ratios in Figure 11 were calculated for cables in voltage classes between 4 to 5 and 34 to 35 kv. In making the necessary calculations, it was noted that conductor size had little influence on the ratios. Small conductors had large series losses and low shunt losses, whereas the large conductors had small series losses and large shunt losses, the $2L/R$ ratios being substantially independent of conductor size.

In using these ratios for estimating

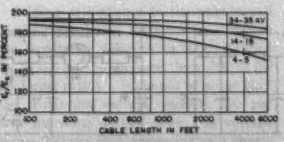

Figure 12. Calculated receiving-end to sending-end voltage ratios for open-end cables

purposes, the lowest natural frequency of the circuit is obtained, including the effects of terminal capacitance. The data in Figure 17 can be used for this purpose. The $2L/R$ ratio corresponding to this frequency and the cable insulation class is then used in the damping factor relation $\epsilon^{-Rt/2L}$. Figure 12 is a plot of the calculated receiving-end to sending-end voltage ratios for cable lengths from 100 to 6,000 feet, including the effects of attenuation. These curves apply for the case of open-end cables, that is, no terminating capacitance, and assume the front of the junction-pothead voltage is less than twice the cable propagation time. These curves are included to show the probable trend of the voltage ratios with cable length and cable insulation class.

Comparison of Anacom and Impulse Laboratory Test Results

Three receiving-end voltage curves are plotted in Figure 13, all applying to the case of a sustained-tail wave applied to a 200-foot cable terminated in a 6,300-micromicrofarad capacitor. The highest voltage shown was calculated and neglects all attenuation. The analogue computer curve was obtained with a 20-*pi* section representation of the cable, and includes the effects of the inherent loss of the computer elements. The Impulse Laboratory curve includes the actual loss in the 15-kv power cable. These results show that the analogue computer and Impulse Laboratory test results check very closely over the first 1.6 microseconds.

The curves in Figure 14 apply for the same case, and compare the analogue computer and Impulse Laboratory re-

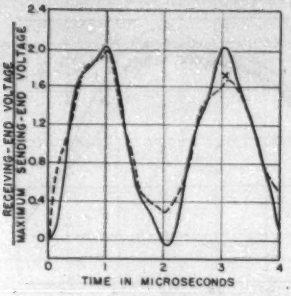

Figure 14. Surge voltage at the end of a 200-foot cable

Solid curve—Analogue computer data
Dashed curve—Impulse Laboratory data
Cross—Analogue computer data, including calculated attenuation

sults over a period of four microseconds. It will be noted that the Impulse Laboratory curve is considerably below the analogue computer curve at the time of the second peak, which is attributed to the lower attenuation in the analogue computer circuits. The cross in Figure 14 represents the second crest obtained by applying attenuation to the first crest of the computer curve. Attenuation was applied on a straight time basis using the simple resistance-inductance-capacitance circuit decrement factor $\epsilon^{-Rt/2L}$. These results indicate that reasonably satisfactory results can be obtained by applying calculated decrement to the analogue computer data, whenever it is necessary to know the general shape of the entire receiving-end voltage curve. It would be possible to include decrement in the computer studies; however, this would require a separate study for each voltage-class cable. Furthermore, it is the authors' opinion that accurate data are not generally required on the magnitude of the second and successive peak voltages.

Figure 15 compares analogue computer and Impulse Laboratory data for a case involving a 1,000-foot cable terminated in a 2,000-micromicrofarad capacitor. The significant difference between these two curves is the rapid rise to maximum voltage as obtained on the analogue computer and the more gradual rise obtained in the Impulse Laboratory. This difference is due to the high losses present in a cable when the applied surge has a short front, and the gradual change to a condition of low loss on the tail. This characteristic of the cable, which was not represented on the analogue computer, is not significant in applications where it is necessary to limit the maximum voltage, irrespective of wave shape, to a prescribed level. However, in applications involving oil-insulated equipment, where it should be possible to take advantage of higher short-time insulation levels, the actual shape of the voltage curves may prove to be important.

Analogue Computer Studies

After it was established that satisfactory agreement could be obtained between analogue computer studies and Impulse Laboratory tests, a general investigation was made on the computer. The analogue of the cable consisted of *pi* sections as shown in Figure 16, a total of 20 being used for cables up to 800 feet in length. An appropriate time base was selected to keep the natural frequencies of the computer circuits within desirable limits, so that the losses would not exceed those expected in an actual power cable. The complete analogue depended upon the ratio of the cable propagation time to the front F. The circuit in Figure 16(A) was used for those cases where this ratio was more than 0.5. The capacitor C_1 is charged through resistor R_1 by closing switch S_1. When the voltage across C_1 reaches the desired level, switch S_2 is closed to hold the voltage across C_1 constant. The battery voltage is large by comparison to the maximum cable-input voltage in order to produce a relatively uniform rate-of-rise of voltage. The capacitance C_1 is large in order to prevent reflections from changing the input voltage appreciably. With this analogue the voltage across the input end of the cable has the wave shape illustrated in Figure 2(B).

The analogue in Figure 16(B) was employed in those cases where the ratio of cable propagation time to the front F was

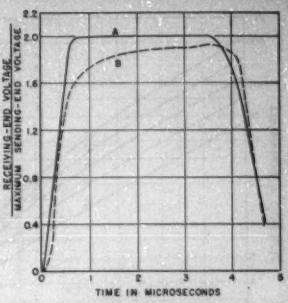

Figure 15. Surge voltage at the end of a 1,000-foot cable

A. Analogue computer data
B. Impulse Laboratory data

less than 0.5. Capacitor C_1 is charged through resistor R_1 by closing switch S_1. The voltage across C_1 is applied to the cable-input terminals through resistor R_2, which represents the overhead line surge impedance. When the voltage across the cable terminals reaches the desired level, switch S_2 is closed to hold the voltage constant. Capacitor C_2 is large enough to prevent reflections from altering the voltage established by battery V_2. It should be noted that, with this analogue, reflections from the remote end of the cable can influence the voltage across the cable-input terminals until switch S_2 is closed.

The computer studies were based on a 25-ohm cable and terminating capacitance values from zero to 12,800 micromicrofarads. A front F of 0.4 microsecond was represented in all cases. The cable length was varied between 25 and 800 feet.

In selecting these limits, it was realized that the basic variables in the problem were the surge propagation time of the cable, the duration of the front F, and the time constant of the circuit consisting of the cable surge impedance and the terminating capacitance C. As all of these basic variables can be expressed

Figure 16. Basic circuits used in analogue computer studies

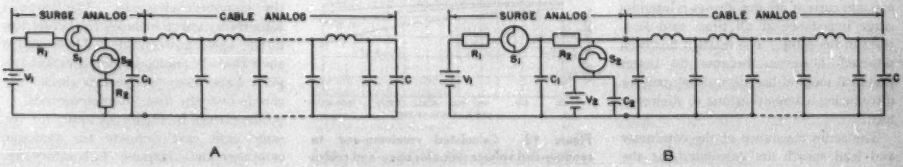

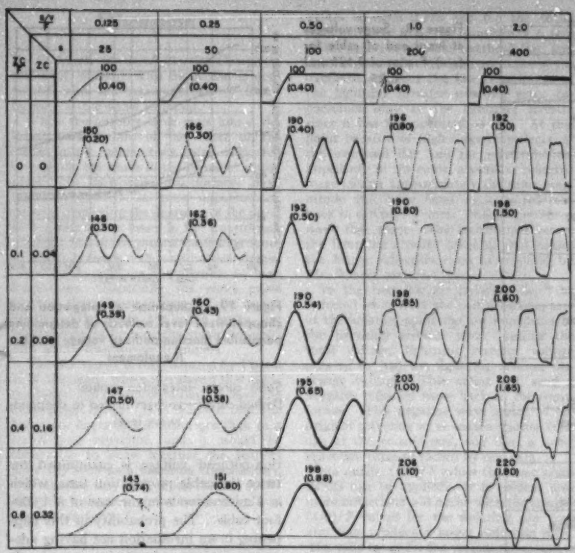

Figure 17. Typical oscillograms obtained in analogue computer studies

in microseconds, generalization of the computer data is possible.

Let:

s = cable length in feet

v = velocity of surge protection in the cable in feet per microsecond

Z = cable surge impedance in ohms

C = terminating capacitance (effective capacitance of terminating equipment) in microfarads

F = front in microseconds of the voltage across the cable input terminals, neglecting reflections

Then

s/v = cable propagation time in microseconds

ZC = time constant in microseconds of the circuit consisting of the cable and terminating equipment

If the cable propagation time and the circuit time constant are divided by the front F, these two quantities will be expressed in per unit, where one per unit time is the length of the front F. They also may be expressed as ratios to the front, obtaining the ratios $(s/v)/F$ and ZC/F. These two ratios are, in effect, the only two fundamental variables involved. Reducing the five variables encountered in cable applications to two fundamental variables permits generalization of the computer data obtained with a 0.4-microsecond front and a 25-ohm cable.

General Data. Typical oscillograms obtained in the computer studies are shown in Figure 17. The upper line of oscillograms is the voltage across the input terminals of the cable, neglecting reflections from the remote end. In each case this voltage rises to 100 per cent in 0.4 microsecond. As reflections do not alter the input voltage when the $(s/v)/F$ ratio is greater than 0.5, based on the assumptions made in this study, the upper line of oscillograms is also the actual voltage across the cable-input terminals for $(s/v)/F$ ratios of 0.5, 1.0, and 2.0. The input voltages, as modified by reflections, are shown in Figure 18 for $(s/v)/F$ ratios of 0.125 and 0.25.

The second line of oscillograms in Figure 17 shows the voltage across the remote end of the cable for the case of zero terminating capacitance. The succeeding lines illustrate the general shape of the receiving-end voltages with ZC/F ratios up to 0.8.

Adding capacitance to the remote end of the cable has a tendency to decrease the maximum voltages for $(s/v)/F$ ratios below 0.5 and to increase the voltages for the larger ratios. It should be noted that the maximum voltage exceeds 200 per cent for some of the cases, the voltage above 200 per cent appearing as a short-duration pip. These pips are more pronounced in these studies than in the Impulse Laboratory studies, indicating that they suffer high attenuation in an actual cable. As practical ZC/F ratios will be less than 0.4, these pips are not too significant in the over-all protection problem.

The lines in Figure 17 are labeled in terms of ZC/F ratios, and also ZC products based on a 0.4-microsecond front. The column headings include $(s/v)/F$ ratios, and also cable length in feet based on a 0.4-microsecond front and a velocity of propagation of 500 feet per microsecond. The upper figure of the individual records is the maximum voltage expressed in per cent of the input voltage. The figure in parentheses is the time to maximum voltage in microseconds, assuming a 0.4-microsecond front and velocity of propagation of 500 feet per microsecond. For other fronts these times will vary directly with the front.

Figure 5 summarizes the maximum receiving-end voltages obtained in the computer studies. The voltages are expressed as ratios to the maximum voltage at the sending or input-end of the cable.

Integration Method

In the integration method of evaluating the effect of surge voltages on oil-insulated transformers, the disruptive effect of the surge is defined by the equation

$$DE = \int (e - K_1)^{K_2}\, dt,$$

where

DE = disruptive effect

e = volt-time curve of the applied surge

K_1, K_2 = constants fixed by the standard transformer test voltages

This relation was established on the general basis that transformer insulation could withstand some constant voltage K_1 for an extended period of time (a few hundred microseconds) without suffering ill effects. It was realized that the disruptive effect of a surge is a function of both voltage magnitude and time, but that these two factors are not of equal importance. Introducing the exponent K_2 allows some variation in the relative weight given to magnitude and time. The constants in the disruptive-effect equation can be evaluated from the standard tests for transformers, if the assumption is made that the tests are of equal sever-

Table XIII. Constants Used in Integration Equation

Insulation Class, Kv	Basic Insulation Level, Kv	K_1	K_2	Disruptive Effect
5.0	75	73.5	0.579	1.27
8.66	95	90.5	0.997	8.34
15.0	110	98.8	1.808	3.6×10^{9}
23.0	150	46.5	6.75	2.78×10^{14}
34.5	200	90.0	5.65	2.90×10^{13}

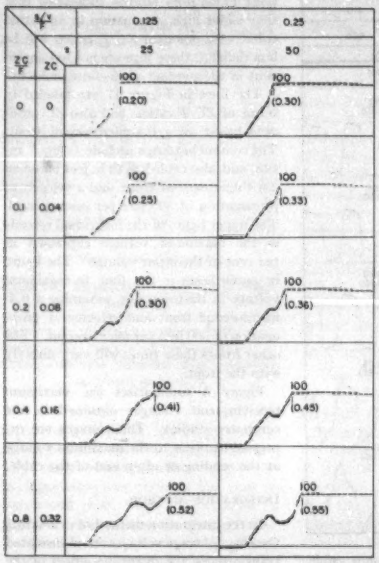

Figure 18. Surge voltages at input end of cable for (s/v)/F ratios of 0.125 and 0.25

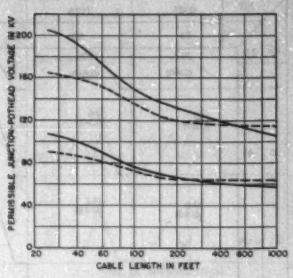

Figure 19. Comparison of integration and chopped-wave level methods of determining permissible junction-pothead voltage for Class II equipment

Solid curves—integration method
Dashed curves—voltages limited to chopped-wave level

ity. This assumption should be reasonable from a general application standpoint because transformers must be designed and built to withstand these standard tests. The general form of the equation requires that the constants be evaluated by a cut-and-try procedure. The constants have been evaluated for insulation classes up to and including 34.5 kv, and are given in Table XIII. The disruptive effect, obtained by substituting any one of the three standard test waves in the equation, is also included in the table.

As the equation gives the same disruptive effect for the three standard test waves, which vary over a wide range in magnitude and duration, it should give acceptable accuracies in determining whether particular nonstandard waves are more, or less, severe than the standard test waves. Judgment, however, is required in evaluating oscillatory waves as experienced on circuits involving transformers connected to overhead lines through cable. The authors have integrated only the first cycle of such oscillations, because the second cycle is usually of appreciably reduced magnitude, and because the condition of the insulation probably improves some during the period of low voltage between the first and second crests of the oscillation.

Figure 19 is a comparison of the permissible junction pothead voltages for Class II equipments for two methods of interpretation of the basic data. The dashed curves are based on limiting the surge voltages to the equipment chopped-wave levels, and the solid curves are based on the integration method. It should be noted that the solid curves are based on a front F of 0.4 microsecond, rather than on a surge current having a 4,000-ampere-per-microsecond rate-of-rise. Assuming a constant front of 0.4 microsecond makes these curves somewhat more conservative, especially with the shorter cables.

The integration method permits higher voltages with short cables, and slightly lower voltages with the longer cables. This should be expected because the times associated with the overvoltages with short cables are less than the minimum times to flashover used in chopped-wave testing, whereas with long cables the reverse is true. The curves would indicate that the equipment voltages should be held below the chopped-wave levels with the longer cables. Practical considerations, however, will show that this requirement is not necessary. First, the differences even with 1,000-foot cables are only 7 per cent. Second, the analogue computer studies were based on the assumption that the maximum junction-pothead voltage is maintained for twice the cable propagation time, which is 4 microseconds in the case of a 1,000-foot cable. The probability of this happening in an installation not having adequate equipment-insulation margin is considered too small to be a significant factor.

Although the integration method indicates that the surge voltages at the equipment may be permitted to exceed the chopped-wave levels, the authors decided not to take advantage of this possibility at this time. It was felt that further study should be given to the influence of wave shape on the permissible maximum voltages before co-ordinating with anything higher than the chopped-wave levels.

References

1. Dielectric Strength and Protection of Modern Dry-Type Air-Cooled Transformers, P. L. Bellaschi, Edward Beck. *Electrical Engineering (AIEE Transactions)*, volume 64, November 1945, pages 759–63.

2. Transmission Line Design and Performance Based on Direct Lightning Strokes, E. L. Harder, J. M. Clayton. *AIEE Transactions*, volume 68, part I, 1949, pages 439–49.

3. Lightning Protection for Rotating Machines, G. D. McCann, E. Beck, L. A. Fizzi. *AIEE Transactions*, volume 63, 1944, pages 319–33.

4. Lightning Investigation on the 25-Kv System of the West Penn Power Company, W. C. Bowen, E. Beck. *AIEE Transactions*, volume 66, 1947, pages 831–36.

5. Characteristics of Chlorinated Impregnants in D-C Paper Capacitors, L. J. Berberich, C. V. Fields, R. E. Marbury. *AIEE Transactions*, volume 63, 1944, pages 1173–79.

6. A Large-Scale General-Purpose Electric Analog Computer, E. L. Harder, G. D. McCann. *AIEE Transactions*, volume 67, part I, 1948, pages 664–73.

Discussion

P. A. Abetti (General Electric Company, Pittsfield, Mass.): This discussion is concerned with the representation of transformers at the cable terminal.

While the authors have gone into a detailed investigation of the effect of the losses in the cable, they have neglected completely the losses in the terminal equipment. In particular, transformers have been represented as pure capacitances, thereby neglecting the damping of the oscillations due to the losses in the transformer winding, and in the capacitances to ground, to shield, between coils, and between turns. These losses may be considerable at high frequencies. Especially for short cable lengths, these internal losses of the transformer, rather than the cable losses, are instrumental in limiting the maximum voltages at the transformer terminals.

This statement is corroborated by Figure 10 of the paper, where it is shown that cable insulation and capacitor insulation have the same power factor. It is believed that the losses are larger in a transformer than in a commercial capacitor, and it would be interesting to know whether the authors have any such data taken on transformers, and whether they have made tests to determine the reduction of the terminal voltage due to this factor.

W. L. Teague and **L. B. Rademacher** (Westinghouse Electric Corporation, Sharon, Pa.): The paper presents pertinent data in a very useful and concise form. By using Table II and III of the paper, the maximum cable length permissible for general applications is given directly. For more specific applications, the curves, Figures 3 and 4 of the paper, and the basic application data permit a more detailed study. The tables and figures mentioned above are derived from Figure 5 of the paper which contains the basic data for the complete investigation.

During 1947 and 1948 a similar investigation was made at Sharon and the data obtained, Figure 1 of the discussion, are superimposed on Figure 5 of the paper. For this study either an actual transformer or a simulated transformer and a 37-ohm cable were used to give a ZC/F value of 0.195. By starting with a 200-foot cable and cutting to the desired length, the length was varied from 200 to 50 feet. Initially the tests were made using several ratings of completely assembled lightning arresters and the 200-foot cable. The action of the lightning-arrester isolating gap caused erratic fronts which made interpretation difficult. Like the authors tests, the isolating gaps were removed and the major part of the study was made without the lightning arrester gap. The data presented in Figure 1 of the discussion are for the gap removed.

Over a $(s/v)/F$ factor of 0.25 the two sets of data are in good agreement. Below this value, Sharon's data show a lower reflection ratio (E_R/E_S) for corresponding values. This difference is attributed to the omission of the lightning arrester isolating gap. Theoretically, this error should occur at 0.5 and become predominately greater as the ratio decreases. With the isolating gap in lightning arrester and for $(s/v)/F$ values between 0.125 and 0.5 the initial reflected wave from the transformer e_1 sees at the junction of cable, overhead line, and lightning arrester the high impedance of the overhead line and the low capacitance of the lightning arrester isolating gap; capacitance only at the lightning arrester since it has not operated as yet. At this point because of high-surge impedance of the overhead line and the relatively low impedance of the cable, a positive reflected wave having approximately the same magnitude and wave front as e_1 is reflected back to the transformer. It is this reflected wave that reaches the transformer before the lightning arrester operates that causes the higher reflection ratio as reported by Mr. Witzke and Mr. Bliss.

In the case for no isolating gap, the reflected wave from the transformer e_1 sees at the junction point the low impedance of the lightning arrester block limiting the total voltage, lightning arrester voltage plus e_1, to just the lightning arrester discharge voltage. This action will send a negative reflected wave back to the transformer. This negative wave added to the original traveling wave causes a lower voltage at the transformer, and thus a lower reflection ratio as shown by our data.

For smaller $(s/v)/F$ values the same arguments can be applied. It is evident how more reflections will occur with the smaller $(s/v)/F$ values for the isolating gap case and thus produce a larger reflection ratio. The valid range for the various approximate equations for calculating the reflection ratio are given as

$$\frac{E_R}{E_S}=\frac{4}{3}\left(1+\frac{s/v}{F}\right)0.5\geq\frac{s/v}{F}\geq0.125 \qquad (1)$$

$$\frac{E_R}{E_S}=\frac{6}{5}\left(1+\frac{2s/v}{F}\right)0.125\geq\frac{s/v}{F}\geq0.056 \qquad (2)$$

$$\frac{E_R}{E_S}=\frac{8}{7}\left(1+\frac{3s/v}{F}\right)0.056\geq s/v\geq0.0315 \qquad (3)$$

By using equations 1, 2, and 3 it can be seen that Witzke's and Bliss' data below 0.25 are correct. Above this value the two sets of data agree, which is most gratifying since the two investigations were carried out independently and in different laboratories. The agreement of the data also shows the value of the analogue computer which is much easier and less time-consuming to use provided the actual circuit constants are known.

From the paper it should be apparent that for cable-connected equipment careful consideration should be given to proper surge protection. It also points out that the practice of installing lightning arresters at the junction between overhead lines and cable is sound for many applications.

H. A. Cornelius (Public Service Company of Northern Illinois, Chicago, Ill.): Evaluation of many factors which must be considered in the problem of providing satisfactory lightning protection for cable-connected electric equipment has been needed in the industry for a long time. The paper by Mr. Witzke and Bliss is considered a major contribution which will be of great value to protection engineers and to the industry at large.

With the Witzke and Bliss data available, it will be possible to make lightning-arrester applications with greater assurance that the results will be satisfactory, than has been possible in the past.

A. M. Opsahl (Westinghouse Electric Corporation, East Pittsburgh, Pa.): For years the hazards of double voltage reflections at the ends of cables tied to overhead lines have been pointed out. Witzke and Bliss have made a very adequate study of the problem and have assigned very definite values to the factors involved.

Flashovers do occur at the ends of cables, but no extensive surveys have been made to evaluate the percentage of trouble. The authors express the estimated hazard in terms of the average number of years per outage at a given location. One outage in 40 years at a given location seems safe, but expressed in another way, one flashover in 40 installations, even with the recom-

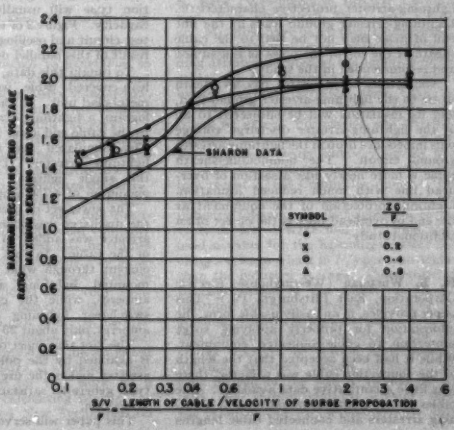

Figure 1. Maximum receiving-end voltages expressed as a ratio to the maximum sending-end voltage. Sharon data superimposed on Figure 5 of the paper

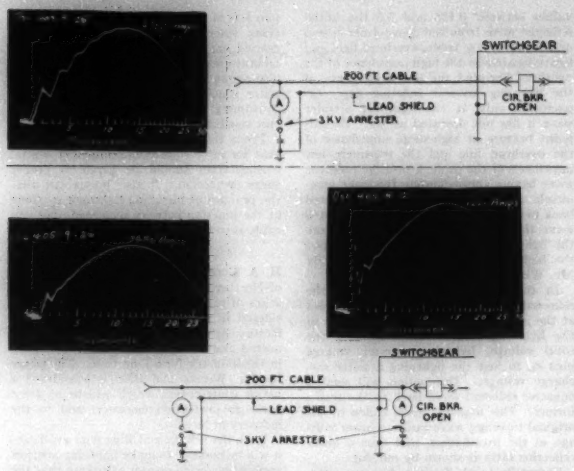

Figure 2. Top oscillogram shows the discharge through a single set of pole-mounted lightning arresters. In the lower oscillograms the discharge duty is shared by the pole and switchgear lightning arresters

mended protection may not seem so safe. There are alleviating circumstances however. The second cable connected to the same terminal equipment in many installations eliminates the over-voltage reflection. Cable entrances would be more common in the densely-populated areas where lightning exposure of the line is low, and there may be lightning arresters on the line near the cable entrance. Slower rates of rise of surge voltage and current than those in the study will decrease the magnitude of the reflections on the shorter cables. As opposed to these alleviating conditions, the older installations will have questionable co-ordination between insulation and the lightning-arrester protective characteristic. Lightning-arrester ground leads at the line end of cable may not be tied to the cable sheath at the top of the poles as is assumed and recommended in the study.

Nonmetallic-sheath cable has no sheath to tie to the lightning-arrester ground lead, and its insulation will be subjected to all of the lightning-arrester discharge voltage plus impedance drop in the lightning arrester ground circuit. The nonmetallic-sheath cable is more nearly like a section of overhead line with much reduced insulation. Lightning protection of the equipment at the end of overhead lines is the object of an additional study.

H. B. Wortman (Westinghouse Electric Corporation, East Pittsburgh, Pa.): This paper provides, in an easily usable form, the information for properly applying surge protection to cable-connected equipment. While it had been accepted that the length of the connecting cable was a factor, there was little quantitative data available. The tables showing the combinations of lightning arresters and connected cable lengths and formulas for the calculation of surge behavior for a given set of conditions will be very helpful.

There has been an increasing interest in the need for lightning-arrester protection of individual circuits. The information contained in this paper will determine the amplitude of the surge voltage possible at the switchgear end of the circuit. If this exceeds the basic insulation level rating, then consideration should be given to the capacity of the switchgear lightning arresters.

Since the switchgear lightning arresters share the discharge burden with the pole-mounted lightning arresters, the distribution type will usually provide adequate capacity. Figure 2 of the discussion shows a test circuit and oscillograms illustrating the result of this parallel discharge circuit.

To obtain this data, a 200-foot length of lead-covered cable was connected to a metal-clad unit. In the first test and oscillogram, a lightning arrester was connected to the cable end away from the switchgear. This simulated the usual pole-mounted lightning arrester. The current through this single lightning arrester reached a maximum of 4,750 amperes.

The lower set of oscillograms shows how the discharge was shared when a lightning arrester was added to the switchgear end of the cable. In this case, the maximum current through what would be the pole-mounted lightning arrester was 3,480 amperes, while the current through the switchgear lightning arrester was 1,220 amperes, only about 25 per cent of the total.

The fact that most of the discharge duty is assumed by the pole-mounted lightning arrester makes the use of the distribution-type generally satisfactory for switchgear protection.

This paper will serve as a guide to more complete protection of metal-clad switchgear connected to overhead lines. If lightning arresters are necessary, adequate and more economical protection can usually be obtained through the use of distribution-type lightning arresters. In cases when more discharge capacity is needed, station-type lightning arresters should, of course, be used.

E. M. Hunter (General Electric Company, Schenectady, N. Y.): This paper was of considerable interest to a group of us in the General Electric Company, because over a year ago we undertook to study this same problem. From our work, application guides for the protection against lightning of metal-clad switchgear and unit substations were formulated and presented in a paper in March 1949.[1] It is of interest to compare the results obtained by these two independent investigations.

The following general conclusions can be drawn from each investigation, that where exposure is through a short length of cable and there is an adequately installed lightning arrester at the junction of the cable and overhead line:

1. Additional lightning arresters are required in the metal-clad gear if the application is in the 13.2-kv class.

2. No lightning arresters are required in the gear if the application is in the 4.16-kv class.

These similar results were obtained through somewhat different assumptions. In this paper, the decision on whether or not additional lightning arresters were required was based on whether the lightning-arrester characteristics with their plus tolerances together with lightning-arrester lead drop exceeded the demonstrable impulse strength of the switchgear. In our investigation, we also used plus tolerances on the lightning arresters, but these were somewhat larger than they would be today because of downward industry changes in these values. Our criterion was that these lightning-arrester characteristics must be 80 per cent or less of the demonstrable impulse strength of the switchgear. This 20 per cent margin was intended to cover such variables as lead lengths, multiple strokes, and the other factors that are present in every application and are not known with preciseness.

Because of these differences in assumptions, our solution of "how long is a short cable" is somewhat more conservative than the results given in this paper, but in general, the actual results have little practical differences in them. There is a minimum length cable that can be used in any given application, and this length is dictated by the height of the pole on which the cable user is located at the junction of the cable and overhead line, and the location of the pole with respect to the substation site. So regardless of whether 20 feet or 34 feet, to take a specific example, are specified each of these cable lengths are shorter than can be practically installed.

With regard to the type of lightning arresters to be used in metal-clad switchgear, this type of gear should have the best available. We feel definitely that the station-type lightning arrester should be used. We have developed a type of porcelain housing for this lightning arrester for

this application which can be mounted on close centers in these equipments where space is at a premium. Each feeder position in the metal-clad switchgear has room for a cable pothead and a set of lightning arresters so no additional compartment is necessary if station lightning arresters are specified.

In general, I would like to commend the authors on their work on the propagation of surges through cable. In general, there appears to be a dearth of information on this subject, and the work they have done will undoubtedly pave the way for further investigations.

REFERENCE

1. LIGHTNING PROTECTION OF METALCLAD SWITCHGEAR AND UNIT SUBSTATIONS CONNECTED TO OVERHEAD LINES. Committee on Application of Lightning Arresters to Switchgear. *General Electric Review* (Schenectady, N. Y.), March 1949.

F. E. Andrews and **W. H. Hatch** (Public Service Company of Northern Illinois, Chicago, Ill.): The authors have presented a useful analysis of a problem of considerable importance, and of which there has been some lack of understanding. This analysis appears to be confined to paper-insulated cable with complete metallic covering such as provided by a lead sheath.

It would be desirable to have similar information on types of cable coming into more general use on distribution systems having only partial metallic covering. With the advent of buried cable for rural service and the demand for underground distribution in certain classes of housing developments and subdivisions, the use of cable interspersed in overhead distribution systems is rapidly increasing. Aerial cable should also be considered, as it also may be connected to open overhead conductors and will involve a wide range of cable lengths.

These buried and aerial cables are commonly of oil-base rubber-compound insulation and will have partial metal coverings. In the buried cable this may take the form of a number of spiral strands with some spacing between them. In the aerial cable, it will consist of the messenger and the spiral metal binding tape which holds the rubber-insulated conductors to the messenger. In both cases, this metallic covering will generally be the neutral conductor. Associated with this cable will be overhead distribution transformers and fused cutouts of the 5-kv insulation class.

The possible effects of the partial metal covering and the different impulse characteristics of the rubber-compound insulation are added factors which make the analysis of the problem difficult for the distribution engineer. It is hoped that the authors, in their published closing discussion will include comments and some information, at least qualitative, on the above aspects of the cable protective problem.

E. L. Harder (Westinghouse Electric Corporation, East Pittsburgh, Pa.): I would like to comment on the use of the computer in this problem. It requires no very great imagination to realize the enormous potentialities opened to us as electrical engineers with the advent and perfection of large-scale computing machinery. However, as with most activities, those of us working closely with this equipment have these potentialities impressed on us more vividly than otherwise.

It is only five or six years since the first studies of the type just described were made on equipment which was the forerunner of the analogue computer. These studies were for open-wire line rather than cable but involved a distance between the lightning arresters and the transformers. The studies were made by H. S. Kirschbaum and myself as part of a joint study with the Philadelphia Electric Company directed toward improving the lightning protection in the 230-kv Plymouth Meeting station. A line section, lightning arrester, and transformer were represented on the computer to test out the method and check it against theoretical analysis, and then the complete station was represented to determine the degree of protection afforded by lightning arresters in various locations.

The computer equipment and techniques used in these studies were generally the same as had been devised and used earlier by Evans, Monteith, and Witzke[1] for study of recovery voltages and switching transients on power system. The only difference was the introduction of lightning waves, scaled down in time, in place of the 60-cycle voltages and the use of inductor coils of lower loss. These had been developed for studying mechanical systems. Nonlinear elements also were introduced for representing the lightning-arrester characteristic.

Since that time the lightning protection of a number of particular substations has been studied by this technique, for example, substations of the Potomac Edison system and of the Metropolitan Edison system.

This is a perfectly practical thing to do and quite useful if one wishes to obtain a clear picture of what goes on when surges enter a particular substation. It requires analysis, based on the line construction and exposure, as to what surges must be considered as entering the station, an analysis similar to that which Witzke and Bliss have so ably carried out in connection with the cable problem.

There is a definite need for two kinds of studies.

1. General studies of typical situations which are simple enough to generalize so that the results can be widely applied and can form the basis for industry standardization of practice. The study just outlined by Witzke and Bliss is in this category.
2. Specific studies of particular stations. Seldom are two stations exactly alike. The exposures differ. The arrangements and spacings differ. Each one requires consideration of some different aspect of the protection problem. We must not under-estimate the value to an individual company and to the industry of these specific studies of important or typical stations. In addition to providing a much more accurate picture of the individual case, they show up the importance of practical station design practices which can later be incorporated into the general studies. They reveal what general situations should be subjected to study by the industry as a whole. Computers are available for this work on a similar basis to a-c calculating boards.

In a paper entitled New Techniques on the Anacom[2] an analogue or representation for corona was described, so that it is now possible to represent accurately the effect of corona on the travelling waves entering stations and affecting the protection problem.

Both corona and transformer saturation are being represented in current studies of switching transients on high-voltage lines.

Other new types of studies taking place on large scale computers which I believe might be of interest in pointing out the potentialities of computers are:

Series capacitors—the complex action of currents and voltages when protective gaps are operating during line faults. How else would one study the relaying currents and voltage prior to the actual installations?

Carrier current—during the year studies were made of carrier propagation over a 5-terminal line. A smooth line representation over the entire carrier frequency spectrum were obtained by the use of 150 pi sections. The 50 to 150 kc was scaled down about 100 to 1.

Transient performance of potential devices for various burdens and faults can be analyzed.

Gas flow, fluid flow, and so forth all can be handled now in addition to electric current flow since general nonlinear elements are available.

The open phase and fault to ground or the simultaneous faults on twin circuit lines need no longer be a mystery as a general method of solution by computer is now available for this problem.

These potentialities of the analogue computer are quite unlimited and are something to stir the imagination indeed.

REFERENCES

1. POWER-SYSTEM TRANSIENTS CAUSED BY SWITCHING AND FAULTS, R. D. Evans, A. C. Monteith, R. L. Witzke. *Electrical Engineering* (*AIEE Transactions*), volume 59, August 1939, pages 386–97.

2. NEW TECHNIQUES ON THE ANACOM, E. L. Harder, J. T. Carleton. *AIEE Transactions*, volume 69, part I, 1950, pages 547–56.

E. Beck (Westinghouse Electric Corporation, East Pittsburgh, Pa.): Mr. Witzke and Mr. Bliss have based their recommendations on certain characteristics of the lightning arresters located at the junction of the cable and the overhead line. For distribution lightning arresters they have assumed the maximum industry figures with which we agree. For station and line-type lightning arresters they have used values that are the average industry figures plus one-half the industry tolerance published in a recent AIEE Committee report.[1] For station lightning arresters, for example, the industry tolerance in that report is 15 per cent, so Mr. Witzke and Mr. Bliss have used a value for the lightning-arrester discharge voltage which is $7^1/_2$ per cent higher than the industry average. Consequent to the publication of the AIEE report, the lightning protective devices section of the National Electrical Manufacturers Association announced new tolerances for the discharge voltages of station and line-type lightning arresters, namely 10 and 15 per cent instead of the former 15 and 20 per cent. For station lightning arresters then, the value used by Mr. Witzke and Mr. Bliss

is really three-fourths of the maximum industry tolerance. NEMA also has suggested a protective level for use as a basis in insulation co-ordination problems, found by adding to the average two-thirds of the maximum tolerance in the case of station arresters. This would be the average performance plus $6^2/_3$ per cent.

It is probably subject to further discussion and debate whether these suggestions are practical or whether the full industry tolerances should be used. If Mr. Witzke and Mr. Bliss had used the new tolerance of 10 per cent for station lightning arresters, the cable lengths would have been a little more conservative. It seems to me, and this is now opinion and not complete conviction, that Mr. Witzke's and Mr. Bliss' suggestions are conservative. They should be. However, it has not been brought to our attention that lightning damage to cable-connected equipment with lightning arresters installed only at the pothead, is prevalent; perhaps the result of the as yet imponderable probabilities mentioned by Mr. Witzke and Mr. Bliss. Since these are still undetermined it seems to me that information from the users of cable-connected equipment regarding their experience would be most helpful in providing some kind of a confidence factor, and I would recommend that such information be accumulated.

For example, from Table VI of the paper, it appears that line insulation can be a potent-factor and that on a highly insulated line, 1,000 kv for example, the installation of a protective device which would spark at 250 kv, located 125 feet from the pothead, would decrease the chances of lightning damage to the cable-connected equipment, since for strokes beyond the protective device on the line and for strokes on the other side in the vicinity of this protective device this line-type protective device will operate and the duty on the lightning arrester at the pothead and therefore the terminal equipment will be reduced. This is only one of the probability factors that may well operate in practice to give a conservative tinge to the recommendations. Considering these factors, the practical picture may actually not be altered much by using the present maximum industry tolerances or the NEMA suggestion for station and line-type lightning arresters instead of the compromise adopted by Mr. Witzke and Mr. Bliss. However, the use of the maximum tolerance with some allowance for the probabilities would be another method. The question affectively boils down to this, the user of cable-connected equipment must weigh the risks and his experience and the consequence of possible lightning damage in the equipment. The data on past experience would be of much value in this connection.

REFERENCE

1. PERFORMANCE CHARACTERISTICS OF LIGHTNING PROTECTIVE DEVICES, AIEE Committee Report. *AIEE Transactions*, volume 68, part II, 1949, pages 1330–33.

R. L. Witzke and T. J. Bliss: The discussion by Mr. Andrews and Mr. Hatch, as well as the one by Mr. Opsahl, points out the need for surge-protection application data for installations involving cables without a metallic sheath, or with a partial metallic covering. The authors agree that this information is desirable, and additional studies should be made in the near future. With no metallic sheath, the cable surge impedance and the velocity of surge propagation are more difficult to determine, because these constants depend upon the location of the conductors relative to ground, or metal ducts. Careful consideration also must be given to the resistance of the lightning arrester ground.

Mr. Beck's comments relative to the installation of additional lightning arresters on the line, at some distance from the cable pothead, is pertinent. Surges originating beyond this point will be limited in magnitude by this second set of lightning arresters, and the duty on the junction-pothead lightning arresters will be reduced considerably. In many applications the installation of additional lightning arresters one or two spans from the cable junction may be preferable to the installation of lightning arresters at the equipment end of the cable. This is particularly true in those cases where the installation of lightning arresters at the equipment is difficult because of space limitations.

Mr. Hunter recommends the use of station-type lightning arresters in switchgear assemblies on the basis that the best available lightning arrester should be used. The data presented by Mr. Wortman show that the duty on the lightning arresters in the switchgear is moderate, because the junction-pothead lightning arresters discharge a large part of the total current. For this reason distribution lightning arresters should be generally satisfactory for this service.

Mr. Abetti has asked whether or not transformer losses have any important influence on the surge voltages at the transformer terminals. Our investigations indicate that these losses should have less influence than the cable losses, which we concluded were of secondary importance for cable lengths up to 1,000 feet. Investigations made by Mr. Teague and Mr. Rademacher showed no appreciable difference in results between tests made with actual and simulated transformers.

The Metrotype System of Digital Recording and Telemetering

G. E. FOSTER
ASSOCIATE AIEE

Synopsis: A measuring system has been developed which will automatically measure and record in numerals at predetermined intervals items which can be measured electrically. The readings may be telemetered over a single channel for any distance. The paper describes briefly, with the aid of block diagrams, the process by which the instrument measures, telemeters, and prints the readings on a "log sheet."

THE years since the war have been highlighted by ever increasing costs of production. With such a condition existing, the need for automatic devices to monitor and/or control processes becomes increasingly urgent. The need for devices to provide data is felt even more pressingly. If additional labor to read curves, instruments, and so forth, can be eliminated and the data obtained in numerical form, even further advantages can be obtained.

The Metrotype is a system of making measurements and recording them in digital form. If telemetering is required, each reading is transmitted singly and recorded in tabulated form. Only one transmission channel is required and this can be of telegraph quality. The name Metrotype is derived from the Greek words metron, to measure, and typo, to mark.

There are several ways in which an electrical quantity may be measured. The usual ways are an indicating instrument or a curve-drawing instrument. The method of making a measurement by the direct writing of the numbers has not been generally used other than in digital counting machines (the cash register or adding machine). Before the war, several machines which printed electrical measurements were built and used,[1] but they were subject to many difficulties. A machine such as the Metrotype which can make sequential readings and transmit these readings to a distant point is an improvement on the prewar machines.

The machine to be described will select in sequence the quantities to be measured, make the measurement, transmit these readings as far as desired, and record them in numerical form properly tabulated. A complete 3-digit reading can be measured and recorded in 0.8 second. It combines the electronic computer technique with that of the printing telegraph. The result is a measuring instrument which makes readings automatically in numerical form. Standard paper with as many copies as desired may be used.

System Arrangement

The block diagram of Figure 1 indicates the interrelationship of the various components. The master control is inherent in the teletype (*TTY*) transmitter. This unit controls a line relay which in turn will operate a standard teletype printer. It is started by a clock, manual switches, or any other starting circuit, and generates the teletype codes[2] as required by the master switch and the number mixing relays.

In order to sequence the operations properly, a master switch is provided. Stepping of the master switch is controlled by the *TTY* transmitter. The master switch establishes the proper framing functions for the printer. It determines when the circuit selector will operate. It provides a method for homing the circuit selector to the proper starting point, and it controls the operation of the print sequence control. At the end of the printing cycle it turns off the printer and equipment.

The print sequence control is initiated by the master switch after the printer has been properly framed. As it runs, it selects the circuit to be measured, clears the electronic counters, pulses the step voltmeter, operates the digital sequence of the number mixer, and inserts the space function following the numbers.

The quantity to be read enters through the circuit selector and appears as a voltage at the step voltmeter. The latter generates a number of pulses proportional to the voltage being measured. The pulses are counted by the electronic counters and held in the form of an electrical condition in the various stages of the counter.

The number mixer consists of relays and

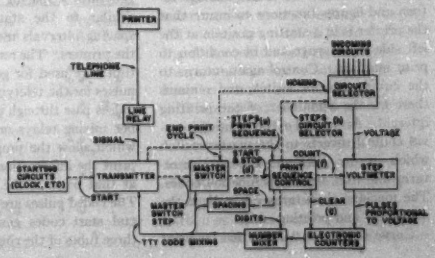

Figure 1. System diagram

Paper 50-84, recommended by the AIEE Instruments and Measurements Committee and approved by the AIEE Technical Program Committee for presentation at the AIEE Winter General Meeting, New York, N. Y., January 30–February 3, 1950. Manuscript submitted November 2, 1949; made available for printing December 8, 1949.

G. E. Foster is Chief Engineer with the Metrotype Corporation, Chicago, Ill.

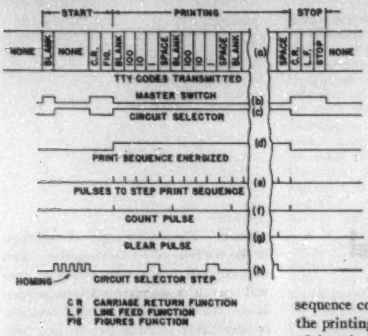

Figure 2 (left). Time relations

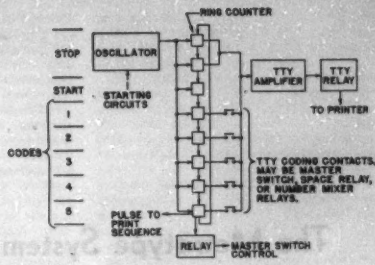

Figure 3 (right). Teletype transmitter

tubes which receive control information from the electrical conditions of the electronic counters and the print sequence control and translates this information into teletype code. The teletype code appears on the contacts on the number mixer relay where it is read by the teletype transmitter and transmitted to the printer. The space function also is inserted at the proper time by means of relay a controlled by the print sequence control.

Timing Sequence

The timing of some of the more important events in the printing sequence is shown in Figure 2. The upper row *a* shows the teletype codes transmitted during the starting interval, the printing interval, and the stopping interval. The selection of events is controlled by either the master switch or the circuit selector switch. The controlling element is shown as curves *b* and *c* of Figure 2. Following the sequence of events, the start of the master switch puts out a blank interval to start the printer, and then cuts in the circuit selector and waits until the circuit selector has reached home position. During this interval no codes are transmitted. When the circuit selector reaches home position, control reverts to the master switch which then transmits carriage return and figures functions to insure that the printer is in a starting position at the left side of the page and in condition to print numbers. Control again returns to the circuit selector switch and remains there for the remainder of the printing interval. At the end of the printing interval control reverts to the master switch which, in turn, transmits the carriage return, line feed, and stop function codes. The machine then turns off at both the measuring and printing ends.

Curve *d* of Figure 2 shows that the print sequence control is energized only during the printing interval. This prevents any of the print sequence functions from interfering with the framing functions as determined by the master switch. The pulses which step the print sequence control are shown as curve *e* of Figure 2. Curve *f* shows that a pulse to the step voltmeter occurs at the beginning of the blank interval of each printing cycle. This blank interval provides a time interval for the step voltmeter to make the measurement. It is 0.16 second in duration. As indicated by curve *g*, a clearing pulse is transmitted to the various counters at the beginning of the space interval to remove the previous count from the counters before a new count is received. Curve *h* of Figure 2 shows when the circuit selector steps. During the homing interval it steps rapidly until it reaches home. During the remainder of the printing cycle it steps at the beginning of the space function.

Teletype Transmitter

Figure 3 is a block diagram containing the essential information on the operation of the teletype transmitter. The principal component is a tube arrangement which acts like a ring counter of eight tubes operated one at a time under the control of an oscillator. The first two tubes of the ring counter generate a marking interval for the teletype printer and the next tube generates a spacing interval. These are similar to the standard marking and spacing intervals used for synchronizing the printers. The remaining five counting tubes are used for generating the coding pulses for the teletype printer. The code pulses pass through contacts of the number mixing relays or the master switch, which allow the proper codes to pass to print the information or function desired at that point in the operation sequence. The coded pulses are mixed with the stop and start codes generated by the first three tubes of the ring counter and passed to an amplifier which in turn controls the transmitting relay. On the contacts of this relay appear normal teletype pulses used for control of the telephone line circuit connecting to the printer. Although a mechanical transmitter could be used in place of the electronic transmitter outlined, the need for auxiliary control pulses to operate other electronic equipment makes an electronic pulse generator more desirable than a mechanical one. This is due to the difficulty of obtaining mechanical contacts with no chatter or bounce. An electronic pulse is derived from the tube which generates the fifth code impulse to operate a relay which in turn steps the master switch, and in addition provides a pulse to the step print sequence control.

Print Sequence Control

The print sequence control operates in a manner analogous to that of the transmitter. However, it contains only five counters in the ring instead of eight. It is triggered by the pulses received from the transmitter. These pass through a control circuit (operated by the master switch) before reaching the print sequence tubes in order that operation can occur only during the printing interval. Figure 4 shows a block diagram of the essential features. As the ring counter steps,

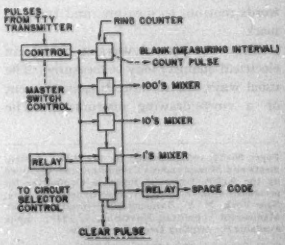

Figure 4. Print sequence

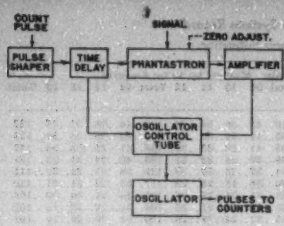

Figure 5. Step voltmeter

various auxiliary conditions are controlled. The blank interval is provided to permit time for the measurement. If three digits are to be printed the tubes of the 100's mixer are energized. The next step energizes the 10's mixer, the fourth step energizes the 1's mixer and also the auxiliary relay which energizes the coil of the circuit selector stepping relay. In the fifth step the circuit selecting relay moves to the next position. At the instant the print sequence is transferred to the first step a pulse is transmitted to the step voltmeter giving the command to make a measurement.

The Step Voltmeter

The actual measurement is performed during the blank interval of the print sequence by the step voltmeter, shown in the block diagram of Figure 5. On receipt of the count command pulse from the print sequence control, a pulse is generated by the pulse shaper which in turn causes the time delay tube[2] to function. The time delay tube does two things. It starts a phantastron,[3] and it also operates the oscillator control tube to hold the oscillator in an off position. At the end of the delay interval the oscillator control tube turns on the oscillator. Meanwhile, the phantastron has been started and it runs for a time interval determined by the d-c signal voltage applied to its plate. It operates through an amplifier to turn the oscillator control tube off. As the oscillator runs, a number of pulses will be generated proportional to the voltage being measured. The zero set is a voltage introduced into the phantastron to permit its running time with no signal to exactly equal the time delay interval, and thus, with no signal, the oscillator never starts.

Counting and Number Mixer

The pulses obtained from the oscillator are counted by four tube binary counters arranged in decades.[4] As many decades are provided as are required by the digits needed. Figure 6 indicates the general arrangement. The number mixer permits the selection of the proper digit as commanded by the print sequence control and, in addition, as determined by the count existing in the selected decade of the counters.

Voltages from the number mixer operate through the number mixer amplifier to operate the number mixer relays. It can be seen readily that with four relays ten possible contact arrangements can be provided. These contacts therefore set up the teletype codes required for each digit from one to zero. Table I shows the relays operated for each number from zero to nine.

Arrangement of Components

A complete machine is shown in Figure 7. This machine in addition to performing the functions outlined previously also will accumulate totals, shift ranges, and print on two machines. Two machines were required since the user desired more columns than were available on one machine. This can be carried as far as desired. In the rack from top to bottom are located a control panel, the tube circuits, the transmitting relays, the circuit selecting relays, and the power supply. Although the teletype machines are shown alongside the rack, they may be located at any distance provided a satisfactory communications link is used for interconnection.

A section of one of the log sheets obtained from one of the machines during a test period is shown in Table II. The machine was designed to read current in the outgoing lines of a distribution center and to accumulate totals for zone loads. The vertical columns are the readings in tens of amperes for a given line or total and the horizontal readings were made automatically once each half-hour. In this particular case the form for a log

Table I

Digit or Function	Relays Operated	TTY Code 1	2	3	4	5
1	DA	●	●	●		●
2	DB	●	●			●
3	DAB	●				
4	CD		●		●	
5	ACB					●
6	BCD	●		●		●
7	ABCD	●	●	●		
8	BC		●	●		
9	ABC				●	●
0	D		●	●		●
C.R.	Master Sw.				●	
Fig.	Master Sw.	●	●		●	●
L.F.	Master Sw.		●			
Stop	Master Sw.			●		●
Space	Spacing			●		

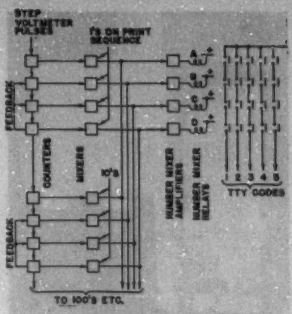

Figure 6. Number mixer

sheet is preprinted. Approximately 20 vertical columns can be printed on a page. Such features as automatic page advance at the end of the day can be readily obtained. These readings were made at the control center of the supervised distribution substation.

Fields of Usefulness

The usefulness of this instrument is most apparent on any continuous flow processes, such as electric power generation and transmission, gas transmission, oil storage or transmission, steel making, paper making, oil refining, chemical processes, and so forth. A portable type can be used in testing new installations. The readings of many different quantities related to the process such as time, temperature, pressure, flow, voltage, current, counting, integrated flows, and so forth, may all be assembled in a related manner on a single instrument and on a single log sheet. The record may be made at the most essential point whether feet or miles intervene. It is particularly useful in those operations which are fully automatic or where the man power available is low, or desired to be lowered.

The use of this instrument permitting the elimination of the human element results in a more accurate and legible record. All readings are taken as scheduled either by clock contacts or by some element of the process whether or not the operator is busy on other duties.

Where records are used in more than one office for various purposes the instrument will produce up to 20 good carbon copies. Copies containing vast amounts of data are readily mailed or stored. If more than 20 copies are required, a ditto carbon or ribbon may be used and up to several hundred copies may be obtained.

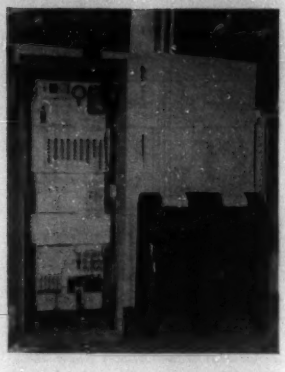

Figure 7. Rack and two printers producing 40 columns with totals and subtotals

In addition, if readings must be obtained at two or more locations, as many additional printers as desired may be used.

The Metrotype system for digital recording and telemetering is a measuring system which produces records in the form of columns for separate quantities, lined up automatically for time or some other factor. Transmission may be made any distance and may include totals or any other computation as required. The following are incidental benefits from the use of the Metrotype: greater accuracy, greater legibility, duplicate records, uniform timing of readings, and each reading distinct from all others.

References

1. Automatic Printing Ammeter, T. G. LeClair. *Electrical Engineering (AIEE Transactions)*, volume 60, March 1941, pages 93–99.

2. Standard Handbook for Electrical Engineers (book), A. E. Knowlton. McGraw-Hill Book Company, New York, N. Y., eighth edition, 1949.

3. Waveforms (book), Chance. Radiation Laboratory Series, volume 19, McGraw-Hill Book Company, New York, N. Y., 1949.

4. Electronic Counters, I. E. Grosdoff. *RCA Review* (New York, N. Y.), volume VII, September 1946, page 438.

Discussion

N. G. Larson (Commonwealth Edison Company, Chicago, Ill.): This discussion is restricted to describing an application of the device in the power field. In Chicago, the Commonwealth Edison Company is using a number of these machines, principally to record ampere load readings of 12,000-volt lines originating in various generating stations or 66,000-volt substations. The 4,000-volt radial distribution system throughout the city is supplied from step-down 12,000/4,000-volt distribution substations. These substations are geographically grouped together by 12,000-volt tie lines and the group supplied by radial 12,000-volt lines originating at one supply center. This center is the 12-kv switchhouse at either a generating station or 66,000-volt substation. The number of 12,000-volt supply lines per group varies from three to eight.

Table II. Metrotype Systems Record

Location—Glenwood Substation

No. Time	Line Current and Group Totals; Multiply by 10 for Amperes																			
	01	02	03	04	Total	05	06	07	08	Total	09	10	11	12	Total	13	14	15	16	Total
12:30	13	25	38	29	105	28	37	17	28	110	43	30	34	33	140	44	26	37	25	132
1:00	13	26	39	29	106	27	35	16	27	105	42	29	33	32	136	42	25	36	24	125
1:30	12	24	37	27	100	27	35	16	27	105	41	29	33	32	135	41	25	35	24	127
2:00	12	23	35	27	097	25	33	15	26	099	39	28	32	31	130	40	24	34	23	121
2:30	11	21	33	25	090	24	32	14	24	094	37	26	30	29	122	38	23	32	22	115
3:00	11	21	32	24	088	23	30	14	23	090	36	25	28	28	117	36	22	31	21	110
3:30	10	20	31	23	084	23	29	14	23	089	35	24	28	27	114	35	21	30	20	106
4:00	10	19	30	23	082	22	28	13	22	085	33	23	27	26	109	34	20	29	19	102
4:30	10	19	30	22	081	22	28	13	22	085	33	24	27	26	110	34	20	29	19	102
5:00	10	19	30	23	082	22	28	13	22	085	33	23	27	26	109	34	20	29	19	102
5:30	10	19	30	23	082	22	28	13	22	085	33	24	27	26	110	34	20	29	19	102
6:00	10	19	32	24	085	23	30	14	23	090	36	25	28	28	117	36	21	31	21	109
6:30	11	21	32	24	088	23	30	14	23	090	36	25	28	28	117	36	22	31	21	110
7:00	11	22	33	25	091	24	32	15	24	095	37	26	30	29	122	38	22	32	21	113
7:30	12	23	35	27	097	26	34	15	26	101	39	28	31	31	129	40	24	34	23	121
8:00	12	24	37	28	101	27	35	16	27	105	41	29	33	32	135	42	25	35	24	126
8:30	12	24	38	29	103	28	36	17	28	109	41	28	31	32	132	42	25	36	23	126
9:00	11	22	33	25	091	25	32	15	24	096	38	27	30	29	124	38	23	32	22	115
9:30	11	21	32	24	088	23	30	14	23	090	35	25	29	28	117	36	22	30	21	109
10:00	10	19	30	23	082	22	29	13	22	086	34	24	27	26	111	34	20	29	21	104
10:30	12	23	35	26	096	26	34	15	25	100	36	26	30	30	122	38	23	33	22	115
11:00	14	27	42	32	115	31	40	18	31	120	48	34	38	37	157	49	29	41	28	147
11:30	14	28	44	33	119	32	42	19	32	125	49	35	39	38	161	50	30	43	29	152
12:00	11	22	34	26	093	25	33	15	25	098	39	27	31	30	127	39	23	33	22	117
12:30	11	22	34	26	093	25	33	15	25	098	38	27	31	30	126	39	23	33	22	117
1:00	13	25	39	29	106	28	37	17	28	110	44	31	35	34	144	44	26	38	23	133
1:30	13	25	39	29	106	28	37	17	28	110	44	31	34	33	142	44	26	37	25	132
2:00	14	27	42	31	114	30	40	18	30	118	47	33	37	36	153	48	28	40	27	143
2:30	14	27	42	31	114	30	40	18	31	119	47	33	37	36	153	48	28	40	27	143
3:00	15	29	45	34	123	33	43	19	33	128	50	35	40	39	164	51	30	43	29	153
3:30	15	30	46	35	126	33	44	20	34	131	52	36	41	40	169	52	31	45	30	158
4:00	15	30	46	35	126	33	44	20	34	131	52	36	41	40	169	53	31	44	30	158
4:30	15	30	46	35	126	34	44	20	34	132	52	36	41	40	169	53	31	44	30	158
5:00	13	25	38	29	105	28	37	16	28	109	43	30	34	33	140	44	26	37	25	132
5:30	13	25	38	29	105	28	37	16	28	109	43	30	34	33	140	44	26	37	25	132
6:00	13	25	38	29	105	28	37	16	28	109	43	30	34	33	140	44	26	37	25	132
6:30	13	25	38	29	105	28	37	17	28	110	43	30	34	33	140	44	26	37	25	132
7:00	15	31	48	36	130	35	46	20	35	136	57	40	45	44	186	58	34	49	33	174
7:30	16	32	51	38	137	37	48	22	37	144	57	40	46	44	187	58	34	48	33	173
8:00	16	33	51	39	139	37	48	22	37	144	57	40	45	44	186	58	34	49	33	174
8:30	16	32	51	38	137	37	49	22	37	145	57	40	45	44	186	58	34	49	33	174
9:00	16	31	47	36	130	34	45	20	34	133	53	37	42	41	173	54	31	45	30	160
9:30	15	29	45	34	123	33	43	19	33	128	51	36	41	39	167	52	30	44	29	155
10:00	15	29	45	34	123	32	41	19	32	124	49	35	39	38	161	50	29	42	28	149
10:30	14	27	41	31	113	30	39	17	30	116	46	32	37	35	150	47	27	39	26	139
11:00	13	26	40	30	109	28	38	17	29	112	45	31	36	34	145	45	26	38	25	134
11:30	13	25	40	30	108	28	37	16	28	109	43	30	34	33	140	44	25	37	25	131
12:00	12	24	37	28	101	27	35	16	27	105	41	29	33	32	135	42	25	36	24	127

In stations where manual recording is used, the sequence of line readings on the data sheet is determined by the location of the line ammeters on the instrument panel. Consider, for example, an 8-line substation group. In this case the lines are supplied from eight different line busses at the 12-kv switchhouse. The readings are necessarily scattered throughout the data sheet, resulting in a considerable time interval between the first and last reading, particularly in large stations having as many as 50 outgoing lines. The determination of the group maximum from the data sheet at any particular hour requires the use of a special template, and the determination of the daily maximum requires considerable cut-and-try computation.

In stations where machine recording is used, all lines to the same substation group are grouped together on the automatic meter. This results in: more reliable coincident group maximum because of a very large reduction in time interval required to record all of the line readings; simplification in comparing individual line readings; elimination of need for cut-and-try computation in determining group maximums since the group line readings are automatically totalized; insurance that readings are taken on scheduled time; and the ability to take special readings at any time by merely pushing a button.

The machine has been found to be particularly useful in the case of large unattended supervisory controlled 66,000-volt substations. Substation groups are supplied from these stations by 12,000-volt radial lines in the same manner as from generating stations. The line-ampere readings are teletyped to the remote supervisory center, and are there recorded. The operators at the control center can obtain special readings at any desired time.

Our load dispatchers make frequent use of these special readings. For example, such readings are taken at supervisory control center and relayed by telephone to load dispatcher whenever it is required to take a line out of service, or during times of unscheduled line outage. With system data readily available, proper action can be taken immediately by the dispatchers. If these data were not available, it would be necessary to dispatch a travelling operator to the unattended substation and wait for his report, and usually to perform insurance operating in the interim.

New Techniques on the Anacom—Electric Analog Computer

E. L. HARDER
FELLOW AIEE

J. T. CARLETON
ASSOCIATE AIEE

Synopsis: The paper outlines the direct-analog approach used on the Anacom and describes the sigma amplifier which combines adding, integrating, delay, and other operations into a single computer amplifier and results in an improved computing technique. Examples include a speed-regulating system, and systems of simultaneous differential equations such as the aerodynamic equations of flight of an airplane. An adjustable nonlinear resistor and other functional devices are described, together with their use in analogs of fluid flow, saturating iron cores, magnetic amplifiers, and hysteresis. An analog for corona is given.

THE Anacom[1] was designed as a general purpose electric analog computer based on several years' experience with smaller scale and special purpose computers. These were the electric transients analyzer,[2] the servo analyzer,[3] the mechanical transients analyzer,[4] and the pilot model of the general purpose computer.[5] These transient computers, or solvers of ordinary and partial differential equations had in turn been built up from a background of experience with the d-c and a-c network calculators,[6] machines primarily for solving the short-circuit, steady-state, and stability problems of electric power systems.

The general purpose electric analog computer, the Anacom, was started in 1946 and completed in 1948. However, because of its compartmented character, problems were started before its final completion. In the approximately $1^1/_2$ years of its operation some 43 different types of problems have been solved, involving a total of 141 distinct problems.

Most of these problems have had to do with the design, application, or operation of electric and mechanical machinery and equipment or with studies of switching transients and lightning phenomena in electric power systems. These are all physical problems that are reducible to mathematics. However, several purely mathematical problems have been solved, which, though they may have physical interpretations, did not arise directly therefrom.

In the course of this work the analog techniques have been vastly improved resulting in a more systematic approach of great power and flexibility. It is the purpose of this paper to outline some of these techniques and to indicate their use in typical problems.

The Direct-Analog Method

The Anacom is a general purpose computer composed of a multiplicity of integral computing elements and thus can be used to solve problems by a variety of techniques. However, it is particularly powerful in the direct-analog approach[7] which now will be described.

Figure 1 (B) illustrates the same problem analyzed by the conventional analog approach, and also by the direct-analog method, Figure 1(C). In the direct-analog method all elements of the physical system, or nearly all, have their counterparts in the analog and as such are under the direct and independent control of the operator. To study the effect of varying a certain element of the system the operator need only vary the corresponding element of the analog. In rare cases this may involve a lessened mathematical generality and the use of a few

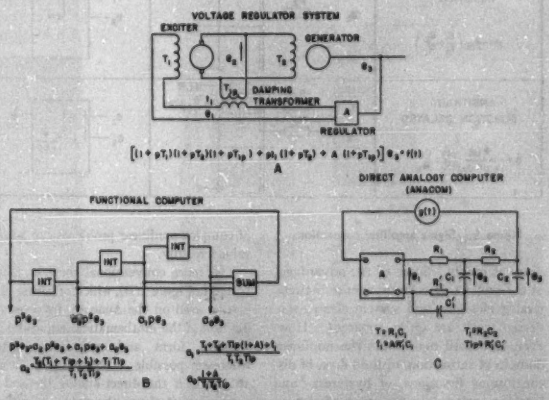

Figure 1. Analogs of a simple regulating system

(A). Voltage regulating system; (B). Functional or indirect analog; (C). Direct analog

Paper 50-85, recommended by the AIEE Computing Devices Committee and approved by the AIEE Technical Program Committee for presentation at the AIEE Winter General Meeting, New York, N. Y., January 30–February 3, 1950. Manuscript submitted November 2, 1949; made available for printing November 30, 1949.

E. L. HARDER is Technical Director of the Anacom, and J. T. CARLETON is Anacom Operating and Design Engineer, both with the Westinghouse Electric Corporation, East Pittsburgh, Pa.

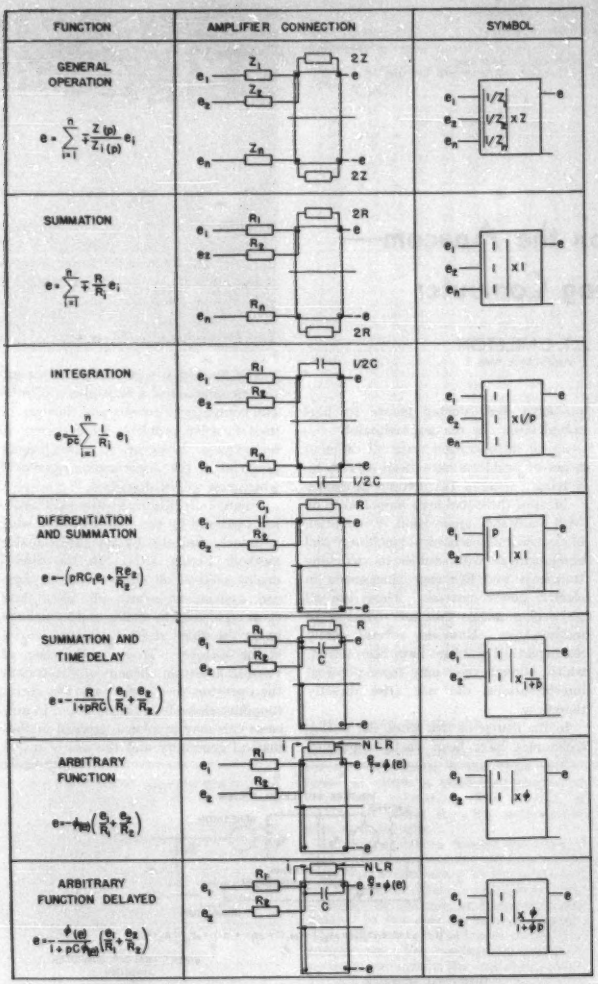

Figure 2. Sigma amplifier connections

more elements. Some of the advantages of a direct 1-to-1 correspondence between analog elements and system elements in design work are quite apparent. However, not until one enters the nonlinear domain of saturation, of fluid flow, of discontinuous functions, of hysteresis, and limiting action does the great advantage of the direct-analog method become truly evident. Rapid and accurate solutions of complex nonlinear problems can be obtained readily.

The more conventional method, illustrated in Figure 1(B), which of course also can be used on the Anacom, involves reduction of the mathematical equations to simplest form and combining terms wherever possible. This step is desirable even if the direct-analog method is used, since it shows the actual combination of parameters on which the solution depends. The highest order derivative is usually integrated by successive integrators until all the required derivatives have been obtained. These then are operated upon by addition, multiplication, and other functional processes as indicated by the equation so that the highest order derivative, which had been assumed at the start to be available, is thus generated, as shown in the figure. The computer as thus connected is a direct analog of the equation but is an indirect analog of the system.

This method has the distinct advantage of a systematic mathematical approach and has been most successful in many years of operation of the differential analyzer.[8–10] Also, in many scientific and mathematical problems the direct analog does not have the same advantages that it has in design work. For example, in solving the complex equations of cosmic-ray paths the direct-analog method is certainly not indicated.

One would be foolhardy to attempt to delineate the precise field of applications of these two methods, as they depend a great deal on the computer characteristics, the nature of information sought, whether a general or specific problem is studied, the relative costs of preparation and interpretation as compared with actual computer costs and many other factors. However, with a high-speed computer, and engineering problems of design and application, the direct analog, wherever it can be devised readily, offers considerable advantage. In design particularly, the designer may have only two or three of a total of fourteen or fifteen system parameters at his disposal to vary. The direct analog enables these to be varied with a minimum of effort, preparatory computation, and subsequent interpretation. It makes possible the direct determination of optimum solutions obtainable with the variables under the designer's control. This will become more evident in the example to follow. Practically all of the problems on the Anacom to date have been solved by the direct-analog method.

The Sigma Amplifier

The use of the feedback amplifier as a computer or simulator element is well known and will not be discussed here except to show the particular type, and the use made of it, in the Anacom. The general functional relationship obtainable between output and input voltages is indicated in the top row of Figure 2. The resulting relationships for various input and feedback impedances are given in the subsequent rows, together with the

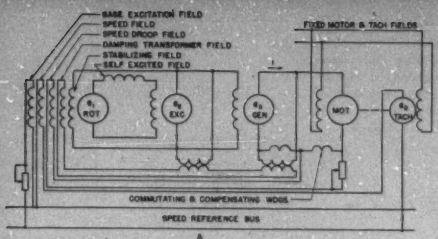

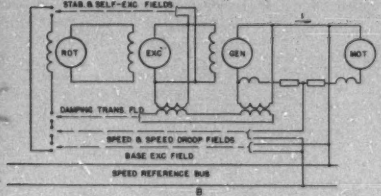

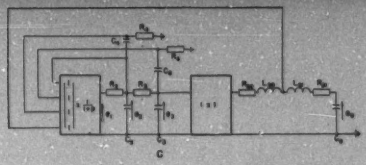

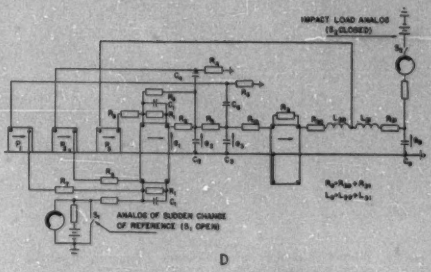

Figure 3 (above). Speed regulator analog

(A). Regulating system. (B). Simplified equivalent. (C). Schematic analog. (D). Complete analog connection diagram. (Analogous relations are listed in Table I)

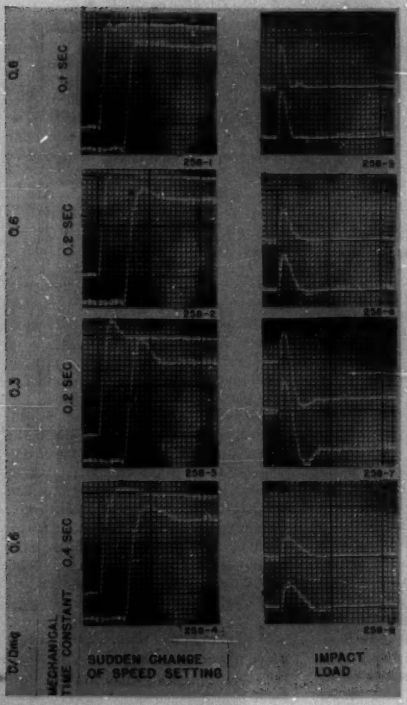

Figure 4 (left). Typical generator voltage traces for regulating system of figure 3

Upper traces—Damping number 1. Lower traces—Damping number 2

Figure 5 (below). Effect of exciter hysteresis on speed regulator transient performance

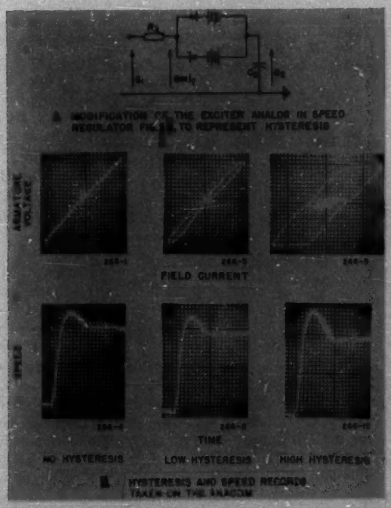

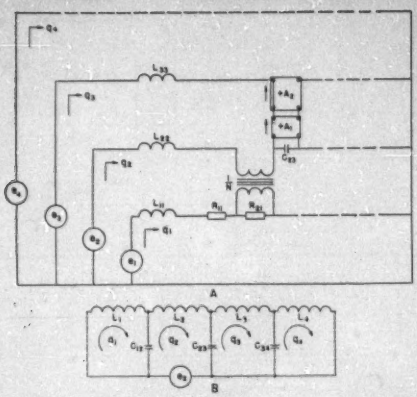

Figure 6. Illustrative analogs for simultaneous equations

(A). General simultaneous equations

$$f_1(t) = A_{11}\frac{d^2y_1}{dt^2} + B_{11}\frac{dy_1}{dt} + B_{12}\frac{dy_2}{dt} + \ldots$$

$$f_2(t) = A_{22}\frac{d^2y_2}{dt^2} + B_{22}\frac{dy_2}{dt} + B_{21}\frac{dy_1}{dt} + \ldots$$

$$f_3(t) = A_{33}\frac{d^2y_3}{dt^2} + B_{33}y_3 + \ldots$$

$$f_4(t) = \ldots$$

Analogous relations

$e_1 \equiv f_1(t)$ $\qquad \frac{1}{C_{23}}A_3A_3 + \ldots \equiv B_{33}$

$L_{11} + \ldots \equiv A_{11}$ $\qquad q_1 \equiv y_1$

$R_{11}R_{21} + \ldots \equiv B_{11} \ldots$

$\frac{R_{21}}{N} + \ldots \equiv B_{12}$ $\qquad q = change$

(B). Limited simultaneous equations in four variables; analog for spring-connected masses

$$\frac{d^2\theta_1}{dt^2} + \frac{K_{12}}{I_1}(\theta_1 - \theta_2) = 0$$

$$\frac{I_2}{I_1}\frac{d^2\theta_2}{dt^2} + \frac{K_{12}}{I_1}(\theta_2 - \theta_1) + \frac{K_{23}}{I_1}(\theta_2 - \theta_3) = F_2(t)$$

$$\frac{I_3}{I_1}\frac{d^2\theta_3}{dt^2} + \frac{K_{23}}{I_1}(\theta_3 - \theta_2) + \frac{K_{34}}{I_2}(\theta_3 - \theta_4) = 0$$

$$\frac{I_4}{I_1}\frac{d^2\theta_4}{dt^2} + \frac{K_{34}}{I_1}(\theta_4 - \theta_3) = 0$$

Analogous relations

$e_2 \equiv F_2(t)$

$\theta_1, \theta_2, \ldots \equiv q_1, q_2, \ldots$

$L_1 \equiv I_1$

$1/C_{12} \equiv K_{12}$

symbolic representation used in computer schematic analogs. Note that the operator $p = d/dt$ is utilized to symbolize differentiation, $1/p$ integration, $(1+p)$ advance through a time constant, $1/1+p$ delay of a time constant, and so forth.

The particular amplifier used for this purpose can be supplied with either push or pull input signals and supplies both push and pull outputs. It thus obviates the need for separate sign-reversing amplifiers. This differential input arrangement also makes possible operation of the amplifier grounded although neither side of the input voltage is grounded. Because of its multiplicity of uses, one of which is as an adding amplifier, and for want of a better name, this device has come to be known as a Sigma amplifier.

Through its use, ungrounded operation of amplifiers, multipliers, and other electronic gear, as well as the use of transformers in the analogs, has been largely eliminated. Voltages are developed to ground and added in adding amplifiers instead of in series loops as was common in earlier analogs. This greatly simplifies the electronic equipment making possible common power supplies, simplifies shielding, and results in a more systematic procedure for determining the analog.

Speed Regulator Analog

The four steps usually present in the over-all solution of a problem by electric analog may be illustrated by the four parts of Figure 3. The problem here is the determination of speed versus time for impact loads and for sudden changes of the speed setting. Solutions are required for a large number of values of the parameters, and so the analog method is to be used.

The system shown consists of a d-c motor with fixed field supplied by a generator whose field is controlled by a Rototrol through an intermediate exciter. The Rototrol responds to deviations of the speed (tachometer voltage) from the reference voltage setting. Speed droop with motor load is provided by feeding back the commutating and compensating field drop into a separate Rototrol field. Stabilization is afforded by degenerative feedback from the exciter and by damping transformers which feed back derivative functions of exciter and generator voltage. Base excitation is supplied through still another Rototrol field to reduce the unregulated speed error and hence increase the accuracy of regulation for a given regulator gain.

It is a matter of machine and regulator theory requiring a specialist in this field to reduce this system to its equivalent, Figure 3(B), and its corresponding equations. It is an important matter, sometimes overlooked, that between the actual physical problem and its mathematical expression, with such approximations as are permissible in the particular art, lies a whole field of knowledge with which the operator of a general purpose computer will not in general be familiar. The mathematical expression of the problem is strictly a function of the specialist in the field of the problem, working of course in conjunction with the computer staff to express the problem in proper form and with sufficient information. Practically, there is considerable overlap in these two functions since analog computers have usually started as special purpose computers for particular problems, and the computer engineer is, or soon becomes, skilled in the art in question.

Figure 3(C) gives the schematic analog which obeys the same differential equations as the system in question. It is made up by reference to tables of basic

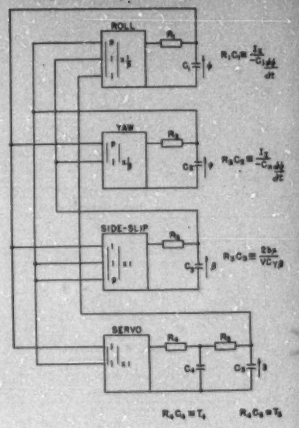

Figure 7 (right). Sigma amplifier analog for representing the aerodynamic equations of flight of a high-speed airplane

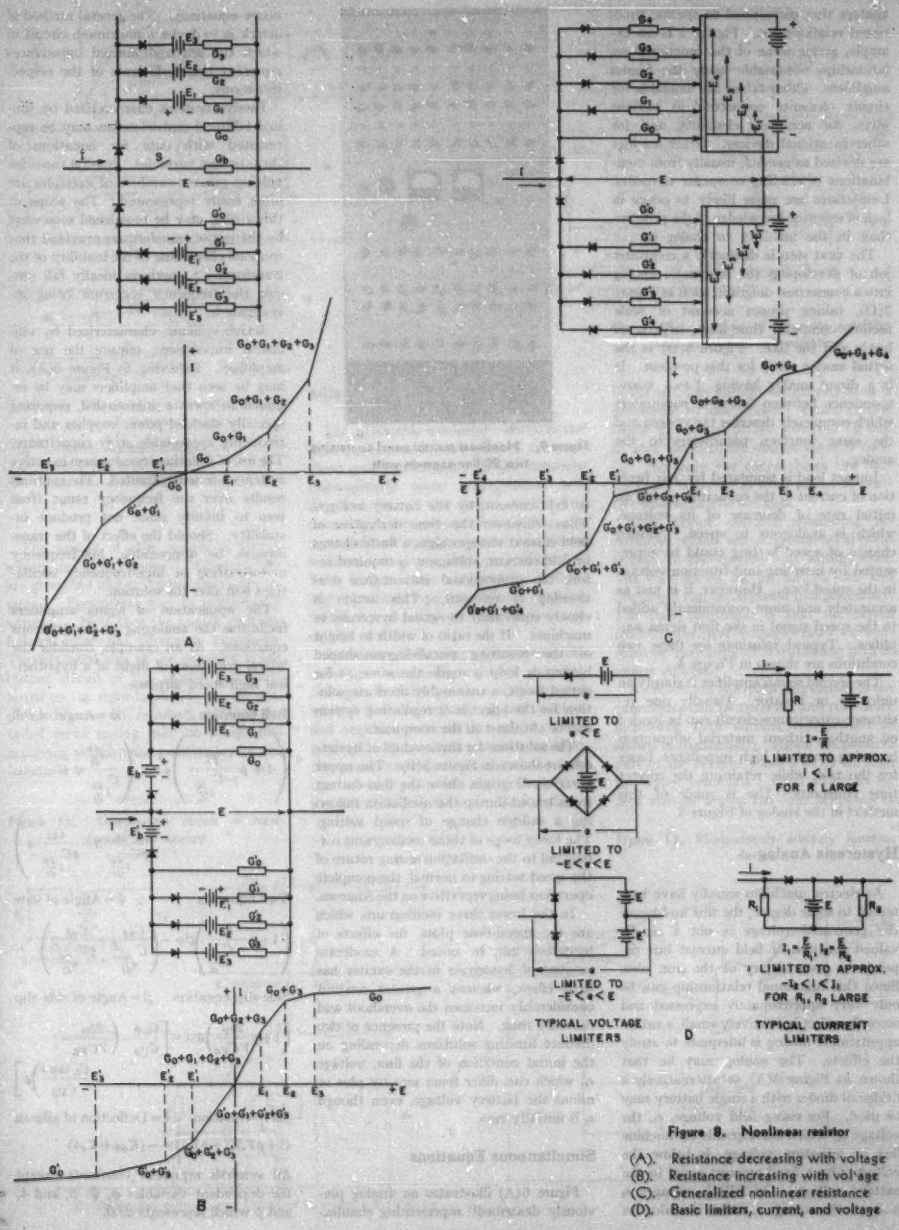

Figure 8. Nonlinear resistor

(A). Resistance decreasing with voltage
(B). Resistance increasing with voltage
(C). Generalized nonlinear resistance
(D). Basic limiters, current, and voltage

analogs that correspond to specific functional relationships. Figure 2 is an example, giving some of the functional relationships obtainable using the Sigma amplifiers. Other tables are available for circuit elements connected in various ways, for nonlinear elements, and for other functional devices. Other analogs are devised as needed, usually from combinations of existing computer elements. Limitations are more likely to occur in lack of essential knowledge of the problem than in the inability to analog it.

The next step is distinctly a computer job of developing the schematic analog into a connection diagram, such as Figure 3(D), taking proper account of scale factors, computer time base, impedance levels and the like. Figure 3(D) is the actual analog setup for this problem. It is a direct analog having 1-to-1 correspondence between fourteen parameters which completely describe the system and the same fourteen parameters in the analog.

Impact load is simulated by unit function of current in the capacitor, giving an initial rate of decrease of its voltage, which is analogous to speed. Sudden change of speed setting could be represented by inserting unit-function voltage in the speed loop. However, it is just as accurately and more conveniently added to the speed signal in the first sigma amplifier. Typical solutions for these two conditions are shown in Figure 4.

The second sigma amplifier is simply an unloader or isolator. Usually one resistance-capacitance circuit can be loaded on another without material interaction by using low and high impedance bases for the two, while retaining the correct time constants. Use is made of this method in the analog of Figure 3.

Hysteresis Analog

As electric machines usually have hysteresis to some degree, the flux and hence the generated voltage is not a single-valued function of field current but depends on past history of the iron also. Since this functional relationship can be only very approximately expressed and since the effect is relatively small, a rather approximate analog is adequate to study the effects. The analog may be that shown in Figure 5(A), or alternatively a bridge of diodes with a single battery may be used. For rising field voltage, e_1, the voltage e_2, which corresponds to machine flux or armature voltage, is below the voltage e by a fixed amount equal to the battery voltage. On falling voltages e_2 is above the voltage e, which is analogous

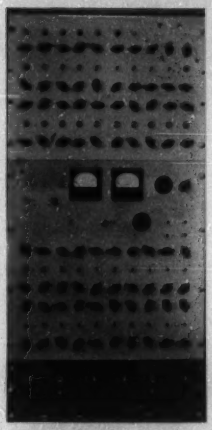

Figure 9. Nonlinear resistor panel containing two 20-line-segment units

to field current, by the battery voltage. Thus whenever the time derivative of field current changes sign, a finite change in field current, voltage e, is required before the proportional current-flux relationship is resumed. This action is closely equivalent to actual hysteresis in machines. If the ratio of width to height of the resulting parallelogram-shaped hysteresis loop is made the same as for actual loops, a reasonably accurate solution for the effect in a regulating system can be obtained on the computer.

The solutions for three values of hysteresis are shown in Figure 5(B). The upper three oscillograms show the flux-current locus traced during the oscillation following a sudden change of speed setting. The lower loops of these oscillograms correspond to the oscillation during return of the speed setting to normal, the complete operation being repetitive on the Anacom.

In the lower three oscillograms which are the speed-time plots, the effects of hysteresis can be noted. A moderate amount of hysteresis in the exciter has little effect, whereas a greater amount considerably increases the overshoot and recovery time. Note the presence of two distinct limiting solutions depending on the initial condition of the flux, voltage e_3, which can differ from zero by plus or minus the battery voltage, even though e_1 is initially zero.

Simultaneous Equations

Figure 6(A) illustrates an analog previously described[11] representing simultaneous equations. The general method of attack is to devise a multimesh circuit in which the self and mutual impedances represent the coefficients of the respective terms.

Passive systems characterized by limited bilateral mutual terms may be represented with ease for equations of three or less variables. Special cases involving greater numbers of variables are often easily represented. The scope of this analog may be broadened somewhat by the use of transformers provided that spurious effects due to the inability of the transformer to perform ideally fall outside the frequency spectrum being investigated.

Active systems, characterized by unilateral impedances, require the use of amplifiers. Referring to Figure 6(A), it may be seen that amplifiers may be required to operate ungrounded, requiring specially shielded power supplies and introducing appreciable stray capacitance. The use of isolating transformers in active systems is seriously limited. The spurious results over the frequency range from zero to infinity must not produce instability. Should the effect of the transformers be appreciable, low-frequency motorboating or high-frequency oscillations will alter the solution.

The application of sigma amplifiers facilitates the analoging of simultaneous equations. As an example, consider the lateral equations of flight of a hypothetical high-speed airplane.

Roll equation ϕ = Angle of roll

$$\left(1+p\frac{I_x}{-C_{l\frac{d\phi}{dt}}}\right)\phi=-\left(\frac{C_{\frac{d\psi}{dt}}}{C_{l\frac{d\phi}{dt}}}\psi+\frac{C_{l\beta}}{pC_{l\frac{d\phi}{dt}}}\beta+\frac{C_{l\delta}}{pC_{l\frac{d\phi}{dt}}}\delta\right)$$

Yaw equation ψ = Angle of yaw

$$\left(1+p\frac{I_z}{-C_{n\frac{d\psi}{dt}}}\right)\psi=-\left(\frac{C_{n\phi}}{C_{n\frac{d\psi}{dt}}}\phi+\frac{C_{n\beta}}{pC_{n\frac{d\psi}{dt}}}\beta\right)$$

Side-slip equation β = Angle of side slip

$$\left(1+p\frac{2b\mu}{VC_{Y\beta}}\right)\beta=-\left[\frac{C_{L\phi}}{C_{Y\beta}}-\left(\frac{2b\mu}{VC_{Y\beta}}-\frac{C_L\tan\nu}{C_{Y\beta}}\right)\psi\right]$$

Servo equation δ = Deflection of aileron

$$(1+pT_4)(1+pT_5)\delta=-(K_\phi\phi+K_\psi 4)$$

All symbols represent constants except the dependent variables ϕ, ψ, β, and δ, and p which represents d/dt.

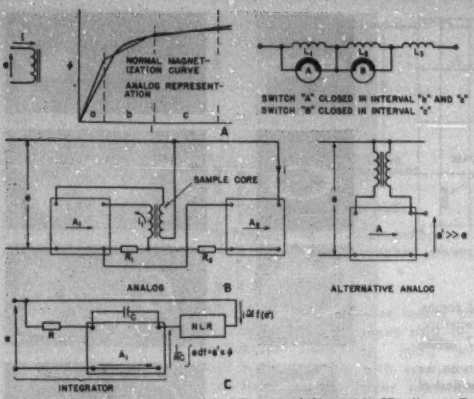

Figure 10. Analogs of a saturating, iron-cored inductance

(A). Switched inductance analog
(B). Sample core analog
(C). Integrator and nonlinear resistor analog

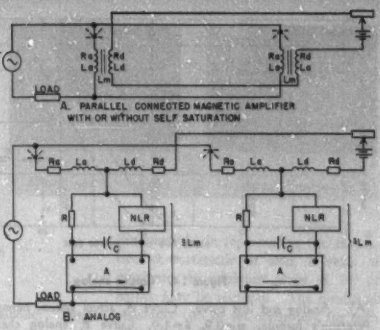

Figure 12. Analog of magnetic amplifier with or without self-saturation

The analog of this system is shown schematically in Figure 7. All amplifiers are grounded and no transformers are required. Parameters may be individually adjusted. Note that the analog logically follows from the foregoing equations. The left-hand side of the equation is the output circuit of the amplifier and the terms on the right-hand side are the amplifier inputs. If required, a more detailed servo analog may be substituted involving velocity and position limits and backlash.

Figure 11. T-equivalent circuit of transformer and analog

Adjustable Nonlinear Resistor

The adjustable nonlinear resistor is the basis for a considerable part of the nonlinear problem solution on the Anacom. Consequently some consideration will be given first to the device itself. The circuit is a connection of rectifying elements, direct voltage sources, and linear resistors, connected as shown in Figure 8. With it monotonic (continually increasing) functions can be closely approximated by a series of straight line segments.

Resistance decreasing with current is obtained as shown in Figure 8(A). If switch S is open, positive portions of the current wave I flow through the upper resistors and negative portions through the lower resistors. For positive currents the effective conductance is G_0 as long as the voltage is 0 to E_1. In this region no current flows in G_1, G_2, G_3 since E_1, E_2, and E_3 act to the left, but current in this direction is prevented by the diodes. Above E_1 but below E_2 current divides between G_0 and G_1 and the effective conductance is $G_0 + G_1$. Similarly the curve shows the conductance effective in each region of positive and negative voltages.

This device permits simulating resistances which are unsymmetrical with respect to the current and voltage axes. The voltages E_1, E_2, E_3, E_1', E_2', E_3' and the slopes can be adjusted independently. The only limitation is that the slopes (current per-unit voltage) must be constant or increasing with increasing plus or minus voltage.

By reversing the rectifying elements the curvatures can be reversed and resistance increasing with current represented as shown in Figure 8(B). Again the positive part of the current wave I flows through the upper branches. E_4 is adjusted for zero voltage across the four branches at

Figure 13. Photoelectric arbitrary function device

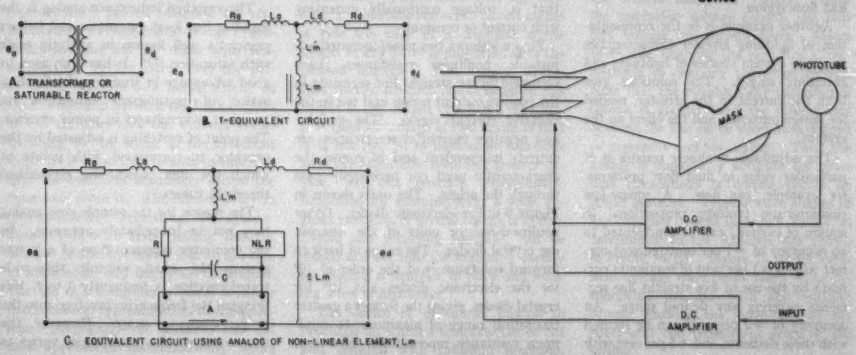

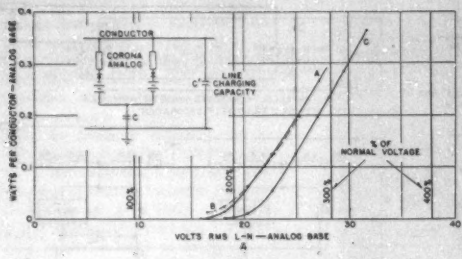

Figure 14. Corona analog

(A). Analog and loss curve. Curve *A*, actual system, normal corona, Peterson's formula, $m=0.9$, $\delta=1.0$; Curve *B*, analog characteristic; Curve *C*, actual system, heavy corona, $m=0.945$, $\delta=1.17$

(B). Wave shapes of line-charging current with corona, taken on the Anacom. The critical disruptive voltage equals 132 per cent of the peak of the normal line to neutral voltage

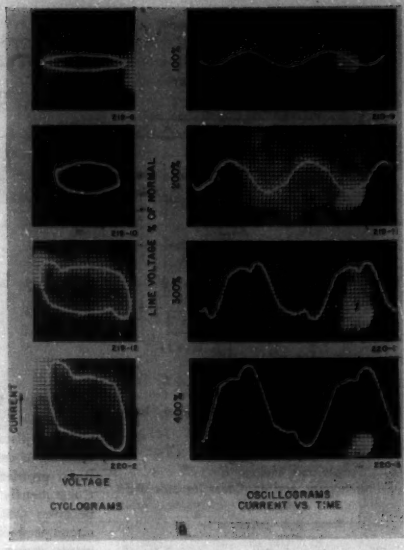

zero current, I. Then as the current I increases G_1 cuts out at E_1, G_2 at E_2, and G_3 at E_3. The conductance effective in each region is shown on the associated curve.

For convenience potentiometers are used in place of the multiple batteries. Diodes are arranged for reversal so that functions having reversals of curvature can be represented as shown in Figure 8(C). Again the conductances effective in each region are indicated on the associated characteristic curve. As the voltage E is raised certain conductances cut in and others cut out, producing any desired variation of conductivity G with E or I.

An example of the use of the nonlinear resistor is the analog of a deisel engine lubricating system. The characteristic to be represented for many of the passages is linear in the laminar flow region and approaches square law in the turbulent flow region.

Another example is in the representation of lightning arrester characteristics in power system studies of lightning and switching surges. The solutions give both the current in the arrester, needed for design purposes, and the effect on the system.

The adjustable nonlinear resistor is of particular value in fluid flow problems, for example, gas flow. A square-law characteristic (voltage proportional to square of current) can be represented to an accuracy of ±1 per cent (current correct within ±1 per cent of maximum current) by the use of five straight line segments covering any desired range. An accuracy of ±2 per cent can be secured with three elements, and ±5 per cent with two elements. Actual results are somewhat better than these theoretical figures which are based on sharp intersection of the straight lines. Other uses will be illustrated later in the paper.

The nonlinear resistor degenerates in the simplest cases to current- and voltage-limiter circuits, typical arrangements of which are illustrated in Figure 8(D). These are useful for representing backlash, hysteresis, limiting action, and other types of discontinuities.

In general this device provides an arbitrary function of either dependent or independent variables with the sole restriction that the function be monotonic, that is, voltage continually increasing with current or constant.

Figure 9 shows two panel-mounted adjustable nonlinear resistances, each equipped for ten straight-line segments in the positive current region and ten in the negative current region. The positive and negative current characteristics are entirely independent and of course the characteristic need not necessarily pass through the origin. The units shown in Figure 9 utilize electronic diodes. Other nonlinear-resistor units of the Anacom use crystal diodes. The range of back to forward resistance is of the order of 10^5 for the electronic diodes and 10^3 for crystal diodes, giving the former a greater theoretical range of maximum to minimum resistance represented. However, not all of this increased range is usable and the lower forward resistance of crystal diodes is advantageous in some analogs.

Analog of a Saturating Iron-Cored-Inductance Magnetic Amplifier[13]

Three basic analogs which have been used to represent the functional relationships involved in a saturating or saturable iron-cored inductance are shown in Figure 10. In two of these, (A) and (C), the normal magnetization curve is represented, whereas in the third, (B), hysteresis is represented, but a small sample of the actual iron is required.

The switched inductance analog is the simplest but least automatic and follows principles well known in analytic work with saturation.[13,14] It has been used to good advantage in studying the limiting action of transformer saturation on transient overvoltages in power systems. The point of switching is adjusted by the operator to correspond with points at which the flux passes the established threshold values.

The reason for the sample core analog may not be immediately apparent. In the computer representation of a power system the most suitable time-scale transformation is frequently 1-to-1, this bringing the frequencies involved into the proper computer range. However, the time constant of a transformer varies as

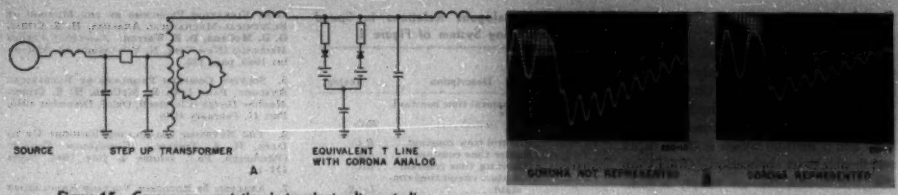

Figure 15. Corona representation in transient voltage studies

(A). Schematic single-line diagram of transmission line, one end open
(B). Oscillograms of voltage on phase A during line de-energizing operation

the square of its linear dimensions. Thus a 2-inch model of a 200-inch-high transformer would have a time constant 10^4 too low, or the winding resistance is 10^4 too high. The circuit of Figure 10(B) eliminates this resistance from consideration.

The integrator-nonlinear-resistor analog of Figure 10(C) combines flexibility with automatic operation and has been used in magnetic amplifier studies described recently.[13] As would be expected, it has been found quite adequate for study of saturation phenomena when representation of the normal magnetization curve is sufficient and not adequate if the phenomenon is dependent, to an important extent, on hysteresis.

The analog of a core with two windings is shown in Figure 11 and follows the conventional T representation of a 2-winding transformer. The magnetizing branch has been separated into linear and nonlinear inductances corresponding to mutual flux inside and outside of the iron core, to provide direct correlation with iron characteristics and coil form.

The use of this basic analog in the complete analog of a parallel-connected magnetic amplifier with or without self-saturation is shown in Figure 12. This representation proved adequate for representation of amplifiers without self-saturation but not for those with self-saturation. In the latter case the performance depends to a major extent on the relationship between the back current of the rectifiers and the current corresponding to the width of the hysteresis loop. It is important to note in this case that the computer accurately solved the equations given it. The difficulty lay in mathematically expressing the system. Comparison with tests quickly brought out this deficiency, resulted in an increase in knowledge, and improved techniques. The use of a computer requires accurate mathematical representation of the problem. Frequently the problem has not been approached mathematically before the computer became available. Thus the techniques must be developed cooperatively, initial solutions being checked with experience and tests to assure proper representation in later studies.

In machine studies the generated voltage produced by rotation is proportional to flux instead of to its time derivative. The analog for saturation is then more simple and is indicated in the lower row of Figure 2. Use of a nonlinear resistor, as described here, in the feedback position fulfills the equations in this case. It may be noted simply that both the ratio of armature to field voltage and the time constant are reduced by saturation at the higher voltages, as occurs in machines and as represented by the equations given, the function being the flux-current relationship.

Photoformer

The oscillographic arbitrary-function device,[14,16,17] which has been called a Photoformer, is a new technique of considerable promise in the analog computer field. It consists of the elements shown in Figure 13. As the beam is moved horizontally in accordance with one variable, a phototube and servo circuit makes it ride the edge of a template whose height at any point is proportional to the desired function. The vertical deflection voltage which is proportional to this height is the output or desired function.

A chief advantage of this device is that it is not limited to monotonic functions as is the adjustable nonlinear resistor device, but can generate trigonometric functions, for example, over a wide angular variation of several complete cycles. Useful and recurring functions can be stored and set into the computer merely by slipping a template in place and making a few adjustments.

The device is, of course, limited to functions for which a template can be cut and oriented with sufficient precision. For example, in representing the saturation characteristic of iron, a ratio of maximum to minimum slope of 10^3 or higher may be required. The nonlinear resistance can be set accurately for such ratios but the Photoformer template would be extremely sensitive to orientation with such steep slopes. Also where large numbers of nonlinear elements are required, the simplicity and economy of the resistor type dictates its use. There thus appears to be a definite need for both devices in the general purpose computer.

Corona Analog

A most interesting analog is that for corona on high-voltage transmission lines shown in Figure 14, which has been valuable in studying the action of corona in limiting transient overvoltages. Space does not permit the detailed theory to be given, but its principle of operation is as follows. As the voltage of a wire rises, no corona current flows until a critical disruptive voltage is exceeded. From this point until crest voltage a current flows, producing a space charge about the conductor. After crest there is no further current until the conductor potential falls to twice critical voltage below the crest voltage, when corona current flows until the next crest.

In the analog the batteries are set for the critical disruptive voltage. Until the conductor voltage exceeds the battery voltage, no current flows. Above this value, charging the capacitor C corresponds to charging the space charge. Note that the possible daily variation of corona is greater than the discrepancy between the loss curve which it is desired to represent and its analog. Thus the analog is sufficiently accurate for practical calculations of corona effects on power systems. Typical wave shapes of line-charging current including corona, as determined on the Anacom, are shown in Figure 14(B). Figure 15 shows transient voltage wave forms taken when de-energizing the line with and without corona, showing the magnitude of the effect and the consequent value of the analog.

Conclusions

Analog computer work is admittedly still in its infancy and the only conclusion that seems indisputable is that this is a very powerful method of computation of a wide range of complex engineering problems and a method which is quite rapid and flexible in its application. Other than this, our conclusions are simply a summary of some of the important points of the paper.

1. The direct-analog technique has distinct advantages in engineering design and application problems and has been used almost exclusively on the Anacom.

2. The sigma amplifier technique with consequent operation of all electronic equipment grounded is a major improvement in the direct-analog method. It simplifies problems of shielding and power supply, largely eliminates transformers and systematizes analog procedures.

3. The adjustable nonlinear resistor device is the preferred arbitrary function of a dependent variable provided the function to be represented is monotonic. Square-law representation within ±1 per cent is possible with five line segments, ±2 per cent with three segments, and ±5 per cent with two segments.

4. For other single-valued functions and certain double-valued functions the Photoformer presents a very useful solution. The ability to retain templates of important functions for subsequent use is of considerable value.

5. Studies of nonlinear systems have included representation of lightning arresters, transformer saturation, saturable reactors (magnetic amplifiers), saturation in machines, lubrication (fluid flow), hysteresis, corona, backlash (dead zone), limiting action, and other phenomena. Some of these have involved partial differential equations solved by the difference equation method. In this nonlinear field, computation by other means is extremely difficult and the analog computer is opening up vast new fields of information.

Table I. Analogous Relations in Speed Regulating System of Figure 3

Quantity in Actual System	Description	Analog
T_3	Mechanical time constant, $\frac{RI^*}{bg}$	R_3C_3
T_1	Rototrol time constant	R_1C_1
T_2	Exciter time constant	R_2C_2
T_5	Generator time constant	R_5C_5
T_4	Armature circuit time constant	L_a/R_4
T_6	Commutating and compensating field time constant	L_n/R_{11}
T_{p2}	Exciter damping transformer primary time constant	R_2C_6
k_{s02}	Exciter damping transformer mutual time constant times loop gain	$R_2C_6P_2\frac{R_1}{2R_3}$
T_{p5}	Generator damping transformer primary time constant	R_5C_8
k_{s05}	Generator damping transformer mutual time constant times loop gain	$R_5C_8P_5\frac{R_1}{2R_3}$
D/D_{mE}	Ratio of the speed droop, D, to the unregulated speed droop, D_{mE}	$\frac{R_{11}}{R_3}$
A	Speed loop gain	$P_5\frac{R_1}{2R_3}\frac{R_9}{R_{10}}$
N	Negative feedback loop gain (stabilizing and self-exciting fields)	$\frac{R_1}{2R_{11}}$

* R = Armature circuit resistance
I = Moment of inertia
b = Torque per ampere
g = Volts per radian per second

References

1. A Large-Scale General-Purpose Electric Analog Computer, **E. L. Harder, G. D. McCann.** *AIEE Transactions*, volume 67, part I, 1948, pages 664–73.

2. System Recovery Voltage Determination by Analytical and A-C Calculating Board Methods, **R. D. Evans, A. C. Monteith.** *Electrical Engineering (AIEE Transactions)*, volume 56, June 1937, pages 695–705.

3. Solution of the General Voltage Regulator Problem by Electrical Analogy, **E. L. Harder.** *AIEE Transactions*, volume 66, 1947, pages 815–25.

4. A New Device for the Solution of Transient Vibration Problems by the Method of Electrical-Mechanical Analogy, **H. E. Criner, G. D. McCann, D. E. Warren.** *Journal of Applied Mechanics* (New York, N. Y.), volume 12, September 1945, page 135.

5. Solving Complex Problems by Electrical Analogy, Part I, **G. D. McCann, H. E. Criner.** *Machine Design* (Cleveland, Ohio), December 1945, Part II, February 1946.

6. The Network Calculator Brought Up to Date, **H. A. Travers.** *Westinghouse Engineer* (Pittsburgh, Pa.), volume 4, July 1944, pages 111–14.

7. Analysis of Rototrol Voltage Regulators by Electrical Analogy, **J. T. Carleton.** *Proceedings*, National Electronics Conference (Chicago, Ill.), volume 4, 1948, pages 272–78.

8. The Differential Analyzer—A New Machine for Solving Differential Equations, **V. Bush.** *Journal*, Franklin Institute (Philadelphia, Pa.), volume 212, 1931, page 447.

9. A New Type of Differential Analyzer, **V. Bush, S. H. Caldwell.** *Journal*, Franklin Institute (Philadelphia, Pa.), volume 240, October 1945, pages 255–326.

10. Mathematical Tables and Aids to Computations. *National Research Council* (Washington, D. C.), volume 2, 1946–1947, page 89.

11. Electronic Techniques Applied to Analogue Methods of Computation, **G. D. McCann, C. H. Wilts, B. N. Locanthi.** *Proceedings*, Institute of Radio Engineers (New York, N. Y.), volume 37, August 1949, pages 954–61.

12. Some Considerations in the Lateral Stability of High Speed Aircraft, **Leonard Sternfield.** *Technical Note Number 1282*, National Advisory Committee for Aeronautics (Washington, D. C.), May 1947.

13. Magnetic Amplifier Studies on the Analog Computer, **E. L. Harder, W. H. Hamilton, D. E. Aldrich, J. T. Carleton, F. N. McClure.** *Proceedings*, National Electronics Conference (Chicago, Ill.), volume 5, 1949.

14. Mathematical Analysis of Non-Linear Circuits, **A. Boyajian.** *General Electric Review* (Schenectady, N. Y.), volume 29, September 1931, page 531.

15. Peak Voltages on Saturating Reactances in Three Phase Circuits, **E. L. Harder.** *Electric Journal* (East Pittsburgh, Pa.), volume 29, March 1932, page 124.

16. Arbitrary Electrical Function Device, British Patent Number 607,397, February 1946.

17. Photoelectric Wave Form Generator, **David E. Sunstine.** *Electronics* (New York, N. Y.), volume 22, February 1949, pages 100–03.

18. Application of the California Institute of Technology Electric Analog Computer to Nonlinear Mechanics and Servomechanisms, **G. D. McCann, C. H. Wilts, D. N. Locanthi.** *AIEE Transactions*, volume 68, part I, 1949, pages 652–60.

No Discussion

Design and Control of Ferroalloy Furnaces

F. V. ANDREAE
ASSOCIATE AIEE

FERROALLOY furnaces form a special group of electric furnaces in which the electrodes are buried in the charge instead of standing over a bath of molten metal as they do in the steel-melting furnaces.

The main part of the energy is used to perform chemical reactions, such as the reduction of ores and the subsequent combination of the resulting elements with iron or other elements such as carbon.

Among their most important products are ferrosilicon, high-carbon ferromanganese and ferrochrome, silico manganese, calcium silicide, ferro phosphorus, and calcium carbide.

In contrast to steel-melting furnaces, ferroalloy furnaces are stationary. However, recently it has been proposed to install the furnace on a table which rotates very slowly around its vertical axis. The idea behind this invention is to avoid any freezing of the charge at any place of the furnace.

Electrically, ferroalloy furnaces are built for one, two, or three phases, see Figure 1.

Single-phase furnaces are either of the 1- or 2-electrode type. In the 1-electrode type, the current returns through the bottom of the furnace. In the 2-electrode type, the two electrodes are in series and the current passes from one electrode to the bath and from there to the other electrode.

Electrically, single-phase furnaces with return through the bottom are very simple. They have been developed in sizes up to 15,000 kw. In this case the return circuit is divided into several parallel branches distributed around the circumference of the furnace to reduce the reactance.

Two-phase furnaces may have two or four electrodes. They are not very frequent because they require special Scott-connected transformers and have no special advantages over the 3-phase type.

The 3-phase type is the one found most frequently, at least in the United States. It has three electrodes arranged either in line or in triangle. By combining two furnaces in one tank it can be designed with six electrodes.

The great majority of ferroalloy furnaces are open on the top, and the raw material is charged around the electrodes either by hand or by means of chutes fed from overhead bins and controlled from the furnace platform.

If the gases have a potential value, the furnaces can be provided with a roof and the vapors collected in suitable mains.

This is the case for ferrophosphorus furnaces where a part of the phosphorus, instead of being combined with iron, is volatilized and collected either as phosphorus or as phosphoric acid. In certain cases, also, the carbon monoxide resulting from the reduction of the ore is collected and used either as a fuel or as the starting point of various chemical compounds.

In size, ferroalloy furnaces range from a few hundred to 50,000 kw.

A furnace installation consists of the transformer, bus bars, flexibles, electrodes and holders, furnace, and collecting and controlling equipment, Figure 2.

A short description of the various parts of the installation will help in discussing design and control procedure.

Transformer

Transformers must be designed individually for the job. While the primary voltage is fixed by the power company, the low voltage must be specified by the customer from his own experience. Each product requires a special voltage which also depends upon the size of the furnace. On account of the unavoidable variations in the primary voltage and in the secondary due to the demands of the furnace, taps must be provided above and below the specified voltage. These taps are installed on the primary side. In general, tap changes are made with the load off, and the tap changers are of relatively simple construction.

Since the secondary voltage is low, very heavy currents must be handled in the conductors which result in tremendous forces acting between them. Coils and leads must be braced carefully.

Since the reactance of the bus and electrodes is relatively high, the impedance of the transformer must be made as low as possible.

The arrangement of the low-tension terminals is generally specified by the customer to fit the design of his bus bars.

Bus Bars

The bus bars form the stationary link between transformer and electrodes. In order to carry the heavy current with as little voltage drop as possible, the reactance of the bus bars must be low. Their design is a nice problem which requires considerable experience.

To reduce reactance as much as possible, outgoing and incoming conductors of the same phase are laid close together. On account of the heavy currents, the circuits are divided into several parallel branches. All these branches bundled together have led to the name "interlaced" bus. This interlacing is carried as far as possible and stops at the flexibles which

Paper 50-86, recommended by the AIEE Chemical, Electrochemical, and Electrothermal Applications Committee and approved by the AIEE Technical Program Committee for presentation at the AIEE Winter General Meeting, New York, N. Y., January 30–February 3, 1950. Manuscript submitted May 13, 1948; made available for printing December 7, 1949.

F. V. Andreae is with the Southern Ferro Alloys Company, Chattanooga, Tenn.

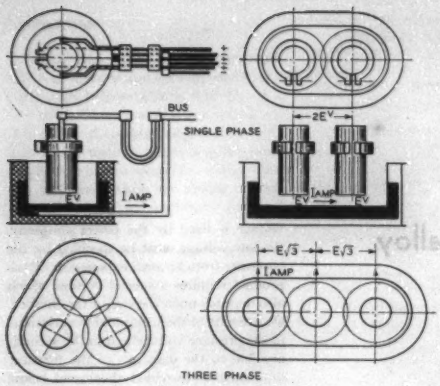

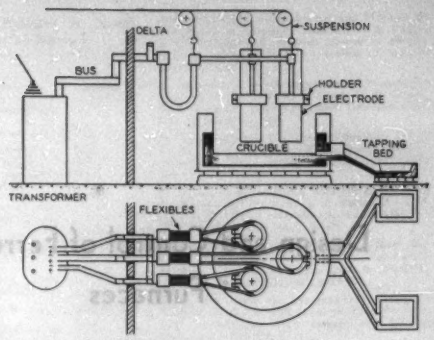

Figure 1 (left). Single and 3-phase furnaces

Figure 2 (above). Typical ferroalloy furnace

are placed as close to the furnace as heat permits.

In 3-phase furnaces where the electrodes are in line, it is impossible to make all three reactances equal. This is due to the delta connections and the fact that the noninterlaced portion of the leads are more or less in the same horizontal plane. This inequality in the three reactances is the cause for the well-known dead phase. An easy way to explain the dead phase is by means of the following reasoning. If three conductors are in the same plane, the mutual inductance of the two outside conductors in relation to the center one are equal and larger than the mutual between the two outside conductors in relation to each other. A certain and considerable amount of power passes from phase 1 to phase 2 in the center and the same amount from phase 2 to phase 3, a much smaller amount however returns from phase 3 to phase 1. These amounts are in direct proportion to the mutual inductances.

It follows therefore that, if all three phases receive equal amounts from the transformer, phase 1 will deliver considerably less power at its extremity than phase 3, and phase 2 will deliver an amount half way between phase 1 and phase 3. Phase 1 is the dead phase.

This phase can be recognized easily by the smaller amount of raw materials it consumes and by the slower consumption of electrodes. If the currents are maintained equal in the three phases, the three tip voltages will be different: low in phase 1, average in phase 2, and high in phase 3.

To equalize reactances, the electrodes are arranged in a circle and the bus so designed that the noninterlaced parts of each phase are exactly alike. This involves more copper, but results in a balanced furnace and also in a better power factor, with a saving in losses because the currents are proportionally smaller.

Flexibles

Since the furnace loads are controlled by moving the electrodes up and down, a flexible member must be inserted between stationary bus and moving leads. Several methods are used to provide the necessary flexibility. Those most frequently used are copper cables designed especially to give maximum flexibility. In many cases the cables are water cooled which permits placing them closer to the furnace and reducing their number. Bundles of thin copper strips sometimes replace the copper cables.

Either strips or cables must be relatively long in order to permit the necessary up and down travel of the electrodes.

To shorten the path of the current, a swinging bar with short flexibles on one end and a rotary contact on the other end would reduce the reactance. It is difficult to design a satisfactory rotary contact for large currents. When the cables are water cooled they can be carried directly to the electrode holder through the hot gases of the furnace.

Electrode Holders or Clamps

The holder transmits the current from the copper leads to the electrode. Besides this it must carry the weight of the electrode and keep it from slipping. Holders are naturally water cooled. Each furnace designer has evolved some special type, and it is probably in this part of the installation that most ingenuity is displayed.

Electrodes

The electrodes carry the current into the reaction zone where the temperatures are extremely high, in the order of 2,000 degrees centigrade. There is only one material, namely carbon, which possesses all the necessary characteristics. It is a good conductor of electricity and is chemically resistant at the highest temperatures. Electrodes in most ferroalloy furnaces are made of amorphous carbon, prepared from anthracite coal, tar, and pitch and subsequently baked. Graphite electrodes are used only when particularly pure products are desired and where the ash content of the amorphous carbon electrode would be too high. The reactions in the furnace consist principally in the reduction of some oxide by means of carbon which is charged into the furnace in the shape of coke, coal, or charcoal. It is inevitable that the electrodes also take part in the process to a certain extent. Even if this consumption is small in comparison with the consumption of the normal reducing agents in the charge, the cost is high because the price per unit of carbon is very much larger in the electrodes. It is about 10-to-1 for amorphous carbon and 20-to-1 for graphite. There is, therefore, a serious economic factor in favor of the choice of amorphous carbon.

Instead of ready-baked electrodes, use is also made of so-called self-baking electrodes. This type of electrode, known under the name of their inventor, Soederberg, consists of large metallic

cylinders of the desired diameter in which green electrode paste is dumped. The heat of the furnace does the baking. The cost of green paste is much lower than the cost of prebaked electrodes, but the installation costs are somewhat higher.

Electrodes are suspended from the superstructure by means of cables or chains leading to electric winches or hydraulic motors which control their movements.

Furnace

The furnace is simply a large crucible, generally of carbon, built of cut blocks or formed with paste. In some cases the ore used in the process is used for the crucible, for instance in the manufacture of ferrochrome or calcium carbide. When carbon is used it must be backed by refractory brick in order to keep the heat from escaping.

The amount of heat insulation depends upon the viewpoint of the designer, his knowledge of the process, and of the existing temperatures. There is a balance between the costs of insulation and the amount of power saved. Even with an infinitely large amount of insulation, there will be losses, because though the temperature difference between shell and surrounding atmosphere becomes infinitely small the area is infinitely large.

Collecting Installation

The liquid product which is tapped at regular intervals is led into tapping beds or tapping cars which are made of various materials, depending on the product, such as cast iron, sand, graphite, or copper. If valuable gases are generated, the furnace is covered and the gas led to collecting tanks through suitable gas mains.

In a typical ferroalloy furnace, there is a deep crucible into which dip suitably-placed electrodes around which the raw materials are charged either by hand or by means of chutes fed from overhead bins. While the raw materials descend slowly they are preheated by the rising gases and the heat generated in the electrode. At the tip of the electrode, where the highest temperature exists, the reaction takes place. The liquid products collect at the bottom of the furnace while the gases seep through the charge and escape on top of the furnace. The change in volume is worth mentioning. From one pound of ore and half a pound of carbon which occupy together something like 0.014 cubic feet one-half pound of metal and one pound of carbon monoxide is obtained. At the reaction temperature this pound of gas occupies, at standard pressure, about 100 cubic feet. It is, therefore, necessary for the charge to be quite porous to permit these enormous amounts of gas to escape rapidly without creating too much pressure. While the speed of the raw materials is figured in feet per hour that of the gases is given in feet per second.

The temperature of the electrode plays an important part in the energy balance of the furnace. In an infinitely long electrode entirely exposed to the air the heat generated in the resistance will be dissipated along the cylindrical surface. The higher the current, the higher the temperature. This temperature, which is determined by the heat transfer coefficient to the atmosphere, limits the carrying capacity of the electrode. It must stay below the point at which the electrode will burn in air. The condition applies approximately to the part of the electrode above the charge. Below the charge the electrode is in presence of the charge whose temperature increases with the depth. In order to dissipate heat the electrode must be hotter than the surrounding materials; the coefficient of heat transfer determines the temperature difference between electrode and charge. It is evident that the temperature of the electrode increases with the depth and also with the length, and also depends on the temperature existing at the point where the electrode enters the charge and on the current, see Figure 4.

The temperature at the tip of the electrode varies with its position. It determines in large measure the temperature of the reaction because it represents the starting point at the hearth level. We see that a change in electrode position, if of long enough duration, affects the energy balance in the furnace.

The current that leaves the electrode passes through the surrounding narrow zone which acts as a resistor in which the electric energy is transformed into heat energy. Before this is done the energy is useless. From this small zone which is the heart of the furnace the energy radiates and does its useful work. There is a beautiful balance between furnished and consumed energy which is easily upset.

Electrical Characteristics of Furnace

Basically the furnace is an electric circuit with constant reactance and variable resistance. The reactance is determined by the characteristics of the transformer and the design of the bus bars including electrodes. Unfortunately for the operator, resistance and reactance are not far apart.

For rectangular furnaces the reactance at 60 cycles increases from around 0.001 ohm per phase for a 2,000-kw furnace to about 0.0014 ohm for 8,000 kw (not including the transformer). On the other hand the resistance decreases from about 0.0025 to about 0.0012 for 8,000 kw.

It becomes evident that for large rectangular furnaces the reactance becomes larger than the resistance. If the power factor is to be above 85 per cent the

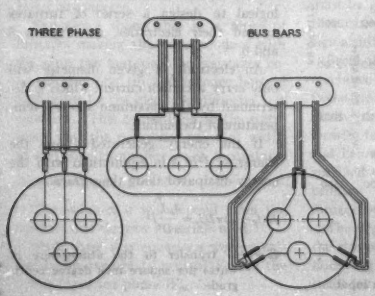

Figure 3 (left). Typical 3-phase bus bar arrangements

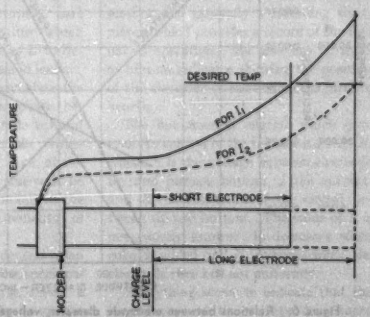

Figure 4 (right). Distribution of temperature in electrode

$$K(t_e - t_a)\pi DL = \frac{4\rho L}{\pi D^2} I^2$$

$$D^3 = \frac{4\rho I^2}{\pi K(t_e - t_a)} = b^2 I^2$$

$$R \times \pi D = \text{CONSTANT}$$

$$E_g = IR = \frac{1}{b} D^{3/2} \times \frac{c}{D}$$

$$W_{ph} = I^2 R = \frac{D^3}{b^2} \times \frac{c}{D}$$

$$\text{ACTIVE AREA DIAMETER} = \phi = \alpha D$$

$I = \frac{1}{b} D^{3/2}$
$R = \frac{c}{D}$
$E_g = \frac{c}{b} D^{1/2}$
$W_{ph} = \frac{c}{b^2} D^2$
$\phi = \alpha D$

Figure 5 (left). Design equations

$$\text{MAXIMUM POWER} \quad W_{MX} = \frac{E_{ph}^2}{2X} \qquad \frac{W}{W_{MX}} = \sin 2\phi$$

$$\text{MAXIMUM CURRENT} \quad I_{MX} = \frac{E_{ph}}{X\sqrt{3}} \qquad \frac{I}{I_{MX}} = \sin \phi$$

$$\text{RESISTANCE} \quad R = \frac{X}{\tan \phi} \qquad \frac{R}{X} = \frac{1}{\tan \phi} = \cot \phi$$

$$\text{IMPEDANCE} \quad Z = \frac{R}{\cos \phi} \qquad \frac{R}{Z} = \cos \phi$$

REQUIRED	R=	R=	W=	I=	X=	VA=	X=
ϕ FUNCTION	COS ϕ	COT ϕ	SIN 2ϕ	SIN ϕ	TAN ϕ	SEC ϕ	COSEC ϕ
FACTOR	$\times Z$	$\times X$	$\times \frac{E_{ph}^2}{2X}$	$\times \frac{E_{ph}}{X\sqrt{3}}$	$\times R$	$\times W$	$\times Z$

Figure 7 (right). Operating equations

size of rectangular furnaces is limited to about 4,000 kw. In some cases such as phosphoric acid where R is high, the limit is higher.

Round furnaces can be designed with much lower reactance. This is true because the leads between the end of the interlaced bus to the electrode can be made shorter and because the delta is closed at the electrode instead of being closed at the end of the interlaced bus. See Figure 3.

In the calculation of electric furnace circuits the following set of equations has been found very useful. See Figure 7.

The maximum power input, W_{max}, into the furnace is reached when $R = X$ and is equal to $E^2/2X$, if E is the low-tension voltage between phases at no load. The actual power input W is equal to $W_{max} \sin 2\phi$.

The maximum possible current, I_{max}, is $E/X\sqrt{3}$.

The actual current

$$I = \frac{E}{Z\sqrt{3}} = I_{max} \sin \phi$$

$$\text{Cos } \phi \text{ is equal to } \frac{R}{Z} \text{ or } \frac{\text{kilowatts}}{\text{kilovolt-amperes}}$$

$$\text{Tan } \phi = \frac{X}{R}$$

By means of these relations it is easy to determine any desired unknown from given values. All that is necessary is a table of functions containing cos ϕ, sin ϕ, tan ϕ, and sin 2ϕ. See Figure 8.

For instance, knowing the reactance of a furnace and the voltage between phases, we can figure the power at which the power factor will be, say, 85 per cent.

We find in our table that for cos $\phi = 0.85$, sin $2\phi = 0.89553$, therefore $W = 0.89553\ E^2/2X$.

For cos $\phi = 0.85$, sin $\phi = 0.52679$, therefore

$$I = 0.52679 \frac{E}{X\sqrt{3}}$$

Another problem is to find the power factor of a furnace, at constant load, under varying voltage, either due to change of tap or change in the primary line voltage.

In this case we calculate a series of values of sin 2ϕ by dividing $2XW$ by E^2. The corresponding values of cos ϕ give the desired power factor.

If E becomes low enough the value sin 2ϕ is larger than 1 which is an impossibility. With sin $2\phi = 1$ we have reached the point of maximum power input. Without the table such calculations would be extremely tedious.

Design of Electric Furnaces

In designing a series of furnaces of various capacities for the same product one is interested in knowing the diameter of the electrode, the current, the voltage, the power input, and the size of the crucible. Of all these elements the size of the electrode is the only factor which varies in steps. The standard diameters of amorphous electrodes are 17, 20, 24, 30, 35, 40, and 45 inches. It is therefore logical to design a series of furnaces around their electrodes, see Figures 5 and 6.

An electrode of given diameter will only carry a certain current which is determined by the maximum allowed temperature of the surface.

If the energy generated above the charge as I^2R is in equilibrium with the energy dissipated along the surface

$$K(t_e - t_a)\pi DL = \frac{4\rho L}{\pi D^2} I^2$$

K = heat transfer to the atmosphere in watts per square inch degree centigrade

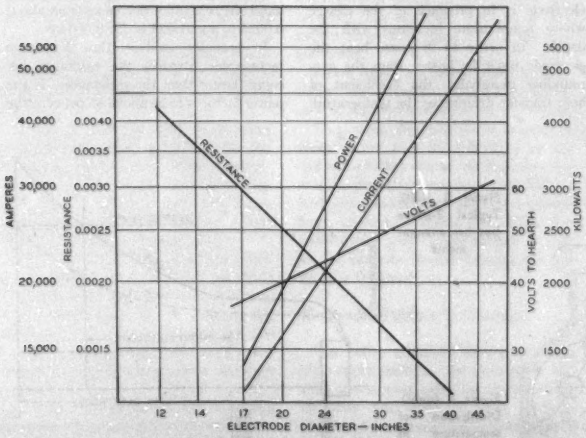

Figure 6. Relations between electrode diameter, voltage, current, and power input

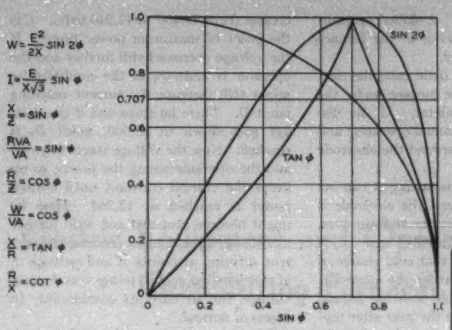

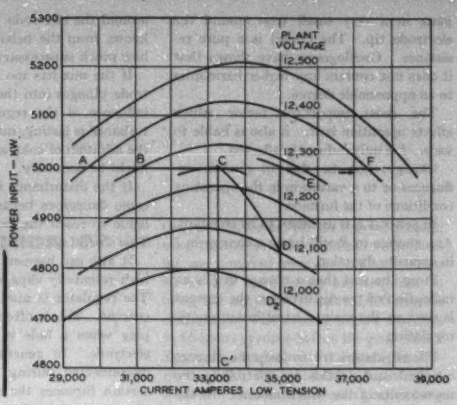

Figure 8 (above). Trigonometrical relations

Figure 9 (right). Power input and current for varying voltage

t_e = temperature of the electrode surface in degrees centigrade
t_a = temperature of the atmosphere in degrees centigrade
D = diameter of the electrode in inches
L = length of the section in inches
ρ = resistivity of the electrode in ohms per inch per square inch
I = current in amperes

Above a certain temperature the electrode burns in contact with the air so that t_e cannot exceed a certain limit. For a given value of t_a, K and ρ are constant, so that the formula becomes

$$D^2 = b^2 I^2 \quad \text{or} \quad I = D^{3/2}/b$$

For very long electrodes, such as the ones in closed furnaces, the value of t_e must be chosen relatively low, otherwise the temperature at the tip becomes abnormally high. See Figure 4.

A 30-inch electrode which in ordinary furnaces will carry 30,000 amperes was found to be good for only 19,000 amperes in a furnace where the electrode extended ten feet under the roof.

In normal cases, the value of b^2 is around 30×10^{-6} when D is in inches and I in amperes.

Experience shows that in a series of furnaces making the same product with the same raw materials the resistance between electrode tip and furnace bottom multiplied by the electrode diameter is a constant. This comes back to the statement that the resistance per unit width of electrode circumference is a constant.

$$R \pi D = \text{constant}; \quad R = c/D$$

The value of c will depend upon the product and the raw materials used.

With these two equations we can calculate the voltage to neutral E_g and the power input per phase W_{ph}.

$$E_g = IR = \frac{1}{b} D^{3/2} \frac{c}{D} = \frac{c}{b} D^{1/2}$$

$$W_{ph} = I^2 R = \frac{D^3 c}{b^2 D} = \frac{c}{b^2} D^2 \text{ in watts}$$

For a 3-phase furnace the power input in kilowatts is $\frac{3c}{b^2} \frac{D^2}{1{,}000}$

Considering that the energy flows from the electrodes along the radius of concentric circles it is logical to assume that the active zone around an electrode will be circular with an area proportional to the power input, and since the power input is in direct proportion to the square of the electrode diameter the radius of the active area will be directly proportional to the electrode diameter. A good rule is to assume this active radius equal to the electrode diameter.

We now have determined all the factors necessary for the design of the furnace. The thickness of the lining will be chosen with the idea of making the sum of the cost of losses and amortization a minimum. In choosing refractories, care must be given to the temperature which they can stand. The next step is to design a suitable set of bus bars and leads.

From this design one can calculate the reactance and resistance per phase between transformer and electrode tip and finally the phase voltage at the transformer terminals. Several taps above and below the theoretical value will be specified to take care of variations in the primary voltage and requirements of furnace operation.

The type of bus bars will depend upon the size of the furnace and the specifications regarding power factor. For a small furnace a layout as shown on the left of Figure 3 will be satisfactory; for a large furnace, 6,000 kw or more, it will be necessary to use an arrangement such as indicated on the right with the delta closed at the electrode holders.

Control of Furnaces

Many factors affect the operation of the furnace. The raw materials must have the proper analysis and be of suitable size; they must be mixed in the right proportion. Their speed must be constant so that they reach the crucible without interruption. There they must find the right temperature and the correct current and voltage.

If one of these factors is wrong, operation is spoiled. The duty of the operator is to diagnose the trouble correctly and to apply the proper remedy. The outward sign of a disturbance is generally a change in the electrical conditions.

In order to be able to see what is going on the operator has before him a panel with ammeters, voltmeters, and wattmeters, and generally a recording wattmeter, which provides a record of the furnace's operation. He also has in front of him an indicator showing the position of the electrode in relation to the furnace hearth.

The fundamental relation which governs the control of the furnace is $I = E/R$, where E is the voltage between electrode tip and furnace bottom, I the current, and R the resistance of the circuit between tip and bottom. The value of R is not exactly known. It decreases when coke is added and it increases when the electrode rises but not uniformly.

Everything seems to indicate that the largest part of the voltage drop takes

place in a very small zone around the electrode tip. The circuit is a pure resistance. Oscillograms have shown that it does not contain any higher harmonics to an appreciable degree.

The most important factor which affects operation is R. E also is liable to vary. I is only indirectly affected.

Changes can be due to outside influences or to a variation in the operating conditions of the furnace.

In general E is assumed to be constant. Any change in R will bring a change in I in opposite direction.

From the fact that a change in I is an indication of the disturbance, the current is used as the main control in automatic regulation.

The regulators try to keep the current constant and do this by controlling the movements of the winch motors. In the simplest kinds of regulators this is done by means of contactors; in more recent regulators the current circuit passes through an amplidyne set mounted on the shaft of the winch motor. As long as the current is normal the motor is quiet; if the current drops below normal the motor lowers the electrode, decreasing the resistance in the furnace and bringing I back to normal. If the current rises above normal the motor reverses and lifts the electrode.

In normal operation there are two reasons for change in R: the electrode is consumed in the furnace; and the path between electrode tip and neutral is shortened by the slow accumulation of metal between taps.

In both cases the regulator automatically takes care of the change in R and restores normal current.

If an electrode position indicator is used it must be adjusted to the electrode consumption which is known. An adjustment at the end of each shift is sufficient. When an electrode is slipped and the indicator is connected to the holder a corresponding adjustment must be made.

More irregular variations in R are due to changes in the mix, more especially in the coke distribution. If due to improper mixing the proportion of coke increases at the tip of the electrode, the resistivity of the resistor decreases and I increases. The regulator lifts the electrode. If the variation is only temporary, the regulator is kept in operation. The electrode will rise momentarily, later coming back to its normal position when the disturbance disappears. If the effect is lasting it might be necessary to operate manually for a while, at the same time reducing the coke in the mix, or charging raw mix around the electrode. A skilled operator knows from the behavior of the furnace how much is necessary.

If the mix has too little coke the electrode plunges into the furnace under the influence of the regulator. If the disturbance is lasting, manual operation and the addition of coke around the electrode might be necessary.

If the disturbance is lasting it can become dangerous because the electrode is liable to reach the bottom and tip over. This should not be allowed.

It also can happen that cold charge of high resistivity slips under the electrode. The regulator is unable to bring normal current. This is often the case after tapping when a hole is created under the electrode. In general, the regulator is disconnected during tapping time. In certain furnaces the recovery after tapping is so slow that regulators are not used at all and the furnace is operated entirely by hand.

If the voltage is constant a regulator controlled by the current will maintain constant power input.

The current can also change due to a change in the voltage. The change in E can come from a disturbance inside of the furnace. Even if the three delta voltages do not change the voltages to ground might vary considerably. The neutral may travel inside the triangle due to disturbance in the metallic neutral, but most changes in E are caused by variations in the primary voltage. These might be caused by changes in load distribution in the feeding circuit or by intentional variations; for instance, lowering of voltage at night when industrial customers are idle and rises in residence voltages must be avoided. These changes of voltage cause serious problems.

Since most contracts contain a demand clause, the operator tries to keep his load as constant as possible. When the primary voltage decreases the current must be increased. As long as the variations are reasonably small the equipment can take care of the increase in current. However, when the variations are large, two difficulties arise. The first one is an excessive heating of the bus and electrodes, the second is a decrease in power factor which at the limit reaches 0.707. At this point, the power input into the transformer is a maximum, and any current increase beyond this point results only in a decrease in power.

Some rather peculiar conditions have been observed, especially with inexperienced operators.

Referring to Figure 9, the line ABC represents conditions as the voltage decreases from 12,400 to 12,240 volts. C is the point of maximum power input. If the voltage decreases still further and the operator is unaware of the condition he might still increase the current reaching point D. There he stops and if the voltage goes down to 12,000, point D_2 is reached. Now the voltage starts to go up and the operator seeing the power go up keeps the current constant until normal power is reached at 12,280. Here he might become confused and with further increasing voltage might increase the current arriving at points E and perhaps F at which he has normal power with normal voltage, but at currents considerably in excess of normal.

To avoid such errors the operator can be furnished with a table giving him the highest current that he should carry at any time, in this case C'.

If the furnace plant is at the end of a long feeding line the voltage drop in the line increases the effect of a voltage drop at the substation. The station operator may think that his line is good and that the variations are small, but by the time they reach the plant they are greatly multiplied. To remedy this situation, a bank of capacitors will improve conditions and a voltage regulator at the plant will maintain constant voltage at the furnace transformer. Such equipment is very expensive, and since it is difficult to express the advantage of constant voltage in dollars and cents, it is hard to convince the management that it is necessary. The power company, however, may see the advantage of a capacitor in increased revenue from higher loads.

Many contracts contain a power factor clause, which states that the monthly demand (generally 30 minutes) will be adjusted for the power factor existing at the time of the demand. Under normal voltage conditions the power factor might be entirely satisfactory. If, however, at the time of the demand the voltage was low, the power factor might very easily be below the contract power factor and the consumer is penalized for a condition entirely out of his control. The power factor clause should contain an arrangement that it should be adjusted for the voltage.

The control of an electric furnace requires constant attention and long experience. The operator at the switchboard has a considerable responsibility because the proper running of the furnace depends on his reactions.

No Discussion

Electric Equipment and Operation of Graphitizing Furnaces

EDWARD R. COLE
ASSOCIATE AIEE

THE method of graphitizing amorphous carbon by accidently overheating silicon carbide was discovered by Dr. Edward G. Acheson. The silica was volatized out and pure carbon or graphite remained. A lubricant had been made from an abrasive material. His conclusions were that to produce graphite a carbide had to be made first and then reduced by heating. Subsequent tests showed that the purest form of carbon (petroleum coke) could be graphitized without adding sand.

Another theory exists today on the formation of graphite in the electric furnace. It is believed that pure carbon at about 2,600 degrees centrigrade has a better affinity for its like than for any other element and the pure particles of carbon combine to form a new material approaching the real density of themselves. Further proof is presented as objects shrink a very definite amount during graphitization. By the addition of enormous pressure to the graphite while at the temperature of 2,600 degrees centigrade, a pure white diamond has been made experimentally. The graphite changed from black to white and its physical properties from a lubricant to an abrasive.

Usual Process of Manufacture of Graphite Electrodes

The usual steps in the manufacture of graphite electrodes are to load the green, or pitch bound preformed electrodes, into a ring or other type of fuel-fired baking kiln, where they are baked to the amorphous or raw state, by heating slowly to a maximum temperature of 1,300 degrees centigrade. After they have cooled down to room temperature they are unloaded, inspected, and reloaded into an electric furnace for graphitizing.

Dow Process

Figure 1 illustrates the arrangements of graphitizing furnaces and transformers at the Dow Chemical Company. The greens are baked and then graphitized in the same furnace on a continuous run. This eliminates the backing kiln and the labor, to load and unload kilns, together with the necessary fuel to heat the material up to 1,300 degrees centigrade the second time. There is no raw electrode inventory or kiln and storage buildings. Five handlings are saved and time of production is reduced as much as eight weeks.

The baking is accomplished by a 400-kva tap-changing transformer in an Acheson-type resistance furnace. Interlaced secondary bus bars, in trenches, with proper switching arrangements, conduct the current from the 400-kva transformer to any furnace in its group. The switchboard attendant follows a predetermined schedule of temperature increase from room temperature to approximately 1,300 degrees centigrade, by changing the taps on the primary winding under load. This baking time may be as much as 200 hours, depending on the size of the electrodes and the weight of charge in the furnace. The secondary voltage is variable under load, between 40 and 120, with one interruption, to change the secondary switch from multiple to series-multiple position.

After the baking period, the 400-kva transformer is switched to another furnace and the 1,600-kva graphitizing transformer is moved into place and connected to the furnace. Before applying the load, however, all the thermocouples, used to indicate temperature while baking, are removed from the furnace. From 80 to 100 more hours are required to bring the temperature up to 2,600 degrees centigrade. The cooling period amounts to 85 hours or more before the graphitized electrodes can be removed from the furnace. Each 400-kva baking transformer serves four furnaces and each graphitizing unit requires two bakers or eight furnaces to keep it running full time.

The graphitizing transformer is rated 13,800 volts, 1,600 kva—40/80—40,000/-20,000 amperes, 60 cycles, with 16 steps on ratio adjuster. By means of a secondary switch the coils can be connected series-multiple, thus making the full voltage range 40/160 volts, variable by 32 steps of near equal value. The secondary winding has full 1,600-kva rating for all taps of the ratio control.

Operation Without Power Factor Correction

Operation at the Dow Plant was started without any power factor correcting device. It was found that when the secondary current rose above 20,000 amperes the power factor decreased rapidly until at 40,000 amperes its value was down to 0.41. The load had to be raised to 3,200 kva, to secure a kilowatt load high enough to produce graphitization. The secondary voltage reached 63 volts at this load. As the graphitizing transformers operate single phase, a very bad condition was set up at the power house and on the transmission lines, due to this overload and low power factor. However, the transformer was liberally designed and withstood the 100 per cent overload for a few hours, at the end of 50 runs, without overheating or otherwise being damaged.

Paper 50-97, recommended by AIEE Chemical, Electrochemical, and Electrothermal Applications Committee and approved by the AIEE Technical Program Committee for presentation at the AIEE Winter General Meeting, New York, N. Y., January 30–February 3, 1950. Manuscript submitted February 20, 1949; made available for printing December 6, 1949.

EDWARD R. COLE is with the Dow Chemical Company, Midland, Michigan.

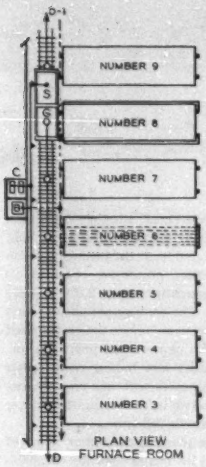

Figure 1 (left). Arrangement of furnaces, transformers, power line, and capacitors

B—400-kva baking transformer
G—1,600-kva graphitizing transformer has portable side bars as shown on Number 8 furnace
S—2,200-kva series capacitor transformer. *G* and *S* are carried on same motor-driven car
C—Capacitors in adjacent room. Can be connected to series transformers, at each furnace, from bus circuit (solid line)
D—13.8-kv single-phase power conductor. Circles at each furnace represent isolator switches
Bus bars to furnaces 5, 6, 7, and 8 dotted in trench, with eight 1,000,000-circular-mil cables under furnace as shown in Number 6 for return circuit on baking units
One graphitizer is connected to phase *A*, the second one to phase *B* (*D-1*), and the four 400-kva bakers to phase *C* to secure the best balanced load possible

Figure 3. Connections to portable side bars

Installation of Series-Capacitor Power-Factor Corrector

A series-capacitor transformer rated 2,200 kva with operating voltage on a primary winding of 40 volts and 2,420 volts secondary across the capacitors was installed. There are 140 individual capacitor units, each rated 15 kva at 2,300 volts. The total reactance value of this series capacitor is 0.0015 ohm. It does not produce full unity power factor as the total reactance in the secondary circuit, including bus bars, series transformer, and furnace, totals 0.00207 ohm.

The secondary terminal connections of all the transformers (400 kva and 1,600 kva) used in the process are brought out through the top of the case with alternate terminals of like polarity. This allows interlacing of the bus bars from transformer to the load. The connection of the series transformer into the furnace circuit is accomplished in the shortest possible distance and is a permanent assembly carried on the transformer truck. See Figures 2 and 3. As the graphitizing transformer can be brought to within five feet of the furnace head, the length of the secondary circuit is only 35 feet long, Figure 4.

Portable side bars are hung along the side of the furnace, as return circuit, for the graphitizing transformer, as shown in Figures 5 and 6. They are spread apart to envelope as much of the furnace surface as possible. This arrangement is the same for each furnace regardless of its location in the furnace room. Had the customary system of stationary graphitizing transformer been used, some 400 feet of bus, consisting of 32 1/2 inch by 6 inch copper bars or other bus bar metals, would have been required together with 16 switching stations of 40,000 amperes' capacity. The inductance and resistance thus added would have further reduced the power factor and efficiency of the secondary circuit below 0.41.

High Tension Power Supply

Single-phase power is brought from the switch room to the graphitizing trans-

Figure 2 (left). Permanent connection of series transformer

Figure 4 (right). Positive and negative flexible connectors and transformer bus bars

Figure 5. Side bars and connections to grounded furnace head

Figure 7. Control board, panels

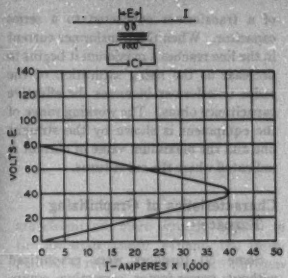

Figure 8. Typical volt-ampere characteristic curve of transformer connected in series capacitor circuit

former in conduit, hung from the ceiling, for the full length of travel of each of the 1,600-kva graphitizing transformers, see Figure 1. A bayonet-type toggle-operated isolator switch is located at each furnace for connecting the graphitizer transformer to the 13,800-volt power line. The capacitor units are located in a room adjacent to the transformer bay. A bus extends from them full length of run of the transformer with which they are used, with terminal boxes in which flexible leads from a series transformer are connected. Doors to these terminal boxes and the operating handle of the isolator switch are interlocked with the transformer's oil switch to prevent its being closed until all contacts have been made. When the oil switch is closed the truck motor's circuit is blocked out to prevent the possibility of moving the truck while the transformer is furnishing power to a furnace.

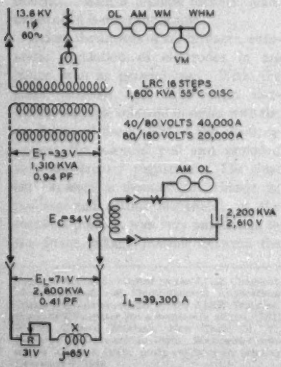

Figure 6. One-line electrical diagram of graphitizing transformer circuit

Operation Control

Figure 6 is a 1-line electrical diagram of the complete circuit of a graphitizing furnace.

In Figure 7 is shown the control board. The control consists of an ammeter, voltmeter, wattmeter, and watt-hour meter in the primary circuit together with a Selysn tap position indicator. The only secondary intrument is a voltmeter. The secondary voltmeter and the wattmeter are indicating-curve drawing instruments. Each 400-kva baking transformer also has a 6-point indicating and curve drawing, automatic circuit changing, temperature recording instrument.

During the baking period the load is increased on a temperature schedule up to 1,000 degrees centigrade, at which point the thermocouples are removed from the furnace. Beyond that the load on the furnace is increased, according to a kilowatt load curve, as determined by experience, until 2,600 degrees centigrade is reached.

The 1,600-kva graphitizing units have in addition an ammeter in the secondary circuit. Its current transformer operates a relay that turns on a red light, when current reaches 38,000 amperes, to warn the operator; and also an overload relay which trips the oil circuit breaker if current is allowed to reach 40,000 amperes. Should the operator fail to reduce the load the circuit is automatically opened at this point to prevent oversaturation of the series transformer. Figure 8 shows a typical volt-ampere characteristic curve

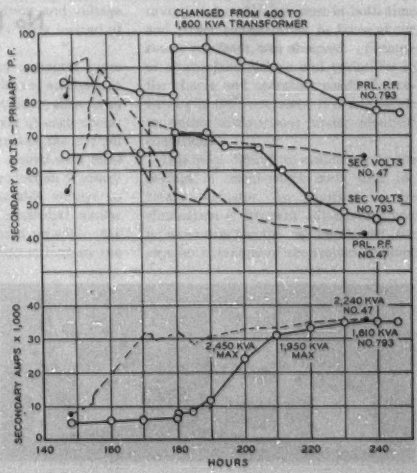

Figure 9 (right). Current, voltage, and power factor versus running hours of graphitizing furnace

Run Number 47 (without capacitors), charge 37,900 pounds. Run Number 793 with capacitor, charge 43,000 pounds

of a transformer connected to a series capacitor. When the transformer current in the line reaches a maximum it begins to decrease as the rising saturation of the series transformer increases the effective capacitance ohms. The working range of the equipment is shown by the straight line and the maximum value of current is indicated where the curve turns.

Characteristics of Graphitizing Furnace

Some 50 furnaces were graphitized without power-factor correcting equipment. Figure 9 shows running conditions without and improvements obtained with a capacitor power-factor correcting device.

The curves for Number 47 (dotted lines) represent data from run without corrector. Run Number 793 (solid lines) shows improvements after installing series transformer.

Note particularly that in addition to improving the power factor from 0.41 to 0.77 the furnace charge has been increased from 37,900 pounds to 43,000 pounds. The secondary voltage also improved to such an extent that it is no longer necessary to change the secondary switch connection from parallel to series multiple; thus in a new installation the cumbersome 40,000-ampere series-parallel switch can be eliminated.

Experience has shown that an exact duplicate of this circuit, on 25-cycle power, gives a power factor of 0.85, without using series transformer for correction.

Changing Taps under Load

Tap changing under load is justified as changes on a graphitizer are made about twice an hour; 777 runs showed a total of 16,770 tap changes on the graphitizing transformers alone. The 400-kva bakers change taps more frequently. With six transformers in operation at once it would require several men to manually change taps. To do this the load would have to be taken off. When the power is discontinued for a short period, especially when the furnace has reached 1,500 degrees centigrade or above, excessive radiation starts.

The lost heat must be returned to furnace charge by supplying extra power to re-establish a progressive increase in the heating schedule.

Due to the fact that atmospheric conditions around the graphitizing transformers are extremely dusty, with large quantities of graphite dust settling on everything, junction box potheads were used on transformers for incoming cables. A special packing device of water repellent material was made around the secondary terminals to break the dust layer into vertical sections to prevent short-circuiting. The entire unit is washed down frequently to remove the graphite dust deposit, as blowing with compressed air still leaves the surfaces covered with a thin film of graphite.

Economics of the Series Capacitor

Had the operation been continued without the power-factor correcting device, a new 3,200-kva transformer costing $32,000 would have been necessary, as 1,500 kw is required at the end of graphitizing run. The transmission lines were too light, as were the oil circuit breaker and current transformers. Our new series transformer cost $22,000, giving a saving of $10,000 for that item. Referring to Figure 9, the operating conditions show a drop in load from 2,240 kw without series capacitor, and with power factor of 0.41, to 1,610 kw with a power factor of 0.77 at the end of runs Numbers 47 and 793.

When the 13.8-kv system with the transmission line, transformers, and turbines is considered, the cost of the series capacitor device is saved many times over each year. The lessening of the burden on the 13.8-kv system is difficult to evaluate. If only one graphitizer with two 400-kva bakers is in service, all running single phase, it is impossible to balance the load on each phase. Generating capacity equal to about three times the kilovolt-ampere load had to be supplied. With two 1,600-kva graphitizers and four 400-kva bakers the phase balance was improved. To operate all these transformers without correcting the power factor, the new equipment would have cost well over $150,000.

No Discussion

Electrode Control and Associated Operating Mechanisms

E. A. HANFF
ASSOCIATE AIEE

THE history of the development of the control or regulation of furnace electrodes has been interesting. In this paper, it is not intended to discuss the technical features of the various methods of control in use; as such details are covered quite ably and fully in papers presented by engineers engaged in the design and manufacture of such equipment.

Essentially, the electrode regulator is required first to establish arcs from the electrodes to the metal in the furnace and then to adjust the arcs to admit a uniform flow of power into the furnace under widely varying conditions at different phases of the melting process. Except for occasional manual adjustment of the voltage and rate of input; the control is fully automatic.

On the earlier furnaces, operating single phase, regulation by hand was not too difficult. With a 3-phase furnace, manual control is not practicable.

Before the advent of arc furnaces, automatic regulation of electrodes in arc lamps was in general use. With the small currents and light-weight electrodes, a simple solenoid in series with the arc balanced the weight of the electrode against the solenoid pull and provided very satisfactory regulation. The time lag between a demand for change in position and actual movement to the required position was very small, due to the direct linkage possible between the electrode and the solenoid armature.

In furnaces, an intermediate power-driven mechanism is necessary, of course, to move the electrodes. One of the principal problems in developing a satisfactory regulator is to control this power operated mechanism so that the electrode will be moved to its correct position with minimum loss of time and with the least amount of overtravel in either direction.

The Thury regulator was one of the earliest successful types. This regulator employed mechanically-operated contactors which energized the electrode motors in a series of impulses in either direction. This type was succeeded by the magnetic-contactor type, such as the Seede regulator, and by later modifications, including the well-known "balance beam" regulator which utilizes both current and voltage elements in the primary relay instead of current elements only.

Since the Thury and contactor types make use of primary relays or solenoids to energize the motor contactors, there is an appreciable time interval at each operation. This time lag makes the control more irregular than is desired with ideal control. With the introduction of rotary regulators applying variable voltage to the electrode motors; somewhat similar to the old Ward Leonard principle, the current and voltage fluctuations in the arc circuit are more directly applied to the electrode motor without the intervention of relays or contactors. Furthermore the speed and direction of rotation of the motors are controlled directly by these arc fluctuations. The electrodes therefore are moved more steadily in the required direction at a speed roughly proportional to the magnitude of the variation from the desired current value; instead of in a series of impulses as with the contactor type of regulator.

In order to present a comparison between the contactor and rotary regulators, comments and data obtained through the helpful co-operation of representatives of manufacturers and users of both types have been assembled. This information is given in Table I to show the advantages of the two types. Only the more important items are shown, although the table could be expanded to include many other features.

In certain installations it has been possible to get comparative data by operating the same or duplicate furnaces with both types of regulators. On one large installation equipped with switches for transfer from one type to the other, an average saving of 3 to $3^1/_2$ per cent in both time and power consumption, in favor of the rotary regulator, was observed. Because of unavoidable delays and variations in the charge and operating conditions occurring in different heats, it is impossible to obtain comparisons under identical conditions.

It is quite difficult to evaluate fully the savings in maintenance costs with the rotary regulator. In addition to the elimination of frequent adjustments and replacements for the regulator itself, the steadier operation of the motors, without

Figure 1. Upward travel (left) and slack cable (right) limit switches

Paper 50-88, recommended by the AIEE Chemical, Electrochemical and Electrothermal Applications Committee and approved by the AIEE Technical Program Committee for presentation at the AIEE Winter General Meeting, New York, N. Y., January 30–February 3, 1950. Manuscript submitted March 8, 1948; made available for printing December 7, 1949.

E. A. HANFF is Chief Engineer of the Swindell-Dressler Corporation, Pittsburgh, Pa.

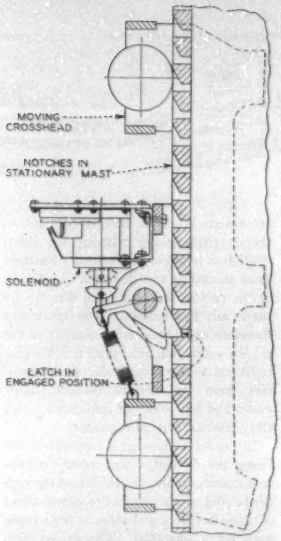

Figure 2. Notch and latch-type electrode safety stop

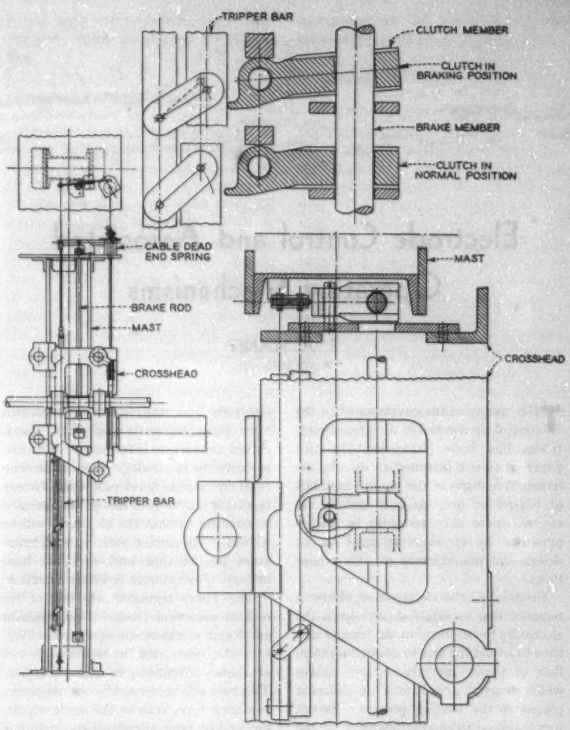

Figure 4. Details of tripper-bar operated clutch-type safety stop

the repeated starts and stops under dynamic braking, tends to reduce the maintenance costs on the motors and driving mechanism.

The remainder of the paper will discuss certain associated mechanisms which concern the operation of the furnace electrodes.

Most arc furnaces are operated by d-c motors geared to wire rope drums. For many years a combination of worm gear and open spur gears has been used, but recent preference has been for completely-enclosed gear sets, usually of the double-reduction worm type.

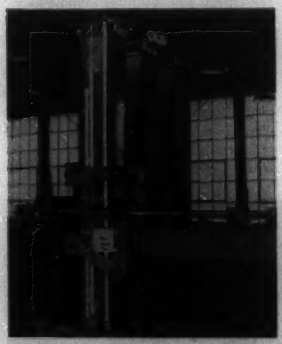

Figure 3. Shop view of clutch-type safety stop in holding position

Since all wire rope has a certain amount of elasticity, it is desirable to keep the rope length to a minimum so that the rope stretch will not affect the accuracy of control unduly. This effect is less noticeable with the rotary regulator because of the smoother acceleration and deceleration.

Hydraulic cylinders are in use to some extent in place of motors, particularly in European practice. Hydraulic drives have their peculiar advantages and disadvantages; but since the extensive adoption of the rotating regulators, there appears to be less interest in the use of hydraulic equipment for electrode operation.

In handling electrodes by means of hoisting ropes, it is advisable to provide means to prevent damage from overtravel. The upward movement is limited by the height of the masts which support the electrodes. In the lowering direction, if the moving structure reaches the limit of travel, or if the electrode comes to rest on solid scrap in the furnace with little or no flow of current, the hoist rope will become slack or unwind from the drum. To prevent damage or delays resulting from such overtravel, limit switches are often used. Figure 1 shows these switches as mounted at the top of the masts. The switch at the left stops the upward travel when the moving crosshead lifts the vertical rod to engage the hatchway switch lever. In the slack cable switch at the right, the hoist rope is anchored to the guided member at the top of the heavy compression spring. The weight of the electrode system normally compresses the spring and the limit switch contacts remain closed. If the electrode is prevented from moving down for any reason, the

spring releases and the contacts open.

Under normal conditions, the electrode hoisting ropes give long service, but, as with any wire rope, they will wear out eventually or may be damaged from some unusual occurrence. When a rope fails, the electrode and its supporting arm will drop and may damage the electrode arm or the furnace roof. If it only breaks the electrode, delay and expense may result because of the labor required to remove the broken pieces and from contamination of the molten metal with excess carbon.

The best insurance against such accidents is to maintain close inspection of the ropes and replace them before they reach the danger point. As an additional safety feature, furnaces now are being equipped with a device which prevents the electrode arm from dropping even if the rope fails.

One of the first devices of this description is shown schematically in Figure 2. In this design a steel latch is mounted on the movable crosshead and arranged to travel in line with a series of notches built into the mast structure. The latch is held out of engagement with the notches by means of a solenoid, the coil of which is energized through contacts of the slack cable switch. In case of a rope failure, the slack cable switch opens the solenoid circuit, releasing the latch, which engages the nearest notch in the mast. The crosshead is brought to rest immediately and is safely held until a new rope can be installed. As an improvement on this design, eliminating the electric solenoid, the friction clutch or sprag arrangement shown in Figure 3 was developed. In this design a vertical round rod, serving as a brake member, is mounted on the mast structure parallel to the vertical axis. A tiltable clutch member, carried on the crosshead, is provided with a hole slightly larger than the brake rod which passes through the hole. Figure 4 shows the construction more clearly. The clutch member normally clears the brake rod, but upon failure of the cable, the mechanism causes the clutch to tilt sufficiently to grip the sides of the brake rod. The action is so rapid and positive that the crosshead is stopped before it has accelerated appreciably, thus limiting the shock. Since the movement is stopped by friction, there is a small amount of slipping and the stopping is not as abrupt as with the notch and latch type just shown. It has been found, however, that the device will stop a large crosshead with a heavy electrode within a small fraction of an inch.

Table I. Comparison of Contactor and Rotary-Type Regulators

	Contactor Type	Rotary Type
Performance		
General performance	Satisfactory	Excellent
Smoothness of operation	Somewhat rough	Very smooth
Arc and overload power interruption	Frequent	Infrequent
Motor resistor power losses	Yes	No
Motor generator set stand-by losses	No	Yes
Kilowatt-hour energy consumption	100 per cent	94–99 per cent*
Total time of heat	100 per cent	91–95 per cent*
Electrode consumption	100 per cent	95–100 per cent*
Maintenance		
Complexity of control system	Quite simple	Rather complicated
Diagnosis and correction of trouble	Easily located	More obscure
Inspection and adjustment	Frequent	Seldom required
Spare part requirements	Inexpensive parts	Spare motor generator set
Rotating machine maintenance	Motors only	Motors and motor generator sets
Type of supervisory personnel	Average	Highly skilled
Cost Comparison		
Regulator only, 100 to 5,000 kva	100 per cent	150–165 per cent*
Regulator only, 6,000 to 12,000 kva	100 per cent	180–190 per cent*
Total furnace cost, 100 to 5,000 kva	100 per cent	103–101 per cent*
Total furnace cost, 6,000 to 12,000 kva	100 per cent	101–100.7 per cent*

* Approximate averages based upon figures supplied by several sources.

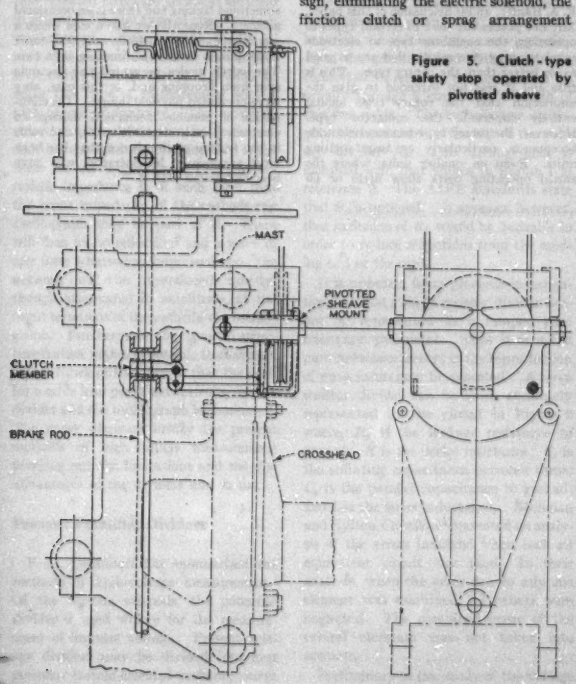

Figure 5. Clutch-type safety stop operated by pivotted sheave

In a modification of the design, shown in Figure 5, a different method of tripping the clutch is employed. In this arrangement the sheave on the crosshead is mounted in a pivotted cradle. Normally, the weight of the electrode system keeps the sheave and cradle in a vertical position. When the rope breaks, a powerful spring tilts the sheave cradle and a connecting link to trip the clutch member. This arrangement, being simpler and having fewer parts is preferred over that shown in Figure 4.

In order to meet the increasingly important demand for furnaces and equipment which will produce more output with less labor and material, the furnace and electric equipment manufacturers must be alert to develop new devices and improvements in existing designs. In this brief discussion it has been possible to describe only a few of these developments.

Discussion

J. R. Lee (Pittsburgh Lectromelt Furnace Corporation, Pittsburgh, Pa.): Mr. Hanff has presented an interesting paper on several phases of arc furnace design and operation. We would like to point out several things that should not be overlooked in considering electric furnaces as a whole.

As brought out in this paper, it is true that 3-phase arc furnaces require automatic electrode control almost invariably unless they happen to be of a character such as electro-smelting furnaces used on charges and processes where the resistance changes very slowly. For many operations a very much simplified control is justified from an economic point of view.

The statement by the author is correct to the effect that the relay-type regulator is lower in first cost, but requires more regular adjustments as the contacts wear away than does the motor-generator (or so-called rotary-type) regulator. While the rotary-type regulator requires less frequent adjustments and repairs, trouble shooting requires more highly skilled attention and the supply parts and repairs are of a more expensive type. We have found it advisable to stock a complete spare motor-generator unit in addition to various resistors and rectifiers which can fail for a number of reasons. It has been our experience that when the relay-type regulators are in proper adjustment, the operating results are practically as good as with the rotary-type regulator. In fairness, we should add that it is sometimes very difficult to impress the average maintenance man with the advantages to be gained by proper setting of the regulator. Reports indicate that wear and tear on the winch motors, electrode supporting gears, rams and sheaves is slightly less with the rotary-type regulator.

The rotary regulator built according to standard design is very well adapted to use on steel-type furnaces where the load is of a very highly fluctuating nature. There is reason to doubt that it does as good a job as the contactor-type on bare bath, submerged arc, or deep slag operations unless its standard design is considerably modified.

The author discusses several schemes for preventing drop of arms in case of cable breakage. These are of the well known safety stop type which have been in use on elevators in various varieties for many years past. However the height of the lift of the electrodes is so small, the danger to human life so remote, and the liability of drop so very infrequent, that the vast majority of furnace men feel that proper inspection of the cables is a better substitute.

It is proper to note that with the counterbalanced electrode cable drive and the so-called friction-bite attachment of the cable to the drum, that the limit stops for both up and down travel are eliminated entirely and thus the arm travel is held, by the friction bite scheme, within safety limits to a small fraction of an inch.

The paper discusses the elasticity of the hoisting cables. Our experience has not indicated even the slightest difficulty due to such cause where the electrode arms are properly mounted on truly machined masts, fitted with hardened rollers and running on antifriction roller bearings. In other words the difficulty seems to be purely theoretical and with little if any effect on the practical performance of the furnace.

E. A. Hanff: In his discussion of this paper, Mr. Lee points out that in certain types of operation, the contactor type of electrode regulator may give results that are as good as, or better than, the rotary type. This is true and it was not intended to give the impression that the rotary type should entirely supersede the contactor type. However, the rotary type has received wide acceptance, particularly on large melting units. Even on smaller units, where the actual operating costs show little or no saving and where the proportionate initial cost is much greater, there has been a marked preference for the rotary type. Perhaps this preference is partly psychological owing to the unobtrusive, smooth performance of the rotary regulator as compared with somewhat noisy and jerky action of the contactor type.

The friction-bite attachment mentioned by Mr. Lee is an adaptation of an old principle used widely in hoisting and haulage equipment. As applied to hoists, such as furnace door hoists, the drum and counterweight can be mounted close to the load with a minimum of guide sheaves and with short cable length. On an electric melting furnace, the hoist drum and counterweights are usually mounted away from the furnace, resulting in rather long cables and a complex system of guide sheaves.

Contrary to Mr. Lee's experience, we have found that the elasticity of the hoisting cables has a noticeable effect. Tests made by one of the regulator manufacturers demonstrated that the momentary stretch or "bounce" is measureable and has an appreciable effect on the magnitude of the instantaneous current peaks. This effect would be less noticeable where there is enough friction in the sheaves or electrode arm system to "damp out" the bounce.

It was pointed out in the paper that maintenance of close inspection of the hoisting ropes is the best insurance against cable breakage. However, such maintenance is sometimes lacking and there is an occasional accident. Recently, we had a case where a workman carelessly held an acetylene torch flame near a hoist rope, burning it in two. The safety device prevented the electrode arm from dropping and, in this case, may have prevented physical injury. The elimination of possible mechanical damage to electrode joints, electrode arms, and roofs is the feature of the device that has been most appreciated by operators who have become familiar with it.

Impulse Measurements by Repeated-Structure Networks

C. L. DAWES
FELLOW AIEE

C. H. THOMAS
ASSOCIATE AIEE

A. B. DROUGHT
STUDENT MEMBER AIEE

SURGE testing of dielectrics and electric apparatus with impulse voltages having steep-wave fronts has recently become important and has necessitated a much higher degree of accuracy in the measurement of such impulse voltages. It is the purpose of this paper to show that repeated-structure networks are ideal in principle for any type of surge-voltage measurement. Experimental study of prototype networks and tests on a larger-scale model indicate that it is possible to make this type of measurement with a high degree of accuracy. The repeated-structure network has a realizable characteristic impedance termination that is the same for all frequencies. This characteristic impedance is of such form that the input impedance of the cathode-ray oscillograph may be part of it. There will then be no reflections and a wave of any form whatsoever impressed upon the network will be reproduced exactly, though attenuated in amplitude, at the input terminals of the cathode-ray oscillograph. Furthermore, the repeated-structure feature makes it possible to construct this network of such length that the need for a cable lead per se between the voltage divider and the oscillograph is eliminated. The paper discusses briefly the present methods of high-voltage measurement pointing out the limitations and the disadvantages of the dividers now in use.

Present Potential Dividers

F. M. Defandorf has summarized the methods of high-voltage measurement.[1] Of the various methods, the potential divider is used widely for the measurement of impulse voltage. Present voltage dividers may be divided into four groups: corona-shielded resistor; surge resistor; capacitor divider; and capacitance-shielded and guarded resistor.

The corona-shielded resistor tends to increase stray capacitance and for this reason is undesirable. At the present time the surge resistor type of divider shown in Figure 1 is commonly used. This consists of a large number of resistors bifilar wound on cards, all connected in series. A voltage tap across a portion R_a of the grounded end of the resistor is connected to another voltage divider R_b usually through a considerable length of shielded cable. The cathode-ray oscillograph is connected to the tap of the voltage divider R_b. This arrangement is identical with that shown in Figure 1 of reference 2. The AIEE standards state that R_a is optional. It appears, however, that inclusion of R_a would be desirable in order to reduce reflections from the sending end of the cable.

It is apparent from previous investigations[3,4,5] that a surge resistor divider cannot be represented as a lumped pure resistance parameter. Since it is not a pure resistance, errors in the reproduction of wave forms may be expected. A surge resistor divider can be more accurately represented by the circuit in Figure 2 where, R_g is the leakage resistance to ground; R is the series resistance; C_s is the shunting capacitance between turns; C_p is the parallel capacitance to ground; and L is the series inductance. Böchman and Hylten-Cavallius[4] presented an analysis of the errors involved when such an equivalent circuit was used. In their analysis, when the error due to any one element was examined, all others were neglected. The combined error of the several elements was not taken into account.

Preliminary to the study of the voltage divider described in this paper an investigation was made of the surge-resistance card type of divider. This consisted of 10 bifilar wound cards as elements, each having a resistance of 500 ohms. The several parameters shown in Figure 2 were determined by appropriate measurements.

As will be shown later, there was a substantial phase displacement between the input and output voltage, when the applied frequency became high.

In an attempt to minimize the effect of inductance and extraneous capacitance, the capacitor type of divider is sometimes used.

The usual circuit arrangement for a capacitor divider is shown in Figure 3. This consists of a single high-voltage capacitor in series with a ground capacitor of low-voltage rating. It is extremely difficult to compute the divider ratio even when the capacitance of the units are known, since when high-voltage capacitors are used, large spacings are involved, and the capacitances to ground may be as large or larger than the capacitance between the two electrodes of the high-voltage capacitor. J. H. Hagenguth[6] points out that in laboratories where capacitor dividers were used rather extensively, it was found necessary to calibrate the divider with an auxiliary resistor divider. Furthermore it is difficult to connect the cathode-ray oscillograph in a satisfactory manner to a capacitor divider. A cable lead with resistance termination

Paper 50-89, recommended by the AIEE Instruments and Measurements Committee and approved by the AIEE Technical Program Committee for presentation at the AIEE Winter General Meeting, New York, N. Y., January 30–February 3, 1950. Manuscript submitted September 19, 1949; made available for printing December 5, 1949.

C. L. Dawes is Associate Professor and C. H. Thomas is Instructor of Electrical Engineering at Harvard University, Cambridge, Mass. A. B. Drought is Assistant Professor of Electrical Engineering, Marquette University, Milwaukee, Wis.

The authors wish to thank J. H. Hagenguth of the High-Voltage Engineering Laboratory of the General Electric Company at Pittsfield, Mass., for suggesting the voltage divider as a problem for this research performed in partial fulfillment for the degree of Doctor of Science by A. B. Drought. We appreciate the loan by Mr. Hagenguth of a wire-wound resistor card which became the basic unit in the surge-resistor type of divider which was constructed. We also are indebted to F. L. Bellaschi who followed the research closely and recommended a presentation of this work.

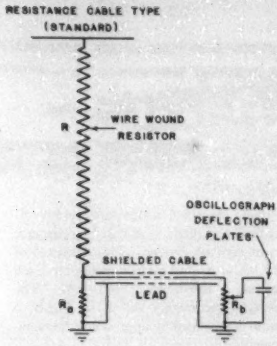

Figure 1. Surge resistor voltage divider

is undesirable, since this tends to prevent the voltage across the low-voltage capacitor from following the wave form of the impressed voltage. Location of the cathode-ray oscillograph near the divider for direct connection across the low-voltage capacitor also is undesirable, since this introduces stray capacitance and inductive effects on the cathode-ray beam.

In the capacitance-shielded and guarded-resistor type of divider, capacitance shielding has been accomplished in two ways:

1. Höhl[8] placed a capacitor and resistor divider in parallel and made the time constants of the two sections thus formed identical.

2. The Allmanna Svenska Elektriska Aktiebolaget (ASEA)[4] investigated the divider with a screen, sometimes termed a "doughnut" or a "pie-plate," on the upper end of the divider.

Either of these methods seem to eliminate the undesirable effects of the capacitance to ground. If one considers the response of such a compensated divider without the cable lead, however, it is found to be limited in accuracy by the inductance. The uncompensated surge-resistor divider may be nearly as satisfactory if careful attention is paid to the spacing of the equipment in the laboratory. The ASEA also added a nonlinear resistive element around the measuring resistor to equalize the nonlinearity of the capacitance voltage distribution. It would seem that such a resistance would tend to increase the inductance.

In all of these types of compensated dividers the cable lead is still a part of the circuit and cannot be properly terminated under all conditions, and hence must contribute to the over-all error.

Analysis of the Repeated-Structure Network

Since electrical impulse measurements are concerned with the recording or observing of transitory voltages or currents, a transient analysis of any network used to make such measurements is desirable. The method of the Laplace transformation offers a powerful and relatively simple means for such analysis and will be used throughout.[7]

Simplified Attenuating Network

In Figure 4(A) is shown a simple network in which the output voltage $e_o(t)$ can be made an attenuated replica of the input voltage $e_i(t)$ if the impedance of the cathode-ray oscillograph is neglected. This may be seen readily from the following analysis.

By definition

$$E_i(s)=\int_0^\infty e_i(t)\epsilon^{-st}dt \tag{1}$$

and

$$E_o(s)=\int_0^\infty e_o(t)\epsilon^{-st}dt \tag{2}$$

where $E_i(s)$ is the Laplace transformation of the input time signal $e_i(t)$; $E_o(s)$ is the Laplace transformation of the output response $e_o(t)$; and $s=\sigma+j\omega$ a complex variable.

For no initial energy storage in the network

$$E_o(s)=\frac{Z_2(s)}{Z_1(s)+Z_2(s)}E_i(s) \tag{3}$$

where the impedance functions are

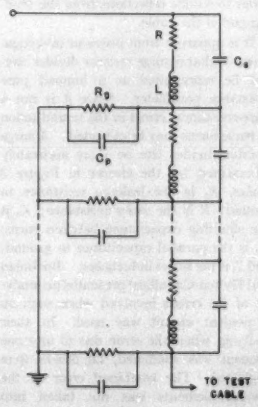

Figure 2. An equivalent circuit of the surge resistor

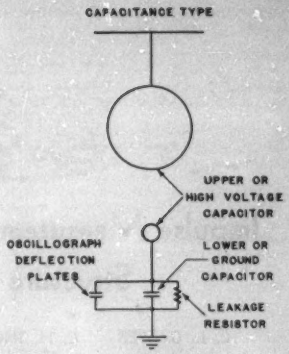

Figure 3. Capacitor voltage divider

$$Z_1(s)=R_1\frac{L_1C_1s^2+\left(R_1C_1+\frac{L_1}{R_1}\right)s+1}{L_1C_1s^2+2R_1C_1s+1} \tag{4}$$

and

$$Z_2(s)=R_2\frac{L_2C_2s^2+\left(R_2C_2+\frac{L_2}{R_2}\right)s+1}{L_2C_2s^2+2R_2C_2s+1} \tag{5}$$

Now if

$$R_1C_1=\frac{L_1}{R_1} \tag{6}$$

and

$$R_2C_2=\frac{L_2}{R_2} \tag{7}$$

then

$$Z_1(s)=R_1 \tag{8}$$
$$Z_2(s)=R_2 \tag{9}$$

Hence

$$E_o(s)=\frac{R_2}{R_1+R_2}E_i(s) \tag{10}$$

Since $e_o(t)$ is the inverse Laplace transformation of $E_o(s)$, equation 10, it is apparent that

$$e_o(t)=\frac{R_2}{R_1+R_2}e_i(t) \tag{11}$$

Equation 11 shows that $e_o(t)$ is exactly of the same form as $e_i(t)$ but of reduced amplitude.

If s is set equal to $j\omega$ in equation 10 where ω is interpreted as angular frequency, there may be written

$$\frac{E_o(j\omega)}{E_i(j\omega)}=\frac{R_2}{R_1+R_2} \tag{12}$$

Equation 12 represents the relative amplitude and phase of output to input when the input is a sinusoidal voltage.

This ratio is a constant independent of frequency.

Any attempt to observe or measure the output voltage $e_o(t)$ by means, for example, of a cathode-ray oscillograph alters the terminating impedance $Z_2(s)$ as expressed by equation 9 and the condition expressed by equation 11 no longer holds. Some deviation of the output observed from that of the input may be expected.

For simplification, assume the input to the cathode-ray tube to be represented by a pure capacitance C_o. Combining C_o with the impedance $Z_2(s)$ to form $Z_2'(s)$, the input and output then are related by

$$E_o(s)=\frac{Z_2'(s)}{Z_1(s)+Z_2'(s)}E_i(s) \tag{13}$$

where

$$Z_2'(s)=\frac{R_2}{R_2C_os+1} \tag{14}$$

On substituting equations 8 and 14 in equation 13 there is obtained

$$E_o(s)=\frac{R_2}{R_1+R_2}\frac{1}{\dfrac{R_2}{R_1+R_2}R_1C_os+1}E_i(s) \tag{15}$$

Some measure of the closeness with which $e_o(t)$ follows $e_i(t)$ may be determined by assuming $e_i(t)$ to be a step function of amplitude V. For such an input

$$e_o(t)=\frac{R_2}{R_1+R_2}V(1-e^{-t/T}) \tag{16}$$

where

$$T=\frac{R_2}{R_1+R_2}R_1C_o \tag{17}$$

The ratio $R_2/(R_1+R_2)$ must be chosen to give the desired voltage division, hence for the undesired transient term to be of minimum duration the product R_1C_o must be minimized. By minimizing the time constant T this divider may be satisfactory for the measurement of voltages which have no discontinuities as in a step function and which do not exceed a specified maximum rate of change with time.

To adapt this network to high-voltage impulse measurements it may be altered as shown in Figure 4(B). The terminating resistance R_2' must be the characteristic impedance of the cable (assuming the cable to be lossless). There are some reflections, however, since the cable is not lossless. To minimize reflections from the sending end of the cable R_2 also should approximate the cable characteristic impedance. This assumes that $R_1 \gg R_2$ so that a large voltage division is attained. This type of network may prove satisfactory where the accuracy requirements are not too stringent; but however, it does not appear that the inherent difficulties could be overcome for very short impulse measurements.

A Universal Voltage Division Network

A network constructed of simple-T sections is shown in Figure 5. The following analysis indicates that by proper choice of the components in each section an attenuating network results which has the property of passing any kind of signal without alteration of form. The Laplace transformation of voltage and current at the nth section is (see appendix)

$$E(s,n)=E(s,0)\cosh\beta(s)n-Z_o(s)\,I(s,0)\sinh\beta(s)n \tag{18}$$

$$I(s,n)=I(s,0)\cosh\beta(s)n-\frac{E(s,0)}{Z_o(s)}\sinh\beta(s)n \tag{19}$$

At the nth section output terminals, the termination, the voltage and current transforms are related by

$$E(s,N)=Z(s)I(s,N) \tag{20}$$

where $Z(s)$ is the terminating impedance function. By setting $n=N$ in equations 18 and 19 and substituting in equation 20 the input current to the network is found to be

$$I(s,0)=\frac{\cosh\beta(s)N+\dfrac{Z(s)}{Z_o(s)}\sinh\beta(s)N}{Z(s)\cosh\beta(s)N+Z_o(s)\sinh\beta(s)N}\times E(s,0) \tag{21}$$

Eliminating $I(s,0)$ between equations 18 and 21

$$E(s,n)=\frac{Z(s)\cosh(N-n)\beta(s)+Z_o(s)\sinh(N-n)\beta(s)}{Z(s)\cosh N\beta(s)+Z_o(s)\sinh N\beta(s)}\times E(s,0) \tag{22}$$

Writing equation 22, in equivalent exponential form

$$E(s,n)=\frac{e^{(N-n)\beta(s)}+\gamma(s)e^{-(N-n)\beta(s)}}{e^{N\beta(s)}+\gamma(s)e^{-N\beta(s)}}\times E(s,0) \tag{22A}$$

where

$$\gamma(s)=\frac{Z(s)-Z_o(s)}{Z(s)+Z_o(s)} \tag{23}$$

the reflection ratio function.

If the terminating impedance is identical to the characteristic impedance, the reflection ratio function is zero. In this event equation 22A becomes

$$E(s,n)=e^{-n\beta(s)}E(s,0) \tag{24}$$

Under the same condition for which the characteristic impedance is realizable at the termination, the function $e^{-n\beta(s)}$ is independent of s. Equation 67 of the appendix then becomes

$$e^{-n\beta(s)}=(\nu-\sqrt{\nu^2-1})^n=\left(\frac{1}{k}\right)^n \tag{67}$$

where k is a constant and may be defined as the attenuation per section. The function ν (equation 59 of the appendix) becomes independent of s if the impedance ratio functions α, μ, and λ are made independent of s. The complete voltage transform solution then is

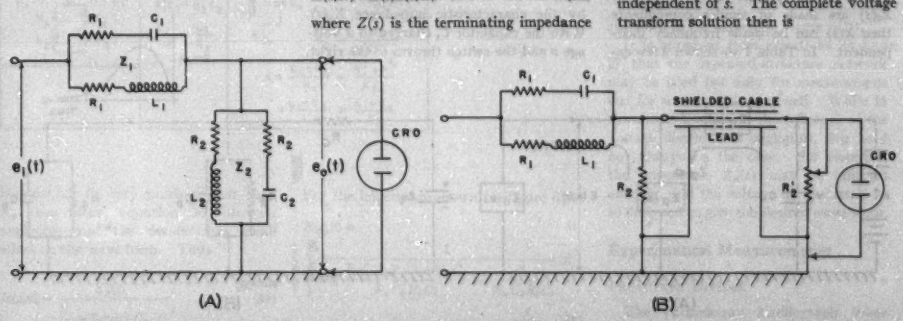

Figure 4. (A) Simplified attenuating network (B) Schematic arrangement for remote location of the cathode-ray oscilloscope

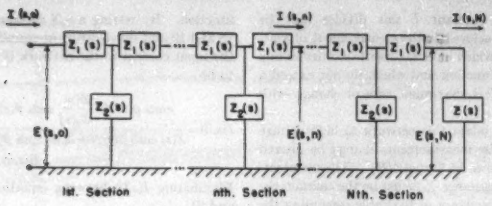

Figure 5. Repeated-structure network composed of T sections

$$E(s,n)=\left(\frac{1}{k}\right)^n E(s,0) \tag{25}$$

which has the inverse Laplace transformation

$$e(t,n)=\left(\frac{1}{k}\right)^n e(t,0) \tag{26}$$

This simple relation shows that the voltage at the output terminals of any section is identical in form to the input voltage $e(t,0)$. The voltage across the terminating characteristic impedance is

$$e(t,N)=\left(\frac{1}{k}\right)^N e(t,0) \tag{27}$$

which is the voltage desired to be observed or recorded.

If the repeated-structure network is composed of simple-T sections, as shown in Figure 5, the characteristic impedance is

$$Z_o(s)=Z_2(s)\sqrt{\lambda^2(s)-1} \tag{28}$$

where

$$\lambda(s)=\nu(s)=\frac{Z_1(s)+Z_2(s)}{Z_2(s)} \tag{29}$$

If the impedance ratio function $\lambda(s)$ is made frequency independent, the characteristic impedance becomes physically realizable at the termination. By equation 29 it is apparent that if $Z_1(s)$ and $Z_2(s)$ are made of similar components then $\lambda(s)$ can be made frequency independent. In Table I are shown a few examples where λ is but a numerical constant. If the vertical plates of a cathode-ray tube are connected directly across the terminating impedance and the network is of the type A, C, or D shown in Table I, the capacitance of the plates may be considered as part of the required termination, thus permitting the ideal condition of including the recording instrument as part of the characteristic impedance termination.

A simple and convenient means for precision adjustment of the section parameters exists. Setting $s=j\omega$ in equation 25 gives

$$\frac{E(j\omega,n)}{E(j\omega,0)}=\left(\frac{1}{k}\right)^n \tag{30}$$

This expression shows the network to be capable of passing sinusoidal signals without phase shift, and that the amplitude ratio of output to input voltage is a constant for all frequencies.

Impulse Generator with Repeated-Structure Voltage Divider

In Figure 6(A) is shown a schematic arrangement for generating a transient voltage of prescribed form. With the repeated-structure network properly terminated the divider may be represented by the characteristic impedance $Z_o(s)$. With the capacitor C_v charged to a voltage v and the switch thrown to the right, the Laplace transformed voltage $E(s,0)$ may be obtained from the mesh equation

$$\left[\frac{1}{C_v s}+Z_g(s)+Z_p(s)\right]I_g(s)-Z_p(s)I(s,0)=\frac{v}{s} \tag{31}$$

$$Z_o(s)I(s,0)=E(s,0) \tag{32}$$

$$Z_p(s)[I_g(s)-I(s,0)]=E(s,0) \tag{33}$$

From these relations

$$E(s,0)=\frac{Z_p(s)}{\left[Z_g(s)+Z_p(s)+\frac{1}{C_v s}\right]}\times\left[1+\frac{Z_p(s)}{Z_o(s)}\right]-\frac{Z_p(s)}{Z_o(s)}Z_p(s)\ \frac{v}{s} \tag{34}$$

Since $e(t,0)$ is the inverse Laplace transformation of $E(s,0)$, equation 34, and

$$e(t,N)=\left(\frac{1}{k}\right)^n e(t,0) \tag{27}$$

it follows that the desired testing wave form may be obtained by adjusting the impedances $Z_g(s)$ and $Z_p(s)$, and the observed voltage $e(t,N)$ will be exactly of the same form. Note that the characteristic impedance of the voltage divider will influence the shape of the testing wave. The relative effect of $Z_o(s)$ may be controlled to almost any desired amount by proper choice of the impedances $Z_p(s)$ and $Z_o(s)$.

To illustrate, assume that a network of type A, Table I, was chosen for both $Z_p(s)$ and $Z_o(s)$ as shown in Figure 6(B). Then the impedance ratio

$$\frac{Z_p(s)}{Z_o(s)}=\frac{R_p\,R_oC_os+1}{R_o\,R_pC_ps+1} \tag{35}$$

If $R_oC_o=R_pC_p$

$$\frac{Z_p(s)}{Z_o(s)}=\frac{R_p}{R_o} \tag{36}$$

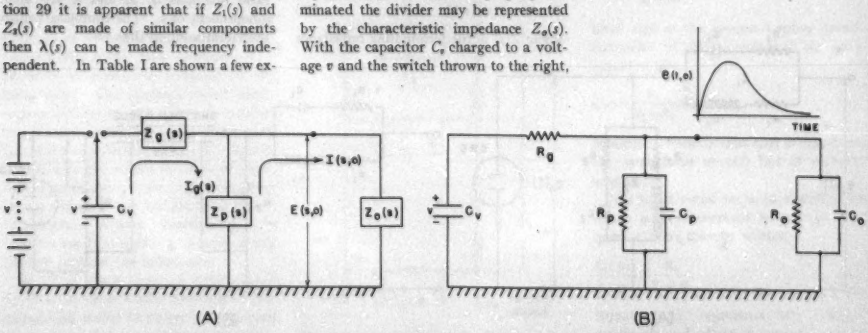

Figure 6. (A) Schematic arrangement for producing a testing wave (B) Circuit for producing a particular type of impulse

Table I. T-Section Networks

TYPE	RESTRICTIONS	CHARACTERISTIC IMPEDANCE
(A) 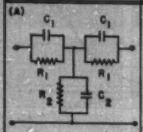	$R_1C_1 = R_2C_2$	$Z_0(s) = \frac{R_0}{R_0C_0s+1}$ $R_0 = R_2\sqrt{\lambda^2-1}$ $C_0 = \frac{C_2}{\sqrt{\lambda^2-1}}$ $\lambda = \frac{R_1+R_2}{R_2} = \frac{C_1+C_2}{C_1}$
(B) 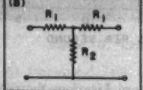	NONE	$Z_0(s) = R_0$ $R_0 = R_2\sqrt{\lambda^2-1}$ $\lambda = \frac{R_1+R_2}{R_2}$
(C)	NONE	$Z_0(s) = \frac{1}{C_0s}$ $C_0 = \frac{C_2}{\sqrt{\lambda^2-1}}$ $\lambda = \frac{C_1+C_2}{C_1}$
(D) 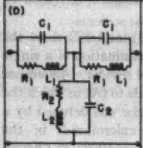	$R_1C_1 = R_2C_2$ $\frac{L_1}{R_1} = \frac{L_2}{R_2}$	$Z_0(s) = \frac{L_0s+R_0}{L_0C_0s^2+R_0C_0s+1}$ $R_0 = R_2\sqrt{\lambda^2-1}$ $L_0 = L_2\sqrt{\lambda^2-1}$ $C_0 = \frac{C_2}{\sqrt{\lambda^2-1}}$ $\lambda = \frac{R_1+R_2}{R_2} = \frac{L_1+L_2}{L_2} = \frac{C_1+C_2}{C_1}$
(E) 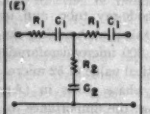	$R_1C_1 = R_2C_2$	$Z_0(s) = R_0 + \frac{1}{C_0s}$ $R_0 = R_2\sqrt{\lambda^2-1}$ $C_0 = \frac{C_2}{\sqrt{\lambda^2-1}}$ $\lambda = \frac{R_1+R_2}{R_2} = \frac{C_1+C_2}{C_1}$
(F) 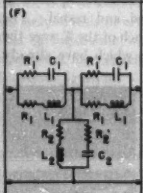	$\frac{R_1'}{R_1} = \frac{R_2'}{R_2}$ $R_1'C_1 = R_2'C_2$ $\frac{L_1}{R_1} = \frac{L_2}{R_2}$	$Z_0(s) = \frac{(L_0s+R_0)(R_0'C_0s+1)}{C_0s(L_0s+R_0)\ R_0'C_0s+1}$ $R_0 = R_2\sqrt{\lambda^2-1}$ $R_0' = R_2'\sqrt{\lambda^2-1}$ $L_0 = L_2\sqrt{\lambda^2-1}$ $C_0 = \frac{C_2}{\sqrt{\lambda^2-1}}$ $\lambda = \frac{R_1+R_2}{R_2} = \frac{R_1'+R_2'}{R_2'} = \frac{L_1+L_2}{L_2} = \frac{C_1+C_2}{C_1}$

Table II. Various Sections Derived from the Parallel-T

TYPE SECTION	CHARACTERISTIC IMPEDANCE	IMPEDANCE RATIO FUNCTION
PARALLEL T 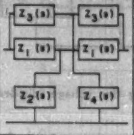	$Z_0(s) = \frac{\mu^2-1}{1+a\frac{\mu^2-1}{\lambda^2-1}}\frac{Z_3(s)}{\sqrt{\lambda^2-1}}$	$\nu = \frac{\mu+a\lambda\frac{\mu^2-1}{\lambda^2-1}}{1+a\frac{\mu^2-1}{\lambda^2-1}}$
BRIDGED T 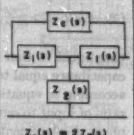 $Z_4(s) = 2Z_3(s)$	$Z_0(s) = Z_3(s)\sqrt{\frac{\lambda^2-1}{1+2\frac{Z_1(s)}{Z_3(s)}}}$	$\nu = \frac{\lambda^2+\frac{Z_1(s)}{Z_3(s)}\lambda-1}{\lambda^2+\frac{Z_1(s)}{Z_3(s)}-1}$
SINGLE T 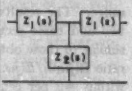	$Z_0(s) = Z_2(s)\sqrt{\lambda^2-1}$	$\nu = \lambda$
PI 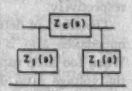 $Z_4(s) = 2Z_3(s)$	$Z_0(s) = \frac{Z_2(s)}{\sqrt{\lambda^2-1}}$	$\nu = \frac{Z_1(s)+Z_2(s)}{Z_1(s)}$

By making R_s very much greater than R_p their ratio, equation 36, becomes negligible and the divider has small effect on the wave form. Thus

$$E(s,0) = \frac{Z_p(s)}{\frac{1}{C_ps}+Z_0(s)+Z_p(s)}\frac{v}{s} \tag{37}$$

For the impedance shown in Figure 6(B)

$$E(s,0) = \frac{1}{s^2+\frac{R_pC_s+R_pC_0+R_sC_p}{R_sC_pR_pC_s}s+\frac{1}{R_sC_pR_pC_s}} \times \frac{v}{R_pC_p} \tag{38}$$

This expression may be written

$$E(s,0) = \frac{1}{\left(s+\frac{1}{T_1}\right)\left(s+\frac{1}{T_2}\right)}\frac{v}{R_pC_p} \tag{39}$$

where the two time constants may be adjusted so that $T_1 \gg T_2$. The inverse Laplace transformation of $E(s,0)$, equation 39, is of the form

$$e(t,0) = K(e^{-t/T_1} - e^{-t/T_2}) \tag{40}$$

as shown in the sketch of Figure 6(B).

It is apparent from equations 34 and 27 that the repeated-structure network may be used not only for measurement but for wave shaping as well. While in the above illustration the influence of the voltage divider was negligible, this need not always be the case. For example, the impedance $Z_p(s)$ may be omitted entirely, and the voltage divider itself be so designed to give the desired wave form.

Experimental Measurements

Prototype Divider

The cathode-ray oscillograph when used with some suitable voltage-divider

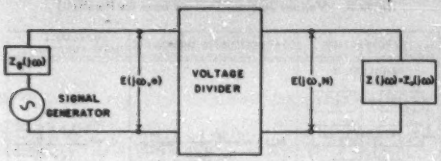

Figure 7 (above). Test circuit for measuring the voltage divider frequency response

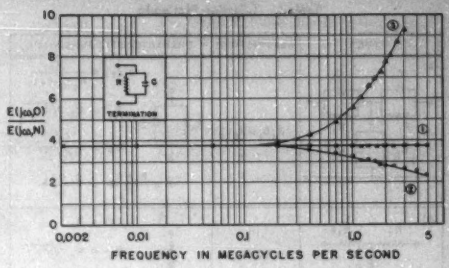

Figure 8 (right). Frequency response of one section, network A, Table I

(1) $R=R_o$ $C=C_o$ (2) $R=R_o$ $C<<C_o$ (3) $R=R_o$ $C>>C_o$

has been generally accepted as the instrument best adapted for the measurement of surge voltages. The input impedance to the vertical plates of a cathode-ray tube may be represented by a parallel combination of resistance and capacitance, similar in form to the characteristic impedance of network A, Table I. The equivalent parallel resistance, caused by convection currents between the plates, is sufficiently large to be neglected in most instances.

A prototype divider consisting of three T-sections, network A, Table I, was constructed. The T-section was chosen for experimental study because of its simplicity. Each branch of the T was composed of a special carbon-type resistor of 10,000 ohms ±1 per cent, in parallel with a capacitor of 90 micromicrofarads, ±0.5 micromicrofarad. The resistive element in the termination was adjusted to a value of 17,350 ohms (R_o, Table I). The capacitive element in the termination consisted of the vertical plates of a cathode-ray tube and the input capacitance to a vacuum-tube voltmeter. In addition a variable air capacitor was connected in parallel with the above combination, and by means of an impedance bridge the total capacitance was adjusted to 52 micromicrofarads (C_o, Table I).

This prototype divider was tested as suggested by equation 30. The essential elements of the test circuit are shown in Figure 7. The output and input voltages, $E(j\omega, N)$ and $E(j\omega, 0)$ respectively, were measured by means of two vacuum-tube voltmeters over the frequency range zero to 5 megacycles. The ratio of input to output voltage as a function of frequency was thus obtained. Measurements were made on each of the three sections separately, then on two sections in cascade, and finally on all three sections in cascade. A plot of amplitude ratio as a function of frequency for a typical set of tests on a single section is shown in Figure 8. Curve 1 was obtained with the shunt resistor of the termination having resistance equal to that of R_o, and the shunt capacitance equal to C_o, the values which according to equation 30 give a constant ratio of input to output voltage, and zero phase displacement between these voltages. It will be noted that the ratio remains constant over the entire frequency range. The results of measurements on two and three sections in cascade were similar to those obtained with one. The ratio $E(j\omega,0)/E(j\omega,N)$ remained constant within ±2 per cent from 0 to 5 megacycles, the ratios then being 13.93 and 52 respectively.

The effect of detuning the terminating impedance also is shown in Figure 8. When too little capacitance was present, the voltage ratio decreased at high frequencies as shown by curve 2; and when too much capacitance was present, the voltage ratio increased at high frequencies as shown by curve 3. Detuning the terminating capacitor by 10 micromicrofarads had no significant effect on the voltage ratio over the frequency range zero to 5 megacycles; however, a slight phase shift became noticeable at 5 megacycles, as shown in the oscillogram Figure 10(A). Oscillograms were taken at the same time the measurement of the voltage ratio was made on the divider.

The input voltage $E(j\omega,0)$ was applied to the horizontal plates and the output voltage $E(j\omega,N)$ was applied to the vertical plates of a cathode-ray tube. The resulting pattern was a Lissajous figure which was a straight line when both voltages were in time phase. Oscillograms were taken for one, two, and three sections, but oscillograms are shown for one section only, since with more than one section the ratio was so great that only a small vertical deflection could be obtained.

Photographs of Lissajous figures were taken at frequencies of 200 kc, 1 megacycle, and 5 megacycles per second and are shown in Figures 9(A), (B), and (C) respectively. No evidence of phase shift is observable. Figures 9(D), (E), and (F) are photographs of Lissajous figures taken with the same test circuit and at the same frequencies but with the type A voltage divider replaced by a surge-resistor divider of the conventional type. For this conventional divider considerable phase shift above 1 megacycle is present. In addition, the attenuation increased by a significant amount.

Figures 10(A), (B), and (C) show the effect of improper termination of a single section of the type A divider. Reference has already been made to (A) in which the terminating impedance was detuned by a change of 10 micromicrofarads in the capacitance. In Figure 10(B), at 1 megacycle no terminating capacitance is present excepting that of the vertical plates of the cathode-ray tube, and in Figure 10(C) also taken at 1 megacycle, the termination is 200 micromicrofarads rather than the critical value of 52 micromicrofarads. The phase shifts in (A), (B), and (C) show the importance of proper termination of the network.

A resistor divider of type B, Table I, also was constructed and tested. The resistors in each branch of the T were the 10,000-ohm resistors which have already

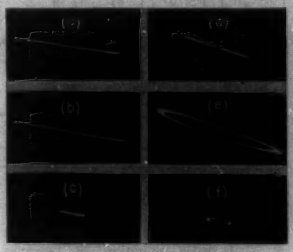

Figure 9. Lissajous figures

(A) Network A, Table I, 200 kc
(B) Network A, Table I, 1 megacycle
(C) Network A, Table I, 5 megacycles
(D) Surge resistor divider, 200 kc
(E) Surge resistor divider, 1 megacycle
(F) Surge resistor divider, 5 megacycles

Figure 10. Lissajous figures

(A) Network *A*, Table I, 5 megacycles, terminating capacitor detuned by 10 micromicrofarads
(B) Network *A*, Table I, 1 megacycle, terminating capacitor much less than required value
(C) Network *A*, Table I, 1 megacycle, terminating capacitor much greater than required value
(D) Network *B*, Table I, 1 megacycle, correct resistance termination
(E) Network *D*, Table I, 1 megacycle, correct termination
(F) Large-scale model (Network *D*, Table I), 1 megacycle, correct termination, attenuation of 22

Figure 11 (right). Frequency response of one section

(A) Network *B*, Table I,
(B) Network *C*, Table I,
(C) Network *D*, Table I

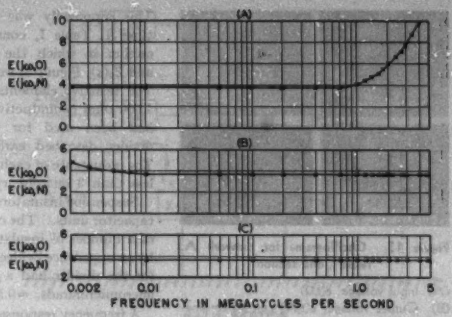

been described. Measured voltage ratio as a function of frequency is shown in Figure 11(A). This result is similar to that shown by curve 3, Figure 8, where the terminating capacitance was too large. The small capacitance of the cathode-ray tube, vacuum-tube voltmeter, and leads come into effect at the higher frequencies. It may be concluded that in a divider network consisting only of resistor arms, correct termination is impossible when the measuring equipment has capacitive impedance. A Lissajous figure for 1 megacycle is shown in Figure 10(D). The resulting large phase shift is obvious.

A divider of type *C*, Table I, also was constructed using 90-micromicrofarad capacitors and terminated by a total capacitance equal to C_e. Figure 11(B) shows the amplitude ratio of a typical test made in one section. Deviation of the voltage ratio from the ideal value at the lower frequencies is caused by convection currents between the plates of the cathode-ray tube. It is thus evident that in a divider network consisting of capacitance arms only, correct termination is impossible when the impedance of the measuring equipment has a resistive component.

A 3-section divider of type *D*, Table I, also was constructed and tested. The resistors and capacitors were the same as those already described. Inductors of approximately 500 microhenrys were placed in series with the resistors. As in the preceding cases the divider was terminated in its characteristic impedance and tested. The constancy of the voltage ratio with frequency for one section is shown in Figure 11(C). The appearance of the Lissajous figure, Figure 10(E), is typical of the condition in which there is no phase shift. The results for the other sections individually and for two and three sections in cascade were equally good. This indicates that although considerable inductance is present in the arms of a divider network, by correct design and termination a good voltage divider may be realized.

Finally a network of type *E*, Table I, was constructed and tested. The results show that this type of network would not be satisfactory, as may have been expected from the foregoing discussion. The characteristic impedance could not be realized with the cathode-ray tube connected across the termination. For the same reason this eliminates the possibility of realizing a good voltage divider of type *F*, Table I, if the value of R_1 is at all appreciable.

The type *A* divider, Table I, was next tested for transient response. The output terminals of the wave-shaping circuit shown in Figure 12 were connected to the input terminals of the divider. The capacitor C_e was charged from a d-c source and then discharged through thyratrons V_b and V_e and the associated circuit. The wave shape was controlled by the resistors R_e and R_b. The sweep in each case was carefully calibrated by a timing wave and could be measured accurately to about 0.2 microsecond. Figures 13(A) and (B) show oscillograms taken of input voltage $e(t,0)$ and output voltage $e(t,N)$ for correct termination. Figures 13(C) and (D) show oscillograms taken of the output voltage for incorrect termination. When the network is incorrectly terminated, the output wave shape is far from being a reproduction of the input wave. Photographic enlargements of Figures 13(A) and (B) were made and the input wave was plotted in Figure 14.

Points obtained from the output wave were multiplied by the theoretical attenuation factor and also are shown on the same figure. The fact that the points computed from the output wave lie almost directly on the input wave shows the high degree of accuracy in wave reproduction which may be obtained with a correctly designed and terminated voltage-divider network.

In Figure 15 are shown oscillograms of the input and the output transient voltages for one section of the type *D* network with the correct value of terminating impedance. Note that each output response is a replica of the input wave, the

Figure 12. Wave shaping circuit for transient tests

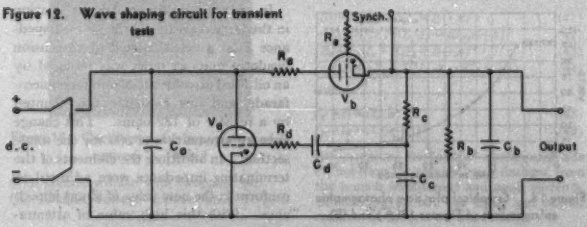

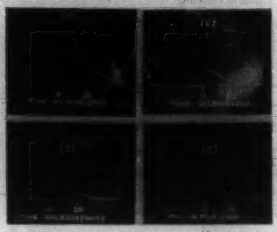

Figure 13. Oscillograms for network A, Table I, one section

(A) Input voltage $e(t,0)$
(B) Output voltage, $e(t,N)$ correct termination
(C) Output voltage, $e(t,N)$ $R=R_0$ $C \ll C_0$
(D) Output voltage, $e(t,N)$ $R=R_0$ $C \gg C_0$

network itself introducing no apparent distortion.

In Figure 16 is shown a schematic arrangement for switching an impulse repeatedly onto the voltage divider input terminals.[8] By repeating the transient in this way it was possible to obtain photographs of both input voltage $e(t,0)$ and output voltage $e(t,N)$ for a relatively fast sweep. The input circuit was closed in consecutive intervals by allowing mercury drops falling under the influence of gravity to act as a switch when bridging two contacts. The cathode-ray oscillograph sweep, exponential in form, was initiated by the mercury switch. The time axis of the cathode-ray oscillograph was calculated from the known values of resistance and capacitance in the cathode-ray oscillograph sweep circuit. A cable, T_4, introduced sufficient time delay to allow the sweep to begin before the impulse arrived at the divider input terminals. Figure 17 shows input and output voltages where the divider consisted of one section of network D, Table I. No deviation of output from input is observable.

Large Scale Model

A larger model capable of measuring up to 50,000 volts peak was constructed.

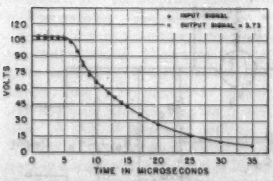

Figure 14. Graphical plot from photographic enlargements of Figures 13(A) and (B)

This supposedly was a network of the type A, Table I, consisting of a single section in which the impedances $Z_1(s)$ and $Z_2(s)$, Figure 5, were made identical. The resistive elements consisted of the 1,000 ohm noninductive resistors which had been used for the surge-resistor divider described earlier in the paper. The inductance of each 500-ohm card was less than 3 microhenrys.

Suspension insulators were used for the capacitor units. The capacitance of each of a number of insulators was measured by an impedance bridge and those selected for the divider had a capacitance of 39 micromicrofarads, ±0.5 micromicrofarad.

A frequency response test was made, as was done with the prototype dividers, and the results were unsatisfactory. It was found that the length of leads was extremely critical. It was found possible, however, to obtain satisfactory results if the lengths of the leads in each section element were made identical. The foregoing essentially noninductive resistors were then replaced by some wire-wound ceramic coated resistors. These resistors had an over-all length of about 15 inches and a resistance of 20,000 ohms plus appreciable inductance. With these resistive-inductive elements the results were excellent. The voltage ratio was constant with frequency, and no phase shift was detectable.

The reason for the improvement is the fact that the inductance of the leads was appreciable and the divider was thus of the type D rather than of the type A. The inductance of the leads was more or less indeterminate so that it was difficult to obtain the correct values of L_1 and L_2 for the type D divider of Table I. However, the inductance of the ceramic-coated resistor units was large compared with the inductances of the leads and since the inductances of the units were essentially equal, the type D divider was readily produced. This, we believe, emphasizes one advantage of the network-type divider, that is, the stray inductances of the leads need not in any manner vitiate the ideal characteristics of the divider.

In order to obtain greater attenuation in the large-scale model the shunt impedance $Z_2(s)$ which consisted of suspension insulator units in series was replaced by an oil-filled capacitor of 5,850 micromicrofarads, and this capacitor was shunted by a resistor of 133 ohms. This change gave an attenuation of 300 for the single section. In addition, the elements of the terminating impedance were adjusted to conform to the new value of shunt impedance. With this high value of attenuation it was not possible to compare input and output voltages. However, an oscillogram of the output response was taken for a surge rising slowly to 27,200 volts and applied to a chopping gap, Figure 18(A). A surge generator of the conventional type was used. The 27,200 volt peak recorded on the oscillogram, Figure 18(A) was within 2 per cent of the mean breakdown voltage for the sphere spacings of the chopping gap.

Figure 15. Oscillograms for network D, Table I, one section with correct termination

(A) Input voltage
(B) Output voltage for input (A)
(C) Input voltage
(D) Output voltage for input (C)

The surge-generator circuit was then adjusted to produce a $1^1/_2$ by 40-microsecond wave, the maximum value of which was 29,000 volts. The oscillogram of the output wave is shown in Figure 18(B). The sweep was not fast enough to delineate the wave front too clearly, but so far as the oscillogram can be analyzed, the output response corresponded with the $1^1/_4$-microsecond wave front.

In order to test this large-scale model more completely, both a cold-cathode type of oscillograph and a glass-tube type each with a very fast sweep that can be synchronized with the surge generator are needed. With instruments of this type the model can be tested with impulse of very short duration, and the input and output can be accurately computed.

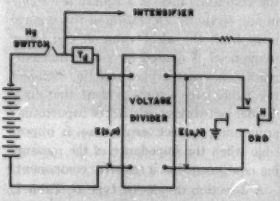

Figure 16. Schematic diagram of arrangement for placing an impulse repeatedly onto the input terminals of the voltage divider

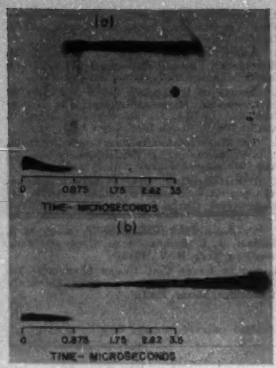

Figure 17 (left). (A) Divider input voltage, (B) resulting output voltage

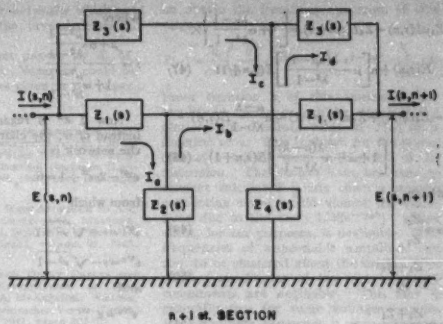

Figure 19 (right). One section of a parallel-T repeated-structure network

This work is being undertaken at the present time.

Conclusions

1. Present-day methods of surge testing as well as a review of the literature shows that there is a need for increasing the accuracy of the present methods of measuring impulses of very short duration.

2. The repeated-structure network described in the paper has been shown by rigorous analysis to possess the ideal characteristic of an attenuating network for passing any kind of signal whatsoever without distortion. Experimental results from tests made on the simple T-structure are sufficiently favorable to indicate that a practical improved high-voltage divider of high accuracy may be constructed. When a cathode-ray oscilloscope is used as the measuring instrument and its input impedance becomes a part of the terminating impedance, networks of type *A*, *D*, and possibly *C* are particularly suitable.

3. The effect of the impedances of the connecting leads was not explicitly accounted for in the analysis, but it is apparent that any possible effects can be disregarded if the impedances of the leads be included in the required impedances of the arms of the network and if all connection lead impedances are made negligible with respect to the branch impedances.

4. The effect of stray capacitance to ground can either be compensated for or made negligible by proper choice of the circuit parameters in the networks of type *A*, *C*, or *D* in Table I.

5. In the past, improvement in dividers for high-voltage measurements has been accomplished by such means as: reduction of inductance by using bifilar wound resistors; minimizing stray capacitance by isolation of the divider; and reduction of the input capacitance to the cathode-ray tube by using a specially designed tube. In the repeated-structure network type of voltage divider, however, the presence of inductance as part of the resistive elements may be desirable; stray capacitance may be either compensated for or neglected; and the input capacitance to the cathode-ray tube may be incorporated as part of the terminating impedance.

6. The need for a cable lead to the measuring instrument is eliminated since the divider itself can be made of sufficient length so that the measuring instrument and similar equipment may be located at a remote distance from surge generator.

Figure 18. Oscillograms for large-scale model, network D, Table I

(A) Output voltage with chopping gap
(B) Output voltage approximately $1^1/_2 \times 40$ wave

7. The practicability of the network type of voltage divider for very high voltage, 1,000,000 volts and higher, has so far been given only general consideration by the authors. The theory is completely presented and only the practical design remains. While suspension insulators may be used for the capacitive system, the authors feel that capacitor units having much greater values of capacitance and which are less affected by humidity would be preferable. Since the requirements for the capacitive system are only moderate, the cost should not be excessive. Because of less exacting requirements the resistor units can be made at less cost than the present ones. Moreover, the divider may be so designed that the largest part of the voltage drop occurs in the first section making the voltage rating of subsequent sections only moderate. We realize that the elimination of stray capacitance and inductive effects may present some problems for the first section, at least.

Appendix. Derivation of the Laplace Transform Solution of the Repeated-Structure Network

Consider a repeated-structure network consisting of parallel-T sections having impedances as shown in Figure 19. For no initial energy storage within the network, the Maxwell mesh equations are

$$[Z_1+Z_3]I_a-Z_3I_b=E(s,n) \tag{41}$$
$$-Z_3I_a+[Z_1+Z_3]I_b=E(s,n+1) \tag{42}$$
$$[Z_3+Z_4]I_c-Z_4I_d=E(s,n) \tag{43}$$
$$-Z_4I_c+[Z_3+Z_4]I_d=-E(s,n+1) \tag{44}$$

where

$$I_a+I_c=I(s,n) \tag{45}$$
$$I_b+I_d=I(s,n+1) \tag{46}$$

All quantities are Laplace transformed, the (s) notation for brevity being dropped from the branch impedances and mesh currents. Eliminating all but the input and output currents of the section there results

$$Z_{\omega\mu}I(s,n)-Z_4I(s,n+1)=\left[1+\alpha\frac{\lambda\mu-1}{\lambda^2-1}\right]\times E(s,n)+\alpha\left[\mu-\frac{\lambda(\lambda\mu-1)}{\lambda^2-1}\right]E(s,n+1) \quad (47)$$

$$-Z_4I(s,n)+Z_{\omega\mu}I(s,n+1)=\alpha\frac{\mu-\lambda}{\lambda^2-1}E(s,n)-\left[1+\alpha+\alpha\frac{\lambda(\mu-\lambda)}{\lambda^2-1}\right]E(s,n+1) \quad (48)$$

where

$$\alpha=\frac{Z_4}{Z_2} \quad (49)$$

$$\lambda=\frac{Z_1+Z_2}{Z_2} \quad (50)$$

$$\mu=\frac{Z_3+Z_4}{Z_4} \quad (51)$$

Equations 47 and 48 are algebraic equations in s and difference equations in n. Interpolating the points of $E(s, n)$ and $I(s, n)$, section voltage and current transforms respectively, by a jump function[7]

$$Z_{\omega\mu}\int I(s,n)-Z_4\int I(s,n+1)=\left[1+\alpha\frac{\lambda\mu-1}{\lambda^2-1}\right]\int E(s,n)+\alpha\left[\mu-\frac{\lambda(\lambda\mu-1)}{\lambda^2-1}\right]\int E(s,n+1) \quad (52)$$

$$-Z_4\int I(s,n)+Z_{\omega\mu}\int I(s,n+1)=\alpha\frac{\mu-\lambda}{\lambda^2-1}\int E(s,n)-\left[1+\alpha+\alpha\frac{\lambda(\mu-\lambda)}{\lambda^2-1}\right]\times\int E(s,n+1) \quad (53)$$

By definition

$$\mathcal{L}\left[\int E(s,n)\right]=\mathcal{E}(s,w)$$

$$\mathcal{L}\left[\int I(s,n)\right]=\mathcal{I}(s,w) \quad (54)$$

The Laplace transformation of equations 52 and 53 with respect to n is

$$Z_{\omega\mu}\mathcal{I}(s,w)-Z_4e^{w}[\mathcal{I}(s,w)-I(s,0)P(w)]=\left[1+\alpha\frac{\lambda\mu-1}{\lambda^2-1}\right]\mathcal{E}(s,w)+\alpha\left[\mu-\lambda\frac{\lambda\mu-1}{\lambda^2-1}\right]\times e^{w}[\mathcal{E}(s,w)-E(s,0)P(w)] \quad (55)$$

$$-Z_4\mathcal{I}(s,w)+Z_{\omega\mu}e^{w}[\mathcal{I}(s,w)-I(s,0)P(w)]=\alpha\frac{\mu-\lambda}{\lambda^2-1}\mathcal{E}(s,w)-\left[1+\alpha+\alpha\lambda\frac{\mu-\lambda}{\lambda^2-1}\right]\times e^{w}[\mathcal{E}(s,w)-E(s,0)P(w)] \quad (56)$$

Solving equations 55 and 56 for $\mathcal{E}(s,w)$ and $\mathcal{I}(s,w)$ respectively

$$\mathcal{E}(s,w)=\frac{[e^{w}-\nu]E(s,0)-\dfrac{Z_4[\mu^2-1]}{1+\alpha\dfrac{\mu^2-1}{\lambda^2-1}}I(s,0)}{e^{2w}-2\nu e^{w}+1}\times e^{w}P(w) \quad (57)$$

$$\mathcal{I}(s,w)=\frac{[e^{w}-\nu]I(s,0)-\dfrac{1+\alpha\dfrac{\mu^2-1}{\lambda^2-1}}{Z_4[\mu^2-1]}[\nu^2-1]E(s,0)}{e^{2w}-2\nu e^{w}+1}\times e^{w}P(w) \quad (58)$$

where

$$\nu=\frac{\mu+\alpha\lambda\dfrac{\mu^2-1}{\lambda^2-1}}{1+\alpha\dfrac{\mu^2-1}{\lambda^2-1}} \quad (59)$$

Now if e^{w} is regarded as the variable instead of w, the characteristic equation of the network is

$$e^{2w}-2\nu e^{w}+1=0 \quad (60)$$

from which

$$e^{w_1}=\nu+\sqrt{\nu^2-1}$$

$$e^{w_2}=\nu-\sqrt{\nu^2-1} \quad (61)$$

and

$$e^{w_2}=e^{-w_1}$$

Expanding equations 57 and 58 in partial fractions, as described in reference 7, Chapter IX, the inverse Laplace transformation with respect to w is

$$E(s,n)=E(s,0)\frac{e^{w_1n}+e^{-w_1n}}{2}-Zo(s)I(s,0)\frac{e^{w_1n}-e^{-w_1n}}{2} \quad (62)$$

$$I(s,n)=I(s,0)\frac{e^{w_1n}+e^{-w_1n}}{2}-\frac{E(s,0)}{Z_o(s)}\frac{e^{w_1n}-e^{-w_1n}}{2} \quad (63)$$

where

$$Z_o(s)=\frac{Z_4[\mu^2-1]}{1+\alpha\dfrac{\mu^2-1}{\lambda^2-1}\sqrt{\nu^2-1}} \quad (64)$$

Replacing w_1 by a more suitable term $\beta(s)$, the propagation function, the solution may be written

$$E(s,n)=E(s,0)\cosh\beta(s)n-Z_o(s)I(s,0)\sinh\beta(s)n \quad (65)$$

$$I(s,n)=I(s,0)\cosh\beta(s)n-\frac{E(s,0)}{Z_o(s)}\sinh\beta(s)n \quad (66)$$

From equation 61 it may be seen that $e^{w_2n}=e^{-w_1n}$, and

$$e^{-n\beta(s)}=\left[\nu-\sqrt{\nu^2-1}\right]^n \quad (67)$$

The bridged T-section is obtained from the parallel T-section upon setting $Z_4=\infty$ (or $Z_1=\infty$); the simple T is obtained upon setting $Z_3=\infty$ (or $Z_1=\infty$); and the pi section is obtained upon setting $Z_3=0$ and $Z_4=\infty$ (or $Z_4=0$ and $Z_3=\infty$). This fact is illustrated in Table II.

If the impedance ratio functions α, μ, and λ are made independent of frequency, the realization of the characteristic impedance at the termination of the above described repeated-structure networks is possible. This is demonstrated in Table I for the simple T.

References

1. The Measurement of High Voltage, **Francis M. Defandorf**. *Journal*, Washington Academy of Sciences (Menosha, Wis.) volume 38, number 2, February 15, 1948, pages 33–60.

2. American Standards for Measurement of Test Voltage in Dielectric Tests. *AIEE Standard Number 4*, 1942, pages 1–23.

3. Short-Time Sparkover of Gaps, **J. H. Hagenguth**. *Electrical Engineering* (*AIEE Transactions*), January 1937, volume 56, page 67.

4. Errors in Measuring Surge Voltages by Oscillograph, **Marius Böchman, Nils Hylten-Cavallius**. *ASEA Journal* (Vesterås, Sweden), number 7084E, March 1946, pages 1–16.

5. The Measurement of High Surge Voltages, **P. L. Bellaschi**. *AIEE Transactions*, volume 52, June 1933, pages 544–52.

6. Der Hochspannungtheiler beim Kathodenstrahloszillographen, **H. Höhl**. *Archiv für Electrotechnik*, (Berlin, Germany), volume 36, 1942, pages 329–331.

7. Transients in Linear Systems (book), **M. F. Gardner, J. L. Barnes**. John Wiley and Sons, Inc., New York, N. Y., 1942.

8. Single Layer Coil Under Electrical Impacts, **Karl Lerstrup**. *Thesis*, Harvard University (Cambridge, Mass.), 1942.

Discussion

P. A. Abetti (General Electric Company, Pittsfield, Mass.): The authors are to be commended for a thorough and accurate analysis of the voltage transfer characteristics of repeated-structure networks. The solution of the difference equations which arise from such types of networks is greatly facilitated by the Laplace transformation of jump functions, as was done by the authors. The electrical engineer therefore finds a familiar tool employed on rather unfamiliar equations, usually treated separately in the "difference calculus", which is not generally taught in engineering schools.

I think that a more general approach to the problem investigated by the authors might clarify the physics of the phenomena. Briefly, it is desired to investigate, analytically and experimentally, various types of networks for surge-voltage measurement. These networks should, ideally, reproduce faithfully the impulse voltage shapes in reduced scale, without any form of distortion.

Network theory gives assurance of this characteristic of the network under investigation, for all impulse voltages, of any shape, by either one of the two equivalent tests:

1. At all frequencies, from zero to infinity, the amplitude ratio of output to input voltage must be constant, and the phase shift must be zero. This is equation 30 of the paper. Actually, since amplitude and phase characteristics are interdependent, only one of these requirements is sufficient in theory.
2. A unit impulse function must be transmitted undistorted by the network.

It is easily seen that these two requirements are equivalent, by observing that the Fourier spectrum of the unit impulse function $U(t)$ contains all frequencies, all with the same amplitude. This is shown by the complex form of its Fourier integral

$$U(t)=\Re e\left[\frac{1}{\pi}\int_0^\infty e^{jwt}dw\right]$$

The authors, instead, used for their transient tests applied waves as that of Figure 13(A). Assuming for simplicity, that this wave may

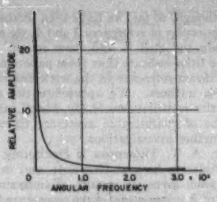

Figure 1. Amplitude spectrum of 0x15 microseconds wave

be represented as a decaying exponential

$$V(t)=\epsilon^{-\alpha t}$$

of tail length 0.693 $1/\alpha$, its Fourier integral expression is given by

$$V(t)=\mathcal{R}e\left[\frac{1}{\pi}\int_0^\infty \frac{e^{j\omega t}}{\alpha+j\omega}d\omega\right]=\frac{1}{\pi}\int_0^\infty \frac{\omega \sin \omega t+\alpha \cos \omega t}{\alpha^2+\omega^2}d\omega$$

The amplitude spectrum of the impulse wave is

$$S(\omega)=(\omega^2+\alpha^2)^{-1/2}$$

an expression which is a function of α, and therefore of the wave-tail. For a tail length of 15 microseconds, which corresponds to the wave of Figure 13(A), the amplitude spectrum is plotted, according to this equation, in Figure 1 of the discussion. It is seen that only the lower frequencies are present, and that their amplitude is not constant.

Thus the fact alone that this particular wave was reproduced satisfactorily by the divider does not guarantee that all other impulse waves will be reproduced in the same manner.

Although the unit impulse function may not be obtained in practice, it may be approximated in a satisfactory manner by the modern "pulse testing" techniques[1,2,3] which have found useful application in the fields of communication and electronic engineering.

As explained before, the steady-state measurements for all frequencies and the "pulse tests" are equivalent. It is therefore expected that the latter will take the place of the former for the determination of the characteristics of those networks which are used principally in the investigations of transients.

Finally, I think that papers by A. M. Angelini[3] and by S. A. Nazarov[4] could be added to the references given in the paper.

References

1. The Impulse Response of Electrical Networks with Special References to the Use of Artificial Lines in Network Design, M. Levy. *Journal*, Institution of Electrical Engineers (London, England), volume 90, 1943, part III, pages 153–64.

2. Pulse Response: A New Approach to A-C Electric Network Theory and Measurement, C. Cherry. *Journal*, Institution of Electrical Engineers (London, England), volume 92, 1945, part III, pages 183–96.

3. Voltage Dividers and Delay Cables for the Oscillographic Registration of Fast Transient Phenomena, A. M. Angelini. *Bulletin*, Schweizerischer Elektrotechnischer Verein (Zürich, Switzerland), volume 32, 1941, pages 305–15.

4. Distortionless Divider of Impulse-Voltages, S. A. Nazarov. *Elektrichestvo* (Moscow, Russia), 1948, Number 8, pages 28–33.

A. T. Thompson (Harvard University, Cambridge, Mass.): The potential dividers, introduced by the authors in this most interesting paper, have been tested to 5 megacycles. That this frequency testing range is quite adequate is briefly discussed here.

Consider the general surge of Figure 2 of the discussion. This is a $a\times10^6\times\frac{1}{2}(a+b)\times10^6$ wave, since it reaches its peak value E in $a\times10^6$ microseconds, and takes $\frac{1}{2}(a+b)\times10^6$ microseconds to reach $\frac{1}{2}E$ on the wave tail. The expression for this surge is

$$\epsilon=f(t)=\begin{cases}0, & -\infty<t<0\\ \frac{E}{a}t, & 0<t<a\\ \frac{E}{a-b}(t-b), & a<t<b\\ 0, & b<t<\infty\end{cases} \qquad (a<b) \qquad (1)$$

By use of the Fourier transform,

$$F(\omega)=\int_{-\infty}^{\infty} f(t)\epsilon^{-j\omega t}dt \qquad (2)$$

we obtain the frequency spectrum of this surge

$$F(\omega)=\frac{E}{a\omega^2}\left(\frac{b}{b-a}\epsilon^{-j\omega a}-\frac{a}{b-a}\epsilon^{j-b\omega}-1\right) \qquad (3)$$

From equation 3 of this discussion, the amplitude spectrum can be obtained by plotting the absolute value of $F(\omega)$ as a function of ω. This is shown for the severe case of a 1/4×5 wave in Figure 3 of the discussion. The dashed lines are used to connect calculated points since a smooth connecting curve would violate the variations due to the term $1/38\epsilon^{-j\omega b}$, whose effect, for our purposes, is negligible. The frequencies of appreciable amplitude are seen to be clustered about the origin. The relative amplitudes of the high-frequency components are negligible. This fact is generally true for surge voltages because the amplitude spectrum is inversely proportional to ω^2, as shown by equation 3 of the discussion. For this reason, then, it is concluded that a frequency testing range of 5 megacycles is adequate.

J. H. Park (National Bureau of Standards, Washington, D. C.): This paper contains a very thorough and desirable treatment on the use of the Laplace transform in obtaining solutions for repeated-structure networks. It also clearly indicates how such a treatment can be used in obtaining a theoretical analysis for certain special types of voltage divider networks. However, as in practically all theoretical treatments of a voltage divider for measuring high-voltage surges, the conditions imposed by the theory are difficult if not impossible of attainment in the laboratory. The type of T-section most nearly attainable in the laboratory conforms to D shown in Table I. The restriction, $L_1/R_1=L_2/R_2$, is possible of fulfillment if sufficient care is exercised. However, since C_1 must include stray capacitance from all parts of the high-voltage sections of the "T" to ground the restriction, $R_1C_1=R_2C_2$, is not attainable unless a high-voltage capacitor is actually inserted at C_1 with sufficient capacity to swamp out stray capacitance. Since, in any full-scale high-voltage surge testing equipment the physical size of at least some of the T-sections must

Figure 2 (below). A general surge voltage

Figure 3 (right). Amplitude spectrum of 1/4x5 surge

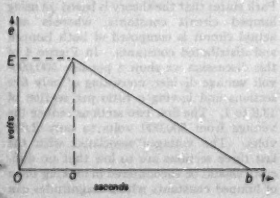

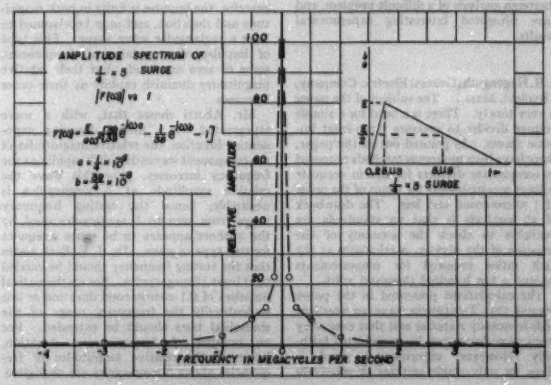

be large, stray capacitance to surrounding grounded objects is quite large and somewhat variable depending on the location of the adjacent grounded objects. Thus, to eliminate the effects of stray capacitance, several capacitors capable of withstanding nearly the full peak surge output voltage of the generator would be needed. Even after obtaining such capacitors the troubles are not entirely eliminated because such capacitors are of necessity large physically and even in the best designs contain inductive residuals, the inductive effect predominating at frequencies above 2 megacycles, in most cases. It is the general conclusion of this writer that theoretical treatments are most helpful but can only be used as a guide in predicting the qualitative performance of high-voltage surge dividers.

An experimental approach is needed for evaluating the quantitative performance characteristics of any high-voltage divider. The writers of the present paper have made a good start in this direction but in the end results should be based on measurements made on a full scale high-voltage divider because it is readily seen that the effect of stray capacitance increases vary rapidly with increase in size of the circuit elements. It also is the opinion of this writer that steady-state measurements to be meaningful should include a range of frequency extending at least as high as 15 megacycles with suitable equipment. This is necessary because of the high-frequency superposed oscillations always present in a high-voltage surge generator.

The authors of this paper conclude that the main advantages of using a repeated-structure network as a voltage divider are that it would eliminate the use of a cable to the cathode-ray oscillograph and would permit exact matching of the cathode-ray oscillograph deflecting plate circuit. These deductions are based on theory using lumped circuit constants, whereas any actual circuit is composed of both lumped and distributed constants. Where the length of the circuit begins to be comparable or greater than the wave length of the highest frequency component of the voltage being measured, the adequacy of lumped circuit theory must be checked experimentally.

The authors of this paper are to be congratulated on their presentation of a thorough analysis of a difficult problem, and have presented interesting experimental results.

J. H. Hagenguth (General Electric Company, Pittsfield, Mass.): The subject of the paper is very timely. There is a need for a simple voltage divider to measure steep-front impulse waves. As pointed out in the paper, there have been numerous methods proposed to compensate dividers for use in accurate voltage measurements for times of the order of 1 microsecond and less. The drawback of all methods is that no standards are available to check the accuracy of the response of the divider, particularly at the high ratios required for measurements beyond a few hundred thousand volts.

The calculations presented in the paper suggest that T-networks have an excellent high-frequency response and that even very steep wave fronts can be transmitted faithfully. However, experimental proof is given for only single sections or relatively low divider ratios. It is hoped that such measurements are practical for higher ratios.

As pointed out in the paper, accurate reproduction of all branch constants is needed to eliminate distortion. Network D, Table I, appears to have given the best experimental results. For high voltages of the order of 500,000 volts or more, the first capacitance elements to ground may have relatively high inductances in series, and these will have to be matched throughout the structure.

A voltage divider for practical laboratory impulse work should have the following characteristics:

1. Accurate reproduction of wave shape between 0.1 microsecond and several hundred microseconds.
2. Occupy small space.
3. Not be influenced by external fields.
4. Ratio must be readily adjustable in small steps.
5. Influence the wave shape as little as possible.
6. Possible to connect directly across the test specimen.

These are the principal requirements. If methods can be developed to check divider ratio and phase shift for the higher ratios required, the divider described in the paper should be very useful to the industry.

C. L. Dawes, C. H. Thomas, and **A. B. Drought:** It is gratifying to the authors to learn that those who have discussed the paper substantiate its theoretical basis, and up to the limits of our experimentation give general approval of the results which so far have been obtained. Many of the limitations, and suggestions which have been made for further experimental study were realized early by the authors; and research in these directions has been conducted for some time.

Mr. P. A. Abetti shows by the Fourier integral that the unit impulse function $U(t)$ contains all frequencies, all of which have the same amplitude. This is known as the Dirac impulse function and goes to infinity and returns to zero, all in zero time while enclosing a unit area, a condition which is not realizable in practice. In practice, the impulse is finite in both magnitude and duration, and may be assumed to have a rectangular wave shape. This type of impulse also contains all frequencies, some of zero amplitude, but their relative magnitudes diminish rapidly as their order increases.

Mr. Abetti shows that, with a wave represented by a simple decaying exponential function, the relative magnitudes of the component waves diminish rapidly as the frequency increases. For this wave the relative amplitude at 5 megacycles is negligible, hence the testing frequency range from zero to 5 megacycles used by the authors appears to be quite adequate for this type of wave. Dr. J. E. Park states that the testing frequency should be carried to at least 15 megacycles. For mathematical impulses of 0.1 microsecond duration or less undoubtedly the frequency range of the sinusoidal tests should be extended. For an impulse of 1-microsecond duration, however, the relative amplitudes of frequencies above 5 megacycles are negligible.

Although, so far, we have been unable to obtain copies of references 3 and 4, we shall be only too glad to add them to our list, as the titles indicate that these papers must have direct reference to the work described by the authors. We appreciate the constructive contributions of Mr. Abetti, which will be of considerable assistance to us in our further investigations.

Mr. A. T. Thompson is continuing the investigation here at Harvard; and in his discussion gives the results of analyzing a 1/4 by 5 microsecond wave represented by two straight lines, using a method of analysis similar to that used by Mr. Abetti. This curve shows that for this particular wave, all frequencies above 1.5 megacycles are entirely negligible.

Dr. Park points out that the paper clearly shows the method of obtaining a divider that will reproduce faithfully the input voltage, but states that the theoretical conditions are difficult, if not impossible of attainment in the laboratory. We can appreciate the difficulties which he describes, and realize that the stray capacitances and other stray parameters inherent in a high-voltage divider, which necessarily occupies a large space, are not easily determined. However, the first step in the production of an ideal high-voltage divider is to determine the values of the parameters which it must have. This sets the goal toward which practical design can be directed. The paper at least does this. We agree with Dr. Park that the type-D section most nearly conforms to the requirements of a practical divider and this type of section is most readily attainable. The stray capacitances certainly cannot be exactly determined; but at least they can be approximated. It would not be necessary to make C_3 so large as to "swamp" out the entire stray capacitances, but rather to insert a known capacitor of sufficiently large capacitance to make negligible the errors incurred in determining the values of the stray capacitances. This, we feel, should produce an accuracy which is much greater than is attainable with the present-type divider in which the stray capacitances and the other stray parameters are entirely uncontrolled. The principal method now used is to attempt to eliminate them, and unsuccessfully, we believe. The paper describes how readily a 50-kv divider was produced with ordinary resistors, and capacitors consisting only of suspension-insulator strings. The resistors which had the higher values of associated inductance produced the greater accuracy because this inductance was "controlled" and is inherent in the type-D section. At the present time, we are constructing a divider for a voltage much higher than 50 kv and do not anticipate any insurmountable difficulty.

In the matter of eliminating the use of a cable to the cathode-ray oscillograph, Dr. Park states that the theory is based on using lumped circuit constants, whereas any actual circuit is composed of both lumped and distributed constants. In Figure 4 of this discussion we show a possible 500,000-volt voltage divider, consisting of only five sections and having a ratio per section of 13.8 to 1. The first two sections reduce the voltage from 500,000 volts to only 2,620 volts. The voltages associated with the last three sections are so low that no difficulty should be encountered in making them of lumped constants whose magnitudes can

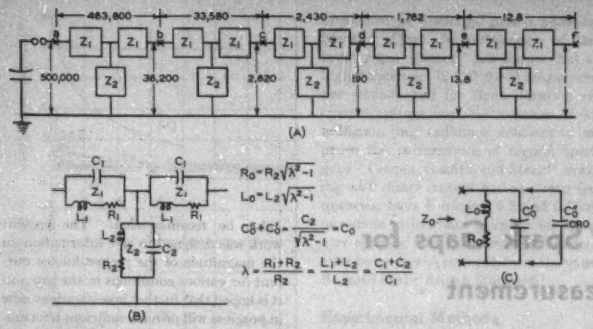

Figure 4. (A) High-voltage divider, attenuation 13.8 per section (B) Circuit elements of each section (C) Termination, Z_0

be large compared with any distributed constants which will be encountered. These could form the oscillograph lead. As a matter of fact, at low voltage the units are small in size and the stray parameters also will be small and thus can be made definite, and by measurement the elements of each T-section can be adjusted to correct value.

Mr. Hagenguth states that in the paper, experimental proof is given only for single sections of the divider. This is true of the figures. However, with reference to Figure 8, it is stated in the paper that tests were conducted with two and three sections also, and results similar to those of Figure 8 were obtained. The same is true for the results shown in Figures 10 and 11. He also correctly points out that the ratio must be readily adjustable in small steps. The divider shown in Figure 4 of this discussion shows that a ratio of 13.8 to 1 per section can be readily obtained. With a divider made up of nine T-sections, the first two of which operate above 20,000 volts, a section ratio of 5-to-1 is easily attainable, thus giving a voltage ratio change by a factor of five per step. However, it is not at all difficult to provide a gradual change of voltage ratio at any of the low-voltage sections, such as dividing the 190 volts at the termination of the third section in Figure 4. Work now is being conducted on this phase of the divider, and it is hoped that it will be published in the near future.

In his last statement Mr. Hagenguth points out one great experimental difficulty, that of being able to check directly the ratio and phase angle. Obviously, in order to do this there must be a primary measuring device responsive to the input voltage, which may be as high as 500,000 volts or higher. So far as we know, at this time there is no such measuring device available. Obviously no voltage-reduction apparatus can be used, for it is the errors in such apparatus that are being studied. As more equipment becomes available we hope to be able to provide a type of direct-measuring apparatus which may respond perhaps to 100,000 volts at least. This same experimental difficulty occurs, even with low-voltage measurements. As sections are added and the ratio increases, the measuring apparatus, such as cathode-ray oscillographs, must be able to respond with the input and the output voltages directly applied to their deflection plates. No voltage reduction device and no amplifier can be used. Hence, the voltage ranges of the cathode-ray oscillographs which were available to us limited our experiments to three sections. The extension of the ratio by which direct measurement of the input and output voltages can be made is a problem on which we now are conducting research; and we are certain to extend the range far beyond our present limits.

We are appreciative of the interest taken by those who have discussed the paper and also of the analyses and suggestions which have been made.

The Irradiation of Spark Gaps for Voltage Measurement

D. R. HARDY
NONMEMBER AIEE

J. D. CRAGGS
NONMEMBER AIEE

THE American, British, and German standards relating to the measurement of high voltages by means of sphere gaps recommend that in certain circumstances, in order to ensure consistency of measurement, the gaps should be suitably irradiated. The amount of irradiation required is not specified in definite terms. However, it is known[1,2] that while insufficient irradiation may cause the gap to behave in an erratic manner as the result of excessive time lags, too much irradiation will introduce a space charge in the gap with a consequent lowering of sparking voltage. It is desirable, therefore, to know the optimum amount of irradiation for any given spark gap.

The effect of irradiation is to cause a prebreakdown current to flow in the gap. Experiments designed to determine this current have been carried out and are described in the paper. Ultraviolet and gamma irradiation have been used as these methods are recommended in the various standards, and appear to be the most suitable for such purposes.

From a knowledge of prebreakdown currents the number of electrons liberated per microsecond in the gap can be estimated and hence an indication given of the probable statistical time lag of the gap when subjected to impulse voltages.

Information is given of a new but obvious method of irradiation of spark gaps, that is, the use of a radioactive cobalt (Co60) which from preliminary tests would appear to be particularly suitable for this purpose.

It is recognized by several leading authorities (the American, British, and German standards), that irradiation in some form is necessary for certain gap dimensions but there is little agreement as to the nature and method of application of this irradiation. The value of the prebreakdown current set up in the gap as a result has been estimated by many workers in this field, but no attempt seems to have been made to correlate the value of this current with the form of irradiation used and the breakdown voltage obtaining.

Section 4-67 of the American Standards for Measurement of Test Voltage in Dielectric Tests[3] recommends irradiation by ultraviolet light and discusses in some detail the type of lamp to be used and its position relative to the gap. Little mention is made of the material and surface condition of the electrode apart from the fact that it should be kept clean. Several workers[4,5,6] in this field have measured the breakdown voltage for various gaps irradiated in this manner and have expressed their results as a function of intensity of illumination at the electrode surface. As shown in this paper, this is of little value since a variation of photocurrent (for the same light intensity) of as much as 200 times has been obtained under normal laboratory conditions. A very much smaller variation is claimed to produce appreciable errors in the value of breakdown voltage, particularly with impulse voltages, and it is in this respect that the present work is considered to be of value to other workers in this field.

The British Standard Rules for the Measurement of Voltage with Sphere Gaps[7] revised in 1939, recommends irradiation by "radioactive or other ionizing media" while the German Standard suggests ultraviolet light irradiation and polished copper spheres as electrodes.

Such diverse opinions would suggest that further information is required regarding the relative merits of these methods of irradiation and that some optimum value be recommended. The present work was designed to give information on the magnitude of the prebreakdown current for various conditions in the gap and it is hoped that further investigations now in progress will provide sufficient information to enable suggestions for the modification of the various standards to be made.

The Effect of Irradiation on Discharge Gap Breakdown

The formation of a spark discharge in a uniform electric field between parallel plate electrodes at the minimum breakdown voltage is preceded by an electron avalanche which crosses the gap from cathode to anode. The electron avalanche may be itself initiated by a single electron. Consequently, for the development of a spark in a discharge gap, at least one electron capable of initiating an avalanche must appear in the gap and preferably in the region of the cathode. The breakdown of a discharge gap is, of course, also dependent on the value of the applied voltage. If, say, an impulse voltage of a 2-microsecond duration is applied to the gap, the possibility of breakdown is remote unless free electrons occur frequently, that is, at the rate of at least 5×10^8 electrons per second, which corresponds to a current of 8×10^{-14} amperes.

Such a supply of free electrons may be provided if the gap is irradiated by any of the following agents:

1. Ultraviolet light, which is known to produce an appreciable amount of photocurrent from the surface of the electrodes.

Paper 50-90, recommended by the AIEE Instruments and Measurements Committee and approved by the AIEE Technical Program Committee for presentation at the AIEE Winter General Meeting, New York, N. Y., January 30–February 3, 1950. Manuscript submitted July 18, 1949; made available for printing December 5, 1949.

D. R. Hardy and J. D. Craggs are both with the University of Liverpool, Liverpool, England.

The experimental work described in this paper was carried out by D. R. Hardy and used as the basis for a thesis submitted to the University of London in fulfillment of the requirements for a Master of Science Degree.

The authors wish to express their appreciation of the assistance given and facilities provided by Professor Meek of the Electronics Department and Professor Teago of the Electrotechnics Department of the University of Liverpool.

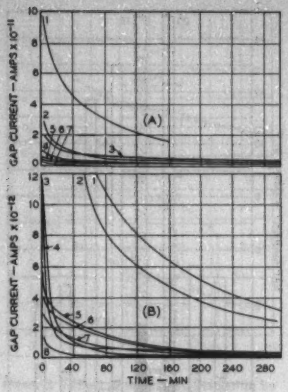

Figure 1. Photoelectric fatigue of electrodes

(A). After initial polish with emery paper
Curve 1. Zinc electrode; Curve 2. Magnesium electrode; Curve 3. Tin electrode; Curve 4. Copper electrode; Curve 5. Brass electrode; Curve 6. Aluminium electrode; Curve 7. Steel electrode.

(B). After repolish with emery paper
Curve 1. Zinc electrode; Curve 2. Aluminium electrode (polished emery paper and powder); Curve 3. Magnesium electrode; Curve 4. Tin electrode; Curve 5. Brass electrode; Curve 6. Copper electrode; Curve 7. Aluminium electrode (polished with emery paper, powder, and liquid polish)

2. A radioactive material, whose radiations ionize the gas between the electrodes and possibly also cause the emission of electrons from the electrodes.

3. A nearby corona or spark discharge which produces ultraviolet radiations and so ionizes the test gap and causes photoemission from the electrodes.

Corona has been used for the irradiation of spark gaps in lightning arresters. Sparks have been found to be a very effective source of irradiation and Street and Beams[8] showed that in certain conditions the voltage to sparkover, if maintained for 1 microsecond, could be reduced some 16 times when the gap was irradiated by a nearby spark.

The scope of this present paper is limited to the effects produced by ultraviolet light irradiation and radioactive materials since these methods are specifically mentioned in the American, British, and German Standards, and, furthermore, because they appear to be the more convenient from the point of view of quantitative measurement, which is desirable if standardization is to be obtained.

A summary of previous work on the breakdown of discharge gaps is given by Meek.[14] Since the publication of this latter paper Cooper[15] has shown that at high frequencies (2,800–9,800 megacycles per second) and for short duration recurrent voltage impulses a source of 0.2 milligram (mg) radium is sufficient to improve the performance of certain spark gaps. Cooper, Garfitt, and Meek[17] working with direct current and at power frequencies, have employed 0.2 and 0.5 mg of radium to irradiate 2-centimeter diameter spheres, and their final calibrations vary by up to $4^1/_2$ per cent, from the value declared in the British Standard.[7]

Experimental Methods

The measurements may be conveniently arranged in two main classes: those in which the spark gap is irradiated by ultraviolet light from a quartz mercury vapour lamp,[18] and those in which a radioactive source is used.

For each class of measurement a high voltage power supply was connected across a spark gap having parallel plate or spherical electrodes and the current flowing in the gap measured by means of an electrometer triode.[19] For the amounts of radium used, the plateau (or saturation) value of gap current for gap lengths of 1 centimeter occurred at about 100 volts. This value was subsequently chosen as the arbitrary level at which the two classes of measurement were to be compared.

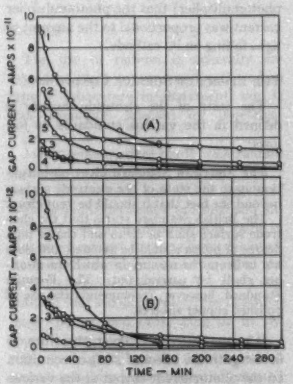

Figure 2. Fatigue curves for electrodes having same polish

(A). Zinc electrode
Curves 1 and 2. Polished with emery paper; Curves 3, 4, and 5. Polished with emery paper and powder

(B). Copper electrode
Curve 1. Polished with emery paper; Curves 2, 3, and 4. Polished with emery paper and powder

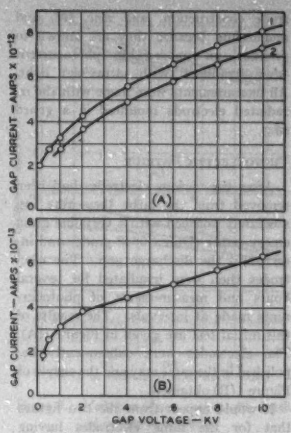

Figure 3. Effect of voltage on gap current—gap length, 1 centimeter

(A). Zinc electrode
Curve 1. Taken some six days after initial polishing during which time the electrode was irradiated in all for about 20 hours; Curve 2. Taken 1 hour later than curve 1

(B). Copper electrode

When radium was in use it was usually enclosed in the anode but some tests were made with the source enclosed in the cathode. The activity of a radioactive cobalt cathode also was investigated.

Irradiation by Ultraviolet Light

The photoelectric current from an electrode surface is dependent upon several factors, the most important of which are the nature of the irradiating source, the electrode material, and the state of the electrode surface. Previous workers in this field have chosen to ignore some of these factors and, as will be seen, this is not permissible.

It is well known that the photocurrent from an irradiated surface decreases with time producing what is known as the "fatigue effect,"[20,21] but little consideration appears to have been given to the effect of this fatigue on the prebreakdown current in the discharge gap—which itself effects the minimum breakdown voltage.

The materials chosen for these tests were brass, copper, steel, and aluminum because they are frequently used in elec-

trode construction, and zinc, tin, and magnesium because they are known to produce an appreciable photocurrent when irradiated with ultraviolet light. All measurements were made with the irradiated electrode mounted in a guard ring.

Photoelectric Fatigue

After the various electrodes had been removed from the lathe they were immediately polished with a very fine grain emery paper (Durex 0/48 grade) and inserted in the discharge gap. The electrodes then were irradiated for several hours and measurements of photocurrents made at intervals. The results of this initial test are given in Figure 1(A). The electrodes were subsequently repolished in the same way and the curves of Figure 1(B) obtained.

It would appear from the two figures that for the same electrodes having nominally the same surface treatment there exists an appreciable variation in the rates of decrease of photocurrent. This matter was further investigated and several tests were made with each electrode material. Typical results are shown in Figure 2. The photoelectric fatigue does not appear to be a simple exponential phenomenon and is not consistent from test to test.

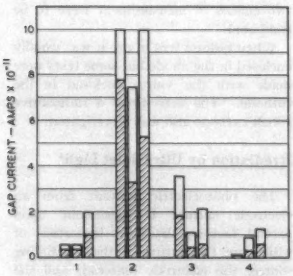

Figure 4. Effect of polish on photoelectric current

Each material represented by block of three columns. First column. Fatigue in first test after initial polishing with fine emery paper; Second column. Fatigue after further application of polishing powder; Third column. Fatigue after further application of liquid polish

Steps in columns indicate photoelectric current after ultraviolet irradiation for 25 seconds and ten minutes

Block 1. Brass electrode; Block 2. Zinc electrode; Block 3. Magnesium electrode; Block 4. Copper electrode

The Effect of Gap Voltage

The saturation or plateau value of current defines the state of ionization existing in a discharge gap before breakdown takes place, so that it is this value which is of importance when considering the effects of irradiation.

Tests were carried out on the various electrodes and the gap current measured for increasing voltages up to 10 kv. Typical curves are shown in Figure 3.

It is considered impossible to compare the "plateau" currents accurately for the various electrodes since their values obviously depend on the state of the electrode surface at the time the measurement is made and it has already been seen that the same repeated physical treatment of the surface of an electrode does not produce the same photocurrent output. It should be emphasized that, for the practical engineering uses to which sphere gaps are submitted, refined methods of treating the surfaces are not practicable.

The Effect of Light Intensity

It has been shown by many workers[20,21] that the photoemission from an electrode surface is proportional to the intensity of the incident light, and this was confirmed with the present apparatus on the assumption (justified by the recent work of Engstrom[22] on the same type of photomultiplier) that the photomultiplier current was proportional to the amount of light falling on its cathode.

The Effect of Surface Condition

The state of the electrode surface is defined in the various standards as follows:

The American Standard gives no indication as to the state of the electrode surface beyond the fact that it should be kept clean.

The British Standard states that the electrode surface shall be clean and that a high degree of polish should be avoided, but does not indicate the manner in which the cleaning shall be carried out. The German Standard, however, recommends the use of polished copper spheres.

It is considered of interest, therefore, to investigate the effect of surface condition on the photocurrent output of the various electrodes.

The electrodes were each tested after polishing with emery paper, a polishing powder, and a liquid polish which contained an abrasive and mineral spirits. Typical results obtained are shown in Figure 4. The results obtained for the materials tested are in no way consistent and since, in any case, it is unlikely that the same surface condition could be reproduced exactly, the diagram indicates only the order of photocurrent to be expected.

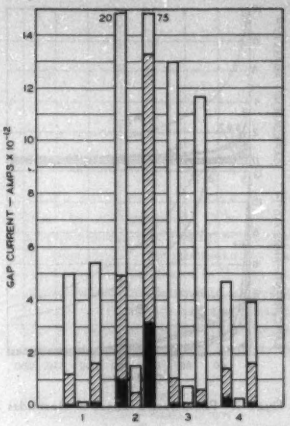

Figure 5. Effect of period of inactivity on photoelectric current

Each material represented by block of three columns. First column. Fatigue in last test prior to inactivity period; Second column. Subsequent fatigue (without repolishing) after inactivity period of two weeks; Third column. Effect of immediate repolishing on fatigue rate. Steps in columns indicate photoelectric current after ultraviolet irradiation for 25 seconds, 10 minutes, and 5 hours respectively. Method of polishing-fine emery paper and powder in lathe at about 1,500 rpm

Block 1. Brass electrode; 2. Zinc electrode; 3. Magnesium electrode; 4. Copper electrode

The Effect of a Period of Inactivity

It is considered likely that in an engineering laboratory some appreciable time may elapse between measurements and it is, therefore, of interest to investigate the effect of such a period of inactivity upon the photocurrent output.

After polishing, the electrodes were each irradiated with ultraviolet light for a period of five hours and then allowed to stand in the laboratory for a period of two weeks. They were then rubbed lightly with cotton wool to remove grease and dust and retested without further repolishing. The electrodes were then again repolished and further tests carried out. The results obtained are shown in block diagram form in Figure 5. A large reduction of photocurrent (10 to 30 times for the particular tests carried out) may be effected if the electrode is initially

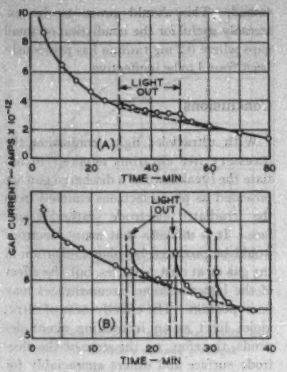

Figure 6. Effect of interrupted irradiation by ultraviolet light

(A). Copper electrode
(B). Zinc electrode

polished, irradiated, and then allowed to stand unirradiated for some time. If, as might be the case in practice, the electrodes were not used for voltage measurements until some minutes after polishing the reduction in photocurrent would be perhaps some four or five times for the above conditions.

The Effect of Interrupted Irradiation

To investigate the above effect further, tests were carried out on zinc and copper electrodes with interrupted irradiation. The results are shown in Figure 6. Both electrodes appear to recover their photoelectric properties and upon further irradiation tend to follow the original fatigue curve. The copper electrode, Figure 6(A), appears to fatigue less rapidly when the ultraviolet light source is cut off.

Irradiation with Radioactive Substances

It is well known that the ionization which occurs in the proximity of a radioactive substance may be due, in varying degrees depending on circumstances, to the emission of α, β, or γ rays. The α-particles (helium nuclei) ionize very heavily along their paths in a gas but are, therefore, so easily absorbed that they do not emerge from the usual radium capsules. With thin electrode coatings of, for example, polonium, the α-particles are able to produce strong ionization in a spark gap.[34,35] The β and γ rays (respectively fast electrons and very hard electromagnetic radiation) cause less ionization per centimeter path per particle, than do the α rays. The γ rays are by far the least efficient.

Most of the natural β rays from radium are stopped by about 1 millimeter of copper and so the use of radium capsules (usually with nickel or nickel-alloy envelopes) in general restricts the ionization effects in a spark gap to those caused by the γ rays. With these the direct air ionization is relatively unimportant compared with the ionization caused by the secondary electrons ejected from the electrodes by the γ rays.

Previous workers have made use of some or all of these effects as sources of irradiation. Berkey[33] obtained some favorable results using a radium solution (the content of which was not specified); Garfitt[34] employed a polonium-coated cathode; while Dillon[35] used a polonium alloy, but in each case the active life of the ionizing agent was comparatively short. Van Cauwenberghe[36] employed a radium capsule which ensured a stable performance and long life but the ionizing power was much reduced since the α-rays and the greater part of the β-rays would be absorbed by the capsule itself.

The authors have shown, however, that an activated cobalt[28,29] electrode is possessed of the required characteristics of a long stable life and appreciable activity.

Radium

The use of radium is generally accepted as most convenient for the usual type of laboratory measurement, and it was, therefore, selected for investigation.

Measurements were made with radium capsules containing 0.1, 0.2, 0.5, and 1 mg in the cathode and in the anode of various metal electrodes, polished and unpolished, but little difference was found in measured current for the electrodes used. At first, the cathode was arranged as the central electrode of a guard ring but it was realized that secondary electrons liberated from the earthed outer ring or in the space between the cathode and guard ring, would pass into the cathode, which was at a slightly higher potential (about 1 millivolt per 10^{-13} ampere), due to the current flowing through the electrometer grid resistance, and thereby cancel part of the true gap current. The order of magnitude of this effect can be seen from Figures 10 and 11(A). An apparent reduction in gap current of some 10 times occurs for the radioactive cobalt cathode and for the radium irradiated cathode.

The location of the radium in the

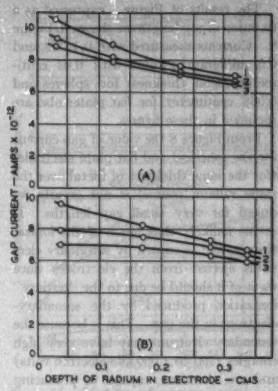

Figure 7. Variation of gap current with depth of radium in electrode

(A). Spheres 2 cm diameter. Material—brass. Gap voltage 100 volts, 1 mg radium (in anode)
Curve 1. Gap length 1.0 cm; 2. Gap length 0.1 cm; 3. Gap length 0.01 cm
(B). 2 cm diameter. Flat plates. Material brass, gap voltage 100 volts, 1 mg radium (in anode)
Curve 1. Gap length 1.0 cm; 2. Gap length 0.1 cm; 3. Gap length 0.01 cm

cathode (curve 2, Figure 11(A), where thickness of metal to radium is 0.068 centimeter) and in the anode (curve 3, Figure 11(A), where the thickness of metal to radium is 0.038 centimeter) shows little difference in the order of current measured. With a guard ring, however, the apparent current was found to reverse (that is, the effect of secondary emission was to swamp the real gap current) when the thickness of metal between the radium and the gap was increased to some 0.5 centimeter.

It was expected that the depth of the radium source in the electrode (that is, thickness of electrode between source and gap) would affect the gap current, and this is confirmed in Figure 7.

With 2-centimeter diameter spheres and 2-centimeter diameter flat plates as electrodes, the gap current at 100 volts and with gap length 0.01, 0.1, and 1.0 centimeters, was measured for metal thickness from about 0.03 to 0.3 centimeter, the irradiating source being 1 mg radium situated in the anode.

The currents measured for the two sets of electrodes is seen to be of the same order, about $2\text{–}3\times10^{-13}$ amperes per square centimeter of electrode projected area.

The results of Figure 7 expressed as a function of gap length are shown in Figure 8. Currents measured with 0.1, 0.2, and 0.5 milligram radium with 0.03 centimeter metal thickness for spheres and 0.038 centimeter for flat plates also are included in these figures.

From Figure 8 the value of gap current for the spherical and flat plate electrodes (for the same thickness of metal over the same radium source) is not greatly reduced for very small gap lengths. It seems unlikely that much of the ionization current is caused by secondary electrons ejected from the electrodes since most of it should be due to the "tertiary" ionization produced by the secondary-electrons in the gap. This is because the secondary electrons may have very high energies (100 to 1,000 kilo-electron volts) and are, therefore, capable of producing many "tertiary" ion pairs. The curves of Figure 8 were, however, taken at constant gap voltage so that for very small gap lengths the voltage gradient would be very high (10 kilovolts per centimeter at 0.01 centimeter) and, therefore, due to this change of voltage gradient, the effect of secondary emission could not be followed. In Figure 9 results were taken at a constant value of voltage gradient and these curves indicate that the ionization current is caused by the liberation of "tertiary" electrons in the air gap, for at small gap lengths the gap current approaches zero.

From the curves of Figure 8 it will be seen that 1 mg radium enclosed by a thin skin of metal in the anode produces a current of the order of 10^{-11} amperes for the electrode considered with a gap length of 1 centimeter and voltage 100 volts. This current is equivalent to approximately 1 electron per 0.016 microsecond. These electrons appear at random through out the gap but in a uniform field only an electron appearing near the cathode will initiate an electron avalanche leading to the formation of a spark when the gap is subjected to a voltage just sufficient to cause breakdown. If one assumes that say 10 per cent of the electrons are produced in the region close enough to the cathode to be effective in initiating the spark breakdown of the gap, then the number of such initiating electrons is one per 0.16 microsecond for the above conditions. Consistent behavior of the particular gap when subjected to impulse voltages of magnitude slightly in excess of the d-c breakdown value may, therefore, be expected when the duration of the impulse is about 1 microsecond for flat plate electrodes and perhaps 10 microseconds for spherical electrodes (since perhaps 10 per cent of the projected area of the spherical electrode is effective for sparking). Erratic behavior may, therefore, be expected for impulses of less than 0.1-microsecond and 1-microsecond respectively.

Radioactive Cobalt

Radioactive cobalt which now can be produced in fairly large quantities in uranium piles, can be used for the purpose of sphere gap irradiation with certain advantages over other methods. It is relatively cheap; electrodes can be machined from it and then irradiated in a pile so that the defects of thin polonium layers[24] are overcome; the half life is 5.3 years; the γ-ray energies are 1.3 and 1.1 mega-electron volts and the β rays (0.3 mega-electron-volts maximum) also should be of use in cases where the γ rays, which liberate more electrons from the electrodes than from the air or other gas in the interelectrode space of the gap, do not give sufficient ionization.

The current produced in the gap by the activated cobalt is shown in Figures 10 and 11. Here it is seen that an activity equivalent to about 10 mg of radium is obtained. This should prove to be extremely useful for the irradiation of small gaps where 0.2 mg radium has previously been found to be ineffective.

Conclusions

With ultraviolet light irradiation the necessary free electrons required to initiate the breakdown of a discharge gap are provided as photoelectrons emitted from the irradiated electrode (cathode) surface. It is unlikely that many electrons would be produced by photoionization in the gas or at dust particles, but the effect of the latter in some circumstances may be important. The effectiveness of ultraviolet light as an irradiating agent depends, therefore, on the state of the electrode surface and differs appreciably for different electrodes. The fatigue of the electrode surface which is found to occur to some degree for all the materials tested, and especially the inconsistency of this quantity, suggests that it is impossible to estimate with accuracy in ordinary laboratory conditions (which are not those of advanced vacuum physics) the

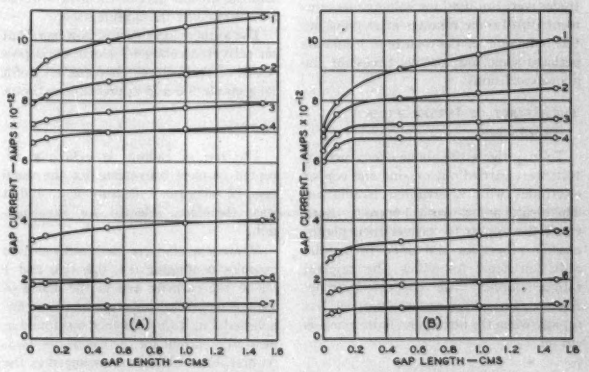

Figure 8. Variation of gap current with gap length (radium irradiation)

(A). 2 cm diameter spheres. Material—brass, gap voltage 100 volts
Curve 1. 1 mg radium. Depth of radium in electrode (anode) 0.030 cm; Curve 2. 1 mg radium. Depth of radium in electrode (anode) 0.112 cm; Curve 3. 1 mg radium. Depth of radium in electrode (anode) 0.228 cm; Curve 4. 1 mg radium. Depth of radium in electrode (anode) 0.318 cm; Curve 5. 0.5 mg radium. Depth of radium in electrode (anode) 0.030 cm; Curve 6. 0.2 mg radium. Depth of radium in electrode (anode) 0.030 cm; Curve 7. 0.1 mg radium. Depth of radium in electrode (anode) 0.030 cm

(B). 2 cm diameter flat plates. Material—brass, gap voltage 100 volts
Curve 1. 1 mg radium. Depth of radium in electrode (anode) 0.038 cm; Curve 2. 1 mg radium. Depth of radium in electrode (anode) 0.170 cm; Curve 3. 1 mg radium. Depth of radium in electrode (anode) 0.277 cm; Curve 4. 1 mg radium. Depth of radium in electrode (anode) 0.338 cm; Curve 5. 0.5 mg radium. Depth of radium in electrode (anode) 0.038 cm; Curve 6. 0.2 mg radium. Depth of radium in electrode (anode) 0.038 cm; Curve 7. 0.1 mg radium. Depth of radium in electrode (anode) 0.038 cm

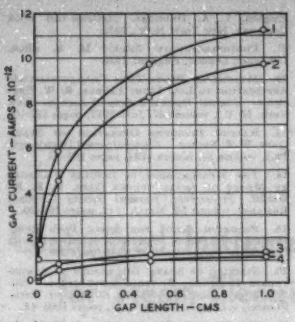

Figure 9. Variation of gap current with gap length at constant voltage gradient

Gap voltage varied to maintain 100 volts per centimeter gradient. Brass electrodes
Curve 1. 2 cm diameter spheres. 1 mg radium in anode. Depth of radium in electrode 0.030 cm; Curve 2. 2 cm diameter flat plates. 1 mg radium in anode. Depth of radium in electrode 0.038 cm; Curve 3. 2 cm diameter spheres. 0.1 mg radium in anode. Depth of radium in electrode 0.030 cm; Curve 4. 2 cm diameter flat plates. 0.1 mg radium in anode. Depth of radium in electrode 0.038 cm

prebreakdown current existing in a particular discharge gap. Unless irradiation by ultraviolet light is to be supplied to such an extent that makes polishing unnecessary, it is considered that over a period of time the accuracy of voltage measurement will deteriorate appreciably. This requirement will probably necessitate a source of great intensity, especially at the higher voltages because of the greater distance required between lamp and electrodes, but too high an irradiation is to be avoided since it tends to lower the value of voltage required to spark-over. Meek[17] has calculated values for the lowering of breakdown voltage for various gap currents, and it appears that, for a zinc electrode where the gap current was observed to vary from 10^{-10} to 5×10^{-12} amperes per square centimeter, under certain circumstances, a lowering of breakdown voltage of up to 5 per cent may be expected.

Radioactive materials can form very stable sources of irradiation and produce an ionization which is largely independent of surface conditions and to a large extent of the gap voltage. Since the γ rays give their effect by first producing at the metal surfaces fast secondary electrons which then cause the major part of the ionization, it would be expected that some influence of the nature of the electrodes would be apparent. In the present experiments such effects appear to be too small to be observed. As the gap length is increased at a constant voltage, the gap current increases and appears to attain a maximum value which, in the case of radium, varies in magnitude with the amount of radium present.

In the radium source used the monel-metal capsule and the electrode thickness cuts off the α rays and probably most, if not all, of the β rays. As these are known to be more effective ionizing agents than the γ rays, it would appear that the radioactive cobalt has the more desirable characteristics for spark gap work. Because the ionization produced by the radium decreases with increasing distance, it is considered necessary to locate the radium source at the cathode rather than at the anode so that a maximum ionization in the cathode region is obtained with a minimum amount of radium. Where it is anticipated that a nonuniform field form will exist and breakdown of the gap may be initiated at or near the high voltage electrode irrespective of polarity, it may be more effective to locate the radium capsule in the high-voltage electrode.

The radioactive cobalt proved to be a very stable source of ionization and in view of its high activity should prove to be a most useful means of spark gap irradiation.

For these reasons it would appear that in general spark-gap work radioactive substances provide a more satisfactory means of irradiation than ultraviolet light.

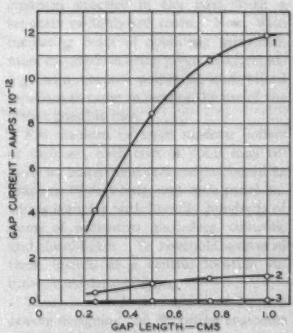

Figure 10. Effect of guard ring on gap current

Gap voltage 100 volts, flat plate electrodes. Lower electrode (cathode) surrounded by earthed guard ring (brass) internal diameter 1.3 cms, external diameter 3.0 cms
Curve 1. Radioactive cobalt cathode 1.08 cm diameter; Curve 2. Cobalt cathode 1.22 cm diameter. 1 mg radium in anode; depth of radium in electrode 0.175 cm; Curve 3. Cobalt cathode 1.22 cm diameter. 0.1 mg radium in anode. Depth of radium in electrode 0.175 cm

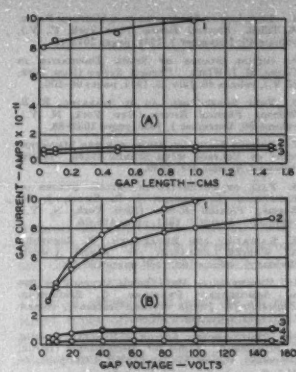

Figure 11. Variation of gap current with gap length and gap voltage

(A). Flat plate electrodes. Brass anode 2 cm diameter. Gap voltage 100 volts
Curve 1. Radioactive cobalt cathode 1.08 cm diameter; Curve 2. Cobalt cathode 1.22 cm diameter, 1 mg radium in cathode. Depth of radium in electrode 0.068 cm; Curve 3. Cobalt cathode 1.22 cm diameter, 1 mg radium in anode. Depth of radium in electrode 0.038 cm
(B). Flat plate electrodes. Brass anode 2 cm diameter
Curve 1. Radioactive cobalt cathode 1.08 cm diameter. Gap length 1.0 cm; Curve 2. Radioactive cobalt cathode 1.08 cm diameter. Gap length 0.1 cm; Curve 3. Cobalt cathode 1.22 cm diameter, 1 mg radium in cathode. Depth of radium in electrode 0.068 cm. Gap length 1.0 cm; Curve 4. Cobalt cathode 1.22 cm diameter, 1 mg radium in cathode. Depth of radium in electrode 0.068 cm. Gap length 0.1 cm; Curve 5. Cobalt cathode 1.22 cm diameter, 0.1 mg radium in cathode. Depth of radium in electrode 0.068 cm. Gap length 0.1–1.0 cm

References

1. Variation of Sparking Potential with Intense Ultra-Violet Illumination, H. J. White. *Physical Review* (New York, N. Y.), volume 48, July 15, 1935, pages 113–17.

2. Effect of Intense Illumination on Time Lag in Static Spark Breakdown, H. J. White. *Physical Review* (New York, N. Y.), volume 49, April 1, 1936, pages 507–12.

3. American Standard for Measurement of Test Voltage in Dielectric Tests. *AIEE Standard Number 4*, 1942, page 7.

4. Time-Lag of Sparkover in a Uniform Field, **A. Tilles.** *Physical Review* (New York, N. Y.), volume 46, December 1, 1934, pages 1015–22.

5. Initial Stages of Spark Discharge in Gases, **H. J. White.** *Physical Review* (New York, N. Y.), volume 46, July 15, 1934, pages 96–106.

6. Very Short-Time-Lag of Sparking, **R. R. Wilson.** *Physical Review* (New York, N. Y.), volume 50, December 1, 1936, pages 1082–88.

7. British Standard Rules for the Measurement of Voltage with Sphere Gaps. *British Standard Number 358*, 1939.

8. Fall of Potential in Initial Stages of Electrical Discharges, **J. C. Street, J. W. Beams.** *Physical Review* (New York, N. Y.), volume 38, August 1, 1931, pages 416–26.

9. Radiation and Breakdown, **W. Rogowski, A. Walkoff.** *Zeitschrift für Physik* (Berlin, Germany), volume 102, 1936, pages 183–200.

10. Lowering of Breakdown Voltage of Air at Atmospheric Pressure, **C. Brinkmann.** *Zeitschrift für Physik* (Berlin, Germany), volume 111, 11–12, 1939, pages 737–46.

11. Photoelectric Action of Electric Sparks, **C. Brinkmann.** *Archiv für Electrotechnik* (Berlin, Germany), volume 33, January 16, 1939, pages 1–22.

12. Sparking Distance Increase Due to Radiation Impulse and Radiation Brightness of Impulse Sparks, **M. Toepler.** *Physikalische Zeitschrift* (Leipzig, Germany), volume 40, March 15, 1939, pages 206–16.

13. Effect of Spark Type (Length) and Electrode Material on Sparking Distance Increase Due to Ultra-Violet Illumination with Impulse Sparks, **M. Arnold.** *Physikalische Zeitschrift* (Leipzig, Germany), volume 40, November 15, 1939, pages 687–95.

14. The Influence of Irradiation on the Measurement of Impulse Voltages with Sphere Gaps, **J. M. Meek.** *Journal*, Institution of Electrical Engineers (London, England), part II, volume 93, April 1946, pages 97–115.

15. Experiments on the Electric Strength of Air at Centimetric Wavelengths, **R. Cooper.** *Journal*, Institution of Electrical Engineers (London, England), part III, volume 94, September 1947, pages 315–24

16. A Note on the Measurement of Short Duration Recurrent Voltage Impulses by Means of Spark Gaps, **R. Cooper.** *Journal*, Institution of Electrical Engineers (London, England), volume 95, part II, August 1948, pages 378–82.

17. Calibration of 2 Centimeter Diameter Sphere Gaps, **R. Cooper, D. E. M. Garfitt, J. M. Meek.** *Journal*, Institution of Electrical Engineers (London, England), volume 95, part II, June 1948, pages 309–11.

18. A Compact Source Projection Lamp, **H. K. Bourne.** *Journal of Scientific Instruments* (London, England), volume 22, June 1945, pages 107–10.

19. Portable Thermionic Electrometer for Glass-Electrode Potentials, **C. Morton.** *Journal of Scientific Instruments* (London, England), volume 9, September 1932, pages 289–93.

20. Photoelectric Phenomena (book), **A. L. Hughes, L. A. Dubridge.** McGraw-Hill Book Company, New York, N. Y., 1932.

21. Photoelectricity (book), **H. S. Allen.** Longman, London, England, 1925.

22. Multiplier Photo-Tube Characteristics Application to Low Light Levels, **R. W. Engstrom.** *Journal*, Optical Society of America (New York, N. Y.), volume 37, June 1947, pages 420–31.

23. Radium Improves Operation of Spark Gaps, **W. E. Berkey.** *Electric Journal* (Pittsburgh, Pa.), volume 31, March 1934, pages 101–03.

24. The Measurement of Impulse Voltages by Means of Small Sphere Gaps, **D. E. M. Garfitt.** *Proceedings*, Physical Society (London, England), volume 54, March 1942, pages 109–20.

25. Polonium Alloy for Spark Plug Electrodes, **J. H. Dillon.** *Journal of Applied Physics* (Lancaster, Pa.), volume 11, 1940, page 291.

26. Striking of Spark Discharges at Atmospheric Pressure, **R. van Cauwenberghe.** *Bulletin de la Société Française des Electriciens* (Paris, France), volume 7, October 1937, pages 1005–44.

27. The Electric Spark in Air, **J. M. Meek.** *Journal*, Institution of Electrical Engineers (London, England), volume 89, August 1942, pages 535–56.

28. The Microwave Spark, **D. Q. Posin.** *Physical Review* (New York, N. Y.), volume 73, March 1948, pages 496–509 and May 1948, page 1118.

29. Use of Radioactive Cobalt for Sphere Gap Irradiation, **D. R. Hardy, J. D. Craggs.** *Nature* (London, England), volume 164, August 27, 1949, page 356.

No Discussion

Centralized Instrumentation and Controls for Steam Electric Power Stations

B. C. MALLORY
NONMEMBER AIEE

THE ultimate in centralization of instrumentation and controls for a steam electric power station might be considered as having only one operator for the whole station, with this operator sitting in a quiet air-conditioned office with one load indicator, and with one control to start, adjust load, and stop each main turbine generator. The boiler for each unit and all other equipment would operate automatically and the operator's only duties would be to operate the load controls in accordance with telephoned instructions from the system load dispatcher. However, this ultimate in simplification is neither economical nor feasible for present-day steam turbine generators, boilers, and auxiliary equipment.

Once started and put on the line, a turbine with its boiler and complete set of auxiliaries may be so equipped today that it can be operated automatically. But, present-day equipment and controls are not sufficiently troublefree even with the best of maintenance programs, and are not to be trusted to operate satisfactorily without adequate attention. Nor, so far as the writer knows, have automatic controls been devised to start either a turbine or a large high-pressure boiler from a cold condition without manual assistance and careful checking by operators.

There is a vast amount of thought and effort that should be applied to developing reliable controls for automatic starting of boilers and turbines, especially from an overnight stand-by condition. Managements are asking engineers to consider seriously some automatic time clock device, possibly with temperature and vibration sensitive adjustments to co-ordinate starting procedures properly, both from the viewpoint of uniformity of operations and ease of control.

According to Cybernetics as described recently by Norbert Wiener,[1] "automatic factories without human agents, are only so far ahead of us as is limited by our willingness to put such a degree of effort into their engineering as was spent, for example, in the development of the technique of radar in the second world war".

Separate control points for each turbine generator and each boiler have been common practice in the past, with a separate switchboard room. Now, with increasing costs of operating personnel, more emphasis is being given to aggregating main control points at centralized locations in order to require the use of the fewest possible men.

For medium or large modern boilers or turbines, each control point may require an instrument and control board as much as 30 feet long, and each panel becomes complex with literally hundreds of items of indicators, recorders, controls, and alarm lights. To assemble several of these boards at a central location requires considerable space.

There is a wide divergence of opinion among designing and operating engineers with regard to the amount of centralization of control that is practicable. The problem of the extent of advantageous centralization revolves about the number of manual controls that can be handled by one man in time of trouble. The cartoon, Figure 1, illustrates and emphasizes what happens when there is trouble.

One operator can supervise many controls while everything is functioning properly and units are neither being put on nor taken off the line, but in times of trouble the number and complexity of the controls that one operator can handle depend to a large extent on the panel layout and the ability of the man. The number can be increased safely to some extent by a logical arrangement and use of different types of control handles for different types of control, so that routine adjustments become simplified and, in emergencies, the operator acts from habit without having to think out each step of what he should do.

Too often the artistic appearance or the space needed in the back of the panels for instruments has governed the board layouts. There is a need for miniature mechanical instruments comparable to those on electrical boards or to those used for large airplanes. Furthermore, for ease and reliability of operation, the instruments and controls should be segregated to permit manipulating the vital controls from a central point, with those having minor manual adjustments for efficiency and the historical items located at some less strategic point.

The advantages of complete centralized control with the switchboard located in the control room include:

1. Reduction in number of operators which minimizes cost of operating personnel.

2. Presentation of all pertinent data to one operator to give a better understanding of the plant as an integrated co-ordinated unit.

3. Ability of the operator to take corrective action simultaneously for two or more operations, should conditions demand.

4. Avoidance of communication errors.

5. Improvement in quality of operation. The better operating conditions of the centralized control room attract a higher type personnel. This means more than better thermal efficiency as it should give better maintenance of load during upset conditions, quicker restoration after an interruption, and better judgment in preventing an interruption.

Paper 50-91, recommended by the AIEE Power Generation Committee and approved by the AIEE Technical Program Committee for presentation at the AIEE Winter General Meeting, New York, N. Y., January 30-February 3, 1950. Manuscript submitted November 4, 1949; made available for printing December 22, 1949.

B. C. MALLORY is Chief Mechanical Engineer with the Stone and Webster Engineering Corporation, Boston, Mass.

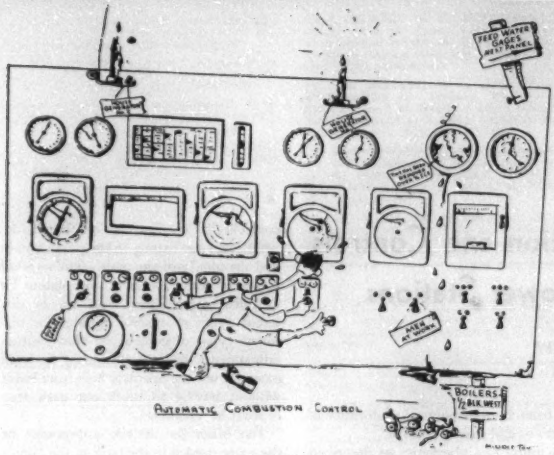

Figure 1. Preliminary operation

6. More automatic controls may be required, which tend to free the operator from details and permit more supervision.

The disadvantages of complete centralized control with the switchboard located in the control room include:

1. Space required for control room in heart of station. Adds to initial construction cost by adding building space and may add it for the full height of the station.

2. Each additional instrument and control adds equipment to be maintained and each is a potential source of trouble because it may function incorrectly.

3. Complexity of many instruments, controls, alarms, and lights requires a considerable training period for operators, especially if the mechanical and electrical men have to substitute for one another. With two mechanical men and one electrical man in a control room, this substitution might easily be required.

4. Added cost, due to either duplication of controls, or longer runs of instrumentation and control leads and the space required for them.

5. Higher rate of pay for operators having greater responsibility.

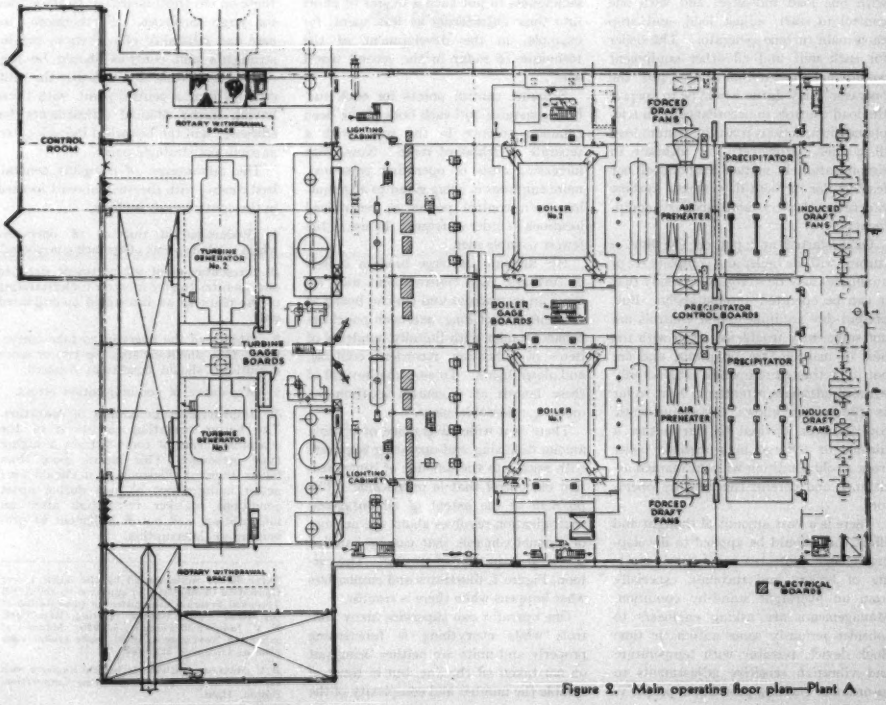

Figure 2. Main operating floor plan—Plant A

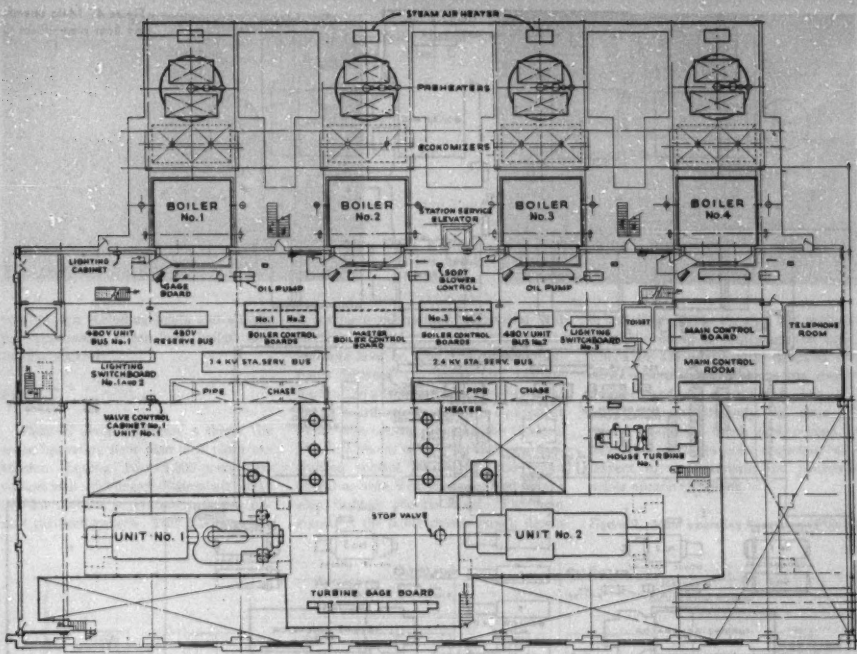

Figure 3. Main operating floor plan—Plant B

Four stations designed since the war, each with two 40,000-kw or larger turbine generators illustrate differing amounts of centralization of control.

Plant A

Plant A given in Figure 2 shows the main operating floor plan of a new station which has two 850-pound-per-square-inch 900-degree-Fahrenheit 80,000-kw units and two coal-fired boilers. The two boiler panels have been combined so that the men operating the boilers have a common control point. The two turbine generators have been located with their steam ends together so that the turbine operators have control points close together. The electrical control room is separate, just outside the turbine room, and approximately centered on the expected ultimate station of four or five units.

Operations are limited to two floor levels with a few minor exceptions. The forced and induced draft fans and the precipitator controls are located on the operating floor grade for ease of operation. The 440-volt switchgear also is on the operating floor and shown cross-hatched in Figure 2. Boiler feed pumps and their controls are located on the ground floor with the condensate and booster pumps. Boiler feed pump controls are duplicated on the boiler boards.

The complexity of even this relatively minor centralized arrangement may be emphasized from the following data: These two boiler panels are each 19 feet long, or a total of 38 ft for the two, and each has 42 indicators, 18 recorders, six controllers and 25 sets of start-and-stop pistol grip control switches, usually with three lights per switch. There are over 300 items for the two boilers. Each turbine panel is 13 feet long and has seven indicators, ten recorders, eight sets of start-and-stop push buttons, usually with three lights per switch. Communication between the electrical control room and the boiler and turbine rooms is by telephone and telautograph.

One company preferred this arrangement and objected to combining the boiler and turbine gauge boards on the basis that boiler and turbine operators are not readily interchangeable, each having very different duties. In some localities, with the arrangement shown, a boiler operator with a helper to patrol the boiler operating floor, and a turbine operator with a helper are required so that combining the boiler and turbine boards, or placing them close together in a separate room would not decrease the number of operators.

Plant B

Plant B given in Figure 3 shows the main operating floor plan of a new station with two 850-pound-per-square-inch 900-degree-Fahrenheit 60,000-kw turbine generators and four oil- and gas-fired boilers. The station has recently been extended with two more 60,000-kw units. Here the electrical control room was placed in the aisle between the boilers and the turbines at turbine operating floor grade and is centrally located in the completed station. The boiler boards are grouped together as are the turbine boards. For the equipment in the picture there are 110 linear feet of mechanical gauge boards which have over 300 functions for indicating, recording, and con-

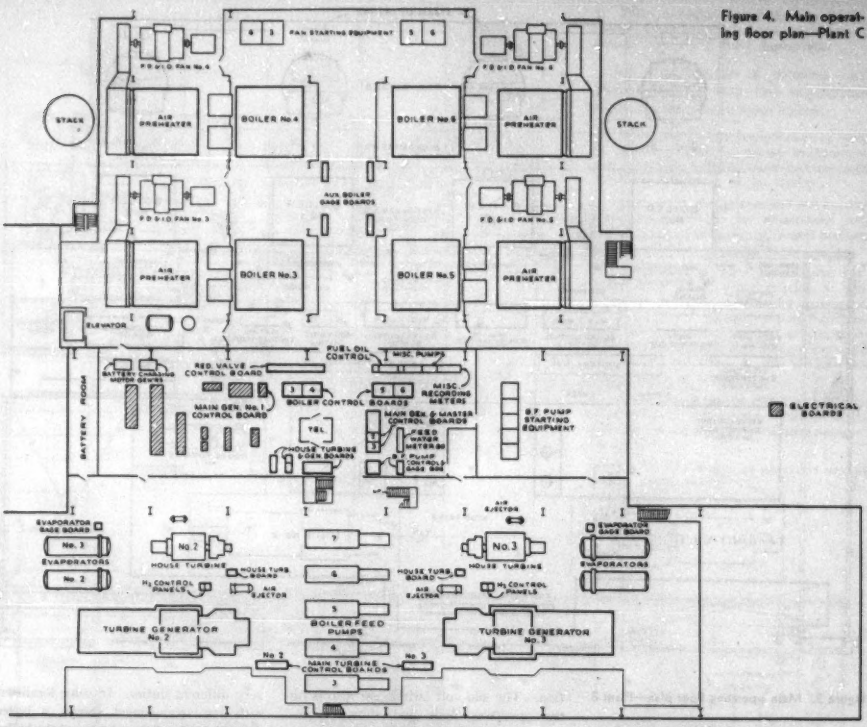

Figure 4. Main operating floor plan—Plant C

Figure 5 (left). Control room—Plant C

Figure 6 (above). Master panel—Plant C

Figure 7 (left). Boiler boards—Plant C

Figure 8 (right). Electrical boards—Plant C

trolling, not including lights and alarms for condensate, boiler feed, boiler, and turbine controls.

Plant C

Plant C given in Figure 4 shows the main operating floor plan of a plant extension having two 1,300-pound-per-square-inch 950-degree-Fahrenheit 100,000-kw turbine generators and four oil- and gas-fired boilers. This extension has a complete centralized mechanical and electrical control room located at operating floor level so that it is at the crossroads between the boiler and turbine rooms. In addition, there are individual gauge boards at the various equipment items. The control room is 40 by 130 feet. Figure 5 shows a view through the centralized control room from the boiler operating aisle, with the boiler feed pumps seen through the far door. The man stands at the boiler master panel, shown in detail in Figure 6, and the enclosed telephone booth is shown on the right. There are 378 annunciator drops in this room. Some control rooms are soundproofed and air-conditioned, but this utility soundproofs only the glass enclosed telephone booth and prefers to have the operators noise conscious with respect to characteristic and abnormal noises around the plant.

Figure 9. Main operating floor plan—Plant D

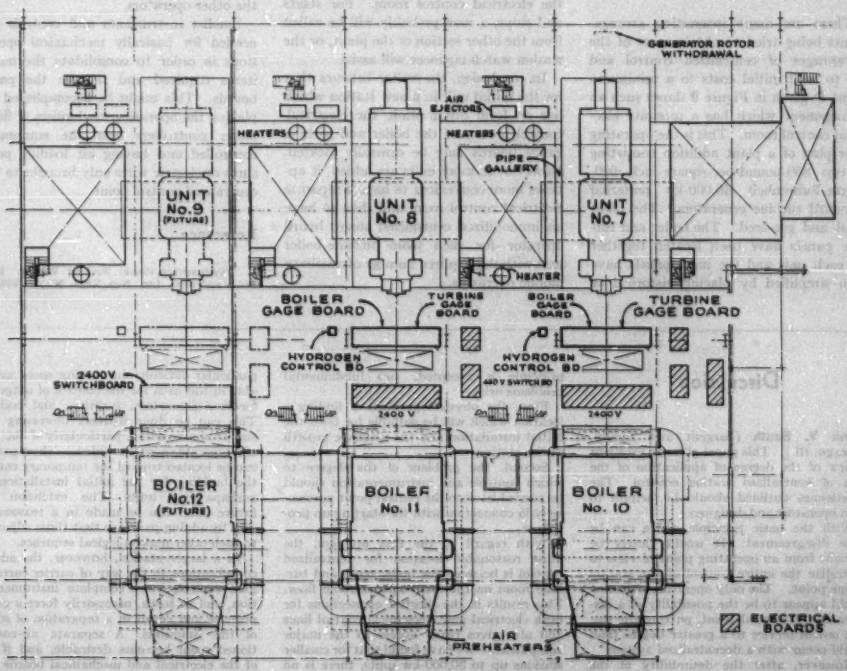

A separate panel is located in this control room for each boiler and each turbine including each house generator. Figure 7 shows the individual boards for two of the four boilers. In addition, there are miscellaneous mechanical instruments and controls on another long panel. In all, there are about 100 linear feet of panel for basically mechanical, and about 76 linear feet for basically electrical controls.

Figure 8 shows part of the electrical boards. Note that there are several rows of panels.

Each control room operator is given considerable training in what should be done in emergencies. The men are expected to operate both basically electrical and mechanical controls and after they have become trained in handling the controls it is thought that seven men per shift can operate the entire station.

There now appears to be a trend towards the single boiler-single turbine installation, which would have considerably reduced the number of instruments and controls.

Plant D

There are many interesting arrangements being tried to obtain most of the advantages of centralized control and yet to hold initial costs to a minimum. Plant D given in Figure 9 shows such an arrangement which has a separate electrical control room. This is the operating floor plan of a plant addition consisting of two 850-pound-per-square-inch 900-degree-Fahrenheit 40,000-kw preferred standard turbine generators. The plant is oil- and gas-fired. The boiler and turbine panels have been located together for each unit and the main panels have been simplified by placing historical or efficiency instruments on other panels, and locating only the instruments and controls necessary for start-run-stop operation at the central point. For each unit this centralized boiler-turbine board is about 24 feet long. Many indicating gauges have been combined in multipointer-type dials like multipointer draft gauges that have decreased the length of the panels.

A bench-board type of panel was investigated for this application, but it was found to require more building space as it required a mezzanine below the board for initial installation of pipes and wires, and for maintenance of the instruments and controls.

When the first unit of Plant D starts initial operation, it is expected that only three men per shift will be added to operate the gas-fired boiler, the turbine generator, and their auxiliaries, one of whom will be immobilized at the central steam control board and the others will circulate throughout the station; and a few months later when the second unit goes into service, one more man per shift will be added, making a total of four. No additional operators will be required in the electrical control room. For starts and stops, a man probably will be called from the other section of the plant, or the station watch engineer will assist.

In conclusion, the writer believes that for the initial unit in a new station which has no local distribution, the electrical control room and the boiler and turbine gauge boards may be centrally located. However, as more units are added, it appears more convenient to have a separate electrical control room and then to have an immobilized centralized steam board operator for each main turbine-boiler unit with the required number of auxiliary mobile operators.

An operator or group of operators can care for one turbine-boiler unit and ordinarily do a good job in case of trouble, but if they have more than one to cover there is a chance that any complication of difficulties may develop into a serious outage.

Many of the advantages of a centralized control room may be gained, and some of the disadvantages eliminated, by having a centralized point for the control of each single boiler-single turbine located between the boiler and turbine at the main operating floor level with the switchboard in a separate room where the electrical controls for several such single boiler-single turbine units and those of the outgoing lines would be located. The writer favors this latter idea on the premise that a good operator should be able to control a single boiler-single turbine unit gauge board, but that anything more than that with present-day equipment and controls does not give adequate care in times of trouble. This one man must have assistance in starting the unit and when the unit is running for circulating through the plant. The control board operator should be in close contact with the other operators.

Smaller instruments and controls are needed for basically mechanical operations in order to consolidate the many items required and shorten the panel boards. This might be accomplished by placing the operating mechanism of flowmeter controllers near the equipment controlled and having air loading pressures or electric wires only brought to the centralized control point.

Reference

1. Cybernetics, (book), Norbert Wiener. John Wiley and Sons, Inc., New York, N. Y., 1948.

Discussion

Frank V. Smith (Sargent and Lundy, Chicago, Ill.): This paper gives an excellent review of the degree of application of the idea of centralized station control. The experiences outlined should be helpful to both operators and designers.

With the basic principle, there can be little disagreement. It would clearly be efficient from an operating point of view to centralize the entire control of the station at one point. The only operating objection would appear to be the possibility of a disaster at this central point, putting the station out of service to a greater degree than would occur with a decentralized system.

However, after the desirability of the principle is accepted, two fundamental problems arise.

First, the physical problem of finding a location which will be suitable for both the initial installation and the ultimate growth of the station.

Second, the problem of the degree to which controls and instrumentation should be carried back to the central point particularly in connection with the starting up procedure.

With regard to the first problem, the most reasonable location for centralized control is between the boiler room and turbine room on the main turbine room floor. This results in the shortest connections for both electrical and mechanical control lines and also gives ready access to the major equipment. We have found that for smaller stations up to 30,000-kw units, there is no particular difficulty in making space available in this area for the control of outgoing feeders, generators, turbines, and boilers. This can be done without increasing the size of the building, particularly if the use of a separate room is avoided. These panels can be located toward the temporary end of the building for the initial installation of perhaps two units. The extension for future units can be made in a reasonable way by adding panels so that those adjacent to each other make a logical sequence.

In a larger station, however, the added complications in the way of carrier current, load control, more complete instrumentation, and so forth, necessarily force a compromise and result in a separation of some of the functions. A separate air-conditioned room becomes desirable, and if all of the electrical and mechanical boards are

located together, a room of at least 30 or preferably 40 feet wide is necessary. This probably result in adding to the size of the building which will be a costly procedure since the entire height of the building is involved.

It is because of this fact that practically all stations have been forced to separate some of the elements and the following separations have been used:

1. Feeder, generator, turbine, and boiler controls for one unit or a pair of units have been placed in a separate room from the next unit or a pair of units.
2. Feeder controls have been moved to a separate location from the generator, turbine, and boiler controls.
3. Feeder and generator controls have been moved to a separate location from the turbine and boiler controls.
4. Relays for feeders and generators have been moved to a separate location from the feeder, generator, turbine, and boiler controls.

In this connection, we have found that most operators seem to feel that:

1. All electric feeder controls should be in one location so that the operator will be fully aware of what is happening on all outgoing lines.
2. All electric generator controls should be in one location so that the operator can be aware of load division between units, excitation problems, and so forth; in general, but not necessarily, this location should be the same as the feeders.
3. Boiler and turbine controls should be all together for the entire station or, if separated, should be in convenient groups of related units for stations built on the unit system.

These preferences indicate that unless it is possible to so design the centralized control that the electrical board can be essentially continuous for the ultimate development of the station, it is better to move the electrical control to a separate room and centralize only the turbines and boilers.

When a separate room is chosen for the electrical control, its cost is less than that required to widen the space between the boilers and turbines since it is located in a smaller building at the side or end of the station.

The second problem as to the degree to which controls should be brought back to the central point revolves around the extent to which manpower can be saved by additional expenditures. It is apparent that the simple process of grouping together electrical boiler and turbine controls at one point will reduce the number of operators from that required if all of these functions are in separate places, although a higher type of operator will be needed.

However, there is considerable difference of opinion as to the degree to which the number of operators around the plant can be reduced by bringing back controls for starting equipment. Studies made on two roughly similar situations showed that while the initial investment was increased appreciably by motorizing valves, installing position indicators and bringing back other electrical devices and alarms to the control room so as to avoid the necessity of operators having to be at equipment during starting or for frequent inspection, one operating company felt that this would permit a saving of sufficient operators around the plant to justify the additional expenditure, while another operating company felt that no appreciable reduction would occur.

It appears that while there is no question that complete instrumentation should be provided in the centralized control room, there is some difference of opinion as to whether any great expenditure should be made to carry back to this point sufficient controls for starting major items of equipment without operators at the equipment involved. We will all look forward to further operating experience in this field.

Design and Operation of Central Control Rooms

B. F. BORGEL
NONMEMBER AIEE

Synopsis: A description of the experiences leading to the adoption of the central control system in the Warren, Pa. plant of the Pennsylvania Electric Company, the design features incorporated in this room; the operating experiences with this type of control to date; the basic changes which have been indicated by actual operation; and the costs involved in this type of control.

THE central control room of the Warren, Pa. station of the Pennsylvania Electric Company is basically a balanced combination of control and supervisory rooms, and is a result of that company's extensive investigation into the field of centralized control, as well as an indication of a firm belief in the advantages and economics of this type of plant control.

This particular installation is serving as a proving ground for various changes which will be incorporated in future plant design, and will therefore be used to illustrate the engineering policy being followed by the Pennsylvania Electric Company in this and future plants, and to bring forth the experiences encountered in the operation of this room. Though the soundness of the design has been amply proved in operation, experience has indicated several desirable basic changes which will be incorporated in future installations.

Due to the peculiar operating problems encountered on this system, the need for faster communication between the various operators on duty in a station has long been recognized. This system, which is spread over a mountainous area 300 miles in extent, is subjected to severe disturbances from electrical storms, which frequently isolate a generating station from the system, causing the loss of all the load except that in the immediate area.

During these conditions, the plant facilities must be maintained in such a manner which will permit immediate load pickup when tie lines are reclosed, and aggravating this situation is the fact that several of the stations are located in metropolitan areas, and other sections in which are located customers such as oil refineries, rayon mills, electric furnaces, and so forth.

In order to take advantage of the low generating costs represented by the Company's mine-mouth plants, power is frequently transmitted as much as 200 miles into the metropolitan areas. During these periods, the area plant must be able to pick up load from minimum to maximum in the event of any tie line disturbance, and to accomplish this without any objectionable drop in voltage or frequency.

Attempts have been made in the past to effect faster internal plant communication by various means. The first attempt was the installation of telephone stations at key operating positions. This led to the use of common loud-speaker systems, arranged to provide coverage of all operating locations.

The third move in this direction, was the location on boiler control boards of the governor control of the turbine served by that boiler, thus turning over to the boiler operator the control of turbine load. These moves definitely speeded operation during emergencies, and indicated more efficient operation during normal periods, but underlined the necessity for one key operator to be constantly cognizant of the condition of all equipment in the plant that he might properly co-ordinate the actions of the other operators.

To meet this demand, the central control room system was investigated and adopted to the particular needs of this company, as illustrated in Figure 1. It was not felt that a control room in which control of all equipment in the plant was concentrated was feasible, since experience had indicated that sufficient operators must be used to permit satisfactory operation of the plant manually upon loss of one or more controls.

It was felt that it would be advantageous to concentrate in a central control room sufficient indicating and alarm systems which would furnish the operator a full picture of plant operation at all times, as well as full control of all equipment required during periods of emergency operation. With this end in mind, the room was designed to incorporate as shown in Figure 2, the necessary equipment for:

1. Operation of boilers, generators, and station auxiliary power supply.
2. Indicating and recording supervision of turbines, hydrogen systems, and feedwater systems.
3. Annunciator alarms on miscellaneous plant equipment such as water screens, service pumps, storage tank levels, air compressors, and so forth.

Experience had indicated the desirability of control boards arranged for maximum ease of operation, and particular attention was paid to this phase of the design, as shown in Figure 2. Operation is facilitated by grouping of associated equipment and locating the various groups in a functional sequence.

For example, the sequence of operation of each boiler panel is from left to right, starting with the induced draft equipment, followed by the forced-draft equipment, and the two sets of pulverizers. Vertical segregation of all equipment has

Paper 50-92, recommended by the AIEE Power Generation Committee and approved by the AIEE Technical Program Committee for presentation at the AIEE Winter General Meeting, January 30–February 3, 1950. Manuscript submitted October 31, 1949; made available for printing January 6, 1950.

B. F. Borgel is with the Pennsylvania Electric Company, Johnstown, Pa.

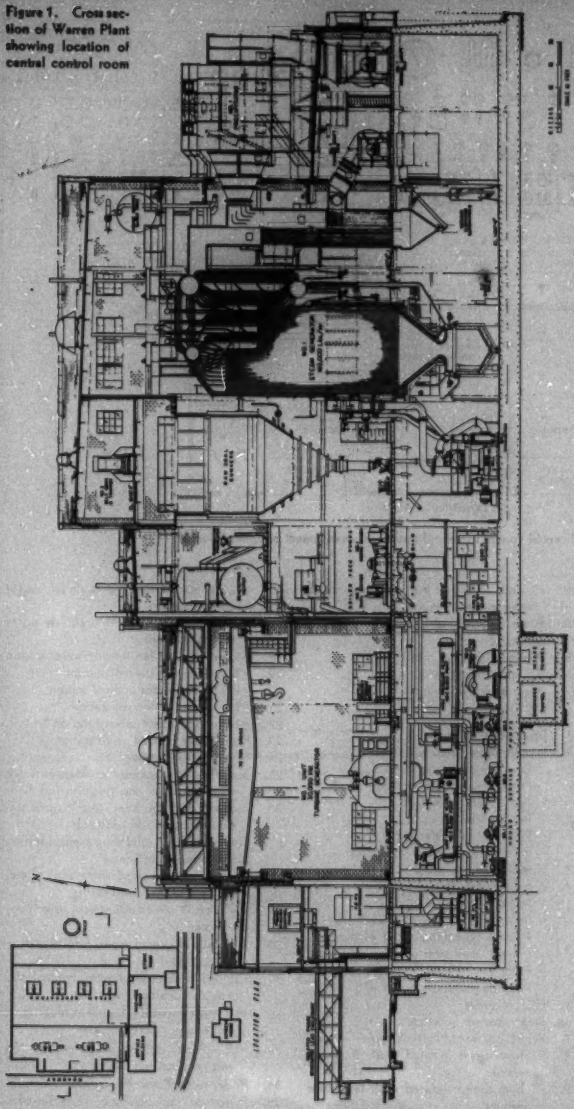

Figure 1. Cross section of Warren Plant showing location of central control room

been followed. Thus, the remote control station and position indicators for the induced draft inlet vane drive unit are directly below the induced draft fan motor control stations and ammeters. All start-stop stations are in a horizontal line at one level, and all remote control stations are in a horizontal line at another level on the panel board.

On the station power boards, the switch controls are arranged horizontally by voltages and vertically by sequence of operation, as pictured in Figure 3. Maximum usage has been made of all available types of handles for control stations. Thus pistol grip denotes circuit breaker control, oval is used on remote operating controls, round smooth on governor and field controls, round knurled on current and potential transfer switches.

The instruments and draft gauges which indicate the changes resulting from control operation are located vertically above the corresponding control stations on the panel boards. The primary objective throughout was to provide a layout that would help the operator to think and to follow the correct sequence of operation.

Figure 4 shows the arrangement and relative locations of one boiler control board, and the turbine, hydrogen, and generator panels. Figure 5 illustrates the arrangement and location of the station power bench board, one boiler control panel, and the master combustion control panel.

The Warren plant was placed in service on August 15, 1948, and operation since that time has amply justified the faith of the engineers in the advantages of a central control room. The plant was manned with experienced operators in the central control room, and new operators with no previous power plant experience in all other operating posts.

No misoperation by the new operators, who work directly under orders of the control operator has resulted to date. During the start-up period we had a total of 17 trip-outs of the machines at full load due to staged relay testing and accidental trip-outs.

In all cases, the machine was resynchronized and the plant returned to full load in less than five minutes elapsed time. The best record for this performance was 1 minute, 30 seconds, in which case the operator did not trip out any mills, but being able to see at a glance the condition of the plant, resynchronized the generator and put on load, allowing his safety valves to open and dump the excess steam for the required period.

This operating condition was duplicated in another plant of this system which is identical in design with Warren, lacking only the central control room, and a minimum of 11 minutes was required from trip-out of the generator to re-establishment of full load on the unit.

Since the Warren control room was the first effort by the Pennsylvania Electric Company toward the use of centralized control in generating plant operation it,

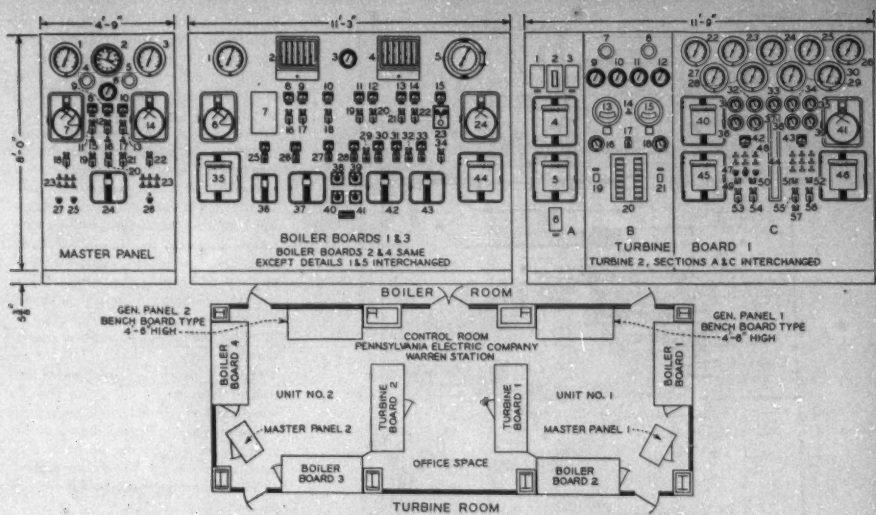

Figure 2. Plan view of central control room and instrument arrangement of control boards

MASTER PANEL

1. Steam header-pressure gauge
2. Clock
3. Feed-water header pressure gauge
4. D-c alarm horn
5. A-c alarm horn
6. Air supply pressure gauge
7. Feed-water flowmeter
8. #1 and #4 boiler feed pump motor ammeter
9. #2 and #5 boiler feed pump motor ammeter
10. #3 and #6 boiler feed pump motor ammeter
11. #1 and #4 boiler feed pump motor control station
12. #2 and #5 boiler feed pump motor control station
13. #3 and #6 boiler feed pump motor control station
14. 3-pen pressure recorder
    Point 1—feed-water pressure
    Point 2—steam pressure
    Point 3—fuel oil pressure
15. #1 boiler feed pump light load indicating lights
16. #2 boiler feed pump light load indicating lights
17. #3 boiler feed pump light load indicating lights
18. #1 and #3 boiler lead motor-operated valve control station
19. #3 and #6 boiler feed pump by-pass valve control station
20. #2 and #5 boiler feed pump by-pass valve control station
21. #3 and #6 boiler feed pump by-pass valve control station
22. #2 and #4 boiler lead motor-operated valve control station
23. Alarm system signal lights
24. Master controller
25. Alarm system reset button
26. D-c failure reset switch
27. Alarm system test button

BOILER BOARD

1. Drum pressure gauge
2. 6-point boiler draft gauge
    Point 1—air heater inlet
    Point 2—air heater outlet
    Point 3—furnace draft
    Point 4—boiler outlet
    Point 5—air heater outlet
    Point 6—induced draft fan inlet
3. Combustion rate gauge
4. 6-point mill draft gauge
    Point 1—mill inlet #1A
    Point 2—exhauster inlet #1A
    Point 3—exhauster outlet #1A
    Point 4—mill inlet #1B
    Point 5—exhauster inlet #1B
    Point 6—exhauster outlet #1B
5. CO_2 recorder
6. Steam flow-air flowmeter
7. Retractable soot blower control
8. #1 low speed induced draft fan motor ammeter
9. #1 high speed induced draft fan motor ammeter
10. #1 forced draft fan motor ammeter
11. #1A mill motor ammeter
12. #1A feeder speed indicator
13. #1B mill motor ammeter
14. #1B feeder speed indicator
15. Feed-water control valve position indicator
16. #1 low speed induced draft fan motor control station
17. #1 high speed induced draft fan motor control station
18. #1 forced draft fan motor control station
19. #1A mill motor control station
20. #1A feeder motor control station
21. #1B mill motor control station
22. #1B feeder motor control station
23. Feed-water control valve station
24. Drum level recorder
25. Superheat temperature condenser valve control station and position indicator
26. Induced draft fan inlet vane control station and position indicator
27. Forced draft fan inlet vane control station and position indicator
28. #1A mill exhauster damper control station and position indicator
29. #1A feeder speed adjustment lever control station
30. #1A mill hot air damper control station and position indicator
31. #1B mill exhauster damper control station and position indicator
32. #1B feeder speed adjustment lever control station
33. #1B mill hot air damper control station and position indicator
34. Boiler feed shutoff valve control station
35. Superheat temperature recorder-controller
36. Superheat temperature micromax electric control relay
37. Air flow controller
38. Transfer valve
39. Combustion control selector switch
40. Load adjustment valve

41. Fuel-air ratio rheostat
42. Furnace pressure controller
43. Totalizing fuel feed controller
44. 8-point boiler temperature recorder
    Point 1—gas leaving boiler
    Point 2—gas leaving air heater
    Point 3—air leaving air heater
    Point 4—air entering air heater
    Point 5—coal-air mixture #1A mill
    Point 6—coal-air mixture #1B mill
    Point 7—feed water entering boiler
    Point 8—spare

TURBINE BOARD

1. Station service kilowatt-hour meter
2. Deaerating heater water level indicator
3. Generator kilowatt-hour meter
4. Generator field temperature recorder
5. 10-point generator stator temperature recorder
    Point 1—generator coil #1
    Point 2—generator coil #2
    Point 3—generator coil #3
    Point 4—hydrogen out #1
    Point 5—hydrogen out #2
    Point 6—hydrogen in #1
    Point 7—hydrogen in #2
    Point 8—exciter air in
    Point 9—exciter air out
    Point 10—test
6. Station service kilowatt-hour meter
7. A-c alarm horn
8. D-c alarm horn
9. Generator hydrogen temperature gauge
10. Generator hydrogen low pressure gauge
11. Generator hydrogen high pressure gauge
12. Vacuum oil treating gauge
13. Generator fan pressure gauge
14. Emergency pump signal light
15. Density meter gauge
16. Generator gland seal oil gauge (turbine end)
17. Hydrogen pressure selector switch
18. Generator gland seal oil gauge (collector end)
19. D-c power switch
20. Hydrogen alarm system
21. A-c power switch
22. #2 bleed point pressure gauge
23. #3 blood point pressure gauge
24. #4 bleed point pressure gauge
25. #5 bleed point pressure gauge
26. House service water pressure gauge
27. Throttle pressure gauge
28. Primary pressure gauge
28. Primary inlet pressure gauge
29. Impulse chamber pressure gauge
30. Exhaust pressure gauge
31. Steam flow limit control gauge
32. Bearing oil pressure gauge
33. Main oil pump suction gauge
34. Main oil pump discharge gauge
35. Auxiliary oil pump discharge gauge
36. Governing impeller discharge gauge
37. Governing secondary controller gauge
38. Gland water pressure gauge.
39. Gland steam seal pressure gauge
40. 8-point condensate temperature recorder
    Point 1—condensate leaving #5 bleed point heater
    Point 2—condensate leaving evaporator condenser
    Point 3—feed water leaving daerating heater
    Point 4—feed water leaving #3 bleed point heater
    Point 5—feed water leaving #2 bleed point heater
    Point 6—circulating water—condenser inlet
    Point 7—circulating water—condenser outlet #1A
    Point 8—circulating water—condenser outlet #1B
41. Condensate flowmeter
42. Turbine speed indicator
43. Turning gear ammeter
44. Vacuum mercury column
45. 6-point conductivity recorder
    Point 1—saturated steam #1 boiler
    Point 2—saturated steam #2 boiler
    Point 3—check point
    Point 4—condensate leaving #1 condenser
    Point 5—boiler feed water
    Point 6—evaporator distillate
46. 5-point vacuum condensate temperature recorder
    Point 1—vacuum
    Point 2—condenser condensate
    Point 3—oil to oil cooler
    Point 4—oil from oil cooler
    Point 5—test
47. Alarm system test button, d-c failure reset switch, alarm system reset button
48. 14-point alarm system lights
49. #1A circulating water pump signal lights
50. #1B circulating water pump signal lights
51. #1A condensate pump signal lights
52. #1B condensate pump signal lights
53. #1 turbine lead valve control station
54. #1 condensate storage transfer pump control station
55. #1 turning gear oil pump control station
56. #1 feeder extractor pump control station
57. #1 turning gear signal lights

---

was recognized that actual operation would indicate desirable basic changes in design which could be incorporated in future planning. These changes are as follows:

1. Concentration on the board fronts of only those indicating instruments which are required for minute-to-minute operation.

The board fronts on a central control room are by far the most expensive surface per square foot in the station, and such valuable space should be utilized only for instruments and controls which are vital to station operation. Recorders, which primarily register trends and provide permanent records should be located on the backs of the control cubicles, or in a location adjacent to the control room which would be readily accessible to the operator for periodic checking.

A common monitoring system covering all points of temperature on the equipment will be used, permitting constant checking by the operator. Investigations now are being made regarding the use of small indicating instruments in parallel with recorders such as steam flow-air, flow, water level, and so forth, on the board fronts, as well as the development of smaller meters for pressures and drafts.

It is felt that unless the board fronts in a control room are kept to such a length as will permit normal coverage by one operator, the major benefit resulting from central control design will be lost. Application of these principles of design would shorten the Warren boards by 30 per cent.

It is not beyond the realms of possibility that the future control room will comprise a bank of airplane-type instruments and miniature controls, so arranged that a station will be monitored and operated from a control seat.

2. Relocation of the generator hydrogen indicating and signal panel to a location adjacent to the actual hydrogen equipment, to provide guidance for the operator in making adjustments to the hydrogen supply to the generator, and to eliminate the hazard of hydrogen leakage into the control room.

3. Use of pressure transmitting devices with the sender located at the boiler drum or other pressure point and multiple indicating units in the control room and at other required locations, to avoid the danger of a pressure blowout in the control room, with the attendant disruption of electrical control circuits.

4. Phase-angle control of tie line loading and frequency applied directly to combustion control as well as to the governor control of the turbine. This will be done by employing a 2-element master combustion control, the primary element receiving its impulse from the phase-angle control and changing combustion rate simultaneously with changes in turbine loading, and the secondary element working on header steam pressure and correcting this pressure at a predetermined rate.

5. The control room will be rearranged to permit greater visibility of the plant by the control room operator. Experience has indicated that it is inducive to better operation if the operator is able to see the equipment he is operating.

6. Further studies of the lighting problems in connection with control

Figure 3. Generator, exciter, and station auxiliary power control benchboard

Figure 5. Relative location and arrangement of station auxiliary power benchboard, boiler panel, and master combustion control panel

Figure 4. Relative location and arrangement of boiler, turbine, hydrogen, and generator panels

rooms. At Warren, the lighting intensity in the control room is high in comparison to the rest of the plant to decrease eyestrain on the part of the operators.

Reference to Figure 3 will show that this has led to a condition in which the Thermopane glass enclosing the room acts as a mirror and hampers outside vision.

The Warren control room has served a secondary purpose aside from the operating advantages described previously, in providing data permitting a judgment on the economic advisabilities of this type of design to be made. This plant consists of two 30,000-kw namepate rating generators operated on a continuous basis at 40,000 kw each.

The plant is operated with six operators per shift, and a total force, including supervisors, of 53 men. Accurate cost data of the control room versus conventional design has been compiled, and show the additional cost of the Warren design to be $60,000.00 or $1.00 per kilowatt of nameplate capacity.

The direct savings accruing from this expenditure is the elimination of two shift operators, evaluated at $35,000 per year total. No attempt has been made to date to evaluate the return represented by faster and more efficient operation of the plant when required, but this has been a sizable amount.

In conclusion, this company is convinced of the economic feasibility of the modified central control room, when it is engineered to meet a specific purpose in a definite plant, and that capital invested in such construction provides a high continuing rate of return on the investment.

Discussion

C. P. West (Westinghouse Electric Corporation, East Pittsburgh, Pa.): The operation of this plant departs from commonly-used practices in that control of the loading and excitation of the generators is chiefly placed in the hands of boiler-room operators rather than directly under the control of the operator handling the primary switchgear. This arrangement is claimed to be better because of close co-ordination of boiler control and generator output during emergencies. Under normal conditions when switching operations and load changes are planned in advance, communication between operators by telephone is said to be adequate. In many new plants, all these functions and the required operators are in one large control room. It would appear that this arrangement, with the proper grouping of switches and instruments on control boards in one location with specific operators responsible for each functional unit, would give the best contact between them with no increase in personnel.

The author emphasizes the need for smaller instruments for indicating and recording electrical, steam, and combustion conditions. This is necessary to bring these devices as close together as possible to facilitate operation and reduce the number of people required. The possible future use of miniature instruments and control devices is predicted. There have been other plants planned where the tendency has been toward large indicating instruments, as apparently space consideration was not a controlling factor. It appears to me that standard control switches, electrical indicating instruments about 4 inches square, and boiler and combustion control instruments as near to this as possible gives the best arrangement. Such indicating devices can be plainly seen and yet are not too bulky. Smaller instruments may be less accurate and are harder to read. Small

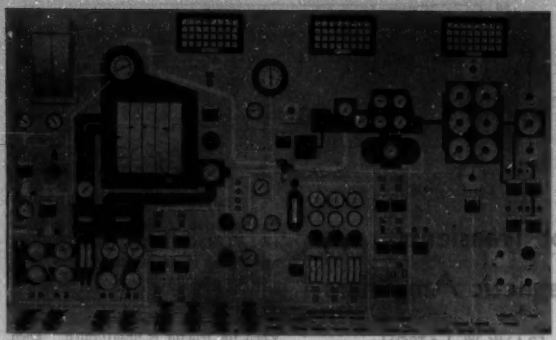

Figure 1 (left). Front view of control board

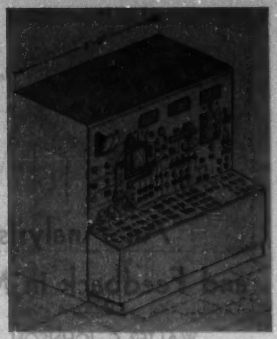

Figure 2 (right). Isometric view of control board enclosure

switching devices often require interposing relays with consequent complication of circuits and the increased hazards of more contacts and operating parts. A move toward either extremely large or extremely small devices appears to have little to recommend it.

A. H. Burkhalter (Ebasco Services Incorporated, New York, N.Y.): Mr. Borgel is to be commended for his work of reducing the size of control room equipment and the contribution which that size reduction has made toward greater accessibility to the operator of indications and controls.

We marvel at the similarity of his suggestions in paragraphs 1 and 3 of his summary to the basic design which we have embodied in a compact control board which we are using regularly to control the boiler, turbine, and generator of our new unit type stations of sizes up to and including 60,000-kw preferred standard turbine generators.

Figure 1 of this discussion shows this control board. It is only eight feet in length and has a front bench section. It is of tunnel-type construction with all electrical recorders, watthour meters, and relays for the boiler turbine generator unit mounted on the rear panel. All of the large recorders which, in the past, have required piping of such primary quantities as steam, water, and fuel gas, have been replaced by remote electrical retransmitting devices. The only space then required on the board for indication of these quantities is that required for the electrical receiving indicators from these retransmitting devices. The high-pressure gauges on the control board are replaced by 0–15 pounds-per-square-inch gauges operating by pneumatic retransmission from the primary elements located at the most convenient point on the boiler or turbine. These 0–15 pounds-per-square-inch gauges are of the small type mentioned in Mr. Borgel's paper. They, and the above electrical receiving instruments, are also part of a retransmitting system as suggested in the paper.

The drafts and pressures at various points in the air stream through the furnace are all read on airplane-type pressure gauges as suggested in the paper.

Annunciation is provided on the front panel of the board for the boiler, the turbine, and the generator by use of a 32-point luminous-window type annunciator for each.

The control switches used are standard rotary type mounted with minimum spacing wherever necessary. Supervisory control was avoided in order to maintain maximum simplicity and reliability.

The significance of any indication or control facility is indicated by its position in the mimic representation of the boiler, the turbine, or the generator. This mimic representation is carried on to include all primary piping or bus work associated with these primary divisions of the unit.

Figure 2 of the discussion shows an isometric view of an earlier model of the control board. This shows more clearly the bench and tunnel-type construction. It also illustrates the compactness of the board.

As mentioned earlier, this board has on it all the indications and controls necessary for operation of a 1,350-pounds-per-square-inch boiler with its fuel control and condensate handling equipment, a turbine with its condensing equipment, and a 60,000-kw preferred standard generator with its electrical auxiliaries. This is in sharp contrast to the several massive gauge boards and control boards which have heretofore been a part of any centralized control arrangement. This compact control board makes it possible for one operator to control more than one unit by concentrating all the controls which he needs into such a small area. This eliminates any question of vertical versus horizontal centralization, since it accomplishes both.

The first two of these boards were designed to control two 20,000-kw units in the new Morgan Creek Steam Electric Station of Texas Electric Service Company. These boards are practically fabricated.

The next one is designed for control of one 60,000-kw unit in the new Handley Steam Electric Station of the same company. This one is ordered and has passed the drawing for approval stage.

The next four are designed for control of 60,000-kw units of the Middle South Utilities Corporation. These are to be located as follows: Two in the Hamilton Moses Steam Electric Station of Arkansas Power and Light Company; one in the Natchez Steam Electric Station of Mississippi Power and Light Company and one in the Ninemile Point Steam Electric Station of Louisiana Power and Light Company. These are ordered and have passed the preliminary drawing stage.

One is ordered for control of the 60,000-kw unit at Goldsboro Steam Electric Station of Carolina Power and Light Company.

Two more are being engineered for control of new 60,000-kw units.

Figure 1 of the discussion is a full-scale model which was made earlier and which is used as a standard with minor modifications for all subsequent jobs.

An Analysis of Transients and Feedback in Magnetic Amplifiers

WALTER C. JOHNSON
MEMBER AIEE

FRANK W. LATSON
STUDENT MEMBER AIEE

Synopsis: This paper presents an analysis of the steady-state and transient characteristics of the magnetic amplifier without feedback, with external feedback, and with one commonly-used type of self-feedback. Comparisons with experimental data indicate that the accuracy of the analysis is well within the limits that may be expected for nonlinear circuits.

THE terms saturable reactor, d-c controllable reactor, transductor, and magnetic amplifier have been used to denote an iron-cored inductor in which the a-c impedance can be controlled by magnetically saturating the core with an auxiliary d-c winding. In this paper, the term saturable reactor will be used to denote the iron-cored inductor itself, and the term magnetic amplifier will be applied to the entire circuit which makes use of the properties of the saturable reactor in order to amplify a signal. In many practical magnetic amplifiers, positive feedback is used to increase the amplification.

The steady-state characteristics of the saturable reactor have been discussed in many papers, and its properties have been related to the nonlinear characteristics of the core in a number of different ways by different investigators.[1-3] The purpose of this paper is to show how the steady-state characteristics of the saturable reactor, whether computed or determined experimentally, can be used to determine the effect of feedback on both the steady-state and the transient properties of the device. The illustrative computations given in this paper are based on the steady-state analysis given in reference 1, but the general methods can be applied equally well to the steady-state characteristics as found by any other means, including experimental methods.

Paper 50-94, recommended by the AIEE Electronics Committee and approved by the AIEE Technical Program Committee for presentation at the AIEE Winter General Meeting, New York, N. Y., January 30-February 3, 1950. Manuscript submitted October 27, 1949; made available for printing December 2, 1949.

WALTER C. JOHNSON is Professor of Electrical Engineering with Princeton University, Princeton, N. J., and FRANK W. LATSON is with the Kellex Corporation, New York, N. Y.

The investigation presented in this paper was supported in part under a contract with the General Electric Company.

The Steady-State Load Line

A useful method of presenting the characteristics of a saturable reactor is to plot a family of curves of rms voltage across the reactor terminals versus either the rms or the average current through the reactor, one curve being given for each of a number of values of control current. An example of this is shown in Figure 1 for a commercial saturable reactor with a 4-legged silicon-steel core. This particular reactor was chosen for a number of these experiments because its comparatively large current-handling capacity facilitated accurate measurements of current and voltage. The quantity labeled I_m on the graphs is the net d-c magnetizing current referred to the control winding. For steady-state operation without feedback, this is equal to the control-winding current. The advantage of the type of presentation shown in Figure 1 is that it is not restricted to any particular value of supply voltage or to any particular value or type of load impedance. However, these graphs must be measured or computed on the basis of a particular waveshape of applied voltage, usually a sinusoidal one. The question is whether, because of the nonlinearity of the device, the curves so obtained can be applied to the operation of the reactor when connected to a load, for here the reactor voltage will not be sinusoidal.

When a saturable reactor is connected in series with a load impedance as shown in Figure 2, the load current will be small when the reactor is unsaturated. Then the voltage drop across the load will be small, and the reactor voltage will be nearly sinusoidal. On the other hand, when the reactor is saturated, the load current and load voltage will be large, and the reactor voltage will be nonsinusoidal. However, it has been shown previously[4] that, under the saturated condition, the characteristic curves of the reactor are affected only a little by the waveshape of the terminal voltage. Hence, we may expect that the characteristic curves will apply reasonably well to the loaded condition, and that a load line based on linear circuit theory can be traced on the characteristics of the reactor. The foregoing conclusion has been checked experimentally for various load lines on different reactors, and the results found to be uniformly satisfactory.

If the load impedance shown in Figure 2 is a resistance, and if the reactor is temporarily considered as a linear inductance, the relationship between the reactor voltage and the rms current is the ellipse

$$\left(\frac{E_s}{E_a}\right)^2+\left(\frac{I}{E_a/R_L}\right)^2=1 \qquad (1)$$

where

E_s = rms voltage across the saturable reactor
E_a = rms applied voltage
I = rms current in the circuit
R_L = load resistance

Thus, the load line is an ellipse with the intercepts E_a and E_a/R_L, as shown in Figure 3. The load line for a purely inductive load would be a straight line connecting the intercepts E_a and E_a/X_L, where X_L is the reactance of the load.

A typical calculated result, which was obtained with the load line of Figure 1, is shown in Figure 4. Comparison with the experimental points shows that the calculated result is reasonably accurate, particularly considering that the curves of Figure 1 were computed by the methods of reference 1 rather than measured.

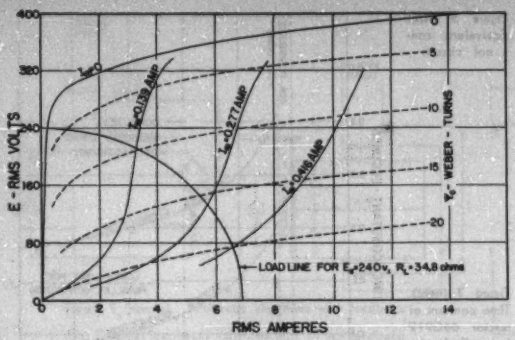

Figure 1. Characteristic curves calculated for reactor 66G912; a-c coils in series. For parallel a-c coils, multiply abscissae by 2 and divide ordinates by 2

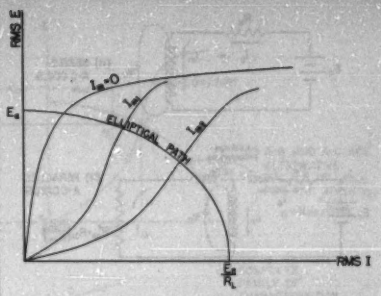

Figure 3. Load line for a resistive load

Transient Operation Without Feedback

This section presents an equivalent circuit for the computation of transients in the absence of feedback, and discusses the factors that influence the speed of response.

Calculated results are compared with experimental data.

Equivalent Control Circuit

When the a-c coils of the saturable reactor are connected in series, as shown in Figure 2, a change in the flux that links the control circuit will induce equal and opposite voltages in the two a-c coils, and these coils are therefore open circuited insofar as changes in the control circuit are concerned. The equivalent control circuit for this condition is shown in Figure 5(A) in which i_c represents the current in the control winding and ψ_e represents the flux linkage of this winding. The current in the control winding is here the only current that produces a d-c magnetomotive force, and so it is equivalent to the magnetizing current I_m of Figure 1.

When the a-c coils of the reactor are connected in parallel, they form a short-circuited coil around the control winding.[7] The resulting equivalent circuit, as obtained from the well-known coupled-circuit theory, is shown in Figure 5(B). In this circuit, R_{ac} represents the resistance of the series path through the two a-c coils, N_{ac} represents the number of turns on one a-c coil, and N_{dc} represents the number of turns on the d-c control winding (if the reactor is built with two separate cores, N_{dc} represents the number of control-winding turns on one core). The current i_m represents the magnetizing current that supplies the flux ψ_e, and i_i represents the effect of the current induced in the a-c coils. As before, i_c is the current in the control winding, but this now is equal to the sum of i_m and i_i.

Figure 5(C) shows the equivalent circuit for parallel-connected a-c coils, reduced to a more convenient form by Thévenin's theorem. The time lag introduced by the leakage fluxes is generally much smaller than that caused by the main control flux, ψ_e, and so, for simplicity, the leakage inductances have been neglected in the last diagram. The effective resistance for transient changes in i_m is the parallel combination of R_c and R_{ac}'.

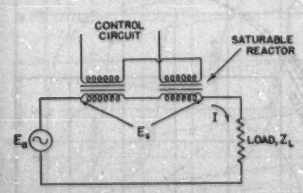

Figure 2. Saturable reactor connected in series with a load impedance

Control-Circuit Flux Linkage

The transients caused by changes in the system will depend on the relation between the control-winding flux linkage, ψ_e, and the magnetizing current i_m. The main time lag is caused by the slowness of change of the flux that links the control winding, and so we shall assume that the steady-state load line is followed during transient conditions. The flux linkages of the control winding, as computed by the method of reference 1, are shown as dashed curves in Figure 1. By following along the load line, one can plot the relation between the magnetizing current and the flux linkage of the control circuit. This plot is shown in Figure 6 for the load line of Figure 1.

In using the universal curves of reference 1, it should be observed that the quantity plotted there is the d-c flux linkage of one a-c coil. This quantity must be multipled by two (because of the two a-c coils) and further multiplied by the turns ratio N_{dc}/N_{ac} to obtain ψ_e.

The foregoing graph of ψ_e versus i_m was drawn for a given load line. If a transient is caused by a sudden shift from one load line to another (change in applied voltage or in load impedance), the transition will take place along a line of constant ψ_e in Figure 1; this will determine the initial condition for the transient.

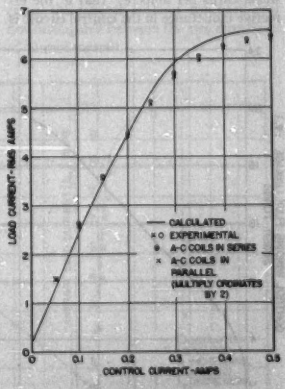

Figure 4. Load current versus control current along the load line of Figure 1

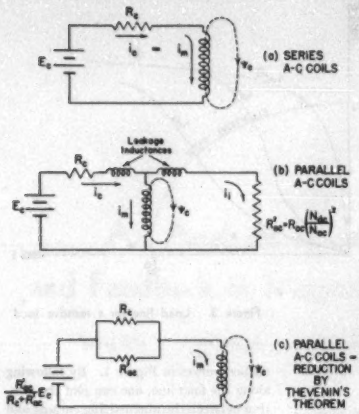

Figure 5 (left). Equivalent control circuits

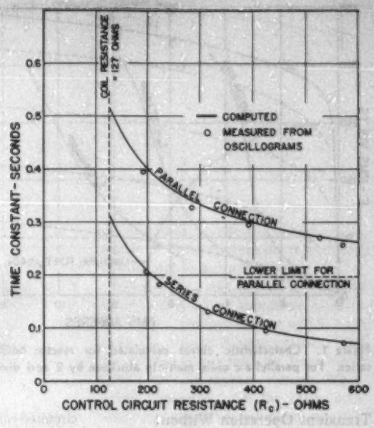

Figure 7 (right). Time constant of reactor 66G912 for small changes in the neighborhood of 0.200 ampere control current

Transient Response

If the changes that take place are small enough in magnitude so that they traverse only a substantially linear segment of the control-circuit magnetization curve, the transient will be nearly exponential and a time constant can be defined. The average slope of the magnetization curve between the two points in question, expressed in weber-turns per ampere, is the effective inductance of the control winding, L_c henrys. The effective time constant is then L_c/R henrys, where R is the effective resistance of the control circuit as obtained from the appropriate equivalent circuit of Figure 5. For example, at a current of 0.2 ampere in Figure 6, the slope of the graph is approximately 41 weber-turns per ampere; that is, the effective inductance in the control circuit is 41 henrys. The effective resistance in the control circuit then determines the time constant. It will be observed in Figure 5 that, with series a-c coils, the time constant can be decreased indefinitely by increasing the resistance of the control circuit, R_c. But, with the a-c coils in parallel, the effective resistance for the transient is composed of R_c in parallel with R_{ac}', and so there is a lower limit for the time constant which is determined by R_{ac}'. This is illustrated in Figure 7, which shows calculated and experimental time constants for reactor *66G912* for small changes in the neighborhood of 0.2 ampere control current. As observed before, the effective inductance here is 41 henrys. The value of R_{ac}' was 209 ohms, and the resistance of the control winding itself was 127 ohms.

When the change in control current is so large that it involves considerable curvature in the characteristics, the transient will not be exponential and the concept of

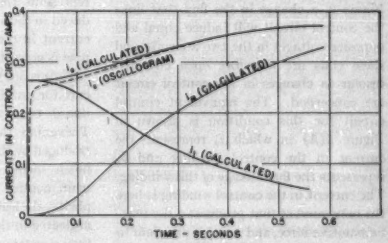

Figure 6 (left). Control-winding magnetization curve for the load path of Figure 1

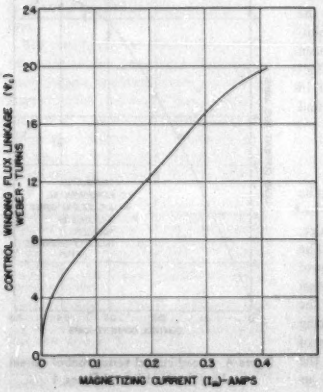

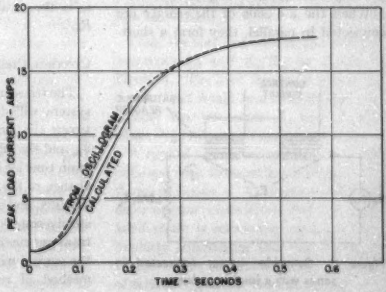

Figure 8 (right). Comparison between calculated and test results: reactor 66G912 with a-c coils in parallel, full control voltage applied abruptly

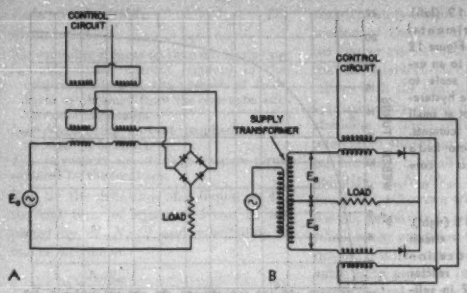

Figure 9 (above). Magnetic amplifiers with feedback

(A) External feedback; (B) One type of self feedback

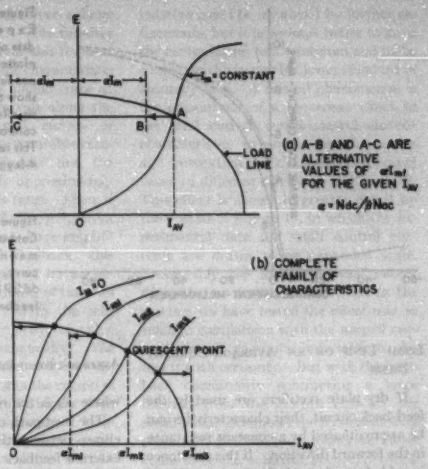

Figure 11 (right). Graphical construction for determining control current with feedback

a time constant loses much of its usefulness. In spite of this, it may sometimes be useful to estimate a mean value for the inductance and compute an approximate time constant. If more accurate results are desired, they can be obtained with a step-by-step integration of the magnetizing-current transient. A suitable graphical method is given in the Appendix. The results of a typical calculation, using this method, are shown in Figure 8 for parallel-connected coils. The magnetizing current was first determined as a function of time, then the load currents corresponding to various values of the magnetizing current were read from the load line of Figure 1. The load current was plotted in terms of peak values to facilitate comparison with an oscillogram. As shown by the equivalent circuit of Figure 5(B), the control-winding current is equal to the magnetizing current plus the induced current i_i. The latter can be found from the equivalent circuit when i_m is known as a function of time. The graph of actual control current in Figure 8 is rounded off slightly at the beginning. This is caused by the leakage inductance which was neglected in the calculations. The comparison between computed and experimental results in Figure 8 is typical of the many measurements that have been made.

Steady-State Operation With Feedback

Feedback circuits for the magnetic amplifier exist in great variety. Basically, the a-c load current is rectified and is applied to the magnetic core in such a way as to aid the saturation that is produced by the control current; in this way, the steady-state amplification can be increased to the point of instability. Figure 9(A) shows a magnetic amplifier with "external" feedback; that is, the feedback winding is separate from the load-current winding. Other magnetic amplifiers use "self" feedback, in which one set of windings serve as both load-current and feed-back windings. One of these circuits is shown in Figure 9(B). Since it is the average value of the rectified load current that is effective in feedback, the subsequent discussion will be based on the average-current characteristic curves of the saturable reactor. A set of average-current curves for reactor *66G912*, as computed by the methods of reference 1, are shown in Figure 10. The values of I_m on the curves are shown with ± signs because the reactor without feedback can not distinguish between the two directions of control current.

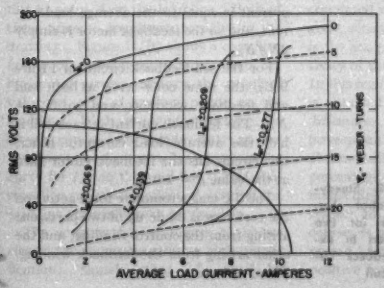

Figure 10 (left). Characteristic curves for reactor 66G912 on an average - current basis (a-c coils in parallel)

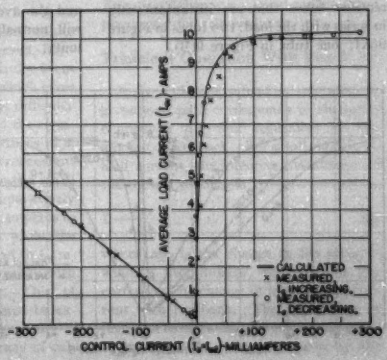

Figure 12 (right). Steady-state control characteristic for reactor 66G912 in self-feedback circuit

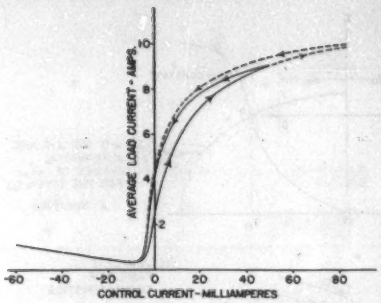

Figure 13 (left). Experimental data of Figure 12 plotted to an expanded scale to show the hysteresis effect at small control currents. This reactor had a 4-legged core

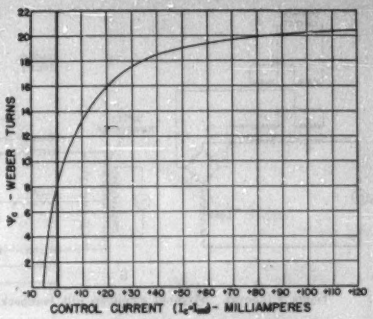

Figure 15 (right). Control - circuit magnetization curve; reactor 66G912 in self-feedback circuit

Load Line on an Average-Current Basis

If dry-plate rectifiers are used in the feed-back circuit, their characteristics can be approximated by a constant resistance in the forward direction. If this resistance is added to that of the load itself, the intercepts of the load line can be found as for the rms-current case, Figure 3, except that the intercept on the current axis is replaced by

$$\frac{E_a}{1.11\ R_L} \text{ average amperes}$$

where R_L is the apparent load resistance including the forward resistance of the rectifiers.

When gas-tube rectifiers are used, the voltage drop across each tube is nearly constant during conduction, and this introduces a further non-linearity into the analysis. Reasonable results are obtained by determining the intercepts of the load line as follows

$$\text{Voltage intercept} = E_a - V_t \qquad (2)$$

where V_t is the tube drop through the rectifier tubes that are instantaneously in series with the load: two tubes in Figure 9(A); one tube in Figure 9(B).

$$\text{Average-current intercept} = \frac{E_a/1.11 - V_t}{R_L} \qquad (3)$$

where R_L is the resistance of the load.

The load path can then be drawn as an ellipse between these intercepts. In the external-feedback circuit of Figure 9(A) the a-c coils can be connected either in series, as shown, or in parallel. The load line is then drawn on the appropriate characteristic curves. In the self-feedback circuit of Figure 9(B), the appropriate average-current curves are essentially the same as those of the parallel-connected reactor. Note, however, that there is no path for an induced circulating transient current, and so the equivalent circuit of Figure 5(A) is applicable for transients.

Effect of Feedback on Control Current

The effect of feedback will be expressed in terms of a feedback factor, β, which will be based on the magnetizing ampere turns that act on one core of a 2-core unit, or on one a-c flux path of a 3- or 4-legged single-core unit. It will be defined as the ratio between the d-c feedback ampere turns and the average a-c ampere turns, and will normally range between zero and unity.

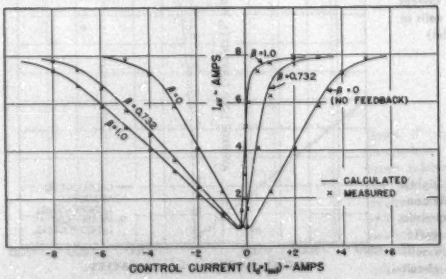

Figure 14. Steady-state control characteristics for two transformers in external-feedback circuit

It will be convenient to base the formula for β on the total number of a-c turns in series between the a-c terminals of the complete reactor N_{ac}. This will be equal to twice the number of turns on one a-c coil for the series coil connection, and will be equal to the number of turns on one coil for the parallel connection.

If the a-c coils are connected in series, the number of a-c turns on one core will be $N_{ac}/2$. On the other hand, with a parallel connection, only half the average load current will flow through each coil. Hence, for either connection, the feedback factor can be written as

$$\beta = 2\frac{N_f I_f}{I_{av} N_{ac}} \qquad (4)$$

where

I_{av} = average value of the load current
I_f = d-c current through the feedback winding
N_f = number of turns on the feedback winding.

When two separate cores with separate magnetizing windings are used, the number of turns for either the control winding or the feedback winding should be counted on one core only, for two separate series coils could be replaced by one coil surrounding both cores.

With an external feedback circuit such as that of Figure 9(A), the d-c feedback current is equal to the average load current, and so the feedback factor is simply $2N_f/N_{ac}$.

For the self-feedback circuit of Figure 9(B), the same coils serve as both load and feedback windings, and so $N_{ac} = N_f$. The feedback current in each coil is half the average load current; hence, this circuit has the feedback factor fixed at the value $\beta = 1.0$.

The d-c magnetomotive force acting on the core now is made up of two parts, one arising from the control winding, and the other arising from the feedback winding. Thus, we have

$$N_{dc}I_m = N_{dc}I_{mf} + N_fI_f, \tag{5}$$

where

N_{dc} = number of turns on the control winding

I_m = magnetizing current required in the control winding in the absence of feedback, as obtained from the characteristic curves of the reactor

I_{mf} = magnetizing current required in the presence of feedback

N_fI_f represents the average ampere-turns supplied by the feedback

But, by the definition of β (equation 4), the last term of equation 5 can be replaced by $\beta I_{av}N_{ac}/2$, and so equation 5 can be written as

$$I_{mf} = I_m - \beta\frac{I_{av}N_{ac}}{2N_{dc}} \tag{6}$$

This equation can be used to compute the control current required to produce any given value of I_{av} along the load line. It was noted that the reactor without feedback cannot distinguish between the two directions of control current, and that the values of I_m assigned to the curves of Figure 10 can therefore be taken to be either positive or negative currents. For a given value of I_{av}, this produces two different values of I_{mf} from equation 6. The positive value of I_m corresponds to positive feedback; the negative value to negative feedback.

The variation of control current along any given load line, and the effect of different load lines, can be visualized by the method shown in Figure 11. Equation 6 can be written in the form

$$\alpha I_{mf} = \alpha I_m - I_{av} \tag{7}$$

where $\alpha = 2N_{dc}/\beta N_{ac}$. Figure 11(A) shows one of the characteristic curves of the reactor for a constant value of I_m. The intersection of this curve with the load line (point A) determines a value of I_{av} as shown. To find the corresponding value of control current, two lines are drawn on opposite sides of the vertical axis, each located αI_m units away as measured on the horizontal current scale. Then, as shown by equation 7, either of the lines A-B or A-C represents a value of αI_{mf} that will produce steady-state operation at point A on the load line. Both of these currents are shown negative in the drawing. Figure 11(B) shows a complete family of characteristic curves, and the horizontal arrows indicate the required values of αI_{mf} at various points on the load line. With zero control current, the circuit comes into steady state at the quiescent point where αI_m intersects the curve for I_m on the load line. This construction makes the effect of varying the load line especially easy to visualize.

The construction of Figure 11 shows clearly the requirement for a high amplification: namely, that αI_m shall be approximately equal to I_{av} over a large portion of the load line. This requires the proper choice of α, and also requires that the intersections of the characteristic curves with the load line should come at approximately equal intervals along the abscissae. The universal curves of reference 1 show that, if a saturable reactor has only a small "air-gap" line, the quantity I_mN_{dc}/N_{ac} is approximately equal to $I_{av}/2$ over a wide range. Then, if $\beta = 1.0$, we have $\alpha I_m = 2I_mN_{dc}/\beta N_{ac} \approx I_{av}$, which is the condition for a large amplification. With external feedback, this value of β must be obtained by an accurate control over the number of turns on the feed-back winding. With the self-feedback circuit of Figure 9(B), the value $\beta = 1.0$ is obtained automatically. The amplification of the device will be very sensitive to the value of β in the region of 1.0,[8] and the values slightly higher than this will produce a double-valued load-current characteristic, which may be useful in some applications.

Experimental Results

Experimental results for the self-feedback circuit of Figure 9(B) are shown in Figure 12, together with the corresponding computed values. The computations were made by applying equation 6 to the characteristic curves and load line of Figure 10, using $\beta = 1.0$. For example, at $I_m = \doteq 0.277$ ampere, the corresponding value of I_{av} in Figure 10 is 8.80 amperes. With $\beta = 1.0$, $N_{ac} = 230$ turns for one a-c coil, and $N_{dc} = 4{,}000$ turns on the control winding, equation 6 becomes

$$\begin{aligned} I_{mf} &= \doteq 0.277 - 0.500 \times 8.80 \times \frac{230}{4{,}000} \\ &= \doteq 0.277 - 0.253 \\ &= 0.024 \text{ ampere or } -0.530 \text{ ampere} \end{aligned}$$

These values, together with the value $I_{av} = 8.80$ amperes, determine two points on the solid curve of Figure 12.

The calculated results shown in Figure 12 are seen to check the measured values quite well. It should be observed, however, that a computational difficulty is encountered when β has a value which gives great sensitivity, and that this difficulty is the analytical counterpart of the sensitivity of the device to small changes in β. In this region, the required control current is obtained from equation 6 as the small difference between two comparatively large quantities; one subtracts amperes to obtain milliamperes. Hence, while the percentage accuracy with respect to I_m remains high, the percentage accuracy with respect to I_{mf} becomes poorer. This, of course, is a difficulty which must be expected of devices with large amounts of positive feedback. The accuracy of calculation could be improved by further refinements, but it is perhaps better to keep the computation to a minimum and to be content with a somewhat lower standard of accuracy here. A related phenomenon is the appearance of a hysteresis effect in the load current versus control current characteristic, as shown by the circles and crosses that mark experimental points taken in different directions in Figure 12. This effect is shown in greater detail by the graphs of Figure 13, in which the experimental data for small control currents are drawn to an expanded scale. Presumably the hysteresis was present when there was no feedback, but in the reactors we have tested the effect was so small in comparison with the normal currents that it was quite impossible to detect it with certainty. But with the feedback consistently subtracting a large fraction from the control current, the small remainder shows the hysteresis loop prominently. The large hysteresis effect seems to be characteristic of cores in which there is a portion of the d-c flux path that is not traversed by a-c flux. The 4-legged core used in reactor *66G912* was of this type.

Experimental results for external feedback that compare directly with the previous curves can not be given, as the reactor *66G912* did not have the required additional winding. Figure 14 shows a comparison between calculated and experimental results for a magnetic amplifier made up of two transformers. The feed-back winding was tapped, which made possible the use of several different values of β, and the graphs show the results for $\beta = 0$, 0.732, and 1.00. The computed curves were obtained by determining a set of characteristic curves similar to those of Figure 10, and then drawing a load line corresponding to the applied voltage and the load resistance. Equation 6 then was applied as illustrated previously for self feedback.

Transient Operation With Feedback

A given change in load current along a given load path corresponds to the same change in d-c flux regardless of the amount of feedback. For small changes in load current, the effective inductance of the control winding is

$$L = \frac{\Delta\psi_c}{\Delta i_{mf}} \tag{8}$$

where $\Delta\psi_c$ is the change in the control-winding flux linkage, and Δi_{mf} is the corresponding change in magnetizing current with feedback. The application of feedback reduces Δi_{mf} for a given $\Delta\psi_c$, and so increases the inductance seen by the

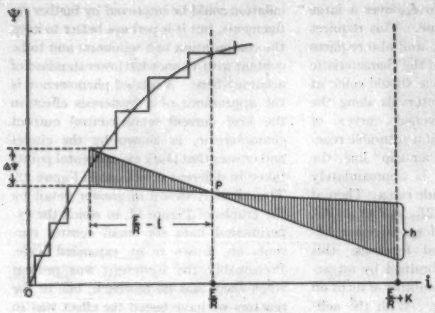

Figure 16. Graphical construction for a single step

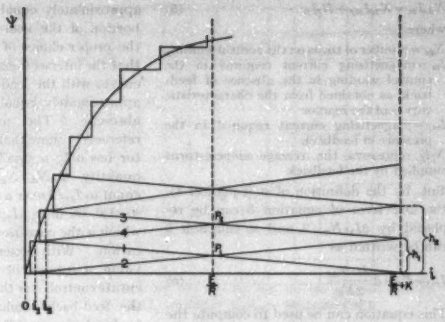

Figure 17. Sequence of graphical constructions

control circuit. If the same resistance is maintained in the control circuit after feedback is applied, the time constant L/R_c will be increased proportionately to the amount that the sensitivity of the amplifier is increased. To keep the time constant the same after feedback is introduced, the control-circuit resistance must be increased. The effect can be shown as follows

$$\text{Time constant: } t_c = \frac{L}{R_c} = \frac{\Delta\psi_c}{R_c \Delta i_{mf}} = \frac{\Delta\psi_c}{\Delta e_c} \quad (9)$$

For small changes along any given part of the load path, the time constant varies inversely with the required increment in control-circuit voltage, Δe_c. If R_c is increased in the same proportion as Δi_{mf} is reduced, both Δe_c and the time constant will remain constant. The sensitivity to changes in control current now is greater than without feedback, but the sensitivity to changes in control voltage is the same as before.

Analysis

The computation of transients in the feedback amplifier follows the same principles outlined earlier for the magnetic amplifier without feedback. The main difference is that the feedback changes the control current for a given control-winding flux linkage so that Figure 6 no longer applies. A graph of flux linkage versus control current is given in Figure 15 for reactor *66G912* operating in a self-feedback circuit. This graph is obtained by reading the flux linkage at various points on the load line of Figure 10, and then referring to Figure 12 to find the corresponding control-winding currents.

The time constant for small changes can be found as described for the reactor without feedback. An equivalent inductance is first found for the control winding, by determining the slope of the flux-linkage graph in weber-turns per ampere. For example, for a change in control current from zero to 9 milliamperes, the flux linkage in Figure 15 changes almost linearly from 8.2 to 12.9 weber-turns. The mean inductance here is approximately

$$L \approx \frac{\Delta\psi_c}{\Delta i_{mf}} = \frac{12.9-8.2}{9\times10^{-3}} \approx 520 \text{ henrys}$$

It is important to realize that, because of the inherently smaller accuracy in computing control currents for large amounts of feedback, and because of the uncertainty introduced by the hysteresis effect, the foregoing calculation has a lower accuracy than the corresponding one without feedback. The time constant is observed experimentally to depend to some extent on the direction of change of the current and on the direction and magnitude of previously existing control currents, as would be expected from the hysteresis loops of Figure 13. Using the foregoing calculated value of inductance, a resistance of 139 ohms in the control circuit would produce a time constant of $L/R_c = 520/139 \approx 3.7$ seconds in the region between zero and 9 milliamperes control current. An oscillogram of a transient between these two points showed an approximately exponential variation which had a time constant of about 3.3 seconds. This result, with the calculated value 12 per cent higher than the measured value, is typical of the time constants that have been checked. The error has generally been of the order of 10 to 15 per cent, with the calculated result being high. It should be emphasized that the foregoing results were computed by starting with the a-c saturation curve of the core, and that no experimental corrections were used at any stage of the calculations.

Table I

Control Current, Amperes	Time Constant, Seconds Calculated	Measured
Zero (rising)	2.1	1.9
0.25 (rising)	1.7	1.5
0.23 (falling)	1.7	1.5
0.50 (falling)	1.4	1.2

If desired, the path of a transient that spans a markedly nonlinear portion of the flux-versus-current graph can be computed graphically by the step-by-step method described in the Appendix. The main error here is caused by the uncertainty introduced into the initial condition by the hysteresis effect.

If a comparatively large control voltage is used to force the control current to change rapidly to a point well above the knee of the control-circuit magnetization curve, the $i_m R_c$ drop can be neglected during most of the change in flux, and the time required for the flux linkages to change an amount $\Delta\psi_c$ is only slightly greater than $\Delta\psi_c/E_c$, where E_c is the suddenly-applied control voltage. For example, reactor *66G912* connected in the self-feedback circuit was started at $\psi_c = 6$ weber-turns ($I_{av} = 0.8$ ampere), and an electromotive force of 47 volts was suddenly applied to the control winding. This was sufficient to produce a steady-state control current of 300 milliamperes, which is well above the knee of the curve of Figure 15; see also Figure 12. The final value of ψ_c is, from Figure 15, about 21 weber-turns ($I_{av} = 10.2$ amperes). Therefore, the approximate time of rise is $\Delta\psi_c/E_c = (21-6)/47 = 0.32$ second. An oscillogram showed that the load current rose almost linearly to 10 amperes in 0.31 second.

Calculations similar to the foregoing

ones also have been made for the external-feedback circuit whose steady-state control curves are given in Figure 14. A typical comparison between computed and measured time constants for a feedback factor of 0.732 is given in Table I. These experimental data were obtained by applying a control-circuit voltage of moderate size and measuring on an oscillogram the instantaneous values of di/dt at various instantaneous control currents.

Appendix. Graphical Computation of Nonlinear Transient

A graphical method now will be described for the step-by-step integration of a nonlinear differential equation of the form

$$\frac{d\psi}{dt}+Ri=E \tag{10}$$

where ψ is a nonlinear function of i. Expressed approximately in terms of finite differences, equation 10 is

$$\frac{\Delta\psi}{\Delta t}+Ri=E \tag{11}$$

This equation can be rewritten in the form

$$\frac{\Delta\psi}{E/R-i}=R\Delta t \tag{12}$$

Now consider Figure 16, which shows a graph of the function $\psi(i)$. A vertical line is erected on the i-axis at the value E/R, and a second vertical line is erected at the value $E/R+K$, where K is any convenient number, either positive or negative. (For a current rising from zero to the value E/R, a convenient value of K is E/R. For a current dropping toward zero, a convenient value of K is the negative of the initial value of the current.) Imagine that the graph of ψ versus i is made up of small steps, as shown in the figure. Consider the step whose vertical height is labeled $\Delta\psi$, and the point P which is located anywhere on the vertical line that was erected at $i=E/R$. A straight line is drawn from the top of the step through the point P, and is extended to the second vertical line. A second straight line is drawn from the bottom of the step through the point P, and is extended to the second vertical line. The two shaded triangles formed by this construction are similar, and so we have

$$\frac{\Delta\psi}{E/R-i}=\frac{h}{K} \tag{13}$$

where h is the height of the right-hand triangle measured on the ψ-scale. Comparison with equation 12 shows that the time required for the change $\Delta\psi$ is given by

$$\Delta t=\frac{h}{KR} \tag{14}$$

The location of the point P is immaterial, and so is the value of K except that it should lend itself conveniently to the scale of the drawing.

In order to determine the complete path of a transient, it is necessary to add the amounts of time for each step in the graph, starting with a known initial current. The addition can be done graphically as shown in Figure 17, which assumes for purposes of illustration that the current starts initially from zero. The construction lines are drawn in the sequence 1,2,3,4,... The first is drawn from the top of the first step so that it intersects the right-hand vertical line at zero on the ψ-scale. This establishes the point P_1, and the second construction line is drawn from the bottom of the first step through this point. The height h_1 determines the time required for the current to reach the value i_1 (see equation 14). The construction proceeds upward step by step, and, at any point, the net height h_k determines the time required to reach the corresponding current i_k: $t_k=h_k/KR$.

The foregoing method can be used for computing either increasing or decreasing transients, starting with any initial value. For increasing currents, the quantity $E/R-i$ in equation 13 will be positive, and K should be a positive quantity for convenience. For decreasing currents, $E/R,-i$ will be negative, and the construction is generally more convenient with K chosen as a negative quantity.

References

1. Universal Curves for D-C Controllable Reactors, Walter C. Johnson, B. C. Merrill, R. E. Alley, Jr. *AIEE Transactions*, volume 68, part I, 1949, pages 31–37.

2. The Transductor (D-C Pre-Saturated Reactor) (book), Uno Lamm. *Ersslie Ahlsbolag*, Stockholm, Sweden, 1943.

3. An Analysis of Interlinked Electric and Magnetic Networks with Application to Magnetic Amplifiers, D. W. Ver Planck, M. Fishman. *Proceedings*, Institute of Radio Engineers, volume 37, September 1949, pages 1021–27.

4. An Analysis of Magnetic Amplifiers with Feedback, D. W. Ver Planck, M. Fishman, D. C. Beaumariage. *Proceedings*, Institute of Radio Engineers, volume 37, August 1949, pp. 862–866.

5. Self Saturation in Magnetic Amplifiers, W. J. Dornhoefer. *AIEE Transactions*, volume 68, part II, 1949, pages 835–50.

6. An Experimental Verification of a Method of Calculating the Characteristics of Saturated Iron-Cored Reactors, Reuben E. Alley, Jr. Master of Science Thesis, Department of Electrical Engineering, Princeton University, June 1938.

7. Some Fundamentals of D-C Controlled Reactors with Resistive Load, H. F. Storm, *AIEE Transactions*, volume 68, part I, 1949, pages 188–94.

8. Effect of Core Material on Magnetic Amplifier Design, A. O. Black, Jr. Presented at the National Electronic Conference, Chicago, Ill., November 1948.

Discussion

L. A. Finzi (Carnegie Institute of Technology, Pittsburgh, Pa.): The analysis of the transient response of magnetic amplifiers with feedback presented in this paper implies that the coupling between signal windings and feedback windings is neglected. Actually changes of direct components of core fluxes, that follow any variations of the signal, induce in the feedback windings voltages which do not cancel, as is the case, for example, in series-connected a-c windings of simple amplifiers without feedback. For instance, in an amplifier with positive feedback a decrease of the signal induces in the feedback windings a voltage acting in the direction of rectifier conduction. Therefore, at least in some portions of the cycle, induced currents flow in the feedback windings and the transient response, according to Lenz's law, is delayed in a manner similar to the one observed in no-feedback amplifiers with parallel connected a-c windings. As a matter of fact, voltages induced in opposition to the direction of rectifier conduction, as they arise for instance for an increase of signal in amplifiers with positive feedback, also affect the transient response as they act against the flow of feedback currents that would be expected from simple steady-state considerations.

It is conceivable that these induced voltages in some instances may be small in comparison with the crest of the voltage impressed by the a-c source across the feedback rectifiers; then, of course, the simplifying assumption implied may be acceptable. On the other hand, however, the very nature of the feedback action, as recognized also by Johnson and Latson in their paper, is based on a very sensitive balance among ampere-turns of the various windings and simplifying assumptions concerning instantaneous values of currents in the feedback windings have to be weighed very carefully.

Walter C. Johnson and **Frank W. Latson**: As Mr. Finzi states, the signal and feedback windings are magnetically coupled, and a change in signal will induce a voltage in the feedback winding. The main question is the order of magnitude of this voltage as compared with the other voltages existing in the same circuit.

If the voltage across the control winding is suddenly changed an amount Δe_c, a voltage approximately equal to $N_f\Delta e_c/N_{ac}$ will be induced in the feedback winding, where N_f is the number of turns on the feedback winding and N_{ac} is the number of turns on the control winding. The voltage in the feedback circuit with which this should be compared will depend on whether or not the load impedance is included in the circuit in which this voltage acts. The magnitude of Δe_c itself will depend on whether the amplifier is used in a continuous-type control such as a servomechanism or whether it is used in an on-off type of application.

In the circuit of Figure 9(A), the rectifiers that are not conducting are biased off by a voltage that is equal to the normal voltage drop through the feedback winding plus the forward voltage drop in one rectifying element. A decrease in signal will induce a voltage in the feedback winding that is in the proper direction to produce a short-circuit current through two rectifier elements, but this path will be inoperative

unless the induced voltage exceeds the bias voltage across the nonconducting rectifier element. Otherwise, the voltage induced in the feedback winding acts in series with the load, and its effect in the circuit can be judged by comparing it with the applied electromotive force, E_a, or with the normal load voltage. An increase in signal results in an induced voltage that does not tend to produce a short-circuit current through the rectifiers, and which therefore always acts in series with the load. For the circuit of Figure 9(B) or for a circuit similar to that of Figure 9(A) but with the load directly in series with the feedback winding, there is no potential short-circuit path for either direction of signal change, and the induced voltage acts in series with the main applied electromotive force.

Therefore, the voltage induced in the feedback winding should be compared with two other voltages. The first comparison will be with the normal voltage existing across the feedback winding, to determine whether short-circuit conduction is likely to occur for decreasing signals in the circuit of Figure 9(A). The second comparison will be with either the applied electromotive force or the normal load voltage to determine the effect of the induced electromotive force in the absence of a short-circuit path.

The ratio of the induced voltage in the feedback winding to the normal voltage drop through the winding can be written as

$$\frac{\text{Induced voltage}}{\text{IR drop}} = \frac{\Delta i_c N_f}{I_L R_f N_{dc}} = \frac{\Delta i_c R_c N_f}{I_L R_f N_{dc}} \qquad (1)$$

where Δi_c is the eventual change in control-winding current, R_c is the resistance of the control circuit, I_L is the average load current, and R_f is the resistance of the feedback winding. If we assume that the load and feedback windings operate at the same current density and have approximately the same mean length of turn, we have very nearly $R_f \approx R_{ac} N_f / N_{ac}$. Also, if the control and load windings occupy approximately the same amount of space, we shall have very nearly $k R_c / N_{dc}^2 \approx R_{ac} / N_{ac}^2$, where k is the fraction of the control-circuit resistance that is contained in the control winding itself. Making these substitutions into the foregoing ratio, we find its order of magnitude to be

$$\frac{\text{Induced voltage}}{\text{IR drop}} \approx \frac{\Delta i_c N_{dc}}{k I_L N_{ac}} \qquad (2)$$

In a magnetic amplifier with positive feedback, the ampere-turn ratio $\Delta i_c N_{dc} / I_L N_{ac}$ will be very much less than unity. Unless the fraction k is made very small by the use of an extremely large "forcing" resistor, the foregoing ratio will be small. This indicates that short-circuit conduction through the rectifiers of Figure 9(A) is likely to occur only for very short intervals during the cycle, and then only in the case of decreasing signals of large magnitude.

Generally, then, the voltage induced in the feedback winding will be forced to act in series with the load, and its effect can be judged by comparison with the normal load voltage. To obtain the ratio of the induced voltage to the normal load voltage, we multiply the ratio (2) by R_f / R_L. Using the former approximation $R_f \approx R_{ac} N_f / N_{ac}$, we obtain

$$\frac{\text{Induced voltage}}{\text{Load voltage}} \approx \frac{1}{k}\left(\frac{\Delta i_c N_{dc}}{I_L N_{ac}}\right)\left(\frac{R_{ac}}{R_L}\right)\left(\frac{N_f}{N_{ac}}\right) \qquad (3)$$

As was observed previously, the ampere-turn ratio is generally much smaller than unity.

The third factor, R_{ac}/R_L, is the per-unit resistance of the load winding, and is a very small fraction. The last factor, N_f/N_{ac}, will rarely exceed unity. Hence, the ratio will almost always be a very small quantity indeed, and the effect of the induced voltage will be inappreciable.

To take a specific example with some moderately unfavorable data: consider the reactor *66G912*, which was used in some of the experiments described in the paper. As shown in Figure 12, a load current of 9 amperes is produced by a control-winding current of approximately 30 milliamperes. The resistance of the control winding itself was 127 ohms. Assuming an external forcing resistance of 373 ohms, the total control-circuit resistance would be 500 ohms. The required control-circuit electromotive force for this condition would be $0.030 \times 500 = 15$ volts. Assuming that the amplifier is initially in a quiescent condition and that this voltage is applied suddenly in the control circuit, and using the values $N_{ac} = 230$, $N_c = 4{,}000$, we compute the induced voltage in the feedback winding to be

$$15 \times 230/4{,}000 = 0.86 \text{ volt}$$

The value of the peak of the impressed electromotive force here is about 162 volts, which is nearly 200 times a s large. A smaller external resistance in the control circuit, or a smaller change in control voltage, will produce a correspondingly larger ratio.

The conclusion is that the voltage induced in the feedback winding by changes in the signal voltage will not generally be a factor of major importance.

A Magnetic Amplifier Frequency Control

L. J. JOHNSON
ASSOCIATE AIEE

H. G. SCHAFER
NONMEMBER AIEE

Synopsis: A frequency control system utilizing a magnetic amplifier is described. The frequency control is applied to a dynamotor where the accuracy must be ±0.1 per cent over a range of temperature, input voltage, and load. A qualitative description of the system is given, along with performance data gathered from tests on a prototype model.

FOR the operation of certain types of equipment aboard ship, an accurate source of frequency-regulated alternating current is required. This need has been met by the use of small motor-driven alternators or dynamotors of 1-kva capacity or less. These alternators run on the ship's d-c power supply, and frequency control is accomplished usually by a frequency-sensing device and a servomechanism, which, in turn, control the motor field current and the frequency.

Electromechanical control systems have some disadvantages, the most important of which are vacuum-tube amplifiers and moving mechanical parts. These systems also are slow in response and sensitive to shock and vibration.

In order to overcome the limitations of existing frequency regulating devices, the magnetic-amplifier type regulator described herein was developed. This new regulator system has no moving parts, is extremely accurate in performance, and is not affected by shock and vibration.

Description

General—A magnetic amplifier frequency control is shown in the schematic diagram of Figure 1. The system consists of the following components:

A. A dynamotor for d-c to a-c conversion. (In this particular system, the dynamotor output rating is 80 volt-amperes at 115 volts and 60 cycles. The d-c voltage supply is 115 volts.)

B. A small permanent magnet a-c pilot generator attached to the dynamotor shaft.

C and *D*. A pair of series resonant circuits with bridge rectifiers.

E. A magnetic amplifier, consisting of two toroidal reactors and two self-saturation rectifiers.

F. A control field rectifier.

Operation

In operation, two series resonant circuits (*C* and *D*) are excited by the output of a pilot generator (*B*), and supply rectified control currents to the magnetic amplifier (*E*). The magnetic amplifier controls the current flow to the control field rectifier (*F*), which, in turn, supplies rectified current to the control field of the dynamotor.

The circuit components (*A* to *F*) in Figure 1 comprise a closed servomechanism loop. In addition to the principal circuit components, an electrical damping circuit is utilized, and consists of capacitor C_1, and two auxiliary windings on the magnetic amplifier cores. The purpose of the damping circuit is to achieve high stability together with high sensitivity.

Two frequency-sensing circuits, shown at (*C*) and (*D*) in Figure 1 are used to maintain the system at constant frequency. These circuits are tuned above and below the 240-cycle pilot generator frequency as shown in Figure 2.

The system operates at the cross-over point of the two resonance curves, and this point is accurately maintained by the use of temperature-stable circuit components. The use of a 240-cycle pilot generator and corresponding resonant circuits for frequency sensing has two important advantages, namely:

1. The size of the resonant circuit com-

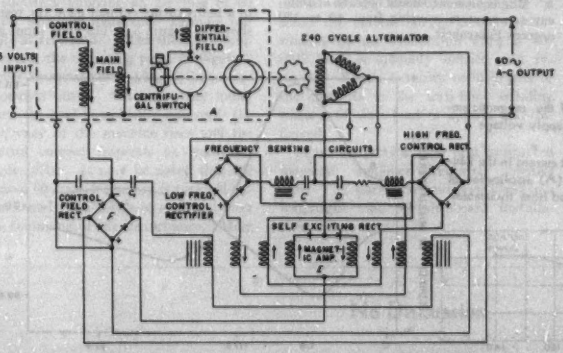

Figure 1. Schematic diagram of a magnetic-amplifier frequency control unit

Paper 50-95, recommended by the AIEE Electronics Committee and approved by the AIEE Technical Program Committee for presentation at the AIEE Winter General Meeting, New York, N. Y., January 30–February 3, 1950. Manuscript submitted November 2, 1949; made available for printing December 13, 1949.

L. J. JOHNSON and H. G. SCHAFER are both with the Naval Research Laboratory, Washington, D. C.

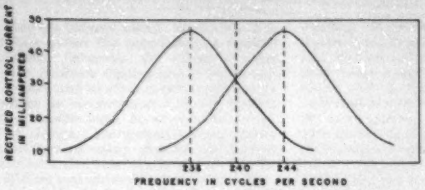

Figure 2. Resonance curves of the frequency-sensing circuit, showing crossover at 240 cycles

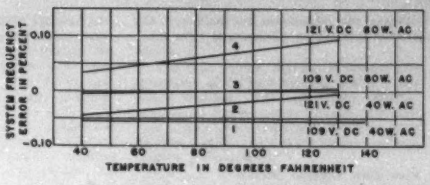

Figure 4. Temperature characteristics of the magnetic amplifier and dynamotor at various temperatures, loads, and supply voltages

ponents can be made smaller than those required for 60 cycles.

2. The frequency-sensing circuits are independent of the voltage regulation of the main alternator.

The type of core material used in the resonant circuit inductors has an important effect on the stability of the system. The most stable reactors were wound on Permalloy dust toroidal cores, known as *Mu-125* material. The capacitors used were of a high grade mica type having a small temperature coefficient.

The Magnetic Amplifier

Referring to Figure 1, the magnetic amplifier component, E, of the system is seen to consist of two saturable reactors, each of which has one power winding, two control windings, a damping winding, and two half-wave selenium rectifiers for self-saturation.

The directions of the magnetic fluxes are as indicated by the arrows on the diagram. When the outputs of the two frequency-sensing rectifiers are equal (at a dynamotor frequency of exactly 60 cycles) the ampere-turns in the control windings are equal and opposite. Any disturbance of the ampere-turn balance in the control windings due to a change in frequency will cause the reactance of the magnetic amplifier to increase or decrease as a function of the net control currents delivered by the sensing circuits. The magnetic amplifier reactors in turn regulate the current to the control field coils of the dynamotor in such manner as to restore the frequency to normal value.

The Anti-Hunt Circuit

The anti-hunt or transient-feedback circuit (damping winding), shown in Figure 1, consists of a large capacitor C_1 and a winding on each of the saturable reactors of the magnetic amplifier. This anti-hunt circuit is connected in parallel with the control field winding and produces a magnetomotive force in the magnetic amplifier which is a function of the rate of change of voltage across the rectifier. This additional magnetomotive force acts in a direction to stabilize the frequency of the system.

Design Requirements

The operating requirements for this regulated a-c power supply dictated the following specification limits:

1. A magnetic amplifier control having no moving parts should be ultimate objective.

2. The control system should maintain a constant frequency within ±0.1 per cent, with a load variation of 100 per cent, and an input voltage variation of ±5 per cent.

3. The equipment should operate at ambient temperature varying from 40 to 130 degrees Fahrenheit.

4. Because of the small size of the machine to be regulated, the efficiency of the regulator system should be kept high.

5. In order to keep the power rating of the amplifier at a low value the shunt field of the dynamotor should be designed to incorporate a separate control field in conjunction with a fixed shunt field. By this means, the control field power only would be regulated by the magnetic amplifier. As a means to reduce further the burden on the control field and the amplifier, the dynamotor should be designed to incorporate a differentially compound winding to give good speed regulation without external control. The frequency control need then be only large enough to compensate for the deficiency of the differentially compounded motor as a constant speed device. A centrifugal switch was used to by-pass the differential field during the starting period.

Performance Results

A detailed description of the design procedure for each of the components involved in this control system is beyond the scope of this paper. It is believed, however, that the evaluation data shown in Figures 3 and 4 will be an indication of the kind of results to be expected from this and similar systems.

Temperature Stability

A test on the complete system enclosed in a temperature cabinet gave the results shown in Figure 3 at 115 volts input and

Figure 3 (below). Temperature characteristic of the magnetic amplifier and dynamotor at normal load and supply voltage

Figure 5 (right). Oscillogram of rectified transient current in the 244-cycle frequency-sensing circuit, resulting from (A) application of a 60-watt a-c load, and (B) from removal of load from dynamotor

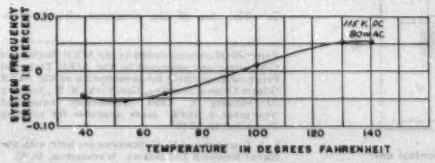

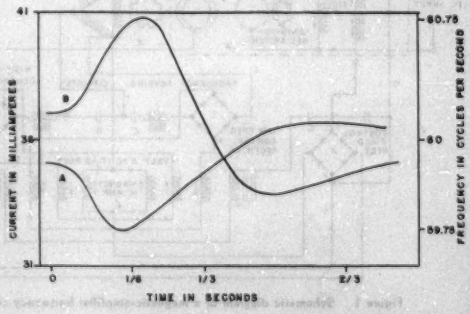

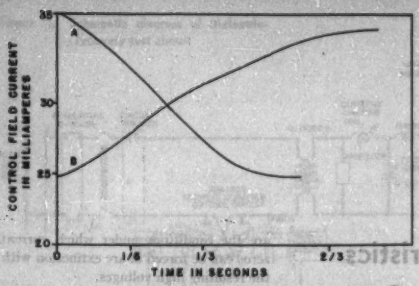

Figure 6 (above). Oscillogram of transient current in the dynamotor control field, (A) upon application of a 60-watt a-c load, and (B) upon removal of load from dynamotor

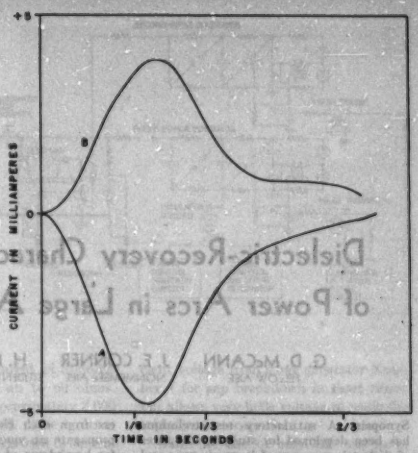

Figure 7 (right). Oscillogram of current in the damping circuit, (A) upon application of a 60-watt a-c load, and (B) upon removal of load from dynamotor

80 watts output. At other supply voltages, the frequency error is as shown in Figure 4. It may be noted that at no time did the error exceed 0.1 per cent, and at the more usually encountered ambient temperatures the frequency error was 0.05 per cent or less.

Transient Response

The effectiveness of the control in quickly restoring stable operation after an external disturbance to the system is shown in the oscillograms of Figures 5 to 7. The two oscillograms in this Figure 5 show the rectified control current in the higher frequency resonant circuit. Since this current is a function of frequency, it is used to indicate the transient departure from the normal frequency. In Figure 5(A) the oscillogram shows the effect of suddenly applying an a-c load of 60 watts with the dynamotor running initially at zero load. When there is a drop in speed, the operating point in Figure 2 moves downward on the higher frequency resonance curve. On the other hand, when the load is suddenly removed, the frequency of the machine rises and the control current responds as shown in Figure 5(B). It may be noted that the normal 60-cycle frequency is restored approximately two-thirds of a second after the beginning of the disturbance. Most of this time delay can be attributed to the inertia of the dynamotor. Figure 6 shows the current surges in the control winding of the dynamotor when a 60-watt load is suddenly applied and removed. Figure 7 shows oscillograms of the currents in the anti-hunt winding when a 60-watt load is applied and removed.

Figure 8. Assembled magnetic-amplifier frequency-control unit and dynamotor

Figure 8 shows a view of a completed magnetic amplifier frequency control unit. This particular unit is enclosed in a watertight case for shipboard installation.

Conclusion

An example of a successful magnetic amplifier design has been given in this paper.

The system described is believed to be smaller, lighter, and more effective than other frequency controls designed for the same purpose. At normal temperatures the system gives frequency regulation of the order of one part in 5,000 or better. This accuracy of performance is achieved without the aid of a tuning fork or quartz crystal.

No Discussion

Dielectric-Recovery Characteristics of Power Arcs in Large Air Gaps

G. D. McCANN
FELLOW AIEE

J. E. CONNER
NONMEMBER AIEE

H. M. ELLIS
STUDENT MEMBER AIEE

Synopsis: A satisfactory test technique has been developed for studying the rates of dielectric recovery of large air gaps and other types of power-system insulation. This permits the accurate control of the fault conditions so that all practical types of fault currents can be studied. These are: (1) very high magnitude short-duration surges typical of lightning currents; (2) currents of power-system frequencies; and (3) intermediate duration currents such as those which might result from high-frequency current zeros produced by natural system oscillations.

Results are presented showing the rate of dielectric recovery of 3-, 6-, and 11-inch standard rod gaps for power frequency fault currents up to 700 amperes. Electrode cooling effects were found important at 3-inch gap spacings but not at six inches or above. The 11-inch gap data are proportionately higher than the 6-inch data, indicating that the results can be extrapolated. The data show that for arcs of a few cycles actual duration has little effect on rate of recovery. A range of current magnitudes from 50 to 700 amperes causes only about a 2-to-1 variation in rate of recovery. For the normal ratios of transmission-line insulation level to operating voltage (about four to one) minimum delay times of from 0.025 second for 100-ampere faults to 0.05 second for 700 ampere faults are required before the recovery voltage reaches the magnitude of the normal applied voltage. Time intervals of 0.05 to 0.08 second are required before the voltage strength has built up to twice this level or one-half the initial gap strength. This is contrasted with a corresponding time interval of only 2- to 3,000-microseconds for very short duration lightning-surge currents.

High-speed camera studies of the arcs show that for power-frequency faults of one-half to one-cycle duration, visible luminous gases are present in the gap space for times after current zero up to 0.07 or 0.08 second. The illustrations and voltage breakdown curves show that subsequent breakdowns will occur through the region of brightest photographic luminescence if such still exists in the gap space. Under these conditions breakdown is started by initial streamers from each electrode which, however, propagate at much slower velocities than for breakdown of air under normal conditions. Time intervals as high as 30 or 40 microseconds are required for a low-impedance path to be established.

This research program is being extended to other insulating media and fault conditions and fundamental studies are being made of the dielectric-recovery mechanism.

KNOWLEDGE of the dielectric-recovery characteristics of power-system insulation following flashover or breakdown is of fundamental importance in determining and improving power-system performance. However, relatively little fundamental data have been obtained because of the complexity of the phenomena and the difficulty of performing significant tests on representative insulation media. The bulk of the data that have been gathered apply only to the circuit breaker arc or to small gaps where electrode effects dominate.

Studies of the primary insulations are important in determining probabilities of insulation failure resulting in sustained faults, permissible reclosing times for circuit breakers, and the performance of disconnect switches. A study of the performance of simultaneous arcs through similar and dissimilar insulating media and at various distances apart on systems is required for better co-ordination of such protective devices as deion protector tubes. Dielectric-recovery studies are also of great importance in determining the characteristics of system transients during such faults as arcing grounds. The conditions under which arc extinction and reignition occur determine the characteristics and magnitudes of the resulting system transient voltages. Of particular importance in this connection are the conditions under which current zeros can be forced in arc extinction with the resulting high voltages.

Recognizing this to be a general field of considerable importance at the present time, a co-operative research program on dielectric recovery has been instigated at the High Voltage Laboratory of the California Institute of Technology. This program is being sponsored by the Department of Water and Power of the City of Los Angeles, the Kelman Electric and Manufacturing Company, and the Southern California Edison Company. The first phase of this program, discussed in this paper, deals with air insulation at normal atmospheric conditions. This medium was chosen first since it is the most fundamental one of the practical insulations and is subject to the least number of controlling factors. A limited amount of data had been obtained elsewhere on large air gaps[1,2] by artificially producing faults and determining system conditions under which reignition did or did not occur. Also safe circuit-reclosing times have been determined from staged tests under a limited range of conditions.[3,4] Such techniques, however, permit a very limited variation in the important parameters and require so long that either insufficient data are obtained or important variations have occurred in the conditions during the period of the test. Also many such staged tests are performed by closing in on an artificially produced or fused fault. Accurate timing of the start of the fault current thus is not obtained, and vaporized metal may be produced in the gap by the fused element.

A testing technique has been developed

Paper 50-96, recommended by the AIEE Transmission and Distribution Committee and approved by the AIEE Technical Program Committee for presentation at the AIEE Winter General Meeting, New York, N. Y., January 30–February 3, 1950. Manuscript submitted November 2, 1949; made available for printing December 2, 1949.

G. D. McCANN, J. E. CONNER, and H. M. ELLIS are all of the California Institute of Technology, Pasadena, Calif.

The authors wish to acknowledge the valuable assistance rendered by B. N. Locanthi in the development of the electronic equipment, Sol Matt and L. H. Tejada in helping to obtain the test data, and A. T. Puder who helped with equipment construction.

Figure 1. Schematic diagram of dielectric-recovery test circuit

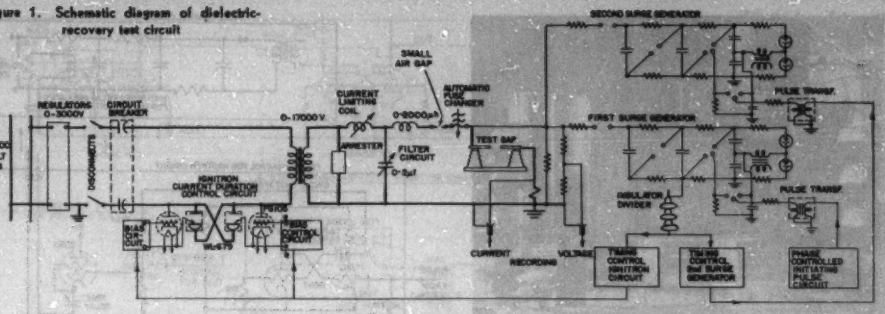

which overcomes these difficulties and is an extension of work performed earlier on lightning current faults.[5] The insulation medium is first broken down by a surge generator, the fault current allowed to flow a specified time and then shut off, after which the dielectric strength of the insulating medium is tested over a wide range of time delays with a second surge generator. By this means data for complete dielectric-recovery curves can be obtained for a wide range of fault-current magnitudes and durations. Because of the very flat breakdown characteristics of air insulation, particularly while still under the influence of a predischarge, such data are applicable to all practical types of system overvoltages. This technique permits the accumulation of a large mass of data so that effects of the various important parameters can be studied and quantitative correlations made with theoretical approaches to the problem.

Test Circuits and Techniques

The main test and auxiliary control circuits are of interest not only because they represent a new technique for studying dielectric-recovery phenomena, but also because of certain new control methods that are being applied to surge-generator testing. A general schematic diagram of the test circuit is shown in Figure 1. Figure 2 shows the main power circuit. This part of the test circuit is shown by heavy lines in Figure 1. Sixty-cycle power is supplied from a 17-kv bus through a single-phase induction regulator. This energizes a bank of four 150-kva 8.6- to 2.4-kv transformers which supply the actual test circuit. By various combinations of series or parallel connections a range of power currents and voltages can be supplied to the test gap. A further fine control of the fault current is obtained with the current-limiting inductor which can be varied in approximately one-ohm steps up to 60 ohms. Fault currents up to approximately 3,000 amperes can be obtained. The ignitron circuit shown in Figure 1 is used to control the fault-current duration if the self-extinguishing characteristics of the circuit are not to be studied directly.

To start a fault condition, the test gap is first broken down by the surge generator designated as Number 1. Its firing time is accurately synchronized with the main 60-cycle power source by means of the phase-shifting selsyn peaking-transformer trip circuit shown in Figure 3. Thus fractions or multiples of half-cycles of fault current can be accurately duplicated. As shown in Figure 3, radar pulse transformers, rated 8 to 30 kv, have been used with excellent results for tripping the surge generators.

The facilities of the California Institute of Technology High-Voltage Laboratory include two 100-kv surge-generator charging circuits and two separate 10-bank, 1,000-kv surge generators that can be used as two separate generators or as one 2,000,000-volt generator. In this test the two separate units comprised generators Numbers 1 and 2.

When the main 60-cycle power circuit of Figure 1 is energized, the test-gap shunt resistors are isolated by means of a small air gap to reduce their required power rating. For breaking down the test gap, surge generator Number 1 is adjusted to cause gap flashover on the wave front and thus produce a very short duration voltage pulse which (due to its high effective frequency) can be kept out of the main power circuit by means of the filter circuit shown in Figure 1. The inductor and capacitors of this circuit are shown in Figure 2 together with the test-gap and power transformers. At high frequencies this circuit is a high impedance as viewed from the test gap and thus permits sufficient voltage from surge generator Number 1 for gap breakdown in short times, but allows very little voltage to reach the transformer terminals.

With the use of only the one surge generator and by blocking cut-off of the ignitron circuit, it is possible to study directly the reignition characteristics of the test gap over a limited range of system recovery voltages and frequencies, as indicated by the range of variation of voltage and filter-circuit constants shown in Figure 1. Natural system frequencies from 300 to 7,000 cycles per second can be obtained.

The Number 2 surge generator is used for the second type of dielectric-recovery study in which the insulation strength of the test medium is tested at various time intervals following the end of a controlled fault current. The Number 2 surge generator and ignitron circuit are both timed by a pulse taken from the Number 1 generator as shown schematically in Figure 1. The ignitron bias control and timing-control circuits are shown in Figure 4. The pulse from the Number 1 generator is applied to a single-shot multivibrator circuit whose time delay in sending out a pulse can be controlled by the variable capacitor shown. This pulse is applied to the grid of a *2050* thyratron whose plate circuit supplies current to high-speed relays in the bias-control circuits of the *F6105* ignitron control thyratrons, see Figure 4. These relays have a delay time of only five milliseconds so that the ignitron circuit can cut off the fault current at any desired current zero. For fractions of a half-cycle it was found readily possible to trip the *F6105* grid-bias circuit by an induced pulse from the Number 1 generator. Thus the ignitrons are immediately conditioned to block off at the first current zero. The duration of fault current then is varied by the initial trip time of the Number 1 generator.

Figure 2. View of main power circuit showing test gap in foreground and power transformers in background. Capacitors and inductor of filter circuit are on right side

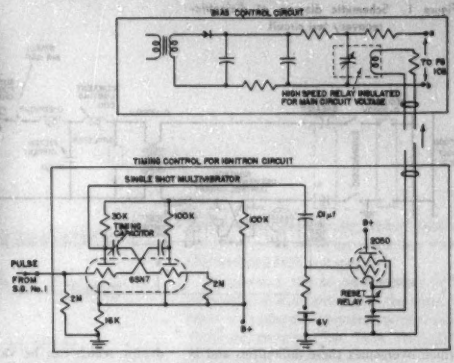

Figure 4. Timing and bias-control circuits for main ignitron fault-duration control circuit

Ten-Stage Scale-of-Two Counting Circuit

It is desired, of course, to control accurately the time of firing of the Number 2 surge generator to study the dielectric-recovery properties of the test medium over a wide range of times after the end of the fault current. For this purpose a binary or scale-of-two flip-flop circuit[8] was developed which counts pulses from a variable frequency square-wave generator. This circuit is shown in Figure 5 with its schematic diagram in Figure 6.

Each stage of the counting circuit consists of two tubes which have two stable states and can be changed from one to the other by the appropriate trigger pulse, the two stable states being distinguished by which tube is conducting. The terminal Out of one scale-of-two is connected directly to the terminal In of the next scale-of-two and so on for 10 stages. When *T-2*, Figure 6, of the preceding stage becomes conducting, a negative signal is applied to the plate of the Off tube and through the resistance-capacitance cross coupling to the grid of the On tube, which causes the flip-flop to pass to its other stable state. When *T-2* of the preceding state becomes nonconducting the resulting positive pulse has no effect on the following scale-of-two. Each scale-of-two produces one negative pulse for each two that are applied to it from the preceding stage, so that for 10 stages a total of 2^{10} or 1,024 pulses input to the first stage is required to produce a complete operation of the counting circuit. Thus, by varying the frequency applied to the counting circuit a varying time delay can be obtained. The oscillator driving the square-wave generator will apply frequencies up to 80 kc, and thus for 10 stages time delays from over one minute and down to about 13,000 microseconds can be obtained. Less stages are used for shorter delays. Values less than 100 microseconds can be reproduced.

The counting circuit is triggered by a pulse from the firing of the first surge generator which changes the stable state of the *6SN7* gate control tube, thus putting a positive bias on the *6SJ7* amplifier tube and allowing this tube to supply square waves to the first scale-of-two. The stable state of the gate-control tube is returned again to its cut-off state by a negative pulse from the counting circuit

Figure 3 (below). Control pulse circuits for timing surge-generator trip circuits

Figure 5 (right). View of timing control circuit for the number 2 surge generators showing oscillator, square wave generator, and binary counting or delay circuit

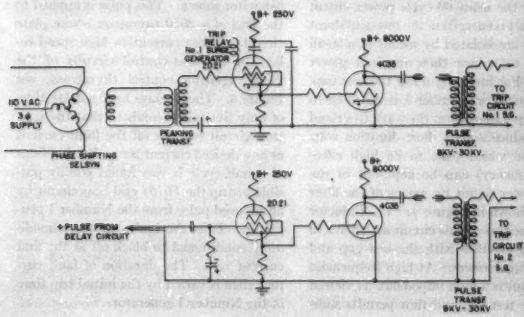

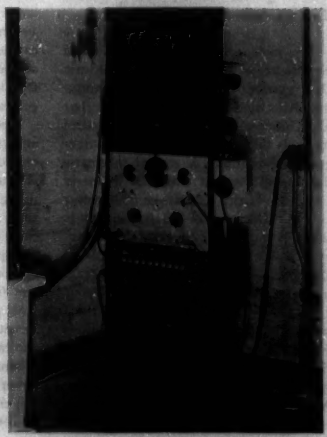

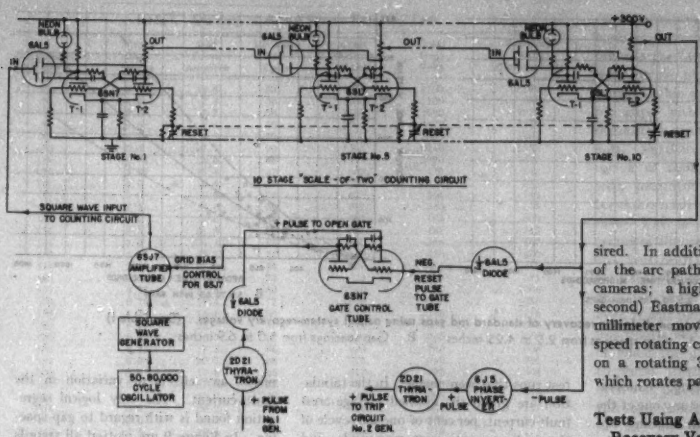

Figure 6. Schematic diagram of timing control circuit for number 2 generator

at the end of its operation which in turn negatively biases the *6SJ7* to cut-off and resets the counting circuit for its next operation. The control pulse out of the counter is fed to the Number 2 surge-generator trip-pulse circuit shown in Figure 3.

Automatic Fuse Changers

Although the inductance-capacitance filter of the main power circuit, Figure 1, presents sufficient impedance for the short-duration pulse of the Number 1 generator, it is not very practical to have a filter of sufficient impedance to allow a conventional surge generator to produce a full wave with a tail of 40 microseconds or more. It was found quite easy, however, to use a series-fused gap so co-ordinated as to allow the fault current to flow but to insulate against the discharge of the Number 2 generator. An automatic fuse changer was developed to allow continuous operation without shutting off the main power circuit between test shots. This is shown in Figure 7. The device pulls a small diameter copper wire from a spool around and between gap terminals at the top. The fuse holder is driven through an insulated shaft by a limit-switch position-controlled motor that accurately positions each quarter-turn of the fuse-holder rotor.

Recording Equipment

The complete circuit is suitable for testing insulating media with initial insulation levels up to about 300 or 400 kv. As shown in Figure 1, shunts are used for measuring the gap current and voltage. Low-frequency records are obtained with a magnetic oscillograph and high-speed records with a Westinghouse cold-cathode cathode-ray oscillograph with both electrostatic sweep control and a high-speed drum-type film holder. The cathode-ray oscillograph can be tripped from the Number 1 or Number 2 generator as desired. In addition, photographic studies of the arc path can be made with two cameras; a high-speed (3,000-frame-per-second) Eastman prism shutter-type 16-millimeter movie camera and a high-speed rotating camera with film mounted on a rotating 3,600 rpm 12-inch drum which rotates past a fixed lens.

Tests Using Actual System-Recovery Voltage

Standard rod gaps were used in all studies reported here. The test-circuit insulation levels are adequate for studying gap spacings up to about 15 inches. Previous data on lightning surge currents[8] had been obtained at gap spacings of 6 and 11 inches. Most of the data discussed here were obtained at the same spacings to correlate with those tests. In addition 3-inch gaps were studied.

When using the actual system-recovery voltage of the circuit supplying the fault current, the logical procedure is to vary one of several possible parameters until critical reignition is reached. A point on a dielectric-recovery curve then can be obtained by the crest magnitude and time to crest of the system-recovery voltage when the arc just fails to restrike. The parameters which can be varied are the time constant of the circuit to control the rate of rise of the system-recovery voltage, the applied circuit voltage to control the magnitude of the recovery voltage, the magnitude of the fault cur-

Figure 7 (left). Automatic fuse changer for series gap in main power circuit

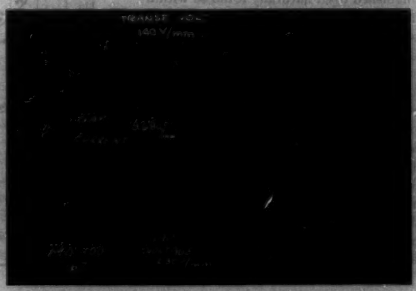

Figure 8 (right). Typical fault-current recovery-voltage oscillogram for tests using natural system-recovery voltage. (Test 167 of Table I)

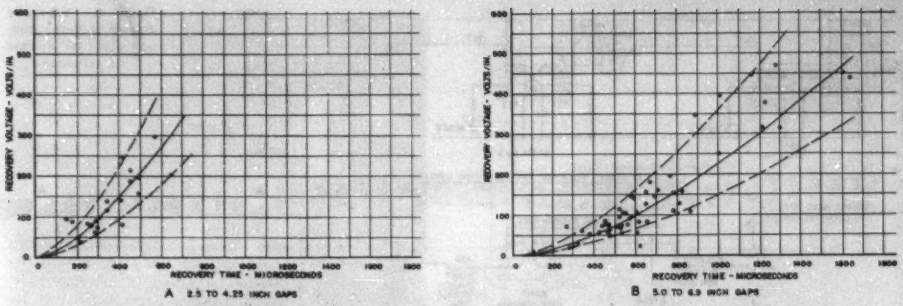

Figure 9. Data on dielectric recovery of standard rod gaps using natural system-recovery voltages. (See Table I)
A. Gap spacings from 2.5 to 4.25 inches B. Gap spacings from 5.0 to 6.9 inches

rent, and the gap spacing. Unfortunately, it is difficult to vary any one of the above parameters without causing appreciable changes in one or more of the others. Variation of circuit voltage or system natural frequency at a fixed fault current produces a very slow test procedure since it requires an accurate readjustment of the current-limiting reactor. The best test procedure found was to set the circuit voltage, natural system frequency, and limiting reactor and then vary the gap spacing until the critical reignition condition is reached.

With gaps of the order of three to six inches, it was found that the circuit voltage had to be reduced to the order of 1,000 volts rms, or less, before arc extinction would occur naturally with fault currents of practical magnitudes. This was true with system natural frequencies as low as 300 cycles per second. Even then the currents were below 50 amperes. Therefore this phase of the study necessarily was confined to currents of this magnitude or less. Under these conditions the arc drop was appreciable and, as is to be expected, accurate reproduction of test conditions was difficult. It was found in all cases that if the arc extinguished itself naturally it did so within the first half-cycle or at the first current zero. However, for any two faults with identical settings of the controllable parameters the magnitude and duration of fault current from its start to the first current zero varied considerably. This erratic characteristic therefore requires so many tests to get a mean critical condition that enough points for even a portion of a dielectric-recovery curve can not be obtained in a short enough time so that the effects of variations in atmospheric conditions can be eliminated or studied.

Table I lists 76 sets of critical reignition test runs that were made. In the tabulation are given the applied voltage-crest fault current, per cent of one-half cycle of the fault current, crest magnitude, and time to crest of the system-recovery voltage. The current data apply to the actual oscillograms from which the recovery voltage point was scaled at the test shot on which the circuit just recovered. A typical oscillogram from which these data were obtained is shown in Figure 8. As shown in Table I, the crest current ranges from 7 to 52 amperes and the time to current zero from 18 per cent to 100 per cent of a half-cycle. Various analyses of the data were attempted, such as segregating into groups of limited current variation, but the spread in the points as plotted on dielectric-recovery curves completely masks any effects of variation in the fault current. The only logical segregation found is with regard to gap spacing. In Figure 9 are plotted all records segregated into two groups of gap spacings. These data will be discussed in more detail later.

Tests Using Two Surge Generators

With the ignitron circuit and sufficiently high circuit voltages so that arc drop is not a factor, accurate control of the magnitude and duration of the fault current is obtained. Individual tests can be made at the charging rate of the surge generator or 1-minute intervals. Thus the study of the effects of the controlling factors becomes practicable since the circuit test conditions can be accurately

Figure 10. Comparison of time-lag or volt-time curves (obtained by two generator tests) for 3-inch rod gap with no predischarge and predischarge of one-half cycle 250-ampere crest

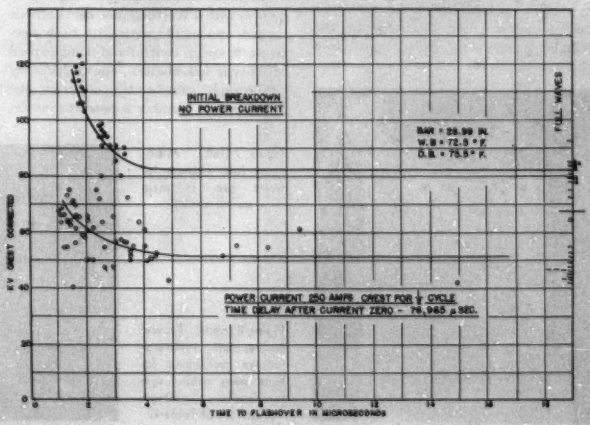

Table I. Summary of Actual System Recovery Tests

Oscillogram Number	Test Gap, Inches	Gap Crest, Amperes	Per Cent Half-Cycle	Crest Transformer, Volts	Crest Gap, Volts	Recovery Time, Microseconds
75	6.0	18.8	50	1750	2700	1160
78	6.0	7.2	50	1530	2100	895
80	6.5	7.7	50	1585	1660	1010
85	6.5	8.4	50	1590	2475	1290
87	6.5	11.3	72	1560	2060	1305
116	6.5	21.7	90	1565	3140	1285
119	6.75	24.0	86	1580	2920	1640
138	6.75	11.4	27	608	420	943
139	4.0	10.4	36	609	372	286
141	3.0	23.0	59	630	255	248
142	2.5	19.6	59	637	240	145
149	3.5	12.6	32	601	195	209
150	3.5	21.8	59	627	437	343
151	3.0	24.1	63	640	548	437
153	2.75	38.7	71	640	675	430
154	2.63	27.6	64	625	375	410
155	2.56	41.4	73	635	765	571
167	6.75	21.8	86	1740	3080	1605
176	6.75	13.4	77	1600	2680	1016
184	6.75	15.1	86	1310	2145	1314
187	6.75	22.1	55	1310	1287	870
193	6.75	25.0	82	906	1065	650
195	6.75	17.3	68	396	740	508
199	6.0	20.7	68	875	940	781
200	6.0	19.6	55	947	880	694
202	6.0	27.6	77	947	1200	770
241	6.75	23.0	73	1040	1085	710
253	3.5	20.2	50	806	260	257
254	3.5	12.1	18	806	279	262
255	3.5	19.4	50	806	316	171
257	3.5	16.1	50	867	224	286
258	3.5	10.3	36	867	403	344
263	3.75	11.4	23	806	281	294
265	3.75	16.1	45	947	300	417
271	3.69	29.9	64	932	794	455
279	3.94	17.2	36	940	152	214
283	3.94	27.6	68	804	386	305
290	4.25	34.4	59	934	837	498
297	5.0	36.3	50	793	105	286
298	5.0	56.5	50	793	216	271
299	5.25	56.5	50	806	291	381
301	5.25	19.4	27	778	71	105
302	5.25	44.4	45	804	185	328
306	5.25	48.4	50	804	306	617
307	6.0	52.3	50	764	435	506
309	6.0	48.4	50	793	425	530
396	2.56	32.2	90+	700	404	496
438	5.75	21.8	90+	1032	486	621
441	5.88	27.6	90+	1032	649	785
444	5.63	22.3	90+	1025	735	814
449	6.88	27.6	90+	985	760	884
452	6.38	25.3	90+	962	680	553
454	6.0	20.7	90+	962	513	456
456	5.94	33.9	90+	962	868	585
462	5.38	34.6	90+	962	870	829
471	4.50	33.8	90+	962	924	644
506	5.63	30.2	90+	1202	813	595
513	6.75	36.8	90+	1147	876	657
527	6.75	28.7	90+	1019	726	540
528	6.75	28.7	90+	1019	799	723
539	6.75	27.2	90+	941	671	585
544	6.75	29.9	90+	941	664	520
545	6.75	24.8	90+	941	535	460
551	6.75	25.3	90+	941	638	572
559	6.75	17.9	90+	941	388	468
561	6.75	23.0	90+	941	513	458
563	6.75	23.2	90+	941	583	660
565	6.75	25.3	90+	835	398	530
566	6.75	34.5	90+	835	518	534
567	6.75	18.4	90+	835	168	303
568	6.75	39.1	90+	835	513	440
571	6.75	30.3	90+	835	403	430
572	6.75	36.8	90+	835	535	473
573	6.75	32.2	90+	835	495	469
575	6.75	32.2	90+	835	488	530
576	6.75	26.4	90+	835	358	475

duplicated and many test points obtained during essentially constant atmospheric conditions.

The method of testing the gap, at a given time interval following the end of the fault current, is to raise the voltage applied by the Number 2 generator until breakdowns occur. Then oscillograms are obtained over a sufficient voltage range to produce a volt-time or time-lag curve. It is not considered necessary to use a standard $1^1/_2$ by 40-microsecond wave. The volt-time curves under the conditions of a predischarge are much flatter than with no predischarge and unaffected by large variations in the tail of the test waves. This had been observed previously for the lightning surge studies.[8] Typical volt-time curves both with and without a predischarge are shown in Figure 10. Two things of interest are illustrated by this figure. One is the more random nature of the data when the medium is recovering from a fault. The other is the fact that although the volt-time curves plotted through points obtained in this way have less turn-up than for gaps without a predischarge, the breakdown can occur at much longer time lags. Further, it was found that for a region of time intervals (that increase with magnitude of the fault current) breakdown can occur at a relatively slow rate. This is illustrated by the oscillograms of Figure 11. This same phenomena had been observed when studying gaps recovering from high-current short-duration surge currents.[5] There, however, it was found only for time intervals less than about 100 or 200 microseconds or when the gap is still carrying small currents. In the case of one or two half-cycles of power-frequency fault current this region extends to about 40,000 microseconds for 100-ampere faults and to about 70,000 microseconds for currents as high as 700 amperes. The percentage of such slow breakdown records decreases at the longer intervals. However, even though all breakdowns are at this slow rate there still exists a definite critical voltage below which breakdown will not occur. Because of this type of breakdown and the possibility of the media not supporting voltages below the apparent critical, it was considered desirable to use as long tail test waves as practicable. Surges with a time to half-value of about 80 microseconds were used for the data in all of the dielectric-recovery curves except the highest point on the 11-inch gap curve, Figure 14(B). As shown by Figure 11, partial breakdowns were also recorded at the shorter time delays after current zero.

High-Speed Camera Studies

Much valuable information has been obtained from the high-speed photographic studies, particularly from the records obtained with the 3,000-frame-per-second movie camera. Portions of one of the more interesting of these records are shown in Figure 12. The first group of frames shows the first 2,300 microseconds of the fault-current arc. The second group shows the luminous gases present in the arc 0.013 second after the start of the fault or 0.0043 second after the end of current flow. The third group shows the luminous gas in the arc just prior to the flashover produced by the Number 2 surge generator 0.041 second after the start of the fault or 0.0322 second after the end of the fault-current flow. In all cases photographed the luminous gases either moved out of the

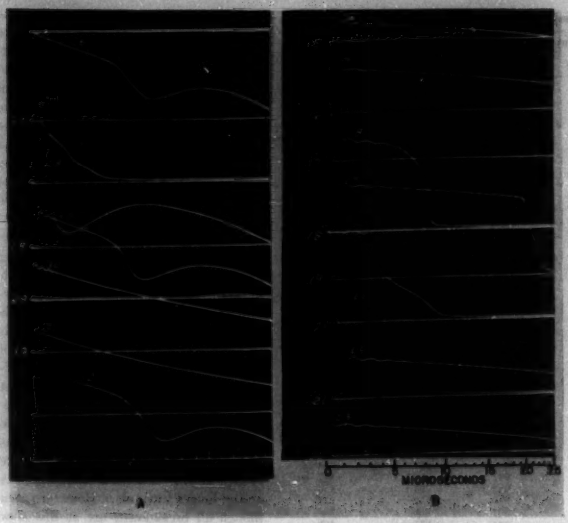

Figure 11. Typical oscillograms showing slow breakdown characteristics obtained when number 2 generator voltage is applied at short time intervals

center of the gap toward the electrodes or the gases near the electrode remained luminous longer. As shown in the third group of records in Figure 12, there still remains a faint path of luminosity in the gap through which the second discharge occurred. In all recorded cases the period in which visible luminous gas remains in the central region of the gap corresponds to the maximum delay for which slow voltage breakdown is observed. The fourth group shows the second discharge, and the fifth, the luminosity which still persisted at one terminal after 0.12 second. Faint traces of luminous gas are visible in such a record as long as 0.15 to 0.17 second after the end of the fault current even though no second discharge is applied.

Detailed examination of such records shows that extensive motion in the arc path occurs even during the half-cycle of fault current. The arc develops, then expands radially (in, of course, a tortuous corkscrew path) with visible diameters of two or three inches. The luminous area shown in the frames reaches its maximum at the crest of the fault current and diminishes only slightly by the time

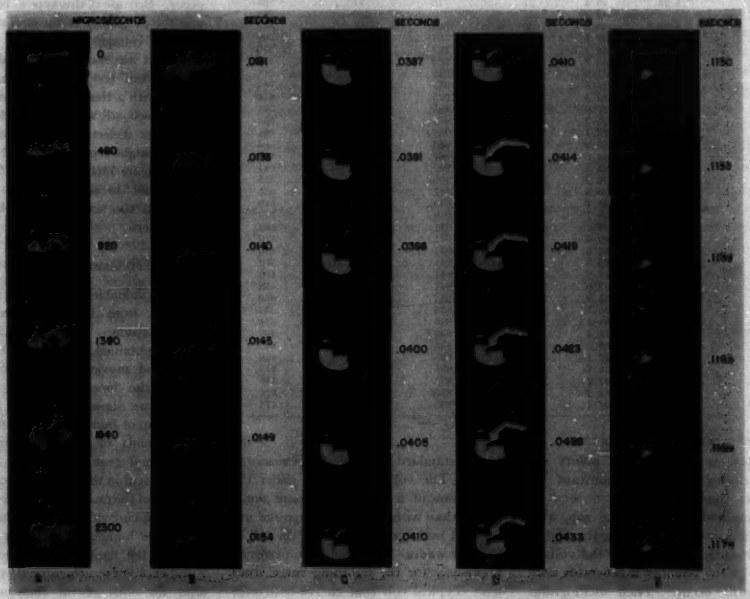

Figure 12. High-speed movie camera record of 3-inch gap discharge. Initial fault current one-half cycle of 100-ampere crest
A—Start of fault current. B—During second half-cycle of time from start of arc. C—Period just prior to second discharge. D—Period just after second discharge. E—Period toward end of visual luminescence showing ionized gas in region of one terminal only

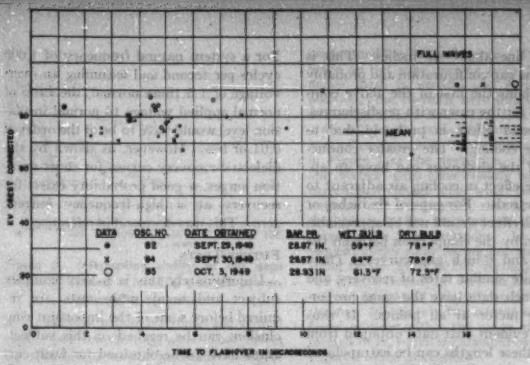

Figure 13 (above). Volt-time data for three separate runs showing effect of varying atmospheric conditions

Six-inch rod gap, $^1/_2$-cycle 10-ampere crest fault current. Time delay after current zero 77,000 microseconds

Figure 14 (below). Dielectric-recovery curves obtained with two generator tests

A. Three-inch standard rod gaps B. Six- and 11-inch gaps

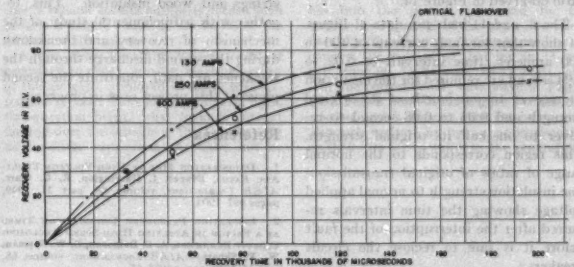

A 3" STANDARD ROD GAP – $\frac{1}{2}$ CYCLE OF FAULT CURRENT

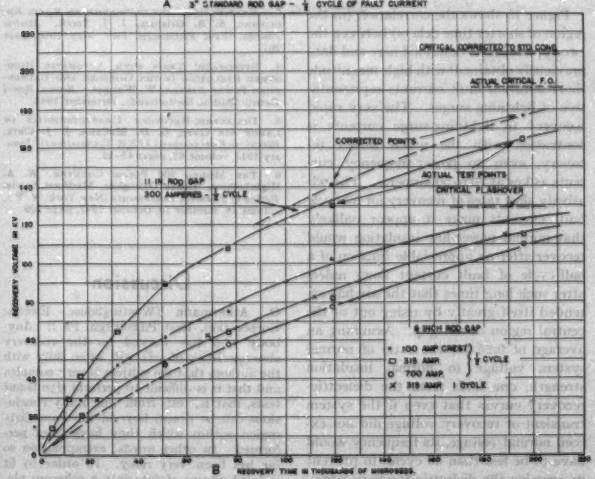

B

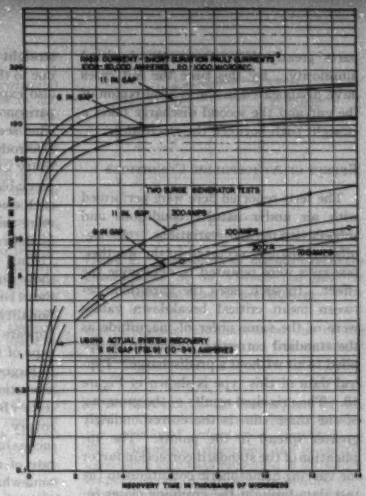

Figure 15. Comparison of dielectric-recovery characteristics of standard rod gap for different types of predischarge

the fault current reaches zero. For half-cycle faults it is quite intense for three or four more half-cycles. However, it does not drift out or away from the general region of the gap in the period that it is photographically visible.

The record in Figure 12 is of particular interest since it shows that a large time interval was required for the second discharge to build up to maximum intensity. This corresponds to the slow rate of breakdown mentioned previously. The first frame of the fourth set shows initial streamers propagating from each electrode through the trail of luminous gas. The next frame shows the intense return streamer that completes the discharge. Of these two initial streamers the one passing through the gas of greatest luminosity is more intense itself. The time interval between these two frames is about 400 microseconds, but of course about 300 microseconds of time is lost by the shutter action and the first faint trace may have started just before the shutter closed. Thus the actual time of build-up can not be determined from such a record. Actually the longest times for breakdown to develop as recorded with the oscillograph were of the order of 30 or 40 microseconds. This was true even for very short time intervals between the end of the fault current and the application of the test voltage.

The photographic records showed that for time intervals above 70- or 80,000-microseconds, the second discharge de-

parts greatly from the path of visual luminosity. By this time the hot gases have disappeared in the central region of the gap and the second discharge takes a straight path between the electrodes.

Effect of Atmospheric Conditions

The tests reported here were performed with air under natural conditions and subject to normal variations. As significant changes occurred in the weather, test runs were repeated to determine the effect. In such cases the variations between mean critical breakdown values were of the same order of magnitude as the standard correction factors to be applied to air without a predischarge. Typical data of this type is shown in Figure 13. The principal results o' the grouping of the three runs is the correspondingly greater spread in the points. The application of the standard correction factor for varying atmospheric conditions to the test data brought the grouping closer together. In most of the data presented here, such correction factors amount to only three or four per cent at the most. Under these conditions they were applied to the data but probably have no significance. Only the two points shown in Figure 14(B) had larger correction factors.

Dielectric-Recovery Curves

Thirty-five or forty test points appear to be adequate for establishing a critical point on a dielectric-recovery curve. However, two to four such runs were made at each time interval in an attempt to establish accurately the dielectric-recovery curves presented here. Thus each point is the result of 70 to 150 actual tests. The data obtained for longer time intervals is plotted in Figure 14 for 3-, 6-, and 11-inch horizontal rod gaps. As shown, the bulk of the data has so far been obtained for one-half cycle of power current. Shorter duration arcs have not yet been studied in detail. It has been found that the rate of recovery is relatively insensitive to longer durations. Points obtained with one or two cycles of fault current are not appreciably different than those for one-half cycle.

Comparison of the three-inch and six-inch gap data in Figure 14 shows that not only is the strength of the three-inch gap proportionately higher at any time interval but its relative rate of recovery is more rapid. Examination of critical breakdown curves for rod gaps without a predischarge shows that the relative strength of a 3-inch gap is greater than a 6-inch gap whereas the curve becomes a straight line above six inches. This is due to the gap configuration and probably also explains the first of the above comparisons for the cases with predischarges. The second effect is probably due to electrode cooling. The greater conductivity of the electrodes can have an appreciable effect in cooling air adjacent to each electrode. For gaps of six inches or more this effect should not be appreciable as shown by the comparison between the 11-inch and 6-inch gap curves. These show quite similar rates of recovery and the 11-inch data have the same proportionality factor at all points. It thus appears evident that data obtained from gaps of these lengths can be extrapolated to larger gap spacings. These same considerations apply to data of Figure 9 for tests obtained using natural system recovery. Here gaps in the region of three inches have about twice the proportionate rate of recovery as 6-inch gaps. This is somewhat higher than the proportionate ratio observed in Figure 14.

The 6- and 11-inch gap data of Figure 14 show that for fault currents of 100 to 700 amperes, time intervals of 0.02 to 0.04 second are required for the insulation to recover to one-fourth of its original strength and 0.05 to 0.08 second to recover to one-half its original strength. This region corresponds to the normal range of ratios of original transmission-line insulation strength to normal applied voltage showing the time intervals required after the interruption of the fault before it is safe to reclose the circuit breakers.

Figure 15 shows the correlation (in the region of shorter time delays) between the two types of tests described here and data previously obtained[5] with high-magnitude short-duration fault currents representative of lightning surges. The very rapid recovery to lightning-surge currents is contrasted with the much slower recovery, even to power-frequency currents as low as 20 to 50 amperes. The relatively slow rates of recovery for 60-cycle fault currents make it appear unlikely that normal power-line insulation would recover after an appreciable fraction of a half-cycle of fault current flows unless after such long times that the arc has extended itself greatly by rising out of the central region of the gap. Assuming an average of 0.25 for the ratio of normal system voltage to normal insulation strength, one finds from the dielectric-recovery curves that even if the system transient or recovery voltage did not exceed normal voltage, its frequency would have to be less than 60 cycles to prevent its crossing the dielectric-recovery curve. For a system natural frequency of 1,000 cycles per second and assuming an overvoltage of 1.5 times normal, the ratio of normal applied voltage to normal insulation level would have to be of the order of 0.01 or less. However, as shown by the dielectric-recovery curves for short-duration surges, a good probability exists for recovery at a high-frequency current zero. This was discussed in reference 5.

Future Tests

Unfortunately this is a very complex subject and many more tests are required before some of the important conclusions can be reached on this subject. Data have to be obtained for fault-current durations between the range of the short-duration lightning surges and appreciable fractions of one-half cycle of power frequency. The effects of appreciable air velocities and of gap positions must be studied and similar data obtained for other media such as insulator strings and wood insulation. This, together with a fundamental study of the mechanism of recovery and breakdown during the second discharge through the weakened arc path, constitute the second phase of this project now in progress.

References

1. Dionization Time of High-Voltage Fault-Arc Paths, **Everett J. Harrington, E. C. Starr.** *AIEE Transactions*, volume 68, part II, 1949, pages 997–1004.

2. Insulation Flashover Dionization Times as a Factor in Applying High-Speed Reclosing Circuit Breakers, **A. C. Boisseau, B. W. Wyman, W. F. Skeats.** *AIEE Transactions*, volume 68, part II, 1949, pages 1058–67.

3. Keeping the Line in Service by Rapid Reclosing, **S. B. Griscom, J. J. Torok.** *Electric Journal* (East Pittsburgh, Pa.), May 1933, page 201.

4. Systematic Tests with Automatic High-Speed Reclosing in the Gossgen and Laufenburg Power System, **W. Wanger.** *Brown Boveri Review* (Baden, Switzerland), December 1945.

5. Dielectric-Recovery Characteristics of Large Air Gaps, **G. D. McCann, J. J. Clark.** *Electrical Engineering* (*AIEE Transactions*), January 1943, volume 62, pages 45–52.

6. The Model 200 Pulse Counter, **W. A. Higinbotham, James Gallagher, Matthew Sands.** *Review of Scientific Instruments* (New York, N. Y.), volume 18, number 10, October 1947, page 706.

Discussion

O. Ackermann (Westinghouse Electric Corporation, East Pittsburgh, Pa.): Anybody who has worked on the recovery characteristics of arcs will agree fully with the authors that the subject is very complex and that it is difficult to perform significant tests, that is, tests from which any conclusions can be drawn beyond the immediate region within which they have been performed. In other words, extrapolation so far has been very risky. In order to fit isolated groups of data into a coherent pic-

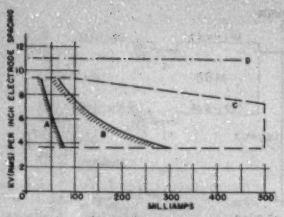

Figure 1. Interrupting ability of rod gaps (5.5 to 11 inches) at low 100-per cent power-factor 60-cycle currents

A. Applying to both horizontal and vertical gaps: limit for clearing within four cycles
B. Applying to vertical gaps only: limit for clearing at all, sometimes after as much as 30 cycles
C. Limit of explored area; horizontal gaps clear anywhere within this range, sometimes taking up to 70 cycles
D. Average gradient for initial breakdown of rod gap

ture, a reliable core or outline is needed such as now is taking shape in the hands of the authors of this paper.

A few years ago the writer found it necessary to check into the clearing ability of the air gaps employed in series with expulsion-type arresters for transmission lines, the question being, what leakage current flowing over the outside of the tube or over an insulator supporting the tube can be interrupted by the series gap. Tests were made on rod gaps ranging from $5^1/_2$ to 11 inches, both in vertical and in horizontal position; the currents were limited to 500 milliamperes and less. The data were coordinated on the basis of kilovolts rms per inch of gap spacing; the results are shown in Figure 1 of the discussion. Horizontal and vertical gaps clear equally well in the current and voltage range where the clearing requires only a few cycles, that is, while the arc still is in the more or less direct line between the two electrodes. In the subsequent cycles some flaring out and lengthening occurs even in the vertical arc, but the process cannot go very far and the arc will not clear at all unless it can do so within the first 30 cycles. Horizontal arcs never failed to clear within the range of the performed tests, which is indicated by line *C* in Figure 1 of the discussion.

In all these tests the current was entirely resistance limited; therefore, after current zero, the voltage reappeared across the gap in the form of a symmetrical 60-cycle sine wave, starting from zero. In the critical clearing tests indicated by line *A* in Figure 1 of the discussion, the dielectric-recovery curve of the gap must have more or less followed that sine wave. To see how this fits into the picture presented by the authors in Figure 15 of the paper, we select the 5-kv 66-milliampere point of our line *A*, convert the voltage to that for an 11-inch gap, that is, 55 kv rms, 78-kv crest, and plot the corresponding sine wave in Figure 15. This is done in the Figure 2 of the discussion, and it appears that the new curve, although arrived at by an approximative method, fits fairly well into the general pic-

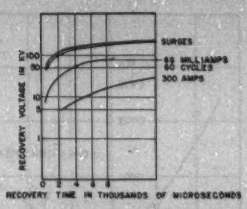

Figure 2. Comparison of dielectric-recovery characteristics of an 11-inch rod gap for different types of predischarge

ture and adds information on one of the numerous fringe areas to this extensive problem.

G. D. McCann, J. E. Conner, and H. M. Ellis: The authors were happy to receive the additional information provided by Mr. Ackermann's discussion and to see the agreement with data presented in the paper. As pointed out by Mr. Ackermann, the very great complexity of this subject makes it extremely risky to rely on a few isolated points for reliable information on dielectric recovery or try to extrapolate into unconfirmed regions.

It was for these reasons that so much effort has been devoted by the authors to the development of a reliable and sufficiently rapid dielectric-recovery testing technique that makes possible a comprehensive study of this subject.

Total and Incremental Losses in Power Transmission Networks

J. B. WARD
MEMBER AIEE

J. R. EATON
MEMBER AIEE

H. W. HALE
ASSOCIATE AIEE

THE FIRST development of a loss formula wherein total transmission losses are expressed in terms of source loadings was presented by E. E. George[1] in 1943. In a recent paper[2] a formula of this type was used to co-ordinate losses and station costs in obtaining optimum operating economy. An appendix in this latter paper describes a modification of George's original method, adapted to the use of the network analyzer for evaluating the constants. The present paper describes an extension or generalization of George's original formula, together with improved techniques of evaluating the constants by use of the analyzer. A simple relation which gives the incremental loss incurred in transferring a block of generation from one source to another is derived from the total loss formula.

The loss formula is derived by an application of the principle of superposition. Two basic approximations are involved. First, for a given total load each individual substation load is represented as a certain current which has a constant magnitude and fixed relative angular position with respect to other load currents, regardless of the manner in which the total generation is apportioned among the sources. Second, as the total system load varies the magnitude of each individual load current varies proportionately and maintains its fixed relative angular position with respect to other load currents. Suitable values of load currents may be obtained from a selected, typical, intermediate power-flow condition which is taken as the normal or reference condition.

The complete process of developing a loss formula for a system is explained through the medium of an example worked out for a sample system.

Determination of Loss Formula for a Sample System

The method of determining a loss formula is illustrated in detail on the sample system shown in Figure 1. This system is purely hypothetical and is relatively simple in order to minimize the space required to explain the calculations. However, the system is sufficiently representative and complete to serve as a guide for applying the method to larger systems.

Impedances are given in per cent on a 100 megavolt-ampere base. Off-nominal transformer ratios are indicated as per cent deviation from nominal ratio. Note that ratios in the two transformer banks supplying the 66-kv system are not the same, as frequently occurs in practice. In such instances, the difference in ratios is usually small or the loop impedances are large, resulting in small circulating current due to the residual turn ratio. The transformer ratios are retained at the values shown for subsequent tests.

Complete network analyzer readings for the operating condition chosen as the basis for deriving the formula constants are shown in Table I. It should be emphasized that the algebraic signs associated with the vector current readings in Table I have no significance except in relation to the analyzer plugging diagram

Table I. Normal Power Flow Condition

Circuit	Voltage, Per cent	Angle,* Degrees	P,** Megawatts	Q,** Megavolt-amperes Reactive	Current,† Per unit
Generator 1	105	42	190	93	$-1.977-j0.039$
2	105	32.5	60	14	$-0.585-j0.045$
Tie Line 3	101	35.6	−25	0	$+0.228+j0.083$
4	100	0	0	0	0 0
Load 1	105	42	40	19.5	$0.425+j0$
3	104.5	30.5	45	17.8	$0.465+j0.050$
4	102	30.5	60	16.5	$0.620+j0$
5	102	28.2	30	0	$0.282+j0.058$
6	101.5	29	10	4.5	$0.102-j0.020$
7	97	28.2	30	14.5	$0.335-j0.072$
Line 1–3			115	48	$1.160+j0$
1–4			34	13	$0.348+j0.010$
3–5			27	6	$0.263+j0.010$
3–7			13	11.2	$0.143-j0.068$
5–6			−2.9	4.7	$-0.020-j0.048$
2–6			13.2	0.6	$0.121+j0.031$
2–7			18.4	6.5	$0.182-j0.010$
2–4			28.8	7.0	$0.280+j0.020$
Transformer 1			−150	−50	$-1.470-j0.050$
3			86.5	44.5	$0.970-j0.122$
4			33	12	$0.355+j0.010$

* Arbitrary reference.

** Positive P and Q in sources denote real power and lagging reactive power input to the system.
Positive values in loads denote power and lagging reactive power withdrawn from the system.
Positive values in line 1–3, for example, indicate power flow and reactive power flow (lagging) from bus 1 to bus 3, values being measured at the first-mentioned terminal, bus 1.
Positive values in transformers indicate real and lagging reactive power flow from the high side to the low side, as measured on the high side.

† Reference is the total generator and tie-line current. Signs depend on initial polarity of circuits.

Paper 50-97, recommended by the AIEE System Engineering Committee and approved by the AIEE Technical Program Committee for presentation at the AIEE Winter General Meeting, New York, N. Y., January 30–February 3, 1950. Manuscript submitted October 31, 1949; made available for printing December 2, 1949.

J. B. Ward, J. R. Eaton, and H. W. Hale are all of Purdue University, Lafayette, Ind.

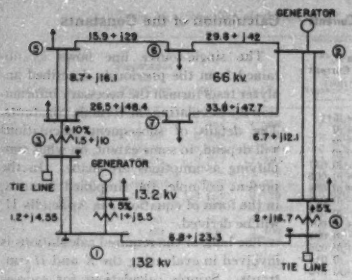

Figure 1 (left). Sample system

Impedances are given in per cent on a 100-megavolt-ampere base

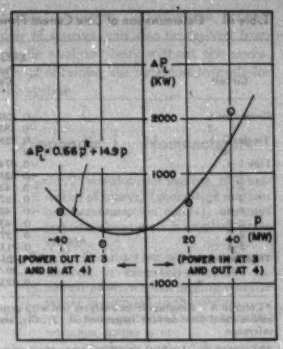

Figure 3 (right). Incremental loss formula for power flow from tie-line 3 to 4

Initial loadings are: $P_1 = 167$ megawatts, $P_2 = 60$ megawatts, $P_3 = P_4 = 0$

Points indicate calculated incremental losses from check studies

which is not shown. The important point is to maintain consistently throughout all tests the same circuit polarity. The vector reference used for these readings is the total source current (generators and tie-lines).

In addition to the normal power-flow study, a number of other operating conditions were established on the analyzer, readings taken, and losses calculated line by line to serve as checks on the formula results. Some of these conditions are summarized in Table II. These check studies were adjusted in the conventional manner, with loads maintained at scheduled values of real and reactive power.

The simplified form of the loss formula, as given by equation 7 in Appendix II, is derived for this sample system in the following paragraphs. An incremental loss formula for through transfer between the interconnection points at Stations (3) and (4) is derived from the total loss coefficients. The formula for total transmission loss is given in Appendix IV, together with the assumed values of constant source voltage and power factor. Comparison of the results yielded by this formula with the results of calculated losses in the check studies is shown in Figure 2. The check studies listed in Table II are noted on the diagram.

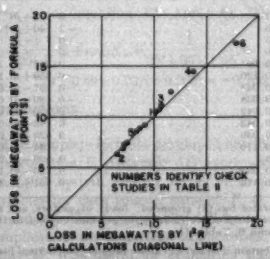

Figure 2. Comparison of calculated and formula results

Figure 3 gives the incremental loss formula, the corresponding parabolic curve, and several points calculated from the check studies.

Determination of Separate Line Flows

Certain analyzer tests are required in addition to the normal base power-flow condition. These additional tests are simple to perform, since they are all made with load and capacitor circuits opened. Their purpose is to determine what the current in each line would be if the normal-flow load and capacitor currents were supplied by one source at a time. These line currents are derived indirectly by an application of the principle of superposition. This expedient is taken to avoid the difficult task of reproducing these separate-source line flows directly on the analyzer.

The first step is to select one source, preferably a centrally located major source, as the key or reference point. In the present example, the low-voltage bus at Station (1) is chosen for this purpose. With load and capacitor circuits opened on the analyzer setup, and with transformer taps on normal settings, the following operations are performed:

1. Connect the selected key bus (Station (1)) to neutral through a metered jumper circuit which is polarized in the same way as Station (1) generator circuit. Open the generator at Station (1).

2. Connect a high-impedance buffer circuit in series with each of the other sources. Energize these sources and adjust them so that the vector current in each, with respect to a common reference, is the same as the corresponding vector current in the normal-flow condition, Table I. It is desirable to

Table II. Source Loadings and Calculated Losses from Check Studies

Test Number	Source Number	P, Megawatts	Q, Megavolt-amperes reactive	V, Per unit	Calculated Total Loss, Kilowatts
1 (Normal)	1	190	93	1.05	
	2	60	14	1.05	10,060
	3	− 25	0	1.01	
	4	0	0	1.00	
2	1	112	68	1.05	
	2	60	14	1.06	6,530
	3	50	0	1.04	
	4	0	0		
3	1	194	87	1.05	
	2	60	19	1.04	10,710
	3	0	0		
	4	− 25	0	1.03	
4	1	221	101	1.05	
	2	60	18	1.03	13,790
	3	0	0		
	4	− 50	0	0.97	
5	1	166	80	1.05	
	2	60	14	1.06	8,360
	3	− 20	0	1.01	
	4	20	0	1.02	
6*	1	237	149	1.05	
	2	0	0	0.93	17,920
	3	0	0		
	4	0	0		

Note: In establishing these conditions on the network analyzer, loads were adjusted to normal power and reactive values, generator voltages were held approximately constant, and tie-line flows were held at unity power factor. Additional studies, not shown here, are plotted in Figure 2.

* Transformer tap was changed at Station 1 to boost the 132-kv bus 12.5 per cent.

Table III. Determination of Line Current Flow with Station (1) Supplying Normal Load Currents

Circuit	Column A,* Per-Unit Current	Column B,** Per-Unit Current ($a_{31}+jb_{31}$)
Generator 1	0.420 − j0.039†	−2.397 + j0††
2	−0.585 − j0.048	0 + j0
Tie line 3	0.228 + j0.082	0 + j0
4	0 + j0	0 + j0
Line 1–3	−0.074 + j0.031	1.234 − j0.031
1–4	−0.325 + j0.007	0.673 + j0.003
3–5	−0.143 − j0.024	0.406 + j0.034
3–7	−0.127 − j0.022	0.270 − j0.046
5–6	−0.143 − j0.024	0.123 − j0.024
2–6	0.143 + j0.024	−0.022 + j0.007
2–7	0.127 + j0.022	0.055 − j0.032
2–4	0.311 + j0.006	−0.031 + j0.026
Transformer 1	0.401 − j0.035	−1.871 − j0.016
3	−0.297 − j0.052	1.267 − j0.070
4	−0.325 + j0.007	0.680 + j0.003

* Column A: Readings from analyzer test with generator (1) bus grounded, all loads and capacitors opened, and normal-flow current impressed at (2), (3), and (4). All readings taken with respect to a common reference.

** Column B: Derived line flow giving the current distribution if source (1) alone supplied normal load currents. To obtain the values in this column, subtract the readings of column A from corresponding normal-flow measured values.

† Current in metered jumper used to ground bus (1). This metering circuit is polarized the same as the generator circuit it replaces.

†† This value, 2.397, is the value of C_1 used in evaluating the loss formula constants.

have the buffer impedances as large as possible in order to make the adjustment of each source current nearly independent of the others. Read and record all line currents as shown in Table III, column A. In the event that full value would produce currents in excess of circuit or instrument ratings, all of the impressed source currents may be reduced to one-half or one-quarter value, and then the resulting line currents corrected to full value.

In the presence of off-nominal turn ratios in the network, the current in the grounding circuit at the reference bus may differ from the sum of impressed currents in other sources. Note that such a difference appears in the data of Table III, column A.

Column B of Table III is obtained by subtracting values in column A from the corresponding currents in Table I. All source currents except (1), the key or reference bus, vanish, and the line currents are the correct values for Station (1) alone supplying normal load currents. This follows from the fact that since the two sets of line currents, namely normal flow and those in column A, separately satisfy Kirchhoff's laws in the network, the currents resulting from their superposition must also satisfy Kirchhoff's laws. As a result of the superposition, all source currents vanish except at source (1). The line flow of column A contributes nothing to loads, since it was taken with loads off. Hence, the resulting combined line currents represent the condition of source (1) alone supplying normal load currents.

3. Next, it is desired to determine the line currents when source (2) alone is supplying normal load currents. To this end, a simple additional test is made. Open all sources except number (2), leaving loads and capacitors off and generator (1) bus grounded. Energize source (2) and adjust it so that the current in the grounding jumper at bus (1) is equal and opposite to the source (1) current appearing in column B, Table III; that is, the source (1) current when this source alone supplies normal load currents. Again it may be necessary to limit the current to a lower value. Read and record the line currents as shown in column AA, Table IV. Column BB of Table IV is obtained by adding column AA to column B of Table III. All source currents except (2) vanish, and the resulting line currents are the values for station (2) alone supplying normal load currents.

4. Repeat step 3 for each other source.

In a larger system it may be more convenient to record current readings directly on a 1-line diagram rather than in tabular form.

The combination of different sets of line currents could also be carried out directly on these diagrams.

Calculation of the Constants

The single-source line flows as obtained from the previously described analyzer tests furnish the necessary information for calculating the formula constants. The details of subsequent calculations will depend, to some extent, on what simplifying assumptions are made. In the present example, the simplified formula, in the form of equation 7 in Appendix II, will be derived.

The bulk of the required calculations is involved in evaluating the K and H constants. Sample calculations for sources (1) and (2) are shown in Table V. Column 1 lists identification of the lines and transformers and column 2 the corresponding per cent resistance. The scalar magnitudes of line currents for source (1) alone energized, as obtained from Table III, column B, are entered in column 3. The square of each line current multiplied by the corresponding per cent resistance is entered in column 4. The sum of all values in column 4 is used to obtain the value of K_{11}, as shown in the sample calculation at the bottom of Table V.

Next, cross-products of the real components of single-source line flows associated with sources (1) and (2) are multiplied by corresponding line resistances, as indicated in column 5. Similar cross products of the quadrature components are shown in column 6. The totals of columns 5 and 6 produce the K_{12} constant as indicated at the bottom of Table V.

The operations involved in obtaining the elements of columns 7 and 8 are indicated in literal form in the column

Table IV. Determination of Line Currents with Station (2) Alone Supplying Normal Load Currents

Circuit	Column AA,* Per-Unit Current	Column BB,** Per-Unit Current ($a_{32}+jb_{32}$)
Generator 1	2.397 + j0	0 + j0
2	−2.140 + j0	−2.140 + j0†
Tie line 3	0 + j0	0 + j0
4	0 + j0	0 + j0
Line 1–3	−1.052 − j0.094	0.182 − j0.125
1–4	−1.232 + j0.120	−0.559 + j0.123
3–5	−0.513 − j0.042	−0.107 − j0.008
3–7	−0.459 − j0.038	−0.189 − j0.084
5–6	−0.513 − j0.042	−0.390 − j0.066
2–6	0.514 + j0.043	0.492 + j0.050
2–7	0.467 + j0.039	0.522 + j0.007
2–4	1.165 − j0.110	1.134 − j0.094
Transformer 1	2.280 + j0	0.409 − j0.016
3	−1.052 − j0.094	0.215 − j0.164
4	−1.231 + j0.119	−0.551 + j0.122

* Column AA: Readings from analyzer test with generator bus (1) grounded; loads, capacitors, and all other sources except (2) opened. Source (2) is adjusted to produce (2.397 + j0) per-unit current in the grounding circuit at (1). This value is taken from column B, Table III.

** Column BB: Derived line flow giving current distribution if source (2) alone supplied the normal load currents. To obtain these values, add the readings of column AA to the corresponding line currents in column B of Table III.

† This is the value of C_2.

Table V. Sample Calculation of K^* and H^{**} Constants

1 Line	2 Resistance in Per Cent	3 i_{k1}	4 $i_{k1}^2R_k$	5 $a_{k1}a_{k2}R_k$	6 $b_{k1}b_{k2}R_k$	7 $a_{k1}b_{k2}R_k$	8 $b_{k1}a_{k2}R_k$
1–3	1.24	1.234	1.895	0.279	0.005	−0.191	−0.007
1–4	6.80	0.673	3.090	−2.560	0.002	0.561	−0.010
3–5	8.70	0.406	1.440	−0.378	−0.003	−0.029	−0.032
3–7	26.50	0.273	1.980	−1.352	0.102	−0.600	0.231
5–6	15.90	0.124	0.245	−0.762	0.025	−0.129	0.147
2–6	29.80	0.023	0.016	−0.321	0.010	−0.032	0.097
2–7	33.80	0.064	0.139	0.970	−0.007	0.012	−0.565
2–4	6.70	0.041	0.011	−0.234	−0.015	0.017	0.199
Transformer 1	1.00	1.871	3.502	−0.784	0	0.029	−0.006
Transformer 3	1.50	1.266	2.400	0.408	0.017	−0.311	−0.022
Transformer 4	2.00	0.680	0.927	−0.749	0.001	0.166	−0.003
Total			15.645	−5.463	0.137	−0.507	0.029

Note: From Table III, $C_1=2.397$; From Table IV, $C_2=2.140$

$$* K_{11}=\frac{10}{C_1^2D}\sum i_{k1}^2R_k=\frac{10}{(2.397)^2\times 100}\times 15.645=0.273$$

$$* K_{12}=\frac{20}{C_1C_2D}\sum(a_{k1}a_{k2}R_k+b_{k1}b_{k2}R_k)=\frac{20}{2.397\times 2.140\times 100}(-5.463+0.137)=-0.208$$

$$** H_{11}=\frac{20}{C_1C_2D}\sum(a_{k1}b_{k2}R_k-b_{k1}a_{k2}R_k)=\frac{20}{2.397\times 2.140\times 100}(-0.507-0.029)=-0.021$$

headings. The totals of these two columns yield the H_{12} constant.

The complete set of K and H constants requires computations of the type indicated in column 4 for each source and in columns 5–8 for each pair of sources. The H_{12} constant is included in Table V to illustrate the computations; however, the H constants were neglected in obtaining the B constants of Appendix IV. Note also that the summation of column 6 contributes very little to the value of K_{12}. With fairly uniform load-power factor and line resistance-to-reactance ratios, the quadrature component of single-source flows might be neglected altogether. This would reduce the computations to a single column for each source and each pair of sources.

In the present example additional assumptions are made to the effect that source bus angles may be neglected and that source voltages and power factors remain constant at values listed in Appendix IV. A sample calculation of B_{12} is given here (equation 10, Appendix II)

$$B_{12}=\frac{1}{2V_1V_2}(1+r_1r_2)K_{12}=\frac{1}{2\times 1.05\times 1.05}\times(1+0.49\times 0.23)(-0.208)=-0.105$$

Conclusions

The complete formula developed herein (see equation 5, Appendix II) expresses the total system loss in terms of four variables for each source, namely, P, Q, V, and ϕ. This form usually will be too complicated for practical applications. However, it is useful for evaluating the effects of simplifying assumptions. The assumption of constant values for ϕ is necessary from a practical viewpoint, since relative angular displacements of source bus voltages are not obtainable from system log sheets, nor are they easily estimated in complex networks. It is felt that the assumptions employed in the numerical example will yield satisfactory results on most systems. A few check studies should always be made to furnish a check on calculations as well as the assumptions.

A basic assumption of the method is that during the normal cycle of system load variation all loads vary in proportion. If a major load does not conform with the pattern of variation followed by the rest of the system, this load may be treated as a negative source and introduced as an additional variable in the formula. In the event that many loads vary in a nonuniform manner, it may be necessary to develop two or three sets of constants in order to cover the entire daily load cycle.

In choosing the source points which will appear as variables in the loss formula, it is desirable to hold the total number to a minimum. Generators within a station can usually be combined, and small plants may sometimes be eliminated by combining with local loads. It may be feasible to combine separate plants which are close together electrically.

The parabolic incremental loss formula may be useful for certain applications. Considering the difficulty of analyzing incremental losses, this formula is capable of showing quite well the pattern of variation in losses resulting from power interchange between pairs of stations or interconnection points. This formula, for any pair of sources, can also be derived from simple analyzer tests without the necessity of obtaining the total-loss formula for the system.

Appendix I. Nomenclature

$P_1, P_2, \ldots P_s$ = real power loading, in megawatts, of sources (generating stations or interconnection points); assumed positive when power is supplied to the system.

$Q_1, Q_2, \ldots Q_s$ = reactive power loading of sources, in megavolt-amperes; assumed positive when lagging reactive power is supplied to the system.

$V_1, V_2, \ldots V_s$ = magnitude of source terminal voltages, in per unit.

$\phi_{mn}=\phi_m-\phi_n$ = phase angle difference between terminal voltages of sources m and n.

$r_n=Q_n/P_n$ = tangent of power factor angle.

P_L = total I^2R transmission loss in kilowatts.

ΔP_L = incremental transmission loss in kilowatts.

p_{kj} = block of generation, in megawatts, transferred from source j to source k, that is, P_j is decreased and P_k is increased by p_{kj}.

K_{mn}, H_{mn} = constants of the complete loss formula.

B_{mn} = constants of the simplified form of loss formula.

A_1 and A_2 = constants of the incremental loss formula.

D = power base, in megavolt-amperes. Currents and impedances are expressed in per cent or per unit on this base.

R_k = resistance of line k, in per cent on base D.

G = magnitude of the summation of all vector source currents in reference power flow condition. Expressed in per unit on base D.

$i_k=a_k+jb_k$ = current in line k, in per unit on base D, under any general operating condition.

$g_n=c_n-jd_n$ = current in source n under any general operating condition, in per unit on base D. Vector reference is the same as that used for source voltage angles ϕ_n.

C_n = magnitude of source n current, in per unit, when this source alone supplies normal-flow load currents. In the absence of off-nominal transformer tap settings G and C_n are equal.

$i_{kn}=a_{kn}+jb_{kn}$ = per unit current in line k when source n alone supplies the normal-flow load currents. Vector reference is the corresponding source n current, C_n.

Appendix II. Derivation of Loss Formula

Consider a special type of network, as shown in Figure 4, in which each individual load current is a constant fraction of the total load current and maintains a fixed relative phase position with respect to other load currents. The total load current may be apportioned in any way among the s sources. Autotransformers may appear in

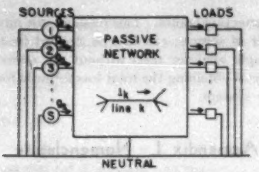

Figure 4. Idealized network

the network, and in their presence the total load current will not necessarily be equal to the total source current. It is assumed that the network connections remain intact.

The following development is exact for the network of Figure 4. With certain approximations and in the range of normal operation, the single-phase diagram of a power system may be visualized as a network of this nature.

Let $i_{kn} = a_{kn} + jb_{kn}$ denote the per-unit current in line k when source n alone supplies a specified set of load currents. The vector reference of i_{kn} is taken as the source n current C_n.

Let $g_1, g_2, \ldots, g_s$ represent per-unit source currents resulting from some arbitrary apportionment of the total load among the s sources of the system. These source currents are referred to an arbitrary, common vector reference. The resulting current in line k may be obtained by superposition

$$\begin{aligned} i_k = i_{k1}(g_1/C_1) + i_{k2}(g_2/C_2) + \ldots + \\ i_{ks}(g_s/C_s) = (a_{k1}+jb_{k1})(c_1-jd_1)/C_1 + \\ (a_{k2}+jb_{k2})(c_2-jd_2)/C_2 + \ldots + \\ (a_{ks}+jb_{ks})(c_s-jd_s)/C_s \end{aligned} \quad (1)$$

Expand the products in equation 1, and separate the real and imaginary parts. The square of the magnitude of i_k is obtained by taking the sum of the squares of these real and imaginary parts. Upon collecting terms in the resulting expression, we obtain

$$\begin{aligned} i_k^2 = a_k^2 + b_k^2 = (c_1^2+d_1^2)(a_{k1}^2+b_{k1}^2)/C_1^2 + \\ (c_2^2+d_2^2)(a_{k2}^2+b_{k2}^2)/C_2^2 + \ldots + \\ (c_s^2+d_s^2)(a_{ks}^2+b_{ks}^2)/C_s^2 + \\ 2(c_1c_2+d_1d_2)(a_{k1}a_{k2}+b_{k1}b_{k2})/C_1C_2 + \\ \ldots + (\text{similar terms for each pair of sources}) + 2(c_1d_2-d_1c_2)(a_{k1}b_{k2} - \\ b_{k1}a_{k2})/C_1C_2 + \ldots + (\text{similar terms for each pair of sources}) \end{aligned} \quad (2)$$

The loss in kilowatts is obtained by multiplying the square of the current in line k by $10DR_k$, and total loss is the sum of the losses in the individual lines; that is

$$P_L = 10D\sum_k i_k^2 R_k \quad (3)$$

Source currents may be expressed in terms of real and reactive power loadings and terminal voltages. If the source terminal voltages (vector expressions) are given with the same reference as source currents, then

$$\begin{aligned} c_n &= (P_n \cos\phi_n + Q_n \sin\phi_n)/V_nD \\ d_n &= (Q_n \cos\phi_n - P_n \sin\phi_n)/V_nD \end{aligned} \quad (4)$$

where positive value of Q_n denotes lagging reactive power supplied to the system.

Upon substituting expressions 4 for c and d in equation 2, the total power loss in kilowatts, equation 3, may be written

$$\begin{aligned} P_L = \frac{P_1^2+Q_1^2}{V_1^2}K_{11} + \frac{P_2^2+Q_2^2}{V_2^2}K_{22} + \ldots + \\ \frac{P_s^2+Q_s^2}{V_s^2}K_{ss} + \frac{P_1P_2+Q_1Q_2}{V_1V_2}\times \\ [K_{12}\cos\phi_{12} - H_{12}\sin\phi_{12}] + \ldots + \\ \frac{P_{s-1}P_s+Q_{s-1}Q_s}{V_{s-1}V_s}[K_{(s-1)s}\times \\ \cos\phi_{(s-1)s} - H_{(s-1)s}\sin\phi_{(s-1)s}] + \\ \frac{P_1Q_2-Q_1P_2}{V_1V_2}[H_{12}\cos\phi_{12} - K_{12}\sin\phi_{12}] + \\ \ldots + \frac{P_{s-1}Q_s-Q_{s-1}P_s}{V_{s-1}V_s}\times \\ [H_{(s-1)s}\cos\phi_{(s-1)s} - K_{(s-1)s}\times \\ \sin\phi_{(s-1)s}] \end{aligned} \quad (5)$$

where

$\phi_{12} = \phi_1 - \phi_2$; $\phi_{13} = \phi_1 - \phi_3$; and so forth

$$K_{nn} = \frac{10}{C_n^2 D}\sum_k (a_{kn}^2 + b_{kn}^2)R_k$$

$$K_{mn} = \frac{20}{C_mC_nD}\sum_k (a_{km}a_{kn} + b_{km}b_{kn})R_k$$

$$H_{mn} = \frac{20}{C_mC_nD}\sum_k (a_{km}b_{kn} - b_{km}a_{kn})R_k \quad (6)$$

The summations in equations 6 are taken over all lines in the network.

Equation 5 gives the total loss in the network as a function of four variables for each source, namely: P, Q, V, and ϕ. The number of additive terms in equation 5 is equal to the square of the number of sources. This expression is rigorous for the hypothetical network of Figure 4. It holds true approximately for power networks in so far as their characteristics conform approximately with those of the idealized network of Figure 4. For adaptation to practical power-system problems, the following simplifications are suggested to obtain a more usable loss formula. The effects of these assumptions may be analyzed for a given system, and a reasonable combination chosen to fit the requirements.

1. Assume the source bus voltage angles remain fixed at the value attained in some typical, intermediate operating condition. Then each quantity in brackets in equation 5 may be treated as a single constant.

2. If the magnitudes of source bus voltages remain essentially constant, then the voltages in equation 5 may be absorbed in the constants.

3. The jb_{kn} components of separate-source line flows will be negligibly small when load power factors are fairly uniform, line resistance-to-reactance ratios are essentially uniform, and loops containing transformers close with regard to turn ratio. This means that the H constants may be neglected and scalar current distribution used for i_{kn}.

4. A convenient form of loss formula is obtained if in addition to items 1 and 2 it is assumed that each source operates at a constant power factor, thus making the ratios Q_n/P_n constant.

$$\begin{aligned} P_L = P_1^2B_{11} + P_2^2B_{22} + \ldots + P_s^2B_{ss} + \\ 2P_1P_2B_{12} + 2P_1P_3B_{13} + \ldots + \\ 2P_{s-1}P_sB_{(s-1)s} \end{aligned} \quad (7)$$

$$P_L = \sum_{m=1}^{s}\sum_{n=1}^{s} P_mP_nB_{mn} \quad (8)$$

where

$$B_{nn} = \frac{(1+r_n^2)}{V_n^2}K_{nn} \quad (9)$$

$$\begin{aligned} B_{mn} = B_{nm} = \frac{1}{2V_nV_m}\{[(1+r_mr_n)\times \\ \cos\phi_{mn} - (r_n - r_m)\sin\phi_{mn}]K_{mn} + \\ [(r_n - r_m)\cos\phi_{mn} + (1+r_nr_m)\times \\ \sin\phi_{mn}]H_{mn}\} \end{aligned} \quad (10)$$

$r_n = Q_n/P_n$

The data calculated from these equations is shown in Appendix IV.

Appendix III. Differential and Incremental Losses

The form of loss formula given in equation 7 or 8 leads to useful relations for an approximate analysis of incremental losses.

Assume that a very small (differential) increase in total load is imposed on the system and that this increase is supplied by source n. The change in total loss is obtained by differentiating equation 7, or 8

$$\begin{aligned} dP_L = \frac{\partial P_L}{\partial P_n}dP_n = [2P_1B_{1n} + 2P_2B_{2n} + \ldots + \\ 2P_nB_{nn} + \ldots + 2P_sB_{sn}]dP_n \\ = \left[2\sum_{j=1}^{s} P_jB_{jn}\right]dP_n \end{aligned} \quad (11)$$

Equation 11 is approximate for finite increments. For an incremental increase in loads, supplied by source n, the change in total loss is obtained by substituting the increased loading of source n, $(P_n + \Delta P_n)$, in equation 7 to obtain a new loss, P_L'. Then

$$\Delta P_L = P_L' - P_L = (\Delta P_n)^2B_{nn} + \left[2\sum_{j=1}^{s} P_jB_{jn}\right]\Delta P_n \quad (12)$$

The first term of equation 12, $(\Delta P)^2B_{nn}$, is an additive correction to equation 11 for finite increments. This correction may be interpreted as the loss which would be incurred if source n alone supplied the system with loads equal to the increment increase only.

It is frequently of interest to investigate the change in loss caused by shifting a block of generation from one source to another, with loads and other sources held constant. Let P_n be increased by increment p_{nm} megawatts, and at the same time let P_m be decreased by the same amount. Neglecting the effects of the incremental loss in so far as it modifies the total generation, the following relation is obtained for the incremental loss. In equation 7 substitute $(P_n + P_{nm})$ for P_n and $(P_m - p_{nm})$ for P_m to obtain the new loss, P_L'. The increase in loss due to the shift of generation is

$$P_L = P_L' - P_L = A_1 p_{nm}^2 + A_2 p_{nm} \quad (13)$$

where

$$A_1 = B_{nn} + B_{mm} - 2B_{nm}$$

$$A_2 = 2\sum_{j=1}^{s} P_j (B_{nj} - B_{mj}) \quad (14)$$

P_j is the initial loading of source j.

The second term in equation 13 may be interpreted as the total differential of equation 7 with P_n and P_m as variables, and the first term is a correction for finite increments. The first term in equation 13 is the loss incurred in sending P_{nm} megawatts (at normal voltage) from n to m over the unloaded transmission network. This interpretation neglects, as a second-order effect, the appearance of the incremental loss in the source loadings of the system.

Appendix IV. B Constants

A complete set of the B constants for the simplified loss formula have been calculated by the use of equation 10 in Appendix II. The values calculated are as follows:

$B_{11} = 0.306$	$B_{13} = 0.138$
$B_{22} = 0.667$	$B_{24} = -0.006$
$B_{33} = 0.229$	$B_{34} = -0.110$
$B_{44} = 0.362$	$B_{23} = 0.166$
$B_{12} = -0.103$	$B_{14} = -0.036$

Inserting these values in equation 7 of Appendix II, the loss formula becomes

$$P_L(\text{kw}) = 0.306P_1^2 + 0.667P_2^2 + 0.229P_3^2 + 0.362P_4^2 - 0.210P_1P_2 + 0.276P_1P_3 - 0.012P_1P_4 - 0.220P_2P_3 + 0.332P_2P_4 - 0.072P_3P_4$$

In computing the B constants, the H constants and the voltage angles ϕ were neglected. Assumed values of constant bus voltage and source power factor are as follows:

Source	V, Per unit	r
1	1.05	0.49
2	1.05	0.23
3	1.00	0
4	1.00	0

The quantity r equals Q/P or the tangent of the power-factor angle.

References

1. Intrasystem Transmission Losses, E. E. George. *AIEE Transactions*, volume 62, 1943, pages 153–58.

2. Co-ordination of Fuel Cost and Transmission Loss by Use of the Network Analyzer to Determine Plant Loading Schedules, E. E. George, H. W. Page, J. B. Ward. *AIEE Transactions*, volume 68, part II, 1949, pages 1152–63.

Discussion

W. R. Brownlee (Commonwealth Services, Inc., Jackson, Mich.): The simplifications developed by the authors for dealing with incremental transmission losses are of material value, especially the not too obvious omission of changes in losses due to changes in reactive kilovalt-ampere flows. While it is true that an incremental flow of kilowatts will actually result in a counter flow (incremental) of reactive kilovolt-amperes, the changes in losses due to the reactive kilovolt-ampere flow difference will be partly compensating. This is based on maintaining approximately constant voltages at generating plants, and departure from this assumption would cause greater changes in indicated losses than the omission reactive kilovolt-amperes from the loss formula.

The need for a thorough understanding of incremental loss calculations is highlighted by the difficulties of securing a check based on actual system readings. Most systems provide hourly readings of generator output, but in some instances the corresponding hourly readings on the low-voltage busses of transmission substations are not available. When these are available, a reasonable indication of total transmission losses might be obtained, but a check of incremental losses would be quite difficult. On the other hand, a high degree of accuracy in loss calculations may not be justified because of changes in syste .l load distribution and voltage differences.

Still further simplification is highly desirable in planning generating-unit additions and even for the more usual operating engineering analyses. In this simplified procedure, a direct comparison is required between two generating plants. The complete system with its many loads and generating stations then may be reduced to an equivalent load and generation at each of these two points, with an equivalent single-line impedance joining them. Since the fuel differences are in per cent, the incremental losses may best be expressed as a per cent of the incremental or transferred power. If the equation given in Figure 3 of the paper is divided by the incremental power, an expression for incremental losses in terms of per cent of the transfer power is secured, this formula being a constant times the transferred power plus another constant. The first term is a linear function of the transferred power times the equivalent line resistance, expressed in per cent on a base, divided by the system base. The second, or constant, term is secured by multiplying the initial equivalent power flow by the per cent equivalent line resistance and dividing by the system base.

L. K. Kirchmayer (General Electric Company, Schenectady, N. Y.): The authors have presented a very good exposition of their method of calculating total and incremental losses stating many of their simplifying assumptions. The method of superposition proposed in their paper avoids a number of the difficulties involved in obtaining the network analyzer data by previous methods in which the output of a given source, with the remaining sources open circuited, is adjusted to a value resulting in approximately 100-per cent current.

A study of the results obtained by making the various simplifications in the calculations proposed by the authors has been made for a 4-generator system. The results indicate that the accuracy obtained is not appreciably affected by the following simplifications which were suggested by the authors:

1. Neglecting the effect of ϕ_{mn} and the H_{mn} terms in the calculation of the power loss coefficients B_{mn}.

2. Neglecting $\sum_k b_{km} b_{kn} R_k$ in the calculation of K_{mn}.

In the authors' discussion of their method it appears that all shunt capacitors, including those representing line charging, are treated in a manner similar to the loads. Is it to be inferred that the assumption has been made that as the total system load varies, the magnitude of the line-charging currents is also considered to vary proportionally?

H. B. Smith (Niagara Hudson Power System, Buffalo, N. Y.): The authors have presented a very interesting paper. I think all will agree with the statement under the section on Conclusions that equation 5 is too complicated for practical applications. However, the authors are to be thanked for developing and presenting this equation as a basis for simplifying assumptions.

Referring to equation 2 of the paper and the simplifying assumptions of Appendix II, I think it is worth while to point out that if all the $j\delta_{kn}$ components are negligible (assuming uniform load power factors, uniform ratios of r/x in the lines, no transformers in the network), then i_{kn} can be obtained by means of a d-c board. Furthermore, if C_n is kept equal to 1.0 per unit in each set of board readings, then all C_n^2 and $C_n\ C_m$ factors disappear in equation 2. In the case of the Niagara Hudson 115-kv transmission system, the foregoing assumptions are easily justified and therefore a d-c board is satisfactory for obtaining data for a loss formula. As I see it, the general form of equation 2 and the equations for determining the constants for the simplified loss formula (equation 7) then become

$$i_k^2 = a_k^2 + b_k^2 = (c_1^2 + d_1^2)a_{k1}^2 + (c_2^2 + d_2^2)a_{k2}^2 + \ldots + (c_s^2 + d_s^2) \times a_{ks}^2 + 2(c_1c_2 + d_1d_2)a_{k1}a_{k2} + \ldots$$

$$K_{nn} = \frac{10}{D}\sum_K a_{kn}^2 R_k$$

$$K_{mn} = \frac{20}{D}\sum_K a_{km}a_{kn}R_k$$

$$B_{nn} = \left(\frac{1 + r_n^2}{V_n}\right)K_{nn}$$

$$B_{mn} = \frac{1}{2V_nV_m} \times [(1 + r_mr_n)\cos\phi_{mn} - (r_n - r_m)\sin\phi_{mn}]K_{mn}$$

E. E. George (Ebasco Services, Inc., New York, N. Y.): This paper is of extreme interest because it removes one of the major difficulties in making accurate loss formulas on extended transmission systems, namely, that of maintaining proper load currents at substations remote from the single source of generation required in previous methods of determining a transmission-loss formula by the principle of superposition.

Although no opportunity to use this new method has arisen in our organization, an

effort will be made to try it out in the near future. The basic idea seems fundamentally sound and practical and may have application in connection with another approach to the calculation of transmission-loss formulas which is now engaging the attention both of the authors and of the discusser.

The assumptions required to be made are not particularly restrictive when one is studying good operating conditions on a system, either from the standpoint of low transmission loss or low delivered cost of power, because in such cases the angles between generating plants will never be very large.

There is still one moderate disadvantage in making transmission loss formulas by the superposition method. This disadvantage is the large amount of calculation, after the board work is completed, in making the coefficients in the loss formula. While this is simple algebra and arithmetic, it becomes very tedious in the case of systems having many generating plants. The work varies as the cube (or a higher power) of the number of generating plants. Any comments by the authors on possibilities of reducing this work would be welcome.

The authors are to be commended on the particularly clear and concise manner in which the paper was presented.

J. B. Ward, J. R. Eaton, and **H. W. Hale:** The authors wish to thank the discussers for their interest in the paper and for their comments and suggestions.

In answer to Mr. Kirchmayer's question regarding line charging, the method of the paper assumes that line-charging currents vary in the same manner as load currents. This is obviously not the correct representation for an essentially constant-voltage system; however, no other satisfactory method of treating line charging separately has occurred to the authors.

The large amount of calculation required, as pointed out by Mr. George, is very imposing when the method is applied to a widespread system. The time and amount of work required to make the calculations of constants (equation 6) may be appreciably reduced by proper subdivision of the several steps in the procedure. Furthermore, certain sums of products may be evaluated directly by analyzer measurements.

A Voltage Gradient Meter

R. L. TREMAINE
ASSOCIATE AIEE

R. C. CHEEK
MEMBER AIEE

EARLY in the studies now in progress on the Tidd 500-kv test lines at Brilliant, Ohio, it was thought that the voltage gradient at the earth's surface might have an important effect on corona and radio influence.[1] Since the phase conductors on a grounded neutral transmission system are grounded for d-c potentials through the transformers, the earth's gradient cannot cause a change in the potential of the conductors. However, it does induce a static charge on the conductors of such polarity and magnitude as to exactly nullify the potential which would exist in space if the conductors were not present. The presence of this induced static charge establishes a gradient on the surface of the conductors which theoretically is superimposed upon the gradient produced by the applied a-c voltage and therefore may alter the corona and radio influence performance of the line.

It was decided to include in the Tidd 500-kv test program studies of the effect of the earth's gradient. No gradient meter satisfactory for use on this project was available, so it was necessary to undertake the design and construction of a suitable instrument. The resulting device has a number of features which have not been available in any such instrument described previously in the literature and it is believed that a description of this instrument will be of value to other investigators.

This paper is devoted exclusively to the design and construction of the gradient meter itself. The studies of the effect of the earth's voltage gradient on corona and radio influence have not yet been completed, and the results will be reported at a later date.

Methods of Measuring Ground Gradients

Voltage gradient has been measured with a variety of methods. Generally speaking they fall into two classes. The more common type has a carefully insulated member which assumes the potential in space at which it is located, and its voltage with respect to ground is measured, usually with an electrometer. The insulated member may be a long wire parallel to the ground,[2,3] a Kelvin water dropper,[3] or some device employing a "collector." This may be a glowing fuse, or a radioactive element such as ionium, radio-thorium or polonium, the latter being more common. The action of the collector is to reduce the time required for the insulated member to assume the potential in space. The insulation requirements in this type of gradient meter are extremely severe, making the instrument sensitive to contamination. Such an instrument requires considerable attention.

The other common type of voltage gradient meter has provision for alternately exposing and shielding a grounded member from the earth's field. The change in the charge is a measure of the voltage gradient. In the earliest types the grounded member was a plate mounted level with earth or a sphere mounted on a hinged rod so that it could be raised or lowered.[4] The change in the charge was measured with a capillary electrometer. An improvement on this method is the so-called generator-type gradient meter which has a continuously rotating member.[5,6] The instrument described in this paper is of this type.

Extremely high voltage gradients may be measured by determining the current in the discharge from a sharp point.[7]

Design Considerations of the Gradient Meter

It was felt that a gradient meter suitable for use in the Tidd studies would have to meet the following specifications:

NECESSARY FEATURES

1. It must be suitable for use as either a graphic or indicating instrument.
2. It must indicate the polarity of the field.
3. It must cover a wide range on a single scale.
4. It must have sufficient scales so that fields of any magnitude likely to be encountered could be measured.
5. It must be insensitive to the a-c gradient from the test line which may be several times the d-c gradient.
6. It must be able to operate continuously in all weather.
7. It must have stable calibration.
8. It must be able to operate on 115 ± 10 volts alternating current.

DESIRABLE FEATURES

9. The ability to measure electric fields accurately without being partially buried.
10. Low insulation requirements.
11. Minimum distortion of the electric fields in the vicinity of the detection element.
12. Simple mechanical design.

The above requirements indicated thet a generator-type instrument should be designed.

Requirement number 5 is peculiar to this application, as the instrument is used in the vicinity of the Tidd experimental transmission lines which are operated at voltages up to 500 kv.

Paper 50-98, recommended by the AIEE Instruments and Measurements and the Transmission and Distribution Committees and approved by the AIEE Technical Program Committee for presentation at the AIEE Winter General Meeting, New York, N. Y., January 30–February 3, 1950. Manuscript submitted November 1, 1949; made available for printing December 2, 1949.

R. L. TREMAINE and R. C. CHEEK are both with the Westinghouse Electric Corporation, East Pittsburgh, Pa.

The authors wish to acknowledge the assistance of C. F. Wagner, S. B. Griscom, and H. T. Akers in the design of this instrument and to thank A. R. Jones and J. S. Kinney for their work in the actual construction and operation of this instrument. They also wish to acknowledge the co-operation of American Gas and Electric Service Corporation.

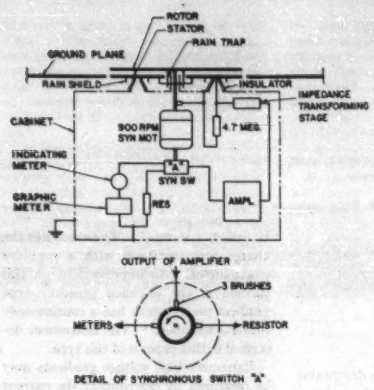

Figure 1 (left). Schematic diagram of electric voltage gradient meter

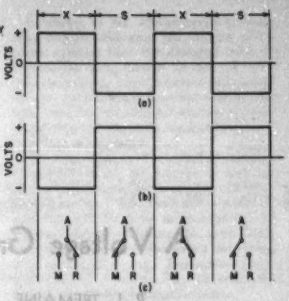

Figure 3 (above). Operation of gradient meter during one revolution of rotor

(a) and (b) show the voltage of the stator for positive and negative fields respectively, and (c) shows the action of the mechanical switch. X and S indicate that the rotor is exposing and shielding the stator from the earth's field respectively. A = amplifier, M = meters, R = resistor

Description of Instrument and Its Operation

The exposed components of the instrument are the detector plates (stator) mounted in the center of the ground plane, and the rotor, which alternately shields and exposes the stator to the earth's electric field. These parts are mounted above the water and dust tight steel cabinet which houses the amplifier, motor, synchronous switch, and recorder. Figure 1 is a schematic diagram. Figure 2 gives a plan view of the rotor and detector element (stator).

For simplicity the explanation of the operation of this instrument will be given as if the stator were solidly grounded, starting with the completely covered position. When the stator is covered, there is no voltage gradient at its upper surface and hence its charge is zero. As the stator is uncovered, it is exposed to the earth's electric field and hence a voltage gradient is present over an increasing portion of its surface. A current flows through the ground connection of such magnitude that the charge distribution in the stator is that which is dictated by the voltage gradient on its surface. By the time the stator is fully exposed, sufficient current has flown through the ground connection so that the charge on the plates is that determined by the gradient at the surface of the earth. Since the charge on any conducting body is a function of the gradient at its surface, the charge on the stator per unit area may be calculated, if the gradient is known, by the equation

$$F = 4\pi q \qquad (1)$$

where

F = statvolts per centimeter

q = statcoulombs per square centimeter

The detector plates have an area of 364.9 square centimeters. The rotor is turned at 900 rpm so the plates are uncovered in 0.01667 second. If a voltage gradient of 100 volts per meter is assumed, equation 1 may be used to show that the current which would flow through the ground connection is 0.001936 $\times 10^{-4}$ amperes.

This current is much too small to be measured directly, so the stator is actually grounded through a 4.7-megohm resistor, and the voltage appearing across this resistor is fed into a special amplifier. The voltage which appears on the stator in the presence of a field of 100 volts per meter is 0.00910 volt. Distortion of the electric field by this voltage is negligible.

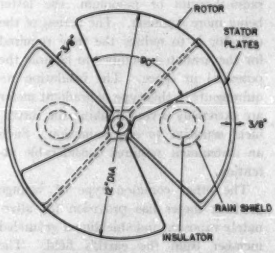

Figure 2. Plan view of rotor and stator which are in the middle of the ground plane

Clearance between stator and ground plane is 3/8 inch

The presence of the 4.7-megohm resistor does not in any way affect the theory of the operation of the instrument, except insofar as the voltage of the stator does not remain at zero.

The distributed capacity of the stator and the leads to the resistor and the amplifier have been kept at a minimum, and is less than 100 micromicrofarads. However, as the stator is covered by the rotor the capacity of the stator circuit increases 300 micromicrofarads. This variation in capacity gives the stator circuit a time constant which varies from less than 0.0005 to less than 0.002 second. These times are very small in comparison with the repetition rate of 30 cycles per second, so the charge on the stator is essentially a function of the position of the rotor.

The voltage on the stator (input to the amplifier) is shown in Figures 3(A) and 3(B) for fields set up by positively and negatively charged clouds respectively. Referring to Figure 3(A), with the stator completely exposed a negative charge is bound on its surface in the presence of a positive cloud. As the stator is covered (shielded) this bound charge is released and flows to ground through the 4.7-megohm resistor. During this period the stator is negative by a voltage equal to the product of the current and the resistance. The opposite condition takes place as the stator is exposed to the electric field. When the stator is uncovered the bound charge must be replaced by a current flowing in the opposite direction and the plates are positive. It is important to note that the average voltage of the stator is zero.

A comparison of Figures 3(A) and 3(B) shows that regardless of the polarity of the electric field the input to the amplifier is exactly the same in magnitude, but displaced by 180 degrees (1/4 revolution) in time. Thus the only intelligence which may be used to determine polarity is time. A mechanical switch is so connected that the output of the amplifier is fed into the graphic and indicating instruments while the plates are being covered and is fed to ground through a resistance equal to that of the meters when the plates are being uncovered. The mechanical switch is a d-c commutator with the segments shorted to form two 180-degree arcs. The action of the commutator is shown in Figure 3(C) and its details in the insert of Figure 1. The brushes are silver-graphite type, Stackpole Carbon Company *WNS-140*, which have low contact drop and low friction making them ideal for this application. An indicating meter and a graphic meter are connected in series with the output of the amplifier so that either or both may be used. The graphic instrument is a standard Westinghouse *5 MA D-C* recording meter.

The gradient meter has been made insensitive to 60-cycle a-c fields by use of a synchronous rotor speed of 900 rpm. Since the rotor and stator are both 90-degree sectors, each incremental area of the stator is exposed to the 60-cycle a-c field for one full cycle and then covered for one full cycle, and the net effect is zero. This statement cannot be exactly true in a practical meter because of the fringing of the electric field around the edges of the rotor. Also, the mechanical switch cannot operate at exactly 180 degrees, because the brushes have physical width and allowance must be made for insulation. The net effect of these departures from an ideal circuit on this meter was that the meter indicated up to ±2 per cent of the crest value of the a-c field in a sinusoidal manner, depending on the phase relation between the a-c field and the rotor. This was reduced to ±1 per cent by filing about 3/32 inch off the edges of the rotor. This minimized the fringing effect. The meter was made completely insensitive to a-c fields by a final adjustment at the test site of the rotor position relative to the a-c field. There is no change in the indication of the instrument in the presence of an a-c field 100 times the magnitude of the unidirectional field.

The meter is housed in a water- and dust-tight metal cabinet. The stator plates are mounted on two large steatite lead-in bowl insulators. The insulators are shielded from rain and are readily accessible for cleaning. They are kept above ambient temperature, to prevent dewing on their surface, by the heat generated within the cabinet. Although the insulation requirement of the insulators is not high, since their resistance need only be large in comparison with 4.7 megohms, these precautions were taken to eliminate any possible error from this source.

A ground plane 4 feet by 4 feet is mounted on top of the cabinet exactly level with the stator plates. It was originally thought that this ground plane was sufficiently large so that the gradient on the surface of the stator would be the same as on the surface of the earth. A flux map of the electric field in the vicinity of the ground plane showed that this hypothesis was not true, and indicated that the ground plane should be extended several feet in all directions. At the time the illustrations shown in Figure 6 were taken this had not been done. The use of an extended ground plane is preferable to burying the instrument so that the stator is level with the surface of the ground. The cabinet itself is grounded to a driven ground rod.

Distortion of the field in the vicinity of the stator is reduced to a minimum by mounting the ground plane level with the stator, by keeping the voltage change of the stator to a minimum, and by mounting the rotor close to the stator. Strictly speaking, the distortion present is not important provided that it is exactly the same when the instrument is calibrated as it is in the presence of the earth's field.

The instrument was calibrated by placing an artificial cloud, a chicken wire screen 8 feet by 8 feet, 9 inches above the ground plane and parallel to it, and applying d-c voltages to the artificial cloud. The ratio of height to width of this set-up was such that the field at the stator was essentially uniform and the artificial cloud was sufficiently high so that any distortion of the field by the rotor would be the same as for a natural field.

The artificial cloud is relatively inconvenient to use, so a quick means of obtaining a check on the calibration of the

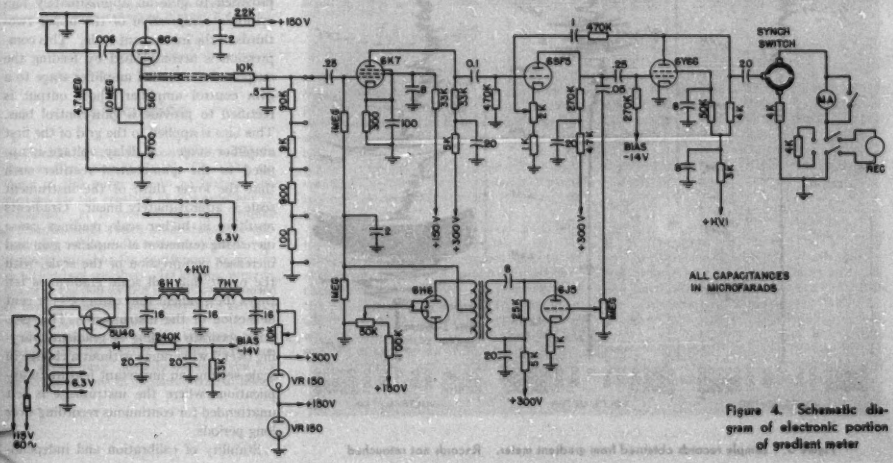

Figure 4. Schematic diagram of electronic portion of gradient meter

instrument was devised. This consists of a metal bushel basket, with an insulated metal plate mounted inside, which can be placed over the rotor and grounded to the ground plane. Provision is made for varying the potential of the plate and for reversing its polarity so that several points on the calibration of the instrument, both positive and negative, may be checked. The check calibrating device is shown in Figure 6(C).

The necessary mechanical components of the instrument were reduced to a minimum by selecting a ball-bearing 900-rpm synchronous motor with a 6-inch shaft at each end. The bearings are sufficiently heavy to take the additional weight of the mechanical switch and the rotor with the motor operating with the shaft vertical. The shafts were sufficiently long so that the rotor could be mounted on one end and the mechanical switch on the other. Standard brush-holders are used. These are supported by a rocker ring mounted directly on the motor frame. Thus all gears, extra shafts, and bearings are eliminated. It was only necessary to mount the motor so that its shaft was in the correct position relative to the stator. A brush is used to ground the shaft.

The instrument is reasonably portable. The ground plane and its supporting brackets can be removed quickly. Loops are provided through which carrying bars are placed and the instrument can be moved like a Chinese carrying chair. All parts except the ground plane remain in place.

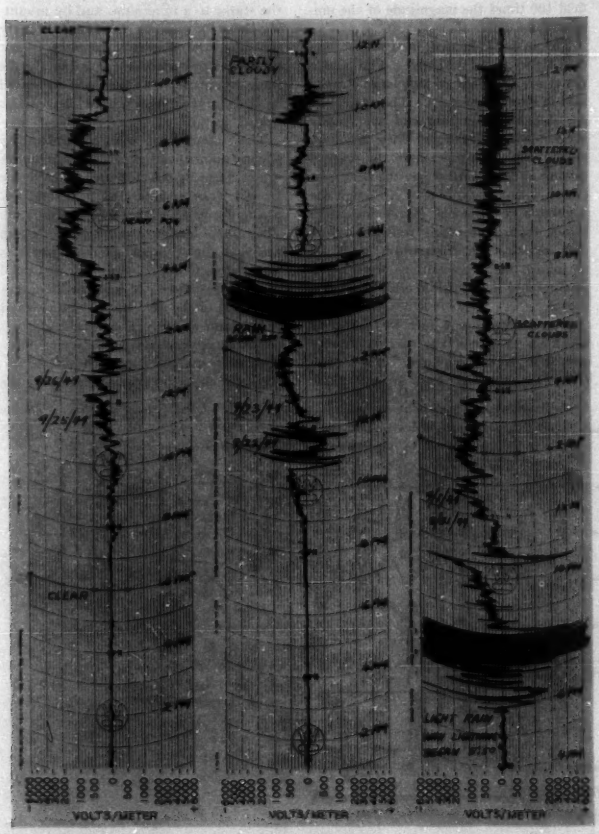

Figure 5. Sample records obtained from gradient meter. Records not retouched

Amplifier

The electronic portion of the instrument consists of two parts, an impedance transforming pick-up unit, located close to the stator detector plates, and a 3-stage resistance-coupled amplifier unit located at the bottom of the instrument cabinet. These are shown schematically in Figure 4.

The pick-up unit is a cathode-follower stage, which serves to convert the stator voltage, which is at a high-impedance level with respect to ground, to a low-impedance level for connection to the main amplifier input. The necessity for running several feet of high-impedance lead from the detector plates to the first-stage grid is thus avoided.

The input circuit of the amplifier proper contains a resistance-capacitance filter which provides an attenuation that increases rapidly with frequencies above 30 cycles, giving the amplifier added immunity to strong 60-cycle fundamental and harmonic fields. A decade attenuator is used at the input to the first amplifier stage to provide full-scale meter deflection at gradients of 40,000, 4,000, 400, and 40 volts per meter.

The measured overall voltage gain of the amplifier proper, including the input filter, is approximately 20,000 or 85 decibels with minimum inverse feedback adjustment.

An automatic gain control circuit is provided to give an approximately logarithmic compression of the upper two-thirds of the instrument scale. This compression is accomplished by feeding the output of the second amplifier stage to a gain control amplifier whose output is rectified to provide a gain-control bias. This bias is applied to the grid of the first amplifier stage. A delay voltage is applied to the gain-control rectifier such that the lower third of the instrument scale is approximately linear. Gradients resulting in higher scale readings cause increasing reduction of amplifier gain and increased compression of the scale, with the result that full scale gradient is ten times the gradient that causes 30 per cent deflection of the instrument. This permits accurate reading of gradients varying over a wide range without a change in scale setting, an important feature in applications where the instrument is left unattended for continuous recording over long periods.

Stability of calibration and independ-

ence of tube changes is obtained by the use of inverse feedback from the output circuit to the cathode of the second amplifier stage. The amount of feedback is made adjustable to provide a small range of over-all gain control for initial calibration.

To insure freedom from motorboating and to reduce the sensitivity of the instrument to supply voltage changes, the plate voltage for the pick-up unit and the first two amplifier stages is regulated. Heavy decoupling is used in the plate circuits of all stages.

Results and Conclusions

At the time this paper was written, the instrument had been in successful operation for three months. Figure 5 shows some sample records which have been obtained, together with the weather conditions at the time of these records. The instrument is shown in Figure 6.

The authors believe that in this instrument they have combined the desirable features of a number of instruments as well as having added a few new ones. The authors do not know of any other instrument which meets all of the specified requirements, and many of these requirements have been more highly refined than on previous instruments. The operation of this instrument has been completely satisfactory and it appears to be ideally suited for its application.

Figure 6. (a) Instrument in operation. (b) Close-up of instrument with door open. (c) Artificial cloud in position for calibration; check calibrating device shown at side. (d) Close-up of amplifier

References

1. Corona Considerations on High-Voltage Lines and Design Features of Tidd 500-Kv Lines, **C. F. Wagner, Anthony Wagner, E. L. Peterson, I. W. Gross.** *AIEE Transactions*, volume 66, 1947, pages 1583–90.

2. Electric Thunderstorm Field Researches, **H. Norinder.** *Electrical World* (New York, N. Y.), volume 83, 1924, pages 223–26.

3. Atmospheric Electricity (book), **B. F. J. Schonland.** Methuen and Company, Ltd., London, England, 1923.

4. On Some Determinations of the Sign and Magnitude of Electric Discharges in Lightning Flashes, **C. T. R. Wilson.** *Proceedings*, Royal Society of London, London, England, volume 92A, 1915–16, page 555.

5. An Electric Field Meter for Use on Airplanes, **R. C. Waddel.** *Review of Scientific Instruments* (New York, N. Y.), volume 19, January 1948.

6. A Recording Generating Voltmeter for the Study of Atmospheric Electricity, **E. J. Workman, R. E. Holzer.** *Review of Scientific Instruments* (New York, N. Y.), volume 10, May 1939.

7. The Distribution of Electricity in Thunderstorms, **George Simpson, F. J. Scrase.** *Proceedings*, Royal Society of London (London, England), Series A, Number 906, volume 161, August 1937.

Discussion

O. Naef (American Gas and Electric Service Corporation, New York, N. Y.): The authors of this paper are to be highly commended for the creation of this excellent instrument. It is one of the few graphic gradient meters which are suitable for outdoor use. Its special features make it particularly suitable for continuous operation in all kinds of weather. Its graphic records, taken at the 500-kv test project over a period of several months, have proved to be very accurate and consistent.

The construction of this gradient meter was inspired by a desire to know all the factors which may possibly explain the observed variations in measured corona losses. Such known factors are the atmospheric pressure, temperature and humidity, rain, sleet, snow and fog, and the condition of the surface of the conductor as influenced thereby.

But even under conditions which are seemingly identical the loss caused by corona is found to vary considerably from test to test.

The atmospheric gradient is one such factor which has been known to vary, but because no measuring instrument was available its effect on corona and radio interference could not be studied. It is hoped that the tests now in progress will in time show whether it has any marked influence, or whether we must be on the lookout for another, hitherto unknown variable.

Meanwhile we welcome the new gradient meter as the latest addition to our large family of recording instruments, which consists of wattmeters, voltmeters, indicators of temperature, atmospheric pressure and humidity, a rain gauge, radio influence meters, and an automatic camera, which takes pictures of moisture collecting on a sample conductor.

R. L. Tremaine and **R. C. Cheek:** The authors are pleased with Mr. Naef's discussion of the gradient meter which we designed and installed at the Tidd 500-kv corona test site. We sincerely hope that it will continue to function as successfully in the future as it has thus far, and that it may provide an answer to the question of whether corona on a practical transmission line is affected by atmospheric voltage gradient.

Solderless Commutator Joints for High-Temperature Operation of Railway Traction Armatures

J. R. REED
MEMBER AIEE

THE advent of the diesel-electric locomotive and its rapid large-scale acceptance by the railroads of the United States have brought to the fore many problems for which solutions must be found. Among the problems related to this tremendous increase in heavy d-c electric traction equipment is that of adequate joints between coil leads and commutator bars in motors subjected to severe operating conditions. This is a problem of long standing in motors operated at high temperatures, but it has become much more acute with the development and use of insulating materials that will withstand more and more heat. The first substantial increase in permissible operating temperatures of such equipment was brought about a number of years ago by the introduction of full class *B* insulation to replace the then standard class *A* or composite insulation. This permissible temperature now has been further increased by the acceptance of class *H* (Silicone)[1] insulation as standard in certain types of traction motors.

For traction motors operated at normal temperatures, the conventional solder joints between coil leads and commutator bar made with lead-tin alloys have proved satisfactory when an area large enough to provide a satisfactory conductivity of the joint is available. However, as operating temperatures have increased in value and design restrictions have decreased the available space for the commutator joint, the factor of safety thus afforded has been reduced to the danger point. This paper describes a method of eliminating entirely easily-fusible material from joints of this type.

As noted, the chief source of difficulty in commutator joints is high temperature of operation. All lead-tin solders between $2^1/_2$ and 85 per cent lead with the single exception of the eutectic alloy (37 per cent lead) have what is known as a plastic range. This is a range of temperature over which the alloy is in the form of a mush or suspension of unmelted crystals in molten metal. This is shown graphically in the lead-tin constitution diagram,[2] Figure 1. At temperatures above this range the alloy is completely liquid, and at temperatures below it, the alloy is completely solid. The eutectic alloy melts abruptly at the lower limit of this range which is constant for all alloys of these two metals within the limits mentioned. This temperature is 361 degrees Fahrenheit. It is at this temperature that these lead-tin alloys soften and begin to flow; and thus, it is at this temperature that the mechanical protection of any lead-tin solder is lost or greatly impaired regardless of the "hardness" of the solder.

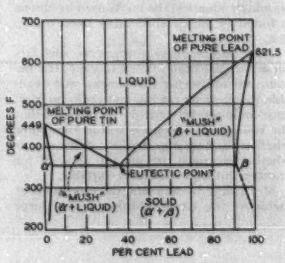

Figure 1. Lead-tin constitution diagram

In armature work where full class *BBB* windings are used with a permissible operating temperature up to, or even in excess of, 300 degrees Fahrenheit, it is obvious that a solder which gives little or no protection above 361 degrees Fahrenheit leaves a negligible factor of safety for overload or other unusual conditions. This situation is further aggravated by the possibility of a high-resistance electrical joint which will cause still additional heat to be generated in the contact area of the solder.

For this reason, it has been customary to use solders with higher melting points for this class of work. Unfortunately, however, such solders are very limited in both availability and desirable properties. The most satisfactory of these has been a solder consisting of pure tin or 95 per cent tin and 5 per cent antimony. Both of these solders give protection to approximately 450 degrees Fahrenheit and are quite satisfactory for use where temperatures never exceed this limit. With the pure tin the plastic range is eliminated entirely, and in the case of the tin-antimony alloy it is reduced to a range of about 5 degrees Fahrenheit. Because of the desirability of some plastic range for ease of working, the tin-antimony alloy is most popular where hand soldering is employed. In addition, the antimony is thought to give a solder which will alloy to a greater extent with the copper being soldered, thus giving a better joint. Pure tin is used prin-

Paper 50-100, recommended by the AIEE Land Transportation Committee and approved by the AIEE Technical Program Committee for presentation at the AIEE Winter General Meeting, New York, N. Y., January 30–February 3, 1950. Manuscript submitted October 27, 1949; made available for printing December 8, 1949.

J. R. REED is a resident engineer with the National Electric Coil Company of Columbus, Ohio, at Pasadena, Calif.

The investigation of solderless commutator connections was made by the author at the San Bernardino, Calif., shops of the Atchison, Topeka and Santa Fe Railway. The author expresses his indebtedness to the Atchison, Topeka and Santa Fe Railway for their valued assistance, general supervision, and making possible the investigation and road testing; and for permission to submit this paper

cipally in solder-pot applications. These are the two solders used most widely in present practice on heavy high-speed diesel-electric traction armatures.

Even though pure tin or tin-antimony solders used with care in either hand-soldering or pot-soldering give a joint which is reasonably satisfactory for armatures insulated with standard class *B* components and operated at normal temperatures, they are not adequate for armatures insulated with class *H* (Silicone) components and operated at the still higher temperatures consistent with this type of insulation.

At present, temperatures are often attained in the operation of these armatures which exceed the melting point of this type of solder. In fact, well over 50 per cent of all armatures returned to the shops of at least one large railway have high-resistance commutator solder joint readings, and over 20 per cent require resoldering. Because of this, much work has been done to develop a solder with a still higher melting point. A number of these solders have been produced and used, particularly during the recent war when the use of tin was restricted; but, for a number of reasons, they have not been satisfactory.

Most of the high-temperature solders are primarily high-lead solders. Analysis of one solder in this class shows lead, 87.50 per cent; tin, 10 per cent; silver, 1.50 per cent; bismuth, 0.50 per cent; antimony, 0.50 per cent. Another solder has: lead, 97.25 per cent; silver, 2.50 per cent, copper, 0.25 per cent.[8] The first of these has a plastic range of 540 to 548 degrees Fahrenheit and the other has a plastic range of 550 to 580 degrees Fahrenheit. Although the melting points of these solders indicate that, from the standpoint of temperature, they are satisfactory for most applications, they still do not leave much factor of safety under present operating conditions even if they are applied with perfect results.

In practice, however, this type of solder is extremely difficult to use with consistently satisfactory results. This is primarily because of the poor spread factor, characteristic of high-lead solders. The spread factor is defined as the area in square centimeters that will be covered on clean copper when one gram of the solder is melted completely. This factor for the high-lead solders averages only about one-fifth that of the high-tin solders. For this reason, these solders are extremely difficult to flow into contacts where there is even a reasonably tight fit, such as is the case with high-speed traction armatures. However, they can be and, in fact, are being used with good results in certain types of d-c armatures where space requirements and general design are more liberal. They also are used with good results in soldering steel-wire coil retaining bands.

In the case of a particular high-speed diesel-electric armature, the electrical conductivity of the commutator joint is only about 1.5 times that of the armature bar, even when a perfect solder job has been accomplished with this type of solder. In practice, however, it has not been possible to obtain consistent soldering results which will give assurance of more than half of this amount, and even this requires careful attention to all details of cleaning, fluxing, and soldering operations with high-lead solders. For this reason, it is not possible with these high-temperature solders to obtain connections in the high-speed traction armatures under discussion, which will be consistently low in electrical resistance. As a consequence of this, heat in excess of the operating heat of the armature is liberated in the very joint which is particularly vulnerable to the effects of the high temperature; and a considerable part, if not all, of the advantage of the higher melting points of the solders is thus nullified. Furthermore, these solders are subject to oxidation as the temperature is increased, and the tendency is to produce joints eventually to high-electrical resistance. In severe operation, this brings on a vicious circle of events.

Although the use of other solders in the high-temperature range has been attempted, this has been without much success up to the present time. This is primarily because of the difficulty of getting an alloy which will flow readily into the small spaces involved and adhere properly to the copper bars with fluxes that are available for soldering operations on electric apparatus at these relatively elevated temperatures.

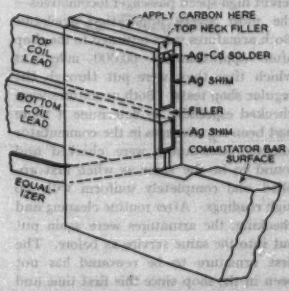

Figure 2. Sketch showing the use of the silver shim to tighten the coil leads in the commutator risers

The silver-cadmium solder is used to bond the top filler to the commutator risers

Tests were made with low-temperature brazing to determine if this might not possibly be a satisfactory solution to the problem. This was ruled out, however, by a number of factors. Chief among these is that the temperatures involved are destructive to the commutator insulation where such a sizable joint must be made so deep in the commutator bar as is the case with short riser bars characteristic of high-speed traction armatures where equalizer coils must often be connected actually below the level of the commutator surface. In addition to this, the work involved in milling out these connections, even if they were feasible, would so increase the cost of a subsequent rewind that this alone would make the method prohibitive.

With brazing thus ruled out, and since no suitable solder in the temperature range above 600 degrees Fahrenheit and below 700, or possibly 750 degrees Fahrenheit was available, tests were undertaken to determine if a suitable soft joint could be obtained by the use of silver plating and the complete elimination of a fused connection. With this in mind, two sets of special armature coils were manufactured incorporating a heavy silver-plated lead section in place of the then standard tinned leads. Two armatures were prepared for these coils and the commutator risers were thoroughly cleaned of all residual solder and tinning by means of a pneumatic disk sander with fine grit. Care was taken to preserve as nearly as possible the original surface of the copper bar and to avoid an irregular surface which might interfere later with the plane surface contact which it was hoped would be obtained.

After the risers were thoroughly cleaned in this manner, the inside surfaces of the riser slot were silver-plated by means of a portable silver-plating apparatus using controlled direct current and a silver-cyanide electrolyte. The current was controlled by means of surface pressure and voltage so that as nearly as possible, a bright plate was obtained. The silver was built up to a thickness of approximately 0.0005 inch and the commutator thoroughly cleaned with pure water and then baked and tested for bar-to-bar resistance. Satisfactory cleaning was achieved with the first attempt.

Following this preliminary preparation,

Figure 3. Bearing failure which allowed armature to rub on the pole pieces and practically wreck itself

the armature was wound in conventional manner with the special coils, with the exception that the commutator risers were blocked ahead of the leads being laid, and the connections were shimmed to produce a very tight circle of the risers. The material used for this shimming was fine silver shim stock rolled to a thickness of 0.003 inch and inserted in approximately every fourth or fifth riser as was needed to maintain the tight fit. The silver was used in the annealed form and was inserted as a U-shaped piece placed around the coil lead as it was driven into place in the commutator riser, as shown in Figure 2. The leads were driven into place as tightly as possible without causing appreciable upsetting of the copper. No shims were used with the equalizer winding, and these leads were actually upset into the bottom of the riser slots so as to produce a tight fit without shims. This was possible because of the relative difference in the dimensions of the equalizer leads as compared to the main coil leads and their location at the bottom of the slots.

As the winding progressed, first the equalizers and then the bottom main coil leads were "mudded in" with inorganic filled Silicone compound. This material was used to fill completely the space back of the risers to eliminate the possibility of varnish getting into the joint in subsequent impregnation. Finally as the top coils were laid as described, the remaining space behind the risers and the spaces at the ends of the cores were filled with inorganic filled Silicone compound and the armatures hot banded and wedged.

After checking the armatures for resistance in the standard manner, the remaining space in the riser slots above the top coil leads was filled in for mechanical reasons and to present a smooth contour. In the first armature this was done by brazing a copper filler into the opening with a phosphorus silver alloy material. However, as pointed out previously, this introduced the rather serious problem of stripping the armature for subsequent rewinding, and although this has not yet been done, it is evident that a softer filler would be of considerable advantage from this standpoint. For this reason, the second armature was finished by soldering the top filler into the risers with a special alloy consisting of 95 per cent cadmium and 5 per cent silver, and having a melting point between 640 and 740 degrees Fahrenheit. This solder was heated by incandescent carbon applied from the top under pressure and was fluxed with an acid-type flux used very sparingly. Actually, a small piece of the soldering alloy was placed in the slot under the filler which was deep enough to extend above the top of the risers. The carbon was applied to this filler and held until the solder melted and the filler settled into its place, see Figure 2. The results obtained in this way were very satisfactory and produced a mechanically strong bond at the top of the risers to prevent radial movement of the coil leads. The fillers could still be driven out much as the standard soldered fillers, and did not require milling or sawing as did the brazed fillers. A simple jig and carbon holder was arranged so that very little time was required for this operation.

Both armatures were vacuum pressure impregnated in the usual manner with the exception that special precaution was taken to prevent the varnish level in the tanks from coming up over the risers during the process. Final tests were completed and the resistance readings, indicating the relative conductivities of the commutator connections, showed them to be completely uniform and fully as low as the best of the solder jobs which were being tested with the same equipment.

The two armatures were placed in different high-speed passenger locomotives—the most severe application available. Both armatures were returned to the shop after approximately 60,000 miles, at which time they were put through the regular shop tests. Both armatures were checked especially to determine if there had been any changes in the commutator joints. Resistances were checked and found to be the same as when first applied and completely uniform with no high readings. After routine cleaning and checking, the armatures were again put out into the same service as before. The first armature to be rewound has not been in the shop since this first time and now has a mileage of more than 300,000 miles.

The second armature, however, was returned again after an additional 50,000 miles when the second locomotive to

Figure 4. Close-up of commutator risers of the armature shown in Figure 3

Even though commutator temperature was raised to approximately 700 degrees Fahrenheit or more, as was evidenced by the melting of the cadmium-silver solder in the top fillers, no damage was done to the riser connections

which it had been applied was in the shop for an annual overhaul. The armature was again checked carefully, and all resistance readings were found to be excellent and uniform, indicating that there had been no deterioration in the conductivity of the riser connections. There was no evidence of any excessive or localized heating as is evident in a majority of soldered armatures operated under the same conditions, even though they may not have failed. After routine cleaning and checking and reimpregnation, the armature again was placed in service on a similar locomotive where it remained in service for an additional 95,000 miles. After this additional mileage, it was returned to the shop following a complete bearing failure which allowed the armature to drag on the pole pieces and wreck itself, as is shown in Figures 3 and 4. This failure, after 206,000 miles of severe service, was not in any way the result of a winding failure, but rather was caused by a mechanical failure.

Fortunately, the commutator risers were not destroyed by the failure and were left in excellent condition for detailed inspection and study. At the time of the failure, the temperature of the commutator was in excess of 700 degrees Fahrenheit as was evidenced by the fact that the cadmium-silver solder in the top fillers had melted and run. All of the external varnish had been charred or entirely burned out. The glass-base bakelite wedges had been charred or burned out entirely. In spite of this, as was to be expected, the riser connections showed no signs of damage from the heat. There had not been any movement of the bars in the risers even at the time of failure, though the coils had been thrown from the slots in about one-fourth of the armature and had dragged on the pole pieces.

After external inspection, the coils were

cut off behind the risers and the risers themselves carefully stripped to study the nature and condition of the contact. It was found that there had been some cold welding of the silver surfaces in all of the slots while some, especially on the equalizer coils,[4] had considerable cold welding. This latter was probably due to the tighter fit of the equalizers caused by the upsetting of the copper during winding. This caused a much higher contact pressure in the constricted bottom portion of the riser slot than was obtained in the less restricted upper portions of the slots where the coils were merely wedged tightly. Some of the equalizer leads were welded so tightly that they required sawing to remove them from the slots.

There was only slight evidence of oxidation of the contact surfaces, and in no case was there any evidence of contact burning as so frequently takes place in soldered connections. There was considerable varnish in many of the contacts. This was probably due to capillary action during impregnation, by which the varnish filled the open spaces in many slots leaving free only those surfaces that were actually in solid contact. This condition should be prevented or at least minimized by more care in sealing behind the commutator before impregnation. It may possibly have been caused by improper care in one of the impregnations to which the armature was subjected during its life, and greater care in this respect also might be indicated. Actually, the presence of a varnish film in a portion of the contact area is of little consequence, because conductivity equivalent to that of the armature bar can be maintained in the commutator contact, if over 90 per cent of the available area is unused. In other words, with silver-to-silver contact, the designed factor of safety of the connection with respect to electrical conductivity is about 15 as compared to approximately 1.5 for a perfect solder contact.

In addition to this much greater factor of safety, is the fact that silver oxide between silver surfaces breaks down to pure silver at temperatures above 356 degrees Fahrenheit.[5] For this reason, it seems that electrical conductivity of the silver joint would be improved materially following subjection to temperatures which would destroy a soldered contact. These higher temperatures, if they were attained, also would tend to destroy any varnish film that might be in the contact. It also seems that repeated oxidation and reduction of even a portion of the silver surfaces accelerates to a large degree the welding of the silver to a more solid contact. This, of course, would complement the natural cold-welding characteristics of the silver which also are accelerated as the temperature is increased.

As a further practical test of this type of commutator connection, it is proposed that another ten armatures be wound in this manner and put into service under severe operating conditions as were these two.

Certainly there will be refinements in technique to improve the contacts as well as to reduce the labor involved in making them. The use of new or rebuilt commutators manufactured with silver-plated riser slots in place of tinned slots would be a big step in this direction. However, even with the present methods described in this paper, it is expected that a definite saving can be shown in labor as compared with standard soldered joints.

On the basis of the preliminary tests which have been conducted, and on the basis of the performance of the two test armatures in actual road service, it seems safe to conclude that this method of making commutator connections, although a radical departure from accepted practice, offers a practical step toward the much-needed solution to the problem of furnishing a satisfactory connection between commutator and coils for operation at temperatures above the limits of soldered joints in equipment which does not lend itself to the application of brazing. The problem, as stated previously in this paper, is becoming increasingly acute as insulations are being adopted which will materially increase the temperature limits for traction armatures. Even with the present standard insulations, a high percentage of electrical failures are caused by weaknesses of soldered connections. The high percentage of failures will certainly increase rapidly with each small increase in loading made possible by improved insulation if steps are not taken to correct the condition.

References

1. Introduction to AIEE Standards. AIEE Standard Number 1, June 1947.

2. The Constitution of Lead-Tin Alloys, D. Stockdale. *Journal*, Institute of Metals (New York, N. Y.), volume 49, 1932, page 267.

3. Substitute Solders, F. N. Rhines, W. A. Anderson. *Metals and Alloys* (New York, N. Y.), November, 1941, pages 704–11.

4. Silver in Industry (book), Lawrence Addicks. Reinhold Publishing Company, New York, N. Y., 1940, page 197.

5. Ibid, page 187.

No Discussion

Synthetic Load for Testing Rectifiers

C. L. TETHEROW
MEMBER AIEE

WHEN metallic rectifiers are designed specifically for providing charging currents for electric storage batteries the selection of satisfactory test loads presents somewhat different problems from those normally encountered. The conventional type of ordinary variable resistance load proved unsatisfactory for this application and the need for some type of standard test load for this class of rectifier was indicated with the development of the so-called "fast-rate" battery chargers.

When speaking of "fast-rate" battery chargers, reference is made to the popular portable rectifiers which have been designated to charge the ordinary type of 6-volt automobile storage batteries at rates of from 70 to 100 amperes. Colloquially speaking, these chargers are claimed to "charge your battery while you wait". Actually they are designed to charge the average automobile battery in 40 to 60 minutes. For convenience they are provided with a pair of battery clips attached to suitable lengths of heavy-duty flexible leads so that the battery may be charged without removing it from the automobile and the connection to the source of energy is usually obtained from a generous length of power supply cord with attachment plug cap for connection to ordinary 15-ampere 125-volt outlet receptacles.

Because of the inherent low efficiency (over-all efficiency usually less than 50 per cent) of these devices, their input requirements generally border on the 15-ampere maximum allowed for portable equipment which is intended to receive its energy from ordinary 15-ampere 125-volt outlet receptacles. If input currents in excess of 15 amperes are indicated, the equipment must be provided with supply cords and attachment plug caps of suitable rating (usually 20 amperes or more) which will not fit 15-ampere outlet receptacles. Since the input requirements of this type of rectifier are dependent upon the output load, careful consideration of the proper output load is necessary in order to ascertain the input current rating.

Prior to the introduction of this particular type of rectifier, ordinary variable resistance loads had been utilized for testing rectifiers. Apparently this type of load had proved satisfactory previously and output name-plate ratings were taken at their face value when determining the output load to be used for testing purposes. The justification of the use of an ordinary variable resistance test load for "fast-rate" battery chargers was questioned and consequent investigations indicated that test procedures established previously were inadequate for this type of rectifier.

In conducting investigations, attempts have always been made to utilize test procedures which simulate as nearly as practical the actual operating conditions of the device in the field. A sincere effort also is made to maintain a minimum of discrimination between various manufacturers of similar classifications of equipment by establishing standard test procedures which are applied to all devices of a particular classification. Therefore, the problem at hand was to establish a standard test procedure for this type of rectifier which would satisfactorily maintain the foregoing policies.

Since applications were being received for investigations of "fast-rate" battery chargers with rated outputs of six volts at 100-ampere direct current, the question arose as to what minimum output voltage was actually required to charge a 6-volt battery at a 100-ampere rate. An investigation of considerable length was conducted using various sizes and ages of batteries in various conditions from completely-charged to completely-discharged status. No definite conclusions could be established from these results so as to specify any minimum charging voltage.

However, it was determined that most batteries in healthy condition (no excessive sulphation of plates or not worn out to the point where they would no longer maintain a useful charge) could be charged at a 100-ampere rate by the application of a potential from 7.2 to 8.5 volts. One exception was noted under special conditions when an output potential of approximately 6.9 volts was sufficient to charge a particular battery at a 100-ampere rate. It also was noted that under various conditions of sulphated plates, rectifier output potentials considerably in excess of 8.5 volts were required. However, when the plates of these particular batteries were sufficiently desulphated, the majority of them could be charged at a 100-ampere rate with rectifier output potentials of 8.5 volts or less.

The results of these tests indicated that the standard procedure of utilizing an ordinary variable resistance load adjusted for rated name-plate output of six volts at 100-ampere direct current was unsatisfactory. Comparative tests between resistance loads and battery loads utilizing the same rectifier at the same output potentials and currents indicated entirely different operating characteristics of the rectifier. Widely different input characteristics were noted, as well as variations in operating temperatures and efficiency. The use of an ordinary variable resistance load was thus proved to be unsatisfactory for the testing of "fast-rate" battery chargers since field operating conditions could not be satisfactorily approximated.

The only obvious alternative apparent

Paper 50-102, recommended by the AIEE Domestic and Commercial Applications Committee and approved by the AIEE Technical Program Committee for presentation at the AIEE Winter General Meeting, New York, N. Y., January 30–February 3, 1950. Manuscript submitted October 13, 1948; made available for printing December 8, 1949.

C. L. Tetherow is with the Underwriters' Laboratories, Inc., Chicago, Ill.

The author wishes to express his gratitude to H. Worthman of Hammet Electric Manufacturing Company for his assistance in this work.

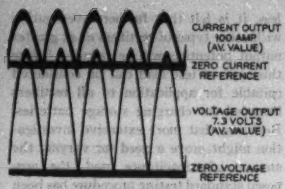

Figure 1. Resistance load

at this time was the use of some type of standard batteries as a test load. In order to assure minimum satisfactory margins of safety, it appeared from previous test results that a set of standard batteries was needed which would require rectifier output potentials of approximately 8.5 volts in order to charge them at a rate of 100 amperes. Obtaining such a set of batteries was impractical for several quite obvious reasons.

Experience gained from attempting to determine what potential was required to charge a battery at a 100-ampere rate indicated that it was extremely difficult and certainly impractical to obtain two batteries with similar charging characteristics. It was further noted that any specific battery exhibited different charging characteristics each time it was charged. An investigation indicated that the following variable conditions have a distinct bearing on the charging characteristics for any given battery, namely: age of the battery; number of times cycled; rate of discharge; amount of discharge; length of time allowed to stand between charges; and condition of the battery solution.

Since so many variables of battery conditions affect their charging characteristics, the idea of attempting to use batteries for a test load was questionable. The battery load was abandoned at this time as it was apparent that there was no assurance that similar loads and test procedures would be applied to devices received from different manufacturers, or, for that matter, to different models received from the same manufacturer. It was apparent at this point that some type of test load was required which would simulate the characteristics of a battery and still maintain stable control features.

It was suggested that a high capacitance in parallel with a variable resistance could be made to approach the characteristics of a battery load. This seemed possible as it was pointed out that the capacitors would tend to retain a potential across the load at all times, thus simulating to some extent the potential maintained across the output terminals by the battery. Because of the extremely low resistance characteristics of the load, a considerable amount of capacitance is required to maintain an appreciable amount of potential across the output terminals of the rectifier. The problem of obtaining the necessary amount of capacity was not too difficult since low-voltage capacitors could be used.

Electrolytic capacitors rated at 25 volts in 10,000 microfarad capacity units were obtained. These units are contained in metal cans approximately 3 inches in diameter by $4^1/_2$ inches high. A unit containing ten of these capacitors can be housed in an enclosure having approximate over-all dimensions of 6 by 7 by 17 inches. With such a unit it was possible to experiment with capacitances of from 10,000 to 100,000 microfarad in 10,000-microfarad steps.

The entire 100,000-microfarad capacitance was found to give extremely satisfactory results from several standpoints. For identical output values of current and voltage, with identical input voltages, it was noted that the input current variation between the battery load and the capacitance-resistance load was less than 1 per cent in all cases. Comparative temperature tests were conducted and final constant temperature variations did not exceed 2 degrees centigrade in any instance. Three different types of metallic rectifiers were used during these tests and it was noted that the capacitance-resistance load caused no appreciable variations in any of the operating characteristics of the devices investigated. Reducing the capacitance from 100,000 microfarads to 50,000 microfarads caused very little variation in the input current requirements; however, oscilloscope pictures indicated some variation in output voltage wave characteristics.

Reference is made to Figures 1, 2, and 3 for typical output current and voltage wave characteristics for the three types of loads discussed. Figure 1 illustrates the wave shapes characteristic of a resistance load. The expected symmetry of wave shape is shown and it is noted that extremely high potential peaks are required in order to offset the momentary zero values and maintain an average voltage equivalent to that obtained for the other two types of test loads.

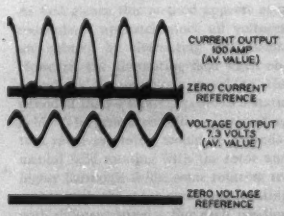

Figure 2. Capacitance-resistance load, 100,000 microfarads

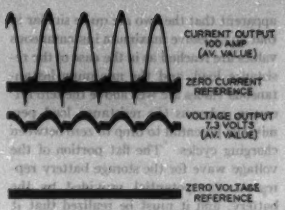

Figure 3. Storage battery load

The wave characteristics typical of a capacitance-resistance load are illustrated in Figure 2. Features of these wave characteristics noteworthy of attention are the increased peak values of the current as compared to the resistance load, the small reverse currents, the peculiar current wave shapes in the vicinity of the zero current reference line, the low-peak values of the voltage wave as compared to the resistance load, and the minimum instantaneous voltage values as compared to the zero voltage reference line. It is interesting to note that maximum instantaneous current values of the capacitance-resistance load are approximately 40 per cent greater than those of the resistance load, whereas the exact reverse is true of the maximum instantaneous voltage values.

An analysis of Figure 3, which illustrates the typical wave characteristics obtained for a storage battery load, indicates some rather interesting features. A comparison of this current wave with that obtained in Figure 2 for the capacitance-resistance load shows a rather high degree of similarity with respect to maximum instantaneous values and general wave shape.

In fact, a careful analysis of the two current waves is required in order to distinguish any variations. The most pronounced difference in these two current waves appears to be in the amount of reverse current occurring during the momentary time between charging cycles. This difference is so small and of such short duration that it is considered relatively unimportant.

Although there is considerable difference between the general wave shapes of the voltages for these two loads, it is

apparent that the two are quite similar in that no excessive maximum instantaneous values are reached as in the case of the resistance load, and the minimum instantaneous values are well above the zero reference, whereas the resistance load permits the potential to drop to zero between charging cycles. The flat portion of the voltage wave for the storage battery represents the potential provided by the battery, and it must be realized that it would be impractical to supply a sufficient amount of capacitance to approach duplication of this characteristic.

A decrease in the amount of capacitance used caused an increase in the amount of variation between the maximum and minimum instantaneous voltage values and smaller reverse currents between charging cycles. Increasing the amount of capacitance used caused a decrease in the amount of variation between the maximum and minimum instantaneous voltage values and larger reverse currents between charging cycles. Therefore, it appears that the larger the capacitance used the nearer the approach can be made to the wave characteristics of the storage battery load. However, further analysis of the wave characteristics of capacitance-resistance load shows the current leading the voltage by a small angle. In order to prevent too large a phase difference between the current and voltage the amount of capacitance used must be limited accordingly. On the assumption that the power factor of the load should be maintained within certain limits, it would be necessary to vary the capacitance used in accordance with the charging rate. This would probably be considered necessary for certain research problems. It is not the purpose of this paper to attempt to establish specified amounts of capacitance for particular test loads, since the requirements for various particular problems will undoubtedly be subject to considerable variation.

Test results have actually indicated that the amount of capacitance used is not very critical. As far as input currents and temperature characteristics are concerned for the particular problem, the practical results from a 50,000-microfarad capacitance was almost as satisfactory as those obtained from a 100,000-microfarad load. Recent results obtained from a low-rate battery charger of the metallic-rectifier type have caused considerable doubt to be cast upon the importance of maintaining a specified limit on phase relationships. The entire 100,000-microfarad capacitance was used in experimenting with a battery charger whose rated output was 5 amperes, and as far as could be determined there was no appreciable effects on the operating characteristics of the rectifier. Oscilloscopes indicated an acceptable degree of similarity in output wave characteristics, and input and temperature characteristics were not appreciably affected. The phase relationship in most cases is believed to be relatively unimportant. It appears that it is more important to ascertain that sufficient capacitance is provided to maintain a substantial value of minimum instantaneous potential across the output terminals of the rectifier between the charging cycles.

Time did not permit an extension of the investigation to the point where determination could be made of what minimum amounts of capacitance might conceivably give satisfactory results or what variations in amounts of capacitance might be indicated for various charging rates. Although this particular investigation was limited to metallic-type rectifiers with maximum output potentials of 15 volts or less, it is felt that further investigation with other types of rectifiers or at greater output potentials will be required before this type of test load can be considered suitable for application to all rectifiers intended for charging storage batteries. Realizing that more extensive investigation might prove a need for varying the amount of capacitance used, the proposed standard testing procedure has been arranged to read as follows: "A suitable resistance shall be connected in parallel with the proper capacitance in such a manner as to produce output wave characteristics similar to those obtained when charging a storage battery at the prescribed rate."

Although the use of the synthetic (capacitance-resistance) load has not been formally adopted at this time, it appears to be an effective method for establishing a uniform test procedure for metallic rectifiers intended for battery-charging purposes. It is realized that the synthetic load described does not perfectly simulate the characteristics of a storage battery load; however, it appears to be considerably superior to the resistance load method, and it provides a positive means of controlling the load which is impractical to obtain by the use of storage batteries. It also provides a standard test procedure, thus enabling application of identical testing methods and loads to all equipment of this classification. In addition to the foregoing advantages it eliminates the problem and inconvenience of storing and properly maintaining a large number of various sizes of storage batteries. It is believed that the problem of selecting a satisfactory test load for metallic rectifiers intended for charging storage batteries has been satisfactorily solved by the use of the synthetic or capacitance-resistance type load.

No Discussion

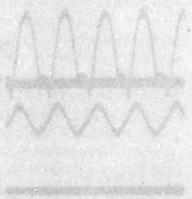

Static Accuracy Performance of the Selsyn Generator Control-Transformer System

G. KRONACHER
ASSOCIATE AIEE

THE selsyn-generator control-transformer system, as shown in Figure 1, electrically transmits an angular position. The function of the generator or transmitter is to transform the angular position of its rotor shaft into an electrical signal. The selsyn generator is built like a synchronous 3-phase generator with laminated rotor, having either a concentrated or distributed rotor winding. The rotor winding is connected to an a-c power supply. Thus to each rotor position corresponds a definite set of three voltages between the stator winding terminals. This set of voltages is the electrical signal transmitted by the generator.

The function of the control-transformer or receiver is to transform this electrical signal into an angular position of its shaft. The control-transformer impedances are higher than those of the generator, otherwise the control-transformer is built like a generator. The rotor winding terminals are generally connected to the input of an amplifier. The signal voltages of the generator produce three currents in the 3-phase stator winding of the control-transformer. Assuming perfect conditions, the axis of the magnetic field produced by these currents would be parallel to the generator rotor axis. Therefore, the voltage induced in the rotor-winding is a measure of the angle between the generator rotor and the control-transformer rotor. Particularly, a zero rotor-voltage indicates that the control transformer rotor is at right angles with the generator rotor. This position of the control transformer rotor is defined as its position of correspondence. To obtain only one position of correspondence, the sign of the variation of the rotor-voltage when moving the rotor from its position of correspondence also must be defined.

At standstill this system would work without error if all windings were sinusoidally distributed, if the air gap were uniform and if the 3-phase system were balanced. In reality these conditions are not fulfilled, partly because of the design limitations and partly because of inaccurate manufacturing. The errors caused by inaccurate manufacturing shall not be discussed in this paper. The purpose of this paper is to calculate the inherent errors of generator and control-transformer with respect to the design data. Both the physical reason for these inherent errors as well as formulas for their calculation will be given.

The primary cause for the inherent error is the nonsinusoidal distribution of the windings. A secondary cause for errors, only attenuating or intensifying that of the primary cause, is due to the slot openings.

The following development is based mainly on the revolving field theory. At first glance this method appears as a roundabout approach since all voltages are induced by alternating axial fields. However, the alternating field when observed in time-intervals equal to the period of the a-c input appears as a static field. The generator field, corresponding to a revolving rotor, would be a fundamental field rotating with the rotor and higher harmonic fields, some rotating together with the rotor and some rotating with different speed. For each position θ of the generator rotor, Figure 1, the fundamental field together with all higher harmonic fields may be replaced by one equivalent fundamental field, which would produce the same voltage signal. In Figure 1, the real fundamental field is represented by the vector $\boldsymbol{B}_1$ and the equivalent fundamental field is represented by $\boldsymbol{B}_e$. The angle ϵ_g between these two vectors is the error of the generator. Looking at the control transformer field, there can be seen a fundamental field $\boldsymbol{B}_1'$ revolving parallel with the equivalent generator field $\boldsymbol{B}_e$ and higher harmonic fields revolving either forwards or backwards. Due to the higher harmonic fields the voltage induced in the rotor winding is not zero for a rotor position 90 degrees ahead of the vector $\boldsymbol{B}_1'$, but at an angle 90 degrees $+\epsilon_c$ ahead of B_1'. The angle ϵ_c through which the control transformer rotor has to be turned ahead of its theoretical position of correspondence with respect to the voltage signal in order to obtain zero flux-linkage in its rotor winding is the control transformer error. The sum of the generator error ϵ_g and the control-transformer error ϵ_c is the total error. It is evident that the generator error also depends on the generator load, since the voltage drop in its stator winding may influence the voltage signal.

As outlined before, the revolving field theory is the basis for the further considerations. This theory represents the total air gap field of a machine, generally a nonsinusoidal field which, while revolving, changes periodically its size and shape, in terms of a series of harmonic sinusoidal fields, each field being constant in time, but rotating in space with its proper speed. The first step in order to obtain this kind of representation is to

Paper 50-103, recommended by the AIEE Feedback-Control Systems and Rotating Machinery Committees and approved by the AIEE Technical Program Committee for presentation at the AIEE Winter General Meeting, New York, N. Y., January 30–February 3, 1950. Manuscript submitted April 27, 1948; made available for printing December 8, 1949.

G. Kronacher was with General Electric Company, Schenectady, N. Y., at the time this paper was written. He now is with Air Associates, Inc., Teterboro, N. J.

The author acknowledges and appreciates the encouragement and co-operation given by A. E. Blume, D. B. Harrington, and R. W. Votaw.

Nomenclature

A_ν = νth harmonic space vector of the stator point
B = air gap flux density
$\mathbf{B}_\nu$, B_ν = vector and amplitude of νth harmonic flux density distribution
$\mathbf{B}_e$, B_e, $(B_\nu)_1$ = vector and amplitude of equivalent fundamental field
C_0, C_{1s}, C_2 = Fourier coefficients of air gap permeance
$\mathfrak{F}$ = magnetomotive force
$\mathfrak{F}_c$ = magnetomotive force of one coil
$\mathbf{\mathfrak{F}}_\nu$, $\mathfrak{F}_\nu$ = vector and amplitude of νth harmonic magnetomotive force
k_ν = νth harmonic reduction factor
i_a, i_b, i_c = phase currents
n = any positive integer number
p = air gap permeance per unit area
p_0 = air gap permeance of a machine without slots
s_ν = skew factor
t = number of turns per phase of a winding
w_c = number of turns of a coil
w_s = number of series conductors of a coil side
$\mathbf{W}_\nu$ = νth harmonic winding vector
z_r, z_s = number of rotor or stator teeth
Z_l, Z_d, Z_q = load impedance, direct axis impedance, quadrature axis impedance
α = stator co-ordinate
α_n = co-ordinate of coil side "n"
β = rotor co-ordinate
γ = rotor pole arc
γ_i = ideal rotor pole arc
ϵ_g, ϵ_c = generator error, control transformer error
θ = position angle of axis of rotor coil in generator
θ' = position angle of axis of rotor coil in control transformer
$\theta_0 = \theta + \epsilon_g$
λ = mutual skew angle between rotor and stator slots
Δ = position angle of fundamental magnetomotive force field produced by a 3-phase winding
ν = order of a harmonic component of a periodic curve
$\psi_{\nu\alpha}$ = flux linkage between a νth harmonic field and a winding if both axes form an angle α

establish the flux-density distribution produced by each coil of one phase. Next the curves representing the flux densities are resolved into its Fourier components. Then all Fourier components of equal period are added together. Thus one Fourier series representing the total air gap flux of one phase is obtained. The total air gap field, created by all the phases of the winding, is obtained by superimposing the various phasefields, considering at the same time that one standing oscillating magnetic field may be represented by two equal fields constant in time and rotating in space in opposite directions. In order to consider the effect of the permeance-variations caused by the slot openings, the corresponding distortion is considered separately for each component of the resultant Fourier series. In the following development it was not necessary to consider time harmonics in the induced voltage, caused by the magnetic nonlinearity of the iron, since the position of correspondence of the control-transformer is determined by the fundamental rotor voltage only.

The Air-Gap Field

The magnetic field of a salient-pole, open-circuited generator is first analyzed under the assumption of a smooth stator surface. Later on care is taken of the distortion of the field caused by the stator slot openings. Figure 2 represents the flux-density distribution B along the rotor. In order to obtain quickly an approximate expression for the flux density, a rectangular flux-density distribution, as shown in Figure 2, is assumed. The width γ_i of this rectangle, the ideal pole-length, is determined by the condition that the total flux represented by the rectangle is equal to the real flux. For reasons of symmetry the magnetic potential drop is $+\mathfrak{F}$ for one air gap and $-\mathfrak{F}$ for the other if the total magnetomotive force for both air gaps is $2\,\mathfrak{F}$. If p_0 represents the air gap permeance per unit area the air gap flux density may be written as a Fourier-series as follows

$$B_\mathfrak{F} = \frac{4\mathfrak{F}p_0}{\pi}\left[\sin\frac{\gamma_i}{2}\cos\beta + \frac{1}{3}\sin\frac{3\gamma_i}{2}\cos 3\beta + \frac{1}{5}\sin\frac{5\gamma_i}{2}\cos 5\beta + \dots\right] \quad (1)$$

Often it is advantageous to eliminate completely a certain harmonic field. Equation 1 shows that the harmonic field of order ν disappears, if $\gamma_i\nu$ is an integer multiple of 2π. Considering that $(2\pi)/\nu$ represents the wave-length of the field of order ν, it can be stated that the harmonic field of order ν is zero, if the ideal pole-length γ_i is an integer multiple of its wave-length. Changing from rotor co-ordinates β to stator co-ordinates α according to the relation

$$\beta = \alpha - \theta \quad (2)$$

and making use of the following abbreviation

$$B_\nu = \frac{4\mathfrak{F}p_0}{\pi\nu}\sin\left(\frac{\nu\gamma_i}{2}\right) \quad (3)$$

equation 1 reads as follows

$$B_\mathfrak{F} = B_1\cos(\alpha-\theta) + B_3\cos 3(\alpha-\theta) + B_5\cos 5(\alpha-\theta) + \dots \quad (4)$$

Distortion of Magnetic Field by Stator Slot Openings

The effect of the slot-openings on a magnetic field as represented by equation 4 is two-fold. First, the permeance-variation, periodically repeating along the stator, produces ripples in the various harmonic field curves; and, second, an uneven number of stator slots destroys the original symmetry of both poles, so that the magnetic potential is no longer the same for both poles. The magnetomotive force of one air gap may be written as $+\mathfrak{F}+f$ and that of the other as $-\mathfrak{F}+f$. The value of f is determined by the condition that the total flux leaving the rotor is zero. The additional flux-density B_f corresponding to the addi-

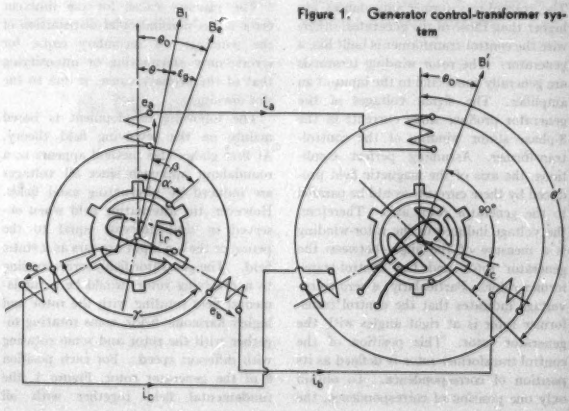

Figure 1. Generator control-transformer system

tional magnetomotive force f, still neglecting the ripples is

$$B_f = \frac{f p_0}{\pi}\left[\gamma_i + 2 \sin \gamma_i \cos 2(\alpha-\theta) + \ldots\right] \quad (5)$$

Since f is small compared with $\mathfrak{F}$, only the first and second terms of the corresponding Fourier-series, shown in equation 5, is taken into account. Introducing the abbreviation

$$B_0 = \frac{f p_0 \gamma_i}{\pi} \quad (6)$$

equation 5 can be written

$$B_f = B_0 + B_0 \frac{2 \sin \gamma_i}{\gamma_i} \cos 2(\alpha-\theta) \quad (7)$$

The mathematical expression for the flux density curve containing the ripples caused by the slot openings is obtained by first adding equations 4, and 7 and then multiplying this expression by p/p_0. p is a periodic function of α representing the permeance between a smooth round rotor and a slotted stator. The following development is carried along for the specific case of a 15-slot stator. For that special case p/p_0 can be written as

$$\frac{p}{p_0} = C_0 + C_{15} \cos 15\alpha + C_{30} \cos 30\alpha + \ldots \quad (8)$$

Only the three terms given in equation 8 are considered in the following development. The actual value of the factors C_0, C_{15}, C_{30} may best be found from a flux plot. With equations 4, 7, and 8, the flux density can be written

$$B = \left[\left\{B_0 + B_0 \frac{2 \sin \gamma_i}{\gamma_i} \cos 2(\alpha-\theta)\right\} + \{B_1 \cos(\alpha-\theta) + B_3 \cos 3(\alpha-\theta) + \ldots\}\right] \times [C_0 + C_{15} \cos 15\alpha + C_{30} \cos 30\alpha] \quad (9)$$

The total flux per unit rotor length and radius leaving the rotor is given by the integral

$$\int_0^{2\pi} B d\alpha$$

Equaling this integral to zero, the following equation for B_0 is obtained

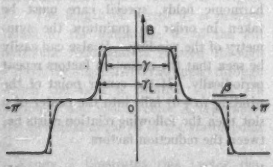

Figure 2. Flux density distribution in salient-pole machine

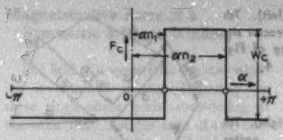

Figure 3. Magnetomotive force per unit current produced by a coil of w_c turns

$$0 = B_0 C_0 2\pi + \frac{B_{15} C_{15}}{2} 2\pi \cos 15\theta \quad (10)$$

$$B_0 = -\frac{B_{15} C_{15}}{2C_0} \cos 15\theta \quad (11)$$

First the distortion of the fields of the second parenthesis of equation 9 is to be discussed. The original νth harmonic field is transformed into the following expression

$$B_\nu \cos \nu(\alpha-\theta)\frac{p}{p_0} = C_0 B_\nu \cos \nu(\alpha-\theta) + \frac{B_\nu C_{15}}{2}\left[\cos\left\{(15+\nu)\left(\alpha - \frac{\nu\theta}{15+\nu}\right)\right\} + \cos\left\{(15-\nu)\left(\alpha + \frac{\nu\theta}{15-\nu}\right)\right\}\right] + \frac{B_\nu C_{30}}{2}\left[\cos\left\{(30+\nu)\left(\alpha - \frac{\nu\theta}{30+\nu}\right)\right\} + \cos\left\{(30-\nu)\left(+\frac{\nu\theta}{30-\nu}\right)\right\}\right] \quad (12)$$

From equation 12 it can be seen that the effect of the slot openings on the νth harmonic field is: first; to reduce slightly the original field rotating together with the rotor—C_0 is slightly smaller than 1; second, to create a field of order $(15+\nu)$ rotating in the same direction as the rotor with $\nu/(15+\nu)$ times its speed and a field of order $(15-\nu)$ rotating opposite to the rotor with $\nu/(15-\nu)$ times its speed; and third, two fields of order $(30+\nu)$ and $(30-\nu)$ respectively, one rotating forward and the other backward.

The product of the first parenthesis of equation 9 by p/p_0 can be written, considering at the same time equation 11, and neglecting the product $C_{30}B_0$ since B_0 is already a small value

$$B_0\left(1 + \frac{2 \sin \gamma_i}{\gamma_i} \cos 2(\alpha-\theta)\right)\frac{p}{p_0} = -\frac{B_{15} C_{15}}{2C_0}\left[\cos(15\theta)(C_0 + C_{15} \cos 15\alpha) + \frac{2 \sin \gamma_i}{\gamma_i} \cos 2(\alpha-\theta) \times \cos 15\theta(C_0 + C_{15} \cos 15\alpha)\right] \quad (13)$$

After some trigonometric transformations, equation 13 reads as follows

$$B_0\left(1 + \frac{2 \sin \gamma_i}{\gamma_i} \cos 2(\alpha-\theta)\right)\frac{p}{p_0} = -\frac{B_{15} C_{15}}{2C_0}\left\{C_0 \cos 15\theta + \frac{C_{15}}{2} \times [\cos 15(\theta+\alpha) + \cos 15(\theta-\alpha)] + \frac{\sin \gamma_i}{\gamma_i}\left[C_0\left(\cos 2(\alpha+13\theta/2) + \cos 2(\alpha-17\theta/2)\right) + \frac{C_{15}}{2}\left(\cos 17(\alpha+13\theta/17) + \cos 17(\alpha-\theta) + \cos 13(\alpha-\theta) + \cos 13(\alpha+17\theta/13)\right)\right]\right\} \quad (14)$$

Equation 14 shows revolving 2nd, 13th, 15th, and 17th harmonic fields. The intensity of these fields is proportional to the original 15th harmonic field. Summing up, the following expression for the total flux density is obtained

$$B = \sum_{\nu=2k+1} C_0 B_\nu \cos \nu(\alpha-\theta) + \frac{C_{15}}{2}\sum_{\theta=2k+1} B_\nu \times \left[\cos\left\{(15+\nu)\left(\alpha - \frac{\nu\theta}{15+\nu}\right)\right\} + \cos\left\{(15-\nu)\left(\alpha - \frac{\nu\theta}{15-\nu}\right)\right\}\right] + \frac{C_{30}}{2}\sum_{\nu=2k+1} B_\nu\left[\cos\left\{(30+\nu) \times \left(\alpha - \frac{\nu\theta}{30+\nu}\right)\right\} + \cos\left\{(30-\nu)\left(\alpha + \frac{\nu\theta}{30-\nu}\right)\right\}\right] - \frac{B_{15} C_{15}}{2}\left[\cos 15\theta + \frac{\sin \gamma_i}{\gamma_i} \times \left(\cos 2(\alpha+13\theta/2) + \cos 2(\alpha-17\theta/2)\right)\right] - \frac{B_{15} C_{15}}{4C_0}\left[\cos 15(\theta+\alpha) + \cos 15(\theta-\alpha) + \frac{\sin \gamma_i}{\gamma_i}\left(\cos 17(\alpha+13\theta/17) + \cos 17(\alpha-\theta) + \cos 13(\alpha-\theta) + \cos 13(\alpha+17\theta/13)\right)\right] \quad (15)$$

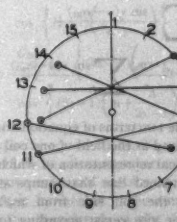

Figure 4. Winding diagram of one phase of a 3-phase 15-slot winding

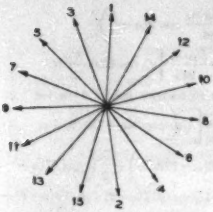

Figure 5 (left). 7th harmonic vector star for winding of Figure 4

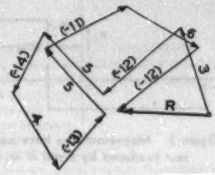

Figure 6 (right). 7th harmonic vector polygon for winding of Figure 4

Magnetic Field Produced by a Distributed Winding

In the theory of rotating machinery it is usual practice to calculate the magnetic field of a distributed winding by using harmonic reduction factors. The field of a distributed winding is compared to that of a concentrated winding and the ratio between the νth harmonic fieldintensity of the distributed winding and that of a concentrated winding is called differential factor. The differential factor is calculated as the product of pitch factor and distribution factor. This method is very convenient when dealing with the ordinary type of windings. The design of selsyns, however, also requires the study of irregular windings with coils of different number of turns or different coil pitches. To determine the harmonic reduction factors for odd and even harmonics of these windings a more general method is needed. It was found most convenient to study these special windings with a graphical method. The only restriction made with respect to the distribution of the coil sides is that the winding is symmetric to its axes.

Figure 3 illustrates the magnetomotive force per unit current produced by a coil of w_c turns in a round rotor machine. α_{s1} and α_{s2} are the angular distances of the coil sides from the symmetry point "O" of winding. The magnetomotive force $\mathfrak{F}_c$ per unit current of this coil can be written as

$$\mathfrak{F}_c = \frac{w_c}{\pi}\sum_{\nu} + \frac{\sin \nu(\alpha-\alpha_{s1})}{\nu} + \frac{(-w_c)}{\pi}\sum_{\nu}\frac{\sin \nu(\alpha-\alpha_{s2})}{\nu} \qquad (16)$$

Each of the two terms of equation 16 may be considered as the field of one coil side, the graphical representation of which is a straight inclined line that jumps at the center of the coil side from $w_c/2$ to $(-w_c/2)$ or vice versa, according to the direction of the current. The magnetomotive force $\mathfrak{F}$ produced by a winding is obtained by adding all partial magnetomotive forces of its coil sides. If the number of turns and position angle of any coil side are w_n and α_n the magnetomotive force per unit current can be written

$$\mathfrak{F} = \frac{1}{\pi}\left\{\sum_{n}\frac{(\pm w_n)\sin(\alpha_n-\alpha)}{1} + \frac{1}{2}\sum_{n}(\pm w_n)\sin 2(\alpha_n-\alpha) + \frac{1}{3}\sum_{n}(\pm w_n)\sin 3(\alpha_n-\alpha) + \ldots\right\} \qquad (17)$$

The positive sign in front of w_n applies to a coil side current directed away from the observer and the negative sign to a current directed towards the observer. Since the magnetomotive force is symmetric to the axes of the winding, or respectively to the origin "O" of the coordinates, $\mathfrak{F}$ also may be written in the form

$$\mathfrak{F} = \mathfrak{F}_1 \cos\alpha + \mathfrak{F}_2 \cos 2\alpha + \mathfrak{F}_3 \cos 3\alpha + \ldots \qquad (18)$$

Equalling α to zero in equations 18 and 17 and comparing the correspondent terms, the following expression results for $\mathfrak{F}$

$$\mathfrak{F}_\nu = \frac{1}{\pi\nu}\sum_{n}(\pm w_n)\sin(\nu\alpha_n) \qquad (19)$$

The total number of turns t of the winding equals one half the number of the sum of conductors per coil side.

$$t = \frac{1}{2}\sum_{n} w_n \qquad (20)$$

Introducing the harmonic reduction factor or, simply, reduction factor of order ν according to the following definition

$$k_\nu = \frac{\sum_{n}(\pm w_n)\sin \nu\alpha_n}{2t} \qquad (21)$$

equation 18 can be written in the form

$$\mathfrak{F} = \frac{2t}{\pi}\left\{\frac{k_1}{1}\cos\alpha + \frac{k_3}{2}\cos 2\alpha + \frac{k_3}{3}\cos 3\alpha + \ldots\right\} \qquad (22)$$

The νth harmonic reduction factor k_ν can be calculated from equation 21 or found by a graphical method. This method shall be explained by the example of a 15-slot winding as illustrated in Figure 4. The first step is to plot the "vector-star" of order ν. In this vector star the electrical angle, which is ν times the geometrical angle, of each slot is represented by a unit vector. The angle of the axis of the winding is assumed as zero. Figure 5 represents the vector star of order 7 for the 15-slot winding of Figure 4. Next a vector polygon is plotted as shown in Figure 6. Each side of this vector polygon corresponds to a coil side of the winding. The length of each polygon side is proportional to the number of conductors of the corresponding coil side and the direction is given by the corresponding unit vector of the vector star. The sense of the polygon side is the same as that of the unit vector if the current flows away from the observer and is reversed when the current flows towards the observer. For reasons of symmetry, the resultant of the vector polygon is prependicular to the unit vector representing the axis of the winding. The length of the resultant is proportional to the expression

$$\sum_{n} \pm w_n \sin \nu\alpha_n$$

The length of the vector polygon is proportional to twice the total number of turns, or $2t$. The length of the resultant of the vector polygon divided by the length of the vector polygon is therefore equal to the reduction factor k_ν as defined by equation 21. k_ν is positive if the resultant is turned through 90 degrees clockwise with respect to the winding axis and is negative if the resultant is turned counterclockwise. According to Figure 6, k_7 is equal to (-0.087). It can be seen from Figure 6 that k_7 becomes zero if the number of turns of the coils 3 to 12 and 5 to 14 are reduced to 63 per cent of their original value. Thus the vector polygon in general indicates how a certain reduction factor may be made zero by using coils of different number of turns. When reducing the number of turns of several coils in order to eliminate higher harmonic fields, special care must be taken in order to maintain the symmetry of the winding. It also can easily be seen that the reduction factors repeat periodically. If the center point of the winding $(\alpha = 0)$ falls into the center of a slot then the following relation exists between the reduction factors

$$k_\nu = -k_{(nz-\nu)} = k_{(nz+\nu)} \qquad (23)$$

n is any integer positive number and z is

the number of teeth of the punching, assuming equally spaced teeth. According to equation 23 the reduction factor of order 8, k_8, of the winding of the foregoing example is $+0.087$.

A similar relation exists if the center point of the winding falls into the center of a tooth. The relation is as follows

$$k_\nu = -(-1)^n k_{(nz-\nu)} = (-1)^n k_{(nz+\nu)} \qquad (24)$$

It can be seen from equation 23 and 24 that the absolute value of the reduction factors of order $(nz \pm 1)$ is equal to that of the first harmonic. All other reduction factors can be kept small or made zero by distributing the coils properly, eventually, by using coils of different number of turns. The physical reason why the reduction factors of order $(nz \pm 1)$ cannot be reduced, is that the harmonic fields of these orders are caused by the discrete distribution of the winding. These harmonics, which shall be called step-harmonics, and the steps in the graphical representation of the magnetomotive force are correlative. The reduction factors of order (nz) are all equal to zero.

$$k_{(nz)} = 0 \qquad (25)$$

Vector Representation of a Sinusoidal Field

Equation 22 represents the magnetomotive force per unit current produced by a winding symmetric to the point $(\alpha = 0)$; for instance winding "a" in Figure 1. If the axis of a winding passes through the point α_0 the expression of its magnetomotive force per unit current is as follows

$$\mathfrak{F} = \frac{2t}{\pi}\left\{\frac{k_1}{1}\cos(\alpha-\alpha_0) + \frac{k_3}{2}\cos 2(\alpha-\alpha_0) + \frac{k_3}{3}\cos 3(\alpha-\alpha_0) + \ldots\right\} \qquad (26)$$

Each of the harmonic fields of equation 26 can be represented by a vector diagram. In this diagram the magnetomotive force of the νth harmonic field at any point α is represented by the projection of a νth harmonic field vector $\mathfrak{F}_\nu$ on a νth harmonic unit space vector A_ν (Figure 7). The length of vector $\mathfrak{F}_\nu$ is proportional to the amplitude $\mathfrak{F}_\nu$ of the νth harmonic field and is rotated through ν-times the angle (electrical angle) through which the field is rotated. The νth harmonic unit space vector A_ν represents the electrical angle $\nu\alpha$ of the stator point α.

Figure 7 illustrates this vector diagram representing the second harmonic field of phase b of Figure 1.

Magnetomotive Force of a Symmetric 3-Phase Winding

The field of a symmetric 3-phase winding is obtained by superimposing the three single-phase fields, considering at the same time that the axes of two consecutive phases form an angle of 120 degrees. $\mathfrak{F}_a$, $\mathfrak{F}_b$, $\mathfrak{F}_c$ are the magnetomotive forces of the windings a, b, c and $\mathfrak{F}_{a1}$, $\mathfrak{F}_{b1}$, $\mathfrak{F}_{c1}$, are the amplitude of the fundamentals of the fields. Then the expression for the νth harmonic resultant field $\mathfrak{F}_{\nu_a}$ is, considering, equation 22

$$\mathfrak{F}_{\nu_a} = \mathfrak{F}_{a_1}\frac{k_\nu}{\nu k_1}\cos\nu\alpha + \mathfrak{F}_{b_1}\frac{k_\nu}{\nu k_1}\times\cos\nu(\alpha-120°) + \mathfrak{F}_{c_1}\frac{k_\nu}{\nu k_1}\times\cos\nu(\alpha-240°) \qquad (27)$$

The three single-phase magnetomotive forces can be written in the following form

$$\mathfrak{F}_{a_1} = \mathfrak{F}_0 + \mathfrak{F}_A\cos_A \qquad (28A)$$

$$\mathfrak{F}_{b_1} = \mathfrak{F}_0 + \mathfrak{F}_A\cos(A+240°) \qquad (28B)$$

$$\mathfrak{F}_{c_1} = \mathfrak{F}_0 + \mathfrak{F}_A\cos(A+120°) \qquad (28C)$$

Representing the three fields of equation 27 in a vector diagram, and considering equation 28, one finds the following results for the 3-phase field. The amplitude of the fields the order of which is an integer multiple of three is equal to 3 $F_0\, k_{3n}/3_n k_1$ and they are symmetric to the three phases

$$\mathfrak{F}_{3n_a} = 3\mathfrak{F}_0\frac{k_{3n}}{3nk_1}\cos(3n\alpha) \qquad (29)$$

According to equation 28, if the 3-phase currents i_a, i_b, i_c add up to zero with a star-connection $\mathfrak{F}_0$ is equal to zero. The amplitude of any other field $\mathfrak{F}_\nu$ is equal to $3/2\ \mathfrak{F}_A\ (k_\nu/\nu k_1)$. The fundamental field is rotated through the angle A with respect to phase a, while the fields of order $(3n-2)$ are rotated through the angle $+A/(3n-2)$ and the fields of order $(3n-1)$ are rotated through the angle $(-A)/(3n-1)$. In other words, the higher harmonic fields rotate slower than the fundamental field in proportion to their order and rotate alternately in the same and opposite direction as the fundamental field.

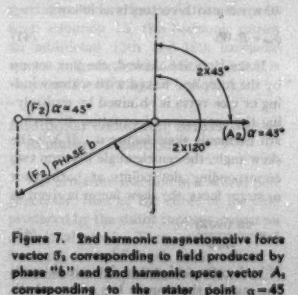

Figure 7. 2nd harmonic magnetomotive force vector $\mathfrak{F}_2$ corresponding to field produced by phase "b" and 2nd harmonic space vector A_2 corresponding to the stator point $\alpha = 45$ degrees

$$\mathfrak{F}_{(3n-1)\alpha} = \frac{3}{2}\mathfrak{F}_A\frac{k_{(3n-1)}}{(3n-1)k_1}\cos\left(\alpha + \frac{A}{3n-1}\right) \qquad (30)$$

$$\mathfrak{F}_{(3n-2)\alpha} = \frac{3}{2}\mathfrak{F}_A\frac{k_{(3n-2)}}{(3n-2)k_1}\cos\left(\alpha - \frac{A}{3n-2}\right) \qquad (31)$$

Magnetic Field Distortion Caused by the Slots

The magnetic flux density of a round rotor machine is obtained by multiplying the magnetomotive force by the permeance. To each harmonic magnetomotive force-field corresponds a magnetic field of the same order plus additional higher harmonic fields conditioned by the periodic permeance variations. These shall be called permeance harmonics. Assuming a 3-phase stator winding imbedded in a punching of z slots, the permeance can be written as follows

$$p = p_0[C_0 + C_z\cos z\alpha + C_{2z}\cos 2_z\alpha + \ldots] \qquad (32)$$

In the following development, the permeance distortion of the fundamental wave only shall be considered. The magnetic field corresponding to the fundamental magnetomotive force is according to equations 31 and 32

$$\mathfrak{F}_{1\alpha}p = \frac{3}{2}p_0\mathfrak{F}_A\{C_0\cos(\alpha-A) + C_z\cos(\alpha-A)\cos(z\alpha) + C_{2z}\cos((\alpha-A\cos(2z\alpha) + \ldots\} \qquad (33)$$

Transforming trigonometrically this equation

$$\mathfrak{F}_{1\alpha}p = \frac{3}{2}p_0\mathfrak{F}_A\{C_0\cos(\alpha-A)\} + \frac{C_z}{2}\left[\cos\left\{(z+1)\left(\alpha-\frac{A}{z+1}\right)\right\} + \cos\left\{(z-1)\left(\alpha+\frac{A}{z-1}\right)\right\}\right] + \frac{C_{2z}}{2}\left[\cos\left\{(2z+1)\left(\alpha-\frac{A}{2z+1}\right)\right\} + \cos\left\{(2z-1)\left(\alpha+\frac{A}{2z-1}\right)\right\}\right] \qquad (34)$$

Comparing equations 34, 30, and 32, it is seen that the permeance harmonics are of the same order and angular orientation as the step harmonics. The sum of both shall be considered as slot harmonics. Assuming that the phase axes pass through the center of slots, and consider-

ing equation 23, the following expression results for the slot harmonics flux density B_s

$$B_s = \frac{3}{2}\rho_0 \mathfrak{F}_A \left\{ \begin{array}{l} \left[\frac{C_z}{2} - \frac{1}{(z-1)}\right] \times \\ \cos\left[(z-1)\left(\alpha + \frac{\Lambda}{z-1}\right)\right] + \\ \left[\frac{C_z}{2} + \frac{1}{(z+1)}\right] \times \\ \cos\left[(z+1)\left(\alpha - \frac{\Lambda}{z+1}\right)\right] + \\ \left[\frac{C_{2z}}{2} - \frac{1}{(2z-1)}\right] \times \\ \cos\left[(2z-1)\left(\alpha + \frac{\Lambda}{2z-1}\right)\right] + \\ \left[\frac{C_{2z}}{2} + \frac{1}{2z+1}\right] \times \\ \cos\left[(2z+1)\left(\alpha - \frac{\Lambda}{2z+1}\right)\right] + \\ \cdots\cdots\cdots\cdots \end{array} \right\}$$

Equation 35 shows that the permeance harmonics partly intensify and partly attenuate the step harmonics. This effect may be so strong that some of the step-harmonics are completely compensated while others are doubled.

Flux Linkages of the Air Gap Field

The flux linkage of the air gap field with a coil is the air gap flux through the part of the air gap area enclosed by the coil multiplied with the number of turns, w_c, of the coil. The flux linkage is positive if the air gap flux is of the same sense as a flux produced by a positive current in the coil. The flux linkage per unit rotor radius and width with a coil, $\psi_{\nu w}$, of a νth harmonic field symmetric to the winding axis and of amplitude B_ν is: (see Figure 3)

$$\psi_{\nu w} = w_c \int_{\alpha_{n1}}^{\alpha_{n2}} B_\nu \cos(\nu\alpha) d\alpha \tag{36}$$

and evaluating this integral

$$\psi_{\nu w} = \frac{B_\nu}{\nu}[w_c \sin \nu\alpha_{n2} - w_c \sin \nu\alpha_{n1}] \tag{37}$$

The expression of the flux linkage ψ_ν of the total winding per unit rotor radius and width with the νth harmonic air gap flux is consequently

$$\psi_\nu = \frac{B_\nu}{\nu} \sum \pm w_n \sin \nu\alpha_n \tag{38}$$

w_n is the number of conductors of the nth coil side and the positive sign applies to a positive coil side current flowing away from the observer, while the negative sign applies to a current directed towards the observer.

Introducing the harmonic reduction factor k_ν as defined by equation 21, the

Figure 8. Vector representation of the equivalent generator air gap field

flux linkage can be written as follows

$$\psi_\nu = \frac{B_\nu 2t}{\nu} k_\nu \tag{39}$$

If the magnetic field axis is turned through an angle α with respect to the winding axis, the flux linkage $\psi_{\nu\alpha}$ is as follows

$$\psi_{\nu\alpha} = (B_\nu)\left(2t\frac{k_\nu}{\nu}\right) \cos \nu\alpha \tag{40}$$

It can be seen from equation 40 that the flux-linkage of a νth harmonic flux with a symmetric winding may be represented as the scalar product of two vectors. One vector, $\boldsymbol{B}_\nu$, represents the νth harmonic field as explained previously and the other vector represents the winding. This vector shall be called the νth harmonic winding vector, $\boldsymbol{W}_\nu$. The length of this vector is equal to $2tk_\nu/\nu$ and its sense and direction is that of the νth harmonic unit space vector corresponding to the axis of the winding. The angle between $\boldsymbol{B}_\nu$ and $\boldsymbol{W}_\nu$ is ν-times the geometrical, or electrical angle, between the winding axis and the flux axis. Equation 40 written with vectors is as follows

$$\psi_{\nu\alpha} = \boldsymbol{B}_\nu \boldsymbol{W}_\nu \tag{41}$$

If the slots are skewed, the flux set up by the rotor and linked with stator winding or vice versa is obtained by multiplying the expression of equation 42 with a νth harmonic skew factor s_ν. If λ is the skew angle, the centric angle between two corresponding slot points at both rotor or stator faces, the skew factor is given as

$$s_\nu = \frac{\sin(\nu\lambda/2)}{\nu\lambda/2} \tag{42}$$

If both rotor and stator slots are skewed, the mutual skew angle has to be substituted in equation 42. The general expression for the flux linkage of a skewed winding is consequently

$$\psi_{\nu\alpha} = s_\nu(\boldsymbol{B}_\nu \boldsymbol{W}_\nu) \tag{43}$$

The Equivalent Flux

Comparing, on base of a vector diagram, the three flux linkages of a 3-phase winding produced by a revolving fundamental flux with the flux linkages produced by a revolving higher harmonic field, the following relation can be established: considering the flux linkages of a symmetric 3-phase winding, a νth harmonic field of amplitude B_ν and rotated through the angle α_ν is equivalent to a first harmonic field $(\boldsymbol{B}_\nu)_1$, of amplitude $(B_\nu\ s_\nu k_\nu)/(\nu s_1 k_1)$ rotated through an angle $(\nu\alpha_\nu)$ in the same direction if ν is equal to $(3n\text{-}2)$ and in the opposite direction if ν is equal to $(3n\text{-}1)$. A revolving field of order $\nu = 3n$ produces equal flux linkages in all three phases.

$$(B_\nu)_1 = \frac{B_\nu s_\nu k_\nu}{\nu s_1 k_1} \tag{44}$$

Thus replacing all higher harmonic fields by their respective equivalent fields, the whole nonsinusoidal field may be replaced by one fictitious equivalent fundamental field. Generally the vector representing this equivalent field is not in line with the axis (if there is any) of the nonsinusoidal field. Only if the axis of the nonsinusoidal field lines up with one of the phase axes the equivalent field is in line with the nonsinusoidal field.

Errors Caused by the Generator

First it shall be assumed that the generator is connected to a balanced load, the impedance of which is high compared with that of the generator. In that case the stator armature reaction may be neglected. Then the error caused by the generator simply is the angle between the rotor axis and the axis of the equivalent rotor field. The calculation of this error shall be shown on an example, considering only the 1st, 5th, and 7th harmonic of the rotor field. Figure 8 shows the vector diagram of the 1st harmonic field B_1 and the equivalent fields of the 5th and 7th harmonics $(B_5)_1$, and $(B_7)_1$. According to the vector diagram, the error is a function of 6θ. The analytic expression for this error angle $(\epsilon_\theta)_6$ is

$$\tan\ (\epsilon_\theta)_6 = -\frac{(B_5)_1 \sin 6\theta + (B_7)_1 \sin 6\theta}{B_1 + (B_5)_1 \cos 6\theta + (B_7)_1 \cos 6\theta} \tag{45}$$

With equation 44 and considering that $(\epsilon_\theta)_6$ is a small angle and that $(B_5)_1$ and

$(B_7)_1$ are small compared to B_1, equation 45 may be written as follows

$$(\epsilon_g)_4 \approx \left\{ -\frac{B_5 k_5 s_5}{5B_1 k_1 s_1} + \frac{B_7 k_7 s_7}{7k_1 s_1 B_1} \right\} \sin 6\theta \qquad (46)$$

Assuming a generator winding as shown in Figure 4, a skew angle of 24 degrees, and a salient pole rotor of 90-degree pole arc, the parameters of equation 46 are as follows

$$B_7/B_1 = -1/7; \quad k_1 = 0.916; \quad k_5 = 0; \quad k_7 = -0.087; \quad s_1 = 1.0; \quad s_7 = 0.68$$

Substituting these values into equation 47, the maximum 6th harmonic generator error results in 0.0013 radian.

All errors caused that way are of the order $3n$. This is a consequence of the symmetries of a 3-phase winding. The general expression for the error of order $3n$ is

$$(\epsilon_g)_{3n} = \left\{ -\frac{B_{(3n-1)} k_{(3n-1)} s_{(3n-1)}}{B_1 (3n-1) k_1 s_1} + \frac{B_{(3n1+)} k_{(3n+1)} s_{(3n-1)}}{B_1 (3n+1) k_1 s_1} \right\} \sin (3n\theta) \qquad (47)$$

If there is a distributed winding on the rotor, the ratios $B_{(3n-1)}/B_1$ and $B_{(3n+1)}/B_1$ may be expressed by harmonic reduction factors according to equation 22. If the index r refers to the rotor and s to the stator, equation 47 transforms into

$$(\epsilon_g)_{3n} = \left\{ -\frac{k_{(3n-1)r} k_{(3n-1)s} s_{(3n-1)}}{(3n-1)^2 \; k_{1r} k_{1s} s_1} + \frac{k_{(3n+1)r} k_{(3n+1)s} s_{(3n+1)}}{(3n+1)^2 k_{1r} k_{1s} s_1} \right\} \sin (3n\theta) \qquad (48)$$

Equation 48 shows that in order to obtain a good selsyn generator, the products of the harmonic reduction factors of rotor and stator should be small. In other words, the stator winding should be insensitive to all harmonics to which the rotor winding is sensitive.

Additional Generator Errors Caused by the Slot Openings of the Rotor

As can be seen from equation 34 and the subsequent discussion, the main effect of the rotor slots is to intensify one part of the step-harmonics and to attenuate the other part. Consequently, the errors caused by these step harmonics are intensified or attenuated in proportion. This effect has to be taken into account if one wants to compensate against each other the errors caused by two step harmonics. For instance, according to equation 48, both the 11th and 13th field harmonic of a 12-slot rotor cause a 12th harmonic generator error. It would be possible to choose the reduction factors of the stator-winding so that both errors cancel each other. However, the slot openings may, for instance reduce considerably the 11th harmonic field and increase the 13th harmonic field, changing thereby the picture completely. In this special case, equation 48 is unreliable. Equation 47 has to be used and the intensity of the 11th and 13th harmonic fields has to be calculated according to equation 35. If however, according to equation 48, the error caused by a certain field harmonic is zero, the slot openings do not change this. Likewise, if the error of a certain harmonic is very small, the slot openings do not cause much change and may be neglected. In order to keep the slot harmonic errors small, these harmonics must be either matched with very low stator-reduction factors or the slots must be skewed so as to obtain a small skew factor.

Additional Generator Error Caused by the Stator Slot Openings

Equation 15 shows the additional revolving harmonic fields, caused by the slot openings of a 15-slot stator. Replacing the additional fields, caused by a νth harmonic rotor field, by their equivalent fields, it can be seen that they cause an error of the same order as does the νth harmonic field. The effect of the stator slots, therefore, is merely to intensify or attenuate the errors caused by the original rotor field harmonics. Mostly this effect is weak and may be neglected. Only the error due to original harmonics, the order of which equals that of the stator slot harmonics, may be changed considerably by this effect. In that case, several of the additional fields are of the 1st order and therefore may cause a strong additional error.

The error caused by the 15th harmonic, generally by a harmonic of order equal to the number of stator teeth, needs special consideration. As can be seen from equation 15, this harmonic causes an additional 12th and 18th harmonic error. In general this additional error is very small and may be neglected.

Additional Generator Errors Due to Armature Reaction

The armature reaction in a salient pole generator, that is, the effect of the field produced by the stator currents, causes an additional error. There are two causes for such an additional error. First, a fundamental magnetomotive force in the stator produces beside a fundamental magnetic field also higher harmonic fields. These higher harmonic fields rotate together with the rotor and are practically in time phase with the rotor field because of the inductive generator load. Therefore, they simply intensify or attenuate the corresponding rotor harmonic fields as well as the errors caused by them. Obviously, this effect only becomes important if the strength of the field produced by the stator approximates that of the rotor, that is, at very low generator load-impedance.

Secondly, an additional error is caused by the assymmetry of the generator reactances. The quadrature reactance of a salient pole machine is considerably less than its direct axis reactance. The fundamental field of the rotor magnetizes in the direct axis, whereas the errors are caused by fields or field components magnetizing in the quadrature axis. The corresponding direct and quadrature currents are inversely proportional to the total direct and quadrature impedances of the system. If the load impedance is Z_l, the generator direct and quadrature impedances respectively Z_d and Z_q, the generator error under load ϵ_{gl} is, assuming all impedances as mainly inductive

$$\epsilon_{gl} \approx \epsilon_g \frac{Z_l + Z_d}{Z_l + Z_q} \qquad (49)$$

Errors Caused by the Control Transformer

The currents induced by the equivalent generator field produce a corresponding field in the control transformer. The field of an ideal control transformer would be sinusoidal and its axis would be parallel to that of the equivalent generator field. Then the position of correspondence of the control transformer rotor, position for zero rotor voltage, would be exactly $\pi/2$ ahead of the equivalent generator field. However, the control transformer stator windings also produce, beside the fundamental field, higher harmonics. The rotor position for zero flux-linkage, θ', is therefore ahead of the equivalent generator field by an angle equal to $(\pi/2+\epsilon_c)$; ϵ_c is the control transformer error. The position angle of correspondence of the control transformer is therefore

$$\theta' = (\theta + \epsilon_g) + (\pi/2 + \epsilon_c) \qquad (50)$$

The position angle of the equivalent generator field $(\theta+\epsilon_g)$ shall be written as θ_0.

$$\theta_0 = \theta + \epsilon_g \qquad (51)$$

The control transformer error can be calculated by establishing the expression of the rotor flux-linkage ψ_r' and equating

it to zero. In the following the rotor flux linkage caused by the fundamental flux $\boldsymbol{B}_1$ and the harmonics of order $(3n+1)$ $\boldsymbol{B}_{(3n+1)}$ and of order $(3n-1)$, $\boldsymbol{B}_{(3n-1)}$, shall be considered. If $\boldsymbol{W}_1$, $\boldsymbol{W}_{(3n-1)}$ and, $\boldsymbol{W}_{(3n-1)}$ are the respective winding vectors of the rotor winding, the flux linkage can be written according to equation 41 as

$$\psi_r' = s_1\boldsymbol{B}_1\boldsymbol{W}_1 + s_{(3n+1)}\boldsymbol{B}_{3n+1}\boldsymbol{W}_{3n+1} + \boldsymbol{B}_{(3n-1)}\boldsymbol{W}_{(3n-1)}s_{(3n-1)} \quad (52)$$

Figure 9 shows the vector diagrams corresponding to equation 52. According to these diagrams, the condition for zero rotor flux linkage is

$$0 = B_1k_{1r}s_1\cos(\theta'-\theta_0) + \frac{B_{(3n-1)}k_{(3n-1)r}s_{(3n-1)}}{3n-1}\times \cos(\theta_0+(3n-1)\theta') + \frac{B_{(3n+1)}k_{(3n+1)r}s_{(3n+1)}}{3n+1}\times \cos(\theta_0+(3n+1)\theta') \quad (53)$$

With equations 50 and 51 and considering that $B_{(3n+1)}$ and $B_{(3n-1)}$ is small compared with B_1 and ϵ_e is a very small angle, the control transformer error of order $3n$ results as

$$(\epsilon_e)_{3n} \approx \left\{\frac{B_{(3n-1)}k_{(3n-1)r}s_{(3n-1)}}{B_1\quad(3n-1)k_{1r}s_1} - \frac{B_{(3n+1)}k_{(3n+1)r}s_{(3n+1)}}{B_1\quad(3n+1)k_{1r}s_1}\right\}\times \sin\left(3n\theta_0+\frac{3n\pi}{2}\right) \quad (54)$$

Expressing the ratios $B_{(3n+1)}/B_1$ and $B_{(3n-1)}/B_1$ by harmonic reduction factors according to equation 22 and writing θ instead of θ_0, since ϵ_e is a very small angle, the control transformer error can be written as follows

$$(\epsilon_e)_{3n} \approx \left\{\frac{k_{(3n-1)}k_{(3n-1)r}s_{(3n-1)}}{(3n-1)^2\,k_{1r}k_{1r}s_1} - \frac{k_{(3n+1)}k_{(3n+1)r}s_{(3n+1)}}{(3n+1)^2\,k_{1r}k_{1r}s_1}\right\}\times \sin\left(3n\theta+\frac{3n\pi}{2}\right) \quad (55)$$

Equation 55 for the control transformer error is very similar to equation 47 for the generator error. If both the generator and control transformer of a selsyn system have the same windings, except of its total number of turns, then the maximum error of a given order is the same for both machines. The errors of order $(12n-6)$ add, that is the maximum system error is twice the maximum error of either machine. The errors of order $(12n)$ cancel each other. The errors of order $(6n-3)$ add in quadrature, that is the generator errors are sine functions of θ and the control transformer errors are cosine functions. The corresponding system error is $\sqrt{2}-$ times the error of either machine.

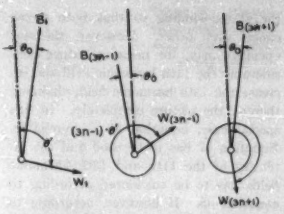

Figure 9. Representation of the magnetic field vectors B_1, $(B_{(3n-1)})_1$, and $(B_{(3n+1)})_1$, and of the winding vector W_1, $(W_{(3n+1)})$, $(W_{(3n-1)})$ for a control transformer

Additional Control Transformer Error Caused by Stator Slot Openings

According to equation 35 the effect of the stator slot openings is either to intensify or attenuate several step harmonics. This means that the errors, the order of which is an integer multiple of the number of stator slots are either intensified or attenuated. If the rotor winding is insensitive to the stator slot harmonics, then the slot openings do not cause any additional error.

Additional Control Transformer Error Caused by the Rotor Slot Openings

The main effect of the rotor slot openings is to distort the fundamental field. If the rotor has z_r teeth, then the fundamental field will be accompanied by a pair of harmonic fields of order (z_r+1) and (z_r-1) and another pair of order $(2z_r+1)$ and $(2z_r-1)$ and so forth. These additional fields rotate together with the fundamental field and induce in the stator windings an additional voltage. For instance, the 13th harmonic field caused by a 12-slot rotor acts on the stator like an equivalent fundamental field revolving forward with 13 times the rotor speed. The voltage induced by this equivalent field causes an opposite fundamental field. This field is somewhat weaker than the equivalent field because of the leakage reactance and the generator reactance. From the previous explanations, it is obvious that this field causes an additional 12th harmonic error. Generally it can be stated that the rotor slot openings either increase or decrease the errors, the order of which is an integer multiple of the number of rotor teeth. If the stator winding is insensitive to the rotor slot harmonics, then the rotor slot openings do not cause any additional error.

Summary

The design of an accurate selsyn generator or control transformer may be accomplished by considering equations 47 and 48 or 55 respectively. The slot openings only increase or decrease certain errors given by these formulas. If according to these formulas a certain harmonic error is small or zero, the slot openings also cause a small or zero additional error. Exception of this rule has to be made only in the case that the errors caused by two different harmonic fields cancel each other. All errors of order $(6n-3)$ can be avoided by making the rotor or stator winding insensitive to even harmonics. Therefore the winding also has to be symmetric to a line vertical to

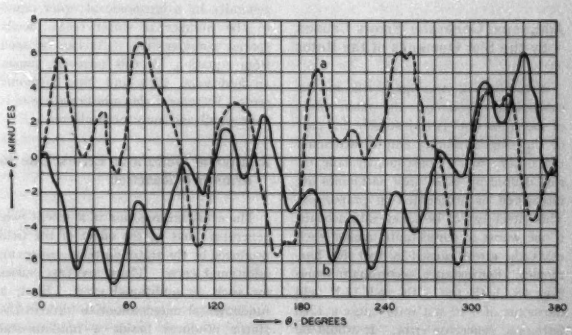

Figure 10. Generator error curve b and control transformer error curve a

its axis. This is only possible if the punching contains an even number of slots.

Curve *a* in Figure 10 shows a control transformer error curve. It corresponds to a control transformer with a 2-slot round rotor and a 15-slot stator winding, as shown in Figure 4. The 6th-harmonic error is caused by a 7th-harmonic flux and should reach, according to equation 55, an approximate maximum of 0.0013 radian, or 4.5 minutes. The actual 6th-harmonic error is 3.7 minutes. Curve "*b*" shows the error curve of a generator with a 15-slot stator winding and a salient pole rotor of 90-degree pole arc. The 6th-harmonic error has been eliminated by using a stator as before but coils of different number of turns. Thus it was possible to obtain a 7th harmonic reduction factor equal to zero. The 12th-harmonic error is caused by the 11th-harmonic field. The 2nd-harmonic error is caused by manufacturing inaccuracies.

The inherent error of the differential selsyn, that is, a selsyn with 3-phase winding on stator and rotor, can be treated by the same method. Moreover, it may be mentioned that an additional accuracy error is caused by manufacturing errors. Also an inherent dynamic error is present if the selsyn generator moves with considerable speed or acceleration.

However, it was not intended to discuss these additional phenomena in this paper. References 2 and 3 discuss some of these aspects.

References

1. Slot Harmonics of Turbine Generators, F. Moldenhauer. *Jahrbuch der AEG Forschungen* (Berlin, Germany), volume 7, December 1940, pages 169–75.

2. Electrical Accuracy of Selsyn Generator—Control Transformer System, Harold Chestnut. *Electrical Engineering (AIEE Transactions)*, volume 65, August–September 1946, pages 570–76.

3. Selsyn Design and Application, T. C. Johnson. *Electrical Engineering (AIEE Transactions)* volume 64, October 1945, pages 703–08.

4. Fundamental Concepts of Synchronous Machine Reactances, B. R. Prentice. *AIEE Transactions*, volume 56, 1937, pages 1–21 in supplement.

Discussion

A. E. Blume and R. W. Votaw (General Electric Company, Schenectady, N. Y.): Mr. Kronacher is to be commended on a very general and rigorous treatment of the inherent errors present in selsyn generators and control transformers. The use of the revolving-field theory has one outstanding feature. If we have a flux component (using Kronacher's symbols) $B_{n,m}\cos(n\alpha-m\theta)$, n determines the maximum number of flux linkages in the secondary and so determines the maximum induced voltage. m determines how this voltage varies with θ, and so determines the order of the error caused. The harmonic reduction factors for all harmonics can be determined by calculating those for the first $z/2$ harmonics (z even) or the first $(z-1)/2$ harmonics (z odd). The skew factor for any harmonic is easy to calculate. Then K_nS_n/K_1S_1 determines the flux linkages and therefore the voltage induced by $B_{n,m}\cos(n\alpha-m\theta)$ as compared to the fundamental voltage produced by $B_1\cos(\alpha-\theta)$.

There are several points that should be made about the second and third sections of the paper. In the first place the condition that

$$\int_0^{2\pi} B d\alpha = 0$$

is true but not enough. The selsyn generator, like most a-c machines, is nearly a constant flux machine. Thus, in addition to the above condition, there should be a condition that

$$\int_{-\pi/p}^{\pi/p} B d\beta = \text{constant}$$

Stated in words, the flux out of a pole at the same time every cycle on the exciting current wave is constant. What happens is that the exciting current can and will vary when the total reluctance seen by the primary changes. Thus the magnitudes of the various magnetomotive-force components can change when the rotor of a generator is revolved.

In the section on The Air-Gap Field, Mr. Kronacher discusses the variation of the ideal pole-length, γ_i. In the section on Distortion of Magnetic Field by Stator Slot Openings, Mr. Kronacher carries along γ_i, but it is no longer a variable, since the equations are for a smooth, round rotor, which means a rotor with a pole are approaching 180 degrees. For a salient-pole rotor the permeance considering both the rotor and a slotted stator would be

$$p = [p_0 + p_2\cos 2(\alpha-\theta) + p_4\cos 6(\alpha-\theta) + \ldots]$$
$$[c_0 + c_{15}\cos 15\alpha + c_{30}\cos 30\alpha + \ldots\ldots]$$

p_2 is roughly half of p_0 and p_{2n} is approximately equal to p_2/n, so that the first series does not converge very fast. These additional permeance terms would make the equations for the salient pole case much more complicated than those for the round rotor. Furthermore, there is a question as to the validity of the conditions

$$\int_{-\pi/p}^{\pi/p} B d\beta = \text{constant}, \qquad \text{and}$$

$$\int_0^{2\pi} B d\alpha = 0 \text{ in the salient pole case}$$

The flux must leave or enter the pole face at right angles, or practically so. However, if r is the radius from the center of the rotor to the pole face, there is no particular necessity for the flux to cross the circle of radius r at right angles between the poles. It would appear that there might be some modification (and probably a very complicated one) that must be made to the two conditions.

All of these points are relatively unimportant as far as the merit of the paper is concerned. Mr. Kronacher has shown how inherent error can be avoided. Practical windings have been developed by the General Electric Company following the principles developed in Mr. Kronacher's paper and machines using these windings now are in production. The 6th harmonic of error is not present in these machines; in fact, there is effectively no inherent error.

There remain, however, two problems which must be solved before the reduction in inherent or design errors so obtained can be fully exploited. In the first place, errors due to asymmetries such as mechanical eccentricities, out-of-roundness, unbalanced resistances, and so forth, which are unavoidable in the actual machine are frequently as great or greater than the design errors in even a machine using a conventional stator winding with the same pitch and number of turns for each coil. This problem can be attacked by changing mechanical design or improving production methods and control or possibly by electrical means of reducing the effect of mechanical asymmetries.

Even if this problem is solved, an additional difficulty is caused in practice by the so-called "null voltage" at correspondence. Theoretically, correspondence is the position of the control transformer rotor at which the control transformer output voltage is zero, a condition which never occurs in an actual machine. There always remains a voltage, consisting partly of higher time harmonics and partly of fundamental voltage in time quadrature with the normal rotor output voltage at a position off correspondence. In theory, servo amplifiers can be designed to reject such signal inputs from the selsyn system, but in modern practice, with the emphasis on reduction of the size and weight, nonlinearities exist in the amplifier which cause it to respond to these extraneous signals. This second selsyn problem is then the old story of "increasing the signal-to-noise ratio."

Past practice has been to reduce the transmitted error and increase the signal-to-noise ratio by using a 2-speed selsyn system where one generator-control transformer pair is operated at higher than load speed for fine control and another pair is operated at load speed to remove the possibility of the first pair being in correspondence while the director and load are not. Until practical solutions for the two additional problems discussed above are obtained, 2-speed systems will continue to be necessary for accurate work.

G. Kronacher: I studied with great interest the thorough discussion presented by A. E. Blume and R. W. Votaw.

I agree with their first statement that the flux passing through the rotor is constant. The selsyn error, however, is not dependent on the amount of flux but only on its distribution. The flux distribution may change with the magnitude of the flux because of iron saturation effects. It can, indeed, be observed that the angle of the selsyn generator signal slightly varies with the magnitude of the input voltage.

The equations of the section Distortion of the Magnetic field by Stator Slot Openings were intended to be valid both for salient-pole and round-rotor generators. As pointed out by Blume and Votaw, equation 8 is correct for points under the pole arc only and is completely wrong for points of the interpole space. However, it was stated previously that the flux of the interpole space shall be neglected. This assumption was introduced mathematically by expressing the flux density for a smooth stator in a Fourier series representing the rectangular curve shown in Figure 2. The final flux density distribution is obtained as a product of two functions, namely the rectangular flux density distribution expressed by equation 5 and the ratio between the real permeance and that for a smooth stator as expressed by equation 8. It does not matter that the second factor is wrong for all points of the interpole space because the first factor is zero for all these points of the interpolar spaces. Of course the method used in this scheme is an approximation only.

I agree with Blume and Votaw that it is of equal importance to minimize errors caused by manufacturing tolerances and to reduce the null voltage. An analysis of the causes of these errors would certainly be very interesting, but is beyond the scope of this paper.

Electrical Hazards to Farm Stock

W. B. BUCHANAN
MEMBER AIEE

THIS paper is a brief summary of various points of interest in the supply of electric power to stock farms. Cases of data given are derived from actual field experience and should be of interest to inspectors and consumer service representatives. The need for careful study is emphasized not only in the initial installations but for periodic reinspections to ensure maintenance in safe condition.

About six years ago this subject was presented to the AIEE as a problem which seemed to warrant a more critical study than had, at that time, been given to it by this Institute. The channel through which the request was made indicated that many important groups, having high responsibilities, were interested and the interest would be widespread, possibly even global.

A subcommittee was organized under the Committee of Domestic and Commercial Applications and the co-operation of a group of engineers solicited, some of whom were not members of the Institute. Named only as a fact-finding committee, it was not only advisable but necessary to be content with passing on such information to those in authoritative positions for interpretation in action at their own discretion.

Information has been obtained from many sources. The writer's most intimate knowledge of the problems arose from the fact that during the year 1943 a large number of cases occurred in the Province of Ontario, Canada, where valuable cattle were killed while standing in their stalls and investigations were made by The Hydro-Electric Power Commission of Ontario to determine the causes in each case. These cases were apparently very similar to other cases reported from areas where climatic conditions and dairying practices closely parallel those in Ontario, namely, Wisconsin and Minnesota.

A study of the various components of this problem led to a further continuous study of various features of its distribution system by The Hydro-Electric Power Commission of Ontario. This paper constitutes simply a plea for more and better engineering in the supply of electric power to farm buildings. There has been evidence of a rather widely held opinion that extension of electric service to farms has been merely an extension of the practices and standards of construction common in urban centers, regardless of local conditions, and there seems to have been some justification for such a view.

The majority of fatalities reported were derived from the modern practice in dairy stables of supplying drinking water to the stalls through iron pipe, the use of metal piping for operating milking machines and the use of steel stanchions as enclosures. Such conditions present a 24-hour-a-day hazard in case of electric potential being set up at the stanchions and an animal cannot possibly withdraw to safety. Cases have occurred with animals in other locations and human fatalities also have occurred.

While the owner is normally the principal financial loser in these cases the utility and also the general public are vitally concerned with the safety to life and property involved in the distribution of electric power. Codes for standard practice have been developed and in some cases have statutory authority for their enforcement. We know something of the efforts of Code committees to formulate standards that may prove workable and of value. Notwithstanding all effort of the part of officials to ensure installations free from hazard, it has been well-nigh impossible to eliminate risk even on new equipment. Where the various deteriorating effects due to age, and so forth, are added the need for careful inspection and possibly test by the owner or his adviser becomes apparent. An intelligent inspection requires some knowledge of basic data and ability to estimate conditions in quantitative terms. Some of these features have been studied in considerable detail.

Safe Limits of Voltage and Current

Popular opinion seems to indicate that standard distribution voltages can be handled with little care but this is unwarranted; a large number of bathroom fatalities testify to that fact.

A great deal of investigation has been conducted toward determining what might be adopted as safe currents and voltages and at what values such units might prove fatal. For obvious reasons it is not permissible to go to the limit in experiments on human beings. Valuable information on maximum let-go currents, body-resistance, and so forth, have been obtained on normal men and women and this type of test can be repeated in almost any well-conducted laboratory.

Experiments have been made on animals up to and including lethal dosages in connection with studies on resuscitation. Further studies have been made on a comparison of body-weights to anticipate what a lethal dosage for a human being might be, but such a method of substitution is too highly conjectural to be reliable.

A summary of investigations made where farm stock have been killed tends to indicate that 32 volts (less than one-third of normal service voltage) applied between the nose or shoulders of a cow and her feet may prove fatal; that 20 volts (less than one-fifth normal service voltage) between metal stanchions and the floor of the stalls has set up violent commotion among the animals in a stable

Paper 50-104, recommended by the AIEE Safety Committee and approved by the AIEE Technical Program Committee for presentation at the AIEE Winter General Meeting, New York, N. Y., January 30–February 3, 1950. Manuscript submitted February 9, 1950; made available for printing February 9, 1950.

W. B. Buchanan is Research Adviser with The Hydro-Electric Power Commission of Ontario, Toronto, Ontario, Canada.

and that about 12 volts (or less than one-tenth normal service voltage) between a drinking trough and the floor of a stall is sufficient to prevent an animal drinking and hence interfere with proper feeding and milk production.

Other records tend to indicate that for healthy adult human beings, maximum let-go currents are of the order of 12 to 15 milliamperes (less than 1/50 of the current taken by a 100-watt lamp) with lethal values anywhere above 25 milliamperes even with current interrupted at frequent intervals. Involuntary muscular response, however, occurs at as low current as $1^1/_2$ to 2 milliamperes (less than 1/500 of the current taken by a 100-watt lamp) and in hazardous locations might initiate a serious accident.

These figures are introduced to emphasize the need for absolutely preventing the straying of current by devious and unauthorized paths, hence the need for high quality of installation and maintenance, and the advisability of adhering to recognized codes insofar as these codes deal with safety in operation. A breakdown in the insulation of a conductor may enliven metallic parts with which man or beast normally comes readily in contact and such locations may be quite remote from the fault itself.

Earth Potentials and Current Paths

There are a number of features associated with electrical hazards that do not appear to be well understood, certainly not where all the various ramifications of the problems are taken into account. The most important of these probably is associated with so-called grounding of circuits and other metallic parts of electric equipment.

The conductivity of earth varies over a wide range of values and also, so far as this problem is concerned, with seasonal changes. If current is discharged to ground, it is practically impossible to prevent it taking unauthorized and frequently dangerous routes in its return circuit. These sneak currents and voltages are particularly hazardous because they are usually unsuspected and their action very prompt. The difficulties of the engineer arise from the fact that earth conductivities are usually sufficient to carry the lethal currents noted above but not high enough to cause interruption of the power supply by blowing fuses or opening circuit breakers. Fire hazards also can be created with very low values of stray current and voltage.

An assumption frequently made is that if current is led to earth by metallic rods or water pipes it would therefore be harmless. As a matter of fact the current must dissipate through fairly large areas of earth before the voltage drop around such grounding metals can be entirely neglected. For this reason a high concentration of voltage drop or voltage gradient may occur adjacent to rods or pipes of small diameter.

The practical application of this phenomena has many ramifications, for example, a lightning rod ground should be separated at least six feet from the ground rod to which any conduit or motor frame may be attached. Otherwise a lightning stroke can cause, and has resulted in a breakdown of the insulation of the wiring in such conduit.

The flexible steel-armour of a 2-wire circuit was installed under a floor in a cottage and was grounded at both ends, yet sufficient stray current passed through this steel armour to heat it and set fire to adjacent wood work on two occasions.

A cow was walking quietly through a gateway alongside a barn and dropped to the ground and expired. A piece of loose iron wire was found embedded in the surface of the earth over which she walked, and one end of the wire was attached to conduit on the wall of the barn. The insulation on a wire of the circuit in the conduit had failed and the conduit and wire were electrically alive.

A fault on a range in a residence caused potential to be applied to a waterpipe which led underground (in contact with soil) about 200 feet to the stable. Fifty volts was measured between the waterpipe, which was attached to the stanchions, and the floor of the stalls where six cattle had been killed.

Water-Piping for Grounding Purposes

The value of water-piping for grounding purposes in rural services is frequently much over-rated, if considered at all. In addition to the low conductivity to earth as indicated in the example previously noted, various objectionable conditions such as the following have been discovered.

Many such water-systems have no contact with earth whatever, some only slightly and then in fairly dry locations. It is quite common to find the water-piping carried overhead from its entrance to the stable to its termination at the stalls.

Electrical discontinuities occur in the piping due to various causes. Breaks in malleable T-couplings have been mended with tape. One hundred ohms was measured between the incoming and outgoing pipes from a float-tank from which water-bowls were supplied; unions and other couplings may have high resistances. In fact it is possible to assemble a union in a 1/2-inch pipe to introduce 100 ohms when full of water; the piping to and from either wooden or concrete tanks may not be directly connected at all; grounding clamps unless carefully cleaned and fitted may be found to result in quite high resistances to the pipe.

Other cases, associated with summer cottages perhaps to a greater extent than on farms, have indicated lethal hazards where none were suspected. A boy swimmer in a river attempted to grasp the suction pipe to an electrically-driven pump while there was a breakdown in the motor insulation and was electrocuted. Ninety volts was measured within the length of his body adjacent to the pipe.

A collie dog stepped on a water pipe which led from a cottage out along the sandy beach into the water for some distance and was killed. The motor had for some years been removed in the fall and replaced in the spring and the insulation at the terminals had become weakened and failed.

A grounding pipe installed at a boathouse was driven into the soil below about five feet of water and was in contact with water directly for that five feet as well. With 115 volts applied, however, this ground would not permit enough current to flow to blow fuse wire of 1-ampere rating.

Deterioration

There are certain features and practices which seem to be more characteristic of rural installations and though the immediate risk may be negligible, the effect of deterioration of insulation and other material should be given some thought. It would be difficult to list these in the order of their importance nor would the list be complete, but some items of more than passing interest may be mentioned.

Pump-motors have been found installed in wells, metallically connected to piping. Insulation on such motors also has failed, with temporary wiring offered as an explanation. Other installations of a safer type involve separation of the motor from the pump by wooden platform and belt-drive or by wooden operating rod on the pump jack.

The humid atmosphere occurring at times in stables has a deteriorating effect on insulation at various locations but

principally if moisture is allowed to collect in conduit leading in from colder atmosphere. The best simple remedy against collection of moisture seems to be to avoid any possible traps in the conduit, or provide automatic drainage.

The merits of nonmetallic sheathed cable versus metal conduit is a subject of controversy. As a matter of fact, it should be possible to do a good job using either system but the essential requirements cannot be ignored. Among other things, nonmetallic sheath should be fungus-resistant, have good abrasion and shock resistance and have slow flammability. The insulation over-all should be moisture-resistant, have good tensile strength and reasonable life. One case occurred recently where a 1/2-inch water pipe wore through the insulation of a nonmetallic sheath cable and 18 purebred cows were electrocuted. This wiring had been installed about six years.

More than ordinary care is necessary to ensure good current carrying capacity in conduit. Corrosion of joints between conduit and boxes may be accelerated by the application of lime or other disinfecting washes used in stables. A recent field investigation showed that 45 volts existed across a length of less than three feet where three such joints were involved. Had these joints, and the others in the conduit run, been of good conductivity, undoubtedly the animals in the stables would have been subjected to voltages of dangerous magnitude. The cause of this stray voltage was found to be a corroded connector between the high-voltage neutral conductor and the grounding lead.

Another class of trouble arises from conductors so loosely supported that they may be whipped together in the wind or otherwise make accidental contact with exposed metal parts. Loosely strung lines across the yard may develop a short circuit. Hazards are multiplied when barns or other buildings are covered with metallic siding.

One outstanding criticism may be made which would be applicable to many of the cases reported, for example, an attempt to make alterations or additions to the system without due regard to all conditions as they existed at the time, in effect, incorrect procedure due to incomplete or incorrect diagnosis. This may be observed all up the line from the amateur who installs a single-pole switch in the neutral or grounded lead of a circuit to more complex cases in which the work was carried out by experts. One such case occurred when eight cows were killed. The contractor very conscientiously provided a grounding wire (third conductor) and connected it from the frame of the milking machine back to the switch panel at the entrance to the stable. The conduit carrying the power wires was grounded but not connected to the neutral. Insulation failed in the conduit and potential was carried by way of the frame of the milking machine to the stanchions where 80 volts was set up within length of any one animal.

Another case resulted in the electrocution of two cows because the contractor made wrong assumption as to the manner in which the utility normally brought out terminals and neither party actually made check tests before enlivening the circuit.

Strange as it may appear some of the installations made over 30 years ago with the knob-and-tube-system of open wiring were in better condition than many with metalclad wiring less than ten years old.

It should be evident from this brief examination of factors involved in the problem of supplying electric power with safety that very little carelessness can easily introduce a high degree of hazard. Various proposals for protection have been made, some of which are of doubtful value. Others have controversial aspects which are desirable under some conditions and undesirable under others. A proper appraisal of the various factors becomes quite an involved problem—a job for specialists. Even when all is done that can possibly be accomplished by standardization and mandatory codes, it appears that hazards will still continue. Many of these will doubtless be repetitions of what has occurred before and new types may develop.

Whatever else may be done to improve safety, it seems clear that periodic inspection of equipment by specially-trained inspectors would be desirable. In any case alertness and continual vigilance should be exercised by those who recognize hazardous conditions to see that any such hazards be brought to the attention of the proper authority.

No Discussion

Protective Grounding of Electrical Installations on Customer's Premises

A. H. SCHIRMER
MEMBER AIEE

THE problem of electrical safety in rural areas is one of providing adequate insulation on circuits and equipment, and effective grounding and bonding. Providing adequate insulation presents no particular problems. However, there is some confusion as to what constitutes effective grounding and bonding. This paper briefly discusses the various factors which must be taken into account. The discussion is limited to a-c circuits.

Purpose of Grounding

The purpose of grounding is: to limit or reduce potentials that would otherwise exist between conductors and equipment; to limit the voltage between conductors and their metal enclosures; and to provide a path for fault currents of sufficient magnitude to cause overcurrent devices to operate and de-energize the circuit.

It is well known that limiting potentials reduces the likelihood of electrical shock to persons and animals, and much emphasis has been placed on this point. What is not so well known is that limiting or preventing potentials by grounding, reduces the possibility of insulation failure and arcing, and thus also reduces the fire hazard.

Voltages Involved

There are ordinarily three sources of voltages for which protection must be provided: (1) lightning; (2) primary distribution, 2400 volts or above; and (3) secondary distribution, that is, 120–240 volt circuits.

Relative Importance of Protection from Primary and Secondary Voltages

In the early days when electricity was used primarily for lighting and convenience outlets, and appliances were practically unknown, the main reason for grounding secondary circuits was to reduce the hazard resulting from primary voltages. Today, with better transformers and transformer protection, as well as improved pole line construction, faults involving primary circuits are relatively rare. On the other hand, more and more appliances are being used in the home and factory so that protection from low-voltage faults has become the more important consideration. It seems wise, therefore, to discuss low-voltage protection in detail, particularly since the grounding and bonding required for adequate low-voltage protection is in general adequate for primary voltage and lightning protection.

The National Electrical Code[1] requires secondary circuits to be grounded if they can be so grounded that the maximum voltage to ground does not exceed 150 volts. Except in public water pipe areas it is in general not practicable to secure a grounding electrode which has a resistance of less than 10 ohms. In view of this, satisfactory low-voltage protection cannot ordinarily be obtained where separate grounding electrodes are used for circuits and equipment. This is illustrated by the following examples. The conduit mentioned in these examples may be considered as any metallic enclosure for conductors or equipment.

EXAMPLE 1

Conditions

Neutral of 120–240 volt circuit connected to a 10-ohm grounding electrode. Conduit connected to a 20-ohm grounding electrode. Fault between live conductor and conduit.

Result

Fault current 4 amperes; 15-ampere fuse did not operate. Conduit remained energized at 80 volts.

Remarks

This method of grounding is obviously unsatisfactory for low-voltage protection. Additional secondary grounds at the transformer or elsewhere on the secondary system would not help the situation since the current would remain under 6 amperes.

EXAMPLE 2

Conditions

Neutral of 120–240 volt circuit and conduit connected to a common 25-ohm electrode. Fault between live conductor and conduit.

Result

Fault caused a short circuit; fault current large; fuse blew quickly; voltage on conduit small.

Remarks

This method provides adequate low-voltage protection.

EXAMPLE 3

Conditions

Neutral of 120–240 volt circuit and conduit connected to a common grounding electrode having a resistance R_1 ohms. In addition, a grounding electrode having a resistance of R_2 ohms is connected to the neutral at the transformer pole. Fault between live conductor and conduit.

Results

Fault caused a short circuit, fault current large; fuse blew quickly. If the resistance of the electrode at the service (R_1) is large compared to the resistance of the electrode at the transformer (R_2) the voltage of the conduit to ground may

Paper 50-105, recommended by the AIEE Safety Committee and approved by the AIEE Technical Program Committee for presentation at the AIEE Winter General Meeting, New York, N. Y., January 30–February 3, 1950. Manuscript submitted March 8, 1950; made available for printing March 15, 1950.

A. H. SCHIRMER is with the Bell Telephone Laboratories, Inc., New York, N. Y.

approach 60 volts, that is one-half of the secondary voltage until the fuse blows.

Remarks

This method also provides low-voltage protection.

Common Grounding Electrode

From the foregoing example it is evident that to have good low-voltage protection, it is necessary to have a common ground for circuits and equipment at each building served. Section 2554 of the 1947 edition of the National Electrical Code makes such common grounding mandatory.

The use of a common grounding electrode is important from the standpoint of lightning and also for faults involving primary circuits in order to prevent excessive voltage between conductors and equipment enclosures. It might be pointed out that insulation failures resulting from lightning, where separate grounding electrodes are used for circuits and equipment, are a frequent cause of conductor or equipment enclosures becoming and remaining energized from secondary voltages.

Interconnection of Grounding Electrodes

Safety may be further improved by so arranging the grounding that all metallic structures, which can be touched or to which arcing might occur, are connected to or from part of the same grounding electrode used for grounding the circuit. If all grounded-metallic structures within a building are connected to the grounding electrode used for grounding the electric circuits, no large difference in potential can develop within the building. In recognition of this fact, it has long been the practice of power companies to bond together all metallic parts within a generating or substation area. Such interconnection also is approximated where a water piping system is used as the grounding electrode, as discussed below.

Reason for Using Water Pipe Grounds

In urban areas, the use of underground metallic piping systems as a grounding electrode is well established. The reasons why such water pipes provide the best grounding electrode and why it is necessary to use them for grounding the circuit are well expressed in a paper, Electrical Grounds on Water Pipes, by H. S. Warren.[3]

He states as follows:

"The reason why a continuous metallic public supply water piping system makes the best ground is not because such pipes have water in them but is due to the fact that such a piping system has by far the largest contact surface with the conducting material of the earth. In fact, where such a piping system exists, it is the earth, electrically speaking, for all practical purposes. The hazard to be protected against arises from the fact that voltages may accidentally be set up between different metallic objects in the house and that persons may be subjected to these voltages. Water pipes appear at numerous points through the house and are interconnected or in contact with steam pipes, gas pipes, and so forth, so that they offer numerous chances for people to get in contact with them. If some other grounding electrode were employed instead of the water pipes, the voltages between electric wiring, apparatus, and so forth, and this extensive system of pipes might be much larger and, hence, the hazard much greater. The very presence of these piping systems in a house increases the importance of using them as grounding electrodes."

Where so-called private water systems, that is systems supplied from local wells, are used, the presence of the water piping system in a building presents, in varying degrees, the same situation as outlined in Mr. Warren's statement. It is recognized that, in general, the resistance to ground of such systems will be materially larger than for public systems. It is nevertheless important to use such a system as the grounding electrode or to bond it to any other electrode which may be used.

There are several reasons:

1. The use of such piping systems for grounding purposes, regardless of their resistance to ground, reduces the likelihood of difference of potential within a residence.

2. If the water system is not used as the grounding electrode, large differences of potential may occur between the electric wiring and the piping system due to lightning, particularly in rural areas. Since it is difficult to have large separations between the water pipes and electric wiring, arcing due to lightning will occur at points of small separation. Such arcing, with power arc follow-up, constitutes a greater fire hazard than lightning alone where power wires are not involved.

3. Most private water systems today have an electric pump with the motor frame in contact with the piping system. If the wiring system is not connected to the water piping systems, large potentials may develop between the winding and the frame of the motor due either to lightning or a fault involving the primary circuit. Such potentials frequently cause insulation failure and a cross between the live circuit conductor and the frame. Where the resistance of the water pipe is more than a few ohms, such a fault will not operate the branch fuses and the water pipe will remain energized at a voltage approaching 120 volts.

Interconnection of Primary and Secondary Neutral

It is evident, of course, that the grounding connection should have a resistance as low as it is practicable to obtain. Bonding the secondary neutral to a multigrounded primary neutral reduces the resistance of the secondary neutral to ground and has definite advantages both from the standpoint of lightning and faults involving a primary distribution circuit. With properly designed multigrounded primary circuit, the normal potentials due to load currents are ordinarily small. At any rate, if the potential to ground due to normal load current is larger than seems wise, the answer is to improve the grounding on the primary neutral circuit, rather than to separate secondary and primary. The National Electrical Safety Code[2] permits the interconnection of the primary and secondary neutrals. It states in Rule 285c:

"Primary and secondary circuits may utilize a single conductor as a common neutral if such a conductor has at least four ground connections in each mile of line. Ground connections at individual services are to be counted only if made to underground water piping systems."

Section 2632-a-2 of the National Electrical Code also provides for such interconnection.

Farm Barns

While the writer does not claim to have complete statistics on farm animal fatalities, such cases as have come to his attention were largely due to sustained secondary voltages on conduits or piping systems. These sustained voltages resulted from the fact that the circuit, conduit, and equipment were not grounded to a common grounding electrode at the barn. In rural areas it is important that the circuit and enclosures be grounded at each substantial building served. In many of the cases the failure of the conductors in the service conduit (at the barn) caused the sustained potential. These failures in the service conduit were probably caused by high lightning potentials between conduit and conductors resulting from the fact that the circuit either was not grounded at the barn or was not commonly grounded to the conduit grounding electrode.

Potentials which persist for only a very short time do not ordinarily constitute a substantial hazard, and there is very little evidence that such momentary potentials have been a major factor in farm animal electrocutions. It must be admitted, however, that in a dairy barn

where the stalls are provided with automatic drinking cups, the likelihood of electric shock to cattle is greater than it would be without the automatic cups. If there is concern, the way to solve the problem is to bond and ground all extensive metallic structures in a barn and place in each stall or group of stalls some metallic structure under or in the floor and bond such structure to the piping system. The metallic structure should be so located that the potential at the rear of the stall will be the same as at the front of the stall. With such an arrangement the cow may be at a substantial voltage above ground, but there would be no damaging current through the body of the cow.

References

1. National Electrical Code. National Fire Protection Association (Boston, Mass.), 1947.

2. Electrical Grounds on Water Pipes, H. S. Warren. *Journal*, New England Water Works Association (Boston, Mass.), volume XLVIII, September 1934, pages 350–58.

3. National Electrical Safety Code. *Handbook H-32*, National Bureau of Standards (Washington, D. C.), 1941.

No Discussion

Rural Neutral Potentials

J. H. WAGHORNE
NONMEMBER AIEE

THIS paper covers the results of an investigation of potentials occurring on the neutrals of the rural distribution lines of The Hydro-Electric Power Commission of Ontario. Having regard to the potentials under normal operation, unusual loads, primary faults, and lightning surges, the conclusion drawn is that the common multigrounded neutral is the safest and most reliable ground available in the distribution system and that normally all metallic enclosures should be connected to it.

Background of the Investigation

The Commission's Rural Systems

The Hydro-Electric Power Commission of Ontario owns and operates 32,000 miles of rural distribution lines serving 260,000 consumers. Approximately 55 per cent of this mileage carries 25 cycles-per-second power, and the balance 60 cycles per second. About 8 per cent of the total mileage has single-phase distribution transformers connected phase-to-phase on a grounded-star 3-wire system, but this is gradually being displaced by using the multigrounded neutral common to primary and secondary. This neutral is grounded at each distribution transformer, and on each consumers' premises. Although the lines have an average of more than eight consumers per mile, some sections are ungrounded for as much as two miles.

All of the 8 per cent phase-to-phase distribution is at 4,000 volts, along with 44 per cent of total mileage with multigrounded neutral. These lines serve the more densely populated areas. The 8,000-volt system (4,600 volts phase-to-neutral) covers 43 per cent of the rural mileage at present, and in time will replace more of the 4,000-volt system. For long lines in more sparsely populated areas, 12,000 volts (6,900 volts phase-to-neutral) is generally used. At present, this includes 5 per cent of the total mileage.

Grounding Regulations

Before 1931 the consumers' grounds were not connected to the neutral even on grounded neutral lines. Service boxes, conduit, and all other metallic enclosures were required to be connected to a driven ground for "safety." Service entrance boxes installed since 1931 have been connected not only to a driven ground but also to the neutral. Distribution boxes in other buildings continued to be connected to "safety" grounds but not to the neutral until 1947. This means that all metallic enclosures connected to the service entrance boxes during this period have been tied to the common neutral while those not so connected have been protected only by "safety" grounds. Since 1947 revised wiring regulations for rural areas require that all metallic enclosures be connected to both the neutral at the distribution box and a driven ground rod.

Reason for Investigation

Primarily to investigate the extent of the hazard involved in the connection of metallic enclosures to the neutral, the Electrical Research Department of the Commission has been and is investigating the primary neutral potentials which exist or can occur on its rural lines. The use of a common primary and secondary neutral obviously applies any primary neutral potential to whatever metallic enclosures are connected to it.

If metallic enclosures are not connected to the neutral but only to driven rods for "safety" the sum of the driven rod resistance to earth and the secondary neutral to earth resistance must be low enough to clear secondary fuses in case of secondary faults. This means a maximum combined resistance of less than five ohms. If this is not obtained, a fault from a 110-volt conductor to any metallic enclosure may fail to blow the fuse and the fault is sustained. Depending on the ratios of resistances involved, some fraction of the 110 volts remains on the enclosure. Where water systems and steel stanchions in stables are connected to such enclosures this voltage can prove fatal to farm stock. The Commission, as well as others, has had first-hand experiences of this nature.

The investigation of neutral potentials has included four different conditions: normal operation; unusual loads; primary faults; and lightning surges.

Normal Operation

Survey of Farm Areas

A survey in 1945 indicated that lethal voltages do not normally exist on the primary neutrals throughout farm areas. In general, where land is good for farming, creating heavy electrical loads, it is also good for grounding; conversely, where grounding is poor due to rock or light soil, farming is less productive and farm electrical loads lighter. The search for possible neutral potentials was made through a farming area about 100 by 350 miles. Two graphic voltmeters were used to obtain fortnightly charts at 20 locations where the largest neutral potentials would be expected and an indicating voltmeter was used to check an additional 56 lines.

The maximum potential recorded near the end of a line was 17 volts. This was found in dairy farming country and was the result of a combination of factors: large milking machine and grain grinding load, too small neutral conductor, and very few consumer grounds connected to the neutral, as the line was one of early

Paper 50-106, recommended by the AIEE Safety Committee and approved by the AIEE Technical Program Committee for presentation at the AIEE Winter General Meeting, New York, N. Y., January 30–February 3, 1950. Manuscript submitted March 8, 1950; made available for printing April 19, 1950.

J. H. Waghorne is with The Hydro-Electric Power Commission of Ontario, Toronto, Ontario, Canada.

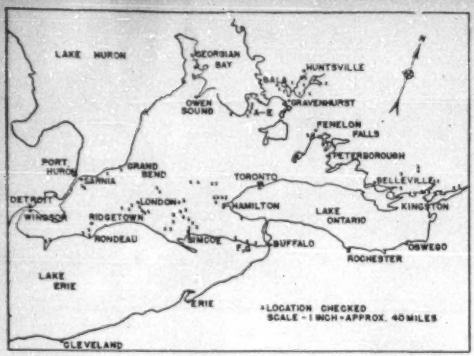

Figure 1. Map of Southern Ontario showing locations of rural neutral potential measurements

construction. Regulation of the line was very unsatisfactory, hence this condition would not normally be permitted to continue. Adjacent to the distribution station, 19 volts was found at one location and 16 volts at another, which calls attention to the fact that voltage can appear at either end of a line. At the load end of the lines from these stations, no appreciable voltage was measured.

One other line was found with a maximum of seven volts but all others checked in farm areas were below five volts.

Summer Resort Areas

In 1946, the survey of neutral potentials was concentrated on lines serving summer resort areas. For this survey, 15 graphic voltmeters with ranges of 14 and 28 volts were purchased. In resort areas the possibility exists of poor grounding due to rock or sand and gravel, while the electrical loads during the summer may be heavy. Graphic voltmeter measurements were made at 31 locations where load and grounding suggested the possibility of neutral potentials, and in 1948 an additional 10 locations were checked. From this total of 41 locations, nine were found with voltages at times reaching values above 10 volts. Three of these reached above 25 volts, one of which was above 28 volts for 5 per cent of the time, see Figure 1.

Reduction of Neutral Potentials

In many areas throughout the province where grounding is poor, sand or gravel overlies clay. If ground rods are driven through the sand or gravel into the clay, good grounding is usually obtained. For this purpose extension rods are used, threaded at both ends to permit them to be fastened together with a short coupling. Driving is done with a standard gasoline-driven pavement breaker adapted to fit the threaded ground rods. The longest rod driven to date was 210 feet. Laboratory and preliminary field tests indicate that hardened steel tips and just a tapered fit for couplings instead of threads would facilitate driving considerably.

Long rods were driven on the only farm line found with appreciable voltage, one to a depth of 94 feet, and the maximum neutral potential was reduced from 17 to 11 volts. At one of the two distribution stations found with appreciable neutral voltage, four ground rods were driven to a depth of more than 50 feet. At two summer resort locations, long rods were used to bring down the neutral potentials in 1948.

In 1949 the use of long rods was extended, 4,912 feet of rod being driven at about 100 locations in the area including Deanlea, Wymbolwood, New Wasaga, Wanakawening, and Nottawa beaches. The voltage at these locations before improvement is shown in Figure 2. Checks after improvement showed none of these going above five volts.

At one summer resort location where as high as 28 volts was recorded, grounding is poor because bedrock is only a few feet below the surface. No holes or crevices in the bedrock can be readily located near enough to be effective. In this instance the single phase is to be changed to 3-phase, which will reduce the primary neutral current. However, a heavier primary neutral conductor would also have been effective in reducing the neutral voltage to a safe value.

Considerable confidence has been gained through this investigation in the possibility of maintaining all rural neutrals at safe potentials under normal load conditions. If an exception be found, isolation of the secondary neutral from the primary could be a second choice.

Unusual Loads

Open-Star-Open-Delta

At one location a 40-horsepower 3-phase load was supplied from two phase conductors and the neutral through an open-star-open-delta transformer bank. This line ran about five miles from a 3-phase supply to this load but a maximum of eight volts was measured on this neutral at the end of the line and nine volts was measured at the distribution station.

Ground-Return Circuit

In another area a few miles of single-phase circuit with transformers connected from primary to grounded neutral using underground cable is fed from a 3-wire 3-phase distribution line several miles from the distribution station. As the star point at the station was grounded all the neutral current from the single-phase grounded section was forced to return to the station via the earth. Only one volt was measured on this section of neutral.

Wide Separation of Phases

Where two different phases travelled by widely separated routes as single-phase lines from the distribution station to within one-half mile of each other no appreciable neutral potential was found on the end of either line.

Large Concentrated Single-Phase Load

The Village of Newburgh is fed single-phase power from an 8,000-volt 3-phase line by carrying the 4,600 volts phase-to-neutral about three-quarters of a mile to the village limits. At this point a 75-kva single-phase transformer reduces the line voltage to 2,300 volts and the line then continues for three-quarters of a mile to the village center where the main part of the load is located. The conductor in the 2,300-volt section is number 2 copper and when carrying the maximum load, a drop of about 30 volts is produced along this neutral. Since the neutral resistance is less than one ohm and the grounding resistance at the transformer is much greater than this, there is no appreciable current carried in the earth.

As only one point on a conductor carrying current can be at true ground potential, this neutral cannot be maintained at a low potential throughout its length. The need to change to 3-phase for a concentrated load of this magnitude is indicated.

Fault Conditions

In evaluating the possible hazards from common neutral potentials, the results of primary faults must be considered. The most serious types of fault are phase-to-neutral short circuits, breaks in the neutral, and the combination of both.

Line Used for Experiment

The line serving a farm area around Roseville, was found from the survey as having unfavorable grounding and was chosen for fault tests. This line is 3-phase for $1^1/_2$ miles and then single-phase for an additional $4^1/_2$ miles, number 6 copper phase and neutral, operating at 2,300 volts. It is an old line and consequently has few consumer grounds. In the last 1.7 miles of single-phase there are nine transformers with a ground at each having resistances ranging from 4 to 100 ohms.

Phase-to-Neutral Short

With a short circuit between phase and neutral applied through a 15-ampere fuse at the end of the line, 370 volts was measured on the neutral for 0.8-second duration. With 15 extra consumer grounds connected (as there would be under more modern construction) 204 volts was measured.

A short circuit applied 1.7 miles from the end of the line with no extra consumer grounds connected produced 220 volts at the point of application and 135 volts at the end of the line for a duration of 0.4 second.

Phase-to-Neutral Short Plus Open Neutral

With the neutral broken 1.7 miles from the end of the line short circuits were again applied at the end and 445 volts was measured on the neutral without extra consumer grounds and 225 volts with such grounds.

Primary Neutral Open

Under normal load with the neutral broken 1.7 miles from the end of the line, 19 volts would be the maximum neutral potential. At another location where the neutral was accidentally broken, leaving only three transformers on the end section feeding summer cottages, the neutral potential measured was only 2.4 volts.

Lightning Surges

Surge Voltage Recorder

The development of a simplified klydonograph-recording unit in the Commission's laboratories has greatly facilitated the collecting of field data on surges. In two rural areas a total of 400 units has been serviced for three lightning seasons.

Installations

In order to determine the frequency of surges on the rural neutrals 76 klydonograph installations were made from neutral to a separate ground connection at the distribution transformers and 70 installations between neutral and ground at consumers' equipment.

Results

These records have been plotted in two curves, as shown in Figure 3, showing the frequency of occurrence of surges larger than a given value on the primary neutral and also at the consumers' equipment. As the majority of these surges originate on the primary, attenuation is evident by the time they reach the consumers' equipment. This is particularly the case with the larger surges which would have steeper wave fronts and tails. Equipment located close to the transformers would be subjected to the surges indicated at the transformer, hence this curve should be used to determine possible frequency of surges on secondary equipment connected to the neutral.

It can be seen from the curves that 38 per cent of equipment will receive surges above 10,000 volts each year, 15 per cent above 20,000 volts, and 6 per cent above 30,000 volts.

Evaluation of Hazard from Neutral Potentials

The classification of voltages is still not very definite with respect to degree of nuisance, or probable lethal effects. The accumulation of information of this type is necessarily slow, as for obvious reasons lethal limits for human beings cannot be set by experiment and would be expensive to obtain for the larger domestic animals. A few cases have arisen where evidence of neutral potential has been given by cattle refusing to drink from water bowls that were connected through

Figure 2. Potentials measured with graphic voltmeter on rural neutrals at lettered points shown on map of Figure 1

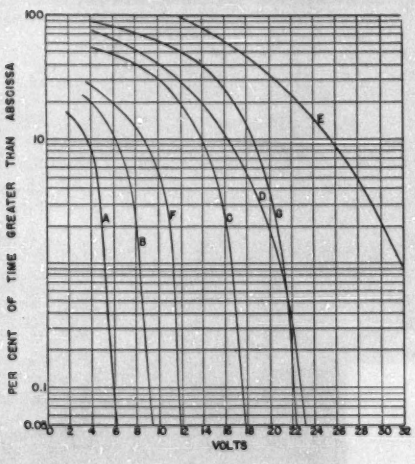

Figure 3. Frequency of lightning surges measured with klydonographs between the rural neutral and an independent ground

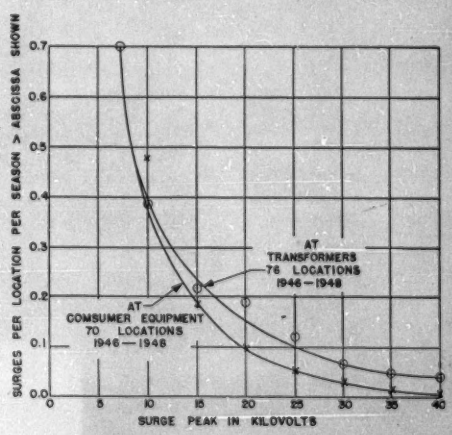

the private water system to the neutral. The lowest voltage recorded to date causing this nuisance is seven volts.

For sustained power frequency voltages where the exposure may be severe as in stables or around water pumping systems, and so forth, a fair amount of evidence has accumulated in favor of a classification such as:

0–7 volts, possible nuisance
7–25 volts, probable nuisance
25–50 volts, possibly lethal
50–110 volts, probably lethal

The hazards involved in exposures of short duration are even more highly conjectural than for sustained potentials. The amount of evidence available is more scanty and is somewhat conflicting. However, very much larger voltages apparently can be safely withstood for periods of the order of a fraction of a second than for sustained periods. Against this is some evidence that the phase of the heart cycle at the instant of application of the shock is a controlling factor on the result.

The hazards may be evaluated under the four operating conditions:

Normal Operation: Under normal operation, neutral potentials can be maintained at safe values without undue expense.

Occasionally potentials will be experienced large enough to be a nuisance. In these cases if it is not practical to reduce the maximum potential to less than seven volts separation of primary and secondary neutrals can be used. If in the future the neutral potential condition is remedied reconnection can be made easily.

Unusual Load Conditions: While no unusual load conditions producing serious neutral potentials have been found on the Commission's rural systems during these tests it would not be safe to conclude that such instances will not arise. Hence all such conditions should be individually checked.

Fault Conditions: If primary phase-to-neutral faults were sustained they would no doubt lead to lethal voltages. However, when their slight probability of occurrence is multiplied by the small probability of the existence of severe exposure and by a reduction factor resulting from their short duration, the chance of the neutral potential having lethal consequences is reduced to a very small undetermined value. As the Commission has been operating with a small percentage of the consumers' metallic enclosures connected to the common neutral for 17 years with only a single fatality as yet from this cause, some confidence has been gained that the hazard involved is very slight.

Lightning: Much the same arguments apply with regard to lightning as for fault conditions. One additional factor is that the most severe lightning surges will flash over to metallic enclosures even without interconnection, and have been doing so for years without adding any fatalities to our records.

Conclusion

Nearly all fatalities of farm stock investigated by the Commission from 1943 to 1949 resulted from a sustained fault to metallic enclosures on consumers' equipment. These metallic enclosures were connected to driven rods as "safety" grounds which failed to clear the circuits. Such faults would have cleared the circuit had the enclosure also been connected to the neutral.

Investigation of neutral potentials indicates that the common primary and secondary multigrounded neutral can be safely used for grounding purposes.

Wiring regulations for rural areas in the Province of Ontario were amended in 1947 to require all metallic enclosures on future installations to be connected to the common neutral and to driven grounds.

Discussion

W. B. Buchanan (The Hydro-Electric Power Commission of Ontario, Toronto, Ontario, Canada): This paper is a contribution to the work of the fact-finding committee in which the writer has been interested during the last few years. It serves to call attention to various factors involved in the problem rather than to establish limiting conditions.

It is only fair to point out that the operators of the system on which these results were taken have been highly alert to the grounding problem in all its ramifications for at least 25 years to the writer's knowledge, and from the point of view of maintenance the system might be considered as one of the best if not the best in existence.

In the interests of safety, however, it seems prudent to call attention to some possibilities which indicate that the cases given do not warrant final conclusions as to operating practice.

The writer personally investigated a case of a break in the primary neutral, where 110 volts persisted through most of an afternoon from the primary and secondary neutrals to ground at periods of light loads. Shocks were obtained by operators at gasoline pumps and the condition existed some days before being reported. This was in a moderately well settled suburban section with grounds mainly in clay loam. Fortunately, no serious accident resulted from this case.

It would be unfortunate from the point of view of safety to disregard the possibility of lethal potentials occurring on primary neutrals. The writer has definite information of two unsuspecting linemen (other cases have been reported) being fatally shocked by coming in contact with the primary neutral and ground only. There are very definite reasons for the use of guards on ground wires and other suitable protection of man or beast in exposed locations.

One may not assume that transient overloads of the nature of short circuits will always be of negligible duration. Arcing-grounds can be rather vicious in setting up potentials in and around so-called grounded structures.

Care must be taken that bonding of all metallic objects in contact with earth does not become a fetish rather than sound engineering. There is frequently a great deal of metal equipment around farms that has nothing whatever to do with the electric service and which, if tied in therewith, could introduce serious potential hazards. Those entrusted with the formulation of mandatory codes should recognize such conditions as being possible and not put the electrical inspector in the embarrassing position of having to violate code regulations in order to make equipment safe. Waghorne mentions the fact that the primary and secondary neutrals could be separated as a second choice.

Obviously, there is need for a permissive clause on this point in regulations; also for one to provide for isolation of the iron-piping in the stables if that should prove to be the best and safest solution.

The listed values of nuisance and lethal values require some analysis. Data available indicate that seven volts is a nuisance if applied to an animal under certain conditions, also that 30 volts is a lethal value. The terms "possibly" and "probably" thus refer to the chance that an animal (or person) may make contact in such manner as to allow the voltage to become fully effective. The writer had occasion some years ago to take measurements on the equipment used for electrocuting dogs and cats. The sustained potential between a metal collar around the dog's neck and the metal floor on which it sat was only 60 volts. The hair and skin of the neck was wetted to improve contact conductivity. There was never any doubt as to whether 60 volts was lethal or not.

AIEE Transactions Index for Part I, Volume 69, 1950

1. Technical Subject Index

Accounting System, Fundamentals of the Automatic Telephone Message. Meszar....255–68; disc. 269
Accuracy Performance of the Selsyn Generator Control Transformer System, Static. Kronacher.....645–54; disc. 653
Air Gaps, Dielectric Recovery Characteristics of Power Arcs in Large. McCann, Conner, Ellis.....616–24; disc. 624
A-C Generators with Suddenly Applied Loads, Regulation of. Part II. Harder, Cheek, Clayton.....395–405; disc. 405
(Part I—1944)
A-C Lead Networks for Servomechanisms, Improvements in the Characteristics of. McDonald. 293–300
A-C Servo Systems with Compensation for Carrier Frequency Changes, Phase Lead for. Notthoff.....285–91; disc. 291
A-C Turbine Generators, Liquid Cooling of. Part II. Fechheimer.....165–71; disc. 171
(Part I—1947)
Alco-GE 4,500-Horsepower Gas-Turbine Electric Locomotive, The. Morey.....504–07
Aluminum Industry, The Theory of the Current Transductor and Its Application in the. Specht, Wagner.....441–52; disc. 452
Amplifier Frequency Control, A Magnetic. Johnson, Schafer.....613–15
Amplifiers, An Analysis of Transients and Feedback in Magnetic. Johnson, Latson.....604–11; disc. 611
Amplifiers, An Analysis of Transients in Magnetic. VerPlanck, Finzi, Beaumariage.....498–503
Anacom—Electric Analog Computer, New Techniques on the. Harder, Carleton.....547–56
Analog Computer, New Techniques on the Anacom—Electric. Harder, Carleton.....547–56
Analogue Computer for Flight Simulation, A Generalized. Hall.....308–20
Analogue Computer for Multicomponent Fractionation Calculations. Goelz, Calvert.....97–103
Analysis of Transients and Feedback in Magnetic Amplifiers. Johnson, Latson.....604–11; disc. 611
Analysis of Transients in Magnetic Amplifiers, An. VerPlanck, Finzi, Beaumariage.....498–503
Analyzing and Synthesizing Contactor Servomechanisms, A Frequency Response Method for. Kochenburger.....270–83; disc. 283
Apparatus, Quick and Accurate Production Testing on Large D-C. Baldwin, Barnhart.....136–8
Application and Handling of Very Large Power Transformers on the System of the Bonneville Power Administration. Stevens.....158–63; disc. 163
Application of Electronic Motor Drives to Printing Presses. Johnson, Stacey.....216–19
Arcs in Large Air Gaps, Dielectric Recovery Characteristics of Power. McCann, Conner, Ellis.....616–24; disc. 624
Armatures, Solderless Commutator Joints for High Temperature Operation of Railway Traction. Reed.....638–41
Arrester Protective Levels and Transformer Insulation, Margins Between Lightning. Vogel.....110–12; disc. 112
Arrester Standard, New Lightning. Stewart, Defandorf.....525–6
Arresters as a Criterion for Insulation Levels, Lightning. Rorden.....84–91; disc. 91
Audible Noise of Power Transformers. Gordy.....45–50; disc. 50
Audio Noise in Transformers in Residential and Commercial Areas. Baugh.....121–6; disc. 126
Audio Noise Investigation, Harmonic Index—A Tool for Transformer. Mutschler, Madden. 115–18; disc. 118
Automatic Telephone Message Accounting System, Fundamentals of the. Meszar...255–68; disc. 269
Auxiliary System, Bus Transfer Tests on 2,300-Volt Station. Johnson, Thompson....386–90; disc. 390

B

Bandwidth, The Direct Measurement of. Ammerman.....27–31
Basic Patterns for Arrangement of Electric Power Systems for Steel Mills. Finison.....54–9; disc. 59
Basic Theory Underlying Bell System Facilities Capacity Tables. Gracey.....238–43; disc. 243
Bell System Facilities Capacity Tables, Basic Theory Underlying. Gracey.....238–43; disc. 243
Beta Rays, Noncontacting Thickness Gauge Using. Clapp, Bernstein.....488–90
Bonneville Power Administration, Application and Handling of Very Large Power Transformers on the System of the. Stevens.....158–63; disc. 163
Breaker, A New 69-Kv Oil-Blast Circuit. Rietz, Balentine.....416–23; disc. 423
Breaker, Development and Testing of an Improved High-Voltage, High-Capacity Impulse Circuit. Rietz.....15–25; disc. 25
Breakers for 5,000,000- to 10,000,000-Kva Interrupting Capacity, High-Voltage Oil Circuit. Leeds, Friedrich.....70–6; disc. 76
Buck-Boost Voltage Regulator on Steady-State Power Limit, Effect of. Concordia.....380–4; disc. 384
Burner Safety Devices, Flame Detectors for Domestic Fuel. Deubel.....220–5
Bus Transfer Tests on 2,300-Volt Station Auxiliary System. Johnson, Thompson.....386–90; disc. 390
Bushing-Type Current Transformers, A New Line of Orthomagnetic. Farr.....424–8
Bushing-Type Current Transformers for Metering Purposes, A Survey of. Camilli.....429–40

C

Cable-Connected Equipment, Surge Protection of. Witzke, Bliss.....527–38; disc. 539
Cable, Development of Improved Luminous Sign. Roehmann, Greenfield.....350–5; disc. 355
Cable Ducts and Duct Assemblies, Heat Transfer Study on Power. Greebler, Barnett....357–64; disc. 364
Cables, A Two-Channel Carrier Telegraph System for Short Submarine. Newell, Cramer.....61–5
Cables and a Surrounding Pipe or Duct Wall, The Thermal Resistance Between. Buller, Neher.....342–7; disc. 347
Calculations, Analogue Computer for Multicomponent Fractionation. Goelz, Calvert.....97–103
Calculations of Single-Phase Induction Motors, Suggested Improvements in the Performance. Thacker, Gopalakrishna.....1–6; disc. 6
Capacity, High-Voltage Oil Circuit Breakers for 5,000,000 to 10,000,000-Kva Interrupting. Leeds, Friedrich.....70–6; disc. 76
Carrier Frequency Changes, Phase Lead for A-C Servo Systems with Compensation for. Notthoff.....285–91; disc. 291
Carrier Telegraph System for Short Submarine Cables, A Two-Channel. Newell, Cramer.....61–5
Central Control Rooms, Design and Operation of. Borgel.....598–602; disc. 602
Centralized Instrumentation and Controls for Steam Electric Power Stations. Mallory. 591–6; disc. 596
Changes, Phase Lead for A-C Servo Systems with Compensation for Carrier Frequency. Notthoff.....285–91; disc. 291
Channel Carrier Telegraph System for Short Submarine Cables, A Two-. Newell, Cramer.....61–5
Characteristics of A-C Lead Networks for Servomechanisms, Improvements in the. McDonald. 293–300
Characteristics of Power Arcs in Large Air Gaps, Dielectric Recovery. McCann, Conner, Ellis.....616–24; disc. 624
Characteristics of Some Magnetic-Fluid Clutch Servomechanisms. Parziale, Tilton.....150–7
(Chemical) Design and Control of Ferroalloy Furnaces. Andreae.....557–62
(Chemical) Electric Equipment and Operation of Graphitizing Furnaces. Cole.....563–6
(Chemical) Electrode Control and Associated Operating Mechanisms. Hanff.....567–70; disc. 570
Circuit Breaker, A New 69-Kv Oil Blast. Rietz, Balentine.....416–23; disc. 423
Circuit Breaker, Development and Testing of an Improved High-Voltage, High-Capacity Impulse. Rietz.....15–25; disc. 25
Circuit Breakers for 5,000,000 to 10,000,000-Kva Interrupting Capacity, High-Voltage Oil. Leeds, Friedrich.....70–6; disc. 76
Clampers in Video Transmission. Doba, Rieke. 477–87
Clutch Servomechanisms, Characteristics of Some Magnetic-Fluid. Parziale, Tilton.....150–7
Coefficients for Hydrogen-Cooled Rotating Electric Machines, Surface Heat-Transfer. Snell, Norris, Buckland.....174–85; disc. 185
Coefficients of Synchronous Machines and Their Application, Spring and Demping. Kilgore, Whitney.....226–9; disc. 229
Combined Phase and Ground Distance Relaying. New.....37–42; disc. 42
Commercial Areas, Audio Noise in Transformers in Residential and. Baugh.....121–6; disc. 126
(Committee Report) Maximum Short-Circuit Current of D-C Motors and Generators. (50-23)....146–9
(Committee Report) Sensitive Ground Protection. (50-70).....473–5; disc. 475
(Communication) A Frequency Response Method for Analyzing and Synthesizing Contactor Servomechanisms. Kochenburger....270–83; disc. 283
(Communication) A New Electronic Telegraph Regenerative Receiver. Ostendorf....32–6; disc. 36
(Communication) A Printing Telegraph Tape-to-Page Translator. Frost.....79–83
(Communication) Basic Theory Underlying Bell System Facilities Capacity Tables. Gracey.....238–43; disc. 243
(Communication) Fundamentals of the Automatic Telephone Message Accounting System. Meszar.....255–68; disc. 269
(Communication) The Number 5 Crossbar Dial Telephone Switching System. Korn, Ferguson..244–54
Computer for Flight Simulation, A Generalized Analogue. Hall.....308–20
Computer for Multicomponent Fractionation Calculations, Analogue. Goelz, Calvert.....97–103
Computer, New Techniques on the Anacom—Electric Analog. Harder, Carleton.....547–56
(Computing Devices) An Electronic Simulator for Nonlinear Servomechanisms. Edwards, Johnson.....300–06; disc. 306
Commutator Joints for High Temperature Operation of Railway Traction Armatures, Solderless. Reed.....638–41
Concepts of Thyratron Deionization Time, Statistical Nature and Physical. Romanowitz, Dow..368–79
Connected Equipment, Surge Protection of Cable-. Witzke, Bliss.....527–38; disc. 539
Consideration of Requirements and Limitations of Relaying and High-Speed Reclosing on Long and Heavily Loaded Transmission Lines. Parks, Brownlee.....103–07; disc. 107
Constant Using the Susceptance Variation Principle, An Improved Method of Measuring Dissipation Factor and Dielectric. Miller, Whelan.....491–7
Contactor Servomechanisms, A Frequency Response Method for Analyzing and Synthesizing. Kochenburger.....270–83; disc. 283
Control, A Magnetic Amplifier Frequency. Johnson, Schafer.....613–15
Control and Associated Operating Mechanisms, Electrode. Hanff.....567–70; disc. 570
Control of Ferroalloy Furnaces, Design and. Andreae.....557–62
Control of Large D-C Motors Supplied from Ignitron Rectifiers. Livingston.....205–10
Control Rooms, Design and Operation of Central. Borgel.....598–602; disc. 602
Control System for a 4,500-Horsepower Gas-Turbine Electric Locomotive. Warrick.....508–13
Control System Synthesis by Root Locus Method. Evans.....66–9
Control Transformer System, Static Accuracy Performance of the Selsyn Generator. Kronacher.....645–53; disc. 653
Controls for Steam Electric Power Stations, Centralized Instrumentation and. Mallory...591–6; disc. 596
Cooled Generators at Elevated Gas Pressures, Loading of Hydrogen-. Snell.....186–99; disc. 199
Cooled Rotating Electric Machines, Surface Heat-Transfer Coefficients for Hydrogen-. Snell, Norris, Buckland.....174–85; disc. 185
Cooling of A-C Turbine Generators, Liquid. Part II. Fechheimer.....165–71; disc. 171
(Part I—1947)
Crossbar Dial Telephone Switching System, The Number 5. Korn, Ferguson.....244–54
Current of D-C Motors and Generators, Maximum Short-Circuit. (Committee Report).....146–9
Current Transductor and Its Application in the Aluminum Industry, The Theory of the. Specht, Wagner.....441–52; disc. 452
Current Transformers, A New Line of Orthomagnetic Bushing-Type. Farr.....424–8
Current Transformers, A Primary Method of Measuring the Ratio and Phase Angle of. Brownlee....459–60

Current Transformers for Metering Purposes, A Survey of Bushing-Type. Camilli.....429–40
Customer's Premises, Protective Grounding of Electrical Installations on. Schirmer.....657–9

D

Damping Coefficients of Synchronous Machines and Their Application, Spring and. Kilgore, Whitney.....226–9; disc. 229
Deionization Time, Statistical Nature and Physical Concepts of Thyratron. Romanowitz, Dow.....368–79
Design and Control of Ferroalloy Furnaces. Andreae.....557–62
Design and Operation of Central Control Rooms. Borgel.....598–602; disc. 602
Design and Test on Electronic Exciter Supplied from Common Shaft-Driven Generator. Colaiaco, Johnson, Reilly.....328–35; disc. 335
Detectors for Domestic Fuel Burner Safety Devices, Flame. Deubel.....220–5
Development and Testing of an Improved High-Voltage, High-Capacity Impulse Circuit Breaker. Rietz.....15–25; disc. 25
Development of Improved Luminous Sign Cable. Roehmann, Greenfield.....350–5; disc. 355
Device for Metal-Clad Switchgear, A New Grounding and Testing. Krida, McCurry.....407–12; disc. 412
Devices, Flame Detectors for Domestic Fuel Burner Safety. Deubel.....220–5
Dial Telephone Switching System, The Number 5 Crossbar. Korn, Ferguson.....244–54
Dielectric Constant Using the Susceptance Variation Principle, An Improved Method of Measuring Dissipation Factor and. Miller, Whelan.....491–7
Dielectric Recovery Characteristics of Power Arcs in Large Air Gaps. McCann, Conner, Ellis.....616–24; disc. 624
Digital Recording and Telemetering, The Metrotype System of. Foster.....543–6; disc. 546
D-C Apparatus, Quick and Accurate Production Testing on Large. Baldwin, Barnhart.....136–8
Direct-Current Dynamos, Transient Response of. Koenig.....139–44; disc. 144
D-C Motor Drives, Rectifier Equipment for Electronic. Mulhern, Crawford.....211–15
D-C Motors and Generators, Maximum Short-Circuit Current. (Committee Report).....146–9
D-C Motors Supplied from Ignitron Rectifiers, Control of Large. Livingston.....205–10
Direct Measurement of Bandwidth, The. Ammerman.....27–31
Dissipation Factor and Dielectric Constant Using the Susceptance Variation Principle, An Improved Method of Measuring. Miller, Whelan.....491–7
Distance Relaying, Combined Phase and Ground. New.....37–42; disc. 42
Domestic Fuel Burner Safety Devices, Flame Detectors for. Deubel.....220–5
Drives, Rectifier Equipment for Electronic D-C Motor. Mulhern, Crawford.....211–15
Drives to Printing Presses, Application of Electronic Motor. Johnson, Stacey.....216–19
Dry-Type Insulation for Instrument Transformers, A New. Pfuntner, Franck, D'Entremont.....453–8
Duct Wall, The Thermal Resistance Between Cables and a Surrounding Pipe or. Buller, Neher.....342–7; disc. 347
Ducts and Duct Assemblies, Heat Transfer Study on Power Cable. Greebler, Barnett.....357–64; disc. 364
Dynamos, Transient Response of Direct-Current. Koenig.....139–44; disc. 144

E

Effect of Buck-Boost Voltage Regulator on Steady-State Power Limit. Concordia.....380–4; disc. 384
Electric Analog Computer, New Techniques on the Anacom—. Harder, Carleton.....547–56
Electric Equipment and Operation of Graphitizing Furnaces. Cole.....563–6
Electric Equipment for a Gas-Turbine Electric Locomotive, Rotating. Coho.....514–18
Electric Fences—Their Hazards, Types, Regulations, and Safe Application. Dalziel.....8–15
Electric Locomotive, Control System for a 4,500-Horsepower Gas-Turbine. Warrick.....508–13
Electric Locomotive, The Alco-GE 4,500-Horsepower Gas-Turbine. Morey.....504–07
Electric Machines, Surface Heat-Transfer Coefficients for Hydrogen-Cooled Rotating. Snell, Norris, Buckland.....174–85; disc. 185
Electric Power Stations, Centralized Instrumentation and Controls for Steam. Mallory.591–6; disc. 596
Electric Power Systems for Steel Mills, Basic Patterns for Arrangement of. Finison.....54–9; disc. 59
Electrical Hazards to Farm Stock. Buchanan.....654–6
Electrical Installations on Customer's Premises, Protective Grounding of. Schirmer.....657–9
Electrification, Rectifier-Type Motive Power for Railroad. Hibbard, Whitaker, Ames.519–23; disc. 523
Electrode Control and Associated Operating Mechanisms. Hanff.....567–70; disc. 570
Electronic D-C Motor Drives, Rectifier Equipment for. Mulhern, Crawford.....211–15
Electronic Motor Drives to Printing Presses, Application of. Johnson, Stacey.....216–19
Electronic Excitation and Regulation of Electric Generators as Compared to Conventional Methods, Excitation Improvement—. Phillips, Lambert, Pattison.....538–40; disc. 340
Electronic Exciter Supplied from Common Shaft-Driven Generator, Design and Test on. Colaiaco, Johnson, Reilly.....328–35; disc. 335
Electronic Simulator for Nonlinear Servomechanisms, An. Edwards, Johnson.....300–06; disc. 306
Electronic Telegraph Regenerative Receiver, A New. Ostendorf.....32–6; disc. 36
(Electronics) A Magnetic Amplifier Frequency Control. Johnson, Schafer.....613–15
(Electronics) An Analysis of Transients and Feedback in Magnetic Amplifiers. Johnson, Latson.....604–11; disc. 611
(Electronics) An Analysis of Transients in Magnetic Amplifiers. VerPlanck, Finzi, Beaumariage.498–503
(Electronics) The Direct Measurement of Bandwidth. Ammerman.....27–31
(Electronics) Statistical Nature and Physical Concepts of Thyratron Dionization Time. Romanowitz, Dow.....368–79
Equipment and Operation of Graphitizing Furnaces, Electric. Cole.....563–6
Equipment for a Gas-Turbine Electric Locomotive, Rotating Electric. Coho.....514–18
Equipment for Electronic D-C Motor Drives, Rectifier. Mulhern, Crawford.....211–15
Equipment, Surge Protection of Cable-Connected. Witzke, Bliss.....527–38; disc. 539
Excitation Improvement—Electronic Excitation and Regulation of Electric Generators as Compared to Conventional Methods. Phillips, Lambert, Pattison.....338–40; disc. 340
Excitation System Performance with Motor-Driven Exciters. Mellor, Temoshok.....321–7
Exciter Supplied from Common Shaft-Driven Generator, Design and Test on Electronic. Colaiaco, Johnson, Reilly.....328–35; disc. 335
Exciters, Excitation System Performance with Motor-Driven. Mellor, Temoshok.....321–7

F

Facilitites Capacity Tables, Basic Theory Underlying Bell System. Gracey.....238–43; disc. 243
Factor and Dielectric Constant Using the Susceptance Variation Principle, An Improved Method of Measuring Dissipation. Miller, Whelan.....491–7
Farm Stock, Electrical Hazards to. Buchanan.....654–6
Feedback in Magnetic Amplifiers, An Analysis of Transients and. Johnson, Latson.....604–11; disc. 611
Fences—Their Hazards, Types, Regulations, and Safe Application, Electric. Dalziel.....8–15
Ferroalloy Furnaces, Design and Control of. Andreae.....557–62
Flame Detectors for Domestic Fuel Burner Safety Devices. Deubel.....220–5
Flight Simulation, A Generalized Analogue Computer for. Hall.....308–20
Fluid Clutch Servomechanisms, Characteristics of Some Magnetic-. Parziale, Tilton.....150–7
Fractionation Calculations, Analogue Computer for Multicomponent. Goela, Calvert.....97–103
Frequency Changes, Phase Lead for A-C Servo Systems with Compensation for Carrier. Notthoff.....285–91; disc. 291
Frequency Control, A Magnetic Amplifier. Johnson, Schafer.....613–15
Frequency Response Method for Analyzing and Synthesizing Contactor Servomechanisms, A. Kochenburger.....270–83; disc. 283
Fuel Burner Safety Devices, Flame Detectors for Domestic. Deubel.....220–5
Fundamentals of the Automatic Telephone Message Accounting System. Meszar.....255–68; disc. 269
Furnaces, Design and Control of Ferroalloy. Andreae.....557–62
Furnaces, Electric Equipment and Operation of Graphitizing. Cole.....563–6

G

Gaps, Dielectric-Recovery Characteristics of Power Arcs in Large Air. McCann, Conner, Ellis.....616–24; disc. 624
Gaps for Voltage Measurement, The Irradiation of Spark. Hardy, Craggs.....584–90
Gas Pressures, Loading of Hydrogen-Cooled Generators at Elevated. Snell.....186–99; disc. 199
Gas-Turbine Electric Locomotive, Control System for a 4,500-Horsepower. Warrick.....508–13
Gas-Turbine Electric Locomotive, Rotating Electric Equipment for a. Coho.....514–18
Gas-Turbine Electric Locomotive, The Alco-GE 4,500-Horsepower. Morey.....504–07
Gauge Using Beta Rays, Noncontacting Thickness. Clapp, Bernstein.....488–90
GE 4,500-Horsepower Gas-Turbine Electric Locomotive, The Alco-. Morey.....504–07
Generalized Analogue Computer for Flight Simulation, A. Hall.....308–20
Generator Control Transformer System, Static Accuracy Performance of the Selsyn. Kronacher.....645–53; disc. 653
Generator, Design and Test on Electronic Exciter Supplied from Common Shaft-Driven. Colaiaco, Johnson, Reilly.....328–35; disc. 335
Generator Rating of Induction Motors. Smith.....129–35
Generators as Compared to Conventional Methods, Excitation Improvement—Electronic Excitation and Regulation of Electric. Phillips, Lambert, Pattison.....338–40; disc. 340
Generators at Elevated Gas Pressures, Loading of Hydrogen-Cooled. Snell.....186–99; disc. 199
Generators, Liquid Cooling of A-C Turbine. Part II. Fechheimer.....165–71; disc. 171
(Part I—1947)
Generators, Maximum Short-Circuit Current of D-C Motors and. (Committee Report).....146–9
Generators with Suddenly Applied Loads, Regulation of A-C. Part II. Harder, Cheek, Clayton.....395–405; disc. 405
(Part I—1944)
Gradient Meter, A Voltage. Tremaine, Cheek.....633–7; disc. 637
Graphitizing Furnaces, Electric Equipment and Operation of. Cole.....563–6
Ground Distance Relaying, Combined Phase and. New.....37–42; disc. 42
Ground Protection, Sensitive. (Committee Report).....473–5; disc. 475
Grounding and Testing Device for Metal-Clad Switchgear, A New. Krida, McCurry.407–12; disc. 412
Grounding of Electrical Installations on Customer's Premises, Protective. Schirmer.....657–9

H

Harmonic Index—A Tool for Transformer Audio Noise Investigation. Mutschler, Madden.....115–18; disc. 118
Hazards to Farm Stock, Electrical. Buchanan.....654–6
Hazards, Types, Regulations, and Safe Application, Electric Fences—. Dalziel.....8–15
Heat-Transfer Coefficients for Hydrogen-Cooled Rotating Electric Machines, Surface. Snell, Norris, Buckland.....174–85; disc. 185
Heat Transfer Study on Power Cable Ducts and Duct Assemblies. Greebler, Barnett.....357–64; disc. 364
High-Speed Reclosing on Long and Heavily Loaded Transmission Lines, Consideration of Requirements and Limitations of Relaying and. Parks, Brownlee.....103–07; disc. 107
High-Voltage, High-Capacity Impulse Circuit Breaker, Development and Testing of an Improved. Rietz.....15–25; disc. 25
High-Voltage Oil Circuit Breakers for 5,000,000 to 10,000,000-Kva Interrupting Capacity. Leeds, Friedrich.....70–6; disc. 76
High-Voltage Transmission Lines, Relay Protection for Medium Length. Kinghorn.....461–5; disc. 465
Horsepower Gas-Turbine Electric Locomotive, Control System for a 4,500-. Warrick.....508–13
Horsepower Gas-Turbine Electric Locomotive, The Alco-GE 4,500-. Morey.....504–07
Hydrogen-Cooled Generators at Elevated Gas Pressures Loading of. Snell.....186–99; disc. 199
Hydrogen-Cooled Rotating Electric Machines, Surface Heat-Transfer Coefficients for. Snell, Norris, Buckland.....174–85; disc. 185

I

Ignitron Rectifiers, Control of Large D-C Motors Supplied From. Livingston.....205–10
Improved Luminous Sign Cable, Development of. Roehmann, Greenfield.....350–5; disc. 355
Improved Method of Measuring Dissipation Factor and Dielectric Constant Using the Susceptance Variation Principle, An. Miller, Whelan.....491–7
Improvement—Electronic Excitation and Regulation of Electric Generators as Compared to Conventional Methods, Excitation. Phillips, Lambert, Pattison.....338–40; disc. 340
Improvements in the Characteristics of A-C Lead Networks for Servomechanisms. McDonald.293–300
Improvements in the Performance Calculations of Single-Phase Induction Motors, Suggested. Thacker, Gopalakrishna.....1–6; disc. 6

Impulse Circuit Breaker, Development and Testing of an Improved High-Voltage, High-Capacity. Rietz ..... 15–25; disc. 25
Impulse Measurements by Repeated-Structure Networks. Dawes, Thomas, Drought ..... 571–80; disc. 580
Incremental Losses in Power Transmission Networks Total and. Ward, Eaton, Hale ..626–31; disc. 631
Index—A Tool for Transformer Audio Noise Investigation, Harmonic. Mutschler, Madden ..... 115–18; disc. 118
Inductances of Synchronous Machines, Per-Unit Kirschbaum 231–4
Induction Motors, Generator Rating of. Smith..129–35
Induction Motors, Suggested Improvements in the Performance Calculations of Single-Phase. Thacker, Gopalakrishna ..... 1–6; disc. 6
(Industrial) Basic Patterns for Arrangement of Electric Power Systems for Steel Mills. Finison ..... 54–9; disc. 59
Industry, The Theory of the Current Transductor and Its Application in the Aluminum. Specht, Wagner ..... 441–52; disc. 452
Installations on Customer's Premises, Protective Grounding of Electrical. Schirmer 657–9
Instrument Transformers, A New Dry-Type Insulation for. Pfunitner, Franck, D'Entremont 453–8
Instrumentation and Controls for Steam Electric Power Stations, Centralized. Mallory ..591–6; disc. 596
(Instruments) A Voltage Gradient Meter. Tremaine, Cheek ..... 633–7; disc. 637
(Instruments) Noncontacting Thickness Gauge Using Beta Rays. Clapp, Bernstein 488–90
(Instruments) The Metrotype System of Digital Recording and Telemetering. Foster ..543–6; disc. 546
(Instruments) The Theory of the Current Transductor and Its Application in the Aluminum Industry. Specht, Wagner ..... 441–52; disc. 452
(Insulated Conductors) Development of Improved Luminous Sign Cable. Roehmann, Greenfield ..... 350–5; disc. 355
(Insulated Conductors) Heat Transfer Study on Power Cable Ducts and Duct Assemblies. Greebler, Barnett ..... 357–64; disc. 364
(Insulated Conductors) The Thermal Resistance Between Cables and a Surrounding Pipe or Duct Wall. Buller, Neher ..... 342–7; disc. 347
Insulation for Instrument Transformers, A New Dry-Type. Pfunitner, Franck, D'Entremont 453–8
Insulation Levels, Lightning Arresters as a Criterion for Rorden ..... 84–91; disc. 91
Insulation, Margins Between Lightning Arrester Protective Levels and Transformer. Vogel ..... 110–12; disc. 112
Interrupting Capacity, High-Voltage Oil Circuit Breakers for 5,000,000 to 10,000,00-Kva. Leeds, Friedrich ..... 70–6; disc. 76
Investigation, Harmonic Index—A Tool for Transformer Audio Noise. Mutschler, Madden ..... 115–18; disc. 118
Irradiation of Spark Gaps for Voltage Measurements The. Hardy, Craggs 584–90

J

Joints for High Temperature Operation of Railway Traction Armatures, Solderless Commutator. Reed 638–41

L

(Land Transportation) Control System for a 4,500-Horsepower Gas-Turbine Electric Locomotive. Warrick 508–13
(Land Transportation) Rectifier-Type Motive Power for Railroad Electrification. Hibbard, Whittaker, Ames ..... 519–23; disc. 523
(Land Transportation) Rotating Electric Equipment for a Gas-Turbine Electric Locomotive. Coho..514–18
(Land Transportation) Solderless Commutator Joints for High Temperature Operation of Railway Traction Armatures. Reed 638–41
(Land Transportation) The Alco-GE 4,500 Horsepower Gas-Turbine Electric Locomotive. Morey..504–07
Lead for A-C Servo Systems with Compensation for Carrier Frequency Changes, Phase. Notthoff ..... 285–91; disc. 291
Lead Networks for Servomechanisms, Improvements in the Characteristics of A-C. McDonald 293–300
Levels and Transformer Insulation, Margins Between Lightning Arrester Protective. Vogel ..... 110–12; disc. 112
Levels, Lightning Arresters as a Criterion for Insulation. Rorden ..... 84–91; disc. 91
Lightning Arrester Protective Levels and Transformer Insulation, Margins Between. Vogel ..... 110–12; disc. 112
Lightning Arrester Standard, New. Stewart, Defandorf 525–6
Lightning Arresters as a Criterion for Insulation Levels. Rorden ..... 84–91; disc. 91
Limit, Effect of Buck-Boost Voltage Regulator on Steady-State Power. Concordia ..... 380–4; disc. 384
Limitations of Relaying and High-Speed Reclosing on Long and Heavily Loaded Transmission Lines, Consideration of Requirements and. Parks, Brownlee ..... 103–07; disc. 107
Line Protection of Short Lines of the Metropolitan Area of a Typical System, Transmission-. Marter ..... 468–71; disc. 471
Lines, Consideration of Requirements and Limitations of Relaying and High-Speed Reclosing on Long and Heavily Loaded Transmission. Parks, Brownlee ..... 103–07; disc. 107
Lines, Relay Protection for Medium Length High-Voltage Transmission. Kinghorn ....461–5; disc. 465
Liquid Cooling of A-C Turbine Generators. Part II. Fechheimer ..... 165–71; disc. 171
(Part I—1947)
Load for Testing Rectifiers, Synthetic. Tetherow ..642–4
Loading of Hydrogen-Cooled Generators at Elevated Gas Pressures. Snell ..... 186–99; disc. 199
Loads, Regulation of A-C Generators with Suddenly Applied. Part II. Harder, Check, Clayton ..... 395–405; disc. 405
(Part I—1944)
Locomotive, Control System for a 4,500-Horsepower Gas-Turbine Electric. Warrick 508–13
Locomotive, Rotating Electric Equipment for a Gas-Turbine Electric. Coho 514–18
Locomotive, The Alco-GE 4,500-Horsepower Gas-Turbine Electric. Morey 504–07
Locus Method, Control System Synthesis by Root. Evans 66–9
Losses in Power Transmission Networks, Total and Incremental. Ward, Eaton, Hale..626–31; disc. 631
Luminous Sign Cable, Development of Improved Roehmann, Greenfield ..... 350–5; disc. 355

M

Machines and Their Application, Spring and Damping Coefficients of Synchronous. Kilgore, Whitney ..... 226–9; disc. 229
Machines, Per-Unit Inductances of Synchronous. Kirschbaum 231–4
Machines, Potier Reactance for Salient-Pole Synchronous. Mikhail 235–8
Machines, Surface Heat-Transfer Coefficients for Hydrogen-Cooled Rotating Electric. Snell, Norris, Buckland ..... 174–85; disc. 185
Magnetic Amplifier Frequency Control, A. Johnson, Schafer 613–15
Magnetic Amplifiers, An Analysis of Transients and Feedback in. Johnson, Latson ..604–11; disc. 611
Magnetic Amplifiers, An Analysis of Transients in. Ver Planck, Finzi, Beaumariage 498–503
Magnetic-Fluid Clutch Servomechanisms, Characteristics of Some. Parziale, Tilton 150–7
Margins Between Lightning Arrester Protective Levels and Transformer Insulation. Vogel ..... 110–12; disc. 112
Maximum Short-Circuit Current of D-C Motors and Generators. (Committee Report) 146–9
Measurement of Bandwidth, The Direct. Ammerman 27–31
Measurement, The Irradiation of Spark Gaps for Voltage. Hardy, Craggs 584–90
Measurements by Repeated Structure Networks, Impulse. Dawes, Thomas, Drought..571–80; disc. 580
Measuring Dissipation Factor and Dielectric Constant Using the Susceptance Variation Principle, An Improved Method of. Miller, Whelan 491–7
Measuring the Ratio and Phase Angle of Current Transformers, A Primary Method of. Brownlee..459–60
Mechanisms, Electrode Control and Associated Operating. Hanff ..... 567–70; disc. 570
Message Accounting System, Fundamentals of the Automatic Telephone. Meszar..255–68; disc. 269
Metal-Clad Switchgear, A New Grounding and Testing Device for. Krida, McCurry ..... 407–12; disc. 412
Meter, A Voltage Gradient. Tremaine, Cheek ..... 633–7; disc. 637
Metering Purposes, A Survey of Bushing-Type Current Transformers for. Camilli 429–40
Method, Control System Synthesis by Root Locus. Evans 66–9
Method for Analyzing and Synthesizing Contactor Servomechanisms, A Frequency Response. Kochenburger ..... 270–83; disc. 283
Method of Measuring Dissipation Factor and Dielectric Constant Using the Susceptance Variation Principle, An Improved. Miller, Whelan 491–7
Method of Measuring the Ratio and Phase Angle of Current Transformers, A Primary. Brownlee..459–60
Metropolitan Area of a Typical System, Transmission-Line Protection of Short Lines of the. Marter ..... 468–71; disc. 471
Metrotype System of Digital Recording and Telemetering, The. Foster ..... 543–6; disc. 546
Mills, Basic Patterns for Arrangement of Electric Power Systems for Steel. Finison ..... 54–9; disc. 59
Motive Power for Railroad Electrification, Rectifier-Type. Hibbard, Whittaker, Ames..519–23; disc. 523
Motor-Driven Exciters, Excitation System Performance with. Mellor, Temoshok 321–7
Motor Drives, Rectifier Equipment for Electronic D-C. Mulherin, Crawford 211–15
Motor Drives to Printing Presses, Application of Electronic. Johnson, Stacey 216–19
Motors and Generators, Maximum Short-Circuit Current of D-C. (Committee Report) 146–9
Motors, Generator Rating of Induction. Smith..129–35
Motors, Suggested Improvements in the Performance Calculations of Single-Phase Induction. Thacker, Gopalakrishna ..... 1–6; disc. 6
Motors Supplied from Ignitron Rectifiers, Control of Large D-C. Livingston 205–10
Multicomponent Fractionation Calculations, Analogue Computer for. Goetz, Calvert 97–103

N

Nature and Physical Concepts of Thyratron Deionization Time, Statistical. Romanowitz, Dow..368–79
Networks for Servomechanisms, Improvements in the Characteristics of A-C Lead. McDonald..293–300
Networks, Impulse Measurements by Repeated Structures. Dawes, Thomas, Drought..571–80; disc. 580
Networks, Total and Incremental Losses in Power Transmission. Ward, Eaton, Hale..626–31; disc. 631
Neutral Potentials, Rural. Waghorne..660–3; disc. 663
New Lightning Arrester Standard. Stewart, Defandorf 525–6
New Line of Orthomagnetic Bushing-Type Current-Transformers, A. Farr 424–8
New 69-Kv Oil Blast Circuit Breaker, A. Rietz, Balentine ..... 416–23; disc. 423
New Techniques on the Anacom—Electric Analog Computer. Harder, Carleton 547–56
Noise in Transformers in Residential and Commercial Areas, Audio. Baugh ..... 121–6; disc. 126
Noise Investigation, Harmonic Index—A Tool for Transformer Audio. Mutschler, Madden ..... 115–18; disc. 118
Noise of Power Transformers, Audible. Gordy ..... 45–50; disc. 50
Noncontacting Thickness Gauge Using Beta Rays. Clapp, Bernstein 488–90
Nonlinear Servomechanisms, An Electronic Simulator for. Edwards, Johnson ..... 300–06; disc. 306
Number 5 Crossbar Dial Telephone Switching System, The. Korn, Ferguson 244–54

O

Oil Blast Circuit Breaker, A New 69-Kv. Rietz, Balentine ..... 416–23; disc. 423
Oil Circuit Breakers for 5,000,000 to 10,000,000-Kva Interrupting Capacity, High-Voltage. Leeds, Friedrich ..... 70–6; disc. 76
Operating Mechanisms, Electrode Control and Associated. Hanff ..... 567–70; disc. 570
Operation of Central Control Rooms, Design and. Borgel ..... 598–602; disc. 602
Operation of Graphitizing Furnaces, Electric Equipment and. Cole 563–6
Operation of Railway Traction Armatures, Solderless Commutator Joints for High Temperature. Reed 638–41
Orthomagnetic Bushing-Type Current Transformers, A New Line of. Farr 424–8

P

Patterns for Arrangement of Electric Power Systems for Steel Mills, Basic. Finison ..... 54–9; disc. 59
Per-Unit Inductances of Synchronous Machines. Kirschbaum 231–4
Performance Calculations of Single-Phase Induction Motors, Suggested Improvements in the. Thacker, Gopalakrishna ..... 1–6; disc. 6
Performance of the Selsyn Generator Control Transformer System, Static Accuracy. Kronacher ..... 645–53; disc. 653
Performance with Motor-Driven Exciters, Excitation System. Mellor, Temoshok 321–7
Phase and Ground Distance Relaying, Combined. New ..... 37–42; disc. 42
Phase Angle of Current Transformers, A Primary Method of Measuring the Ratio and. Brownlee 459–60
Phase Lead for A-C Servo Systems with Compensation for Carrier Frequency Changes. Notthoff ..... 285–91; disc. 291
Physical Concepts of Thyratron Deionization Time, Statistical Nature and. Romanowitz, Dow..368–79
Pipe or Duct Wall, The Thermal Resistance Between Cables and a Surrounding. Buller, Neher ..... 342–7; disc. 347

Pole Synchronous Machines, Potier Reactance for Salient-Pole. Mikhail....235–8
Potentials, Rural Neutral. Waghorne. 660–3; disc. 663
Potier Reactance for Salient-Pole Synchronous Machines. Mikhail....235–8
Power Area in Large Air Gaps, Dielectric Recovery Characteristics of. McCann, Conner, Ellis....616–24; disc. 624
Power Cable Ducts and Duct Assemblies, Heat Transfer Study on. Greebler, Barnett....357–64; disc. 364
Power for Railroad Electrification, Rectifier-Type Motive. Hibbard, Whittaker, Ames. 519–23; disc. 523
(Power Generation) Bus Transfer Tests on 2,300-Volt Station Auxiliary System. Johnson, Thompson....386–90; disc. 390
(Power Generation) Design and Operation of Central Control Rooms. Borgel....598–602; disc. 602
(Power Generation) Design and Test on Electronic Exciter Supplied from Common Shaft-Driven Generator. Colaiaco, Johnson, Reilly...328–35; disc. 335
(Power Generation) Excitation Improvement—Electronic Excitation and Regulation of Electric Generators as Compared to Conventional Methods. Phillips, Lambert, Pattison....338–40; disc. 340
(Power Generation) Excitation System Performance with Motor-Driven Exciters. Mellor, Temoshok..321–7
(Power Generation) Regulation of A-C Generators with Suddenly Applied Loads. Part II. Harder, Cheek, Clayton....395–405; disc. 405
(Part I—1944)
Power Limit, Effect of Buck-Boost Voltage Regulator on Steady-State. Concordia....380–4; disc. 384
Power Stations, Centralized Instrumentation and Controls for Steam Electric. Mallory..591–6; disc. 596
Power Systems for Steel Mills, Basic Patterns for Arrangement of Electric. Finison....54–9; disc. 59
Power Transformers, Audible Noise of. Gordy....45–50; disc. 50
Power Transformers on the System of the Bonneville Power Administration, Application and Handling of Very Large. Stevens....158–63; disc. 163
Power Transmission Networks, Total and Incremental Losses in. Ward, Eaton, Hale...626–31; disc. 631
Premises, Protective Grounding of Electrical Installations on Customer's. Schirmer....657–9
Presses, Application of Electronic Motor Drives to Printing. Johnson, Stacey....216–19
Pressures, Loading of Hydrogen-Cooled Generators at Elevated Gas. Snell....186–99; disc. 199
Primary Method of Measuring the Ratio and Phase Angle of Current Transformers, A. Brownlee....459–60
Principle, An Improved Method of Measuring Dissipation Factor and Dielectric Constant Using the Susceptance Variation. Miller, Whelan....491–7
Printing Presses, Application of Electronic Motor Drives to. Johnson, Stacey....216–19
Printing Telegraph Tape-to-Page Translator, A. Frost....79–83
Production Testing on Large D-C Apparatus, Quick and Accurate. Baldwin, Barnhart....136–8
Protection for Medium Length High-Voltage Transmission Lines, Relay. Kinghorn..461–5; disc. 465
Protection of Cable-Connected Equipment, Surge. Witzke, Bliss....527–38; disc. 539
Protection of Short Lines of the Metropolitan Area of a Typical System, Transmission-Line. Marter....468–71; disc. 471
Protection, Sensitive Ground. (Committee Report)....473–5; disc. 475
(Protective Devices) Lightning Arresters as a Criterion for Insulation Levels. Rorden....84–91; disc. 91
(Protective Devices) New Lightning Arrester Standard. Stewart, Defandorf....525–6
Protective Grounding of Electrical Installations on Customer's Premises. Schirmer....657–9
Protective Levels and Transformer Insulation, Margins Between Lightning Arrester. Vogel....110–12; disc. 112

R

Railroad Electrification, Rectifier-Type Motive Power for. Hibbard, Whittaker, Ames. 519–23; disc. 523
Railway Traction Armatures, Solderless Commutator Joints for High Temperature Operation of. Reed....638–41
Rating of Induction Motors, Generator. Smith..129–35
Ratio and Phase Angle of Current Transformers, A Primary Method of Measuring the. Brownlee....459–60
Rays, Noncontacting Thickness Gauge Using Beta-Clapp, Bernstein....488–90
Reactance for Salient-Pole Synchronous Machines, Potier. Mikhail....235–8
Receiver, A New Electronic Telegraph Regenerative. Ostendorf....32–6; disc. 36
Reclosing on Long and Heavily Loaded Transmission Lines, Consideration of Requirements and Limitations of Relaying and High-Speed. Parks, Brownlee....103–07; disc. 107
Recording and Telemetering, The Metrotype System of Digital. Foster....543–6; disc. 546
Recovery Characteristics of Power Area in Large Air Gaps, Dielectric. McCann, Conner, Ellis....616–24; disc. 624
Rectifier Equipment for Electronic D-C Motor Drives. Mulhern, Crawford....211–15
Rectifier-Type Motive Power for Railroad Electrification. Hibbard, Whittaker, Ames....519–23; disc. 523
Rectifiers, Control of Large D-C Motors Supplied from Ignitron. Livingston....205–10
Rectifiers, Synthetic Load for Testing. Tetherow....642–4
Regenerative Receiver, A New Electronic Telegraph. Ostendorf....32–6; disc. 36
Regulation of A-C Generators with Suddenly Applied Loads. Part II. Harder, Cheek, Clayton....395–405; disc. 405
(Part I—1944)
Regulation of Electric Generators as Compared to Conventional Methods, Excitation Improvement—Electronic Excitation and. Phillips, Lambert, Pattison....338–40; disc. 340
Regulations, and Safe Application, Electric Fences—Their Hazards, Types. Dalziel....8–15
Regulator of Steady-State Power Limit, Effect of Buck-Boost Voltage. Concordia....380–4; disc. 384
Relay Protection for Medium Length High-Voltage Transmission Lines. Kinghorn..461–5; disc. 465
(Relay) Transmission-Line Protection of Short Lines of the Metropolitan Area of a Typical System. Marter....468–71; disc. 471
Relaying and High-Speed Reclosing on Long and Heavily Loaded Transmission Lines, Consideration of Requirements and Limitations of. Parks, Brownlee....103–07; disc. 107
Relaying, Combined Phase and Ground Distance. New....37–42; disc. 42
(Relays) Sensitive Ground Protection. (Committee Report)....473–5; disc. 475
Repeated Structure Networks, Impulse Measurements by. Dawes, Thomas, Drought...571–80; disc. 580
Requirements and Limitations of Relaying and High-Speed Reclosing on Long and Heavily Loaded Transmission Lines, Consideration of. Parks, Brownlee....103–07; disc. 107
Residential and Commercial Areas, Audio Noise in Transformers in. Baugh....121–6; disc. 126
Resistance Between Cables and a Surrounding Pipe or Duct Wall, The Thermal. Buller, Neher....342–7; disc. 347
Response Method for Analyzing and Synthesizing Contactor Servomechanisms, A Frequency. Kochenburger....270–82; disc. 283
Response of Direct-Current Dynamos, Transient. Koenig....139–44; disc. 144
Rooms, Design and Operation of Central Control. Borgel....598–602; disc. 602
Root Locus Method, Control-System Synthesis by. Evans....66–9
Rotating Electric Equipment for a Gas-Turbine Electric Locomotive. Coho....514–18
Rotating Electric Machines, Surface Heat-Transfer Coefficients for Hydrogen-Cooled. Snell, Norris, Buckland....174–85; disc. 185
(Rotating Machinery) Loading of Hydrogen-Cooled Generators at Elevated Gas Pressures. Snell....186–99; disc. 199
(Rotating Machinery) Quick and Accurate Production Testing on Large D-C Apparatus. Baldwin, Barnhart....136–8
(Rotating Machinery) Spring and Damping Coefficients of Synchronous Machines and Their Application. Kilgore, Whitney....226–9; disc. 229
(Rotating Machinery) Transient Response of Direct-Current Dynamos. Koenig....139–44; disc. 144
Rural Neutral Potentials. Waghorne..660–3; disc. 663

S

Safety Devices, Flame Detectors for Domestic Fuel Burner. Deubel....220–5
(Safety) Electric Fences—Their Hazards, Types, Regulations, and Safe Application. Dalziel....8–15
(Safety) Electrical Hazards to Farm Stock. Buchanan....654–6
(Safety) Protective Grounding of Electrical Installations on Customer's Premises. Schirmer....657–9
(Safety) Rural Neutral Potentials. Waghorne....660–3; disc. 663
Salient-Pole Synchronous Machines, Potier Reactance for. Mikhail....235–8
Selsyn Generator Control Transformer System, Static Accuracy Performance of the. Kronacher....645–53; disc. 653
Sensitive Ground Protection. (Committee Report)....473–5; disc. 475
Servo Systems with Compensation for Carrier Frequency Changes, Phase Lead for A-C. Notthoff....285–91; disc. 291
Servomechanisms, A Frequency Response Method for Analyzing and Synthesizing Contactor. Kochenburger....270–83; disc. 283
Servomechanisms, An Electronic Simulator for Nonlinear. Edwards, Johnson....300–06; disc. 306
Servomechanisms, Characteristics of Some Magnetic-Fluid Clutch. Parziale, Tilton....150–7
Servomechanisms, Improvements in the Characteristics of A-C Lead Networks for. McDonald...293–300
Shaft-Driven Generator, Design and Test on Electronic Exciter Supplied from Common. Colaiaco, Johnson, Reilly....328–35; disc. 335
Short-Circuit Current of D-C Motors and Generators, Maximum. (Committee Report)....146–9
Short Lines of the Metropolitan Area of a Typical System, Transmission-Line Protection of. Marter....468–71; disc. 471
Sign Cable, Development of Improved Luminous. Roehmann, Greenfield....350–5; disc. 355
Simulation, A Generalized Analogue Computer for Flight. Hall....3–8–20
Simulator for Nonlinear Servomechanisms, An Electronic. Edwards, Johnson....300–06; disc. 306
Single-Phase Induction Motors, Suggested Improvements in the Performance Calculations of. Thacker, Gopalakrishna....1–6; disc. 6
Solderless Commutator Joints for High Temperature Operation of Railway Traction Armatures. Reed....638–41
Spark Gaps for Voltage Measurement, The Irradiation of. Hardy, Craggs....584–90
Spring and Damping Coefficients of Synchronous Machines and Their Application. Kilgore, Whitney....226–9; disc. 229
Standard, New Lightning Arrester. Stewart, Defandorf....525–6
Static Accuracy Performance of the Selsyn Generator Control-Transformer System. Kronacher....645–53; disc. 653
Station Auxiliary System, Bus Transfer Tests on 2,300-Volt. Johnson, Thompson....386–90; disc. 390
Stations, Centralized Instrumentation and Controls for Steam Electric Power. Mallory...591–6; disc. 596
Statistical Nature and Physical Concepts of Thyratron Deionization Time. Romanowitz, Dow....368–79
Steady-State Power Limit, Effect of Buck-Boost Voltage Regulator on. Concordia....380–4; disc. 384
Steam Electric Power Stations, Centralized Instrumentation and Controls for. Mallory...591–6; disc. 596
Steel Mills, Basic Patterns for Arrangement of Electric Power Systems for. Finison....54–9; disc. 59
Structure Networks, Impulse Measurements by Repeated. Dawes, Thomas, Drought..571–80; disc. 580
Study on Power Cable Ducts and Duct Assemblies, Heat Transfer. Greebler, Barnett....357–64; disc. 364
Submarine Cables, A Two-Channel Carrier Telegraph System for Short. Newell, Cramer....61–5
Suddenly Applied Loads, Regulation of A-C Generators with. Part II. Harder, Cheek, Clayton....395–405; disc. 405
(Part I—1944)
Suggested Improvements in the Performance Calculations of Single-Phase Induction Motors. Thacker, Gopalakrishna....1–6; disc. 6
Surface Heat-Transfer Coefficients for Hydrogen-Cooled Rotating Electric Machines. Snell, Norris, Buckland....174–85; disc. 185
Surge Protection of Cable-Connected Equipment. Witzke, Bliss....527–38; disc. 539
Survey of Bushing-Type Current Transformers for Metering Purposes, A. Camilli....429–40
Switchgear, A New Grounding and Testing Device for Metal-Clad. Krida, McCurry...407–12; disc. 412
(Switchgear) A New 69-Kv Oil Blast Circuit Breaker. Rietz, Balentine....416–23; disc. 423
(Switchgear) Development and Testing of an Improved High-Voltage, High-Capacity Impulse Circuit Breaker. Rietz....15–25; disc. 25
Switching System, The Number 5 Crossbar Dial Telephone. Korn, Ferguson....244–54
Synchronous Machines and Their Application, Spring and Damping Coefficients of. Kilgore, Whitney....226–9; disc. 229
Synchronous Machines, Per-Unit Inductances of Kirchbaum....231–4
Synchronous Machines, Potier Reactance for Salient-Pole. Mikhail....235–8
Synthesis by Root Locus Method, Control System. Evans....66–9
Synthesizing Contactor Servomechanisms, A Frequency Response Method for Analysing and. Kochenburger....270–83; disc. 283
Synthetic Load for Testing Rectifiers. Tetherow..642–4
System, Bus Transfer Tests on 2,300-Volt Station Auxiliary. Johnson, Thompson....386–90; disc. 390
System for a 4,500-Horsepower Gas-Turbine Electric Locomotive, Control. Warrick....508–13
System for Short Submarine Cables, A Two-Channel Carrier Telegraph. Newell, Cramer....61–5
System, Fundamentals of the Automatic Telephone Message Accounting. Mestar...255–68; disc. 269
System of Digital Recording and Telemetering, The Metrotype. Foster....543–6; disc. 546

System Performance with Motor-Driven Exciters, Excitation. Mellor, Temoshok.....321–7
System, Static Accuracy Performance of the Selsyn Generator Control Transformer. Kronacher.....645–53; disc. 653
System Synthesis by Root Locus Method, Control. Evans.....66–9
System, The Number 5 Crossbar Dial Telephone Switching. Korn, Ferguson.....244–54
Systems for Steel Mills, Basic Patterns for Arrangement of Electric Power. Finison.....54–9; disc. 59
Systems with Compensation for Carrier Frequency Changes, Phase Lead for A-C Servo. Nothhoff.....285–91; disc. 291

T

Tables, Basic Theory Underlying Bell System Facilities Capacity. Gracey.....238–43; disc. 243
Tape-to-Page Translator, A Printing Telegraph. Frost.....79–83
Techniques on the Anacom—Electric Analog Computer, New. Harder, Carleton.....547–56
Telemetering, The Metrotype System of Digital Recording and. Foster.....543–6; disc. 546
Telegraph Regenerative Receiver, A New Electronic. Ostendorf.....32–6; disc. 36
Telegraph System for Short Submarine Cables, A Two-Channel Carrier. Newell, Cramer.....61–5
Telegraph Tape-to-Page Translator, A Printing. Frost.....79–83
Telephone Message Accounting System, Fundamentals of the Automatic. Meszar.....255–68; disc. 269
Telephone Switching System, The Number 5 Crossbar Dial. Korn, Ferguson.....244–54
(Televison) Clampers in Video Transmission. Doba, Rieke.....477–87
Temperature Operation of Railway Traction Armatures, Solderless Commutator Joints for High. Reed.....638–41
Test on Electronic Exciter Supplied from Common Shaft-Driven Generator, Design and. Colaiaco, Johnson, Reilly.....328–35; disc. 335
Testing Device for Metal-Clad Switchgear, A New Grounding and. Krida, McCurry..407–12; disc. 412
Testing of an Improved High-Voltage, High-Capacity Impulse Circuit Breaker, Development and. Rietz.....15–25; disc. 25
Testing on Large D-C Apparatus, Quick and Accurate Production. Baldwin, Barnhart.....136–8
Testing Rectifiers, Synthetic Load for. Tetherow..642–4
Tests on 2,300-Volt Station Auxiliary System, Bus Transfer. Johnson, Thompson...386–90; disc. 390
Theory of the Current Transductor and Its Application in the Aluminum Industry, The. Specht, Wagner.....441–52; disc. 452
Theory Underlying Bell System Facilities Capacity Tables, Basic. Gracey.....238–43; disc. 243
Thermal Resistance Between Cables and a Surrounding Pipe or Duct Wall, The. Buller, Neher.....342–7; disc. 347
Thickness Gauge Using Beta Rays, Noncontacting. Clapp, Bernstein.....488–90
Thyratron Deionization Time, Statistical Nature and Physical Concepts of. Romanowitz, Dow..368–79
Time, Statistical Nature and Physical Concepts of Thyratron Deionization. Romanowitz, Dow.....368–79
Tool for Transformer Audio Noise Investigation, Harmonic Index—A. Mutschler, Madden.....115–18; disc. 118
Total and Incremental Losses in Power Transmission Networks. Ward, Eaton, Hale..626–31; disc. 631
Traction Armatures, Solderless Commutator Joints for High Temperature Operation of Railway. Reed.....638–41
Transductor and Its Application in the Aluminum Industry, The Theory of the Current. Specht, Wagner.....441–52; disc. 452
Transfer Coefficients for Hydrogen-Cooled Rotating Electric Machines, Surface Heat-. Snell, Norris, Buckland.....174–85; disc. 185
Transfer Study on Power Cable Ducts and Duct Assemblies, Heat. Greebler, Barnett..357–64; disc. 364
Transfer Tests on 2,300-Volt Station Auxiliary System, Bus. Johnson, Thompson.....386–90; disc. 390
Transformer Audio Noise Investigation, Harmonic Index—A Tool for. Mutschler, Madden.....115–18; disc. 118
Transformer Insulation, Margins Between Lightning Arrester Protective Levels and. Vogel.....110–12; disc. 112
Transformer System, Static Accuracy Performance of the Selsyn Generator Control. Kronacher.....645–53; disc. 653
Transformers, A New Dry-Type Insulation for Instrument. Plunniner, Franck, D'Entremont.....453–8
Transformers, A New Line of Orthomagnetic Bushing-Type Current. Farr.....424–8
Transformers, A Primary Method of Measuring the Ratio and Phase Angle of Current. Brownlee.....459–60
Transformers, Audible Noise of Power. Gordy.....45–50; disc. 50
Transformers for Metering Purposes, A Survey of Bushing-Type Current. Camilli.....429–40
Transformers in Residential and Commercial Areas, Audio Noise in. Baugh.....121–6; disc. 126
Transformers on the System of the Bonneville Power Administration, Application and Handling of Very Large Power. Stevens.....158–63; disc. 163
Transient Response of Direct-Current Dynamos. Koenig.....139–44; disc. 144
Transients and Feedback in Magnetic Amplifiers, An Analysis of. Johnson, Latson....604–11; disc. 611
Transients in Magnetic Amplifiers, An Analysis of. VerPlanck, Finzi, Beaumariage.....498–503
Translator, A Printing Telegraph Tape-to-Page. Frost.....79–83
Transmission, Clampers in Video. Doba, Rieke..477–87
(Transmission) Dielectric-Recovery Characteristics of Power Arcs in Large Air Gaps. McCann, Conner, Ellis.....616–24; disc. 624
Transmission-Line Protection of Short Lines of the Metropolitan Area of a Typical System. Marter.....468–71; disc. 471
Transmission Lines, Consideration of Requirements and Limitations of Relaying and High-Speed Reclosing on Long and Heavily Loaded. Parks, Brownlee.....103–07; disc. 107
Transmission Lines, Relay Protection for Medium Length High-Voltage. Kinghorn..461–5; disc. 465
Transmission Networks, Total and Incremental Losses in Power. Ward, Eaton, Hale...626–31; disc. 631
Turbine Electric Locomotive, Control System for a 4,500-Horsepower Gas-. Warrick.....508–13
Turbine Electric Locomotive, Rotating Electric Equipment for a Gas-. Coho.....514–18
Turbine Electric Locomotive, The Alco-GE 4,500-Horsepower Gas-. Morey.....504–07
Turbine Generators, Liquid Cooling of A-C. Part II. Fechheimer.....165–71; disc. 171 (Part I—1947).
Two-Channel Carrier Telegraph System for Short Submarine Cables, A. Newell, Cramer.....61–5

V

Variation Principle, An Improved Method of Measuring Dissipation Factor and Dielectric Constant Using the Susceptance. Miller, Whelan.....491–7
Video Transmission, Clampers in. Doba, Rieke..477–87
Voltage Gradient Meter, A. Tremaine, Cheek.....633–7; disc. 637
Voltage Measurement, The Irradiation of Spark Gaps for. Hardy, Craggs.....584–90
Voltage Regulator on Steady-State Power Limit, Effect of Buck-Boost. Concordia....380–4; disc. 384

W

Wall, The Thermal Resistance Between Cables and a Surrounding Pipe or Duct. Buller, Neher.....342–7; disc. 347

2. Author Index

Abetti, P. A. Disc.....539, 580
Ackermann, O. Disc.....624
Ames, E. W.; L. J. Hibbard, C. C. Whittaker. Rectifier-Type Motive Power for Railroad Electrification. (50–81).....519–23; disc. 523
Ammerman, Charles R. The Direct Measurement of Bandwidth. (50–5).....27–31
Andreae, F. V. Design and Control of Ferroalloy Furnaces. (50–86).....557–62
Andrews, F. E.; W. H. Hatch. Disc.....54
Asbury, C. E. Disc.....466, 47
Attura, George M. Disc.....29

B

Baldwin, M. J.; H. D. Barnhart. Quick and Accurate Production Testing on Large D-C Apparatus. (50–21).....136–8
Balentine, C. J.; E. B. Rietz. A New 69-Kv Oil Blast Circuit Breaker. (50–61).....416–23; disc. 423
Barnett, Guy F.; P. Greebler. Heat Transfer Study on Power Cable Ducts and Duct Assemblies. (50–55).....357–64; disc. 366
Barnhart, H. D.; M. J. Baldwin. Quick and Accurate Production Testing on Large D-C Apparatus. (50–21).....136–8
Baugh, C. E. Audio Noise in Transformers in Residential and Commercial Areas. (50–19)..121–6; disc. 127
Beaumariage, D. C.; D. W. VerPlanck, L. A. Finzi. An Analysis of Transients in Magnetic Amplifiers. (50–76).....498–503
Beck, E. Disc.....113, 141
Beck, E.; A. M. Opsahl. Disc.....92
Beckwith, Sterling. Disc.....185
Bellaschi, P. L. Disc.....92, 143
Bernstein, S.; C. W. Clapp. Noncontacting Thickness Gauge Using Beta Rays. (50–73).....488–90
Bishop, E. A. Disc.....414
Bliss, T. J.; R. L. Witzke. Surge Protection of Cable-Connected Equipment. (50–83)..527–38; disc. 539
Blomqvist, E. A. Disc.....126
Blume, A. E.; R. W. Votaw. Disc.....653
Borgel, B. F. Design and Operation of Central Control Rooms. (50–92).....598–602
Brancato, E. L.; J. Cybulski. Disc.....144
Bretch, Edward. Disc.....7
Brownlee, Allan L. A Primary Method of Measuring the Ratio and Phase Angle of Current Transformers. (50–67).....459–60
Brownlee, W. R. Disc.....631
Brownlee, W. R.; J. A. Elzi. Disc.....591
Brownlee, W. R.; C. E. Parks. Consideration of Requirements and Limitations of Relaying and High-Speed Reclosing on Long and Heavily-Loaded Transmission Lines. (50–16)....103–07; disc. 109
Buchanan, W. B. Electrical Hazards to Farm Stock. (50–104).....654–6
Buchanan, W. B. Disc.....663
Buckland, Mrs. B. O.; R. H. Norris. Disc.....347
Buckland, Mrs. B. O.; D. S. Snell, R. H. Norris. Surface Heat-Transfer Coefficients for Hydrogen-Cooled Rotating Electric Machines. (50–29).....174–85; disc. 185
Buller, F. H. Disc.....365
Buller, F. H.; J. H. Neher. The Thermal Resistance Between Cables and a Surrounding Pipe or Duct Wall. (50–52).....342–7; disc. 349
Burkhalter, A. H. Disc.....603
Burrell, R. W. Disc.....347, 364

C

Calvert, J. F.; G. W. Goelz. Analogue Computer for Multicomponent Fractionation Calculations. (50–15).....97–103
Camilli, G. A Survey of Bushing-Type Current Transformers for Metering Purposes. (50–63)...429–40
Carleton, J. T.; E. L. Harder. New Techniques on the Anacom—Electric Analog Computer. (50–85).....547–56
Carothers, B. M. Disc.....413
Cheek, R. C.; E. L. Harder, J. M. Clayton. Regulation of A-C Generators with Suddenly Applied Loads. Part II. (50–58).....395–405; disc. 406 (Part I—1944)
Cheek, R. C.; R. L. Tremaine. A Voltage Gradient Meter. (50–98).....633–7; disc. 637
Chipman, J. F. Disc.....414
Clapp, C. W.; S. Bernstein. Noncontacting Thickness Gauge Using Beta Rays. (50–73).....488–90
Clayton, J. M.; E. L. Harder, R. C. Cheek. Regulation of A-C Generators with Suddenly Applied Loads. Part II. (50–58).....395–405; disc. 406 (Part I—1944)
Cobb, E. E. Disc.....385
Coho, O. C. Rotating Electric Equipment for a Gas-Turbine Electric Locomotive. (50–79)....514–18
Colaiaco, A. P.; A. A. Johnson, J. E. Reilly. Design and Test on Electronic Exciter Supplied from Common Shaft-Driven Generator (50–50).....328–35; disc. 336
Cole, Edward R. Electric Equipment and Operation of Graphitizing Furnaces. (50–87).....564–6
Concordia, C. Effect of Buck-Boost Voltage Regulator on Steady-State Power Limit. (50–57).....380–4; disc. 384
Conner, J. E.; G. D. McCann, H. M. Ellis. Dielectric Recovery Characteristics of Power Arcs in Large Air Gaps. (50–96).....616–24; disc. 624
Cornelius, H. A. Disc.....539
Craggs, J. D.; D. R. Hardy. The Irradiation of Spark Gaps for Voltage Measurement. (50–90)..584–90
Cramer, C. H.; E. L. Newell. A Two-Channel Carrier Telegraph System for Short Submarine Cables. (50–10).....61–5
Crawford, S. N.; M. J. Mulhern. Rectifier Equipment for Electronic D-C Motor Drives. (50–33)..211–15
Cybulski, J.; E. L. Brancato. Disc.....144

D

Dalziel, Charles F. Electric Fences—Their Hazards, Types, Regulations, and Safe Application. (50–2).....8–15
Dawes, C. L.; C. H. Thomas, A. B. Drought. Impulse Measurements by Repeated-Structure Networks. (50–89).....571–80; disc. 580
deBellis, A. M. Disc.....77
Defandorf, F. M.; H. R. Stewart. New Lightning Arrester Standard. (50–82).....525–6
de Koning, Th. Disc.....172, 201

D'Entremont, F. R.; R. A. Pfuntner, R. E. Franck. A New Dry-Type Insulation for Instrument Transformers. (50-66)....453–8
Deubel, Justin A. Flame Detectors for Domestic Fuel Burner Safety Devices. (50-35)....220–5
Doba, S., Jr.; J. W. Rieke. Clampers in Video Transmission. (50-72)....477–87
Dovjikov, A. Disc....384
Dow, W. G.; H. A. Romanowitz. Statistical Nature and Physical Concepts of Thyratron Deionization Time. (50-56)....368–79
Drought, A. B.; C. L. Dawes, C. H. Thomas. Impulse Measurements by Repeated Structure Networks. (50-89)....571–80; disc. 580

E

Eager, G. S., Jr. Disc....355
Eaton, J. R.; J. B. Ward, H. W. Hale. Total and Incremental Losses in Power Transmission Networks. (50-97)....626–31; disc. 631
Edwards, Charles M.; E. C. Johnson, Jr. An Electronic Simulator for Nonlinear Servomechanisms. (50-47)....300–06; disc. 306
Ein, S. Disc....59
Ellis, H. M.; G. D. McCann, J. E. Conner. Dielectric Recovery Characteristics of Power Arcs in Large Air Gaps. (50-96)....616–24; disc. 624
Elzi, J. A.; W. R. Brownlee. Disc....391
Evans, Walter R. Control System Synthesis by Root Locus Method. (50-11)....66–9

F

Farr, John W. A New Line of Orthomagnetic Bushing-Type Current Transformers. (50-62)....424–8
Fechheimer, Carl J. Liquid Cooling of A-C Turbine Generators. Part II. (50-28)..165–71; disc. 171
(Part I—1947)....
Fechheimer, Carl J. Disc....185
Ferguson, J. G.; F. A. Korn. The Number 5 Crossbar Dial Telephone Switching System. (50-41)..244–54
Finison, Harvey J. Basic Patterns for Arrangement of Electric Power Systems for Steel Mills. (50-9)....54–9; disc. 60
Finzi, L. A. Disc....611
Finzi, L. A.; D. W. VerPlanck, D. C. Beaumariage. An Analysis of Transients in Magnetic Amplifiers. (50-76)....498–503
Fischer, E. G. Disc....126
Floyd, G. D. Disc....77
Foster, G. E. The Metrotype System of Digital Recording and Telemetering. (50-84)....543–6
Fountain, L. L. Disc....471
Franck, R. E.; R. A. Pfuntner, F. R. D'Entremont. A New Dry-Type Insulation for Instrument Transformers. (50-66)....453–8
Frederickson, C. W. Disc....43
Friedrich, R. E.; W. M. Leeds. High-Voltage Oil Circuit Breakers for 5,000,000 to 10,000,000-Kva Interrupting Capacity. (50-12)....70–6; disc. 77
Friend, O. A. Disc....269
Frost, A. E. A Printing Telegraph Tape-to-Page Translator. (50-13)....79–83
Fugill, A. P. Disc....50

G

Gay, F. W. Disc....392
George, E. E. Disc....631
Goeis, G. W.; J. F. Calvert. Analogue Computer for Multicomponent Fractionation Calculations. (50-15)....97–103
Goldman, J. E. Disc....51
Goldsborough, S. L. Disc....43
Gopalakrishna, H. V.; M. S. Thacker. Suggested Improvements in the Performance Calculations of Single-Phase Induction Motors. (50-1)..1–6; disc. 7
Gordy, T. D. Audible Noise of Power Transformers. (50-8)....45–50; disc. 53
Gordy, T. D. Disc....126
Gracey, A. L. Basic Theory Underlying Bell System Facilities Capacity Tables. (50-40)....238–43
Graff, J. M. Disc....413
Greebler, Paul. Disc....348
Greebler, Paul; G. F. Barnett. Heat Transfer Study on Power Cable Ducts and Duct Assemblies. (50-55)....357–64; disc. 366
Greenfield, E. W.; L. F. Roehmann. Development of Improved Luminous Sign Cable. (50-53)....350–5; disc. 356
Gross, Eric T. B. Disc....452, 476

H

Hagenguth, J. H. Disc....582
Hale, H. W.; J. B. Ward, J. R. Eaton. Total and Incremental Losses in Power Transmission Networks. (50-97)....626–31; disc. 631
Hall, Albert C. A Generalized Analogue Computer for Flight Simulation. (50-48)....308–20
Halperin, Herman. Disc....199
Hanff, E. A. Electrode Control and Associated Operating Mechanisms. (50-88)....567–70; disc. 570
Harder, E. L. Disc....541
Harder, E. L.; J. T. Carleton. New Techniques on the Anacom—Electric Analog Computer. (50-85)....547–56
Harder, E. L.; R. C. Cheek, J. M. Clayton. Regulation of A-C Generators with Suddenly Applied Loads. Part II. (50-58)....395–405; disc. 406
(Part I—1944)
Hardy, D. R.; J. D. Craggs. The Irradiation of Spark Gaps for Voltage Measurement. (50-90)..584–90
Hatch, W. H.; F. E. Andrews. Disc....541
Hayford, B. I. Disc....413
Herskind, C. C. Disc....523
Hibbard, L. J.; C. C. Whittaker, E. W. Ames. Rectifier-Type Motive Power for Railroad Electrification. (50-81)....519–23; disc. 523
Hill, A. W. Disc....423
Horstman, C. C. Disc....51
Howard, S. B.; W. A. McMorris, J. R. Meador. Disc....95
Hunt, Lloyd F. Disc....475
Hunter, E. M. Disc....540

J

James, W. Gordon. Disc....164
Jeanne, P. A. Disc....108, 523
Johnson, A. A.; A. P. Colaiaco, J. E. Reilly. Design and Test on Electronic Exciter Supplied from Common Shaft-Driven Generator. (50-50)....328–35; disc. 336
Johnson, A. A.; H. A. Thompson. Bus Transfer Tests on 2,300-Volt Station Auxiliary System. (50-59)....386–90; disc. 393
Johnson, E. Calvin, Jr.; C. M. Edwards. An Electronic Simulator for Nonlinear Servomechanisms. (50-47)....300–06; disc. 306
Johnson, I. B.; L. E. Saline. Disc....94
Johnson, J. A.; E. M. Stacey. Application of Electronic Motor Drives to Printing Presses. (50-34)..216–19
Johnson, L. J.; H. G. Schafer. A Magnetic Amplifier Frequency Control. (50-95)....613–15
Johnson, Walter C.; F. W. Latson. An Analysis of Transients and Feedback in Magnetic Amplifiers. (50-94)....604–11; disc. 611

K

Kennedy, L. F. Disc....475
Kidder, A. H. Disc....348
Kilbourne, C. E.; D. S. Snell. Disc....171
Kilgore, Lee A.; E. C. Whitney. Spring and Damping Coefficients of Synchronous Machines and Their Application. (50-36)....226–9; disc. 229
Kinghorn, J. H. Relay Protection for Medium Length High-Voltage Transmission Lines. (50-68)....461–5; disc. 465
Kinghorn, J. H.; F. M. Porter. Disc....340
Kirchmayer, L. K. Disc....631
Kirschbaum, H. S. Per-Unit Inductances of Synchronous Machines. (50-38)....231–4
Kochenburger, Ralph J. A Frequency Response Method for Analyzing and Synthesizing Contactor Servomechanisms. (50-44)....270–83; disc. 283
Koenig, H. E. Transient Response of Direct-Current Dynamos. (50-22)....139–44; disc. 145
Korn, F. A.; J. G. Ferguson. The Number 5 Crossbar Dial Telephone Switching System. (50-41)..244–54
Krida, H.; E. T. McCurry. A New Grounding and Testing Device for Metal-Clad Switchgear. (50-60)....407–12; disc. 414
Kronacher, G. Static Accuracy Performance of the Selsyn Generator Control-Transformer System. (50-103)....645–53; disc. 653

L

Lambert, W. H.; A. H. Phillips, D. R. Pattison. Excitation Improvement—Electronic Excitation and Regulation of Electric Generators as Compared to Conventional Methods. (50-51)..538–40; disc. 340
Landsman, Gerald....306
Langstaff, H. A. P. Disc....335
Larson, N. G. Disc....546
Latson, Frank W.; W. C. Johnson. An Analysis of Transients and Feedback in Magnetic Amplifiers. (50-94)....604–11; disc. 611
Lee, J. R. Disc....570
Leeds, W. M. Disc....25
Leeds, W. M.; R. E. Friedrich. High-Voltage Oil Circuit Breakers for 5,000,000 to 10,000,000-Kva Interrupting Capacity. (50-12)....70–6; disc. 77
Linders, J. R. Disc....475
Livingston, O. W. Control of Large D-C Motors Supplied from Ignitron Rectifiers. (50-32)..205–10
Lowerison, Cort. Disc....108

M

MacLeod, D. R. Disc....523
Macpherson, R. H. Disc....107
Madden, T. F.; W. H. Mutschler, Jr. Harmonic Index—A Tool for Transformer Audio Noise Investigation. (50-18)....115–18; disc. 120
Mallory, B. C. Centralized Instrumentation and Controls for Steam Electric Power Stations. (50-91)....591–6
Marter, W. E. Transmission-Line Protection of Short Lines of the Metropolitan Area of a Typical System. (50-69)....468–7; disc. 472
Mason, V. V. Disc....199, 364
Mathews, C. A. Disc....471
McCann, G. D.; J. E. Conner, H. M. Ellis. Dielectric Recovery Characteristics of Power Arcs in Large Air Gaps. (50-96)....616–24; disc. 624
McConnell, A. J. Disc....465
McCreary, Harold J. Disc....36
McCurry, E. T.; H. Krida. A New Grounding and Testing Device for Metal-Clad Switchgear. (50-60)....407–12; disc. 414
McDonald, Donald. Improvements in the Characteristics of A-C Lead Networks for Servomechanisms. (50-46)....293–300
McMorris, W. A.; S. B. Howard, J. R. Meador. Disc....95
Meador, J. R.; W. A. McMorris, S. B. Howard. Disc....95
Mellor, A. G.; M. Temoshok. Excitation System Performance with Motor-Driven Exciters. (50-49)....321–7
Mellor, A. G.; M. Temoshok. Disc....390
Meszar, John. Fundamentals of the Automatic Telephone Message Accounting System. (50-42)....255–68
Mikhail, Saad L. Potier Reactance for Salient-Pole Synchronous Machines. (50-39)....235–8
Miller, C. Frank; F. G. Whelan. An Improved Method of Measuring Dissipation Factor and Dielectric Constant Using the Susceptance Variation Principle. (50-74)....491–7
Morey, A. H. The Alco-GE 4,500-Horsepower Gas-Turbine Electric Locomotive. (50-77)....504–07
Morgan, W. A. Disc....108
Mulhern, M. J.; S. N. Crawford. Rectifier Equipment for Electronic D-C Motor Drives. (50-33)..211–15
Murray, C. S. Disc....52, 118
Mutschler, W. H., Jr.; T. F. Madden. Harmonic Index—A Tool for Transformer Audio Noise Investigation. (50-18)....115–18; disc. 120

N

Naef, Otto. Disc....26, 537
Nagel, G. A. Disc....405
Nau, Robert H. Disc....76
Neher, J. H. Disc....365
Neher, J. H.; F. H. Buller. The Thermal Resistance Between Cables and a Surrounding Pipe or Duct Wall. (50-52)....342–7; disc. 349
New, Warren C. Combined Phase and Ground Distance Relaying. (50-7)....37–42; disc. 44
Newell, E. L.; C. H. Cramer. A Two-Channel Carrier Telegraph System for Short Submarine Cables. (50-10)....61–5
Noest, John G. Disc....384, 391, 405
Norris, R. H.; Mrs. B. O. Buckland. Disc....347
Norris, R. H.; D. S. Snell, B. O. Buckland. Surface Heat-Transfer Coefficients for Hydrogen-Cooled Rotating Electric Machines. (50-29)....174–85; disc. 185
Notthoff, Arthur P., Jr. Phase Lead for A-C Servo Systems with Compensation for Carrier Frequency Changes. (50-45)....285–91; disc. 292

O

Opsahl, A. M. Disc....113, 539
Opsahl, A. M.; E. Beck. Disc....92
Ostendorf, B., Jr. A New Electronic Telegraph Regenerative Receiver. (50-6)....32–6; disc. 36

P

Park, J. H. Disc....581
Parks, C. E.; W. R. Brownlee. Consideration of Requirements and Limitations of Relaying and High-Speed Reclosing on Long and Heavily-Loaded Transmission Lines. (50-16)....103–07; disc. 109
Parziale, A. J.; P. D. Tilton. Characteristics of Some Magnetic-Fluid Clutch Servomechanisms. (50-24)....150–7

Pattison, D. R.; A. H. Phillips, W. H. Lambert. Excitation Improvement—Electronic Excitation and Regulation of Electric Generators as Compared to Conventional Methods. (50-51)..338-40; disc. 340
Pfuntner, K. A.; K. E. Franck, F. R. D'Entremont. A New Dry-Type Insulation for Instrument Transformers. (50-66).....453-8
Philbrick, George A. Disc.....283
Phillips, A. H.; W. H. Lambert, D. R. Pattison. Excitation Improvement—Electronic Excitation and Regulation of Electric Generators as Compared to Conventional Methods. (50-51)..338-40; disc. 340
Porter, F. M. Disc.....201
Porter, F. M.; J. H. Kinghorn. Disc.....340

R

Rademacher, L. B.; W. L. Teague. Disc.....539
Ramsaur, O. Disc.....466
Reed, J. R. Solderless Commutator Joints for High Temperature Operation of Railway Traction Armatures. (50-100).....638-41
Reilly, J. E.; A. P. Colalaco, A. A. Johnson. Design and Test on Electronic Exciter Supplied from Common Shaft-Driven Generator. (50-50).....328-35; disc. 336
Rieke, J. W.; S. Doba, Jr. Clampers in Video Transmission. (50-72).....477-87
Rietz, E. B. Development and Testing of an Improved High-Voltage, High-Capacity Impulse Circuit Breaker. (50-3).....15-25; disc. 26
Rietz, E. B.; C. J. Balentine. A New 69-Kv Oil Blast Circuit Breaker. (50-61).....416-23; disc. 423
Roehmann, L. F. Disc.....523
Roehmann, L. F.; E. W. Greenfield. Development of Improved Luminous Sign Cable. (50-53).....350-5; disc. 356
Romanowitz, H. A.; W. G. Dow. Statistical Nature and Physical Concepts of Thyratron Dionization Time. (50-56).....368-79
Rorden, Harold L. Lightning Arresters as a Criterion for Insulation Levels. (50-14).....84-91; disc. 95
Rosch, S. J. Disc.....356
Ross, M. D.; R. A. Towne. Disc.....199

S

St. Clair, H. P. Disc.....77
Saline, L. E.; I. B. Johnson. Disc.....94
Schafer, H. G.; L. J. Johnson. A Magnetic Amplifier Frequency Control. (50-95).....613-15
Schirmer, A. H. Protective Grounding of Electrical Installations on Customer's Premises. (50-105).....657-9
Shepherd, R. V. Disc.....229
Smith, H. B. Disc.....631
Smith, Otto J. M. Generator Rating of Induction Motors. (50-20).....129-35
Snell, D. S. Loading of Hydrogen-Cooled Generators at Elevated Gas Pressures. (50-30)..186-99; disc. 202
Snell, D. S.; C. E. Kilbourne. Disc.....171
Snell, D. S.; R. H. Norris, B. O. Buckland. Surface Heat-Transfer Coefficients for Hydrogen-Cooled Rotating Electric Machines. (50-29)..174-85; disc. 185
Specht, T. R.; R. N. Wagner. The Theory of the Current Transductor and Its Application in the Aluminum Industry. (50-64).....441-52; disc. 452
Stacey, E. M.; J. A. Johnson. Application of Electronic Motor Drives to Printing Presses. (50-34)..216-19
Starr, E. C. Disc.....91, 112
Stevens, Richard F. Application and Handling of Very Large Power Transformers on the System of the Bonneville Power Administration. (50-26).....158-63; disc. 163
Stewart, H. R.; F. M. Defandorf. New Lightning Arrester Standard. (50-82).....525-6
Streifus, C. A.; F. Von Roeschlaub. Disc.....42
Suhr, F. W. Disc.....6

T

Taylor, D. W. Disc.....392
Teague, William L. Disc.....94
Teague, W. L.; L. B. Rademacher. Disc.....539
Temoshok, M.; A. G. Mellor. Excitation System Performance with Motor-Driven Exciters. (50-49).....321-7
Temoshok, M.; A. G. Mellor. Disc.....390
Tetherow, C. L. Synthetic Load for Testing Rectifiers. (50-102).....642-4
Thacker, M. S.; H. V. Gopalakrishna. Suggested Improvements in the Performance Calculations of Single-Phase Induction Motors. (50-1)..1-6; disc. 7
Thomas, C. H.; C. L. Dawes, A. B. Drought. Impulse Measurements by Repeated Structure Networks. (50-89).....571-80; disc. 580
Thompson, A. T. Disc.....581
Thompson, H. A.; A. A. Johnson. Bus Transfer Tests on 2,300-Volt Station Auxiliary System. (50-59).....386-90; disc. 393
Tilton, P. D.; A. J. Parziale. Characteristics of Some Magnetic-Fluid Clutch Servomechanisms. (50-24).....150-7
Tomlinson, C. M. Disc.....269
Towne, R. A.; M. D. Ross. Disc.....199
Tremaine, R. L.; F. C. Cheek. A Voltage-Gradient Meter. (50-98).....633-7; disc. 637

V

Valentine, C. E. Disc.....384
VerPlanck, D. W.; L. A. Finzi, D. C. Beaumariage. An Analysis of Transients in Magnetic Amplifiers. (50-76).....498-503
Vikoren, O. B. Disc.....412
Vogel, F. J. Margins Between Lightning Arrester Protective Levels and Transformer Insulation (50-17).....110-12; disc. 114
Von Roeschlaub, F.; C. A. Streifus. Disc.....42
VonVoigtlander, F. Disc.....119
Votaw, R. W.; A. E. Blume. Disc.....653

W

Waghorne, J. H. Rural Neutral Potentials. (50-106).....660-3
Wagner, R. N.; T. R. Specht. The Theory of the Current Transductor and Its Application in the Aluminum Industry. (50-64).....441-52; disc. 452
Ward, J. B.; J. R. Eaton, H. W. Hale. Total and Incremental Losses in Power Transmission Networks. (50-97).....626-31; disc. 631
Warrick, T. J. Control System for a 4,500-Horsepower Gas-Turbine Electric Locomotive. (50-78)..508-13
Webb, R. L. Disc.....391
Wentz, E. C. Disc.....452
West, C. P. Disc.....602
Whelan, Frederick G.; C. F. Miller. An Improved Method of Measuring Dissipation Factor and Dielectric Constant Using the Susceptance Variation Principle. (50-74).....491-7
Whitney, E. C. Disc.....405
Whitney, Eugene C.; L. A. Kilgore. Spring and Damping Coefficients of Synchronous Machines and Their Application. (50-36)..226-9; disc. 229
Whittaker, C. C.; L. J. Hibbard, E. W. Ames. Rectifier-Type Motive Power for Railroad Electrification. (50-81).....519-23; disc. 523
Wilder, Willard S. Disc.....475
Wilkinson, R. I. Disc.....243
Wiseman, R. J. Disc.....348, 363
Witzke, R. L.; T. J. Bliss. Surge Protection of Cable-Connected Equipment. (50-83)..527-38; disc. 539
Wolfe, W. A. Disc.....44
World, R. W. Disc.....475
Wortman, H. B. Disc.....540

Preface

The 1950 TRANSACTIONS (volume 69) of the American Institute of Electrical Engineers is published in two parts. Part I contains technical program papers and related discussions presented at the Winter General Meeting, New York, N. Y., January 30–February 3, 1950.

Part II of the 1950 volume contains approved papers and related discussions presented at the following meetings:

North Eastern District Meeting, Providence, R. I., April 26–28, 1950.
Great Lakes District Meeting, Jackson, Mich., May 11–12, 1950.
Summer and Pacific General Meeting, Pasadena, Calif., June 12–16, 1950.
Middle Eastern District Meeting, Baltimore, Md., October 3–5, 1950.
Fall General Meeting, Oklahoma City, Okla., October 23–27, 1950.

Part I of Volume 69 contained an index covering only the first half of the year. A complete multi-entry index for 1950 (Parts I and II) is included in this volume beginning on page 1737. The Report of the Board of Directors and the list of Officers and Committees for 1950–1951 also are included in Part II.

The original number assigned each paper by the Technical Program Committee is given in the author index.

Statements and opinions given in papers and discussions published in TRANSACTIONS are the expressions of contributors for which the American Institute of Electrical Engineers assumes no responsibility.

Analysis of Synchronous Machine Short Circuits

ROBERT D. CAMBURN
ASSOCIATE AIEE

ERIC T. B. GROSS
FELLOW AIEE

Synopsis: Representation has been made of synchronous machines and power systems by α-, β-, and 0-networks which are basic for the analysis of various types of short circuits. New expressions for the characteristic synchronous machine reactances in α-, β-, 0-components, or Clarke components, are derived. It is found that these characteristic reactances are constant so that the use of Clarke component networks does not compare unfavorably with other methods of short-circuit analysis.

IN RECENT years a number of papers have been published[1,2,3] dealing with a new type of substituted variables to supplement symmetrical components. These new components are α-, β-, and 0-components or "Clarke components" as they will be called here following a suggestion which was discussed at some length before a meeting of the AIEE.[4]

α-components are equal in phases b and c; they are there opposite in sign and half the magnitude of the α-component in phase a.

β-components are equal in phases b and c but of opposite sign; in phase a they are zero.

0-components are equal in all three phases.

Current components of this nature were first used in 1917 by W. W. Lewis[5] for the analysis of short circuits occurring on the high-voltage side of a delta-Y transformer. Figure 1(A) shows that a line-to-line fault on the Y-side of a delta-Y transformer causes β-currents in the Y-connected windings and α-currents in the leads to the delta-connected windings. From Figure 1(B) it can be seen that a line-to-neutral fault on the wye side of a delta-Y transformer causes α and 0-currents in the Y-connected windings, and β-currents in the leads to the delta-connected windings. A third condition which results in a flow of Clarke component-type currents, is the line-to-line fault as shown in Figure 1(C). In his discussion, however, Lewis made no attempt to establish a system of components which could be generally applied to the analysis of unbalanced 3-phase circuits.

Edith Clarke was the first to present a complete definition of these components and to describe their usefulness in the solution of system engineering problems. Later, E. W. Kimbark[3] presented a paper on the applications of "2-phase co-ordinates," a slightly modified form of Edith Clarke's α-, β-, and 0-components. These two papers[1,2] and the discussions[4] contain the basic material on Clarke components, though the same or similar components have been used by others in the solution of special problems.[3,4]

Clarke components can be used in the analysis of any unbalanced 3-phase circuits, however, their application is presently limited because the well-established symmetrical components may be used with equal or perhaps greater facility in many cases. Clarke components allow a more direct solution where any of the unbalances sketched in Figure 1 are involved. They can be used in the system recovery voltage determination by transient analyzer methods when symmetrical components are not applicable, as will be shown in a paper in preparation.

It is the purpose of this paper to derive new expressions for synchronous machine reactances in Clarke components. In the same manner as symmetrical component analysis is undertaken, Clarke component networks representative of a synchronous machine will be developed, and methods of using these networks to solve for the various types of short-circuit currents and voltages will be indicated. Of particular interest is the analysis of generator reactances when a line-to-line fault occurs on the high-voltage side of a Y-delta transformer (the generator being connected to the delta side) as this does not seem to be contained in known references.

An underlying motive for undertaking this analysis was the belief that Clarke component currents have a direct physical significance from the standpoint of synchronous machinery. It was expected that Clarke component analysis would not involve varying impedances (that is to say, varying with the type of unbalanced faults) such as negative sequence generator impedance.[10] The results of this investigation seem to indicate this advantage of Clarke components.

The reasoning behind these presumptions may be indicated by considering an idealized synchronous machine. In Figure 2, it is shown that α-current magnetizes only the vertical or "α"-axis of the stator. In Figure 3, it is shown that β-current magnetizes only the horizontal or "β"-axis. Thus, the problem of analyzing a 3-phase machine by means of Clarke components is equivalent to the analysis of a 2-phase machine with stator windings in quadrature. The faults shown in Figure 1 would each be short circuits on only one of the two phase windings.

As is done in symmetrical component analysis, the machine will be represented by component networks consisting of driving voltages and internal impedances which may be interconnected to solve for various types of short circuits. In de-

Paper 50-37, recommended by the AIEE Rotating Machinery Committee and approved by the AIEE Technical Program Committee for presentation at the AIEE Winter General Meeting, New York, N. Y., January 30–February 3, 1950, and at the North Eastern District Meeting, Providence, R. I., April 26–28, 1950. Manuscript submitted March 21, 1949; made available for printing December 22, 1949.

ROBERT D. CAMBURN is with Commonwealth Services, Inc., Jackson, Mich., and ERIC T. B. GROSS is with Illinois Institute of Technology, Chicago, Ill.

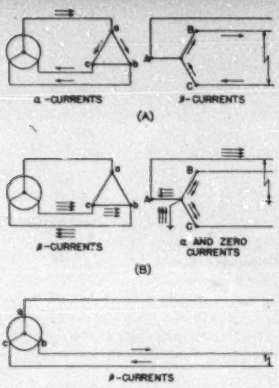

Figure 1. Distribution of Clarke component currents under fault conditions

(A) Line-to-line fault on high-voltage system. (B) Line-to-ground fault on high-voltage system. (C) Line-to-line fault on generator leads

riving component impedance expressions R. H. Park's analysis[6,7] of the two reactances theory of synchronous machines is applied. However, a slightly modified treatment of Park's work, following W. A. Lewis,[8] is used. It is assumed here that the quadrature axis is 90 degrees behind the direct axis so that $I_a = I_q + jI_d$. In Park's papers, the quadrature axis is defined to be 90 degrees ahead of the direct axis.

Fundamental Relationships

The relations between Clarke components phase currents and voltages are defined as follows:

$$I_a = I_\alpha + I_0$$

$$I_b = -\frac{1}{2}I_\alpha + \frac{\sqrt{3}}{2}I_\beta + I_0$$

$$I_c = -\frac{1}{2}I_\alpha - \frac{\sqrt{3}}{2}I_\beta + I_0$$

$$V_a = V_\alpha + V_0$$

$$V_b = -\frac{1}{2}V_\alpha + \frac{\sqrt{3}}{2}V_\beta + V_0$$

$$V_c = -\frac{1}{2}V_\alpha - \frac{\sqrt{3}}{2}V_\beta + V_0 \qquad (1)$$

$$I_\alpha = \frac{2}{3}\left(I_a - \frac{I_b + I_c}{2}\right)$$

$$I_\beta = \frac{1}{\sqrt{3}}(I_b - I_c)$$

$$I_0 = \frac{1}{3}(I_a + I_b + I_c)$$

$$V_\alpha = \frac{2}{3}\left(V_a - \frac{V_b + V_c}{2}\right)$$

$$V_\beta = \frac{1}{\sqrt{3}}(V_b - V_c)$$

$$V_0 = \frac{1}{3}(V_a + V_b + V_c) \qquad (2)$$

Symbols in the equations may be interpreted either as phasor, or as instantaneous quantities. Modified networks having twice the usual zero sequence currents and one-half zero sequence impedance are employed to simplify the analysis of some types of short circuit.

The General Component Network

For purposes of calculation, the synchronous machine is usually pictured as an internal electromotive force in series with an impedance network. Similarly, the Clarke component networks representative of a synchronous machine are composed of electromotive forces and some network of impedances. Figure 4 shows such circuit of the most general nature having all possible combinations of self and mutual impedance. The voltage E_α, E_β, and E_0 at the left in the figure are component electromotive forces (driving voltages). At the right, V_α, V_β, and V_0 are component terminal voltages.

Writing circuit equations for this network gives

$$\begin{aligned} E_\alpha - V_\alpha &= I_\alpha Z_{\alpha\alpha} + I_\beta Z_{\alpha\beta} + I_0 Z_{\alpha 0} \\ E_\beta - V_\beta &= I_\alpha Z_{\beta\alpha} + I_\beta Z_{\beta\beta} + I_0 Z_{\beta 0} \\ E_0 - V_0 &= I_\alpha Z_{0\alpha} + I_\beta Z_{0\beta} + I_0 Z_{00} \end{aligned} \qquad (3)$$

It is then necessary to determine the independent variables in equation 3, the driving voltages and the various impedances.

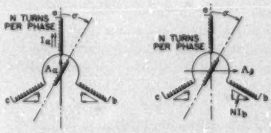

Figure 2 (left). Flux produced in the machine by α-currents

$$\Lambda_\alpha = NI_a + 2\frac{1}{4}NI_a = \frac{3}{2}NI_\alpha$$

$$\Lambda_\beta = 0$$

Figure 3 (right). Flux produced in the machine by β-currents

$$\Lambda_\alpha = 0$$

$$\Lambda_\beta = 2\frac{\sqrt{3}}{2}NI_b = \sqrt{3}NI_b = \frac{3}{2}NI_\beta$$

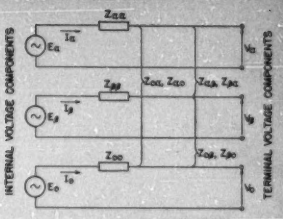

Figure 4. General Clarke component network for the representation of a synchronous machine

Components of Generated Electromotive Force

Since only balanced 3-phase voltages are generated in the machine, the internal voltages may be found at once from equation 2. That is, since

$$E_a = E_a e^{j0}$$

$$E_b = E_a e^{j\frac{4\pi}{3}}$$

$$E_c = E_a e^{j\frac{2\pi}{3}} \qquad (4)$$

we have

$$E_\alpha = \frac{2}{3}\left(E_a - \frac{E_b + E_c}{2}\right) = E_a$$

$$E_\beta = \frac{1}{\sqrt{3}}(E_b - E_c) = -jE_a$$

$$E_0 = \frac{1}{3}(E_a + E_b + E_c) = 0 \qquad (5)$$

Component Network Impedances

The component impedances for the network shown in Figure 4 can be found analytically by assuming certain currents to be circulated by an external source, while the field is open or short circuited and the machine driven at synchronous speed. Under actual test, reactances measured with the field open circuited would be synchronous reactances. With the field short circuited, the result would be transient reactance. Further, if the effect of a damper winding were included, the result would be subtransient reactance. Here, the distinction will not be evident, and so the symbol X_d may be interpreted as any of the three.

Since there now is no generated electromotive force, equation 3 becomes

$$\begin{aligned} -V_\alpha &= -I_\alpha Z_{\alpha\alpha} - I_\beta Z_{\alpha\beta} - I_0 Z_{\alpha 0} \\ -V_\beta &= -I_\alpha Z_{\beta\alpha} - I_\beta Z_{\beta\beta} - I_0 Z_{\beta 0} \\ -V_0 &= -I_\alpha Z_{0\alpha} - I_\beta Z_{0\beta} - I_0 Z_{00} \end{aligned} \qquad (6)$$

By comparison of the derived expressions for component terminal voltages with equation 6, the component impedances may be determined.

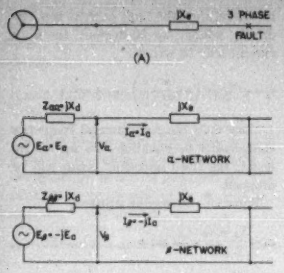

Figure 5. Clarke component networks for the analysis of 3-phase fault

(A) Single-line diagram. (B) Clarke component networks. jX_e is a reactance external to the generator

Component terminal voltages now can be found in the following way:

1. Define the currents to be circulated in the generator leads and transform them into direct and quadrature axis currents.

Since the quadrature axis is defined to lag the direct axis by 90 degrees, the rotation of positive field flux in the direct axis generates a positive voltage in the quadrature axis, or, $E_q=\omega\Lambda_d=E_t$. It is convenient to choose the quadrature axis voltage as the reference to give $\mathbf{E}_a=E_q+jE_d=E_t+j0$ at no load. Then $\mathbf{I}_a=I_q+jI_d$.

The expressions for instantaneous direct and quadrature axis, and zero sequence currents are[9]

$$i_d=\frac{2}{3}\left[i_a\cos\sigma+i_b\cos\left(\sigma-\frac{2\pi}{3}\right)+i_c\cos\left(\sigma-\frac{4\pi}{3}\right)\right]$$

$$i_q=\frac{2}{3}\left[i_a\sin\sigma+i_b\sin\left(\sigma-\frac{2\pi}{3}\right)+i_c\sin\left(\sigma-\frac{4\pi}{3}\right)\right]$$

$$i_0=\frac{1}{3}[i_a+i_b+i_c] \tag{7}$$

where σ is the electrical angle between the axis of phase a and the direct axis. Then $\sigma=\omega t+\sigma_0$, where σ_0 is the rotor position at $t=0$.

2. Find the flux linkages of the direct, quadrature, and zero windings. There is no field current so that the flux linking each coil is self induced.

Thus

$$\Lambda_d=L_d i_d$$
$$\Lambda_q=L_q i_q$$
$$\Lambda_0=L_0 i_0 \tag{8}$$

L_d, L_q, L_0 are the direct axis, quadrature axis, and zero sequence inductances of the machine found directly from test data.

3. Differentiate and add the flux linkages to find direct axis, quadrature axis, and zero sequence voltages. The equations for these voltages are

$$v_d=\frac{d\Lambda_d}{dt}+\Lambda_q\frac{d\sigma}{dt}$$
$$v_q=\frac{d\Lambda_q}{dt}-\Lambda_d\frac{d\sigma}{dt}$$
$$v_0=\frac{d\Lambda_0}{dt} \tag{9}$$

The armature resistance is neglected as is common practice in short-circuit analysis of synchronous machines.

4. Transform the voltages in equation 9 into phase voltages, and then into Clarke components. It is shown in reference 9 that

$$v_a=v_d\cos\sigma+v_q\sin\sigma+v_0$$
$$v_b=v_d\cos\left(\sigma-\frac{2\pi}{3}\right)+v_q\sin\left(\sigma-\frac{2\pi}{3}\right)+v_0$$
$$v_c=v_d\cos\left(\sigma-\frac{4\pi}{3}\right)+v_q\sin\left(\sigma-\frac{4\pi}{3}\right)+v_0 \tag{10}$$

By substituting these voltage expressions in equation 2, it will be found that

$$v_\alpha=\frac{2}{3}\left\{v_d\left[\cos\sigma-\frac{1}{2}\cos\left(\sigma-\frac{2\pi}{3}\right)-\frac{1}{2}\cos\left(\sigma-\frac{4\pi}{3}\right)\right]+v_q\left[\sin\sigma-\frac{1}{2}\sin\left(\sigma-\frac{2\pi}{3}\right)-\frac{1}{2}\sin\left(\sigma-\frac{4\pi}{3}\right)\right]\right\}=v_d\cos\sigma+v_q\sin\sigma$$

$$v_\beta=\frac{1}{3}\left\{v_d\left[\cos\left(\sigma-\frac{2\pi}{3}\right)-\cos\left(\sigma-\frac{4\pi}{3}\right)\right]+v_q\left[\sin\left(\sigma-\frac{2\pi}{3}\right)-\sin\left(\sigma-\frac{4\pi}{3}\right)\right]\right\}=v_d\sin\sigma-v_q\cos\sigma$$

$$v_0=v_0 \tag{11}$$

It then is necessary to circulate currents in the windings similar to the various types of fault current which might occur and carry out the procedure outlined to find the component terminal voltages. The resulting expressions will be compared with equations 6 to determine the character of the Clarke component impedances.

Clarke Component Impedance Networks

For each type of short circuit which seems to be of major practical importance from the standpoint of network analysis, the nature of the Clarke component impedances will be analyzed and methods of solution for short circuit currents and voltages indicated.

The 3-Phase Fault

To analyze the component impedances for a 3-phase fault, balanced 3-phase currents must be circulated in the machine. Let

$$i_a=\sqrt{2}I\sin(\sigma+\phi)$$
$$i_b=\sqrt{2}I\sin\left(\sigma+\phi-\frac{2\pi}{3}\right)$$
$$i_c=\sqrt{2}I\sin\left(\sigma+\phi-\frac{4\pi}{3}\right) \tag{12}$$

By substituting these currents in equations 7, it is found that

$$i_d=\sqrt{2}I\sin\phi$$
$$i_q=\sqrt{2}I\cos\phi$$
$$i_0=0 \tag{13}$$

Then, from equations 8

$$\Lambda_d=L_d i_d=L_d\sqrt{2}I\sin\phi$$
$$\Lambda_q=L_q i_q=L_q\sqrt{2}I\cos\phi$$
$$\Lambda_0=0 \tag{14}$$

From equations 9, the direct and quadrature axis voltages are

$$v_d=\frac{d\Lambda_d}{dt}+\Lambda_q\frac{d\sigma}{dt}=\omega L_q\sqrt{2}I\cos\phi$$
$$v_q=\frac{d\Lambda_q}{dt}-\Lambda_d\frac{d\sigma}{dt}=-\omega L_d\sqrt{2}I\sin\phi$$
$$v_0=\frac{d\Lambda_0}{dt}=0 \tag{15}$$

since $\sigma=\omega t+\sigma_0$ and, therefore, $d\sigma/dt=\omega=2\pi f$. The quantities ωL_d and ωL_q are the direct and quadrature axis reactances of the machine X_d and X_q.

From equations 11, the voltages in equations 15 may be transformed into Clarke component voltages. Thus

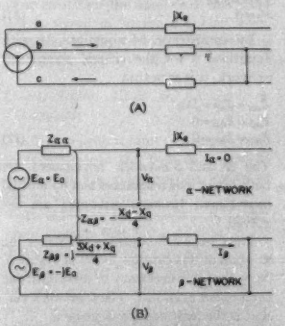

Figure 6. Clarke component networks for the analysis of line-to-line fault on generator terminals

(A) 3-phase circuits. (B) Component networks

$$v_\alpha = X_q\sqrt{2}I\cos\phi\cos\sigma - X_d\sqrt{2}I\sin\phi\sin\sigma$$
$$v_\beta = X_q\sqrt{2}I\cos\phi\sin\sigma + X_d\sqrt{2}I\sin\phi\cos\sigma$$
$$v_0 = 0 \tag{16}$$

In short circuit analysis, it is usually assumed that the fault current lags the driving voltage by $\pi/2$, that is, the impedance between the generated electromotive force and the fault is entirely reactive. Internal electromotive force of the generator may be written $E_a = \sqrt{2}E\sin\sigma$. The fault current in phase a will then be $i_a = \sqrt{2}I\sin(\sigma - \pi/2)$, or, $\phi = -\pi/2$.

Equations 16 become, upon setting ϕ equal to $-\pi/2$

$$v_\alpha = X_d\sqrt{2}I\sin\sigma$$
$$v_\beta = -X_d\sqrt{2}I\cos\sigma$$
$$v_0 = 0 \tag{17}$$

Transforming the assumed currents in equations 12 into Clarke components gives

$$i_\alpha = -\sqrt{2}I\cos\sigma$$
$$i_\beta = -\sqrt{2}I\sin\sigma$$
$$i_0 = 0 \tag{18}$$

again assuming $\phi = -\pi/2$

Substitutions are made from equations 18 into equations 17 to find

$$v_\alpha = -i_\beta X_d$$
$$v_\beta = i_\alpha X_d$$
$$v_0 = 0 \tag{19}$$

or, in phasor form

$$V_\alpha = -I_\beta X_d$$
$$V_\beta = I_\alpha X_d$$
$$V_0 = 0 \tag{20}$$

Equations 20 may be rewritten, using the fact that for balanced 3-phase currents $I_\alpha = jI_\beta = I_a$, to find

$$V_\alpha = jI_\alpha X_d$$
$$V_\beta = jI_\beta X_d$$
$$V_0 = 0 \tag{21}$$

By comparison of equations 21 with equations 6 for the general component network, it is seen that

$$Z_{\alpha\alpha} = Z_{\beta\beta} = jX_d$$
$$Z_{\alpha\beta} = Z_{\beta\alpha} = 0$$
$$Z_{\alpha 0} = Z_{\beta 0} = 0 \tag{22}$$

The α- and β-network impedances are both direct axis reactances and no mutual impedances between networks are involved.

The Clarke component networks for the solution of this case are shown in Figure 5. Note that it is necessary to solve only one component network. The α-network current is the fault current in phase a.

Line-to-Line Fault on Generator Terminals; Line-to-Ground Fault Beyond a Delta-Y Transformer with Grounded Neutral

A line-to-line fault on the generator terminals or a line-to-ground fault behind a delta-Y transformer (with grounded neutral) will cause β-currents in the generator as shown in Figures 6 and 7.

To derive the component impedances, β-currents will be circulated in the machine. Then

$$i_a = 0$$
$$i_b = \sqrt{2}I\sin(\sigma+\phi)$$
$$i_c = -\sqrt{2}I\sin(\sigma+\phi) \tag{23}$$

Transforming these currents into direct and quadrature axis currents by equations 6 gives

$$i_d = \frac{2}{3}\sqrt{2}I\sin(\sigma+\phi)\left[\cos\left(\sigma - \frac{2\pi}{3}\right) - \cos\left(\sigma - \frac{4\pi}{3}\right)\right] = \frac{\sqrt{2}}{\sqrt{3}}I\,[\cos\phi - \cos(2\sigma+\phi)]$$

$$i_q = \frac{2}{3}\sqrt{2}I\sin(\sigma+\phi)\left[\sin\left(\sigma - \frac{2\pi}{3}\right) - \sin\left(\sigma - \frac{4\pi}{3}\right)\right] = \frac{\sqrt{2}}{\sqrt{3}}I\,[\sin\phi + \sin(2\sigma+\phi)]$$

$$i_0 = 0 \tag{24}$$

The flux linkages are found and differentiated as before to find

$$v_d = \frac{2X_d - X_q}{\sqrt{3}}\sqrt{2}I\sin(2\sigma+\phi) - \frac{X_q}{\sqrt{3}}\sqrt{2}I\sin\phi$$

$$v_q = \frac{X_d - 2X_q}{\sqrt{3}}\sqrt{2}I\cos(2\sigma+\phi) - \frac{X_d}{\sqrt{3}}\sqrt{2}I\cos\phi$$

$$v_0 = 0 \tag{25}$$

Converting these to Clarke component voltages by equations 10 gives

$$v_\alpha = \frac{2X_d - X_q}{2\sqrt{3}}\sqrt{2}I[\sin(3\sigma+\phi) + \sin(\sigma+\phi)] - \frac{X_q}{\sqrt{3}}\sqrt{2}I\cos\sigma\sin\phi + \frac{X_d - 2X_q}{2\sqrt{3}}\sqrt{2}I\,[\sin(3\sigma+\phi) - \sin(\sigma+\phi)] - \frac{X_d}{\sqrt{3}}\sqrt{2}I\sin\sigma\cos\phi$$

$$v_\beta = \frac{2X_d - X_q}{2\sqrt{3}}\sqrt{2}I\,[\cos(\sigma+\phi) - \cos(3\sigma+\phi)] - \frac{X_q}{\sqrt{3}}\sqrt{2}I\sin\sigma\sin\phi - \frac{X_d - 2X_q}{2\sqrt{3}}\sqrt{2}I\,[\cos(\sigma+\phi) + \cos(3\sigma+\phi)] + \frac{X_d}{3}\sqrt{2}I\cos\sigma\cos\phi$$

$$v_0 = 0 \tag{26}$$

The driving voltage behind a line-to-line fault is E_{bc} which lags the voltage in phase a by 90 degrees. If it is assumed, as before, that the fault current lags the driving voltage by 90 degrees, the fault current may be written

$$i_b = \sqrt{2}I\sin\left(\sigma - \frac{\pi}{2} - \frac{\pi}{2}\right), \text{ or, } \phi = -\pi$$

Since only the fundamental frequency components in equations 26 are of interest, the third harmonic terms will be dropped.

Equations 26 may be written

$$v_\alpha = \frac{X_d - X_q}{2\sqrt{3}}\sqrt{2}I\sin\sigma$$

$$v_\beta = \frac{3X_d + X_q}{2\sqrt{3}}\sqrt{2}I\cos\sigma$$

$$v_0 = 0 \tag{27}$$

Converting the assumed currents to component form gives

$$i_\alpha = 0$$

$$i_\beta = \frac{2}{\sqrt{3}}i_b = -\frac{2\sqrt{2}}{\sqrt{3}}I\sin\sigma$$

$$i_0 = 0 \tag{28}$$

Eliminating the α- and 0-component current terms, the general equations 6 become

$$V_\alpha = I_\beta Z_{\alpha\beta}$$
$$V_\beta = I_\beta Z_{\beta\beta}$$
$$V_0 = I_\beta Z_{0\beta} \tag{29}$$

By changing equations 27 and 28 to phasor form and substituting them in equations 29, it will be found that

$$\frac{X_d - X_q}{2\sqrt{3}}I = -\frac{2}{\sqrt{3}}IZ_{\alpha\beta}$$

$$-j\frac{3X_d + X_q}{2\sqrt{3}}I = -\frac{2}{\sqrt{3}}IZ_{\beta\beta}$$

$$0 = -\frac{2}{\sqrt{3}}IZ_{0\beta} \tag{30}$$

Thus, it is seen that

$$Z_{\alpha\beta} = -\frac{X_d - X_q}{4}$$

$$Z_{\beta\beta} = j\frac{3X_d + X_q}{4}$$

$$Z_{0\beta} = 0 \tag{31}$$

Figure 6 shows the component network for the analysis of a line-to-line fault on the generator terminals. It is necessary to solve only one network for current distribution since there is no α-current. The voltages induced in the α-network by β-current flow may be easily calculated after an analysis of the β network is completed. The induced voltage will be in phase with the β current since $Z_{\alpha\beta}$ is a resistance.

Figure 7 shows the component network for the analysis of a line-to-ground

short circuit beyond a delta-Y transformer with grounded neutral. The representation of the transformer is discussed in Appendix II.

Line-to-Line Fault beyond a Delta-Y Transformer

A line-to-line fault beyond a delta-Y transformer causes α-currents to flow in the generator as shown in Figure 8. The currents to be circulated to analyze the impedances are written

$$i_a=\sqrt{2}I\sin(\sigma+\phi)$$

$$i_b=i_c=-\frac{\sqrt{2}}{2}I\sin(\sigma+\phi) \tag{32}$$

The direct and quadrature axis currents are found to be

$$i_d=\frac{\sqrt{2}}{2}I\,[\sin\phi+\sin(2\sigma+\phi)]$$

$$i_q=\frac{\sqrt{2}}{2}I\,[\cos\phi-\cos(2\sigma+\phi)]$$

$$i_0=0 \tag{33}$$

The flux linkages of the direct and quadrature axis windings are found and differentiated as before to find

$$v_d=\frac{2X_d-X_q}{2}\sqrt{2}I\cos(2\sigma+\phi)+\frac{X_q}{2}\sqrt{2}I\cos\phi$$

$$v_q=\frac{2X_q-X_d}{2}\sqrt{2}I\sin(2\sigma+\phi)-\frac{X_d}{2}\sqrt{2}I\sin\phi$$

$$v_0=0 \tag{34}$$

By equations 11

$$v_\alpha=\frac{2X_d-X_q}{4}\sqrt{2}I\,[\cos(\sigma+\phi)+\cos(3\sigma+\phi)]+\frac{X_q}{2}\sqrt{2}I\cos\sigma\cos\phi+\frac{2X_q-X_d}{4}\sqrt{2}I\,[\cos(\sigma+\phi)-\cos(3\sigma+\phi)]-\frac{X_d}{2}\sqrt{2}I\sin\sigma\sin\phi$$

$$v_\beta=\frac{2X_d-X_q}{4}\sqrt{2}I\,[\sin(3\sigma+\phi)-\sin(\sigma+\phi)]+\frac{X_q}{2}\sqrt{2}I\cos\phi\sin\sigma-\frac{2X_q-X_d}{4}\sqrt{2}I\,[\sin(\sigma+\phi)-\sin(3\sigma+\phi)]+\frac{X_d}{2}\sqrt{2}I\sin\phi\cos\sigma$$

$$v_0=0 \tag{35}$$

The driving voltage behind such a fault is in phase with the voltage of phase a. If it is assumed that the fault current lags the driving voltage by 90 degrees, the current in phase a may be written

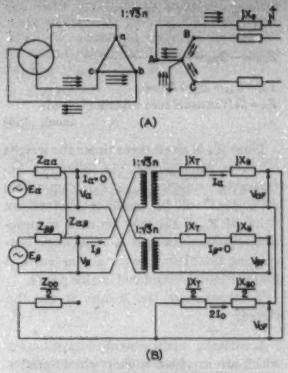

Figure 7. Clarke component networks for the analysis of line-to-ground fault beyond delta-Y transformer with solidly grounded neutral

(A) 3-phase circuit. (B) Component networks. jX_T is the reactance of the transformer, per phase, referred to high-voltage side. The transformer turn ratio per leg is 1:n

$$i_a=\sqrt{2}I\sin\left(\sigma-\frac{\pi}{2}\right)$$

$$\phi=-\frac{\pi}{2}$$

Neglecting the third harmonic components and setting $\phi=-\pi/2$

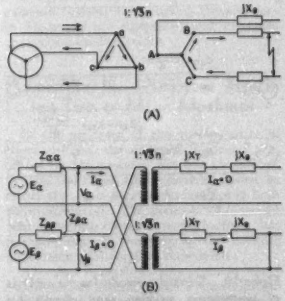

Figure 8. Clarke component network for the analysis of line-to-line fault beyond delta-Y transformer

(A) 3-phase circuit. (B) Component networks

$$v_\alpha=\frac{3X_d+X_q}{4}\sqrt{2}I\sin\sigma$$

$$v_\beta=-\frac{X_d-X_q}{4}\sqrt{2}I\cos\sigma$$

$$v_0=0 \tag{36}$$

The components of the assumed currents are, from equations 2

$$i_\alpha=i_a=\sqrt{2}I\sin\left(\sigma-\frac{\pi}{2}\right)$$

$$i_\beta=0$$

$$i_0=0 \tag{37}$$

Under this condition, the general network equations 6 become

$$V_\alpha=I_\alpha Z_{\alpha\alpha}$$
$$V_\beta=I_\alpha Z_{\beta\alpha}$$
$$V_0=I_\alpha Z_{0\alpha} \tag{38}$$

or

$$Z_{\alpha\alpha}=\frac{V_\alpha}{I_\alpha}$$

$$Z_{\beta\alpha}=\frac{V_\beta}{I_\alpha}$$

$$Z_{0\alpha}=\frac{V_0}{I_\alpha} \tag{39}$$

Converting equations 36 and 37 to phasor form and making a substitution in equations 39, it is found that

$$Z_{\alpha\alpha}=j\frac{3X_d+X_q}{4}$$

$$Z_{\beta\alpha}=\frac{X_d-X_q}{4}$$

$$Z_{0\alpha}=0 \tag{40}$$

Again it is necessary to find current distribution in only one network, the α-network, and then calculate the voltages induced in the β-current. An equivalent circuit for the analysis of this problem is shown in Figure 8. The representation of the delta-Y transformer is discussed in Appendix II.

Line-to-Neutral Fault on the Generator Terminals

A line-to-neutral fault on the generator terminals causes the flow of α- and 0-currents in the generator, as shown in Figure 9.

As indicated in equations 8, α-currents produce flux linkages only in the direct and quadrature axis windings and 0-currents produce flux linkages only in the zero sequence winding. Since there is no interaction between the two components, they may be considered separately.

The α- and β- networks will be the same as in the previous section, and the 0-network will be the usual network.

Thus

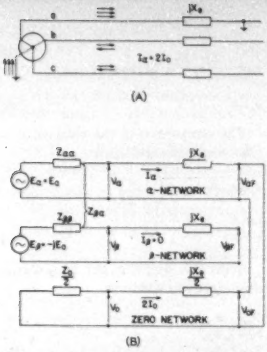

Figure 9. Clarke component networks for the analysis of single line-to-neutral fault at the generator

(A) 3-phase circuit. (B) Component networks

$$Z_{\alpha\alpha}=j\frac{3X_d+X_q}{4}$$
$$Z_{\beta\alpha}=\frac{X_d-X_q}{4}$$
$$Z_{\alpha\beta}=Z_{\gamma\alpha}=0$$
$$Z_{00}=Z_0 \qquad (41)$$

The interconnection of the networks for this analysis is shown in Figure 9.

A 2-line-to-neutral fault on generator terminals will not be considered here since such a fault occurs rarely and does not seem to be of primary importance. If such a fault were to occur on the high-voltage side of a delta-Y transformer, of course, only β-currents would flow in the generator windings.

Conclusions

Upon examination of the results of the preceding development, it may be seen that the Clarke component network representative of a synchronous machine for the purposes of short circuit analysis takes on two forms, one being a simplification of the other.

Figure 10(A) shows the Clarke component network to be used in the analysis of a balanced 3-phase short circuit. The characteristic impedances of this network are

$$Z_{\alpha\alpha}=Z_{\beta\beta}=jX_d$$
$$Z_{\alpha\beta}=Z_{\beta\alpha}=Z_{0\alpha}=Z_{\alpha 0}=0 \qquad (42)$$

Figure 10(B) shows the Clarke component network to be used in the analysis of all other types of short circuits considered here. The characteristic impedances of this network are

$$Z_{\alpha\alpha}=Z_{\beta\beta}=j\frac{3X_d+X_q}{4}$$
$$Z_{\alpha\beta}=-Z_{\beta\alpha}=-\frac{X_d-X_q}{4}$$
$$Z_{0\alpha}=Z_{\alpha 0}=Z_{0\beta}=Z_{\beta 0}=0$$
$$Z_{00}=Z_0 \text{ (the usual zero sequence impedance)} \qquad (43)$$

Since X_d is given three times the weight of X_q in equation 43, the difference between the values for $Z_{\alpha\alpha}=Z_{\beta\beta}$ in equations 42 and 43 will be small so that either value of $Z_{\alpha\alpha}=Z_{\beta\beta}$ may be used in practical applications and a-c network calculating board studies for all the various kinds of faults considered in this paper.

To summarize the results it can be stated:

1. Clarke component impedances which are involved in short circuit analysis do not vary with the type of unbalanced fault. For a 3-phase fault, the appearance of the network seems to change but upon examination it is seen that this is but a simplification of the more general network allowable for this one case.

2. Expressions for all component impedances are relatively simple with the exception of the mutual impedances between the α- and β-networks. It appears that this is a nonreciprocal mutual impedance ($Z_{\alpha\beta}=-Z_{\beta\alpha}$). From the standpoint of short circuit analysis by means of a network calculator, this would appear to be a disadvantage. However, it

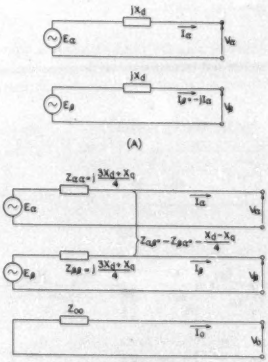

Figure 10. General networks for the analysis of synchronous machine short circuits by means of Clarke components

(A) Network for 3-phase fault analysis. (B) Network analyzing all types of faults, except double-line-to-neutral fault on generator terminals

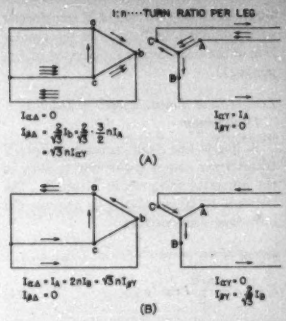

Figure 11. Clarke component current distribution in delta-Y transformer

(A) α-currents on Y side produce β-currents on delta side, and (B) vice versa

is shown in Appendix III that it is permissible to analyze either the α- or the β-network independently and introduce later the effect of the mutual impedance. For instance, suppose the β-network is short circuited as in Figure 13. Current distribution is found in the β-network neglecting the very small effect of $I_\alpha Z_{\beta\alpha}$. Later the voltage induced in the α-network, $I_\beta Z_{\alpha\beta}$, may be calculated and its effect upon the α-network examined.

3. In each case considered, the number of Clarke component networks which must be solved for current distribution is less than, or equal to, the number of component networks which would have to be so solved if symmetrical components were used.

4. From the results of the analysis of component impedances, it would seem that Clarke components do have some physical significance, more so, at least, than the negative sequence reactance.[19]

Appendix I. Terminology

a, b, c, n = designation of the phase and neutral in a 3-phase system

α, β, 0 = designation of Clarke component quantities and networks

I_a, I_b, I_α = phasor currents in subscript conductor

V_a, V_b, V_α, E_a, E_b = phasor voltages on subscript conductor. (The symbol E implies a generated or driving electromotive force)

i_a, i_α, v_a, v_α, e_a = instantaneous currents and voltages

i_d, i_q, e_d, e_q = instantaneous direct and quadrature axis currents and voltages, respectively, of a synchronous machine

Λ_a, Λ_d, and so forth = flux linkages of subscript winding

σ = electrical position of direct axis with respect to the axis of phase a

ϕ = phase angle between fault current and driving voltage

$Z_{\alpha\alpha}$, $Z_{\beta\beta}$, and so forth = self impedance between subscript networks

$Z_{\alpha\beta}$, $Z_{\beta\alpha}$, and so forth = mutual impedance between subscript networks. The first subscript is the network acted upon, thus, $V_1 = I_k Z_{1k} + \ldots$

L_d, L_q, X_d, X_q = direct and quadrature axis inductances and reactances respectively, of a synchronous machine

X_s = a symmetrical 3-phase reactance between generator terminals and fault position

Appendix II. Clarke Component Analysis of a Delta-Y Transformer

The delta-Y transformer has often entered in the preceding discussion and its analysis in terms of Clarke components is included here to complete the picture.

It can be seen from Figure 11(A) that β-currents flow in the leads to the delta-connected windings when α-currents are circulated in the Y-connected windings. It is shown there that the ratio between the component currents in the leads on either side of the transformer is merely the effective turn ratio of the transformer. That is

$$I_{\alpha Y} = I_A,\ I_{\beta Y} = 0$$
$$I_{\alpha\Delta} = 0,\ I_{\beta\Delta} = \sqrt{3}nI_A = \sqrt{3}nI_{\alpha Y} \tag{44}$$

Similarly, Figure 11(B) indicates that β-currents flowing in the Y-connected windings cause the flow of α-currents in the phase wire on the delta side. It is shown that

$$I_{\alpha Y} = 0,\ I_{\beta Y} = \frac{2}{\sqrt{3}} I_B$$
$$I_{\alpha\Delta} = 2nI_B = \sqrt{3}nI_{\beta Y},\ I_{\beta\Delta} = 0 \tag{45}$$

From these relationships, it is evident that the α- and β-networks are cross-connected and coupled by transformers of a turn ratio $\sqrt{3}n$:1 to represent the delta-Y transformer.

The nature of the component transformer impedances may be examined by considering the delta terminals to be short circuited while currents are circulated in the Y side. Then, if α-currents circulate in the Y-connected windings as shown in Figure 11(A)

$$E_A = I_A Z_T$$
$$E_B = E_C = -\frac{1}{2} I_A Z_T \tag{46}$$

where Z_T is the transformer impedance per leg, referred to Y-side voltage.

By changing these voltages and currents to Clarke components

$$E_{\alpha Y} = I_A Z_T$$
$$I_{\alpha Y} = I_A \tag{47}$$

or

$$Z_{\alpha Y} = \frac{E_{\alpha Y}}{I_{\alpha Y}} = Z_T \tag{48}$$

The α-loop impedance of the transformer is positive sequence impedance.

Similarly, from Figure 11(B)

$$E_{\beta Y} = \frac{2}{\sqrt{3}} I_B Z_T$$
$$I_{\beta Y} = \frac{2}{\sqrt{3}} I_B \tag{49}$$

or

$$Z_{\beta Y} = \frac{E_{\beta Y}}{I_{\beta Y}} = Z_T \tag{50}$$

The β-loop impedance also is positive sequence impedance.

The network which satisfied equations 44 and 45 and includes the transformer impedances is shown in Figure 12. The zero network is familiar from symmetrical component analysis.

In this treatment, the terminals of the transformer are not marked in the conventional manner to give a phase shift of 30 degrees between correspondingly marked phases. Rather, they have been marked for convenience in short circuit analysis. For this purpose, the notation of the terminals is of no significance as long as consistency is maintained.

If a per-cent or per-unit method of calculation is used, the coupling transformers in Figure 12 are eliminated and the cross connection made directly.

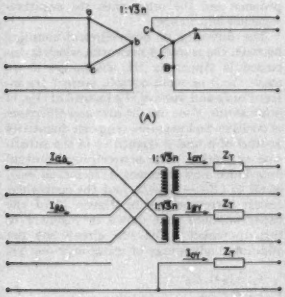

Figure 12. Clarke component network of delta-Y transformer

(A) 3-phase circuit. (B) Component network. Z_T is the transformer reactance per leg referred to the Y side voltage

Appendix III. Analyses Involving Two or More Machines

In the analyses of the various cases of short circuits, the effect of a second generator on the systems was not considered. It was assumed that currents flowed in either the α- or β-networks but not in both simultaneously. The presence of a second source closes both the α- and β-loops so that currents may be induced in the network previously considered to have none.

An exact analysis of this problem would be somewhat difficult since a nonreciprocal mutual impedance, $Z_{\alpha\beta} = -Z_{\beta\alpha}$, becomes involved. Therefore, the examinations of a particular example in order to obtain a conception of relative values and determine what simplifying assumptions may be made will be valuable.

Consider the case shown in Figure 13 of two generators connected by a transmission line which is faulted line-to-line at some point.

Writing circuit equations for the component networks in Figure 13 gives

$$0 = I_\alpha(Z_{\alpha\alpha 1} + Z_{\alpha\alpha 2} + Z_1 + Z_2) + I_{\beta 1} Z_{\alpha\beta 1} - I_{\beta 2} Z_{\alpha\beta 2}$$
$$E_\beta = I_{\beta 1}(Z_{\beta\beta 1} + Z_1) + I_\alpha Z_{\beta\alpha 1}$$
$$E_\beta = I_{\beta 2}(Z_{\beta\beta 2} + Z_2) - I_\alpha Z_{\beta\alpha 2} \tag{51}$$

The first of equations 51 may be rearranged to find

$$I_\alpha = \frac{-I_{\beta 1} Z_{\alpha\beta 1} + I_{\beta 2} Z_{\alpha\beta 2}}{Z_{\alpha\alpha 1} + Z_{\alpha\alpha 2} + Z_1 + Z_2} \tag{52}$$

To make this case most extreme, set Z_1, Z_2, and $Z_{\alpha\beta 1}$ equal to zero. This means that the generators are connected together on one bus and number one is a cylindrical rotor machine. Then equation 52 becomes

$$\frac{I_\alpha}{I_{\beta 1}} = \frac{Z_{\alpha\beta 2}}{Z_{\alpha\alpha 1} + Z_{\alpha\alpha 2}} \tag{53}$$

Values of typical machine reactance may be assumed and the ratio of I_α to $I_{\beta 1}$ evaluated. For example, if

$$X_{d1} = 40 \text{ per cent}$$
$$X_{q1} = 40 \text{ per cent}$$
$$X_{q2} = 70 \text{ per cent} \tag{54}$$

Then

$$\frac{I_\alpha}{I_{\beta 1}} = -j0.086 \tag{55}$$

Introducing this ratio into the third of equations (51)

$$E_\beta = \underbrace{I_{\beta 1} j47.5}_{I_{\beta 1} Z_{\beta\beta}} - \underbrace{I_{\beta 1} j0.65}_{I_\alpha Z_{\alpha\beta}} \tag{56}$$

Thus, it is seen that even in extreme cases the influence of the α-circulating currents on the β-network is very small and may be disregarded. It is only necessary in such cases to find the current distribution in the β-network and then calculate induced voltages and circulating currents in the α-network. A similar examination of the case of α-fault currents would show the same result.

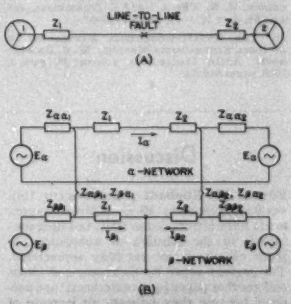

Figure 13. Clarke component networks for a 2-generator system

(A) Single-line diagram. (B) Component networks

References

1. Problems Solved by Modified Symmetrical Components, **Edith Clarke.** *General Electric Review* (Schenectady, N. Y.), volume 41, 1938, pages 488–95 and 545–49.

2. Two-Phase Co-ordinates of a Three-Phase Circuit, **E. W. Kimbark.** *AIEE Transactions*, volume 58, 1939, pages 894–904.

3. Circuit Analysis of A-C Power Systems (book), **Edith Clarke.** John Wiley and Sons, New York, N. Y., volume 1, chapter 10 and references, page 362, 1943.

4. Discussions by **A. Boyajian, W. A. Lewis,** and **E. W. Kimbark** of Two-Phase Co-ordinates of a Three-Phase Circuit, **E. W. Kimbark.** *AIEE Transactions*, volume 59, 1939, pages 904–06 and 909–10.

5. Short Circuit Currents on Grounded Neutral Systems, **W. W. Lewis.** *General Electric Review* (Schenectady, N. Y.), volume 20, 1917, pages 524–27.

6. Two Reaction Theory of Synchronous Machines, Part I, **R. H. Park.** *AIEE Transactions*, volume 48, July 1929, pages 716–27.

7. Two Reaction Theory of Synchronous Machines, Part II, **R. H. Park.** *AIEE Transactions*, volume 52, June 1933, pages 352–54.

8. The Principles of Synchronous Machines, **W. A. Lewis.** *Lecture Notes*, Illinois Institute of Technology (Chicago, Ill.), 1948.

9. Ibid, chapter 9.

10. Single-Phase Short Circuit Calculations, **W. W. Lewis.** *General Electric Review* (Schenectady, N. Y.), volume 28, 1925, page 478.

11. Calculations of Single-Phase Short Circuits, **A. P. Mackestras.** *General Electric Review* (Schenectady, N. Y.), volume 29, 1926, pages 218, 468.

12. Short Circuits in High Voltage Systems (book), **J. Biermanns.** Julius Springer, Berlin, Germany, 1926.

13. Transmission Line Engineering (book), **W. W. Lewis.** McGraw-Hill Book Company, New York, N. Y., 1928.

14. Determination of Voltages and Currents During Unbalanced Faults, **Edith Clarke.** *General Electric Review* (Schenectady, N. Y.), volume 41, 1937, pages 511–13.

15. Symmetrical Component Impedance Notation, **E. W. Kimbark.** *Electrical Engineering*, volume 57, 1938, page 431.

16. Power System Stability (book), **E. W. Kimbark.** John Wiley and Sons, New York, N. Y., volume 1, chapter 6, 1948, pages 245–49.

17. Analysis of Synchronous Machine Short Circuits in Clarke Components, **R. D. Camburn.** *Thesis*, Illinois Institute of Technology (Chicago, Ill.), 1948.

18. Transients in 2-Phase Synchronous Machines, **N. E. Wilson.** *AIEE Transactions*, volume 68, part II, 1949, pages 1360–67.

19. The Negative-Sequence Reactances of an Ideal Synchronous Machine, **W. C. Duesterhoeft.** *AIEE Transactions*, volume 68, part I, 1949, pages 510–14.

Discussion

Edward W. Kimbark (Northwestern University, Evanston, Ill.): Clarke components were introduced in 1938, but their usefulness in the solution of unbalanced 3-phase circuits is not yet fully appreciated. The present paper by Camburn and Gross and another paper by Duesterhoeft[1] are welcome because they indicate an increase of interest in Clarke components. There are still promising opportunities, however, for further work in exploring the application of these components to both steady-state and transient problems, either as substitutes for, or as adjuncts to, Fortescue's symmetrical components and Park's direct- and quadrature-axis components.

Camburn and Gross show that the α and β networks of a synchronous machine are as given in their Figures 6 and 10(B): with electromotive forces, E_α and E_β equal to one another in magnitude and 90 degrees apart in phase, with equal self-impedances

$$Z_{\alpha\alpha} = Z_{\beta\beta} = j(3X_d + X_q)/4 \qquad (1)$$

and with nonreciprocal mutual impedances

$$Z_{\alpha\beta} = -Z_{\beta\alpha} = -(X_d - X_q)/4 \qquad (2)$$

The same results could have been obtained more briefly by starting with equations 2B of my 1939 paper,[2] which (after changing the notation to agree with Miss Clarke's) give the Clarke impedances of a 3-phase rotating machine in terms of the Fortescue impedances as

$$Z_{\alpha\alpha} = Z_{\beta\beta} = (Z_{11} + Z_{22})/2 \qquad (3)$$

$$Z_{\alpha\beta} = -Z_{\beta\alpha} = j(Z_{11} - Z_{22})/2 \qquad (4)$$

Here Z_{11} and Z_{22} are the positive- and negative-sequence self-impedances, respectively. Let us substitute into equations 3 and 4 for the positive-sequence impedance

$$Z_{11} = jX_d \qquad (5)$$

and for the negative-sequence impedance its common value

$$Z_{22} = j(X_d + X_q)/2 \qquad (6)$$

In equations 5 and 6, X_d and X_q have been written instead of x_d'' and x_q'' for the sake of agreement with the notation in the paper under discussion. More will be said about this later. The value of Z_{22} given by equation 6 is correct for sinusoidal negative-sequence current.[1] Upon substituting, we obtain expressions for the Clarke impedances identical with those found by Camburn and Gross (equations 1 and 2 of this discussion).

It seems preferable, however, because of the variation of both Z_{11} and Z_{22}, to leave the expressions for the Clarke impedances of a rotating machine in the form of equations 3 and 4 instead of obtaining equations 1 and 2 by substitution of equations 5 and 6. Consider first the variation of negative-sequence impedance Z_{22}. It is well known that the negative-sequence reactance of a synchronous machine varies with the external circuit conditions, such as the type of short circuit, the highest value of this reactance occurring for sinusoidal negative-sequence current, the lowest value for sinusoidal negative-sequence voltage, and various intermediate values for line-to-ground, line-to-line, and 2-line-to-ground short circuits. Camburn and Gross claim that, by contrast, the Clarke impedances of a synchronous machine are independent of the type of short circuit. I believe, however, that this claim is based on fallacious reasoning. The authors have assumed in their derivations that, during every type of short circuit, the Clarke currents are sinusoidal. In consequence, they have obtained Clarke impedances (equations 1 and 2) which implicitly contain the corresponding value of negative-sequence reactance, equation 6. They should have found the actual wave form of the Clarke currents for each type of fault and then should have taken the fundamental-frequency components of such currents for use in determining the impedances. For example, Duesterhoeft gives the β current during a line-to-line short circuit in his equation 24 and the fundamental component in his equation 25. From this fundamental current and the sinusoidal β electromotive force, we obtain the β self-impedance as

$$Z_{\beta\beta} = j(x_d'' + \sqrt{x_d'' x_q''})/2 \qquad (7)$$

This value is the one that is obtained by substituting into equation 3 of this discussion

$$Z_{11} = jx_d'' \text{ and } Z_{22} = j\sqrt{x_d'' x_q''} \qquad (8)$$

the latter being the value of negative-sequence impedance of a machine during a line-to-line short circuit according to previous papers.

Second, consider the variation of the positive-sequence impedance Z_{11} both with power factor and with time-rate of change of positive-sequence current. As power factor varies, Z_{11} varies between jX_d and jX_q. If we restrict the power factor to zero, as it is very closely during short circuits with negligible external resistance, Z_{11} equals jX_d, as given by equation 5. However, X_d can still vary with the rate of change of positive-sequence current from the subtransient value, written x_d'', through the transient value x_d', to the synchronous value x_d. Regardless of which value of X_d is used for positive-sequence impedance, the X_d and X_q associated with the negative-sequence impedance should always be the subtransient values x_d'' and x_q''. So equations 1 and 2 really combine into one symbol two values of X_d which may very well differ, one being associated with the positive-sequence impedance and the other with the negative-sequence impedance.

The difficulty of nonreciprocal coupling between the α and β networks, which is discussed in Appendix III, disappears if we make the β network contain current jI_β instead of I_β and voltage jV_β instead of V_β, in other words, if we use the sum and difference of positive- and negative-sequence quantities instead of α and β quantities in the substitute networks. The nonreciprocal mutual impedance now becomes a reciprocal one, equal to $(Z_{11} - Z_{22})/2$, and the equivalent circuit corresponding to Figure 13 of the paper becomes that shown in Figure 1 of this discussion. The new circuit has the additional advantage of using only one set

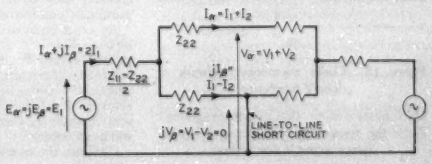

Figure 1. Substitute networks corresponding to Figure 13 of the paper but with reciprocal mutual impedances

of electromotive forces in the two substitute networks. Another example of the use of the sum and difference of positive- and negative-sequence quantities to a problem in rotating machinery connected to an unbalanced circuit is contained in Problem 3 and Figure 1 of my 1939 paper.[2]

REFERENCES

1. See reference 19 of the paper.
2. See reference 2 of the paper.

R. D. Camburn and Eric T. B. Gross: We are indeed grateful to E. W. Kimbark for his discussion, since he emphasizes a few points which may be by-passed by the reader. This is especially true with regard to the values (x_d, x_d' and x_d'', x_q and x_q'') that should be assigned to X_d and X_q, as is mentioned in the paper in the section on Component Network Impedances under Fundamental Relationships.

In our opinion, it is more than a matter of taste whether reference is made to Blondel-Park 2-reaction reactances, or to some kind of derived quantities, as for example, sequence reactances. It appears that Blondel-Park reactances are basic quantities which have real physical meaning. This viewpoint leads to the desire to derive expressions for Clarke reactances directly, and without the detour through symmetrical components.

It now is generally understood (see ASA Standard C 42, 10.35.170)[1] that "the negative sequence reactance is the ratio of the fundamental component of reactive armature voltage, due to the fundamental negative-sequence component of armature current, to this component of armature current at rated frequency." Therefore, it is logical and in line with present day practice[2,3] to follow the procedure outlined in our paper, that is, to assume circulating sinusoidal currents for the derivation of Clarke reactances expressed by Blondel-Park reactances.

The variation of negative sequence reactance values has been discussed in detail by W. A. Lewis,[4,5] and he found five different values for the "negative sequence" reactance for short circuits at the terminals. However, system short circuits, as considered in the paper, involve substantial external impedances which minimize the harmonic effects. Furthermore, since x_d'' and x_q'' are very nearly equal for modern machines with adequate damper circuits, the harmonics will normally be very small in any case. Thus the assumption of sinusoidal currents is usually justified. It is well known, as stated by Kimbark, that the assumption of harmonic currents or sinusoidal voltages will lead to other reactance values,[4] but these are by no means the "true" ones, or of greater significance than the values in his equations 1 and 2. Of course, Kimbark's remarks are a most welcome supplement to our paper.

The modification suggested in the last paragraph of Kimbark's discussion may serve as a beautiful example of simplification through a slight variation of Clarke components.

REFERENCES

1. AMERICAN STANDARD DEFINITIONS OF ELECTRICAL TERMS. *ASA Standards Number C-42*, American Standards Association (New York, N. Y.), section 10.35.170, 1942.
2. THE NEGATIVE SEQUENCE REACTANCES OF AN IDEAL SYNCHRONOUS MACHINE, W. C. Duesterhoeft. *AIEE Transactions*, volume 69, part I, 1949, pages 510–13.
3. Discussion by W. A. Lewis of reference 2, page 514.
4. See reference 8 of the paper, chapters 10 and 11.
5. Discussion by W. A. Lewis of reference 2, page 513.

Power Factor Measurements on Polyphase and Multiconductor Cable Using Single-Phase Bridges

E. W. GREENFIELD
MEMBER AIEE

THE accurate measurement of dielectric losses in modern, low-loss power cable is generally accomplished by means of various types of bridge circuits. Perhaps the most accurate and useful circuit for high-voltage cable testing is the Schering bridge in one form or another. Such bridges are capable of operation at very high voltages depending only upon the voltage limitation of the reference standard capacitor. When provided with suitable shunts, they also can measure a wide range of cable sizes and lengths.

Figure 1 shows a highly developed form of Schering bridge utilized in the author's company for the measurement of power factor and capacitance of high-voltage cable. Using a compressed gas reference capacitor, the bridge is capable of operating up to 150 kv and can handle charging currents from 0.014 to 10 amperes through a system of 13 shunts in the low-voltage arm. Accuracy in power factor (actually the bridge reads directly in dissipation factor) is the larger of 1 per cent of the reading or 10 microradians over the range 0-10 per cent dissipation factor; capacitance accuracy is ±0.5 per cent. The bridge is provided with a balancing guard circuit system substantially at ground potential which eliminates strong pick-up and end influences and permits accurate definition of the electrode system under test.

Limitation of Bridge Circuits in Polyphase Systems

All such bridges are essentially single-phase devices and normally cannot be used with multiphase voltage sources—for example, in a 3-phase system, to determine the 3-phase power factor of a 3-conductor cable. It is quite possible however through proper use of the bridge's guard circuit, to measure the polyphase power factor of any polyphase system using single-phase voltages. It also is possible to determine the mutual phase angles and capacitances between any system of conductors in a multiconductor cable from single-phase measurements properly taken.

It is the purpose of this paper to illustrate how this may be accomplished and to that end, two very important examples will be described. The first of these is the 3-conductor metallic-sheathed belted cable for which it will be shown how a guarded bridge circuit using single-phase voltage may be employed to obtain 3-phase power factor. The second example is the 2-conductor metallic-sheathed nonbelted cable which is used widely in many specialized circuits. Here the objective will be the determination of power factor and capacitance under operating conditions of voltage distribution.

The 3-Conductor Belted Cable

Measurement of 3-Phase Power Factor by Single-Phase Bridge

There is obviously no problem or question with regard to the power factor measurement for 3-conductor shielded cables. There also is no question involved for 3-conductor nonshielded cables providing the measurement is made with 3-phase equipment. A Y-connected 3-wattmeter method will always give total true power absorbed by a Y load and if the load is balanced, a phase power factor can always be determined which applies to the system as a whole. Unfortunately wattmeters cannot be used for measuring power factors of cables since they are far too insensitive. A 3-conductor belted cable has unshielded conductors and application of a single-phase bridge measuring device must take into account the mutual field configuration when connected to its normal voltage source.

When single-phase voltage and measurement are to be used, two important questions arise at once:

1. What values of voltage shall be applied between sheath and conductors as compared with that between conductors?
2. How shall equivalent 3-phase power factor be computed?

Definition of 3-Phase Power Factor

No answer to these questions can be attempted until the term "equivalent 3-phase power factor" is acceptably defined. Three-phase power factor may be defined as follows: "three-phase power factor is that parameter which when multiplied by the line (or phase) current and the phase voltage (in a Y-connected system) will give the true watt power consumed per phase."

This definition is completely adequate so long as the system is balanced as to voltages and loads. For unbalanced systems there is no single parameter that may be defined as 3-phase power factor.

Based on the foregoing, it is thus required that "equivalent 3-phase power factor" be understood to mean that value computed from single-phase measurements which yields 3-phase power factor as defined above. With this interpretation the answers to the questions raised

Paper 50-107, recommended by the AIEE Insulated Conductors and approved by the AIEE Technical Program Committee for presentation at the AIEE North Eastern District Meeting, Providence, R. I., April 26-28, 1950. Manuscript submitted June 22, 1949; made available for printing March 2, 1950.

E. W. Greenfield is Supervisor of the Electrical Laboratory, Anaconda Wire and Cable Company, Hastings-on-Hudson, N. Y.

Figure 1. Commercial form of high-voltage high-current Schering bridge

above are found by simple but rigorous analysis of the belted cable circuit.

Voltage Stresses

When a nonshielded cable (belted) is connected to a 3-phase source (assumed Y-connected) the voltages across its structure are as follows:

1. Between conductors:—line voltage.
2. Conductor to sheath:—phase voltage (line voltage $\div \sqrt{3}$).

Hence the dielectric between conductors is stressed by a factor equal to $\sqrt{3}$ times the potential across the dielectric between any individual conductor and sheath.

Formula for Equivalent 3-Phase Power Factor

Consider a nonshielded (belted) cable connected to a 3-phase balanced wye source. The cable is the load; the energy consumed in the cable is supplied by the source. Energy is consumed in the cable as a result of its dielectric losses which arise from the fact that various portions of its dielectric structure are subjected to electrical stresses.

Figure 2 shows such a nonshielded cable connected to its 3-phase source. For balanced conditions, the total watts

Figure 2. 3-phase belted cable

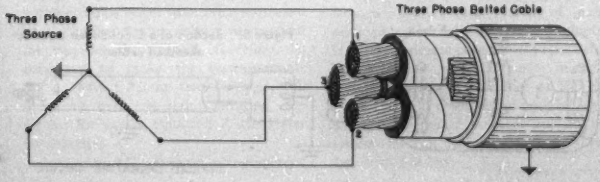

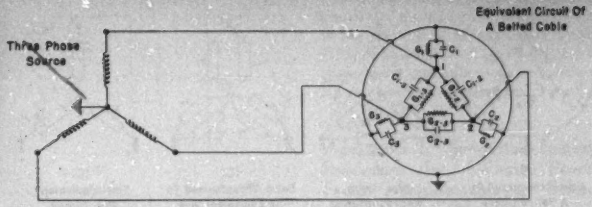

Figure 3. Equivalent circuit of a belted cable

absorbed by the cable load is equal to three times the power consumed per phase. The cable load may be represented schematically as shown in Figure 3. Here the dielectric between conductors and to sheath are represented by appropriate admittances (Y). There are three similar admittances between conductors and three similar admittances to sheath. The cable load is thus seen to be composed of a wye circuit in parallel with a delta circuit, Figure 3. Such a circuit can be treated readily by transposing the delta circuit to an equivalent wye and then adding the resulting paralleled wye circuits together to form a single equivalent wye. The steps are given in detail in Appendix II. The final computation is based on a perfectly symmetrical cable structure.

The single admittance in each phase of the equivalent wye load, Figure 3(D) is made up of conductance (G) and capacitance (C) values for both conductor-to-sheath dielectric and conductor-to-conductor dielectric paths. From these values one readily computes the phase power factor which as defined above is the true 3-phase power factor of the cable. Appendix II shows the computation in detail with the results as follows

$$\text{3-phase power factor} = \frac{3C_{12}DF_{12}+C_1DF_1}{3C_{12}+C_1} \quad (1)$$

where:

C_{12} = capacitance between conductor 1 and 2
DF_{12} = dissipation factor between conductor 1 and 2
C_1 = capacitance between conductor 1 and sheath
DF_1 = dissipation factor between conductor 1 and sheath

For values over 10 per cent, the power factor should be corrected from tan ϕ to cos θ as indicated in Appendix II.

Computation of 3-Phase Power Factor From Single-Phase Measurements

Equation 1 can be used to determine 3-phase power factor when C_{12}, DF_{12}, C_1, and DF_1 are known. These values are measured readily by single-phase voltages and a guarded Schering bridge. Guard circuits are necessary so as to eliminate all but the desired dielectric path from the measurement. It is recalled here that bridges read directly in dissipation factor not in power factor.

The capacitance and dissipation factor between conductors are determined at the stresses corresponding to those specified; namely, 20 and 100 volts per mil.* The single-phase voltages used must be computed on the basis of the total insulation thickness between conductors. The capacitance and dissipation factor from conductor to sheath are determined at single-phase voltages which correspond to phase stresses; namely, the conductor-to-conductor voltages divided by $\sqrt{3}$.

Equation 1 is based on a perfectly symmetrical cable. For actual cable, it may be desired to use the average "between-conductor" value and the average "conductor-to-sheath" value. These values may be obtained by three "between-conductor" measurements and one "conductor-to-sheath" measurements. The "between-conductor" measurements are made from one conductor to a second conductor, placing the third conductor and sheath in the guard circuit. The "conductor-to-sheath" measurement is made from the three paralleled conductors to the sheath. Equation 1 then becomes

$$\text{3-phase power factor} = \frac{(C_{12}+C_{23}+C_{31})(DF_{12}+DF_{23}+DF_{31})+C_s\times DF_s}{3(C_{12}+C_{23}+C_{31})+C_s} \quad (2)$$

*Industry specifications for impregnated paper power cables require that the power factor be determined at two insulation stress levels. These are generally at 100 volts per mil and at 20 volts per mil average stress.

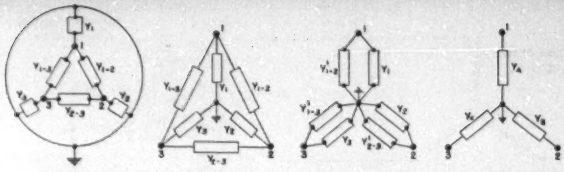

Figure 4. Analysis of electrical circuits of a 3-phase belted cable

where

C_s and DF_s = the measured capacity and dissipation factor between all three conductors in parallel to sheath.

When $(C_{12}+C_{23}+C_{31})=C_s$, equation 2 reduces to

$$\text{3-phase power factor} = (DF_{12}+DF_{23}+DF_{31}+DF_s)/4 \quad (3)$$

Equation 3 indicates simply that the dielectric between conductors and sheath contributes only 25 per cent to the over-all 3-phase power factor.

Suggested Factory Procedure for Single-Phase Tests

It is felt that symmetry of construction and uniformity of materials in present-day cable manufacture preclude the necessity of making four separate measurements as prescribed by the averaging method given by equation 2. Two measurements only are felt to be necessary, namely:

1. Conductor-to-conductor: 1 versus 2 and 3, with sheath to guard.
2. 3 conductors-to-sheath: 1, 2, 3, versus sheath.

These measurements will automatically average 67 per cent of the dielectric paths between conductors, and 100 per cent of those between conductors and sheath.

Appendix I gives in detail the suggested factory procedure for determining 3-phase power factor from single-phase bridge measurements based on the above, also a formula for 60-cycle loss.

The 2-Conductor Sheathed Cable

Measurement of Working Parameters by Single-Phase Bridge

It is often required to measure the power factor and capacitance of a metallic sheathed 2-conductor cable. Such cable when classified for power usage finds wide application in series lighting service and other fields where single-phase power is required with full conductivity "go" and "return." For communication and control the shielded twin must be used for all balanced line services. For power application there may or may not be a belt over the conductor insulations; for communication or control no belt is used.

In almost all uses of this type of cable, the two conductors operate as nearly balanced to ground as possible. Power sources are of the center-tap-grounded variety, so that the voltage between conductors is twice the voltage of either conductor to sheath, which, of course, is solidly grounded.

The determination of power factor and capacitance of such a cable has significance only if evaluated under the same conditions of operation, namely the balanced-to-ground condition. This means it is required to evaluate the input impedance of such a cable looking directly into the two conductors with sheath grounded and voltages properly distributed. The usual Schering bridge is essentially a one-grounded-point network and cannot measure the cable impedance under the balanced condition required. However, by making several measurements it is possible to determine the separate impedances between conductors and between conductors and sheath. These may then be combined to give the power factor and capacitance sought.

Analysis of 2-Conductor Metallic-Sheathed Cable

Figure 5 shows a section of a 2-conductor metallic-sheathed cable. The dielectric paths between components are shown as capacitances shunted by conductances. There are three such admittances and their values combine to give the cable its operating characteristics.

Figure 6 (A) is the equivalent electrical circuit. The admittance seen between terminals 1 and 2 determines the operating power factor of the cable. This admittance is made up of the direct admittance between the two conductors paralleled by the admittance of each conductor to sheath in series. This network is readily reduced to an equivalent conductance in shunt with an equivalent capacitance.

Using the notation given in Figure 6 and assuming $C_a = C_b$ and $DF_a = DF_b$, the equations for operating capacitance and power factor of the cable are

$$C = \frac{C_a+2C_{12}}{2} \quad (4)$$

$$PF = \frac{C_aDF_a+2C_{12}DF_{12}}{C_a+2C_{12}} \quad (5)$$

Appendix IV gives the complete derivation of these equations.

To evaluate the operating capacitance and power factor of the cable, it is necessary to determine C_a, C_{12}, DF_a, and DF_{12} at the electric stresses existing during operation. This means that the measurement between conductor and sheath must be limited to the voltage corresponding to that which would normally exist across this region when the operating voltage is applied between conductors. For the 2-conductor sheathed cable operating balanced-to-ground, the voltage between each conductor and sheath will be one half that between conductors.

Measurement of Power Factor and Capacitance

Using a standard, guarded, high-voltage Schering bridge it is possible to measure the constants required by equations 4 and 5. To measure DF_a and C_a, the two conductors are joined and one half the operating voltage applied between these and the sheath. This will give an average of the dissipa-

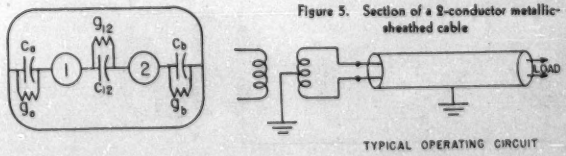

Figure 5. Section of a 2-conductor metallic-sheathed cable

tion factors between conductors and sheath and the sum of each conductor's capacitance to sheath. Dividing the latter by two gives the average capacitance to sheath. This method of measuring to-sheath dissipation factors and capacitances is justified since the cable geometry is symmetrical to better than a few per cent.

C_{12} and DF_{12}, the direct capacitance and dissipation factor between conductors, can be measured by making the cable sheath part of the bridge guard circuit. This measurement is made with full operating voltage between conductors. Since the sheath will, during guard balancing, be brought to the same potential as the low conductor for the duration of the measurement there will be twice normal voltage across the conductor-to-sheath insulation.

In certain bridge systems it will be found impossible to make the between-conductor measurements using the guard circuit as described before. In this case it will be necessary to measure between one high conductor and the second conductor connected to sheath. A second measurement may be made with the conductors reversed and the two sets of results averaged. The capacitance and dissipation factors so obtained, C_e and DF_e are made up of the impedance between conductors, in parallel with the impedance from the high conductor to sheath. Knowing the impedance between conductor and sheath from the first measurement (C_a and DF_a) it then is possible to compute C_{12} and DF_{12} as follows

$$C_{12} = C_e - C_a \tag{6}$$

$$DF_{12} = \frac{C_e DF_e - C_a DF_a}{C_e - C_a} \tag{7}$$

These are then substituted in equations 4 and 5 as previously. A note of caution must be entered here regarding equation 7. Since the values of C_e and DF_e are determined with the same voltage between conductors as between conductors and sheath, it is required that the C_a and DF_a to be used in equation 7 be those for that voltage. Capacitance has negligible change with voltage; the dissipation factor, DF_a, however, may change with voltage and be larger than when measured at one half operating voltage as required for equation 5. It will, therefore, be necessary to make the measurements for C_a and DF_a, at two voltages, full operating and one half operating, the former for use in equation 7, the latter for equation 5.

Appendix III gives a recommended

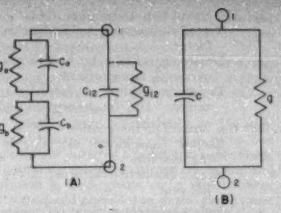

Figure 6. Equivalent electrical circuits of a 2-conductor metallic-sheathed cable

factory test procedure based on the above analysis. Data for an actual, full reel length cable are included as an example of the method and the computations.

If it is desired to measure the true power factor of the cable at a high stress, for example 100 volts per mil, with the Schering bridge, it must be remembered that during the period of measurement the insulation between conductors and sheath will be subjected to 200 volts per mil when no belt insulation is present. This is generally not good practice and should be avoided.

Field Configuration

It may be asked purposefully how the field configurations in the cable differ when single-phase voltages are used for example, in place of 3-phase sources and how such differences might affect power factor values.

An anisotropic media such as a belted impregnated paper-insulated cable which also is subject to local ionizing regions might be expected to show losses which are more dependent on the electric field configuration than on over-all potential differences.

A qualitative analysis of single-phase fields versus 3-phase fields indicates that the space distributions between conductors and conductors and sheath are not essentially different. The time-phase differences in a 3-phase source system bring the individual conductors to maximum potential differences at 1/6th of a cycle intervals. However, in any one cycle all conductors each have one positive and one negative maximum potential difference. During each instant of maximum potential difference, one conductor is at its maximum potential and the other two are at a lower (opposite in sign) but equal potential. Hence at this instant the field configuration is the same as for single-phase voltages applied between one high conductor and the other two joined as low.

Since the space shape of the fields is similar and the net ionizing time per cycle is the same, it is expected that power factor values obtained by means of the single-phase methods described before are valid for 3-phase operation.

Appendix I. Suggested Factory Procedure for 3-Phase Power Factor Measurements on Belted Cable*

1. Measure conductor 1 versus 2 and 3 with sheath on guard circuit. Use 20 and 100 volts per mil (vpm) calculated from two times the insulation thickness on conductor. Call these voltages $E_{20\ \mathrm{vpm}}$ and $E_{100\ \mathrm{vpm}}$.

(a). Record capacitance, C_g.
(b). Record dissipation factor, DF_g.

2. Measure three conductors to sheath. Use E_{20} vpm/$\sqrt{3}$ and E_{100} vpm/$\sqrt{3}$ for the two voltages.

(a). Record capacitance, C_s.
(b). Record dissipation factor, DF_s.

3. Calculate true 3-phase power factor from

$$PF = \frac{9C_e DF_e + 2C_s DF_s}{9C_e + 2C_s} \tag{8}$$

4. Calculate total 3-phase loss at 60 cycles per second from

$$\text{Watts} = 0.628 \times KV^2 \times PF(9C_e + 2C_s) \tag{9}$$

Where KV = line-to-line voltage in kilovolts, C_e and C_s are expressed in microfarads, and PF = 3-phase power factor from equation 8, expressed in per cent.

Bridge measurements actually give dissipation factors rather than power factors; that is, tan ϕ rather than cos θ. Below 10 per cent, the two have negligible differences. Above 10 per cent, the tan ϕ readings should be corrected to power factor (cos θ). In equation 8 bridge readings, regardless of value, are substituted into the equation. If the resulting solution is greater than 10 per cent it should be corrected from tan ϕ to cos θ.

Appendix II. Derivation of Equivalent 3-Phase Power Factor of a 3-Phase Belted Cable

The cable dielectric is represented by equivalent admittances; that is, conductances in parallel with capacitances. The admittances of the equivalent circuit for a 3-phase belted cable shown in Figure 4(A) are as follows:

CONDUCTOR-TO-CONDUCTOR:

Conductor 1 to 2: $G_{12} + jwC_{12} = Y_{12}$
Conductor 2 to 3: $G_{23} + jwC_{23} = Y_{23}$
Conductor 1 to 3: $G_{13} + jwC_{13} = Y_{13}$

*Based on balanced voltages and load; no harmonics in neutral; Y-connected source.

CONDUCTOR-TO-SHEATH:

Conductor 1 to sheath: $G_1+jwC_1=Y_1$
Conductor 2 to sheath: $G_2+jwC_2=Y_2$
Conductor 3 to sheath: $G_3+jwC_3=Y_3$

Figure 4(B) indicates how the conductor-to-conductor dielectric forms a delta circuit which is in parallel with the wye made up of conductor-to-sheath dielectrics. In Figure 4(C), the delta circuit is transformed to its equivalent wye. The transformation gives

$$Y_{12}'=Y_{12}Y_{13}\left(\frac{1}{Y_{11}}+\frac{1}{Y_{21}}+\frac{1}{Y_{12}}\right)$$

$$Y_{23}'=Y_{23}Y_{13}\left(\frac{1}{Y_{11}}+\frac{1}{Y_{22}}+\frac{1}{Y_{13}}\right)$$

$$Y_{13}'=Y_{13}Y_{23}\left(\frac{1}{Y_{12}}+\frac{1}{Y_{23}}+\frac{1}{Y_{13}}\right)$$

For a symmetrical load (as is the case)

$$Y_{12}=Y_{23}=Y_{13}$$

also

$$Y_1=Y_2=Y_3$$

and the above equations simplify as follows

$$Y_{12}'(=Y_{23}'=Y_{13}')=3Y_{12}(=3Y_{23}=3Y_{13})$$

Figure 4(C) thus shows the equivalent belted cable circuit made up of two wye circuits in parallel which are readily combined to give the single wye circuit shown in Figure 4(D). Here the phase admittances are assumed all equal and are given by

$$\begin{aligned}Y_A(=Y_B=Y_C)&=3Y_{12}+Y_1\\&=3(G_{12}+jwC_{12})+(G_1+jwC_1)\\&=(3G_{12}+G_1)+jw(3C_{12}+C_1)\end{aligned} \quad (10)$$

but

Dissipation factor:—$\tan\phi=\dfrac{G}{wC}$

Substituting dissipation factors for conductances in equation 10, we get

$$Y_A=w[(3C_{12}\tan\phi_{12}+C_1\tan\phi_1)+j(3C_{12}+C_1)] \quad (11)$$

from which

$\tan\phi_A$ (3-phase dissipation factor)

$$=\frac{3C_{12}\tan\phi_{12}+C_1\tan\phi_1}{3C_{12}+C_1} \quad (12)$$

For dissipation factors less than 10 per cent

3-phase power factor:—PF_A

$$=\frac{3C_{12}DF_{12}+C_1DF_1}{3C_{12}+C_1} \quad (13)$$

Appendix III. Recommended Factory Test Procedure for Measuring Capacitance and Power Factor of 2-Conductor Metallic Shielded Cable Using a Schering Bridge

1. Refer to Table I for circuit connections and voltages.

2. Use connection designation AA:
   Record capacitance and dissipation factor.
   Divide capacitance by two to obtain: C_a in microfarads.
   Designate dissipation factor obtained: DF_a (in per cent).

3. Use connection designation C_{12}:
   Record capacitance as: C_{12} in microfarads.
   Record dissipation factor as: DF_{12}, per cent.

4. Calculate cable capacitance and power factor from

$$C=\frac{C_a+2C_{12}}{2}\text{ mfd} \quad (14)$$

$$PF=\frac{(C_aDF_a+2C_{12}DF_{12})}{C_a+2C_{12})}\text{ per cent} \quad (15)$$

5. Where the type of bridge guard employed does not permit balancing of the C_{12} circuit, use:

6. Connection designation AA':
   Record capacitance and dissipation factor.
   Divide capacitance by two to obtain: C_a', microfarads.
   Designate dissipation factor as: FD_a', per cent.

7. Use designations CA and CB:
   Record capacitances and dissipation factors.
   Designate these as: C_{ca}, C_{cb}, DF_{ca}, and DF_{cb}.
   Average C_{ca} and C_{cb} to obtain: C_c, microfarads.
   Average DF_{ca} and DF_{cb} to obtain: DF_c, per cent.

8. Calculate C_{12} and DF_{12} from

$$C_{12}=C_c-C_a'\text{ mfd} \quad (16)$$

$$DF_{12}=\frac{C_cDF_c-C_a'DF_a'}{C_c-C_a'}\text{ per cent} \quad (17)$$

9. Having C_{12} and DF_{12}, substitute these in equations 14 and 15 to obtain the desired capacitance and power factor.

EXAMPLE:

Factory order, 2-conductor, flat, number 6, American wire gauge, solid, 14/64-inch paper, 7/64-inch lead. Length 2,013 feet. Tested September 20, 1945 by the Cable Test Department of the Anaconda Wire and Cable Company.

Using circuit AA:

$C_a=1/2\times0.2032=0.1016$ microfarad
$DF_a=0.413$ per cent

Using circuit C_{12}:

$C_{12}=0.0068$ microfarad
$DF_{12}=0.66$ per cent

Using equation 14

$$C=\frac{C_a+2C_{12}}{2}=\frac{0.1016+2\times0.0068}{2}=$$

0.0576 microfarad

Using equation 11

$$\text{Power factor}=PF=\frac{C_aDF_a+2C_{12}DF_{12}}{C_a=2C_{12}}=$$

$$\frac{0.1016\times0.413+2\times0.0068\times0.66}{0.1016+2\times0.0068}=$$

0.445 per cent

Should the bridge not balance with the C_{12}

Table I. Test Circuits for the Measurement of Capacitance and Power Factor of 2-Conductor Metallic-Sheathed Cable

Connection Designation	Voltage High to Low	Capacitance and Dissipation Factor Readings	Test Circuit
AA	1/2 operating	$2C_a$ DF_a	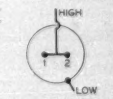
C_{12}	operating	C_{12} DF_{12}	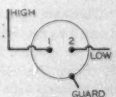
AA'	operating	$2C_a'$ DF_a'	
CA	operating	C_{ca} DF_{ca}	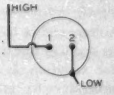
CB	operating	C_{cb} DF_{cb}	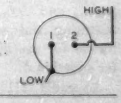

circuit, then use circuits AA', CA, and CB.

Using circuit AA'

$2C_a' = 0.2032$ microfarad
$DF_a' = 0.6695$ per cent

Using circuit CB

$C_{cb} = 0.1084$ microfarad
$DF_{cb} = 0.666$ per cent

Using circuit CA

$C_{ca} = 0.1084$ microfarad
$DF_{ca} = 0.672$ per cent

Average the results of circuits CA and CB

$C_c = 0.1084$ microfarad
$DF_c = 0.669$ per cent

Now use equation 16

$$C_{12} = C_c - C_a' = 0.1084 - 0.1016 = 0.0068 \text{ microfarad}$$

And equation 17

$$DF_{12} = \frac{C_c DF_c - C_a' DF_a'}{C_c - C_a'} = \frac{0.1084 \times 0.669 - 0.1016 \times 0.6695}{0.1084 - 0.1016} = 0.662 \text{ per cent}$$

Having C_{12} and DF_{12} use equations 14 and 15 as previously. The two methods are found to agree within better than 1 per cent.

Appendix IV. Derivation of Equivalent Circuit of a 2-Conductor Metallic-Sheathed Cable

Figure 5 shows the cable section with its component interadmittances. Equivalent electric circuit is shown in Figure 6(A).

Assuming perfect cable symmetry, $C_a = C_b$; $g_a = g_b$.

Figure 6(A) then readily reduces to 6(B)

$$g = \frac{g_a}{2} + g_{12}$$

$$C = \frac{C_a}{2} + C_{12}$$

$$\tan\phi = \frac{g}{wC} = \frac{g_a + 2g_{12}}{w(C_a + 2C_{12})} = \frac{C_a \tan\phi_a + 2C_{12}\tan\phi_1}{C_a + 2C_{12}} \quad (18)$$

Since $\tan\phi = PF$ for values under 0.10 and using the designation, DF, for $\tan\phi$, we have

$$PF = \frac{C_a DF_a + 2C_{12} DF_{12}}{C_a + 2C_{12}} \quad (19)$$

Discussion

Wm. A. Del Mar (Phelps Dodge Copper Products Corp., Yonkers, N. Y.): One cannot help wondering why Mr. Greenfield is resurrecting that relic of bygone days, the belted cable and reviving, as something new, the single-phase method of testing it, which was abandoned long before the belted cable itself passed into oblivion.

The single-phase method gives low power factors, as compared with the 3-phase method because it neglects losses due to tangential stresses.

Another error is introduced by the artificial voltage relations, because when one conductor is tested against two conductors, the voltage between the one conductor and ground is much greater than that between the pair and ground due to the capacitance effect.

Tests were made on a 15 foot length of belted cable (12/64 by 6/64) by setting a spark-gap between conductor and sheath and noting the voltage applied between conductors when the spark-gap flashed. It was found that when one conductor was connected to the high-tension terminal of the transformers, the voltage between sheath and the one conductor was twice that between sheath and the two conductors.

When the single conductor was grounded and the pair connected to the transformer, the voltage relation became 61 to 39 instead of 2 to 1.

W. B. Kouwenhoven (The Johns Hopkins University, Baltimore, Md.): Dr. Greenfield has presented a clear analysis of the 3-phase power cable loss problem, and has provided a tool for the determination of the 3-phase loss by single-phase measurement technique.

I would like to know if there is much difference in the results when the measurements are taken between conductor 1 and conductor 2–3, between 2 and 1–3, and between 3 and 2–1.

I also would like to know if any measurements have been made that will give the magnitude of the loss in the insulation which is caused by the rotating electrostatic field set up by the 3-phase voltages.

E. W. Greenfield: Mr. Del Mar is apparently under the impression that I have "resurrected that relic of bygone days, the belted cable . . .". Mr. Del Mar, being in the cable manufacturing business, should well know that the belted cable has not "passed into oblivion." There are many miles of belted cable in various moderate voltage operating systems with long-time successful records. Occasional replacements and system expansion have always and do now provide a sizeable proportion of paper cable orders.

Mr. Del Mar also accuses me of "reviving" as something new, "the 1-phase method of testing belted cables" which, he goes on to say "was abandoned long before the belted cable itself passed into oblivion." Obviously if belted cables are being manufactured today, they must be tested. The current edition of the Association of Edison Illuminating Companies' specifications as did its predecessors, provides that power factor measurements shall be made on belted cable having ratings of 8 kv or above. Either 3-phase or 1-phase methods are permitted but no details of the test method are given.

Older methods of testing belted 3-conductor cable generally involved a 3-phase scheme using a compensated wattmeter. With the advent of the Schering bridge (and others) as used first in Europe and then in this country, it was found at last, that precision phase-angle measurements were possible. In consequence the old 3-phase wattmeter methods were abandoned therefore in favor of the more accurate bridge method. Few cable manufacturers or users employ the 3-phase wattmetric method today since excellence of modern materials and assembly almost make a shielded bridge mandatory. The contribution of my paper is that it sets down, for the record, the measuring methods and formulations whereby 1-phase measurements can be converted to 3-phase measurements.

I do not know of any previously published similar material.

Mr. Del Mar states that the 1-phase method neglects losses due to tangential stresses and therefore gives values of power factor lower than that obtained by the 3-phase method. This statement does not appear to be valid since the electric field between high and low conductors in the 1-phase case meet the cable structure at angles which are the same as in the 3-phase case.

This also is true of the high conductors to the sheath.

The tests using sphere gaps, of which Mr. Del Mar speaks, appear to have to do with a "floating" conductor cable. This has little or no revelancy to the problem at hand. In the 1-phase method both the low conductors and the sheath are always at or practically at ground potential. To summarize, the 1-phase method, by selecting proper voltages and bridge connections, can employ the principle of superposition to add up the losses in the variously stressed portions of the cable structure and give a net result practically equivalent to that obtaining in a 3-phase system.

Prof. Kouwenhoven asks what differences in power factor are found when measuring between the various conductors of a modern 3-conductor belted cable. The maximum difference I can find in a survey of belted cable tests extending back for several years is about 10 per cent. In most cases the differences appear to be between 2 and 6 per cent, with a possible average of 5 per cent.

A typical belted cable tested at room temperature and operating voltage has values as follows: conductor 1 versus 2 and 3; 0.7 per cent, conductor 2 versus 1 and 3; 0.72 per cent, and conductor 3 versus 1 and 2; 0.69 per cent.

With regard to the 3-phase field in such a cable, this much can be said: With 3-phase voltage applied, each conductor attains one positive maximum, and one negative maximum potential with respect to the sheath per cycle. Therefore in any one cycle the insulation between each conductor and sheath is under maximum stress twice per cycle. Also, each conductor attains two maximum differences of potential with respect to the other conductors per cycle, making a total of six maximum differences of potential between conductors per cycle. Hence the three insulation paths between conductors are each under maximum stress twice per cycle. Further, during the instant of maximum potential difference between conductors, two of them are at exactly the same voltage with respect to sheath. In the 1-phase methods described, the insulation

paths between conductors and sheath are each stressed to the same maximum value twice per cycle as is the insulation paths between conductors. Therefore, as far as maximum ionizing stresses are concerned, the 1-phase test method duplicates conditions under 3-phase operation.

The net ionizing time per cycle also is important in assessing dielectric losses. This may be loosely defined as the product of stress and time per cycle for a given pair of conductors. When the 3-phase case and the 1-phase method are analyzed on this basis the net ionizing time for both turns out to be the same.

A New High-Accuracy Counter-Type Tachometer

T. M. BERRY
ASSOCIATE AIEE

C. L. BEATTIE
NONMEMBER AIEE

Synopsis: Recent advancements in highly efficient power machinery have created demands for super accurate speed measurements. Developments in magnetic recording and high-speed electronic counters have made extremely accurate speed measurements possible. A tachometer, accurate to better than ±0.03 per cent, is described in this paper.

ALTHOUGH rotational speed measurements have been made for many years, it has not been until recently that accuracies within 1 per cent and better have been required. The 1 per cent point is approximately the ultimate accuracy for simple tachometers and is, therefore, the point where special means must be employed for higher accuracies. Simple tachometers employ such principles as the magnetic drag cup as is used in automobile speedometers, the liquid column supported by a rotary pump, and the flashing light on a rotating disk with alternate black and white sections.

This tachometer consists of three units. A pulse generator, Figure 3, is driven by the rotating machine and feeds into the electronic counting unit. The counting unit controls the remote indicator, Figure 1. When photographed, the speed indication was 15,081 rpm as shown in direct numerical form. The indicator can be read from distances up to 30 feet.

The special means used in this precision tachometer is the counting of electrical pulses from a special high-frequency generator for a precise period of time. The generator frequency and counting period are arranged so that the total count is equal to the speed in revolutions per minute. The total count is used to control the illumination of the proper number stencils whose images are presented on an opal glass screen. Although the accuracy of this tachometer is within 0.03 per cent, it can be modified so that its accuracy is much greater. A feature of the tachometer which actually limits its accuracy is that it averages the speed over a period of time instead of giving an instantaneous value.

The system does not count partial pulse periods from the generator and these pulses are not synchronized with the counting period. Because of this, a complete pulse may be included in the counting period when only part of the corresponding pulse period was included. This action occurs when the counting period starts immediately before a pulse occurs and closes immediately after the last pulse occurs. In this way, it is possible for one too many pulses to be counted. Similarly, if the counting period starts just after a pulse occurs and ends just before a pulse occurs, one too few pulses would be counted. This variation of one pulse corresponds to a variation of 0.1 rpm in speed indication for speeds up to 4,000 rpm and a variation of 1.0 rpm for speeds between 4,000 and the designed speed of 15,000 rpm. The timing element is a precision tuning fork accurate to 0.002 per cent.

Besides being inherently accurate, the system is such that frequent calibration is not necessary, and the human element is essentially eliminated because the operator has only to read or copy the indicated number instead of interpolating between divisions of a calibrated scale. Furthermore, an electric typewriter unit or other printer may be coupled to the system which will record the speed automatically.

Applications and proposed applications of the counter-type tachometer will illustrate the need for high accuracy speed measurements. In steam and gas turbine design and development, accurate speed measurement is of primary importance in the determination of efficiency. It has been found that, in testing duplicate designs over a period of time, there occurs a standard deviation in efficiency which is attributed to deviations in test equipment and the human element in taking readings. These turbines are highly developed, and often the expected improvement in efficiency, as a result of a design change, is about equal to this standard deviation. To detect changes in efficiency of 1 per cent or less, all test equipment should be accurate to 0.1 per cent or better.

A second application requiring extreme accuracy is the development testing of refrigerator compressor motors. The requirements are for an instrument which requires no calibration or zero setting, has no operator errors, and is accurate to within 2 rpm at 1,800 rpm and below, and to within 0.1 per cent of reading at speeds above 1,800 rpm. Hermetic refrigerator motors operate at such levels of efficiency that the per-cent error in motor losses is about double the per-cent error in the speed reading.

A third application for this type of tachometer is in the testing of governors for paper and textile mills where accuracies of speed control within 0.01 per cent may be required.

Operation

The operation of the unit may be described with the aid of Figure 2. At the beginning of each one second counting cycle a control voltage from the timing counter opens the electronic gate. Pulses flow from the pickup through the shaper and gate to the pulse counter where they are counted electronically. After 0.8

Paper 50-109, recommended by the AIEE Instruments and Measurements Committee and approved by the AIEE Technical Program Committee for presentation at the AIEE North Eastern District Meeting, Providence, R. I., April 26–28, 1950. Manuscript submitted November 10, 1949; made available for printing February 27, 1950.

T. M. Berry and C. L. Beattie are both with the General Electric Company, Schenectady, N. Y.

Figure 1 (left). Remote indicator of tachometer in use

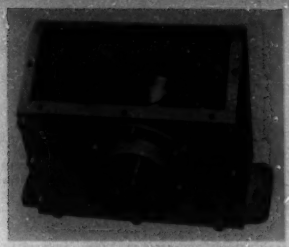

Figure 3 (right). Pulse generator cover removed

second has elapsed, the timing counter closes the gate and operates the reset relay through the power tube. The reset relay is energized for 0.1 second during which time the relay unit is released from its previous count and allowed to make any changes detected by the counter-position senser. When the reset relay is de-energized, it locks the relay unit and operates the counter resetter which resets the pulse counter to zero. The relay unit transforms the total count of the pulse counter to a speed indication by connecting power to the proper indicator lamps which illuminate number stencils. The above completes one cycle. At the 1-second point, the gate opens again and another cycle begins. The indicator indication remains fixed during each counting period. The variations of the control voltages from the timing counter for a 1.0-second cycle are shown by the square waves on Figure 2.

Pulse-Generator

Any form of pulse generator may be used which can develop an exact number of pulses per revolution. A photoelectric type was considered but the permanent magnet a-c generator was chosen for its simplicity and ruggedness. A photoelectric type would be used if no torque were available from the machine whose speed is to be measured. The rotor of the generator, as shown in Figure 3, consists of an aluminum alloy disk with magnetic wire wound on its periphery. With the rotor turning in its own bearings, the wire was ground smooth. Two stationary magnetic pickups are mounted above individual tracks of the magnetic surface.

To accommodate the speed range, maintain the required accuracy of 0.05 per cent, and keep the signal frequency within practical limits, it was necessary to divide the speed range into two sections; 400 rpm to 4,000 rpm, and 4,000 rpm to 15,000 rpm. At 400 rpm, the accuracy required is 0.2 rpm. Therefore, it was necessary to indicate speed to tenths of a revolution per minute. At 4,000 rpm, the required accuracy is down to 2 rpm, and the pickup signal frequency has reached 50 kc; so another track was made on the generator rotor with one-tenth the number of poles. The switch-over is automatic as will be described later. The number of poles in the track for the upper speed range is such that the total number of pulses counted for 0.8 second will be equal to the speed in revolutions per minute. At 4,000 rpm on the upper range, 5,000 cycles per second are generated. This signal is counted for 0.8 second so 4,000 pulses are counted. Seventy-five cycles per revolution of the rotor produces this result. On the low range, 750 cycles per revolution are used so 50,000 cycles per second are generated at 4,000 rpm. In 0.8 second, 40,000 pulses are counted with the last digit representing tenths of a revolution per minute.

The system shown schematically in Figure 4 was used to magnetize the drum. The system output is a current in the record head whose value varies sinusoidally with respect to zero as the selsyn rotor, *R-A* and *R-B*, is rotated. One cycle of current variation in the record head occurs for each revolution of the selsyn rotor. Assume *R-A* and *R-B* to be a center tapped rotor winding of the selsyn and *S* to be a stator winding whose induced voltage is equal to the voltage across half the rotor. The voltage across the rotor will remain constant but the stator voltage varies with the rotor position and reverses 180 degrees relative to the supply voltage as it goes through zero. If the rotor is rotated so that the stator voltage is maximum and points "1" of *R-A* and "2" of *S* are both positive at the same time, a maximum rectified current will flow through rectifier *D-1* and half of the recording head. No current flows through *D-2* because the voltage in *R-B* and *S* are equal and opposite.

As the rotor is turned, the stator voltage decreases to zero at 90 degrees movement and current *Y* due to voltage in *R-B* through *D-2* increases to equal current *X* which has decreased to half its initial value at zero degrees. Since currents *X* and *Y* are equal and opposite, the resultant flux in the head is zero. As the rotor is turned further to 180 degrees the voltage in *S* reverses and begins to aid the voltage in *R-B* and oppose the voltage in *R-A*. This increases current *Y* and decreases current *X* to zero. At 270 degrees, the currents are again equal due to zero voltage in *S*. At 360 degrees the initial condition is reached which completes one sinusoidal cycle of flux in the recording head for one revolution of the selsyn rotor. The capacitors and choke produce the desired filtering. The selsyn rotor and the pickup drum are coupled together through worm gearing of the proper ratio. The whole unit is driven by an electric motor.

Figure 2. Block diagram of complete system

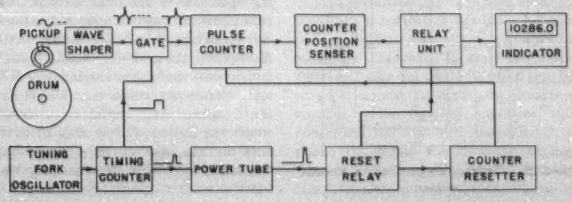

Timer Unit

The purpose of the timer unit is to produce accurately timed voltages to control the remainder of the system. The basic timing element is a precision tuning

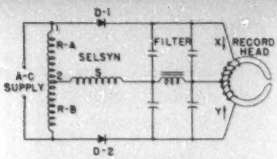

Figure 4. Circuit for magnetizing pulse generator drum

fork which operates at 1,000 cycles per second. This fork controls the frequency of an oscillator whose output drives three electronic binary decade counters through a square wave and differentiating circuit. Each decade unit divides the frequency by 10. Therefore, the output of the third decade unit is one cycle per second. Voltages which occur at the 0.8 second, 0.9 second, and 1.0 second points in the third decade unit are used to control other units of the system.

The decade circuit used may be described with the aid of Figure 5. Each of the binary sections is as shown in Figure 7. The cross connections between the anodes and grids of the triodes produces an effect similar to a lever pivoted at its middle and below its center of gravity with the ends represented by the anodes. In other words, when the potential of the anode of *V1* is high, the potential of the anode of *V2* must be low and vice versa with no stable point in between. As negative pulses are applied at the input, they trigger the section so that the anode voltage of *V1* alternately goes up and down while the anode voltage of *V2* goes down and up. One pulse causes the section to flip one way and the next pulse flips it back. Each time the anode voltage of *V2* decreases, it delivers a negative pulse at the output which triggers the next section. Since two input pulses causes one complete cycle of the circuit operation and one output pulse is produced, the section divides the input frequency by two.

Four of these sections connected as shown in the outline diagram, Figure 5, constitute a decade counter. The four sections are connected in series by capacitors *A*, *B*, and *C*. Each section is designated by the corresponding number in the binary sequence: 1, 2, 4, and 8. The first pulse applied to section 1 turns its neon lamp on. The second pulse turns section 1 off which applies a pulse through capacitor *A* to section 2 which turns 2 on. This pulse is obtained from the sudden decrease in plate voltage of *V1* (see Figure 7) as transmitted through capacitor *C1*. A third pulse turns 1 on again indicating a total count of two plus one or three. A fourth pulse turns 1 off which turns 2 off which turns 4 on. The fifth pulse turns 1 on. The sixth turns 1 off and 2 on. The seventh turns 1 on and the eighth turns 1, 2, and 4 off and 8 on. The ninth pulse turns 1 on. The tenth pulse turns 1 off which passes a pulse through capacitor *D* to 8, which turns 8 off. In going off, 8 passes a pulse back to 2 through capacitor *E* which keeps 2 from coming on so no sections are on. When 8 went off it passed a pulse to the input of the next decade which turned on its section 1 which is an indication of a count of 10.

Wave Shaper, Gate and Pulse Counter

As in the timer unit, a square wave and differentiator circuit is used to shape the input signal from the pickup. The output of the differentiator goes through an electronic gate, Figure 6, before the signal goes to the pulse counter. This electronic gate is essentially a double triode tube and one resistor connected similar to a cathode follower. One grid is connected to the incoming signal and the other grid is connected to the timing counter which opens and closes the gate. The voltage at the cathode of the gate essentially follows the voltage of the highest grid. Therefore, to close the gate, it is only necessary to raise the voltage of the control grid higher than the highest voltage on the signal grid. The control grid is connected to the plate of one of the frequency dividing elements in the timing counter which is at its high voltage between the 0.8 and 1.0 second time. During the remainder of the 1.0 second cycle, this voltage is lower and is below the lowest value of signal grid voltage. Therefore, the cathode voltage follows the signal grid voltage and the gate is open.

The pulse counter consists of six binary decade units each of which divides the frequency by 10. At the end of a counting period, a count is registered on each decade unit by four neon lights in binary form and is the value of the digit

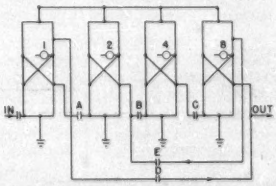

Figure 5. Outline diagram of a decade counter

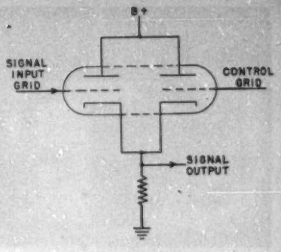

Figure 6. Electronic gate

in the total count corresponding to its position relative to the other counters. In other words, if the first decade unit has registered on it a count of four, the second a count of two, the third a count of one, the fourth a count of three, and the fifth a count of one, the speed indication would be 1312.4 rpm.

Counter Position Senser

It is possible to read the speed indication by means of the neon lamps, but it was considered too difficult to be used for this application. To improve the readability and to provide remote indication, a circuit is used which senses the count of the decade units and controls a relay system. This relay system transforms the binary of each decade into a digit which forms part of the final numerical speed indication. An extra triode was used for each binary section to isolate the relays from the counter units. The grid of the triode is connected to a grid of the binary section, and the relay coil is connected in the plate circuit of the triode as shown in Figure 7. *KA* is the reset relay whose contacts are open between the time 0.8 and 0.9 second of each cycle as controlled by the timing counter through *V4*. *KB* is the transformation relay. When the reset relay *KA* opens, the transformation relay *KB* is allowed to change positions if necessary to correspond to the count on the binary section. To further explain the operation, assume that the neon lamp (*N*) was out, and on a succeeding operation of the reset relay it happened to be lit. Before relay *KA* opened, *KB* would be in the position shown. When *KA* opened, the grid of *V3* would be high and current would flow through coil *KB*, and operate its contacts. When *KA* closed again, there would be a circuit which would lock *KB* in this position, until at the end of some succeeding counting period when the neon lamp was out.

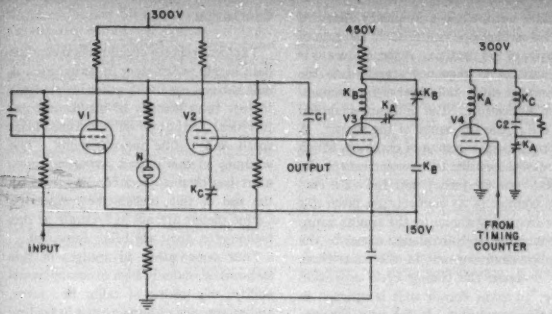

Figure 7. Binary section and associated relay circuits

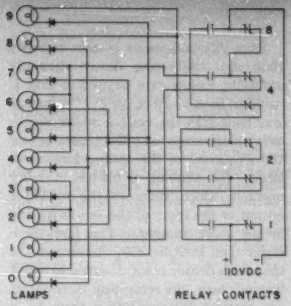

Figure 8. Relay and indicator lamp circuit for one digit

Power Tube, Reset Relay, and Counter Resetter

As shown in Figure 2, the power tube receives its signal from the timing counter. This signal voltage is high during the period 0.8 to 0.9 seconds and controls current through the power tube which has the reset relay coil in its plate circuit, Figure 7. The reset relay operation allows the relays in the relay unit to change during the 0.1-second period during which it is energized. As the reset relay *KA* closes, one set of its contacts closes a circuit from the plate supply voltage through the counter resetter relay, coil *KC*, and a capacitor, *C2*, in series to ground. The capacitor charging current is sufficient to close the counter resetter relay for approximately 0.05 second. The normally closed contacts of *KC* upon opening interrupt the current in the cathode lead of all triodes corresponding to *V2* in all binary sections. This interruption forces all the counters to their zero count position in preparation for the next counting period.

Automatic Range Changer

As mentioned previously, the pulse generator has two tracks of magnetic poles on its rotor with a pickup above each track. At 4,000 rpm the system automatically switches from the high-frequency pickup to the low-frequency pickup to decrease the signal frequency. To account for this frequency decrease of 10 to 1, the signal is applied to the units decade instead of the tenths decade. In this way, the decimal point remains fixed. The only difference is that the tenths decade always registers zero at speeds above 4,000 rpm, and the indication is accurate to 1 rpm. The transfer is automatically accomplished by detecting when the speed reaches 4,000 rpm. A voltage is available in the thousands decade which gives a negative pulse each time this decade unit reaches a count of four. This negative pulse is used to trigger a 2-section binary counter. Each of the two binary sections controls a relay in the same manner as the other counters. The 2-section counter was used because at 4,000 rpm one pulse occurs, and at 14,000 rpm, another pulse occurs, which turns the first section "off" and the second section then goes "on." Therefore, if either of the binary sections are "on," the relay connected to that section serves as a control for the range transfer relay. Since the relays of the 2-section counter are controlled the same as the other counter relays, they cannot change except during a regular reset period. In this way, no error occurs due to the transferring action.

Relay Unit and Indicator

Figure 8 shows the circuit for transforming the binary count on the decade units to a direct-numerical type of presentation. This circuit shows the operation for a single digit. The four sets of relay contacts on the right are connected to indicator lamps such that the proper lamp is lit to indicate the value of the digit as registered on the decade unit. By using a d-c power supply and the rectifiers, this simple circuit using few relay contacts was found desirable.

The indicator could have been made by providing a column of ten labeled lamps per digit. With this type of indication, it would be necessary to scan the whole panel and pick out the light which was lit in each column to make the complete reading. This type of indication was considered too awkward and difficult to read. To simplify the indicator reading, number stencils were illuminated with the lamps and the images of each column of ten stencils were focused at a single spot on an opal glass screen. This was accomplished by mounting the optical tubes, each containing a lamp, a stencil, and a lens; on a cylindrical surface whose axis is horizontal. Figure 9 shows the inside of the indicator. The tubes are threaded into an aluminum plate which allows for focus and alignment adjustments. The numbers at the bottom and top of the cylindrical frame appear somewhat elongated when viewed on the screen but it was not considered objectionable. This could have been corrected by changing the shape of the numbers. An acceptable material found for the screen was flashed opal glass. The indicator is readily readable in ordinary room light, but the contrast is increased if no direct light falls on the indicator screen. Several indicators may be used simultaneously.

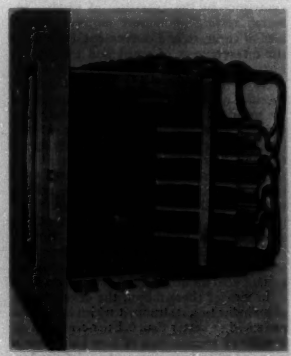

Figure 9. Top view of indicator removed from case

Calibration

Since this tachometer is more accurate than any calibration device normally available, means were devised so that it could be used to check itself. One means was built into the system which checks everything except the pulse generator and the frequency of the tuning fork oscillator. By pressing a button, a relay operates which connects the oscillator output to the input of the tenths decade in the pulse counter. The first three digits then indicate 800. Since the ten thousands decade is not designed to count beyond three, the remaining three digits are checked by connecting them to a point in the tenths decade where the 1,000-cycle oscillator frequency is divided by five. Therefore, since each group of three counters counts for 0.8 second, the reading should be 160800 exactly. This checking relay also disconnects the output of the third decade from the input of the fourth decade. Several means are available for checking the tuning fork frequency.

One way is to connect both the oscillator output and a frequency standard to an oscilloscope and observe the rate of change of the pattern. A second means is to connect a frequency standard to the generator cable and observe the tachometer indication. The indication should be 0.8 of the frequency of the supply. A more elaborate system of checking, which checks the entire tachometer except the 1,000-cycle frequency and the sixth decade counter is to connect the generator low-frequency signal to the timing counter and the high-frequency signal to the regular counting unit at the same time. To decrease the timing cycle repetition rate, an extra decade unit is inserted in the timing counter. In this way, the generator controls the timing period as well as the pulses counted, and the tachometer reading should be the same regardless of speed. The timer unit will require 10,000 counts per cycle and will allow counts to accumulate in the main counter during 8,000 counts. Since the high frequency is accumulated in the main counter, the indication will be 80,000. The system can be checked over a wide range of frequency by varying the generator speed.

Conclusion

The performance of this tachometer has been highly satisfactory in actual use. A unit is being used with other instruments to test the efficiency of steam and gas turbines. Output power is obtained from speed and torque measurements. The accuracy of this output power measurement has been appreciably improved by the use of this tachometer. Although torque meters are not as accurate as this tachometer, they are being improved.

Four outstanding advantages of this tachometer, namely high accuracy, readability, minimizing of calibration error, and minimizing of human error in reading make it desirable for many applications in development testing, production testing and in use as a calibrating standard for other tachometers.

References

1. A Four-Tube Counter Decade, J. T. Potter. *Electronics* (New York, N. Y.), June 1944, pages 110–13.

2. Electronic Digital Counters, Warren H. Bliss. *Electrical Engineering*, volume 68, April 1949, pages 309–14.

Discussion

C. M. Gardiner (General Electric Company, Schenectady, N.Y.): It has long seemed strange to this writer that accurate measurements of such fundamental things as speed, torque, and electric power should be as difficult as they are. During a number of years of active work in conducting acceptance tests on large steam turbine-generator sets, it was found that, in almost every case, one of the most significant errors affecting the net result was that incurred in measuring electrical output. Subsequent experience in the operation of turbine research testing equipment emphasized the lack of accurate and convenient devices for the measurement of speed and torque. A system had been developed for measuring speed by recording the time required for a specified number of revolutions, with which, by using an accurate time recorder, and counting a sufficiently large number of revolutions, a very good value of average speed could be obtained. The work of computing the results from the recorded times, however, was inconvenient, and since results were not available until a run had been completed, they could not be used to adjust speed, or to indicate variations therein during a test. No device of any type was available which could consistently measure torque with an accuracy of 0.1 per cent.

In view of these things, the development of an indicating instrument which can measure speed to better than 0.1 per cent, and do it without reservations of any kind over a range of 40-to-one, represents a definite forward step in the measuring art. While the device itself appears complicated, its designers seem to have done a good job of keeping the complications within the machine, and of safeguarding it so that failures which might occur can be readily detected and will not result in erroneous readings.

This instrument should be valuable to large research organizations which have frequent demands for a means to measure speed accurately. It also should have an application in places where a number of tests are running concurrently, each of which requires a measurement of speed. In many such cases an accurate indication as often as once per minute would be adequate, and by attaching a pulse generator to each unit whose speed is to be measured, and wiring these all to one counting element, this element could, with some modifications, be made to print the speed of each unit once per minute on a paper tape and, if desired, also to indicate the speed at one or more remote points on the same type of indicator as described in the paper. At a rate of once per minute, it could indicate and record the speeds of 60 different machines.

The basic elements of this tachometer also should find application in the precise control of speed or frequency. Information could be obtained to indicate deviation of speed from any desired standard, and a measure of the deviation could be supplied to corrective mechanisms; or with equal facility, information could be obtained to indicate the total accumulated angular error, and corrections could be applied to hold this to a small value.

Undoubtedly control systems and research investigations will continue to have need for increasingly accurate speed measurements and the tachometer described in this paper should fill many needs which previously could not be met with commercially available equipment.

Frank D. Olney (General Electric Company, Fort Wayne, Ind.) Experience in testing fractional-horsepower motors with an electronic counter-type tachometer similar to the one described in this paper suggests the following points:

1. In comparison with other types of tachometers, the counter-type is very near to a primary standard in that it counts revolutions for a certain interval of time instead of converting rotational speed into voltage or spring force or some other secondary quantity—that is, the counter-type tachometer is a digital computer rather than an analogue computer. By the method described in this paper, a tenfold improvement in accuracy has been made possible, so that the speed reading becomes the most accurate test quantity instead of the least accurate as has previously been the case.

2. The authors state that a neon lamp indicator composed of ten labeled lamps per digit is too awkward and difficult to read. In order to simplify the indicator reading, they provided a fairly complicated projection system using illuminated stencils focused at a single spot on a glass screen. While this is a novel solution of the problem, our experience shows that it is not difficult to read a 4-digit number in which each digit is in a separate column, and that the neon lamp indicator gives satisfactory results with a considerable saving in cost over the projection system.

3. An important feature of this tachometer where industrial usage is concerned is that any electron tube may be replaced

without affecting the speed reading, since the counting circuit is of the "on-off" type.

4. Since each speed reading is spaced one second apart, this tachometer can be used to make accurate speed-time deceleration curves simply by removing power from the rotating machine and calling off each speed reading into a recording machine. This application of the tachometer was suggested by one of our engineers who is interested in obtaining values of windage, bearing friction, and core loss of small motors without the necessity for taking oscillograms.

5. This tachometer can be used as a time-interval meter to measure the time-interval between two events by counting the oscillations from the tuning fork during the interval. At an oscillation rate of 1,000 cycles per second, a unit on the indicator scale will represent an elapsed time of one millisecond.

6. By reading the speed of a small synchronous motor, this tachometer can be used to measure line frequency more accurately than can be done by the usual frequency meter. On one large power system, the frequency swing is from 59.9 to 60.1 cycles per second during the day, which causes a spread of six rpm in the full-load speed of a 4-pole motor operated from the power line. Correction for this frequency deviation should be made in development testing where extreme accuracy is required.

7. With further development of binary counting circuits which were first used extensively for radar applications, it seems reasonable to expect that the cost and physical size of the electronic counter tachometer will be drastically reduced in the future.

C. L. Beattie: Mr. Olney has made several interesting comments and suggestions for special applications of the tachometer.

The projection type of number system was used for convenience and to facilitate the reading of the indicated speed values every second. This is particularly desirable for long tests to prevent eye strain and fatigue.

In many applications a conventional type of indicating decimal counting unit may be used.

A Direct Reading High-Voltage Capacitance Bridge

A. H. FOLEY
ASSOCIATE AIEE

Synopsis: In contrast with the conventional Schering bridge, the network described in this paper is direct reading for both dissipation factor and capacitance, has a fixed guard adjustment, and hence simplified operation. A unique method of phase-angle compensation employs adjustment of the effective phase angle of the standard capacitor. This compensation may be either positive or negative as required. Design is simplified since compensation for stray wiring capacitances is easily accomplished. Simplified operation and elimination of all calculations permit substantial reductions in unit testing time and operation by nontechnical personnel without sacrifice of accuracy.

A GENERAL survey of high-voltage capacitance bridges in use throughout the electrical industry has shown the need for a bridge specifically designed for production measurement of capacitors and similar devices. For this purpose a bridge has been developed which is direct reading in both capacitance and dissipation factor and which does not require a guard balance for most measurements. The use of this bridge should result in the saving of several thousand dollars per year where large quantities of capacitors must be checked daily as on a production line or in the development laboratory.

It was with a view toward increasing testing efficiency that the direct reading bridge described in this paper was developed. Though the Schering bridge network is in quite general use for capacitance and dissipation factor measurements at high voltage, especially at low frequencies, and provides accurate test data, the conventional arrangement of the network does not generally provide direct readings for both capacitance and dissipation factor. At least one of these quantities usually must be computed from the readings obtained. These factors led to the development of the direct reading bridge network, which, though similar fundamentally to the Schering network, differs from the Schering bridge in a number of technological details.

The development also has been directed toward a unit package containing, as far as possible, all components of the bridge. Examples of direct reading capacitance bridge designs for large capacitances are shown in Figures 1 and 2. The unit shown in Figure 1 was designed for the measurement of power factor correction capacitors at rated voltage and frequency on the factory production line. Here, a capacitance accuracy of ±0.1 per cent and a dissipation factor accuracy of better than ±0.0001 is maintained for rapid production measurements by nontechnical personnel.

The principle objective of this paper is to introduce the direct reading capacitance bridge network. The discussions which follow, though principally theoretical, often present the practical side of the bridge design.

Comparison of the Direct Reading and Schering Bridge Networks

The basic circuit of the direct reading bridge is shown in Figure 3(A). For purposes of comparison the Schering bridge network is shown in Figure 3(B). In these two figures C_s represents the standard capacitor while C_x and ρ represent, respectively, the capacitance and effective series resistance of the capacitor under test. The bridge balance detector is indicated as G.

The remaining elements, all operating at low potential, complete the two networks and are either fixed or adjustable resistances and capacitances employed in balancing the bridges. In the discussion to follow it will be assumed that a power source of fixed frequency is used, a condition most generally met in practice.

The Schering Bridge Network

A brief review of the Schering bridge network[1] will clear the way for a quicker understanding and appreciation of the advantages of the direct reading network. Referring to Figure 3(B), when the network is balanced the capacitance of the test capacitor is

$$C_x = \frac{C_1 R_3}{R_2} \tag{1}$$

while the dissipation factor (tangent of the defect angle) is

$$D_x = \omega C_1 R_3 \tag{2}$$

where

$\omega = 2\pi f$

If it is chosen to make the Schering bridge read capacitance directly, capacitance balance can be made by adjusting either C_x or R_3. Since C_x is usually a guarded high-voltage air capacitor it is impractical, all points considered, to construct it to have a continuously variable capacitance. Furthermore, manipulation of this high-voltage element is generally undesirable from a safety point of view. This quickly rules out the use of C_x as an adjustable element for balancing capacitance when measurements are to be made at high voltages. On the other hand R_3, operating entirely at low potential, is easily made variable over a wide range. Since R_3 is a direct function of C_x, the controls on R_3 may be calibrated to read capacitance directly. If this is done, however, two variables, C_1 and R_3, are involved in determining the dissipation

Paper 50-110, recommended by the AIEE Instruments and Measurements Committee and approved by the AIEE Technical Program Committee for presentation at the AIEE North Eastern District Meeting, Providence, R. I., April 26–28, 1950. Manuscript submitted November 18, 1949; made available for printing March 7, 1950.

A. H. Foley is with the General Electric Company, Pittsfield, Mass.

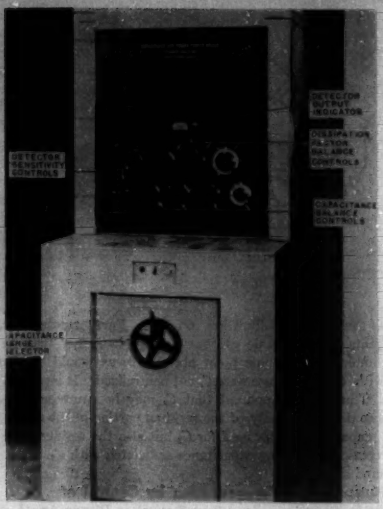

Figure 1. A 13.8-kv direct reading capacitance bridge designed for the measurement of power factor correction capacitors on the production line by nontechnical personnel

factor of the test capacitor. A direct calibration of C_3 for dissipation factor is not possible. With such an arrangement dissipation factors must be computed employing equation 2.

A direct calibration of C_3 for D_x can be made only when R_4 is fixed. It then becomes necessary to adjust R_4 in order to make a capacitance balance, but since R_4 is an inverse function of C_x, a direct capacitance calibration cannot conveniently be made without employing special resistance controls. One form of such control for R_3 is the conductance decade. While conductance decades can be calibrated to read capacitance directly, it is very difficult to construct a system of decades which will cover a wide range of resistance such as 10,000-to-1 or greater, and at the same time permit readings of four or five significant figures to be taken at any point in the range. An additional difficulty is the problem of maintaining good phase-angle characteristics for R_4 over this extremely wide resistance range. A third difficulty arises when large capacitances are to be measured, particularly at high voltage; the charging currents become quite large, hence switch contacts and heating of the resistance elements must be given special attention.

It is to be concluded from the foregoing discussion that, in general, the Schering bridge conveniently can be made to read directly for one quantity only, either capacitance or dissipation factor. One of these must be computed from the bridge readings. While this discussion makes no pretense at covering all possible modifications of the Schering bridge network, it is believed that a more general discussion will lead essentially to the same conclusion.

The Direct Reading Network

Having thus reviewed the basic Schering bridge circuit, the direct reading bridge network now can be considered in some detail. Referring to Figure 3(A) it will be noted that a resistance potentiometer, comprised of resistances R_1 and R_2, replaces resistance R_2 of Figure 3(B). Capacitances C_1 and C_2 effect phase angle compensations in a manner to be discussed later. It can be shown that, very closely, when the network is balanced

$$Cx = \frac{C_3 R_3}{R_2} \tag{3}$$

and, for proper phase-angle compensation

$$Dx = \omega C_1 (R_1 + R_2) \tag{4}$$

It is a simple matter to arrange the resistance potentiometer so that R_2 is proportional to the potentiometer dial settings. Hence, by suitable choice of R_3, the potentiometer controls can be calibrated to read C_x directly.

Since resistances R_1 and R_2 comprise a

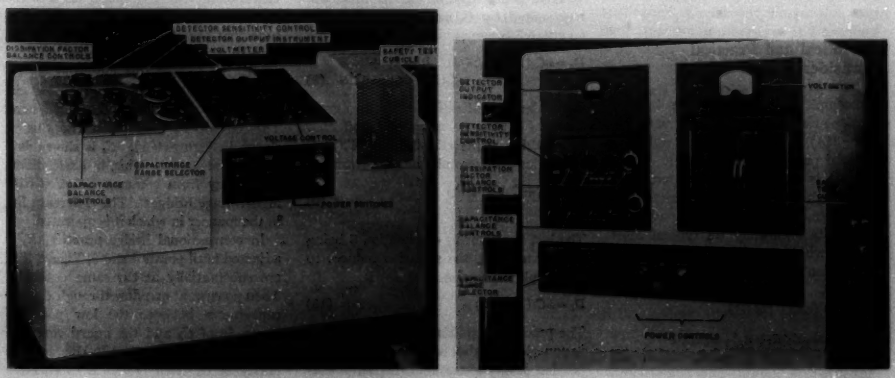

Figure 2 Examples of portable 2-kv direct reading capacitance bridges for (left) quality control measurements, and (right) developmental measurements on small a-c capacitors. Both units are complete with power supplies and safety test cubicles

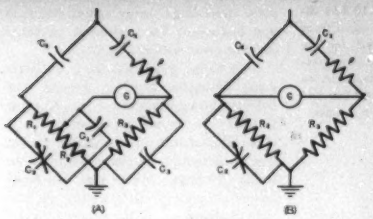

Figure 3 (left). Basic bridge networks. (A). Direct reading. (B). Schering

Figure 4 (right). (A). The direct reading bridge network with standard capacitor guard system. (B). The standard capacitor phase angle control network

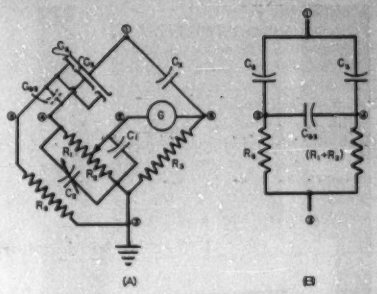

potentiometer, the sum of the two is a constant. If $R_1+R_2=R_p$, equation 4 can be rewritten

$$Dx=\omega C_3Rp \tag{5}$$

Only one variable, C_3 is involved in determining the dissipation factor hence a direct calibration for D_x can be made on the dials controlling C_3.

Direct readings for both C_x and D_x can thus be obtained without making R_3 continuously variable. In covering a wide capacitance range, say 100-to-1 or more, it is desirable to vary R_3 but this most conveniently can be done in decade steps thus preserving the direct reading feature, as regards significant figures, of the R_3 calibration.

The use of decade step values for R_3 also makes it unnecessary to vary R_2 through more than a 10-to-1 range no matter how wide the total capacitance range of the bridge might be. This provides still another advantage; capacitance readings of any desired number of significant figures at any point in the bridge capacitance range can be obtained by employing a decade potentiometer system for (R_1+R_2) and simply providing a single decade for each desired significant figure.

Theoretical and Practical Considerations

A complete solution of the balance equations for the direct reading network, Figure 3(A), is unwieldy and would serve no useful purpose in the present discussion. It is sufficient to say that after certain high order terms are omitted the capacitance, C_x, of the test capacitor is given quite accurately (in typical cases the error will be less than 0.001 per cent) by equation 3. Similarly the dissipation factor, D_x, is very closely (error generally less than 0.00001)

$$Dx=\omega Cxp=\omega C_x(R_1+R_2)+\omega C_3R_1+\omega C_1R_2-\omega C_3R_3 \tag{6}$$

Equation 6 takes into account all of the parameters shown in the circuit of Figure 3(A). The terms on the right of the equation are, respectively, the tangents of the phase angles created by C_3 in combination with (R_1+R_2), R_1 in series with C_x, C_1 across R_3 and C_3 across R_3. Thus the effect of R_1 in series with C_x is to destroy the purity of the standard capacitor. Also, C_1 across R_3 further increases the phase-angle error on the left-hand side of the network, Figure 3(A). However, if C_1 is made equal to C_x, equation 6 becomes

$$D_x=\omega C_3(R_1+R_2)+\omega C_x(R_1+R_2)-\omega C_3R_3 \tag{7}$$

Since C_x and (R_1+R_2) are constant the second term on the right of equation 7 becomes constant and can be completely neutralized by making $C_3R_3=C_x(R_1+R_2)$. In fact, the sole function of C_3 in the network of Figure 3(A) is that of phase-angle error compensation. Another, and more satisfactory, means of compensation will be described later.

To be thoroughly practical, C_3 should be considered as composed of two parts: the minimum or residual capacitance below which C_3 cannot be set; and the variable component of C_3. If these are represented by C_r and C_d, respectively, equation 7 becomes

$$D_x=\omega C_d(R_1+R_2)+\omega C_r(R_1+R_2)+\omega C_x(R_1+R_2)-\omega C_3R_3 \tag{8}$$

Complete neutralization of the two error terms of equation 8 now can be affected by making $C_3R_3=C_r(R_1+R_2)+C_x(R_1+R_2)$. Thus, for zero phase-angle error

$$C_3=\frac{(C_x+C_r)(R_1+R_2)}{R_3} \tag{9}$$

The last three terms of equation 8 being thus eliminated, the equation reduces to the simple expression

$$D_x=\omega C_d(R_1+R_2) \tag{10}$$

The practical significance of including C_r in equation 8 is that only the straight line portion of any variable air capacitor employed for C_3 needs be calibrated. A linear scale is thus provided for the dial calibration on C_3. Furthermore, the scale can start at $D_x=0$ rather than at some point above zero as would be the case were C_r not neutralized. It is at once apparent that C_r may be composed not only of the residual portion of the capacitor used for C_3 but also the residual wiring capacitance associated with C_3.

Compensation by Control of Standard Capacitor Phase Angle

The use of C_3 for phase-angle compensation is unsatisfactory particularly in a wide range capacitance bridge. Though R_3 may be changed in decade steps, a wide range bridge may employ a large number of such steps and each would have to be shunted with a suitable value of C_3. For bridges designed to measure high capacitances R_3 may be quite low and the associated value of C_3 very large; in some cases tens of microfarads.

A unique and improved method of compensation, one which eliminates the use of C_3 altogether, makes use of adjustments of the effective phase angle of the standard capacitor, C_s. The method is such that the effective phase angle of C_s may be adjusted with precision in either a positive or negative direction, as required, and should find application in circuits other than those considered here. The circuit for accomplishing this is shown in Figure 4(A). C_s is shown as a guarded capacitor. This, in itself, differs in no way from common practice with high-voltage bridges. The difference lies in the manner in which it is operated.

In conventional bridge practice, R_g is adjusted until points 4 and 5, Figure 4(A) are substantially at the same potential. Then no current can flow through C_{gs}, the capacitance between the low potential electrode of C_s and the guard ring surrounding that electrode. In this way the purity of C_s, with reference to effective phase angle, is preserved.

In the method of compensation under

discussion here, points 4 and 5 are not operated at the same potential. It will be shown, however, that the effective phase angle of C_s can be adjusted precisely in either a positive or a negative direction from the angle obtained when points 4 and 5 are at equal potentials and that the phase angle so obtained can be employed to compensate for the sum of all other constant phase angle errors in the network.

An approximate analysis is presented here in order to give a clearer physical picture of the compensation circuit performance. If the left-hand side of the network is examined, three capacitances will be observed to be involved in the standard capacitor system, namely, C_s, the direct capacitance between high-and low-voltage electrodes, C_g, that between the high-voltage electrode and the guard ring, and C_{gs}, that between the guard ring and the low-voltage electrode. Tracing the left-hand side of the network between points 1 and 3 it is seen that the network of Figure 4(B) is obtained if C_1 and C_3 are omitted. Since, in practice, the ratio of the reactance of C_s to resistance (R_1+R_2) is quite high (1,000-to-1, or more in typical cases) the component of voltage across (R_1+R_2), due to current through C_s, is closely

$$E_{3-4}=j\omega C_s(R_1+R_2)E_{1-3} \tag{11}$$

Likewise, the voltage across R_g, due to current through C_g, is

$$E_{3-5}=j\omega C_gR_gE_{1-3} \tag{12}$$

Equations 11 and 12 hold closely because, in practice, the difference between potentials E_{3-5} and E_{3-4} is impressed across C_{gs} and causes a current to flow through C_{gs} which is quite small compared to currents flowing through C_s and C_g.

Consider, separately for the moment, the current through C_{gs}. This current flows principally around through (R_1+R_2) and R_g thus creating a component of voltage across (R_1+R_2) which is closely

$$E_{3-4}'=j\omega C_{gs}(E_{3-5}-E_{3-4})(R_1+R_2) \tag{13}$$

Substituting equations 11 and 12 in equation 13

$$E_{3-4}'=\omega^2C_{gs}E_{1-3}[R_1+R_2][C_s(R_1+R_2)-C_gR_g] \tag{14}$$

Equation 14 shows that we can get a component of voltage across (R_1+R_2), due to current flow through C_{gs}, which is essentially in quadrature with the principal component across (R_1+R_2). If C_gR_g is greater than $C_s(R_1+R_2)$, E_{3-4}' is negative.

Clearly then, the effect of E_{3-4}' on the total voltage drop across (R_1+R_2) is to

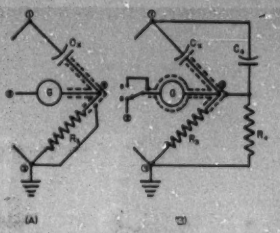

Figure 5. Methods of guarding. (A). For high-capacitance bridges. (B). For low-capacitance bridges

shift its phase by a small angle, ϕ_s. This angle, which can be defined as the effective phase angle of C_s, is closely

$$\phi_s=\tan^{-1}\frac{E_{3-4}'}{E_{3-4}} \tag{15}$$

Upon substituting equations 11 and 14 in equation 15

$$\phi_s=\tan^{-1}\omega C_{gs}[R_1+R_2-\frac{C_g}{C_s}R_g] \tag{16}$$

From this equation the value of R_g, for any desired small value of tan ϕ_s, is

$$R_g=\frac{C_s[\omega C_{gs}(R_1+R_2)-\tan\phi_s]}{\omega C_gC_{gs}} \tag{17}$$

Referring again to equation 8, it is seen that the magnitude of the angular error for which neutralization is required is $\omega C_r(R_1+R_2)+\omega C_s(R_1+R_2)$. These terms express the tangents of the error angles discussed previously, each representing a constant phase angle at fixed frequency. Clearly then, if these terms are to be neutralized by adjusting the effective phase angle of C_s, tan ϕ_s must be made equal in magnitude and opposite in sign to their sum. Thus, for correct compensation

$$\tan\phi_s=-\omega C_r(R_1+R_2)-\omega C_s(R_1+R_2) \tag{18}$$

Substituting equation 18 in equation 17

$$R_g=\frac{C_s(R_1+R_2)(C_s+C_{gs}+C_r)}{C_gC_{gs}} \tag{19}$$

Note that R_g is independent of frequency. When the conditions of equation 19 are satisfied, equation 8 again reduces to the simple expression

$$D_x=\omega C_s(R_1+R_2) \tag{10}$$

The Service Guard Circuit

At this point those familiar with high-voltage bridge practice will raise the question concerning a guard circuit for use when measuring guarded test specimens. R_g having been fixed for compensation purposes, the circuit, as shown in Figure 4(A), is without a service guard. The practical answer to this question is determined by the range of capacitances to be measured.

For large capacitances, say of the order of 0.1 microfarad and greater, guarded capacitors are seldom encountered. They are almost invariably two terminal units. For such units there is no need for a service guard. There is a need, however, for a shield around the low-voltage lead which connects the test capacitor to point 6 as shown in Figure 5(A). The shield is simply connected to point 3, commonly grounded. The added capacitance which this arrangement places across R_g is usually negligible since, for large capacitances, R_g is small (typically less than one ohm).

The circuit arrangement shown in Figure 5(A), which is for the measurement of large capacitances, has the important advantage of not requiring a guard balance each time a capacitor is measured. This very materially simplifies the bridge operation and permits measurements to be made on large quantities of capacitors with substantial reductions in time. Examples of designs of direct reading bridges taking advantage of this feature are shown in Figures 1 and 2.

For the measurement of small capacitances, a service guard is definitely needed. For this purpose an auxiliary high-voltage capacitor, C_4, and an adjustable resistance, R_4, are required as shown in Figure 5(B). The question of cost of the auxiliary high-voltage capacitor, C_4, invariably arises. Since a guarded capacitor is not needed for this application, a relatively inexpensive vacuum capacitor or other type of 2-terminal capacitor usually will be satisfactory.

Standard Capacitor Design

The practical application of phase-angle error compensation by means of standard capacitor phase-angle control requires, among other factors, that the voltage across R_g, Figure 4, be stable. Hence a few words concerning the design of the standard air capacitor are in order.

It is common practice to design guarded air capacitors with only three terminals, one for the high-voltage electrode, one for the low-voltage electrode and one for the guard rings or cylinders. In some designs of this type there can be an appreciable leakage both through and over the surfaces of the supporting insulation between the high-voltage electrode and the

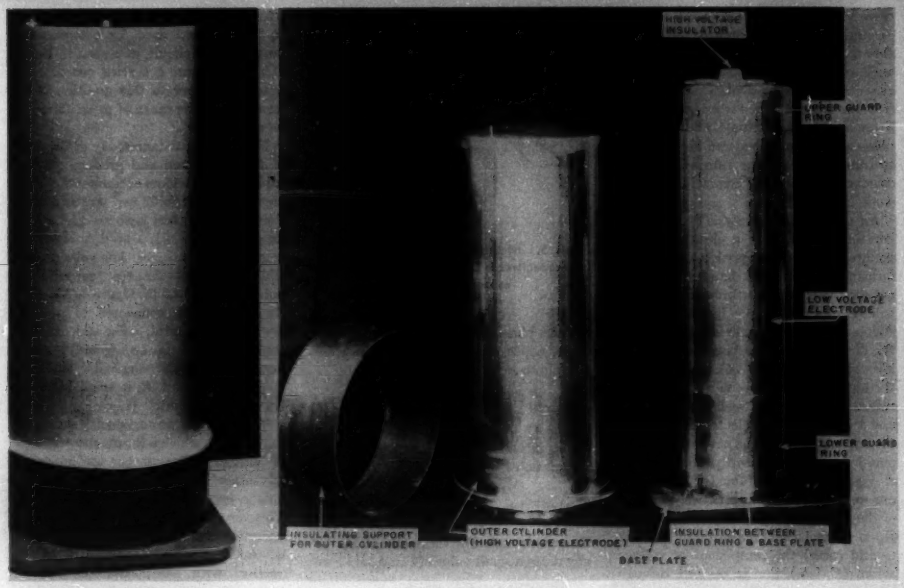

Figure 6. A 13.8-kv 4-terminal standard air capacitor suitable for use with the direct reading capacitance bridge. (Left) assembled unit (Right) component parts

guard rings. Such leakage may not be stable. In any case it causes an additional current to flow through R_x and thereby alters the potential drop across this resistor.

This effect can be satisfactorily overcome by employing a 4-terminal standard, that is, one with a leakage interceptor electrode between the high-voltage electrode and guard rings. This fourth terminal generally can be connected to the low-potential supply line (point 3 in Figure 4(A)). An example of 4-terminal guarded air capacitor design is shown in Figure 6. The capacitor is of the concentric-cylinder type with the high-voltage electrode supported on insulators from a steel base plate. The lower guard cylinder, see Figure 6(B), is insulated from the base plate on insulation independent from that supporting the high-voltage cylinder. The base plate thus becomes the interceptor of any leakage through or over the surfaces of the high-voltage insulation.

Adjustment of C_1 and R_x

It has already been shown that, in order to hold certain of the network phase angles constant, C_1 must be equal to C_x, the standard capacitor. A part of C_1 easily may be in the form of distributed wiring capacitance across R_3. A portion also may exist between point 2 of the detector and point 3 (usually ground). An experimental method of adjusting C_1 makes it unnecessary to know the magnitude of these stray capacitances.

The method is based on the requirement that the slope of the curve of dissipation factor calibration versus C_x, with C_x as the abscissa, be zero. In other words, if D_x is held constant at any point and C_x varied, there should be no change in the setting of C_3. Equation 6 shows that this condition can be realized only when $C_1 = C_x$.

For bridges designed to measure capacitances in the range between, say, 100 and 1,000 micromicrofarads, two guarded air capacitors having a ratio of some three to one or more (but not more than ten to one) between their respective capacitances will be useful in adjusting C_1. The lower unit preferably should have a capacitance between 100 and 300 micromicrofarads so that, when the unit is connected to the bridge as C_x and the bridge balanced, the ratio of (R_1+R_3) to R_2 approaches ten. When the larger of the two guarded capacitors is in place and the bridge balanced, this ratio should approach unity. Then, if both capacitors have equal or zero dissipation factors, the setting of C_3 will remain unchanged for the two measurements only if C_1 is properly adjusted. It is simply a matter of experimentally adjusting C_1 until the slope is zero.

A particularly useful type of guarded air capacitor for adjusting the direct reading bridge is shown in Figure 7. This is a guarded decade air capacitor having ten steps of 100 micromicrofarads each. A selector switch is provided for setting the capacitance. Only the low-voltage electrodes are switched. Electrodes not in use for direct capacitance are simply switched into the guard circuit as the selector switch is set.

With the aid of this type of guarded air capacitor, a most thorough check can be made of the setting of C_1 and, at the same time, any variations in the phase angle of R_3 can be evaluated. Such variations cause the curve of dissipation factor calibration versus C_x to depart from a straight line.

An added advantage of employing

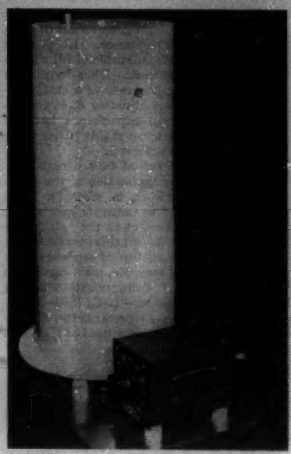

Figure 7. A 2-kv 1,000-micromicrofarad 4-terminal decade standard air capacitor. Very thorough phase angle checks can be made on capacitance bridges with the aid of this unit. (Left) assembled unit (Right) component parts

guarded air capacitors having dissipation factors of essentially zero in the manner described before is that, once C_1 has been set, R_g can also be set for proper phase-angle compensation. This is done simply by setting C_3 to the point arbitrarily calibrated as $D_x=0$ and then adjusting R_g and R_3 until the bridge is balanced. This procedure makes it unnecessary to determine the magnitudes of either C_p, C_{gs}, or R_g.

For direct reading bridges designed to measure only large capacitances a somewhat different procedure must be followed in adjusting C_1. The method consists, essentially, in choosing a number of capacitors such as, for example, the impregnated-paper type, all having the same nominal capacitance. The capacitance and dissipation factor of each is measured on the bridge just as it stands before adjustment of C_1. The capacitors are then connected in parallel in groups of two, three, and so forth, and remeasured on the bridge. The results of the group measurements are then compared with the value of capacitance and dissipation factor as computed from the individual readings.

An example will make the procedure more readily understood. Suppose R_3 is set so that the bridge will measure capacitances between 1 and 10 microfarads. Ideally a group of ten 1-microfarad capacitor would be employed for a very thorough check but this would call for an excessive number of measurements. It would be more practical to choose, say, four 2.5-microfarad capacitors. When all four units are in parallel they can still be measured on the same range of the bridge, as set by R_3. If the individual measurements give results as shown in Table I, then the dissipation factors of parallel combinations of capacitors may be computed from the equation

$$D' = \frac{C_1D_1 + C_2D_2 \ldots + C_nD_n}{C_1 + C_2 \ldots + C_n} \qquad (20)$$

Substituting the figures in Table I in equation 20 yields the results shown in Table II.

The procedure now is to measure the parallel groups as arranged for the computation. If the measured dissipation factors differ from the computed values, C_1 must be adjusted, experimentally, to bring about an agreement. Note that any adjustment of C_1 also will affect the dissipation factor readings as taken on the individual units. After each adjustment of C_1 a complete new set of readings must be taken and computations made. Convergence, however, generally is rapid and two or three "runs" usually is sufficient to adjust C_1 for the required zero slope.

The Bridge Balance Detector

In general, any detector suitable for use with the Schering bridge network is suitable for use with the direct reading bridge. Detector systems composed of a tuned amplifier and an output meter are especially good if designed so that inductive elements are not included in the low-level signal circuits. A particularly satisfactory type of circuit[2] employs a high gain resistance coupled amplifier in conjunction with a resistance-capacitance twin-T network through which selective negative feedback is obtained. Detector systems of this type have the advantages of low susceptibility to pickup from magnetic fields, fast response, high discrimination against harmonics (virtually always present in any power bridge), high signal sensitivity, and ruggedness.

Table I

Unit Number	Capacitance, Microfarads	Dissipation Factor (D_x)	C_xD_x
1	2.489	0.00307	0.00764
2	2.507	0.00343	0.00860
3	2.510	0.00299	0.00751
4	2.480	0.00331	0.00821

Table II

Unit Combination	Total Capacitance (C')	Composite Dissipation Factor (D')
1, 2	4.996	0.00325
1, 2, 3	7.506	0.00316
1, 2, 3, 4	9.986	0.00320

Summary

The direct reading bridge network, while retaining the advantage of the Schering bridge network by keeping all adjustable elements in the low potential arms, has the additional advantage of providing direct readings for both capacitance and dissipation factor. Furthermore, large amounts of stray wiring and other capacitances are easily compensated for without knowing their magnitudes. A useful feature in checking the bridge performance, one not common to the Schering bridge when R_3 is employed for the capacitance balance (as is most generally done), is that the bridge can be balanced when the test capacitor arm is completely open. If any stray capacitance exists across this arm it then can be read directly from the bridge dials.

These desirable features, together with the complete absence of an adjustable guard where large capacitances are to be measured, make the direct reading bridge exceptionally easy and fast to operate, even by nontechnical personnel, at no sacrifice in accuracy and without the necessity for any computations.

References

1. Alternating Current Bridge Methods (book), B. Hague. Sir Isaac Pitman and Sons, Ltd., London, England, 1943.

2. A New Type of Selective Circuit and Some Applications, H. H. Scott. *Proceedings*, Institute of Radio Engineers (New York, N. Y.), volume 26, February 1938, pages 226–35.

Discussion

E. H. Povey (Doble Engineering Company, Belmont, Mass.): There seems to be a prejudice against the use of any bridge circuit which cannot be resolved simply and with mathematical rigor. In the case of the circuit described in this paper, the peculiar advantages offered by the circuit should go far in overcoming any such prejudice. The author has done an effective job in designing the circuit from the viewpoint of the operator.

The description of the bridge leaves the impression that the phase angle control network shown in Figure 4(B) is necessarily associated with the construction of the standard capacitor. However, C_g and C_{g2} can be separate components. For phase control in one direction only and at a fixed frequency, these capacitors may be replaced by resistors.

In some bridge applications it may not be feasible to keep the residual capacitance C_3 very small, and phase angle errors will be introduced as decade arm R_3 is switched. These errors can be avoided by the use of shields and a guard balance as shown in Figure 5(B). Another method is to compensate for the errors by proper adjustment of the phase angle control network. The adjustment is most simply made by changing the value of R_g, and if the switch for performing this function is mechanically linked to the R_3 switch, the adjustment will be automatic.

A. H. Foley: Mr. Povey has pointed out a certain lack of completeness in the paper on a direct-reading capacitance bridge. It was not the author's intention to give the impression that the phase angle control network, Figure 4(B), is necessarily associated with the construction of the standard capacitor. In fact there usually is a definite advantage in padding C_{g2} by means of additional external capacitance. In practice C_{g2} is perhaps the least stable of all the parameters in the network. Thus by placing some additional capacitance of a stable nature across C_{g2} and readjusting R_g in accordance with the total capacitance between points 4 and 5, a more stable phase-angle control usually is achieved.

C_g and C_{g2} can indeed be separate components. A useful application of the phase angle control network is where a small voltage is required in accurate quadrature relationship with respect to the voltage between points 1 and 3. In this case the entire network can be made up of separate components using, for example, mica capacitors as C_x, C_g, and C_{g2}. Using equation 17, tan ϕ_g must be set equal to $-[\omega C_x(R_1 + R_3) + \tan \phi_{cx}]$ where tan ϕ_{cx} represents the dissipation factor of the capacitor used as C_x. This results in the equation

$$R_g + C_3 \frac{\omega(R_1+R_3)(C_{g2}+C_3)}{\omega C_g C_{g2}} + \tan \phi_{cx}$$

for a pure quadrature voltage across $(R_1 + R_3)$.

While C_g and C_{g2} may be replaced with resistors, the direction of phase-angle control which can be obtained is opposite to that required for compensation of the error terms considered in the paper. Also, the resistor replacing C_g would have to operate at high voltage and might pose a practical problem as regards construction and stability.

Mr. Povey's suggestion to mechanically link the R_3 switch and a switch controlling R_g to obtain correct compensation for phase-angle errors in R_3, where several values of R_3 are used, seems practical and should further help to realize direct readings and eliminate the necessity for applying corrections.

Power Measurement by the Hook-On Method

A. J. CORSON
MEMBER AIEE

A. L. NYLANDER
NONMEMBER AIEE

THE "hook-on method" is here defined as the measurement of an electrical quantity, where the current component of such measurement is obtained by encirclement of the current-carrying conductor by a removable magnetic structure. This magnetic structure provides a circuit for the magnetomotive force, which force is a unique function of the current and is applied to a secondary winding, or directly to an instrument mechanism. Available self-contained instruments are limited to current measurement. Some of these instruments have independent potential circuits, such as the hook-on voltammeter, illustrated in Figure 1. The authors recently became interested in extension of this measurement method to active and reactive power. This paper is a summary of the development of the self-contained hook-on wattmeter, illustrated in Figure 2. It was necessary that this instrument meet exacting requirements as to accuracy, weight, simplicity of operation, and range of full-scale capacities, 3 to 300 kw.

The Measurement Problem

Since power measurements involve circuits, which will preserve phase-angle relationships, it was evident that a direct application of ammeter magnetic circuits would not necessarily be satisfactory.

Investigation of one such design by application of the secondary voltage to either the fixed or moving coils of an electrodynamic wattmeter showed that only 1/3 of the measurement range of 3 to 300 kw could be covered with acceptable accuracy. The computed and measured phase-angle errors were excessive for the entire measurement range. For this and other reasons, as stated later, the direct acting principle was adopted, even though the development expense was increased some ten-fold by this decision.

The Direct-Acting Instrument

The preferred construction then consisted of a ferrodynamic wattmeter, the field of which is energized by the current carrying conductor through the magnetic hook shown in Figure 3.

The basic torque equation[1] for any electrodynamic (air core) 2-coil system is

$$t_y' = i_1' i_2' dM/dY \qquad (1)$$

where

t_y' = torque at angle Y in dyne centimeters
i_1' = field current in centimeter-gram-second units
i_2' = moving coil current in centimeter-gram-second units
Y = deflection in radians
M = coefficient of mutual induction to centimeters

The application of this equation to a ferrodynamic 2-coil system, with spring-controlled moving system, involves the following considerations:

1. The torque t_y' is translated in angular deflection by the control.

2. For linear scales, the space rate of change of mutual inductance dM/dY must be constant.

An important, but nonrelated observation, is the fact that the scale capacity is directly proportional to potential circuit resistance over a wide current range, and

Figure 1 (left). Hook-on voltammeter

Figure 2 (below). Portable $3^1/_2$-pound hook-on a-c wattmeter with single knob switching for six ranges from 3 to 300 kw, 120 to 600 volts

Paper 50-111, recommended by the AIEE Instruments and Measurements Committee and approved by the AIEE Technical Program Committee for presentation at the AIEE North Eastern District Meeting, Providence, R. I., April 26–28, 1950. Manuscript submitted November 23, 1949; made available for printing March 9, 1950.

A. J. CORSON and A. L. NYLANDER are both with the General Electric Company, West Lynn, Mass.

The authors gratefully acknowledge the assistance of several associates in the development of this instrument, particularly, S. C. Haley, who did much of the original work including the compensation for reluctance torque errors.

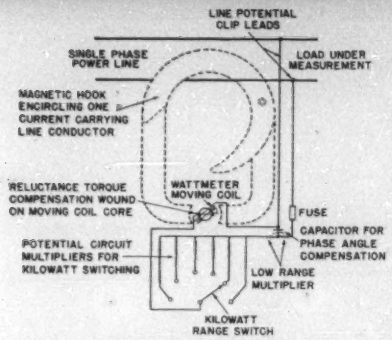

Figure 3 (left). Schematic diagram of hook-on wattmeter. Connections for single-phase power measurement also are shown

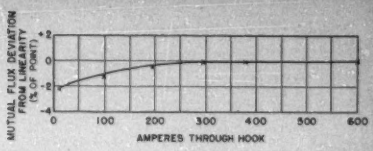

Figure 5 (above). Linearity deviation characteristic of hook-on wattmeter mutual flux

that range changing can be accomplished by potential switching alone.

The Magnetic Circuit

Returning to the magnetic circuit, it is required that this circuit deliver an appropriate value of useful flux, as a linear function of current, and without a substantial shift in phase angle over a range of 15 to 600 amperes, in order to make equation 1 valid. This was accomplished as follows:

1. The concept of a central core of useful magnetic material, plus a leakage sleeve, was adopted. See Figure 4. The cross section of the leakage sleeve is as close to proportionality with the leakage flux, as manufacture will permit. This objective was closely attained, as shown by the relative flux densities.

2. Air gaps are interposed, as illustrated in Figure 4. The reluctance of these gaps is sufficiently high to dominate the magnetic circuit, and incidentally, to provide insulation between current and potential circuits.

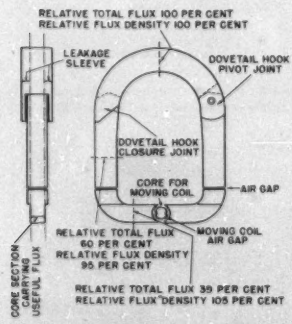

Figure 4. Hook-on Nicalol magnetic structure, showing cross-sectional area proportioned to carry useful flux and leakage flux

3. The magnetic hook must be in such mechanical form, that it can be opened and closed. The effect of the resultant discontinuity in the magnetic circuit is minimized by the use of a long dove-tail joint, as illustrated in Figure 4. This is particularly important where, under difficult conditions, the hook may remain slightly open, due to foreign material or mechanical interference. Also, the resultant flux concentration, with or without partial opening, will limit the maximum principal flux density to values considerably less than the values indicated by the saturation curve of the material used.

It is shown in the Appendix that the required mutual flux is

$$\Phi = T_v \frac{981}{NI} \frac{\pi}{4} \tag{6}$$

Numerical values of the necessary mutual flux are computed by substituting reference condition values in equation 6.

There is an appreciable lagging phase displacement of the mutual flux, with respect to the current over the range of 15-600 amperes. The corresponding phase angle of the potential circuit is practically nil and compensation is therefore necessary. Of the several possible methods, the introduction of a similar phase displacement in the moving coil current by a shunt capacitor is used.

Design Constants and Performance Data

The instruments constants and performance data, Table I, in general, substantiate the predicted values. These test results on a hand-made preproduction sample may be modified when data on significant quantities of tool-made instruments are available. The instrument covers a measurement range of 3 to 300 kw in full scale rating. The equivalent scale length, obtained by multiplying geometrical scale length by the number of ranges, is 15 inches. The low-weight of $3^1/_2$ pounds is obtained by use of the direct-acting principle and suitable proportioning of the hook, as shown in Figure 4. A factor of merit $T/W^{1.5}$ of 0.86, together with a free period of 0.5 second and a damping constant of 2.2 dyne centimeters per radian per second, are ample values for quick, accurate indication, even under adverse conditions of use. The instrument is magnetically damped. The potential circuit rating is dictated by the sensitivity requirement on the one hand and permissible temperature rise on the other. The volt-ampere consumption of the potential circuit is negligible for power system measurements.

Calibration

As for any instrument, there is general agreement as to the use of initial or basic accuracy, plus a tolerance for unusual operating conditions, such as extremely high or low ambient temperature, abnormal wave form, and so forth. The performance data on this instrument are so arranged. Care in the basic design, plus compensation already discussed, result in satisfactorily minimizing errors due to particular conditions. The influence of conductor position in the hook is $2^1/_2$ per cent maximum when using a $^1/_2$-inch diameter conductor in extreme positions. This results from changes, with the conductor position, of the magnetic circuit mmf distribution and leakage patterns.

The scale distribution of the instrument is substantially linear, and departures from linearity, see Figure 6, are a measure of imperfections in alignment of the core, with respect to the pole pieces. Main-

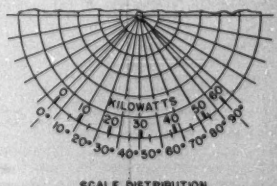

Figure 6. Scale distribution based on mean characteristic of all ranges for best tracking

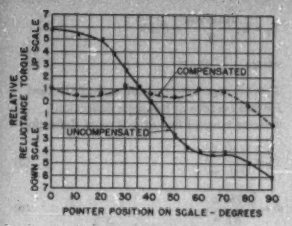

Figure 7. Reluctance torque effect

Potential circuit alone energized at 150 volts on 3-kw range

tenance of this alignment should insure adequate control of distribution in production. The scale tracking on the six scale ranges is influenced by two factors: magnetization curve of the hook already discussed, and the moving coil reluctance torque. This reluctance torque is due to the circumstance that the total flux linking the moving coil, as a result of moving coil magnetomotive force only, is a function of the coil position. It is a second order effect and is usually negligible in a construction of this kind. In the hook-on wattmeter, however, with its necessarily wide range of moving coil magnetomotive forces, the error is appreciable, when operating under the worst condition, Figure 7. Compensation therefore is necessary.

The reluctance torque is essentially zero at center scale and increases as the scale extremities are approached. Its direction is such that the moving coil tends to return to its central position. Compensation consists of a series magnetizing winding centrally located on the core, Figure 3, thus producing a counter torque of approximately the same relationship as the reluctance torque. Both the reluctance torque and the compensating torque will vary as the voltage squared, so compensation is independent of the applied potential. The necessary concentration of the compensating winding, however, prevents an exact duplicate of the reluctance torque curve; hence, approximate compensation is achieved.

Application

The resulting hook-on wattmeter, illustrated in Figure 2, is applicable to active and reactive power measurements in single and polyphase circuits. Connections are similar to those of the conventional single-phase wattmeter, allowing for the circumstance that the hook surrounds the current carrying conductor. In addition, a 3-phase balanced power measurement, made possible by the hook-on method, is accomplished by the reversed current connection, shown[2] in Figure 8. The current lead number 1 goes through the hook in a direction opposite to that of number 2, resulting in vector addition of the currents and voltages, as shown in the vector diagram.

When V_{13} is applied to the potential circuit, and currents 1 and 2 magnetize the hook, as indicated $(-I_1+I_2)$ at unity power factor, the resultant line voltage and $\sqrt{3}$ times line current are in phase. At any power factor, $\cos\theta$, the instrument will read $\sqrt{3}I_{line}V_{line}\cos\theta$ and is thus direct reading for 3-phase balanced power.

Table I. Instrument Constants and Performance Data

General	Instrument Constants
Power range, full scale, kw	3/6/20/60/200/300
Voltage range, volts	100–600
Current range, amperes	15–600
Size, inches	14 1/2 long by 4 wide by 2 1/4 deep
Diameter of hook opening, inches	2
Weight, complete, pounds	3.5
Scale	
Pointer radius, inches	1.623
Scale angle, degrees	90
Scale length	2.5
Moving System	
Full-scale torque, gram millimeter	0.40
Weight of moving element, grams	0.60
Ratio: full scale torque/weight	0.67
Ratio: full scale torque/weight$^{1-5}$	0.86
Free period, seconds	0.60
Critical damping constant	4.8
Per cent critical damping	31
Damping factor	2.8
Response time, seconds	1.3
Potential Circuit	
Multiplier resistance per kilowatt of scale capacity, ohms	6,000
Multiplier total resistance, megohms	1.8
Potential circuit phase-angle compensation. Lag of moving coil current with respect to line potential, degrees	2.1
Performance	**Instrument Performance**
Accuracy classification (per cent of full scale	3–5
Frequency error 55–65 cycles, per cent	0.2
Power factor error, power factor 0.5 lagging to 0.5 lagging to 0.5 leading over 6 to 200 kw range, per cent	±1
Maximum sustained operation influence, per cent full scale	—0.7
Ambient temperature error ±10°C	±0.5%
Temperature rise	Hot spot °C —47°C
High potential test, rms a-c volts hook to potential circuit	4,000
Wave form error, per cent full scale	—0.3% with 10% 3rd and 10% 5th harmonics

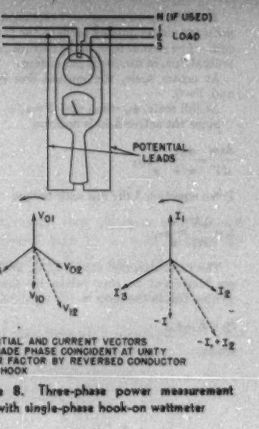

Figure 8. Three-phase power measurement with single-phase hook-on wattmeter

Conclusion

This development has resulted in the extension of the hook-on method of measurement to include single and polyphase power.

It has been accomplished by the development of an accurate, light-weight, portable, single-phase hook-on wattmeter, having wide measurement range. Simple switching and direct reading scales have resulted in one-hand operation and minimum possibility of error in use.

Appendix

The relationship between the torque and mutual flux is developed as follows:

For a constant permeability magnetic circuit, the coefficient of mutual inductance M' is, by definition, equal to the flux linkages in the moving coil circuit per ampere in the hook circuit, or

$$M' = \phi_m \frac{N}{i_1} \qquad (2)$$

where

ϕ_m = mutual flux, maxwells
N = moving coil turns

substituting in equation 1

$$t_y' = i_2' N \frac{d\phi m}{dY}$$

We now substitute practical units by letting

t_y = torque at angle Y in gram millimeters = $ty'/98.1$
i_2 = current in amperes = $i_2' \times 10$

$$t_y = \frac{(i_2 N)}{981} \times \frac{(d\phi m)}{dY} \qquad (3)$$

The first term, equation 3 represents the potential circuit ampere turns in the moving coil. The second term is the current circuit mutual flux, in maxwells per radian.

At center scale, the mutual flux $\phi_m = 0$ and $Y = 0$.

At full scale, $\phi_m = \phi_{m1}$ and $Y = \pi/4$.

Since the active field is uniform

$$\frac{d\phi m}{dY} = \frac{\phi_{m1}}{\pi/4} = \frac{4}{\pi}\phi_{m1} \tag{4}$$

From equation 3 the full scale torque

$$t_y = \frac{i_2 N}{981} \times \frac{4}{\pi}\phi_{m1}$$

The instantaneous values t_y, i_2, and ϕ_{m1} are converted to rms values by first rewriting this in the form

$$t_{y_1} = K_1 i_2 \phi_{m1}$$

where

$$K_1 = \frac{4}{981\pi}$$

at unity power factor

$$i_2 = I_{max} \sin \omega t$$
$$\phi_{m1} = \Phi_{max} \sin \omega t$$

where

I_{max} = maximum current at full scale
Φ_{max} = maximum flux at full scale

If the free period of the instrument greatly exceeds the period of the current and flux, the average torque

$$T_y = \frac{K_1}{T}\int_0^T i_2 \phi_{m1} dt$$

$$= \frac{K_1}{T}\int_0^T I_{max}\Phi_{max} \sin^2 \omega t dt$$

$$T_y = K_1 \frac{I_{max}\Phi_{max}}{2} = K_1 I \Phi$$

where

T_y = average torque at full scale deflection
I = rms current at full scale deflection
Φ = rms mutual flux at full scale deflection

$$T_y = \frac{(IN)}{981}\frac{4}{\pi}\Phi \tag{5}$$

$$\Phi = T_y \frac{981}{NI}\frac{\pi}{4} \tag{6}$$

References

1. Electrical Measurements (book). Frank A. Laws. McGraw-Hill Book Company, New York, N. Y., 1938, page 64.

2. Commercial A-C Measurements (book). G. W. Stubbings. Chapman and Hall, Ltd., London, England, 1930, page 67.

No Discussion

Determination of Effective Oil Temperature in a Transformer

MARTIN F. BEAVERS
MEMBER AIEE

TOP oil temperature and winding temperature by resistance are determined by direct measurements when a heat run is made on a transformer in accordance with the American Standards Association Test Code[1] for transformers. However, the average oil* temperature is not directly measureable. The test code states that the average oil temperature may be approximated by subtracting one-half of the tank temperature gradient (as determined by measurement of the temperature at the top and bottom surfaces of the external cooling means) from the top oil temperature.

Since it is the oil immediately surrounding the windings which cools the windings, it is logical to assume that if the load on the transformer is suddenly reduced to zero, the windings will immediately begin cooling to the temperature of the surrounding oil which is effectively cooling the winding. In other words, the effective oil temperature is the temperature to which the winding is cooling at the instant of shutdown of a heat run.

This paper shows how the data obtained in taking several hot-resistance measurements on the windings immediately following shutdown of a continuous heat run on a transformer can be used to determine the effective oil temperature and time constant of each individual winding, as well as the winding temperature at instant of shutdown.

This paper also gives the results of analysis of heat runs on several transformers. The study shows that the average oil temperature as determined in accordance with the Test Code is in fairly close agreement with the effective oil temperature obtained from the resistance-time data methods as described herein.

If the true effective oil temperature is established by one of these methods, it is very probable that a developmental investigation will show that a simple system of tank and/or cooling-tube temperature measurements may be used to calculate the effective oil temperature more directly.

In this respect, the methods are offered as useful tools in the search for a better understanding of transformer thermal characteristics.

Resistance-Time Cooling Curve of Winding

One of the methods recognized by American Standards Association[1] in obtaining the temperature of windings at instant of shutdown is to take several hot-resistance readings at different time intervals. By plotting this resistance-time data on linear co-ordinate paper and extrapolating back to zero time (instant of shutdown), the resistance at instant of shutdown may be obtained. The winding temperature at shutdown is then determined from this value of resistance.

If the first of several hot-resistance readings on a winding is sufficiently close to the instant of shutdown to permit accurate extrapolation of the cooling curve back to zero time, the resistance (R_0) at instant of shutdown may be determined quite accurately as shown by the high-voltage coil curve in Figure 1.

If, however, the cooling curve must be extrapolated from two or three minutes back to shutdown, the value of R_0 is subject to an appreciable error by this method as illustrated by the dashed part of the low-voltage coil curve in Figure 1. For such cases, two alternate methods are suggested later for a more accurate determination of the value of R_0.

Windings Cool Exponentially

It has been well established[2,3,4] that windings cool in accordance with the general relation

$$K\theta^n dt = -Cd\theta \qquad (1)$$

where

θ = temperature rise of winding over oil at any time t after start of cooling period
K = heat transfer coefficient, winding to oil
t = time after start of cooling
C = heat storage capacity of winding

If a winding cools linearly as a function of the heat loss, the solution of this equation is

$$\theta = \theta_0 e^{-t/\tau} \qquad (2)$$

where θ_0 is the winding rise over oil at start of cooling period and τ is the time constant of the winding.

If a winding cools as a function of (loss)^n, where n is any value other than 1, the solution of equation 1 is

$$\theta = \theta_0\left[1+(n-1)\frac{t}{B}\right]^{-\frac{1}{n-1}} \qquad (3)$$

where $B = \theta_0 C/K\theta_0^n$

After analyzing the resistance-time data on several different types of transformers, it was concluded that when the value of n was not over about 1.25, the results using equation 2 were sufficiently accurate to justify the use of equation 2 in the majority of the cases analyzed. Equation 2 lends itself to relatively simple mathematical manipulation and permits a satisfactory solution whereas the solution by equation 3 may be extremely difficult.

For these reasons, the methods pre-

*All references to "oil" in this paper include synthetic liquids as well as mineral transformer oil.

Paper 50-112, recommended by the AIEE Transformers Committee and approved by the AIEE Technical Program Committee for presentation at the AIEE North Eastern District Meeting, Providence, R. I., April 26–28, 1950. Manuscript submitted January 23, 1950; made available for printing February 27, 1950.

MARTIN F. BEAVERS is with the General Electric Company, Pittsfield, Mass.

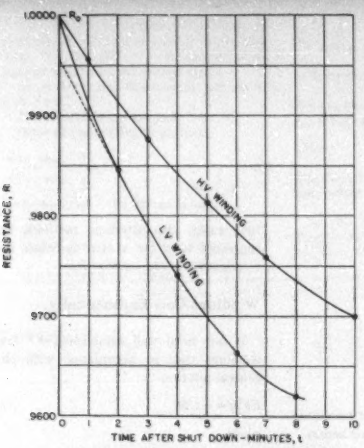

Figure 1. Resistance-time cooling curves of windings having exponential decay characteristics

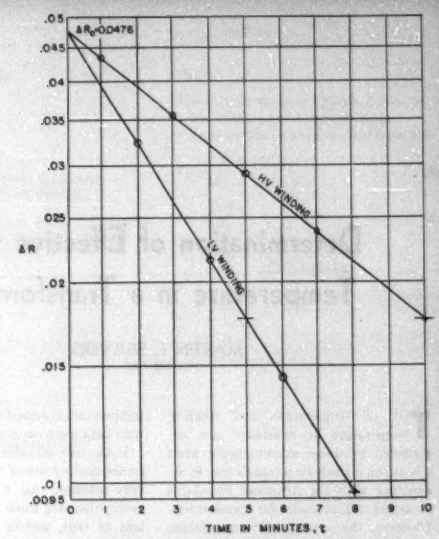

Figure 2. Resistance increment, ΔR, versus time t, for windings which cool exponentially, plot as a straight line on semilogarithmic co-ordinate paper

sented in this paper assume that all windings cool in accordance with equation 2.

Since resistance changes are directly proportional to temperature changes, the differential ΔR between the hot resistance R and the resistance R_e to which the winding is cooling at instant of shutdown will vary exponentially, that is,

$$\Delta R = R - R_e = \Delta R_o e^{-t/\tau} \qquad (4)$$

where R_e, called hereafter "effective resistance," is the resistance corresponding to the effective oil temperature.

ΔR_o is the resistance differential at instant of shutdown, that is, $\Delta R_o = \Delta R$ when $t=0$, or $\Delta R_o = R_o - R_e$ where R_o is the hot resistance at instant of shutdown.

Exponential Curve Plots as Straight Line on Semilogarithmic Co-ordinate Paper

Any data having an exponential relationship will plot as a straight line on semilogarithmic co-ordinate paper.[3,4]

As an illustration, consider the case of a hypothetical transformer having the characteristics shown in Table I.

From the data shown in Table I, the relation of ΔR and t may be tabulated as shown in Table II.

These data are plotted on semilog paper as shown in Figure 2 and it will be observed that all of the points fall on a straight line. Extrapolating the lines back to zero time, the value of ΔR_o for both high-voltage and low-voltage windings is observed to be 0.0476 which, when added to $R_e = 0.9524$, results in the value of $R_o = 1.0000$ (the originally assumed value of the shutdown resistance).

This illustrates, therefore, that the resistance differential (ΔR) versus time (t) of a winding which cools exponentially will plot as a straight line on semilog co-ordinate paper if the values of R and R_e are accurately determined.

Table I

	High Voltage	Low Voltage	Top Oil	Eff. Oil
Temperature rises, degrees centigrade	55.0	55.0	45.0	40.0*
Time constant of winding*, minutes	10.0	..	5.0	
Resistance measurements:**				
Cold (at 25 C)	0.8250		0.8250	
Hot resistance (R),				
At 1 minute†	0.9955			
At 2 minutes	0.9843			
At 3 minutes	0.9877			
At 4 minutes	0.9738			
At 5 minutes	0.9813			
At 6 minutes	0.9668			
At 7 minutes	0.9761			
At 8 minutes	0.9620			
At 10 minutes	0.9609			

*The time constants and effective oil temperature are normally unknown, but for the purpose of establishing data for the hypothetical transformer, the values shown were used. The solution of the problem should result in these values.

**All resistance values are calculated on the basis of $R_o = 1.0000$ at 80 degrees centigrade (=55 degree-centigrade rise+25 degree-centigrade ambient). Hot resistance values are calculated according to the relation $R = (\Delta R + R_e)$ where $R_e = 0.9524$ that is, R_e is the resistance corresponding to 65 degrees centigrade (=40 degree-centigrade rise+25 degree-centigrade ambient) effective oil temperature and $\Delta R = \Delta R_o e^{-t/\tau}$. In this case, $\Delta R_o = (1.0000 - 0.9524) = 0.0476$.

†The resistance-time data are plotted in Figure 1.

Determination of Effective Oil Temperature and the Resistance R_e at Shutdown

For the purpose of the illustrative hypothetical transformer just described the value of effective resistance R_e was known to be 0.9524. However, the resistance-time data taken immediately at the termination of a heat run do not immediately disclose the value of R_e. In fact, it is this value which is to be determined.

As indicated previously, the basic assumption in this paper is that a winding cools exponentially from its temperature at instant of shutdown to the mean temperature of the oil which is effectively cooling the winding at the time of shutdown. Since the oil temperature change very slowly after the load is removed very little change will occur during the

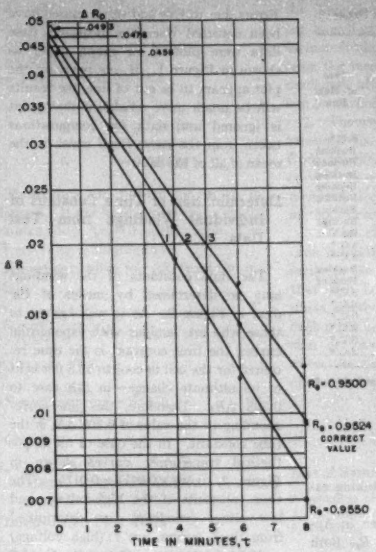

Figure 3 (left). Resistance increment, ΔR, versus time t for various values of effective resistance, R_o. Time constant is 5.0 minutes

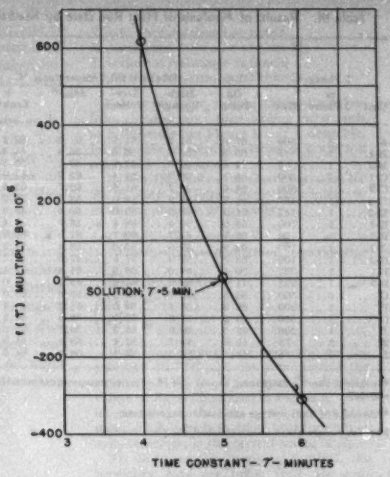

Figure 5 (right). Graphical determination of the time constant τ of a winding. See text for $f(\tau)$

five to ten minutes usually required to obtain several hot-resistance readings on the windings.

Proceeding on this basic assumption, it is only necessary to find, by trial and error, the value of R_o which, when subtracted from the various values of R, will produce a straight-line plot of ΔR $(=R-R_o)$ versus time (t) on semilog paper.

Such a procedure is illustrated in Figure 3 for the low-voltage winding resistance-time data of the hypothetical transformer referred to previously. Assume, for example, that the first selection of a value of R_o is 0.9550. A plot of ΔR versus t on semilog paper is shown by curve 1. It will be observed that the points in the long-time region are below a straight line drawn through the two points nearest zero time. This indicates that the value of R_o is too high. Now assume that $R_o=0.9500$ is chosen. The plot of ΔR versus t for this value is shown by curve 3. It will be observed that the points in the long-time region are now above the straight line through the first two points, indicating that the value of R_o is too low. The correct value of R_o is obviously between 0.9500 and 0.9550. Another try or two will show that a value of $R_o=0.9524$ will cause all of the points to lie on a straight line, indicating that 0.9524 is the correct value of R_o.

It is interesting to observe that even with a relatively large change in value of R_o, the value of R_0 (the resistance at instant of shutdown) is not greatly in error. For example, curve 1 in Figure 3 gives a value of $\Delta R_0=0.0456$ and $R_0=0.9550+0.0456=1.0006$, while curve 3 gives a value of $\Delta R_0=0.0493$ and $R_0=0.9500+0.0493=0.9993$, whereas the correct values from curve 2 are $\Delta R_0=0.0476$ and $R_0=0.9524+0.0476=1.0000$.

Referring to the usual linear plot of R versus t shown in Figure 1, the dashed

Figure 4. Resistance increment, ΔR, versus time t for various values of effective resistance, R_o. Time constant is 30.0 minutes

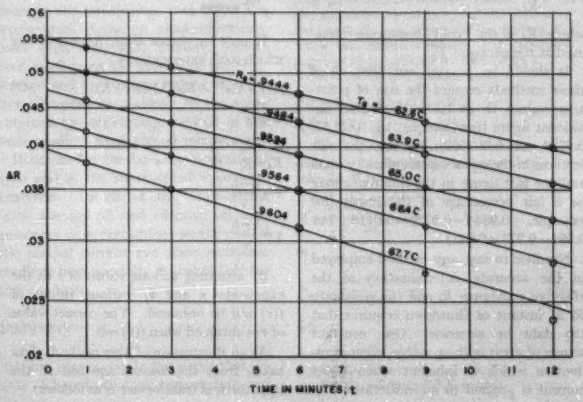

Table II

High Voltage Winding		Low Voltage Winding	
Time t, Minutes	$\Delta R=(R-R_o{}^*)$	Time t, Minutes	$\Delta R=(R-R_o{}^*)$
1	0.0431	2	0.0310
3	0.0353	4	0.0214
5	0.0280	6	0.0144
7	0.0237	8	0.0096
10	0.0175		

* $R_o=0.9524$.

Table III. Results of Analysis of Heat Run Data by Methods Described in this Paper

Unit	1 Phase or 3 Phase	Kva	Top Oil Temp.	Effective Oil Temperature, °C High-Voltage	Low-Voltage	Avg.**	Tank†	Time Constant, Minutes High-Voltage	Low-Voltage	Type of Heat Run
A	3	500	67.0	61.2	61.7	61.5	62.1	9.5	10.3	S.C.*
B-1	1	75	60.8	56.8	56.0	56.4	58.9	13.8	16.8	Bucking
B-2	1	75	61.6	55.3	58.9	57.1	59.6	18.8	13.1	Bucking
C-1	1	500	68.1	63.9	61.4	62.7	64.0	5.3	7.8	Bucking
C-2	1	500	68.6	63.7	61.6	62.7	63.8	5.7	4.7	Bucking
D-1	1	167	63.0	58.2	58.0	58.1	58.2	7.3	4.6	Bucking
D-2	1	167	64.2	60.2	59.0	59.6	59.9	6.6	4.8	Bucking
E-1	1	100	65.0	59.4	58.4	58.9	59.4	11.1	5.4	Bucking
E-2	1	100	66.3	61.7	60.7	61.2	61.3	12.5	6.4	Bucking
E-1	1	100	62.9	57.8	55.0	56.4	57.2	10.4	7.4	S.C.*
E-2	1	100	63.2	57.3	57.3	57.3	57.2	11.8	6.7	S.C.*
F-1	1	333	70.1	62.0	66.8	64.4	63.4	7.7	6.3	Bucking
F-2	1	333	71.2	63.9	63.4	63.7	66.0	7.5	6.7	Bucking
G	3	300	63.5	58.7	59.2	59.0	60.0	8.2	8.7	S.C.*
H	1	200	60.2	54.4	54.0	54.2	54.4	9.2	5.9	S.C.*
I	1	500	63.5	57.8	59.7	58.8	59.2	8.2	6.0	S.C.*
J	1	200	59.5	49.9	51.5	50.7	55.0	12.4	9.1	S.C.*
K	3	75	59.3	59.7	52.4	56.1	54.9	11.6	11.5	S.C.*
L	3	75	58.1	58.6	53.3	56.0	54.0	12.4	10.1	S.C.*

*In case of short-circuit tests, top oil and effective oil temperature was determined at end of normal current run only.

**Average of high-voltage and low-voltage values.

†Top oil temperature minus one-half the tank gradient.

curve for the low-voltage winding illustrates that a value of $R_0 = 0.9970$ might result from a long extrapolation of the plot back to zero time.

It should be pointed out that for the sake of accuracy, the hot-resistance readings should be taken over a period of time approximately as long as the time constant of the winding under test.

For example, if the time constant of a winding is 30 minutes, resistance readings out to only eight or nine minutes will result in a straight-line plot of ΔR versus t on semilog paper for a wide range of values of R_e. This is illustrated in Figure 4. It will be observed, however, that readings plotted at 12 minutes will more definitely indicate the correct value of R_e. Readings at 20 to 30 minutes will give even better results.

When resistance readings have to be taken over a very long period, consideration must be given to the drop in effective oil temperature which will occur during the extended period of readings. In other words, if the oil temperature is one degree lower at the time a certain value of hot resistance is obtained, this resistance reading should be corrected to a value corresponding to one degree higher temperature. Thus, all of the hot-resistance values so obtained will correspond to the condition of a constant oil temperature.

It has been observed that the effective oil temperature changes very nearly the same amount as the top oil temperature, therefore correction for change in effective oil temperature may be made in accordance with top oil temperature changes during the period of taking extended resistance-time data.

Two other methods are given in Appendix for the determination of R_e. Both of these methods require a precise determination of the shutdown resistance R^0.

Two alternative methods are also given in the Appendix for the determination of R_0 which may be useful when a long extrapolation of the usual resistance-time plot on linear co-ordinate paper might give chance to an appreciable error in R_0.

Knowing the correct value of R_e, the effective oil temperature T_e may be determined from the relation

$$T_e = \frac{R_e - R_c}{R_c}(T_c + 234.5) + T_c \qquad (5)$$

where R_c is the "cold" resistance measured at temperature T_c.

It should be pointed out that all of these methods require the use of resistance values to at least the fourth significant figure (for example, 186.6, 11.17, 0.9726, or 0.007562) because the differences in the equations are usually small and the last figure in the difference may be a fair percentage of the result (for example, $0.9844 - 0.9726 = 0.0118$ but $0.984 - 0.973 = 0.011$).

Needless to say, any method employed in the accurate determination of the effective resistance R_e and the resistance R_0 at instant of shutdown requires that the data be accurate. One constant source of error is the possible effect of induction which is inherent when direct current is applied to an inductance coil. Errors due to this and other causes have been detected when the resistance-time data were plotted on graph paper as shown in Figure 1. If one point on the plot appears to be out of line, the results will be much more reliable if that point is ignored and data for computations taken from the curve itself which is the mean of all of the data.

Determination of Time Constant of Individual Windings from Test Data

The time constants of the windings may be determined by means of the data in Figure 2. As is well known to those who are familiar with exponential curves, the time constant is the time required for the coil to cool to 36.8 per cent of its ultimate change—in this case to 0.368 ΔR_0. Therefore, the time corresponding to the value of 0.368 ΔR_0 is the time constant. In the case of the hypothetical transformer curves shown in Figure 2, $0.368 \times 0.0476 = 0.0175$. The time constants of the high-voltage and low-voltage windings, as determined from these curves, are τ (high voltage) $= 10.0$ minutes and τ (low voltage) $= 5.0$ minutes, which are the originally assumed values.

The time constant also may be determined by substituting the correct value of R_e in the equation

$$\tau = \frac{0.434t}{\log \dfrac{R_0 - R_e}{R - R_e}} = \frac{0.434t}{\log \dfrac{\Delta R_0}{\Delta R}} \qquad (6)$$

For the case just cited, τ for the high-voltage coil is

$$\tau = \frac{0.434 \times 5}{\log \dfrac{0.0476}{0.0289}} = \frac{2.170}{\log 1.65} = 10.0 \text{ minutes}$$

It may be shown that, for a winding which cools exponentially

$$f(\tau) = K_1 e^{-x} - K_2 e^{-y} + (K_2 - K_1) \qquad (7)$$

where

$K_1 = R_1 - R_2$

$K_2 = R_1 - R_3$

$x = \dfrac{t_2 - t_1}{\tau}$

$y = \dfrac{t_3 - t_1}{\tau}$

By assuming various values of τ in the exponents x and y, various values of $f(\tau)$ will be obtained. The correct value of τ is obtained when $f(\tau) = 0$.

As an illustration of this method, data taken from the low-voltage coil of the hypothetical transformer is as follows:

$R_1 = 0.9843$ $\quad t_1 = 2$ minutes
$R_2 = 0.9738$ $\quad t_2 = 4$ minutes
$R_3 = 0.9620$ $\quad t_3 = 8$ minutes
$K_1 = 0.9843 - 0.9738 = 0.0105$
$K_2 = 0.9843 - 0.9620 = 0.0223$

τ	$f(\tau)$
4	0.000617
5	0.000004
6	−0.000316

These data are plotted as shown in Figure 5. It will be observed that $\tau = 5.02$ minutes where $f(\tau) = 0$ on the graph. The correct value is 5.0 minutes.

Knowing τ, solve for ΔR_0 from the relation

$$\Delta R_0 = \frac{R_1 - R_2}{e^{-t_1/\tau} - e^{-t_2/\tau}}$$

In the case cited

$$\Delta R_0 = \frac{0.0105}{e^{-2/5} - e^{-4/5}} = 0.0476 \qquad (8)$$

Solve for

$$R_e = R - \Delta R_0 e^{-t/\tau}$$
$$= 0.9843 - 0.0476 e^{-2/5} = 0.9524$$

Transformer Test Data

Resistance-time data taken from heat-run test records on several transformers of various ratings have been analyzed by the methods outlined in this paper and the results on typical ratings are shown in Table III.

It will be observed that the effective oil temperature as determined from the high-voltage coil data is, in most cases, different from the value as determined by the low-voltage coil data. This indicates, as might be expected, that the size of the ventilating ducts, relative position of the windings to each other and to the core, as well as the division of losses in the transformer, may affect the temperature of the oil which effectively cools each individual winding. However, in all cases, the average of the high-voltage and low-voltage values of effective oil agrees very closely to the value obtained by subtracting one-half of the tank gradient from top oil temperature.

Heat runs of the bucking (opposition) type and of the short-circuit type were analyzed. In all of the short-circuit tests, the top oil and effective oil temperatures were determined at the end of the normal current run since resistance readings were normally available only for this condition.

Summary

It has been shown in this paper that:

1. The effective oil temperature and the thermal time constant of each winding, as well as the winding temperature at instant of shutdown, can be determined from the resistance-time data taken immediately after the shutdown of a heat run on a transformer.

2. The average oil temperature as determined in accordance with the Test Code checks, within limits of test accuracy, the effective oil temperature determined by the resistance-time data methods described in this paper.

3. The effective oil temperature for each individual winding may not necessarily be the same value. This indicates that such factors as size of ventilation ducts, relative position of the windings to each other and to the core, and the division of loss in the transformer, may affect the temperature of the oil which effectively cools each individual winding.

Appendix

List of Symbols

θ = winding rise over oil at time t after shutdown of heat run
θ_0 = winding rise over oil at instant of shutdown
e = 2.718
R = hot resistance measured at time t after shutdown of heat run
R_0 = resistance at instant of shutdown
R_e = effective resistance, that is, the resistance corresponding to the effective oil temperature
ΔR = resistance differential, that is, $(R - R_e)$
ΔR_0 = resistance differential at instant of shutdown, that is, $(R_0 - R_e)$
τ = time constant of winding, minutes
t = time after shutdown of heat run, minutes

Determination of Shutdown Resistance R_0

Since a long extrapolation of the resistance-time cooling curve back to zero time may give chance to an appreciable error in the shutdown resistance, R_0, the following two methods are suggested for finding R_0. These two methods assume that the windings cool in accordance with equation 2.

Solve for R_0 in the expression

$$\left(\frac{R_0 - R_1}{R_0 - R_2}\right)^2 = \frac{R_0 - (2R_1 - R_{21})}{R_0 - (2R_2 - R_{22})} \qquad (9)$$

This expression may be reduced to a quadratic of the form $ax^2 + bx + C = 0$, the solution of which is

$$X = \frac{-b \pm \sqrt{b^2 - 4ac}}{2a}$$

or

$$R_0 = \frac{-b \pm \sqrt{b^2 - 4ac}}{2a} \qquad (10)$$

where

$a = R_{22} - R_{21}$
$b = R_1(R_1 - 2R_{22}) - R_2(R_2 - 2R_{21})$
$c = R_1^2(R_{22} - 2R_2) - R_2^2(R_{21} - 2R_1)$

and where

R_1 is the hot resistance at time t_1
R_{21} is the hot resistance at time $2t_1$
R_2 is the hot resistance at time t_2
R_{22} is the hot resistance at time $2t_2$

Values of R for various times are taken from the resistance-time cooling curve such as is illustrated in Figure 1. It is desirable, for the sake of accuracy, to select t_1 and t_2 a reasonable time apart.

Rather than solve the above equation for R_0, it may be found more convenient to solve the problem graphically.

Let $A = R_0 - R_1$, $B = R_0 - R_2$
$C = R_0 - (2R_1 - R_{21})$, $D = R_0 - (2R_2 - R_{22})$

Then, for equation 9

$$\left(\frac{A}{B}\right)^2 = \frac{C}{D}$$

Plot two curves, one representing the quantity $(A/B)^2$ and one representing the quantity C/D, as a function of assumed values of R_0, as illustrated in Figure 6. The intersection of the two curves occurs at a value of R_0 which satisfies both quantities and, therefore, is the correct value of R_0.

To illustrate this graphical method, the necessary data are taken from the low-voltage coil curve in Figure 1 and are tabulated as follows:

$R_1 = 0.9843$, $\quad t_1 = 2.0$ minutes
$R_{21} = 0.9738$, $\quad 2t_1 = 4.0$ minutes
$R_2 = 0.9738$, $\quad t_2 = 4.0$ minutes
$R_{22} = 0.9620$, $\quad 2t_2 = 8.0$ minutes

$A = R_0 - R_1 = R_0 - 0.9843$
$B = R_0 - R_2 = R_0 - 0.9738$

$C = R_0 - (2 \times 0.9843 - 0.9738) = R_0 - 0.9948$
$D = R_0 - (2 \times 0.9738 - 0.9620) = R_0 - 0.9856$

$$\left(\frac{A}{B}\right)^2 = \left(\frac{R_0 - 0.9843}{R_0 - 0.9738}\right)^2 \cdot \frac{C}{D} = \frac{R_0 - 0.9948}{R_0 - 0.9856}$$

Substituting various assumed values of R_0 in the foregoing equations, Table IV is obtained.

The curves for R_0 versus $(A/B)^2$ and R_0 versus C/D are plotted in Figure 6. The intersection of these curves occurs at $R_0 = 1.0000$, the correct value.

Determination of the Effective Resistance R_e

The effective resistance, R_e, also may be determined by calculations for windings which cool exponentially. Two methods are suggested as follows:

(1). From equation 4, it can be shown that

$$\frac{1}{\tau} = \frac{2.303}{t_1} \log \frac{R_0 - R_e}{R_1 - R_e} \qquad (11A)$$

Table IV

R_0	$(A/B)^2$	C/D
0.9948	0.250	0
0.9960	0.278	0.115
0.9980	0.320	0.258
1.0000	0.360	0.360
1.0020	0.394	0.439

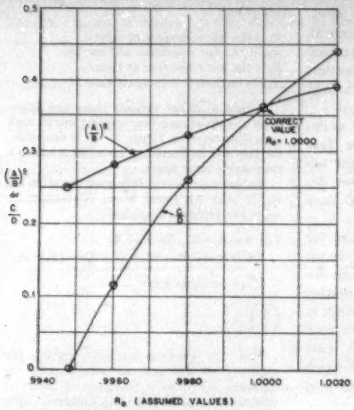

Figure 6. Graphical determination of the resistance R_e at instant of shutdown. See text for A, B, C, and D

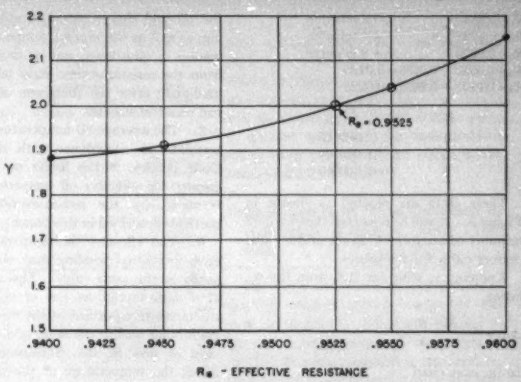

Figure 7. Graphical determination of effective resistance, R_e. See text for Y

$$\frac{1}{\tau}=\frac{2.303}{t_2}\log\frac{R_0-R_e}{R_2-R_e} \qquad (11B)$$

Equating (11A) and (11B), we obtain the relation

$$\frac{t_2}{t_1}=\frac{\log(R_0-R_e)-\log(R_2-R_e)}{\log(R_0-R_e)-\log(R_1-R_e)}=\frac{\log\Delta R_0-\log\Delta R_2}{\log\Delta R_0-\log\Delta R_1}=Y \qquad (12)$$

By substituting various values of R_e in equation 12, a different value of Y will be obtained. Plot R_e versus Y as shown in Figure 7. The value of R_e from this curve, corresponding to $Y=t_2/t_1$, represents the correct value of R_e which satisfies both equations 11A and 11B.

As an illustration of this method, an example is given using the low-voltage winding data of the hypothetical transformer in "Exponential Curve Plots As Straight Line On Semilogarithmic Co-ordinate Paper" of the paper:

$R_0=1.0000$, $R_1=0.9843$, $R_2=0.9738$
$t_1=2.0$ minutes, $t_2=4.0$ minutes.

Prepare tabulation as follows and substitute various values of Re in equation 12. Solve for Y:

R_e	$\Delta R_0 = R_0 - R_e$	$\Delta R_1 = R_1 - R_e$	$\Delta R_2 = R_2 - R_e$	$\log \Delta R_0$	$\log \Delta R_1$	$\log \Delta R_2$	Y
0.9400	0.0600	0.0443	0.0338	0.7782–2	0.6464–2	0.5289–2	0.2493/0.1318 = 1.89
0.9450	0.0550	0.0393	0.0288	0.7404–2	0.5944–2	0.4594–2	0.2810/0.1460 = 1.92
0.9500	0.0500	0.0343	0.0238	0.6990–2	0.5353–2	0.3766–2	0.3224/0.1637 = 1.97
0.9550	0.0450	0.0293	0.0188	0.6532–2	0.4669–2	0.2742–2	0.3790/0.1863 = 2.03
0.9600	0.0400	0.0243	0.0138	0.6021–2	0.3856–2	0.1399–2	0.4622/0.2165 = 2.13

Plot R_e versus Y as shown in Figure 7. The value of R_e corresponding to $t_2/t_1=4.0/2.0=2.0$ is found to be 0.9525. 0.9524 is the correct value.

(2). The maximum change in hot resistance (ΔR_0) in cooling from the resistance of the winding at instant of shutdown (R_0) to the resistance corresponding to the effective oil temperature (R_e) is

$$\Delta R_0=(R_0-R_e)=\frac{R_0-R_1}{2-\dfrac{(R_0-R_2)}{(R_0-R_1)}} \qquad (13)$$

where R_1 is the resistance at time t_1 from instant of shutdown and R_2 is the resistance obtained from the resistance-time cooling curve at time $2t_1$.

To illustrate this method, the resistance-time cooling curve for the high-voltage winding in Figure 1 will be used. From this curve, the following data are obtained:

$R_0=1.0000$, $R_1=0.9877$ at $t_1=3.0$ minutes
$R_2=0.9786$ at $2t_1=6.0$ minutes

Substituting these values in equation 13

$$\Delta R_0=\frac{1.0000-0.9877}{2-\dfrac{(1.0000-0.9786)}{(1.0000-0.9877)}}=\frac{0.0123}{2-\dfrac{0.0214}{0.0123}}=\frac{0.0123}{0.260}=0.0473$$

$R_e=R_0-\Delta R_0$, therefore, $R_e=1.0000-0.0473=0.9527$ which is in close agreement with the correct value of 0.9524.

The effective resistance also may be obtained by the trial and error method suggested in "Determination of Effective Oil Temperature and the Resistance R_0 at Shutdown" of the paper for the determination of R_e. This method also may be used as a check on the accuracy of the value of R_e obtained from methods (1) or (2) above.

References

1. Test Code for Distribution, Power, and Regulating Transformers, C57.22. American Standards Association (New York, N. Y.), 1948.

2. Temperature Limits for Short-Time Overloads for Oil-Insulated Neutral Grounding Reactors and Transformers (part II), **V. M. Montsinger, J. E. Clem.** *AIEE Transactions*, volume 65, 1946, pages 966–73.

3. Measuring Transformer Winding Temperatures Continuously with the Transformer Carrying Load, **A. M. Lockie, G. M. Stein.** *AIEE Transactions*, volume 67, part II, 1948, pages 1608–17.

4. Thermal Characteristics of Transformers, **V. M. Montsinger.** *General Electric Review* (Schenectady, N. Y.), July 1946, page 30.

5. Heating of Transformers under Short-Circuit Conditions, **V. M. Montsinger, G. H. Halsey.** *AIEE Transactions*, volume 68, part II, 1949, 947–54.

6. Cooling of Oil-Immersed Transformer Windings After Shutdown, **V. M. Montsinger.** *AIEE Transactions*, volume 36, 1917, pages 711–34.

Discussion

Paul Narbutovskih (Westinghouse Electric Corporation, Sharon, Pa.): The average temperature of transformer oil has been, in a certain sense, a subject very much like the weather: it has been frequently mentioned mostly as a somewhat hypothetical quantity, but very little has been done about it. It is a quantity elusive of experimental determination, and yet it is of considerable theoretical and practical importance in view of the fact that the recognized and the most reliable measurement of the copper temperature by resistance yields the average temperature result. Because of this, the paper by Mr. Beavers is certainly a welcome addition to the literature on the subject. A reliable and a practically simple method of determining average oil temperature by test

will go a long way toward ascertaining the thermal characteristics of a transformer.

The definition itself of the average oil temperature does not as yet appear to be sufficiently clear cut. It is natural that a practical definition of a physical quantity should be dependent upon the method available for its measurement. Since the average oil temperature in a transformer appears to be measurable as the limiting average temperature of copper after time of shutdown, this may well be accepted as the workable definition for the average oil temperature, at least for the purpose of determining a true winding to oil gradient. It must be appreciated, however, that the temperature thus defined will not be entirely adequate for other purposes, such as estimating the heat loss from transformer cooling surfaces.

In establishing any new method of measurement, the weight of experimental data is of prime importance. The writer has analyzed a considerable number of cooling curves of the transformer windings. The results, with possibly a few exceptions, are in agreement with the basic proposition stated in Mr. Beavers' paper, namely that transformer windings cool approximately according to an exponential law

$$\theta = \theta_0 \epsilon^{-t/\tau} \tag{1}$$

where

θ = temperature difference between average winding and average oil temperature at time t, minutes after shutdown

θ_0 = initial temperature difference, as above, at time of shutdown (average winding gradient)

τ = time constant of the winding, minutes

ϵ = base of natural logarithms

The method of analysis used by the writer was, however, somewhat different from that used by Mr. Beavers, and since it seems to have certain advantages, it is presented below along with some of the experimental data.

After the resistance values versus time after shutdown are obtained, instead of plotting the difference $(R-R_e)$ versus time on a semilog paper for different values of R_e—a time consuming operation, the resistance value R is directly plotted versus ratio t/τ on an exponential transient coordinate paper.[1] Since the value of the time constant τ is not known, a convenient figure may be chosen for τ, such as 5, 10, or 20 minutes. If the chosen value of τ were equal to the time constant of the winding, the plot would be approximated by a straight line. Generally, however, a considerable deviation from a straight line will exist as shown by curves A and B of Figure 1 of the discussion, of which the first one is plotted for $\tau=10$, and the second is plotted for $\tau=5$ minutes. Two such curves can be extrapolated with a fair accuracy to the time of shutdown $(t/\tau=0)$, and to time when the ultimate winding temperature (that is, average oil temperature) is reached $(t/\tau=\infty)$, taking advantage of the fact that the terminal points of all such curves are the same.

In many cases, after the curves A or B are drawn, no second approximation will be necessary. If such is desired, however, it may be determined without any random guessing at the proper value of τ required to give a straight line plot of the data. Using a straight edge laid between the first approximations of points R_0 and R_e Figure 1 and Figure 2, two values of the abscissa t/τ are noted for some convenient value of resistance R, for example, X and X_1 of which X belongs to one of the curves, while X_1 belongs to the straight line. The correct second approximation for the copper time constant, τ_1, is then calculated as

$$\tau_1 = \tau \frac{X}{X_1} \tag{2}$$

The above procedure applied to the data on Figure 1 of the discussion results in the value of the time constant $\tau=7.43$ minutes and curve C. It may be noted that the latter is not quite a straight line, indicating that the transient change in the copper temperature does not exactly conform to the exponential law. However, using this plot an extrapolation of the curve to the terminal points is probably as accurate as the original test data.

Most of the cooling curves of copper examined by the writer deviate somewhat from the exponential law, some quite appreciably. Relatively few behave in such a well-trained manner as the example given by Mr. Beavers or that given in Figure 1. In view of this the test data should extend for a period of time equal to about twice the time constant of the winding and preferably even longer. If the deviation from an exponential curve is present, the use of data extending over a period of one time constant, or less, may lead to a considerable error in the determination of the ultimate temperature of the cooling copper. This, of course, is also true when the semilog paper, or an analytical method, is employed, such as is described by Mr. Beavers, since, in this case, one must rely on a long range extrapolation, using an assumed law which may not and usually does not apply.

For accurate results a correction is required in the values of the copper resistance to compensate for any appreciable drop in the oil temperature during the test. A precise theoretical correction required is difficult to make. A reasonably accurate correction can be simply made, however, if it is assumed that the oil temperature drops linearly with time after shutdown, at least for the limited duration of the test. Furthermore, it may be assumed that the nature of the rapid transient in the copper to oil temperature differential is not affected by the relatively slow change in the oil temperature. On these assumptions the correction to be added to the experimental values of resistance may be calculated by

$$\Delta R = \frac{R_e t}{234.5+\theta_e}\left(\frac{d\theta}{dt}\right) \tag{3}$$

where

ΔR = additive correction for the test resistance values

R_e = cold winding resistance at temperature θ_e

$\frac{d\theta}{dt}$ = rate of oil temperature change during the test, degrees centigrade per minute (Top oil temperature measurements may be used)

t = time after shutdown, minutes

This correction is rather important, and even as few as $1^1/_2$- or 2-degrees centigrade oil temperature change during the test, if neglected, may lead to an appreciable error in the windings temperature gradient to oil and its time constant.

The writer had a chance to verify the foregoing method on transformers with forced circulation of oil. In many cases the oil turnover is so rapid that there is only a small temperature differential between the incoming and outgoing oil, and it may be safely assumed that the average oil temperature is equal to the arithmetic mean of the two. Applied to these transformers the method of determining the average oil temperature just described, gave results agreeing very closely with the oil temperature measured by thermocouples. As an example, in Table I of the discussion values

Table I. Values of Oil Temperature, Degree Centigrade

	Winding Number	Average Oil, θ_e	Mean Oil, In and Out of Coolers
167 per cent load	1	64	63.5
	2	65.5	66
	3	65	62
	4	61.5	62.5
133 per cent load	1	65.4	64
	2	60.5	61.5
	3	62.5	60.5
	4	64	62.5
100 per cent load, self-cooled	1	59	57.1
	3	53.5	52.5

are given obtained on a 25,000-kva shell form transformer, enclosed in a form fit tank.

In the 100 per cent load heat runs given in Table I, an appreciable difference between top and bottom oil temperature existed. Nevertheless, the mean value

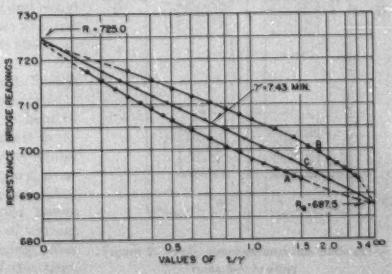

Figure 1. Variation of winding resistance in a 1,000-kva, forced air transformer, plotted versus ratio t/τ on an exponential coordinate paper

seems to be in a good agreement with the average oil temperature determined as an asymptotic average temperature of the cooling copper.

REFERENCE

1. SIMPLIFIED GRAPHICAL METHOD OF COMPUTING THERMAL TRANSIENTS, P. Narbutovskih. *AIEE Transactions*, volume 66, 1947, pages 78–83.

Andrew Hvizd, Jr. (Yonkers, N. Y.): The method proposed for determining the effective oil temperature shows possibilities of being useful not only for developmental investigations as mentioned in the paper, but also for commercial heat-run tests.

Having used this method on several heat-run tests, I should like to stress that the resistance readings taken at the culmination of a heat run be extended to a period of time greater than $1^1/_2$ times the time constant of the winding for the best results. An extension of these readings to 1/2-hour would suffice in the majority of cases.

It is specified in the paper that this method is most applicable in those instances where the n of the equation 3 is less than 1.25. Ordinarily, the value of n is unknown. Consideration should be given to a modification of the proposed method to cover all possible values of n. This could be done by observing the characteristic manner into which the test points will align themselves on semilogarithmic co-ordinate paper for values of n greater than 1.25, and some sort of criterion devised which would select the correct value of R_e. As it stands, there is no indication of the accuracy of the results while n remains unknown.

M. F. Beavers: The method suggested by Mr. Narbutovskih of plotting the resistance values of R versus the ratio of t/τ on a special exponential co-ordinate paper illustrates an interesting version of the same basic idea presented in my paper. As may be seen from equation 4 of the paper, $R = R_e + (R_0 - R_e)^{-t/\tau}$. This may be rearranged to $R = R_0 - (R_0 - R_e)(1 - \epsilon^{-t/\tau})$. By constructing the scale on the abscissa as a function of t/τ in the expression $(1 - \epsilon^{-t/\tau})$ the resistance of a winding which cools in accordance with equation 1 of the discussion will plot as a straight line on this co-ordinate paper.

For those cases where the winding cools as a function of (loss)^n, where n is any value other than 1, the cooling data will not, as pointed out by Mr. Narbutovskih and Mr. Hvizd, plot as a straight line on semilog paper. This also is true for such data plotted on the co-ordinate paper suggested by Mr. Narbutovskih. If the value of n is not substantially different from 1, the deviation of the data from a straight line in either case will not, for practical purposes, be serious. However, when n is substantially different from 1, it is necessary, as suggested, to take hot-resistance readings for a period of time equal to twice or three times the time constant of the winding. I have found that readings extending over a 30-minute period after shutdown is usually sufficient in the majority of cases.

The correction suggested by Mr. Narbutovskih in equation 3 of his discussion is essentially the same as was used by the author in correcting for drop in oil temperature during the extending period when hot-resistance readings were being taken.

Mr. Hvizd comments on the fact that the value of n in equation 3 of the paper is usually unknown for the particular winding under consideration. This is, to some degree, true. However, a little experience with this method will indicate the characteristic manner in which the points align themselves for different values of n, and as more test data are analyzed, the correct value of n for various types of windings will be obtained.

Transverse Flux Induction Heating

ROBERT M. BAKER
MEMBER AIEE

For several years following 1941, the author was engaged in the development of radio-frequency induction heating for the flow-brightening of electrolytic tin plate. In this method, the steel strip (approximately 0.01-inch thick and 30 inches or more wide) is passed through rectangular helical copper coils supplied with radio-frequency (approximately 200 kc) currents. Lines now are in operation melting the electrolytically-deposited tin coating at speeds of 1,300 feet per minute, with a power input of 1,200 kw to the strip. This method of induction heating will be called longitudinal flux induction heating because the magnetic flux is directed along the length (longitudinal to) the strip.

During the early stages of this development, it was recognized that an equally large potential field of application for induction heating existed in the heating of nonferrous strip like aluminum, brass, copper, and magnesium. It also was soon realized that longitudinal flux heating, so admirably suited to the heating of magnetic steel strip, was not satisfactory for heating nonferrous strip or stainless steel strip which does not have ferromagnetic properties. Reasoning that the limitations of longitudinal flux heating were due to the fact that the small cross-section of the nonferro-magnetic strip intercepted only a very small percentage of the flux through the inducing coil, a special method of induction heating was devised to overcome this difficulty. The method will be called transverse flux induction heating because magnetic flux is directed perpendicular to the surface and through the strip instead of along its length, as in longitudinal flux heating. Although this method of heating has not been publicized, two 300-kw pilot line installations have been made.

It is the purpose of this paper to describe the method of transverse flux heating, and to provide a mathematical analysis sufficient for design and application.

Description of Method

Transverse flux heating is accomplished by passing the strip between two opposing laminated pole structures such as shown in Figure 1. The field coils supplied with alternating current are so polarized that at any instant opposing poles have opposite sign and force flux through the strip. From the analysis to follow, it will become evident that the frequency and geometry of the pole structures will depend on the physical and electrical properties of the strip to be heated. A pole structure and coil assembly of a 300-kw 60-cycle installation is shown in Figure 2. This was designed and used to heat aluminum strip 0.040-inch thick and 54 inches wide. Frequencies used in transverse flux heating will range from 60 cycles to 10,000 cycles. The first experimental coil built and tested in 1943 was designed to operate at a frequency of 10,000 cycles and is shown in Figure 3.

The alternating magnetic field through the strip causes voltage to be generated in the strip, and currents flow to heat it. As shown in Figure 4, the currents in the strip tend to concentrate under stator slots, and if the strip is stationary, overheating will occur in these regions. Any point in a moving strip, however, moves through the various regions of current concentration and the averaging effect results in uniform heating of the strip, except near the edges. Special compensation must be provided to obtain uniform heating out to the edge of the strip, as will be explained later.

Quantitative Considerations

One could, of course, arbitrarily choose a pole structure, wind coils into the slots, and apply various frequencies to see what heating effects were obtained in a given strip, but this would obviously not be a practical or desirable procedure. It is necessary to analyze the effect of such variables as air-gap, slot dimensions, pole pitch, strip thickness and resistivity, and frequency to arrive at formulas from which an optimum design can be made.

The writer has chosen a rather formal approach to this problem, and one versed in the mathematics of skin effect will see great similarity between equations derived for transverse flux heating and those currently used to calculate longitudinal flux heating effects.

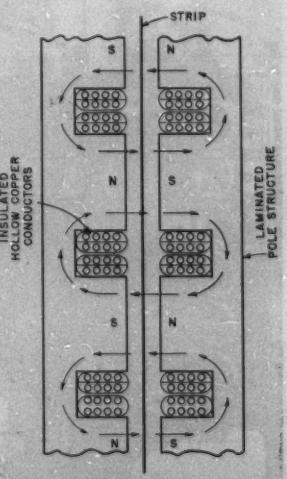

Figure 1. Pole structure and flux path transverse flux heating

Paper 50-113, recommended by the AIEE Electric Heating Committee and approved by the AIEE Technical Program Committee for presentation at the AIEE North Eastern District Meeting, Providence, R. I., April 26–28, 1950. Manuscript submitted January 26, 1950; made available for printing March 2, 1950.

Robert M. Baker is with the Westinghouse Electric Corporation, Baltimore, Md.

A definition of terms and units is included in the paper. The centimeter-gram-second system of practical units will be used, and all sinusoidally varying quantities like current, voltage, magnetizing force, flux-density, and total flux will be represented as vector quantities.

Basic Assumptions and Equations

To simplify the mathematical calculations, the following assumptions are made. (See Figure 5).

1. Because of symmetry, conditions under only one pole pitch need be considered.
2. Lines of flux in the air-gap are straight lines perpendicular to the pole faces and to the surfaces of the strip.
3. The current paths are as shown in Figure 5(B). This neglects edge effect and is justified because corrective measures must be taken in practice to obtain uniform heating.
4. The discontinuity due to slot openings can be neglected.
5. The strip is equal in width to the pole structures.
6. The magnetic drop in the steel pole structure may be neglected.
7. There is one field coil of (T_c) turns on each pole. The magnetomotive force of two of these coils is therefore active across the air-gap between each pair of poles.

On the basis of these assumptions, conditions are ideally represented in Figure 5 and one may proceed as follows:

The flux through the rectangle $ABCD$ is

$$\phi = 2b\int_0^x \boldsymbol{H}dx \tag{1}$$

The voltage induced around the loop $ABCD$ is

$$\boldsymbol{E} = -j\omega\phi 10^{-8} \tag{2}$$

The current density at distance (x) from the center of the pole pitch is

$$\boldsymbol{I} = \frac{-j\omega\phi 10^{-8}}{2b\rho} = \frac{-j\omega 10^{-8}}{\rho}\int_0^x \boldsymbol{H}dx \tag{3}$$

Differentiating equation 3 gives

$$\frac{d\boldsymbol{I}}{dx} = -j\frac{\omega \boldsymbol{H} 10^{-8}}{\rho} \tag{4}$$

Another equation relating ($\boldsymbol{I}$) and ($\boldsymbol{H}$) is

List of Symbols

DIMENSIONS

b = width of pole structure or strip, both assumed equal, centimeters
l = pole pitch, centimeters (See Figure 4)
s = width of slot, centimeters (See Figure 10)
h = depth of slot, centimeters (See Figure 10)
g = air-gap, centimeters (See Figures 5 and 10)
t = strip thickness, centimeters
x = a variable distance, centimeters (See Figures 5 and 10)
x_0 = half pole pitch, centimeters

MISCELLANEOUS

T_c = number of turns in field coil
ρ = electrical resistivity of strip, ohm centimeters
j = operator $\sqrt{-1}$
k = a parameter defined under equations 7 and 9
f = frequency (cycles per second)
θ_1 = internal power-factor angle (See equation 24)
θ_0 = terminal power-factor angle (See Figure 11)
$M(kl)$ = a function of (kl) (See equation 22)
$N(kl)$ = a function of (kl) (See equation 22)
$F(kl)$ = a function of (kl) (See equation 20)
R_1 = apparent resistance of a field coil produced by air-gap flux, ohms
R_2 = ohmic or self-resistance of field coil including iron loss, ohms
X_1 = apparent reactance of a field coil produced by air-gap flux, ohms
X_2 = slot leakage reactance of a field coil, ohms
$\omega = 2\pi f$
A = a constant of integration
B = a constant of integration
P = power input to strip per pole pitch, watts
W_a = average power density generated in strip, watts per cubic centimeter
f_0 = optimum frequency, cycles per second (See equation 39)

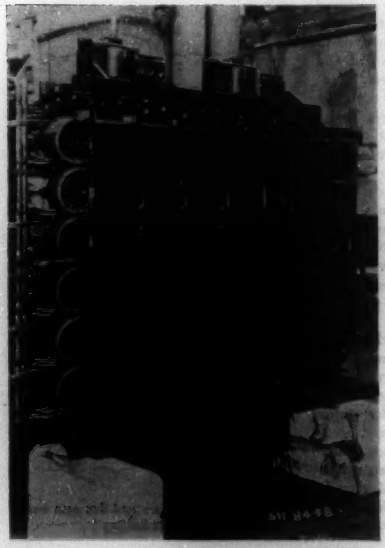

Figure 2 (left). 300-kw 60-cycle transverse flux coil (one pole structure)

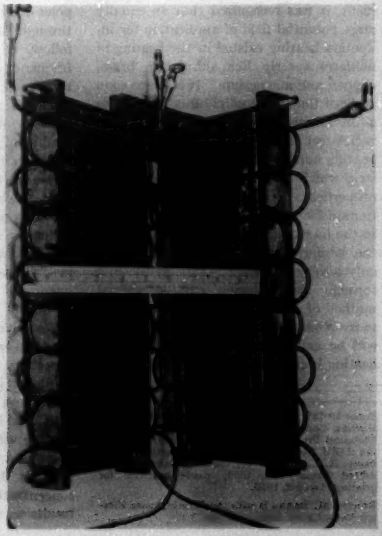

Figure 3 (right). Laboratory model 10,000-cycle transverse flux coil

$$\frac{dH}{dx} = -\frac{0.4\pi I t}{g} \tag{5}$$

Differentiating equation 5 gives

$$\frac{d^2H}{dx^2} = -\frac{0.4\pi t}{g}\frac{dI}{dx} \tag{6}$$

VECTOR QUANTITIES

All sinusoidally varying quantities are represented as vectors with a magnitude equal to the peak value of the sinusoidally varying quantity. Absolute values of the vector quantities are represented in the conventional manner. For example, the absolute value of magnetizing force (H) is represented as H.

I_e = current in a field coil, amperes
H = magnetizing force at any point in the air-gap, oersteds
H_0 = magnetizing force at the edge of a pole pitch, oersteds
H_s = magnetizing force at any point in a slot, oersteds
I = current density at any point in the strip, amperes per square centimeter
I_0 = current density in the strip at the edge of a pole pitch, amperes per square centimeter
ϕ = total flux, Maxwell's
ϕ_0 = total air-gap flux per pole pitch, Maxwell's
$-E_t$ = voltage generated in a field coal by air-gap flux, volts
E_1 = component of total applied coil voltage resulting from air-gap flux, volts
E_s = component of total applied coil voltage resulting from slot leakage flux, volts

Eliminating I between equations 4 and 6 gives

$$\frac{d^2H}{dx^2} - j2k^2H = 0 \tag{7}$$

where

$$k = \sqrt{\frac{4\pi^2 f 10^{-8}}{\rho g}}$$

Differentiating equation 4 gives

$$\frac{d^2I}{dx^2} = -\frac{j\omega 10^{-8}}{\rho}\frac{dH}{dx} \tag{8}$$

Eliminating H between equations 5 and 8 gives

$$\frac{d^2I}{dx^2} - j2k^2I = 0 \tag{9}$$

where

$$k = \sqrt{\frac{4\pi^2 f 10^{-8}}{\rho g}}$$

Equations 7 and 9 are the basic equations which, with the proper boundary conditions inserted, can be used to calculate current density distribution in the strip, magnetizing force in the air-gap, total flux over a pole pitch and all the other quantities and relationships needed for a complete analysis of the problem.

Distribution of Flux Density and Current Density

The magnetizing force at any point in the air-gap is the resultant of the magnetizing effect of the field coils and of the circulating currents in the strip. The effect of the circulating currents in the strip is predominantly opposed to that of the field coils, so the net magnetizing force and flux density toward the center of the pole pitch will be less than it is near the edges of the pole pitch. In fact, at the extreme edges of the pole pitch there is no effect from the currents in the strip and the magnetizing force is simply the value H_0 produced by the field coils acting across the air gap, g.

$$H_0 = \frac{0.4\pi(2T_c)I_e}{g} \tag{10}$$

The general solution of equation 7 is

$$H = Ae^{(1+j)kx} + Be^{-(1+j)kx} \tag{11}$$

Since H is an even function of (x) this can be written

$$H = 2A\cosh(1+j)kx \tag{12}$$

Inserting the boundary conditions

$$x = -x_0,\ x = x_0,\ H = H_0$$

one obtains for the magnetizing force at any point in the air-gap

$$H = H_0\frac{\cosh(1+j)kx}{\cosh(1+j)kx_0} \tag{13}$$

The absolute value of magnetizing force determined from equation 13 is

$$H = H_0\sqrt{\frac{\cosh 2kx + \cos 2kx}{\cosh kl + \cos kl}} \tag{14}$$

From this equation, one can plot a family of curves as shown in Figure 6, which shows the variation of H over a pole pitch for various (kl) values. The reader should look closely at the parameter (kl) since it will appear again and again in the following analysis. It is a dimensionless index of the degree of crowding of flux and current toward the edges of a pole pitch. In looking at Figure 6, it helps to visualize what is happening if one assumes that the current in the field coils is held constant to hold H_0 at the edge of a pole-pitch constant, and that the value of (kl) is increased simply by increasing the frequency.

In this case, the curves represent flux-density distribution across a pole pitch for different applied frequencies. Actually, of course, the value of (kl) may vary as a result of varying air-gap, pole pitch,

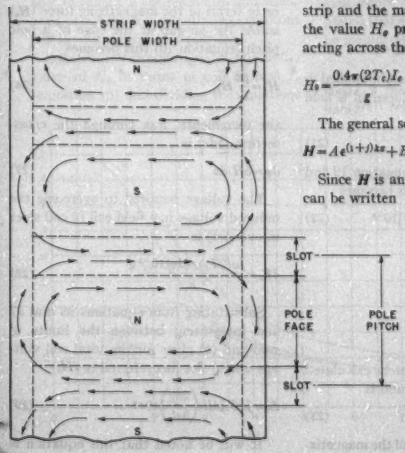

Figure 4 (left). Current paths in strip-transverse flux heating

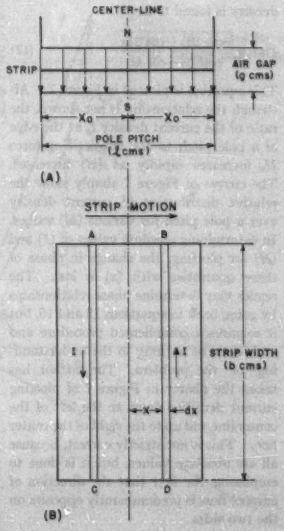

Figure 5 (right). Calculation of flux and current density in one pole pitch

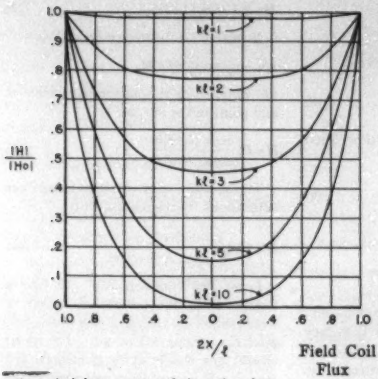

Figure 6 (left). Distribution of magnetizing force in air gap

Figure 7 (right). Distribution of current density in strip

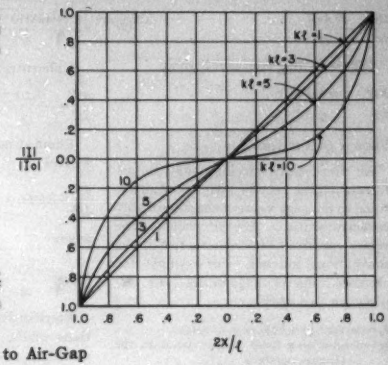

strip resistivity, or any of the other factors which it includes.

The general solution of equation 9 will have the same form as equation 11 but since (I) is an odd function of (x), its solution must be written

$$I = 2A \sinh (1+j)kx \tag{15}$$

Inserting the boundary conditions

$x = x_0, I = I_0$ and $x = -x_0, I = -I_0$

one obtains the following equation for the current density in the strip

$$I = I_0 \frac{\sinh (1+j)kx}{\sinh (1+j)kx_0} \tag{16}$$

from which the absolute value of current density is found to be

$$I = I_0 \sqrt{\frac{\cosh 2kx - \cos 2kx}{\cosh kl - \cos kl}} \tag{17}$$

This equation is plotted in Figure 7. Although the relationship is not shown, the ratio of the current density I_0 at the edge of a pole pitch to the magnetizing force H_0 increases rapidly as (kl) increases. The curves of Figure 7 simply show the relative distribution of current density over a pole pitch for various (kl) values. In determining absolute values of (I) and (H) for plotting, the change in phase of these quantities with (x) is lost. The reader may determine phase relationships by going back to equations 13 and 16, but it requires a complicated procedure and adds little or nothing to the understanding of the problem. The author has taken the liberty in Figure 7 of plotting current densities down to the left of the center line and up to the right of the center line. This is not strictly correct, because all are absolute values, but it is done to emphasize the fact that the direction of current flow is predominantly opposite on the two sides.

Field Coil Voltage Due to Air-Gap Flux

The total flux across a pole pitch is

$$\phi_0 = 2b \int_0^{x} H dx \tag{18}$$

Substituting the value of (H) from equation 13 and carrying out the integration gives

$$\phi_0 = \frac{2bH_0}{(1+j)k} \frac{\sinh (1+j)kx_0}{\cosh (1+j)kx_0}$$

which upon expanding, rationalizing, and substituting (kl) for $(2kx_0)$ becomes

$$\phi_0 = \frac{bH_0}{k} \frac{(\sinh kl + \sin kl) - j(\sinh kl - \sin kl)}{\cosh kl + \cos kl} \tag{19}$$

From equation 19 the absolute value of total flux is found to be

$$\phi_0 = blH_0 F(kl) \tag{20}$$

where

$$F(kl) = \frac{\sqrt{2}}{kl} \sqrt{\frac{\cosh kl - \cos kl}{\cosh kl + \cos kl}}$$

The voltage E_1 which must be applied to overcome the voltage induced in a field coil by the air-gap flux is

$$E_1 = j\omega T_c \phi_0 10^{-8} \tag{21}$$

Substituting (ϕ_0) from equation 19 and using H_0 as a reference this becomes

$$E_1 = \omega T_c blH_0 [M(kl) + jN(kl)] 10^{-8} \tag{22}$$

where

$$M(kl) = \frac{1}{kl} \frac{\sinh kl - \sin kl}{\cosh kl + \cos kl}$$

$$N(kl) = \frac{1}{kl} \frac{\sinh kl + \sin kl}{\cosh kl + \cos kl}$$

The absolute value E_1 can be calculated directly from equation 20 and is

$$E_1 = \omega T_c blH_0 F(kl) 10^{-8} \tag{23}$$

The vector relationship of the magnetizing force (H_0), the coil current (I_c), the total air-gap flux (ϕ_0), the induced voltage $(-E_1)$, and the voltage (E_1) are shown in Figure 8. The internal power factor, or the cosine of the angle (θ_1) between the voltage (E_1) and the coil current (I_c) is from equations 22 and 23

$$\cos \theta_1 = \frac{M(kl)}{F(kl)} \tag{24}$$

For ready use in calculations, the functions $F(kl)$, $N(kl)$, and $M(kl)$ are plotted in Figure 9.

Field Coil Voltage Due to Slot Flux

Referring to Figure 10, the magnetizing force across a slot is

$$H_s = \frac{0.4\pi(2T_c)I_c x}{hs} \tag{25}$$

or in terms of the magnetizing force (H_0) across the air-gap at the edge of a pole pitch (equation 10) this becomes

$$H_s = \frac{gx}{hs} H_0 \tag{26}$$

the incremental flux through the cross-section (bdx) is

$$d\phi = bH_s dx \tag{27}$$

The voltage required to overcome the induced voltage in a field coil (2 coil sides in one slot) is

$$dE_2 = \frac{j\omega(2T_c)x(d\phi)10^{-8}}{h} \tag{28}$$

Substituting from equations 26 and 27 and integrating between the limits of zero and (h) gives for the total coil voltage due to slot flux referred to (H_0)

$$E_s = j\omega T_c blH_0 \left(\frac{2hg}{3sl}\right) 10^{-8} \tag{29}$$

It will be noted that this equation is

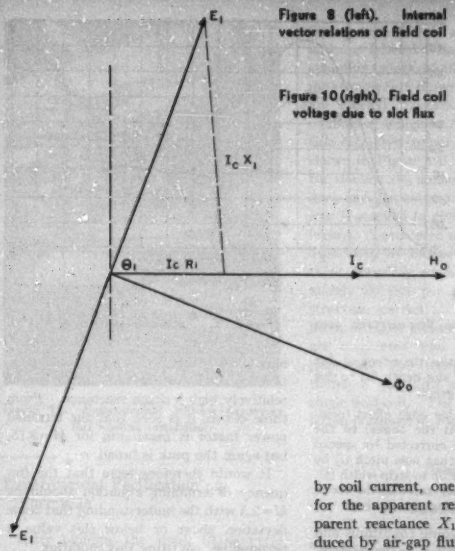

Figure 8 (left). Internal vector relations of field coil

Figure 10 (right). Field coil voltage due to slot flux

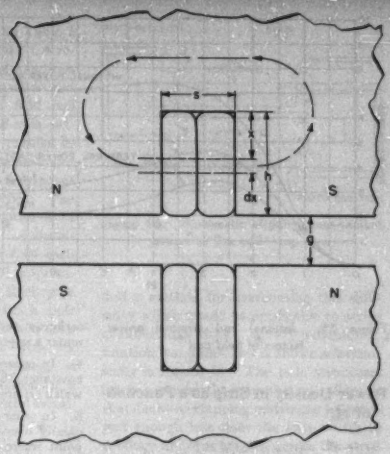

written in a way to show its similarity to equation 22.

The total coil voltage except for the small ohmic resistance drop, which can generally be neglected, is obtained by adding equations 22 and 29.

Resistance and Reactance of a Field Coil—Over-all Efficiency

It is sometimes advantageous to be able to calculate the resistance and reactance of a field coil directly, so equations will be derived for this purpose.

Substituting in equations 22 and 29 the value of H_0 in terms of coil current I_c (equation 10) and dividing the equations by coil current, one obtains expressions for the apparent resistance R_1 and apparent reactance X_1 of a field coil produced by air-gap flux, and the reactance X_2 of a field coil produced by slot flux

$$R_1 = \frac{0.8\pi\omega T_c^2 bl}{g} M(kl) 10^{-8} \tag{30}$$

$$X_1 = \frac{0.8\pi\omega T_c^2 bl}{g} N(kl) 10^{-8} \tag{31}$$

$$X_2 = \frac{0.8\pi\omega T_c^2 bl}{g}\left(\frac{2hg}{3sl}\right) 10^{-8} \tag{32}$$

The self or ohmic resistance R_2 of a field coil can be calculated by conventional methods with due consideration of skin effect when necessary. It is suggested that iron loss in the pole structures be included as an increase in R_2. A total vector diagram for a field coil is shown in Figure 11. Resistance R_2 should always be small in comparison to R_1, X_1, and X_2 and can therefore be neglected in calculating total coil impedance. It is, however, all important in determining efficiency.

The conversion efficiency of the individual coils and therefore that of the over-all coil and core assembly will be

$$\text{Per cent efficiency} = \frac{100R_1}{R_1 + R_2} \tag{33}$$

Figure 9 (below). Functions $F(kl)$, $M(kl)$, and $N(kl)$

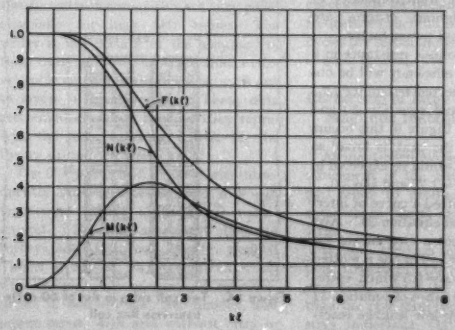

Figure 11. Complete vector diagram of field coil

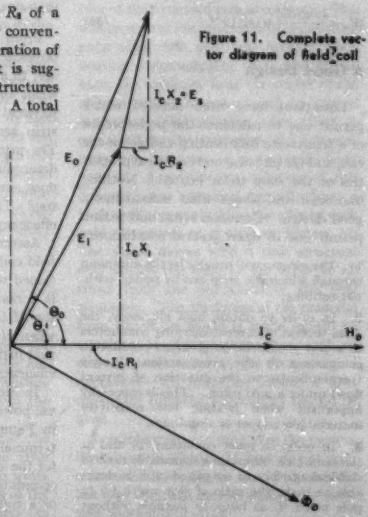

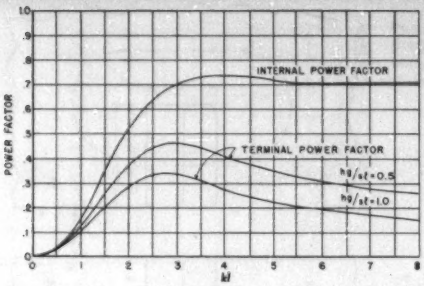

Figure 12. Internal and terminal power factors of field coil

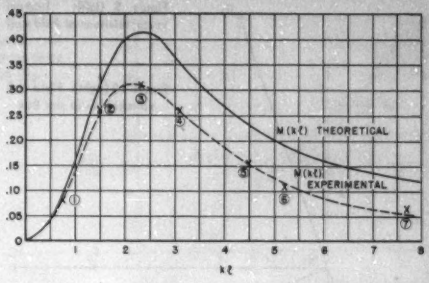

Figure 13. Experimental check of $M(kl)$

Power Density in Strip as a Function of $\overline{H}_1$

Because there are two field coils per pole pitch, the power input to the strip per pole pitch is

$$P = E_1 I_c \cos \theta_1 \tag{34}$$

The average power density in the strip is therefore

$$W_a = \frac{E_1 I_c \cos \theta_1}{blt} \tag{35}$$

Substituting in equation 35 from equations 23 and 24 and expressing (I_c) in terms of (H_0) (equation 10) one obtains the very important equation

$$W_a = \frac{2.5 g f H_0^2}{t} M(kl) 10^{-9} \tag{36}$$

A Good Design

Equations have been derived which permit one to calculate the performance of a transverse flux heating coil given the coil, and the physical and electrical properties of the strip to be heated. Nothing has been said about what constitutes a good design. Common sense and reason permit one to draw general conclusions.

1. The air-gap will usually be the minimum through which the strip can be passed without rubbing.

2. In order to obtain high efficiency, the cross-section of current-carrying conductors in a slot should be as great as possible in comparison to the cross-section of strip (perpendicular to the direction of current flow) under a pole pitch. This is especially important when heating low resistivity material like copper or aluminum.

3. In order to meet condition (2) and at the same time maintain a reasonable ratio of slot-leakage flux to air-gap flux, it is desirable to make the ratio of slot width (s) to pole pitch (l) as large as possible without seriously reducing the flux-carrying area under a pole pitch.

4. In order to minimize the effect of slot reactance, the ratio of slot depth (h) to slot width (s) must not be great.

5. In order to minimize edge effect (principally over-heating at the edges) to the point where it can be corrected by special means, it is desirable that pole pitch (l) be made small in comparison to strip width (b). This condition generally excludes the use of transverse flux for heating narrow strip.

Weighing the foregoing conditions and limitations and drawing on experience, the writer sets forth below some typical ratios of dimensions helpful in approaching a design. These are only guides and may vary somewhat from one design to another.

$$\left.\begin{array}{l} s/g = 1.0 \\ s/l = 0.25 \\ h/s = 2.0 \\ b/l = 4.0 \text{ or greater} \end{array}\right\} \tag{37}$$

From the above, it is seen that the physical dimensions of a pole structure are, to a considerable extent, established when one agrees on an air-gap. The physical and electrical properties of the strip are fixed by the job to be done. The principal unknown remaining to be determined is therefore frequency. How does one then decide what frequency to use? The two obvious criteria are efficiency and terminal power factor.

Assuming a fixed ohmic resistance in a field coil, maximum efficiency will be obtained when the reflected resistance (R_1) is a maximum. From equation 30 and the $M(kl)$ curve of Figure 9, this occurs when $kl = 2.25$, but the peak is broad so that little difference would be expected in efficiency between $kl = 1.75$ and $kl = 3.0$.

In Figure 12 is plotted a curve of internal power factor from equation 24. Also in Figure 12 are shown two curves for terminal power factor. The one is plotted for the condition $hg/sl = 0.5$ which corresponds to the typical ratios of equation 37 or a coil of relatively low leakage reactance. The other is plotted for the condition $hg/sl = 1.0$ which indicates a coil of relatively high leakage reactance. From these curves it is seen that the terminal power factor is maximum for $kl = 2.75$, but again the peak is broad.

It would therefore seem that the frequency determining equation should be $kl = 2.5$ with the understanding that some deviation above or below this value is permissible. Writing this condition

$$kl = 2.5 = l\sqrt{\frac{4\pi^2 f 10^{-9}}{\rho g}} \tag{38}$$

and solving, one obtains an equation for optimum frequency

$$f_0 = \frac{1.58 \rho g}{l^2} 10^9 \tag{39}$$

As mentioned earlier, the required frequency will generally fall in the range between 60 cycles and 10,000 cycles per second. In arriving at a final design, it will be desirable to juggle the dimensions of the pole structure to permit the use of some standard frequency such as 60 cycles, 960 cycles, 3,000 cycles, or 9,600 cycles.

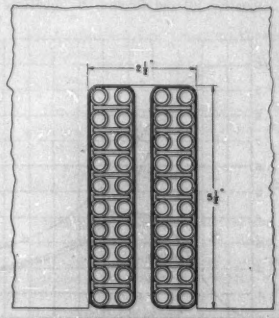

Figure 14. Two coil sides in slot of 60-cycle transverse flux coil

Figure 15. Experimental 300-kw transverse flux heating installation

Experimental Verification of Formulas

After building the small 10,000 cycle coil shown in Figure 3, it was tested with various strips to verify equation 36. All factors in the equation except M (kl) were measured and from these M (kl) was calculated. The resulting curve is shown in Figure 13 marked "Experimental." The theoretical M (kl) curve shown in Figure 9 is reproduced in Figure 13 for comparison. The marked points on the experimental curve correspond to measurements made on the following strips:

1. Lead strip 0.0014-inch thick.
2. Aluminum strip 0.00072-inch thick.
3. Copper strip 0.0011-inch thick.
4. Aluminum strip 0.003-inch thick.
5. Brass strip 0.010-inch thick.
6. Copper strip 0.005-inch thick.
7. Aluminum strip 0.020-inch thick.

It is seen that the agreement between theory and measurement is not very good, especially for high (kl) values. The writer is not certain of the accuracy of these data and it is suspected that a considerable amount of the discrepancy is due to errors in measurement. These data are included mainly because they represent the most extensive check on the theory up to the present time.

The 60-cycle coil of Figure 2 was subsequently built and tested, and although tests were made only for (kl) values around 1.75, the agreement between theory and test was nearly perfect. Values of M (kl), R_1, R_2, and (X_1+X_2) were calculated from averaged measurements of coil voltage, coil current, and power input, with and without strip in the air-gap. These are listed in Table I and are labeled "Experimental." Corresponding values calculated from equations in the paper are shown for comparison and are labeled "theoretical." A field coil consists of ten turns of two 3/8-inch outside diameter copper tubes in parallel as shown in Figure 14. The dimensions of the slot are $2^1/_2$ inches wide by $5^1/_2$ inches deep and the air-gap is $2^3/_4$ inches. The iron is stacked to give a core width of 54 inches. Tests were made heating aluminum strip 54 inches wide by 0.04 inch thick traveling at a speed of approximately 30 feet per minute. Each pole structure carries six poles with a pole pitch of eight inches. The 12 field coils are connected two in series with six parallels. The terminal impedance is therefore one-third the impedance of a single field coil. The experimental installation is shown in Figure 15.

Table I

	Experimental	Theoretical
kl	1.74	1.74
M (kl)	0.34	0.36
R_1	0.041	0.044
R_2	0.009	0.005
(X_1+X_2)	0.159	0.159

The theoretical value of coil resistance R_1 is low because it was calculated simply from the cross-section and length of copper without considering eddy currents or skin effect. Also, iron loss was not included and iron loss automatically appears in the experimental value of R_2.

From these data it would appear that the equations derived in this paper are quite accurate. It also will be noted from the experimental values of R_1 and R_2 that an efficiency of better than 80 per cent can be expected. The fact that the equations developed in this paper have been used so successfully for designs at widely different frequencies such as 60 cycles and 10,000 cycles per second indicates that the theory is quite general.

Correction of Edge Heating—Magnetic Instability

As mentioned earlier in this paper, the movement of the strip through the air-gap tends to produce uniform heating everywhere except near the edges of the strip.

If the strip is narrower than the pole structures, the edges of the strip over-heat; and if the strip is much wider than the pole structures, the edges of the strip underheat. It was necessary to find a method for overcoming this difficulty which would be applicable to strips of different widths. A very satisfactory solution was found and is shown schematically in Figure 16. The pole structures are independently mounted on rollers so that their overlapping width can be made just enough less than the strip width to produce uniform heating across the strip. By looking closely at Figure 3, it will be noted that this pole structure was equipped with both vertical and horizontal rollers designed to run on suitable tracks. The pole structures also were equipped with independent photoelectric systems which automatically maintained a fixed distance between the edge of a pole structure and the edge of the strip.

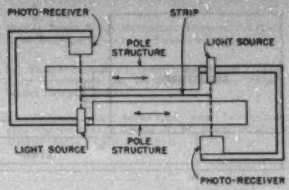

Figure 16. Automatic aligning arrangement transverse flux coil—top view

This method proved satisfactory except for one very serious trouble. The current flow near and parallel to the edge of the strip (see Figure 4) tended to pull the edge of the strip down against the iron of the extended pole structure. This was an unexpected and surprising phenomenon when first observed because when heating a nonmagnetic strip like aluminum, the tendency near the center of the pole structure is and should be one of centering. The peculiar edge effect is explained by the attraction of a current-carrying conductor to a magnetic body near it. A satisfactory solution of this difficulty was obtained by attaching a U-shaped copper shield to the edge of each pole structure, as shown in Figure 17. The shield moves with a pole structure and shields the edge of the strip at all times from the attraction of the pole structure. The thickness of the material from which the shield is made should be equal to or greater than the depth of current penetration at the frequency of operation. To minimize losses, a low-resistivity material like copper should be used.

It is interesting to note that the system illustrated in Figures 16 and 17 not only automatically adjusts for strip width, but also will take care of weaving or sidewise motion of a strip.

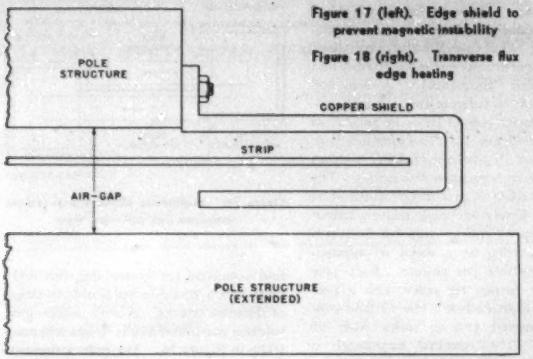

Figure 17 (left). Edge shield to prevent magnetic instability

Figure 18 (right). Transverse flux edge heating

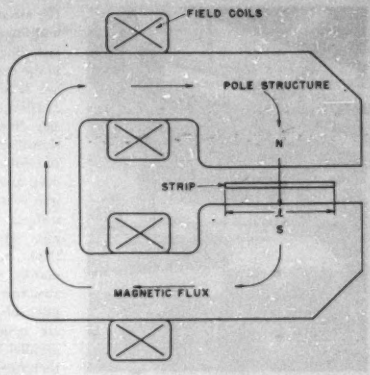

Making a Design

Given a strip of specified dimensions and material to heat to a specified temperature at a specific linear speed, steps in making a design may be listed as:

1. Calculate the total power in watts required to heat the strip from purely thermal considerations, making suitable allowance for losses by radiation and convection.

2. Assume a length of pole structure (in direction of strip travel), and calculate the watts per cubic centimeter which must be generated in the strip.

3. Decide upon the air-gap necessary from mechanical considerations and, using the typical ratios of equation 38, arrive at suitable slot dimensions and pole pitch.

4. From equation 39 calculate the optimum frequency to use. If the calculated frequency is not readily obtainable, consider using a standard frequency near the calculated value and investigate the effect of the changed (kl) value by referring to the power-factor curves of Figure 12 and the power input function $M(kl)$ of Figure 9. It may be necessary to adjust the pole pitch to obtain a reasonable compromise.

5. From equation 36 calculate the value of magnetizing force H_0 required. Reasonable values of H_0 vary from 4,000 oersteds at 60 cycles to 1,000 oersteds at 10,000 cycles. If the value of H_0 falls outside this range, it may be necessary to lengthen the pole structures by adding more poles.

6. Using equations 22 and 29, proceed by a cut and try process to arrive at the number of turns in a field coil and the grouping of field coils to permit operation at the voltage of the chosen power source. It will usually be desirable to wind the coils from hollow copper tubing to permit water cooling.

7. Design the magnetic circuit, providing enough depth behind the slots to carry the total air-gap and slot-leakage flux without saturation and without undue iron loss. The thickness of laminations will be dictated by the frequency used. It may be necessary to provide ducts through the iron (across laminations) for forced air cooling.

8. Knowing the magnetizing force H_0 and the number of turns per coil, calculate coil current and copper loss. Knowing the flux density in various parts of the magnetic core and frequency, calculate iron loss. Knowing total loss and power input to the strip, calculate the expected conversion efficiency.

All of the derivations of this paper and the steps outlined above for making a design are carried out as if the strip was just as wide as the pole structures, and are furthermore based on the assumption that edge effects are corrected to produce uniform heating across the strip. Likewise, the curves of power factor, Figure 12, are valid only for this condition.

When the pole structures are shifted (as shown in Figure 15) to heat strip considerably narrower than the pole structures, the terminal power factor, the efficiency of conversion and the terminal impedance will all be reduced somewhat. Approximate corrections may be made, if desired, by using formulas in this paper.

Effect of Magnetic Permeability in Strip

It has been tacitly assumed throughout that the strip being heated is not ferromagnetic. Ferromagnetic strip like steel can be heated with transverse flux, although this is not generally recommended. The derived equations will be slightly in error for two reasons.

1. The presence of the ferromagnetic strip effects a slightly lower reluctance in airgap.

2. Some flux will be diverted through the strip from one pole to an adjacent pole on the same side of the strip. In so doing, a certain amount of longitudinal flux heating is produced. Using the optimum frequency for transverse flux heating calculated from equation 39, this effect is generally small because the strip saturates before much flux can be diverted, and the depth of current and flux penetration for longitudinal flux heating is large compared to strip thickness.

A Special Application of Transverse Flux Induction Heating

Whereas the aim thus far has been to produce uniform heating in a moving strip, there are some applications such as in the heating of skelp for making seam-welded steel pipe, where it is actually desirable to overheat the edges of a strip of metal.

Based on the foregoing analysis, it is obvious that such heating can be obtained by passing the strip between a pair of poles, as indicated in Figure 18. If the pole is long in the direction of strip travel compared to the width of the strip, the average power density may be calculated from equation 36. However, in determining (kl), one must take (l) as the width of the strip. The distribution of current density across the width of the strip will be a function of (kl) as shown in Figure 7. The power density distribution can be obtained for any (kl) value simply by plotting current-squared curves from those of Figure 7. If one wishes the major part of the heating to occur near the edges of the strip, the frequency must be chosen to make (kl) large.

Conclusions

1. Transverse flux induction heating provides a practical and efficient method for the continuous heat-treating of nonferromagnetic strip like aluminum, brass, copper, magnesium, or stainless steel.

2. Formulas derived in this paper allow one to design a transverse flux installation and predict performance with good accuracy.

3. Frequencies used will generally fall in the range between 60 and 10,000 cycles per second, and depend on the physical and electrical properties of the strip to be heated.

4. An efficiency of 80 per cent or better can be expected in most applications.

5. Special means can be provided to

accommodate various strip widths and insure uniform heating.

6. Transverse flux heating also is applicable to certain edge-heating applications.

References

1. Induction Heating of Moving Magnetic Strip, R. M. Baker. *Electrical Engineering* (*AIEE Transactions*), volume 64, April 1945, pages 184–89.

2. Heating of Non-Magnetic Electric Conductors by Magnetic Induction, R. M. Baker. *Electrical Engineering* (*AIEE Transactions*), volume 63, June 1944, pages 273–78.

3. Inductive Heating of Longitudinally Moving Metal Strip, R. M. Baker, et al.—United States Patent 2,448,009.

4. Induced Heating of Continuously Moving Metal Strip With Pulsating Magnetic Flux, R. M. Baker, et al.—United States Patent 2,448,012.

5. Transverse Flux Induction Heating Furnace Structure, R. M. Baker, et al.—United States Patent 2,448,010.

6. Method and Apparatus for Induction Heating of Metal Strips, R. M. Baker, et al.—United States Patent 2,448,011.

No Discussion

Classification of the Reference Frames of a Synchronous Machine

GABRIEL KRON
MEMBER AIEE

THIS is the second part of a series of studies on the steady-state stability calculation of long-distance transmission systems as influenced by voltage regulators. The physical and hypothetical reference frames of a synchronous machine hitherto used or now contemplated are reviewed and classified from a dynamical and geometrical point of view. It is found that among the large number of possible reference frames, there exists one frame—representable by an equivalent circuit—possessing the remarkable properties that for any complex transmission system the sum of its i^2r losses is equal to the damping torques and the sum of the i^2x powers is equal to the synchronizing torques of the various generators. The significance of the tensorial formulation of the equations of hunting and the role played by the Riemann-Christoffel curvature tensor in the above physical picture is outlined.

The Limitations of Long-Distance Transmission of A-C Power

Present-day economics indicate the practicability of long-distance power transmission in many localities for distances greater than 300 miles. One of the important characteristics of an a-c transmission system is its steady-state stability limit. That is at some particular steady-state load and system condition, when the synchronous machine is still able to supply more power across the line, the system nevertheless loses synchronism. This is interpreted physically that the generator has no longer enough "synchronizing torque" to keep it in synchronism against small disturbances that continually arise.

It has been known that a voltage regulator attached to the field of the generator raises the steady-state stability limit to a higher value. The mechanism of this process has not been quite clear. No satisfactory physical theory of the small oscillations of a transmission system exists as yet and all attempts to explain physically the magnitudes of positive and negative damping and synchronizing torques of even such a simple system as a synchronous machine connected to an infinite bus, have led only to very complicated expressions without any clear-cut physical picture.

Purpose of the Paper

It is one of the purposes of this series of papers to develop a consistent and fairly simple physical theory of hunting of a transmission system that is correct dynamically and is useful as well in practice. Such a development requires a critical examination of the basic role played by the concept of "reference frame" in the physical pictures the engineer constructs to visualize the behavior of a rotating machine. Unlike conventional mechanical systems, an electrodynamical system offers different basic concepts and different physical pictures by a change of the relative velocities of the reference frames. While one reference frame gives the most satisfactory pictures for say sudden-short-circuit problems, another reference frame is needed to visualize in a simple manner the phenomenon of hunting. And the passage from one reference frame to another is not so simple a step as it is in a mechanical problem.

The purpose of the present paper is to point out the automatic appearance of new concepts and new physical entities as the relative angular velocities of the reference frames of a synchronous machine are varied, in order to lead up logically to the right reference frame to be employed in the study of hunting. In other words a search is instituted for a new type of reference frame in which, during hunting, some fluxes behave as springs (positive T_S), other fluxes behave as masses (negative T_S), and in which the resistances behave as frictions (positive and negative T_D). The actual study along the new reference frame will be undertaken in a subsequent paper.

Electrodynamics in Words of Many Syllables

Electrodynamics is a young and still very little developed or understood subject. Even such a simple topic as the electromagnetic field of free space viewed from a reference frame in uniform translation leads to 4-dimensional relativity with all its mystic connotations and formulae. Though in a synchronous machine the velocities are small compared to the speed of light, and though only magnetic fields, electric currents and rotating magnetic and conducting media appear, nevertheless the reference frames and the media have different relative angular velocities. This difference in rotational speed between conductors, magnetic materials and the observers themselves (the reference frames) leads to an electrodynamics that has no longer any parallel with conventional particle dynamics of moving material bodies. However the parallelism is still maintained with modern differential geometry whose development was instigated by this very need of electrodynamics for a unified treatment, though in fields other than electric machinery. Nevertheless any logical study of electric machinery must also necessarily lead to the same basic

Paper 50-114, recommended by the AIEE Basic Sciences Committee and approved by the AIEE Technical Program Committee for presentation at the AIEE North Eastern District Meeting, Providence, R. I., April 26-28, 1950. Manuscript submitted August 26, 1949; made available for printing February 27, 1950.

GABRIEL KRON is Consulting Engineer with the General Electric Company, Schenectady, N. Y.

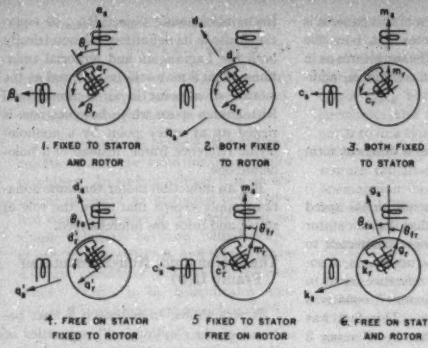

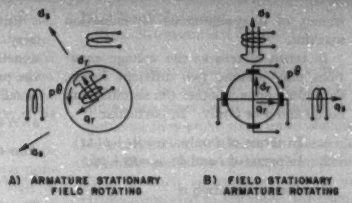

Figure 1 (left). Six physical, rectangular reference frames of a synchronous machine

Figure 2 (right). Two points of view of a synchronous machine

concepts that appear in the electrodynamics of moving elementary particles, namely to multidimensional non-Riemannian spaces, to the "Riemann-Christoffel curvature tensor," to "nonholonomic" reference frames, and to similar euphonious polysyllabic expressions that modern geometry has invented for use in electrodynamics.

Whether the electrical power engineer likes it or not, he has no other choice. Only these strange-sounding creations of physicists and geometers fit the logic of the peculiar behavior of electric machines, and unfortunately even these creations are still very fragmentary and insufficient. Future progress in the theory of electrical power utilization lies clearly along these very channels and the engineer must necessarily stumble through these same pathways either blindfolded or with an intelligent understanding of their peculiarities and pitfalls. The engineer may and undoubtedly will eventually replace these words with something more pronounceable and practicable, but not the basic concepts the words stand for. These basic concepts and the equations they occur in, are among the very few concepts and equations that form the very foundations of modern physics.

The Reference Frames

It has been argued that there are only two industrially important a-c rotating machines, namely the synchronous machine and the induction machine; and for that reason it is not worthwhile to build up an elaborate theory for their analysis. The flaw in the argument is that there are not two, but only one type of a-c rotating machine. The transient equations of both structures are identical (if the role of the stator and rotor are interchanged) and the saliency, frequency, or speed are only incidental characteristics in the construction of a basic theory.

As a matter of fact the transient equations of all rotating electric machines are basically identical, be they direct or alternating current, synchronous or induction or commutator machines, and irrespective of whether their leads, brushes or slip rings are connected in shunt or series, in singly or in arbitrary combination. The difference between the various types of machines and even the difference between the various theories of any one particular machine, may be reduced to the statement that it is all a question of point of view, or technically speaking, it is all a question of the "reference frame" assumed.

The Primitive Synchronous Machine

That particular single machine, from which all other machines differ only by the reference frame assumed, will be called—for the present limited purpose—the "synchronous machine." (In other publications the author called it the "primitive" machine.) For purposes of simplicity a 2-phase machine will at first be considered, having a salient-pole rotor and smooth stator structure. The stator windings are identical along the two phases, those of the rotor differ. The existence of zero-sequence currents will be ignored for the time being.

Having settled that the electrical engineer needs to write down the transient equation of only one 2-phase machine consisting of one stationary and one rotating magnetic structure, each with two sets of windings at right angles to each other, Figure 1, his troubles are about to begin. Even forgetting the brushes, slip rings, the possible shunt and series connections and simply concentrating on isolated windings in each axis, numerous possibilities arise in deciding the elementary question whether the reference frames should be rigidly connected to the magnetic structure or should be free of them. (The conducting windings themselves are rigidly connected to their respective magnetic structures.) Four such different possibilities are enumerated in the order of their increasing physical complexity and the reasons for their selection discussed, see Table I.

The Holonomic Riemannian Reference Frame I

The most obvious assumption for the analysis of a synchronous machine is that the reference axes of all stator windings should be rigidly connected to the stator iron and copper and those of the rotor windings should be rigidly connected to the rotor iron and copper. In this frame the physics of the phenomenon is very simple and the transient voltage equation along each axis has the form

$$e = Ri + p\psi$$

This is the reference frame (although written for three phases instead of two) which is used by Park as a starting point in the development of his equations. This also is the reference frame along which books on physics and electrotechnics employ the "holonomic" form of the dynamical equations of Lagrange

$$f_\alpha = \frac{d}{dt}\left(\frac{\partial T}{\partial\left(\frac{dx^\alpha}{dt}\right)}\right) - \frac{\partial T}{\partial x^\alpha} + \frac{\partial F}{\left(\frac{dx^\alpha}{dt}\right)} \qquad (1)$$

accompanied by the statement that these equations represent the dynamical theory of "all" electric machines. This dynamical theory originally was developed by Maxwell almost a century ago and until recently no progress has been made by electrical engineers to extend it to commutator machines or to other reference

frames of a synchronous or induction machine.

In terms of tensors the voltage equations may assume two different forms, depending upon whether the variables are both i and ψ or i only. In particular

1. In terms of i only: $e = Ri + p(Li)$.
2. In terms of i and ψ: $e = Ri + p\psi$.

The torque equation is

$$f = \frac{1}{2}\frac{\partial}{\partial\theta}(i^* Li) = \frac{1}{2}\frac{\partial}{\partial\theta}(i^*\psi) \tag{2}$$

The resultant tensor equation, that includes both voltage and torque equations, is written as

$$e_\alpha = R_{\alpha\beta} i^\beta + L_{\alpha\beta}\frac{di^\beta}{dt} + [\beta\gamma,\alpha] i^\alpha i^\gamma \tag{3}$$

Here $[\beta\gamma,\alpha]$ is the "holonomic" form of the Christoffel symbol defined as

$$[\beta\gamma,\alpha] = \frac{1}{2}\left(\frac{\partial L_{\gamma\alpha}}{\partial x^\beta} + \frac{\partial L_{\alpha\beta}}{\partial x^\gamma} - \frac{\partial L_{\beta\gamma}}{\partial x^\alpha}\right) \tag{4}$$

where $L_{\alpha\beta}$ is the "metric tensor" representing all the self and mutual inductances and the rotor inertia. This tensorial equation can be derived from the dynamical equation of Lagrange[1] by simply replacing T by $L_{\alpha\beta} i^\alpha i^\beta/2$. Expressed in another way equation 4 is an "explicit," form of the Lagrangian equation itself. (Since it is assumed that the variables i^α are complex functions, the spin indices are shown in bold-face type instead of placing a bar over them.

Since the dynamical equation of Lagrange will soon prove helpless when other reference frames are to be introduced it is necessary to give a geometrical interpretation to the above two dynamical equations. Geometrically the equations represent the motion of a point particle in an n-dimensional Riemannian space expressed along a holonomic reference frame. The geometrical language will rescue dynamics from an apparent breakdown.

The Nonholonomic, Riemannian Frame II(a)

Of course electrical engineers are aware that the previous equations can be used only in exceptional cases because of the analytical complexity introduced by the cos θ, sin θ terms in the metric tensor L Blondel and later on Park introduced a new, more practical set of equations in which these trigonometric functions no longer occur, by assuming that both stator and rotor reference frames are rigidly connected to the rotor only. This theory now is called the "2-reaction theory."

From the point of view of this paper it is very important to note that now the equations do not have the same form as in the previous frame but contain an additional speed term $p\theta_r$ as

$$e = ri + p\psi_d - \psi_q p\theta_r$$

Also the torque assumes a different form

$$f = i^q\psi_q - i^q\psi_d$$

The appearance of an additional speed term is due to the fact that the new stator reference frame, no longer connected to the stator magnetic structure, is a so-called "nonholonomic" reference frame to which the usual "holonomic" equations 1 to 3 no longer apply. This fact was recognized by the author in reference 3 showing that the Park-Blondel equations correspond exactly to the "nonholonomic" form of the dynamical equations of Lagrange given in many advanced books on dynamics

$$f_\alpha = \frac{d}{dt}\left(\frac{\partial T}{\partial\left(\frac{dx^\alpha}{dt}\right)}\right) - \frac{\partial T}{\partial x^\alpha} + \frac{\partial F}{\partial\left(\frac{dx^\alpha}{dt}\right)} + \frac{\partial T}{\partial\left(\frac{dx^\alpha}{dt}\right)} \times \left(\frac{\partial C_k^{\ b}}{\partial x^n} - \frac{\partial C_n^{\ b}}{\partial x^k}\right) C_\alpha^{\ k} C_\beta^{\ n}\left(\frac{dx^\beta}{dt}\right) \tag{5}$$

The transformation tensor $C_\alpha^{\ \alpha'}$ always appears in such equations and relates the nonholonomic frame to the holonomic one. The term containing it, namely

$$\Omega_{\alpha\beta}^{\ \ b} = \left(\frac{\partial C_k^{\ b}}{\partial x^n} - \frac{\partial C_n^{\ b}}{\partial x^k}\right) C_\alpha^{\ k} C_\beta^{\ n} \tag{6}$$

is the so-called "nonholonomic object," a nontensor geometric object, that will play an important part later on.

In terms of tensors the voltage and torque equations are (if γ is the "coefficient of rotation" containing only ± 1)

In terms of i only: $e = Ri + Lpi + \gamma Lp\theta_r i$

In terms of i and ψ: $e = Ri + p\psi + \gamma\psi p\theta_r$

$$f = i^* \gamma Li = i^* \gamma\psi \tag{7}$$

In these equations γ is not a tensor. The resultant tensorial equation is

$$e_\alpha = R_{\alpha\beta} i^\beta + L_{\alpha\beta}\frac{di^\beta}{dt} + [\beta\gamma,\alpha] i^\beta i^\gamma \tag{8}$$

where $[\beta\gamma,\alpha]$ is now the "nonholonomic" form of the Christoffel symbol, containing the nonholonomic object $\Omega_{\beta\gamma,\alpha}$ of equation 6 also in its definition. Geometrically both the Lagrangian and tensorial equations 5 and 8 may still be pictured as the motion of a point in an n-dimensional Riemannian space which however now is rigged up at every point by a nonholonomic reference frame, instead of a holonomic one.

For an induction motor the same equations apply except that often the role of stator and rotor are interchanged.

The Holonomic, Non-Riemannian Frame II(b)

It was shown in reference 3 that because of the "cylindrical" properties of the variables (for instance the relations between the currents, namely $C_\alpha^{\ \alpha'}$, are functions only of θ) there is nothing in the new equations to indicate that they were derived from some holonomic frame. For that reason it is possible to consider them on their own strength as basically new equations having their own special physical interpretation. Such a reformulation is accomplished by considering the expression in equation 6 defining the nonholonomic object $\Omega_{\alpha\beta,\gamma}$, not a nontensor object, but a tensor, the so-called "torsion tensor" $S_{\beta\gamma\alpha}$. In consequence γ in equation 7, the voltage, also becomes a tensor, the "rotation tensor."

Although this reformulation becomes mathematically useful only in going over to a new reference frame (as $S_{\beta\gamma\alpha}$ has a different law of transformation from that of $\Omega_{\beta\gamma,\alpha}$) it becomes physically important even in this particular reference frame. Since ψ is always a tensor and γ becomes now a tensor (because of the redefinition) their product $\gamma\psi$ must necessarily also be a tensor, a new physical entity, the so-called "flux-density" B of the armature. This is the same physical concept B that occurs in Maxwell's field-equations. (The flux-linkage ψ that occurred hitherto corresponds to the vector-potential A of Maxwell.) The new tensorial voltage and torque equations become

In terms of i only: $e = Ri + Lpi + Gip\theta_r$

In terms of i and ψ: $e = Ri + p\psi + \gamma\psi p\theta_r$

Table I. Rectangular Reference Frames of a Synchronous Machine

Attachment of Stator and Rotor Reference Frames	Actual Machine Physical	Actual Machine Hypothetical	Equivalent Circuit Physical	Equivalent Circuit Hypothetical
I.....One fixed to rotor, one to stator.....	1	7	13	19
II.....Both fixed to rotor.....	2	8	14	20
Both fixed to stator.....	3	9	15	21
III.....One fixed to rotor, one free.....	4	10	16	22
One fixed to stator, one free.....	5	11	17	23
IV.....Both free.....	6	12	18	24

In terms of i, ψ, and B: $e = Ri + p\psi + Bp\theta_r$

$$f = i^* Gi = i^* \gamma\psi = i^* B \quad (9)$$

In these equations of is a tensor. This physical reinterpretation has several advantages, among others:

1. It enables to assume that the new equations also are valid for commutator machines. In such machines it is an absolute necessity to introduce both physical concepts ψ and B, as there exist no simple relations between "flux-linkage" ψ and "flux-density" B, and they must be and are considered independent of each other. (That is in commutator machines B is no longer expressible as $\gamma\psi$.)

2. The torque can now be expressed as a generalization of the force equation of Maxwell, namely of $f = iB$.

3. The concept of B enables the construction of equivalent circuits on a more logical basis. In assuming symmetrical components, it is possible to measure on the equivalent circuit the components of B as differences of potential. (In assuming the physical axes d and q, the equivalent circuits allow to measure ψ but not B.)

4. During small oscillations an additional new physical entity, a flux-linkage, may be derived from B (as γB) corresponding to the much sought after "spring" that keeps the machine in synchronism.

A further advantage of the reinterpretation is shown later on.

It is emphasized that all three forms of the equations (containing i only, or i and ψ or i, ψ and B) are equivalent mathematically and their choice depends on convenience only. One form may be sometimes shorter, the other may give a more visual physical picture. For instance if the field axes of a synchronous machine are permanently eliminated by the use of operational impedances then the use of i and ψ requires the least number of symbols.

Unfortunately conventional rigid dynamics has no equations—analogous to the Lagrangian forms, equations 1 and 5, —that could represent this new dynamical system containing B or, for that matter, that could represent a d-c machine with commutators. Geometry now comes to the rescue. The resultant tensorial equation (including both voltage and torque equations), can be written in the form of a shortest line between two points

$$e_\alpha = R_{\alpha\beta} i^\beta + L_{\alpha\beta} \frac{di^\beta}{dt} + \Gamma_{\beta\gamma,\alpha} i^\beta i^\gamma \quad (10)$$

This equation also is sometimes called the generalized Lagrangian equation as it is derivable from a variational principle. Here $\Gamma_{\beta\gamma,\alpha}$ is called the "affine connection" and contains besides the holonomic Christoffel symbol $[\beta\gamma,\alpha]$ also the torsion tensor $S_{\beta\gamma\alpha}$ in its definition. (If time harmonics also are considered, $[\beta\gamma,\alpha]$ is not zero in a synchronous machine.)

Geometrically the new equation represents the motion of a point in a non-Riemannian space rigged up with a holonomic frame (instead of a Riemannian space with nonholonomic frames). That the frame still may be considered as holonomic, is seen from the fact that all the reference axes are still connected rigidly to one of the magnetic structures. The appearance of the non-Riemannian space (a space with "torsion") is due to the motion of the conductors with respect to the reference axes. That is even though the observer sees the current-density wave stationary, the conductors themselves replace one another in succession. (The "metallic metabolism" of Hoffman, reference 5.)

The "Electromagnetic-Field Tensor"

The appearance of a new physical entity due to the reinterpretation is shown more emphatically by the introduction in the last tensor equation of a skew-symmetric "electromagnetic-field" tensor $F_{\alpha\beta}$ containing B (for the voltage) and $-B$ (for the torque). In terms of this important tensor the equation of motion of a synchronous machine, equation 10 becomes

$$e_\alpha = R_{\alpha\beta} i^\beta + L_{\alpha\beta} \frac{di^\beta}{dt} + [\beta\gamma,\alpha] i^\beta i^\gamma + F_{\alpha\beta} i^\beta \quad (11)$$

where $[\beta\gamma,\alpha]$ is the holonomic Christoffel symbol. This equation is exactly the same as equation 3 except for the presence of the added term $F_{\alpha\beta} i^\beta$. Hence a physical entity is made to appear or disappear at will by a mere change in the reference frames.

If e_α and $R_{\alpha\beta}$ are made equal to zero this last equation also represents the classical or relativistic motion of a charged particle in an electromagnetic field. This tensorial equation of motion also plays a basic role in the theories of elementary particles of nuclear physics.

Summarized, from the new point of view the equations of a synchronous generator or induction motor become identical in form with those of a commutator machine, either alternating or direct current.

A more detailed discussion of the foregoing reinterpretation is given in reference 5.

The Nonholonomic, Non-Riemannian Frame III

While the physical concepts i, ψ and B appear to be sufficient for steady-state and sudden short-circuit (constant speed) problems, they prove to be unsatisfactory for acceleration problems, in particular for small oscillation (hunting) problems. That is when all reference frames are rigidly connected to the rotor, the frames also oscillate when the rotor does and at least two disadvantages follow:

1. If a transmission line is connected to the stator of the synchronous machine, the oscillatory stator reference axes introduced extra generators into each mesh of the line.

2. Even if no line is connected to it, no clear-cut physical picture can be developed for the damping and synchronizing torques of a synchronous machine, as the many unsuccessful trials indicate. There is something missing from the theory.

Both of these difficulties are removed if the stator reference-frame is divorced from the rotor and is allowed to rotate uniformly. Separating the stator reference frame from the rotor magnetic structure is again equivalent to the introduction of a nonholonomic reference frame. In analogy to equation 7 an additional speed term $p\theta_f$ appears (in addition to the rotor speed $p\theta_r$), so that a representative circuit equation has the form

$$e = Ri + p\psi + Bp\theta_r + \varphi(p\theta_f - p\theta_r)$$

where φ is a new type of flux density produced by the currents passing through the nonoscillating stator reference frame. The rotor reference frame still oscillates with the rotor structure.

The tensorial voltage equation now assumes four different forms

$$\begin{aligned} e &= Ri + Lpi + Gipe_r + Vi(p\theta_f - p\theta_r) \\ e &= Ri + p\psi + \gamma_1\psi p\theta_r + \gamma_2\psi(p\theta_f - p\theta_r) \\ e &= Ri + p\psi + Bp\theta_r + \gamma_2\psi(p\theta_f - p\theta_r) \\ e &= Ri + p\psi + Bp\theta_r + \varphi(p\theta_f - p\theta_r) \end{aligned} \quad (12)$$

It so happens that in a synchronous machine the second form simplifies to

$$e = Ri + (p + \gamma_2 p\theta_f)\psi = Ri + p\psi$$

since γ_1 (a tensor) is equal numerically to γ_2 (a nontensor). The cancellation of two equal terms having opposite signs is not allowable from a tensorial (physical) point of view and it would lead to a non-visualizable hunting equation unless B and φ are reintroduced somehow during the manipulations. Due to the simplicity of its derivation this last form will be used in the development of the equivalent circuit of hunting of a synchronous machine.

When the rotor velocity $p\theta_r$ is zero, then the new moving reference frame is identical with that used in the first part of this series of studies in connection with stationary networks (reference 1). If in the above four equations $p\theta_r$ is made equal to zero, the equations derived here are reduced to the simplicity of those given in reference 1 for a stationary network with no capacitors.

Along the new, uniformly rotating reference frame the torque equation remains unchanged while the resultant tensorial equation, representing also the generalized Lagrangian equation assumes the form

$$e_\alpha = R_{\alpha\beta} i^\beta + L_{\alpha\beta} \frac{di^\beta}{dt} + \Gamma_{\beta\gamma,\alpha} i^\beta i^\gamma \qquad (14)$$

where the affine connection $\Gamma_{\beta\gamma,\alpha}$ contains now the nonholonomic form of $[\beta,\gamma,\alpha]$, hence the nonholonomic object $\Omega_{\beta\gamma,\alpha}$, in addition to the torsion tensor $S_{\beta\gamma\alpha}$. Geometrically the equations describe the motion of a point in a non-Riemannian space rigged up with a nonholonomic reference frame.

It is emphasized that it is not at all an absolute necessity to introduce four physical concepts i, ψ, $\boldsymbol{B}$ and φ even in this particular reference frame. Also it is possible to consider the uniformly rotating frame still as a nonholonomic, Riemannian frame containing only two physical concepts i and ψ, by starting with frame number 1 and immediately passing to frame number 4, giving an equation of voltage analogous to equation 7

$$e = Ri + p\psi + \gamma\psi p\theta_r \qquad (15)$$

Here γ is a nontensor geometric object. However by leaving out frame number 2 as an intermediary step the simplified physical picture of hunting disappears.

A Better Physical Picture

A more visual physical picture of the three physical concepts may be given by assuming the field stationary and the armature rotating with $p\theta_r$ (Figure 2). Then frame number II is represented by stationary brushes and frame number III is given by assuming the brushes to oscillate around their stationary position in unison with the rotor oscillation with $p\theta_f - p\theta_r$. Then:

1. ψ is the flux-linkage of all windings, that induces voltages while the rotor and the reference frames all are stationary and the currents vary in time.

2. $\boldsymbol{B}$ is the flux-density of the armature windings that is cut by the rotor velocity $p\theta_r$, assuming the frames stationary and the currents constant. It lies at right angles in space from ψ_r of the armature.

3. φ is the flux-density that oscillates with the brush velocity $p\theta_f - p\theta_r$ and cuts both stator and rotor conductors, assuming the rotor stationary and the currents constant. This flux-density is produced only by the currents passing through the oscillating brushes.

Additional Flux Concepts and the Synchronizing Torques

If this last physical reference frame is used with its three flux concepts ψ, $\boldsymbol{B}$, and φ, then during hunting two additional flux-concepts appear that separate the resultant synchronizing torque into positive and negative components. The two additional fluxes are:

1. $\boldsymbol{B}\dagger$ is a flux-linkage at right angles in space to $\boldsymbol{B}$, hence numerically equal to the negative of the armature flux-linkage ψ_r

$$B\dagger = -\gamma B = -\gamma Gi = Ki = \psi_r \qquad (16)$$

This is a flux that acts as a spring to bring the rotor back to its original position when displaced by $\Delta\theta_r$. This flux is responsible for the existence of a permanent synchronizing torque in the absence of a voltage regulator or even in the

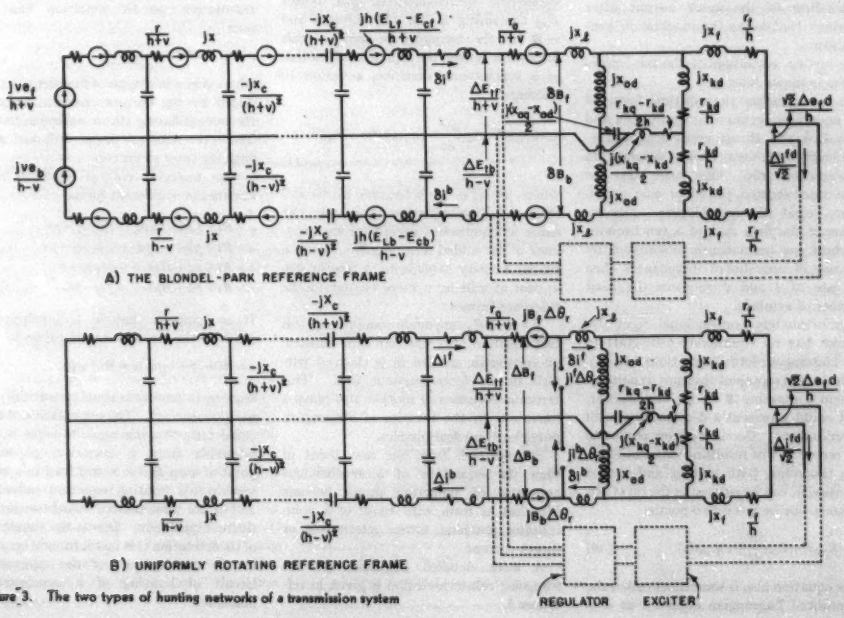

Figure 3. The two types of hunting networks of a transmission system

absence of hunting-frequency currents. The coefficient of i, namely K, is the "curvature-tensor." The tensor of valence four $K_{\alpha\beta\gamma\delta}$ built up from K (for the voltage) and $-K$ (for the torque) is the "Riemann-Christoffel curvature tensor."

The statement that the curvature tensor is an approximate measure of the steady-state stability of a synchronous machine is analogous to a similar generalization made by engineers about the short-circuit ratio.

2. $\varphi^{\dagger}$ is a flux-linkage at right angles in space to φ

$$\varphi^{\dagger} = \gamma\varphi = \gamma V i = G\Gamma i \tag{17}$$

This is a flux that acts as an apparent increase in the rotor moment of inertia, responsible for the appearance of a negative synchronizing-torque component during hunting.

When engineers talk about improving steady-state or transient stability by reducing the "transient reactance," or redesigning the voltage regulator, their statements are equivalent to expressing the coefficient of i, namely $G\Gamma$, in simple practical terms. (Not being a tensor, the latter has no single symbol or distinctive name.)

Additional Current Concepts and the Damping Torques

It is interesting that none of these flux concepts has any bearing upon the positive and negative damping torque components. The latter depend upon new current concepts that however appear only during small oscillations and then only along the last reference frame number III.

In the first two reference frames, Figure 3(A) the current concept i introduces during hunting the sole concept δi. But in frame number III, Figure 3(B) three new currents appear during hunting. In particular:

1. In the synchronous machine flows δi. It is a tensor, the so-called "absolute change" in i.

2. In the machine resistances and in the transmission line flows Δi (not a tensor).

3. Their difference $\Gamma i \Delta\theta_r$ (not a tensor) flows in a shunt between the machine and the line (when represented by an equivalent circuit)

$$\delta i = \Delta i - \Gamma i \Delta\theta_r \tag{18}$$

In the presence of this tensorially correct redistribution of currents all resistances act as positive or negative frictions tending to damp out or enlarge any small oscillations that arise.

A Still More General Frame IV

In analyzing the small oscillations of a polyphase induction motor, the conventional reference frame number III stationary with respect to the stator (the "cross-field" theory) introduces sinusoidal steady-state currents of fundamental frequency f along each axis. During hunting two sets of equations must be written, however, one set having $f+h$ frequencies, the other set $f-h$ frequencies. If now a uniformly rotating frame is assumed on both stator and rotor that rotates with the steady-state field and does not take part in the oscillations, then:

1. All steady-state currents are direct current (zero frequency).

2. Only one set of h frequency currents appears.

The analysis of hunting becomes thereby parallel to that of a synchronous machine (see reference 2, page 118). Dynamically and geometrically their theory may be assumed to be the same as those of frame number III. Or at least no need arose as yet to investigate whether additional physical concepts might be desirable in frame number IV.

The 24 Basic Reference Frames

In connection with each of the foregoing four types of physical reference frames (extended to six by interchanging the roles of stator and rotor) it is possible to introduce hypothetical "symmetrical component" frames (positive- and negative-sequence frames) provided the real variables i are replaced by complex variables even in the transient equations. These additional six frames are shown in the second column of Table I. Several of these were already used on previous occasions leading to simpler equations and more visual physical pictures.

In connection with each physical and each hypothetical frame it is possible to introduce still another reference frame that allows the equations to be represented by a stationary electrical network. This possibility doubles the number of frames of a synchronous machine, as shown in Table I, columns 3 and 4.

The Remarkable Properties of Reference Frame Number 22

While the physical frame number 4 (belonging to group III) separates the fluxes into equivalent springs and masses, and the resistances into positive and negative frictions, nevertheless the actual *magnitudes* of the various damping and synchronizing torques still are not clearly brought out in that frame. However there exists among the four reference frames of group number III one set that correctly gives the magnitudes of the individual torque components also. That particular frame is number 22 which also allows the representation of the synchronous machine and its connected power system in the form of a stationary network along the forward and backward (f and b) sequence axes.

Considering any large transmission system consisting of several synchronous machines, voltage regulators, transmission lines and other connected apparatus, —all expressed along reference frame number 22—the following relations exist between the power flow in the transmission system and the machine torques.

1. The damping torque T_D of each machine is the sum of the i^2r losses in the various portions of the system.

2. Similarly the synchronizing torque T_S of each machine is the sum of the i^2x powers stored in the various portions of the system.

It is interesting and important to note that none of the other reference frames of groups number I to number III mentioned hitherto is capable of this elegant physical interpretation. In the Blondel-Park frame number II, even though it is expressed in the form of an equivalent circuit along frame number 20 (Figure 3(A), the i^2r losses have nothing whatever to do with the damping torques, nor have the i^2x powers any connection with the synchronizing torques. By inference from Figure 3(B), however, some isolated relations may be established for 3(A) also.

Moreover it cannot be sufficiently emphasized that it is not adequate merely to express the equations of the synchronous machine along frame number 22. The equations must be developed in a strictly tensorial form involving the Riemann-Christoffel curvature tensor. It is possible to express the equations of frame number 22 in a conventional manner and develop even an equivalent circuit for it. But there exist no simple relations between torques and powers and the equivalent circuit is devoid of such simple physical meanings.

The physics of small oscillation of rotating electric machines, or of any dynamical system for that matter, is intimately connected with the curvature tensor. Without it the physics of the phenomenon must be expressed in terms of artificial, nontensorial concepts that do not lend themselves to easy visualization.

The derivation of this interesting equivalent circuit of a synchronous machine, Figure 3(B), representing reference frame number 22 in a tensorial formulation, will be the subject matter of a subsequent paper.

Doubling the Number of Reference Frames

To each of the 2-phase axis of a winding belongs a third, the zero-sequence axis, that hitherto has been ignored since it does not take part in the transformations. However on both stator and rotor of each of the 24 types of reference frames it is possible to assume three axes at 120 degrees from each other, representing a 3-phase winding. Even though the analysis itself is usually performed in terms of 2-phase axes, in many cases the final results must be reinterpreted in terms of the actual 3-phase winding.

Practically all problems can be and should be analyzed first in terms of the simpler 2-phase (and zero sequence) frame to save labor, and then only should the results be transformed to the actual 3-phase frame. Similarly since all transformations are easier to perform from a 2-phase to another 2-phase frame, consequently 3-phase transformations should be avoided if at all possible. However these precautions were not followed by Park in his basic work, who performs his transformation from frame number 1, considered as 3-phase axes, to frame number 2 considered as 2-phase axes. The apparent difficulty of his work is partly due to his going from the $\boldsymbol{a}$, $\boldsymbol{b}$, $\boldsymbol{c}$ to the $\boldsymbol{d}$, $\boldsymbol{q}$, $\boldsymbol{o}$ axes without first changing to the 2-phase axes $\boldsymbol{\alpha}$, $\boldsymbol{\beta}$, $\boldsymbol{o}$ on the same holonomic physical frame. (The author in his book[1] performs all transformations always from $\boldsymbol{\alpha}$, $\boldsymbol{\beta}$ to $\boldsymbol{d}$, $\boldsymbol{q}$ or vice versa. He denotes $\boldsymbol{\alpha}$ and $\boldsymbol{\beta}$ by $\boldsymbol{a}$ and $\boldsymbol{b}$.)

Some More Reference Frames

When a reference frame is not connected rigidly to the structure but is free to move, several possibilities may arise. The reference frame may be accelerated or may have an arbitrary uniform velocity. It may follow the motion of some other structure or of the rotating flux. Also the stator reference frame may rotate with speeds different from those of the rotor frame.

The number of possible reference frames increases greatly if the angle between the axes changes from 90, or 120, degrees. (A shaded-pole induction motor is an example.) If the various axes of the stator and rotor also are interconnected in shunt or series (as in a-c and d-c commutator machines) the possible number of frames grows by leaps and bounds. When several machines and stationary networks are interconnected and when other than electrodynamical systems also are interlinked into one unit, the number of possible reference frames becomes inexhaustible. It cannot be sufficiently emphasized that it is possible to establish equations for any one reference frame by starting with those of any other frame. From a mathematical point of view all reference frames are of equal value (all form one "group") though the use of any one particular frame is dictated by some practical necessity.

The Evolutionary Growth of Electrodynamic Concepts

One other characteristic of electrodynamical systems must be pointed out. Because of the cylindrical properties of the variables it was possible to introduce two sets of physical concepts along frame number II. In going over to a new reference frame number III, either of the two sets of physical entities may be carried along. Moreover since it is possible to arrive to frame number III from frame number I without the intermediary step of frame number II, it is possible to attribute to frame number III at least three different sets of physical entities, each associated with a different type of physical picture. The situation is complicated by the fact that in returning from frame number III to frame number II the original set of equations and physical entities need not necessarily be re-established.

It has to be recognized that in electrodynamics it is not sufficient merely to state what reference frame is being used. It also is necessary to define all the intermediary reference frames, the physical interpretation (type of geometrical space) attributed to the intermediary frames, also the original starting frame and equations that have been employed in arriving to the working equations.

In other words, a characteristic of electrodynamics is that the history of the succession of reference frames and geometrical spaces employed leaves its imprint upon the nature of the physical entities that happen to exist along any particular type of reference frame.

The Elementary Books on Tensor Analysis

It is rather unfortunate that most introductory books on tensor analysis only cover the study of 3-dimensional holonomic Euclidean and Riemannian spaces, all of which are practically useless to represent the physical concepts dealt with by the electrical power engineer. What is worse, even in these restricted spaces the authors assume only real transformations (in electric machinery during steady state and during hunting the currents are complex, not real). In addition usually all transformations occur only between equal number of variables (nonsingular transformations) while in interconnecting electric machines and networks most transformations are singular (the interconnected system has fewer number of variables). Needless to say that all such books are also full of geometrical theorems that are of no earthly use to the power engineer.

It is emphasized though that such restricted analysis of a holonomic Riemannian space with real variables and nonsingular transformations is still valuable to the engineer who is interested in conventional 2- and 3-dimensional field problems such as heat-flow, fluid dynamics, electromagnetic fields, et cetera. For him tensor analysis represents, however, only an improved presentation of the concepts of conventional vector analysis. But outside of serving as a short introduction to the more advanced concepts of tensor analysis the electrical power engineer, interested in circuits and machines as opposed to fields, will find a more than cursory study of elementary books on tensors disappointing and a waste of time.

The Advanced Concepts of Tensor Analysis

Although each winding of a rotating electric machine is a 2-dimensional field and an entire machine is a collection of such interconnected 2-dimensional fields, the spaces described by the currents in the windings are not holonomic and Riemannian, but nonholonomic and non-Riemannian, as demonstrated previously. Moreover a transmission system is not merely an n-dimensional space, it is rather a conglomeration of interconnected and interlinked zero-, 1- and 2-dimensional Euclidean, Riemannian, and non-Riemannian spaces, all rotating, sliding and intertwining with each other. The concept of "interconnection of spaces" transgresses the boundaries of "differential geometry" and encroaches upon the territory of "topology."

The writer knows of only two books[6,7] that cover the geometry of the general spaces and the type of transformations

that arise in electrical power engineering. (The geometrical analogues of resistances, capacitances and impressed forces are still absent in these books, so is the concept of interconnection of different types of spaces.) Curiously enough, one of their authors, Schouten, the creator of several of these spaces, was himself originally an electrical engineer specializing in rotating electric machinery. (Several of his engineering contributions are to be found in the Elektrotechnische Zeitschrift.) In his search for a co-ordinating engineering tool more general than vector analysis, he became interested in tensor analysis and never again did he turn back to vector analysis or to engineering. Schouten has been applying these non-Riemannian spaces during the last three decades to the study of the atomic nucleus and its elementary particles in place of electric machinery.

The electrical engineer will be surprised to find how the very same tensorial concepts mentioned in these pages turn up over again in the study of the motion of the elementary particles of nuclear physics or of the stars of distant nebulae (cosmology) as a glance through any issue of the Physical Review would show. These fascinating analogies are additional driving forces behind the authors insistence upon the rigorous tensorial formulation of each new physical entity he is called upon to employ. These analogies from the world of atoms and of stars serve as inexhaustible sources of information and inspiration for the further extension of knowledge concerning the behavior of such man-made creations as electrical power networks and power machinery.

References

1. Stationary Networks and Transmission Lines Along Uniformly Rotating Reference Frames, G. Kron. *AIEE Transactions*, volume 68, part I, 1949, pages 690–96.

2. The Application of Tensors to the Analysis of Rotating Electrical Machinery, (book), G. Kron. *General Electric Review* (Schenectady, N. Y.), 1938.

3. Non-Riemannian Dynamics of Rotating Electrical Machinery, G. Kron. *Journal of Mathematics and Physics* (Cambridge, Mass.), 1934, pages 103–94.

4. Two-Reaction Theory of Synchronous Machines, R. H. Park. *Electrical Engineering* (*AIEE Transactions*), volume 48, July 1929, pages 716–27.

5. Kron's Non-Riemannian Electrodynamics, B. Hoffmann. *Reviews of Modern Physics* (New York, N. Y.), volume 21, Number 3, July 1949, pages 535–40.

6. Einführung in die Neueren Methoden der Differentialgeometrie, J. Schouten, D. J. Struik. Volumes I and II, Noordhoff (Groningen, Holland), 1940.

7. Theory of Linear Connections, D. J. Struik. Ergebnisse der Mathematik, Band III Heft 2, Julius Springer, Berlin, Germany, 1934.

No Discussion

The Calculation of the Capacitance of Coaxial Cylinders of Rectangular Cross-Section

GEORGE M. ANDERSON
ASSOCIATE AIEE

IN A recent paper, T. J. Higgins and R. D. Teasdale,[1] using experimental techniques, have made a thorough study of the capacitance per-unit length of copper bus-bars set in concrete cells.

A cross-section of a typical arrangement is shown in Figure 1. The cylindrical conductor of rectangular cross-section, at line potential, is arranged symmetrically within a concrete cell assumed to be at zero potential. Results of the investigation show graphically the variation of capacitance per centimeter with side lengths. An empirical relation also is given for the case of square cross-sections.

The purpose of the present paper is to develop analytical formulas and methods for calculating the capacitance per-unit length of configurations of this type. The field problem is assumed to be two dimensional; that is, it does not depend on the long dimension of the cylinders. The cylinders themselves are assumed to be equipotentials and their orientation with respect to each other is as shown in Figure 1.

Two approaches are presented: (1) an exact solution based on the work of Bergman,[2,3] which permits the calculation of capacitance from a simple formula for a square coaxial cylinder or for the rectangular case provided the side lengths in the latter case satisfy a given restraining condition, and (2) an approximate calculation for those cases where the exact solution does not apply.

Part III, the section on Comparison of Calculated and Experimentally-Determined Values of Capacitance compares, in a few instances, calculated values of capacitance with the experimentally-determined values of Higgins and Teasdale. Their experimentally-determined values appear to have an error of from 4 to 8 per cent, always high.

I. An Exact Solution

The calculation of the capacitance of configurations in which the field is two dimensional can often be effected with the aid of conformal transformations of a complex variable. A suitable transformation transforms the given problem into a new problem for which the solution is known or can be found. When the boundary of the configuration is a closed polygon of straight sides, the Schwarz-Christoffel integral offers a systematic approach to finding the desired transformation.

Bergman,[2,3] using this method, has investigated the magnetic field in a single-phase transformer. With the aid of certain simplifying assumptions, he reduced the transformer problem to that of the "L" of Figure 2(A), in which AF and CD are magnetic equipotentials and ABC and DEF are lines of magnetic flux.

From symmetry considerations it is apparent that the capacitance problem of the rectangular cylinders may be reduced to determining the capacitance of the "L" of Figure 2(A), in which AF and CD now are taken as lines of electric flux and ABC and DEF are electric equipotentials. The capacitance of the cylinders is then four times the capacitance of the "L." Bergman's work may therefore be applied directly.

The details of the analysis are contained in the Appendix.

The results of the analysis, which apply only when equation 4 is fulfilled, show that the capacitance of the rectangular cylinders of Figure 1 may be computed from*

$$C = 2\varepsilon_0 \frac{K(x')}{K(x)} \tag{1}$$

where $K(x)$ and $K(x')$ are complete elliptic integrals of the first kind[4,5,6,7] to the moduli x and x' respectively. (The prime notation is used to designate the complimentary modulus. Thus $x'^2 = 1 - x^2$.)

The modulus x is given by

$$x^2 = \frac{k_2^2}{k_1^2} \frac{(1-k_1^2)}{(1-k_2^2)} \tag{2}$$

where k_1 and k_2 are also moduli of complete elliptic integrals of the first kind determined in terms of the side lengths of one of the four "L's" of the rectangular cylinders by

$$\frac{K(k_1)}{K(k_1')} = 2\left[\frac{(AB)-(CD/2)}{(AF)}\right];$$
$$\frac{K(k_2)}{K(k_2')} = \frac{1}{2}\left[\frac{DC}{(BC)-(AF)/2}\right] \tag{3}$$

The condition of restraint mentioned above requires that k_1, k_2, and the side lengths satisfy

$$\frac{K(k_2)}{K(k_1')} = \frac{(DC)}{(AF)} \tag{4}$$

This condition is always satisfied when there is symmetry, that is when $(AB) = (BC)$ and $(DE) = (EF)$. (In this case $k_1^2 + k_1'^2 = 1$.) If equation 4 is not satisfied this method is not applicable.

Paper 50-115, recommended by the AIEE Basic Sciences Committee and approved by the AIEE Technical Program Committee for presentation at the AIEE North Eastern District Meeting, Providence, R. I., April 26–28, 1950. Manuscript submitted November 15, 1949; made available for printing February 27, 1950.

GEORGE M. ANDERSON is with the Carnegie Institute of Technology, Pittsburgh, Pa.

The author wishes to express his thanks to Professor B. R. Teare for his encouragement during the course of this work and for his helpful comments and suggestions in the preparation of the paper. Thanks also are extended to Professor A. Heins for a useful discussion of the problem and to Professor G. Handelman for reference 3.

*The dielectric is taken to be air. Meter-kilogram-second rationalized units are used throughout this paper. In this system $\varepsilon_0 = (10^{-9})/36\pi$.

Approximations to the Elliptic Integrals

For extreme values of the modulus, x, in equation 1, it is desirable to use approximations to $K(x)$ and $K(x')$. A particularly suitable approximation, since it deals directly with the ratio of $K(x)$ to $K(x')$, is given by Whittaker and Watson.[8]

If $k^2<0.5$, then

$$\frac{K(k')}{K(k)}=\frac{1}{\pi}\log_e(1/q) \tag{5}$$

where

$$q=\varepsilon+2\varepsilon^4+15\varepsilon^9+150\varepsilon^{16}+\ldots$$

and

$$2\varepsilon=(1-\sqrt{k'})/(1+\sqrt{k'})$$

ε has a maximum value

$$\varepsilon_{max}=0.087$$

so that

$$q\approx\varepsilon$$

with an error of less than eight parts per million, and

$$\frac{K(k')}{K(k)}\approx\frac{1}{\pi}\log_e 2(1+\sqrt{k'})/(1-\sqrt{k'}) \tag{6}$$

If $k^2>0.5$, it is similarly established that

$$\frac{K(k)}{K(k')}\approx\frac{1}{\pi}\log_e 2(1+\sqrt{k})/(1-\sqrt{k}) \tag{7}$$

Approximations to the Moduli of the Elliptic Integrals

Equations 6 and 7 can, of course, be inverted to find the modulus when the ratio of the integrals is known as required in equation 3. The advantage, of course, being that the cut and try process necessary with the elliptic integral tables is eliminated and the result is expressed in terms of the more elementary functions.

Let

$$\frac{K(k)}{K(k')}=y$$

If $y<1$, then from equation 6

$$k'=\sqrt{1-k^2}\approx\left[\frac{1-2e^{-\pi/y}}{1+2e^{-\pi/y}}\right]^2=\tanh^2\left[\frac{(\pi/y)-\log_e 2}{2}\right] \tag{8}$$

and if $y>1$, from equation 7

$$k\approx\left[\frac{1-2e^{-\pi y}}{1+2e^{-\pi y}}\right]^2=\tanh^2\left[\frac{\pi y-\log_e 2}{2}\right] \tag{9}$$

Example

To illustrate the numerical calculations consider the case of a square coaxial cylinder with dimensions

$$\frac{(AB)}{(EF)}=3.0;\quad (AB)=(BC);\quad (DE)=(EF)$$

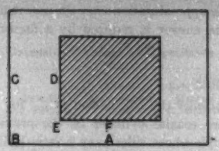

Figure 1. Cross section of rectangular cylindrical capacitor

From equation 3

$$\frac{K(k_1)}{K(k_1')}=\frac{K(k_2')}{K(k_2)}=\frac{[(AB)/(EF)]+1}{[(AB)/(EF)]-1}=2.0$$

K. Hayashi[7] gives a table of $K(k)/K(k')$ from which k_1 and k_2 may be determined directly.

If this table is not available, k_1 and k_2 can be found after some experimentation using the tables for $K(k)$.

Let

$$k_1=k_2'=\sin\theta$$

then

$$k_1'=k_2=\cos\theta$$

and from the tables

$$\theta=80 \text{ degrees } 6 \text{ minutes}$$

From equation 2

$$x^2=(k_1/k_1')^4=\cot^4\theta=0.03046$$

Using the elliptic integral tables directly we find

$$K(x)=1.571;\quad K(x')=4.879$$

and from equation 1

$$C=2\varepsilon_0\frac{K(x')}{K(x)}=\frac{2(10^{-9})}{36\pi}\,\frac{4.879}{1.571}$$

$$=54.91 \text{ micromicrofarads per meter}$$

This result also can be obtained using the previously described approximations to the elliptic integrals and their moduli.

From equation 9

$$k_1=\left[\frac{1-2e^{-2\pi}}{1+2e^{-2\pi}}\right]^2=[(1-2e^{-2\pi})(1-2e^{-2\pi}+4e^{-4\pi}-\ldots)]^2$$
$$=1-8e^{-2\pi}+32e^{-4\pi}+\ldots$$
$$=0.98517$$

Again, from equation 2, x is found to be

$$x=\frac{k_2^2}{k_1^2}=\frac{1}{k_1^2}-1=0.03031$$

The ratio $K(x')/K(x)$ is determined from equation 6 with x replacing k

$$\frac{K(x')}{K(x)}=\frac{1}{\pi}\log_e 2(1+\sqrt{x'})/(1-\sqrt{x'})$$

$$=\frac{1}{\pi}\log_e\frac{2(1+\sqrt{x'})^2(1+x')}{x^2}$$

$$\frac{K(x')}{K(x)}=\frac{2}{\pi}\log_e(4/x) \text{ for } x \text{ near zero}$$

$$=\frac{2}{\pi}(4.883)$$

and from equation 1

$$C=2\varepsilon_0\frac{K(x')}{K(x)}=\frac{2(10^{-9})}{36\pi}\,\frac{2}{\pi}(4.883)$$

$$=54.97 \text{ micromicrofarads per meter}$$

II. An Approximate Solution

In the event that the exact solution described in Part I is not applicable, an approximate calculation, using conformal transformation methods, is possible in most cases. It is convenient, here again, to make use of symmetry and to consider the rectangular cylinder of Figure 1 to be composed of four "L" sections.

The most important and best known approximation to the finite "L" of Figure 3(A) is the infinite "L" (sides extend to infinity in both directions) of Figure 3(B). Historically this approximation was first used in estimating the additional capacitance in the bend of a Leyden jar. Jeans[9] uses this approximation to compute the capacitance of a finite "L" whose side lengths are large compared with the distances between the conductors.

When the side lengths are not large compared to these distances another procedure must be used. The lines of electric flux in the region near the bend have approximately the shape shown in Figure 3(B). Consider the particular section bounded by the flux lines $(H'D')$, $(G'F')$, and the conductors $(G'B'H')$ and $(D'E'F')$. If DE equals $D'E'$ and EF equals $E'F'$, then the capacitance of the section $G'B'H'D'E'F'G'$ will be less than that of the "L," $ABCDEFA$, and is accordingly designated $C_-/4$, where $C/4$ is the capacitance of the "L."

Similarly the capacitance of the section $A'B'C'I'E'J'A'$ will be greater than $C/4$ and is designated $C_+/4$. The four factor is included so that C may represent the capacitance of the rectangular coaxial cylinder of Figure 1 consisting of four "L" sections.

The transformation which maps the interior of the infinite "L" into the upper half of the t plane is

$$z=\frac{2}{\pi}\left[a\tan^{-1}\sqrt{\frac{\alpha^2t-1}{t+1}}+b\tanh^{-1}\frac{1}{\alpha}\sqrt{\frac{\alpha^2t-1}{t+1}}\right] \tag{10}$$

where

$$\alpha=a/b$$

The correspondence between points

in the z plane and the transformed points in the t plane is indicated in Figure 3; the primed points of Figure 3(B) go into the double primed points of Figure 3(C). The curved flux lines in the z plane transform into the semicircles in the t plane.

The points E'' and B'' correspond to $t=-1$ and $t=1/\alpha^2$ respectively. Let η, λ, ρ, and μ represent the particular values of t at the points A'', C'', D'', and F'' respectively. To determine C_+ and C_- it is necessary to compute these constants. This is done with the aid of the transformation (equation 10). For example, μ is given by the solution of the equation

$$(BA)+jb=\frac{2}{\pi}\left[a\tan^{-1}\sqrt{\frac{\alpha^2\mu-1}{\mu+1}}+b\tanh^{-1}\frac{1}{\alpha}\sqrt{\frac{\alpha^2\mu-1}{\mu+1}}\right] \quad (11)$$

It should be observed that η, λ, ρ, and μ are bounded by the relations

$$\begin{aligned} -\infty<\mu<-1 \qquad & 0<\lambda<1/\alpha^2 \\ -1<\rho<0 \qquad & 1/\alpha^2<\eta<+\infty \end{aligned} \quad (12)$$

The transformation

$$w=u+jv=\log_e t \quad (13)$$

maps the upper half of the t plane into the infinite strip between $v=0$ and $v=\pi$ in the w plane, with the positive real axis going into $v=0$ and the negative real axis into $v=\pi$. $C_+/4$ and $C_-/4$ are readily determined in the w plane since they are simply sections of an infinite parallel-plate capacitor.

The capacitance approximations C_+ and C_- are therefore obtained from the expressions

$$C_+=\frac{4\varepsilon_0}{\pi}\log_e(\eta/\lambda);\ C_-=\frac{4\varepsilon_0}{\pi}\log_e(\mu/\rho) \quad (14)$$

C_+ and C_- provide upper and lower bounds for C, the capacitance per meter of the cylinder of Figure 1, and therefore permit the calculation of maximum error. An average value of C_+ and C_- provides a better approximation since the uncertainty of the answer is reduced by a factor of two.

Example

Consider the calculation of C_- for the square coaxial cylinder of the previous example whose sides have a ratio $[(AB)/(EF)]=3.0$. From equation 14 μ and ρ are to be determined. Substituting in equation 11, $\alpha=(a/b)=1$ and $a=b=(AB)-(EF)$, we find

$$\left[\frac{(AB)}{(AB)-(EF)}+j\right]\frac{\pi}{2}=\tan^{-1}\delta+\tanh^{-1}\delta \quad (15)$$

where

$$\delta=\sqrt{\frac{|\mu|+1}{|\mu|-1}}>1 \text{ since } -\infty<\mu<-1 \quad (16)$$

The $\tanh^{-1}\delta$ may be evaluated from the identity

$$\tanh^{-1}\delta=\frac{1}{2}\log_e\frac{(1+\delta)}{(1-\delta)}=\frac{1}{2}\log_e\frac{(\delta+1)}{(\delta-1)}+\frac{j\pi}{2}+j\pi m \quad (17)$$

where m is an integer. It must be chosen so as to select the correct branch of the multiple valued arc hyperbolic tangent. Substituting equation 17 in equation 15, we obtain

$$\left[\frac{3}{2}+j\right]\frac{\pi}{2}=\tan^{-1}\delta+\frac{1}{2}\log_e\frac{(\delta+1)}{(\delta-1)}+\frac{j\pi}{2} \quad (18)$$

for $m=0$. This is a real, transcendental equation in δ which must be solved by approximation methods.

Solution gives

$\delta=1.09979$
$\mu=-10.54$

The equation corresponding to equation 11 for ρ is, after substituting $\alpha=1$ and $a=b=(AB)-(EF)$

$$\left[1+j\frac{(BC)}{(AB)-(EF)}\right]\frac{\pi}{2}=\tan^{-1}(j\gamma)+\tanh^{-1}(j\gamma) \quad (19)$$
$$=\tan^{-1}(j\gamma)+j\tan^{-1}\gamma$$

where

$$\gamma=\sqrt{\frac{1+|\rho|}{1-|\rho|}}>1 \text{ since } -1<\rho<0 \quad (20)$$

The $\tan^{-1}(j\gamma)$ is evaluated using

$$\tan^{-1}(j\gamma)=j\tanh^{-1}\gamma=\frac{j}{2}\log_e\frac{(1+\gamma)}{(1-\gamma)}$$
$$=\frac{j}{2}\log_e\frac{(\gamma+1)}{(\gamma-1)}+\frac{j}{2}(j\pi+j2\pi n) \quad (21)$$

Substituting equation 21 in equation 19 gives

$$\left[1+j\frac{3}{2}\right]\frac{\pi}{2}=\frac{j}{2}\log_e\frac{(\gamma+1)}{(\gamma-1)}-\frac{\pi}{2}(2n+1)+j\tan^{-1}\gamma \quad (22)$$

for which $n=-1$ selects the desired branch of the arc tangent. Equation 22 in γ is the same equation as 18 in δ, so that $\gamma=\delta$, and from equations 16 and 20 $\rho=1/\mu$. From equation 14

$$C_-=\frac{4\varepsilon_0}{\pi}\log_e\mu^2=\frac{8(10^{-9})}{36\pi^2}\log_e(10.54)$$
$$=52.9 \text{ micromicrofarads per meter}$$

Another Approximate Method

Another method of approximating the finite "L" problem using conformal transformations is given in a paper by Cockcroft.[18] This method requires that only one pair of sides go to infinity. While it is less restrictive than the method pre-

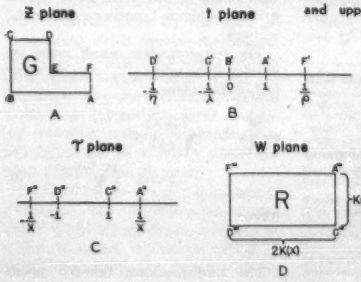

Figure 2 (left). (A) "L" section of Figure 1. Region "G" is mapped successively into: (B) real axis and upper half of t plane; (C) real axis and upper half of τ plane; (D) rectangular region R of w plane

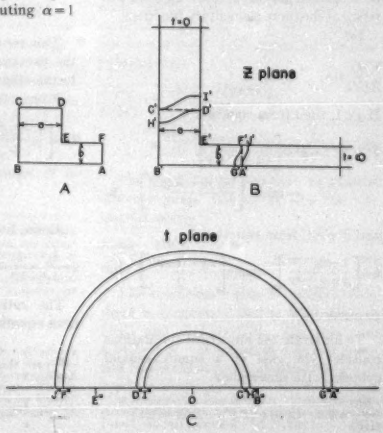

Figure 3 (right). (A) "L" section of Figure 1. (B) Infinite "L" approximation to the finite "L" of (3A). Boundary and interior are transformed into (C) real axis and upper half of t plane

Table I. Comparison of Calculated and Experimentally Determined Values of Capacitance

$\frac{(AB)}{(EF)}=\frac{(BC)}{(DE)}$	Part I C, mmf/m	Part II C_+, mmf/m	Part II C_-, mmf/m	Part II C_{av}, mmf/m	Exper. Determined C, mmf/m	Relaxation Method C, mmf/m
1.18	412.8	412.4	412.4	412.4	429	
1.47	170.3	170.1	170.1	170.1	180	
2.0	90.4	90.7	89.9	90.3	97.5*	92.5
3.0	54.9	56.9	52.9	54.9	57.5*	53.6
5.62	34.1	39.1	29.2	34.2	37.6	

*These values were not determined directly but were computed from an empirical formula based on other measurements.[11]

sented, it appears to be much more difficult to apply.

III. Comparison of Calculated and Experimentally-Determined Values of Capacitance

Capacitance calculations, using the methods of Parts I and II, were performed for several cases of square cross-sections; that is, $(AB)=(BC)$ and $(DE)=(EF)$. Table I shows these values compared with the experimentally-determined values of Higgins and Teasdale.[11] The latter were derived from resistance measurements based on the mathematical equivalence of the electrostatic and current flow fields.

The final column shows values of capacitance as computed by a relaxation process. These values were used by the authors[12] as check points. It is to be noted that the capacitance values determined by experiment are all above the calculated values and are also above the values determined by relaxation process.

The approximation method of Part II yields surprisingly good results when the average of C_+ and C_- is used. In the case where the sides are in the ratio 5.62-to-1 the average value of capacitance is still very close to the correct value.

Appendix

Summary of Previous Work

The transformation

$$z=\alpha\int_0^t \frac{dt}{\sqrt{t(1+\eta t)(1+\lambda t)(1-t)(1-\rho t)}} \tag{23}$$

maps the upper half of the t plane in Figure 2(B) into the region G, Figure 2(A), in the z plane, and carries the points A', B', C', D', F' into the corresponding points A, B, C, D, F and the infinite point into E.

The difficulty in applying the method attends the determination of the branch points of the integral η, λ, and ρ and the evaluation of the integral in terms of known functions. Bergman,[8,9] using a theorem due to Jacobi, has reduced the hyperelliptic integral (equation 23) to two elliptic integrals of the first kind for the special case where the branch points satisfy the relation

$$\rho=\eta\lambda \tag{24}$$

Using the successive transformations

$$p=(1+\eta\lambda t^2)/t \tag{25}$$

and

$$r^2=\frac{p-(1+\eta\lambda)}{p-2\sqrt{\eta\lambda}};\quad s^2=\frac{p-(1+\eta\lambda)}{p+2\sqrt{\eta\lambda}} \tag{26}$$

the integral (equation 23) is reduced to

$$z=\frac{\alpha}{2}\left[\int_{r_0}^{r}\frac{dr}{\sqrt{(1-r^2)(1-k_1^2r^2)}}+\int_{s_0}^{s}\frac{ds}{\sqrt{(1-s^2)(1-k_2^2s^2)}}\right] \tag{27}$$

where

$$k_1^2=\frac{(\sqrt{\eta}+\sqrt{\lambda})^2}{(1+\eta)(1+\lambda)};\quad k_2^2=\frac{(\sqrt{\eta}-\sqrt{\lambda})^2}{(1+\eta)(1+\lambda)} \tag{28}$$

As t varies from $-\infty$ to $+\infty$ along the real axis the point in the z plane moves around the boundary of the "L." The sides of the "L" are related to the elliptic integrals of the first kind from equation 27. The moduli k_1 and k_2 are therefore determined by the dimensions of the "L." The relations are

$$\frac{K(k_1)}{K(k_1')}=2\left[\frac{(AB)-(CD)/2}{(AF)}\right];$$
$$\frac{K(k_2)}{K(k_2')}=\frac{1}{2}\left[\frac{(DC)}{(BC)-(AF)/2}\right] \tag{29}$$

To satisfy equation 24 it is necessary that k_1, k_2 and the sides of the "L" satisfy

$$\frac{K(k_2)}{K(k_1')}=\frac{(DC)}{(AF)} \tag{30}$$

Application to the Capacitance Problem

Since the preceding transformations are conformal, they can be applied to the capacitance problem. In this problem, as explained earlier, ABC and DEF are equipotentials and CD and AF are lines of electric flux. To determine the capacitance we must retransform the upper half of the t plane into the interior of the region R of the w plane of Figure 2(D). To facilitate the final transformation, it is convenient first to transform the upper half of the t plane into the corresponding region of the τ plane using the transformation

$$v=\frac{(\sqrt{\lambda}+\sqrt{\eta})(1+\sqrt{\eta\lambda}t)}{(\sqrt{\lambda}-\sqrt{\eta})(1-\sqrt{\eta\lambda}t)} \tag{31}$$

The correspondence between points in the two planes is indicated in Figure 2; the primed points in Figure 2(B) go into the double primed points in Figure 2(C).

The upper half of the τ plane is finally mapped into the rectangular region R, Figure 2(D), in the w plane by the transformation

$$w=\int_0^{\tau}\frac{d\tau}{\sqrt{(1-\tau^2)(1-x^2\tau^2)}} \tag{32}$$

The modulus, x, of the elliptic integral (equation 32) is determined in terms of the original branch points η and λ from

$$x^2=\left[\frac{1-\sqrt{\eta\lambda}}{1+\sqrt{\eta\lambda}}\right]\left[\frac{\sqrt{\lambda}-\sqrt{\eta}}{\sqrt{\lambda}+\sqrt{\eta}}\right]^2 \tag{33}$$

Using equations 28 and 33, x is expressible in terms of k_1 and k_2 as

$$x^2=\frac{k_2^2(1-k_1^2)}{k_1^2(1-k_2^2)} \tag{34}$$

Since capacitance is invariant under the conformal transformations, the capacitance per unit length of the "L" of Figure 2(A), is equal to that of the parallel-plate capacitor of Figure 2(D). There are four "L's" in parallel making up the cylindrical capacitor of Figure 1. Therefore

$$C=4\epsilon_0\left[\frac{K(x')}{2K(x)}\right]=2\epsilon_0\frac{K(x')}{K(x)} \tag{35}$$

gives the capacitance per meter of coaxial cylinders of rectangular cross-section.

References

1. Experimental Determination of the Capacitance of Heavy-Current Busses Comprised of Solid or Tubular Rectangular Conductors, T. G. Higgins, R. D. Teasdale. *AIEE Transactions*, volume 67, part 1, 1948, pages 653–59.

2. Uber die Berechnung des Magnetischen Feldes in Einem Einphasen-transformator, S. Bergman. *Zeitschrift fur Angewandte Mathematic und Mechanik* (Berlin, Germany), volume 5, 1925, pages 319–31.

3. Partial Differential Equations—Advanced Topics, S. Bergman. *Notes*, summer session, 1941, Brown University (Providence, R. I.), June 23–September 13, 1941, pages 168–73.

4. Tables of Functions (book), E. Jahnke, F. Emde. Dover Publications, New York, N. Y., fourth edition, 1945, page 85.

5. Elliptic Integrals of Large Moduli, H. B. Dwight. *Electrical Engineering* (*AIEE Transactions*), volume 54, July 1935, pages 700–11.

6. Auxiliary Tables of Complete Elliptic Integrals, E. L. Kaplan. *Journal of Mathematics and Physics* (Cambridge, Mass.), volume 25, 1946, page 26.

7. Tafeln der Besselchen, Theta, Kugel und Anderer Functionen (book), K. Hayashi. Julius Springer, Berlin, Germany, 1930.

8. Modern Analysis (book), E. T. Whittaker, G. N. Watson. Cambridge University Press (Cambridge, England), fourth edition, 1940, page 480.

9. The Mathematical Theory of Electricity and Magnetism, Sir James Jeans. Cambridge University Press (Cambridge, England), fifth edition, 1943, pages 277–79.

10. The Effect of Curved Boundaries on the Distribution of Electric Stress Round Conductors, J. D. Cockcroft. *Journal*, Institution of Electrical Engineers (London, England), volume 66, 1927–1928, page 390.

11. See reference 1, table III, page 655.

12. See reference 1, page 658.

No Discussion

A New Device for Calibrating Watt-Hour Meters

H. F. ROBISON
MEMBER AIEE

W. H. WICKHAM
MEMBER AIEE

A NEW device has been developed to provide a better means of calibrating watt-hour meters, particularly in the field. With this device the field testing of watthour meters is made much faster and easier as compared to the conventional methods of counting or timing of disk revolutions. It is faster because an instantaneous and continuous visual indication of meter accuracy is obtained. It is easier because the indication is definite and clear. The tester is subjected to less eye strain than in the close observation of meter disks. In general, closer adjustment to correct registration is obtained than by the methods involving successive trials. The device is portable. No special disks, disk markings, or the like are required for its application.

Other methods, such as the stroboscopic methods and automatic counting of revolutions, have been developed for laboratory and shop use and have some of the same advantages. While these methods are a great improvement over the conventional methods of counting or timing of disk revolutions, they are not applicable to field testing because they require that the meters be mounted in a special stand, or jig, and furthermore, the equipment is too elaborate and cumbersome.

The new device compares the speed of the disk of the meter under test with that of a standard watt-hour meter by photoelectric means. An instantaneous and continuous comparison of speeds is indicated on the screen of a cathode-ray tube.

Both the standard and test watt-hour meters are equipped with a light source, a system of lenses and mirrors, and a photocell. Serrations on the disk of each meter interrupt the light on the photocells as the disks rotate. Serrated disks are standard on most modern watt-hour meters. The variation of current in the photocell on the standard meter is utilized to control the horizontal sweep circuit of a cathode-ray tube, and on the test meter to produce a vertical deflection on the screen of the cathode-ray tube. The resulting trace is stationary when the disks of both meters are rotating at the same speed, and moves across the screen when the two speeds differ. The action of the trace is used to obtain an "as found" check by varying the voltage on the standard to match its speed to that of the meter under test. It also is used to obtain correct registration of the meter under test by varying the speed of that meter, by adjustment, to match the speed of the standard.

Description of Device

The standard watthour meter is permanently equipped with an optical system and photocell. For the test meter, a spare cover of the type on the meter under test is equipped with a bracket on which a similar optical system and photocell can be mounted. This cover temporarily replaces the regular meter cover for test purposes. This optical system is shown in Figure 1(A). Light is directed by lenses and mirrors along the path indicated by the dotted lines to project an enlarged image of the disk teeth on the light shield of the photocell. The holes in this shield are in a horizontal line and are spaced so that the distances between centers of the holes are equal to the distances between centers of the magnified tooth images. Figure 1(B) is a section of watt-hour meter disk showing the toothed edge and Figure 1(C) is a section of the light shield of the photocell showing the holes with the disk tooth images superimposed. As the watt-hour meter disk revolves, the holes in the light shield of the photocell are alternately covered and uncovered by the disk tooth images. This causes the photocell to pass a periodic current, the frequency of which is proportional to the speed of rotation of the watt-hour meter disk.

The photocells used in this apparatus also are electron multipliers. The periodic photocell currents are passed through suitable resistors to produce periodic voltages. The method of comparison of the frequencies of the voltage waves from the test unit on the standard meter and from the test unit on the meter under test is shown in a block diagram in Figure

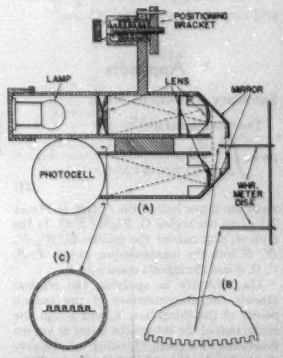

Figure 1 (A). Optical system and photocell. (B) Section of watt-hour meter disk. (C) Section of photocell light shield

Paper 50-116, recommended by the AIEE Instruments and Measurements Committee and approved by the AIEE Technical Program Committee for presentation at the AIEE North Eastern District Meeting, Providence, R. I., April 26–28, 1950. Manuscript submitted November 15, 1948; made available for printing February 27, 1950.

H. F. ROBISON and W. H. WICKHAM are both with the Commonwealth Edison Company, Chicago, Ill.

The authors are indebted to J. D. Sallemi and R. I. Ward for their helpful suggestions and co-operation in this development.

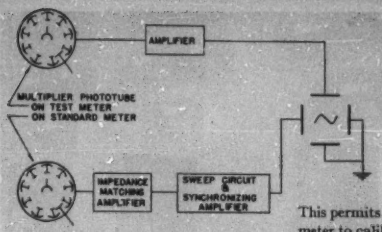

Figure 2 (left). Block diagram of electronic circuit

Figure 3 (right). Test connections for calibration of watt-hour meter

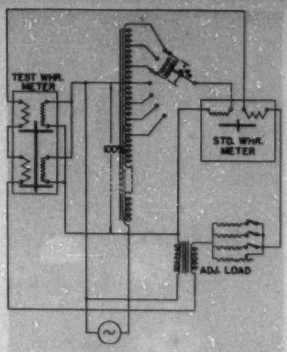

2. The periodic voltage from the test unit on the standard meter is amplified by an impedance-matching amplifier and used to synchronize the adjustable frequency linear sweep circuit. Thus the sweep frequency of the trace on the cathode-ray tube is controlled by the disk speed of the standard meter. The voltage from the test unit on the meter under test is amplified and impressed on the vertical deflection plates of the cathode-ray tube. In this way a single wave is produced on the screen of the tube that remains stationary when the disks of the two watt-hour meters are running at the same speed. When the disk speeds differ, the wave will travel across the screen in a horizontal direction. The direction of travel indicates whether the test meter is running faster or slower than the standard. Note that, because of "anti-creep" holes, the speed of a watt-hour meter disk is not constant throughout a revolution. Because of this variation in speed the wave will not remain perfectly stationary, but will move back and forth, and equal average speeds are indicated by zero net travel of the wave. This effect is more noticeable at the lower disk speeds, but in no case does it seriously impair the accuracy. A difference of 0.1 per cent in disk speeds can be detected. Since the cathode-ray oscilloscope is used as a null detector, that is, to detect zero difference in disk speeds, the accuracy of detection is independent of the calibration of the detector. It is not essential that the frequencies of the periodic voltages produced by the rotation of the two disks be the same since the latitude of adjustment of the resistance-capacitance components in the sweep circuit is sufficient to permit adjustment to one-half or one-third of the frequency of the voltage from the standard meter. The sweep will then lock at every second or third cycle of the voltage from the standard. Conversely, if the frequency of the voltage from the test meter is an integral multiple of the frequency of the voltage from the standard, such as 2 or 3 and so forth, 2 or 3 cycles will appear on the cathode-ray screen. This permits the use of the same standard meter to calibrate meters having different numbers of disk teeth and different disk constants.

In order to vary the speed of the disk of the standard watt-hour meter to match the speed of the disk of the meter under test as required for an "as found" check, the potential coil of the standard is energized through a combination of two autotransformers, one tapped, and one continuously variable as shown in Figure 3. The main autotransformer has three taps spaced at $2^1/_2$ per cent intervals each side of the 100 per cent point. The auxiliary autotransformer can be connected across alternate taps of the main autotransformer by a tap switch as shown, so that the voltage impressed on the standard meter can be varied from $92^1/_2$ per cent to $107^1/_2$ per cent of the voltage impressed on the meter under test. The tap switch on the main transformer and the dial on the auxiliary transformer are calibrated in per cent voltage impressed on the standard, which is the same as per cent registration of the meter under test. The phase angles of the autotransformers have been measured and found to be negligible, therefore the same scale markings on the dials are used for loads at unity and 50 per cent power factors, the usual check points.

All equipment necessary to calibrate a watt-hour meter by this method, except the adjustable load, is installed in one metal case. This includes the standard watt-hour meter with the optical system attached, the ammeter, the two autotransformers and the electronic detecting equipment. The test unit for use on the watt-hour meter under test is equipped with a flexible lead and polarized plug to be plugged into the side of the case. Figure 4 shows the top panel of this metal case along with the optical system, or test unit, to be attached to the meter under test.

Operation of Device

The operation of the device is very simple and with a small amount of practice, the meter tester is able to calibrate watt-hour meters quickly and accurately. Figure 5 shows the calibrating device with the test unit mounted on a switchboard meter and with all connections made for calibration. With the device connected as shown in Figure 5 for calibration at a desired load point, or speed, the test unit on the meter under test is positioned so as to produce maximum vertical deflection on the cathode-ray screen. The frequency of the sweep circuit is adjusted to approximate the frequency of the periodic voltage produced by the rotation of the disk of the standard, at which point the synchronizing voltage from the standard controls the frequency of sweep. The "as found" check on the meter being tested is obtained by adjusting the speed of the standard to the speed of the test meter as indicated by a stationary trace on the cathode-ray screen. The per cent registration of the meter under test is then read directly from the dials of the autotransformers.

If the "as found" check shows a need for adjustment of the meter being tested, the dials of the autotransformers are set for the desired registration, taking into account the ratio correction factors of the instrument transformers supplying the meter being tested, and the calibration of the standard watt-hour meter. This will cause the trace on the screen of the cathode-ray tube to travel across the screen, the direction of travel depending on whether the meter being tested is faster or slower than the standard. The trace on the screen is again brought to a stationary position by changing the adjustments on the meter being tested.

Operating Experience

The new watt-hour meter calibrating device has been used for calibrating sta-

Figure 4 (left). Panel view of device

Figure 5 (right). Device connected for watt-hour meter calibration

tion meters for a period of about eight months. In this time it has been found that accurate calibration by this method requires only one-third as much time as the conventional method of counting revolutions. The device detects erratic disk motion such as caused by defective bearings or by foreign material on the disks or magnets much more readily than the conventional method. It has been found that the tester can observe the action of the trace on the cathode-ray screen over long periods of time with no appreciable eye strain.

The sensitivity of the detecting device is such that meters can be calibrated with an accuracy of 0.1 per cent. Numerous checks have been made in the laboratory comparing the accuracy of the new method against the conventional method of counting revolutions. It has been found that these methods are within 0.1 per cent of agreement.

Watt-hour meter adjustments are more accurately made with this new device because the meter under test is adjusted accurately to the desired registration on the first trial rather than within previously established limits after successive trials.

References

1. Modern Methods of Meter Testing, T. Snell. *Electric Light and Power* (Chicago, Ill.) November 1937, pages 66–69.

2. Stroboscopic Timing of Rotating Meter Disks, E. Bradshaw. *Royal Technical College Journal* (Glasgow, Scotland), January 1939, pages 542–50.

3. Photo Electric Tester Modernizes Meter Testing, T. A. Abbott. *General Electric Review* Schenectady, N. Y.), June 1940, pages 244–47.

4. Stroboscopic Meter Testing Saves Time and Effort. *Electrical World* (New York, N. Y.), June 29, 1940, pages 31–32.

5. Watthour Meters Compared by Magic-Eye Wink, H. S. Bull. *Electrical World* (New York, N. Y.), November 27, 1943, pages 40–41.

No Discussion

Equivalent Circuits of the Shaded-Pole Motor with Space Harmonics

GABRIEL KRON
MEMBER AIEE

EQUATIONS and equivalent circuits are developed for the shaded-pole motor including the space-harmonics introduced by the stator windings. Uneven airgap, also an impressed voltage on the shaded coil are assumed, while the parameters include the ratio of turns and the angle of shift of the shaded coil. The equations and equivalent circuits cover both the cross-field and the revolving-field theories.

Derivation from the Primitive Machine

There are at least four different points of view in which a shaded-pole motor may be assumed to differ from a split-phase induction motor with uneven airgap, or rather from the primitive machine with three stator windings, Figure 1.

1. The shaded pole is represented by a winding shifted by an angle α from the direct axis, Figure 2(A).

2. The shaded pole is assumed to be wound on both axes, in particular with $\cos\alpha$ turns on the direct axis and with $\sin\alpha$ turns on the quadrature axis, Figure 2(B).

3. The main winding is shifted by an angle α, Figure 2(C).

4. The main winding is wound on both axes, Figure 2(D).

It will be shown that the first two (or last two) points of view may be so treated as to be indistinguishable from each other. The writer in a previous publication (reference 10, page 47) followed the first point of view. Here the same method will be extended to be reducible to equivalent circuits.

Reactance Calculation of the Shaded Coil

The shaded coil lies at an angle α from the main-pole axis (direct axis). The reactances are calculated in the following manner:

1. The shaded coil is assumed to lie at first in the direct axis, $\alpha=0$, Figure 3(A).

Its leakage reactance x_{ds1}, its mutual leakage reactance with the main-pole winding is x_{mds} and its mutual reactance with the rotor is X_{md}.

2. The shaded coil is assumed to lie next in the quadrature axis, $\alpha=90°$ Figure 3(B). Its leakage reactance is x_{qs1} which may be different from x_{ds1} and its mutual reactance with the rotor is X_{mq}, which may be different from X_{md}.

Its resistance in either axis is r_{s1}. Also the shaded coil is assumed to have the same number of turns as the main pole winding (and the rotor). Any difference in their turn ratio, also any outside impedance in series with the shaded coil will enter into the analysis later on.

The Sequence of Steps

The following steps will be made in the derivation of the equivalent circuits:

1. First the equation of the actual shaded pole motor with windings at an angle α are derived, using the cross-field theory.

2. Next the actual machine is replaced by an equivalent split-phase induction motor whose windings are at right angles from each other. The reactances of this hypothetical motor are expressed in terms of those of the shaded-pole motor assuming the angle of shift "α" and the ratio of turns "α" as parameters. Its equations in the cross-field theory are found.

3. The equations of the equivalent motor in the revolving-field theory are found.

4. The equivalent circuit of the hypothetical motor are found by the revolving-field theory.

5. The equivalent circuits in the cross-field theory are developed.

6. The presence of space-harmonics is considered in both types of equivalent circuits.

Part I. Equations of the Actual Machine

The Primitive Machine

Let it be assumed that two identical shaded coils exist on the stator, in particular one along the direct axis (d_{s1}) and one along the quadrature axis (q_{s1}). Then the Z of the primitive machine (Figure 1) with three stator and two rotor windings (each having the same number of turns) is

$$Z=\begin{array}{c|c|c|c|c|c|}
 & d_{s2} & d_{s1} & q_{s1} & d_r & q_r \\
\hline
d_{s2} & r_{ds2}+jX_{ds2} & jX_{ms} & & jX_{md} & \\
\hline
d_{s1} & jX_{ms} & r_{s1}+jX_{ds1} & & jX_{md} & \\
\hline
q_{s1} & & & r_{s1}+jX_{qs1} & & jX_{mq} \\
\hline
d_r & jX_{md} & jX_{md} & X_{mq}v & r_r+jX_{dr} & X_{qr}v \\
\hline
q_r & -X_{md}v & -X_{md}v & jX_{mq} & -X_{dr}v & r_r+jX_{qr} \\
\hline
\end{array} \qquad (1)$$

The coefficients of v are the torsion tensor G

$$G=\begin{array}{c|c|c|c|c|c|}
 & d_{s2} & d_{s1} & q_{s1} & d_r & q_r \\
\hline
d_r & & & X_{mq} & & X_{qr} \\
\hline
q_r & -X_{md} & -X_{mc} & & -X_{dr} & \\
\hline
\end{array}$$

Paper 50-117, recommended by the AIEE Rotating Machinery Committee and approved by the AIEE Technical Program Committee for presentation at the AIEE North Eastern District Meeting, Providence, R. I., April 26–28, 1950. Manuscript submitted January 18, 1950; made available for printing March 6, 1950.

GABRIEL KRON is Consulting Engineer with the General Electric Company, Schenectady, N. Y.

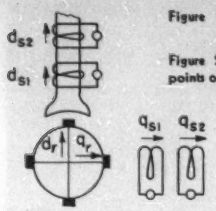

Figure 1 (left). The primitive machine

Figure 2 (right). Four different points of view of the shaded-pole motor

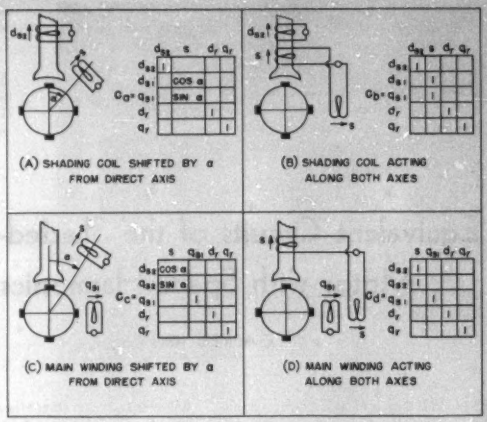

In terms of leakage reactances x_{ds1}, x_{ds2}, x_{dsm}, x_{qs1}, X_{md}, X_{mq}, x_r (Figure 3) the self-inductances are defined as

$$\begin{aligned} X_{ds2} &= X_{md}+x_{ds2} & X_{ms} &= X_{md}+x_{dsm} \\ X_{ds1} &= X_{md}+x_{dsm}+x_{ds1} & X_{dr} &= X_{md}+x_r \\ X_{qs1} &= X_{mq}+x_{qs1} & X_{qr} &= X_{mq}+x_r \end{aligned} \qquad (2)$$

The equations of the primitive machine are $\boldsymbol{e}=\boldsymbol{Z}\boldsymbol{i}$ and $T=\boldsymbol{i}^*\boldsymbol{G}\boldsymbol{i}=\boldsymbol{i}^*\boldsymbol{B}$ where $\boldsymbol{B}=\boldsymbol{G}\boldsymbol{i}$.

The Actual Machine

In going from the primitive machine to the actual machine, two different points of view may be used, each leading to the same set of equations:

1. Let only one shaded coil exist shifted by an angle α from the direct axis, Figure 2(A) and having "a" number of turns where

$$a=\frac{\text{Number of turns of shaded coil}}{\text{Number of turns of main winding}}$$

The relation between the old and new currents are $\boldsymbol{i}=\boldsymbol{C}_1\boldsymbol{i}_1$ where

$$\boldsymbol{C}_1=\begin{array}{c|c|c|c|c|}
 & m & s & d_r & q_r \\ \hline
d_{s2} & 1 & & & \\ \hline
d_{s1} & & a\cos\alpha & & \\ \hline
q_{s1} & & a\sin\alpha & & \\ \hline
d_r & & & 1 & \\ \hline
q_r & & & & 1 \\ \hline
\end{array} \qquad (3)$$

By $\boldsymbol{C}_{1t}\boldsymbol{Z}\boldsymbol{C}_1$ the new impedance matrix and torque tensor are

$$\boldsymbol{Z}_1=\begin{array}{c|c|c|c|c|}
 & m & s & d_r & q_r \\ \hline
m & r_{ds2}+jX_{ds2} & jX_{ms}a\cos\alpha & jX_{md} & \\ \hline
s & jX_{ms}a\cos\alpha & a^2r_{s1}+jX_{ds1}a^2\cos^2\alpha+jX_{qs1}a^2\sin^2\alpha & jX_{md}a\cos\alpha & jX_{mq}a\sin\alpha \\ \hline
d_r & jX_{md} & jX_{md}a\cos\alpha+X_{mq}v\,a\sin\alpha & r_r+jX_{dr} & X_{qr}v \\ \hline
q_r & -X_{md}v & jX_{mq}a\sin\alpha-X_{md}v\,a\cos\alpha & -X_{dr}v & r_r+jX_{qr} \\ \hline
\end{array} \qquad (4)$$

$$\boldsymbol{G}_1=\begin{array}{c|c|c|c|c|}
 & m & s & d_r & q_r \\ \hline
d_r & & X_{mq}\,a\sin\alpha & & X_{qr} \\ \hline
q_r & -X_{md} & -X_{md}\,a\cos\alpha & -X_{dr} & \\ \hline
\end{array}$$

The current vector is

$$\boldsymbol{i}_1=\begin{array}{c|c|c|c|}
m & s & d_r & q_r \\ \hline
i^m & i^s & i^{dr} & i^{qr} \\ \hline
\end{array} \qquad (5)$$

where i^s is the actual shaded-coil current and i^m the main-winding current. The impressed-voltage vector is

$$\boldsymbol{e}_1=\begin{array}{c|c|c|c|}
m & s & d_r & q_r \\ \hline
e_m & e_s & 0 & 0 \\ \hline
\end{array} \qquad (6)$$

where e_s is the actual shaded-coil impressed voltage and e_m is the main-winding impressed voltage.

2. Let two shaded coils exist. One, along the direct axis, has $a\cos\alpha$ turns, the other, along the quadrature axis, has $a\sin\alpha$ turns (Figure 1). Then

$$\boldsymbol{C}_1'=\begin{array}{c|c|c|c|c|}
 & d_{s2}' & d_{s1}' & q_{s1}' & d_r' & q_r' \\ \hline
d_{s2} & 1 & & & & \\ \hline
d_{s1} & & a\cos\alpha & & & \\ \hline
q_{s1} & & & a\sin\alpha & & \\ \hline
d_r & & & & 1 & \\ \hline
q_r & & & & & 1 \\ \hline
\end{array} \qquad (7)$$

$$\boldsymbol{C}_1''=\begin{array}{c|c|c|c|c|}
 & m & s & d_r & q_r \\ \hline
d_{s2}' & 1 & & & \\ \hline
d_{s1}' & & 1 & & \\ \hline
q_{s1}' & & 1 & & \\ \hline
d_r' & & & 1 & \\ \hline
q_r' & & & & 1 \\ \hline
\end{array} \qquad (8)$$

Performing simultaneously the two transformations the resultant matrix

$$\boldsymbol{C}_1=\boldsymbol{C}_1'\boldsymbol{C}_1'' \qquad (9)$$

is identical with $\boldsymbol{C}_1$. Hence the two points of view of Figures 2(A) and 2(B) are indistinguishable from each other mathematically.

The equations $\boldsymbol{e}_1=\boldsymbol{Z}_1\boldsymbol{i}_1$ and $T=\boldsymbol{i}_1^*\boldsymbol{G}_1\boldsymbol{i}_1$ represent the basic equations of the shaded pole motor in the cross-field theory, as given by the author in reference 10 (the same equations also appear in reference 9). The equations of references 3, 4, and 5 are also of the same general nature. All these equations have the disadvantage that the d and q axes are all mixed up in them. Hence they are not well adapted for the introduction of symmetrical components nor for the development of equivalent circuits.

The two coils are connected in series, Figure 2(B) by

Replacing Currents of Individual Windings by Resultant Magnetomotive Forces Along the Axes

The equations may be brought to a simpler, more practical and also more familiar form by replacing the actual winding currents i^m and i^s by another set of variables i^{ds} and i^{qs}

$$i^{ds} = i^m + i^s a \cos \alpha$$
$$i^{qs} = i^s a \sin \alpha \tag{10}$$

representing the resultant direct-axis magnetomotive force of both windings and the quadrature-axis magnetomotive force of the shaded coil respectively. That is, let the inverse matrix of transformation be

$$C_s^{-1} = \begin{array}{c|cc|c|c|} & m & s & d_r & q_r \\ \hline d_s & 1 & a\cos\alpha & & \\ q_s & & a\sin\alpha & & \\ \hline d_r & & & 1 & \\ q_r & & & & 1 \\ \hline \end{array} \tag{11}$$

Then its inverse is

$$C_s = \begin{array}{c|cc|c|c|} & d_s & q_s & d_r & q_r \\ \hline m & 1 & -\cot\alpha & & \\ s & & 1/(a\sin\alpha) & & \\ \hline d_r & & & 1 & \\ q_r & & & & 1 \\ \hline \end{array}$$

$$i^m = i^{ds} - i^{qs} \cot \alpha$$
$$i^s = i^{qs}/(a \sin \alpha) \tag{12}$$

where i^s is the shaded-coil current (it should be noted that in the special case when $\alpha = 0$ then $\sin \alpha = 0$ and C_s has no existence. Hence the following equations are not valid in the special case when $\alpha = 0$).

By $C_s Z_1 C_s$, $C_s G_1 C_s$ and $C_s e_1$,

$$Z_s = \begin{array}{c|c|c|c|c|} & d_s & q_s & d_r & q_r \\ \hline d_s & r_{ds1} + jX_{ds1} & -(r_{ds2} + jx_{ds2}) \cot \alpha & jX_{md} & \\ q_s & -(r_{ds2} + jx_{ds2}) \cot \alpha & \begin{array}{c} r_{qs1} + jX_{qs1} + \\ (r_{ds2} + jx_{ds2} + \\ r_{ds2} + jx_{ds2}) \cot^2 \alpha \end{array} & & jX_{mq} \\ d_r & jX_{md} & X_{mq}v & r_r + jX_{dr} & X_{qr}v \\ q_r & -X_{md}v & jX_{mq} & -X_{dr}v & r_r + jX_{qr} \\ \hline \end{array} \tag{13}$$

$$G_s = \begin{array}{c|c|c|c|c|} & d_s & q_s & d_r & q_r \\ \hline d_r & & X_{mq} & & X_{qr} \\ q_r & -X_{md} & & -X_{dr} & \\ \hline \end{array}$$

$$e_s = \begin{array}{c|c|c|c|c|} & d_s & q_s & d_r & q_r \\ \hline & e_m & e_s/(a\sin\alpha) - e_m \cot\alpha & & \\ \hline \end{array} \tag{14}$$

Reactances of the Equivalent Split-Phase Motor

The equations of the shaded-pole motor with stator windings at an angle α, Figure 4(A), have hereby been brought to the form of those of an unsymmetrical split-phase induction motor having windings along the direct and quadrature axes, Figure 4(B). The only difference is that now mutual impedances exist between the two stator windings at right angles in space.

The equivalence is made clearer by replacing the actual shaded-pole machine reactances by those of the equivalent split-phase motor. (The latter will be denoted by a prime.) Only the stator resistances and leakage reactances are different, the airgap and rotor quantities are identical. In particular, Figure 4(C)

$$r_{ds}' = r_{ds2}(1 - \cot \alpha)$$
$$x_{ds}' = x_{ds2}(1 - \cot \alpha) + x_{dms}$$
$$r_{qs}' = r_{qs1} + r_{ds1} \cot^2 \alpha + r_{ds2} \cot \alpha (\cot \alpha - 1)$$
$$x_{qs}' = x_{qs1} + x_{ds1} \cot^2 \alpha + x_{ds2} \cot \alpha (\cot \alpha - 1)$$
$$z_m' = (r_{ds2} + jx_{ds2}) \cot \alpha \tag{15}$$

It should be noted that the angular shift α appears only as a single ratio of turns

$$\cot \alpha = b = \frac{\cos \alpha}{\sin \alpha} = \frac{\text{number of turns on direct axis}}{\text{number of turns on quadrature axis}}$$

Equations of the Equivalent Split-Phase Motor

In terms of the primed reactances Z_2 of the equivalent motor becomes

$$Z_2 = \begin{array}{c|c|c|c|c|} & d_s & q_s & d_r & q_r \\ \hline d_s & r_{ds}' + jX_{ds}' + z_m' & -z_m' & jX_{md} & \\ q_s & -z_m' & r_{qs}' + jX_{qs}' + z_m' & & jX_{mq} \\ d_r & jX_{md} & X_{mq}v & r_r + jX_{dr} & X_{qr}v \\ q_r & -X_{md}v & jX_{mq} & -X_{dr}v & r_r + jX_{qr} \\ \hline \end{array} \tag{16}$$

$$e_2 = \begin{array}{c|c|c|c|c|} & d_s & q_s & d_r & q_r \\ \hline & e_{ds} & e_{qs} & & \\ \hline \end{array}$$

In terms of the known actual motor impressed voltages e_m and e_s the voltages to be impressed on the equivalent motor are

$$e_{ds} = e_m$$
$$e_{qs} = e_s/(a \sin \alpha) - e_m \cot \alpha \tag{18}$$

$$i_2 = \begin{array}{c|c|c|c|c|} & d_s & q_s & q_r & q_r \\ \hline & i^{ds} & i^{qs} & i^{dr} & i^{qr} \\ \hline \end{array} \tag{19}$$

In terms of actual motor currents i^m and i^s

$$i^{ds} = i^m + i^s a \cos \alpha$$
$$i^{qs} = i^s a \sin \alpha \tag{20}$$

Hence, if the equations $e_2 = Z_2 i_2$ of the equivalent motor are solved for i_2 then the actual machine currents are found from those of the equivalent motor by

$$i^m = i^{ds} - i^{qs} \cot \alpha$$
$$i^s = i^{qs}/(a \sin \alpha) \tag{21}$$

These equations are identical with those of a split-phase induction motor (or of the primitive machine having two stator and two rotor windings) with the following complications:

1. The two stator windings have an additional self and mutual impedance equal to z_m'.
2. The airgap is unequal along the two axes.

The Revolving Field Theory

Since the losses in the rotor of induction motors are mostly of double frequency, it is useful to set up the equations along the symmetrical component (forward and backward) axes.

If the following matrix of transformation is assumed

$$C_3 = \begin{array}{c|c|c|} & s & r \\ \hline s & C_s & \\ r & & C_s \\ \hline \end{array} \qquad C_s = \frac{1}{\sqrt{2}} \begin{array}{c|c|c|} & f & b \\ \hline d & 1 & 1 \\ q & -j & j \\ \hline \end{array} \tag{22}$$

$$G_3 = \begin{array}{c|c|c|c|c|} & d_s & q_s & d_r & q_r \\ \hline d_r & & X_{mq} & & X_{qr} \\ q_r & -X_{md} & & -X_{dr} & \\ \hline \end{array} \tag{17}$$

then the formula $C_3^*, Z_3 C_3$ gives the impedance matrix $Z_3 =$

	f_s	b_s	f_r	b_r
f_s	$\frac{Z_{ds}'+Z_{qs}'}{2}+z_m'$	$\frac{Z_{ds}'-Z_{qs}'}{2}-jz_m'$	$\frac{j(X_{md}+X_{mq})}{2}$	$\frac{j(X_{md}-X_{mq})}{2}$
b_s	$\frac{Z_{ds}'-Z_{qs}'}{2}+jz_m'$	$\frac{Z_{ds}'+Z_{qs}'}{2}+z_m'$	$\frac{j(X_{md}-X_{mq})}{2}$	$\frac{j(X_{md}+X_{mq})}{2}$
f_r	$(1-v)\frac{j(X_{md}+X_{mq})}{2}$	$(1-v)\frac{j(X_{md}-X_{mq})}{2}$	$r_r+(1-v)\frac{j(X_{dr}+X_{qr})}{2}$	$(1-v)\frac{j(X_{dr}-X_{qr})}{2}$
b_r	$(1+v)\frac{j(X_{md}-X_{mq})}{2}$	$(1+v)\frac{j(X_{md}+X_{mq})}{2}$	$(1+v)\frac{j(X_{dr}-X_{qr})}{2}$	$r_r+(1+v)\frac{j(X_{dr}+X_{qr})}{2}$

(23)

By $C_3^* e_2$ the impressed voltage vector is

$$e_3 = \frac{1}{\sqrt{2}} \begin{array}{cccc} f_s & b_s & f_r & b_r \\ \hline e_{ds}+je_{qs} & e_{ds}-je_{qs} & & \end{array} \qquad (24)$$

The coefficients of v (or $C_3^* G_2 C_3$) give the torsion tensor

$$G_3 = \begin{array}{c|cccc} & f_s & b_s & f_r & b_r \\ \hline f_r & \frac{-j(X_{md}+X_{mq})}{2} & \frac{-j(X_{md}-X_{mq})}{2} & \frac{-j(X_{dr}+X_{qr})}{2} & \frac{-j(X_{dr}-X_{qr})}{2} \\ b_r & \frac{j(X_{md}-X_{mq})}{2} & \frac{j(X_{md}+X_{mq})}{2} & \frac{j(X_{dr}-X_{qr})}{2} & \frac{j(X_{dr}+X_{qr})}{2} \end{array} \qquad (25)$$

The equations $e_3 = Z_3 i_3$ and $T = i_3^* G_3 i_3$ represent the basic equations of the shaded-pole motor in the revolving field theory. Again they are analogous to the equations of the split-phase motor with the generalizations mentioned.

Part II. Equations of the Equivalent Circuits

The Revolving Field Equivalent Circuit

In order to establish an equivalent circuit along the sequence axes it is necessary to reduce the currents and voltages in all meshes of the actual machine to the same frequency base by multiplying both Z_3 and e_3 (but not i_3 or G_3) by the inverse of the "absolute frequency tensor" n, representing the actual frequency of the currents with respect to the conductors in each winding.

$$n^{-1} = \begin{array}{c|cccc} & f_s & b_s & f_r & b_r \\ \hline f_s & 1 & & & \\ b_s & & 1 & & \\ f_r & & & 1/(1-v) & \\ b_r & & & & 1/(1+v) \end{array} \qquad (26)$$

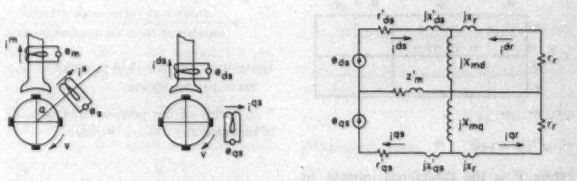

Figure 4 (A, B, C, D). The equivalent split-phase induction motor at standstill

$e_{ds} = e_m$	$i^m = i^{ds} - i^{qs} \cot a$
$e_{qs} = \frac{e_s}{a \sin a} - e_m \cot a$	$i^s = \frac{i^{qs}}{a \sin a}$
$r'_{ds} = r_{ds2}(1-\cot a)$	
$x'_{ds} = x_{ds2}(1-\cot a) + x_{dsm}$	
$r'_{qs} = r_{qs1} + r_{ds1} \cot^2 a + r_{ds2} \cot a(\cot a - 1)$	
$x'_{qs} = x_{qs1} + x_{ds1} \cot^2 a + x_{ds2} \cot a(\cot a - 1)$	
$z'_m = (r_{ds2} + jx_{ds2}) \cot a$	

(D) RELATIONS BETWEEN ACTUAL AND EQUIVALENT MOTOR

Figure 3. Reactances of the shaded-pole motor

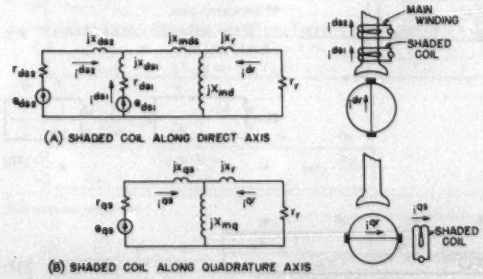

Figure 5. Equivalent circuit of the shaded-pole motor (revolving field theory)

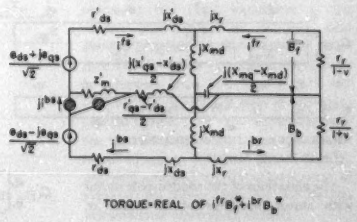

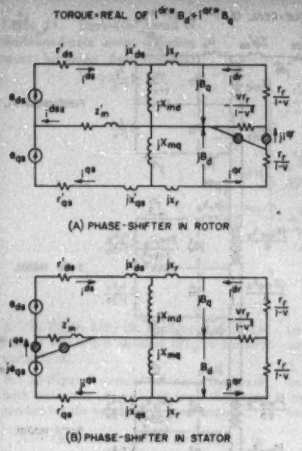

Figure 6 (left). Equivalent circuit of the shaded-pole motor (cross-field theory)

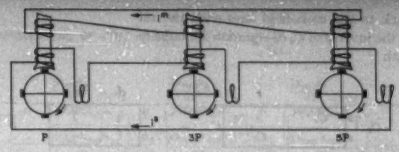

Figure 7 (top right). Interconnection of three shaded-pole motors having P, $3P$, and $5P$ pair of poles

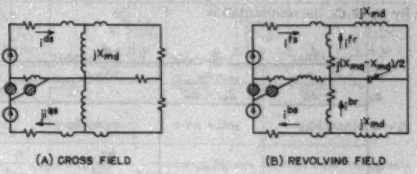

Figure 8 (center right). Arrangement for space harmonics

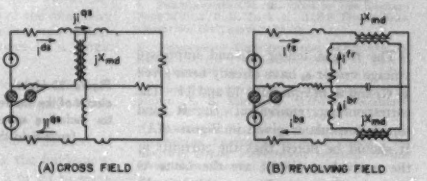

Figure 9 (lower right). Isolating stator from rotor meshes

The resultant impedance matrix and impressed voltage vector become by n^{-1} $\mathbf{Z}_3$ and $n^{-1}\mathbf{e}_3$

	f_s	b_s	f_r	b_r
f_s	$\frac{Z_{ds}'+Z_{qs}'}{2}+z_m'$	$\frac{Z_{ds}'-Z_{qs}'}{2}-jz_m'$	$\frac{j(X_{md}+X_{mq})}{2}$	$\frac{j(X_{md}-X_{mq})}{2}$
b_s	$\frac{Z_{ds}'-Z_{qs}'}{2}+jz_m'$	$\frac{Z_{ds}'+Z_{qs}'}{2}+z_m'$	$\frac{j(X_{md}-X_{mq})}{2}$	$\frac{j(X_{md}+X_{mq})}{2}$
f_r	$\frac{j(X_{md}+X_{mq})}{2}$	$\frac{j(X_{md}-X_{mq})}{2}$	$\frac{r_r}{1-v}+\frac{j(X_{dr}+X_{qr})}{2}$	$\frac{j(X_{dr}-X_{qr})}{2}$
b_r	$\frac{j(X_{md}-X_{mq})}{2}$	$\frac{j(X_{md}+X_{mq})}{2}$	$\frac{j(X_{dr}-X_{qr})}{2}$	$\frac{r_r}{1+v}+\frac{j(X_{dr}+X_{qr})}{2}$

(27)

$$e_4=\frac{1}{\sqrt{2}}\begin{array}{cccc} f_s & b_s & f_r & b_r \\ \hline \multicolumn{2}{|c|}{e_{ds}+je_{qs}} & \multicolumn{2}{c|}{} \end{array} \qquad (28)$$

The multiplication of $\mathbf{Z}_3$ by n^{-1} consists simply in dividing the third row by $1-v$ and the fourth row by $1+v$. Also $\mathbf{e}_4=\mathbf{e}_3$ and $\mathbf{G}_4=\mathbf{G}_3$.

The corresponding equivalent circuit is shown in Figure 5. The torque is found as usual by subtracting the negative sequence rotor losses from the positive sequence rotor losses. That is

$$T=i_4^*G_4i_4=i_4^*B_4 \qquad (29)$$

where the flux densities $\mathbf{B}_4$ appear in the equivalent circuit as voltages across the rotor resistances.

If the direction of rotation of the rotor (from d to q) is assumed to occur counterclockwise, then

$$e_4=\frac{1}{\sqrt{2}}\begin{array}{cccc} f_s & b_s & f_r & b_r \\ \hline \multicolumn{2}{|c|}{e_{ds}-je_{qs}} & \multicolumn{2}{c|}{e_{ds}+je_{qs}} \end{array}$$

Similarly

$$i^{fs}=\frac{i^{ds}-ji^{qs}}{\sqrt{2}}$$

and so on.

The Phase-Shifter

It should be noted that the expression $z^{m\prime}$ (representing a mutual impedance between the stator direct and quadrature axes) does not occur in a symmetrical manner in the upper left hand corner of $\mathbf{Z}_4$. While analytically only a change in sign occurs in $jz^{m\prime}$, physically a phase shifter must be placed in the equivalent circuit. Its role is to rotate the current and the voltage by 90 degrees in the same direction.

In writing, for instance, the voltage equation for mesh b_s the actual voltage drop across z_m is from left to right $-(i^{fs}-ji^{bs})z_m$. Shifting this voltage to the other side of the phase-shifter into the mesh of b_s, it now becomes $(-j)[-(i^{fs}jz_m+i^{bs}z_m)]=i^{fs}jz_m+i^{bs}z_m$. This is in the same form as given by the second equation.

On the a-c board it is not necessary to use an actual phase-shifter. The use of two generators and their cut-and-try adjustment is sufficient. The cut-and-try adjustment of the generators may be avoided by the use of open-circuit and short-circuit measurements.

The Cross-Field Equivalent Circuits

The equivalent circuit along the cross-field is found by simply transforming the equations of the revolving-field network

back to the cross-field axes with the aid of the inverse of C_3 of equation 22, namely with

$$C_z = C_z^{-1} \begin{array}{c|cc|} & s & r \\ \hline s & C_s^{-1} & \\ r & & C_r^{-1} \\ \hline \end{array} \quad C_z^{-1} = \frac{1}{\sqrt{2}} \begin{array}{c|cc|} & d & q \\ \hline f & 1 & j \\ b & 1 & -j \\ \hline \end{array} \tag{30}$$

By $C_u^* Z_4 C_b$, the resultant Z_5 is

$$Z_5 = \begin{array}{c|c|c|c|c|} & d_s & q_s & d_r & q_r \\ \hline d_s & Z_{ds}' + z_m' & -z_m' & jX_{md} & \\ q_s & -z_m' & Z_{qs}' + z_m' & & jX_{mq} \\ \hline d_r & jX_{md} & & \frac{r_r}{1-v^2} + jX_{dr} & \frac{jvr_r}{1-v^2} \\ q_r & & jX_{mq} & -\frac{jvr_r}{1-v^2} & \frac{r_r}{1-v^2} + jX_{qr} \\ \hline \end{array} \tag{31}$$

The torque tensor G_5 and impressed voltage vector e_5 have already been given as G_3 and e_3 in equations 13 and 14. The corresponding equivalent circuit and torque formula is given in Figure 6(A). It should be noted that the currents in the equivalent circuit are the same as those in the equivalent machine itself. The phase-shifter occurs in the rotor

$$i_5 = \begin{array}{|c|c|c|c|} d_s & q_s & d_r & q_r \\ \hline i^{ds} & i^{qs} & i^{dr} & i^{qr} \\ \hline \end{array}$$

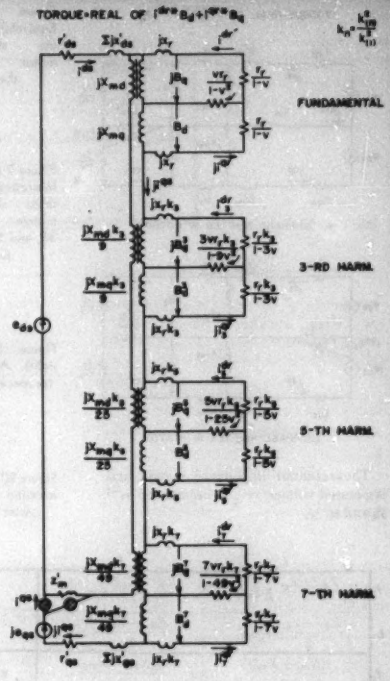

Figure 10 (right). Equivalent circuit of the shaded-pole motor including space harmonics (cross-field theory)

SHIFTING PHASE-SHIFTER TO STATOR

The rotor meshes in the network may be brought to more familiar form if along the quadrature axes ji^{qs} and ji^{qr}, are introduced as variables in place of i^{qs} and i^{qr} by

$$C_4 = \begin{array}{c|c|c|c|c|} & d_s & q_s & d_r & q_r \\ \hline d_s & 1 & & & \\ q_s & & -j & & \\ d_r & & & 1 & \\ q_r & & & & -j \\ \hline \end{array} \tag{32}$$

Then $C_4^* Z_5 C_4$ multiplies each q column by $-j$ and each q row by j, giving

$$Z_6 = \begin{array}{c|c|c|c|c|} & d_s & q_s & d_r & q_r \\ \hline d_s & Z_{ds}' + z_m' & jz_m' & jX_{md} & \\ q_s & -jz_m' & Z_{qs}' + z_m' & & jX_{mq} \\ \hline d_r & jX_{md} & & \frac{r_r}{1-v^2} + jX_{dr} & \frac{vr_r}{1-v^2} \\ q_r & & jX_{mq} & \frac{vr_r}{1-v^2} & \frac{r_r}{1-v^2} + jX_{qr} \\ \hline \end{array} \tag{33}$$

$$i_6 = \begin{array}{|c|c|c|c|} d_s & q_s & d_r & q_r \\ \hline i^{ds} & ji^{qs} & i^{dr} & ji^{qr} \\ \hline \end{array} \tag{34}$$

$$e_6 = \begin{array}{|c|c|c|c|} d_s & q_s & d_r & q_r \\ \hline e_{ds} & je_{qs} & & \\ \hline \end{array} \tag{35}$$

Now the phase-shifter is in the stator as shown in Figure 6(B). This form of the network is better adapted for the introduction of space harmonics.

Part III. Space-Harmonic Equivalent Circuits

SPACE-HARMONICS OF THE STATOR

Each stator current (i^m and i^s) produces a series of fluxes with P, $3P$, $5P$, $7P$, ... and so forth, pairs of poles. Each of these fluxes cuts the rotor producing in it a current-density and flux-density wave having the same number of pairs of poles as the stator flux producing them. Hence each shaded-pole motor may be looked upon as consisting of several motors with different number of pairs of poles whose stator windings are connected in series (Figure 7).

For each motor an equivalent circuit may be developed using either the cross-field or the revolving-field reference frames. For each harmonic:

1. The rotor resistance r_r and leakage reactances x_r differ by the factor k_n

$$k_n = \frac{k_{(n)}^2}{k_{(1)}^2}$$

where $k_{(n)}$ is the nth harmonic pitch-factor.

2. The mutual impedances X_{md} and X_q, differ by k_n and also by $1/P^2$.

3. The stator leakage-impedances (functions of the angle of shift α) differ by unspecified amounts that depend on the particular design.

4. The rotor speeds v differ by P.

In order to be able to connect the stator windings of the equivalent circuits in series, it is necessary to rearrange the circuits of Figure 5 and 6 in two successive steps.

Figure 11. Equivalent circuit of the shaded-pole motor including space harmonics (revolving-field theory)

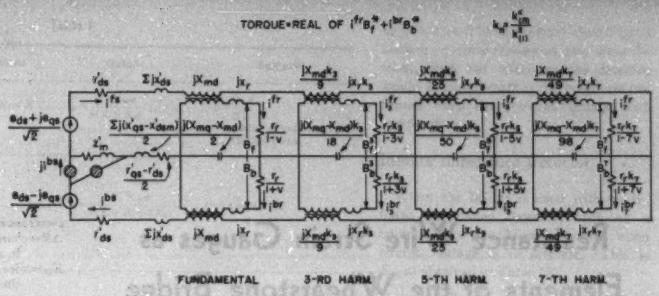

A. In Figure 8(B) the configuration of the coils of Figure 5 is changed (Figure 6 is left unchanged).

B. In Figure 9 some of the stator meshes of both networks are isolated from the rotor meshes by the use of ideal transformers.

Now the stator circuits are ready to be connected in series as shown in Figures 10 and 11. The resultant networks give the fundamental and harmonic rotor currents and torques as shown. It should be especially noted that no quantity in the harmonic meshes depends on the angle of shift α. The latter influences only the stator resistances and the leakage reactances.

Solution of the Network

The network Figure 11 of the cross-field theory is better adaptable for numerical calculation. In particular:

1. All quadrature axis meshes of the rotor may be eliminated in succession by a simple mesh-star transformation.

2. In the remaining network each transformer may be replaced by a single mutual coil.

3. All direct axis meshes of the rotor may be eliminated in succession by simply replacing two parallel impedances by a single impedance.

With the above simple steps the harmonic network has been reduced to two meshes only.

An approximate but quick method of solution consists of using the fundamental networks of Figures 5 or six to solve for the stator currents. Knowing the stator currents, the harmonic networks of Figures 10 and 11 may be solved easily for each rotor current.

Bibliography

1. Capacitor Motors with Windings Not in Quadrature, A. F. Puchstein, T. C. Lloyd. *Electrical Engineering* (*AIEE Transactions*), volume 54, November 1935, pages 1235–39.

2. Analysis of Unsymmetrical Machines, W. V. Lyon, C. Kingsley. *Electrical Engineering* (*AIEE Transactions*), volume 55, May 1936, pages 471–76.

3. An Analysis of the Shaded-Pole Motor, P. H. Trickey. *Electrical Engineering* (*AIEE Transactions*), volume 55, September 1936, pages 1007–14.

4. Performance Calculations of the Shaded-Pole Motor, P. H. Trickey. *AIEE Transactions*, volume 66, 1947, pages 1431–38.

5. Analysis of Unsymmetrical Machines, K. Burian. *AIEE Transactions*, volume 67, part I, 1948, pages 643–46.

6. The Field Fluxes of the Shaded-Pole Motor, E. E. Kimberly. *AIEE Transactions*, volume 68, part I, 1949, pages 273–77.

7. Per-Determination of Shaded-Pole Induction-Motor Performance, H. L. Beyer. *Det Kongelige Norske Videnskabers Selskabs Skrifter* (Trondheim, Norway), 1947, Number 5.

8. A Mathematical Theory of Shaded-Pole Motors, E. Morath. *Transactions, Royal Institute of Technology* (Stockholm, Sweden), 1949, Number 26.

9. Single Phase Induction Motor with Short Circuited Auxiliary Winding, J. Kucera. *Revue Generale de l'Electricite*, (Paris, France), volume 58, May 1949, pages 185–91.

10. The Application of Tensors to the Analysis of Rotating Electrical Machinery, G. Kron. *General Electric Review* (Schenectady, N. Y.), 1938, pages 153–59, 244–50, 448–54.

11. Equivalent Circuit of the Primitive Rotating Machine, G. Kron. *General Electric Review* (Schenectady, N. Y.), March 1946, pages 43–49.

12. Steady-State Equivalent Circuits of Synchronous and Induction Machines, G. Kron. *AIEE Transactions*, volume 67, part I, 1948, pages 175–81.

No Discussion

Resistance Wire Strain Gauges as Elements of the Wheatstone Bridge

VINCENT J. PETRUCELLY
ASSOCIATE AIEE

ALMOST invariably, in the use of the resistance wire strain gauge, the instrument engineer employs the gauge as an element of the Wheatstone Bridge.[1-7] To use the gauge to maximum advantage, the engineer should be able to determine beforehand the behavior of the bridge circuit.

This usually requires the use of rather lengthy and unwieldy bridge equations. Further, most of the desired material is scattered throughout the literature, and is not easily available. It is the purpose of this paper to derive and assemble various characteristics of the Wheatstone Bridge, such as the output equations, condition for maximum sensitivity, and so forth, and present them in simplified form for direct application to wire strain gauges.

Consider the Wheatstone Bridge shown in Table IA.

R_1, R_2, R_3, R_4 are four arms of the bridge in ohms.

R_g is the resistance of the galvanometer detector in ohms.

V is the input voltage in volts, with polarity as shown. This source is assumed to have zero resistance.

I_g is the galvanometer or output current, in amperes.

At balance, I_g is zero. The balanced condition is

$$\frac{R_1}{R_2}=\frac{R_3}{R_4} \tag{1}$$

For an unbalanced condition, the solution for the output current can be obtained by the application of Thevenin's theorem, as follows:

Referring to Table IA, the resistance between the points cd, with R_g disconnected and the source V short-circuited, is

$$R_{cd}=\frac{R_1R_2}{R_1+R_2}+\frac{R_3R_4}{R_3+R_4} \tag{2}$$

The open-circuit voltage at cd, when the short circuit is removed from V, is E_{cd}

$$E_{cd}+I_3R_4-I_1R_2=0$$

$$E_{cd}=V\left[\frac{R_2}{R_1+R_2}-\frac{R_4}{R_3+R_4}\right] \tag{3}$$

Therefore, by Thevenin's Theorem

$$I_g=\frac{E_{cd}}{R_{cd}+R_g}=\frac{V\left[\frac{R_2}{R_1+R_2}-\frac{R_4}{R_3+R_4}\right]}{\frac{R_1R_2}{R_1+R_2}+\frac{R_3R_4}{R_3+R_4}+R_g}$$

$$I_g=\frac{V(R_2R_3-R_1R_4)}{R_1R_2R_3+R_1R_2R_4+R_1R_3R_4+R_2R_3R_4+R_g(R_3+R_4)(R_1+R_2)} \tag{4}$$

Equation 4 may be simplified as follows: (Refer to Table IA.)

Let $R_1=R_2=R_3=R_4=R$. Let the branch containing R_2 change in resistance by $\pm\Delta R$. Then the output current I_g becomes

$$I_g=\frac{V(\pm\Delta R)}{4R^2\pm3R\Delta R+2R_g(2R\pm\Delta R)}$$

$\pm\Delta R$ may be neglected in the denominator

$$I_g=\frac{V(\pm\Delta R)}{4R^2+4RR_g} \tag{5}$$

The strain acting on a strain gauge is expressed in terms of the resistance R of the gauge, the change in resistance R caused by the strain, and the wire gauge factor K_w, as follows

$$\epsilon=\frac{\Delta R/R}{K_w} \tag{6}$$

where

R = resistance of the strain gauge in ohms

ϵ = strain in inches per inch

ΔR = change in resistance of R in ohms, due to ϵ

K_w = wire gauge factor, usually supplied by the gauge manufacturer

Equation 6, when substituted in equation 5, yields

$$I_g=\frac{V\epsilon K_w}{4(R+R_g)} \tag{7}$$

from which it can be shown if more than one gauge of the same bridge circuit is active, that

$$I_g=\frac{V\epsilon K_w n}{4(R+R_g)} \tag{8}$$

where n represents the number of active gauges.

Often R_1 and R_2 are two strain gauges, only one of which is active, and R_3 and R_4 are fixed resistances, in which case[9] I_g may be found as follows:

Let $R_1=R_2=R$. Let $R_3=R_4=R_0$ = fixed resistances. Let R_2 change in resistance by $\pm\Delta R$. (Refer to Table IA.) Then

$$I_g=\frac{V(\pm\Delta R)}{2R^2\pm2R\Delta R+R_0(2R\pm\Delta R)+2R_g(2R\pm\Delta R)}$$

$\pm\Delta R$ may be neglected in the denominator

$$I_g=\frac{V(\pm\Delta R)}{2R(R+R_0+2R_g)}$$

from which it can be shown that

$$I_g=\frac{V\epsilon K_w n}{2(R+R_0+2R_g)}$$

where n is either one or two, depending upon whether one or both gauges are active.

Optimum Galvanometer Resistance

The best galvanometer resistance for maximum power in the galvanometer,

Paper 50-118, recommended by the AIEE Instruments and Measurements Committee and approved by the AIEE Technical Program Committee for presentation at the AIEE North Eastern District Meeting, Providence, R. I., April 26–28, 1950. Manuscript submitted June 1, 1948; made available for printing February 27, 1950.

VINCENT J. PETRUCELLY, is with the American Machine and Foundry Company, Brooklyn, N. Y.

Table I

Circuit	Bridge Elements	Output	Remarks
A 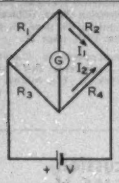	$R_1=R_2=R_3=R_4=R$	$I_g=\frac{V_eK_wn}{4(R+R_g)}$	$\epsilon=\frac{\Delta R/R}{K_w}$ n = number of active gauges K_w = gauge factor
	$R_1=R_3=R$ $R_2=R_4=R_0$ R_0 = fixed resistance	$I_g=\frac{V_eK_wn}{2(R+R_0+2R_g)}$	Same as above
B 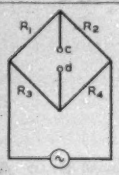	$R_1=R_2=R_3=R_4=R$ or $R_1=R_4=R$ and $R_2=R_4=R_0$	$E_{cd}=\frac{V_eK_wn}{4}$	Same as above c-d feeds into infinite impedance detector

for a given bridge arrangement, is given in equation 2. This satisfies the condition that the load be equal to the source impedance.

Often it will not be possible to match the galvanometer to the bridge circuit for maximum power transfer. However, the resistance of the galvanometer can differ from the resistance of the external circuit by a ratio of 6 to 1 with a loss of only 30 per cent. This can be demonstrated as follows:

If the galvanometer coil does not change in size or position with changes in the number of turns, and if the galvanometers to be compared are alike in all other respects, then it can be shown[10] that the deflection of a galvanometer is proportional to the current and the square root of its resistance, as shown below

$$\delta_g=K_1I_g\sqrt{R_g}$$

The galvanometer current is

$$I_g=\frac{V_eK_w}{4(R+R_g)}=\frac{K_2}{R+R_g}$$

therefore

$$\delta_G=\frac{K_1K_2}{R+R_g}\sqrt{R_g}$$

The greatest deflection is obtained when $R=R_g$

$$\delta_{g1}=\frac{K_1K_2}{R+R}\sqrt{R}=\frac{K_0\sqrt{R}}{2R}=\frac{0.5K_0}{\sqrt{R}}$$

For $R_g=6R$

$$\delta_{g2}=\frac{0.35K_0}{\sqrt{R}}$$

$$\delta_{g1}-\delta_{g2}=0.149K_0/\sqrt{R}$$

As a per cent

$$\text{Per cent}=\frac{0.149}{0.5}\times100$$

which is a 30 per cent loss in deflection.

The Galvanometer Current

A knowledge of the direction of the output current for tensile or compressive stresses in the arms of the Wheatstone Bridge is essential when using strain gauges in pairs. For instance, once the polarity of the output current is known under various conditions, it is possible to place gauges in the bridge so that compensation for temperature variation may be obtained, or so that the gauges will respond to axial strain and not bending strain, and so forth. As an example, assume that R_1 is in compression and that R_2 is in tension, also that $R_1=R_3=R_2=R_4$. If R_1 is in compression then it assumes some value $R-\Delta R$ and R_2 becomes $R+\Delta R$. For $R-\Delta R$

$$I_g=\frac{V(R\,\Delta R)}{4R^3-3R^2+4R^2R_g-2RR_g\,\Delta R}$$

which by inspection is positive.

For $R+\Delta R$

$$I_g=\frac{V((R+\Delta R)R-R^2)}{3R^2(R+\Delta R)+R^2+R_g(2R)(R+R+\Delta R)}$$

which also is positive.

Thus it can be seen, that for the condition where R_1 is in compression and R_2 in tension, the currents are additive. It follows that if both resistors should be in tension or compression at the same instant, their net effect on the detector would be zero, which is the condition obtained when the resistors change with temperature.

Infinite Impedance Detector

When the bridge is used with an infinite impedance detector, such as a vacuum-tube amplifier, only the open circuit voltage is of interest. This is E_{cd} as obtained in Table IB.

$$E_{cd}=V\left(\frac{R_3}{R_1+R_3}-\frac{R_4}{R_2+R_4}\right)$$

This, too, can be simplified for strain gauge work.

Let R_2 change by $\pm\Delta R$. Let $R_1=R_3=R_3=R_4=R$.

$$E_{cd}=\frac{V(\pm\Delta R)}{4R\pm2\Delta R}$$

Neglecting ΔR in denominator

$$E_{cd}=\frac{V(\pm\Delta R)}{4R}=\frac{V_eK_w}{4}$$

in general

$$E_{cd}=\frac{V_eK_wn}{4}$$

J. Avins[11] shows that the greatest sensitivity is obtained when $R_1=R_2$ and $R_3=R_4$, but the upper and lower arms need not equal each other as for the case where the detector draws current.

Usually when a vacuum-tube amplifier is used as a detector, the source of the voltage V is alternating at audio frequency, in which case the above quantities are vector quantities.[12] With alternating current the bridge is no longer phase sensitive. However, this can be overcome by operating the bridge slightly off-balance and utilizing a bridge rectifier arrangement in the output to detect a shift towards or away from balance, or by using a double balanced bridge, or ring demodulator, in which the carrier serves as a polarizing medium by virtue of its relation to the modulated carrier. The use of the ring circuit introduces other desirable features, such as operation of the bridge at zero balance, instead of off-balance, and reduction of noise, because it is double-balanced.[13,14]

For convenience, the circuits discussed are presented in Table 1.

References

1. Stress Measurement by Electrical Means, R. E. Kern, S. B. Williams. *Electrical Engineering (AIEE Transactions)*, volume 65, March 1946, pages 100–07.

2. The Galvanometer and the Bridge. *Weston Engineering Notes* (Newark, N. J.), volume 1, number 1, February 1946.

3. Wheatstone Bridge—List of Circuit Equations. *Weston Engineering Notes* (Newark, N. J.), volume 2, number 5, October 1947, page 6.

4. Absolute Measurements in Electricity and Magnetism (book), **Andrew Gray.** Macmillan Company, London, England, second edition, 1921, pages 133–41 and 333–40.

5. Electrical Measurements (book), **Frank Arthur Laws.** McGraw-Hill Book Company, Inc. New York, N. Y., second edition, 1938, pages 179–85.

6. Mechanical Measurements by Electrical Methods (book), **Howard Creighton Roberts.** The Instruments Publishing Company, Inc., Pittsburgh, Pa., 1946, pages 130 and 201–29.

7. A-C Bridge Methods (book), **B. Hague.** Sir Isaac Pitman and Sons, Ltd., London, England, fifth edition, 1946, page 61.

8. On the Best Arrangement of Wheatstone's Bridge for Measuring a Given Resistance with a Given Galvanometer and Battery, **O. Heaviside.** *Philosophical Magazine* (London, England), volume 45, 1873, page 114.

9. Application of Strain Gages to Aircraft Design Problems. *Proceedings*, Society for Experimental Stress Analysis (Cambridge, Mass.), volume 2, number 1, 1944, page 60.

10. Electricity and Magnetism for Advanced Students (book), **Sydney George Starling.** Longmans Green and Company, New York, N. Y., fifth edition, 1929, page 73.

11. A Wide Range Wheatstone Bridge, **Jack Avins.** *Electronics* (New York, N. Y.), July 1939, page 38.

12. Universal Chart for Unbalanced A. C. Bridges, **R. C. Paine.** *Electronic Industries* (New York, N. Y.), November 1936, page 72.

13. Phase-Sensitive Indicating Devices, **H. C. Roberts.** *Radio and Television News* (Chicago, Ill.), volume 7, number 1, July 1946, page 16, and volume 7, number 2, August 1946, page 12.

14. Copper Oxide Modulators in Carrier Telephone Systems, **R. S. Caruthers.** *Bell System Technical Journal* (New York, N. Y.), volume 18, April 1939, pages 315–77.

No Discussion

Variable Speed Drive, Constant Frequency Alternator

G. G. GOULD
MEMBER AIEE

E. KRUPOTICH
ASSOCIATE AIEE

A CLUTCH-DRIVEN alternator, which will maintain its output frequency constant within 1 per cent although the input driving speed varies more than 80 per cent, has been developed at the Naval Ordnance Laboratory. This development resulted from the need for a source of constant-frequency alternating current in ordnance equipment wherein adequate mechanical power is available for driving a generator but where a constant speed driving source is not available, similar to conditions encountered when generators are driven from aircraft or automotive engines. Two different methods are employed to convert the variable drive shaft speed to a constant alternator speed; one is by means of a centrifugal friction slip clutch, the other by means of a centrifugally-governed magnetic-fluid clutch. The units are completely self-contained, requiring no external excitation or reference frequency and are capable of limited frequency adjustment. Their chief limitation is the loss of power in the clutches as heat, this loss being dependent on the range of driver speed variations to be accommodated.

Clutch Principles

One method of converting variable shaft speed to constant shaft speed is by means of the centrifugal friction slip clutch illustrated in Figure 1. Driving torque is transmitted to the generator through the friction coupling of six spring-loaded friction shoes slipping on a revolving driver drum. When the driver drum is rotated at the regulating speed, the difference between spring forces and the centrifugal forces due to the shoe holders is just sufficient to produce the torque required to drive the alternator. If the speed of the driver drum is increased above regulating speed, the friction shoes will slip on the driver drum maintaining constant alternator speed. In normal operation, there is always relative slip between the driver drum and friction shoes in order to accommodate both increases and decreases in driving speed. The regulating speed is set by preadjusting the spring forces.

The second method of obtaining constant speed from a variable speed shaft is by means of the magnetic-fluid clutch illustrated in Figure 2. In this clutch, a mixture of fine iron powder and oil fills the space between the two relatively moving ferrous drums. This magnetic fluid is made more or less viscous by a controllable magnetic field, whose excitation is obtained directly from the alternator through a small, full-wave dry disk rectifier. To insure alternator starting, even with no clutch exciting current, a small permanent magnet is mounted on the clutch output shaft to provide the requisite starting torque and to permit excitation build-up as in ordinary d-c generators. A later model employs a centrifugal switch instead of the permanent magnet for starting. Automatic frequency control is obtained by regulating the amount of clutch current by use of a Lee type centrifugal governor in the clutch circuit. At a predetermined speed, depending on the governor setting, the governor contacts tend to open due to centrifugal force; however, since this tends to reduce the control current and in turn the governor speed, the generator maintains constant speed for any further drive speed increase. The regulating speed is chosen by preadjustment of a small backing screw on the governor so as to accommodate both normal increases and decreases in driving speed.

Figure 3 shows a complete, self-contained clutch-driven alternator having an output of 200 watts at 200 cycles. Either a centrifugal-friction clutch or a magnetic-fluid clutch is incorporated in the housing.

Frequency Regulation

The alternator output frequency varies slightly with slip speed as shown in Figure 4. Slip speed, which is defined as the difference between the driver and regulating speeds, is plotted as per cent of the regulating speed, while the frequency variation is plotted as the per cent change from the frequency at 30 per cent slip speed. For the friction clutch, the change in output frequency is due to the change in the coefficient of sliding friction with slip speed. For the magnetic-fluid clutch, the output frequency is independent of slip speed, except at high values of slip where heating alters the magnetic-fluid viscosity. Even with this slip effect it is seen that at constant electric load the alternator frequency remains constant within 1 per cent for large changes in driver speed.

Changes in alternator load have a more pronounced effect on frequency than changes in slip speed. Figure 5 shows the effect of change of load on the friction clutch, where a change in load from full load to no load caused the frequency to rise 1.2 per cent. The magnetic-fluid clutch is not as sensitive to load changes as the friction clutch; the frequency remains within one half per cent for all load changes.

The frequency versus time trace for a typical 1-hour run is shown in Figure 6, where the drive speed is varied every ten minutes and frequency continuously re-

Paper 50-119, recommended by the AIEE Rotating Machinery Committee and approved by the AIEE Technical Program Committee for presentation at the AIEE North Eastern District Meeting, Providence, R. I., April 26–28, 1950. Manuscript submitted November 4, 1949; made available for printing March 24, 1950.

G. G. GOULD is with the Naval Ordnance Laboratory, White Oak, Maryland, and E. KRUPOTICH, formerly with the Naval Ordnance Laboratory, is with the United States Bureau of Reclamation, Casper, Wyo.

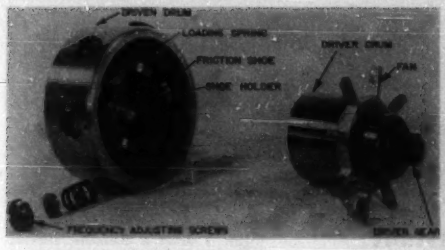

Figure 1. Centrifugal friction slip clutch, disassembled

Figure 3. Self-contained clutch-driven constant frequency alternator

corded. Although the frequency for both clutches remained constant within 1 per cent, the friction clutch shows its characteristically slow frequency decrease with time due to wear of the friction material and of heating, while the magnetic-fluid clutch shows failure to regulate above 100 per cent slip speed due to centrifugal packing of the iron powder.

Excellent response to transient speeds is characteristic of both types of clutches. There is neither hunting nor overshooting during the transient period even though the driver speed is rapidly varied. The alternator frequency responds to the drive speed change, but remains constant within one half per cent. Similarly, the "warm-up" time from a cold start is of short duration; the generator frequency is up to 1 per cent of steady frequency as fast as the prime mover can come up to speed.

Limitations

Since the clutches must accommodate both decrease as well as increase in driving speed, there will always be slip between driver and driven members. Consequently, power is continuously dissipated in the clutch as heat, the amount of such power being equal to the ratio of slip speed to regulating speed times the power output. This limits the size of generator that can be driven by the clutches. For the two clutches shown, the temperature rise is about 40 degrees centigrade above ambient at full load.

In the friction clutch, wear of the friction shoes requires their replacement after about 20 hours of running. Although the proper choice of friction shoe and driver drum materials will help minimize the wear encountered, it is not possible to eliminate wear entirely. The manifestation of wear is the gradual decrease in regulating frequency of approximately 1 per cent after five hours of running.

The magnetic-fluid clutch is not troubled with wear, but it does require periodic maintenance because of loss of oil from the iron-oil mixture. Due to centrifuging, the iron tends to separate from the oil; while due to heat, the oil is driven out of the clutch. Thus, the clutch characteristics are slowly changed in time. Although adequate life tests have not been performed, it appears that this clutch can be operated for at least 20 hours without requiring servicing.

Considerably longer service-free life can be obtained readily with both types of clutches by increasing clutch sizes. The units built are intended for short life, intermittent duty, and hence are small physically.

Design Factors

The alternator is of conventional design, incorporating a permanent magnet rotor and a wound stator, with the number of poles chosen to permit the highest possible drive speed in keeping with the strength of the Alnico rotor and the desired frequency. Since high centrifugal forces yield improved speed regulation for the friction clutch, and, furthermore, since high speeds yield smaller generator size, the clutch was designed to regulate at 6,000 rpm, and driven at 6,500 to 12,000 rpm. The magnetic-fluid clutch, however, was designed to regulate at the lower speed of 4,000 rpm and driven at 4,200 to 8,000 rpm because of separation of iron from oil due to centrifugal forces. This decreased regulating speed reduced the maximum generator output by one third.

Changes in drive speed, load, and temperature affect the coefficient of sliding friction in the friction clutch. Even for constant speed and constant shoe pressure, the friction force available for driving the generator will vary with time when the clutch is brought up to speed from a cold start. For good speed regulation it is necessary to choose a combination of friction shoe material and driver drum material which exhibits the least change in friction due to temperature, pressure, or slip speed. By experimental means, it was determined that the best clutch operation was obtained by using a copper-base, sintered friction shoe material, of the type commonly used for clutch or brake applications, mating against a chromium-plated steel drum.

Figure 2. Magnetic-fluid clutch parts and generator housing

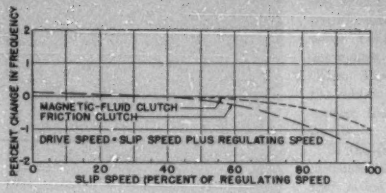

Figure 4 (left). Change in alternator frequency as drive speed is changed at constant full load

Figure 5 (right). Change in alternator frequency as load is changed at constant drive speed

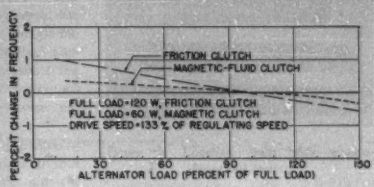

This combination of materials yields a high coefficient of sliding friction which is relatively constant, and further does not result in excessive wear of either the shoe or the drum.

As noted previously, centrifuging and sealing are the primary problems encountered with the magnetic-fluid clutch. The separation of iron powder from the oil can be minimized by judicious design and by the use of the correct quantity of magnetic-fluid based on the design. As to sealing, standard type shaft seals have been found to be satisfactory for retaining the iron particles; nevertheless, the oil does gradually disappear from the magnetic fluid.

Frequency Setting

By use of a calibrated spring scale, each of the six compression springs of the friction clutch is set accurately to a specified loading, thereby ensuring that all friction shoes take an equal load. Tests have shown that it is possible to preset the regulating frequency of the generator within an accuracy of two per cent. To effect minor changes in frequency, each of the six adjusting screws is rotated by an equal amount, thereby slightly increasing or decreasing the force of each spring by an equal amount.

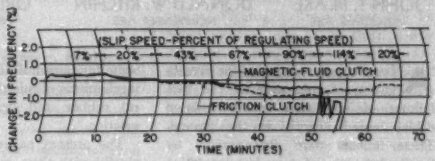

Figure 6. Frequency variation with time, as drive speed is changed every ten minutes

For the magnetic-fluid clutch, frequency setting is readily accomplished by merely adjusting the governor spring backing screw. With the centrifugal governor used, it is possible to set the regulating frequency to any value between 150 and 220 cycles per second.

Applications

The clutches and associated control systems described are suitable for many applications where a constant output speed is desired from a source of variable speed power. The simplicity of control and the excellent transient response of the clutches commend their application in fractional horsepower equipment, provided the losses due to clutch heating can be tolerated. In addition to the use of the clutches as frequency regulating devices, they have been successfully used as accurate voltage regulating devices on d-c generators driven from variable speed shafts.

Other applications that have been suggested, especially for aircraft or for automotive use, are as constant speed drives for pumps and fans.

Discussion

P. H. Trickey (Vickers Electric Division, Vickers Inc., St. Louis, Mo.) Mr. Gould and Mr. Krupotich are to be commended for their development of a constant frequency drive from a variable speed source. It may be of interest to know that the magnetic fluid clutch which they have used in a small size for short life, has now been developed successfully by Vickers Incorporated for use on much larger sizes, and for normal life of thousands of hours.

G. G. Gould and **E. Krupotich:** Mr. Trickey's comments are appreciated, especially since he is well cognizant of the many detailed problems which had to be solved to produce a successful clutch. It is gratifying to note that the magnetic fluid clutch has been applied successfully to larger units than the ones developed at the Naval Ordnance Laboratory, as this justifies the confidence placed on the system for speed regulation. The short, service-free life of the units developed does not necessarily indicate unsatisfactory characteristics. The clutches were specifically designed for maximum load at the expense of longer life, and further required to accommodate unusually large driver speed variations. The service-free life of both types of clutches can be extended appreciably by increasing the size of the units or, even for the same size, by decreasing the slip speed.

Failures of Rubber Insulation Caused by Soil Microorganisms

JOHN T. BLAKE
ASSOCIATE AIEE

DONALD W. KITCHIN
NONMEMBER AIEE

ORISON S. PRATT
NONMEMBER AIEE

AN earlier paper[1] reported the investigation of the cause of the rare failures of nonleaded rubber-insulated cables buried directly in the ground. These failures were characterized by localized regions of very low insulation resistance. The absorbed water content was no greater than in adjacent regions of high insulation resistance, and the physical properties were usually normal. Drying the failed insulation raised the resistance several decades, but brief exposure to moisture restored the low values. It was suspected that these failures had been caused by the action of soil microorganisms.

A study was made in the laboratory with conditions favoring microbial activity. By exposing thin walls of insulation to soil of high microbe content, adjusted to neutral or slightly alkaline pH, and kept moist and warm, it was possible to accelerate the action so that failures like those occasionally found after ten or more years under actual service conditions were produced in a few weeks. Parallel tests in active soil, sterilized soil, and water showed conclusively that the drastic loss of insulation resistance in active soil was due neither to water absorption nor to the action of soil chemicals, but to attack by living microorganisms.

In the actual operation of underground cables the most favorable combination of conditions necessary for producing failure by microbial attack occur only rarely.

Since certain soil microbes can consume the natural rubber hydrocarbon, failure of natural rubber insulation is usually accompanied by visible surface pitting. Synthetic rubber insulation shows no visible signs of attack even after a six decade drop in resistance. This suggests some fundamental difference between the mechanisms of microbial attack on natural rubber and synthetic rubber insulation.

The present paper is concerned principally with these mechanisms and with the composition and structure that tend to make rubber insulation vulnerable to such attack. Experimental evidence is given to show that the *GR-S* and butyl hydrocarbons are not consumed by soil microorganisms, and that the invisible faults leading to electrical failure occur only where microbes eat out other materials present in the synthetic insulating compound.

Methods of Locating Faults

To study the faults in rubber produced by microorganisms it is necessary to locate them precisely. Searching along a failed wire sample with a test probe is neither sensitive nor precise enough. Several methods of locating such faults are described below.

Use of Electrolyte with a Color Indicator

A simple method of locating faults is to immerse the failed sample in an electrolyte containing phenolphthalein. The conductor is made negative to the bath. Voltages from 100 to 500 volts may be used. At any faults sufficiently leaky the development of alkali produces a red color. Figure 1 shows a failed sample on which 65 color spots could be counted. This method does not mark the faults permanently nor reveal their nature directly.

D-C Corona Test

A more sensitive and rapid method is to stress a wet failed wire sample with about 5,000 volts (conductor negative) under reduced air pressure. Figure 2 shows a sample with five corona spots. Another sample showed over 20 such spots. The resistance of a single typical fault is of the order of 10 megohms, whereas that of the surrounding intact region is usually of the order of 10,000,000 megohms per foot of sample. Thus the leaky spots act like point electrodes to produce stress concentrations which break down the air near them. Considerably higher voltage is required to produce corona over-all, so that the effect is clean-cut. Alternating stress would be much less effective because the capacitive current through the whole insulation would mask the leakage current through the faults.

Electrodeposition of Copper in Faults

Some faults produced by microbes in rubber insulation can be located and permanently marked by immersing failed wire samples in a copper sulfate solution and making the conductor 100 to 500 volts negative to the solution. After a period of several days surface specks of metallic copper appear at some of the faults. If the treatment is continued these specks grow to copper nodules, while new small specks may appear, Figure 3. In a number of samples insulated with laboratory-mixed stock certain faulty regions showed hundreds of fine copper specks after this treatment, Figures 4 and 5.

When the insulation was sliced off to various depths, particles could be found all the way through the wall. These were too minute to be seen by unaided eye, but their color made them visible at a

Paper 50-121, recommended by the AIEE Insulated Conductors Committee and approved by the AIEE Technical Program Committee for presentation at the AIEE North Eastern District Meeting, Providence, R. I., April 26–28, 1950. Manuscript submitted January 27, 1950; made available for printing March 22, 1950.

JOHN T. BLAKE, DONALD W. KITCHIN, and ORISON S. PRATT are all with the Simplex Wire and Cable Company, Cambridge, Mass.

Figure 1. Locating faults with color indicator

magnification of 100 X. To obtain good photographs it was necessary to intensify the specks in the cut layers by additional plating, Figure 6.

Of these three methods of locating faults the electrodeposition of copper on failed samples has shown the most about the nature and distribution of faults. As a quick routine means of counting faults the d-c corona is more convenient.

Since the first copper ions have to traverse the wall of insulation before they are deposited, the copper filament grows from the conductor outwards. It is extremely fine. After it reaches the surface further deposition leads only to nodule formation without thickening the filament inside the pore. The copper-bearing channels are not always radial, but sometimes run in many directions, a fact which suggests the existence in the insulation, before microbial attack, of paths more vulnerable than the surrounding insulation.

In the copper-treated faults no continuous, solid filaments have been found that would cause a short circuit. Instead the pores contained practically single-file aggregates of microscopic copper particles. It was not possible by dissolving the rubber away to leave any continuous copper filaments since they were too fragile.

Figure 2. Locating faults with d-c corona

In the previous paper the presence of invisible faults in *GR-S* insulations that had failed was demonstrated, but the structure of these faults was not established. Two alternatives were suggested, namely that these faults were either: regions of insulation degraded by diffused microbial products until the rubber there had extremely low resistivity; or actual holes through the insulation. The results of the copper deposition test show that the faults are holes.

Evolution of Hydrogen in Faults

Some failed samples did not show copper specks even though the measured microampere-hours passed through the insulation in the copper sulfate solution were equivalent to an appreciable deposit. If copper were present, but merely too finely distributed to be seen, it could be recovered by electrodeposition on a platinum wire and weighed. Careful experiments failed to detect any copper in these samples. The leakage current had been carried by ions other than copper ions. Hydrogen ions seemed the most likely carriers. To test this a sample which had failed to show deposited copper after several days in the copper sulfate bath was placed in the same electrolyte in a glass tube where the hydrogen was collected and measured. After a week a few copper specks appeared, but about 90 per cent of the current through the sample was accounted for by the evolved hydrogen.

Microorganisms could hardly produce a pore with a diameter smaller than that of a copper ion. It is more probable that hydrogen gas evolved at the conductor forms bubbles in the pores that markedly reduce the leakage current. One failed sample showed a four-decade rise in resistance during a prolonged electrolytic test. Soaking in hot water without voltage allowed the hydrogen to diffuse out and restored the initial low resistance.

Two Types of Microbial Attack

When wire samples which have failed in the accelerated laboratory soil exposure test are inspected the most obvious difference is that the surface of the natural rubber insulation is usually badly pitted, that of the *GR-S* rubber insulation not at all. This suggests a fundamental difference between the modes of attack on the two types of rubber.

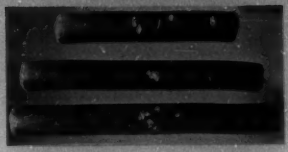

Figure 3. Locating faults with electrodeposited copper

The severe microbial pitting so far found in natural rubber insulation, but not in the synthetics, is the more obvious action, Figure 7. Its progress can be noted visually long before there is any decrease in insulation resistance. Dielectric strength tests would be expected to show impending failure, but to produce drastic loss of sample resistance the microbes have to eat all the way through to the conductor. The breach in the insulation may eventually become a rather coarse hole rather than a micropore, since there is no reason for the microbes to prefer a radial direction when they can consume the insulation in bulk. It has been shown[1-7] that a number of soil microorganisms can readily consume natural rubber either as the pure rubber hydrocarbon or as a part of a vulcanized compound. Unless a natural rubber insulation is protected by adequate preventives, the microbes can eventually eat through the wall. This type of attack appears to be little affected by differences in physical texture imparted by variations in processing.

The mechanism of the microbial attack which creates micropores is more obscure. This occurs in both natural and synthetic rubber insulation. In natural rubber the microporous regions are much less numerous than the pitted regions, yet the samples fail through the micropores long before any pits reach the conductor. Figures 4 and 7 illustrate this point. They show two regions of a sample of natural

Figure 4. Electrodeposited copper showing micropores in natural rubber insulation

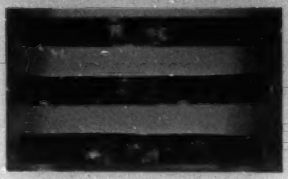

Figure 5. Electrodeposited copper showing micropores in GR-S insulation

rubber insulation which had failed in the accelerated laboratory soil test. The electrodeposited copper in Figure 4 shows the presence of many pores that traverse the wall all the way to the conductor. Before the copper treatment this spot showed no visible signs of attack. This was the only microporous region observed. On the other hand, there were very many pitted regions like those shown in Figure 7. Although these regions had been exposed to exactly the same conditions no copper specks were found in these pits nor signs of leakage by any other tests. The wall of insulation under the pits appears to have remained sound. To cause failure by pitting the microbes have to consume the bulk insulation all the way to the conductor. This is a process which seems to be much slower than the one which creates the micropores.

Figure 6 shows the same microporous region as Figure 4 after 70 per cent of the wall had been sliced off and the copper filament ends, visible only under the microscope at 100 X, had been intensified by additional copper plating.

Since microbial attack on *GR-S* insulation does not create pits, visual examination does not show whether it has failed or not. Failure is detected by loss of insulation resistance. To locate the faults one of the tests described above is required. Figure 8 shows samples of failed *GR-S* insulation after copper deposition. Although these samples had suffered a loss of resistance of six decades or more the surface remained smooth and shiny. The existence of the micropores is revealed by the electrodeposited copper.

In *GR-S* insulation that failed the absence of surface erosion, the random direction of the pores, and their minute size imply that the insulation is not uniformly vulnerable, but that even before exposure to soil microorganisms, it contains "imperfections" in otherwise inert material. These are minute veins of microbe food scattered in a random manner throughout a medium that microbes cannot consume. This microbe food is neither water-soluble nor hygroscopic, since control samples in water maintain normal resistance indefinitely. Soil microbes eat out the insoluble food and leave in its place some hygroscopic material. This makes the resistance of the pores very low when the sample is wet, but very high when it has been allowed to dry.

Evidence of the Existence of Imperfections

There is a variety of evidence for the existence of these imperfections. If the bulk insulation could be consumed by soil microorganisms, we should expect, after prolonged soil exposure and failure, to find both severe surface erosion and much larger pores. There would also be no reason for the peculiar orientation and the zigzag course of the pores so often observed when samples are examined after copper deposition. The electrical evidence relating to these imperfections is especially interesting. Considerable light is thrown on the probable structure both by the trend of insulation resistance versus soil exposure when the test is continued several months after initial failure, and by the d-c breakdown values on samples not exposed to soil but simply soaked in hot water.

Figure 9 shows the peculiar trend of resistance of *GR-S* insulation when exposure to soil is continued after failure. These accelerated laboratory soil exposure tests were made on ten samples of number 14 solid wire with a 3/64-inch wall of a *GR-S* compound having low water absorption. The samples were consecutive 5-foot lengths from the same length of wire run in the factory. Ten samples in soil all failed in ten months or less. Four control samples in water maintained normal resistance.

The course of the attack is presumably as follows. Some soil microorganisms, not yet identified, consume food in the minute streaks. Until the first micropore reaches the conductor the effect on the sample resistance is negligible. As soon as the pore passes all the way through the wall, the resistance drops several decades. After this first drop the decrease

Figure 6. Section of insulation shown in Figure 4 with copper deposits in micropores intensified by further plating

Figure 7. Characteristic pitting of natural rubber

is very gradual. As more pores traverse the wall they decrease the resistance relatively little. For example, ten faults having equal leakage lower the sample resistance only one decade more than a single fault. If a pore kept increasing in diameter because the microbes could consume the surrounding medium the sample would soon be practically short circuited. This levelling off of the sample resistance after the first sharp decrease, together with the extreme minuteness of the pores and the absence of any visible surface erosion seem to be convincing proof of the correctness of the postulated structure of the imperfections.

There is other independent evidence. Visual tests described later in this paper show that the *GR-S* hydrocarbon does not support microbe growth, but that raw *GR-S* contains materials that do. These materials and others added in the compounding are believed to be the food in the imperfections.

Effect of Processing on Stability of GR-S Insulation in Soil and On D-C Breakdown after Hot Water Soak

Whether a given rubber insulating compound is processed in the factory or in the laboratory the regular physical and electrical tests usually show no significant difference in quality. In the soil exposure tests, if the insulation is not inherently resistant, or made so by the addition of effective preventives, wire samples made in the laboratory have almost invariably proved to be more vulnerable than those made in the factory. Thus the structure, as influenced by the processing, that is, the thoroughness and uniformity of mixing, is an important factor in determining the stability in soil.

One of the most effective means of testing rubber insulation for structural imperfections not revealed by low resistance is to make d-c breakdown measurements on samples which have been soaked several days in hot water. If fissures, micropores, or poorly bonded interfaces extend only partly through the wall their effect on the insulation resist-

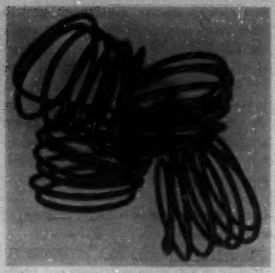

Figure 8. Copper deposits on *GR-S* sample. (Note absence of erosion)

ance may be negligible. Direct voltage stress causes breakdown at the weakest spot. It is a local, not a bulk effect. After a few days soaking in water at 158 degrees Fahrenheit an imperfection in only a fraction of the wall thickness can lower the d-c breakdown considerably. Water which diffuses to an imperfection acts like a sharp electrode to produce high local stress concentration and breakdown.

In the following experiment, *GR-S* insulation having abnormal vulnerability to soil microbes also showed low d-c breakdown strength. Samples were prepared of number 14 solid wire with 3/64-inch wall of *GR-S* insulation having low water absorption. The formulation was identical in all samples, but the processing in the three groups was thus:

1. Insulation processed entirely in the factory.
2. Insulation mixed in the factory, extruded and vulcanized in the laboratory.
3. Insulation processed entirely in the laboratory.

The usual tests for insulation resistance versus soil exposure were made on samples from each group. Table I shows the initial megohms and the megohms after four months in soil (five feet buried length). Another set of samples from the same groups was soaked three days in water at 158 degrees Fahrenheit and then broken down by d-c stress.

Control samples for the soil tests showed no drop in insulation resistance in water. Samples from each group, after being dried two days at 185 degrees Fahrenheit showed an average value of 2,300 volts per mil apparently not significantly affected by the variations in processing. Thus the major physical factor affecting both stability in soil and d-c breakdown strength is the completeness of mixing. Although the low d-c breakdown voltages and the rapid failure in soil may not both be caused by the same imperfections, it is evident that the kind of mixing that produces the highest d-c breakdown after hot soak also increases the stability in active soil. It is not surprising that the factory mixing should prove superior.

The difference with regard to stability in soil is one of degree only. The results in Figure 9 and those in the third column of Table I were obtained with samples from the same length of factory-run wire. The better mixing thus merely delayed failure. These were only 5-foot lengths, yet in one sample the d-c corona test revealed 20 micropore faults. It seems unlikely that any amount of mere physical processing would guarantee unlimited stability in service lengths of thousands of feet, which a few microbe faults might put out of operation. On the other hand, certain types of *GR-S* insulation made inherently resistant by the addition of effective microbe preventives have been stable in soil even when the processing is not thorough enough to produce optimum d-c breakdown strength after hot water soaking. The d-c breakdown strength after hot water soaking is thus an index of structural integrity, regardless of inherent resistance to microbe growth. The visual fungus test described later shows whether the material is inherently resistant to microbe attack without regard to the thoroughness of mixing. These two tests are entirely independent.

The ideal insulation is one combining maximum resistance to microbe growth with the best possible physical structure.

Protection of Insulation by Jackets—Staggered Imperfections

Tough neoprene jackets are commonly used over the insulation of nonleaded

Table I. Effect of Processing on Stability and Breakdown

Laboratory Mixed and Insulated	Factory Mixed Laboratory Insulated	Factory Mixed and Insulated
Initial Megohms in Soil		
2,700,000	2,100,000	2,500,000
2,700,000	2,200,000	3,000,000
2,700,000	2,300,000	3,100,000
2,900,000	2,200,000	3,500,000
Megohms after 4 Months in Soil		
400	3,300,000	2,000,000
8	2,900,000	2,100,000
3	3,100,000	2,300,000
4	700	2,400,000
Volts Per Mil D-C Breakdown after 3 Days in Water at 158°F		
750	1,000	1,100
750	1,200	1,200
700	1,100	1,300
700	1,200	1,200

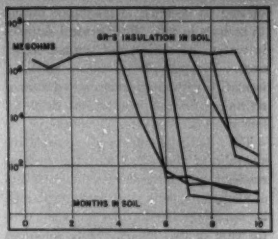

Figure 9. Dielectric resistance versus time of exposure to soil

underground cables to provide mechanical protection and weather resistance. It is desirable that they should also protect the insulation against attack by soil microorganisms. It is not satisfactory to test the resistance of neoprene jacket compounds to microbial attack by extruding them directly on a copper conductor and measuring insulation resistance versus soil exposure. The resistivity of such compounds is inherently low, and this tends to mask the effect of failures produced by microorganisms.

The most significant laboratory test is carried out by coating wire with insulation known to be susceptible to microbes, applying a layer of neoprene compound over this, burying the samples in soil, and making periodic megohm measurements between conductor and soil. The resistance of the jacket is so low that it does not interfere with the measurement.

Since two different mechanisms of attack had been observed in the failures of natural rubber and *GR-S* insulation, it was of interest to test the effect of neoprene jackets over both types. Ten five-foot samples of number 14 solid wire with 3/64-inch wall of a natural rubber insulation and a 25-mil wall of neoprene jacket compound were buried in soil and four were immersed in water. Those in water showed normal high resistance during 13 months. All ten soil test samples failed in 9 to 13 months with an average drop in insulation resistance of three decades. This is less than that observed when the insulation is directly exposed to soil. Even an imperfect jacket delays the attack and restricts it to a small fraction of the total area. These failures indicate that the microbes traverse the neoprene jacket, presumably through food streaks or imperfections. When they reach the natural rubber at any point they can cause failure by consuming the bulk insulation.

In a parallel test ten samples with similar jackets but with *GR-S* insulation

showed no decrease in resistance during 15 months in soil. Four control samples in water also maintained normal resistance. Two samples of the same *GR-S* insulation without jackets showed normal resistance for ten months but drops of four to six decades after 13 months.

The marked difference in relative stability of the *GR-S* and the natural rubber insulation under neoprene jackets of identical type is most easily explained by applying the imperfection theory to the case of two layers. Since microbes cannot consume the bulk material of either neoprene or *GR-S* they have to find imperfections in both to cause failure. Even when these are numerous the probability of an imperfection in the jacket registering exactly with one in the insulation is small. If this does happen the sample should eventually fail. In general the imperfections would be expected to be staggered in such a way that failures in jacketed *GR-S* samples would be rare.

In another experiment to test this idea a 2-layer *GR-S* insulation is being compared for stability in soil with a single layer of the same thickness.

The statement in the earlier paper that neoprene compounds appear to be inherently resistant to soil exposure is true only in the sense that like *GR-S* they do not show visible results of microbe attack. If a neoprene jacket contains food streaks microbes can eat through it and attack susceptible natural rubber under it.

In a preliminary experiment samples of wire insulated with a 15-mil wall of vulcanized latex covered with a 20-mil wall of a neoprene jacket compound were exposed to soil until they had failed. The jacket was stripped from short pieces and these were quickly placed on sterile nutrient agar. In a few days white colonies starting from the wire spread gradually over the agar surface. The microorganism was identified as a species of Fusarium.

Experiments of this type are valuable both to show that microbes can traverse the jacket and also to identify those that do.

Figure 10. Visual fungus test on raw *GR-S* with additives

Figure 11. Fungus on raw *GR-S*

Accelerated Visual Test of Microbial Attack

The decisive laboratory test of the stability of underground cable insulation is the periodic measurement of insulation resistance of samples buried in soil for long periods under conditions most favorable to microbial attack. In this test susceptible samples fail in a few months. As compounds more resistant to soil exposure are developed the time to failure may become excessively long. A means of quickly showing whether a compound is inherently resistant to soil microbes is of great advantage.

A simple visual test provides such a means. Small pieces of material, which may be either vulcanized insulation or raw rubber or other polymer are placed on a thin layer of soil sprinkled over moist sand. The test may be accelerated by dusting the sample lightly with dried soil. The amount of material for such a test is very small and much processing time is saved.

Most susceptible materials show considerable fungus growth in a week or two. For example, the *GR-S* insulation on the samples of Figure 9, some of which took ten months to fail electrically, showed profuse fungus growth in about two weeks on the visual test. This test shows whether the insulating compound is inherently resistant and is independent of the degree of mixing.

One use of this visual test is illustrated in Figure 10. The samples are pieces of raw *GR-S 65* with various additives. At the left is a blank containing no additives. All samples had equal milling. Figure 11 shows an unmilled lump of *GR-S* after several weeks in a closed bottle over inoculated water. Without other tests the profuse growth of fungus on the raw *GR-S* could be misleading. When the same type of *GR-S* has been acetone extracted it shows no fungus growth after many months on this test. Even if the *GR-S* is badly oxidized after extraction by prolonged heating, it does not support growth. The *GR-S* hydrocarbon is not a source of microbe food. When the acetone extract is evaporated on aluminum foil and exposed to soil, heavy fungus growth appears, Figure 12. The immunity of purified *GR-S* supports the imperfection theory of failure of *GR-S* insulation. It accounts for the absence of surface erosion.

Growth of fungus on a particular insulation in the visual test does not prove that failure in soil of that insulation was directly caused by fungus. The fungus serves as an indicator which shows whether the compound is attractive to microorganisms in general. In doubtful cases the visual test may not be a sufficient criterion. On the other hand, an insulation that supports profuse fungus growth would be a poor risk for underground cable insulation. A large number of unpromising materials can be screened out with little effort. To-date the routine soil exposure tests on rubber insulation have confirmed the predictions of the visual test.

A practical application of this test is illustrated in Figures 13 and 14. Both samples have similar *GR-S* insulation of low water absorption, but with different combinations and amounts of preventives. Compound *A* showed visible fungus growth in one week. Compound *B* showed no growth during nine months test. Thus the implication of the visual test was that compound *A* would be unstable in soil, *B* stable.

To check this, 5-foot lengths of number 14 solid wire with 3/64-inch wall of insulation were prepared. Four samples of each type were buried in active soil, four in sterilized soil, and four immersed in

Figure 12. Fungus on acetone extract of raw *GR-S*

Figure 13. Visual fungus test on GR-S compound A

water. In water and in sterilized soil all samples have maintained normal resistance for a year. In active soil all four samples of compound *A*, which showed fungus in the visual test in one week, failed after three to five months. The four samples insulated with compound *B*, which showed no growth on the visual test, have maintained normal high resistance for one year. These results confirmed the predictions of the visual test for these particular compounds.

A similar confirmation was obtained with the natural rubber samples jacketed with a particular neoprene compound. The jacket showed profuse fungus growth on the visual test. The corresponding ten samples failed in the accelerated soil exposure test.

Visual fungus tests on individual materials aid in the choice of compounding ingredients. It is not safe, however, to use these results to predict the stability of complete insulating compounds. For example, although raw neoprene, both as received and after extraction with alcohol, shows no fungus growth in this test, a typical neoprene jacket compound may support profuse growth within a week. Certain insulating compounds may show no growth in the unvulcanized condition, but abundant fungus after vulcanization. The interaction of compounding ingredients during vulcanization may change susceptibility to microorganisms. The only safe test is one made on the final insulation. If a compound shows no appreciable fungus growth, the visual test should be followed up by making periodic measurements of insulation resistance on wire samples buried in soil.

Pure natural rubber hydrocarbon supports growth of microorganisms. In the visual test the first growth seems to be Actinomycetes appearing wherever the sample contacts the soil. This is followed by fungus growth. Raw butyl rubber generally shows little or no fungus growth. A slight growth of an organism cultured and identified as a species of Tricoderma was observed on some samples, but acetone extracted butyl rubber shows no growth at all. Butyl rubber severely oxidized after acetone extraction also fails to show growth of fungus. Paraffin wax and Heliozone show excessive growth. A high paraffin content tends generally to make compounds more susceptible to microbial attack. In neoprene compounds the effect of paraffin is peculiar. It blooms rapidly to the surface where it supports heavy fungus growth. A number of preventives that are effective in insulating compounds do not inhibit such growth on neoprene compounds, presumably because they are not sufficiently soluble in the paraffin layer. They also may reach the surface more slowly than the paraffin. If the microorganisms merely ate off the paraffin film without further action, this would not be cause for concern. It is not safe to rest on that assumption. This is shown by the failure of the samples jacketed with neoprene compounds that showed fungus growth in the visual test.

Summary

The failure of rubber insulation brought about by soil microorganisms can best be detected by a decrease of several decades in the insulation resistance. To study the mechanism of attack and the physical structure that makes rubber insulation vulnerable to such attack it is necessary to have means of locating and marking the failed spots. Several methods of doing this have been described. The electrodeposition of copper in the micropores created by microbes affords the most insight into the physical structure of the faults. Two distinct modes of attack have been shown. The simpler one which is characteristic of natural rubber, is a progressive eating away of the bulk insulation. The second more obscure type creates micropores through the wall, but without any visible surface erosion. This mode is typical of the synthetics in which the base hydrocarbon or polymer, if freed of extraneous microbe food, does not support microbe growth. The imperfections consist of streaks of microbe food scattered in a random manner through otherwise inert material. Their distribution is affected by physical processing. These streaks are not hygroscopic and do not lead to failure in prolonged immersion in either hot or cold water. They do, however, tend to lower the d-c breakdown of samples after several days soaking in hot water. Thus with a given susceptible compound it is possible to predict which processing will produce the greatest stability in soil by breakdown tests on samples not exposed to soil. The breakdown tests relate to physical structure. To test the inherent resistance of a material to soil exposure the simple visual fungus test is very convenient. The validity of this test as a criterion of stability has so far been confirmed by the routine resistance tests after accelerated laboratory soil exposure. It is not safe to predict the stability of a complete compound from the results of visual tests on the base material. The vulcanized insulation must be tested. Insulating compounds shown to be promising by the visual test should be given a thorough soil exposure test.

The testing of preventives is a field in itself. It is not simple. Materials which are strongly antiseptic in water may not be so when mixed in a rubber compound. Many of them would be completely unsuitable in rubber insulation. Some preventives are effective in a compound before it is vulcanized but not afterwards. Some are completely inactivated by certain other necessary or desirable ingredients. Others may leach out in time and cease to protect the material. Oxidation inactivates some preventives. A nicely balanced compound is required to produce insulation with sufficient stability in soil, proper physical characteristics, and high electrical quality.

Figure 14. Visual fungus test on GR-S compound B

References

1. Effect of Soil Micro-organisms on Rubber Insulation, J. T. Blake, D. W. Kitchin. *Industrial and Engineering Chemistry* (Easton, Pa.), volume 41, 1949, pages 1653–41.

2. Role of Moulds, Actinomycetes, and

Bacteria in the Decomposition of Rubber, B. O. Kalinenko. *Microbiology* (Russia), volume 7, 1938, pages 119–28.

3. Bacterial Decomposition of Rubber, D. M. Novogrudski. *Microbiology* (Russia), volume 1, 1932, pages 413–21.

4. Decomposition of Rubber by Microbes, N. L. Sohngen, J. G. Fol. *Centralblatt für Bakteriologie* (Germany), volume 40, section II, 1914, pages 87–93.

5. Bacterial Decomposition of the Rubber in Hevea Latex, D. Spence, C. B. vanNiel. *Industrial and Engineering Chemistry* (Easton, Pa.), volume 28, 1936, pages 847–50.

6. The Deterioration of Rubber Products by Micro-organisms, C. E. ZoBell, J. D. Beckwith. *Journal*, American Water Works Association (New York, N. Y.), volume 36, 1944, pages 439–52.

7. Action of Micro-organisms on Hydrocarbons, C. E. ZoBell. *Bacteriological Reviews* (Baltimore, Md.) volume 10, numbers 1–2, March-June 1946.

Discussion

F. E. Kulman (Consolidated Edison Company of N. Y., Inc., New York, N. Y.): This paper presents evidence that rubber insulations fail by microbiological deterioration and describes a mechanism by which the materials are damaged. Rubber compounds in which the base polymer may or may not be inert to microorganisms contain imperfections, scattered in a random manner throughout the medium, which are nutrient to microorganisms. When the food particles are consumed the damage appears as micropores which can be located and marked by the deposition of copper in them. The concept of the formation of micropores, as described by the authors, represents an advance in our knowledge of the limitations of cable materials and provides the opportunity of producing better cable insulations and jackets. Since raw neoprene which is used so widely as a jacket base in network cables is apparently immune to microorganisms, improvements in these cables can be expected.

Since the spring of 1948, the microbiological services of a research laboratory have been engaged by the Consolidated Edison Company of New York to investigate the bacterial corrosion of metals and the microbiological deterioration of nonmetallic protective coatings and jackets which are applied to underground feeder pipes and lead sheaths for corrosion prevention.

Samplings of the soils in New York City have shown the presence of five types of bacteria which may influence metal corrosion and at least 23 species of fungi and actinomyces which may cause coating deterioration. Quantities of the soil have been removed to the laboratory and short sections of coated pipes and cables placed therein. Similar specimens of pipes and cables were placed in steam-sterilized soil as controls. Periodic measurements of insulation resistance are being made to determine whether the materials are deteriorating. Preliminary results showed severe deterioration of cellulose or cellulose derived coatings.

Visual tests of nutrient inertness, conducted in accordance with Joint Army-Navy specifications, were found to be useful in screening out inferior coating materials. The visual tests are made in glass jars at 28 degrees centigrade and 95 to 98 per cent relative humidity with the spores of four prescribed types of aggressive fungi sprayed on the test materials. These tests can be made in as short a period as two to four weeks.

To assure long life of underground pipes and cables it is most desirable to select a coating material which is nutriently inert to microbiological damage. Insufficient work has been done on incorporating fungicides in coating or jacketing materials which are not inherently inert. The results of our tests to date have shown that the coatings being used on the pipes containing high voltage feeders or carrying high pressure gas in New York are inherently inert. Microbiological tests should be required on the new synthetic materials before they are accepted for widespread underground use as jackets or coatings.

The authors of this paper have made a significant contribution to electrical engineering and it is hoped that the investigational work which they have done so capably can be continued to completion.

Kenneth S. Wyatt (Phelps Dodge Copper Products Corporation, New York, N. Y.): The authors have opened up a new field of study in electrical insulation. They have devised ingenious techniques for detecting the attacks of microorganisms and for observing their mechanisms. The paper is stimulating because it is a bright example of what can be done by able investigators by carefully conceived methods thoroughly executed.

Microbial attack of cable insulation appears widespread in the tropics. When in Caracas, Venezuela, three years ago, and on subsequent trips, I was puzzled by the failure of long lengths of 5-kv rubber cable in the foothills after only a year or two of service. The same thing happened at Mercedes several hundred miles southeast. The bitumenized Hessian finish on cable standing in the yard for six months or less would crumble to powder in the fingers. This and other considerations led me to the conclusion that the trouble was due to bacteria. I now began to look for these troubles as I travelled about. I found they were highly localized. Conditions of humidity, temperature, and pH value have to be just right. My limited observations indicated little or no trouble on the islands of Aruba or Curacao, which are volcanic with a surrounding coral formation. There is some trouble in Puerto Rico and Jamaica, and I believe Maracaibo is bad. I am considering not only microbial attack of buried cable but fungus attack of aerial cable.

Knowing what microbial attack looks like, one begins to observe cable troubles due to this cause in our own country in subtropical areas, such as Florida and the Gulf Coast. I have seen control cable troubles further north in power stations where temperature humidity (moist ducts) and pH were favorable.

As to materials, rubber was most vulnerable, although neoprene was reported attacked. Vinylite cannot be used because the plasticizer evaporates off in the hot tropical sun. Polyethylene was resistant to airborne fungi in Jamaica, and is believed resistant to soil bacteria.

For these tropical areas it begins to be clear that cable should be especially designed. It is useless to ship out jute coverings. Rubber must have special attention and protection. But we have to guard against not only soil bacteria and aerial fungi, but also against white ants and termites which will corrode through steel tapes and then drill the insulation; flying beetles which bore holes in the lead sheath; in lakes and rivers, teredos which riddle rubber, neoprene and vinylite; and greatly accelerated corrosion because of the high temperature. A rubber-insulated cable, shielded for the higher voltages but without cotton tapes, protected against borers by a soft untinned bronze tape quarter-lapped, and protected against bacteria and fungi (and against corrosion) by a continuous pigmented polyethylene sheath, would appear to answer the tropical cable problem.

In investigating susceptibility of insulating materials to soil bacteria and aerial fungi, there are pitfalls into which many have stumbled. The methods employed by the authors appear to me to have great merit.

Robert J. Wiseman (The Okonite Company, Passaic, N. J.): The authors of this interesting paper have added another item to the list of possible causes of failure of rubber-insulated cables, thereby removing another item from "cause unknown." We all have observed occasionally a failure of a rubber cable, and could not assign a cause after making check tests on the voltage breakdown of an adjacent sample, power factor tests and physical tests. We are indebted to the authors for reporting on their findings, yet we must be careful in drawing conclusions. We are in the early stages of this approach to the operation and life of rubber insulation and, therefore, must not be hasty in believing that because microorganisms attack some rubber insulations, we must abandon its use. We all know there are many millions of feet of rubber insulated cables in duct and directly buried which are giving excellent service. In a majority of cases we can determine the cause of a failure. If we could reivew past failures on the basis of attack by microorganisms, I venture to state that the percentage will be extremely small and, therefore, let us not get excited about it. Rather let us take advantage of this approach and try to learn more about its mechanism, such as: what kind of organisms attack rubber or rubber-like material? What are the kinds of so-called food that they like? Can we geographically determine where the attack is most likely to occur? We know during World War II that the South Pacific area was a nightmare to all kinds of materials due to bacteria action. Are warm localities more subject to attack than cooler climates? What is the effect of partially moist soil, that is, not bone dry and not water saturated? What is the degree of alkalinity necessary to get the greatest effect? Why,

according to the authors, do we get a pitting action on the surface of rubber insulation made with natural rubber and not with synthetic rubber? Apparently, it is not the pitting that will cause a failure, but the micropores that exist for both natural and synthetic rubbers. Therefore, neither is better than the other in resisting attack. The authors report that *GR-S* raw rubber showed attack, but after it was treated with acetone it showed a very high degree of resistance and the extract did show the microorganism could attack it. Does this mean it is necessary to treat all raw *GR-S* with acetone before usage? Imagine the cost! What effect does prior treatment on raw rubber have on its resistance to attack? Some cable manufacturers do not bother to wash the raw rubber before compounding. We, at Okonite do, as we consider it essential to obtain a uniform product. Perhaps we unconsciously have been carrying out some of the requirements for good resistance to microorganisms.

The authors suggest considerations be given to adding something—we will call it "*X*" to a rubber compound to overcome the effect of bacteria. Let us go slowly on this. As soon as the composition of a rubber compound is changed, its physical and electrical characteristics also are liable to change. So we can be worse off than what we are trying to correct. This effect cannot be evaluated in the laboratory under accelerated conditions, but must be watched in the field under operating conditions which takes years before reliable conclusions can be drawn.

The authors infer that because of their findings, natural rubber should be abandoned for synthetic rubber, because both natural and synthetic rubber showed micropores to occur and it is the latter that causes failure, principally, as I understand it, because they found pitting of the surface of natural rubber compounds. I am not in accord with their viewpoint. It is based on too little and doubtful evidence. Furthermore, it must be recognized that many years of excellent service experience with properly manufactured natural rubber insulated cables irrefutably testify to their worth, whereas cables made with synthetic rubber are only a few years old; in fact, actually since World War II because *GR-S* made during the war was far from a suitable material. The constant changing by some manufacturers of the composition of their synthetic rubber compounds before any worthwhile field experience has been obtained is puzzling. Years ago we went through these growing pains with natural rubber compounds. Some of us fared better than others. Today we furnish a long life, natural rubber insulation which can be subjected to all the variables that cables are prone to and it is known where we stand. I do not feel that this is true for synthetic rubber insulation. It appears that each year a new composition is proposed so that we are constantly in a state of hope or wishful thinking that we have a satisfactory rubber insulation.

Let us continue the study reported by the authors and we are indebted to them for reporting it to us, but it also is important that we do not draw hasty conclusions that we will regret later.

J. T. Blake, D. W. Kitchin, and **O. S. Pratt:** The experiments and findings described in the discussions of F. E. Kulman and K. S. Wyatt are valuable contributions to the general problem of protection against underground hazards. In this and our earlier paper[1] the study was confined to microbial attack on rubber and rubber-like materials. The extremely interesting description by Mr. Wyatt of the other hazards met in the tropics and the methods of overcoming them covers another aspect of the problem.

Dr. Wiseman's discussion presents several interesting points of view. We are in hearty agreement with some of these but not with others. In neither of our papers is there any recommendation that rubber be abandoned for underground use. Dr. Wiseman stresses the fact that failures from microbe attack in service have been very rare. In both papers, particularly in the earlier one, we emphasized strongly their infrequency and explained it.

Some of the questions asked by Dr. Wiseman about the effect of different environmental conditions are covered earlier in the paper. We have shown that failure of even such vulnerable insulation as thin natural rubber vulcanized latex was absent or greatly retarded in dry, flooded, or cold soil. Partially moist, fertile, neutral, or slightly alkaline soil is the most active in causing failure. The question about the likelihood of failure in various geographic regions is very well covered in Mr. Wyatt's interesting discussion.

The questions: "What kind of organisms attack rubber or rubber-like materials? What kinds of so-called food do they like?" are at least partially answered in our two papers. We found, as did several earlier investigators, that natural rubber can be consumed in bulk by certain bacteria, actinomycetes, or fungi. We have not observed so far any direct consumption of acetone extracted raw *GR-S* or butyl rubber, or of raw neoprene by any of the foregoing microorganisms. The so-called foods are the acetone soluble soaps, fatty acids, paraffin, and other waxes.

The question of why there is pitting on natural rubber insulation but not on synthetic rubber insulation, we believe to be explained in the section on the two types of microbial attack. The microbes can consume bulk natural rubber but not *GR-S* or butyl rubber. The experiment with acetone extracted raw *GR-S* demonstrated this fact. No suggestion was made that *GR-S* be acetone extracted for cable usage.

Dr. Wiseman's deduction that, because failure in a particular natural rubber sample occurred sooner by micropores than by pitting, neither natural nor synthetic rubber is better in resisting attack, is one with which we cannot agree in the light of our experimental results. There is no reason to suppose that the slower process of direct consumption of natural rubber is somehow arrested before failure.

A striking and practical illustration of the difference between natural rubber and *GR-S* insulation is given by the results on neoprene-jacketed wire samples of identical construction except that one set had natural rubber insulation, the other *GR-S* insulation.

The tests are described in the section on jacket protection and staggered imperfections. As stated, all ten natural rubber samples failed in soil in nine to 13 months. In the corresponding *GR-S* set the two unjacketed controls failed in 11 months and now are down five decades (21 months). Of the ten jacketed samples in soil nine are still normal at 21 months. Only one started to drop at 16 months, and this levelled off at three decades down where it has remained for the last four months. This is attributed to geometric protection which one would expect on statistical grounds. It is a fact that the minute vulnerable food streaks in the insulation and in the jacket coincide extremely seldom. With uniformly vulnerable natural rubber this geometric or statistical protection is completely absent. Since the *GR-S* samples had no added preventive and those without jacket failed drastically, it seems reasonable to ascribe the observed protection to the geometry.

Dr. Wiseman's warning to go slowly on the addition of preventives is quite in line with the final paragraph of our summary, except for his objection to accelerated laboratory tests. The development of inherently resistant compounds would be greatly retarded if we had to wait 15 to 20 years each time a new compound or preventive was tried.

Similar arguments could be advanced pro and con for all other accelerated laboratory tests. Very few research or development laboratories would consent to abandon such tests or give up a valuable tool in their constant striving to develop improved rubber insulating compounds.

REFERENCE

1. See Reference 1 of the paper.

Series-Connected Saturable Reactor with Control Source of Comparatively Low Impedance

H. F. STORM
MEMBER AIEE

Synopsis: The object of this analysis is to shed light onto the mechanics of magnetic-amplifier operation and to derive simple, and yet reasonably accurate, formulas. The analysis deals with the effects of various parameters, such as voltage, frequency, load resistance, and feedback. The various mathematical expressions are condensed into a nondimensional, normalized master graph which completely describes the steady-state operation of the magnetic amplifier under consideration. Speed of response and its relation to the gain are also investigated. The formulas and conclusions are verified by test data.

ONE FORM of magnetic amplifier uses saturable reactors whose load windings are connected in series. Besides other variables, operation of the magnetic amplifier is influenced by the relative magnitude of currents induced into the control windings from the load windings. These induced currents become larger as the outer control-circuit impedance decreases and therefore are largest when the outer control-circuit impedance is zero; conversely, for very high outer control-circuit impedance, the induced currents become practically zero. Consequently, the series-connected saturable reactor may be divided into one category where the outer control-circuit impedance is comparatively small (with respect to the referred load resistance), and another where the outer control-circuit impedance is relatively high. While the latter category has been analyzed in another paper of the author,[1] the following analysis deals with the case where the control-circuit impedance is very small. Such reactors are widely used in industry, for instance, in theater-lighting controls, speed controls, and voltage regulators.[2,3,4]

A rigorous analysis of saturable-reactor circuits becomes quite difficult due to the presence of nonlinear and multivalued functions. The following analysis relinquishes some rigor in return for a quicker and clearer understanding of the fundamentals. In addition, it permits the performance to be calculated simply and yet with a reasonable degree of accuracy. To this end, simplifications are made so that good agreement is obtained between theoretical calculations and actual test results. It should be kept in mind, however, that simplifications, by their very nature, result in solutions which are accurate only as long as the simplifications closely approximate real conditions. This reservation should be kept in mind when interpreting the results of this paper.

One approximation consists in reducing the hysteresis loop to a single-valued function; this is often permissible, if, as in our case, the core losses of the reactor are not considered. The wide present-day use of grain-oriented steels and other square-loop materials permits a further simplification since the magnetization characteristic can be represented by three straight lines,[5] Figure 1(A). If the magnetic intensities in the core of the saturable reactor are much larger than H_s (see Appendix for definitions of symbols), a further simplification is possible by reducing H_s to zero, resulting in the rectangular characteristic of Figure 1(B): this approximation becomes increasingly accurate with core materials of high differential permeabilities (50,000 gauss per oersted or more), as previously mentioned. Leakage reactance of the load windings is considered negligible in comparison with the load resistance. The resistance of the load windings, the feed-back windings, and the feed-back rectifier is included in the load resistance R_L, and the resistance of the control windings is lumped into the control-circuit resistance R_C. By premise, the control-circuit resistance R_C' is small with respect to the load resistance R_L, when referred to the same side of the saturable reactor.[6] The reverse current of the feed-back rectifier is to be assumed zero.

The magnetic amplifier described in the following consists of two magnetic circuits (Figure 2) arranged in such a manner that voltages of fundamental frequency and odd harmonics are cancelling each other in the control circuit.[7] The two magnetic circuits may consist of two separate units, A and B as shown, or they may be embodied in a 3- or 4-legged construction without change of basic performance. Each of the two units exhibits the essentials of a single-phase transformer: an iron core, one winding, $X1$-$X2$, connected as load winding; a second winding, $Y1$-$Y2$, used as control winding; and a third winding, $Z1$-$Z2$, used as feed-back winding. The load current i_L flows through load winding $X1$-$X2$ of unit A, from there through part of the rectifier, and into an ammeter which reads the average value I_L; then, depending upon the position of switch S, the current either flows directly through the remaining part of the rectifier, or if switch S connects points 7 and 8, the load current will flow first through the feed-back windings, $Z1$-$Z2$, of the two units A and B before emerging from the rectifier. From here the current flows through the load winding, $X1$-$X2$ of unit B, and into the load resistance R_L. Increasing the control voltage E_C will strengthen the

Paper 50-123, recommended by the AIEE Electronics Committee and approved by the AIEE Technical Program Committee for presentation at the AIEE Great Lakes District Meeting, Jackson, Mich., May 11-12, 1950. Manuscript submitted February 9, 1950; made available for printing March 20, 1950.

H. F. STORM is with the General Electric Company, Schenectady, N. Y.

control current I_C and result in a larger load current I_L. As will be shown later, control current and load current are proportional over a wide range and, therefore, this circuit is suitable for measurement purposes; within limits, this proportionality, which is a fundamental feature of saturable reactors, is obtained despite variations of line voltage, frequency, and load resistance.

The dots in Figure 2 signify winding polarities. A current is called positive when it flows through the winding in a direction away from the dot. The magnetomotive force F is called positive when derived from a positive current, and the positive direction is indicated by arrows F_A and F_B. The voltage across the winding is defined as positive when the terminal with the dot is more positive than the other terminal. The a-c supply voltage e is counted positive when the a-c bus with the dot is the more positive.

Voltage, Flux, and Current Wave Shapes

Let switch S be in the position shown in Figure 2 and consider the magnetic amplifier to be in steady-state operation. As will become clearer shortly, there is good reason to assume that at $\theta=0$ the flux ϕ_A in core A equals Φ_1 and the flux Φ_B in core B equals the saturation flux Φ_s, the operating point at this instant being right at the knee of the magnetization line, Figure 1(B). The line voltage e will cause a magnetizing current to flow through the load windings $X1$-$X2$ of units A and B. With a rectangular magnetization line, this current will be very small (theoretically zero) and, hence, its voltage drop in the load resistor is negligible. The voltage of point 4, therefore, is practically identical with the voltage of bus 5. Thus the line voltage is applied to the two units A and B in series, and because of the identity between units A and B, one-half of the line voltage will appear across $X1$-$X2$ of unit A and the other half across $X1$-$X2$ of unit B, Figure 3(D).

As a result of the application of the voltage $e/2$, a flux change $\phi_{\Delta,A}$ will now occur in core A

$$\frac{e}{2}=\frac{d\phi_{\Delta,A}}{dt}N_L10^{-8} \tag{1}$$

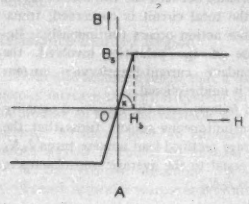

Figure 1 (left). (A). Magnetization line represented by three straight lines. (B). Rectangular magnetization line

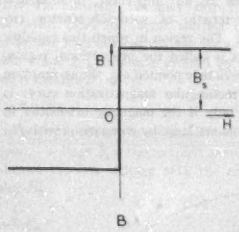

Figure 2 (below). Elementary circuit diagram of magnetic amplifier

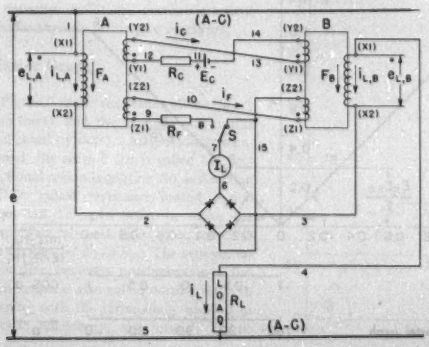

Figure 3 (right). Theoretical wave shapes of voltage, flux, and current

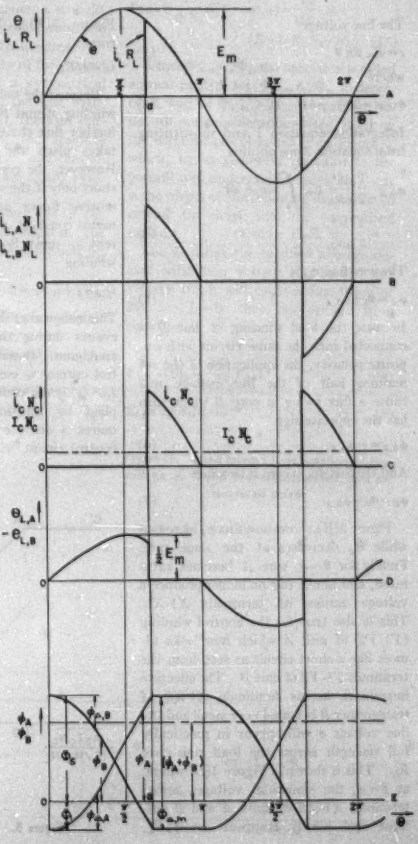

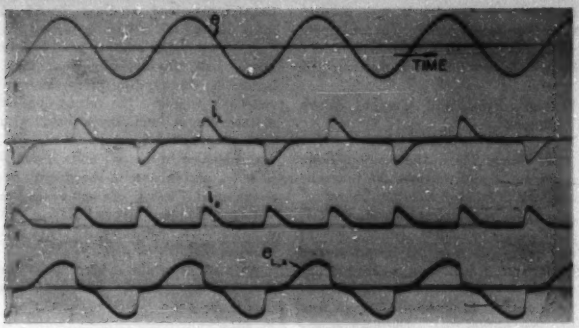

Figure 4. Oscillogram showing the wave shapes of line voltage e, load current i_L, control current i_C, and voltage $e_{L,A}$ across load winding of unit A

The line voltage

$$e = E_m \sin \theta \tag{2}$$

where

$$\theta = \omega t = 2\pi f t \tag{3}$$

Integrating equation 1 and substituting from equation 2 one obtains

$$\phi_{\Delta,A} = \frac{1}{2}\frac{10^8}{\omega N_L} E_m \int_0^\theta \sin\theta \, d\theta$$

$$= \frac{1}{2}\frac{10^8}{\omega N_L} E_m (1 - \cos\theta) \tag{4}$$

The core flux ϕ_A is

$$\phi_A = \Phi_1 + \phi_{\Delta,A} \tag{5}$$

Because the load winding of unit B is connected into the same circuit with opposite polarity, the application of the remaining half of the line voltage will cause a flux swing in core B which also has the opposite sign

$$\phi_{\Delta,B} = -\phi_{\Delta,A} \tag{6}$$

And the flux ϕ_B in core B becomes

$$\phi_B = \Phi_2 - \phi_{\Delta,A} \tag{7}$$

Figure 3(E) shows how flux ϕ_A increases while ϕ_B decreases at the same rate. Finally for $\theta = \alpha$, core A becomes saturated, and hence can no longer produce a voltage across its terminals $X1$-$X2$. This is also true for the control winding ($Y1$-$Y2$) of unit A which now looks almost like a short circuit as seen from the terminals $Y1$-$Y2$ of unit B. The effective impedance across terminals $X1$-$X2$ of transformer B becomes very small and the line voltage e will appear in practically full strength across the load resistance R_L. This is shown in Figure 3(D) where, at $\theta = \alpha$, the sinusoidal voltages across terminals $X1$-$X2$ of units A and B collapse and jointly reappear across R_L, Figure 3(A). The load current becomes

$$i_L = e/R_L \tag{8}$$

Because the voltage $e_{L,B}$ across the load winding of unit B is zero for $\alpha < \theta < \pi$, no further flux change (equations 1 and 6) takes place and ϕ_B remains constant. However, the core flux can remain constant only if the sum of all the magnetomotive forces acting on the core remains constant, which means that a current i_C must flow through the control winding

$$i_{L,B} N_L + i_C N_C = 0 \tag{9}$$

This is shown in Figures 3(B) and 3(C). The events during the next half-cycle are analogous. It will be seen that the control current i_C contains a d-c component I_C. This d-c component cannot be supplied by transformer action, but requires a discrete voltage source in the control circuit, $E_C = I_C R_C$. This last requirement is the closing link in the chain of events so far discussed.

The oscillogram of Figure 4 shows the close agreement between the theoretical wave shapes of Figure 3 and the actual observation.

The Law of Equal Ampere Turns (Proportional Region)

The phenomenon of equal but opposing ampere turns (equation 9) is closely related to the function of a-c transformers; however it differs from it by the fact that in the saturable reactor, this action takes place during only one half-cycle. However, there are two saturable reactors in the circuit, and while the transformer action takes place during only one half-cycle per core, this transformer action alternates between the two cores. As far as the total circuit is concerned, transformer action occurs continuously. Because of the polarities involved, the secondary current-transformer current (i_C) is unidirectional.

It follows from the numerical equality of instantaneous ampere turns that the average rectified-load ampere turns $I_L N_L$ are equal to the average control ampere turns $I_C N_C$.

$$I_C N_C = I_L N_L \tag{10}$$

This is an important fundamental characteristic of saturable-reactor circuits. The region in which this equality occurs is called the proportional region. As previously pointed out, the assumption of a rectangular magnetization curve is valid only if the magnetic intensities in the core are large by comparison with H_s.

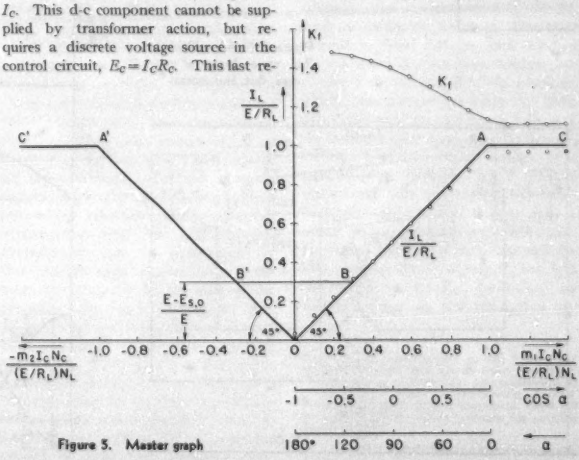

Figure 5. Master graph

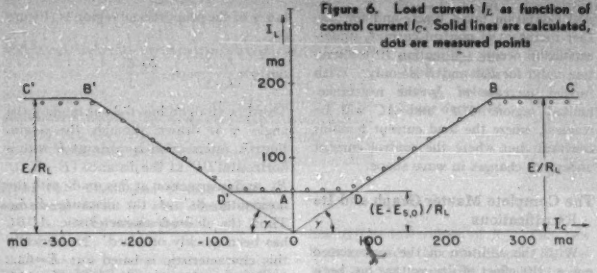

Figure 6. Load current I_L as function of control current I_C. Solid lines are calculated, dots are measured points

Therefore equation 10 and its ramifications should not be applied to the vicinity of $I_L N_L = 0$; for instance, for zero control ampere turns, the load current cannot become zero because this would require an infinite reactance, which cannot be realized.

Resistance-Limited Region

It will also become evident that a continuous increase of control current cannot produce an unlimited increase of load current. As shown later, an increase in control current I_C causes an increase of Φ_1 in the positive direction. When $\Phi_1 = \Phi_s$ each saturable reactor is saturated over π radians, which means that the total impedance of both load windings in series theoretically becomes zero. At this point (and for larger control currents), the load current reaches its maximum value $I_{L,m}$, which is limited by the load resistance R_L only:

$$I_{L,m} = E/R_L \tag{11}$$

This region is called the resistance-limited region. Voltage E is the rectified average value of the line voltage with the crest value E_m.

$$E = \frac{2}{\pi} E_m \tag{12}$$

Actually, maximum current is a little smaller because of air-core reactance.

Master Graph

Figure 5 shows the results of the theory (full lines), and the experimental results (indicated by dots). As previously mentioned, the section OA is called the proportional region (equation 10) and section AC is called resistance-limited region (equation 11). In order to make the graph general, both sides of equation 10 are divided by $N_L E/R_L$. The representation then becomes nondimensional and such graph is also called normalized. In keeping with the terminology applied to electric machinery, the ratio $I_L/I_{L,m}$ is called the per-unit load current, and the ratio $m_{1,2} I_C N_C/(I_{L,m} N_L)$ the per unit ampere turns, where m_1 or m_2 as defined later, and equal to unity for the case of no feedback. Then the relation between per unit ampere turns and per unit load current becomes a straight line, which for identical scales, subtends an angle of 45 degrees with the axes.

A reversal in the polarity of the control voltage E_C will produce a symmetrical characteristic $OA'C'$. In the case without feedback ($m_1 = m_2 = 1$), the load current depends only upon the absolute value of the control current, and characteristics OAC and $OA'C'$ are axially symmetrical.

In places where the power loss in the resistance R_L becomes of interest, the effective value $I_{L,eff}$ can be expressed by the form factor k_f

$$k_f = I_{L,eff}/I_L \tag{13}$$

of which experimental values are plotted in Figure 5.

The rectified average current becomes

$$I_L = \frac{1}{\pi}\int_\alpha^\pi i_L d\theta = \frac{1}{\pi}\frac{E_m}{R_L}\int_\alpha^\pi \sin\theta\, d\theta = \frac{1}{\pi}\frac{E_m}{R_L} \times (1+\cos\alpha) \tag{14}$$

where α is the angle of retard (Figure 3). From equation 12

$$I_L = \frac{E}{2R_L}(1+\cos\alpha) \tag{15}$$

and from equation 10

$$\cos\alpha = 2\frac{I_C N_C}{I_{L,m} N_L} - 1 \tag{16}$$

The angle of retard α and its cosine are plotted on separate axes in Figure 5.

Overexcitation and Overexcited Region

The maximum flux swing $\Phi_{\Delta,m}$, Figure 3(E), is obtained from equation 4, substituting $\theta = \alpha$ from equation 16, and from equation 12

$$\Phi_{\Delta,m} = \frac{10^8}{8fN_L} E(1-\cos\alpha) = \frac{10^8}{4fN_L} \times (E - I_C R_L N_C/N_L) \tag{17}$$

When $\Phi_{\Delta,m} = 2\Phi_s$, the operation is called normal excited, for $\Phi_{\Delta,m} < 2\Phi_s$, underexcited, and for $\Phi_{\Delta,m} > 2\Phi_s$, overexcited. So far, all our considerations were based on the wave shapes obtained from Figure 3, which, by its geometry, pertains to the normal and underexcited cases only. It is the object of the following discussion to extend the range into the overexcited region.

Let us define the rectified average no-load saturation voltage $E_{s,0}$ as the line voltage which will cause a flux swing of $2\Phi_s$, for $I_C = 0$, then one obtains from equation 17

$$\Phi_{\Delta,m} = 2\Phi_s = \frac{10^8}{4fN_L} E_{s,0} \tag{18}$$

$$E_{s,0} = 8f\,\Phi_s N_L\, 10^{-8} \tag{19}$$

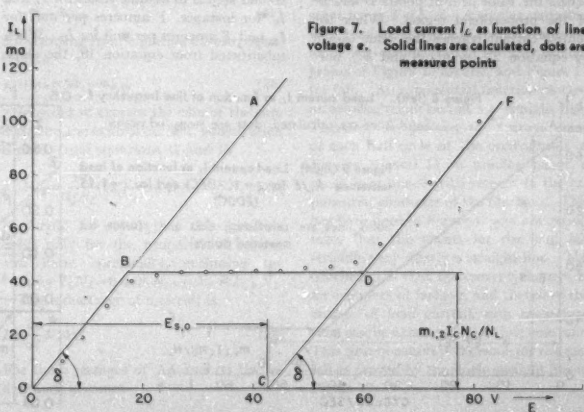

Figure 7. Load current I_L as function of line voltage e. Solid lines are calculated, dots are measured points

If the line voltage is raised above $E_{s,0}$ the saturable reactor may operate in a different fashion, depending on its degree of loading. Suppose $I_C=0$ and

$$E=\xi E_{s,0} \tag{20}$$

where ξ is called the per unit excitation. The flux swing $\Phi_{\Delta,m}$ cannot physically become larger than $2\Phi_s$, and therefore the reactor cannot hold a larger voltage than $E_{s,0}$ (equation 19). The balance $E-E_{s,0}$ is driving the minimum current $I_{L,\min}$ through the load resistance

$$I_{L,\min}=\frac{E-E_{s,0}}{R_L} \tag{21}$$

Increasing the control current from $I_C=0$ will not increase the load current $I_{L,\min}$ until the control current succeeds in producing a flux swing $\Phi_{\Delta,m}=2\Phi_s$ according to equation 17

$$\Phi_{\Delta,m}=\frac{10^8}{4fN_L}(E-I_CR_LN_C/N_L)=2\Phi_s$$

$$=\frac{10^8}{4fN_L}E_{s,0} \tag{22}$$

and

$$\frac{I_CN_C}{(E/R_L)N_L}=\frac{E-E_{s,0}}{E} \tag{23}$$

The control current can be increased from zero to the value of equation 23 without causing a change in the load current $I_{L,\min}$ of equation 21. This region is called the overexcited region, and its representation becomes a horizontal line $B'B$ in the normalized graph of Figure 5. The overexcited characteristic takes priority over the proportional characteristic $B'OB$.

During overexcited operation ($B'B$) the angle of retard α is constant and equals the value of α at points B and B' of the proportional region. When the control current reaches the value shown by equation 23 (points B and B'), normal excitation takes place, and for further increases of control current, underexcitation occurs. Equation 10 is therefore valid for BA and $B'A'$ only. With further increase of I_C the resistance-limited regions $C'A'$ and AC will be reached, where the load current remains constant, but where the control current undergoes changes in wave shape.

The Complete Master Graph and Its Ramifications

With the addition of the overexcited region, the effect of line voltage has been added to the normalized characteristic of Figure 5. Because $E_{s,0}$ is also a function of the line frequency (equation 19), the latter is thereby represented in the normalized graph (equation 21).

We see now that the operation of the saturable reactor is completely described by the per unit excitation ξ and the per unit ampere turns. These relations are of particular importance when model laws are to be evolved and when comparisons among different reactors are made. The normalized graph of Figure 5 embodies all circuit parameters (even feedback, to be discussed later) and therefore constitutes a master sheet from which the steady-state performance of the saturable reactor can be predicted for any set of circumstances.

Load Current Versus Control Current

Suppose the object is to predict the load current I_L as a function of the control current I_C, with line voltage, frequency, and load resistance remaining constant. The first step is to multiply the axes of Figure 5 by E/R_L. The second step is to assume scales for I_L and I_C, for instance, Y amperes per unit for I_L, and X amperes per unit for I_C. When substituted from equation 10, the slope $\tan\gamma$ of the proportional region is (Figure 6)

$$\tan\gamma=\frac{I_L/Y}{I_C/X}=m_{1,2}\frac{N_C}{N_L}\frac{X}{Y}$$

Third, a straight line OB subtending the angle γ is drawn through the origin. Fourth, intersection is made at D with a horizontal DD' at the distance $(E-E_{s,0})/R_L$, and intersection at B is made with the horizontal BC at the distance E/R_L. Thus the desired characteristic $ADBC$ has been quickly obtained. Numerically this characteristic is based on: $E=62.2$ volts, $E_{s,0}=42.8$ volts, $N_C=400$, $N_L=592$, $R_L=346$ ohms, $X=Y=0.1$ ampere per unit, $\tan\gamma=0.676$. A check by actual measurement has been made and the dots of Figure 6, representing the measured points, indicate the close agreement between calculation and observation.

Load Current Versus Line Voltage

The effect of line voltage on the load current is quite interesting. By freezing all parameters in the normalized graph except E, the load current I_L can be obtained by a geometric manipulation, which, because of its simplicity, is not further described. The practical procedure, however, is illustrated: Assume scales for I_L and E, for instance Y amperes per unit for I_L, and X volts per unit for E. The slopes of OA and CF (Figure 7) follow from

$$\tan\delta=\frac{1}{R_L}\frac{X}{Y}$$

The starting point C of CF is for $E=E_{s,0}$. A horizontal line BD is drawn at the distance $m_{1,2}I_CN_L/N_C$. The total characteristic is now $OBDF$. The line voltage can change theoretically by $E_{s,0}$ volts without causing a change in load current. This is an important feature in d-c measuring devices. The characteristic shown in Fig-

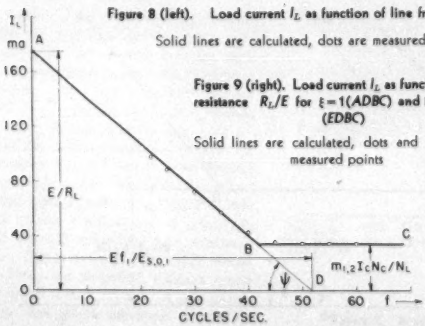

Figure 8 (left). Load current I_L as function of line frequency f

Solid lines are calculated, dots are measured points

Figure 9 (right). Load current I_L as function of load resistance R_L/E for $\xi=1$ (ADBC) and for $\xi=1.25$ (EDBC)

Solid lines are calculated, dots and crosses are measured points

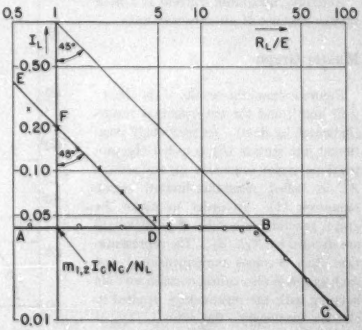

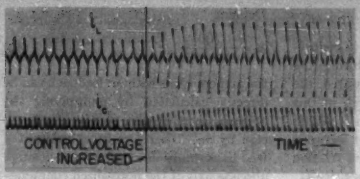

Figure 10. Oscillogram of load current I_L and control current I_C, when control voltage E_C was increased

Figure 11 (right). Oscillogram of load current I_L and control current I_C, when control voltage E_C was decreased

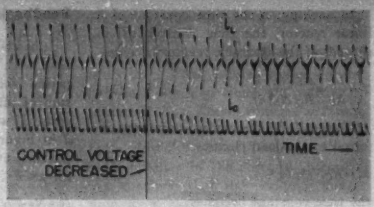

ure 7 is based on: $E_{s,0}=42.8$ volts; $N_C=400$; $N_L=592$; $R_L=395$ ohms; $I_C=64$ milliamperes; $X=20$ volts per unit; $Y=0.04$ ampere per unit; tan $\delta=1.266$. The dots in Figure 7 show measured points.

Load Current Versus Line Frequency

Next the effect of frequency on the load current will be demonstrated (Figure 8): Suppose the no-load saturation voltage $E_{s,0,1}$ is known for the frequency f_1, then point D on the abscissa axis has the value $Ef_1/E_{s,0,1}$. The straight line AD has a slope

$$\tan\psi=\frac{1}{R_L}\frac{E_{s,0,1}}{f_1}\frac{X}{Y}$$

with X cycles per second per unit and Y amperes per unit. Point A could alternatively be obtained from its ordinate value of E/R_L. Intersection at B is obtained by a horizontal line BC at the distance $m_{1,2}\ I_CN_C/N_L$, with $m_{1,2}\ I_CN_C/N_L$ not to exceed E/R_L. The total frequency characteristic is now ABC and it can be seen that an increase of frequency beyond point B will not change the load current. The characteristic of Figure 8 is based on: $E_{s,0,1}=42.8$ volts; $f_1=60$ cycles per second; $N_C=400$; $N_L=592$; $R_L=210$ ohms; $I_C=50$ milliamperes; $X=10$ cycles per second per unit; $Y=0.04$ ampere per unit; tan $\psi=0.849$. Again good agreement is obtained between the theoretical and measured points.

Load Current Versus Load Resistance

The effect of load resistance on the load current can also be derived from the normalized characteristic and can be conveniently plotted on log-log paper (Figure 9). The straight line $1C$ is inclined under 45 degrees with the axes. For $\xi\leq 1$ the load current is represented by the horizontal AB until intersection occurs with $1C$ at B; then, with increasing R_L, the load current declines along BC. For $\xi>1$ the load current follows another 45-degree line ED at low values of R_L. This new locus intersects the ordinate axis ($R_L/E=1$) at $1-1/\xi$ (point F); specifically for $\xi=1.25$, point F is at 0.2. Starting at low values for R_L, the load current decreases (ED) with increasing load resistance. Then the plateau DB is reached and the load current follows the pattern for $\xi\leq 1$ (DBC). We see that over a certain range, the load resistance does not affect the load current.

The theory has again been verified by measurements, and two cases are shown in Figure 9, one for $\xi=1$ and the other for $\xi=1.25$. $E_{s,0}=42.8$ volts; $f=60$ cycles per second; $N_C=400$; $N_L=592$; $I_C=60$ milliamperes. The measured points are indicated by dots for $\xi=1$ and by crosses for $\xi=1.25$. The minimum value for R_L is given by the resistance of the load windings. Good agreement between calculated and measured values has again been obtained.

Apparent Inductance

The sum of the core fluxes follows from equations 5 and 7

$$\phi_A+\phi_B=\Phi_1+\phi_{\Delta,A}+\Phi_s-\phi_{\Delta,A}=\Phi_1+\Phi_s \quad (24)$$

and is a constant quantity. Φ_1 is seen from Figure 3(B).

$$\Phi_1=\Phi_s-\Phi_{\Delta,m} \quad (25)$$

Substituting from equation 25 into equation 24

$$\phi_A+\phi_B=2\Phi_s-\Phi_{\Delta,m} \quad (26)$$

In order to express the sum of the core fluxes by the control current, substitution is made from equations 17 and 18

$$\phi_A+\phi_B=\frac{10^8}{4fN_L}(E_{s,0}-E+I_CR_LN_C/N_L) \quad (27)$$

It should be noted that this equation holds only for the proportional region, and more specifically, excluding the vicinity $I_LN_L=0$ and $m_{1,2}\ I_CN_C \geqslant I_{L,m}N_L$.

The inductance of a circuit is

$$L=\frac{d\phi}{di}N10^{-8} \quad (28)$$

For finite changes of $\Delta\phi$ and Δi the inductance becomes

$$L\doteq\frac{\Delta\phi}{\Delta i}N10^{-8} \quad (29)$$

Because of the average character of I_C, differences according to equation 29 should be introduced instead of differentials, and ΔI_C is considered averaged over 1/2 cycle. The apparent inductance of the control circuit follows from equations 27 and 29

$$L_C=\frac{\Delta(\phi_A+\phi_B)}{\Delta I_C}N_C10^{-8}=\frac{1}{4f}R_L\frac{N_C^2}{N_L^2} \quad (30)$$

One obtains the rather surprising result that the inductance of the control winding is proportional to the load resistance R_L and inversely proportional to the frequency, while the core permeability which is of paramount importance in linear reactors does not even appear in equation 30. For I_LN_L nearly zero, the actual operation of the saturable reactor is entirely different and equation 30 cannot be applied.

Time Constant

In the case of an ordinary linear inductance L connected in series with a resistor R, the sudden change in the driving voltage will cause an exponential variation of current with time, the time constant being $T=L/R$. A similar variation with time takes place in the saturable reactor as demonstrated by the oscillograms of Figure 10 for rise, and Figure 11 for fall. An exponential function plotted on semilog paper becomes a straight line. Therefore, by plotting the average value of each half-cycle of the oscillograms of Figures 10 and 11 on semilog paper, a check is obtained with respect to the exponential character of the function. This has been done in Figure 12 and one recognizes that the points for rise and fall straddle very closely a straight line. The conclusion is that the current changes in an exponential fashion, and therefore the change of load current with respect to time can be expressed by a time constant. This time constant is the same for rise and fall as proved by the single straight line of Figure 12.

In analogy to the time constant of a linear reactor, the time constant T in seconds of the saturable reactor becomes

$$T=\frac{L_C}{R_C}=\frac{R_L}{R_C}\frac{N_C^3}{N_L^2}\frac{1}{4f} \tag{31}$$

If we call R_C' the control resistance referred to the load circuit

$$R'=R_C N_L^2/N_C^3 \tag{32}$$

the time constant becomes

$$T=\frac{1}{4f}\frac{R_L}{R_C'}\text{ seconds} \tag{33}$$

One recognizes that the load resistance and control-circuit resistance affect the time constant in inverse manner: an increase in control circuit resistance speeds up the response, whereas an increase in load resistance slows down the response. The time constant is also inversely proportional to the frequency, becoming shorter with an increase of frequency. This fact can also be expressed by stating that the time constant measured in cycles depends on resistance ratio only

$$T=\frac{1}{4}\frac{R_L}{R_C'}\text{ cycles} \tag{34}$$

For the case shown in Figures 10 and 11 ($R_L=1{,}600$ ohms, $R_C=5.2$ ohms, $N_L=910$, $N_C=200$), T follows from equation 34 as 3.7 cycles; the measured value of T from Figure 12 is 3.8 cycles.

It should be pointed out that for time constants of less than one cycle, equation 34 becomes inaccurate and indicates too small values for T. Furthermore, equation 34 will yield too small results if the cores are not well saturated during part of the cycle. Such condition is encountered when the per unit load current is very small; under these circumstances the time constant may become many times larger than expressed by equation 34.

Feedback

It has been previously stated in connection with equation 9 that during the period when one core is unsaturated, the sum of all ampere turns is zero in this core. If we change the position of switch *2* in Figure 2 to make contact between points *7* and *8*, the ampere turn relation for $\alpha<\theta<\pi$ now becomes for positive i_C

$$i_{L,B}N_L+i_F N_F+i_C N_C=0 \tag{35}$$

The winding *Z1* and *Z2* are called feed-back windings and have N_F turns per winding. This case is illustrated in Figure 13.

If one assumes that the feed-back rectifier has no reverse current

$$i_F=-i_{L,B}=i_L \tag{36}$$

Hence

$$i_L(N_L-N_F)=i_C N_C \tag{37}$$

and in analogy to equation 10

$$I_L(N_L-N_F)=I_C N_C \tag{38}$$

With a positive control voltage E_C, the feed-back ampere turns are aiding the control ampere turns and hence this feed-back is called positive. It is well to recognize the very important fact that, with positive feedback, a much smaller control current is sufficient to obtain the same load current as without positive feedback.

When comparing the case with positive feedback to the case without feedback, the following relation between the control ampere turns of the two cases can be obtained from equations 10 and 38

$$(I_C N_C)_{\text{no feedback}}=(I_C N_C)_{\text{pos. feedback}}\times\frac{N_L}{N_L-N_F} \tag{39}$$

Defining

$$m_1=\frac{N_L}{N_L-N_F} \tag{40}$$

the ampere turns without feedback can be directly calculated by multiplying the ampere turns of the positive feedback case by m_1. Therefore by attaching the feed-back multiplier m_1 to the positive abscissa axis of the normalized characteristic (Figure 5), it also becomes valid for positive feedback. The case without feedback is characterized by $N_F=0$, in which case m_1 degenerates to unity.

By reversing the polarity of the control source E_C, core *A* will now be unsaturated for $\alpha<\theta<\pi$. In analogy to equation 35, we obtain

$$i_{L,A}N_L+i_F N_F+i_C N_C=0 \tag{41}$$

where

$$i_F=i_{L,A}=i_L \tag{42}$$

Hence

$$i_L(N_L+N_F)=-i_C N_C \tag{43}$$

Substituting average terms

$$I_L(N_L+N_F)=-I_C N_C \tag{44}$$

Disregarding the negative sign of $I_C N_C$, one recognizes that more control ampere turns are now needed with feed-back than without, and hence this feed-back is called negative. In analogy to the preceding, a feed-back multiplier m_2 is defined for negative feedback

$$m_2=\frac{N_L}{N_L+N_F} \tag{45}$$

By attaching the feed-back multiplier m_2 to the negative abscissa axis of the normalized characteristic (Figure 5) its range is extended into the negative feed-back range.

Figure 12 (below). Load current changes, obtained by averaging load current from Figures 10 and 11 over one half-cycle

Figure 13 (right). Theoretical wave shapes for ampere turns for positive feedback

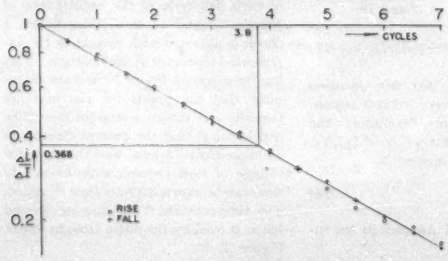

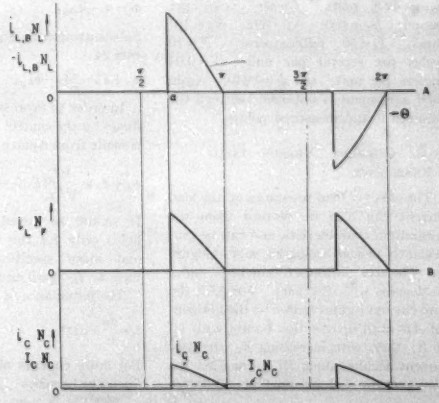

Because the characteristics in Figures 6, 7, 8, and 9 were derived directly from the master graph (Figure 5), it is obvious that Figures 6, 7, 8, and 9 also embody feedback. The positive feed-back multiplier m_1 is larger than unity and the negative feed-back multiplier m_2 is smaller than unity. In the characteristics shown in Figures 6, 7, 8, and 9, selection between m_1 and m_2 has to be made depending on whether the feedback is positive or negative, and the notation $m_{1,2}$ means either multiplier.

The effect of feedback is demonstrated in Figure 14 for the case of $N_F=400$, $N_L=592$, otherwise having the same parameters as the case I_L versus I_C. By comparison with Figure 6 (no feedback), the slope of the proportional region OB for positive feedback is $m_1 \cdot 0.676$ (in Figure 14) and the slope of the proportional region OA' for negative feedback is $m_2 \cdot 0.676$.

While the characteristics without feedback (Figure 6) are symmetrical with respect to the ordinate axis, the characteristics with feedback become unsymmetrical. For large values of m_1, the measured characteristic OB is shifted somewhat to the left of the theoretical position due to the finite magnitude of the magnetizing ampere turns (see Figure 5, vicinity of O) which are now amplified by the positive feed-back circuit, and also due to the width of the hysteresis loop.

If the reverse current in the feed-back rectifier is not zero, the current flowing through the feed-back winding is smaller than the load current. As a result the effective value of m_1 appears somewhat smaller than calculated from equation 40. For large values of m_1 the control ampere turns are small and become comparable to the magnetomotive force necessary to produce a given flux in the core. In this case, our assumption of infinite slope of the magnetization curve up to saturation flux density is no longer a valid assumption. The numerical accuracy of the various expressions will be lessened, but the general trend is still correctly reflected by equation 40: as the number of feed-back turns N_F is increased the gain of the saturable reactor is increased and may reach infinity. If the number of feed-back turns is increased beyond this point, snap action sets in and the saturable reactor behaves somewhat similar to a latch type relay.

Response with Feedback

The application of feedback also has a significant effect upon the response of the saturable reactor. The total flux swing $\Phi_{\Delta,m}$ (equation 17) now becomes

$$\Phi_{\Delta,m}=\frac{10^8}{4fN_L}(E-m_{1,2}I_C R_L N_C/N_L) \qquad (46)$$

and the apparent inductance L_C

$$L_C=m_{1,2}\frac{\Delta(\phi_A+\phi_B)}{\Delta I_C}N_C 10^{-8}=m_{1,2}\frac{R_L}{4f}\frac{N_C^2}{N_L} \qquad (47)$$

With the reservations set forth in the following paragraph the time constant in cycles becomes proportional to the multiplier $m_{1,2}$ and therefore it can be expressed by the following equation

$$T=m_{1,2}\frac{1}{4}\frac{R_L}{R_C''} \qquad (48)$$

In the preceding, where only two coupled circuits on each reactor were involved, the time constant for rise and fall is the same (Figure 12). With the application of feedback, a third winding is introduced and, in combination with the feed-back rectifier, transient currents can flow which have not been accounted for in the previous considerations.

Suppose positive feedback is applied and the control voltage is suddenly raised. By this action a voltage is induced in the feed-back windings which is positive at terminals Z_1. This voltage attempts to drive a current through the following path (Figure 2): *15-10-9-8-7-6*, but the circuit cannot be closed from *6* to *15* because of the blocking action of the rectifier. Thus, a transient current in the feed-back circuit cannot flow for a rise of control voltage, and therefore the expression of equation 48 for the time constant is applicable.

Now, let the control voltage E_C suddenly drop. This induces voltages in the feed-back windings which are positive at terminals Z_2. These voltages are now driving a transient current through the path: *15-6-7-8-9-10-15*, passing the feed-back rectifier in the forward direction. We conclude that the decaying flux is now interlinked with two windings in parallel, namely the control winding and the feed-back winding. As seen from the core, the resistance of the control winding has been reduced by paralleling it with the resistance of the feed-back winding, referred to the control winding. The effect of this apparent reduction of R_C' is an increase of the time constant (equation 48) for the fall direction. One concludes that in the presence of feedback two different time constants exist for rise and fall. For positive feedback and rise, $R_C''=R_C'$ (equation 32); for fall, R_C'' is equal to R_C' and R_F' in parallel, where

$$R_F'=R_F\frac{N_L^2}{N_F^2} \qquad (49)$$

A portion of the rectifier forward resistance should be included in R_F.

For negative feedback (region OA', Figure 14) a rise in negative control voltage will cause a transient current through the feed-back circuit and therefore R_C'' equals the parallel connection of R_C' and R_F'. For a drop of negative control voltage, the double interlinkage is prevented by rectifier blocking and therefore $R_C''=R_C'$.

As in the case without feedback, equation 48 does not hold for very small per unit load current. In this region the response is delayed to a far greater measure than expressed by equation 48.

When operated in the overexcited region (DD' in Figures 5, 6, and 14), no change in net flux occurs, and therefore the response is practically instantaneous.

Figure 14. Load current I_L as function of control current I_C with feedback

Solid lines are calculated, dots are measured points

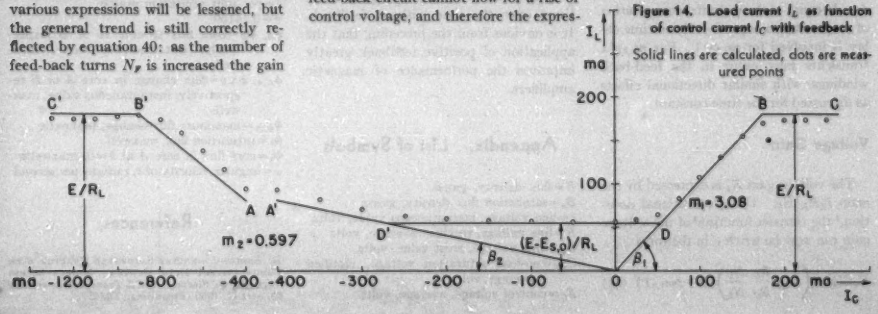

Rectifier Rating

The current rating of the feed-back rectifier is determined by the magnitude of the load current I_L. The voltage rating is determined by the peak-inverse voltage. Suppose the load current is flowing at this moment from *2* (Figure 2) to *6*, through the instrument, *7-8*, feed-back windings, and *15* to *3*. The current flowing from *6* to *3* causes voltage drops in the resistance of the various components just listed and also in the leakage reactance of the feed-back windings. These voltage drops appear as peak inverse voltage on the rectifier cell between *6* and *3*, and an equal amount between *15* and *2*. It will be observed that these voltage drops are small in comparison with the line voltage. In order to make the a-c component of i_C, see Figure 13, flow through the control circuit with its resistance R_C, an alternating voltage must be induced in the control windings. The feed-back windings are linked in the same way as the control windings, and therefore the alternating voltages are also induced in the feed-back winding. The net peak inverse voltage across the rectifier is obtained by the joint action of the voltage drops and induced voltages. Practically, this net peak-inverse voltage is usually very small by comparison with the line peak voltage and therefore a single selenium rectifier cell in each branch of the bridge rectifier is often sufficient where the line voltage is 115 volts rms. One recognizes that the rating, size, and cost of the feed-back rectifier will be only a fraction of the power rating of the magnetic amplifier.

Current Gain

It is defined by

$$K_i = \frac{I_L}{I_C} = m_{1,2}\frac{N_C}{N_L} \tag{50}$$

as can be verified from equations 38 and 44. Because of the instantaneous relation of ampere turns (equation 9), no time delay is involved for $m_{1,2}=1$. For $m_{1,2}\neq 1$ transients may occur in the feed-back windings, with similar directional effects as discussed for the time constant.

Voltage Gain

The voltage gain K_e is expressed by the ratio $I_L R_L/E_C$. Using operational notation,[8] the transfer function[9] of the voltage gain can now be written in the form

$$K_e G(p) = \left(m_{1,2}\frac{R_L}{R_C}\frac{N_C}{N_L}\right)/(1+pm_{1,2}T) \tag{51}$$

It should be pointed out that the multiplier $m_{1,2}$ affects gain and effective time constant in the same manner.

Power Gain

This gain is defined as the ratio of output power over control power

$$K_p = \frac{I_L^2 R_L k_f^2}{E_C I_C} = \frac{I_L}{I_C}\frac{I_L R_L}{E_c}k_f^2 = K_i K_e k_f^2 \tag{52}$$

Substituting from equations 51, 52, and 32

$$K_p = m_{1,2}^2 k_f^2 R_L/R_C' \tag{53}$$

The application of positive feedback increases the steady-state power gain to m_1^2 times. The effective time constant is increased to m_1 times; it should be remembered that the time constants T are different for rise and fall, and therefore two different values for the time constant T exist. The following remarks are directed to the rise of positive control voltage.

A speed-up of response can be obtained by placing an external resistance in series with the control winding, thus effectively increasing R_C. The result is a reduction of time constant and a proportional reduction of power gain.

If a saturable reactor is supplied with positive feedback m_1, and at the same time an external resistor is placed in series with the control winding such that the total control-circuit resistance becomes $m_1 \cdot R_C$, the time constant of the saturable reactor remains the same

$$m_1 \frac{R_L}{m_1 R_C'}\frac{1}{4f} = T \tag{54}$$

Under these circumstances the power gain K_p of the saturable reactor is

$$K_p = m_1^2 k_f^2 R_L/R_C' m_1 = m_1 k_f^2 R_L/R_C' \tag{55}$$

Comparing the saturable reactor without feedback to the one with feedback, we see that for equal time constants, the positive feedback results in a power gain of m_1 times over the case without feedback. It is obvious from the preceding that the application of positive feedback greatly improves the performance of magnetic amplifiers.

Appendix. List of Symbols

B = flux density, gauss
B_s = saturation flux density, gauss
e = line voltage, instantaneous value, volts
E = line voltage, rectified average, volts
E_m = line voltage, crest value, volts
$E_{s,0}$ = no-load saturation voltage, rectified average, volts
E_C = control voltage, average, volts
E_C' = control voltage referred to load winding, average, volts
$e_{L,A}, e_{L,B}$ = voltage across load winding A or B respectively, instantaneous value, volts
f = line frequency, cycles per second
F_A, F_B = magnetomotive force in core A or B respectively, gilberts
$G(p)$ = a function of p
H = magnetic intensity, oersted
H_s = magnetic intensity at which saturation flux density occurs, oersted
i_L = load current, instantaneous value, amperes
I_L = load current, rectified average, amperes
$I_{L,m}$ = maximum load current, rectified average, amperes
$I_{L,min}$ = smallest possible load current, average, amperes
$I_{L,eff}$ = load current, rms, amperes
$i_{L,A}, i_{L,B}$ = current in load winding A or B respectively, instantaneous value, amperes
i_C = control current, instantaneous value, amperes
I_C = control current, average, amperes
i_F = current in the feed-back winding, instantaneous value, amperes
I_F = current in the feed-back winding, average, amperes
K_e = voltage gain, unity
K_i = current gain, unity
K_p = power gain, unity
k_f = form factor, unity
L = inductance, henrys
L_C = apparent inductance of complete control circuit, henrys
m_1 = feed-back multiplier for positive feed-back, unity
m_2 = feed-back multiplier for negative feed-back, unity
$m_{1,2}$ = either feed-back multiplier, unity
N_C, N_L, N_F = number of turns of one control winding, one load winding, and one feed-back winding, respectively
p = operator d/dt
R_L = load-circuit resistance, ohms
R_C = control-circuit resistance, ohms
R_C' = R_C referred to load winding, ohms
R_F = resistance of feed-back circuit, ohms
R_F' = R_F referred to loading winding, ohms
R_C'' = effective resistance of control windings and feed-back windings during transient operation, as seen from load winding, ohms
t = time, seconds or cycles
T = time constant, seconds or cycles
α = angle of retard, degrees or radians
θ = electrical angle, degrees or radians
ξ = per unit excitation, unity
π = 3.14159
ϕ_A, ϕ_B = core flux in core A or B respectively, instantaneous value, maxwells
$\phi_{\Delta,A}$, $\phi_{\Delta,B}$ = flux change in core A or B respectively, instantaneous value, maxwells
$\Phi_{\Delta,m}$ = maximum flux change, maxwells
Φ_s = saturation flux, maxwell
Φ_1 = core flux in core A at $\theta=0$, maxwells
ω = angular velocity of θ, radians per second

References

1. Series-Connected Saturable Reactor with Comparatively High Control Source Impedance, H. F. Storm. *AIEE Transactions*, volume 69, part II, 1950 (*Proceedings T0205*).

2. Theory of D-C Excited Iron-Core Reactors and Regulators, **A. Boyajian.** *AIEE Transactions*, volume 43, June 1924, pages 919–36.

3. Saturable Reactors for Automatic Control, **W. D. Cockrell.** *Electronic Industries* (New York, N. Y.), December 1948, page 48.

4. The Application of the Saturable Reactor in Modern Engineering (translated from Russian), **L. A. Bessonov.** *Elektrichestvo* (Moscow, Union of Soviet Socialist Republics), number 5, 1948, pages 7–21.

5. Mathematical Analysis of Non-Linear Circuits, **A. Boyajian.** *General Electric Review* (Schenectady, N. Y.), 1931, pages 531–37, 745–51.

6. Magnetic Circuits and Transformers (book), **Massachusetts Institute of Technology Staff.** John Wiley and Sons, Inc., New York, N. Y., 1945, page 271.

7. Some Fundamentals of D-C Controlled Reactors with Resistive Load, **H. F. Storm.** *AIEE Transactions*, volume 68, part I, 1949, pages 188–94.

8. Heaviside's Operational Calculus (book), **E. J. Berg.** McGraw-Hill Book Company, Inc., New York, N. Y., 1936, page 164.

9. Principles of Servomechanisms (book), **G. S. Brown, D. P. Campbell.** John Wiley and Sons, Inc., New York, N. Y., 1948, page 84.

10. An Analysis of Transients in Magnetic Amplifiers, **D. W. VarPlanck, L. A. Finzi, D. C. Beaumariage.** *AIEE Transactions*, volume 69, part I, 1950, pages 498–503.

11. Magnetic Amplifiers, **A. G. Milnes.** *Proceedings*, Institution of Electrical Engineers (London, England), June 1949, volume 96, part II, pages 329–38.

12. A Theoretical and Experimental Study of the Series-Connected Magnetic Amplifier, **H. M. Gale, P. D. Atkinson.** *Proceedings*, Institution of Electrical Engineers (London, England), June 1949, volume 96, part II, pages 349–54.

13. An Analysis of Transients and Feedback in Magnetic Amplifiers, **Walter C. Johnson, Frank W. Latson.** *AIEE Transactions*, volume 69, part I, 1950, pages 604–12.

No Discussion

Effects of Supply Line Unbalance on the Filtered Output Ripple of Polyphase Rectifiers

C. K. HOOPER
ASSOCIATE AIEE

C. H. McADIE
ASSOCIATE AIEE

RECTIFIERS are often used when direct currents are obtained from a-c sources. Some of these d-c loads require a minimum of ripple in the applied voltage. This is particularly true in the case of electronic communication equipment, for example broadcast transmitters. Output filters in the direct current are practically always used in these cases, as the inherent ripple normally present in the output of rectifiers is too great to be tolerated.

For the larger loads, polyphase rectifiers are preferred to single-phase rectifiers. One of the reasons for this is that the d-c voltage at the output of a polyphase rectifier has a lower value of a-c component than in the d-c output of a corresponding single-phase rectifier. Another advantage of the polyphase rectifier is that the lowest frequency of a-c component in the direct current is normally higher than for a single-phase rectifier.

The inherent condition of low-ripple voltage and high-ripple frequency simplifies the filtering problem. The results of this can readily be observed by comparing the filter components of a polyphase rectifier with those of a single-phase rectifier of the same rating and output ripple. The filter components used with the polyphase rectifier are much smaller. But, in the case of a polyphase rectifier, if the a-c supply line voltages are not exactly balanced, then additional components of ripple voltage will be present in the d-c output and these added components will have a frequency lower than that normally present when the a-c supply voltages are balanced.

In most power distribution systems in use today, the polyphase voltages are quite well balanced. Any slight unbalance which may exist is therefore frequently ignored in the design and application of polyphase rectifiers. However, particularly in the case of rectifiers having filtered output, the effects of line unbalance, even of the small amounts commonly encountered, are such as to often result in unsatisfactory rectifier performance. In particular, the magnitude of the ripple voltage in the d-c output may be much higher than expected.

As an example standard *TR-101-A* published by the Radio Manufacturers Association (RMA)[1] states in paragraph 16b(2) that . . . "for 3-phase power supplies the full load voltage from phase-to-phase shall be within 2 per cent of the average of the three phases. . ." The radio transmitter performance is expected to comply with all operating standards under these conditions of supply line unbalance. This same requirement also appears in RMA standard *TR-104* for Electrical Performance of Television Broadcast Transmitters.[2]

Polyphase rectifiers using filters of the types commonly required in broadcast service will show a marked increase in output ripple voltage as the line unbalance changes from 0 to the 2 per cent limit permitted by the RMA standards. Actually the amplitude of the ripple voltage may increase over 400 per cent as the line unbalance increases from 0 to 2 per cent. It therefore can be seen that the effects of line unbalance of even small amplitude should not be neglected in polyphase rectifier filter designs.

The following discussion applies specifically to 3-phase double-way rectifiers. However, the same equations and curves also apply to 6-phase single-way rectifiers. Most applications requiring polyphase filtered power supplies use either of these two types of rectifier circuits. Methods of determining the effect of line unbalance on the output ripple of a filter rectifier are given. The required filter modifications also can be determined should it be desired to overcome the effects of line unbalance. The relative amplitude of the original ripple component and that of the lower frequency component resulting from line unbalance also can be determined readily for various values of line unbalance.

A conventional circuit of a 3-phase double-way rectifier having a single section choke input filter is shown in Figure 1. The direct voltage appearing in the output of a 3-phase double-way rectifier without being filtered is shown in Figure 2. The solid line shows the envelope of the direct voltage. This envelope is not a straight line but is seen to consist of periodic pulsations each of equal amplitude and similar shape. The lowest frequency component of these pulsations is six times the supply line frequency and the rms amplitude of this lowest frequency component is 4.04 per cent of the average direct current. This relationship is well known and is derived in standard texts on this subject.[3] Figure 3 is an oscillogram of the unfiltered rectified output obtained with a balanced supply. Figure 4 is similar to Figure 2 except that the a-c supply voltage is shown as unbalanced. In this case it can be seen that while the d-c envelope contains pulsations as before, the successive pulsations are no longer identical. As an approximation, the variations in successive pulsations can be represented as

Paper 50-125, recommended by the AIEE Electronic Power Converters Committee and approved by the AIEE Technical Program Committee for presentation at the AIEE Great Lakes District Meeting, Jackson, Mich., May 11-12, 1950. Manuscript submitted February 9, 1950; made available for printing March 24, 1950.

C. K. HOOPER and C. H. McADIE are both with the Westinghouse Electric Corporation, Baltimore, Md.

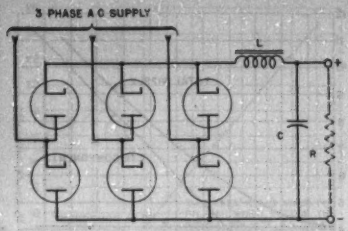

Figure 1 (left). Diagram of a 3-phase double-way rectifier with a single section low pass filter

Figure 2 (right). Envelope of 3-phase double-way rectifier output voltage with balanced supply line

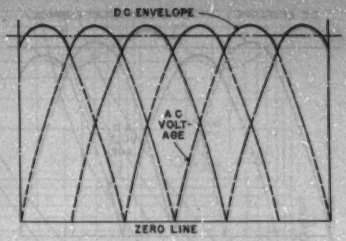

the equivalent of uniform pulsations plus a superimposed pulsation of lower frequency as shown by the dotted line. This lower frequency pulsation is seen to have a frequency of two times the supply line frequency. Also the amplitude of this lower frequency component can be seen to vary with the amount of line unbalance being zero for a balanced line. Figure 5 is an oscillogram of the unfiltered rectified output obtained with an unbalanced supply.

The relationship between the amplitude of this double frequency component and amount of unbalance is given in equation 4 of the Appendix. (The development of this equation and those which follow are given in the Appendix. The numbers of equations in this section refer to similar equations appearing in the Appendix.)

$$E_{2p} = K \tag{4}$$

where E_{2p} is the rms amplitude of the $2fo$ component in per cent of direct voltage, K is the amount of line unbalance expressed in per cent, and fo is the frequency of the supply line.

The curves on Figure 6 show the $2fo$ and $6fo$ components of ripple in the output of a 3-phase double-way rectifier as a function of line unbalance. The combined value of the $2fo$ and $6fo$ component also is shown as this same figure.

If the supply line is balanced, the relationship between the filter constants and the desired output ripple amplitude can be expressed by

$$E_{4a} = \frac{4.04}{(6\times 2\pi fo)^2 LC - 1} = \text{output ripple voltage (rms, in per cent of the average direct voltage)} \tag{7}$$

where

fo = supply line frequency
L = inductance in henrys
C = capacity in farads

Higher frequency components are appreciably smaller and can be neglected in this over-all rms relationship: Now if the a-c supply line voltage is unbalanced there will then be present in the d-c output a ripple component E_{2a} of frequency $2fo$ and this will be in addition to the output ripple E_{4a} of frequency $6fo$.

E_{2a} is determined as follows

$$E_{2a} = \frac{K}{(2\times 2\pi fo)^2 LC - 1} = 2fo \text{ component of output rms voltage resulting from line unbalance. (Expressed as a per cent of the average direct voltage)} \tag{8}$$

The basis $6fo$ component is unaffected by the amount of line unbalance and the resulting rms output ripple is the combined total of E_{4a} and E_{2a}.

Let the ratio

$$N = \frac{E_{1a}}{E_{4a}}$$

where E_{1a} is ratio of total output ripple voltage under conditions of line unbalance to the output ripple under conditions of balanced line. Approximately, for conditions applying when the output is well filtered this ratio N can be expressed by

$$N = \sqrt{5(K)^2 + 1} \tag{12}$$

It is thus seen that the increase in output ripple in terms of the ripple existing under balanced conditions is dependent only on the degree of unbalance. The supply line frequency and the filter constants have no effect on this relationship. Figure 10 shows this relationship in curve form. For example, it can be seen that for a 2 per cent unbalance, the resulting output ripple is 4.5 times the value which would be obtained with a balanced supply.

Figures 7, 8, 9 are oscillograms showing the filtered output for various amounts of unbalance. Since all oscillograms were taken to the same scale it will be seen that a large increase in ripple results from a comparatively small increase in unbalance.

The curve shown on Figure 10 also can be used to determine how much additional filtering is required to overcome the effect of a given amount of supply unbalance. For example, assume that an output ripple of 0.05 per cent maximum is required for all values of line unbalance up to 3 per cent. From Figure 10 it is seen that at 3 per cent line unbalance the ripple amplitude is 6.7 times as great as for zero unbalance. Thus a filter must be designed which will limit the ripple to 0.05/6.7 or 0.0075 per cent at zero unbalance. From fundamental relationships or from filter calculation charts[4,5] it can be determined that the inductance-capacitance product to give 0.0075 per cent ripple is 100 for a 60-cycle supply. That is the product of the inductance in henrys, times the capacity in microfarads, must equal at least 100. For balanced line conditions, however, the inductance-capacitance product corresponding to 0.05 per cent ripple is only 16. Thus, since the size and cost of a filter is roughly proportioned to its inductance-capacitance product, then a 3 per cent line unbalance is seen to require about 100/16 or 6.3 times as much filter.

As the line unbalance increases, the percentage of $2fo$ component in the filtered output increases rapidly in comparison with the basic $6fo$ component. For example, an unbalance of 1 per cent will result in the $2fo$ component being about 90 per cent, and the $6fo$ component being about 40 per cent of the total output ripple. Figure 11 shows in curve form the distribution of the $2fo$ and $6fo$ components for various values of line unbalance. The relationship expressed in equation 12 and Figure 10 is approximate only. It is, however, reasonably accurate whenever filters having comparatively large attenuations are used. When filters of moderate or small attenuations are used the curve becomes less accurate. For example: if a filter having an inductance-capacitance product

Figure 3. Oscillogram of unfiltered 3-phase double-way rectifier output voltage with balanced supply line

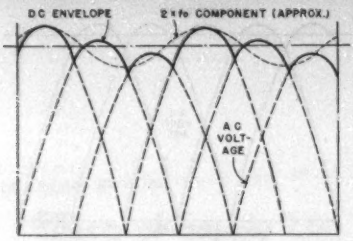

Figure 4 (left). Envelope of unfiltered 3-phase double-way rectifier output voltage with unbalanced supply line

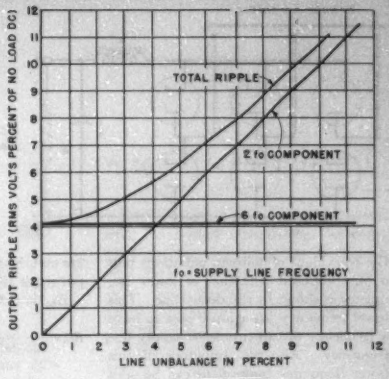

Figure 6 (right). Output ripple voltage from a 3-phase double-way rectifier as a function of line unbalance

of 15 is used with a 60-cycle supply, then the approximate methods give an output ripple of 0.0525 per cent for a balanced line and 0.24 per cent for a 2 per cent line unbalance. If a more accurate analysis is made the output ripple under balanced conditions is 0.053 per cent and 0.27 per cent for 2 per cent unbalance. The error resulting from the use of approximate methods is seen to be small in this case and can usually be neglected.

Consider, however, a filter having an inductance-capacitance product of three with a 60-cycle supply. In this case the approximate methods give an output ripple under balanced line conditions of 0.26 per cent and for a 2 per cent line unbalance, 1.20 per cent. However, if a more accurate calculation is made, the corresponding ripple amplitudes are 0.28 per cent for balanced conditions and 2.85 per cent for a 2 per cent unbalance. For the filter combinations assumed in the later case, the discrepancy between the values obtained by approximate methods and those obtained by more accurate methods are probably too great for practical use. This is particularly true when line unbalance conditions exist.

As a practical consideration, however, in most cases where filtered direct current is required, the effectiveness of the filter is usually large enough so that the Figure 10 can be used with reasonable accuracy.

Figure 12 shows the value of output ripple as affected by the size of the filter components and for several values of supply line unbalance. This curve is more limited in scope and is less convenient to use than the curve shown in Figure 10. However, if because of small filter requirements the assumptions upon which Figure 10 is based are not valid, then a more correct result can be obtained from Figure 12.

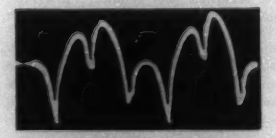

Figure 5. Oscillogram of unfiltered 3-phase double-way rectifier output voltage with 2.7 per cent line unbalance

Appendix

Ripple measurements made on a 3-phase double-way test rectifier with a harmonic analyzer indicate that the amount of $2fo$ components varies linearly with line unbalance. It can be represented by

$$E_2 = 1.35 \times \frac{K}{100} \times E_{avg} \qquad (1)$$

where

E_{avg} = rms line-to-line voltage (average of the three line-to-line values)
K = per cent maximum deviation from E_{avg}
E_2 = $2fo$ ripple rms volts
fo = supply line frequency

In order to put this in terms of the no load direct voltage, the following standard relations between the input alternating voltage and output direct voltage of a 3-phase double-way rectifier are used

$$E_{dc} = 1.35 E_{avg} \qquad (2)$$

$$\therefore E_2 = \frac{K}{100} E_{dc} \qquad (3)$$

or dividing by E_{dc} and multiplying by 100 to get E_2 as a percentage of the no-load d-c voltage.

$$E_{2p} = K \qquad (4)$$

where E_{2p} is the rms amplitude of the $2fo$ component in per cent of the direct current.

The amplitude of the $6fo$ component was found by the harmonic analyzer to remain essentially constant for varying amounts of line unbalance, therefore is the same as the theoretical amount at zero line unbalance.

$$E_{6p} = 4.04 \text{ per cent} \qquad (5)$$

where E_{6p} is the rms amplitude of the $6fo$ component in per cent of the no load direct current.

The total rms ripple is made up of a combination of the $2fo$ and $6fo$ components which since they are of different frequencies combine to give

$$E_t = \sqrt{E_{2p}^2 + E_{6p}^2} = \sqrt{16.4 + K^2} \qquad (6)$$

E_t = total rms ripple amplitude as a per cent of the d-c voltage.

Effects of Filtering

If a filter is used of a type shown in Figure 1, the amplitude of the output ripple with a

Figure 7. Oscillogram of the filtered output of a 3-phase double-way rectifier with balanced supply line

Figure 8. Oscillogram of the filtered output of a 3-phase double-way rectifier with 0.7 per cent line unbalance

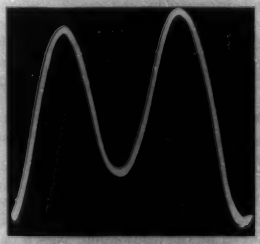

Figure 9. Oscillogram of the filtered output of a 3-phase double-way rectifier with 14.0 per cent line unbalance

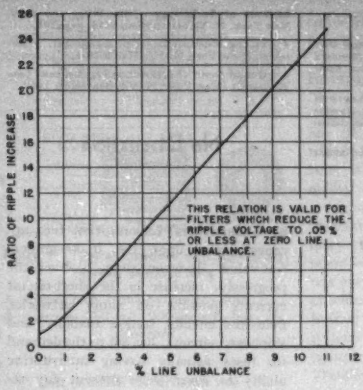

Figure 10 (left). Ratio of ripple voltage increase in the filtered output of a 3-phase double-way rectifier as a function of line unbalance

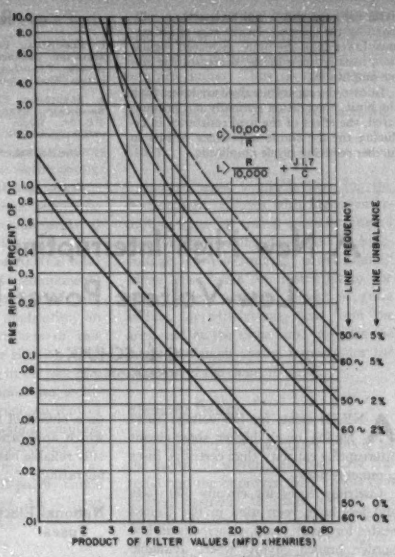

Figure 12 (right). Output ripple from a single stage low pass choke input filter used with a 3-phase double-way rectifier as a function of filter constants

balanced supply line is attenuated and is given[2] by

$$E_{4a} = \frac{4.04}{(6\times 2\pi fo)^2 LC - 1} \tag{7}$$

where

E_a = the rms amplitude of the $6fo$ component as a per cent of d-c voltage
L = the inductance in henrys
C = the capacity in farads
$R > 1/(2\times 2\pi foC)$

If the supply line is unbalanced then an additional component of ripple appears in the output of the filter and its amplitude is given by

$$E_{2a} = \frac{K}{(2\times 2\pi fo)^2 LC - 1} \tag{8}$$

where E_{2a} = the rms amplitude of the $2fo$ component in terms of d-c voltage.

As a simplifying approximation, if $(2\times 2fo)^2 LC$ is large compared with one, then E_{4a} and E_{2a} can be combined in a manner similar to equation 6 to give

$$E_{1a} = \frac{1}{(2\times 2\pi fo)^2 LC} \times \sqrt{K^2 + \left(\frac{4.04}{9}\right)^2} \tag{9}$$

where E_{1a} is the rms amplitude of the total output ripple as a per cent of the direct voltage.

If the filter under balanced conditions is effective in reducing the ripple to 0.05 per cent or less (a value commonly used in electronic applications) then the values obtained from equation 9 are accurate to within about 10 per cent.

Equation 9 simplifies to the following for 60-cycle and 50-cycle cases.

$$E_{1a(60\ cy)} = \frac{1.79}{LC'} \sqrt{K^2 + 0.2} \tag{10}$$

L = inductance of filter choke in henrys
C' = capacitance of filter capacitor in microfarads

$$E_{1a(50\ cy)} = \frac{2.54}{LC'} \sqrt{K^2 + 0.2} \tag{11}$$

By dividing equation 9 by itself with K, set equal to zero we obtain the ratio of increase in filter output ripple with increases in line unbalance.

$$N = \frac{E_{1a}}{E_{4a}} = \sqrt{\frac{K^2 + 0.2}{0.2}} = \sqrt{5(K)^2 + 1} \tag{12}$$

This equation is plotted as Figure 10.

It should be noted that the actual filter values and line frequency disappear from this relation, thus giving the ratio of increase in filter output ripple as a function of line unbalance only.

A simple relation between $2fo$ and $6fo$ components is obtained by dividing equation 7 by equation 8

$$\frac{E_{2a}}{E_{4a}} = \frac{9}{4.04} K = 2.23K$$

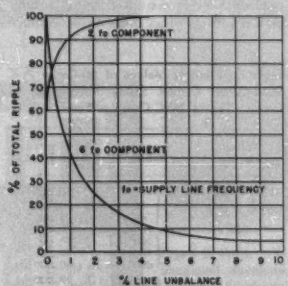

Figure 11. Relative amplitude of ripple components in the filtered output of a 3-phase double-way rectifier as a function of line unbalance

which shows that the ratio of $2fo$ and $6fo$ component is 2.23 times the line unbalance.

The percentage that each of the ripple components represent of the total is found by dividing equations 7 and 8 by equation 9. The percentage of $2fo$ in the total ripple, dividing equation 8 by equation 9 is

$$P_2 = \frac{\dfrac{K}{(2\times 2\pi fo)^2 LC} \times 100}{\dfrac{1}{(2\times 2\pi fo)^2 LC}\sqrt{K^2 + 0.2}} = \frac{K \times 100}{\sqrt{K^2 + 0.2}} \tag{13}$$

and the percentage of $6fo$ in the total ripple dividing equation 7 by equation 9 is

$$P_6 = \frac{\dfrac{4.04}{(6\times 2\pi fo)^2 LC} \times 100}{\dfrac{1}{(2\times 2\pi fo)^2 LC}\sqrt{K^2 + 0.2}} = \frac{45}{\sqrt{K^2 + 0.2}} \tag{14}$$

In each of these cases the final minus one in the denominator of equation 7 and 8 has been dropped.

Where less effective filters are used, resulting in output ripple amplitude larger than 0.05 per cent the approximations previously made are no longer sufficiently accurate. In these cases the amplitudes of the $2fo$ and $6fo$ ripple components must be individually calculated from equations 7 and 8, and then the total ripple will be obtained by taking the square root of the sum of the components.

Values calculated in this manner for 50- and 60-cycle supply line frequencies and for 0, 2 per cent, and 5 per cent line unbalance are shown on Figure 12. Where the values of capacitance and inductance of the filter are less than those set by the limits indicated on

Figure 12, the ripple will be less than indicated by the curves. In the case of inductance lower than the limit, increased regulation, usually undesirable, decreases the ripple amplitude.

In case the capacity values are lower than the limit, a condition normally not encountered, the effect of the load resistance in reducing the a-c shunt impedance results in further reducing ripple amplitude.

References

1. Electrical Performance Standards for Standard Broadcast Transmitters. *Standard Number TR-101-A*, Radio Manufacturers Association (Washington, D. C.).

2. Electrical Performance of Television Broadcast Transmitters. *Standard Number TR-104*, Radio Manufacturers Association (Washington, D. C.).

3. Applied Electronics (book), Massachusetts Institute of Technology. John Wiley and Sons, New York, N. Y., first edition, 1943, page 291.

4. Filter Ripple Chart, C. K. Hooper. *Electronics* (New York, N. Y.), March 1948.

5. Choke-Input Filter Chart, Reuben Lee. *Electronics* (New York, N. Y.), September 1949.

No Discussion

A New High Interrupting Capacity Low-Voltage Power Fuse

C. L. SCHUCK
ASSOCIATE AIEE

A NEED exists for low-voltage fuses having much higher short-circuit interrupting capacity than cartridge fuses commonly used.

Cartridge fuses for circuits 600 volts and less have been used in the United States for many years, principally in low burden branch circuits where available fault currents were relatively low. They are produced by numerous manufacturers, and practically all makes satisfy the National Electric Code through compliance with the Standard for Fuses[1] of Underwriters' Laboratories, Inc.

In the matter of short-circuit interrupting ability, the Standard for Fuses includes a d-c test with 10,000 amperes available, the rate of rise of the Underwriters' Laboratories New York City testing circuit being approximately 2,000,000 amperes per second. While most applications of cartridge fuses are on a-c circuits, this d-c short-circuit test is, even today, the only criterion in use for determining the acceptability of fuses for application on either a-c or d-c circuits.

However, no direct inference is valid concerning the a-c short-circuit interrupting ability of a fuse which has passed this particular test. Table I shows limiting values of 60-cycle symmetrical available short-circuit current safely interrupted by members of a typical line of cartridge fuses, all of which passed the Underwriters' d-c 10,000 ampere short-circuit acceptance test.[2] These were nonrenewable, nonindicating fuses.

Conversely, the a-c short circuit interrupting ability demonstrated for a fuse is not a reliable indication of its ability to interrupt a d-c short circuit. Although some efforts have been made to establish a theoretical relation between a-c and d-c interrupting ability,[3] interruption tests on a circuit of the same type as that on which applications are intended are the only reliable basis for assigning interrupting ratings.

National Electric Code Cartridge Fuses

Cartridge fuses as manufactured in the United States, through standardization of dimensions and melting time-current and temperature rise specifications of the Standard for Fuses have become extremely low cost devices. Practically all makes employ a link of zinc wire or strip surrounded by a granular or powder filler (or merely air) and are enclosed in a rolled paper or fiber tube with brass or copper ferrules. Some makes incorporate special features such as time-lag in the melting characteristic, field renewability, and so forth, but with one recent exception,[4] none of the numerous manufacturers, to the writer's knowledge have published a-c or d-c interrupting ratings or d-c ratings other than those implied by Underwriters' Laboratories, Inc., approval based upon the 10,000-ampere test value. In recent years, however, the progressive increase in the short-circuit currents possible on many networks, industrial circuits, station auxiliary, and shipboard circuits, has led to the demand for fuses actually having interrupting ability to cover these present day requirements, which are in many cases greatly in excess of 10,000 amperes rms.

Table I. Limiting Values of 60-Cycle A-C Short-Circuit Current Safely Interrupted by Typical NEC Cartridge Fuses

Voltage Rating	Ampere Rating	Rms Current Interrupted
250	15	20,000
	30	4,000
	60	5,000
	100	6,000
	200	15,000
	400	25,000
	600	30,000
600	50	20,000
	30	3,000
	60	3,000
	100	6,000
	200	15,000
	400	25,000
	600	30,000

European Developments

In Europe, and principally in Great Britain and Germany, cartridge fuses of proved high-interrupting capacity have been in use for some years. Their development evidently was spurred by efforts to conserve strategic materials, leading to their application in many cases where it is the American practice to use circuit breakers. Also, there do not appear to have been available in Europe any counterparts of the mass-produced low-cost National Electric Code fuses. Fuse development in England was accompanied by considerable research on the fuse design factors and circuit parameters to determine their effect on interrupting ability, with the result that the high-capacity fuse designed according to these findings could justly be described by Gibson[5] as "in its more advanced forms a reliable piece of apparatus with a precision performance."

The European high-capacity fuse for low-voltage service was of the same basic construction as the current limiting fuses already well established for high-voltage applications,[7] having metallic links embedded in a granular inert filler. The current limiting manner of interruption resulting from this construction when properly designed, minimized the energy dissipated in the fuse cartridge to the ex-

Paper 50-127, recommended by the AIEE Switchgear Committee and approved by the AIEE Technical Program Committee for presentation at the AIEE Great Lakes District Meeting, Jackson, Mich., May 11–12, 1950. Manuscript submitted February 14, 1950; made available for printing March 24, 1950.

C. L. Schuck is with the General Electric Company, Philadelphia, Pa.

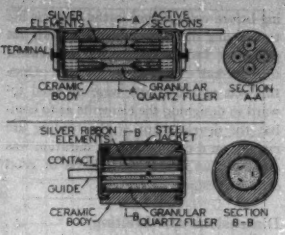

Figure 1. Typical European high interrupting capacity cartridge fuses

A—British high rupturing capacity fuse
B—German 350-volt 200-ampere fuse for shipboard

tent that external disturbance was eliminated and interrupting ratings could be assigned of 44,000 symmetrical rms amperes for 660-volt circuits.

Although no standardization of dimensions had been found practical in Great Britain, "high-rupturing-capacity" fuses were developed to occupy minimum space, and for given ampere ratings have diameters of the same order as American National Electric Code fuses, but shorter cartridge lengths. The cartridges usually are made of heavy-walled ceramic material, having separate holes isolating the parallel element components and the resulting arcs formed during interruption. The holes are filled around the elements with granular quartz similar to that used in high-voltage current limiting fuses, Figure 1(A). The transient pressure must still have constituted a considerable problem in view of the thickness of ceramic used. In German fuses for submarines, a substantial portion of the cartridge length was reinforced with a steel jacket, Figure 1(B).

Interrupting Rating

In commencing the development of a line of high-interrupting capacity cartridge fuses suitable for manufacture here, it was realized that interrupting ability beyond the 44,000-rms ampere rating of the British designs would be necessary to satisfy the requirements of many American industrial and shipboard circuits. A rating of 100,000 total rms amperes, (including d-c component) appeared to be the most satisfactory objective, so as to permit application on systems where circuit breakers of this rating are required in some circuits. The 100,000-rms ampere rating in the case of a 3-pole circuit breaker implies an available symmetrical short circuit current of 80,000-rms amperes, the factor accounting for the d-c component and average current among the phases being 1.25, as explained in a recent AIEE paper, Guide for Applying Low-Voltage Air Circuit Breakers.[8] (See Appendix I).

Tube Material

Efforts toward obtaining the desired interrupting capacity were aided considerably by the availability from several American manufacturers of glass-cloth-base, heat-resistant resin-impregnated insulation in tube form. The strength and resilience of such tubes was found more than adequate to withstand the transient pressures occurring during interruption with even more than the maximum element section usable, as determined from time-current melting, and maximum temperature limits. Thus the problems associated with thick-walled ceramic tubes, reinforcement, and so forth were avoided.

Filler

Another asset available here for the development of fuses with higher interrupting capacity was a specially graded granular quartz filler developed for high-voltage current-limiting power fuses,[9] where grain sizes are restricted to the range which provides maximum grain surface for withdrawing heat from the arcs, and at the same time provides the intergranular air spaces required for the dispersal of the element metal.

Element Design

In addition to advantages gained by the use of the woven glass base tube material and the improved filler, it was considered desirable to make use of any further advances that might result from improvements in the element proportions. As a general conclusion based on interrupting test results, it was found that substantial length was not required in the arc paths for the low-circuit voltages involved. This differs from findings in high-voltage fuse developments.[9] As circuit voltage was causing no particular hardship, the minimization through the use of short active element sections of the amount of metal which became involved in the arcs could be credited with much of

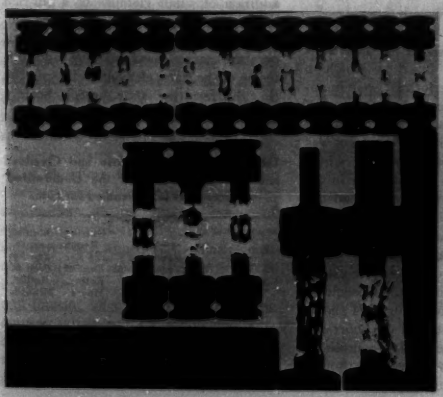

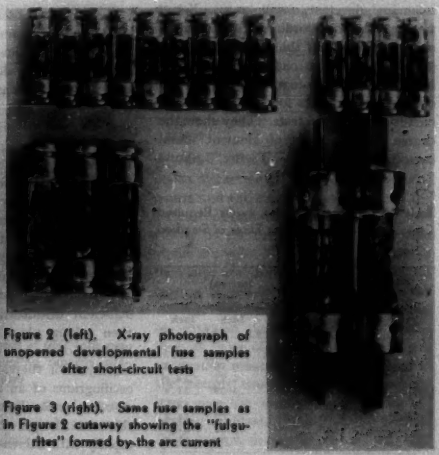

Figure 2 (left). X-ray photograph of unopened developmental fuse samples after short-circuit tests

Figure 3 (right). Same fuse samples as in Figure 2 cutaway showing the "fulgurites" formed by the arc current

the improvement obtained in interrupting ability.

The division of the element section required for a given ampere rating into a number of spaced parallel paths was found to aid in the prompt development of arc voltage, in limiting transient pressure in the cartridge, and thereby in further increasing the interrupting ability.

The degree of division of element section when carried sufficiently far was found to provide interrupting ability well above the 100,000-rms ampere objective. Carried too far, extreme subdivision with the required spacing between elements calls for more fuse tube cross-section than would be practical or economical. For adequate interrupting ability, with an acceptable pattern of element spacing, the number of parallel arc paths was found to be significant.

It was found that the number of rated amperes per single element necessary for the safe interruption of 100,000-rms amperes should be substantially less than the amperes per element of European designs. This further reduction in the amount of element metal which becomes involved in any one arc path is the factor believed chiefly responsible for the greater interrupting ability found possible.

These factors, together with the spacing between arcs, and from any arc to the inner surface of the fuse tube, were investigated in a series of d-c short-circuit tests, using samples in which the element designs differed from one sample to the next by definite increments. As criteria of the difficulty with which the fuse sample opened the circuit, use was made of the temperature rise of the cartridge following the test, oscillograms, X-ray photographs, and ordinary photographs and examination of the fuse samples cut-away to show the elements. Figure 2 shows an X-ray photograph of typical unopened test samples following d-c short-circuit interruption tests. They show the degree of dispersion of element metal caused by the arcing. Figure 3 shows

Table II. Available Space versus Required Capacities of NEC Cartridge Fuses of Standard Dimensions

Voltage Rating	Ampere Rating	Kva	Internal Volume in Cubic Inch	Kva Per Cubic Inch
250	30	7.5	0.20	37.5
	60	15	0.70	21.4
	100	25	1.71	14.6
	200	50	4.39	11.4
600	30	18	1.31	13.7
	60	36	2.52	14.3
	100	60	2.82	21.2
	200	120	7.76	15.5

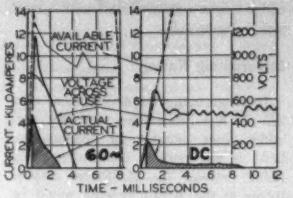

Figure 4. Comparable d-c and a-c short-circuit tests. Sustained voltage prolongs arc current in d-c test

Frequency	60 Cycles	D-C
Test voltage	600 v. rms	525 v.
Available amperes	60,000 rms	30,000
Melting time, seconds	0.0003	0.0006
Arcing time, seconds	0.0026	0.0083
Total time, seconds	0.0029	0.0089

the same samples cut-away with excess quartz removed to expose the remains of the elements. By study of the size of "fulgurite" or slag formation where the arcs had fused the granular quartz filler, and the other means mentioned previously the influence of each of the several factors was assessed, and conclusions were reached concerning:

1. Number of elements (arcs in parallel).
2. Number of reduced sections (arcs in series).
3. Spacing between parallel arcs.
4. Spacing between arcs in series.
5. Spacing of any arc to inner wall of fuse tube.
6. Mass of terminals—path to ferrules.
7. Type of filler.

From these observations followed the optimum dimensions and other data around which a line of high-capacity fuse elements could be designed.

A d-c circuit was employed for these tests in view of results of numerous earlier short-circuit tests in which a given fuse design performed well in interrupting an a-c circuit, but not as well in a d-c circuit. The salient factor making for greater severity in the d-c tests was evidently the sustained voltage, which caused arc current to persist, while in the a-c tests the falling voltage enabled the fuse to force current to zero at or before the first voltage zero following melting, sufficient deionization of the arc paths then taking place to prevent re-establishment of the arcs during the subsequent half cycle or thereafter. Figure 4 shows oscillograms of an a-c and d-c short-circuit test on developmental fuse samples of the same design, the arc current falling rapidly with decreasing voltage and ceasing before voltage zero in the 60-cycle a-c test, arcing time being 0.0026 second, but persisting for 0.0083 second (equivalent to a full half cycle) in the d-c test. Once this was noted, efforts were directed toward so designing the elements as to combat the development of the trailing arc current on d-c tests, and its duration was employed as one of the criteria of good element design.

Dimensions and Melting Requirements

Based on the data accumulated, it appeared that it would be perfectly possible to make the line of high-interrupting capacity cartridge fuses in the same cartridge sizes as conventional National Electrical Code fuses, even in the case of the 250-volt 30-ampere rating which appeared to be the "tightest" on the basis of the values in Table II.

In order fully to meet the requirements of the Standard for Fuses,[1] elements had to be so designed as to melt within specified times at given percentages of overload current, and on normal current to generate heat at a rate sufficiently low so as not to overheat the fuses themselves nor connected devices such as knife switches, contactors, and so forth. The requirements are summarized in Table III.

"M" Effect

With respect to active element section required, the above specifications are contradictory, requiring a large cross section for the 110 per cent cool-running requirement, and a small cross section for the overload prompt-melting requirement. This problem was solved by use of the so-called "M" effect,[16] obtained by the addition of small globules of a tin-rich alloy to the active sections of the elements. On overload, the elevated temperature causes local alloying and diffusion of the silver element metal into the tin, the resulting alloy having both a

Table III. Temperature Rise and Overload Melting Requirements of the Underwriters' Laboratories Inc., Standard for Fuses

Ampere Rating	Temperature Rise Requirement 110 Per Cent of Rated Current	Overload Melting Requirements* 135 Per Cent of Rating, Hours	200 Per Cent of Rating, Minutes
Up to 30	Max. Temp. rise	1	2
31 to 60	of 50°C on any	1	4
61 to 100	part of the fuse	2	6
101 to 200		2	8

* Fuse must operate within times listed.

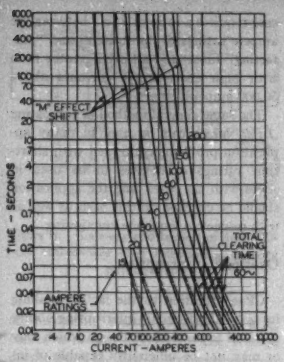

Figure 5. Melting time-current curves. Improved overload protection results from "M" effect shift

higher resistance and a lower melting point than the silver alone. This permits the element to melt and separate at a current 30–35 per cent lower than would be required if the element consisted simply of silver. Since this metallurgical process requires time for its accomplishment, the time-current curves of the fuses are not affected in the high-current short-time region, but do show displacement toward lower currents in the low-current long-time region. This is evident in the melting time-current curves shown in Figure 5.

Short-Circuit Performance

With element sections adjusted to meet the foregoing specifications, and designed on the basis of the studies made after the earlier a-c and d-c short-circuit tests, acceptable short-circuit interrupting ability was demonstrated with fuses designed in standard cartridge sizes. Figure 6 shows reproductions from oscillograms taken during a-c short-circuit tests of the maximum ampere ratings in the four standard sizes: 30, 60, 100, and 200 amperes.

These records and many similar ones taken at different available short-circuit currents and angles of inception, fully substantiate an interrupting rating of 80,000 symmetrical or 120,000 total rms amperes. (See Appendix I). The records also furnish information useful in making applications. The extent of the current-limiting effect as a function of the ampere rating and the available short-circuit current can be obtained simply by measurement of the peak values of current passed, Figure 6. These, plotted as a function of available current for each ampere rating, give the current-limiting curves of Figure 7. Such test results as are shown in the current traces of Figure 6 form the "anchor points" of the current-limiting curves of Figure 7, and were checked and "smoothed" by calculation.[9] These maximum currents and their effective values and durations passed by given ampere ratings of fuses at available short circuit currents of interest establish the short-time capacities required by series connected devices. Examples are: contactor coils (magnetic stress), the contacts themselves (thermal duty), switch contacts, connections, and other fuses or interrupters in co-ordinated protective schemes. Thus the arcing time and current along with the melting time and peak currents already mentioned, are of importance in making applications.

"Let-Through" Current

Melting

As a measure of the current and time passed by a fuse in interrupting a fault, the heating effect or $\int i^2 dt$ during both the melting and arcing periods should be evaluated. In the records of Figure 6, the clear time current areas are taken as melting periods, and the subsequent time current areas (cross hatched) as arcing. Calculations indicate that the elements had sufficient heat developed in them by the passage of current to reach the melting point considerably before the times of the peak currents appearing on the oscillograms. This phenomenon was found to occur only with very high short-circuit currents, the peak currents and times for moderate available currents correspond-

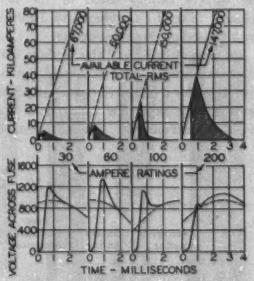

Figure 6. Short-circuit tests at 660 volts rms, 60 cycles of high interrupting capacity cartridge fuses

Melting time-current areas—clear; arcing time-current areas—cross hatched; generated voltage—dotted

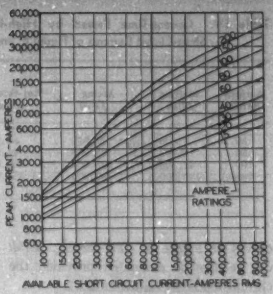

Figure 7. Current limiting curves for fuses of Figures 5 and 6

ing more closely to calculated values for melting. This indicates that current continues to rise following melting on high available short-circuit current, until sufficient arc resistance has developed to cause the substantial reduction in current characteristic of the operation of current limiting fuses.

With the available short-circuit current known as a function of time, a complete description of the instantaneous current versus time leading up to melting can be calculated. However, a disparity between this mathematical description of the current during the melting period and the actual current is evident in the current traces of Figure 6. The slope of the available current is not followed by the actual current, but is reduced by the resistance of the fuse. This effect is more evident in the case of the lower current ratings which have higher resistance. Assignment of melting time and current in the short-circuit tests of Figure 6 was made using the slope of the actual current measured from the oscillograms rather than the slope of the theoretically available current.

Arcing

While current prior to melting depends almost entirely on the circuit constants and the character of the fault, the arc current following melting is influenced chiefly by the fuse, that is, by the shape of the arc voltage it produces. Although the shape and duration of arc current can be constructed by assuming values of arc voltage,[9] factual data on arc current can be obtained directly from oscillograms such as those of Figure 6. Arcing times are readily measured, and when added to the melting times for given ampere ratings, give the total clearing curves appearing as dashed lines at the bottom (high-current-fast-time) ends of the

Table IV. Current-Time Passed by High-Interrupting Capacity Fuses on High Available Short-Circuit Currents of Figure 6, and Heating Effect on Connected Wire

Ampere Rating	Melting $\int i^2dt$	+	Arcing $\int i^2dt$	=	"Let-through" $\int i^2dt$	Temperature Rise—C° Wire No.	Rise	Wire No.	Rise
30	1,600		17,970		19,570	8	2.7°	10	6.8°
60	10,000		34,960		44,960	4	1.0°	6	2.4°
100	42,000		218,000		260,000	1	1.4°	3	3.5°
200	130,000		1,190,000		1,320,000	200,000 cm.	1.2°	0	4.3°

curves of Figure 5. The arcing $\int i^2dt$ can readily be evaluated provided the current has some simple form.

If arc current falls linearly from a value i_a to zero during a time Δt, it can be shown that $\int i^2dt = i_a^2\ \Delta t/3$. More generally, if the arc current falls linearly from a value i_a to a value i_b during a time interval of Δt, it can be shown that

$$\int i^2dt = \frac{\Delta t}{3}\{i_a^2 + i_a i_b + i_b^2\} \qquad (1)$$

By use of this expression, with time and current values measured from the oscillograms, the arcing $\int i^2dt$ was computed for the tests of Figure 6. These values (in ampere-squared-seconds) are listed in Table IV, together with $\int i^2dt$ required to cause melting on a short-time no-heat-loss basis. Their sum gives the total "let-through" current-time passed by each ampere rating in interrupting a large short-circuit current.

This "let-through" $\int i^2dt$ must be tolerated by all devices connected in series with a given fuse. Depending on the resistance of the device, heat will be developed in it, and a rise in temperature will result. As a measure of the short-circuit protection afforded wire sizes commonly used with these ampere ratings in making motor branch circuit connections, the temperature rises resulting from the passage of the "let-through" $\int i^2dt$ were computed and are included in Table IV. These were calculated assuming no heat loss from the wire to its surrounding insulation during the short time interval of the "let-through."

Another use that can be made of these melting and arcing $\int i^2dt$ values is the determination of suitable ampere ratings to use in co-ordinated protective schemes. In addition to choosing ratings so that the desired sequence operation is assured in the range of times in which co-ordination schemes are usually laid out (0.1 to 200 seconds), see Figure 5, it must also be ascertained whether the "protecting" fuse can complete the work of interrupting the circuit without damaging the element of the "protected" fuse through the range of available short-circuit current involved in the application. This in turn requires that the $\int i^2dt$ passed by the "protecting" fuse in both melting and arcing shall be less than the $\int i^2dt$ required to melt the "protected" fuse.

Calculations similar to those on which were based the $\int i^2dt$ values appearing in Table IV were carried through to obtain the melting, arcing, and total $\int i^2dt$ at several levels of available short-circuit current for all the ampere ratings appearing in time-current curves of Figure 5.

Fuse-to-fuse Co-ordination

Comparisons of the resulting values yielded Table V in which are listed the minimum ampere ratings to "back-up" the ampere ratings listed in the first column. The $\int i^2dt$ values and Table V are all based on 60-cycle circuits.

The ratings listed in Table V show that successive ampere ratings should not be used in series if selective operation is desired, except in a few cases with low available fault current. The more general case requires a ratio of 2 to 1 between the ampere ratings of "protected" and "protecting" fuses, and an even greater ratio with high short-circuit currents above 50,000-amperes rms.

The same general method of comparing $\int i^2dt$ values can be used in many application problems concerned with short-time ratings of devices to be used in series with the fuses, and the application should be checked on this basis as well as with respect to sequence functioning.

Overload Interruption

Close attention to the factors making for good short-circuit interrupting ability can lead to an element design which may or may not be inherently capable of interrupting the circuit safely in the event of an overload condition. In view of this a series of overload tests were made at 60 cycles on the "final designs" of each rating with the results shown in Table VI. Some of these tests were made outdoors in cold weather, and durations in these cases were longer than those given by the melting time-current curves of Figure 5.

In these tests, particularly those in which the duration was more than ten minutes, all parts of the fuse had had ample time to assume temperatures substantially as high as those obtainable at any value of overload current. With somewhat higher current, the duration is less and the fuse does not have time to get up to temperatures as high as the empirical optimum at 150–160 per cent of the ampere rating. At less current, although the duration is longer, the wattage developed is less, and the fuse parts do not reach temperatures as high. The tests of Table VI cover the region from 146 to 204 per cent of rated current with most tests in the 150–160 per cent region producing maximum temperature rises.

Transient Recovery Voltage

The conversion of the fuse from a good conductor prior to and during melting, to

Table V. Minimum "Back-up" Ampere Ratings

Ampere Rating	Available Asymmetrical Short Circuit Current, Rms 15,000	25,000	50,000	75,000	100,000
15	30	30	30	40	40
20	30	30	40	60	60
30	60	60	60	80	80
40	60	60	80	100	100
60	100	100	100	150	150
80	150	150	150	200	
100	200	200			

Table VI. Overload Test Data

Test No.	Voltage Rating	Ampere Rating	Test Current, Amperes	Test Duration, Minutes	Seconds	Recovery Voltage	Performance
1		30	44	13	10	250	
2	250	60	92	4	20	250	No
3		100	185	13	4	250	Disturbance
4		200	348	14	8	250	
5		30	49	12	30	600	
6	600	60	101	10	43	600	No
7		100	200	4	50	600	Disturbance
8*		200	408	15	24	600	

* Section of element of this rating subsequently reduced better to comply with the requirements of the Standard for Fuses.

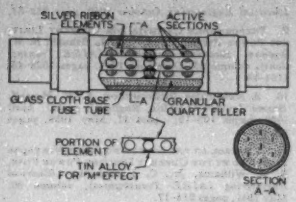

Figure 8. Cutaway and section of new 600-volt 100-ampere high interrupting capacity cartridge fuse

an increasing resistance during arcing, causes a radical increase in the voltage drop across the fuse after peak current. During approximately the next 500 microseconds the voltage as measured across the fuse rises, reaching its crest at a time when current has been reduced substantially from its peak value, in many cases by as much as 50 per cent. This relatively slow development of arc resistance and arc voltage results in a relatively lower peak voltage for these low-voltage fuses as compared to voltage peaks obtained with high-voltage current limiting fuses, in which the arc resistance is caused to develop more rapidly, producing a voltage peak while current is still practically at its peak value.[11] Peak voltage values measured from the traces of Figure 6, which are typical of records of many similar tests, average to 1,190 volts, bearing a ratio to the crest of 600 volts of only 1.4. For present fuses ratio is 2 to 3.

Line of Low-Voltage Power Fuses

Figure 8 shows the construction of a typical rating of the new line of fuses designed according to the experience gained in the short-circuit and other tests described above, and to comply with the requirements of the Standard for Fuses. The 600-volt ratings of the four standard sizes, 30, 60, 100, and 200 amperes, are shown in Figure 9. While having the limiting dimensions of standard cartridge fuses, the mechanical design includes certain features which make possible the use of special clips which will not accept fuses of lesser interrupting capacity. These features consist of grooves in the ferrules of the ferrule-type ratings, see Figure 9, and a shorter body in conjunction with a projection at the base of the blade in the blade-type ratings.

Conclusions

1. The need in the United States for fuses with high interrupting capacity for use on low-voltage circuits, now can be satisfied with specially-designed fuses of the current-limiting type.

2. A line of such fuses has been developed satisfying in every respect the Standard for Fuses of the Underwriters' Laboratories, Inc.

A. Through compliance with standardized dimensions, fuses of the new line have the same physical sizes as conventional cartridge fuses.

B. Through compliance with heating and melting requirements of the Standard for Fuses, ratings of the new line provide proved overload protection, and can therefore be applied, rating for (ampere) rating in the same way as conventional cartridge fuses.

3. Interrupting ability in excess of 100,000-amperes rms at 250 and 600 volts, 60 cycles, results from use of special materials and design factors established in controlled a-c and d-c short-circuit tests.

4. D-c interrupting ability, not completely determined through the range of rates of rise of current (inversely proportional to circuit inductance) occurring in d-c circuits, also has been demonstrated to be a considerable advance over the d-c interrupting capacities provided heretofore.

5. Measurements from oscillograms taken during short-circuit tests make possible the evaluation of the heating effect, $\int i^2 dt$ of current-time "let-through" by the fuse.

6. Determination of the melting and arcing portions of the total "let-through" forms a basis for matching short-time ratings of other devices with the short-time fuse characteristics.

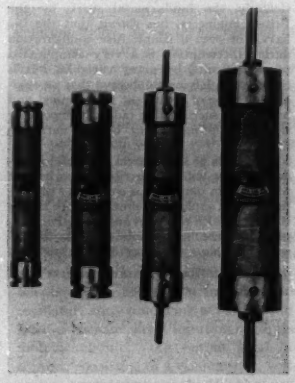

Figure 9. Representative 600-volt ratings of new high interrupting capacity low-voltage power fuses

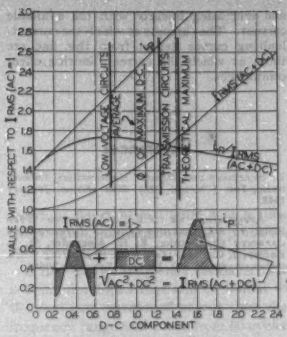

Figure 10. Numerical relations between peak and rms values of a-c short-circuit currents having both a-c and d-c components

7. Co-ordinated protective schemes in which members of such a series of current ratings of high interrupting capacity fuses are applied one ahead of (nearer the source) another, call for the use of ampere ratings having a ratio of 2 to 1 or greater for large available short-circuit currents.

8. The transient recovery voltage associated with the current limiting character of such a line of fuses, is relatively slow-rising and reaches peaks in the order of only 1,200-1,400 volts, easily tolerated by the insulation ordinarily used in 250- and 600-volt circuits, and an improvement in this respect also over voltage transients produced by conventional cartridge fuses.

Appendix I

Shown in Figure 10 are the numerical relationships between the rms value of a symmetrical a-c short-circuit current, taken as 1.0, and the offset current resulting from various amounts of a d-c component added to the alternating current. In addition to the theoretical maximum of direct-current present to the same amount as the peak value of alternating current, ($\sqrt{2}$), with total rms value 1.732, well accepted[13] factors of 1.6 for transmission circuits (momentary rating for circuit breakers—also total rms current for power fuses) and 1.25 for low-voltage circuits are shown. In the latter case the maximum rms current possible in one phase would be 1.5 compared to the rms value of the alternating current alone of 1.0, the 1.25 factor being the results of averaging three phases. The ratio of peak value to the total rms (1.68 for low-voltage circuits) was used in plotting the current-limiting curves of Figure 7, in which the curve for each ampere rating becomes tangent to the line starting at 1,680 peak amperes for the 1,000-rms ampere short circuit,

and increasing linearly with the available current. The currents at which the current-limiting curves depart from this line are those at which the current limiting effect commences.

References

1. Standard for Fuses. Underwriters' Laboratories, Inc. (Chicago, Ill.), fifth edition, January 1948.

2. Application of N.E.C. Cartridge Type Fuses to A-C Circuits from an Interrupting Capacity Standpoint, E. H. Alexander, N. L. Hadley, J. C. Page. *Industrial Engineering News*, (Schenectady, N. Y.), January–February 1944.

3. Criteria of Severity in the Short-Circuit Testing of Fuses, A. W. Metcalf. *Beama Journal* (London, England), August 1938, page 38–43.

4. Amp-Trap—A New Era of Protection of Low Voltage Circuits. *Leaflet*, The Chase-Shawmut Company, Newburyport, Mass.

5. The High-Rupturing-Capacity Cartridge Fuse with Special Reference to Short-Circuit Performance, J. W. Gibson. *Journal*, Institution of Electrical Engineers (London, England), volume 88, part II, February 1941, pages 2–40.

6. United States Patent 2,439,674, C. L. Schuck. April 13, 1948.

7. The Current Limiting Power Fuse, D. C. Prince, E. A. Williams, Jr. *Electrical Engineering* (*AIEE Transactions*), volume 60, February 1941, pages 77–80.

8. Guide for Applying Low-Voltage Air Circuit Breakers, AIEE Committee Report. *Electrical Engineering*, October 1949, page 853–54.

9. Performance Criteria for Current Limiting Power Fuses, I and II, C. L. Schuck, E. W. Boehne. *Electrical Engineering* (*AIEE Transactions*), volume 65, December 1946, pages 1028–48, 1191–94.

10. A New Fuse Phenomenon, A. W. Metcalf. *Beama Journal* (London, England), part I, April 1939, pages 109–12; part II, May 1939, pages 151–52.

11. Control of the Switching Surge Voltages Produced by the Current Limiting Power Fuse, E. A. Williams, Jr., C. L. Schuck. *Electrical Engineering* (*AIEE Transactions*), volume 60, May 1941, pages 214–17.

12. System Short Circuit Currents, W. M. Hanna, H. A. Travers, C. F. Wagner, C. A. Woodrow, W. F. Skeats. *Electrical Engineering* (*AIEE Transactions*), volume 60, September 1941, pages 877–81.

Discussion

R. H. Kaufmann (General Electric Company, Schenectady, N. Y.): The new high-speed current limiting low-voltage fuse with an a-c interrupting rating of 100,000 amperes as reported by Mr. Schuck fills a long felt want. Among industrial plants, commercial buildings, and small shops fed from low-voltage city networks, there is an extensive field for application in which the available fault current levels range from 20,000 to 75,000 amperes. It now becomes possible to apply fuse interrupters for low-voltage branch circuit protection on a sound engineering basis.

The new fuse unit alone, however, is not the complete solution. An essential associated auxiliary is a line switching unit which serves to make and break circuit normal currents (below the fuse protective level) and also allows the fuse assembly to be de-energized for fuse replacement.

The requirements for a safe switching device are quite exacting. During fuse operation, the current surge should not weld the switching contacts. Neither should a flash occur at the switch contacts which could ignite an unrestricted fault arc ahead of the protective fuses with disastrous consequences. These requirements apply whether the switch is in the fully closed position or is being closed on a faulted circuit. The switching unit must also be capable of interrupting any current magnitude below that which will produce prompt automatic interruption by the fuse unit.

The fuse clip design also is an important consideration. An arc flash could ignite an unrestricted fault arc at the source terminals of the fuse unit with disastrous results.

The crest magnitude of current passed by the fuse increases as the available fault becomes greater as illustrated in Figure 7. It is entirely possible that a particular switch and fuse clip construction may show signs of distress at an available current somewhat in excess of 50,000 amperes. The permissible interrupting rating which could be assigned to that combination fuse assembly would be limited to 50,000 amperes even though the fuse unit itself is rated 100,000 amperes.

The behavior pattern of pressure contacts in the presence of large short time current impulses is not sufficiently understood to be able to predict the performance with any degree of certainty. Only by full scale testing can the actual ability of combination equipments be established. Co-ordination testing is already in progress which will form the basis for legitimate interrupting ratings on composite equipment incorporating the new fuse unit.

N. L. Hadley (General Electric Company, Schenectady, N. Y.): While it has been generally assumed that better interrupting performance was inherently possible in the National Electrical Code dimensions, the problem has not seemed to be an easy one to solve. Some earlier work, and particularly the fundamental work by the British engineers, has shown that the behavior of even a simple fuse configuration during interruption is a very complicated process affected by many variables. It is therefore satisfying to observe that an engineering type of treatment was applied and has so well succeeded in radically improving the interrupting ability of the cartridge fuse.

This class of fuse should be useful in industrial low-voltage distributions where it will assist in obtaining a continuity of protection and application practice more nearly consistent with the rules and objectives employed in the higher voltage parts of systems. Perhaps the most difficult problem in the secondary distribution has been the selection of a device for protecting small circuits and devices in a high capacity system. The unsatisfied requirement was not simply one of economics, but was a real need for a fast low energy interrupter capable of protecting loads in addition to the supply.

C. L. Schuck: It is gratifying to note from Mr. Kaufmann's discussion that joint short-circuit testing of the new high-interrupting capacity fuses with contactors and other line switching devices is already in progress. The position assumed by the new fuse in the low-voltage protective field will be determined in large measure by the results of such tests translated into recommendations for proper application.

With regard to Mr. Hadley's comment on the need for a fuse with improved interrupting capacity, some further explanation of the data given in Table I is in order. The short-circuit current values listed describe "worst" rather than "average" performances by the lots of fuses tested, and it is felt that interest should center in such values in a subject like circuit protection where reliability and safety are issues. These tests, and all short-circuit tests referred to in the body of the paper, were made single phase, with full line-to-line voltage across a single fuse unit. In many cases, when conventional cartridge fuses have been called upon to clear faults on 3-phase systems, they have afforded protection and interrupted without disturbance, being aided by the fact that the duty was divided, the fuses in two of the three phases being effectively in series. While this favorable situation can exist for certain types of faults, there is no assurance that it will, and good engineering practice demands that an essentially single phase interruptor such as a fuse be capable of clearing faults under the most severe conditions possible.

Modern Carrier Current Test Equipment and Its Application

R. L. BRINTON
ASSOCIATE AIEE

DURING the past 20 years the carrier system of the Pacific Gas and Electric Company has advanced from two simple carrier circuits serving a total of seven terminals to the present complex system consisting of 45 circuits serving nearly 100 terminals. Originally the carrier system provided only telephone service. At present, in addition to the greatly expanded telephone facilities, the system includes relay carriers, telemetering, and remote alarm systems.

The carrier transmitting and receiving equipment now in use as a whole is not uniform in type or design. Some installations employ simple amplitude modulation and transmit the carrier and both sidebands, while other installations transmit only one sideband and suppress the carrier. Also, there are installations using frequency modulation. The power output of the transmitting equipment varies from 100 watts for the long-haul power line carriers down to 0.05 watt for the short-haul telephone line carriers.

When the carrier system was simple and consisted of only a few circuits, conventional vacuum-tube voltmeters and a cathode-ray oscilloscope were adequate as the principal tools for most maintenance and installation problems. As the equipment became more complex and the number of carrier channels on each metallic circuit were increased, the simple vacuum-tube voltmeter and the oscilloscope became entirely inadequate. Most power line carriers have a test meter panel that enables the attendant to read jack currents of the various tubes in the transmitting and receiving equipment. This method of trouble shooting is relatively slow and cannot be conducted effectively by the average substation operator. Moreover, the fault, except when it happens to be a bad tube which can be readily corrected by simply changing all the tubes in the equipment, is frequently in external apparatus of the carrier such as filters, couplers, or line trouble. Installing and maintaining this apparatus requires special test equipment such as tunable voltmeters and carrier-frequency oscillators. For example, at one major substation there are now more than 15 carrier frequencies that can be detected by a conventional vacuum-tube voltmeter connected across a tuning unit.

Several test and maintenance instruments have been developed to meet the needs of the carrier system of the Pacific Gas and Electric Company and most of these are finding wide acceptance and usage among other power utilities and the communication companies as well. For use as a signal source and for frequency determinations, an oscillator capable of delivering 5 watts in the frequency range from 20 cycles per second to 200 kc per second has been found invaluable. This instrument, referred to as the carrier frequency oscillator, provides both balanced and unbalanced output with provisions for matching impedances of 50, 200, 500, and 5,000 ohms. It will be noted from the block diagram of the oscillator shown in Figure 1 that the instrument also contains a modulator for voice frequency modulation of the oscillator output from an external source. A portable magneto telephone can be used to modulate the oscillator, thus producing a voice-modulated carrier for direct insertion on to the metallic circuits. An output level indicator, consisting of a vacuum-tube voltmeter connected across the 500-ohm output winding of the matching transformer, is included in the design. The oscillator, shown at the right in Figure 4, is a relatively small instrument, readily portable, and operates from 115 volts, 60 cycles.

A new carrier frequency oscillator now is being developed that will be similar to the one just mentioned except that the frequency range will cover from 50 cycles per second to 500 kc per second.

For measurement purposes, a carrier frequency voltmeter (designated model *101*) has been designed and manufactured to measure voltages at any selected frequency in the range from 20 kc to 500 kc. The instrument is actually a radio receiver with the d-c output from the final detector operating an indicating meter on the front panel, calibrated to show the values of the voltages applied to the input terminals. The voltmeter operates with a fixed gain and is therefore a voltage measuring device at the frequency to which it is tuned.

A telephone jack is provided on the front panel for use of a headset, to listen to incoming signals. The headset is energized from an audio amplifier, the audio level of which is adjustable from a front panel level control.

A block diagram is included, Figure 2, to explain the functions of the voltmeter. As shown, the signal input first passes through a section which includes the variable attenuator and an input filter, before arriving at the grid of the first detector. The input filter is of the band pass variety with a pass band from 20 kc to 500 kc. The variable attenuator reduces in ten decibel steps the signal arriving at the grid of the first detector so as to increase the voltage measuring range of the instrument and make possible the measurement of relatively large voltages. As shown, the steps of the attenuator between +40 and +10 are connected ahead of the band pass filter and those between −60 and +10 follow the filter.

Paper 49-211, recommended by the AIEE Carrier Current Committee and approved by the AIEE Technical Program Committee for presentation at the Pacific General Meeting, San Francisco, Calif., August 23–26, 1949, and at the AIEE Summer and Pacific General Meeting, Pasadena, Calif., June 12–16, 1950. Manuscript submitted May 27, 1949; made available for printing April 26, 1950.

R. L. BRINTON is with the Pacific Gas and Electric Company, San Francisco, Calif.

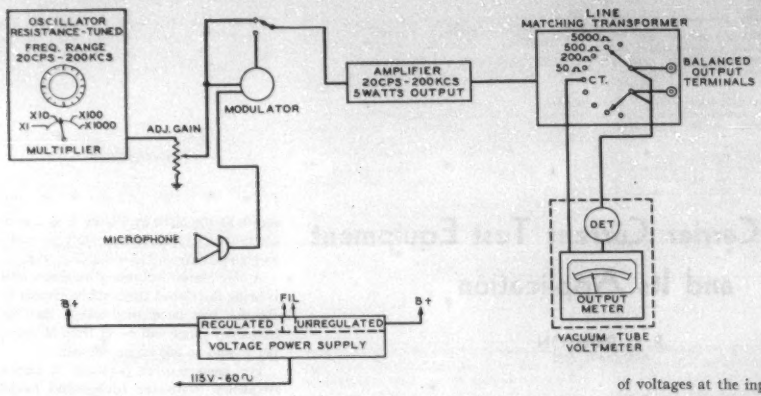

Figure 1. Block diagram of carrier frequency oscillator

The tuning dial on the front of the voltmeter controls the frequency of a variable frequency oscillator over a range of 1,000 kc to 1,480 kc. The output of this oscillator combines with the incoming signal in the first detector to produce an intermediate frequency (I.F.) of 1,500 kc.

Likewise, the 1,500-kc signal, after passing through the I.F. amplifier, combines in the second detector with the 1,675-kc crystal controlled oscillator frequency to produce a second intermediate frequency of 175 kc. The output of the 175-kc amplifier goes directly into the diode detector, the d-c output of which operates the indicating meter.

An injection oscillator, which operates at 100 kc, is included in the voltmeter. This oscillator provides a fixed known amplitude signal of 0.77 volt rms (1 milliwatt into 600 ohms or 0 decibels) which can be switched to the input circuit and substituted for the incoming signal for calibration purposes. The injection oscillator circuit contains a vacuum-tube voltmeter, which can be switched to the output meter, for monitoring the amplitude of oscillations to insure an accurate injection signal amplitude. The harmonics of this oscillator provides a means for checking the frequency calibration of the main tuning dial at the 200-, 300-, and 400-kc points on the dial.

The voltmeter also can be calibrated externally by substitution of a signal frequency in the region of the frequency under measurement. The sensitivity control is adjusted by means of a control on the front panel marked I.F. gain.

The voltage measuring range of the voltmeter is from 77 microvolts to 77 volts, or 80 decibels below to 40 decibels above zero level (one milliwatt into 600 ohms). The indicating meter on the front has a 0–200-microampere range, but the scale is calibrated in decibels. The calibrations indicate in decibels the ratios of voltages at the input terminals to the receiver.

The voltmeter has sharp tuning characteristics. The selectivity characteristics of the model *101* are approximately 6 decibels down at 1 kc off resonance, 18 decibels down at 3 kc off resonance, and 40 decibels at 4 kc off resonance. The input impedance is 10,000 ohms in the rejection band and 20,000 ohms in the pass band between 20 kc and 500 kc.

A second model carrier frequency voltmeter (designated model *103*) has been manufactured to measure voltages at any selected frequency in the range from 3 kc to 40 kc. In other respects, this model is similar to the model *101*, except that it has provision for reception of suppressed carrier transmission.

As shown in block diagram, Figure 3, the tuning dial controls the frequency of a variable frequency oscillator over a range of 85 kc to 122 kc. The output of this

Figure 2. Block diagram of carrier frequency voltmeter model 101

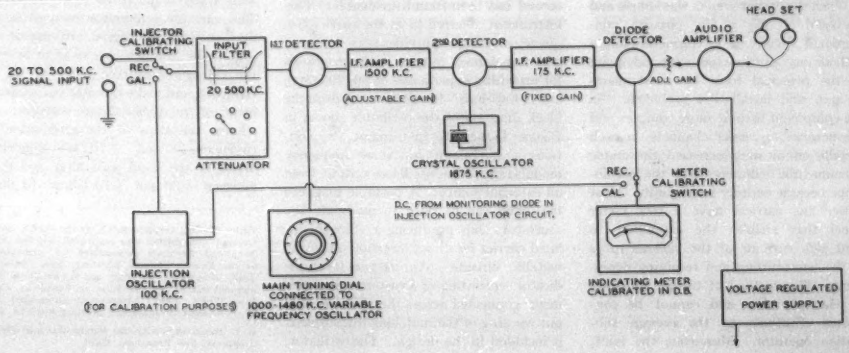

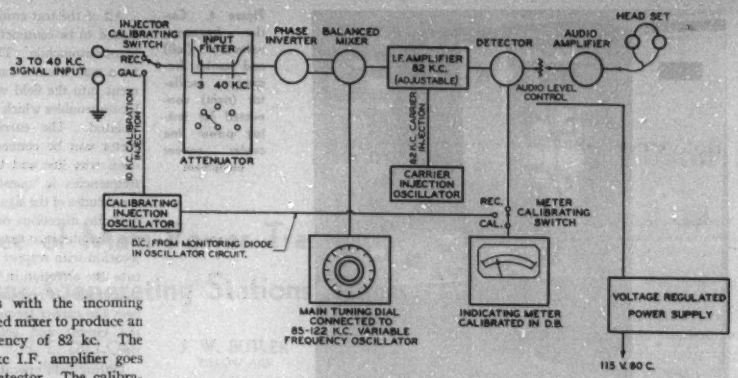

Figure 3. Block diagram of carrier frequency voltmeter model 103

oscillator combines with the incoming signal in the balanced mixer to produce an intermediate frequency of 82 kc. The output of the 82-kc I.F. amplifier goes directly into the detector. The calibration injection oscillator operates at 10 kc and provides an output of 0.77 volt or 0 decibel. The harmonics of this oscillator also provide a means for checking the frequency calibration of the main tuning dial at the 20-, 30-, and 40-kc points on the dial.

In order to make voice transmission intelligible while using the headset for monitoring suppressed carrier transmission, the voltmeter is equipped with a carrier injection oscillator which replaces the suppressed carrier in the incoming signals. This oscillator operates on 41 kc, and provides a strong second harmonic at 82 kc which is injected into the second stage of the I.F. amplifier. Two listening jacks are provided for use of a headset to listen to incoming signals. One of the two jacks is intended for listening to ordinary amplitude modulated signals, the other for listening to suppressed carrier signals which has the carrier replaced.

The measuring range of the model *103* voltmeter also is 77 microvolts to 77 volts with the selectivity 10 decibels down at 1 kc off resonance, 21 decibels down at 2 kc off resonance, and 50 decibels down at 4 kc off resonance.

A third instrument frequently used in testing and maintenance is an untuned vacuum-tube voltmeter with special built-in features to meet the particular needs of the system. This instrument consists of a standard vacuum-tube voltmeter to which is added a set of terminals for connection to a cathode-ray oscilloscope. The signals are amplified in the vacuum-tube voltmeter circuit, thus making it possible to view relatively weak signals. A telephone jack also is included in the instrument for use of a standard headset to enable the user to make audible inspection. This instrument has a high input impedance and is principally useful for monitoring audio frequencies without upsetting the balance of the hybrid circuits.

Other test equipment of a less specialized nature, used in the maintenance of the carrier systems, are frequency meters, standard tube testers, and volt-ohmmeters. These instruments, with the specialized equipment just mentioned, make it possible for carrier maintenance personnel to maintain communication circuits and equipment in good working order and make routine performance checks so that incipient troubles can be located before actual failures occur. These facilities have materially aided in maintaining a degree of performance of the carrier systems not otherwise possible prior to the availability of these test instruments.

The carrier-frequency spectrum now is so congested that each carrier and its associated equipment should be tuned to within a hundred cycles of its assigned frequency, otherwise adjacent channel interference may result. At the present time there are no frequency meters on the market that cover the carrier-frequency spectrum. Carrier-frequency oscillators now in production are not sufficiently stable to be used for tuning line traps, tuning units, and carrier transmitters and receivers.

The Pacific Gas and Electric Company has purchased a number of army-type *BC-221* and navy-type *LM* frequency meters from war surplus stores. These particular models are the type that can be tuned to frequencies as low as 125 kc, consequently when tuning equipment on frequencies below 125 kc it is customary to heterodyne a second or third harmonic of the carrier-frequency oscillator against the *LM* or *BC-221* frequency meter.

Another test equipment problem that may arise in the near future is the need for a field strength meter to measure radiation of power line carrier circuits. The design of a new instrument, to be known as the very Low Frequency Field Intensity Meter, has just been completed for the United States Navy. This instrument is a highly sensitive low-frequency radio receiver operating as a selective radio frequency voltmeter over the 14- to 250-kc portion of the radio spectrum. It is capable of accurately measuring field intensities from one microvolt per meter to one volt per meter, depending on the antenna used. This equipment will be available commercially within a few months under the type number *NM-10A*.

The general procedure for the installation of new carrier equipment requires that extensive tests be performed on the proposed metallic circuit to determine its characteristics and to predict the performance requirements of the new installation. In making the tests it is common practice to use the carrier frequency oscillator as a carrier transmitter at one end of the circuit and the carrier frequency voltmeter as a receiver at the opposite end. The modulation features of the oscillator make it possible for the engineers to communicate between terminals during tests, which simplifies the procedure and permits more rapid progress. Usually the frequency characteristics of the circuit do not follow predictions, some frequencies showing greater or less attenuation than expected. These variations may be due to a number of causes, the most usual being the effects of branch circuits. Noise levels, also often surprisingly high, are easily measured and are usually due to cross-coupling with other lines bearing carrier communica-

Figure 4. Carrier frequency voltmeter (left) and carrier frequency oscillator (right) connected for testing power line carrier current equipment

tions, or pick-up from radio transmitting stations. All of this information is usually necessary before installation and successful operation of new circuits.

A carrier frequency oscillator, a vacuum-tube voltmeter, and a frequency meter normally are required to tune line traps. The oscillator furnishes the signal for the trap tuning but is frequently calibrated against the frequency meter in order to eliminate any error due to temperature drift. This same equipment also is used for tuning carrier transmitters.

A carrier frequency voltmeter is required to adjust line tuning units. A signal is fed into the tuning unit from either the carrier transmitter or test oscillator. Resonance of the circuit can be determined by inserting a small piece of resistance wire of about one ohm in series with each leg of the line tuning unit, and connecting the carrier frequency voltmeter across the resistance.

In the application of the test equipment to correction of faulty carrier circuit operation, it is usual for the maintenance man to first examine the condition at the nearest circuit terminus. By connecting the carrier frequency voltmeter across the circuit terminals and tuning to the frequency of the local transmitter, he is able to check the output level and modulation. Tuning to the frequency of the remote transmitter enables him to obtain the same information relative to the signal arriving from the opposite terminus. A similar use of the carrier frequency oscillator connected across the terminals will indicate if the receiver at each terminus is functioning properly In case it is necessary for the maintenance man to communicate with the opposite end of the circuit, the features of the test equipment which enable their use for communication purposes will serve his needs.

All of the test equipment has been designed to be compact and easily portable in an automobile. This makes it possible for a maintenance man to take his equipment into the field where he can readily locate troubles which cannot otherwise be isolated. The carrier frequency voltmeter can be connected directly to an open wire line and tuned to the carrier frequencies in question. The relative amplitudes of the signals arriving from the opposite directions on the circuit enable the maintenance man to determine his location with respect to a fault and indicate the direction in which to make further tests. If necessary he also can connect the carrier frequency oscillator onto the circuit and establish communication.

During field operations the test equipment is powered from a vibrator-type inverter connected to the automobile battery.

The volt-ampere capacity of any of the equipment is small enough to be powered from standard-type inverters.

During the past 20 years much advancement has been made in the design of carrier current communication system. However, little, if any, advancement has been made in the design of specialized test equipment for carrier current equipment until the last two years. Power companies and communication companies now are relying on carrier current equipment for dependable communication circuits and for other equally important functions. In order to provide these dependable circuits it is essential that suitable test equipment, such as the carrier frequency oscillator, carrier frequency voltmeter, the special vacuum-tube voltmeter, and the other test equipment described here be available to carrier engineers and maintenance personnel.

No Discussion

The Choice of Main Power Transformers for Generating Stations

N. E. DILLOW
MEMBER AIEE

J. W. BUTLER
FELLOW AIEE

Synopsis: In the past few years some lack of confidence has existed when the engineer is confronted with the task of specifying the main power transformer at generating stations. The proper choice of rating—cooling method, kilovolt-ampere size, voltage, insulation, and so forth—requires an approach which can be rationalized as good engineering. This necessitates not only an economic choice but one based on adequacy of electrical and mechanical requirements. It is the purpose of this paper to present an approach whereby the factors that affect the selection of main power transformers at generating stations may be evaluated.

IN THE early days of power plant projects, the selection of the main power transformer was a comparatively simple procedure. Generating units were generally small and being air-cooled had only one rating. In the power transformer the engineer had little to choose from in the methods of cooling, voltages, and size in kilovolt-amperes. At that time almost any choice would be a satisfactory one as the generating units were small, transmission voltages were low, and fuel and labor costs were at a considerably lower level than they are today.

However, at the present time the engineer is faced with at least six practical methods of transformer cooling. The transformers may be single- or 3-phase, and the kilovolt-ampere size should be suitable to match the generator rating. Transmission voltages as high as 360 kv are being considered. In addition, there is some latitude in the choice of impedance. These and other factors affect the selection of the main power transformer and will be considered so as to develop an approach to effect a proper application of the transformer.

Paper 50-128, recommended by the AIEE Transformers Committee and approved by the AIEE Technical Program Committee for presentation at the AIEE Summer and Pacific General Meeting, Pasadena, Calif., June 12–16, 1950. Manuscript submitted March 14, 1950; made available for printing April 6, 1950.

N. E. DILLOW is with the General Electric Company, Schenectady, N. Y.; J. W. BUTLER is with the General Electric Company, Pittsfield, Mass.

Types of Transformer Cooling

The types of cooling now available are as follows:

1. Type *OA*, self-cooled.
2. Type *OW*, water-cooled.
3. Type *OA/FA*, self-cooled/forced-air-cooled. This type of unit has 100 per cent self-cooled rating and a continuous rating of 125 per cent obtained with small fans (low-velocity air) according to present standards (125 per cent is applicable to transformers rated 3,333 kva and above).
4. Type *OA/FA/FA*, self-cooled/forced-air-cooled. This type of unit, now referred to as the super-fan-cooled transformer, has 100 per cent self-cooled rating and continuous ratings of 125 per cent and 167 per cent by the use of two sets of large fans (high-velocity air). The fans are arranged and so controlled from a winding temperature relay that they are operated in two successive steps to produce the two air-cooled ratings. As an alternate approach, certain manufacturers offer forced-oil circulation to obtain one of the upper ratings resulting in a designation of type *OA/FA/FOA*.
5. Type *FOA*, forced-oil-air-cooled. This type of unit has no self-cooled rating. Pumps circulate the oil, and heat is removed by a number of unit air coolers mounted on the sides or ends of the tank. In general, transformers are equipped with unit coolers arranged in two groups. Operation of one of the unit cooler groups permits realization of at least 70 per cent of the rating with normal temperature rise.
6. Type *FOW*, forced-oil-water-cooled. This type of unit has no self-cooled rating. Pumps circulate the oil and heat is dissipated by external oil-water heat exchangers mounted on the sides or ends of the tank. Operation of one group of heat exchangers permits realization of at least 70 per cent of the rating with normal temperature rise.

It is of interest to note that industry standards on oil-immersed transformers state in substance that transformers of all types of cooling shall have a continuous rating with an average winding temperature rise not to exceed 55 degrees centigrade and the hottest spot temperature rise not to exceed 65 degrees centigrade.

Choice of Transformer Cooling

The choice of the method of cooling for a transformer may depend on consideration of load-cycle requirements, first cost, losses, reactance, installation cost, maintenance cost, shipping limitations, and other factors. However, in general, the choice of the type of cooling should be based on the most economical transformer, the one having the minimum total capitalized cost or minimum annual cost depending on one's point of view. This cost is composed of: first cost; capitalized loss evaluation; installation costs; and capitalized maintenance costs. For consideration in this paper, the economic approach to the choice of the type of cooling will be evaluated on the annual cost basis.

Capitalized loss evaluation is probably the most variable and elusive item associated with the choice of a transformer. Many viewpoints have been expressed with considerable variation in values. However, an approach deemed reasonable although giving a somewhat conservative loss evaluation is to assign both a demand and energy charge. The demand charge can be based on the installed cost of generation. The energy charge can be based on the incremental cost of power consisting primarily of fuel costs and incremental labor and operating costs. Other means of obtaining comparative loss evaluation may be desired by the engineer, and he should apply the capitalization method which he feels best fits the problem.

The economic approach to the choice of the type of cooling can best be illustrated by an example. For consideration, assume it is desired to choose the

Table I. Example of Economic Comparison for Choice of Type of Transformer Cooling

	Type of Cooling			
	OA-T	OA/FA-T	OA/FA/FA-T	FOA-T
Rating, kva*	82,500	66,000/82,500	49,500/82,500	82,500
Impedance, per cent	7.5 at 82.5 mva	7.5 at 66 mva	7.5 at 49.5 mva	11.25 at 82.5 mva
Exciting current, per cent	2.9 at 70 mva	2.4 at 70 mva	2.0 at 70 mva	2.2 at 70 mva
Basic Loading, kva	70,000	70,000	70,000	70,000
First cost**	$215,000	$192,000	$163,000	$148,000
No-load loss, kw	163	139	113	125
Load loss at 70 mva, kw	150	206	300	280
Fans and/or pump loss, kw	——	9	26	25
Total kw loss	313	354	439	430
I^2X loss, kvar	4,460	5,570	7,430	6,680
Excitation loss, kvar	2,030	1,680	1,400	1,540
Total kvar loss	6,490	7,250	8,830	8,220
Transformer carrying charge at ten per cent	$21,500	$19,200	$16,300	$14,800
Capacity Loss at $140/kw at ten per cent	$4,380	$4,960	$6,150	$6,020
Energy Loss at 2.5 mils:				
No load loss for 8,400 hrs	$3,420	$2,920	$2,375	$2,625
Load loss for 5,977 hrs. (80 per cent load factor with 68 per cent equivalent hrs)	$2,250	$3,090	$4,500	$4,200
Kvar loss at $6/kvar at ten per cent†	$3,900	$4,350	$5,300	$4,930
Total transformer annual cost, ten per cent	$35,450	$34,520	$34,625	$32,575

* Transformer rating considered for use with 60,000/66,000-kw preferred-standard turbine generator.

** Transformer cost based on 3-phase 60-cycle 138,000 grounded Y/13,200 (115-kv insulation class) with four $2^1/_2$ per cent taps.

† Reactive kilovolt-ampere loss evaluation is optional depending on system conditions.

Table II. Example of Economic Comparison for Choice of Transformer Kilovolt-Ampere Rating

	FOA-T Type of Cooling	
Rating, kva*	75,000	82,500
Impedance, per cent	11.25 at 75 mva	11.25 at 82.5 mva
Exciting Current, per cent	20 at 70 mva	2.2 at 70 mva
Basic Loading, kva	70,000	70,000
First cost**	$137,000	$148,000
No-Load Loss, kw	117	125
Load loss at 70 mva, kw	317	280
Fans and/or pump loss, kw	23	25
Total kw loss	457	430
I^2X loss, kvar	7,350	6,680
Excitation loss, kvar	1,400	1,540
Total kvar loss	8,750	8,220
Transformer carrying charge at ten per cent	$13,700	$14,800
Capacity loss at $140/kw at ten per cent	$6,400	$6,020
Energy Loss at 2.5 mils:		
No-load loss for 8,400 hrs	$2,460	$2,625
Load loss for 5,977 hrs. (80 per cent load factor with 68 per cent equivalent hours)	$4,740	$4,200
Kvar loss at $6/kvar at ten per cent†	$5,250	$4,930
Total transformer annual cost, ten per cent	$32,550	$32,575

* Transformer rating considered for use with 60,000/66,000-kw preferred-standard turbine generator.

** Transformer cost based on 3-phase 60-cycle 138,000 grounded Y/13,200 (115-kv insulation class) with four $2^1/_2$ per cent taps.

† Kilovolt-ampere loss evaluation is optional depending on system conditions.

transformer for use with a 60,000/66,000-kw preferred-standard turbine-generator to be installed in a conventional unit plan, that is, the generator and transformer are to be in series with no switching at the generator voltage. Further, let it be assumed the transformer maximum rating is 82,500 kva and the transmission voltage is 138 kv. Table I indicates an economic comparison of the types of cooling, this approach to the problem being one deemed rational. For this example, typical values are used for demand charge at $140 per kilowatt, energy charge at 2.5 mils per kilowatt-hour, and annual carrying charge at 10 per cent. For a particular application, one might choose other values for these charges. It is the approach and not the quantities tabulated that it is intended the example will illustrate.

A basic loading of 70,000 kva is presupposed as the usual operating level for the unit. It is the loading many operators consider reasonable for a 60,000/66,000-kw machine. This does not preclude the possibility that occasionally system conditions will make it necessary to operate the unit at higher loadings, especially during emergency conditions. But it is not considered good economics to base an evaluation on emergency or abnormal loading conditions. It appears, therefore, rational to use a basic loading for the evaluation rather than the maximum transformer rating for the generating station application.

On certain systems a considerable portion of the reactive requirements is supplied by the generators. Where this is the case, it is logical to include the reactive kilovolt-ampere loss charge against the transformer. This item in the loss evaluation, therefore, becomes an optional one, being included when the reactive capabilities of the generator are necessary for normal system operation.

The total annual transformer cost for the example considering first cost and losses is indicated in Table I. To this may be added the capitalized annual cost of installation and maintenance. The engineer may include these items upon estimating these expenditures for a given application. Hence, this example in Table I can serve as a guide for comparing the economics of the types of cooling available.

A limitation on the choice of the type of cooling exists in the lower kilovolt-ampere ratings. Forced-oil-air-cooled or forced-oil-water-cooled transformers are generally not considered economical under 30,000 kva, in either single-phase or 3-phase units. Self-cooled/forced-air-cooled transformers (type *OA/FA/FA*) are not considered economical under 10,000 kva at this time in either 3-phase or single-phase units. No lower limitation exists in the available kilovolt-ampere ratings for self-cooled (type *OA*), water-cooled (type *OW*), and self-cooled/forced-air-cooled (type *OA/FA*) transformers. The shipping limitation sets the maximum kilovolt-ampere rating for all types of cooling.

Choice of Transformer Kilovolt-Ampere Rating

The choice of the transformer size in kilovolt-amperes depends on the interpretation given to the various ratings and intended loadings in service of the boiler, turbine, generator, and transformer. Since the investment in transformer capacity is low relative to that in steam-generating equipment and turbine generators, it does not appear to be good judgment to be unnecessarily conservative in the choice of the main power-transformer size. Consideration of the problem will indicate that it appears reasonable to consider the maximum capabilities of the generator when choosing the transformer kilovolt-ampere rating. Practically all steam-turbine driven generators of 15,000 kva and above are now hydrogen-cooled and rated at 1/2-pound

Table III. Transformer Ratings for Preferred-Standard Turbine Generators

Turbine Generator Rating			Transformer Rating	
Nameplate, Kw	Air or 1/3-lb H_2, Kva	15-lb H_2, Kva	Type of Unit	Rating, Kva
20,000	23,529	27,058	OA	27,500
			OA/FA	22,000/27,500
30,000	35,294	40,588	OA	41,250
			OA/FA	33,000/41,250
			FOA*	41,250
40,000	47,058	54,117	OA/FA	44,000/55,000
			FOA	55,000
60,000	70,588	81,176	OA/FA	66,000/82,500
			FOA	82,500

* Type *FOW* could be substituted for type *FOA* in the table.

hydrogen pressure with capabilities of 115 per cent at 15-pound hydrogen pressure. Experience has indicated that selecting a transformer kilovolt-ampere size in the order of the 15-pound capability of the generator has proved to be a sound selection. It is recognized that an increasing number of installations obtain auxiliary power from the terminals of the main generator, but selection of a transformer kilovolt-ampere size on the aforementioned suggested basis results in a transformer rating which best matches the plant capabilities. Certain large generators are being designed for base ratings at a 15-pound hydrogen pressure. In these cases the transformer kilovolt-ampere rating should be selected on the basis of the maximum expected capability of the generator.

The choice of the kilovolt-ampere rating can be predicated on the economic factors previously considered. Without regard to the maximum loading requirements, the economics of the choice of kilovolt-ampere size is illustrated by the example shown in Table II. Again it is assumed it is desired to choose the transformer for use with a 60,000/66,000-kw preferred-standard turbine generator to be installed in a conventional unit plan. For comparison, a 75,000-kva type-*FOA-T* transformer is considered in relation to a 82,500-kva type-*FOA-T* unit. The form of the cost comparison is the same as that used for the comparison for choice of the type of cooling. The assumed basic loading for the generator-transformer combination is the same for both sizes of transformers. Reference to the total annual transformer cost comparison in Table II will indicate that the total cost is independent of the kilovolt-ampere size for the range considered. Furthermore, choice of the larger transformer rating will provide lower transformer reactance at the basic loading of the unit, and hence offers advantages in system regulation. With other factors evaluated, such as the lower reactance and the turbine-generator capabilities, a comparatively small increase in annual cost can generally be justified. The analysis of Table II is representative and further illustrates that the choice of a transformer kilovolt-ampere rating to match the 15-pound hydrogen-cooled kilovolt-ampere rating of the generator can be justified from an economic viewpoint.

From economic studies of preferred-standard turbine generators and the step-up power transformers in a unit scheme, it has been determined that the turbine-generator and transformer ratings and types of cooling listed in Table III are preferable. The choice of the type of cooling should be determined by an analysis as previously outlined.

The choice of a 3-phase unit or three or four single-phase units for the main power transformer is a question of customer preference. However, the old argument of better service continuity when using three or four single-phase units has largely disappeared due to the demonstrated reliability of modern power transformers. Because of the excellent service record, lower cost, lower losses, and lower exciting current of 3-phase units, and because of the greater installation expense of single-phase units, the trend of the industry is to 3-phase main power transformers.

The analyses employed in the examples illustrated by Tables I and II are equally applicable to single-phase and 3-phase units. Hence, this method of comparison can be used to evaluate 3-phase versus single-phase banks.

Table IV. Step-Up Power Transformers*

Generator Rated Voltages	Transformer Voltage Rating of Low-Voltage Winding
2,400/2,500**	2,300; 2,400
2,400/4,160Y	2,300; 2,400
2,500/4,330Y	
4,800; 5,000	4,600; 4,800
6,900	6,600
11,500	11,000
12,500	12,000
13,800	13,200
14,400	13,800

* Values in this table are from reference 1.

** Generator rated voltages under 11,500 volts are generally applied to low kilovolt-ampere rating machines. Thus in this range the transformers are generally self-cooled or self-cooled/forced-air with low velocity fans (Types OA or OA/FA).

Choice of Transformer Voltage Rating

Main power transformers at generating stations are oftentimes subject to special voltage requirements to fill all the application conditions required by the system design. These application conditions dictate the secondary-voltage (high-voltage) ratings. However, the transformer primary-voltage rating should be properly co-ordinated with the generator voltage rating. Table IV shows the voltage co-ordination established by the Edison Electric Institute and the National Electrical Manufacturers Association.[1] The turn ratio should be chosen to allow both transformer and generator to operate within their prescribed ratings as established by American Standards Association Standards. This is usually accomplished by choosing the primary voltage of the transformer approximately 5 per cent below the generator voltage rating.

Choice of Transformer Impedance

Power transformers are furnished with a range of impedance values available for choice by the engineer and usually found sufficient to fulfill all application requirements. The minimum and maximum values available for self-cooled transformers are indicated by Table VI. It is noted the ranges are divided into three

Table V. Approximate Base Price and Impedance Comparison

	Type of Cooling	Fully Insulated (230 Kv B.I.L.), Per Cent	Next Lower Ins. Class with Ord. Neutral Insulated (196 Kv B.I.L.), Per Cent
Base price	OA-T	100	75
	FOA-T	100	75
Minimum standard impedances	OA-T	11	9
	FOA-T	16½	13½

Table VI. Standard Impedance Limits*

Rated High Voltage	Rated Low Voltage	Fully Insulated Min.	Fully Insulated Max.	Reduced Insulation Class or Reduced Neutral Insulation Min.	Reduced Insulation Class or Reduced Neutral Insulation Max.	Reduced Insulation Class and Reduced Neutral Insulation Min.	Reduced Insulation Class and Reduced Neutral Insulation Max.
2400–15,000	440–15,000	4.5	7				
15,001–25,000	440–15,000	5.5	8				
25,001–34,500	440–15,000	6	8				
	15,001–25,000	6.5	9				
34,501–46,000	440–25,000	6.5	9				
	25,001–34,500	7	10				
46,001–69,000	440–34,500	7	10				
	34,501–46,000	8	11				
69,001–92,000	440–34,500	7.5	10.5	7	10		
	34,501–69,000	8.5	12.5	8	11.5		
92,001–115,000	440–34,500	8	12	7.5	10.5	7	10
	34,501–69,000	9	14	8.5	12.5	8	11.5
	69,001–92,000	10	15.5	9.5	14	9	13
115,001–138,000	440–34,500	8.5	13	8	12	7.5	10.5
	34,501–69,000	9.5	15	9	14	8.5	12.5
	69,001–115,000	10.5	17	10	16	9.5	14
138,001–161,000	440–46,000	9	14	8.5	13	8	12
	46,001–92,000	10.5	16	9.5	15	9	14
	92,001–138,000	11.5	18	10.5	17	10	16
161,001–196,000	440–46,000	10	15	9	14	8.5	13
	46,001–92,000	11.5	17	10.5	16	9.5	15
	92,001–161,000	12.5	19	11.5	18	10.5	17
196,001–230,000	440–46,000	11	16	10	15	9	14
	46,001–92,000	12.5	18	11.5	17	10.5	16
	92,001–161,000	14	20	12.5	19	11.5	18

* Impedance limits apply to self-cooled, water-cooled, or self-cooled/forced-air-cooled transformers at the self- or water-cooled continuous rating of the largest capacity winding. For forced-oil-cooled units, impedance limits of 150 per cent of values listed in the table apply in each case. This impedance will apply at maximum continuous kilovolt-ampere rating. Unless otherwise specified, transformers will usually be designed to have the minimum values tabulated.

groups: (1) fully insulated where the full winding is insulated for the line-to-line voltage class; (2) reduced insulation class of one step or reduced neutral insulation where the neutral end of the winding is graded to a minimum class of 15 kv; and (3) reduced insulation class and reduced neutral insulation.

For forced-oil-air-cooled or forced-oil-water-cooled transformers, the values of Table VI are increased to 150 per cent of those values. Generally, transformers are furnished for the minimum values tabulated. It should be noted that a change in impedance will result in a change in the load and no-load losses of the transformer.

Miscellaneous Application Criteria

Omission of Transformer Voltage Taps

For many years it has been the practice to request four taps on 2-winding transformers and six taps on 3-winding transformers. These are the maximum permissible number of taps manufacturers will provide without a price increase. However, in many applications of main power transformers, experience has indicated that voltage taps are not required. If all taps are omitted, a saving of 4 per cent in the base price of the transformers results. With modern analytical methods, such as the a-c network analyzer, system performance can be accurately determined in the planning stage, and as a result one does not need to specify extra taps to take care of the operating contingencies as has been past practice. If the transformer primary voltage rating was chosen in accordance with Table IV, the necessity of voltage taps is eliminated as the generator can be used to compensate for the voltage and reactive kilovolt-ampere loss in the transformer.

Reduced-Insulation Philosophy

With transformers for transmission voltages 115 kv and higher, the philosophy of reducing the insulation class at the line end and grounding the neutral directly with a still lower insulation class at the neutral end is a rational engineering trend.

This presupposes, of course, the use of lightning arresters rated for use on an effectively grounded system and connected in close shunt relation with the transformer. The reduction of the insulation class not only results in an attractive price saving, but also results in a lower reactance at the standard price.

Where stability is a problem, special low-reactance generators are sometimes specified. It can be shown that over-all low system reactance can be obtained also economically in transformers. The use of the reduced-insulation philosophy, at both line and neutral ends, is in this direction. As an example, a price and impedance comparison is shown in Table V.

This indicates a saving of approximately 25 per cent in the base price for reduced insulation class as well as a substantial reduction in impedance for both self-cooled and forced-oil-air-cooled transformers.

Concluding Example

It is of interest to note the contribution toward decreased costs of the main power transformer occasioned by use of the practices previously presented. For example, a 82,500-kva main power transformer bank for 13.8 kv/138 kv (engineered in accordance with prewar thinking) would probably have the following characteristics: four self-cooled 27,500-kva single-phase transformers, 138 kv grounded Y (138-kv insulation class), 13.2-kv primary rating (to be used with 13.8-kv generator), with at least four $2^1/_2$ per cent taps in the high-voltage winding. The total price would be $325,000.

Based on current trends in main power transformer application, a functionally equivalent transformer could have the following characteristics: one forced-oil-air-cooled 82,500-kva 3-phase transformer, 138 kv grounded Y (115-kv insulation class), 13.2-kv primary rating (to be used with 13.8-kv generator), with no taps. The total price is $143,000 and the savings are $182,000 or 56 per cent.

To this saving in price of the main power transformer should be added the smaller physical size, lower weight, and reduced installation expense of the forced-oil-cooled unit.

It is recognized that all main power-transformer applications cannot make use of all the price-reducing features considered. However, the example does indicate the spread in costs that are available. This requires the system and application engineer to consider the application in detail.

Summary

1. The choice of the main step-up power transformer for generating stations warrants a complete economic study.

2. Choice of the type of cooling can rationally be predicated on an economic analysis based on first cost and a loss evaluation.

3. Choice of the kilovolt-ampere size should match the maximum capability of the turbine generator. Generally, the transformer should be in the order of the

15-pound hydrogen-cooled kilovolt-ampere rating of the generator.

4. Choice of voltage rating should be such that the primary voltage rating is approximately 5 per cent below the generator voltage rating. Occasionally all taps can be eliminated and a price reduction realized.

5. Choice of impedance within the standard range is sufficient for most applications. Insulation requirements will determine standard impedances.

6. Reduced insulation philosophy is based on sound principles of engineering.

7. Large investment savings are possible by evaluation of the application requirements.

Reference

1. Preferred Voltage Ratings for A-C Systems and Equipment, Joint Edison Electric Institute-National Electrical Manufacturers Association Report. *EEI Publication Number R-6, NEMA Publication Number 117* (New York, N. Y.), May 1949.

Discussion

Lester B. LeVesconte (Sargent and Lundy, Chicago, Ill.): The authors have given a good analysis of methods for estimating the real cost of transformers. While they have emphasized that they are illustrating the approach to the problem rather than actual values, one might be led to conclude that there is one particular type of transformer most suitable for a given application and set of conditions and that any engineer should be able to determine that type. Unfortunately, this does not seem to be the case because of an accounting reason rather than an engineering reason.

The authors stated that "Capitalized loss evaluation is probably the most variable and elusive item" and Table I of the paper is a good example to illustrate the truth of this statement and the lack of uniformity that exists in this field today, not only between companies but within companies.

As indicated in the paper, the charge for reactive-kilovolt-ampere loss is optional and often not included. Some also claim that the rating of generating stations would not be changed because of the transformer loss and no demand charge should be considered. Some consider the cost of energy only as the incremental cost of fuel and so forth, approaching the 2.5 mils per kilowatt-hour used in this paper while others include maintenance, overhead, and so forth, at a higher figure like 5 mils per kilowatt-hour. Some companies use carrying charges higher than the 10 per cent used by the authors while others use as low as $7^1/_4$ per cent. It is interesting to note the effect of just two factors, carrying charge and energy cost values given in Table I, using exactly the same transformer design and application. The resulting total annual costs on this basis are given in Table I of this discussion.

From these figures it will be noted that within the accounting limits given, the total annual cost can be figured to be anywhere from $17,525 to $41,500. In all cases the type-*FOA-T* indicates the lowest cost. But suppose that the type-*FOA-T* is ruled out of consideration for some other reason and a choice must be made between the other three types. In some cases the type-*OA/FA/FA-T* shows the lowest cost while in other cases it shows the highest cost. In some cases the type-*OA/FA-T* shows the lowest cost with less than $300.00 difference between it and the type *OA-T*. Thus the choice can depend on these accounting procedures.

From this it appears evident that while methods are available for the economic comparison of transformer types, as set forth in this paper, there is a crying need of more uniformity in the theory of evaluation of costs and losses.

Table I. Total Transformer Annual Cost Based on Table 1 of the Paper

	Type of Cooling			
	OA-T	OA/FA-T	OA/FA/FA-T	FOA-T
$7^1/_4$%—2.5 Mills				
Energy only	$21,270	$19,910	$18,675	$17,525
Including demand	24,450	22,590	23,135	21,895
Including kvar	27,280	25,750	26,975	25,475
$7^1/_4$%—5.0 mils				
Energy only	26,940	25,920	25,550	24,350
Including demand	30,120	29,520	30,010	28,720
Including kvar	32,950	32,680	33,850	32,300
10%—2.5 mils				
Energy only	27,170	25,210	23,175	21,625
Including demand	31,550	30,170	29,325	27,645
Including kvar	35,450	34,520	34,625	32,575
10%—5.0 mils				
Energy only	33,840	31,220	30,050	28,450
Including demand	37,220	36,180	36,200	34,470
Including kvar	41,120	40,530	41,500	39,400

Selection, Design, and Operation of Power Transformers on American Gas and Electric Company System

F. A. LANE
MEMBER AIEE

I. W. GROSS
FELLOW AIEE

P. S. PUGH
ASSOCIATE AIEE

Synopsis: This paper discusses briefly the philosophy underlying power transformer practices on the American Gas and Electric Company system. It includes power transformers used in generating, transmission, and distribution stations. It does not include transformers generally used on distribution lines to serve residential customers, or special purpose transformers not directly associated with the transmission and distribution of power.

The size and extent of the interconnected electric system on which the transformers are used are described, and the requirements of such a system discussed. Considerations entering into the selection of transformers, their general design requirements, operation, and maintenance, including principles of loading, flexibility of use, and spare transformer practices, are amplified in considerable detail. Over-all economics are emphasized.

The power transformer is a most important piece of apparatus in modern electric power systems, being second only to the generator. It makes possible the widespread use of power. In larger sizes it is the largest, heaviest, and most costly piece of electric equipment, except for the generator. In total rated capacity it far outranks all other elements; hence it is worthy of the utmost attention in our search for construction and operating economies.

Fortunately, the present-day power transformer is a most dependable piece of electric equipment. It has become so reliable that interruptions to service because of transformer failure are rare. Notwithstanding, however, there is great need for less costly transformers that are still more reliable and require less maintenance. These are the goals we seek.

American Gas and Electric Company System

THE American Gas and Electric Company system is an outgrowth of many originally isolated systems of diverse origin and characteristics. It serves 1,100,000 customers in more than 2,000 communities. Well integrated and thoroughly interconnected with 16 neighboring systems at 36 different points, its transmission extends over an area with a population of approximately 4,000,000 people in seven states. Power is served to some of the most highly industrialized portions of the nation, albeit about one-third of its customers live in rural areas.

System-generating capacity of over 2,200,000 kw is available through transmission and subtransmission networks of various voltages, essentially all operated with solidly grounded neutrals. These diverse voltages (154-, 132-, 110-, 88-, 66-, 44-, 33-, 27-, 22-kv, as well as numerous lower voltages for distribution use) make the power transformer problem a complicated one, although some of the voltages are restricted to small areas.

System Transformer Requirements

While all transformers, regardless of specific use, present many similar basic problems, different factors are stressed depending on the specific application.

Generator Transformers

Transformers used to step up generator output to transmission voltages as a general rule will be larger units than those used for other purposes. They will be be fully loaded when initially placed in service and unlikely to be required, during their existence, to handle more load. Not only is this so, but they may have to carry that load for many consecutive hours or even months with little variation. We select such transformers with sufficient capacity for any load of which the combined boiler plant and turbo-generator unit is capable without penalizing transformer life. Our practice is to specify generator transformers larger than the generator, to provide for the inherent plant capabilities above nameplate rating. We do not believe it is good practice to overload such transformers and thereby appreciably decrease their life expectancy.

Generator step-up transformers often will have more than two transmission voltages, and sometimes a winding will be included for station auxiliary supply, if the economics of transformer design do not bar it. Such a transformer is shown in Figure 1.

Step-Down Transformers

Our usual step-down station serves a growing load. Initially we install a transformer of such size that it will not have to be replaced or supplemented before a reasonable economic period has elapsed. This transformer can take the normal increases in loads until it is no longer economic to load it further even with the benefit of auxiliary cooling. Such transformers usually do not have a sustained maximum demand for more than one or two hours a day. We take advantage of this to overload the unit during such periods. There are many rules evolved for operating transformers with overloads, but in large measure the determination of how these transformers shall be operated is one of operating judgment coupled with the advice of the designer in critical cases. Transformers, generally speaking, will readily take 20 to 25 per cent overloads daily without any apparent harm so long as such overloads do not last more than a short time.

Paper 50-129, recommended by the AIEE Transformers Committee and approved by the AIEE Technical Program Committee for presentation at the AIEE Summer and Pacific General Meeting, Pasadena, Calif., June 12–16, 1950. Manuscript submitted March 14, 1950; made available for printing April 6, 1950.

F. A. Lane, I. W. Gross, and P. S. Pugh are all with the American Gas and Electric Service Corporation, New York, N. Y.

Figure 1. Four-winding single-phase generator transformer, 132Y/27/11/2.3-kv delta 40,000 kva, forced-oil and forced-air-cooled type

Three comprise a 120,000-kva bank; each is shipped completely assembled. The interior assembly has essentially been placed on its side, and the bushings depressed and tilted to limit over-all height. There are two sets of radiators with cooling fans, one in the foreground and the other at the opposite end of the transformer. This bank connects the 85,000-kw generator at the Twin Branch Plant of the Indiana & Michigan Electric Company to the 132-kv and 27-kv systems, and supplies auxiliary power to the generator through the 2.3-kv windings

Large units are required to step down from the transmission voltage to subtransmission and distribution voltages at load centers. Initially transformers in such stations have considerable capacity for load growth, differing in this respect from generator step-up transformers. We are careful not to make the transformer banks too large in order not to tie up too much capacity, relative to the load served, in a single unit. Our problem in this respect is much the same as that which determines the size of a generating unit. Such a station takes the place of a generating station in serving a community. In the ultimate setup of the station there will be two or more transformer banks so that the station capacity is not all in one bank. Usually this is a natural progression, since these stations tend to grow in size until a point is reached where diverse technical and economic conditions dictate additional stations to serve the area.

Barring other necessities, two winding units will be used, but just as often they will be transformers which step down to both a subtransmission and a distribution voltage, or perhaps two subtransmission voltages simultaneously. Considerable economy results by combining these functions into one transformer.

Transformers in large stations serving single industrial customers generally will be 2-winding transformers.

Our conventional distribution station utilizes 2-winding transformers of standard design. Single-phase units will range from 100 kva up to 5,000 kva, while 3-phase transformers will be rated from 300 kva up to 10,000 kva. They can be moved readily from one station to another as required; the majority can be connected for either 4-kv Y or 12-kv Y as needed.

Many transformers rated 1,000 to 10,000 kva are used for stepping down directly from 132 kv to distribution voltages or to subtransmission voltages in small load centers. These are 3-phase units, and the general setup of such a station will not be different from that stepping down from a lower voltage except that we omit 132-kv circuit breakers and fuses. A typical station of this type is shown in Figure 2. Usually a single 3-phase unit is the initial installation which may be replaced later with a larger one, or preferably supplemented by another similar unit as required to provide assurance against serious disarrangement of service in time of trouble.

Station Auxiliary Transformers

Power transformers ranging in size from 5,000 to 10,000 kva are used to supply generating station auxiliaries. With the unit system, it is our practice to carry

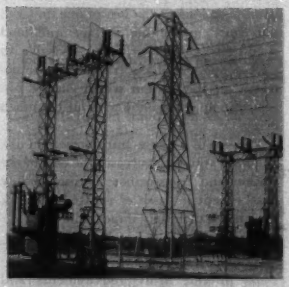

Figure 2. Transformer rated 1,500 kva 3-phase 132-kv Y/4-kv Y, stepping down to a distribution system

This transformer is tapped directly to the 132-kv line through motor-operated airbreak switches, without intervening circuit breaker or high-voltage fuses. Note the close coupled 109-kv lightning arrester mounted on the transformer tank

Figure 3. Three 3-phase 132Y/13.2-kv delta generator transformers at the new Philip Sporn Plant

They supply power from a 152,500-kw generator to the 132-kv system. Two units are rated 62,500 kva, and one unit 52,500 kva. Two larger transformers connect to the double-winding low-pressure generator and the smaller transformer connects to the single-winding high-pressure generator

the auxiliary load from two 3-phase transformers connected directly to the generator leads. Two units are used because our large generators have two independent windings, and load is best balanced in that way. It reduces risks and enables us to economize by the use of lower rated auxiliary switchgear. To provide an outside source while starting and stopping generating units and to meet emergencies, a 3-phase unit stepping down directly from 132 kv or other transmission voltage to either a single or two auxiliary voltages is provided. Such transformers are like those used in distribution step-down stations and have a capacity for the auxiliary requirements of a generating unit. Usually only one such unit is provided for a station.

Transformers for Synchronous Condensers

While synchronous condensers are sometimes provided with transformers that have no other function, most often they are connected to a tertiary winding on a main station transformer bank. Compensators are eliminated and switching simplified by using starting taps in the transformer winding. When it is necessary to have a tertiary winding for other reasons, sufficient capacity is provided to allow for the future installation of a synchronous condenser or static capacitors.

System Grounding

In stepping down from a higher to a lower voltage we usually prefer a Y-connected low-tension winding to establish a system ground so as to get the best

Figure 4. Railway portable transformer rated 15,000 kva temporarily installed at Carswell, W. Va., to supply a customer from our 132-kv lines while permanent facilities are being constructed

lightning protection and relay operation. Sometimes, however, this is not possible inasmuch as we need a Y connection on the high side, and the phasing of the system requires a delta connection on the low side. A grounding transformer on the low side then is used. Offsetting this, however, there is often a reduction in the cost of the main transformer by reason of the Y connection on the high side. Such situations require a rather complete study to determine which is the more economical and satisfactory arrangement. Generally speaking, where the higher voltages are concerned, we use the Y-connected high-tension winding for economy. If we do not provide the Y connection on the high voltage, we will have to use expensive potential transformers for relaying.

Inasmuch as our system neutrals are grounded for the most part, it is customary wherever possible to use high-voltage transformers with graded insulation, and thereby take advantage of economies in design, economics of lightning protection, and the best relaying practices.

Considerations in Selecting Transformers

Single-Phase and 3-Phase Units

Formerly, generator transformer banks, and large transformer banks stepping down from the transmission voltage to subtransmission voltages, were nearly always three single-phase units with a spare, because the physical size of a 3-phase transformer at that time made such a unit extremely difficult, if not impossible, to handle. Single-phase transformers, with a spare unit that may be connected in quickly, offers a very effective solution as far as reliability is concerned. The spare transformer and its appurtenances, however, involve a substantial idle investment at all times. With increased reliability and decrease in physical size of modern transformers, the 3-phase transformer offers a number of valuable advantages. A single 3-phase transformer without a spare involves a lower first cost but poses a problem when failure occurs. One effective answer is to utilize two 3-phase transformers, either one of which alone is capable of taking care of 60 to 70 per cent of the total requirements. When there are several generator units of similar characteristics and size, 3-phase transformers are used in each case with a single spare unit which is available for a number of generators even at different plants.

The transformer itself is not the sole consideration. Its connections must be considered, and often a 3-phase unit is not only most economical in first cost, but also in its leads, structures, and other associated appurtenances. The banking of single-phase transformers requires complicated connections, whereas a 3-phase transformer can be connected by simple direct leads. Where generating units have multiwindings or multigenerators, a 3-phase unit for each winding or generator is simplest and most economical. See Figure 3.

With our expanding system, the subtransmission networks are often fed by two or more step-down transformer stations. Thus, 3-phase transformers may be used so long as the loss of one unit will not cause intolerable voltage and load conditions. However, it is advisable to have a spare 3-phase transformer somewhere on the system which can be obtained in an emergency without too much delay.

The use of 3-phase transformers in distribution stations decreases the cost of the station and transformer so considerably that, except in cases of isolated stations, their use is definitely indicated.

Mobile Transformer Units

To provide spare requirements and meet emergencies, mobile transformers are available on our system. Five 3-phase transformers, complete with lightning arresters, are permanently mounted on drop center railroad cars. These units have all bushings permanently installed. Three of these units, with a capacity of 15,000 kva each, have a high-voltage winding of 132-kv Y and step down to

Figure 5. Portable station temporarily at Scio, Ohio, rated 2,500 kva 33/66-kv 2.4/4.16Y/7.2/12.47Y-kv supplying a load for which a station is being rebuilt

110-, 88-, and 66-kv Y, to 44-, 33-, 27-, and 22-kv Y or delta, and to 13.2- and 11.5-kv delta. All of these connections are made available by internal terminal boards which also allow 180-degree change in phase relationship. The other two units of 17,000-kva capacity each have high voltages of 88 kv, 66 kv, 44 kv, and 33 kv stepping down to low voltages of 44 kv, 33 kv, 27 kv, 22 kv, 13.2 kv, and 11 kv. These units, which are the result of many years' thought and discussion, were ordered in 1939. Although held up by the war, they became available in 1942. Although these mobile transformers were planned initially for emergen-

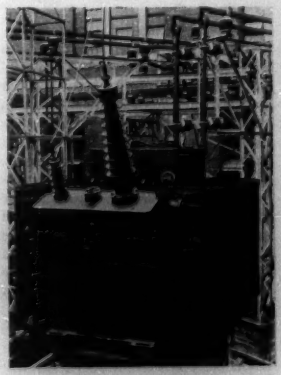

Figure 6. Generator transformer rated single-phase 40,000 kva, forced-oil- and forced-air cooled type 132Y/11 kv

Three units comprise a 120,000-kva bank. Installed at Philo plant of The Ohio Power Company in 1941, this is the first large power transformer to use forced oil and forced air cooling, and compact design. Note low head room, duplicate oil pumps and coolers, and low over-all height

Figure 7. A modern, single-phase 42,500-kva, forced-oil and forced-air-cooling type transformer

This unit is one of a bank connecting the 13.8-kv Number 2 double-winding generator at The Ohio Power Company's Tidd Plant to the 132-kv transmission system. On this unit, note close coupled lightning arresters, the compactness of the unit, and the installation of CO_2 piping for fire protection

Figure 8 (right). The same transformer as in Figure 7 during a test discharge of the CO_2 fire protection system

cies, they proved extremely useful in supplying sizeable war plant loads during the war, and in partially alleviating power-transformer shortages after the war. One of these mobile car-mounted units is shown in Figure 4.

We now are studying the possibilities of units of about 50,000 kva similarly mounted.

In order to provide quickly available capacity for distribution stations, we have on our system 11 portable stations. Each consists of a 3-phase transformer, with high-voltage airbreak switches, fuses, low-voltage oil circuit breaker, and control and protective equipment all mounted on a pneumatic-tired trailer. Each of these stations is capable of supplying power at 2.4/4-kv Y, or 7.2/12-kv Y. These have one of the following high-voltage ratings: 33/66 kv, 44 kv, 33 kv, 27/33 kv, or 22 kv. All of these are 3,000 kva except the 33/66-kv unit, which is 2,500 kva, see Figure 5. This 3,000-kva size has proved to be the largest which we can conveniently transport over the roads because of state highway regulations. We plan, however, that with progress in the art of building lightweight portable transformers, the use of 5,000- and 6,000-kva units for this purpose in the near future will be possible. Forced oil and forced air cooling is used in all of these cases to obtain lightweight and compact transformers.

These portable stations, in addition to furnishing quickly available spare capacity, also are invaluable for by-passing stations during maintenance or station changes, and for feeding unexpected load demands while permanent facilities are being constructed.

Autotransformers

Autotransformers are used wherever the ratio of transformation is between 1 and 2 and the systems to be interconnected are in phase. Autotransformers are much cheaper, smaller in size, and have lower impedance and losses than corresponding 2-winding transformers. All of our autotransformer banks are Y-connected with a delta tertiary. This tertiary winding has been used for synchronous condensers or static capacitors, subtransmission voltage supply, and generator input. The major autotransformations are from 154 to 132 kv, 132 to 110 kv, 132 to 88 kv, 132 to 66 kv, and 66 to 33 kv.

Transformer Impedances

Each combination of high- and low-voltage rating, together with the method of cooling, has a corresponding band of impedance within which the most economical transformer can be designed. For transformers stepping down to distribution voltages, an impedance at the lower limit of the economical band is selected. This facilitates the paralleling of transformer banks, when necessary, without loss of capacity. For transformers stepping down to subtransmission voltage where more than one station feeds an interconnected subtransmission system, impedances have to be selected so that the stations will divide the load in proper proportion. The transfer of large blocks of power on the transmission system complicates this problem and a thorough calculating board study of the system in these cases is made to determine the optimum impedances for the transformers. When selecting impedances for 3-winding units transforming to a subtransmission system with the tertiary winding used for a static capacitor or synchronous condenser, the impedances are selected so that the capacitance will be electrically close to the system we wish to regulate. When the subtransmission voltage is the one to be regulated, this impedance relationship falls within the natural economic design of the transformer, but when the transmission system is to be regulated, it entails special arrangement of windings with consequent higher cost, weights, and losses.

On 4-winding transformers, the equivalent impedances are determined and calculating board studies made on the effect of each system on the others. This is done with the different possible economic combinations of impedance. The proper selection and use of such a 4-winding transformer entails very close cooperation between the users, engineers, and transformer designer.

Transformer Cooling

Until about twenty years ago, our large generator step-up transformers were, in the majority of cases, water-cooled. One of the major reasons for this was to keep the physical size of the transformer down to a point where it could be handled readily. Even then, many of the large units were constructed in double-section tanks with the top section removed for shipment. Subsequent to 1930, with one exception, no water-cooled transformers have been purchased, but by 1941 developments in forced oil, forced air cooling made it possible for us to obtain a 120,000-kva generator transformer bank, the single-phase units of which were shipped completely assembled with all bushings in place. To obtain maximum reliability, the power supply for the fans and pumps is contained within the main power transformer, and is provided in duplicate so that either supply can operate all fans and pumps. The fans and pumps also are divided into two similar groups so that in case of trouble with either group, the

transformer will still carry 70 per cent load.

Other developments that contributed to the small and compact size of this unit were the use of oriented grain steel for the core, the placing of the core on its side instead of upright, and constructing the tank so that it conformed to the core very closely. Figure 6 shows the first such unit installed, and Figure 7 a later unit.

Oil-immersed self-cooled transformers, while employing the most expensive type of cooling, offer the greatest reliability and overload capacity. One of the greatest advantages of using self-cooled transformers is that if they are called upon to carry overloads in an emergency, the addition of portable high-velocity fans will increase greatly the capacity of these units. In emergencies, water often has been used directly on the cooling surfaces of a transformer to increase its capabilities. Forced-air-cooled transformers are often given additional overload capacity by changing the initial fans to higher velocity units. Each specific case requires study of the factors involved, and it is not satisfactory to follow arbitrary rules.

Our experience with applying fan cooling to self-cooled transformers and calculating the hot-spot temperature of the windings from the original heat run gives much higher permissible loads than indicated by the rule-of-thumb method set down by National Electrical Manufacturers Association standards.

Overload Provisions

While no specific requirements have been made as to the ability of transformers to carry overloads, this thought is always in the picture.

Any transformer that reaches an overload condition which cannot be relieved immediately is subjected to detailed study to determine the possibilities. Usually some expedient can be found to carry the load required. In the case of multiwinding transformers, light loading on one of the windings enables the others to carry substantial overloads.

Tap Changing Under Load

In designing larger distribution stations where bus regulation is required, we find it most economical to include low-voltage tap changing under load in 3-phase transformers where the capacity is 5,000 kva or more. In smaller size stations, it is often more economical to use a separate step-voltage regulator for bus regulation.

Fire Protection of Transformers

Special fire protection for transformers has been used only in relatively few cases. Generally speaking, these involve generator step-up transformers. In a few instances we have installed automatic sprinkler systems, using spray nozzles to extinguish the fire.

We have installed a larger number of protective schemes on generator transformers using carbon dioxide as the extinguishing agent. This has been done notably at all our most recent generating stations. In many cases fire barriers have been built between adjacent transformers when they were located in important installations. Figure 8 shows a test discharge on the transformer shown in Figure 7.

For the most part, however, special fire protective barriers and extinguishing systems have not been applied to power transformers. The fire protective and extinguishing equipment supplied for a station as a whole has been selected to be adequate for transformer fire protection. Generally speaking, it consists of water available in the form of spray, or foam supplied either through fixed or portable equipment. In the smaller transmission and distribution stations the fire protective equipment for transformers is generally no more than is available for other risks.

Transformer Design

Lighter Weight

The modern transformer is more economical in its use of material than was the case a few years ago. It is therefore lighter and has smaller dimensions than formerly. This is reflected directly both in the cost of the transformer initially and in the lower costs of installation. Less costly foundations are required, less expensive structures will suffice. The lighter weight and smaller dimensions also enable complete factory assembly so that it can be installed directly on its foundations without any appreciable assembly work. This further contributes to economy of installation.

Multiwinding Transformers

While most transformers are of the 2-winding type, it often has been found economical to utilize transformers having three or four windings, and consideration has been given to units having five windings.

As the number of windings increases, design problems become more difficult. Only in the larger size transformers is it feasible to have these extra windings because of the lack of space on the outside of the transformer to locate the various bushings and other accessories. There is a distinct saving in first cost when transformer capacity is attained by including additional windings, and an equally attractive saving in foundations, structures, and simplified switching. When any one of the windings is less than one-fourth the capacity of the largest winding, the economics of including the smaller winding should be questioned.

Transformer Taps

The mistake of not having enough transformer taps is more often made than that of having too many. In the higher voltage transformers it is customary to place a sufficient number of taps in the high-voltage winding to cover the range of voltages which is likely to be encountered. Except in rare cases, this range will not exceed 10 per cent of the rated voltage, nor will more than five taps be required. In the lower voltage and the smaller transformers, it has been necessary to consider past practice in arriving at taps and tap ranges. Many years ago most distribution systems were based on 2,200 volts, or in the higher voltages some multiple of 110 volts. Transformers customarily were purchased with a given high voltage and four or five taps at $2^1/_2$ per cent intervals below that voltage. As voltage standards increased, 2,200 volts were changed to 2,300, later to 2,400, and then to 2,500. It was necessary in buying new transformers that they parallel in

Figure 9. A single-phase unit of an autotransformer bank rated 105,000 kva, forced-oil and forced-air-cooling type

The over-all height of this transformer has been kept to a minimum by the location of the bushings in pockets on the sides of the tank and the use of a special lightning arrester composed of two separate vertical stacks connected in series

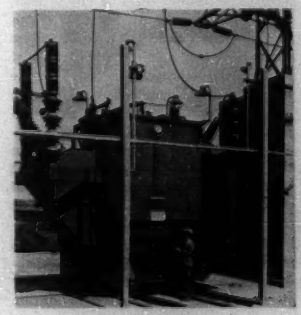

some degree, at least, the old ones. Consequently, through the years our specifications have been changed so that the new transformers would parallel at least partially with the old ones, but at the same time attempts were made to keep the tap range and the number of taps within standards which would not penalize us on first cost. Fortunately, this situation has now worked out so that the taps and tap ranges generally used by the industry are applicable to our purposes and will parallel with the older transformers without too much difficulty.

In a 2-winding transformer the tap situation is relatively simple. One winding need have no taps at all, and the other can be designed to cover the voltage range which the transformer must serve. There is usually not too much difficulty in arriving at a choice in this matter. In 3- or 4-winding transformers taps are needed in all but one of the windings to provide the same flexibility attained in 2-winding transformers.

Lightning Arrester Application

The impulse or lightning protection of transformer insulation has received serious consideration on our system for some thirty years. As field research determined the characteristics of natural lightning and laboratory work disclosed the effects of lightning on transformer insulation, and, further, as the protective characteristics of lightning arresters were better understood, it was possible to co-ordinate all factors on an engineering basis.

In the early 1930's it became apparent that lightning arresters, which in some cases previously had fallen into disrepute, were not capable of protecting the then existing transformers; the lightning-arrester protective levels were too high, and the transformer insulation strength was too low. As the result of a careful study made at that time, it was decided to reduce lightning-arrester ratings over the entire high-voltage system and this resulted in marked improvement in transformer performance against lightning surges.

The success of this forward step was followed by further study of the possibility of reducing transformer insulation below the then accepted industry standards of impulse values of full rated insulation, and co-ordinating the transformer strength with lightning-arrester protective levels was undertaken. This resulted, in 1934, in adopting the so-called reduced insulation on a 30,000-kva 132-kv transformer bank where a lightning arrester of reduced rating was mounted directly on the transformer bank; see

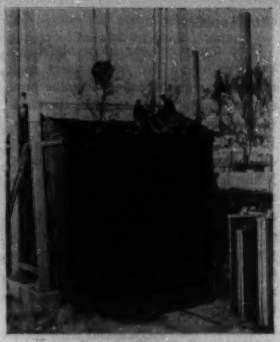

Figure 10. A portable tent attached to steel A frame for weather protection during field repair of a transformer

This tent and an electric hoist are portable and fit a number of different A frames, and are moved to locations as needed. The top of tent rolls back for untanking transformers

Figure 9. In this way, it was possible to use 115-kv class insulation for the transformers and a 75 per cent lightning arrester on our 132-kv grounded neutral system with an over-all saving in the order of 15 to 20 per cent. This practice has been continued up to the present time with complete transformer protection and entire satisfaction.

During the last 16 years, there have been installed on the American Gas and Electric Service Company system, nearly 3,750,000 kva of transformer capacity in the range of 88, 132, and 154 kv, all having reduced insulation, that is, one level below the standard basic impulse level values. 180,000 kva have been on 154-kv lines, over 40,000 kva on 88-kv lines, and approximately 3,500,000 kva on the 132-kv system. Practically all of this kilovolt-ampere capacity has been impulse-tested at the factory to the extent that one transformer, at least, of any bank has received the factory test, and in some cases all transformers comprising the bank. In almost all cases where reduced insulation is used in the transformer windings, bushings likewise have a reduced insulation rating. The saving in first cost of the transformers alone, to date, by the use of reduced insulation as described here, has been estimated at $1,500,000.

Commercial factory impulse tests have been a valuable and indispensable means of proving that the transformer strength specified actually is obtained. In 12 cases of transformer failures that occurred on factory tests, defects in the design or faulty workmanship or material were found in every case. To our knowledge some 500,000 kva (13 per cent) of transformers capacity-tested have failed during the factory impulse tests mentioned.

At the present time, in adapting lightning-arrester protection to transformers, all important cases are checked to make sure that the lightning arrester properly fits the application as regards providing an adequate lightning arrester (60-cycle rating), and maintaining a margin between the lightning-arrester protective level and the transformer-tested strength.

We have not carried reduced insulation into or below the 66-kv class of transformers, as no transformer cost reduction has been indicated by the manufacturers up to the present time.

In all cases where reduced transformer insulation has been applied, the system has been grounded solidly, although quite a few cases exist where the transformer is delta-connected. The system overvoltages under fault conditions, however, are such that reduced rated arresters, in the order of 75 per cent, have been applied with some 30 per cent margin or more between the lightning arrester protective level and the transformer full-wave tested strength.

Transformer Accessories

Transformer accessories, such as thermometers, oil gauges, hot spot indicators, alarm signals, tap changers, radiator valves, drain valves, explosion relief devices, fans, oil pumps and controls, trucks and nitrogen gas control equipment, do not have the same reliability and long life as the transformer windings themselves. These devices usually require more maintenance over long periods of time than the other parts of the transformer. In the last 20 years considerable improvement has been made in respect to oil gauges, valves, explosion relief devices, tap changers, and nitrogen gas control equipment, but all such accessories still require considerable maintenance and there is room for further improvement.

On large transformer banks, bushing current transformers are provided on all line bushings for operating the transformer differential protection. An extra set of bushing current transformers is also provided on the high-voltage bushings where the transformer is connected to the 132-kv system without a circuit breaker; these are used for high-speed carrier current relaying.

At small distribution stations, bushing current transformers are provided on the low-voltage bushings to operate thermal demand meters. This has proved the

least expensive method of transformer load indication.

Considerable progress has been made in preventing leaks in transformer tanks. The main steps in this direction have been the elimination of gasketed joints by welding, wherever possible, and the substitution of properly designed gasket joints using synthetic rubber instead of cork, where such joints are necessary.

Oil Preservation

Our experience through the years with the different methods of oil preservation has indicated that the use of a cushion of nitrogen gas over the oil, maintained by a bottle of nitrogen gas under pressure, is the most satisfactory. This gives maximum preservation of the oil, has less chance of rupturing the tank and causing a fire from an internal explosion, and leaves the tank cover free of obstacles such as conservators which interfere with the high-voltage lead connections.

Transformer Operation

Field Servicing of Transformers

No matter how well the transformer aspects of an electric system may have been worked out, designs perfected, overvoltage protection supplied, and construction carried out satisfactorily, there is always the problem of field maintenance after the transformer is put into use. Field servicing during the useful life of equipment is a very important element of transformer operation.

About 1932, in connection with the power-factor field testing of bushings, we started in a small way similar insulation testing of the larger power transformers. This test work has expanded steadily, and numerous conditions hazardous to safety and continuous operation of transformers have been found in this way and corrected before costly failures occurred. Field power-factor testing of large power transformer insulation is now on a routine basis. Tests are being made periodically at approximately 3-year intervals. These tests include not only transformer windings but also transformer bushings and oil. We also use a special field test set, developed by us, to determine oil neutralization number and color where the oil is questionable. In addition, dielectric tests of the oil are made at much more frequent intervals. In cases where field tests have shown the oil questionable, a detailed oil analysis is made in our laboratory and, based on our laboratory recommendations, the oil is reconditioned or reserviced as required.

Oil Handling

Over the years our ideas about the handling of oil for transformers have undergone a great change. At the present time our object is to make the facilities for handling oil as simple as possible. It is necessary to supply clean and dirty oil tanks at nearly all large stations. While formerly we used very elaborate fixed pumping systems, with large amounts of pipe laid in the ground, much of this has been eliminated. Our general practice now is to utilize portable pumping and filtering equipment which can be moved directly to the apparatus being treated and to use flexible tubing or other portable piping. This transition from the elaborate oil handling and purifying schemes of the past has resulted in a tremendous saving not only in equipment but in building space.

Reclamation of oil is carried out by filtering through fuller's earth when necessary.

Transformer Protection

All of the larger transformers have differential relay protection. Generator transformers do not have overload protection; but, generally speaking, the transformers in step-down stations do. Frequently, generator transformers will have not only a separate differential relay system but also differential relay protection to include both the generator and the transformers.

Although Buchholz relays have been used to a large degree in Europe, and we have given them serious consideration, they do not appear to us to have sufficient advantages to justify their use.

Transformers in the large sizes and especially those with forced oil, forced air cooling have been provided with thermal relays which function if operating temperatures are exceeded (which may result from loss of air or oil pressure). While some advocate tripping the transformer off the line when these relays operate, we have felt that it is preferable to use the alarm to give a warning signal only.

Switching Spare Transformers

Although it was general practice in past years to move spare transformers to replace a damaged unit, the time and effort required resulted in serious delays in restoring service. As a result of our experience we now arrange the spare transformer so that it can be cut in and out of service to replace any regular transformer without physically moving it.

In case of a delta connection, this can be done readily by using hot-line clamps to connect the spare transformer to the proper extended delta bus. For a Y connection, one terminal of the spare transformer is permanently connected to the neutral, and a jack bus extending from the other terminal permits replacing any transformer of the bank. Where two banks are used a single spare, in the same way, can serve both. Anything more elaborate than this is not warranted.

In a few isolated cases, substitution of the spare transformer for one of the others has been carried out without de-energizing the transformer bank by using hot-line tools. A great deal of care is necessary in carrying out such an operation, and except in emergencies, it is not generally recommended, although experience has proven that it can be carried out successfully.

Field Repair of Transformers

When necessary to repair transformers, serious consideration is given to whether or not the work will be done at the transformer location. Minor repairs are carried out at the site. For major repairs, the transformer is usually moved to a location where there are adequate shop facilities. Such facilities are available on the American Gas and Electric Company system at a few of the older major stations. Experience has shown, however, that these were seldom used; hence, in later stations they have not been furnished. Major transformer rebuilding or repair is best handled by transporting the transformer to the factory or manufacturer's service shop. On a system such as ours, which is spread over a very wide area, it is more economical to handle the situation in this manner than to have a central service shop requiring the maintenance of an organization and facilities.

Transformer Overhaul

It has never been possible to determine how frequently large power transformers should be given periodic overhauls. Although this subject has been studied for many years, our conclusion is that such overhaul should be undertaken only when it is indicated that the transformers need it. While it is somewhat difficult to tell just when they do need an overhaul, data obtained from Doble power-factor testing, from the use of meggers, and by testing the oil usually is sufficient to give us a clue as to overhaul requirements. An inspection without untanking sometimes will suffice.

Most field overhauling of large transformers has been carried out by the use of *A* frames and temporary shelters. At a

number of points on the system it was customary in years gone by to install permanent *A* frames, usually at large transformer stations. This is not the present practice. It is more economical to set up temporary wood pole *A* frames with canvas shelters for carrying on this work. A typical *A* frame and portable canvas shelter is shown in Figure 10.

Smaller size transformers are best moved to a point where hoisting and other facilities are available for handling that kind of work. This may be the manufacturer's service shop or a company service shop.

Summary and Conclusions

Among the highlights of our transformer practice described in this paper are the following:

1. The rating of generator transformers always exceeds the generator nameplate rating in order to take advantage of the overload capabilities of the generator.

2. By improvement of transformer iron, forced oil cooling, and the reduced insulation we use on our 132-kv system, the over-all weight, dimensions, and cost of large transformers have been basically lowered.

3. Autotransformers are used, where applicable, because of their greater efficiency and lower weight and cost, where transformation ratios do not exceed 2-to-1.

4. Three-phase transformers are now used in many locations because of decreased cost, a high degree of reliability, and because their use simplifies installation arrangements.

5. About $1,500,000 in initial transformer costs has been saved during the past 16 years by the use of reduced insulation (one level lower than industry standard) for transformers on our 132-kv system, with complete satisfaction and without a single transformer failure resulting from this practice.

6. Some transformers arranged for tap changing under load have been used, and the practice has become more prevalent. These are applied generally in the distribution range of 4 to 12 kv; so far it has not been found necessary above 44 kv.

7. The practice of using multiwinding transformers, for example, three and four windings, is quite prevalent and has resulted in considerable economies.

8. Field servicing of large transformers was formerly done on the site. At the present time, where major repairs are required, usually it is done at the manufacturer's plant or at the service shop.

9. The size and characteristics of our system require that transformer reactances, in many cases, be chosen to fit each application. In such cases, we make calculating board studies of the system setup to predetermine the required transformer reactances to produce the desired power flow under stable and transient conditions.

10. Portable railroad car mounted transformers in a high-voltage range of 33 to 132 kv now are available for use on our system. These are 15,000- to 17,000-kva 3-phase units, and have proved invaluable during and after the war to supply emergency loads and provide temporary service while new stations were being built.

11. Eleven portable substations for highway transportation, consisting of 3-phase transformers, switching, and protective equipment are in use. In general, these are 3,000 kva, with voltage ratings from 22 to 66 kv on the high side, stepping down to distribution voltages. The availability of these portable substations eliminates the necessity of providing spare transformers in many small distribution stations. They also are used to by-pass stations during repair and serve emergency loads.

Discussion

F. L. Snyder (Westinghouse Electric Corporation, Sharon, Pa.): The authors have thoroughly and concisely outlined the principles followed by the American Gas and Electric Company in the selection, design, and operation of power transformers. I would like to briefly point out the savings in capital investment in transformers which can be achieved through the medium of the principles outlined in the paper.

Assuming that the cost of four single-phase transformers for a 75,000-kva generating station and a transmission voltage of 138,000 volts is 100 per cent, or a base cost of approximately $322,000, the following reductions in capital investment can be made by taking advantage of certain principles in the design and operation of the transformers for such a station:

1. At generating stations, the use of two 3-phase transformers instead of four single-phase transformers reduces the cost $51,000, or 15 per cent.

2. The use of one 3-phase transformer instead of four single-phase transformers reduces the cost an additional $40,000, or an additional 15 per cent, or to 72 per cent of the base.

3. The use of water-cooled transformers instead of self-cooled transformers reduces the cost another $38,000, or 17 per cent, or to 60 per cent of the base.

4. The use of forced-oil cooling with an oil-to-air cooler reduces the cost an additional $30,000, or 15 per cent, or to 51 per cent of the base.

5. If an oil-to-water cooler is used instead of an oil-to-air cooler, additional savings of $14,000 to $149,000, or 47 per cent of the base, will be achieved.

6. The use of a graded insulation with full basic impulse levels makes possible a further reduction of $7,000 to $142,000.

7. Reducing the insulation level from one full voltage class achieves a further cost reduction of $15,000, or roughly 10 per cent.

8. At switching or receiving stations where, because of higher low voltage the base cost may be $381,000, the use of an autotransformer instead of a 2-winding transformer at the step-down stations on the transmission line makes possible an ultimate reduction in cost to 30 per cent of the base, assuming that the transformation ratio is 138,000 volts to 69,000 volts.

The trend towards the use of 3-phase transformers rather than single-phase transformers is illustrated by production statistics, which show that whereas 20 years ago two-thirds of all large power transformers were single-phase and only one-third 3-phase, today two-thirds of all such transformers are 3-phase and only one-third are single-phase.

Today approximately 50 per cent of all large power transformers are forced-oil cooled, approximately 25 per cent have auxiliary forced-air cooling, and approximately 25 per cent are straight self-cooled—whereas, prior to World War II, practically all large power transformers were straight self-cooled, either with or without auxiliary forced-air cooling.

It is recognized that it may not be possible nor practical to take advantage of all of these principles on any one particular installation, but it should be possible to take advantage of one or more in the great majority of large power transformer applications, as the authors have done.

Eric T. B. Gross (Illinois Institute of Technology, Chicago, Ill.): This paper should be of considerable interest to the power systems' engineer since it indicates present-day practices of a large company. Of particular value are references to previous practice, as for example the comparison between 3-phase transformers of today and banks of single-phase transformers used before the war. I am not too certain, however, that the size of the 3-phase transformer prevented its application, since I remember that 3-phase units of 75 megavolt-amperes rating were in use in Europe in 1935, and these were designed for 50 cycles.

It is noted that transformers with a nitrogen cushion above the oil level is given preference. However, it seems that the experts are not unanimous in the opinions as to the value of this method and the conservator type. In Canada, for example, conservators are used without exception,[1] and recent Swedish research seems to indi-

cate that inhibitors used with conservators preserve the oil excellently.[3]

It is interesting that bushing current transformers of the transformer proper are used for differential protection, thereby limiting the zone of protection to the inside of the tank, and excluding the leads to the circuit breakers and the outside of the transformer cover.

The statement that gas- and pressure-relays do not appear "to have sufficient advantages to justify their use" needs some qualification, especially in the light of recent experiences in Canada with such relays,[4,5,6,7] and with reference to the report on Relay Protection of Power Transformers[7] which contained the following recommendations:

"The value of gas accumulator relays for detecting incipient faults has been underestimated generally in the United States.

"Substantial experience in Canada has demonstrated the value of gas accumulator relays to detect conditions such as turn-to-turn faults, core insulation failures, and defective joints.

"Objections commonly raised to the gas accumulator method of detecting faults can be overcome largely by suitable application and proper interpretation of relay indications.

"The present commercially developed gas detector relays are limited in application to conservator-type transformers. Experimental installations indicate that devices may be developed for extending gas detection principles to other types of transformers."

"The wider application of pressure protection offers considerable promise: (a) to provide supplemental protection with sensitivity greater than usually obtained with conventional differential schemes alone; (b) for protection, when used with overcurrent relays, where it is not feasible to provide a satisfactory differential scheme; (c) to solve inherently difficult application problems, such as with step regulators and rectifier transformers; and (d) for fast, low cost protection and reclosing lockout of feeder voltage regulators."

References

1. *Discussion* by **A. M. Doyle** of Relay Protection of Power Transformers, **AIEE Committee Report**. *AIEE Transactions*, volume 66, 1947, page 915.

2. The Effect of Inhibitors on the Oxidation of Transformer Oil, **H. Liander, G. Ericson**. *Technical Achievements of Asea Research*, Allmanna Svenska Elektriska Aktiebolaget (Vasteras, Sweden), 1947, pages 174–86.

3. Typical Transformer Faults and Gas Detector Relay Protection, **J. T. Madill**. *AIEE Transactions*, volume 66, 1947, pages 1052–60.

4. Shipshaw Relay Protection, **J. T. Madill, F. H. Duffy**. *AIEE Transactions*, volume 68, part I, 1949, pages 50–55.

5. Simplicity in Transformer Protection, **Eric T. B. Gross**. *Electrical Engineering*, volume 66, June 1947, pages 564–69.

6. Philosophy of Relaying, **E. W. Knapp, Ben C. Hicks**. *Electrical Engineering* (*AIEE Transactions*), volume 65, November 1946, pages 735–41, 1135.

7. Relay Protection of Power Transformers, **AIEE Committee Report**. *AIEE Transactions*, volume 66, 1947, pages 911–15, and discussions by **A. M. Doyle, F. L. Lawton, E. E. George**, pages 915–16.

A. N. Garin (General Electric Company, Pittsfield, Mass.): This very comprehensive paper by one of our leading utilities will undoubtedly stimulate an exchange of views and will be studied and discussed by the engineers of other operating companies. I am sure, however, that engineers of various transformer manufacturing companies will be even more interested in what amounts to a very first systematic exposition of the present ideas on transformers, by the users of transformers.

A power transformer is a wonderful piece of apparatus, with a very long and impressive history back of it. It possesses inherent flexibility, and offers great opportunities for still further development. The progress in the design and manufacturing of power transformers over the last half century has been truly extraordinary. Naturally, this progress has been directed simultaneously at quite a few somewhat divergent, but fortunately not completely irreconcilable, objectives. Modern transformers, as contrasted with their prototypes, are not only smaller, lighter, less costly, more efficient, and more reliable, but also incorporate many features that were absent in the original product. These features have been built into transformers to utilize them as (to quote a comparison that has been used before) "universal joints" in a power transmission system. I need only mention means for adjusting the turn ratio or the phase angle of transformation at no load, or without interruption of the load, various reactance relations in multiwinding transformers that fit, or complement, the reactances of the transmission system itself, and so forth.

Undoubtedly, simultaneous progress in all of these directions can continue for a long time to come. Better understanding of the fundamental electromagnetic and thermal phenomena in transformers, better materials, and better manufacturing techniques will result in transformers becoming more efficient, reliable, less costly, and smaller in weights and dimensions, and incorporating to an even greater degree various special features that make the transformer such a versatile link in the power system. It must be realized, however, that if the objectives were more clearly defined in the order of their importance, much more rapid progress could be achieved by concentrating on a few of the very many desirable characteristics.

Obviously, it is up to the operating people to define the objectives that are foremost in their mind. To quote from the paper: "There is great need for less costly transformers that are still more reliable and require less maintenance."

If we accept this statement as a directive indicating the preferred line of advance, then some general observations can be made. It must be recognized that minimum cost, maximum reliability and minimum maintenance are, of necessity, somewhat inimical to the requirement of flexibility in application. To illustrate, a design with load ratio control or manual taps permitting the operation of a transformer at a number of different transformation ratios cannot be, in the nature of things, as economical in the first cost, as reliable, or require as little maintenance as a similar transformer without taps. Similarly, a transformer with considerable overload or over-excitation capacity built into it cannot possibly show the same degree of utilization of materials in its construction as a transformer of similar rating but designed for operation at constant excitation and constant load. The oil conservator has proved itself, in the opinion of many operating companies, to be an entirely adequate method of oil preservation for modern power transformers, and yet the brief paragraph in the paper under the title Oil Preservation states a definite preference for gas cushion transformers.

It is important that purchasers of transformers realize, as transformer designers do, that a gas cushion design requires a taller tank than an oil conservator design; therefore, the preference expressed stands in conflict not only with the objective of minimum maintenance, but also with the objective of obtaining minimum weights and dimensions and maximum kilovolt-ampere ratings capable of shipment without disassembling.

This line of reasoning can be carried farther. For instance, maximum inspectability of the transformer core and coils or maximum accessibility of various parts of the transformer for repair work will, in some cases, militate against compactness and economy of design. Obviously, no academic approach can be taken in connection with such an eminently practical and vital piece of equipment as a transformer, and none of the practical requirements could be neglected or disregarded for the sake of spectacular progress in some selected characteristics. Nevertheless, it would be very helpful, both for the users and manufacturers of transformers, to give this matter of somewhat conflicting requirements more thought than perhaps has been given in the past.

The question of emphasis on some characteristics at the expense of others is particularly important when transformers for more or less special applications are under consideration. As an example, generator transformers referred to on the first page of the paper are a specific case where maximum economies, reliability, and kilovolt-ampere capacities within the limits of permissible weights and dimensions can be obtained by a clear-cut policy of limiting the number of windings to two, eliminating all the taps, and permitting a free choice of the voltage rating of the low-voltage winding, on the basis of a concept defining a step-up transformer as an integral part of the generator.

Another example along the same lines is the case of mobile units referred to in the paper. On the assumption that the two primary objectives in mobile units are obtaining maximum capacity within the limits of weights and dimensions imposed by transportation facilities, and obtaining maximum flexibility of connections to make these units suitable for application at as many points of a system as possible, it follows that some other characteristics and requirements, normally expected of stationary transformers, must be sacrificed. These characteristics may be the level of losses, the sound level, the reactance level, the insulation level, and the temperature rises. However, a reduction in insulation level might be particularly undesirable in a piece of equipment that must be relied on in emergencies.

An increase in the temperature rises may be equally unacceptable because of its bearing on the probable useful life of the equipment. Increased reactances may affect undesirably the usefulness of the portable transformer as an emergency link in the

system or may necessitate extra wide tap ranges in the windings to compensate for the high regulation drop, thus resulting in larger, rather than smaller, size and weight per kilovolt-ampere of output. It is obvious, therefore, that any sacrifice in any one of these directions may be objectionable and should be a matter of explicit consideration and complete agreement between the purchaser and the manufacturer.

Broadly speaking, we are in complete agreement with the comments on impulse testing. It cannot be stressed too much, however, that not only the value of commercial impulse testing, but the advisability itself of subjecting transformers to commercial impulse tests, depend completely on the reliabilty of failure detection. Thus, the statement: "Commercial factory impulse tests have been a valuable and indispensable means of proving that the transformer strength specified actually is obtained" is true statistically, but the possibility is not excluded that some of the transformers, particularly in the early years of impulse testing, that apparently passed the test had actually failed without the failure being detected. The next statement to the effect that: "In 12 cases of transformer failures that occurred on factory tests, defects in the design or faulty workmanship or material were found in every case," could also be amplified. The greatest concern of transformer designers and manufacturers in connection with impulse tests does not lie in the possibility that the tangible cause for failure of a given unit on impulse test will not be found, but in the possibility of damaging the transformer by the impulse test without any indication of this damage within the scope of the failure-detection means incorporated in the regular commercial testing procedure. Only the gradual advance in the art of impulse testing from this particular viewpoint and the present reliability of detection justify the widespread practice of subjecting transformers to commercial impulse tests. Engineers of the American Gas and Electric Company have always been outstandingly willing to co-operate with transformer designers in discussing the specific objectives and requirements of the more complicated transformers.

As pointed out in the paper, one example of a situation where such discussions can result in very substantial savings and improvements in quality of the product is the case of multiwinding transformers referred to in the paper. A 3-winding transformer has three values of short circuit impedance between windings, a 4-winding transformer has six, and a 5-winding has ten. A system study may indicate certain preferred values of these reactances and normally this information is passed on to the transformer manufacturer with the request that he provide a design which will satisfy all of these impedance values. Now, a transformer is a very flexible device and a good transformer designer is a very skillful manipulator of shapes, dimensions, and arrangements of windings so that usually he can arrive at a design to satisfy all of these impedance requirements within the accepted American Standards Association tolerances. It would be a miracle, however, if such a design should also give maximum economy and reliability. Very often slight departures from specified impedance values, so slight that they would not affect the usefulness of the transformer on the system, result in a much better design.

F. A. Lane: Mr. Snyder's comments add emphasis to some of the points brought out in the paper. Most of his data have to do with the first cost of the transformer. It is important, however, not to lose sight of other costs, many of which have a strong bearing on the final installed cost of the transformer, which, in the end, is the thing we are after. It may be found that the transformer which is sold at the lowest price is not the most economical one when finally installed. For example, the connections to a transformer or bank of transformers may be simple or very complex. A complex arrangement may cost a great deal of money, and whether it is simple or complex may depend on the type of transformer. It is often found that a more expensive transformer will result in a simpler connection layout and lower installed cost. Hence, while attention must be paid to the design of a transformer from the first cost angle, this should not be to the exclusion of other factors which will enter into the final installed cost and which, if not carefully surveyed, may result in a higher final cost than is warranted.

Mr. Eric T. B. Gross points out that large-size 3-phase transformers were in use in Europe at least as early as 1935. In this country we could have used larger 3-phase transformers than were used had we so desired. At that time, however, the reliability of transformers had not been as well established as it is now, and a great many large transformer banks were made up of single-phase units in order to guard against loss of transformer banks for extended periods. Spare transformers were usually immediately available in case of failure.

Mr. Gross also comments on the use of bushing current transformers in the transformer proper for differential relay protection, thereby limiting the zone of protection to the inside of the tank. This practice has not proved to be disadvantageous and it may be noted that it is inside the tank where most destructive results occur. The loss of a bushing or the loss of connections external to the transformer is not a serious matter, as these can be replaced with relative ease and at relatively low cost. Damage inside the transformer, however, is another matter and may have extremely serious consequences.

Reference is made to the use of gas relays and it may be noted that this type of relay has been known in this country for a great many years. It has been given a great deal of consideration. Many of us, however, are far from convinced that the gas relay has a great deal to offer that we cannot get some other way.

Mr. Garin brings out in his remarks the necessity for compromise in design of a transformer to meet all of the requirements. It cannot be too strongly emphasized that the best results can only be in the nature of a compromise. All angles of the problem must be studied, and frequently it is necessary to discuss the transformer itself in great degree with the manufacturer. As users we are not designers and do not have the understanding of the fine points of transformer design that are within the grasp of those whose specialty is to design and build transformers. By getting together with these people, however, and by exchanging points of view between the user and designer, it is possible to bring out the effect of various changes in design on the results which the user wishes to obtain. In this way a compromise design may often be arrived at, with more satisfactory results than would have been the case had such conference not been had. It is always helpful if all those concerned can discuss the problems involved.

Mr. E. T. B. Gross and Mr. Garin raised a question about the gas cushion transformer. It should be made clear that we do not question the ability of the conservator-type transformer to give us good results with the insulating oil. For a long time we went on the assumption that both conservator and gas cushion designs gave essentially the same protection to the oil. Accumulated experience now indicates that the gas cushion is superior in this respect.

It is pointed out that the transformer with the gas cushion has a taller tank than that of the conservator type. It might be questioned that the over-all height of the two transformers is vastly different when we get all through with them. The conservator tank has been found to interfere seriously with a proper installation of a transformer. Emphatically it is in the way. Getting leads from the various bushings so placed that clearances will be adequate has proved, time and again, to be a most embarrassing problem. Elimination of this conservator tank largely eliminates that problem. For this reason more than any other, the conservator tank has become an unwelcome portion of a transformer.

In addition, the point is often made that the conservator tank supplies a head of oil to feed the flames of fires that are started at the time of bushing failures which result in fracture, allowing oil to escape and catch fire. While this has often been the case, it may be reasonably argued that it has not taken place sufficiently often to be a major factor. However, it is a substantial one in the eyes of many users.

It may be noted that the writers of the paper feel very strongly that impulse tests of new transformers have been amply justified by the results. There has been some tendency to question this. The record, however, can speak for itself, and there is no question but that the results of impulse testing have shown the way to detect design and construction defects in transformers, and to give us a product that is highly reliable.

Thirteen-Year Lightning Performance of Boulder 287.5-Kv Transmission Lines

T. M. BLAKESLEE
FELLOW AIEE

E. L. KANOUSE
MEMBER AIEE

THIS paper presents the lightning performance data that have been accumulated on the 287,500-volt Hoover Dam-to-Los Angeles transmission lines over the first 13-year period these lines have been in operation. The design data for these circuits have been presented to the Institute[1] and a comparison with other high-voltage lines in this country on features pertinent to lightning performance will be found in an AIEE committee report presented in 1946.[2] Figure 1 shows a standard single-circuit suspension tower and indicates the dimensions pertinent to lightning performance. Figure 2 presents the general geographic layout of the three transmission circuits, their terminals, and switching stations.

The line passes from cultivated land around Los Angeles through valleys, foothill sections, mountain ranges, and long stretches of desert to Hoover Dam. The line elevation varies from practically sea level to a maximum of 4,862 feet to give an average of 2,400 feet. The isokeraunic level varies from 30 near Hoover Dam to approximately five for the Los Angeles vicinity. The heaviest lightning season for the lines is during the summer and early fall.

Lightning Recording Devices and Their Use

The performance data are obtained through the medium of four types of lightning recording equipment:

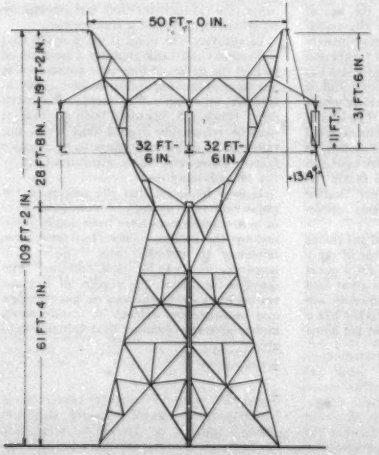

Figure 1. Standard single-circuit suspension tower

1. Counterpoise gaps[1] are installed on three legs of the Victorville–Receiving Station E section and on all four tower legs of the remainder of the line. These gaps, installed primarily to prevent corrosion, have proved a reliable means for recording lightning data. They are used to determine the comparative intensity and probable number of lightning strokes on the line. Figure 3 shows the two types of gaps used.

2. Magnetic links (surge-crest ammeters[3]) are installed at select locations along the line totaling 30 miles, where lightning storms are prevalent.

3. Surge recorders with paper indicators are installed on all lightning arresters at the terminals of the lines. While these offer a positive indication of current discharge, they are not accurate for estimating current values. The lightning arresters are equipped also with the magnetic links.

4. Copper lightning rods in series with fusible copper wires, together with magnetic links, are used on the lightning-diverter towers at the Hoover Dam terminal and at the intermediate switching stations. These rod and fuse indicators are installed also on a small number of transmission-line towers.

During the month of May, the transmission lines are practically free of lightning, so this month has been used generally to examine and recondition the installed lightning recording equipment. A lightning year, as designated in this paper, begins about the middle of May and ends about the end of April. Exception to this was the year 1936, which includes some data from the 1934–35 season when the first circuits were under construction.

Since the counterpoise gaps are installed throughout the line, they are relied upon for a good part of the data. Prior to 1943–1944 these gaps were surveyed once a year, but since that time the gaps have been inspected several times a year by the line patrolmen. After the first few years of experience a coding

Paper 50-130, recommended by the AIEE Transmission and Distribution Committee and approved by the AIEE Technical Program Committee for presentation at the AIEE Summer and Pacific General Meeting, Pasadena, Calif., June 12–16, 1950. Manuscript submitted March 17, 1950; made available for printing April 6, 1950.

T. M. Blakeslee and E. L. Kanouse are with the Department of Water and Power, Los Angeles, Calif.

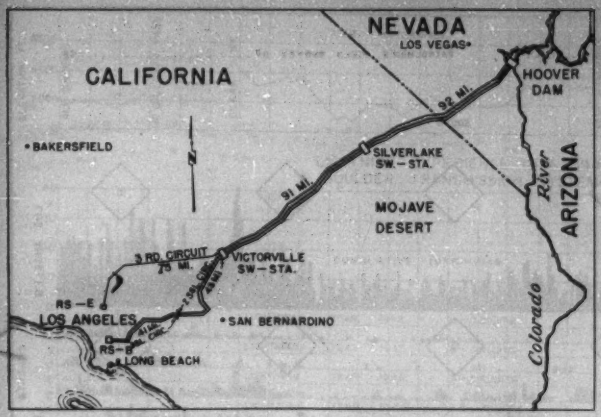

Figure 2. Map showing geographical location of Boulder 287.5-kv transmission lines

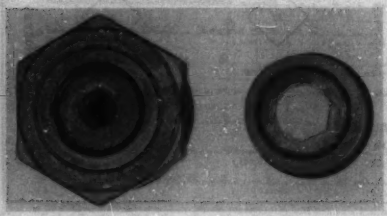

Figure 3. Counterpoise gaps used on the Boulder lines

system was developed to facilitate inspection and report. A sample of the code sheet is shown in Figure 4, and a counterpoise gap survey sheet is shown in Figure 5. For the past three years the average number of flashed gaps per year was 1,250 and at least 15 per cent of these gaps were found to have been flashed over more than once in the same year.

The estimation of the number of lightning strokes from the counterpoise gap data requires some judgment, as a lightning stroke may be direct, involving several towers, or it may be indirect, causing a small burn on only one gap. This is the reason for the designation "probable lightning strokes" used in this paper.

Lightning Performance Data

Figure 6 presents a chart showing the probable number of lightning strokes per line mile per year and the cumulated number of strokes for the 13-year period. The line profile is also shown on this chart, and the correlation between high elevation and high number of strokes is evident from the data, exemplified particularly by conditions in the vicinity of Clark Mountain.

From Boulder switchyard to Victorville the three 287,500-volt circuits have a normal separation of 265 feet. From a lightning standpoint these circuits are treated as one line. From Victorville to Los Angeles, circuit *III* traverses a dif-

Figure 4. Boulder 287.5-kv transmission system lightning survey—counterpoise gap code sheet used by field forces

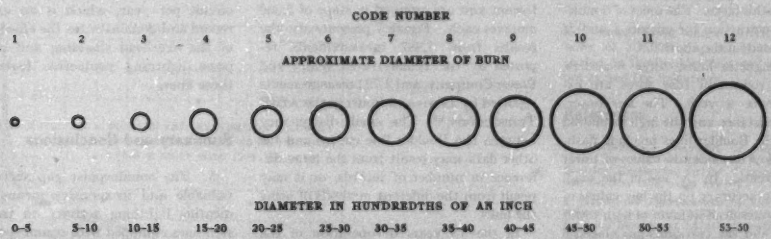

In coding, Numbers 1 to 12 denote diameter of burn in 20th of an inch.
Numbers standing alone indicate smoked or burned areas without molten metal. Example: 2.
M denotes molten metal. For melted spots use number and *M*. Example: 3*M*.
MS denotes molten metal that has been blown or splashed out.
A denotes a general pitted area. Denote size of such area by numbers and *A*. Example: 3*A*.
G denotes beads or globules of metal.
F indicates solidly fused gap. Use number with *F* to denote diameter of fused column. Example: 2*F*.
M^2 denotes a molten burn. Example: $2M^2$, or $3A^3$, or $2G^4$.
If any type burn occurs inside another type, circle the inner burn. Example: 4*M*(2*G*), meaning 4*M* with 2*G* inside it.

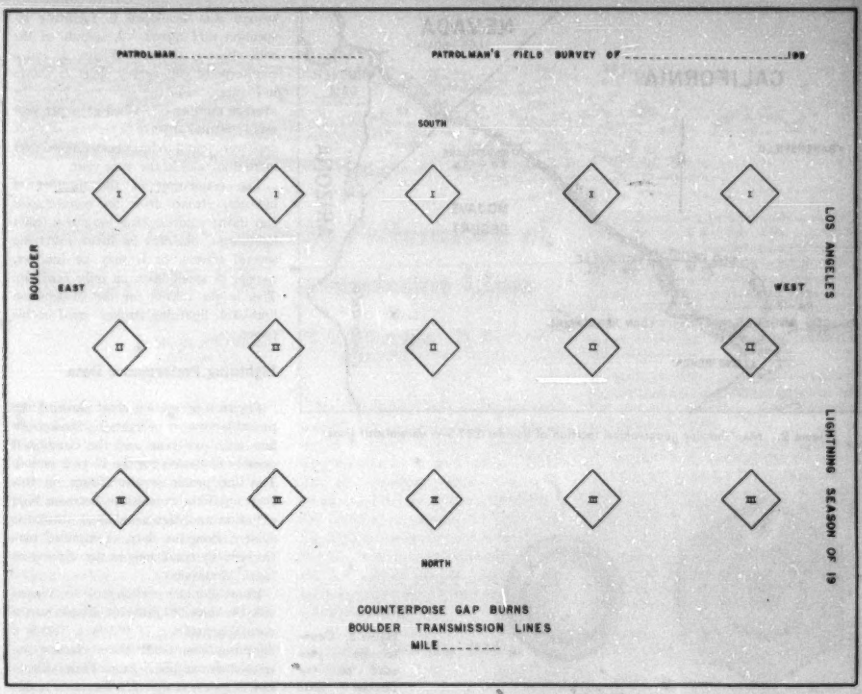

Figure 5. Counterpoise gap service sheet used to collect data

ferent route, as shown in Figure 2; this section is therefore treated as another line, and the data of Figure 6 are presented on this basis. The miles of double-circuit construction for circuits *I* and *II* are indicated on the chart.

The magnetic links, surge recorders, lightning rods, and fuse wires are examined once a year. The low tower footing resistance and the high insulation level on the Boulder lines preclude flashovers on low or moderate values of tower surge currents. In the use of the magnetic links, accuracy on the low values of current is sacrificed in favor of high tower currents, and the two links are placed 6 and 18 inches from the center of gravity of the tower leg instead of the usual three and nine inches. On lightning-rod installations distances for the links of 9 and 27 inches are used.

Since the magnetic-link installations cover only a small portion of the transmission line, the results obtained from them are limited. The curve of Figure 7 presents the data available. The currents plotted are from magnetic-link measurements on all four legs of 107 towers, and are grouped in steps of 5,000 amperes each. Figure 7 presents also the results from 1,987 measurements reported by the Pennsylvania Water and Power Company, and 2,721 measurements reported by Lewis and Foust in the AIEE Transactions.[4,5] The small discrepancy between the Boulder line curves and the other data may result from the large difference in number of records, or it may result from the different methods of using the links.

In the 13 years of operation of the Boulder lines, there have been only two circuit trip-outs attributed to lightning, and one trip-out which probably resulted from lightning but for which the evidence is not definite. The chart of Figure 6 shows that the probable number of strokes to the lines during this period was 2,568, which represents an average of 198 strokes per year. On the basis of three trip-outs resulting from lightning, this is only 0.072 outage per 100 miles of line per year, and 0.032 outage per 100 miles of circuit per year, which is an excellent record and demonstrates the effectiveness of the overhead shielding and counterpoise lightning protective features of these lines.

Summary and Conclusions

1. The counterpoise gap serves as a valuable and inexpensive means of indicating lightning activity on transmission lines equipped with counterpoise.

2. The excellent lightning performance of the Boulder 287.5-kv transmission lines, over the first 13 years of operation, of 0.072 outages per 100 miles of line per year demonstrates the effectiveness of overhead ground wires and continuous counterpoise system.

3. Data from a limited number of magnetic-link installations indicate:

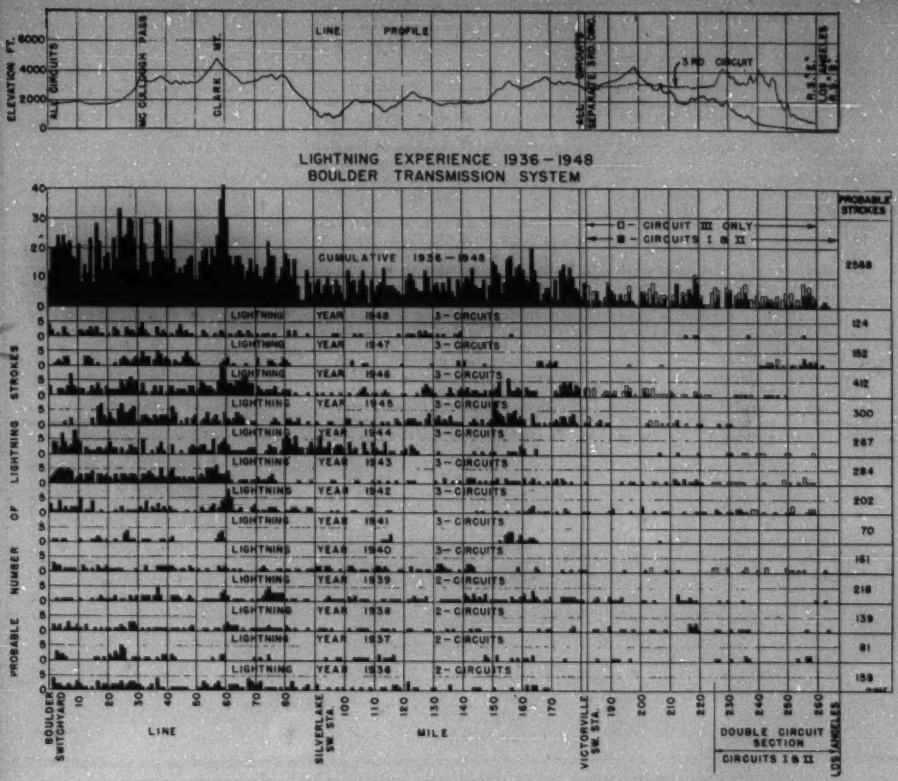

Figure 6. Chart showing probable number of lightning strokes to transmission lines per mile for 13-year period

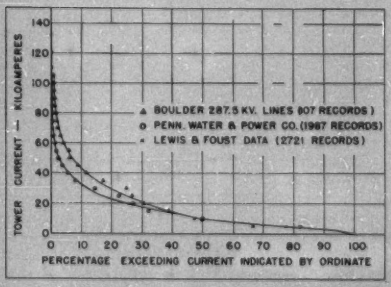

Figure 7. Distribution of tower lightning currents measured by magnetic links

(a). Oscillatory surge currents predominate over unidirectional currents.

(b). Cloud polarity is predominately negative.

(c). The percentage distribution with respect to magnitude of tower currents compares favorably with published data from other sources.

(d). Tower surge currents are generally not divided equally in the four tower legs.

(e). Some tower surge currents in the order of 100,000 amperes have been recorded on the Boulder line, and these have not caused line flashovers.

References

1. Engineering Features of the Boulder Dam—Los Angeles Lines, E. F. Scattergood. *Electrical Engineering (AIEE Transactions)*, volume 54, May 1935, pages 494–512.

2. Lightning Performance of 220-Kv Transmission Lines—II, AIEE Committee Report. *Electrical Engineering (AIEE Transactions)*, volume 65, February 1946, pages 70–6.

3. Direct Measurement of Surge Currents. C. M. Foust, J. T. Henderson. *Electrical Engineering (AIEE Transactions)*, volume 54, April 1935, pages 373–8.

4. An Eight-Year Investigation of Lightning Currents and Preventive Lightning Protection on a Transmission System, E. Harrison, S. K. Waldorf. *Electrical Engineering (AIEE Transactions)*, volume 63, May 1944, pages 251–8.

5. Lightning Investigation on Transmission Lines—VIII, W. W. Lewis, C. M. Foust. *Electrical Engineering (AIEE Transactions)*, volume 64, March 1945, pages 107–15.

Discussion

Abe Tilles (Pacific Gas and Electric Company, San Francisco, Calif.): The excellent record of the line here reported over a long period in quite heavy lightning territory is certainly a heartening evidence that high-voltage circuits can be protected from service interruption due to lightning. Certain questions come to mind.

What are the tower footing resistances on the line with and without the effect of the counterpoise?

Has there been any difficulty in some of the bad soils traversed due to corrosion of the buried counterpoise?

Those of us who may have to keep the "box score" on a well-protected line on which lightning interruption has been reduced practically to the vanishing point meet a problem in exact identification of outages due to lightning. In the two cases listed as sure, and the one doubtful, what evidence pointed to lightning? The authors with their counterpoise gaps, have more evidence than is otherwise available. Did the lightning outages occur during readily identified lightning storms? Was there positive evidence of flashover location additional to the gaps, such as conductor or arcing ring burns, cracked insulators, and so forth?

Was there any indication as to why these three strokes out of the 2,568 hitting the line caused flashovers? How did they compare in current magnitude with others not causing flashover? Were they at insulator strings that might be presumed to be earlier damaged, unusually dirty, or on towers of higher footing resistance than usual?

T. M. Blakeslee and E. L. Kanouse: The authors agree with Dr. Tilles that the Boulder line experience indicates that lightning proof operation of high-voltage lines can be very closely approached. The use of continuous counterpoise on these lines resulted in a maximum measured footing resistance of 7.5 ohms, whereas a limited number of footing measurements made without counterpoise indicated 150 ohms maximum. In a few line locations the buried copper wire has entirely disappeared, leaving a green stain through the soil some two to three inches in diameter. This corrosion, apparently due to corrosive elements in the soil, has not to date resulted in altered line performance. Lightning experience in these localized areas will be watched with a great deal of interest.

It is extremely difficult to prove absolutely the case against lightning in the instances where line flashovers have been laid to that cause. The existence of lightning in the area at the time, the character and size of counterpoise gap burns on adjacent towers, the nature of the burns on the arcing horns, and the lack of any other reasonable cause or evidence, have all had a part in the assignment of cause of flashover in the three cases.

In every case the indication of 60-cycle power follow current given by the counterpoise gap was verified by conditions around an insulator string on that tower. But no indication was had as to the possible terminus of a stroke to the tower or ground wire. Since the flashovers never occurred on towers equipped with magnetic links, no idea of current magnitudes was provided by measurements, and hence no reasons can be advanced as to why the three particular instances appeared in our experience records. Immediate tower footing resistance measurements showed nothing significant.

Automatic Control of Ignitron Rectifier Stations

E. J. CHAM
ASSOCIATE AIEE

W. A. DERR
MEMBER AIEE

THIS paper discusses ignitron rectifier station equipment, operating procedures, and the factors involved in applying automatic control. Reclosing, voltage control, protection, and ground detection are discussed. Considerations involved in applying supervisory control to automatic ignitron rectifier stations are presented. Typical schematic diagrams indicating the components required and the operating procedures established are described for single-unit battery-controlled pumped and sealed ignitron rectifiers with and without anode circuit breakers.

An automatic rectifier station is one in which the rectifier is started and connected to load following an impulse received from a single control device. The operating method established for the rectifier station determines the origin of the starting impulse. The starting impulse may be given by a local operator, by remote operator through supervisory control equipment, by a time switch, or by a load- or voltage-responsive element.

Station Elements

The basic elements of an ignitron rectifier installation consist of a rectifier, a rectifier transformer, and the necessary switchgear equipment. Figure 1 shows these three basic elements. The rectifier transformer is shown at the left, the rectifier in the screened enclosure, and the switchgear at the right. The rectifier and the rectifier transformer remain the same whether the station is automatically or manually controlled. The amount of switchgear equipment is determined by the method of operation, automatic or manual.

Ignitron Rectifiers

The fundamental purpose of an ignitron rectifier is to change electric energy from alternating current to direct current. The ignitron rectifier consists of an assembly of gas-tight evacuated steel containers in each of which there is a graphite main anode, a cathode of mercury, an ignitor, and an auxiliary anode or grid. The individual containers are tied together to form a common cathode for the assembly.

The ignitor is used to initiate the cathode spot for each cycle. Once the cathode spot is started the anode will pick up the current if it is positive with respect to the cathode. The d-c output voltage is determined by the phase connection and secondary voltage of the rectifier transformer, the conduction period, and the small arc drop of the tubes.

The ignitron rectifier has been used for a large percentage of the a-c to d-c conversion installations in the last decade in the mining, railway, industrial, and electrochemical fields. The voltage ranges are for the most part between 250 and 750 volts. However, there has been an increasing number of installations of the 1,500–3,000-volt class.

To provide the necessary vacuum required for operation of an ignitron rectifier the individual containers are either connected to a vacuum system in continuous operation or they are evacuated and permanently sealed. These fundamental methods of maintaining a vacuum have resulted in the common usage of the terms "pumped" and "sealed" ignitrons.

Figure 2 shows a large pumped-type ignitron installation. Figure 3 shows a typical sealed-type ignitron installation. The equipment to maintain a vacuum for a pumped-type ignitron rectifier consists of pumps, equipment for the measurement of pressure, and the necessary protective devices. Economic considerations determine whether pumped or sealed ignitrons are used for a given installation. While the sealed type requires eventual replacement, it does not need vacuum maintaining equipment.

A cooling system is required for all rectifiers to dissipate the heat of the arc and to control the mercury vapor pressure in the ignitron tube. Some form of recirculating water system is used unless a sufficient quantity of clean noncorrosive water at suitable pressure is available for direct cooling.

Rectifier Transformers

Rectifier transformers are essentially power transformers that have been modified to make them suitable for rectifier service. Rectifier transformers are subjected to more severe stresses at frequent intervals than are power transformers because of rectifier arcbacks. Consequently the transformer must be sufficiently braced to handle these repeated stresses. The number and arrangement of windings is determined by the circuits of the rectifier. Voltage, power factor, and regulation depend upon the rectifier-transformer connection and characteristics. The most common connections are the delta 6-phase double-Y and the Y 6-phase double-Y. The delta 6-phase double-Y connection is illustrated in Figure 4.

Most rectifier transformers are provided with taps to compensate for a-c system voltage changes. Taps may also be provided for raising or lowering the voltage applied to the rectifier. The tap-changing equipment may be either the no-load type or underload type and may be automatic or manual.

Paper 50-131, recommended by the AIEE Substations Committee and approved by the AIEE Technical Program Committee for presentation at the AIEE Summer and Pacific General Meeting, Pasadena, Calif., June 12–16, 1950. Manuscript submitted March 18, 1950; made available for printing April 6, 1950.

E. J. Cham and W. A. Derr are with the Westinghouse Electric Corporation, East Pittsburgh, Pa.

Figure 1. Typical pumped-type ignitron rectifier installation showing rectifier transformer, rectifier, and switchgear

Figure 2. A large pumped-type ignitron rectifier installation

SWITCHGEAR

The switchgear includes the d-c circuit breakers, the a-c circuit breaker, and the protective and control relays. In the application of the switchgear equipment, consideration must be given to the fact that rectifiers are subject to arcbacks. An arcback is failure of the check-valve action, permitting a reversal of current flow between the cathode and the anode. The occurrence of arcbacks in rectifiers is random in nature. Up to the present time it has not been found possible to absolutely eliminate arcbacks. Therefore, the switching means provided for a rectifier must be arranged to prevent damage to any of the components of the installation and minimize service interruptions due to arcbacks.

In early ignitron installations d-c circuit breakers were used only in the cathode circuits. This is still acceptable for many applications. However, during recent years circuit breakers have been used in anode circuits where the rating dictates the desirability of fast fault removal from the transformer or where it is necessary to maintain uninterrupted service during arcbacks. An anode circuit breaker is a multiple-pole device having a circuit-interrupting element equipped with a reverse current device for each anode circuit.

High-speed or semihigh-speed switching is provided for a rectifier depending on the direct voltage, the kilowatt rating of the individual rectifier, and the full-load rating of the station bus. High-speed or semihigh-speed switching can be provided by either cathode or anode circuit breakers.

It is standard practice to provide an a-c circuit breaker capable of interrupting the circuit in 0.13 second or less. The manufacturers have not as yet established definite circuit-interruption times for high-speed or semihigh-speed d-c circuit breakers.

The control relays are applied to fit the operating methods adopted for the station. They govern the starting and stopping sequences employed. Protective devices provide for shutdown of the ignitron rectifier for conditions which could result in damage to equipment if maintained. The number and type of protective devices used is determined by the size and operation of the installation.

Single-Line Diagram

Figure 4 indicates the main power connections for a typical single-unit single-way 6-element ignitron rectifier, with a delta 6-phase double-Y transformer. This diagram applies to either the pumped- or sealed-type ignitron rectifier. Instrumentation for local quantities is simple. Alternating and direct current and voltage are quantities of interest. Either a-c or d-c kilowatt-hours are usually metered. The telemetering transmitters which would be used for a station operated by supervisory control are not shown on the diagram.

An interphase transformer is not effective when there is no load on the rectifier and a higher direct voltage results. With reference to Figure 4, this higher voltage occurs since the rectifier transformer functions as a delta 6-phase star rather than as a delta 6-phase double-Y, with no load on the rectifier. Therefore, when an interphase transformer is used, a light-load voltage suppressor is necessary to limit the voltage rise when there is no connected load. The value of this resistor is such that it applies a lead of less than 1/2 per cent of the kilowatt rating of the ignitron rectifier. The light-load application relay, device 37 (see Appendix), is sometimes omitted on units of small kilowatt rating and the light-load voltage suppressor is then permanently connected to the output terminals.

Figure 3. Typical sealed-type ignitron rectifier installation

Figure 4. Single-line diagram of a single-unit ignitron rectifier station

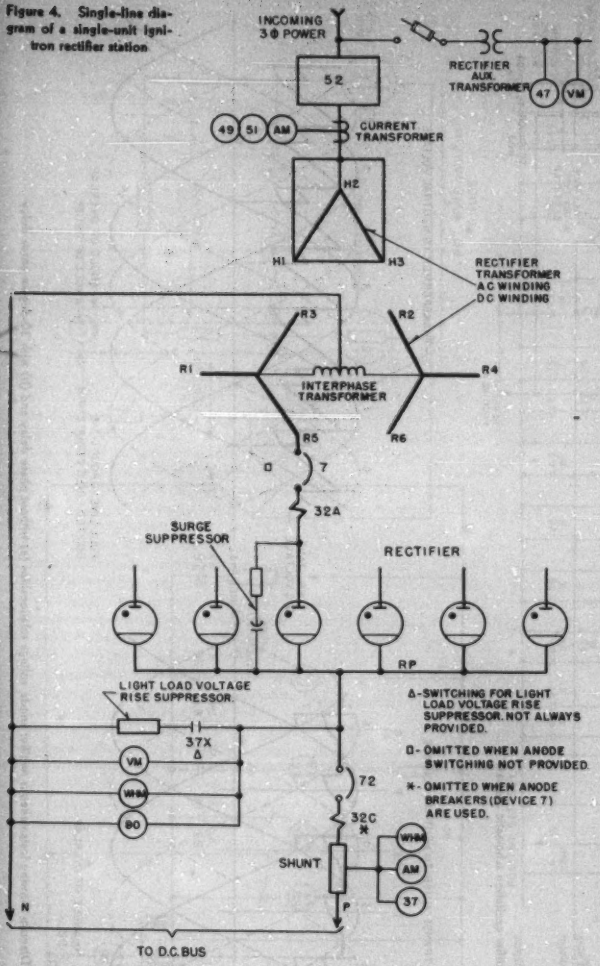

Excitation and Cooling System Circuits

Figure 5 shows a typical saturating reactor-capacitor network excitation circuit for a pumped or sealed ignitron, as well as the recirculating water pump contactor. All the devices on this diagram are connected to the 3-phase rectifier auxiliary transformer, the primary of which is connected to the line side of the a-c circuit breaker *52*. The excitation system should be connected to the same source as the main transformer since the excitation must be synchronized with the anode voltages.

The feed transformers, *P1*, *P2*, *P3*, supply the energy in the correct phase relationship to the network. The firing capacitor *CF* is charged through phase shifting reactor *XPS*. The capacitor voltage is continuously applied to the saturating reactor *XS* until the current reaches a value at which the reactor *XS* saturates. At this point the capacitor is discharged through reactor *XS* and a large peak current passes through the ignitor. This peak current or ignitor impulse creates the cathode spot within the ignitron. By the use of dry-type rectifier units it is possible for one circuit to supply two ignitrons which are diametrically opposite in phase position in the rectifier circuit.

The variable-voltage transformer is used to apply voltage to the full-wave dry-type rectifier. This makes it possible to vary the saturating current in the d-c coil of the phase-shifting reactor *XPS*, which results in a change of the phase position of the ignitor impulse.

With transfer switch *43* in the degas position, contacts of device *31*, connected between the saturating reactor *XS* and the ignitor dry-type rectifiers, short-circuit the ignitors when the coil of device *31* is energized by the closing of contact *63VX* on high ignitron tank pressure. Degassing is the process of removing occluded gases from internal parts of the ignitron by passing current through it. The liberated gases are removed by the vacuum pumps. Degassing is required only on initial installation or when a tank has been opened for inspection or repair. Since, during degassing, tank pressure is erratic, it is not desirable to shut down the rectifier completely each time tank pressure is high; therefore, the ignitors are merely short-circuited by device *31*. This stops rectification. After the tank pressure returns to normal, the coil of device *31* is de-energized by the opening of contact *63VX*. Contacts of device *31* open and the short circuit across the ignitors is removed. The coil circuit of device *31* can be modified so that certain operating conditions short-circuit or release the ignitors to start or stop rectification without circuit breaker operations.

To insure that the anodes pick up current when the ignitor pulse occurs, a voltage is impressed on the auxiliary anode or grid, leading the no-delay ignition impulses by a fixed number of degrees. The grid transformers in Figure 5 have a resistor in series with each grid to limit the current. A lamp connected across the resistor will give misfire indication. During each cycle that the main anode fails to conduct current because of a misfire of the ignitor, no current will flow in the grid circuit. The lamp will thus not be energized on a misfire. When a rectifier station is operated by supervisory control, the lamps can be replaced by relays to provide an alarm following a sustained misfire.

Figure 6(A) shows the voltage relations of a delta 6-phase double-Y rectifier circuit. As previously mentioned, the

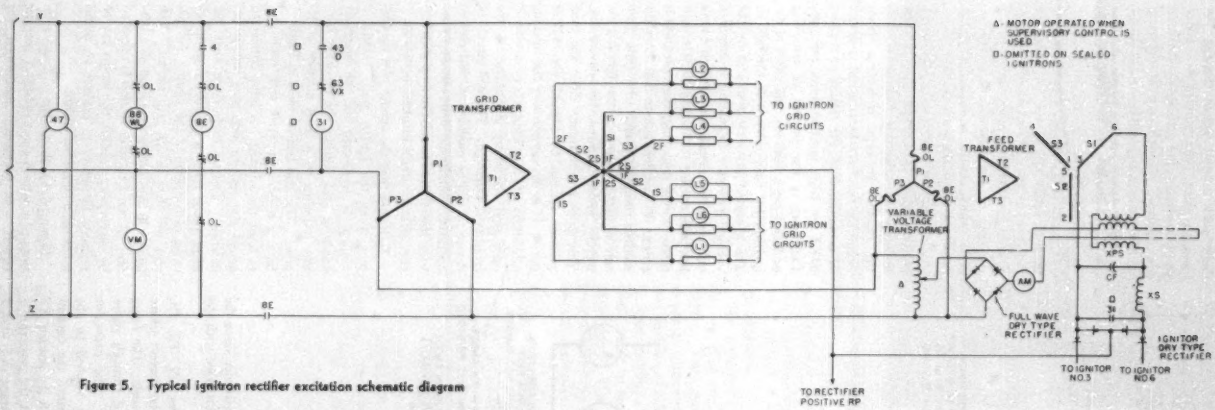

Figure 5. Typical ignitron rectifier excitation schematic diagram

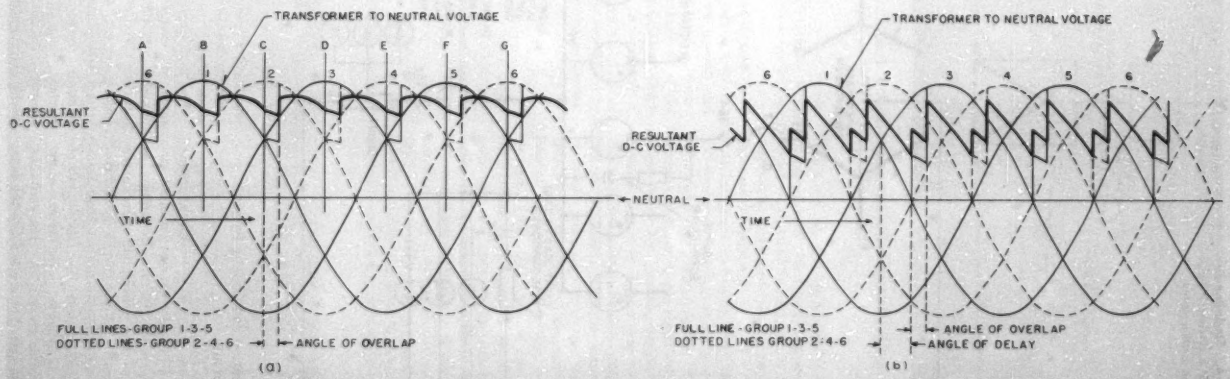

Figure 6. Diagram showing instantaneous rectifier anode voltage relationships (a) without phase delay and (b) with 30-degree phase delay

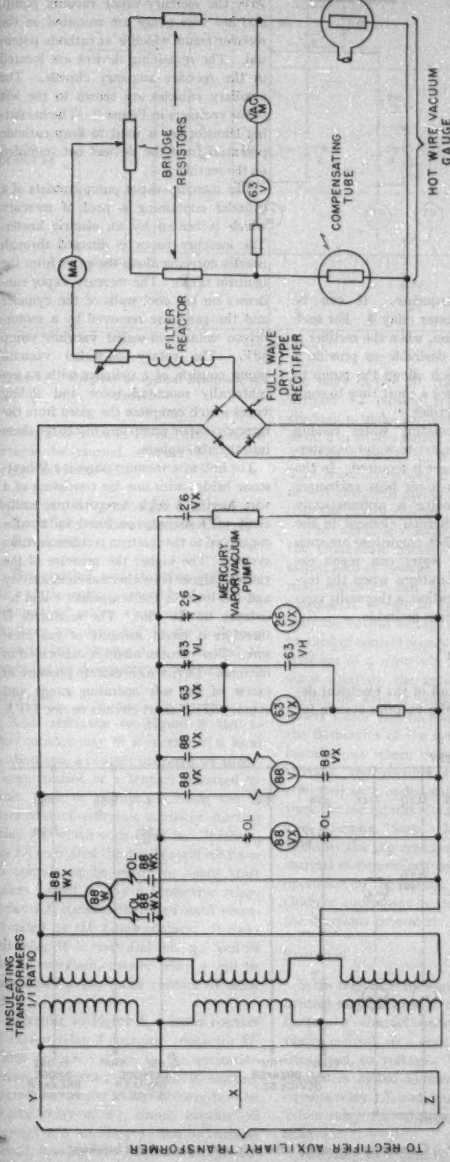

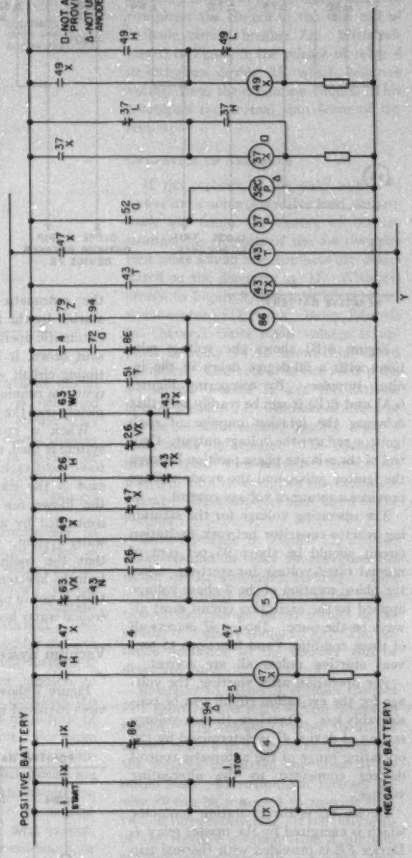

Figure 7 (above). Typical vacuum system control for pumped-type rectifiers

Figure 8 (right). Partial control schematic diagram applying for ignitron rectifiers with and without anode circuit breakers

ignitor is used to initiate the cathode spot for each cycle. Once the cathode spot is started, the anode will pick up the current if it is positive with respect to the cathode. With no firing delay, a cathode spot is formed in the ignitron at times *A*, *B*, *C*, *D*, *E*, *F*, and *G*, and the current will transfer consecutively from ignitrons *5* to *1*, *1* to *3*, *3* to *5*, *5* to *1*, and so forth, for group *1-3-5*, and *6* to *2*, *2* to *4*, *4* to *6*, *6* to *2*, and so forth, for group *2-4-6*. The resultant direct voltage is the average of the direct voltage produced by group *1-3-5* alone and the direct voltage produced by group *2-4-6* alone.

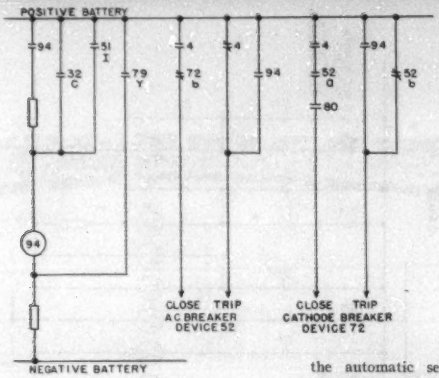

Figure 9. Circuit breaker control schematic without anode circuit breakers

Figure 6(B) shows the voltage relations with a 30-degree delay in the ignitor impulse. By comparing Figures 6(A) and 6(B) it can be readily seen that delaying the ignition impulse of each ignitron reduces the voltage output. Control of the relative phase position between the ignitor pulses and the anode voltage provides a means of voltage control.

The operating voltage for the saturating reactor-capacitor network excitation circuit should be above 95 per cent of normal rated voltage for starting. Also, the phase rotation of the 3-phase voltage applied to the excitation circuit must always be the same. Device *47* detects all of these conditions and functions to prevent starting unless all are correct.

For operation after starting, the voltage for the excitation circuit can be considerably less. Therefore, the low-voltage setting of device *47* is determined by the operating range of the automatic control devices connected to the alternating voltage.

Device *8E* is the excitation contactor which is energized by the master relay *4*. Device *8E* is provided with thermal trip elements to de-energize the excitation circuit whenever the input-current magnitude indicates a fault in the excitation circuit. An open-circuited ignitor results in high unbalanced currents in the excitation circuit which, if allowed to continue, would damage the equipment.

The simplest method of operation when a recirculating water pump is required is to have the pump run continuously. This method is shown in Figure 5 where device *88WX* is the motor contactor. The pump motor device *88W* is shown in Figure 7. The pump motor can also be individually controlled or its starting and stopping can be incorporated as part of the automatic sequence. It can be started by the master relay *4*. For such automatic operation, when the rectifier is shut down, it is desirable to provide a timing circuit which allows the pump to continue running for a short time to completely cool the rectifier.

When a recirculating water cooling system is used, a water-to-water or water-to-air heat exchanger is required. In the case of the water-to-air heat exchanger the blower-fan motor is automatically controlled by a thermal element in the water system. When conditions are such that the cooling water can reach extremely low temperatures when the rectifier is not in operation, a thermally controlled water heater is desirable.

Vacuum System

Figure 7 shows all of the electrical devices involved in the vacuum system for pumped-type rectifiers as well as the recirculating water pump motor previously mentioned. Devices *88VX*, *88V*, *26V*, the mercury-vapor vacuum pump, and hot wire gauge are mounted on the rectifier frame which is at cathode potential. The remaining devices are located in the rectifier auxiliary cubicle. The auxiliary cubicles are shown to the left of the rectifiers in Figure 2. The insulating transformer is used to keep cathode potential from the devices not mounted on the rectifier.

The mercury-vapor pump consists of a cylinder containing a pool of mercury which is heated by an electric heater. The mercury vapor is directed through nozzles carrying along the gases from the ignitron tanks. The mercury vapor condenses on the cool walls of the cylinder and the gases are removed by a motor-driven rotary oil-sealed vacuum pump *88V*. The rotary oil-sealed vacuum pump consists of a cylinder with an eccentrically mounted rotor and sliding vanes which compress the gases from the mercury-vapor pump and discharge them into the atmosphere.

The hot-wire vacuum gauge is a Wheatstone bridge with one leg consisting of a wire having a high temperature coefficient of resistivity enclosed in a tube connected to the ignitron rectifier vacuum system. The higher the pressure of the gas, the higher is its thermal conductivity and the lower is the temperature and resistance of the wire. The resistance is therefore a direct measure of gas pressure. The vacuum meter is calibrated in microns. Device *63V* detects pressure in excess of the safe operating range and contact *63VH* short-circuits device *63VX*

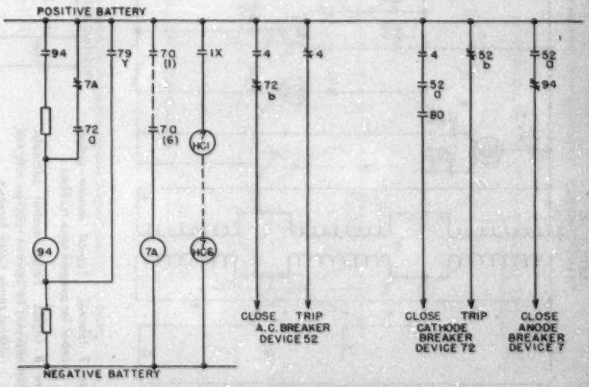

Figure 10. Circuit breaker control schematic with anode circuit breakers

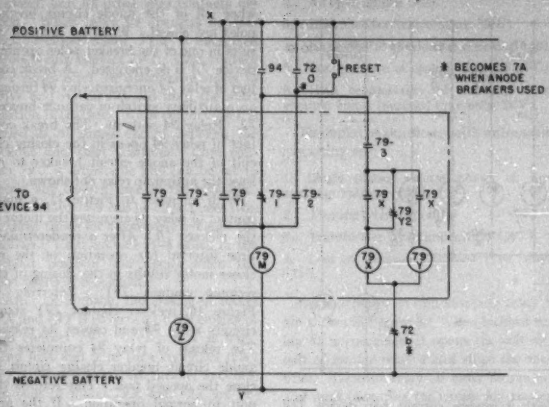

Figure 11. Diagram of typical automatic recloser

causing it to release. When the pressure returns to normal, contact *63VL* energizes device *63VX*.

Automatic Sequence for Ignitron Rectifiers without Anode Circuit Breakers

The starting and stopping sequences for a single ignitron assembly of either the pumped or sealed type without anode breakers are described in the following paragraphs. Figures 4, 5, 8, 9, and 11 apply for the description to be given.

Starting

With reference to Figure 8 the *1-start* contact may be a contact of a local pushbutton, a contact operated by supervisory control, or a contact actuated by time, load, or voltage. Closing the *1-start* contact energizes auxiliary starting relay *1X* which seals itself in. With relay *1X* energized the rectifier will continue to operate or be ready to again start unless locked out by a protective relay. Relay *1X* remains energized until short-circuited by the *1-stop* contact. If lockout relay *86* is reset and relays *5* and *94* are de-energized, master relay *4* will be energized by the make contact of relay *1X*.

Referring to Figure 5, a make contact of master relay *4* energizes contactor *8E* which applies voltage to the excitation circuit. Referring to Figure 9, another contact of master relay *4* energizes the closing relay of a-c circuit breaker *52* through a *b* auxiliary switch of cathode circuit breaker *72*. When voltage appears on the rectifier terminals to energize d-c relay device *80*, the cathode circuit breaker *72* closing relay is energized through a make contact of master relay *4*, an *a* auxiliary switch of circuit breaker *52*, and a make contact of device *80*. This sequence places the ignitron rectifier in complete operation and connects it to the load or system.

The variable-voltage transformer in the phase-shift circuit can be varied to adjust load or voltage. A voltage or current regulator can be applied in the phase-shift circuit to control automatically the output voltage or current. This method of control is only used for changes that are of a relatively small magnitude since delaying the rectifier ignition to reduce the load or voltage decreases the power factor and increases amplitude of the harmonics of the system. For large installations where power factor is important, the rectifier transformers are equipped with underload tap changers to vary the a-c input voltage to the rectifier and thereby vary the d-c output. Whether the tap changer is automatic or manual is determined by the method of operation for the station. The use of tap-changer equipment is not considered in the diagrams presented.

Stopping

With reference to Figure 8, the *1-stop* contact may be a contact of a local pushbutton, a contact operated by supervisory control, or a contact actuated by time, load, or voltage. When the *1-stop* contact is closed momentarily, it short-circuits relay *1X* and causes it to release. When relay *1X* releases, it de-energizes relay *4*.

Referring to Figure 9, a break contact of relay *4* completes the circuit to the trip coil of a-c circuit breaker *52*. A *b* auxiliary switch of a-c circuit breaker *52* completes the circuit to the trip coil of cathode circuit breaker *72*. With reference to Figure 5, the release of relay *4* de-energizes device *8E* which removes voltage from the excitation circuit. This completes the normal shut-down of the rectifier.

Operation of Arcbacks

If the rectifier is the only source of power for a nonregenerative load, an arcback will cause the closing of the instantaneous contacts of the a-c overcurrent relay *51*. These contacts are designated on the diagrams as *51I*. With reference to Figure 9, device *94* is energized when contact *51I* closes. Relay *94* seals in. Several times rated voltage is applied to relay *94* to insure high-speed operation. Contacts of device *94* trip the a-c circuit breaker *52* and the cathode circuit breaker *72*. Another contact of device *94* short-circuits master relay *4* and causes its release. The release of master relay *4* de-energizes device *8E* which in turn de-energizes the excitation circuit. This completes shut down of the rectifier.

With reference to Figure 11, another make contact of relay *94* energizes the motor of the automatic recloser. After a predetermined time interval the operation of the recloser motor results in the closing of recloser contact *79Y*. The detailed operation of the recloser will be described later.

Referring to Figure 9, recloser contact *79Y* short-circuits relay *94* and causes its release. The release of relay *94* allows master relay *4* to again be energized and the rectifier is started the same as on initial start. The automatic recloser device *79* can be arranged to provide one, two, or three reclosures. If the shutdown of the rectifier resulted from a random arcback, experience has indicated that service will be restored with a single reclosure. If the shutdown of the rectifier resulted from a permanent fault, repeated reclosures may result in possible damage to equipment. Therefore, it is customary to provide for only a single automatic reclosure.

With reference to Figure 8, it will be noted that a circuit to the lockout relay *86* is completed through contacts of relay *94* and auxiliary reclosing relay *79Z*. If reclosing is unsuccessful, both of these contacts will be closed to energize the lockout relay. Lockout relay *86* opens the circuit to master relay *4* and prevents restarting of the rectifier until the lockout relay *86* is manually reset.

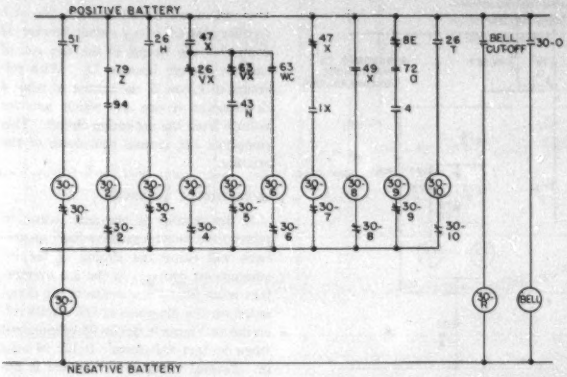

Figure 12. Typical annunciator schematic diagram

If the rectifier is not the only source of power, an arcback results in the operation of reverse current device *32C*, shown in Figure 4. Reverse current trip device *32C* is provided as a part of the cathode circuit breaker mechanism and its actuation trips the cathode circuit breaker in a minimum of time. All of the other operations including the tripping of the a-c circuit breaker and operation of the recloser are the same as just described for the condition with nonregenerative load.

Automatic Sequence for Ignitron Rectifiers with Anode Circuit Breakers

The starting and stopping sequences for a single ignitron assembly of either the pumped or sealed type with anode breakers are described in the following paragraphs. Figures 4, 5, 8, 10, and 11 apply for the description to be given. Figure 10 is based on an anode circuit breaker with six individual poles with a single motor-operated closing mechanism. Each pole has an individual latch-holding coil which must be energized to keep the pole in the closed position after it has been closed by the motor-operated mechanism. Operation of the motor-closing mechanism of the anode circuit breaker will close any number of poles that are open. The latch-holding coils are devices *7HC1* to *7HC6* inclusive. These latch-holding coils are usually energized by a contact of the starting relay *1X* as shown in Figure 10. In some cases these latch-holding coils are left continuously energized. Each pole of the anode circuit breaker is also equipped with a reverse current trip device *32A* as shown in Figure 4. On reverse current, device *32A* overcomes the flux of the latch-holding coil to trip the pole.

Starting

The starting sequence is exactly the same as previously detailed for ignitron rectifiers without anode circuit breakers except for the additional operation of closing the anode circuit breaker. The closing mechanism of the anode circuit breaker is energized as soon as the a-c circuit breaker is closed through an *a* auxiliary switch of the a-c circuit breaker *52*, and a break contact of device *94* as shown in Figure 10. The closing of the cathode circuit breaker is determined by device *80* just as in the case without anode circuit breakers.

Stopping

The stopping sequence is the same as previously described for ignitron rectifiers without anode circuit breakers except for the additional operation of opening the anode circuit breaker by de-energizing the latch-holding coils *7HC1* to *7HC6*, inclusive.

Operation on Arcbacks

Operation on arcback is the same whether the rectifier is the only source of power or if it is paralleled with other sources of power. In either case the current reverses in one or more of the individual ignitron tubes. This results in operation of the reverse current devices *32A* which trip the anode circuit breaker poles connected to the faulted ignitrons. All of the unfaulted ignitrons remain in service and continue to supply load.

With reference to Figure 10, it will be noted that device *7A* is energized only when all of the anode circuit breaker poles are closed. When an arcback results in one of the breaker poles opening, device *7A* is de-energized. A break contact of relay *7A* energizes relay *94* through an *a* auxiliary switch of cathode-breaker *72*. Relay *94* seals in. The break contact of relay *94* opens in the closing circuit of the anode circuit breaker to release the antipump relay not shown.

With reference to Figure 11, a make contact of relay *94* energizes the motor of the recloser *79*. After a predetermined time interval the operation of the recloser motor results in the closing of the recloser contact *79Y*. Referring to Figure 10, recloser contact *79Y* short-circuits relay *94* and causes its release. The release of relay *94* completes the anode circuit breaker closing circuit to close the opened pole. This returns the unit to normal operation. If the arcback repeats within a definite time interval, the anode pole connected to the faulted ignitron will again open as just described.

The automatic recloser *79* can be arranged to provide one, two, or three reclosures. It is customary to provide only one reclosure to prevent possible damage to equipment. Assume the automatic recloser device *79* is arranged for a single automatic reclosure. Then relay *79Z* in Figure 8 will still be closed if the anode circuit breaker pole trips within a definite time interval after the first reclosure. With relay *94* being again energized by the break contact of relay *7A*, a circuit is completed to lockout relay *86* in Figure 8. Lockout relay *86* opens the circuit to master relay *4* which stops the rectifier as previously described. Lockout relay *86* must be manually reset before the rectifier can be restarted. It should be noted that neither the a-c circuit breaker nor the cathode circuit breaker operates on arcback. The a-c circuit breaker and the d-c circuit breaker only provide back-up protection on arcback. The cathode circuit breaker does not have a reverse current trip device.

Automatic Recloser

The automatic recloser *79* consists of a synchronous motor-driven set of cams and relays *79X* and *79Y*. The cam contacts are designated as *79-1* to *79-4*. The circuits are arranged so that once the synchronous motor *79M* is energized it will continue to run until the start or lockout position is reached. When the recloser is in the start position it is ready to effect a reclosure.

In the start position, cam contact *79-1*

is closed and all other cam contacts are open. When relay *94* operates on arcback, recloser motor *79M* is energized through cam contact *79-1*. Cam contact *79-2* closes after the mechanism starts to move and remains closed until the start position is reached. Cam contact *79-1* is closed at all times except between the lockout and start positions. Cam contact *79-3* is adjustable and can be set to obtain the desired time of the reclosure. Cam contact *79-3* can be closed one, two, or three times for a complete cycle of the recloser. Cam contact *79-4* closes in the lockout position and opens when the start position is reached.

After an arcback, the closing of relays *79X* and *79Y* is governed by the closing of cam contact *79-3*. Relay *79X* is energized first and it in turn energizes relay *79Y*. When the circuit breaker recloses, the coils of relays *79X* and *79Y* are de-energized. However, a latching arrangement prevents relay *79Y* from completely releasing until cam contact *79-3* opens. This latching arrangement allows reclosing contact *79Y* to open but keeps contact *79Y1* closed and contact *79Y2* open. Thus, relay *79Y* is only energized for as many times as cam contact *79-3* closes during a complete cycle and prevents pumping of the circuit breaker.

If the circuit breaker remains closed after a reclosure, the recloser is run to the start position through cam contact *79-2*. If the circuit breaker trips after being reclosed before the recloser reaches the start position, it is run to the lockout position through the cam contact *79-1* and a make contact of relay *94*. After the lockout position is reached, the reset push button must be operated to run the recloser to the start position.

Protection

In addition to the protective devices required to detect arcback and result in the interruption and subsequent automatic restoration of service, an automatic rectifier installation requires other protective devices. These protective devices are usually arranged to either lock the unit out of service until manual reset of a lockout relay or to stop the unit with automatic restarting allowed when the trouble no longer exists.

The following listings indicate for a typical installation the trouble conditions which initiate lockout and those which merely stop the rectifier with automatic starting allowed. Examples of shutdown and lockout are:

1. A-c overcurrent for a definite time interval (*51T*).
2. An open ignitor (*8E*).
3. High rectifier temperature (*26H*).
4. Unsuccessful automatic reclosing (*79*).
5. Low pressure of cooling water (*63WC*).
6. High temperature of mercury-vapor vacuum pump (pumped type only, *26V*).

Examples of shutdown with automatic restarting are:

1. Single phase, reverse phase, or low auxiliary voltage (*47*).
2. Thermal overload (*49*).
3. Transformer overtemperature (*26T*).
4. Loss of vacuum (pumped type only, *63V*).

Lockout relay *86* and stopping relay *5* are shown in Figure 8. When lockout relay *86* is energized, it opens the coil circuit of master relay *4* and stops the rectifier. Lockout relay *86* must be manually reset to restore the circuit for master relay *4*. A make contact of stopping relay *5* short-circuits the coil of master relay *4* and causes it to release. When stopping relay *5* is de-energized, master relay *4* will be again energized if the contact of lockout relay *86* is closed and the starting relay *1X* is energized.

Lockout relay *86* is directly energized by the protective circuits for a-c overcurrent, unsuccessful automatic reclosing, and for an open ignitor. When oil-filled rectifier transformers are used, lockout relay *86* is also directly energized by a low oil level contact. The protection for low transformer oil level is not shown in Figure 8. It is to be noted that the protective circuits for high rectifier temperature (*26H*), high temperature of the mercury-vapor pump (*26VX*), and low cooling water pressure (*63WC*) are connected to the lockout relay *86* through a make contact of relay *43TX* and to stopping relay *5* through a break contact of relay *43TX*. Relay *43TX* is an auxiliary to timing relay *43T*. This arrangement is provided so that operation of devices *26H*, *26V*, and *63WC* results in shutdown and lockout if the rectifier has been in service for a definite period of time (usually ten minutes), but only prevents starting for this time interval if the rectifier has been shut down because of loss of or low alternating voltage. This is done to avoid a lockout when during shutdown the latent heat of the rectifier units may operate devices *26H* and *26V*. Likewise, device *63WC* may operate because of low voltage on the pump motor.

Stopping relay *5* is energized by the protective circuits for thermal overload, transformer overtemperature, loss of vacuum, and improper a-c auxiliary voltage.

Device *47*, which detects single-phase, reverse-phase, and low auxiliary voltage, has a *47H* contact which closes only if all voltage conditions are correct and the magnitude of the voltage is at least 95 per cent of normal. If the voltage conditions are not correct and the voltage magnitude is less than 85 per cent of normal, contact *47L* will close. Contacts *47H* and *47L* are connected to auxiliary relay *47X* so that 95 per cent of normal voltage must be available for starting, and, if the voltage drops to less than 85 per cent after starting, the rectifier is shut down.

Device *49*, which detects thermal overload of the rectifier installation, has a contact *49H* which closes on high temperature and energizes device *49X*. De-

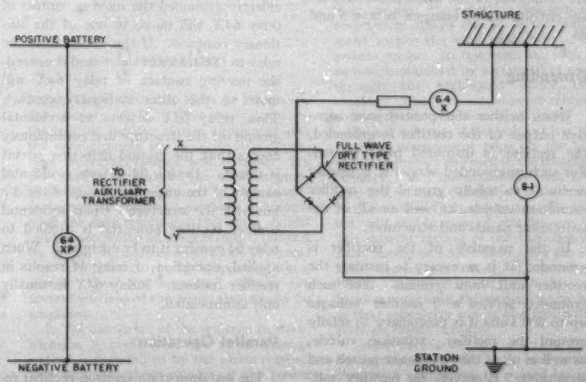

Figure 13. Ground detection schematic which applies when structure is insulated from ground

vice *49X* energizes relay *5* which shuts down the rectifier in the usual manner. When the rectifier unit cools sufficiently, contact *49L* of device *49* short-circuits device *49X* which releases relay *5* to allow restarting.

A contact of auxiliary vacuum relay *63VX* will energize stopping relay *5* for poor vacuum if the degassing switch is in the normal operating position. The degassing switch contact is used in this circuit to avoid shutdown during degassing when vacuum conditions are erratic.

Device *37*, which detects loads of less than one-half per cent of normal rating, has a *37L* contact which closes under such a condition to energize device *37X*. Device *37X* applies the light-load voltage suppressor to the rectifier. When the output of the rectifier exceeds one-half per cent of normal rating, contact *37H* closes to short-circuit device *37X* and causes it to release and disconnect the light-load voltage suppressor.

All of the conditions which result in shutdown of a rectifier are usually annunciated. A typical annunicator arrangement is shown in Figure 12. The annunciator *30* consists of drops and a latching alarm relay. Closing of any of the protective circuits energizes an individual drop in series with the operating coil *30-0* of the latching relay. Operation of the annunciator drop opens its circuit. Operation of relay *30-0* completes a circuit to an alarm bell. Closing the bell cutoff contact energizes the reset coil *30-R* of latching relay and silences alarm.

A different annunciator arrangement is sometimes used to reduce the number of protective relay contacts required. In this arrangement the annunciator drops are connected in the same protective relay circuits which energize relays *5* and *86*.

Grounding

When neither the positive nor negative output of the rectifier is grounded, the rectifier is insulated from ground. For such ungrounded service it is usually desirable to solidly ground the rectifier excitation cubicle, as well as all of the switchgear panels and structures.

If the negative of the rectifier is grounded, it is necessary to insulate the rectifier unit from ground. For such grounded service a d rectifier voltages up to 300 volts it is customary to solidly ground the rectifier excitation cubicle, as well as all of the switchgear panels and structures. However, for rectifier voltages above 300 volts it is customary to insulate the rectifier excitation cubicle, as well as all of the switchgear panels and structures, with a single connection to ground being provided through a high-resistance ground detecting relay circuit.

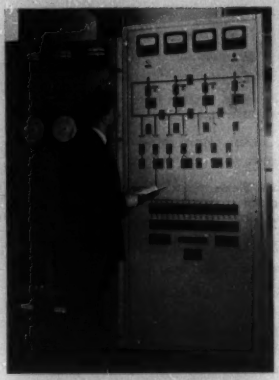

Figure 14. Front view of supervisory control dispatching office cabinet for the control of a large ignitron rectifier station

Figure 13 shows devices to detect accidental grounding or contact of the rectifier excitation cubicle, switchgear panels, or structure with the ungrounded side of the rectifier output. Device *64X* detects an accidental ground. The moving contact of relay *64X* maintains a position between two stationary contacts when there is no ground on the structure and when there is no break in the circuit from the relay to the structure or to ground. If the structure becomes accidently grounded the moving contact of relay *64X* will move to one of the stationary contacts. If the circuit from the relay to the structure or ground is opened, the moving contact of relay *64X* will move to the other stationary contact. Thus, relay *64X* detects an accidental ground on the structure and continuously checks that the ground detecting circuit is intact. Device *64* detects accidental contact of the ungrounded side of the d-c bus with the structure. Upon accidental contact rectifier potential is applied to relay *64* causing it to be energized. When applied, operation of relay *64* results in rectifier lockout. Relay *64X* is usually only annunciated.

Parallel Operation

The arc drop of an ignitron rectifier remains essentially fixed from light load to rated load. The major voltage drop is due to the resistance and reactance of the transformer. Both the reactance and resistance drops are directly proportional to the load currents. Therefore the regulation curve of an ignitron rectifier is virtually a straight line. This simplifies paralleling of several rectifiers as well as paralleling with other conversion equipment.

Parallel operation may be accomplished by matching the voltage regulation characteristics of the rectifier with the paralleled apparatus, or by automatically adjusting the voltage output of the rectifier to that of the paralleled apparatus by the means of a voltage regulator.

Supervisory Control

Economic considerations often result in the use of supervisory control equipment to provide the necessary controls and indications for an automatic rectifier station.

Supervisory control equipment can be operated over a single pair of telephone wires, a power-line carrier channel, or a microwave radio channel. A single channel is all that is required regardless of the number of controls, lamp indications, and selective telemetered indications required. Following is a list of typical supervisory control functions for an ignitron rectifier station:

1. Control and supervision of master starting relays of the rectifiers.
2. Control of each rectifier output with simultaneous telemetering of rectifier amperes or kilowatt output.
3. Control of each rectifier voltage with simultaneous telemetering of rectifier voltage.
4. Control and supervision of d-c feeder circuit breakers.
5. Control and supervision of all a-c circuit breakers other than the rectifier circuit breakers.
6. Supervision of cathode circuit breakers.
7. Supervision of anode circuit breakers.
8. Supervision of rectifier lockout.
9. Supervision of annunciator (if any quantities are annunciated that do not shut down rectifiers).
10. Supervision of ignitron misfire.
11. Supervision of local-remote transfer switch.
12. Communication.

The supervisory control at the rectifier station is usually incorporated as part of the local switchboard.

Figure 14 shows the front of a supervisory control dispatching office unit for the control of a rectifier station. It will

be noted that the plates which mount the supervisory control keys and lamps are located in a mimic bus arrangement.

Conclusions

Ignitron rectifiers are well suited for automatic operation since the starting and stopping sequences are quite simple. Hence, automatic control is employed in a large percentage of ignitron rectifier installations.

Devices are available to provide for any reasonable operating requirements. Supervisory control and telemetering operating over line wires, power-line carrier, or microwave radio channels makes it possible to obtain many desirable operating features for completely unattended installations.

Developments in equipment and methods of operation in recent years have made it possible to improve the service factor of rectifier installations and have made operation and maintenance simpler.

Appendix. Devices Designated in Illustrations

1—Start-stop elements
1X—Auxiliary starting and stopping relay
4—Master relay
5—Automatic stopping relay
7—Anode circuit breaker
7A—Auxiliary relay operated when all anode circuit breaker poles are closed
7HC—Anode circuit breaker latch-holding coils
8E—Excitation contactor
26H—Rectifier thermal device
26T—Rectifier transformer thermal device
26V—Mercury vacuum thermal device
26VX—Auxiliary relay to device *26V*
30—Annunciator relay
30-1 and so on—Individual drops
30-0—Operate coil to sound alarm
30-R—Reset coil to silence alarm
31—Ignitor shorting relay
32—Reverse current device
32A—Anode circuit breaker
32C—Cathode circuit breaker
32P—Polarizing coil
37—Light-load application relay
37H—Closes on high current
37L—Closes on low current
37P—Polarizing coil
37X—Auxiliary contactor to device *37*
43—Transfer switch
43D—Closed in degas position
43N—Closed in normal operating position
43T—Timed lockout transfer relay
43TX—Auxiliary relay to device *43T*
47—Single, reverse-phase and low-voltage relay
47H—Closes for normal voltage conditions
47L—Closes for reverse phase, single phase and low voltage
47X—Auxiliary to device *47*
49—Thermal overload relay
49H—Closes for high temperature
49L—Closes for normal temperature
49X—Auxiliary to device *49*
51—A-c overcurrent relay
51I—Instantaneous element
51T—Timed element
52—Rectifier a-c circuit breaker
63V—Vacuum relay
63VH—Closes high pressure
63VL—Closes on normal pressure
63VX—Auxiliary to device *63V*
63WC—Circulating water pressure
64—High-resistance structure-grounding relay
64X—Structure ground-detection relay
64XP—Polarizing coil
72—Cathode circuit breaker
79—Reclosing relay
79-1 to *79-4*—Motor-operated cams
79M—Synchronous motor
79X—Recloser relay element
79Y—Recloser relay element
79Z—Auxiliary reclosing relay
80—Rectifier voltage indication relay
86—Lockout relay
88V—Vacuum pump motor
88VX—Vacuum pump motor contactor
88W—Recirculating water pump motor
88WX—Recirculating water pump motor contactor
94—Arcback relay
CF—Firing capacitor
L1-L6—Misfire indication lamps
XPS—Phase-shifting reactor
XS—Saturating reactor

References

1. Protection of Electronic Power Converters, AIEE Committee Report. *AIEE Transactions*, volume 69, part II, 1950, pages 813-29.

2. Rectifier Transformer Characteristics, AIEE Committee Report. *AIEE Transactions*, volume 68, part II, 1949, pages 1305-11.

3. Automatic Control for Mercury Arc Rectifiers, H. Bany, M. E. Reagan. *Electrical Engineering (AIEE Transactions)*, volume 55, January 1936, pages 100-09.

Discussion

Ralph Siegel (General Electric Company, Schenectady, N. Y.): This paper describes the ignitron rectifier station equipment and the arrangements for its automatic operation, switching, control, and relaying. Its presentation is based on the methods practiced by one manufacturer. Other manufacturers have different methods to accomplish the same results and this paper should not be interpreted as the practices employed by them. In addition, the mode of operation is subject to change, depending upon specific user requirements. There are several portions of this paper that should be amplified.

In the discussion of the ignitron rectifier, mention is made that the direct voltage output is determined by the phase connection and secondary voltage of the power transformer, the conduction period, and the arc-drop of the tubes. In addition, the system impedance is often extremely important. Poor regulation or unexpected voltages will result when it is not taken into consideration. This factor is especially important in the chemical and building service industry and where low direct voltages, such as the 250-volt class, are required.

The authors state that economic considerations determine whether pumped or sealed ignitrons are used for a given installation. In the final analysis this is true, but other factors do enter into the application or selection of a rectifier. Of prime consideration is the current-carrying ability of the tubes or tanks at a particular direct voltage. Larger blocks of power can be concentrated in the pumped tanks with a resultant decrease in material, ease of handling, and concentration of control than if functionally similar sealed tubes are used.

The subject of the operation of the rectifier with arc back requires some amplification. Arc back as described by the authors is random in nature. However, it is an infrequent occurrence that manifests itself near the end of the tube life or at the time when the tanks need reconditioning. More on this subject can be read in the paper by J. W. Seaman and L. W. Morton presented in 1942.[1]

When a power circuit breaker and separate protective relays are required in the primary of a rectifier transformer rated above 600 volts alternating current, these relays should be of the induction disk overcurrent type. Adjustable time delay relays are more satisfactory than the instantaneous type because they can be set lower than the instantaneous relays in order to override the transformer magnetizing inrush. They will also allow more selectivity with the d-c circuit breaker. Better performance can, therefore, be obtained by using time delay overcurrent relays.

When anode circuit breakers are not used these low set relays should be of short time delay type in order to clear the a-c system in the shortest possible time when arc back occurs. Instantaneous attachments, high set, can also be used to clear a-c system faults or internal transformer faults.

When high-speed anode circuit breakers with built-in reverse current tripping devices are used, the induction disk time delay overcurrent relays can be of the standard speed to give the same protection as other system relays. In this case, arc back protection is obtained by a reversal of current through the high-speed anode circuit breaker. Thus the overcurrent relays are not required to function on arc back.

On a-c systems of 600 volts or less, dual-magnetic overcurrent trips on the circuit breaker are generally used in the transformer primary. The instantaneous trips in this case are set high enough so that the circuit breaker will not trip on magnetizing inrush, but will trip in case of rectifier arc back. The current setting of the time delay element should be adjusted to carry the short-time overcurrent rating of the rectifier. When an overcurrent cathode circuit breaker is present, the setting can be higher so that selectivity can be obtained with the cathode circuit breaker.

Under the subject of protection, an item for persistent misfire has been omitted. Persistent misfire can be caused by any of the following:

1. Gassy tube or tank.
2. Short-circuited or wetted ignitor.
3. An open circuit of the ignition system (covered by the paper).

Such a condition should cause the rectifier to shut down and lock out if not cleared within a definite time.

In general the conditions that cause shut down and lock out are:

1. Arc back.
2. Misfire for longer than a predetermined time.
3. Incompleted sequence of operation.
4. Severe a-c overcurrent.
5. D-c short circuit not cleared by sectionalizing equipment.

While conditions causing a temporary outage, holding the rectifier in readiness to automatically come on the line as soon as the condition has been rectified are:

1. Improper water pressure or loss of water.
2. Temperature of cooling water too high or too low.
3. Insufficient vacuum (pumped rectifiers).
4. Transformer overtemperature.
5. Low, single phase, or reverse phase sequence for a-c supply voltage.

The authors have stated that high rectifier temperature, low cooling water pressure, and high temperature of the mercury vapor pump cause shut down and lock out. This is not necessary as the facilities are available to allow these conditions to be automatically corrected. Of course, if the rectifier is not temporarily shut down while the conditions are automatically taking care of themselves, then the rectifier will arc back and cause shut down and lock out.

The subject of parallel operation should be amplified. It is necessary to match the voltage characteristics of the rectifier with the paralleled apparatus as explained by the authors.

However, this is not the only item to be taken into consideration when a rectifier is paralleled with other equipment. Insofar as the a-c circuit is concerned the addition of a rectifier does not change the interrupting requirements of the a-c circuit breaker. On the d-c equipment this is not true and the additional contributions must be reckoned with. The interrupting requirements are usually increased when a rectifier is paralleled on a bus with other d-c generating or conversion apparatus.

REFERENCE

1. A NEW MULTIPLE HIGH-SPEED AIR CIRCUIT BREAKER FOR MERCURY-ARC RECTIFIER ANODE CIRCUITS AND ITS RELATION TO THE ARC-BACK PROBLEM, J. W. SEAMAN, L. W. MORTON. *Electrical Engineering* (*AIEE Transactions*), volume 61, November 1942, pages 788–96.

E. J. Cham and **W. A. Derr:** A large part of Mr. Siegel's discussion is either confirmation or amplification of some of the statements made in our paper.

Most of Mr. Siegel's discussion requires no comments. We will only comment on the items which Mr. Siegel has questioned or on any of his amplifications with which we do not agree.

With reference to the first paragraph of Mr. Siegel's discussion, it should be noted that throughout the paper we referred to the diagrams as typical. Obviously, special applications require special consideration and were not intended to be within the scope of this paper.

Mr. Siegel's statement, "In addition the system impedance is often extremely important" is an overstatement. We have found it only occasionally important in paralleling of rectifiers with other conversion equipment. We have found it important on one installation within the last eight years.

Mr. Siegel states that better selectivity with the d-c circuit breaker can be obtained on systems of 600 volts or more, by the use of adjustable time delay relays instead of instantaneous relays. It should be noted that this selectivity is obtained at the expense of delayed tripping during arc back which is the most damaging fault to which rectifiers are subjected. If during arc back the high current is allowed to continue it may damage the tube and/or the rectifier transformer. There are two requisites for best protection under arc back conditions: high speed and selectivity. This is true regardless of voltage. Using an instantaneous trip gives maximum high-speed operation under arc back conditions. There are some cases in which the setting of the instantaneous trip element is rather critical to obtain selectivity. When anode circuit breakers are used the instantaneous trip is omitted, (Figure 10 of our paper) as rectifiers equipped with anode circuit breakers possess a very high degree of selectivity.

The following sentence is quoted from a recent report[1] AIEE entitled Protection of Electronic Power Converters by the Committee on Electronic Power Converters: "Instantaneous element (50) to trip quickly in case of tube arc back or transformer fault. This relay should be set slightly in excess of the transformer current inrush and the short time rating of the rectifier".

It is to be noted that our paper is in accord with this AIEE Committee recommendation.

Figure 5 of our paper shows misfire indicating lamps. Our paper also states that these lamps may be replaced by relays to provide an alarm following a sustained misfire. This relay would give an alarm on sustained misfire regardless of the cause; that is, wetted ignitor, gassy tube, and so forth. Using an alarm instead of shutting down and locking out allows the rectifier to continue to carry reduced load until such a time that the tube can be replaced or repaired.

The sequence for a rectifier from the time the starting impulse is received to the time that the sequence is completed is a matter of seconds. If the sequence is incomplete, indication is given quickly by the failure of the cathode circuit breaker to close. Consequently, a complete sequence check adds very little to the over-all operation, and is not required.

Mr. Siegel suggests that the conditions of high rectifier temperature, low cooling water pressure, and high temperature of the mercury vapor pump not be allowed to shut down and lock out since facilities are available to allow these conditions to be automatically corrected. It is unfortunate that Mr. Siegel did not disclose what these facilities were to enable us to comment on them. Experience has indicated that after a rectifier has been in service for a period of time, trouble occurring as a result of these three items is not of a temporary nature and is not self-corrective. The scheme suggested by Mr. Siegel would cause the rectifier to "pump" and eventually arc back and lock out.

In our paper, high rectifier temperature, low cooling water pressure, and high temperature of the mercury vapor pump results in shut-down and lockout if the rectifier has been in service for a definite period of time (usually 10 minutes), but only prevents starting for this time interval if the rectifier has been shut down due to loss of or low alternating voltage. This is done to avoid a lockout when during shut-down the latent heat of the rectifier units may operate the contacts that detect high rectifier temperature and high temperature of the mercury vapor pump, or low voltage cause the water pump motor to fail to keep sufficient water pressure. This arrangement does not allow the unit to "pump."

Mr. Siegel in questioning our omission of a statement regarding the interrupting duty required of the d-c circuit breaker during paralleling failed to note that in the first portion of our paper we stated "high-speed or semihigh-speed switching is provided for a rectifier depending on the d-c voltage, the kilowatt rating of the individual rectifier, and the full load rating of the station bus." This statement would normally be interpreted that the rating of the station bus is determined by the paralleled equipment.

REFERENCE

1. See reference 1 of the paper.

Protection of Electronic Power Converters

AN AIEE COMMITTEE REPORT

THIS report discusses the protection of electronic power converters operating as power rectifiers. It treats specifically the problems of protection arising from the occurrence of faults, such as overloads and short circuits in the load circuits to which the rectifier is connected, and arc-back within the rectifier.

Electronic power converters must be provided with adequate protective gear in order to prevent damage to the various components of the rectifier unit from overload or fault currents. Protective gear also is required to limit the extent and duration of the disturbance in a-c and d-c systems at the time of fault.

The report is devoted primarily to the problem of protection of power rectifiers of the size and type usually encountered in railway, electrochemical, and general industrial applications, see American Standard ASA C34.1—1949.[1] In such rectifiers, reactance is usually the dominant factor in determining the magnitude of fault currents. Correction factors are given for resistances up to values numerically equal to the reactance.

While overvoltages and surges may occur as a result of the flow and interruption of fault currents in the rectifying elements and other parts of the rectifier circuit, they do not usually affect the problem of protection to any considerable degree. The factors to be considered and the measures required for overvoltage protection are, therefore, omitted from this report.

The report is based on the experience of manufacturers and users of electronic power converters, accumulated over many years. The material is derived from published literature, theoretical analyses, and factory and field tests. A list of references is given at the end of the report.

Historical Review

The general principles of protection of electronic power converters have not changed greatly through the years, but many improvements have been made in the character and performance of protective systems.

Early rectifiers were protected by conventional a-c and d-c switchgear of the type used on comparable rotating equipment. As the size of rectifiers and rectifier installations increased, it became necessary to increase the speed of interruption and limit the ceiling values of fault currents. These improvements have been accomplished by the use of arc suppression, anode circuit breakers, and higher transformer reactance. Arc suppression provides high-speed interruption of the fault current in the normal anodes of the rectifier. Anode circuit breakers provide fast interruption of the fault current in the faulty anode and at the same time make it possible to maintain essential service with the rest. High transformer reactance reduces the ceiling value of damaging fault currents.

Metalclad switchgear now is widely used and has improved the safety of rectifier installations. Increased speed of circuit breaker interruption has not only been a great advance in isolating faults and reducing damage to equipment but has improved service and reduced outage time. In the larger rectifier sizes, the use of anode circuit breakers has added materially to the protection of rectifiers and increased the quality of uninterrupted service to the load.

Nature of Problem

The purpose of this section is to provide a basis for analyzing the problem of protection. The basic factors which enter into this problem are formulated. The effects of the various types of faults on the rectifier unit, the a-c system, and the d-c system are qualitatively stated. The analysis of rectifier circuits under normal conditions is thoroughly covered in the references cited and a fair working knowledge is assumed.

Principles of Operation

The circuit diagram for a typical polyphase electronic power converter unit is shown in Figure 1. The unit consists of a rectifier transformer, a group of rectifier tubes, and the a-c and d-c circuit breakers. The a-c winding of the rectifier transformer is connected to the 3-phase a-c system by the a-c circuit breaker. The d-c winding is connected to the d-c system through the tubes and the d-c circuit breaker.

The rectifier transformer shown is the 6-phase double-Y, and is the most commonly used for large power rectifiers. The methods for determining fault currents outlined in this report are based on this circuit.

The operation of the electronic power converter is based on that characteristic of the mercury-arc rectifier which normally permits current flow in only one direction, namely, from the anode to the cathode.[2,3] The tubes act merely as switches and the currents are determined by the connected circuits. Current flow in any tube takes place when a positive voltage is impressed on the anode with respect to the cathode after the tube is made conductive. This is done by establishing a cathode spot on the surface of the mercury pool and applying a suit-

Paper 50-133, recommended by the AIEE Electronic Power Converters Committee and approved by the AIEE Technical Program Committee for presentation at the AIEE Summer and Pacific General Meeting, Pasadena, Calif., June 12–16, 1950. Manuscript submitted March 3, 1950; made available for printing April 7, 1950.

Personnel of the Working Group of the Subcommittee on Electronic Converter Circuits: C. C. Herskind, *Chairman*; J. L. Boyer, I. K. Dortort, D. C. Hoffmann, G. F. Jones, H. V. Nye, M. E. Reagan, A. Schmidt, Jr., H. Winograd.

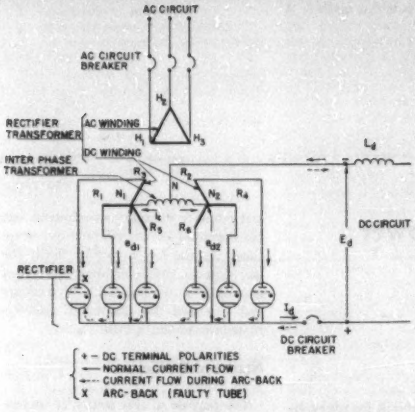

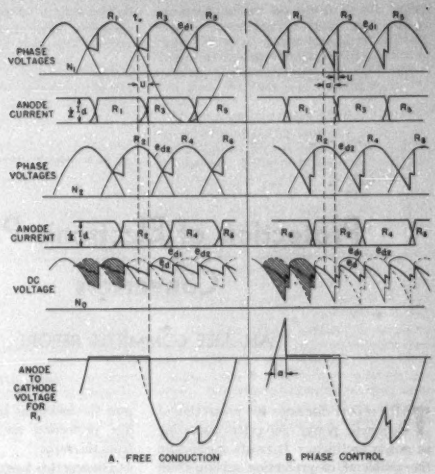

Figure 1 (above). Typical 6-phase double-Y rectifier circuit

Figure 2 (right). Rectifier voltage and current wave forms

able potential on the grid (if present). The start of conduction may be controlled by means of either an ignitor, which starts the cathode spot, or a grid, which controls the passage of electrons to the anode, depending on the type of tube. This is known as phase-control. Once the current flow in the tube has started, it will continue until it is brought to zero by the action of the external circuit, as the grid has no influence on the current and can regain control of conduction only after it has reached zero. The resumption of current flow in succeeding cycles may be prevented by rendering the tube nonconductive by means of ignitor or grid control, or by the interruption of excitation. This action is called arc-suppression.

In the 6-phase double-Y circuit the rectifier transformer d-c winding is connected in two 3-phase groups, or wyes, with their neutral points interconnected by an interphase transformer. Each Y and the tubes connected to it constitute a commutating group which carries a direct current I_e. The two commutating groups operate in parallel, and each carries one-half of the total direct current I_d.

A graphic analysis of the circuit action is given in Figure 2, which shows the phase voltages, the direct voltage, the anode currents, and the anode-to-cathode voltages in the 6-phase double-Y circuit.[4]

Figure 2(A) shows the action under the condition of free conduction where each anode is permitted to start firing as soon as its voltage becomes positive with respect to the cathode. The direct voltage, or output voltage of the rectifier, e_d is the average of the direct voltages of the two commutating groups e_{d1} and e_{d2}. The difference between the voltage waves of the two commutating groups is shown by the shaded area. This voltage difference appears across the interphase transformer as an alternating voltage having a fundamental frequency three times that of the phase voltages.

Commutation, or current transfer, requires a definite time, or commutating angle u, which depends upon the transformer reactance and the commutating voltage, that is, the voltage difference between two commutating phases. The transformer reactance which controls the transfer of current between phases of a commutating group is called the commutating reactance. The commutating angle increases with increasing commutating reactance or increasing commutated current and decreases with increasing commutating voltage.

The anode-to-cathode voltage wave of phase R_1 is shown in Figure 2. During the conducting period, the anode is positive with respect to the cathode by the amount of the arc-drop. During the nonconducting period, the anode is negative with respect to the cathode.

Figure 2(B) shows the action with phase control. Under this condition, anode R_1 continues to carry current despite the fact that its voltage is lower than that of anode R_3. The output voltage of the rectifier may be reduced by means of phase control, the average value of the direct voltage decreasing as the angle of retard, α, is increased. The commutation process with phase control is similar to that for the free rectifier except that the commutating angle is smaller because of the increased voltage effective for commutation.

The natural voltage regulation of the rectifier unit is determined to a large degree by the commutating reactance. The effect of the overlapping conduction during commutation is to decrease the average value of the direct voltage. The direct voltage is reduced further by resistance drop in the transformer and arc-drop in the tubes. Under rated loads the inherent d-c voltage regulation curve for a rectifier unit deviates only slightly from a straight line as the commutating reactance and resistance voltage drops are linear and the arc-drop is essentially constant. The area between heavy overloads and short-circuit has not yet been fully analyzed.

The duty on the tubes is determined by the wave shapes of the anode current and the anode-to-cathode voltage. These wave shapes depend on the rectifier circuit used and operating conditions such as voltage, current, and amount of phase control.[5] A rectifying device must be a good conductor during the conducting period of each cycle and a good insulator capable of withstanding the anode-to-cathode voltage during the inverse period. The transition from a conducting to an insulating state occurs at the conclusion of each conducting period. Most arc-backs are initiated during this transition.

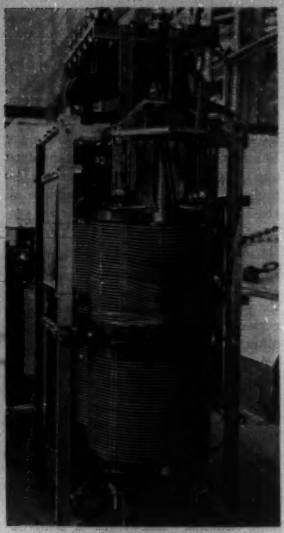

Figure 3. Delta 6-phase parallel double-Y connected rectifier transformer damaged by repeated arc-backs

Nature of Faults

Overload and Short Circuit. The operation of the rectifier on moderate overload is the same as at rated loads except that the commutating angle increases with increasing load current. This modifies the anode current and voltage waves and so changes the duty on the tubes.[6]

As the impedance at the d-c terminals of the rectifier approaches zero, the current delivered by the rectifier increases to a limiting value determined by the constants of the rectifier circuit. The conduction period of the tubes increases to 180 degrees or more on d-c short circuit.

The mode of operation of the rectifier circuit also changes so that the anode current waves are substantially sinusoidal instead of flat-topped.

The direct current delivered by a rectifier unit to a bolted short-circuit usually ranges from 10 to 20 times its rated current. Its magnitude is determined primarily by the reactance of the rectifier transformer and the a-c supply system.

Arc-Back. Faults may occur within the rectifier unit as the result of arc-back.[7,8] An arc-back is the failure of the rectifying action resulting in the flow of a principal electron stream in the reverse direction due to formation of a cathode spot on an anode.

When an arc-back occurs, fault current flows from the other transformer phases and their connected anodes to the faulty anode as shown by the broken arrows in Figure 1. If the d-c circuit to which the rectifier is connected has other d-c voltage sources, the current flow at the positive terminal of the rectifier will reverse and a fault current will flow from the positive terminal through the faulty tube and its transformer winding to the negative terminal as indicated by the broken arrows.

If there is no feedback from the d-c circuit and all the reverse current to the faulty anode comes from the other anodes of the rectifier, the fault current is determined only by the impedance of the transformer and a-c supply system and by the arc-drop. It usually attains its maximum value in the first cycle and its magnitude is generally comparable to that of the d-c short-circuit current.

If there is feedback from the d-c circuit into the faulty anode, the fault current is determined by the inductance and resistance of the fault path. The rate of rise of d-c fault current is determined largely by the inductance of the circuit, and its ultimate value by the circuit resistance, tube arc-drop and voltage regulation of the current source. In most rectifier installations, the circuit constants are such that the feedback current requires several cycles to reach sustained values. Ultimate fault currents of 25 to 100 times the rated current of the tube and the transformer winding to which it is connected may be obtained.

Effects of Faults on Rectifier Unit

Overloads and Short Circuits. Mercury pool tubes may usually be operated at loads above their continuous or short-time ratings without causing immediate structural failure. However, they do have definite limitations and such operation may impair them and shorten their life.

The rating of an electronic power converter usually includes overloads of specified magnitudes for specified periods of time, to take care of service requirements for particular applications. Standard overload ratings for electrochemical, industrial, and several classes of railway applications have been established.[1] Two types of overload ratings are specified: overloads of 2-hours' duration and overloads of 5-minute or 1-minute duration.

Forward currents in excess of specified overload rating, up to short-circuit values may have some or all of the following effects on the tubes of an electronic power converter:

1. *Temperature.* Temperatures of the anodes and other internal parts in the arc path will be raised by the increased losses and may be drastically increased by local heating.

2. *Vacuum.* The increased temperatures and increased ion current to the anode during the inverse period may cause the liberation of gases and impairment of the vacuum.

3. *Contamination.* The increased arc-drop voltage may start intermediate cathode spots on the metal or graphite surfaces in the arc-path or adjacent to it. Such cathode spots erode the surfaces and produce metal vapor or graphite powder, which may deposit on insulating surfaces and ultimately impair the operation of the rectifier.

4. *Surges.* If a rectifying device carries high forward current with insufficient mercury vapor to provide the needed ionization, high-voltage surges may result due to so-called "arc starvation": this might be detrimental to the insulation of the rectifier transformer, cables, wiring, or other connected equipment.[9] Such surges are likely to occur on suddenly applied overloads if the rectifier is too cold.

5. *Arc-Backs.* The occurrence of arc-back in a mercury arc rectifier is basically random in nature. However, it is influenced by the magnitudes and shapes of the current and voltage waves impressed on the anode and the conditions within the rectifier. During overloads, the probability of arc-back is increased as a result of the greater ionization produced by the overload current. It also may be increased by the physical conditions listed above.[6,7,8]

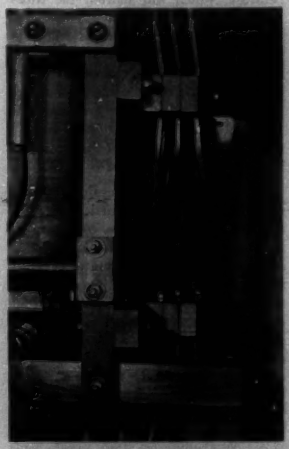

Figure 4. Bus-bar leads deflected during arc-back tests

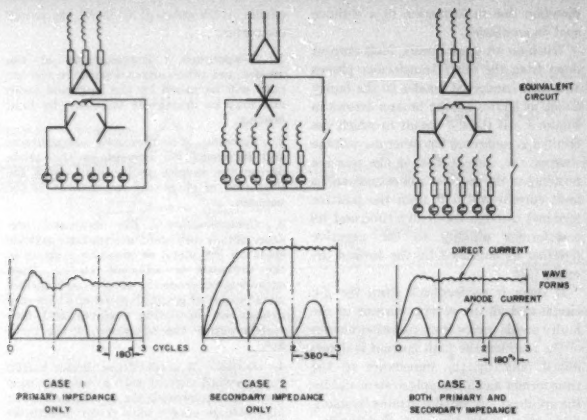

Figure 5. D-c short-circuit, idealized conditions

The over-all effect of overloads and repeated short-circuits on the rectifier tubes is to decrease their reliability and increase the cost of maintenance. A pumped rectifier subjected to such overloads may have to be reconditioned more frequently. The operating life of sealed tube rectifiers subjected to such overloads may be shortened.

Excessive overloads will raise the operating temperature of the rectifier transformer windings above the rated temperature, which will shorten the transformer life. Too frequent application of the short-time rated overload will have the same effect. Excessive overloads also may increase the maintenance cost of the switchgear, due to overheating of circuit breaker contacts or due to an increase in the number of operations to clear faults if the frequency of faults on the rectifier is increased by the overloads.[10]

Arc-Back. Arc-backs result in forward fault currents in the normal anodes and the transformer windings connected to them, of the same order of magnitude as obtained on d-c short circuit. In addition, the faulty anode and its transformer winding carry a reverse current which considerably exceeds that incurred on d-c short circuit. The effects of arc-back currents are similar to those of short-circuit currents except for the action of the reverse current on the faulty anode. The arc-back current, if sustained too long, will cause pitting and overheating of the anode, will impair the vacuum, and may damage the anode insulator and vacuum seals.

Because of their high magnitude, the repeated occurrence of arc-backs is attended by an increasing hazard of thermal of mechanical failure of the rectifier transformer. Severe mechanical stresses are imposed on the coils, leads, and even the core. Figure 3 shows a 3,000-kw 600-volt delta-parallel double-Y rectifier transformer which was tested to destruction by the repeated application of artificial arc-backs in the laboratory. The repeated impacts caused mechanical failure of the upper coils of the a-c winding. Figure 4 illustrates the need for adequate strength and bracing in bus-bars and leads.[11]

Figure 6. Arc-back, idealized conditions

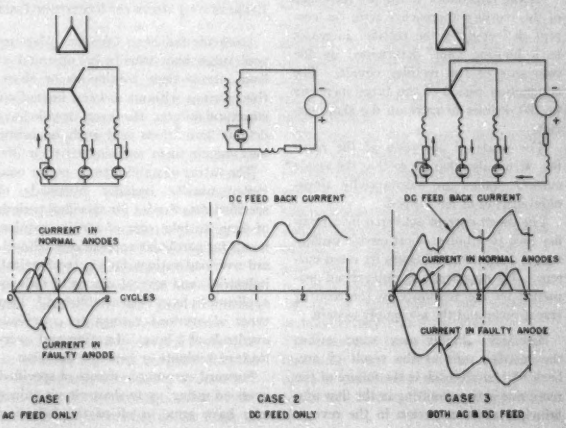

Effects of Faults on Systems

Fault currents flowing in the d-c windings of the rectifier transformer during short-circuit or arc-back are reflected in the a-c windings and supply system. There is no flywheel effect between the a-c and d-c sides, the disturbances are limited only by the impedances involved and the speed of the protective gear. D-c faults on a rectifier therefore produce all the harmful disturbances on the a-c system that would be produced by a fault of the same magnitude occurring directly on the a-c system.

Short circuits and arc-backs produce the same kind of disturbance on the connected d-c system as similar faults on other types of equipment. Flashover may result on parallel rotating equipment and sympathetic arc-backs may occur on parallel rectifiers.

Determination of Fault Currents

This section presents analyses of the circuit action during faults and outlines the procedure for the determination of fault currents. Knowledge of both the character and magnitude of fault currents is important in the selection and design of protective systems.

The complete and accurate determination of the fault currents in rectifier circuits under all conditions is not possible at the present time, as existing analyses do not cover adequately the wide variety of circuits and their many modes of operation. However, it is the object of this section of the report to describe typical circuit action during faults in rectifier circuits under usual service conditions and to present a procedure for the

approximate determination of fault currents for the double-Y circuit. A number of sample computations are given in Appendix II.

Rectifier faults may be resolved into two general types, namely, d-c short circuit and arc-back. The nature of the rectifier fault currents under idealized conditions are shown on Figures 5 and 6. During d-c short circuit, the circuit action is determined by the relative magnitude and location of the various impedances in the rectifier unit and short circuit path. Figure 5 shows three idealized cases and their equivalent circuits and wave forms. During arc-back, the circuit action is determined primarily by the number of sources of voltage producing the fault current. The action may be resolved into the three cases illustrated in Figure 6.

The equivalent circuit shown on Figure 7 indicates the various impedance elements which may be present in a typical 6-phase double-Y rectifier circuit. In the general case all of these impedances must be considered in determining fault currents. However, in actual practice, one or two of these impedances usually play a dominant role and the others may either be neglected or allowed for by a small correction. In the usual rectifier the d-c windings associated with each phase of the transformer are interlaced, the anode leads are generally short, and current limiting reactors in the anode leads are seldom used. Under these conditions all the a-c circuit reactance may be considered located in the a-c supply line.

D-C Short Circuit

The form and magnitude of the direct current obtained when a rectifier is short circuited at its load terminals determines the duty imposed on d-c circuit breakers, the forces on d-c conductors, and the possibilities of destructive damage. Of interest is the rate of rise of d-c short-circuit current, its maximum instantaneous value and the final or sustained value. Similarly, the corresponding values of the reflected fault current in the a-c system determine the duty on the a-c circuit breaker. The magnitude of the tube currents under short circuit also is important, as it determines the duty imposed on the tubes, consequently the probability of tube arc-back or damage, and the forces on transformer windings and conductors.

The circuit action in a rectifier during d-c short circuit depends upon the location of the impedance. When the circuit impedance is in the transformer primary or supply line, the fault currents are similar to those in a standard power transformer on a-c short circuit. The two anodes connected to diametrically opposite phases act as a pair and carry current alternately. With the impedance located in the transformer secondary the anodes act independently and each carries current for more than one half of the cycle. Three cases are considered in the analysis of d-c faults, namely: primary impedance only; secondary impedance only; and both primary and secondary impedance.

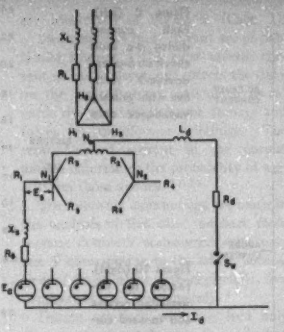

Figure 7. Equivalent circuit during d-c short circuit

The symbols used in the formulas which follow are defined in Appendix I. The circuit constants are defined and their determination described in the section on circuit constants.

Case I. Short Circuit With Primary Impedance Only

The following assumptions are made in the derivation of the formula which apply to a 6-phase double-Y transformer: a-c windings are perfectly interlaced (all impedance in a-c windings and supply line).

There is no impedance in anode leads (usual types of current-dividing reactors do not contribute to the impedance). There is a bolted d-c short circuit (zero resistance and inductance) and free conduction (no phase control).

Typical wave forms of the current obtained during d-c short circuit are shown in Figure 8. The anode current waves are sinusoidal and add to produce the d-c fault current.

Under sustained short circuit the two anodes connected to diametrically opposite phases fire alternately to produce symmetrical a-c flow in the a-c winding.[9,12,13] The sustained anode current is

$$i_{ss} = \frac{\sqrt{2}\,E_s}{Z_s} \text{ (crest value)} \tag{1}$$

The sustained direct current is

$$I_{ds} = \frac{2\sqrt{2}}{\pi}\frac{VA}{E_s Z_{c\,pu}} = 0.900\frac{VA}{E_s Z_{c\,pu}} \text{ (average value)} \tag{2}$$

The sustained fault current also may be expressed in terms of the rated direct current I_{dn} by

$$I_{ds} = \frac{2\sqrt{3}}{\pi}\frac{I_{dn}}{Z_{c\,pu}} = 1.10\frac{I_{dn}}{Z_{c\,pu}} \tag{3}$$

This current has a ripple whose fundamental frequency is six times the a-c supply frequency. The crest value of the sustained direct current is $\pi/3$ or 1.047 times its average value, or $2\,i_{ss}$.

The sustained supply line current is

$$I_{Ls} = \frac{I_{Ln}}{Z_{c\,pu}} = \frac{VA}{\sqrt{3}\,E_L Z_{c\,pu}} \text{ (rms value)} \tag{4}$$

On a bolted short circuit, the transient fault current will reach a peak higher than the sustained crest value during the first cycle. This peak is caused by d-c transient components in one or more anode currents.[14] This transient decreases exponentially as a function of the resistance/reactance ratio and generally has little effect beyond the first peak of the a-c wave. The ratio resistance/reactance is the sum of the equivalent resistances of the transformer, supply line, and arc-drop, to the sum of the transformer and supply line reactances, all expressed either in ohms or per-unit quantities.

A correction factor, K, a function of resistance/reactance, is applied to the sustained crest values to obtain the value of the first, or transient, peak of the anode, a-c system, and d-c fault currents. K is plotted against resistance/reactance in the curve of Figure 9. K cannot be greater than two and very seldom exceeds one and a half.

Transient peak of anode current

$$i_{sf} = K\,i_{ss} \tag{5}$$

The transient peak of supply line current

$$I_{Ls}' = \sqrt{2}\,K\,I_{Ls} \tag{6}$$

Transient peak of direct current

$$I_{ds}' = K\frac{\pi}{3}I_{ds} \tag{7}$$

The rate of rise of direct current in the fault varies with the switching angle and attains maximum value on a bolted short-circuit with no inductance. The peak I_{ds}', is reached along a composite curve in one-half to two-thirds cycles.

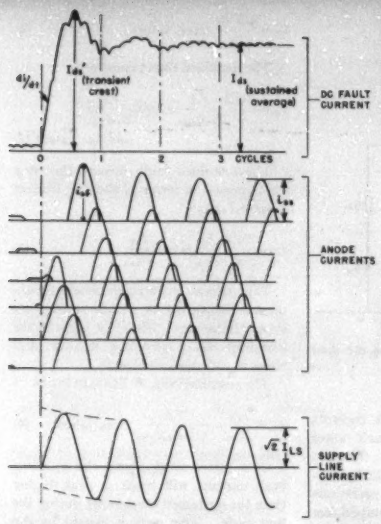

Figure 8 (left). Fault currents during d-c short circuit on 6-phase double-Y rectifier with primary impedance only

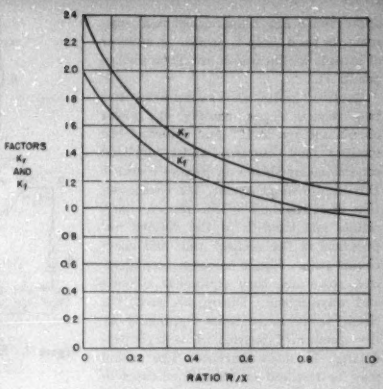

Figure 10 (right). Factors for determining reverse and forward current during arc-back with a-c feed only

The initial rate of rise is $\pi f I_{ds}'$ but the average rate of rise to the first major peak is $2fI_{ds}'$. Since the fastest circuit breakers available do not begin to limit the current appreciably in less than one-third cycle, it is suggested that an average value for this period be taken as

$$\frac{di}{dt_{as}} = \frac{1}{2}\sqrt{3}\,\pi f\, I_{ds}' \text{ (amperes per second, approximate)} \quad (8)$$

This formula gives reasonably accurate values of current up to 90 per cent of the peak.

Case 2. Short Circuit With Secondary Impedance Only

In this case the following assumptions are made which apply to a 6-phase double-Y transformer, with all impedance in anode leads. There is a bolted d-c short circuit (zero resistance and inductance), and free conduction (no phase control).

This is an idealized case rarely realized in practice. With no mutual impedances, each phase (anode) acts independently, carrying current more than 180 degrees as determined by circuit constants. If there are no losses, the current will flow 360 degrees in the form of a fully displaced sine-wave. A typical wave-form of the anode current is shown in Figure 5. The current in the fault is the sum of six such anode currents spaced 60 degrees apart. It is to be noted that the short-circuit current does not drop off after the first peak as in Case 1. The displacement transients that cause this peak are repeated in each cycle.

A sustained direct current, assuming no losses, is

$$I_{ds} = K\sqrt{2}\frac{VA}{E_n Z_{c\,pu}} = \frac{K\sqrt{3}\, I_{dn}}{Z_{c\,pu}} \text{ (average value; approximate)} \quad (9)$$

this value is π times that obtained for the sustained current in Case 1 with zero resistance. Theoretically, the conduction period of each anode is 360 degrees. Losses decrease the conduction period and the short-circuit current to values intermediate between those given by equation 2, and equation 9.

Figure 9 (below). Transient factor for determining crest value of transient current on d-c short circuit

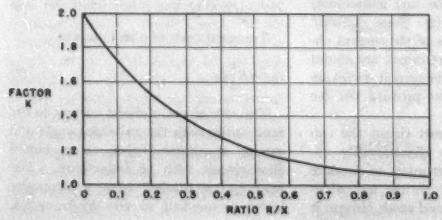

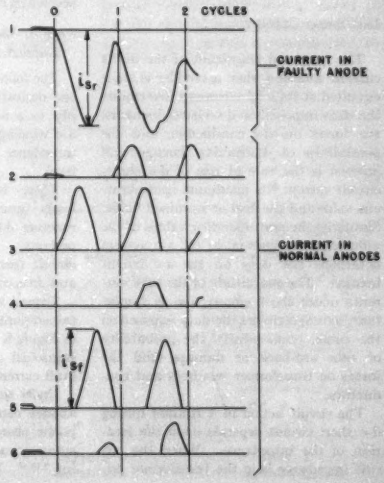

Figure 11 (right). Fault current during arc-backs in 6-phase double-Y rectifier with no external d-c feed

Case 3. Short Circuit with Both Primary and Secondary Impedance

This is a general case which is encountered in practice. The analytical treatment is similar to that for Case 1 with primary impedance only except for a greater complexity of circuit action. Exact analyses for this case have not been completed.

Usually, most of the circuit reactance is in the primary, while the major part of the resistance, consisting of the transformer d-c winding, the anode leads, and the tube arc-drop, is located in the secondary. Secondary resistance must be considered in the determination of fault currents: However, since its effect on circuit action is generally small, it is permissible to transform and add it directly to the primary resistance. Fault currents are then computed as in Case 1.

Equivalent Machine Constants. In setting up a d-c system problem on a calculating board, it may be desirable to represent the rectifier as a machine having a known induced voltage, internal resistance, and inductance. For specific cases it is possible to determine and assign values based on the short-circuit currents and rate of rise as obtained above. Some work has been done along this line, but it is felt that no recommendations should be made until the subject has been explored further.

Arc-Back

An arc-back in a rectifier constitutes a short circuit of both the a-c and d-c circuits. The current in the faulty anode under arc-back conditions is the sum of the current delivered by the normal anodes of the rectifier and the current fed back from the d-c system. The currents which flow in a 6-phase double-Y rectifier during arc-back are indicated in Figure 1 by the broken arrows.

In analyzing the fault currents during arc-back, it is helpful to consider idealized cases where only one component of feed to the faulty anode is present, before proceeding to the general case where both a-c and d-c feed are present.

Case 1. Arc-Back with A-C Feed Only

This type of fault is approximated when arc-back occurs in a rectifier supplying a resistance load with no other source of d-c power in parallel. If the current contribution from the other Y is neglected, the circuit reduces to a single Y with one faulty anode carrying reverse current and two normal anodes carrying forward currents. The equivalent circuit and typical fault current wave forms are illustrated in Figure 6 (Case 1).

Two values of fault current are of particular interest. The crest reverse current in the faulty anode affects the duty on the faulted phase particularly as regards the possibility of tube damage and forces on transformer windings. The crest forward current in the normal anodes determines the probability of arc-back on those anodes.[12,13,14]

The following assumptions are made in the analysis of this case: no back feed; 6-phase double-Y transformer with only one Y contributing to the fault; saturation of transformer core neglected; free conduction (no phase control).

During arc-back with a-c feed only the crest reverse current in a faulted anode is

$$i_{sr} = \frac{K_r \sqrt{2}\, E_s}{Z_c} \tag{10}$$

and the crest forward current in normal anodes is

$$i_{sf} = \frac{K_f \sqrt{2}\, E_s}{Z_c} \tag{11}$$

Values of the reverse current factor K_r and the forward current factor, K_f, for various resistance/reactance ratios are given in Figure 10. The resistance/reactance ratio should include the resistance of the rectifier transformer and the equivalent resistance of the rectifier tube. These factors give the crest values of the fault current obtained during the first cycle when arc-back occurs immediately after forward conduction of the anode. The current may increase to some extent during subsequent cycles but sufficient information for most system studies is generally provided if the values of reverse and forward current obtained during the first cycle are known.

The fault current waves obtained in a 6-phase double-Y rectifier during arc-back with no d-c feed except that from the anodes of the normal Y are shown on Figure 11. These fault current waveforms show that the arc-back current in the faulty anode is supplied principally from the other two anodes of the same Y. The current contribution of the anodes in the normal Y is limited to a relatively low value, because of the impedance of the interphase transformer, the interlacing of the two secondary coils of each phase of the rectifier transformer, and the long conduction period of the anodes of the faulted Y. Since the anodes in the normal Y of a double-Y rectifier do not begin to feed any appreciable current into the fault until the second cycle, their contribution may be neglected without appreciable error in most cases.

Case 2. Arc-Back with D-C Feed Only

This condition is obtained in practice when all the normal anodes of the rectifier are prevented from firing at the time of the fault, as when arc-suppression is instantly applied to the faulted rectifier. It also is approximated to a limited extent if several rectifiers are connected in parallel and are supplied through a common line reactance so that the loading on the parallel rectifiers reduces the anode voltages on the faulty rectifier and thereby reduces the a-c feed from the normal anodes on the faulted Y.

The equivalent circuit for this idealized case and the waveform of the current in the faulty anode are shown in Figure 6 (Case 2).

Reverse Current. For the most severe condition when arc-back is initiated at the instant of voltage reversal[13] the instantaneous reverse current i_d in the faulty anode is given with fair accuracy by the equation

$$i_d = \left[\frac{E_d'}{R_d} - \frac{\sqrt{2}\, E_s}{Z_d}\right]\left[1 - e^{\frac{-R_d t}{L_d}}\right] + \frac{\sqrt{2}\, E_s}{Z_d} \times [1 - \cos \omega t] \tag{12}$$

The time t is measured from the beginning of the negative half cycle of a-c voltage wave.

The reverse current attains peak values at the end of the first, third, fifth, and succeeding half cycles. The crest value at the nth peak is

$$i_d = \left[\frac{E_d'}{R_d} - \frac{\sqrt{2}\, E_s}{Z_d}\right]\left[1 - e^{\frac{-R_d}{L_d f}\left(n - \frac{1}{2}\right)}\right] + \frac{2\sqrt{2}\, E_s}{Z_d} \tag{13}$$

Case 3. Arc-Back with Both A-C and D-C Feed

The case of arc-back with both a-c and d-c feed is the one most commonly met in practice. It is obtained whenever arc back occurs among parallel rectifiers or in a rectifier supplying a counter-electromotive-force load.[14,15] Figure 12 shows the fault currents obtained on a 6-phase double-Y rectifier during arc-back with both a-c and d-c feed. The circuit action is quite complex and a complete solution including the current contribution of all the normal anodes has not been made. However, several approximate methods for determining the fault currents have been developed.

Method 1. The analysis of the fault currents during arc-back with both a-c and d-c feed is simplified by representing the faulted Y as a simple 3-phase rectifier and treating the action as a combination

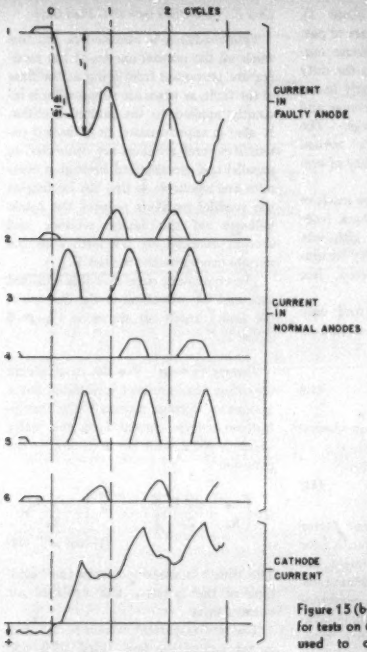

Figure 12 (left). Fault currents during arc-back with both a-c and d-c feed in a 6-phase double-Y rectifier

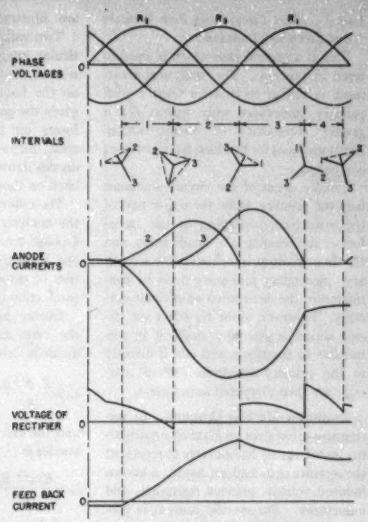

Figure 14 (right). Circuit action during arc-back with both a-c and d-c feed in 3-phase Y rectifier

of a-c feed from the two normal anodes and d-c feed from a single source consisting of all other anodes and parallel sources. The equivalent circuit is shown in Figure 13 together with all the circuit impedances which are considered in the analysis. The inductance of the d-c circuit external to the rectifier, including the inductance of the source of feed-back, the inductance of the d-c leads and the "air-core" inductance of one-half the interphase transformer (where the rectifier circuit includes one) is represented by L_{d1}. R_{d1} represents the corresponding resistance. L_c and R_c are the commutating inductance and resistance per phase. R_c includes the arc-drop resistance.

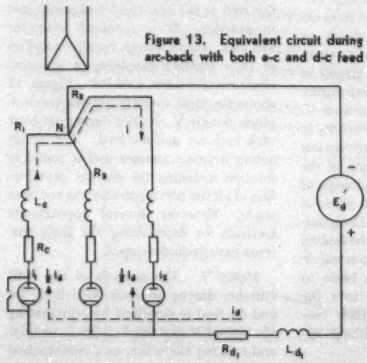

Figure 13. Equivalent circuit during arc-back with both a-c and d-c feed

Figure 15 (below). Power circuit and constants for tests on 6-anode 200-kw 300-volt rectifier used to check sample computations in Appendix II

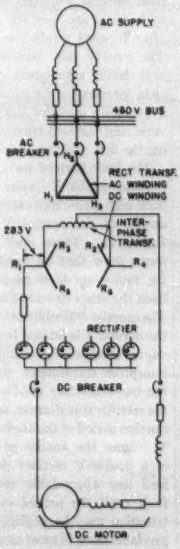

CIRCUIT CONSTANTS

SUPPLY LINE
X = .0250
R = .0031
(PER UNIT VALUES ON 230 KVA BASE)

RECTIFIER TRANSFORMER
- 60 CYCLE - 230 KVA CONT. AT 45° C RISE - 480/283 V L TO N.
- IMPED. Z = 5.97% AT 480/283 V AND 75° C
- COMM. REACT. X_c = .080 OHMS L TO N.
- LOAD LOSSES: P_r = 3707 WATTS AT RATED CURRENT I_{dn} = 667 AMPS
- RESISTANCE AC WIND. R_p = .0241 OHMS PER COIL
DC WIND. R_s = .00632 OHMS PER COIL

INTERPHASE TRANSFORMER
- 180 CYCLES - 78 KVA OUTPUT AT 45° C RISE - 236 - 118 VOLTS
- LOAD LOSSES = 346 WATTS AT RATED CURRENT
- RESISTANCE = .00316 OHMS ACROSS FULL CO

ANODE CABLES
- RESISTANCE = .003 OHMS PER PHASE

RECTIFIER TUBES (ARC DROP)
- EQUIV. RESISTANCE = .0015 OHMS PER TUBE

LOAD CIRCUIT
CABLE LEADS
- RESISTANCE = .0034 OHMS
- INDUCTANCE = 79.5 X 10^{-6} HENRYS
DC MOTOR (EQUIVALENT MACHINE)
- RESISTANCE OF ARMATURE CIRCUIT = .0170 OHMS
INDUCTANCE OF ARMATURE CIRCUIT = 46 X 10^{-6} HENRYS
- VOLTAGE E_d' = 290 VOLTS OPEN CIRCUIT

For purposes of defining the circuit action, the time during a cycle is divided into four intervals corresponding to the different current flow patterns obtained during the successive conduction periods of the two normal anodes. The dotted lines in Figure 13 indicate the components of the currents which flow in the circuit during the interval when anode 2 is conductive. The circuit action and the waveforms of the transient currents in the faulty anode, the normal anodes, and the d-c feed obtained in a typical example are shown in Figure 14. In this example, the action is that obtained during the first cycle when the arc-back occurs at the end of conduction and it is assumed that the rectifier is operating without phase control so the anodes are free to conduct at any time. The current in subsequent cycles may be obtained by dividing them similarly into four intervals and assuming larger currents in the faulty anode at the beginning of each cycle. This step-by-step method of analysis also may be used where the initial conditions are different and phase control is applied.

Method 2. The foregoing analysis illustrates a method of attack that can be applied to obtain results of good accuracy. However, it is too cumbersome for general use and a more practical solution may be obtained by assuming that the circuit action is equivalent if one normal anode in the Y is assumed to feed into the arc-back throughout the entire cycle. The a-c voltage effective in the d-c circuit is then $1/2\ E_e$ and the equivalent resistance and reactance are $1/2\ R_e$ and $1/2\ X_e$ since the feedback flows through two phases in parallel. The procedure is then as follows:

1. Calculate the normal and faulty anode currents for arc-back with a-c feed only as in Case I.
2. Calculate the current for arc-back with d-c feed only as in Case 2, using $1/2\ E_e$, $1/2\ R_e$, and $1/2\ X_e$.
3. Add one-half of the d-c feed (step 2) to current calculated for the faulty anode in step 1, and subtract 1/2 from the normal anode current.

Method 3. For many problems it is sufficient to know the ceiling values of the fault currents. These may be determined by the following rules:

1. The current in the normal phases will never exceed that obtained with a-c feed only, as given in Case 1.
2. The current from the d-c source generally will not exceed that obtained with d-c feed only, as given in Case 2, unless sympathetic arc-backs occur in additional anodes. The d-c switchgear should interrupt the feedback before this occurs.
3. The current in the faulty anode cannot, in the usual case, exceed the sum of the maximum current in one normal phase and the maximum feedback.

It should be recognized that the values estimated by this method are ceiling values and will exceed those obtained in practice.

Added Circuit Effects

The procedure for calculating rectifier fault current which has been outlined involves many simplifying assumptions which are not fully realized in practice. Two of the more important factors which must be considered are the characteristics of the feedback source and the effects of phase control.

Effect of Feedback Source. The characteristics of the source of d-c feedback affect both the transient and sustained currents obtained during arc-back. The following discussion covers some of the important cases:

Double-Y Circuit. The analysis for Case 3 covers the action in a single Y. The normal Y of a double-Y rectifier is treated as a source of d-c feed. As stated in Case 1, the amount of d-c feed from the normal Y is limited by the coupling between the transformer windings in the normal and faulted wyes and also by the inductance of the interphase transformer. At the initiation of the fault, the build-up of current from other sources of d-c feed is delayed until the interphase transformer becomes saturated. The time required for such saturation to become effective depends on the design of the interphase transformer, the rectifier load at time of arc-back, and the phase of arc-back. Usual values range up to 80 degrees at supply line frequency.

Motor Load. The reactance of a general purpose motor load is generally high compared with the reactance of the rectifier transformer windings. In such cases, the a-c components of current in the d-c circuit may be neglected and the current may be calculated by assuming the motor to be short circuited at its terminals by series inductance and resistance equal to one-half of the inductance and resistance of one d-c winding of the rectifier transformer, this being a close approximation of the average inductance and resistance in the fault circuit over the entire cycle.

Parallel Rectifiers. When two or more rectifiers are operated in parallel and one of them arc-backs, the inductance of the d-c circuit feeding the fault is of the same order of magnitude as the inductance of the transformer windings in the fault. In such cases, the amplitude of the a-c component of d-c fault current is considerable and may not be neglected. This observation also applies in the case of a rectifier supplying low-inductance motors such as machines with pole face windings.

Effect of Phase Control

The effect of phase control on the fault currents is neglected in the foregoing analyses. It is assumed that the anodes are free to conduct at any time. This assumption is usually justified in the determination of fault currents in connection with the problem of protection as it gives maximum or ceiling values. While the rectifier anodes are not free to conduct at all times in most rectifiers, because of the nature and characteristics of the excitation circuits, conduction is usually not limited sufficiently to greatly reduce the fault current. When a double-Y rectifier is operated with free conduction, anode current flow starts at the 30 degree point of the voltage wave. Under short-circuit conditions, conduction is retarded so that the phase angle of conduction is $\tan^{-1} X/R$. As excitation is usually maintained for an appreciable part of the cycle, the anodes actually operate without phase control during the short circuit. Under arc-back conditions, the feed from the normal anodes may be reduced somewhat by phase retard.

Other Circuits

The general analytical procedure which has been outlined for the double-Y circuit may be used in the determination of fault currents in other rectifier circuits. The large variety of circuits and circuit parameters precludes a comprehensive treatment at the present time.

Circuit Constants

When making fault current calculations, it is essential that the proper values of circuit reactance, resistance, and impedance be used. The circuit data which are usually available are reviewed and the procedure for determining the equivalent circuit constants from these data is described.

Circuit Data

Transformer Constants. Factory tests on rectifier transformers usually provide the following information:[1]

The per cent impedance of the rectifier transformer is stated on its nameplate. It is determined in the usual manner by short-circuiting the total d-c winding and

is calculated on the basis of rated volt-amperes (VA) of the rectifier transformer at the a-c terminals.

The value of the commutating reactance of the rectifier transformer in ohms referred to the d-c winding also is given on the transformer nameplate. It is determined by short circuiting the total a-c winding and applying a sinusoidal voltage between two terminals of the d-c winding where commutation occurs. See ASA C-34.1-1949, section 5.304.

Load losses (P_r) and the resistances of the windings, including the interphase transformer, are usually measured during factory tests and may be obtained from the manufacturer.

Typical values of commutating impedances and resistance/reactance ratios (for the transformer only) as encountered in practice are given in Table I. They vary widely and should be used for estimating purposes only.

Supply Line Constants. The resistance and reactance of the supply line are usually expressed in per cent on a nominal kilovolt-ampere base. They also may be given in ohms per line. When no other information is available the minimum reactance of the supply line may be estimated from the interrupting rating of the a-c circuit breaker.

The supply line impedance may range from a fraction of 1 per cent to 10 per cent based on the rectifier transformer rating and rarely exceeds the latter value.

Rectifier Constants. The rectifier arc-drop is generally unimportant in short circuits but may have considerable effect on arc-back currents, particularly below 600 volts. The arc-drop varies with the type of tube, the relative current magnitude, current wave shape, direction of current flow, and other factors. In some cases it is nearly constant over a considerable current range and in others it varies directly with instantaneous current.

In making fault current calculations, arc-drop may be represented as either an equivalent resistance, a counter electromotive force, or a combination of both. The choice of method depends upon the accuracy desired, the fidelity with which a particular arc-drop may be represented, and mathematical convenience. In general, arc-drop is most readily represented by an equivalent resistance which may be added directly to the other resistance elements in the rectifier circuit.

It is not possible to give concise data on arc-drop at fault current values for the various types of rectifier tubes because of the meager data available at the present time. However, test data on one type of sealed tube give an equivalent resistance of 0.0015 to 0.0025 ohm. Data on one type of pumped tank give an equivalent resistance of 0.002 to 0.004 ohm.[14,15]

Table I. Typical Values of Constants for 6-Phase Double-Y Rectifier Transformers

Application	Voltage, D-C Volts	Type of Tube	Size of Unit, Kw	Z_{epu}	R/X
General industrial	250	Sealed	75–500	0.055–0.10	0.19–0.39
General industrial	250	Pumped	500–1,500	0.04–0.08	0.15–0.43
Railway class I	275	Sealed	200–500	0.06–0.10	0.19–0.26
General industrial	600	Pumped	1,000–3,000	0.05–0.08	0.13–0.28
Electrochemical	600	Pumped	1,000–3,000	0.05–0.09	0.11–0.28
Railway class II and III	600	Pumped	1,000–3,000	0.05–0.08	0.13–0.28

Notes:—The above values apply for a-c line voltages of 550 volts to 66 kv in ratings up to 1,500 kw and 6.6 kv to 66 kv in higher ratings.

The values of impedance are somewhat higher at voltages above 22 kv than at lower voltages.

The ratio of per-unit commutating reactance to the per-unit 3-phase short-circuit reactance usually ranges from 1.02 to 1.10.

Load System Constants. The resistance and inductance of the load system is determined from the constants of the parallel rectifiers, rotating machines and other voltage sources and of the connecting leads. Each parallel rectifier may be represented as an equivalent machine consisting of a voltage source with series resistance and inductance. The other voltage sources may be represented in a similar manner. Generally a d-c system consisting of several parallel voltage sources may be represented by a single large equivalent machine. The regulation of the d-c system may be entered into the computations as an equivalent series resistance.

Equivalent Circuit Constants

The equations for determining the fault currents have been derived on the basis of equivalent circuits with lumped constants. To use them, the impedances of the various elements must be added to obtain total values.

It is frequently necessary to convert impedance values from ohms to per unit and vice versa. The following equation gives the relations between ohmic and per-unit values of reactance in 3-phase circuits

$$X = \frac{E_L^2}{VA} X_{pu} = \frac{3E_a^2}{VA} X_{pu} \tag{14}$$

Similar expression may be written for resistance and impedance.

Total Commutating Reactance in Ohms

The total commutating reactance is the sum of the reactances of the transformer, supply line and other elements in the a-c circuit. To determine its value in ohms referred to the d-c winding proceed as follows:

1. Obtain ohmic value of commutating reactance of rectifier transformer from its nameplate. If it is not known, an approximate value may be determined from equation 14 using the 3-phase impedance Z_{pu} as the per-unit reactance.

2. Determine the ohmic value of the supply reactance X_L. If the supply line reactance is given in per-unit X_{Lpu} referred to a nominal volt-ampere base VA_1, the ohmic value may be determined from equation 14. If no other information is available the minimum reactance of the supply line may be estimated from the interrupting rating of the a-c circuit breaker by the relation:

$$X_L = \frac{E_L^2}{VA_{brr}} \tag{15}$$

3. Transform the ohmic value of supply line reactance to ohms referred to the rectifier transformer d-c winding by the transformation formula

$$X_{cL} = \left(\frac{E_a^2}{E_a}\right) X_L \tag{16}$$

4. Add the ohmic values determined in 1, and 3 to obtain X_c.

Total Commutating Reactance in Per Unit

All per-unit quantities are based on the rated volt-amperes VA input to the rectifier transformer a-c terminals. To determine the per-unit values, X_{pu}, corresponding to the ohmic values, X, divide the ohmic values by the value of unit reactance

$$\frac{3E_a^2}{VA}$$

which results in

$$X_{pu} = \frac{VA}{3E_a^2} X \tag{17}$$

Total Resistance

The total resistance of the a-c circuit is the sum of the effective resistances of the transformer and supply line and the equivalent resistance of the rectifier. Since the resistance of the rectifier tubes may exceed that of the transformer windings the total per-unit resistance must be

calculated in order to determine the resistance/reactance ratio.

The per-unit resistance of the transformer may be calculated by the equation

$$R_{pu} = \frac{P_r}{VA} \tag{18}$$

The equivalent per-unit resistance of the rectifier tube may be determined from its equivalent ohmic resistance by the relation

$$R_{epu} = \frac{VA}{3E_a^2} R_a \tag{19}$$

Total Commutating Impedance

The total commutating impedance of the rectifier transformer, rectifier, and supply line in either ohmic or per-unit values may be determined by vector addition of total resistance and reactance.

Protective Systems

Essentially, the protective system of an electronic converter is designed to protect the converter against the harmful effects of faults occurring within the unit and without. For obvious reasons the switch gear employed for this purpose also is used to accomplish normal switching functions, and other features are added to prevent operation under improper conditions that might endanger the equipment or personnel. This section of the report discusses the various factors entering into the selection, design and operation of the protective system and equipment.

Functions of the Switchgear

The protective switchgear for an electronic power converter must perform two basic functions: limit the duty on the rectifier so as to prevent damage from overloads and faults; and limit the disturbance in the a-c and d-c systems during faults.

Ideally, in order to protect the rectifier, transformer, and other parts of the rectifier unit, the protective switchgear must function to limit:

1. The duration of overloads and the frequency of application of rated overloads; the desired action may be obtained by interrupting the rectifier a-c or d-c circuits, reducing the rectifier output voltage by phase control, or other means.

2. The duration of d-c short circuit or the magnitude of the short circuit currents; this may be accomplished by interruption of the a-c or d-c circuit, arc-suppression of the rectifier, insertion of resistance in the d-c circuit, application of phase control to the rectifier, or similar means.

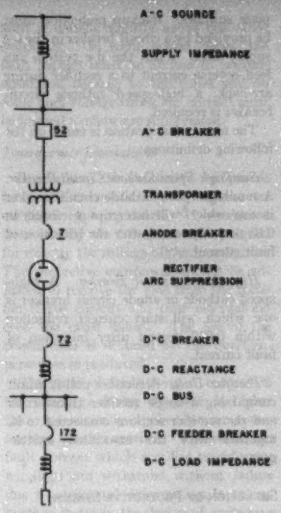

Figure 16. Single-line diagram of main protective system

3. The duration and magnitude of arc-back currents.[17,18] The current flow to the faulty anode must be completely interrupted. This requires the interruption of both the feedback from the d-c circuit and feed from the a-c circuit. The feedback current from the d-c circuit can be interrupted by interrupting any part of the circuit through which this current flows or by removing the sources of d-c voltage. The current flowing to the faulted anode from the other anodes of the rectifier can be interrupted by removing their phase voltages, or making them nonconductive by means of arc-suppression. The arc-back current arising from both the d-c circuit and the other anodes also may be interrupted by opening only the circuit of the faculty tube.

In order to limit and minimize the disturbance in the supply and load circuits, the protective switchgear must perform several functions in addition to those required for the specific protection of the rectifier unit. First, it must have suitable sensitivity and speed of interruption to obtain selective circuit breaker operation and limit the extent of the system disturbance. Second, it must provide backup protection in the event of failure of a protective device or circuit which might endanger equipment or personnel. For some applications it must be adaptable to automatic control with provisions for load resistance measurement, automatic reclosure, and similar features. The various functions must be co-ordinated so as to obtain a definite planned behavior for a large variety of circumstances.

Elements of Protective System

The protective system of an electronic converter includes all devices required in the installation to interrupt fault currents together with the relays that actuate them, as well as those components of the converter and connected systems whose inherent characteristics serve to limit the magnitude or rate-of-rise of fault current. Also for the purpose of the report, the protective system will include elements provided to protect the unit against improper operating conditions, as well as protection against overloads which do not reach fault proportions. All the elements shown on Figure 16 are considered a part of the protective system, and may be used in various combinations to effect the desired results. The main protective elements may be divided into two general classes; one class being those devices which protect by interrupting or preventing current flow, and the other being those which limit the current flow by virtue of their impedance. Referring to Figure 16, the elements in the first class are:

1. The a-c circuit breaker, which interrupts the a-c circuit *52*.

2. The anode circuit breaker, used in the anode circuits to interrupt both the a-c and d-c circuits on arc-back *7*.

3. The d-c circuit breaker which interrupts the d-c circuit *72*.

4. The rectifier, which, when controlled by suitable arc-suppression devices, can interrupt the flow of forward current.

The elements in the second class are:

1. The impedance of the supply source.

2. The transformer impedance.

3. The inductance and resistance of the d-c circuit, which limit the rate of rise and maximum value of short circuit and feedback currents.

Classes of Protective Systems

In order to classify the various arrangements of protective schemes, the following classes are suggested for adoption and use. They are based on the time of current limitation and point of circuit interruption when faults occur due to short circuits and arc-backs.

Five general classes are proposed (see Figure 17):

Class I—Interruption at the a-c and d-c terminals of the unit with medium-speed a-c and d-c circuit breakers.

Class II—Interruption at the a-c and d-c terminals of the unit with medium-speed a-c

circuit breaker, and high-speed d-c circuit breaker.

Class III—Interruption within the unit by the use of medium-speed anode circuit breakers.

Class IV—Interruption within the unit by the use of high-speed anode circuit breakers.

Class V—Interruption within the unit by the use of arc-suppression.

Class I is the simplest and oldest form of protective system. It is used widely for all types of service on small and medium size units, particularly in transportation, mining, and general industrial applications. It also is used extensively in large isolated units when fault currents are limited.

Class II is used when higher speed interruption of the d-c feed back circuit is required than is provided by the medium-speed d-c circuit breaker. It is used for large kilowatt rated units as well as on the higher d-c voltages—1,500- and 3,000-volt classes, for transportation service. It provides an economical protective means when rapid interruption is required to prevent the tripping of other units in parallel. In some cases, arc-suppression also is included to reduce the duty on the transformers and a-c circuit breaker as well as to lessen the disturbance to the a-c system. D-c reactors also may be provided to reduce the rate of rise of feedback current from the d-c system.

Class III provides an economical protection system for small and medium size units connected to high-voltage a-c systems. A few applications have been made in mining and transportation services. Additional protection is required for the transformer in the form of fuses or remote feeder circuit breakers.

Class IV usually is adapted to large-capacity units when maximum protection of rectifier and rectifier-transformer from damaging over-current is required. It is used in essential service applications when continuity of power flow is required. Typical applications include large electrochemical, transportation, and heavy industrial installations. It also is used for electronic exciters of large generators. Additional a-c and d-c circuit breakers are provided either as part of the unit, or in the a-c and d-c systems in order to obtain necessary operational features as required.

Class V utilizes arc-suppression for interrupting short circuit and arc-back currents in applications having no d-c feedback. The usual applications are rectifiers in service where high d-c voltages are used to supply resistance-type loads such as frequency changers and radio plate supplies. Backup protection must be provided by a circuit breaker in the a-c supply line. When the d-c system can feed reverse current to a rectifier during arc-back, a high-speed cathode circuit breaker is required.

The above classification is based on the following definitions:

Semihigh-Speed Cathode Circuit Breaker. A semihigh-speed cathode circuit breaker is one which will interrupt a circuit in 0.03 to 0.05 second after the initiation of fault current.

High-Speed Circuit Breaker. A high-speed cathode or anode circuit breaker is one which will start current reduction within 0.017 second after initiation of fault current.

Rectifier Unit. A rectifier unit is a unit comprising a single rectifier transformer and the rectifier sections connected to it, together with the associated switchgear.

Selection of Protective System

The selection of the protective system for electronic converters is based on the grade and character of performance required and the capabilities and limitations of the converters, transformers and, protective devices which are available. The characteristics and capabilities of the various elements of the protective system must be co-ordinated to obtain the operation desired in a sound and economical manner.

Minimum interrupting ratings of the switchgear are determined by the fault current calculations developed in the section on Determination of Fault Currents of this report. However, switchgear must protect itself as well as the converter unit. To do so, it must be capable of interrupting the maximum fault that can develop across its own terminals. Any other scheme must be used with great caution. Here we will discuss additional factors which must be considered in the selection of protective devices, and the preparation of specifications.

Service Requirements

The basic protective requirements for a rectifier unit are satisfied by protective gear consisting of an a-c circuit breaker and a d-c circuit breaker. The a-c circuit breaker is relayed to trip on time delay for the lower values of overcurrent and instantaneous for higher values of overcurrent. The d-c circuit breaker is tripped by instantaneous reverse current. Such equipment is adequate for most applications of a single unit of moderate capacity, where protection of the converter equipment is the prime consideration. These minimum requirements may be satisfied by a-c circuit breakers having opening speeds up to eight cycles (at 60 cycles) and d-c circuit breakers with interrupting speeds of three to five cycles. A large number of installations of this type have been made, and are in successful operation. Longer interrupting times are very undesirable, and good practice favors shorter times. Good practice has thus established this minimum equipment on the basis of apparatus which is available in standard manufacture, and is in use for protecting other types of electric generating and load equipment.

The selection of switchgear with other features should be based on the need for meeting further service requirements or providing additional protection for the rectifier unit to obtain the most economical arrangement. Where single units are installed and short-time outages are not objectionable, minimum protective gear consisting of a-c and d-c circuit breakers is adequate. Where continuity of d-c

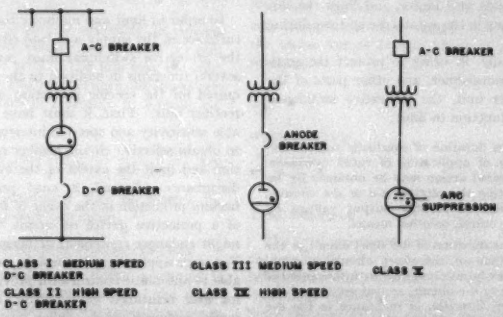

Figure 17. Single-line diagram of the five classes of protective systems

power flow is essential, anode circuit breakers capable of opening and automatically reclosing only the faulty anode circuits and maintaining power flow on the normal anode circuits are required. Some rectifier units are constructed with two rectifier sections operating from a common transformer. At the time of arc-back, the faulty section is cleared by means of an anode circuit breaker so that power flow is maintained on the normal section.

Where two or more rectifiers operate in parallel in essential service applications, it is desirable that d-c power flow to the load be maintained during arc-back. This requirement makes it necessary at the time of arc-back to clear the faulty rectifier before the overload on the parallel units causes them to arc-back. This requirement may be met by the use of suitable high-speed circuit breakers.

Rectifier Limitations

The characteristics of the rectifier tubes limit the overload and fault currents which can be permitted. The overload capacities of rectifier tubes are determined by thermal overload, fault current limit, control limit, and damage currents.

The thermal overload limit of the pool-type tube determines what overloads can be carried for longer than momentary swings. This allowable load is usually sufficiently above the thermal overload limits of the transformer so that the protective relay settings can be set just slightly above the guaranteed 2-hour rated overload. On 600 volts and higher, the tubes usually arc-back before the thermal limit is reached.

The fault current limit is the maximum current which a tube is able to conduct for one cycle without arc-back. If this limit is exceeded on the normal anodes during arc-back, sympathetic arc-backs will occur and the fault will be extended.

The control limit is the value of current which causes the tube to fail to control. This limit must not be exceeded where arc-suppression is to be used.

The damage currents at which the internal parts of tubes are damaged is usually so high that such currents are not the limiting factor in determining the overload ratings of the rectifier unit.

Ordinarily, it can be assumed on low-voltage, pumped, single-anode tubes that the tube characteristics do not determine the permissible overload or fault currents as long as the other rectifier equipment is protected. However, on sealed tubes, the short time overload capacity is lower and the tube characteristics determine the permissible overloads. This limit is usually slightly above the rated overloads. On some sealed tubes, the fault current must be limited to prevent structural damage to the tubes and on some high-voltage tubes, the current must be limited to allow arc suppression.

Transformer Limitations

In selecting the protective equipment for a rectifier installation, the transformer overload capacity must be considered since usually the transformer is designed for exactly the ratings of the installation. The protective equipment should be adjusted to remove the load from the rectifier if the current and time interval exceed the rated values. The life of the transformer is reduced by the overtemperatures so produced.

The ratio of fault-to-rated current in the windings during arc-back is higher than for normally applied power transformers in other services. The maximum fault current which rectifier transformer windings can withstand without failure due to structural deformation is an important factor in the design of protective systems. Allowance also must be made for the effect of repetitive faults in causing hammering and wear of coil insulation.

Circuit Breaker Requirements

Switchgear for rectifier equipment must be capable of reliable operation with low maintenance despite a relatively high frequency of faults.

Some of the factors which will determine the selection of the proper switchgear devices are listed below:

A-C Circuit Breaker

1. Voltage and frequency of the a-c system.
2. The supply line current at the 2-hour rating of the rectifier.
3. Maximum fault current which the a-c system can deliver with a fault or short-circuit applied on the load side of the circuit breaker.
4. Interrupting time.
5. Derating factors due to reclosing requirements and frequency of operation.
6. Atmospheric conditions and altitude.

D-C Circuit Breaker

1. The d-c voltage rating of the rectifier unit.
2. The two-hour current rating of rectifier unit.
3. Maximum fault current delivered by the rectifier on d-c short circuit, or maximum feedback current which the d-c system can deliver at the time of arc-back, whichever is greater.
4. Current limiting and interrupting time.
5. Frequency of operation.
6. Atmospheric conditions and altitude.

Anode Circuit Breaker

1. The d-c voltage rating of rectifier unit.
2. The secondary current at the 2-hour rating of rectifier.
3. Maximum half-cycle fault current delivered by both a-c and d-c system during arc-back.
4. Interrupting time.
5. Rectifier circuit, and type of transformer connection.
6. Atmospheric conditions and altitude.

Protective Relaying

Overload

The ideal overload protective system would disconnect the converter whenever the magnitude or duration of an overload exceeded the values specified in the rating of the converter. This cannot be fully accomplished by means of overload and timing relays commercially available, and neither the cost nor complexity of the devices required for such protection have been found justified.

Inverse time overload relays afford protection only above the short-time (one or five minute) rating of the machine, and commercially available thermal overload relays afford protection only above the 2-hour rating. Since the 2-hour rating is seldom used except during emergencies, a compromise setting of the thermal relay is usually adopted or the relay is omitted.

Transformer overtemperature and hot-spot indicators give some added measure of protection to the transformer on the 2-hour rating. The rectifier has too short a thermal time constant to be effectively protected by the transformer overtemperature indicator.

Fault Detection

Fault-current detection is provided by means of external relays or built-in devices. For tripping primary a-c circuit breakers, at least in the larger ratings, use is generally made of separate overcurrent relays connected to current transformers. These relays are usually a combination of inverse time and instantaneous elements.

Primary voltages of 600 volts or less permit the use of low-voltage air circuit breakers, which will normally have built-in direct-acting trip attachments. Separate inverse-time relays may be used for purpose of selectivity.

Anode circuit breakers have reverse current (in some cases, an overcurrent series trip) coil built into each pole. Most anode circuit breakers today employ flux-shifting type tripping devices which

are connected for reverse current tripping to afford protection on arc-back.

Primary circuit overcurrent relays might be used to trip anode circuit breakers but the individual series trips on each pole of the circuit breaker should be retained if the advantage of this type of circuit breaker on arc-back is to be realized.

There is a high fault-to-normal current ratio occurring in the faulted anode circuit during arc-back. This ratio is between 25 to 50, in most cases, and may exceed 50.

The selection of the d-c machine circuit breaker depends on the presence of other protective devices.

Selectivity

To insure the maximum protection without sacrificing continuity of service, the protective system must possess a high degree of selectivity. Faults can be generally classified as internal and external. In the ordinary converter installation, the most common internal fault is the arc-back. External faults are usually short circuits of various degrees on the connected d-c system or internal faults in parallel units. The protective system is designed to differentiate between internal and external faults.

For a unit operating alone, the a-c system currents during an arc-back or a solid d-c short circuit are of the same order of magnitude. Selectivity between a-c circuit breaker and d-c feeder circuit breakers is obtained by the use of inverse time and instantaneous overcurrent tripping. In general, the more units there are operating in parallel, the easier it is to obtain good selectivity since each unit will contribute less to an external fault or a fault in one of the other units.

Since the arc-back is the most damaging fault to which converters are liable, instantaneous overcurrent devices (when used) are set as low as operating conditions will permit. The inrush current of the rectifier transformer is generally the limiting factor. Selectivity is lost, however, when the d-c fault results in an alternating current exceeding the setting of the instantaneous overcurrent devices, causing the a-c circuit breaker to trip. In some cases, such tripping may be avoided by the use of special inverse time overcurrent relays with just enough time delay to permit the d-c feeder circuit breaker to trip and yet not permit excessive damage to the tube elements.

As explained previously, arc-backs are most easily recognized by reverse current devices in the anode circuits. Converters equipped with anode circuit breakers, therefore, possess a very high degree of selectivity.

In the absence of the anode circuit breaker and where the d-c system produces feedback during arc-back, the reverse current trip on the d-c circuit breaker can often be utilized to provide excellent selectivity. If the reverse current tripping of the d-c circuit breaker is arranged to trip the a-c circuit breaker, fast clearing of the arc-back is obtained.

Selectivity can be obtained by means of arc-suppression initiated by an arc-back detecting device in the anode or cathode circuit. The anode circuit provides most rapid response and a positive signal in all cases, but requires a multiplicity of devices. The cathode circuit is, therefore, frequently preferred where operating conditions permit.

Tripping Means

The power source for tripping the circuit breakers of a rectifier installation must be completely reliable and the circuits so arranged that this power will always be available when the rectifier is in service. Lacking this reliability, arrangements must be made to trip all circuit breakers and disconnect the rectifier whenever the voltage of the tripping power source drops below the minimum safe operating value for any of the trip coils.

In large important installations station batteries are available for operating the circuit breakers, or at least for tripping service. Such batteries, properly maintained, have been found sufficiently reliable.

In smaller installations, particularly in small industrial plants, building service and coal mines, battery maintenance is not, in general, up to the required standard and it is better to use some other source of tripping power. For low-voltage circuit breakers under 600 volts, the safest protection is afforded by built-in direct acting overload trips. When direct-acting overload relays on the a-c circuit breaker are not desirable, current transformer trip coils normally shunted out by normally closed contacts of overload relays, provide a very reliable tripping means. Shunt or undervoltage a-c trip coils then are used for control switching operations of the a-c and d-c circuit breakers.

A-c shunt trip coils can be used with overload relays, but the circuit breaker must be provided with an undervoltage trip device. Both the shunt and undervoltage coils must be connected to the same power source. They must be so designed and adjusted that the low-voltage operating limit of the shunt trip is less than the drop-out voltage of the undervoltage device by a safe margin. An arc-back or severe short circuit may depress the voltage of the a-c power source below the minimum required to operate the shunt trip, and the undervoltage trip must then drop out, or the rectifier unit will be severely damaged.

Capacitance tripping devices have been used, consisting of a condenser charged through a small metal-plate rectifier. The charged condenser supplies the required tripping power. This system involves several vulnerable components and must be adequately protected or backed up.

Circuit Breaker and Relay Settings

A-C Overcurrent

1. Time Delay Element *51:* Set only high enough so that d-c feeder circuit breakers, or d-c rectifier circuit breaker if there are no feeders, will trip first on d-c overloads or short circuits. Usual setting is just slightly above short-time rating of the rectifier and for as short a time as the service will permit.

2. Instantaneous Element *50:* Set only high enough to over-ride the transformer inrush current. The lower it can be set, the better the protection afforded against arc-back and transformer fault.

Note:—Random arc-backs may occur when there is nothing wrong with any part of the equipment. One circuit breaker reclosure will restore service quickly in that event. Should the circuit breaker trip out again immediately due to some type of permanent fault, a second reclosure might result in further damage. Only one automatic reclosure is recommended.

D-C Overcurrent

1. D-c Overloads and Faults: Where d-c feeder circuit breakers are used either the overcurrent trip is omitted or time delay tripping is used on the rectifier d-c circuit breaker. When there are no d-c feeders, an overcurrent device *76* is provided on the rectifier d-c circuit breaker, except for electrolytic service. Device *76* should be set between the 2-hour and short-time ratings of the rectifier, as low as service requirements will permit. When d-c overload protection is omitted or set too high, the unit will be cleared by the a-c circuit breaker through the operation of *51*.

2. Feeders: When a fault or overload occurs on a distribution d-c feeder, the feeder circuit breaker is caused to

trip by an instantaneous tripping device, *176*, affording selectivity and maintaining uninterrupted service on unaffected feeder circuits. In railway, mining, and some industrial services, reclosing systems automatically restore normal service to feeders as soon as the trouble is cleared.

Reverse Current (Arc-Back)

1. Reverse Current: Under normal operating conditions, reverse current in a rectifier is not possible. In case of arc-back, most installations are capable of furnishing considerable reverse current and the cathode circuit breaker is equipped with a reverse current tripping device *32*. Where anode circuit breakers are used, the reverse current trip on the cathode circuit breaker is usually omitted. When there is no source of reverse current and no anode circuit breaker, the a-c overcurrent relays *50* are used for arc-back protection. Reverse currents above approximately 15 per cent of normal output will trip the cathode circuit breaker.

2. Anode Circuit Breakers: In installations employing high-speed anode circuit breakers, individual pole tripping is employed in many cases, eliminating service interruptions to the load. Since opening the anode lead, in case of arc-back, interrupts the a-c as well as the d-c fault path, the short-time opening of the individual pole may be followed by a successful reclosing and return to normal service. In such cases, it is unnecessary and undesirable to open the a-c and cathode circuit breakers. High-speed anode circuit breakers are usually equipped with built-in tripping means designed to trip on reverse currents less than rating.

3. Arc-Suppression: In some heavy-duty installations when no anode circuit breakers are used, methods of high-speed arc-suppression on all tubes are used to prevent the unfaulted tubes from feeding current into the arc-back. High-speed devices (half-cycle operation or better on basis of 60 cycles) are essential for satisfactory operation. Back-up protection is desirable.

Thermal (Long-Time Overload) Protection

1. Transformer: Thermal protection for the transformer is provided by a thermal relay or thermostat whose setting depends on the transformer design. Some transformers, particularly the air-cooled variety, are equipped with temperature detecting coils. Additional transformer protection may be obtained by a replica thermal relay operating from current transformers.

2. Rectifier: Thermal protection of the rectifier provides protection against inadequate cooling rather than overloading. Protection is obtained by a thermostat set in accordance with the manufacturer's recommendations.

Undervoltage Protection

1. Incoming Line: To protect the ignition circuits and all a-c closing devices and motors, a polyphase reverse phase sequence and undervoltage relay may be used *47*. This is usually set to permit starting if there is 95 per cent of normal voltage available, and to take the equipment out of service in case the voltage drops to 85 per cent or below. (A short-time delay is used here to prevent tripping on momentary voltage dips.)

2. Excitation Circuits: Should excitation fail on one or more tubes and not re-establish within a given time, the rectifier unit is taken out of service or an alarm is sounded.

3. D-C Circuit: A voltage relay *80* is connected between the positive and the negative terminals of heavy-duty pumped rectifiers. Relay *80*, when energized, permits the cathode circuit breaker to close. In starting, the failure of the cathode circuit breaker to close within a given time will lock the rectifier unit out of service by means of device *48*.

Other Protective Devices

1. Rectifier: In addition to thermal protection mentioned previously, protection is provided, as required, against low water pressure *63W*, overtemperature *26R*, and undertemperature *26L* of the rectifier, and poor vacuum *63V*. Where used, the settings of these devices should follow the manufacturer's recommendations.

2. Grounding of D-C Structures: In services 301 volts direct current and above and when one side of the d-c circuit is grounded, it is recommended that the d-c structure (metal housing or supporting metal framework) be grounded through a protective relay *64*.

3. Light Load Resistor: Where interphase transformer windings are used and low loads (not enough to excite the windings) are possible, some means of preventing abnormally high d-c voltages are desirable. The protection often takes the form, in the smaller sizes, of a permanently connected resistor across the d-c end of the rectifier but, in larger installations, the resistor is commonly switched in and out of service as required.

4. Regenerative Resistor: Some installations supply loads which may be regenerative in character, such as cranes, machine shops, elevators, rotating machines, and railways. When the system cannot absorb this regenerated power, resistors of suitable capacity are usually automatically connected across the d-c bus and disconnected after the regeneration has ceased.

Auxiliaries

1. Excitation Circuits: Protection is usually provided for ignitor misfire (which may result from faulty circuits or ignitors).

2. Protection of Auxiliaries: For pumped tubes, the mercury pump is protected by a thermostat. All auxiliary circuits, such as firing or excitation circuits, water pumps, oil pumps, vacuum pumps, fans, and water heaters, have their energizing contactors protected by thermal trip elements.

Appendix I. Nomenclature

The symbols which appear in the equations are defined as follows:

α = phase control angle of retard
u = commutation angle of overlap
$\omega = 2\pi f$, where f = frequency of a-c power system
E_a = arc-drop voltage
E_d = average d-c voltage under load
E_d' = average voltage of d-c source during feedback
E_L = a-c system line-to-line voltage in rms volts
E_m = a-c system line-to-neutral voltage in rms volts
E_s = transformer d-c winding line-to-neutral voltage in rms volts
i_d = instantaneous direct current
i_{sf} = crest forward anode current in amperes—first half-cycle
i_{ss} = crest forward anode current in amperes—sustained
i_{sr} = crest reverse current in amperes—first half-cycle
I_d = d-c load current of the rectifier in average amperes
I_{ds} = rated direct current of rectifier
I_{ds} = sustained short circuit current in average amperes
I_{ds}' = crest short-circuit current in amperes during transient period
I_{La} = rated current in rms amperes at a-c terminals of rectifier transformer at rated volt-amperes
I_{La} = sustained short-circuit current in rms amperes at a-c terminals of rectifier transformer
K = transient factor
K_f = forward current factor
K_r = reverse current factor
L_d = total inductance in henrys, of fault path during d-c feedback
P_r = rectifier transformer resistance loss in watts
R_a = equivalent resistance of rectifier arc-drop in ohms
R_c = commutating resistance in ohms per phase

Table II

Circuit Element	R, Ohms	L, Henrys
Supply line $R=0.0031\times1.042$	0.00334	
$L=0.025\times1.042/377$		69.1×10^{-6}
Rectifier transformer $(3707/230\times1,000)$ 1.042	0.0168	
$0.0575\times1.042/377$		159.0
Interphase transformer	0.0016	
Estimated inductance, fully saturated		15.8
Anode cable	0.003	
Rectifier tube arc-drop (Not included—arc-back simulated by switch)		
D-C cable	0.0034	79.5
D-C motor	0.0170	46.0
Total	0.0450	369.4×10^{-6}

R_d = total resistance in ohms of fault path during d-c feedback

t = time in seconds measured from beginning of the negative half-cycle of a-c voltage wave

X = reactance in ohms

X_s = commutating reactance in ohms per d-c winding phase

X_{sL} = commutating reactance of a-c supply line in ohms referred to the d-c winding of the rectifier transformer

X_L = reactance of a-c supply line in ohms per line

VA = rated volt-amperes of rectifier transformer at terminals of a-c winding

VA_{bkr} = circuit breaker interrupting rating in volt-amperes

Z_s = commutating impedance in ohms per phase

Z_d = total impedance in ohms of fault path during d-c feedback

Note: Per-unit quantities are indicated by subscript "pu," for example: X_{pu}, X_{spu}, Z_{spu}, and so forth. They are usually based on the primary rating, VA, of the rectifier transformer.

Appendix II. Examples of Fault Current Calculations

The procedure for calculating rectifier fault currents is illustrated by the following examples. These calculations apply to a 6-phase, 200-kw 300-volt sealed ignitron rectifier unit operating in a power circuit with constants as given in Figure 15. Tests results are given for comparison.

D-C Short Circuit

For calculating the impedances the per-unit base is 230 kva.

$$\text{Unit Impedance}=\frac{3E_s^2}{VA}=\frac{3\times283^2}{230\times1000}=1.042 \quad \text{ohms}$$

The sustained direct current is

$$I_{d3}=0.9\times\frac{VA}{E_sZ_{c\,pu}}=\frac{0.9\times230\times1000}{283\times0.0860}=8,500 \quad \text{amperes (average value)}$$

The transient direct current = ratio $R/X=0.0243/0.0825=0.295$. From Figure 9 $K_p=1.41$.

$$I_{d3}'=1.41\times\frac{\pi}{3}\times I_{d3}=12,500 \quad \text{amperes (crest value)}$$

Tests show the fault currents obtained during d-c short circuit with a bolted short. The comparative values are:

	Calc., Amperes	Test, Amperes
Average sustained current	8,500	7,700
Crest transient current	12,500	11,000

Arc-Back With A-C Feed Only

The calculated per-unit impedances are the same as for d-c short circuit except that the resistance of the interphase is omitted since no current flows in it and the resistance of the tube is assumed to have two-thirds value since a switch was used to simulate the faulty tube. The total per-unit impedances are then

$R=0.0226$ $X_{pu}=0.0825$ and $Z_{c\,pu}=0.0855$

The ohmic value of commutating impedance is

$$Z_c=\frac{3E_s^2}{VA}.Z_{c\,pu}=1.042\times0.0855=0.0890 \quad \text{ohm}$$

The ratio $R/X=0.0226/0.0825=0.274$. From Figure 9, $K_r=1.61$ and $K_f=1.35$.

Crest reverse current is

Circuit Element	R_{pu}	X_{pu}
Supply line (for values see power circuit diagram)	0.0031	0.0250
Rectifier transformer $X_{s\,pu}=X_s/1.042=0.060/1.042$		0.0575
$R_{pu}=P_r/VA=3,707/230\times1,000$	0.0161	
Interphase transformer $R_{pu}=P_i/3\,VA=346/3\times230\times1,000$	0.0008	
Anode cables $R_{pu}=0.003/1.042$	0.0029	
Rectifier tubes (arc-drop) $R_{pu}=0.0015/1.042$	0.0014	
Total	0.0243	0.0825

$$\text{Total } Z_{c\,pu}=\sqrt{R_{pu}^2+X_{pu}^2}=0.0860$$

$$i_{sr}'=K_r\frac{\sqrt{2}E_s}{Z_c}=\frac{1.61\times\sqrt{2}\times283}{0.089}=7,220 \quad \text{amperes}$$

The crest forward current

$$i_{sf}'=K_f\frac{\sqrt{2}\,E_s}{Z_c}=6,230 \text{ amperes}$$

The comparative values of the fault current with a-c feed only with the rectifier operating on only three anodes are:

	Calc., Amperes	Test, Amperes
Crest reverse current (faulty anode)	7,220	7,440
Crest forward current (normal anodes)	6,230	6,370

Arc-Back With D-C Feed Only

In calculating the fault current in this case, the total ohmic resistance and the total inductance are determined by adding the values for the various elements in the d-c fault path. The calculated impedances are shown in Table II.

The total impedances are then

$R_d=0.0450$

$X_d=L=377\times369.4\times10^{-6}=0.139$ ohm

$Z_d=\sqrt{R^2+X^2}=0.146$

Ratio $R_d/X_d=0.324$ ratio $R_d/L_d=121.6$

The approximate values of current in the faulty anode at the successive peaks at the end of the first, third, and fifth half-cycles are given by the equation

$$i_d'=\left[\frac{E_d'}{R_d}-\frac{\sqrt{2}\,E_s}{Z_d}\right]\left[1-\epsilon^{-\frac{R_d}{L_d}\frac{1}{f}\left(n-\frac{1}{2}\right)}\right]+\frac{2\sqrt{2}\,E_s}{Z_d}$$

Substituting

$$\frac{E_d'}{R_d}=\frac{2,800}{0.045}=6,230 \text{ amperes}$$

$$\frac{\sqrt{2}\,E_s}{Z_d}=\frac{2\times283}{0.146}=2,740 \text{ amperes}$$

The approximate currents in the faulty anode at the end of the first, third, and fifth half-cycles are shown in Table III.

Table III

Cycle $(n-1/2)$	$\left[1-\epsilon^{-\frac{R_d}{L_d}\frac{1}{f}\left(n-\frac{1}{2}\right)}\right]$	Current i_d', Amperes
1/2	0.632	7,680
1 1/2	0.950	8,790
2 1/2	0.995	8,960

No test results were obtained for this condition. It is included here to illustrate the method.

Arc-Back With Both A-C and D-C Feed

If it is assumed that on the average, two phases are conducting and that the average

Table IV

Circuit Element	R, Ohms	L, Henrys
Supply line 0.5×0.00324	0.00162	
$0.5\times69.1\times10^{-6}$		34.5×10^{-6}
Rectifier transformer 0.5×0.0168	0.0084	
$0.5\times159.0\times10^{-6}$		79.5
Interphase transformer	0.0016	15.8
Rectifier tube arc-drop (Not included—arc-drop simulated by switch)		
Anode cable 0.5×0.003	0.0015	
D-C cable	0.0034	79.5
D-C motor	0.0170	46.0
Total	0.03352	255.3×10^{-6}

Table V

Cycle $(n-1/2)$	Currents in Amperes: D-C Source	Currents in Amperes: Faulty Anode
$^1/_2$	7,280	10,860
$1^1/_2$	9,960	12,000
$2^1/_2$	10,340	12,200

Table VI

	Calc., Amperes	Test, Amperes
Reverse current in faulty anode		
At end of 1st half cycle	10,660	8,680
At end of 3rd half cycle	12,000	12,300
At end of 5th half cycle	12,200	12,900
Maximum d-c feedback	6,230*	7,030

* Value calculated for arc-back with d-c feed only.

a-c voltage in the circuit is one-half E_a, then the impedances of the circuit are shown in Table IV.

The total impedances are

$$R_d=0.0335 \text{ ohm} \quad X_d=L=377\times255.3\times10^{-6}=0.096 \text{ ohm}$$

$$Z_d=\sqrt{R^2+X^2}=0.101 \text{ ohm}$$

Ratio $R_d/X_d=0.348$ $R_d/L_d=131.4$

Substituting in the equation used in the previous section, gives the approximate currents in the d-c source at the end of the first, third, and fifth half cycles. Note that $E_a/2$ is used in making the calculation. The approximate current in the faulty anode is obtained by adding half of the current in the d-c source to the value of current in the faulty anode for arc-back with a-c feed only (See section on Arc-Back With A-C Feed Only). These values are shown in Table V.

$$\frac{E_d'}{R_d}=\frac{280}{0.0335}=8{,}400 \text{ amperes}$$

$$\frac{\sqrt{2}\,E_d}{2\,Z_d}=\frac{\sqrt{2}\times283}{2\times0.101}=1{,}980 \text{ amperes}$$

The effect of the time taken for saturation of the interphase transformer was not considered in the calculation and the calculated value of current for the first half cycle is, therefore, too high. Comparative values are shown in Table VI.

References

1. Pool-Cathode Mercury Arc Power Converters. *C34.1-1949*, American Standards Association (New York, N. Y.), 1949.

2. Principles of Mercury-Arc Rectifiers and Their Circuits (book), D. C. Prince, P. B. Vodges. McGraw-Hill Book Company, New York, N. Y., 1927.

3. Mercury-Arc Power Rectifiers (book), Othmar K. Marti, Harold Winograd. McGraw-Hill Book Company, New York, N. Y., 1930.

4. Analysis of Rectifier Circuits, E. F. Christensen, C. H. Willis, C. C. Herskind. *AIEE Transactions*, volume 63, 1944, pages 1048–58.

5. Rectifier-Circuit Duty, C. C. Herskind. *Electrical Engineering* (*AIEE Transactions*), volume 63, March 1944, pages 123–28.

6. The Relation of Residual Ionization to Arc-Back in Thyratrons, K. H. Kingdon, E. J. Lawton. *General Electric Review* (Schenectady, N. Y.), volume 42, November 1939, page 474.

7. Backfires in Mercury-Arc Rectifiers, J. Slepian, L. R. Ludwig. *AIEE Transactions*, volume 51, March 1932, pages 92–104.

8. Back-Firing in Mercury-Arc Rectifiers, J. E. White. *Journal of Applied Physics* (New York, N. Y.), volume 11, July 1940, page 507.

9. High Voltage Surges in Rectifier Circuits A. W. Hull, F. R. Elder. *Journal of Applied Physics* (New York, N. Y.), volume 13, June 1942 page 372.

10. Maintenance of Rectifiers in Electrochemical Installations, J. E. Housley, G. N. Hughes. *Electrical Engineering* (*AIEE Transactions*), volume 64, July 1945, pages 436–41.

11. Rectifier Transformer Characteristics, A. J. Maslin, R. A. Nelson, F. D. Kaiser, W. C. Sealey. *AIEE Transactions*, volume 68, part II, pages 1305–11.

12. Rectifier Fault Currents, C. C. Herskind, H. L. Kellogg. *Electrical Engineering* (*AIEE Transactions*), volume 64, March 1945, pages 145–50.

13. Anode-Circuit-Breaker Design and Performance Criteria, R. W. Beckne, W. A. Atwood. *Electrical Engineering* (*AIEE Transactions*), volume 64, June 1945, pages 337–45.

14. Rectifier Fault Current, II, C. C. Herskind, A. Schmidt, Jr., C. E. Rettig. *AIEE Transactions*, volume 68, part I, pages 243–52.

15. Arc-Backs in Rectifier Circuits—Artificial Arc-Back Tests, R. D. Evans, A. J. Maslin. *Electrical Engineering* (*AIEE Transactions*), volume 64, June 1945, pages 303–11.

16. Calculation of the Back-Firing Phenomenon in Rectifiers, H. Forssell. *Technical Achievements of A.S.E.A. Research* (Vasteras, Sweden), 1946, pages 58–64.

17. A Fast Circuit Breaker, D. I. Bohn, Otto Jensen. *Electrical Engineering* (*AIEE Transactions*), volume 61, March 1942, pages 165–68.

18. Discussion of, A New Multipole High-Speed Air Circuit Breaker for Mercury-Arc Rectifier Anode Circuits and Its Relation to the Arc-Back Problem, J. W. Seamen, L. W. Morton. *AIEE Transactions*, volume 61, 1942, pages 1057–61.

No Discussion

Selection and Application of Power Transformers

HOWARD P. SEELYE
FELLOW AIEE

THE CHOICE of a power transformer for use on a power system is governed quite largely by the characteristics of that system, the precedents set by previous purchases, and the established standards of the industry. It follows, therefore, that any discussion of the selection of transformers must deal to a considerable extent with the matter of standards, both those for the individual company and those for the country as a whole. This paper will, therefore, take up several of the more important features of power transformers with particular attention to the relation between the needs of the operating system and some of the standardization activities now in progress.

Standardization

Power transformers have been standardized to a considerable degree for many years. These standards have been developed and improved continuously. Recently, however, there has been a strongly directed effort toward the revision and extension of these standards on a national industry-wide basis. The Joint Edison Electric Institute-National Electrical Manufacturers Association Committee completed its work and published its report on Preferred Voltage Ratings for A-C Systems and Equipment[1] in May 1949, including therein proposed voltage ratings for power transformers. The Subcommittee on Standardization of Power and Distribution Transformers of the American Standards Association Sectional Committee on Transformers (C-57) is now actively engaged in working on standards for the various features of these transformers, including the application of the preferred voltage ratings. The author of this paper has been closely connected with both of these activities.

The major problem for those who are setting up standards is to determine those items and details which will best fulfill the wishes and the real needs (these may not be synonymous) of the greatest majority. The problem of the user is first to participate in the formulation of the standards to the extent of having his ideas and practices fully considered, and thereafter to find means, if possible, for adopting the established standards for his own purposes and thereby join the majority in getting the price savings which should result.

The chief purpose of standardization is, of course, reduction in cost. This is accomplished mostly by a reduction of varieties, and a concentration on the most advantageous types, the increased volume in these allowing economies in production, distribution, and stocking. To realize this objective, standards adopted should be as broad and flexible as feasible in order to cover the real needs of the greatest possible number of users. Furthermore, they should not be so restrictive as to stifle further improvement and development in design and practice. In a field such as power transformers, where a considerable variety in the requirements of the users is well established, it is obviously impossible to set up standards which will be universally acceptable. If, however, a standard corresponds with the existing practice of a fair majority of the users, there will be some of the users who can adopt it by minor changes in their ideas, and who will be induced to do so if they can thereby gain a cost advantage. There will, of course, be certain systems which will not find it practical to use a standard without changes in their practice, which would outweigh any possible saving. Sometimes users in this latter class will complain that they are being penalized if standards are not set up in accordance with their particular needs. They should recognize, however, that a real standard cannot be effected merely by committee action but only by the concerted agreement of a number of users.

It is to be hoped that the new standards for power transformers can be established on a broad enough basis so that those users, who find it impossible to accept all of the features of the complete standard units, can still partake to some extent in the advantages by using standard features and parts as far as allowable under their own restricting conditions. If standardization is properly effected, the over-all result should be a tangible saving in cost not only to those who can conform with the standard but also to those who cannot fully conform. The cost of unavoidable "specials" should, on the other hand, not be greater, because of the existence of standards, than they would be if there were no such standardization.

Voltage Ratings

The voltage ratings for power transformers proposed by the Joint EEI-NEMA Committee on Preferred Voltage Ratings were the result of extensive studies of the ratings and operating voltages existing in the industry. Practice in this regard is considerably confused because of the fact that previous ratings corresponded with voltages used during the period of progress from multiples of 110 volts, to 115, 120, and 125 volts, with numerous variations thereof. A transformer is, however, essentially a ratio device. A transformer which will step down from 23,000 to 2,300 volts will

Paper 50-134, recommended by the AIEE Transformers Committee and approved by the AIEE Technical Program Committee for presentation at the AIEE Summer and Pacific General Meeting, Pasadena, Calif., June 12–16, 1950. Manuscript submitted March 13, 1950; made available for printing April 7, 1950.

HOWARD P. SEELYE is with the Detroit Edison Company, Detroit, Mich.

Table I. High-Voltage Rating and Tap Voltages on 34.5-Kv Transformers

Previous Design*		Preferred Voltages**			
		Group I		Group II	
Ratio	2,400 Volts Low Voltage	Ratio	2,520 Volts Low Voltage	Ratio	2,400 Volts Low Voltage
15.06	34,650			15.08	36,200
14.71	33,825			14.71	35,300
14.34	33,000	14.36	36,200	14.33	34,400
13.95	32,175	14.01	35,300	13.96	33,500
13.62	31,350	13.65	34,400	13.58	32,600
13.30	30,525	13.29	33,500		
12.91	29,700	12.94	32,600		

* 33,000 volt rating with $2^1/_2$ per cent taps.

** From reference 1.

also step down from 24,000 to 2,400 volts, or from 25,000 to 2,500 volts provided other characteristics are suitable. It was naturally impossible for the committee to arrive at standards which would match exactly all of the variety of ratios in use. The choice was made, therefore, to fit as closely as possible to the predominating historical ratios, with the belief that these could be adopted without undue penalty by most of those whose customary ratios were similar, although differing somewhat numerically.

The surveys indicated that, in general, a total range of taps of approximately 15 per cent on the high-voltage side of the transformer is needed in the industry. It appeared, however, that this whole range is not required by a large enough portion of the users to warrant the expense of including it in a single standard—the majority would be penalized for the advantage of the few. Most of the applications can be divided into two distinct groups. In one of these, either the high-side voltage is relatively low or a comparatively high voltage is desired on the low side for general distribution circuits, both of these conditions needing transformer ratios in the lower part of the total range mentioned. In the other group, a higher range of ratios is required for locations where the high-side voltage is relatively high or where a lower order of low-side voltage is preferred, as is the case for many industrial plants.

Two alternative designs, therefore, seemed to be the most economical answer. High-voltage ratings and taps would be exactly the same for both. Low-voltage ratings would be 2,520 for one group and 2,400 volts for the other (or multiples thereof). The nominal voltage designation of a transformer would correspond to the "preferred nominal system voltage," 34.5 kv for example. The rating upon which performance characteristics of the transformer should be specified would, however, for convenience be made the mid-point of the tap range, which may or may not be the same as the nominal voltage designation. In selecting the actual tap voltages, prevailing practice was taken into account and also the desirability of covering as fully and adequately as possible the full range of operating voltages indicated by the surveys. The steps between taps were, for simplicity and consistency, made in even voltage amounts rather than in percentages of some rating.

It is hoped and expected that most users will find either one or the other (or both) of the alternatives adaptable to their needs, their choice being based on ratios rather than specific tap-rating figures. Table I shows, for a 34.5-kv transformer, the various ratios provided by the taps on these alternative designs, and how these ratios compare with those for previous designs having taps of $2^1/_2$ per cent on 33,000 volts.

Figure 1 indicates graphically the various voltages on both high-voltage and low-voltage sides which may be obtained with these ratios, within the usual operating range of voltages for 34.5-kv and 2,400-volt systems (the "tolerable zone" of the Preferred Voltage report). The group-I (2,520-volt) design will produce 2,520 volts from 32,600 to 36,200 volts on the high side, and will also give 2,400 volts for applied voltage as low as 31,000. On the other hand, a group-II transformer (2,400-volt) will put out 2,400 volts from 32,600 to 36,200 volts applied, and will also give 2,500 volts from 33,900 to 37,000 on the high side. It is recognized that the losses for a 2,520-volt transformer will not be the same when producing full kilovolt-amperage at 2,400 volts as they might be in a transformer designed for 2,400 volts with the same high voltage applied—copper loss will be higher and core loss lower. It is believed, however, that the practical difference will not be great and will be outweighed by the cost advantages of standardization.

As an example of adaptation of the preferred voltage recommendations, on the Detroit Edison system a full tap range of 15 per cent for the system as a whole has been utilized in the past, being obtained by a secondary tap in the transformers in most cases. It is anticipated that in the future transformers can be used from group I for those units located where transmission voltage tends to be in the lower part of the system spread, and from group II for those where the transmission voltage is generally higher. The 23-kv (nominal) "preferred" tap voltages appear suitable except for certain uses where a variation of 40 kv is needed.

The ASA C57 Subcommittee previously mentioned is now in process of fitting the preferred voltage ratings to standard kilovolt-ampere ratings, and for 3-phase transformers to the phase connections—delta or wye—most commonly required. All of the various possible voltage ratings will, of course, not be included in all sizes and all phase connections. The recognized standards should be selected as only those which have sufficient demand to allow savings by quantity production. Others may be considered allowable variations or special designs according to the degree of their departure from the standards.

Kilovolt-Ampere Ratings

On any one system, it is desirable for simplicity and economy to standardize on as few kilovolt-ampere ratings as feasible. In the past, the standard ratings offered by the manufacturers have been in steps which were unnecessarily small for an individual user. These ratings for 3-phase transformers, with the steps between them in per cent of the lower rating of each step, are shown in Table II. It seems probable that for national standards the number of ratings can be reduced, resulting in appreciable economy in manufacture by concentrating on fewer sizes. The problem, which is being studied by the ASA C57 Subcommittee,

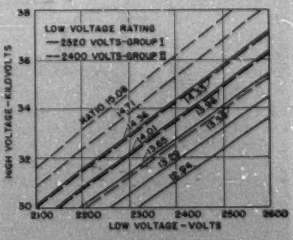

Figure 1. Preferred voltage ratings for 34.5-kv transformers

is to discover the most generally acceptable series of steps and ratings. The Detroit Edison Company has, for example, used for many years a step of approximately 60 per cent between sizes, shown in Table II. Although this series is quite consistent as to size of steps and has been found entirely practical, it is recognized that the 4,000-kva and 6,000-kva ratings are not largely used by other companies, and some intermediate sizes may be more generally favored. The last columns in Table II show another series which has been proposed. It would seem obvious that some such simplification would lead to worth-while savings and would justify a serious attempt by users to compromise on the fewer ratings.

Table II. Three-Phase Power-Transformer Kilovolt-Ampere Ratings

Present Ratings		Detroit Edison Ratings		Proposed Ratings	
Kva	% Step	Kva	% Step	Kva	% Step
750		(750)*		750	
1,000	33	(1,000)*	33	1,000	33
1,500	50	1,500	50	1,500	50
2,000	33				
2,500	25	2,500	67	2,500	67
3,000	20				
3,750	25			3,750	50
		4,000	60		
5,000	33			5,000	33
6,000	20	6,000	50		
7,500	25			7,500	50
10,000	33	10,000	67	10,000	33
12,000	20				
15,000	25	15,000	50	15,000	50
13 ratings: average 28.5%		8 ratings: average 53.9%		9 ratings: average 45.8%	

* 750- and 1,000-kva ratings have not been used by The Detroit Edison Company.

Oil Preservation

Modern practice calls for the exclusion of air from free access to the oil in a power transformer because of its deteriorating action on the oil. This exclusion is accomplished in several different ways. The objectives of the design in each of these is, in addition to excluding the air, to avoid excessive positive or negative pressures within the tank throughout the probable range of temperatures produced by the transformer's operation.

The simplest method is the sealed-tank design in which the tank is completely sealed with a cushioning space of proper proportions above the oil or in an auxiliary gas expansion tank. This space is filled initially with nitrogen or with air from which the oxygen will be eventually absorbed by the oil. This design was formerly limited to the smaller sizes of transformers but has more recently been extended to larger ones. Its simplicity commends it for all sizes for which it can be justified by design, tests, and experience. It has been used successfully on the Detroit Edison system for ratings up to 30,000 kva. The "gas oil seal" design is an available alternate to the sealed tank using an auxiliary tank on the manometer principle.

For larger transformers, the "gas pressure regulated" system, the "conservator system," and also the "gas oil seal" design have been usual practice. The first maintains a positive gas pressure in the tank from a separate inert gas source. The "conservator" employs an auxiliary oil tank to keep the transformer tank full of oil under positive pressure. The "gas pressure regulated" system or "gas oil seal" system are favored by those who wish to avoid a head of oil above the top of the tank.

Noise

The present NEMA standard for noise levels for power transformers was developed about 1939. It was based on reasonably good practice at that time, although it was felt by some users that transformers could and should be built with lower noise levels than the standards allowed.

The changes introduced in materials and designs in recent years, while producing marked improvement in other directions, have seemed to tend toward more noise.

From the user's standpoint, noise from transformers frequently means greater cost for installation. As residential loads become larger and more concentrated, it becomes necessary to put larger and larger transformers in densely populated areas in close proximity to residences. On the Detroit Edison system, several 10,000-kva units are located in substations in residential districts, and two 60,000/100,000-kva transformers were recently installed in a substation in such an area. When the noise level is low enough, say, 60 decibels or less, it is probable that a transformer without special screening will not be found objectionable in such a location. If the noise is higher than this, some means to screen or enclose the noise source may be required. Up to about 75 decibels, wall enclosures, open at the top, have been used satisfactorily. For the higher levels, complete enclosure with the attendant complication of ventilation is likely to be necessary. Although there are many locations away from residences where transformer noise, even of a relatively high level, is not objectionable, nevertheless when a transformer is bought for general system use, the possibility that it may be installed in one of the more critical locations cannot be ignored. It is very desirable that all practical means for reducing transformer noise levels be developed as a means of minimizing the trouble and expense which the users must incur in their application.

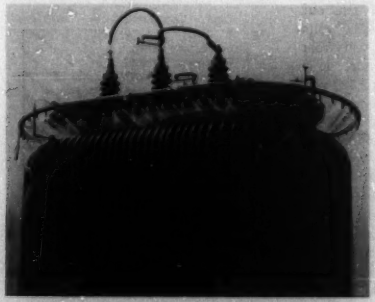

Figure 2. Water-spray cooling of transformer

Transformer Loading

The load-temperature characteristics of a transformer have a direct bearing on the economy of its application and operation. For the most effective use of capacity, the loading should be related to

operating temperatures. The latter are a function of not only the kilovolt-amperes carried, but also ambient temperatures and duration of load, that is, the characteristics of the load curve. In Detroit Edison practice, the allowable load on a substation is, in general, that which can be carried by the transformers in the station without overheating, either day-to-day or when the largest one is out of service because of a failure. The temperature criterion used for emergency loading is that which will produce a loss of one per cent of the life of the insulation under the emergency loading over one daily peak load period. Load characteristics, prevailing ambient temperatures, and individual transformer characteristics are taken into account in the calculations developed for the purpose from well-known published methods.

A typical example of such a case would be a substation with two 6,000-kva transformers serving a residential and commercial load. With self-cooled units, the maximum allowable emergency load for one of these might be 150 per cent of the name-plate rating of the unit, or 9,000 kva. Supplementary cooling by fans can increase this considerably. A simple water spray, such as that shown in Figure 2, is very effective in certain cases in increasing the emergency rating, up to perhaps 12,000 kva for the case cited, where such an increase is not limited by allowable voltage or other conditions. Such a spray is not very desirable if used regularly, however, so where a day-to-day loading above the self-cooled capability is anticipated, fan cooling is preferable.

Forced oil cooling has been increasing in popularity because of its relatively low cost as compared with self-cooled designs. Usually water cooling for the heat exchanger is cheaper than fan cooling where adequate and economical cooling water is readily available, but the advantage can be easily offset by any considerable amount of piping or cost for water. Forced oil cooled transformers are best suited to attended stations where the continuous operation of pumps and fans is under immediate supervision, and to applications where the loading is more or less fixed and not subject to the large increases in emergency, which were described in the foregoing example. Although some over-name-plate capability is available for short times, they do not offer the opportunity for increasing this capability by supplementary means, which is inherent in the self-cooled unit.

Other Features

There are numerous other features which must be considered in the choice of a transformer for a specific case—impedance, losses, insulation strength, bushings, accessories, details of construction, and other factors. The standardization program which has been mentioned includes those upon which a consensus of opinion seems feasible and for which such concentration is likely to have a material influence on the cost of transformer production. The individual user's chief objective in selecting his transformer is, naturally, to promote good service and economy on his own system. It may well be that his conditions are such that established standards are not acceptable or that the higher cost of a nonstandard unit is entirely justified by savings accomplished otherwise by its use. As a rule, however, most users will derive appreciable eventual benefit from the existence of sound and comprehensive standards in the industry. Such standards can only be accomplished by the willing and understanding co-operation of all users and manufacturers in their preparation and in their use thereafter to the fullest practicable extent in the choice of transformers to be purchased.

Reference

1. Preferred Voltage Ratings for A-C Systems and Equipment, Joint Edison Electric Institute-National Electrical Manufacturers Association Report. *EEI Publication Number R-6, NEMA Publication Number 117* (New York, N. Y.), May 1949.

No Discussion

Long-Distance Power Transmission

S. B. CRARY
FELLOW AIEE

THIS paper presents the results of recent studies to determine the performance characteristics of long-distance transmission systems. The analysis is directed toward a consideration of straightaway transmission systems of 600 miles in length, a distance which is representative of transmission now under study and actual development.[1,2,3] The system characteristics and requirements for economic transmission outlined in this paper may be used to furnish a guide for the future development of long-distance as well as moderate-distance transmission systems.

The first part of the paper is devoted to straightaway transmission of 600 miles and considers the effect of intermediate switching stations, series-capacitor compensation, intermediate synchronous condenser and shunt capacitor compensation, fault switching times, excitation system characteristics, and generator and receiving system reactances and inertias.

The second part gives consideration to this same distance, but with intermediate generation. Long-distance power transmission systems of the order of 600 miles may have intermediate generation which can provide a point for interconnection.[1,2] To determine the effect of intermediate generation on the over-all transmission of power it was assumed that this generation or system capacity exists at the halfway point. Several general conclusions can be drawn from these results, which may be used to indicate an expected trend in the development of such long-distance transmission systems.

Although the paper is confined mostly to the determination of stability characteristics, an indication is given of the relative economics for the various methods of increasing the power limits.

Paper 50-135, recommended by the AIEE Transmission and Distribution Committee and approved by the AIEE Technical Program Committee for presentation at the AIEE Summer and Pacific General Meeting, Pasadena, Calif., June 12–16, 1950. Manuscript submitted March 14, 1950; made available for printing April 7, 1950.

S. B. CRARY is with the General Electric Company, Schenectady, N. Y.

The author wishes to acknowledge the assistance of the Network Analyzer and Differential Analyzer staffs of the General Electric Company and in particular the contributions of his associates: Charles Concordia; L. K. Kirchmayer; F. J. Maginniss; G. M. Miller; L. W. Robbins; and M. W. Sheets.

Summary of Results

From the results of this analysis of 600-mile transmission, the following summary can be made. The first two points are essentially a reaffirmation of previous studies.[2,4,5,6]

1. Intermediate switching stations constitute a very effective and practical way to increase the transmission-line loadings and reduce the cost of transmission.

2. Special means to overcome the stability limitations (commonly called "compensation means") are also necessary to reduce the cost of long-distance straightaway transmission.

3. Series capacitors may be used as a basis for evaluating quite accurately the expected cost of long-distance transmission.

4. Other methods of compensation such as intermediate synchronous condensers and controlled shunt capacitors may be comparable in cost to that of series capacitors. Their application will depend upon the particular system under consideration and particularly on the amount of intermediate loading.

5. Interconnection to intermediate system capacity is an entirely practical and economic method to increase the power limits of long-distance transmission systems. When such intermediate capacity already exists this means may constitute the most economic method of attaining low transmission costs.

6. A measure of the transmission-system economy is the design loading of the circuits. There appears to be no longer any justification for design or maximum loadings below the surge impedance loading for any circuit, even for the circuits with lengths as great as 600 miles and even when the system is required to withstand the loss of any one transmission line section.

7. The higher voltages, 287 kv and 360 kv, with their high kilowatt loadings for optimum economy, will be essentially limited in their use for delivery of power to large integrated systems capable of absorbing large blocks of power, such as 400 to 800 megawatts per pair of circuits. (See Table I).

8. With the continued growth, development, and interconnection of electric systems, the ability to absorb large blocks of transmitted energy is increasing.

9. Comparisons of a-c transmission with other methods of transmitting energy long distances should be persistently reappraised in view of the continued progress in the transmission art and the development of electric systems.

Discussion of Results

The following gives the results of some of the studies which have been made recently of long-distance transmission systems. These results are selected to present the information used to arrive at the foregoing summary which bears most directly on the development of long-distance power transmission systems. The first part of these results is confined to straightaway transmission at a distance of 600 miles. In the second part the results obtained with mid-point generation are discussed.

I. 600-Mile Transmission Without Intermediate Generation or Load

1. Comparison of 200-Mile and 600-Mile Straightaway Transmission System Power Limits. Figure 2 gives the results of differential analyzer studies of the power limit of 200-mile, Figure 2(A), and 600-mile, Figure 2(B), transmission systems. These studies were made for a double-circuit system with an intermediate switching station every 100 miles. The system used for Figure 2 and Figure 8 is shown in Figure 1 except that for the case of Figure 2(A) the transmission is limited to 200 miles rather than 600 miles as shown, and the series capacitors (indicated by the dotted lines) were used only for the case of Figure 8. The

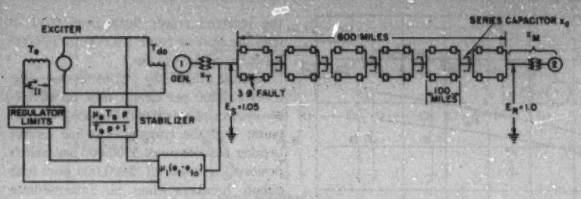

Figure 1. The 600-mile transmission system

All quantities expressed in per unit are on a kilowatt and kilovolt-ampere base of $5(kv)^2$; for a 287-kv transmission system this corresponds to 412,000 kw and 412,000 kva. The system constants are

Generator:
- $x_d = 0.63$ per unit
- $x_q = 0.42$ per unit
- $x_d' = 0.21$ per unit
- $H_g = 5$ seconds
- $T_{do} = 5$ seconds

Transformer:
- $x = 0.10$ per unit

Line:
- $x = 0.8$ ohm per mile per line
- $r = 0.12$ ohm per mile per line
- $y = 5.2 \times 10^{-6}$ mhos per mile per line

System:
- $x_m = 0.2$ per unit (includes receiving end transformer reactance)
- $H_s = 50$ seconds

Regulating System:
- $\mu_1 = 20$
- $\mu_2 = 4$
- $T_e = 0.47$ sec. for 200-mile line
- $= 0.93$ sec. for 600-mile line
- $E_{max}' = +2.25$ per unit regulator limits
- $E_{min}' = -0.30$ per unit regulator limits

System Damping:

Torque Coefficients	Fault On	Fault Cleared
T_{d1s}	1	4
T_{d2s}	0	3
T_{d3s}	0	3
T_{d4s}	15	18

results of Figure 2 are for an uncompensated line or $x_c = 0$. The differential analyzer method of analysis is described in reference 7. Figure 2 shows the effect of fault-clearing time on the power limit, where the power limit is given in per unit sending end power on a $5 \times kv^2$ base. For example, per unit power for a 287-kv system is $5 \times (287)^2$ or 412,000 kw. See Table I.

The results shown can be interpreted directly for any single conductor per phase circuit from Table I which gives the per unit kilowatts and kilovolt-amperes for the higher voltages. If dual conductors are used, then the per unit power and kilovolt-amperes will be increased approximately 25 per cent.[8] Accordingly, the results given in this paper can be interpreted also for dual conductors per phase although all the results are given directly for single conductors per phase.

As shown in Figure 2(A) for the 200-mile line the power limit for 0.06 second fault-clearing time and an exciter time constant of 0.68 second (per unit response of approximately unity) is 1.065 in per unit or 440,000 kw for a 287-kv system (692,000 kw for a 360 kv system and, if 360 kv with dual conductors, 866,000 kw). This represents a fairly good loading for a double-circuit 200-mile system. Figure 2(B) for the 600-mile uncompensated line ($x_c = 0$) with the same amount of connected generation as for the 200-mile system has a power limit equal to 0.735 per unit or 303,000 kw for the 287-kv system. Therefore, the 600-mile line has a power limit of only 69 per cent of

Table 1

Circuit (kv)	Per Unit kw and kva* $[5(kv)^2]$
360	650,000**
287	412,000
230	264,000
161	130,000
115	66,000
69	24,000

*This column corresponds to the total surge impedance kilowatt loading of two circuits when each circuit has a surge impedance of 400 ohms.

**If a dual conductor[1,8] is used, then the per unit kilowattage is increased approximately 25 per cent above the values shown so that at 360 kv the per unit power becomes 813,000 kw.

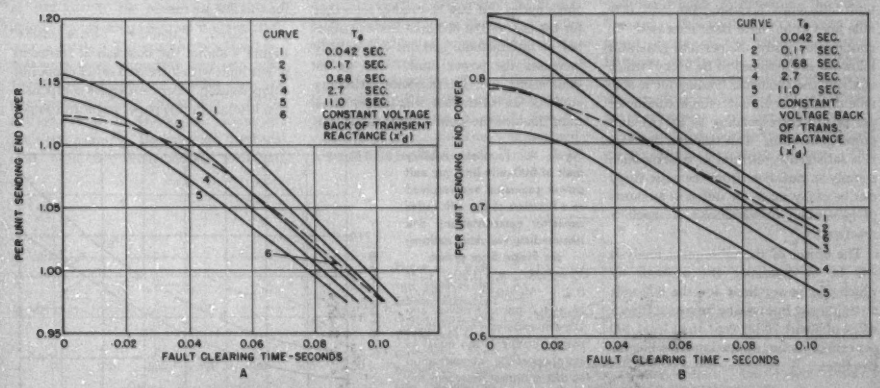

Figure 2. Sending-end power versus fault-clearing time for stability

Three-phase fault at sending end. Illustrating effect of excitation system time constant. Intermediate switching station every 100 miles. See Figure 1 for system

A. 200-mile line B. 600-mile line

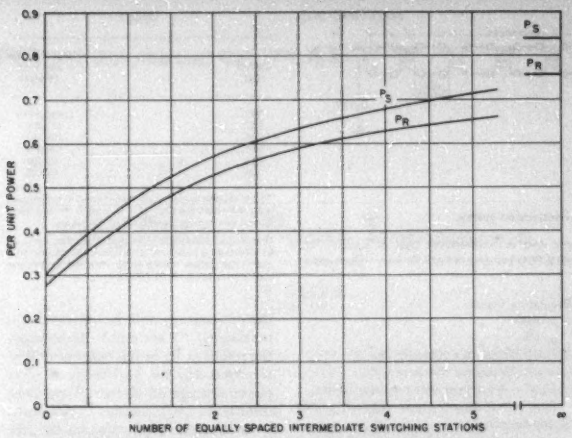

Figure 3. Effect of intermediate switching station on transient stability limit for 600- mile transmission system similar to that of Figure 5 with exception that number of intermediate switching stations was varied and series and shunt compensation was not used

$V_R = V_S = 1.0$; $H_g = 5.0$; $H_m = \infty$; $x_g = 0.30$; $x_m = 0.25$; per unit power and kilovolt-amperes $= 5(\text{kv})^2$; fault clearing time $= 0.05$ second

the 200-mile line, other conditions being kept constant. It should be noted that this comparison is on the basis of the same sending-end reactance for each case, or for the same equivalent generation. If the generation had been reduced correspondingly to the reduced limit for the 600-mile case, in order to maintain the same per unit reactance per kilovolt-ampere of generating capacity, the power-limit difference between 200- and 600-mile lines would have been increased. In making this study, the per unit generator kilowatts are assumed to be $5 \times \text{kv}^2$ which is about the economic loading for a 600-mile double-circuit line (single conductor per phase) corresponding to 1.0 per unit power generation. It is believed that this is a satisfactory method of making such a study as variations from the basic study can be easily made for different amounts of generation or variations in machine reactance.

The object of the subsequent analysis will be to determine the methods by which the power limit for the 600-mile straightaway line may be increased from a value of about 70 per cent to at least 100 per cent of its surge impedance loading for two lines.

2. Effect of Intermediate Switching Station. In the above comparison of 200- versus 600-mile transmission, the results are presented for the case of using intermediate switching stations every 100 miles, as this was considered to be in the region of the most economic number of intermediate switching stations.

Figure 3 shows how the power limit increases with increasing number of switching stations. For this case the system shown in Figure 5 was used, assuming an equivalent voltage behind transient reactance (x_d') and a total fault duration of three cycles. It can be readily seen that for the case of the 600-mile line the number of intermediate stations appreciably increases the power limit. The power limit using five intermediate switching stations, as contrasted with none, more than doubles the power limit, increasing the received power limit from 0.30 to 0.65 per unit or from 124,000 to 268,000 kw for a 287-kv system.

Assume that the transmission line costs $30,000 per circuit mile for a 287-kv system, $36,000,000 for the two circuits; and the transmission line circuit breaker positions cost $200,000 per switch position, a total of $800,000 for four circuit breakers when no intermediate stations are used and $4,800,000 for 24 circuit breakers when five intermediate stations are used.

Then the cost per kilowatt for the transmission, not including the terminal transformers and their circuit breakers, is $36,800,000/124,000 kw = $297 per kilowatt, with no intermediate switching stations and $40,800,000/268,000 kw = $152 per kilowatt, with five intermediate switching stations. This fully demonstrates the value of intermediate switching stations.

This result is not surprising as it is well known that the use of intermediate switching stations is an economical means to increase the reliable power limit of high-voltage transmission systems.[3,4] In this study intermediate stations were assumed to be spaced every 100 miles. For a double-circuit line it may be economical to space them even closer. However, this was thought to be close enough to the optimum spacing particularly when there will usually be the practical future possibility of adding an additional parallel circuit in the normal development of a transmission system. The next step in this example is to further reduce the cost of transmission below $152 per kilowatt for this 287-kv case.

3. Series Capacitor Compensation. Figure 4 shows the increase in transient power limit with increased series capacitor compensation. Per cent series compensation is taken in this paper to mean the per

Figure 4. Transient stability limit of 600-mile line, per unit power generated and received as a function of per unit series capacitor compensation; five intermediate switching stations; see Figure 5 for system

$V_S = 1.05$; $x_g = 0.30$; $x_m = 0.25$; $V_R = 0.95$; $H_g = 5.0$; $H_m = \infty$; per unit power and kilovolt-amperes $= 5(\text{kv})^2$; shunt reactor compensation equal to series-capacitor compensation so that at normal frequency the surge impedance of the compensated line is 400 ohms. Fault-clearing time is 0.05 second. Capacitor reinsertion time is assumed to be zero

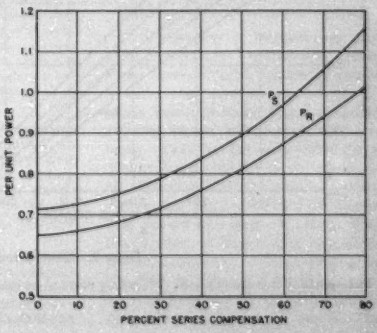

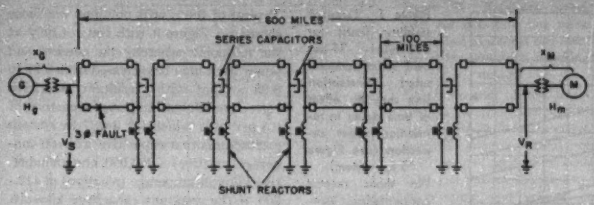

Figure 5. System diagram

cent compensation of the reactance of the line, that is, for a 600-mile double-circuit line with 0.8 ohm reactance per mile, 75 per cent compensation distributed in five intermediate stations corresponds to

$$x_c = \frac{600 \times 0.8 \times 0.75}{2 \times 5} = 36 \text{ ohms per phase}$$

per station or 0.18 per unit on a kilovolt-ampere base of $5 \times kv^2$. Figure 5 is the system studied for this case. At 75 per cent line compensation, the sending-end power is 1.10 per unit kilowatt and the receiving end is 0.98 per unit kilowatt. Seventy-five per cent compensation of the line, therefore, results in practically 1.0 per unit power transfer. For a 287-kv system this is a delivered power of $0.98 \times 412{,}000 = 403{,}000$ kw.

Previous studies[5,9] have indicated that systems may be built with as much as 75 per cent compensation and satisfactory operation can be expected. Seventy-five per cent line compensation of this system requires about 0.90 reactive kilovolt-ampere of series capacitors and 0.90 reactive kilovolt ampere of shunt reactors or 370,000 reactive kilovolt-amperes of each at 287-kv. If the series capacitor and shunt reactor compensation is assumed to cost a total of $12 per one reactive kilovolt-ampere of capacitor plus one reactive kilovolt-ampere of reactor then the compensation for a 287-kv line is $370,000 × 12 or about $4,500,000. Using the previous example, the cost for transmission with five intermediate switching stations (excluding the terminal transformers and their circuit breakers) plus the compensation, is $40,800,000 plus $4,500,000 or $45,300,000. The received power limit is increased from 268,000 kw to 403,000 kw. The cost per kilowatt is accordingly reduced from $152 to $112. This figure of $112 per kilowatt can therefore be used in comparison with other methods of increasing the power limit.

Studies of this system with series capacitors were made also without shunt reactors. Interestingly enough, the power limits were very close to the same values when shunt reactors are used along the line. It appears therefore that the shunt reactor's primary function is to maintain essentially normal voltage along the line. Without the use of shunt reactors, the voltage rises to 115 per cent of normal voltage at no load near the receiving end and the same voltage rise occurs under load near the sending end, for the conditions of 1.05 sending end high-tension bus voltage and 0.95 receiving-end high-tension bus voltage, with a sending-end line section out. See Figure 6(A). Distribution of the series capacitor and the reactor compensation reduces the voltage rise along the line as is evident by Figure 6(B), which is a typical illustration of the effect of distributed compensation on the voltage gradient.

Figure 7 shows the effect of time delay in reinserting the series capacitors, measured from the time of fault clearing where the fault-clearing time was assumed to be of 0.05 second or three cycles. It is advantageous to make the reinsertion as quickly as possible. The curves of Figure 7 indicate the influence of change in generating and receiving reactance as well as the generator inertia for the case of a 600-mile line (system of Figure 5) with five intermediate stations, no shunt reactor compensation, and series line compensation of 75 per cent.

Figure 8 is a summary of a differential analyzer study which shows the variation in per unit power limit as a function of switching time and exciter time constant for a 600-mile line (system of Figure 1) with 75 per cent series capacitor compensation and without shunt reactor compensation.

When Figure 8 and Figure 2(B) are compared, a good comparison is obtained of the effect of series capacitor compensation, as all of the other system characteristics (Figure 1) were kept constant except for a change in voltage regulator stabilizer time constant (T_s). The sending-end power limit for a fault-clearing time of 0.06 second and an exciter time constant of $T_e = 0.68$ second has been increased from a P_S of 0.735 to 1.07. The latter value is practically the limit obtained under the same conditions for a 200-mile uncompensated line, Figure 2(A). In other words, the effect of 75 per cent series capacitor compensation has in effect increased the power limit of the 600-mile line to that of an uncompensated 200-mile line.

4. Intermediate Synchronous Condenser Compensation. A study of the effect of intermediate synchronous-condenser capacity was made to determine the effectiveness of this method in increasing the power limits of the 600-mile system. Previous steady-state stability studies[10] have indicated the desirability of keeping the transient reactance of the intermediate synchronous condenser as low as practicable and distributing the synchronous-condenser capacity along the line. The

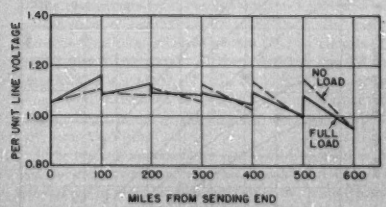

Figure 6. Voltage gradient for 600-mile double-circuit line with 75 per cent series capacitor compensation. System shown in Figure 5

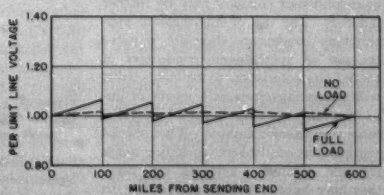

A. No shunt reactor compensation, with one of the sending-end 100-mile sections out; $V_S = 1.05$; $V_R = 0.95$; $P_S = 1.10$; $P_R = 0.95$
B. With distributed shunt reactor compensation; all line sections in; $V_S = 1.0$; $V_R = 1.0$; shunt reactor reactive kilovolt-amperes = series capacitor reactive kilovolt-amperes at unit load; $P_S = 1.10$; $P_R = 0.95$

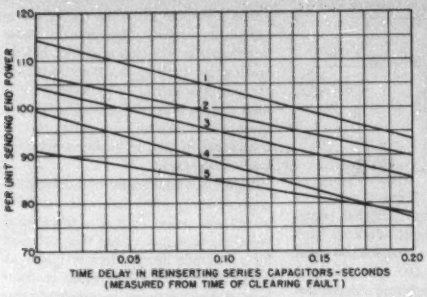

Figure 7. Transient stability limits for 600-mile 75-per cent series-compensated transmission line showing effect of time delay in reinserting series capacitors (see Figure 5 for system)

No shunt reactor compensation; $V_S = 1.05$; $V_R = 0.95$; series capacitors bypassed on occurrence of fault and reinserted at time shown on abscissa after fault has been cleared; fault-clearing time is 0.05 second

Curve	x_l	x_m	H_g
1	0.30	0.15	4
2	0.30	0.25	6
3	0.30	0.25	4
4	0.30	0.25	2
5	0.40	0.25	4

present transient stability study of the 600-mile line case also showed the desirability of keeping the reactance as low as practicable, and distributing the available capacity at more than one intermediate location. The optimum distribution for the transient case is dependent, among other factors, on the location of the faulted line section. For example, if an intermediate synchronous condenser for the system of Figure 5 (without either series or shunt compensation) is placed at the midpoint, having a per unit rating of 1.25 and a transient reactance including its high-voltage transformers of 0.25 on its own rating, the sending power limit is increased from 0.71 per unit ($x_g = 0.30$) to 0.90. If the same condenser capacity is equally distributed at the five intermediate stations, the sending-end power limit is increased to 0.98. If the synchronous condensers were distributed to obtain the highest power limit for a given system, the received power limit would be still further increased to at least 1.03 for this particular amount of synchronous-condenser capacity.

The foregoing limits are based on calculations using constant voltages behind the transient reactances for all the synchronous machines. If quick response excitation systems are used, particularly at the intermediate synchronous condenser locations, the required synchronous condenser capacity may be further reduced. The use of intermediate synchronous condensers therefore requires the use of synchronous condensers of special characteristics, to be competitive with series capacitors as a means of improving the stability limits of long-distance transmission circuits. When special synchronous condensers, including quick response excitation systems, are used, they may have a rating comparable to that of series capacitors for the same power limits.

If the system has intermediate loads requiring synchronous-condenser voltage and reactive-kilovolt-ampere control at these intermediate points, then the benefits of the synchronous condenser are increased.

5. *Intermediate Shunt Reactive Control Using Static Capacitors.* Consideration has also been given to the possibilities of using intermediate controlled shunt reactive kilovolt-amperage for increasing the power limits. Dr. E. F. W. Alexanderson has proposed the use of special arrangements of reactors and capacitors to obtain voltage control whereby the correction can be applied smoothly rather than in sudden large increments.[11]

Consideration of such schemes indicates that, if the intermediate correction is distributed, higher power limits are obtained for a given total corrective capacity. Typical of the results obtained are those shown on Figure 9 with control only at the midpoint, whereby the sending-end power limit may be increased from 0.71 to 0.95 per unit, with a resultant capacitive corrective kilovolt-amperage (reactive) of 0.5 per unit which for a 287-kv system corresponds to a capacitive kilovolt-amperage (reactive) of 206,000, and an inductive kilovolt-amperage (reactive) of 412,000, if the resultant capacitive kilovolt-amperage (reactive) is to be controlled by variation of the inductive kilovolt-amperage (reactive). In the calculation, it was assumed that there were available equal amounts of lagging and leading reactive kilovolt-amperage at the midpoint and that they were applied instantaneously and smoothly so as to obtain a change in corrective current up to the limit of the capacity assumed for each case, with a regulation characteristic of 0.20 per unit for each 0.01 per unit deviation from normal voltage.

II. 600-Mile Transmission With Mid-Point Generation

The following presents some of the results of a study of 600-mile power transmission with and without mid-point generation. The systems studied are shown in Figure 10. Figure 10(A) shows the system which may be considered the initial development of a transmission system with a generating station 300 miles from its load center with three transmission lines and two intermediate switching stations. Figure 10(B) shows the same system but with another generating station located 600 miles from the load center and interconnected into the transmission system at the first generating station. From a study of the system of Figure 10(A), it is found, for the representative reactances chosen, that the power limit

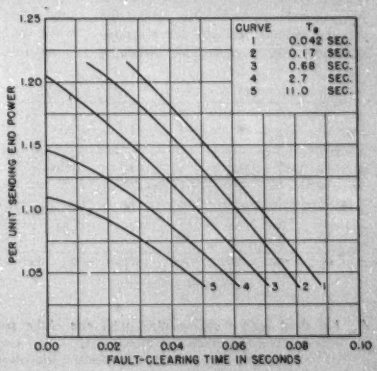

Figure 8. Transient power limit for 600-mile 75-per cent series-compensated line

System conditions the same as Figure 1 except capacitors as shown dotted in Figure 1 assumed to be in circuit (75-per cent line compensation, $x_c = -0.18$ at each intermediate switching station)

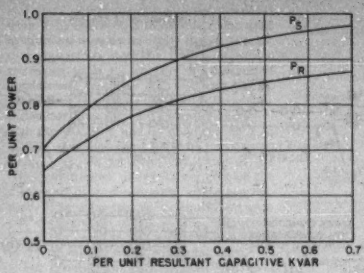

Figure 9. Transient power limit for 600-mile line using controlled capacitors and reactors at the mid-point switching station

System consists of five intermediate switching stations similar to Figure 5. Corrective reactive kilovolt-amperes of 0.20 per unit applied for each 0.01 per unit of voltage variation from unit voltage at mid-point. Resultant kilovars equal to capacitive reactive kilovolt-amperes shown on abscissa. $H_p = 4.0$; $X_m = 0.25$; $V_R = V_S = 1.0$; $x_p = 0.30$; $H_m = \infty$; base kilowatts = base reactive kilovolt-amperes $= 5(kv)^2$

of the sending-end power for a 3-phase fault near the sending-end bus of a duration of four cycles is 1.33 per unit, that is, on the kilowatt base of $5 \times kv^2$, for a 287-kv system, this is 550,000 kw.

The effects of variation in the receiving-end reactance were also studied. The power limit was reduced almost 15 per cent by a 100 per cent increase of the receiving-end reactance. It is significant that the receiving-end reactance is quite important in determining the maximum power transfer and that in the design of a system for receiving large blocks of power from distant stations it is essential for good economy to keep this receiving-end equivalent reactance as low as is practical by a rational circuit arrangement. It becomes particularly effective to bus all high-voltage circuits near the receiving end directly together. Fortunately this can now be more readily accomplished with the development and increasing use of high interrupting-capacity circuit breakers.[19]

Keeping the output of the mid-station generator number *1* at 1.33 per unit, corresponding to its maximum power limit with three lines, the Figure 10(B) system was analyzed to determine the maximum total sending-end power that could be transmitted with stability. This limit was found to be 1.73 with 1.33 from generator number *1* and 0.4 from generator number *2*. This corresponds to a loading on the two circuits from the distant generating point of 160,000 kw for a 287-kv system. The total received power (P_R) for this case is $1.62 \times 5.0 \times (287)^2 = 666{,}000$ kw. As this is a relatively light loading, means were considered as to how to obtain an increase in the loading particularly from the distant station.

If the mid-station reactance was halved and the inertia was doubled, which would correspond in effect to interconnecting to a moderate amount of system capacity at this point, see Figure 10(C), the power limit for the distant generating station was increased from 0.4 per unit to 0.85 per unit. If the mid-station reactance was further reduced to one-third of its original value and its inertia trebled, the power limit for the total generating station was increased to 0.9. At this loading the critical fault moves from location number *1* at the mid-station to location number *2* at the distant generating station. With this doubling or trebling of the equivalent capacity at the mid-point, the power limits of the system approach those which may be considered reasonable from an economic standpoint. For a 287-kv system the mid-generating station remains at 550,000 kw and the output of the distant station is 370,000 kw. It is estimated that the loadings of Figure 10(C) would be realized if the tie is made to generating capacity of twice that of generator number *1* and with an autotransformer bank capacity of about 300,000 kva for a 287-kv system. The additional power delivered to the load from the 600-mile distant source of the Figure 10(C) system as compared with system 10(A) is 0.76 per unit. This was obtained by the addition of 900 circuit miles of line, approximately 22 circuit breaker positions, and a 300,000-kva autotransformer bank.

Assume again for a 287-kv system the additional power delivery is 315,000 kw. The cost of the additional transmission circuits at $30,000 per mile is $27,000,000; the 22 circuit breakers at $200,000 per position are $4,400,000; the autotransformer bank installed at $3.00 per through kilovolt-ampere installed is $900,000. This gives a total of $32,300,000. Transmission costs $32,300,000/315,000 kw = $101 per kw. This figure, although only approximately obtained, indicates that the connection to intermediate system capacity when possible compares quite favorably with the straightaway compensated transmission cases previously considered and may result in the most economic transmission system.

It may be concluded here that a system of substantial line loadings per circuit can be realized even for 600 miles if the high-tension lines are tied directly together and full use is made of generation or system capacity along the line of the order of two to four times the capacity of the distant generator source. It should be kept in mind that intermediate switching stations and a low-reactance receiving system are also quite necessary. The important conclusion is that by rational system design heavy line loadings are realizable at relatively small increase in cost, resulting in important reductions in the cost per kilowatt for transmission.

Effect of Series Capacitors and Mid-Point Generation (600-Mile Transmission)

The following present some results of the studies made to determine the influence of series capacitors used with mid-point generation, keeping the mid-point generation again at a value corresponding to the power limit of 1.33 per unit, Figure 10(A). Using series capacitors in the system of Figure 10(B) to compensate for 50 per cent of the line reactance from the mid-generating point to the distant generating point and shunt reactors to obtain essentially unity power factor at the terminals of the distant generating station, the power limit of the distant generating station was only increased to 0.5 per unit as contrasted with 0.4 per unit with no compensation.

Using the Figure 10(D) system which has a fifth circuit from generator number *1* to the load, with 70 per cent series capacitor compensation of the two circuits from generating station number *1* to generating station number *2*, and sufficient shunt reactors to obtain unity power factor at the terminals of generator number *2*, the power limit of the distant generator was increased to 1.0 per unit. Accordingly, by the use of 70 per cent series capacitor compensation in the lines to the distant station with an equal reactive kilovolt-amperage of shunt reactors and the addition of two 600-mile circuits, it is possible to obtain a reasonable loading of the distant station. P_R increased from 1.25 per unit for the system of Figure 10(A) to 2.10 per unit for the system of 10(D) giving an increase of received power of 0.85 per unit. For the case of Figure 10(D), again assuming a 287-kv system with the previously assumed costs, the following tabulation may be made up:

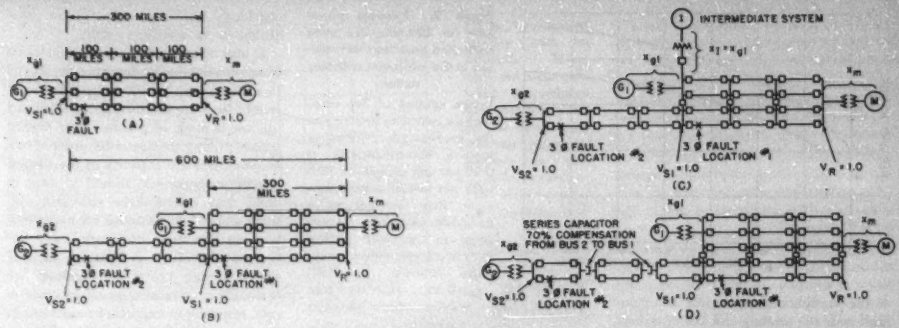

Figure 10. Transmission systems studied to determine effect of mid-point generation

Base kilowatts = base kilovolt-amperes = $5(kv)^2$

A. Initial system development. Power limit: $P_{G1} = 1.33$; $P_R = 1.25$

B. Initial system development plus extension of system for transmission of power from 600 mile distant source. Power limit: $P_{G1} = 1.33$; $P_{G2} = 0.40$; $P_S = P_{G1} + P_{G2} = 1.73$; $P_R = 1.62$. Critical fault: location number 1

C. System B with intermediate system interconnection assumed equivalent to halving x_{g1} and doubling H_{g1}. Power limit: $P_{G1} = 1.33$; $P_{G2} = 0.85$; $P_S = P_{G1} + P_{G2} = 2.18$; $P_R = 2.01$

D. System using series capacitors and additional 300-mile circuit added to that used by system of B. Power limit: $P_{G1} = 1.33$; $P_{G2} = 1.00$; $P_S = P_{G1} + P_{G2} = 2.33$; $P_R = 2.10$

Line:

$x = 0.8$ ohm per mile

$r = 0.08$ ohm per mile

$y = 5.2$ micromhos per mile

Receiving End System:

$$X_M = \frac{0.50}{\text{number of receiving end circuits}}$$

$H_m = \infty$

Generators (Generator kva rating assumed equal to kilowatt output at stability limit):

$x_{g1} = 0.30$ on kilovolt-ampere rating

$x_{g2} = 0.30$ on kilovolt-ampere rating

$H_{g1} = 5.0$ on kilovolt-ampere rating, seconds

$H_{g2} = 5.0$ on kilovolt-ampere rating, seconds

Fault:

Three-phase, 0.067 second or four cycles

1,200 circuit miles at $30,000 per mile = $36,000,000

28 circuit breakers at $200,000 per position = 5,600,000

175,000 reactive kilovolt-amperes of capacitors and 175,000 reactive kilovolt-amperes of shunt reactors at $12 per reactive kilovolt-ampere = 2,100,000

Total cost = $43,700,000

Increase in received power realized by above investment = $0.85 \times 5(287)^2 = 350{,}000$ kw

Transmission cost per kilowatt from 600 mile source = $\frac{\$43{,}700{,}000}{350{,}000 \text{ kw}} = \$125.$

This cost per kilowatt corresponds sufficiently close in relation to the previous costs per kilowatt to warrant the conclusion that there may be several system designs achieving heavy line loadings which may need consideration for any given case. These studies confirm the conclusion that the use of series capacitors with shunt reactors may be used as a benchmark for estimating long-distance transmission line costs. More detailed and complete studies of any given system will reveal possible further improvements which may result in substantial savings.

References

1. The Swedish 380-Kv System, **Ake Rusck, Bo G. Rathsman.** *Electrical Engineering*, volume 68, December 1949, pages 1025–9.

2. The Proposed Colorado River Developments, **William S. Peterson.** *Electrical Engineering*, volume 66, December 1947, pages 1184–93.

3. Hydro-Electric Developments in the Nile Valley, **Abdel Aziz Ahmed.** *Proceedings*, International Conference on Large Electric High-Voltage Systems (Paris, France), volume III, 1948, report number 332, 26 pages.

4. Stability Limitations of Long-Distance A-C Power Transmission Systems, **Edith Clarke, S. B. Crary.** *AIEE Transactions*, volume 60, 1941, pages 1051–1059.

5. Series Capacitors for Transmission Circuits, **E. C. Starr, R. D. Evans.** *AIEE Transactions*, volume 61, 1942, pages 963–973.

6. Economics of Long-Distance A-C Power Transmission, **S. B. Crary, I. B. Johnson.** *AIEE Transactions*, volume 66, 1947, pages 1092–1099.

7. The Differential Analyzer as an Aid in Power System Analysis, **C. Concordia.** To be presented at the International Conference of Large Electric High-Voltage Systems (Paris, France), June 29–July 8, 1950.

8. Relative Surface Voltage Gradients of Grouped Conductors, **M. Temoshok.** *AIEE Transactions*, volume 67, part II, 1948, pages 1583–1589.

9. Self-Excited Oscillations of Capacitor-Compensated Long-Distance Transmission Systems, **R. B. Bodine, C. Concordia, G. Kron.** *Electrical Engineering (AIEE Transactions)*, volume 62, January 1943, pages 41–44.

10. Long-Distance Power Transmission as Influenced by Excitation Systems, **C. Concordia, S. B. Crary, F. J. Maginniss.** *AIEE Transactions*, volume 65, 1946, pages 974–987.

11. Electronic Stabilizer for Power Transmission, **Ernst F. W. Alexanderson, David C. Prince.** *AIEE Transactions*, volume 66, 1947, pages 950–953.

12. Development and Testing of an Improved High-Voltage, High-Capacity Impulse Circuit Breaker, **E. B. Rietz.** *AIEE Transactions*, volume 69, part I, 1950, pages 18–26.

Discussion

J. G. Holm (New York, N.Y.): In his very interesting paper Mr. Crary gives an up-to-date presentation of the long-distance power transmission problem. Mr. Crary gives his data specifically for single conductors but mentions that these data may be used also in the study of dual-conductor lines. Since there has been lately an increased interest in bundle-conductor lines, as indicated by five papers presented on this subject at the 1950 International Conference on Large High-Voltage Electric Systems meeting in Paris and by actual application of bundle conductors on 220- and 380-kv lines now being erected in Sweden, it may perhaps be of interest to discuss briefly the bundle-conductor lines.

To find out where we stand in this subject, I made a study of bundle-conductor lines comparing single-circuit single-, dual- and triple-conductor lines transmitting power at 345 kv over distances of 100, 300, and 500 miles.

In each case four conductors were taken: two copper conductors of the *HH*-type of two different cross-sections, and two ACSR (aluminum cable steel reinforced) expanded conductors of cross-sections of the same equivalent copper as the corresponding copper conductors. The diameters of dual and triple conductors were so chosen that the total fair-weather corona loss per mile, determined for a certain altitude and temperature, was the same in the single-, dual- and triple-conductor lines. Disruptive critical voltages and gradients were calculated,

and then conductor diameters determined from data given by Temoshok.[1] The dual conductors were horizontally spaced at a 15-inch separation, and the triple conductors were located at the corners of an inverted equilateral triangle with 15-inch sides. Thus while the copper conductors for single-conductor lines were 1.5 inches in diameter, and the ACSR's had a diameter of 1.75 inches, the diameters of dual conductors were about 68 per cent and those of the triple conductors, about 53 per cent of the diameters of corresponding single conductors. The total copper, or equivalent copper, cross-section of the bundle conductors was taken equal to the copper cross-section in corresponding single-conductor lines.

For conductors thus selected the electrical design of lines was made, and their kilowatt rating established. The bundle conductors have a smaller reactance and greater line capacitance than single conductors. In order that this characteristic can be made use of to full advantage, a correspondingly greater generating capacity was assumed at the sending end. The lines were provided with receiving-end synchronous condensers for full-load to no-load operation, with the condensers supplemented by receiving-end reactors where this was economical for the absorption of the excess lagging kilovolt-amperes. The lines have no series-capacitor compensation. System power limits were determined, and the line ratings were established sufficiently below the power limits to give assurance of stability in the steady state. Thus the ratings of all dual-conductor lines were uniformly about 21 per cent and those of the triple-conductor lines, about 37 per cent above the ratings of corresponding single-conductor lines. Total system losses were calculated in both the line and the terminal equipment. In order to reduce the no-load losses and the mid-point no-load voltages in the 500-mile lines, all these lines were equipped with mid-point reactors.

In all systems conductors were supported by steel structures of the rotating type. All mechanical calculations were made for heavy-loading conditions, with simultaneous ice and wind loads taken on all conductors.

All systems were suitably protected by ground wires, counterpoises, and so forth. The pull on insulators in the bundle-conductor lines was calculated, and mechanically stronger units, as well as additional parallel insulator strings, were placed on those lines where this was required. On the dual- and triple-conductor lines with the ACSR conductors, armor rods were placed on each conductor. Spacers were placed on all bundle-conductor lines according to practice adopted in Swedish lines.[2]

System capital and annual costs were calculated for the entire system, comprising the line, terminal substations and the mid-point reactor substation (in the 500-mile lines). The cost of the right-of-way was omitted. Costs were those prevailing during the first quarter of 1949. Estimates were made of the specific hardware required by the bundle conductors. The line erection costs for the dual-conductor lines were taken at a higher figure than for single-conductor lines, and at still higher figure for the triple-conductor lines. The expenses for maintenance and operation of the bundle-conductor lines were taken at figures higher than those for single-conductor lines. The cost of all system losses, including those at no-load, was included.

Table I

Conductors	Line Length, Miles	Average Per Cent Lower Cost Per Kw	Maximum Per Cent Lower Cost Per Kw (in one case)
Dual	100	4.4	9.0
	300	5.3	8.8
	500	5.7	8.3
Triple	100	9.8	14.8
	300	10.1	14.8
	500	10.9	14.1

Table II

Conductors	Line Length, Miles	Cost of Generating Capacity A $/Kw: Average Per Cent Lower Cost Per Kilowatt-hour	Cost of Generating Capacity A $/Kw: Maximum Per Cent Lower Cost (in one case) Per Kilowatt-hour	Cost of Generating Capacity 35.3 A $/Kw: Average Per Cent Lower Cost Per Kilowatt-hour	Cost of Generating Capacity 35.3 A $/Kw: Maximum Per Cent Lower Cost (in one case) Per Kilowatt-hour
Dual	100	3.5	8.0	2.4	6.2
	300	3.3	6.3	1.7	4.1
	500	3.0	6.2	1.4	4.0
Triple	100	7.9	12.5	6.0	10.0
	300	7.1	9.7	3.8	6.3
	500	6.0	10.1	2.3	5.8

For the four cases, the average capital cost per mile of the transmission line alone for the dual-conductor lines was 12.2 per cent greater than the average cost of single-conductor lines, with a maximum of 15.1 per cent in one case. In the case of triple-conductor lines, the average increase was 21.4 per cent, with a maximum increase of 28.3 per cent in one case. The Swedish calculations, reported in 1950,[3] for one case of a 380-kv dual-conductor line show an increase of 19.8 per cent, compared with a single-conductor line, per kilometer.

For the loadings used, capital costs of the entire system, per kilowatt transmitted, for the dual- and triple-conductor lines were lower than for single-conductor lines, for all the three distances investigated. The decrease in costs for the four cases studied are given in Table I of this discussion.

The annual costs of the entire system, per kilowatt-hour, for the dual- and triple-conductor lines were also lower than for single-conductor lines, for all three distances. The average percentage decrease in costs for the four cases studied, for two different costs of generating capacity are given in Table II of this discussion.

The Swedish calculations,* reported in 1948,[4] for one case of a dual-conductor 380-kv line show capital costs for the entire system, per kilowatt, 8.5 per cent smaller than for the 380-kv single-conductor system. They also show annual costs for the entire system to be 3.3 per cent less than for the single-conductor system. In these calculations losses are included.

* It is not clear if calculations were made for a 280-mile line, or for a line of twice this length.

The costs given in this discussion are in good agreement with the Swedish costs so far referred to. However, the Swedish engineers,[3] in discussing the annual costs of an entire 380-kv dual-conductor system ("with stability", as they say), state that the costs on this system for a 300-mile line are 9.2 per cent less and for a 600-mile line, 11.9 per cent less than the annual cost of a 380-kv single-conductor system of corresponding length. These are very high figures. In my total of 48 cases they have been approached, or exceeded, only four times. Moreover, it is indicated in their paper that the annual economy of a dual-conductor system increases as the length of the line increases, varying from 5.1 per cent on a 125-mile system to 11.9 per cent on a 600-mile system. Even though this dual-conductor Swedish line has 30 per cent more equivalent copper than the single-conductor line, calculations made on the basis of their assigned ratings place in doubt the indication that relative economy increases with the length of the line. It is possible that the figures they reported in 1950 may be affected by the fact that their system is State-owned, so that the cost of hydro-generation is very small, and taxes none. Their annual charges are a little more than half the annual charges applied by private public utilities in this country.

In general, while the data here reported show that under some conditions there are significant economies for bundle conductors, the comparison may be reversed for other conditions. If the amount of power to be transmitted is fully within the capacity of a single-conductor line having a sufficient amount of copper, or equivalent copper, then it is possible that it will be more economical than the inherently higher capacity and more expensive dual- or triple-conductor line. Many variables, such as for example the general national price level or possible differences in the engineering approach, may produce some changes in the relation between single- and bundle-conductor costs and cause appreciable deviations from the average percentage values. Therefore, it is my opinion that the question of whether, and to what an extent, the bundle-conductor lines are more economical must be decided on the merits of each particular case.

Whatever the economic features of bundle conductors may be, their technological advantages and disadvantages must be given full consideration. No attempt will be made at this place to discuss this phase of the subject.

References

1. Relative Surface Voltage Gradients of Grouped Conductors, M. Temoshok. *AIEE Transactions*, volume 67, part II, 1948, pages 1583–91.

2. Series Capacitor and Double Conductors in the Swedish Transmission System, Ake Ruck, Bo G. Rathsman. *Electrical Engineering*, volume 69, January 1950, pages 53–57.

3. A Comparison of Costs for Power Transmission at 220 and 380 Kv, G. Nilsson, U. Sandstrom. *Report Number 405*, International Conference on Large High-Voltage Electric Systems (Paris, France), 1950.

4. The Swedish 380-Kv System, W. Borgquist, A. Vrethem. *Report Number 412*, International Conference on Large High-Voltage Electric Systems (Paris, France), 1948.

W. A. Morgan (United States Bureau of Reclamation, Denver, Colo.): I want to

congratulate the author on his worthwhile and timely analysis of factors affecting the design of a long-distance power transmission system. The general problem Mr. Crary has assumed is a practical one, and the analytical treatment he has given it establishes several fundamental ideas to be considered in any system of this type.

The Bureau of Reclamation is currently making studies of the proposed power system which will be required when power developments above Hoover Power Plant are built. If all the power potentialities within 300 miles upstream from Hoover Power Plant are utilized, this new power would amount to 2,500,000 kw to 3,000,000 kw capacity in three or four power plants. The purpose of these studies is to establish nominal voltage and arrangement of transmission lines for the ultimate development, and then to determine the program for development of this system as each power plant is to be built so that the initial system will fit into the pattern of a well-designed ultimate system.

It is brought out by the author that series capacitors may be used as a basis for evaluating quite accurately the expected cost of the long-distance transmission. Also, the 75 per cent compensation in capacitors is assumed to be lumped at the intermediate switching stations. Have the technical difficulties of relaying for line faults with such an installation been overcome as yet?

It is understood that in the Swedish application the series capacitors are located in the middle of a line section, and the value of compensation is less than 30 per cent, thereby assuring correct directional relaying with the presently available distance-type line relays. Would the author care to comment on the conservative approach of the Swedish engineers in regard to the application of series capacitors?

Are there any other design problems in connection with a high-voltage series capacitor installation, such as arc-gap bypass switch protection, that will require further developmental work before the manufacturers will be willing to guarantee satisfactory performance of a series capacitor installation?

It is noted that the power limit of a transmission line may be increased approximately 25 per cent if dual conductors are used. It would appear that there might be justification for dual conductors on 287-kv lines, particularly for single circuit construction, as well as on 360-kv lines as they are presently being applied. Are cost data and analysis available to demonstrate whether dual conductors are justified for 287-kv lines, either for single- or double-circuit construction?

There are two comments that are believed to be pertinent with regard to Figures 3 and 5 and the discussion of the value of intermediate switching stations. One is that it may not be practical to extrapolate the conclusion to include the case where as many as 12 transmission lines may be required. The other is that cost comparisons on an initial cost basis only may not give the full picture and that it may be more accurate to consider the total annual costs which would include operation and maintenance, amortization of investment over a period of years, and annuity for replacement.

With regard to the first point, there definitely is no disagreement regarding the value of intermediate switching stations where only two transmission lines are concerned. In this case, without the intermediate switching stations, the impedance is doubled when one line is tripped out of service; whereas with five intermediate switching stations, the impedance is increased only 17 per cent for loss of a line section.

Table III

	Transmission Line	Substation Equipment
Amortization*	0.03887 (3 per cent, 50 years)	0.03887 (3 per cent, 50 years)
Annuity†	0.01027 (100 per cent replaceable, 45 years)	0.01529 (90 per cent replaceable, 28 years)
Operation and maintenance**	0.00750	0.02750

* From *Reclamation Law*.

† *Bulletin F*, United States Treasury Department.

** From *Reclamation Manual*.

However, if there are 12 transmission lines, the benefits of intermediate switching stations is diminished. For example, if one line of the 12 is tripped, the impedance is increased about 9 per cent, without intermediate switching stations; whereas it is increased about $1^1/_2$ per cent for loss of a line section with five intermediate switching stations.

With two lines the intermediate switching stations are beneficial in reducing this change in impedance from 100 per cent to 17 per cent, which is a substantial improvement. However, considering the many assumptions that must be made in a study of a system of this size, it may be more difficult to justify reducing the change in impedance from 9 per cent to $1^1/_2$ per cent by intermediate switching stations in the case of 12 lines.

With regard to the second point, it is necessary to consider the total costs in comparing any two schemes and they may be put on an annual basis considering amortization of initial investment, annuity for replacement reserve, and operation and maintenance. The significant point here is that the factor for operation and maintenance of substations is over three times that for transmission lines, and the replacement annuity is only one and a half times that for a transmission line.

To illustrate the point, let us assume that 2,500,000 kva could be transmitted with equivalent stability 300 miles with either 13 287-kv transmission lines without two intermediate switching stations, or 12 transmission lines with two intermediate switching stations. Considering the large number of circuit breakers and the higher operation and maintenance cost factor, it would be less costly to use the system with 13 lines and no intermediate switching stations than with 12 lines and two intermediate switching stations. This is arrived at using the factors, shown in Table III of this discussion, which are to be multiplied by the initial cost to obtain the annual costs.

This method of comparing schemes on a total annual cost instead of only the initial costs is proposed.

The cost of a long distance power transmission system is so great that advantage should be taken of every means that will improve system performance and thereby reduce this cost, such as the full interconnection with generation at intermediate points and the reduction of reactance at the receiving end terminal which Mr. Crary points out. Some preliminary work we have done indicates that the reduction of receiving terminal reactance and interconnection with intermediate generation may amount to a savings of millions of dollars in over-all system costs.

In conclusion, it is desired to emphasize that papers such as Mr. Crary's are very important in bringing forth discussion and outlining the principles to follow in designing a long-distance power transmission system.

C. H. Prior (Department of Water and Power, The City of Los Angeles, Calif.): Mr. Crary's paper is of considerable interest to those of us in Southern California where large blocks of power must be transmitted over long distances. For this reason, the author's studies on the stability limits of the 600-mile system with mid-point generation and with series capacitors were of great interest, and they stimulated the desire to determine the power limits of the systems shown in Figures 1 and 2 of this discussion.

When transient stability analyses were made of the system shown in Figure 1 of this discussion, using the Department's network analyzer, it was found that with no compensation of the two 287-kv lines from the sending end to the mid-point, with 75 per cent compensation of the three 287-kv lines from the mid-point to the receiving end, and with 540,000-kw generation at the mid-point, the maximum delivered power was about 775,000 kw, with a net delivery of about 265,000 kw from the 600-mile source.

Using the author's cost-estimating data, the transmission cost for this 265,000 kw is as follows:

600 circuit miles at $30,000 per mile	$18,000,000
12 circuit breakers at $200,000 per position	2,400,000
561,000 kvar of capacitors and 561,000 kvar of shunt reactors at $12 per kvar	6,732,000
	$27,132,000
Transmission cost per kilowatt from 600-mile source	$ 102

In order to increase further the power limits of the system, 75 per cent series capacitor compensation was used in the two lines from the sending end to the mid-point

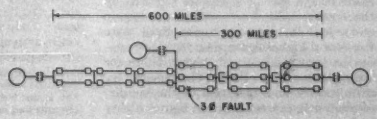

Figure 1. 600-mile 287-kv transmission system with mid-point generation and with 75-per cent series compensation between the mid-point and the receiving end

as shown in Figure 2 of this discussion. For this case the maximum delivered power was 996,000 kw, with a net delivery of 484,000 kw from the 600-mile source.

The cost for this 484,000 kw is as follows:

600 circuit miles at $30,000 per mile	$18,000,00
12 circuit breakers at $200,000 per position	2,400,000
1,470,000 kvar of capacitors and 1,470,000 kvar of shunt reactors at $12 per kvar	17,640,000
	$38,040,000
Transmission cost per kilowatt from 600-mile source	$ 79

These studies indicate the heavy line loading that can be obtained by using series capacitor compensation; however, further studies are required to determine if such heavy loading is desirable.

W. F. W. Alexanderson, and **D. C. Prince** (General Electric Company, Schenectady, N. Y.) and **C. H. Willis** (Princeton University, Princeton, N. J.): Mr. Crary has kindly included mention of our work using shunt saturable reactors and capacitors to give a continuous voltage control. There are some differences in operation between shunt and series capacitor control which should be noted. When series capacitors neutralize line reactance, the line angle is reduced. Large changes of load occur for small angular displacements between the two ends of the line. Also, of course, large voltages appear across the capacitors under fault conditions, unless protective devices are used.

With shunt compensation, on the other hand, the line angle is increased and large phase displacements accompany changes in load. It is interesting to examine the application of shunt compensation, instead of the series capacitors, to Mr. Crary's case of a 600-mile line with five intermediate switching stations. Using the same kilovolt-amperes of capacitors and twice the reactive kilovolt-amperes employed by Mr. Crary, in the section on Series Capacitor Compensation, gives approximately 0.9 for the per-unit power. (This value is obtained by extrapolating the sending-end-power of Figure 9 of Mr. Crary's paper.) This corresponds to a cost per kilowatt of power transmitted of $128.00 as compared to $112.00 for the same capacitive kilovolt-amperes used in series compensation. In computing the line cost, an appropriate addition has been made on account of the added shunt reactor.

It should be noted that the above-mentioned curve assumes the shunt kilovolt-amperes applied at the center of the line. When the shunt kilovolt-amperes used for compensation are applied at several points, as was the case for the series compensation, the comparison becomes more favorable to the shunt compensation as is stated in the paper. Since curves are not given which show the per-unit load for this line with shunt compensation applied at 100-mile intervals, no exact comparison of the relative cost of the two schemes is apparent; but the discrepancy will be somewhat less than shown in the comparison given above.

Series and shunt compensation may be compared analytically by considering the effect of the compensation on the surge impedance and line angle which will be considered loss-less to simplify the discussion. The analytical expressions for the surge impedance and angle of a Pi section are well known.

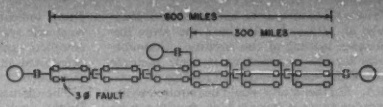

Figure 2. 600-mile 287-kv transmission system with mid-point generation and with 75-per cent series compensation of the entire line

When series compensation is used, the series impedance is reduced to a fixed lower value by the series capacitive reactance added. This reduces the surge impedance and the line angle. The maximum power transfer is increased because the surge impedance is reduced and the phase difference between the ends of the line is also reduced because the line angle is reduced.

When shunt compensation is used, the shunt impedance is increased if the compensation is inductive; but, if the compensation is capacitive, it is reduced. This permits a wide range of variation of the surge impedance and, since the compensation varies automatically to maintain a constant line voltage, the line operates at surge impedance loading over a wide range of load. The load limit is increased as in the series capacitor case, because the surge impedance is reduced by capacitive shunt compensation. This method of describing the operations may, of course, be applied to any operating scheme which maintains the same voltage at the two ends of the line under transient conditions.

S. B. Crary: The discussors have made very worthwhile contributions to the subject, some of which require no comment.

Mr. Holm has made a rather thorough study of the economics of dual-conductor lines versus single-conductor lines and, as he points out, the economic justification for dual versus single conductor lines is relatively small and may be dependent upon the particular local conditions. Mr. Holm may have avoided some of the complications of his analysis if he had assumed that the dual-conductor circuit had a resistance per mile proportional to its surge impedance, that is, $R_d = (Z_d/Z_s)R_s$ where R is resistance per mile and Z is the surge impedance. The subscript s indicates a single conductor per phase and d a dual conductor per phase. If this assumption is made it follows rather directly that the dual-conductor line can be justified (keeping all other factors equal) when the cost per mile does not exceed the ratio of the surge impedances of the two lines being compared; $C_d < C_s\ (Z_s/Z_d)$, where C is the cost per mile of the transmission line. This particular relationship is discussed in reference 1 of this discussion.

The above relationship applies when considering single-circuit lines at a single-voltage level. If the additional considerations of twin-circuit and single-circuit tower lines, including the variation in circuit voltages, the reliability, cost of right-of-way, and so forth are included then the comparison can no longer be as simple as indicated by the preceding relationship.

Apparently Mr. Holm has restricted himself, in this discussion at least, to a relatively simple comparison and it would have been helpful if he had given the line costs for the dual and single conductor lines as this appears to be the most important factor in determining the relative economy for the simple type of comparison which he has attempted to make.

Mr. Morgan has raised some very pertinent questions. We wish to assure Mr. Morgan that the relaying of the line faults will be solved as an essential requirement for the use of series capacitors, particularly when large values of compensation are used.

Mr. Morgan asks in regard to the conservative approach of the Swedish engineers in regard to the application of series capacitors. It appears from a recent paper[4] that the Swedish engineers have applied series capacitors primarily for load balancing of the 230-kv lines to decrease the real and reactive losses of the system and thereby increase the transmission capacity of lines already built. They also have indicated that this step is preliminary to possible application to the 380-kv lines. It must be kept in mind that the European transmission system design philosophy differs from that in this country in that the hydroelectric generators with their associated transmission circuit are not designed for firm power transfer, as an outage on the high-voltage line may result in loss of generating capacity. Therefore the application of series capacitors to European systems may be expected to differ in some respects from the requirements of the equipment developed for use in this country. Mr. Morgan also has asked in regard to the development of an arc-gap by-pass switch protection. We are pleased to state that such equipment has been under development and the manufacturers are in a position to quote on such equipment to meet rational system requirements.

Mr. Morgan is correct that the results shown in Figures 3 and 5 do not apply to the case of 12 parallel transmission circuits as these were made for the case of two parallel circuits. In the case of additional parallel circuits, the number of switching stations which can be economically justified would decrease for a given distance. Mr. Morgan's point is well made, that in order to make a more complete economic picture, it will be necessary to determine the cost per kilowatt-hour for transmission (mills per kilowatt-hour) rather than the investment cost (dollars per kilowatt). In the paper the investment costs per kilowatt were taken as a simple measure or indication of the relative economy of the various systems of transmission. This comparison seemed justified inasmuch as the stable loadings did not exceed appreciably the surge impedance loading of any one circuit. As other studies have indicated, it is economic to at least load the circuit up to this point. However, if the loadings of the lines are to exceed appreciably the surge impedance loadings, then it becomes necessary to make an evaluation in terms of cost per kilowatt-hour in order to determine the most economic loading and system transmission.

This comment particularly applies to Mr.

Prior's discussion as he had considered loadings of 1.25 and 1.61 times the surge impedance loading of the circuits. Undoubtedly for the assumed costs some increase above the surge impedance loading is justified. Further study would be required to determine to what extent these circuits can be economically loaded. Such a study would involve, among other things, a determination of the most economic conductor size. Mr. Prior's point is certainly a good one in that the loadings given on Figure 10 of the paper for the four systems shown may actually be increased by even greater amounts of compensation. This would require an economic study in more detail than that attempted in this paper, but may, as Mr. Prior indicates, result in an even more economic system. This would require more complete economic consideration than was attempted in the paper or in Mr. Prior's discussion.

The discussion by Messrs. Alexanderson, Prince, and Willis points out the desirability of considering the shunt compensation method. As has been emphasized, some form of compensation is fully justified, particularly for long straightaway transmission. The problem in any case, because of the large investments involved, is to determine the most economic as well as the most reliable method. In order to make such comparisons rather complete information needs to be available as to the relative costs, operating characteristics, and efficiency of the different types of equipment. One of the most encouraging features is that the transmission engineer now has available many different methods by which it is possible to overcome the stability limitations of long-distance transmission.

References

1. Economic Studies of Long Distance A-C Power Transmission, S. B. Crary. *Report Number 414*, International Conference on Large High-Tension Electric Systems (Paris, France), 1948.

2. The Series Capacitor with Special Reference to its Application in the Swedish 220-Kv Network, G. Jancke, K. F. Åkerström. *Report Number 332*, International Conference on Large High-Tension Electric Systems (Paris, France), 1950.

The Bridge River Hydroelectric Development

T. INGLEDOW
MEMBER AIEE

J. H. STEEDE
MEMBER AIEE

THE Bridge River development is a relatively high-head hydroelectric project on the eastern side of the coastal range in the Fraser River drainage area in the southern part of British Columbia. It is being constructed by the British Columbia Electric Railway Company to serve the greater Vancouver and lower Fraser Valley area. The project lends itself to economical development in progressive stages to an ultimate capacity approaching 750,000 hp. Three 62,000-hp units are now in operation. Ultimate capacity of the main project will be ten such units in a power house on the shore of Seton Lake. There are a number of novel features about this development which make it of particular interest at this time.

Location and Geographical Features

The Bridge River rises almost due north of Vancouver, approximately 110 miles distant, and flows in a generally easterly direction from near the height of land of the Cascade mountains to join the Fraser River five miles above the town of Lillooet, and 200 miles from the mouth of the latter river. In its upper reaches it is a turbulent mountain stream. At a lower stage after juncture with several tributaries, it flows through two flat basins between towering mountain ranges, then plunges downward over 1,400 feet in the last 15 miles of its course to join the Fraser.

Just above this last precipitous section the river bends southward and approaches within less than three miles of Seton Lake at an elevation almost 1,200 feet above the lake. Such is the natural setting for this high-head diversion project.

Watershed and Stream Flow Conditions

The watershed area is estimated to be 1,350 square miles, the greater part of it more than 3,000-feet elevation above sea level, and extending to mountain peaks of 7,000 to 9,000 feet. Precipitation varies over a considerable range from 18 inches or less in the valleys to considerably more at the higher elevations where it is mostly in the form of snow. As the water supply is mainly derived from those higher elevations, run-off is at a maximum in the late spring and early summer, continuing at a high level until early autumn. Low run-off occurs during January, February, and March, when temperatures even in the valleys may normally reach 10 to 20 degrees below zero. The stream flow, therefore, varies over a very wide range, the ratio of maximum to minimum daily flow recorded being of the order of 160-to-1, indicating the necessity for extensive storage facilities to take advantage of the average yield of the watershed, which is of the order of 3,400 cubic feet per second. Stream flow records compiled from measurements taken under the supervision of the Dominion Government Water & Power Bureau are available back to 1913.

Early History

The power possibilities of the site were first realized in 1912 by Captain Geoffrey Downton, a land surveyor, who discovered the difference in elevation between the river and Seton Lake, and their close proximity to each other. Subsequently, surveys and investigations were carried out sufficient to establish the power capabilities of the site, and the Bridge River Power Company was formed for the purpose of developing it. Due to a lack of market for the power, however, little or no action was taken until 1925. At that time an option was taken on the rights and properties of the Bridge River Power Company by the British Columbia Electric Railway Company, which then was giving extensive study to various projects to meet the future long-term power requirements of the Vancouver area. After a thorough investigation of the whole project, the property and assets of the Bridge River Power Company were purchased in 1926. Rate of system load growth at that time appeared to justify proceeding with construction and accordingly in 1927 preparatory work was started in connection with the driving of the first diversion tunnel.

To parallel the development of Bridge River at various stages, development of an additional plant on the Stave River relatively close to Vancouver was planned, such a plant to be utilized largely for peaking purposes when operated in conjunction with the Bridge River plant, as in its early stages particularly, Bridge River is capable of relatively high load factor operation. The first Ruskin unit as part of this Stave development was brought into service in the late autumn of 1930.

With the general depression in business which began to have its effect about that time, load growth was greatly reduced and later ceased altogether. In view of this falling off in load when the diversion tunnel was completed in December 1931, work on the Bridge River development was suspended. Prior to the outbreak of war in 1939, load conditions had not justified resumption, system capacity in the interim being obtained by further development at Ruskin. Lack of

Paper 50-136, recommended by the AIEE Power Generation Committee and approved by the AIEE Technical Program Committee for presentation at the AIEE Summer and Pacific General Meeting, Pasadena, Calif., June 12–16, 1950. Manuscript submitted March 13, 1950; made available for printing April 10, 1950.

T. INGLEDOW and J. H. STEEDE are both with the British Columbia Electric Railway Company, Ltd., Vancouver, B. C., Canada.

Figure 1. Bridge River Valley, looking eastward toward the diversion dam

materials and manpower precluded Bridge River construction during the war years, but early in 1945 detailed engineering was put in hand. There resulted considerable modification of the original design to take advantage of recent engineering developments and to more nearly meet the changing needs of the system. The overall scheme of development was not changed materially, however. Actual construction on the site was resumed in June 1946, the first unit being brought into operation eight months ahead of initial schedule on October 23, 1948. The second followed on May 6, and the third on December 14, 1949.

Component Parts of the Project

The component parts of the project at its present stage are as follows: a diversion dam in the Bridge River Valley to create a regulating pond and maintain a head of water over the tunnel intake; a 13,200-foot tunnel through Mission Mountain to divert the water from the Bridge River Valley to the mountainside above Seton Lake; steel penstocks some 2,100 feet in length down the side of Mission Mountain and crossing under the main line of the Pacific Great Eastern Railway; a building housing three vertical impulse turbines with generators and associated hydraulic and electric controls and servicing facilities, this building being designed for extension to accommodate seven additional units at a later date; a switching structure on several levels on the rapidly rising ground at the rear of the powerhouse; a 130-mile 230-kv steel tower transmission line terminating at Horne-Payne Substation in Vancouver; a rock-fill storage dam some 35 miles up the Bridge River Valley from the tunnel intake which will ultimately provide 570,000 acre-feet of storage. Reference will be made later to the additional features which will form part of the ultimate development; a second storage dam in the vicinity of the tunnel intake and a second tunnel through Mission Mountain parallel but on the east side of the present one.

Relative locations of all the present facilities are shown in Figure 2, both in relation to one another and to Vancouver. The various parts of the development now are described in some detail.

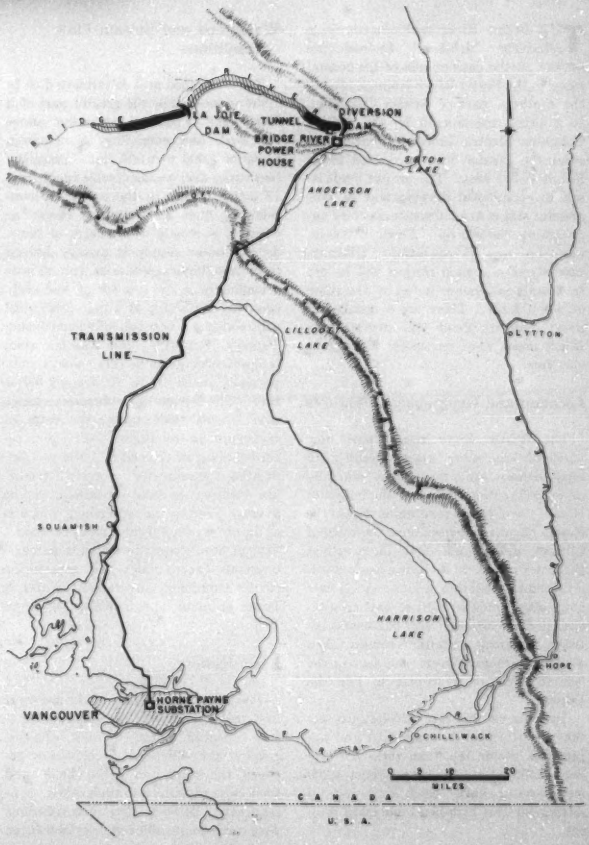

Figure 2. Map showing Bridge River Development in relation to Vancouver

The Diversion Dam

This is an earth- and rock-fill dam with an impervious clay core, just over 60 feet high at the center of the old stream bed

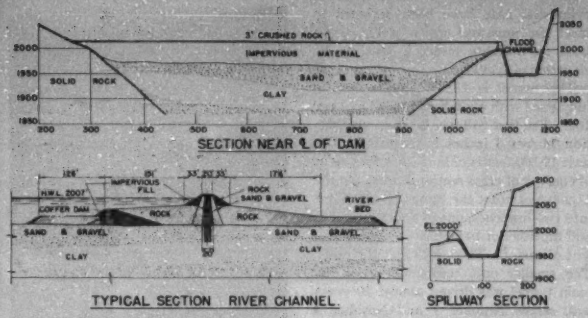

Figure 3. Diversion dam, sectional views

and having a crest length of 820 feet. An unusual feature is its width as compared with the crest length, it being over 600 feet from toe to heel as indicated in Figure 3, which shows a cross-sectional view. This width was necessary owing to the foundation conditions. While the walls of the valley, which assume canyon-like proportions at this point, are of solid granite, no bedrock foundation was found in the narrow channel although test boring was carried out to a considerable depth, both at the dam location and for two or three miles downstream. Materials underlying the dam consists of a deposit of silt, sand, gravel, and boulders varying in depth up to 50 feet overlying a bed of blue clay 30 to 35 feet thick. Owing to the nature of this underlying clay, it was essential that consolidation due to the superimposed weight of the dam take place very gradually and, accordingly, the side slopes had to be made unusually flat to avoid abrupt changes in loading.

Figure 4 (left). Plan of diversion dam

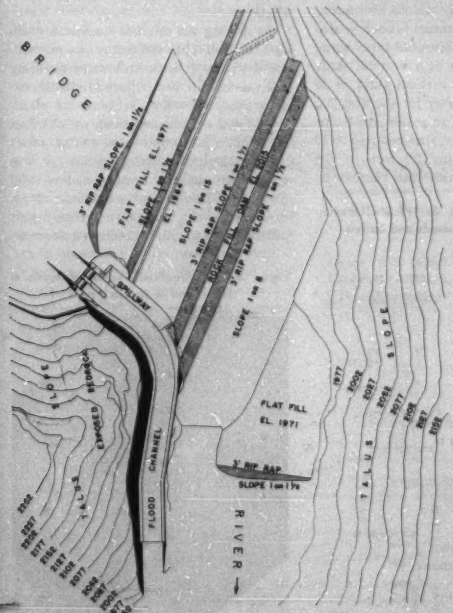

Figure 5 (below). Profile of tunnel

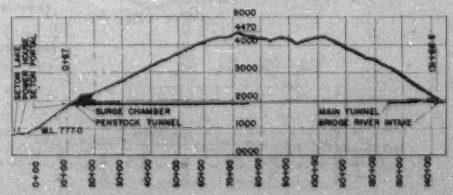

As shown in Figures 3 and 4 a concrete-lined spillway channel is provided to carry flood water downstream. This channel excavated through the solid rock of the south abutment is 50 feet wide and 900 feet long. Discharge is controlled by two sluice gates 25 feet wide by 40 feet high, and the dam is protected from overtopping by a concrete overflow spillway weir 250 feet wide, 15 feet lower than the crest of the dam. The excavation of the spillway provided 209,000 cubic yards of rock, all of which went into the dam and comprised about two-thirds of the total rock fill used, the remainder being obtained from nearby rock slides. Talus fill amounting to nearly 70,000 cubic yards was trucked one mile. It was necessary, however, to go 29 miles up the valley to find material for the clay core amounting to 26,000 cubic yards.

Work on the dam site commenced on June 4, 1946. Construction of the diversion channel continued without interruption throughout the winter of 1946, it being essential that it be completed to permit the river to be diverted through it before the 1947 spring freshet, in order that work could proceed on the body of the dam. Diversion of the river took place on April 28. On June 13, 1947, driving of sheet-steel piling for the cut-off trench on the dam center line was commenced and was followed by the placing of the first clay for the core, coffer dams having been previously completed on the upstream and downstream sides of the dam area. The clay core was completed on August 18, 1948, and the sluice gates were closed for the first time on November 10, 1948.

Care was used during construction to determine that the underlying clay strata was not stressed unduly. Piezometers were established in the upstream coffer dam before the commencement of rock fill, and in addition a number of settlement plates were established at the bottom of the fill downstream on the dam center line, and also downstream from the dam center line. Frequent readings were taken during the progress of construction, and upon completion of the dam further piezometers were established on the

dam center line and downstream from the dam center line as the original piezometers in the upstream coffer dam were under water. Subsequently, additional monuments were established on the dam center to permit periodic readings to be taken to determine the extent of settlement.

This dam with spillway elevation of 2,000 feet backs up the water for $7^1/_2$ miles, impounding approximately 18,000 acre-feet, roughly half of which is available for regulating purposes and provides a head of water on the tunnel intake.

Tunnel, Tunnel Intake and Outlets

The tunnel intake is in the form of a massive tower structure two miles above the diversion dam, provided with two entrance bays with water passages through the base and leading up into the interior of the tower, and thence into the tunnel. The control gate is of balanced cylindrical type, 20 feet in diameter with open bottom, and sits in an upright position on an annular ring encircling the water opening in the base of the tower. In its closed position the water from the regulating pond rises to its level inside the cylinder but, being contained within the cylinder, is prevented from flowing into the tunnel. Screen racks are fitted and outside the screens a heavy grillage of concrete columns and beams extending up to high-water level protects the screens from coarse debris or floating ice. To provide for the possibility that the future lower storage dam will be downstream from this intake, the base is designed to be capable of extension to a height of 217 feet. All features of the intake and cylindrical gate have been designed to meet the pressures which would result from an ultimate reservoir level at an elevation of 2,140 feet.

The tunnel is 13,200 feet in length, fully lined with a gradient of 0.73 foot per 100. The first 640 feet is of circular section 14 feet 3 inches in diameter. The next 10,560 feet is of horseshoe shape but of equivalent cross-sectional area. At the 11,200-foot point the tunnel breaks down into two branches, one of 8 feet 10 inches and the other of 10 feet 10 inches equivalent diameter. These also are fully lined. The smaller one, completed when the main tunnel was driven almost 20 years ago, serves Number 1 and Number 2 units; the larger branch was just completed in 1949 and will serve units Number 4 and 5 as well as the present Number 3.

In the initial branch a surge chamber was formed by enlarging the cross-sectional area of the tunnel for a distance of 185 feet and by driving a vertical shaft 300 feet long with a lined diameter of 7 feet to the ground surface. The design of this surge chamber was based on the use of smaller units than those now utilized, which may necessitate enlarging the vertical shaft at some later date. Operating experience up to this time has not indicated that there is any serious limitation.

The recent larger tunnel branch is also provided with a differential-type surge chamber in the form of a vertical shaft through rock. This vertical shaft is 20 feet 6 inches in diameter for the first 205 feet of its rise, with an inside steel pipe riser 9 feet in diameter, then reduces to 10 feet for the remaining 90 feet to the ground surface. In this case there is no enlarged section in the tunnel adjoining the vertical shaft. Instead of the branch tunnel being extended to the portal at full diameter, however, necessitating a manifold or a complicated pipe structure to serve three pressure pipes, the branch tunnel breaks down to three 6 foot 3 inch tunnels at the base of the surge shaft. This arrangement, as well as a plan of the smaller 8 foot 10 inch tunnel, is shown in Figure 6.

In driving the original tunnel 20 years ago, considerable difficulty was encountered with soft rock and water entering the tunnel bore under pressure to the extent that a 430-foot section was abandoned and a fresh start made on an offset to avoid the trouble zone. The offset section also proved troublesome but was eventually pushed through to more solid ground. The soft and crumbling nature of the rock throughout the greater part of the tunnel length necessitated the com-

Figure 7. Gantry for hoisting and placing penstock sections

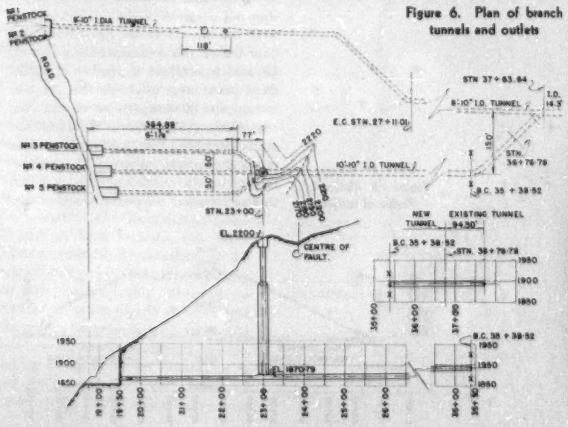

Figure 6. Plan of branch tunnels and outlets

Figure 8. Fifty-four-inch spherical valve at lower end of pressure pipe

Figure 9. Turbine nozzle body assembly number 1 unit

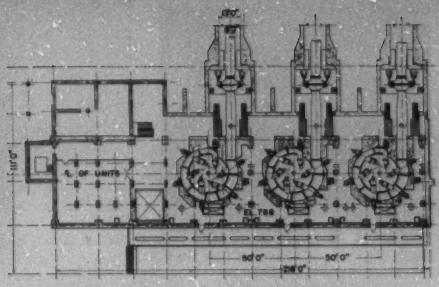

Figure 11. Plan view of powerhouse at turbine level

plete lining which had not been contemplated. In driving the new tunnel branch in 1949, conditions proved to be worse than those encountered in the first tunnel branch and an extremely bad section persisted for a distance of approximately 300 feet. Progress of tunnelling through this section was heartbreakingly slow, taking slightly over six months or an average of less than two feet per day.

Penstocks

In the initial branch tunnel the penstock steel commences 340 feet inside the tunnel and extends to the portal where there is a Y with a butterfly valve on each of the individual pressure pipes supplying the number 1 and 2 units. The steel liner in the tunnel is 106 inches in diameter and of uniform thickness, $1^{3}/_{16}$ inches.

In the new tunnel branch, the number 4 and 5 tunnels were not lined except for a short section between the base of the surge chamber and the location of bulkheads which were installed in each of these tunnels to close them off until they are required for units number 4 and 5. Number 3 tunnel was lined to the commencement of the penstock section, which is steel pipe $73^{7}/_{8}$ inches inside diameter and 13/16 inch in thickness, and extends 80 feet inside the tunnel portal. A butterfly valve also is installed in this penstock outside the portal at the top of the pressure pipe. In each pipe there is a venturi section about 100 feet below the butterfly valve. The valve is designed to close automatically in case of a break downstream, being actuated from a differential pressure device operating on this venturi section, or it can be closed by push button from the powerhouse. The valve-operating mechanism is an oil-pressure type controlled electrically by a d-c motor.

The pressure pipes are 2,100 feet in length, $75^{1}/_{8}$ inches constant outside

Figure 10 (below). Cross-sectional view of powerhouse

Figure 12 (right). One-line diagram, generating station

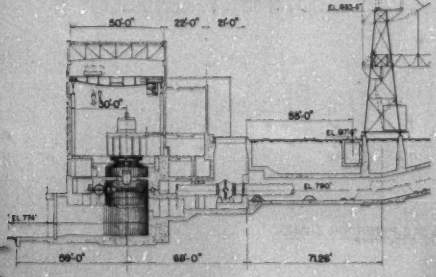

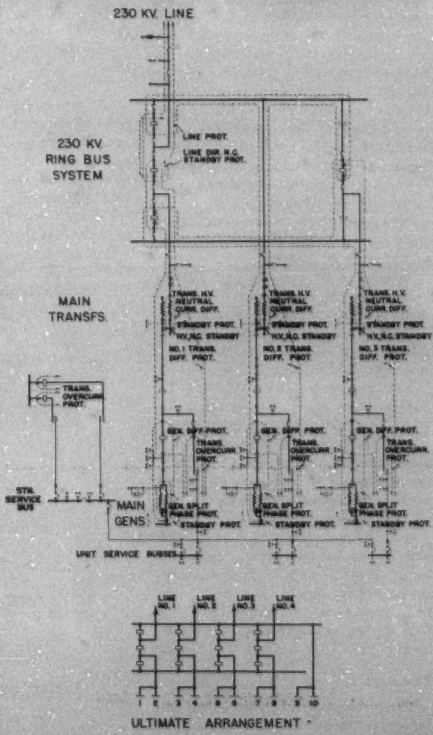

Figure 13. View of switchyard from above, Seton Lake beyond

diameter varying in thickness from 7/8 inch at the top to $1^{13}/_{16}$ inches at the bottom. Joints between sections of the tunnel liner were field-welded and -tested by gamma rays, photographic film being wrapped around the outside of the pipe and a lead capsule containing radium passed along the inside. Joints between sections of the pressure pipe were made with Dresser couplings, giving an expansion joint every 40 feet on the hillside. Designed for 1,000-pound-per-square-inch pressure in shop test, a coupling remained tight at 1,500-pound pressure. We are advised by the manufacturer that this is the first time that these couplings have been applied at such pressures. Three weights of coupling are used, all utilizing formed rubber continuous ring gaskets 5/8 inch by $2^1/_4$ inches compressed under an inner steel cylindrical ring by two 3-inch by 3-inch steel followers drawn up by bolts, 60, 80, or 90 in number, depending on the weight of coupling.

Erection of the pressure pipe sections weighing up to 30 tons each on a steep mountain side, the slope of which reached 41 degrees, presented a problem which was solved by the use of a gantry running on steel rails laid on top of the penstock footings and hauled up the the hill by an electric hoist above the portal. The gentry in operation is shown in Figure 7.

Each pressure pipe terminates in a spherical valve, the purpose of which is to provide a seal at that point to permit work to be carried out on the turbine whenever this may be necessary. This is a 54-inch plug-type valve, Figure 8, which with trunnions but without operating levers weighs 37 tons. It embodies a retractable joint capable of four inches in and out movement to permit uncoupling from the penstock for removal or replacement.

Turbines

The turbines are of vertical-shaft impulse type, equipped with six nozzles and rated 62,000 hp at 1,118 feet net head and 300 rpm. The six nozzles are supplied by a single spiral casing, comprised of eight steel castings. The largest, containing the number 1 nozzle, has an inlet diameter of 66 inches and weighs nearly 12 tons after machining. Diameter of each nozzle is $10^1/_2$ inches. The runner has 20 buckets, each $26^1/_2$ inches wide and weighing 550 lbs. They are bolted to a solid steel disc 6 inches thick. Outside diameter of this runner is $117^1/_2$ inches, pitch diameter 95 inches. Power is delivered to the generator by the 24-inch diameter turbine shaft.

The turbine is controlled by a Woodward-type governor which transmits the proper impulses through a conventional servomotor arrangement to a rockshaft linkage which actuates individual jet controllers of hydraulic piston type, one to each nozzle. Jet deflectors are provided to operate automatically in the event of sudden loss of load.

These units are believed to be the largest vertical impulse turbines ever built, and except for certain parts, were manufactured in Vancouver to design of a well-known American turbine manufacturing firm.

These units represent not only a forward step in impulse turbine design in point of size, but have broken new ground in the efficiencies obtained. Gibson tests run on number 2 unit after it went into service have indicated an efficiency as high as 92 per cent at 60 per cent load and efficiencies in excess of 90 per cent from 33 to 93 per cent of rated output.

Certain bucket trouble experienced on number 1 unit after nine months' operation and on number 2 after much less time was found to be due to faulty foundry work, which was remedied by the installation of new buckets.

Generators

The generators are rated 50,000 kva, 0.9 lagging power factor, 13,800 volts, 3-phase, 60 cycle, 300 rpm, 60-degree Centigrade rise and have class-B insulation. They are of conventional design; weight of both generator and turbine being supported by a Kingsbury thrust bearing with upper and lower guide bearings. They are totally enclosed with eight water coolers mounted on the periphery of the stator absorbing the generator heat loss from the circulating air. Facilities for a water spray controlled by a manually operated valve are provided for use in the event of fire developing in the windings. The main exciter, pilot exciter, and permanent magnet generator for operating the governor mechanism are located above the upper bracket and are direct connected to the generator shaft. Due to the comparatively high speed and small number of poles for waterwheel-driven generators of this capacity, the units occupy a floor space only 20 feet square, but the over-all height is 23 feet above the stator foundations. For the same reasons the efficiency is quite high, the manufacturer's guarantees being 97.8 per cent at full load, 97.3 per cent at three-fourths load and 96.4 per cent at one half load, all at 0.9 power factor lagging.

Stability studies simulating conditions on the system as a whole indicated that while the rest of the system was stable, being relatively closely coupled electrically, there was a tendency for Bridge River to swing out of synchronism during system faults, and for this reason a higher than normal short-circuit ratio was speci-

Figure 14. Elevation through switchyard

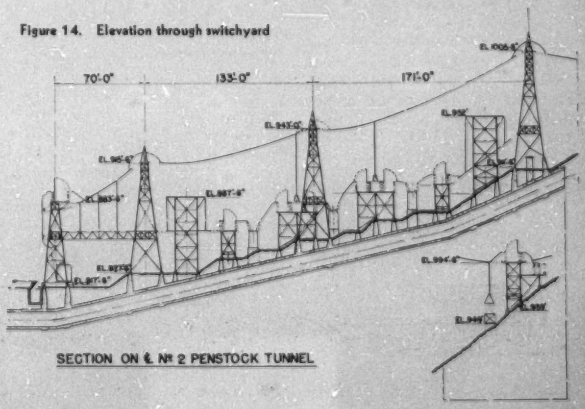

fied. Under initial conditions also, with only one transmission line, a greater spread in operating voltage was required, it being specified that each machine should operate satisfactorily over a range from 14.5 down to 11 kv. Prior to the installation of a synchronous condenser at the receiving station, this range of generator voltage was covered under normal operating conditions.

Design characteristics of the generators are as follows:

Synchronous reactance:	$X_d = 100$ per cent
Transient reactance:	$X_d' = 30$ per cent
	$X_q' = 53$ per cent
Subtransient reactance:	$X_d'' = 25.6$ per cent
	$X_q'' = 25$ per cent
Negative sequence reactance:	$X_2 = 25.3$ per cent
Short-circuit ratio = 1.18	
Calculated flywheel effect (WR^2) = 7,625,000 pounds times square feet	

The stator windings are Y-connected with the neutral fully insulated from ground. For ground detection in the windings, three special potential transformers arranged with grounded-Y primary, open-corner-delta secondary are connected to the line leads. The stator winding is in two parallels with six line and six neutral leads brought outside the machine, permitting the use of double primary current transformers with primaries in opposition for split-phase protection. Additional current transformers on the phase and neutral terminals are utilized for differential protection.

Indication and record of winding temperatures are obtained from 10-ohm resistors imbedded between coils in the stator slots.

The 24 pole rotors are conventional in design, with the pole pieces dovetailed into slots in a laminated rim which in turn is shrunk on a cast steel spider, the whole being designed for twice normal speed. Rotor diameter is 155¼ inches. Bearings are water cooled and equipped with temperature detectors which operate an alarm if the temperature of any bearing exceeds a predetermined value. Brakes are provided under the rotor designed to bring the unit to rest in 15 minutes after water has been shut off the turbines, although normally each unit is stopped by a jet of water projected onto the back of the turbine buckets. The brake mechanisms can also be utilized as hydraulic jacks to lift the rotor off the thrust bearing to permit adjustments or maintenance of the component parts of the bearing.

Figure 15. View of transmission line indicating rugged nature of country traversed

Each main exciter is rated 250 kw, 250 volts, and the pilot exciter 10 kw, 250 volts.

Figure 10 shows a cross section of the powerhouse through number 2 unit.

Transformers

Main transformers are 3-phase and match the generating units in capacity. Each is rated 50,000 kva, 13.8-kv delta to 230-kv Y with high-voltage neutral solidly grounded. The high-voltage winding has full capacity taps at 250, 240, and 220 kv and one of reduced capacity at 210 kv. Two forced-oil water-cooled heat exchangers per unit external to the transformer provide the necessary cooling, each cooler alone being capable of keeping the transformer in operation at three-quarter load. The heat exchangers are located below the transformers and the oil pressure inside the transformer normally is adjusted to exceed the water pressure, thus reducing the possibility of water entering the transformer in the event of a leak developing in the water piping.

These 3-phase transformers, complete with oil, weigh 171 tons each, both weight and dimensions being practically the maximum which could be transported to the site.

Switching and Control

Figure 12 is a 1-line diagram of the station. On the low-voltage side of the transformers it will be noted that a circuit breaker and a separate station service transformer are provided for each unit. The switchgear is of metal-clad type with an oil circuit breaker of 15 kv, 3,000 amperes, 1000-megavolt-amperes interrupting rating. The service transformers are 3-phase, 300 kva with load ratio control on the primary supplying 460 volts for the normal operation of all auxiliaries. Provision is made on the secondary side for synchronizing with the station service supply so that station service can be supplied from any generator or, alternatively, the auxiliaries of any unit can be operated from the separate station service supply, should this be required. The station

Figure 16. An indication of the transmission line maintenance problems

service supply is presently obtained through a 2,300/460-volt step-down from a small 4,000-kva hydrogenerating unit, which was installed some years ago adjoining the new plant for construction power and local service.

The main transformers are located in the switchyard behind the powerhouse. The leads from the low-voltage switchgear are 150 feet long in underground ducts and consist of two 2,500,000-circular mil lead-covered cables in parallel on each phase.

The high-voltage side of each transformer is connected through a motor-operated disconnecting switch to a 230-kv ring bus with four oil circuit breakers, as shown in the 1-line diagram, Figure 12. The insert in Figure 12 indicates present plans for the ultimate development when all ten units are installed, which makes provision for four outgoing transmission lines. At this stage two generating units through their individual transformers are connected to one position in the ring.

The 230-kv oil circuit breakers are operated by compressed air and rated 800 amperes with an interrupting rating of 3,500-megavolt-amperes and a fault clearing time of three cycles.

Protective Relaying

Each generator is provided with split-phase, differential, and overspeed protection with an impedance relay connected for stand-by. This relay has a double set of elements with each set supplied from a separate source of potential to prevent operation should potential in one set of elements be lost for any reason, such as blowing of a potential transformer fuse.

Each main transformer has phase-differential and ground-differential pro-

tection with an impedance relay for phase stand-by, also of the double element type, and an over-current relay for ground stand-by. A gas pressure relay is fitted into the cover of each transformer tank to disconnect the transformer from generator and line if an arc or explosion should increase the oil pressure rapidly.

For protection of the transmission line, impedance relays are installed on the phases and directional overcurrent relays for ground-fault protection controlled by carrier-current equipment of standard type which also blocks tripping of the line under out-of-step conditions. Overcurrent relays of the nondirectional type are used for stand-by ground protection. The respective relay zones are indicated by the dotted lines in Figure 12.

Figure 18. La Joie Dam under construction showing stream flow diverted through tunnels

TRANSMISSION LINE

The main feature of this line is the rugged nature of the country through which it passes which posed various access and construction problems. Leaving the power plant, the line follows the route of the Pacific Great Eastern Railway along the shore lines of Seton and Anderson Lakes westward, then up the Gates River Valley across the main divide of the Cascades and down the Birkenhead River Valley to cross the Lillooet River at Pemberton, then up the Green River Valley over a further divide in the vicinity of Alta Lake, down the Cheakamus River traversing the Cheakamus Canyon to tidewater at Squamish. After following the rugged shore of Howe Sound for some 10 miles it turns inland up Furry Creek to cross into the valley of the Capilano River, thence down that valley across the top of North Vancouver Municipality to the Second Narrows over Burrard Inlet to Vancouver City.

A total of 704 steel towers is utilized between the power plant and Horne-Payne Substation, the actual distance being 126.88 miles. The maximum and minimum spans are 2,500 and 192 feet respectively, with an average span of 960 feet. A right-of-way was acquired of sufficient width to accommodate a second circuit at a later date. Single-circuit towers have been utilized for the greater part of the route, therefore, on this initial line, except where it is not practicable to construct two parallel tower lines when double-circuit towers have been used. There are 49 such double-circuit towers at the Vancouver end of the line where it traverses built-up areas.

The conductor is a 795,000-circular-mil steel-reinforced aluminum cable utilizing 54 strands of aluminum on 7 strands of

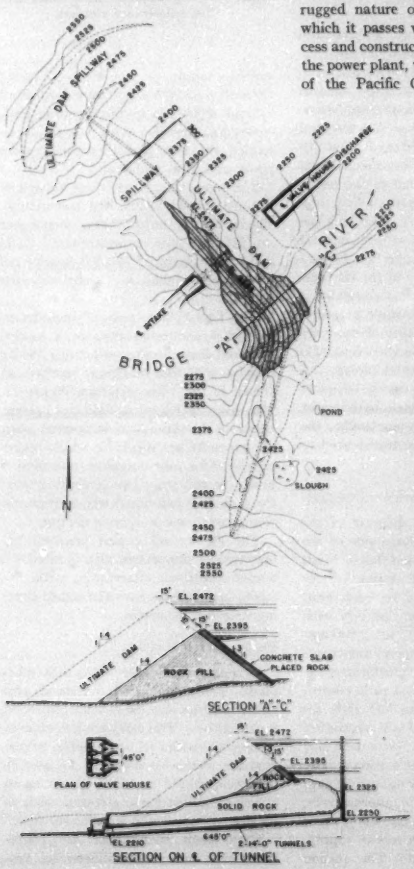

Figure 17 (left). Plan and elevation of La Joie Dam

Figure 19 (below). La Joie Dam under construction showing facing

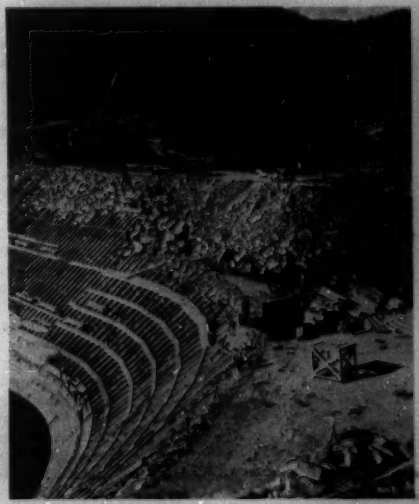

steel, and having an over-all diameter of 1.093 inches strung with a horizontal spacing of 26 feet. Transpositions at 6- to 12-mile intervals are relatively frequent, as the line parallels communication circuits along the Pacific Great Eastern Railway for the greater part of the route. Sixteen 11,000-pound insulator units are used per suspension string and sixteen 25,000-pound units for strain purposes. As lightning is relatively infrequent in the areas traversed, ground wires are installed for a short distance only at the power plant and receiving station.

Construction of the line was begun in June 1946 and completed in October 1948. To complete it in this time it was necessary to carry on tower erection all through the winter of 1947–48 in the face of all sorts of weather conditions. In spite of the close proximity of the railway from Squamish to the power plant, 142 miles of access roads were built in connection with its construction. Experience is presently being obtained with maintenance of the line; one of the various factors which has to be considered is the heavy seasonal precipitation in the coastal areas which not only results in rapid growth of brush and tree cover but frequently causes slides and swells the rivers and streams with resultant washouts of bridges and maintenance roadways. Keeping such roadways open in deep snow in some of the rugged narrow valleys also presents a problem. A helicopter is used regularly for inspection of the line and 4-wheel-drive jeep trucks for ground patrol.

Storage Dam at La Joie Falls

Reference was made previously to the high ratio of maximum to minimum flow of the Bridge River, making it necessary to provide storage facilities to operate the plant at the required load factor during the season of restricted runoff. For the initial stages of development, these storage facilities are provided on the upper valley of the Bridge River. After investigation of several sites, a storage dam was chosen at La Joie Falls, approximately 35 miles above the diversion tunnel intake.

The ultimate dam at this site will be approximately 275 feet in height above the original river bed, 3,500 feet along the crest with a width of 680 feet at the widest part of the base, and will impound 570,000 acre-feet of water. The extent of the ultimate dam is shown by the broken lines in both plan and elevations in Figure 17. The crest will be at an elevation of 2,472 feet.

The first stage contemplated for use with these generating units is shown in heavy lines in Figure 17 with a crest elevation of 2,395 feet. This is a rock-filled structure approximately 1,450 feet long on the crest, with maximum depth in the river bed of 200 feet, a maximum width on the base of 470 feet, and having a slope of the upstream face of 1.3-to-1, downstream face of 1.4-to-1. Foundation offers no problem at this site.

Preparatory work of erecting a camp and clearing the dam site was begun in June 1947. In September, excavation of the discharge channel for the diversion tunnels was commenced and was followed by excavation of an intake channel and the excavation of the spillway channel. Driving of the two parallel diversion tunnels began on March 9, 1948. These tunnels are 645 feet in length, driven 17 feet and lined to 14 feet inside diameter. At the outlet end, the last 72 feet of tunnel was lined with steel pipe one inch in thickness, which provides for a reduction in size from each 14-foot diameter tunnel to two 4-foot diameter Howel Bunger valves. The final reducer section from 10-foot diameter to 4 and the Bunger valves were not installed at that time, however, as it was later necessary to divert all of the spring runoff through the tunnels while the placing of the dam foundations in the old river bed was carried out.

At the intake end the foundation for a gate structure was built and this structure was raised in 10-foot lifts. After construction of a coffer dam 700 feet in length to a 2,284-foot elevation, the river was diverted on February 11, 1949, to the first tunnel and later to both tunnels as the runoff began to increase.

In the meantime, quarrying operations had been going on at a site about one mile northeast of the dam. This site had been chosen after study of the geological features of the area as the best source of a suitable supply of rock fill for the dam. To obtain this rock, which is an augite diorite, it was necessary to build 7,000 feet of roadway suitable for heavy traffic between quarry and dam site. Wastage from the quarry was utilized to a very considerable extent for this purpose.

As it was essential that some storage be provided for the 1949–50 winter season the work of placing the rock fill was pressed during the spring and early summer months. As originally designed, the dam was to be sealed on the upstream side by a reinforced concrete paving keyed into the foundation rock at the toe of the slope. However, a timber facing was substituted for the concrete facing, which substitution was considered desirable in view of the fact that facing would have to follow immediately on the rock fill without any time for settlement. The timber sleepers for this facing were placed vertically, the facing planks 4 by 12 inches were placed horizontally in two layers with lean concrete placed between the sleepers to provide support for deck planking, and underneath, where the unevenness of the rock fill required it.

Storing of water commenced in mid-August 1949, and for the next six weeks the water level rose steadily, following closely on the placing of the facing. On October 23, all work was suspended. Rock fill had been placed to a 2,370-foot elevation, involving in all some 572,000 cubic yards; the intake concrete was completed to an elevation of 2,370 feet and the dam capable of storing water to an elevation of 2,365 feet. Maximum water level was reached on December 20 at a 2,356-foot elevation.

Preparations are being made to recommence operations and a decision recently has been made to increase the height of the dam to beyond the 2,395-foot elevation visualized in the stage indicated in Figure 17 to permit storage of water to an elevation of 2,405 feet. This may call for some revision of the plans in so far as the location of the spillway is concerned, and will require increasing the spillway height above the planned 2,380 feet of the initial stage.

Future Development

The raising of La Joie Dam to its ultimate level of 2,472 feet to provide 570,000 acre-feet of storage will coincide with the installation of units Number 4 and 5 at the Bridge River Plant. These units can be accommodated by the present diversion tunnel through Mission Mountain, but will require construction of additional transmission facilities to the load area.

For the next stage a second diversion tunnel as large or possibly slightly larger than the existing one to supply units 6 to 10 will be required. The storage required for year-round operation of these units will be provided by the lower storage dam previously referred to. Choice of a final site for this lower storage dam has not been made, although considerable study has been given to the subject.

A location almost immediately below the present diversion dam has much to offer in that the canyon walls would lend themselves to a dam of relatively short crest length, but there exists the foundation problem referred to in connection with the diversion dam. Experience with this present dam during the next several years will doubtless aid in

assessing the foundation requirements of a higher dam at this point. Another possible site exists two miles farther down the river, but such is the fall in the river bed that to obtain an equivalent amount of storage would necessitate a 130-foot higher dam. A site above the intake also has been given some study. As the valley is considerably wider in this locality, however, a dam of considerably greater volume would be required and there would be a sacrifice in ultimate head on the plant at Seton Lake.

In so far as transmission is concerned, as noted previously, the switching structure at the plant is laid out with space provision for four outgoing circuits. There are three possible routes for the three additional circuits. At some stage a second line will be built on the route of the existing line, as this is the shortest route to the load area. Two other routes remain, one eastward along Seton Lake and Seton Creek to the Fraser River and down through the Fraser Canyon to the Lower Fraser Valley; the other westward, paralleling the existing line as far as Pemberton, then south paralleling Lillooet Lake and Lillooet River and via Harrison Lake to the same termination. Studies of the various factors involved have not been carried sufficiently far at this time to determine whether both or only one of these routes will be utilized.

Conclusion

A few words with regard to the system of which the Bridge River Development forms a part may be of interest in concluding this paper. The total generating capacity on the British Columbia Electric Lower Mainland system now is 313,600 kw in six hydroelectric plants. Two additional projects are presently under development, a Number 3 unit of 35,000 kw at Ruskin on the Stave River, and the replacement of seven small units in the Buntzen Number 1 plant with a new 50,000-kw unit, the combined effect of which will be to increase the system peaking capability to 377,600 kw by October 1951.

Since mid-1949, surplus power above system load requirements at a monthly rate of 15,000,000 kilowatt-hours or more has been transmitted to a group of other member utilities of the North West Power Pool over a 230-kv interconnection from Vancouver to Arlington, Wash.

No Discussion

Hydroelectric Generator Excitation Experience at Grand Coulee

C. L. KILLGORE
MEMBER AIEE

N. G. HOLMDAHL
MEMBER AIEE

THE Grand Coulee Power Plant located in central Washington is the largest concentration of hydroelectric generating capacity in the world, having a presently installed capacity of 1,316,000 kw and an ultimate capacity of 1,974,000 kw. This plant is being built and operated by the Bureau of Reclamation as a major feature of the Columbia Basin Project.

The Grand Coulee Power Plant differs from most modern hydroelectric plants in that only 12 of its 18 108,000-kw main units have direct-connected exciters, while the other six, which are to be used to drive 12 65,000-kw synchronous pump motors as well as to furnish commercial power, have separate motor-driven exciters. Since these six main units have exciters whose motors are driven by two 10,000-kw station-service generators, the problem of loss of generator excitation is an important consideration. This paper covers the experiences obtained from consideration of the original power layout for these exciter motors and the development of the final plans for insuring the power supply to these motors. It also covers experiences with loss-of-field relays and excitation under heavy load rejections.

Motor-Driven Exciters

The 6,900-volt station-service system consists of two 10,000-kw station-service generators feeding into a complete 6,900-volt double-bus system with double breakers for all generators and all feeders. The feeder breakers are controlled so that only one breaker can be closed at a time unless the busses are paralleled through a generator breaker. In that case both feeder breakers can be closed momentarily in order to transfer a feeder from one bus to the other. The exciter motors for generators *L-1* through *L-6* are fed from the switchgear. In the early years of operation when these six units were the only ones installed, or, even now, when they still form a major portion of the generation, loss of excitation on the units constituted a major outage, not only to this plant but usually to the Northwest Power Pool, of which this plant forms a part. Because of this potential hazard to the system, considerable study was given to the problem of insuring the power supply to the exciter motors. Station-service generator differential relays were moved to a location where there was little chance of accidental tripping. Also, the control system was changed so that the exciter feeder breakers would automatically transfer from one 6,900-volt bus to the other in case of loss of potential on the feeder. This scheme offered protection should a bus fault or failure of the station power source occur, or should a feeder breaker fail to clear. As the exciter motors are synchronous, across-the-line starting, and rated at 600 horsepower and 6,900 volts, considerable experimenting was done to determine the effect of dropping the loaded exciter from one bus and picking it up on another. This automatic transfer was tested under variable conditions of main generator load, the results of which are shown graphically on Figures 1, 2, 3, and 4. Figure 1 illustrates the effect of transferring the exciter motor without any load on the exciter, while the others show the effect with various conditions of load on the main generators.

The following information is pertinent to the proper interpretation and evaluation of the oscillograms. Under normal starting of the exciters, the machine is closed in on the 6,900-volt system with the motor field short-circuited. The machine comes up to a speed as an induction motor, and after a predetermined length of time necessary for the pilot exciter voltage to build up (about 13 seconds), the motor-field circuit breaker is closed, connecting the pilot exciter output to the field of the motor. The motor pulls into synchronism with a minimum of disturbance upon the application of the field. The high motor current on the oscillograms for such a long period, after closing the unfaulted breaker and then the reduction to the initial valve, is caused by the machine being run as an induction motor for about 13 seconds before application of the field.

It will also be noted that the exciter-motor voltage does not exhibit rapid decay until about ten cycles before the motor is closed-in on the opposite bus. This is caused by the motor operating as a synchronous machine with its field breaker still closed until the undervoltage relay operates and trips the breaker connected to the faulty 6,900-volt bus. This action in turn trips the motor field thereby causing it to act as an induction generator rotated by the kinetic energy of its rotor.

From the oscillograms, it was determined that an exciter motor-generator set could be removed from one power source and closed in on another without requiring removal of the main generator from the system. The controls on the exciter sets were then changed to incorporate this feature on all of the six units containing motor-driven exciters.

However, this arrangement was not entirely satisfactory as the control circuits were somewhat complicated because a number of control switch and relay contacts are required to operate in

Paper 50-137, recommended by the AIEE Power Generation Committee and approved by the AIEE Technical Program Committee for presentation at the AIEE Summer and Pacific General Meeting, Pasadena, Calif., June 12–16, 1950. Manuscript submitted March 13, 1950; made available for printing April 10, 1950.

C. L. KILLGORE is with the Bureau of Reclamation, Denver, Colo.; N. G. HOLMDAHL is with the Bureau of Reclamation, Coulee Dam, Wash.

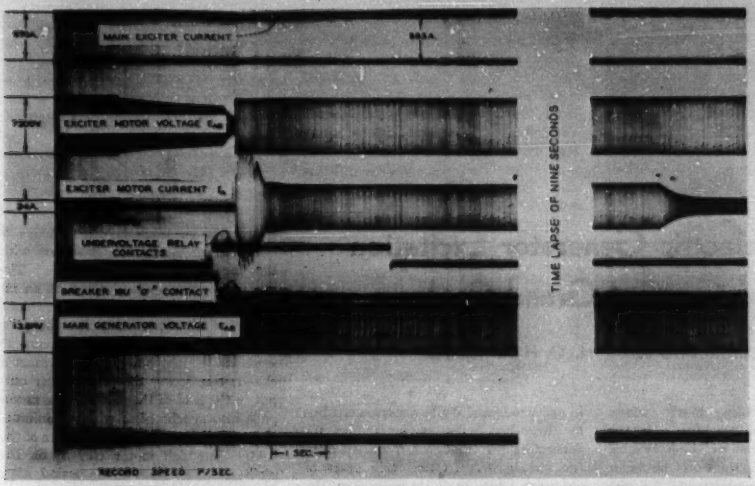

Figure 1. Automatic transfer of *L*-5 exciter motor from upstream to downstream station-service bus with zero load on main unit, Grand Coulee Power Plant

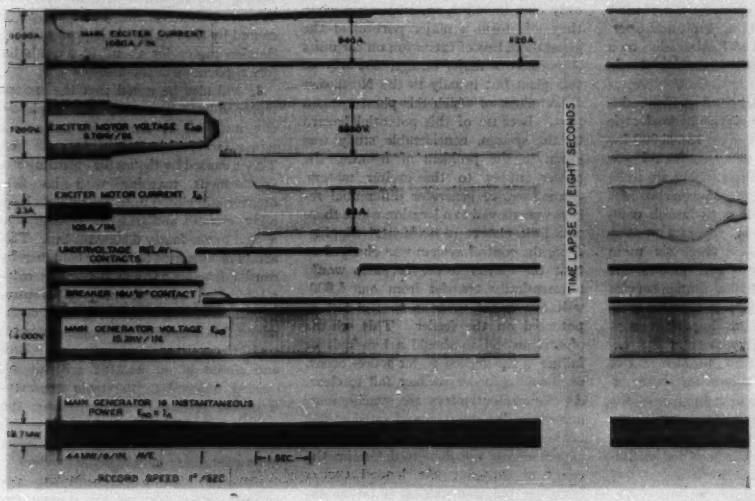

Figure 2. Automatic transfer of *L*-5 exciter from upstream to downstream station-service bus with 25-megawatt load on main unit

the correct sequence. Then, too, the problem was affected by the decision to install a ring bus for all main units at Coulee[1] and by plans to install the third 10,000-kw station-service generator for commercial and local power. The ring bus affected this problem because the system was designed so that ultimately a loss of one 230-kv bus section (three units and two transmission lines) would not cause instability on the system. Under that condition, the loss of three exciters together with the loss of their three associated generators would not be as serious as it was when these units formed the major portion of the plant's capacity. The addition of the third station-service generator to the plant also eased the loss-of-excitation problem because it added another source of supply for the exciter motors and thereby decreased the probability of loss of power source. By using the surplus power from these generators for local and commercial use, some additional hazard was added because of the connection of the station-service system to the main transmission system. This additional hazard was partially compensated for by having two additional power sources in case of loss of the station-service generators. As a protection against the main system speed swings, an over-and-under-frequency relay will be

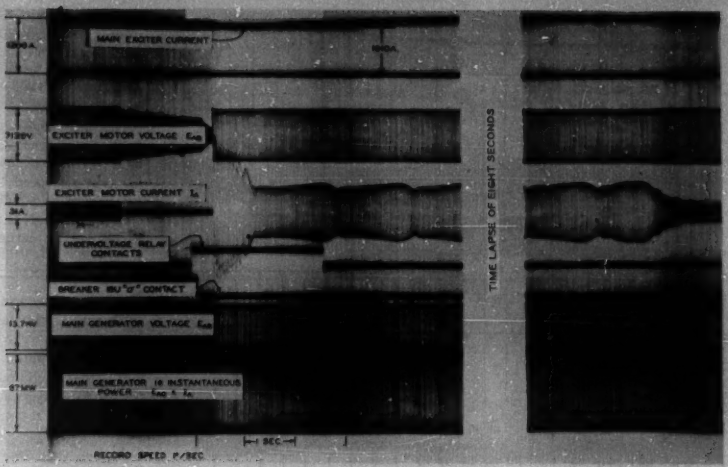

Figure 3. Automatic transfer of *L*-5 exciter motor from upstream to downstream station-service bus with 104-megawatt load on main unit

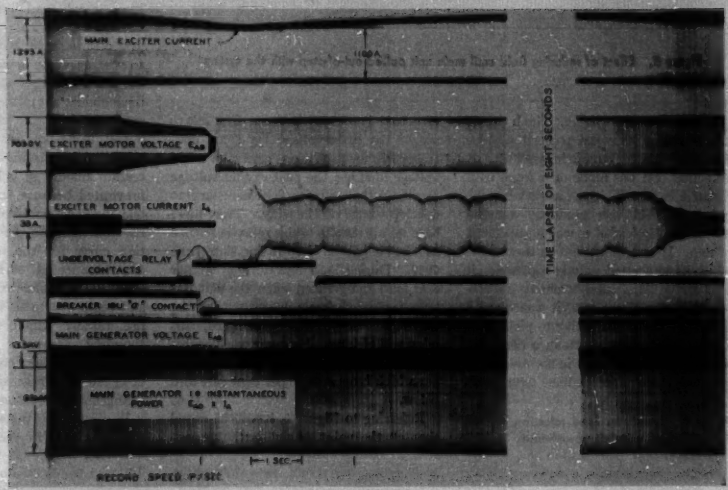

Figure 4. Automatic transfer of *L*-5 exciter from upstream to downstream station-service bus with 129-megawatt load on main unit

installed on feeders *0* and *23*, which connect the station-service bus to the main transmission system, so that the main power system and the station service will be separated in the event of any major system speed fluctuation. The third station-service unit, together with the autotransformer banks for transmitting the excess power, are scheduled for installation in 1950. In the meantime, both busses are operated in parallel with both generator breakers closed, with three exciters on each bus, and with the automatic transfer in operation.

Loss-of-Field Relays

As originally designed, the Grand Coulee units were equipped with differential relay protection only. It was foreseen that the loss of field on a main unit would cause the unit to go out of step as the field decayed, resulting in some voltage disturbances as well as producing large currents in the damper windings and field windings of the generator rotor. Such a condition might continue for an appreciable length of time before the unit was either removed from the system or the field restored, thereby causing considerable damage. System disturbances from such loss of field might be serious if it occurred at time of heavy loads. It was to protect against these possibilities that loss-of-field relays are being installed on all main units. In order to in-

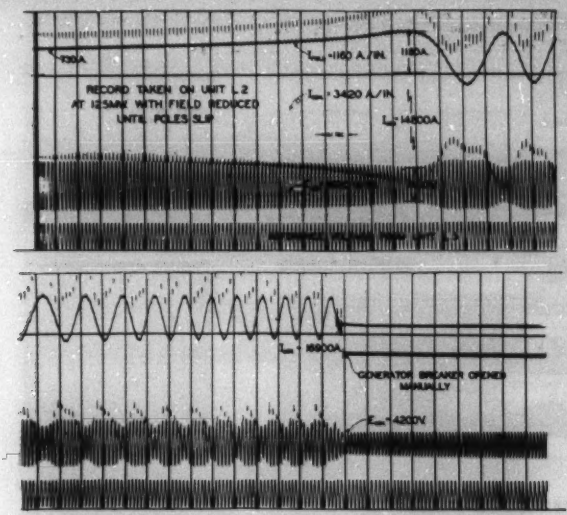

Figure 5. Effect of reducing field until main unit pulled out-of-step with the system

stall a loss-of-field relay, which would trip a unit if the field reached a value where it could not remain in synchronism, an actual test was made on a main unit. Figure 5 is an oscillogram made when the generator field was gradually reduced until the fully loaded machine pulled out of step. It was found that on these units which have a rated voltage, open circuit field current decreased to about 700 amperes. From these data, it was decided to set the loss-of-field relay to pick up at 800 amperes of field current, a condition which should not be met in normal operation unless there are extreme overspeeds or actual loss of excitation. The relays are of the undervoltage type, are controlled from the main generator field voltage, and use the pilot exciter voltage to set up the opposing field necessary to develop torque on the relay. There have been no operations of this relay in service as it has only been in operation since June 1949. During load rejections of 75 per cent load and greater, when the unit has been separated from the system or the unit is free to go over rated speed, this relay will pick up. However, such operation is blocked by a contact on the governor which is open at 20 per cent gate and below.

Referring to Figure 5, it will be noted that at the point of pull-out, the generator voltage was reduced to 7,400 volts from a normal of 13,800 volts, and the generator current increased to 14,800 amperes from a normal of about 5,200 amperes.

Experience with one unit with non-connected damper windings, when its field was lost while carrying full load, indicates that the unit will reach about 25 per cent overspeed before the governor can recover and reduce the wicket gate opening and turbine output to the value which can be carried as an induction generator.

Generator Voltage Regulation During Disturbances

During the initial test period of each unit at the Grand Coulee Plant, a series of tests of load rejections were made to determine the operation of the governor, the pressures developed in the penstock due to hydraulic surges, and the operation of the voltage regulating equipment. Rejections of full load during such tests and during commercial operation cause the generator voltage to rise considerably and to reach a value some 30 per cent above the rated voltage. Although this rise in itself should not cause any undue harm to equipment in first-class condition, this overstressing of insulation should be eliminated or reduced if possible. A certain amount of voltage rise cannot be prevented because, as soon as the electric load is removed, the voltage will rise to a point on the open-circuit saturation curve for the machine. Also, for direct-connected exciter machines, the speed of the pilot exciter, main exciter, and main generator rotors will begin to rise rapidly which will cause a corresponding generator voltage increase. Voltage-regulation equipment should be designed to compensate for these voltage changes within reasonable limits.

Recently, the installation of a Silverstat regulator in the pilot exciter field

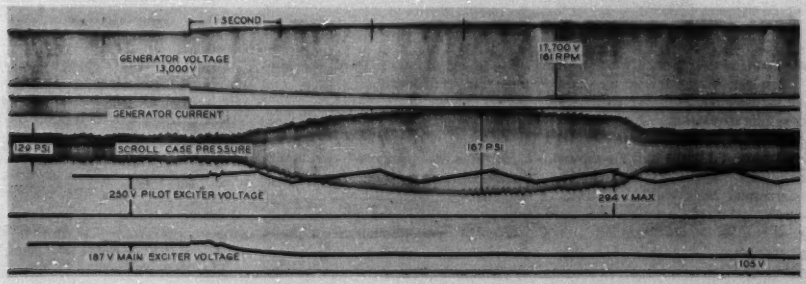

Figure 6. Maximum load rejection test on main unit, left powerhouse

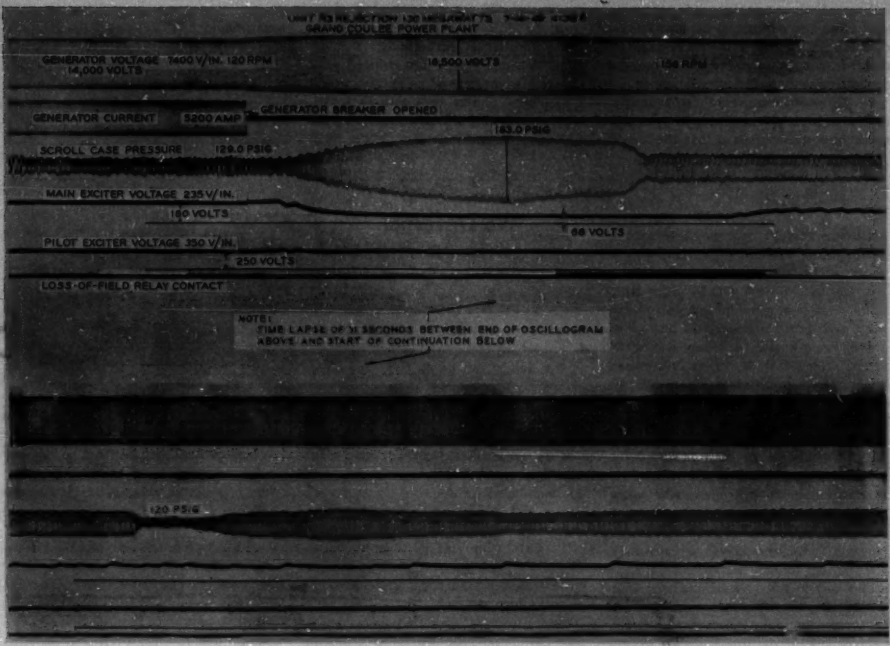

Figure 7. Maximum load rejection test on main unit, right powerhouse

has caused the pilot exciter voltage to remain practically constant during system disturbances as can be seen by a comparison of the traces shown in Figures 6 and 7.

Figure 6 shows load rejection of a unit which has the normal type of pilot-exciter voltage regulation, namely, an overvoltage relay which inserts a block of resistance in the pilot exciter field at a predetermined pilot exciter voltage. The repeated operation of this relay accounts for the zig-zag shape of the pilot exciter voltage trace. Figure 7 is a test on a similar unit but has a continuous step regulation of the pilot exciter field. Practically uniform pilot exciter voltage is maintained throughout the various speed changes of the unit. This factor helps to reduce the peak of the main generator voltage by reducing the amount of pilot exciter voltage available to supply excitation to the main exciter. In each case the unit was separated from the system while carrying a load of 130 megawatts. The generator voltage rises immediately to the open-circuit saturation curve, and then gradually rises further as the rotor speed increases due to the time required for the turbine gates to close from wide open to the speed-no-load point. The time for such operation is four seconds. However, as soon as the voltage rises over 0.5 per cent, the main exciter rheostat control on the voltage regulator attempts to bring the voltage back to normal.

At two per cent above the rated voltage the high-speed lowering contact on the regulator operates to insert a block of resistance in the main exciter field. This action accounts for the first step in the main exciter voltage after separation from the system. The high-speed lowering relay then remains energized continuously until the voltage is reduced to about ten per cent above normal when intermittent operation begins.

From analysis of tests made to date on three units with the overvoltage relay-type of pilot exciter voltage control against the continuous regulation type of control, it appears that peak voltages have been reduced about 1.5 kv to a maximum of about 16.5 kv. However, the peak voltage reached will depend upon the amount of excitation just prior to the loss of load.

Analysis of these oscillograms also indicates that the main exciter voltage reduces to a practically constant value during the overspeed, which condition is believed to be caused by the resistance controlled by the high-speed lowering regulating relay not being large enough to further reduce the main exciter voltage.

It is planned to run further tests on this phase during load rejections on a future machine. Additional resistance will be inserted in the main exciter field in an attempt to further reduce the main exciter voltage and thereby reduce the generator terminal voltage. However, it does not appear that the peak voltage will be reduced very much because of the time necessary to operate the generator voltage regulator and the time necessary for the main generator field to decay.

Summary

1. Experience with the motor-driven exciter at the Grand Coulee Power Plant

indicates that automatic transfer of power sources to the motor can be successfully done under full load by removing the motor from a faulty power source and reconnecting it to another power source.

2. However, experience also indicates that the best protection is to provide sufficient power sources so that the loss of one source will not cause the loss of excitation.

3. Additional pilot-exciter voltage-regulation equipment has reduced peak voltages on the generators approximately 1.5 kv on a 13.8-kv base with the possibility of reducing this still further by the addition of more resistance in the high-speed lowering relay circuit in the main exciter field.

Reference

1. Development of the 230-Kv Ring Bus for Grand Coulee Power Plant, N. G. Holmdahl, C. L. Killgore. *AIEE Transactions*, volume 67, part II, 1948, pages 1369–81

No Discussion

Expansion of the System of the Southern California Edison Company

A. A. KRONEBERG
FELLOW AIEE

THE BEGINNING of the Southern California Edison Company's system may be traced back to 1893 when two 250-kw 2,200-volt generators were installed for local use near Redlands, Calif., approximately 75 miles from Los Angeles. From this small beginning the company expanded to become one of the ten largest privately-owned electric utilities in the United States. The company's system serves directly some 75 incorporated cities and 150 unincorporated communities and outlying rural territories. It also supplies electric energy to four municipalities for redistribution and to other utilities on a wholesale basis. The territory served includes large areas devoted to farming and fruit growing, which are made possible by irrigation. Among the more important industries served are those engaged in the production and refining of oil, production of motion pictures, fruit packing, the manufacture of cement, rubber tires, chemicals, airplanes, oil-well equipment, automobiles, and the production and fabrication of iron and steel. In addition, the company serves two electric railway systems operating in and around the city of Los Angeles.

The expansion of the company's system is the direct result of population growth in southern California. Figure 1 shows this growth of population in the present service area of the company during the first half of the twentieth century. Population figures for 1900, 1910, 1920, 1930, and 1940 were obtained from the Federal census reports and are accurate. Population figures for other years were estimated on the basis of average daily attendance records of school districts. It may be noted that the population approximately doubled during each decade except during that from 1930 to 1940. This rapid growth of population is due to immigration and was but temporarily retarded by the depression of the 1930's. The primary effect of the population growth is an increase in the number of customers. One metered service is required for every three people. Thus it is estimated that by the end of 1950, the company will be serving a population of approximately 3,000,000 through nearly 1,000,000 meters. The per capita use of energy also is showing a growth which, although adversely affected during the decade of 1930–1940, resulted in a net increase from 1,600 kilowatt-hours in 1920 to more than 2,500 kilowatt-hours in 1949. Figure 2 illustrates the total annual energy use in the service area of the company.

The maximum demand upon the generating facilities of the company also has grown at a comparable rate. However, a substantial improvement in annual load factor took place concurrently with expansion of the system. This improvement is due to greater diversification of energy use. From an estimated 40 per cent in the early years of the system's growth, the annual load factor improved to 50 per cent in 1920, to 60 per cent in 1930, and to 65 per cent in 1949. Figure 3 illustrates the maximum demand in the service area of the company.

Generating Capacity

Two alternatives are available to the company in providing generating capacity for supplying this rapidly growing load. One is the continuation of the development of the upper San Joaquin River which is known as Big Creek, and the other is the construction of steam-electric plants at the load. A brief review of the development of the major generating sources follows. The development of the upper San Joaquin River was begun in 1913 with 64,000 kw of hydroelectric generator capacity in powerhouses number 1 and Number 2. From then until 1928, the chain of Big Creek powerhouses was increased to five with nearly 400,000 kw of generating capacity. The plans of development at that time contemplated an ultimate project of 18 powerhouses, totaling approximately 1,070,000 kw of capacity. Operating experience of 1924, the year of minimum water resources in the history of the Southern California Edison Company, demonstrated the need of balancing hydroelectric developments in California with steam-electric plants of no less capacity than 40 per cent of the hydroelectric plant capacity. The rapid improvement in steam plant economy during the decade from 1920 to 1930, and the concurrent decline in price of fuel in southern California, caused the company to defer, in 1928, the further development of the Big Creek hydroelectric project. Revised plans at that time contemplated the construction of the Long Beach Number 3 Steam Plant which was designed for an ultimate capacity of 800,000 kw. The business depression of the early 1930's halted this development after two 100,000-kw units had been completed and placed in operation. With the older steam plants in operation on the system, this addition provided 465,000 kw of steam plant capacity to be combined with a total hydroelectric capacity of 493,000 kw in operation at Big Creek and in miscellaneous river flow plants on the system of the company in 1931.

In 1939 the company began receiving power from the Hoover powerhouse of the United States Bureau of Reclamation.[2] Under the terms of various con-

Paper 50-138, recommended by the AIEE System Engineering Committee and approved by the AIEE Technical Program Committee for presentation at the AIEE Summer and Pacific General Meeting, Pasadena, Calif., June 12–16, 1950. Manuscript submitted March 3, 1950; made available for printing April 10, 1950.

A. A. KRONEBERG is Senior Electrical Engineer with the Southern California Edison Company, Los Angeles, Calif.

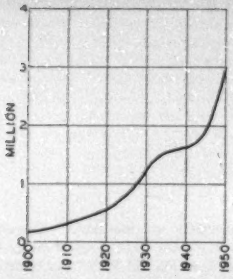

Figure 1. Population in the territory served by the Southern California Edison Company

tracts with the Bureau of Reclamation, the company operates a part of the powerhouse as an agent of the government, and receives and pays for energy allocated to it. In addition, the company is entitled to receive and pay for 40 per cent of energy allocated to but not used by certain other allottees, and is entitled to receive and pay for 40 per cent of surplus energy (secondary). The maximum capacity of the portion of the Hoover powerhouse connected to the system of the Southern California Edison Company directly and through the transmission system of the Metropolitan Water District of Southern California is 465,000 kw.

The additions of generating capacity to the company's system since 1945 include gains in capacity of old generating units due to the change of system frequency from 50 to 60 cycles,[4] the addition of a 35,000-kw unit at Big Creek Number 3, the addition of Redondo Steam Plant having an operating capacity of 280,000 kw, and the construction of Big Creek Number 4, now under way, which is expected to add 84,000 kw to the 1,730,000 kw of capacity in operation on the company's system on January 1, 1950. For planning purposes, this installed capacity must be discounted by: (a) hydroelectric capacity rendered idle by deficiency of river flow; (b) hydroelectric capacity rendered idle because of shortage of water in storage reservoirs; (c) generating capacity removed from service for maintenance and repair; (d) prudent reserve. The remaining capacity is the capability of the system in a dry year and must be expanded to remain equal to the expected maximum demand of the load.

Transmission System

The transmission system of the Southern California Edison Company is an interconnection of 220-kv transmission lines linking the Big Creek hydroelectric plants, the Hoover powerhouse of the United States Bureau of Reclamation, and the steam plants.[1] Two 106,000-kw 60-cycle steam-electric units at the Long Beach Steam Plant Number 3 are directly connected to the 220-kv transmission lines.[2] All other steam-electric units are connected to 66-kv subtransmission systems which in turn are connected to the 220-kv system through 220/66-kv transformers. Figure 4 is a map of the company's transmission system showing existing plants and lines, authorized plants and lines under construction, the 220-kv line of the Metropolitan Water District of Southern California, and the service area of the company.

This transmission system evolved from the two parallel 150-kv 240-mile transmission lines constructed in 1913 for transmitting Big Creek power to Southern California. At the time these lines held the distinction of being the longest lines in the world and of being operated at the highest voltage. In 1923, following the lead of the Pacific Gas and Electric Company, the voltage of these lines was changed to 220 kv, the towers were raised to provide added clearance to ground, insulators were added, and 220/150 kv autotransformers were connected at the terminals to maintain connections with existing equipment. The load-end terminals of the lines were connected to a grid of 66-kv transmission lines interconnecting the distribution substations of the company. With the growth of the system, the duty on 66-kv oil circuit breakers exceeded their interrupting capacity and many explosions and station fires occurred from time to time. This led to the adoption in 1928 of the fundamental principle underlying the planning of the system and its operation.

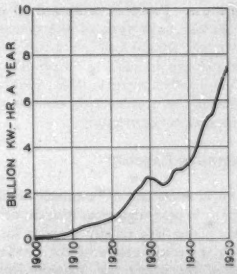

Figure 2. Energy generated for use in the service area of the Southern California Edison Company

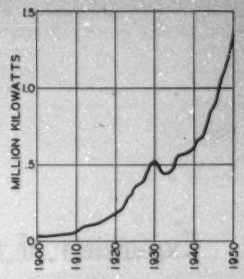

Figure 3. Demand on generators in the service area of the Southern California Edison Company

This principle is the establishment of a "backbone" transmission system from which a number of subtransmission systems are supplied through 220/66-kv transformer banks. Except for having only the 220-kv system as a common source of supply and having some emergency 66-kv tie lines to adjacent systems, each one of these subtransmission systems is independent of the other. From some four such systems originally obtained by splitting the 66-kv grid into sections, the number of subtransmission systems and areas served by them has increased to 13. The number of major substations supplying subtransmission systems has increased from three in 1924 to 12 in 1949. The purpose of this is to limit to 225,000 kva the capacity of 220/66-kv transformers operating in parallel to a short circuit (12 per cent impedance). The effects of system growth upon the interrupting duty of circuit breakers and the resultant program of modernization and replacement of circuit breakers are confined to the 220-kv transmission system by this method of expansion and system operation.

The capacity of each 220-kv transmission line is nominally 200,000 kva, but the normal loading is not in excess of 165,000 kva for reasons of stability of operation. The system is planned for operation near 75 per cent of the steady-state stability limit when all the equipment is in service. Coupled with the program of modernization of circuit breakers, this makes the system stable during all but the most severe 3-phase short circuits that occur on the system. It also is possible under this method of loading to remove from service occasionally, sections of line for repairs and rebuilds without curtailing generation. In addition to the 12 transformer substa-

tions, three switching stations are provided at the approximate mid-points between the three major sources of generation. The purpose of these stations is to limit the length of line sections to a maximum of 140 miles for stability reasons and to provide facilities for high-voltage interconnections with other systems.

Distribution

The term "distribution" in its broader meaning includes subtransmission systems, transformer substations, high-voltage distribution lines, primary distribution lines, line transformers, and secondaries. Each of these groups of system equipment must be expanded at approximately the same rate as the expected growth of load to maintain the established standards of service, quality, and continuity, to retain existing margins in load carrying capacity and thus to be prepared for sudden local load increases, and to provide for safety of employees and the public.

Figure 5 presents a diagrammatic summary of capacity of transformers interconnecting the various groups or systems of the Southern California Edison Company as reported on January 1, 1950. Some 1,190 megawatts of generating capacity is connected directly to the 220-kv transmission system. From the 220-kv transmission system, power is delivered to the 13 subtransmission systems through 220/66-kv transformers totalling 1,750 megavolt-amperes. The excess of step-down capacity over the capacity of generators is due in part to seasonal diversity of load in the various subtransmission systems and in part to capacity required to interconnect local generation with the 220-kv system, and to provide standby for this generation from the 220-kv system. Included in the subtransmission group is a small 33-kv system which is an extension of one of the 66-kv systems through autotransformers totalling 60 megavolt-amperes.

From the several subtransmission systems, power is delivered directly to ten large industrial customers, to one municipality for resale, to primary distribution systems (4 and 7 kv), and to high-voltage distribution systems (11 and 16.5 kv). The total stepdown capacity of 1,900 megavolt-amperes indicates a diversity of 1.1 in relation to the total generating capacity of 1,730 megawatts, and a diversity of 1.52 with respect to the "net" system peak of 1949, the latter being the demand in the service area of the company only. Approximately three-fourths of the stepdown capacity from the subtransmission systems is to high-voltage distribution. The high-voltage distribution systems are divided into two voltage groups. The service area within 50 miles of the Pacific Ocean and to the west of the 220-kv transmission system is served at 16.5 kv; while all the remaining area is served at 11 kv. Approximately one-third of the transformer capacity connected to the high-voltage distribution systems is installed at distribution substations stepping down to primary distribution voltage (4 kv). The other two-thirds of transformer capacity are supplying customers directly through customer substations or through line transformers. The prevailing arrangement of all distribution systems is that of radial feeders with occasional loops and double line arrangements when serving larger distribution substations. Primary distribution is used in cities and towns. A total capacity of 1,030 megavolt-amperes of transformers is installed at substations supplying primary circuits. Some 1,260 megavolt-amperes of line transformers supply customers from the primaries, indicating a diversity of 1.22 in primary distribution systems. The over-all annual efficiency of the system is 85 per cent. It has been raised slowly to this value from 80 per cent in 1929.

Reactive Power Supply and Demand

When power is transmitted through the inductive circuits of a power system, there is created a demand for reactive power which is similar to the real power losses in the system. Such a demand also is created in customer's equipment beyond the meter. This demand is in part composed of the magnetizing current taken by ironclad machines such as transformers and induction motors, and in part of the I^2X loss in series impedances. This demand must be supplied from sources of generation of reactive power in much the same manner as real power is supplied from generators. The company long ago abandoned the use of power factor meters as a means of control of reactive flow and instituted the metering and dispatching of reactive power on its system. The chief source of generation of reactive kilovolt-amperes on the system is synchronous condensers, operating on the 66-kv busses of the major substations. At the conclusion of World War II, the synchronous condenser capacity at the major substations was deficient by some 200 megavars (mvar) because no additions could be made during the war. Because of this deficiency, the required reactive power had to be generated on power generators and on frequency changers. To do so required operation of transmission lines on voltage gradients much steeper than originally intended, and operation of transformers on taps of

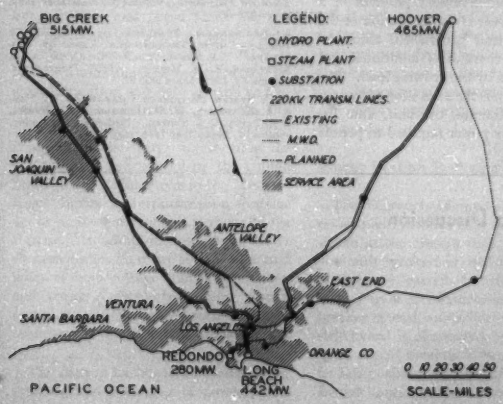

Figure 4 (left). Transmission system of the Southern California Edison Company

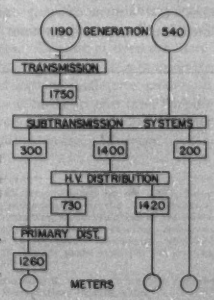

Figure 5 (right). Summary capacity diagram of the system of the Southern California Edison Company

Figures in circles—megawatts

Figures in boxes—megavolt-amperes

lowest ratio. To remedy this shortage of reactive capacity, the following programs were undertaken:

1. A program of installing each year approximately 50 mvar of static capacitors on distribution lines was begun in 1947. As reported on January 1, 1950, 170 mvar have been installed on distribution lines and on substation busses. Installation of 50 mvar has been budgeted for 1950.

2. An increase in capacity of existing synchronous condensers was obtained incident to conversion from 50-cycle to 60-cycle operation. The initial total capacity of 583 mvar was thus increased to 674 mvar.

3. A total of 120 megavolt-amperes of frequency changer capacity was released following conversion of the system from 50 to 60 cycles. The net gain in synchronous-condenser capacity resulting from uncoupling the frequency changers has been 228 mvar.

4. Four synchronous condensers have been purchased for installation at major substations. Of the total 220 mvar ordered, one 60-mvar machine has been installed and placed in operation. The remaining three machines are in various stages of construction.

The system demand of reactive power in 1949 is estimated in round figures to consist of the following: (a) customer demand beyond meters—450 mvar; (b) magnetizing requirement of all transformers operating on the company's system—270 mvar; (c) series losses in subtransmission lines, distribution lines, and transformers—400 mvar; (d) series losses in 220-kv transmission lines—360 mvar; (e) series losses in generator transformers and 220/66-kv transformers—200 mvar. The total demand was approximately 1,680 mvar.

To supply this demand the company had the following: (a) synchronous condensers—962 mvar; (b) a frequency changer normally operated as a condenser, but retained as an emergency connection for three 50-cycle machines at Long Beach Steam Plant Number 1—60 mvar; (c) 170 mvar of static capacitors; (d) 400 mvar charging capacity of 220-kv lines; (e) 70 mvar charging capacity of lines in subtransmission systems.

Table I. Supply and Demand of Reactive Power on the System of the Southern California Edison Company in 1949

	Megavars
Generating Capacity	
Hydro plants	90
Steam plants	280
Synchronous condensers	1,022
Static capacitors	170
220-kv transmission lines	400
66-kv transmission lines	70
Total available	2,032
Demand	
Customer demand	450
Transformer magnetization	270
Distribution loss	400
Transmission line loss	360
Generator and 220-kv transformer loss	200
Total demand	1,680
Planned Additions to Generation	
Synchronous condensers	160
Static capacitors	50
Fourth Big Creek 220-kv line	65
Total addition	275

The above supply capacity totals 1,662 mvar. In addition to the capacity of facilities for direct generation of reactive power, the real power generators are capable of delivering some reactive power to the system without overload. Thus 90 mvar may be obtained from hydroelectric plants, and 280 mvar from steam-electric plants, bringing the total available capacity up to over 2,000 mvar. Table I illustrates the supply and demand of reactive power on the company's system. Therefore, it may be concluded that the company has overcome the post-war deficit in reactive generating capacity, has kept pace with the growth of reactive demand, and has provided for the growth of reactive demand during the next two or three years.

Conclusion

The first and foremost problem of a planning engineer is the expansion of the system to permit generation, transmission, and distribution of additional real power required by the growing load. The second problem is the expansion of system facilities to generate, transmit, and distribute reactive power required to permit transmission of real power. The supply of reactive power is inseparable from the problem of proper voltage control on the system. Voltage control of the company's system is exercised at three points along the route from generator to the customer meter. First, voltage is controlled at the generator terminals by well-known methods of excitation control. The second point of control is on the 66-kv busses of major substations. Tap changers under load are provided on nearly all 220/66-kv transformer banks, and synchronous condensers are installed at nearly all major substations. Voltage at generating stations and at major substations is maintained in accordance with established schedules, usually ranging from 69 kv during the day to 65 kv at the time of minimum load. The third point of voltage control has been brought as near as practicable to the customer using voltage-sensitive equipment. The 4-kv primary circuits are equipped with voltage regulators compensated beyond the feed point of the circuit, that is, the point where the circuit branches off in all directions.

The problems of relay protection and system operation are not a planning engineer's direct responsibility. However, the system he has planned must be operable and protectable. For this reason the planning of the system of the Southern California Edison Company has always stressed simplicity. A simple system is easy to operate, it is easy to protect, and in the long run, it is easy to expand.

References

1. Master System Planning, N. B. Hinson, H. W. Tice. *Electrical World* (New York, N. Y.), 1931, pages 384–88.

2. Switching at Long Beach Plant Number 3, A. A. Kroneberg, O. R. Bulkley, W. A. Andree. *Electrical Engineering*, volume 52, December 1933, pages 826–30.

3. Engineering Features of the 230-Kv Boulder-Chino Transmission Line of the Southern California Edison Co., Ltd., A. A. Kroneberg, E. M. Hunter. *AIEE Transactions*, volume 59, 1940, pages 982–87.

4. A System Frequency Change, H. W. Tice, A. A. Kroneberg, W. N. Johnson, J. D. Enofer, E. E. Tugby, C. L. Sidway. *Electrical Engineering*, volume 67, September 1948, pages 866–81.

No Discussion

Relaying Practices and Economical Switching Station Arrangements of the Bureau of Reclamation

W. A. MORGAN
MEMBER AIEE

R. W. WORLD
ASSOCIATE AIEE

THE high-voltage transmission systems serving the western half of the United States are characterized by longer line sections between substations than is common in the eastern half, where the population density is greater. The relaying of the power systems of the Bureau of Reclamation, United States Department of the Interior, presents, therefore, somewhat different problems than usual. It is the purpose of this paper to describe some of the relaying schemes used by the Bureau and the philosophy underlying them.

The Bureau has designed and constructed power plants having 3,054,400 kw of hydroelectric generating capacity, and 3,997 miles of transmission lines of nominal voltages from 33 to 230 kv. The generating units are as large as 108,000 kva, and the first power plant was put into operation in 1909. At most plants, the electric energy is made available as part of a multipurpose project which includes irrigation and flood control as mutual benefits. In recent years, the Bureau has also been designated as marketing agent for the energy developed at the power plants constructed by the United States Corps of Engineers in the Missouri River Basin, and transmission systems are being designed for this purpose by the Bureau. In addition, throughout the 17 western states, there are several thousand miles of high-voltage transmission lines, and many hydroelectric power plants, pumping plants, and substations under construction or authorized at the present time.

The Bureau has several isolated power systems, and a number of power plants interconnected with large power systems owned and operated by others. The transmission voltages are 230 kv, 161 kv, and 115 kv, in general, while the distribution voltages are 115 kv, 69 kv, and 34.5 kv. On some systems, the 115-kv lines are functionally transmission circuits, while on others the 115-kv lines serve as distribution circuits, as there are small substations connected to the lines without high-voltage circuit breakers. It is not economical to have a standard practice for such a diversified group of electrical installations. One of the objectives in Bureau power system designs is the obtaining of maximum amount of power system for the last expenditure. This is accomplished without jeopardizing the protection of equipment. So, in some designs, it has been recognized that transformer faults and high-voltage bus faults are a rare occurrence, and it is not worthwhile to try to sectionalize for such faults to prevent an interruption to service. However, when service reliability is paramount, two busses or the equivalent are used.

Power Station Relaying Practice

The diagram in Figure 1 shows a typical power plant arrangement as might be designed at the present time. A minimum of circuit breakers is used in the interest of economy, current transformer circuits are not transferred when the spare circuit breaker is used, and a line position in the switchyard is eliminated by putting the spare circuit breaker in one of the transfer bus positions of a transformer circuit. In this case, the spare circuit breaker is provided with a set of line relays connected to its bushing current transformers, and the relays may be used for any of the circuits by adjusting the settings. The spare circuit breaker is put in a transformer circuit position because of the low probability of transformer or generator faults, as a fault in the transformer circuit when the spare breaker is being used for a line circuit would interrupt both circuits.

Arrangements without a low-voltage bus for generators have been used at a number of the large power plants. Separate transformer and generator differential relays are always provided to gain the advantage of more sensitive and faster protection for the generator. Often the generator differential relay zone is overlapped by the transformer differential relays if the current transformer arrangement can be simplified by doing so. Standard-speed induction-type ratio differential relays almost always are used for both the transformer and generator differential relays, instead of high-speed relays requiring special methods of adding restraint to prevent tripping on inrush transients and heavy faults external to the protected zone. The standard speed relays are usually sufficiently fast to coordinate with 15-cycle time delay of remote line relays.

Experience has shown that the relays have operated properly for all major faults in station equipment and it is believed that backup protection against equipment faults is unnecessary in attended stations. The individual relay elements provide backup to each other as, usually, a heavy fault will pick up the relays in at least two phases. The use of overcurrent relays as backup protection is undesirable since a setting that is effective under fault conditions is likely to give false tripping under overloads, remote faults, or other system disturbances. However, gener-

Paper 50-140, recommended by the AIEE Relay Committee and approved by the AIEE Technical Program Committee for presentation at the AIEE Summer and Pacific General Meeting, Pasadena, Calif., June 12–16, 1950. Manuscript submitted February 20, 1950; made available for printing April 10, 1950.

W. A. MORGAN and R. W. WORLD are both with the Bureau of Reclamation, Denver, Colo.

ator overcurrent relays are provided where necessary to protect otherwise unprotected zones resulting from use of current transformers for differential protection that do not overlap the circuit breaker, or where it is impractical to have differential protection on the station bus.

At smaller plants, the transformer differential zone sometimes includes the station service transformer, which is given no other protection. This, of course, is not selective protection but is considered adequate if a solid fault at the low-voltage terminals draws fault current in excess of relay operating current. At larger plants, separate differential protection or fuses are provided for the station service transformers. Thermal devices in the main generator and transformers are connected to give alarm only. Protection against overload is at the discretion of the plant operator.

The high-voltage main bus invariably is given differential protection with induction-disk overcurrent relays having short-time characteristics. These simple relays have been found satisfactory for reasons similar to those given for simple transformer protection. Linear couplers or other special bus differential relays are being considered for 230-kv busses where fault currents are unusually high, but, so far, calculations have shown that they are not required to prevent false operation and their advantage would be to give faster relay operation, if obtainable at no additional cost, complication or loss of reliability.

Bus differential relaying becomes complicated where the bus may be sectionalized and it is desirable to obtain selective tripping for all operating arrangements. In these cases, it has been thought desirable to find a way of omitting bus protection. A ring bus, as shown in Figure 2, is one way of eliminating the need for bus differential relaying where there are only a few circuits. The ring bus requires less switchyard space than a double bus. The ring bus may be more applicable to a load substation than a power plant switchyard, because the need for keeping the ring intact in order to retain proper selectivity in clearing faults has resulted in low-side generator circuit breakers at one power plant where the ring bus will be used. Also, the 3-winding transformer type of transformer differential relay has been found necessary since the maximum fault current through the high-voltage current transformers is large compared to the rated current of each generating unit.

Station-service power for large power plants such as Hoover, Grand Coulee, and Shasta, has been furnished by two or more relatively small hydroelectric generating units normally operated as a system entirely separate from the main generating units. However, at the smaller power plants, and in the designs of recent fairly large plants up to 300,000 kw in capacity, station power is obtained usually from the main power system by some variation of the scheme shown in Figures 1 and 2. An electrical interlock prevents paralleling the two generators through the station-service system, and, by means of undervoltage relays, load is automatically transferred from one generator to the other.

At some power plants with the unit system, the high-voltage bus differential relays are connected to shut down the generating units in addition to tripping all high-voltage circuit breakers; see Figure 3. This is necessary in order to protect the zones between current transformers located in the transformer bushings and circuit breakers and is considered preferable to the addition of other relays for the sole purpose of protecting these zones.

At power plants using the unit system but serving two transmission systems at different voltages, it has been our practice to furnish 3-winding transformers for some or all of the generating units. A disconnecting switch for each generator connected to a 3-winding transformer permits transfer of energy between the two transmission systems when the generator is not running.

The arrangement shown in Figure 3 is the result of a practice that has developed of avoiding the transferring of current transformer circuits in taking a circuit breaker out of service. A system of utilizing the spare circuit breaker in the transfer bus position by automatically transferring the trip circuit is used to economize on double circuit breakers. For example, if one of the line circuit breakers were to be taken out of service, the auxiliary switches, operating when that particular line transfer bus disconnect switch is closed, will connect the trip circuit for the line relays so that they would trip the circuit breaker in the spare or transfer bus position. Sufficient current transformers are provided so that no switching of current transformer secondary circuits is necessary. This usually requires wound-type current transformers in each line. However, an extra line position in the switchyard is avoided for the so-called bus-tie or spare circuit breaker, and, of course, double circuit breakers are not required.

Another arrangement which eliminates the necessity for transferring current transformer circuits without the expense of a full double circuit breaker installation is shown in Figure 4. In this case, the current transformers provided with the oil circuit breakers are utilized wherever possible and wound-type current transformers are installed in the vacant oil circuit breaker positions. This arrangement is used at Grand Coulee Power Plant where the cost of 230-kv 10,000,000-kva interrupting capacity circuit breakers made it desirable to consider a modification of the double circuit breaker arrangement.

The unit system has been used at a number of the large power plants with a trend toward 3-phase unit transformer banks where the physical size is within transportation limitations. Ground

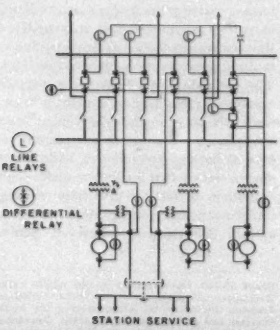

Figure 1. Typical busing arrangement for a power plant using a minimum number of circuit breakers

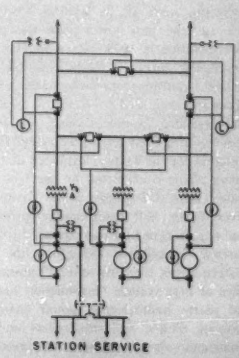

Figure 2. Ring bus for a power plant using a minimum of circuit breakers; is applicable where there are few circuits

faults in the generator voltage system are detected by a voltage relay energized from a potential transformer or distribution transformer connected between generator neutral and ground. When a distribution transformer is used, a secondary resistor provides an in-phase component of fault current roughly equal to the reactive component due to capacitance to ground. This method of grounding the generator neutral is used where selective tripping of circuits for ground faults is not required. In some existing plants the older installation of a potential transformer between each generator neutral and ground has been replaced with a distribution transformer with secondary resistor. All new power plants of the unit system will have this method of neutral grounding, which gives less transient overvoltage than an isolated neutral or potential transformer. With either method, the detection of a ground by means of a voltage relay is the same, and the current at the fault is of the same order of magnitude, much too small for the operation of differential relays. Originally, in many of the power plants, the ground detector relays gave only an alarm but lately have been reconnected to trip the circuit breaker and shut down the unit the same as for a differential relay operation. The ground detector relay is usually of the induction type set to pick up for grounds down to 10 per cent of the generator winding at the neutral end. Tripping the unit off, instead of giving alarm only, permits using a sensitive relay without need for protecting the relay against a continuous overvoltage. Although Figures 1, 2, and 3 show the unit system of a transformer bank for each generator unit, actually the Bureau has many power plants where two or more generators are connected to a single transformer bank. Sometimes these generator busses have circuits connected to them for serving local communities or station service. In power plants having generator-voltage busses where selective tripping is required for ground faults, the generator neutrals are grounded through neutral circuit breakers and reactors which limit fault current in generator windings to a value slightly less than a 3-phase fault current.

Transmission Line Protection

The 3-zone type of distance relay is used for protection against multiphase faults on nearly all transmission lines of 115 kv and higher voltage and also on lines of lower voltage where there is insufficient difference between maximum load current and minimum fault current to permit the use of overcurrent relays. Both the conventional distance relays and long-line type of distance relays having phase-angle discrimination are used as required. As a general rule, the conventional type is preferred because of the faster speed of operation wherever the long-lines type minimum ohms would require a current transformer ratio that was higher than required by load current. On 115-kv lines, it has been calculated that line lengths usually must be in excess of 100 miles before the long-lines type distance relay should be considered.

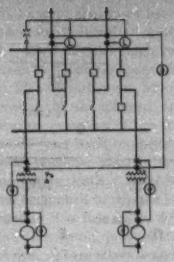

Figure 3. Use of wound-type current transformers in line circuits

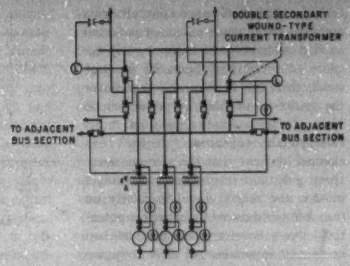

Figure 4. Use of wound-type current transformers in transfer bus position

Carrier-current pilot relaying with terminal circuit breaker arranged for reclosing in 20 cycles is usually applied to all transmission lines rated 115 kv or greater. Distance-type carrier relaying is usually more applicable on our systems than the current phase-comparison type since fault currents are in general too small for a good application of the latter. The simplicity of the current phase-comparison relaying scheme has certain advantages and an attempt to apply it to Bureau systems is made wherever possible. However, so far we have found only one 80-mile 230-kv line sections where carrier relaying and fast reclosing circuit breakers were required and where the fault currents were high enough to allow the application of current phase-comparison relays. Other 230-kv lines on this system will have distance-type carrier. The backup relays on the line with phase-comparison relays will be distance relays and product-type induction-disk ground relays. It is expected that experience with this line will indicate whether current phase-comparison relays will have greater application on Bureau lines in the future.

Some of the special relay characteristics required for long high-voltage lines were described in a previous paper.[1] The high frequency residual current transient that is likely to occur when a long transmission line is energized is of sufficient magnitude and duration to cause undesirable operation of carrier-current ground relays. However, a transient shunt has been developed which allows only 60-cycle current to enter the ground fault relay, and this has obviated this difficulty without increasing the relay operating time.

The Bureau's practice has been to install capacitor potential devices for relaying instead of potential transformers wherever there is a saving in initial cost, except where potential transformers are required for revenue metering. Capacitor potential devices have a cost advantage at 115 kv and higher voltages, and also at 69 kv if coupling capacitors are to be furnished for carrier-current purposes. The problem of adjusting the devices has been solved by use of apparatus for compensating for the reactance drop in power transformers under load conditions and comparing the output of the capacitor potential device with the compensated voltage from a low-side potential transformer.[2] Where it is convenient to unload the power transformers, reactance drop compensation is unnecessary.

Bus potential is preferred for the restraint for distance relays and is provided for this purpose at substations having a single main bus. In double-bus arrangements where either bus may be de-energized while the other bus serves the transmission lines through the same sets of protective relays, it is believed that line potential is preferable to the complications of switching between bus potentials. With automatic reclosing circuit breakers, the use of line potential may result in failure to trip or in slow tripping after reclosing on a close-in permanent fault. Mechanical interlocks are provided between line disconnecting switches and line grounding switches to prevent operating errors from causing faults. Al-

though standard distance relay elements are sensitive to small values of potential so that probability of failure to trip because of insufficient potential is quite small, there has been some concern over the omission of backup protection in view of the possibility of solid faults close to the substation. It has been claimed by some that the extreme sensitivity of distance relays has disadvantages in that the relays may trip falsely on transients introduced by capacitor potential devices; however, the Bureau has had no direct experience of false tripping from this cause.

The Bureau has been operating three separate 115-kv systems protected by ground-fault neutralizers without overhead ground wires. However, on two of these systems the transformer neutrals now are being changed to a solidly grounded connection, and the ground-fault neutralizer coils will be salvaged. At the same time, overhead ground wires are being installed on the 115-kv transmission lines; and on some of the line sections carrier-relaying and 20-cycle reclosing circuit breakers are being added. The ground-fault neutralizers have been effective in clearing about 80 per cent of the total number of faults on the 115-kv lines so protected, leaving about six faults per 100 miles per year to be cleared by relay action. On 161-kv lines with overhead ground wires for which records are available, the number of faults has averaged about 0.5 per 100 miles per year.

The tapping of 115-kv and lower voltage lines is common practice with the Bureau since in most such cases there is only one long line traversing the area. Tapping that line is the only economically feasible method of serving loads at intermediate points, and transmission lines of this voltage sometimes serve as "Distribution" lines. The current phase-comparison type of carrier relaying cannot be readily applied to tapped lines because an extremely high minimum pickup current is required. It is considered essential that all types of faults should be protected against, including 3-phase faults at the end of long lines.

Tapping of transmission lines gives rise to a number of relaying problems with regard to reclosing terminal circuit breakers in 20 cycles, especially where the circuit fed from the tap has an appreciable amount of connected synchronous machine capacity, either small local generators or irrigation pump motors. Available data indicate that a current as small as 5 amperes fed to the fault on the 115-kv line from a tap on the line may delay the deionization sufficiently to prevent successful reclosure. Relaying with primary currents of this magnitude would be difficult where normal load current is several times as great. One possibility is that of using undervoltage relays at the tap substation, but for completely reliable relaying such a scheme would require transmitting a continuous carrier-blocking signal from one of the main terminals. Besides the disadvantage of not being able to use the carrier channel for other purposes, there would be complications in preventing false tripping in the event that carrier failed.

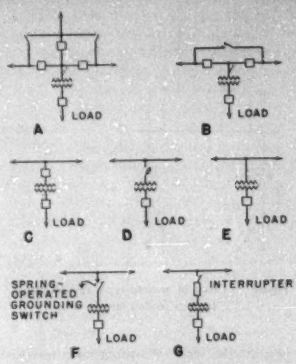

Figure 5. Arrangements at small substations

Studies indicate that sequential tripping is the fastest that can be obtained with current actuated relays for most lines tapped with synchronous machinery loads, and reclosing times in excess of 20 cycles must be accepted in these cases.

Transmission lines that are merely feeders to isolated loads are not furnished with carrier relaying. Such lines usually have circuit breakers arranged for automatically reclosing three times. Where the line may be energized from the load, undervoltage relays energized from line potential are provided to assure that the line is de-energized before reclosing.

Ground relays of the distance type are being considered for circuits which require fast clearing of all faults but which for some reason do not permit use of carrier relaying. One example is a transmission line including a section of high voltage cable in which the attenuation is too great for a good application of a carrier-current relaying channel. Distance ground relays may also be advantageous where one of the line terminals at times has an ungrounded neutral, but for this application the relays must be of a type that is actuated by the total current in the faulted phase rather than the zero-sequence component.

Line protection is provided at a station which does not have high-voltage circuit breakers by means of low-voltage current transformers and capacitor potential devices connected to the high-voltage side of the transformers. This arrangement is preferred because it allows a greater percentage of the line to be protected by first zone of the distance relays, while still protecting the transformer bank at the station. If the power transformers have load ratio control or equivalent, the effective current transformer ratio is a variable and must be given special consideration in setting the relays.

The Bureau has applied transformer impedance drop compensators for adapting low-voltage potential sources to distance relaying of transmission lines. In accordance with the manufacturer's recommendation, the compensators are adjusted to compensate for only 90 per cent of the voltage drop in the power transformers, in order to assure against overcompensation which would cause incorrect directional element operation for close-in faults. In calculating the relay settings, a correction is made for the error in the compensator caused by the potential circuit burden of the relays. Since the compensators are no more accurate than the distance relays themselves, we have found that there is nothing gained in using compensators where the power transformer carries the total fault current, for it is just as effective to omit the compensators and include the transformer impedance as part of the impedance of the protected line section. Where the transformers carry a variable major fraction of the fault current fed from the station, a first-zone setting based on the calculated minimum value of this fraction has proved satisfactory without resorting to transformer drop compensators.

In some installations where relay coordination is quite simple, three zone elements of distance relays are available for protection of the line itself without need of providing backup protection against faults in adjacent sections, and settings have been used which assist in the location of the fault by means of relay target indication. Though this method of setting the relays gives an unnecessarily short reach to the first-zone element, the second- and third-zone time settings can be quite fast.

Induction-disk relays operated from the residual line current are provided on all lines of solidly grounded neutral systems for protection against ground faults. These relays are directional if this feature

is required, usually polarized by transformer neutral current. Either the product-type or directional overcurrent-type of directional ground relay is used, depending on which best suits the station design. Where the line current transformers are low-ratio bushing type, the lower burden of the product-type ground relay is preferred. However, at the larger power plants it has been found that the large number of product-type ground relays has placed an excessive burden on neutral current transformers, and the directional overcurrent type would be preferred. It has been calculated that co-ordination can be obtained with either type of relay, but the product type is more difficult for the man in the field to calculate.

Substation Protection

The arrangement of the substations varies with the size and importance of the loads, and the number of high-voltage circuits terminating there. Thus, the arrangements shown in Figures 1, 2, and 3 for power plant switchyards also apply to the larger receiving substation switchyards. However, Figure 5 shows seven arrangements that are more generally used for load substations of about 30,000 kva or less in capacity.

In Figure 5(A) and 5(B), the transformer differential relays trip all of the circuit breakers for either transformer or bus faults. It is believed that the omission of the transformer circuit breaker on the high-voltage side is justified in most cases by the infrequency of transformer faults. No spare circuit breaker is provided, since a line circuit breaker can be removed for maintenance after a by-pass switch is closed between lines. This type of by-pass is preferred to a by-pass switch between bus and line, since transformer differential protection can be retained and the two transmission lines can be relayed as a 3-terminal line. Figure 5(C) shows a method frequently proposed as an alternative to 5(B) for an unimportant load served from an important transmission line. Reliable transformer protection is still furnished while saving one high-voltage circuit breaker, but the line must be relayed as a 3-terminal line. However, if the transformer capacity is relatively small without a grounded high-side neutral and if the load feeds back no fault current to line faults, this substation can be practically ignored in setting the line relays at remote terminals, and no line relays need be provided at this substation. The arrangement in Figure 5(D) has been used quite extensively. It is the same as 5(C) except that fuses have been substituted for differential protection to save the cost of the high-voltage circuit breaker. There has been some opposition to high-voltage fuses by operating men because of unexplained operations and because operation of one fuse causes the transformer bank to operate single-phase with possible damage to synchronous machinery loads. Phase-balance relays can be applied to trip the low-side circuit breaker if a fuse blows for any reason, and thus would prevent damage to machines. These relays would detect an unbalance in current or voltage or both, depending on the characteristics of the connected loads. The elimination of all transformer protection at the substation as shown in Figure 5(E) seldom is used except on radial lines terminating in transformers. Distance relays at the source terminal must be set to reach low-voltage faults at all load substations, and good protection and relay co-ordination are possible if the reach is approximately the same to low-voltage 3-phase faults at all substations. A carrier-current transferred-tripping scheme for transformer protection could be used with the arrangement shown in Figure 5(E), but our experience with this type of protection has not been good as it has been found difficult to prevent false tripping. Figure 5(F) has been applied when it is desired to force operation of line relays at the terminals. Here a spring-operated grounding switch protects the transformer against internal faults by means of differential relays and also protects the transformer against overheating as a result of carrying sustained ground-fault current to line

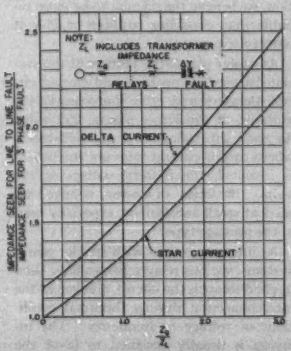

Figure 6. Loss of relay reach for line-to-line faults on far side of delta-Y transformer bank as compared to 3-phase faults upon which calculations are usually based

faults when the neutral is grounded. The neutral current relay must have sufficient time delay to allow the normal operation of remote relays to clear the fault. The grounding switch protects the transformer adequately, but has the disadvantage of causing an interruption to service on the line. Figure 5(G) makes use of a 3-phase interrupter disconnecting switch for removing the transformer from the lines where the fault duty is 500,000 kva or less. The interrupter is new and the Bureau does not have any in service as yet. Its cost is less than that of a circuit breaker and it has operating advantages over fuses by being 3-phase in operation, and over grounding switches because it would not disrupt service on the transmission line. Its use appears promising where the interrupting duty is low enough to allow its application.

The high-voltage switching at these substations influences the choice of whether or not to ground the high-voltage neutral of the substation transformers. In Figures 5(A) and (B) with a Y-connected high-voltage winding, grounding the transformer neutral is definitely desirable, since relaying of faults on the transmission line would be improved. In 5(C), (D), (E), (F), and (G), the opposite is true from a relaying viewpoint even though common practice is to ground the neutral in order to save the cost of increased transformer insulation. Figure 5(D) is particularly objectionable and is never used in protecting a transformer having a grounded high-voltage neutral. We have one transformer installation at a line tap where the neutral of the Y-connected high-voltage winding is ungrounded in order to permit use of fuses and, by increasing ground fault current at the main terminals, to improve the carrier relaying required for simultaneous tripping and 20-cycle reclosing of circuit breakers. With a grounded neutral at the tap, the arrangement shown in Figure 5(C) is generally used and the transformer circuit breaker is arranged to be reclosed immediately after tripping for a line fault. Figure 5(G) would be less objectionable than 5(F) for a grounded-neutral transformer bank, since an operation of the neutral current relay would cause an outage on the tap circuit and not on the line itself, assuming that the main terminal circuit breakers were immediately reclosed and the fault was transitory.

At the larger and more important substations that are main junction points in a high-voltage network, a circuit breaker is furnished for each circuit including transformer circuits, and the bus is protected by differentially-connected over-

current relays separate from the transformer protection. Complete reliance is placed in the differential relays. Backup protection provided by distance and residual current relays at near and remote terminals of transmission lines is incidental and, in many cases, incomplete since it is believed desirable to avoid setting high-voltage line relays to reach into low-voltage power systems connected to the substation. The relaying on these low-voltage systems is usually of the time-delay overcurrent type, making co-ordination difficult especially where the low-voltage system is owned and operated by a customer. The problem of securing complete transformer backup protection by line relays is further complicated because of the mutual impedance effect if the substation is fed fault current from more than one transmission line.

At some of the substations of line taps, calculations have shown that fuses would be slower than the primary transmission-line distance and ground relays in clearing either high-voltage or low-voltage transformer faults, and the fuses have been omitted with reliance being placed on the terminal relays. Since with delta-Y transformer connections the transformer blocks the passage of zero-sequence current, the ground relays for the transmission line will not provide any protection against low-voltage faults, and consequently such faults must be cleared by the distance relays. If the transformers are Y-delta or delta-Y connected, which gives a phase shift, the reach of the distance relays will be greater for 3-phase faults than for line-to-line faults on the low-voltage side. This is usually not appreciated by the relay engineer. As indicated by the curve in Figure 6, the difference in the reach for the two types of fault is a function of the ratio of the impedance from internal machine voltage to relay location to the impedance from the relay location to the fault. It is apparent that the second- or third-zone elements of the relays must be given a long reach in order to give complete protection against all types of transformer faults, especially if some allowance is made for impedance at the fault and for part-winding faults. Consideration also must be given to maximum load currents in order to prevent false tripping with the longer setting required to reach low-voltage line-to-line faults. Careful calculations must be made, therefore, if transformers are to be protected by the line relays at remote terminals, but the protection has been considered adequate for new transformers as a temporary expedient at substations where ultimately a high-voltage circuit breaker and differential relays will be provided.

At important unattended substations it is planned to provide automatic reclosing of line circuit breakers and to provide supervisory control of all circuit breakers and of some motor-operated disconnecting switches. Where necessary, dead-line-check voltage relays and synchronism-check relays are used with the automatic reclosing; but on feeder circuits where these check relays are not needed, the reclosing relay recloses the circuit breaker three times before locking out. Where carrier relaying and 20-cycle reclosing are provided, either the slower type reclosing or the supervisory control is usually omitted, but one of these methods is available for reclosing the circuit breaker after clearing transitory line faults when carrier relaying is out of service.

At small substations where the cost and maintenance of a battery cannot be justified, current transformer tripping is the preferred method for tripping the circuit breakers for multiphase and close-in ground faults on feeder circuits. For remote ground faults drawing current too small to operate a current trip coil, an alternating current shunt trip coil is furnished, energized from a line-to-line potential of a potential transformer or station service transformer. A line-to-line potential will not be reduced by ground faults as much as a line-to-neutral potential might be reduced. Three circuit-opening overcurrent phase relays and one circuit-closing overcurrent ground relay are furnished for each feeder. If calculations indicate that this scheme will protect against all faults in the protected section, we believe the scheme to be more reliable than capacitor tripping or 24-volt battery tripping.

At power plants the voltage of the station battery for opening and closing circuit breakers and other purposes is 125 volts or, at the larger plants, 250 volts. At main substations and any substation where carrier-current relaying equipment is installed, the battery voltage is 125 volts. Batteries of lower voltage are used at small substations, especially ones of the package type.

At interconnections with smaller power systems, various relay schemes have been applied to open the circuit breaker at the interconnection during abnormal conditions of voltage or frequency. The relaying is usually designed to favor the smaller of the two interconnected systems because it is undesirable for small generators to attempt to supply the loads or charging current on the long high-voltage lines. Automatic tripping of the circuit-breaker is desirable only if there is high voltage or an excessively low frequency accompanying a reversal of power to the smaller system. Simultaneous pickup of a reverse power relay and an underfrequency relay is a definite indication that opening the interconnection would improve the frequency on the smaller receiving system. The Bureau has used instantaneous overvoltage relays to protect generators on the small power systems against becoming self-excited while charging the high voltage transmission line. Where a sudden overvoltage can result without reversal of power flow or increase in frequency, there is usually no need for interlocking with other relays. Overvoltage relays, which are used for protection against overvoltage resulting from overspeeding of hydroelectric generators when a major part of the load is suddenly dropped, must have frequency compensation.

Conclusions

1. Economies in switching arrangement at power plants and receiving substations may be made by omitting unnecessary high-voltage circuit breakers and taking advantage of the infrequency of transformer and high-voltage bus faults.

2. Transfer of line protection to the spare circuit breaker may be accomplished automatically without transferring current transformer circuits with possible false tripping.

3. Equipment may be adequately protected against all types of faults with a minimum of circuit breakers and relays and give adequate service reliability and dependability.

References

1. Relaying Difficulties Disclosed by Staged-Fault Tests, **W. A. Morgan, Byron Evans.** *AIEE Transactions*, volume 67, part I, 1948, pages 73–82.

2. New Instrument Adjusts Capacitor Potential Devices, **Ferber R. Schleif.** *Electrical World* (New York, N. Y.), volume 128, number 7, August 16, 1947, pages 74–75.

Discussion

Eric T. B. Gross (Illinois Institute of Technology, Chicago, Ill.): This paper is a valuable contribution to the art of protective relaying since it describes the practices used in a number of large systems at various voltages and because simplicity seems to be one of the guiding principles in the selection of appropriate protective schemes.

I am wondering if "gas and pressure protection" has been considered for relatively small transformers where differential protection is far too expensive. Gas-alarm relays are also helpful to supplement differen-

tial protection of large transformers since they are much more sensitive than any other type of transformer protection.[1] This question seems particularly timely since I happen to know of some recent transformer breakdowns which were due to core faults, for example, where failure of insulation between laminations was responsible. This is a type of unbalance which is too small for detection by differential relays. Turn-to-turn faults, which are sometimes the beginning of winding failures, are a similar unbalance.

Since the ground fault neutralizers in the 115-kv systems seem to have given satisfactory service, it should be of interest to learn if together with the grounding other changes of some of these systems are also contemplated.

It is noted that ground distance relaying is being considered for circuits which do not permit carrier relaying. This type of distance relaying deserves much wider application than it has had in the past.

The use of capacitor potential devices on bus bars is an interesting application of such equipment. It would be helpful if the authors would comment in more detail on their experiences with potential devices in general, and on the advantages of this arrangement.

REFERENCE

1. RELAY PROTECTION OF POWER TRANSFORMERS, AIEE Committee Report. *AIEE Transactions*, volume 66, 1947, pages 911–15, and discussions by A. M. Doyle, E. E. George, and F. L. Lawton, pages 915–16.

W. A. Morgan and R. W. World: We appreciate the comments of Professor Eric T. B. Gross, as he has touched upon parts of the paper that should receive further discussion.

Gas and pressure protection would be given greater consideration if it were made available for sealed-tank transformers. We have one gas accumulation relay in service on a 3,000-kva conservator-type transformer, to give an alarm only. The relay was added after a core fault occurred. We are looking forward to the further development of these relays in this country, but because of the impressive record of transformers as regards faults we have not actively encouraged their development. It is difficult to understand the reluctance of manufacturers to promote the gas relays, in view of their excellent performance record in Canada and Europe.

Ground fault neutralizers are being removed from service because the systems are expanding and are becoming networks consisting of many hundreds of miles with one or more loops which would require many coils. The existing coils are of the 10-minute rating type with automatic by-pass switches. On two systems, they will be replaced by overhead ground wires and solidly grounded transformers sometime this year.

On one system, they will be retained as long as possible because this sytem will be free of interconnections to solidly grounded systems for several years and the cost of adding the overhead ground wires can not be met at this time. Overhead ground wires and 20-cycle reclosing circuit breakers will eliminate the need for the ground fault neutralizers, which will be modified and relocated on systems of lower voltage.

Capacitor potential devices are furnished in place of potential transformers on busses where burden permits. It is found that one 3-phase bank of potential devices rated 150 watts per phase can carry the burden of the instruments and relays of at least three transmission lines. Contrary to previous thinking it has been found that potential device performance is improved when the devices are loaded to near their rating. It is believed that some users of capacitor potential devices may have blamed the devices for incorrect relaying where line potential is used and where automatic circuit breaker reclosing is applied. However, it is believed that present-day analysis shows that the relays themselves are likely not to operate correctly when the circuit breaker recloses on a permanent fault and line potential is used, whether this potential is supplied by potential transformers or capacitor potential devices.

Desert Measurements of Corona Loss on Conductors for Operation Above 230 Kv

W. S. PETERSON
FELLOW AIEE

BRADLEY COZZENS
FELLOW AIEE

JOSEPH S. CARROLL
FELLOW AIEE

Synopsis: This paper reports corona loss measurements made under desert conditions on 1.25-inch and 1.4-inch type-HH copper conductor and 1.4-inch conductor. The variations from wattmeter equipment are discussed. Conditions and losses measured indicate that factors, yet unknown, exist in some desert areas that cause corona loss values to occur at considerably lower voltages than would have been anticipated from previous tests in coastal climates. The tests indicate the necessity for use of added liberality in selecting conductor diameter or confirmation by extended field tests of the existence or absence of the phenomena described. The 1.4-inch type-HH conductor showed adequate liberality for desert operation. The 1.4-inch stranded cable, though adequate in coastal or under normal climatic conditions, showed losses which might prove uneconomical under conditions encountered in the desert areas. The 1.25-type-HH cable appeared definitely inadequate for use in desert areas.

IN 1938 the operation of the 287-kv Boulder Dam transmission lines of the Department of Water and Power up to that date was recorded before the Institute.[1] It was reported that studies then were in progress in the desert area in the vicinity of Victorville measuring corona loss on 1.25-inch and 1.4-inch type-HH cable and on 1.4-inch steel-reinforced aluminum cable. These studies essentially were for basic information in connection with the design of the third circuit from Hoover Dam to Los Angeles.

The present interest in transmission at higher voltages in other parts of the United States and Europe, and the feasibility of going beyond 220 kv for high-load interconnecting circuits, prompts the presentation of this information for such value as it may be in the design of lines for these higher voltages.

Purpose

From studies which have been conducted at Stanford University[2,3] and subsequent theoretical analysis,[4] it was indicated that 1.4-inch diameter conductor would operate satisfactorily at 287 kv and that the segmental-type cable carried some liberality above the diameter necessary for operation at 287 kv. This diameter initially had been established as a result of studies conducted primarily on stranded-type cables so that at the time specifications were issued for conductor on the first two Boulder transmission lines there were not sufficient data to permit establishing a differential in diameter between segmental- and stranded-type cables.

Results of tests later conducted at Stanford[5] indicated that the 1.25-inch diameter cable might operate satisfactorily at 287 kv with resultant reduction in capital investment in both conductor and towers. Contrary to this, however, observations on the desert in the vicinity of Victorville had indicated that under certain climatic conditions not involving storms, corona was visible on 1.4-inch diameter conductors in amounts appreciably more than would have been expected from the measured loss values or visual observations made at Stanford. Victorville is located at the base of a gradual slope on the northeastern side of the Sierra Madres at an elevation of approximately 2,800 feet. These phenomena of unusual corona loss were not observed generally in the desert and did not exist at elevations between 3,000 and 4,000 feet. Little value would have been gained by testing 1.25-inch diameter conductor at the Ryan High Voltage Laboratory since there had been interjected the question of desert surroundings as an item affecting corona loss. It was of utmost importance, therefore, that tests be made on the desert, and in so far as possible in the vicinity where the unusual corona conditions had been observed.

The fundamental purposes of the tests, therefore, were to determine: first, whether or not 1.25-inch diameter segmental cable could be utilized satisfactorily at 287 kv; second, the relation of diameter between stranded- and segmental-type cable for the same corona loss levels; and third, to determine the exact losses which were existing under the desert conditions upon 1.4-inch HH and other conductors and, if possible, the cause for the apparent increase in corona loss above that observed under atmospheric conditions at Ryan Laboratory.

Test Location

It was highly desirable that any test location established be adjacent to one of the two switching stations, either Victorville or Silver Lake, in order that the connection might be made to a switch rack rather than tying into the transmission lines at a regular tower structure. The decision to utilize Victorville was determined for several basic reasons. The voltage rise which would be available at Victorville, 183 transmission-line miles from the generator end, was such that with slight overvoltages on the generators at Boulder it was possible to develop 365 kv for test purposes at Victorville. It was decided early to use the water-column

Paper 50-141, recommended by the AIEE Transmission and Distribution Committee and approved by the AIEE Technical Program Committee for presentation at the AIEE Summer and Pacific General Meeting, Pasadena, Calif., June 12–16, 1950. Manuscript submitted March 15, 1950; made available for printing April 10, 1950.

W. S. Peterson and Bradley Cozzens are with the Department of Water and Power, The City of Los Angeles, Calif.; and Joseph S. Carroll is with Stanford University, Stanford, Calif.

Figure 1. Suspension and dead-end structures for supporting test spans

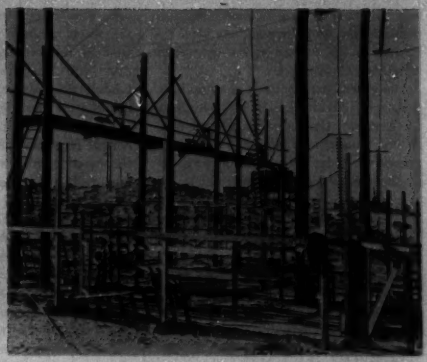

Figure 2. Arrangement of wattmeter multipliers and test connections

resistor-type wattmeter multiplier as used for the previous laboratory tests.[3,5] It was found that water available from a well at Victorville had a specific resistance approaching 3,000 ohms per centimeter cubed which was suitable for use in such water resistors, while the water at Silver Lake carried a high chemical content and very low resistance which would have required the use of distilled water had that location been selected. The fact that the unusual corona conditions had been observed only 14 miles to the east of Victorville and the proximity of Victorville to Los Angeles, allowing for easy transportation of material and test crews, coupled with the other factors mentioned, established this as the location for test. A section of right-of-way extending westerly from the switching station, which was eventually to be utilized for the third circuit from Hoover Dam to Los Angeles, was available upon which to erect the test line.

Physical Arrangement

Victorville switching station is the second sectionalizing station between Hoover Power Plant and Los Angeles and is located adjacent to a transcontinental highway. The station structure from which takeoff could be most readily accomplished terminated a portion of the buss tying directly to the section of transmission line extending between Victorville and Silver Lake Station to the East. A single span carried across the State highway to the start of the test line was the only construction necessary in addition to that required for the test specimens. The test line thus electrically became a portion of the line between Victorville and Silver Lake so that under any fault conditions it would be relayed as a portion of that section of line. Under normal test conditions it was the Victorville end of such line with no switching at Victorville. To provide for emergency de-energizing, switching was accomplished over the carrier current relay circuit to Silver Lake. This switching though provided was never required during the test, normal switching being carried out by the regular supervisory control from Hoover Power Plant.

Four spans were provided for the erection of test conductors, the first two totaling 800 feet and the second two totaling 700 feet. These dimensions were selected because of irregularities in the terrain and in order to provide as nearly as possible similar ground clearance in all of the test spans and to accommodate the specimens available. The structures were of wood poles with latticed steel channel cross-arms and with guy supports to the tops of the poles to form an H-frame structure. Conductor spacing was $32^1/_2$ feet horizontally on a 65-foot cross-arm identical with the Boulder lines. Ground wires, rather than being spaced 50 feet as on the Boulder line construction, were carried on the top of the poles at a separation of $32^1/_2$ feet but at elevations of 30 feet above the conductor, to this extent duplicating the Boulder construction. Suspension and dead-end structures as they appeared during stringing operations are shown in Figure 1. The slight variation in ground-wire spacing from that existing on the Boulder transmission circuits was determined to produce negligible change upon the voltage gradient at the conductor surface, and therefore the difficulty of providing identical spacing was considered unjustified.

For the initial tests the two spans adjacent to the metering connection carried 800-foot specimens of 1.25-inch type-HH cable and the next two spans carried the 700-foot specimens of the 1.4-inch steel-reinforced aluminum cable conductor. Jumper loops between the two specimens were provided for quick removal so that the combined losses from the two samples could be measured followed promptly by the measurement of the losses from the specimen adjacent to the meters. The loss from the more remote specimen could then be determined by subtraction.

Metering

For metering the losses at this location the fundamental circuit used was that described for measuring corona loss at the Ryan High Voltage Laboratory, Stanford University.[2,3]

The scheme essentially uses a water resistor as a high-voltage multiplier for the voltage circuit of the standard low-power factor wattmeter. The actual current into the conductor under test is carried through the current coils of this meter. Particular care is taken that all leads and the meters themselves are shielded to the point where losses are intended to be measured. Unlike the laboratory tests, this circuit used a fixed size of water resistor with resistance varying slightly with current and resultant temperature rather than maintaining constant current through the resistor as was the practice at the Ryan Laboratory. It was necessary at Victorville, therefore, to measure the resistance of the water entering the water column, the current actually flowing in the water column, and the water temperature in order to deter-

mine the heat being generated, the temperature rise, and the resultant total resistance of the column at the time each measurement was taken.

The general arrangement of equipment is shown in Figure 2. The down-leads at the center of the jumper loop and connecting tubes over to the wattmeter assembly under the platform carry shielded leads from the wattmeters located on top of the water resistor shield to the dead-end string, the first point where corona loss is measured. Observers during test runs were stationed on the platform above each wattmeter assembly, reading through telescopes the wattmeters and milliammeters showing conductor current. Figure 3 shows a single water column assembly. The shield at the top of the water column was approximately six feet in diameter with the outer edges composed of 2-inch iron pipe. Additional rings or loops were provided extending beyond the insulator supports. This large metal surface at the top with the capacitance of the insulator stacks provides a relatively uniform field along the water column hanging vertically from the center of the shield. The water resistors were made of capillary tubing approximately 1/8 inch in diameter. The water flow through this tubing was at the rate of from 15 to 20 gallons per minute and the maximum current somewhat below 50 milliamperes. For the voltages involved the energy dissipated in this column was at the rate of between 10 and 12 kw. Wattmeters were located in screen shielding cages on top of the shielding members. In addition to the wattmeter and charging current readings, the current through the water resistors, approximate line voltage from coupling capacitors, resistance and temperature of water entering the water column, generator voltage at Boulder received by telephone, wet and dry bulb temperatures for humidity, barometric pressure, and noise measurements were recorded with each reading loss. The water-flow quantity and the normal resistance of the water in each of the water columns was measured between each test. The relation of the meters and measuring and shielding equipment is pictured in the circuit schematic diagram of Figure 4. Although voltage indication was available from coupling capacitors, its accuracy was not considered sufficient for these tests. The line voltage was actually determined from the computed resistance of the water column and the measured milliampere current through that column. Three of these measurements were available providing considerable check upon errors in meter reading.

Metering Accuracy

Wattmeters

The wattmeters used for these tests were the same meters previously used at the Ryan High Voltage Laboratory. Calibration of these meters was checked after their transportation to Los Angeles by several methods and by comparison with calibrated standards. Insignificant changes had occurred from the corrections previously applied so that values as actually read by scale divisions would correspond identically with those as determined under the Stanford conditions. Two sets of meters were necessary because of the two lengths of cable involved. The meters being read through telescopes practically eliminated any error due to parallax. Reading was attempted to 0.1 of a division. Estimate was probably within 0.1 of a division of the actual deflection. With some meter swing at the time of reading, the average readings probably were within 0.2 division of the actual value. This would correspond to 14 watts and 32 watts per phase respectively on the low- and high-range meters being used.

Shunting Capacities

Any capacities shunting the meter coils could affect the accuracy of the reading. The shielded lead, carried approximately 50 feet from the dead-end insulator string through copper cable or copper tubing back to the meter, has capacitance to this tubing which is, in effect, shunting the current coil of the meter. A study made to determine the possible magnitude of this error showed that the maximum voltage across the coil was approximately 3.37 volts for 60-cycle frequency, which would produce a theoretical error reading of only 0.01 division. Although harmonic voltages would produce error readings in proportion to their frequency, their existence is in relatively smaller magnitude. Computations indicated that even at higher frequencies this error of 0.01 to 0.02 of a division probably would not be exceeded. Tests have been made at Stanford[3] with balancing impedance and a shielded lead circuit such that the voltage drop through this shunting impedance

Figure 3. Water-resistor wattmeter multiplier for one phase

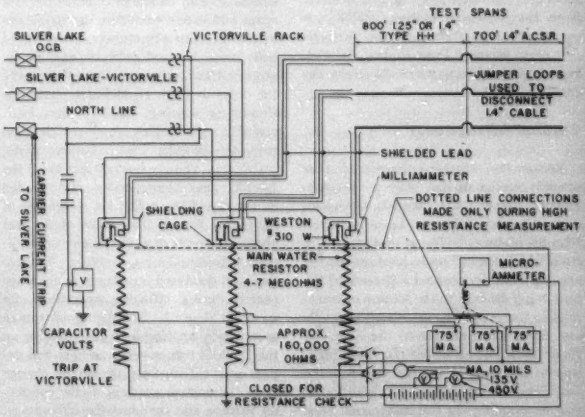

Figure 4. Schematic diagram of metering circuits showing relation to transmission line and test circuit

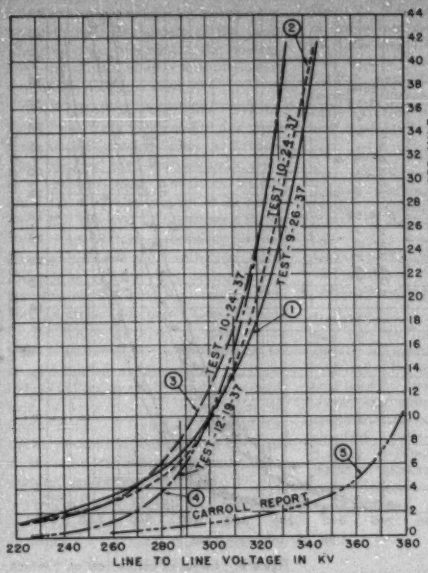

Figure 5. Curves of corona loss on 1.25-inch type-HH cable

Data from Victorville Tests

Curve	Test Date, 1937	Condition	Cable Temp., °F	Corrected to °F
(1)	9–26	As erected	102	—
(2)	10–17	Weathered 3 weeks	98	—
(3)	10–24	2 days after interior flush and external wash	94	100
(4)	12–19	8 weeks after wash	68	100
(5)		Curve extrapolated from Stanford tests		100, 27.5 inches high

would have the same percentage and phase angle as the voltage drop through the current coils of the meter. With between 80 and 100 feet of shielded lead between the meters and the loss specimen, the balancing impedance could be cut in or out of the circuit with no visible movement of the meter needle. These checks and other computations indicated that shunting capacities were not producing measurable errors in either the Stanford or the Victorville tests.

Voltage Measurements

Since variation in burden on coupling capacitors and saturation effects of iron components at the overvoltages involved made it questionable to rely upon this source for voltage measurement, voltage was determined at the test site by milliammeter readings of current and corresponding resistance of the main wattmeter resistors. Temperature of the water entering the base of each column was read with each two or three voltage readings. Coming from a large source there was little fluctuation in the temperature. Readings were taken to the nearest 1/2 degree. Water flow was measured before and after each group of readings, but since regulated pressure was maintained, the flow also showed little variation. Since water has a finite temperature resistance characteristic, the resistance of the water column varied materially with the voltage and consequent current and heating of the water. Current readings were made for each of the multipliers for each voltage applied. The error in these readings again was probably not over 0.2 milliampere, but since the normal reading was as low as 20 milliamperes, the error could thus be one per cent, or the equivalent of approximately three kv. Since three meters were read and compared, these errors probably averaged less than the above amount.

The formula derived for the computation of the resistance of the water column from resistance, temperature, and current readings was as follows

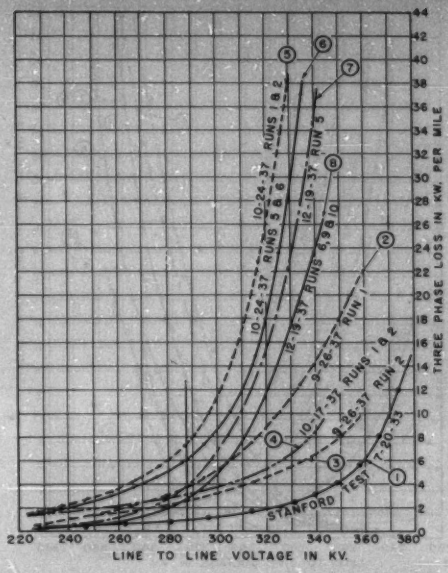

Figure 6. Curves of corona loss from 1.4-inch steel-reinforced aluminum cable

Data from Victorville and Stanford Tests

Curve	Test Date, 1937	Condition	Cable Temp., °F	Corrected to °F
(1)		Stanford Tests		100, 97.5 inches high
(2)	9–26	Run 1 Victorville test	106	100
(3)	9–26	Run 2 Victorville test	106	100
(4)	10–17	Runs 1 and 2 three weeks later	95	100
(5)	10–24	Runs 1 and 2 after water washing	94	100
(6)	10–24	Runs 5 and 6 after water washing	92	100
(7)	12–19	Run 5 two months later	70	100
(8)	12–19	Runs 6, 9, and 10 two months later	63–68	100

$$R=\frac{-Q(83.68-4.84T)}{I^2}+$$

$$\frac{\sqrt{Q^2(83.68-4.184T)^2-335R_{30}(L/a)QI^2}}{I^2}$$

in which

R = the resistance of the column
R_{30} = the specific resistance at 20 degrees centigrade
Q = the flow in cubic centimeters per second
T = the water temperature in degrees centigrade
L and a = length and area of the water column in centimeter units
I = the current through the water column in amperes

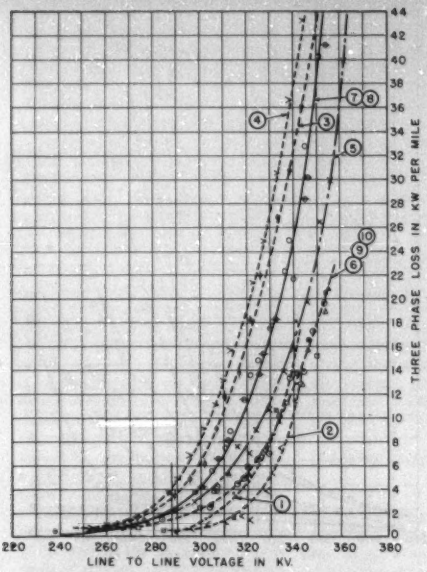

Figure 7. Curves of corona-loss comparison of 1.25-inch HH and 1.4-inch steel-reinforced aluminum cables

Data from Victorville Test of December 19, 1937, Eight Weeks after Washing—Corrected to 70 Degrees Fahrenheit

Run No.	Cable	Temperatures, °F Dry Bulb	Wet Bulb	Cable	Rel. Humid., %
(1)	1.4-in. ACSR	44-45	33-38	46-52	61-50
(2)	1.4-in. ACSR	46-47	38	52	50-46
(3)	1.25-in. HH	54-57	42-44	61-62	34-30
(4)	1.25-in. HH	57-59	44	62-67	30-27
(5)	1.4-in. ACSR	61.0	46.0	70-72	30
(6)	1.4-in. ACSR	61.0	45.5	72-70	28
(7)	1.25-in. HH	62.0	46.0	70-68	27
(8)	1.25-in. HH	62.0	46.0	68	27
(9)	1.4-in. ACSR	60.5	45.5	65-63	20
(10)	1.4-in. ACSR	60.2	45.2	63	29.5

From studies of literature and measurements of the actual water being used, the formula, $R_{50} = [(20 + T)/40]R_t$, was confirmed. By plotting the resistance values thus computed as a function of current, it was possible to establish a smooth curve relation, correct error readings, and be assured of a much higher accuracy than that for any single reading. It is believed that voltage determinations were within one per cent accuracy.

Results of Tests

Type-HH 1.25-Inch Cable

Tests on the 1.25-inch type-HH cable were conducted on four days extending over a period of nearly twelve weeks—September 26, October 17, October 24, and December 19. With the possible exception of December 19, the data for the several runs on individual days correlated so closely that a single curve can be plotted for each day and be truly representative of the entire group of data. Typical curves for these data are presented in Figure 5. Temperature corrections were made only where the cable temperature was greater than 102 degrees Fahrenheit by the first power relation of the air density factor. Data within this range were used without correction.

The first test conducted on September 26 was on the cable as received, having been washed and rinsed exteriorly only before shipment. The loss at 287 kv was in excess of 6 kw per mile. After approximately four weeks of weathering, the test conducted on October 17 showed very little change in the loss, being only slightly lower in the lower region and a fraction higher in the region above 300 kv. At this time it was evident that the excess dye grease or lubricant carried on the inside of the cable was beginning to seep through the joints between the segments. Dust was collecting at these locations and it was indicated that any reduction in loss resulting from weathering was being counteracted by these dust deposits and by small dust precipitation areas. These dust precipitation areas were novel to the authors, were generally elliptical in shape, and occurred both on segmental- and stranded-type cables. They were determined to be deposits of dust, the result of precipitator action in the immediate vicinity of a corona brush, estab-

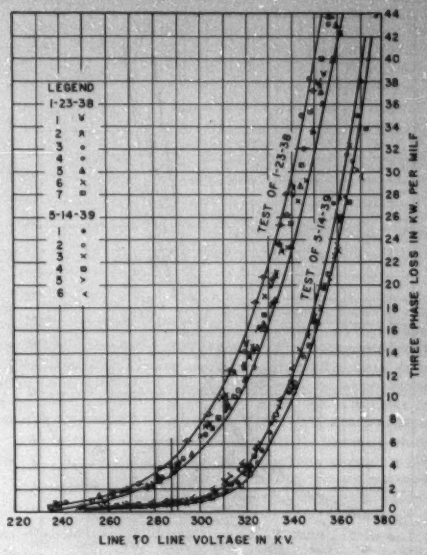

Figure 8. Curves of corona loss on 1.4-inch type-HH cable

Data from Victorville Tests Corrected to 70 Degrees Fahrenheit

Run No.	Temperatures, °F Dry Bulb	Wet Bulb	Cable	Rel. Humid., %
Tests of 1-23-38				
(1)	54.0	45.9	67.5	48.5
(2)	55.5	45.5	70.0	46.5
(3)	61.0	46.5	80.0	34.0
(4)	61.5	46.0	81.0	30.0
(5)	61.5	45.5	74.5	26.0
(6)	61.5	45.0	71.5	24.0
(7)	60.7	44.5	68.0	22.5
Tests of 5-14-39				
(1)	73.5	56.0	90.0	32.0
(2)	75.5	56.5	93.0	29.0
(3)	82.0	57.5	86.0	22.5
(4)	81.0	57.5	81.8	26.0
(5)	76.0	56.5	76.5	29.0
(6)	74.5	57.0	76.0	34.0

Line curves represent approximate extreme variations.

lished either by a rough spot or some contamination on the surface of the cable. These were also observed on the Boulderline conductors, but after several years of weathering no longer exist.

The 1.25-inch cable was lowered, flushed internally with gasoline and given the external gasoline, soap, and water wash identical with that normally given to conductors under laboratory tests.[2,5] Since the 1.4-inch stranded cable previously had received this treatment at the Ryan High Voltage Laboratory, it was given an external wash with clear water through a ring of high-pressure jets. Immediately following the washing treatment, October 24, the 1.25-inch cable, though indicating a slight reduction in loss in the lower loss range, had an increased loss of approximately 1 kw per mile at 287 kv, or a shift along the voltage axis of approximately 10 kv. In the upper range or high-loss range of the curve, the shift approached ten kv; that is, the same loss occurred at ten kv lower voltage than before.

Final test on this cable was conducted on December 19, two months later. At this time the loss had reduced somewhat, indicating slightly less than six kw per mile at 287 kv for 100 degrees Fahrenheit cable temperature, but in carrying into the higher voltage range the loss was still somewhat above that determined under the initial erection conditions of the cable. For comparison a curve also is shown extrapolated from tests on 1.4-inch and 1.65-inch type-HH cable conducted at Stanford University which would indicate that for that location the corona loss on 1.25-inch type-HH cable at normal operating voltage of 287 kv would be less than one kw per mile. This change in loss is equivalent to a shift in voltage of over 50 kv in the lower loss range, while in the upper range of the curve a voltage shift of nearly 70 kv is necessary to produce the same loss. The particular significance of these tests is that by comparison with tests at the Ryan High Voltage Laboratory some unknown factors are present in this area of the desert which cause corona to start at a voltage of 50 to 70 kv below that at which it is experienced on corresponding conductors at the Ryan Laboratory.

In addition, contrary to the experience at the Laboratory, the internal and exterior washing of the cable did not produce the normal reduction in loss previously experienced. The loss figures remained almost identical with those of the initial test actually showing a slight increase immediately following washing and then with weathering dropping somewhat below the losses experienced under initial test conditions.

Figure 9. Summary of corona-loss data on 1.25- and 1.4-inch type-HH and 1.4-inch steel-reinforced aluminum cable—Victorville and Stanford Tests

Victorville Tests: 1.25-inch HH and 1.4-inch steel-reinforced aluminum cable weathered two months after washing—1.4-inch HH weathered 16 months after washing

Stanford Tests: 1.4-inch HH 15 days after washing—1.25-inch HH extrapolated from above and similar tests on 1.65-inch type-HH cable—1.4-inch steel-reinforced aluminum cable 16 days after washing

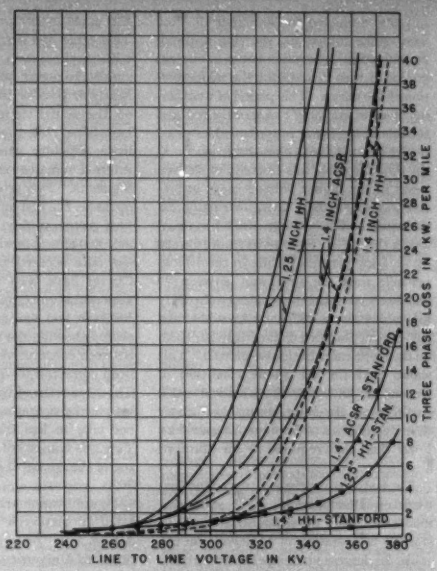

Tests on 1.4-Inch Steel-Reinforced Aluminum Cable

Tests conducted on 1.4-inch steel-reinforced aluminum cable are shown in Figure 6 and cover the identical dates mentioned for the previous conductor tests. The loss on this cable was determined of necessity by making a combined loss measurement on the two sections, including the 800 feet of 1.25-inch cable and the 700 feet of 1.4-inch steel-reinforced aluminum cable conductor and then subtracting the loss computed for the former from the combined loss measurement. Since temperature variations were usually very slight between consecutive runs and since the loss values as determined for the 1.25-inch cable showed little variation between runs on the same day, it was possible to use the loss values for the run immediately preceding or immediately following the combination run and thus be assured of a high degree of accuracy. It is of interest to note that the two runs on September 26 showed somewhat different results in the higher loss regions. The loss at normal operating voltage, 287 kv, for these two tests was between 2.5 and 4 kw per mile, corresponding to a voltage shift between the two tests of approximately 20 kv, while in the region approaching 10 kw per mile the curves showed a voltage separation of nearly 35 kv for the same loss. Tests conducted four weeks later on October 17 showed very little difference between consecutive runs and the loss values were approximately midway between the two tests of September 26.

Following the test of October 17, the conductor was given an external rinse with a circle of high-pressure water jets carried along the cable on a small trolley. Whether or not a surface condition had developed as a result of the treatment and storage at Stanford University, which was removed as a result of this washing, or whether dust accumulation in the desert during the short period of testing and after washing had modified the surface condition, is not known. Immediately following this washing treatment on October 24, four test runs were taken. All of these runs fell within close limits, as indicated by the curves, but showed a very material increase in the loss over the earlier tests. The loss at 287 kv was now in the vicinity of six kw per mile, corresponding to a voltage shift from the earlier tests of approximately 50 kw and very near that of the 1.25-inch HH cable. The two groups of runs taken on this date were less than ten kv apart in the upper range and approaching 5-kw separation in the range of 287 kv and below.

Tests conducted on December 19 again were quite consistent, showing approximately a 5-kv separation between various groups of runs throughout the major portion of the curve. This period of weathering of approximately two months reduced the loss in the lower range to values practically identical with those experienced at the time the cable was erected but showed losses in the higher voltage range appreciably greater than those originally experienced. The voltage shift for equal loss in the 287-kv region was from 10 to 20 kv (2–4 kw per mile) while in the 10-kw-per-mile area the shift was between 40 and 60 kv, the curves rising very abruptly for values above 287 kv. An additional curve from Stanford tests of July 20, 1933, on the identical cable is also plotted. This shows that for the stable condition of December 19, 1937, the identical cable would show the same corona loss under desert conditions at between 50 and 60 kv lower than that required in the Stanford area.

The last test on these two conductors, made on December 19, 1937, showed a moderate range of temperature from a starting temperature of 46 degrees on the cable, 36 degrees air temperature through a maximum of 72 degrees on the cable, 61 degrees air temperature, and concluding with 63-degree cable temperature and 60.2-degree air temperature. A curve sheet, Figure 7, has been plotted covering these data correcting all to the approximate maximum value of temperature recorded, namely 70 degrees on the cable. No correction was made for tests 5 and 6 or 7 and 8 which are within two degrees of the correction temperature. Curves of Figure 7 are corrected using the first power of the air-density correction factor. Although data from Stanford tests indicated the use of 2/3 power as a more accurate correction for conditions at that location, it was considered that the other factors being introduced on the desert would not justify this refinement.

Tests on 1.4-Inch Type-HH Cable

Immediately following the tests on the 1.25-inch type-HH cable and 1.4-inch steel-reinforced aluminum cable, these cables were removed and replaced by three 800-foot sections of 1.4-inch type-HH cable as used on the Boulder circuits. This cable had been given external wash with gasoline, soap, and water in order to speed the aging process and yet be as nearly as possible like the cable as erected on the actual circuits. Since this cable had been closed with a soap solution, little difficulty was contemplated from internal greases exuding between the segments. Two groups of tests were performed—the first on January 23, 1938, the final group on May 14, 1939, following 16 months of weathering. Figure 8 covers the data secured from these two tests. Curves have been drawn indicating the approximate extreme limits of these data for each test and plotted points are included showing the manner and variation between consecutive runs. All data have been corrected to 70 degrees Fahrenheit. The 16 months of weathering reduced the loss in the operating range from four kw per mile to less than one kw per mile. This was equivalent to a horizontal shifting of the curves of somewhat in excess of 30 kv.

Figure 9 summarizes the data accumulated at Victorville and includes typical curves from previous measurements at Stanford University, corrected to Victorville conditions for the 1.4-inch type-HH and steel-reinforced aluminum cable conductors, and 1.25 inch data as extrapolated. The Victorville data are plotted as areas or limits within which losses may be expected after normal weathering conditions. The advantage of the segmental-type conductor, both for desert operation as well as for conditions existing near the Ryan High Voltage Laboratory, is clearly indicated. The differential, however, is not as great under desert conditions as was previously contemplated.

Conclusions

Although tests at the Ryan Laboratory, Stanford University, had indicated by extrapolation of data from larger conductors that 1.25-inch HH or segmental-type conductor would operate satisfactorily at 287 kv, the tests here reported under desert conditions indicated that operation at this voltage was so close to the knee of the loss curve that uneconomic losses could easily result from variations in weather or atmospheric conditions, changes in altitude, or roughened surface conditions of the cable.

Tests on 1.4-inch type-HH cable, though not showing the liberality originally contemplated, indicated that operation at 287 kv was sufficiently below the knee of the curve to be within the economic loss range even for the atmospheric conditions experienced at Victorville, at higher elevations, or with possible higher voltages experienced near the generating source. These losses under Victorville conditions varied from 0.5 to 0.9 kw per mile.

Tests on 1.4-inch stranded conductor showed that losses in the normal operating range occurred under Victorville conditions at from 50 to 70 kv lower than the voltage required to produce corresponding losses at Stanford. This is approximately the same differential in voltage as was found for segmental-type cables. Likewise, it was found that corresponding losses were produced on stranded-type cable at from 20 to 25 kv below the voltage carried to produce the same loss on segmental-type cable. Again, this shift was similar to that experienced at Stanford.

Loss values found to exist under desert atmospheric conditions dictate the use of liberality in the selection of conductors to operate in such regions, or the establishment by test, prior to the selection of conductor diameter, that similar unusual atmospheric conditions are not present in the area to be traversed.

References

1. Symposium on Operation of the Boulder Dam Transmission Line—Corona Experience on Transmission Line, **Bradley Cozzens, Wm. S. Peterson.** *Electrical Engineering (AIEE Transactions)*, volume 58, April 1939, pages 137–40.

2. Corona Loss Measurements on a 220-Kv 60-Cycle Three-Phase Experimental Line, **Joseph S. Carroll, Leland H. Brown, D. P. Dinapoli.** *AIEE Transactions*, volume 50, March 1931, pages 36–46.

3. Corona Loss Measurements for the Design of Transmission Lines to Operate at Voltages Between 220 Kv and 330 Kv, **Joseph S. Carroll, Bradley Cozzens.** *AIEE Transactions*, volume 52, March 1933, pages 55–62.

4. Discussion by **Wm. S. Peterson** of reference 3, pages 62–3.

5. Corona Losses from Conductors of 1.4-Inch Diameter, **Joseph S. Carroll, Bradley Cozzens, Theo. M. Blakesley.** *AIEE Transactions*, volume 53, 1934, pages 1727–33.

Discussion

Abe Tilles: (Pacific Gas and Electric Company, San Francisco, Calif.): This valuable and intriguing paper gives answers to some questions and raises others. It is demonstrated that the voltage corona loss curve is shifted markedly under some desert conditions. The general amount of this shift, some 60 kv, is established by careful field measurements. It is interesting that in this case "Mahomet has been brought to the mountain." To obtain the needed results the experience, techniques, and precision of measurement which have been developed over a period of two decades of corona measurements in the laboratory have been transferred "on location" to accomplish in

the field a precision measurement of a laboratory nature. The factors of safety in the original design are shown to be well chosen, and the specific problems here involved are satisfactorily bracketed to provide an engineering solution.

At the same time, of course, a general problem of very large scope is forcefully introduced. The present paper presents it but does not solve it. The basic cause of this corona increase is not established, nor is its possible extent in various other situations delimited. It is observed that variation in loss with washing and weathering is partly masked by unknown variables. In a way it is not surprising that new phenomena are being uncovered, since frontiers are being pushed forward in two directions.

For one thing, as the voltage is raised above 230 kv, even though steps are taken, such as using larger conductor radius to keep voltage gradients small in the main, possibilities of corona discharges are increased very greatly, nevertheless. For another thing, the desert is still on uncharted territory. Literally, as can be seen on the map, it is still largely uncharted; and figuratively, as attested in a great variety of lore and legend, the desert is unknown, it is different. The dryness, the large unbroken spaces, the dust and wind, the motion of large air masses, the unobstructed blaze of the sun—the desert is different. All that have been there have felt it, and they will find it interesting, but possibly not surprising, that the differences produce effects that can be measured on wattmeters and plotted on charts.

Certainly it is enough for one paper to raise clearly, as has been done, the question of corona increase in the desert; but the important questions then remain as to causes and limits of such increase, and these deserve further study.

The authors, in their paper proper, have not undertaken to speak on these further matters. It would be of great interest if, in discussion, they would care to point the way by giving such partial answers, clues, and speculations as they can on some of the questions that come to mind. How does the corona loss correlate with general atmospheric density of total ionization and with presence of ions of different sign and mobilities? How does the loss vary with day and night and intensity of sunlight, with seasonal variation in ultraviolet intensity of sunlight? How does it vary with content and variety of solid and gaseous air borne impurities? How does it vary with wind velocity and possible frictional electrification? How does it vary from place to place? Does the extra corona loss seem to be caused by varying meteorologic conditions or by local concentration of radioactive materials? Comment along these lines would certainly be of interest.

Otto Naef (American Gas and Electric Service Corporation, New York, N. Y.): We have every reason to be grateful to the authors of this paper for their decision to make known the results of these important tests, which influenced the final selection of conductors for the third circuit of the 287-kv Hoover Dam–Los Angeles line. Though carried out some ten years ago, these tests have lost nothing of their value.

An important revelation made in this paper is the statement, that after all known corrections for differences in barometric pressure and temperature were applied, the tests made at Victorville showed considerably higher corona losses than those carried out in the laboratory at Stanford on identical conductors. Apparently no explanation so far has been found of this strange phenomenon, which seems to be neither a consequence of desert climate nor altitude alone, as it was not observed in other parts of the desert, nor at higher altitudes.

Anyone who is selecting conductors for an extra high voltage transmission line may therefore be asking himself whether the projected line is likely to traverse territory where unknown climatic factors produce increased corona losses. Since field tests on a large scale are in progress at the 500-kv Test Project of the American Gas and Electric Service Corporation at Brilliant, Ohio, it was only natural for us to compare the results of our own measurements with those indicated in the paper. It was reassuring to find that our results seem to correspond to the lower values of corona loss measured at Stanford Laboratory.

A direct comparison is only possible in the case of the 1.40-inch type-*HH* conductor because all other single conductors tested at Brilliant are of larger diameter. This particular conductor was tested only single phase. After converting the measured loss into 3-phase loss and making allowance for the difference in air density factor, this conductor, when new, produced a 3-phase loss of 1 kw per mile at 347 kv, and the same loss at 386 kv after five months of aging. The sharp bend in the curve of the aged conductor begins only at 390 kv which is an 80-kv shift from the corresponding curve shown in Figure 9 of the paper for the 1.40-inch type-*HH* conductor tested at Victorville.

All the tests described in the paper were carried out in good weather, because the test installation evidently did not readily permit taking measurements under adverse weather conditions. The suitability of a conductor for operation at a specified voltage is judged, from a corona viewpoint, by the distance between the sharp upward bend in the voltage-loss curve and the point on the curve at operating voltage. At Brilliant, where the losses are recorded continuously at operating voltage, average and peak losses in all kinds of weather are readily obtained, and the suitability of a conductor is judged rather by its actual performance than by the shape of its fair-weather "Loss versus Voltage" curve.

The graphic records bring out facts that are not easily obtained by other methods. The "Stanford" curves in Figure 9, for instance, indicate that the 1.25-inch type-*HH* conductor is superior to the 1.40-inch steel-reinforced aluminum cable conductor. A similar relation was found to exist between the 1.65-inch type-*HH* and the 2.00-inch steel-reinforced aluminum cable stranded conductors at Brilliant if tested in fair weather. However, the results so far obtained from the graphic records at constant voltage, in all kinds of weather, indicate a reversal of this relation; the average loss of the 2.00-inch steel-reinforced aluminum cable conductor being smaller because it seems to be less effected by heavy rain.

The determination of corona loss on transmission lines is a complicated and difficult problem because of the many variables involved. The information presented in the authors' paper is a valuable contribution towards a better understanding of some of these problems.

Engineering Staff (Anaconda Wire and Cable Company, Hastings-on-Hudson, N. Y.): This paper reports corona-loss measurements made in the California desert some 12 to 13 years ago using the same techniques, equipment, and cables previously employed for similar tests at Stanford University. The results indicate considerably higher losses in the desert than were anticipated from the measurements near the coast. No explanation of the causes of these increased losses is suggested in the paper.

Neglecting for the moment the possibility of some unusual influence present at the desert location, three other possible causes of the difference in results suggest themselves:

Inaccuracies in Measurements

The very formidable problems in making such measurements make one look for some data regarding the accuracy of the test method. Other investigators[1,2,3] have employed several methods for the loss measurements so that possible errors could be eliminated by continuous cross-checking. Apparently, in these tests, the authors have depended only on obtaining a very approximate agreement between successive test runs under apparently similar conditions.

If additional tests had been made on short (approximately 10 feet) lengths of each conductor in a corona cylinder using the Schering bridge technique, this might have served as a direct check on the data obtained through the rather indirect and cumbersome water resistance-wattmeter method used.

It also is suggested that sphere gap sparkover measurements of desert air during the test runs may have served a useful purpose in interpreting the data.

The effect of harmonics, both generated and produced by corona, is not clearly analyzed. In the setup described, harmonic voltages can cause significant errors—these increasing with increase of line voltage. The water resistance values, too, may have errors due to the presence of harmonics.

The equation given for water resistance as a function of current, temperature, flow, and so forth, is indeterminant as written since two solutions are possible. It would be of value to restate the derivation of this equation since it is so important in obtaining the final results.

Inaccuracies in Analysis

For purposes of comparison, the curves of test data are "corrected" to some reference conditions (temperature and barometric pressure), presumably by the procedures expounded in 1937 by Carroll and Rockwell.[4] These procedures were devised empirically to agree with observed data from the Stanford tests. Possibly these procedures are not universally applicable.

In view of the rather wide variations in observed loss on a given conductor run, the method adopted for determining the losses in the 1.4-inch steel-reinforced aluminum cable is somewhat questionable. Subtract-

ing the 1.25-inch type-*HH* data from the combined losses of 1.25-inch type-*HH* and 1.4-inch steel-reinforced aluminum cable conductors can only lead to still wider variations. This is evident upon comparing Figures 5 and 6 and noting the much wider spread of curves in Figure 6. Comparing such indirectly determined losses of a round-wire conductor (steel-reinforced aluminum cable) with directly measured losses of a segmental conductor (type-*HH*) is hardly fair.

Insufficient Data

The 1.25-inch type-*HH* and 1.4-inch steel-reinforced conductors were tested over a 3-month period. During this time, four individual runs were made, representing as-received and washed conditions. Natural aging processes were therefore interfered with considerably. On the other hand, the 1.4-inch type-*HH* conductor was tested only twice, immediately after erection and after 16 months of natural weathering. The decrease in corona loss pattern obtained was therefore more typical of actual service. It is questionable whether or not direct comparisons of the three conductors can be made—the data may not be comparable at all.

An examination of the continuously-recorded data from the Tidd tests[6] shows the great variation in corona from day to day under nearly the same apparent conditions. In view of this it does not appear that, based on the Victorville tests (two groups of tests, each made during a single day, separated by an elapsed time of about 18 months) the authors can conclude "The advantage of the segmental conductor . . . is clearly indicated." Other investigators have arrived at the opposite conclusion.[7,8]

REFERENCES

1. BUNDEL LEITUNGEN, **F. Busemann, W. V. Mangoldt.** *Siemens Zeitschrift* (Berlin, Germany), 1942.

2. INSTRUMENTATION AND MEASUREMENT—TIDD 500-KV TEST LINES, **R. L. Tremaine, G. D. Lippert.** *AIEE Transactions*, volume 66, 1947, pages 1624–31.

3. NEW INVESTIGATIONS OF THE CORONA LOSSES OF A TRANSMISSION LINE, **F. Beldi.** *Report Number 401*, Conference on Large High-Voltage Electric Systems (Paris, France), 1948.

4. 400-KV TEST STATION AT CHEVILLY—LOSS MEASUREMENT AND INVESTIGATION OF CORONA EFFECTS, **D. Renaudin.** *Report Number 409*, Conference on Large High-Voltage Electric Systems (Paris, France), 1948.

5. EMPIRICAL METHOD OF CALCULATING CORONA LOSS FROM HIGH-VOLTAGE TRANSMISSION LINES, **Joseph S. Carroll, Mabel MacFerran Rockwell.** *Electrical Engineering* (*AIEE Transactions*), volume 56, May 1937, pages 558–65.

6. PROGRESS REPORT ON 500-KV TEST PROJECT OF THE AMERICAN GAS AND ELECTRIC COMPANY CORONA, RADIO INFLUENCE, AND OTHER FACTORS, **Philip Sporn, A. C. Monteith.** *AIEE Transactions*, volume 69, part II, 1950, pages 891–99.

7. INFLUENCE OF THE CONSTITUTION OF THE EXTERNAL LAYER OF HIGH-TENSION CONDUCTORS ON THE AMOUNT OF CORONA LOSS, **J. Biermanns.** *Elektrotechnische Zeitschrift* (Berlin, Germany), volume 48, number 37, 1927, page 1331.

8. CORONA LOSSES OF CONDUCTORS AT A-C VOLTAGES, **K. Potthoff, B. Mathiesen.** *Elektrotechnische Zeitschrift* (Berlin, Germany), volume 56, number 1, 1935, page 3.

W. S. Peterson, Bradley Cozzens, and **Joseph S. Carroll:** In addition to the general comments regarding the measurements and information contained in the paper, Mr. Tilles poses several questions which can be answered in part as a matter of conjecture and part by observations made at the time of the test and at subsequent intervals. Most of this information, however, is not substantiated by rigorous observations and tests and, therefore, was considered as not proper for inclusion in the paper.

Mr. Tilles questions the correlation between air density, total ionization, ionization of various polarities, and mobilities. The air density correction factors applied were based upon first power correction of the normal air density ratios rather than the two-thirds power as has been indicated by some laboratory tests. The differences in temperature and normal air densities were not sufficient, nor was the test setup sufficiently flexible to carry on a study of this variable. Although antennas were erected to measure d-c voltages as a result of accumulated ion charge, little correlation was established between corona noise levels and the rapidity with which this charge would accumulate or the polarity of the charge. These measurements did establish the fact, however, that large quantities of charged particles are present in the desert atmosphere giving rise to accumulations of potentials on insulated conductors or objects and assisting in the precipitation of dust particles upon insulators and conductors.

Mr. Tilles questions the variation in loss between day and night and as affected by sunlight or ultraviolet radiation. Again, no direct measurements were made of these conditions, but from noise observations, which correlate quite well with corona loss, and from visual observations of corona brushes, there seemed to be little change and in many cases an increase rather than a reduction in the noise level with darkness. Of course, no reasonable comparison of corona brush length could be obtained between daylight and dark periods. Regarding the effect of wind velocity and electrification of the atmosphere, the audible noise in some cases tended to increase with winds. When dust particles were blown of sufficient quantity and possibly carrying electric charges, both the 287-kv and adjacent 138-kv lines have been seen to exhibit aggravated corona conditions. This is attributed to the discharge between the charged dust particles and the conductor. This latter phenomena can occur at practically any location in the dry desert area. The phenomena as described in the paper, however, namely the observed corona streams, occurred largely in the area adjacent to Victorville which is approximately 100 miles (90 miles air line) from Los Angeles and was most frequently present following a north wind. Subsequent tests indicated precipitation of dust particles following such north winds which carried some radioactive material, but laboratory tests in which conductors were coated with radioactive materials did not correlate with observed conditions in this area. As time permits, it is hoped that additional studies can be progressed along these lines.

Mr. Naef indicates that by comparison the tests conducted by the American Gas and Electric Corporation and co-operating agencies at Brilliant, Ohio, correlate closely with the values of corona loss obtained at Stanford University rather than those experienced under desert conditions. It was the surmise of the authors that this phenomena was associated largely with the dry desert atmosphere which carries with it highly ionized dust particles and because of the lack of moisture is subject to maintaining larger accumulations of these charges as a result of wind friction and dust movements. The more humid atmospheres of the midcontinent and east coast, as well as that in the vicinity of Stanford University, are not conducive to maintaining these charges.

As stated by Mr. Naef, it is necessary to consider climatic conditions in the selection of the conductor diameter and surface. In the case of the Hoover transmission lines, the major portion of these circuits traverse a desert area which has an average rainfall of from 1 to 4 inches per year. The presence of rain or high humidity is so relatively infrequent that it was not feasible to attempt to conduct tests under these conditions and likewise the percentage of time which they are present is so small they need be given little consideration in the over-all economics of the transmission system. Mr. Naef and his organization are to be complimented on their extensive studies under varying weather conditions which when completed will furnish sufficient information to evaluate these factors in connection with the design of future high-voltage transmission lines.

Several questions regarding the accuracy of measurements and methods used, as well as the ultimate results, were raised in the discussion presented by the engineering staff of the Anaconda Wire and Cable Company.

First, the suggestion that duplicate methods of measurement be used, of course, presents appreciable difficulty when making full-scale field studies both from the time involved and the cost of such procedure.

The reference to the use of short sections of conductor utilizing Schering bridge methods and concentric cylinder arrangement is ideal for basic theoretical studies in the laboratory. It is questionable, however, whether this would have confirmed the conditions being investigated for several reasons. First, if the conductor is maintained at high potential, the space charge established between the conductor and cylinder, as a result of corona upon the conductor and the physical dimensions of the test equipment, is of material effect in determining the nature and actual corona loss which exists. Any atmospheric phenomena which would be present and which would be influencing the corona loss probably would be swept clear of the area within the cylinder and would be overshadowed by the space charge established between conductor and cylinder. Second, if the cylinder is maintained at high potential and the conductor at ground potential, the atmosphere surrounding this cylinder would most assuredly be cleared of ionized or other materials which might be affecting the corona loss. The use of the water resistor multiplier method gave direct comparison with the studies previously conducted at Stanford without having to attempt field balancing and adjustment of bridge circuits.

The suggestion of sphere gap determination of dielectric strength of desert air would be subject to the same conditions as mentioned regarding concentric cylinders. If moderate-sized spheres and voltages up to

approximately 100 kv were used, the spacing between spheres would be of such magnitude that ionized particles would be swept out of the gap area during each half cycle. To go to larger spheres would be a cumbersome and difficult problem and of questionable value, particularly when using a voltage source at the generating end of a transmission line some 180 miles distant as a means of controlling voltage. Tests have been made up to 50 kv using sphere gaps which showed no measurable variation from the normal calibration value.

The question of harmonics is also raised. Cathode-ray oscillograph observations indicated the presence of limit harmonic voltages. The wave, however, was not mathematically analyzed. Losses resulting from normal harmonics through the seventh would be accurately measured by the water column wattmeter method and would correspond to those normally encountered on an operating transmission system.

Space does not permit the development of the equation for temperature correction and water flow. The fundamental formula for resistivity change with temperature was verified. Applying this to a straight water column carrying a definite current results in the equation developed.

Regarding temperature air density corrections, voltage values were corrected by direct application of the air density ratio, with the exception of those tests which were within 2 degrees Fahrenheit of the actual value to which correction was being referred. Since many of the tests were within 5 to 10 degrees Fahrenheit of the actual corrected values, little error can be introduced by the application of air density corrections using this direct ratio.

It is agreed it would have been much more desirable had time and equipment permitted to have made tests measuring losses on all cables independently without subtractions. During certain periods of the day, however, the losses on the cable specimen adjacent to the wattmeters was very constant, consecutive curves being almost identical. We feel justified, therefore, in using these data as accurate in establishing by subtraction the loss on the more remote sample and neglecting those tests during the early morning and late evening hours when some variations did exist. The wide variations referred to during the day observations of the Tidd tests (reference 6 of the previous discussion) largely occurred as the result of high humidity, fog or rain, which conditions were not present at Victorville.

The discussion refers to early tests in Europe (references 7 and 8 of the previous discussion) reported in 1927 and 1935 in which stranded cable is reported to have lower corona loss than segmental-type of the same diameter.

The segmental-type cables which were used at this early date and which were studied even earlier at Stanford[1] were of the rectangular flat-strip spiral-wound type or involved segments with sharp edges. Even the lock-wire tramway-type cable investigated in 1924[1] after being erected did not present a completely smooth surface. The individual strands rise slightly above the true circular contour and present sharp edges upon which corona forms at relatively low voltage. Investigators have reported that under rain conditions the losses on segmental-type cable may be equal or higher than those found on stranded-type conductors. The climatic conditions experienced on the transmission line, therefore, should be investigated very carefully. In connection with the Hoover Dam–Los Angeles transmission lines of the Department of Water and Power, the length of circuit over which rain is experienced frequently is relatively small, the major portion traversing desert areas where rains are very infrequent. Under these climatic conditions there is little question of the definite advantage of the type-*HH* segmental conductor both as established by tests at Stanford University and those conducted at Victorville.

References

1. Power Measurements at High Voltages and Low Power Factors, Joseph S. Carroll, Thomas F. Peterson, George R. Stray. *AIEE Transactions*, volume XLIII, October 1924, pages 1130–38.

A 5,000-Kva Underground Substation

JOSEPH F. SINNOTT
MEMBER AIEE

LARGE increases in electrical usage in a relatively small area of downtown San Diego began overtaxing the 4-kv underground radial feeders of the San Diego Gas and Electric Company supplying it. Furthermore, Substations A and C, the source stations for the overloaded feeders, were carrying full capacity and were 4,560 feet and 2,080 feet respectively from the distressed loads.

After lengthy consideration, it was decided to establish a new substation close to the center of the load, taking advantage of the fact that two lightly loaded 12-kv 500,000-circular mil 3-phase tie lines ran close by. These tie lines originated at Station B, a generating station with a capacity in excess of 100,000 kw, serving among others the two substations mentioned previously.

Since real estate values in downtown San Diego are high, it was agreed to install the substation underground, provided that a location with adequate ventilation could be obtained or built. Investigation soon revealed that no ready-made vault space could be obtained in any of the larger buildings nearby, and that a new vault would have to be constructed.

The district to be served was already fairly well built up, making large load increases rather unlikely. Consequently it was not deemed unreasonable to install a 5,000/6,667-kva capacity substation to feed the 4,890 kva in transformers installed in the area. It also was decided to feed the load with three 4-kv underground radial feeders of about 2,000-kva capacity each.

Area and Method of Serving Load

The load to be served, consisting mainly of office buildings and stores, is concentrated under the crosshatching on Figure 1, a portion of the street map of the city of San Diego. This figure also shows the location of Substation C at 4th and Ash Streets, Station B (the generating plant) at Kettner Boulevard and Broadway, and Substation A at 10th Street and Imperial Avenue. These are the three stations related to our discussion, others in downtown San Diego not being shown in order to simplify the picture.

Figure 2 is an enlarged map of the crosshatched area of Figure 1, showing the feeders serving it before the new substation was installed. From Substation C, 2,080 feet away, there were five single-phase and three 3-phase feeders to the area, whose cable sizes ranged from number 4/0 on the main leads, to as small as number 6 on some of the smaller branches. These feeders also fed some loads nearby.

Substation A, 4,560 feet away, had two 3-phase feeders serving this load, circuit *A-7*, a number 4/0 feeder; and circuit *A-4*, a 500,000-circular-mil cable. As in the case of the feeders from Substation C, there were loads outside the area on both circuits.

Figure 2 also shows the two 12-kv tie lines running between the generating plant (Station B) and Substation A, with the taps to Substation C. These tie lines were at one time the main source of energy for Substation A and emergency feeds for Substation C, but since the new Silver Gate Generating Station was built, they had been operated as emergency tie lines only, making them ideal for feeding any new substation close by.

Taking into account the location of the load, the proximity of the two 12-kv cables and the fact that the San Diego Gas and Electric Company garage was located within a block of the area to be served, it was decided to locate the new substation in a vault under the garage floor and call it the Electric Building Substation.

Figure 3 shows the three 4-kv feeder from the new Electric Building Substation to the area, one each on 5th, 6th, and 7th Streets. Each feeder has suitable ties and sectionalizing switches which are not shown in the figure. Whenever the old feeders from Substation A and Substation C remained in service, it was only to supply alternate emergency power to some of the larger buildings. The only load outside the area to be supplied by the Electric Building Substation was the Fox Theater at the corner of 7th and B Streets.

Substation Site

The new substation was built in a vault dug in the rear of the garage, because of the advantages of this location. These advantages were briefly:

1. It was wholly on San Diego Gas and Electric Company property.

2. The back of the garage abutted the company office building, whose basement provided easy access to the new vault from the air compressor room.

3. There was an old incinerator in the basement of the office building which was no longer used. The incinerator stack which was on the other side of the office building wall from the vault location provided an ideal exhaust flue for the vault, it being $3^1/_2$ feet by 4 feet in cross-section, and rising eight floors above street level.

4. By drawing the necessary cooling air for the transformer from the office building basement and exhausting it up the flue, we could greatly improve the basement ventilation as well as maintain proper transformer temperatures.

Figure 4 shows a plot plan and general layout of the office building basement and garage (at street level). The vault is located at the west end of the garage adjacent to the office building wall. The incinerator flue also can be seen on this

Paper 50-142, recommended by the AIEE Substations Committee and approved by the AIEE Technical Program Committee for presentation at the AIEE Summer and Pacific General Meeting, Pasadena, Calif., June 12–16, 1950. Manuscript submitted March 13, 1950; made available for printing April 10, 1950.

JOSEPH F. SINNOTT is with the San Diego Gas and Electric Company, San Diego, Calif.

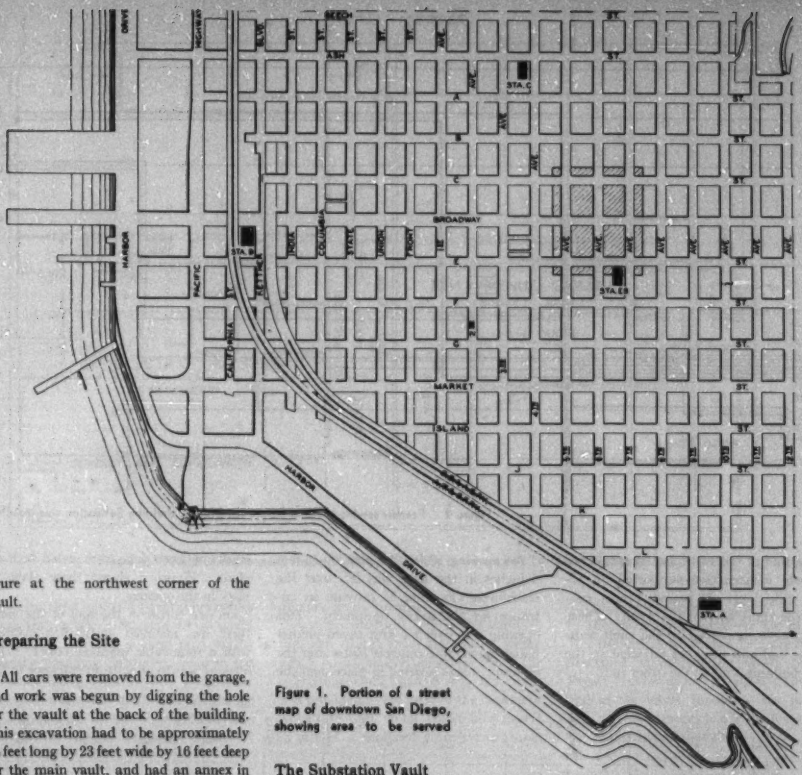

Figure 1. Portion of a street map of downtown San Diego, showing area to be served

figure at the northwest corner of the vault.

Preparing the Site

All cars were removed from the garage, and work was begun by digging the hole for the vault at the back of the building. This excavation had to be approximately 45 feet long by 23 feet wide by 16 feet deep for the main vault, and had an annex in which the blowers for the ventilating system were located which was about 7 feet wide by 23 feet long and varied in depth between 8 and $10^1/_2$ feet.

Because of the limited clearance between the garage floor and the lowest roof trusses, about 12 feet, it was necessary to dig the hole with a gasoline-driven Hoe-back. The Hoe-back would deposit the dirt on the garage floor from where it was lifted into waiting trucks by a pneumatic-tired High-lift. Trucks entered the north door of the garage, were loaded, and then departed through the south door.

The excavation was completed in 24 hours, working three shifts, and it was another 12 days before the vault was completed and temporary planking placed over the equipment opening so that cars could once more use the garage.

During the period of vault construction, the underground ducts from the future substation to the street also were installed and the garage floor resurfaced.

The Substation Vault

The vault itself is of reinforced concrete construction with walls one foot thick on three sides, utilizing the existing office building wall on the fourth side.

Before the floor slab was poured, a ground grid of number 1/0 wire was installed at the bottom of the floor slab excavation and connected to eight copperweld ground rods driven 10 feet into the moist soil.

Two 5-inch 6.7-pound channels also were imbedded in the floor slab and accurately leveled. These channels provided mounting supports for the transformer and metal-clad switchgear, eliminating the necessity of shimming or grouting the transformer or metal-clad equipment in order to make them line up. The channels also were used as a screed for leveling the concrete on the floor slab. Figure 5, a plan view of the vault proper, shows the location of the ground grid and mounting channels.

It is sometimes rather difficult to line up the channels in the floor slab and keep them lined up while the slab is being poured; however, the method used in this vault gave good results.

After reinforcing steel had been put in place, holes were dug in the dirt below the slab excavation with a posthole digger along the line on which the channels were to be installed. Bolts, long enough to extend about two inches above the channel surface, were then set in the holes, the holes filled with concrete. When the concrete was set, the channels were installed and leveled with a transit, using a nut on the top and bottom of the bolts to hold the channels firmly in place.

It was found that the channels remained in place very well during the pouring of the floor slab, and when the slab had set, it was a simple matter to cut or burn off the extra length of bolt extending above the channel.

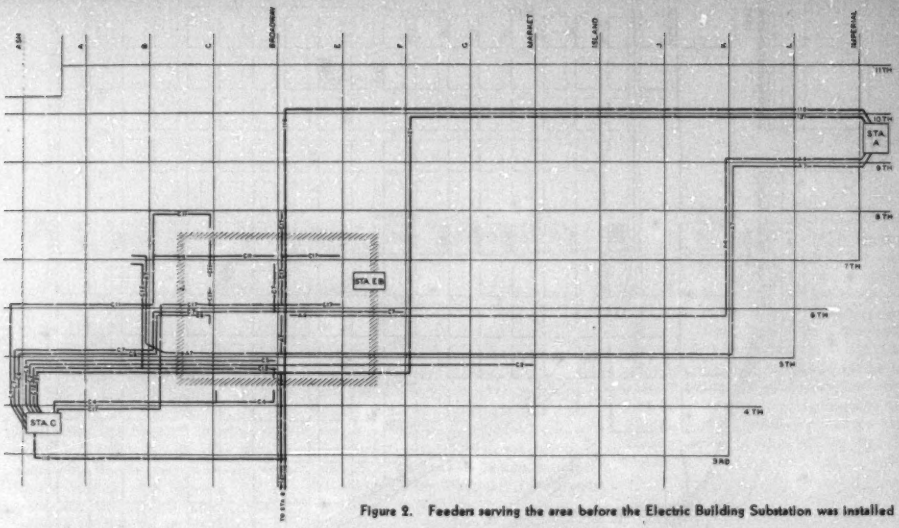

Figure 2. Feeders serving the area before the Electric Building Substation was installed

The roof of the vault was of reinforced concrete construction supported by 12-inch wide-flange 58-pound beams running the short way of the vault. These beams were supported by the vault walls on one end and piers set adjacent to the office building wall on the other end.

An opening 10 feet 4 inches by 14 feet 6 inches in the clear was left over the transformer location to provide an entrance for the heavy equipment. This opening was covered with seven precast 6-inch removable concrete slabs after the equipment was lowered in place, and the cracks between slabs were sealed with asphalt. Figure 6 shows these slabs in place in the opening.

On one corner of the roof of the vault there was installed an 18-inch opening with a removable manhole cover. This opening was to provide an entrance to the

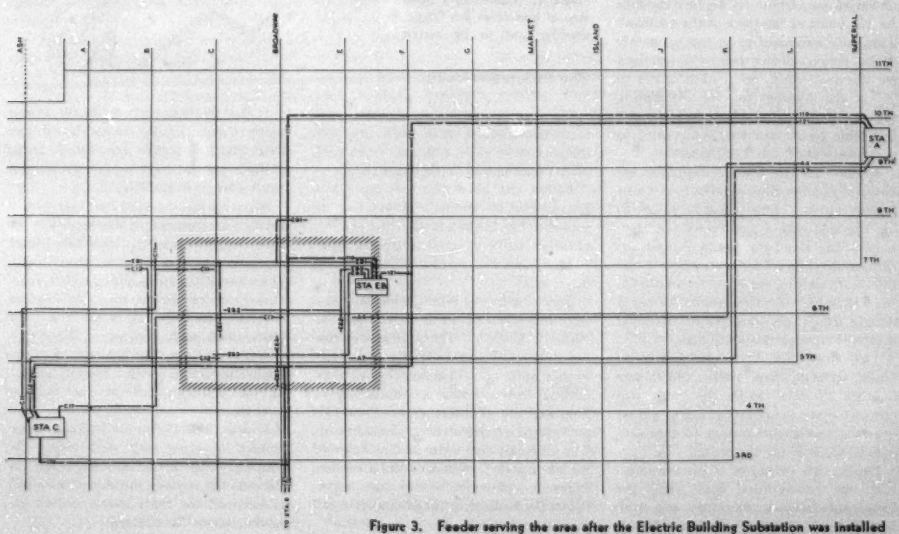

Figure 3. Feeder serving the area after the Electric Building Substation was installed

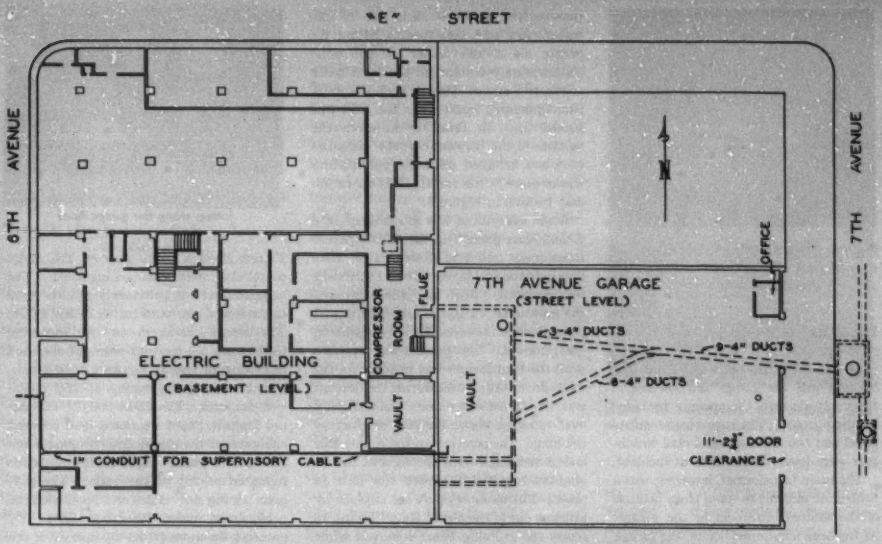

Figure 4. Plot plan and general layout of Electric Building basement and 7th Street Garage (at street level)

vault for the 12-kv and 4-kv rubber cables from the mobile substation which could be used to pick up a good part of the Electric Building Substation load in the event of transformer failure. The mobile substation could be parked in the garage and connected to the underground substation in various ways by means of dummy circuit breakers.

A sump was provided in the vault to take care of any small amounts of water which might inadvertently seep into the substation vault, and a $4^1/_2$-inch curb was provided at the door to the basement to be sure that no oil could flow into it in case of a ruptured transformer tank.

The 2 by 9 foot opening from the vault to the incinerator stack for air exhaust and the ventilating fan annex previously described complete the vault proper. Figure 7, showing an elevation of the west end of the vault, including the fan annex, will show more clearly the location of the elements just described.

Figure 5. Plan view of vault, showing mounting channels and ground grid

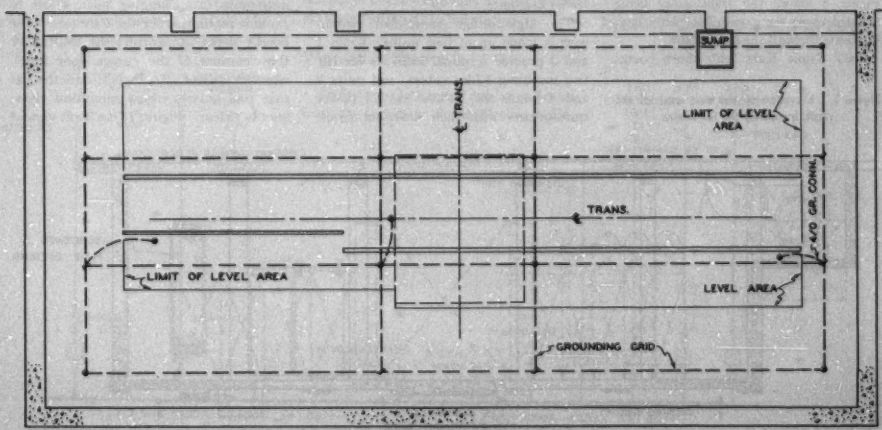

Figure 6. View of removable precast concrete slabs in place in the opening through which the apparatus was lowered

Installing the Equipment

All of the substation equipment was brought into the garage and lowered in the vault through the opening provided for the purpose. The supervisory control panel and two units of metal-clad switchgear were lowered first without incident.

The main transformer, however, was a little more difficult to set in place because of the limited headroom in the garage. As has been mentioned before, the garage door lintel is 11 feet, $2^3/_4$ inches in the clear above the floor at the lowest point. The transformer is 11 feet $1^5/_8$ inches high to the top of the pressure relief device, leaving very little clearance for handling under the door lintel.

The transformer was unloaded in the street and skidded into the garage on greased steel angles. Wooden cribbing, 12 by 12, was installed in the vault below the opening until the cribbing was flush with the garage floor. The transformer was then skidded onto the cribbing. Figure 8 shows the transformer being skidded along the garage floor after having come through the south door.

Two Krane Kars with short booms were set in place on each side of the transformer and their booms bolted together above the center of the unit. Cables were run between the front axles of the two Krane Kars to keep the axles from spreading apart when the load was picked up. In order to improve the balance of the transformer, the radiators were not installed until the transformer was in place in the vault. This operation may be seen in Figure 9.

When everything was in readiness, the Krane Kars picked up the 35,000-pound transformer and held it suspended while the skids and first layer of 12 by 12 cribbing was removed. Then the cranes lowered the unit about 12 inches and held it suspended while the second layer of cribbing was removed. This process was repeated until the transformer was in place on the vault floor. At no time during the descent was the transformer more than slightly over 12 inches above the very substantial cribbing. The positions of the Krane Kar booms remained fixed throughout the 36 minutes required to lower the unit in place. The radiators were set in place by utilizing one of the Krane Kars. Figure 10 shows the cribbing being removed while the transformer is lowered through the opening.

The Substation Proper

Figure 11 is a 1-line diagram of the indoor metal-clad master unit substation which was installed in the vault. It will be noted that there are two incoming 12-kv circuits, operating in parallel to feed a main 3-phase power transformer, which in turn feeds a main 4-kv bus from which three outgoing feeders and a transfer feeder originate.

The high-voltage metal-clad switchgear is made up of four units. Units 1 and 3 provide terminal facilities for the two incoming 12-kv cables, and units 2 and 4 house the 10-kva control power transformers with their draw-out fuses.

Figure 8. Skidding the main power transformer along the garage floor

Figure 12 is a front view of the 12-kv metal-clad switchgear as installed. The sump referred to previously may be seen in the lower left-hand corner of the figure. The circuit breakers on the incoming feeders are a-c-rectifier solenoid-operated draw-out air circuit breakers with a published interrupting rating of 250 megavolt-amperes. The 12-kv 500,000 circular mil 3-phase paper insulated lead covered cables enter the metal-clad compartments through 3-phase right-angle potheads mounted on top of the units. The pothead wiping sleeves are on a level with the cable ducts under the garage floor. By entering the units at the top instead of the bottom, the necessity of draping the cables along the walls of the vault was eliminated. As is usual on indoor metal-clad equipments, instruments, relays, and so forth, are mounted on the face of the doors of the circuit-breaker compartments, as can be seen in Figure 12.

The main 12-kv 1,200-ampere bus is throat-connected to the 3-phase 12,500/-4,330-volt power transformer. This unit is rated 5,000/6,667 kva and has $2\text{-}2^1/_2$ per cent hand taps above and below 12,500 volts as well as $\pm 7^1/_2$ per cent automatic tap changing under load to provide regulation for the 4-kv bus. The height of the transformer was limited by the clearance of the garage door lintel, which is 11 feet, $2^3/_4$ inches, and the garage roof trusses whose minimum clearance is 12 feet. Figure 13 is a front view of

Figure 7. Elevation of the west end of the vault, including the fan annex

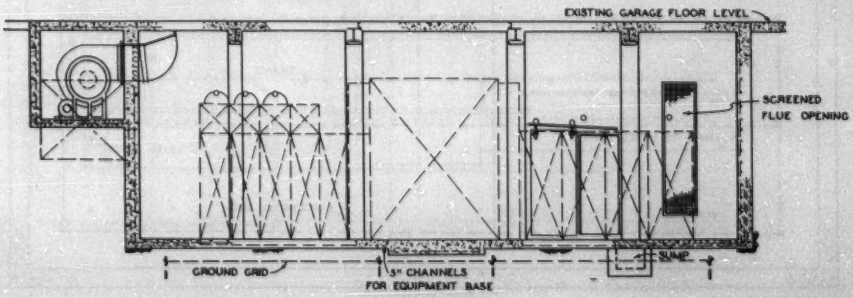

Figure 9. Transformer ready to be lowered into the vault

the transformer, showing the tap changer compartment with the controls mounted below inside the door. The 4-kv switchgear is in the distance.

In order to obtain the maximum cooling efficiency for the transformer, the radiators were all mounted at the back of the unit and the stream of ventilating air is directed on them by adjusting the louvres on the air intake ducts. Figure 14 shows the air intake ducts on the south wall with the louvres set to direct the air stream downward toward the transformer radiators, from which the picture was taken.

The transformer proper and tap-changing compartment of the unit are both oil-filled. At the time the specifications for the substation were being written considerable thought was given to the use of askarel instead of oil as a cooling medium because of the lesser fire hazard. But inasmuch as oil was required in the tap-changing compartment, the place where trouble is most likely to occur if there is any trouble, and because it would be a simple matter to contain the oil from a ruptured transformer in the vault, it was decided that it would not be worth while to use a half askarel, half oil unit.

From the transformer a throat connection leads to the low-voltage metal-clad switchgear which consists of five units housing 1,200-ampere 4-kv main and transfer busses. There are three 4-kv feeder units with their a-c-rectifier solenoid-operated 100-megavolt-ampere interrupting capacity air circuit breakers and interlocked disconnecting switches to permit connecting the outgoing feeder to the 4-kv transfer bus. There also is a 4-kv transfer feeder unit which contains the 4-kv transfer air circuit breaker, similar to the feeder circuit breakers. The fifth unit, an auxiliary compartment, houses the 48-volt battery, metering current and potential transformers and station power and light throwover. The 4-kv metal-clad switchgear is shown clearly in Figure 15.

The 4-kv transfer circuit breaker is provided to permit testing and maintenance on the three outgoing feeder circuit breakers and controls without the necessity of transferring the feeder load to some other substation.

As in the case of the 12-kv potheads, the 4-kv right angle potheads are mounted on the top of the metal-clad switchgear. The 4-kv transfer bus is located in a compartment with the transfer disconnecting switches at the top of the switchgear. The transfer bus compartment and back of the 4-kv potheads can be seen clearly in Figure 15.

The last major item in the substation is the code selector supervisory control equipment. The relays which form the integral part of this type of supervisory control are mounted on a separate panel set up in one corner of the vault and connected to the metal-clad switchgear by means of overhead conduits. The control station for the Electric Building Substation is in the dispatcher's office, which is located adjacent to Substation A.

Ventilation System

Air for ventilation and cooling is drawn from the basement of the Electric Building through a $5^1/_2$ by 6 foot grilled opening near the ceiling of the stationery department storage room by means of two 30-inch fans each driven by a 2-horsepower 220-volt 3-phase motor, and discharged into the vault through two openings each about 2 feet square. By providing such a large opening from the stationery department to the ventilating fan annex and by providing screens instead of a solid wall in the upper part of the basement partitions, it was possible to keep drafts in the stationery and other departments quite low, even though providing 300 cubic feet per second of air to the vault.

Figure 10. Removing the cribbing from beneath the transformer as it was being lowered into the vault

Figure 11. One-line diagram of the Electric Building Substation

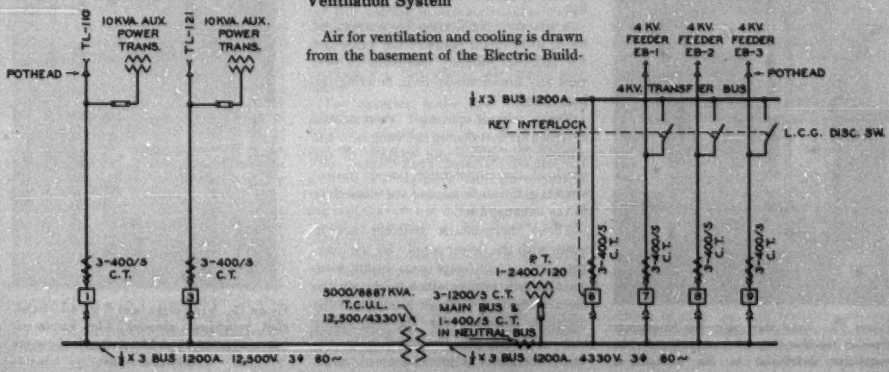

Figure 12. Front view of 12-kv metal-clad switchgear

Two fans were provided instead of one larger one in order to be sure of some ventilation and cooling air even though one fan should fail.

The 2 by 2 foot intake openings for the vault are located near the ceiling and are provided with louvres tending to direct the stream of air toward the transformer radiators where the transformer fans pick up the cool air and carry it through the radiator bank, still maintaining the same direction of flow. Finally, the warmed air is discharged through the incinerator flue. Figure 14 shows these openings.

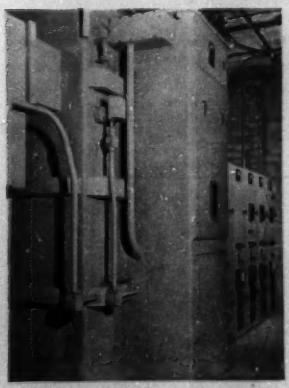

Figure 13. Front view of power transformer showing tap-changing compartment and 4-kv metal-clad switchgear in the background

Figure 14. View of air intake openings taken from the top of the transformer radiators. The 4-kv outgoing cables appear in the center of the picture

The fan motors are equipped with pushbuttons located in the vault to the right of the door as you enter. These pushbuttons operate magnetic switches next to the motors in the annex. Energy for the fan motors is obtained from the Electric Building power supply and not from the substation control power transformers.

Over each intake opening, a 3/16-inch metal door is suspended and held open by a magnetic latch which can be shut in event of a fire. This device will be described more in detail later.

So far with about 4,200 kva on the transformer bank the maximum recorded temperature has been 40 degrees centigrade, a very reasonable figure for a vault transformer operating at 84 per cent load.

Fire Protection

In any substation in which oil-filled electric equipment is installed, there is always present the danger of an oil fire. To cut this possibility to a minimum, several precautions have been taken in the Electric Building Substation.

In the first place, the 12-inch beams supporting the roof of the vault were incased in concrete in order to prevent damaging them in the event of an oil fire.

A fire door, held open by a magnetic latch, is installed between the vault and the Electric Building basement to prevent any fire or smoke from entering the basement.

Two circuit-opening thermostatic switches are installed in the vault near the ceiling, one above and slightly to the north of the transformer proper (downstream in the air flow), and the other close to the exhaust flue.

These thermostatic switches are in series with the power supply for the magnetic latch which keeps open the fire door, the magnetic latches which hold open the metal doors over each air intake, and the magnetic switches for the ventilating fans. Should the temperature in the vault rise above a predetermined value, the fans are shut down, the air intake closed off and the fire door to the basement closed at once. Operation of this equipment sounds an alarm in the dispatcher's office over the supervisory control equipment.

In the event of a serious fire, the cover can be removed from the opening in the northeast corner of the vault which was installed to take the emergency leads from the mobile substation and the vault flooded with CO_2 brought in from an outside source.

Circuit Relaying and Control

Both 12-kv incoming feeders are operated with their circuit breakers closed on the Electric Building bus at all times, so that the failure of either source will not result in an outage to the substation. As has been mentioned earlier, the 12-kv lines feed from Generating Station B to Substation A, Substation C, and the Electric Building Substations. Two-wire differential-type pilot wire relays

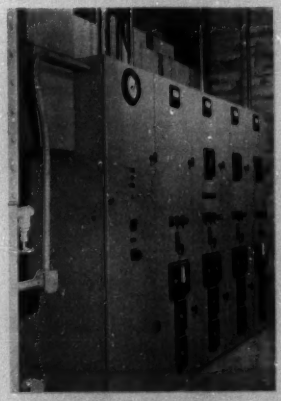

Figure 15. View of the front of the 4-kv metal-clad switchgear, showing 4-kv transformer bus compartment and 4-kv potheads above the switchgear proper

which are normally not recommended for application to lines having more than three terminals have been applied to these 4-terminal lines. Knowing that normal or even most abnormal operation would never require more than three of the line terminals to be closed at one time, the pilot wires to the three receiving substations were carried through "a" auxiliary switches at those substations so that the idle relay would not shunt the active relays when its breaker was open.

The transformer bank itself is protected with induction overcurrent relays equipped with instantaneous trip attachments connected to trip both incoming 12-kv oil circuit breakers, which can be set half or three-fourths of the way through the transformer bank.

The relaying on the 4-kv feeders is conventional 3-phase relays and a residual or ground relay, all equipped with instantaneous trip attachments to clear high current faults as soon as it is possible.

Each circuit breaker is equipped with a supervisory-local transfer switch by means of which the control of the individual units may be changed from supervisory control to control by the pistol grip control switches on the panels. It might be noted that the control is wired in such a way as to permit circuit breakers to be tripped locally no matter what the position of the supervisory-local switch might be, but only permits the circuit breaker to be closed locally when the supervisory-local switch is in the local position.

Instantaneous single-shot reclosing relays are installed on the 4-kv feeder circuit breakers which are in service whether the substation is on supervisory or local control, it being considered important to limit outages to these feeders to a bare minimum. Even though the feeders are all underground and faults probably would be of a permanent nature when they occur, the reclosers were installed to re-energize the feeders on the chance that some faults might be self-clearing. Incorrect co-ordination between the relay instantaneous trip attachments and distribution fuses during high-current faults might be considered a self-clearing fault.

Summary

The Electric Building Substation whose design and installation has been outlined is operating very satisfactorily. Transformer operating temperatures are very low, and voltage regulation throughout the area served is well within allowable limits.

The company was extremely fortunate in being able to take advantage of the incinerator flue to exhaust the heated air from the transformer vault, as this is always one of the major difficulties to be overcome on any large vault installation.

Discussion

Ray K. Klumb (Southern California Edison Company, Los Angeles, Calif.): I have studied Mr. Sinnott's paper with considerable interest and am pleased to find there are other people who believe in the practicality of the underground substation for multicircuit distribution service. The San Diego Gas and Electric Company was indeed fortunate in having structural conditions so well suited and are to be commended on seeing the advantages of the situation and putting it to such good use. This application points a way for other utilities in that their own structures may be part of the answer to providing service facilities in the more congested areas.

It appears that increased load density in the area was the necessity for the substation, and I wonder if the station was made large enough in physical size to take care of future increase. The thought being that provision for future capacity is relatively easy when building a new substation of this type, but oftentimes extremely difficult after the station is on the line. Load within reach of the substation, but not now served from the substation may in the future reach values that will make it desirable to feed from this point rather than from the existing source. When such conditions occur, and they do quite often, it is a comfortable feeling to have sufficient room to add the necessary facilities.

I would like to mention a few points that the Southern California Edison Company feel are important in underground substation application and operation.

When an underground substation is dictated plans should be laid for at least an ultimate of the capacity needed for the area that can be economically served from that point to the extent that carrying charges on structural space are within the cost of an addition or a new substation. Another factor to consider in deciding upon a definite capacity is whether or not the load can be satisfactorily served if additions or replacements are necessary. Maintenance has to be considered, in that facilities to handle maintenance without load interruption are needed. Also reasonably good protection should be available when various parts of the substation are out of service for maintenance. Testing facilities for relays and circuit breakers are a part of the plan, and the cost of handling the maintenance should be reasonable.

Mr. Sinnott mentioned the provision for getting cables from a mobile substation into the vault in case of transformer failure, and he stated that the mobile substation could pick up a good part of the substation load. Is it best practice to put reliance in a single transformer in an underground substation? Also, when the time arises to overhaul the tap changer, how will it be done and service maintained? Within our company, we do not feel justified in making installations of this kind without switching facilities for disconnecting the equipment, and also we do not feel secure without a spare or means of carrying the load should the largest unit fail.

Tap changing under load transformers feeding more than one circuit requires balancing circuit loads in order to deliver correct voltage at all points on the feeders. This condition and requirement has deterred us from handling more than two circuits in this manner in the areas where circuit loading is of the order of 1,500 kva or better. I would be interested in Mr. Sinnott's comments on this point.

Provision for fire protection as covered in Mr. Sinnott's paper is from the exterior and with the use of outside equipment. This I do not believe would be satisfactory in case of fire. We prefer fully automatic fire protection using CO_2 saturation, with control from suitably placed thermostats.

The Southern California Edison Company has operating one completely-underground 16/4-kv substation with 9,000-kva capacity, feeding six 4-kv individually-regulated circuits. The transformers at present consist of three 2,000-kva and three 1,000-kva single-phase units. Ultimate capacity for which room has been provided is six 2,000-kva single-phase units. A spare 2,000-kva transformer is maintained in the Alhambra warehouse to cover the large bank. The station is fed at present by two 16-kv circuits and the third circuit is being added. Switchgear is all metal-clad using oil circuit breakers. The protection employs directional overcurrent on the incoming lines and overcurrent and ground on the 4-kv circuits. The station is fully automatic. Incoming lines are self-restoring and 4 kv circuits are equipped with reclosers. Alarm signals are transmitted over wired circuits to the nearest attended substation.

Transformers are protected with differential relays and an automatic CO_2 fire extinguishing system is provided. Cooling is provided by fans operating on thermostat control from room temperature. The operation of this station has been satisfactory, but in an attempt to reduce the cost of such installations, a new design is on the drawing board for an eight circuit 18,000-kva 16/4-kv underground substation using four 3-phase tap changing under load transformers so rated and arranged that two will carry the total load over the peak if necessary. Arrangement is such that normally one transformer carries two circuits. In case of failure of one transformer the circuits carried from the bad order unit are automatically picked up on two of the remaining transformers. Control and protection will be arranged to cover failure at any one point and still carry the load. The station will be automatic and self-sustaining for all conditions of operation and maintenance and nothing except complete failure of the 16-kv switchgear should shut it down. Each transformer will have 4,000-volt capacitors

provided with automatic switching facilities for voltage level control. Control power will be supplied for all operating functions by a 125-volt storage battery. The substation will be constructed in connection with an office building, the basement of which will contain a portion of the equipment, but the rear area will be completely underground with the roof used for parking. Access to the station, both by stairway and hatchway, will be from the parking area. Only one half of the substation equipment will be installed initially, and the other half will be installed when load conditions dictate. Arrangement and connections will be such that additions can be made with only part of the equipment out of service at one time. Cooling air will be provided with low velocity fans to keep down the noise level outside the substation.

I wish to compliment Mr. Sinnot on his paper, particularly on the detail with which he covered the subject. I would like my remarks to be accepted merely as thoughts and ideas on underground substations. It is evident that the compelling forces of congestion will necessitate more underground substations. Criticism and ideas will be most welcome.

J. F. Sinnott: In his discussion, Mr. Klumb questions as to whether or not the substation was made large enough in physical size to take care of future increase.

There were several reasons for limiting the size of this substation.

1. As pointed out in the paper, the area to be served is fairly well built up, making large load increases rather unlikely.

2. A larger substation would require more cooling air, increasing the velocity through the flue to the point where the noise of the exhaust would be objectionable. Furthermore, the air intake problem would become complicated.

3. When the new substation becomes loaded, it is planned to shorten the extent of the three feeders and feed the far ends from existing or new stations that would not have to be installed underground.

Whenever it becomes necessary to maintain the tap changer, the far ends of the three 4-kv feeder loads will be picked up on feeders from Substations A and C through tie switches, and the bulk of the load carried on the mobile substation. This can be done without an outage to any load and with very little voltage disturbance.

We have found modern 3-phase transformers extremely reliable and can see no reason for dividing the load between two units as long as the feeders can be tied to other substations in an emergency and so long as we have a mobile unit available.

That the longest 4-kv feeder is less than 900 feet in length and that all the load is of similar nature makes, in our opinion, individual feeder regulation unnecessary.

Progress Report on Tidd 500-Kv Test Project of the American Gas and Electric Company—Corona, Radio Influence, and Other Factors

PHILIP SPORN
FELLOW AIEE

A. C. MONTEITH
FELLOW AIEE

Synopsis: The field test project for studying corona, radio influence, and other technical features of electric power transmission in the extra-high-voltage range now has been in progress on The Ohio Power Company system of the American Gas and Electric Company at Brilliant, Ohio, for over two years. This paper is a progress report of this activity. It presents problems that are unique in the study of corona, particularly the effects of the conductor surface and weather upon the corona loss. It emphasizes the importance of foul weather in determining the average loss for use in evaluating the economic aspects of corona loss. Extensive tests also have been made of the effects of corona upon radio communication services. Radio influence is probably the factor limiting the choice of a satisfactory conductor for extra-high voltages.

DURING the past two years a great deal of information of value on the technical features of high-voltage line design has been obtained from the field research which is being carried out by the American Gas and Electric Service Corporation in co-operation with eight manufacturers of high-voltage equipment. This program was fully described in a symposium of seven papers in 1947.[1–7] The objectives and test facilities for carrying on the field test work were covered in considerable detail in that series of papers.

The broad objective is to obtain additional, more extensive, and more precise information on some of the technical problems involved in extra-high-voltage transmission. It was feared that the satisfactory solution of some of these problems possibly might act to put a limit on the voltage one might otherwise choose in seeking ways to improve the economics of transmitting large blocks of electric energy which are certain to be needed in the relatively near future.

In brief, the test facilities consist of a 5,000-kva bank of three single-phase transformers which can vary the 3-phase line-to-line voltage in steps from 265 to 532 kv. Three test lines, two 1.4 miles long and one 800 feet long, are available. Supersensitive metering equipment is used to indicate and record corona loss. The metering also includes indicating and graphic radio-influence meters, commercial amplitude-modulated and frequency-modulated receivers, a television set, a voltage gradient meter,[8] and graphic meters to record temperature, barometric pressure, precipitation, and humidity. In addition, an automatic camera, set to photograph sample conductors and insulators every 20 minutes, is used in the determination of general weather conditions, such as rain, snow, sleet, and fog. A setup is also provided to measure the loss on a string of insulators. Line conductors from 0.92 inch to 2.0 inches in diameter have been tested. A view of the field test station is shown in Figure 1.

The great amount of data already obtained from the field tests has been analyzed partially but still requires further study and correlation before arriving at definite conclusions. However, it was felt that although the analysis and field test work are not complete at this time, a presentation of the progress being made and some of the high points of the results obtained would be justified in being presented now because of the interest. This report accordingly has been prepared to fulfill this objective. It is planned within the next year to follow this brief presentation with more complete results and analysis giving detailed test data and summarized results. It needs to be emphasized, therefore, that the data presented here must be considered as preliminary; complete analysis of data already obtained and further work now in progress may modify the results.

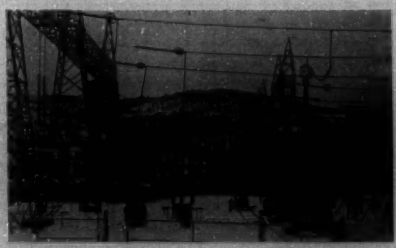

Figure 1. General view of 500-kv test station at Tidd

At right center is 5,000-kva transformer bank supplying the three test lines at 265 to 532 kv. Equipment for corona-loss measurements is in cabinets on top of bushings. Meters are read from observation booth at left center, by high-power telescope. Servicing of meters is done from moving elevated platform: center, background

Paper 50-143, recommended by the AIEE Transmission and Distribution Committee and approved by the AIEE Technical Program Committee for presentation at the AIEE Summer and Pacific General Meeting, Pasadena, Calif., June 12–16, 1950. Manuscript submitted March 14, 1950; made available for printing April 10, 1950.

PHILIP SPORN is President of the American Gas and Electric Service Corporation, New York, N. Y., and A. C. MONTEITH is a Vice-President with Westinghouse Electric Corporation, Pittsburgh, Pa.

Figure 2. Typical correlated graphic data on corona loss, radio influence, weather, and so forth, obtained or derived from continuously recorded field measurements

The test lines here were energized at 454 kv line-to-line

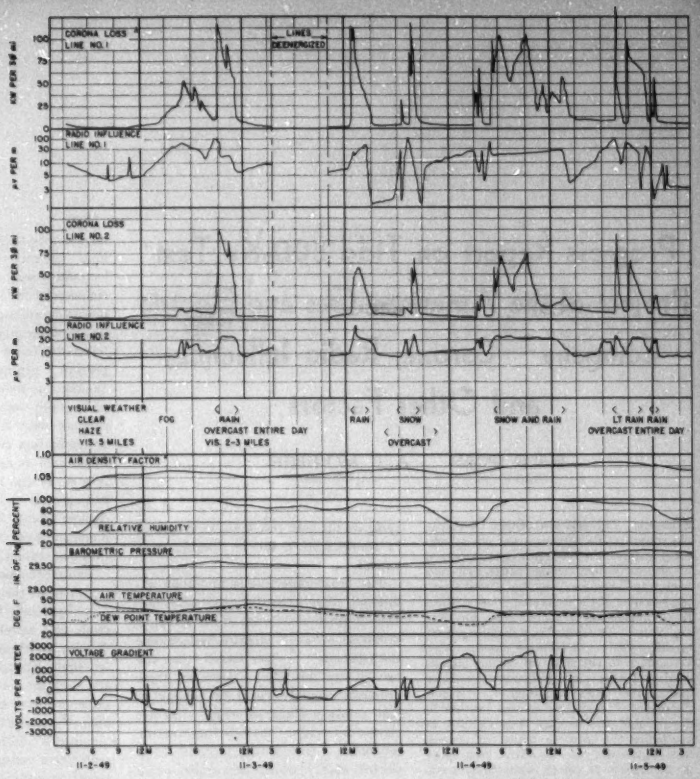

Figure 3 (below). Change in corona loss of a conductor with time at phase-to-phase line voltages of 376, 454, and 532 kv, during fair weather over a period of almost two years

The conductor spacing was 45 feet up to July 18, 1949, at which time it was changed to 32 feet

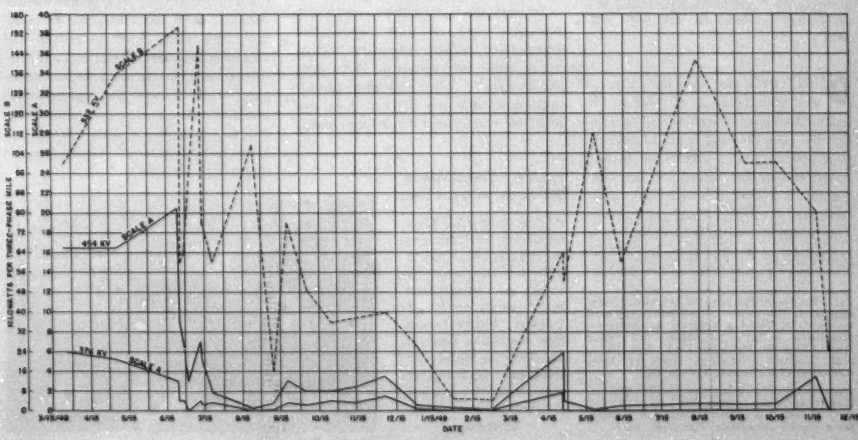

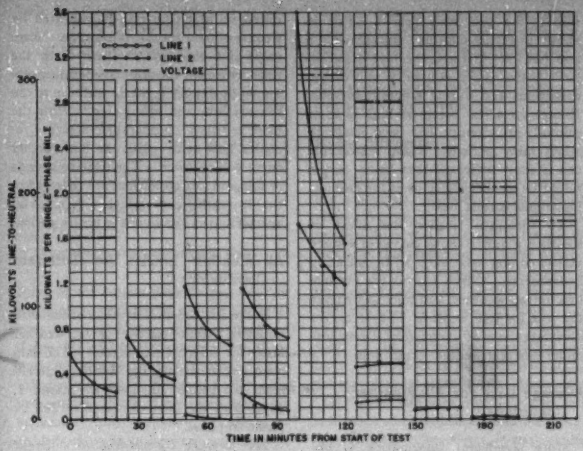

Figure 4. Change in corona loss on different conductors as affected by duration of energization

The lines had been de-energized for several days prior to this test

Corona-Loss Test Program

In the corona-loss studies emphasis has been placed on establishing a method of estimating the magnitude of the annual corona loss on various conductor and line designs, and the manner in which the corona loss might be expected to vary with voltage and weather. Information upon which to base estimating procedures can be obtained by recording the corona loss on a full scale line at different voltages over long periods that include all kinds of weather. The corona test program has been planned to obtain the fundamental data required to meet these objectives.

Because of the many variables involved, and the fact that weather conditions cannot be controlled, the procedure was adopted of recording, for later analysis, those factors which are considered important, rather than depending upon making individual tests under a variety of weather conditions. Figure 2 illustrates typical information that has been obtained thus, or can be derived from the field graphic charts.

In order to provide information on the full voltage range over which the conductors might be expected to operate, the lines were energized continuously, and the applied voltage was changed every few days. Voltages of 280, 345, 396, and 452 kv phase-to-phase have been used. In addition to obtaining graphic records of corona loss at these four voltages, voltage-versus-corona-loss runs were made every four weeks using indicating instruments. These tests were made under both single- and 3-phase conditions. Most voltage runs were made under fair-weather conditions so that the results of successive tests could be compared. Some tests under adverse weather were made, but these tests are not readily comparable as rainfall is rarely constant for a sufficient time to obtain a complete test under constant conditions.

Factors Producing High Values of Corona Loss

Great variance was observed in corona loss measurements as noted by previous investigators.[8, 10, 11, 12, 13] The factors influencing this variance can be divided into two categories: first, those associated with the conductor surface, and second, those associated with weather conditions. Thus different conductors might have comparable corona loss under fair-weather conditions but different losses after aging or during foul weather.

Surface Factors

The surface of an energized conductor undergoes a change with time such that the loss usually decreases, the magnitude of the change varying with the particular type of conductor. From the fair-weather runs made periodically over a period of almost two years, the loss values corresponding to the 532-, 454-, and 376-kv points are plotted in Figure 3 for the 1.65-inch Heddernheim conductor. This figure shows how much loss might be expected on a new conductor when it is first placed in service.

The effect of continuous energization of the conductor is indicated in Figure 3 for 454 and 376 kv. In determining the time required for a conductor to stabilize, the 532-kv curve in Figure 3 may not be significant because the conductors have never been energized for long periods of time at this voltage.

The wide range of loss readings which are obtained at a given voltage on successive fair-weather voltage runs indicates that comparisons of conductors should not be based on single observations.

Another surface effect is the temporary increase in the corona loss on a conductor after it has been de-energized for a day or more. If the conductor is energized again, the initial value of the loss is considerably higher than normal, and the loss immediately starts to decrease, requiring several hours or more to become constant. Because of this effect, the corona starting voltage of a given conductor might be 100 kv or more below its normal value. Conversely, although to a much lesser extent, if a conductor is energized at a voltage high enough to produce profuse corona, the loss at a lower voltage is temporarily reduced.

This effect is shown in Figure 4, which presents the results of a single-phase test. With increasing and then decreasing voltages, each voltage being applied for a period of 20 minutes, readings were taken every five minutes. Each time the applied voltage was increased, the conductor on line 1 showed a marked decrease in corona loss from its initial value for the interval, but when the voltage was reduced, it showed a slight increase in loss above the initial value for the interval. At the lower voltages the conductor on line 2 was not in corona, but at higher voltages a loss decrement with time can be observed which is similar in character to the conductor on line 1 but different in magnitude. Therefore, to obtain consistent results it was found necessary to precondition the conductors by energizing them at maximum voltage for about 15 minutes prior to testing. This procedure unfortunately yields values which are lower than the loss which would exist if the conductors were energized continuously at each test voltage.

Weather Factors

Of the weather factors causing high corona loss, rain, sleet, and snow are the

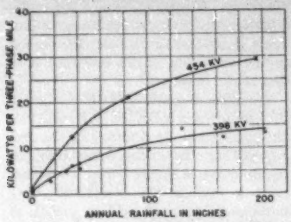

Figure 5. Correlation between rate of rainfall and corona loss, both averaged for periods of 48 hours to several days of operation at constant voltage

most important. High corona loss has been recorded during fog, but it is believed that this condition was caused by condensation of moisture on the surface of the conductor which is not likely to occur on an operating line. Temperature, humidity, barometric pressure, and atmospheric voltage gradient have an effect which is small compared to that of rain. Figure 2, in which most of these factors are recorded, is a typical example of how they vary. Separation of weather factors requires detailed analysis of a large number of records because several of the weather factors change together.

Preliminary analysis shows a consistent correlation between corona loss and average rate of rainfall.[16] Remarkably smooth curves are obtained if the corona loss, averaged over periods of from 48 hours to several days of operation at constant voltage, is plotted against average rate of rainfall for the same period. This is shown in Figure 5 for line voltages of 398 and 454 kv. These curves are based on data taken under a variety of weather conditions and during different seasons. Except for a few points at high rates of rainfall, no attempt has been made to select rainy periods. Their remarkable consistency indicates that such curves might be an acceptable basis for estimating annual corona loss.

To illustrate further the effect of weather, Figure 6 shows curves of voltage versus corona loss taken with indicating instruments. Curve 1 gives the average loss for fair weather, and the other curves the loss for foul weather. These curves illustrate the wide variation of corona loss under different weather conditions.

Average Loss for All-Weather Conditions

More significant information is obtained from the graphic records of all-weather corona loss than from individual fair-weather voltage runs. From graphic records, the annual corona loss can be estimated and its economic importance determined. From an analysis of corona-loss graphic records and weather charts, examples of which are shown in Figure 2, curves of the type illustrated in Figure 7, which show the per cent of time that the loss exceeds values given by the ordinate, can be plotted. It will be observed that the fair-weather losses are small and that for periods of known rainfall the losses are high.

"Fair weather" in this figure is a condition in which no rain is indicated by a conventional graphic rain gauge. "Rain only" is a condition as observed by the test men during the day and operating personnel during the night, in addition to the records from the rain gauge. With the more sensitive photographic weather recorder now being used, the fair-weather curve will be lower. The relative periods of fair and rain conditions are reflected in the all-weather curve which is obtained by averaging the loss over the entire period.

All-Weather Losses for Different Conductors

Table I is a résumé of some of the data obtained from curves of all-weather losses for different conductors. The data were taken during the 3-month period from November 29, 1948 to March 1, 1949, with the lines energized at 390 kv phase-to-phase.

The average corona loss of different

Table I. Three-Phase Corona Loss on Conductors at 390 Kv Phase-to-Phase

Line Conductor	Kw/3φ Mile Max.	20%*	50%†	Avg.	Test	C. Curve No.
Group 1—11/29/48 to 12/29/48—2.82″ of Rain						
1.65″ HH	90	8.0	2.0	5.2	3φ¶¶	225–1
1.65″ ACSR	120	8.1	2.1	7.4	¶	227–1
2.0″ ACSR	50+††	3.3	1.7	3.4	3φ¶¶	226–1
2.0″ ACSR	111	3.0	1.8	4.1	¶	229–1
2×0.92″—20″	131	22.5	2.3	8.1	**	228–1
Group 2—12/29/48 to 1/25/49—1.5″ of Rain						
1.65″ HH	74	2.6	1.5	4.8	3φ¶¶	214–1
1.65″ ACSR	99	3.0	1.8	4.4	¶	215–1
2.0″ ACSR	90	2.6	1.5	2.9	¶	217–1
2.0″ ACSR	25	1.5	0.8	1.6	3φ¶¶	212
2×0.92″—20″	96	3.0	1.8	5.6	**	216–1
Group 3—1/25/49 to 3/1/49—1.7″ of Rain						
1.65″ HH	98	5.7	1.0	5.3	3φ¶¶	197–1
1.65″ ACSR	133	4.8	1.9	6.3	¶	218–1
2.0″ ACSR	117	3.0	1.8	3.9	¶	222–1
2.0″ ACSR	46	1.8	0.8	2.9	3φ¶¶	206–1
2×0.92″—20″	132	6.0	1.8	7.8	**	197–1

* Values exceeded 20% of time.
† Values exceeded 50% of time.
¶ Outside phase of 3-phase line with different conductor.
** Middle phase of 3-phase line with different conductor.
†† Meters went off scale. This is an estimated value.
¶¶ Conductors have 45-foot horizontal spacing.

Values given for conductors tested under conditions ¶ and ** are three times the per-phase values obtained. This procedure theoretically yields low values when the outside phase is used and high values when the middle phase is used.

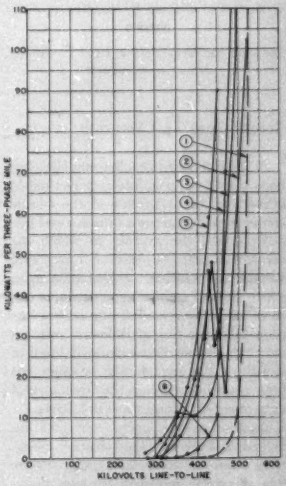

Figure 6. Three-phase corona loss under different weather conditions

Curve 1—Mean of 20 fair-weather curves. Curve 2—Light rain; conductor spacing 45 feet. Curve 3—Light rain; conductor spacing 32 feet. Curve 4—Rain; conductor spacing 45 feet. Curve 5—Heavy fog, conductor surface wet; spacing 45 feet. Curve 6—Snow flurries; spacing 45 feet.

Data for curves 5 and 6 were taken single-phase, and have been converted to 3-phase based on surface gradients for 45 feet flat spacing

Table II. Three-Phase Corona Loss at 390 Kv* Phase-to-Phase

For 3 Months 11/29/48 to 3/1/49

Conductor	Kw/3φ Mile Max.	20%†	Avg.
1.65" HH-Cu 3φ	98	5.4	5.1
1.65" ACSR 1φ	133	5.3	6.0
2-0.92—20" 1φ	133	10.7**	7.2
2.0" ACSR 3φ	50+††	1.7	2.6
2.0" ACSR 1φ	117	1.7	3.6

* See Notes at bottom of Table I.

† Values exceeded 20% of time.

** This value high because of data in Curve 228-1, Table I.

†† Estimated value—meters went off scale.

types of conductors depends not only on the applied voltage but also on the relative duration of fair and foul weather. Table II, which summarizes the three months' data of Table I, shows how the information can be tabulated, but does not contain information extending over sufficiently long periods to permit a reliable comparison between conductors. The conductors were tested at other voltages during the periods indicated, but this table presents only the information obtained at 390 kv. Records of this nature have been continued and still are being made.

The average values of corona loss, such as given in Table II, can be expected to be the same on operating lines as they are on the test lines. However, for lines of practical length the maximum value of corona loss will be much less than on test lines because extremes of weather are not likely to exist all along a line simultaneously. An evaluation of the weather conditions along a proposed right-of-way is necessary before an attempt to estimate the average and maximum values of corona loss can be made.[9]

Radio Influence

When this investigation was started, the published information available on radio-influence characteristics of transmission lines was believed to be insufficient for the prediction of these characteristics for a line designed to operate at voltages appreciably higher than the voltages used at the present time. The most recent publications[8, 10, 13, 14, 15] present most of the information available and have been published since the Tidd project was planned and started. Because of the clearly indicated need for the consideration of radio influence in the design of extra-high-voltage lines, it was decided to undertake a major study of radio influence using the Tidd test lines. A laboratory test program is also in progress to co-ordinate laboratory and field data.

The radio-influence problem consists essentially of two parts: the determination of the radio-influence factors of transmission lines, and the evaluation of these factors in terms of their effects on the communication services. One practical approach to the second part is the evaluation of data and experience on existing high-voltage lines as a bench mark.

Scope of Tests

It was planned to determine the effect of voltage and weather on radio influence for various conductor types, sizes, and spacings over long periods of time using graphic radio-influence meters so that average fair-weather and all-weather data would be available for analysis. Measurements have been made over the frequency range of 0.015 to 400 megacycles per second. Some of the data over this portion of the radio spectrum have consisted of manual readings, generally obtained during fair weather. Fair weather is considered to be any weather other than fog, rain, sleet, or snow environment around the conductors, and with conductor surfaces free of water, ice, or snow. Lateral and longitudinal profiles of radio influence have been made with the available portable meters. The effect of line voltage on radio influence has been investigated both with portable meters and with the graphic radio-influence meters.

Test Equipment

The equipment for radio-influence measurements consists of standard radio noise and field intensity meters[16, 17, 18] and a trailer equipped with amplitude-modulated, frequency-modulated, and television receivers.

Figure 7 (below). Corona loss record for one month on line 2 at 395 kv line-to-line during fair, rain, and all weather conditions

Ordinate indicates per cent time losses exceed the abscissa

Figure 8. Radio influence variation with line voltage at distances of 0 to 160 feet at right angles to line 1

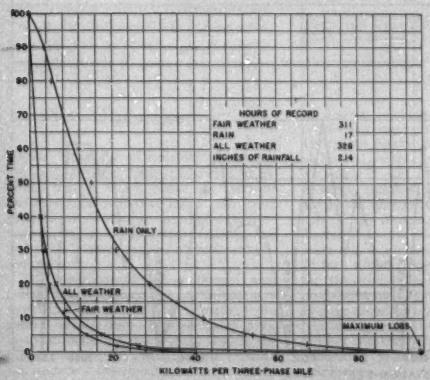

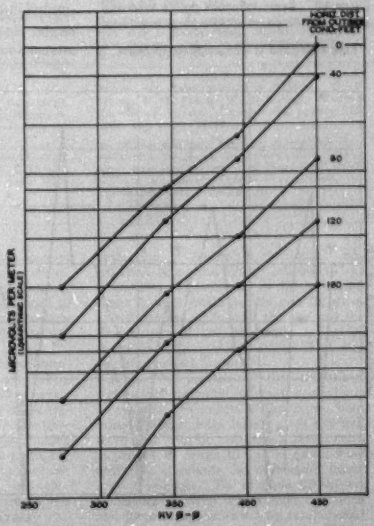

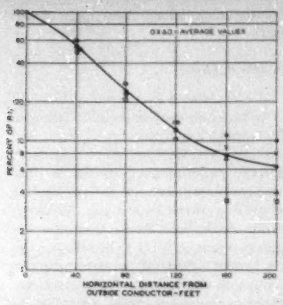

Figure 9. Attenuation of radio influence in per cent of values measured directly below outer phase conductor for line voltages from 138 to 450 kv phase-to-phase

Some Typical Data

The variation in radio influence with weather is being recorded with graphic meters at several voltages and for two conductor sizes. A portion of chart record for each of two lines is shown in Figure 2. It can be seen from this figure that snow and rain increase radio influence. The relative values of radio influence for the short period of time shown in this chart are not necessarily the same as would be obtained over a long period. There are considerable variations in radio influence during fair weather, and the causes for these variations have not been completely determined.

Radio Influence and Line Voltage

The relative change in radio influence with line voltage for different horizontal distances from the outside conductor is shown in Figure 8. The rapid rise of radio influence with increase of line voltage is apparent, as is the drop with increase in horizontal distance from the conductor. The slope of radio influence curve with voltage, for conductors of this size, is approximately the same as obtained by other investigators.[9,10]

Radio-Influence Attenuation with Lateral Distance from Outer Phase Conductor

Measurements of the lateral attenuation have been made at several frequencies with lines energized both single-phase and 3-phase. Some of the data obtained are shown in Figure 9. These data are from 62 tests at voltages of 138 to 450 kv line-to-line. The small spread of the test points indicates that the lateral attenuation is practically independent of line voltage.

Radio Influence Along the Line

Measurements obtained under the center-phase wire at 475 kv are shown in Figure 10. The variations of radio influence along the line are believed due to shielding by towers, change in conductor height, and reflections. The apparent attenuation is probably due to a change in radio influence during the three hours required for the test.

Radio Influence and Frequency

Measurements of radio influence over the frequency range show that radio influence values vary somewhat inversely as the frequency. Tests with amplitude-modulated, frequency-modulated, and television receivers indicate that radio influence may affect amplitude-modulated broadcast reception without appreciably affecting frequency-modulated and television reception.

Factors Affecting Tolerable Radio-Influence Levels

The evaluation of the effects on the communication services and tolerable limits of radio influence requires consideration of the characteristics of radio influence obtained and its effect on the various communication receivers, available signal intensities along the line, satisfactory signal-to-noise ratios, effects of weather, number and type of receivers in vicinity of line, distances of receivers from the line, transfer of radio influence to lower voltage circuits, and means for improvement of reception at a particular receiver.[19,20] It seems reasonable to permit higher levels of radio influence on extra-high-voltage transmission lines than on lower voltage lines for several significant reasons: 1. the direct coupling to receiver antennas will generally be less; 2. there will be fewer receivers near the line; and 3. there will be fewer parallels and cross-overs.

Figure 10. Radio-influence profile measured along test line under middle-phase conductor

Line energized at 475 kv phase-to-phase

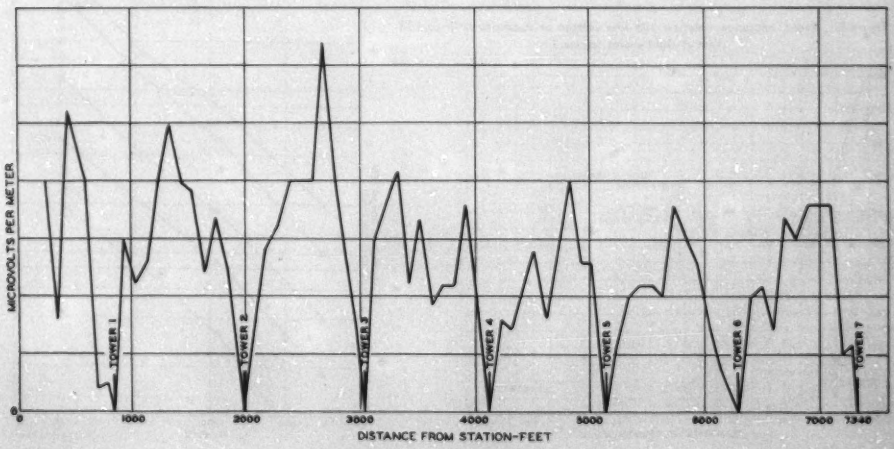

Continuation of Investigation—Evaluation of Test Data

While some test data still remain to be recorded, most of the information has been obtained. The large amount of work involved in analyzing and correlating these data still remains to be done.

A summary of the large amount of data which has been obtained at the field test location may be of interest. Up to January 1, 1950, over 12,000 feet of graphic records from corona loss and radio influence instruments have been obtained. Over 200 corona-loss-versus-voltage runs have been made, including 3-phase and single-phase tests. In addition, all weather recording meters have been in almost continuous operation but are not included in the foregoing summary of graphic records.

By February 1950 only part of the data thus far obtained in the field had been analyzed and correlated. For this reason only typical data are presented in this report and the conclusions drawn must be considered tentative. Definite conclusions cannot be drawn at this time, but must await the more complete analysis of all significant data.

A series of complete reports giving detailed analyses of the data obtained on conductors tested and information on the application of these data to extra-high-voltage line design is planned for presentation before the AIEE in the near future.

Tentative Conclusions

1. Voltage-corona-loss runs are primarily of theoretical interest, and in general are less significant for comparing conductors than voltage tests of long duration. The all-weather corona loss of conductors is believed to be of more significance in studying the economic value of corona loss on a high-voltage line.

2. Corona loss is a function of the combined effect of surface and weather factors. New conductors generally produce more corona than aged conductors.

3. The radio-influence problem involves the determination of radio-influence factors to be expected on a line of specific design, and the evaluation of these factors in terms of their effects on communication services to be encountered. Much work has been done on both phases of the problem. Serious consideration must be given to this problem in the design of extra-high-voltage lines.

4. While some definite values on corona loss and relative figures on radio influence are presented in this paper, they must be considered tentative. A series of reports to be presented in the near future will give complete information on both corona loss and radio influence, and on the application of these data to extra-high-voltage transmission line design.

References

1. Transmission of Electric Power at Extra High Voltages, **Philip Spore, A. C. Monteith.** *AIEE Transactions*, volume 66, 1947, pages 1871–82.

2. Corona Considerations on High-Voltage Lines and Design Features of Tidd 500-Kv Test Lines, **C. F. Wagner, Anthony Wagner, E. L. Peterson, I. W. Gross.** *AIEE Transactions*, volume 66, 1947, pages 1583–91.

3. Transformers and Lightning Arresters—Tidd 500-Kv Test Lines, **F. A. Lane, J. K. Hodnette, P. L. Bellaschi, Edward Beck.** *AIEE Transactions*, volume 66, 1947, pages 1613–18.

4. Insulators and Line Hardware for Tidd 500-Kv Test Lines, **I. W. Gross, R. L. McCoy, J. M. Shoadel.** *AIEE Transactions*, volume 66, 1947, pages 1592–1602.

5. Line Conductors—Tidd 500-Kv Test Lines, **E. L. Peterson, D. M. Simmons, L. F. Hickernell, M. E. Noyes.** *AIEE Transactions*, volume 66, 1947, pages 1603–12.

6. Instrumentation and Measurement—Tidd 500-Kv Test Lines, **R. L. Tremaine, G. D. Lippert.** *AIEE Transactions*, volume 66, 1947, pages 1624–31.

7. Switchgear Equipment for Tidd High-Voltage Test Lines, **F. A. Lane, B. W. Wyman.** *AIEE Transactions*, volume 66, 1947, pages 1619–23.

8. A Voltage Gradient Meter, **R. L. Tremaine, R. C. Cheek.** *AIEE Transactions*, volume 69, part I, 1950, pages 633–37.

9. The Swedish 380 kv System, **W. Borquist, A. Vrenthem.** Appendixes by **B. Henning, S. Skagerlind, S. Bylund.** *Paper number 412*, International Conference on Large High-Voltage Electric Systems (Paris, France), June 24–July 3, 1948.

10. Mecanisme de l'Effet Couronne sur les Lignes de Transport d'Energie en Courant Alternatif, **F. Cahen, R. Pelissier, D. Renaudin.** *Bulletin*, Societe Francaise des Electriciens (Paris, France), series 6, volume IX, number 89, February 1949.

11. L'Emploi de Conducteurs en Faisceaux Pour L'Armement des Lignes a Tres Haute Tension, Resultats D'Essais de la Station Experimentale a 500 kv de Chevilly. *Bulletin*, Societe Francaise des Electriciens (Paris, France), series 6, volume VIII, number 79, March 1948, pages 111–160.

12. Influence, sur L'Effet de Couronne, du Diametre et du Profil des Cables des Lignes Aeriennes a Tres Haute Tension, **F. Cahen, R. Pelissier.** *Revue Generale de l'Electricite* (Paris, France), July 1949, volume 58, pages 279–90.

13. Recherches Experimentales sur le Comportement des Conducteurs des Lignes a 400 kv, **F. Cahen, R. Pelissier.** *Bulletin*, Societe Francaise des Electriciens (Paris, France), series 6, volume IX, number 99, December 1949.

14. Radio Influence from High-Voltage Corona, **Gordon R. Simon.** *AIEE Transactions*, volume 68, part I, 1949, pages 199–205.

15. Radio-Noise Influence of 230-Kv Lines, **H. L. Rordes.** *AIEE Transactions*, volume 66, 1947, pages 677–83.

16. Methods of Measuring Radio Noise, **Joint Report of EEI, NEMA, and RMA.** *Publication G-9*, Edison Electric Institute (New York, N. Y.), 1940.

17. Specification for Ultra-High Frequency Radio Noise Meter, **Committee on Television Interference.** *Radio Manufacturers Association* (New York, N. Y.), 1939.

18. Proposed American Standard Specification for a Radio Noise Meter, .015 to 25 Megacycles. *C63.2*, American Standards Association (New York, N. Y.).

19. Effect of Radio Frequencies of a Power System on Radio-Receiving Systems, **C. V. Aggers, W. E. Pakala, W. A. Stickel.** *Electrical Engineering* (*AIEE Transactions*), volume 62, April 1943, pages 169–72.

20. Measurements Pertaining to the Coordination of Radio Reception With Power Apparatus and Systems, **C. M. Foust, C. W. Frick.** *Electrical Engineering* (*AIEE Transactions*), volume 62, June 1943, pages 284–91.

Discussion

P. L. Bellaschi (Consulting Engineer, Portland, Oreg.): Although lacking in essential details, which presumably will be forthcoming in reports to follow, this paper presents substantiating data and new findings relating to the problems of corona loss and radio influence at the higher transmission voltages.

The variations of radio influence with voltage and with distance from the line, presented in Figures 8 and 9 of the paper, are in general accord with the findings of prior investigators. We concur, too, that at the higher transmission voltages radio influence can become a determining factor, probably limiting the permissible operating voltage for a given conductor or limiting choice of satisfactory conductor for a given voltage. The paper further indicates that possibly higher radio-influence levels might need to be accepted for the higher transmission voltages; this is a point on which some differences in viewpoint can exist.

It is well recognized now that radio influence and corona loss are accentuated by foul weather (rain, snow, sleet, and so forth). In fact, where precipitation is a major factor, the annual rainfall, as the French have established, is a good index in determining average annual corona loss. However, the relationship between average corona loss and rainfall, remaining fair weather, and other influencing factors, does not appear to be a simple one.

A factor we consider of significance in the evaluation of corona is the annual distribution of corona loss in relation to the availability of power and to the peak load. Other factors which hardly can be overlooked are the altitude of the line and the temperature of the conductor. For instance, in the Northwest, altitude is a factor requiring consideration.

A practical approach to the problems of corona loss and radio influence naturally is to evaluate the results of experience from existing high-voltage lines; these can well serve as a valuable criterion or bench mark in projecting design to and in establishing operating standards for the higher transmission voltages. For example, 230-kv experience in a given region, duly evaluated and further supplemented by fundamental studies in the field and laboratory at 230-kv

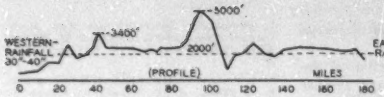

Figure 1. Ambient and climatic conditions

and higher voltages, will provide a valuable basis in projecting transmission-line design in that region to higher voltages; that is, 288 kv or 345, or possibly 360 or 380 kv, as the case and economics may require.

The results of research studies and experience at Chevilly, France, in Sweden, on the Los Angeles 288-kv lines, from the special investigations in course in various quarters, and those now becoming available from the Tidd test project, are providing a more secure basis in the development of transmission-line design for the higher voltages and in arriving at the more economical solutions for long-distance power transmission.

Tables I and II and Figure 1 of this discussion illustrate the approach in estimating the performance of larger conductors "B" and "C" for operation at correspondingly higher transmission voltages, where conductor "A" serves as a bench mark or reference for 230 kv. The corona losses for the entire line (conductor "A") are determined by test over a sufficiently long period of time to establish an annual corona-loss distribution curve. Thus, the tests integrate the combined effects due to climate (rainfall, snow, sleet, and so forth), surrounding conditions, altitude, and other influencing factors present in the region and route traversed by the lines.[1, 2] Similar tests need be made, of course, with reference to radio-influence effects. The evaluation of radio influence in projecting transmission-line design to higher voltages is understandably much more difficult than corona losses. With the larger conductors this inherently is the case, because even small irregularities on the conductor proper, or rain or deposits, are conducive to concentrated streamer formation or discharges with resulting radio-influence effects of corresponding high levels resulting therefrom.

The corona-loss data presented in Tables I and II of the paper have been analyzed, consideration being given to the factors which influence corona loss, namely: a. the conductor and conductor arrangement; b. precipitation; c. altitude; d. temperature of air at conductor; e. spacing of conductors; and so forth. Two cases have been considered: one where precipitation corresponds to conditions in the East and altitude (profile of the line) does not exceed 1,000 feet; the other, where the average altitude is 2,000 feet and the rainfall 15 inches for one-half of the line and 40 inches for the other half.

In the light of these and similar analyses, the data presented in the Tidd Report indicate that:

1. On the basis of an annual corona loss of 5 to 6 kw per mile, a line designed and equipped with single 2.0-inch diameter steel-reinforced aluminum cable (ACSR) (expanded) conductors, spaced 40 to 45 feet, should be satisfactory for operation at 380 kv. The French, in their investigations at Chevilly, have found a 1.92-inch diameter ACSR conductor adequate for 380/-400 kv but not as favorable as a 2×1.04-inch bundle conductor spaced 16 inches.[3, 4]

2. On the same basis of corona loss, a 1.65-inch diameter ACSR conductor should be suitable for 345 kv.

3. In the Tidd Report, the 2×0.92-inch bundle conductor spaced 20 inches does not compare favorably to the 1.65-inch diameter conductors. This is due in part apparently to the choice in the spacing. Either a smaller spacing (less than 20 inches) or a larger diameter would have been more appropriate.

4. Finally, based on the statement in the Tidd Report that radio noise is the determining factor at the higher voltages, over and above corona-loss considerations, it then would appear that a conductor greater than 1.65 inches in diameter but less than 2.0 inches might be required for 345-kv operation.

In conclusion, a technique is rapidly in course of development which, when completed, should provide a more secure, straightforward, and more economically sound basis of transmission-line design at the higher voltages. Contributions such as the present one are providing valuable fundamental data in establishing this technique.

Table I. Annual Corona-Loss Distribution for "A" and "B" Conductors

Per Cent of Time	Corona-Loss Distribution for "A" Conductor at 230 Kv, Kilowatts Per Mile (Actual)	Corona-Loss Distribution for "B" Conductor at 287 Kv, Kilowatts Per Mile (Estimated)
0.8	11.6	27
7.7	8	18.6
20	4	9.3
8.5	2	4.7
63 (fair weather)	1.25	2.9
Average kilowatts per mile	2.45	5.70

Table II. Relative Operating Voltage as Determined from Geometric, Gradient and Stranding Factors of "A," "B," and "C" Conductors

$E_{L-L} \propto (r/n\ s/r)$ (Gradient Factor Stranding Factor)

Conductor	r/n	s/r	Gradient Factor	Stranding Factor	Relative Operating Voltage
"A"	3.50	1.00	0.80	0.80	230 kv
"B"	4.24	0.98	0.93	0.93	282 kv
"C"	5.76	0.947	0.95	0.95	382 kv

REFERENCES

1. Discussion by E. C. Starr of 500-Kv Experimental Station at Chevilly. Results of a Year's Tests—Use of Bundle Conductors; Corona Effects; Clearances, Pierre Ailleret, Francois Cahen. *Transactions*, International Conference on Large High-Voltage Electric Systems (Paris, France), volume I, 1948, pages 491–92.

2. See reference 9 of the paper.

3. See reference 13 of the paper.

4. The Choice of Conductors for the Equipment of 380–400-Kv Lines According to Tests Carried Out at the 500-Kv Chevilly Substation, P. Ailleret, F. Cahen. *Report 411*, International Conference on Large High-Voltage Electric Systems (Paris, France), June 29–July 8, 1950.

Engineering Staff (Anaconda Wire and Cable Company, Hastings-on-Hudson, N. Y.): The quantity of data which has been accumulated thus far in the Tidd project experiments is truly staggering. No interpretations or conclusions are attempted in this paper since, as frankly stated, no systematic analysis of any considerable quantity of the data has been made as yet. The sample data presented in the paper stimulates one's interest in the promised series of complete reports. Of particular interest is the authors' statement that single measurements of corona loss are misleading and that continuous, long-time tests are required to establish annual losses.

The general pattern of results appears consistent with data obtained by other investigators, as evidenced by these facts:

1. The long-time decrease of corona due to weathering has been reported, without exception, by all experimental investigators here and abroad.

2. The short-time surface effect is confirmed by Ailleret and Cahen.[1]

3. Automatic records of corona loss versus weather, similar to Figure 2 of the paper, were presented by the Germans[2,3] and by the French[1,4] and confirm the authors' findings.

4. The overwhelming importance of precipitation in corona loss is amply proved by the data presented. The Swiss[5] have done considerable work to appraise the individual effects of humidity, fog, rain, snow, and frost upon corona. They too found rain to be of paramount importance.

5. The consistent curves of corona loss versus rate of rainfall check well with similar curves by Cahen[6] of corona loss versus height of rain water. (It would be of interest to know the type of conductors, line spacing, and so forth, applying to curves in Figure 5 of the paper.)

However, one outstanding point of difference is noted. In the entire literature on bundle conductors it is accepted that bundles have not only higher corona starting voltage but also lower corona losses, for a given voltage, as compared with an equivalent single conductor. In every case, these results were based not only on calculations but confirmed by measurements by German, Swedish and French investigators.[1,2,3,4] Figures were published by Henning and Skagerlind[3] indicating that the ratio of operating voltages for equal corona loss on 2-conductor bundles and single conductors of the same diameter is approximately 1.4-to-1.

The 2×0.92-inch bundle conductor spaced 20 inches, referred to in Table I of the paper, means that the subconductors were spaced somewhat greater than the theoretically optimum spacing. If the subconductors are spaced too far apart, one simply adds up the corona losses of the individual (smaller) subconductors, which losses can be quite high. Ailleret and Pelissier[4] show that twin bundles with subconductors of 411 square millimeters (810,000 circular mils) give much lower losses than large single conductors (1.77- to 1.97-inch diameter), if the bundle

subconductors are spaced from 8 to 16 inches apart.

Referring to the Tidd tests, we appreciate that it is not possible to test all conductors simultaneously in order to obtain a direct comparison and that Tables I and II of the paper probably are not intended to offer such a comparison, but the very form in which the information is presented makes it inevitable that such comparison will be attempted by the uninitiated. Data on the effect of conductor size and construction upon corona are too meager to permit definite conclusions. Only these comparisons seem valid:

1.65-inch Heddernheim (HH), 3-phase, 45-foot spacing, versus 2.0-inch ACSR, 3-phase, 45-foot spacing.

1.65-inch ACSR, outer phase, versus 2.0-inch ACSR, outer phase.

No data are reported for the 2.0-inch type HH, 1.65-inch I beam, and bundle conductors for three and four conductors per phase.

Tables I and II of the paper indicate that the 1.65-inch HH conductor was measured 3-phase, the 1.65-inch ACSR phase-to-phase, the 2.0-inch ACSR both ways, and the bundle conductor only phase-to-phase. The spread of results as shown is not given in a form which would enable one to evaluate the conversion of single-phase measurements to 3-phase losses. If the standard deviation of each test conductor run were given it would help considerably. Both 2.0-inch ACSR conductor sets of values show as much difference from each other as do the other comparable conductors. This may be due to inherent inaccuracy of the conversion or to different spacing, although it is not clearly stated. Conversion of the corona losses of 1-phase measurements to 3-phase values is based on the assumption that the same electrical gradient gives rise to an equivalent corona current. To evaluate the field gradient for the conversion requires a knowledge of the ratio of the capacitance of the single-phase bundle conductor to its 3-phase operating capacitance. Since no data are given for capacitances, it is presumed that these were calculated and so used in the conversion formula.

We also wonder if some of the variations under normal dry conditions may be ascribed to variations in the electron density in free space about the conductor. Such electron density variations may be brought about by cosmic ray showers, sun spot activities, Aurora Borealis phenomena, magnetic storms, and the like.

References

1. 500-Kv Experimental Station at Chevilly. Results of a Year's Tests—Use of Bundle Conductors; Corona Effects; Clearances, Pierre Alliaret, Francois Cahen. *Report 410*, International Conference on Large High-Voltage Electric Systems (Paris, France), 1948.

2. Bundel Leitungen, F. Busemann, W. V. Mangoldt. *Siemens-Schuckertwerke* (Berlin, Germany), part II, 1942.

3. New Investigations of A-C Corona on Conductors, H. Laepple. *Electrotechnische Zeitschrift* (Berlin, Germany), 1944, page 25.

4. See reference 13 of the paper.

5. New Investigations of the Corona Losses of a Transmission Line, F. Boldi. *Report 407*, International Conference on Large High-Voltage Electric Systems (Paris, France), 1948.

6. Results of Tests Carried Out at the 500-Kv Experimental Station of Chevilly (France), Especially on Corona Behavior of Bundle Conductors, Francois Cahen. *AIEE Transactions*, volume 67, part II, 1948, pages 1118–27.

7. High-Voltage A-C Transmission Over Bundle Conductors, G. Marki, B. Mangele. *Elektrotechnik und Maschinenbau* (Vienna, Austria), volume 50, 1933, page 293.

8. See reference 9 of the paper, Appendix A, Section III, by B. Henning and S. Skagerlind.

M. Temoshok (General Electric Company, Schenectady, N. Y.): From dual conductor theory three factors tend to cause lower corona losses on dual conductors than on single conductors:

1. For equivalent areas of dual and single conductors, the maximum voltage gradients on the surface of the dual conductors is less than for the single conductors.[1]

2. Because of the relative location of the dual conductors, a varying gradient exists around the periphery of each conductor with the minimum gradient appreciably less than the maximum gradient.[1]

3. With conductors having the same surface gradient the losses tend to vary as the square of the radii.[2] First, let it be stipulated that the cross-sectional area per phase for dual and single conductors be equal, and second, that the surface voltage gradient be equal in each case. The corona loss of each dual conductor modified by the square of the ratio of conductor radii would have one-half the loss of the single conductors. But because of two conductors per phase, the losses in each case should be equal. But experimental data appear to indicate that small diameter conductors in general tend to have less loss than large diameter conductors when both have identical surface voltage gradients and have losses modified to a common conductor radius base.

Keeping areas per phase equal, instead of 1.65-inch diameter and 2.0-inch diameter single conductors, dual conductors of 1.17-inch diameter and 1.414-inch diameter respectively could be used with resulting lower corona losses. To attain equal losses the dual conductor diameters must be less than those just mentioned.

An interesting comparison of the results presented in Tables I and II of the paper may be made with the work presented in reference 13 of the paper. Based on the conductor outside diameters of Tables I and II, the ratio of areas of the single conductors (1.65-inch and 2.0-inch diameter) to the combined area of the dual conductors (0.92-inch diameter each) is 1.61 and 2.36 respectively. Investigators in reference 13 of the paper arrived at a conclusion indicating that if the ratio of areas was 1.65, the losses of the single and dual conductors would be approximately equal, depending on the spacing between the dual conductors. These relationships are borne out in this paper. The 20-inch spacing between dual conductors is fairly large, and if it could be decreased to 15–18 inches, even less corona loss should result.

References

1. Relative Surface Voltage Gradients of Grouped Conductors, M. Temoshok. *AIEE Transactions*, volume 67, part II, 1948, pages 1583–89.

2. Technical and Economic Aspects of the Transmission of Electrical Energy Over Long Distances, W. J. Wanger. *Journal*, Institution of Electrical Engineers (London, England), volume 95, part I, August 1948, pages 340–51.

Philip Sporn and **A. C. Monteith:** The authors appreciate the interest shown and value the comments of all the discussers. Questions are raised concerning the insufficiency of the data. A progress report by its very nature is limited in the completeness of the data presented. As mentioned in the paper, subsequent papers giving much greater detail will be presented. It is hoped that the future papers will answer in much more detail than is possible in a discussion of this nature the questions raised by the discussers.

The use of a 20-inch separation for the study of bundle conductors is questioned. Actually other separations also were tested and little difference in the results was observed. Mr. Temoshok in particular suggests that a separation of 15 to 18 inches instead of 20 inches would have resulted in less corona loss. Analytical studies made by a number of investigators have shown very little difference in loss for separations between 15 and 20 inches in a 2-conductor bundle. For two 1-inch conductors, Mr. Temoshok shows only a difference of 1.3 per cent in surface gradient for a change in separation from 15 to 20 inches. The final choice of separation between subconductors of a bundle should not be selected to obtain the minimum value of the maximum gradient around the periphery. On the basis of such additional factors as reduced reactance, sleet-loading, charging kilovolt-amperes and sticking of conductors resulting from short-circuit currents, a larger than optimum separation determined on the basis of corona loss only should be selected. A design should be chosen that balances these factors against increased loss and radio influence with increasing separation.

Power-System Planning in the City of Los Angeles

A. L. WILLIAMS
ASSOCIATE AIEE

E. L. KANOUSE
MEMBER AIEE

THE phenomenal past and continuing growth of the electrical industry and its transition from a luxury to a necessity for living, business, and industry make long-range planning imperative. While it may not seem as urgent, planning for the future expansion of a power system is fully as important as supplying the present load, and the responsibility it entails is probably even greater.

One responsibility of a system-planning group is to recommend a power-system arrangement that gives maximum reliability consistent with reasonable annual costs, that is capable of economical extension for load and community growth, and that can utilize current advances in equipment and methods, all without future costly reconstruction or excessive obsolescence. To meet this responsibility, it is necessary to have some idea of what the amount of community load growth may be, what its general characteristics will be, and where its various component parts will appear in the community to be served. Only with this knowledge can the system additions needed for immediate growth be made with assurance that these additions will continue to function as a proper part of tomorrow's system.

The Department of Water and Power of the City of Los Angeles has attempted to estimate the probable future load, and its distribution, from studies of population, land use, and feeder demand. With a reasonable estimate of future load and its probable location established, the problem of formulating a basic plan of system arrangement is simplified, and a suitable long-range program of expansion may be initiated. Periodic re-estimate of the basic quantities involved is desirable, as is a continuing study to insure that each addition of generating capacity, with its attendant transmission and distribution facilities, adheres to the long-range plan.

Electrical Load Demands of the City of Los Angeles

In 1924 the Department undertook a survey to determine the electrical power demands of the city by load classes and by geographical areas. The method used was essentially a field survey of land use by the various classes of load, coupled with an application of electrical load demands which are related to unit square miles of the load class. Similar surveys were made in 1934 and 1944 and have furnished very interesting information on trends in Los Angeles which can be utilized to advantage in making long-range forecasts for the city.

Field Survey of Land Use

The initial phase of each survey began in the field, and consisted of estimating the land use of 1/4-square-mile areas in terms of some 12 different load classifications. The work usually was done by driving through the various areas and estimating what percentage of that area was devoted to each of the various types of activities. When this was accomplished, the 16 maps making up a 4-square mile area were totalled by load classes, and the square miles devoted to each of the 12 classifications were tabulated. In this way the land use of each 4-square-mile area of the city was determined, and the initial phase of the survey was completed.

The land use of the entire city area as of 1944, comprising some 453 square miles, has been tabulated in Table I. This table was prepared by totalling the results of each 4-square-mile area, and gives considerable insight into the manner in which land is used in the community. While it is of course impractical to include here the results of the survey for each unit area, it should be remembered that these have been determined, and are available for considering the need for stations and lines in the various sections of the city.

Loading Value Determinations

The second phase of the survey involved the estimating of kilowatt demands of a square mile of each of the 12 load classifications. Such estimates were made by relating actual typical areas to the electrical demands on feeders serving these areas. Analysis of individual feeders sometimes made it possible to utilize actual meter readings, where it could be shown that a feeder served a well-defined load area of substantially one classification. It was soon apparent that for some classifications the economic character of the area influenced the electrical demands per square mile. In such cases two demand figures were used, referred to as "high"- or "low"-load density areas. The low loading applied to old or small homes, businesses, or districts, while larger secondary business districts and new homes might be put into the high-load density class.

Table II shows average loading values determined in each of the three surveys, expressed in feeder demand per square mile of the individual classes tabulated.

Feeder Demands by Load Classes and Areas

With the land use per-unit area of the city available from the survey, and with determinations at hand of the electrical loading values for each square mile of such

Paper 50-144, recommended by the AIEE System Engineering Committee and approved by the AIEE Technical Program Committee for presentation at the AIEE Summer and Pacific General Meeting, Pasadena, Calif., June 12–16, 1950. Manuscript submitted March 15, 1950; made available for printing April 10, 1950.

A. L. Williams and E. L. Kanouse are both with the Department of Water and Power, The City of Los Angeles, Los Angeles, Calif.

Table I. 1944 Land Use, City of Los Angeles

Description	Square Miles	Per cent of Area
Single-family residences	78.5	17.42
Standard flats	21.0	4.65
Apartments, under 4 floors	1.7	0.37
Large apartments over 4 floors	0.1	0.03
Commercial, 2 floors or less	11.5	2.57
Heavy commercial, 4 floors or more	0.7	0.16
Wholesale or small industrial	1.2	0.26
Heavy industrial	2.4	0.53
Individual heavy industrial	7.3	1.61
Vacant	130.8	28.92
Vacant subdivided	64.8	14.31
Cultivated farm land	98.8	21.83
Miscellaneous: parks, schools, golf courses, and so forth	33.2	7.34
Total	452	100.00

land use, the final step in the analysis was simply one of multiplication. As an illustration, the kilowatt demands of the various load classifications as found in the most recent survey (1944) have been totalized and tabulated in Table III. It is of interest to note that the total value of 733,347 kw of feeder demand, when corrected for diversity back to the central receiving stations, checked within 18,000 kw of the metered receiving-station simultaneous-peak output in 1944. This is a 3-per cent error, and was on the low side.

Long-Range Load Forecasting

The results of these three surveys, conducted over a 20-year period, were most helpful in indicating trends for current long-range load forecasting work.

On the premise that the electrical demands of a metropolitan area are almost wholly dependent on two factors—population, and the activities of that population, or land-use—trends in these factors were analyzed for the metropolitan area.

Population Estimates

If population is estimated on the basis of trend curves alone, there is no limit to the ultimate value that may be assumed. In most areas, however, there will be found some limiting factor that can be used to determine a possible ceiling. In the semiarid coastal plain on which Los Angeles is situated, it appears to be water supply. After a careful analysis of water available to the metropolitan area from the Owens Valley and Colorado River aqueducts and from local pumping sources, a possible future population for the area was assumed at 6,250,000. It must be recognized that ample opportunity will be afforded in the coming decades to revise that figure if other factors, unknown or discounted today, later show such revision to be warranted. The population of 6,250,000 was established on a metropolitan area basis in order to obtain the statistical advantages of working with larger quantities and to eliminate the troublesome problem of dealing with irregularly-shaped city boundaries.

In order to estimate the population in the city area only, reference was made to past trends and census data with respect to persons living within and outside of the city. Figure 1 shows the trends indicated by past census data, and also shows the assumed extensions of these trends to establish a basis for determining the probable future city population. This study indicates that the population of the city proper may be approximately 3,850,000 when the population for the metropolitan area reaches 6,250,000. This represents an increase of approximately 1,850,000 over the city's estimated 1949 population of 2,000,000.

Housing Requirements

Studies of the living habits of the people in the metropolitan area gave some indication of the possible housing necessary to supply the population, expressed in terms of single-family or multiple-dwelling units. Analysis of past trends in housing indicated that Southern Californians prefer individual homes, more than 50 per cent of the population being housed in single-family dwellings in 1944. It was recognized, however, that industrialization of the area will bring to bear economic factors which will force a somewhat larger percentage of the people into multiple housing in the future. Federal Census Bureau housing statistics were utilized to determine the number of persons per occupied-dwelling unit of the various types, and values of per cent vacancy, in order to relate area requirements with the number of persons to be housed in each type of dwelling. Figure 2 shows in graphical form the answers obtained and the past trends from which they were extrapolated.

Table II. Average Loading Values Per Square Mile

Description	Feeder Demand Per Square Mile Kilowatts 1944	1934	1924
Single-family residences	2,000	1,500	1,000
Standard flats	5,700	4,500	3,000
Apartments, under 4 floors	20,000	15,000	10,000
Large apartments over 4 floors	40,000	40,000	10,000
Commercial, 2 floors or less	8,000	8,000	5,000
Heavy commercial, 4 floors or more	65,000	60,000	50,000
Wholesale or small industrial	7,000	7,000	4,000
Heavy industrial	35,000	30,000	30,000
Vacant	0	0	0
Vacant subdivided	0	0	0
Cultivated farm land			
Miscellaneous: parks, schools, golf courses, and so forth			

Table III. 1944 Load Demands, City of Los Angeles

Description	Feeder Maximum Demand Kilowatts	Per cent of Total
Single-family residences	132,216	18.03
Standard flats	101,350	13.82
Apartments, under 4 floors	28,905	3.94
Large apartments over 4 floors	2,854	0.39
Commercial, 2 floors or less	82,887	11.30
Heavy commercial, 4 floors or more	40,131	5.47
Wholesale or small industrial	7,406	1.01
Heavy industrial	260,929	35.59
Vacant	0	0
Vacant subdivided	0	0
Cultivated farm land	1,640	0.22
Miscellaneous: parks, schools, golf courses, and so forth	75,020	10.23
Total	733,347	100.00

Commercial and Industrial Land-Use Requirements

In like manner the trends in the commercial and industrial load classes, as related to population, may be utilized to gain some insight into the square miles of these categories required by an increasing number of people. In these cases reference was made to average values of other large metropolitan areas, adjusted for the individual characteristics of this particular Southern California area. The results of these studies are shown in Figures 3 and 4, the upward trend of the curve in Figure 4 reflecting to some extent the tendency of industrial concerns to include large parking areas for employees as a part of the plant.

Future Land Use, Los Angeles City

The total land-use requirements of the city, as determined by this type of reasoning and analysis, are shown summarized in Table IV. Data from each individual 4-square-mile area of the city has been summarized to produce this information. For this particular table it was of interest to separate the San Fernando Valley area of the city in view of the extremely rapid growth and development there. It should be noted that in order to care for a population of nearly 4,000,000 in the city proper, with housing as indicated, it was necessary to consider San Fernando Valley as housing approximately a third of that portion of the people living in single-family dwellings. This is not at all

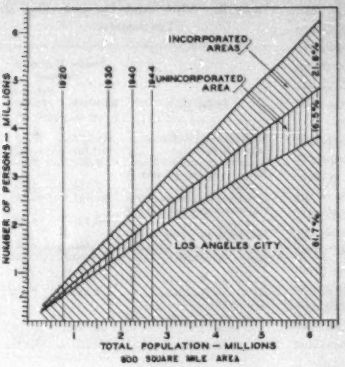

Figure 1 (left). Estimated trends in population distribution in 900-square-mile metropolitan area

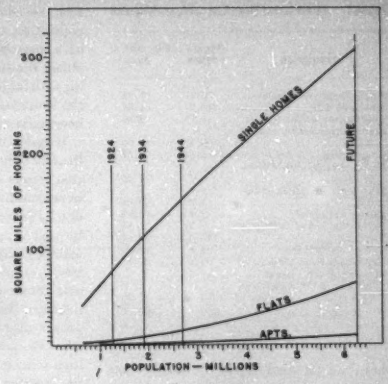

Figure 2 (right). Estimated trends in land use for residential load classification, metropolitan area

illogical, in view of the type of development, zoning ordinances, and so forth, prevalent in that district today.

Electrical Load Demands of the Various Classifications

The values of future electrical load demands per square mile for each type of land use, and for high- and low-loading densities, were assumed after a careful study of past trends, present and possible future saturation values of various types of electric utilization equipment, and probable new applications, increasing lighting intensities, and so forth. The average values of these assumed demands are tabulated in Table V.

The total feeder demand of the future city was estimated by obtaining the product of the square miles devoted to each of the various load classifications, and the applicable assumed feeder loading per square mile. Table VI shows the results obtained, with a total feeder demand of 2,780,000 kw resulting. It is of interest and importance to realize that this feeder demand, when present values of diversity factors and losses are utilized, represents a receiving station demand of 2,198,000 kw, a distributing station demand of 2,417,000 kw, and a required generation of 2,303,000 kw. These required generating capabilities are those which just meet the estimated requirements, and do not include the necessary additions essential for normal reserve capacity or for protection against the effects of depleted water conditions in periods of low river flows.

Summary

Electrical load surveys of the type outlined provide the information for the development of a basic power-system plan adequate for the future load requirements and capable of accomplishment through step-by-step construction processes. The segregation of the load requirements as to load classes enables the drawing of probable system load curves, the determination of kilowatt-hour requirements, and estimates of possible revenues. Furthermore, the unit area survey provides data for detailed study of the requirements of the receiving station, distributing station, and local feeder load areas.

Development of a Basic Power Plan

As a result of the 1924 electrical load survey, the Department developed a basic system plan for the then-estimated future load requirements of 1,250,000 kw. In formulating such a basic plan it was recognized that for a city covering more than 400 square miles and relying to a large extent on hydroelectric power developed in large blocks and transmitted over long distances, consideration must be given to methods of consolidating and distributing the power in the load area. The plan devised is illustrated in Figure 5.

This plan provided that the future load be distributed from not less than six receiving stations, each of a maximum capacity of 240,000 kw, and each to be supplied with a source of power approximately equal to the load distributed from that station. Every receiving station with its power source and its 34.5-kv distribution system was to be considered an isolated power system, and each such isolated power system was to be connected to a common bus, or belt circuits, through suitable reactors. The proper voltage for the belt circuits and receiving station primaries was determined to be 138 kv. Connections between receiving stations and their power sources were to be at the most economical voltage, and if transformation was required it was to be accomplished with autotransformers located at or near the receiving station and incorporated as a part of the transmission line.

Steam sources, where they constituted

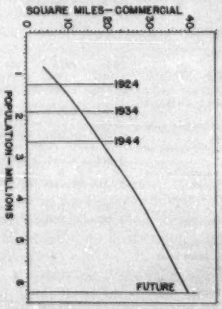

Figure 3 (left). Estimated trends in land use for commercial load classification, metropolitan area

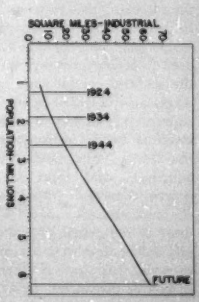

Figure 4 (right). Estimated trends in land use for industrial load classification, metropolitan area

Table IV. Future Land Use Estimate, City of Los Angeles

	Los Angeles City		Los Angeles City Less San Fernando Valley Area		San Fernando Valley Area of Los Angeles City	
	Square Miles	Per cent of Total	Square Miles	Per cent of Total	Square Miles	Per cent of Total
Single-family residences	164.8	36.5	85.5	35.7	79.3	37.4
Standard flats	40.3	8.9	34.9	14.6	5.4	2.6
Apartments, under 4 floors	5.8	1.3	5.3	2.2	0.5	0.2
Large apartments over 4 floors	1.2	0.3	1.2	0.5	0	
Commercial, 2 floors or less	23.1	5.1	18.0	7.5	5.1	2.4
Heavy commercial, 4 floors or more	1.9	0.4	1.8	0.7	0.1	
Wholesale or small industrial	5.2	1.1	1.5	0.6	3.7	1.8
Heavy industrial	22.0	4.9	18.7	7.8	3.3	1.6
Vacant	81.2	17.9	32.0	13.3	49.2	23.1
Vacant subdivided	35.6	7.9	15.9	6.6	19.7	9.3
Cultivated farm land	31.5	7.0	0.2	0.1	31.3	14.8
Miscellaneous: parks, schools, golf courses, and so forth	39.4	8.7	24.9	10.4	14.5	6.8
Total	452.0	100.0	239.9	100.0	212.1	100.0

a power source or stand-by, were to feed into the 34.5-kv bus of the receiving stations and were also to furnish reactive kilovolt-amperes in lieu of synchronous condensers at such stations. Studies on which this plan was based indicated that, with 8-per cent reactors (on a 100,000-kva base) between each 138-kv load and belt bus, this arrangement would limit maximum circuit breaker duties on the belt line busses to 4,000 megavolt-amperes; on the 138-kv load busses to 2,500 megavolt-amperes; 1,500 megavolt-amperes on the receiving station 34.5-kv busses; and 1,000 megavolt-amperes on the 34.5-kv bus at the distribution stations.

The advantages inherent in this plan are:

1. The limited capacity interconnection between systems reduces the necessity for duplicate transmission circuits to each system.

2. It may not be possible or economical to have the power development, and transmission circuits or power available, equal to the demand of its corresponding distribution system. The difference can be equalized by the other systems over the belt circuits.

3. Because of periods of low water, it may be desirable to have one or two steam-generating stations as reserve. The interconnection over the belt lines not only makes steam reserves available, but greatly reduces the total steam stand-by capacity required.

4. During periods of growth, the belt-line interconnections permit a receiving station to be established in advance of the power source for the station, the belt lines acting as a supply during the initial years.

5. Additional receiving stations may be given belt-line support either through looped-in lines between existing stations or through new lines tapped off from an existing receiving station bus.

This basic plan was adopted in 1926, when only three receiving stations existed, and when city-owned generating capacity totalled less than 120,000 kw. It is the plan toward which all construction since 1926 has been aimed, and with the exception of certain expedients resulting from construction work done before the plan existed, or from acquisition of some private utility properties, the original plan has been very closely followed. However, the growth of the city has not been uniform by geographical areas, and all six receiving stations were needed considerably in advance of the load development. The sixth receiving station was put in service in 1943, and the loads on several existing stations are rapidly approaching ultimate design capacity.

Table V. Average Loading Values Per Square Mile

Description	Feeder Demand Per Square Mile Kilowatts			
	Future	1944	1934	1924
Single-family residences	4,000	2,000	1,500	1,000
Standard flats	12,000	5,700	4,500	3,000
Apartments, under 4 floors	50,000	20,000	15,000	10,000
Large apartments over 4 floors	95,000	40,000	40,000	10,000
Commercial, 2 floors or less	12,000	8,000	8,000	5,000
Heavy commercial, 4 floors or more	110,000	65,000	50,000	50,000
Wholesale or small industrial	8,000	7,000	7,000	4,000
Heavy industrial	35,000	35,000	30,000	30,000
Vacant	0	0	0	0
Vacant subdivided	0	0	0	0
Cultivated farm land	0			
Miscellaneous: parks, schools, golf courses, and so forth				

Table VI. Estimated Future Electrical Demands, City of Los Angeles

Description	Feeder Maximum Demand	
	Kilowatts	Per cent of Total
Single-family residences	578,000	20.8
Standard flats	419,000	15.1
Apartments, under 4 floors	275,000	9.9
Large apartments over 4 floors	115,000	4.1
Commercial, 2 floors or less	241,000	8.7
Heavy commercial, 4 floors or more	257,000	9.2
Wholesale or small industrial	42,000	1.5
Heavy industrial	772,000	27.8
Vacant	0	
Vacant subdivided	0	
Cultivated farm land	0	
Miscellaneous: parks, schools, golf courses, and so forth	81,000	2.9
Total	2,780,000	100.0

Considerations Indicating Need for Current Review of the Basic Plan

On completion of the 1944 load survey, with the clear indication it provided of the greatly increased growth expectancy of the city, and in view of the imminent need for expanding the existing receiving station system, it was realized that the basic plan should be reappraised to determine its adequacy for a power system with peak demands approximately twice those considered probable in 1926. Developments in the art of power generation and transmission during the past 24 years have had pronounced effects on the short-circuit duties imposed on circuit breakers, and the importance of these effects on the ratings of hundreds of switches in the subtransmission and distribution system could not be minimized. The more important of these developments that have affected the Department's power system are:

1. The use of higher speed circuit breakers requiring such circuit breakers to open the circuit higher on the current decrement curve.

2. Lower reactance hydroelectric generators.

3. Increased speed and lower subtransient reactance of steam-electric generators.

4. Connection of steam generation sources directly to the 138-kv bus instead of to the 34.5-kv system.

5. Use of 138-kv underground cable in belt circuits and transmission lines.

Relative economic advantages to be obtained with various hydroelectric-to-steam-electric ratios are on a somewhat different basis than that contemplated in 1926, and certain technological changes in the art warrant consideration because of their important effects on the economics to be obtained.

For all of these reasons it was deemed

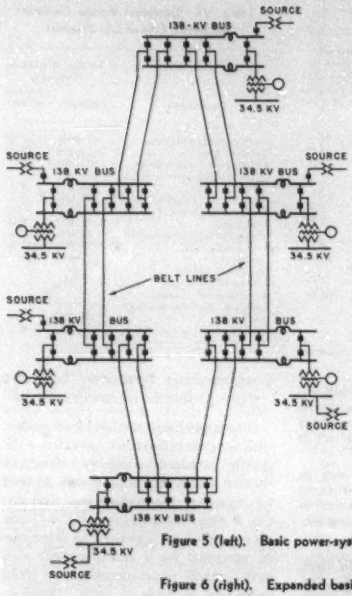

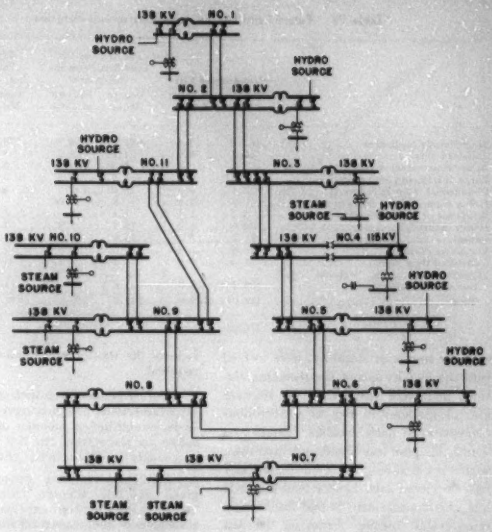

Figure 5 (left). Basic power-system plan for serving 1,250-megawatt load from combined hydroelectric and steam generation

Figure 6 (right). Expanded basic plan for distributing future city load from combined hydroelectric and steam generation totaling 2,400 megawatts

desirable to re-evaluate the basic plan, particularly since the load study data furnished indication of the approximate location of the future load increases.

The Basic Plan Applied to a 2,400-Megawatt Power System

In order to determine the possible limitations of the basic plan when applied to a power system nearly double the size originally contemplated, an a-c network analyzer study was made of an assumed 2,400-megawatt system constructed in accordance with the basic plan. By this means reliability, flexibility, voltage regulation, reactive kilovolt-ampere requirements, and short-circuit duties were determined and evaluated, and many operating problems were posed and answered.

In building up the assumed power system for such a check on operation, the following four broad principles were followed:

1. The system under study was made adequate to care for the presently estimated future demands of the City of Los Angeles, having a generating capability of approximately 2,400 megawatts, including approximately 250 megawatts of spinning reserve.
2. The study was made directly applicable to the existing power system by adding receiving stations, belt-line connections, and power sources, in accordance with the principles of the basic plan. Such additions were made with the results of the load study trends at hand, showing the probable location of future load growth.
3. For purposes of comparison, the system being checked had some new receiving stations connected to the present system by lines tapped off receiving station busses, and some stations connected by looping into the belt circuits; and steam plant power was fed into some stations at 34.5 kv and into others at 138 kv.
4. Hydroelectric power or steam-electric power was assumed as power sources for the various new receiving stations, in order to determine the various electrical requirements accompanying the use of each.

The resulting assumed power system is shown in 1-line diagram form in Figure 6. The receiving stations were assumed located geographically at the centers of the load areas served, and in developing the impedance diagrams of the transmission system a realistic view was taken of the probability of underground or overhead construction being used for the various connections.

Dozens of power-flow studies were made of the power system shown schematically in Figure 6, under normal, single-contingency, and multiple-contingency conditions of operation. The results of the studies clearly indicated the basic plan to be sound, to contain reliability and flexibility elements highly prized by the operating engineers, and to be capable of application to a very large power system. However, short-circuit duties were found to be excessive, amounting to 5,000 megavolt-amperes or more on the belt-line side of the bus reactors at several of the stations. This was true even though reactor sizes were increased from eight to ten per cent in each of the 138-kv busses at every receiving station.

It was recognized that circuit breakers could be built to meet these requirements, but the use of such circuit breakers would require eventual replacement of nearly all existing 138-kv circuit breakers. In addition, the hundreds of circuit breakers in the 34.5-kv distribution system also would require replacement if the switch duties on the high side of the receiving station banks were allowed to exceed the limiting values assumed for the basic plan. These low-voltage circuit breakers have been purchased to date in accordance with those values set forth in the section on Development of a Basic Power Plan, and in many instances space would not permit larger circuit breakers to be

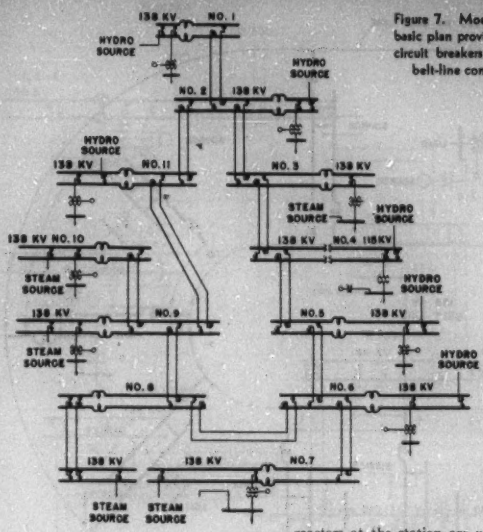

Figure 7. Modification of basic plan providing single circuit breakers in 138-kv belt-line connections

Table VII. Comparative Circuit-Breaker Interrupting Duties

Three-Phase Duties, Millions of Kva

Station	Bus	Double Circuit-Breaker Operation (Figure 6)	Single Circuit-Breaker Operation (Figure 7)
Number 1	132-kv belt	2.76	1.32
	132-kv load	2.20	2.20
Number 2	132-kv belt	4.72	2.90
	132-kv load	2.48	2.48
	132-kv stub	2.48	2.48
	110-kv stub	2.20	2.20
Number 3	132-kv belt	4.40	2.22
	132-kv load	2.27	2.27
Number 4	132-kv belt	4.47	2.22
	110-kv load	2.67	2.67
Number 5	132-kv belt	2.47	2.10
	132-kv load	2.52	2.52
Number 6	132-kv belt	5.00	3.04
	132-kv load	2.64	2.64
Number 7	133-kv belt	2.76	1.23
	132-kv load	2.64	2.64
	132-kv stub	1.94	1.94
Number 8	132-kv belt	5.00	2.27
	132-kv supply	2.10	2.10
Number 9	132-kv belt	5.63	3.27
	132-kv load	3.38	3.38
Number 10	132-kv belt	4.54	2.48
	132-kv load	3.25	3.25
Number 11	132-kv belt	5.25	2.87
	132-kv load	2.64	2.64

installed without costly reconstruction of existing stations.

Modification of the Basic Plan

After due consideration of the results discussed previously, and on analysis of the fault-current contributions from the various sources of energy available to the belt-line busses, a simple expedient was found which not only made remarkable reductions in the short-circuit duty on the belt-line circuit breakers at every station, but actually reduced the capital investment represented in the power-system plan as studied. This expedient was to omit half of the circuit breakers in the belt-line connections at each station, tying each belt line to only one of the two busses.

The single-line diagram of Figure 7 shows the connections resulting, and a comparison of 3-phase short-circuit duties obtained with the double-bus and single-bus method of operation is shown in Table VII.

This remarkable reduction of belt-line short-circuit duties is accomplished without undue sacrifices in flexibility or reliability. It is obvious that under normal conditions the removal of one circuit breaker from each of the four line positions at a receiving station has no electrical effect on the operation. However, if a fault occurs on a belt-line bus, the short-circuit current is very greatly reduced because the two current-limiting reactors at the station are no longer in parallel.

The connections indicated in Figure 7 can be simplified by presentation as in Figure 8. Extensive network analyzer power-flow studies showed the plan to have completely satisfactory flexibility and reliability characteristics, and there is indication that, from a short-circuit duty standpoint, the plan may be capable of still further extension. It is quite apparent that the 3,500,000-kva interrupting-duty circuit breakers being purchased for the present needs of the power system can continue to be utilized on the greatly expanded system.

The Los Angeles 1950 Power System

The extent to which the basic plan has been followed to date is indicated by Figure 9, which shows schematically the present power system of the Department of Water and Power. Reference to this diagram will show how effective use has been made of the belt lines to equalize power sources and load demands, to provide for stations having no power source of their own, and to make steam stand-by available to all of the receiving station systems. Stations *A*, *E*, and *F* have been equipped with 115-kv belt-line connections as an expedient arising out of: 1. the use of a section of the original San Francisquito transmission lines as part of the belt system; and 2. the acquisition of certain Los Angeles Gas and Electric Company properties, including the Seal Beach Steam Plant and its associated 115-kv transmission lines.

Although the diagram of Figure 9 is a schematic 1-line drawing of the Department's present power-system connections, it has been drawn to represent approximately the geographical arrangement of the several stations. A distance of 33-line miles separates Receiving Station *E*, at the north of the city in the San Fernando Valley, and Receiving Station *C* at the south in the harbor area. The air-line distance between Stations *D* and *F* is 4.8 miles. At the present time the entire area of the city, comprising 452 square miles, is served from the 34.5-kv distribution systems fed from the six receiving stations shown. It will be apparent that the backbone of the basic plan has been constructed, and that the future load growth of the city can be served from additional stations, constructed to augment the existing system and connected to it in either of the two possible ways permitted by the plan. The results of the study of the expanded system offer reasonable assurance that operation will be highly satisfactory and that 3-phase short-circuit duties on the various circuit breakers will not exceed the ratings of most existing circuit breakers or those presently being purchased.

No zero-phase sequence network was developed for the expanded power system studied, and phase-to-ground fault duties were not investigated. However, studies of single-phase-to-ground fault duties on the existing system have shown

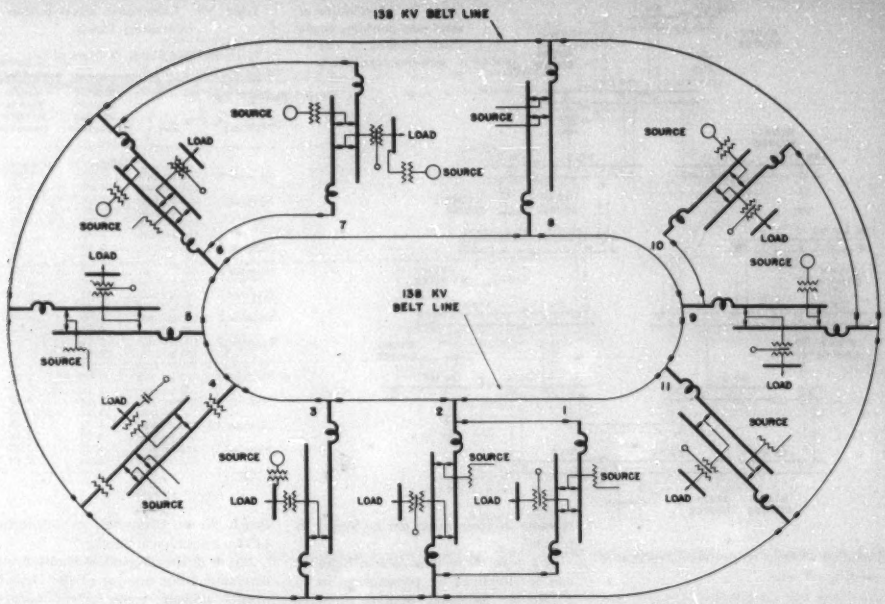

Figure 8. Double-bus, single-circuit-breaker receiving station connections

them to be considerably higher in some locations than the corresponding 3-phase duties. This condition has resulted from the practice of employing literally solid-grounded neutral connections. As the system is expanded, a continuation of the practice would undoubtedly increase circuit-breaker short-circuit duties to values above those tabulated in Table VII. It was recognized that the single-phase-to-ground short-circuit duties could be reduced by increasing either the positive-sequence impedance or the zero-sequence impedance. However, the positive-sequence impedance is the one through which power flows from the source to the load, and any increases in this quantity beyond those absolutely necessary for the control of 3-phase fault currents are detrimental to normal system operation. The zero-sequence impedance is that impedance offered to the flow of fault current in the system neutrals, and plays no part in the normal system operation, becoming a factor only under unbalanced conditions arising out of system trouble. Three-phase duties having been controlled satisfactorily by means of the connections employed, it was believed desirable to limit phase-to-ground fault currents by inserting impedance in the neutral connections.

Table VIII. Zero-to-Positive-Sequence Reactance Ratios

Station	Bus	Condition A*	Condition B**
Receiving Station A	34.5 kv	0.73	
	110 kv	1.56	
Receiving Station B	34.5 kv	0.90	1.25
	132 kv	0.67	1.26
Receiving Station C	34.5 kv	0.97	1.79
	132 kv	1.14	1.31
Receiving Station D	34.5 kv	1.04	1.25
	132 kv	0.88	1.05
Receiving Station E	34.5 kv	1.09	1.35
	132 kv	0.74	1.07
Receiving Station F	34.5 kv	0.87	1.22
	132 kv	0.75	1.12

*Condition A: Maximum fault current
**Condition B: Maximum neutral reactor voltage.

The insertion of impedance in system neutrals results in a voltage drop across that impedance under fault conditions, the magnitude of such drop depending on the ratio of zero-to-positive-sequence reactance. This ratio was determined on the a-c calculating board for two conditions: A. for conditions producing maximum fault current; and B. for conditions producing maximum neutral reactor voltage. Maximum fault current will usually occur with all transformer banks in service, while maximum neutral reactor voltage will be obtained with some of the bank capacity disconnected. Table VIII shows the ratios found on the power system represented by Figure 9, except that double circuit-breaker operation of the belt-line busses was assumed. Neutral reactors of five per cent (100,000-kva base) were used in most of the receiving station load bank neutrals, both high and low sides, and on the Boulder Dam auto-transformer banks at the line terminals.

It should be noted that the ratios ex-

Table IX. Maximum Voltage across Neutral Reactors

Station	Banks	Volts
Receiving Station B	Boulder Dam	16,000
	132-kv load	10,300
	34.5-kv load	6,230
	Boulder Dam tertiary	2,820
Receiving Station C	132-kv load	17,150
	34.5-kv load	5,840
Receiving Station D	132-kv load	12,350
	34.5-kv load	6,250
Receiving Station E	Boulder Dam	14,900
	132-kv load	12,000
	34.5-kv load	6,350
	Boulder Dam tertiary	2,610
Receiving Station F	132-kv load	12,800
	34.5-kv load	6,000

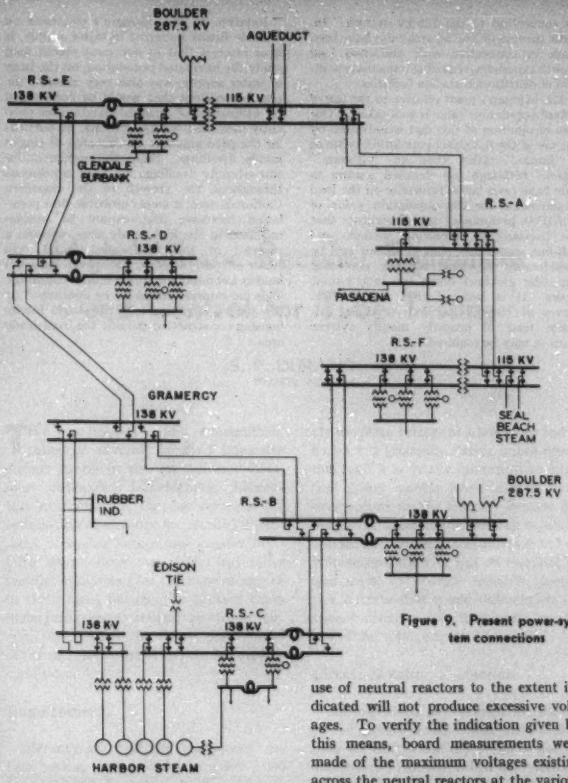

Figure 9. Present power-system connections

isting under condition B, giving maximum neutral reactor voltage, are well below 2.0 in all instances. In view of the tentative designation of 3.0 as the maximum ratio for which the term "solidly-grounded system" applies, this is indication that the use of neutral reactors to the extent indicated will not produce excessive voltages. To verify the indication given by this means, board measurements were made of the maximum voltages existing across the neutral reactors at the various stations under fault conditions. These are tabulated in Table IX.

Since the Department's transformers have all been purchased with insulation, on the grounded ends of the windings, tested for more than twice the maximum voltage possible with the neutral reactors indicated, there is no doubt but that neutral reactors may be safely utilized. The studies outlined above have indicated no hazards in employing this method for reducing short-circuit duties, and the advantages are numerous. In addition to the reduction of short-circuit duty which it accomplishes, impedance in the neutral connections is favorable to system stability under certain types of faults.

Conclusions

1. Land-use surveys provide basic information necessary for forecasting with considerable assurance the amount, character, and location of future electrical load growth. With these three growth factors determined, adequate plans may be made for meeting future generation, transmission, and distribution requirements.

2. Such land-use surveys, made at suitable and regular intervals, provide a continuing check of load growth forecasts and enable any required modification of the basic transmission and distribution plan to be made in sufficient time to avoid construction inapplicable to the ultimate system, and to best utilize existing plant without unnecessary obsolescence.

3. Power-system connections can be devised whereby numerous large power sources can be consolidated in a single load area without imposing excessive 3-phase short-circuit interrupting-duty requirements on the system circuit breakers. Series reactors in such system connections may be applied in a manner permitting them to function as current limiters during periods of short circuit without introducing serious voltage drops or energy losses during normal or contingency operation.

4. Where 3-phase short-circuit interrupting duties are maintained at nominal levels, the use of neutral reactors provides a suitable method for the control of single-phase fault currents.

Discussion

Berton S. Rice (Niagara Mohawk Power Corporation, Buffalo, N. Y.): This paper presents a very logical and apparently new method for determining the power system requirements for a large city, thus enabling the system planners to more adequately meet the needs for future growth.

In areas having heavy industrial loads such as electrolytic processes and rolling mills, it might be necessary to make surveys oftener than every ten years. It will be interesting to see where the results of a 1954 survey will fall in relation to the forecasts indicated in this paper.

The authors are to be complimented on their logical approach to what, at its best, is a difficult problem. The methods and ideas set forth can be easily adapted to any other city or to a combined metropolitan and rural area system.

W. A. Morgan (Bureau of Reclamation, Denver, Colo.): I would like to raise the question of whether it is safe to base an estimate of power use on a fixed population of 6,225,000 people in a location such as Southern California with its ever-increasing population. Apparently this figure is based primarily on available water supply that is anticipated in the future as being the limiting factor.

I do not feel that we should accept such a limit. Engineers will solve this problem of water limitation in some way, if there is a sufficient demand for it.

There is also the possibility that, as more people live in Los Angeles, the high percentage of single-family dwellings will be reduced, which would allow a denser population and larger use of power. In addition, it is likely that the use of power per capita

may be greater in the future than was assumed.

This all leads up to the question I have for the authors. How is it planned to take care of the contingency of having to supply a load in the Los Angeles area substantially greater than that assumed in the paper? For example, say that 10,000,000 people instead of 6,225,000 people made their homes in Los Angeles in the future.

A. L. Williams and **E. L. Kanouse:** The authors appreciate comments made by Mr. Rice and Mr. Morgan, and are pleased at the indication of agreement with the load study method as a system planning tool.

Relative to comment by Mr. Rice, unusually heavy industrial loads to be served might well involve special study as to their connection. The Department's only experience with a load of this type resulted in its connection to the 138-kv system. Interim surveys of limited areas also have been made in connection with abnormal load growth experience requiring immediate addition of distribution station facilities.

Mr. Morgan's point relative to the use of a fixed population value is well taken. Our own recognition of this fact is indicated by the use of the 6,250,000 population value as a "future," rather than an "ultimate," figure. Although our detailed studies to date have been based primarily on the load requirements for the population value of 6,250,000, preliminary studies indicate that the transmission, receiving station, and belt-line connection plan described can be considerably expanded without exceeding our basic assumed limits for short-circuit duties. It is believed that the periodic survey of 10-year intervals provides sufficient time to properly modify system plans as may be required.

Relative to Mr. Morgan's comment on possible future increases of water supply, it is of interest that in our most recent load study the estimated population, on the basis of water supply, was also very close to the population limit that would be determined by utilization of available land under presently indicated habits of living, in particular the predominance in this area of single-family dwellings. Since the preference for single-family dwellings has been continuous throughout the growth of the Southern California area, it seems probable that population increases that cannot be accommodated in the load study area, without a reversal of this established trend, will locate in outlying districts where sufficient land is available for single-family dwellings. This assumption seems to be confirmed by the recent large increases in single family housing construction outside the load study area.

High-Voltage Rectifier Equipment and Control for Tube Testing

S. R. DURAND
MEMBER AIEE

THE testing of radio transmitting tubes of several hundred kilowatts output rating in the RCA-Victor Company Advanced Development Laboratory at Lancaster, Pa., has required the installation of mercury-arc rectifier equipment of higher rating and greater flexibility and voltage range than any other rectifier equipment for this type of service in the United States. To protect tubes undergoing tests, several electronic circuits have been developed for control of the rectifier under all types of operating conditions.

Requirements

Mercury-arc rectifier equipment for tube testing was needed to provide 2,000 kw at 12,000 d-c volts with two 6-phase rectifier units connected in parallel, and 2,000 kw at 24,000 d-c volts with the two units in series. With each connection, 12-phase rectification was desirable and could be obtained by effectively displacing the d-c side transformer windings 30 electrical degrees.

A wide range of voltage adjustment was also an important requirement. To obtain this, a step regulator connected between the power-line circuit breaker and the paralleled a-c side windings of the two rectifier transformers was specified for reducing the voltage over an 80-per cent range in 32 steps to a minimum value of 2,000 d-c volts. Phase control by means of grids in the mercury-arc rectifier units then would permit regulation to lower values or fine adjustment of voltage between steps of the regulator. The basic circuit of the rectifier equipment installation is shown in Figure 1.

When testing new designs of high-power transmitting tubes, it is desirable to apply d-c plate voltage at a low value and to increase it gradually during initial operation, and it is vitally important to interrupt power quickly when internal flashovers occur in the tubes. Because the per cent impedance of the step regulator and rectifier transformers increases at low-voltage operation, it was an essential requirement to provide sensitive protective circuits that would differentiate between normal and fault currents, regardless of the voltage applied to a tube.

Circuit-Breaker Protection

An important requirement for the a-c power circuit breaker was that a tripping control circuit be designed for instantaneous response when a preselected overload current value was reached, regardless of the a-c phase or the part of the sine wave in which the current first attained this value. The circuit breaker is a metal-enclosed air-blast type in which the intense cooling and turbulence produced in the arcing zone by the sudden expansion of compressed air causes extremely rapid deionization of the arc path and arc extinction at the first current zero. An electronic overload tripping circuit is provided to take advantage of this high-speed characteristic of the circuit breaker so as to keep the over-all time a minimum from the occurence of a fault until its interruption. The circuit is shown in Figure 2.

The air-blast circuit breaker, *52*, is equipped with two trip coils, one of which (not shown in the diagram) is operated in the normal manner from any one of three inverse-time overload relays, *51*, and a 48-volt battery. The other trip coil, *52T2* is actuated much more rapidly by release of the energy stored in a 50-microfarad capacitor. The charge in this capacitor normally is maintained from the low-voltage auxiliary supply circuit by means of a selenium rectifier. It is released by conduction of a thyratron tube when the control grid of this tube receives a positive triggering potential. This potential emanates from the fault current first produced in any one of the three a-c power-supply lines through current transformers connected to 1/2-ohm adjustable resistors, step-up transformers and cold-cathode discharge tubes. The potential applied to the control grid of the thyratron tube thus is determined by the discharge voltage level of the cold-cathode tubes so that a positive triggering potential of definite magnitude is obtained regardless of the direction or phase in which the overload current first reaches fault value in the a-c power-supply lines. Adjustment to cause tripping of the circuit breaker at any desired overload setting is made by means of contacts on the 1/2-ohm resistors and a positive bias applied to the anodes of the cold-cathode tubes.

Step-Regulator Voltage Control

The transformer windings of each phase of the Y-connected 3-phase regulator are designed with two coils so that both a buck and a boost connection can be made between them by means of the operating mechanism. This contact-making mechanism employs the principle of compressing and releasing springs to obtain a quick make-and-break action when moving between the contact sectors of each position under load. The two moving contacts of each phase are connected to a center-tapped reactor which limits the circulating current when these contacts overlap between two tapped positions. This enables the contact mechanism to be designed so that the circuit is never broken.

The contact positions cover an effec-

Paper 50-145, recommended by the AIEE Electronic Power Converters Committee and approved by the AIEE Technical Program Committee for presentation at the AIEE Summer and Pacific General Meeting, Pasadena, Calif., June 12–16, 1950. Manuscript submitted March 13, 1950; made available for printing April 11, 1950.

S. R. DURAND is with the Allis-Chalmers Manufacturing Company, San Francisco, Calif.

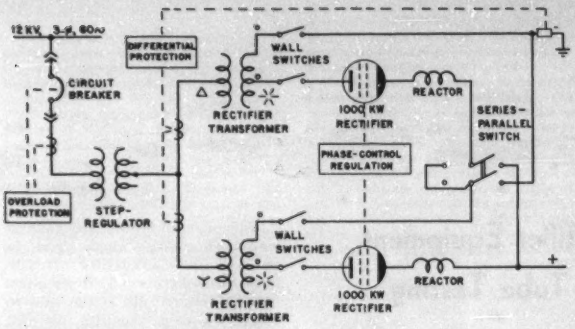

Figure 1. Basic power circuit of rectifier installation

tive range of 16 taps on the series coil of each phase while it is connected in bucking relationship with the magnetizing coil. At the midvoltage position, a reversing switch operates so that the same taps of the series coil may be utilized while it is connected in boosting relationship, thus economizing on the construction of both the electrical and mechanical parts. Actually, only eight taps are brought out from the series windings and connected to eight contact sectors, each alternate position of the stepping mechanism functioning to interconnect two adjacent contact sectors through small center-tapped reactor so as to obtain a voltage halfway between them. With 32 effective positions each of $2^3/_4$ per cent, the voltage can be varied by means of the regulator in 320-volt steps.

Transformer Connections

The transformers for each 1,000-kw rectifier can be used to provide several different types of d-c side circuit connections such as 6-phase diametrical, 3-phase Y series or parallel, 3-phase delta series or parallel, and 3-phase zigzag. All these circuits can be set up readily because each end of the six d-c side phase windings are connected to high-voltage single-pole, double-throw wall switches, and jumpers are provided for interconnections between the switches.

One transformer is equipped with a delta a-c side winding and the other with a Y and tertiary winding so that equivalent 12-phase rectification will be obtained with normal 6-phase operation of each rectifier in either the parallel or series output d-c connection. The transformers, step regulator, and metal-enclosed switchgear are located outdoors in a fenced-in section adjacent to the laboratory building, and the rectifiers, filters, wall switches, and control equipment are installed within the building.

Rectifier Units

Each mercury pool rectifier unit is a 6-phase pump-evacuated steel-tank type mounted on an insulated frame which also includes the control cubicle and a water-to-water heat exchanger. In order to insulate the water supply circuit, cooling water is run through a porcelain insulating coil mounted adjacent to each frame. It also is essential to insulate the 3-phase 230-volt auxiliary power supply for the rectifiers and control equipment. This is accomplished by insulating transformers designed for 95-kv dielectric test between windings.

Each anode of the mercury-arc rectifier units is equipped with two graphite grids. Each grid has a terminal connection so that separate phase-control circuits may be used for the upper and lower grids to control the regulation of d-c output voltage. A phase shifter is mounted in each control cubicle and each phase shifter is driven through an insulating shaft by a small geared motor mounted on a front grounded-steel control panel. Instruments located in the control cubicle at high voltage above ground potential may be viewed through a glass window in the front steel panel.

Phase-Control Voltage Regulation

Another interesting electronic control scheme employed in this installation is a phase-control circuit for d-c output rectifier voltage regulation. This circuit uses thyratron tubes for applying positive impulse potentials to the mercury-arc rectifier grids, and for setting a small advance angle to the potentials applied to the lower ionizing grids with respect to the potentials applied to the upper control grids. The essential elements of this circuit are shown in Figure 3, the diagram being drawn to show the control-tube connections completed through current-limiting resistors to only one set of grids associated with one main anode of a rectifier unit. A negative biasing voltage with respect to the cathode of the mercury-arc rectifier is maintained continuously on all grids by means of a selenium rectifier equipped with output filter. Each upper and lower rectifier grid is permitted to become positive only by triggered voltage impulses from the thyratron tubes controlled (in phase relation to the potentials applied to the rectifier anodes) by means of the phase shifter previously mentioned. Steep wave-front impulse potentials are obtained by applying 60-cycle sine-wave voltages to the anodes of the control tubes 60 electrical degrees in advance of the filtered sine-wave voltages applied to the control-tube grids. The positive-impulse potentials impressed cyclically on the main rectifier grids in this manner offset the negative bias so that each pair of grids regulates the firing instant of its anode with accurate timing control.

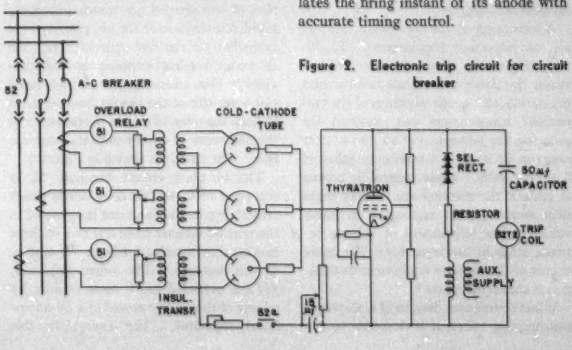

Figure 2. Electronic trip circuit for circuit breaker

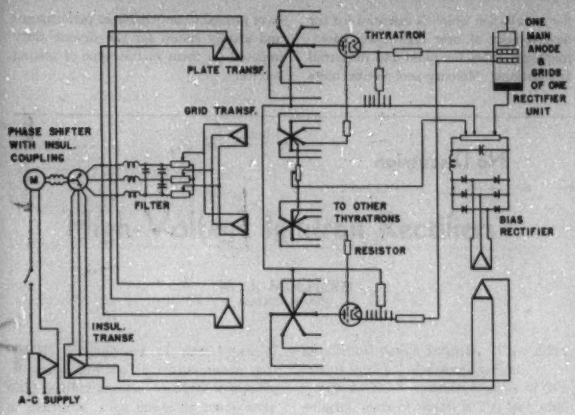

Figure 3. Phase-control voltage regulation circuit

A slight angle of advance is applied to each lower ionizing grid with respect to the associated upper control grid by means of a resistor inserted in the neutral lead of the grid transformer of the control tubes for the upper main grids. This causes the negative bias for the grids of these control tubes to be greater than that for the grids of the lower control tubes, and thus results in an angular delay in firing sequence of the order of one electrical degree. More accurate pickup and control of firing of the anodes of the main rectifier units is attained in this manner.

Regulation of the d-c output voltage of the rectifier units is controlled by operation of the geared motors driving the phase shifters to advance the relative angular setting to obtain higher values or to retard it to obtain lower values. The control is very flexible because it can be operated in conjunction with the step regulator for applying precise values of d-c plate voltage to transmitting tubes. Portable stands with instruments and multiconductor cable connections are provided so that complete starting and stopping control and voltage regulation can be set up at any place in the laboratory.

Differential Protection Circuit

Sensitive high-speed overload protective equipment is required to differentiate between normal and backfire fault currents that might be only slightly different in magnitude when operating at low voltage. This circuit differentiates between the a-c input and d-c output current so as to cause the circuit breaker to be tripped instantly should a backfire occur even at a relatively low voltage.

A rectified d-c current is obtained from the 3-phase a-c input side of each rectifier unit by means of current transformers, three center-tapped insulating transformers, and selenium rectifiers. A direct current in the main output circuit is obtained from a resistor of 1-kw heat dissipation rating inserted in the grounded side of the rectifier equipment, the loss in this resistor being insignificant in comparison to the output rating of the installation. A rheostat enables one direct-current to be adjusted in relation to the other in order to set the initial balance condition. The two currents are about equal and opposed to each other under normal loading of the rectifier equipment so that no current flows through the coil of a sensitive high-speed relay unless a backfire occurs. In this case the current values on the a-c and d-c sides will be radically different, and the relay will operate to cause the a-c circuit breaker to be tripped.

Arc Suppression

In addition to high-speed tripping of the main circuit breaker by means of the electronic overload circuit or the differential protection circuit, it also is possible with rectifier units of this type to utilize electronic circuits to prevent some of the main anodes from firing into a fault after it occurs. Thus, the anodes carrying current at the instant of a surge or overload will continue to carry the fault current until it is extinguished, but the other anodes that would normally conduct current in successive order can be prevented from firing into the fault.

When a flashover occurs in a tube undergoing test, the voltage across the tube will collapse instantly so that if a reactor is connected in series with the tube, nearly full voltage will appear accross the reactor. An auxiliary winding on the reactor insulated from the main winding for a high-insulation voltage level thus can be utilized to transmit an impulse-triggering voltage to electronic tubes. These tubes function to prevent ionization of the arc paths between the mercury pool and any anodes that are not carrying current in the main rectifier, and thus limit the magnitude and duration of a fault current. Other types of load fault detecting equipment also can be utilized to effect high-speed protection.

When circuits of this type are employed, it is essential to use electronic devices throughout to gain full advantage with respect to the extremely short time in which an air-blast circuit breaker can interrupt power. Because the fault-detecting equipment may be located in the circuit effectively at ground potential whereas the mercury cathodes of the rectifier units may be several thousand volts above ground, it is necessary to transmit impulse voltages through insulating transformers between the detecting and electronic-actuating devices.

By means of separate insulating-transformer windings and electronic-impulse control circuits, it is possible to restore power when desired by manual control or by a timing device. In some cases flashovers may reoccur instantly each time an attempt is made to automatically restore power, so that it is desirable to have a means of limiting the number of successive attempts to resume operation. This can be provided by use of a proportioning stepping relay. If only one or two steps are made and then normal operation is successfully reattained, the relay will eventually reset itself automatically to its initial position, but if the preset number of successive steps is completed due to inability to restore normal operation, the relay will cause the circuit breaker to be tripped to open the power-supply circuit.

If fault-responsive circuits are employed for arc suppression in the rectifier units, they must respond at a more sensitive setting and function at a lower value of current than that set for the electronic circuit for circuit-breaker tripping. Otherwise, the main air-blast circuit breaker always will be opened regardless of the

nature or magnitude of the existing fault.

Electronic-control and protective circuits provide some of the most useful and important features of this 2,000-kw rectifier installation which is essential for the development of new high-power radio-frequency tubes for radio and industrial applications. Mercury-pool rectifier units have proved to be reliable in performance and ideally suited for the diverse duty imposed on them in this type of testing service.

No Discussion

High-Voltage Ignitron Rectifiers

M. J. MULHERN
ASSOCIATE AIEE

THE development of new types of sealed ignitron tubes has made possible rectifier equipment which is capable of delivering high power at moderately high direct voltages. These tubes permit the design of high-voltage equipment which has the same reliability in operation as its low-voltage counterparts. The practically unlimited emission of the pool cathode, the long life of the tube, and the lack of moving parts are other characteristics of this equipment. These features bring to the high-voltage field the same power ratings, high efficiency, and high grade of performance that are found in the low-voltage rectifier equipment, which is used widely in general industrial service.

This paper discusses the circuits, design factors, and operating features of two high-voltage rectifiers. Each of the rectifiers described is a typical design for its rating. The first rectifier is designed to deliver 17,000 volts at a load of 2,500 kw, and uses 50-ampere sealed ignitron tubes. The other rectifier is designed to deliver 17,000 volts at a load of 7,500 kw and uses 150-ampere sealed ignitron tubes.

General Description of Equipment and Tubes

The general arrangement of the cubicles in each rectifier is indicated in Figure 1. The 6-phase double-way power circuit is used in both rectifiers. This power circuit permits mounting the ignitron tubes in pairs, together with their associated circuit components. The tubes which are paired conduct current during alternate half-cycles of the supply voltage. This type of mounting of the tubes and circuit components permits a unit-type of cubicle assembly, and results in a more simple mechanical arrangement and reduces floor space requirements. The two machines have similar electrical and mechanical design features. They differ mainly in physical size and weight.

The 2,500-kw rectifier consists of five cubicles, each of which is $2^1/_2$ feet wide and four feet deep. There are three tube cubicles, a control cubicle, and a d-c cubicle. A-c power is connected through bushings in the rear of the control cubicle, and d-c power is delivered through bushings extending from the side of the d-c cubicle. The 7,500-kw rectifier consists of four cubicles, each of which is six feet wide and five feet deep. There are three tube cubicles and a control cubicle. A-c power is connected through three bushings located in the top of each tube cubicle. D-c power is delivered through a bushing in the top of the control cubicle with one side of the d-c grounded.

Both rectifiers employ similar excitation systems.[2] The actual circuits differ slightly because of the different characteristics of the two ignitron tubes. These machines incorporate a water-to-water heat exchanger for removing the arc-losses from the tubes. The correct tube temperatures are maintained at any value of load by the temperature regulating controls. Electrical control circuits provide for operation of the rectifier auxiliaries and for proper starting and stopping sequence.

The 50-ampere sealed ignitron tube[2] which is used in the 2,500-kw rectifier is shown in Figure 2 and in the diagram of Figure 3. The over-all height of the tube, excluding the length of the anode lead, is 22 inches and the tube is $5^1/_2$ inches in diameter. It weighs approximately 25 pounds. The internal structure of this tube is similar to other types of sealed ignitrons except for the addition of the grids. The mercury pool cathode, ignitor, and excitation anode elements are the same as in the low-voltage tubes. Current flow is initiated by the ignitor and control grid voltages. The ignitor establishes the cathode spot and starts emission, while the control grid voltage determines the instant at which anode conduction begins. An important feature of this tube is the second grid located between the control grid and the anode. This is called the gradient grid[1] and effectively divides the anode-cathode space into two regions. Its purpose is to control the anode-cathode potential gradients during nonconducting periods and this construction results in a tube which will withstand much higher inverse and forward voltages. The baffle below the control grid structure serves to deflect mercury droplets away from the grid structure. It also aids in deionizing the grid-cathode space after current conduction ceases. This ignitron carries a continuous direct current rating of 50 amperes at 20,000 volts.

The 150-ampere sealed ignitron tube[1] which is used in the 7,500-kw rectifier is shown in Figure 4 and the diagram of Figure 5. The internal structure of this tube is similar to the 50-ampere ignitron except that it employs three grids, and it is much larger in size. It is 42 inches in over-all height, excluding the anode lead, and it is nine inches in diameter. It weighs approximately 100 pounds. From the cathode the grids are, first, the shield grid; next, the control grid; and then the gradient grid. The shield grid assists in deionizing the space near the control grid immediately after conduction. The other elements provide the same functions as in the smaller tube. The tube carries a continuous d-c rating of 150 amperes.

Both tubes are operated with control (and shield) grid voltages negative with respect to the cathode except during the conducting period. The gradient grids are operated at some intermediate value of the actual anode-to-cathode voltage, usually 50 to 65 per cent. Each ignitron

Paper 50-146, recommended by the AIEE Electronic Power Converters Committee and approved by the AIEE Technical Program Committee for presentation at the AIEE Summer and Pacific General Meeting, Pasadena, Calif., June 12–16, 1950. Manuscript submitted March 16, 1950; made available for printing April 11, 1950.

M. J. Mulhern is with the General Electric Company, Schenectady, N. Y.

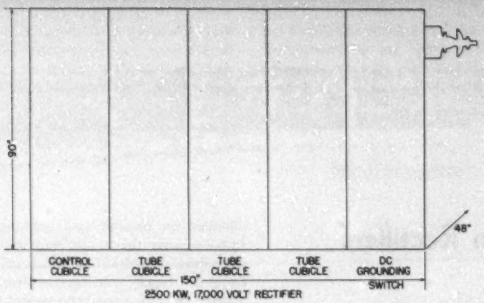

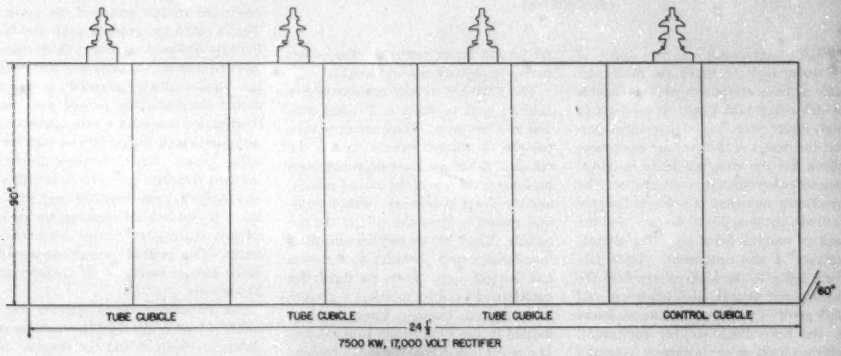

carries a momentary surge current rating approximately 30 times its continuous rated value.

Circuit

The power and excitation circuits are shown in Figure 6. The double-way power circuit delivers twice the direct voltage of a double-Y circuit for the same rectifier transformer secondary voltage. The circuit also requires only three secondary windings on the rectifier transformer and only three high-voltage a-c connections between the transformer and the tubes. The double-way connection results in better utilization of transformer capacity and requires less insulating material on the a-c side than other rectifier circuits.

The symmetry of the power circuit allows several possible circuit arrangements on the d-c side. The d-c busses may be ungrounded, or either bus may be grounded according to the particular installation requirements. The equipments shown in Figure 1 illustrate two possible arrangements. The 7,500-kw unit has a single d-c bushing with provision for internally grounding either the positive or the negative bus. The 2,500-kw unit is provided with two d-c bushings and an internal grounding switch. Either of the d-c busses may be grounded externally as required. The switch provides a safety precaution by grounding both d-c busses in order to discharge the external circuits which are connected to the rectifier before any cubicle doors are opened.

The surge filter shown in the circuit diagram provides a discharge path for the stored energy in the rectifier transformer secondary windings during tube commutation intervals. The filter is a 3-phase

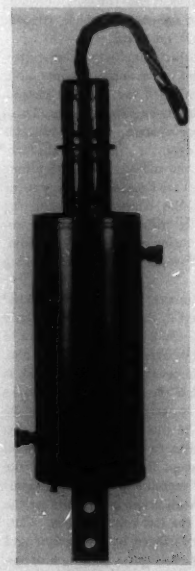

Figure 1 (above). Arrangement of high-voltage rectifier equipment

Figure 2 (left). 50-ampere sealed ignitron tube for use in 20,000-volt circuits

Figure 3 (below). Construction of 50-ampere sealed ignitron tube

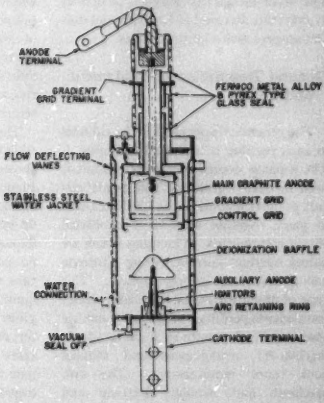

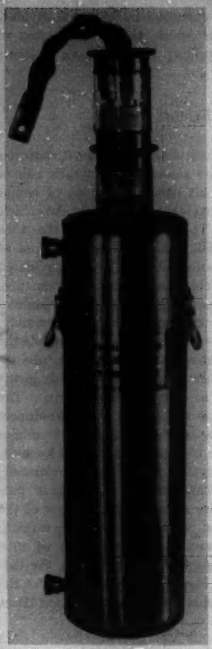

Figure 4 (left). 150-ampere sealed ignitron tube for use in 20,000-volt circuits

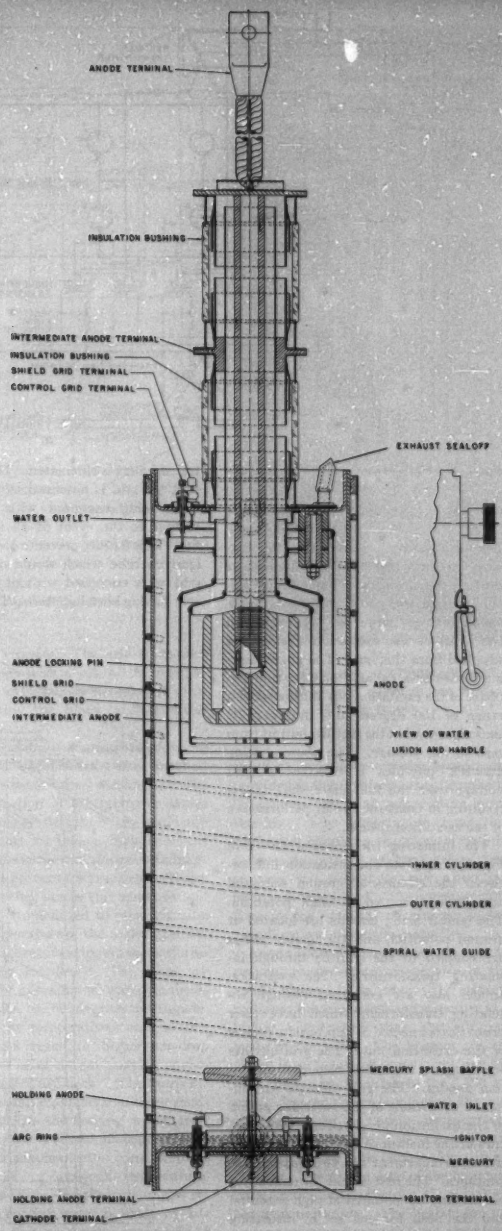

Figure 3 (right). Construction of 150-ampere sealed ignitron tube

resistance capacitance network with circuit constants chosen for critical damping. The inductance corresponds to the commutating reactance at the transformer secondary terminals. The value of inductance depends upon the per-unit reactance of the transformer and the per-unit reactance of the power system. The surge filter limits the transient voltages which are produced by the commutation of the load current from tube to tube. These voltages, if undamped, would be sufficiently high to damage the transformer winding insulation, particularly when the rectifier is operated with large amounts of phase retard. The combined resistance losses are approximately 1 per cent of the rectifier rating. This, however, results in a power loss of 3.5 kw per resistor assembly in the 2,500-kw machine. The resistor assembly is, therefore, rather large since this is an appreciable wattage.

The excitation system provides ignitor, excitation anode, and grid voltages for each of the tubes. The circuit components employed are all static devices which have long life and require low maintenance. The excitation system also includes a phase shifting network which

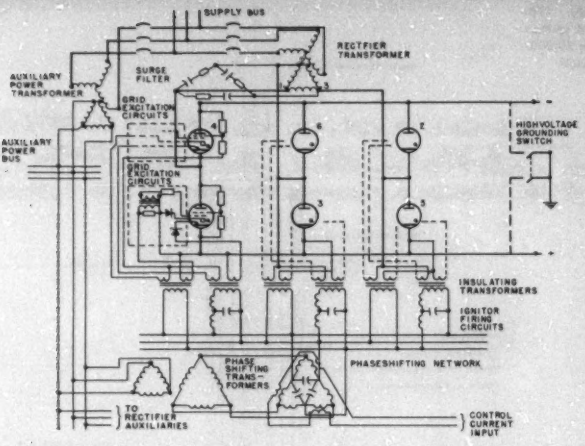

Figure 6. High-voltage rectifier circuit diagram

provides continuous control of the phase of all of the tube excitation voltages. Excitation power is derived from the auxiliary bus through a set of adjustable phase shifting transformers. These transformers energize the phase shifting network which delivers power to the excitation bus. All of the excitation circuits are supplied from this bus. The phase shifting network is capable of adjusting the phase of the excitation bus voltages over a range of 150 degrees and thus permits smooth control of the rectifier output from zero to full voltage. The phase shifting network provides a constant output voltage over the full phase shift range, resulting in constant circuit performance of the excitation system.

The insulating transformers shown in Figure 6 indicate the insulation line between the circuits at ground potential and those mounted at high potential. The ignitor firing circuits are located at ground potential, and the ignitor pulses are coupled to the ignitors through insulating transformers. The excitation anodes also are energized through insulating transformers which have their primaries connected to appropriate phases of the excitation bus. The grid circuits are energized from their respective excitation anodes. The grid voltages are obtained as a result of the switching action in the excitation anode circuit which occurs at the instant of ignitor firing. This circuit arrangement has two distinct advantages. The first is that the entire grid circuit may be mounted at high potential and the need for one set of insulating transformers is eliminated. The second is that the grid is automatically prevented from being energized with a positive voltage in the event of an ignitor misfire. This feature prevents damage to the ignitron tube which would occur if the grid were energized without a cathode-spot having been initiated. The gradient grids are energized by potential dividing resistances which supply a fraction of their respective anode-cathode voltages to them.

Design Factors

The circuit diagram, Figure 6, indicates the circuits associated with each pair of tubes. This natural grouping of circuit components is the basis of the tube cubicle design. The circuits within the tube cubicles fall into three groups, those at ground potential, and those associated with the cathode potential of each tube. The circuits connected to the cathode of one tube are made as a single assembly, insulated from the frame, and include the sealed ignitron mounting. The tube assemblies are mounted side by side in the cubicles in the 7,500-kw unit. The smaller size and weight of the 50-ampere ignitron permits mounting the assemblies one above the other in the 2,500-kw unit. The excitation insulating transformers, ignitor firing circuits, and water pipe headers are mounted on the floor of the cubicles in both rectifiers. The internal arrangement of the two types of tube cubicle assemblies is shown by the diagrams of Figures 7 and 8. The grid circuits are mounted in fully shielded boxes

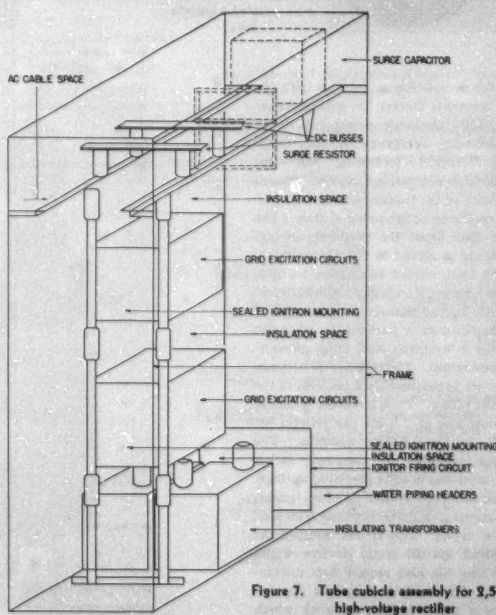

Figure 7. Tube cubicle assembly for 2,500-kw high-voltage rectifier

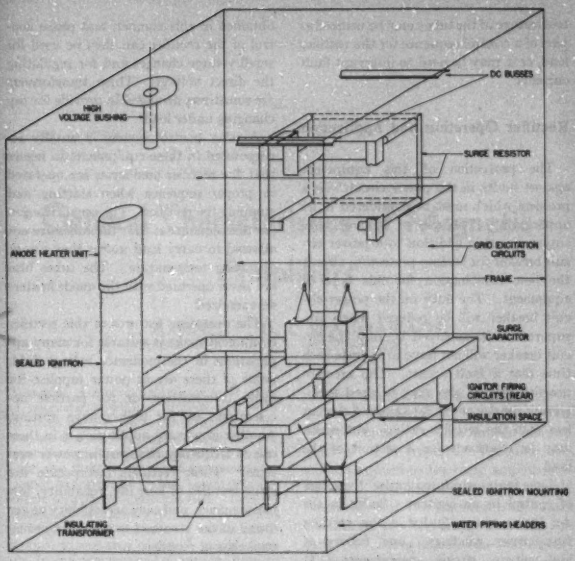

Figure 8. Tube cubicle assembly for 7,500-kw high-voltage rectifier

Figure 9. Front view of 17,000-volt rectifier rated 2,500 kw and operating from 3-phase 13.8-kv supply

which minimize the transient voltages that would otherwise appear at the ignitron grids. The water jackets of the sealed ignitrons must be insulated from the grounded cooling system. This is provided by an insulating water column that connects the tubes to the water pipe headers. Distilled water of high resistivity is used in a closed, recirculating system. The water column is made of 30-foot lengths of neoprene hose, which is wound in a flat spiral and mounted adjacent to the tube mountings. Electrolytic targets are provided at each end of each hose to protect the fittings from electrolysis. The magnitude of the electrolytic current which flows will be 250 to 500 microamperes, depending upon the condition of the cooling water. The inlet and outlet hoses are wound together in one assembly in the 7,500-kw machine, and they are mounted in the insulating space to the right of the tube mountings. The inlet and outlet hoses are wound separately in the 2,500-kw machine and are mounted in the insulating spaces on either side of the tube mounting. The hoses are visible in Figure 9.

The cubicles in both machines have doors both front and rear. This affords complete accessibility to the tubes and excitation circuits. The grid boxes also are equipped with doors in the rear, so that these circuits may be checked without removing the tubes or their water connections.

The excitation insulating transformers have dual secondaries with internal shields between the windings. The switching action of the ignitrons causes their cathode potentials to suddenly shift, tending to induce high transient voltages across the transformer windings. The shields prevent the transient voltages from appearing across the windings and from being transmitted to other circuits.

The temperature of the sealed ignitron tubes has a direct bearing on the performance of the rectifier.[1,3] The tubes are designed for operation at water temperatures of 30 to 60 degrees centigrade. Operation at temperatures outside this range would result in higher arc-drop voltage, or loss of current carrying capacity, or frequent arc-back. The temperature regulating equipment in these rectifiers maintains the cooling water temperature between 35 and 45 degrees centigrade and automatically corrects itself for changes in ambient temperature. Correction of the temperature of the recirculated cooling water is made by adjusting the flow on the raw water side of the heat exchanger. Water heaters are provided so that the tubes may be quickly brought to operating temperature when starting. The temperature regulating equipment circulates 18 gallons of coolant per minute in the 2,500-kw machine, and requires ten gallons of raw water per minute at rated load. The corresponding flows for the 7,500-kw machine are 30 and 10 gallons per minute respectively.

Anode heaters are provided in order to prevent condensation of mercury in the anode region of the tube. The heaters maintain the anode seal and structure at a higher temperature than the adjacent parts of the tube. The heaters are enclosed in an insulated assembly which fits over the top of the tubes in the 7,500-kw unit. Heater power is supplied through the excitation insulating transformers. The heaters in the 2,500-kw unit are mounted on the tube cubicle doors in reflectors. The anode seals of the ignitrons have individual reflectors to distribute the heat uniformly. The heaters are energized at ground potential and, therefore,

permit the use of a smaller size of insulating transformer in the 2,500-kw rectifier.

Key operated door interlocks are provided on all cubicles which enclose high voltage a-c and d-c busses and tubes. A mechanical key sequence is provided which requires that all a-c switchgear and d-c switches be operated to a de-energized position and locked, before any high-voltage cubicle doors can be unlocked and opened. Additional electrical interlocks in the doors control the excitation system and the rectifier auxiliaries.

Operating Features

The control of the direct voltage output of the rectifier is obtained by adjusting the phase of the ignitor pulse. The phase of the ignitor pulse and the other ignitron excitation voltages is controlled by the phase shifting network. A direct current signal applied to the saturable reactors in the network is the means of control. This current may be obtained from a small d-c source and adjusted manually with a rheostat. This would provide manual control of the voltage. The control current may be obtained from a voltage regulator instead, and thus provide automatic regulation of the direct voltage.[6] The network provides a continuous function and the direct voltage output of the rectifier may be adjusted from maximum to zero.

An important feature of the ignitron tubes is their ability to rapidly interrupt the load current. The conduction in any one of the ignitrons will cease after the first current zero if the ignitor impulse is removed. The tubes will then "hold off" and prevent current flow until the ignitor impulse is again restored. The permissive action of the grid circuit is useful under these conditions, since the absence of a cathode-spot results in a negative voltage being impressed on the grid. The simplest means of interrupting the ignitor pulses is to short circuit the primary windings of the ignitor insulating transformers with a set of high-speed relay contacts. This relatively simple means of arc-suppression results in both ignitor blocking and grid blocking of the tubes to prevent conduction. This additional control feature of the tubes may be utilized as part of a control sequence for the rectifier load, or it may be used to interrupt fault currents.

Rectifier Operation and Application

The protection of this equipment against faults in the power circuit[4,7] is a problem which must be considered in its application. The use of ignitron arc-suppression[10] in addition to a power circuit breaker for backup protection affords the best combination for this type of equipment. The duty on the power circuit breaker will be reduced when arc-suppression is employed because the circuit breaker will not have to operate each time that a fault occurs. The arc-suppression feature also may be used to interrupt the d-c power for values of current less than the rectifier ratings, but which may be overloads for a section of the load.

Some faults which may arise[7,8] are, loss of control in an ignitron; faults in the d-c load circuit; faults in the rectifier transformer windings; and failure of high-voltage circuit components. It should be noted that very few failures in the ignitrons will result in sustained fault currents on the power system. The ability of the ignitron to recover after a fault is generally good, and permanent damage to the tubes or equipment is not likely.

The load regulation characteristic of the rectifier is a straight line in these machines. The maximum voltage drop from no load to full load depends solely upon the reactances of the rectifier transformer and the power system feeder. This regulation characteristic may be made flat over the load range by using a voltage regulator which will supply the control current to the phase shifting network.

There are some applications in which the poor direct voltage waveform of a rectifier operated at large phase retard cannot be used. In these cases, a regulating autotransformer is connected ahead of the rectifier transformer and it is used to raise and lower the supply voltage. Large changes in the direct voltage output are obtained in this manner, and phase control of the rectifier can then be used for small voltage changes and for regulating the direct voltage. These transformers are sometimes arranged to provide for tap changing under load.

A relay control system is usually incorporated in these equipments to insure that the rectifier auxiliaries are operated in proper sequence when starting and stopping the rectifier. The usual criterion for this sequence is that the tubes are not allowed to carry load unless they are at operating temperature. The tubes also are never operated with the anode heaters de-energized.

The operating features of this rectifier equipment make it suitable for many applications in the moderate voltage field. Some of these are as power supplies for radio transmitters, or for particle accelerators, or for high-voltage testing. Another important application is in their use as frequency changers in power systems.[5] These rectifiers incorporate the same features of long life, reliability, low maintenance, and easy accessibility as are found in the standard low-voltage industrial class of rectifier.

References

1. Pentode Ignitrons for Electronic Power Converters, H. C. Steiner, J. L. Zehner, H. E. Zuvers. *Electrical Engineering* (*AIEE Transactions*), volume 63, October 1944, pages 693–97.

2. Sealed Ignitrons for Radio-Transmitter Power Supplies, H. E. Zuvers. *Proceedings*, National Electronics Conference (Chicago, Ill.), volume 3, 1947.

3. The Relation of Residual Ionization of Arc-Back in Thyratrons, K. H. Kingdon, E. J. Lawton. *General Electric Review* (Schenectady, N. Y.), volume 42, 1939, page 474.

4. Rectifier-Circuit Duty, C. C. Herskind. *Electrical Engineering* (*AIEE Transactions*), volume 63, March 1944, pages 123–28.

5. Design of an Electronic Frequency Changer, C. H. Willis, R. W. Kuenning, E. F. Christensen, B. D. Bedford. *AIEE Transactions*, volume 63, 1944, pages 1070–78.

6. Rectifier Fault Currents, C. C. Herskind, H. L. Kellogg. *Electrical Engineering* (*AIEE Transactions*), volume 64, March 1945, pages 145–50.

7. Rectifier Fault Currents—II, C. C. Herskind, A. Schmidt, Jr., C. E. Rettig. *AIEE Transactions*, volume 68, part I, 1949, pages 243–52.

8. Protection of Electronic Power Converters, AIEE Committee Report. *AIEE Transactions*, volume 69, part II, 1950, pages 813–29.

9. Excitation, Control, and Cooling of Ignitron Tubes, C. C. Herskind, E. J. Remscheid. *Electrical Engineering* (*AIEE Transactions*), volume 65, October 1946, pages 632–35.

No Discussion

General Characteristics of Magnetic Amplifiers

L. A. FINZI
MEMBER AIEE

D. C. BEAUMARIAGE
ASSOCIATE AIEE

Synopsis: A general analysis of basic types of magnetic amplifiers without and with feedback is presented in dimensionless form. The use of a simplified approximation of the normal magnetization curve with a hyperbolic sine function permits a comparatively simple treatment of a most comprehensive nature on a purely analytical basis. General dimensionless characteristics are obtained which apply, without need for further calculations, to any kind of design specifications and to any core material of not too abruptly varying incremental permeability. Thus the influence of factors of design and materials on the performance is made evident. This approach also yields a practical method of accounting for the simultaneous conduction of the feedback rectifiers (commutation) in terms of a correction factor which is applied to the feedback ratio. Numerical values of this correction factor are calculated for some significant instances.

Introduction

In a recent study[1] an analysis has been presented for the determination of the steady-state characteristics of magnetic amplifiers in terms of data of design. The method is to apply Kirchhoff's and Faraday's laws to the electric circuits of the amplifier and to use Ampere's law to relate the magnetic field intensities and currents, expressing the empirical relationship between field intensities and flux densities by means of some convenient analytical expressions.

The procedure is facilitated by the use of simplifying assumptions: leakage fluxes, hysteresis, and eddy currents are neglected. The core fluxes are assumed to vary sinusoidally in time. Rectifiers as used in feedback amplifiers are assumed to have infinite resistance in the reverse direction and a constant small resistance in the forward direction.

When the normal magnetization curve of the core material can be approximated by a power series with a limited number of terms, or by hyperbolic functions, the method applied to the basic amplifiers of Figure 1 yields comparatively simple expressions for the instantaneous values of currents in the various amplifier circuits.[1,2,3] These expressions are in terms of the direct component B_0 and the crest of the alternating component B_{max} of flux density in the cores, and are checked quite well by experimental results. If for instance, the normal magnetization curve is approximated by a representation of the type $H = U \sinh uB$, $H = U \sinh uB + vB$, or the sum of two sinh terms, the currents are expressed in the form of harmonic series whose coefficients are modified Bessel functions for which tabulations are available.[4] Thus characteristic curves expressing output currents (rms or also rectified average values) in terms of the direct component of signal current and of the sinusoidal voltage applied are obtained, which also agree very closely with experimental checks.

This agreement also is obtained for feedback amplifiers, as the analysis[1] expresses accurately the differences in wave form of the output and feedback currents, which appear in portions of the cycle during which all of the feedback rectifiers conduct simultaneously. The time average value of feedback currents is accordingly increased, with effects which are particularly pronounced for instance when a forcing resistor is used in series with the signal circuit in order to improve the speed of response.

It is the purpose of this paper to elaborate further upon the findings of the previous analysis. The results are presented in the form of general dimensionless characteristics, that can be used directly for the amplifiers of Figure 1 without need for calculations, other than the simple ones required to convert the dimensionless data to the actual values corresponding to any specific design and core material.

Dimensionless Curves

The full line curves shown in Figure 2 represent in general dimensionless form the relationship between the alternating voltage across the amplifier terminals and the rectified average value of load current for different values of the total time average magnetomotive force due to signal, bias, and feedback currents for any of the amplifiers of Figure 1.

The calculations from which these curves result are based on an approximation of the normal magnetization curve of the core with a simple hyperbolic sine function

$$H = U \sinh uB$$

and they are intended to apply for those core materials (hypernik, hypersil, and similar improved transformer steel alloys) for which the simplifying assumptions already mentioned are valid.

This function may yield somewhat less close approximations to the experimental magnetization curve than those obtainable with some of those used in reference 1. However, the simplified approximation chosen is advantageous as it allows for a comparatively simple dimensionless treatment of a most general nature in pure analytical form. Samples of experimental checks, as shown later, indicate that the results are still satis-

Paper 50-148, recommended by the AIEE Electronics Committee and approved by the AIEE Technical Program Committee for presentation at the AIEE Summer and Pacific General Meeting, Pasadena, Calif., June 12–16, 1950. Manuscript submitted March 14, 1950; made available for printing April 13, 1950.

L. A. Finzi and D. C. Beaumariage are both with the Carnegie Institute of Technology, Pittsburgh, Pa.

This work was done in part under a contract with the Office of Naval Research, and in part by D. C. Beaumariage in partial fulfillment of the requirements for the degree of Doctor of Science at Carnegie Institute of Technology.

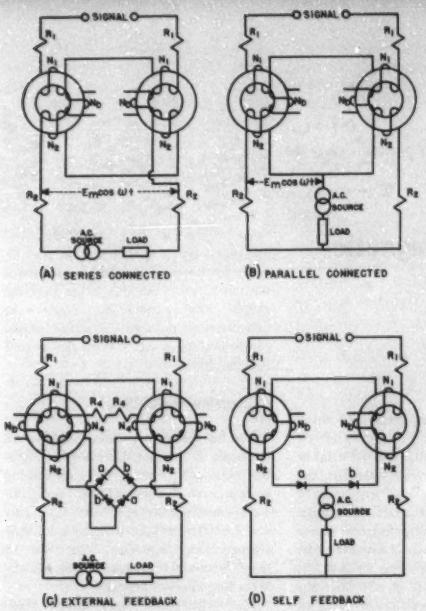

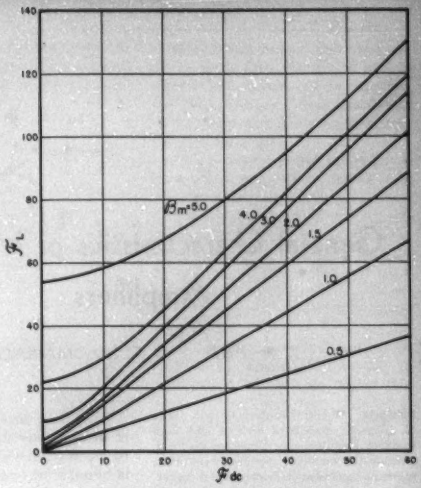

Figure 1 (left). Typical magnetic amplifiers

Figure 3 (above). General dimensionless transfer characteristics of magnetic amplifiers

factory within the range of accuracy expected in problems of this nature.

The dimensionless ordinates of the curves of Figure 2 are

$$\mathcal{B}_m = uB_{max} = u\frac{E_m}{N}\frac{1}{\omega A} \tag{1}$$

where B_{max} (for example, in webers per square meter) is the crest of the component of the flux density in the core alternating at frequency f (cycles per second), E_m/N is the crest value of the corresponding volts per turn, $\omega = 2\pi f$ and A is the cross sectional area of one core (square meter). (For the amplifiers of Figures 1(A) and (C), $N = 2N_2$; for the amplifiers of Figures 1(B) and 1(D), $N = N_2$.)

The dimensionless abscissae are defined as

$$\mathcal{F}_L = \frac{1}{U}\frac{NI_{L\,ave}}{l} \tag{2}$$

where l is the mean length of the magnetic path (meters) and $I_{L\,ave}$ is the current measured by a rectified average ammeter in the output circuit.

Moreover the parameter $\mathcal{F}_{dc}$, is defined as

$$\mathcal{F}_{dc} = \mathcal{F}_1 + \mathcal{F}_b + \mathcal{F}_f \tag{3}$$

where

$$\mathcal{F}_1 = \frac{1}{U}\frac{N_1 I_{1\,ave}}{l}, \quad \mathcal{F}_b = \frac{1}{U}\frac{N_b I_{b\,ave}}{l},$$

$$\mathcal{F}_f = \frac{1}{U}\frac{N_f I_{f\,ave}}{l} \tag{4}$$

$I_{1\,ave}$, $I_{b\,ave}$, and $I_{f\,ave}$ are direct components (time average values) of the currents that flow in signal, bias and feedback windings, and N_1, N_b, and N_f are correspondingly their number of turns (per core). The convention is used that N_b is a positive or negative number according to whether the bias magnetomotive force $N_b I_b$ is such to aid or to oppose the magnetomotive force $N_1 I_{1\,ave}$, of the signal. A similar sign convention is used for N_f which will be a positive quantity in the case of positive feedback, but shall be negative for negative feedback action.

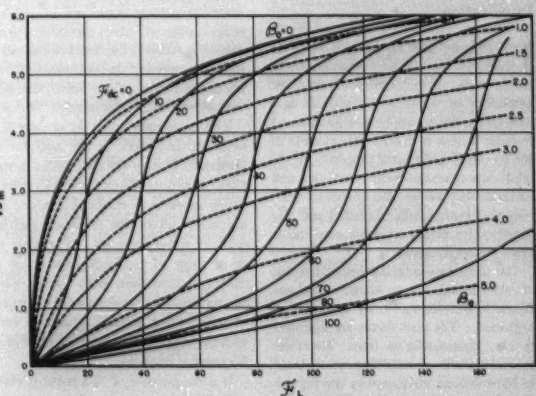

Figure 2. General dimensionless output characteristics of magnetic amplifiers

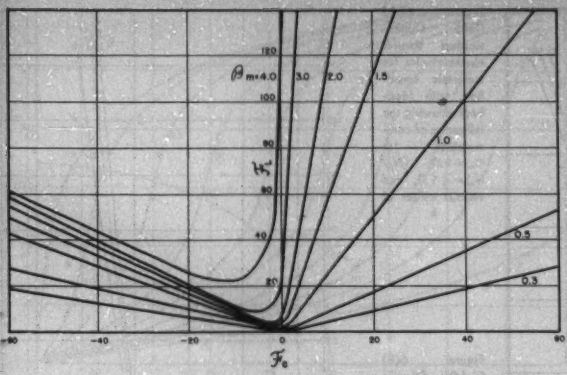

Figure 4. Dimensionless transfer characteristics for magnetic amplifiers with feedback, negligible commutation and feedback ratio $(N_f/N_s) = 1$ for various values of $\mathcal{B}_m$

Thus for the external feedback amplifier of Figure 1(C), $N_f = \pm N_t$, while for the self feedback of Figure 1(D), in which feedback and output windings coincide, $N_f = \pm N_2$.

The full lines of Figure 2 have been calculated from equations 17 and 18 of Appendix I. The abscissa $\mathcal{F}_L$ has been chosen as in equation 2 on the basis of rectified average value of output currents as the curves convey in this form more directly usable information on the performance of feedback amplifiers, as shown later. If so desired, similar dimensionless curves in terms of rms or of peak output currents can be plotted from equations 15 or 16. More simply these curves also may be obtained from the average value currents of Figure 2 by means of the no-load form factor and peak factor curves shown in Figure 12. (It may be of interest to note that such form and peak factors do not depend on the average value of core flux density if an hyperbolic sine function is used to represent the experimental normal magnetization curve.)

The dotted curves of Figure 2 represent in general dimensionless form the same relationship between $\mathcal{B}_m$ and $\mathcal{F}_L$ for different values of the parameter $\mathcal{B}_0 = \mu B_0$ where B_0 is the direct component of core flux density. These curves are calculated using equation 18 of Appendix I and are plotted in Figure 2 as they are useful for the study of commutation phenomena as discussed in Appendix I. (They also can be useful in the analysis of transients, in which the growth or decay of the direct component of the average core flux is essential, as indicated for example in reference 5.) The representation of Figure 2 evidences also that $\mathcal{B}_0$ depends not only on $\mathcal{F}_{de}$ but on $\mathcal{B}_m$ as well.

By crossplotting the full line curves of Figure 2, Figure 3 is obtained in which $\mathcal{F}_L$ is plotted as function of $\mathcal{F}_{de}$ for various values of $\mathcal{B}_m$. The curves show the limitations of the so-called "turns ratio law."[3] This law states an approximate equality of ampere turns per core of rectified average output currents and of average ampere turns per core of signal, bias, and feedback current; that is, in our notation $(1/2)\,\mathcal{F}_L = \mathcal{F}_{de}$. It is seen actually that for high enough values of $\mathcal{F}_{de}$, these curves are nearly straight lines, whose slopes however vary for different values of $\mathcal{B}_m$, (as expressed also by equation 19 in Appendix I). In other terms the turns ratio law, obtained on the assumption of so-called square magnetization curves, may not apply too well to materials with gradually varying incremental permeability with which this analysis is concerned.

Amplifiers Without Feedback

The full line curves of Figure 2 allow the immediate evaluation of the operating point of any amplifier without feedback, (Figures 1(A) and 1(B), for which $N_f = 0$), for any specific instance for which data of design (resistance, number of turns of the various windings, core cross section and mean length) and magnetization curve of the material (expressed in terms of the parameters U and u) and for which signal and bias currents and alternating voltage across the output windings are given.

"Load lines" expressing the possible points of operation of a magnetic amplifier for various values of signal current and fixed a-c supply voltage and load also can be plotted in dimensionless form on the chart of Figure 2. For instance the known elliptical load lines that result for a resistive load R_L under the approximate assumption of sinusoidal output current can be represented on the chart also with ellipses whose axes coincide with the coordinate axes. The intercept $\mathcal{B}_{mi}$ of such ellipses with the ordinate axis is the value of $\mathcal{B}_m$ corresponding to zero output current (infinite "reactance" of the output windings). Thus if the supply voltage is V_{rms} it follows from equation 1.

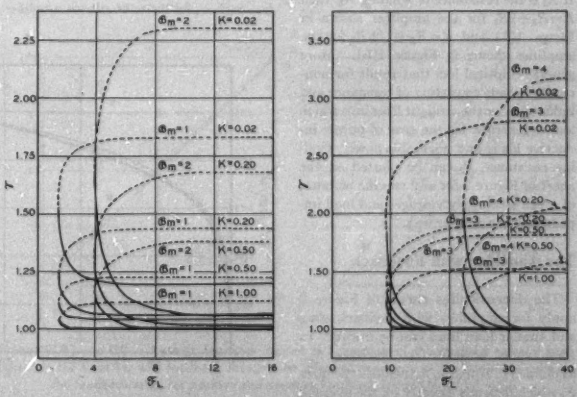

Figure 5. The feedback correction factor γ as a function of $\mathcal{F}_L$ for various values of $\mathcal{B}_m$ and k for $(N_f/N_s) = +1.0$ in full line and $(N_f/N_s) = -1.0$ in dotted line

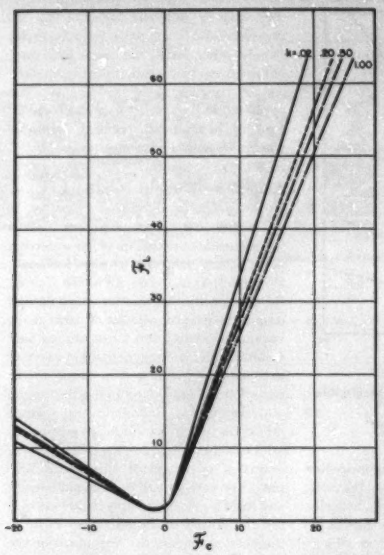

Figure 6(A) (left). Dimensionless transfer characteristics for magnetic amplifiers with feedback showing the influence of commutation for $\mathfrak{B}_m = 1.0$, $(N_f/N_3) = +1.0$, and various values of k

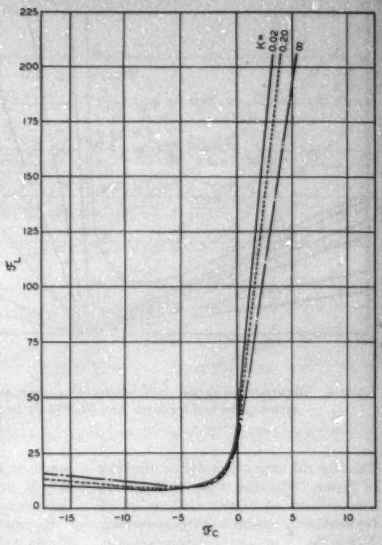

Figure 6(B) (right). Dimensionless transfer characteristics for magnetic amplifiers with feedback showing the influence of commutation for $\mathfrak{B}_m = 3.0$, $(N_f/N_3) = +1.0$, and various values of k

$$\mathfrak{B}_{mt} = u\frac{\sqrt{2}V_{rms}}{N}\frac{1}{\omega A} \tag{5}$$

On the other hand the intercept with the abscissae axis is

$$\mathfrak{F}_{Lt} = \mathfrak{B}_{mt}/\mathfrak{R} \tag{6}$$

where

$$\mathfrak{R} = uU\frac{\pi}{2}\frac{l}{N^2\omega A}R \tag{7}$$

If R_3 is the resistance of winding N_3, then $R = R_L + 2R_3$ for the amplifier shown in Figure 1(A) and $R = R_L + 1/2\ R_3$ for the amplifier shown in Figure 1(B). More general elliptical loci that result for non-rectified loads consisting of resistance and inductance or the straight lines into which loci degenerate for the case of purely inductive loads and negligible power winding resistance R_3 can be plotted on the chart of Figure 2 for any specific instance of given a-c supply voltages and load impedances in a similar way.

The Amplifier with Feedback

The dimensionless curves of Figure 2 apply for amplifiers with feedback also, and similar load lines can be drawn. In these cases however the variable $\mathfrak{F}_{de}$, as defined in equation 3, includes the term $\mathfrak{F}_f$ which depends directly on the average value $I_{f\,avg}$ of current flowing in the feedback windings.

Transfer curves, expressing $\mathfrak{F}_L$ as function of the dimensionless control magnetomotive force $\mathfrak{F}_C = \mathfrak{F}_1 + \mathfrak{F}_b$ for given values of $\mathfrak{B}_m$ are obtained immediately from the curves of Figure 3, whenever the assumption can be made that

$$I_{f\,avg} = I_{L\,avg} \quad \text{for the external feedback amplifier} \tag{8}$$

and

$$I_{f\,avg} = \frac{1}{2}I_{L\,avg} \quad \text{for the self-feedback amplifier.}$$

The dimensionless magnetomotive force $\mathfrak{F}_C$ of the control windings (bias and signal) is then related to $\mathfrak{F}_{de}$ by

$$\mathfrak{F}_C = \mathfrak{F}_1 + \mathfrak{F}_b = \mathfrak{F}_{de} - \frac{N_f}{N_1}\frac{1}{2}\mathfrak{F}_L \tag{9}$$

where for the external feedback case $N_f = \pm N_4$ and for the self feedback case $N_f = \pm N_3$. The curves of Figure 4 have been obtained under the assumption given in equation 8 for a "feedback ratio" $N_f/N_3 = 1$.

As shown later quantitatively, condi-

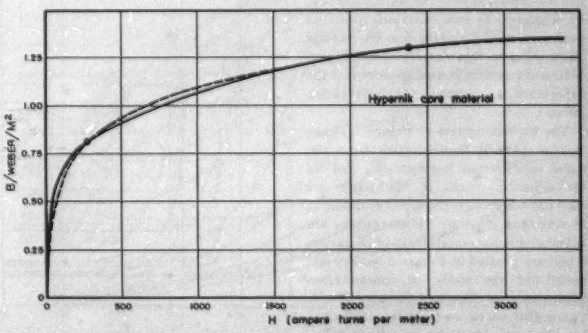

Figure 7. Normal magnetization curve (full line) and its analytical approximation $H = U \sinh uB$ (dotted line). $U = 12.7$ ampere turns per meter; $u = 4.6$ square meters per weber

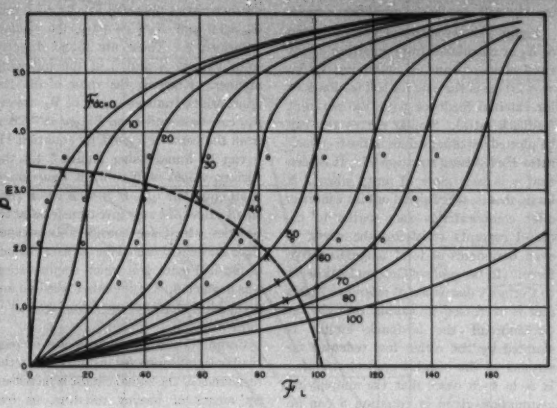

Figure 8. General dimensionless output curves with samples of experimental checks

The circled points check the no load curves and the crossed points are for the elliptical load line

tions may arise however for which I_{fave} is greater than the value given in equation 8. This phenomenon has been recognized already in the early papers of T. Buchhold,[4] and has been mentioned also in a discussion of references 3 and 7 by D. B. Corbyn. In the wording of Corbyn, the feedback circuit is highly inductive and hence a decaying current may be expected to continue flowing through some of the feedback rectifiers when the other feedback rectifiers have already initiated conduction. (This phenomenon is not to be confused with the reverse conduction that may be due to imperfect rectifiers.) This simultaneous conduction of all feedback rectifiers (called "commutation") is explained in the analysis[1] considering that the assumption of a sinusoidally alternating core flux superposed on a direct component of flux implies the need of even harmonics of magnetomotive forces. In the simple amplifier (Figure 1A) these magnetomotive forces are supplied by even harmonic currents flowing in the signal windings, while for the amplifier (Figure 1B), harmonic currents are induced in the signal windings as well as in the external loop of the output windings in the inverse ratio of the resistances and in the direct ratio of the number of turns. Likewise for the amplifiers (Figures 1C and 1D) a contribution to the total need of even harmonics of magnetomotive force should be expected to be provided by current flowing in the feedback windings, this contribution being dictated by ratios of resistances and numbers of turns and being not necessarily coincident with the even harmonics which result simply from the rectification of the currents supplied by the a-c source.

The detailed analysis established in reference 1 does not need to be repeated here. In Appendix I however it has been found convenient to elaborate upon the results of the previous analysis, and a correction factor γ has been calculated for the feedback ratio so as to take into account the rather involved commutation phenomena in a directly usable form. With the introduction of this factor, equation 9 is modified into the more general form

$$\mathcal{F}_C=\mathcal{F}_1+\mathcal{F}_b=\mathcal{F}_{dc}-\gamma\frac{N_f}{N_L}\frac{1}{2}\mathcal{F}_L \tag{10}$$

which no longer requires the not always acceptable assumption $I_{fave}=I_{Lave}$ or $(1/2)$ I_{Lave} as indicated in equation 8.

The factor γ depends on the number of turns of the signal, bias, and feedback windings and the resistance of their cir-

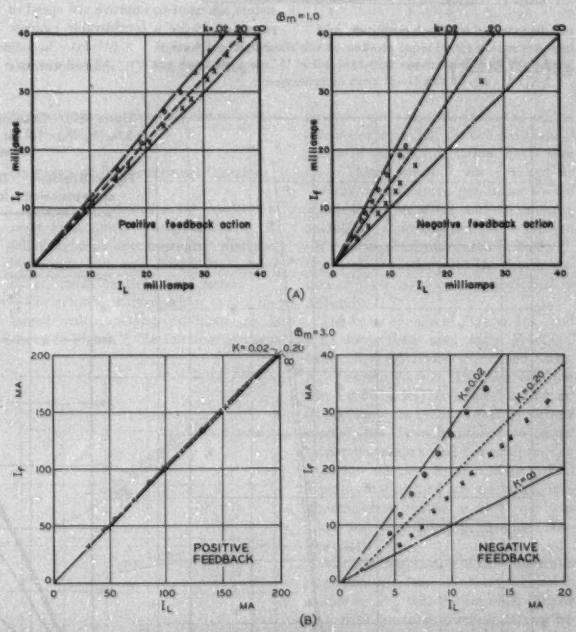

Figures 9(A) and (B). Average feedback current as a function of the rectified average load current in the amplifier with feedback showing the effect of resistance of the control circuits on the feedback ratio, for positive and negative feedback action $(N_f/N_L)=\pm 1.0$

The dotted points are for $k=0.02$ and the crosses for $k=0.20$. Figure 9(A) is for $\mathcal{B}_m=1.0$ and Figure 9(B) is for $\mathcal{B}_m=3.0$

cuits. Moreover, it is a function of the direct and alternating components of core flux densities. As shown in equations 18 and 25 of Appendix I, γ can be conveniently expressed in terms of the variables $\mathcal{B}_m$, $\mathfrak{F}_L$, and k. Here

$$k=\left(\frac{N_1}{N_f}\right)^2\left(\frac{R_f}{R_C}\right) \tag{11}$$

R_f is the resistance of the feedback circuits during commutation; $R_f=2R_4+R_r$ for the external feedback amplifier and $R_f=2R_4+2R_r$ for the self feedback amplifier where R_r is the forward resistance of one rectifier arm. R_C is the resistance of the combined signal and bias circuits as given by

$$\frac{1}{R_C}=\frac{1}{2R_1}+\left(\frac{N_b}{N_1}\right)^2\left(\frac{1}{2R_b}\right) \tag{12}$$

where $2R_1$ and $2R_b$ are the resistances of the signal and bias circuits respectively. Thus in the case of no bias windings

$$k=\left(\frac{N_1}{N_4}\right)^2\left(\frac{2R_4+R_r}{2R_1}\right)$$

for the external feedback amplifier, and

$$k=\left(\frac{N_1}{N_3}\right)^2\left(\frac{R_3+R_r}{R_1}\right)$$

for the self feedback amplifier circuit.

Figure 5 shows values of γ as a function of $\mathfrak{F}_L$ as calculated from equation 25 for fixed values of k and $\mathcal{B}_m$, assuming $N_f/N_2=+1.0$ (as is the case for self feedback or for external feedback with 100 per cent feedback ratio). Similar curves also can be plotted for other values of the feedback ratio N_f/N_2 using equation 25. It is seen that γ is very close to unity when k is large, that is, when signal or bias windings offer comparatively easy paths to induced currents satisfying the needs of even harmonics of total magnetomotive force. (In the reply of Gale and Atkinson to Corbyn's discussion of reference 7, this fact is expressed by saying that the inductance of the feedback circuit is shunted by the rather low reflected resistance of the coupled control circuits.) It is in such cases that the simplifying assumption given in equation 8 can be accepted, that is commutation phenomena are ignored. On the other hand, small values of k (as they may occur in feedback amplifiers in which forcing resistors are used to improve the speed of response), cause a considerable increase of feedback action.

Figures 6(A) and 6(B) indicate transfer characteristics obtained for $\mathcal{B}_m=1.0$ and $\mathcal{B}_m=3.0$ and $N_f/N_2=+1.0$, for various values of k. These are found directly from Figures 3 and 5 in the following manner. Knowing the value of $\mathcal{B}_m$ the appropriate transfer curve of $\mathfrak{F}_L$ versus $\mathfrak{F}_{d.c.}$ can be found from Figure 3. Then from the value of k given by equation 11, γ can be found using Figure 5 for the various values of $\mathfrak{F}_L$. $\mathfrak{F}_C$ is then found from equation 10. It is seen again that small values of k may give transfer characteristics which are considerably steeper than the ones obtained for the same values of $\mathcal{B}_m$ in Figure 4 in which commutation was neglected. On the other hand no appreciable differences are found when k is large ($k\geq 1.0$).

Commutation phenomena are of particular significance, for instance, when the resistance of the signal circuit is increased by means of forcing resistors, as frequently used to improve the speed of response. For the case of positive feedback, the forcing resistor shifts upon the feedback windings the burden of providing the $\mathfrak{F}_{d.c.}$ needed for a given output $\mathfrak{F}_L$. That is, as $\mathfrak{F}_f$ increases, the need for $\mathfrak{F}_1$ decreases (as shown clearly by the increased slope of the transfer characteristics of Figure 6).

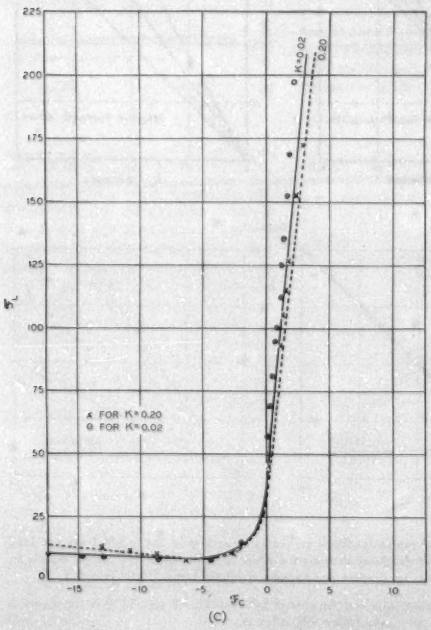

(C)

Figure 9(C). Calculated dimensionless transfer characteristics for $\mathcal{B}_m=3.0$, $(N_f/N_1)=1.0$ for $k=0.20$ and $k=0.02$ showing the influence of commutation with experimental points

Figure 10 (below). The ratio of the second harmonic to the fundamental of magnetomotive force as a function of $\mathcal{B}_m$ for various values of $\mathcal{B}_m$

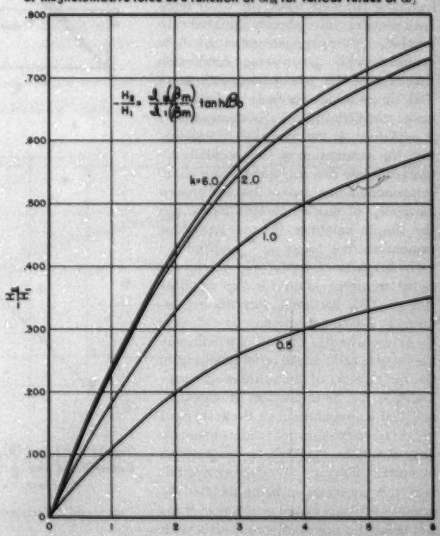

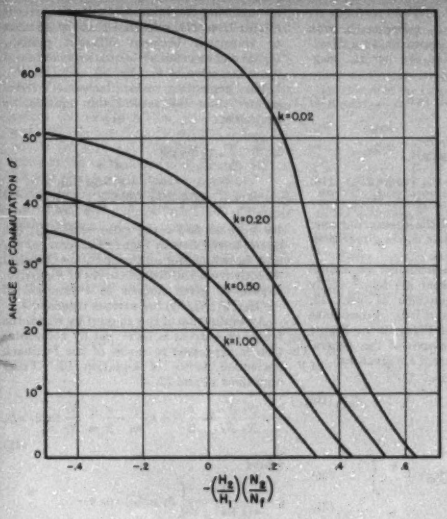

Figure 11. The angle of commutation σ as a function of $-(H_2/H_1) \times (N_2/N_f)$ for various values of k as calculated using equation 24

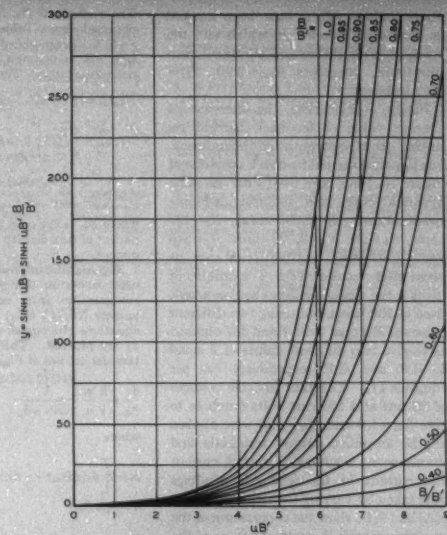

Figure 13. Hyperbolic sine co-ordinate paper for the determination of the constants u and U in the analytical approximation of the normal magnetization curve $H = U \sinh uB$

In fact somewhat particular conditions may even be thought of, for which the use of a forcing resistor results in an increase of power gain. A phenomenon of this kind is obtained for instance for the following conditions

$\mathfrak{G}_m = 1.0$, $\mathfrak{F}_L = 40$, thus $\mathfrak{F}_{id} = 35.9$ (from Figure 3)

With $(N_4/N_3) = 1.0$, $k = 1.0$ and no forcing resistance, $\mathfrak{F}_f = 20.5$ and $\mathfrak{F}_C = 15.4$. Assuming a bias $\mathfrak{F}_b = 12.5$, then $\mathfrak{F}_1 = 2.9$.

If now a forcing resistor is used to increase the resistance of the signal circuit five times, for very large resistance of the bias circuit (as needed if fast speed of response is wanted) $k = 0.20$ and $\mathfrak{F}_C$ decreases to 13.8 as shown in Figure 6. In this case $\mathfrak{F}_f$ is increased to $\mathfrak{F}_f = 22.1$ and for unchanged bias $\mathfrak{F}_b = 12.5$, $\mathfrak{F}_1$ reduces to $\mathfrak{F}_1 = 1.3$. Hence the power loss in the signal circuit is decreased in spite of the increase of circuit resistance.

On the other hand, commutation phenomena may be reduced considerably, if so desired (for example, in order to lessen the burden of the feedback rectifiers) by connecting a capacitor of large enough value directly across the signal or bias windings, thus providing an easy path for the even harmonics of currents through such windings.[6] The resistance of the signal or bias circuit to be used in the expression for k is then only the resistance of the windings.

Samples of Experimental Checks

Samples of experimental results are given as obtained on amplifiers with the following core specifications: material, Hypernik; core area $A = 4.2\ 10^{-4}$ square meter; mean length $l = 0.181$ meter.

The normal magnetization curve, obtained with a moving coil fluxmeter, is shown in Figure 7. In the dimensionless analysis, the magnetic properties of the core are expressed by the two constants U and u of the approximation $H = U \sinh uB$. These constants are obtained as $U = 127$ ampere turns per meter $u = 4.6$ square meter per weber, and the resulting analytical approximation is compared with the experimental curve in Figure 7. (Convenient methods for the determination of these constants are indicated in Appendix II.)

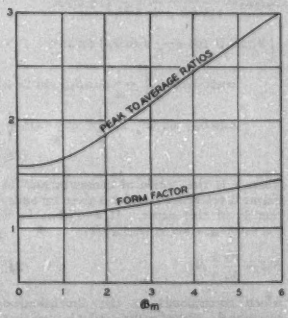

Figure 12. No load form factor and peak factor curves as a function of $\mathfrak{G}_m$

The basic circuits of Figures 1(A) and 1(B) have been used with $N_1 = 2{,}000$ turns, $R_1 = 100$ ohms, $N_2 = 2{,}000$ turns, $R_2 = 120$ and $N_b = 0$. The rms volts per turn (at 60 cycles) have been varied from 0 to 0.12 and the rectified average output current has been measured for fixed values of average signal current I_1 varying from 0 to 200 milliamperes. A few typical experimental values are converted into dimensionless values as per equations 1 to 4 and plotted then on the dimensionless chart.

An additional sample of experiments on operation with load also is represented in Figure 8. For this the amplifier (Figure 1A), with the same winding data as before, has been used with a series load resistance $R_L = 5{,}040$ ohms and with a fixed 60-cycle supply voltage of 338 volts rms. The output currents corresponding to various values of signal, after reduction to

dimensionless values, have been marked as crosses in Figure 8 in which also the corresponding theoretical elliptical locus ($\mathfrak{B}=0.033$, intercepts $\mathfrak{B}_{m1}=3.40$, $\mathfrak{F}_{L1}=102$) is shown.

Figure 9 evidences the increase of average value of feedback current resulting from commutation phenomena. For this the external feedback amplifier of Figure 1(C) has been used with the same hypernik cores and following winding specification: $N_1=2{,}000$ turns, $R_1=120$ ohms, $N_b=20$, $N_f=2{,}000$ turns, $R_f=216$ ohms (including rectifier resistance as given after equation 11). The number of turns in the signal windings has been kept fixed at 500 turns, but using two different values of R_1 equal to 33.7 and 337 ohms so as to give two different values of k equal to 0.20 and 0.02 respectively (as per equation 11). Constant 60-cycle voltages of 98 rms and 294 rms volts (such as to give $\mathfrak{B}_m=1.0$ and $\mathfrak{B}_m=3.0$) were applied at the amplifier output terminals and simultaneous readings of output current and current in the feedback windings were taken by varying the signal. Figures 9(A) and 9(B) show the comparison of the experiment with theoretical values of the analysis for the two values of k and for positive and negative feedback action. The 45-degree line plotted corresponds to the simplified case of no commutation ($k=\infty$). Figure 9(C) presents experimental checks on the over-all influence of this commutation phenomena upon the transfer curves.

Appendix I

Tables II and III of reference 1 give expressions for the instantaneous values of currents in the windings of the feedback amplifiers (Figures 1A and 1C). These expressions result from the simultaneous solution of magnetomotive-force equations for each of the three periods shown in Figure 2 of reference 1.

The time average values of the currents are related by

$$N_{d_0}I_{d_0\,\mathrm{avg}}=N_1I_{1\,\mathrm{avg}}+N_bI_{b\,\mathrm{avg}}+N_fI_{f\,\mathrm{avg}}=lH_0 \quad (13)$$

$$NI_{L\,\mathrm{avg}}=\frac{4}{\pi}l\left[H_1+\frac{1}{3}H_3+\frac{1}{5}H_5+\ldots\right] \quad (14)$$

where $N_{d_0}I_{d_0\,\mathrm{avg}}$ is the total direct component of magnetomotive force of each core and $NI_{L\,\mathrm{avg}}$ is the rectified average output magnetomotive force as defined initially. Similarly the rms value is

$$NI_{L\,\mathrm{rms}}=\frac{2}{\sqrt{2}}l\sqrt{H_1^2+H_3^2+H_5^2+\ldots} \quad (15)$$

while the peak value is

$$NI_{L\,\mathrm{peak}}=2l[H_1+H_3+H_5+\ldots] \quad (16)$$

The coefficients H_0, H_1, H_3 and so forth are obtained from Table I, reference 1, with $v=0$, if the simplified approximation $H=U\sinh uB$ is adopted for the normal magnetization curve. Thus

$$N_{d_0}I_{d_0}=lU\mathfrak{g}_0(uB_m)\sinh(uB_b) \quad (17)$$

$$NI_{L\,\mathrm{avg}}=\frac{4}{\pi}lU2\left[\mathfrak{g}_1(uB_m)-\frac{1}{3}\mathfrak{g}_3(uB_m)+\ldots\right]\cosh(uB_b) \quad (18)$$

where B_m is the crest of the alternating component of flux density and B_b the direct component.

The significant dimensionless quantities used earlier in this paper are immediately recognizable from equations 17 and 18, namely NI/lU, uB_m, and uB_b. From these equations the curves of Figure 2 (or Figure 3) are plotted. The slopes of the general transfer curves of Figure 3 are given by

$$\frac{\mathfrak{F}_L}{\mathfrak{F}_{d_0}}=\frac{8}{\pi}\frac{m}{n}\frac{1}{\tanh uB_b} \quad (19)$$

where

$$m=2\left[\mathfrak{g}_1(uB_m)-\frac{1}{3}\mathfrak{g}_3(uB_m)+\ldots\right] \quad (20)$$

$$n=\mathfrak{g}_0(uB_m) \quad (21)$$

For large values of $\mathfrak{F}_L$ and $\mathfrak{F}_{d_0}$ this ratio $\mathfrak{F}_L$ to $\mathfrak{F}_{d_0}$ approaches constant values as seen in Figure 3.

In order to relate $N_{d_0}I_{d_0}$ to the signal and bias ampere turns, N_fI_f must be determined. In fact the simultaneous conduction of all feedback rectifiers that occurs during commutation periods results in an increase of the instantaneous values of the current in the feedback winding, above the values of instantaneous rectified output during such periods. Thus the average feedback current $I_{f\,\mathrm{avg}}$ is greater than $I_{L\,\mathrm{avg}}$ in the external feedback amplifier and is greater than (1/2) $I_{L\,\mathrm{avg}}$ in the self feedback amplifier. The time average feedback current, including the effect of commutation, results from equations 19 or 24 of reference 1 for the amplifiers of Figures 1D and 1C respectively and is given in both cases by

$$N_fI_{f\,\mathrm{avg}}=\frac{2lU}{\pi(1+k)-2\sigma}\left\{\frac{N_f}{N_2}(1+k)2\times\left[\mathfrak{g}_1(uB_m)\cos\sigma-\frac{1}{3}\mathfrak{g}_3(uB_m)\cos 3\sigma+\ldots\right]\times\cosh(uB_b)+2\left[-\frac{1}{2}\mathfrak{g}_2(uB_m)\sin 2\sigma+\frac{1}{4}\mathfrak{g}_4(uB_m)\sin 4\sigma-\ldots\right]\times\sinh(uB_b)\right\} \quad (22)$$

where σ is the "angle of commutation" of Figure 2, reference 1, and k is given by equation 11 of this paper. If $\sigma=0$(that is, if the commutation is negligible)

$$N_fI_f=\frac{N_f}{N_2}\frac{1}{2}NI_L \quad (23)$$

which corresponds to the dimensionless equation 8. However for $\sigma\neq 0$ it is seen that $N_fI_f>(N_f/N_2)(1/2)(NI_L)$.

An additional expression results for N_fI_f by matching the values of feedback currents (Table II or III, reference 1) at the instants of transition between different periods. Hence a transcendental equation is obtained for σ in terms of k, (N_f/N_2) and (H_2/H_1). Upon neglecting even harmonic terms greater than the second this equation is written as

$$-\frac{H_2}{H_1}\frac{N_2}{N_f}=(1+k)\times\frac{2\cos\sigma-[\pi(1+k)-2\sigma]\sin\sigma}{\sin 2\sigma+[\pi(1+k)-2\sigma]\cos 2\sigma} \quad (24)$$

In order to find σ the ratio $-(H_2/H_1)$ has been plotted now in Figure 9 in terms of $\mathfrak{B}_m$ and $\mathfrak{B}_0$ (which, for any output, are obtained directly from the dotted curves of Figure 2). Figure 10 gives then σ as a function of $-(H_2/H_1)(N_2/N_f)$ for various values of k.

An evaluation of the amount by which the feedback current is increased by commutation is expressed in terms of the feedback correction factor of equation 10. From equations 18 and 22

$$\gamma=\frac{N_2}{N_f}\frac{N_fI_f}{NI_L}=\frac{\pi}{2}(1+k)\frac{p}{m}-\frac{\pi}{2}\frac{q}{m}\frac{N_2}{N_f}\tanh uB_b \quad (25)$$

where

$$p=\frac{4}{\pi(1+k)-2\sigma}\left[\mathfrak{g}_1(uB_m)\cos\sigma-\frac{1}{3}\mathfrak{g}_3(uB_m)\cos 3\sigma+\ldots\right]$$

$$q=\frac{4}{\pi(1+k)-2\sigma}\left[\frac{1}{2}\mathfrak{g}_2(uB_m)\sin 2\sigma-\frac{1}{4}\mathfrak{g}_4(uB_m)\sin 4\sigma-\ldots\right] \quad (26)$$

For any given $\mathfrak{B}_m$, γ can be evaluated for various k as function of $\mathfrak{B}_0$ or, using the dotted curves of Figure 2, also as function of $\mathfrak{F}_L$ as plotted in Figure 5.

Appendix II. The Constants U and u of the Core Material

The magnetic properties of the core material appear in the dimensionless quantities of this analysis in the form of the two constants U and u of the approximation $H=U\sinh uB$ chosen to fit the normal magnetization curve. Two points of this experimental curve are sufficient to determine such constants. Their choice has to be made with some judgment as the resulting fitting function truly will coincide with the experimental data at the origin and at these two points only. Two points, one (H',B') in the region of higher magnetizing intensity and the other (H'',B'') somewhere slightly "below the knee" are likely to provide a stisfactory fit.

The determination of the unknown values of U and u appearing in the two simultaneous equations $H'=u\sinh uB'$ and $H''=U\sinh uB''$ is facilitated by the use of the chart of Figure 13, in which $y=\sinh uB=\sinh uB'(B/B')$ is plotted as a function of uB' for given constant values of the ratio (B/B'). The abscissa of a vertical line intercepting the two curves $(B/B')=(B''/B')$ and $(B/B')=1$ at two values y'' and y' such that

$(y'/y'') = (H'/H'')$, gives the wanted uB' and thus u.

Moreover U is found as $U = (H'/y') = (H''/y'')$. As an example the determination of U and u for the experimental curve of Figure 7 is obtained on the basis of the two points ($H' = 2{,}440\ AT/m$, $B' = 1.290\ w/m^2$) and ($H'' = 266\ AT/m$, $B'' = 0.775\ w/m^2$) for which $(y'/y'') = 9.8$. In Figure 13 the abscissa of the vertical line in this case is $uB' = 5.9$ and thus $u = 4.6$ and also $U = 12.7$.

Additional attempts to fit the experimental curve also can be tried for different initial choices of the points (H',B') and (H'',B''). Actually for magnetic materials such as hypernik and similar silicon steel alloys, for which the simplifying assumptions of the analysis[1] apply best, comparable over-all accuracy seems to result from calculations based on apparently different fits, as long as the fitting function is reasonably close to the experimental normal magnetization curve in the range of higher magnetizing intensities.

References

1. Analytical Determination of Characteristics of Magnetic Amplifiers with Feedback, D. W. VerPlanck, L. A. Finzi, D. C. Beaumariage. *AIEE Transactions*, volume 68, part I, 1949, pages 565–70.

2. Universal Curves for D-C Controllable Reactors, W. C. Johnson, B. C. Merrell, R. E. Alley, Jr. *AIEE Transactions*, volume 68, part I, 1949, pages 31–39.

3. Magnetic Amplifiers, A. G. Milnes. *Proceedings*, Institution of Electrical Engineers (London, England), volume 96, part I, number 99, May 1949.

4. A Five-Figure Table of the Bessel Function $I_0(x)$, H. B. Dwight. *Electrical Engineering (AIEE Transactions)*, volume 60, March 1941, pages 135–136.

5. An Analysis of Transients in Magnetic Amplifiers, D. W. VerPlanck, L. A. Finzi, D. C. Beaumariage. *AIEE Transactions*, volume 69, part I, 1950, pages 498–503.

6. Uber Gleichstromvormagnetisierte Wechselstromdrosselspulen und deren Rückkopplung, T. Buchhold. *Archiv für Electrotechnik*, volume 36, 1942, page 221.

7. A Theoretical and Experimental Study of the Series-Connected Magnetic Amplifier, H. M. Gale, P. D. Atkinson. *Proceedings*, Institution of Electrical Engineers (London, England), volume 96, part I, number 99, May 1949.

No Discussion

Underground Hydroelectric Power Stations in Sweden

ÅKE RUSCK
NONMEMBER AIEE

G. WESTERBERG
NONMEMBER AIEE

SWEDEN has practically no resources of coal, oil, or natural gas. There are comparatively large resources of peat, but it has not yet proved economically possible to utilize it on a large scale. Water power resources, however, are large and it has been estimated that the resources capable of economic development amount to about 50,000 million kilowatt-hours a year, corresponding to a little more than 7,000 kilowatt-hours per head of the population. By the end of 1949, the power stations already in existence were capable of producing approximately 16,000 million kilowatt-hours a year, about 30 per cent of the economically available resources.

A fairly low head is generally utilized in Swedish water power stations. The head is frequently less than 150 feet and only in rare cases exceeds 300 feet. The natural falls are often very extended in length, with the result that a gathering of the head must be brought about. The mean flow of water in the larger rivers amounts to about 10,000 cubic feet per second at the mouth. The water flow to be developed at the plants amounts to an average of 1.5 or 1.6 times the average flow of water. The amount of water to be developed, which is then relatively great, is spread over only a few (2 to 4) units. Kaplan turbines have hitherto been used for heads up to 110 feet, and for greater heads, Francis turbines are used. The biggest units now under installation will have a capacity of about 100,000 kw.

The General Layout of a Power Station

When planning and constructing a power station, all efforts are made to utilize the head of the falls and rapids of the river in the best possible way, and to obtain the lowest possible annual costs. In the economic calculation, the interest on the capital outlay, the cost of normal operation, maintenance costs, and depreciation are taken into account.

In order to find the most economical position for the dam, a preliminary survey is made in which are calculated the cost of constructing the dam, and the headrace and tailrace for different alternatives. In order to make the final choice between the various alternatives, the annual costs for all parts of the plant are compared, as they will vary according to the dam-site. Account is then taken of the value of the head and the storage reservoir, the price that will have to be paid for the land to be flooded, the cost of the coffer dams and diversion of the river during construction, the cost of log flumes, the machine station, mechanical and electric equipment and power transmission to the switchyard, the surge basin, and so forth. When a rock-fill dam has been constructed, the most economical results were sometimes achieved when it was so situated that the rock blasted out for other purposes sufficed as filling for the dam.

When comparing underground and surface power stations, it must be remembered that maintenance costs for tunnels and rock rooms are lower than for the corresponding parts of a surface station where concrete has to be employed to a great extent. This also is true of depreciation, as rock has a far longer life than concrete. In Sweden, we reckon on an annual maintenance expenditure and depreciation of 1 per cent of the cost of construction for rock work, while the corresponding figure for concrete work is 1.7 per cent.

The progress of the last few decades in the technique of digging and blasting have made it economically possible to concentrate the head of falls and long rapids in a single power station. Swedish rivers are, however, not usually of such a nature as to permit high dams to be built. The river banks are seldom more than a few meters higher than the natural water level and are surrounded by farm land and built-up areas which are too valuable to submerge on a large scale. These obstacles do not occur in the mountainous districts, but owing to the great width of the valley floors, high dams are not usually constructed there. Normally, therefore, the concentration of the greater part of the head must be done by means of river-bed clearances, tunnels, and canals.

The water intake is often placed at the dam itself, but on occasions it has been found more convenient to conduct the water via a headrace canal to an intake situated so as to give a shorter length of the conduits from the intake to the turbines or downstream from the power station, thereby reducing the conduit costs and, when the penstocks are shortened, also simplifying the regulation of the turbines. Penstocks are employed except for very low heads. If the ground is composed of good rock and its surface is on a sufficiently high elevation, the machine station is constructed underground, and the tailrace either partially or wholly as a rock tunnel. The penstocks are in that case, for the main part, placed vertically. If the ground is earthy, it is necessary to conduct the water through sloped penstocks and place the power station further from the intake, so that it will be situated at the ground surface, with no discharge tunnel being required. It is not usually necessary to construct large power stations in this way in Sweden.

Paper 50-149, recommended by the AIEE Power Generation Committee and approved by the AIEE Technical Program Committee for presentation at the AIEE Summer and Pacific General Meeting, Pasadena, Calif., June 12–16, 1950. Manuscript submitted March 16, 1950; made available for printing April 13, 1950.

ÅKE RUSCK is President, and G. WESTERBERG is Chief Director, Civil Engineering Department, with the Swedish State Power Board, Stockholm, Sweden.

Figure 1 (left). Machine hall with uncovered rock walls

Figure 2 (above). Machine hall with uncovered rock walls

If, in rocky ground, a surface station was to be built instead of an underground station, it would be necessary either to maintain the turbines in deep shafts as in the underground station and place the generator hall only at the ground surface, or to construct the station somewhat like that described for a station in earthy ground, using sloping penstocks and a tailrace canal. A station with deep turbine pits and long driving shafts is usually more expensive to construct than an underground station in rock and is, in addition, less advantageous from the operational point of view. A station with long penstocks makes regulation of the turbines more difficult (relief valves are often required) and the additional cost for the extended length of the penstocks on account of a sloped location is usually considerably greater than the saving which results from having a shorter or no discharge tunnel. The cost of the power station itself also must be taken into account when making a comparison. This will not be more expensive when located down in the rock than at the surface, as the expense of blasting out the larger masses of rock is partially compensated for by the diminished cost for walls and roofing. When planning an underground station, however, allowance must be made for the cost of transport arrangements to the ground surface and, when there are long tunnels, also for surge basins.

There is no general rule as to whether a station should be built as an underground station or not. For the sake of clarity, however, it should be mentioned here that in every case where an underground station has been built in Sweden, it has been because it was the most economic solution for the power plant as a whole. The improved safety attained thereby in time of war was only a welcome extra advantage and not the primary reason.

The cost for power plants with underground power stations recently built, or at present under construction, is calculated at about $80 per kilowatt maximum output for stations with a capacity of 100,000-300,000 kw based on the 1949 year's price level and at an exchange rate of $1 = 5.18 Swedish kronor.

The Design of the Underground Hydroelectric Power Stations

Intakes and Penstocks

For underground stations, the intakes are constructed on much the same principle as for surface stations.

As mentioned previously, the penstock shafts are usually placed vertically for underground stations. They are equipped with steel tubes, either detached from the rock surface, or embedded in concrete. The lower horizontal part of the tube, which needs to be rigidly anchored, is always embedded in concrete. In certain cases where the rock was particularly good, steel tubes have been dispensed with altogether to a depth of approximately 250 feet below the upstream water level and the rock surface of the shaft lined with reinforced concrete instead.

Machine Stations

When constructing an underground station, the removal of blasted rock from the machine station and the discharge tunnel has often been done by trucks through special transport tunnels. When these tunnels also could be used as an entry for rotors, turbines, and so forth, a considerable saving was effected as lifts were not then necessary for this purpose. In those cases, the heavy machinery was transported to the machine hall directly from the nearest railway station on special trailers drawn by tractors.

As in a surface station, heating is generally supplied by the surplus heat from the transformers, but the need for heat in underground stations is less than in surface station. The supply of fresh air, on the other hand, requires more complicated arrangements. The fresh air is introduced usually either through a special shaft or through a shaft which also performs another function. Ar-

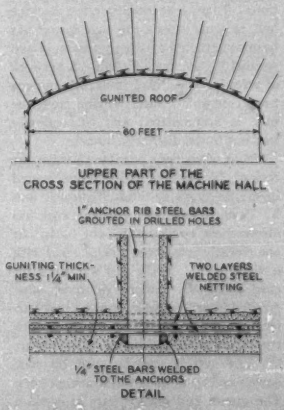

Figure 3. Rock roof covered with reinforced gunite

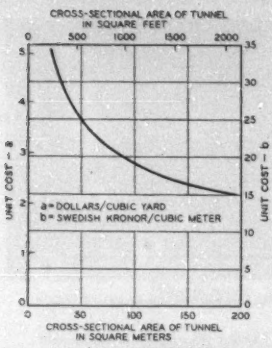

Figure 4. Tunneling unit cost, based on the 1949 year's price level

The costs comprise drilling, blasting, ventilation, mucking, transport (by trucks) and dumping, drainage, electric energy and administration, but not interest of outlay during the construction period, or costs of such transport arrangements as, for instance, transport tunnels

rangements are sometimes made for the air to be lead over a cold water surface, for instance, the surge basin, in order to reduce its moisture. The generators generally have a closed water-cooling circuit and the transformers also are water cooled insofar as their surplus heat is not employed for heating purposes. Large quantities of fresh air are therefore not required.

The problem of drainage has not caused any great difficulty in underground stations. To prevent leakage in the machine hall, in some cases a drainage tunnel has been constructed a little upstream, of and parallel to, the machine hall. A network of holes is then drilled from the drainage tunnel in which water seeping from the rock is accumulated and subsequently lead out to the discharge tunnel.

It has often been possible to leave the rock of the machine hall walls uncovered in underground stations, Figures 1 and 2. Protective or reinforcement work has always been employed for the roofs. In one recently completed machine hall with a width of 60 feet, the roof was strengthened with long anchor rib steel bars, grouted in drilled holes, and the rock surface covered with gunite, reinforced with two layers of welded steel netting, Figure 3. The netting was fastened by rock dowels and by welding to the anchor bars. The gunite and anchor bars replaced a concrete arch, but were considerably cheaper.

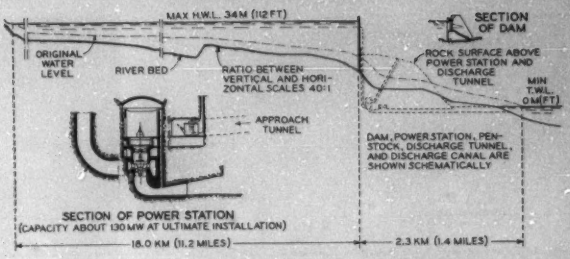

Figure 5. Underground station with comparatively low head

Discharge Tunnels and Surge Basins

Lifts are seldom used for removing blasted rock from the rock rooms and tunnels. It is removed by diesel-engine trucks directly from the blasting place to the dump site. When driving a long tunnel, special transport tunnels are blasted out which are usually given a slope of about 1 to 8 (in one case 1 to 7). The transport tunnel is usually made wide enough to permit trucks to meet at any point, so that as many trucks can be brought to the cutting face as the excavator is able to load. It is therefore the capacity of the excavator which determines the time of loading, and consequently it is of great importance to obtain the most suitable excavators.

Tunnels with a cross-sectional area of up to about 1,200 square feet are blasted out by the full face method. When the tunnel section is larger than this and the rock is very good, the lower portion of the tunnel sometimes is first blasted out by this method and the excavation is subsequently extended up to full height. If the rock is not quite so good, the upper section is blasted out first and the lower section afterwards, as this avoids the necessity of cleaning the roof twice. When the upper section is the last to be blasted out, the bulk from this portion can be removed continuously, but this advantage is lost when the lower section is the last to be blasted. Usually the bottom of the tunnels are given a slight slope towards the drainage pumps to minimize the trouble from seepage during construction.

The cost of excavating a tunnel of say, 1,000 square feet cross-sectional area is usually about $2.90 per cubic yard. Figure 4 illustrates the variation in the cost per unit of volume to tunnel area when the cost of possibly needed reinforcement is excluded. The cost of reinforcement generally has not exceeded 5 per cent of the cost of excavation, but in one case the cost has been as high as 25 per cent.

When the downstream water level varies greatly, the whole of the discharge tunnel is usually placed below the lowest water level so as to prevent a large ineffective cross-sectional area to come up at low water levels. When the downstream water level varies within narrow limits and the tunnels are short, they have in some cases been placed sufficiently high to obtain a free water level and to avoid the necessity of a surge basin. In other cases, the surge basin has been placed downstream of the machine station either by increasing the height of the tunnel a sufficient length immediately downstream of the draft tubes, or by blasting out a special basin with connection to the discharge tunnel near the outlet of the draft tubes. The connection between the surge basin and the discharge tunnel has sometimes been choked. The cost of constructing the surge basin on the downstream side of an underground station is partially compensated for by the fact that because the penstocks become short the devices for diminishing rises in pressure and surge on the upstream side are simplified.

The Transformer Rooms and Switchyards

Immunity to aerial bombardment is highly valued at the more important power stations. When the machine hall is located below the ground, thereby giving the units a high degree of protection, the transformers are usually also placed in rock rooms so that all the vital parts of the installation are equally well protected from air attack.

In power stations with a voltage stepped up to 200 kv or more, it is usually more expensive to place the transformers in rock rooms than on the surface, although in the latter case it is customary to surround them with splinterproof protection. The choice of placing the transformers in rock-rooms is attributed sometimes to the fact that at low generator voltage it may be cheaper to draw up

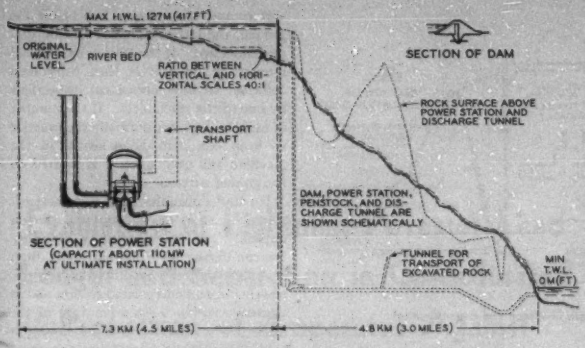

Figure 6. Underground station with comparatively long tailrace tunnel

high-tension cables rather than low-tension cables to the ground surface. High-tension switchyards, on the other hand, are never located in the rock as the great space required makes the cost of blasting prohibitive.

The simplification of the operation usually is the determining factor in placing the control room. It is, therefore, as a rule placed near the machine hall.

Description of Some Power Plants

A description of some of the underground stations is shown in the following, in order to illustrate whenever it has been considered advisable to place them underground. The plants are shown in Figures 5 to 8. The profile of the rivers have been made on a horizontal scale 40 times less than the vertical scale. The detail of the power station on the drawings is on the same scale as the vertical scale of the river profile, but the cross-section of the dam is on one half of this scale. In all cases, the surface of the tail water level has been taken as zero.

Plant 1

Plant 1, Figure 5 is in operation. The site for the dam was determined by the fact that the river bed narrows here and that the ground was of rock. The spillway occupies nearly the whole length of the dam. The intake is placed in the dam and the water is conducted to the turbines by penstocks that are mainly vertical. The rock downstream of the dam is so low that only part of the machine station has a rock covering. An arch-shaped reinforced concrete roof has been constructed near the ground surface over the machine hall and the control department. It would have been possible to have made the whole station underground by moving the machine station further inland, but the cost of the whole plant would thereby have been increased. The tailrace is a rock tunnel 0.6-mile long, and a canal in earthy soil is 0.8-mile long. Access to the machine station is via a sloping tunnel. The transformers are located in rock rooms beside the machine hall and from here, 200-kv oil-pressure cables run up to the switchyard on the ground surface.

Plant 2

Plant 2, Figure 6, is in operation. The machine hall is placed in the rock near the dam. The ground slopes steeply downstream from the dam, and the cost of the dam would have increased considerably more than the cost of the tunnel would have decreased if the dam had been placed further downstream. A 3-mile long tunnel forms the tailrace. Removal of the blasted rock during construction was carried out partly through a lift shaft at the power station, partly by a transport tunnel from the middle of the tailrace tunnel, and partly by way of a sloping road at the downstream end of the tailrace tunnel. Access to the machine hall is by a lift shaft. The control room and transformers are placed on the ground surface.

Plant 3

Plant 3, Figure 7, is under construction. The dam is of the rock-fill type with an impervious core. The tailrace consists of a tunnel 1.8-miles long with a cross-sectional area of 2,040 square feet. The most advantageous site for the dam proved to be where the excavated rock from the tunnel and power station most nearly sufficed for the supporting parts of the dam. Mainly vertical penstocks lead from an intake situated in the dam down to the machine station in the rock. In the river bed a short distance upstream from the dam a marked fault zone runs through the rock and this has resulted in the dam and the power station being placed somewhat further downstream than would otherwise have been desirable. A railway track runs right up to the plant. Access to the machine hall is via a lift shaft with an unloading hall on the ground surface. The transformers and control room are situated underground beside the machine hall, and the transformers are connected to the switchyard by 380-kv oil-pressure cables.

Plant 4

Plant 4, Figure 8, is under construction. It will be possible to shorten the conduits by transferring water from one arm of the river to another. The head-race tunnel will be 2.3 miles long with a free water surface and the tailrace tunnel will be 1.7 miles long and placed below the lowest downstream water level. The reason why the head-race tunnel is given a free water surface is that the tunnel is

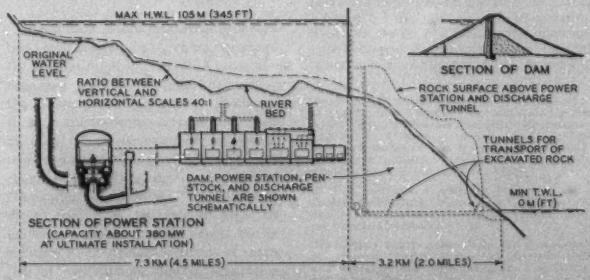

Figure 7. Underground station with comparatively high rockfill dam

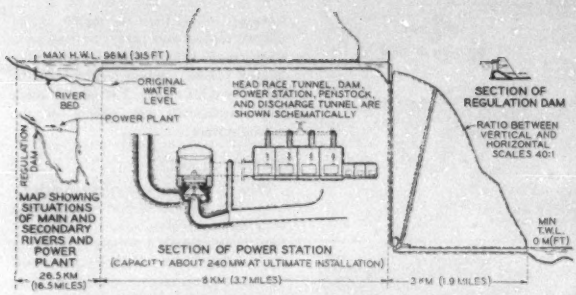

Figure 8. Underground station with both headrace and tailrace tunnel

intended to be used also for logging operations. The rock is good for the main part, but reinforcement proved necessary for parts of the roof and walls of the machine hall. Access to the machine hall, which is nearly 300 feet below the ground surface, is for heavy machinery by means of the transport tunnel used for removing blasted rock during the construction period. For transport of lighter equipment and persons there will be installed elevators. The transformer and control rooms are being constructed as for Plant 3.

Operational Experiences

As the center of power production has been moved to the northern part of the country, a great many operational problems have arisen. The power plants in the northern part of Sweden are generally developed to a less degree in relation to the average water flow than those in the southern part, and the plants are continuously operated at full capacity for long periods. It is therefore necessary that they have great operational reliability and that only short standstill times are needed.

The attendance of an underground station does not differ essentially from that of a surface station. It cannot be pointed out any direct disadvantage in the operation or maintenance of an underground station in comparison with a surface station.

In a large power station two machinists are normally on duty at each shift, regardless if the station is located above or below the ground surface. One man remains continuously in the control room, while the other is employed inspecting the turbines, generators, auxiliary machinery, dam, and so forth. In those cases when the control room is on the ground surface and the machine hall below the ground, the latter is not always continuously manned. If the station has a small number of units it is then considered sufficient to have occasional inspections by one of the machinists. If the number of units is great it is normally the practice to keep one man permanently in the machine hall even when it is located on the ground surface.

No staff difficulties have been noticed. A machinist in an underground station naturally has no opportunity of seeing the sun during his shift, but apart from this, there should be no difference between working in an underground station and in a surface station. An advantage of the underground station worth mentioning is that the climatic conditions are more constant. It is conceivable that psychological factors may have some influence, but no such difficulties have hitherto arisen with the staff.

It should be mentioned in this connection that there is a vast difference between the conditions under which a power station machinist works and, for example, a miner. The former worksin a dry, well heated, ventilated and illuminated place which is hardly to be distinguished from a normal room while the latter suffers discomfort from dampness, darkness, cold and rough rock faces. As a further proof that work in underground stations does not imply any discomfort, may be cited the fact that there is no noticeable tendency among the staff to apply for a discharge or transfer to a surface station. The staff of the underground station, have the same working hours, holidays, and social advantages as any other power station staff.

No Discussion

Evaluation of Lightning-Arrester Lead Length and Separation in Co-ordinated Protection of Apparatus Against Lightning

T. J. CARPENTER
ASSOCIATE AIEE

I. B. JOHNSON
MEMBER AIEE

L. E. SALINE
ASSOCIATE AIEE

CO-ORDINATED protection of station equipment against lightning damage has proved to be a vital factor in system operating economics. Now, however, with increasing acceptance of the reduced insulation concept in voltage classes of 115 kv and above, the co-ordinated protective approach merits more exact quantitative appraisal of the over-all protective scheme.

It generally is known that the voltages at the insulation to be protected may be above the protective level held at the lightning arrester.[1,2,3,4] These overvoltages can be attributed primarily to the following causes:

1. The lightning-arrester lead length; that is, the length of lead joining the top of the lightning arrester to the overhead line plus the length of lead joining the bottom of the lightning arrester to the lead or mat between the lightning arrester and the protected apparatus.

2. The lightning-arrester separation; that is, the horizontal distance from the lightning arrester to the protected apparatus.

3. The degree of grounding of both the lightning arrester and the protected apparatus.

Hence, for maximum protection the lightning arrester should be connected directly across the insulation to be protected. In actual practice, however, this is not always done, and an evaluation of the probability of whether or not the insulation will be protected by the lightning arrester in these cases has been largely a qualitative one, based to some extent on past operating experience.

The purpose of this paper is to extend the knowledge on lightning-arrester performance and application for lightning arrester installations on transmission systems of 115 kv and higher, giving particular consideration to the effects of circuit configuration and lightning-arrester discharge currents. Field and laboratory investigations have been made of the effect of circuit configuration, but these have been limited in scope. This investigation has utilized the differential and transient analyzers in making possible, conveniently and economically, a generalized evaluation of a large number of different combinations of circuit geometry, lightning-arrester discharge currents and system voltage levels. As a result, it is hoped that the application of arresters can be placed on a more quantitative basis.

Summary and Conclusions

In addition to lightning arrester separation, lead length, and ground resistance, the evaluation of the degree of protection necessary for a given station depends on the anticipated lightning discharges through the lightning arrester and these, in turn, are a function of isokeraunic level, system shielding and grounding, and other surge-limiting devices or factors. Generally, the results of the study indicate that it is desirable to place the lightning arrester directly across the insulation to be protected to avoid undue risk of overvoltages due to separation, lead length, and ground resistance. This is more important with reduced insulation levels.

Most of the results are derived from lumped constant concept and analysis and were based on the results from experimental investigations; see the section on Analytical Investigation. And in general, also, these results of protected insulation overvoltages caused particularly by the lightning-arrester lead length and separation are considered conservative in so far as they are based largely on an elementary circuit configuration and do not include a bus having several connected circuits.

Based on a lightning-arrester discharge current of 5,000-ampere crest, 1.6×16.5 microseconds (5,000 amperes per microsecond effective rate-of-rise), the specific results from the study are as follows:

For the elementary circuit (that is, one which includes only the lightning arrester connected by conductors to the incoming overhead line and to the capacitor simulating the protected apparatus) there are these conclusions:

1. With typical lightning-arrester connections, the voltage appearing at the capacitor will tend to be a damped oscillatory voltage that increases in maximum value as the lead length in the T-connection, separation, ground resistance, and steepness of front of the impulse current wave increase and the initial capacitor charge and impulse capacitance decrease. For severe discharge currents and the circuit configurations studied the capacitor voltage in per unit of sparkover voltage of the lightning arrester (herein assumed a constant equal to 40 kv per 12-kv station-type lightning-arrester unit) varies between 1.2 and 1.85 for 288-kv systems and between 1.4 and 2.4 for 115-kv systems. These values do not include the effect of initial charge or the attenuation that may be inherent in protected apparatus, Figure 8.

Paper 50-150, recommended by the AIEE Protective Devices Committee and approved by the AIEE Technical Program Committee for presentation at the AIEE Summer and Pacific General Meeting, Pasadena, Calif., June 12–16, 1950. Manuscript submitted March 14, 1950; made available for printing April 14, 1950.

T. J. CARPENTER is with the General Electric Company, Pittsfield, Mass., and I. B. JOHNSON and L. E. SALINE are both with the General Electric Company, Schenectady, N. Y.

The authors wish to acknowledge the assistance of the General Electric Differential Analyzer staff and several of their associates in the Transformer and Allied Products Divisions of the General Electric Company.

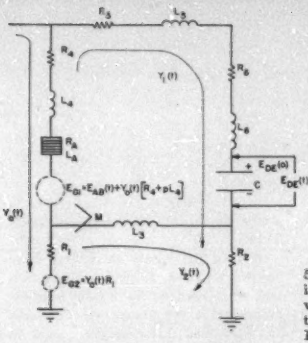

Figure 1. Final equivalent circuit representing lightning-arrester protecting apparatus simulated by impulse capacitance = C. Lightning discharge current is $Y_0(t)$. M is the mutual coupling between loops 1 and 2

R_1, R_2 = equivalent ground resistance
L_3 = equivalent ground inductance
R_A, L_A = equivalent lightning-arrester resistance and inductance
R_4, L_4 = equivalent resistance and inductance of lightning-arrester lead
R_5, L_5 = equivalent resistance and inductance of overhead conductor between lightning arrester and protected apparatus
R_6, L_6 = equivalent resistance and inductance of apparatus lead
C = equivalent impulse capacitance of protected apparatus

See Appendix I and the section on Analytical Investigation for methods used in arriving at the foregoing equivalent parameters

2. The time-to-crest of the capacitor voltage increases as the impulse capacitance of the protected apparatus, lead length, and separation increase. The time-to-crest of the capacitor voltage is practically independent of ground resistance and wave shape for the values assumed in the study and varies between 0.16 and 1.25 microseconds, Figure 9.

3. As the system voltage level increases, the per-unit capacitor voltage decreases, as shown in Figure 8.

4. Of primary importance in controlling the overvoltage at the capacitor is the lightning-arrester capacitor separation, Figure 4. The separation range from 0 to 10 feet is particularly critical:

a. The effective loop inductance associated with each foot of lead length in the T-connection increases critically from zero to approximately 0.28 microhenry per foot in the range of separations from 0 to 10 feet and then increases slowly for larger separations from 0.28 microhenry per foot at 10 feet to 0.304 microhenry per foot at 50 feet, Figure 3.

b. With the V-connection (zero lead length) the capacitor voltage does not exceed double the maximum voltage drop across the lightning arrester for separations greater than 10 feet.

5. The length of the lightning-arrester lead is important since the lead is effectively a voltage source that contributes to the capacitor voltage in proportion to its length, Figure 5.

6. In the connection of the lightning arrester to the overhead line and the protected apparatus through appreciable lengths of conductor, the V-connection should be used rather than the T-connection. This becomes of increasing importance in applications to apparatus designed with reduced insulation.

7. Studies of a variety of transformers indicate that the representation of a transformer by an impulse capacitance gives the correct natural oscillations, but the magnitudes of the oscillations obtained with a transformer are of the order of 25 per cent less than those obtained with the equivalent capacitor due to inherent transformer attenuation.

8. The effect of the oscillatory voltage on the apparatus insulation is important in determining the breakdown of the insulation; that is, for transformer insulation, a test wave composed of a 1.5×40-microsecond full wave of 1.0 per-unit crest plus a superimposed oscillation (4 to 5 cycles) of 0.3 per unit is equivalent to a chopped wave with a crest of 1.15 per unit.

In a complex circuit typical of a large modern station having several lines and transformer banks connected to a common bus, Figure 12, the lines and transformers connected in parallel at the bus will reduce the severity of the effect of the surge entering the station, Figure 14. However, a lightning arrester is desirable at each transformer in addition to those on the line side of the line circuit breakers to protect against:

1. Line strokes if all the lines and transformers are not connected to the station.

2. Failure of direct-stroke shielding between the main bus and transformers.

3. Switching surges.

Experimental Basis for Analysis

To establish some basic facts pertaining to the discharge of current surges through lightning arresters, some laboratory experiments were performed involving a surge-current generator and a rectangular loop. In one vertical leg of the loop there was inserted a capacitor and in additional tests a transformer; in the other vertical leg there was inserted a lightning arrester. The current discharge used in these tests had a wave shape of 1.6×16.5 microseconds with an effective rate-of-rise exceeding 5,000 amperes per microsecond. These tests indicated the following:

1. The voltage appearing across the capacitor consisted of a damped oscillatory wave superimposed upon a unidirectional impulse similar to that expected in a circuit consisting of lumped constants of inductance, capacitance, and resistance. Similar results have been reported from other laboratory and field experiments.[2,4,9]

Figure 2 (below). Characteristics of 12-kv station-type lightning-arrester unit

Figure 3 (right). Effective loop inductance assigned to lightning-arrester lead as a function of lead length, l, and separation, D, for conductor radius ρ = 0.5 inch

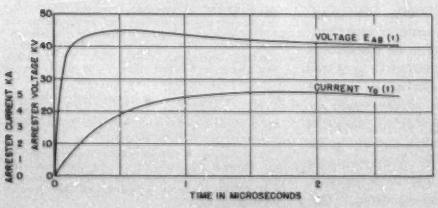

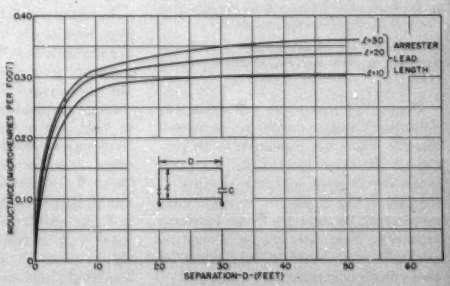

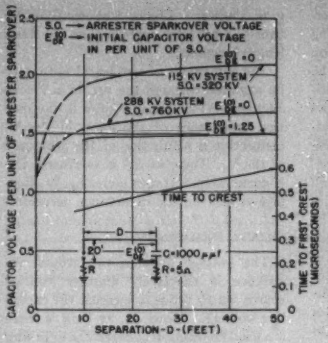

Figure 4 (left). Capacitor voltage and time-to-first-crest as a function of separation *D*. Lightning current discharge = 5,150 amperes, 1.6× 16.5 microseconds

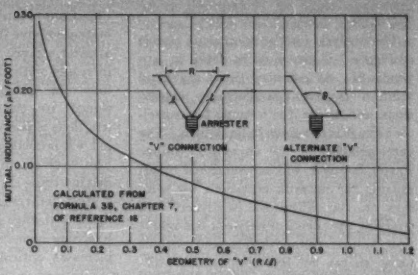

Figure 6 (right). Mutual inductance of equal leads in V-connection of lightning arrester

2. The laboratory results could be checked and predicted analytically from lumped circuit concepts and from known and calculated circuit constants based on the geometry of the loop.

3. A transformer can be represented by a lumped capacitance as far as natural oscillations are concerned, but the first crest of the oscillatory component of the voltage at the transformer is approximately 25 per cent less than that obtained with an equivalent capacitor substituted for the transformer. Transformer impulse capacitances were measured from the order of several hundred to several thousand micromicrofarads.

4. The initial charge on the capacitor due to any charging voltage from the surge preceding the sparkover of the lightning arrester tends to decrease the magnitude of the oscillatory component of the voltage at the capacitor resulting from the current discharge through the lightning arrester and its leads after sparkover. It is to be expected that some initial charge is obtained in the majority of cases in service.

5. The magnitude of the oscillatory component of voltage at the capacitor may be appreciably decreased if a V-connection instead of a T-connection at the lightning-arrester line terminal is used, particularly if the length of the vertical lead in the T-connection is such that the inductive drop in the lead is appreciable relative to the drop across the lightning arrester.

Analytical Investigation

Equivalent Circuit

Since the results of experimental investigations demonstrate that the problem of lightning-arrester protection as affected by circuit configuration can be solved for some practical cases using the lumped constant theory, the equivalent circuit employed in further studies by analyses is shown in Figure 1 and is the result of considerations in the succeeding paragraphs and in Appendix I.

The lightning-arrester lead length, as already defined, is represented by the lumped inductance L_4, which is calculated in conjunction with L_4 as outlined in Appendix I. To include some damping due to the nonlinear thyrite lightning arrester, its resistance R_A is assumed constant at 4 ohms per lightning-arrester unit. The nonlinearity of the thyrite was considered in the voltage drop in the resistance of the lightning arrester by measuring the voltage $E_{ab}(t)$ for a lightning-arrester discharge current $Y_0(t)$. Typical current and voltage curves are shown in Figure 2 and were employed in the analysis as explained subsequently. The resistances R_1 and R_3, together with the inductance L_3, represent a metallic ground connection between the lightning arrester and the transformer or protected apparatus. The equivalent leakage resistances R_1 and R_3 to ground were assumed to be equal and given a value of 5 ohms. It should be recognized, however, that R_1 and R_3 are actually variable quantities that will depend on the nature of the impinging wave. The inductance L_4 of the ground was chosen as the lumped inductance of a solid conductor connecting the transformer and lightning-arrester ground leads, and it was calculated as explained in Appendix I. Also a mutual inductance, M, coupling the loop involving the overhead line with the loop involving the ground lead joining the protected apparatus to the lightning arrester is calculated as explained in Appendix I. The resistances of the lightning-arrester lead, transformer lead, and transmission line were calculated for an average frequency of 700,000 cycles per second as outlined in Appendix I. The values of impulse capacitance C were chosen as 200 micromicrofarads, 1,000 micromicrofarads, and 3,000 micromicrofarads, which are representative for bushings,[7] circuit breakers, and a wide range of transformer ratings.

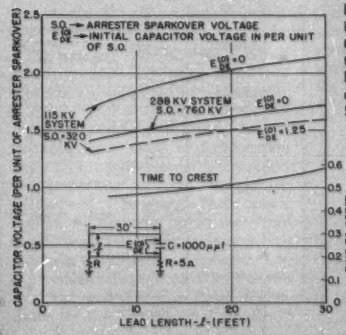

Figure 5 (left). Capacitor voltage and time-to-first-crest as a function of lightning-arrester lead length *l*. Lightning current discharge = 5,150 amperes, 1.6× 16.5 microseconds

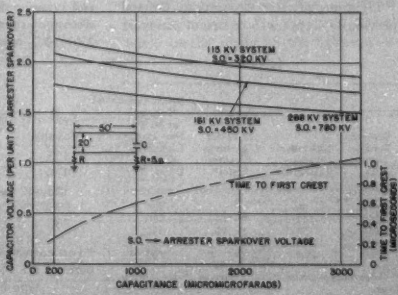

Figure 7 (right). Capacitor voltage and time-to-first-crest as a function of impulse capacitance, C. Lightning current discharge = 5,150 amperes, 1.6× 16.5 microseconds

Analysis of Equivalent Circuit

The analysis for the equivalent circuit of Figure 1 is presented in detail in Appendix II. As indicated there, a general solution involves cumbersome expressions, and, hence, the formula for capacitor voltage is not given in final form. The determination of the capacitor voltage $E_{DR}(t)$, however, was accomplished by arranging the network equations for solution on the differential analyzer[4] and studying the effects of network configuration, system voltage levels, and various wave shapes of lightning-arrester discharge currents. Also the equivalent circuit was set up in miniature on the transient analyzer[5,6] to check the differential analyzer study and to extend the study to other conditions and more complex circuits.

It is to be noted in Figure 1 that the effect of the lightning current $Y_0(t)$ discharging through the lightning arrester and its leads to ground is represented, for the purpose of analysis, by an equivalent voltage generator in each loop, where the generated voltage in one loop consists of the sum of the lightning-arrester voltage $E_{ab}(t)$ and the lead-length drop $E_{01}(t)$ while in the other loop the voltage consists of the ground-resistance voltage drop $E_{02}(t)$.

Results

The results of the analyzer studies are illustrated and discussed in this section. The voltages on the capacitor simulating the protected apparatus are expressed in per unit of the spark-over voltage of the lightning arrester, and this is assumed to be a constant of 40 kv per 12-kv lightning-arrester unit regardless of the nature of the lightning discharge. The lightning-arrester ratings associated with the various voltage levels are for effectively grounded systems, as shown in Table I.

Lightning-Arrester Separation

Lightning-arrester separation, defined previously, appears to be one of the most important factors in determining the overvoltages above those held at the lightning arrester. Since the inductance of a loop increases with the area enclosed by the loop, the inductance that may be assigned to the lightning-arrester lead length as a part of the circuit being studied will increase with the arrester separation, as shown in Figure 3. Thus, a specified lightning current discharging through a given lightning-arrester lead length induces a voltage in the loop involving the lightning arrester and capacitor which increases critically for lightning-arrester separations in the range from 0 to 10 feet and increases slowly for separations greater than 10 feet. Figure 4 illustrates this for two voltage levels, showing also the effect of an initial charge $E_{DR}(o)$ on the capacitor at the time of sparkover of the lightning arrester. From Figure 8 it should be noted that even for a V-connection overvoltages exist, hence, for finite separations, regardless of lead length, overvoltages can be expected to occur. It is interesting to note that the time-to-crest increases nearly linearly with separation.

Table I

System Voltage Level, Kv	Lightning-Arrester Rating, Kv	Proposed Number of 12-Kv Lightning-Arrester Units*	Spark-over Voltage at 40 Kv Per 12-Kv Lightning-Arrester Units, Kv*
115	96	8	320
138	117	9.75	390
161	135	11.25	450
230	180	15	600
288	228	19	760

* "Lightning-arrester units" refers to 12-kv station type.

Lightning-Arrester Lead Length

The lightning-arrester lead is effectively a voltage source that contributes to the capacitor voltage in proportion to its lead length, as shown in Figure 5. Actually the importance of this additional voltage source per foot of lightning-arrester lead depends on the separation and the length of the lead, as shown in Figure 3. There it is shown that for a given separation the inductance per foot increases nearly 20 per cent as the lead length increases from 10 to 30 feet. The induced voltage acting on the circuit due to the lightning-arrester lead also depends on the steepness of the front of the lightning current discharged through the lightning arrester. Figure 5 shows that the time-to-crest also increases as the lead length increases.

The equivalent of zero lead length may be attained through the use of a V-connection. As shown in Figure 6, the mutual inductance of the leads in the V-connection is a function of the geometry of the V. Thus, as R/l is increased, the V-connection becomes increasingly effective as the mutual inductance decreases.

Ground Resistance

The voltage drop in the ground resistance is effectively another voltage source which tends to increase the capacitor voltage. However, as long as there is a good connection between the lightning arrester and protected apparatus grounds, the ground leakage resistance, R_1 and R_2 of Figure 1, is not critical. It can be shown analytically that the time-to-crest is practically independent of the ground resistance.

Impulse Capacitance

For the circuit configurations and discharge currents studied here, the capacitor voltage decreases slowly as the impulse capacitance increases, as shown in Figure 7. However, for certain combinations of lightning-arrester transformer separations, lightning-arrester voltage characteristics, and impulse capacitances the capacitor voltage can vary as the impulse capacitance as previously reported in a discussion of reference 5.

Figures 7 and 9 indicate that the time-to-crest of the capacitor voltage increases with capacitances and actually the time-to-crest increases according to the square root of the impulse capacitance.

It is to be emphasized that the results given herein for a capacitor representation of a transformer are pessimistic to the

Figure 8. Capacitor voltage as a function of separation, lead length, capacitance, and system voltage for lightning-arrester discharge current = 5,150 amperes, 1.6×16.5 microseconds and initial capacitor voltage = 0

System Voltage	Lightning-Arrester Spark-over Voltage	Lightning-Arrester Voltage Drop*
115	320	360
138	390	437
161	450	507
230	600	675
288	760	856

* For current discharge of 5,150 amperes, 1.6×16.5 microseconds (station-type lightning arrester)

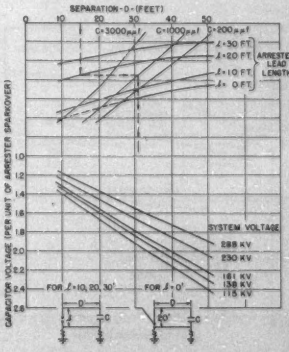

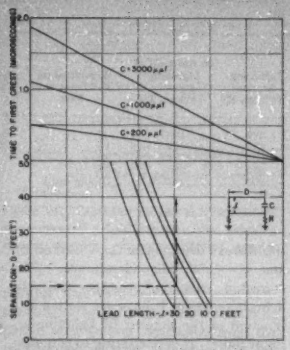

Figure 9. Time-to-first-crest as a function of separation, lead length, and capacitance for all system voltage levels and lightning discharge current 5,150 amperes, 1.6×16.5 microseconds

extent that the oscillatory component of the voltage be decreased by the order of 25 per cent at the first crest due to transformer attenuation.

Initial Capacitor Charge

If there is an initial charge on the capacitor due to the impinging wave, it has been shown analytically and demonstrated experimentally that the capacitor voltage after lightning-arrester spark-over is less than when there is no initial capacitor charge, as shown in Figures 4 and 5. Since the initial voltage at the capacitor is a function of the wave shape of the surge voltage prior to lightning-arrester spark-over and since specific information is not available on the correlation between the wave shape of the lightning arrester current and the pre-sparkover voltage, the results presented here are for zero initial voltage and are consequently conservative.

Composite Characteristics

The complete relation between circuit geometry, system voltage level, and capacitor voltage is illustrated graphically in Figure 8 for a lightning current discharge through the lightning arrester having a wave shape of 5,000-ampere crest, 1.6×16 microseconds and an effective rate-of-rise of 5,720 amperes per microsecond. The graphical data include separations from 10 to 50 feet, lead lengths from 0 to 30 feet, impulse capacitors from 200 to 3,000 micromicrofarads, and system voltage levels 115 kv to 288 kv. The dashed line on Figure 8 illustrates the use of the curves for $D=15$ feet, $l=20$ feet, and $C=1{,}000$ micromicrofarads.

Figure 9 gives the complete relationship for time to first crest for the same circuit geometry, and is independent of system voltage level.

Figure 10 shows the components of capacitor voltage due to the lightning arrester, lead length, ground resistance, and initial charge for a high-voltage system using 16 lightning-arrester units. These data are based on a discharge current of 10,000 amperes, 1.6×16.5 microseconds showing somewhat more severe voltages than would be obtained with a similar wave of 5,000-ampere crest.

Wave Shape of Lightning Current Discharge

The choice of a representative wave shape of lightning current discharged by the lightning arrester on which to base protection studies is somewhat arbitrary, depending on the probability of occurrence and the degree of protection economically feasible and desirable. Involved in these considerations are the isokeraunic level, system shielding, system grounding and other protection or surge-reducing factors. Based on field data gathered at stations[2,10,11,12] the lightning-arrester discharge currents include the values shown in Table II.

Figure 11 illustrates the decrease in the capacitor voltage as the effective rate-of-rise of the lightning current wave discharged through lightning arrester becomes smaller.

For the capacitor voltages, the time-to-first-crest and the time-to-maximum-value are the same for current impulses having steep fronts but may be different for current impulses with relatively slowly rising fronts. In the case for $C=200$ micromicrofarads the maximum value may occur on the second or third voltage crest for slow-front waves. Since the maximum crest value differs only slightly from the value at first crest for most cases, the time-to-crest is generally given as the time-to-first-crest. The physical implication of the first crest of the capacitor voltage appearing in time before the crest of the lightning-arrester voltage is that the capacitor voltage will be sustained for a larger number of cycles than if the first crest voltage across the capacitor appears in time after the crest of the lightning-arrester voltage.

System Voltage Level

As the system voltage level increases, the per-unit capacitor voltage decreases as shown in Figure 8. This is so because, percentage-wise, the induced voltage resulting from the lightning-arrester lead length and the voltage drop in the ground resistance becomes proportionately smaller relative to the increase in maximum voltage drop across the lightning arrester as the system voltage and the number of lightning-arrester units increase. Another interpretation of the results is that the geometry of the lightning-arrester-protected apparatus network is less critical the higher the system level for any given discharge current.

The time-to-crest of the oscillatory overvoltage is essentially independent of voltage level and is given in Figure 9 for various circuit configurations.

System Configuration

The elementary circuit which was considered in all of the foregoing represents the simplest setup or station. It is the purpose in this section to discuss the surge phenomena in a more complex station arrangement. The station circuit arrangement chosen is shown in Figure 12 and was set up in miniature on the transient analyzer[8,9] as shown in Figure 13.

The 16-unit station-type lightning arrester at point 1 in Figure 12 is assumed to discharge a 5,150-ampere, 1.6×16.5-microsecond current wave and the voltage at point 1, E_1, is composed of the voltage drop across the lightning arrester and the induced voltage resulting from the vertical lead in the T-connection. It is desired to determine the voltage at the various circuit breakers and transformers for different numbers of lines and transformers connected to the main 230-kv bus. In the study all the lightning ar-

Table II

Crest, Amperes	Wave Shapes, Microseconds	Effective Rate-of-Rise, Amperes per Microsecond (10 Per Cent–90 Per Cent)	$\left[\frac{di}{dt}\right]_{t=0}$, Amperes per Microsecond	Maximum Voltage Drop Across One 12-kv Lightning Arrester Unit, Kv
5,150	1.6×16.5	5,720	14,600	44.7
5,000	4.5×16	1,730	2,500	43
4,600	10×20	550	1,000	39.2

resters except the one located at point 1, Figure 12, were disconnected during the discharge of the lightning arrester at point 1. This was done in order that the voltages measured at the other lightning-arrester locations would indicate the actual voltages against which the disconnected lightning arresters must protect.

The impedance Z in Figure 13 is a surge impedance representing additional lines and transformers, since it was found that the addition of lines and transformers to the main bus was effectively the same as the addition of a surge impedance of 400 ohms for each of the lines or transformers connected to the bus.

The results of the study are summarized in Figure 14. Some typical oscillograms for one line and one transformer connected to the main bus are shown in Figure 15. These do not include the effect of attenuation due to transformer damping or the initial charges on the apparatus at the time of sparkover of the lightning arrester.

Although it is indicated that the effect of surges entering a station from a transmission line is decreased as the number of pieces of apparatus and the number of lines connected to the main bus are increased, it should be mentioned that lightning arresters also are necessary at the transformers, as well as at the line circuit breakers, to protect against:

1. Line strokes if all the lines and transformers are not connected to the station.
2. Failure of direct-stroke shielding between the main bus and transformer.
3. Switching surges.

Relation of Overvoltage to Volt-Time Characteristic of the Apparatus

The exact interpretation of the effect of the oscillatory overvoltage on the protected insulation necessitates voltage characteristics of the insulation obtained with damped oscillatory waves. It has been shown[13] that a test wave composed of a 1.5×40-microsecond full wave of 1.0 per-unit crest plus a superimposed oscillation (4 to 5 cycles) of 0.3 per unit is equivalent to a chopped wave with a crest of 1.15 per unit. Since the American Standards Association chopped-wave test is 1.15 per unit of the American Standards Association full-wave test, it is concluded[13] that a damped high-frequency oscillation of 0.3 per unit can be superimposed on the full-wave of 1.0 crest without stressing the transformer major insulation greater than the American Standards Association chopped-wave test (1.15 per-unit crest).

It is of interest, therefore, to consider the maximum separation (for V-connection in the elementary circuit) which would limit the oscillatory voltage to 0.3 per unit of the lightning-arrester voltage for a discharge current of 5,150 amperes, 1.6×16.5 microseconds. Figure 16 presents the oscillatory component of capacitor voltage (calculated by subtracting lightning-arrester voltage from the results of Figure 8) corrected for 25-per cent transformer damping for the V-connection and C = 1,000 micromicrofarads. This corrected capacitor voltage and the lightning-arrester voltage are plotted as a function of the number of lightning-arrester units. It is interesting to note that the oscillatory component increases until approximately 15 lightning-arrester units are employed and then decreases as more lightning-arrester units are used in the circuit. The decrease beyond 15 lightning-arrester units can be attributed to the damping resistance which increases approximately linearly with the number of lightning-arrester units. The oscillatory component would be zero if the number of lightning-arrester units were increased to the point of critical damping for the circuit configurations considered.

From the data in Figure 16 it is possible to derive a table of separations for the elementary circuit which results in a 30-per cent overshoot; see Table III.

For oscillations limited to 30 per cent of the lightning-arrester voltage (due to a discharge current of 5,150 amperes, 1.6×16.5 microseconds) the separations for the V-connection and with assumed transformer damping of 25 per cent are plotted on Figure 16. These separations do not consider any reductions of capacitor voltage which might arise from the initial charge on the capacitor or from complex station configurations. It is

Table III

System Voltage Level, Kv	Lightning-Arrester Rating, Kv	Proposed Number of 12-kv Lightning-Arrester Units	Lightning-Arrester Voltage, Kv	30 Per Cent of Lightning-Arrester Voltage, Kv	Separation for V-Connection, Feet
115	96	8	360	108	9
138	117	9.75	437	131	15
161	135	11.25	507	152	20
230	180	15	675	202	38
288	228	19	856	257	70 (by extrapolation)

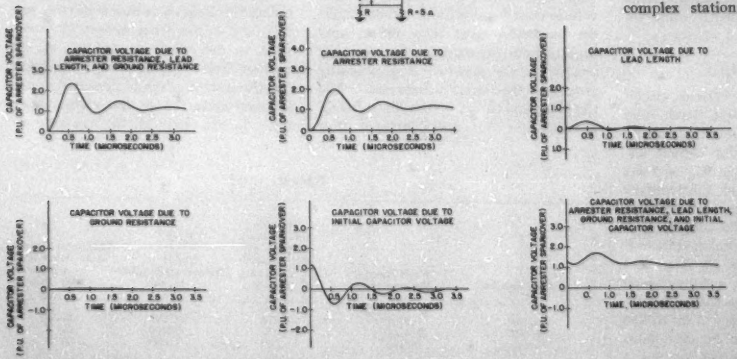

Figure 10. Component capacitor voltages for discharge of 10,000 amperes, 1.6×16.5 microsecond - wave through 16-unit station-type lightning arrester. Arrester spark-over = 640 kv. P.U. = Per Unit

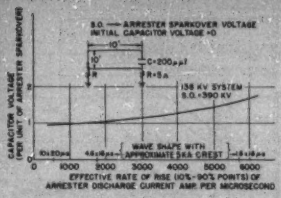

Figure 11. Capacitor voltage as a function of wave shape of a 5,000-ampere crest lightning current discharge through lightning arrester

possible that with complex station configurations the lightning arrester could be placed at a greater separation from the transformer without exceeding the 30-per cent oscillatory overshoot.

Appendix I. Considerations of Parameters for Equivalent Network

Resistance Calculations

For solid conductors the resistance[14] at very high frequencies (R_∞) may be expressed as

$$R_\infty = \frac{R_S}{2\pi r_0} \text{ ohms per meter}$$

where

$$R_S = \frac{1}{\sigma\delta} = \text{surface resistivity}$$

σ = conductivity in mhos per meter
δ = depth of current penetration in meters
r_0 = conductor radius in meters

Consider copper conductor at a frequency of 700,000 cycles per second. (Range in study 0.4 to 3.0 megacycles per second.)

$$\delta = \frac{0.0660}{\sqrt{f}} = \frac{0.0660}{\sqrt{700{,}000}} = 0.0000788 \text{ meter}$$

$$\sigma = 5.8\times10^7 \text{ mhos per meter}$$

$$R_S = \frac{1}{\delta\sigma} = \frac{1}{(5.8\times10^7)(0.0000788)} = 2.19\times10^{-4}$$

For

$$r_0 = 1/4 \text{ inch} = 0.0063 \text{ meter}$$

$$R_\infty = \frac{R_S}{2\pi r_0} = \frac{2.19\times10^{-4}}{2\pi(0.0063)} = 5.55\times10^{-5}$$

ohms per meter $= 1.69\times10^{-5}$ ohms per foot

Inductance Calculations

Consider the general circuit of Figure 17. The electromagnetic image[15] of a current is that current, or system of currents, which, when placed at proper positions behind a surface, produce the same magnetic effect in front of the surface, in the region containing the original current, as actually is produced by the induced magnetization upon the surface. When the bounding surface is a plane, the electromagnetic images coincide in position with the optical images of the original current which would be produced if the surfaces were mirrors with their silvered surfaces presented toward the region which contains the current. In the case under consideration the bounding plane is the zero current plane which is assumed to be parallel to the conductors 1 and 2. Hence, the images of conductors 1 and 2 are shown in their proper positions where

$$D_{ac} = D_{bd} \quad \text{and} \quad D_{ab} = D_{cd}$$

and the i_1 and i_2 are loop currents as indicated. Thus the zero current plane has been removed effectively from the picture and the inductances can be calculated without regard for the zero current plane.

Reference 16 gives formulae for calculating the total inductance or the equivalent inductance of each conductor side of the rectangular loop which is l centimeters long and d centimeters wide and has conductor of radius ρ centimeters. Such rectangles might be loops 1 and 2 of the circuit under consideration. It is shown here that the inductance of a rectangle of length a and breadth b is

$$L = 2(L_a + L_b - M_a - M_b) \qquad (1)$$

where L_a and L_b are the self-inductance of the two sides of length a and b taken alone, M_a and M_b are the mutual inductances of the two opposite pairs of length a and b respectively.

The self-inductance of one side may be determined from

$$L = 0.002\left[l \log_e \frac{l+\sqrt{l^2+\rho^2}}{\rho} - \sqrt{l^2+\rho^2} + \frac{l}{4} + \rho\right] \text{ microhenrys} \qquad (2)$$

where

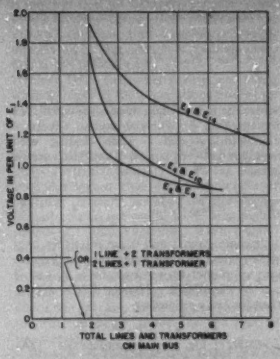

Figure 14. Transformer and circuit-breaker voltage as a function of lines and transformers on main 230-kv bus in per unit of crest E_1 = 740 kv

E_1 = Lightning-arrester voltage plus induced voltage due to current discharge of 5,000 amperes, 1.6×16.5 microseconds through 15 feet of lead length in the assumed T-connection

Subscripts on voltages correspond to measuring points on Figures 12 and 13

ρ = radius
l = length of wire in centimeters

The mutual inductance of two parallel filaments is given as

$$M = 0.002\left[l \log_e \frac{l+\sqrt{l^2+d^2}}{d} - \sqrt{l^2+d^2} + d\right] \text{ microhenrys} \qquad (3)$$

where ρ = radius
l = length
d = separation of the wires in centimeters

The total inductance L calculated in equation 1 could be proportioned to the sides a and b, according to the values of L_a, L_b, M_a, and M_b. The principle illustrated in equation 1 also is employed in the calculation of L_4 and L_5 of Figure 1.

Figure 12. One-line schematic diagram of a high-voltage switching station. Circled numbers represent measuring points

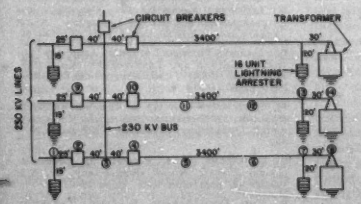

Figure 13. Equivalent miniature circuit of Figure 12 for study on transient analyzer

Actual pi-section constants: L = 320 microhenrys and C = 900 micromicrofarads
Lightning-arrester resistance = 10 + R_A = 600, C_1 = 500 micromicrofarads and C_2 = 1,000 micromicrofarads
Circled numbers correspond to measuring points on Figure 12

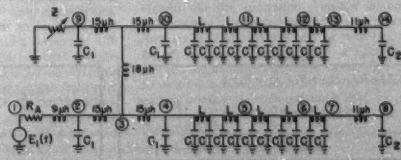

The mutual effect between loops 1 and 2 is

$$M_{12} = M_{ab} - M_{ac} + M_{cd} - M_{bd} = 2M_{ab} - 2M_{ac} \tag{4}$$

where the mutual inductances are calculated by equation 3. For the mutual effects of conductors a and b when dealing with voltages between a and b and the current plane

$$M = \frac{M_{12}}{2} = M_{ab} - M_{ac} \tag{5}$$

If conductors 1 and 2 are relatively long with respect to their height above the zero current plane, then equations 1, 2, and 3 can be simplified. Hence, if $l \gg d \gg \rho$, then for l in centimeters

$$L = 0.002\, l \left[\log_e \frac{2l}{\rho} - \frac{3}{4} \right] \text{ microhenrys} \tag{2A}$$

and

$$M = 0.002\, l \left[\log_e \frac{2l}{d} - 1 \right] \text{ microhenrys} \tag{3A}$$

However, if the permeability of the conductor is μ and that of medium outside is unity

$$L = 0.002\, l \left[\log_e \frac{2l}{\rho} - 1 + \frac{\mu}{4} \right] \text{ microhenrys} \tag{2B}$$

and for high frequency ($\mu = 0$)

$$L = 0.002\, l \left[\log_e \frac{2l}{\rho} - 1 \right] \text{ microhenrys} \tag{2C}$$

If in equation 1 $L_b = M_b = 0$, if equations 2A and 3A are substituted for L_a and M_a, and if L is divided by $2l$, then the standard equation for the inductance of a long line $d/2$ centimeters above the zero current plane is approximately given by

$$L_{ll} = 0.004 \log_e \frac{d}{\rho} \frac{\text{microhenrys}}{\text{centimeter}} \tag{1A}$$

Similarly the mutual inductance for two conductors a and b with positions above the zero current plane as defined in the figure can be approximated from equations 3A and 5 to find that

$$M = 0.004 \log_e \frac{D_{ac}}{D_{ab}} \frac{\text{microhenrys}}{\text{centimeter}} \tag{5A}$$

Appendix II. Analytical Solution of Figure 1

From Figure 1 the following loop equations in matrix form from which the voltage across the capacitor C is to be determined may be written as

$Y_1(p)$	$Y_2(p)$
$(R_1+R_2+R_A+R_4+R_5+R_6)+p(L_A+L_4+L_5+L_6)+\frac{1}{pC}$	$pM+R$
$pM+R$	$R_1+R_2+pL_3$

$$= \frac{E_{G1}(p) - \dfrac{E_{DE}(0)}{p} + E_{G2}(p)}{E_{G2}(p)}$$

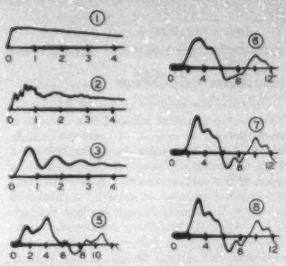

Figure 15. Typical oscillograms of voltages measured with one line and one transformer on main bus. Time scale in microseconds. Numbers on oscillograms refer to measuring points on Figures 12 and 13

If

$r = R_1 + R_2 + R_A + R_4 + R_5 + R_6$
$L = L_A + L_4 + L_5 + L_6$
$R = R_1 + R_2$

and solving for $Y_1(p)$, there results

$$Y_1(p) = \frac{\left[E_{G1}(p) - \dfrac{E_{DE}(0)}{p}\right][R + pL_3] + E_{G2}(p)[p(L_3 - M)]}{\Delta(p)}$$

Solving for the voltage across the capacitor

$$E_{DE}(p) = \frac{1}{pC} Y_1(p) + \frac{E_{DE}(0)}{p}$$

$$= \frac{\left[E_{G1}(p) - \dfrac{E_{DE}(0)}{p}\right][R + pL_3] + E_{G2}(p)[p(L_3 - M)]}{C\, LL_3 \left[\left(1 - \dfrac{M^2}{LL_3}\right)p^3 + \left(\dfrac{R}{L_3} + \dfrac{r}{L} - \dfrac{2MR}{LL_3}\right)p^2 + \left(\dfrac{rR}{LL_3} + \dfrac{1}{LC} - \dfrac{R^2}{LL_3}\right)p + \dfrac{R}{LL_3C}\right]} + \frac{E_{DE}(0)}{p}$$

where

$E_{G1}(p) = [E_{ab}(p) + Y_0(p)(pL_4 + R_4)]$
$E_{G2}(p) = R_1 Y_0(p)$
$E_{DE}(0)$ = initial voltage on capacitor
M = mutual inductance between loops 1 and 2.

The inductances L_3, L_4, L_5, and L_6 are determined from the equations in Appendix I, considering loops 1 and 2 as separate rectangular circuit loops with their images below the zero current plane. Similarly the mutual inductance M between loops 1 and 2 may be calculated from the equations in Appendix I.

The voltage across the capacitor as a function of time is obtained by taking the inverse Laplace transform as

$$E_{DE}(t) = \mathcal{L}^{-1} E_{DE}(p) = \mathcal{L}^{-1}\left(\frac{Y_1(p)}{pC} + \frac{E_{DE}(0)}{p}\right)$$

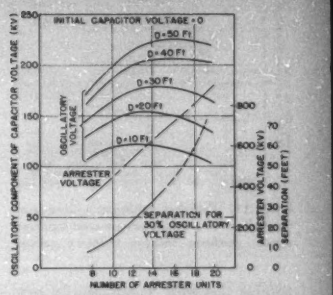

Figure 16. Oscillatory component of capacitor voltage as a function of separation and lightning-arrester units for V-connection and corrected for transformer damping = 25 per cent

Separation curve with V-connection to limit oscillatory voltage to 30 per cent of lightning-arrester voltage as a function of lightning-arrester units

References

1. Protection of Station Equipment on High Voltage Transmission Lines, **K. B. McEachron.** *General Electric Review* (Schenectady, N. Y.) volume 31, May 1928, pages 230–37.

2. Field Tests on Thyrite Lightning Arresters Using Artificial Lightning of 1,500,000 Volts, **K. B. McEachron, E. J. Wade.** *AIEE Transactions*, volume 50, June 1931, pages 479–89.

3. Field Investigation of Lightning Surges at Substations, **I. W. Gross, G. D. McCann.** *AIEE Transactions*, volume 66, 1947, pages 569–76.

4. Coordination and Protection of Station Insulation Against Lightning, **P. L. Bellaschi.** *International Conference on Large High-Voltage Electric System* (Paris, France), volume III, 1939.

5. Lightning Arresters as a Criterion for Insulation Levels, **Harold L. Rorden.** *AIEE Transactions*, volume 69, part I, 1950, pages 84–96.

6. Margins Between Lightning Arrester Protective Levels and Transformer Insulation, **F. J. Vogel.** *AIEE Transactions*, volume 69, part I, 1950, pages 110–14.

7. Equivalent Circuits of Transformers and Reactors to Switching Surges, **L. V. Bewley.** *AIEE Transactions*, volume 58, 1939, pages 797–802.

8. Analyzers, **H. A. Peterson, C. Concordia.** *General Electric Review* (Schenectady, N. Y.), volume 48, September 1945, pages 29–37.

9. The Oscillograph Electric Transient

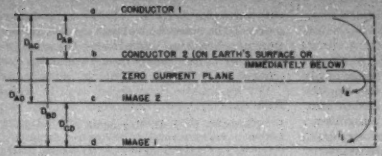

Figure 17. General circuit for calculation of inductance of transmission line and ground connection in presence of ground. (See Appendix I)

ANALYZER, N. Rohats. *General Electric Review* (Schenectady, N. Y.), volume 39, March 1936, pages 146–49.

10. LIGHTNING CURRENTS IN ARRESTERS AT STATIONS, I. W. Gross, W. A. McMorris. *Electrical Engineering* (*AIEE Transactions*), volume 59, August 1940, pages 417–22.

11. FIELD RESEARCH ON LIGHTNING ARRESTER DISCHARGES, G. D. McCann, Edward Beck. *AIEE Transactions*, volume 66, 1947, pages 625–30.

12. LIGHTNING INVESTIGATION ON THE 25-KV SYSTEM OF THE WEST PENN POWER COMPANY, William C. Bowen, Edward Beck. *AIEE Transactions*, volume 66, 1947, pages 831–37.

13. PROPOSED BASIC IMPULSE INSULATION LEVELS FOR HIGH-VOLTAGE SYSTEMS, J. E. Clem, J. R. Meador, W. J. Rudge, A. H. Powell. *AIEE Transactions*, volume 69, part II, 1950, pages 953–63.

14. FIELDS AND WAVES IN MODERN RADIO (book), Simon Ramo, J. R. Whinnery. John Wiley and Sons, New York, N. Y., 1944.

15. ELECTROMAGNETIC PROBLEMS IN ELECTRICAL ENGINEERING (book), B. Hague. Oxford University Press, Oxford, England, 1929.

16. INDUCTANCE CALCULATIONS (book), F. W. Grover. D. Van Nostrand Company, Inc., New York, N. Y., 1946.

Discussion

J. R. Meador (General Electric Company, Pittsfield, Mass.): This timely paper contains a very thorough analysis of the pertinent factors involved in the important problem of lightning-arrester location. While it has been apparent from theoretical considerations that lightning arrester lead length and separation from the transformer should be kept to a minimum for maximum protection, the numerical values have not been available.

It is obvious from this paper that more field data on rates of current rise through lightning arresters in stations are needed. As these data become available for the various conditions of station and line shielding, the authors' method of calculation can be used to arrive at an increasingly-accurate appraisal of proper lightning arrester location.

The authors bring out an interesting point in showing that separation between lightning arrester and transformer has an effect that increases rapidly up to a separation of ten feet, and beyond ten feet increases more slowly. Thus, if the permissible separation is ten feet or more under one set of conditions, a reduction in oscillation voltage will permit a disproportionately large increase in separation. This fact makes the effect of initial capacitor charge assume greater importance since the precharge reduces the magnitude of the oscillation substantially.

In a station-type lightning arrester where the gap sparkover and resistance voltage are of the same order of magnitude, it would appear that a substantial precharge on the capacitor would exist before the surge current discharged through the lightning arrester. Calculations showing permissible separation with different amounts of precharge would be of interest.

The transformer acts as a capacitor only as seen from its terminals and for a relatively small number of microseconds. For longer times the inductance and resistance become more important. However, for the separations and rates of rise of current considered in the paper, the oscillation frequencies are accurate for a few cycles if the transformer is treated as a capacitor.

The assumption of a permissible 30 per cent superimposed oscillation is correct if the period of the oscillation is less than one or two microseconds. If considerably longer separations are considered, the period will increase, and it may be necessary to limit the magnitude of the oscillation to less than 30 per cent.

A. M. Opsahl (Westinghouse Electric Corporation, East Pittsburgh, Pa.): The authors state that it has been shown that transformer insulation of a given basic impulse level (BIL) will withstand a short superimposed oscillation 30 per cent above the full-wave test. The stress on the insulation is no greater than in the chopped-wave test which is a test voltage 15 per cent above the BIL. Table III of the paper gives recommendations on the maximum separation that should be permitted between the lightning arrester and transformer in a substation. This table is developed on the basis of limiting the voltage oscillation at the transformer to 30 per cent above the lightning-arrester discharge voltage. There is no explanation given for the transition from BIL as a base for the permissible overvoltage oscillation to the lightning-arrester discharge voltage as a base for the permissible over-voltage oscillation at the transformer terminals. Presumably a margin has been assumed between the voltage as limited by the lightning arrester and the voltage that the transformer will withstand. Take for example the 115-kv system voltage. The lightning-arrester voltage is given as 360 kv but the BIL of 115-kv class insulation is 550 kv and the BIL of 92-kv class insulation is 450 kv, 53 and 25 per cent above the lightning-arrester voltage respectively. No values of transformer insulation level are given in the table but it looks like the only combination considered is the reduced rating lightning arrester, reduced insulation level in the transformer, and about 25 per cent margin between the transformer insulation strength and the voltage as limited by the lightning arrester. The margin of 53 per cent between insulation level of a full rating transformer and the characteristic of a reduced rating lightning arrester is not reasonable if it requires that all lightning arresters must be within nine feet of the transformer on 115-kv circuits. Full insulation transformers on 115-kv circuits is common practice at the present time.

Table III of the paper is very misleading when so many of the assumptions leading up to its conclusions are omitted.

W. A. McMorris (General Electric Company, Pittsfield, Mass.): Operating experience has shown that current practices of applying lightning arresters for the protection of station apparatus have been highly successful. Some operators have demonstrated that where transformer insulation levels have been properly co-ordinated with the protective levels afforded by lightning arresters, the insulation levels can be reduced one full class below the normal values, resulting in large savings in the cost of transformers.

Because of the increasing trend toward reduced transformer insulation and the large economies that are possible through close co-ordination of insulation at the higher voltage levels, it is desirable to reexamine critically the margins between lightning-arrester protective levels and transformer insulation strengths. These margins are determined in part by lightning-arrester application practices.

In their analysis the authors have assumed relatively severe conditions. They have indicated, however, that lightning voltages at a protected transformer would be reduced by the connection of additional lines or transformers to the bus, or by precharge on the capacitance of the transformer at the instant of lightning-arrester sparkover.

The probability of the assumed condition of zero precharge, on which Figure 16 and Table III of the paper are based, would appear to be rather remote. Where recommended types of construction have been used, the precharge would approach the lightning arrester sparkover value for any practical rates of rise of voltage and separations between lightning arresters and transformers. This would reduce the voltage oscillation at the transformer far below the value for zero precharge. It would permit a substantial increase in lightning-arrester lead lengths and separations between lightning arresters and transformers without exceeding the suggested maximum value of 30 per cent oscillation.

Regardless of what wave shapes may be established as a basis for co-ordination studies, the operator who desires to obtain the widest possible margin of protection, or to retain a normal margin for severe conditions, should use the V-connection. This was demonstrated by tests which were reported by K. B. McEachron and E. J. Wade in 1931,[1] and has been advocated since that time for installations where the lowest protective level is desired. Also, he should use the minimum possible separation between lightning arresters and transformers, and at stations with several transformer banks, he should install a lightning arrester immediately adjacent to each transformer bank as well as on the line side of the circuit breaker on each incoming line.

REFERENCE

1. See reference 2 of the paper.

E. Beck (Westinghouse Electric Corporation, East Pittsburgh, Pa.): The authors' paper on lightning arrester location, and another by R. L. Witzke and T. J. Bliss[1] contribute considerably to the analysis and resolving of the problem. They are not in agreement. This is a good thing as it means that the matter will be studied further and a sound conclusion reached. The authors' paper requires considerable study to uncover the various assumptions and steps and relations assumed between BILs, lightning-arrester voltages, and voltages at the equipment. Considering for the moment only their basic assumption of lightning arrester voltage in Figure 2 and experience in the field, it is my opinion that their conclusions are too conservative for high-voltage equipment shielded in the manner described in a paper on insulation levels.[2]

Considering the author's assumption of a lightning arrester discharge current of 5,000 amperes per microsecond, together with their Figure 2 and the lightning arrester discharge voltage characteristics indicated there, it would seem that to produce the assumed current rise in the lightning arrester, a voltage would have to be impressed at the lightning arrester terminals immediately after lightning arrester sparkover with an initial rate of rise of some 40 kv in 0.125 of a microsecond per 12 kv of lightning arrester. On a 115-kv system with a 97-kv lightning arrester, this would be about 2,560 kv per microsecond. On a 230-kv system with the 180-kv lightning arrester proposed by the authors, it would be about 4,800 kv per microsecond. What do the authors estimate the probability of such rates of rise of surge voltage in a station shielded in the manner considered in the plans for co-ordination?

The authors appear to have neglected what happens before lightning-arrester sparkover. The paper is not clear on this matter, if they have considered it. It is considered in the Witzke and Bliss paper.

Without shielding, we agree that there is no problem, the lightning arresters should be applied as close to the equipment as possible.

In view of the tendency to install lightning arresters near the transformers, a practice with which we concur, especially where reduced insulation levels are used on high-voltage transformer, another aspect of the question is the voltages ahead of the lightning arresters and their effect on switchgear or metering equipment insulation. This may become the more important question. It should receive attention, and offhand looks like a simpler problem.

REFERENCES

1. Co-ordination of Lightning Arrester Location with Transformer Insulation Level, R. L. Witzke, T. J. Bliss. *AIEE Transactions*, volume 69, part II, 1950, pages 964–73.

2. See reference 13 of the paper.

J. H. Hagenguth (General Electric Company, Pittsfield, Mass.): The paper explains in detail how traveling waves affect voltages in stations with lightning-arrester protection, principally where only one line enters the station. Previously[1] it has been shown in a general way that large differences in voltage to ground and rate of voltage rise can exist in stations with many incoming lines and extended station bus. This point was recently illustrated by the study of a particular station, the results of which are of interest.

Through the courtesy of Mr. I. W. Gross it was possible to obtain a station diagram of the 138-kv Roanoke Station of the Appalachian Power Company. This station has two busses, normally connected together, each 220 feet long. The transformer bank with its lightning arrester is approximately 400 feet from the nearest line. A potential transformer with its lightning arrester has a distance of 240 feet. Between each circuit breaker and its connected circuit, coupling capacitors are connected between two of the phases and ground for carrier-current communication. The electrical circuit equivalent for transients was set up and studied with the transient analyzer.

Based on traveling wave crests of about 800 kv, the maximum voltage permitted by the line insulators, 0.5x40 microseconds waves were applied and the voltages at various points in the station were measured. It is possible to give only a few of the results.

With a traveling wave coming in over only one line, the voltage at the station entrance was about equal to the traveling wave voltage, about 720 kv. The rate of rise of voltage at this point was 1,900 kv per microsecond. At the potential transformer the voltage was 470 kv with a much slower rate of rise of 905 kv per microsecond, while at the power transformer the voltage was 370 kv, with a still slower rate of rise of 310 kv per microsecond. These results are obtained without lightning arresters connected in the circuit. When lightning arresters are connected to the potential and power transformer, the maximum voltage at the station entrance is not changed. The voltages at the transformers are reduced to the lightning-arrester protective level which was about 350 kv in the model.

Some of the lines are double circuit lines on one tower, and the possibility exists that the same phase of both lines is involved in a lightning transient, particularly from back flashover from a tower with high ground resistance.

In this case conditions at the station entrance of both lines are essentially the same as before, but without lightning arresters the potential and power transformer voltages reach 540 kv and 810 kv respectively. With lightning arresters, the voltages are, of course, again held to about 350 kv. The rate of voltage rise is of the order of 900 and 500 kv per microsecond respectively.

If the lightning arresters are connected at the station entrance and not near the transformers, and the same phase of two circuits is impulsed, voltages of 400 kv and 560 kv are obtained at the potential and power transformer respectively, even though the arrester is still holding about 350 kv at its terminals.

Such studies show that in stations with many lines connected to the bus, considerable differences in voltages to ground and rate of voltage rise can exist at various points in the station.

While the most favorable location of the lightning arrester is near the transformer to obtain a minimum protective level at that point, location of the lightning arrester even 400 feet away from the transformer holds the voltage to about the impulse test level of this particular system. However, if one or more of the lines were disconnected at the time of a lightning disturbance, the impulse test level of the transformer would be exceeded.

REFERENCE

1. *Discussion* by J. H. Hagenguth of Lightning Investigation of 132-Kv System of American Gas and Electric Company, I. W. Gross, G. D. Lippert. *AIEE Transactions*, volume 64, 1945, pages 475–76.

L. A. Finzi (Carnegie Institute of Technology, Pittsburgh, Pa.): This paper presents a skillful study of transient phenomena in terms of a lumped-parameter analysis and gives interesting conclusions on the basis of rather typical values of the constants of the equivalent circuit.

It may be pointed out however that an accurate evaluation of the various sinks of energy in the equivalent circuit is most essential as it is their damping action that intervenes to limit appreciably the first overvoltage crest at the apparatus terminals and to further dictate the decay of the subsequent crests. Indeed the total energy to be dissipated in the transient is generally very small—a few watt seconds—but the time available for a safe damping is also exceedingly short, as seen from the insulation volt-time curves.

A most important sink of energy is represented by the lightning arrester nonlinear resistors; for these the authors suggest the use of a value of 4 ohms per lightning-arrester unit. Actually this value may vary considerably for various types of discharge; this circumstance seems to confirm the need for a better agreement upon reasonable standard current surges that was raised from various parts in the discussion of a companion paper.[1]

Another important sink can be seen in the drainage by gradual propagation into the transformer, that is in the inherent transformer attenuation. This attenuation should be expected to vary depending on the size and type of transformer.

REFERENCE

1. See reference 13 of the paper.

D. D. MacCarthy (General Electric Company, Pittsfield, Mass.): This paper reports the results of an extensive study of the effect of lightning-arrester lead length on the voltage at the terminals of the protected apparatus. In the past this subject has not received the attention that it deserves.

Figure 16 and Table III of the paper show the separation permissible between a lightning arrester and a transformer in order that the short-duration oscillatory voltage at the transformer does not exceed the voltage at the lightning arrester by more than 30 per cent under the specified conditions. These conditions include: a lightning arrester discharge current of 5,000 amperes crest rising at an effective rate of 5,720 amperes per microsecond; a single overhead line that terminates at the transformer; and a lightning arrester connected in "V." The authors have chosen a lightning arrester discharge current and the basic circuit as being representative of conditions that give high voltages at the transformer but which might

occur in service. A limit of 30 per cent overvoltage at the transformer was selected as a voltage of short duration that preserves the same margin of protection below the transformer strength as exists at longer values of time between the discharge voltage of the lightning arrester and the strength of the transformer demonstrated by American Standards Association tests. The "V" connection was selected since it is the best connection for minimizing the effect of the lightning-arrester leads.

However, power transformers have operated satisfactorily for years with the lightning arresters connected in "T," with longer lightning-arrester lead lengths, and with separations many times larger than shown in Figure 16. There are several factors that account for the excellent operating record of these transformers even though the margins of protection were less than they would have been had the practices recommended in this paper been followed. Lightning-arrester discharge currents rising as fast as 5000 amperes per microsecond are probably rare, although available data are few. In service the circuits are usually more complex than the basic circuit for which Figure 16 applies. More than one line is usually connected to the transformer bus. The capacitance of the bus is usually greater than that provided by a single transformer, and this also may reduce the voltage of the transformer.

Another factor that will reduce the voltage at the transformer is the presence of a charge on the transformer capacitance at the instant of lightning arrester gap spark-over. While Figure 16 indicates a separation of 9 feet between the transformer and a V-connected lightning arrester for a 115-kv circuit, this is for no charge on the capacitor and it is well to consider other data in the paper on the effect of capacitance charge. By allowing for the effect of a charge on the transformer capacitance, the lightning arrester and the transformer may be separated by 50 feet using the data in the paper. The effect of this charge is discussed in the paper and is shown in Figures 4 and 5.

The effect of charge on the voltage at a 115-kv transformer is illustrated by an example calculated from Figure 4 using these circuit constants:

"T" connection of 8-unit lightning arrester
Lead length (l) = 20 feet
Separation (D) = 50 feet
Capacitance (C) = 1,000 micromicrofarads

These calculations are shown in Table I of the discussion.

If the transformer capacitance is charged to 400 kv, the oscillatory voltage allowing for damping is 90 kv, which is only 83 per cent of the value permissible. Under this assumption, it is permissible to connect the lightning arrester in "T," with a lightning-arrester lead of 20 feet and a separation of 50 feet. However, if no initial charge exists on the transformer capacitance, the oscillatory voltage is 234 kv, which is 217 per cent of the permissible value. Hence, it is clear that the permissible lead length greatly depends upon the charge on the transformer capacitance. It would be helpful if the authors would present data similar to that in Figure 16, indicating recommended maximum separations between transformers and lightning arresters for both the T- and V-connections, assuming reasonable values of capacitor charge.

R. L. Witzke and **T. J. Bliss** (Westinghouse Electric Corporation, East Pittsburgh, Pa.): The general method of analysis used in the paper involves a number of assumptions that limit greatly the value and applicability of the results. The separation distances between the lightning arrester and the transformer appear to be unrealistic and are not substantiated by field experience.

The studies reported were made by considering the conditions only after the lightning arrester starts to conduct current. This makes it necessary to neglect the initial charge on the capacitor used to represent the transformer, or to assign some arbitrary value to the initial charge. This charge has a very important influence on the voltage at the transformer as is evident from Figures 4 and 5 of the paper.

In our investigation[1] we assumed an incoming voltage surge having a constant rate of rise. The voltage at the lightning-arrester location was permitted to increase to a value corresponding to the lightning-arrester voltage before the elements used to represent the lightning arrester were connected to the circuit. This procedure gives due consideration to the transients before the lightning arrester gap operates, and does not require an assumption relative to the initial charge on the capacitor used to represent the transformer.

The incoming-line surge impedance has an important influence on the circuit voltages in those cases where reflections return from the transformer to the lightning-arrester location before the lightning arrester gap operates. It is therefore necessary to represent this circuit element in any complete investigation.

In problems of the nature reported in this paper, which involve a number of probabilities, misleading conclusions are reached if all assumptions are conservative. The assumptions of 5,000 amperes per microsecond in the lightning arrester, a plus $6^3/_4$ per cent lightning arrester tolerance and a 20 per cent margin lead to unrealistic separation distances.

REFERENCE

1. CO-ORDINATION OF LIGHTNING ARRESTER LOCATION WITH TRANSFORMER INSULATION LEVEL, R. L. Witzke, T. J. Bliss. *AIEE Transactions*, volume 69, part II, 1950, pages 964-75.

T. J. Carpenter, I. B. Johnson, and **L. R. Saline:** It should be emphasized that these comments are primarily based on evaluating the over-all lightning arrester protective scheme in relation to the reduced insulation concept in voltage classes 115 kv and above. Specifically, the voltage classes, lightning arrester ratings, and the corresponding BIL values upon which the lightning arrester study was made are shown in Table II of this discussion.

The authors are in agreement with Mr. Meador's comments that more complete and more accurate statistical field data are required at the voltage levels studied on the rates of rise of voltage surges entering stations and on the rates of current rise through lightning arresters before a more accurate appraisal of proper lightning-arrester location can be made. Also such data should be evaluated in terms of the degree of shielding of both the station and the line, of the insulation level of the line and of the effect of the station configuration. Consequently, in considering costly equipment using reduced insulation, the authors felt justified in being conservative in the evaluation of the necessary assumptions.

Also, in Mr. Meador's discussion a request is made for lightning arrester separation as a function of capacitor charge at the time of lightning arrester sparkover. The results of the study indicated, with zero lightning arrester lead length (that is, with a V-connection), the permissible separations were 50 feet or more when the initial charge on the capacitor, at the time of lightning-arrester sparkover, was approximately equal to the lightning-arrester sparkover voltage; as contrasted to separations given in Table III of the paper for the same conditions but with zero initial capacitor charge on the capacitor.

As presumed by Mr. Opsahl a margin has been assumed between the voltage limited by the lightning arrester and the BIL level of the protected transformer in deriving the separations recorded in Table III of the paper. The BIL values chosen were reduced insulation values corresponding to those given in Table II of this discussion. One of the primary arguments for providing margin is to allow for the multishot strength of the transformer. Since some transformers fail as a result of a single impulse during the factory test, transformers which do not fail do not necessarily have additional strength to enable them to withstand a large number of impulses. Consequently, to assure a multishot strength for all transformers, some margin is necessary between

Table I

Initial Charge on Capacitance	1.25 PU	0
Capacitance voltage	1.5×8×40 = 480 kv	2.1×8×40 = 672 kv
Voltage across lightning arrester	8×45 = 360 kv	8×45 = 360 kv
Oscillatory voltage	120 kv	312 kv
75 per cent of oscillatory voltage	90 kv	234 kv
Permissible oscillatory voltage	0.30×360 = 108 kv	108 kv

Table II

System Voltage Level, Kv	Lightning Arrester Rating, Kv	BIL 1.5×40 Voltage Value, Kv
115	96	450
138	117	550
161	135	650
230	180	825
285	228	1050

the protective level and the demonstrated strength of the transformer.

The authors wish to reiterate some of Mr. McMorris' comments that the operator who desires to obtain the widest possible margin of protection should, ideally, approach the V-connection and the minimum possible separation between lightning arresters and transformers.

Mr. Beck comments on the results of our paper and the comparable results from a similar paper by Witzke and Bliss[1] and concludes they are not in agreement. However, as it will be shown later, the results from the two studies are not as different as it first may appear.

With regard to Mr. Beck's questions on our assumptions as related to field experience we wish to make several comments. First, the events preceding sparkover were not neglected, the effect being included as an initial charge on the capacitor or transformer at the instant of lightning-arrester sparkover. The effect of this initial charge is illustrated in Figures 4 and 5 of the paper. However, in setting up Table III of the paper the initial charge was set equal to zero, introducing a conservative assumption, perhaps, for most cases in view of the limited field data available. Second, with regard to rates of rise of lightning-arrester discharge currents and lightning-arrester discharge voltages, the lightning-arrester discharge voltage should initially rise almost instantaneously in response to the voltage already existing at the lightning arrester to cause sparkover. Similarly, if it is assumed that the circuit elements in the discharge path are entirely resistive, the initial rate of rise of lightning-arrester discharge current should be almost instantaneous at the time of lightning-arrester sparkover.

Further, from conclusions 3 and 6 of reference number 2 of this discussion of a field study, it is indicated:

1. That the wave shapes of lightning-arrester discharge currents were of the same general character as for direct strokes but with the fronts times to half value and durations markedly shorter.
2. That the wave fronts of lightning-arrester discharge currents are characterized by an initial high rate of rise as the lightning arrester starts to discharge.
3. That surge voltage values at the transformer were measured as large as 32 per cent greater than at the lightning arrester for the same surge.

Also, from reference number 3 of this discussion on lightning-arrester discharge currents in 132-kv stations, we wish to quote the following: "Although the maximum value of lightning arrester current measured in this investigation was only 4,100 amperes, on another part of the system a maximum lightning arrester current of 16,000 amperes was measured in an arrester on the 132-kv system—the result of a stroke within 400 feet of the station."

The 16,000-ampere lightning-arrester discharge occurred on a line and station that was shielded. Since the distance between the lightning arrester and the stroke makes it possible to consider it almost a direct stroke phenomena it is feasible that the effective rate of rise of the lightning-arrester discharge current exceeded that assumed in our study. The analysis given in the discussion of reference number 3 by Mr. Hagenguth would tend to support this possibility.

Mr. Hagenguth's discussion on the effect of many incoming lines and extended station bus substantiate in general a similar study on station configuration as recorded in the section on System Configuration of our paper. The effect of surges entering a station from a transmission line is decreased as the number of lines and number of pieces of apparatus is increased.

Mr. Finzi points to an accurate evaluation of the various sinks of energy in the equivalent circuit as most essential. This depends on complete and accurate lightning discharge data to begin with. With regard to the energy sink represented by the transformers, it was found experimentally for a number of transformers of different sizes that a transformer can be represented by a lumped capacitance as far as natural oscillations are concerned but the first crest of the oscillation of the voltage at the transformer is approximately 25 per cent less than that obtained with an equivalent capacitor substituted for the transformer. Also, for a transformer, the decay of the oscillations is almost complete in the order of 3 to 4 cycles.

In Mr. MacCarthy's comments on past satisfactory operation of power transformers with relatively long lead lengths and separations we wish to emphasize again that we are primarily concerned with transformers with reduced insulation with which there is limited field experience. We agree with Mr. MacCarthy's interesting discussion on the effect of the initial charge on the capacitor. At these higher voltages relatively long increases in lightning arrester lead length result in relatively small increases in voltage at the protected transformer.

R. L. Witzke and T. J. Bliss state that "The separation distances between the lightning arrester and the transformer appear to be unrealistic and are not substantiated by field experience."

Let us look at the record from an operator's point of view and experience, keeping in mind that we are discussing reduced insulation transformers only. Thus, from reference number 4 we quote:

"This resulted, in 1934, in adopting the so-called reduced insulation on a 30,000-kva 132-kv transformer bank where a lightning arrester of reduced rating was mounted directly on the transformer bank. (See Figure 9.) In this way, it was possible to use 115-kv class insulation for the transformers and a 75 per cent lightning arrester on our 132-kv grounded neutral system with an over-all saving in the order of 15 to 20 per cent. This practice has been continued up to the present time with complete transformer protection and entire satisfaction.

During the last 16 years, there have been installed on the American Gas and Electric Company system, nearly 3,750,000 kva of transformer capacity in the range of 88, 132, and 154 kv, all having reduced insulation—that is, one level below the standard BIL values. 180,000 kva has been on 154-kv lines, over 40,000 kva on 88-kv lines, and approximately 3,500,000 kva on 132-kv system."

Again, from Mr. Gross' closing discussion in reference number 2 it is stated that failure of station equipment is intolerable even though it may be the result of a possible infrequent high voltage at the transformer exceeding the voltage held by the lightning arrester.

And again from Mr. Sporn's discussion in this same reference number 2 it is stated that some 13 years prior to 1947 there was placed in service on the 132-kv system a transformer with closely coupled lightning arresters, the lightning arresters being mounted directly on the transformer tank and that the practice of closely coupling lightning arresters to equipment is now standard practice in this company. It is also stated that it seemed proper protection involves three important elements:

"1. Knowledge of the insulation strength of the transformer.

"2. Knowledge of the lightning arrester protective level.

"3. A relationship between the two to allow an appropriate margin between them."

In the comparable separations given by Witzke and Bliss for reduced insulation transformers and zero lightning arrester lead length, Table III of reference 1 shows separations of 53, 67, 92, 69, and 80 feet for system voltages of 115, 138, 161, 230, and 287 kv, respectively. These are to be compared with the separations recorded in Table III of our paper. One of the differences in assumptions in these results was the allowance of margin or no margin between the over-voltage appearing at the transformer due to separation and its equivalent voltage on the volt-time curve of the transformer insulation. Whereas it appears Witzke and Bliss have assumed no margin, we in our study have assumed some margin as necessary. Consequently, if instead of holding the oscillatory overshoot at the transformer due to separation to 30 per cent it is allowed to reach 50 per cent, then the lightning-arrester separations at 115 kv, 138 kv, and 161 kv become 55 feet, 65 feet, and 100 feet, respectively. These are to be compared with 53 feet, 67 feet, and 92 feet from the results by Witzke and Bliss which include the length of the down lead from the overhead line to the transformer whereas our separations do not.

We cannot agree with some of the statements made by Witzke and Bliss in the second paragraph of their discussion. Our study considered the conditions not only during and after lightning-arrester sparkover but those preceding it. It was not necessary nor was it done to neglect the initial charge on the capacitor used to represent the transformer. It is not necessary to arbitrarily assign a value to the initial charge. Our lumped circuit method of analysis is a simple approach in which the initial conditions at the time of lightning-arrester operation can be accurately calculated from assumptions pertaining to the rate of rise of the surge voltage causing lightning-arrester sparkover.

References

1. See reference 1 of preceding discussion.
2. See reference 3 of the paper.
3. Lightning Investigation on 132-Kv System of American Gas and Electric Company, I. W. Gross, G. D. Lippert. *Electrical Engineering* (AIEE Transactions), volume 64, February 1945, pages 76–84.
4. Selection, Design, and Operation of Power Transformers on American Gas and Electric Company System, F. A. Lane, I. W. Gross, P. S. Pugh. *AIEE Transactions*, volume 69, part II, 1950, pages 786–93.

Field Testing a Microwave Channel for Voice Communication, Relaying, Telemetering, and Supervisory Control

D. R. PATTISON
FELLOW AIEE
S. C. LEYLAND
MEMBER AIEE

M. E. REAGAN
FELLOW AIEE
F. B. GUNTER
MEMBER AIEE

COMMUNICATION channels, for transmitting the various types of intelligence necessary for operation of a power system, are becoming increasingly important to the utility industry because of the trend toward centralized system control. Pilot wire and power line carrier channels are already used widely to accommodate the many items of information necessary for efficient system operation. Microwave channels are the most recent addition to the means of communication available for this purpose.

A microwave channel[1] is a beamed high-frequency radio communication medium which can be used to transmit from point-to-point the intelligence required in the normal operation of a power system. Relaying, telemetering, supervisory control, and voice communication are some of the functions which can use such a channel. The large number of items of information which can be transmitted simultaneously over a microwave channel makes it particularly valuable at locations where communication traffic is heavy.

It is the purpose of this paper to describe an experimental installation of a microwave channel and terminal equipment which accommodate simultaneously three voice conversations, two different types of protective relaying, two telemetered quantities, and supervisory control of eight points. A feature of considerable interest on this installation is the use of a reflector to provide a continuous path for the microwave beam between the terminal stations, where line of sight was not available. The use of the reflector eliminated the need for $2^1/_4$ miles of cable originally planned to connect one of the terminal stations to a point where line of sight to the other station was possible.

The installation is on the system of the Pennsylvania Electric Company and ties together the main generating plant at Seward and the operating headquarters at Johnstown, Pa. A joint test program has been carried out during the past year by the Pennsylvania Electric Company and the Westinghouse Electric Corporation.

The Problem

The Seward Generating Plant is the terminus for power line carrier communications, telemetering, and supervisory control equipment for the entire power system. The efficient operation of the system depends on adequate and reliable communication facilities between the system operator in Johnstown, approximately 12 miles distant, and the Seward Plant. The use of wire lines in the past has not been satisfactory because of outages and inferior service caused by extreme conditions, such as landslides, icing, automobile accidents, and gunshots.

The problem, therefore, was to prove that microwave and audio multiplex equipment provides a reliable channel which is suitable for voice communications, telemetering, supervisory control, and relaying.

It was decided that three 2-way telephone circuits, two 1-way telemetering circuits, one 2-way supervisory control circuit, and two relaying circuits would be provided for in the tests.

The Equipment Used

A block diagram of the equipment located at each terminal is shown in Figure 1. The microwave equipment and audio multiplex equipment are suitable for transmitting four voice frequency channels in each direction. Three of these channels are used for the telephone circuits and the fourth circuit has a number of tones applied to it which are keyed to perform the other functions. The microwave equipment and audio multiplex equipment, Figure 2, provide the means for the simultaneous handling of the circuits required by the various functions being used in the field tests. The microwave transmitters and receivers with the associated antennas and the reflector provide a radio beam capable of modulation over a band of about 30 kc. The multiplex equipment divides this broad band into several narrow bands by a system of frequency division. Each of these narrow bands can be used as a separate communication circuit and all can be used simultaneously. The equipment shown in Figure 2 provides four such bands, but is capable of being extended to seven. Each band can be further subdivided by the use of audio frequency tones to handle telegraphic types of service. The microwave and multiplex equipment is described in more detail in reference 2 of the bibliography.

Relaying

The directional-comparison-distance type[5,6] and the phase-comparison type[8] of "carrier" relaying are both used in this installation. The distance-type relays are connected to protect one of a pair of parallel 25-kv lines between Seward Generating Station and Broad Street Substation, and the phase-comparison relays are connected to protect the other. The Broad Street Substation is located

Paper 50-151, recommended by the AIEE Carrier Current Committee and approved by the AIEE Technical Program Committee for presentation at the AIEE Summer and Pacific General Meeting, Pasadena, Calif., June 12–16, 1950. Manuscript submitted March 14, 1950; made available for printing April 14, 1950.

D. R. PATTISON is with the Pennsylvania Electric Company, Johnstown, Pa. and M. E. REAGAN, S. C. LEYLAND, and F. B. GUNTER are all with the Westinghouse Electric Corporation at East Pittsburgh, Pa., Newark, N. J., and Baltimore, Md., respectively.

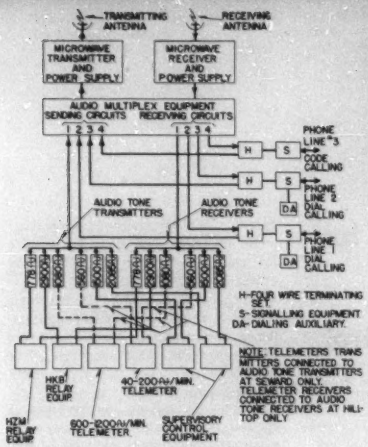

Figure 1 (left). Block diagram of the microwave, multiplex, communication relaying, telemetering, and supervisory control equipment used at the Seward and Johnstown (Hilltop) terminals of the experimental microwave channel. The telemetering transmitters are located at Seward and the receivers are at Johnstown

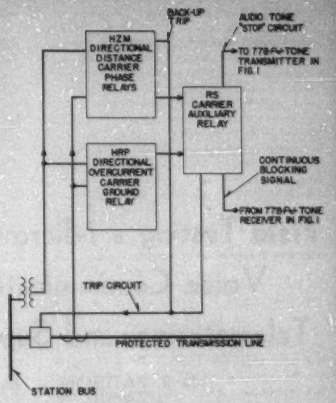

Figure 3 (right). Block diagram of the components to obtain the communication facilities required by a directional comparison, distance type of "carrier" relaying over a microwave channel. Note that under normal system conditions, a continuous blocking signal is present. The relaying equipment operates to "stop" the blocking signal on the occurrence of an internal fault

remote from the microwave equipment; therefore, the control circuits between the relays and the multiplex equipment are carried on underground control wires. In each case the signals required by the relaying system are transmitted and received on audio tones operating in conjunction with one of the subcarriers in the audio multiplex equipment, and the subcarriers in turn operating the microwave transmitter-receiver.

The units involved for the directional-comparison-distance type of carrier relaying are shown in block diagram in Figure 3. In this case the audio tone is transmitted continuously during normal power system conditions thereby providing continuous restraint on the receiver relay. The phase and ground relays are arranged to stop the tone transmission on the occurrence of an internal fault. This is the equivalent of a "continuous" carrier scheme as contrasted with the "intermittent" carrier scheme used in conventional carrier relaying applications. A means of continuous supervision of the channel for transmitting signals required by the relays is provided by this method of operation. The transmission of a continuous signal also eliminates the necessity for the relays to start a blocking signal on external faults, and it is therefore, not necessary to set the third zone of the distance relays to "look out" of the protected line section as required of an intermittent carrier scheme. Loss of the blocking signal under normal system conditions would not result in an incorrect tripout, as the phase and ground relays supervise tripping, and would not operate unless a fault existed on the system within their setting range. Backup tripping for phase faults is included in the phase relays. Backup ground relays were not provided for the test.

The phase-comparison system of relaying,[8] when used over a microwave channel is shown in the block diagram of Figure 4. The signals required by this relaying system also are handled on an audio tone. Since this is an

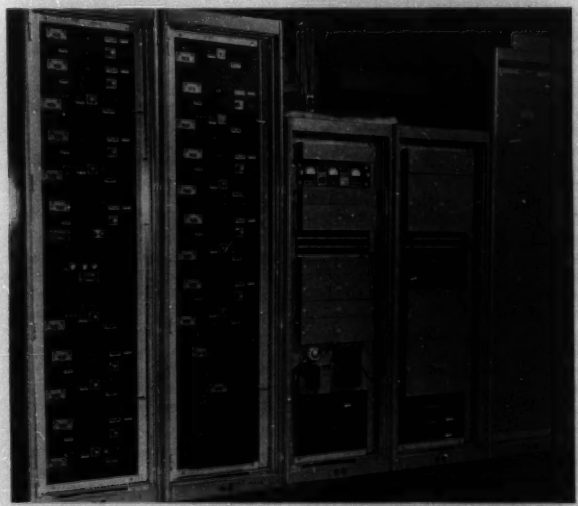

Figure 2. The microwave and multiplex equipment and the power supply components at Seward Generating Station. The two left-hand cabinets contain the audio-tone equipment, the next cabinet contains hybrids and signalling equipment, the next contains the frequency division equipment, and the cabinet on the right contains the microwave transmitter, receiver, and power supply units

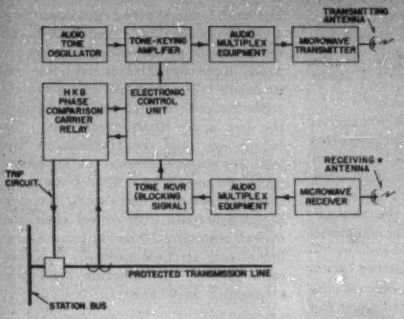

Figure 4. Block diagram of the components to obtain the communication facilities required by a phase-comparison type of "carrier" relaying over a microwave channel. This is an intermittent system with the relaying intelligence, being carried over a 2,900-cycle audio-tone channel

"intermittent" carrier system, signals are transmitted only when a fault occurs on the power system. In addition, the blocks of "carrier" required for operation of this system must be transmitted at the power frequency. To accommodate this keying speed, a 2,900-cycle tone is used, and the control of this tone by the relays is through an isolating amplifier. Using this relatively low frequency to carry the relaying signals, resulted in a phase shift of about 55 degrees (60-cycle-per-second basis) in the received blocking signal and required the use of a delay filter in the circuit controlling the operating voltage of the relay. In other words, on an external fault, the half cycle block of "carrier" initiated at one end of the protected line to block the opposite end from tripping, after going through the receiving equipment would be 55 degrees behind the half cycle block of operating energy and depending on the phase position of the fault currents. This 55-degree shift could result in an incorrect operation on either an internal or an external fault.

Proper co-ordination of the relays for both the directional-comparison and phase-comparison systems using audio tones as the means of transmitting the necessary intelligence has been thoroughly checked on an artificial transmission line in the laboratory. Confirmation of these results is expected in the field experience which will be gained from this installation.

Staged fault tests are being planned to check the performance of the relaying equipments.

The two sets of relays for protecting one end of the two 25-kv lines are mounted on a common panel, Figure 5, along with the conventional-impulse-rate type of telemetering transmitter. A transmitter for an experimental frequency-type telemetering system is mounted on the rear of the panel.

Telemetering

Impulse-rate (frequency) type telemetering,[6,7] of two kinds is used in the trial installation. The impulse-rate type telemeter operating over a range of 40 to 200 impulses per minute is one kind, and an experimental electronic impulse rate (or frequency) system operating over a range of from 600 to 1,200 impulses per minute (10 to 20 cycles per second) is the other kind. As shown in Figure 1, the former is operating over a 560-cycle audio-tone channel, and the latter over a 1,080-cycle channel. The telemetering transmitters key the audio tone transmitters, and the telemetering receivers are fed from the audio tone receivers. Both transmitters are located at Seward Generating Station and the receivers are at Johnstown.

Supervisory Control

Two types of supervisory control systems[8,9,10,11,12] are used in this trial installation. One is the standard Visicode system and the other is the revertive pulse type as described in reference 12. Both are all-relay systems which provide for the control of any required number of individual pieces of equipment. The relays originate and receive impulses in coded groups to select the equipment to be controlled, to perform the operation, and provide an indication that the operation has taken place. Indications are also provided in the event of automatic operation of equipment.

One of the actual equipments used is shown in Figure 6, and consists of an 8-point assembly. This unit is used to control six 25-kv circuit breakers at Seward and to provide telemetering of a-c volts and a-c amperes from Seward to the dispatcher's office. Reference to Figure 1 shows the supervisory control equipment operating over 1,500- and 2,085-cycles-per-second audio-tone channels. In general, any tone frequency within the audio spectrum may be used; however, the speed of pulsing may make some frequencies at the lower end of the band undesirable.

Supervisory control has been used previously in conjunction with microwave equipment on an experimental installation made in 1943 on a frequency of 53 megacycles.[3] In this installation direct keying of the high frequency was used, as contrasted with the use of an audio tone channel working through audio multiplex equipment in the present installation.

Selection of Microwave Antenna Sites

The selection of antenna sites required considerable study, since microwave equipment requires a line-of-sight transmission path from the transmitting antenna to the receiving antenna. In addition, in order to eliminate serious fading the line-of-sight path should clear all obstacles by at least 50 feet. The topography between Johnstown and Seward showed that the line-of-sight path between the system operations office and the Seward plant goes about 1,000 feet underground. This ruled out the use of a direct path between the two points. Study of the terrain and charts indicated that a line-of-sight path did exist from a 200-foot tower at the Hilltop Substation near Johnstown (Figure 7) to a property at Armagh which was about $2^1/_2$ miles from the Seward plant. Further investigation of maps and terrain located a relatively inaccessible knoll which had line-of-sight paths to both Hilltop and the Seward plant. A repeater station located at this point would have satisfactory path clearance to both terminals. However, the lack of an available source of power, and inaccessibility of this location in bad weather led to the consideration of a reflector instead of an electronic repeater. Since there was no previous information available upon which to base a decision as to the practicability of the reflector, a mathematical analysis and field test program were laid out to prove the application.

Mathematical Analysis of Transmission Loss

The free space transmission loss of microwave energy over a given path can be calculated from formulas[13] derived to determine the maximum range over which a signal of a certain strength could be received from a transmitter of a given

power. For convenience these formulas have been rearranged as follows:

$$\text{Free space transmission} = 10 \log_{10} \frac{P_T}{P_R} \quad (1)$$

where

$$\frac{P_T}{P_R} = \left(\frac{4\pi R_0}{\sqrt{G_T G_R}\, \lambda} \right)^2 \quad (2)$$

and

$$G = \frac{4\pi A_{eff}}{\lambda^2} \quad (3)$$

where transmitting and receiving antennas are identical, equation 2 reduces to

$$\frac{P_T}{P_R} = \left(\frac{4\pi R_0}{G\lambda} \right)^2 \quad (4)$$

where

P_T = transmitter power in watts
P_R = received power in watts
R_0 = distance between antennas in meters
G_T = gain of transmitting antenna
G_R = gain of receiving antenna
λ = wavelength in meters
G = antenna gain
A_{eff} = approximately one-half of the projected area of the antenna in square meters

The total loss between a transmitter output and a receiver input includes other factors in addition to the free space transmission loss. In planning an application, allowance must be made for fading and also transmission line (in this case coaxial cable) losses between the equipment and the antennas.

The amount of fading that can be expected is a function not only of the amount of clearance obtained along the transmission path, but also of the weather. Fading is most severe during the summer months. Based on data previously taken[14] a fading loss figure of 1/2 decibel per mile is used for planning 940-to-960-megacycle installations, and this much fading is expected to occur only 1 per cent of the time. Transmission line (coaxial cable or the equivalent) loss depends on the type of transmission line and its length. The total loss for a given installation can be predicted by adding: the free space transmission loss; the fading loss; and the transmission line loss. For example, assume two 950-megacycle equipments with 42-inch diameter antennas located 20 miles apart, having a line-of-sight path with 50-foot clearance over all obstacles, 100 feet of transmission line at each terminal using *RG-17/U* coaxial cable. The following maximum attenuation would exist:

	Decibels
Free space transmission loss	87.1
Fading loss 20 miles × 1/2 db/mile	10.0
Transmission line loss	8.0
	105.1

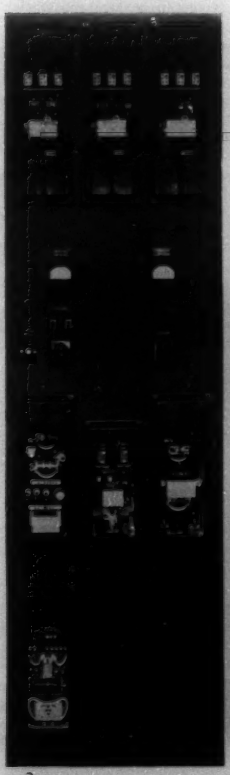

Figure 5 (left). Switchboard panel at the Seward Station on which the relays for the distance-type and phase-comparison type of carrier relaying are mounted. A conventional impulse rate telemeter transmitter is mounted at the lower left, and an experimental electronic telemeter transmitter is mounted on the rear of the panel

Figure 6 (below). Supervisory control equipment located in the Seward Generating Station. Dispatching equipment of similar appearance is located at Hilltop Substation. Six circuit breaker control stations and two telemetering points are being used

Figure 7 (right). The 200-foot high frequency-modulation radio tower at Hilltop Substation, showing the microwave transmitting and receiving antennas mounted about three quarters of the way up

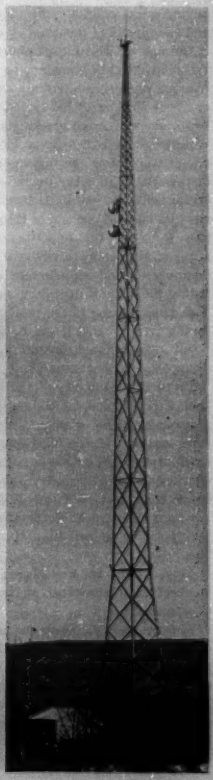

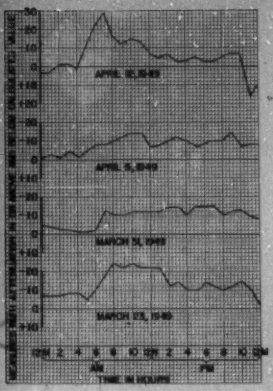

Figure 8. A comparison of the measured and calculated path attenuation between Armagh and Hilltop. The distance is 11.3 miles, frequency 955.5 megacycles, and the antenna gain 58. Levels above the zero line represents lower losses than the calculated values

Figure 10. The temporary reflector at Armagh used to check the calculations. The dish antenna on the left-hand pole was used in obtaining the data for Figure 8. The garage at the left was used to house the terminal equipment, and a temporary power line was constructed to supply the power for the equipment

These losses can be decreased by any or all of the following:

1. Increasing size of antennas, 2. Using lower loss transmission line. 3. Mounting the equipment closer to the antennas.

Where the loss between two terminals exceeds the permissible ratio between transmitter power output and minimum receiver input power, the transmitter output power can be increased or repeater stations installed. Where no line-of-sight path exists, reflectors can be used if the additional loss caused by the reflection does not increase the path loss beyond the maximum permissible attenuation for the equipment being used.

The increase in path transmission loss caused by the use of reflectors also can be calculated. In making calculations involving the use of reflectors, it is assumed that a plane reflector acts in the same manner as two parabolic antennas having areas equivalent to the projected area of the reflector in the two directions. The path loss can then be calculated by applying equation 2 twice: first, between the transmitter and the reflector to determine the equivalent amount of energy received at the reflector; and second, between the reflector and the receiver assuming that the reflector acts as a transmitter.

For a single reflector, equation 2 can be expanded to give directly the ratio of transmitter power to receiver input power as follows

$$\frac{P_T}{P_R} = \left(\frac{16\pi^2 R_1 R_2}{\sqrt{G_1 G_2 G_3 G_4}\,\lambda^2}\right)^2 \qquad (5)$$

where

R_1 = distance from transmitter to reflector in meters
R_2 = distance from reflector to receiver in meters
G_1 = gain of transmitting antenna
G_2 = equivalent gain of reflector in direction of transmitter
G_3 = equivalent gain of reflector in direction of receiver
G_4 = gain of receiving antennas
λ = wavelength in meters

The foregoing equations were used to calculate the expected loss with a reflector between Hilltop and Seward. From equation 5 the loss was calculated to be 115 decibels. This corresponds to the zero levels shown in Figure 8. The calculations also showed that a 20-foot square reflector would be required to meet this figure of 115 decibels. This would provide adequate margin of safety over the permissible path loss of 125 decibels with the type of microwave equipment being used. However, before proceeding with

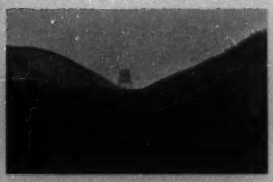

Figure 9. A view from the temporary reflector location at Armagh looking toward Hilltop substation. The tower in Figure 7 is at the center of the notch between the two hills in the center background. The permanent reflector is shown

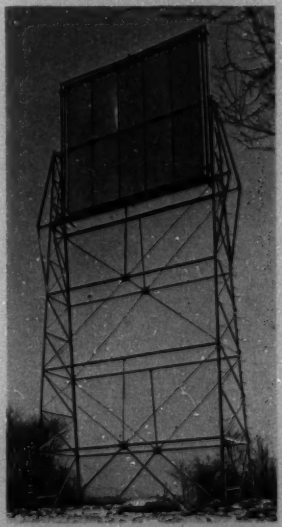

Figure 11. The permanent reflector. This is a rear view of the reflector looking toward the Hilltop Substation. This design is capable of withstanding 100-mile-per-hour winds or 60-mile-per-hour winds with ice coating which closes the perforations in the reflecting surface

a permanent installation of a reflector, it was decided that a test program would be carried out to determine the variation in signal strength at the reflector location, and try out a temporary reflector 20-feet square to check the calculations.

A microwave transmitter-receiver assembly was installed at Hilltop Substation and another at Armagh with recording voltmeters indicating received signal strength at Hilltop. Continuous recordings of field strength were made for a 6-week period. These data were converted into terms of the total attenuation between transmitter output and receiver input and an analysis made taking readings once an hour for the period.

A comparison between the measured data and the transmission loss calculated from the foregoing equations was made using measured values for coaxial cable losses. The following conclusions were reached:

1. That the measured path attenuation did not exceed the calculated data for more than 0.99 per cent of the hours during which data was taken. This calculated data included an allowance for fading of 1/2 decibel per mile of path.

2. That the measured path attenuation did not exceed the calculated data for more than 3.87 per cent of the time if no allowance is made in the calculated data for fading.

3. That although the maximum attenuation figures were not greater than would be expected from the calculations, the minimum attenuation figures were considerably less than would be expected.

The signal strength was found to vary considerably during a day. A plot of the hourly variation for several typical days during the test period is shown in Figure 8. The average level at the receiver was considerably greater than expected and fading about this average level was also greater than expected. The wide variations due to fading were attributed to multipath transmission of signals to the receiver, with alternate cancellation and reinforcement, possibly due to the terrain, Figure 9, as the several signals went in and out of phase.

Based on the calculated data it appeared feasible to use a reflector to get the signal to Seward, providing 6-foot diameter antennas were used at each terminal.

The first step in the reflector test program was to install a receiver and a 42-inch receiving antenna at Seward to determine if a signal reflected from natural surfaces was being received from Hilltop. In a series of tests made over a 2-day period, no measurable signal was received from any direction or at any polarization. Next a signal was transmitted from the Armagh transmitter and the signal level was checked at Seward. The measured loss was quite high indicating that line-of-sight did not exist, even though a study of the topographical maps had showed clear line-of-sight. It was decided, however, to install the temporary reflector, Figure 10, at Armagh and check the reflected signal level at two points on the highway where line-of-sight to the reflector could be obtained. This necessitated mounting the receiving equipment in a light truck equipped with a motor generator set so that readings could be taken at the side of the highway. The following results were obtained:

1. The measured beam width of the energy reflected from the screen was 2.4 degrees.

2. The total measured path attenuation to a point 2.75 miles away from the reflector (total path 14.05 miles) was approximately 115 decibels which is 10 decibels less than the maximum permissible with the type *FB* equipment.

3. Additional tests were made at a point 3.75 miles from the reflector where the maximum attenuation was approximately 133 decibels. Under these conditions voice

Figure 12. Topographical and contour map of the microwave path from Johnstown to Seward via the permanent reflector at Armagh. The location of the temporary reflector also is shown

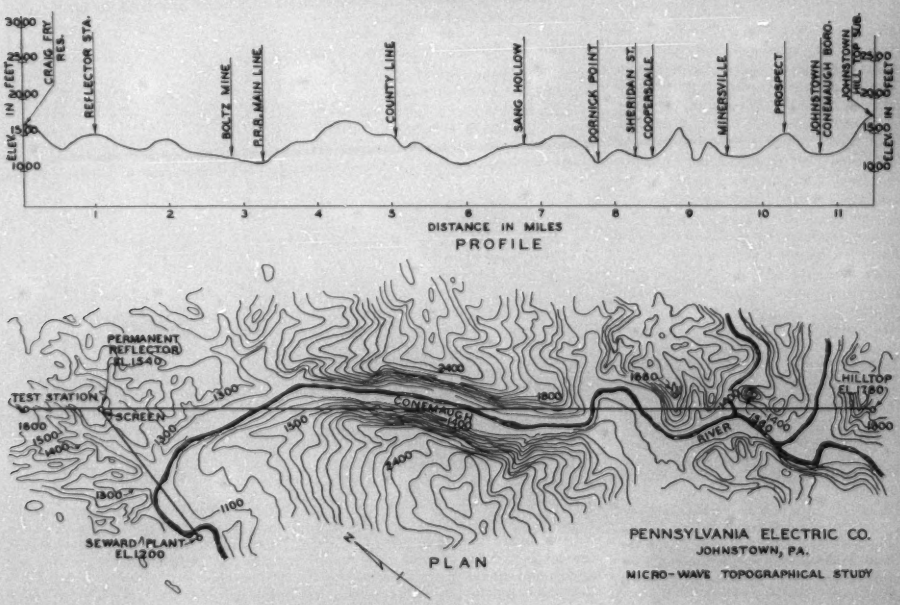

communication over the circuit was very good, with slight noise in the background.

Based on the foregoing calculations and field data, it was decided to install a permanent reflector made of perforated sheet aluminum. This reflector is shown in Figure 11. It is mounted in a different location than the temporary reflector of Figure 10, and has a clear line-of-sight path to both Hilltop and Seward as shown in Figure 12. The tower support is 60 feet high and the center of the 20-foot square reflector is 50 feet from the ground. The reflector and tower are designed for use in 100-mile-per-hour winds and in 60-mile-per-hour winds with ice coating which close up the perforations. Because of the sharp beam of energy reflected from a surface of this size, it is of utmost importance that the reflector be positioned so a perpendicular to its center bisects both the vertical and horizontal angles subtended by the antennas at the terminal stations. For ease of this adjustment the reflector is mounted in gimbals, which permit it to be moved as much as ±10 degrees in both vertical and horizontal planes.

Results of Tests to Date

During the test period it has not been necessary to replace any tube on an emergency basis. No internal defects have developed such as a short circuit between tube elements or an open heater.

The experience to date on tube life is not conclusive; however, indications are that satisfactory life will be obtained. The microwave portion of the equipment has been operating continuously since February 1949, and replacement of tubes has been at about the same average rate as for power line carrier and mobile radio equipment. There have been no component failures. The multiplex equipment has been in operation since August 1949 with similar experience.

A direct lightning strike on the tower at Hilltop had no effect on the operation of the microwave equipment. Operation was not affected during the worst conditions of weather including heavy snow, sleet, and rain, indicating that sufficient margin of safety has been used. It is interesting to note that the maximum variation in path attenuation occurs on clear days in the morning and evening hours, and this is apparently the result of temperature inversion.

Data on noise and crosstalk, and distortion on the three telephone channels obtained by the microwave and the audio-multiplex equipment is given in Table I.

Table I

	Noise and Crosstalk, Decibels Below 1 Milliwatt	Distortion
Telephone channel Number 1	−41	Less than 1 per cent
Telephone channel Number 2	−40	Less than 1 per cent
Telephone channel Number 3	−43	Less than 1 per cent

The audio response of the three multiplexed channels is not over 6 decibels down from response at 1,000 cycles at 250 cycles and at 2,800 cycles.

Conclusions

The microwave and multiplex equipment have proved entirely satisfactory for service on power systems where reliability of performance is most important. Tube life in tests to date has been equivalent to that encountered in other electronic equipment used by power companies. As a result of the tests, plans are being made to permanently control the entire Seward Station switchyard from the load dispatcher's office at Johnstown using this microwave channel. When this is done a diesel-engine-driven generator will be provided at each terminal for emergency power.

The experience gained in the use of the reflector to provide a dog-leg path opens up an entirely new field of application possibilities for microwave channels. It is, however, desirable to check calculations and data taken from topographical maps by actual field measurements.

The type of reflector (powerless repeater) used in this installation eliminates the need for a power supply and therefore can be located in places which are physically difficult to get at.

The measured path losses were close enough to the calculated values to show that the formulas used are entirely practical for use in studying microwave applications.

Staged fault tests are planned to check the performance of the relaying equipment. Also the continuing test program anticipates a thorough check of the telemetering and supervisory control equipment.

The reliability of performance of the equipment on the tests opens up the possibility of using a microwave channel as the means of obtaining a transfer-trip type of protective relaying.

References

1. Microwave Channels for Power System Applications, AIEE Committee Report. *AIEE Transactions*, volume 68, part I, 1949, pages 40–43.

2. A Low Noise and Distortion Audio Multiplexing Equipment with High Stability Carrier Source, F. S. Beale. *AIEE Transactions*, volume 69, part II, 1950, pages 1028–38.

3. A Distance Relay with Adjustable Phase-Angle Discrimination, S. L. Goldsborough. *Electrical Engineering* (*AIEE Transactions*), volume 63, November 1944, pages 835–38, 1471.

4. A New High-Speed Distance-Type Carrier-Pilot Relay System, E. L. Harder, B. E. Lenehan, S. L. Goldsborough. *Electrical Engineering* (*AIEE Transactions*), volume 57, January 1938, pages 5–10, 291–94.

5. A New Carrier Relaying System, T. R. Halman, S. L. Goldsborough, H. W. Lenzner, A. F. Dromp. *Electrical Engineering* (*AIEE Transactions*), volume 63, August 1944, pages 568–72.

6. An Improved High Rate Impulse Telemeter System, C. Oman. *Electric Journal* (East Pittsburgh, Pa.), August 1934, page 313.

7. A Telemeter Transmitter Without Moving Contacts, C. Oman. *Westinghouse Engineer* (East Pittsburgh, Pa.), May 1948, page 92.

8. A Self-Checking System of Supervisory Control, M. E. Reagan. *Electrical Engineering* (*AIEE Transactions*), volume 57, October 1938, pages 600–05.

9. Channels for Operation of Supervisory Control Equipment, W. A. Derr, M. J. Brown. *AIEE Transactions*, volume 67, 1948, pages 1654–60.

10. By a Flick of the Finger (Supervisory Control), W. A. Derr. *Westinghouse Engineer* (East Pittsburgh, Pa.), November 1949, page 162.

11. The Combination of Supervisory Control with Other Functions on Power Line Carrier Channels, R. C. Cheek, W. A. Derr. *Electrical Engineering* (*AIEE Transactions*), volume 64, May 1945, pages 241–46.

12. A New Two-Signal Synchronous Supervisory Control System, W. A. Derr. *AIEE Transactions*, volume 68, part II, pages 857–63.

13. Propagation of Very Short Waves, D. E. Kerr. *Electronics* (New York, N. Y.), January 1948, page 124.

14. Microwave Propagation Tests over 40 Miles Overland Path, A. L. Durkee. *Proceedings*, Institute of Radio Engineers (New York, N. Y.), February 1948, page 200.

Discussion

R. H. Miller (Pacific Gas and Electric Company, San Francisco, Calif.): This paper is of particular interest due to the fact that it presents actual problems that were met in the establishment of a microwave communication system. The most unusual feature of the system described is the use of an inert repeater for completing a microwave path that does not provide line of sight. The successful use of this technique opens up many possible applications for such systems at locations that have previously been considered impracticable.

The microwave system discussed is very representative of the applications that are

of interest to power utilities in that voice, telemetering, supervisory control, and relaying channels were all provided.

The results of the tests, as discussed by the authors, indicate a high degree of reliability. The question is raised as to whether or not, where such a concentration of important communication and control channels are operated over a single link, duplicate microwave equipment with automatic transfer might be justified. It is also noted on Figure 8, the comparison of measured and calculated path attenuation that all of the data indicated was taken in a period of approximately one month. It would be of interest to know whether or not further measurements have been made to determine if there are seasonal variations in the microwave propagation properties.

O. A. Starcke (Kansas City Power and Light Company, Kansas City, Mo.): The authors are to be congratulated upon a concise yet complete report of a field test of a microwave channel. Present-day microwave theory, experience with similar multiple channels on carrier equipment, and laboratory tests of the microwave equipment itself, indicate that a multiple-use channel should operate successfully and reliably. The reasonably close check between the actual experimental results and calculated performance is a big boost in our confidence of our ability to forecast what microwaves will do in actual practice. However, since such an installation is expensive and the ultimate of reliability is required, it is believed that a test should be made of the transmission path before installation. It is believed that a test equipment of this nature could very easily be made available by the manufacturer for such testing purposes as a readily portable type of equipment.

The use of a reflector to cover a dog-leg path between the transmitter and receiver is an important contribution and should extend the use of microwave equipment considerably. It is particularly encouraging to find that the operation of such a reflector could be forecast with a reasonable degree of accuracy.

One of the great drawbacks to the rapid application of microwave equipment since the war has been the fact that military secrecy delayed or withheld the publication of the large amount of data accumulated on microwave transmission during the war years. The data is not always applicable since it was obtained primarily for predicting radar performance which usually depends upon the reception of reflected pulses of energy from various targets instead of direct reception of continuous waves. Publication of tests of the kind described in this paper will go far toward relieving the shortage of information on microwave operation.

D. R. Pattison: I wish to thank R. H. Miller and O. A. Starcke for their discussion of the subject paper. In closing this paper I would like to emphasize the following points:

Mr. Starcke comments on the lack of data on microwave performance. As he has pointed out, there has been very limited published data regarding the performance of microwave equipment. The data regarding the practical application of multichannel microwave equipment would no doubt be entirely different than that experienced by the radar application, primarily due to the wide band as applied in our communication application. Although the formulas used by us in our investigation have been published for quite some time, we still feel they are sufficiently accurate to predict actual performance.

I wish to emphasize the statement made in the paper regarding routing of microwave channels. Very little dependence can be put in United States geographic maps and actual line-of-sight survey should be carried out as suggested in the paper.

In answer to Mr. Miller's comment, we do believe that the reliability of such microwave channel does justify our reliance in such a system for the operation of this important equipment. We have considered the installation of duplicate equipment and the automatic transfer feature. However, to date we have not been able to justify it. Experience will eventually indicate whether the duplicate equipment is necessary or not.

It is true that our comparisons were taken over a period of approximately one month. However, we have made a continuous record of the channel performance. Although a distinct improvement has been made in the performance by the use of voltage regulation, larger dishes and proper focusing, the curves as shown on Figure 8 are fairly indicative. We are continuing to collect this data and no doubt it will be available to those who are interested.

Proposed Basic Impulse Insulation Levels for High-Voltage Systems

J. E. CLEM
FELLOW AIEE

J. R. MEADOR
MEMBER AIEE

W. J. RUDGE
MEMBER AIEE

A. H. POWELL
MEMBER AIEE

SINCE the establishment of basic impulse insulation levels (BIL)[1] there has been essentially no change in the values up to the present time. On the other hand, there have been improvements in the method of operating systems, increased knowledge of the lightning discharges, and better understanding of the surge behavior of apparatus and its insulation. Several industry committees are at present investigating the factors which determine the BIL. It is in the hope of successfully culminating a part of this work that this paper is being presented. Since the greatest need for a review in the industry at present is associated with the transmission voltages 115 kv and above, this paper is confined to the BIL applying to these voltages.

Object

The purpose of this paper is to make an evaluation of the essential factors upon which the selection of BIL can be based, and to propose a series of BIL for adoption by the industry, based upon these considerations.

The Factors

It generally is recognized that the principal factors to be evaluated in the establishment of BIL are: nominal system voltage; system neutral grounding; lightning-arrester rating and performance; lightning-arrester location and system arrangement; impulse strength of equipment; and required margin.

Nominal System Voltage

The Joint Edison Electric Institute–National Electrical Manufacturers Association Report on Preferred Voltage Ratings for A-C Systems and Equipment[2] gives the results of an industry survey of system operating practices and sets the nominal and maximum tolerable zone voltages. The maximum voltage of the tolerable zone was used as a basis for this study.

A review of the general problem of impulse insulation levels indicates that the circumstances and conditions pertaining to the required impulse insulation levels are different in the distribution range of voltages of 15 kv and below than in the subtransmission range of 15 kv to 69 kv inclusive, and that both of these are different than in the high-voltage transmission range of 115 kv and higher. In this paper only the high-voltage transmission range is considered.

System Neutral Grounding

Part II of Present-Day Grounding Practices on Power Systems[3] which covered a total of 567 systems, shows that of the companies reporting nearly 100 per cent of power systems 115 kv and above are operating with neutrals grounded and that 95 per cent of these are "effectively grounded" according to the commonly accepted definition.[5,12] In Table XIX of the report[3] it may be seen that for circuits rated 93 kv to 165 kv most systems have X_0/X_1 ratios less than three, although there are a few in which the ratio goes as high as four. Above 166 kv the systems have ratios ranging from zero to one. Of the effectively grounded systems having circuit voltages 93 kv and higher, only one had an R_0/X_1 ratio in excess of one, and that did not exceed a ratio of two. Since this is the practice, it is logical for standardization purposes to select lightning-arrester ratings based on grounded-neutral operation.

It may be necessary to use higher lightning-arrester ratings and insulation levels at nongrounded substations which may be removed from the grounded portion of the system.

Selection of Lightning-Arrester Rating

As is indicated in reference 3, for circuit voltages of 115, 138, and 161 kv the systems are effectively grounded, and hence the rating of the lightning arrester can be 80 per cent of the line-to-line voltage. For these systems the voltage on the two unfaulted phases will not rise over the line-to-neutral voltage for the case of single line-to-ground faults by more than 40 per cent. While this rise in voltage may be lowered in some cases where lightning arresters are located at the transformers, it should be recognized that for lightning arresters located on the line side of a circuit breaker in the open position the conditions may be such as to require the full 80-per cent rating for the lightning arrester. There may also be cases for which the full 80-per cent lightning-arrester rating is required for transformers. Hence, the 80-per cent lightning-arrester ratings were chosen for this study for systems operating at voltages of 115, 138, and 161 kv.

For system voltages of 230 kv and up, however, the X_0/X_1 and R_0/X_1 ratios are generally less than for the 115- to 161-kv range, and the overvoltages on the unfaulted phases will not, except in unusual cases, exceed 30 per cent of the line-to-

Paper 50-152, recommended by the AIEE Protective Devices Committee and approved by the AIEE Technical Program Committee for presentation at the AIEE Summer and Pacific General Meeting, Pasadena, Calif., June 12–16, 1950. Manuscript submitted March 10, 1950; made available for printing April 17, 1950.

J. E. Clem is with the General Electric Company, Schenectady, N. Y., J. R. Meador and W. J. Rudge are with the General Electric Company, Pittsfield, Mass., and A. H. Powell is with the General Electric Company, in Philadelphia, Pa.

The authors are grateful for the permission of the Consumers Power Company, Jackson, Mich., to use the heretofore unpublished data on lightning arrester discharge currents included in Figure 1; for the assistance of S. B. Howard of the General Electric Company, Pittsfield, Mass., for the probability calculations in connection with lightning arrester performance; and to several others for their suggestions and comments.

neutral voltage. Therefore, it appears logical to select lightning-arrester ratings for these higher circuit voltages which are 75 per cent of the line-to-line voltage. For circuit breakers at these higher voltages it probably will be necessary to use an 80-per cent lightning arrester, particularly on the line side, although the transformer lightning arrester in the same station can be a 75-per cent one.

The following table of lightning-arrester ratings for the different systems was therefore selected on the basis of even multiples of 3 kv as the minimum increment of rating.

Table I

Preferred Nominal System Voltage, Kv	Maximum Tolerance Zone, Kv	Lightning-Arrester Rating, Kv: Non-grounded Neutral, 100 Per cent Lightning Arrester	Grounded Neutral, 80 Per cent Lightning Arrester	Grounded Neutral, 75 Per cent Lightning Arrester
115	121	120	96	
138	145	144	117	
161	169	168	135	
230	242	240	192	180
288	302	300	240	228
345	360	360	288	270
360	378	378	303	282

Lightning-Arrester Performance Values and Tolerances

At the request of AIEE Standards Co-ordinating Committee Number 8 (Insulation Co-ordination), the arrester manufacturers reviewed their production records to determine if it would be feasible to reduce the maximum tolerance of lightning-arrester performance as given in the report Performance Characteristics of Lightning Protective Devices.[4] The NEMA Lightning Protective Devices Committee, after reviewing the matter, replied that a review of the present-day manufacturing practice and performance values for station- and line-type lightning arresters has shown that the plus tolerances relating to impulse spark-over and discharge voltage drop in the resistance can be reduced by 5 per cent, as shown in Table II.

Table II

Type of Lightning Arrester		New Tolerance, Per cent	Present Tolerance,[4] Per cent
Station:	impulse spark-over	+15	±20
	discharge voltage drop	+10	±15
Line:	impulse spark-over	+20	±25
	discharge voltage drop	+15	±20

Note: These tolerances may also apply to the current wave later discussed in this paper.

In addition to the tolerances shown in Table II, the committee pointed out that approximately 95 per cent of the lightning arresters supplied have performance values which do not exceed the average plus two-thirds of the stated maximum tolerance.

The NEMA Committee recommended that the protective level of the lightning arrester be taken as a value which is the average value plus two-thirds of the stated maximum tolerance.

Lightning-Arrester Discharge Currents in Service

A review of the data obtained in several separate investigations[5,6,7,8] of discharge currents through lightning arresters in stations resulted in the average discharge expectancy curve shown in Figure 1. For the study reported in this paper a crest value of 5,000 amperes was chosen as a reasonable reference base. It will be noted that a discharge current exceeding this value will occur only once in about 70 lightning-arrester years.

A further review of the data from three separate investigations[6,7,9] giving the time-to-crest for currents discharged through lightning arresters in stations resulted in the average expectancy curve, Figure 2. The data did not show any direct or definite correlation to exist between the time-to-crest or rate-of-rise and the crest current, although it was noted that many of the fast rates-of-rise occurred with low crest values of current. The highest recorded rate-of-rise is approximately 5,000 amperes per microsecond[10] (10-per cent and 90-per cent points), and was associated with a crest current of 7,900 amperes. This data was obtained on a 23-kv system which had no ground wire shielding. It appears reasonable from the review of these data to use as the basis for this study a rate-of-rise of 5,000 amperes per microsecond, and to associate with this a crest value of 5,000 amperes. This gives a wave having an effective front of 1.0 microsecond, based on measurements of the time between the 10 and 90 per cent of crest value points.

This choice of 5,000 amperes and 5,000 amperes per microsecond presumes that the overhead line leading into the station, and the station itself, will be protected by overhead ground wires. The ground wires should extend for a distance of approximately $^1/_2$ mile from the station steel.

If it is assumed that the time-to-crest is 1.2 times the time of the effective front it may be seen from Figure 2 that a time-to-crest of 1.2 microseconds, or an effective front time of one microsecond, occurs once in five lightning-arrester years.

Separation Between Lightning Arrester and Transformer

The difference in the voltage at a transformer, or other protected equipment from the voltage at the lightning arrester, when there is some circuit distance between them, has been investigated in several studies.* An evaluation of the effect of the circuit distance is given in the paper by Carpenter, Johnson, and Saline;[11] since this subject is fully discussed there, it is not dealt with at length in this paper. The relation between the lightning-arrester protective levels and proposed BIL is based on using a V-connection, as defined in reference 11, and limiting the separation between the lightning arrester and protected equipment. The circuit distance, or separation, between the lightning arrester and the protected equipment may cause an oscillatory increase in the voltage at the protected equipment above the lightning-arrester discharge voltage. The limiting separations given later are

* See companion paper by Carpenter, Johnson and Saline,[11] and the references therein.

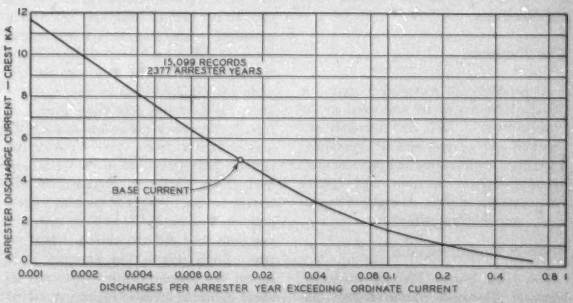

Figure 1. Discharge currents measured through lightning arresters in stations

chosen so that the crest value of the first cycle of the oscillatory voltage at the protected equipment does not exceed the lightning-arrester discharge voltage by more than 30 per cent. These limiting separations are considered representative of single line stations because the analysis upon which they are based considered only an elementary circuit configuration and did not include the effect of a bus or additional incoming lines.

Number and Magnitude of Surge Voltages Applied to Protected Equipment in Excess of the Base Voltage

If the discharge voltages of a station lightning arrester at 5,000 amperes per microsecond and various crest currents are compared with its impulse spark-over voltage (AIEE wave), using average performance values plus two-thirds of the industry maximum tolerances, it is found that the crest value of lightning-arrester discharge currents below 5,000 amperes will produce lightning-arrester discharge voltages less than the lightning-arrester spark-over voltage. Therefore, the maximum lightning-arrester discharge voltage for these discharges will be determined by the lightning-arrester spark-over voltage and will be independent of the crest value of the current.

Conversely, only currents in excess of 5,000-ampere crest will produce discharge voltages in excess of the lightning-arrester discharge voltage chosen for the basis of this study, or as it may be termed, the reference discharge voltage. It was felt that the probability of voltages in excess of the reference discharge voltage should be estimated so that the effect on equipment insulation could be studied. By combining the lightning-arrester volt-

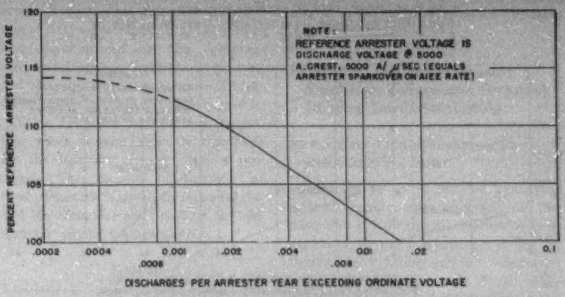

Figure 3. Calculated impulse discharge voltage above reference lightning-arrester voltage at lightning arresters in stations

ampere characteristics with the lightning-arrester-discharge current expectancy curve of Figure 1, the expectancy curve of lightning-arrester discharge voltages shown in Figure 3 is obtained. This curve shows that only a limited number of the lightning-arrester discharge voltages will be above the reference lightning-arrester discharge voltage.

To determine the number of times that these higher voltages will occur at a given lightning arrester, a calculation was made assuming that the discharge current of 5,000 amperes, and the wave front of 5,000 amperes per microsecond, are concurrent and that all currents exceeding 5,000 amperes have the same rate-of-rise. There is no field data to substantiate this, and accordingly it is a very conservative assumption which places the calculated voltages above those expected in service.

For example: for such a calculation it is most convenient to consider a group of 100 single-pole lightning arresters operating over a period of 30 years, or 3,000 lightning-arrester years. From Figure 3 (0.015×3,000) or 45 of the discharges in this 30-year interval will cause discharge voltages higher than the reference lightning-arrester voltage.

Calculations were made to determine the proportional part of the total number of lightning arresters, 100, which might have one, two, or three current discharges during the 30-year period capable of producing a discharge voltage higher than the reference discharge voltage used in this study. The probability expression used is

$$P_m(n) = \frac{e^{-mp}(mp)^n}{n!}$$

where

$P_m(n)$ = probability of n discharges through one unit in m total discharges

m = number discharges (45 above reference lightning-arrester voltage)

$p = \dfrac{1}{\text{number lightning arresters}}$ (0.01 for this calculation)

The calculations show that 29 per cent of the lightning arresters will have one current discharge which will produce a lightning-arrester discharge voltage in excess of the reference lightning-arrester voltage; 6.5 per cent, two such discharges; and less than one per cent, three such discharges in the 30-year period.

The results of similar calculations for 105 per cent, 110 per cent, and so forth, of reference lightning-arrester voltage are shown in Figure 4. These curves show only one lightning arrester out of a hundred might be expected to have one discharge exceeding 114 per cent of the reference lightning-arrester voltage, or three exceeding 100 per cent, over the 30-year period. These factors are considered in selecting the margin later in the paper.

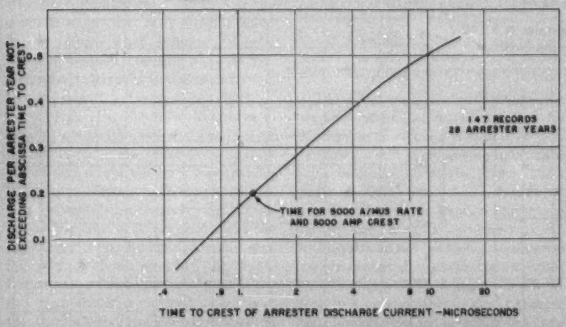

Figure 2. Time-to-crest value of discharge currents measured through lightning arresters in stations

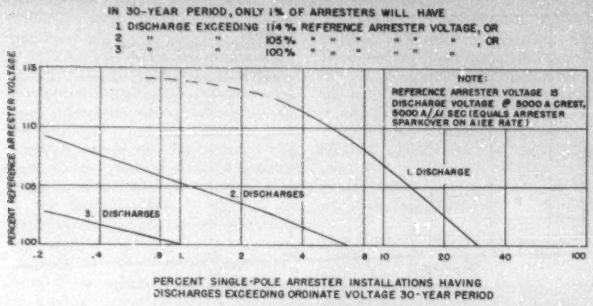

Figure 4. Probability of lightning-arrester discharge voltage exceeding reference lightning-arrester voltage in a 30-year period

Impulse Strength of Equipment

The American Standards Association impulse test on high-voltage transformers consists of a full (1.5×40) wave at BIL value and two waves at 15-per cent higher level chopped in not less than 3.0 microseconds.

A front-of-wave test sometimes is made to demonstrate the volt-time turn-up of the transformer insulation. Test results show[13] that the impulse puncture strength of the major insulation used in transformers is constant from about 3.0 microseconds to several hundred microseconds or more. For shorter times the impulse strength increases. At 0.5 microsecond the breakdown is about 50 per cent greater than 3.0 microseconds. This volt-time relationship, which has been used to determine the front-of-wave test for transformers in the NEMA Transformer Standards, is shown as Curve 1 in Figure 5.

Other parts of the transformer, such as oil spacings, creepage paths, and so forth, have other volt-time curves. However, the minimum envelope of these curves tends to follow a volt-time curve similar to Curve 2 in Figure 5. Thus, the over-all transformer volt-time curve can be represented best by a composite broken curve going from 0.5 microsecond to 3.0 microseconds along Curve 1, and from 3.0 microseconds to longer times along Curve 2. The plotted points represent the ASA full-wave and chopped-wave tests. The exact point along Curve 1 for showing the NEMA front-of-wave test depends on the insulation test level of the transformer, since this test is made with a voltage rising at approximately 1,000 kv per microsecond. All transformers designed to meet the ASA impulse tests are also designed for this front-of-wave test.

The impulse insulation strength of switchgear is usually checked, when required, by full-wave impulse withstand tests at BIL value. During the design and development of power circuit breakers, chopped-wave tests also are made. These tests are made at values 35 to 50 per cent above the full-wave withstand values. However, as switchgear equipment contains no windings, the magnitude of the test voltage is of more importance than the rate of change of the voltage wave.

Effect of Superimposed Frequency Oscillations on Transformer Insulation

Since the circuit separation between the lightning arrester and the transformer results in a high-frequency oscillation being superimposed upon the voltage wave which appears at the transformer terminals, it is necessary to determine the effect such a voltage would have on the transformer insulation. Since the superimposed oscillations are of very short duration, relative to the 1.5×40 microsecond test wave, it is apparent from Figure 5 that the Curve 1 portion of the transformer volt-time curve will be most affected by them. A few spot tests have indicated that insulations of the type represented by Curve 2 are not appreciably affected by them.

To get an estimate of the effect of these oscillations on transformer insulation, samples having a volt-time curve similar to Curve 1, Figure 5, were selected for these tests. These samples consisted of heavily-insulated conductors taped together and immersed in oil. When tested with smooth 1.5×40 waves the curve in Figure 6 was obtained. The similarity to Curve 1, Figure 5, is apparent.

Similar samples were tested with 1.5×40 (negative polarity) waves having damped superimposed high-frequency oscillations. There were three variables in

Figure 5 (below). Transformer volt-time curves

Figure 6 (right). Volt-time curve of insulation samples (1.5×40 negative polarity) representative of transformer major insulation

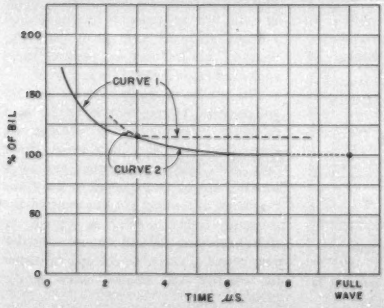

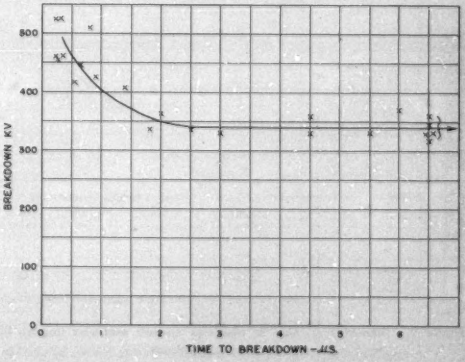

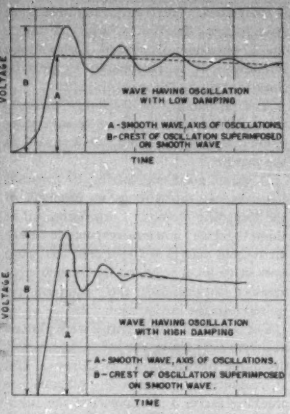

Figure 7. Representative voltage waves used for tests on insulation samples

addition to the magnitude of the 1.5×40 wave: a. period of oscillation; b. degree of damping; c. per cent "overshoot" of the oscillation. Typical voltage waves are shown in Figure 7. The test results are shown in Figure 8. The points are plotted to show how much, for equal severity on the insulation, the magnitude of the smooth 1.5×40 wave upon which the oscillations are superimposed must be reduced as the magnitude of the superimposed oscillation (overshoot) is increased. On the assumption that these insulation samples are reasonably representative of transformer major insulation, a significant conclusion can be drawn.

From Figure 5 it is apparent that transformer major insulation puncture strength will withstand a full wave at the chopped-wave level. The problem, then, is to determine what oscillations can be superimposed on the full wave at the BIL value to have the same destructive effect as a smooth full wave at the chopped-wave level. On Figure 8, the curve is drawn through the minimum points to be conservative. This curve goes through 87-per cent magnitude for a wave having 30-per cent overshoot. The conclusion is that a damped high-frequency oscillation, whose first crest is 30 per cent above the smooth wave, may be superimposed on the full wave without stressing the transformer major insulation to a greater extent than the ASA chopped wave, since the ASA full-wave test is 87 per cent of the chopped-wave test. For this reason the permissible separation between lightning arrester and transformer used in this selection of BIL was so chosen that the oscillation superimposed on the lightning-arrester voltage was limited to 30 per cent and therefore would not require the addition of any insulation to take care of it.

Table III gives the maximum separation which is permissible on this basis for the lightning-arrester ratings proposed. The method of arriving at these distances is given in reference 11, and the distances are based on the elementary circuit configuration.

Table III

Lightning-Arrester Rating, Kv rms	Number of 12-Kv Units	Maximum Separation, Feet
96	8.0	9
117	9.75	15
135	11.25	20
180	15.0	38
238	19.0	72

Ratio of Single to Multishot Strength of Transformer

It is necessary to evaluate the long-time strength of transformers that are periodically subjected to transient voltages. A carefully considered answer must weigh several factors, some of which are:

A. Laboratory investigations of the effect of repeated applications of impulse voltages are, of necessity, compressed into a relatively short period of time. A transformer in service may be subjected to only one or two high-impulse voltages in one year, thereby having long-time intervals to recover. Therefore, the ratios of single-to-multishot strength determined from laboratory test results probably are not directly indicative of the multistrength of the transformers when in service.

B. During factory impulse testing, transformers are sometimes subjected to many times the required number of impulse voltages and it is extremely rare for these additional applications of voltage to cause failure.

C. If a transformer being tested is near breakdown, this condition is often detectable by modern, sensitive testing technique.

These factors tend to deprecate the need for additional margin to allow for repeated application of voltage in service. However, a strong argument can be made for a multishot allowance. Since it is a known fact that some transformers fail as a result of a single impulse during the factory test, it cannot be said that the units which do not fail have an additional margin of strength to enable them to withstand a large number of impulses. Therefore, it is unreasonable to expect that all transformers passing the factory test have multishot strength. For this reason some margin is necessary between the protective level and the demonstrated strength of the transformer.

Reference Lightning-Arrester Discharge Voltage and Required Impulse Insulation Levels

Reference Lightning-Arrester Discharge Voltage

Since the published data on lightning-arrester performance are given on the basis of a 10×20 microsecond wave, it is necessary to use a correction factor to derive the lightning-arrester discharge voltage for a different wave shape. This point was brought up for discussion at the meeting of an AIEE Subcommittee of the Protective Devices Committee, and the manufacturers stated that the crest value of discharge voltage for a 5,000-ampere, 5,000-ampere-per-microsecond discharge current is approximately the same as the crest value of the discharge voltage for a 10,000-ampere 10 × 20 discharge current. On this basis the reference lightning-arrester discharge voltage, or protective level, for station-type lightning arresters of representative voltage ratings, on the basis of a 5,000-ampere discharge current, is as shown in Table IV.

Discharge voltages are for a current discharge having a crest value of 5,000 amperes. These values are shown on Curve A, Figure 9.

By using the method contained in ASA Standards Z1.1, Z1.2, and Z1.3[14,15,16] it can be shown that as lightning-arrester units are stacked in series the effective plus tolerance for the entire stack is decreased with the number of units in

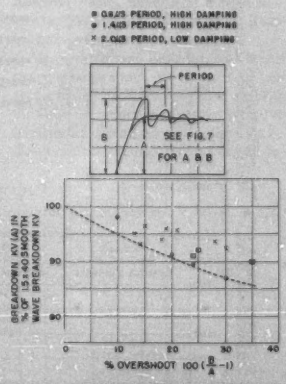

Figure 8. Effect of superimposed oscillations on strength of insulation samples

the stack, and that the discharge voltage then is given by the equation

$$E_d = E_a N\left(1+\frac{0.067}{\sqrt{N}}\right)$$

where

E_d = Minimum reference lightning-arrester discharge voltage
= Minimum protective level

E_a = Average lightning-arrester discharge voltage given in the published data for a 12-kv rating

N = Number of 12-kv ratings connected in series

0.067 = Plus tolerance for one 12-kv rating

Therefore, the minimum reference lightning-arrester discharge voltage, protective level, is not a linear function of rating but has a slight curvature. Discharge voltages calculated from the formula are shown as Curve *B* on Figure 9. This curve was used in the determination of the minimum protective levels which the lightning arrester could be expected to provide. It should be noted that the Minimum Reference Lightning-Arrester Discharge Voltage or the synonomous Minimum Protective Level always includes the positive tolerance, and thus the meaning of the term "minimum" is by definition restricted accordingly.

Required Margin

When choosing the margins these factors should be considered:

A. The deviations in lightning-arrester performance.

B. Effect of separation between lightning arrester and protected equipment.

C. The single and multishot strength of equipment.

Table IV. Station-type Lightning Arresters

Lightning-Arrester Voltage Rating	Lightning-Arrester Discharge Voltage or Protective Level	
	10×20 Microsecond, Kv	5,000 Amperes Per Microsecond, Kv
12	43	47
96	345	373
120	430	467
240	860	931

D. Possible occurrence of impulse currents above 5,000 amperes and 5,000 amperes per microsecond.

The lightning-arrester manufacturers have made allowance for the deviations in lightning-arrester discharge voltages in recommending a protective level to be determined by adding a factor of two-thirds the plus tolerance to the average performance values. Therefore, it is felt that no additional margin is required to take care of this factor.

The superimposed oscillation in the voltage across the equipment being protected causes an increase in voltage above the protected level maintained by the lightning arrester. By imposing limits on the separation between the lightning arrester and the protected equipment this factor is adequately taken care of.

The transformer strength is demonstrated by two applications of a chopped-wave test, but sometimes several applications of the test are made before the test is completed. The transformer insulation strength may deteriorate in service due to the application of several high-voltage impulses. It is reasonable to provide some margin for these contingencies.

The probability of discharge currents through the lightning arrester exceeding 5,000 amperes also should be included in the margin.

It is not good engineering to pyramid the separate safety margins for each of the foregoing factors. Considering all of them together, it seems reasonable to use an over-all margin of 20 per cent above the protective level provided by the lightning arrester to establish the minimum required impulse insulation levels.

Curves *C* and *D* in Figure 9 were plotted at 20 per cent above the lightning-arrester discharge voltage shown by Curves *A* and *B*, respectively. Curve *D* evaluates the stacking factor and represents the minimum required impulse insulation levels obtained from this analysis.

Table V gives the required impulse insulation levels for systems with nominal system voltages 115 to 360 kv, using the lightning-arrester ratings from Table I.

During the preparation of Table V, these facts were brought out:

A. There are no preferred system voltages above 230 kv. However, there is a system already operating in this country at 288 kv (sometimes listed as 287.5 kv).

B. The system voltage of 360 kv is listed instead of 345 kv as in the BIL report[1] because it is the highest system voltage that can use the present standard BIL of 1,300 when operated as an effectively grounded system.

C. The standard BIL for the listed 345-kv reference class is 1,550 and the value of

Figure 9. Lightning-arrester discharge voltage and required insulation level versus lightning-arrester rating kilovolts rms

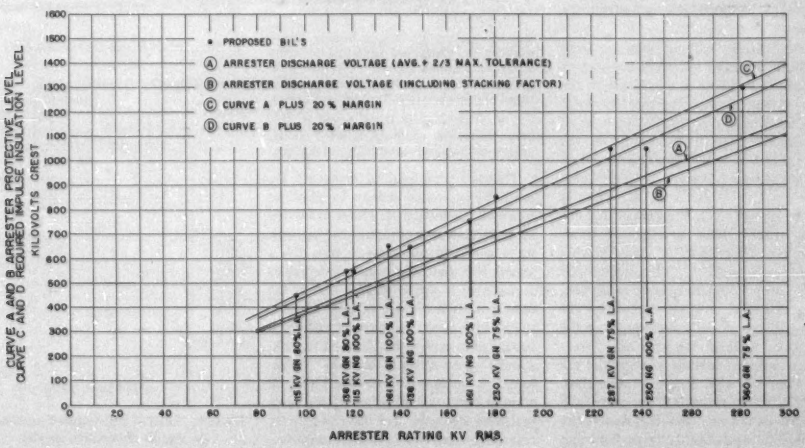

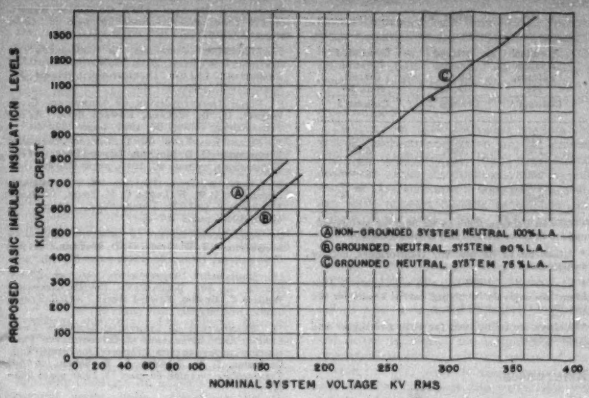

Figure 10. Proposed BIL values versus nominal system voltage

1,615 given for the 360-kv nominal system voltage is consistent with the present array of BIL.

Selection of BIL

The Effect of Small Changes in BIL Values on Transformer Design

It should be realized that the strength of insulation is not predictable to within two or three per cent. Turn insulation, spacings between coils, the thickness and number of insulating barriers, and so forth, cannot be changed in extremely small increments. A great deal of testing and experience is required to achieve just the right balance in these components for each BIL value. These components become standardized building blocks for the designer to use for a given BIL value even though practically all high-voltage transformers are purchased with ratings or characteristics which require different design layouts.

This standardization of the components used to secure a given BIL has contributed greatly to transformer reliability and lower cost by permitting repetitive use of certain insulation structures. It would require a long time and involve considerable expense to gain back the loss entailed in changing to new BIL which are only slightly different from those now in use.

Requirements for Ungrounded Installations

There may be occasions when transformers and circuit breakers supplied on systems 115 kv, 138 kv, and 161 kv may be called upon to operate on ungrounded neutral circuits. Accordingly, it is desirable to have levels suitable both for grounded-neutral system operation and also for isolated neutral operation for these circuit voltages. It is not anticipated that this requirement will exist for system voltages 230 kv and higher and, accordingly, only impulse insulation levels suitable for grounded neutral operation are required in this range.

Insulation Levels of Switchgear

Circuit Breakers

Power circuit breakers present different problems than do transformers when considering the problem of reducing their insulation, because the voltages at their terminals is not always subject to the same degree of control as those at transformer terminals.

Earlier in this paper it was pointed out that most systems operating at voltages 230 kv and higher are operated with their neutrals very well grounded. Circuit breakers with reduced insulation levels have been used successfully on these systems for a number of years. However, it is desirable to give further study to these systems.

Systems operating at 115, 138, and 161 kv are discussed as a group, since they represent additional special problems. It is noted that a large per cent of these systems are at times operated ungrounded, or so that the X_0/X_1 ratios are greater than 3.0. Loss of ground may also occur on the opening of some of the line circuit breakers. Thus a grounded-neutral rated lightning arrester could not, in these cases, be used to protect circuit breakers used on systems operating at 115, 138, and 161 kv.

In consideration of the various circuit conditions that may be present, and the desirability of retaining a margin in a circuit interrupting device, it is concluded that the circuit breaker must be capable of interrupting 87 per cent of its rated interrupting capacity at full line-to-line voltage. Therefore, the circuit-breaker interrupter would not be changed, and material reduction in circuit breaker or switch parts would be negligible and not justify the necessary new designs and additional ratings.

External Porcelain Insulation

The life of bushings and insulators which are used with circuit breakers, switches, bus supports, and so forth, probably will not be reduced by operating them at higher 60-cycle voltages than at present. Such a condition would result if the low frequency wet and dry withstand tests were reduced in the same proportion as the reduction in impulse levels.

However, creepage and strike distances over the exposed surface must be reviewed very carefully before reducing the size of these parts. The present values appear to be satisfactory, although wet flashover values have little margin and greater creepage has been required if excessive contamination is expected.

Air switches are designed with open gap distances which are at least 10 per cent greater than the insulator striking distance. A reduction in insulation could be reflected in reduced switch dimensions. However, the material savings would be

Table V

Nominal Circuit Voltage, Kv	Impulse Insulation Level: Isolated Neutral	Grounded, 80 Per Cent Lightning Arrester	Neutral, 75 Per Cent Lightning Arrester	Present BIL, Kv
115	540,562*	432,450*		550
138	645,675*	518,542*		650
161	750,788*	605,630*		750
230			810,850*	1,050
288			1,025,1062*	1,300
360			1,268,1331*	(1,615)

* The minimum value for the required impulse insulation level represents that which could be used if the lightning arrester was given full credit for the stacking factor. The larger value is obtained when the stacking factor is ignored completely.

small, and problems involving corona and radio noise would be amplified. Smaller open break distances would also reduce the isolating safety factor of the switch.

It is questionable if any reductions in the size of the external porcelain insulating part of equipment used on circuits operating at 115, 138, and 161 kv can be justified, even with effectively grounded neutrals.

It is concluded from the foregoing considerations that the impulse insulation levels for both circuit breakers and external porcelain insulating parts, including bus insulations, should be those associated with the use of the 100-per cent lightning arrester.

The Proposal

Based on the foregoing considerations and analysis, we propose that the values shown in Table VI be adopted as BIL for equipment used on systems operating at nominal voltages 115 kv and higher. These values are shown in Figure 10 and are on the basis of the standard 1.5×40 microsecond impulse voltage wave.

They have been determined on the basis that the circuit distance between the lightning arrester and the protected equipment will not exceed the maximum values shown in Table III.

Table VI

Nominal System Voltage, Kv Column 1	Isolated Neutral Circuit BIL, Kv Column 2	Grounded Neutral Circuit BIL, Kv Column 3
115	550	450*
138	650	550*
161	750	650*
230		†850**
288		1,050**
360		1,300**

Values in Column 2 are to be used for switchgear, and for transformers, if and when necessary.

* Values are to be used for transformers, not for switchgear.

† A lower value of 825 could be reasonably derived from this analysis by giving partial credit for the benefit of the stacking factor.

** Values are to be used for both switchgear and transformers.

References

1. Standard Basic Impulse Insulation Levels, **Joint Edison Electric Institute—National Electrical Manufacturers Association Report.** *EEI Publication Number H-8, NEMA Publication Number 109* (New York, N. Y.), January 1941.

2. Preferred Voltage Ratings for A-C Systems and Equipment, **Joint Edison Electric Institute—National Electrical Manufacturers Association Report.** *EEI Publication Number R-6, NEMA Publication Number 117* (New York, N. Y.), May 1949.

3. Present-Day Grounding Practices on Power Systems, Third AIEE Report on System Grounding, **AIEE Committee Report.** *AIEE Transactions*, volume 66, 1947, pages 1525–51.

4. Performance Characteristics of Lightning Protective Devices, **AIEE Committee Report.** *AIEE Transactions*, volume 68, part II, 1949, pages 1333–36.

5. Lightning Currents in Arresters at Stations, **I. W. Gross, W. A. McMorris.** *Electrical Engineering (AIEE Transactions)*, volume 59, August 1940, pages 417–22.

6. Field Investigations of Lightning, **C. F. Wagner, G. D. McCann, Edward Beck.** *AIEE Transactions*, volume 60, 1941, pages 1222–30.

7. Field Research on Lightning Arrester Discharges, **G. D. McCann, Edward Beck.** *AIEE Transactions*, volume 66, 1947, pages 625–30.

8. Lightning Investigation on Transmission Lines—VIII, **W. W. Lewis, C. M. Foust.** *Electrical Engineering (AIEE Transactions)*, volume 64, March 1945, pages 107–15.

9. Field Investigation of Lightning Surges at Substations, **I. W. Gross, G. D. McCann.** *AIEE Transactions*, volume 66, 1947, pages 569–76.

10. Lightning Investigation on the 25-Kv System of the West Penn Power Company, **William C. Bowen, Edward Beck.** *AIEE Transactions*, volume 66, 1947, pages 831–37.

11. Evaluation of Lightning-Arrester Lead Length and Separation in Co-ordinated Protection of Apparatus Against Lightning, **T. J. Carpenter, I. B. Johnson, L. E. Saline.** *AIEE Transactions*, volume 69, part II, 1950, pages 933–44.

12. Neutral Grounding Devices. *AIEE Standard Number 32*, June 1942.

13. Co-ordination of Power Transformers for Steep-Front Impulse Waves, **V. M. Montsinger.** *Electrical Engineering (AIEE Transactions)*, volume 57, April 1938, pages 183–95.

14. Guide for Quality Control. *Publication Number Z1.1–1941.* American Standards Association (New York, N. Y.), 1941.

15. Control Chart Method of Analyzing Data. *Publication Number Z1.2–1941.* American Standards Association (New York, N. Y.), 1941.

16. Control Chart Method of Controlling Quality during Production. *Publication Number Z1.3–1942.* American Standards Association (New York, N. Y.), 1942.

Discussion

A. M. Opsahl (Westinghouse Electric Corporation, East Pittsburgh, Pa.): The authors take a value of 43 kv as the lightning arrester discharge voltage or protected level on a 5,000-ampere 10x20-microsecond wave, and 47 kv on a 5,000-ampere-per-microsecond 5,000-ampere wave for a 12-kv lightning arrester. The kilovolt values are given without regard to time. I think this could be amplified. The valve lightning arrester characteristic is such that at crest discharge current the voltage is dropping. There is also another characteristic of valve lightning arresters that at high rates of rise of current, the discharge voltage reaches a higher crest. These two characteristics are tied together in the crest value and shape of the lightning-arrester discharge voltage during a surge test. The voltage crest is reached on the rise in current rather than at crest current so the rate of rise of current rather than its magnitude determines the voltage crest. For instance, a discharge current having a crest of 5,000 amperes and one having a crest of 20,000 amperes produce about the same discharge voltage crest across the lightning arrester if the rates of current rise in amperes per microsecond are the same. The 5,000-ampere 5,000-ampere-per-microsecond current wave has substantially the same rate of rise of current as the 20,000 ampere 10x20 wave and approximately the same crest voltage will be obtained in both cases.

The effect of steep front current waves on lightning-arrester discharge voltage was discussed at a Subcommittee meeting of the AIEE Protective Devices Committee as stated by the authors. However the minutes of that meeting do not bear out the authors' statement that: "The manufacturers stated that the crest value of discharge voltage for a 5,000 ampere 5,000-ampere-per-microsecond discharge current is approximately the same as the crest value of discharge voltage for a 10,000 ampere 10x20 discharge current."

The duration of the crest discharge voltage is dependent upon the total time that the current continues to rise at a given rate. The voltage peak on a 5,000-ampere test would have about one fourth the duration of the voltage peak on a 20,000-ampere test.

Another comparison can be made between the discharge voltage at a given crest current using a steep-front current wave and a slow-front current wave. Such a comparison is made in the three oscillograms shown in Figure 1 of this discussion. The left-hand oscillogram shows the lightning-arrester discharge voltage "V" and the 5,000 ampere 10x28 microsecond discharge current wave "I." The center oscillogram shows the characteristic of the same lightning arrester on a 5,000 ampere 3x23 microsecond current wave. The crest

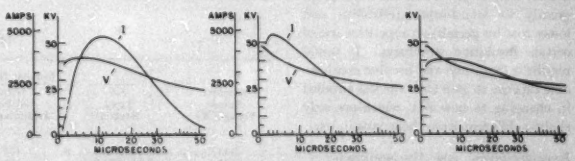

Figure 1. Lightning-arrester discharge voltages on slow-front and steep-front 5,000-ampere surges

Left—10×28 microsecond current wave
Center—3×23 microsecond current wave
Right—Discharge voltages superimposed

voltage is higher. For direct comparison, the same tests were run again and the two voltages recorded on the film on the right. This shows that the lightning-arrester discharge voltage on the steep-front current wave may be higher in crest value but falls rapidly so that after 4 microseconds it is below the lightning-arrester discharge voltage on the slow-front wave. The authors give careful consideration to the strength of transformer insulation on chopped waves and on full waves with superimposed short time overvoltages, but ignore the fact that the lightning-arrester crest voltage on which they base their co-ordination system is only a short duration peak on a long tail wave.

To be good protectors, valve lightning-arrester discharge voltages of necessity fall in a fairly narrow band for a wide range of discharge currents. The effects due to current wave shape fall in this same band of voltages. A co-ordination system can better be based on the discharge voltage of the lightning arresters on a 10x20 microsecond current wave shape. Allowance for the effect of steep front waves can then be made in the margins, if it is found that the probability of occurrence of such rates of rise is sufficiently high.

C. F. Wagner (Westinghouse Electric Corporation, East Pittsburgh, Pa.): The evaluation of the magnitude and the rate of rise of lightning-arrester discharge currents is fundamental to the whole problem of insulation co-ordination. Other discussions of these papers have attempted to evaluate these quantities by analyzing the available data pertaining to actual lightning-arrester discharge currents. The present discussion attempts to arrive at these values by analytical means using the available lightning stroke current data as a starting point.

The vast majority of transmission lines in this country operating at 115 kv and above have ground wires installed over them either for their entire length or for a distance about a mile from each substation.

A working group of the Institute under the chairmanship of Dr. E. R. Whitehead in a recent unpublished report outlined a method for determining the lightning performance of transmission lines. In this report it is assumed that the stroke currents having values in excess of 30 to 40 kiloamperes can be represented by a 4x40 wave, that is, a wave that rises to crest in 4 microseconds and decays to half value in 40 microseconds. Lightning in striking a tower raises the tower top voltage and if sufficiently great will cause flashover of the insulator string. From information obtained from E. L. Harder and J. M. Clayton, who made the analogue computer study for the above-mentioned report, the wave shape of the tower top voltage for a 1,000-foot span has the general form indicated by the upper curves shown in Figure 2 of this discussion. These curves for the present purpose can be regarded as typical of other span lengths also. Assuming a 30 per cent coupling factor, before flashover the conductor voltage is 0.3 of the tower top voltage and the voltage across the supporting insulator string is 0.7 of the tower top voltage. Depending upon the magnitude of the stroke current, flashover occurs at different times. The minimum voltage that still causes flashover occurs near 4 microseconds. Using as unit voltage the 1.5x40 insulation level of the line, Figure 2 of this discussion shows the relative values of various voltages concerned in this analysis for flashovers occurring if the flashover occurs at 2 or 4 microseconds.

Figure 3 of this discussion depicts the voltage and current waves on the ground wire and conductor for the 4-microsecond flashover. Prior to flashover the current wave in the conductor is zero and the voltage wave appears because of mutual coupling with the ground wire. After traveling one or two spans, that part of the current wave in the ground wire (and its associated voltage wave) disappears by drainage to ground. One can, therefore, neglect those portions of the voltage and current waves before the instant of flashover. At the instant of flashover the ground wire potential drops suddenly, the magnitude being dependent upon the relative values of conductor, tower, and footing impedances. For present purposes the reduction was taken as 10 per cent. At the same time the conductor rises to the same potential as the ground wire. These equal potentials are designated in Figure 3 as E.

After traveling one or two spans the voltage on the ground wire disappears but the current component in the phase conductor continues with unattenuated magnitude. The relative values of currents and voltages are shown for the position B in Figure 3.

The foregoing premised the flashover of a string of insulators at one tower only. Actually, when the tower-top voltage is sufficiently great to cause flashover at 2 microseconds, flashovers at adjacent towers are likely to occur. At the instant of flashover at the struck tower the ground wire and conductor voltages become equal. Equal voltage waves propagate along the ground wire and conductor. When the next tower is reached, however, the ground wire voltage drops suddenly and a difference in voltage builds up across the insulator string of sufficiently high value to cause flashover. This is the same phenomena depicted in Figure 3 which shows that the conductor voltage at the adjacent tower is reduced to 70 per cent of its value at the struck tower. If the voltage on the ground wire drops to substantially zero, the voltage across the string of insulators at the adjacent tower will be about 140 per cent of the insulation level of the line—sufficient to cause flashover of the insulators at adjacent towers. It would appear then that the conditions in Figure 2(A) for the flashover of one tower should be limiting. One would not expect voltages that are much greater than these to appear on the system.

If the lightning arrester is represented simply by a device having a drop E_a, independent of current, the lightning-arrester current at any instant can be determined by the expression given in Figure 3. If, further, a so-called 80 per cent lightning arrester (0.84xnominal system voltage) is assumed and since the voltage drop across the blocks is 3.67xlightning arrester voltage rating (at 5,000 amperes discharge current) then the lightning-arrester discharge current can be determined in terms of E and the system voltage by the expression also given in Figure 3.

Transmission lines for both 115 kv and 230 kv (to cover the range above 92 kv) are in existence having insulation levels that vary between 500 kv and 1,500 kv. Using the crest values of voltage E obtained from Figure 2, the maximum lightning arrester discharge currents shown in Table I of this discussion were obtained. While the values for a time to flashover of 4 microseconds are the important ones, the values for 2-microsecond flashover are also included. Corona and earth resistivity slope the wave front of incoming voltage surges considerably. The available data indicate that in one mile a square-front surge would be sloped so that its crest would be slowed to 2 microseconds in fair weather. Figure 2 gives an idea of the extent to which the wave front would be distorted and attenuated. The closer the strokes to the station, the higher the rate of rise of lightning-arrester discharge current. The eighth row of Table I, based upon a front retardation of 2 microseconds per mile, gives the distance in miles in which the stroke must occur to produce rates of rise of lightning-arrester discharge currents in excess of 5,000 amperes per microsecond. The great majority of strokes occur during a rain storm, for which condition corona and

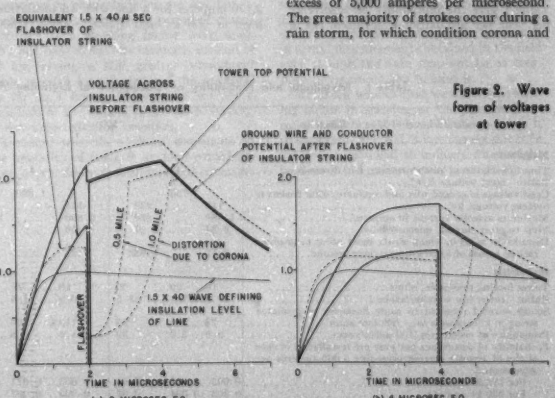

Figure 2. Wave form of voltages at tower

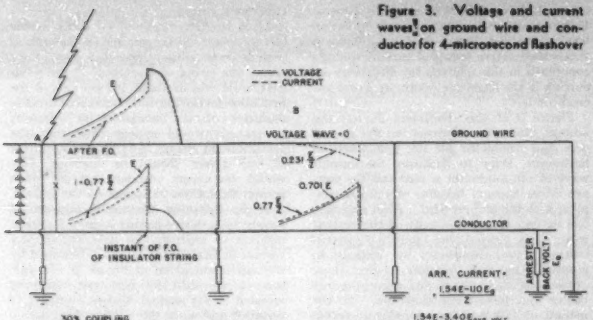

Figure 3. Voltage and current waves on ground wire and conductor for 4-microsecond flashover

attenuation will be greater. The seventh row gives the time to attain the crest current or the approximate duration of the high rate of rise of current. Lightning arrester engineers state that the crest of the lightning-arrester drop is largely dependent upon the rate of rise of current. For a conventional 10x20 wave at which lightning arresters are usually tested, for a 5,000-ampere crest, the maximum rate of rise is approximately 1,000 amperes per microsecond. A 5,000-ampere-per-microsecond current wave produces a voltage drop that is 15 to 20 per cent higher. The discussion by Mr. Opsahl discusses this point in more detail.

The magnitude and rate of rise of the lightning-arrester discharge current is not the entire story. The frequency with which these currents can be obtained must be taken into consideration. From the lightning performance report, values of the ratio of tower-top voltages to stroke current were obtained for several values of tower footing resistance. From this number the stroke currents required to produce flashover were obtained. Then with the aid of the stroke-probability curve the probability of occurrence per 100 miles per year was obtained. The last two rows in Table I give the probability of occurrence per year per installation of a rate of rise of lightning arrester current exceeding 5,000 amperes per microsecond.

The first significant conclusion to draw from Table I is the desirability, because of its effect upon the probability factor, of holding the tower footing resistances to 20 ohms or lower for the first mile from the station. Considering only the 10- and 20-ohm footings, for the 1,500-kv levels the probability of occurrence of a 5,000-ampere per-microsecond discharge is extremely low. In the 500-kv levels, while the probability is somewhat higher, the duration of the high rate (row 7) is so short that it can have little effect upon transformer insulation.

There still remains the consideration of side flashes—strokes that strike the conductor directly instead of the ground wire On a well-laid-out ground wire system, this will represent about 0.1 of one per cent of the strokes or about 0.001 stroke per mile per year. High current side flashes flash the insulator string but there is a limiting value of current below which flashover will not occur. This current is very low and, using the same wave shape as the Lightning Performance Working Group, it will have a 2x40 wave shape. Using the same surge impedance as the working group (460 ohms) this limiting current will be 500x2/460 or 2,170 amperes for a line with an insulation level of 500 kv and 1,500x2/460 or 6,500 ampere for a 1,500-kv line. For the 500-kv level this limit represents 98 per cent of the strokes and for the 1,500-kv level about 80 per cent. These strokes perform essentially the same as strokes to the ground wire, perhaps a little less severe as they do not possess the sharp discontinuity illustrated in Figure 3(B). In any event they add a negligible amount to the probability of occurrence. The remaining side flashes produce a 2x40 wave that in the limit gives rise to a lightning-arrester discharge current of about 4,000 amperes in 2 microseconds for the 500-kv insulation level and to 12,000 amperes in 2 microseconds for the 1,500-kv level. Considering the probability of occurrence of a side flash within the first half mile (0.0005), the fact that 2 per cent of these for the 500-kv level and 20 per cent for the 1,500-kv level do not cause flashover and that only a portion of these produce currents as high as 12,000 amperes in 2 microseconds, the contribution of side flashes to the probability of occurrence of lightning-arrester discharges of the order of 5,000 amperes is negligible.

In conclusion it must be borne in mind that a great element of judgment is present in determining the basic assumptions to use in insulation co-ordination. Pyramiding the most severe conditions for all assumptions leads to ridiculous results. In selecting a lightning-arrester discharge current the probability of the simultaneous occurrence of the worst condition for other factors, such as location of protected device, length of down lead and tower footing resistance, must be considered. Bearing in mind these other fortuitous factors and the short duration of the higher lightning-arrester voltage associated with high rates of current rise, it appears that the probability of occurrence (about one per 200- to 500-lightning arrester locations per year) of rates of rise of currents of 5,000 amperes per microsecond is too infrequent to use as a basis of co-ordination. The lightning arrester characteristic corresponding to the conventional 10x20 wave is sufficiently representative.

E. Beck (Westinghouse Electric Corporation, East Pittsburgh, Pa.): The paper follows the pattern of a memorandum pre-

Table I. Magnitude and Probability of Occurrence of Lightning Arrester Discharge Currents

Insulation Level of Line in Kilovolts	500						1,500					
Magnitude												
Time to flashover of insulator string, microseconds		4			2			4			2	
Ratio: crest voltage E/IL		1.5			2.15			1.5			2.15	
Crest voltage of ground wire and conductor after flashover		750			1,080			2,250			3,230	
System voltage, kv	115	....	230	115	....	230	115	...	230	115	...	230
Maximum arrester current in amperes	1,680	....	830	2,800	....	1,900	6,700	...	5,900	10,000	...	9,100
Time to crest current, microseconds	0.34	....	0.17	0.56	....	0.38	1.38	...	1.18	2	...	1.82
Distance in miles in which stroke must occur to produce rate in excess of 5,000 amperes/microsecond	0.17	....	0.083	0.28	....	0.19	0.67	...	0.59	1.0	...	0.91
Probability												
Tower footing resistance, ohms	10	20	50	10	20	50	10	20	50	10	20	50
Ratio: tower-top voltage/stroke I	10.9	17.4	33.5	10.9	17.4	33.5	10.9	17.4	33.5	10.9	17.4	33.5
Stroke current required to cause flashover of insulator string in kiloamperes for 1,000-foot span	78	49	25	110	69	36	230	150	80	330	210	100
Probability of occurrence/100 miles/year	2.6	5.0	30	1.0	3.8	18	0	0.3	2.6	0	0	1.4
Probability of occurrence per year per installation of rate of rise of arrester current exceeding 5,000 amperes per microsecond:												
For 115-kv systems	0.005	0.009	0.05	0.003	0.011	0.05	0	0.002	0.02	0	0	1.4
For 230-kv systems	0.002	0.004	0.03	0.002	0.007	0.03	0	0.002	0.02	0	0	1.4

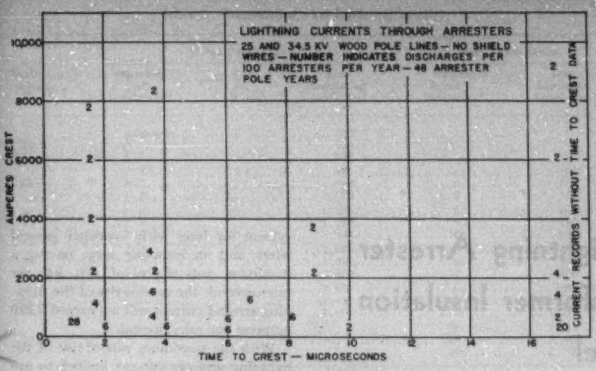

Figure 4. Lightning currents through lightning arresters

sented by Mr. Clem for the National Electrical Manufacturers Association group, to the Edison Electric Institute and AIEE groups of the Triple Joint Committee on Insulation Co-ordination. It did not represent the opinion of all manufacturers, and the Lightning Arrester engineers of my company registered objection because we felt sufficient consideration had not been given to several items before conclusions were adopted. Thus we also find ourselves not in agreement with some of the steps discussed in the paper.

I would like to see a more detailed discussion of the method used to arrive at the curve of Figure 2 of the paper. I am cited twice in Figure 2 of the paper as a reference for the data. I wish it understood clearly that I am not a party to the curve of the authors' Figure 2. In my opinion it is not logical to lump all data on wave fronts in a curve regardless of corresponding crest currents and I am inclined to believe that this is what the authors have done. Nor does it appear to me logical to apply the data in the references cited, obtained on unshielded wood pole lines in highly exposed locations to the shielded lines considered in the paper.

A more significant way of presenting the data is shown in Figure 4 of this discussion prepared by Mr. Opsahl from the data obtained in our field investigations. It shows the number of discharges of recorded crest current and wave front per 100 lightning-arrester years. It is to be noted that there are 28 records with fronts of 1 microsecond but they are all less than 500 amperes, hence of no practical interest in co-ordination. What we are interested in is the probability of occurrence of high currents with short fronts. This is not frequent even on lines without shielding, and I wish to repeat that the data in Figure 4 of this discussion consist only of measurements on unshielded wood pole lines.

It has been found that the probability of short-front currents of appreciable magnitude on shielded lines is much less.

Therefore I am of the opinion that the 5,000-ampere-per-microsecond 5,000-ampere crest is not a realistic figure for 115-kv systems and higher, that are shielded as indicated in the paper. The use of this discharge current also colors the conclusions in the companion paper on the evaluation of lightning-arrester lead lengths by Carpenter Johnson and Saline,[1] cited in Table III of the authors' paper. These conclusions are too conservative.

In reference to taking advantage of a stacking factor in lightning arresters, we are of the opinion that this is not good practice because it has been found that the variations in characteristics are not purely random except over a long period of manufacture. If a stacking factor were used, why not base it on 3-kv elements instead of 12 kv, giving a still greater advantage? Why was 12 kv selected by the authors? As far as I know, 12-kv units are not a standard of the industry, for either station- or line-type lightning arresters.

I concur with the authors' comments on the necessity of keeping in mind considerations of wet 60-cycle flashover and creepage.

Reference

1. See reference 11 of the paper.

W. J. Rudge: None of the discussions of our paper indicate any disagreement with the values of basic impulse insulation levels proposed in our paper. This is very gratifying. Apparently there is a misunderstanding in reference to the discharge voltage of a 12-kv lightning arrester rating for a 5,000-ampere crest 5,000-ampere-per-microsecond, current discharge wave. In our paper we said "the manufacturers stated" that this discharge voltage was the same as for a 10,000-ampere 10x20-microsecond current wave. We made this statement in good faith because our notes taken at the meeting in question indicate that the statements were made.

Most of the discussions questioned our choice of the lightning-arrester discharge current upon which we based our study. We knew that a rate of current rise of 5,000 amperes per microsecond will occur very seldom, and in going over the available field data we noted that the higher rates of current rise were frequently associated with relatively low crest values of discharge current. We chose the current wave shape after careful consideration with full understanding that it was conservative.

In view of the fact that there was very little data available we felt, and still feel, that we were justified in being conservative. If further statistical data becomes available indicating that a slower rate of rise is preferable, we will be agreeable to using that which can be justified.

The oscillograms submitted by Mr. Opsahl (Figure 1 of the discussion) confirm our preference for a wave faster than the 10x20 microsecond wave. In the oscillogram giving the 3x23 current wave it is noted that the voltage wave is close to a 1x20 wave. The current wave we used is about a 2x20 wave and gives about a 0.5x30 voltage wave. Both of these are much closer to the standard 1.5x40 voltage wave upon which impulse tests are based than is the voltage wave given by the 10x20 current wave.

Mr. Wagner has presented a theoretical discussion outlining a method of estimating the number of occurrences of a rate of rise exceeding 5,000 amperes per microsecond. He gets figures ranging from zero to one in 0.7 of a year. We prefer to use the results of actual measurements obtained in the field even though the data may not be as complete as we would like to have it.

Mr. Beck implies that we used the stacking factor in arriving at the proposed impulse insulation levels. We did not use it to determine the BIL's but merely put it in for information and to indicate what might be done if full credence was given to it.

Co-ordination of Lightning Arrester Location with Transformer Insulation Level

R. L. WITZKE
MEMBER AIEE

T. J. BLISS
ASSOCIATE AIEE

THE location of lightning arresters, relative to the equipment being protected, must be given careful consideration if adequate protection is to be provided at reasonable cost. This is particularly true if equipment having reduced insulation levels is used for economy reasons. Unfortunately, a large number of factors must be considered in determining the number and location of lightning arresters in most substations. The more important factors include the number, insulation level and shielding of lines entering the station; substation shielding; length of individual bus sections; distances between bus and equipment; capacitance of circuit breakers, transformers and other equipment; lightning arrester lead lengths; equipment insulation levels; and magnitude and rate-of-rise of surges entering the station. All of these factors, as well as others, must be considered in any complete evaluation of economical substation protection. The authors are of the opinion that each case must be studied individually if adequate protection is to be provided at a minimum cost. Individual studies of large, high-voltage substations on an analogue computer, or by other means, are certainly justified. In the case of the smaller or lower voltage stations, extensive studies cannot be justified, and protection must be based on established rules, which of necessity must be quite conservative.

In view of the complicated nature of the substation protection problem, the authors have limited the scope of their investigation to the relatively simple case of a single overhead line terminated in a single transformer bank. The results of this study, as summarized in this paper, will be conservative when applied to stations having a multiplicity of circuits. Several special studies were made to show the influence of additional circuits on the transformer protection provided. All studies reported were made on the Anacom, or analogue computer.[1]

Summary and Conclusions

The general studies reported in this paper are limited to the surge protection of a liquid-filled power transformer located at the end of a transmission line as shown in Figure 1. The results are expressed in terms of the distance s, the maximum permissible distance between the transformer bushing and the lightning arrester lead tap to the bus, point a, in Figure 1. The summary tables included in this section are based on 35 feet of lead between the lightning arrester and the bus; however, the general computer data may be used to evaluate protection with other lightning arrester lead lengths.

It has been concluded that protection based on an incoming surge having a maximum rate-of-rise of 500 kv per microsecond is adequate, if the station is provided with shielding against direct strokes[2] and the overhead line is provided with properly located ground wires,[3,4] for at least one-half to one mile out from the station. Under these conditions, it appears reasonable to assume that the lightning arrester current is limited in magnitude by the line insulation level and surge impedance. Based on a line surge impedance of 450 ohms, which is typical for lines with overhead ground wires, and an incoming surge having a maximum rate-of-rise of 500 kv per microsecond, the rate-of-rise of the lightning arrester current will not exceed 2,220 amperes per microsecond.

With the maximum rate-of-rise of the lightning arrester current limited to approximately 2,220 amperes per microsecond, satisfactory co-ordination is obtained by using the maximum 10×20 lightning arrester discharge characteristics and the transformer chopped-wave level, in determining the permissible distance between a lightning arrester and a transformer. It should be noted that the voltage at the transformer may exceed the chopped-wave level if the rate-of-rise of lightning arrester current is as high as 2,220 amperes per microsecond and the lightning arrester has maximum discharge characteristics. However, due to the wave shape of the surge voltage applied to the transformer, the impulse level of the transformer is not exceeded. This conclusion gives due consideration to the duration, as well as the magnitude, of the voltage at the transformer.

It has been concluded that station ground resistance is a negligible factor, at least in the general case. Most stations will be provided with a ground mat having a low resistance to ground. In all cases, good engineering practice will dictate connecting lightning arresters and all apparatus tanks to a common ground in order to equalize potentials within the station for safety reasons. With the lightning arrester ground and the transformer tank interconnected by a counterpoise system, all of the resistance between the counterpoise and ground will not be effective in increasing the voltage across the transformer. The transformer tank will rise above ground potential,

Paper 50-153, recommended by the AIEE Protective Devices and the Transmission and Distribution Committees and approved by the AIEE Technical Program Committee for presentation at the AIEE Summer and Pacific General Meeting, Pasadena, Calif., June 12–16, 1950. Manuscript submitted March 15, 1950; made available for printing April 17, 1950.

R. L. Witzke and T. J. Bliss are both with the Westinghouse Electric Corporation, East Pittsburgh, Pa.

Table I. Transmission Line Insulation Levels

System Voltage, Kv	Wood-Pole Lines: Number of Insulators*	Wood-Pole Lines: Feet of Wood	Wood-Pole Lines: Line Insulation Level, Kv†	Steel-Tower Lines: Number of Insulators*	Steel-Tower Lines: Line Insulation Level, Kv†
34.5	Pintype	3	500		
			600		
			700		
69	4	5.5	970	4	430
	5		1,020	6	600
	6		1,070	8	760
115	6	6	1,130	6	600
	8		1,220	8	760
	10		1,330	10	930
138	8	7	1,330	8	760
	9		1,380	10	930
	11		1,490	12	1,100
161	9	7.5	1,450	9	850
	10		1,490	11	1,020
	12		1,600	14	1,270
230				14	1,270
				16	1,440
				20	1,780

*Middle figure is most common number, upper and lower figures indicate range for modern lines.

†Minimum level based on $1^1/_2 \times 40$ positive waves.

Table II. Suggested Maximum Distance Transformer to Lightning Arrester-Lead Tap—Full Transformer Insulation

System Voltage	Line Construction	Lightning Arrester	Maximum Distance—Feet: 100 Per Cent Lightning Arrester	Maximum Distance—Feet: 80 Per Cent Lightning Arrester
34.5	wood	station type	22	52
69	wood		22	66
	steel		32	82
115	wood		31	107
	steel		44	133
138	wood		33	94
	steel		46	126
161	wood		39	84
	steel		52	122
230	steel		59	187
34.5	wood	line type	*	18
69	wood			19
	steel			29

*Lightning arresters should be mounted adjacent to, and preferably on transformer.

Table III. Suggested Maximum Distances Between Transformer and Lightning Arrester Lead Tap When Transformer Has Reduced Insulation

System Voltage, Kv	Line Insulation Level, Kv*	Transformer BIL, Kv	Lightning Arrester Rating, Kv	Distance—Feet, Arrester Lead Length: 0	Distance—Feet, Arrester Lead Length: 35 Ft.
115	760	450	99**	53	33
			93‡	75	45
138	930	550	117**	67	45
			111‡	92	60
161	1,020	650	135**	92	65
			129‡	117	85
230	1,440	900	195**	79	65
			183‡	119	90
		825§	183‡	69	49
287	1,610†	1,050	243**	60	50
			228‡	80	68
345	1,780†	1,800	273‡	120	98

*Minimum insulation level based on $1^1/_2 \times 40$ wave.

†These line insulation levels have never been used in practice.

**80 per cent lightning arrester.

‡75 per cent lightning arrester.

§This BIL is not included in the current standards, but is being considered by the industry.

which partially offsets the increase in voltage produced by the lightning arrester current discharging into the resistance between the ground mat and ground. If the lightning arrester has a separate ground of appreciable resistance, the voltage across this resistance must be considered in surge-protection problems.

Application Guides

The application guides included in this section are limited to the surge protection of power transformers located at the end of a transmission line as shown in Figure 1. The guides are in the form of tables giving suggested maximum distances between the transformer bushing and the lightning arrester lead tap to the bus (distance s in Figure 1). The limiting distances are based on the following assumptions:

1. Any surge reaching the station has a maximum rate-of-rise of 500 kv per microsecond. This requires that the station be provided with adequate shielding against direct strokes,[3] and the overhead line be provided with properly located ground wires[5,6] for at least one-half to one mile out from the station.

2. Lightning arrester current is limited by the line insulation level and line surge impedance.

3. The overhead-line insulation levels do not exceed the values in Table I.

4. Lead between lightning arrester and bus does not exceed 35 feet.

5. The transformers have full insulation unless otherwise specified.

6. Station ground resistance is neglected.

In using these tables it is necessary to know the transformer basic impulse insulation (BIL) and the type and rating of the lightning arrester. The lightning arrester rating is, of course, determined by the system voltage and grounding conditions. The maximum distances given in the tables are measured between the transformer bushing and the lightning arrester tap to the line or bus. If the suggested distance is exceeded in a particular case, special study is required. General data are included in later sections for more detailed investigations where these are necessary.

The data in Table II are based on transformers having full insulation and standard 80 or 100 per cent lightning arresters. The data in Table III are based on transformers with reduced insulation and special lightning arrester ratings. The lightning arrester ratings were obtained by taking 80 per cent or 75 per cent of 1.05 times system voltage to obtain a minimum lightning arrester rating. The added restriction that the ratings be a multiple of three increases most of the

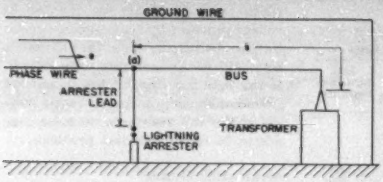

Figure 1 (left). Circuit studied in general investigation

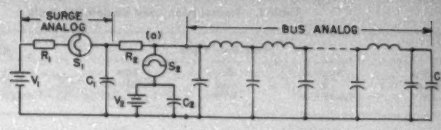

Figure 3. Basic circuit used in analogue computer studies

(a) = lightning arrester location
C = equivalent capacitance of transformer
S_2, V_2, C_2 = lightning arrester analogue

ratings above the calculated minimum values. These ratings should not be applied without giving careful consideration to the dynamic voltage across the lightning arrester during fault or unusual system conditions.

The effect of varying the rate-of-rise of the incoming surge and the lightning arrester lead length is indicated by the results in Table IV.

The influence of a second line entering the station is indicated by the data in Table V. These results apply for the case of a 200-foot separation between the arrester and the transformer (distance s in Figure 1), an overhead line surge impedance of 500 ohms, and a front F of 0.8 microsecond, neglecting the second line. The second line was terminated at the lightning arrester, at the transformer and at 50-foot intervals between these limits. The results are given in terms of the voltage at the transformer, expressed as a ratio to the voltage at the lightning arrester. The equivalent surge capacitance was varied between zero and 0.0032 microfarad. It will be noted that the second line has considerable influence on the voltage ratios, particularly if the termination is close to the transformer. This illustrates the need for considering all factors in any complete study of substation protection.

Basis of General Investigation

The general study reported in this paper was limited to the case of a single overhead transmission line terminated at a transformer bank as illustrated in Figure 1. It is assumed that the station is adequately protected against direct strokes, and the transmission line is provided with properly located ground wires, for at least one-half to one mile out from the station. It is assumed that any surge reaching the lightning arrester originates out on the line and that the lightning arrester current is limited by the line surge impedance. The station bus is treated as an extension of the line and no distinction is made between horizontal and vertical runs. The distance s, between the lightning arrester location and the transformer, is taken as the total distance between the lightning arrester lead tap to the bus and the transformer bushing. In these studies the transformer is represented by an equivalent surge capacitance C, which is permissible for surges of short duration.

The studies were based on an incoming surge voltage e having a uniform rate-of-rise de/dt. Unit voltage, or 100 per cent voltage, is defined as the maximum surge voltage at the lightning arrester location. The voltage at the lightning arrester location is assumed to rise to this unit voltage and then to remain constant at least until the maximum voltage at the transformer is reached.

Unit time, referred to in this paper as F, is defined as the maximum surge voltage at the lightning arrester location divided by the rate-of-rise of the incoming surge. If the distance between the lightning arrester and the transformer were unusually long, the voltage at the lightning arrester would reach its maximum voltage before reflections returned from the transformer. In this case, and based on the assumptions made, the voltage at the lightning arrester location would follow the solid line in Figure 2, and F would be the time to maximum voltage. In the more practical cases, negative reflections will return from the transformer before the voltage at the lightning arrester location reaches its maximum value. The voltage at the lightning arrester is then modified as indicated by the dashed line in Figure 2, and the time to maximum voltage is increased. These reflections, however, do not influence the basic definition of unit time F. These definitions of unit voltage

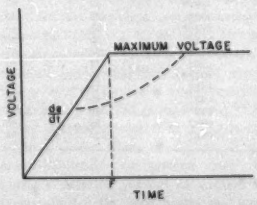

Figure 2. Voltage at lightning arrester location as assumed in general studies

and unit time were selected to permit generalization of the data obtained in the analogue computer studies.

Let

v = velocity of surge propagation in feet per microsecond.
Z = line or bus surge impedance in ohms.
F = maximum voltage at the lightning arrester location divided by the rate-of-rise of the incoming surge.

Then

s/v = time required for surge to travel from lightning arrester location to transformer.
ZC = time constant in microseconds of the circuit consisting of the bus and the terminating capacitance.

The times F, s/v, and ZC are the only variables that need be considered in the problem. Dividing s/v and ZC by F reduces the problem to two fundamental variables $(s/v)/F$ and ZC/F.

Analogue Computer Studies

The analogue computer studies were made using the analogue in Figure 3. The overhead line between the lightning arrester location and the transformer was represented by pi-sections, and the transformer by a capacitor C.

The transmission line entering the station was represented by the resistor R_2 having a resistance equal to the line surge impedance. It was assumed that the overhead line and bus surge impedances were equal. Capacitor C_1 was charged through resistor R_1 by closing switch S_1. The voltage across C_1, which had a uniform rate-of-rise, was applied to the station bus through the transmission line surge impedance R_2. The voltage at point (a) was allowed to increase until it was equal to the battery voltage V_2, at which time switch S_2 was closed to hold the voltage constant at this point.

The voltages at the lightning arrester location (a) and across the transformer represented by C, were measured with a cathode-ray oscilloscope. The circuit lengths and terminating capacitance

values used in the studies were selected to cover a range of $(s/v)/F$ and ZC/F ratios expected in practice.

General Data

Typical oscillograms obtained in the Anacom studies are included in Figures 4 and 5. The upper line of oscillograms in each figure shows the voltages that would be obtained at the lightning arrestor location with no reflections from the transformer. These records were obtained by replacing the capacitor C by a resistance equal to the line surge impedance. One per unit time F is defined as the time to the maximum voltage on these records. The second line of oscillograms in Figure 4 shows the voltage at the lightning arrester location with zero terminating capacitance, that is, with an open-end line. The successive lines illustrate the voltages at the lightning arrester location with ZC/F ratios up to 2.0.

The second line of records in Figure 5 is the voltage at the end of an open-wire circuit. The succeeding lines illustrate the voltages at the transformer with ZC/F ratios up to 2.0. It should be noted that attenuation was neglected in obtaining these results. Practical attenuation values will have little influence on the magnitude of the first crest, but will reduce the second and successive crests appreciably.

Figure 6 summarizes the maximum receiving-end voltages (voltages at transformer) as obtained in the computer studies. These voltages are expressed as a ratio to the maximum voltage at the lightning arrester location. Table VI is a summary of the E_r/E_s and T/F ratios obtained. In this table, T is the time to maximum voltage at the transformer.

Table IV. Influence of Lightning Arrester Lead Length and Rate-of-Rise of Incoming Surge on Maximum Distance Transformer to Lightning Arrester Lead Tap

System Voltage, Kv	Line Insulation Level, Kv	Rate-of-Rise of Incoming Surge, Kv Per Microsecond	Maximum Distance, Feet — Lead Length 0 Feet	35 Feet
34.5	600	250	244	154
		500	122	52
		1,000	61	8
138	930	250	352	297
		500	176	126
		1,000	88	45
230	1,440	250	460	417
		500	230	187
		1,000	115	65

Note: Above distances are based on the following: full transformer insulation; and standard 90 per cent station-type lightning arresters.

Integration Method

In surge protection problems involving appreciable lead length between the protective device and the protected equipment, consideration must be given to the wave shape, as well as the magnitude, of the surge voltage applied to the equipment. Apparatus insulation levels are expressed in terms of test waves having definite shapes. If the wave shape of the surge applied to equipment deviates from these test wave shapes, considerable judgment must be exercised in estimating the permissible magnitude of the surge. The industry is in need of an acceptable method of evaluating the influence of surge voltages of nonstandard wave shape on electric apparatus. Any method finally adopted should be substantiated by laboratory test results.

In the paper Surge Protection of Cable-Connected Equipment,[8] the authors proposed an integration method of evaluating the effect of surge voltages of nonstandard wave shape on oil-insulated transformers. In this method the disruptive effect of the surge is defined by the equation

$$DE = \int [(e(t) - K_1)]^{K_2} dt \qquad (1)$$

where

DE = disruptive effect
$e(t)$ = surge voltage expressed as a function of time
K_1, K_2 = constants fixed by transformer test voltages

This relation was established on the basis that the transformer insulation could stand some constant voltage K_1 for an extended period of time without distress. It was realized that the disruptive effect of a surge is a function of both voltage magnitude and time, but that these two factors should not be given equal weight. The constant K_2 was introduced to allow some variation in the relative weight given to magnitude and time. The constants K_1 and K_2 can be evaluated from the standard impulse tests for transformers if the assumption is made that the full-wave, chopped-wave, and front-of-wave tests are of equal severity. The constants are obtained by solving the following relations

$$\int [(e_1(t) - K_1)]^{K_2} dt = \int [(e_2(t) - K_1)]^{K_2} dt \qquad (2)$$

$$\int [(e_2(t) - K_1)]^{K_2} dt = \int [(e_3(t) - K_1)]^{K_2} dt \qquad (3)$$

In these equations $e_1(t)$, $e_2(t)$, and $e_3(t)$ are the full-wave, chopped-wave, and front-of-wave test voltages, respectively, expressed as a function of time. The general form of the equations is such that a cut-and-try solution is required. After K_1 and K_2 have been determined, the disruptive effect of a standard test wave is determined by substituting one of the standard test waves in equation 1. All three test waves should give the same DE when used in equation 1.

As the equation gives the same disruptive effect for the three standard test waves, which vary over a wide range in magnitude and duration, it should give acceptable accuracy in evaluating the nonstandard wave shapes normally encountered in surge-protection applications. Judgment, however, must be used in evaluating oscillatory waves as experienced in cases involving appreciable lead length between the lightning arrester and the transformer. The authors have integrated only the first cycle of these oscillations because the second cycle is of appreciably reduced magnitude, and because the stresses in the transformer insulation are relieved to some extent during the period of low voltage between the first and second crests of the oscillation.

The authors evaluated K_1, K_2, and DE for insulation classes between 5.0 and 34.5 kv, and included them in Table XIII of the paper referred to previously. Since then it has been discovered that the integration method, based on equation 1, has a limitation when used at the higher circuit voltages because no combination of the constants K_1 and K_2 will give the same DE for all three test waves. In order to retain the method, at least until a better approach to the problem is developed, an approximation had to be introduced. This consisted of setting K_1 equal to zero and then finding K_2 by solving equation 2, which is based on the full-wave and chopped-wave transformer tests. This procedure gave results for 138-kv class insulation as follows:

$K_1 = 0$
$K_2 = 10.3$
$DE = 660 \times 10^{10}$

These constants give the same DE for the full-wave and chopped-wave test volt-

Table V. Influence of Second Line Entering Station

Location of Second Line Termination in Feet from Arrester	E_r/E_s — Capacitance C in Microfarads 0	0.0008	0.0032
0	1.2	1.39	1.66
50	1.15	1.38	1.55
100	1.10	1.28	1.50
150	1.05	1.23	1.45
200	1.00	1.18	1.37
No second line	1.43	1.60	1.70

Note: Above data based on 200 feet between lightning arrester and transformer, overhead line surge impedance of 500 ohms and a front F of 0.8 microsecond, neglecting the second line.

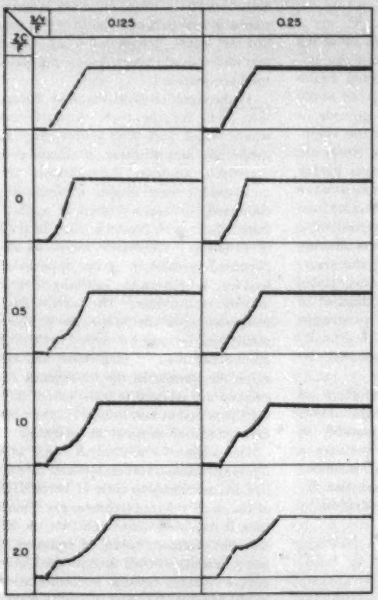

Figure 4. Typical voltages at lightning arrester location as obtained on Anacom

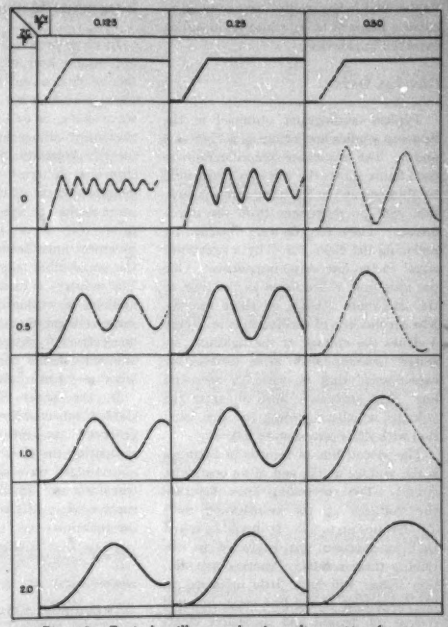

Figure 5. Typical oscillograms showing voltages at transformer

ages, and a second value for the front-of-wave test voltage. The integration method, based on these constants, will permit a front-of-wave test voltage approximately 5 per cent higher than the standard test for 138-kv class insulation. This error, however, was of little practical importance in the cases included in this paper because the surge voltages permitted had magnitudes much closer to the chopped-wave than the front-of-wave levels.

The integration method permits expressing a surge voltage of nonstandard wave shape in terms of an equivalent chopped-wave or full-wave voltage. For example, the voltage in Figure 7 consists of a combination of the chopped-wave and full-wave test voltages for 138-kv class transformers. The voltage rises to 750 kv in $1^1/_2$ microseconds, decreases to 650 kv at 3.0 microseconds and then follows the tail of a $1^1/_2$x40 wave. The *DE* of this voltage is $1{,}183 \times 10^{33}$, which is the same as the *DE* of a 689 kv $1^1/_2$x40 voltage wave. It is concluded that this voltage is approximately equivalent to a $1^1/_2$x40 voltage, 6 per cent higher than the 650-kv full-wave test voltage.

Insulation Co-ordination

As discussed in the previous section, consideration should be given to the wave shape of surge voltages applied to transformers. In co-ordinating lightning arrester characteristics with transformer insulation levels, consideration also should be given to the rate-of-rise of current in the lightning arrester because this influences the magnitude and wave shape of the lightning arrester discharge voltage. The authors, however, have concluded that satisfactory results can be obtained if the 10x20 lightning arrester discharge characteristics are co-ordinated with the chopped-wave level of the transformer. This conclusion is limited to those cases involving appreciable lead between the lightning arrester and the transformer. It also assumes that the maximum rate-of-rise of current in the lightning arrester does not exceed approximately 2,220 amperes per microsecond.

The basis for this conclusion is discussed in connection with the following example: The maximum permissible distance between a 138-kv class transformer and the lightning arrester location (distance *s* in Figure 1) is 132 feet, assuming a 121-kv lightning arrester and 35 feet of lead between the lightning arrester and the bus. This distance was calculated by using the 10x20 lightning arrester characteristics and co-ordinating with the transformer chopped-wave level of 750 kv. Under the assumed conditions, as outlined in the detailed example in a later section on the application of the computer data, the lightning arrester current is 3,580 amperes and the rate-of-rise of lightning arrester current is 2,220 amperes per microsecond. The latter value assumes a 500-kv per microsecond surge reaching the station over a 450-ohm line. The lightning arrester discharge voltage used in obtaining the permissible distance of 132 feet was 429 kv, which was based on a 3,580-ampere, 10x20 discharge current.

An 8,900-ampere, 10x20 discharge current has a rate-of-rise of approximately 2,220 amperes per microsecond. The maximum voltage across a 121-kv lightning arrester at this current is 473 kv, which is 10 per cent higher than used in the above example. Increasing the arrester voltage to this value, and leaving

Table VI. E_r/E_s and T/F Ratios Obtained in Analogue Computer Studies

ZC/F	$(s/v)/F$ 0.01	0.031	0.0625	0.125	0.25	0.50	1.0	2.0
0	1.01	1.03	1.10	1.22	1.46	1.88	2.00	2.00
	(0.5)	(0.5)	(0.57)	(0.62)	(0.75)	(1.09)	(1.25)	(1.5)
0.25	1.08	1.14	1.25	1.38	1.58	1.94	2.05	2.06
	(0.85)	(0.81)	(0.95)	(1.1)	(1.07)	(1.38)	(2.25)	(4.25)
0.5	1.10	1.22	1.32	1.43	1.63	1.94	2.11	2.10
	(0.93)	(1.08)	(1.2)	(1.45)	(1.5)	(1.75)	(2.5)	(4.75)
1.0	1.12	1.26	1.34	1.47	1.70	1.98	2.13	2.23
	(1.25)	(1.4)	(1.56)	(1.82)	(1.8)	(2.38)	(3.0)	(5.0)
2.0	1.12	1.26	1.37	1.50	1.72	1.97	1.98	2.21
	(1.65)	(1.9)	(2.2)	(2.5)	(2.6)	(3.13)	(3.5)	(5.75)
4.0	1.04	1.27	1.37	1.51	1.71	1.97	1.98	2.00
	(2.27)	(2.7)	(2.9)	(3.29)	(3.6)	(4.12)	(5.25)	(6.5)

Note: Upper value is E_r/E_s ratio, and lower value (in parenthesis) is T/F ratio.

the distance between the transformer and the arrester location equal to 132 feet, increases the voltage at the transformer to 807 kv, which is 7.5 per cent above the transformer chopped-wave level. The general shape of the transformer voltage is illustrated by the oscillogram in Figure 5 for an $(s/v)/F$ ratio of 0.125 and a ZC/F ratio of 1.0. The time to maximum voltage is approximately 2.30 microseconds based on the data in Table VI. This voltage, with a crest of 807 kv, is equivalent to a chopped-wave test voltage of only 744 kv. This equivalence gives due consideration to the duration as well as the magnitude of the voltage applied to the transformer, and was obtained by means of the integration method discussed in the previous section.

It is concluded that it is permissible to use the published 10x20 lightning arrester characteristics and the transformer chopped-wave level in determining the permissible distances between lightning arresters and transformers. This conclusion assumes that the maximum rate-of-rise of current in the lightning arrester does not exceed approximately 2,220 amperes per microsecond, which appears to be a reasonable upper limit if the station and incoming lines are adequately shielded.

Incoming Surge Voltage

In this investigation it is assumed that the maximum surge voltage reaching the lightning arrester is limited by the insulation level of the transmission line. In all cases considered, the crest voltage at the transformer is reached in less than 3.0 microseconds. To obtain the maximum voltage at the transformer, it is necessary to maintain the voltage at the lightning arrester location until crest transformer voltage is reached, or for times approaching 3.0 microseconds. For this reason it was decided to base the magnitude of the incoming surge on a line insulation level approximately equal to the 3.0-microsecond flashover value. However, the line full-wave level is usually known, a line level 20 per cent above the full-wave level was used. This is very close to the 3.0-microsecond flashover value of wood-pole and steel-tower lines as normally designed and built.

The rate-of-rise of the incoming surge is of considerable importance in evaluating the influence of lightning arrester location on the protection afforded. For this reason, some conclusion must be reached regarding the front of the incoming surge. Brune and Eaton,[6] in field tests with artificial surges, showed that the time to crest voltage of an 850-kv surge increased from 2.0 microseconds at the point of surge application to 5.0 microseconds after traveling 1.4 miles. The maximum rate-of-rise of voltage decreased from approximately 1,000 kv per microsecond to 133 kv per microsecond in the same distance. Rorden[7] applied an 800-kv surge, having a front of less than $^1/_2$ microsecond, to a 1-mile open-wire circuit, and measured a time to maximum voltage of approximately 2.0 microseconds at the open end. The results of these tests and of analytical calculations[8] show that corona has considerable influence in sloping surge voltages high enough to be of importance in station-protection problems. However, insufficient statistical data are available to prepare a satisfactory probability curve on the fronts of surges reaching stations. The authors have based their suggested protection, as given in the tables in the application guides, on a rate-of-rise of 500 kv per microsecond. This appears to be a reasonable upper limit for surges originating at some distance from the station. However, the general data included in this paper permits a consideration of other rates-of-rise.

Surge Voltage at Lightning Arrester Location

The surge voltage at the lightning arrester location is a function of the following factors:

1. Lightning arrester discharge voltage (IR drop).
2. Lightning arrester lead drop.
3. System dynamic voltage.
4. Station ground resistance.

Each of these items, as well as factors affecting them, will be discussed in this section.

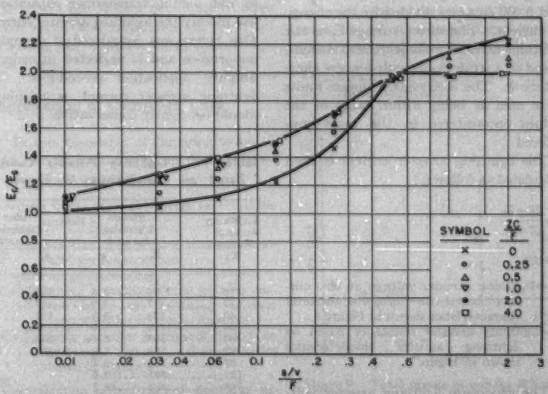

Figure 6. Maximum voltage at transformer expressed as a ratio to the maximum voltage at the lightning arrester location

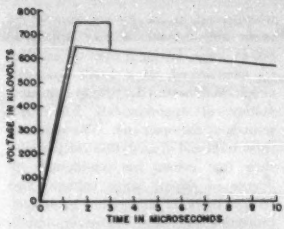

Figure 7. Combination of chopped-wave and full-wave test voltages for a 138-kv class transformer

Lightning Arrester Voltage

The current in a lightning arrester located at the end of a line is usually calculated using the following relation:

$$I=\frac{2e-e_a}{Z}$$

where

I = maximum lightning arrester current
e = crest value of incoming surge voltage
e_a = lightning arrester voltage

This equation has the limitation of requiring the lightning arrester voltage, which depends on the lightning arrester current, before finding the current. In order to eliminate the need for a cut-and-try solution, the authors have used an equation based on a lightning arrester analogue consisting of a d-c voltage and a resistance. The lightning arrester is assumed to have volt-ampere characteristics as illustrated in Figure 8. The lightning arrester resistance R is taken as the change in discharge voltage between 3,000 and 5,000 amperes divided by the change in current. The direct voltage E_0 is the lightning arrester voltage at zero current, based on a straight-line volt-ampere characteristic. The 3,000–5,000 ampere limits were used as being within range of the values encountered in the cases considered.

The lightning arrester current is then calculated as follows:

$$I=\frac{2e-E_0}{Z+R}$$

where

E_0 = lightning arrester voltage at zero current based on lightning arrester characteristics shown in Figure 8
R = lightning arrester resistance based on lightning arrester characteristics shown in Figure 8

The maximum lightning arrester voltage is then equal to E_0 plus IR.

The lightning arrester constants E_0 and R are given in Table VII for line and station lightning arresters between 30 and 242 kv. These values are based on average lightning arrester discharge voltages plus 10 per cent for station lightning arresters and plus 15 per cent for line lightning arresters. These maximum tolerances have been agreed upon by the members of the Lightning Protective Devices Committee of the National Electrical Manufacturers Association, and should eventually replace the present maximum tolerances of 15 per cent for station lightning arresters and 20 per cent for line lightning arresters.

Lead Drop

The voltage drop in the lightning arrester lead depends on the lead inductance and the rate-of-change of lightning arrester current. A lead inductance of 0.4 microhenry per foot is assumed in this paper as being typical. Lead lengths of 35 feet are used in the illustrative cases included; however, other lengths can be used with the data included.

The lead voltage is determined as follows:

$$L\frac{di}{dt}=\frac{2Lde/dt}{Z}$$

where

$\frac{di}{dt}$ = rate-of-rise of current in kiloamperes per microsecond

$\frac{de}{dt}$ = rate-of-rise of incoming surge in kilovolts per microsecond

L = lead inductance in microhenrys

In practical cases the circuit between the lightning arrester and the transformer, as well as the transformer capacitance, will modify the lightning arrester current. This factor was considered of secondary importance and is neglected in order to simplify application procedures. The lightning arrester current as calculated should be slightly conservative.

Table VII. Lightning Arrester Constants Based on Characteristics in Figure 8

Lightning Arrester Rating, Kv	Station Lightning Arrester E_0	Station Lightning Arrester R	Line Lightning Arrester E_0	Line Lightning Arrester R
30	96	2.8	122	3.5
37	117	3.9	143	5.8
40	128	3.9	151	6.9
50	159	5.0	189	8.6
60	195	5.0	235	8.6
73	234	7.2	284	11.5
97	314	8.3		
121	391	10.5		
145	464	14.3		
169	546	15.4		
195	629	16.5		
242	782	20.9		

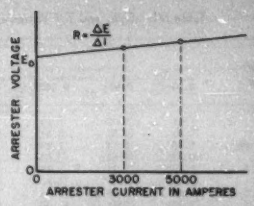

Figure 8. Lightning arrester characteristics assumed in calculating lightning arrester current

Dynamic Voltage

In applications involving appreciable lead length between the lightning arrester location and the transformer, consideration should be given to the system dynamic voltage. If the dynamic voltage is of a polarity opposite to the polarity of the incoming surge, the change in voltage at the lightning arrester location is the sum of the lightning arrester voltage, lead voltage and the dynamic voltage. This change in voltage at the lightning arrester location increases the maximum voltage at the transformer over what it would be if dynamic voltage were neglected. This factor can be taken into account in using the computer data in Figure 6, if E_s is defined as the maximum change in voltage at the lightning arrester location. In this case E_s is obtained by adding normal line-to-ground crest voltage to the lightning arrester plus lead voltages.

If system dynamic voltage is included in E_s, then E_r, as used in Figure 6, is the maximum change in voltage at the transformer, and not the maximum voltage to ground. The maximum voltage change permitted at the transformer terminals depends on the magnitude and polarity of the system dynamic voltage at the time a surge reaches the transformer. In all cases the total voltage between the line terminals and ground must not exceed the transformer impulse level. If the dynamic voltage is equal to zero, the surge voltage applied should not exceed the transformer impulse level. However, if the dynamic voltage is equal to line-to-ground crest voltage, and of a polarity opposite to the surge polarity, E_r can be as high as the transformer impulse level plus line-to-ground crest voltage, without producing a total voltage to ground at the transformer terminals higher than the transformer impulse level. In using the data in Figure 6, normal line-to-ground crest voltage is added to the transformer impulse level in obtaining E_r. If dynamic voltage is included in E_r, it must be included in E_s.

Table VIII. Influence of Counterpoise on Transformer Voltage

F, Micro-Seconds	C, Micro-farads	E_r/E_s Counter-poise Neglected	E_r/E_s Counter-poise Included
0.8	0	1.46	1.46
	0.0008	1.63	1.68
	0.0032	1.72	1.80
1.2	0	1.28	1.28
	0.0012	1.46	1.50
	0.0048	1.54	1.60

Station Ground Resistance

Station ground resistance should be a negligible factor, at least in the general case. The larger stations will be provided with an extensive ground mat having a low resistance to ground. In all cases, good engineering practice will dictate connecting lightning arresters and all apparatus tanks or housings to a common ground in order to equalize ground potentials within the station for safety reasons. If the lightning arrester ground and the transformer case are interconnected by means of a counterpoise, all of the resistance between the counterpoise and ground is not effective in increasing the voltage across the transformer insulation. The transformer tank will rise above ground potential, which partially offsets the increase in voltage produced by the lightning arrester current discharging into the resistance between the counterpoise and ground.

A special computer study was made to show the influence of a counterpoise on the voltages across a transformer. In the case considered, 200 feet of lead was assumed between the lightning arrester location and the transformer. The ground end of the lightning arrester was connected to the transformer tank with a single buried conductor 200 feet long, having a surge impedance of 167 ohms and a leakage resistance to ground of 10 ohms. Several values of F and C were considered. The results in Table VIII give the voltages at the transformer, expressed as a ratio to the voltages at the lightning arrester location, with and without the counterpoise. In the latter case, without the counterpoise, station ground resistance was neglected entirely. The data in Table VIII shows that the counterpoise system does not increase the voltage at the transformer more than 5 per cent above the voltages obtained with a perfect station ground. In more practical cases, involving shorter distances between the lightning arrester and the transformer, and lower counterpoise-system surge impedance and leakage-resistance values, the effects will be even less than indicated by the data given in Table VIII.

If the lightning arrester has a separate ground of appreciable resistance, the voltage across this resistance should be added to the lightning arrester and lead voltages in obtaining the maximum voltage at the lightning arrester location.

Total Voltage Change at Lightning Arrester Location

The total voltage change E_s at the lightning arrester location is equal to the sum of the lightning arrester discharge voltage, lead voltage, and system dynamic voltage. This assumes that the lightning arrester ground resistance is negligible. Figure 9 illustrates the addition of the voltages included in E_s. The front F is obtained by dividing E_s by the rate-of-rise of the incoming surge voltage de/dt.

Circuit Constants

The circuit constants used in connection with Figure 6 are the overhead circuit surge impedance Z and the equivalent surge capacitance C of the transformer. If these constants are known, they can be used directly in the ZC/F ratio. A surge impedance of 450 ohms is used in calculations made in this paper, this value being typical for circuits with ground wires.

The surge capacitance of a transformer is considerably lower than the total capacitance of the winding to ground, and depends on the transformer design. In the absence of data on this capacitance, it is satisfactory to use the upper curve in Figure 6, this curve defining the maximum E_r/E_s ratio that can be obtained irrespective of capacitance. Considering practical ZC/F ratios, the use of this curve will introduce a maximum of 5 per cent error, and eliminates the need for knowing the capacitance in specific applications.

Application of Computer Data

In this discussion of the application of the computer data in Figure 6, the following symbols are used:

e = crest value of surge voltage entering the station

$\frac{de}{dt}$ = rate-of-rise of incoming surge in kilovolts per microsecond

Z = line surge impedance

E_a = lightning arrester voltage at zero current based on lightning arrester characteristics shown in Figure 8

R = lightning arrester resistance based on lightning arrester characteristics shown in Figure 8

$\frac{di}{dt}$ = maximum rate-of-rise of lightning arrester current in kiloamperes per microsecond

I = maximum lightning arrester current in kiloamperes

$L\frac{di}{dt}$ = lightning arrester lead voltage in kilovolts

E_4 = line-to-neutral crest system voltage in kilovolts

E_s = maximum voltage change at lightning arrester location

E_r = maximum voltage change at transformer

$F = \frac{E_s}{de/dt}$

E_s and E_r are obtained as follows:

$E_r = E_4 +$ transformer chopped-wave test voltage.

$$E_s = E_a + IR + L\frac{di}{dt} + E_4$$

where

$$I = \frac{2e - E_4}{Z + R}$$

$L = 0.4 \times$ lightning arrester lead length in feet

$$\frac{di}{dt} = \frac{2de/dt}{Z}$$

In using the computer data, E_r/E_s is first obtained and then $(s/v)/F$ is taken from Figure 6. In the absence of specific data on the transformer capacitance C, the upper curve in Figure 6 should be used. The permissible circuit distance s, between the lightning arrester tap and the transformer, is then obtained by multiplying $(s/v)/F$ by 1,000 F.

The following example will illustrate the procedure:

A 138-kv steel tower line with nine insulators enters a station protected with 121-kv station-type lightning arresters. The lightning arresters are connected to the bus through 35 feet of lead. Determine the maximum distance that should be permitted between the lightning arrester lead tap to the bus and the bushings of a 138-kv class transformer having a 750-kv chopped-wave level.

e = 1,020 kv (1.2 × full-wave impulse level of nine insulators)

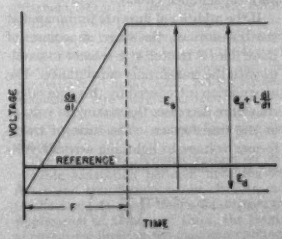

Figure 9. Total change in voltage at lightning arrester location neglecting reflections from transformer

$\frac{de}{dt} = 500$ kv per microsecond (assumed)

$Z = 450$ ohms

$E_s = 391$ kv (from Table VII)

$R = 10.5$ ohms (from Table VII)

$L = 0.4 \times 35 = 14$ microhenrys

$$Ed = \frac{\sqrt{2}}{\sqrt{3}} 138 = 113 \text{ kv}$$

$$\frac{di}{dt} = \frac{2 \times 500}{450} = 2.22 \text{ kiloamperes per microsecond}$$

$$I = \frac{2 \times 1{,}020 - 391}{450 + 10.5} = 3.58 \text{ kiloamperes}$$

$IR = 3.58 \times 10.5 = 37.5$ kv

$$L\frac{di}{dt} = 14 \times 2.22 = 31.1 \text{ kv}$$

$E_s = 391 + 37.5 + 31.1 + 113 = 572.6$ kv

$E_r = 113 + 750 = 863$ kv

$E_r/E_s = 1.51$

From Figure 6, $(s/v)/F = 0.115$

$$F = \frac{573}{500} = 1.15 \text{ microseconds}$$

$s = 1{,}000 \times 1.15 \times 0.115 = 132$ feet

This length of circuit will limit the maximum voltage at the transformer to 750 kv.

Influence of Additional Lines

The data presented in Table V showed that a second line entering the station has considerable influence on the voltage at the transformer, and consequently on the permissible distance between the lightning arrester and the transformer. This section discusses a method of estimating the influence of one or more additional lines terminated at the lightning arrester or at the transformer. In this method the circuit between the lightning arrester and the transformer, and the transformer capacitance, is treated as a simple inductance-capacitance circuit.

If the additional lines are terminated at the transformer, the surge impedance of these lines is treated as a resistor in parallel with the transformer capacitance. The attenuation introduced by this equivalent resistance decreases the maximum voltage at the transformer. The ratio of transformer voltage to lightning arrester voltage is calculated as follows:

$$E_r'/E_s' = 1 + \epsilon^{-T/2Z'C}\left(\frac{E_r}{E_s} - 1\right)$$

where

E_r/E_s = voltage ratio as given in Figure 6, which neglects additional lines

Z' = equivalent surge impedance of additional lines in parallel

T = time to maximum transformer voltage neglecting additional lines

Values of T are given in Table VI, expressed as a ratio to the front F. These values must be multiplied by F to obtain the time to maximum voltage in microseconds.

In these calculations, conservative results will be obtained if a capacitance of 0.0032 microfarad is assumed in the absence of specific data. Smaller capacitance values will result in lower voltage ratios.

As an example, consider the following case: 200 feet between lightning arrester and transformer; overhead line surge impedance of 500 ohms; transformer capacitance of 0.0032 microfarad; front F of 0.8 microsecond. One additional line terminated at transformer.

Then

$$\frac{s/v}{F} = \frac{200/1{,}000}{0.8} = 0.25$$

$$\frac{ZC}{F} = \frac{500 \times 0.0032}{0.8} = 2.0$$

$2Z'C = 2 \times 500 \times 0.0032 = 3.2$

From Figure 6, $E_r/E_s = 1.7$, and from Table VI, $T/F = 2.6$

$T = 2.6 \times 0.8 = 2.08$

Substituting these values in the foregoing equation gives a voltage ratio of 1.37, as compared to a ratio of 1.37 obtained in a study of the same case on the analogue computer. Table IX is a summary of measured and calculated values for a number of special cases studied on the computer.

If the additional lines are terminated at the lightning arrester, the initial rate-of-rise of the voltage at the lightning arrester will be modified and the front F will be decreased. In this case the front F can be modified before entering Figure 6.

Table IX. Influence of Additional Lines on Transformer Voltage

Number of Additional Lines	Lines Terminated at	E_r'/E_s' Measured	E_r'/E_s' Calculated
0	transformer	1.70	
1		1.37	1.37
2		1.15	1.19
3		1.05	1.10
0	lightning arrester	1.70	
1		1.56	1.60
2		1.40	1.52
3		1.22	1.47

Note: Above values are based on overhead line surge impedances of 500 ohms, a capacitance of 0.0032 microfarad, and 200 feet between lightning arrester and transformer.

Let

F = front neglecting additional lines

F' = equivalent front including effect of additional lines

N = number of additional lines

Then

$$F' = \frac{N+2}{2} F$$

Assuming the same conditions as used in the above example, determine the voltage at the transformer with one additional line terminated at the lightning arrester.

$$F' = \frac{1+2}{2} \times 0.8 = 1.2 \text{ microseconds}$$

$$\frac{s/v}{F} = \frac{200/1{,}000}{1.2} = 0.167$$

From Figure 6, $E_r'/E_s' = 1.60$, which should be compared to the measured value of 1.56 given in Table IX. Comparisons between measured and calculated values are given in the table for 1, 2, and 3 additional lines. The calculated values are conservative because the influence of the additional lines on reflections from the transformer is neglected.

Lines Without Ground Wires

The data in Figure 6 can be used to estimate the transformer protection provided in cases where the overhead line is not protected with ground wires. The assumption of adequate shielding of the substation against direct strokes must still be made.

If the overhead line is not equipped with ground wires, the probability of strokes directly to a phase conductor in the vicinity of the station is high enough to warrant consideration. If such strokes occur, reflections from the station can prevent a line flashover, and the lightning arrester current can approach the stroke current in magnitude and rate-of-rise. In these cases, the initial rate-of-rise de/dt of the voltage at the lightning arrester location is equal to one-half the line surge impedance multiplied by the rate-of-rise of stroke current.

References

1. A Large-Scale General-Purpose Electric Analog Computer, E. L. Harder, G. D. McCann. *AIEE Transactions*, volume 67, 1948, pages 664–73.

2. Shielding of Substations, C. F. Wagner, G. D. McCann, C. M. Lear. *Electrical Engineering (AIEE Transactions)*, volume 61, February 1942, pages 96–100.

3. Shielding of Transmission Lines, C. F. Wagner, G. D. McCann, G. L. MacLane, Jr. *AIEE Transactions*, volume 60, 1941, pages 313–38.

4. Transmission Line Design and Performance Based on Direct Lightning Strokes, E. L. Harder, J. M. Clayton. *AIEE Transactions*, volume 68, part I, 1949, pages 317–24.

5. Surge Protection of Cable-Connected Equipment, R. L. Witzke, T. J. Bliss. *AIEE Transactions*, volume 69, part I, 1950, pages 527–42.

6. Experimental Studies in the Propagation of Lightning Surges on Transmission Lines, O. Brune, J. R. Eaton. *AIEE Transactions*, volume 50, 1931, pages 1132–38.

7. Lightning Arresters as a Criterion for Insulation Levels, Harold A. Rorden. *AIEE Transactions*, volume 69, part I, 1950, pages 84–96.

8. Electrical Transmission and Distribution Reference Book. Westinghouse Electric Corporation (East Pittsburgh, Pa.), third edition, chapter 11, 1944.

Discussion

H. W. Hartzell (Commonwealth Services Incorporated, Jackson, Mich.): This paper, while dealing largely with lightning-arrester protection for transformers, indirectly brings to attention the possible lack of protection resulting in many substations for equipment located near the circuit boundaries of these stations. This equipment includes the line entrance air break switches, busses, circuit breakers, and many other items that may be located at some distance from lightning arresters installed to protect the more costly transformers.

This problem was recognized many years ago in our organization as well as others and a great deal of consideration has been given to the protection of "boundary equipment" in substations, both large and small. Protection of this equipment, however, has not received the general attention which it would seem to deserve.

Tables II, III, and IV of the paper list suggested maximum distances between lightning arrester lead taps and protected transformers. A little consideration of these distances will show that it is often quite impractical to design substations so that all electrical components will be within the suggested circuit distances. In fact, it is sometimes very difficult to locate the lightning arresters within the suggested distances of the transformers themselves unless the lightning arresters are mounted on or directly adjacent to the transformers. This of course results in less effective protection for other substation equipment.

Protection of the other electric equipment then depends on how much risk of equipment failure the designer is willing to assume. His solution is usually a compromise based on the use of:

1. Standard basic impulse insulation levels.
2. Auxiliary surge protective equipment such as some form of spill gap.
3. Lightning arresters.
4. Various combinations of (1), (2), and (3).

The designer has a choice in his selection of insulation levels and may accordingly use higher levels for the boundary equipment in an effort to reduce the risk of failure. He may use valve-type lightning arresters located at each line entrance so as to provide additional protected areas within the station similar to that provided by the transformer lightning arresters. This will generally result in an excess of protection because not all surges coming into the station will have characteristics assumed by the authors of this paper and others when determining protection requirements for transformers. Only a small percentage of surges have these characteristics.

The spill gap then seems to have a logical place in the protective scheme for boundary equipment. Because its spark-over characteristics are somewhat similar to those of equipment depending primarily on air for insulation, the installation of gaps at line entrances to substations will provide protection areas around equipment which the severe steep front surges first encounter on coming into the station. A spill-over across the gap will then prevent a flashover in the circuit entrance equipment.

Our experience over a period of more than 15 years has shown that protection of both transformers and boundary equipment may be effectively achieved when transformer lightning arresters are applied in accordance with the principles suggested in this paper and simple line entrance gaps are applied for protection of the other station components. For most surges, the lightning arresters protect the whole station, even the line entrance gaps, and thereby prevent unnecessary line trip-outs. For the more occasional severe surge, a discharge of the line entrance gap provides the necessary boundary protection.

I. B. Johnson and **L. E. Saline** (General Electric Company, Schenectady, N. Y.): In view of differences of approach to the problem of lightning-arrester location it is of interest to compare the results in the authors' paper with those in a similar study by Carpenter, Johnson and Saline.[1] Whereas Witzke's and Bliss' results are initiated from traveling wave concepts and analysis, the results from the similar study referred to are derived from lumped circuit concepts and analysis.

For comparison, consider the separations from Table III of the paper for zero lightning arrester lead length and reduced transformer insulation with those given in Table III, of reference 1. These tabulated results in the reference paper were based on zero lightning arrester lead length and the preservation of a margin between the protective level held by the lightning arrester and a reduced transformer insulation level corresponding approximately to those given in a companion paper[2] for grounded neutral circuit. Table I of this discussion gives a comparative tabulation.

In arriving at these distances a number of different assumptions were made in each study. Among these was one of allowance of margin or no margin between the overvoltage appearing at the transformer due to separation and its equivalent voltage on the volt-time curve of the transformer insulation. Whereas it appears that Witzke and Bliss have assumed no margin, reference paper 1 assumed some margin as necessary. Consequently, if instead of holding the oscillatory overshoot at the transformer due to separation to 30 per cent it is allowed to reach 50 per cent, then the lightning arrester separations at 115 kv, 138 kv, and 161 kv become 55 feet, 65 feet, and 100 feet, respectively. These are to be compared with 53 feet, 67 feet, and 92 feet from the results by Witzke and Bliss.

Table I

System Voltage, Kv	Lightning Arrester Distance,* Feet (Witzke and Bliss)	Lightning Arrester Separation,** Feet (Carpenter, Johnson and Saline)
115	53	9
138	67	15
161	92	20
230	69	38
287	80	70

* Includes down lead to transformer.

** Does not include down lead to transformer.

Among the other differences in assumptions are these:

1. Magnitude and polarity of charge on the impulse capacitance of the transformer at the time of lightning arrester operation.
2. Magnitude and rate of rise of lightning arrester discharge currents particularly at the higher voltages.
3. Effect of transformer attenuation on the overvoltages at the transformer resulting from lightning arrester separation.

In general, the conclusions from the two studies are believed to be conservative inasmuch as they are based on an elementary circuit and do not include a bus having several connected circuits. At the higher voltages it may be that the results from the elementary circuit are also somewhat conservative insofar as they are derived from initiating conditions based on insufficient statistical data with regard to wave shapes of surges reaching stations and to magnitude and rates of rise of lightning arrester discharge currents. However, where costly equipment using reduced insulation is involved, conservatism is justified until and unless a larger field experience with reduced insulation, more complete statistical data on the nature of surges at the higher voltages, and more complete evaluation of the effect of various surge wave shapes applied to the insulation indicate otherwise.

References

1. Evaluation of Lightning-Arrester Lead Length and Separation in Co-ordinated Protection of Apparatus Against Lightning, T. J. Carpenter, I. B. Johnson, L. E. Saline. *AIEE Transactions*, volume 69, part II, 1950, pages 933–44.

2. Proposed Basic Impulse Insulation Levels for High-Voltage Systems, J. E. Clem, J. R. Meador, W. J. Rudge, A. H. Powell. *AIEE Transactions*, volume 69, part II, 1950, pages 953–63.

J. R. Meador (General Electric Company, Pittsfield, Mass.): There are several points in the authors' paper that require further discussion and clarification. One of these is the question of margin between the factory impulse test on the transformer and the protected level in the field. Do the authors recommend zero margin between the transformer test voltage and the "disruptive effect" resulting from a severe lightning discharge?

The effect of the dynamic voltage on permissible separation between lightning arrester and transformer is not clear to me. In the example given under the section on Application of Computer Data, the length of circuit for limiting the maximum voltage at the transformer to 750 kv is 132 feet. If the dynamic voltage E_d is taken as zero, then

$E_s = 459.6$ kv
$E_v = 750$ kv
$E_v/E_s = 1.63$

From Figure 6,

$$\frac{S/V}{F} = 0.175$$

$$F = \frac{460}{500} = 0.92$$

$$S = 1{,}000 \times 0.92 \times 0.175 = 161 \text{ feet}$$

On this basis 161 feet of circuit will limit the maximum voltage at the transformer to 750 kv. Is this the proper interpretation?

The authors' use of an equation for "disruptive effect" is interesting but of very questionable accuracy. The complex phenomena involved in the breakdown of insulation by voltages of the type being considered here do not appear to be susceptible to such a simplified treatment. The results of our tests[1] on insulation samples gave very little hope that an equation of this form could be used with any confidence.

Until such time as the effect on insulation of superimposed oscillations is better understood, and more field data on rates of current rise through lightning arresters are obtained, it appears that considerable conservatism should be employed in separating the lightning arrester from the transformer. This is particularly true if the transformer has reduced insulation.

REFERENCE

1. PROPOSED BASIC IMPULSE INSULATION LEVELS FOR HIGH-VOLTAGE SYSTEMS, J. E. Clem, J. R. Meador, W. J. Rudge, A. H. Powell. *AIEE Transactions*, volume 69, part II, 1950, pages 953–63.

P. A. Abetti (General Electric Company, Pittsfield, Mass.): As in a previous paper,[1] the authors have represented the transformer as a pure capacitance, thereby neglecting the damping of the oscillations due to the losses which are present in the transformer winding, in the capacitances to ground, to shield, between coils and between turns.

The authors state that damping particularly affects oscillations subsequent to the first one. While this is undoubtedly true, reductions of practical importance are obtained also in the first peak, which is generally the highest. Carpenter, Johnson, and Saline[3] have taken into account this damping effect, by a 25 per cent reduction of the maximum voltages at the transformer. Do the authors think that such a factor should be taken into account? If they agree on some reduction factor, how would it modify the maximum lead lengths obtained in their investigation?

The surge capacitance, C, of the transformer was first obtained by L. F. Blume and A. Boyajian in 1919,[2] who stated

$$C = \sqrt{C_g C_s} = \frac{C_g}{\alpha} \text{ with } \alpha^2 = \frac{C_g}{C_s}$$

where C_g is the capacitance to ground and C_s the intercoil capacitance. These may be readily computed from the transformer design data. C is "considerably lower" than the capacitance to ground if $C_s << C_g$, or $\alpha >> 1$ which is not always the case.

The "suggested maximum distances between transformer and lightning arrester lead-tap when transformer has reduced insulation," as given by Table III of the paper, are plotted in Figure 1 of this discussion for zero lead length and for recommended lightning arrester levels. It appears very peculiar that separation should be less for 287-kv system voltage, than for 230 kv and 345 kv. It also appears questionable that separation should be almost the same for 230 kv and 345 kv. The corresponding data of Carpenter, Johnson, and Saline[3] show a consistent increase in separation as the system voltage increases, as may be seen from the dotted curve of Figure 1 of this discussion. In comparing the two curves, it must be remembered that Witzke's and Bliss' distances include the down lead to the transformer, but Carpenter's, Johnson's, and Saline's do not.

REFERENCES

1. See reference 5 of the paper and discussion thereof by P. A. Abetti.

2. EVALUATION OF LIGHTNING-ARRESTER LEAD LENGTH AND SEPARATION IN CO-ORDINATED PROTECTION OF APPARATUS AGAINST LIGHTNING, T. J. Carpenter, I. B. Johnson, L. E. Saline. *AIEE Transactions*, volume 69, part II, 1950, pages 933–44.

3. ABNORMAL VOLTAGES WITHIN TRANSFORMERS, L. F. Blume, A. Boyajian. *AIEE Transactions*, volume 38, 1919, pages 577–610.

W. A. McMorris (General Electric Company, Pittsfield, Mass.): The qualitative results obtained by Carpenter, Johnson, and Saline[1] are in agreement with those obtained by Witzke and Bliss. They show that lightning arrester lead length and separation between lightning arresters and transformers should be minimized, and that in any particular case, the protective margin achieved will depend upon the wave shapes of the lightning discharges involved. The quantitative results obtained by the two groups are not in agreement because their calculations and tests have not started with the same assumptions.

Perhaps the weakest point in both studies is the lack of statistical field data on rates of rise of lightning currents discharged through lightning arresters in stations, and the rates of rise of voltage at stations prior to lightning-arrester sparkover. Such data have not been obtained in a quantity comparable to that obtained with the surge crest ammeter on the crest values of lightning-arrester discharge currents, because no equally accurate and low-cost measuring instruments have been available. There is great need for the development of such instruments which are low enough in cost to permit installation in large numbers, so that data can be obtained for a variety of representative operating conditions. It will then be necessary for the industry to review the wave shapes to be used for insulation coordination studies, in order to determine the best compromise between reliability and cost of apparatus.

The wave shapes assumed by Witzke and Bliss are probably as severe as will be encountered in most cases where recommended practices have been followed with regard to overhead ground wires, low footing resistance, and shielding of stations from direct strokes. If adequate shielding is not used, sneak strokes that get in under the ground wires may result in even more severe rates of rise of current than the 5,000 amperes per microsecond assumed by Carpenter, Johnson, and Saline.

REFERENCE

1. EVALUATION OF LIGHTNING-ARRESTER LEAD LENGTH AND SEPARATION IN CO-ORDINATED PROTECTION OF APPARATUS AGAINST LIGHTNING, T. J. Carpenter, I. B. Johnson, L. E. Saline. *AIEE Transactions*, volume 69, part II, 1950, pages 933–44.

R. L. Witzke and **T. J. Bliss**: Mr. Hartzell's discussion is very interesting in that it pre-

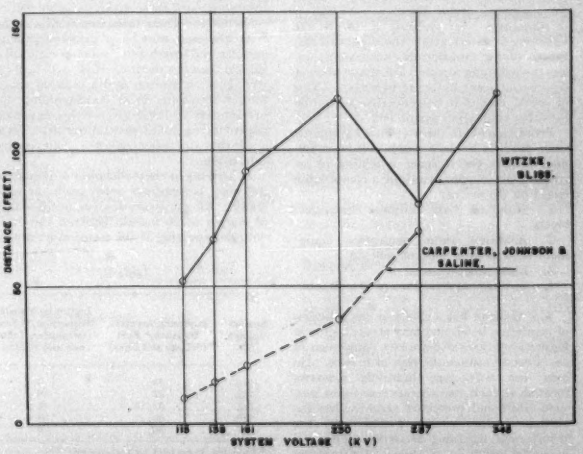

Figure 1. Maximum lightning arrester distance as a function of system voltage

sents the views of an operating company that has given careful study to the surge protection of station equipment. Our investigation was limited to the protection of transformers and did not include a consideration of other apparatus, such as circuit breakers, air switches, and so forth. We believe that individual studies of the larger stations are necessary to obtain the most economical protection, at least at this stage of the art.

The permissible separation distances given in the Carpenter, Johnson, and Saline paper[1] are very short by comparison to the values given in Table III of our paper. The discussion presented by I. B. Johnson and L. E. Saline attributes these differences to assumed margins. A careful analysis of the two papers will show that the assumptions relative to lightning arrester voltage, dynamic voltage, transformer capacitance, permissible transformer voltage and decrement are of more importance than margin. This fact is illustrated in Table II of this discussion for the case of a 450-kv BIL transformer protected with a 96-kv lightning arrester.

Procedure I is based on the Carpenter, Johnson, and Saline assumptions, whereas Procedure II is based on our assumptions. In both cases, protection is provided for an incoming surge having a rate-of-rise of 500 kv per microsecond, and the calculations are made by the method outlined in our paper.

The lightning arrester voltage under Procedure I was taken from Table III of the Carpenter, Johnson, and Saline paper. As dynamic voltage is neglected, E_t is equal to this lightning arrester voltage. The ZC/F ratio is based on the assumed 1,000 micromicrofarad transformer capacitance used in the section on Relation of Overvoltage to Volt-Time Characteristic of the Apparatus of the above paper. Carpenter, Johnson, and Saline limited the oscillation in the voltage at the transformer to 30 per cent, but allowed for 25 per cent damping. The undamped oscillation permitted is therefore 40 per cent, making E_T/E_s equal to 1.40 when attenuation is neglected. Referring to Figure 6 of our paper, a ZC/F ratio of 0.625 and an E_T/E_s ratio of 1.4 gives an $(s/v)/F$ ratio of 0.10, from which we obtain a separation distance of 72 feet.

The lightning arrester voltage under Procedure II assumes an overhead line having a full-wave insulation level of 760 kv, and is calculated as outlined in our paper. As we include dynamic voltage, E_s is higher than the lightning arrester voltage by 94 kv, the crest line-to-neutral voltage of a 115-kv system. Adding this dynamic voltage to 520 kv, the chopped-wave level of the assumed transformer, gives an E_t value of 614 kv. As data are not generally available on the effective surge capacitance of transformers, we chose to use the upper curve in Figure 6 of our paper, this curve being based on a ZC/F ratio of 4.0 in the region of interest in the present comparison. We also chose to neglect loss because this varies with the circuit and transformer characteristics, and because insufficient data are available on this factor. With these assumptions, we obtain a separation distance of only 55 feet under Procedure II as compared to 72 feet under Procedure I. We, therefore, conclude that our procedure is more conservative even though we include no margin.

Table II

	Procedure I	Procedure II
E_{arr}	360 kv	341 kv
E_d	0	94
E_s	360	435
F	0.72 microsecond	0.87 microsecond
E_t	468 kv	614 kv
C	1,000 micromicrofarads	
$\frac{ZC}{F}$	0.625	4.0
E_T/E_s (with loss)	1.30	
E_T/E_s (no loss)	1.40	1.41
$\frac{s/v}{F}$	0.10	0.063
s	72 feet	55 feet

It should be noted that the foregoing comparison is based on providing protection against an incoming surge having a rate-of-rise of 500 kv per microsecond. It is our opinion that some assumption must be made relative to the incoming surge before permissible separation distances can be evaluated. Carpenter, Johnson, and Saline neglected the all-important transients that occur prior to the time the lightning arrester gap operates, which was necessary in the absence of assumptions regarding the incoming surge. The short distances given in the section, on Relation of Overvoltage to Volt-Time Characteristic of the Apparatus of their paper, are due to neglecting these transients rather than to including margin.

Mr. Meador's interpretation of our application procedures is correct. If dynamic voltage is neglected the separation distances will be longer. We, however, feel that dynamic voltage should be considered if conservative results are to be obtained. We agree that the breakdown of insulation is a complex phenomena that cannot be accurately represented by a simple equation. As stated in our paper, the industry is in need of an acceptable method of evaluating the influence of surge voltages of nonstandard wave shape on electric apparatus, and that the method finally adopted should be substantiated by laboratory test results. The laboratory tests, however, must be more extensive than the major insulation tests in the Clem, Meador, Rudge, Powell paper.[2]

Our results neglect the damping introduced by the transformer as mentioned by Mr. Abetti. These losses vary with the circuit and transformer characteristics, and should not be given too much weight in surge protection applications until more test data are available. The results in Table III of our paper do not show a consistent increase in the permissible separation distances because the established basic insulation levels are inconsistent. It should be noted that the BIL-to-system voltage ratios used in Table III are 3.92, 3.66, and 3.76 for system voltages of 230, 287, and 345 kv, respectively. The lower ratio at 287 kv is reflected in our results, but not in the Carpenter, Johnson, and Saline paper.

Mr. McMorris emphasizes the fact that the weakest point in studies such as reported in our paper is the lack of statistical field data on the characteristics of surges that reach stations. Until such data are available, protection must be based on reasonable assumptions that give due consideration to experience.

References

1. Evaluation of Lightning Arrester Lead Length and Separation in Co-ordinated Protection of Apparatus Against Lightning, T. J. Carpenter, I. B. Johnson, L. E. Saline. *AIEE Transactions*, volume 69, part II, 1950, pages 938–44.

2. Proposed Basic Impulse Insulation Levels for High-Voltage Systems, J. E. Clem, J. R. Meador, W. J. Rudge, A. H. Powell. *AIEE Transactions*, volume 69, part II, 1950, pages 953–63.

Development of the Standard for Neutral Grounding Devices

J. E. CLEM
FELLOW AIEE

PRIOR to the time AIEE Standard number 32[1] was first published there were no standards for neutral grounding devices, information on them being included in other standards as supplementary information. There was a definite need to have all the material in reference to grounding devices in the same place and AIEE Standard number 32 was prepared to satisfy this need.

The standard for neutral grounding devices is different from other standards in that it is a functional standard. It is a standard covering the characteristics of several types of devices when used for grounding purposes. The purpose of this paper is to outline briefly the factors reviewed in the preparation of the standard for neutral grounding devices.

When the group appointed to prepare the standard took up its work, it quickly became evident that the terminology required some clarification.

The definition of "rated circuit voltage" ASA C42-15.10.100[2] was considered to be definitely in error on two counts:

1. Systems do not have a rated circuit voltage in the same sense that equipment has a rated voltage.

2. According to the definition, the rated circuit voltage of a system would change each time a transformer was connected to the system which had a secondary voltage higher than the transformer already there.

Accordingly, the group took a realistic attitude and discarded the term and its definition completely. The various systems were identified by another term "circuit voltage class", which was used in the selection of insulation class designations for neutral grounding devices. This action culminated with the later adoption by the Edison Electric Institute—National Electrical Manufacturers Association Joint Committee in Preferred Voltage Ratings for A-C Systems and Equipment[3] of the term "nominal system voltage" for the purpose of convenient designation of the voltage class of a circuit or system.

The terms indicating the various methods of grounding were selected and defined. The term "effectively grounded" was tied down securely and made quantitative by putting numbers in the definition to associate the term with limiting impedance ratios.

Before the standard was written, it was customary to base the thermal and mechanical short-time current ratings of neutral grounding devices on the "rms value of the current, including the d-c component." This appeared to be an unwieldy manner of handling this simple feature. The heating of a neutral grounding device, for the rating times considered in this standard, is practically independent of the initial offset of the ground fault current flowing through the device.

The mechanical forces depend upon the maximum crest value of the first displaced cycle. Since the decrement of the fault current may vary, not only among systems, but also among various points on the same system, some assumption of offset for the first cycle was required to establish standards for the mechanical current rating.

When a fault occurs, the fault current is initially a function of the subtransient reactance and is displaced giving rise to the d-c transient. After a few cycles, it is a function of the transient reactance. Although a displaced current will have a greater heating effect than a symmetrical current, the effect is practically negligible when the time element is ten seconds or more. Therefore, it became obvious that the use of the rms value of the symmetrical fault current, calculated using the transient reactance, for the thermal current rating was not only reasonable but also logical.

There was considerable discussion when the proposal was made to express the mechanical current rating on the rms value of the fault current and accordingly on same basis as the thermal current rating. The reason for this proposal is this: calculations of the fault current, for the determination of the thermal current rating, are made in a manner for which the result is obtained as an rms symmetrical current. If this value of fault current is used without modification but with an assumed value of offset, the procedure is simplified.

The use of the rms value of fault current to express both the thermal current rating and the mechanical current rating is simple and direct. To do this it was necessary to stipulate in the standard that the device be capable of withstanding the mechanical forces set up by the current on the basis that the current wave is completely offset. In addition, it was necessary to make allowance for the fact that the calculations of fault current for the thermal current rating are made using the transient reactance of the generators, while the fault current which determines the mechanical forces is determined by the subtransient reactance, and accordingly is higher during the first few cycles. This difference was checked for several representative cases and it was found that a difference of 20 per cent in the two values of current would include a large enough proportion of possible occurrences to justify its use in the standard. Accordingly, in the interest of simplification, the standard requires that the mechanical current rating of a neutral grounding device be 1.2 times the thermal current rating.

Paper 50-154, recommended by the AIEE Protective Devices Committee and approved by the AIEE Technical Program Committee for presentation at the AIEE Summer and Pacific General Meeting, Pasadena, Calif., June 12–16, 1950. Manuscript submitted March 13, 1950; made available for printing April 17, 1950.

J. E. CLEM is with the General Electric Company, Schenectady, N. Y.

The voltage rating of neutral grounding devices was carefully analyzed. It seemed reasonable to use, as the basis of the voltage rating, the voltage developed across the device during a fault. There were two cases for which an exception appeared justified. For resistor neutral grounding devices it was thought desirable to make the voltage rating the same as the line-to-neutral voltage of the circuit on which it was used whenever the impedance voltage at 25 degrees Centigrade exceeded 80 per cent of the circuit line-to-neutral voltage. This was done because of the increase in resistance due to increase of temperature. And quite obviously, the voltage rating of a grounding transformer should be the same as the line-to-line voltage of the circuit on which it is used, because it is directly connected to the circuit.

The question of the time rating involved much discussion. Prior to the writing of the standard, neutral grounding devices had been specified for various time intervals between ten seconds and two minutes. A careful review of the essential performance requirements of the devices indicated that a rated time of one minute would be adequate for all cases except one and for all devices except ground fault neutralizers. The review indicated that neutral grounding devices used for grounding the neutral of generators need not require in many instances, the 1-minute time rating, a 10-second rating being sufficient.

The review also showed that practice in the use of ground fault neutralizers required a short-time rating longer than one minute, and a long-time rating shorter than continuous. Ten minutes was chosen for the short-time rating and 90 days for the long time, the latter being designated as "extended time."

Ground fault neutralizers are required to be capable of carrying continuously a circulating current equal to 30 per cent of their rating without exceeding a 55-degree Centigrade rise. This results in a well-co-ordinated thermal design between the continuous capability and the time rating. When the standard was being prepared there was some question as to whether this value of circulating current might be too small, or too large. Consequently a survey was undertaken after the standard was finished to answer this question. The results of the survey have been reported[4] and indicate that the value chosen for the standard was about the optimum, being high enough to cover nearly all the cases and not so low as to require costly transpositions. The investigation included economic factors.

In establishing the temperature limits, a new concept was introduced for those devices using class-A and class-B insulation. Previously equipment standards merely required that the equipment be capable of withstanding a specified value of fault current for a specified time. An analysis was made to check the relative aging during the heating-up period, the specified time, and the cooling-off period, which revealed some very startling results.

For example, one standard states that a fault current of 25 times rated value must be withstood for two seconds, and 16.6 times for four seconds, and this is coupled with the requirement that the starting temperature be assumed as 95 degrees Centigrade and the limiting temperature be 250 degrees Centigrade for class-A material. Nothing is said about how often this may occur. It is absurd to say that 250 degrees Centigrade for four seconds produced by 16.6 times current is no worse than 250 degrees Centigrade for two seconds produced by 25 times current, and it is equally absurd to neglect the frequency of occurrence.

Actually, there were some who maintained that the 250-degrees Centigrade temperature for four seconds should be incorporated in the standard for neutral grounding devices, because its presence in the other standard indicated that "experience had proven it to be satisfactory." It was a simple matter to show that a temperature of 250 degrees Centigrade for four seconds would cause, in one occurrence, the insulation to deteriorate slightly more than in one year's normal operation. Further, calculations proved conclusively that the equipment in question had thermal characteristics such that it was impossible to attain the 250-degrees Centigrade limiting temperature at the specified current, even if the fault continued for the time mentioned in the standard.

It was easy to demonstrate that most, about 95 per cent usually, of the aging of the insulation occurred during the cooling period of the temperature cycle. The obvious next step is the recognition of the fact that a device that has a slow rate of cooling should have a lower limiting temperature, if the aging in the two cases is to be comparable.

Prior to the initiation of the work on this standard, it was commonly accepted throughout the industry that cooling was always a logarithmic function. This is true only for those devices for which the temperature rise is directly proportional to the losses. However, the temperature rise of devices immersed in a cooling liquid is not directly proportional to the losses but varies as an exponential function with the exponent different from unity. Thus

$$\theta = kw^n$$

In this equation n is always less than unity down to a value of about 0.7. Because of this neither the heating nor the cooling is a logarithmic function.

Once the concept that the rate of cooling and the permissible maximum temperature should be correlated, it was easy to pass on to the next forward step of setting the maximum temperature limitation on the basis of the relative aging over a definite period of time. Aging data[5] for class-A insulation as determined by laboratory tests at various temperatures are available. The relative aging is based upon the reduction in mechanical strength. This information does not enable one to estimate the useful life of a transformer or of any other equipment. It does enable one to estimate how much more rapidly the insulation used in equipment will lose its mechanical strength when the temperature to which it is subjected is increased.

It has been customary to consider that the rate of aging for class-A insulation when used in transformers doubles with each 8-degrees Centigrade increase in temperature. The information in reference 5 indicates that the temperature increment which doubles the rate of aging at 95 degrees Centigrade is much less than 8 degrees Centigrade. The series of temperature increments, 2, 2.5, 3, 3.5, 4, 5, 6, 7, 8, . . ., starting at 95 degrees Centigrade, gives closely the same over-all increase in rate of aging for a wide range in temperature as does the data in reference 5. Rate-of-aging curves were prepared using these increments, and extending over the range of temperatures under consideration.

The exponent n of the heating characteristic for liquid-insulated devices is not constant. Apparently it will increase when the insulation thickness is increased, and apparently it is reduced at higher temperatures because of the lowered viscosity of the oil. All such factors were considered when the cooling curves upon which the aging calculations, used in establishing the temperature limits, were prepared. Calculations were made of both the heating and cooling periods and compared with test results for different conductors, thickness of insulation, and temperatures of the cooling oil. The analytical formula was first used, but was modified as the study progressed by empirical factors and procedure until the agreement was very, very close.

Considerable thought was given to the question of the relative aging upon which to base the temperature limits. This would be dependent, of course, upon the number of times the device might be called upon to function and upon the relative loss of life which might be considered reasonable. An investigation was made and it appeared that ten operations per year would be sufficient to cover all except the most severe operating conditions. It seemed reasonable also to expect these devices to have about the same life expectancy as power and distribution transformers.

The rate-of-aging curves, and the heating and cooling curves, were used together to establish temperature limits and the associated initial rate of cooling, such that ten events per year would give about the same loss of life in one year as occurs in a transformer when operated at full load in a 30-degrees Centigrade ambient temperature for one year.

Prior to the development of the standard it was customary, in checking the temperature rise on the occurrence of a fault, to neglect the insulation associated with the conductor and to assume that all the heat was stored in the copper. This assumption was conservative for the heating-up period, but would have been suicidal for the cooling period. Even when the insulation was considered, the formula used for the combined thermal capacity had no sound basis.

In working out the heating and cooling curves previously mentioned, an empirical formula for the thermal capacity of the copper conductor and its associated insulation was developed. The development of this formula was closely and directly associated with the development of the empirically modified heating and cooling formulas previously mentioned. Since its use with the correct method of calculating heating and cooling curves gives correct results, it is reasonably and logically considered to be correct for the high-temperature conditions allowed in the standard for neutral grounding devices.

Since limiting temperature is dependent upon the rate of cooling, it is necessary to have a uniform method of quickly checking the cooling rate. This is affected by several factors, some of which, such as the temperature rise at the start of the cooling period, can be directly evaluated, and others, such as the exponent of the heating characteristic, cannot. Accordingly, a simple expression containing an empirical factor was developed. This expression gives very good results over the range of temperatures for which it is used. The use of this empirical formula provides a ready and simple means of making sure that the thermal design of any specific device is reasonably correct.

The establishment of a limiting maximum temperature and the corresponding cooling required an extended analytical investigation, together with an extensive experimental investigation. Part of this experimental and analytical investigation was reported by Montsinger and Clem[6] and part by Montsinger and Halsey.[7]

An outline of some of the analytical work is given in the appendix to this paper.

Methods of demonstrating that the temperature limits are fulfilled in the design came in for considerable discussion. It was agreed that the 10-second and 1-minute ratings could be demonstrated adequately by calculations and that the 10-minute and extended time ratings should be demonstrated by tests. Therefore, formulas for calculating the temperature rise were developed and placed in the standard for the various conditions and types of devices. To be on the conservative side, these calculations are made on the basis of all heat stored and with the eddy-current loss neglected. When eddy currents are present the increase in resistance as the temperature rises reduces the eddy-current portion of the losses. The high-temperature rises allowed for neutral grounding devices results in a high rate of cooling. Accordingly, the requirement that a cooling curve be taken on the temperature on each device was included in the standard as applicable to the 10-second and the extended time ratings.

Prior to the development of this standard, the problem of selecting the proper dielectric test was a rather difficult one. This problem was analyzed for a considerable time and tabulations were prepared with accompanying instructions which will result in the selection of the same dielectric test irrespective of who makes the selection.

As mentioned earlier, the standard for neutral grounding devices is on a somewhat different basis than other equipment standards, because the functional performance of the device is of prime importance. There has been included in the standard a considerable amount of information on the selection and application of neutral grounding devices. It was felt desirable to do this because the frequency of use of these devices is much less than of other equipment, and with this information available in the body of the standard the application engineer will not be called upon to do research work elsewhere.

The correlation of the temperature limits with the rate of cooling and the reliability of the empirical expressions for the thermal capacity of the conductor together with its associated insulation, and for the rate of cooling, places the thermal design of neutral grounding devices on a sound, uniform, and clean-cut engineering and commercial basis. The engineering establishment of varying limiting temperatures, as dependent upon the rate of cooling and a reasonable aging for a specified time, is an outstanding development.

It is felt that this standard is a forward contribution to the list of standards prepared by the Institute and that by adopting the principle of selecting the maximum limiting temperature on the basis of the rate of cooling, a precedent has been set which should be followed in the standards for other types of equipment.

Appendix

Heating and Cooling Curves—General Equation

At any point on the heating curve of a device, the increment in temperature will be determined by the energy supplied in the increment of time and the thermal capacity. As an analytical expression

$$\Delta\theta = \frac{(W_s - W_r)\,\Delta t}{C}$$

where

$\Delta\theta$ = increment in temperature
W_s = rate of heat supply
W_r = rate of heat loss
Δt = increment of time
C = thermal capacity, properly associated with the units in which W_s and W_0 are given

$$W_s = (1 + \alpha_0\theta)\,W_0$$

where

α_0 = temperature coefficient of resistance at the starting temperature, θ_0
θ = temperature increase above the starting temperature at time t
W_0 = initial watts input at zero time

$$W_r = K\theta^n$$

where

K = empirical constant, depending upon the design
n = empirical exponent, varies from about 1.5 to 1.0 depending upon the design, temperature, and possibly other factors

Neither K nor n are themselves constant over the range of temperatures encountered in neutral grounding device design, but are essentially constant for the temperature range in the design of transformers.

Cooling Curve

The differential equation

$$d\theta = \frac{-W_r}{C}\,dt$$

The solution

$$t = \frac{C\theta_1}{W_1}\,\frac{1}{1-n}\,(1-r^{1-n})$$

where

θ_1 = temperature rise at start of cooling period
W_1 = watts loss corresponding to θ
r = ratio of θ to θ_1

The writer first derived this expression many years ago and quickly found that, while it applied very well for the usual temperatures of transformer windings and oil, it became increasingly unreliable as the temperatures increased.

If n is unity, the solution is

$$t = \frac{C\theta_1}{W_1}\log\frac{\theta_1}{\theta}$$

$$\theta = \theta_1 e^{-at}$$

$$a = \frac{W_1}{C\theta_1}$$

These are the so-called standard cooling curve equations and the quantity a represents what has been referred to as the time constant.

A better way of calculating a cooling curve at high temperatures is to determine the heating characteristic, that is, the curve showing the temperature rise θ as a function of watts loss W_r. Then use the equation

$$\Delta t = -\frac{C}{W_r}\Delta\theta$$

and take reasonably small decrements in θ, reading W_r for the midpoint of the decrement, at the same time compensating the thermal capacitance for the change in temperature. This is the method that was used in deriving the temperature limits and the required rate of cooling which were adopted for the standard.

Heating Curves-Constant Current

No Radiation—No Eddy Current

The differential equation

$$d\theta = \frac{W_0}{C}\,dt$$

The solution

$$t = \frac{C}{\alpha_0 W_0}\log(1+\alpha_0\theta)$$

$$\theta = \frac{1}{\alpha_0}(e^{at}-1)$$

$$a = \frac{\alpha_0 W_0}{C}$$

The translation of these expressions into those given in the standard is simple and straightforward.

No Radiation—with Eddy Current

The differential equation

$$d\theta = \left\{(1-m)(1+\alpha_0\theta)W_0 + \frac{mW_0}{1+\alpha_0\theta}\right\}\frac{dt}{C}$$

where

m = per-unit eddy-current loss, referred to the total initial loss W_0

The solution

$$t = \frac{1}{a}\log\left\{(1-m)(1+\alpha_0\theta)^2+m\right\}$$

$$\theta = \frac{1}{\alpha_0}\left\{\sqrt{\frac{e^{at}-m}{1-m}}-1\right\}$$

$$a = \frac{2\alpha_0(1-m)W_0}{C}$$

A comparison of the equation for the time given here with that given for the preceding case shows quite clearly that the presence of eddy currents does increase the time to attain any specified temperature. Therefore, neglecting the eddy current loss gives conservative results.

Radiation—No Eddy Current

The differential equation, when the exponent n is taken as unity

$$d\theta = \left\{(1+\alpha_0\theta)W_0 - K\theta\right\}\frac{dt}{C}$$

The solution

$$t = \frac{\theta_1 C}{W_0}\log\frac{1}{1-r}$$

$$\theta = \theta_1(1-e^{-at})$$

In these equations

θ_1 = ultimate temperature rise
r = ratio of temperature θ at time t to ultimate temperature rise $= \frac{\theta}{\theta_1}$

$$a = \frac{W_0}{\theta_1 C}$$

Radiation—with Eddy-Current Loss

Analytical

The differential equation, when the exponent n is taken as unity

$$d\theta = \left\{\frac{(1-m_1)(1+\alpha_0\theta)}{1+\alpha_0\theta_1} + \frac{m_1(1+\alpha_0\theta_1)}{1+\alpha_0\theta} - \frac{\theta}{\theta_1}\right\}\times\frac{W_1}{C}\,dt$$

In this equation m_1 is now the per-unit eddy-current loss referred to the total ultimate loss W_1.

The solution

$$t = \frac{C\theta_1(1+\alpha_0\theta_1)}{W_1(1+2m_1\alpha_0\theta_1)}\times\left\{\log\frac{1}{1-r} + \frac{m_1\alpha_0\theta_1}{1+m_1\alpha_0\theta_1}\log\frac{a}{a-cr}\right\}$$

$$a = 1+2m\alpha_0\theta_1+m(\alpha_0\theta_1)^2$$

$$c = -\alpha_0\theta_1 - m(\alpha_0\theta_1)^2$$

Step by Step

The differential equation may be put in the form

$$\Delta t = \frac{C}{(1-m)(1+\alpha_0\theta)W_0 + \frac{mW_0}{1+\alpha_0\theta} - W_r}\,\Delta\theta$$

As was done for the cooling curve, the procedure is to establish the heating characteristic, take reasonable increments of temperature, determine the heat supplied and radiated, adjust the thermal capacity for the actual temperature, and then calculate the corresponding increment of time.

The step-by-step method was used for the calculations for the oil-immersed devices, and additional spot checks by the analytical method were obtained for the dry-type devices.

Heating Curve—Constant Voltage

The differential equation

$$d\theta = \frac{W_0}{C(1+\alpha_0\theta)}\,dt$$

The solution

$$t = \frac{C\theta}{W_0\left(1+\frac{\alpha_0\theta}{2}\right)}\,dt$$

$$\theta = \frac{1}{\alpha_0}\left\{\sqrt{\left(1+\frac{2\alpha_0 W_0 t}{C}\right)}-1\right\}$$

In these equations the eddy-current loss has been neglected and the translation into the form given in the standard is simple and straightforward.

References

1. Neutral Grounding Devices. *AIEE Standard Number 32*, June 1942.

2. Definitions of Electrical Terms, *ASA Standard Number C421-1941*, AIEE, 1941.

3. Preferred Voltage Ratings for A-C Systems and Equipment, Joint Edison Electric Institute—National Electrical Manufacturers Association Report. *EEI Publication Number R-6, NEMA Publication Number* 117 (New York, N. Y.), May 1949.

4. Report on Survey of Unbalanced Charging Currents on Transmission Lines as Affecting Ground-Fault Neutralizers, *AIEE Committee* Report. *AIEE Transactions*, volume 68, part II 1949, pages 1328–39.

5. Factors Affecting the Mechanical Deterioration of Cellulose Insulation, F. M. Clark. *Electrical Engineering (AIEE Transactions)*, volume 61, October 1942, pages 742–49.

6. Temperature Limits for Short-Time Overloads for Oil-Insulated Neutral Grounding Reactors and Transformers—II, V. M. Montsinger, J. E. Clem. *AIEE Transactions*, volume 65, 1946, pages 966–73.

7. Heating of Transformers Under Short-Circuit Conditions, V. M. Montsinger, G. H. Halsey. *AIEE Transactions*, volume 68, part II, 1949, pages 947–54.

No Discussion

Indicating Instruments at the Servomechanism Frequencies

WILSON S. PRITCHETT
ASSOCIATE AIEE

ROBERT M. SAUNDERS
MEMBER AIEE

Synopsis: Tests on indicating instruments excited with sinusoidal signals at the servomechanism frequencies show that under certain conditions they are the same useful and time-saving tools as when used at the power frequencies. These conditions are determined by the motional characteristics of the instrument and the desired accuracy. This paper describes the performance of conventional indicating instruments at these low frequencies, discusses what can be done to these instruments to make them more suitable for this service, and gives one example of what can be expected when an indicating instrument is designed expressly for servo system use.

WITH the advancing application of sinusoidal analysis to servo systems, the need has arisen for instruments that will measure a-c steady-state quantities in the frequency range of usual servo operation, either by use of conventional portable instruments or by the development of new instruments. At the present time the oscillograph and oscilloscope are the most commonly used tools in the analysis of servo systems. If the indicating instrument could be used, it would make the analysis of oscillograms unnecessary, and would thereby represent a considerable saving in the time required for a-c steady-state servo analysis.

Most commercial a-c indicating instruments are designed for optimum performance in the range from 25 to 133 cycles per second. As the frequency applied to the terminals of such instruments is reduced, the behavior of the instrument is characterized by three zones:

Zone A—Where the pointer remains motionless or has a small excursion on either side of the average deflection.

Zone B—Where the pointer follows the impressed wave without amplitude or phase angle error.

Zone C—The zone lying between zones A and B.

In most instruments zone A extends downward from the power frequencies and the readings represent the effective values of the impressed wave, while zone B extends upward from zero frequency or direct current and the maximum reading of the instrument represents the maximum value of the wave. Either zone A or B operation of the instrument will result in reliable indications of either the maximum or the effective value of the wave in question. Zone C operation is completely unreliable. Frequently a-c instruments which have a low stated error on direct currents give a larger deflection on one half than on the other half of the cycle when used in zone B, but the average of the two maximum readings usually can be used. It is the object of this paper to: determine the ranges of zones A, B, and C in commercial instruments available today; explore the means of modifying conventional instruments toward extending zone A downward, zone B upward, and compressing zone C; and to consider the design features of an instrument that will extend zone A beyond that now encountered in conventional instruments.

Conventional Instrument Characteristics

The amplitude response versus frequency characteristic of a given instrument will provide one with the information needed to determine where the described zones lie.

In this paper the per-unit change in scale reading is defined as the ratio of the actual change in reading to the reading corresponding to the maximum value of the impressed electrical quantity. When the per-unit change in scale reading is unity, the instrument is following the impressed wave precisely without amplitude error, as described for zone B. As the frequency of the impressed wave increases, although the amplitude remains constant, the per-unit response begins to fall off until the per-unit change in reading becomes very small, say within approximately 5 per cent; this is defined as the beginning of zone A which then extends upward to the power frequencies

Figure 1 shows the amplitude response characteristics of several conventional instruments when subjected to such a constant amplitude but varying frequency voltage. The ideal instrument, whose characteristic curve is shown at the left of Figure 1, would have a zone C of negligible width; thus the width of zone C becomes a figure of merit for instruments contemplated in this service. It is noted that the electrodynamometer instrument follows the wave up to 0.07 cycle per second and then begins to drop off. At 1.0 cycle per second, the excursion on either side of the average reading is within 5 per cent so that the average position of the pointer now is indicating the effective value of the wave. Thus for this instrument zone A extends downward to 1.0 cycle per second; zone B extends upward to 0.07 cycle per second, and zone C extends from 0.07 to 1.0 cycle per second. The D'Arsonval instrument (which has no zone A) and the full-wave rectifier instrument have characteristics very similar to each other even though the applied torque waves are not the same function. Zone C is about two decades wide for these instruments. Since zone B extends to the same upper frequency as

Paper 50-155, recommended by the AIEE Instruments and Measurements Committee and approved by the AIEE Technical Program Committee for presentation at the AIEE Summer and Pacific General Meeting, Pasadena, Calif., June 12–16, 1950. Manuscript submitted March 13, 1950; made available for printing April 17, 1950.

WILSON S. PRITCHETT and ROBERT M. SAUNDERS are both with the Division of Electrical Engineering, University of California, Berkeley, Calif.

The authors wish to express their appreciation to F. F. Davis for his many contributions to the design and construction of the low-frequency instrument described herein.

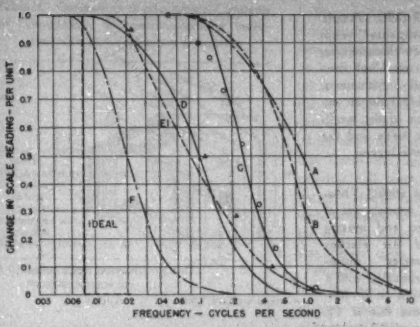

Figure 1. Amplitude response versus frequency characteristics for conventional instruments, the ideal instrument, and the low-frequency instrument described in the paper. The instruments associated with each curve are described in Table I

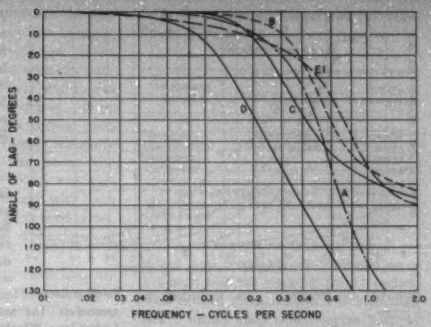

Figure 2. Phase angle versus frequency characteristics for some of the instruments shown in Figure 1

for the electrodynamometer type, these instruments are not as attractive since their zone *C* is much wider. The general characteristic of the moving vane instrument is shown as curve *E1* in Figure 1. The particular instrument shown here is one which was chosen for later modification. The thermocouple instrument was selected because of its relatively long zone *A* although its zone *C* is about five octaves. The instrument whose design is described later in this paper is shown for comparison purposes as curve *F*, and shows what can be expected from an instrument expressly designed for this service. It should be pointed out that the ordinate is plotted in terms of change in scale reading, not change in deflection. In this paper deflection is defined as the angle of motion of the movement, whereas the scale readings are those values which appear on the face of the instrument. If the curves were plotted in terms of the change in deflection, they would all be of the same general type as that for the D'Arsonval instrument. However, because of the nonlinear scales on a-c instruments, the curve of change in reading is very steep at the upper end.

Table I summarizes and collects the pertinent data for the various instruments tested. These instruments were believed to be typical examples of the portable instruments found in most laboratories. It was found that all tests of instruments of a particular type (for example, electrodynamometer) resulted in the same general curve although the curves might be displaced slightly to the right or left depending upon the manufacturer.

All but one of the instruments tested used eddy current damping of some type, and an auxiliary additional means of damping was employed as described in the column labeled "Special Damping Medium." Instrument *F* solely employed an oil whose viscosity was 38 seconds, Saybolt Universal Viscosity (SUV) at 100 degrees Fahrenheit. The time constant is defined as the time required for the deflection to reduce to 37 per cent of its initial value.

In most cases the amplitude response characteristic is of more significance; however, in the interest of completeness, the curves showing the angle of lag of the maximum deflection of the pointer with respect to the impressed wave as a

Table I. Data for Instruments Shown in Figure 1, 2, and 3

Instrument	Instrument Type	Accuracy Class Per Cent	Manufacturer	Manuf. Type	Special Damping Medium	Time Constant, Seconds	Moment of Inertia, gm-cm²	Zone $\overline{C}$, Cycles Per Second	Spring Constant, gm-cm/radian
A	Permanent magnet-moving coil	0.2	Gen. Elec.	*DP2*	None	*	*	0.06–10	*
B	Full-wave rectifier	4	Weston	*430*	None	*	*	0.06–5	*
C	Electrodynamometer	0.2	Gen. Elec.	*P3*	None	0.06†	13.8	0.06–0.8	0.14
D	Thermocouple	0.5	Weston	*412*	None	1.0	*	0.005–0.55	*
Not shown	Moving vane, 270-degree scale	1.0	Westinghouse	*KA24*	None	*	*	0.01–1.5	*
E1	Moving vane (radial scale)	1.0†	Gen. Elec.	*H*	None	1.2	73.8	0.015–0.80	0.59
E2					Oil (10 sec SUV)	2.8	73.8	0.012–0.30	0.59
E3					Oil (200 sec SUV)	23	73.8	0.007–0.035	0.59
E4					Oil + small vane (10 sec SUV)	4.3	*	0.0015–0.20	0.59
E5					Oil and large vane (10 sec SUV)	7.5	95	0.007–0.12	0.59
E6					Oil and large vane (200 sec SUV)	38	95	0.007–0.09	0.59
F	Electrodynamometer	1.0**	Univ. of Calif.	*P5042*	Oil (38 sec SUV)	7.5	2300	0.006–0.07	0.18

Notes:
*These values were not determined for this instrument. †Estimated. **Ammeter service; voltmeter, milliammeter, wattmeter service, 0.5 per cent.

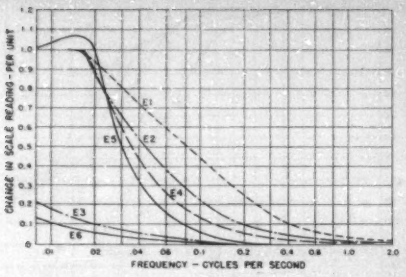

Figure 3 (left). Amplitude response versus frequency characteristics for the modified conventional instruments. See Table I for an explanation of the modifications made and the curve legend

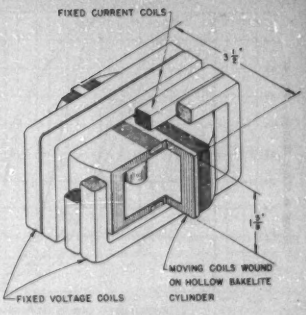

Figure 4 (right). Mechanical arrangement of the fixed and moving coils of the electrodynamometer instrument constructed with a large moment of inertia for use on low frequencies. The tank, whose size is 11 inches long, 8 inches wide, and 5 inches deep, is not shown

function of frequency are included in Figure 2.

It is possible to compute the characteristics shown in Figure 1 and 2; however, these instruments probably will be used for investigation of control system response to a-c signals. In such cases it is quite likely that there will be a low-frequency oscillator available so that the actual frequency response curve can be obtained for the contemplated instrument. This procedure is considered to be somewhat simpler than calculating the curve. As is shown in equation 8, Appendix I, the upper and lower limits of the deflection of an electrodynamometer movement are obtainable from

$$\theta = I_f I_M \frac{dM}{d\theta} \left\{ \frac{\cos\phi}{K} + \frac{1}{\sqrt{(K-4\omega^2 J)^2 + (2\omega D)^2}} \sin(2\omega t + \lambda) \right\} \quad (8)$$

The first term represents the mean deflection whereas the last term represents the excursion on either side of the mean. Graybeal[1] has examined this latter term in considerable detail, and one may make use of his work to reduce the labor involved in calculating the response curves. In order to use Graybeal's curves, it is necessary to know the natural frequency and the relative damping. The natural frequency can be obtained in most cases by removing the lid of the air damping box or by removing the damping magnets so that the number of oscillations per given length of time can be found. In some cases the relative damping can be determined by use of Graybeal's Figures 8 and 9 for which one must know the ratio of the successive maximum swings, if oscillatory, or the time it takes for the deflection of the instrument to become 50 and 25 per cent of the initial value if it is overdamped. In some cases this relative damping cannot be ascertained without the use of special equipment because the instrument may move too fast for visual observation. However, it may be assumed that β lies between 0.7 and 1.0 for most instruments since the manufacturers make every attempt to cause their instruments to register the final reading in a minimum length of time and with minimum oscillation.

Calculated points for the curve pertaining to the electrodynamometer instrument are shown as circles in Figure 1. In the case of the moving vane instrument or any other in which the torque is a nonsimple function of the position of the movement, the calculations become involved. However, one may sometimes make the simplifying assumption that the torque varies as the square of the applied current, and obtain curves that check reasonably well with test. Such a set of points for a moving vane in air are plotted as triangles in Figure 1. It will be noted that one may calculate curves closely approximating the test curves.

Modifications to Conventional Instruments

As was mentioned previously, there are some modifications that can be made to conventional instruments that will shift zones *A*, *B*, and *C* to the left. Damping is one such modification. Curves *E1*, *E2*, *E3*, of Figure 3 show how zone *A* can be extended as the time constant of a given instrument is increased from 1.2 to 23 seconds. Curves *E2* and *E3* are for liquid damping, the whole instrument being set in insulating oils of 10 and 200 SUV. The authors feel that increasing the damping is not an especially desirable method of extending zone *A* because zone *C* becomes extremely wide, and the transient response is very much impaired when heavy damping is employed. In collecting the data for curve *E3*, it was noted that it took nearly five minutes for the needle to come to its final deflection after being energized with a 1-cycle-per-second wave. Ordinarily this extremely long time constant cannot be tolerated.

Curves *E4*, *E5*, and *E6* of Figure 3 show the effects of decreasing the natural frequency by increasing the moment of inertia. As is shown by Graybeal[1] the natural frequency

$$f_n = \frac{1}{2\pi}\sqrt{\frac{K}{J}} \quad (1)$$

where K is the spring constant and J is the moment of inertia of the movement.

Since, for a given instrument, the spring constant cannot be reduced without jeopardizing the electrical to frictional torque ratio, the only other possibility is to increase the moment of inertia. However, the increase in that quantity can only be effected by adding weight to a movement. This results in added load on the bearings, a condition that will lead also to faulty operation. Hence, it is concluded that modification to conventional instruments is not as attractive as designing an instrument for use at the frequencies encountered.

A Special Low-Frequency Instrument

An instrument overcoming the objections mentioned previously and having a Zone A throughout Zone C of conventional a-c instruments has been constructed. At the outset it was decided to use construction as nearly conventional as possible and to employ commonly available springs, pivots, and jewels. Rapid response together with low per-unit change in scale reading was afforded by a high moment of inertia moving system with damping slightly below critical.

Since the moment of inertia and consequently the weight required was many times that of conventional instruments, means other than jewels and pivots alone were needed to support the extra burden.

Table II. Comparison of Mechanical Contants of Conventional Electrodynamometer Instrument with Low-Frequency Instrument

	Conventional Instrument	Low Frequency
Spring constant, gm-cm/radian	0.18	0.18
Weight of moving system, gram		
In air	3.2	215
On bottom pivot	3.2	2 (approx)
Undamped natural periods, seconds	1.0	23*
Moment of inertia, gm-cm²	4.5*	2,300

* Computed from measured constants.

This was accomplished by winding the moving coils upon a hollow bakelite cylinder and immersing the entire instrument mechanism in an insulating liquid. The cylinder was designed so that the residual weight of the moving system when submerged was well within the normal capacity of the pivots and so that the moment of inertia was correct for the springs used. Table II compares the mechanical constants of the low-frequency instrument with those of a high-quality commercially available instrument.

Appendix II describes the design requirements which led to the choice of the mechanical constants given. Use of the electrodynamometer principle permitted calibration of the low-frequency instrument on d-c and afforded greater flexibility in application. Advantage was taken of the needed weight of the moving system to use as many turns of comparatively large wire as possible since the pivots were not required to carry the burden. The low frequencies for which the instrument was intended made the resulting large inductance acceptable. Both of these factors offered uncommon possibilities in securing excellent sensitivity for instruments of the electrodynamometer type. In this instance, it was possible to design the moving coil for both good current sensitivity and good voltage sensitivity. That is, the number of turns could be made large enough to permit the instrument to be connected as a sensitive voltmeter and at the same time the resistance could be kept low enough to permit the instrument to be connected as a low-loss ammeter. A separate set of fixed coils, however, was required for each of the two connections. If the moving coil had been designed for either the voltmeter or the ammeter alone the sensitivity could have been appreciably improved. Figure 4 shows the arrangement of the fixed and moving coils for the compromise design.

Since instrument transformers are not suitable for use at the very low frequencies it was decided to provide four ranges on both the voltmeter and ammeter connections. Accordingly, four multipliers for the voltmeter were required. Four shunts together with eight current coils which were wound to have approximately the same average position about the moving coil were required for the ammeter. Heavy brass terminals with links were provided to make the desired series, parallel, or series-parallel connections of the current coils.

Figure 5 shows the schematic diagram and the circuit constants of this low-frequency electrodynamometer. The series connection of the current coils is shown in the figure. It is seen that additional provisions have been made for connecting the instrument either as a multiple-range wattmeter or as a single-range milliammeter. Also the instrument can be used as a separately excited electrodynamometer for harmonic analysis or phase angle studies. The small resistor connected to the wattmeter potential coil terminal "$\pm W$" permits using the same multipliers and terminals for the wattmeter potential circuit connection as are used for the voltmeter connection. The letters "A", "M", "V", and "W" refer to the terminals to be used for the ammeter, milliammeter, voltmeter, and wattmeter connections respectively. The larger terminals are for the current circuit and the smaller terminals for the potential circuit. Both pairs of terminals, "AM" and "A" are closed with links for the ammeter connection. For the milliammeter connection, only the terminals "AM" are closed, and all current coils are connected in series. The scale is calibrated for all four services.

Table III gives the full scale reading and the power consumption at this reading for each connection. The data are for the "1X" range of the ammeter, the voltmeter, and the wattmeter, and for the single range of the milliammeter.

Table III. Calibrated Ranges and Full Scale Power Consumption of Low-Frequency Indicating Instrument

Instrument Connection	Full Scale Range	Power Consumption
Ammeter	1.5 amperes	0.5 watts
Milliammeter	100 milliamperes	0.5 watts
Voltmeter	75 volts	1.4 watts
Wattmeter	75 watts	1.5 watts*

* For one ampere in the current coil connected for "1X" range and for the "1X" range of the potential circuit in use.

The instrument mechanism and all resistors and terminals are mounted on a 1/2-inch bakelite panel 8 by 11 inches. This in turn mounts upon a welded steel box 5 inches deep which serves both as magnetic shield and case. With the exception of an air chamber contained in the inspection cover above the upper pivot, the whole is filled with the insulating fluid. Neoprene gaskets prevent leaks between adjoining parts. About $1^1/_2$ gallons of fluid is required. This fluid surrounding all coils and resistors prevents significant inequalities in temperature of the parts, hence, the temperature compensation is more easily controlled. An 8-hour test at full scale voltage on the "4X" range (300 volts and 5.6 watts) showed that the temperature rise of the fluid was 3 degrees centigrade.

Future Considerations

The authors are currently considering other possibilities for low-frequency instrument design such as the thermal instrument having a very long time constant along the lines described by Lincoln[3], and the use of a high moment of inertia magnetically-suspended moving system.[2] They also are considering the problem of using vacuum-tube amplifiers with these instruments for measurements on low-power level servo systems, and demodulators for adapting these instruments to the measurement of error-modulated signals.

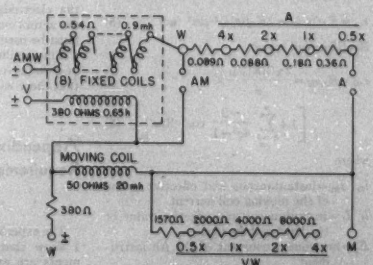

Figure 5. Connection diagram and circuit constants of low-frequency instrument shown in Figure 4

Conclusions

As a result of these investigations, it is concluded that:

1. Conventional instruments will perform accurately from direct current to approximately 0.01 cycle per second, and excepting the permanent magnet-moving coil instrument, above 1.0 cycle per second.

2. The electrodynamometer instrument damped to the slightly oscillatory condition gives the narrowest unreliable zone C.

3. When zone B operation can be sacrificed, and a long time constant can be tolerated, zone A operation can be extended by heavy damping of conventional instruments.

4. Increasing the moment of inertia and decreasing the spring constant is not feasible in conventional instruments.

5. An instrument expressly designed with a large natural period and proper damping affords the opportunity of bridging the zones where conventional instruments are unreliable.

Appendix I. Motional Equations of Instrument Movements

The equations of motion of the pointer can be derived from the following fundamental equation of motion

$$J\frac{d^2\theta}{dt^2}+D\frac{d\theta}{dt}+K\theta=\tau_e \tag{2}$$

where

J = moment of inertia
D = damping constant
K = spring constant
θ = instantaneous angle of deflection
τ_e = instantaneous electrical torque

The electrical torque developed by the various instruments when used to measure sinusoidal quantities is given by the following group of equations

Permanent magnet-moving coil

$$\tau_{eA}=K_A i_M=\sqrt{2}K_A I_M \sin(\omega t) \tag{3}$$

Electrodynamometer

$$\tau_{eD}=i_f i_M\frac{dM}{d\theta}=2I_f I_M\frac{dM}{d\theta}\sin(\omega t)\times\sin(\omega t+\phi) \tag{4}$$

Moving-iron

$$\tau_{eI}=K_I f(\theta)i_f^2=2K_I f(\theta)I_f^2\sin^2(\omega t) \tag{5}$$

Rectifier (full wave)

$$\tau_{eR}=K_A i_M=\frac{2\sqrt{2}K_A I_M}{\pi}\times\left[1+\sum_{q=1}^{n}\frac{-2}{4q^2-1}\cos(2q\omega t)\right] \tag{6}$$

where

i_m, I_m = instantaneous and effective value of the moving coil current
i_f, I_f = instantaneous and effective value of the fixed coil current
K_j = instrument constant of the jth instrument
$f(\theta)$ = function depending upon the deflection alone
ϕ = phase angle between the currents i_m and i_f
M = mutual inductance between the fixed and moving coils

It has been shown[1] that the a-c steady-state solution of equations 2 and 3 for the D'Arsonval instrument is (Graybeal's equation 6)

$$\frac{\Delta R}{R_{max}}=\frac{1}{\left[\left(\frac{2\omega}{\omega_n}\beta\right)^2+\left(1-\frac{\omega^2}{\omega_n^2}\right)^2\right]^{1/2}} \tag{7}$$

where ΔR is the maximum minus the minimum reading and R_{max} is the reading corresponding to the maximum value of the impressed electrical quantities. Thus the curves in Graybeal's paper apply to the performance of the D'Arsonval instrument under these conditions.

Solving equations 2 and 4 results in the a-c steady-state solution for the electrodynamometer instrument

$$\theta=I_f I_M\frac{dM}{d\theta}\left\{\frac{\cos\phi}{K}+\frac{1}{\sqrt{(K-4\omega^2J)^2+(2\omega D)^2}}\sin(2\omega t+\lambda)\right\} \tag{8}$$

From which the total change in deflection

$$\Delta\theta=\frac{2CI_f I_M}{K\sqrt{\left[2\frac{2\omega}{\omega_n}\beta\right]^2+\left[1-\left(\frac{2\omega}{\omega_n}\right)^2\right]^2}} \tag{9}$$

if $dM/d\theta$ is assumed to remain constant. Since the reading is proportional to the square root of the deflection, the per-unit change in reading can be written as

$$\frac{\Delta R}{R_{max}}=\frac{(\theta_{max}+\Delta\theta)^{1/2}-(\theta_{max}-\Delta\theta)^{1/2}}{\sqrt{2}\theta_{max}^{1/2}} \tag{10}$$

where $\Delta\theta$ is described by equation 9 and

$$\theta_{max}=\frac{2CI_f I_M}{K} \tag{11}$$

These equations were employed in obtaining the calculated results shown in Figure 1, for the electrodynamometer instrument.

The solution of the moving-iron equations results in an equation that is very similar to those for the electrodynamometer instrument except that some assumption regarding $f(\theta)$ must be made. The authors have found that the assumption that $f(\theta)$ is constant leads to fairly reliable results in this case. When this simplifying assumption is made, the calculations are very similar to the electrodynamometer case except that the actual curve of reading versus deflection must be used to obtain the ratio $\Delta R/R_{max}$.

The rectifier instrument solutions will appear to be very similar to equation 8 except that there will be an infinite series involved.

Appendix II. Mechanical Design Requirements of Low-Frequency Instrument

The experimental data exhibited in Figure 1 show that several conventional instruments are available for zone B operation up to approximately 0.07 cycle per second. This frequency, therefore, marks the lower boundary of zone A of a low-frequency instrument needed for use in zone C of these instruments. Based upon laboratory observations the lower end of zone A has been arbitrarily limited to a per unit change in reading of 0.05. For instruments having approximately a square-law scale, such as an electrodynamometer voltmeter, this change in reading corresponds very nearly to a per-unit change in deflection of 0.10.

From equations 9 and 11

$$\frac{\Delta\theta}{\theta_{max}}=\frac{1}{\sqrt{\left[2\frac{2f}{f_n}\beta\right]^2+\left[1-\left(\frac{2f}{f_n}\right)^2\right]^2}} \tag{12}$$

Solving this equation for f_n

$$f_n=f\sqrt{\frac{1}{1-2\beta^2\pm\sqrt{4\beta^2(\beta^2-1)+\left(\frac{\theta_{max}}{\Delta\theta}\right)^2}}} \tag{13}$$

Substituting $f=0.07$, $\Delta\theta/\theta_{max}=0.1$ and $\beta=1$, results in an undamped natural frequency of 0.047 cycle per second for the low-frequency instrument.

If the spring constant is specified, the required moment of inertia can be computed from equation 1. For a spring constant, K, of 0.18 gram-centimeters per radian, which was selected because of availability, the moment of inertia required is about 2,000 gram-centimeters squared. The foregoing steps give the procedure used in determining the basic mechanical requirements of the low frequency instrument.

The final mechanical design requirement remaining was to specify a shape and size for the moving system which would have the required moment of inertia and at the same time be largely supported by the insulating liquid. A readily available clear mineral oil and pearl oil, a combination frequently used in magnetic oscillograph galvanometers, was chosen to serve as the supporting fluid because these two could be combined to give a wide range in viscosity for adjusting the damping with very little change in density. Also from preliminary tests no detrimental effects of these liquids on the insulation and other materials in the instrument could be discovered.

Because of the ease of fabrication and of balancing, the shape chosen for the coil form of the moving system was that of a right circular cylinder. This resulted in a rectangular shape for the moving coil. To keep the electrical losses in this coil to a minimum, the decision was made to allocate as much of the weight as possible to the coil and to keep the ratio of the length of the coil (diameter of the cylinder) to the height of the coil (height of the cylinder) within a reasonable value. The initial estimates on the shape and size of the moving system were made by assuming the cylinder to be solid and to have an effective density the same as that of the fluid. For this system the moment of inertia is

$$J=(1/2)WR^2 \tag{14}$$

The weight, W, of the moving system is

$$W=\pi R^2Hd \tag{15}$$

where R is the radius, H is the height both in centimeters and d is the density of the cylinder. From these relationships and the required moment of inertia it follows that

$$HR^4 = \frac{5{,}000}{\pi} \tag{16}$$

It is seen that if a small R is chosen, the cylinder becomes extremely long and of considerable volume, and if a large R is chosen, the cylinder becomes very thin. Either of these results in a greatly elongated moving coil. An initial choice in which H was set equal to R was made; in this case 4.36 centimeters which gave a moving coil with length of 3.45 inches and height of 1.72 inches.

As more complete computations were made taking into account an estimate of the maximum weight of wire consistent with minimum safe cylinder thickness and the actual moment of inertia of this wire together with that of the remaining hollow cylinder, very few changes in the dimensions were deemed advisable. Figure 4 shows the final dimensions.

For construction purposes about 5 per cent more wire than actually needed was specified for the first model of the instrument. Most of this extra wire was subsequently removed a small amount at a time from each side of the moving coil in turn to obtain balance and proper weight of the moving system when submerged.

References

1. Frequency Response Characteristics of Recording Instruments, T. D. Graybeal. *AIEE Transactions*, volume 67, 1948, pages 755–66.

2. Rates and Rate Making, Paul M. Lincoln. *AIEE Transactions*, volume 34, part II, 1915 pages 2279–2360.

3. Magnetic Suspension of the Watt-Hour Meter Rotor, H. F. Trekell, L. I. Mendelsohn, J. H. Wright. *AIEE Transactions*, volume 67, 1948, pages 1180–85.

No Discussion

The Extension of Amplistat Performance by A-C Components

R. E. MORGAN
MEMBER AIEE

H. M. OGLE
ASSOCIATE AIEE

V. J. WATTENBERGER
NONMEMBER AIEE

APPLYING amplistats to exacting control problems often reveals that effects normally considered of a secondary nature determine the actual performance limits. By studying these effects, it is usually possible to design circuits which avoid these limitations. In some cases, by controlling the effect, it is possible to considerably extend the performance of certain control systems. Circuits for amplistats and other magnetic amplifier systems have been well covered in previous papers.[1-3] Most work in this field has been concerned with pure d-c signals and a true sine wave power supply. In practical amplifiers designed to give high gain, fast response, and stable operation, these conditions are rarely met. This paper will study some of the effects normally encountered and will suggest possible means to control these effects.

It has been shown that the firing angle of a self-saturated magnetic amplifier is controlled by the time integral of the voltage applied to a winding linking the core.[4,5] This is the case when any number of windings link the core and includes, therefore, both control and output windings (account must be taken, of course, of the number of turns of each of the windings and any appreciable voltage drop). Any variation in the wave shape of the power supply occurring before the firing point will, therefore, have the same effect upon the firing time as a corresponding variation in signal. Any variation in the wave shape of the power supply occurring after the firing point will not affect the firing time. Either of these possibilities will influence the average value of the output current, but variations occurring before the firing point will have their effect amplified by the action of the amplistat and are usually far more important. It is possible, then, to cause a large change in the output of an amplistat by varying the wave shape of the power supply. This can often be done with no change in the rms value of the power supply voltage.

A study of the effects of pulses of voltage applied to amplistat windings is, therefore, desirable to gain a more complete understanding of the proper methods of application.

Procedure

For simplification, let us consider an amplistat element connected in a circuit shown in Figure 1. (For an experimental setup, the amplistat consists of two such circuits, but only one need be instrumented.)

Let us first consider the operation of this circuit with a square wave a-c supply in order to more easily interpret the results. The output curve of this circuit element with a d-c signal would be as shown in Figure 2.

With no signal, the circuit operation is as illustrated by Figure 3.

The line voltage appears across the reactor (*a-b*) until saturation, after saturation the voltage drop across the reactor falls (*b-c*) and current flows and approximately full-line voltage appears across the load (*b-c-d*). The current flows continuously until the line voltage reverses (*d-e*) at which time the voltage across the reactor reverses due to the decay of flux. Current cannot flow in this direction due to the blocking action of the rectifier and the voltage drop disappears from across the reactor after the collapse of flux is complete and appears across the rectifier (*f-g*). Figure 4 illustrates the same conditions with a sine wave supply.

If we apply a negative d-c signal to the reactor, we can move along the hysteresis loop, Figure 5, until we reach a point at which the reactor no longer saturates. The signal may be increased until the entire supply voltage appears across the reactor. At this point where the output is a minimum, the reactor is operating about the points on the hysteresis loop designated as *d-e-f-g*, Figure 5.

Discussion

When the core is saturated, there is very little coupling between the signal winding and the load winding. When the core is unsaturated, however, nearly perfect transformer coupling exists between these circuits. This is illustrated by Figure 6 which shows a 400-cycle a-c signal applied to the test reactor with a 60-cycle square wave supply. When pulse signals are considered, it is convenient, therefore, to consider the circuit in terms of several different equivalent circuits as shown in Figure 7.

In Figure 7(A), a simplified equivalent circuit is given for the operation during part of the negative half cycle of the supply voltage (*f-g* in Figure 3). For positive signal pulses or small negative signal

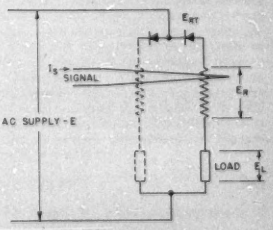

Figure 1. Amplistat test circuit

Paper 50-156, recommended by the AIEE Electronics Committee and approved by the AIEE Technical Program Committee for presentation at the AIEE Summer and Pacific General Meeting, Pasadena, Calif., June 12–16, 1950. Manuscript submitted March 17, 1950; made available for printing April 17, 1950.

R. E. Morgan, H. M. Ogle, and V. J. Wattenberger are all with the General Electric Company, Schenectady, N. Y.

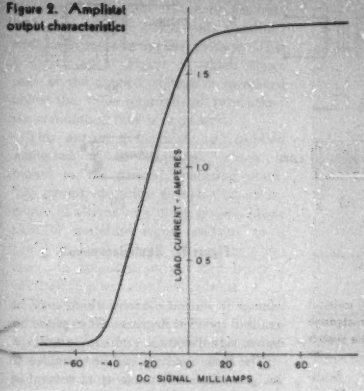

Figure 2. Amplistat output characteristics

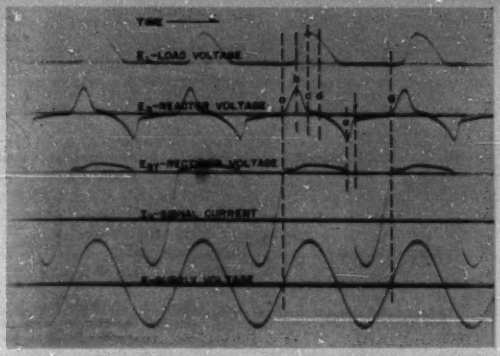

Figure 4. Amplistat wave shapes with no signal and with sine-wave supply

pulses, the circuit acts the same as a transformer with an open-circuited secondary winding. For large negative signal pulses, the circuit of Figure 7(B) must be used. If the induced voltage in the load winding is equal to or greater than the instantaneous value of the supply voltage, the rectifier will become conductive and further flux change in the core will be resisted by an induced current in the load circuit. The effects of large negative pulses occurring during this period is thereby limited.

That any effect at all occurs from pulses during this period can be explained by an examination of the hysteresis loop, Figure 5. The core will usually be at a point on the hysteresis loop slightly to the left of the vertical axis (point a) because of rectifier leakage and possible flux leakage. A current pulse will now take the core through a minor hysteresis loop and cause it to end at some different condition. For example, for a negative pulse a-b-c or for a positive pulse a'-b'-c', this will affect the time of firing (point b, Figure 3) of the next half cycle. It is to be noted that small negative pulses will, in general, have more effect than equal positive pulses because of the shapes of the minor hysteresis loops. It is worth reiterating that changing the amplitude of the negative pulse will have an effect only up to the point where the induced voltage in the load winding is equal to the instantaneous value of the supply voltage: voltage E, Figure 7(B).

Investigation has shown that the change in output current is a direct function of the length of the pulse in the half cycle preceding firing (f-g, Figure 3). This is due to the fact that the flux cannot change in the core instantaneously because of eddy currents. It takes a finite time to move to a new point on the hysteresis loop.

Negative pulses occurring during the period g-a, Figure 3, are in much the same category as those in the period f-g, except that the voltage E, in equivalent circuit Figure 7(B), is being reduced during this time. However, this is the region of possible maximum effect for a positive signal pulse, due to the fact that the core is moved to a region nearer saturation by the pulse (point b', Figure 5) and may not be allowed to complete its travel around the minor loop. This is due to the fact that supply voltage may reverse while the pulse is in effect, resulting in a change of the firing angle of the reactor.

After passing point a, Figure 3, the rectifier becomes conducting and the equivalent circuit of Figure 7(C) must be considered. From here until firing point b, any pulse in the signal winding current will be opposed by an induced current in the load circuit and will, therefore, have a greatly reduced effect. The amount of this reduction is obviously a function of the load impedance.

After firing, point c, Figure 3, the core is saturated and no coupling effect exists between windings and the signal current is no longer induced into the load winding. The equivalent circuit for this condition would be as shown in Figure 7(D), where the signal would be impressed upon an equivalent impedance.

Oscillograph records were taken of a reactor operating under these various conditions. For example, let us consider the reactor with a pulse signal of varying

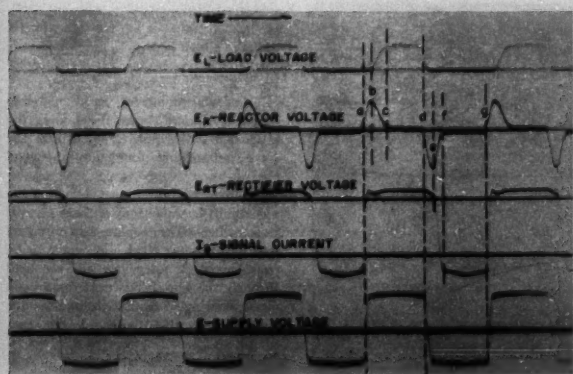

Figure 3. Amplistat wave shapes with no signal and with square-wave supply

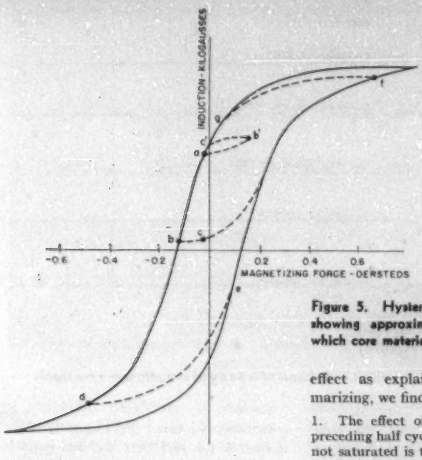

Figure 5. Hysteresis loop for core material showing approximate minor loops through which core material is driven by pulse signals

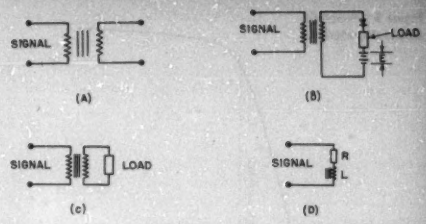

Figure 7. Equivalent circuits

polarity and phase. If we consider a pulse time which is short compared to the a-c supply, it is possible to illustrate the effects described.

Figure 8 illustrates a negative pulse signal at the point of maximum effect for a reactor with a sine wave supply. As expected, this occurs at the point of maximum instantaneous supply voltage in the half cycle preceding saturation because of the varying effect of rectifier leakage. If we utilize a square wave a-c supply as illustrated by Figure 9, we can determine that the pulse d-c signal will have the same effect at any time from f to g in the preceding half cycle. Figure 10 illustrates a positive signal at its point of maximum effect as explained previously. Summarizing, we find the following:

1. The effect of the pulse signal in the preceding half cycle during which the core is not saturated is to drive it around a minor hysteresis loop to a new position. The new position will be determined by the pulse height and by the length of the pulse for any core with appreciable eddy currents.

2. The induced voltage in the load winding, when the core is not saturated, is a function of the signal current times the turns ratio of the windings. It is limited, however, to a value slightly greater than the instantaneous value of the supply voltage.

If we extend our study to varying d-c pulse lengths and to sine wave a-c signals, it can be shown that these effects continue to apply. The factor that is important is that the final position on the hysteresis loop is determined by the summation of voltage time integrals applied during the previous half cycle. Figures 11 and 12 illustrate the appreciable change in output current which may be realized by a few degrees shift in phase between signal voltage and supply voltage.

The same analysis can be extended to include amplistats made up of several of the fundamental elements described.

Applications

The proper utilization of the effects described extends the efficiency of the amplistat in circuit operation. For example, amplistat voltage and frequency regulators have been built with flat or even negative regulation with loads of varying power factor. This is accomplished by using phase shift of ripple components for primary control and the additional use of wave shape changes for regulator droop compensation. By means of this compensation, the regulator is more stable because high-loop gain is not required.

Voltage Regulator

The voltage regulator consists of three main parts, as illustrated by the circuit, Figure 13:

1. Saturated transformer—voltage regulator element.
2. Phase shift network—compensator.
3. Amplistat—amplifier.

The characteristic of the regulator is based on the amplistat, recognizing the phase shift of ripple components; the wave shape change; and the d-c control current.

The regulation is obtained by use of the phase shift in the output of the saturated transformer. The regulation is improved by compensation taken from wave shape changes of the alternator and supplied through the bias. This was done by a phase shift network of C_1 and R_4 in the circuit, Figure 13.

Saturated Transformer

The output of the saturated transformer after saturation is constant when

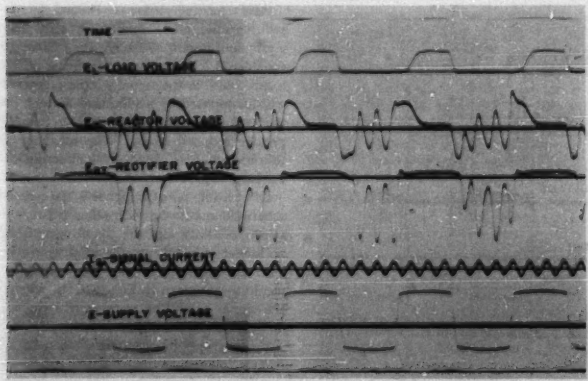

Figure 6. Amplistat wave shapes transformer action with 400-cycle signal

measured by a meter. However, the output is an effective phase shift (leading) with an increase in applied voltage. This is illustrated by Figure 14 which shows that as the applied voltage is increased above the value required for saturation, the conducting time is decreased.

This output is rectified and applied unfiltered to an amplistat which is biased to the desired operating point. The circuit operation is such that an increase in alternator voltage gives a phase shift of amplistat signal current to a position of less effect. This gives a decrease in amplistat output and hence a decrease in alternator field current.

The circuit is such that the bias need not be a constant direct current, but can be derived from alternator voltage. Therefore, this bias also was used to supply alternator wave shape changes for droop compensation.

Droop Compensation

The small amount of wave shape change that occurs in most alternators can be shifted to the most sensitive phase and used as an ideal compensator which varies with load only. Although the distortion may be only 1 per cent, it is still very useful. The distortion usually changes from no load to full load. As load is applied, there are dips that occur in part of the alternator's voltage wave shape, while rises appear in other parts. The effective dips usually occur in one 90-degree section, while the effective rises usually occur in the other 90-degree section of each half cycle in the alternator voltage. In the oscillogram of Figure 15, the average of the dips occurred in the lagging 90 degrees, while the average of the rises occurred in the leading 90 degrees. Both the dips and rises could have been used by shifting the rises lagging and the dips leading. That is, shifting each into the most sensitive phase for an amplistat. However, the dips gave sufficient compensation for voltage regulation. So capacitor C_1, Figure 13, was used to shift the dips to the most sensitive phase for a positive signal in the amplistat.

Also, the phase shift caused by the wave shape change was used. This was an effective phase shift leading as load was increased which decreased the output of the 2-stage amplifier and the alternator field current. Thus an effective control was designed using change in both amplitude and phase shift of the alternator's output wave shape. With this particular circuit, it was possible to obtain a regulation of −0.5 per cent; however, this is seldom required so this circuit is used to obtain regulations of 1.5 per cent with

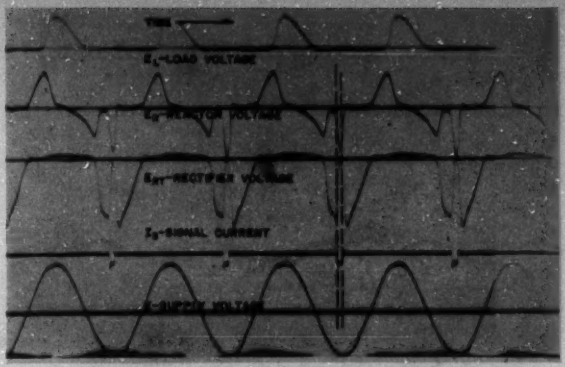

Figure 8. Amplistat wave shapes with negative pulse signal and with sine-wave supply

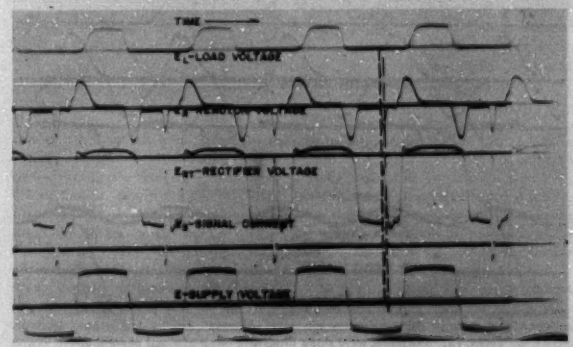

Figure 9. Amplistat wave shapes with negative pulse signal and with square-wave supply

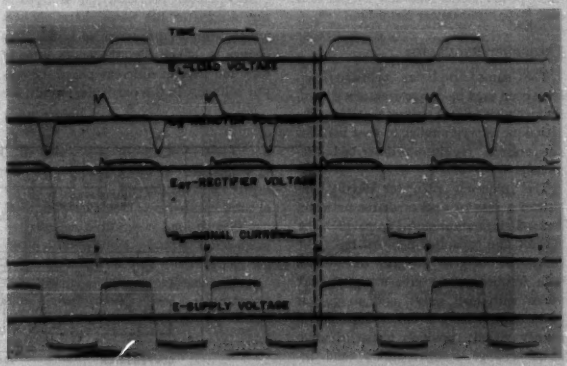

Figure 10. Amplistat wave shapes with positive signal—point of maximum effect

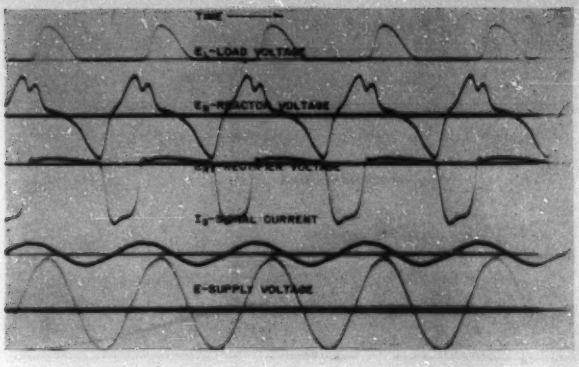

Figure 11. Amplistat wave shape illustrating effect of signal phase shift

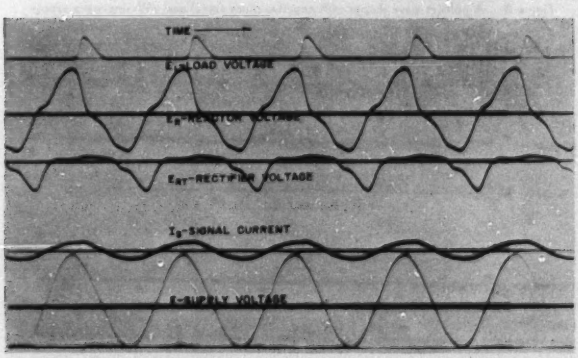

Figure 12. Amplistat wave shape illustrating effect of signal phase shift

unity power factor load and 1.3 per cent with 80 per cent power factor load.

Frequency Regulator

The same amplistat characteristics have been used to design frequency regulators with flat characteristics. The technique is very similar to that used for the voltage regulators described previously.

The frequency regulator circuit consists of a resistor and capacitor network, and a 2-stage amplistat, Figure 16. The resistor and capacitor network has three functions: to give a signal that varies with frequency; to give a signal that varies with load only; and to give a phase shift so as to position phase of frequency signal; position phase of wave shape change compensation; and increase effective amplification of the amplistat.

As discussed previously, the output of any alternator has wave shape changes which occur as a function of load. This change is, effectively, the appearance of dips and rises at different phases of output voltage. In this particular circuit, the dips and rises were shifted to the most sensitive phase in the amplistat characteristic by a resistor-capacitor network.

The same network was used to form a frequency circuit. This was accomplished by circuit elements R_1, C_1, C_6, C_5, and R_5 of Figure 16 which supplied I_c. The result is that as the load was increased, the tendency of frequency to decrease caused I_c to decrease. Also, the dips increased, thus I_c was further decreased with a resultant decrease in the output of the 2-stage amplistat and motor field current.

The rises in the alternator wave shape, due to wave shape change, were shifted lagging and fed in as part of I_R. By shifting, the effect of I_R was made to increase as frequency decreased and load increased. Therefore, the total effect of I_R and I_c gave a push-pull signal from both frequency changes and load changes (wave shape changes). This also cancelled the influence of voltage changes in both circuits.

The frequency regulation was further improved by use of phase shift in both the frequency circuit and the compensator circuit. I_R was shifted leading by a decrease in frequency. The shift leading of I_R was in the same direction as the shift of the saturating phase in the first amplistat stage. Since the amplistat recognizes phase shift in its signals, the phase shift of I_R is in the direction to increase the effect of a frequency change.

In addition, the wave shape change of the alternator voltage produced a rise in the leading edge and a dip in the trailing edge, as load was increased. That is, effectively, a leading phase shift. Therefore, as the load increased, this shift in phase had a similar effect on the amplistat as a drop in frequency. As a result, the phase shift, as well as amplitude, in both the frequency circuit and the compensator circuit, was used to improve the regulation.

The signal I_c also was used to aid in the phase shift. This was accomplished by

Figure 13. Voltage regulator circuit

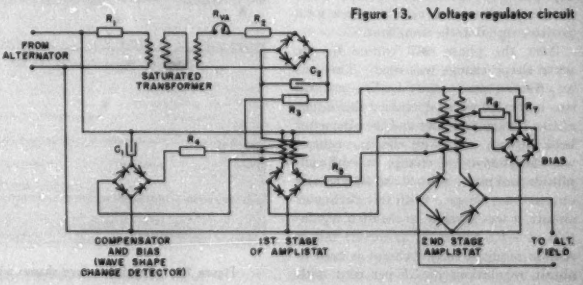

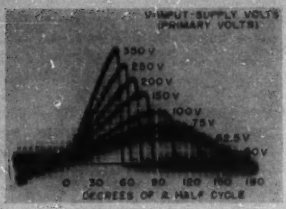

Figure 14. Saturating transformer characteristic

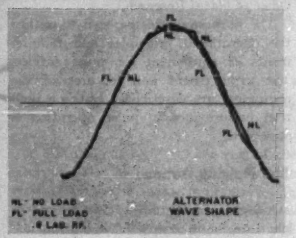

Figure 15. Alternator wave shape

Figure 16. (right) Frequency regulator circuit

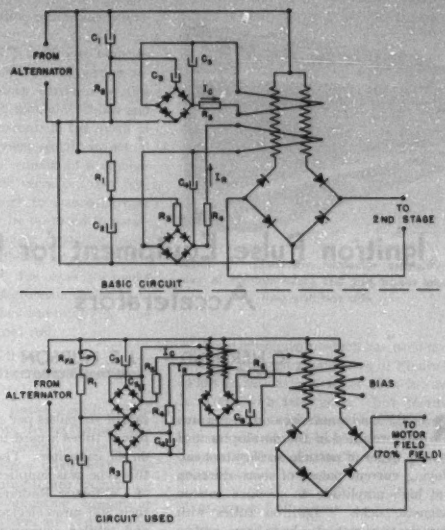

shifting I_c slightly leading of the optimum phase for a negative signal. Therefore, as the frequency decreased, I_c shifted more leading. Thus, the effect of I_c decreased and caused the output of the first stage to increase further. Therefore, the above resulted in increasing the output of the first stage and decreasing the output of the second stage in the amplistat. That decreased the motor field sufficiently to hold speed as load increased. The inverse is true with an increase in frequency.

The amplistat is sensitive to both the magnitude and the phase of the ripple which appears in the signal. In this particular circuit, these factors have been used to an advantage by the proper selection of C_4, R_4 and C_4, R_4, to give additional gain.

If any of the foregoing factors are applied incorrectly, stabilizing problems may enter. In fact, if enough of them are applied incorrectly, it may be impossible to get good regulation under various load conditions.

Additional Circuit Problems

With multistage amplifiers, trouble is sometimes encountered because of the common power supply. As stated previously, the amplistat is sensitive to changes in either supply voltage or signal current during the time the core is being driven around a minor hysteresis loop. The power stage will frequently put a sharp dip in the power supply voltage during firing. This dip may adversely affect the input stage or stages.

One method of overcoming this limitation for sensitive amplifiers is to use a carefully controlled square wave as a power source. Such square waves may be obtained by clipping sine wave power supplies with either conventional clipping circuits or with circuits involving series-connected saturable core reactors. Permanent magnet biased saturable reactors have been successfully used in circuits of this type.

Conclusion

In addition to the control effect of d-c signals, amplistats can be controlled by a-c components. Anything which changes the condition of the core material prior to the start of build-up of load current can cause a large effect. During build-up of load current, and before saturation, a-c components in the signal can only produce a much smaller effect. After saturation, they can produce no effect. Therefore, the phase of a-c or pulse signals is of major importance.

In general, a negative signal will have its maximum effect in the half cycle preceding saturation at the point where the instantaneous value of supply voltage is greatest.

A positive signal has its maximum effect during the time of the supply voltage reversal which immediately precedes firing.

References

1. The Amplistat—A Magnetic Amplifier, R. E. Morgan. *Electrical Engineering*, volume 68, August 1949, pages 663–67.

2. Self-Saturation in Magnetic Amplifiers, W. J. Dornhoefer. *AIEE Transactions*, volume 68, part II, 1949, pages 835–46

3. The Transductor, H. B. Rex. *Instruments* (Pittsburgh, Pa.), volume 20, December 1947, pages 1102–09.

4. The Transductor (book), Ulo Lamm. *Etsolis Aktiebolag* (Stockholm, Sweden), second edition, 1948.

5. Saturable Reactors and Magnetic Amplifiers, F. G. Logan. *Electronics* (New York, N. Y.), volume 21, October 1948, pages 104–09.

6. Magnetic Amplifier Circuits, Neutral Type, A. S. Fitzgerald. *Journal, Franklin Institute* (Lancaster, Pa.), volume 244, October 1947, pages 249–65.

7. Transductor Fundamentals, S. E. Hedstroem, L. F. Borg. *Electronics* (New York, N. Y.), volume 21, September 1948, pages 88–93.

No Discussion

Ignitron Pulse Equipment for Particle Accelerators

C. C. HERSKIND
FELLOW AIEE

J. E. HUDSON
NONMEMBER AIEE

RECENT advances in atomic research have resulted in the development of various types of particle accelerators employing current pulses of short duration and high amplitude to produce intense magnetic fields. Ignitron tubes with mercury pool cathodes have been used as switching devices in the power circuit to apply such current pulses.

The choice of the ignitron tube is based on its ability to carry current pulses having crest values of 5 to 15 times sustained ratings. The use of the ignitron tube also permits accurate control of the time at which the current pulses occur. This is necessary in order that the magnetic field may be properly timed in relation to the other physical processes associated with the particle accelerator operation.

A very intense magnetic field providing high energy levels may be obtained with low continuous energy input and a substantial saving in equipment by exciting the magnet coils of the particle accelerators by pulses of current.

A number of applications have been made. One application employs a total of four sealed ignitrons of type *GL506* connected to operate in pairs with each pair carrying a crest pulse current of 5,300 amperes at 17 kv. The current pulse which is produced by the discharge of a capacitor bank through one pair of tubes is a half sine wave of 1/120-second duration. It is applied at a repetition rate of six pulses per second. The second pair of tubes is used to reverse the charge on the capacitor. The first equipment of this type was supplied to the University of California Radiation Laboratory for their 300 mega-electron volt synchrotron and similar equipments have been furnished to others.

A second application employs four pumped ignitrons of 16-inch diameter. These tanks deliver a crest pulse current of 30,000 amperes at 6 kv. The current pulse and repetition rate are the same as for the first application. The capacitor charge is reversed by switches. One equipment of this type has been installed by the University of Illinois for their pulsed betatron.

A third application consists of 12 type *GL506* sealed ignitrons with eight tubes connected in parallel to provide a magnet current of 28,000 amperes at 20 kv. The remaining four tubes reverse the capacitor charge through a separate reactor. The magnet current pulse is a half sine wave of 1/1,200-second duration. The equipment is designed to operate at repetition rates up to 60 pulses per second. In order to permit operation at high current levels, the tubes are provided with commutating reactors. This equipment will supply power to the 300 mega-electron volt nonferromagnetic synchrotron being built by the General Electric Company Research Laboratory under the sponsorship of the Office of Naval Research.

The purpose of this paper is to outline the operational principles and requirements of equipment for pulse service. The arrangement and features of the equipment are described. Data on ignitron performance in pulse operation is presented.

The Pulsing Action

A high current pulse of 0.01 second or less duration is desired for energizing the magnet coil of some types of particle accelerators. In order to minimize the load demand and maintain an essentially constant drain on the a-c power supply, a large capacitor bank is used to store energy for producing the current pulse. This capacitor is charged to a high direct voltage by means of a rectifier connected to the a-c power supply. At the desired time, the capacitor is connected in series with the magnet coil by means of an ignitron tube and the current discharge through the coil takes place.

A typical power circuit for producing current pulses is shown in Figure 1. The operation of the circuit is as follows: The capacitor bank is first charged to a fixed direct voltage by means of a high-voltage rectifier. The current drawn from this rectifier is limited by means of impedance elements such as a diode limiter and a d-c reactor. At the desired time the ignitron discharge tube is made conductive and the capacitor is permitted to discharge through the magnet coil. The subsequent circuit action is shown by current and voltage wave forms in Figure 2.

The magnitude and duration of current pulse are determined by the capacitor voltage and the impedance of the capaci-

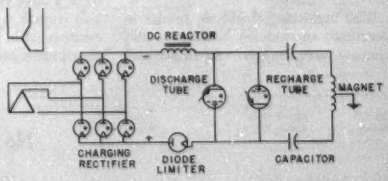

Figure 1. Power circuit

Paper 50-157, recommended by the AIEE Electronic Power Converters Committee and approved by the AIEE Technical Program Committee for presentation at the AIEE Summer and Pacific General Meeting, Pasadena, Calif., June 12–16, 1950. Manuscript submitted March 16, 1950; made available for printing April 17, 1950.

C. C. HERSKIND and J. E. HUDSON are both with the General Electric Company, Schenectady, N. Y.

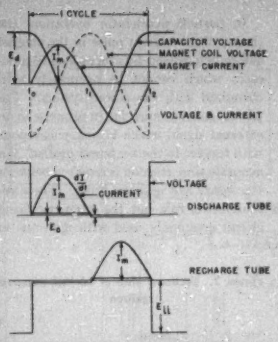

Figure 2. Circuit wave forms and tube duty

tor and magnet coil. At the end of the current pulse in the discharge tube, the voltage of the capacitor is negative. In order to reverse the polarity of the capacitor and rechange it to its original voltage, the recharge tube is made conductive and the capacitor is discharged in the reverse direction. Since the resistance of the circuit is low and little energy is dissipated in the magnetic field, the capacitor voltage at the end of the second current pulse is but slightly less than its original value. The capacitor voltage is brought back to normal by the charging rectifier before the succeeding current pulse.

The recharge current flows through the magnet coil in the circuit shown in Figure 1. The capacitor voltage also may be reversed by recharging through a separate reactor or by providing means for reversing connections.

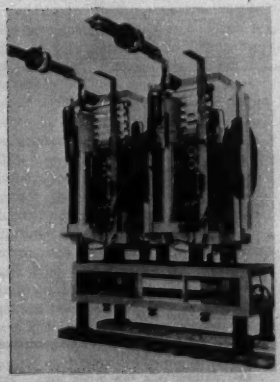

Figure 3. Electronic contactor assembly—view of ignitron tube and grid boxes taken from tube side

Current pulses of 5 to 30 kilo-amperes are required for some types of particle accelerators. To obtain currents of this magnitude by using available tubes and to limit the fault currents in the event of tube failure, the power circuit in actual installations usually consists of a number of parallel tubes or circuits. By providing anode reactors to insure current division, tubes may be operated in parallel to discharge a single capacitor bank. An alternative paralleling arrangement is obtained by dividing the capacitor banks into a number of sections corresponding to the number of tubes and totalizing tube currents in the magnet coil.

Description of Electronic Contactor

The part of the power circuit equipment which performs the switching function, that is, the electronic contactor, consists of the ignitron tubes with their excitation and temperature regulating equipment (also evacuating equipment when pumped ignitrons are used). The excitation equipment, which is assembled in a grid box, and the ignitron tubes are mounted on a common frame which is usually insulated from ground. Insulating power and signal transformers are, therefore, required for energizing the excitation circuit and controlling tube firing. Insulating hose or pipe is likewise required for carrying cooling water to the tubes as the temperature regulating equipment is usually mounted at ground potential.

The general appearance of the tube and grid box assembly is shown in the figures. Figure 3 shows an assembly of two tubes with grid boxes viewed from the tube side of the equipment. Figure 4 shows an assembly of eight tubes viewed from the grid box side. The draw-out type construction is used for the grid boxes as this provides a compact assembly which is readily accessible for servicing. Figure 5 shows a grid box in the draw-out position with a portion of the excitation circuit exposed to view.

Ignitron Tubes

Two types of ignitron tubes have been used for these applications. One of these is the sealed ignitron *GL506* having a nominal inside diameter of 8 inches. A sectional view of this tube is shown in Figure 6. For rectifier operation this tube has a continuous rating for industrial service of 150 amperes average (450-ampere crest) at 20-kv peak inverse. This tube is fitted with three grids.

Figure 4. Electronic contactor assembly—view of ignitron tubes and grid boxes taken from grid box side

The other ignitron which has been used is of the pumped type shown in Figure 7. It has an inside diameter of 16 inches and is fitted with two grids. For rectifier operation this tank has a continuous rating for railway service of 200 amperes average (600-ampere crest) at 7,500-volts peak inverse.

Excitation Equipment

The excitation equipment is an essential and major part of the electronic contactor. Its functions are to establish the conditions for conduction in the power ignitron and to control the start of conduction. In greater detail, the excitation circuit must provide means for obtaining the following action:

1. Initiate a cathode spot on the mercury pool. The cathode spot may be produced by passing a suitable pulse of current through the ignitor.
2. Maintain the cathode spot and spread

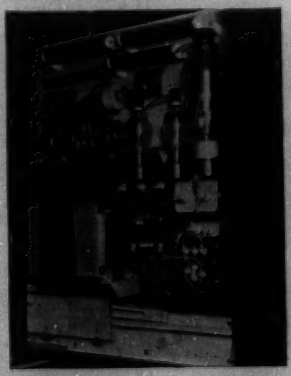

Figure 5. Electronic contactor grid box—view of grid box in draw-out position with excitation panel partly exposed

ionization. Since the ignitor current pulse is usually of short duration, means must be provided for maintaining the cathode spot after the ignitor has ceased firing. The necessary holding current is obtained by means of the excitation anode.

3. Start conduction of the main anode. Conduction of the main anode may be started by applying a positive voltage to the grid of the ignitron tube.

4. Prevent conduction without cathode excitation. Means should be provided for holding the ignitron grid negative until after a cathode spot has been established on the mercury pool. If this is not done, the anode voltage may produce a spot on the tube side wall. Such a spot causes faulty operation and deterioration of the ignitron tube as a result of gassing and erosion of the metal surface.

5. Clean up ionization and regain control. Following the end of anode conduction, a negative voltage must be applied to the ignitron grids to hasten the clean up of ionization and regain grid control. This function must be completed before the main anode goes positive.

In particle accelerator operation, the timing of the current pulse in the magnet coil is determined by other physical processes which cannot be accurately synchronized with the power system. The power ignitrons must fire in response to an external signal which is nonsynchronous with respect to the a-c power system. An accurate time relation is required between the signal and ignitron firing. These requirements rule out the magnetic firing circuit commonly used with ignitrons in

Figure 6. Sectional view of GL506 sealed ignitron

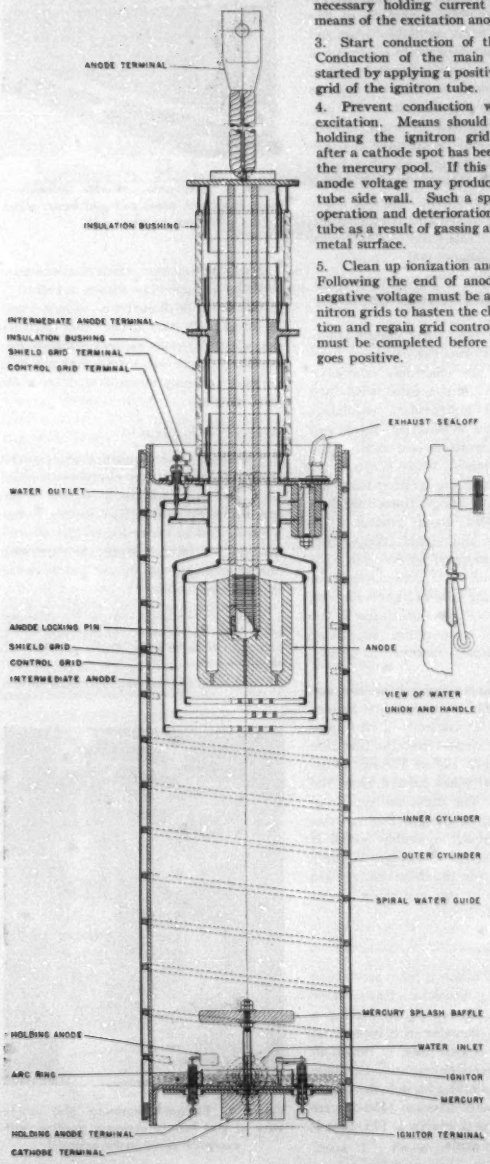

Figure 7. Sectional view of 16-inch pumped ignitron

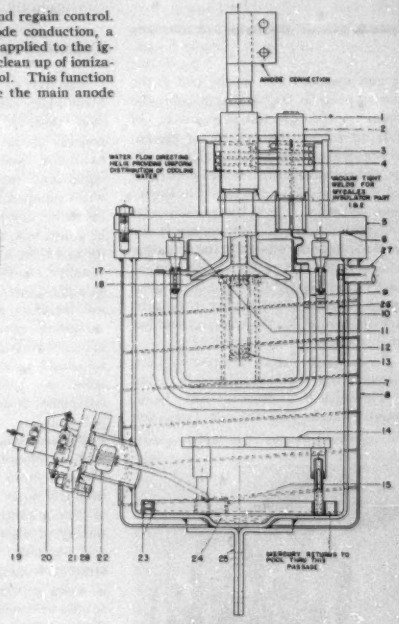

1 MYCALEX ANODE INSULATOR
2 MYCALEX INSULATOR (GRID)
3 ANODE HEATER COVER
4 ANODE HEATER
5 VACUUM CHAMBER COVER
6 TWO (2) ALUMINUM GASKETS
7 VACUUM CHAMBER
8 WATER JACKET
9 INNER GRID
10 OUTER GRID
11 INSULATOR
12 GRAPHITE ANODE
13 ANODE STUD
14 MERCURY SPLASH BAFFLE
15 IGNITOR TIP
16 INDIVIDUAL VACUUM VALVE
17 HEAT SHIELD
18 ANODE SPACER
19 MYCALEX INSULATOR FOR IGNITOR & RELIEVING ANODE LEADS
20 ADJUSTING SCREWS FOR PT 15
21 FLEXIBLE DIA (AND ADJUSTING SCREWS PT 20) PERMIT ADJUSTMENT OF IGNITOR IMMERSION IN MERCURY POOL TO CORRECT VALUE FROM OUTSIDE TANK
22 RELIEVING ANODE FOR IGNITOR TIP
23 MERCURY SEPARATORS
24 MERCURY POOL (CATHODE)
25 CATHODE CONNECTION
26 EXHAUST BAFFLE
27 EXHAUST PIPE
28 GASKETS (INNER - FORMVAR) (OUTER - ALUMINUM)

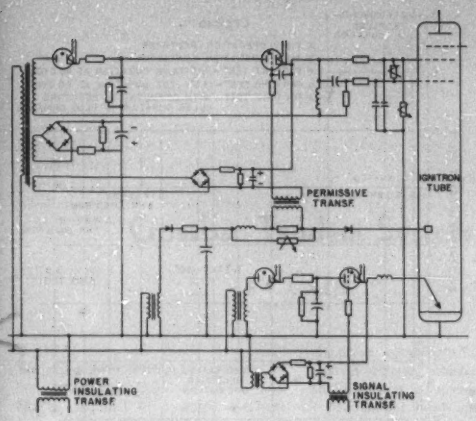

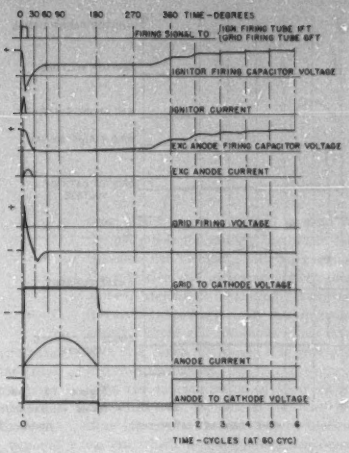

rectifier service and necessitate use of excitation circuits employing vacuum tubes.

Two excitation circuits for use with electronic contactors have been developed. While they are quite similar and operate on the same principles one is designed for operation at repetition rates of 5 to 10 pulses per second while the other will operate at repetition rates up to supply line frequency. The choice of circuit depends upon the application requirements. While the second circuit possesses definite advantages over the first in that it provides for higher frequency operation and greater accuracy of firing, these advantage are obtained at the expense of increased number of firing tubes, complexity, and cost.

A schematic diagram of ignitron excitation circuit number 1 is shown on Figure 8 and the wave forms and firing sequence of the various electrodes on Figure 9. In this circuit, firing is initiated by an external signal which trips the ignitor firing tube. A current pulse produced by an inductance and capacitance discharge then flows in the ignitor. As soon as a cathode spot has been established by the ignitor, the excitation anode fires. Its current pulse also is produced by an inductance and capacitance discharge. Current flow in the excitation anode trips the grid firing tube through the permissive transformer. The grid firing tube applies a positive voltage to ignitron grid and ignitron tube becomes conductive.

All timing is determined by the one signal which trips the ignitor firing tube. The time at which the ignitron tube starts current conduction will be subject to a small jitter since the grid firing time depends upon that of the ignitor. In the

Figure 8 (above). Excitation circuit number 1

Figure 9 (right). Wave form and firing sequence in excitation circuit number 1

present design, the ignitor firing voltage and current have been selected to limit the ignitor jitter to 200 microseconds.

This excitation circuit permits parallel operation of two tubes. This is accomplished by providing the two tubes with individual ignitor and excitation anode circuits and using a common grid firing tube to energize the grids of both ignitron tubes. By connecting the output windings of the permissive transformers in series so that the sum of their voltages is required to trip the grid firing tube, the firing of both ignitron tubes is permitted only when cathode excitation has been established in each. Anode current division during conduction may be insured by the use of anode reactors.

The second excitation circuit is shown in Figure 10. It is designed to operate at repetition rates up to 60 pulses per second and provides accurate firing free from ignitor jitter. Wave forms describing the circuit action are shown in Figure

Figure 10. Excitation circuit number 2

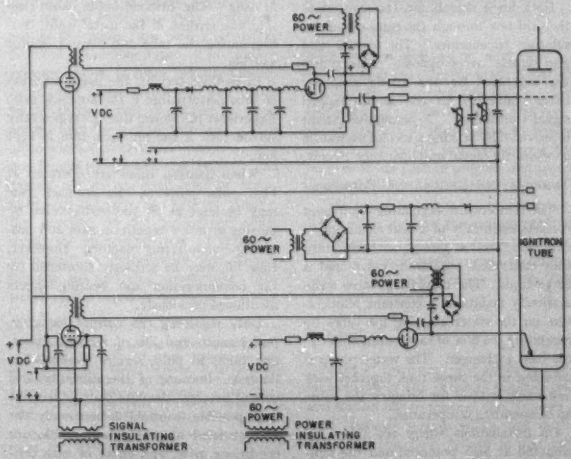

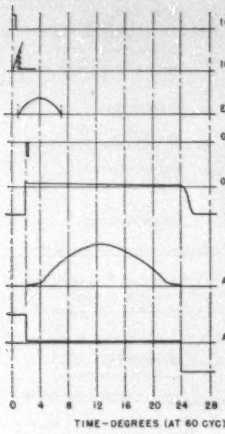

Figure 11 (left). Wave forms in excitation circuit number 2

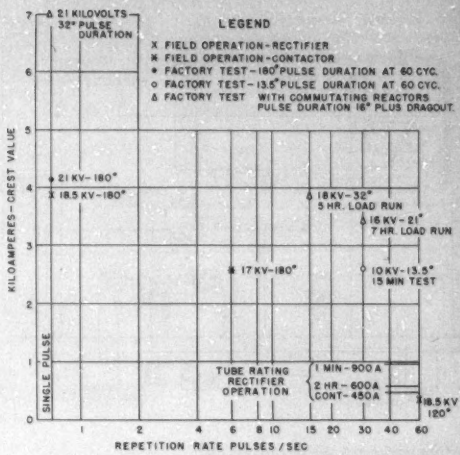

Figure 12. Pulse data on *GL506* sealed Ignitron

11. The action is similar to that of the first circuit. However, firing is initiated by two separate voltage impulses from the signal circuit. The first of these is positive and trips the ignitor firing tube thus firing the ignitor and excitation anode in turn. The second impulse is negative and follows the first by a short time interval to allow sufficient time for the ignitor to fire. The grid firing tube, which is tripped by the second impulse, discharges an artificial transmission line to produce a square voltage pulse. This pulse is of sufficient amplitude to overcome the fixed negative grid bias and fire the grid of the ignitron.

Both firing signals are transmitted to the grid box through the same signal insulating transformer. The ignitor and grid signals are of opposite polarity and are separated by the triode amplifier tubes connected to the center tapped signal transformer. A permissive circuit is provided by putting a second excitation anode in the signal amplifier tube circuit.

Temperature Regulating Equipment

The temperature regulating equipment consists essentially of a heat exchanger, a circulating water pump, a thermostatically-controlled regulating valve and a surge tank. The regulating valve automatically maintains a constant temperature on the water entering the tubes by regulating the flow of raw cooling water to the heat exchanger. The water pump is mounted in the surge tank together with immersion heaters for bringing the tubes up to operating temperature.

On installations where the tubes are mounted at high potential and the temperature regulating equipment is mounted at ground potential, insulation between tubes and heat exchanger is obtained by lengths of rubber hose or porcelain water coils. Pure water of high resistivity is used in the recirculating system. Electrolytic rods are provided to prevent corrosion of piping system by electrolysis.

Tube Performance

Tests and observations on ignitron tubes operated at high pulse currents show that the arc-drop rises and cathode spots form on the tube walls. The increased arc-drop may cause severe local heating. The cathode spots cause gassing and erosion of the metal walls, contaminating the tube and causing ignitor wetting.

In rectifier service, the usual criterion of tube performance is the arc-back rate. Experience has shown that life is generally satisfactory if the arc-back rate is kept low.

When ignitron tubes are operated at high pulse currents, the arc-back rate may be kept at an acceptable value by pulsing at a low repetition rate and providing commutating reactors. However, tube life may be seriously shortened by the contamination and heating effects mentioned previously.

Data regarding the current capacity, performance and life of ignitron tubes, and tanks in pulse service is somewhat limited. Because of the difficulty and cost of making adequate tests, it has not been possible to establish accurately the current level at which undesirable arc conditions arise, and effect of such conditions upon tube performance and life.

The results of experience obtained on the *GL506* sealed ignitron in field operation and factory tests are shown in Figure 12. This figure shows the currents which have been successfully carried without excessive arc-back. The following conclusions are indicated by the data:

1. The current capacity of the tube in single pulse operation with half sine wave (180 degrees) pulses at 60 cycles is approximately ten times its continuous capacity in rectifier service.

2. The crest current carried by the tube may be further increased by using commutating reactors and shortening the current pulse to provide current dragout at the end of conduction before application of the inverse voltage.

Summary

The power ignitron has been successfully applied in pulse service. This service imposes new operating conditions and has required the development of new excitation circuits.

References

1. Pentode Ignitrons for Electronic Power Converters, H. C. Steiner, J. L. Zehner, H. E. Zuvers. *Electrical Engineering (AIEE Transactions)*, volume 63, October 1944, pages 593–97.

2. Rectifier Capacity, C. C. Herskind, H. C. Steiner. *Electrical Engineering (AIEE Transactions)*, volume 65, October 1946, pages 667–70.

No Discussion

Crossbar Tandem System

R. E. COLLIS
MEMBER AIEE

LOCAL telephone traffic in a small community having fewer than 10,000 subscribers' stations can be adequately handled by a single telephone central office. When the number of stations increases beyond 10,000, it is necessary to establish a second office, the equipment for which may or may not be in the same building as that of the first office. In order to complete calls from a subscriber in one office to a subscriber in the other office, so called "direct trunks" are run between the two offices, the number of these trunks depending upon the amount of traffic. As the number of local offices and the distances between them increase, it may be found more economical to provide trunks from each local office to a common point or tandem office, than to run separate groups of trunks between each pair of local offices. Connections between the trunks from the various offices are then established at the tandem point as required.

Traffic between local manual offices through a manual tandem office is completed by the local or "A" operator passing the desired office name orally over a "tandem trunk" to a tandem operator at the tandem office. The tandem operator then tests for an idle trunk in the group of trunks to the required office and by means of a "cord" circuit connects the incoming trunk to the selected idle outgoing trunk. The local "A" operator then passes the called subscriber's number to a "B" operator at the called office who completes the connection to the desired line. It may be noted here that the "A" operator, the tandem operator and the "B" operator must be able to understand each other, that is, must speak a common language; if not it would be necessary for the tandem operator to act as an interpreter or translator between the "A" and "B" operators. Furthermore, the tandem operator must perform the job of selecting the proper outgoing trunk group and also that of selecting which particular trunk she will use to complete the connection.

As manual local operation was replaced by dial operation, it became desirable to replace the manual type of tandem operation by automatic operation. Automatic installations in many of the small offices were of the step-by-step type and it was logical that the automatic tandem equipment for these areas should be of this type. Since in this case it is necessary to deal with only one type of language, namely, decimal pulsing, the tandem switches and the switches beyond the tandem are operated directly by the pulses coming over the trunk. The step-by-step tandem cannot, therefore, act as an interpreter or translator where it is necessary to operate the terminating equipment on some other than the decimal type of pulsing.

In most of the larger cities of the country, the local automatic equipment was of the panel type, and later of the Number 1 crossbar type. Two tandem systems known as office selector tandem (or 2-wire office tandem), and panel sender tandem were developed for these areas. Like the step-by-step tandem, the office selector tandem can operate on only one language, namely, "revertive", and cannot act as an interpreter or translator. In the revertive type of pulsing, the selectors at the terminating office signal the successive steps in their advancement by momentarily short circuiting the tip and ring conductors. The panel sender tandem is more versatile than either the step-by-step tandem or the office selector tandem in that it can translate the incoming information into the revertive, call indicator, step-by-step and call announcer languages. However, it is arranged to receive only one language, namely, panel call indicator which consists of a series of tip and ring reversals in a coded sequence.

As the mechanization of local offices continued at a rapid rate, the need became imperative for an automatic tandem system which would combine such features as:

1. Ability to receive all the various types of pulse languages.
2. Ability to translate any of these languages into any of the others.
3. Adequate trunk capacity.
4. Greater trunking flexibility both as to assignment of the trunks on the trunk switches and as to the number of trunks in the trunk groups, than the existing systems.
5. Ability to complete through any of the other tandem systems.
6. Arrangements for concentration of certain traffic such as time announcements, weather reports, and so forth.
7. High-speed operation.
8. Inherent flexibility to permit the incorporation of new features to meet new conditions as they arise.

With these objectives in mind, the development of the crossbar tandem system was undertaken in the late 1930's. The first phase of this development was completed and a few offices installed before the war. Since the war, continuous development has been in progress and many new features have been added.

This paper describes the crossbar tandem system and how the incorporation of the foregoing basic requirements is enabling the system to fill an ever-expanding field in the mechanization of the Bell Telephone System.

General

Many of the circuit and equipment arrangements of the crossbar tandem system are similar to those of the Number 1 local crossbar system which was introduced by the Bell System in the late

Paper 50-158, recommended by the AIEE Communication Switching Systems Committee and approved by the AIEE Technical Program Committee for presentation at the AIEE Summer and Pacific General Meeting, Pasadena, Calif., June 12–16, 1950. Manuscript submitted March 14, 1950; made available for printing April 18, 1950.

R. E. Collis is with the Bell Telephone Laboratories, Inc., New York, N. Y.

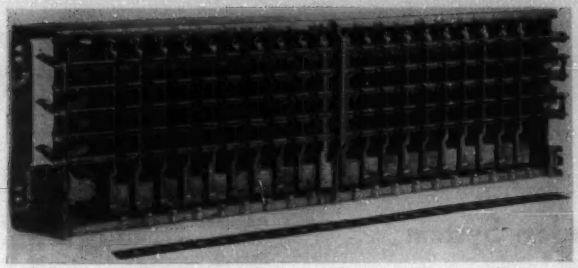

Figure 1. Crossbar switch—front view

1930's and described in detail by F. J. Scudder and J. N. Reynolds in a paper presented to the Institute in January 1939.[1]

Like the Number 1 crossbar system, the basic switching unit is the crossbar switch, Figure 1. Other apparatus employed consists almost entirely of multicontact relays and small relays similar to those employed in other crossbar telephone systems.

In order to perform its job as an intermediary between all varieties of originating and terminating offices, a number of types of senders are provided, each able to receive a different language from the originating point. With the help of a "marker" each sender is able to translate the incoming information into the language required to reach the terminating point.

The major switching operations are controlled by large common circuits or "markers." A marker is used only once per call and it performs its functions so quickly that only a few are required, even in large offices.

As in the Number 1 crossbar system, the markers are arranged to detect short circuits, open circuits, false grounds and other troubles and to check that the connection is properly established before it releases. If trouble is encountered the nature of the trouble is indicated on a trouble indicator and a second trial is made, a feature which is possible only in common control systems.

Types of Office Interconnections

Figure 2 shows the various types of originating and terminating offices which can be interconnected through the crossbar tandem system. As indicated in the figure a separate sender is provided for each type of language which must be received, namely; revertive, dial, or multifrequency pulsing. All senders are arranged with the help of the marker to translate the incoming language into the proper language required by the terminating office.

In panel offices the subscriber dials the code and number into a sender in his local office or the operator at the *DSA* board keys the number on a d-c key pulsing basis into an operator's sender. In either case the sender at the panel office sends the selections, normally used for controlling panel selectors, into the revertive sender at the tandem office. These selections are used by the tandem equipment to set up the connection to the terminating office as explained later.

Operators' dial circuits at either local or toll dial switchboards are connected over the trunk to a dial sender at the crossbar tandem and the operator dials directly into the tandem sender. Certain types of switchboards equipped with d-c key pulsing, first connect to key pulsing senders which receive the keyed number and then automatically out-dial this number over the trunk into the tandem sender.

In step-by-step offices arranged for automatic ticketing,[2] the called code and number are first registered in a ticketing sender in the step-by-step local office. This sender then is connected over the trunk to the dial sender at the tandem office, after which the digits are dialed

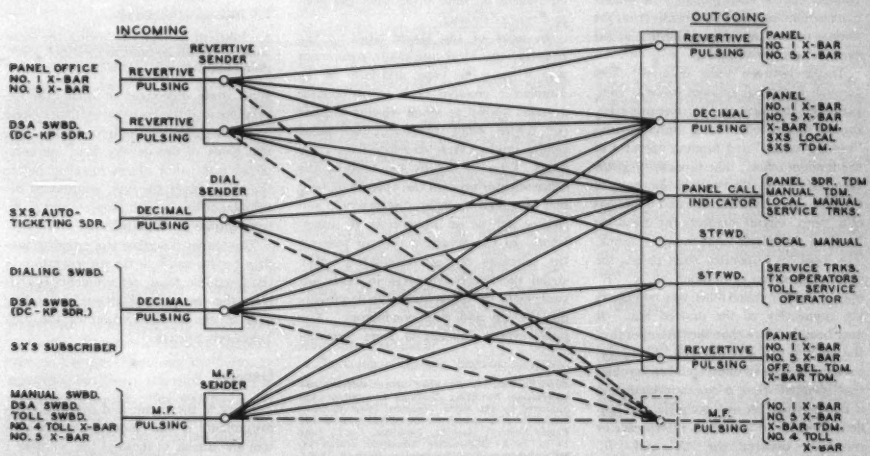

Figure 2. Type of incoming and outgoing trunks which can be interconnected through the crossbar tandem system

automatically by the ticketing sender into the tandem sender.

In some areas advantage is taken of the crossbar tandem to permit step-by-step subscribers to dial panel, Number 1 crossbar and manual offices on a "second dial tone" basis. The subscriber in the step-by-step office after receiving the initial dial tone in the usual manner, dials a single digit which connects his line through the step-by-step switches in the central office over a trunk to a crossbar tandem office. When the tandem sender is ready to receive pulsing it returns a second dial tone to the subscriber who then proceeds to dial the wanted code and number directly into the tandem sender.

Incoming multifrequency pulsing[3] has only recently been introduced into crossbar tandem. This type of pulsing was first used in the Number 1 crossbar sys-system in 1941 and in the Number 4 toll crossbar system[4] in 1943. Switchboards that are equipped with multifrequency key sets are able to key over long toll lines directly into the multifrequency sender. This method of operation is being rapidly expanded in connection with toll terminating traffic since it enables toll operators in distant cities to complete calls without the assistance of operators at the terminating end. Number 5 crossbar offices[5] also may complete through crossbar tandem by the use of multifrequency pulsing.

As indicated in Figure 2, outgoing connections can be completed to all terminations requiring revertive pulsing, call indicator pulsing, and dial pulsing. Completion to manual straightforward positions, service and operator trunks also are provided. Development work now is under way to provide completion on a multifrequency basis as shown dotted in the figure. Further description of outpulsing features is given later.

Apparatus

Crossbar Switch

Since the crossbar switch was described in detail by Scudder and Reynolds,[1] only a brief review of its salient features will be given here.

Figure 1 shows a front view of a 200-point switch. Fundamentally the switch consists of:

1. Twenty separate sets of vertical paths each equipped with a holding magnet.
2. Ten separate sets of horizontal paths each equipped with a selecting magnet.
3. Five selecting bars each capable of assuming two selecting positions.
4. A mechanical means of connecting any one of the ten horizontal sets of circuit paths to any one of the 20 vertical sets of circuit paths by the operation of the corresponding selecting and holding magnets.

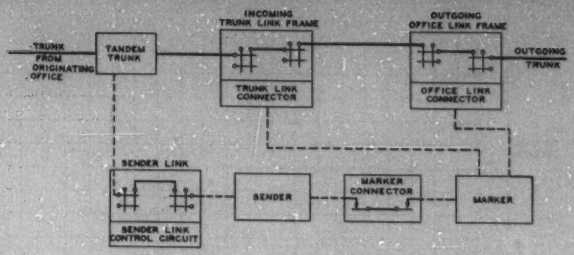

Figure 3. Block diagram of switching units

Any one of the 200 sets of contacts, called "crosspoints," can thus be closed by co-ordinate operation of a selecting magnet and a holding magnet. The contacts are held operated by the holding magnet alone, the selecting magnet being released as soon as the holding magnet is operated. A total of ten connections, one for each set of horizontal paths, can thus be simultaneously established. Each of the crosspoints may consist of from three to six separate "make" contacts, the number depending on the requirements of the circuit.

The switch shown is a 200-crosspoint switch, each crosspoint having three make contacts. This is known as a 200-point 3-wire switch. Other switches having only 100 crosspoints, that is ten vertical units, also are used in this system.

Relays

Multicontact relays having 30, 40, 50, or 60 sets of individually insulated make contacts, the same as in the Number 1 crossbar system are used in the tandem system. These relays are used chiefly in the common connector circuits where a large number of leads must be connected simultaneously.

General purpose relays of the (U) and (Y) type are used throughout the system. These relays may have as many as 24 springs arranged in various combinations of makes, breaks, and transfers. (U) and (Y) type relays are similar in physical construction except the (Y) type are provided with copper or aluminum sleeves and larger pole faces to secure slow operating and releasing characteristics.

A small number of other types of relays such as polar relays are required for special purposes.

Functions of Equipment Units

The general operation of the system may be more easily understood by first describing the principal equipment units and their functions. Figure 3 is a simplified block diagram which shows these units and their interconnection. In general there are six types of equipment units:

1. Tandem trunks.
2. Incoming and outgoing trunk link frames.
3. Senders.
4. Markers.
5. Sender link and controller frames.
6. Connector frames.

A tandem incoming trunk circuit consists of a few small relays, a repeat coil, capacitors, and resistances. These circuits provide supervisory and transmission facilities. An outgoing trunk usually consists only of three conductors, that is, tip and ring which go to the called office and the sleeve which is used for control purposes.

The incoming and outgoing trunk link frames which consist almost entirely of crossbar switches, provide means for connecting the incoming trunks to the outgoing trunks.

The senders consist principally of small relays. They register the called office codes and numbers which are pulsed from the originating offices and transmit the necessary information to the markers and to the terminating offices for completing the connections to the called lines.

The markers are the largest and most important of the common control circuits. They are composed of both small and multicontact relays. From the code of the called office, which is received from the sender, the markers determine the proper trunk group to the called office. They test the trunk group to find an idle trunk and also test to find an idle path or "channel" through the switch frames, after which they operate the proper selecting and holding magnets on the

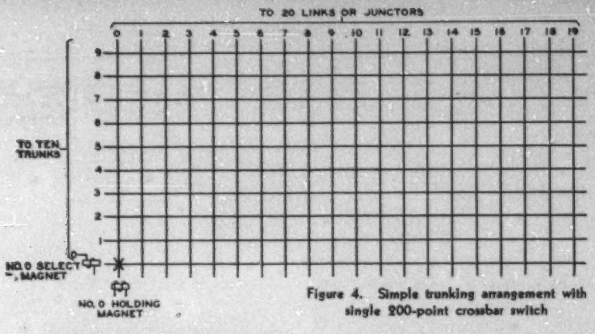

Figure 4. Simple trunking arrangement with single 200-point crossbar switch

crossbar switches to establish the connection from the incoming to the outgoing trunk. The markers also furnish the senders with detailed information such as type of out pulsing and so forth, required to complete the call to the called office.

The sender link and controller frames provide means of connecting the incoming trunks to the senders. The operation of selecting the proper type of sender and connecting it to the trunk is performed by the sender link controller. A sender link frame is required for each 100 incoming trunks.

The marker connector, the trunk link connector, and the office link connector consist mainly of multicontact relays which are used for connecting the markers to the senders and to the link frames. These connectors operate on a lockout basis, that is, only one marker, for example, can connect to an office frame at one time through office link connector.

Trunking Arrangements

The fundamental method of using the switch in a trunking scheme is shown in Figure 4. Each of the horizontal and vertical lines represents the wires, for example, tip, ring and sleeve, of the connecting circuit. When the Number 0 selecting magnet is operated followed by the Number 0 holding magnet the tip, ring and sleeve leads of the circuit on the Number 0 horizontal are connected to the corresponding leads on the Number 0 vertical circuit as shown by the "X."

To obtain the required trunking access, 20 switches are mounted on a frame and interconnected in a primary, secondary arrangement as shown in Figure 5. Two types of trunking frames are used:

1. An incoming trunk link frame called a "trunk frame."

2. An outgoing trunk link frame called an "office frame."

Incoming trunks are connected to the horizontals of the primary switches of the trunk frames and outgoing trunks are connected to the horizontals of the secondaries of the office frames. The system is arranged for a maximum of 20 each of trunk frames and office frames which will accommodate a total of 3,200 incoming trunks and 4,000 outgoing trunks as explained later. Figure 6 shows an incoming trunk frame with associated incoming (or tandem) trunks.

The horizontal circuits on the secondary switches of the trunk frames and on the primary switches of the office frames are separated between the tenth and eleventh verticals, thus providing 20 horizontal circuits per switch instead of ten. These 200 horizontal circuits on the secondary switches of the trunk frame connect, as shown in Figure 5, to the 200 vertical circuits on the primary switches and are called "trunk links." Similarly, the 200 horizontal circuits on the primary switches of the office frame connect to the 200 verticals on the secondary switches and are called "office links." The circuits connecting the trunk frames and office frames are called "junctors." It will be observed that the total number of junctors from a trunk frame is 200. Since each trunk frame must reach each office frame the number of junctors which can be assigned between any two frames will vary depending upon the number of frames in the office.

Normally the horizontals on the secondary switches of the office frame are not divided. In this case only 100 trunks per frame can be accommodated. However, if the traffic density permits, these horizontals may be divided between the tenth and eleventh verticals to provide for additional trunk capacity. Also, if traffic density permits, ten extension secondary switches for the office frame may be provided. These switches have capacity for an additional 100 trunks per office frame. The horizontals of the extension switch are not arranged to be divided. The office links are multipled directly to the verticals of the extension switch as shown. The primary switches of the trunk frames are 200-point 6-wire switches. A special wiring arrangement of these switches permits 16 incoming trunks to be wired to the horizontals, that is, a total of 160 trunks per frame as shown in Figure 7. Each trunk is multipled as indicated to corresponding contacts on all 20 verticals of the switch. Since each horizontal consists of six springs, two incoming trunks of three leads each, that is, the tip, ring and sleeve, can be connected to each horizontal. Only the top eight horizontals are wired to trunks in this fashion, the odd numbered trunks being wired to the right-hand sets of three contacts and the even numbered trunks being wired to the left-hand sets of three contacts as illustrated. If the call originates on an odd-numbered trunk all six of the contacts at that horizontal crosspoint are closed, but only the right-hand set of three contacts is connected to the link. This is accomplished by closing the contacts associated with the Number 1 horizontal, simultaneously with the trunk horizontal contacts. If the call originates on an even-numbered trunk it is connected to the link by the use of Number 0 horizontal contacts. In this way any one of the trunks connected to the horizontals, two to nine, can be connected to any one of the 20 trunk links.

To establish a circuit from an incoming trunk to an outgoing trunk it is necessary to match three idle paths, namely a link on the trunk frame, a link on the office frame and a junctor between the two frames. The proper selecting and holding magnets must then be operated. These functions are performed by the marker as will be described later.

Description of Circuit Operation

The functioning of the system in establishing a connection may be divided into four major stages. These stages are:

1. Operation of the sender link and control circuit in selecting an idle sender of the proper type and connecting the selected sender to the tandem trunk.

2. Receiving and registering the called office code and number in the sender.

3. Operation of the marker in establishing the connection through switches and of furnishing the sender with directions as to how to complete the call.

4. Operation of the sender in transmitting information of the proper type to the called office.

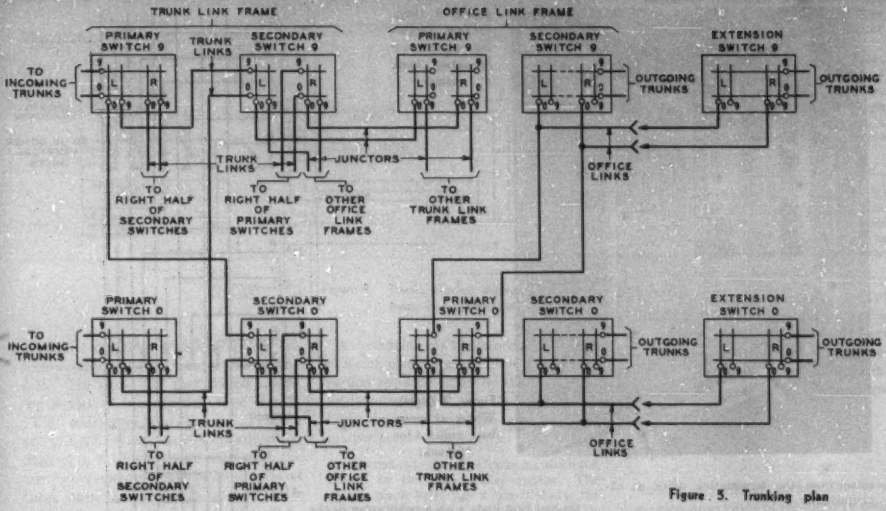

Figure 5. Trunking plan

Although the foregoing is the normal progress of the functioning of the circuits, the operation of the senders can best be described by combining (2) and (4) and treating each sender separately. The operation of the marker will be considered last.

The first major stage is illustrated in Figure 8. When a tandem trunk is selected by the originating office, the sender link control circuit is brought into action. The sender link is a primary—secondary arrangement of crossbar switches. Each incoming tandem trunk is connected to a horizontal on each of two primary switches in order to insure completion of a connection to a sender if one linkage is in trouble. If the trunks are all of one type, 40 senders maximum of the corresponding type are wired to the horizontals of the secondary switches. If the trunks are of two types, two corresponding types of senders (maximum 40 of each) are connected to the secondary switches by dividing the horizontals of the secondary switches.

The control circuit proceeds as follows to connect a trunk to a sender:

1. Locates the horizontal position of the trunk on the primary switch of the sender link frame.

2. Selects an idle sender of the type required by the trunk. If the incoming trunk is of the revertive type, for example, the control circuit will test for an idle sender only in the revertive group of senders.

3. Selects an idle link between the primary and secondary switch.

4. Operates the proper selecting and holding magnets associated with the selected circuits, which establishes the connection from the trunk to the sender.

5. Signals the sender the number of the trunk frame with which the trunk is associated. This frame identification is used later in establishing the connection to the outgoing trunk.

6. Signals the sender the "trunk group" number to which the trunk belongs. All ten trunks appearing on the ten horizontals of a particular primary switch of the sender link frame are treated as a group. Since there are 100 trunks on the sender link frame, there are ten such trunk groups. All ten trunks of a group must be of the same type.

7. The control circuit then releases after checking that the connection between the trunk and the sender has been properly established. If trouble is detected an alternate control circuit is summoned which makes a second attempt to establish the connection.

As soon as the sender link control circuit has finished its functions, which takes but a fraction of a second, the tandem sender signals the originating office that it is ready to receive the pulsing of the called code and number.

The second and fourth major stages in the progress of a call are handled by the senders.

Revertive Pulse Receiving Sender

The revertive sender receives the office brush, office group, incoming brush, incoming group, final brush, final tens, and final units selections, revertively, from the originating sender in the panel or Number 1 crossbar offices and registers these selections on a crossbar switch. The office brush and office group selections represent the code of the terminating office, while the rest of the selections represent the number of the called line. Although there are normally only five office brush selections for panel operation, this number has been increased to ten for crossbar tandem operation by minor changes in the senders of the originating offices. The ten office brush and ten office group selections give 100 combinations or codes which can be transmitted over a single trunk group. By arranging the originating office to reach the tandem office over three separate trunk groups, a total of 300 codes can be recognized. Thus a particular combination of office brush and group selections, for example 37, may be used three times once in connection with each trunk group to represent three terminating codes. The sender link control circuit passes the trunk group number to the sender at the time that it is connecting the trunk to the sender.

The progress of sender operation is as follows:

1. Registers the office brush and group selections.

2. Opens the trunk toward the originating office. This is necessary because further selections after office brush and group must be delayed until the marker has informed the sender what type of outpulsing is required. If the call is to a manual call indicator position, the next trunk closure must

Figure 6 (left). Tandem incoming trunks and incoming trunk frames

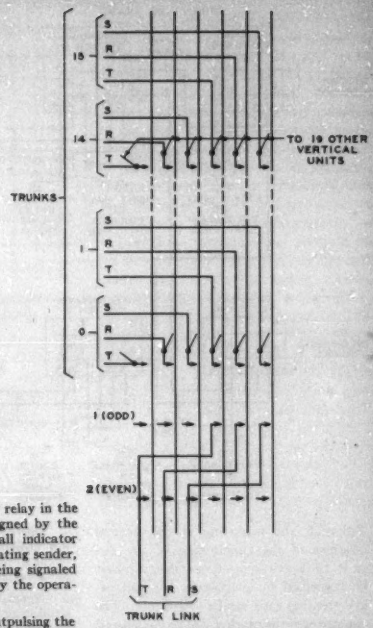

Figure 7 (right). Wiring of crossbar switch for 16 trunks

come from the terminating office as explained later.

3. Connects to a marker by means of a marker connector and passes the office brush and group selections together with the trunk group and trunk link frame numbers to the marker.

4. Waits for the marker to set up the connection to the outgoing trunk.

5. Receives from the marker information as to the type of outpulsing and other information required to complete the call.

6. Releases the marker.

7. On other than call indicator calls, the sender closes the trunk toward the originating office and proceeds to register the incoming brush, incoming group, final brush, final tens, and final units selections sent out on a revertive basis from the originating panel and Number 1 crossbar offices.

8. If the terminating office requires revertive pulsing, the sender closes the trunk toward the terminating office and sends out the incoming brush, incoming group, and so forth, selections as they have been received from the originating office.

9. If the terminating office is of the step-by-step type, the sender translates the incoming and final selections back into thousands, hundreds, tens, and units digits of the called number and proceeds to dial these digits into the step-by-step terminating office. If the marker has so indicated, the sender dials out either one or two arbitrary digits ahead of the numericals. These digits are set up in the sender by the marker and provide switching features which are specially important in step-by-step areas. For example, these digits can be used to steer the call through step-by-step tandem switches or to cause the insertion of repeaters if transmission so requires.

10. If the terminating office requires call indicator pulsing the sender connects the incoming tip and ring leads to the outgoing tip and ring leads with a polar relay in the circuit When the call is assigned by the call indicator operator, the call indicator pulsing is done from the originating sender, the crossbar tandem sender being signaled when the pulsing is complete by the operation of the polar relay.

11. After the completion of outpulsing the sender operates relays in the tandem trunk which set the trunk in talking and supervisory position. The sender then releases from the connection.

Incoming Dial Pulse Receiving Sender

As in the case of the revertive sender, the dial pulse sender registers the incoming digits on a crossbar switch. This sender may be arranged for 2-digit codes, 3-digit codes or combined 2-3 digit codes, depending on the area in which it is used.

This sender is arranged to send out the numerical digits either on a call indicator, revertive or dial pulsing basis. The dial pulses are sent out as received. For revertive outpulsing, the incoming thousands, hundreds, tens, and units digits are translated into incoming brush, incoming group, final brush, final tens, and final units selections. For call indicator pulsing these digits are translated into the call indicator code.

The progress of the call through the dial sender is similar to that of the revertive sender except that the reception of the numerical digits proceeds without waiting for marker completion.

Multifrequency Receiving Sender

The multifrequency sender registers the incoming digits on relays instead of a crossbar switch. Associated with each sender is a multifrequency receiver which receives the multifrequency pulses and changes them into direct current pulses in order to operate the register relays. Five register relays per digit are required. These are operated on a 2-out-of-5 basis to register the ten decimal digits. The multifrequency sender is arranged to send out revertive, step-by-step and call indicator types of pulsing the same as the incoming dial sender.

The progress of the call through the multifrequency sender is similar to that of the dial sender.

Other Sender Features

Both the incoming dial and incoming multifrequency senders are arranged to receive ten "trunk group" signals from the sender link. This class signal is passed to the marker and enables the marker to determine the route and the charge for the call, depending on the class of the originating subscriber.

Both the incoming dial and incoming multifrequency senders are arranged to handle 3-digit service codes as well as "TX" operator codes of the "11X" type. A "TX" code is a special code used in connection with a delayed toll call to reach a

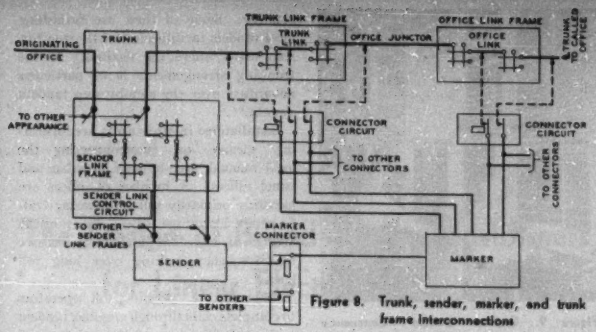

Figure 8. Trunk, sender, marker, and trunk frame interconnections

particular operator who has specific information as to the completion of the call. The two "1's" first dialed enable the sender to identify this type of call. "TX" codes may be of the type "11XX", or "11XXX" where the X's are any of the digits 1 to 0. Two X's are used when the number of operators is from 10 to 100 and three when the number is over 100 as is true in large cities. The senders will be arranged in a particular office for only one of these types of operation.

Marker

The tandem marker is basically the same as the originating marker of the Number 1 system. It is the most important of the common control circuits. Since calls coming into the revertive sender are on a 2-digit basis (plus the trunk group signal) the tandem marker is equipped with a 300-point translator operating in accordance with this information. The dial and multifrequency senders may be on a 2-digit only, 3-digit only, or a combined 2-3 digit basis and therefore the marker is equipped with a translator which will meet these conditions. The marker also has a translator for 90 service codes and 100, or 300 "TX" operators' codes. In addition to the code information, the marker receives from the sender the trunk link frame number and the trunk group number. From this information the marker sets up one of the several translators which results in the selecting of a code point, 1 of 300, 1 of 800, or 1 of 90 depending on which translator is involved. The selection of a code point operates a "route" relay which furnishes all further information required by the marker and the sender for completing the connection through the tandem office. There are a number of route relays in each marker since one is required for each called office route.

A route relay has 12 make contacts each of which controls a certain item of information required either by the marker or sender for setting up the connection. Upon the operation of the route relay the marker proceeds as follows:

1. Connects to the office frame on which the trunks to the called office appear. The marker places battery on a "start" lead to the desired office frame which operates relays individual to the marker on the office link connector circuit. The operation of these relays automatically locks out other markers from that office frame.

2. The marker connects a test relay to the sleeve lead of each of the trunks to the desired office and selects one of the idle trunks as indicated by these test relays. If all trunks tested are busy, a group of overflow trunks will be tested and the connection set up to an idle overflow trunk. If there are more trunks to the desired office than the marker can test simultaneously (40 the maximum) the marker is directed to a second group by a "route advance" feature.

3. The marker also connects by means of a trunk link connector to the trunk link frame on which the incoming trunk appears. The number of this frame was furnished to the marker by the sender. As in the case of the office link connector, only one marker can connect to a trunk frame at a time. The marker determines from "pattern" relays which combinations of links and junctors are allotted for the completion of calls between the particular trunks involved. It tests these combinations (called channels), selects an idle one and proceeds to operate the proper selecting and holding magnets of the two links and the junctor making up this combination. This establishes a connection from the incoming tandem trunk to the selected outgoing trunk.

4. When the marker has completed these operations it checks the connection to assure that it is properly established and that it will hold from the tandem trunk circuit.

5. From information furnished by the route relay, the marker transmits to the sender the following information:

(a) Class of outpulsing—that is, revertive, call indicator or dial.

(b) Compensating resistance. Compensating resistance is necessary for revertive pulsing since the pulsing loops must be kept within certain resistance limits.

(c) Office brush and office group selections. These selections are required by the dial and multifrequency senders when these senders complete through an office selector tandem or through a second crossbar tandem on a revertive basis.

(d) Fifth and sixth step-by-step digits.

6. When the marker has completed its operation, it sends a release signal to the sender which causes the sender to release the marker connector and the marker. The marker on releasing releases in turn the office and trunk link connectors.

Wide flexibility in the assignment of trunks on the office frames and in the size of trunk groups is provided by the marker design. Alternate routing arrangements are also provided which permit the establishment of connections over other routes if the normally used groups are busy.

Trunks

Incoming trunks are arranged for local type loop supervision or for toll type composite, simplex or voice frequency supervision. Trunks used for toll traffic are provided with means to permit re-ring from the originating end, a necessary feature for toll operation.

An important feature provided in trunks coming from panel offices is remote control of zone charging. Zone charging involves the operation of the subscriber's message register one or more times on a single call, depending upon the initial charge for the call and also on the length of the conversation. Although the local panel circuits can be arranged for this feature it is much more economically accomplished by determining the charge at the tandem office and then operating the message register by signals passed over the trunk to the local office. The trunks are arranged to receive information from the marker, through the trunk link connector, as to the charge rate, that is, the number of times the message register should be operated for the initial and overtime periods together with the length of the initial and subsequent talking periods permitted on that call. At the beginning of the initial period the predetermined number of charge signals is sent back to the local tandem office over the tip and ring in such a way as not to disturb the talking circuit.

The tandem trunk also times the conversation and again operates the message register the required number of times for the overtime period. The function of the marker in this connection is to determine

and set up in the trunk the proper charge combinations. This is done in the following manner: a contact on the route relay operates one of 30 "zone" relays, each having ten pairs of contacts, the ten corresponding armatures of these relays are multiplied together and these ten leads, called zone leads, are run to the trunk link frames. Each selecting magnet on the primary crossbar switch of the trunk link frame is associated with an incoming trunk.

By cross-connecting the winding of the selecting magnet to one of the zone leads the incoming trunk can be identified by the marker as coming from one of ten zones. Likewise the outgoing zone is identified by the operated zone relay in the marker. The ten contacts on each of the 30 zone relays (total 300 contacts) are cross-connected to control the setting of the proper charge relays in the trunk.

Maintenance Features

The arrangements for maintenance of crossbar tandem are very similar to those in the Number 1 system. Routine test frames are provided for the senders and outgoing trunks. The incoming trunks can be tested from the trunk test boards of the originating offices and also by means of portable test sets at the tandem office. These test circuits apply marginal operations to the various circuits. The routine test frames perform these tests automatically and if trouble is encountered the tests are stopped and an alarm given to the maintenance force.

The marker is provided with many self-checking features which are applied while a call is being handled. If trouble is encountered, the marker automatically connects momentarily to a recording circuit called the "trouble indicator." Relays operated in the trouble indicator light lamps which enable the maintenance force to locate the trouble.

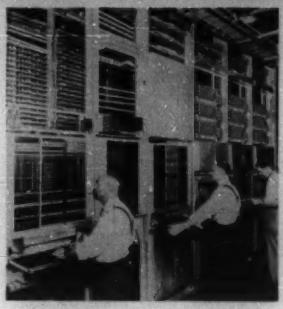

Figure 9. Crossbar tandem maintenance center

Figure 9 shows the crossbar tandem maintenance center. The bays from left to right are sender test, sender make busy, trouble indicator, and three bays of trunk test circuits.

Power Plant

The principal power required by the crossbar tandem is 48 volts, direct current, which is used for the operation of practically all the signaling and transmission circuits. Several other sources of direct current are furnished for miscellaneous purposes. Individual frame filters are connected across the 48-volt power supply leads at the frames where noise-free battery supply is required for talking circuits.

Conclusion

There are at present about 30 installations of crossbar tandem throughout the country. Some of these are furnishing local tandem facilities in strictly step-by-step areas where the flexibility of the trunking arrangements is of particular advantage over the step-by-step tandem system.[6]

Installations in other areas are furnishing means or interconnecting the local manual, step-by-step, crossbar and panel offices. A number of offices are handling primarily toll terminating traffic where advantage is being taken of the ability of crossbar tandem to receive multifrequency pulsing over long toll lines.

This feature permits toll operators to complete calls through crossbar tandem in distant cities without the assistance of terminating operators.

An extensive development program now is in progress to incorporate new features which will still further enhance the usefulness of crossbar tandem in the rapid expansion of automatic switching in the Bell Telephone System.

References

1. Crossbar Dial Telephone Switching System, **F. J. Scudder, J. N. Reynolds.** *Electrical Engineering* (*AIEE Transactions*), volume 58, May 1939, pages 179–92.

2. Automatic Ticketing of Telephone Calls, **O. A. Friend.** *Electrical Engineering* (*AIEE Transactions*), volume 63, March 1944, pages 81–88.

3. Application of Multifrequency Pulsing in Switching, **C. A. Dahlbom, A. W. Horton, Jr., D. L. Moody.** *AIEE Transactions*, volume 68, part I, 1949, pages 392–96.

4. Crossbar Toll Switching System, **L. G. Abraham, A. J. Busch, F. F. Shipley.** *Electrical Engineering* (*AIEE Transactions*), volume 63, June 1944, pages 302–09.

5. The Number 5 Crossbar Dial Telephone Switching System, **F. A. Korn, J. G. Ferguson,** *AIEE Transactions*, volume 69, part I, 1950, pages 244–54.

6. Interexchange Trunking With the Crossbar Tandem in Los Angeles, **W. F. Pfeiffer.** *AIEE Transactions*, volume 69, part II, 1950, pages 1071–79.

No Discussion

The Design of Broad-Band Transformers for Linear Electronic Circuits

H. W. LORD
MEMBER AIEE

WHEN designing linear amplifier circuits, the designers often find it highly desirable to take advantage of the impedance-matching and phase-inverting properties of transformers. However, they sometimes fail to realize that even a well-designed transformer may not be able to pass the required band of frequencies when connected between the available power source and specified load. At other times they may ask for impedance or phase characteristics which are unrealistic or which call for unnecessarily close tolerances.

The designers of the transformers which the electronic circuit designers need do not always appreciate the manner in which certain transformer characteristics influence the over-all frequency response of the combined transformer and linear-amplifier circuit. Another little known factor is the manner in which the transformer contributes to the harmonic distortion.

So long as the electronic circuits were required to handle band widths of only a few kilocycles, this lack of understanding was not serious. However, the advent of high standards of performance for both amplitude modulation and frequency-modulation transmitters and studio equipment soon made this difficulty very apparent. The electronic circuit designers complained that it was very difficult to obtain completely satisfactory transformers for their equipment. They almost invariably had to go through a long series of developmental samples on small units before obtaining satisfactory transformers. On the larger modulation transformers, they usually had to incorporate a series of compensating and equalizing networks in their circuits in order to obtain satisfactory over-all performance. On the other hand, the transformer designers complained that the specifications given them by the electronic engineers were often incomplete or unrealistic. Furthermore, they claimed that their designs would often test satisfactorily in the low-power or equivalent test circuit specified by the electronic engineers and then give unsatisfactory performance under actual operating conditions.

This state of affairs was brought to the attention of the writer in the early part of 1947. A review of the pertinent literature available at that time[1,2] revealed no really satisfactory answer to the general problem, so a project directed toward rectifying this condition was initiated in the General Electric Research Laboratory. A book[3] published several months later covers this subject fairly well. However, the approach to the problem to be described here offers some advantages over that described in these references. One of the objectives of this project was to provide some common meeting ground between electronic-circuit engineers and transformer-designing engineers. Information was to be provided which would enable the designers of broad-band linear amplifier and transmission circuits to determine the practicability of using transformers to obtain certain desired results and to make proper and realistic requirement specifications to convey their needs to the transformer designer. Also, the information was to be such as to enable transformer designers, given these requirement specifications and electronic circuit operating conditions, to determine the feasibility of designing the required transformers and to predict with reasonable accuracy the performance of the transformers when combined with the circuits.

Development of a Terminology

Perhaps the main barrier to the free exchange of information between these two groups of engineers has been that of terminology or language. For example, the electronic-circuit designers use such terms as coefficient of coupling, primary inductance, secondary inductance, and circuit Q to express some of the characteristics of transformers in electronic circuits. Since most audio and power transformers have very tight coupling between the primary and secondary, it is more convenient for the transformer designers to express these characteristics in terms of leakage inductance, magnetizing inductance, and load resistance.

In order to have the analysis cover the most general case, the transformer-coupled modulator with shunt-feed reactor was chosen as representative, since it requires consideration as a coupling net-

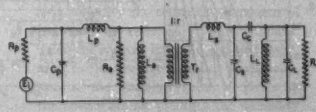

Figure 1. General equivalent circuit of modulator output amplifier, modulation transformer, coupling network, and load

Paper 50-159, recommended by the AIEE Electronics Committee and approved by the AIEE Technical Program Committee for presentation at the AIEE Summer and Pacific General Meeting, Pasadena, Calif, June 12–16, 1950. Manuscript submitted March 13, 1950; made available for printing April 18, 1950.

H. W. LORD is with the General Electric Company, Schenectady, N. Y.

The author acknowledges and appreciates the help of the several associates within the General Electric Company whose co-operation has made this paper possible. These include R. A. Dehn, S. G. Reque, F. A. Pessler, K. Carpenter, Miss W. J. Clelland of the Research Laboratory, C. L. Rounsit of the Electronics Department, C. H. Wells of the Power Transformer Engineering Division, and V. R. Peterson of the Specialty Transformer Engineering Division. Part of the work forming the basis for this paper was supported by contracts with the Signal Corps Engineering Laboratories, Fort Monmouth, N. J.

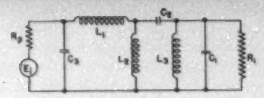

work at both ends of the pass band.

Figure 1 is the general equivalent circuit of such a modulator, where

E_1 = voltage generated in plate circuit of final amplifier tube
R_p = plate resistance of final amplifier tube
C_p = total primary shunt and distributed capacitance
L_p = primary leakage inductance
R_c = equivalent resistance corresponding to core losses
L_m = equivalent magnetizing inductance of primary
T_r = ideal transformer of primary-to secondary ratio of $1/r$
L_s = secondary leakage inductance
C_s = total shunt and distributed capacitance of transformer secondary and modulation inductor
C_c = coupling capacitance between transformer and modulation inductor
L_L = modulation inductor (shunt-feed inductor)
C_L = radio-frequency by-pass capacitor plus capacitance of wiring
R_L = equivalent resistive load of radio-frequency amplifier

If it is assumed that the winding resistances and core losses are negligibly small, that the coefficient of coupling is practically unity, and that any primary-to-secondary capacity effects are negligibly small, then Figure 2 will be recognized as the general equivalent circuit, where all circuit values such as shunt-feed reactor, load, and so forth, are referred to the primary. The circuit elements in Figure 2 are as follows

L_1 = total transformer leakage inductance referred to primary $= L_p + L_s/r^2$
L_2 = primary exciting inductance $= L_m$
L_3 = inductance of shunt-feed reactor referred to primary $= L_L/r^2$

Figure 4. Generalized frequency-response characteristic

Output voltage at low frequencies

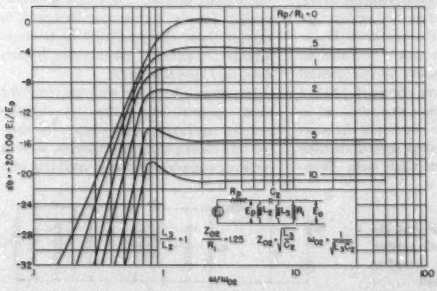

Figure 2 (left). General equivalent circuit of modulation system reduced to unity ratio and referred to the transformer primary

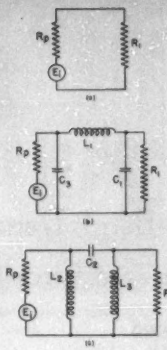

Figure 3 (right). Simplified equivalent circuits for limited frequency ranges

C_1 = total shunt capacitance of load, shunt-feed reactor, and transformer $= r^2(C_S + C_L)$
C_2 = capacitance of coupling capacitor referred to primary $= r^2 C_c$
C_3 = total shunt capacitance of transformer primary and wiring $= C_p$
R_1 = equivalent resistance load referred to primary $= R_L/r^2$

Since the analysis is to apply to transformers having broad-band characteristics, the equivalent circuit can be simplified by dividing the frequency range into three sections—low, medium, and high frequency. The medium-frequency region is the band over which the reactive elements have negligible effect and so the simple circuit of Figure 3(A) holds true. At high frequencies the effect of the series inductances and shunt capacitances are all that need to be considered; hence the equivalent circuit at the high-frequency end of the pass band becomes that of Figure 3(B). At low frequencies only the shunt inductances and series capacitances need to be considered; hence the equivalent circuit of Figure 3(C) is valid. These equivalent circuits now represent the transformer and circuit as relatively simple networks made up of elements of resistors, inductors, and capacitors.

In order to obtain a simple terminology for expressing the interrelationship of these elements, it seemed desirable to avoid the use of such frequency-dependent factors as Q (quality factor) and D (dissipation factor). This can be done if the reactive elements L and C of the networks are treated as elements of an artificial line of characteristic impedance Z_0 defined by the expression $Z_0 = \sqrt{L/C}$. This term is commonly used in connection with pulse-transformer design[4]; so it seems reasonable to apply it to broad-band-transformer design. If the circuit of Figure 3(B) is treated as an artificial line, it will have a characteristic impedance Z_{01} equal to $\sqrt{L_1/C_1}$. Figure 3(C) also can be considered as an artificial line of characteristic impedance Z_{02} equal to $\sqrt{L_3/C_3}$. These circuit constants can be conveniently related to frequency by the equation for electrical resonance. Thus, for the high-frequency circuit, $2\pi f_{01} = \omega_{01} = 1/\sqrt{L_1 C_1}$, and for the low-frequency circuit, $2\pi f_{02} = \omega_{02} = 1/\sqrt{L_3 C_3}$. These terms are applicable even if the capacitor C_3 and inductor L_3 are of such values that they can be neglected.

This terminology for describing the equivalent circuits of the transformer, their relations to each other and to frequency, is easily understood by both electronic circuit designers and transformer designers. It employs nothing which is unfamiliar to the circuit designers since it avoids such terms as magnetizing reactance and leakage reactance. The term characteristic impedance may be new to some transformer designers. However, its definition is relative simple and experience indicates that transformer designers accept this term more readily than they accept the terms Q and D.

Figure 5. Generalized frequency-response characteristic

Output voltage at high frequencies

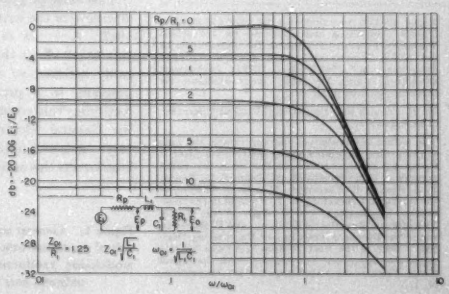

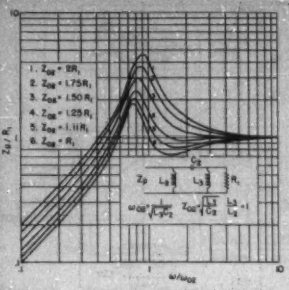

Figure 6. Generalized frequency-response characteristic

Input impedance at low frequencies

Generalized Response Curves

Having established a terminology, the equivalent circuits representing several types of coupling transformers at the high and low regions of the band pass were analyzed relative to such important frequency response characteristics as output voltage, output phase, and input impedance. Because of space limitations, the results of only a few of those analyzed are shown here as examples of this phase of the project.

Perhaps the most important characteristic of the combined amplifier and transformer is the manner in which the ratio of the output voltage to the input voltage varies with frequency. In many instances the allowable variation of this ratio over the useful portion of the pass band must be held to a very constant value. For example, it is not uncommon in audio-amplifier circuits to require that this voltage ratio be held constant within $\pm 1/2$ decibel (± 6 per cent) from 20 cycles to 20,000 cycles. Figures 4 and 5 illustrate the theoretical generalized frequency response curves of this voltage ratio for several ratios of tube plate resistance to equivalent load resistance. Note that the frequency parameter is expressed as a ratio so as to be applicable to any frequency range that may be determined by the equivalent circuit constants. The particular equivalent circuit analyzed to obtain each set of curves is shown schematically in each illustration.

Another important characteristic is the impedance presented to the tube by the combined transformer, coupling network when used, and load. Figure 6 and Figure 7 show the manner in which the impedance characteristic varies with frequency. Large dips in impedance within the normal operating range must be avoided since they tend to increase the distortion in the associated amplifier tubes.[9] However, a large increase in impedance occurring at either end or both ends of the pass band can be tolerated. The curves of Figure 6 and Figure 7 provide means for selecting the proper ratio of the characteristic impedance to the load resistance. They show that when $Z_0/R_1 = 1.25$, the impedance within the normal operating range drops to only 88 per cent of the mid-frequency value. Since this ratio usually provides the best compromise between the impedance characteristic and the output-voltage characteristic, the frequency-response curves which were selected to illustrate this paper are for this optimum ratio.

Except when a feedback loop includes the transformer, the phase angle of the output voltage with respect to the input voltage as a function of frequency is of little importance in many audio amplifiers. This phase angle is important in video amplifier circuits for radar and television. Figure 8 and Figure 9 show frequency response curves of this characteristic.

Specifications Required

In order to design a transformer using these theoretical curves, the circuit designer must provide the transformer designer with certain specifications which adequately describe the circuit in which the transformer is to be used and the overall performance required. An outline of the essential specifications follows:

1. Circuit Characteristics
   - A. Load
     - *i.* Equivalent load resistance
     - *ii.* Total value of shunt capacitances
     - *iii.* Required maximum audio power into load
     - *iv.* Component of direct current into load
   - B. Power Source
     - *i.* Characteristic impedance for a line or cable
     - *ii.* For an amplifier—single-ended; push-pull, class *A*, or class *B*
       - a. Minimum average plate resistance (this should include the effect of feedback in modifying the actual plate resistance)
       - b. Plate current at zero signal and maximum signal; maximum unbalance if push-pull
       - c. Peak plate current
       - d. D-c plate-supply voltage
       - e. Peak-to-peak plate voltage swing
2. Transformer Characteristics
   - A. Secondary
     - *i.* Maximum allowable winding resistance
     - *ii.* D-c component of voltage to ground
     - *iii.* Peak-to-peak voltage swing or rms value of alternating-voltage component
   - B. Primary
     - *i.* Maximum allowable winding resistance
     - *ii.* Normal value of impedance presented to power source with load connected
   - C. Minimum Allowable Efficiency
3. Over-All Performance of Transformer and Circuit
   - A. Frequency-Response Characteristics
     - *i.* Load voltage
       - a. Amplitude versus frequency
       - b. Phase versus frequency when required
     - *ii.* Primary impedance (minimum allowable within operating range, as per cent of normal)
     - *iii.* Signal amplitude (maximum required input signal in per cent of normal as a function of frequency)
   - B. Harmonic Distortion (maximum allowable attributable to the transformer, excluding that caused by impedance effects)

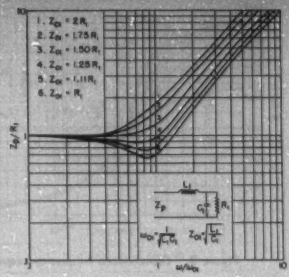

Figure 7. Generalized frequency-response characteristic

Input impedance at high frequencies

Outline of Design Procedure

A design procedure is fairly straightforward when based upon these generalized response curves and a suitable set of specifications covering the transformer and circuit performance requirements. First, the required transformer turns ratio 1/r of the primary to the secondary is calculated from the specified transformer ratings and used to determine an equivalent value for the resistive component of the load as reflected to the primary. Then the ratio of this reflected load resistance to the average effective plate resistance of the amplifier tube, as given by the specifications, provides the necessary

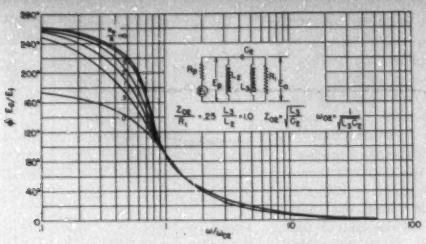

Figure 8. Generalized frequency-response characteristic

Output phase at low frequencies

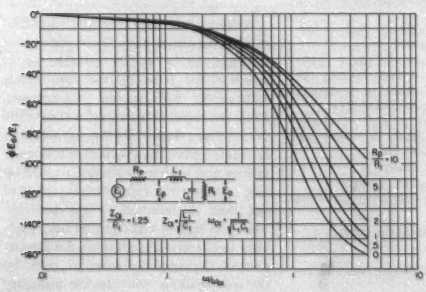

Figure 9. Generalized frequency-response characteristic

Output phase at high frequencies

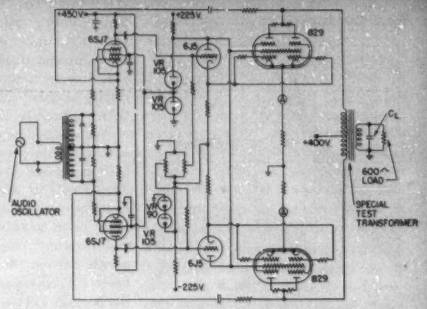

Figure 10. Circuit diagram of push-pull class-B amplifier

Used for harmonic distortion tests

information to select the particular generalized frequency response curve which should be used at each end of the pass band. These two curves are then employed to determine values for the magnetizing inductance, the total leakage inductance, and the allowable secondary shunt capacitance, in the following manner.

For illustrating this procedure, assume the transformer is coupled to the load through a shunt-feed inductor and coupling capacitor. Their equivalent primary values, as well as the transformer magnetizing inductance, can be determined from Figure 4 and the specified low-frequency response characteristic. For example, suppose the reflect load resistance, R_1, is 10,000 ohms, the effective plate resistance, R_p, is 20,000 ohms, and the output voltage must be no more than one decible down at 50 cycles. The curve for the ratio of $R_p/R_1 = 2$ of Figure 4 is then the one to use. The output voltage for this curve is down one decibel from the mid-frequency value of -9.5 decibels at ω/ω_{o2} of 0.72, from which $\omega_{o2} = 2\pi \times 50/0.72 = 437$. Since these curves are for $Z_{o1}/R = 1.25$, then $Z_{o1} = 12{,}500$. The expressions $Z_{o1} = \sqrt{L_1/C_1}$ and $\omega_{o1} = 1/\sqrt{L_1C_1}$ can be combined to give the expressions $L_1 = Z_{o1}/\omega_{o1}$ and $C_1 = 1/Z_{o1}\omega_{o1}$; $L_1 = 12{,}500/437 = 28.6$ henrys is therefore the required reflected value for the shunt-feed inductor. It is desirable that the transformer-primary magnetizing inductance be equal to this same value. The required shunt-feed choke is then $r^2 \times 28.6$ henrys. Also, $C_1 = 1/12{,}500 \times 437 = 0.183$ microfarad is the required reflected value for the coupling capacitor. The required coupling capacitor is then $0.183/r^2$ microfarad. If the primary capacitance is small and so assumed to be negligible, then Figure 5 can be used in a similar manner to determine the total equivalent primary leakage inductance and total allowable secondary and load shunt capacitance. The curve for $R_p/R_1 = 2$ shows the output voltage is down one decible from the mid-frequency value of -9.5 decibels at ω/ω_{o1} of 0.88. If this point is assumed to be specified as the 10-kc point in the specified over-all frequency-response characteristic, then $\omega_{o1} = 2\pi \times 10{,}000/0.88 = 7.14 \times 10^4$. Hence, the total equivalent primary leakage inductance L_1 should be $12{,}500/7.14 \times 10^4 = 0.175$ henry and the total allowable reflected secondary and load shunt capacitance C_1 should be 0.00112 microfarad. If the specifications call for operating with a shunt capacitance across the load of C_L microfarads, then the total shunt and distributed capacitance C_s allowed for the transformer secondary and shunt-feed inductor will be found by the expression $C_s = C_1/r^2 - C_L$ microfarads.

All of the transformer design constants which affect the frequency-response characteristic have now been determined. From here on the design follows the conventional procedure. The problem becomes one of designing a transformer which will have these constants and which will have sufficient core area and copper cross section to handle the power level as specified for certain frequency ranges within the pass band. In general, the core area is determined by the low-frequency requirements; so the trans-

Figure 11. Harmonic distortion characteristics of class-B push-pull amplifier and transformer at high frequencies for different ratios of the leakage inductance measured from one-half primary to one-half primary to that measured from one-half primary to secondary

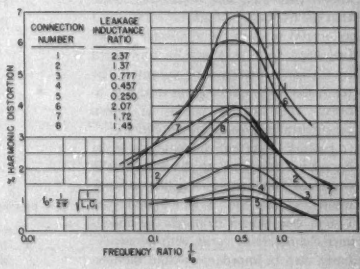

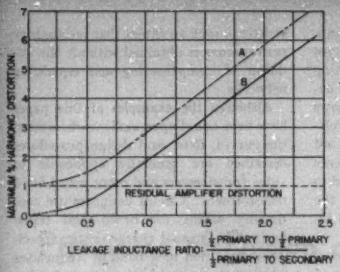

Figure 12. Maximum per cent harmonic distortion at high frequencies as affected by the leakage inductance ratios

(A) Total distortion
(B) Distortion attributable to the transformer

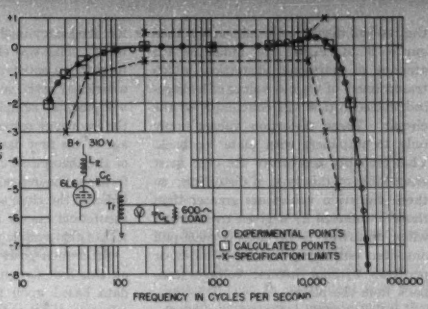

Figure 13. Over-all amplifier frequency response characteristic

Variation of ratio of input voltage to output voltage as measured and as predicted by equivalent circuit analysis

former is first designed with sufficient core area and coil turns to satisfy the specified power conditions at the low-frequency end of the pass band and with the required value of magnetizing inductance. The coil configuration and arrangement of windings are then varied to obtain the required value of leakage inductance. Finally, the secondary distributed and shunt capacitance are calculated. If these turn out to be too high, then the secondary coils may have to be arranged in piles. In order to obtain a satisfactorily low capacitance value without an increase in leakage inductance caused by increasing the spacings between windings and layers, it may be necessary to start a new design with a larger core area.

Harmonic Distortion Attributable to Transformer

Circuit designers must design systems with harmonic distortions below specified maximum values. The transformer, as a component of the system, must be so designed as to contribute only a fraction of the allowable over-all distortion.

It has been recognized for some time in class-*B* push-pull amplifiers[5] that the leakage inductance between the two halves of the primary winding is a source of distortion in the high-frequency portion of the pass band. However, of the only two references found, one[6] assumed linear transfer characteristics for the tubes; hence the theoretical analysis given could not be relied upon for numerical results for a practical amplifier. The other[3] stated that perceptible nicks in the output voltage wave would occur if the ratio of primary-to-primary leakage reactance to average triode plate resistance is four or more. This sort of information is inadequate since modern amplifiers often have tetrodes or pentodes in the output stage and their plate resistance is usually very high. Also, many amplifiers now employ inverse voltage feedback to keep the amplifier distortion low and ten decibels of this type of feedback reduces the apparent plate resistance to a relatively low value[8]. Reduction of this leakage inductance to very low values usually requires complex interleaving of the windings. This is not only expensive but may also introduce undesirable capacity effects between winding sections. It is therefore advantageous to be able to determine with reasonable accuracy a value for this leakage inductance which will keep the distortion caused by it below a specified value.

Since the analytical solution of this problem was complicated by nonlinear circuit elements, it was solved experimentally. A transformer was constructed with several windings of equal turns so that the leakage inductance between halves of the primary as well as that between half-primary and secondary could be varied by changing the winding arrangements. Capacity effects were minimized by operating both primary and secondary at low levels of impedance. The apparent plate resistance of the class-B push-pull amplifier was made very low by operating tubes in parallel and by employing a large amount of inverse voltage feedback from the plates. This feedback also reduced the amplifier harmonic distortion to a relatively small value.

Figure 10 shows the schematic circuit diagram of the test circuit. Leakage inductances for each arrangement of transformer connections were measured and the value of the padding capacitor across the 600-ohm load adjusted so that the equivalent circuit of the transformer and load conformed to that shown on Figure 5. Tests of output voltage of the combined transformer and test circuit as a function of frequency were made for each connection and compared with the theoretical curves as a check of conformity with the equivalent circuit. Harmonic distortion at the high-frequency end of the pass band was then measured for each connection arrangement. Results of the harmonic distortion tests were plotted as shown in Figure 11, using a dimensionless frequency parameter in order to provide a means for readily comparing these data.

Figure 11 indicates that the harmonic distortion in each case reaches a maximum value at a frequency which is approximately one-half the resonant frequency of the circuit and transformer.

Since the leakage inductance between one-half of the primary and the secondary is one of the key values in determining the output voltage versus frequency-response characteristic, it seemed desirable to try to relate the distortion to this parameter also, instead of to the plate resistance of the amplifier. By using the ratio of the leakage inductance between halves of the primary to the leakage inductance between one-half primary and secondary, this parameter can be made dimensionless for purposes of generalization. Curve *A* of Figure 12 was obtained by plotting the harmonic distortion values of the peaks of the curves of Figure 11 against the corresponding inductance ratios for each of those curves. Except for the effect of the small value of residual harmonic distortion due to the amplifier, there is a linear relationship between the inductance ratio and the maximum value of harmonic distortion it produces.

It is frequently assumed that harmonic distortions of these low values can be added and subtracted arithmetically. If

the residual distortion is subtracted, then curve *B* of Figure 12 indicates the amount of harmonic distortion which transformers of various values of leakage-inductance ratios will contribute to the circuit. These distortion values apply only to amplifiers with plate feedback. This probably represents the case most susceptible to this type of distortion; so these distortion values are greater than those introduced by a given transformer when operating from class-*B* push-pull amplifiers employing triodes, tetrodes, or pentodes without inverse voltage feedback from the plates.

Another source of distortion which the transformer may contribute becomes evident at the low end of the pass band. This distortion is caused by the harmonic content in the magnetizing current required by the transformer core. Methods of calculating such distortions have been suggested,[7,8] although they are rather laborious.

Application Results

A series of some 30 generalized frequency-response curves similar to those of Figures 4 through 9 were prepared for the use of designing engineers of the General Electric Company. These were based upon the theoretical analysis of several equivalent circuits and ratio of parameters.

Before turning this information over to the designing engineers, it was deemed advisable to provide some evidence that the information could be used as a basis for designing transformers which would perform as predicted by the theoretical analysis of the equivalent circuits. As a test case, the Electronics Department of the General Electric Company furnished performance specifications for a 3-watt tube-to-line output transformer needed for frequency-modulation studio equipment. This was chosen as they had yet to obtain a satisfactory unit after testing a series of seven successive designs of developmental samples. Figure 13 shows the frequency response of the output voltage of the first design made with the aid of the theoretical curves. Several points from the theoretical curves are included to indicate the close agreement between the theoretical curves and that obtained by test of this sample unit in the circuit.

After such good results were obtained on this first design, the information and data based upon this terminology were released to the transformer and electronics-circuit designing engineers. The suggested terminology was readily accepted by both groups. A format of the specification sheets for audio transformers was modified by the electronic engineers to permit the use of this new approach to the problem. It then became relatively easy for the transformer designers to use the generalized response curves to convert these specifications into design constants for the required transformer. Transformer designers with no previous experience in audio-transformer design are now able to turn out designs which yield a high percentage of satisfactory first models.

Both groups have benefited through the use of these design data. The transformer designers now receive specifications which are complete and which accurately describe the needs of the circuit designers. First developmental models of small units usually perform satisfactorily in the circuit, thus materially shortening the time the circuit designer must spend upon circuit development and testing. The size and weight of large modulation transformers have been reduced. In some cases this size reduction has improved the high-frequency characteristic to such an extent that satisfactory performance is obtained without the addition of compensating and equalizing networks.

Although the examples of this paper have been based upon audio transformers, the curves, data, and design procedures described are generally applicable to video transformers and other broad-band transformers. Circuit designers are continually asking for broad-band transformers of unusual characteristics, specifying operation in a band of frequencies which may lie within the range of a few cycles to several hundred megacycles. The time required to design and develop transformers to meet their needs is materially shortened through application of these techniques.

References

1. Output Transformer Response, **F. E. Terman, R. E. Ingebretsen.** *Electronics* (New York, N. Y.), volume 9, January 1936, pages 30–32.

2. Design of Audio-Frequency Amplifier Circuits Using Transformers, **Paul W. Klipsen.** *Proceedings*, Institute of Radio Engineers (New York, N. Y.), volume 24, number 2, February 1936, pages 219–32.

3. Electronic Transformers and Circuits (book), **Reuben Lee.** John Wiley and Sons, Inc., New York, N. Y., 1947.

4. Pulse Generators (book), **G. N. Glasoe, J. V. Lebacqz.** McGraw-Hill Book Company, Inc. New York, N. Y., 1948.

5. Quasi Transmitents in Class B Audio-Frequency Push-Pull Amplifiers, **A. Pen-Tung Sah.** *Proceedings*, Institute of Radio Engineers (New York, N. Y.), volume 24, number 11, November 1936, pages 1522–41.

6. Control of the Effective Internal Impedance of Amplifiers by Means of Feedback, **H. F. Mayer.** *Proceedings*, Institute of Radio Engineers (New York, N. Y.), volume 27, March 1939, pages 213–17.

7. Harmonic Distortion in Audio-Frequency Transformers, **N. Partridge.** *Wireless Engineer* (London, England), volume 19, September, October, and November 1942, pages 394–400, 451–56, and 503–07.

8. Graphical Harmonic Analysis, **J. A. Hutcheson.** *Electronics* (New York, N. Y.), volume 9, January 1936, pages 16–18.

No Discussion

Principles of Design of Log-Scale D-C Indicating Instruments

ALLEN STIMSON
ASSOCIATE AIEE

C. F. TAYLOR
NONMEMBER AIEE

IN MANY quantities, such as money, equal increments are of equal value regardless of the total amount. In other quantities, the increment is evaluated in relation to the total amount. Physical sensation is one example. According to the Weber-Fechner law, a stimulus which increases in geometric progression, produces a sensation which increases in arithmetic progression. This means that the magnitude of the stimulus determines the importance of its increment. For instance, an increment of one foot-candle added to illumination of five foot-candles would noticeably increase visibility. Yet one foot-candle added to one hundred foot-candles would not be perceptible. The eye is equally sensitive to equal percentage differences. A lightmeter should, therefore, give equal per cent reading accuracy at each scale point. An instrument having this distribution has a logarithmic scale. Sound is also evaluated on a logarithmic basis expressed in the familiar decibel units.

In conventional d-c indicating instruments the scale distribution is linear. Each minor scale division represents an equal increment of current. In an instrument having logarithmic scale distribution, each minor scale division represents an equal per cent of the corresponding scale value.

Log-scale instruments are of value when the entire scale range should be readable with equal accuracy as in an ammeter. For a voltmeter, used on established circuits, the log-scale would be of less usefulness, because only values near the rated voltage would be read.

The advantages of the log-scale distribution may be summarized

1. Equal per cent reading accuracy throughout the scale range.
2. Better reading accuracies in the lower half of the scale.
3. Larger scale ranges are possible.
4. Higher deflection sensitivity near zero for the same full scale rating.
5. The logarithmic scale can function as part of a slide rule with the instrument pointer performing the computation.

Log-scale instruments also have certain disadvantages compared to linear-scale instruments

1. They are more expensive.
2. For equal full-scale rating the log-scale instruments require more power.
3. Unit increments near full scale are not so readable.
4. Variation in magnetic damping with scale deflection may make some dynamic characteristic harder to obtain for certain applications.

Mathematical Background

An electrical indicating instrument which provides equal reading accuracy at all scale points, expressed in per cent of the indicated value, must have a unique scale distribution. The change in scale values per unit angular pointer movement must be proportional to the scale value. If the scale is calibrated for signals x and the pointer deflection is θ, then

$$\frac{dx}{d\theta}=\frac{x}{c_1} \tag{1}$$

or

$$d\theta=c_1\frac{dx}{x} \tag{2}$$

The solution of differential equation 2 is

$$\theta=c_1 \log x+c_2 \tag{3}$$

Equation 3 expresses the general scale law of log-scale instruments.

For the purpose of this discussion it is assumed that an instrument is to be designed having the predetermined scale values defined by equation 3 and shown in Figure 1. The scale has the following characteristics when the base of the system of logarithms is a

Scale range per log cycle $=a$
Number of log cycles in scale range $=n$
Scale range of instrument in log cycles $=a^n$
The scale range in terms of values of the signal x is

$$\frac{x_F}{x_0}=a^n \tag{4}$$

The derivation of equation 3 defines the logarithm to the base e. However, change to any base a merely changes the value of the constant c_1. The example, Figure 1, arbitrarily assumes the base to be $a=2$.

The values of the constants c_1 and c_2 may be determined from the boundary conditions. When

$$x=x_0,\ \theta=0 \tag{5}$$

When

$$x=x_F,\ \theta=\theta_F \tag{6}$$

If the limits of equations 5 and 6 are substituted in equation 3 the constants are found to be

$$c_1=\frac{\theta_F}{\log\frac{x_F}{x_0}} \tag{7}$$

and

$$c_2=-\frac{\theta_F \log x_0}{\log\frac{x_F}{x_0}} \tag{8}$$

From equation 4 it is evident that

$$\log_a\frac{x_F}{x_0}=\log_a a^n=n \tag{9}$$

Paper 50-160, recommended by the AIEE Instruments and Measurements Committee and approved by the AIEE Technical Program Committee for presentation at the AIEE Summer and Pacific General Meeting, Pasadena, Calif., June 12–16, 1950. Manuscript submitted March 13, 1950; made available for printing April 18, 1950.

ALLEN STIMSON and C. F. TAYLOR are with the General Electric Company, West Lynn, Mass.

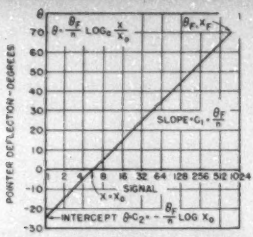

Figure 1. The predetermined scale distribution is defined by this logarithmic relation

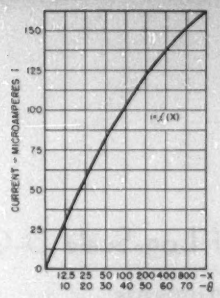

Figure 2. The instrument current is related to the signal by this arbitrary function

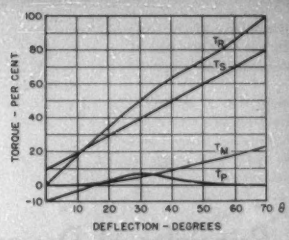

Figure 3. The total restoring torque is the sum of the torques due to control springs, parasitic iron, and ferromagnetic controls

Equations 7 and 9 then become

$$c_1 = \frac{\theta_F}{n} \tag{10}$$

$$c_2 = -\frac{\theta_F}{n} \log x_0 \tag{11}$$

The significance of c_1 is the pointer deflection per cycle, and it is also the slope of the curve of Figure 1. The constant c_2 is the value of θ when $x=1$ and $\log x=0$. Equation 3 may now be written

$$\theta = \frac{\theta_F}{n}(\log_e x - \log x_0) \tag{12}$$

$$\theta = \frac{\theta_F}{n} \log_e \frac{x}{x_0} \tag{13}$$

Equation 13 expresses the general scale law for an instrument having logarithmic scale distribution. It states that equal increments of pointer deflection θ represent equal increments of $\log x$.

In designing an instrument to track equation 13 it is assumed that the signal x is related to the instrument current i by a function

$$i = f_1(x) \tag{14}$$

and which may be an empirical relation of the type shown in Figure 2. In this graph, values of both θ and x are shown according to the relation assumed in Figure 1. For any particular case the function

$$i = f_2(\theta) \tag{15}$$

is also known from Figure 1.

A d-c instrument at steady state indication is subject to the electromagnetic deflecting torque

$$T_D = BSNi \tag{16}$$

From this well-known relation, the flux density may be found. For a log-scale ammeter where the signal is i and the restoring torque is $K\theta$, the flux density from 13 and 16 is

$$B = \frac{T_R}{SNi} \tag{17}$$

$$B = \frac{K}{SNi_0} a_{Bi}^{-\frac{n}{\theta_F}\theta} \tag{18}$$

The graph of this equation is similar to that in Figure 4. For an actual instrument the nonlinear restoring torque of Figure 3 is the sum of several components arising from iron in the moving system in addition to the control springs.

$$T_R = T_S + T_P + T_M \tag{19}$$

The current i may also be nonlinearly related to the signal X as in equation 14. Values of B are calculated point by point from equation 17 using values of i com-

Nomenclature

a = Scale constant (log base)
B = Radial component of magnetic-flux density, gauss
B_1 = Flux density B at angle θ_1, gauss
B_1' = Flux gradient $dB/d\theta$ at angle θ_1, gausses/radian
B_F = Flux density B at full scale, gauss
B_{max} = Maximum flux density at angle $\theta = M$, gauss
C_1 = Scale constant (θ_F/n)
C_2 = Scale constant $\left(-\frac{\theta_F}{n} \log x_0\right)$
C_3 = Damping shell constant $= \frac{D}{B^2}$, $\frac{\text{dyne-centimeter-second}}{(\text{gauss})^2}$
C_4 = Constant $= SNi_1(B_1 - \theta_1 B_1')$, dynecentimeters
D = Damping constant, dyne-centimeter-second
D_1 = Damping constant at angle θ_1, dyne-centimeter-second
f_0 = Undamped frequency of oscillation, $(\text{second})^{-1}$
f_d = Damped frequency of oscillation, $(\text{second})^{-1}$
i = Current in moving coil, ampere
i_1 = Current causing deflection θ_1, ampere
I = Moment of inertia of moving system, gram-centimeter^2
K = Control spring constant, dyne-centimeter/radian
n = Number of log cycles on scale
N = Number of turns on moving coil
S = Torque per ampere turn per kilogauss
T = Torque (general), dyne-centimeters
T_L = Deflecting torque, dyne-centimeters
T_M = Torque due to iron vane on moving system, dyne-centimeters
T_P = Parasitic torque due to magnetic impurities in moving system, dyne-centimeters
T_R = Total restoring torque, dyne-centimeters
T_S = Torque due to control springs, dyne-centimeters
T_1 = T_S at θ_1, dyne-centimeters
W = Weight of moving system, grams
x = Signal calibrated on instrument scale
x_0 = x at $\theta = \theta_0$
x_F = x at $\theta = \theta_F$
θ = Scale angle, radians
θ_F = Full-scale angle, radians
θ_M = Angle at maximum flux B_M, radians

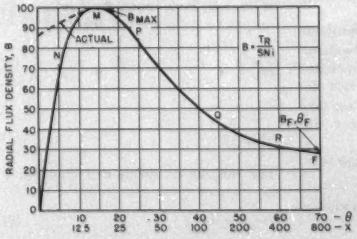

Figure 4. The variation of flux density in the path of the moving coil has a unique pattern for log-scale instruments

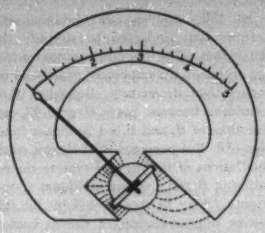

Figure 5. A conventional expanded scale instrument

puted from equations 13 and 14 and values of T_R from equation 19. Figure 4 shows the flux distribution for an actual design.

Design of the Magnetic System

The distribution of the effective flux density B along the path of the moving coil is one parameter which can be controlled. The method of design of the magnetic system will be illustrated by a general example.

The signal x to be measured is manifested by a current i having an arbitrary relation shown in Figure 2. Inasmuch as Figure 1 has shown the desired scale law relating θ and x, the corresponding values of θ are also shown in abscissas in Figure 2.

The instrument mechanism selected for this application has a known torque S per ampere turn per kilogauss of B and a moving coil of N active turns. It is then easy to compute values of the product SNi from the data in Figure 2 for various values of θ.

The instrument mechanism selected may be assigned trial torque characteristics. These are illustrated in Figure 3 and consist of the control spring torque T_R, the parasitic torque T_P due to distributed magnetic impurities in the moving system, and the other torques T_M due to a magnetic vane and possible polarized pivots. At each value of θ the summation of torques T_R has the unique value of equation 19 shown in Figure 3. The numerical values of these torques must be initially assumed for the purpose of evaluating the corresponding flux distribution.

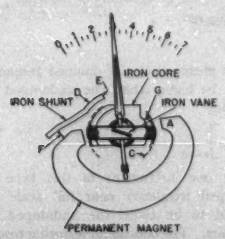

Figure 6. The magnetic structure of a log-scale instrument

The required distribution of the radial component of flux density B is calculated from equation 17 by dividing the values of T_R by the corresponding values of SNi for each value of θ. The resulting unique function of B is plotted in Figure 4.

This distribution of flux in the air gap, Figure 4, is based on assumed torques of Figure 3. The moving-iron torques T_P and T_M are dependent upon the flux distribution and must therefore be recomputed or measured for the actual flux distribution. The new values may demand a second computation of the required flux distribution.

Characteristics of the Flux Distribution

The design of a magnetic system which will provide the flux-density distribution of Figure 4 is limited by several practical considerations. The density cannot be zero at scale zero, $\theta=0$, because there will be a minimum stray field which cannot be avoided. Hence, the actual log-scale distribution must start at some small angle above scale zero. If B were zero at scale zero, initial deflection of the moving system could never result from any current i according to equation 16. The initial deflecting torque would be zero and the response time would be infinite.

The steepness of the gradient of the air-gap flux density $dB/d\theta$ between points P and Q in Figure 4 is limited by the actual length of the path of the moving coil and the value of B_{max}. The longer the path the easier the density can be controlled. The maximum range of the instrument is also limited by the minimum flux density B_P which can be obtained at the full-scale position of the moving coil.

The higher the value of the maximum flux density, B_{max}, the higher the sensitivity of the instrument and the greater the possible scale range. Instruments can be designed for values of B_{max} over 6,000 gausses but the resulting high flux-density gradient increases the highly variable parasitic torques to an uncontrollable level.

The design of the air gap of a conventional expanded-scale moving-coil d-c instrument is shown in Figure 5. This construction can be made to fit part of the characteristic of Figure 4 but only for short scale angles and small ranges. High flux gradients cannot be obtained with this construction in conformance with the required distribution.

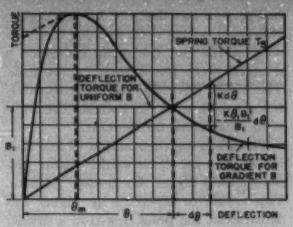

Figure 7. The negative gradient of flux density in a log-scale instrument increases the incremental restoring torque

The sharp peak of flux density at B_{max} Figure 4, indicates that the field magnet should have salient poles as at A in Figure 6. The steep gradient at N, Figure 4, suggests that the core be cut away as at G, Figure 6. To obtain the relatively low density B_P at full scale, both the core and the magnet are spaced away from the locus of the moving coil as at C, Figure 6. The density at C may also be controlled by reducing the depth of the core compared to that at G.

The point of maximum flux density, Figure 4, occurs at about 20-per cent scale deflection. To obtain maximum sensitivity the maximum density should be at zero scale position. It is therefore apparent that a logarithmic-scale distribution gives maximum uniformity of reading accuracy at some sacrifice in sensitivity.

The instrument magnetic system shown

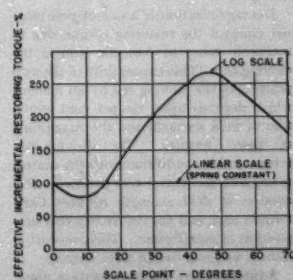

Figure 8. The effective factor of merit of a log-scale instrument is greater than indicated by $T/W^{1.5}$ and varies with scale deflection

in Figure 6 was designed for ten degrees deflection per log cycle with log base two. This means that the signal indication is doubled every ten degrees on the scale. The range covered was approximately seven cycles or 128 to 1 within the limits of its logarithmic distribution.

To obtain log distribution of less than ten degrees per cycle would require proportionately higher flux density gradient. This would be obtained by higher flux densities at the poles A within a smaller angular space and greater air gap at C. Soft iron poles would be helpful in concentrating the flux. To obtain log distribution of more than ten degrees per log cycle, the pole faces A would be broadened and the air gaps at C reduced.

It is obvious that the distribution of flux density can be controlled by shaping either the core or magnet poles. Shaping the core has less influence than shaping the magnet poles. The effective flux density can also be controlled by change in the direction of the flux since only the radial component is effective.

The parasitic torques, due to magnetic impurities distributed throughout the moving system, are not noticeable in concentric gap instruments, but do affect the scale distribution with magnetic systems having an effective flux-density gradient.

Scale Tracking Adjustment

There are several methods of reducing the deflecting torque of a permanent-magnet moving-coil d-c instrument to obtain the desired accuracy. One of the most convenient and widely used methods consists of demagnetizing the permanent magnet by application of an alternating field. This method is also quite satisfactory for log-scale instruments.

Demagnetization of a salient-pole magnet changes the restoring torque due to magnetic vanes or parasitic iron in the moving coil. This causes shift of the zero position of the moving coil by an amount which depends upon the per cent reduction of field strength and the magnitude of these torques. The moving-iron torques are in equilibrium with the control springs at the initial rest position. Reduction of field strength reduces these torques also, and the coil moves to a new position of equilibrium. This zero sift is usually not over two or three degrees.

Adjustment by demagnetization must, therefore, be done in two or more steps. The zero position should be checked or reset after each adjustment. The pointer

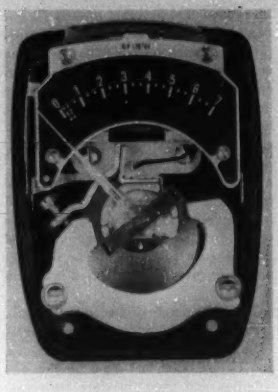

Figure 9. A log-scale instrument mechanism is used in this new exposure meter

zero always shifts down scale in this type of instrument.

Log-scale instruments do not have the consistent distribution that uniform-scale instruments have. Means for adjusting the distribution in one instrument are shown in Figure 6. The soft iron shunt D is pivoted at E and its affect is controlled by varying the air gap at F. This shunt is so located that it affects only the upper half of the scale.

The log-scale instrument can, therefore, be precisely adjusted at two scale points. The first adjustment is demagnetization at a point in the lower quarter of the scale. Second, the shunt is reduced in effectiveness by increasing the air gap F until a point in the upper quarter scale is correct.

Dynamic Characteristics of Log-Scale Instruments

The magnetic damping and incremental restoring torque vary with pointer deflection in log-scale instruments, whereas they are constant in uniform-scale instruments. The difference is due to the variation in flux density illustrated in Figure 4 and Figure 7.

The motion of the moving system obeys the classical differential equation

$$I\frac{d^2\theta}{dt^2}+D\frac{d_\theta}{dt}+K\theta=T_D \tag{20}$$

The coefficient D is the familiar damping constant, and its numerical value is proportional to the square of the flux density B.

$$D=C_3B^2 \tag{21}$$

In this analysis the ferromagnetic torques are neglected to simplify the derivation. The magnitude of the restoring torque is the important consideration rather than its source. Equation 20 is nonlinear because both D and T_D are functions of B, and B is a nonlinear function of θ. For purposes of analyzing small oscillations of the moving system the relation of B and θ shown in Figure 4, and Figure 7 may be represented by the following approximation of B in powers of θ by Taylor's theorem

$$B=B_1+(\theta-\theta_1)B_1' \tag{22}$$

where

$$B_1'=\left.\frac{dB}{d\theta}\right]_{\theta=\theta_1}$$

If it is further assumed that the velocity $d\theta/dt$ as well as the amplitude is small, then also negligible is the contribution of the variation of B^2 to the variation of the product $B^2\,d\theta/dt$. It can therefore be assumed that B in

$$D_1=C_3B^2 \tag{23}$$

does not vary with θ. It is also seen from equations 16 and 22 that

$$SN_{i_1}=\frac{K\theta_1}{B_1} \tag{24}$$

If equations 22, 23, 24, and 16 are combined with equation 20, then

$$I\frac{d^2\theta}{dt^2}+D_1\frac{d\theta}{dt}+\left(K-\frac{K\theta_1}{B_1}B_1'\right)\theta=C_4 \tag{25}$$

This is the familiar equation for damped harmonic motion. From the known solution of equation 25, the damped frequency of oscillation of the moving system is seen to be

$$f_d=\frac{1}{2\pi}\sqrt{\frac{K-K\theta_1B_1'}{I}-\frac{C^2}{4I^2}} \tag{26}$$

and the undamped frequency is

$$f_0=\frac{1}{2\pi}\sqrt{\frac{K}{I}} \tag{27}$$

For values of θ greater than θ_M, Figure 4 shows that $dB/d\theta=B'$ is negative. Therefore for the greater part of the scale

$$\frac{K-K\theta_1B_1'}{I}>\frac{K}{I} \tag{28}$$

This means that the damped frequency may be higher than the undamped frequency

$$f_d>f_1\Big]_{\theta>\theta_M} \tag{29}$$

In one instrument of this type the damped frequency near full scale was found to be twice the undamped frequency. The additional restoring torques which cause the higher damped frequency are shown graphically in Figure 7.

This additional torque also helps minimize the effect of bearing friction.

It is obvious from the form of equation 25 that the total restoring torque for small deflections $d\theta$ of the moving system energized with current i is

$$T = T_1 + K d\theta - \frac{K\phi_1 B_1'}{B_1} d\theta \qquad (30)$$

The ability of an instrument to overcome the affects of bearing friction is frequently judged in terms of the ratio T/W of torque T to weight W of the moving system. The ratio $(T/W)^{1.5}$ is also considered significant. These factor-of-merit concepts were developed for uniform-scale instruments. In instruments having a gradient of flux density, the value of T is not the spring torque alone but has the additional term added to it as shown in equation 30. This total torque is shown in Figure 7 to provide a greater restoring torque for the instrument having a negative flux-density gradient.

The per cent improvement in effective restoring torque due to the flux gradient is shown graphically in Figure 8. Throughout most of the range the incremental restoring torque of the log-scale instrument is higher than that of the linear-scale instrument.

Example of Log-Scale Instrument

One embodiment of the design principles here outlined, is the new exposure meter shown in Figure 9. Logarithmic-scale distribution was desired so that the instrument scale could function as part of the slide rule for computing exposure from the light indication. Conventional instruments require the photographer to read the scale and then find this value on the slide-rule computer. In this new meter, the log-scale distribution permitted synchronizing the instrument pointer deflection with the slide rule so that neither of these reading operations is needed. This improvement reduces the number of operations, time required, and chances for error to half of those of a conventional exposure meter.

For this particular instrument the signal x is the light to be measured. A typical photovoltaic cell converts this signal to current according to the curve in Figure 2. These log-scale instruments have been manufactured by mass-production techniques with no difficulties from scale distribution.

Conclusion

Instruments having logarithmic-scale distribution provide equal (per cent) reading accuracy at all points; and are especially useful where both high threshold sensitivity and large scale range are desired in one device.

The magnetic system of a log-scale instrument can be designed on the basis of mathematical formulae, which are solved point by point, because the quantities involved cannot be represented by simple algebraic expressions. Initial assumptions of instrument characteristics are used to determine the corresponding ideal distribution of flux density. From the nearest practicable approach to this flux distribution, the corresponding instrument torques are recalculated and the design adjusted accordingly.

Adjustment of scale distribution is usually required to obtain reasonable accuracy. One method of securing the distribution adjustment uses a movable soft-iron magnetic shunt. Adjustment for accuracy of the lower quarter of the scale is obtained by demagnetization. Adjustment in the upper quarter of the scale is accomplished by shunting the flux. The mechanism tracks at mid-scale if the moving system is correctly oriented with respect to the salient magnet poles.

The damping is substantially higher at the lower end of the scale than at the high end. The conventional concept of the ratio of torque T to weight W or $T/W^{1.5}$, known as the factor of merit, is not indicative of the effects of possible bearing friction in a log-scale instrument except near the zero position. The gradient of flux density gives effectively higher restoring torques than the static factor of merit indicates and, therefore, greater freedom from bearing friction errors.

The principles outlined in this paper are applicable to general instrument design. They have been illustrated by specific reference to a new exposure meter, manufactured in large quantities.

No Discussion

Interrupting Ability of Horn-Gap Switches

F. E. ANDREWS
FELLOW AIEE

L. R. JANES
FELLOW AIEE

M. A. ANDERSSON
MEMBER AIEE

A HORN-GAP switch has limitations in its ability to successfully open a circuit because of the restricted space available for the arc. As only meager information applicable to switch operation has been found in the technical literature on arc behavior, an investigation including a large number of field tests has been made by the Public Service Company of Northern Illinois with three principal objectives:

1. To study arc behavior on horn-gap switches under various system conditions.
2. To determine magnitude of currents that can be interrupted on existing switches under prevailing system conditions.
3. To determine basic switch design factors for successful operation under specified conditions.

It is the purpose of the authors to describe this investigation and to present the results and conclusions.

Two basic concepts of arc behavior are generally recognized. One is that arc length is proportional to voltage.[1,2,3] The other is that an unconfined arc should always extinguish itself if clearance permits the required growth to a necessary critical length and the gap is wide enough to prevent restriking. Ackerman[1] has given an explanation of the mechanics of arc extinction and the conditions under which an arc attains the critical length at which it goes out. The increasing length is accompanied inherently by an increase in resistance and a decrease in current.

The length of arc is fundamental in relation to the other variables affecting arc behavior. Arc length is defined as the actual complete length of the irregular circuitous arc path.

It is not the length of the arc, but where it goes, or its spread, that is important in horn-gap switch operation. The clearance or free space available for the spread of the arc must be such that it will not form a short circuit between phases or to ground.

"Reach" has been devised as a measure of the spread to provide a criterion for comparison with switch clearances. Arc reach is defined as the distance from a point midway between the arc extremities to the most remote point of the arc at the time of its maximum length. The reach line is not necessarily perpendicular to switch alignment, but may assume any direction thereto. However, the critical direction of reach is usually perpendicular or nearly so to switch alignment.

The test data are presented on a factual basis and analyzed empirically for use in practical application. No attempt has been made at reconciliation with theory of other arc investigations or justification of the results on a theoretical basis.

Limitations in developing firm conclusions from the available test data are recognized. It is believed, however, that the results from these data are reasonably satisfactory for practical application. Additional tests, preferably indoors, under more definitely controlled conditions would be desirable to evaluate the effects of wind and other presently indeterminate factors.

Previous investigations have yielded information helpful in this study and have provided the equivalent of the following expressions in which L is the arc length in feet; V the arc voltage; and I the arc current.

$$L = \frac{VI^{1/2}}{3{,}000} \qquad (1)$$

$$L = \frac{VI^{1/2}}{3{,}200} \qquad (2)$$

It is seen that both of these formulas are of the same general form in which arc length is proportional to the voltage, but varies with the current according to the exponent shown. However, Monseth and Robinson[3] include the statement, "above 800 amperes the arc voltage seems to become practically independent of the current."

The Edison Electric Institute—Bell Telephone System report on power system faults[2] gives data indicating that arc length is proportional to voltage, that the crest voltage per foot decreases as currents increase up to about 100 amperes crest, and that above this value crest voltage per foot averages about 300, equivalent to 4.7 feet per kilovolt rms. These data were based on coincident instantaneous values obtained from measurements taken at intervals during the arcing period.

The foregoing references provide a basis for using the proportionality of arc voltage and arc length in this investigation. However, they lack agreement on relation of current and arc length. This can be seen by referring to Figure 9 in which curves representing equations 1 and 2 have been plotted for comparison with the data of this study.

The most practical approach to the problem of interrupting arcs on horn-gap switches is in terms of the two items of information most readily obtainable in system operating practice, namely the current to be interrupted by the switch and the voltage across the switch after opening. Because of the generalized character of the previous arc investigations, it seemed desirable to obtain data pertaining specifically to horn-gap switch operation by direct measurement of arc length, reach, current, and open-switch voltage, and to make a sufficient number of tests to provide a considerably larger

Paper 50-161, recommended by the AIEE Transmission and Distribution Committee and approved by the AIEE Technical Program Committee for presentation at the AIEE Summer and Pacific General Meeting, Pasadena, Calif., June 12–16, 1950. Manuscript submitted March 14, 1950; made available for printing April 18, 1950.

F. E. Andrews, L. R. Janes, and M. A. Andersson are all with the Public Service Company of Northern Illinois, Chicago, Ill.

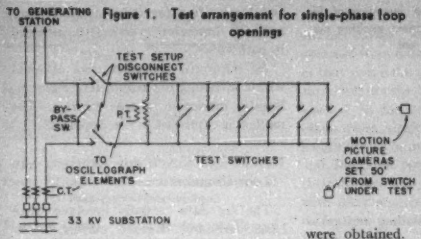

Figure 1. Test arrangement for single-phase loop openings

Figure 2. Equipment shown diagrammatically in Figure 1

1. Horizontal double-break switch
2. Experimental interrupter type switch
3. Vertical lift blade switch
4. Tilting insulator switch with experimental interrupter
5. Tilting insulator switch
6. Potential transformer for recording instruments
7. Bypass switch and test setup disconnects
8. Swinging beam switch

amount of data than was available from the previous tests.

All of the previous work having to do with arc dimensions was related to length and no information was developed relative to reach. As this is the more vital item in switch operation, it seemed especially important to develop data on this factor. It also seemed essential to further investigate how length of arc varied with the current because of the variable conclusions of the earlier work.

General Description of Tests

Tests were made at a frequency of 60 cycles and covered opening horn-gap switches under three general conditions:

1. Opening one side of a 33-kv transmission line loop and transferring its load to parallel paths.
2. Interrupting transformer exciting current at voltages from 12 to 49 kv.
3. Interrupting 132-kv line charging current, with and without gas blast.

Several types of switches were used: the tilting-insulator type with both conventional and quick break horns; the vertical-lift type; and the horizontal double-break type.

In addition, there was provided an arrangement called a swinging beam switch. It consisted of a pair of long horizontal swinging beams operated by ropes and fitted with insulators, contacts, and arcing horns. It was used to rapidly draw arcs out to wide openings in order to study this effect.

As experience soon indicated, arc breaking ability and length of arc were not appreciably affected by the type of switch, so most of the later tests were made with the vertical lift switch which placed the arcs in the best position for photographing.

Tests were generally made in groups of five with the same conditions maintained for each test in the group. Motion pictures were taken of the arcs with two cameras placed at right angles to provide means of obtaining arc dimensions. Oscillograms of arc current and arc voltage were obtained. Average wind velocity varied from about 2 to 20 miles per hour, but equipment was not available for measuring gusts during the actual arcing intervals.

Approximately 400 test openings of all types were made. These produced 273 free arcs suitable for analysis. Data from many tests could not be used because photographic results were unsatisfactory. The work included a number of tests with gas blast and expulsion interrupter devices. These results are not included in this paper as they are outside its scope.

Loop Current and Transformer Exciting Current Tests

Loop Current Test Procedure

A group of test switches was installed in the yard of a large substation and connected as shown in Figures 1 and 2 to interrupt one phase of a 33-kv line between the substation and a nearby generating station. This line was in parallel with an extensive system. During these single-phase test openings, no load was dropped as the current was simply transferred to other parallel paths. Various system arrangements provided different values of loop impedance. These, together with variations in generation, produced a wide range of current and open switch voltage. At this location 72 arcs suitable for analysis were obtained.

Another group of 48 tests was carried out on a 33-kv switch in normal service to obtain a comparison between arcs from 3-phase and single-phase openings at this location. A total of 81 arcs was obtained for measurement. This circuit is shown in Figure 3. A wide range of current and open switch voltage was obtained by phase angle and voltage control on a transformer in the transmission loop. The single-phase tests were obtained by making two phases of the switch inoperative. The loop opening test currents varied from 56 to 312 amperes with 1,000 to 7,600 volts across the open switch gap. The higher voltages were associated with the higher currents. Arcs as long as 25 feet were obtained.

Transformer Exciting Current Test Procedure

The transformer exciting current tests provided 72 free arcs. They were made with the test setup shown in Figure 4. Tests were made at voltages from 12 to 49 kv. Currents ranged up to 35 amperes, with arcs as long as 44 feet. The test switches, arranged for either single or gang operation, were used to obtain data with either single break, or with double break with both switches in series.

Analysis of Test Data

Figures 5 and 6 are views of typical loop and exciting current arcs enlarged from motion picture frames taken at the time of maximum arc length. The greater current in the case of the former is

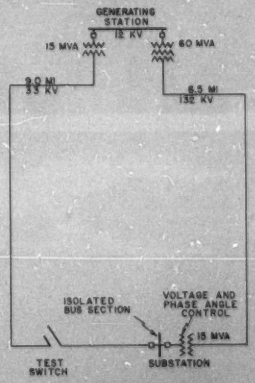

Figure 3. Transmission loop used for single- and 3-phase openings

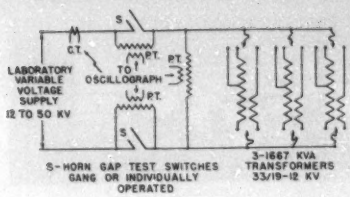

Figure 4. Test arrangement for opening transformer exciting current

seen to produce a much thicker arc. Figures 7 and 8 are typical oscillograms of loop and exciting current interruptions. They illustrate the decrease in current from initial value to zero and the corresponding increase in arc voltage from zero to open circuit value. In the case of the loop openings, the open circuit voltage across the switch depended mainly upon the current interrupted and the impedance of the loop. In the exciting current openings it was the line-to-neutral voltage.

The oscillograms were calibrated in terms of crest values divided by $\sqrt{2}$ to give rms on the assumption that wave shapes were sinusoidal. As they were often nonsinusoidal and peaked, some values used in the analysis were inherently higher than rms. However, since arc persistency is affected by crest rather than rms voltage,[3] the values used were considered satisfactory, as they were proportional to crest.

Arc reach and length were determined from the two corresponding projected motion picture frames showing maximum arc length. This generally occurred just before current interruption and arc extinction. The arcing interval was considered to end with the last frame showing a continuous arc. Actual current interruption may have taken place slightly earlier.[4]

It was originally thought that proper values could be obtained by considering the length as the square root of the sum of the squares of the lengths as traced from the two corresponding right angle views, as has been done by others.[3] However, it was found that this procedure could result in considerable error because: it does not take into account the upward incline of the camera lines of sight; the arc paths are often far from straight lines, and one dimension (vertical) is included in both views.

An improved procedure was adopted which, although not completely rigorous, largely overcame these errors. The method is explained in the Appendix.

Length and Reach for Exciting and Loop Current

The arc data actually involves three basic variables, namely, current, voltage, and length. The data were analyzed by using current at the beginning of the arcing period, voltage just after the arc was out, and length when the arc was longest. By taking advantage of the proportionality of arc voltage and length, the data on these two parameters were reduced to a single variable, feet per kilovolt, leaving current as the other variable. This reduction to two variables permitted all data to be shown with two co-ordinates and greatly aided plotting and study. The data on reach were handled in the same manner.

Length and reach per kilovolt are plotted against current in Figures 9 and 10 respectively. The ratio of reach to length is plotted in Figure 11. Each arc is represented by a separate point. Three-

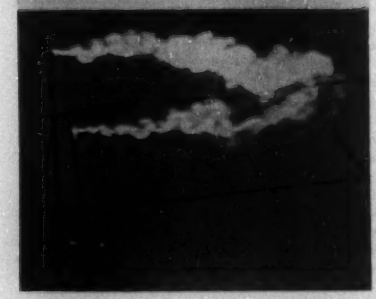

Figure 5 (left). Simultaneous right-angle views of loop current arc

296 amperes, 7.19 kv across the switch, length 19.1 feet, reach 7.2 feet

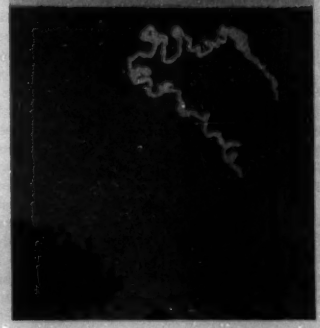

Figure 6 (right). Simultaneous right-angle views of exciting current arc

12.8 amperes, 49.2 kv across the switch, length 21.9 feet, reach 4.5 feet

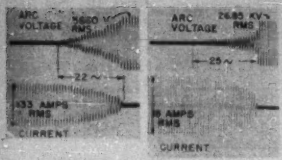

Figure 7 (left). Representative oscillogram of loop current interruption

Figure 8 (right). Representative oscillogram of exciting current interruption

phase openings produced three points.

The values of length and reach per kilovolt are widely spread. This spread is thought to be largely due to variation in atmospheric conditions, magnetic and thermal effects, and errors incident to accurately identifying the devious arc paths when tracing the photographic views.

It was observed that wind conditions greatly affected the shape of an arc and its direction but did not appreciably affect its length. With light wind it tended to be very irregular and circuitous. With strong wind it tended to be blown out horizontally windward, often like an elongated "V." Some of the longest arcs in several current and voltage groupings were obtained with very little wind but these were usually very circuitous. The more circuitous arcs usually had relatively less reach, which produced the low ratios shown in Figure 11.

In Figure 9, a curve has been drawn medially through the points to show the general trend of length per kilovolt with current. Above 120 amperes the trend is essentially flat and conforms fairly well with the EEI-Bell System Report.[3] Much effort failed to produce a mathematical expression that would satisfactorily fit the data throughout its range. Curves plotted from the formulas presented by Ackerman, and by Monseth and Robinson are shown. Ackerman's formula was obtained from data above 70 amperes and in that range the general direction of the curve follows the trend fairly well, but is lower. As his arc measurements were taken from single views low values of length are to be expected. The Monseth and Robinson curve is less similar. As their formula was presented in connection with relay studies, the data used for its derivation probably was obtained from larger currents. Neither curve fits the data in the lower current range. The trend curve levels off at 2.4 feet per kilovolt, equivalent to 417 volts per foot.

A trend curve for reach was similarly drawn in Figure 10, and its shape is about the same as that for length. As the limits of reach provide the vital dimensions in determining switch performance, the trend curve is only of general interest.

For reasonably safe operation, switches must have clearance greater than the probable reach that may be expected normally. It was thought that a simple upper limit above the highest test points would meet this requirement. Such a limit is provided in Figure 10, by a horizontal line at a height of 1.65 feet per kilovolt between 320 and 100 amperes, and below 100 amperes by a straight line dropping to zero with a slope of 0.0165 foot per kilovolt per ampere.

This limit line seems high in the lower range of current. However, the ratio of reach to length was generally lower in this range due to the circuitousness of these arcs. Consequently, because of the possibility of less circuitousness under some conditions, it seems reasonable in practice to use values somewhat higher than the test points. With these small currents, no switching problem exists unless they are associated with a relatively high voltage (line-to-neutral in the case of exciting current) and correspondingly long arcs. As reach per kilovolt from the curve is a multiplier, it seemed desirable that the curve be drawn to provide conservative values of reach when used with higher voltages.

Within the range of Figure 10, it is believed that reach per kilovolt as obtained in practice will rarely exceed values given by these limit lines which are accordingly identified as the limit of probable reach. The upper limits of probable reach can, therefore, be expressed simply as follows:

Range in Amperes	Probable Reach
0 to 100	$0.0165 \times kv \times I$
100 to 320	$1.65 \times kv$

Probable reach is in feet; kv is in rms kilovolts across the separated horns after opening; and I is the current interrupted in rms amperes. Reach on rare occasions under adverse conditions may approach one-half of the arc length and exceed the probable limit given by the foregoing expressions. If this maximum reach does occur, it must be in the general direction of switch alignment where clearance is usually ample. If the switch horns have any appreciable opening prior to arc extinction, the reach, if it occurs in a crosswise direction, is inherently somewhat shorter than that along the switch alignment as explained in the Appendix. Consequently, these expressions normally should be adequate for a design and operating guide. If a greater safety factor is desired, a ratio of one-half can be applied to the higher lengths points in Figure 9 and more conservative reach values obtained.

Comparison of Single-Phase and 3-Phase Openings

As stated previously, one group of loop tests was conducted with the loop shown

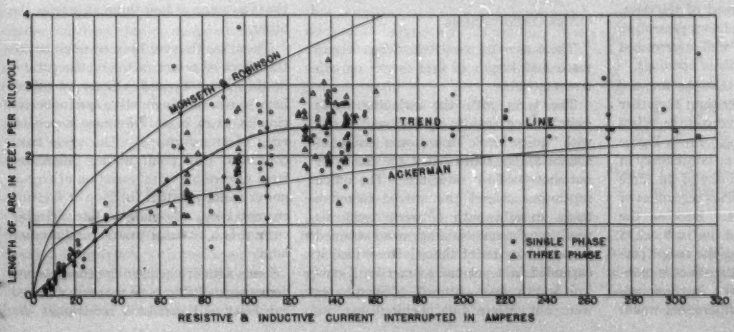

Figure 9. Arc length per kilovolt for resistive and inductive current

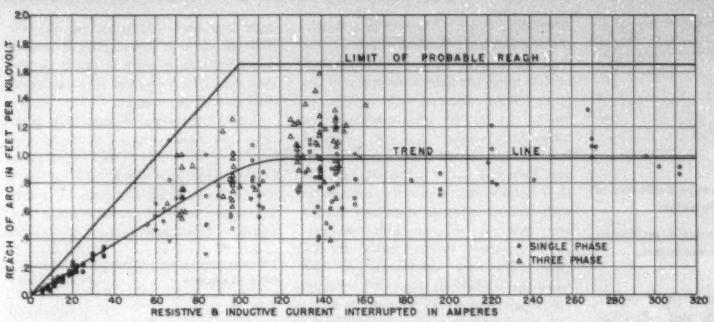

Figure 10. Arc reach per kilovolt for resistive and inductive current

in Figure 3 for the additional purpose of comparing the length and reach of single-phase openings with those of 3-phase. This comparison is shown in Figure 12. Bars in groups of three represent tests of three-phase openings and single bars represent single-phase openings. The length of the arc is represented by the total length of the bar and the reach by the open portion. It can immediately be seen that reach never exceeds half the length.

The voltage across a switch after opening only one phase should be greater than that after simultaneous 3-phase opening of the same current, because the impedance applicable to single-phase opening may be as much as $1^1/_2$ times the normal (positive sequence) 3-phase impedance. A correspondingly longer arc should result from opening only one phase. In this group of tests, the impedance for single-phase opening was calculated to be 10 per cent more than that for 3-phase, and the single-phase arcs should have been correspondingly longer.

The 3-phase openings are identified separately in Figures 9, 10, and 12. The effect of the theoretical 10 per cent overvoltage is not discernible. It was probably masked by the spread of the data. It can be seen that the points representing the 3-phase openings are well interspersed with those of the single-phase openings.

It might be expected that the first arc to go out would be longer than the other two because of the overvoltage effect with single-phase opening. From Figure 12 it is seen that there is no consistency in the order of extinction of any of the three arcs during 3-phase openings regardless of their individual lengths. Because the three arcs are concurrent and subject to 3-phase conditions during the major portion of the arcing time, the effect is probably minimized. However, in these particular tests any such differences would probably not be evident on account of the spread.

The duration bars show, in addition to the duration of each arc, the times of initiation and extinction as determined from the motion pictures. The arcs of greater duration generally have longer length.

The variation in time of initiation of the arcs is of some interest. As the test switch had been checked for good adjustment, this variation in timing and contact separation is probably typical.

The bars showing arc terminal separation represent the separation between the ends of the arcs on the horns at the time of extinction. The arcs often went out before they had traveled to the horn ends and before full opening. The arc terminal separation was usually greater with the longer arcs. It is to be observed that greater separation occurred in the case of single-phase openings than with 3-phase, with the arc durations generally shorter and the length no longer. For the single-phase openings, the switch mechanism was disconnected from two of the phases. This resulted in faster switch operation and apparently shortened the time required for the arc to attain the critical length needed.

Other Observations

There were no consistent differences in reach and length of arcs drawn on different switches.

The tests with the swinging beam switch when rapidly opened and a few with "quick break" horns on a tilting insulator switch showed that the arcs were not shortened by their use. The quick separation caused the arc to follow a fairly straight path between terminals until maximum opening was attained (about 15 cycles of time), after which it expanded in a normal manner until critical length was attained. Short arcs were out before full opening was attained. With the wider opening, reach in a crosswise direction was less for the longer arcs even though they continued to grow after full opening. This latter feature might be made helpful in confining an arc to space within clearance limits.

With wind parallel to the switch alignment, one side of the arc loop may be blown directly across to the opposite horn. This short circuits the arc and prevents or delays its extinction. A long horn away from the wind increases the susceptibility to this effect, as the arc would tend to rise against it.

Occasionally the wriggles of a portion of the arc short circuited. This shortened the arc and caused the arc loop to start growth anew. In these cases the oscillograms showed an abrupt increase of current during a normally decreasing trend. This effect generally increased the time required for extinction.

The double break switch used for some of the loop opening tests and the two switches used during the exciting current tests yielded information on two arcs in series. The lengths of the two arcs in series, when added, approximated the length of a single arc under the same conditions. However, one arc of the pair was sometimes as much as four times as long as the other.

There has thus far been no reference to the effect of power factor of the current in the circuit opened. Tests by others have shown that in resistive and inductive circuits there is no difference in persistency of arcs formed.[2] Our tests have confirmed this point as no differences were discernible with variation of circuit power factor in either the loop or exciting current tests. Opening of line charging current is a separate matter as discussed later.

Tests with arc quenching arrangements demonstrated that both properly directed gas blast and expulsion interrupter de-

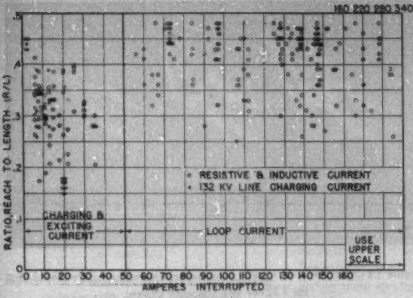

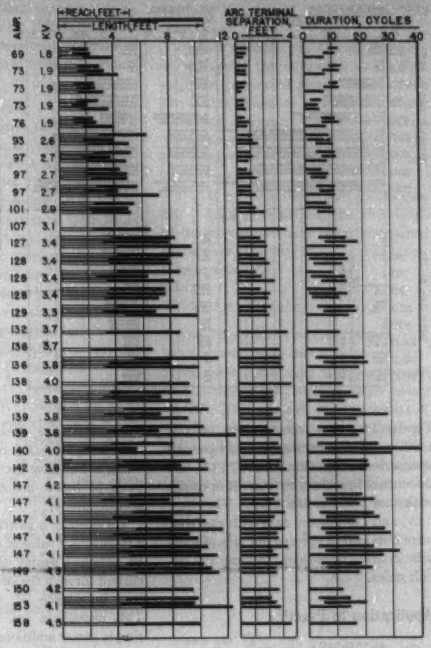

Figure 11 (above). Ratio of reach to length

Figure 12 (right). Reach, length, terminal separation, and duration of arcs for 33-kv single and 3-phase openings

vices have merit for extinguishing horn-gap switch arcs.

Tests at 132 Kv—Loop and Charging Current Opening

132-Kv Line Test Procedure

Tests were performed on 132-kv horn-gap line sectionalizing switches to determine lengths of line that could be safely de-energized. In all cases, motion pictures of the arcs and in a few cases oscillograms were taken. Current values, in most cases, were calculated from the line characteristics and the prevailing voltage.

Of 25 openings, nine provided 27 free arcs suitable for measurement. In these tests, various lengths of line ranging from about 4 to 50 miles were opened. Currents ranged from 2.2 to 20 amperes.

Nine tests were made with gas blast attachments for quenching the arcs. These attachments consist of porcelain tubes mounted on the switch bases through which gas is discharged toward the short stationary horn on which the arc is initiated. The gas was supplied from nitrogen tanks on the ground used to charge auxiliary tanks mounted under each of the three switch bases. Nitrogen at 115 pounds per square inch was discharged by quick opening valves operated from the switch mechanism. Air at 90 pounds per square inch also was used experimentally. These 27 arcs were all measurable.

132-Kv Line Test Results

The length and reach data from these tests are plotted in Figure 13 which includes a comparison with the lower portion of the reach and the length trend curves for resistive and inductive currents from Figure 10. The reach and length per kilovolt were determined by using voltage-to-neutral at the time of the tests and current values either calculated or obtained from oscillograms. It will be noted that both reach and length per kilovolt are generally higher for line charging current than for resistive and inductive current of comparable value. This result is to be expected because of the trapped charge and stored energy in a capacitive circuit which tend to create higher arc voltage and a longer arc before extinction. Tests by other investigators have shown that restriking of long arcs following extinction at current zero occurs only in a capacitive circuit and that the open circuit voltage rises to approximately twice normal.[8]

Figure 14 is a bar chart similar to Figure 12, summarizing the data for the 132-kv line tests.

Currents up to seven amperes were interrupted with reaches which appeared safe for the horizontal phase spacing of 16 feet. Currents of 10, 13, and 20 amperes were also interrupted although resulting reaches were greater than the phase spacing. The favorable oblique wind was responsible for the success of these openings since arc lengths ranged up to

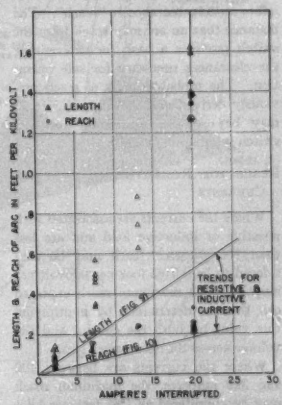

Figure 13. Arc reach and length per kilovolt for 132-kv line charging current

123 feet and arc reaches ranged up to 25 feet. Figure 15 is an enlargement of one of the motion picture views of a 20-ampere opening.

The results of gas blast arc included in

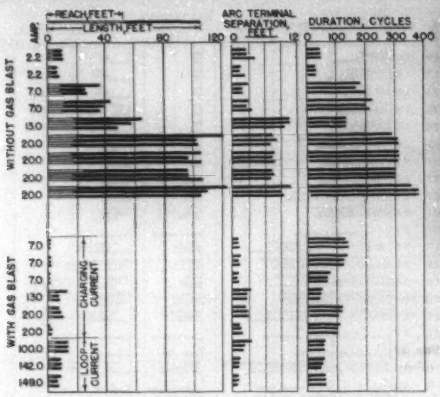

Figure 14 (left). Reach, length, terminal separation and duration of arcs for 132-kv line charging current

Figure 15 (above). Opening 20 amperes of charging current on a 50-mile 132-kv line, length 123 feet, reach 20 feet, switch clearance 16 feet

Figure 14. The effectiveness of this method is demonstrated in this figure by comparison of the data for the 7-, 13-, and 20-ampere line charging current openings with and without the blast. The 100-, 142-, and 149-ampere data with gas blast were obtained in opening one side of a 61-mile double-circuit loop, totaling 122 circuit miles.

Application to Practice

The most practical criterion for adequate switch clearance is "reach". The distance that an arc may reach from the switch provides a basis for determining the clearances necessary for safe operation. The probable limits of reach previously derived and shown in Figure 10 may be used for estimating horn-gap switch interrupting ability.

Reach for Resistive and Inductive Currents

Where the currents are associated with resistive or inductive load and are less than 100 amperes, reach may be considered to be 0.0165 foot per kilovolt per ampere. The maximum reach expected can then be determined by multiplying this value by both the current and the voltage across the open switch gap.

Where the currents are between 100 and 320 amperes, the maximum reach may be considered as 1.65 feet per kilovolt. The maximum reach expected in this case can then be determined by multiplying this value by the voltage across the open switch gap.

Maximum arc reach for opening exciting current of 3-phase transformer banks at various line voltages in common use, based on a factor of 0.0165 foot per kilovolt per ampere, is shown in Figure 16. The curves are for nominal line-to-line voltages but have been calculated on the basis of line-to-neutral voltages which actually apply.

For opening a switch in a loop circuit, a satisfactory value of voltage usually can be obtained simply by multiplying the current through the switch by the equivalent impedance of the loop opened. This impedance can be determined by simple vector additions of the component impedances in the loop. In the unusual case of opening one phase only, impedances must be determined accordingly. If transformers are in the loop, their impedances and ratios must be taken into account. The refinement of taking synchronous machine and load impedances into account does not appear to be normally necessary.

The loop impedances applicable to opening a horn-gap switch in any line often may be predetermined from measurement of voltage and current at an oil switch elsewhere in that line. The voltage across the gap obtained with the oil switch open, divided by the current just prior to opening will give the impedance of the loop regardless of line load at the time of measurement.

After the equivalent loop impedance has been obtained (either calculated or measured), reach can be determined directly from Figure 17 for currents over 100 amperes. This figure shows arc reach for current interrupted with various loop impedances. It is based on the expression, reach equals 1.65xkv, with $IZ/1{,}000$ substituted for kv. For currents less than 100 amperes a chart could be similarly constructed by the same substitution in the expression, reach equals 0.0165 x kv x I.

This basis of estimating the capability of a horn-gap switch is applicable to any loop circuit regardless of operating voltage, as the latter has no particular relationship to the gap voltage.

Switch Design and Operation

For design, or to ascertain if a switch may be safely opened, the expected arc reach should be compared with the proposed or actual switch clearances. The general type and arrangement of some commonly used 33-kv switches is shown in Figure 18. The minimum clearances between phases are shown in Table I. To avoid short circuit, a margin of safety is needed between maximum expected reach and the actual minimum clearance. The amount is largely a matter of judgement. A margin of one foot is believed satisfactory for 33-kv switches under ordinary conditions. Maximum safe reach providing a 1-foot margin also is shown in Table I.

As a convenient operating guide, the horizontal lines in Figure 17 show the maximum safe reaches for the switches in

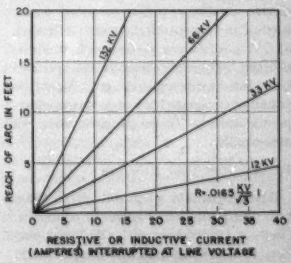

Figure 16. Arc reach for small currents at various line voltages

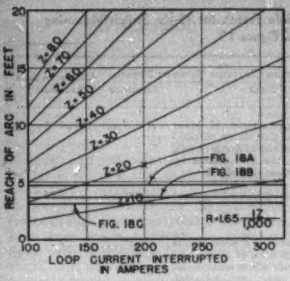

Figure 17. Arc reach for large loop currents in loops with various impedances

Table I. With favorable wind directions, longer reaches may be allowed.

Examples of Reach Determination

Example 1—Interrupting Transformer Exciting Current. A 15,000-kva 132-kv transformer is to be replaced by one of 30,000-kva capacity. The existing horn-gap switch for interrupting the exciting current is of the vertical-lift type with 10.5-feet horizontal separation between phases. It is desired to know whether this switch will have adequate clearance to interrupt the exciting current of the larger transformer. Test data on the proposed transformer gives 2.0 per cent exciting current at rated voltage and 9.0 per cent at 110 per cent rated voltage. It is expected that the line voltage will be 132 kv but that the transformer taps will be set 5 per cent below rating, thus over-exciting the transformer 5 per cent. It is estimated that the exciting current will be 4.5 per cent, or 5.9 amperes. Referring to Figure 16, it is seen that interruption of 5.9 amperes at 132-kv line voltage gives an arc reach of 7.4 feet. This is 3.1 feet less than switch clearance of 10.5 feet. Therefore, the switch should be adequate.

If it is expected that the line voltage may vary from 132 kv, the exciting current should be determined accordingly and the reach obtained from the formula in Figure 16.

Example 2—Opening a Transmission Loop. It was desired to determine if flashover would occur on a horn-gap switch in sectionalizing a line in a 33-kv loop when the current was 200 amperes. The switch had clearance of 4 feet 8 inches (switch arrangement (A) in Table I). Loop impedance was determined by measurement at one terminal of the line. Potential transformers used for synchronizing were available on both sides of the line oil switch. By connecting a voltmeter across the appropriate terminals of the synchroscope, the voltage across the oil switch gap could be measured.

With the oil switch closed the current was 250 amperes. With it open the voltage across the gap was 5,000 volts. The loop impedance was, therefore, 20 ohms. Referring to the "X" in Figure 17, it was seen that interruption of a 20-ohm loop at the expected 200 amperes would have given an arc reach of 6.6 feet. This was above the allowable reach line, designated as Figure 18(A), for this switch. Therefore, opening the horn-gap switch was considered unsafe. The diagram shows that the switch could have been opened safely if the current were not over 142 amperes.

In this example, 5,000 volts was observed across the oil switch gap. This might be considered excessive but it was the vector difference and not the scaler difference between the line-to-neutral voltages on each side of the switch. The line voltages were respectively 34,000 and 31,000 volts.

Had it not been convenient to measure the voltage as described, the impedance of the loop would have been determined by network reduction from line and transformer constants.

132-Kv Line Charging Currents

The 132-kv line charging current tests have demonstrated that about seven amperes, corresponding to charging current of 17 miles of line, may be safely interrupted. This value of current results in arcs having reach shorter than the horizontal phase spacing of 16 feet. The tests demonstrated, however, that under favorable wind direction charging current as high as 20 amperes could be interrupted.

Figure 18 (below). Horn-gap switch arrangements

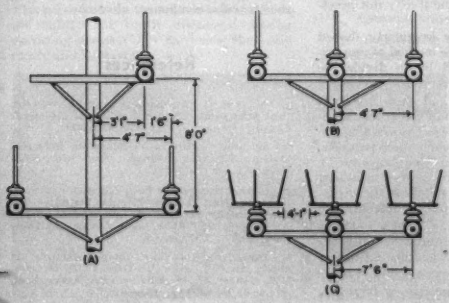

Figure 19 (right). Adapting camera views for measurement

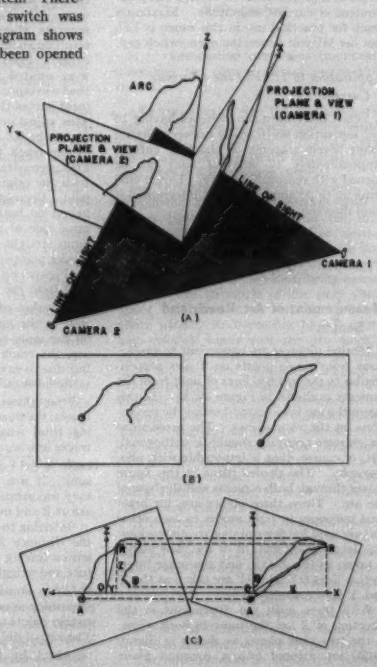

Conclusions

General

1. An open arc formed on adequately separated electrodes will go out if it is free to expand to its critical length.

2. A horn-gap switch will successfully interrupt a current if its dimensions are adequate to permit the arc to grow to its critical length. An exception might be with the wind blowing in line with the arcing horns.

3. With conventional horn-gap switches, arc length and reach are independent of the type of switch and of the speed of operation.

4. Two arcs in series have about the same total length as a single arc produced under the same conditions. One of the pair may be much longer than the other.

5. Arcs are longer when interrupting line charging current than when interrupting a corresponding amount of resistive or inductive current with similar voltage across the switch gap.

Application to Resistive and Inductive Current.

6. Reach for currents below 100 amperes depends on both voltage and current. Maximum reach for practical use in this range is 0.0165 foot per ampere per kilovolt across the open switch gap.

7. Reach for currents from 100 to 320 amperes is proportional to voltage but independent of current magnitude. Maximum reach for practical use in this range is 1.65 feet per kilovolt across the open switch gap.

Application to 132-kv Line Charging Current

8. On 132-kv horn-gap switches having 16 feet separation horizontally between phases, about seven amperes of charging current (approximately 17 miles of line) can be opened with reasonable safety. Larger currents up to 20 amperes can be interrupted if wind direction is favorable.

Table I. Relation Between Clearance and Safe Reach for 33-Kv Switch Mounting Arrangements of Figure 18

Switch	Arrangement Description	Minimum Clearance Between Phases: Path	Minimum Clearance Between Phases: Distance	Allowable Safe Arc Reach
A	Tilting-insulator type, two level mounting. Length of stationary horn, 1'3". Length of movable horn, 1'3". Applies only when bases are not grounded	Between open horns of lower switch and line clamp on moving contact end of upper switch. (Involves the two phases located on same side of pole)	5'8"	4'8"
B	Vertical-lift and tilting-insulator types, all phases on same level. Applies with bases grounded or not grounded	Between open horns of adjacent switches	4'7"	3'7"
C	Double break, horizontal opening, all phases on same level. Blade radius 1'8". Applies with bases grounded or not grounded	Between stationary horn of one switch and horn of open blade of adjacent switch with simultaneous arcs on adjacent switches	4'1"	3'1"

Appendix

Measurement of Arc Reach and Length

Motion pictures are equivalent to projections from single points on planes perpendicular to the inclined lines of sight from the cameras as shown in Figure 19(A). In this figure the arc is indicated behind the projections on the view planes. The projections for extreme accuracy should be orthogonal; but, of course, that is impossible with photography. The shaded plane in this figure passes through both cameras and the base of the arc. These three planes are, for practical purposes, at right angles to each other and are used for determining arc dimensions. The intersection line OZ of the view planes is taken as the Z axis, and the other intersection lines OX and OY are taken as the X and Y axes respectively.

With these axes, arc dimensions in the direction of Z are the same in both views. If the two view planes as shown in Figure 19(B) are rotated into a common plane about line OZ, they appear to be tipped downward by approximately the incline angle of the cameras as shown in Figure 19(C). In this rotation, the X and Y axes fall into the same straight line which is perpendicular to OZ. A method based on this rotation was used in adjusting the views for measurement.

In the actual procedure, the two views were projected on a screen, side by side, by similar motion picture projectors. The machines were each stopped at maximum arc length and their positions adjusted to give the same scale to the two pictures. The known diameter of an insulator in the switch base was usually used to set the scale. The two views were then traced on separate sheets of paper, with one arc terminal encircled on each trace for identification. Prior to measurement, the traces were rotated as shown in Figure 19(C) so that corresponding terminals and the uppermost part of the arc were on horizontal lines. This adjustment was equivalent to rotation about the OZ axis.

The reach was first determined and the axes were drawn on each trace as shown, with the origin midway between arc terminals. Corresponding points have the same height on both traces and must be on the same side of the arc. Reach is the maximum straight line distance from the origin to any point in the arc as shown by line OR in Figure 19(C). It was determined by trial from the two traces to give the maximum value of $\sqrt{x^2+y^2+z^2}$. Trial points were at the same height on both traces and on the same side of the arc. In the actual arc, the reach point is usually uppermost, but due to camera incline it may not necessarily be so on the traces.

From these generally irregularly shaped traces, the most accurate method of measuring total length would be to divide the traces into segments, determine the length of each $\sqrt{dx^2+dy^2+dz^2}$, and then take the sum. It was found that acceptable accuracy was attained, however, by dividing the arc at R and measuring each side separately.

Referring to the YZ trace in Figure 19(C), the distance from A to R was measured with a tracing wheel by following the curvature and wriggles of the path. The distance D_{yz} was considered as $\sqrt{y^2+z^2}$. The x dimension was the horizontal distance between points A and R on the XZ trace. The actual distance between A and R is determined by the relationship $\sqrt{D^2_{yz}+x^2}$. A similar measurement was made of the same side by using the tracing wheel along the line from A to R in the XZ trace and obtaining y from the other. A length $\sqrt{D^2_{xz}+y^2}$ was thus obtained and the value used for the length of the side AR was taken as the average of the two. The other side of the arc from B to R was similarly measured and AR and BR added to give the total length.

In most cases, particularly those having a wide open path, the reach was considerably less than half the length. Occasionally, probably due to more wind velocity, the arc sides were nearly straight and gave ratios of reach to length of nearly one half.

Locus of Maximum Reach Points

Assuming the extreme case for a given arc length where the path has no wriggles and consists of two straight lines from the electrodes to the point of reach, it can readily be seen that the locus of reach points is an ellipsoid. The arc terminals are the foci of the ellipsoid and its long axis equals the arc length. Reach along this axis would be one-half the length if the arc were not interfered with by the intervening horn. That ratio can nearly be attained, however, with reach in the general direction of the long axis. Reach will, in a crosswise direction, be somewhat less by an amount which depends on the spread of the foci or arc terminals. As there is generally less clearance in the crosswise direction, a quick wide spread of arc terminals is beneficial. High speed of separation is necessary, however, if the wide spread is to be effective in reducing the crosswise component of reach.

References

1. A Study of Transmission Line Power Arcs, **Paul Ackerman.** *Engineering Journal* (Montreal, Canada), volume 11, May 1928, page 309.

2. Relay Systems (book), **Monseth, Robinson.** McGraw-Hill Book Company, New York, N.Y., 1938, page 478.

3. Characteristics of Power System Faults to Ground, **Joint Edison Electric Institute—Bell Telephone System Report.** *Engineering Report Number 39, EEI Publication Number E-9* (New York, N. Y.), 1937, page 5.

4. Dielectric-Recovery Characteristics of Power Arcs in Large Air Gaps, **G. D. McCann, J. E. Conner, H. M. Ellis.** *AIEE Transactions*, volume 69, part I, 1950, pages 616–75.

Discussion

H. A. Glover (Electrical Engineers Equipment Company, Melrose Park, Ill.): This paper shows a job of tremendous proportion well done. A well-deserved compliment is extended to the authors and to the Public Service Company of Northern Illinois for the performance of the tests and the thorough and complete paper prepared.

This is the first real guide as to what a horn-gap air-break switch can be expected to do. It is probably the first time formulas, curves, and other data on this subject have been made available to engineers. Since data of this type has never been accumulated previously and uncontrollable factors prevent assigning any guaranteed interrupting ratings to horn-gap switches, this paper should become a part of every substation and overhead line engineer's library.

From the paper it is noted that variations in wind affected arc reach, but not length. Did tests give any indication of effect of temperature or other atmospheric conditions?

Also, some questions in switch design are indicated by these tests, as:

Would a horn-gap switch with extremely long break result in arc of even smaller reach, or could this effect be attained more readily by increased speed of opening, as indicated in tests on single-phase circuits with mechanisms of two poles disconnected?

Can the tests be considered to indicate that a double-break switch, with two arcs in series, would assist in a design to reduce reach of the arc? This would depend on what the reach of the longer of the two arcs in series measured, in comparison to single-break design switches.

Would switch design with contacts and blade tips modified to provide a sphere gap effect in opening be possible, thus eliminating horn? The design would have to prevent burning of main contact points. This appears to have some possibility since photographs indicate horns are not actually required as guides for the arc.

In conclusion, it can be repeated that the paper is complete and should be extremely useful. Certainly, there is no question that little was overlooked in preparing for this study and in the actual carrying out of the tests and preparation of the paper.

G. E. Heberlein (Railway and Industrial Engineering Company, Greensburg, Pa.): This paper raises a question which has been the subject of much discussion among operating people. Let us review the early record and background.

The early expansion of the a-c system was augmented by the introduction of horn-gap switching of load and charging currents. Forty years ago, the Railway and Industrial Engineering Company introduced the air-break switch placed upright, outdoors, and arranged to open the arc, using increased clearances and phase spacing over that needed for a regular isolating hook switch. The arc was severed on horns projected upward and outward and designed to interrupt the arc where no damage could result. Today it hardly seems possible that the first stations were indoor type and the introduction of the air-break switch forced the use of outdoor construction before that construction was dictated by the greater space requirements of higher voltages.

Many thousands of these switches were installed all over the country because operators could not afford the higher cost of circuit breakers for the expected return on investment. While the circuits in the aggregate then were not long, and load and charging currents more limited, yet the air-break switch did its work and is still today the accepted method of switching of many overhead lines.

True, under unfavorable conditions as to winds and loading, they failed to open the arc and in some cases initiated faults. In these cases, the backup circuit breaker cleared the fault, was then again closed, restoring service to the line section. Today there are still thousands of these switching installations in use, sectionalizing, or picking up, or dropping lines or load—the economic answer to the individual problem.

The material presented in the paper should prove of considerable value as a practical guide to system switching with horn-gap switches.

Our companies in the United States and Canada have accumulated records of operating experience gathered through the years. These record the practical experience of operating companies in opening circuits of various voltages and currents with switches of both standard and special types and spacings. This material could not be systematically collated as has been done by the authors as no criteria of agreement between these data could be developed.

From a very general analysis of this background, we have advanced the following recommended practice of operating with horn-gap switches. Each particular case should be analyzed on its own merits evaluating:

1. Current, voltage, and frequency.

2. Atmospheric conditions, that is, prevailing winds.

Figure 1. 115-kv 11-ampere charging current on 16-foot phase spacing. Wind 5 miles per hour

Figure 2. 66-kv 11-ampere charging current on 16-foot phase spacing. Wind about 8 miles per hour

3. Installation conditions (mounting space and the cost of special switch provisions).

As a very rough guide, the standard horn-gap switch at conventional spacing, either of the vertical or horizontal opening type, can be used for successfully breaking up to 5 amperes of line charging current.

For currents in excess of 5 amperes, we recommend the use of switches with a greater tip-to-tip gap when in the fully open position, and greater than normal phase spacing, the basic problem being how much space must be placed between arcing horns to prevent the arc from being carried into the arc terminals of the next phase under the influence of low-velocity cross-phase winds. As borne out by the paper, high-velocity winds cool the arc quickly, while winds of three to six miles per hour carry an arc, thus limiting the amount of charging current successfully handled. For example, a double-rotating side-break switch arranged for 110-degree rotation (rather than 90 degrees) at 132 kv will create an open gap of 8 feet 6 inches when fully open, and will handle up to 9 or 10 amperes on 15-foot phase centers. Mounted on 20-foot phase centers, it could be used up to about 14 amperes charging current.

The striking difference between opening magnetizing and charging current can be seen on Figures 1, 2, and 3 of the discussion, and also illustrates the difficulty of correlating the usual data obtained from various investigators as it is impossible to specify the "reach" in these three cases. The difference in "arc laziness" is easily seen, as well as the effect of the stronger winds.

The authors make no distinction between

Figure 3. 230-kv 5.7-ampere magnetizing current at 25 cycles (two phases already extinguished). Wind 15 miles per hour

standard horn-gap switches. Substantially there is no great distinction but we have found construction factors do influence interrupting ability. For instance, copper horns or copper-clad horns interrupt better than aluminum or galvanized horns. Likewise, on loop circuits in transfer of load with relatively high current at low voltage (under 10 kv), Elkonite arcing tips perform better than copper or copper alloy, permitting the interruption of much higher currents than otherwise possible.

Special switch designs are available with increased open gap clearances. These switches of the 2-insulator double-rotating variety, center break, horizontal opening to 110 degrees or 180 degrees, can give open gap clearances approaching double that of the conventional switch at practically no increase in investment cost. For example, in one group of tests, a special switch of this type opened load currents up to 2,000 amperes at 25 kv.

In Table I of this discussion are examples of interruption with standard side break switches with and without transformer termination.

Table I

Voltage of Line, Kv	Length, Miles	Condition	Length of Arc, Inches	Time of Arcing
44	7	Line open	2	Instantaneous
44	12	Line open	4	Instantaneous
44	31	Line open	12	1/8-second
44	31	3,000-kva transformer unloaded	3	Instantaneous
44	31	6,000-kva transformer unloaded	2	Instantaneous

Concluding, the authors should be commended for their presentation of means to more carefully evaluate operating practice using horn-gap switch interruption. Power companies will undoubtedly use their methods to more rationally evaluate load and charging current interruption, thereby limiting the need for more expensive equipment such as interrupter switches or circuit breakers.

C. S. Beattie and **S. C. Killian** (Delta-Star Electric Company, Chicago, Ill.): For many years there has been a definite need for some means of estimating the interrupting ability of an air switch. This paper provides a bench mark and a quick answer to a question that has been raised over and over again by the users of these switches. The authors are to be congratulated for their fine paper and should be thanked for the enormous amount of time spent on field tests, arc measurements, and calculations. We had the privilege of witnessing some of the tests and can vouch for the carefulness and exactness with which tests and measurements were made.

Two major results are reported. The first covers the relationship between the switch and the arc and states that the interrupting ability of a switch is not determined by the construction of the switch or by its speed of operation. The other result states the importance of arc reach and provides a formula for estimating it. It is of interest to transpose the authors' formula for reach at lower currents into

$$I = \frac{\text{reach in feet}}{0.0165\,\dfrac{\text{KV}}{\sqrt{3}}} \text{ amperes}$$

where KV = line to line voltage

Then, by substituting standard phase spacing for horn-gap switches given in Rule SG8-57.5 of the National Electrical Manufacturers' Association Power Switching Equipment Standards,[1] for the reach, some value of current can be determined which a horn-gap switch should break with fair surety. The authors prefer to add an additional foot to the phase spacing at 33 kv as a safety factor and likely more at high voltages but this is open to debate since the arc would have to lay down in an almost horizontal position in order to fault between phases if the reach were equal to the phase spacing. Table II of this dicussion gives inductive and loop currents which can be interrupted using equation 1 with the reach equal to NEMA phase spacing. There is startling agreement with the rule-of-thumb interrupting value of 10 amperes for standard conditions of switch mounting at higher voltages. This value of 10 amperes has been used by us for years on the basis of inconclusive tests. It also is important to note that contrary to general thinking, the size of the open switch gap does not effect the interrupting ability unless very large changes are made. Rather than widen this open gap on each switch unit, it would be more preferable to add to phase spacing.

It will be interesting to compare the authors' results with those of a nation-wide utility poll being conducted by an existing AIEE subcommittee, questioning each utility company's practice in using air switches as interrupting devices. Early poll results indicate somewhat lower values than those given in Table II of the discussion though agreement is not too bad.

Figure 14 of the paper illustrates the efficiency of the gas-blast type of interrupter as added to an air switch. As further improvements are made on this device, a considerably wider field may be opened for its use, especially in voltages above 69 kv.

Table II

Kv	NEMA Horn-Gap Phase Spacing, Feet	Interrupting Rating, Amperes (Inductive Circuit)
7.5	3	42
15	3	21
23	4	18
34.5	5	15
46	6	14
69	7	11
115	10	9
161	14	9
196	16	9
230	18	8
287	22	8

REFERENCE

1. POWER SWITCHING EQUIPMENT STANDARD. *Publication 49-144*, National Electrical Manufacturers Association (New York, N. Y.), April 1949.

C. J. Beller (Cleveland Electric Illuminating Company, Cleveland, Ohio): Analysis of photographic records of horn-gap switch openings has provided much previously unknown information on the arc behavior. There is considerable evidence to indicate that safe opening of conventional horn-gap switches is limited to relatively low values of charging current and load current.

Tests of our own were recently conducted to establish conditions for the safe operation of horn-gap switches on our 132-kv system. These tests indicate that 2 amperes of 132-kv charging current or 4 amperes of 132-kv transformer exciting current, can safely be interrupted with horn-gap switches under adverse weather conditions.

Mr. Andrews and his associates have opened a door to the investigation of this problem and further study and test will greatly assist in arriving at some factual basis for determining limits of present installations and point the way to further development of better circuit opening devices for use on the higher transmission voltages.

Outdoor color film in better quality movie and still cameras gives a much better photographic record of switch opening arcs than can be obtained with black and white film. Exposures of 1/100 to 1/120 second with lens opening F-1.5 to 2.0 give very good pictures with daylight color film when photographs are taken against early evening north sky. Motion-picture cameras operating at 64 frames per second provide an ideal media for recording switch opening arcs. With this speed, counting of the frames measures the arc time, approximately 1 cycle per frame being recorded.

Eric T. B. Gross (Illinois Institute of Technology, Chicago, Ill): The extensive tests made on the systems of the Public

Service Company of Northern Illinois are of great value to the industry since the problem of arc interruption with disconnecting switches is economically important. This is one of the few publications on this subject. However, many interesting papers are available on free burning arcs. These arcs do not differ fundamentally from those made by the authors though the studies referred to were made for various other purposes, such as: the study of flashovers on insulators produced by overvoltages; destructive effects of free burning arcs on electric equipment, particularly insulators; effect of arc impedance on various types of distance relays; and possibility of self-extinction of arc faults.

Many of the results obtained from these other investigations are directly applicable to the problem investigated by the authors. Reference 2 of the paper is really based on unpublished investigations of A. R. van C. Warrington,[1] who published an early paper on the subject in this country.[2] Other investigations, also based on extensive tests,[3] deal with an analysis of arc voltage and current, and throw light on the power factor of the arc. An interesting investigation concerning arcs with the current nearly in complete quadrature with the voltage also may be mentioned.[4]

The problem of interruption of the magnetizing current of transformers seems to deserve particular consideration. If capacitances are in parallel with the transformer, arc interruption may become easier if the frequency of the circuit formed by the elements to be switched off is near the impressed system frequency of 60 cycles. The problem is then similar to the self extinction of arcing grounds in resonant grounded systems, since the voltage across the former path of the arc starts slowly from zero at arc interruption and permits complete de-ionization without restrikes which otherwise influence the arc duration. It would be of interest to learn if the authors observed the presence of such conditions during the tests.

REFERENCES

1. ARC INTERRUPTION WITH DISCONNECTING SWITCHES, P. A. Abetti. *Thesis*, Illinois Institute of Technology (Chicago, Ill.), January 1948.

2. REACTIVE RELAYS NEGLIGIBLY AFFECTED BY ARC IMPEDANCE, A. R. van C. Warrington. *Electrical World* (New York, N. Y.), volume 98, 1931, pages 502–05.

3. FREE BURNING LONG POWER ARCS AT HIGH VOLTAGE, Eric T. B. Gross. *Schweizer Archiv für Angewandte Wissenschaft und Technik* (Zurich, Switzerland), volume 7, 1941, pages 1916–26.

4. FREE BURNING ARCS IN A-C SYSTEMS, G. T. Trotjak, V. V. Kaplan, E. I. Kender, P. Smouroff. *Report Number 324*, International Conference on High-Voltage Electric Systems (Paris, France), 1935.

5. ARC INTERRUPTION WITH HORN-GAP SWITCHES, J. E. Gerngross. *Thesis*, Illinois Institute of Technology (Chicago, Ill.), January 1949.

P. A. Abetti (General Electric Company, Pittsfield, Mass.): The authors are to be commended for a long and thorough investigation of a problem of practical importance which has been heretofore almost neglected in the literature.

It appears that the main difficulty in reaching a definite formula of arc length versus voltage and current, which would be very useful for theoretical studies and practical applications, lies in the great spread of the test values. This spread appears to be due essentially to random errors, and may therefore be reduced by increasing the number of tests.

Once the variance and mean error of the tests have been established by statistical analysis, one can predict the probability that the reach will be larger than a given value, and, therefore, that a short circuit will occur for a certain switch. The authors have given in Figure 10 of the paper the "limit of probable reach," based empirically on the highest values obtained in their investigation of 225 arcs of resistive or inductive current. From this data it would be interesting to compute statistically:

1. The mean error of all tests.

2. The probability that the "limit of probable reach" will be exceeded, and that this limit plus a given margin, say one foot, will be exceeded.

Once the probability is known, it will be easy to ascertain whether one is willing to take that chance of a short circuit upon opening a certain switch, compared to the advantages which will result from such an operation.

The same considerations can be applied, with less confidence, because the number of tests is smaller, to the interruption of line charging current.

F. E. Andrews, L. R. Janes, and M. A. Andersson: Mr. Glover inquires about any indication of effect of temperature or other atmospheric conditions. There was no discernible effect from atmospheric conditions other than variations in wind. The variations in results indicated by the spread of the data in Figures 9 and 10 includes variations that may have been due to differences in atmospheric conditions. These, of course, could not be segregated from other factors causing variations.

Mr. Heberline states that he has found that copper or copper-clad horns interrupt better than aluminum or galvanized horns. Both copper-covered steel and galvanized horns were used in our tests. There was no discernible difference in their action. If there was any difference, it was apparently less than the spread due to other factors. Elkonite is also mentioned as permitting the interruption of higher currents. The effect of different metals used for arcing electrodes could well stand investigation in connection with application to horn-gap switches. This is one of the items which it would be desirable to include in additional tests under laboratory controlled conditions. Such tests, if made, should be conducted indoors free from the influence of natural wind but with an air stream well controlled with respect to both direction and velocity.

Certain design questions have been raised by Messrs. Glover and Heberline:

1. *The effect of a long switch gap*—It appears that a long switch gap would be beneficial if the opening could be fast enough to prevent a long reach in the critical direction.
2. *Double break with two arcs in series*—The tests made with two arcs in series indicate in some instances that the longer of the two arcs was as much as 80 per cent of the total length. It is the authors' opinion that there is no practical advantage from a double-break switch.
3. *A design to eliminate arcing horns*—As pointed out in the paper, arcing horns in themselves are of no particular benefit in interrupting the arc. Depending upon the switch mounting arrangement, long horns may lessen the critical clearance available for the reach. This is particularly true where a switch has more than one level. In such a case a design without horns or with very short horns would seem to be advantageous.

The analysis of NEMA phase spacing given by S. C. Killian and C. S. Beattie is very interesting. It is hoped that our work may be of value in further horn-gap switch standardization work.

We are glad to have the suggestions by Mr. Beller regarding the technique of arc photography as good quality of photographic work is important in arc studies.

Dr. Gross mentions the question of capacitors in parallel with the transformer to give a circuit having a natural frequency of about 60 cycles.

On a 60-cycle system this amounts to neutralizing the exciting current. No tests of this kind were made. However, our company has been using capacitors in connection with induction regulators for the purpose of offsetting most of their exciting current. This has permitted the use of smaller disconnect switches.

Mr. Abetti calls attention to the problem of establishing a definite relationship of length, current, and voltage because of the great spread of the test values. He suggests that this spread is due to random errors which could be reduced by increasing the number of tests. We consider that the wide spread is due to random variations rather than errors. These variations are probably due to conditions not susceptible to analysis by our methods. While a statistical analysis as suggested by Mr. Abetti would be interesting to evaluate the probabilities and some benefit might be obtained in this direction by a larger number of tests, we believe the greater need is for further investigation of the factors causing the wide variations.

We appreciate the interest as shown by the discussions and hope that further research will be forthcoming.

A Low Noise and Distortion Audio Multiplexing Equipment with High Stability Carrier Supply

F. S. BEALE
ASSOCIATE AIEE

THE equipment described in this paper was the result of conclusions reached while contemplating the problem of how best to utilize the 30-kc audio spectrum offered by the type *FB* microwave-radio equipment. The market for the radio equipment primarily was to be in the electrical utility field. It was proposed as suitable especially for providing telephone, telemetering, load-frequency control, supervisory control, and similar communication circuits over distances up to about 50 miles. It was recognized that with microwave radio, the terrain would be a control factor in the maximum length of a radio circuit without repeater stations. A need exists for a communication facility of multicircuit capacity for such distances, both because of the growing congestion of the power-line carrier frequency spectrum and because of the increasing difficulty of applying carrier to the shorter power lines.

Outstanding conclusions drawn from the study of this problem were the following:

1. Most electrical utilities are forced to provide communication facilities for themselves by the urgency of their emergency communication problem.

2. It has been unusual for them to hire experienced communications engineers and maintenance personnel, or to set up a communications staff. Often persons normally assigned to protective relaying activities have the communications problems added to their work load.

3. While the communication facilities are vital they often do not receive the benefit of well-planned and diligently prosecuted maintenance merited by the investment they serve.

4. The equipment is placed frequently in dusty locations, and practically is never air-conditioned.

5. Some equipment is located in outdoor shelters with no heat except where experience dictates use of some minimum amount of heat.

6. Of those applications where microwave radio can be applied, probably not over 5 per cent will require more than seven voice circuits, or 140 telegraph circuits, or intermediate combinations thereof.

7. Simplicity of technique should be the keynote in the multiplexing equipment design.

8. Complicated adjustments, and frequent readjustments, particularly, of multiplexing carrier frequencies, must be minimized or completely eliminated.[1,2]

9. Vacuum tubes should be used sparingly, conservatively, and should be selected from readily available standard types. No tube type which appears to have an uncertain future should be selected.

10. Variety of vacuum-tube types should be kept to a minimum.

11. Where possible, tube types should be selected from the list of those having industrial counterparts–the "ruggedized" tubes.

12. Building block design necessary to permit adaptability to the greatest variety of problems.

13. It must be mechanically designed to be assembled within an equipment cabinet, yet have a high degree of accessibility to tubes and parts for inspection and maintenance when required.

14. The equipment cabinet design and finish to be compatible with power plant and substation switchgear housings.

15. Standard equipment now in use for multiplexing wire facilities may be in use on some customer's property. To offer the same general type of equipment with the radio will fit into existing maintenance practices more readily.

The two fundamental methods of multiplexing a given communication circuit are frequency division and time division. Frequency division permits all circuits derived by this means to function simultaneously. The useful frequency range of the communication circuit which is to be multiplexed is divided into several frequency bands, each wide enough for handling the function or functions required of it. For telephone service the usual bandwidth is about 2,500 cycles per second—(from 250 to 2,750 cycles) and for a telegraphic service the bandwidth required is a function of the repetition rate of the pulses, and the maximum rise time (steepness of wave front and trailing edges) that can be tolerated by the service. Most telegraphic services can be handled in a 120-cycle bandwidth. The simplest of this form of multiplexing consists of a number of audio oscillators. Each is adjusted to produce a different frequency, and is connected to a common output circuit with all the others. When each is controlled by independent keying devices, we can have a telegraphic circuit and each can transfer information to its respective receiving device independent of the others. The rate at which such information can be transferred depends directly upon the previously-mentioned bandwidth, and therefore is limited by the design for the system.

Since it is not practical to adjust the frequencies of the voices of several people who might want to talk over a multiplexed circuit, to the different frequencies that would permit them to talk simultaneously over this circuit, without mutual interference, it becomes necessary to translate the signals of every but one voice to different parts of the spectrum of the circuit. By the use of well-known methods, several different carrier frequencies are used with individual provi-

Paper 50-162, recommended by the AIEE Carrier Current Committee and approved by the AIEE Technical Program Committee for presentation at the AIEE Summer and Pacific General Meeting, Pasadena, Calif., June 12–16, 1950. Manuscript submitted March 15, 1950; made available for printing April 18, 1950.

F. S. Beale is with the Westinghouse Electric Corporation, Baltimore, Md.

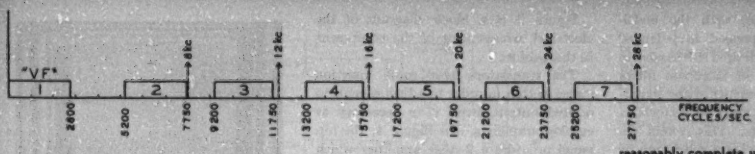

Figure 1. Carrier frequency assignments, spacings, and voice circuit bandwidths for a typical frequency division multiplexing system which will provide reasonably complete utilization of a nominal 30-kc common circuit, whether wire or radio

sions for modulation, each being assigned to handle one voice circuit. The carrier frequencies are spaced to provide a bandwidth of about 2,500 cycles for the voice signals, plus an additional amount to allow for imperfections of one kind or another in the equipment, such as bandpass filters which cannot be made to have either perfectly rectangular attenuation characteristics, or perfect stability with respect to temperature. Any form of modulation may be used on the multiplexing carriers, and its choice will either dictate the maximum number of voice circuits which can be derived from the common circuit, or it will be limited by a requirement imposed on the designer to produce from the common circuit a maximum number of derived voice circuits.

Having produced a system deriving several circuits from a common one, each of which has a bandwidth of about 2,500 cycles, it follows that the previously-mentioned telegraphic services, individually requiring much smaller bandwidths, could be applied to such a voice circuit so long as the telegraph circuit signal frequencies were confined to the voice-frequency band, 250 to approximately 2,750 cycles.

Figure 1 illustrates the application of frequency division multiplexing principles to a wire or radio circuit having essentially a flat frequency response from 0 to 30,000 cycles. It is based upon the use of amplitude modulation of the carrier frequencies with the carrier frequencies suppressed and bandpass filters used to only permit transmission of the lower sideband. Carrier frequency assignments are indicated by dotted lines with arrowheads. The associated lower sideband is indicated by a box to its left containing a number which identifies the circuit so derived. Circuit 1 has no associated carrier frequency assignment. It needs none because it is applied directly to the wire or radio circuit without translation.

The second method, time division multiplexing, involves only one basic difference from the frequency division system in deriving the desired circuits. It transmits over the radio or wire facility only one message at a time. A period of time called the repetition or sampling rate, which is short with reference to the highest frequency present in the voice or signal circuits, is divided into a number of parts, usually equal to one more than the number of signal circuits to be applied to the radio circuit. During a relatively small portion of each such part a connection is electronically made to each of the signal circuits in turn, until all have been sampled. Following this a sample is taken of a reference signal, used for maintaining proper synchronism with the distant demodulation equipment. Each sample is proportional to the signal voltage present in its circuit at the instant the sample is taken. Each sample is used to alter some distinctive characteristic, such as amplitude, or position relative to an index position, of a pulse produced by a local pulse generator. Basically these pulses occur at the repetition rate and are delivered to the modulating equipment where the signal samples modify them. These modulated pulses then are used to modulate the radio carrier.

At the receiving terminal the pulses are sorted out and delivered to their proper demodulators. The outputs of these demodulators, of course, are samples of the original signal voltages, which are passed through a low-pass filter to remove all frequency components higher than the useful frequencies intended to be delivered, and by this process the original signal is synthesized. Obviously the audio fidelity of the recovered signal is almost entirely a function of the repetition rate. It is for this reason that most time division multiplexing systems require bandwidths in the radio spectrum which are much wider than we have been used to in the past. In fact, it is this characteristic combined with the number of derived circuits and repetition rates selected that makes it impractical to apply such systems to conventional wire or cable circuits. Generally, they are applied to high-frequency radio circuits. Where pulses are used with a form of modulation in a system permitting severe filtering, (referred to square-wave pulsing) economies in bandwidth can be obtained which would permit use on wire or cable circuits which are corrected to better than 120 kc.[1]

Referring to Figure 2, the time division system basically involves the equivalent of two distributors connecting the derived circuits together, in succession as they rotate in synchronism, through the common circuit.

General Description of the System

The radio equipment to be multiplexed offered an audio band of about 200 to 30,000 cycles. It operates with carrier frequencies between 950 to 960 megacycles. Due to the choice of seven derived circuits as a maximum, and the bandwidth available, frequency division multiplexing appeared to be the logical selection and is the system which will be described. To be reasonably economical in the use of the 30-kc spectrum, the modulation system selected was ampli-

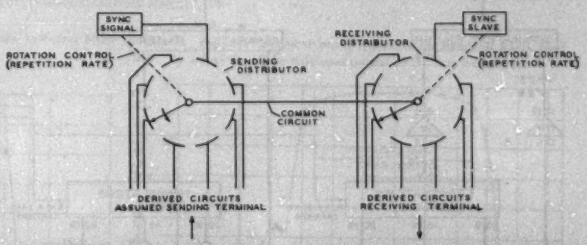

Figure 2. A scheme illustrating the basic theory underlying time-division multiplexing systems. The refinements required to handle speech signals are responsible for the detailed differences between the above and actual systems used. Additional refinements are required where there will be any limitation of bandwidth by the transmission path indicated as the common circuit. Radio usually will provide this circuit

tude, single sideband, with the multiplexing carriers suppressed in balanced bridge circuits. The desired sidebands are selected by the use of bandpass filters having cutoff characteristics giving signal-to-noise ratios better than 50 decibels in all multiplexed circuits. This system has been designed to provide a maximum of six multiplexed circuits, each with a bandwidth of 250 to 2,800 cycles. In addition, of course, the radio can be modulated directly from a seventh circuit, and the bandwidth in this case is 200 to 2,800 cycles. Figure 1 illustrates the band assignments. The radio bandwidth will be responsible for reducing the bandwidth of the direct or voice-frequency circuit, noted previously.

The signals applied to the multiplexing equipment by the connected telephone lines amplitude modulate the multiplexing carrier frequencies in a ring modulator circuit. Copper-oxide rectifiers are the nonlinear elements in this circuit. The circuit has a bridge configuration as far as the signal is concerned in its relationship to the multiplexing carrier. The panels containing these circuits are called frequency translator panels, or translators for short. In Figure 4, which shows one terminal of field test equipment designed to provide for three telephone circuits, and a fourth circuit to be used for telegraphic services, the sending and receiving translator panels are second from the top and fourth from the bottom, respectively, of the rack frame in the cabinet.

Figure 3 is a block diagram of the electrical arrangement of the equipment in this cabinet.

The translators have some insertion losses so that in order to adjust signals to desired output levels it is necessary to employ amplifiers. In Figure 4, the top panel provides a 2-stage amplifier which has a flat amplitude characteristic between 3,000 and 30,000 cycles, and is used to amplify the common output of the sending translator. In Figure 3 this amplifier is indicated by the triangular symbol enclosing the initials *HF*, for high frequency.

For the outputs of the receiving translator, three amplifiers are shown in Figure 3 by the same symbol, but enclosing the initials, *VF*, for voice frequency. In Figure 4 these three amplifiers are on the three bottom panels. For this model, standard audio amplifiers available from stock were used, since they offered satisfactory characteristics and gain.

A third amplifier is indicated in Figure 3, and in Figure 4 it is the panel located immediately below the jackfield panels. This is a compressor amplifier which serves three purposes:

1. It provides amplification for the direct voice-frequency circuit to permit weak signals to properly modulate the radio transmitter.

2. Its gain also compensates for the insertion loss of the low pass section of the separation filter.

3. It is arranged to reduce the dynamic range of speech to permit higher average level of radio transmitter modulation without over modulation.

A standard amplifier was taken from stock and modified for the test equipment.

The multiplexing carriers are obtained from a carrier supply panel, seen in Figure 4 as the panel directly below the compressor amplifier just described. As can be seen from the block diagram, Figure 3, the carrier supply panel provides three carrier frequencies for both the sending and receiving translators and, in addition, de-

Figure 4. Door removed from multiplexing equipment cabinet to show the 4-circuit equipment. Panels are mounted on standard 19-inch rack frame which is hinged to permit access into cabinet and to rear of panels

Figure 3. Block diagram of 4-circuit multiplexing equipment used in the field test program, shown in Figure 4

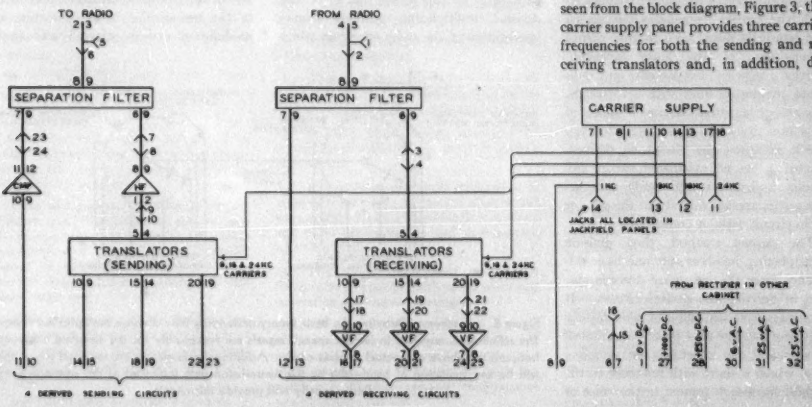

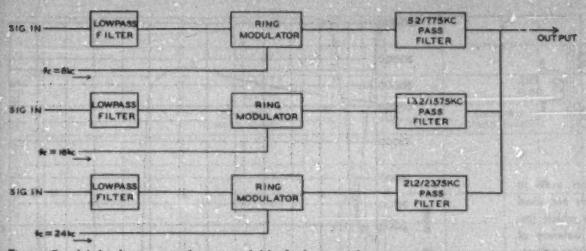

Figure 5. Multiplexing translator panel block diagram showing arrangement of parts, electrically and mechanically, for three multiplexed circuits

livers a 1-kc signal for testing and signaling purposes.

It is interesting to note that this equipment can be operated with but one type of tube, exclusive of the rectifier in the power supply. Present design does not include the compressor amplifier in an average assembly; only the other two kinds of amplifiers and the carrier supply use tubes, and they are the *6SN7* type, which also is available in ruggedized form. No tubes are used in the translators or the separation filter panels.

Two terminals of this model equipment were built and placed in service with a microwave radio system in August 1949. As shown in Figure 3 each terminal provided four 1-way circuits in each direction with all circuits and panels arranged with connections through a jack-field panel. This provided flexibility as well as convenience and speed in testing and in making any temporary rearrangements of circuitry.

Translators

The two translator panels shown in Figures 3 and 4 are identical. Each panel contains three translator circuits that are electrically independent except for a common output circuit. See block diagram, Figure 5. The devices are insensitive to direction and can be used either for sending (modulating signals on carriers) or for receiving (demodulating or recovering signals from incoming signals); thus the output circuit becomes an input circuit when it is used for receiving. The only difference between the translator circuits is in the pass band of the bandpass filter used between the ring modulator circuit and the common output circuit to select the desired sideband. It then becomes obvious that if each translator circuit is used with a different carrier frequency, its bandpass filter must be coordinated to the carrier frequency. The carrier frequencies used in the field test equipment were 8, 16, and 24 kc, and the pass bands of the associated filters were 5.2 to 7.75 kc; 13.2 to 15.75 kc; and 21.2 to 23.75 kc.

Referring again to Figure 5, the signal path for sending is through a low-pass filter to the ring modulator circuit where the signal combines with the carrier frequency. The output of the modulator circuit contains both sidebands, but the carrier is almost entirely absent. The output is delivered to the bandpass filter which is designed to offer only slight losses for frequencies in the lower sideband range, but sharply attenuates all frequencies outside of that range. The low-pass filter is required for the following reasons:

1. To restrict to the required bandwidth the frequencies of those signals to be transmitted.

2. To pass only the desired lower sideband when used in the receiving direction.

3. To prevent undesirable products of modulation from being delivered back toward the source of signals when used in the sending direction.

4. To prevent variations of impedance in the ring modulator circuit from being closely coupled to the external circuits connected through the filter.

The attenuation characteristic typical of the low-pass filters used in this equipment is shown in Figure 6.

The bandpass filters used in this equipment have attenuation characteristics represented by Figure 7, which shows the curve for a filter having a pass band from 13.2 to 15.75 kc. This filter should be used in a translator to which a 16-kc carrier would be supplied.

The ring modulator circuit used in these translators is shown in Figure 8. The use of contact rectifiers is justified by a number of important reasons:

1. They are obtainable with characteristics more uniform than found in vacuum tubes; in some equipment of this type this permits eliminating all ring modulator balance adjustments.

2. They require no plate and filament power.

3. They have no filaments or heaters to burn out.

4. They are not mechanically fragile.

5. They have no cathodes to lose emissivity.

Figure 6. The attenuation characteristic typical of the low-pass filters used in the translator circuits

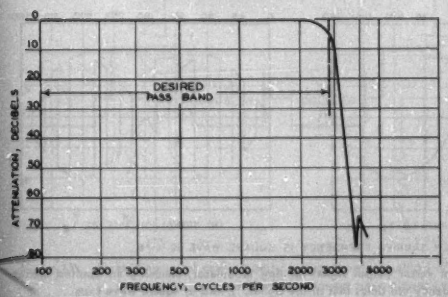

Figure 7. Attenuation characteristic typical of the bandpass filters, used to select the lower sideband output of the ring modulators

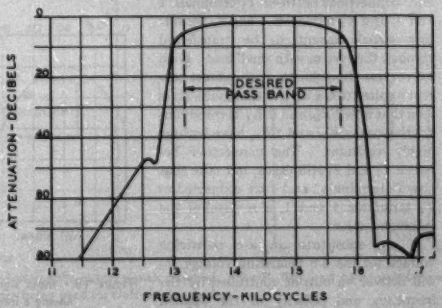

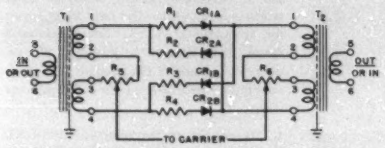

Figure 8 (above). Schematic for ring modulators used in translator panels. Copper-oxide rectifier elements are used in the ring circuit with series-connected resistors which improve both the overload characteristics, and the balance of the bridge circuit. R_5 and R_6 are provided for vernier adjustment of carrier and noise suppression

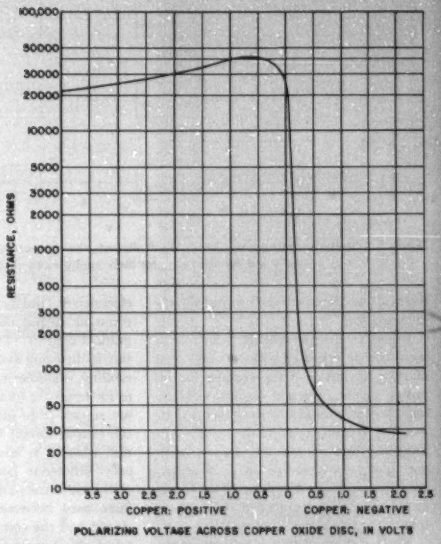

Figure 9 (right). Resistance as a function of applied voltage for a copper-oxide rectifier cell

6. They require an insignificant amount of space.
7. They require no socket.

Technical literature contains a number of articles dealing with the use of copper-oxide rectifier elements as modulators and demodulators.[2–6] Each of the referenced articles contributed to the modulator circuit of Figure 8. Figure 9 is a typical curve of the resistance of a copper-oxide disk as a function of the applied voltage. Perhaps the simplest way of explaining how the modulator operates is to treat the copper-oxide ring unit as a double-pole double-throw reversing switch used to connect the output of T_1 to the input of T_3. This connection is poor if each of the four arms of the ring has the same value of resistance, since they form a shunt across the connection between the transformers, and their unpolarized resistance, 20,000 ohms or more, also is in series in the connection. If direct current is applied to the leads marked "carrier," with polarity and voltage sufficient to cause CR_{1A} and CR_{2B} to become conducting it will be observed that CR_{1B} and CR_{2A} are polarized at the same time so that they are less conducting. In this condition of unbalance CR_{1A} and CR_{2B} form low-resistance connections between T_1 terminals 1 and 4, and T_2 terminals 1 and 4, permitting signal current to be transferred through the system with small loss. Then we reverse the polarity of the direct current applied to the carrier terminals. It is seen that now CR_{1B} and CR_{2A} become conducting and CR_{1A} and CR_{2B} have become highly resistant. The connection between T_1 and T_2 still exists, but note that now T_1 terminals 1 and 4 are connected to T_2 terminals 4 and 1, a reversal of the interconnection.

If we substitute an a-c polarizing voltage for the d-c polarizing voltage, T_2 will deliver an output controlled by the frequency and polarity of the applied alternating voltage. If the alternating voltage effective at the copper-oxide elements approximates a square wave, this output would have the appearance shown in Figure 10. It is necessary that the carrier (polarizing) voltage at all times exceed the drop produced by flow of signal currents when they are of opposite polarity. If this excess has insufficient margin the copper-oxide resistance will increase and cause nonlinearity of signal output. This is recognized as amplitude distortion. The slope of the conducting part of the curve in Figure 9 suggests that such distortion will always be present to some degree. If, in addition to insuring that the carrier voltage is always more than adequate to maintain polarization, fixed resistance is added in series with the copper-oxide element, so setting the minimum resistance in the conducting direction to be large compared to the conducting resistance of the copper oxide, then the small resistance variations can be made to be an insignificant percentage of the total resistance. As a result of employing both of these measures we obtained distortion measurements of 0.5 per cent and less for a voice circuit through a sending and receiving translator system with filters but without amplifiers or radio.

The operation of the ring modulator was compared with the action of a double-pole double-throw switch connected to reverse the polarity of the path between

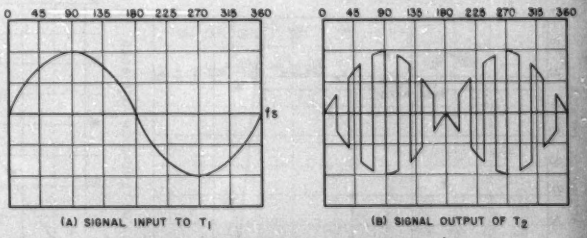

Figure 10. Input signal versus output signal for ring modulator, assuming an applied carrier having a frequency ten times that of the signal, f_s, and of square wave form

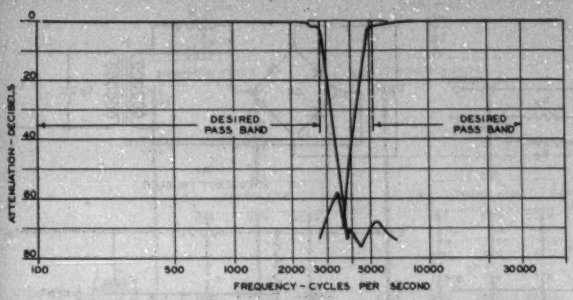

Figure 11. Attenuation characteristic for separation filters. These units are combined low-pass and high-pass filters having common output terminals, but separate terminals for the inputs to low-pass and high-pass sections

input and output. This suggests that the carrier signal applied to the ring modulator should be a square wave carrier. In practice it is customary to use a rather large carrier amplitude, supplying it to the ring modulator through an external resistance which acts as a current limiting device.[6,7] As the ring modulator elements polarize, a carrier current begins to flow and attempts to increase. This results in an increase in the drop across the series resistor, thus limiting the current and producing an approximate square wave carrier drop across the ring modulator elements. It is found, however, that signal currents still must be kept small compared to the carrier.

Mr. Cusack has shown[4] that the nonconducting elements in the ring modulator will overload with a signal less than one-tenth that required to overload the conducting elements. He also shows that the use of resistance in series with each element of the ring can radically reduce this difference.

A further and very important result of the addition of the fixed resistors in the ring modulator is the marked improvement obtained in the balance of the circuit. It can be obtained, of course, only if the resistors used are sufficiently well balanced. It is found that resistors having 1 per cent resistance tolerance gave excellent results. The indirect result of the balance improvement obtained in this manner is the possibility of not requiring ring-modulator copper-oxide elements that are as well balanced as was formerly required.

Filters

Filters are used at several points in this equipment, as can be seen in Figures 3 and 5. In Figure 3, two separation filters are shown. Each consists of a low-pass filter, cutoff at 2,800 cycles, and a high-pass filter with its cutoff at 5,200 cycles. These two filters are combined in one case and have common output terminals but separate input terminals. Their attenuation characteristics are shown in Figure 11.

The separation filter is used to apply a separate or direct voice frequency band to the radio transmitter without frequency translation. By applying it through the low-pass filter, the bandwidth of the voice-frequency circuit is restricted to frequencies below about 2,800 cycles, insuring that no higher frequencies accidentally or intentionally present in the voice frequency circuit will interfere with the high-frequency signals delivered by the translators.

An equally important function also is served. By design the impedances of all filters are about 600 ohms in their pass bands only. Outside of these bands the impedances rise to much higher values. Thus the outputs of two properly designed filters with pass bands in different parts of the spectrum can be paralleled and connected to a 600-ohm circuit without causing the circuit to become a 300-ohm circuit. Such isolating effects are quite important to the frequency response of the derived circuits and for avoiding other undesirable noise effects.

In Figure 5, it is observed that two filters are used in each translator circuit. Again, signals from the voice circuit are passed through a low-pass filter, the ring modulator, and then the bandpass filter. The reasons for their use have already been discussed, but no mention was made of the part the bandpass filters play in permitting the several 600-ohm output circuits to be paralleled and then connected to a 600-ohm load. The attenuation characteristic typical of the bandpass filters used is indicated in Figure 7, while Figure 6 shows the attenuation characteristic of the translator low-pass filters.

Carrier Supply System

It is conventional to use free-running local oscillators for supplying the multi-

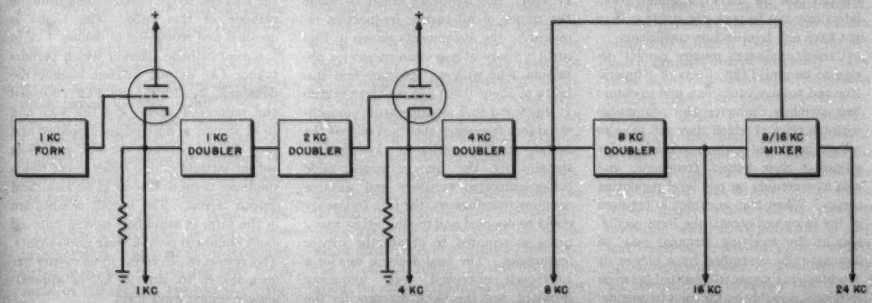

Figure 12. Block diagram of carrier supply system showing method of obtaining the output signals required. The 8-, 16-, and 24-kc outputs are converted to square wave output before being used for multiplexing carriers

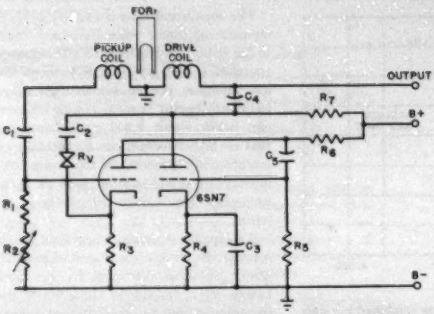

Figure 13 (above). Schematic of fork frequency unit. It consists of a 2-stage resistance coupled amplifier with two feedback paths set up between output and input. One path is through the fork unit and determines the frequency of oscillation; the other employs a varistor in cathode circuit feedback to increase stability and regulate output signal voltage

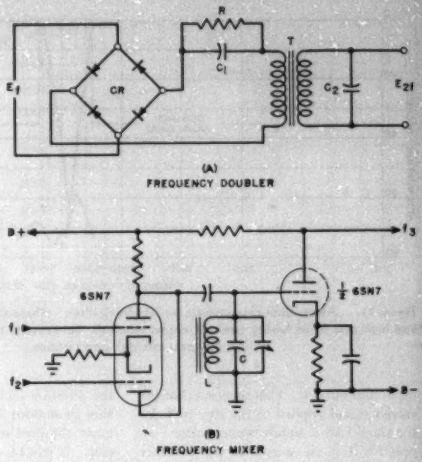

Figure 14. Carrier supply circuitry

(A) When a signal of frequency, f, is applied to the doubler input terminals, a new frequency, $2f$, is obtained at the output

(B) The frequencies, f_1, and f_2, to be mixed, are chosen so that their difference will equal one of them, while their sum equals the desired new frequency, f_3; the filter, L-C, is resonant at f_3

plexing carrier frequencies. Thus the signal frequencies recovered at the receiving terminal in a single-sideband system will differ from the original signal frequencies by the differences between sending and receiving carrier frequency oscillators. Recovery of speech signals is quite satisfactory even though such differences are as high as 20 or more cycles per second. Maintenance adjustment of these oscillators is required only to keep speech intelligible and as natural as the user requires.

Some forms of telegraphic services, when handled over one of the multiplexed voice circuits, cannot tolerate these rather large differences between original and recovered signal frequencies. This is due partly to the narrowness of the receiver filter, which cannot reasonably be broadened. It is further complicated by the fact that the telegraph sending oscillators may not be perfectly stable or may not have zero temperature coefficients.

Carrier oscillators require careful design to minimize the effects of temperature and voltage variations, and to obtain best stability characteristics compatible with the price at which they will have to sell. They must include provisions for adjusting their output frequency, and also may contain output level regulating means. When high accuracy is required of the recovered signal, the local oscillators at the receiving terminal may be automatically controlled by a carrier or synchronizing signal transmitted between terminals, possibly on the pilot frequency. Another method is to transmit some of the sending end carrier over the system and recover it for demodulation purposes at the receiving terminal.

Local oscillators and their associated adjustments and maintenance requirements are not desirable for the type of multiplexing equipment which would be most suitable for use in electric utility communication systems, especially when we considered that it would be rare indeed when telegraphic services would not be handled—telemetering, load-control, even relaying. A carrier supply system should be so precise and stable that it would require no maintenance of frequency. Moreover, there would be no adjustments in the system which could alter any carrier frequency so much that any circuit would fail because of tampering or misadjustment of frequency controls.

With the multiplexing carriers spaced 4 kc apart, this frequency could be made the source of all carrier frequencies required by the assignments shown in Figure 1. Study of ways and means for obtaining 4 kc with an accuracy and stability of about 0.001 per cent was begun. It was found that a temperature compensated fork frequency standard offered the surest, simplest source of the required signal. By the use of copper-oxide bridge-connected rectifiers and suitable coupling transformers, the fork frequency could be doubled and re-doubled as many times as required to obtain the carrier frequencies. The final decision was for a 1,000-cycle-per-second fork frequency standard, and the block diagram for the carrier supply panel took the form shown in Figure 12. The decision on this frequency was based principally upon the availability of a suitable fork operating at 1,000 cycles and using one *6SN7* tube for drive and output. Furthermore, this frequency would be a convenient signal frequency for test purposes, so the plans for the carrier supply included that provision.

Referring to Figure 12, it is seen that the output of the fork unit is applied to a doubler through a cathode follower with the 1-kc test signal output taken from the cathode of this tube. The signal is doubled and redoubled to deliver 4 kc to a second cathode follower which permits taking 4-kc output without loading the doublers. In addition, the 4 kc is doubled and redoubled again, and the 8-kc and 16-kc signals so derived are amplified and then divided between the 8-kc and 16-kc output circuits and a mixer stage which combines them to deliver 24 kc to a third output circuit. The output circuits are in the form of amplifiers having opposed diode shunt clippers in their grid circuits. This results in delivering three carrier frequencies, 8, 16, and 24 kc, of approximately square wave form.

The fork standard unit was purchased as a complete, tested and calibrated as-

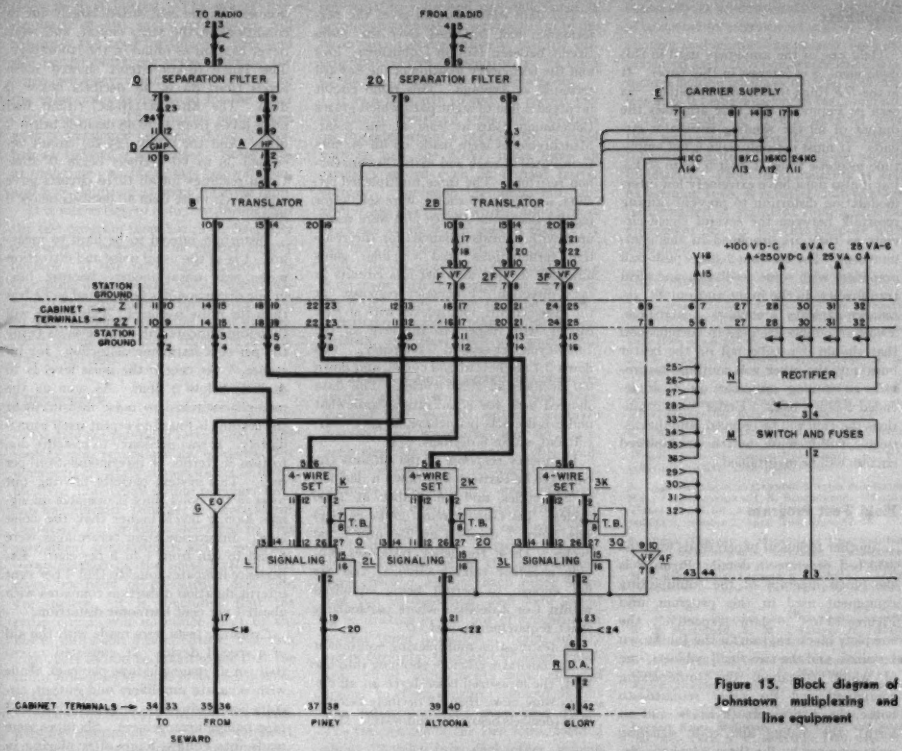

Figure 13. Block diagram of Johnstown multiplexing and line equipment

sembly and was mounted directly upon the carrier supply panel. The fork itself is in a partially evacuated metal container which protects it from atmospheric changes, corrosion, and tampering. It is of bimetallic construction, and the resulting temperature coefficients are better than 0.0001 per cent per centigrade degree between 0 and 100 degrees centigrade. The unit is set to 1,000 cycles per second within 0.0001 per cent at the factory. A vernier frequency adjustment is provided which has a range of about 0.005 per cent, or only 0.05 cycle per second at 1,000 cycles. If another 0.05-cycle error is added for a temperature difference between terminals of 50 degrees centigrade, the total difference in frequency of the forks might be about 0.1 cycle. This amounts to 2.8 cycles for the 28-kc carrier in this system, or an error in the recovered signal frequency of 1.13 per cent for a signal of 250 cycles. The fork is electromagnetically driven, made of a magnetic metal, and polarized by means of a small permanent magnet included in the device. The magnetic flux path links both tines of the fork, a grid or pickup coil and a plate or drive coil. Motion of the tines modulates the flux because the air gaps are being changed, and a small voltage is induced in the two coils. Figure 13 is a schematic of the fork frequency unit.

The schematic of the basic frequency doubler used in this panel is shown in Figure 14(A). C_1 and C_2 are chosen to obtain maximum accentuation of the ripple output of the bridge-connected rectifier, but commercial tolerances are good enough and no adjustments are required to obtain satisfactory operation. The value of R is determined roughly by the safe amount of direct current which can be handled by the rectifier and has little effect upon the ripple amplitude in the range used. It is interesting to note that the $2f$ output voltage of this doubler is about the same as the input voltage across the rectifier. Each doubler used has the same schematic; as frequency increases the transformers, capacitors, and resistors also change correspondingly.

When the desired carrier frequency falls between those obtained by the doubling process, two of the frequencies already obtained are selected and applied to the grids of the mixer circuit of Figure 14(B). Mixing takes place in the plate circuit, and the three frequencies then present are coupled to a high-Q resonant circuit adjusted for the desired frequency. The range of the adjustable capacitor permits peaking, but will not prevent operation on frequency unless it is short circuited. Filtering by this simple circuit is sufficient so that the output of the amplifier contains only insignificant amounts of the two original frequencies. The entire carrier supply system can be placed in operation with no adjustments of any sort required either to obtain correct operating frequencies, or to obtain them so accurately determined that for all known applications no synchronism adjustment need be made.

Amplifiers

Only one of the amplifiers used in this equipment is of interest in this paper. It is the *HF* (high-frequency) amplifier. As seen in Figure 3, this unit amplifies the output of all the sending translator circuits. It must not only have a flat amplitude response from at least 5 kc to 30 kc, but it also must have extremely low intermodulation distortion to prevent causing crosstalk between the several signal circuits as they are amplified in this common unit. The unit is a 2-stage push-pull amplifier, with some feedback, and with transformers in the input and output, resistance-capacity coupled interstage. Two *6SN7* tubes are used in such fashion that should one tube fail or the heater burn out, the other will continue to provide a working amplifier on a single-ended 2-stage basis. Under such conditions the gain will be reduced, and the distortion will increase, but the multiplexed circuits will be maintained.

Field Test Program

Another technical paper[8] deals with the field test program in detail. Figure 3 is the block diagram of the multiplexing equipment used in this program, and Figures 15 and 16 show, respectively, the complete block diagram for the Johnstown terminal, and the two small cabinets, one of which contained the multiplexing equipment and the other required to house the 4-wire sets (hybrids, and so forth), the dialing and code signaling units required by the three telephone circuits to be handled between Johnstown and Seward. These telephone line facilities are not unusual, and their arrangement on Figure 15 is conventional.

It will be seen that the direct or voice-frequency circuit is not provided with a 4-wire set or signaling unit. In the receiving branch, it was equipped with an equalizer amplifier to improve the low-frequency response down to 150 cycles. The field test program included tests of simultaneous operation of all ten audio tones of a line of telegraph equipment, the lowest of which was 150 cycles. From the output of the equalizer amplifier, the receiving branch was connected to the paralleled inputs of the tone telegraph receivers, shown in the block diagram of reference 8. Similarly, the sending branch was connected to the parallel outputs of all ten tone telegraph transmitters. The telegraph circuits thus provided were to be used for several telemetering circuits, two relaying circuits, and for field testing a new supervisory control system.[8]

The data which follows gives the performance first obtained over the radio circuit between Hilltop (Johnstown, Pa.) and the temporary location of the Seward terminal at Armagh. This radio circuit involved a line-of-sight path which grazes Conemaugh Gap at least at one point. Measurements were made on all circuits terminated at each end with 620-ohm carbon resistors. The three multiplexed circuits, as Figure 15 shows, were set up for regular telephone service and were measured with hybrids balanced for the resistive terminations, and amplifier gains adjusted to give zero net-loss circuits in each direction. Frequency response for the Piney circuit, multiplexed with an 8-kc carrier, with respect to the level of the 1,000-cycle-per-second reference, was down 3.7 decibels at 250 cycles, and down 9.0 decibels at 2,800 cycles. The data showed need for equalization, somewhat under 6 decibels per octave, to give a circuit flat within 6 decibels.

Frequency response of the Altoona circuit, (16-kc carrier) was down 6 decibels at 250 cycles, and 5.5 decibels at 2,800 cycles. The Glory circuit (24-kc carrier) was down 7 decibels at 250 and 2,800 cycles. These frequency responses provide excellent talking circuits, and are flat enough to permit being equalized within 1 or 2 decibels where particularly strict requirements exist.

In testing this multiplexing equipment in the laboratory before shipping into the field, the measured noise levels in all circuits were more than 65 decibels below 0 dbm (decibels below one milliwatt). Measurements in the field varied, largely due to conditions in the radio circuit, and were never as good as found in the laboratory. The Piney (8-kc) circuit showed noise levels from 35 to 48 decibels below 0 dbm. The Altoona (16-kc) circuit had noise levels from 41 to 48 decibels below 0 dbm. And the Glory (24-kc) circuit recorded 38 to 60 decibels below 0 dbm. Usual readings for all three circuits gave noise levels more than 40 decibels below 0 dbm.

Figure 16. Doors removed from cabinets housing the multiplexing and line equipment shown in Figure 15

Distortion proved to be hard to measure. Use of the usual noise and distortion meter was unsatisfactory because harmonic distortion has been found to be less than the noise readings. This meter will therefore indicate the noise level as being the per cent harmonic distortion; for instance, 1 per cent if the noise level is 40 decibels below 0 dbm. As soon as the meter is switched to noise measurement the reading is found to repeat itself immediately. It was necessary to measure distortion in terms of intermodulation per cent. This system permits filtering out most of the noise since it operates on signals having levels higher than the noise level. Intermodulation percentages were found to run from 1 to 5 per cent. Experience indicates roughly that 4 per cent intermodulation distortion compares with about 1 per cent harmonic distortion.

Crosstalk tests were made with the aid of a special device. It consisted essentially of six magnetic-tape playback heads with separate amplifiers and output circuits, and a single-drive motor, shaft and tape pulling arrangement. Six tapes were made into endless loops after placing in the machine, and thus any signals recorded in them were played back and repeated as long as the machine was run. The output from one or more speech-recorded tapes was applied to the multiplexing equipment circuits as desired, all at 0 dbm levels to obtain measurements of crosstalk appearing in silent circuits. The noise meter was used to measure any increase in noise level as being the contribution made by crosstalk; at no time was crosstalk responsible for raising the noise level more than 2 decibels. Simultaneous listening tests showed that crosstalk was found to be very slight.

In these comments no mention has been made of the performance of the direct voice-frequency circuit. This is because the use of a special equalizer to boost the 150-cycle-per-second performance also increased the noise output about 15 decibels. This equalizer provided about that much more gain at 60 cycles than it did at 1,000 cycles, and resulted in disproportionately increasing the hum level of the

radio receiver output. The use of pre-emphasis at the radio transmitter will eliminate the need for this equalizer and will permit obtaining noise levels on the voice-frequency circuit, which will be of the same order as indicated for the other three circuits. The original data taken gave a frequency response down 3 decibels at 150 and 2,800 cycles. Noise level at that time was 24 decibels below 0 dbm, and was identified as being 60-cycle hum.

It is interesting to note that throughout the test program there has never been any occasion to question the carrier supply system. It has performed flawlessly in supplying accurate and stable carrier signals. The only tube failures experienced to date evidently were the result of shipment of the equipment from the laboratory to the field.

Conclusions

To date the results of tests made on the multiplexing equipment are evidence that noise and crosstalk requirements of down 50 db or more below 0 dbm reference level can be obtained. Further evidence shows the distortion products delivered by this equipment are extremely small, generally being masked by the noise level so that usual methods of measuring distortion are useless. It is concluded that the radio circuit will introduce most of the noise, distortion and crosstalk, and that great care should be taken to see that the radio line-of-sight path is as nearly ideal as is possible.

Where the full capabilities of the multiplexing equipment are to be required; that is, seven voice circuits, with 50 decibel signal-to-noise and crosstalk ratio, it becomes extremely important to apply the radio circuit conservatively, making certain that 50 feet of clearance is obtained to the line-of-sight for the radio beam.

It is a bit early to put on record any statement regarding tube life. Heaters are operated about 5 per cent below rated voltage, and the *6SN7* tubes have an excellent record even at normal heater voltage. Emission requirements are always less than tube ratings, and in most cases are about 50 per cent of rating. It has not, therefore, been considered economically sound to equip the multiplexing equipment with the ruggedized version of the *6SN7* tube. Since no tube is being operated at a critical point on its characteristics, any good tube will work until emission fails to meet the load.

The carrier supply system has never required any attention. It has been checked for carrier output voltages (loaded) and waveform, and no variations were found. No means was available for checking the accuracy of the frequencies as no ordinary audio oscillator can be used even if especially calibrated because its dial cannot be read with sufficient accuracy. Two carrier-supply panels, one at each end of the radio circuit, were checked against each other when first put in operation, and were found to be drifting in and out of synchronism several times a minute. Again, mostly out of curiosity, the fork frequency standard vernier adjustments were changed enough to effect synchronism and no further adjustment has ever been made. The frequencies of the two forks, located about 12 miles from each other, remain essentially in synchronism over the ranges of temperature experienced to date. Both summer and winter seasons have been experienced and the rooms where the equipment is located normally have no heat, unless work is being done on the test program.

The quality of speech received over this equipment is excellent considering its restriction to a 2,500-cycle-per-second bandwidth. From measurements as well as listening tests, it is better-than-average performance of standard communication equipment in use for this purpose with wire lines.

References

1. Copper Oxide Modulators in Carrier Telephone Systems, **R. S. Caruthers.** *Electrical Engineering (AIEE Transactions)*, volume 58, June 1939, pages 253–60.

2. A Constant-Impedance Modulator, **D. G. Tucker.** British Patent Number 30982, 1946.

3. Rectifier Resistance Laws, **D. G. Tucker.** *Wireless Engineer* (London, England), volume XXV, number 295, April 1948, pages 117–28.

4. Frequency Translation in Wide-Band Transmission Systems, **F. H. Cusack.** *Western Union Technical Review* (New York, N. Y.), volume 2, January 1948, pages 36–44.

5. A 180-Kilocycle Carrier System for Radio Relay Applications, **J. E. Boughtwood.** *Western Union Technical Review* (New York, N. Y.), volume 2, number 2, April 1948, pages 57–65.

6. Field Testing a Microwave Channel for Voice Communication, Relaying, Telemetering and Supervisory Control, **D. R. Pattison, M. E. Reagan, S. C. Leyland, F. B. Gunter.** *AIEE Transactions*, volume 69, part II, 1950, pages 945–52.

7. A Time Division Multiplexing System, **W. P. Boothroyd, E. M. Creamer, Jr.** *AIEE Transactions*, volume 68, part 1, 1949, pages 92–97.

8. Multichannel Open-Wire Telephone Systems for Portugal, **C. G. Mansson.** *Ericsson Review* (Stockholm, Sweden), number 2, 1949, pages 40–53.

9. Electrical Engineers' Handbook, **Harold Pender, Knox McIlwain.** John Wiley and Sons, Inc., New York, N. Y., section 13, 1936, pages 47–51.

Discussion

R. H. Miller (Pacific Gas and Electric Company, San Francisco, Calif.): The multiplexing equipment described by the author is of a much higher degree of stability than the equipment commonly available, and is also characterized by extremely simple circuits.

Both of these factors are of considerable importance to power utilities in that a minimum of attention and adjustment should be required.

The high degree of stability of the carrier supply makes it feasible to install the equipment in unheated shelters, without experiencing excessive frequency drifts due to temperature changes.

In general, the use of frequency division multiplexing should be adequate for most power utility applications of microwave equipment, as the large number of channels available from time division multiplexing rarely will be needed on power utility communication systems, and, in fact, might be a disadvantage due to the concentration of too many channels in one microwave system with the possible loss of the complete system by trouble in one piece of the radio equipment.

The technique described for the measurement of cross-talk is most interesting, and the fact that such an elaborate system of measurement was required should indicate a very low degree of cross-talk in the equipment.

It would be interesting to have the author comment on the reason for the selection of a system using an individual fork drive for each channel, rather than having a single base frequency fork and using harmonics of this fork for controlling the various channel oscillators. In such an arrangement the frequency and phase of each channel would be fixed with respect to each other.

F. S. Beale: The author wishes to express great appreciation for the discussion presented by Mr. Miller.

The reasons for the selection of a single fork frequency standard as the common source for all frequencies used for signaling, and as carrier frequencies for use in deriving telephone circuits, included the following:

1. The stability of all frequencies was determined by that of the fork;
2. Frequency and phase, as Mr. Miller points out, are fixed with respect to each other;
3. Carrier frequencies chosen at 4-kc intervals are in rather common use, and a fork frequency source was compatible with such system;
4. Choice of fork frequency permitted using its output directly for signaling and test purposes, eliminating the need for a separate source which would be required by any telephone signaling system;
5. The accuracy of such signaling frequency was such that it became practical to use a simple bridge circuit to obtain amazingly sharp selectivity in the signaling equipment, positively assuring complete freedom from any false signaling due to

presence in speech of the signaling frequency, even if at high amplitude; and

6. Carrier and signaling frequencies were obtainable without tuning adjustments, eliminating the opportunity such adjustments offer for misadjustment.

In closing, it may be of interest to note that since March 15, 1950, at which time the manuscript for this paper was submitted, the two carrier supply panels undergoing the field test mentioned in the paper have performed with no tube failures, no tubes replaced, and no failure or deviation of output frequencies in the five additional months of service.

The Bonneville Power Administration Relaying and Reclosing Program

CLIFFORD C. DIEMOND
MEMBER AIEE

DONALD L. WYLIE
ASSOCIATE AIEE

EXPERIENCE on the Bonneville Power Administration system has disclosed a number of weaknesses in protective relaying and has shown the need for an extensive high-speed reclosing program on the 230-kv lines.

The initial fault protective devices for the 230-kv system included impedance and reactance distance relays, directional-comparison carrier relaying, and the largest circuit breakers obtainable—2,500,000-kva 230-kv 3-cycle nonreclosing oil circuit breakers. Until quite recently modified-impedance and phase-comparison carrier relaying were not available.

System performance was studied on the Bonneville Power Administration a-c network analyzer for anticipated operating conditions and for actual system breakups which were initiated by simultaneous 230-kv multicircuit outages during lightning storms. The studies disclosed that automatic reclosing at high speed would be of great benefit in maintaining stability, especially during multicircuit outages. These analyzer reviews also established the necessity for replacing the distance relays with modified impedance units and for taking steps to improve the performance of the carrier relaying.

As part of a co-ordinated program to eliminate the difficulties with distance relays, carrier relaying, and circuit breakers and to improve the transmission-system performance, these steps are being taken:

1. Increase transmission capacity by the construction of additional lines, by the use of series capacitors, and by the use of higher nominal as well as higher operating voltages.

2. Improve lightning protective design to decrease the frequency of multiphase and simultaneous multicircuit faults, especially on double-circuit towers.

3. Use modified (restricted impedance) distance relays and high-speed phase-comparison carrier relaying on the long, heavily loaded circuits.

4. Install 3-phase high-speed reclosing circuit breakers in 230-kv line positions.

5. Pursue actively a development program for high-speed relaying using the microwave communications system.

6. Continue and expand the use of automatic high-speed recorders, oscillographs, and automatic fault locators.

7. Continue to encourage the manufacturers in the development of high-capacity high-speed tripping and high-speed reclosing circuit breakers by co-operating in staged tests of new developments.

8. Encourage the manufacturers in the development of new relaying methods and of new relays.

New Transmission Facilities

Figure 1 shows the 230-kv transmission system and the proposed 6-year 230-kv construction program of the Bonneville Power Administration. These needs are based on present knowledge and techniques. It is anticipated that the number of circuits will be reduced and routings changed as a result of technological improvements. Among the new 230-kv lines being considered for construction are some 14 lines from various Columbia River hydroelectric plants to the coastal area, those necessary for completion of the Western Montana–Southern Idaho Loop, the Southwest Oregon lines, and a Southeastern Washington 230-kv loop. Although they are not shown in this diagram, there are also many lower-voltage lines proposed for construction during this same 6-year period.

Series capacitors have been discussed in a previous paper.[1] These present relaying problems which have not yet been completely solved. An installation of series capacitors has been authorized for Chehalis substation. Other applications are being studied.

With regard to higher-voltage transmission, studies and investigations of various phases of the problem are in progress. These include the methods for obtaining the necessary transmission voltages, examination of corona and related problems, and consideration of the various economic questions.

Since construction of transmission capacity has not kept pace with the addition of generation, it will be several years before the remaining points in the program will appreciably reduce investment per unit of system capacity. Meanwhile the program will result in improved service—an extremely important point in itself.

Lightning Protection

Design changes to improve lightning protection should decrease the frequency of multiphase faults and multicircuit outages especially on double-circuit towers. Present efforts are to keep all tower footing resistances low and to use overhead ground wires in certain locations where lightning storms are particularly frequent. Overhead ground wires will continue to be used over the lines for a distance of 0.5 to 1.0 mile from most substations on the system. The primary purpose of these is for the protection of the substation equipment.

Distance Relaying

Limitations imposed on distance relays by the system are brought out in Table I where data, including maximum loadings, are shown for typical Bonne-

Paper 50-164, recommended by the AIEE Relay and Transmission and Distribution Committees and approved by the AIEE Technical Program Committee for presentation at the AIEE Summer and Pacific General Meeting, Pasadena, Calif., June 12–16, 1950. Manuscript submitted March 13, 1950; made available for printing April 28, 1950.

CLIFFORD C. DIEMOND is with the Bonneville Power Administration, Vancouver, Wash.; DONALD L. WYLIE is also with Bonneville at Portland, Ore.

Acknowledgment is due the many engineers of the Bonneville Power Administration who have worked on and contributed to the program described.

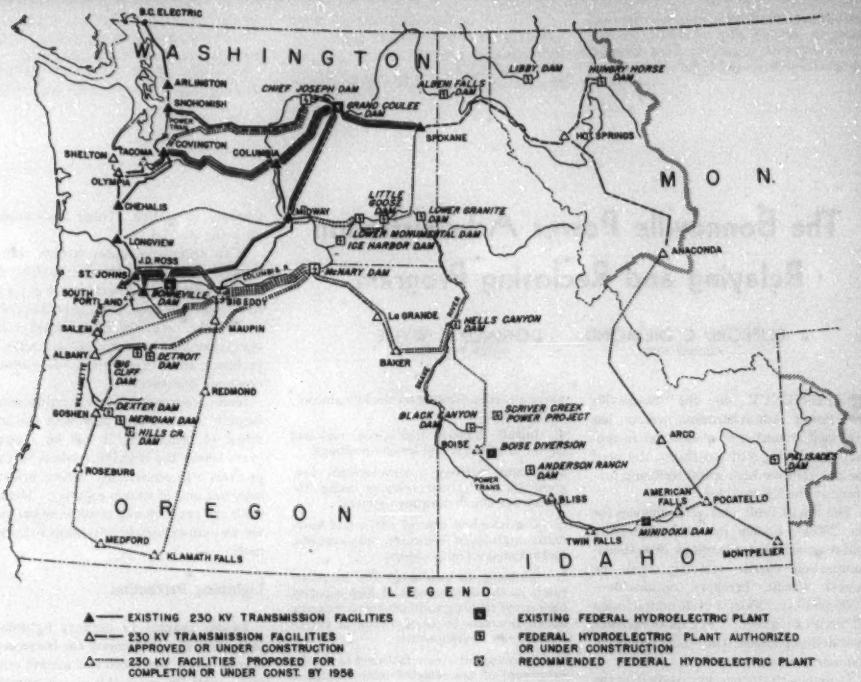

Figure 1. Existing Bonneville Power Administration 230-kv lines and 6-year advance program

Number of circuits shown may be reduced and routings changed as a result of technological improvements now under investigation

ville Power Administration 230-kv lines. These maximum loads are expressed in terms of millivolt-amperes and of approximate apparent impedance (load vectors) seen by distance relays at the line terminal closest to the terminus of the load vector. Consideration of the load vectors and possible surges which could occur without losing system stability demonstrates the urgency of restricting the relay impedance characteristics because the surge vectors are always smaller than the steady state load vectors. Both can be seen to be of a magnitude not much greater than the line impedance. Since surge and load vectors usually appear at nearly unity power factor, the modern modified distance relay[2,3] lends itself ideally as a solution to the problem of restricting tripping to actual faults on the line section. These are capable of being set so that tripping cannot occur for a transient system surge unless the system becomes unstable and the apparent impedance vector[4] passes through the relay impedance characteristic, that is, the system electric center is within the relay reach.

Table I also gives the magnitudes of representative 3-phase faults in megavolt-amperes at 230 kv for a solid fault at the end of the line with the circuit breaker closed and also open at that end. The 3-phase fault impedance seen by distance relays at the line terminal is of course equal to the line impedance Z_1 during these faults.

It is the Bonneville Power Administration plan to use distance relaying for phase faults which is as simple as possible commensurate with the load, fault, and system-surge considerations. It is recognized that if the tripping response of the phase relays is limited to fault and out-of-step conditions, (apparent impedances in the range 45–115-degree lag) a certain degree of complexity must be accepted.

The decision was made to de-activate the out-of-step trip-blocking equipment originally supplied with the distance-relay directional-comparison equipment. It was felt that more satisfactory system operation would be obtained if tripping was permitted by any relay which saw the out-of-step impedance vector within its tripping area. It was considered doubtful that the location of the out-of-step impedance vector could be predicted accurately enough for all load and fault conditions so that tripping could be relied on at selected line locations.

There is little likelihood that out-of-step tripping will open enough lines to completely drop any substation. On the other hand, trip blocking for out-of-step could easily magnify the severity of the disturbance.

The first zones of the modified distance relays are set at 85 per cent of the protected circuit length. Because of the limitations brought out in Table I and covered in the foregoing, the second zones

are set at about 130 per cent of the protected line length with a time delay of 15 or 20 cycles. In order to give the greatest backup for faults on other lines, the third zones are often adjusted to give maximum reach in the reversed direction. By tipping the modified impedance characteristic for all zones away from the system surge vector, the tendency to trip for a swing from which the system can recover is lessened.

The use of modified distance relays gives promise of complete elimination of improper tripouts due to accidental loss of potential. One method of accomplishing this end involves the use of overcurrent fault detectors set above load current in the first-zone trip circuit and offsetting the second- and third-zone elements so that the origin as plotted on an impedance diagram[4] is outside the relay tripping area. This possibility makes the use of bus potential transformers more attractive at all voltages.

Backup ground relaying is provided for most lines by directionally controlled induction overcurrent ground relays equipped with instantaneous trip attachments.

While some of the ground relays now in service are of the product type, it is planned to use no more of these except on short transmission lines, a use which they seem to fit to better advantage than the long-line application. The combination of instantaneous trip attachments in ground relays and phase-comparison carrier relays should give a reasonably fast relaying speed for most faults.

Carrier Relaying

Experience with directional-comparison carrier relaying using the older impedance and reactance relays disclosed several weaknesses in the carrier relaying systems as used on the Bonneville Power Administration lines. The limited reach permissible with the impedance and reactance relays resulted in slow operation of carrier relaying for end-zone faults. There is also considerable doubt that any directional element, whether it is a separate unit or inherent in the distance measuring element, can successfully determine direction when closing in on an electrically close 3-phase fault where the relaying potentials are obtained from the line side of the circuit breaker.

Performance of the directional-comparison carrier ground relaying was also impaired because of mutual coupling between lines for zero sequence currents. For some system operating connections, notably the interleaved Coulee bus,[5] product-type carrier ground relays were subject to improper operations.

The final objections to directional-comparison carrier relaying, as used on the long 230-kv lines of the Administration, lay in its extreme complexity and the dependence of the carrier relaying on proper operation of the distance relays.

Therefore, as a primary system of relay protection, at least until a satisfactory microwave relaying system can be developed, it is planned to replace directional-comparison carrier with modified distance relaying as covered in the foregoing and phase-comparison carrier relaying,[6,7] on the 230-kv network. At the time an adequate microwave relaying scheme is in service, experience and carrier frequency spectrum congestion will dictate further changes to be made.

Phase-comparison carrier is being used in spite of its inability to relay for some 3-phase end-zones faults on long lines. Several considerations are being kept in mind in accepting this restriction. First, the number of 3-phase faults on the 230-kv system is very small. Second, most of these will be cleared quickly by the first zones of the distance relays. The majority of the 3-phase faults which occur in the end zones can be relayed by phase-comparison equipment at the remote end due to the usual increase in fault current (as shown in Table I) after the end nearest the fault has cleared. Finally, if the 3-phase fault current is not large enough to operate the phase-comparison relays, it cannot be classed as a severe fault, so that second-zone relay times of 15 or 20 cycles for perhaps one 3-phase end-zone fault in a total of 500 can be tolerated. The directional-comparison carrier relaying does not do nearly as well for all faults including 3-phase and unbalanced faults.

The phase-comparison relays being current-operated and, independent of voltage, should provide reliable and fast operation for 3-phase faults where failure to trip may occur during a closing in operation with distance or directional-comparison carrier relays. They should not be as subject to the limitations due to mutual impedance as are directional overcurrent ground relays. Of importance is the fact that the phase-comparison equipment is essentially independent of the distance relays, and is mechanically simpler than is the directional-comparison equipment.

Relaying speed with presently available phase-comparison relays should be from two to three cycles for all unbalanced faults including phase to ground, 2-phase to ground, and phase to phase faults. This speed of operation is contrasted with Bonneville Power Administration experience with directional comparison carrier where relaying times of up to 15 cycles have been measured.

At the time of installation of directional-comparison carrier pilot equipment, the equipment was satisfactory for line loadings then considered to be large. It has been since established that line loadings could be raised to much higher levels. With these higher loadings, the older directional-comparison equipment has become inadequate for fault protection where fault and load currents are comparable. Ground fault currents and voltages have also become limiting factors.

Microwave Relaying

Relaying over microwave communications channels[8] shows considerable prom-

Table I. Typical Bonneville Power Administration 230-Kv Lines

Maximum Nonsimultaneous Emergency Loadings Encountered and Typical 3-Phase Fault Data

Line	Length, Miles	Line, Z_1, Ohms	Maximum Emergency Loadings: Load, Mw	Maximum Emergency Loadings: Impedance, Ohms**	3-Phase Faults, End Line†: From	3-Phase Faults, End Line†: Normal, Mva	3-Phase Faults, End Line†: Line Open Mva
Columbia-Coulee Number 1	72.4	60.6	310	163	Columbia	260	630
Columbia-Covington Number 1	110.6	92.4	240	192	Columbia	365	470
Coulee-Midway Number 1	100.4	84.1	300	169	Midway	230	500
Coulee-Snohomish	166.5	96.3*	250	212	Snohomish	410	410
Covington-Chehalis	69.4	58.1	230	200	Chehalis	430	430
Midway-North Bonneville Number 1	133.6	111.6	200	215	No. Bonn.	310	400
North Bonneville-Ross Number 2	36.2	29.4	200	202	Ross	500	1,040
North Bonneville-Troutdale Number 1	21.0	17.4	800	162	Troutdale	435	1,150

*Approximately 55% of the Coulee-Snohomish line is made up of the future Number 2 circuit paralleled with the Number 1 line.

**Impedance as listed is the approximate apparent impedance seen by the distance relays while the line was carrying the indicated loads.

†Representative 3-phase end-line faults shown are those from the line terminal given for both terminals closed, normal system, and with the terminal nearest the fault open, line open. Values are given in megavolt-amperes at 230 kv.

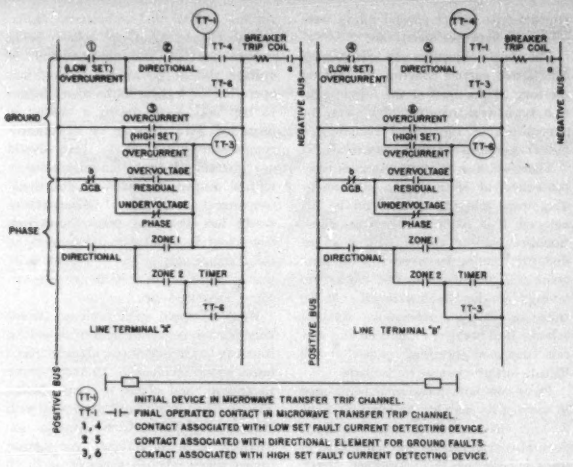

Figure 2. Microwave transfer trip circuits

ise of attaining the goal of clearing all faults in less than four cycles with present-day circuit breakers.

The fundamental advantage of microwave communication facilities for relaying is that since the protected line is not used for signal propagation, the chance of coincident failure of the high-voltage line insulation and of the communication channel can be reduced to a negligible factor. The facilities can be used for at least two general relaying methods—a transfer trip and a differential scheme. There are many variations of these, the two herein discussed are presented simply as possible methods.

For the microwave transfer trip scheme proposed, it is planned to use modified directional distance relays as the basic fault locators for phase faults. The scheme takes advantage of the fact that the zone-*1* distance relay elements at the far terminal will operate for end-zone phase faults, as seen from the near terminal.

For example, in a phase-to-phase fault near line terminal *B*, *TT-6* (transfer trip relay number *6*) in Figure 2 will be energized simultaneously with the trip coil of the circuit breaker at *B* by the first-zone distance relay contact. The *TT-6* contact at line terminal *A* would be closed in a time of one to three cycles permitting the second zone at terminal *A* to trip for this end-zone fault with negligible time delay. The *TT-6* relay at *B* operates the *TT-6* contact at *A* over the microwave facilities and auxiliary interposing relays at *A* and *B*.

There are available distance ground relays[9] which could be used for ground relay transfer trip in the same way as for phase faults. However the relaying system shown in Figure 2 presents a method which requires comparatively simple overcurrent elements.

For ground faults, this scheme provides for the use of two instantaneous overcurrent relays at each terminal. One of these is set to operate for low values of fault current (60 to 200 amperes primary), and the other, a so-called "high-set" overcurrent relay, will close its contacts in the range, 1,000 to 3,000 amperes. In addition, a separate directional element to operate in conjunction with the low-set overcurrent relay is required at each terminal. These relays energize transfer trip functions in a manner similar to that covered in the foregoing under phase relaying so that for most system conditions all ground faults can be relayed at both terminals in one cycle from fault initiation.

To cover those cases when a line is energized from only one end as when testing a faulty circuit, phase undervoltage and residual overvoltage relays interlocked with oil circuit breaker (*OCB*) auxiliary switches are proposed.

In order to attain an over-all clearing time of four cycles using 3-cycle circuit breakers, the fault-sensing relays and the microwave channel are required to completely transmit the transfer tripping or differential relaying intelligence in one cycle or less. This may be easily realized in practice. Bonneville Power Administration microwave equipment will provide full duplex voice channels having a transmission band flat within one decibel from 300 to 3,000 cycles. By the use of tone telegraph submultiplexing equipment, it is possible to subdivide the voice channel into one or more high-speed telegraph channels as shown in Table II. The figures in the table represent the theoretical maximum speed of each telegraph channel when the voice channel is submultiplexed by one or more telegraph channels. The finite delay due to electrical propagation in the microwave link and the delay inherent in relay end devices are neglected. Actually the total time requirements including the relay end devices will be about 0.75 cycle greater than the times shown in Table II.

The microwave transfer trip system, unlike present-day carrier relaying, will only be required to transmit relaying impulses when tripping is necessary. This poses a small problem in that it will probably be necessary to monitor the voice channel. This monitoring may easily be obtained by impressing a pilot tone at the bottom end of the voice band. This tone may be isolated from the relaying channels by[4] suitable electric filters. The microwave radio circuits are equipped with a failure alarm to signal the loss of radio-frequency carrier. Another possibility for monitoring of channel continuity is to use frequency-shift telegraphy in which case all relaying channels will at all times transmit a steady tone, the frequency of the tone being shifted when the channel is required to transmit a relaying signal. In this case, loss of any channel tone at the receiver would signal a channel or equipment failure and steps can then be immediately taken to restore service.

Initial equipment being acquired by the Bonneville Power Administration will not employ frequency-shift operation but will be of the amplitude-modulated on-off keyed carrier type, a type which is simpler in design, requires fewer com-

Table II. Theoretical Speed Capabilities of Submultiplex Microwave Channels

Number of Channels	Effective Bandwidth Per Channel, Cycles	Approximate Channel Transmission Time for Unit Step Impulse, 60-Cycle Basis, Cycles
1	2,700	1/12
2	1,200	1/18
3	750	1/8
4	375	1/4

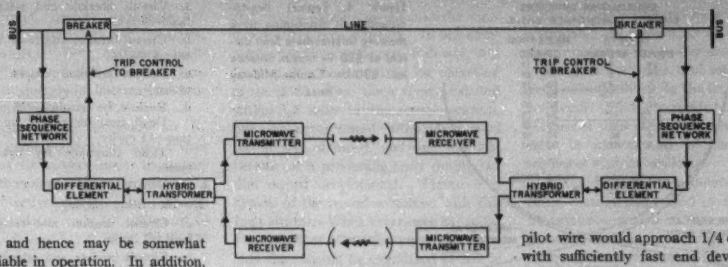

Figure 3. Microwave differential relaying circuits showing pilot-wire system applied to microwave

Arrows denote flow of relaying information

ponents, and hence may be somewhat more reliable in operation. In addition, extensive studies [10] of the relative merits of frequency-shift versus amplitude-modulated telegraph operation indicate that on circuits where the carrier-to-noise level is high and the system is relatively free from signal fading the two systems are essentially equivalent. It is recognized however that, under conditions of low carrier-to-noise ratio and heavy fading, the frequency-shift operation shows a marked improvement over amplitude modulation. This factor will probably be of little importance when operating over microwave radio links. The microwave system exhibits excellent level stability and a high signal-to-noise level at the demodulator output for all carrier-to-noise ratios above the improvement threshold of the system. It is, therefore, likely that except for an occasional outage due to tube failure the microwave relaying channels will be equivalent to or better than power-line carrier in reliability and many times superior to wire lines.

A relatively simple modification of the pilot-wire relay, of which several types are in use in the protection of short Bonneville Power Administration transmission lines, seems to offer a promising field for possible microwave differential relaying. With the microwave system, a 2-way full duplex channel of essentially lossless character may be established for any desired distance, and the limiting factor of present pilot-wire relay systems, namely, line loss, may be eliminated. The limiting distance to which existing pilot-wire relaying systems may be extended is controlled by phase shift of line currents and by the finite propagation delay of the radio channel. The propagation delay may be held to a minimum by delay-compensating networks at each end of the relaying channel, but the total residual delay is always equivalent to at least the line-current phase shift between the two relaying locations. For this reason, it now appears probable that present pilot-wire systems, when adapted to microwave, will find an upper limit of application at line lengths approaching 150 miles. For line lengths in excess of this distance the phase differences between comparison voltages derived from phase-sequence networks at near and distant terminals becomes such that the sensitivity of the relaying system as well as its ability to differentiate between fault and nonfault conditions are greatly reduced.

Figure 3 shows one simple arrangement by which a pilot-wire relaying system designed primarily for operation over wire lines might be successfully adapted to operation in connection with microwave. In order to establish a 2-wire connection at each end of the link it is necessary to employ the hybrids shown. Since the microwave link can transmit intelligence but no significant amount of relay operating power, it is necessary to reduce the normal relay voltages derived from the phase-sequence networks to a low level for transmission to the distant terminal and then employ an amplifier having a fixed gain to raise the received signal to proper level for relay operation. This introduces some complication but with relays of at least one type this can be largely offset, as studies indicate that the relay operating network may itself be used as the hybrid, thus eliminating the two hybrid transformers indicated in the drawing. By simple modifications in circuitry, the microwave channels, which are required to transmit differential relaying intelligence, may be obtained with the lower transmission band extending down to 50 cycles. In this case, by using a low-pass filter to pass frequencies between 50 and 600 cycles the channel may be used to derive simultaneously one pilot-wire channel and four transfer trip channels. Using a pilot-wire channel bandwidth from 50 to 300 cycles, the over-all channel transmission time for the pilot wire would approach 1/4 cycle, and, with sufficiently fast end devices, both ends of the channel could be reasonably expected to initiate breaker tripping in one cycle, which, with 3-cycle high-speed circuit breakers, would give a total line-clearing time of approximately four cycles.

Until experience has been obtained with the microwave facilities and the various relaying schemes tried on an experimental basis, it does not seem advisable to rely on any kind of microwave blocking system. In a blocking system, whether it be of the directional comparison, phase comparison, or of another differential type, a signal must be received from the remote end of an unfaulted circuit to prevent or block operation of the tripping elements for faults external to the line section. Use of two independent microwave channels would probably increase the reliability of a differential blocking system. While this would decrease the complexity of the relaying, it would do so at the expense of the microwave. On the other hand, by use of a transfer trip signal via the microwave channels, the only consequences of microwave failure are to delay clearing of the fault until the backup relays have functioned on the faulted line and possible reclosing failure.

Merely to adapt an existing relaying system to operate in connection with the microwave is not the primary aim of the relaying investigations now being carried on. It is ultimately expected that a completely electronic system will be developed which may in time employ thyratrons as a direct means of circuit breaker tripping with the resultant elimination of most mechanical end devices. There are several arguments for a system of this sort, chief among which may be cited the possibility of imposing almost zero burden on current and potential transformers and the further increase in relaying speed by the elimination of mechanical inertia inherent in present relays. Another argument for development of electronic relays is the ever present desire to achieve a more simple and universal relay operation.

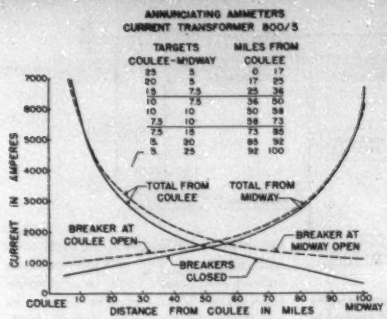

Figure 4. Typical line-to-ground fault distribution curve showing intermediate fault current at 230 kv versus distance for 230-kv Coulee-Midway lines

The vacuum tube with its flexibility and adaptiveness to design offers some important possibilities for investigation[11,12] and members of the Bonneville staff and others are actively exploring this new field. Several interesting electronic relaying systems have already been proposed and present plans call for an active development work in this field concurrent with the expansion of the Bonneville Power Administration microwave system.

Reclosing Program and Circuit Breaker Modernization

Analysis of the several system breakups experienced shows the need for an extensive high-speed reclosing program. In addition, growth of the system requires 230-kv reclosing circuit breakers of at least 10,000,000- and 7,500,000-kva capacity at several substations, many of which are now equipped with 2,500,000-kva nonreclosing breakers. It will be necessary to replace or rebuild a number of breakers for heavier fault-interrupting duty and for reclosing service. Existing equipment which is moved will be used in transformer positions or in other locations where interrupting and reclosing requirements are not severe.

Reclosing on transmission circuits is limited by at least four factors (for lightning-caused faults).

1. The circuit breaker must be capable of high-speed reclosure (12 to 20 cycles).
2. High-speed relaying must be provided which will initiate tripping simultaneously at all terminals of the protected transmission line for highest-speed reclosing.
3. Sufficient dead time must be allowed to permit deionization of the power arc path.
4. Adequate time must be allowed for long duration or repetitive lightning strokes.

Simultaneous high-speed tripping within one cycle of fault initiation must be provided by the relays at all terminals of the faulted transmission line for the fastest reclosing. Phase-comparison carrier relaying at present is not capable of attaining this ideal, but this goal appears possible using relaying over the microwave communication facilities.

Fault-arc deionization appears to be a function of fault duration, fault magnitude, the weather, fault configuration, and magnetic blowout of the arc. Tests indicate that duration and magnitude are the principal factors.[13] High-speed relaying and clearing at three cycles or less at all terminals of the faulted line are essential to successful high-speed reclosure, since these control the duration of the fault.

Data as to the time duration of lightning strokes to transmission circuits are not complete. Investigations involving high structures indicate that a small percentage of lightning strokes have a duration approaching one second in length. Indications are that the great majority of lightning strokes to transmission circuits have a time duration of less than 0.2 second.[14] Deionization time requirements for lightning arcs are believed to be of no appreciable consequence, so that reclosing in 12 cycles (0.2 second) or more will allow for most single repetitive lightning strokes.

Taking all of the above factors into account, it should soon be possible to successfully reach a reclosing time of 15 cycles assuming nearly simultaneous relaying at both line terminals.

To illustrate the importance of high-speed circuit breakers and relays, high-speed reclosing will be compared for limiting conditions—that is, reclosing, for an end of the line fault with high-speed relaying at both terminals and time-delay relaying in 15 cycles.

1. High-speed relaying—3-cycle circuit breakers
   a. Circuit breaker and relay nearest fault—3 cycles
   b. Circuit breaker and relay, far terminal—4 cycles
   c. Reclose terminal nearest fault—15 cycles
   d. Reclose, far terminal—16 cycles
      Dead time for power arc deionization—11 cycles
      Time allowance for lightning—15 cycles
      Line returned to service—16 cycles
2. Time delay relaying
   a. Circuit breaker and relay nearest fault—3 cycles
   b. Circuit breaker and relay, far terminal—18 cycles
   c. Reclose terminal nearest fault—29 cycles
   d. Reclose, far terminal—44 cycles
      Dead time for power arc deionization—11 cycles
      Time allowance for lightning—29 cycles
      Line returned to service—44 cycles

In the foregoing illustrations, the dead-time allowance for arc deionization, 11 cycles, may be longer than necessary where high-speed relaying and clearing is achieved at both terminals. Similarly the dead-time allowance for time-delay relaying may prove to be too short because of the greater deionizing action required for the longer-duration fault. The significant point is that the line cannot be returned to service in less than 44 cycles with 15-cycle relaying.

Fault Location and Automatic Recording

Closely related to system relaying, circuit interruption and reclosing are the problems of fault location and automatic recording. In order to achieve the maximum economy in system operation, transmission circuits must be loaded as heavily as stability considerations will permit. Consequently, it is essential that each point of system fault be investigated immediately after the occurrence of the trouble in order to correct and repair any damage, and, in the case of permanently faulted circuits, to quickly restore the line to service. Since a major portion of the Bonneville system network traverses mountainous terrain where patrol and inspection is difficult even during good weather and especially so during the winter time, and the vast majority of faults are transient in character, it can be seen that methods for quickly locating faults and checking system performance can save much time and money.

Among the devices in use on the Bonneville system for fault location are, of course, patrol by truck, helicopter, and foot; annunciating ammeters; capacitor

fault current devices; magnetic-link fault-current devices;[15] and pulse-type fault locators.[16,17,18,19] Automatic oscillographs[20] are also relied on for fault location and extensively for information about system troubles.

The annunciating ammeters are residual or ground-current-operated devices containing six targets similar in appearance to those found in the trip circuits of most protective relays. These targets and their related coils are calibrated to indicate values of 5, 7.5, 10, 15, 20, and 25 amperes rms.

Data from annunciating ammeters, although easily obtained, are subject to some inaccuracies. They respond to offset currents as well as to those which are symmetrical. Fault resistance is unknown. The current distribution is affected by the sequence of circuit breaker operations. For these reasons, it is necessary to consider other factors than the ammeter indication in estimating the location of a fault on a line.

Nevertheless, experience has been quite satisfactory with this device, considering its inexpensiveness and its simplicity. It is possible to predict successfully the location of faults to within 25 per cent of the line on the average. In some cases, this prediction has been narrowed appreciably from this figure.

Figure 4 shows the line-to-ground fault-current curves for a typical 230-kv transmission circuit. A tabulation of annunciating ammeter reading combinations derived from these curves is also given. As can be seen, a reading of 20 amperes at Coulee and 5 amperes at Midway on the faulted line indicates a fault location between 17 and 25 miles. This estimate, tempered by any other available data on the fault, is given the line patrolmen as the most likely location of the fault. Often because of the difficult-to-evaluate factors mentioned above, it is necessary to patrol several miles beyond the indicated section to actually locate the fault.

Another ground-fault current-measuring instrument in use on the system is one which charges a capacitor through a rectifier in proportion to the magnitude of the fault current. The charge is measured by observing the maximum deflection as the capacitor is discharged through a long time-constant *RC* circuit which includes a microammeter. Current curves similar to Figure 4 are referred to for estimating fault location.

The latest types of fault-location equipment in service include so-called pulse-type devices of various kinds. There have been two types of these in service on Bonneville lines (type *A*[18] and type *C*[17]), and a third is being installed in the summer of 1950 (type *B*[16,18,19]). In one summer's operation of the type-*C* device, of a total of five faults within its operating range of 83 miles, three were predicted within 1.5 miles of the actual location, one was never found, although a good record was obtained, and one was lost because of a processing error during the film record development. Figure 5 is typical of the records obtained with this fault locator. While experience has so far been excellent with these pulse-type locators, they should be considered as still in the development and trial stage. A possible application of the type-*A* instrument to automatic recording of lightning duration and wave shape is also being considered.

All of these pulse-type fault locators provide data only on fault location and not on system stability or performance. As such, failure of the device could result in a complete loss of all data were it the only fault-locating or automatic recorder in service.

Accordingly, it is felt that automatic oscillographs for the recording of currents and voltages in high-voltage transients, especially during system faults, are highly desirable to successful operation. Faults can be successfully located by means of data from these with an average accuracy of approximately five to ten per cent of a given transmission line. Information from these instruments will be invaluable for checking the performance of the other fault locators covered above. In addition, they will be indispensable for analyzing system performance and sequence of electrical events. Such occurrences as relay operations, circuit breaker tripping and reclosing, data on system stability, and machine performance can only be obtained from complete automatic records.

The automatic oscillograph does have limitations. It depends on fault-detecting relays for initiation, and its record length is limited. As a result, it does not completely monitor the power system for all types of disturbances and especially for cases of instability. In the latter, records are usually difficult to relate to each other because of their random nature. This results in inaccuracies in the analyzer studies of system breakups.

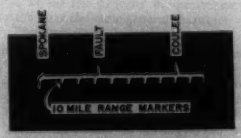

Figure 5. Typical pulse-type fault-locator record, type C

Instrument installed at Spokane substation. Line-to-ground fault on 230-kv Coulee–Spokane number 4 line at 8:43 p.m. on August 3, 1949. Fault estimated to be 33 miles from Spokane and actually found to be 34.5 miles from the station

It would be useful in determining machine characteristics and in deciding on transmission system additions or changes to know what happens to all the system elements for several seconds of a disturbance.

In some cases, the performance data for several minutes after the system trouble would be valuable. It would also be helpful to know the exact sequence of events. Many times after the breakup, out-of-phase switching will occur that causes relay operations which are sources of confusion in analyzing the disturbance. Since this switching is done manually, an automatic oscillograph usually provides little data.

For the above general reasons, Bonneville has been actively investigating the possibilities of a magnetic-tape recording instrument for continuous monitoring of the system. There has been issued an invitation to bid,[21] on a multichannel magnetic-tape recorder. The record which would be obtained from this device would be played into a manually controlled magnetic oscillograph which is operated at a slow speed for long-time records and at a high oscillograph speed for detailed analysis of a given transient.

While this system will be more expensive than automatic oscillographs and it will require more effort to obtain records, there is so much to be gained in improved knowledge of transmission-system performance that it is felt that the investment necessary for several tape recorders is more than justified. The data which can be obtained will be very useful in making complete studies of system disturbances, studies which may involve the future investment of millions of dollars in transmission capacity.

Thought has been given to a short-time 8- to 12-second continuous-loop magnetic-tape recorder. The information which it would provide in addition to that obtained from automatic oscillographs would cover the few cycles immediately preceding the occurrence of the transient which operates the fault-indicating relays. However, it is felt that this small bit of additional data would not warrant the additional complexity of the magnetic-tape system over magnetic oscillographs for short-time recorders.

Future Developments

The Administration will continue its policy of encouragement to relay manufacturers. It is interested in new developments which promise to simplify and to lessen time requirements for relaying, especially on long transmission lines.

When one considers the decrease in costs for 3-cycle 230-kv 7,500,000-kva and 10,000,000-kva reclosing circuit breakers alone, from about $100,000 to $50,000, the development and testing program of the circuit breaker manufacturers, the United States Bureau of Reclamation, and the Bonneville Power Administration can be seen to be more than justified. These lessening costs have been to a large extent attributable to developments which followed and were proved by tests on the Administration system.[23,24,34] This saving will apply to many future installations not only on the Bonneville system but on other transmission networks.

Among the new developments, which the authors believe should be taken under consideration by the manufacturers, is a circuit breaker still faster than the 3-cycle circuit breakers. It does not seem that too many advances need to be made in order to obtain a 2-cycle high-capacity circuit breaker. When the improvements made in interrupting capacity in just the last few years from two and a half million kva to over 10 million kva are considered, this speed-up in interrupting time does not seem at all out of line.

While adequate interrupting capacity is essential, the lower fault-interrupting duties must, of course, be kept in mind. The great preponderance of the fault interruptions required of a 10,000,000 kva circuit breaker on the Bonneville system is in the range from 2 to 25 per cent of interrupting rating. It is as essential that these be interrupted at high speed as for the heavier faults.

The question immediately arises as to the real need for a 2-cycle circuit breaker when 3-cycle equipment is now available. It is believed that the development can be easily justified and is in fact warranted to go along with anticipated relaying improvements. First of all, system stability will be improved. The initial shock due to the fault will be decreased. Bonneville Power Administration studies indicate that fault-arc deionization will be more rapid because of shorter fault duration. Hence it is likely that faster reclosing will be possible. The over-all result is an improvement in stability, an increase in system-load capabilities, and improved service. While the gains appear small percentagewise, they are in actuality large when measured against transmission-system investment.

While it is perhaps oversimplifying a complex subject to apply percentage multipliers to the total system, it can be unhesitatingly stated that faster relaying, fault clearing, and reclosing can be evaluated at several million dollars.

References

1. Characteristics of a 400-Mile 230-Kv Series-Capacitor-Compensated Transmission System, **B. V. Hoard.** *AIEE Transactions*, volume 65, 1946, pages 1102–14.

2. A Distance Relay With Adjustable Phase-Angle Discrimination, **S. L. Goldsborough.** *Electrical Engineering* (*AIEE Transactions*), volume 63, November 1944, pages 835–38.

3. The MHO Distance Relay, **R. M. Hutchinson.** *Electrical Engineering* (*AIEE Transactions*), volume 65, June 1946, pages 353–60.

4. A Graphical Method for Estimating the Performance of Distance Relays During Faults and Power Swings, **A. R. van C. Warrington.** *AIEE Transactions*, volume 68, part I, 1949, pages 608–21.

5. An Analysis to Determine the Optimum Burning Arrangements for Transmission Capabilities at Grand Coulee, **B. V. Hoard, G. W. Bills.** *AIEE Transactions*, volume 63, 1944, pages 1259–64.

6. A New Carrier Relaying System, **T. R. Hallman, S. L. Goldsborough, H. W. Lensner, A. F. Dromps.** *Electrical Engineering* (*AIEE Transactions*), volume 62, August 1944, pages 568–72.

7. Phase-Comparison Carrier-Current Relaying, **A. J. McConnell, T. A. Cramer, H. T. Seeley.** *Electrical Engineering* (*AIEE Transactions*), volume 64, December 1945, pages 825–33.

8. Microwaves Supplement Present Channels, **R. F. Stevens.** *Electrical World* (New York, N. Y.), volume 131, number 1, January 1, 1949, page 39.

9. A New Distance Ground Relay, **S. L. Goldsborough.** *AIEE Transactions*, volume 67, 1948, pages 1442–46.

10. Frequency Shift Telegraphy—Radio and Wire Applications, **J. R. Davey, A. L. Matte.** *AIEE Transactions*, volume 66, 1947, pages 479–93.

11. Electronic Protective Relays, **R. H. Macpherson, A. R. van C. Warrington, A. J. McConnell.** *AIEE Transactions*, volume 67, part II, 1948, pages 1702–08.

12. Electronic Relay Developments, **James J. Loving, Jr.** *AIEE Transactions*, volume 68, part I, 1949, pages 233–40.

13. Deionization Time of High-Voltage Fault-Arc Paths, **E. J. Harrington, E. C. Starr.** *AIEE Transactions*, volume 68, part II, 1949, pages 997–1003.

14. Electrical Transmission and Distribution Book. Westinghouse Electric Corporation (East Pittsburgh, Pa.), Chapter 12, 1944.

15. Fault-Current Measuring Devices, **Martin J. Lantz.** *Electrical Engineering* (*AIEE Transactions*), volume 65, December 1946, pages 839–43.

16. A Transmission Line Fault Locator Using Fault-Generated Surges, **R. F. Stevens, T. W. Stringfield.** *AIEE Transactions*, volume 67, part II, 1948, pages 1168–79.

17. A Transient Fault Locator for High-Voltage Transmission Lines, **L. R. Spaulding, C. C. Diemond.** *AIEE Transactions*, volume 68, part II, 1949, pages 1005–10.

18. Fault Location by Pulse Time Modulation, **R. W. Hughes, Nelson Weintraub.** *Electrical Engineering*, volume 69, November 1950, pages 1009–11.

19. Microwave Application to the Bonneville Power Administration System, **R. F. Stevens, T. W. Stringfield.** *AIEE Transactions*, volume 69, part II, 1950, pages 1088–99.

20. Application of Automatic Oscillographs to High Voltage Transmission Lines, **A. J. McConnell.** *Distribution* (Schenectady, N. Y.), volume 12, January 1950, pages 13–16.

21. Magnetic Tape Recorder. *Invitation to Bid number 5036*, Bonneville Power Administration (Portland, Ore.), February 27, 1950.

22. A 230-Kv 3-Cycle Oil Circuit Breaker for Extra-Heavy Arc Rupturing Duty, **W. M. Leeds, G. B. Cushing.** *AIEE Transactions*, volume 67, part I, 1948, pages 236–42.

23. Unusual Performance of Standard 230-Kv Impulse and Tank-Type Oil Circuit Breakers on Field Tests, **E. B. Rietz.** *AIEE Transactions*, volume 67, part I, 1948, pages 267–70.

24. Field Tests for Development of 10,000,000-Kva 230-Kv Oil Circuit Breakers for Grand Coulee Power Plant, **C. L. Killgore, W. H. Clagett.** *AIEE Transactions*, volume 67, 1948, pages 271–87.

Discussion

W. A. Morgan and **R. W. World** (Bureau of Reclamation, Denver, Colo.): The authors are to be commended on a thorough presentation of a complex subject. Those of us who have heard partial information from time to time on the Bonneville relaying program have had most of our questions answered by this paper.

The Bureau of Reclamation is interested in any new ideas or devices that will improve system performance, because any improvements actually result in large savings in system design costs in the future. The application of microwave channels for speeding up relaying appears to be feasible, and we know of other systems where it may be used if it proves to be practical and economical. Also, the encouragement given to the further development of electronic relays is given a second from the Bureau as this will mean a step toward the goal of maximum speed and simplicity in relaying. When one looks at a complicated mechanism such as a relay or a governor for a hydroturbine, it is not difficult to imagine that these devices with their inertia and friction will some day be replaced by electronic tubes.

With regard to the use of transfer tripping, instead of blocking, on microwave, it appears that there is some advantage for reliable transfer tripping on a 2-terminal line. In fact, it would be desirable to have a transfer tripping scheme sufficiently reliable so that fault detectors would not be required at the receiving terminals. The authors did not bring out the greater advantage of transfer tripping to be found on lines having more than two terminals. The use of these multiterminal lines is an economic necessity in some cases, and it appears that simultaneous tripping would be possible with transfer tripping, whereas sequential tripping is usually all that is possible with blocking-type carrier relaying, because of the mutual impedance effect and

other causes. However, the Bureau has had difficulty with a carrier transfer trip scheme and it is hoped that similar difficulties are not experienced with transfer tripping by microwave.

It is understood that it is planned to have high-speed circuit breaker reclosing on the interim relaying scheme which will use phase-comparison carrier relaying, even though simultaneous clearing for all 3-phase faults will admittedly not be possible. The authors realize they are taking a calculated risk. It is desired to point out that this risk may not be tolerable on other systems where the percentage of 3-phase faults is greater than on the BPA which does not have continuous overhead ground wires. The BPA probably can show data to indicate that perhaps only 2 per cent of their total faults are three-phase. However, other systems having overhead ground wires on steel towers in New York as well as the Tennessee Valley Authority,[1] have records to show that as many as 30 per cent of the total faults are of the 3-phase type and this may be explained by analysis. It is to be recognized, of course, that the total number of faults on a system with overhead ground wires would be only a fraction of that for a system without overhead ground wires for the same lightning frequency. BPA is fortunate in being in a low lightning frequency area, but it is believed that frequent system break-ups might result if this policy were used in a higher frequency lightning area. Thus, it is desired to point out that most systems which have overhead ground wires might find it risky to minimize the importance of 3-phase faults and use phase-comparison carrier rather than the conventional carrier current relaying.

The Bureau of Reclamation's experience with special long-line type distance carrier has been good. It is believed that one of the causes for BPA to turn away from carrier was their experience with improper ground-relay operation because of the interleaved Coulee bus. However, now that the Bureau is installing 10,000,000-kva interrupting duty circuit breakers, all busses will be solidly, electrically connected together at Coulee power plants and the difficulties from use of the interleaved bus should not again occur. So, it is felt that we should not unjustly condemn carrier relaying but should look at the facts on both sides of the case. If this is done it is believed that carrier relaying can do a good job, if given a chance.

The scheme the authors propose for preventing false tripping of distance relays upon accidental loss of potential has possibilities. Where fault currents permit, as on long lines, why not use the overcurrent relays as independent tripping elements and offset all three zone elements to exclude the origin? Then, memory action would no longer be needed; tripping would be fast and positive when closing on a near fault; there would be fewer contacts in series in the tripping circuit; separate directional elements could be eliminated; the characteristic circles of all three zones would be smaller to give better assurance against undesired tripping during power swings without sacrificing speed in clearing faults; incorrect directional element operation resulting from capacitor potential device transients would be prevented; and relay targets would provide greater indication of fault location. The only adverse effect of capacitor potential device transients would be to slow up the distance element pick-up for faults near the balance point, an unimportant consideration on long lines where far-end faults do not greatly depress the station voltage.

In conclusion, I would like to say that the Bureau has recognized the weakness of using line potential as compared to bus potential in that a distance relay cannot distinguish direction when reclosing on a close-in fault using line potential. It has been our policy to use bus potential wherever possible without having to switch bus potential.

Reference

1. Performance of 161-Kv and 115-Kv Transmission Lines, K. E. Hapgood, C. P. Almon, Jr. *AIEE Transactions*, volume 66, 1947, pages 863–69.

J. L. Blackburn and **S. L. Goldsborough** (Westinghouse Electric Corporation, Newark, N. J.): This paper is a valuable contribution in outlining the relay practices and thinking of a large power system for the protection of their major transmission network. There are a number of statements on which more information would be helpful. Other parts require further amplification particularly since they might well lead to false conclusions unless one appreciates the background and reasoning behind them.

Under the section in the paper on Distance Relaying it is stated that out-of-step blocking is being deactivated. This has some merit since, as pointed out, it may be difficult to separate the system at designated points during all operating conditions. On the other hand since the system may be separated at any number of points or several points, it would seem that the dispatcher and operators of the several stations must be well trained to reconnect the system with a minimum of delay.

It is indicated that product-type ground relays are not suitable on long transmission lines for back-up protection. More information on this would be helpful as general experience does not substantiate the authors conclusion. There are two aspects of back-up protection: secondary protection over the primary relays (in this case carrier or pilot wire) for the protected section and: back-up protection for the adjacent line sections.

For the first case, over-all faster relaying times are usually possible with the product-type relays. It should be remembered that all of the several forms of induction-type relays operate on the square of the electrical quantity, or on the product of quantities and as such have the same general characteristics. The degree of inverseness can be controlled within limits as has been done in the conventional induction relays. In the product-type relay only the very inverse type has been made because this characteristic seems best suited to the multiple grounded systems in common use.

In many cases the second type of back-up protection is difficult if not impossible to obtain on multiple grounded systems with any type of induction relay design or curve. This is particularly true where the relays are set to back-up the main section as well as the adjacent section. Instantaneous overcurrent relays can often be applied to protect a major portion of the main line section so that the induction overcurrent relays can be set on the basis of operating for the end zone faults and backing up the adjacent section. For the close-in faults covered by the instantaneous element the induction relay will be operating "off the curve." This is a good compromise as long as the heavy faults do not exceed the short-time thermal limit of the induction relay.

It would be interesting to know whether or not consideration was given to the use of distance relays for ground fault protection.

Under the section on Carrier Relaying it is stated that slow operation of the carrier relaying resulted from the limited reach of straight impedance and reactance relays. It would be well to clarify the meaning of this paragraph. Also it is not clear as to what is meant by the statement that the carrier relaying is dependent upon the proper operation of the distance relays, particularly when they are retained to supplement the phase comparison carrier relays.

The occasional failure of the directional element in the directional comparison carrier scheme to respond to a close in 3-phase fault is treated as a disadvantage of this type of equipment. However, in considering the phase-comparison scheme it is noted that complete 3-phase fault protection may not be possible but in this case several reasons are given as to why this 3-phase failure is not important. It would seem that if this later argument is applied to the directional comparison scheme, then more complete protection would result using the directional comparison scheme.

In this connection there seems to be a feeling that the directional distance carrier scheme is extremely complicated while the phase-comparison carrier scheme is not. This is a matter of relativity. The first scheme has more mechanical elements and contacts while the second has more electronic circuits. Over-all (eliminating the additional back-up elements) both schemes appear about equally complex. Also field experience shows good reliability for both schemes. Hence, where both are applicable, the choice seems to depend largely on whether one prefers to place his "eggs" in an electronic or a mechanical "basket."

The statement is made that times as high as 15 cycles in clearing faults have been measured on the directional comparison carrier relays. It would be helpful to know more specifically the conditions under which these times have been obtained.

The method of transfer trip may have advantages over the carrier blocking schemes as pointed out. Such schemes simplify the relaying circuits but require a considerable amount of electronic equipment which may not be economically justified for relaying alone. The use of the microwave channel for many other functions will make it available for relaying provided the relaying terminals coincide with the terminals for the other services.

C. C. Diemond and **D. L. Wylie:** We thank the reviewers for their comments and suggestions as well as for the questions that were raised.

The experience of the Bonneville Power Administration, with respect to frequency of 3-phase faults on the 230-kv system, is quite different than that reported by W. A. Morgan and R. W. World. A review of the record for a typical pair of long 230-kv lines

for the period November 1946 to May 1950 shows a total of 30 faults. All of these were 1-line-to-ground except one which was 2-phase-to-ground. Data were obtained from automatic oscillographs and are typical for our 230-kv system.

We can recall no more than three 230-kv 3-phase faults during the past three years. The system has been monitored during this time by automatic oscillographs which are applied to about 75 per cent of the 230-kv network and which respond to well over 90 per cent of all 230-kv faults. As previously mentioned in our paper one aim of the line performance improvement program is to reduce multiphase faults through reduction of tower footing resistances and the judicious use of overhead ground wire.

With regard to the risk of minimizing the importance of 3-phase faults, we believe that the combination of long line distance relays and phase comparison carrier will give better performance on our system than most other carrier relaying methods for well over 99 per cent of all faults which might occur. Further, the risk to system operation entailed in relying on second zone distance relays for an extremely rare low magnitude 3-phase fault is not great.

With reference to the comments of Mr. Morgan and Mr. World on the effect of the interleaved bus system on directional comparison carrier ground relay operation, mutual impedance effects remain with us in many places on the system even though the interleaved bus operation is eliminated at Coulee. Even there, with the 230-kv system solidly bussed (no interleaved scheme), mutual coupling between the 115-kv Spokane lines and the 230-kv Coulee-Spokane lines give carrier relaying difficulties similar to those previously encountered with the interleaved 230-kv scheme. Phase comparison relaying should be essentially unaffected.

J. L. Blackburn and S. L. Goldsborough have requested additional information on experience with product-type ground relays. These relays have given serious co-ordination problems on long parallel transmission lines where mutual impedance effects are significant. We agree with their comment that usually faster relaying times are possible with product-type relays. However, where mutual impedance is a problem we have not always been able to obtain these fast relaying times with product-type relays. As an example, in one case on the system where potential polarized product-type relays are used, the relay energy (that is, the product of residual current and residual potential) is essentially identical for a far end of the line fault when the relay must trip and for a near end of the line fault on the parallel circuit where the relay must not trip. If the relaying energy is unchanged between these two faults, no time difference between the two can be obtained regardless of the shape of the relay time current curve.

Carrier relaying has given slow operation, for several reasons, the following of which are believed to be the most probable:

1. Slow operation of distance elements for faults near the balance point. In considering this point, it should be remembered that the discussion in the paper refers to the old style distance relay in which the reach of the third zone distance element, which starts carrier to permit operation of the carrier relaying, is reduced for phase-to-phase faults by 15 per cent, due to the use of Y-current connections. While it is true that this 15 per cent reduction could have been eliminated since we were dispensing with out-of-step trip blocking, other considerations in addition to this one, dictated the need for changes.

2. The possible slow reset of distance elements when energized from line side potentials with its consequent continuance of a carrier blocking signal from the open terminal of the faulted line.

3. The effect on directional or product-type carrier ground relays of zero sequence mutual impedances.

4. The effect on these carrier ground relays of small residual potentials from potential devices.

We cannot agree with the comment about failure of the directional elements in the directional carrier scheme. In the case of directional comparison carrier relaying, failure of the distance relaying for a 3-phase fault could result in absence of tripping by either the carrier or distance relays. On the other hand, the use of phase-comparison carrier with distance relays gives two essentially independent relaying systems for almost 100 per cent of the faults. Three-phase faults which may not be recognized by the distance relays are usually near and of heavy magnitude. Phase comparison relays, being current operated, should respond to these near, heavy magnitude faults. Those 3-phase faults which the phase-comparison equipment may not recognize are of low magnitude and are usually located some distance out on the line. This is the region where the long-line distance relay can be set to operate to best advantage and where all three (phase) distance relays as well as the phase comparison relays must fail in order to result in a failure to trip.

In response to the general questions contained in both discussions about the value of directional comparison carrier relaying, we would like to emphasize that experience indicated that the equipment installed on the long heavily-loaded lines required extensive modification or replacement. We had the choice of using either the newer long-line distance relay directional comparison equipment or phase-comparison carrier. The latter was selected to operate in conjunction with long-line distance relays for reasons given in the paper.

While we recognize that directional comparison carrier has a definite and proper field of application in protective relaying and we expect to use the scheme in certain locations on the system, we feel that the problem of adequately relaying the long heavily-loaded BPA circuits can be better solved by use of the methods proposed in our paper.

Development of Preferred Voltage Ratings for Transformers

H. P. ST. CLAIR
FELLOW AIEE

H. M. JALONACK
MEMBER AIEE

SINCE publication in May 1949 of the Edison Electric Institute—National Electrical Manufacturers Association report on Preferred Voltage Ratings for A-C Systems and Equipment,[1] many requests have been made for further explanation of the basis for the voltage ratings and taps of both power and distribution transformers covered in Tables 9 and 10 of that report. Since it was not feasible to include all of this material in the report itself, the purpose of this paper is to describe the surveys and other studies which led to the adoption of these values.

Historical Background

As pointed out in the Foreword of the 1949 report, the first attempt at voltage standardization of transformers was a report issued by the National Electric Light Association Electrical Apparatus Committee in 1922. After trial use, this was found inadequate and further study by a joint NELA-NEMA committee culminated in the publication of the 1930 Joint Report.[2]

Again it was found after a few years' experience that the transformer ratios and taps recommended in this report were not suitable for a great many, perhaps the majority, of modern systems. For example, intermediate voltage power transformers, 23 kv to 69 kv, stepping down to 2,500 volts, 7,500 volts, and so forth, from the flat ratings of 22 kv, 33 kv, 44 kv, and 66 kv with all taps below, did not give the proper ratios for average system levels in use, such as 24 kv, 34.5 kv, 46 kv, and 69 kv. As a result, utility companies generally were not buying transformers in accordance with the 1930 report. There also were reported some cases of overvoltage complaints from power customers served at one of these transmission voltages where customer-owned transformers had been purchased in accordance with the 1930 report.

Survey Procedure to Determine Existing Practices and Requirements

The new joint EEI-NEMA Committee was set up in 1938 to revise the 1930 report. It was recognized that one of the first requirements of the job would be to find out what voltage levels and transformer ratios were being used generally for power transformer applications throughout the industry. Likewise, in the lower voltages commonly used for distribution, the necessity for revisions and extensions of the 1930 report had been recognized and work by a joint EEI-NEMA Committee on Standards for Distribution Transformers was started at about the same time.

The usual method of making a survey by questionnaire was followed, the first set of questionnaires being sent out late in 1941. Although valuable information was obtained, further study of the transformer problem indicated that additional data would be needed, particularly for the intermediate voltage classes 23 kv to 69 kv. Accordingly, a second questionnaire was circulated covering this group of system voltages and requesting information as follows:

1. Normal operating transmission voltage levels:
   a. At supply points, such as generating stations or substation sources.
   b. At average intermediate points.
   c. At outlying points, extremities of system.
2. Voltage ratings and taps on step-down transformers:
   a. On prevailing types of transformers now in use.
   b. As specified for new purchases.
3. Most frequently used tap setting or settings.
4. Voltage range on low side of distribution supply stations (ahead of feeder regulators if used):
   a. Maximum.
   b. Average.
5. Lamp voltage rating recommended to customers on system.

When the EEI-NEMA Joint Committee on Standards for Distribution Transformers was formed in 1938, it had the benefit of the very considerable amount of thought and study which had been given previously to the study of voltage ratings and voltage taps in the distribution transformer field, all of which was carefully reviewed. The ini-

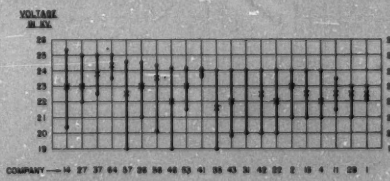

Figure 1. Range of operating voltages for 23-kv systems as reported in questionnaire replies

Average level at intermediate system points indicated by "X"

Paper 50-166, recommended by the AIEE Transformers Committee and approved by the AIEE Technical Program Committee for presentation at the AIEE Summer and Pacific General Meeting, Pasadena, Calif., June 12–16, 1950. Manuscript submitted March 15, 1950; made available for printing May 9, 1950.

H. P. St. Clair is with the American Gas and Electric Service Corporation, New York, N. Y., and H. M. Jalonack is with the General Electric Company, Pittsfield, Mass.

The authors wish to acknowledge the co-operative efforts of all of the other members of the Joint EEI-NEMA Committee on Preferred Voltage, who collaborated in this phase of the Committee's assignment. Particular acknowledgment is made of the large amount of work contributed by the late W. R. Markley and of the more recent participation on the Transformer Working Group by T. J. Brosnan.

Figure 2. Range of operating voltages for 34.5-kv systems as reported in questionnaire replies

Average level at intermediate system points indicated by "X"

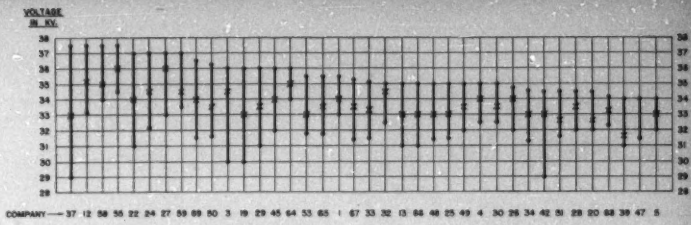

tial scope of the committee work was in the field of high-voltage ratings, 2,400 to 15,000 volts, with low-voltage ratings 600 volts and below. Several reports covering these voltage classes were issued, the first in 1940 on single-phase pole-type units up to 25 kva. Later reports extended the range through 500 kva and included 3-phase as well as single-phase units.

The large amount of data and advice obtained by and made available to this Committee for an intensive and intelligent study of the distribution transformer situation included:

1. Considerable information on usage as reported by the transformer manufacturers.

2. Previous studies of distribution transformer voltages by various operating groups.

3. The substantial background knowledge of the utility members of the Joint Committee.

4. Consultation with the AIEE Subcommittee on Industrial Power Applications.

5. The advice and help through questionnaires of 130 user companies throughout the United States.

6. A final review by the Transmission and Distribution Committee of the Edison Electric Institute.

From all of this it can be said that a great deal of intensive work went into the selection of the ratings chosen and it is believed that all viewpoints were most carefully considered before the standards were established.

Figure 3. Range of operating voltages for 46-kv systems as reported in questionnaire replies

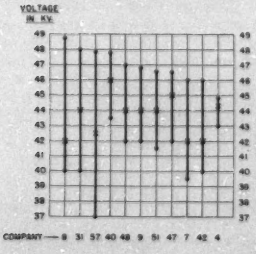

The term "distribution transformer" has been used extensively in statistical and manufacturing classifications to denote transformers for light, power, or general purpose applications in kilovolt-ampere ratings, 500 kva and smaller, regardless of voltage. However, in actual usage the classification is not that clearly defined since transformers over 500 kva may be used for distribution while transformers 500 kva and smaller may be used as substation units in power transmission. In the work of the EEI-NEMA Committee on Preferred Voltage Ratings for A-C Systems and Equipment, it was decided to handle the situation in the following way:

a. To consider as one group those ratings commonly classified as distribution transformers and manufactured in regular quantity production, specifically those 500 kva and smaller, high voltage 15,000 volts and below, low voltage 600 volts and below.

b. To consider as a separate group those transformers, 500 kva and smaller, with high voltages above 15,000 volts, also commonly called "distribution transformers." For this group it was planned to utilize high-voltage ratings and taps consistent with larger sizes for general power purposes, keeping in mind fundamental data available on transformers having low voltages of 600 volts and below.

Results of Survey—Power Transformers

The most effective summary of existing practices with respect to voltage levels, transformer ratios, and taps, and so forth, was obtained by plotting the results of the survey on a series of charts. These proved to be very helpful and will be used in this paper in describing the basis for our final conclusions.

The first basic picture was the range of operating voltage levels, shown in Figures 1 to 4 inclusive. In these figures it will be noted that the range for each company system is indicated by a vertical line, and the average voltage at intermediate points is marked by a cross on this line.

The next picture obtained from the survey covered the ratios and taps in use on existing transformers, the most frequently used taps, and the taps specified for new purchases.

In studying this information as received from questionnaire replies, it was found that many systems used transformer ratios and taps which followed early historical patterns. Except for the 46-kv class, this pattern was based on transformers with 2,300-volt secondaries or multiples thereof and primaries of 22,000, 33,000, and 66,000 volts, with $2^1/_2$-per cent taps, usually all below these values. Since a 2,300-volt secondary has long since been recognized as too low, the 2,400-and 2,500-volt secondaries were adopted, still keeping the same equivalent ratios by increasing the primary voltage ratings in proportion. For example a 33,000/2,300-volt transformer became 35,900/2,500 volts. In the 46-kv systems the basic historical ratio appeared to be 44,000/2,400 volts, giving an equivalent of 45,800/2,500 volts.

In order to summarize these results and present them in a clear, graphical form,

Figure 4 (right). Range of operating voltages for 69-kv systems as reported in questionnaire replies

Average level at intermediate system points indicated by "X"

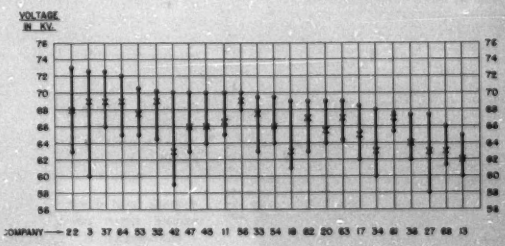

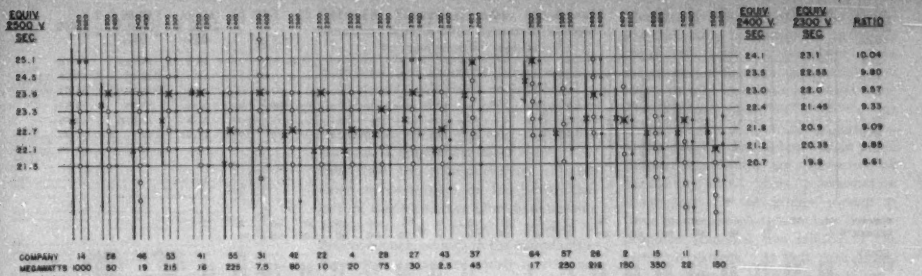

Figure 5. Operating voltage range and transformer taps for 23-kv systems as reported in questionnaire replies

Horizontal lines represent ratios based on historical 2,300-volt secondaries

Figures 5 to 8 inclusive were prepared. It will be noted that the horizontal lines in these figures represent a given ratio which is based on the prevailing historical ratio mentioned above. For example, in Figure 6 showing 34.5-kv systems, the horizontal lines correspond to ratios which for a 2,300-volt secondary would represent primary ratings of 33,000 volts with exact $2^1/_2$-per cent taps. To cover all of the ratings reported, eight horizontal lines are included in the figure. Since these horizontal lines represent fixed ratios, the same lines can be used with equivalent primary voltages to represent transformers with other secondary ratings, such as 2,400 or 2,500 volts. This has been done as indicated on the figures, the equivalent primary voltages for 2,500-volt secondaries being given at the left side of the figure. It will be noted further that the practices of each of the reporting companies were represented on these figures by three vertical lines, the left line being the voltage range, repeated from Figures 1 to 4 inclusive. The center line shows the prevailing pattern of transformer taps now in service, while the line on the right shows the taps currently specified for new purchases. The numbers at the top of the two vertical lines indicate the actual secondary voltage rating used or specified for new purchases. From these figures it is possible to determine the complete voltage rating of the transformer. For example, company number 56 was actually using mostly 2,300-volt secondaries, and by referring to the primary voltage ratings under equivalent 2,300-volt secondary at the right side of the figure, it will be seen that these transformers have 22,000-volt primaries with four $2^1/_2$-per cent taps below. The figure 2,400 at the top of the third vertical line over company 56 indicates that new transformers are being purchased with 2,400-volt secondaries and with primary ratings of 23,000 volts. It should be noted that the secondary ratings at the top of the vertical lines have been shown only in terms of 2,300, 2,400, 2,500 volts, and so forth, even though multiples of these voltages, such as 7,200, 7,500 and so forth, actually were used. Also under each company number at the bottom of the vertical lines is indicated the approximate load of the particular system, or portion of the system, on which these transformers were used. The middle vertical line, showing existing transformer taps, also includes a designation of the most frequently used tap.

Table I. Proposed Preferred Voltage Ratings 23-Kv and 34.5-Kv Classes

Ratio	Group I, 2,500 Volts Secondary	Group II, 2,375 Volts Secondary	6-Tap, 2,500 Volts Secondary	Historical, 2,300 Volts Secondary
10.04		23,900	25,100	
9.80		23,300	24,500	
9.57	23,900	22,700	23,900	22,000
9.33	23,300	22,100	23,300	21,450
9.09	22,700	21,500	22,700	20,900
8.85	22,100		22,100	20,350
8.61	21,500		21,500	19,800
15.08		35,900		
14.72		35,000	36,800	
14.36	35,900	34,100	35,900	33,000
14.00	35,000	33,200	35,000	32,175
13.64	34,100	32,300	34,100	31,350
13.28	33,200		33,200	30,525
12.92	32,300		32,300	29,700
12.56			31,400	

Table II. Proposed Preferred Voltage Ratings 46-Kv and 69-Kv Classes

Ratio	Group I, 2,500 Volts Secondary	Group II, 2,375 Volts Secondary	6-Tap, 2,500 Volts Secondary	Historical, 2,400 Volts Secondary
19.76		47,000		
19.28		45,800	48,200	
18.80	47,000	44,600	47,000	
18.32	45,800	43,400	45,800	44,000
17.84	44,600	42,200	44,600	42,900
17.36	43,400		43,400	41,800
16.88	42,200		42,200	40,700
16.40			41,000	39,600
30.16		71,800		
29.44		70,000	73,600	
28.72	71,800	68,200	71,800	68,000
28.00	70,000	66,400	70,000	64,350
27.28	68,200	64,600	68,200	62,700
26.56	66,400		66,400	61,050
25.84	64,600		64,600	59,400
25.12			62,800	

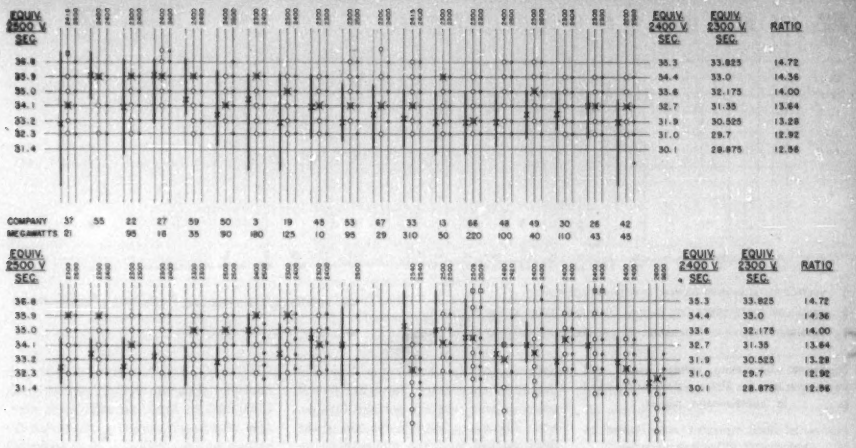

Figure 6. Operating voltage range and transformer taps for 34.5-kv systems as reported in questionnaire replies

Horizontal lines represent ratios based on historical 2,300-volt secondaries

Determination of Voltage Ratings and Taps—Power Transformers

The basic information summarized in these four figures was used as a starting point to discuss possible standards for ratios and taps which would meet the requirements of the greatest possible number of users. In the light of the range of operating voltages and variation in transformer ratios and taps now in use, it was immediately recognized that a single standard transformer with a 10-per cent tap range would not cover all of the industry requirements in any of the four voltage classes. One suggestion for providing a greater range without going above four taps was to use larger steps. For example, four $3^1/_2$-per cent taps would increase the range to $13^1/_2$-per cent, while 4-per cent steps would increase it to 16 per cent. It was the general concensus of opinion, however, based on thorough discussion within the Committee as well as further study of questionnaire replies, that such a departure from present generally used $2^1/_2$-per cent steps would not be acceptable, first, because they would not match existing transformers from a paralleling standpoint, and, second, because the steps were considered by many to be too large. While it is undoubtedly true that the importance of exact matching of transformer ratios in parallel operation is very often overemphasized, nevertheless it was quite evident that adher-

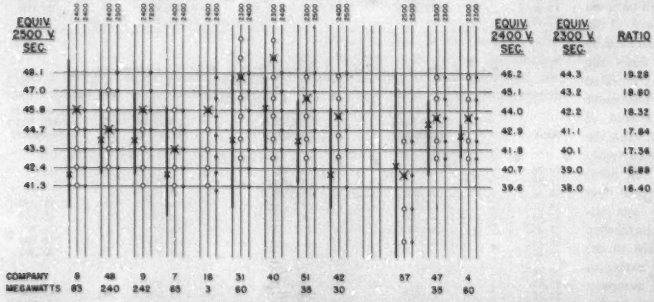

Figure 7. Operating voltage range and transformer taps for 46-kv systems as reported in questionnaire replies

Horizontal lines represent ratios based on historical 2,400-volt secondaries

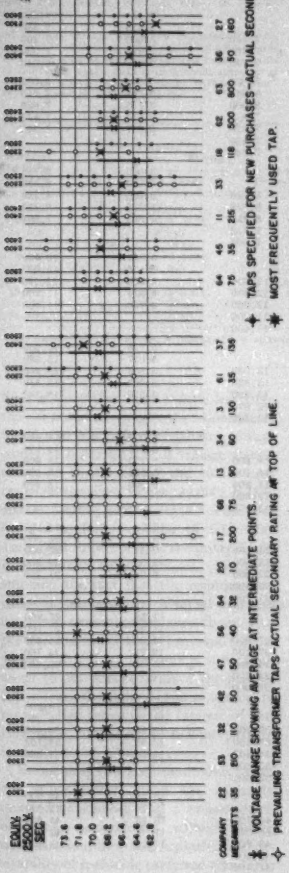

Figure 8. Operating voltage range and transformer taps for 69-kv systems as reported in questionnaire replies

Horizontal lines represent ratios based on historical 2,300-volt secondaries

ence to the traditional $2^1/_2$-per cent taps with ratios based on the actual historical voltage ratios most frequently used would enjoy the greatest acceptance and adoption by the industry.

The next step considered for obtaining in a single standard transformer the necessary tap range to meet the majority of industry requirements was to increase the number of $2^1/_2$-per cent taps above the present standard number of four. At this time the manufacturers, through their representatives on the Joint Committee, made a sincere effort to determine whether or not it would be possible to realize enough savings in the manufacturing cost of a standard widely used transformer to offset the greater inherent cost of supplying five $2^1/_2$-per cent taps or six $2^1/_2$-per cent taps, as against the adoption of two or more standard 4-tap transformers, each covering a different voltage range. Referring again to the figures, it was apparent that a 6-tap transformer would cover practically all of the system requirements reported, and that in two out of the four voltage classes a 5-tap transformer would go a long way in that direction. A choice was not required, however, as the manufacturers, after a thorough study over a considerable period of time, came up with the conclusion that the increased cost of developing and manufacturing even a 5-tap transformer, as against the present 4-tap design, could not be offset by the savings due to standardization even though such a transformer were generally adopted.

At this point, therefore, the Committee worked out, with the aid of the figures, the two groups of 4-tap transformers which appeared best suited to the requirements of the great majority of the operating companies as reported in the replies to questionnaires. These two groups differed only in the secondary voltage ratings, the primary winding and taps being the same for both. The original idea was to use a 2,500-volt secondary (or multiples thereof) for Group-I transformers, those suitable, in general, for distribution supply stations, and to use a secondary winding 5 per cent lower, or 2,375 volts, for Group II, those generally intended to take care of industrial customers requiring lower voltages than distribution systems. Group-II transformers also could be used, on a slightly overexcited basis, on systems where the transmission voltage is somewhat above the average range considered for transformers in Group I.

The reason for suggesting 2,375-volt secondaries for Group II instead of the more common 2,400-volt secondaries was to provide a full 5-per cent difference between the two groups so that the resulting ratios would match correctly on three overlapping tap positions. This feature was believed to be valuable to permit the use of both types of transformers on one system and still retain the possibility of exact parallel operation on three taps. This original proposal for each of the four voltage classes, 23 kv to 69 kv, inclusive, is illustrated in Tables I and II, in which the equivalent ratios are represented on horizontal lines. This representation shows how the two groups overlap at three points and also shows how the new proposed standard was related to the historical pattern. At that time it also was felt desirable to suggest the tap rat-

Table III. Proposed Preferred Voltage Ratings (First Revision) 23-Kv and 69-Kv Classes

Ratio (Average)	Group I, 2,520-Volts Secondary	Group II, 2,400-Volts Secondary	Historical, 2,300-Volts Secondary
10.04	24,100		
9.80	23,500		
9.55	24,100	22,900	22,000
9.3	23,500	22,300	21,450
9.05	22,900	21,700	20,900
8.85	22,300		20,350
8.60	21,700		19,800
15.1	36,200		
14.70	35,300		
14.35	36,200	34,400	33,000
14.0	35,300	33,500	32,175
13.6	34,400	32,600	31,350
13.3	33,500		30,525
12.9	32,600		29,700

Table IV. Proposed Preferred Voltage Ratings (First Revision) 46-Kv and 69-Kv Classes

Ratio (Average)	Group I, 2,520-Volts Secondary	Group II, 2,400-Volts Secondary	Historical 2,300-Volts Secondary
19.75	47,400		
19.25	46,200		
18.80	47,400	45,000	
18.3	46,200	43,800	44,000
17.8	45,000	42,600	42,900
17.3	43,800		41,800
16.9	42,600		40,700
16.40			39,600
30.2	72,200		
29.4	70,600		
28.7	72,200	68,800	66,000
28.0	70,600	67,000	64,350
27.25	68,800	65,200	62,700
26.5	67,000		61,050
25.9	65,200		59,400

Table V. Pattern of Taps for Transformers in Voltage Classes 115-Kv to 230-Kv Inclusive

Voltage Class	Proposed Taps	Voltage Class	Proposed Taps
115-kv	116,000	138-kv	139,200
	113,000		135,600
	110,000		132,000
	107,000		128,400
	104,000		124,800
154-kv	162,400	230-kv	232,000
	158,200		226,000
	154,000		220,000
	149,800		214,000
	145,600		208,000

ings to be used in case a 6-tap transformer was desired by a given customer in spite of failure to include such a transformer as a standard.

Subsequent deliberation by the Committee, and reactions obtained from many users, led to the conclusion that it would be better to retain the familiar 2,400-volt secondary for the Group-II transformers and to increase the Group-I secondary to 2,520 volts, thereby retaining approximately the 5-per cent differential between the two groups. This revision was carried out, still matching historical ratios, simply by increasing the primary voltages of both groups approximately in proportion to the increase in the secondary voltage. The result of this revision is shown in Tables III and IV. The 6-tap transformer was deleted from the table at this time as it was felt that its inclusion would give a false indication of its status as a preferred standard.

In spite of the fact that the range of primary voltages and taps covered by these tables was selected with a view to giving the best coverage of existing requirements as shown in Figures 1 to 8, a subsequent circulation of the proposals among various company groups brought out sufficient data to substantiate a request for a downward adjustment in the voltage ratings of two of the classes, namely, the 46-kv and 69-kv systems. Although this differed from our first interpretation of Figures 7 and 8, it was decided to make this change, particularly since in any case there is a factor of judgment involved in selecting the best tap range for the data given in the figures. Accordingly, in Table IV the top voltage tap was removed and one additional tap added at the lower end of the range for each of these voltage classes.

While reference has been made in all of the preceding discussion to $2^1/_2$-per cent taps, it was decided rather early in the Committee's study that the tap spacings for all of these voltages should be rounded off to fairly even numbers, even though this resulted in ratios which might differ by a fraction of a per cent from the existing historical ratios. In the first place, the practical limitations in design and manufacture do not produce exact ratios without a certain allowable tolerance, and in the second place, a small discrepancy in ratio, even as high as 1 per cent, is not a real handicap for parallel operation and may even be used to advantage to offset moderate differences in transformer reactance. Keeping these considerations in mind, as well as the desirability of obtaining, if possible, a

Table VI.* Step-Down Power Transformers

Preferred Voltage Ratings

Nominal System Voltage, Volts	Transformer Voltage Designation, Kv	Step-down Power Transformers High-Voltage Rating and Tap Voltages: Group I Ratio	Group I 2,520 Volts Low Voltage	Group II Ratio	Group II 2,400 Volts Low Voltage
7,200	7.2			3.15	7,560
				3.075	7,380
		3.000	7,560	3.000	7,200
		2.928	7,380	2.925	7,020
		2.857	7,200**	2.850	6,840
7,620	7.6	2.786	7,020	3.331	8,000
		2.714	6,840	3.254	7,810
		3.174	8,000	3.175	7,620
		3.099	7,810	3.054	7,430
		3.023	7,620	3.017	7,240
		2.948	7,430		
		2.873	7,240		
8,320	8.3			3.640	8,736
				3.523	8,528
		3.466	8,736	3.508	8,320
		3.384	8,528	3.380	8,112
		3.301	8,320	3.293	7,904
		3.219	8,112		
		3.136	7,904		
12,000	12.0			5.250	12,600
				5.125	12,300
		5.000	12,600	5.000	12,000
		4.881	12,300	4.875	11,700
		4.762	12,000	4.750	11,400
		4.643	11,700		
		4.563	11,400		
13,200	13.2			5.775	13,860
				5.637	13,530
		5.500	13,860	5.500	13,200
		5.369	13,530	5.362	12,870
		5.238	13,200	5.225	12,540
		5.107	12,870		
		4.976	12,540		
14,400	14.4			6.000	14,400
				5.875	14,100
		5.714	14,400	5.750	13,800
		5.595	14,100	5.625	13,500
		5.476	13,800	5.500	13,200
		5.357	13,500		
		5.238	13,200		
23,000	23.0			10.04	24,100
				9.79	23,500
		9.56	24,100	9.54	22,900
		9.32	23,500	9.29	22,300
		9.09	22,900	9.04	21,700
		8.85	22,300		
		8.61	21,700		
27,600	27.6			11.58	27,800
				11.29	27,100
		11.03	27,800	11.00	26,400
		10.75	27,100	10.71	25,700
		10.475	26,400	10.42	25,000
		10.20	25,700		
		9.92	25,000		
34,500	34.5			15.08	36,200
				14.71	35,300
		14.36	36,200	14.33	34,400
		14.01	35,300	13.96	33,500
		13.65	34,400	13.58	32,600
		13.29	33,500		
		12.94	32,600		
46,000	46.0			19.25	48,200
				18.75	45,000
		18.33	46,200	18.25	43,800
		17.85	45,000	17.75	42,600
		17.35	43,800	17.25	41,400
		16.90	42,600		
		16.43	41,400		
69,000	69.0			29.42	70,600
				28.67	68,800
		28.02	70,600	27.92	67,000
		27.30	68,800	27.17	65,200
		26.58	67,000	26.42	63,400
		25.88	65,200		
		25.16	63,400		
115,000	115.0			48.33	116,000
				47.08	113,000
		46.03	116,000	45.83	110,000
		44.84	113,000	44.58	107,000
		43.65	110,000	43.33	104,000
		42.46	107,000		
		41.27	104,000		

Notes to Table VI.

* Reproduced from Table IX, reference 1 of this paper.

** Performance characteristics should be specified on the basis of the tap voltage rating shown in bold-face type in the table.

If more than four taps are required for the high-voltage winding, it is recommended that, if possible, the tap voltages given in the table be used with additional taps above or below, using same voltage steps (for example, 900 volt steps for 34.5-kv transformers).

All voltage ratings should be full-rated kilovolt-amperes. Also, in accordance with ASA Standards C-57, the transformers are required to be capable of delivering rated output in kilovolt-amperes at 5 per cent above rated low voltage, without exceeding the specified temperature rise.

If a low-voltage rating higher than 2,520 volts is required, it is recommended that the desired low-voltage rating be chosen for use with the preferred high-voltage rating so as to secure matching overlapping ratios with the transformer having a low-voltage rating of 2,520 volts; for example, a low-voltage rating of 2,940 volts should have three matching overlapping ratios with the transformer having a low-voltage rating of 2,520 volts. If other low-voltage ratings are required, they should be selected in steps of 60 volts, that is, $2^1/_2$-per cent steps on a 2,400-volt basis.

For low-voltage ratings for transformers for use on systems with nominal voltages higher than 2,400, multiples of 126 (5,040 for 40 base voltage, and so forth) should be used for Group-I transformers and multiples of 120 (4,800 for 40 base voltage) should be used for Group-II transformers. The preferred secondary voltages for systems 20 base voltage to 120 base voltage, inclusive, are tabulated below:

Nominal System Voltage	Low-Voltage Rating			
	Group I		Group II	
	Single-Phase	Three-Phase	Single-Phase	Three-Phase
2,400	2,520	2,520	2,400	2,400
4,160	2,520/4,360Y	4,360	2,400/4,160Y	4,160
4,800	5,040	5,040	4,800	4,800
7,200	7,560	7,560	7,200†	7,200†
8,320	5,040/8,720Y	8,720	4,800/8,320Y	8,320
12,000	12,600	12,600	12,000	12,000
12,470		13,090	7,200/12,470Y†	12,470†
13,200	7,960/13,800Y	13,800	7,620/13,200Y	13,200
13,200			13,200	13,200
14,400			14,400	14,400

† For industrial applications, a preferred low-voltage rating is 6,900 or 6,900/11,950Y.

little more rather than a little less than the 10-per cent range, the Committee found that a satisfactory pattern of taps would be obtained for all voltage classes above 23 kv by basing the 10-per cent range on the even values, 24,000, 36,000, 48,000, 72,000, and so forth. This procedure resulted in steps of 600, 900, 1,200, and 1,800 volts for the tap spacings in these four voltage classes. Notwithstanding the fact that the resulting tap range in terms of the nominal voltages for these classes comes out about 10.4 per cent instead of 10 per cent, and for the 46-kv and 69-kv transformers it also exceeds 10 per cent in terms of the highest tap rating, the manufacturers agreed to provide this range in the interest of setting up a simplified, consistent pattern in these voltage classes.

No mention has been made thus far of the 27.6-kv class, which was originally omitted as somewhat of a nonstandard, or at least nonpreferred, voltage. Later consideration, however, indicated the desirability of including preferred standards for this voltage also, since it represents a considerable volume of usage even though concentrated in a few large systems. For this voltage the logical interval between taps was obviously 700 volts, corresponding to a 10-per cent range based on 28,000 volts.

Consideration also was given to voltages above 69 kv, and a considerable amount of information was brought together both from the users and manufacturers bearing on the selection of a pattern of voltage ratings and taps for these higher voltages. Obviously, at these ratings, particularly above 138 kv, the more common voltage transformations would be stepping down to intermediate transmission voltages of perhaps 23 kv and above rather than to the various distribution voltages. In spite of this, however, it was agreed by both the power system and the manufacturers' representatives that it would be highly desirable to continue the same consistent pattern as that adopted for the 23-kv to 69-kv range, extending this to all of the higher voltages, 115 kv, 138 kv, 161 kv, and 230 kv. Table V shows this extended pattern, omitting, of course, the classification into two groups.

In the final preparation of the transformers tables for publication in the Joint Report on Preferred Voltage Ratings it was decided to include only the voltage class up through 115 kv, since this might be considered a dividing line between transformers stepping down to distribution voltages and those stepping down to intermediate transmission. Although the higher voltages were omitted from the tables, the pattern of taps listed in Table V of this paper was agreed upon by both utility and manufacturers' representatives as constituting a sound basis for standards. Thus, this pattern of taps, extended to the higher voltages and approved both by the EEI and NEMA representatives, now is considered as equally standard with units having the conventional four $2^1/_2$-per cent taps, even though the tap range based on the highest tap specified is slightly in excess of 10 per cent.

In Tables I through IV the numerical ratios shown are approximate values based on the historical ratings included in these tables. In the final preparation of figures for Table 9 of the Joint Report, historical ratings were not included and the exact ratios resulting from the even pattern of taps were worked out and shown separately for each group, that is, for the 2,400-volt and 2,520-volt secondaries. As already pointed out, the overlapping taps are not exact but in all cases the deviation is relatively small, usually less than one-half per cent, and in no case in excess of three-fourths of 1 per cent. In regard to the voltage to be designated as the *transformer rating*, it is obvious that the process by which these transformer tap voltages were derived does not provide any one voltage which corresponds exactly with the nominal system voltage class for that transformer. The transformers, however, can still be referred to by the nominal voltage class designation and the matter would be of no further importance except that, from the designer's standpoint, it is necessary to designate one of the actual voltage ratings or taps on which to base his fundamental design characteristics. Since each of these transformers has five voltage connections, any one of which may be used in operation, it is obviously logical to base the transformer design upon the middle voltage and to designate this voltage as the rating at the transformer. This has been done throughout all of the transformer ratings included in Table 9 of the published Joint Report, such ratings being shown in heavy type.

As previously pointed out, in all of the tables and charts and in the final table of the report secondary voltage ratings have been given as 2,520 for Group I and 2,400 for Group II. The same tables, of course, will apply to various other standard distribution voltage ratings, and these are designated for each of the two groups in a separate table included as a footnote to Table 9 in the Report, reproduced herewith as Table VI.

Determination of Voltage Ratings and Taps—Distribution Transformers

In the following discussion reference will be made to the Joint Report on Pre-

ferred Voltage Ratings, Tables 10, 10A, and 10B, which are reproduced in this paper as Table VII A and B.

In determining the voltage ratings of distribution transformers 500 kva and smaller, 15,000 volts and below, certain factors were immediately evident:

1. The 120-volt base was well established and in general use on transformers in this classification.

2. For considerations of economy in manufacture, stocking, handling, and usage, a minimum number of alternate voltage ratings was desirable.

3. Due weight and preference should be given to the well-established primary voltages. A voltage in very small usage would not constitute the basis for standardization merely because it existed.

4. Combination units embracing several primary or secondary voltage classes would be utilized where practical.

5. The size, range, and location of the taps would have to factor the normal and permissible ratings of motor and control equipment.

6. The kilovolt-ampere ratings for each voltage combination would have to be given careful consideration in the interests of economy and because all kilovolt-ampere ratings were not needed in all voltage classes.

Referring to Table VIIA, the first column is that of primary voltages. The 2,400-volt class utilized for 2,400-volt delta systems or 4,160-volt Y systems was an obvious choice—throughout the complete kilovolt-ampere range. The usage of a 4,160-volt delta transformer was rather limited in the larger ratings but there had existed a steady demand in the smaller kilovolt-ampere ratings for this unit for connection line-to-line on a 4,160-volt system and occasionally for line-to-neutral on a 7,200-volt Y system. This unit was, therefore, included through 100 kva.

The 4,800-volt class was also in wide usage and was again an obvious choice. The necessity of units rated 2,400×4,800 volts was carefully reviewed and it was found that a great many companies either operated both systems or were in the process of changing from one system to the other. The double rating 2,400 ×4,800 volts therefore was retained.

The usage of 7,200-volt transformers for either 7,200-volt delta or 12,470-volt Y systems was sufficiently widespread to justify standardization throughout the kilovolt-ampere range. For rural work there had developed a strong demand in the small kilovolt-ampere ratings for a single-bushing transformer designed for use on a 12,470-volt/7,200-volt multigrounded system. This rating therefore was included through 25 kva.

There had been considerable utilization of 7,620-volt transformers for application on 13,200-Y volt systems. This rating therefore was included in the complete range through 500 kva and in the single-bushing grounded-Y rating through 25 kva. The application of this rated unit to existing systems operating at 7,940/13,800-volt Y level will be discussed later.

Long-established systems in the 12,000-volt delta class indicated the necessity of providing a delta voltage standard for this rating.

In the next higher voltage class considerable confusion existed in voltage ratings. For many years there had existed a standard rating of 13,800 volts to 115/230 volts. Later this was superseded by a rating of 13,200 volts to 120/240 volts. However, because of the difference in ratio, many users continued to specify the previous standard. If the previous standard were to be rerated on a 120-volt base, its rating would become 14,400 volts to 120/240 volts. This would match the top level of some systems but would be altogether too high for the systems actually operating at 13,200 volts. On the other hand, the usage hardly justified having two complete sets of ratings all the way through 500 kva. The final result was a compromise in which the two ratings were combined in sizes 3 to 100 kva, providing a voltage spread from 14,400 volts all the way down to 12,540 volts. In the ratings above 100 kva two lines were standardized: a 13,200-volt line with conventional voltage taps, and a 14,400-volt line with taps at 14,100, 13,800, 13,500, and 13,200 volts. Although not a perfect answer, this solution has proved an economical and generally acceptable answer to a rather difficult problem.

Other primary voltages in actual service were considered and left out of the standards because their comparatively limited usage did not justify their addition to a list of distribution transformer ratings already seriously overburdened by a multiplicity of voltages, kilovolt-ampere ratings, and tap combinations. Among the voltages omitted for this reason were 2,080/4,160, 2,170, 2,200/-3,810Y, 3,415, 5,500, 6,900, and 16,500 volts.

The selection of the secondary voltage ratings was considerably easier than that of the primary. The use of 120/240 volts for series, multiple, or 3-wire was widespread in the small and intermediate ratings and of 240/120 volts, 3-wire in the larger sizes. The former combination therefore was standardized through 167 kva, and the latter in ratings 250-500 kva. A 600-volt secondary rating also was necessary for those sections of the country where 550-volt industrial applications were widespread.

In the class between, covering 240-volt and 480-volt applications in a single transformer, the main question was which sizes should be rated 240/480 volts, making them suitable for 240 volts, 480 volts, or 480/240 volts 3-wire. The 3-wire connection was needed by some users in some sizes. Others wanted this connection available for grounding the middle of one leg of the low-voltage delta. On the other hand, this type of secondary requires interlacing of the two halves of the secondary winding which would add materially to the cost in the larger kilovolt-ampere ratings. The alternative rating would be 240 × 480 volts which provides 240 volts or 480 volts but not the 3-wire connection. Here again the advice of a large majority of users indicated a compromise in which sizes up to and including 100 kva were rated 240/480 volts and sizes 167-500 kva were rated 240 × 480 volts.

The final aspect of the voltage rating, and one that was the hardest to determine, was the matter of taps. The problems here were: first, on which standard transformers should taps be omitted altogether; and second, where should the taps be located when included. A range of 10 per cent and a total of four taps were quickly conceded to be adequate except in the 13,200/14,400-volt class already discussed.

It will be noted that in the 2,400-volt, 4,800-volt, and 2,400 × 4,800-volt classes there are lines of standard transformers without taps, the limit being 50 kva in the 2,400-volt and 4,800-volt class and 167 kva in the 2,400 × 4,800-volt class. A very substantial usage of these nontapped transformers has prevailed for many years. Furthermore, such units were obviously simpler and less expensive to build than the tapped units. However, in this voltage and kilovolt-ampere class there also existed the need for tapped units, some users requiring the taps to match older 9-to-1 systems, others to adjust the voltage to that best suited to the various supply requirements on their particular systems. This was recognized in the 2,400-volt and 4,800-volt units by making an alternate standard line with taps. In the case of the 4,160-volt units, the demand was not sufficient to justify both tapped and nontapped units; the tapped units, representing a more universal usage were, therefore, standardized. In the case of the 2,400 × 4,800 transformers the difficulty of making such

Table VII. Distribution Transformers*

Preferred Voltage Ratings

The Joint Committee on Preferred Voltage Ratings concurs with and reproduces herewith the recommendations contained in the Fourth Report[4] of the EEI-NEMA Joint Committee on Standards for Distribution Transformers for voltage ratings of transformers having high-voltage ratings 14,400 volts and below, with low-voltage ratings 600 volts and below; and in sizes up to 500 kva, inclusive.

The low-voltage ratings of these transformers are all on a 120-volt base. In general, where high-voltage taps are provided on units having low-voltage ratings for lighting service (120/240, 240/120, or 208Y/120), the taps are located below rated voltage; and on units having low-voltage ratings for motor service (240, 480, 240/480, 240 × 480, and 600), the taps are located equally above and below rated voltage. Exception is made in the case of 7,620 volts where the taps on units with lighting secondaries are above and below to meet the joint needs of 7,620- and 8,000-volt systems and on 14,400-volt units where definite voltages are selected as shown to combine several classes in ratings 100 kva and smaller and to provide paralleling ratios on larger kilovolt-ampere ratings in the same voltage class. Also, for certain industrial applications involving use of 3-phase units, indoors at load centers or power centers, the taps on transformers with 208Y/120 low-voltage rating are located equally above and below rated voltage.

For voltage ratings of distribution transformers (500 kilovolt amperes and smaller) with low-voltage rating 2,400 volts and above, and also for those with high voltage ratings above 14,400 volts, the preferred voltages are the same as those shown for power transformer in Table VI.

Table VIIA. Single-Phase Distribution Transformers

Transformers with low voltage rated 120/240 volts or rated 240/480 volts are suitable for series or parallel or 3-wire operation at full kilovolt-ampere rating. Transformers, with low voltage rated 240 × 480 are suitable for operation at 240 volts or 480 volts but not suitable for operation at both voltages simultaneously.

Transformers with low voltage rated 240/120 volts are suitable for 3-wire operation at full kilovolt-ampere rating but are not suitable for multiple operation at 120 volts.

High-Voltage Rating	High-Voltage Taps: Above	High-Voltage Taps: Below	Minimum and Maximum Kva Ratings for Low-Voltage Ratings of: 120/240	240/120	240/480	240×480	600
2,400	None	None	3–50				
2,400	None	4–2½%	3–167	250–500			
2,400	2–2½%	2–2½%			3–100	167–500	3–500
4,160	None	4–2½%	3–100				
4,160	2–2½%	2–2½%			3–100		
4,800	None	None	3–50				
4,800	None	4–2½%	3–167	250–500			
4,800	2–2½%	2–2½%			3–100	167–500	3–500
2400 x 4,800	None	None	3–167	250–500	3–100	167–500	3–500
12,470 Grd Y/7,200	None	None	3–5††				
12,470 Grd Y/7,200	None	4–2½%	3–25††				
7,200	None	4–2½%	3–167	250–500			
7,200	2–2½%	2–2½%			3–100	167–500	3–500
13,200 Grd Y/7,620	None	None	3–5††				
13,200 Grd Y/7,620	2–2½%	2–2½%	3–25††				
7,620	2–2½%	2–2½%	3–167	250–500	3–100	167–500	3–500
12,000	None	4–2½%	3–167	250–500			
12,000	2–2½%	2–2½%			3–100	167–500	3–500
13,200	None	4–2½%	167	250–500			
13,200	2–2½%	2–2½%				167–500	167–500
14,400	None	{14,100/13,800/ 13,500/13,200	167	250–500		167–500	167–500
14,400/13,200**	None	{13,800/13,200/ 12,870/12,540†	3–100		3–100		3–100

* Reproduced from Table 10, reference 1 of this paper. ** Electrical performance characteristics shall be at 14,400 volts.

† Transformers in this class, 100 kva and smaller, are designed to cover in one rating the general voltage range 13,000–15,000 volts. The lowest voltage shall be reduced kilovolt-ampere rating. All other voltages shall be at rated kilovolt amperes. †† One high-voltage bushing only.

Table VIIB. Three-Phase Distribution Transformers

Transformers with low voltage rated 208Y/120 volts are suitable for 208Y/120-volt 4-wire operation, but not for 120-volt 3-wire delta operation, and on such transformers for certain applications indoors, at load centers or power centers, the standard high-voltage taps should be 2–2½-per cent full kilovolt-ampere taps below and 2–2½-per cent full kilovolt-ampere taps above rated voltage. Transformers with low voltage rated 240 × 480 volts are suitable for operation at 240 volts or 480 volts but not suitable for operation at both voltages simultaneously.

For certain industrial applications involving the use of 75–500 kva, 3-phase, units used indoors at load centers, low-voltage ratings of 240 volts delta or 480 volts delta or 480Y/277 volts or 600Y/346 volts should be considered as an alternate preferred voltage rating.

To provide for industrial distribution at a level suitable for 6,600-volt motors and control equipment, a high-voltage rating of 6,900 volts used with low-voltage ratings in multiples of 120 volts should be considered an alternate preferred voltage rating for 3-phase transformers. Taps on such units should be the same percentage taps and located similarly to those used for the 7,200-volt high-voltage ratings having the same low-voltage ratings.

High-Voltage Rating	High-Voltage Taps: Above	High-Voltage Taps: Below	Minimum and Maximum Kva Ratings for Low-Voltage Ratings of: 208Y/120	240* Delta or 480 Delta	240×480 Delta*	600 Delta
2,400 volt delta, or						
4,160 Y or	None	None	9–75	9–45	75	9–75
4,800 delta or	None	4–2½%	112½–500			
8,320 Y	2–2½%	2–2½%			112½–500	112½–500
	1–5%	1–5%		9–45	75	9–75
4,160 delta	None	2–5%	9–75			
	None	4–2½%	112½–500			
	None	2–5%	9–75			
7,200 delta	None	4–2½%	112½–500			
	1–5%	1–5%		9–45	75	9–75
	2–2½%	2–2½%			112½–500	112½–500
	None	2–5%	15–75			
12,000 delta or	None	4–2½%	112½–500			
12,470 Y	1–5%	1–5%		15–45	75	15–75
	2–2½%	2–2½%			112½–500	112½–500
13,200 Y	1–5%	1–5%	15–75	15–45	75	15–75
	2–2½%	2–2½%	112½–500		112½–500	112½–500
13,200 delta	None	4–2½%	112½–500			
	2–2½%	2–2½%			112½–500	112½–500
14,400 delta	None	{14,100/13,800/ 13,500/13,200	112½–500		112½–500	112½–500
14,400/13,200 delta**	None	13,800/13,200	15–75	15–45	75	15–75

* For transformers 150 kva and smaller, a 120-volt reduced kva lighting tap shall be available. ** Electrical performance characteristics shall be at 14,400 volts.

units suitable for both series-parallel connection and taps led to the adoption of the simpler units without taps as standard.

In the 7,200-volt and 7,620-volt class, the Second Report[3] of the EEI-NEMA Joint Committee established the smaller kilovolt-ampere ratings as standard without taps. However, this did not prove generally acceptable and a resurvey among users of these voltage classes indicated a preponderant desire for taps even in these smaller ratings. A minority of companies felt that transformers without taps should continue as standard. Therefore, to provide for further observation and study, single-bushing transformers in the 3-kva and 5-kva ratings, 7,200-volt and 7,620-volt ratings, were standardized both with and without taps. In this connection the following comments quoted from the Fourth Report[4] of the Joint EEI-NEMA Committee on Standards for Distribution Transformers are pertinent:

"Although some system conditions make taps a necessity for immediate needs, users are urged to study system voltage levels and auxiliary means of regulating voltage with the objective of obtaining the maximum economies from the use of standard non-tapped transformers. Tapped transformers will be available for those situations where omission of taps appears impractical, but it is urged that the nontapped standard units be used wherever possible."

On the remaining ratings, except as previously noted, taps were standardized throughout in accordance with indicated usage, both as to magnitude and application needs.

The position of the taps on those units where taps are standard is also very important. For units having lighting secondaries, that is, 120/240 volts, there was unanimous agreement that below-normal taps should be provided. Except for one case in the 7,620-volt class, which will be mentioned later, the general standard for such units, therefore, became four $2^1/_2$-per cent taps below rated voltage on the high side.

In considering transformers used to supply motors and control, involving secondaries of 240/480 volts, 240 × 480 volts, or 600 volts, consultation with the AIEE Subcommittee on Industrial Power Applications brought out the need for taps above rated voltage, as well as taps below, in order to deliver a lower secondary voltage which would more nearly match the normal motor and control voltage ratings of 220, 440, and 550 volts. As a result, for such transformers two $2^1/_2$-per cent taps above and two $2^1/_2$-per cent taps below rated voltage were provided. In the earlier Joint Committee Reports these taps were applied only to voltage levels having ratings of 5,000 volts and below. It quickly became evident, however, that the same considerations existed at levels above 5,000 volts so that the practice was extended to higher voltages as well. In the 13,200 and 14,400-volt class, a special range of taps, as previously described, was worked out to adapt a single transformer to both voltage classes.

Although most of the users in the 7,620-volt class actually operated at 7,620 volts to neutral, there existed some usage at 7,980 volts (or 8,000 volts) based on a line-to-line system voltage of 13,800 volts. To obtain the maximum benefits of standardization, it was decided to provide two $2^1/_2$-per cent taps above and below rated voltage on 7,620-volt units regardless of the secondary rating, thereby making one standard unit applicable to either system voltage.

The preceding discussion describes the basis for the selection of voltage and tap ratings on single-phase distribution transformers. The problems involved in a similar selection for 3-phase units were very much the same, although several additional factors were involved. The study and consultation process with users followed the same general pattern as that carried out for single-phase units.

Table VII shows the voltage and tap standards applying to 3-phase units, together with pertinent notes applying to load center applications and to 6,600-volt motor and control installations. In this table it will be noted that these 3-phase primary voltage ratings are substantially the same as those for single-phase units. On the other hand, since the single-phase units, up through 7,620 volts, are designed suitable for either line-to-neutral or line-to-line connections, the corresponding 3-phase units necessarily have such additional primary ratings as 4,160 volts Y, 8,320 volts Y, 12,470 volts Y, and 13,200 volts Y. The delta primary ratings included 2,400 volts, 4,160 volts, 4,800 volts (the 2,400×4,800 volts standard was omitted as being too complicated for 3-phase units), 7,200 volts, 12,000 volts, 13,200 volts, and 14,400 volts, the latter two being combined in one unit for ratings 75 kva and smaller. The 7,620-volt rating was omitted on the basis that there is no recognized usage on delta systems of that voltage.

The low-voltage ratings group themselves naturally into the well-established secondary voltages, 208 Y/120, 240 volts delta, 480 volts delta, and 600 volts delta. In ratings 75 kva and above, the 240-volt and 480-volt units were combined into a single unit rated 240×480 volts delta.

A feature requested by many operators and included in the standard is a 120-volt, reduced kilovolt-ampere lighting tap for such transformers 150 kva and smaller.

The growing usage of 480Y/277 volts or 600Y/346 volts in industrial plants was recognized by the selection of these Y-connected secondary units as alternative standards for such applications.

On 3-phase units in the 2,400-volt delta, 4,160-volt Y, 4,800-volt delta, and 8,320-volt Y classes with ratings 75 kva and smaller, the standard units were established without taps. On other ratings the general pattern was a 10-per cent total tap range, using four $2^1/_2$-per cent taps on ratings $112^1/_2$ to 500 kva and two 5-per cent taps on ratings 75 kva and smaller. This was a natural simplification since there are three times as many taps on a 3-phase unit as there are on a single-phase unit.

The location of the taps on these 3-phase transformers followed substantially the single-phase practice, the taps where provided being above and below rated voltage for transformers with secondary ratings of 240 volts, 480 volts, 240 × 480 volts and 600 volts. The taps for the 208Y/120 volts were obviously all below rated voltage, thereby matching the 120/240 volts and 240/120-volt tap position on the single-phase units.

Conclusions

In describing with as much detail as we have in this paper the step-by-step process of developing preferred voltage ratings for transformers, it is the authors' hope that we have shown convincingly that the resulting standards were not set up in a casual manner, but on the contrary represent the result of a tremendous amount of thought, work, and study carried out over a considerable period of time.

While it goes without saying that these standards are not perfect, nevertheless it is believed that the process of development was such that they will be adaptable to the majority of systems, at least to the maximum extent that can be expected from any set of standards.

While the adoption of these standards in no way prevents users from obtaining ratings other than those specifically listed, at the same time it is desirable that every possible effort be exerted to utilize these standards where they can be applied.

This will result in the greatest economy from an over-all standpoint and will prevent further tendency toward multiplication of voltage ratings, classes, and limits.

Finally, it may well be pointed out that a great deal of progress has already been made by the American Standards Association in incorporating into American standards the work and recommendations of the Joint EEI-NEMA Committee on Preferred Voltage Ratings for A-C Systems and Equipment.

References

1. Preferred Voltage Ratings for A-C Systems and Equipment, Joint Edison Electric Institute—National Electrical Manufacturers Association Report. *EEI Publication Number R-6, NEMA Publication Number 117* (New York, N. Y.), May 1949.

2. Preferred Voltage Ratings for A-C Systems and Equipment, Joint National Electric Light Association—National Electrical Manufacturers Association Report. *NELA Publication Number 043, NEMA Publication Number 100* (New York, N. Y.), 1930.

3. Standards for Distribution Transformers, Joint Edison Electric Institute—National Electrical Manufacturers Association Report. *EEI Publication Number I-9* (New York, N. Y.), 1945.

4. Standards for Distribution Transformers, Joint Edison Electric Institute—National Electrical Manufacturers Association Report. *EEI Publication Number Q-3, NEMA Publication Number 114* (New York, N. Y.), 1948.

Discussion

Howard P. Seelye (The Detroit Edison Company, Detroit, Mich.): As Chairman of the Power Company Group of the Joint Committee on Preferred Voltage Ratings, I was closely connected with the work of transformer standardization which the authors have described. They have done such an excellent job of compressing into a brief but clear and explicit statement the voluminous amount of survey, study, and discussion which was devoted to this work over a 10-year period, that there is little which can be added in that regard. I would like, however, to emphasize three points.

First, that the standardization of transformers was approached from a fundamental basis. The real needs of the users as shown by their operating voltages, in all their variety, were first thoroughly investigated. These were classified and then co-ordinated with certain proposed standards, taking full account of existing equipment, equipment being currently purchased, and the possibilities of moderate modifications in practice in some quarters to eliminate differences between requirements which were more apparent than real. The proposed standards were then carefully refined by reference again to the users and by cost studies of details.

It is believed that the final result represents as nearly a consensus of the true present requirements of the majority of users as it is possible to obtain.

A second point is that the Preferred Voltage Ratings set up a pattern, not only for present detailed standards being developed by the American Standards Association Committee (C57), but also as a basis for future modifications of the standards which may be found necessary in later years under changed conditions. This, again, is due to the fundamental approach.

The third point is that the standardization indicated cannot help but be of very material benefit in reducing the cost of producing transformers. This benefit will be pretty much in proportion to the amount of use which is made of the standards. The authors have brought out very clearly how many differences of opinion were resolved and answers reached which should be generally acceptable if clearly understood. A careful study of this paper is recommended to all those who wish to participate in the cost reductions possible by standardization.

Transformer Oil

E. D. TREANOR
FELLOW AIEE

E. L. RAAB
ASSOCIATE AIEE

THE HIGHLY complex nature of the material, the resulting difficulty in establishing significant tests for evaluation in reasonable time, and the varying conditions of use, have combined to make the study of oils used for the insulation and cooling of transformers a painfully slow process. It is the purpose of this paper to review some of the very extensive efforts made in this study and to draw at least tentative conclusions as to the present status and future possibilities of one of the most important materials in the design, manufacture, and operation of transformers.

Very great progress has been made since inception of the idea of a liquid insulation and heat carrier some 57 years ago. No detailed historical review is intended, but a very brief summary from the standpoint of one manufacturer may be of interest as there may be remnants of earlier practice even yet and memories of early troubles and later progress.

What was called number-6 oil was in extensive use in the first decade of this century in both transformers and switchgear. This and its predecessors, of which little record remains, were essentially commercial lubricating oils of paraffin base and with a high flash point (about 185 degrees centigrade), a viscosity of 100 seconds at 37.8 degrees centigrade and a pour point of −10 degrees. Engineers of outdoor switchgear found it necessary to adopt an additional oil of similar characteristics but with lower pour point—about −40 degrees centigrade—made from low freezing crudes. This was not used in transformers.

After 1910, the need for lower viscosity and better sludging characteristics led to venturesome use of lower flash-point material, and number 8 and number 12 (paraffin base), with characteristics as shown in Table I, came on the scene.

Table I

	No. 8	No. 12	No. 10
Flash point, °C	130	160	140
Fire point, °C	145	175	
Pour point, °C	−10	−10	−10
Gravity, 15.5/15.5°C	.84	86	
Viscosity, SUS at 37.8°C	45	66	52

About 1918, number 10 with intermediate characteristics was adopted to minimize the number of materials, although there was some overlapping due to the fact that some operators had established number 12 as a common material for transformers and circuit breakers.

About 1925, number 10-C was adopted largely to correct troubles with early conservator transformers used in northern climates. Made from low-freezing naphthenic-base crudes, its characteristics are generally stated as follows:

Flash point—minimum 130 degrees centigrade, average 133 degrees centigrade.
Fire point—minimum 145 degrees centigrade, average 148 degrees centigrade.
Pour point—Not higher than minus 40 degrees centigrade.
Viscosity, Saybolt universal seconds at 37.8 degrees centigrade—Maximum 58 seconds, average 57 seconds.
Free sulphur—None
Gravity at 15.5/15.5 degrees centigrade—0.88

With essentially unchanged basic characteristics, although improved from the sludging standpoint, number 10-C has been in use as our one standard for transformers since 1926 and was eventually adopted for the majority of our switchgear. This oil might be classed as oil produced by medium acid refining procedures.

Sludging troubles during the decade of 1920-1930 led to extensive experimentation with highly refined or "water-white" oil. We established a source for and made limited use of number 18 transil oil which had high flashpoint (170), viscosity (85), and freezing point (0 degrees). Eventually, it was concluded that there was little to justify its higher cost and other unsatisfactory characteristics. In passing, it is of interest to note that the extensive use of similar oils in other countries has been abandoned in favor of oils more nearly resembling our own.

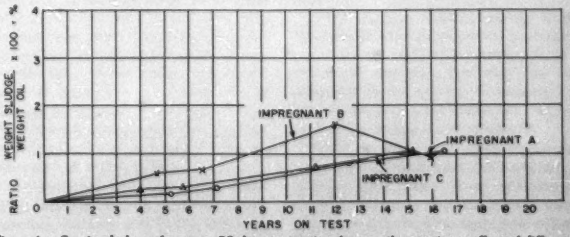

Figure 1. Semisealed transformers—80 degrees centigrade top oil operation—effect of different impregnating materials on sludge formed

Paper 50-165, recommended by the AIEE Transformers Committee and approved by the AIEE Technical Program Committee for presentation at the AIEE Summer and Pacific General Meeting, Pasadena, Calif., June 12–16, 1950. Manuscript submitted March 14, 1950; made available for printing April 27, 1950.

E. D. Treanor and E. L. Raab are with the General Electric Company, Pittsfield, Mass.

The authors wish to express appreciation for much valuable assistance to Mr. F. M. Clark and Mr. G. W. Wade who have been interested and helpful in this study from its inception.

Figure 2 (left). Transformer having impregnant *A*

Figure 4 (right). Two typical transformers operating as a pair

Tests for Evaluation of Oil

During this long use of oil, great effort has been devoted by refiners, apparatus manufacturers, and operators to testing procedures by which various oils could be evaluated and the matter has been and is being continuously studied by the American Society for Testing Materials (ASTM) and other national and international bodies interested in the subject. Ability to judge an oil promptly by agreed-upon tests would obviously be of value in the purchase, application, and development of the material. A wide range of procedures has been proposed here and abroad. Many have been abandoned, many are still in use, and additions are proposed from time to time. It is unfortunate that out of all this effort, there is no unanimity as to the value of these procedures for predicting the life performance of an oil from its initially measurable properties and as to the parallel problem of determining the further usefulness of an oil which has been in service. It is hoped that the data and analysis herein may throw some light on the causes for this situation.

Nonaccelerated Life Tests

At the time this work was undertaken, commonly used tests included color, acidity, saponification, bomb (accelerated oxidation), sludge accumulation, and more recently interfacial tension and power factor have been added. As no entirely satisfactory correlation among these with operating results had been attained and as field data are nearly always indefinite because of uncontrolled conditions and uncertain records, it was decided that it might be of value to run small transformers under approximately normal load conditions indefinitely, so that in the course of time there would be data on actual transformers under controlled conditions and observation by good laboratory methods. These tests were not accelerated except by use of maximum temperature and continuous duty.

Some 30 small transformers with various insulations and treatments and a variety of oils have been under observation for about 15 years. Some of these units have insulating materials representative of those in apparently satisfactory use in power and distribution transformers during the past 20 years, but do not have the oil protective means such as sealing, conservators, and so on, which have been in common use during and preceding that period. Because of the absence of tight sealing, they represent past practice in ordinary distribution transformers or small power transformers, with breathers giving ample access to oxygen, and for brevity are called semisealed transformers throughout this paper.

The coil temperatures were maintained at approximately 95 degrees centigrade (average) and 105 degrees centigrade (hot spot) with a top oil temperature of 80 degrees centigrade, for the principal set of units, to simulate operation at full load in a 40-degree-centigrade ambient.

The procedure for measuring sludge formed, described in detail later, was intended to attain accurate knowledge of this quantity and has not, to our knowledge, been used elsewhere. In retrospect, questions arise as to any possible effect of the washing procedure and the abstraction and replacement with new oil of the samples used for some measurements. No precise answers can be given but it is believed that the conservative extrapolation used in the following discussion leads to valid conclusions.

These transformers after periods up to 15 years have shown various amounts of sludge. If some condition as regards sludging, acidity, and so on, is chosen as an arbitrary end of life, we may say that we have actually measured the full life of oil in a given transformer. For example, the transformer designated as having impregnant *A* in Figure 1 at the end of 15 years shows sludge at one per cent, acidity at one milligram KOH. Its condition after this run is illustrated in Figure 2. Its normal operating characteristics are little affected, but the presence of sludge is obvious and acidity is at a level sometimes considered as limiting. Prudent operation would indicate the desirability of cleaning up a transformer in such condition and replacing or reclaiming the oil. It is to be remembered that this transformer, which used normal oil and well-proved insulating materials, has operated continuously at 80 degrees centigrade top oil temperature with coils at about 105 degrees centigrade (hot spot), conditions representing full load at maximum ambient temperature.

Calculations indicate that under average operating conditions of load and load factor in service, the oil life shown in the

Figure 3. Transformers under life test

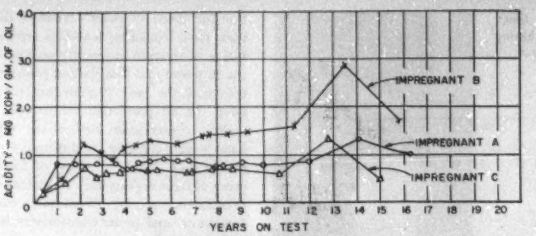

Figure 5. Semisealed transformers—80 degrees centigrade top oil operation—effect of different impregnating materials on measured acidity

continuous run would mean a life of between 20 and 30 years in service before attaining the criterion chosen. As compared with this, the life of class-*A* solid insulation continuously operated at 105 degrees centigrade has been estimated at from five to seven years or at an operating life of from 10 to 14 years on the basis of extrapolation used in the foregoing. This life is, of course, on the basis of an arbitrarily chosen relation of some mechanical property of the material at the end of life to that at the beginning (usually some percentage of initial tensile strength). In the light of common operating experience and the condition of these test units, this figure of 10 or 14 years does not seem realistic, and it seems reasonable to assume that the practical life of the solid insulation is at least as long as that of the oil as shown in these tests.

Some of the transformers under test were subjected to overloads and short circuits after 15 years of test, and the results support the view that the solid insulation, while much embrittled, is intact and the transformers in operating condition.

It should be evident that no one can with certainty set up an estimated or expected life of the oil or solid insulation materials of a transformer in service. Fundamental data on both materials can only be stated on arbitrarily chosen bases. The good mechanical performance of the small transformers reported upon is not likely to be sharply indicative of the performance of power transformers similarly aged. Furthermore, it should be evident that appreciable overloading will have the effect of aging the solid insulations relatively more rapidly than the oil because of the higher temperatures attained in the coils. The well-established laws governing rates of aging show that a change of temperature of the order of eight degrees centigrade can halve or double a life determined by a particular set of conditions. Our purpose here is merely to show that results obtained from very long runs, at normal load under controlled conditions on transformers using good materials, are in line with experience on this type of transformer and to throw more light on things which will affect the life of a transformer.

Life Test Method and Procedure

The 5-kva transformers were operated continuously at 60 degrees centigrade, 80 degrees centigrade, or 100 degrees centigrade top oil temperature. This was achieved by energizing the units in pairs at 230 volts on the low side and paralleling the high sides with the ratio adjusters set apart by two positions. This produced about 120 per cent of full-load current input in each unit. In some cases, units were blanketed with asbestos to realize the desired temperature. Normally, no-load-loss measurements were made semiannually at operating temperature. Power-factor measurements were made annually with a Schering high-voltage bridge at operating and room temperatures. Periodically, oil samples were withdrawn and various characteristics measured. Core and coil assemblies were withdrawn from the tank for inspection and photographing at stated intervals, at which time the total precipitate, total sludge, oil-soluble sludge, and material other than oil sludge was determined. Figure 3 shows some of the transformers under life test. Figure 4 illustrates two typical transformers operating as a pair.

Method of Test

Regarding acidity, the oil acidity is measured in accordance with ASTM methods. In sludge determinations, the transformer was cooled to room temperature, and the core and coils were untanked and drained while being suspended over the tank. Sludge adhering to the core and coils was very carefully washed into the main body of the oil in the transformer tank. The oil and sludge were stirred mechanically until the sludge was evenly distributed throughout the oil and two representative samples of the suspension were taken while the stirring was in progress.

The total precipitate was determined on one sample by washing the sludge with naphtha, drying, and weighing. This included all the precipitate contained in the sample plus that oil sludge which was precipitated out of the oil during the naphtha dilution. The total oil sludge and material other than oil sludge was determined by removing the oil sludge with successive acetone washes. The residue was classed as foreign material other than oil sludge. Percentages are based on the known weight of the oil and the solid material.

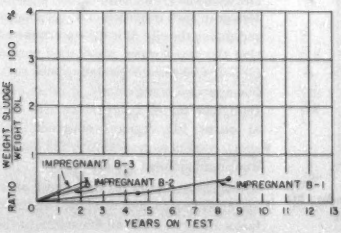

Figure 6 (left). Semisealed transformers—80 degrees centigrade top oil operation—effect of modifications of process using impregnant B (see Figure 1) on sludge formed

Figure 7 (right). Semisealed transformers—80 degrees centigrade top oil operation—effect of modifications of process using impregnant B (see Figure 5) on measured acidity

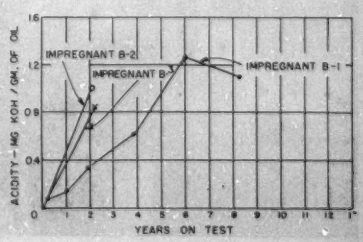

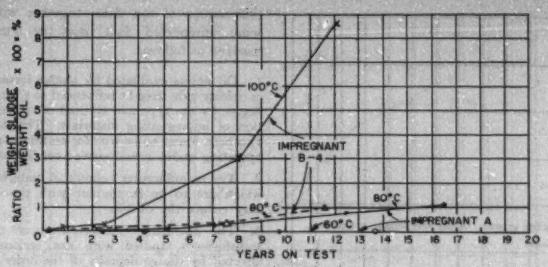

Figure 8. Semisealed transformers—effect of temperature levels for two impregnants on sludge formed

The oil-soluble sludge was determined on a separate sample and is that part of the total sludge which dissolves in the oil at the operating temperature of the transformer. This sample was heated for 48 hours, with shaking, at the operating temperature of the transformer and was then filtered at this temperature to remove excess sludge and foreign material. A weighed sample of the filtered hot oil was then cooled and the sludge determined in the usual manner.

Data on Semisealed Transformers with Normal Oils

Transformer operators are primarily interested in the sludging tendency and the acidity of the oil in their apparatus as these are the characteristics which may actually affect operation. Most other types of tests are a means of gauging changes in the oil quality which are ultimately reflected in increased acidity or sludge deposition, or both. One of the factors influencing the life of an oil as gauged by the amount of sludge deposited in the transformer is the type and method of application of coil-impregnating materials. For the purposes of these studies, 1.0 per cent of sludge by weight of the oil charge has been chosen as the end of life. Figure 1 compares the total oil sludge formed in three similar 5-kva transformers treated with dissimilar types of impregnants designated as *A*, *B*, and *C*. These transformers were operated continuously at 80 degrees centigrade top oil temperature under semisealed conditions.

A common field criterion for oil life is the measurement of the oil acidity. Some operators take the neutralization value of 1.0 milligram of KOH per gram of oil acids produced by normal oxidation as the criterion for reclaiming or changing the oil. Figure 5 compares the oil acidity formed during the life of the three units previously described. In this case, the acidity yields relatively the same information, with impregnants *A* and *C* showing the longest oil life.

In view of the differences shown in life characteristics of the oil when various impregnants were used, a series of units were started with variations of impregnant *B*. Figure 6 illustrates the increased life secured by the modification designated as *B-1* as gauged by the amount of sludge formation. Units impregnated with *B-2* and *B-3* have not been on test sufficiently long to draw any firm conclusions, but at this date do not appear to be as satisfactory. Figure 7, using neutralization number as the guide, again designates impregnant *B-1* as a decided improvement.

In an effort to find the effect of temperature on 10-C oil in contact with several of the more desirable impregnants a series of transformers were operated at 60, 80, and 100 degrees centigrade top oil temperature. Figure 8 shows a typical relation secured as reflected by the amount of sludge formed. It is of interest to note that in a rough sense the 7–10 degree centigrade rule is true in that for approximately each 7–10 degree centigrade rise in temperature, the amount of sludge formed is roughly doubled. Even though the 100 degrees centigrade operating unit containing impregnant *B-4* yielded over 8.5 per cent oil sludge after 12 years on life test, it is still operating satisfactorily and shows no signs of approaching failure. Figure 9 compares the oil acidity formation with life of the same transformers under varying top oil temperature operation. Here, the 7–10 degrees centigrade rule does not seem to hold nor does the value of 1.0 milligram of KOH per gram of oil acidity consistently correspond with the value of 1.0 per cent sludge in terms of years of oil life. This may be due to the effect of soluble materials other than oil oxidation products being present in the oil and will be dealt with in another part of this paper. Relatively speaking, however, impregnant *A* appears to be more desirable than impregnant *B-4*, and the effect of increased top oil temperature is reflected in increased oil deterioration for either impregnant.

The question might be asked as to whether or not the effect of various impregnants on oil life has been noted under actual service conditions. Figure 10 illustrates the effect of several types of impregnants on oil life as judged by the measured oil acidity of samples taken from semisealed transformers operated under severe service conditions of load and ambient temperature. Impregnant *D* is an oxidizing-type varnish long since discontinued, that apparently was incompletely cured before coming in contact with the oil and, as a result, oil deterioration proceeded at a rapid rate as shown by the acidity gain and observed sludge. Similar units refilled with new 10-C oil after several years of preliminary operation yielded a much lower acidity gain coupled with an apparent leveling off. It is presumed that the initial run with the original oil more completely cured the impregnant and that the oil-soluble com-

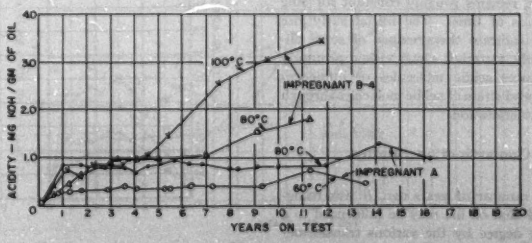

Figure 9. Semisealed transformers—effect of temperature levels for two impregnants on measured acidity

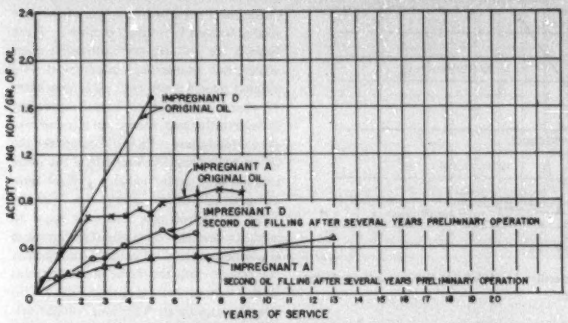

Figure 10. Semisealed transformers—service operation under conditions of severe load and ambient temperature on measured acidity

ponents were largely removed when the oil was changed. Impregnant *A*, while a decided improvement over impregnant *D*, still showed a marked improvement with a second oil filling after several years of preliminary operation of the transformers. This may be due to the removal of detrimental oil-soluble materials during the operational period with the first oil filling. Except for the original oil filling of the transformers containing impregnant *D*, all other variations are well below the neutralization value of 1.0 milligram of KOH per gram of oil. The curves shown in Figure 10 are in each case average values for similar transformers operated under similar conditions in the same location.

It should be noted that throughout this study no attempt has been made to draw smooth line curves in that the determined points occasionally tend to be erratic. This is particularly true for the measured oil acidity values. Figures 5, 9, and 10 indicate that in general the oil acidity tends to level off after an early initial rise and dependent upon operational temperatures, types of transformer impregnants, and so on, the oil acidity value remains roughly constant for long periods of time. The initial early rise may indicate the presence of some oil-soluble material which either promptly produces acidic molecules or influences the production of acidic molecules through oil deterioration.

Oil Contamination Studies

A number of years ago, it was recognized that oil life may be influenced to a large degree by the various transformer materials in contact with it and that some materials may also be affected adversely by being in contact with the oil. Since that time, all materials used in our practice in contact with 10-C oil have been examined under accelerated conditions for physical and chemical contamination of the oil. The effect of the oil on the material is also studied, and no material is used whose electrical, physical, or mechanical properties are affected adversely by being in contact with the oil. Naturally, all types of transformer oils are not affected in a similar fashion by the various solid constructional materials used nor do they all exert the same effect on these various materials.

The 10-C oil after the accelerated aging period is examined for color and acidity changes, as well as various sludging propensities. The solid material is examined for various physical, mechanical, and electrical properties. Additional tests are performed as dictated by the type of material under examination.

Some of the more important findings of this section of our data, together with some unreported data, may be summarized as follows:[4]

1. Oil life as evaluated by sludge formed or acidity gain may be influenced to a large degree by the type and method of application of impregnating materials. This has also been found to be true for transformers operating under actual service conditions.

2. The manufacturer's choice of materials which are to be in contact with the oil may reduce the oil life.

3. The operating characteristics of the transformers studied were not seriously affected by sludge deposits of the order of 1.0 per cent by weight of the oil charge which for noninhibited 10-C oil corresponded in general to an oil acidity value of approximately 1.0 milligram of KOH per gram of oil.

4. Sludge deposits in excess of 7 per cent by weight of the oil charge have not resulted in failure of test transformers.

5. The rate of sludge formation is approximately doubled for every 7–10-degree centigrade rise in top oil temperature throughout the temperature range of 60 to 100 degrees centigrade.

6. For 10-C oil, the rate of sludge formation proceeds in general at a uniform rate.

7. In general, oil characteristics for 10-C oil, such as viscosity, gravity, power factor, saponification, sludge accumulation, resistivity, and so on, while reflecting changes occurring in the oil during its life, are erratic and appear to have little value as indicators of the rate of sludge formation. Acidity levels and color values tend to indicate when sludging is occurring to any marked degree, although the highest acidity level does not necessarily indicate the greatest rate of sludge formation. This apparent discrepancy is attributed to the possible influence of small amounts of certain oil-soluble components secured from various solid insulations on the acidity gain without a corresponding gain in sludge formation. In general, however, an oil acidity of 1.0 milligram of KOH per gram of oil approximately corresponds to 1.0 per cent of sludge formed for 10-C oil.

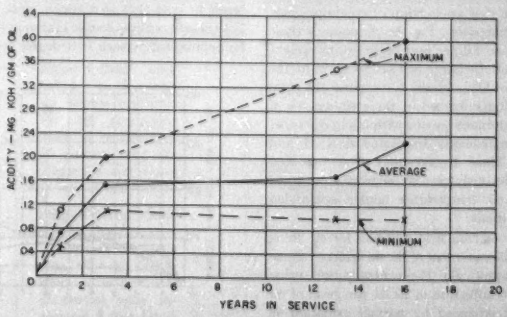

Figure 11. Records of acidity of normal oil in 12 sealed network units during 13 years of service—nitrogen atmosphere substantially maintained

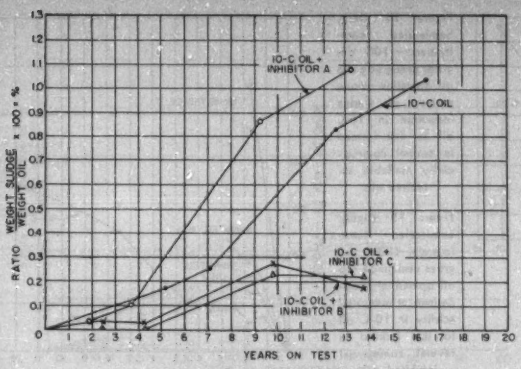

Figure 12. Semisealed transformers—80 degrees centigrade top oil operation—effect of various inhibitors in 10-C oil on sludge formed

8. Oxidation studies may preclude the use of a poor oil, but even a good oil may yield bad service when in contact with solid insulation and materials of poor choice.

Oil Protective Means

Beginning with the conservator, there has been extensive use during the last 35 years of various structures in power transformers designed to limit or prevent the entrance of oxygen, dust, fumes, and water, and to minimize or prevent evaporation. More recently, there has been a trend toward the use of the simplest of these structures in distribution transformers, that is, simple sealing with a gas space sufficient to take the ordinary pressure range. It is not proposed to attempt any comparison of the virtues of the various methods of excluding oxygen. This will doubtless be under continued study in the future. There seem reasonable grounds for the assumption, however, that with these methods and with application of what is known as to materials and processes, the problem of oil as a limiting factor in the life of transformers is a diminishing rather than increasing one.

The tests reported herein throw no light on the matter since none of these structures were used. Indications from field service and laboratory studies indicate, however, that some of these methods have the possibility of extending the life of oil and solid materials by perhaps 50 per cent.

Oil Life When Oxygen Is Minimized or Eliminated

All of the data presented so far have been for transformers operating under semisealed conditions. It is generally recognized that the rate of oil deterioration is materially reduced by various mechanical means of preventing the oil from coming in contact with atmospheric oxygen. Such methods of oil preservation can be classified as conservator protection, hermetic sealing, gas-oil sealing, and nitrogen blanketing. These modern methods of oil preservation have been markedly successful as evidenced by the lack of service complaints due to oil deterioration.

Some service operational data on oil in sealed network units operating under a substantially maintained nitrogen atmosphere are shown in Figure 11. It is noted that the oil acidity for an average of 12 transformers is less than 0.24 and any one unit yielded a maximum oil acidity of 0.40 milligram of KOH per gram of oil. These values are well below the neutralization maximum of 1.0 which is used as a guide by some operators and much less than the acidity values secured under 60 or 80 degrees centigrade continuous semisealed life test conditions for a period of 14 years. (See Figure 9.) Based on the assumption that normal service would yield an oil life of about twice that secured under the accelerated life test conditions, we can project an oil life for transformers with oil protective means far in excess of the expected oil life under semisealed conditions.

Inhibitors

Successful use of inhibitors in other fields, particularly rubber and lubricating oils, led very soon to consideration of similar use in transformer oil. Two objectives were considered. One was to extend the life of normal oil on the assumption that this was not sufficient. The second was to see whether less refined and hence less expensive oils could be made by the addition of inhibitors to give life of the same order as oils properly refined for maximum life. Neither objective has as yet come to fruition. The primary objective of increasing life becomes questionable in view of previous conclusions that transformers of satisfactory design and materials using normal oil and oil protective means will give life equal to or greater than that of the solid insulations. The objective of obtaining oils of lower cost by use of inhibitors in less refined oils is not now believed to be hopeful.

Among the small semisealed units previously referred to were several in which inhibitors were used and directed at each of the objectives mentioned above. Oils underrefined as compared with normal transformer oil, and which had some hope of providing lower costs, were treated with inhibitors which had been sufficiently

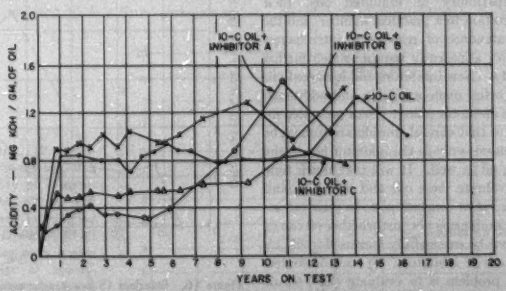

Figure 13. Semisealed transformers—80 degrees centigrade top oil operation—effect of various inhibitors in 10-C oil on measured acidity

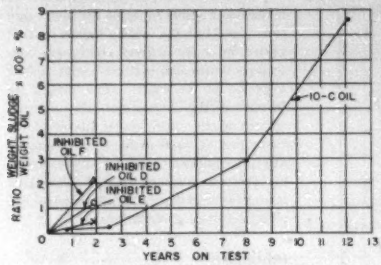

Figure 14 (left). Semisealed transformers — 100 degrees centigrade top oil operation—comparison of sludge formation in 10-C oil to that formed in several commercially available inhibited oils

Figure 15 (right). Semisealed transformers—100 degrees centigrade top oil operation—comparison of measured acidity in 10-C oil to that formed in several commercial inhibited oils

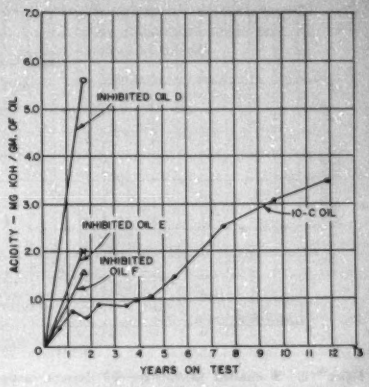

studied at the time to be hopeful. These oils are referred to as distillates in the following data. They were run with other transformers having normal oil similarly treated, and with other variations.

Practical Considerations in Using Inhibited New Oil in New Apparatus

Some presently available inhibitors have properties which will justify careful study from the standpoint of economics and the complexities they unavoidably introduce. If there were available today one or more inhibitors which were considered to be completely satisfactory in a technical sense, the decision to use inhibitors in oil in new apparatus would still be largely influenced by a number of practical considerations for which the present state of knowledge is quite limited. The suitability of such oils for circuit breakers and bushings, the increased cost as opposed to the expected gains, the actual need, if any, in most transformers of modern oil protective design, the eventual problem of reclamation and disposal of the reclaimed inhibited oil, and how to predict and test for its service life must be considered. The compatibility of inhibited oils, their limitation to a practical number, and the maintenance of reasonable interchangeability apparently requires much further study. New inhibitors and inhibited oils are being made available and additional ones are in the offing. Data presented indicate that careful consideration must be given not only to the inhibitor but to the base oil as well. It will take much time to evaluate these oils and inhibitors and to arrive at conclusions as to their merits. The problem is not just whether oil can or cannot be successfully increased in life by the use of inhibitors. It can, of course. The problem is to evaluate the over-all economic, dielectric, chemical, and practical advantages and hazards presented by the use of these oils during years of commercial service.

Semisealed Transformers with Inhibited Oils

Figure 12 compares the effect of various inhibitors in 10-C oil on the sludge formed. The 5-kva transformers were operated at 80 degrees centigrade top oil temperature under semisealed conditions. Of particular interest is the fact that 10-C oil with inhibitor *A* is apparently better than 10-C oil alone from a sludging standpoint in the early stages of the oil life, but is not as effective and may even tend to be detrimental during the later stages of aging. This indicates the necessity for caution in rapid evaluation of an inhibited oil.

Inhibitors *B* and *C* are very effective and approximately equivalent, being well below the 1.0 per cent sludge figure after 14 years of accelerated life. Figure 13 compares the acidity development of these oils. Again we note that inhibitor *A* is quite effective up to six years of accelerated life, but rises rapidly thereafter in terms of acidity and yields values at least as high as the values later obtained by 10-C oil alone. The 10-C oil with inhibitor *B* shows an early sharp acidity rise followed by a leveling off, and viewed in this light is no improvement over 10-C oil alone. The 10-C oil plus inhibitor *C* is a definite improvement over 10-C oil alone whether gauged by sludging or acidity.

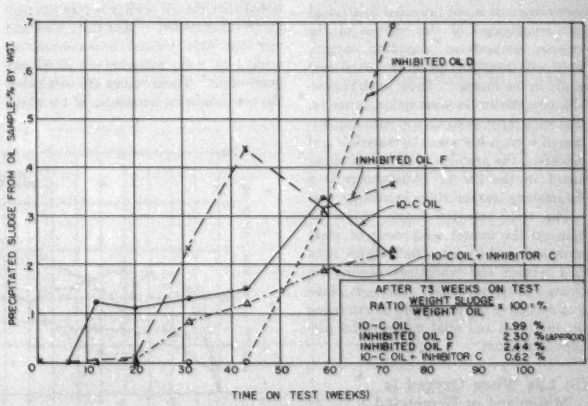

Figure 16. Standard 15-kva transformers with pipe breathers added—100 degrees centigrade top oil operation—comparison of precipitation sludge formed in oil samples from various inhibited oils and 10-C oil

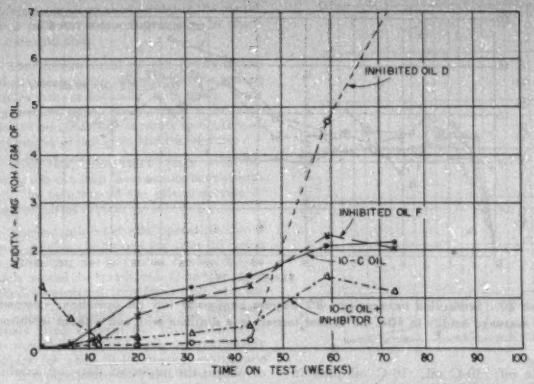

Figure 17. Standard 16-kva transformers with pipe breathers added—100 degrees centigrade top oil operation—comparison of the measured acidity formed in various inhibited oils and 10-C oil

During the course of these studies, a number of inhibited oils have become commercially available. Figure 14 compares three of these inhibited oils to 10-C oil under 100-degree centigrade top oil operation in semisealed transformers of 5-kva design. While it is too early to draw any definite conclusions, the amount of sludge deposited in each case by the inhibited oil is greater than that produced by the 10-C oil alone during the early accelerated life of the transformers. Figure 15 demonstrates the measured acidity secured for these same oils. Of particular interest is the runaway acidity development demonstrated by inhibited oil *D*. In no case, during the early stages of life are any of these oils superior to 10-C oil alone. In the case of inhibited oil *D*, the transformer had to be removed from service due to a runaway temperature rise. The oil after 1.7 years of life had changed in viscosity from 62 to 125 Saybolt seconds taken at 37.8 degrees centigrade. Along with this rapid rise in acidity, the character of the sludge deposited on the core and coils was of a gummy adherent nature which could not be removed by normal oil washing methods. This type of sludge is characteristic of an overly refined base oil. Figures 16 and 17 throw additional light on this type of oil. In these tests, 15-kva transformers with pipe breathers added were operated at 100 degrees centigrade top oil temperatures. Figure 16 compares the precipitation sludge (that is, sludge secured with the oil sample when such samples were periodically withdrawn from the transformers) of several commercially inhibited oils to 10-C oil and to 10-C oil containing inhibitor *C*. Here again we note that inhibited oil *D*, while behaving in a superior fashion in the earlier stages of its life, ran away after 43 weeks of accelerated life and at 73 weeks life was depositing more sludge on a weight basis than any of the other oils. Inhibited oil *F* behaved in a superior fashion for a short time but broke sooner than inhibited oil *D*. The 10-C plus inhibitor *C* again reflected a gain over 10-C oil alone and yielded more resistance towards sludging under prolonged life-test conditions. The table contained in Figure 16 gives the total oil sludge secured in the transformers after 73 weeks of accelerated life, at which time the tests were discontinued. Here we find that 10-C oil plus inhibitor *C* yielded only one-third to one-quarter the amount of sludge as compared to the other oils. The sludge determination of 2.30 per cent for inhibited oil *D* is listed as being approximate in that it was impossible to remove the gummy varnish-like sludge from the coil sections without also removing cellulosic insulation. From previous data, the amount of sludge adhering to the core and coils was estimated to be approximately 20 per cent of the total formed on a weight basis. Inhibited oil *F* is characterized by early sludge formation coupled with a rapid rate of sludge deposition. Figure 17 shows the oil acidity development for this same series of transformers. Relatively speaking, the acidity measurements classify the four oils in the same manner as do the precipitation sludge values. Again we note the early stabilized period for oil *D* followed by an extremely rapid rise in acidity whereas the other three oils appear to be reaching a relatively stable acidity level.

Inhibited oil *D* exhibits the characteristics of an overly refined base oil to which an effective inhibitor has been added. Figure 18 compares the measured acidity of an uninhibited water-white oil, 10-C oil, and inhibited oil *D* during open beaker agings at 75 degrees centigrade of impregnated stamp capacitors operating under 812 volts per mil stress. While 10-C oil shows a slow steady increase in acidity over a 55-week period, inhibited oil *D* yields the characteristic runaway acidity condition which parallels that secured much earlier during this aging study by the water-white oil. The oil viscosity for inhibited oil *D* and for the water-white oil nearly doubled during this period whereas the 10-C oil viscosity increased very slightly. The characteristic gummy adherent sludge was deposited for both the water-white oil and inhibited oil *D*.

A series of 5-kva transformers were operated at 80 degrees centigrade top oil temperature containing a semicrude distillate with and without various added inhibitors. These units were run under semisealed conditions. Figure 19 com-

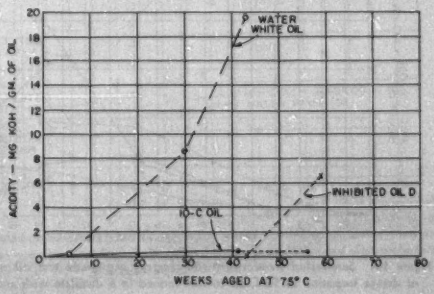

Figure 18. Comparing the measured acidity of a water-white oil to that formed in inhibited oil D and 10-C oil during open beaker agings of impregnated stamp capacitors operating under 812 volts/mil stress

pares the total oil sludge formed by these oils to that formed by 10-C oil. After nearly 14 years on accelerated life test, the distillate oil is exhibiting rapid sludge formation whereas the same crude distillate oil with inhibitor *B* appears to be almost equivalent to 10-C oil. Inhibitor *A* is not as effective as *B* in retarding sludge formation. When we look at Figure 20 which compares the acidity development for these same oils, we find that inhibitor *B* is not as effective as *A*. In fact, we find that the acidity level invariably is higher than that obtained for the semicrude distillate alone. We again note the characteristic early rise in acidity with a subsequent leveling off. In terms of acidity alone, the distillate oil has deteriorated only slightly more than the 10-C oil. Figures 21 and 22 illustrate the performance of a series of inhibited oils operating at 60 degrees centigrade top oil temperature.

Again it is interesting to note the effect of actual service operation on some of the various inhibited oils under discussion. Figure 23 illustrates the behavior of a series of inhibited and noninhibited oils as judged by oil acidity formation while operating in service under conditions of severe load and ambient temperature. These transformers are of semisealed design and all units were given a preliminary operation of several years with 10-C oil before being filled with the oils being reported. All values given are average values for a series of similar transformers operating under similar conditions at the same location. No actual sludge data are available, but from our controlled accelerated life studies, we would predict from the acidity curves that on a comparative basis, the oils would be graded in the following fashion in terms of increasing amounts of sludge present after 13 years of life: water-white oil; 10-C oil; 10-C oil plus inhibitor *B*; semicrude distillate oil plus inhibitor *B*; 10-C oil plus inhibitor *A*; and semicrude distillate oil plus inhibitor *A*. While the water-white oil appears to be behaving satisfactorily from the standpoint of acidity, the fear is always present that such an oil will exhibit the runaway characteristics reported under Figure 18. It has been noted in our controlled accelerated life-test studies that the acidity value of 1.0 milligram of KOH per gram of oil does not correspond to a total oil sludge value of approximately 1.0 per cent for inhibited oils in every case, but may reflect either an approximate value of one per cent or a much lower value. The sludge value was never more than approximately one per cent in any instance for a corresponding acidity of one milligram of KOH per gram of oil for the inhibited oils. From these studies, it would also be predicted that every oil reported on Figure 23 has formed less than one per cent total oil sludge in their respective transformers after 13 years of life.

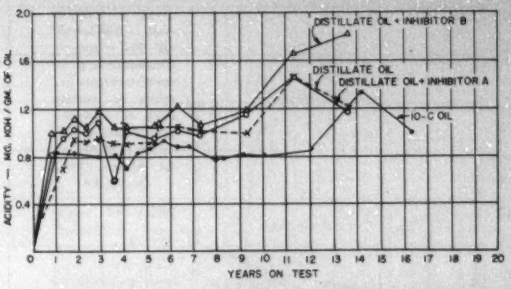

Figure 20. Semisealed transformers—80 degrees centigrade top oil operation—comparison of measured acidity in 10-C oil to that formed in a distillate with and without inhibitors

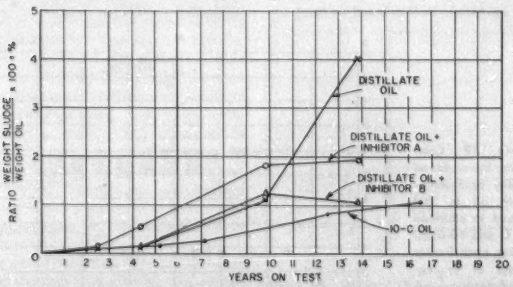

Figure 19. Semisealed transformers—80 degrees centigrade top oil operation—comparison of sludge formation in 10-C oil to that formed in a distillate with and without inhibitors

While the reported data on inhibited oils constitute only a fraction of the work done, some observations and conclusions may be drawn from the data presented.

1. Some inhibitors when added to 10-C oil may retard sludge formation during the oil's early life, although the total sludge formed in the oil's later life may be equal to or slightly more than that produced by the 10-C oil without an added inhibitor.

2. When viewed from the sludging standpoint alone, 10-C oil can be successfully inhibited against sludge formation for long periods of time. This does not mean that such inhibited oils are completely satisfactory in all characteristics nor economically feasible to use.

3. Some of the oil inhibitors when added to 10-C oil retarded sludge formation but promoted acidity formation to a greater degree than is produced by the 10-C oil without an added inhibitor.

4. In general, 10-C oil containing an inhibitor, still shows the characteristic initial rise in acidity which is subsequently followed by a long period when the acidity is comparatively constant. This initial rise in acidity may be due to the effect of oil-soluble material from solid insulation.

5. Several commercially available inhibited oils do not exhibit any superiority over 10-C oil when viewed from the sludging standpoint during the early stages of the oil life under semisealed transformer conditions. Other commercially available inhibited oils which were examined were definitely inferior to 10-C oil when aged for long periods of time under semisealed conditions.

6. One commercially available inhibited oil (inhibited oil *D*) has been shown to exhibit the characteristics of an overly refined base oil to which an effective inhibitor has been added. This oil, however, breaks badly at some point in its life with a runaway acidity and sludge development. The type of sludge formed is also of a different character from that produced by more conventionally refined oil, being of a gummy adherent nature. These characteristics conceivably might make it difficult for an operator to predict when this oil was nearing the danger stage, and should

he already have secured sludging, he would find it difficult, if not impossible, to clean the core and coils.

7. The measurement of the precipitation sludge, which is the sludge secured when oil samples are periodically withdrawn from transformers under study, while a valuable index to oil condition, is rarely indicative of the amount of sludge in the transformer.

8. Short-time laboratory tests with inhibited oils can lead to erroneous conclusions as to the behavior of the oils in service in terms of useful oil life.

9. Various inhibited oils operating under actual service conditions for over 13 years are exhibiting the expected characteristics which would be predicted from the controlled accelerated transformer-life studies.

10. The 7–10-degree centigrade rule previously cited wherein the rate of sludging for noninhibited 10-C oil approximately doubles for each 7–10 degrees centigrade rise in temperature does not hold quite as well for inhibited oils.

11. Laboratory oxidation studies and initial oil characteristics on new inhibited oil yield little indication of the oil's performance in service in terms of years of useful oil life. While such tests may, to some extent, indicate the type of base oil, its degree of refining, and the eventual rate and type of sludge and acidity formation, the inhibitor life period may be considerably shortened by service conditions and the materials with which the oil is in contact.

12. Neither sludge nor acidity formation proceeds at a uniform rate for all inhibited oils and may accelerate markedly when the inhibitor life is ended.

Reclamation of Aged Oil

While these data seem to establish a fairly long life even for semisealed units, there are in the normal course of operation a percentage of transformers, severely overloaded, exposed to unusual ambient temperatures, having past design defects in the way of materials, hot cores, inferior oils, and so on, or failed coils, or simply very old, which give operators constant indication of a problem with a volume of oil, not large as compared with the total in use, but sufficient to justify study of reclamation methods and to raise the fear on the part of operators and apparatus manufacturers that the problem is increasing. We have not found wholly satisfactory reclamation methods but have for many years practiced the fuller's earth reclamation of small quantities of oil where it could be blended or diluted with new oil to such an extent that the objectionable effects of such refinement are lost. New oil contains a certain amount of so-called natural inhibitors which vary, dependent upon the type and the degree of refinement of the oil.

Any refinement by activated adsorbing

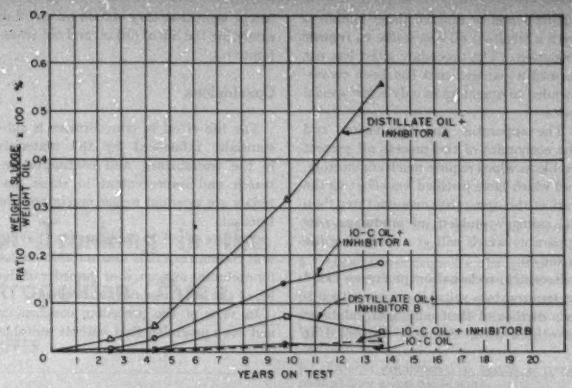

Figure 21. Semisealed transformers—60 degrees centigrade top oil operation—comparison of sludge formation in 10-C oil to that formed in 10-C oil plus various inhibitors and a distillate oil plus various inhibitors

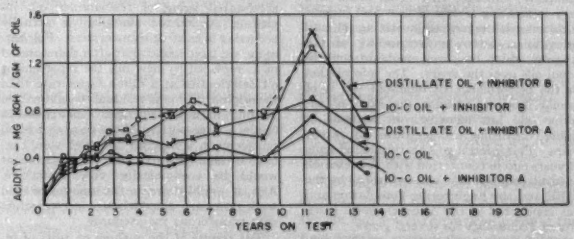

Figure 22. Semisealed transformers—60 degrees centigrade top oil operation—comparison of measured acidity in 10-C oil to that formed in 10-C oil plus various inhibitors and a distillate oil plus various inhibitors

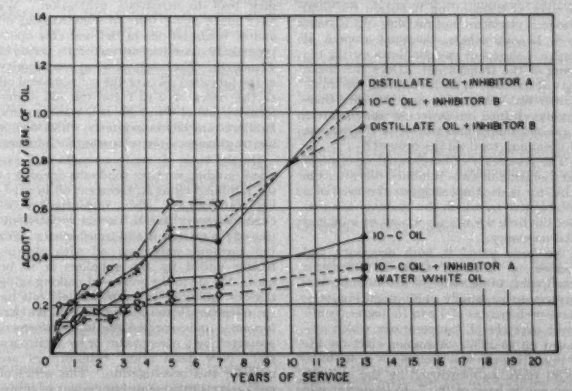

Figure 23. Semisealed transformers—service operation under conditions of severe load and ambient temperature—measured acidity—units refilled with oils as designated after preliminary operation under 10-C oil

agents tends to remove these inhibitors with a resultant oil less stable as regards oxidation. The procedure cited has not seemed a panacea and has been recommended to operators in only a few special cases.

The apparatus, the supervision, and the economics of the process all present problems which require much engineering, and which have justified less effort on the part of the apparatus manufacturer than the primary problem of producing new apparatus which will give very long life of the oil.

Recently, reclamation processes based on treating to a suitable degree with fuller's earth and then adding an inhibitor have been tried. Suitably controlled, it would seem that they should be useful in extending the life of old oil and old transformers.

Conclusions

The life of oil in transformers is substantially influenced by the materials in the transformer, and continuing research and improvement in these materials are essential to get maximum life from oil.

The life of oil in transformers, having well chosen materials and suitable means for excluding oxygen, is of the order of the life of the solid insulating materials.

In view of the preceding conclusions and even assuming that entirely suitable inhibitors are available, their use in new transformers does not yet seem of proved value. We do not believe that final conclusions can be drawn at this time, but results of great importance do not seem to be indicated.

Use of inhibitors in reclamation processes for badly oxidized oil may be of value. Probable costs of the whole process is in the range of 8 to 15 cents per gallon and will indicate to what extent these processes will show economy.

Much has been learned from these tests which will be of value in guiding future work. Some indicated improvements in material and structure of transformers have already been made and others are under study.

Discussion

Herman Halperin (Commonwealth Edison Company, Chicago, Ill.) This paper is a very interesting review of past and present problems with regard to insulating oil, and helps to a better understanding of the progress which has been made in conventional oils over the years. The information on the performance of inhibited oils is of special interest, because the need of superior oils has increased on account of higher operating temperatures in recent years. This interest was also indicated some 12 years ago in connection with the research on insulating oils that was sponsored by the AIEE and the Engineering Foundation and was conducted at the Massachusetts Institute of Technology for several years.

It is of interest to note that precipitation sludge is rarely indicative of the amount of sludge in the transformer. Unfortunately, this is the only sludge test the operator is able to make in periodic checks of transformers, as dismantling to obtain the total sludge is obviously impractical. In Figures 1, 8, 12, and others, the total amount of sludge is shown at various times during the aging of the transformer. Does this mean that at the time of each sampling the transformer was dismantled and the core thoroughly cleaned in order to dissolve the deposited sludge into the oil for the purpose of obtaining total sludge content?

The possibility of accelerated or of rapid deterioration of some inhibited oils after the inhibitor is used up, suggests the need of a reliable test by which the operator can predict the time when replacement of inhibited oil is necessary.

We have found it both necessary and feasible in Chicago, from an economic standpoint, to increase the loading of transformers substantially with resulting temperature increases of 10 to 15 degrees centigrade over the oil temperatures which prevailed up to 1937. Assuming that the life of insulating oils was then of the order of 20 to 30 years, as mentioned by the authors, then on the basis of the 7- to 10-degree rule mentioned in the paper, the life of the oil with these temperatures would be only one-half to one-quarter of the previous life, or as low as five years.

We have found various evidences that accelerated aging of transformer oil, including accelerated sludging, is actually occurring in existing transformers. Furthermore, we have found that after deteriorated oil is replaced by new oil, the replacement oil deteriorates at a much faster rate than the original oil due to residual contamination products in the transformer. Since the labor cost is a large portion of the total cost of oil replacement, a superior oil which would reduce or eliminate frequent oil replacement would be economically very attractive. Also, it would decrease the amount of field work necessary at odd hours in connection with transformer maintenance.

The results of the authors on tests of inhibited oils are very interesting, especially since they show the need of long-time tests to properly evaluate such oils. We agree with the authors that short-time laboratory tests may lead to erroneous evaluation. We have made aging tests of conventional oil and of inhibited oils in old and new open-type distribution transformers for a period of 42 months. The results showed a superiority of the inhibited oil over the conventional oil of the order of 2-to-1 for the old transformers, and of 3-to-1 for new transformers. In short-time laboratory tests, which do not use transformers, the ratio was much higher.

On the basis of our test results and economic studies, we have made the decision to use inhibited oil as replacement oil in existing transformers, when replacements become necessary due to excessive deterioration of the oil now in the transformers. For this purpose, only new oil with the inhibitor added by the suppliers is to be used. We are in the process of making aging tests of inhibited and conventional oils for the purpose of determining the relative performance and expected life in transformers protected by a conservator or by a nitrogen seal. New distribution transformers are used for this investigation. This series of tests relates to present-day designs of transformers.

E. D. Treanor and **E. L. Raab:** In reply to the interesting comments of Mr. Halperin, it is unfortunately true that precipitation sludge is not an entirely satisfactory indicator of the total sludge formed. We adopted the somewhat troublesome method of periodic untanking of the transformers, brushing and washing the deposited sludge into the oil before measurement. It is, of course, not a very practical method for field use. It is possible that interfacial tension now under active study may ultimately prove to be a satisfactory, although indirect, indicator of sludge.

It is, of course, quite true that an increase in oil temperature will decrease its life, roughly by half for each 7 to 10 degrees of increase.

It may be well to recall that the same rather general chemical laws apply to the solid materials in the transformer, and the temperature of some of these solid materials will increase more rapidly than that of the oil and, hence, their rate of degradation will be greater relatively than that of the oil.

The economics of high-load levels and shortened life of transformers is a study for operators in which the manufacturer is a detached, but very much interested, observer.

We believe it is fairly well established that sludge, particularly soluble sludge will catalyze new oil and decrease the effectiveness of inhibitors, so that thorough washing of old transformers is desirable if it can be practiced.

A review of our test data does not offer confirmation of the superiority of inhibited oil which Mr. Halperin reports. This is probably due to the longer duration of our tests and to differences of interpretation and criteria, which we hope can ultimately be reconciled.

The suggested method for a reliable test by which the operator can predict the time when replacement of inhibited oil is necessary is under study by American Society for Testing Materials for new oils, and some modification of any practical method could probably be applied to used oils.

Interexchange Tandem Trunking in the Los Angeles Metropolitan Area

W. F. PFEIFFER
ASSOCIATE AIEE

Synopsis: Twenty-four years have elapsed since the first large-scale machine switching tandem system was designed and installed for service in Los Angeles. As an intermediate switching center, the tandem office enabled operators to use the dial method of operation for establishing interexchange telephone connections over the associated trunking network. During the intervening years, it has facilitated the rapid handling of telephone calls between the various communities in and around the city. Step-by-step tandem equipment was employed and as the volume of calls grew, the trunk capacity was increased by installing additional switching equipment. In 1946 it became evident that the abnormal rate of growth required additions substantially beyond the practical size limit of the step-by-step tandem unit. To solve the resulting problem, it became necessary to reorganize the tandem trunking system and select a multiunit tandem switching plan. It also provided an opportunity to consider the application of the more recently developed crossbar tandem switching system. This paper reviews the factors affecting the general problem of interexchange trunking which have led to the development of the present tandem network in the Los Angeles metropolitan area. It describes the major elements of a system which now employs a total of five tandem switching units, three of which are crossbar tandem offices.

THE provision of telephone service between the communities of a large metropolitan area presents many problems. Appropriate quantities of switching equipment and cable pairs must be provided to carry the expected loads and to perform the functions required for interconnecting telephone users. The resulting plant design must be such that satisfactory service can be provided at a minimum cost to the subscriber. To meet these objectives, operating methods are required which will facilitate the rapid handling of high volume calling. Economical plant design requires efficient operation and an economic balance between the cost of arrangements employed to improve plant efficiency and the value of the savings obtained.

Since forecasts of the volume and distribution of future traffic are the bases for plant design, unpredictable variations in traffic growth and changes in telephone practice are some of the elements of risk associated with planning for growth.

Tandem operation provides one of the principal devices available for improving operating methods and plant efficiency. As an auxiliary switching center it is the hub of trunk plant in a large highly-developed switching network, interconnecting central offices and operating centers. In this capacity it is sensitive to all the unpredictable and changeable elements of advance telephone planning.

Many types of tandem offices are employed throughout the United States and have been described quite thoroughly elsewhere.[1] A step-by-step machine switching tandem system, installed for service in Los Angeles in 1926, was described by F. O. Wheelock and E. Jacobsen in a paper in 1928.[2] A more recent contribution toward the solution of interoffice trunking problems has been the introduction of the crossbar tandem system.

In Los Angeles, where large scale dial tandem trunking is employed only for interexchange traffic, the volume of calls has grown beyond the capacity of the original tandem unit and a multiunit tandem system now is in operation. The accelerated rates of growth in recent years have required an ever-increasing effort to:

1. Provide for total growth in interexchange service.
2. Make adjustments for changes in the rate of growth in individual trunking paths.
3. Provide for changes in the central office numbering plan in order to permit the extension of subscriber dialing on a prefix and number basis.
4. Provide equipment to match a trend toward finer gauge cable pairs.
5. Provide trunk terminating equipment to match the various types employed in connecting offices.
6. Expand from a single-unit tandem system into a multiunit tandem system.
7. Deload the tandem system of traffic that can be handled more economically by other methods.
8. Maintain the most effective trunking methods under the changing conditions.
9. Improve service conditions.
10. Make the most effective use of the types of tandem equipment available.

This paper reviews the basic principles involved in the design of a dial tandem system and traces the development of the Los Angeles metropolitan area interexchange trunking problem. It describes the major elements of the present multiunit tandem system and the function it performs. Reference to minor subtandem switching points and an extensive direct trunking network is avoided deliberately for brevity. The aim is to present interexchange trunking in a growing metropolitan area as a continuing problem driven by service demand and changing technique. Highly flexible facilities are required in order to maintain an economically balanced plant arrangement and satisfy service requirements.

General Background

The serving area of the Los Angeles tandem network now comprises the Los Angeles metropolitan area proper plus

Paper 50-108, recommended by the AIEE Communication Switching Systems Committee and approved by the AIEE Technical Program Committee for presentation at the AIEE Summer and Pacific General Meeting, Pasadena, Calif., June 12–16, 1950. Manuscript submitted March 13, 1950; made available for printing April 26, 1950.

W. F. Pfeiffer is with The Pacific Telephone and Telegraph Company, Los Angeles, Calif.

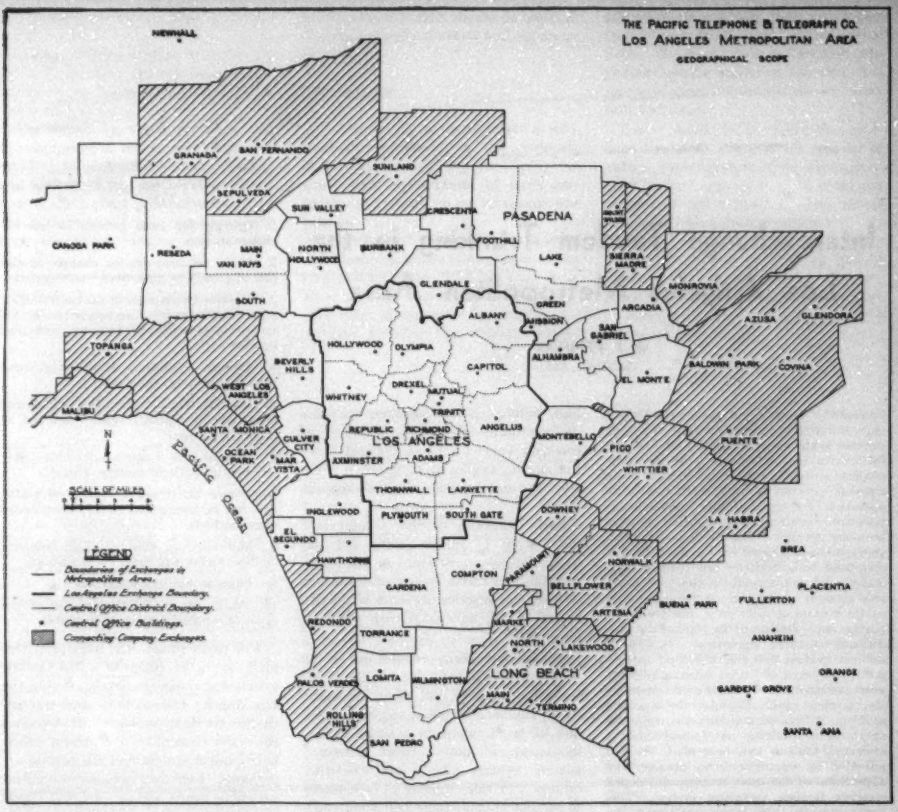

Figure 1. The Los Angeles metropolitan area

additional points described later. The term "Los Angeles Metropolitan Area" has been employed to include Los Angeles and surrounding communities, as shown in Figure 1. The Los Angeles exchange, which is the central core of the area, serves over 800,000 stations in 14 district areas. The development of these district areas varies from 26,000 to more than 132,000 stations. Three of the district areas are subdivided and each employs two central offices that are geographically separated. Other district areas are served entirely from a single central office. The surrounding exchanges each contain from one to five central offices. Within the 35 telephone exchanges involved, there are four manual-type central offices and 75 dial offices that serve approximately 1,600,000 telephones in eight toll center areas. This may be termed the primary serving area of the tandem system.

As in most metropolitan areas, the growth and complexity of the telephone system in the Los Angeles area has followed the industrial and residential development of the communities which comprise it. In the early period, say prior to 1919, the various communities were for the most part separate and distinguishable entities with a relatively light density of population and relatively small community of interest, resulting in a volume of telephone calling which could be handled economically by simple methods. As the area grew, however, under the stimulus applied by the mass influx of population following World War I, and continuing with but slight periods of slackening up to and including the present time, the situation rapidly became more complex. Starting with Los Angeles proper as a center, communities expanded in such fashion as to present in many cases a solid expanse of urban development, with no visible sign to mark the boundary between one community or municipality and the next. Along with this, of course, the population density increased manyfold.

The growth in number of people alone would have produced a volume of telephone calling of such proportions as to have called for a revolution in the manner of handling, even if no change had occurred in other elements affecting the usage of service. But there were other elements operative, so that the increase in the volume of calling was at a rate considerably in excess of linear with re-

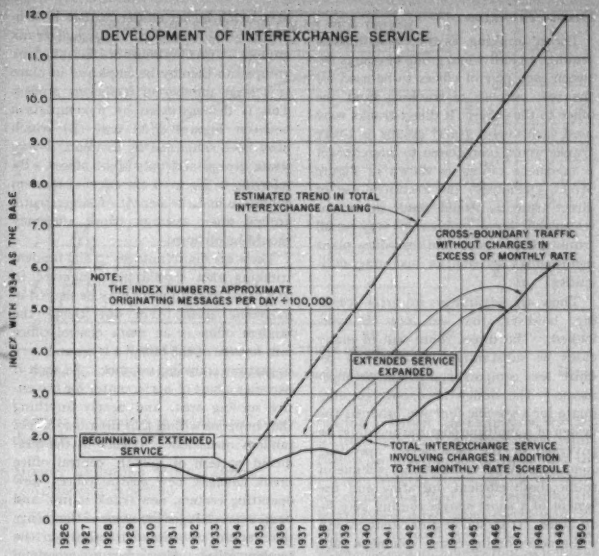

Figure 2. The development of interexchange service

spect both to population and telephone station gain. These elements are several, but perhaps one of the most significant is the almost universal use of the private automobile for passenger transportation. The effect of this has been to soften the limitations of distance on many of the activities within the area, with the result, for example, that industry has been afforded a wider latitude than otherwise in the choice of plant locations, with the assurance that workers may be drawn from a radius limited only by their willingness to travel. As a consequence, industrial activity is widely dispersed throughout the area and, for the same reason, social interests are not limited to the immediate neighborhood of an individual, but may and do extend clear across the area.

The effect of these tendencies on telephone calling has been to increase materially the volume of calls, both business and social, over the longer distances. This effect has been heightened greatly by improvements in the art of telephony which have added immeasurably to the satisfactory quality of telephone communication.

Prior to 1919, interexchange telephone switching was almost exclusively on a manual basis, and calls between exchanges were handled as toll calls through manual toll switchboards interconnected by suitable toll or trunk circuits. With the increase in the volume of calls, however, as the result of the tendencies previously noted, the earlier methods of handling became cumbersome and costly. A significant milestone in the succession of steps taken to solve the problem was the establishment in Los Angeles of the first large scale dial tandem in 1926. Since that time, additional steps have been taken to keep pace with the growing problem and the result is the complex network of circuits and switching arrangements that is in use today.

While not of particular significance as an element affecting the problem at hand, it is of interest to note that the telephone service in the area is provided, each in its own territory comprising a part of the metropolitan area, by four companies, which are: the Pacific Telephone and Telegraph Company, a part of the Bell Telephone System; the Associated Telephone Company, Limited; the California Water and Telephone Company; and Sunland-Tujunga Telephone Company.

In addition to the primary serving area as described, a secondary area comprised of 12 Orange County exchanges is served by the Los Angeles tandem system through interconnecting trunks to and from a small tandem office in Anaheim.

Incoming traffic only is handled from more distant toll centers at Bakersfield, Pomona, San Bernardino, and San Diego. Bakersfield and San Diego, which are located 112 miles to the north and 126 miles to the south, respectively, are the most remote points having access to the tandem facilities for inward traffic to the Los Angeles area.

The traffic to and from points outside the metropolitan area is increasing to such volume that consideration is being given to handling it through a more comprehensive intertoll dial tandem which is being planned for the future. With such an arrangement in the long term picture, the ultimate scope of the metropolitan area tandem network may be restricted to what was described as the primary serving area.

Until automatic ticketing was introduced for interexchange service, all calls handled over the tandem system were operator-dialed by either the "A" operator or by the toll operator. With automatic ticketing, the subscriber is permitted to dial directly all points within the metropolitan area, except for six. Three of these are manual exchanges, and three are dial exchanges not yet arranged for using the universal numbering system. Operator-dialed calls may be directed to all points within the terminating scope of the tandem system.

Traffic is generated within the serving areas of 61 switchboards, 15 automatic ticketing offices, five attended pay stations, and the Orange County tandem office. Each originating unit has access to one or more tandem offices, plus direct trunk groups when justifiable.

Tandem development may be traced to the growing volume of metropolitan area interexchange traffic which is shown graphically in Figure 2. A comparison of traffic increase with respect to station gain may be made by referring to Figure 3. Only a part of the total traffic now is of the type handled over the tandem system as the introduction of the extended class of service, beginning in 1934, permitted calls between nearby exchanges within certain mileage limits to be handled as local calls. This in effect placed a portion of the interexchange traffic on a "free" basis to extended service subscribers.

Direct dialing by these subscribers over cross-boundary cable routes thus absorbed part of the growth that would have otherwise taken place in the type of calls handled by the tandem system. A very small amount of this traffic remains in tandem routes where cross-boundary dialing is not available and operator dialing is substituted. The remaining

portion of the calls are of the type that were all originally classed as short haul toll if placed with the toll operator or "A" board toll if placed with the "O" operator, but now with extended service, a billing schedule of exchange message unit charges has replaced the earlier system of short haul toll charges. "Person to person" or "reverse charge" calls are still classed as toll calls, as are calls involving points beyond the metropolitan area. The kind of traffic handled over the tandem system is therefore practically all of the type that involves a charge in excess of the monthly rate schedule.

Trunking Methods

In the selection of a method for trunking between telephone exchanges within a metropolitan area, there are a number of basic relationships to consider. A heavy volume of calls over any trunk group, for example, will mean that a larger number of calls per trunk can be carried. Conversely, a low volume of calls will result in fewer calls per trunk as shown in Figure 4. As the length of a circuit is increased, the requirements as to size of wire grow progressively more severe. At the same time the terminal equipment becomes more complex and expensive in order to cope with such factors as pulsing, transmission, or supervision. The cost penalties of inefficiency will therefore increase very rapidly as the mileage is extended, unless something can be done to obtain a relatively high volume of calls over each trunk group.

Another element, which is of considerable importance from an operating standpoint, is the effect of the trunking system on switchboard operation. High speed methods are particularly important where large call volume develops. Delay resulting from intermediate manual switching methods may be reduced with automatic dial switching. The number of small trunk groups an operator must search over may be reduced by tandem trunking. It also is desirable to prevent operators' tandem trunk groups from becoming excessively large because the time required to find an idle trunk may adversely affect operation during busy periods. Other factors more directly associated with design details have to be considered also, but the main underlying problem of selecting a trunking method involves a search for greater trunking efficiency, a shorter cable route, or a better method of operation. The various arrangements ordinarily adaptable to the problem are outlined in the following.

Direct Trunking

Direct trunking, as the name implies, requires an individual group of trunks between each pair of offices to be used for the sole purpose of trunking from one office to the other. If direct trunks were used exclusively, $n(n\text{-}1)$ groups of 1-way trunks would be required to interconnect n telephone offices as shown in Figure 5(A). Obviously, the exclusive use of direct trunking would result in an unreasonably large number of very small trunk groups and would introduce plant inefficiencies as well as operating difficulties.

There are advantages in direct trunking, however, that can not be overlooked. The direct route will in many cases be substantially shorter and require less complex equipment arrangements. The design need only be adequate for a specific function, whereas the design of a multipurpose routing must be governed by the most severe operating condition. With a fairly high volume of traffic, both efficient operation and the benefit of a short simple routing may be obtained. It should be noted that growth will produce an increasing volume of calls and the long term trend, therefore, is toward direct trunking.

Tandem Trunking

Tandem operation overcomes to a large extent the disadvantages of direct trunking through the use of strategically centered auxiliary switching equipment which is referred to as a tandem office. When each originating office is provided with tandem trunks, calls may be directed via tandem for completion to any point within its terminating scope. This permits the trunk groups, to and from the tandem, to be relatively large and operate at a much higher efficiency than is ordinarily obtainable with individual trunk groups. A small number of efficient trunk groups can thereby be employed in place of a large number of inefficient groups. This is demonstrated by a comparison between Figures 5(A) and (B) which have been simplified by assuming 1-way trunk groups and only eight offices. By referring to Figure 6, the effect of tandem operation and the benefit of larger trunk groups upon average trunk efficiency should be obvious.

There are disadvantages to dial tandem trunking that should be recognized in order that over-all plans may be shaped to overcome them. For one thing, the tandem office is an extra central office unit located at the hub of a large and very important trunking network. As such it becomes a sort of nerve center for the entire serving area, and nearly anything that happens within that area may affect tandem operation. A shift in the predicted pattern of growth, central office prefix changes, new central offices, new operating centers, new trunk routes, and equipment changes are some of the things that require co-ordinated activity in the tandem office. Also, from an economic standpoint, the cost of the tandem switching equipment is an item offsetting at least a portion of the increased trunk efficiency obtained. As pointed out earlier, the long term trend favors direct trunking, and this means that the economic gain obtained by tandem operation may gradually slip away, and for the heavier routings, direct trunking may become more desirable than tandem operation. A continuing study of the resulting

Figure 3. Station development in the Los Angeles metropolitan area

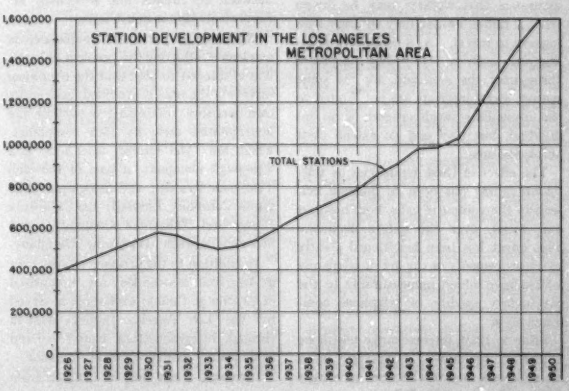

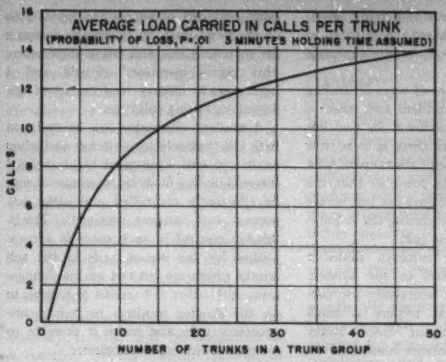

Figure 4. Average load carried in calls per trunk in a trunk group

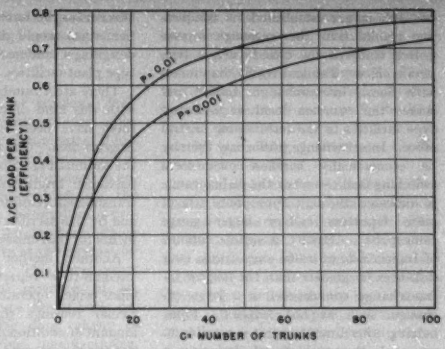

Figure 6. Efficiency of a trunk group

problem is required if a balanced plant design is to be maintained.

Direct Trunking with Tandem Alternate Routing

Direct trunking with tandem alternate routing exploits some rather obvious relationships concerning the distribution of traffic between the individual trunks in a group. If traffic is offered, for example, to a group of ten trunks in an orderly manner, the first choice trunk will have an opportunity to handle all calls. The second choice trunk will have an opportunity to handle all calls except those that found the first choice trunk idle and so on to the last choice trunk. By plotting the resulting distribution of traffic, as in Figure 7, the load carried by each trunk can be observed. In this particular case, more than half the traffic is carried by the first three trunks and they are therefore quite efficient as direct trunks. In larger groups the effect is even more pronounced. The latter choice trunks are progressively less effective on a direct routing basis and a very substantial gain is realized when this traffic is mixed with similar overflow traffic in a large common tandem routing. Direct trunks may be selected so that the least efficient direct trunk carries as much or more traffic than the average tandem trunk, or an economic selection of the load to be carried by the least efficient direct trunk can be made by applying the trunk cost ratio. If, for example, the cost for a direct routing is half as much as for a tandem routing, economic balance is obtained when the least efficient direct trunk carries half as much traffic as the average tandem trunk.

There are a great many factors to consider in the practical application of alternate routing systems which involve consideration of the volume and characteristics of traffic and various other engineering or administrative problems. It is clear, however, that direct trunking with tandem alternate routing is an increasingly important element in metropolitan area plant design. This is to be expected since the advantages of both tandem and direct trunking are thus obtained.

Figure 5. Trunk groups required between eight central offices

(A) Direct trunk plan (56 groups)
(B) Tandem trunk plan (16 groups)

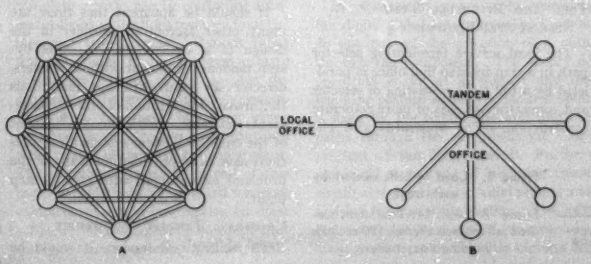

Equipment Available for Dial Tandem Operation

There are three types of equipment that are suitable for dial tandem operation in southern California and features are available in each that provide unique solutions to distinctly different problems. Since the general function of each is equivalent and this fact may obscure the logic of appropriate selection, the relative value of the various features in particular combinations is a subject requiring considerable study. An analysis of the apparent design philosophy can lead to better understanding of the practical applications. The three types of equipment applicable are:

1. Exchange step-by-step equipment.
2. Toll and intertoll step-by-step equipment.
3. Crossbar tandem equipment.

Exchange Type Step-by-Step Equipment

Exchange type step-by-step selector equipment is designed primarily to perform the job of switching intraexchange service calls over relatively short distances. The range has been extended and operation over a much larger area has been made possible through the development of long range pulse correcting repeaters and composite signaling equipment, which have extended the limits imposed by the fact that the switches are operated directly from the impulses of the subscriber's or operator's dial.

In applying exchange type step-by-step equipment to tandem switching,

connections are established via completing trunks into the exchange service switch train of the called party's telephone office. Tandem traffic thus mixes with local intraexchange traffic and shares the common local or exchange type facilities in the terminating central office. Interexchange traffic may thereby be economically handled over local switching facilities when the dialing range is increased through appropriate use of pulse repeaters and/or larger gauge cable pairs. Actually, a sizable amount of interexchange traffic may trunk over distances no greater than the longest intraexchange connections in a large exchange, such as Los Angeles. Thus, barring other limitations, it is possible to approach the problem of designing a metropolitan area tandem system on the basis of merely increasing the range of exchange type facilities.

Transmission limitations also have been extended by improvements in telephone sets and cable facilities, but with advancing standards it is not possible to provide an acceptable talking path over as great a distance as the dialing range will permit unless additional gain is introduced. When gain is provided through use of voice frequency repeaters, the full benefit can not be obtained without furnishing more complex circuits in all connecting facilities to control transmission and permit a proper circuit termination. Exchange plant design, therefore, can not be extended beyond certain limits merely by introducing special equipment on the long trunks since it becomes necessary to redesign the connecting circuits as well.

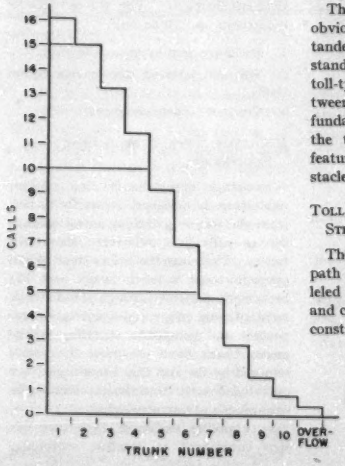

Figure 7. Load in calls carried by each trunk

Erlang "B" basis, 148 equivalent hundred call seconds offered, 180 seconds holding time assumed

Obviously, the latter would bring penalties which would defeat the purpose of designing a tandem system with exchange type plant facilities.

There are a number of ways of dealing with this kind of problem and most of these have been employed in the Los Angeles area. One of these is to narrow the terminating scope of the tandem for a particular originating point so that the transmission requirements are less severe and by this sacrifice reducing the requirements for transmission gain.

Another method employs dialed-in vacuum-tube repeaters in the tandem office which operate selectively for particular routings that require a small amount of additional gain. Since a larger variety of repeater balance conditions are presented maximum gain can not be maintained. As a result, it is either not suitable for as distant an originating point or some part of the terminating area may remain beyond limits.

A third method may employ two grades of trunk groups; namely, a low grade group for calls terminating within a restricted zone and a high grade group for calls switched between outlying points. Various combinations of the preceding also are applicable, but it should be recognized that since we are approaching the problem from the standpoint of extending the range of exchange type plant the inherent limitations remain. Under these circumstances, marginal conditions are continually encountered in expanding the dialing area and a general solution can not be obtained without considering a different approach to tandem plant design.

The problem previously discussed can obviously be eliminated if the design of a tandem system is approached from the standpoint of extending the application of toll-type plant. Interconnections between remotely located subscribers are fundamental to long distance service and the toll plant must therefore provide features to overcome the resulting obstacles.

Toll and Intertoll Type Step-by-Step Equipment

The local service terminating selector path in a step-by-step dial office is paralleled by a toll train consisting of selector and connector switches of more elaborate construction. The apparatus and circuits provided overcome the limitations of the local train by furnishing features for matching line and trunk impedance, plus visual operators' signals and a higher grade battery feed circuit of the 48-volt repeating-coil type.

A tandem office also can be designed with toll-type selector switches and when associated with even more highly refined intertoll dialing facilities transmission can be effectively controlled and other important toll features retained. Transmission control in such cases is accomplished by the use of pads in the toll trunks which are cut out on via connections with other toll trunks or remain in on the shorter routings to reduce unnecessary gain and make it possible to maintain voice repeater balance.

Intertoll selector switches are arranged to pulse directly from a simplex or composite leg, thus eliminating needless conversions from composite dialing to loop dialing and the attendant pulse distortion. As a result, the use of pulse correcting repeaters is avoided, which tends to offset the excess cost of the more elaborate equipment.

The associated equipment arrangements provide a better impedance match between the toll switching trunks and toll circuit, and permit dual use of the toll switching trunk for inward operator routed calls and intertoll dial tandem calls. Two-way operation is possible on the toll circuits.

Thus, step-by-step tandem facilities may be provided for extending either the exchange switch train or the toll switch train. The application depends upon the types of traffic, the relative volume and the geographical development of the area. In the Southern California area both types are employed; however, the Los Angeles metropolitan area system employs the exchange type plant since the character of the traffic and the distances involved more nearly coincide with exchange trunking requirements. A relatively small amount of traffic is handled that eventually will be shifted into toll plant arrangements.

It should be apparent that there are many other factors to consider in the design of a tandem system. Step-by-step tandem equipment without senders, directors or equivalent has limitations that make consideration of other arrangements desirable. With the development of the crossbar tandem system ideal solutions have been provided for many of the problems encountered with step-by-step plant.

Crossbar Tandem Equipment

To facilitate discussion, it would be

well to have in mind at this stage the fundamental difference between the step-by-step and crossbar tandem systems, as employed in the Los Angeles area. In the step-by-step tandem system, the movement of the switches is controlled directly by the impulses from a dial or sender in the originating office, and connections are established through fixed paths determined by the equipment arrangement as installed. Since the impulses are absorbed in switch operation and are not stored, they are not available for any purpose should, for any reason, the first attempt at establishing a connection fail.

The crossbar tandem system, on the contrary, is what may be designated as a common control system. Instead of actuating the switches directly from the impulses, these impulses are recorded in a control circuit, which in turn determines the switch operation necessary. The common control idea is not really new except for its method of application, for manual switching is a form of common control operation. Here the operator receives the desired number from the calling subscriber and, by means of the switchboard cord circuits and jacks, sets up the connection. If trouble is encountered or if the trunks are all busy, the operator can make a second trial or select another routing. An equipment or cable failure may be detected and reported while the subscriber remains utterly unaware of the difficulties experienced in establishing the telephone connection.

In the crossbar tandem system, relays and switches perform the operating function instead of a human operator. After receiving the called number the control equipment proceeds to determine if the first choice path is available and if so, sets up the proper switches; if not, other paths may be tried.

Crossbar tandem equipment may operate into either the step-by-step local train, the toll train or both. Appropriate selections between two or more completing paths can be controlled automatically by indications received from the incoming trunk group. Various other features unique to the common control system are covered in the detailed description of the crossbar tandem system. Equivalent treatment has been given elsewhere to step-by-step equipment and other related elements of telephone plant. The references given at the end of this paper should therefore be noted for more complete sources of information on these subjects. It is suggested, however, that correlated understanding will be facilitated if attention is focused particularly on features affecting trunking flexibility and service protection.

Flexibility

First, let us consider trunking flexibility. With a step-by-step tandem office where a large number of equipment items are assembled at the time of installation in various groups and cross-connected in accordance with a predetermined plan, the exact arrangement is the result of a predicted pattern of development which antedates the maturity of the forecast by roughly three years. This three years includes the normal intervals of six months for the average age of basic development and traffic data, about 18 months for engineering, manufacturing, installation, and testing, and another year from the in-service date to the time that predicted growth will require a subsequent addition for further relief. Even though mass requirements may be predicted quite accurately, excess capacity in one path through a switch train is of no value if an overload develops in another, since routings through the tandem office are controlled directly by the digits received.

The equipment, being assembled into a relatively rigid pattern by what amounts to a phase of manufacturing performed at the customer's premises, can not be readily rearranged except through another construction cycle. Since the trunk and pulse repeater requirements involve the use of a number of different circuit arrangements for matching complementary facilities, minor readjustments frequently require additional apparatus. The normal time required for changes is therefore the controlling element when thinking of flexibility, since maintenance of a proper balance in the system demands the ability to foresee changing conditions sufficiently in advance to satisfy the limitations of construction intervals. From the standpoint of flexibility the application of step-by-step equipment in tandem operation is therefore most favorable when conditions are stable.

In contrast to step-by-step operation the digits dialed into a crossbar tandem do not control the selection of a path through the equipment. The theory of operation is not at all similar and the trunking pattern within the tandem office is fixed by the size of the unit and the paths through the equipment are independent of the digits dialed. Furthermore, only one type of incoming trunk circuit is required for loop dial pulsing and another for composite dialing. The loop dial trunks are also usable for composite dialing when pulse converter circuits are available. In the general case, for this area, outgoing trunk circuits are employed only when a conversion from loop to composite signaling is required. Thus, any change in routing or in individual trunk requirements can usually be handled in crossbar tandem on a routine basis merely by issuing instructions to the maintenance forces.

Adjustments can be made easily in a matter of hours that normally require an extensive construction interval with step-by-step equipment. With only a reasonable anticipation of the kind of situations most likely to be encountered the problem of flexibility is limited only by the maximum call carrying capacity of the unit. The increased flexibility of the crossbar tandem equipment tends to minimize the effect of unforeseeable variations in traffic and provides an important tool for managing the trunk plant. The problem that remains is therefore largely one of predicting the mass requirements.

It should be clear that a large percentage of the total traffic is stable while a lesser part is expected to be more volatile. So if a plan can be developed under which highly flexible facilities are used for the less predictable items of traffic with the more stable items going over the less flexible arrangements, important advantages of both types of plant are utilized. Other points to consider are the number of switching combinations required and the total volume of traffic. Obviously, with only a few switching combinations, where the traffic is divided over a small number of paths or with a relatively low volume of calls, the limited flexibility of step-by-step equipment may be adequate for the conditions encountered. The two systems are not competitive in this respect since each can fulfill the requirements of different circumstances or one may support the other.

Service Protection

The question of service protection can be studied from various angles. Performance statistics may be examined or construction details compared, but a more basic approach should augment such observations. This requires an evaluation of the characteristic differences in the way the two systems operate. For example, with step-by-step equipment the relatively simple circuits respond to battery and ground or their absence, and mechanically follow dial pulses or supervisory signals. Many base metal contacts are used, and because of the sliding action and consequent wear in the switches the maintenance function is organized around the application of system-

atic preventive measures. Periodic cycles of testing, cleaning, lubricating, replacing of worn parts, and adjusting by skilled craftsmen keep the equipment in the best possible working condition.

With crossbar equipment, however, a further step has been taken. The switch employs a relay contact spring type of action, and uses precious metal contacts in voice circuits, permitting quieter connections and eliminating the bulk of manual labor required in searching for potential breakdowns. An even more significant point is the use of special circuits to monitor critical functions and check for proper operation before a call is established. When a failure is detected duplicate circuit elements and retrial features become operative. Further refinement is obtained with automatic testing and monitoring facilities permanently established in the test center, to record troubles and aid the maintenance force in isolating and correcting them. Thus, from a service protection standpoint, there is considerable assurance that crossbar tandem equipment offers advantages that will be of increasing importance in the advancing of future standards of service.

Dial Tandem Network

In the Los Angeles metropolitan area, five tandem offices, as described in the following, are utilized to provide switching facilities for trunking between the various exchanges of the area. Two of the tandem offices are located in Mutual Building which is the wire center for the area. The other three tandem offices are strategically located to provide coverage for particular sectors of the area.

Los Angeles Mutual Step-by-Step Tandem

This unit which is usually referred to as the "long haul tandem" was first placed in service in 1926.[2] Many changes and additions have been required since that time to keep pace with the development of the area, but basically the unit performs the function it was originally designed to accomplish. The present plan employs the following major equipment items:

7,697 selector switches
92 rotary out trunk secondary switch units
3,571 pulse repeaters (20 types)
80 voice frequency repeaters
740 composite sets (7 types)

The voice frequency repeaters are employed on a "dialed in" basis and their use can be controlled by operator's routing instructions that direct the use of a preliminary digit "0" where additional gain is required.

The general transmission plan for this tandem is symmetrical, and Los Angeles exchange connections are limited to a circuit loss between the subscriber and the tandem of 5 decibels for either originating or terminating. The first fringe offices are limited to 6 decibels and those beyond the first fringe are limited to a 7 decibel loss. Thus the over-all service may be established between subscribers in the various exchanges in accordance with the following:

Typical Types of Connections	Transmission Limit, Decibels
Los Angeles to first fringe exchanges	11
Los Angeles to outer exchanges	12
Between fringe exchanges	12
Fringe to outer exchanges	13
Between outer exchanges	14

In addition to the outer exchanges within the metropolitan area this unit connects with the Orange County tandem to serve the following exchanges:

Anaheim	Laguna Beach
Brea	Newport Beach
Buena Park	Orange
Fullerton	Placentia
Garden Grove	Santa Ana
Huntington Beach	Westminster

These exchanges also may reach the Los Angeles exchange and certain others through their operating centers which may dial through the Orange County tandem into the Mutual step-by-step (long haul) tandem.

Incoming trunks are provided for the more distant points; namely, Bakersfield, Pomona, San Bernardino, and San Diego as mentioned previously.

The traffic capacity of this unit is approximately 39,000 calls during the busy hour assuming an average of about three minutes per call. These calls originate over approximately 2,650 incoming tandem trunks.

Since 1926, this tandem unit has been the main switching center for all operator-dialed and automatic ticketing traffic. It is the only unit with complete access to the entire metropolitan area and Orange County points. Experience with the more recently introduced crossbar tandem at Mutual office indicates advantages in ultimately reducing the scope of the step-by-step unit and expanding the coverage of the crossbar unit. This would make the crossbar tandem the main switching center and ultimately reduce the step-by-step unit to the role of a short haul tandem or sector tandem.

Los Angeles Mutual Crossbar Tandem

At present this unit is referred to as the "short haul tandem." It was first placed in service in January 1948 and immediately took over the function of a small step-by-step short haul tandem previously employed for handling traffic between the Los Angeles exchange and Pasadena, Glendale, Beverly Hills, and Culver City. Additional capacity was provided to permit expansion of the area of coverage to include all points within a range of approximately 2,000 ohms trunk resistance. This limited the total scope roughly to Los Angeles and contiguous exchanges.

The reasons for initially limiting the coverage of the crossbar tandem were largely for purposes of expediting the installation. To obtain complete coverage, additional development work would have been required to provide features corresponding to the step-by-step tandem "dialed in" vacuum tube repeater arrangements and to receive more than seven digits or outpulse more than six digits. Since the use of "dialed in" repeaters is gradually being eliminated and a numbering plan has been selected that will not require more than seven digits, the delay and expense associated with the required development work could not be justified to care for what appeared to be a temporary condition.

Progress has been made in expanding the coverage with the crossbar tandem and under the latest plan all dial exchanges within the metropolitan area except two requiring eight digit dialing will be served by completing trunks. The originating side will be expanded as conditions permit until complete coverage of the metropolitan area is obtained.

A full unit of crossbar tandem equipment was installed initially with a capacity of about 28,000 busy hour calls. The quantities of major equipment items are as follows:

2,200 incoming repeated supervision trunk circuits
20 trunk link frames
20 office link frames (with extension frames)
160 dial pulse senders
8 markers

The transmission plan for the Mutual crossbar tandem is identical to the Mutual step-by-step tandem.

Los Angeles Lafayette Sector Step-by-Step Tandem

The Lafayette sector tandem is located in Huntington Park approximately six miles south of Mutual office and is along the route from Los Angeles to such points as Long Beach, Downey, and Compton.

It was first cut into service in May 1949 and has capacity for about 10,000 busy hour calls.

The main purpose behind the sector tandem idea is to eliminate back-haul of traffic and thus permit shorter routes and finer gauge trunk cables. The scope of coverage is limited and in this case includes the central, southerly, and easterly districts of the Los Angeles exchange and outlying points. More specifically the area is as follows:

Los Angeles Exchange

Adams District	Mutual District
Angelus District	Republic District
Axminster District	Richmond District
Drexel District	Thornwall District
Lafayette District	

Other Exchanges

Compton	San Pedro
Downey	Wilmington
Long Beach	

Facilities are provided for 724 incoming trunks and 928 outgoing trunks requiring major equipment items as follows:

1,671 selector switches
20 rotary out trunk secondary units
1,122 pulse repeaters

The transmission design of this and all other sector tandems is limited to 6 decibels inward plus 6 decibels outward. An over-all loss between subscribers of no more than 12 decibels is therefore obtained.

Los Angeles Thornwall Crossbar Sector Tandem

The Thornwall sector tandem is located roughly six miles south of Mutual office and about four miles west of Lafayette. It was first cut into service in November 1949 with a capacity for about 10,000 busy hour calls.

The Thornwall office is along the route from Redondo Beach and Inglewood to central office districts in the central, southerly, and westerly part of the Los Angeles exchange. The following points are within its serving area:

Los Angeles Exchange

Adams District	Republic District
Axminster District	Richmond District
Drexel District	Thornwall District
Lafayette District	Whitney District
Mutual District	

Other Exchanges

Compton	Redondo
Culver City	El Segundo
Hawthorne	Lomita
Inglewood	Torrance

The following major equipment items have been provided for the Thornwall tandem:

1,200 repeated supervision trunk circuits
10 trunk link frames
10 office link frames
54 senders
5 markers

Los Angeles Hollywood Sector Crossbar Tandem

The Hollywood sector tandem was first cut into service in February 1950. It is located 6.7 miles northwest of Mutual office and is along the main route to San Fernando Valley points. It serves exchanges in the sector to the north and west of Mutual office as follows:

Los Angeles Exchange

Axminster District	Republic District
Drexel District	Richmond District
Hollywood District	Whitney District
Mutual District	
Olympia District	

Other Exchanges

Beverly Hills	North Hollywood
Burbank	Reseda
Canoga Park	San Fernando
Crescenta	Santa Monica
Culver City	Van Nuys
Glendale	West Los Angeles

Nearly a full unit of crossbar tandem equipment was installed initially with a capacity for 25,000 busy hour calls. The following major equipment items were provided:

2,160 repeated supervision trunk circuits
18 trunk link frames
18 office link frames (with extension frames)
130 dial pulse senders
8 markers

Summary

Dial tandem facilities are employed in the Los Angeles metropolitan area to permit rapid and economical interexchange telephone service over the wide area of subscriber community of interest. The five major tandem offices are part of an over-all system designed primarily to:

1. Provide operating methods that will permit the handling of calls at a speed comparable to a local grade of service.

2. Permit high trunk efficiency and an economically balanced plant design that is consistent with advanced telephone practice.

3. Allow a less exacting plant design than would be required if toll long-distance type facilities were employed, so that the large volume of calls may be handled at minimum cost to the customer.

Two fundamentally different types of equipment are employed and each contributes important advantages in this area. The step-by-step tandem equipment, which is of the same type employed in the local dial offices and around which the dial tandem network has grown since 1926, is best adapted to stable conditions or small units. The more recently developed crossbar tandem with its highly flexible trunking arrangements is a valuable tool for meeting the requirements of the most volatile service demands. It also includes features which extend the idea of service protection beyond reliance upon high grade preventive maintenance to include the conception of self checking and prompt completion of calls even under many trouble conditions.

While long-term growth tends to increase the effectiveness of direct trunking methods over tandem trunking, other adverse trends are constantly causing additional segregations in the traffic. As the result, the effectiveness of interexchange trunking methods remains dependent upon the tandem switching system.

References

1. Tandem Operation in The Bell System, **F. M. Bronson**. *The Bell System Technical Journal* (New York, N. Y.), volume 15, July 1936, pages 380–404.

2. Tandem System of Handling of Short Haul Toll Calls, **F. O. Wheelock, E. Jacobsen**. *AIEE Transactions*, volume 47, January 1928, pages 9–20.

3. Dial Switching of Connecticut Toll Calls, **W. F. Robb, A. M. Millard, G. M. McPhee**. *Electrical Engineering* (*AIEE Transactions*), volume 55, July 1936, pages 773–83.

4. A General Switching Plan for Telephone Toll Service, **H. S. Osborne**. *The Bell System Technical Journal* (New York, N. Y.), volume 9, July 1930, pages 429–47.

5. An Outline of Step-by-Step Operation **E. D. Butz**. *Bell Laboratories Record* (New York, N. Y.), volume 8, December 1929, pages 174–77.

6. The Toll Train, **E. D. Butz**. *Bell Laboratories Record* (New York, N. Y.), volume 10, December 1931, pages 131–34.

7. Intertoll Dialing with Step-by-Step Selectors, **R. R. Swain**. *Bell Laboratories Record* (New York, N. Y.), volume 18, May 1940, pages 266–68.

8. Step-by-Step Intertoll Dialing, **R. E. King** *Bell Laboratories Record* (New York, N. Y.), volume 19, May 1941, pages 266–69.

9. Thru Selector for Dial Toll Calls, **R. J. Hope**. *Bell Laboratories Record* (New York, N. Y.), volume 20, October 1941, pages 47–51.

10. Automatic Ticketing of Telephone Calls, **O. A. Friend**. *Electrical Engineering* (*AIEE Transactions*), volume 63, March 1944, pages 81–88.

11. Contacts, **P. W. Swenson**. *Bell Laboratories Record* (New York, N. Y.), volume 27, February 1949, pages 50–53.

12. Basic Theory Underlying Bell System Facilities Capacity Tables, **A. L. Gracey**. *AIEE Transactions*, volume 69, part I, 1950, pages 238–44.

13. Crossbar Tandem System, **R. E. Collis**. *AIEE Transactions*, volume 69, part II, 1950, pages 997–1004.

No Discussion

The Universal Director in Strowger Automatic Telephone Systems

J. E. OSTLINE
FELLOW AIEE

FOR more than half a century the Strowger Automatic, or "step-by-step" switching system has been well known to telephone engineers and telephone operating administrations throughout the entire world. Its inherent simplicity, flexibility, and stability in operation have made it suitable for telephone communication requirements in the smallest exchanges as well as the largest metropolitan areas.

The Strowger Automatic switching system, as commonly used, is a "direct" dial controlled system in that each connection is extended on a decimal number basis, stage by stage, by electromechanisms that are under the direct control of the dial at the calling station. This eliminates the need for common controls or registers and thereby offers maximum simplicity and a minimum amount of equipment for a given exchange.

The step-by-step method of operation inherently associates the numbering plan with the switching stages required to establish a connection. In single exchange units up to 10,000 terminals or in small multioffice networks this does not introduce any difficult problems from either a numbering or trunking viewpoint. However, when large multioffice city exchanges or metropolitan multiexchange networks are involved, the direct dial control method is apt to prove somewhat inflexible and sometimes costly. This is particularly true when conditions favor the use of existing tandem trunking routes in a conversion from manual to automatic operation or in a program of interexchange trunking additions or readjustments to meet expanding area requirements.

The problem of providing economical and flexible interexchange trunking with universal numbering, while yet retaining the desirable features inherent in Strowger step-by-step equipment and operation, was met nearly 30 years ago when Automatic Electric Company designed and made available the Strowger Automatic Director. This unit of equipment first was used to meet several complicated interoffice trunking problems in the Havana, Cuba, exchange network in 1924. A year earlier, it had been officially adopted by the British Post Office for the conversion of the telephone network of the London Metropolitan Area from manual to automatic operation.[1] In this network the problem of interoffice trunking was rather complicated due to the fact that the metropolitan telephone network had been built up from a number of isolated manual exchange areas which were consolidated when the British Government assumed ownership of the country's telephone communication systems.

That the Director in conjunction with the basic Strowger Automatic equipment has proved practical and economical is indicated by the fact that Strowger Director operation has since become standard for all metropolitan area telephone networks in Great Britain.

Further Director Developments

The London Director was originally designed to provide only interoffice and tandem trunking controls with universal numbering. It soon became apparent, however, that the Director could be arranged to provide many additional types of services and facilities in Strowger Automatic switching operations. Some of the facilities or controls considered for future use were:

a. Common trunking controls.

b. Alternate routing.

c. Class of service discrimination.

d. Subscriber-dialed short-haul (*AB*) toll service controls with automatic call recording.

e. Operator key-dialed long-distance service controls with semiautomatic call recording (national toll dialing).

Directors containing one or more of the foregoing or any other controls, in addition to the original trunking control functions, now are referred to as Universal Directors.

About 1938, Bell and independent companies providing telephone service in the Los Angeles, Calif., metropolitan area began to consider the possibility of providing subscriber dialing in place of manual operation for short-haul toll calls between the various exchange areas in this network. At this time Automatic Electric Company had already provided a Director-controlled toll dialing and automatic call recording system for the Belgian Telephone Administration. They, therefore, proposed to the independent operating telephone companies in the Los Angeles metropolitan area a Director arranged not only to provide trunking controls for interexchange traffic, but also to control subscriber dialing and automatic call recording for short-haul toll traffic as well as to provide controls for other facilities and services suitable for the area.

After various plans for Director operation had been submitted to and studied by the various companies concerned, the Associated Telephone Company, Ltd., Santa Monica, in 1944 installed and placed in operation a "pilot" installation of Director-controlled automatic short-haul toll ticketing which provided direct

Paper 50-169, recommended by the AIEE Communication Switching Systems Committee and approved by the AIEE Technical Program Committee for presentation at the AIEE Summer and Pacific General Meeting, Pasadena, Calif., June 12–16, 1950. Manuscript submitted March 15, 1950; made available for printing May 11, 1950.

J. E. Ostline is with the Automatic Electric Company, Chicago, Ill.

The author wishes to thank Dr. Arthur Bessey Smith, Mr. C. F. Ffolliott, and other staff members of Automatic Electric Company for their suggestions and assistance in preparing this paper.

Figure 1. Los Angeles metropolitan extended area

The letters "O.A." mean "Office Assignments"

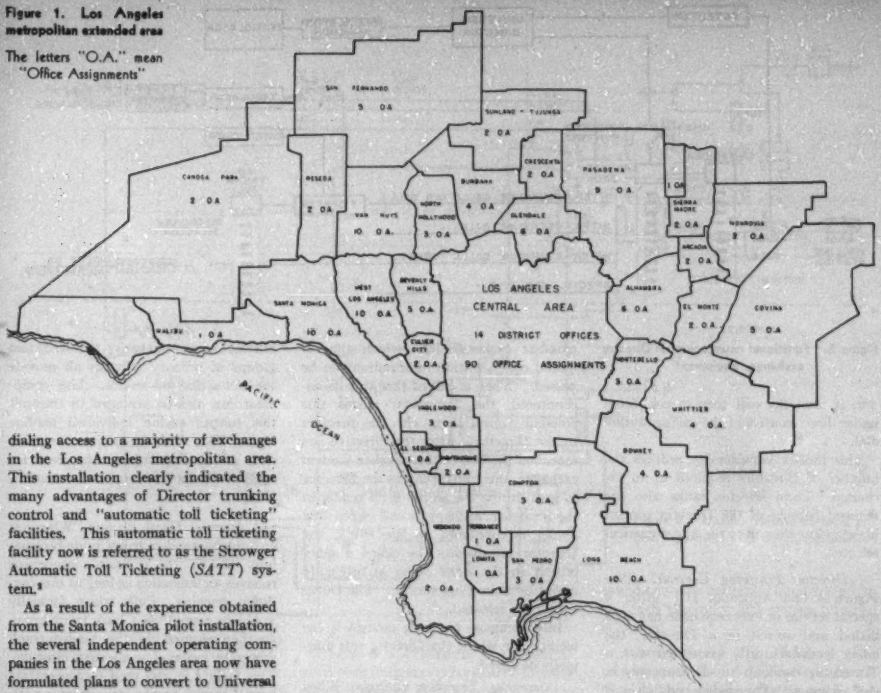

dialing access to a majority of exchanges in the Los Angeles metropolitan area. This installation clearly indicated the many advantages of Director trunking control and "automatic toll ticketing" facilities. This automatic toll ticketing facility now is referred to as the Strowger Automatic Toll Ticketing (*SATT*) system.[3]

As a result of the experience obtained from the Santa Monica pilot installation, the several independent operating companies in the Los Angeles area now have formulated plans to convert to Universal Director operation. One such installation with automatic *AB* toll ticketing and several other facilities recently has been completed for the Sunland-Tujunga Telephone Company, at Sunland, Calif. The Universal Director provided for this installation is described in outline in this paper.

The Universal Director

Facilities

The Director equipment described herein has been designed to provide facilities to meet the various operating requirements encountered in the Los Angeles metropolitan area, Figure 1, which now contains over 1,250,000 stations. Controls for the following facilities are provided:

a. Mixed 6-digit and 7-digit numbering.

b. Director release on local exchange calls.

c. Interexchange trunking with common translators.

d. Secondary trunking.

e. Alternate routing.

f. Class of service discrimination.

g. Line testing.

h. Station identification on party lines.

i. Automatic short-haul toll ticketing (*SATT* system).

j. Emergency directive.

Outline of Director Equipment

The Director and associated equipment is made up of standard Strowger components such as rotary and 2-motion switches and various types of relays. These various units are arranged so as to provide the same easy maintenance facilities which have always been inherently characteristic of all Strowger switching equipment.

In the original (London) Director the translation control was built into each Director. In the Universal Director this facility is provided in a common control unit termed the Translator.

When automatic toll ticketing service is provided in an exchange, several other units of equipment are required besides the Director, as indicated in Figure 2. The detector and dater-timer are units common to the *SATT* operation. Ticketers, tabulators, and associated tape perforators are provided on the basis of short-haul toll traffic.

Outline of Facilities

Mixed Digit Numbering. The Los Angeles area numbering plan will eventually be of the so-called "2 by 5" 7-pull type. At the present time, however, a mixed 6-pull and 7-pull numbering is used. The Director therefore is arranged so that trunking and service controls can be established from dialing 6-pull or 7-pull numbers as well as zero and 3-digit service codes.

Director Release on Local Calls. (See Figure 3 and Appendix I.) All switching components in Director exchanges are of the normal direct-dial control Strowger type, and they can be controlled either directly from station dials or from Directors. Therefore, all Directors are provided with adjustable "strapping" facilities which enable them instantly to recognize local exchange codes. When a local code is dialed the Director releases after the code has been dialed

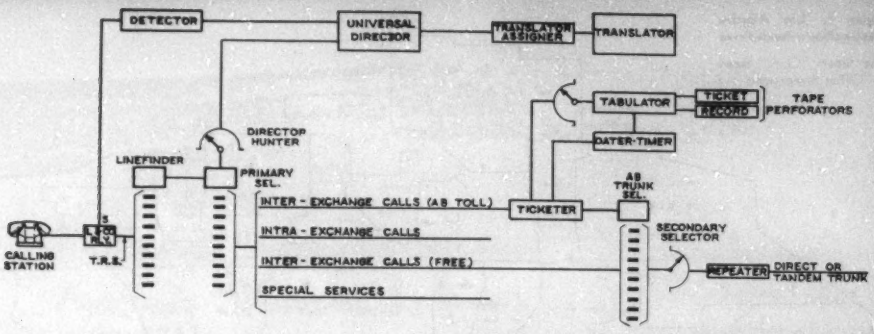

Figure 2. Functional arrangement of Director exchange equipment

nto it, and the call then is completed under direct control of the calling station dial.

This facility considerably reduces the number of Directors required in an exchange. Local selector ranks also are reduced because of the Director control in extending the call to the first numerical selector.

Director Trunking Controls. (See Figure 4 and Appendix II.) After a special service or exchange code has been dialed and stored in a Director, the latter is momentarily associated with a Translator common to all Directors in the exchange. The dialed code then is sent to the Translator, which instantly sends back a "directive" to the calling Director and releases itself. This directive contains the information required for the Director to extend the call to a service operator or the terminating exchange via direct or tandem trunking.

The directive produces from one to five trains of pulses of suitable numerical values. After a terminating exchange is reached, the numerical portion of the called number is transmitted in the same value as registered in the Director. After transmission is completed the Director releases.

The third digit of a called exchange code often is used in tandem trunking. When this is required, the directive does not contain this digit, but it does contain a "C" digit control which causes this digit to be resent from the original called number registration storage in the Director.

Another type of tandem trunking encountered in the Los Angeles area involves passing certain calls via tandem exchanges using crossbar type switching. This requires a search for a register in the crossbar exchange into which the required called station information can be passed. When a call of this type is encountered, the Translator passes this crossbar control along with the directive to the Director. After the directive has extended the call to the crossbar tandem exchange, this control causes the Director to wait during the search for a sender in the crossbar exchange, and when the sender is connected to the trunk, the Director retransmits the called number into it in the same value as originally dialed by the calling station. The Director then is released.

Interexchange trunking control is the facility for which the Director was originally designed.

Secondary Trunking Controls. When desired, the Director can be used to control so-called secondary trunking with 25-trunk or 50-trunk rotary switches. When used in direct-dial controlled exchanges (non-Director), this type of trunking has to be preselective due to the time limitation imposed by the interdigital period. With the Director this interdigital period can be controlled by the switch-through function which takes place in the secondary switch when a free trunk is found. This interdigital period control therefore can be used to provide post-selective secondary trunk selection with continuous hunting. This continuous hunting is limited only by the setting of the time-cut-off facility in the Director.

Class of Service Controls. This is the facility by which the Director controls access to the services to which a calling station is entitled. For instance, Class-1 stations may receive free service to a larger area than Class-2 stations. Therefore, if a Class-2 station dials into a Class-1 free area, the Director will complete the call on an AB toll basis.

The class of service control is transmitted to the Director from the primary selectors on a group basis; that is, certain groups of primary selectors all provide the same class of service. Line equipment can also be arranged to transmit this control on an individual per-line basis. This method permits changes in class of service without the need for transferring the line into another selector group.

Alternate Trunk Routing. Whenever an outgoing tandem trunk group becomes busy (*ATB*), the translator equipment receives an indication as long as this condition remains. Calls which normally would be routed via a busy trunk group are then rerouted via other tandem trunk groups by means of an alternate directive. This facility is also used to concentrate special service trunks into common positions during light load periods. Ordinarily this concentration process requires individual switching of each trunk while it is in a free condition. With the alternate routing facility this change-over can be done at any time regardless of the trunk condition by the operation of one common key.

Line Testing. It is, of course, well known that in both manual and automatic switching systems a partial and sometimes a solid ground on the tip (positive) side of a station line does not seriously interfere with signaling or dialing functions. However, in automatic exchanges using the *SATT* system, ground leaks on station lines must be kept to certain minimums in order to permit correct identification of party stations.

In order to prevent stations on lines with ground leaks beyond a permissible maximum from initiating *SATT* calls on which party identification is required, the Director always tests the line by which it is seized. If a ground fault below the permissible minimum is encountered, this fact is recorded. If the dialed exchange

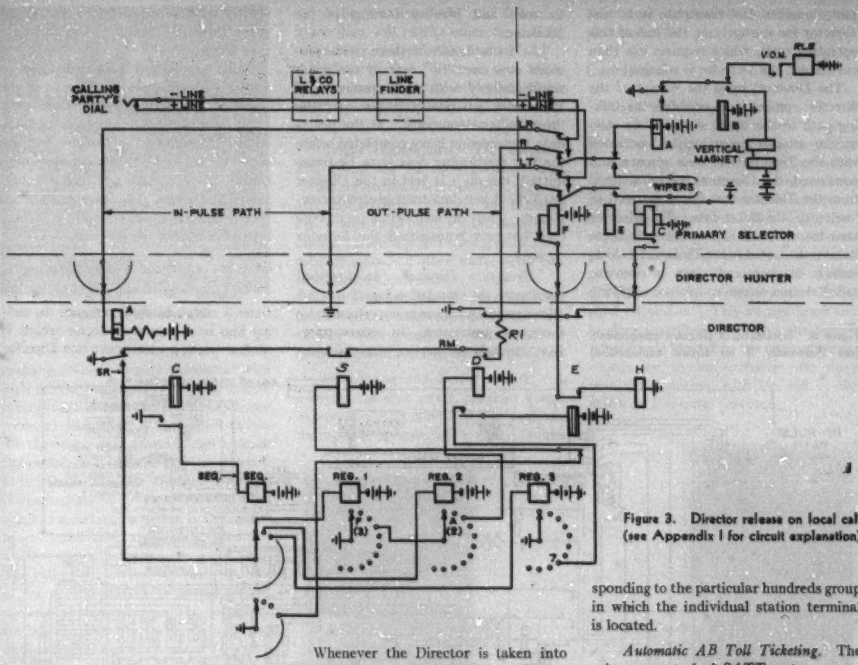

Figure 3. Director release on local call (see Appendix I for circuit explanation)

code and class of service indicates a free call, the Director permits completion of the call in the usual manner. If the dialed code indicates an *AB* toll call, the Director cancels the automatic completion of the call and extends the calling station to a manual operator over a special trunk group. The operator then can complete the *AB* toll call. The call coming in over the special trunk group is an indication of the line fault, which the operator will report to the maintenance staff.

Party Station Identification. In order to provide *SATT* service to 2-party and 4-party stations, means must be provided to identify which particular station on a line is initiating a call. This party station identification facility is provided by means of an "identity" dial, Figure 5, at each of the stations on a party line, and "party group" recording equipment in each Director. Identity dials are ordinary automatic dials as manufactured by Automatic Electric Company with the addition of a party-identity impulse mechanism. This added facility in no way affects the normal function of the dial.

Whenever the Director is taken into use it tests for and registers party-identity pulses, if present, during the dialing of the second code digit. At the end of this digit the Director knows in which group of connector terminals the calling station is located. This party-identity registration is used only if the call is an *AB* toll call and, in such case, this identity control will indicate to the Detector the particular hundreds groups of terminals in which it must search for the calling station terminal number.

Party-identity pulses from station dials do not interfere with the regular dial pulses or the operation of the equipment which is controlled by such dial pulses.

This party-identity facility can also be used, in connection with suitable line equipments, to provide "message metering" for party-line stations.

The fact that a station is located in a particular hundreds group of terminals which serves party-line stations does not always indicate that the station has party-line service. Individual line stations may also be located in these groups to obtain correct traffic loadings throughout an exchange. An individual line station in a party-line service group must, however, be equipped with an identity dial corresponding to the particular hundreds group in which the individual station terminal is located.

Automatic AB Toll Ticketing. The primary control of *SATT* system operation is centered in the Director, see Figure 4. When a calling station dials another station located in a short-haul toll area, the dialed code will indicate this fact to the Translator. The Translator then will include with the returned directive an indication that the call is to be ticketed and also the rate which will apply to the call if completed.

As soon as the Director has the indication that the call is to be ticketed, it prepares itself to transmit "ticket data" to the Ticketer unit which is always included in a toll call trunk path. The first action in this procedure is for the Director to "call in" the Detector. When acknowledgement is received from the Detector, the Director transmits to it the particular hundreds groups in which the Detector must search for the calling station number. This indication is normally Group 1 unless the call is from a party-line station group, in which case the indication will be Group 2, 3, 4, or 5. This party indication is stored in the Director by the calling station identity dial as described previously.

As soon as the Detector has received the group indication it detects the calling

party number and transmits it to the Director for storage. At the end of this operating cycle, which requires less than one second, the Detector is released.

The Director, upon the receipt of the directive, proceeds to establish the talking path to the called station. As soon as the selector permanently associated with the Ticketer has been reached and positioned, the Director receives a signal from the Ticketer that it can proceed to "write up" the ticket data. The Director then transmits in high-speed code these items to be stored in the Ticketer: calling station number and class of service; called station number and rate applying to call; and identity number of the Director.

The transmission of these items proceeds over the "tip" side of the trunk simultaneously with the transmission of the switch positioning pulses over the "ring" side of the trunk. If the ticket-data transmission is not completed before the last positioning digit is to be transmitted, this digit is held in the Director until the ticket-data transmission is completed. When the final switch positioning digit has been transmitted the Director releases.

Emergency Directive. As described previously, the translation function for all Directors in an exchange is performed by a common translator. In order to prevent stoppage of service due to interrupted translator operation, an "emergency directive" facility is provided in each Director.

When a code has been dialed into a Director it calls for a directive from the translator. However, if due to any operating fault no directive is received back within 15 seconds, the Director will extend the call to a *D.S.A.* operator under control of the emergency directive and then release itself. The operator will then take whatever action is required according to local operating practices.

Outline of Director Operation

Station Calls. When a station initiates a call, a linefinder extends the calling line to a primary selector which is similar to a first selector in a non-Director

Figure 4. Schematic of Director components (see Appendix II for circuit explanation)

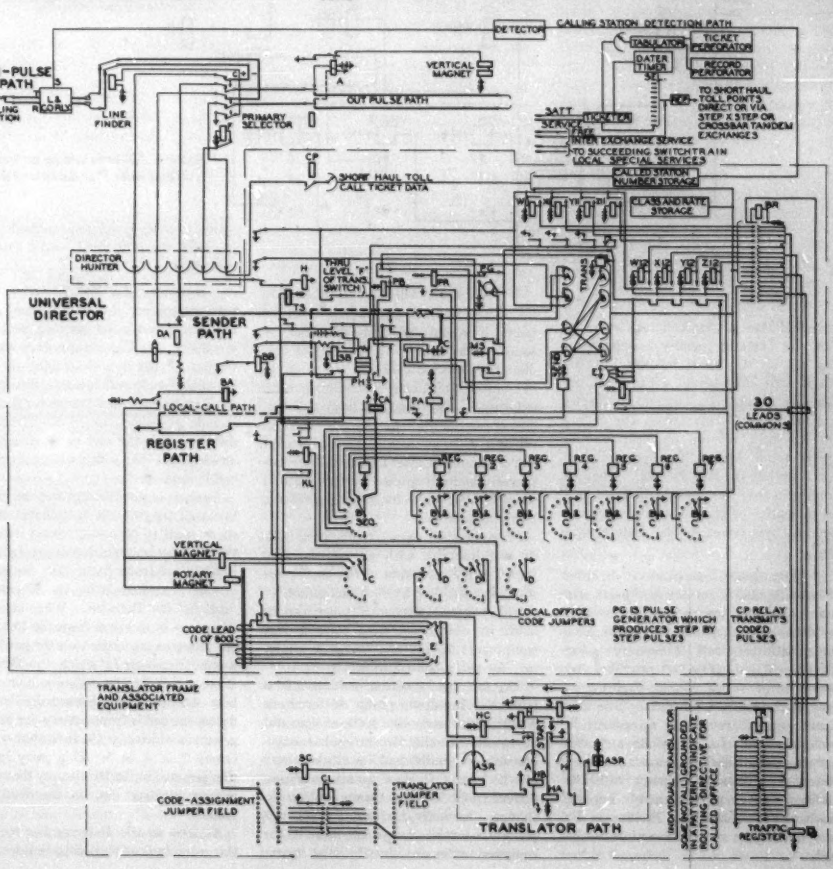

Figure 5. Identity dial

exchange. Permanently associated with each primary selector is a director-hunter rotary switch, the banks of which are wired to Directors. This hunter switch searches for a free Director and extends the calling line and the primary selector to it. On seizure, the Director first tests the calling line for ground insulation, then checks for and registers the class of service to which the calling station is entitled, and finally extends dial tone to the calling line. The calling subscriber now dials the code of the desired station or special service. As soon as this code has been dialed and stored, the Director goes into action as outlined in an earlier section if the call is local, or free to an adjacent exchange area. If call is *AB* toll, it is processed by the Director as already described.

Traffic and Fault Controls. If a Director after seizure fails to completely record a called number or correctly transmit outgoing switch positioning pulse trains, it returns a busy tone to the calling station and gives an alarm. The calling station can release, but the Director will be held busy and locked in the position in which it produced the alarm. This assists the maintenance force in locating the fault.

If the Director is seized by a "short" or "ring-grounded" line, it will, under the control of a suitable time delay device, call in a directive from the Translator which will extend the faulty line to an alarm unit via a level in the primary selector. This will free the Director for normal traffic and alert the maintenance force.

If a nonexisting code is dialed by a calling subscriber, the line is extended either to an operator or to a "no-such-number" tone via a level in the primary selector, and the Director is released.

If dialing of a number is incomplete the time-out facility extends a busy tone to the calling station from the Director, which then will release when the calling subscriber replaces the handset.

If all trunks in a Director hunter bank become busy, the hunter switch stops searching and the calling station receives a "regular" or "all-trunks-busy" tone.

Traffic Registration (Peg Counts). The Translator for each exchange and special service code is arranged to register each call attempt. Correct and detailed traffic data on all traffic routes therefore is obtained from which trunking and equipment changes and other traffic items can be accurately determined.

Each Director also is provided with traffic registers which separately show the number of local calls and the number of outgoing calls processed by each Director.

Monitoring and Test Facilities. A Director monitor panel provides visual observation of all basic Director functions during the progress of a call. "Make busy" and complete test facilities also are provided in this panel.

Conclusion

From the foregoing outline of the Universal Director it will be seen that it is not a fixed or rigid unit of equipment, but that it can be arranged to provide a multitude of service facilities and controls to suit almost every conceivable automatic switching arrangement. Dr. Arthur Bessey Smith states,[8] "We can make the complete Director assembly do whatever is necessary to direct a call to the desired distant office and to connect with the desired telephone." This we now know can be done regardless of whether the desired telephone is located in the originating exchange or in an exchange anywhere within the nation, with the aid of the Strowger Universal Director.

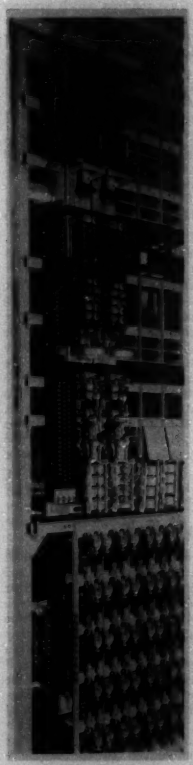

Figure 6 (left). A portion of two Directors

Figure 7 (right). Translator frame

Appendix I

Figure 3 is a functional diagram of an intraexchange call with FAirfax 7 used as local office code.

As depicted, a calling subscriber's line has been extended by way of its line and cut-off relays, linefinder, and primary selector through the director hunter to a Director. The Director is in a seized condition and the selector, though seized and busy, has only its *F* relay operated. Relay *A* in the Director is maintained operated by way of the line loop and subscriber's dial to ground. When the subscriber pulls the dial off normal and releases it for the first digit, relay *A* will pulse following the dial impulses and restore once for each impulse. Relay *C*, when operated, closes a circuit to the motor magnet of the sequence switch, which magnet remains operated for the duration of the digit.

The first digit of the office code, FAirfax 7, will be a 3. When this digit is complete, relay *A* in the Director will resume its operated condition and relay *C* then restores in the interdigital period. Register *1* now has its wiper standing on its fourth bank contact. The restoring of relay *C* allows the sequence switch magnet to restore and to advance its wiper onto its second bank position. On the next digit dialed by the subscriber, relay *A* will follow the dial impulses and relay *C* and the sequence switch will be maintained for the duration of the digit with register *2* taking one step for each dial impulse, which in this case is *2*. When the digit is complete, relay *C* and the sequence switch restore, and register *2* is now standing on its third bank contact. Relay *D* now operates on a circuit through the wipers of registers *1* and *2*. Upon operating, relay *D* closes a circuit from the closed contacts of relay *A* in the Director by way of resistor *R-1* to the number-1 winding of the *A* relay in the primary selector. Relay *A* in the selector operates, closing the circuit to relay *B*, and upon operating, *B* will cause relay *C* to operate and lock to ground at relay *D* in the Director by way of the director hunter.

The third digit dialed by the subscriber, in this case 7, will cause relay *A* in the Director to pulse, relay *C* and the sequence switch remaining operated for the duration of the series, and register *3* stepping in the same manner as registers *1* and *2* stepped on previous digits. However, during the third digit, each restoration of relay *A* on an impulse will open a ground circuit to the *A* relay in the primary selector. The selector *A* relay will restore and, by way of the contacts of its slow release relay *B*, send an impulse to the selector vertical magnet. The selector will take one step for each impulse from the Director *A* relay. This third digit then is impressed on register *3* and the vertical magnet of the primary selector simultaneously. When the digit is complete, relay *A* in the Director resumes its operated condition, relay *C* restores as well as the sequence switch, and a circuit is closed on the bank of register *3* to relay *E*. Relay *E* operates, opens the locking circuit for the primary selector *C* relay so that it may restore and allow the selector to do rotary hunting. Relay *E* also opens the circuit maintained between relay *H* in the Director and relay *F* in the primary selector. These two relays restore and when relay *F* restores, the subscriber's line is connected to the selector equipment in a normal step-by-step manner. Then the Director is released to other subscriber traffic.

If perchance the called office code is one which has its first two digits the same as for local office codes, but the third digit indicates an office code requiring translation and sending, the functions in the Director and primary selector would be the same up to the point where the third digit is complete. Register *3*'s position at the completion of the third digit would be on some bank contact other than *8* and relay *E* would not operate. The sequence switch, when it restores, then closes a circuit to relay *S*, which operates, and by way of contacts not shown, calls for a translation of the dialed code. Relay *S* also opens the circuit to relay *A* in the primary selector. The primary selector, though it has stepped vertically on the third digit, was not able to hunt in the rotary direction due to the fact that its *C* relay was locked to ground at relay *D* in the Director. Relay *A* in the selector restores, opening relay *B* which upon restoration actuates the selector release magnet which restores the shaft. Sending, by way of the primary selector and subsequent switches, will ensue as is normal for translated office codes.

Appendix II

Figure 4 depicts the schematic diagram of the Universal Director and associated component units involved in the registration, translation, and sending of subscriber-dialed calls to be completed on either a free or automatic toll ticketing basis, as well as local special service calls.

Pulse Path

The circuit from the *A* relay in the Director via contacts of relay *F* in the primary selector, the linefinder, line relays, subscriber's line, and instrument is the in-pulse path. All digits dialed to the Director by the subscriber will be "in pulses" on this loop from the subscriber's dial to the *A* relay in the Director. This circuit is established after the line-finder, having found the calling line, extends the line to the primary selector, and the director hunter associated with that selector has found an idle Director. Other equipment in the primary selector is released though it is maintained busy to traffic.

Register Path

Register switches *1* through *7* are used one at a time in sequence to register and store the digits dialed by the subscriber for use in the control and completion of the call. Relay *A*, which is in the in-pulse path, will pulse following dial impulses on each digit, and close ground impulses over the register path by way of the *B* level of the sequence rotary switch to the proper registers, one register at a time. Relay *CA* will operate for the duration of each digit in multiple with the register switch in use, and when operated, relay *CA* closes the circuit to the sequence switch motor magnet. When each digit is complete and relay *CA* restores, the sequence switch is released and its motor magnet restores, driving its wiper ahead one step. When the third digit is complete and the sequence switch advances to its fourth bank contact, the Director has enough information in the 3-digit office code to request a translation and commence sending the directive digits necessary to reach the called office. This function does not require the full seven digits to have been registered. The subscriber will proceed to dial the balance of the digits while at the same time the Director will call for a translation, receive it, and commence sending.

Translator Path

The Translator path is called into the circuit at the completion of the third dialed digit by way of the fourth bank contact of level *C* of the sequence switch. This closes the circuit to relay *S* and relay *S*, when operated, initiates the Translator assigner operation, including the functions of relays *HA*, *HC*, *SC*, and *H*, and when relay *HB* operates, the Translator path is closed by way of the *ASR* bank and the *E* level of register *1* to one of the eight wipers of the Director code switch. The first digit dialed by the subscriber positions registers *1* and this position of register *1* selects which of the eight code switch wipers will be used. The second and third digits of the called office code, besides being registered on register switches *2* and *3*, also cause the vertical and rotary magnets to position the code switch shaft up and in to a position corresponding to the decimal values in the second and third digits. The path thus is closed by one of the eight code switch wipers and one of 800 code leads through the code assignment jumper field to bar relay *CL*, this relay having already been operated by relay *C*. The circuit is complete through relay *CL* and the translator jumper field to that Translator peculiar to the 3-digit office code which was dialed by the subscriber. The Translator relay operates. Certain of the 30 leads connected to the Translator will be grounded when the *TR* relay operates depending upon the directive required to reach the called office and resultant ground strapping on the Translator relay.

Directive Storage

The Director has, as part of its equipment, a group of relays, the purpose of which is to receive and store information from the translator for use as required. Relays *W11*, *X11*, *Y11*, *Z11*, and so forth, as well as the class and rate storage group, make up this equipment. When relay *H* operated on the translator function relay *BR* was closed and it operated. The various grounds closed by the translator over the 30-lead common are extended through the closed contacts of the *BR* relay to the directive and class and rate storage relays. The storage relays connected to those of the 30 leads which are grounded operate and lock, thus their own make contacts to ground at the *BB* relay.

Release of Translator Path

Whenever a Director calls for translation of an office code it is obvious that at least

one directive digit will be necessary to route the call. There may, of course, be other information too, but there must be at least one, and this first digit will be registered and stored in code group 11. Any one of the four relays in code group 11 will close a circuit to relay *SB* in the Director and relay *SB*, when operated and locked, opens the circuit to relay *S* in the Translator path. Relay *S* restores, causing relays *H*, *HA*, *HB*, *HC*, *SC*, *CL*, *TR*, and *BR* to restore. This whole cycle of operation covered under the Translator path, the directive storage, and the release takes but a fraction of one second, and as soon as these various units have been released they are available to other Directors requiring translation and directive information.

Pulse Generation

The Director is equipped with a step-by-step pulse generator designated *PG* on Figure 4, which, by means of its associated *MS* (motor start) relay, is started by the operation of relay *S* when translation was called for. The pulse generator is started as soon as translation is required so that it is up to speed and maintaining a constant speed prior to the time that output impulses are required for sending.

Sender Path

Once the directive has been received by the Director from the Translator, sending of step-by-step impulses by the Director via the primary selector and subsequent switch train may proceed one digit at a time under the control of relays *PA*, *PB*, *PH*, *PC*, and *PR*. The rotary switch designated "Send" is the primary control of each digit transmitted. When relay *SB* operated to initiate the release of the Translator path, it closed a ground-connected circuit over the sender path to the battery connected winding of the *A* relay in the primary selector. The selector *A* relay operates with subsequent selector seizure. The rotary transmission switch, designated "Trans" on Figure 4, has the function of supplying in code to the *C* and *D* levels of the send switch sending control information for each digit to be transmitted. This transmission rotary switch obtains its information one digit at a time by way of its *A*, *B*, *C*, and *D* banks from the code storage group. Having all of its relays in an idle condition after translation has been received, this group will be automatically skipped by the Translator switch when it reaches the bank position peculiar to that idle code group. Thus, no attempt is made by the Director to transmit digits other than those digits which are actually available for transmission. The sending cycle for a digit is as follows: relay *PA* operates from the operation of relay *SB*, closes a direct ground to the sender path and closes a direct ground to the magnet of the transmission switch and closes a pulsing ground to the magnet of the send switch. The transmission switch-magnet is energized and remains so until relay *PB* operates. The send rotary switch commences stepping one step for each operation of the *PR* relay and, after it has taken two steps, the next operation of the *PR* relay, besides advancing the send switch, also opens an impulse out on the sender path to the selector *A* relay. Each succeeding operating cycle of the *PR* relay will step the send switch and pulse the sender path until the send switch encounters on both its *C* and *D* banks indication that the required digit is complete. Relay *PC* will operate on this indication and close *PB*. Relay *PC* also will immediately short those contacts on the *PR* relay which have been impulsing the sender path. Relay *PB* operates and locks to the bank of the send switch *E* level and *PB* remains so locked until the send switch returns to its home (or normal) position. *PB* removes the direct ground from the sender path, places a multiple short across the *PR* relay contact, and leaves the sender path connected to the coil of the *PH* relay and the series resistor to ground. The circuit to relay *PA* also is opened at relay *PB* and relay *PA* restores.

A further result of the operation of relay *PB* is that the transmission rotary switch motor magnet is opened and it is allowed to restore and advance its wipers to the position of the new digit to be transmitted, if any, or, if the digit just completed were the last to be transmitted the transmission switch, by way of its *E* level, would advance to the position which indicates to the Director that sending is complete and that the Director now should release from the connection.

The purpose of relay *PH* in the sending control circuit for the sender path is to make the Director wait for a "sender signal" when a call is extended to a crossbar exchange. As soon as the sender in the crossbar equipment is ready to receive digit information as regards the called office and terminal number, the potential on the sender path is altered in such a manner that the *PH* relay restores. The Director then commences to send the digits as required.

Out-Pulse Path

The first digit transmitted by way of the sender path from the Director is always registered on the primary selector and, when the digit is complete, the primary selector will cut in on the first available trunk to the next switch. The wipers of the selector then are switched through directly to the connection established with the succeeding switch. Impulses of decimal value indicative of called office and terminal number are pulsed over the "ring" side of the out-pulse path to the outgoing trunk repeater. However, when a call has been translated as a short-haul toll call, and the calling subscriber has been identified by the Detector, ticketing information collected up to this moment by the Director must be forwarded to the Ticketer prior to the time that the Director is released from the connection. This data includes the calling station office third-digit code and four-digit terminal number, the class of service of the calling station, the called station office code and terminal number, the rate applicable to that called area, and the identity number of the Director used. This information is pulsed over the "tip" side of the out-pulse path at high speed at the same time that the switch positioning is being extended over the ring side of the out-pulse path to establish the connection. Relay *CP* transmits these coded pulses, which are collected by its associated rotary switch from the various storage points in the Director, such as the called station number storage, calling station number storage relays, and so forth.

Release

As soon as all digits necessary have been transmitted by the Director its presence is no longer required in the connection. Relay *TS* is operated from the *E* level of the transmission switch when all necessary digits have been transmitted. When relay *TS* operates, it opens the circuit which is maintaining the *F* relay in the primary selector operated as well as the *H* relay in the Director. The operation of *TS* and the restoration of relay *H* and of relay *F* in the primary selector will allow the Director to release in its entirety and will replace the calling subscriber's line forward by way of the primary selector in the out-pulse path and succeeding equipment to the final connection at the office wherein is located the desired terminal number. The Director now is available for other subscriber traffic.

References

1. The Post Office and Automatic Telephones, Col. T. F. Purves. *Journal*, Institution of Electrical Engineers (London, England), volume 63, number 343, July 1925.

2. Application of Strowger Automatic Toll Ticketing and Punch Card Accounting in Metropolitan Telephone Networks, J. T. Naylor. *Automatic Electric Technical Journal* (Chicago, Ill.), volume 2, number 2, February 1950.

3. The "Director" for Automatic Telephone Switching Systems, Arthur Bessey Smith. *AIEE Transactions*, volume 67, part 1, 1948, pages 611–19.

No Discussion

Microwave Applications to Bonneville Power Administration System

R. F. STEVENS
MEMBER AIEE

T. W. STRINGFIELD
MEMBER AIEE

THE development of microwave radio has presented the power industry with a tool that promises to be most valuable. For many applications, it possesses important advantages, both economic and technical, over communication means heretofore available. In particular, its development came at a most opportune time for the Bonneville Power Administration (BPA), since use of the power line carrier by BPA and ten major interconnected power utilities had brought the available carrier spectrum practically to the point of saturation.

It was natural then that microwave had a prominent place in the BPA studies undertaken immediately after the war to work out a long-range communication program. These studies, however, were comprehensive in their nature, and considered all available types of channels, including:

1. Toll and Exchange Service
2. Leased Circuits
3. Government-Owned Wire Lines
4. Medium-Frequency Radio
5. Very High Frequency Radio
6. Power Line Carrier
7. Microwave Radio

No single type of channel was found to be superior for all applications. Each type was found to have some job which it could do best in an integrated system.

Toll and Exchange Service

It was obvious from the start that a simple extension from the nearest telephone company exchange was the sole solution needed for many of the small unattended stations. Toll calls from such stations are so infrequent that costs would generally be less than the annual cost on the investment which would be required for facilities to connect to the government system. Reliability and speed of service will vary with location but will generally be adequate for a station of this type. Maintenance men visiting the station will generally have radio equipped cars.

Toll and exchange service also is desired at the larger stations, for communication to points not reached by the government system. It will not constitute the sole or primary communication to such stations for operating purposes, however. Otherwise toll charges to a busy station would be prohibitive and speed of completing calls might not be adequate in emergencies. The importance of most such stations demands at least two alternate methods of communication, at least one of which would not be so susceptible to storm damage as open-wire telephone lines.

Leased Wire Circuits

Leased wire has economic advantages when used over short distances, particularly in urban areas. It has been used in a number of cases for such uses as pilot wire relaying and telemetering. It also is used by some of the interconnected power utilities in the area in providing connections between their dispatcher and the Bonneville communication system.

In many cases the reliability has been disappointing. Open-wire phone lines, and even cables, are more susceptible to damage from storms, floods, and other disasters than the rugged transmission cables used with power line carrier. Trouble, when it occurs, may be at a spot difficult of access, which is seldom the case with carrier. Moreover, in times of disaster, the power utility has its own personnel available on the spot to restore communications and this work is not in competition with work on other customers' services, as is the case for leased wire services.

In spite of this, because of the economic factor, it is expected that the BPA will continue to use a considerable amount of leased wire services for transmission over relatively short distances and in urban areas. However, the development of very high frequency (VHF) equipment provides an alternate which cannot be overlooked, and each application must be studied on its merits, with consideration given to both cost and reliability.

Studies of the BPA, like those of other utilities, have indicated that leased circuits are not competitive in cost with power line carrier over long distances. The same has been found to be true as compared to microwave, when the latter is properly applied.

Government-Owned Wire Lines

Because of susceptibility to storm damage and high maintenance cost, no government-owned wire lines are presently planned. Short sections of underground communication cable will be used, however, between substations and nearby microwave stations for distances of the order of a quarter of a mile.

Medium-Frequency Radio

Medium frequency radio is used by the Administration for communication between fixed stations and mobile units such as line trucks, and has generally been satisfactory. However, because of skip distance effect, the coverage of the region is somewhat erratic and occasional cases of interference have occurred. Two frequencies, 2,222 and 4,880 kc are available one being used for daytime and the other for nighttime reception. This is essentially a 1-channel system and will not be adequate when activities become more extensive and several conversations must

Paper 50-170, recommended by the AIEE Carrier Current Committee and approved by the AIEE Technical Program Committee for presentation at the AIEE Summer and Pacific General Meeting, Pasadena, Calif., June 12–16, 1950. Manuscript submitted March 15, 1950; made available for printing May 8, 1950.

R. F. Stevens and T. W. Stringfield are both with the Bonneville Power Administration, Portland, Oreg.

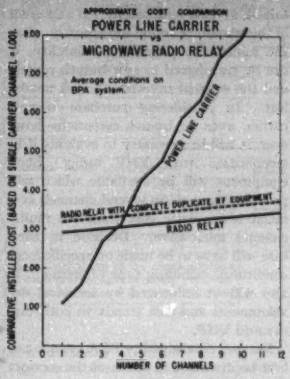

Figure 1. Cost comparison, power line carrier versus microwave, for average conditions on BPA system

Figure 2. Communication facilities for Pacific Northwest Federal Power System, with proposed extensions through 1954

be carried on throughout the region between fixed and mobile units. It is believed that it will be impossible to get assignments of other channels in this band. The amplitude-modulated equipment is susceptible to power line noise and cannot be used in the immediate vicinity of an energized high-voltage line as can frequency-modulated VHF equipment. The medium-frequency equipment also is limited in point-to-point communication for emergency use only and cannot be used for the transaction of ordinary business.

Very High Frequency Radio

VHF, because of its short range and fewer license restrictions, will overcome these disadvantages and the Administration plans to use it in the future for fixed-to-mobile communication. VHF equipment is normally frequency modulated and can be used in the vicinity of transmission lines where reception with our existing medium-frequency equipment would be completely blanked out by noise. An adequate number of channels can be provided. The first cost of each installation is considerably less than for the medium-frequency equipment now in use.

Because of the line-of-sight characteristics of VHF, fixed stations will have to be spaced at closer intervals. Fixed VHF stations will be installed at selected microwave station sites, making use of the existing towers and power facilities. These VHF stations will be connected to channels in the microwave system, thus extending the range of the mobile units to all points of the communication system, including the load dispatcher and other headquarters offices.

VHF, because of its relatively low cost, is well adapted for branches from the multichannel microwave system to substations where only one, or a few channels, are needed.

Power Line Carrier

Power line carrier was formerly the standard means of long distance communication used by most utilities for operation of their systems. Its application must now be evaluated in competition with the new medium, microwave radio, and in some cases, with VHF radio. For this purpose, a cost com-

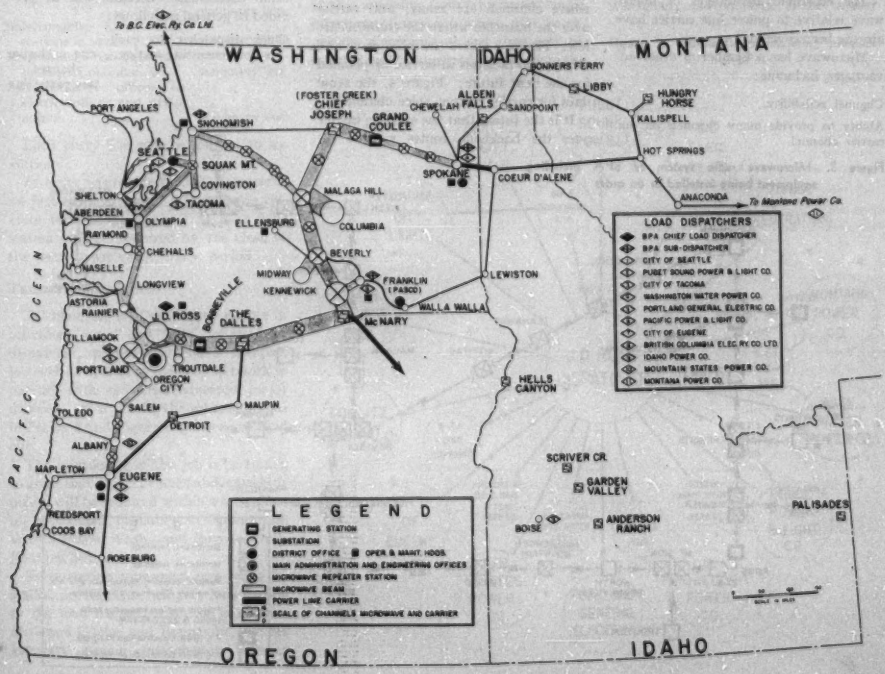

parison was made several years ago, and is summarized in Figure 1. This curve is based on estimates made for running any number of channels from 1 to 12, over a route from Snohomish to Vancouver, Wash., and thence to Spokane. Terminal facilities were included at the important intermediate powerhouses and substations. In Figure 1, the cost of a simple carrier channel is taken as reference. Subsequently, the curve was corrected to reflect recent price decreases in microwave equipment. These curves should, of course, be used with caution by others, as the average conditions of the BPA network may not be typical of other systems. Nevertheless they illustrate the fact that microwave, with its high first cost and low incremental cost per additional channel, is best adapted to applications where many channels follow the same geographic route. Carrier, on the other hand, with its lower fixed cost and high incremental cost per additional channel, is better adapted to routes or branches where only one or two channels are required.

Microwave

The economic advantages of microwave relative to power line carrier have already been covered.

Microwave has a number of other advantages, including:

Channel reliability.

Ability to provide many channels on one carrier channel.

Freedom from interference.

Ease of maintenance.

Superior performance from the standpoint of noise, distortion and attenuation.

Full duplex communication without crowding of spectrum.

Availability of wide spectrum.

Ability to combine relay station sites with VHF for use with fixed-to-mobile communication.

Ability to use during construction prior to completion of connecting transmission line.

The principal disadvantage is that use of multiplex channels puts "more eggs in one basket." This encourages use of duplicate equipment and other means of gaining reliability, which are reflected in the cost.[4,2]

The BPA Communication Program

The most important part of the BPA communication program is shown in the map, Figure 2. This reflects decisions on channel types based on the factors just given, and, in particular, on the carrier-microwave comparison of Figure 1. It will be seen that microwave is to assume the burden over the backbone routes where channels are many, and carrier over the branches where the channels are few. Figure 3 shows the microwave and other radio facilities in service or planned for the near future; Figure 4, the same data for carrier current voice channels.

It is the intent that the existing carrier over the backbone routes will be retained, at least temporarily. If any or all of this should be found unnecessary, after the microwave proves its reliability, it can be transferred to new branch routes, and the original investment need not be lost. In considering purchase of new carrier, even for branch extensions, however, it will be necessary to evaluate it in competition with VHF radio. Such equipment will be available which will provide from one to several channels at a much lower basic cost than the multichannel microwave. Decision in each case will have to be made on specific local conditions, including type of terrain. It also will be influenced by technical developments and cost trends on both carrier and VHF.

Further details of the BPA system can best be discussed in terms of the services provided.

Telephone

Foremost consideration is given to providing circuits for system dispatching. Where economically feasible, telephone circuits will be provided for other functions depending upon access to the microwave system and power line carrier and radio extensions. Circuits will be provided in general as follows:

Chief dispatcher to each major generating station . . . one exclusive channel
one party line

Figure 3. Microwave radio system of BPA including equipment being installed or on order

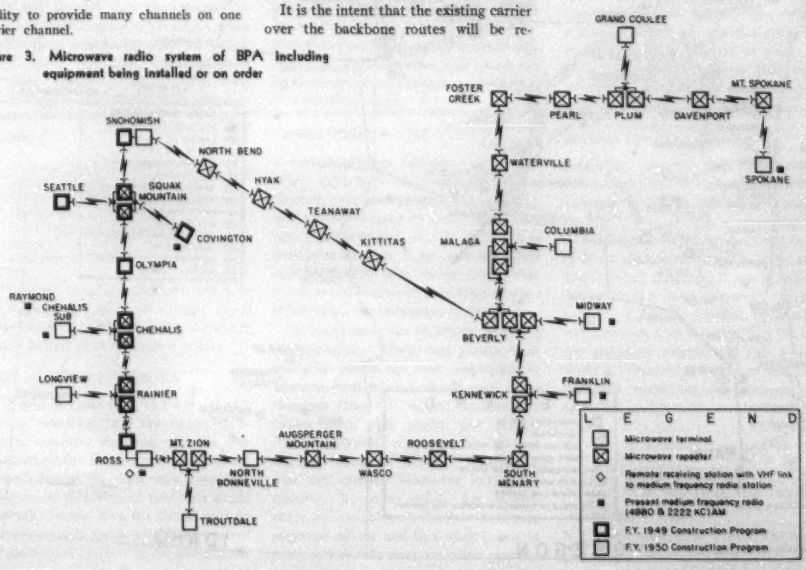

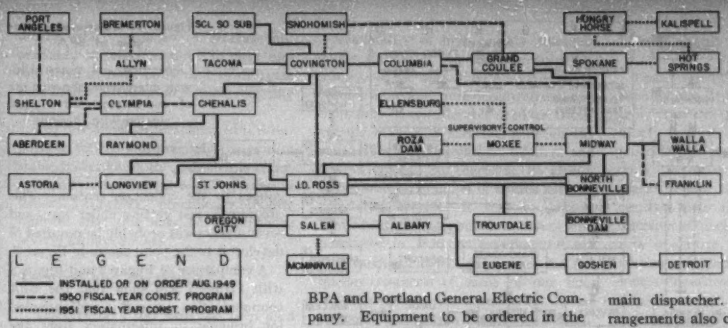

Figure 4. Power line carrier current communication system of BPA, including proposed extensions through fiscal year 1951

Chief dispatcher to small generating station.....two channels either or both of which may be party line

Chief dispatcher to dispatchers of interconnected utilities.....one exclusive channel

Chief dispatcher to each subdispatcher.....two exclusive channels one party line

Subdispatcher to attended stations in area.....one party line

Maintenance headquarters to district maintenance....one party line

Administrative offices to district offices and other points.....one party line

Each party line will be limited to six stations.

In order to provide the telephone service just outlined, about 60 telephone circuits terminating at the J. D. Ross Substation will be required by the close of the next 6-year construction period.

Telemetering-Power

Telemetering is of major importance in providing "eyes" and "ears" for the load dispatcher, particularly for a complex job such as operating the BPA network in parallel with ten interconnected major utilities. As a result, the scheme shown in Figure 5 and Figure 6 has been worked out.

The complexity of the job is becoming so great that at least three subdispatching points will be required within a few years, to be located probably at Snohomish, Wash., Pasco, Wash., and Eugene, Oreg. (Goshen Substation).

Telemetering equipment now being installed provides for bringing information to the load dispatcher on the generation of Grand Coulee and Bonneville, the net kilowatt system interchange between BPA and Portland General Electric Company. Equipment to be ordered in the spring of 1950 will provide for telemetering of interchange with seven of the nine other major utilities. With many of these utilities, Bonneville has several interconnections each. Kilowatt readings of the separate individual interconnections with each utility will be brought to the appropriate future subdispatching point, and there totalized to give the net system interchange, which will be retransmitted to the main dispatcher at Vancouver. In addition, an extra channel will be available in the case of each utility so that a reading from a particular single interconnection point, which may be especially significant at any time may be selected and transmitted separately to the main dispatcher. It is hoped that arrangements also can be made to pick up from the load dispatcher's offices of the various interconnected utilities, readings on total steam generation and total hydro generation to the extent that these are available. These would be transmitted to the main BPA dispatching office, at which point the total steam generation, the total hydro generation, and the grand total generation for the entire Northwest power pool would be indicated and recorded. Channels can be made available to transmit this information back to such interconnected utilities as may desire it. Where outputs from some of the smaller

Figure 5. Schematic telemetering program of BPA

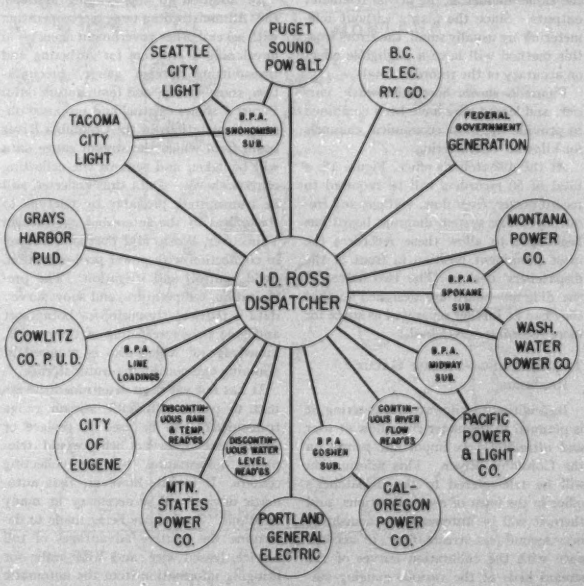

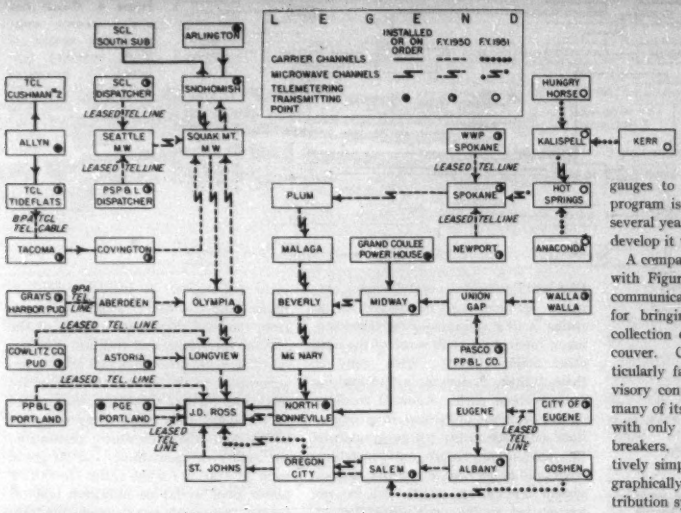

Figure 6. Telemetering program of BPA

Generation and system kilowatt interchange, showing use of microwave, carrier, and leased wire channels

generating plants are not telemetered, the equivalent information on the loads at these plants will be obtained from time to time by telephone and will be simulated by the setting of a potentiometer whose output is fed to the totalizing meters in the same manner as the actual telemeter outputs. Since the plants without telemetering are usually small, the errors from this method will have a negligible effect on accuracy of the recorded totals.

Figure 6 shows how microwave, carrier, and leased wire have been combined to provide the most economical channels for kilowatt telemetering.

At the dispatcher's office, Figure 12, a total of 50 recorders will be required to record power, river flow, voltage, and frequency. The system diagram board has been split to allow these recorders the most prominent position in front of the dispatchers' desks. (The two halves of the diagram board are designed so that they can be further separated as space for more recorders is required.)

Telemetering—Stream Gauge Readings

In addition to kilowatt telemetering, it is planned to telemeter river flow at four and ultimately six important points on the Columbia River. This information will be telemetered to the dispatcher's office in the form of river elevations, and there it will be automatically translated into second-feet-stream flow, in accordance with the calibration curves of the stream beds at the various gauging stations. Stream flow from all six stations will be recorded on a single chart having a semilogarithmic scale, Figure 8. In this way, water released from storage can be conveniently tracked during its passage down the river.

In addition to the gauging stations, the Administration now is co-operating with several other government agencies in developing a program for gathering and transmitting stream gauge, precipitation, snow survey, and temperature data. Figure 7 shows existing and proposed observation stations in the Columbia River basin from which the stream gauge data will be taken and sent to the collecting centers shown. Data thus collected will be transmitted, probably by teletype to the offices of the interested agencies in Vancouver, Wash. and Portland, for use in connection with power pool operation, flood control, and irrigation. The precipitation, temperature, and snow survey data is particularly useful for both short and long time forecasting of the run-off, knowledge of which also is required in planning and controlling water storage.

It has not yet been determined the extent to which automatic stream gauge transmitters will be used to replace or supplement observers who would telephone information to the collecting centers. It is felt, however, that automatic devices will be necessary at many locations. Studies are being made to determine the relative advantages of toll service, leased wire, and VHF radio for bringing information from the automatic gauges to the collection centers. This program is just getting under way, and several years will probably be required to develop it to the point shown in Figure 7.

A comparison of Figure 2 and Figure 3 with Figure 7 will show that the BPA communication system is well adapted for bringing in information from the collection centers to Portland and Vancouver. Conditions on the BPA are particularly favorable to the use of supervisory control. As a wholesale agency, many of its stations are extremely simple with only one or two secondary circuit breakers. Because its stations are relatively simple, and widely dispersed geographically, and because there is no distribution system to maintain, its operating personnel is normally spread quite thin. Many stations have only one operator, who obviously cannot be at the station 24 hours a day, seven days a week. Operation in such cases could definitely be made more reliable by supervisory control.

Some stations now unattended offer chance of improved service at reasonable cost with supervisory control.

Comparatively few supervisory control installations have been made to date, due primarily to lack of suitable channels. With the development of the microwave communication system, this will be remedied to a large degree. Use of VHF also is being studied.

Plans now are under way to increase the number of supervisory control installations from three to five in the fiscal year 1950, with four more to be added in the fiscal year 1951, and 12 in the fiscal year 1952. It is likely that supervisory lamp indication will also be provided in the main dispatcher's office to show position of all line breakers on the main 230-kv grid.

Power Line Relaying

Microwave has a major fundamental advantage over power line carrier as a channel for relaying, namely, because it is not necessary to assume that the channel may be out of service when the power line is faulted.

This permits an approach to the relay problem heretofore impossible—an ap-

proach which promises to decrease appreciably the time required to clear certain lines at both ends, and to decrease even more the minimum possible reclosing time.

The problem is so complex that it is impossible to evaluate precisely the gain in stable power limits throughout the transmission system, and the resulting value in dollars. However, preliminary studies indicate that this may be as much as several million dollars.[3]

Teletype and Facsimile

Teletype on a toll basis has been used for many years for communication between the Portland main office, the various district offices, and the Interior Department in Washington. It is felt that considerable use may be made of commercial facsimile service between Portland and Washington, D. C., should it ever become available on a toll basis. Teletype also is under consideration for bringing in river gauge information from the collecting centers mentioned previously.

Availability of high quality channels makes the use of facsimile also seem attractive, as the work of BPA is expected to become more and more decentralized, and there may be considerable need for transmitting maps and sketches between the main office and the various regional and district offices. Furthermore, its ability to transmit large tables of figures without possibility of error is very important. Three facsimile transmitter-receivers were purchased in 1946 for experimental use over carrier channels. However, the frequency response of most of our long carrier channels was inadequate. Some difficulty also was encountered in maintaining synchronism. These will be installed this summer on the microwave circuits where channel characteristics are more favorable. Studies will be continued to evaluate the usefulness of this and other types of facsimile equipment in power system operation.

Load Control

Load control channels have not yet been required by the Federal power system. The Northwest Power Pool is commonly operated with Grand Coulee powerhouse controlling frequency and with connected utilities using their automatic tie-line load control equipment to regulate their take of power. With the addition of more Federal plants to the two now in service, it is possible that some system may eventually be required to provide automatically for the most desirable division of load between the government plants under various conditions.

Fault Location

One of the most interesting and certainly the most novel BPA microwave application is to power line fault location.

Means have long been available to

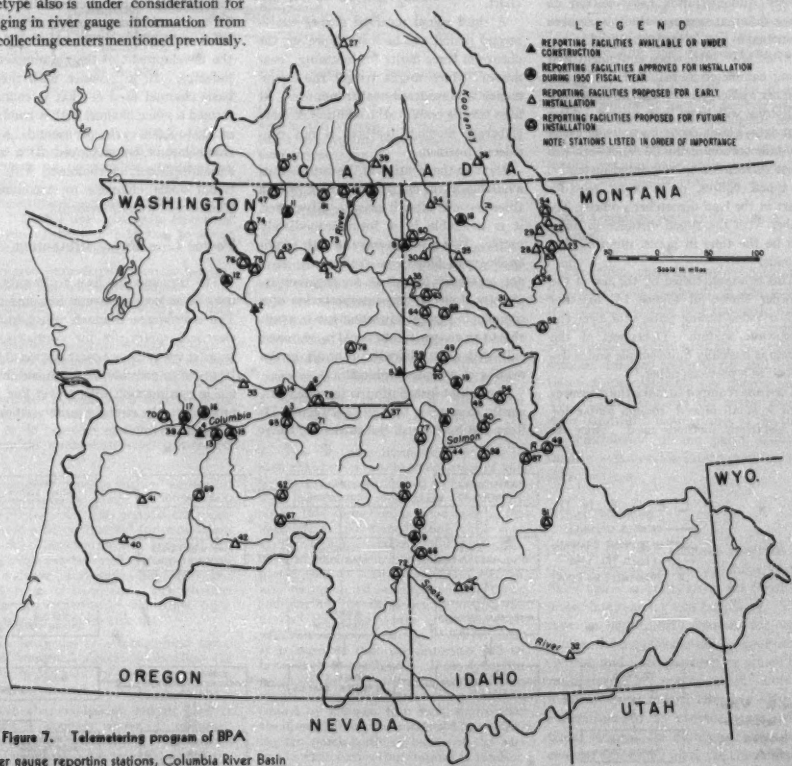

Figure 7. Telemetering program of BPA
River gauge reporting stations, Columbia River Basin

measure quickly, accurately, and conveniently most of the quantities which must be known for the proper operation of a power system. Voltage, current, power frequency, river elevation, and many other quantities can be measured instantly, with great accuracy, and recorded at the site, or telemetered hundreds of miles for the information of the dispatcher.

In contrast, past methods of locating line faults have been almost unique in their slowness, cumbersomeness, and lack of precision. Even today, the commonest way of locating a sustained fault on a long line is to open sectionalizing switches and test line sections in turn until the fault is determined to be in one section, and then patrol that section, which may itself be 50 miles or so in length.

Many investigators here and abroad have been working on this problem in recent years and much progress has been made.[4,5,6] Engineers of the Bonneville Power Administration have worked on three different systems which have been described in part in earlier papers.[7,8]

After May 1950, when equipment now being completed is installed in the dispatcher's office, it is felt that an important milestone will have been passed. After that date, a fault occurring anywhere on a 200-mile section of the BPA network will cause its location to be printed instantly, in typed figures, on a paper recorder chart in the load dispatcher's office. Together with the typed distance in miles will be the time in hours, minutes, and seconds.

This is accomplished by the use of the recorder shown in Figure 15, together with a video timing pulse sent over the microwave system. Operation of the system is basically quite simple and is described in a previous paper.[7]

The time required to make the measurement is small indeed, though ample for the electronic methods used. Since 95 per cent of all faults are of the transient type not re-established when the circuit breakers are reclosed, and since it is desired to locate such faults as well as permanent faults, a measurement must be taken before the arc is extinguished. Since relay time may be less than a cycle (of the 60-cycle wave) and the circuit breaker will operate in less than three cycles, the equipment should be capable of operating in three cycles, or 50,000 microseconds. Actually, the measurement of distance is set up on an electronic counter within a few thousand microseconds.

The setting of the type wheels to correspond to the counter reading, being a mechanical operation, takes about three seconds. But, should another fault occur while the type wheels are being set up and are printing, the counter will receive and "remember" the second reading until the first reading is printed, after which the type wheels will be set to the new value which will be printed in turn on the chart.

A third signal received during the 3-second period will be lost; however, the chanee of three faults (or lightning "near misses" which might trigger the equipment) is considered rather remote. At least for the present, the addition of more elaborate memory features is not considered justified.

Data on the location of the fault is thus available, at the dispatcher's office, within three seconds after it occurs. Moreover, it is available in a form immediately usable. It is not necessary to wait for an oscillograph film to be developed. It is not necessary to call in an engineer especially skilled in the interpretation of a complicated trace. Information is available to an accuracy that could be obtained only with great difficulty, if at all, in the reading of a photographic film.

The initial installation is intended primarily to monitor the lines between J. D. Ross and Snohomish Substations. However, the equipment also will be effective to some degree in locating faults on certain other parts of the high-voltage network, as explained in a previous paper.[7] Complete coverage of the transmission system, however, is not possible with one installation.

It is proposed to add other locators, as the microwave system is extended, as shown in Figure 9. This will not only provide for essentially complete monitoring of the existing 230-kv network, but also will provide for check readings from two or more recorders for a large percentage of transmission faults.

Technical Requirements for Each Type of Service

The wide variety of communication services must each be examined in order to specify the performance of the multichannel microwave system.

In the interest of uniformity, all of the basic channels are specified alike and so far as practical designed to utilize equipment and practices that have evolved in the development of the communications industry. In accordance with this, the basic channel used is what is commonly termed a voice channel with a bandwidth of 300 to 3,000 cycles per second. A voice channel may be employed as a whole, submultiplexed, or combined with additional voice channels to accommodate specific service requirements.

Power Line Relay Protection

The transmission lines to be protected may be as long as several hundred miles. The microwave channels must transmit electrical quantities for comparison or transfer tripping or a combination of both. In order to provide channels suitable for use in conjunction with power line relay protection, the circuit characteristics provided are as follows:

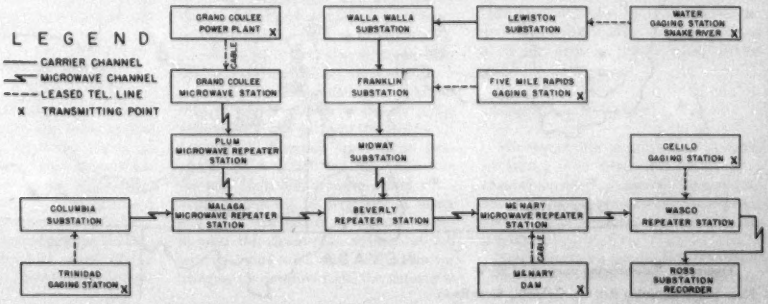

Figure 8. Water flow telemetering program of BPA

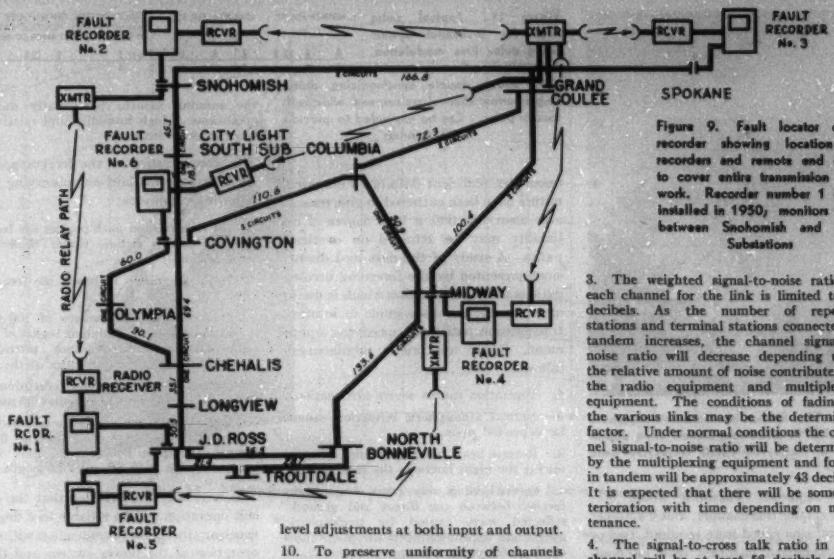

Figure 9. Fault locator chart recorder showing location of recorders and remote and units to cover entire transmission network. Recorder number 1 only installed in 1950; monitors lines between Snohomish and Ross Substations

1. Output level constant within plus or minus 1 decibel over a period of one month to provide a reasonable maintenance schedule.

2. Output level constant within plus or minus 1 decibel when the radio frequency signal varies from plus 6 decibels to minus 30 decibels from the normal.

3. Recover immediately after a momentary loss of signal or power failure.

4. Continuity preserved during primary power outage.

5. Amplitude response linear within 1 decibel over a dynamic range of 30 decibels to allow comparison of electrical quantities.

6. Transient response such that the delay of a suddenly applied tripping signal in rising to 95 per cent of full amplitude is less than one-tenth of a 60-cycle-per-second wave.

7. Frequency response within ±1 decibel over the frequency range of 50 to 3,000 cycles per second. This permits the transmission of a 60-cycle signal for comparison purposes. The channel will transmit signals of frequency below 50 cycles per second with reduced amplitude but does not extend to zero frequency. The channel may be subdivided to provide three high-speed transfer tripping channels.

8. The frequency of a transmitted signal will be preserved absolutely to allow the channel to be used for phase comparison purposes.

9. Each channel has an output level of at least 4 decibels above 1 milliwatt, over a range of inputs of 0 to −12 decibels below 1 milliwatt and is provided with power level adjustments at both input and output.

10. To preserve uniformity of channels the requirements for noise, harmonic distortion and intermodulation distortion are based on telephony requirements which are more severe.

Telephony for Power System Dispatching

The microwave system is designed to provide telephone service over a circuit employing at least 32 repeater stations and six terminal stations connected in tandem over a distance of approximately 1,000 miles, in order to insure good quality communication between points at opposite ends of the Columbia Basin region.

1. Frequency response is flat within ±1 decibel over the range of 300 to 3,000 cycles per second.

2. The total rms harmonic distortion in each channel for one hop consisting of two terminal stations is limited to 3.5 per cent with full channel modulation. Practically all of this distortion is produced in the modulating and demodulating equipment at the terminal stations and practically none in the repeater stations. It is expected that at least six terminal stations may be connected in tandem. With linear addition of the distortion products, the over-all distortion would be 21 per cent; with rms addition it would be 8.6 per cent. It is expected that the distortion will be between these two figures. If the distortion produced in each terminal equipment is similar (same order harmonic), as may be caused by limiters, tests have shown that the distortion may be minimized by polarizing the patch cords to buck out the harmonic when connecting stations in tandem.

3. The weighted signal-to-noise ratio in each channel for the link is limited to 50 decibels. As the number of repeater stations and terminal stations connected in tandem increases, the channel signal-to-noise ratio will decrease depending upon the relative amount of noise contributed by the radio equipment and multiplexing equipment. The conditions of fading in the various links may be the determining factor. Under normal conditions the channel signal-to-noise ratio will be determined by the multiplexing equipment and for six in tandem will be approximately 43 decibels. It is expected that there will be some deterioration with time depending on maintenance.

4. The signal-to-cross talk ratio in each channel will be at least 56 decibels which minimizes the effect of intelligible cross-talk. Since the signal-to-cross-talk ratio is at least 56 decibels, the specified 50-decibel signal-to-noise ratio is protected against unintelligible cross-talk.

Fault Locating on Transmission Lines

The video channel employed for the purpose of fault location on the power transmission system will transmit, when demanded, a single randomly occurring video pulse of approximately two microseconds' duration and with rise and decay times of approximately one microsecond. This channel employs the entire microwave bandwidth momentarily at the time of transmission of the pulse, without causing a noticeable interruption to the other services.

Other Services

All of the basic channels provided by the microwave system will have essentially the characteristics as set forth for power line relaying and telephony. This provides high quality channels for other services such as telemetering, supervisory control, and teletypewriter for which the requirements are not as severe. One or more of the standard channels may be submultiplexed to provide these additional services, the number per standard channel depending upon the transmission

Figure 10. Snohomish microwave station—a typical BPA microwave station using equipment in the 1,700–1,850 megacycle band

speed required. Facsimile would normally employ one channel; but if a higher transmission speed were required, two or more standard channels may be combined.

The versatility and economy of a microwave radio system in meeting diversified communication requirements make the application of microwave to the BPA power system an important contribution to its reliability and efficiency of operation.

Transmission Paths and Profiles

The propagation of radio waves at microwave frequencies through the atmosphere is being studied by many investigators.[9–16] While much is still to be learned about the causes of propagation

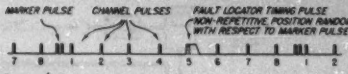

Figure 11. Typical pulse train for 8-channel system using pulse time modulation, as installed on Ross-Snohomish link. Shows double synchronizing pulse, single narrow channel pulses, and wide fault locator pulse. Can be expanded to provide 23 channels

anomalies, sufficient data of an empirical nature have been gathered to give reasonable assurance that a high degree of reliability may be attained on overland paths. A study of the data and discussions presented by the foregoing investigations yields information which is useful and may be used as a guide in locating transmission paths and specifying equipment. These are briefly tabulated as follows:

1. Vegetation causes severe attenuation.
2. Normal atmospheric refraction cannot be depended upon.
3. Reverse beam bending is quite common during the night hours in the summertime.
4. Severe fading may result from interference between the direct and ground-reflected wave caused by tropospheric effects and depending upon the smoothness of the intervening terrain.
5. Severe fading may result from multipaths caused by atmospheric refraction.
6. Frequencies of approximately 7,000 or eight thousand megacycles appear to be the upper limit for protection against excessive attenuation caused by rainfall and employing reasonable radio-frequency.
7. The longer the path, the more severe is the fading caused by atmospheric anomalies.
8. There is a tendency for the fading to be more severe as the wavelength is shortened.
9. During rainy or stormy weather tropospheric conditions are not conducive to fading.
10. Fading occurs more frequently during the summer months particularly during conditions of high humidity and relatively quiet atmosphere.

In consideration of the foregoing, the BPA system was laid out observing the following conditions:

1. All transmission path profiles are based on true earth's radius, rather than 4/3 earth radius.
2. Beam clearance is based on tree-top level.
3. Minimum beam clearance of 100 feet is maintained in the midpoint region of the path with greater clearance provided, when practicable, on the longer paths.
4. Vertical space diversity reception is employed on all paths longer than 30 miles.
5. Equipment is designed to accommodate a 30-decibel fade or a 6-decibel rise from normal free space transmission level over a transmission path 60 miles in length.

As a result, it is believed that the circuit operation will be reliable to a degree necessary for its use in connection with the operation of the power system and that circuit outage due to propagation anomalies will be less than 0.01 per cent of total operating time.

In laying out the transmission paths between points of communication, cost of access roads and site preparation severely limited the choice of sites. Sites therefore were always chosen near existing roads and fortunately, it has been found so far that in such cases commercial power is generally available nearby.

Preliminary selection of sites and transmission paths was made by use of United States Coast and Geodetic Survey maps in conjunction with aerial photographs. Over unsurveyed regions, preliminary

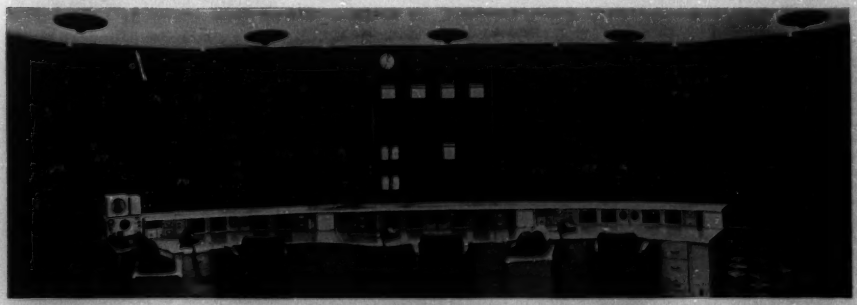

Figure 12. BPA load dispatcher's board showing central location of telemeter recorders. Fault locator to be mounted at right end of dispatcher's desk

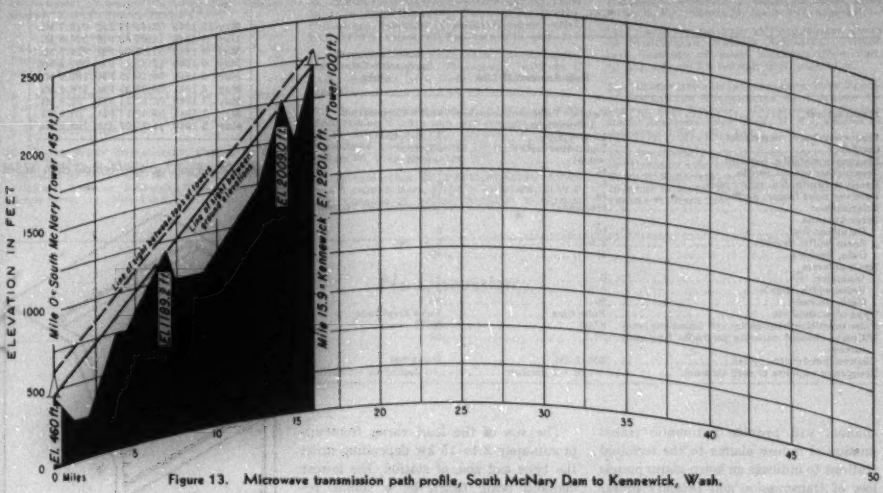

Figure 13. Microwave transmission path profile, South McNary Dam to Kennewick, Wash.

profiles were made by photogrammetric means using aerial photographs and a stereoscopic plotter. All critical points where the amount of clearance was in doubt were then checked in the field. It was found that in general, optical line of sight cannot readily be established or checked by visual observation because of haze or nearby intervening objects which would normally be cleared by the tower. It was found to be most practical to check critical points by accurate instrument survey. Actual propagation tests were not employed, first, because of the expense, and second, to be of value the test should be run for a period of at least one year, since reception of a signal does not necessarily indicate attainment of optical line of site, and certainly would not prove that the desired clearance had been obtained.

Towers

Towers used for all links are the self-supporting steel type. Those in the Vancouver-Snohomish link are of standard Forest Service type with stairways to the top as shown in Figure 10, a design originally selected with the thought the radio-frequency equipment might be mounted at the top of the towers at some stations. When equipment for the other links was placed on order, it was found that the use of fewer and smaller antennas decreased wind loading to the point where smaller towers were practical. At the same time, it was decided to eliminate stairways in favor of ladders with protective guards. The over-all result was a reduction in weight of nearly 50 per cent. Standard policy is to mount all equipment except antennas, on the ground, even though this results in considerable additional cost, in some cases, for coaxial cable or wave guide. It is felt that the saving in extra convenience offsets this added cost.

Buildings

Prefabricated buildings made from aluminum panels are used for the smaller radio station houses. Larger buildings are of concrete block construction.

Radio-Frequency and Multiplexing Equipment

The portion of the system now under construction or on order includes three main links; the Ross-Snohomish link, 200 miles in length, connects the Portland-Vancouver, Wash., headquarters with BPA substations and dispatchers of interconnected systems in the Puget Sound area, also with the BPA Seattle District Office. The Ross-Spokane link connects the Portland-Vancouver area with Spokane by way of the Columbia River federal power plants (Bonneville, McNary, Chief Joseph, and Grand Coulee), other utility dispatchers, and important intermediate substations. The Snohomish-Columbia link connects the north end of the Ross-Snohomish link with an intermediate point on the Ross-Spokane link. This provides a direct routing for protective relay channels for the transmission lines which cross the northern Cascade Mountains. It also completes a loop which makes possible alternate routing of traffic to a large number of the stations on the system, in the event of propagation or equipment failure at any point on the loop.

Equipment for the Ross-Snohomish link was purchased from the Federal Telecommunication Laboratories and will be in operation in June 1950. The equipment for the rest of the system was recently purchased from the Philco Corporation and should be in operation in the fall of 1951. Both companies are supplying pulse modulation systems, that of Federal Telecommunication Laboratories being pulse-time modulated, and that of Philco being pulse-amplitude modulated. The Federal equipment operates in the government band between 1,700 and 1,850 megacycles, and the Philco equipment in the 7,125- to 8,500-megacycle government band. The principal characteristics of the two systems are tabulated in Table I. Figures 10 and 12 show views of a typical station on the Ross-Snohomish link.

Stand-by radio-frequency equipment with automatic change-over in case of failure is provided throughout the system. On the longer paths, the stand-by radio-frequency receiver is connected for vertical space diversity reception.

To facilitate maintenance, a service

Table I

	Ross-Snohomish Link	Ross-Spokane and Snohomish-Columbia Links
Manufacturer	Federal Telecommunication Laboratories, Inc.	Philco Corporation
Frequency band, megacycles	1,700–1,850	7,125–7,425
Oscillator	Lighthouse triode	Klystron
Frequency stability, per cent	±0.05	±0.05
Transmitter output, watts	10	1.0
Receiver bandwidth, megacycles	8	8
Receiver noise factor, decibels	14	14
Polarization	Horizontal	Horizontal and vertical
Large antenna		
Diameter, feet	10	6
Beam width, degrees	3.5	2.2
Gain, decibels	33	40
Small antenna		
Diameter, feet	6	4
Beam width, degrees	5.5	3.5
Gain, decibels	29	36.5
Type of modulation	Pulse time	Pulse amplitude
Pulse repetition frequencies, cps (sampling rate)	8,000	8,000
Ultimate channel capacity per radio frequency carrier	23	32
Channel bandwidth, cycles	300–3,400	300–3,300
Frequency response of each channel	+1 to −2 decibels	+1 decibel to −1 decibel

channel will provide automatic transmission of failure alarms to the terminal stations to indicate on lamp alarm panels loss of transmission and primary power failure at any repeater station with station identification. The service channel also serves as a party line telephone circuit throughout the system. As a supplement to the automatic alarm, it may be used to localize faults to the particular station involved by means of the selective dial system.

Power Supply

Each microwave station will be supplied with primary power either from a commercial source if it is a remote repeater station or from the station service bus of the nearby BPA substation to which it is providing terminal facilities. Because of the likelihood of prolonged power outage at the remote locations during storms, a gasoline engine driven generator set is provided at each repeater station.

The starting time of the gasoline engines ranges from one half to several minutes.

The microwave system will provide channels for power line relay protection of the power transmission lines, and it is therefore essential that it keep operating continuously during the time of system faults.

Since a fault on the BPA power transmission system may affect the station service supply and also the commercial power supply at the repeater stations through interconnection, a means for providing uninterrupted power at the time of system faults must be provided at each microwave station.

The size of the load varies from approximately 2 to 15 kw depending upon the type and size of station, the lowest demand being taken by a simple repeater station and the highest value for a repeater station with several radio branch circuits. Terminal stations and repeater stations with terminal facilities have a power demand between these extremes depending upon the extensiveness of the terminal facilities. Approximately half of this load consists of plate supply and the remaining half of tube heaters. The d-c plate supply voltages range from 200 to over 1,000 volts. The heater load because of thermal storage can withstand switching from one power source to another, but in general, the plate load has insufficient electrical storage to allow a switchover which may be of the order of 0.1 second.

A continuous source of power will be provided by means of a storage battery and a continuously rotating machine consisting of an induction motor, d-c machine and synchronous generator at all stations. At the larger stations, in order to reduce the size of the induction motor, only the d-c plate load is fed from the motor-generator set and the tube heater load is normally fed from the primary station supply. The battery floats on the d-c machine which furnishes a trickle charge. Upon failure of the primary supply, the rotational inertia of the set is sufficient to maintain service until the d-c machine motors. The heater load is automatically transferred to the synchronous generator. At repeater stations the microwave load is automatically transferred from the synchronous generator to the gasoline driven generator after a predetermined time of perhaps 10 minutes. The momentary interruption of approximately 0.1 second during this switching transfer is of no consequence since the power line relaying function should have been accomplished by that time.

May 10 1948	03:45:11 AM	013.7 Mi.
May 9 1948	11:09:53 PM	206.5 Mi.
May 9 1948	07:33:09 PM	206.5 Mi.
May 9 1948	12:31:45 AM	029.9 Mi.
May 8 1948	06:10:35 PM	189.8 Mi.
May 8 1948	06:08:35 PM	168.8 Mi.
May 8 1948	09:20:34 AM	98.9 Mi.
May 7 1948	09:59:17 PM	87.1 Mi.
May 5 1948	11:21:02 AM	125.3 Mi.

Figure 14. Fault locator—typical chart record

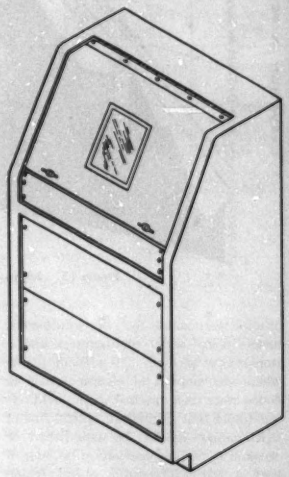

Figure 15. Type-B fault locator chart recorder

References

1. Microwave Channels for Power System Applications, AIEE Committee Report. *AIEE Transactions*, volume 68, part I, 1949, pages 40–43.

2. Discussion of reference 1, R. F. Stevens. *AIEE Transactions*, volume 68, part I, 1949, pages 42–43.

3. The Bonneville Power Administration Relaying and Reclosing Program, Clifford C. Dismond, Donald L. Wylie. *AIEE Transactions*, volume 69, part II, 1950, pages 1039–48.

4. The Linascope—An Echo-Ranging Type Fault Locator for High-Voltage Lines, J. R. Leslie, K. H. Kidd. *AIEE Transactions*, volume 67, part II, 1948, pages 1162–67.

5. Fault Location on High Voltage Overhead Transmission Systems, Wilfred G. Hoyle. *Paper Number 217*, International Conference on Large High Voltage Electric Systems (Paris, France), 1948.

6. The Localization of Fault on Overhead Lines by Means of Impulse Waves, S. Margoulies, P. Fourmarier. *Paper Number 307*,

International Conference on Large High Voltage Electric Systems (Paris, France), 1948.

7. A Transmission Line Fault Locator Using Fault-Generated Surges, R. F. Stevens, T. W. Springfield. *AIEE Transactions*, volume 67, part II, 1949, pages 1168–79.

8. A Transient Fault Locator for High-Voltage Transmission Lines, L. R. Spaulding, C. C. Diemond. *AIEE Transactions*, volume 68, part II, 1949, pages 1005–11.

9. Radio Wave Propagation, Charles R. Burrows, Stephen S. Attwood. *Consolidated Summary Technical Report*, Committee on Propagation of the National Defense Research Committee. Academic Press, Inc., New York, N. Y., 1949.

10. Results of Microwave Propagation Tests on a 40-Mile Overland Path, A. L. Durkee. *Proceedings*, Institute of Radio Engineers (New York, N. Y.), volume 36, February 1948, page 197.

11. Microwave Propagation Experiments, Leland E. Thompson. *Proceedings*, Institute of Radio Engineers (New York, N. Y.), May 1948, page 671.

12. Propagation Studies on 45.1, 474 and 2,800 Megacycles Within and Beyond the Horizon, G. S. Wickizer, A. M. Braaten. *Proceedings*, Institute of Radio Engineers (New York, N. Y.), volume 35, July 1947, page 670.

13. Attenuation of 1.25-Centimeter Radiation Through Rain, Lloyd J. Anderson, John P. Day, Clemens H. Freres, Alfred P. D. Stokes. *Proceedings*, Institute of Radio Engineers (New York, N. Y.), volume 35, April 1947, page 351.

14. Radio Propagation at Frequencies Above 30 Megacycles, Kenneth Bullington. *Proceedings*, Institute of Radio Engineers (New York, N. Y.), volume 35, October 1947, page 1123.

15. Elimination of Interference-Type Fading at Microwave Frequencies with Spaced Antennas, Ross Bateman. *Proceedings*, Institute of Radio Engineers (New York, N. Y.), volume 34, September 1947, page 662.

16. The Effect of Rain Upon the Propagation of Waves in the 1- and 3-Centimeter Regions, Sloan D. Robertson, Archie P. King. *Proceedings*, Institute of Radio Engineers (New York, N. Y.), volume 34, April 1946, page 178.

No Discussion

Microwave Systems for 960 and 2,000 Megacycles

R. V. RECTOR
MEMBER AIEE

W. E. SUTTER
NONMEMBER AIEE

OUR modern civilization has grown extremely dependent upon reliable continuous communications. The vast communication networks of our public utilities will verify this statement. Some have expanded their present communication systems of phone lines, power-line carrier, and mobile radio to a point where additional expansion is extremely difficult. They are turning, therefore, to a fourth system that will help fulfill their expanded requirements. This new system is microwave radio and is the subject of this paper.

Many articles have been written of late on the subject of microwave communications. The words microwave and relaying, multiplexing and pulse modulation have been introduced into our daily conversation and appear in all our current technical literature. Wartime developments in tubes (such as Klystrons, lighthouse tubes, magnetrons, crystal mixers) and in high-frequency circuit design have enabled the communication field to expand into this new frequency spectrum.

The Federal Communications Commission has recognized that microwaves offer a solution to these congested fields. The bands available for point-to-point use by power companies and industrial services are in the 900-, 2,000-, and 6,000-megacycle regions. Present indications tend to make the 952–960 megacycle and the 2,000-megacycle bands the most advantageous. Each band has its own independent applications.

Where a very large number of voice channels are required, it is economical to use the 2,000-megacycle band or higher. The equipment necessarily requires the wide transmission bandwidth available in this region. It seems that for economical reasons, the 2,000-megacycle band is more desirable than the 6,000-megacycle band.

For a number of reasons, the most promising place and the recommended portion of the spectrum for a low cost radio link with a small number of channels and a few relay points appears to be in the 952–960 megacycle region. The equipment has the advantage that it is similar and more closely related to techniques employed in equipment of the low frequencies. It is relatively high frequency, yet standard tubes may still be used. Portions of the 920–960 band are presently assigned for frequency modulation broadcast studio transmitter links. Economical multiplexing of up to seven channels may be obtained on this equipment.

Propagation of microwaves follow very different laws than the waves of the low-frequency bands. They, in general, do not bend nor follow the curvature of the earth. They tend to travel in straight lines similar to beams of light and therefore reliable communications require a line-of-sight path clearing the surface of the earth by some reasonable distance. In actual application, advantage should be taken of hills and tall buildings, see Figure 1.

Because of the short wave lengths, relatively simple antennas can be used to transmit the energy in a beam. Six-foot metallic parabolic reflectors produce beams as narrow as 6 degrees in width at 2,000 megacycles. With this concentration of energy, low power transmitters may be used. Transmitters of 5 to 20 watts are employed enabling simplicity in design and longer trouble free operation. Figures 7 and 8 show a typical transmitter and receiver. Their simplicity will be apparent.

Let us now investigate a typical 2,000-megacycle relay system, such as presented in Figure 2. The major components are:

1. Transmitter Terminal
2. Microwave Transmitter
3. Transmitting Antenna
4. Receiving Antenna
5. Microwave Receiver
6. Receiver Terminal

For simplicity the system shown provides communication in only one direction. A similar system working in the opposite direction would give us 2-way communication. Where greater than line-of-sight distances are to be covered, a relay point or points consisting of a receiver feeding directly into a transmitter may be employed.

When more than one signal is to be transmitted over this system, the signals are said to be multiplexed. This is the function of the terminals. Two systems are available today to accomplish this multiplexing: time division multiplexing; and frequency division multiplexing.

For systems of a small number of channels, frequency division is conventional. For larger systems, time division is used. Here the signals of the various input channels are sampled individually several thousand times a second. The voltage sample at the moment determines some characteristic of the pulse.

Systems using pulse position, pulse amplitude, and pulse length are a few now commercially used. In actual practice, the number of necessary samples can be greatly reduced by passing the demodulated audio voltage through a low-pass filter to attenuate harmonics and thus reduce the distortion at the highest modulation frequencies. Obviously, if the samples are taken at a constant rate, the lower audio frequencies will be sampled

Paper 50-171, recommended by the AIEE Carrier Current Committee and approved by the AIEE Technical Program Committee for presentation at the AIEE Summer and Pacific General Meeting, Pasadena, Calif., June 12–16, 1950. Manuscript submitted March 14, 1950; made available for printing May 10, 1950.

R. V. Rector is with the General Electric Company, Syracuse, N. Y., and W. E. Sutter is with the International General Electric Company, New York, N. Y.

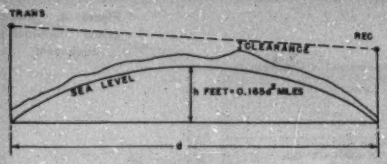

Figure 1. Beam transmission path

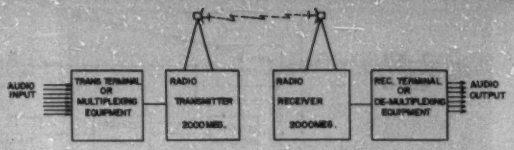

Figure 2. Typical 2,000-megacycle relay system

many more times, in proportion, and thus will inherently have lower distortion. Laboratory measurements have shown that a low-distortion system can be obtained with as few as three samples of the highest modulation frequency. In a practical application for telephone communications, the highest audio frequency is about 3,500 cycles per second, and thus the sampling rate should be about 10,000 times per second.

It is the function of the transmitter terminal to produce all these modulated pulses at the correct time, and feed them to the microwave transmitter, and it is the function of the receiver terminal to take the output of the microwave receiver and route the pulses to the correct output channels.

Let us now take a look at two examples of commercial microwave equipment. First a 2,000-megacycle link. In Figure 3, we see a block diagram of the transmitter terminal. Briefly, the transmitter waveform generator produces waveforms that basically time the over-all system. The timing circuits are all based on a 300-kc crystal controlled oscillator. It then governs the production of the timing pips, sawtooth, and a synchronizing pulse.

The output of the 300-kc oscillator is coupled to a pip generator to produce sharp spikes of voltage. In one branch they are amplified, while in the other they are used to trigger a frequency-divider multivibrator. The frequency divider, triggered at a 300-kc rate, has a 10,000-cycle output and is used to key the synchronizing generator. The synchronizing pulse thus produced is used to trigger the sawtooth generator. The first two waveforms, namely the sawtooth and timing pips, are fed to the respective modulator chassis to be used in the channel selector circuits, along with a variable positive voltage, obtained from a voltage divider.

Each of the channel selectors is arranged to select one particular reference pip. The particular reference pip for each channel triggers the multivibrator to generate a pulse, which is length modulated. Therefore, each channel produces a pulse after each synchronizing pulse in a fixed sequence. The audio signals are fed through an amplifier and limiter stage and coupled to the pulse modulator circuit. The action of this modulating circuit on the pulse generator produces an output that varies in width in accordance with the samples taken of the input signal.

The pulses are mixed in the amplifier shown in the upper right of Figure 3, along with the synchronizing pulse, and are then fed to the transmitter and

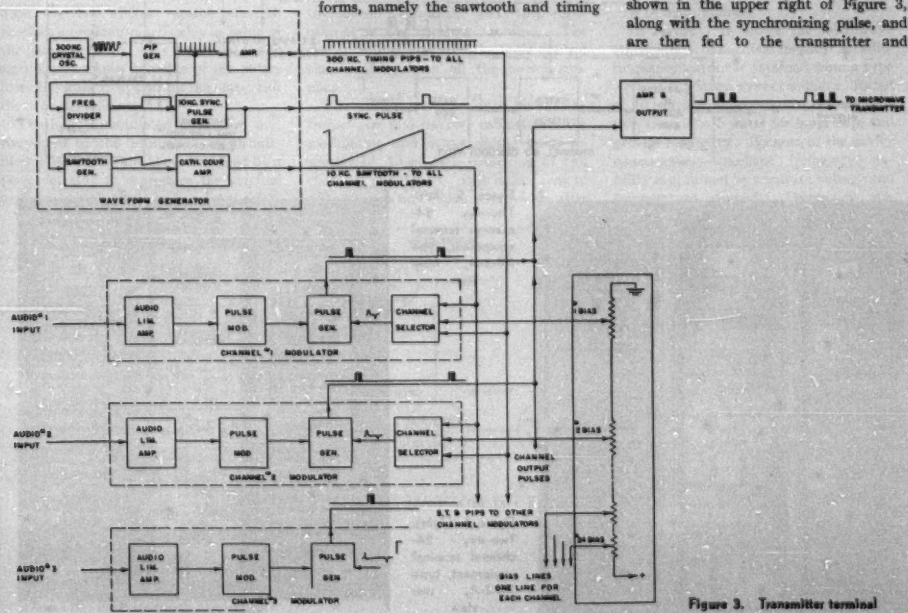

Figure 3. Transmitter terminal

Figure 4. Receiver terminal equipment

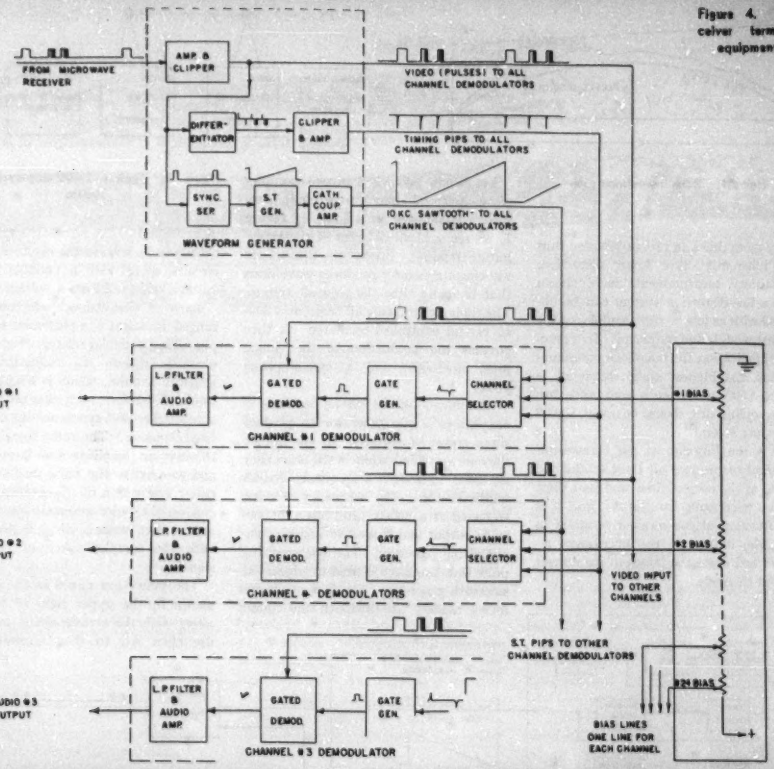

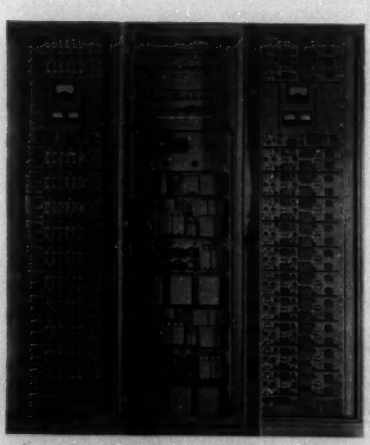

Figure 5 (left). Two-way 24-channel terminal equipment, type *XB-3-A*, front view

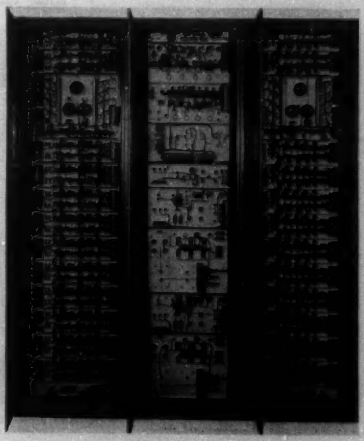

Figure 6 (right). Two-way 24-channel terminal equipment, type *XB-3-A*, rear view

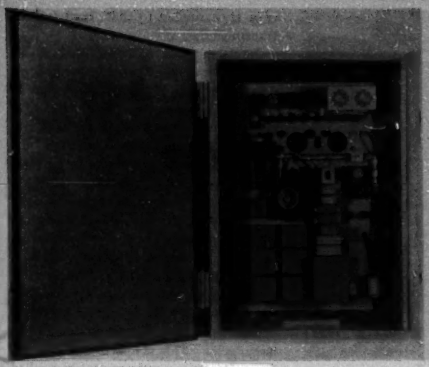

Figure 7. Microwave transmitter mounted in temperature-controlled cabinet

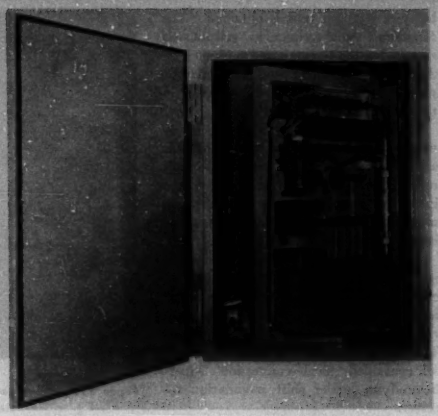

Figure 8. Microwave receiver mounted in temperature-controlled cabinet

beamed to the distant receiver. This signal is then fed to the receiver terminal equipment, Figure 4. Specifically, it is fed to the receiver waveform generator where it is utilized to form timing pips and sawtooth synchronized with the pips and sawtooth at the transmitting terminal.

The sawtooth and timing pips are used, together with a variable bias, to produce a predetermined delay in firing of the gate generator. This gate is fed to the screen, and allows only one of the pulses from the train to appear on the plate, and there be demodulated.

The length modulated pulses are first converted to the equivalent amplitude-modulated pulses and then combined by a peak detector to reproduce the original audio voltage. Audio is then fed through a low-pass filter and coupled through an amplifier to the output lines.

That basically is the multiplexing system. Of course, certain refinements are added, and in Figure 5, the complete terminal is shown. The left cabinet is the transmitter terminal, and the right cabinet is the receiver terminal. The center cabinet contains the basic control chassis along with all the power supplies.

The similar units appearing here in the transmitter and receiver cabinets are the modulating and demodulating units respectively, 12 of each consisting of two channels per chassis. It is rather easy to add channels and expand the system after initial installation. The larger panels in the two outside cabinets provide constant monitoring of input and output channels. In Figure 6, a view of the rear of the three cabinets will show the construction and the availability of parts and ease of maintenance.

In Figure 7 is shown the microwave transmitter. The 2,000 megacycle radio-frequency output is obtained from a type *SRL-7C* Klystron power oscillator. Rated at 10 watts, it is operated in this application from 2 to 5 watts for longer life and greater reliability. Because of the cavity construction, excellent frequency stability is obtained by accurate voltage and temperature control. Frequency sta-

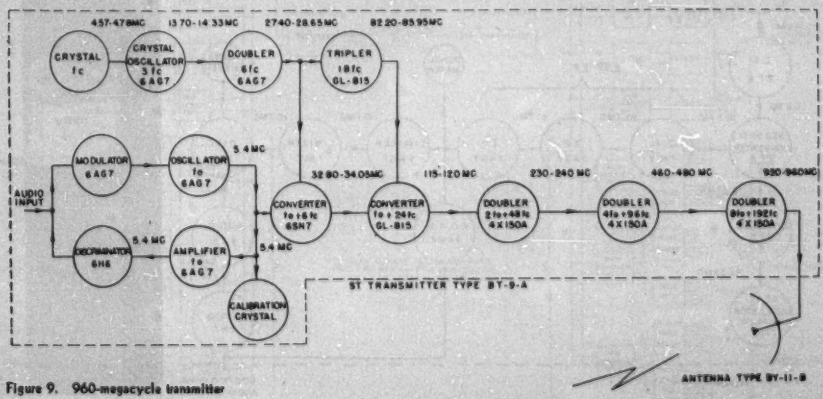

Figure 9. 960-megacycle transmitter

bility of 0.05 per cent is obtained. The Klystron radio-frequency output is matched to the transmitting antenna by a double slug dielectric matcher, and thus no moving finger or contacts are used in the entire radio-frequency system.

Carrier shift modulation (frequency modulation with pulse modulation) is accomplished by modulating the Klystron reflector voltage by the pulses generated in the terminal and amplified by the video modulator. The remainder of the panel is power supplies.

The entire transmitter is housed in an insulated, weather-resistant cabinet equipped with blowers and a thermostatically-controlled damper to automatically maintain the cabinet temperature. The microwave receiver, Figure 8, is a self-contained single-conversion superheterodyne carrier shift modulation receiver.

The *SRL-7C* Klystron is used as the local oscillator. Conversion is accomplished by a silicon crystal located in a specially-designed mixer. The mixer is matched to the antenna with a dielectric matcher.

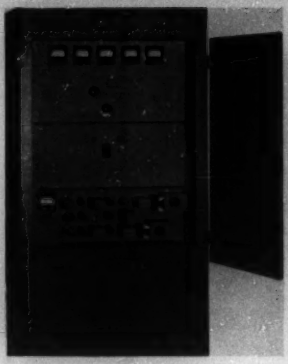

Figure 11. 960-megacycle transmitter, front view

The intermediate frequency amplifier (bandwidth of 8- and 60-megacycle center frequency) provides six stages of intermediate-frequency amplification and two limiter stages. Double fixed tuned circuits are used throughout to provide excellent adjacent channel selectivity. Sensitivity of 95 decibels below 1 watt is obtained.

The receiver is housed in a cabinet of a type similar to that used for the transmitter.

Neglecting the antennas, that covers the basic equipment for a 2,000-megacycle microwave relay system. A system of this nature is capable of transmitting 24 channels of audio (200–3,000 cycles) with less than 3 per cent distortion, and having noise and cross-talk ratios of better than 50 decibels.

Let us briefly compare a typical 960-megacycle relay. In Figure 9, the basic circuits are shown in the block diagram of the transmitter. Basically, it is a typical frequency-modulated transmitter consisting of a reactance tube modulator which frequency modulates an oscillator operating at a center frequency of 5.4 megacycles. This is mixed with a signal derived from a quartz crystal controlled oscillator in two consecutive stages and then fed through three doubler stages. This multiplication gives us a signal of approximately 960 megacycles with a frequency swing of ±75 kc for 100 per cent modulation and output power of 10 watts.

In Figure 10, we have the block diagram of the receiver. The first converter is used to convert the signal power from the carrier to the frequency of the first intermediate frequency, 112 megacycles. This local oscillator is a crystal oscillator with tripler, and doubler stages follow-

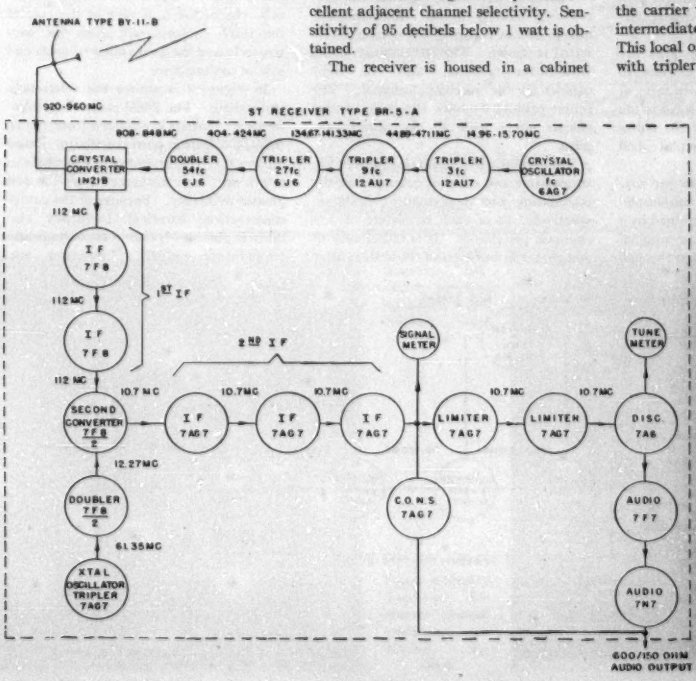

Figure 10 (left). 960-megacycle receiver

Figure 12 (below). 960-megacycle receiver mounted in cabinet with other audio facilities

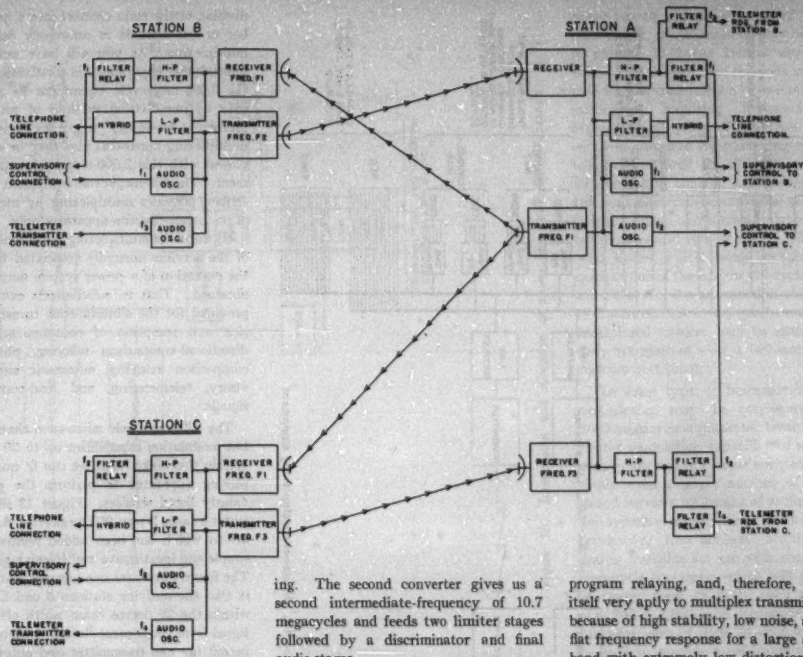

Figure 13 (above). Microwave channel equipment

Figure 14 (below). Microwave multiplexing equipment

ing. The second converter gives us a second intermediate-frequency of 10.7 megacycles and feeds two limiter stages followed by a discriminator and final audio stages.

The performance of this equipment fully meets all the requirements of the Federal Communications Commission for program relaying, and, therefore, lends itself very aptly to multiplex transmission because of high stability, low noise, and a flat frequency response for a large audio band with extremely low distortion. In Figures 11 and 12, we see the manufactured product.

Microwave radio systems have already

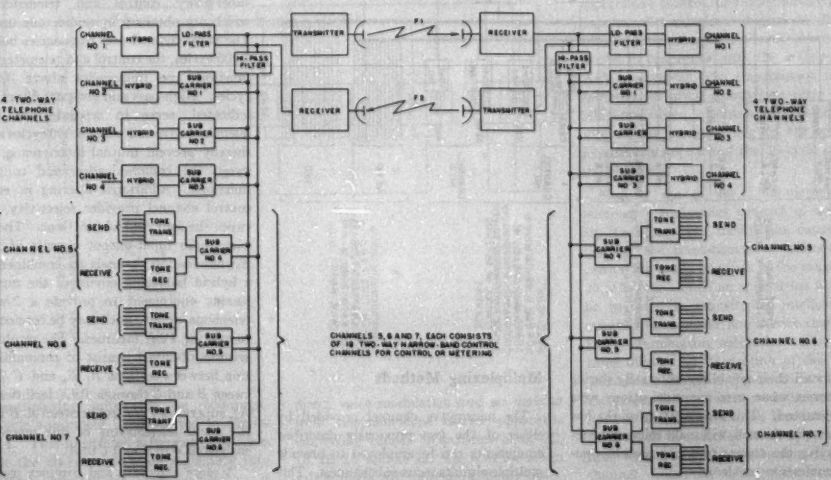

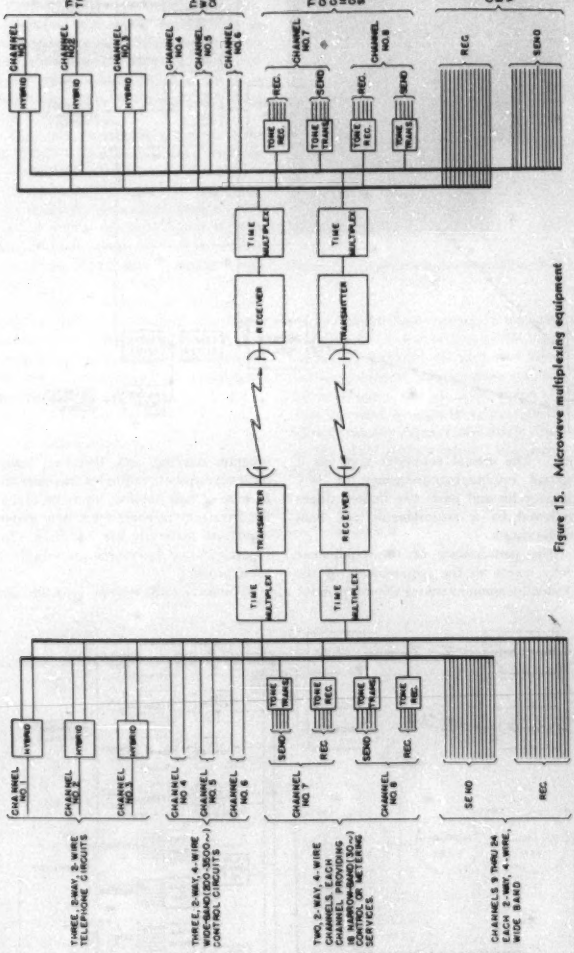

Figure 15. Microwave multiplexing equipment

proved their reliability, especially during storms when wire communications were disrupted. This reliability, plus the low cost per channel, will make microwave relaying the answer to many present communication problems.

Multiplexing Methods

The microwave channel provided by either of the two previously described equipments can be employed to provide multiple simultaneous subchannels. This division of the main channel into a number of subchannels is commonly called multiplexing. As you will have noted, multiplexing equipment is available for the 2,000-megacycle equipment to provide a time-division method of multiplexing. However, frequency-division multiplexing apparatus also may be employed with this 2,000-megacycle equipment. The 960-megacycle equipment described provides multiplexing by means of frequency-division apparatus only.

By means of multiplexing apparatus all of the services normally associated with the operation of a power system may be obtained. That is, subchannels can be provided for the simultaneous transmission and reception of communication, directional-comparison relaying, phase-comparison relaying, automatic supervisory, telemetering, and load-control signals.

The 960-megacycle microwave channel has modulation capabilities up to 30 kc. Within this 30-kc band, we can fit multiplexing apparatus to perform the previously listed services. Figure 13 illustrates a basic 2-way 960-megacycle channel to which has been added relatively simple and inexpensive multiplexing gear. The figure illustrates one unusual feature in that the outlying stations B and C lie within the 20 degree beam width of the signal from the control station A thereby permitting one transmitter and antenna at A to communicate with and control both stations B and C. The multiplexing apparatus in this figure consists of a direct voice channel and four channels of supervisory control and telemetering which are obtained by audio tone units. The voice channel uses frequencies below 3,000 cycles, the control and telemetering functions use frequencies above 3,000 cycles. High-pass and low-pass filters, as indicated, serve to separate the frequencies above and below 3,000 cycles and thereby prevent mutual interference between the communication and control functions. Additional filtering in each control channel provides selectivity between the four control functions. The 4-wire audio input-output circuits of the communication channels are combined in a hybrid balancing circuit of the multiplexing equipment to provide a 2-wire telephone circuit which may be connected to existing *PBX* facilities. The resulting services obtained consist of communication between stations A, B, and C (between B and C through *PBX* facilities at A), supervisory control between A-B and A-C, and telemetering of one quantity each from B to A and C to A.

A more elaborate and complex use of

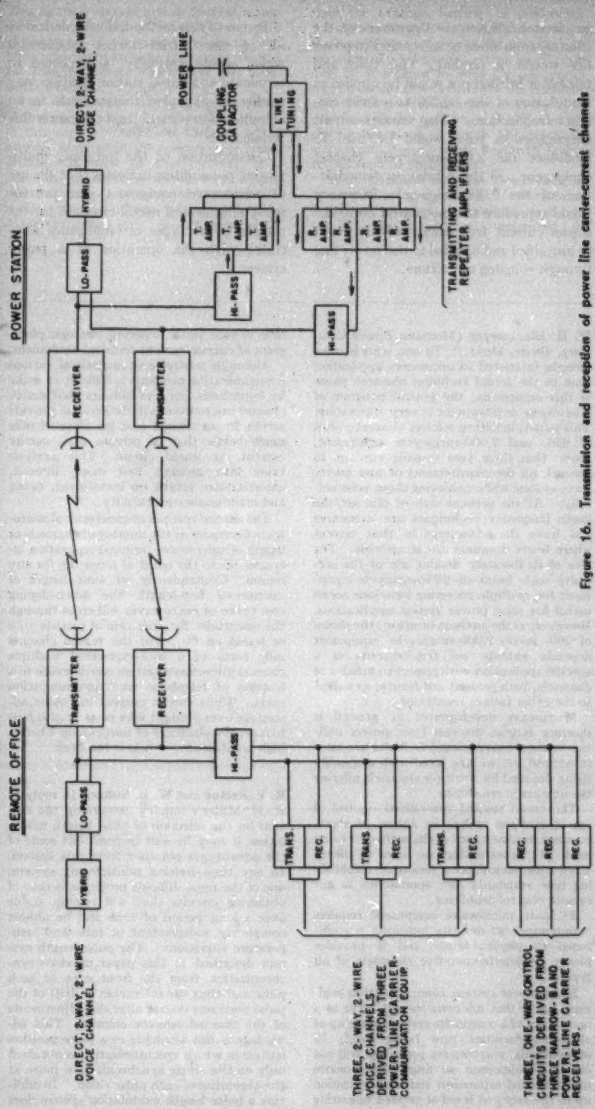

Figure 16. Transmission and reception of power line carrier-current channels

multiplexing apparatus on 960-megacycle equipment is illustrated in Figure 14. This illustrates a frequency division of the 30-kc modulation capability into seven subchannels, one consisting of direct voice modulation and six derived from telephone-type carrier apparatus employing carrier frequencies of 8, 12, 16, 20, 24, and 28 kc. Each of the seven subchannels will provide a 2-way voice circuit having a frequency range of 300 to 2,500 cycles, or each channel may be used to provide 18 2-way control channels. Each of these 18 control channels may be used for the transmission or reception of intelligence requiring frequencies no higher than 30 cycles. This narrow bandwidth is adequate for conveying the intelligence required by all types of telemetering, load control, supervisory control, and directional-comparison pilot relaying. Phase-comparison relaying intelligence would require a bandwidth of ±60 cycles which would occupy the space of two of the narrow (30-cycle) control channels. An examination of Figure 14 illustrates that a very great number of multiplexed services may be simultaneously transmitted over a 960-megacycle microwave channel.

The same type of frequency-division multiplexing may be employed with 2,000-megacycle equipment, however, its greater modulation capability of up to 4 megacycles makes it more economical to obtain even a larger number of multiplexed services by means of a time-division system of multiplexing. As described previously, time-division multiplexing gear is available for use with the 2,000-megacycle equipment which will provide 24 2-way voice channels, each capable of a 200-to-3,500-cycle frequency range. Likewise, each of these 24 channels may be used to provide a maximum of 18 2-way control channels, each of which may be used for the transmission or reception of frequencies up to 30 cycles such as required by telemetering, load control, supervisory control, and directional-comparison pilot relaying. Figure 15 illustrates multiplexing of this type. As mentioned in connection with the 960-megacycle equipment, the transmission and reception of phase-comparison relay intelligence would require a bandwidth of ±60 cycles corresponding to the space requirements of two of the 30-cycle control channels.

Another use of the 2,000-megacycle microwave equipment consists of utilizing its 4-megacycle modulation capabilities for the transmission of power-line carrier-frequency channels in the range of 30 to 200 kc. Such an application would be involved in transferring intelligence received on a power line carrier channel from a terminating substation to an uptown office. An illustration of this application is shown in Figure 16 in which the power-line carrier apparatus, usually located at the transmission line termination, would be installed at an office location within a city. Operation of this channel from the power line to the

substation to office would be as follows:

The carrier frequencies (30-200 kc) conveying three communication channels and three telemeter readings would be taken from the power line through the usual coupling capacitors and applied through radio frequency amplifiers to the microwave channel for sending to the office location. At the office location, the customary demodulation of the 2,000-megacycle signal would again produce the original 30-200 kc carrier frequencies which would be demodulated in the carrier-current equipment to reproduce the required intelligence. Operation of the channel from office to substation to power line would be similar. The voice and telemeter intelligence would be applied as modulation of the 30-200 kc carrier-current frequencies. The carrier-current frequencies in turn would be used to modulate the 2,000-megacycle channel equipment. At the substation demodulation of the 2,000-megacycle frequency would reproduce the modulated 30-200 kc carrier-current frequencies which would be amplified and applied to the power line through coupling capacitors.

By use of this method, it is evident that all of the carrier-current frequencies which would normally be expected to terminate at a power station location may readily be extended to terminate in an office location remote from the power line termination.

Consideration of the foregoing multiplexing possibilities indicates that the use of microwave equipment can provide many reliable and useful channels for the transfer of all types of intelligence associated with the operation of a power system.

Discussion

R. H. Miller (Pacific Gas and Electric Company, San Francisco, Calif.): This paper gives a very good exposition of the relative advantages and limitations of 960-megacycle and 2,000-megacycle microwave systems as well as describing typical commercial versions of presently available equipment for each of these bands.

In the discussion of time-division multiplexing methods a comparison of pulse length, pulse position, and pulse amplitude systems might have been of general interest. It was noted also that no reference was made to pulse code modulation, and this method of muliplexing might have been covered briefly. In the selection of a modulation system for the time-division multiplexing equipment described in the paper, the reasons for the selection of pulse length modulation was not discussed. There must have been certain salient features of this system that led to its selection and an outline of these reasons would have been helpful to the reader.

In discussing the frequency stability of the Klystron oscillator the figure given for stability is 0.05 per cent. This figure seems rather low as compared to lower frequency equipment and the question is raised as to whether or not the figure given is correct or perhaps a typographical error.

In comparing frequency-division and time-division multiplexing methods it should be pointed out that one of the reasons that a favorable signal-to-noise ratio is available from a time-division multiplex system is that all of the energy of the radio signal is available in the channel being sampled while in a frequency-division system the radio-frequency energy is divided among the various channels. This factor itself, as well as bandwidth limitations, on 960 megacycles, limits the number of channels practically usable on a frequency-division multiplexing system.

The authors of this paper have done a particular service in suggesting various applications of microwave equipment in the power industry. By combining voice communications, relaying, telemetering, and so forth in one microwave system, considerable economy can be effected. The only undesirable feature that might be suggested to such a system is the fact that failure of the microwave equipment might prove very serious if many such important functions are carried on one microwave system.

W. H. Blankmeyer (Montana Power Company, Butte, Mont.): To one who is more directly interested in microwave application than in the actual technical research phase of this equipment, the general program of microwave development is very interesting. This paper, in listing relative characteristics of 960- and 2,000-megacycle equipment, shows that these two systems contain, in general, all the requirements of any microwave system while achieving them economically. At the present state of the art, the lower frequency techniques are attractive and have the advantage in that respect where fewer channels are acceptable. The idea of deliberately making use of the normally wide beam of 960-megacycle equipment for multiple receiving locations seems useful for some power system applications. However, as the authors mention, the choice of 960- versus 2,000-megacycle equipment depends entirely on requirements of a specific application with respect to number of channels, both present and future, as well as to the other factors mentioned.

Microwave development in general is meeting intense interest from power utilities because conventional facilities are saturated and yet we are faced with a steadily rising demand for multiple channels offering the utmost in reliability.

The trend toward centralized control of power stations makes us aware of shortcomings in some types of channels now being used. It appears that we have in microwave communication a means of establishing new standards and approaches to our remote control problems.

At least, microwave equipment requires maintenance at definite locations as compared to physical lines, and it provides plenty of interference-free channels of all types.

Most power system communication engineers agree that microwaves will serve as a main stem of a composite system made up of all other facilities now being used. In other words, microwaves probably will not create obsolescence so much as promote much needed expansion and modernization up to the required level of present operating problems.

A microwave feature especially useful in power systems is the idea of piping conventional carrier current frequencies by microwave beam along with other channels. This compares somewhat with the successful practice of transferring carrier current signals directly from power lines to telephone lines or vice versa, to permit strategic placement of carrier current terminal equipment.

Although relative cost analysis of various communication methods is difficult to make by hypothesis, surveys indicate that multichannel microwave installations can provide service at an annual cost per channel mile much below that of private wire, carrier current, or leased circuit. This analysis takes into account first costs, interest, amortization, return on investment, taxes, and maintenance probability.

The annual cost per channel mile of microwave decreases as the number of channels or length of microwave terminal separation increases up to the point of repeating for any reason. Consequently, at some length of microwave hop-length the down-sloping cost curve of microwaves will cross through the essentially flat cost rate of private wire or leased circuit. For this reason channel mile costs of a well-engineered multiple channel microwave system can decrease to a fraction of telephone wire communication costs. While carrier current has some advantage over straight wire costs, it also fails to meet the challenge of microwaves where a high number of channels is involved.

R. V. Rector and **W. E. Sutter:** In reply to R. H. Miller's inquiry concerning the reasons for the selection of pulse-length modulation, it may be well to point out some of the advantages obtained from this system. In any time-division multiplexing system, one of the most difficult problems is that of obtaining circuits that will remain stable over a long period of time and be almost completely independent of tube and temperature variations. The pulse-length system described in this paper provides synchronization from the front edge of each pulse and thus the tolerances or drift of the pulse positions do not alter the adjustments of the channel selector circuits. This advantage is not available in a pulse-position system in which synchronization is obtained only on the single synchronization pulse at the beginning of each pulse chain. In addition a pulse-length modulation system does not require linear amplifiers and does provide good noise elimination characteristics as a result of the pulse-clipper circuits. These advantages are, of course, not available in a pulse-amplitude system.

Mr. Miller also questioned the 0.05 per cent frequency stability figure of the 2,000-megacycle equipment as being rather low.

This figure is correct and in general is considered satisfactory. The wide bandwidth of this type of equipment makes the stability characteristic less important than is the case in systems which have less bandwidth available.

Oral discussion following the presentation of this paper indicated considerable interest in this type of equipment to perform the services required in the operation of utility system. In view of this interest, it is probably advisable to mention some additional features and some of the improvements which have been incorporated in the 2,000-megacycle per second equipment since the original writing of this paper.

Because of numerous inquiries concerning the possibility of transmitting the complete functions of a telephone system, it will probably be of interest to note that the equipment does contain circuits for the transmission of the d-c functions required by automatic telephone exchanges (PAX) and the ringing functions of trunk line telephone circuits and does therefore lend itself readily to this type of application.

This equipment now has been redesigned to provide a more economical arrangement for a small number of channels, such as 2 to 12. The 24-channel equipment described in the paper did not economically lend itself to applications requiring less than 12 channels.

The employment of the Klystron tubes has recently been eliminated in favor of crystal-controlled equipment using less expensive triode tubes. This elimination of the Klystrons permits the use of a less expensive transmitter and receiver housing and permits the equipment to be located at a much greater distance from the antennas. A distance of as much as 350 feet may now be used between the transmitter-receiver and the antennas. In many cases this distance may be increased if necessary.

Ignitron Converters for High Energy Particle Accelerators

J. L. BOYER
ASSOCIATE AIEE

C. R. MARCUM
ASSOCIATE AIEE

THE need for larger magnet power supplies for high energy particle accelerators has resulted in a new application for power conversion equipment. It uses rectifier equipment which can either supply power or return power to a flywheel a-c motor-generator set. The equipment is unusual in that the current flows in one direction, but the polarity of the output voltage is reversed to change the direction of power flow.

The magnet used on a large proton-synchrotron requires the current to build up rather slowly to a maximum value. To save the energy stored in the magnetic field and restart the cycle in a short time, the current in the magnet must be forced to zero by a counter voltage. The acceleration of particles is accomplished in the current build-up period, and this is the most critical portion of the load cycle. In the two units to be described, the current build-up in the magnet is roughly linear with time and the current decay has about the same characteristics.

A rectifier and a-c motor-generator set for a large magnet has been manufactured for the Brookhaven National Laboratory. This equipment has a peak kilowatt rating of about 30,000 kw with a pulse rate of 12 per minute. The second installation is at the University of California Radiation Laboratory in Berkeley, and this unit is rated 100,000 kw peak with a pulse rate of about ten per minute. The rectifier equipments for both of these installations are described in this paper. Since the two installations are so similar, only the data on the University of California equipment will be given.

Paper 50-174, recommended by the AIEE Electronic Power Converters Committee and approved by the AIEE Technical Program Committee for presentation at the AIEE Summer and Pacific General Meeting, Pasadena, Calif., June 12–16, 1950. Manuscript submitted March 16, 1950; made available for printing April 25, 1950.

J. L. Boyer and C. R. Marcum are both with the Westinghouse Electric Corporation, East Pittsburgh, Pa.

Requirements of Magnet Power Supply

The magnet load on the power supply appears as a tremendous inductance in which the time constant is about 15 seconds at small currents. When a direct voltage is applied, the current starts to build up at a constant rate. The build-up time on the University of California unit is approximately 1.9 seconds. After the peak current is reached, it is desirable to bring the current to zero in a minimum time to reduce the losses.

It is necessary to have very accurate control of the direct voltage at the start of the pulse since the injection of the protons occurs at a low magnet current, and the problem of holding the particles is most difficult at this time. The ripple in applied voltage must be low. It was decided that a 12-phase rectifier voltage ripple is satisfactory, but no ignition control can be used because of the increase in harmonics in the d-c output voltage.

Special consideration was required on the problem of never attempting to open the magnet circuit when any current was flowing. The inductance is so high that if any of the equipment would attempt to suddenly change the current, a very high voltage would be produced, and the magnet and other equipment might be damaged.

The load variation taken from the power source had to be kept to a minimum so that the disturbance on the power system would be within the required limits. It was, therefore, necessary to have some energy storage equipment such as flywheels on the motor-generator sets.

Advantages of Rectifiers over D-C Machines

In the original investigation of the best type of power supply for these large magnets, d-c motor-generator sets and rectifiers with a-c motor-generator sets were compared. It was found that the time required to suddenly reverse the polarity of a large d-c machine was so great that a considerable extra loss would result while the magnet current was near the peak value. With rectifiers, the time required to change from rectification to inversion can be as short as 1/2 cycle, and even on the more complicated circuits which correct many mechanical problems, it is only a few cycles.

The problem of completely reversing the field current of a d-c machine twice each pulse and accurately controlling the voltage at the start of each pulse appeared to be extremely difficult if not impossible. With rectifiers, a minimum of field control is used on the a-c generator to make it possible to control the rectified voltage with extreme accuracy at the start of each pulse.

Rectifiers with an a-c motor-generator set proved to be more economical than a d-c motor generator. The higher voltage rating of rectifier tubes make it easier to obtain the high voltages desired for the magnet coils. The type of rectifier which is used on these applications is shown in Figure 1.

Rectifier and Inverter Circuit Operation

Since it was necessary to obtain a rather high direct voltage, four rectifier units are operated in series. Figure 2 shows the complete power circuit for the University of California installation. Two identical units are operated in parallel to give the desired rating.

Each generator Y supplies six ignitron tubes which operate with balance coils to form a 3-phase rectifier. Figure 3 shows

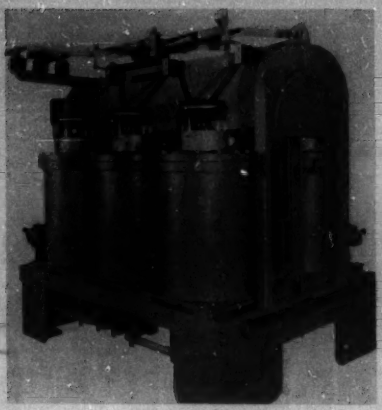

Figure 1 (left). High - voltage ignitron rectifier assembly. Eight such assemblies have peak power output of 100,000 kw

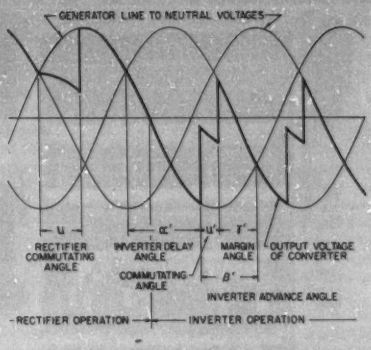

Figure 3 (right). Wave shape of 3-phase ignitron converter direct voltage during changeover from rectifier to inverter operation

the operation of one 3-phase rectifier in the period at the peak current, when the operation is changed from rectifier to inverter. On the left side of this figure, the tubes are operating with zero degrees delay. This current commutates from one tube to the next with a rather long angle because of the relatively high reactance of the generator windings.

The change from rectifier to inverter operation occurs when the ignition point is suddenly delayed approximately 100 degrees. This causes the tube which was conducting the current at that instant to continue for an extra long angle, and the other tubes start to conduct the current mostly on the negative half of their alternating voltage wave.

In the inverter portion of the pulse as indicated on the right of Figure 3, the tubes are fired considerably in advance of the negative crossing point of the alternating voltage waves. This is to allow for a rather long commutation angle and to give the tubes some margin angle so that they will gain control before the anode goes positive. Some extra angle is allowed so that there can be a considerable unbalance in load current between the two units.

Tube Development

The selection of the type of rectifier was based on the requirements for high voltage and heavy direct currents with

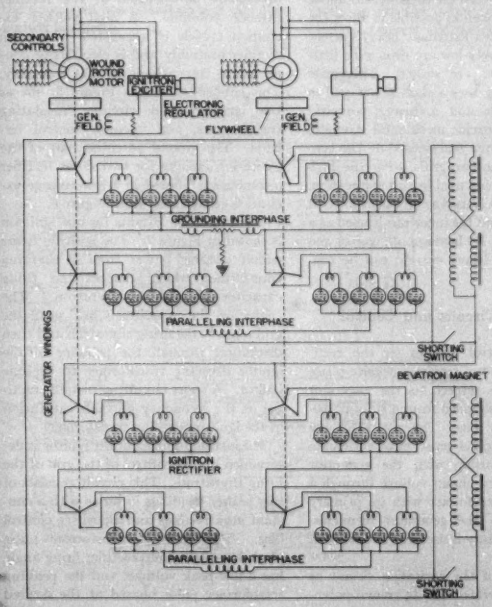

Figure 2 (left). Power circuit of magnet power supply for University of California bevatron

Figure 4 (below). High-voltage pumped-type ignitron

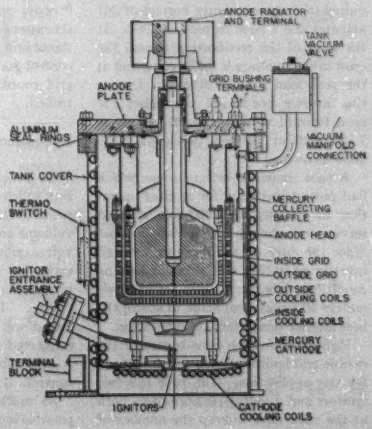

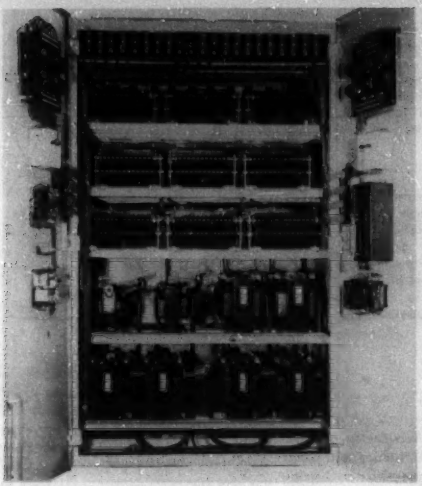

Figure 5. High-voltage excitation cubicle which operates at cathode potential of the ignitron rectifier assembly

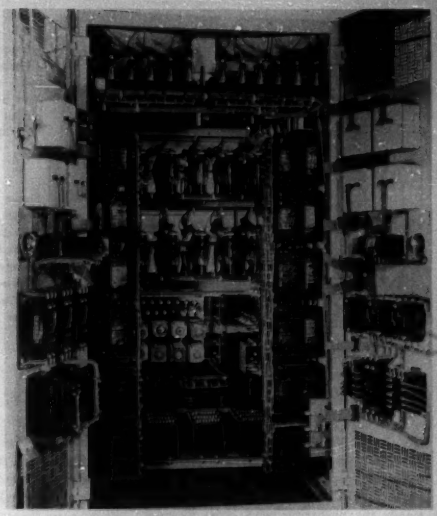

Figure 6. Low-voltage excitation cubicle which operates at ground potential

both rectification and inversion duty. Pumped ignitrons were used rather than sealed ignitrons because pumped tubes have a higher ratio of peak current to average current, will withstand rougher treatment, and have a much longer life. The basic ignitron design is based on a tube which was developed for 3,000-volt railway substation applications.[1]

With the circuit shown in Figure 2, the duty on each ignitron is such that it is required to carry an average current of 261 amperes and a peak current of 2,083. At the start of the rectification period, the crest inverse voltage is 9,430 volts, and at the peak load it is 7,920 volts. During the inverter portion of the pulse, the crest forward voltage on each ignitron is 7,350 volts at the peak load and 9,430 volts at no load.

A tube similar in design to one which had proved successful for rectifier operation in commercial 3,000-volt railroad service was chosen for this application. Since the duty on the ignitron involved inverter operation and unusual loading conditions, laboratory tests for approximately 20 weeks were made to assure the best internal design for this application.

Figure 4 shows the cross-section of the double grid ignitron which was developed for this application. The tube has two ignitors and a voltage is applied to both at the same time to keep the number of ignitor misses to an absolute minimum. All paths between the cathode and anode are made as open as possible to allow the tube to conduct extremely heavy current with a relatively low arc drop with little probability of arc surges. The main anode bushing uses a glass-Kovar seal to hold vacuum and a heavy porcelain bushing to provide mechanical strength.

A glass-Kovar seal is used on the connectors to the two grids. For the high inverter currents used in this application, the outer grid is used as an excitation and shield grid, and the inner one is used as a control grid. By having both ignitor and grid control, heavy current can be controlled.

Excitation Circuits and Control

Those control circuits for the rectifiers which do not require a definite phase relation with respect to the generator voltages are supplied from a station 460-volt auxiliary bus. The power for the excitation circuits must have a definite phase relationship with the generator voltage. They obtain voltage through a step-down transformer with its primary connected to the generator terminals. A station battery is used for the essential control.

As much of the excitation circuit as possible is operated near to ground potential. Certain parts of the circuits must necessarily be operated at the rectifier cathode potential. A high voltage excitation cubicle is associated with each rectifier assembly and is electrically connected to the cathode of that assembly. This cubicle, shown in Figure 5, houses the ignitron grid circuits, insulating transformers, and vacuum control circuits. The ground potential part of the excitation circuits for two series rectifier assemblies is housed in a low-voltage excitation cubicle, shown in Figure 6.

The excitation circuits for one ignitron is shown in Figure 7. The ignitron firing circuit obtains power from a charging transformer which charges the firing capacitor through a thyratron. The charge on the capacitor is held until the grid releases the firing thyratron and then discharges through the primary of the ignitor coupling transformer to fire the ignitor. A short circuiting metallic rectifier on the secondary prevents saturation of the ignitor coupling transformer.

The instant of firing of the ignitor is determined by the control of the grid of the firing thyratron. This circuit consists of two peaker windings in series with a constant negative bias and a positive control bias. The peaking transformer pulse phased at the desired rectifier firing angle has a low-peak voltage, and the peaking transformer pulse phased at the desired

inverter firing angle has a high-peak voltage. With no positive control bias impressed, the negative bias bucks out the low-peak voltage but permits the high-peak voltage to release the tube at an inverter firing angle. When the positive control bias is impressed in series with the negative bias, the resulting bias is reduced so that the low-peak voltage releases the tube at a rectifier firing angle. The phase positions of the peaking transformers are determined by the power connections to the primaries and by a direct current in their phase shift windings.

In order for the ignitron to conduct when the ignitor is fired and its anode voltage is positive, its grids must be released. The outer grid is excited from two windings of the grid insulating transformer which are 90 degrees out of phase and connected through metallic rectifiers. This circuit makes the outer grid positive when the ignitor is fired at either the rectifier or the inverter angle. The inner grid is negatively biased until the outer grid current starts to increase and causes it to be released by a positive voltage on the grid coupling transformer between the outer and inner grid circuits. A misfire light is connected across the inner grid resistor and when lighted indicates that current is flowing to the inner grid. This further indicates that the outer grid has picked up and that the ignitor has fired.

The control and protection of the vacuum and cooling systems and the method of degassing these rectifier assemblies is much the same as for any standard rectifier application and will not be discussed in this paper.[2]

The rapidly increasing current in the magnet during the rectifying period is limited by the length of time that the positive control bias is applied to the excitation circuits. In order to limit the peak current in the magnet, a timing relay with a drop-out time of approximately 110 per cent of the desired rectifying period is de-energized as the positive control bias is applied. If the positive control bias has not been removed within the dropout time of the relay, contacts on the relay will automatically remove it. Further overload protection is obtained from inverse time over-current relays which are connected to the secondary of current transformers on the generator leads.

The generator and the ignitrons must be protected from occasional faults of the ignitrons. In case of an arc-back, there is a local short circuit involving the generator and the rectifier that arced-back caused by some ignitron conducting current in the reverse direction. An instantaneous overcurrent relay connected to the secondary of the generator lead current transformer energizes a relay which short circuits the output of the ignitor excitation circuit and thereby suppresses the arc in the forward-conducting ignitrons which are feeding the short circuit. It is then expected that the inductance of the magnet will force the reverse current in the faulty tube to zero. If the short-circuit current is reduced to a reasonable value, the short-circuiting relay on the excitation circuit will open and allow the ignitrons to operate again. If the short-circuit current is not limited by arc suppression within a few cycles, an inverse time overcurrent relay will energize a switch short circuits the magnet and will trip a high-speed circuit breaker in the field of the generator to remove the voltage from the ignitrons and thereby clear the fault.

If, during the inverter operation, an ignitron should have an arc-through, the current that can flow in the tube is limited to the magnet current. The tube with the arc-through will have a current twice its normal value since the current in the parallel circuit will transfer. Even with twice normal current in the tube, it has a good chance of regaining control the first few cycles after the arc-through occurs, so no instantaneous protection is applied. If the tube should not regain control within a few cycles, a relay, connected through a circuit sensitive to 60 cycles across the d-c terminals of each rectifier assembly, trips the magnet short-circuiting switch and opens the field circuit breaker of the generator.

Arc-back indicators are provided so

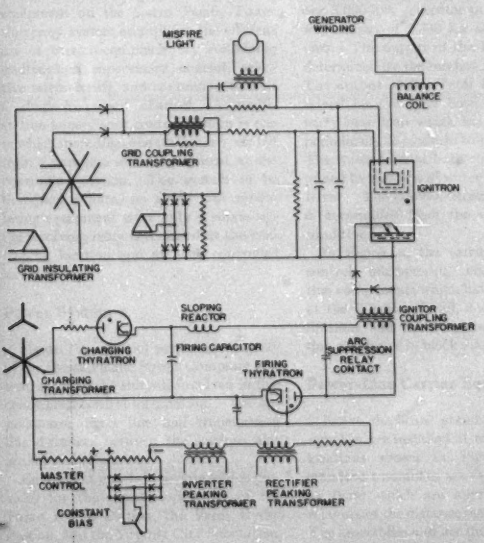

Figure 7 (left). Schematic of excitation circuit for one ignitron tube

Figure 8 (below). Typical load cycle for the University of California magnet power supply

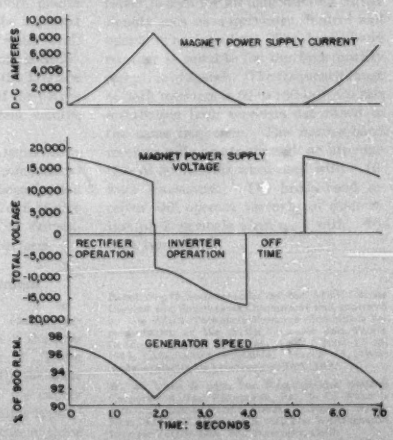

that the number of arcbacks occurring on each ignitron may be recorded. For each ignitron there is a small thyratron with a d-c plate supply and with its grid connected to an impulse coil on the anode lead of the ignitron. Reverse current on the ignitron will release the thyratron and thus record the arcback.

Load Cycle

A typical load cycle for the magnet power supply is shown in Figure 8. The particle acceleration takes place during the rectifier operation which is the first 1.9 seconds of this cycle. This part of the cycle is most critical and must be repeated as closely as possible from cycle to cycle.

Interphase transformers are provided between parallel units so that synchronous operation of the two generators will not affect the output voltage. The interphase transformers are designed with very low exciting currents so that by the time the magnet current reaches a value at which the particles are injected, the interphase transformers are fully excited. An electronic regulator working on an electronic exciter assures that the generator voltage is the same at the start of each cycle.

A master control device applies the positive control bias to start rectifier operation. As the magnet current reaches a predetermined small value, the particles are injected into the vacuum chamber at a speed corresponding to the field strength of the magnet. As the magnet current increases, the master control device causes the particle to accelerate at a rate matching the rate of increase of the magnetic field strength. After the particle has reached the desired speed, it is deflected from the vacuum chamber, and the master control device removes the positive control bias. This allows half of the series units to change to inverter operation. An internal positive bias in the excitation cubicle keeps the other half of the units operating as rectifiers for approximately one-half cycle of the generator shaft resonant frequency. At this time the remainder of the units change to inverter operation. This small time delay accomplished by using a timing commutator on the end of the generator shaft tends to cancel the stresses in the generator shaft that would be obtained with an instantaneous full power reversal. In approximately 2.1 seconds of inverter operation, the magnet current has been brought to zero. With high magnet currents, the inverters must be fired with considerable angle of advance in order to have sufficient deionization time for the tubes. This angle of firing must be delayed as the current approaches zero so that the output voltage of power supply is zero when the current reaches zero. This is accomplished by means of phase shifting windings on the inverter peaking transformers which are controlled by the load current. After the current reaches zero, there is a short off-time and the cycle is repeated.

Conclusions

Although these magnet power supplies are the first of this type and quite large, even larger units can be built without serious complications. Experience obtained with these two installations should give valuable engineering information on the performance of high-voltage pumped-type ignitrons when operating as the total load on an a-c generator.

References

1. High Voltage Ignitron Rectifiers and Inverters for Railroad Service, J. L. Boyer, C. G. Hagenaick. *AIEE Transactions*, volume 65, 1946, pages 463–70.

2. Mercury-Arc Power Converters in North America, AIEE Committee Report. *AIEE Transactions*, volume 67, part II, 1948, pages 1031–37.

No Discussion

Multistation Supervisory Control, Telemetering and Communication on Single-Frequency Carrier Channel

W. A. DERR
MEMBER AIEE

T. C. WREN
NONMEMBER AIEE

J. V. KRESSER
MEMBER AIEE

POWER-LINE carrier and associated equipment was recently placed in service by the Sierra Pacific Power Company for the centralized control of part of the system. In planning this centralized control system, consideration was given to the use of telephone line wires, power-line carrier, and microwave radio to provide the necessary interconnecting channels. Economic considerations led to the selection of power-line carrier.

This first use of power-line carrier equipment on the Sierra Pacific Power Company system exemplifies the efficient use of carrier equipment by combining multistation supervisory control, selective telemetering, and communication on a single-frequency channel. A multistation supervisory control system is one in which more than one station is operated from a common set of equipment at the controlling station. The system to be described requires no audio tone modulating equipment since only a single signal receiving relay is required at the controlling location and at each controlled location.

Power System

Figure 1 is a partial single-line diagram of the Sierra Pacific Power Company system, showing the stations involved in this centralized control installation. The approximate direct line and transmission line distances between the stations also are shown in Figure 1.

Equipment now is in service which provides for the remote operation of the Farad Hydro Station, the Verdi Hydro Station, and the Virginia City Substation. The equipment recently installed provides for the control of these three stations from the Washoe Hydro Station. All system dispatching is done from the Washoe Hydro Station. This remote control system will be extended to include another station in the near future.

The Farad Hydro Station has two 1,750-kva generators providing a normal output of 2,900 kw and 2,100 kilovars. The power house at Farad is shown in Figure 2. The Verdi Hydro Station has one 3,000-kva generator providing a normal output of 2,300 kw and 1,200 kilovars. The output of the Farad Plant is determined by the forebay level at Farad. The output of the Verdi Plant is determined by the river level. Both plants carry base load which must be adjusted periodically to conform to the water level. The water level at both stations is determined by the flow of water in the Truckee River. The kilovar output of the plants is determined from the system voltage conditions.

In Figure 3, the carrier, supervisory control, telemetering, and communication components which have been applied at the Washoe, Farad, and Verdi Hydro Stations and the Virginia City Substation are shown in block diagram form.

Power-Line Carrier Equipment

Exact duplicate standard carrier assemblies are installed at each of the four locations shown in Figure 3. These standard assemblies are exactly the same as those which are applied for carrier relaying of the distance measuring type.[1,2] The assemblies also are duplicate of those used for phase comparison relaying except for the omission of a control unit which is required for phase comparison relaying.[2] All of the carrier equipment is operated from 125-volt station batteries.

The carrier equipment at each location is mounted on a standard relay rack in an indoor-type cabinet. The assembly consists of individual transmitter, receiver, and modulator panels and a test meter unit. Figure 4 shows the carrier cabinet located in the Washoe Hydro Station. The equipment rack shown can be swung open to provide access to the rear of the units.

The transmitter panel consists of a Colpitts oscillator (one tube) and a 6-tube push-pull amplifier. The amplified carrier frequency output is fed into an iron-cored radio-frequency transformer whose secondary couples the carrier to the line through the line tuning unit and coupling capacitor. The transmitter has a frequency range of 50 to 150 kc and a frequency stability of 0.5 per cent. The transmitter has a nominal power output of 10 watts.

The receiver panel consists of a narrow-band saturated receiver and a broad-band receiver. The narrow-band receiver is used for all unmodulated carrier signals such as supervisory control and telemetering impulses. The broad-band receiver is suitable for the high quality reception of speech. The frequency range of both receivers is 50 to 150 kc. On this installation both receivers are tuned to the same frequency. The narrow-band receiver will operate through an attenuation of 30 decibels when used with a 10-watt transmitter. The broad-band receiver will operate through an attenuation of 50 decibels when used with a 10-watt transmitter.

Paper 50-175, recommended by the AIEE Carrier Current and Substations Committees and approved by the AIEE Technical Program Committee for presentation at the AIEE Summer and Pacific General Meeting, Pasadena, Calif., June 12–16, 1950. Manuscript submitted March 15, 1950; made available for printing April 25, 1950.

W. A. Derr is with the Westinghouse Electric Corporation, East Pittsburgh, Pa., T. C. Wren is with the Sierra Pacific Power Company, Reno, Nev., and J. V. Kresser is with the Westinghouse Electric Corporation, San Francisco, Calif.

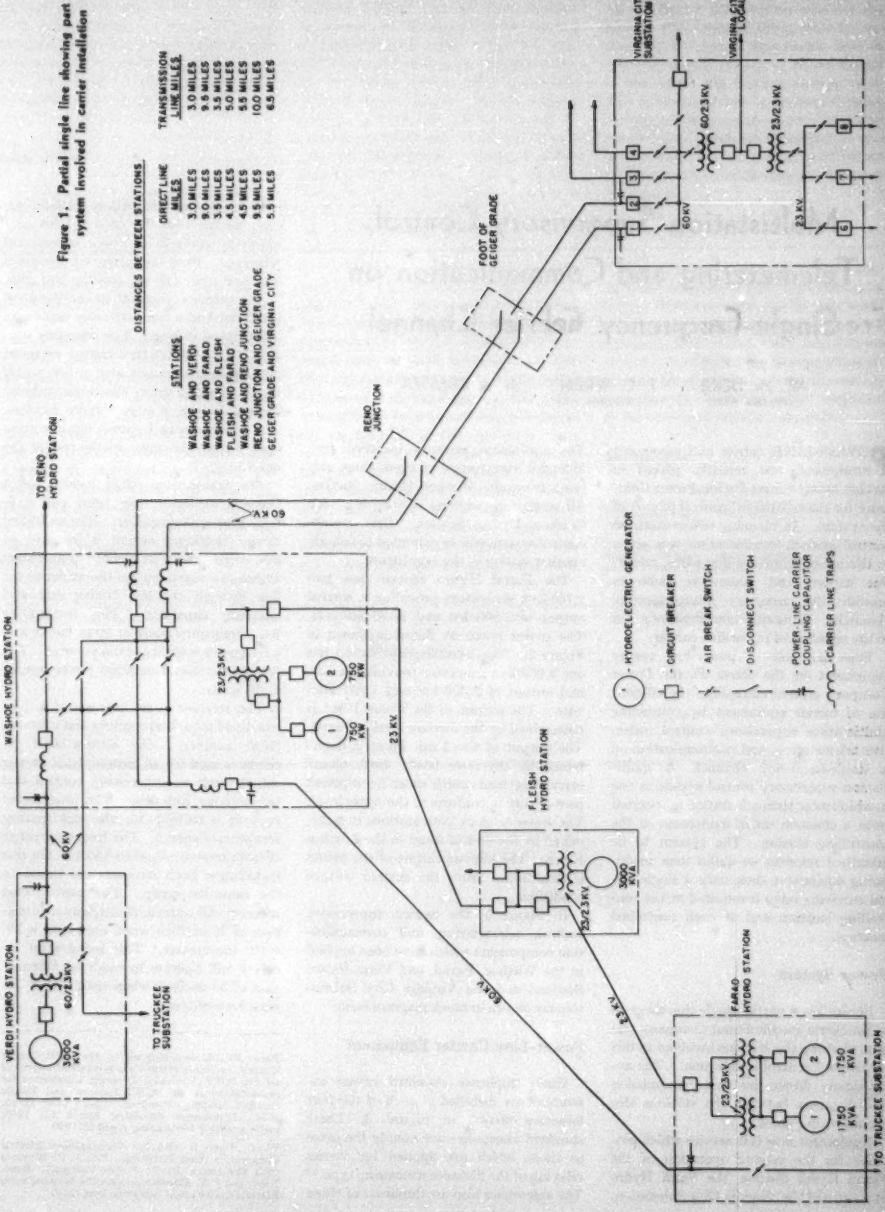

DISTANCES BETWEEN STATIONS

STATIONS	DIRECT LINE MILES	TRANSMISSION LINE MILES
WASHOE AND VERDI	3.0 MILES	3.0 MILES
WASHOE AND FARAD	9.0 MILES	9.5 MILES
WASHOE AND FLEISH	3.5 MILES	3.5 MILES
FLEISH AND FARAD	4.5 MILES	5.0 MILES
WASHOE AND RENO JUNCTION	4.5 MILES	5.5 MILES
RENO JUNCTION AND GEIGER GRADE	9.5 MILES	10.0 MILES
GEIGER GRADE AND VIRGINIA CITY	5.5 MILES	6.5 MILES

Figure 1. Partial single line showing part of system involved in carrier installation

The modulator panel has relays, voltage dropping resistors, and a telephone handset jack mounted on it. It is designed for use with a push-to-talk telephone handset. The voltage dropping resistors furnish proper microphone current and operating voltages for the relays. The various relays and contacts are wired so that the carrier transmitter can be keyed when the telephone push-to-talk key is operated.

The test meter unit is a portable assembly of instruments for routine circuit testing. It can be mounted in the carrier cabinet. The test meter unit is shown near the top of the carrier cabinet in Figure 4. All of the carrier panels have test jacks in the main circuits to provide for the measurement of currents and voltages with the test meter unit.

The power-line carrier equipment operates from phase-to-ground. As shown in Figure 3(A), the carrier transmitter and receiver at Washoe are coupled to the 60-kv lines to Farad as well as to the two 60-kv lines to Virginia City. Single-frequency carrier line traps are installed in each of these lines so that an essentially fixed impedance is presented to all carrier signals regardless of switching operations at Washoe. This is the only location at which carrier line traps are used. The carrier equipment is coupled to both 60-kv lines between Washoe and Virginia City to obtain additional reliability.

Since no attenuation data was available and since there is no other carrier on the system, it was arbitrarily decided to try operation at a frequency of 100 kc. A satisfactory signal was obtained at all locations and the system is still operating at this frequency.

There was no problem involved in tuning the parallel circuits at Washoe. The 4-line tuners are each connected to the carrier equipment by a separate coaxial cable. Each of the lines was tuned independently of the others and it was found that the division of the radio-frequency current was fairly even. No difficulty is anticipated when another line out of Washoe is added to this carrier system for the control of a fourth station.

A satisfactory signal is obtained at Virginia City with either of the two 60-kv lines out of service.

Supervisory Control Equipment

The supervisory control equipment applied is of the direct selection all-relay coded impulse type.[4] This type of system employs a series of impulses transmitted at the rate of approximately 15 per second for all selection and control codes. Check or verification codes are used to insure proper selections. This type of system requires only a single signal receiving element at each station. Only such a single-signal system can be used for the control of several stations on a single-frequency carrier channel.

The supervisory escutcheons are arranged in a mimic bus arrangement at the Washoe Hydro Station to depict the essentials of the power system. An individual escutcheon is provided for the control and supervision of each circuit breaker, for each selective telemetered indication, and so forth. An individual escutcheon for the control of a circuit breaker is shown in Figure 5. The selection pushbutton is located at the bottom of this escutcheon. The selection lamp is above the selection pushbutton and the two upper lamps indicate the circuit breaker position. The position indicating lamps are omitted on the escutcheons for selective telemetering.

Figure 6 shows the supervisory control panels in the Washoe Hydro Station.

Figure 7 shows the supervisory control installation in the Verdi Hydro Station. Part of the power-line carrier cabinet can be seen at the right of this figure.

The supervisory control provides for the control and supervision of the circuit breakers at Virginia City Substation and for all of the essential functions at the Farad and Verdi Hydro Stations. The supervisory control also provides a selective telephone ringing function to each of the controlled stations.

Functions at Verdi Hydro Station

Following is a complete list of the functions provided at the Verdi Hydro Station. Each such complete function is usually referred to as a point of the supervisory control.

1. Start-stop control of generator with supervision of master relay.
2. Control of generator field rheostat with telemetering of kilovar output.
3. Control of generator governor synchronizing motor with telemetering of generator kilowatt output.
4. Control and supervision of 60-kv circuit breaker.
5. Control and supervision of generator circuit breaker.
6. Telemetering of forebay water level.
7. Supervision of alarms for which generator shuts down.
8. Supervision of alarms which do not shut down generator.
9. Telephone ringing.

Telemetering Equipment

Impulse-type telemetering equipment is used for the selective telemetered indications listed previously.[5,6] Rate of impulse telemetering equipment is used for the indications of kilowatts and kilovars.

The rate of impulsing is between 80 and 220 per minute. The left-hand reading on the receiver is obtained with a rate of 80 impulses per minute and the right-hand or full-scale reading is obtained with a rate of 220 impulses per minute.

Since the readings are selective, a single transmitter is used at the Farad and Verdi Hydro Stations for telemetering kilowatts and kilovars. The supervisory control equipment connects the transmitter to the proper potential and current transformer circuits. A reactive component compensator is automatically connected in the potential circuits to the transmitter by the supervisory control equipment for telemetering kilovars.

At the Washoe Hydro Station, a single receiver is provided for all kilowatt indications and a single receiver is provided for kilovar indications.

Duration of impulse-type telemetering equipment is used for the selective indications of water level. The transmitters are of the pressure-bulb type. With this system, the reading obtained is based on the length of impulse transmitted during each 5-second cycle.

Figure 2. Powerhouse at Farad Hydro Station

Automatic Switching Equipment

In providing for the remote operation of the Farad and Verdi Hydro Stations it was necessary to add certain automatic switching and protective equipment at each of these stations.[7] The method of operation provided for the two stations is somewhat different.

At the Farad Hydro Station, an automatic electronic synchronizer, a speed matcher, and a voltage-balance relay are provided. Upon receipt of a starting signal from the supervisory control equipment, all of these devices are automatically connected to the generator to be started. Thus the speed and voltage of the generator are automatically made to match the system frequency and voltage. The automatic synchronizer causes the generator circuit breaker to close when the instantaneous frequency difference and the phase-angle difference are satisfactory for proper synchronizing.

The control of the Verdi Hydro Station is based on all synchronizing being done on the circuit breaker at the Washoe end of the line. Therefore, no automatic synchronizing or speed matching equipment is used at the Verdi Hydro Station. The operator at the Washoe Hydro Station is able to start the generator at the Verdi Hydro Station and to individually control the generator and line circuit breaker. The operator also can control the speed and voltage of the generator at the Verdi Hydro Station to be able to effect manual synchronizing of the circuit breaker at the Washoe Hydro Station.

After the generators at the Farad and

Figure 3. Block diagram showing carrier, supervisory control, telemetering, and communication components at (A) Washoe, (B) Farad and Verdi, and (C) Virginia City

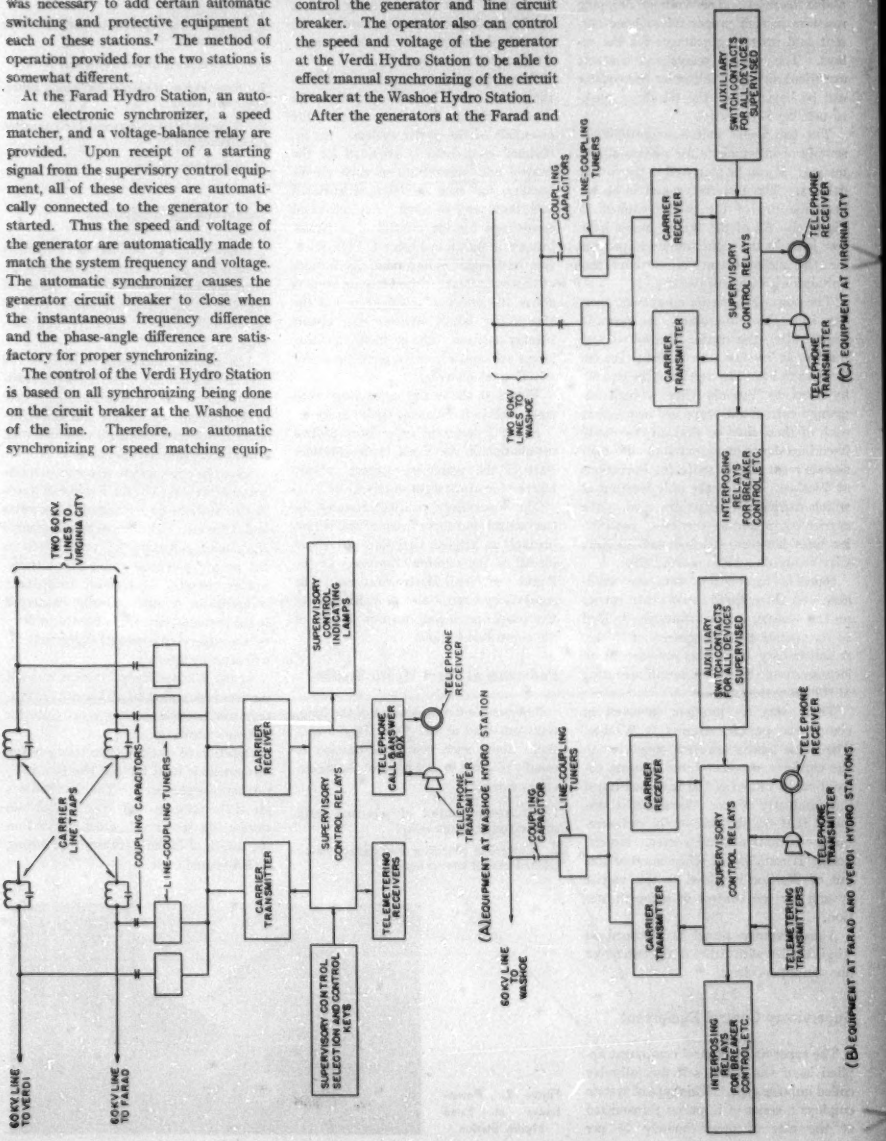

Figure 4. Power-line carrier cabinet in the Washoe Hydro Station

Verdi Hydro Stations are connected to the system, the operator at Washoe can control the kilowatt and kilovar output of the machines.

Operation of Remote Control System

The supervisory control system applied in this centralized control installation can provide for an ultimate of 100 functions or points. Two series of impulses, both of which are automatically checked, are required for the selection of each individual point. The first series of impulses selects a group of ten points and the second series of impulses selects the individual point in the group of ten points. The necessary number of groups to provide for the desired number of functions are assigned to a particular station.

The two series of impulses required for the selection of an individual point are designated as group and point selection codes. The corresponding check or verification codes are designated as group and point check codes. In this installation, the minimum number of impulses for any group selection code is seven. This eliminates the possibility of any actual group selection resulting from random interference which could operate a carrier receiver relay. The corresponding group check codes are in all cases six impulses less than the group selection codes. The point selection and point check codes are the same and may have from one to ten impulses. Since the impulses are transmitted at the rate of approximately 15 per second, the longest selection time for any point of the ultimate system is less than four seconds.

The group selection codes now in use are as follows:

Verdi—7 and 8 impulses.

Farad—9 and 10 impulses.

Virginia City—11 and 12 impulses.

If a selection key is operated at Washoe, the group and point selection codes originate at Washoe and the group and point check codes originate at the station selected. In the case of an automatic operation reporting from one of the remotely controlled stations, the group and point selection codes originate at the remote station and the group and point check codes originate at Washoe.

For control functions and for the supervision of devices, similar series of impulses are used. The number of such impulses is the same for all points since only one point can be selected at a time.

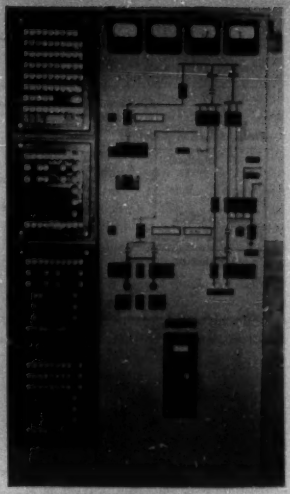

Figure 6. Supervisory control panels in the Washoe Hydro Station

Since the carrier transmitters and receivers are tuned to the same frequency at all locations, keying a transmitter at one or more locations results in operation of the single-carrier receiver relay at every station. This party-line arrangement makes it possible for the supervisory control to select a particular station and to simultaneously lock out all other stations. The group selection code is recognized as a lockout code by all stations except the one being selected. These stations remain locked out until a reset impulse is transmitted from Washoe at the end of a complete function. The re-

Figure 5 (left). Supervisory control escutcheon for control of a circuit breaker

Figure 7 (right). Supervisory control panels and carrier cabinet in the Verdi Hydro Station

Table I. Supervisory Control Impulsing for Typical Operations

Washoe (Controlling Station)	Verdi (Controlled Station)	Farad (Controlled Station)	Virginia City (Controlled Station)
A. Closing of Circuit Breaker at Virginia City From Washoe			
Group Selection Code → (11 Impulses)	Locks Out	Locks Out	
			← Group Selected Group Check Code (5 Impulses)
Group Check Point Selection Code → (3 Impulses)	Remains Locked Out Until Single Long Reset Impulse Received	Remains Locked Out Until Single Long Reset Impulse Received	
			← Point Selected Point Check Code (3 Impulses)
Point Checked Close Control Code → (5 Impulses)			
			← Circuit Breaker Closes Close Supervision Code (5 Impulses)
Lamp Indication Changed Reset Impulse →			
System Restored to Normal At-Rest Condition			
B. Reporting of Automatic Circuit Breaker Trip From Farad to Washoe			
		← Group Selection Code (9 Impulses)	
Group Selected Group Check Code → (3 Impulses)	Locks Out		Locks Out
	Remains Locked Out Until Single Long Reset Impulse Received	← Group Checked Point Selection Code (1 Impulse)	Remains Locked Out Until Single Long Reset Impulse Received
Point Selected Point Check Code → (1 Impulse)			
		← Point Checked Trip Supervision Code (3 Impulses)	
Lamp Indication Changed Reset Impulse →			
System Restored to Normal At-Rest Condition			

set impulse is approximately a quarter of a second long. Receipt of a carrier impulse of this length or longer at any station releases a point which may have been selected at that station or unlocks that station if it had been locked out by selection at another station. A reset impulse restores the entire supervisory control system to its normal at-rest condition so that it is ready for selection of another station.

Table I(A) indicates the impulsing which results if the circuit breaker at Virginia City Substation which is assigned a group selection code of 11 impulses and a point selection code of three impulses is selected and closed. Table I(B) indicates the impulsing for the automatic tripping of a circuit breaker at Farad Hydro Station which is assigned a group selection code of nine impulses and a point selection code of one impulse.

As indicated in block diagram form in Figure 3, the supervisory control relays at each station are interposed between the carrier equipment and all of the services provided. This makes it possible to give preference to the important supervisory control functions rather than to the telemetering or communication services.

Selective Telemetering

Operation of a point selection key for any of the selective telemetered indications, results in the automatic transmission of group selection, group check, point selection, and point check codes of impulses as described for the selection of a circuit breaker control point. However, at the conclusion of the point check code, the proper telemetering transmitter has its keying contact connected to the carrier transmitter and the proper telemetering receiver is connected to receive the carrier impulses. Thus, an indication is obtained immediately after the point is selected.

The circuits are arranged so that the telemetering impulses, which are long with respect to the length of the supervisory control impulses, do not cause the point to be released either at the Washoe controlling station or at the controlled station selected. However, the telemetering impulses do reset the other controlled stations which were locked out when the group selection code was transmitted.

The telemetered indication may be maintained as long as desired. Operation of the reset key results in the supervisory control reset impulse being transmitted at the termination of a telemetering impulse which may have been in progress at the time. Operation of the carrier receiver relay at the station selected without the telemetering transmitter contact being closed results in the selected point being released and the entire system restored to normal.

In the case of points in which a control function is combined with the selective telemetering, the control impulses from the Washoe Hydro Station are transmitted during the off period of the telemetering impulses. The control is of the increment type with the control circuits at the controlled station being energized for a definite period of time for each operation of a control key at the Washoe Hydro Station. An arrangement is provided so that the control increment for each of the devices controlled is individually variable. It is possible for the operator at the Washoe Hydro Station to accurately obtain the desired kilowatt and kilovar output of the generators since a telemetered indication is obtained while the controlling is being done.

Since the continuous transmission of carrier from any station with such a single frequency carrier system would make the entire system inoperative, a timing circuit is provided to automatically disconnect a telemetering transmitter which keys the carrier transmitter continuously due to a failure in the telemetering transmitter or loss of alternating power on the transmitter.

Communication

The supervisory control provides for selective ringing from the Washoe Hydro Station to any of the three stations controlled. It also provides for any of the controlled stations calling the operator at

the Washoe Hydro Station. The telephone ringing is accomplished by points of the supervisory control.

A telephone deskset and a telephone call and answer box is located in the Washoe Hydro Station. The call and answer box has a telephone key and lamp for each of the controlled stations. To initiate a telephone call from Washoe, it is only necessary to operate the telephone call key for the desired station, and to lift the telephone handset from the cradle. This results in the automatic transmission of the proper group and point selection codes from Washoe and the corresponding check codes from the station being called. When the point check code is received at Washoe, a control code is automatically transmitted to ring the telephone bell at the station being called. When the call is answered by the removal of the telephone handset from the cradle at the called station, a supervision code is transmitted which is followed by a reset impulse from Washoe to restore the entire supervisory control system to the normal at-rest condition. When the supervisory control equipment resets, circuits are completed from the telephone to the carrier equipment at Washoe as well as at the station called. This establishes communication of the push-to-talk type between Washoe and the station called. Operating the push-to-talk key on either telephone handset keys the carrier transmitter at that location and the telephone transmitter can then modulate the carrier. This is the same type of communication which is provided on the usual single-frequency carrier protective relaying installation.

Calling the operator at Washoe from one of the controlled stations is accomplished in a similar manner. It is only necessary to remove the telephone handset from the cradle at the controlled station to initiate a call to Washoe. The telephone at the controlled stations is mounted on a supervisory control panel as shown in Figure 7. When the supervision code is received at Washoe, the telephone bell is sounded and the call lamp indicating which station is calling is lighted. To answer the call, the operator removes the telephone handset from the cradle and operates the telephone call key for the station making the call. The supervisory control system than resets automatically and conversation can start.

With this communication system it is possible for the operator at Washoe to perform the necessary ringing functions to establish communication between two or more of the remotely controlled stations.

After communication is established, the supervisory control system is locked out while a telephone push-to-talk key is operated at any of the stations. However, the supervisory takes control at the first instant that no telephone push-to-talk key is operated. Thus, if a circuit breaker is tripped by a protective relay operation at any station, it will report its new position to Washoe in the usual manner at the first pause in the conversation. The first supervisory control impulse disconnects the telephone from the carrier equipment at each station and prevents the starting of carrier by a telephone push-to-talk key until the entire supervisory control function is completed. The conversation can be immediately resumed after the several seconds required to complete the supervisory control function.

The circuits for keying the carrier transmitters with the telephone push-to-talk keys are arranged so that it is only possible to transmit an impulse long enough to constitute a reset impulse for the supervisory control regardless of how short a period of time the push-to-talk key is operated. This makes it impossible to step the supervisory control from its normal at rest condition.

Conclusion

There are many installations of power-line carrier for supervisory control, telemetering, and communication services. In most of these installations a separate channel is used for each one of these services. In quite a number of cases carrier relaying has been combined with any of these three services on a single 2-terminal channel.[8] There also are installations of supervisory control combined with telemetering, and of supervisory control combined with communication on a 2-terminal channel. However, the installation described was the first in which a single-frequency channel was used for multistation supervisory control, telemetering and communication. This provides the most economical possible arrangement since a minimum of carrier equipment is required.

The fact that only a single-carrier frequency is required for this entire system is not particularly important in this instance, since no other carrier is in use on the Sierra Pacific Power Company system. However, this is an extremely important consideration in many sections of the country where it is becoming increasingly difficult to choose new frequencies due to the large number of channels already in use.

The carrier operated remote control installation described, has simplified system dispatching and improved system operation.

References

1. A New High-Speed Distance-Type Carrier-Pilot Relay System, E. L. Harder, B. E. Lenehan, S. L. Goldsborough. *Electrical Engineering (AIEE Transactions)*, volume 57, January 1938, pages 5–10.

2. The Application of Power-Line Carrier, R. C. Cheek. *Power Plant Engineering* (Chicago, Ill.), November, 1945.

3. A New Carrier Relaying System, T. R. Halman, S. L. Goldsborough, H. W. Lenzner, A. F. Dromp. *Electrical Engineering (AIEE Transactions)*, volume 63, August 1944, pages 568–72.

4. By a Flick of the Finger, W. A. Derr. *Westinghouse Engineer* (East Pittsburgh, Pa.), November 1945.

5. Telemetering Circuits—Metallic and Carrier, M. A. Bostwick. *AIEE Transactions*, volume 67, part II, 1948, pages 1081–88.

6. Telemetering System (book), P. A. Borden, G. M. Thynell. Reinhold Publishing Corp., New York, N. Y., 1948.

7. Automatic Control of Hydroelectric Generating Stations, M. J. Brown, W. A. Derr. *AIEE Transactions*, volume 66, 1947, pages 343–55.

8. A Versatile Power-Line-Carrier System H. W. Lenzner, J. B. Singel. *Electrical Engineering (AIEE Transactions)*, volume 63, March 1944, pages 129–33.

Discussion

C. E. Asbury and **C. W. Frederickson** (Commonwealth Associates, Inc., Jackson, Mich.): It is encouraging to see more functions being placed on one carrier channel and further efforts being made to conserve frequency spectrum. Multistation supervisory control on one single-frequency carrier channel should have its economic advantages. However it appears that the application of such a system may be rather limited. Multistation supervisory control over metallic circuits has been in general use for some time and apparently has given satisfactory operation. Multistation communication has also been successfully used for a number of years on single-frequency carrier current channels. It is significant to note that an additional step has been taken to place multistation supervisory control in service on the same carrier frequency which also provides multistation communication. It is hoped that the experience obtained from this application will be favorable and encourage further installations of a similar nature.

In an AIEE paper by R. C. Cheek and W. A. Derr,[1] the authors concluded that it was desirable to use separate channels for multistation simplex communication and supervisory control with joint use of cou-

plling equipment only. The reason given was the excessive amount of equipment and the complicated arrangement that would be necessary. It would be helpful if the authors would point out what changes have been incorporated in this design to simplify it, and hence remove their previous objection to the complicated arrangement.

Multistation equipment is generally applicable on smaller stations where it may not be objectionable to share the control of several stations on one set of dispatching equipment. On larger stations where a number of units are being controlled and supervised, it may be preferable to use one set of control equipment per station. This is often desirable to avoid losing control of all stations in the event the dispatching terminal of the control is out of working order or out of service for maintenance. The same objection is also true where numerous functions (supervisory control, telemetering, and communication) are used on one set of equipment. When the equipment is out of service all functions are inoperative.

The paper mentions that consideration was given to the use of telephone line wires, power line carrier, and microwave radio for the necessary interconnecting channels and that economic considerations led to the selection of power line carrier. Considering the short distance involved and the relatively high cost of the microwave equipment, it is apparent that microwave radio could not be economically justified. On the other hand it is not clear how carrier equipment could be less expensive than leased telephone channels on a system having such short distances between the dispatching point and the outlying stations. It may well be that the stations in question are remote from the present telephone lines in the area. In such a case it may be possible to justify the carrier system rather than resort to the construction of a private telephone channel. It would be interesting to know further details concerning availability, reliability, and rates of telephone channels in the area.

The paper states that no difficulty was experienced in receiving the carrier signal at the receiving stations. This would be expected since the lines are relatively short and all lines are trapped. About the only carrier loss experienced is that due to coupling and the coaxial cables. In applications where the transmission lines are longer and where the network consists of several lines this arrangement would be more difficult to apply since additional trapping would be required and the division of carrier signal between lines might be much less favorable. Sufficient carrier reserve signal should be available in applications of this nature to provide proper operation during adverse weather conditions such as fog, rain, or snow. To assure this reserve signal the carrier installation should be tested using an attenuator pad to determine the reserve range of signal over and above that required for operation during favorable weather conditions. It would be interesting to know if such a test was made in this particular installation, and if so, the decibel range of reserve signal found.

The basis of application of the line traps at the Washoe Hydro Station should be explained. According to Figure 1 of the paper there are six 60-kv lines emanating from this station with the carrier signal being applied to four of the lines. It would seem more practical and less expensive to trap the two lines which are not being used for carrier transmission rather than trap the four lines that are used. This would have the further advantage of not requiring a new trap when the proposed line is added out of Washoe for a fourth station also to be controlled by carrier.

The use of a double carrier channel between the Washoe Station and the Virginia City Substation appears rather difficult to justify. Considering that the line is only 18 miles long, the number of faults on the line per year should not be excessive. If the circuit is adequately protected the line should relay properly, and line damage sufficient to cause an interruption to the carrier channel, should not occur very often. It should further be noted that the only fault that would cause a complete interruption of the carrier channel would be one that would result in the wire being down on the particular phase being used for carrier transmission. A single channel would therefore seem to be adequate.

As stated in the paper, conservation of the frequency spectrum is of extreme importance in certain sections of the country. The use of a single-frequency channel for multistation supervisory control, selective telemetering, and communication is a means of accomplishing this. In many instances, continuous telemetering rather than selective telemetering is desired on a power system. In such a case the use of crystal controlled frequency shift telemetering channels permits the maximum possible number of continuous telemetering channels. This type of equipment has a much greater decibel range than the equipment mentioned in the paper. For this reason it can be used on systems where the telemetering channels have much greater attenuation than the channels listed in the paper. Since the maximum rate of impulse of the supervisory equipment (15 per second) is well within the allowable limits for a crystal controlled frequency shift channel, it would seem desirable to utilize crystal controlled channels for supervisory control. It is suggested that the authors state the possibility of such applications where communication is not required and give the equipment limitations, if there are any.

REFERENCE

1. THE COMBINATION OF SUPERVISORY CONTROL WITH OTHER FUNCTIONS ON POWER-LINE CARRIER CHANNELS, R. C. Cheek, W. A. Derr. *Electrical Engineering* (*AIEE Transactions*), volume 64, May 1945, pages 241–46.

P. W. Schirmer (General Electric Company, Philadelphia, Pa.): The authors have described in their paper what was to them a novel installation combining multistation supervisory control, telemetering, and communication over a single-frequency channel.

There has been such an installation in successful operation in New York State since June 1948. This installation consists of one control station with three outlying stations and includes supervisory control, communication, and selected telemetering over a single-frequency carrier channel.

There are a number of other installations having some of these features but designed to accommodate all if required. In the Midwest there is one installation including all these features, utilizing two relaying channels with a repeater between relaying channels providing the link for supervisory control, communication, and telemetering but still isolating the relay channels. This is not a single-frequency carrier channel over the entire system, but it is more economical as it employs the carrier terminals for a greater number of uses than described in the subject paper.

In conclusion, it should again be pointed out that the system described in the paper does not employ operating principles which are new to the art or which have not been employed previously. However, the authors should be congratulated for calling the public's attention to the rapid strides made in the art of supervisory control in the past few years.

W. A. Derr, T. C. Wren, and J. V. Kresser: We were very glad to receive the discussion of our paper prepared by Mr. Asbury and Mr. Frederickson.

The second paragraph of this discussion refers to statements made in a previous AIEE paper[1] concerning the combination of multistation supervisory control and communication. Note that this previous paper stated that multistation supervisory control should not be combined with a multistation simplex telephone system using separate ringing. However, it also stated that telephone ringing could be provided on a multistation supervisory control system; and this is the scheme used on the Sierra Pacific Power Company installation. Development work done since the previous paper was written in 1945 made it possible to omit the audio tone equipment.

There can be no argument with the statements made in the third paragraph of the discussion. The use of separate sets of equipment for large stations is definitely preferable when it can be economically justified.

With reference to paragraph 4 of the discussion, there are no telephone company lines between the Washoe Hydro Station and the stations controlled. A privately-owned telephone line was available but it was not considered a reliable channel, since it is often out of service during storms. The power line offered a much more reliable channel than the existing telephone line. The construction of a new telephone line of greater reliability was considered but the estimated costs for such a line were greater than the cost of the carrier equipment.

No tests were made to determine the decibel range of reserve signal. However, this equipment has been operated through a severe winter and adequate carrier signals have been obtained at all times.

The application of line traps at the Washoe Hydro Station is questioned in the sixth paragraph of the discussion by Mr. Asbury and Mr. Frederickson. Trapping of the lines to which the carrier is applied maintains more nearly constant characteristics of the carrier channel for all possible switching operations. When operation of a system is dependent on nearly equal division of carrier signals it is desirable to have switching operations change the channel characteristics as little as possible. The original installation offered no economic advantage for either method of trapping. There are

actually two more lines than are shown in Figure 1 at the Washoe Hydro Station.

The use of a double carrier channel between the Washoe Hydro Station and the Virginia City Substation was based on the experience of the Sierra Pacific Power Company with the two power lines. These lines, although only 22 miles long, go through very rugged terrain and are subject to severe storms during the winter. Past operating experience had indicated that permanent faults were to be expected on one or the other of the lines and sometimes on both lines. Quite frequently the lines are sectionalized at Reno Junction and Geiger Grade to locate the trouble. The alternative to the use of a double carrier channel would have been the use of carrier by-pass equipment at Reno Junction and Geiger Grade. Experience during the past winter has indicated that the use of the double carrier channel was justified.

Frequency shift carrier equipment can be used to provide for completely individual operation of each remote station but it cannot provide for telephone communication. It is to be noted, however, that a frequency shift transmitter and receiver are required at the controlling station as well as at the controlled station for each station controlled. Thus for the installation described, three transmitters and three receivers would have been required at the Washoe Hydro Station and no communication could have been possible. A separate frequency shift channel is required for each continuous telemetering indication or recording.

When frequency shift carrier is used for supervisory control operation, it should either be designed for d-c operation, or a battery operated a-c power supply unit should be provided so equipment is not made inoperative due to loss of station power.

It is unfortunate that Mr. Schirmer did not furnish more specific information on the installation mentioned in his discussion. It is impossible to compare this installation with the one described in our paper without such specific information. It is possible to combine functions on a single-frequency carrier channel without obtaining all of the desirable features which we have described in detail. For example, some designs might not give preference to supervisory control functions or they might necessitate the use of audio tone modulating equipment.

It is difficult to reconcile the statement by Mr. Schirmer about an installation made in 1948 with a statement made in 1949 by Mr. Forrest and Mr. Schirmer in an AIEE Paper.[2] The following sentence is quoted from this paper: "A separate additional metering channel is recommended for readings directly associated with a control function, or if a continuous reading of a selected quantity is desired."

In our paper we have described a particular supervisory control installation and we have not discussed the subject of combined functions on carrier channels in general. Where protective relaying is involved, it is of course possible in many instances to make use of consecutive relaying channels for supervisory control operation by providing repeaters between the relaying channels.

With reference to the last paragraph of Mr. Schirmer's discussion, we would like to point out reference 1 of this discussion which was published in 1945. That paper described the principles of multistation operation on a carrier channel. The principles having been thus previously discussed, it was our intention to describe an actual installation in detail and not to present entirely new principles. Our paper indicates the results of development work in recent years which has made it possible to improve the arrangement for the particular case of combined functions described.

References

1. The Combination of Supervisory Control With Other Functions on Power-Line Carrier Channels, R. C. Cheek, W. A. Dietz. *Electrical Engineering* (*AIEE Transactions*), volume 64, May 1945, pages 241–46.

2. Space Code Selector Supervisory System, E. F. Forrest, P. W. Schirmer. *AIEE Transactions*, volume 68, part I, 1949, pages 1312–16.

Amplidyne-Controlled Log Carriage Drive

W. D. VINCENT
ASSOCIATE AIEE

Synopsis: The recently introduced amplidyne-controlled electric log carriage drive is rapidly becoming established in the lumber industry. This paper describes this new drive, explaining those features that make it a real asset to the lumber-mill owner.

FREQUENTLY the term "sawmill" is used loosely to refer to almost any lumber manufacturing plant; however, a more appropriate definition might be "an establishment that cuts planks, boards, and timbers, from logs." There are two general types of sawmills, the portable and the permanent type. The portable mill consists of the bare essential equipment required for cutting rough lumber, and it is transported from spot to spot for the purpose of sawing small tracts of available timber. The permanent type of sawmill, on the other hand, is a large factory-like structure with all of the necessary equipment for converting logs to a finished piece of lumber.

Generally speaking, portable-type sawmills will be found in nearly every section of the country, wherever small isolated tracts of usable timber are grown. However, the permanent-type sawmills will be found only in those areas still having large stands of timber. Most permanent-type sawmills own tracts of timber which have been set up on a perpetual yield basis.

After leaving the woods—either by rail, truck, or water—the logs are transferred to a log pond which is adjacent to the sawmill. From the log pond, the logs are moved into the sawmill either by a conveyor-type log haul or by a lift-type log hoist. Inside the mill the logs are cut to a length suitable for handling in the particular mill involved and are stored on a log deck.

The next step in the lumber-making process consists of cutting the logs lengthwise into long, thick planks and timbers. This is done by the headsaw, consisting of the saw itself, which may be either a circular or band saw, and the log carriage (a rail car upon which the log is supported). One plank after another is cut from the side of the log as long as the lumber is clear and high grade. When the saw begins cutting into the less salable heartwood, the log is rotated 90 or 180 degrees and higher grade planks are again cut. The sawyer in charge of the headsaw operation must decide the most profitable manner for cutting each log. It necessarily follows that the output from the headsaw determines the output of the entire mill. Thus, a leading sawmill must provide the sawyer with the most modern and effective headsaw equipment available.

Planks and timbers from the headsaw fall upon a live roll conveyor. This conveyor is the beginning of an elaborate conveyor system which separates various planks and timbers for proper processing through the mill. Some of the timbers have already been cut to usable dimensions by the headsaw and, hence, are carried directly to storage or shipping areas. However, the majority of the headsaw output must be cut and trimmed to produce rough lumber of standard dimensions. This is done by several different types of circular and band saws.

After the lumber has been cut to rough dimensions it is sorted by hand into groups of like grade and size. Then, the lumber must be thoroughly seasoned to prevent warpage and shrinkage. This is done either in dry kilns or by proper storage in the open air. After seasoning, the lumber may be shipped for use as rough lumber, or it may be processed through a planing mill where it is finished as required for use in lumber products.

Log Carriage

The log carriage for the headsaw consists of a steel or hard-wood framework of very heavy construction mounted on four to eight sets of wheels and riding on two or three steel rails. One of these rails is of V shape so as to keep the carriage on the track. Mounted upon the carriage is all of the necessary equipment for holding the log firmly in place and for accurately positioning the log so that desired thickness may be cut. The positioning and clamping equipment on the carriage may be actuated by levers, air cylinders, or motors, and one or more men ride the carriage for the purpose of manipulating these controls.

The sawyer in charge of all operations associated with the carriage, operates the carriage drive, moving it back and forth past the headsaw as desired. The man or men riding the carriage adjust the log for each cut according to instructions from the sawyer. A special sign language is used for conveying these instructions.

The track upon which the carriage rides must be approximately 20 feet longer than the longest log that will be cut.

Logs are loaded upon the carriage from a loading deck at one end of this track. Each time the sawyer desires to turn the log 90 or 180 degrees, the carriage is returned to this loading deck where a mechanical device (operated by the sawyer) flops the log over to the new position desired. Occasionally, the carriage must be run to the extreme opposite end of the track to facilitate the removal of a board by the "tail sawyer."

Paper 50-176, recommended by the AIEE General Industry Applications Committee and approved by the AIEE Technical Program Committee for presentation at the AIEE Summer and Pacific General Meeting, Pasadena, Calif., June 12–16, 1950. Manuscript submitted March 13, 1950; made available for printing May 9, 1950.

W. D. VINCENT is with the General Electric Company, Schenectady, N. Y.

Figure 1. Diagram showing main components of the amplidyne-controlled log carriage drive

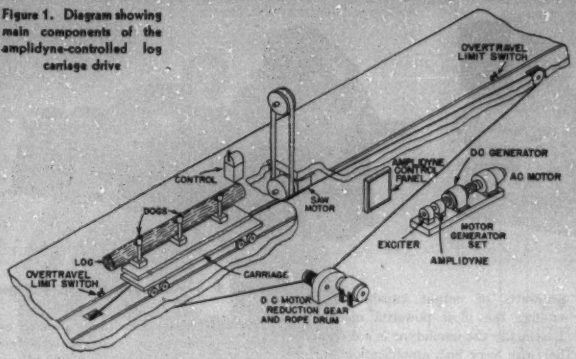

During the sawing of a log, the carriage is normally moved only far enough for the end of the log to clear the saw by about one foot. A very good sawyer will even reverse the carriage in the cutting direction before the trailing edge of the saw has cleared the log. The high production rate demanded can only be maintained if the sawyer is able to control precisely the point of the carriage reversal hundreds of times each hour.

The cutting speed of the carriage is adjusted by the sawyer and depends upon the dimensions, condition, and kind of wood being sawed. Normally, the return speed of the carriage is considerably higher than the cut speed in order to reduce the nonproductive time to a minimum. In some mills the carriage may reach a peak production rate of 15 round trips per minute, averaging nine or ten round trips per minute over an 8-hour shift.

Types of Carriage Drives in Use Today

In general, steam, air, hydraulic, and electric power have all been directly applied for the purpose of driving a sawmill log carriage. Until recently, the only types of drive considered by mill owners for high-production mills were the "steam shotgun" drive and the "steam twin-engine" drive. Compared to the steam drives, the hydraulic, air, and electric drives were all sluggish and incapable of producing the high output demanded by the leading sawmills. However, the recently developed amplidyne-controlled drive is now a serious competitor of the steam drives wherever high production, ease of control, and efficiency are demanded.

The Steam Shotgun. As its name implies, the steam shotgun resembles an actual shotgun both in appearance and performance. The shotgun feed consists of a cylinder up to 50 or 60 feet in length, depending upon the maximum length of log to be cut, made up in sections six or seven feet long and 10 to 16 inches in diameter. In this cylinder there is fitted a piston with a long rod which is attached to the carriage frame. The sawyer controls an operator's lever which by means of specially designed valves will admit steam in or out of either end of the piston, depending upon the direction of travel desired. Steam is admitted to either end of the piston at a pressure of approximately 125 pounds per square inch. The exhaust steam from the piston is generally considered as waste and is discharged into the atmosphere; however, in colder climates this steam is sometimes discharged into the log pond to prevent the formation of ice upon the pond in cold weather.

The Steam Twin-engine Drive. In many of the mills cutting the large fir timber grown on the Pacific Coast, twin-cylinder steam engines are used for driving the carriages. The engines are directly connected to a drum over which is wound several turns of steel cable, the two ends of which are attached to the two ends of the carriage. The twin engine essentially consists of a pair of steam engines with pistons operating upon a common crankshaft, so arranged with respect to each other that any dead spots, or zero-torque points are eliminated in the 360 degrees of travel of the crankshaft. This type of steam drive is more economical in steam consumption than the steam shotgun but also is more sluggish in performance, making acceleration and retardation rates lower and consequently reducing the daily output of the mill.

The Amplidyne-Controlled Log Carriage Drive

Components. The amplidyne-controlled drive *is* designed to achieve optimum performance utilizing the simplest possible combination of electric components. An idea of the simplicity of the electric drive may be gained from the following list of drive equipment:

1. Carriage driving motor
2. Motor-generator set
3. Amplidyne control panel
4. Operator's master control lever
5. Overtravel limit switches
6. A-c motor starters

A schematic diagram illustrating the arrangement of the principal drive components is shown in Figure 1. Carriage drives are available in ten different sizes as shown in Table I.

These mill-type motors (type *MDP*) are designed to operate successfully at more than double voltage and speed, thereby developing more than double of their nominal 230-volt capacity. Furthermore, they are designed to carry high peak loads encountered in steel mill and shovel work, making them exceptionally well suited for sawmill application.

The smaller drive sizes listed are usually applied to small sawmills or to pulp breakdown plants, whereas the larger drives meet all other production demands including the largest sawmills.

The Carriage Driving Motor. The carriage driving motor is a d-c motor built for extra heavy-duty service to withstand severe mechanical strains, high voltage, and large currents. The motor used is the same sturdy motor used so successfully in steel mills for auxiliary and crane service and in surface mining for driving excavation shovels. Heavy steel frames are split and the top half hinged for ease of inspection of the motor. Antifriction-type roller bearings are used for the armature which is also especially designed for low inertia and high-speed operation. Long-life brushes, extra large commutators, and high insulation levels provide extra overload capacity. The motor is completely protected and provided with high temperature rise, class *B* insulation with inorganic silicone-type binders, and the motor is separately forced ventilated with an integrally mounted blower motor to obtain the highest power capacity over the operating speed range of the motor, Figure 2.

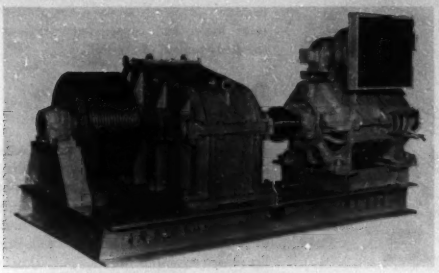

Figure 2. Type-*MDP* blower-ventilated carriage drive motor mounted on a common base with gear reducer cable drum assembly

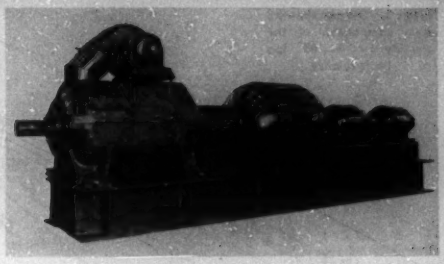

Figure 3. Log carriage drive motor-generator set

Type-*MDP* blower-ventilated generator on left, induction motor in middle, amplidyne and exciter at right (latest design omits blower unit on generator and reduces length of set by mounting amplidyne and exciter on top of generator)

Motor-generator Set. The 4-unit motor-generator set consists of an a-c driving motor, a d-c generator, an exciter, and an amplidyne,[1] see Figure 3. The a-c motor is specially designed with sufficient maximum torque available to meet the requirements of each particular drive and is normally a squirrel-cage induction motor.

The two smallest drives utilize specially designed type *CD* generators. All other drives use type-*MDP* units as generators which are duplicates of the drive motors with the exception of the omission of the blower units. Therefore, the generator is completely capable of supplying the current and voltage demanded by the motor and in the larger sizes the spare-parts problem is reduced to a minimum for these vital components of sawmill production. The exciter provides field excitation for the motor, and control power for the amplidyne control panel.

The amplidyne is similar in appearance to the exciter; however, internally it is so designed that this small piece of equipment becomes the heart of the amplidyne-controlled log carriage drive. In principle, the amplidyne is an externally driven d-c generator, but its unique use of a short circuit and compensating winding creates such precise electrical balance that the smallest electric signals release kilowatts of output capable of controlling the most powerful machinery. Essentially the amplidyne is a d-c amplifier with very high amplification[2]—more than 10,000 to 1—permitting the use of small control devices which are easy to manipulate.

The Amplidyne Control Panel. The control panel for a drive of this type is both simple and inexpensive, as are most amplidyne panels. Since it is controlling small amounts of current, the physical size of the panel is exceptionally small, Figure 4.

Control components consist of adjustable resistors, dry-type selenium rectifiers, electrolytic capacitors, and a small relay. This amplidyne control panel includes no regularly moving devices.

Operator's Master Control Lever. For the sawyer's operation, a simple heavy-duty drum-type master switch with a vertical handle is provided. By means of this master switch, the sawyer controls the direction and speed of carriage motion. Standing by the band saw and facing the carriage, the sawyer simply moves the master switch handle forward to bring the carriage into the cut and moves the master switch handle backward to return the carriage. The type of master switch offered has no points that can be felt by the sawyer and, therefore, the feel of the master switch is substantially the same as that of the steam control levers to which the sawyers have been accustomed over long years of usage. Figure 5 illustrates the simplicity and ruggedness of this control lever.

Safety Limit Switches. An overtravel limit switch is provided for overtravel protection on each end of the carriage travel. Thus, if the sawyer fails to reverse his master switch as the carriage approaches the end of the travel, the tripping of a limit switch takes control away from the master switch, applies a "suicide" connection to the amplidyne, and brings the carriage to a rapid safe emergency stop. Extra track length must be left between the limit switch and the end bumper so that sufficient distance is available for taking up the slack in the cable and decelerating the carriage to a stop as rapidly as the electric equipment will permit.

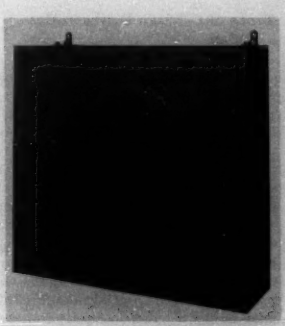

Figure 4. Amplidyne control panel for log carriage drive; approximate 28 inches high, 30 inches wide, and 9 inches deep

Table I. Carriage Drives—Nominal 230-Volt Motor Rating

Equipment Number	Carriage Motor	Hp	RPM	Generator Frame	M-G Set RPM	A-C Motor Hp
1	MDP602	9½	875	CD	1,800	30
2	MDP603	12½	775	CD	1,800	40
3	MDP604	19	700	MDP604	1,800	50
4	MDP606	31½	640	MDP606	1,800	100
5	MDP608	44	565	MDP608	1,200	100
6	MDP610	62½	540	MDP610	1,200	150
7	MDP612	94	510	MDP612	1,200	200
8	MDP614	125	475	MDP614	1,200	250
9	MDP616	187½	450	MDP616	1,200	400
10	MDP618	250	410	MDP618	1,200	500

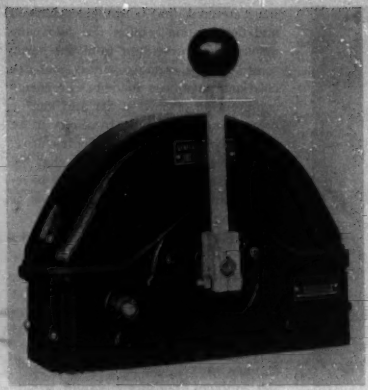

Figure 5 (above). Sawyer's master control lever for log carriage drive; approximately 13 inches wide

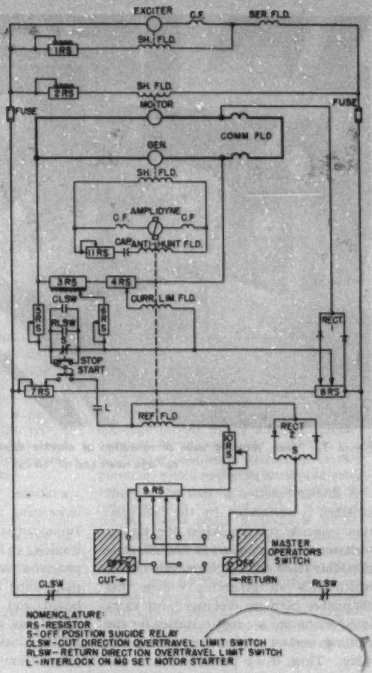

Figure 6 (right). Simplified elementary diagram of amplidyne-controlled drive

A-C Motor Starters. Suitable a-c motor starters are provided for the motor-generator set driving motor and for each of the two ventilating blower motors.

Explanation of Operation. The amplidyne-controlled log carriage drive operates as a d-c adjustable voltage system. A heavy-duty d-c motor drives the carriage through a reduction gear and cable drum. Power for the motor is obtained from a 4-unit motor-generator set driven by an induction motor.

Basically, the operation of the system is quite simple. With fixed field excitation applied to the motor, the carriage speed is essentially proportional to the applied armature voltage. The armature voltage, supplied by the generator, may be changed by adjusting the generator field current. Therefore, the carriage speed increases as the generator field current is increased and decreases as the generator field is decreased. Also, the direction of carriage travel is reversed simply by reversing the current direction in the generator field.

The simplified elementary diagram for the amplidyne-controlled drive is shown in Figure 6. Field excitation for the generator is supplied by the amplidyne. The voltage output of the amplidyne is a function of the net ampere turns produced by the three amplidyne shunt fields. One of these fields is the reference field, the second is the current-limit field, and the third is the antihunt field.

When the sawyer moves his master control switch, essentially, he is changing the number of ampere turns contributed by the reference field. This results in a change in the amplidyne output voltage. Because of the field-forcing action of this reference field, the resulting change in generator voltage would be nearly instantaneous if it were not for the current-limit field. The limiting action of this field limits the maximum armature current in the motor and generator to a safe value. Thus, the resulting rate of armature voltage change (carriage speed change) is the maximum value that can be safely handled by the motor and generator. This current-limiting effect is obtained by comparing the voltage drop across the motor and generator commutating fields with a fixed reference voltage. When this voltage drop exceeds the fixed reference voltage, corrective ampere turns are produced in the current-limit field which correct the net amplidyne excitation to a value corresponding to safe armature current in the d-c driving units. A portion of the generator voltage is also impressed across the current-limit field. This voltage produces ampere turns in the current limit opposing the ampere turns in the reference field. Thus, when the sawyer's master switch is moved to a new position the generator voltage will continue to change until the balance point is reached between these two fields.

The antihunt field is connected in series with capacitors across the amplidyne output. Opposing ampere turns are contributed by this field only when there is a rate of change of amplidyne voltage. Therefore, the corrective action of this field is proportional to this rate of change and eliminates hunting, resulting from the combination of electric and mechanical time constants associated with the drive system. Overtravel limit switches, mounted near each end of the carriage track, will stop the carriage in emergencies. When either of the limit switches is closed, control of the amplidyne output is taken away from the reference field (master operator's switch), and the amplidyne output is suicided to zero through the current-limit field. This is done by applying a portion of the generator output to the current-limit field. The resulting ampere turns are always in the proper direction to reduce the generator voltage, while at the same time the current-limiting portion of the circuit is functioning to limit the maximum armature current.

Figure 7. View showing ease of operation of electric drive, demonstrated by sawyer as carriage nears end of last cut

A similar function to that of the limit switches is performed by the "off-position" suicide relay. When the master operator's lever remains in the off position, this relay sets up the suicide circuit which kills all generator voltage and eliminates carriage creepage. An extra interlock on the a-c motor starter for the motor-generator set is in series with this relay. Thus, if a-c power is lost in the mill, the carriage will be stopped before the saw is damaged.

Results

The first amplidyne-controlled electric log carriage drive was installed prior to the war in 1940.[3] Application of the drive was necessarily slowed down during the war years and subsequent drives were not installed until after the conclusion of the war. There are now installed and in operation a total of 11 of these drives. In addition, six more complete drives are under construction for installation in the near future, Figure 7.

Considering the relatively high initial price of an electric carriage drive and realizing that use of an electric drive is a departure from conventional sawmill practices, there must be some powerful arguments to justify the purchaser's expenditure of the extra money for an electric drive. Valid reasons do exist, and if a user can make the initial investment, he can hardly afford not to buy the electric drive.

For years, sawmill owners have thought of steam as being free power, since it is obtained by burning waste from sawmill operations. However, several factors are influencing a change in this viewpoint. Improved saws and sawing techniques are resulting in less waste. Waste utilization programs such as the manufacture of pulp, wood briquettes, wood flour, fibreboard, and alcohol, have placed a definite dollar value on sawmill waste. In addition, increased production requires more steam for kiln drying. Thus, the elimination of the notorious "steam hogs" of sawmills (the shotgun and twin-engine drives) results in appreciable dollar savings for mill owners.

The amplidyne-controlled drive consumes a comparatively small amount of energy. In each complete round trip of the log carriage, the carriage accelerates to a cutting speed, holds this cutting speed for a definite time, then decelerates to a stop, reverses and accelerates to a return speed, holds this return speed, then decelerates to a stop. The bulk of the power input to the system is required during the two accelerating periods of each cycle. In order to hold the carriage at a constant speed, it is only necessary for the system to supply the electrical and mechanical losses of the carriage and drive components. During the two deceleration periods of the cycle, the stored energy in the carriage motor and gear are converted back into electric energy and pumped back into the consumer's power system. Thus, it is obvious that the total power input required for each cycle is only that amount of power necessary to supply the electrical and mechanical losses in the system. On the other hand, steam-feed drives customarily waste all of their exhaust steam so that both the acceleration and deceleration require the maximum amount of power input from the steam source. Very careful analysis and calculations have been made of the energy consumption of both steam and electric drives, and the results turn out to be startlingly favorable for the electric drive. For example, it can be shown that the entire cost of an electric drive can be recovered in fuel savings alone, in four or five years.

Another striking attraction of the electric drive is the very low maintenance cost. Since there are no regularly moving parts in the control panel, maintenance there will be negligible. The master switch is a very simple device and should require very little attention. The rotating machinery, operating under favorable ambient conditions, should require only occasional maintenance in accordance with the general rules prescribed for that type of apparatus. Actual figures from one installation shows that $35.00 in a typical year covered the total maintenance cost including material and labor for the complete drive.

Safety of operating personnel is a matter of prime importance not only to the personnel involved, but to the management of the company. Assuming that the carriage was traveling at its maximum speed and for some unpredictable reason it was not stopped before reaching the end of the track, the personnel riding the carriage would be in very serious danger. Overtravel limit switches included as a feature of this drive minimize the possibility of this type of personnel injury.

Conclusions

Summarizing, the advantages of the amplidyne-controlled electric log carriage drive are as follows:

1. High drive efficiency resulting in low operating cost.
2. Low maintenance expenses.
3. Snappy acceleration and deceleration matching the performance of the steam shotgun.
4. Ease of operation reduces operator fatigue.
5. Definite speed control during sawing, resulting in improved quality of output.
6. Improved safety for operating personnel —automatic overtravel protection with emergency stop.
7. Automatic emergency stop when a-c power is lost, preventing possible damage to the saw.
8. Smooth nonpulsating cable pull, resulting in long cable life.

References

1. Design Characteristics of Amplidyne Generators, **Alec Fisher**. *General Electric Review* (Schenectady, N. Y.), volume 43, number 3, March 1940, pages 107–113.

2. Dynamoelectric Amplifier for Control Power, **E. F. W. Alexanderson, M. A. Edwards, K. K. Bowman**. *AIEE Transactions*, volume 59, 1940, pages 937–39.

3. Use of Amplidyne Controlled Motor in Drive of Sawmill Log Carriage, **H. B. LaRoque**. *General Electric Review* (Schenectady, N. Y.), volume 44, number 11, November 1941, pages 619–20.

Discussion

H. A. Rose (Westinghouse Electric Corporation, Seattle, Wash.): Mr. Vincent is to be congratulated on his timely and valuable paper on electric log carriage drives. Increasing values assignable to sawmill waste and cost of operation of small steam plants are expected to show increased economic application of the electric drive. This will be particularly true for new and small capacity sawmills.

An important factor in the application of electric drives is the initial direct cost of equipment as compared to that for the steam engine and shotgun. The cost of electric equipment is approximately proportional to the horsepower rating required. This rating and cost for practical purposes is proportional to the total pounds weight (W) accelerated; the square of the maximum speed of the carriage in feet per minute (S^2), and inversely to the time required for acceleration in seconds (ΔT^{-1}). An analysis of these three factors will show that variations in cost by as much as 2-to-1 can be caused by casual specifications calling for performance characteristics not well matched to the actual needs of the particular application. This can easily result in the electric drive being discarded at the outset, when a more careful analysis of requirements would have proved it to be the most acceptable choice.

The importance of the weight factor (W) on cost of electric drives would seem to justify consideration on the part of log carriage builders to reduce weight by design and choice of higher strength materials. This appears particularly promising for the lighter weight lumber cutting carriages.

Mr. Vincent's paper describes a type of drive in which the cable drum is driven through a suitable speed reducer. This arrangement provides a very acceptable type of drive. My company however, in addition to building the "geared" type of drive manufacturers a "gearless" type in which a high-torque low-speed 2-bearing unit-type of armature and cable drum drives the carriage direct. On account of the simplicity and low maintenance of this type of drive, a number of applications have been made in ratings from 30 to 120 horsepower. Two units are presently on order.

W. D. Vincent: Selection of a suitable carriage feed should take into consideration an economic study as well as such nonmeasurable quantities as safety to personnel, ease of operation, and so forth. A complete economic study will, of course, include not only initial costs for all equipment but operating expense, maintenance costs, and replacement costs. Mr. Rose has stated that the rating and direct cost of electric equipment is approximately proportional to weight (W), maximum carriage speed squared (S^2) and inversely to accelerating time (ΔT^{-1}), or that rating and cost are proportional to $(W)(S)^2/(\Delta T)$. This is the familiar formula for the horsepower required to accelerate a weight to a definite speed in a given amount of time. Since the acceleration rate (A) is equal to the final speed (S) divided by accelerating time (ΔT), the foregoing formula may be rewritten as $(W)(A)(S)$. It is frequently more convenient to consider the formula in this form since it is thus readily apparent that for a specified carriage weight and maximum speed the acceleration rate is a direct measure of the power and performance of a drive.

It is common knowledge that both the "geared" and "gearless" types of electric drives are available for various industrial applications. Although, the gearless drive is somewhat simpler mechanically, the author believes the geared drive described in this paper has very definite advantages. The combination of the rugged, heavy duty, mill-type driving motor and the specially designed herringbone gear reduction unit has proved completely reliable for this application, with a negligible amount of maintenance being required. By choosing the optimum gear ratio for each application, the full motor power is available for any specified maximum return speed. Also, the motor designer can build a more powerful motor using less material at the higher speeds, and, for the ratings involved, considerably more horsepower per customer's dollar can be offered. Thus, the "geared" drive provides a faster acceleration rate (more snappy performance) for less cost.

Response Time of Magnetic Amplifiers

E. L. HARDER
FELLOW AIEE

W. F. HORTON
NONMEMBER AIEE

THE magnetic amplifier of modern design, while as much as a hundred times faster than its prewar cousin for the same gain, is nevertheless slower than an electronic amplifier, so that its response time is a vital factor in many of its applications. For example, in servomechanism design a representative time constant for the amplifier must be used. In on-off controls the time from application of the control signal until the output change is substantially complete is of importance. Or, speaking from a steady-state sinusoidal-signal point of view, the magnetic amplifier is a d-c amplifier and operates up to a signal frequency somewhat below its power-supply frequency. As the signal frequency approaches the power-supply frequency, the gain drops off rapidly. The magnetic amplifier is said to require a power-supply frequency "an order of magnitude" higher than the signal frequency.

Standardizing groups are now working on definitions and methods of expressing the performance characteristics of magnetic amplifiers, including response time. It is the purpose of this paper to present theoretical and experimental information on response time, to review the considerations involved, and to make some proposals for the treatment of response time in definitions and standards.

In order to discuss "time constant," it will be tentatively defined as the time for completion of 63 per cent of an output voltage change after a step change in input voltage, in some specified region in which output and input bear a reasonably linear relationship. The further details and qualifications must await the development of the text. The term "response time" will be used in a more general sense to denote the time to respond to any specified degree after a step change of input.

Operation of the reactors of a magnetic amplifier into the saturated region does not in itself preclude a constant "time constant." The time constants of magnetic amplifiers are at least as constant as those of many machines and other devices which are so treated in servomechanism and closed-cycle control system analysis. In fact, the extreme assumption of a 2-straight-line saturation curve, with its very abrupt saturation, results in theoretically constant "time constants" for two important cases. The saturation curve composed of a vertical and horizontal line results in a theoretically constant "time constant" for the simple series-connected amplifier with low control resistance. The saturation curve composed of an almost vertical line and a horizontal line results in a theoretically constant "time constant" for the self-saturating amplifier. Deviations from constancy are thus not caused by the main bend of the saturation curve but by minor effects in some of the more important amplifier circuits.

Since the modes of operation of various magnetic amplifier circuits do vary considerably, with consequent effect on the response time considerations, the theoretical aspects of a number of the common connections will first be reviewed as briefly as possible. The series and parallel connections with and without external feedback and the self-saturating circuit will be treated. These, it is believed, will introduce practically all of the principal considerations involved in the response time of magnetic amplifiers. Because of its importance and, curiously, because of its simplicity, the self-saturating circuit will be considered first. The steady-state operation is well known and will be only briefly stated as a foundation on which to build concepts of transient operation.

Paper 50-177, recommended by the AIEE Electronics Committee and approved by the AIEE Technical Program Committee for presentation at the AIEE Summer and Pacific General Meeting, Pasadena, Calif., June 12–16, 1950. Manuscript submitted March 15, 1950; made available for printing May 12, 1950.

E. L. HARDER and W. F. HORTON are with the Westinghouse Electric Corporation, East Pittsburgh, Pa.

Concepts of Response Time

THE SELF-SATURATING MAGNETIC AMPLIFIER

Steady-State Operation. Operation of the self-saturated amplifier of Figure 2 is as follows. At the beginning of a forward half cycle of supply voltage, in the diode conducting direction, for reactor *1*, let the flux in that reactor have the initial value shown at *a*. The conditions of signal current and other factors that determine this initial flux will be discussed shortly, but for the time being *a* is simply some point on the upper branch of the major hysteresis loop. When forward voltage is applied, the flux, ϕ, rises to saturation, along the line *ab*. For simplicity it will be assumed that the magnetomotive forces below saturation involve currents so low that they cause negligible drop in the load resistance. The entire applied voltage is taken up across reactor *1* until saturation is reached. The flux in rising from *a* to saturation generates a back voltage equal to the applied voltage, this flux change being used up in generating a definite volt-time area. Thus after a voltage area has been generated proportional to the initial flux reduction (saturation flux minus initial flux), the reactor saturates and from this time until the end of the half cycle, voltage is taken up across the load resistor. Thus a linear relation exists between the initial flux reduction in the reactor and the voltage-time area absorbed by the reactor during this half cycle. That is, the average voltage on the load resistor is reduced from its maximum possible value by an amount proportional to the initial flux reduction. The resulting voltage on the load is shown in Figure 2 as e_L. Note that during the next half cycle a similar action occurs in the other reactor while the first returns to its initial flux position.

With a smaller initial flux reduction, when the forward voltage wave is ap-

plied, the flux follows a path such as $a'b'$ and saturation is reached sooner. Thus a smaller area is cut out of the voltage wave proportional to the smaller initial flux reduction, and the larger load voltage e_L' results.

With a greater initial flux reduction the flux follows a path such as $a''b''$. A correspondingly large area is cut out of the voltage wave and a small load voltage e_L'' results. Since the load is resistance, the load current is proportional to the load voltage and of the same wave shape.

Summarizing, in the idealized case, the average load voltage is reduced below a theoretical maximum equal to the full applied voltage by an amount directly proportional to the initial flux reduction. Note that signal current in the forward direction reduces the initial flux reduction (increases the presaturation) and hence increases the load voltage and current. Signal current in the reverse or negative direction increases the initial flux reduction, enabling the reactor to absorb more voltage and correspondingly lowering the load voltage.

This direct proportionality between a change in the initial flux reduction and the change in average output voltage of the self-saturated magnetic amplifier is a basic tenet in much of the discussion of response time that is to follow. It need only be pointed out at this time that since the saturation flux density is fixed, the average flux, that is, the mean of the initial flux and saturation flux, changes by half of any change of initial flux. Changes in average flux, initial flux, and average load voltage are all proportional to each other and are found to appear rather indiscriminately in the response time formulas set forth by different authors. It is, of course, the average flux that, linking the control windings, opposes the change of average control current and determines the time constant. In fact, in the L/R ratio comprising time constant the R is the parallel of all the control winding resistances on a common turns base. The L corresponds to half the slope of the upper branch of the major hysteresis loop between the two initial flux points of interest. These facts will be developed more fully in the course of the paper.

If the initial flux is lowered somewhat below point a'' in Figure 2, the core remains unsaturated throughout the full cycle and only the small unsaturated magnetizing current flows. If lowered further to a''', the current flows in each reactor throughout nearly 360 degrees, with pulses of load current at the end of each half cycle. This mode of operation is entirely different from that just discussed and cannot be analyzed on the basis of the half-wave circuit.

Figure 1. Magnetic amplifier

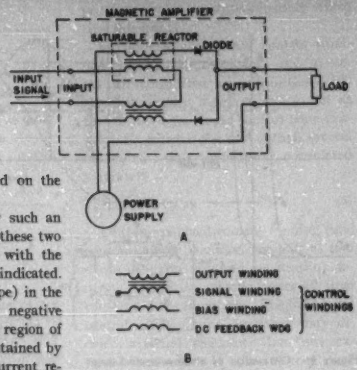

A typical transfer curve for such an amplifier showing operation in these two regions is given in Figure 3, with the operating points a', a, a'', a''' indicated. Note the lower gain (lower slope) in the negative slope region of high negative control. In the positive slope region of the transfer curve control is obtained by the very minute amount of current required to obtain different initial flux reductions on the upper branch of the major hysteresis loop.

Typical wave forms of an actual amplifier are given in Figure 4. The general characteristics of the shapes shown in Figure 2 will be observed although the changes are less abrupt because of the more gradual saturation. Also the unsaturated magnetizing current is not negligible.

Transient Response. Transients in magnetic amplifier circuits are normally treated as slow transients, that is, as a progression through various steady-state operating conditions from one limit of the change to the other. The quantities dealt with, then, are the average applied control voltage, the average flux linkage, and the average output voltage, averages being taken over a cycle. Such treatment is quite satisfactory for transients of several cycles duration.

Transients of short duration become much more complex and depend on many factors which can be safely ignored in the longer transient. For example, in the amplifier just analyzed there is a part of the cycle in which no current flows in the load. A change in control voltage during this interval could obviously have no immediate effect on the load. Thus, very short transients must depend on the point of the cycle at which they are initiated. It is only the so called slow transients involving average quantities that are of much significance and these are the ones that will be treated here. Departures therefrom will be shown experimentally.

The problem of determination of the time constant,[3] $T=2L_s/R_s$, is mainly one of determining the average flux linkages per core per ampere of signal current that constitutes the quantity, L_s. Refer to

Figure 2. The resistance, R_s, is the total signal circuit resistance, L_s is the effective inductance per core.

Or, noting that

$$T=\frac{2L_s}{R_s}=\frac{2\,\Delta\psi_{s\,ave}}{R_s\Delta I_s}=\frac{2\,\Delta\psi_{s\,ave}}{\Delta E_s}\text{ seconds} \qquad (1)$$

where $\Delta\psi_{s\,ave}$ is the average flux linkages per core with the signal winding, the time constant of interest can be determined directly as the ratio of change in average flux linkages to change in signal voltage.

As pointed out previously, for the idealized case of sharp saturation, changes in average flux (hence flux linkages) and average output voltage are proportional. The relation is

$$2\,\Delta\psi_{s\,ave}=\Delta E_L\frac{N_s}{N_L}\frac{1}{2f} \qquad (2)$$

Making this substitution in equation 1

$$T=\frac{\Delta E_L}{\Delta E_s}\frac{N_s}{N_L}\frac{1}{2f}\text{ seconds} \qquad (3)$$

or

$$T=\frac{Av}{2f}\text{ seconds} \qquad (4)$$

where Av is the average voltage gain on a common turns base

$$Av=\frac{\Delta E_L}{\Delta E_s}\frac{N_s}{N_L} \qquad (5)$$

Equation 4 gives a low value as the saturation curve deviates from a flat top, since it is based on a change in average flux only half of the change in flux swing, which generates voltage drop. Using some data from Johnson and Latson[4] for a silicon steel reactor of very gradual saturation

$R_s=139$ ohms
$N_s=4000$ turns
$\Delta I_L=4.0$ amperes (from 4 to 8)
$\Delta I_s=0.02$ amperes approximately

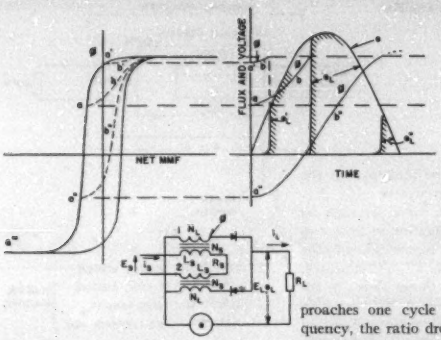

Figure 2. Operation of a self-saturated magnetic amplifier

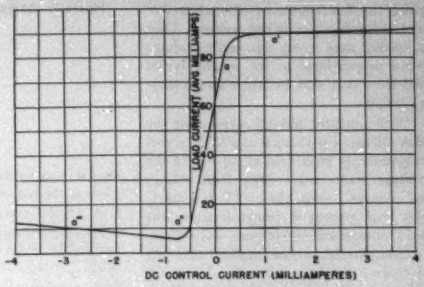

Figure 3. Transfer curve of a typical self-saturated magnetic amplifier

$R_L = 10$ ohms
$N_L = 230$ turns
$\Delta E_L = 40$ volts
$\Delta E_s = 2.78$ volts

$$Av = \frac{\Delta E_L}{\Delta E_s}\frac{N_s}{N_L} = \frac{40}{2.78} \times \frac{4000}{230} = 250$$

$$T = \frac{Av}{2f} = \frac{250}{120} = 2.1 \text{ seconds}$$

The measured value in this region was 3.3 seconds. The value by a more accurate calculation according to equation 1 was 3.7 seconds.

Figure of Merit. Since the time constant is determined as the flux linkages per unit of signal voltage, doubling the signal-circuit resistance will double the voltage required for the same linkages and hence halve the time constant. Also, since twice the signal power (change) is now required for the same output power (change), the power gain A is also halved.

This proportionality between A and T as the signal-circuit resistance is varied is illustrated in Figure 5. It has led to the suggestion of using the ratio A/T as a figure of merit for comparing amplifiers of the same size and type. For operation in a specified region, it would show up in a single figure the beneficial effects of high-permeability iron, low-leakage rectifiers, and quality of design in respect to space utilization in lowering internal resistance, leakage resistance, and so on. It would also afford a more universal constant to associate with amplifiers of various types.

The difficulties lie in adequately specifying all the conditions of test and the inexact nature of the ratio. Note that in Figure 5, A is not exactly proportional to T. In other amplifiers this deviation is considerably greater than shown.

Also note that as the time constant approaches one cycle of the supply frequency, the ratio drops off quite rapidly as the long-transient theory applies less accurately and the lamination and a-c winding delays become a factor. Not shown in this figure are differences in increasing and decreasing transients. If the voltage induced in the a-c windings by the applied signal voltage exceed the back voltage on the one diode, a circulating current can flow for decreasing transients, thereby slowing the response. This does not occur for increasing transients since the induced voltages are counter to the diode conducting directions. Thus, figure of merit will probably remain a useful though inexact amplifier constant which will not receive industry standardization until its limitations have been more thoroughly explored in the various circuits.

Johnson and Latson Method.[4] The complete method described by Johnson and Latson using the generalized curves of an earlier paper[4] involves dead reckoning from the a-c saturation curve, the winding and load resistances, and the turns, to the final performance. The proper set of universal performance curves are picked corresponding to the master saturation curve that best matches the one under consideration. These curves show the average flux linkages for each operating point as well as giving necessary data for the transfer curve (output versus input). Thus, equation 1 above can be used directly since no approximation for flux linkages is needed.

Having plotted the transfer or control characteristic, giving the load current versus control current without feedback, the reduced signal current for any desired percentage of feedback is readily determined, and likewise the signal voltage. For a given operating condition, with feedback, including self-saturation or 100 per cent feedback (50 per cent in their terms), the average flux linkages are determined from the universal curve, the signal voltage determined as explained, and the time constant thereby calculated by equation 1.

For the silicon-steel reactor mentioned, the calculated time constants agreed with experimental values within 10 to 17 per cent (calculations uniformly high) for 73 per cent external feedback, and agreed within 12 per cent (3.7 seconds calculated, 3.3 seconds test) for the self-saturated circuit. Checks were not available for high-permeability materials.

Frequency Response Versus Time Constant

Representation of the magnetic amplifier as a single delay system may be tested by comparing its frequency response with that of a theoretical single delay. Such a comparison is given in Figure 6(B). Note that the theoretical curve for the single delay drops off in voltage response to 50 per cent (voltage) at a signal frequency of 2.55 cycles per second for the test amplifier which has a time constant of 6.5 cycles, measured with a step function. The test amplifier follows the theoretical curve reasonably well, indicating that representation as a single delay is justified.

Table I shows the theoretical possibilities of passing various frequencies. To obtain 87 per cent voltage response (75 per cent power response), even with a 2-cycle time constant, which is about the lower limit of linearity between A and T, the signal frequency must not be over 4.6 per cent of the supply frequency, that is, three cycles per second for a 60-cycle supply. Fifty-per cent power could be obtained at eight per cent or approximately five cycles per second, with 25-per cent power at 13.8 per cent or eight cycles per second. Below this point, power varies inversely as signal frequency squared, or voltage inversely as the signal

Table I. Response of Single Delay System

Output*/Input Voltage or Current, Per Cent	Power, Per Cent	fT**	Signal Frequency/Supply Frequency for Amplifier Time Constants in Cycles of Supply Frequency: 1 cycle	2 cycles	5 cycles	10 cycles
86.6	75	0.092	0.092	0.046	0.019	0.009
70.7	50	0.160	0.160	0.080	0.032	0.016
50	25	0.276	0.276	0.138	0.055	0.028
10	1	1.60	1.60	0.80	0.32	0.16

*Based on 100 per cent for d-c signal.

**$\frac{f}{f_o}$ = signal frequency/supply frequency.

T = time constant in cycles of supply frequency.

frequency. That is, they drop off at six decibels per octave. Thus serious attenuation is encountered unless the supply frequency is at least ten times the signal frequency.

The profit from lowering time constant by increasing signal-circuit resistance is now evident. If the amplifier is putting out 50-per cent power (in terms of that with a d-c signal) at the frequency of interest, a reduction of the time constant to half could not possibly reduce attenuation to half (double the gain), whereas a two-to-one loss in gain (at least) would be suffered in the increased resistance. Below the 25-per cent power, reducing time constant reduces attenuation (raises gain) as the square at the cost of only a first-power loss in the signal-circuit resistances. Obviously some place in between there is an optimum product of d-c gain $\times \frac{\text{gain at signal frequency}}{\text{gain at d-c}}$. Such an optimum amplification occurs at $1=(1/2\pi T)(f_o/f)$ or $(f/f_o)T=0.159$.

Response Time of Small Self-Saturated Magnetic Amplifiers

Practical Considerations. Consider self-saturating amplifiers in the 0–50-watt class, having several control windings and using gapless cores of high-quality magnetic-amplifier steel such as Orthonol, Hipernik V, or others. The practical response time considerations are then as follows.

The natural response time with zero external resistance is of the order of 3–6 cycles if built for moderate gain, up to 30–60 cycles if built for high gain. The delay in output response after a step change of input is occasioned chiefly by the L/R of the control winding, with 1/2 to 2 cycles added delay in laminations and a-c windings.

A typical transfer curve for such an amplifier is given in Figure 3. In general, if response is measured for a step change that runs the output from one end to the other of the high-gain region or some smaller part of it, the response times for 63 per cent or 95 per cent of full response will be nearly independent of the magnitude of change and hence nearly constant. The 63-per cent value can be used as the time constant in control-system calculations with accuracy equivalent to that with small machines and many other devices which also involve some deviations from true time constants. The 95-per cent value is approximately three time constants.

In this case the several control windings, signal, bias, feedback, and so on, may be considered as substantially 100 per cent coupled together and so act as though having a single control time constant, T_c, which is the sum of their several individual time constants considered separately

$$T_c = T_s + T_b + T_f + \ldots\ldots \tag{6}$$

To this combined control-winding time constant must be added one-half to two cycles of lamination and a-c winding delay to obtain the effective over-all time constant of the amplifiers. The individual control-winding time constants may include external resistance but not external inductance if the 100-per cent coupling premise of this simple treatment is to be fulfilled.

Time constant is frequently controlled by using high resistances in the bias and feedback windings, if not open-circuited making T_b and T_f very small. Then T_c is substantially equal to T_s and can be reduced to the desired value by introducing series resistance in the signal winding, at the cost of correspondingly reduced gain.

It may be noted that the control time constant is proportional to the sum of the turns squared per ohm of the several control windings. That is

$$T_c = \frac{L_s}{R_s} + \frac{L_b}{R_b} + \frac{L_f}{R_f} + \ldots\ldots \tag{7}$$

whence

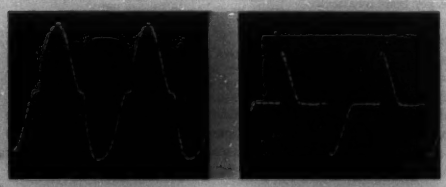

Figure 4 (below). Wave form of load voltage and current for a typical self-saturated amplifier with resistance load

Toroidal Hipernik cores are used

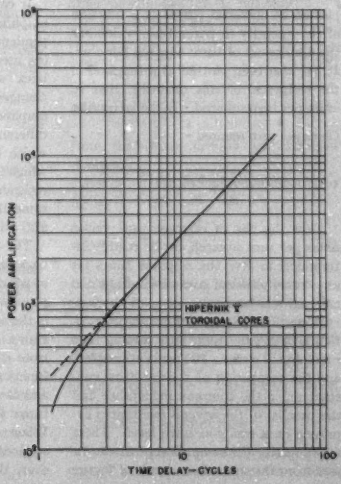

Figure 5 (right). Effect of adding resistance in the control circuit of a magnetic amplifier

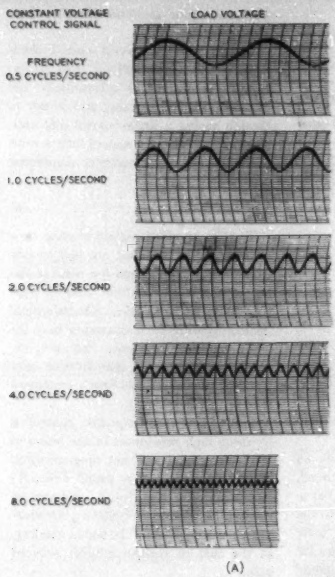

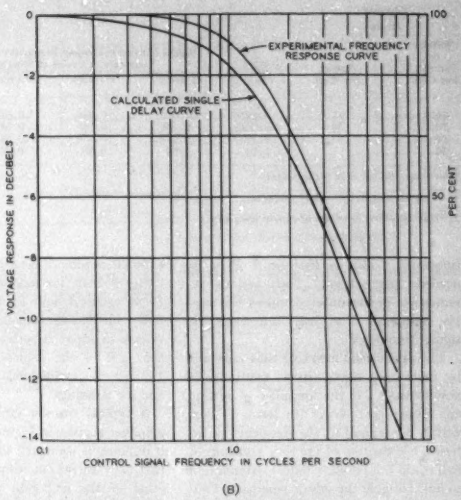

Figure 6. Frequency response of a typical magnetic amplifier

A. Oscillograms. B. Plot of response versus frequency and comparison with an ideal single delay system. Curve calculated from experimental time constant of 6.5 cycles at 60 cycles

$$T_e = P\left(\frac{N_a^2}{R_a} + \frac{N_b^2}{R_b} + \frac{N_f^2}{R_f} + \ldots\ldots\right) \qquad (8)$$

where P is the permeance of the common magnetic circuit.

Hence the response times of a magnetic amplifier can be measured using any combination of control windings and plotted as universal curves as a function of the quantity in parenthesis which has the dimensions of turns squared per ohm. It has also been plotted as a function of the reciprocal of this quantity, that is, ohms per turn squared. In the latter case

Ohms per turn squared =

$$\frac{1}{\dfrac{N_a^2}{R_a} + \dfrac{N_b^2}{R_b} + \dfrac{N_f^2}{R_f} + \ldots\ldots} \qquad (9)$$

Thus the plot of response time versus ohms per turn squared can be readily interpreted to give the response times for any combination of control windings and external resistances.

It may be well to point out the correlation between the concept of adding time constants of circuits 100 per cent coupled, and the computing of a single time constant using the common inductance and the parallel of the several resistances expressed on a common turns base. These are in reality the same concept as can be seen from the equivalent circuit of Figure 7. Since there is but one inductance, there can be but one mode, expressed by a single time constant. As shown in the figure it is the sum of the individual time constants.

It can also be shown that the ratio of amplification to time constant is independent of the turns of the control winding used, assuming that the sum of feedback and bias time constants is not changed. For example, in a magnetic amplifier having three control windings of different numbers of turns, only one of which is to be used, then regardless of which is used, when sufficient external resistance is introduced to achieve the same time constant, the same gain will also exist.

The further addition of bias and feedback will have the same effect regardless of which winding is used in each position, provided only that the per cent feedback is the same and the sum of the time constants is the same. These relations follow from the fact that the response time is a function of control ohms per turn squared, and amplification is a function of ampere turns secured per unit of power input. When a given control ohms per turn squared is secured in any manner whatever, the time constant is fixed. Also, when a given signal winding ohms per turns squared is secured, the application of given ampere turns (hence fixed output) will result in a fixed signal (ampere turns squared).

These fixed ampere turns squared in a fixed ohms per turn squared result in a fixed ampere squared ohms (I^2R) or power input, hence a fixed amplification. Thus it is seen that fixing total control ohms per turn squared, the signal ohms per turn squared and per cent feedback, fixes the response time and gain.

The Series-Connected Magnetic Amplifier with Low Control Resistance

Steady-State Operation. Consider the magnetic amplifier of Figure 8(A), under the following assumptions:

1. Square saturation curve with no hysteresis, as shown in Figure 8(B).
2. Leakage reactances negligible.
3. Control circuit resistance very small compared with load resistance when expressed on same turns base.

The end of each voltage wave finds one reactor completely saturated and the other at some value of flux ϕ_1. Current reaches zero at the voltage zero. This

will become clear later and the reader is asked to accept this starting point.

As the voltage reverses one flux starts downward from saturation and the other upward from ϕ_1. Both reactors are unsaturated and each takes up half of the applied voltage. No current flows until the flux in one reactor has risen from ϕ_1 to saturation flux ϕ_s. As it saturates, it presents a zero impedance on both its output and control windings and thus effectively short-circuits the other reactor as well.

From this time on, the full applied voltage is across the load so that the load current is a part of a sine wave of value e/R_L. As one reactor is unsaturated, it must have equal ampere turns on output and control windings and thus load and control currents are equal at every instant (when expressed on the same turns base). The half cycle ends with current zero at voltage zero and the other reactor having the flux ϕ_1. Note several interesting facts:

1. Since the flux rises in one reactor at the same rate that it falls in the other, the total flux linking the control circuit is constant under steady load. It is $\phi_s+\phi_1$ or if the maximum flux dip below saturation is called ϕ_m it is $2\phi_s-\phi_m$. This is the flux that determines time constant. ϕ_s is constant but ϕ_m will vary with the load.

2. The average load winding voltage is proportional to the flux swing, ϕ_m.

3. The control current I_c must have the average value E_c/R_c. But it must also have the same average value as the load currents (on the same turns base). The firing angle at which a reactor saturates and load current starts to flow adjusts itself until the average load current is equal to the average control current, E_c/R_c.

4. If the load resistance is changed, the firing angle will readjust until the average load current is again equal to the average control current. Thus for a given control current the load average voltage varies directly with the load resistance.

Transient Operation. Thus, in this case, changes in load resistance, load average voltage, and control flux linkage are all proportional, and the time constant is[1]

$$T=\frac{1}{4f}\frac{R_L}{R_c'}\text{ seconds} \tag{10}$$

where R_c' is the control circuit resistance on the output winding turns base

$$R_c'=R_c\frac{N_L^2}{N_c^2} \tag{11}$$

These results hold in the proportional range where the currents are well above unsaturated exciting currents, and hence proportional, but yet are below an average load current of E/R_L, the limit of what

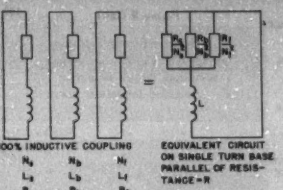

Figure 7. Equivalent circuit of several 100-per cent coupled windings showing that the time constant of the equivalent circuit is the sum of the time constants of the coupled circuits

$$T_s=\frac{L_s}{R_s'},\quad T_b=\frac{L_b}{R_b'},\quad T_f=\frac{L_f}{R_f}$$

$$L=\frac{L_s}{N_s^2}=\frac{L_b}{N_b^2}=\frac{L_f}{N_f^2}$$

$$T_c=\frac{L}{R}=\frac{L}{\dfrac{1}{\dfrac{N_s^2}{R_s}+\dfrac{N_b^2}{R_b}+\dfrac{N_f^2}{R_f}}}$$

$$T_c=T_s+T_b+T_f$$

$$=\frac{L_s}{R_s}+\frac{L_b}{R_b}+\frac{L_f}{R_f}$$

$$=\frac{L}{\dfrac{R_s}{N_s^2}}+\frac{L}{\dfrac{R_b}{N_b^2}}+\frac{L}{\dfrac{R_f}{N_f^2}}$$

$$T_c=\frac{L}{\dfrac{1}{\dfrac{N_s^2}{R_s}+\dfrac{N_b^2}{R_b}+\dfrac{N_f^2}{R_f}}}$$

could be supplied by the given supply voltage.

Since the currents are equal, on a common turns base the resistance ratio is the same as the average voltage gain.

$$\frac{R_L}{R_c'}=Av \tag{12}$$

So that the time constant can also be written as

$$T=\frac{Av}{4f} \tag{13}$$

which is reminiscent of a similar expression for the self-saturated amplifier, equation 4, $T=\dfrac{Av}{2f}$

In the derivation of equation 10, and hence of 13, use is made of assumption 3 (see foregoing section on "Steady-State Operation") that R_c' is very small compared with R_L. Hence any large increase in R_c' to lower T, invalidates the formulas.

Amplification and Transfer Functions.[1] For the previous circuit the voltage gain is

$$K_e=\frac{R_L}{R_c'}\frac{N_L}{N_c} \tag{14}$$

and the voltage transfer function is therefore

$$K_eG(p)=\frac{R_L}{R_c'}\frac{N_L}{N_c}\frac{1}{1+pT} \tag{15}$$

where T is defined in equation 13.

The power gain is

$$K_p=\frac{R_L}{R_c'}k_f^2 \tag{16}$$

where k_f is the form factor and varies from 1.1 for the sine wave maximum currents to approximately 1.5 for the highly distorted minimum currents. As k_f may not be constant throughout the change, there is not strictly a time "constant" for power, although it is nearly a constant for small changes.

The corresponding transfer function is

$$K_pG(p)=\frac{R_L}{R_c'}k_f^2\frac{1}{1+pT} \tag{17}$$

Such an amplifier has an absolute maximum current, which can be delivered with reactors completely saturated, of

$$I_{LM}=\frac{E}{R_L} \tag{18}$$

Storm[1] points out that the time constant as derived in the foregoing applies for any change in the amplifier conditions of operation. Transfer functions for other possibilities are as follows:

For a change in line voltage

$$\Delta I_L=\frac{\Delta E}{R_L}\frac{pT}{1+pT} \tag{19}$$

$$\Delta I_c=\frac{\Delta E}{R_L}\frac{N_L}{N_c}\frac{pT}{1+pT} \tag{20}$$

Note that these involve no sustained changes.

For a change in load resistance R_L to R_L' at $t=0$

$$\Delta I_L=I_L\left(\frac{R_L-R_L'}{R_L}\right)e^{-\frac{t}{T}} \tag{21}$$

That is, there is a sudden current increment that keeps the load voltage constant and this dies out with a time constant T computed from the changed load resistance R_L'.

Series-Connected Amplifiers with High Control Impedance, or Current Transductors

In the current transductor, the control current is fixed entirely by the control

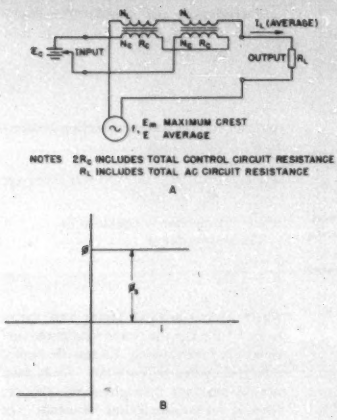

Figure 8 (left)

A. A magnetic amplifier using series connection of output windings, no self-saturation
B. Idealized saturation curve

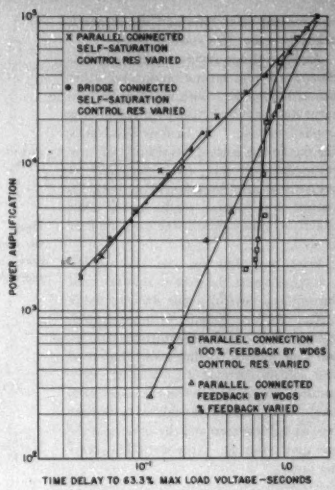

Figure 10 (right). Amplification versus time delay relationships as control resistance is varied

Hipernik V toroidal cores and 440-cycle supply are used

circuit, which may be a high-current d-c bus, for example. In steady operation one reactor is saturated and one unsaturated at all times. Thus on one current half cycle one reactor forces the output ampere turns to equal the control ampere turns, the other reactor being completely saturated. On the next current half cycle, the other reactor forces the equal-ampere-turn relation.

If a control-current change were to occur, the active reactor, at the moment, would continue to force the equal-ampere-turn relationship. Thus the transient response is practically instantaneous.

Parallel-Connected Amplifier

Approximate Time Constant. An approximate expression has been given[2] for the time constant of a parallel-connected magnetic amplifier without self-saturation based on the average reactance in the region of interest. Referring to Figure 9(A), the saturable reactor is assumed to be biased for operation at point *O*. An average reactance is determined, which is

$$X_o = \frac{V_{ao}}{I_{Ao}} \tag{22}$$

From this an effective permeance of the core is determined, since

$$X_o = 2\pi f N_A^2 P_o \tag{23}$$

$$P_o = \frac{X_o}{2\pi f N_A^2} \tag{24}$$

The control coil inductance, using the same permeance, is then

$$L_c = N_c^2 P_o = \frac{N_c^2}{N_A^2}\frac{X_o}{2\pi f} \tag{25}$$

and the time constant is therefore

$$T_o = \frac{L_c}{R_c} = \frac{X_o}{2\pi f R_c}\frac{N_c^2}{N_A^2} \tag{26}$$

Time constants computed according to this formula agreed with tests on a sample amplifier within ±15 per cent. The

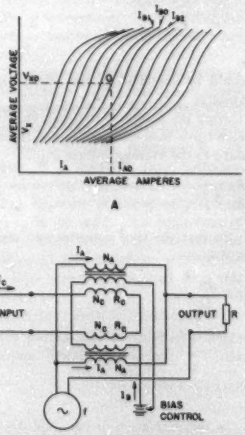

Figure 9. A magnetic amplifier using parallel connection of output windings, no self-saturation

A. Volt-ampere curves of the reactors
B. Circuit diagram

reactor tested was a 3-legged reactor of silicon steel having gradual saturation characteristics.

Similar Operation of Series and Parallel Connections. Several authors[4,6] have shown that the parallel-connected amplifier, steady-state operating mode, is identical with the series-connected amplifier with low control resistance. Either provides a circulating path for the even harmonics. That is, when due account is taken of doubling the voltage, halving the current, and quadrupling the load resistance for the series connection as compared with the parallel connection, the steady operation and hence the control-winding flux linkage is the same.

A difference is encountered, however, in the coupled circuit in the case of the parallel connection, which effectively increases the time constant as discussed earlier for coupled control circuits. The time constant, as compared with the series connection, is increased by the ratio of control circuit resistance to the parallel of control and a-c resistances (loop through two a-c coils) expressed on the same turns base.

Let

$$R_{ac}' = R_{ac}\frac{N_c^2}{N_{ac}^2} \tag{27}$$

This ratio is then

$$\frac{R_s}{\dfrac{R_s R_{ac}'}{R_s + R_{ac}'}} = \frac{R_s + R_{ac}'}{R_{ac}} \tag{28}$$

The time constant is

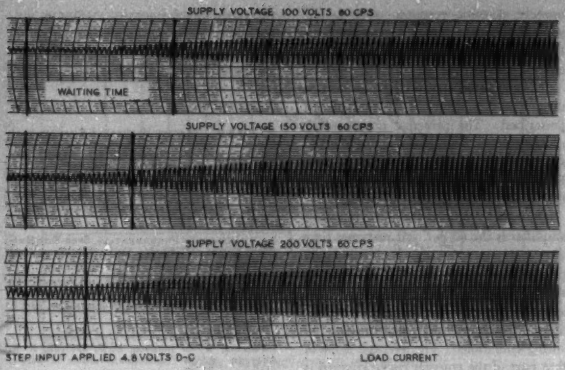

Figure 11. Before-saturation delay of a series-connected magnetic amplifier with several magnitudes of supply voltage but the same step signal voltage, starting from zero signal, with no feedback or bias

$$T = \frac{L_s}{\dfrac{R_s R_{ac}'}{R_s + R_{ac}'}} \tag{29}$$

and approaches L_s/R_{ac}' as a limit as R_s is increased.

This effect is illustrated in Figure 10 in which the performance of the self-saturating circuit with increasing control resistance is compared with a parallel-connected amplifier with external feedback. The A-versus-T relation is the same at low control resistance, but at higher values the parallel-connected amplifier reaches a lower limit of time constant as outlined in the foregoing.

Note also that if time constant is reduced by lowering the percentage feedback, the gain drops off as the square instead of the first power of the time constant. This illustrates the point, now well known, that higher speed for the same gain can be obtained with feedback than without, through the use of control-circuit resistance.

Before Saturation Delay

A concept of response time utilized since the early days of saturable reactors is of interest here in that it represents another aspect of the problem. The circuits considered were the series and parallel circuits without self-saturation, Figures 8 and 9. When control voltage was applied, there was a lapse of time before it seemed to take effect, after which the load current rose rapidly throughout its range to maximum. This time lapse was observed to be twice as long with the parallel circuit as with the series circuit.

The explanation of this phenomenon and the resulting concept of response time is as follows. The most common reactors were in the several hundred watt size used for theater light dimming and other load applications requiring liberal proportioning of iron and turns so as to control down to low reactor exciting currents. Thus the reactors operated at only 10,000 or 12,000 gausses when absorbing the full line voltage at zero control. With the ordinary silicon steels in use up to 1935, the saturation density was about 20,000 gausses.

With no self-saturation, the reactor a-c and d-c ampere turns were equal and amplification resulted simply from the lower direct voltage required as compared with the alternating voltage controlled. Suppose this ratio of direct voltage per core required for full control to average alternating voltage per core was 1/50 on the same turns base. Since a half cycle of the alternating voltage caused a flux change of twice full flux, it would require 50 half cycles of the direct voltage to cause this much change. Thus a large number of cycles were involved until the mean flux had been shifted to the point that the peaks of the a-c flux wave were dipping appreciably into the saturated region. From this point on the mean inductance dropped rapidly, the direct current rose quickly to the E/R value, and the alternating current to the corresponding value.

That the time lapse is twice as long with the parallel connection is explained by the use of approximately equal space for a-c and d-c windings in this type of amplifier. This makes the a-c and d-c winding resistances nearly equal on the same turns base. Thus, as shown in the equivalent circuit, Figure 9(B), only half of the applied voltage appears on the magnetizing branch, so that it requires twice as long to reach saturation.

The development of improved steels such as Hipersil has made possible working much closer to the saturation flux density even with large power size reactors with control to low currents. However, the delay in the relatively unsaturated region is still an important factor. Frequently it involves sacrifice of range or increased size to permit use of sufficient bias to keep partial saturation and avoid excessive delays. For example, in a 200-kva ±10 per cent regulator for a 2,000-kva load, this factor required special consideration. Consequently some provision must be made in nomenclature for description of this before-saturation delay in larger sizes of magnetic amplifiers.

This phenomenon is illustrated in Figure 11, which shows the before-saturation delay for various magnitudes of a-c supply voltage with the same load resistance, for a pair of silicon steel reactors of approximately 200-watt rating.

Conclusions and Recommendations

In view of the considerations set forth in the paper, the following conclusions seem justifiable:

1. The theory of response developed to date is based almost entirely on slow transient theory in which load conditions and core fluxes are assumed to have reached steady a-c operating condition for each instantaneous value of control current.

2. This theory gives very satisfactory accuracy for time constants down to a few cycles of the supply frequency. Below this only experimental results are available.

3. Both series- and parallel-connected amplifiers without feedback have practically constant time constants over a wide operating range.

4. For the series and parallel connections without feedback, analysis based on a theoretical square saturation curve shows the input and output to be linearly related and the time constant to be actually constant. The main bend of the saturation curve is thus not responsible for the variations of time constant that occur in magnetic amplifiers over their useful range.

5. With high feedback or self-saturation the transfer curve (output versus input) shows more curvature and the time constant measured over the full useful region may be down to 60 per cent of that in the steepest portion of the curve.

6. Nevertheless, even for the self-saturated amplifier, and certainly for the amplifiers without feedback, the time constant appears to be fully as constant over a wide operating range as for many of the machines and other

devices which are so treated in regulating and control-system design.

7. While operation is of principal interest in the approximately linear high gain region, magnetic amplifiers have several modes of operation in various regions. For example, the self-saturating amplifier has four recognizable regions with transition zones between. These are high negative control, unsaturated, high gain region, and saturated. Special consideration will need to be given operation in or through some of these other modes. Operation through the saturated region is important in on-off controls.

It is suggested that response time to 30 per cent, 63 per cent, and 95 per cent of full response after a step input be recognized. The 30-per cent response time would adequately describe the before-saturation delay of an amplifier operated into the unsaturated region. The 63-per cent and 95-per cent response times, which correspond to one and three time constants respectively in a linear circuit, adequately describe response over a prescribed operating region, the lower figure being usable as the time constant in most control calculations.

It is suggested that a time constant be defined and a standard method of test prescribed. The principal points which must be covered in such a definition and suggested requirements are as follows. However, these must be subject to further study, and discussion is invited.

The rated time constant of a magnetic amplifier is the 63-per cent response time after a step input voltage with rated supply voltage, frequency, and load resistance. The step change should cover at least 75 per cent of the useful control range possible without violating the following conditions. The average slope of that part of the transfer curve covered is to be not less than 60 per cent of maximum slope. Operation is to be within the 5-per cent and 95-per cent points of the full range of minimum to maximum output. The power gain under the condition of test is to be stated. The type of circuit and percentage feedback are to be stated.

References

1. Series-Connected Saturable Reactor with Control Source of Comparatively Low Impedance, H. F. Storm. *AIEE Transactions*, volume 69, part II, 1950, pages 756–65.

2. A Balanced Amplifier Using Biased Saturable Core Reactors, H. S. Kirschbaum, E. L. Harder. *AIEE Transactions*, volume 66, 1947, pages 273–78.

3. Transductor Fundamentals, Sven-Eric Hedström, Lennart F. Borg. *Electronics* (New York, N. Y.), September 1948, page 88.

4. An Analysis of Transients and Feedback in Magnetic Amplifiers, W. C. Johnson, Frank W. Latson. *AIEE Transactions*, volume 69, part I, 1950, pages 604–12.

5. Universal Curves for D-C Controllable Reactors, W. C. Johnson, B. C. Morrell, R. E. Alley, Jr. *AIEE Transactions*, volume 68, part I, 1949, pages 31–37.

6. An Analysis of Transients in Magnetic Amplifiers, D. W. VerPlanck, L. A. Finzi, D. C. Beaumariage. *AIEE Transactions*, volume 69, part I, 1950, pages 498–503.

Discussion

Walter C. Johnson (Princeton University, Princeton, N. J.): The authors have given a very helpful discussion of the present state of knowledge regarding the speed of response of magnetic amplifiers. As they point out, the time constant varies a remarkably small amount over a considerable range, in spite of the fact that a magnetic core of nonlinear characteristics is essential for the operation of the device. In fact, the sharper the bend in the saturation curve, the more constant is the inductance presented to the control circuit. In many ways, a simple saturable reactor behaves much like a nonlinear amplifier with a large amount of inherent negative feedback.

The ratio of amplification to time constant appears to be a potentially useful figure of merit, provided, of course, that it is specified explicitly with regard to the point of operation. A figure of merit is probably most useful when it is dimensionless, and this could be achieved here by expressing the time constant in cycles of the supply frequency.

When a control voltage is applied to a saturable reactor which had been operating previously in an unsaturated condition, there is a finite time delay before an effect is seen in the output current, as the authors point out. An alternate viewpoint in explaining this phenomenon can be obtained from the universal curves of reference 5 of the paper. When plotted on the *E-I* plane, the curves of constant control flux crowd together at small values of load current. Thus, in this region, a small change in both control current and load current correspond to a large change in control flux. This produces a large effective control-winding inductance when the load current is small. The volt-second product supplied by the control voltage is largely taken up at first in increasing the control flux without any great change in load current. This corresponds to the region of large slope near the origin of the magnetization curve shown in Figure 6 of reference 4 of the paper. The universal curves indicate that the curves of control flux are crowded more closely at small values of terminal voltage; therefore, a lowered supply voltage will lead to a greater time delay.

W. J. Dornhoefer, (Vickers Electric Division, St. Louis, Mo.): As the authors indicate in the introduction, the work of standardizing groups on definitions, performance standards, and ratings of magnetic amplifiers has required both theoretical and experimental information concerning response time. The paper contains much of this information, presented in concise and useful form.

This discussion is intended to supplement certain of the information given in the paper, and to offer comments on several of the conclusions and recommendations. The supplementary information, as well as the discussion in general, refers particularly to the self-saturating magnetic amplifier circuit.

The method of calculating the portion of the response time attributable to the control windings (the slow transient) given in the paper is both accurate and useful. In

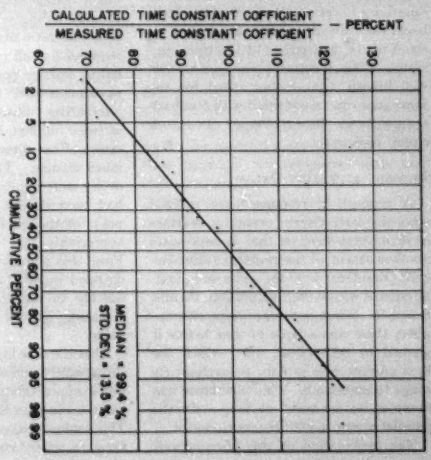

Figure 1. Comparison of measured and calculated values of K_1 for 35 magnetic amplifiers

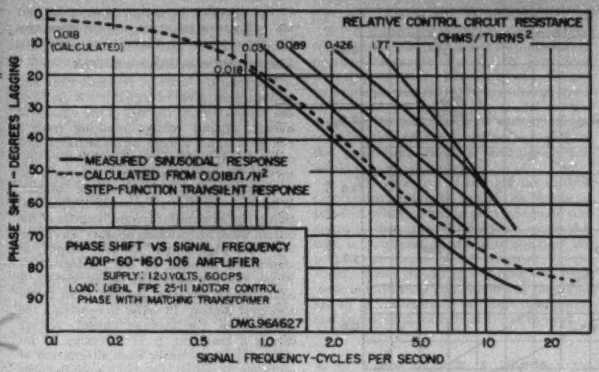

Figure 2. Phase shift versus signal frequency

essence, the change in output voltage is used as a measure of the change in average flux linkages in the cores, thus establishing the value of a fictitious control circuit inductance which then may be associated with the control circuit resistance to give the time constant. This method has proved to give an accurate calculated value of the magnetic amplifier time constant for slow transients, as shown in the example given in the paper. As a matter of fact, it seems likely that the calculation gives a more representative value in many cases, because of the errors inherent in measuring the time constant. These errors include the effects of variation of the phase of the step function switching instant and the resolution limits of recording instruments and medium. The latter is of importance because of the need in a time constant measurement for locating accurately the 63 per cent response point on the envelope of the output peaks or average values.

Data, such as that which follows, can be advanced in support of this argument. The data plotted in Figure 1 of the discussion show the ratio of a calculated time constant coefficient to the measured value for a group of 35 self-saturating magnetic amplifiers. The amplifiers have ratings ranging from 0.020 watt to 12,600 watts; supply frequencies from 60 to 800 cycles per second; core materials including 80 per cent nickel-iron alloy, 50 per cent nickel-iron alloy, and grain-oriented silicon steel; circuits including a-c output, single-phase center-tap d-c output, single-phase bridge, 3-phase half-wave, and 3-phase full-wave. The measured value of the time constant was found by applying step-function changes of voltage to the signal circuit and recording oscillographically the growth and decay of the output response to these signals. These measurements were generally made at nominal supply voltage and frequency, and with rated load resistance. The amplitude of the signal voltage step was adjusted to permit amplifier operation in the linear region of the control characteristic, and generally was sufficient to give approximately 10 per cent change of output. Data was taken for a number of values of relative control circuit resistance and the time constant evaluated for 63 per cent response of the envelope of the output peaks. This time constant was then plotted versus resistance on log-log paper, resulting in a 2-part curve. In the region of slow transients, the curve has a slope of -1, while in the region of fast transients, the slope approaches zero. The value of the time constant as the slope approaches zero is the fixed delay due to the a-c windings, while the location of the curve in the region of -1 slope gives the measured value of control winding time constant, as indicated by equation 1.

$$T = K_1 \frac{N_s^2}{R_s} + K_2 \text{ seconds} \qquad (1)$$

where T, N_s, and R_s are used as in the paper, and K_2 is the constant-delay time.

The calculated value of the time constant is found by the formula given in equation 3 of the paper, with the coefficient as given or modified as required for other amplifier circuit connections. For example, for a 3-phase bridge circuit, the relation is

$$T = \frac{\Delta E_L}{\Delta E_s} \frac{N_s}{N_L} \frac{1}{3f} \text{ seconds} \qquad (2)$$

For this circuit, the value of the coefficient K_1 is found from equation 2 as

$$K_1 = \frac{\Delta E_L}{N_s \Delta I_s N_L} \frac{1}{3f} \text{ ohm-seconds} \qquad (3)$$

Figure 1 of this discussion is a comparison of the measured and calculated values of K_1 for the group of 35 magnetic amplifiers. The ratio of the two values is plotted as ordinate on normal probability paper. The median or average value is 99.4 per cent, showing a difference between measurement and calculation of 0.6 per cent over-all. This is not a significant difference for a sample of this size. From this one can conclude that there is no systematic error in either the calculation or measurement method. The fact that the curve shows a normal distribution (straight line on probability paper) indicates that the errors are random and attributable to measurement. It is estimated that the steady-state measurements required to obtain the calculated value of K_1 are accurate to about 2 per cent. (The principal source of error lies in determining ΔE_L, which is an internal electromotive-force change rather than a change in actual load voltage). It also is estimated that the accuracy of measurement of the time constant is limited to between 10 and 20 per cent, due principally to the necessity of approximating the envelope of the oscillograph transient. The deviation of the measured value from the calculated value shown in Figure 1 of this discussion has an rms value (standard deviation) of 13.5 per cent, which is in approximate agreement with the foregoing estimates. It seems likely that the differences between measured and calculated time constants are due to limitations of the accuracy of the measurement. If this is true, the calculation method affords a direct indication of the actual time constant which could be obtained only from a number of direct time-constant measurements.

Limiting Value of Response Time—K_2

The method of calculating the slow-transient time constant given in the paper is not useful when one is interested in fast response, as the authors have pointed out. It is believed that the use of equation 1, to-

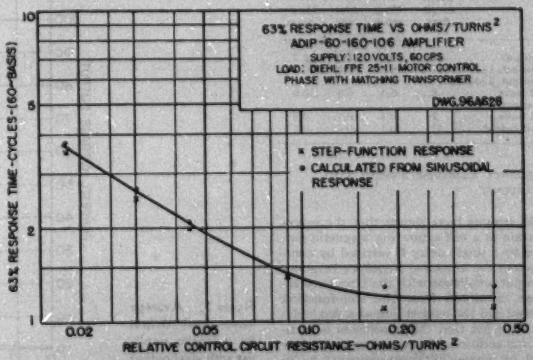

Figure 3. Amplifier time constant as a function of relative control circuit resistance

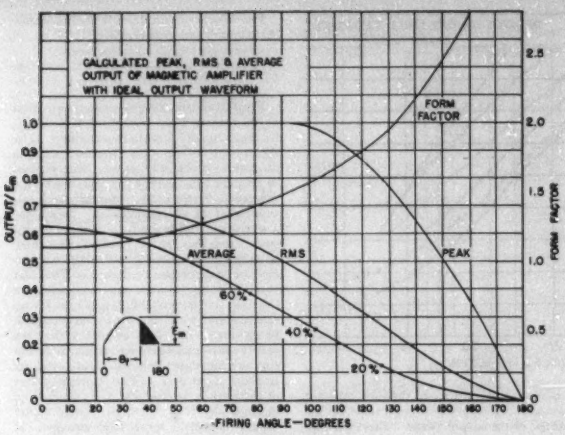

Figure 4. Calculated peak, rms, and average output of magnetic amplifier with ideal output wave form

gether with appropriate values of K_2 will yield sufficiently accurate "fast-transient" results for most practical cases. The range of values which K_2 may have is not known with great accuracy, but it could be determined. The factors, such as rating and geometry, which affect the value of K_2 are known in a general way, and can probably be determined with sufficient accuracy for the purpose, either theoretically or empirically. At present, the possible range of K_2 appears to be slightly wider than the 1/2-to-2-cycle limits suggested in the paper. K_2 values for a group of 44 self-saturating amplifiers of similar diversity to the group of 35 previously described are given in Table I of this discussion.

Table I

	No. of Amplifiers	Values of K_2 in Cycles		
		Minimum	Average	Maximum
A-c output	12	0.5	1.0	2.2
D-c output, 1 phase	17	0.1	0.3	0.8
D-c output, 3 phase, 1/2 wave	8	0.3	0.5	0.9
D-c output, 3 phase, full wave	7	0.5	0.6	0.8
All d-c output	32	0.1	0.4	0.9

Frequency Response Versus Time Constant

The authors have shown that the representation of a self-saturating magnetic amplifier by a single delay is justified by comparison of the measured frequency response of output amplitude with the frequency response calculated from the step-function response and the assumption of a single delay. It is felt that this conclusion is justified, and additional frequency response data based on phase-shift measurements is offered to support it. This phase-shift frequency response data is shown in Figures 2 and 3 of this discussion. Figure 2 shows the measured phase shift of the output envelope of a particular magnetic amplifier plotted versus signal frequency for several values of relative control circuit resistance, and for comparison shows a calculated curve for one value of control circuit resistance. Figure 3 shows two sets of data giving the amplifier time constant as a function of the relative control circuit resistance. One set of data is based on a step-function measurement and the other on phase-shift frequency-response-measurement and the assumption of a single delay in the amplifier.

It is felt that the correspondence found in this phase-shift frequency-response data further justifies the authors' conclusion that the self-saturating magnetic amplifier may be characterized by a single time constant.

Measurement of Response Time

The relation between response time and voltage gain given in equations 3 and 4 of the paper required the use of the change of average output voltage resulting from a change of signal voltage, as the authors have pointed out. For steady-state measurements, the use of simple D'Arsonval instruments makes this a simple matter. When transients are to be studied, the situation is not as straightforward because of the output wave forms which appear. In changing from high output to low output, as shown, for instance, in the oscillogram of Figure 4 of the paper, the output voltage is continuously changing in both form factor and crest factor. In order to construct the envelope of the average output voltage during a transient, it is necessary to integrate the area under each alternation or pulsation of output and plot a smooth curve of the average or integrated output for the duration of the transient. This may then be used in determining the response time. This integration is usually done graphically after the oscillogram of the actual output is made. In special cases, particularly where the transient is relatively slow, the desired result may be obtained directly by the use of an electronic amplifier and an electromechanical recorder with appropriate damping.

It is suggested here that if certain simple precautions are observed, the envelope of the output peaks can be used as a measure of the transient response. This can be done in such a way that the accuracy of the results is not compromised, and at the same time permit a very real saving in the amount of time required and in the cost of making of transient response tests. The data shown in Figure 1 of this discussion are based on peak-value tests and do not appear to include any systematic error, based on the small error apparent in the median value.

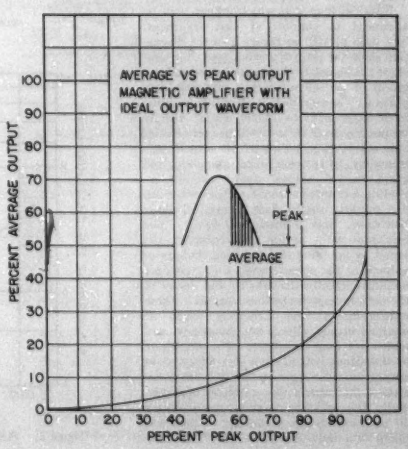

Figure 5. Average versus peak output for magnetic amplifier with ideal output wave form

The precaution that must be observed in peak-value transient response testing is simply that the initial value and amplitude of the transient must be restricted so that the change in average value of the amplifier output is approximately proportional to the change in peak value over the required range. Figure 4 of this discussion is intended to illustrate this point. This figure shows the peak, effective, and average outputs of a single-phase magnetic amplifier with ideal output wave form, plotted versus the firing angle. It is apparent from the curves that the above restriction can be satisfied only in the region up to about 40 per cent average output. It is further apparent that the amplitude of the input step and the resulting output change must be small if reasonable proportionality is to be maintained. The fact that the amplitude of the input step must be relatively small for accurate peak-value response testing is further illustrated by Figure 5 of this discussion, which shows the average output of a magnetic amplifier with ideal output waveform plotted versus the peak output. Here it can be seen that the step should be limited to approximately 10 per cent output change. There is no objection to thus limiting the amplitude of the change, because, as the authors have stated, the response time is virtually independent of the magnitude of the signal change.

Conclusions

1. It is felt that the seven conclusions and recommendations set forth at the end of the paper comprise a sound summary of the facts and the present situation confronting the committees of standardization.

2. It is further felt that the authors final recommendation that a standard method of transient response testing be prescribed should be adopted. It is suggested that the recommendation that the step change cover at least 75 per cent of the useful control range should not be adopted without careful consideration of the fact that accuracy of the peak-value response testing method would thus be compromised.

3. The necessity of keeping the method of transient response testing as simple as possible, while assuring that adequate and accurate data are obtained at reasonable cost, is considered to be one of the most important problems to be resolved by the standardizing committees dealing with magnetic amplifiers. The authors of the paper are to be commended on their informative and stimulating contribution to this work.

E. L. Harder and **W. F. Horton:** The authors wish to acknowledge the discussion by Professor Johnson. His explanation of the before-saturation delay phenomenon in terms of universal curves brings out the mechanism of this phenomenon very clearly.

Mr. Dornhoefer has provided a large amount of experimental evidence corroborating the single-delay concept of the self-saturating amplifier. The fact that the calculated time constant affords a direct indication of the actual time constant, which could only be obtained experimentally with a number of measurements, is also well brought out.

In considering the limiting value of response time K_3, the range of values which K_3 may cover in a particular amplifier will depend on the control switching instant and control voltage magnitude in addition to the factors discussed. Since these control circuit conditions may vary widely the specification of a maximum, minimum, and average value of K_3 is probably a useful concept.

Mr. Dornhoefer has clearly brought out the advantages of crest voltage measurement and a small increment (10 per cent) in transient response testing. Some enlargement on the last paragraph of the paper may serve to present the arguments for a larger increment.

The reasons for the three limits given are that if the response is taken over at least 75 per cent of the useful range, the time constant will be a good average of the high and low values that might otherwise be obtained depending on the portion of the range selected. If limited to the 5 to 95 per cent points it will also give the correct time constant for rectangular loop materials having a practically straight line transfer curve between upper and lower limits. If limited to an average slope not less than 60 per cent of maximum, the stated time constant can never be less than 60 per cent of the maximum, and a safeguard is thus provided in using the value in servo analysis.

Now that the arguments have been quite completely stated the committee should be in a good position to make the best compromise. It may be the use of the largest increment over which crest voltage is a fair measure of average voltage.

Transformer Sound Level Considerations

A. J. MASLIN
MEMBER AIEE

Synopsis: The sound level resulting from the operation of a transformer is an exceedingly complex function of the materials, electrical and mechanical design, construction, service and placement of the unit. Some considerations bearing on the origin, transmission, and resulting aural response to such sounds are presented. Means of reducing the sound level and the economic effects of such reduction are mentioned. The presently recognized rules covering test equipment, test methods, and acceptable levels are briefly discussed.

THE sound level of electric apparatus, particularly transformers, has been subject to scrutiny for somewhat more than 20 years. The published information on the subject appears to indicate periods of emphasis roughly corresponding with the turn of each decade. Actually, however, our engineers, research scientists, and magnetic material suppliers have worked on the problem with steadily increasing devotion throughout most of the entire interval. Apparently this year marks another revival of intense interest in the subject by users and manufacturers alike. These intervals of emphasis coincide approximately with periods of major expansion of operating systems, and point up the changing requirements of new practices resulting from growth of load and load density.

During this interval of two decades there have been a number of significant major changes in transformer materials, design, and manufacture, all in the interest of a better, smaller, lighter, and less-costly product. While the problems involving sound level have not been neglected during this period, it is quite evident that there is lack of agreement concerning the suitability of transformers now being manufactured.[1,2] Some British opinion[3] even favors allowing the sound level of transformers to approach that of running machines to permit the use of higher flux densities with correspondingly reduced weights and cost; if not, the new lower loss core materials will only reduce the cost of cooling equipment and not that of the core and coils. This lack of agreement clearly indicates the wide variation of characteristics deemed essential for satisfactory transformer usage by different people in different places. The importance of these desired characteristics, in specific instances, is evident and undisputed.

A re-evaluation of the transformer sound level situation, taking all possible pertinent factors into account, seems to be indicated. To name and describe some of these factors is the purpose of this paper.

Sound Generation

The sound heard as a result of transformer operation is due to force induced vibrations which are ultimately transmitted to the ear of the observer. The most important forces are found in the core where they give rise to core vibration. These core forces depend primarily on the flux density, the characteristics of the core material, and the core construction.

Magnetostriction is a basic property of magnetic core materials and varies among other things with the flux density. It is one fundamental source of the total core vibration, but by no means the whole of it. The two curves of Figure 1 were obtained from the same ring sample of magnetic material. The change in sound level is due solely to a change in the array of the punchings, hence, is not due to a change in the properties of the material. The per-unit amplitude of vibration in the plane of the punchings of a built-up transformer core is frequently identified as magnetostriction.

This may or may not actually be the case. Magnetostriction is important because it determines the minimum possible core vibration for a given core material and flux density.

Other forces which may produce core vibration are associated with joint gaps, nonuniform flux distribution in the core corners, flux interchange to and from the core frames, and so forth. Reduction of these forces and the resulting vibrations is by no means a straight forward process. However, since these forces are among the very few fundamental stimuli subject to control, their mitigation is actively sought through all expedients not inimical to the absolutely required functions of the core.

The effects of load magnitude and power factor on the core forces are manifest chiefly through the change in flux density and flux distribution which they entail. For commonplace operation these effects are fortunately quite small.

When carrying load there are forces between the turns and coils of the same and other windings. There also are forces acting between the core and the coils which depend to a considerable extent upon the symmetry or balance of the coil arrangement. At the present state of the art, for well-designed transformers, these forces do not contribute significantly to the sound level and will merit attention only after the core forces and vibrations have been greatly reduced.

The centrifugal and impact forces attending the operation of cooling fans, pumps, contactors, and so forth, which may be a part of the complete transformer are also causes of vibrations ultimately evidenced as sound. Fans in particular are important sound generators, sometimes producing a level equal to or greater than that of the transformer. Present methods of mitigation involve the use of fans of reduced output or larger than normal transformers with few fans. Depending on the characteristics of the

Paper 50-178, recommended by the AIEE Transformers Committee and approved by the AIEE Technical Program Committee for presentation at the AIEE Summer and Pacific General Meeting, Pasadena, Calif., June 12–16, 1950. Manuscript submitted February 10, 1950; made available for printing April 26, 1950.

A. J. MASLIN is with Westinghouse Electric Corporation, Sharon, Pa.

transformer there may be as much, or more, room for improvement in cooling fans as there is in the transformer itself.

The vibrations set up by the forces described, particularly those of the core, may be large or small depending upon the mechanical characteristics of the structures on which they act. To limit the amplitude of these vibrations it is evident that the natural periods of the structures must not be the same as the periods of the driving forces. The natural period of some parts of the transformer structure can be predetermined with reasonable accuracy[4] but other parts defy such treatment.

The vibrations so generated are transmitted to the surrounding air by way of the liquid which occupies the space between core and tank, and by means of the mechanical ties between core frames and tank. Transmission is generally achieved with some attenuation. The resulting tank vibrations drive the air. Mechanical resonance must be avoided throughout this transmission path, which, as has been indicated, is in part an empirical procedure.

Sound Level and Aural Response

The relationship between sound level (decibels), intensity level (decibels), loudness level (phons) and loudness (loudness units or sones) for plane wave pure tones of known frequency is relatively direct.[5] Sound level meter reading (A, B, or C weighting) may be converted to intensity level by means of the appropriate response-frequency characteristic.[6] Intensity level is converted to loudness level using the well known equal-loudness contours,[7] and loudness level to loudness through a curve[8] or formula[9] relating these quantities.

For complex sounds, however, the procedure is more complicated and involves the consideration of harmonic components either separately[10] or by bands.[11] The indication of the sound level meter for complex sounds practically defies description in terms of acoustic quantities.[12] It does, however, fulfill a need. Objections to the meter and its use should be supported by constructive recommendations covering the quantity that should be measured in order to minimize such objections. Also due consideration for the equipment and test procedure required to measure this quantity must be given.

Sound Level Reduction

The fundamental approach to sound level reduction is of course by reduction of

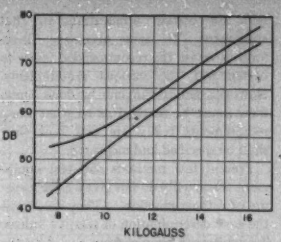

Figure 1. Sound level of a sample of magnetic material for two different arrays of the punchings

the responsible driving forces. Research and material engineers have made every effort to reduce the magnetostriction of the newer magnetic materials with considerable success. Magnetostriction of the core material is at present beyond the control of the transformer design engineer. Every known means consistent with the absolutely essential functions of the various parts of the transformer structure are being employed to reduce the other driving forces. When these other forces are reduced to the minimum attainable magnitudes, and the resulting vibrations likewise held to minimum amplitudes, the flux density is virtually the only variable under the immediate control of the designer.

Reducing the sound level below the recommended standard level[13] by reducing the flux density is more effective and less costly for large transformers than for smaller ones. The curve, Figure 2, indicates approximately the increase in equivalent kilovolt-amperes resulting from reductions of 3, 6, and 9 decibels below the National Electrical Manufacturers Association (NEMA) recommended levels for oil- and air-cooled transformers, when the reduction is effected by lowering the induction in the core.

It is well known that a change of 10 per cent in induction will result in a 2- to 3-decibel change in sound level. Thus, for a 6-decibel reduction, the core weight may be expected to increase about 30 per cent. The larger core, for the same number of turns and the same copper loss, will require about 30 per cent more copper. This increase in weight of active material from 100 to 130 is approximately equivalent to a transformer having a kilovolt-ampere rating of 142 per cent based on the flux density of the original unit which met the NEMA recommended sound level. However, as will be indicated later, the NEMA recommendations permit higher inductions in larger transformers than in smaller ones. This fact, together with other design considerations, causes the equivalent kilovolt-amperes of small transformers to exceed and of large transformer to be less than, the above figure of 142 per cent for 6 decibels. Thus the curve, Figure 2, shows 250 per cent for a 2,500-kva unit having a NEMA level of 65 decibels and 130 per cent for a 25,000-kva unit having a NEMA level of 75 decibels, for the same 6-decibel reduction.

Reduction of the coil driving forces is, in general, limited to providing coil arrangements of maximum symmetry.

Reduction of the vibration of the driven members can be achieved by increasing their mechanical impedance and eliminating resonance. Other factors in the design of the transformer restrict the mechanical impedance of the structure to a relatively narrow range so that the avoidance of resonance is the important means of control. This is done, where possible, by calculation in advance of construction. However, the complexity of the mechanical system defies analysis in many parts, hence, empirical and experimental corrections are frequently required.

Sound level reduction by increasing the attenuation of the mechanical or acoustical circuit between the source and the observer has been repeatedly advocated. The use of isolating or attenuating barriers or suspensions between the core and the tank would be more attractive if they could be effectively and economically applied. If sound attenuation were the only problem to be considered, this solution would doubtless have been long since employed. However, electrical, thermal, physical, and economic factors as well as longevity considerations have discouraged manufacturers from promoting this possibility.

The use of vibration absorbers between the transformer and its supporting foundation is effective only when the foundation transmits vibrations to another sound radiator. Such absorbers are frequently the cure for an intolerable condition when the transformer is located in a building vault, mounted in an overhead structure, or when the foundation communicates directly with bedrock.

Barriers external to the transformer also have been advocated and used.[2,14,15] This solution has taken the form of complete enclosures, roofless enclosures, and partially surrounding walls. To be effective the enclosure must have a low transmission coefficient which usually requires appreciable mass per-unit surface

area. The effectiveness of enclosures is enhanced by lining with a material of high absorption coefficient. Roofless or partial enclosures are less effective particularly at a considerable distance from the source, due to diffraction at their edges. Accurate predetermination of the effectiveness of an enclosure, especially a partial one, does not appear feasible, although there is some information available.[14,15,16,17]

External barriers, in addition to alleviating the sound nuisance of transformer substations, permit camouflage of the installation into esthetic harmony with its surroundings. This factor should be considered when deciding whether the added cost of a quiet installation should reside in the equipment itself, or in an enclosure.

The physical size of transformers has some influence on the sound level at an appreciable distance. If two transformers of different sizes have the same sound level at one foot, the smaller unit will have a lower level than the other at a distance fairly large with respect to its dimensions.[18]

Sound Level Standards

The presently recommended sound levels have been criticized as being too high, as being nonindicative of observer reaction, and as being poorly related to transformer rating. These objections are probably all perfectly valid from particular viewpoints. It must be recognized, however, that wide variations of viewpoint are inherent and justified.

Not all the transformers manufactured are installed where sound level is an important consideration, even though the proportion of such units is increasing. The rating of units installed in residential or business districts is also increasing very rapidly. Not long ago 2,000 kva was considered fairly large, but today units of 20,000 or 30,000 kva or more are located in close proximity to residences and business buildings. Furthermore, there appears to be a tendency to specify substandard levels, whether presently needed or not, as a hedge against possible population growth or relocation of the unit.

To build transformers with lower than standard inherent sound levels is inescapably more costly at the present state of the art than to build units to standard levels. Any "standard" that would require the purchaser to buy a Cadillac when he would be well served by a Chevrolet is unrealistic. Conversely, for example, it is probable that present levels for dry-type transformers are similarly high for certain applications of that equipment. It seems necessary, therefore, to revise the recommended levels to better suit the various requirements. However, before this can be done agreement must be reached as to what these requirements really are and how they shall be specified and measured.

Present test methods and test equipment admittedly do not give a close measure of listener reaction. They do permit the easy determination of relative values. To arbitrarily change from the A to the B or C weighting scale, or to take readings at 5, 10, or 50 feet instead of one foot will not sensibly improve this condition. If the present equipment and procedures are untenable, profound study is required to determine satisfactory objectives and practical means of obtaining them.

Based on certain assumptions it has been shown[19] that the sound level of a transformer may be expressed

$$DB = K_4 + 6.67 \log W$$

where W is the weight of the core and K_4 is a constant determined by design proportions, induction and reference level. Since the relationship between core weight and kilovolt-ampere rating is

$$W = k(KVA)^n$$

substitution affords

$$DB = K + 6.67n \log (KVA)$$

where $K = K_4 + 6.67 \log k$. This relation, for $K = 56$, $n = 0.75$, together with NEMA recommended levels for oil- and air-cooled transformers 69 kv and below, is plotted in Figure 3. The two curves meet at 1 kva and at 100,000 kva. Obviously the NEMA levels for intermediate ratings are lower than the normal relationship. This is one of the reasons why it is relatively so much more costly to reduce the sound level of a small transformer than a large one, as illustrated in Figure 2.

Conclusions

In spite of diligent research on materials, their treatment and use, test analysis, design and model work, all of which has enabled the engineer to design to a specific sound level, with assurance that test results will agree with calculated values with good engineering accuracy, it is still an expensive procedure to produce transformers with substandard sound levels. Since the recommended standard sound levels are not naturally related to transformer rating, the increase in cost for a given reduction below standard levels is greatest for the small and medium sizes of power transformers.

The use of enclosures to afford low sound level is effective and frequently employed, but also is costly. The choice between inherently low level equipment and "standard" equipment with an enclosure, should be based on economic and esthetic considerations.

In view of the steadily increasing requirement for low sound levels it may be desirable to establish at least two sets of standard levels. One set defining levels attending normal equipment which fully utilizes modern materials and technics while meeting the specified electrical, thermal, and other characteristics, another set specifying levels considered acceptable for all considerations, for locations where audible sound is a critical factor.

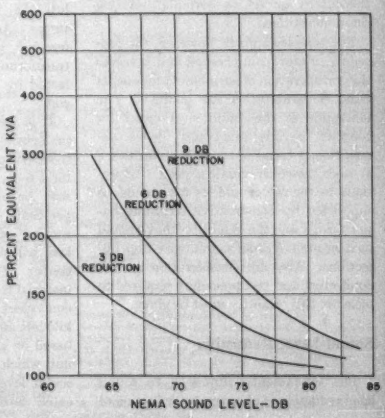

Figure 2. Equivalent kilovolt-amperes required to effect reductions of 3, 6, and 9 decibels below recommended levels by decreasing core induction

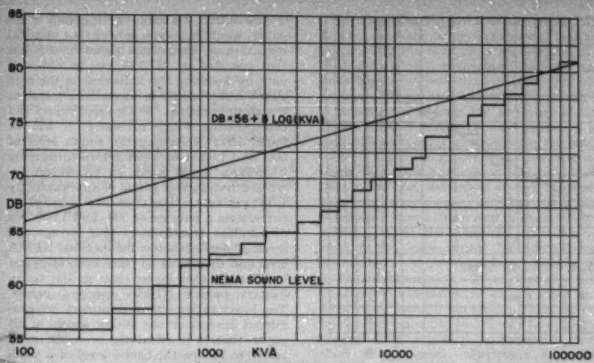

Figure 3. Theoretical variation of sound level with kilovolt-amperes compared with NEMA recommended level

While sound level meters and standard test procedures do not yield an accurate index of aural response under field conditions, and are subject to varied interpretation, a change from present equipment and practice should not be lightly undertaken lest new undesirables be traded for old.

References

1. Transformer Audio Noise Problems on an Electric Power System, **C. S. Murray.** *AIEE Transactions*, volume 68, part I, 1949, pages 740–52.

2. loc cit, discussion, **A. P. Fugill**, pages 747–48.

3. Power Transformers for Systems Operating at 200 Kv and Above, Part II. **H. S. Holbrook.** *BEAMA Journal* (London, England), volume 56, number 148, October 1949, page 351.

4. Natural Modes of Vibration of Simple Frames, **S. Bennon.** *Journal*, Franklin Institute (Philadelphia, Pa.), volume 243, January 1949, pages 13–39.

5. Sound and the Human Ear, **S. Bennon.** *Westinghouse Engineer* (East Pittsburgh, Pa.), volume 9, number 2, March 1949, pages 60–64.

6. American Standard Sound Level Meters for Measurement of Noise and Other Sounds. *ASA Z24.3*, American Standards Association (New York, N. Y.), Figure 1, 1944.

7. American Standard for Noise Measurement, *ASA Z24.2*, American Standards Association (New York, N. Y.), Figure 2, 1942.

8. loc cit, Figure 1.

9. Calculation of the Function of Acoustic Sensation, **G. G. Sacerdote.** *The Engineers' Digest* (New York, N. Y.), volume 10, October 1949, pages 346–48.

10. Loudness, Its Definition, Measurement and Calculation, **Fletcher, Munson.** *Journal*, Acoustical Society of America (New York, N. Y.), volume V, October 1933, pages 82–108.

11. Determination of the Loudness of Noise from Simple Measurements, **Leo L. Beranek and Arnold P. G. Peterson.** *Journal*, Acoustical Society of America (New York, N. Y.), July 1948, page 502.

12. Acoustic Measurements (book), **Leo L. Beranek.** John Wiley and Sons, Inc., New York, N. Y., 1949.

13. NEMA Standards for Transformers, *Publication 48-132* National Electrical Manufacturers Association (New York, N. Y.), September 1948, page 33.

14. Audio Noise in Transformers in Residential and Commercial Areas, **C. E. Baugh.** *AIEE Transactions*, volume 69, part I, 1950, pages 121–28.

15. Quiet Transformer Installations—A Problem for Both Equipment and Substation Designers, **I. S. Mendenhall, F. L. Taylor.** *AIEE Transactions*, volume 69, part II, 1950, pages 1148–53.

16. Some Acoustical Sources—Observer Problems, **S. W. Radfearn.** *Philosophical Magazine* (London, England), series 7, volume XXX, September 1940, page 223.

17. On Sound Diffraction Caused by Rigid Circular Plate, Square Plate, and Semi-infinite Screen, **Sivian and O'Neil.** *Journal*, Acoustical Society of America (New York, N. Y.), volume 3, 1932, pages 483–510.

18. Reference 1, discussion, **S. Bennon**, pages 748–49.

19. The Audio Noise of Transformers, **W. C. Sealey.** *Electrical Engineering* (*AIEE Transactions*), volume 60, March 1941, pages 109–12.

Discussion

T. D. Gordy (General Electric Company, Pittsfield, Mass.): The study of transformer sound levels is a very complex problem, as is shown by Mr. Maslin's paper. Not only is each component of the problem complex, but the way in which the various components are related in an acousto-mechanical-electrical circuit is complicated.[1] The paper discusses major sound generation sources, and comments on the importance of magnetostriction are in order. Sources other than magnetostriction exist, but as is stated in the paper, minimum possible core vibration for a given core material and flux density is determined by magnetostriction.

Mr. Maslin's comments on test methods and test equipment are most timely. These methods and equipment are not perfect for measuring aural effects on the listeners, but they do serve as a tool and guide by which the transformer designer can evaluate his designs. Regardless of the weighting scale used or distance from the transformer to the microphone, methods and equipment do exist that give the designer relative values of sound level. Admitting the weakness of our present transformer noise standards,[2] it is questionable whether present Standards should be changed until more study is given to the various weighting scales and sound meters.

Derivation of the equation

$$DB = 56 + 5 \log (KVA) \quad (1)$$

of Figure 3 and its relation to curves of Figure 2 are somewhat confusing.

The equations

$$DB = K_4 + 6.67 \log W \quad (2)$$

$$W = k(KVA)^n \quad (3)$$

should apply to a certain kilovolt-ampere range of transformers, but it is doubtful if they apply to transformers from 1 to 100,000 kva. Combining equations 2 and 3, there results the equation

$$DB = C_1 + C_2 \log (KVA) \quad (4)$$

in which C_1 and C_2 are constants. Generally speaking, transformers from 1 to 300 kva or 1 to 500 kva are built differently from those larger than 300 or 500 kva. Stepped changes in NEMA sound level limits become effective at 300 kva, because below that value, a level of 56 decibels is permitted for any kilovolt-ampere value. Only between 300 kva and 100,000 kva do NEMA sound levels vary with the kilovolt-amperes. Hence, to evaluate C_1 and C_2 of equation 4, select these two end points of the NEMA limits. Imposing oil-to-air cooled transformers (69 kv and below), boundary conditions of 300 kva, 56 decibels and 100,000 kva, 81 decibels on equation 4, solving simultaneously for C_1 and C_2, then substituting values of these constants back into equation 4, there is obtained

$$DB = 31.5 + 9.9 \log (KVA) \quad (5)$$

This equation plots as shown in Figure 1 of this discussion.

It is seen that this normal relationship of equation 5 agrees very closely with the NEMA levels. Even if equation 5 be extrapolated to smaller kilovolt-amperes, where it justly should not be used, results are reasonably close to actual sound levels obtained. For a 1-kva transformer, the sound level of 31.5 decibels is obtained. This is much closer to the noise level of 1-kva transformers than is 56 decibels as given by equation 1. The conclusion may be drawn that equation 1 is not necessarily a normal relationship between decibels and kilovolt-amperes; but when appropriate constants are obtained for this form of equation, a relation is obtained that not only follows the general equations 2 and 3 but gives results that are close to tested transformer sound levels, and agree with the NEMA levels.

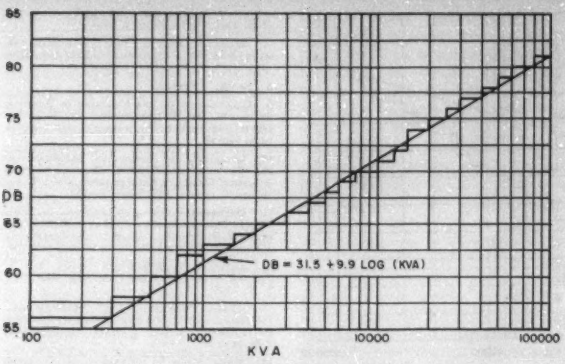

Figure 1. Modified theoretical variation of sound level with kilovolt-amperes compared with NEMA recommended level

Curves of Figure 2 of the paper show a very large variation of per cent equivalent kilovolt-amperes with NEMA sound level for 3-, 6-, and 9-decibel reductions. This is difficult to understand when the ordinate of the curves is expressed in per cent kilovolt-amperes. Assume that a 3-decibel reduction in sound level is desired. Let the core cross-sectional area and copper cross-sectional area be held constant. To obtain a 3-decibel reduction, flux density would have to be reduced 10 per cent. To obtain the original rated voltage, winding turns would have to be increased 10 per cent. Each of these extra turns would have the same copper cross-sectional area as each of the original 100 per cent turns. Hence, the winding kilovolt-amperes in terms of the original 100 per cent kilovolt-amperes becomes 110 per cent. To accommodate these extra 10 per cent turns, a slightly larger core window would be required, but this would change the decibel level by a small amount. In an actual design, both turns and core cross-sectional area would be changed so that the net result would be about 10 per cent increase in equivalent kilovolt-amperes for a 3-decibel reduction.

In the foregoing discussion, kilovolt-ampere rating was not introduced. Hence, the equivalent kilovolt-amperes expressed as a per cent is not a function of the kilovolt-ampere rating of the transformer. Therefore, curves of Figure 2 in the paper should be essentially horizontal. More than likely when covering the NEMA sound level range from 60 to 85 decibels, a change in winding voltage would be encountered; and necessarily, some changes in the basic type of design would be made. These changes probably would tend to make the per cent equivalent kilovolt-ampere versus NEMA sound level curves not horizontal and would give them a slight curvature of the type shown in Figure 2. It is difficult to understand how the per cent equivalent kilovolt-amperes given by Figure 2 can be obtained when a change of from 2 to 3 decibels for 10 per cent change in voltage is the starting point for determination of the curves.

Mr. Maslin has covered the important points of transformer sound level considerations as viewed by the manufacturer. Some of these viewpoints conflict with users' viewpoints as would be expected. Close cooperation between manufacturers and users of transformers appears to be a most logical way to bring the conflicting viewpoints into compromise.

References

1. Audible Noise of Power Transformers, T. D. Gordy. *AIEE Transactions*, volume 69, part I, 1950, pages 45–53.

2. See reference 13 of the paper.

C. S. Murray (Consolidated Edison Company of New York, Inc., New York, N. Y.): The author states that engineers, research scientists, and others have worked on the problem of apparatus sound level for over 20 years. This is not to be questioned, but let us look at what has been accomplished in the field of transformer noise.

Sound level measurements were made on a number of the larger 3-phase transformers installed on our system which have been in service for from 15 to 20 years. These transformers range in kilovolt-ampere ratings from 22,500 to 70,000 and in voltage from 27 to 132 kv. They were purchased without any regard to noise level. In all cases the tests were made with the transformers in service and carrying load and in many instances these transformers are in close proximity to large reflecting surfaces. And yet, in a majority of the tests, the average sound level was from 8 to 10 decibels below the values now specified by NEMA Standards. It is questionable whether transformers purchased today under similar conditions will be as quiet.

There is no doubt that there has been great improvements in transformer materials and design over the last few years. There is some doubt, however, as to whether the problem of noise was given just consideration. When better core material was made available, the core was made smaller and worked at higher flux densities. This resulted in a smaller physical size and reduced weight of transformer but in many cases the noise level was increased.

The author, by means of Figure 2 of his paper, would have you believe that material reduction of transformer sound level below that specified by NEMA can be obtained only by lowering the induction in the core which would result in increased equivalent transformer rating. Using these curves and extrapolating where necessary, it will be found that decreasing the sound level of 500- and 1,000-kva 3-phase transformers by 9 decibels would mean an equivalent increased transformer rating of approximately 1,000 per cent. Yet there are installed on our system a number of 500- and 1,000-kva distribution transformers that have sound levels 10 decibels below the specified NEMA level and they have no more iron, no better iron, or are they larger than similar transformers having NEMA specified values. The lower ratings of transformers are considered here since the author shows in his paper that it is relatively so much more costly to reduce the sound level of a small transformer than a large one.

Others[1,2] have given their experiences for transformers of higher rating and the results are similar.

These results indicate that it is possible to build transformers with a sound level considerably below that specified by the NEMA without resorting to the "brute force" method of lowering the induction in the core and without appreciable cost to either the manufacturer or the user.

The author discusses the sound level meter and states that it has fulfilled a need. It is a fact that without the sound level meter many of the acoustical problems that have arisen in the operation of electric equipment would have gone unsolved. However, those of us who have made considerable use of the meter over a period of years believe that the time has come for something better. It has been the practice in our organization for some time to use a sound analyzer in connection with the sound level meter when making noise tests on any apparatus on the system. Considerable data have been obtained which show that a particular component of the noise emitted by the apparatus is usually the cause for a noise complaint at a remote distance. And yet that component may be such that its presence does not change the indication of the sound level meter. There are a number of cases wherein the hum from a transformer could be easily heard several hundred feet from it and was considered objectionable. The indication of the sound level meter, however, remained the same when the transformer was de-energized.

For each and every one of us to set down our requirements for a meter would probably result in as many different sets of requirements as the number of persons submitting them. It is up to some standardizing body such as the American Standards Association to recognize and arrive at a solution to the problem. It is felt that the standardization of a sound analyzer with proper filter circuits is of great importance at this time. Once the sound analyzer is standardized and greater use made of it by the power engineer, the requirements for a noise meter may be better defined.

References

1. Quiet Transformer Installations—A Problem for Both Equipment and Substation Designers, I. S. Mendenhall, F. L. Taylor. *AIEE*

Transactions, volume 69, part II, 1950, pages 1148–53.

2. See reference 14 of the paper.

A. J. Maslin: Mr. Gordy's discussion is most welcome because it emphasizes some of the more important points made in the paper. Concerning some others there is evident misunderstanding.

Mr. Gordy has obtained his equation 4 from equations 2 and 3 of the discussion. Thus, the constants C_1 and C_2 are, in turns of $K_4 k$ and n

$$C_1 = K_4 + 0.67 \log k$$

$$C_2 = 6.67n$$

In going to equation 5 therefore Mr. Gordy says

$$n = 1.485$$

From equation 3, however, n is the exponent which applied to the kilovolt-ampere rating gives proportionality with core weight. As is well known to all transformer designers, $n = 0.75$ for any geometrically similar line of transformers. This is readily demonstrated theoretically and is borne out in practice. When the range of kilovolt-ampere rating is large enough that geometrical similarity no longer exists the value of n is less than 0.75. Mr. Gordy's value $C_2 = 9.9$, which was chosen arbitrarily to make the slope of his curve match that of the NEMA levels, therefore cannot be justified. If Mr. Gordy prefers to locate his curve so that it passes through 56 decibels at 300 kva it must then pass through 68.6 decibels at 100,000 kva. The important point, however, as brought out in the paper, is that the relationship between kilovolt-amperes and sound level as prescribed by NEMA is not a natural one. In practice this means that the core induction for medium-sized transformers must be lower than the induction for very large, or very small, units if NEMA levels are to be met.

In discussing Figure 2 of the paper Mr. Gordy presents some interesting figures. By holding the core cross section and the copper cross section constant, reducing the induction by 10 per cent, and increasing the number of turns by 10 per cent, he has built a transformer having 100 per cent of the rating, 110 per cent of the load loss and a 3-decibel lower sound level than the reference unit. This transformer does indeed have an equivalent rating of about 110 per cent; that is, at the induction of the reference unit the transformer described by Mr. Gordy will have 110 per cent of the reference rating. What the customer wants, however, is the same rating, 3-decibels lower sound level and the same load loss referred to the reference unit. To achieve this it is necessary to increase the copper cross section by at least 10 per cent. Thus, on the basis of the example Mr. Gordy has chosen, the winding capacity is increased more than 20 per cent. Obviously it is impossible to put 110 per cent turns of 110 per cent cross section in the original core window, so the equivalent ratings of the core and winding are still further increased. In practice, of course, core cross section, number of turns, and copper cross section would all be changed, but the increase in equivalent kilovolt-ampere ratings is not reduced thereby. The curves, Figure 2 of the paper, were actually obtained from a large number of designs covering a wide range of kilovolt-ampere ratings and voltage classes. Quite obviously one curve cannot apply to all voltage classes, hence, as stated in the paper, Figure 2 indicates approximately the increase in equivalent kilovolt-amperes resulting from the stated decibel reductions.

Mr. Murray's discussion is valuable since it reflects the thinking of a user of transformers. He takes the manufacturer to task for building noisier equipment today than he did 15 years ago. It is, of course, true that improved materials and design have permitted higher flux densities. These higher flux densities have been used in ordinary circumstances up to a limiting value imposed by sound level standards. It is Mr. Murray's contention that this should not have been done. However, there is another factor to be considered. During the past ten years labor and material costs to the manufacturer have increased from 80 to 90 per cent. The cost of transformers to the user, on the other hand, has only increased about two-thirds that amount. This state of affairs has been made possible by using the improved materials and design mentioned by Mr. Murray, and by hewing closer to the standard sound levels. If the cost of transformers to the user had been allowed to match the increase in labor and material costs, present-day transformers would be at least as quiet as the older units Mr. Murray mentions. With these factors in mind it is questionable whether all users will agree with Mr. Murray.

The discussion of Figure 2 of the paper has been covered before. However, it should be emphasized that extrapolation of the curves is not permissible because for small units the equivalent rating decreases again. The equivalent kilovolt-ampere rating is a function of the ordinate between the two curves of Figure 3 of the paper. Quite obviously there is something seriously amiss in the noisier 500- and 1,000-kva units mentioned by Mr. Murray if the quiet and the noisy units compare as stated.

Mr. Murray's comments concerning sound level meters point toward an ideal which would be most welcome. The design, construction, and use of such a "calibrated ear" meter must present unusual difficulties, otherwise we could reasonably expect that one would have been developed. Such an instrument should, for example, eliminate the need for telephone interference factors as well as satisfy the requirements of the power engineer. It is hoped that a more satisfactory meter will be made available and that satisfactory performance of transformers sound-wise will be forthcoming through the co-operative effort of all concerned.

Quiet Transformer Installations—A Problem for Both Equipment and Substation Designers

I. S. MENDENHALL
MEMBER AIEE

F. L. TAYLOR
NONMEMBER AIEE

Synopsis: The problem of achieving quiet installations of transformers at substations is one that requires the efforts of both the equipment designer and the substation designer for successful solution.

This paper describes remedial and preventive measures that have been taken by The Detroit Edison Company to solve the noise problem in substations. The most effective method that was tried was to enclose the transformers on four sides with a 12-inch masonry wall, this effecting a sound reduction of about 24 decibels. Other measures, which were less effective acoustically, also are described and data given.

THE problem of the reduction of the noise emanating from substations is one that is being faced by many electrical utilities, and it is one that is likely to become more acute in the future. The problem arises from several causes, among them being the necessity for locating substations in or adjacent to residential areas; an increase in the size of transformers and regulators, due to increasing load densities; and a seeming trend on the part of some manufacturers toward producing transformers having higher noise levels than previously. Figures 1, 2, 3, and 4 are aerial photographs showing the locations of four substations of The Detroit Edison Company with respect to residential and commercial areas.

It is recognized that it may never be economically feasible to build the larger transformers so quiet that they could safely be installed in residential areas without provision for reducing the sound level. The problem, therefore, must be attacked both by the equipment manufacturer, particularly of transformers, and by the substation designer.

This paper discusses measures that have been taken by The Detroit Edison Company to confine the sound that originates in outdoor transformers and regulators, and does not consider the problem of the abatement of noise from other sources, such as air-blast equipment or rotating machinery. Similar measures with some modifications would be of value, however, in other applications.

The first and most obvious approach to the problem of the reduction of noise from substations is to attempt to get quieter transformers and regulators from the manufacturers. This suggestion has been made in other papers[1] and its importance should be stressed again. Experience has shown that it is possible to build a transformer having a noise level many decibels below the value specified in the National Electrical Manufacturer's Association (NEMA) standards, without appreciable increase in cost. For example, The Detroit Edison Company, in the period of 1938 to 1940, received transformers of 1,500-, 2,500-, 4,000-, and 6,000-kva capacity, having sound levels respectively of 56, 57, 60, and 62 decibels. The corresponding sound levels permitted by the NEMA standards are 63, 65, 66, and 68 decibels. It is obvious that there is an opportunity, as well as a need, for the manufacturers to acquire sufficient experience and data so that they can consistently build transformers having sound levels as low as the best units that are built occasionally.

Paper 50-179, recommended by the AIEE Transformers Committee and approved by the AIEE Technical Program Committee for presentation at the AIEE Summer and Pacific General Meeting, Pasadena, Calif., June 12–16, 1950. Manuscript submitted November 15, 1949; made available for printing April 26, 1950.

I. S. MENDENHALL and F. L. TAYLOR are both with The Detroit Edison Company, Detroit, Mich.

Shrubbery

A method that has proved satisfactory, under some conditions, is the planting of evergreens and shrubbery around a substation. In one instance, an outdoor substation was built facing a main highway, in a high-income suburban residential area. Readings of noise showed that the sound level at the highway, due to the substation equipment was about 43 decibels, whereas the intermittent sound level at that point, due to traffic was about 75 decibels. The nearest house was on the opposite side of the highway from the substation and about 200 feet distance from the latter, but nevertheless there were complaints about the noise from the substation.

A heavy planting of evergreens, shrubbery, and trees was made around three sides of the substation fence, see Figures 5 and 6. This reduced the noise sufficiently so that the complaining customer was satisfied, and in addition the appearance of the installation from the highway was greatly improved. Unfortunately, from the standpoint of obtaining data, the transformers were changed out for load reasons shortly thereafter so that no noise readings were obtained that would indicate the actual effectiveness of the shrubbery in reducing noise. This method is worth considering, however, where the noise problem is not severe.

Masonry Walls

The next method that was tried was to surround the transformer and the bus regulator with a masonry enclosure. This was done by using the rear wall of the substation building as one side of the enclosure and completing it with three walls of cinder block, with a brick veneer on the outside to match the building. The walls are 12 inches thick and high enough to extend about five feet above the top of the transformer tank. The enclosures

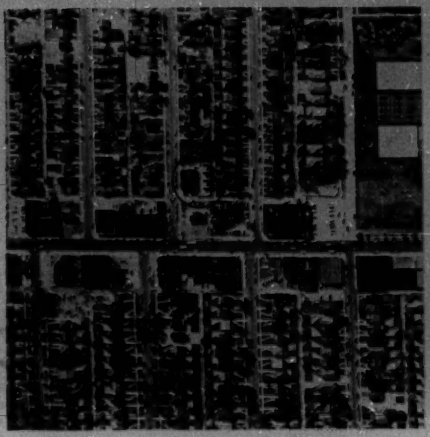

Figure 1. Aerial view of Turner Substation and environs

Figure 3. Aerial view of Cortland Substation and surrounding area

Figure 2. Aerial view of Balfour Substation and vicinity

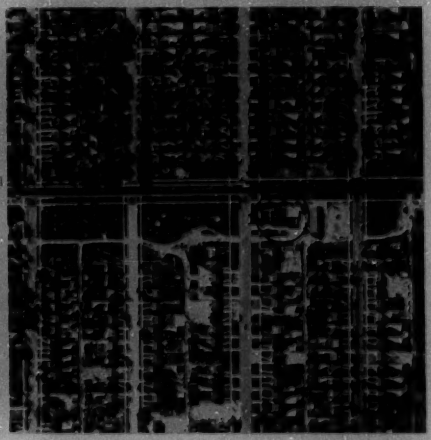

Figure 4 (above). Aerial view of Puritan Substation and vicinity

Figure 5 (below). Rear view of Franklin Substation

are open at the top, although in some cases they are covered with screening to prevent the entrance of birds. The space between the transformer or regulator and the walls is three to six feet. No difficulties have been experienced with overheating of the equipment.

There is a service door for access to each enclosure, but the removal of a transformer or regulator necessitates tearing down a part of the wall. To facilitate this operation, "through-joints" are provided in the wall at two places so

Figure 6 (left). Franklin Substation as seen from the highway

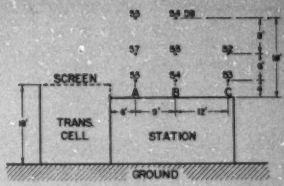

Figure 8 (right). Elevation of Coolidge Substation, with sound readings

that a panel may be removed independently of the remainder of the wall.

Figure 7 shows the transformer enclosures at a substation having this type of construction. Figures 8, 9, and 10 show the sound readings at this location.

A variation of this type of installation that is used where noise reduction is less of a consideration, but nevertheless some noise insulation as well as protection is needed, consists of a masonry enclosure as above, having a removable sheet-metal panel for the removal of equipment. A typical design utilizes 20 gauge sheet-steel roof decking which has ribs formed in the material for stiffness. Removable panel area is divided into independent sections weighing a maximum of 125 to 150 pounds each for facility in erection and removal. The panel sections are bolted to suitable steel members which, in turn, are removable, thus leaving a clear opening of adequate size to move the equipment in or out.

The removable steel panels have an advantage over the masonry panels in initial cost, removal and replacement cost, and in the time required to remove and replace them. The steel panels, however, are somewhat less effective than masonry in reducing sound transmission.

An installation of removable steel panels is shown in Figures 11 and 12.

Sound readings taken at a substation of this type are given in Table I. See also the diagram in Figure 13.

In an effort to improve the sound insulating characteristics of the removable panels, while retaining their advantages, an installation of panels filled with glass fibers was made. These panels have glass fiber batts two inches thick, completely enclosed in 20 gauge sheet steel.

Table I

	Decibels
Transformer sound level, measured in the open	66
Average sound level inside the enclosure, adjacent to the steel panels	69
Average sound level outside the enclosure, 3 feet from the steel panels	67
Average sound level outside the enclosure, 12 feet from the steel panels	52
Sound reduction through panel	12

Table II

	Decibels
Transformer sound level, measured in the open	69
Average sound level inside the enclosure, adjacent to the removable panel	67
Average sound level outside the enclosure, 5 feet from the panel	48
Sound reduction through panel	19

They were made in sizes such that they can readily be handled during erection, the maximum weight being about 150 pounds. They are held in place by through-bolts attaching them to removable steel members which extend across the opening in the wall. Figure 14 shows an installation of this type.

This material proved to be considerably better than sheet steel as a sound insulator, as was expected, and was almost as effective as a masonry wall. Sound level readings taken at this installation are shown in Table II.

Figure 15 is a diagrammatic plan of an installation of this kind, showing the complete set of sound readings that were taken.

Comparison of Panel Types

The practical value of any new development must always be determined on the basis of the benefits as compared with the costs. Each of the three types of closure for transformer enclosures has certain advantages and other disadvantages.

The removable steel panels have the minimum initial cost and may be quickly and cheaply removed and replaced, but their noise insulation capabilities are inadequate, for many locations.

The removable section of brick wall has the second lowest initial cost and the best sound absorption of the three types. The initial cost plus the cost of one removal and replacement, however, is as great as that of the most expensive type of panel (glass fibers), and after two or more removals and replacements the total cost becomes the highest of all.

The removable glass fiber panels have the highest initial cost, but this becomes equal to the cumulative cost of the brick panels after one removal, and becomes less after two or more removals. The sound absorption is only slightly less than is provided by brick. For most substations in residential areas, where good noise insulation is a necessity and provision must be made for changing the transformers to larger sizes, the glass fiber panels appear to be the best compromise that has been developed so far.

Table III gives a comparison of the sound insulating qualities and of the relative costs of the three types of panels, as determined from the experience of The Detroit Edison Company. The costs are for the panels only, installed in place, and do not include the cost of the masonry walls for the remainder of the enclosure.

Figure 9. Elevation of Coolidge Substation, with transformer enclosure partially covered by a tarpaulin. Sound readings are given

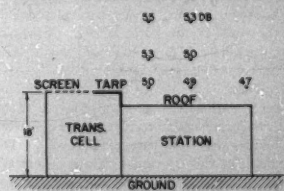

Figure 7. Transformer and bus regulator enclosures built of masonry block and brick

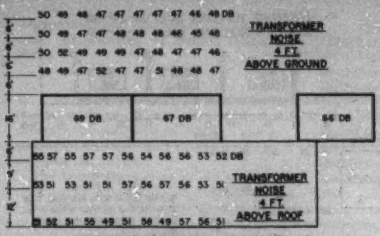

Figure 10 (left). Plan view of Coolidge Substation, with sound readings

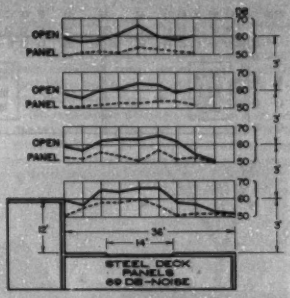

Figure 13 (right). Plan view of Inkster Substation, with sound readings

Figure 11 (left). Removable steel panels in transformer and bus regulator enclosure, Inkster Substation

The curves shown on Figure 18 summarize the results of tests of sound attenuation through panels of the three types, with various sound levels inside the enclosures.

Case History of One Substation

At the substation shown in Figure 1, the three transformers were originally installed in an open yard. Each unit was of 6,000-kva capacity. Although the location was such that there were residences within about 50 feet of the transformers, no noise complaints were received from the neighbors due to the fact that the quietest available units had been selected for this substation. These transformers had an average sound level of 60 decibels.

It became necessary to change the transformers to 10,000-kva units because of load growth, and immediately thereafter the nearest neighbor complained that the noise from the transformers disturbed him. A check of the sound level in the area showed that the complaint was justified. Masonry walls, 20 feet high, were built around three sides of the transformers, the open side of the enclosures being toward the substation building and away from the houses. Following this, sound level readings, and interviews with the complaining customer and others in the area, disclosed that the sound level was very satisfactory.

Figure 16 shows this substation, with a partial view of the masonry cells that were added. Figure 17 is a diagram and plan view of the substation, which shows the readings of sound level that were taken before and after the construction of the masonry cells.

Method of Sound Measurement

In this discussion it is assumed that those interested in the subject of noise abatement are familiar with noise meters and their use. The meter used on these tests was of standard design, and provided with an air blown whistle for overall calibration. 40-decibel weighting was used on all tests, regardless of the sound levels encountered. Measurements were made on the ground, and also in the air above one station, see Figure 8, but like locations were not measured at each station. Conditions also varied from station to station. In some cases, noise was measured before and after installing panels, while at other locations the noise was measured only after completing the enclosure. More data would have been desirable but weather conditions and lack of time interfered.

The curve given in Figure 18 was drawn from data obtained in the field, after it was noticed that similar walls did not always provide the same decibel attenuation. The origin of the curves is at zero decibels and from these curves it would appear that the attenuation for a given wall varies with the intensity of the transformer noise level. The attenuation shown is less than given in data published previously.[3] This condition is probably due to leakage over the top of

Table III

	Brick Panel	Sheet Steel Panel	Fiber Glass Panel
Reduction in sound level through panel at 70 decibels	24	12	20
Relative initial cost, installed	100	75	205
Cumulative cost after one removal	206	85	214
two removals	312	95	223

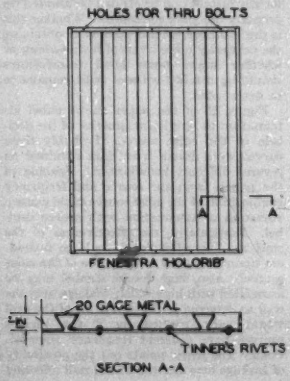

Figure 12 (left). Details of removable steel panels

Figure 14 (right). Removable glass fiber panels in transformer and bus regulator enclosures at Evergreen Substation

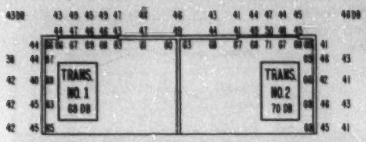

Figure 15 (left). Plan view of Evergreen Substation, with sound readings

Figure 16 (left). Partial enclosures of transformers at Turner Substation

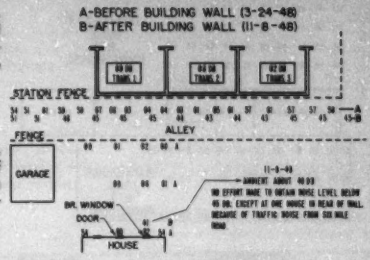

Figure 17 (right). Plan view of Turner Substation with sound readings

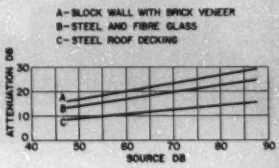

Figure 18 (right). Curves of sound attenuation through panels of masonry, glass fiber batts, and ribbed sheet steel

the wall. Further investigation to supplement the data contained in the curves would be desirable.

Conclusions

The problem of minimizing the noise that is emitted from substations is becoming increasingly acute to electrical utilities. A satisfactory solution that has been evolved by this company consists of enclosing the outdoor transformers and regulators with masonry walls. Removable panels are provided in the walls to allow removal of the equipment.

Three types of material have been used for the removable panels: masonry block, ribbed sheet steel, and glass fiber batts enclosed in sheet steel. The order of effectiveness of the three types in reducing sound transmission is: 1. masonry block; 2. glass fibers; 3. ribbed steel.

References

1. Transformer Audio Noise Problems on an Electric Power System, C. S. Murray. *AIEE Transactions*, volume 68, part 1, 1949, pages 740–53.

2. Transmission of Sound Through Wall and Floor Structures, V. L. Chrisler, W. F. Snyder. *Journal of Research* (National Bureau of Standards, Washington, D. C.), volume 2, March 1929, pages 551–52.

Discussion

R. R. Peck (Southern California Edison Company, Los Angeles, Calif.): This paper is of particular interest to utilities now seeking a solution to the noise problem. The study shows that the use of masonry walls for sound barriers is an effective method of quieting transformer noise. The use of the removable metal-fiber glass panels is important, since it makes the exchange of transformers possible without destroying the barrier. This has been one of the major drawbacks in the use of heavy masonry construction.

Barriers, however, should not be considered as the ultimate solution to all noise problems because of their many disadvantages:

1. A barrier, to be effective, must "fit" the noisy transformer. A new transformer of larger size or of different dimensions may require a different barrier. A change in a masonry barrier is expensive and time-consuming.

2. The optimum distance between the noise radiating surface and the barrier is about four feet. In some cases, considerably more operating space is required and at times the transformer cooling may be impaired by the proximity of the barrier.

3. An efficient sound barrier is not necessarily a thing of beauty, and unless considerable work and money are spent to improve the appearance, it may be unsightly and overcome the advantages gained by the lower noise level.

4. The cost of the barrier adds to the cost of the substation and, hence, changes the economics of the over-all distribution system. In isolated cases, this may not appear to be a problem, but as the number of applications grows it becomes a major consideration.

The manufacturers have offered a transformer with a noise level of 10 decibels less than the National Electrical Manufacturers Association (NEMA) standard for an additional charge of 25 per cent on the transformer price. This 10-decibel reduction below NEMA standards is rarely adequate in itself, and usually requires a further expenditure to make it acceptable.

It is our opinion that the NEMA standard for outdoor transformers to be installed in residential areas is too high and should not have a stair-step rating. If a noise is objectionable it makes little difference whether the noise comes from a 2,000- or 3,000-kva transformer, whether it is rated 69 kv or 132 kv. Ultimately transformers used in this class of service should have a flat decibel rating.

The problem now returns to the design engineer with the request for much quieter transformers at a cost that will make their use feasible from an economical standpoint.

T. D. Gordy (General Electric Company Pittsfield, Mass.): Mr. Mendenhall and Mr. Taylor have contributed data on transformer enclosures which is important to system engineers placing transformers in commercial and residential areas. Even though lower-than-present noise level transformers are desired from manufacturers, the paper demonstrates that present transformer installation levels can be lowered by properly designed enclosures. Whether this is the most economical method of obtaining the necessary noise levels of installations, or whether lower noise level transformers should be installed without walls, remains to be determined.

Figure 18 of the paper shows panel attenuation to be a linear function of the decibels of the noise source. Probably these curves were drawn from data obtained on several different installations. Spacing of the panels from the source and frequency composition of the noise source could cause a variation of attenuation with source decibel. Particularly, the effectiveness of the steel and fiber glass panel would be dependent upon frequency composition of the noise source. Also, high source decibel may be associated with high walls; leakage over the wall as detected in the proximity of the wall would vary, particularly if the various sources have different frequency compositions. The paper points out the possibility of leakage over the top of the wall affecting

attenuation, and the effect of frequency could be included in further investigations.

A. J. Maslin (Westinghouse Electric Corporation, Sharon, Pa.): The authors have presented a wealth of valuable data and constructive comment on the subject of sound nuisance alleviation.

The trend, mentioned in the paper, toward higher sound levels on the part of some transformer manufacturers appears to me to be quite natural. For transformers built with the older or poorer grades of hot rolled silicon iron, the normal flux density was determined by the no-load loss or excitation guarantees at a relatively low value. The sound level, though low, was incidental. With the introduction of newer, better iron alloys, particularly oriented silicon iron, the flux density for a given loss or exciting current could be increased materially. While for a given induction the new materials are generally better sound-wise than the old, the increase in flux density permitted by lower loss and higher permeability more than offsets this. As a result, new transformers tend to be smaller, lighter, and louder than their precedents. However, a point that is frequently overlooked is that the user has profited by this change.

During the past ten years the cost of labor and materials has increased about 85 per cent. The increase in price of finished transformers, on the other hand, is from 25 to 50 points below this figure, and the transformers are better in all respects except possibly sound level. Even with these subnormal price increases transformer sound levels have in general been kept equal to or slightly below the industry recommendations. The manufacturer has a great incentive to reduce the sound when using these newer core materials for, when he learns how to accomplish this, higher flux densities and still smaller transformers will follow.

The authors refer to exceptionally low level units that are built occasionally as if by accident. Our recent experience does not support this contention. The sound level of the completed transformer can be and is predicted with good engineering accuracy, and the variation between units is small. In fact, sound levels can be more accurately calculated than can exciting current. Under these circumstances a substandard sound level requirement inevitably involves a more costly transformer.

It is unfortunate that the authors could not present data on the effectiveness of shrubbery in reducing sound transmission, because this esthetically acceptable barrier should be welcomed in any residential area. The data on masonry walls and steel panels are a valuable addition to the meager information available concerning these barriers. However, the variation of attenuation with source intensity shown in Figure 18 of the paper gives rise to question. Perhaps this variation could be due to differences in spectrum with level, or to obscuring influence of the outside ambient level. The authors' comments on this point would be welcome.

I. S. Mendenhall and **F. L. Taylor:** Mr. Peck's discussion indicates that other utilities are facing the same transformer noise problems that were discussed in the paper. It also points out many of the disadvantages of installing sound barriers in connection with the installation of noisy transformers in residential areas. Most of these disadvantages are economic in the ultimate analysis, and indicate the need for studies of the costs of minimizing transformer noise by various means, including changes in the design by the manufacturer, use of different core materials, and the construction of enclosures or sound barriers by the utility.

It would be ideal, as Mr. Peck suggests, to have all transformers, regardless of size, so quiet that no sound barriers would ever be needed at any location. In the present state of the art, however, it is apparent that the cost of building one of the larger transformers of, for instance, 10,000-kva capacity so that it would have a 50-decibel sound level would be prohibitive.

Mr. Gordy offers several possible explanations for the variance of the data in Figure 18 from other published data. The curves were drawn from readings taken at several different locations, as he suggests. All of the data that entered into the drawing of each curve, however, were obtained from locations where the walls were between 18 and 20 feet in height, of the same thickness, and enclosed essentially the same space. Furthermore, most of the attenuation values were obtained from sound level readings that were taken about one foot inside the panel and one to four feet outside.

No measurements were made of the frequency composition of the noise. It is recognized that the attenuation afforded by a given panel will vary with the frequency and this may account for the unexpected behavior of the curves. Each curve is the result of a considerable number of tests, however, which it was thought would average out the frequency effect. It is planned to study the frequency composition of the sound when further tests of this kind are made.

Mr. Maslin points out that the new transformers are superior to the old in size, weight, and cost in comparison with other items. The utilities appreciate these advantages, and urge the manufacturers to continue the attack on transformer noise as vigorously as on other design problems.

It is thought that some manufacturers have difficulty in designing a new transformer for a definite sound level. As an example, the Detroit Edison Company since 1946 has purchased transformers of from 2,500- to 10,000-kva capacity, some of which had sound levels up to 8 decibels above the industry standard for the respective sizes of units. Fortunately this condition is not general and most manufacturers seem to be able to design to closer limits than this, although the noise levels are not as low as we would like.

The possible effects of the frequency composition of the noise on the curves of Figure 18 have been discussed in the foregoing. All noise tests were made late at night and every effort was made to take readings only when the ambient noise was at a minimum. It is thought, therefore, that ambient noise was not a factor in the results indicated by Figure 18.

In closing, the authors wish to express their appreciation to the discussors for their interest and many pertinent suggestions. It is hoped that further attention will be given to this problem by the engineers of both the utilities and the manufacturers, to the end that it may eventually be solved most equitably for all.

Locomotive Wheel-Slip and Wheel-Lock Protection

R. M. SMITH
ASSOCIATE AIEE

CERTAIN characteristics of the diesel-electric locomotive emphasize the importance of wheel-slip and locked-axle protection. This presents an important problem. The first step in its solution is an analysis of the fundamental phenomena of wheel and rail contact. This is supplemented with a study of tests made on locomotives in service. Together, they form a basis for setting up the requirements for a complete scheme of locomotive wheel-slip detection and protection.

Locked-Axle Problem

Accidents have occurred within recent years because of the locking of driving axles on diesel-electric locomotives, as reported in the minutes of the eleventh annual meeting of Locomotive Maintenance Officers Association, September 19–22, 1949. In some instances, the traction-motor armature bearings locked, and in others, the motor-suspension bearings on the axle locked. In some cases, the motors had been electrically disconnected from their generators, thus making the wheel-slip protective feature inoperative.

Various thermal devices have been suggested to detect overheated bearings before they lock. The relative inaccessibility of the bearings, their large number, and the desirability of furnishing protection against a locomotive starting with a locked (but cold) bearing, have made it seem more desirable to use axle speed rather than bearing temperature as a basis of detection.

High-speed wheel slip is one cause of locked armatures. A system of protection to measure and warn of differences between locomotive speed and axle speed would detect this. Necessary corrective measures could then be taken, either automatically or by the engineer, in time to prevent a locked axle developing from this cause.

Need for Wheel-Slip Protection

The diesel electric locomotive appears to require a degree of protection against wheel slip, never felt necessary in straight electric or steam locomotives. Recently the discovery of wheel slip occurring at speeds over 60 miles per hour has aroused new interest in detection systems of an inclusive character. The reasons for having a complete wheel-slip detection system are:

1. To prevent excessive traction-motor and locomotive speeds.
2. To allow the operator to detect slip on trailing units which are out of normal hearing distance.
3. To obtain optimum locomotive performance, that is, tractive effort, at all speeds.
4. To prevent derailment due to locked axles.
5. To prevent false forward transition.
6. To prevent wheel slide during braking.

Types of Wheel Slip

Wheel slip may be divided generally into two classes: those cases which occur at 20-miles per hour or less, and those which occur at higher speeds. At low speeds, it is possible for the motor torque to give tractive-effort levels greater than the weight on the locomotive axle multiplied by the normal factor of adhesion. At some speed around 20-miles per hour (depending upon the torque characteristics of the motor under consideration) the motor torque falls to a level such that the factor of adhesion must be greatly reduced in order to precipitate wheel slip.

Under very favorable conditions, factors of adhesion of 40 per cent at speed have been observed. Under very adverse conditions, factors as low as 4 or 5 per cent occur at standstill. These, however, represent extreme cases and occur because of some unique rail conditions. Only general causes of wheel slip will be discussed.

Causes of High-Speed Wheel Slip

It is commonly assumed that a locomotive driving wheel in motion, but not slipping, has a static friction lock with the rail and that when this friction lock is broken, the factor of adhesion drops very rapidly as slip increases. That this is not altogether an accurate picture can be seen from the curve of adhesion versus rate of slip, Figure 1.[1] If the curve of adhesion values is continued back to zero slip, a value of about 22 per cent is obtained. It is well known that in starting, values of 25 per cent with dry rail are normally obtained and values of up to 40 per cent can be reached under special conditions. Why, then, must the high-speed rolling friction given by this curve

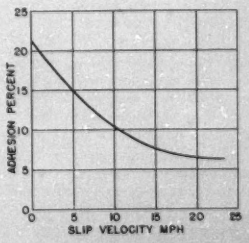

Figure 1. Adhesion versus slip velocity

Paper 50-181, recommended by the AIEE Land Transportation Committee and approved by the AIEE Technical Program Committee for presentation at the AIEE Summer and Pacific General Meeting, Pasadena, Calif., June 12–16, 1950. Manuscript submitted March 14, 1950; made available for printing April 26, 1950.

R. M. Smith is with the General Electric Company, Erie, Pa.

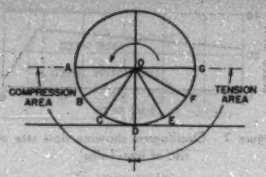

Figure 2. Driven wheel rolling on rail

be less? This is due to the fact that a rolling wheel always has a small amount of slip associated with it.

Consider for a moment a wheel as shown in Figure 2. As torque is applied about the center, *o*, the sections *AB*, *BC*, and *CD* are under compression, whereas sections *DE*, *EF*, and *FG* are under tension. A sketch of the area of contact, shown in Figure 3, reveals that the front section of the area is under compression whereas the rear section is actually under tension. The fact that part of the wheel tread is under compression requires that the wheel make more revolutions per mile than would be indicated by simply considering the distance moved per revolution as the circumference of the wheel. This factor[3] may be calculated as follows

Forces at the point of contact =

$$\frac{\text{coefficient} \times \text{velocity of creep}}{\text{velocity of roll}}$$

If a steel wheel is considered, a representative value of the coefficient equals

$$3{,}500 \sqrt{\text{diameter of the wheel (inches)} \times \text{weight on axles (pounds)}}$$

For the purpose of illustration, assume a 50-inch wheel and 50,000-pound axle loading. If the rail and wheel were in a static lock, which we are attempting to show is not true, we could expect to develop 12,500-pound tractive effort. The coefficient now equals 5,530,000 and the velocity of creep equals 0.227 per cent. Thus, the locomotive in moving one mile actually causes its wheel to rotate 1.00227 miles.

A second factor, indicating that the rolling condition is actually one of small slip, is the taper applied to the wheel tread. Curves or irregularities in the track cause the wheels to move laterally on the rails from one side to the other. If the flange on one wheel is against the rail, then the opposite wheel must be running on a circle of smaller diameter, hence one of the wheels must slip as the axle moves to center itself. Note that the degree of this inherent slip is dependent on speed and that at lower speeds higher factors of adhesion are more common.

The tractive effort characteristics of a diesel-electric locomotive are shown in Figure 4. This curve cannot be expected to match the change in the factor of adhesion shown in Figure 1. If a wheel can be accelerated enough to move onto the sharply decreasing portion of the factor of adhesion curve, and no change in friction characteristics takes place, the wheel will accelerate until a new balance between the torque characteristics of the motor and the friction characteristics of the wheel takes place. This represents an idealized case and will occur only in unusual circumstances when track conditions and axle loadings remain constant. That this is possible, however, is shown by Figure 5, taken from track tests on a gas-turbine electric locomotive in which the axle accelerated and then stabilized itself at a speed approximately 13-miles per hour greater than the running speed. A more common type of slip is for the wheel to vary widely in speed as the action of the truck equalizers alters axle loadings.

Additional Factors Causing Slip

At high speeds, there are a number of factors which, singly or in combination, can cause the weight on the driving axle to be reduced momentarily. These same factors are present on steam and electric locomotives, but because of the greater inertia involved, the slip does not have time enough to reach a value at which the factor of adhesion is seriously reduced. Among the factors which can cause a temporary reduction in the weight on a driving axle are:

1. Unbalance in the driving wheel itself.
2. Eccentricity of the driving wheel.
3. Irregularities in the track, particularly switch frogs and crossings.
4. Journal boxes cramped in their guides.
5. Poor operation of the equalizers.
6. High gradient equalizer springs.
7. Weight shift.
8. Any vertical oscillation caused by resonance in the spring system.

It is very difficult to assess these factors quantitatively. For example, measured accelerations of 5 *g* to 13 *g*, *g* being the acceleration of gravity, have been obtained on the ends of axles moving through crossings at high speed. The duration of these accelerations is short, however, and by themselves they do not normally cause wheel slip. It is probable that a combination of the foregoing factors is necessary to cause high-speed wheel slip.

The other cause of high-speed wheel slip is momentary reduction of the factor of adhesion with constant axle loading. This may occur from changes in rail surface conditions caused by: mist or dew; mill scale occurring on newly laid rail; and oil, fertilizer, insects, wet leaves, and other foreign substances on the rail.

Low-Speed Slip

Low-speed slip can be started by either of the basic methods; that is by temporarily unloading an axle, or by decreasing the coefficient of adhesion. Dynamic factors such as wheel unbalance are insignificant. The subject of low-speed wheel slip, particularly the causes of low adhesion, has been reported elsewhere.

Detection of Wheel Slip

At present, there are available a number of schemes for detecting locomotive wheel slip. These are:

1. The detection of electrical unbalance between traction motors.
2. The measurement of residual motor voltage.

Figure 3 (below). Area of contact between driven wheel and rail

Figure 4 (right). Speed-tractive effort curve, 1,500-horsepower Diesel-electric freight locomotive

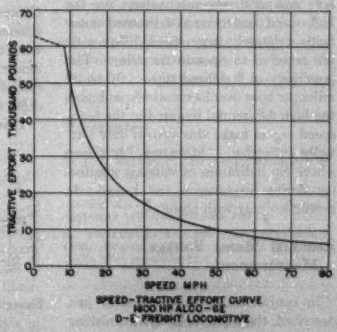

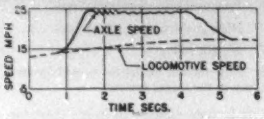

Figure 5. Oscillogram showing stable slip

3. The frequency-sensitive system.
4. Various acceleration schemes.
5. The axle-mounted commutator and brush system.
6. Individual axle generators.
7. The axle-mounted centrifugal switches.

Differential Voltage Detection

The one in most common use employs a relay connected as shown in Figure 8(A). This relay measures the unbalance in current which exists between traction motors during slip conditions. If one motor should speed up, its current drops, thereby unbalancing the bridge circuit and actuating the relay.

This system has the advantage of low cost, and since it measures electrical quantities, it is easily connected in the cab. It detects wheel slip, and a locked axle only when power is on. It does not detect overspeed, nor does it furnish locked-axle protection when the motor is disconnected.

Figure 8(B) shows the same type relay connected so as to measure differential armature voltage.

In both of these circuits the relay is subject to transient voltages due to current surges in the motors. These in turn are caused by changes in track surface causing relative movement between field and armature, commutation phenomena, and so forth.

In order to care for transient voltages and normal electrical differences in motors, it is necessary to make these relays comparatively insensitive. In the high-speed connection with shunted motor fields, relatively large speed differentials are required to operate the relay. The possibility of stabilized slips of 10 to 20 miles per hour over locomotive speed, plus the high differential required in the high-speed region make this system only partially effective. Moreover, it gives wheel-slip indication of varying sensitivity during acceleration and locked-axle protection only with power on.

Residual Motor Voltage Measurement

In conjunction with the system just described, there is a method of furnishing locked-armature protection by measuring residual motor voltage. A relay is connected across each traction motor armature. As long as residual voltage exists the relay is picked up. If, as in the case of a locked armature, no residual exists, this relay drops out.

One type of General Electric traction motor widely used on diesel-electric locomotives has a maximum residual voltage of 21.9 volts at 2,280 rpm. At 5 per cent speed, the lowest residual voltage is 0.5 volt. Thus, the relay measuring the residual must be able to operate on 2.05 per cent of the maximum voltage applied across it.

Actually, if power is taken off while moving, energy to pick up the relays comes partly from the inductive energy stored in the motor fields. If a locomotive should start with a locked axle, the protective relays could not be expected to pick up until a much higher speed was reached than that at which drop-out occurs. These relays provide locked-axle protection with power off. Occasional malfunctioning due to variations in residual voltage can be expected.

It would be possible to add a third set of relays to check on motor overspeed. Still others might possibly be included to cover rolling slip during braking (either air brakes or dynamic brakes). Such a system would offer complete protection by means of apparatus and connections entirely within the cab. The number of components required for complete wheel-slip, wheel-slide, overspeed, and locked-axle protection would be great and would probably result in unreliable operation under certain conditions.

An integrated system, independent of the traction motor power, is inherently more reliable for complete protection.

Frequency Detection

The Metropolitan Vickers Electrical Company, Ltd. has in operation one scheme in which an auxiliary pole-face winding is incorporated in the traction motor. The output frequency is then compared with frequency signals from the other traction motors.

This approach could be made to give complete protection. The high premium put on winding space within the traction motor, however, makes it unlikely that this scheme will be widely adopted in this country.

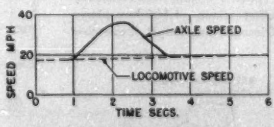

Figure 6. Oscillogram showing rapid rate of rise of wheel slip

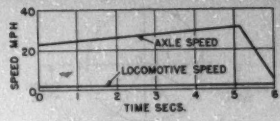

Figure 7. Oscillogram showing slow rate of rise of wheel slip

Acceleration Measurement

Various acceleration measuring methods have been suggested. At least two such devices are in fairly common use on passenger cars to prevent slide flats during braking. Deceleration rates in this service are in the order of 25 miles per hour per second during wheel sliding. By contrast, rates of acceleration during locomotive wheel slip may range from 3 to 20 miles per hour per second as shown in Figures 6 and 7. Accelerations in the lower ranges would cause unreliable operation of such devices. In addition, starting a train with a locked wheel would obviously give no indication of acceleration. It is apparent, therefore, that a measurement of velocity is necessary.

Speed Differential Measurement

One device which could be adapted to measuring locomotive wheel slip consists of a fixed commutator and a rotating brush mounted on the journal box and driven by the axle. This device measures the difference in rotative speed between any two axles. It depends upon the improbability of any two axles slipping or sliding at the same rates. If the two axles being compared have their driving motors connected in series, this is very likely true. If two traction motors are connected in series across a fixed voltage, a speed-up of one motor will cause it to develop more than half the supply voltage across its terminals. This will be accompanied by a reduction in voltage and torque, shown in Figure 9, on the other motor. Although this voltage shift does not limit the acceleration on the slipping axle, it does insure that under ordinary rail conditions the second axle will not slip. The cost of this system is high compared to the differential relay protection commonly employed. It also is probable that there will be an appreciable maintenance problem on the commutator and brush rigging.

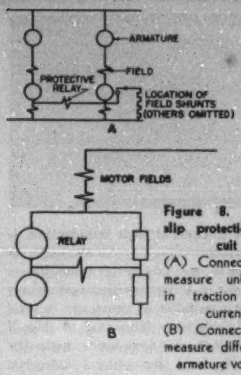

Figure 8. Wheel slip protection circuit

(A) Connected to measure unbalance in traction motor current

(B) Connected to measure differential armature voltage

Variations of this system would allow complete protection.

Locked-Axle Protection

There has very recently come onto the market another system known as the King wheel slide indicator which gives protection only against locked axles. This consists of axle-mounted centrifugal switches. As the locomotive reaches a predetermined speed, one of the axle switches (designated as the master switch) closes and applies power to similar switches mounted on all the other axles. If each of the other axle switches has tripped, indicating that all axles are turning, a light relays this information to the engineer. This device furnishes only locked-axle protection and must be coordinated with one of the other systems described in order to give complete wheel-slip protection.

Individual Axle-Generator Protection Scheme

The Alco-GE gas-turbine electric locomotive was built to study the application of a gas turbine to locomotive service. One of the factors under observation was the wheel slip characteristics of the unusual axle arrangement. The system installed consisted of individual axle-mounted generators, of the same type as those used for controlling transition on Alco-GE locomotives, with a relay to detect the difference in voltage between each generator and the average for all eight generators. Specifications were that the system should operate on a speed differential of 5 miles per hour. This was to allow for normal differences in wheel diameter. Since the generators are of the permanent-magnet type, the system is independent of any locomotive power supply. It is possible to protect against motor overspeed by measuring the absolute value of generator voltage. This system answered the requirement of furnishing complete protection, but the cost of the axle generators makes its widespread use doubtful.

Requirements for Complete Protection

A study of the oscillograms of actual slips obtained on the Alco-GE gas-turbine electric locomotive and also diesel-electric switchers and road locomotives allows a consideration of the deficiences existing in the present methods of wheel-slip detection and makes it possible to draw up a tentative set of specifications for a complete wheel-slip protection system. The system should furnish four types of protection: (1) wheel-slip protection during acceleration; (2) wheel-slip protection during braking (air or dynamic); (3) locked-wheel protection; and (4) overspeed protection.

At low speeds, the protective devices should operate at speed differentials of about 5 miles per hour. At speeds of 40 miles per hour or greater, the allowable slip should be increased to permit a slip equal to 10 to 15 per cent of locomotive speed. The reason for this tapering of sensitivity at higher speeds is to allow self-recovery due to changes in rail condition. It has already been pointed out that starting of high-speed slip is usually a transient phenomenon. Therefore, if normal rail conditions are restored, wheel slip will often stop without requiring corrective action, with its attendant loss in tractive effort. In any case, if the rate of rise should exceed 10 miles per hour per second, corrective action would be taken regardless of the actual speeds involved. A study of the various oscillograms taken reveals no case of recoverable slip occurring at acceleration rates greater than this. Before locked-axle protection can function, the locomotive must attain some finite speed sufficient to determine that an axle is actually locked. A fair compromise for this figure seems to be 5 miles per hour.

During dynamic braking, it is desirable to be able to load each wheel up to the maximum available factor of adhesion. If the traction motors are properly connected, it is not possible to lock wheels during dynamic braking because at zero speed, the power output of the motor is zero. The fact that there is little likelihood of damaging the traction motor or the wheels during small values of slide in

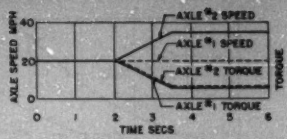

Figure 9. Torque loss on series-connected motors

dynamic braking, coupled with the desire to get maximum braking effort from the locomotive should allow higher values of permissible slide to be established. A value may be tentatively set at 20 per cent of the locomotive speed or 10 miles per hour, whichever is higher.

The overspeed feature of the system should be set at whatever value the manufacturer recommends for the motor with which the locomotive is equipped.

The correction initiated by such a wheel-slip scheme should be automatic and should be limited to the unit affected. In any practical control scheme requiring action by the engineer, he can only correct slipping on any one unit by reducing the power on all. The resultant loss in tractive effort is undesirable. In overspeed, the time lag occurring between the signal to the engineer and the actual reduction in power could be great enough to allow permanent damage to the motor, hence the requirement for automatic correction. A cab indication of slip is necessary to warn the engineer of repeated slips so that he can reduce power. Locked-axle protection definitely requires a cab indication.

Two approaches to this problem exist. One is to add more devices to the schemes already used to provide partial protection. The other is to develop one integrated system for the whole protective function.

Modifications to existing systems have been made by several railroads, and these are now undergoing tests. The idea of a single protective system has been tried on a much smaller scale. Only further experience in actual service can prove the superiority of either of these two approaches.

References

1. Wheel Slip and What Can Be Done About It, C. L. Ekergian. *Air Brake Association* (Chicago, Ill.), September 21, 1949.

2. Track Tests of Electric Locomotives. *Railway Age* (New York, N. Y.), 101, number 2, September 1936, pages 374–80, 412–18.

3. Vibration of Rail and Road Vehicles, B. S. Cain. Pitman Publishing Company, New York, N. Y., 1940, pages 152–53.

No Discussion

A New Resilient Class-H Material for the Insulation of Traction Motor Field Coils

J. ROSS REED
MEMBER AIEE

J. J. TYNER
NONMEMBER AIEE

THE rapid shift by the railroads of this country to the diesel-electric locomotive as standard motive power and the consequent tremendous increase in heavy d-c traction equipment has brought to the fore many problems to vex both the designers of the original equipment and the maintenance men who must keep it in economical operation. Among these problems is that of finding electrical insulation for traction motors which will withstand for long periods of time the rigors incident to the severe conditions of operation encountered in railway service. Much has already been done to develop and utilize electrical insulating materials with a high degree of thermal stability, and class-*H* materials[1] are now standard on a large percentage of traction motor armatures in service. Class-*B* materials,[1] however, are still universally used for the insulation of traction motor field coils, and their shortcomings for this application contribute heavily to the cost of maintenance in this class of equipment. This paper describes the development and application of a new resilient class-*H* insulating material which is being used successfully on field coils by at least one of the major American railroads.

Standard class-*B* materials are not best suited to meet the conditions of service imposed on high-speed railway traction motors. In the first place, temperatures are normally encountered which reduce the effective life of these materials to a point where they soon constitute a weak link in the chain of components making up the present-day traction motor. As the life of the electrical insulation is spent, the coils become progressively more vulnerable to the effects of shock and vibration which are an inescapable part of railway service. Any shrinkage of the insulation allows relative motion between the coils and the pole-piece mountings. This movement of the coils soon produces abrasion of both the insulation and the pole piece or coil support flange itself. Figure 1 illustrates a typical example of the results of loose field coils abrading the metal flange on which the coils are secured.

In addition to promoting looseness of the coils, this loss of life in the insulation is accompanied by a serious increase in brittleness and resultant decrease in resistance to abrasion. Thus, a vicious circle of events is produced and electrical failure of the insulation is the inevitable result. To make the situation even more serious, the insulation cracks as it becomes brittle. This allows conducting contaminants, such as carbon dust and moisture, to permeate the insulation and destroy its effectiveness as a dielectric protection for the electric conductors in the body of the coil.

The use of class-*H* materials for the insulation of field coils of many types of motors has been practiced successfully for a number of years. Conventional class-*H* insulating materials give adequate protection against heat and provide a long life insulation for the average motor in the commonly encountered conditions of severe industrial operation. Here the problems of severe shock and high-amplitude vibration are of relatively minor importance. Under these conditions, a hard finished coil, which will maintain its rigid dimensions for long periods of time at high temperature, is satisfactory.

When the need for better insulation on field coils in heavy traction motors was evident a number of years ago, several sets of fields were fabricated to class-*H* specifications in accordance with the standards used for general industrial motors. Rigid coils of the type mentioned previously were manufactured and installed in test motors which were placed in high-speed passenger service for actual road testing. The results of these tests have been highly satisfactory and show conclusively that these coils have much to offer over the standard class-*B* coils for this type of service. One of the test motors equipped with these fields now has in excess of 750,000 miles of service to its credit. The fields of this motor at the last shopping showed no apparent deterioration after 742,000 miles of service. All of the coils were still tightly seated and the insulation was still pliable with no signs of external cracking.

The condition of the coils contrasts strongly with that of standard field coils in the same type motors operated under the same conditions. The average insulation life for standard coils is between 500,000 and 600,000 miles. After that amount of service, the external ground insulation of the coils is dry, brittle, and cracked, and usually must be replaced for further service.

Though the type of class-*H* coil described has definite advantages over the standard class-*B* insulated coils, even in railway applications, it was evident that coils with greater inherent resiliency would offer still further advantages in such service. Because of the unusual properties of silicone rubbers, experiments were initiated to determine if some member of this general class of material might

Paper 50-182, recommended by the AIEE Land Transportation Committee and approved by the AIEE Technical Program Committee for presentation at the AIEE Summer and Pacific General Meeting, Pasadena, Calif., June 12–16, 1950. Manuscript submitted March 16, 1950; made available for printing May 1, 1950.

J. Ross Reed is with the National Electric Coil Company of Columbus, Ohio, at Altadena, Calif., and J. J. Tyner is with the Dow-Corning Corporation, Los Angeles, Calif.

Figure 1 (left). Metal field coil flange showing coil tape abrasion marking resulting from motion between coil and flange

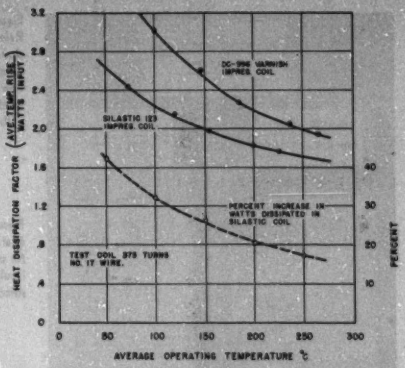

Figure 2 (right). Thermal conductivity of Silastic versus silicone varnish impregnation

be adaptable to this application. It was obvious that a coil mounted between rubber "springs," which would maintain their resilience for long periods of time at high temperatures, would be more easily tightened in place and made to remain tight than would a rigid coil, which must of necessity be built to very close mechanical tolerances to obtain a tight fit. It also was recognized that silicone rubbers possessed several other properties which indicated unique suitability for this application. These materials have found wide industrial application because of their chemical resistance, high thermal conductivity, extreme moisture resistance, and good dielectric properties, along with the fact that they maintain these properties over a temperature range from −70 degrees Fahrenheit to 500 degrees Fahrenheit.

Silicone rubbers have dielectric properties comparable to the best resilient insulating materials at room temperatures and far superior to them at high temperatures.

Unlike resinous coatings and insulating materials, these rubbers do not become progressively more brittle at high temperatures and have virtually unlimited life at 400 degrees Fahrenheit. Silicone rubbers have exceptional resistance to electric arcs and flashes even under conditions of high humidity, and give a surface that will not carbonize to produce a resultant low-resistance track.

In addition to these properties, silicone rubbers have characteristically high thermal conductivities as compared to resin-bonded insulating materials. Curves showing this relationship are given in Figure 2. From this it may be seen that a coil insulated with silicone rubber will operate about 15 per cent cooler than a comparable coil insulated with resin-bonded materials. Thus, the temperature resistance of silicone rubber is augmented by the lower temperature of operation of coils insulated with it, as compared with standard insulated coils operated under the same conditions. This will, of course, still further increase the life expectancy of such a coil.

To adapt a silicone rubber for use as insulation on field coils, it was necessary to produce the materials in such form that it could be easily applied to form a sealed sheathe around the coils. It was recognized that this covering must be continuous, leaving no openings that would admit moisture or other contamination. The use of silicone rubber in paste form was considered and rejected because of the many mechanical difficulties involved. To apply the silicone rubber in a precured form introduced the equally serious problem of sealing any joints which would be formed. After considerable experimentation, it was decided that a pressure sensitive tape would be ideal to form a solid mass of insulation, free from voids and unsealed joints. A Silastic tape was developed that consisted of Fiberglas cloth coated and impregnated with silicone rubber. On one side of this tape the silicone rubber is completely cured, while on the other side, it is only partially cured and remains tacky, subject to subsequent vulcanization. This material proved admirably suited for application to field coils and other rigid sections. The presence of the reinforcing glass fabric gives the tape sufficient strength to allow considerable tension in application without any appreciable reduction in thickness or other mechanical distortion. Actually, the 20-mil tape, as finally developed, has a tensile strength of 80 pounds per inch of width, while a similar tape 12 mils in thickness has a tensile strength of 60 pounds per inch of width.

This tape can be vulcanized and cured in an air-circulating oven, or even in use, if operating temperatures are sufficiently high, although this latter method is not suitable for field coil applications where compressive strength is required at the time of application of the coils to the motor frame. Actual curing time, of course, will vary with the mass of the unit taped and with the thickness of the taped section. However, satisfactory vulcanization of the tape can be obtained in 15 minutes at 260 degrees Fahrenheit after the materials have attained that temperature. Following the initial vulcanization, it also was found desirable to give the tape an after cure in an air-circulating oven at a temperature above the maximum operating temperature of the coil, or at 350-400 degrees Fahrenheit, whichever is higher.

To produce complete vulcanization of the tape into a solid mass, it also was found that pressure between laps was desirable in addition to that obtained in taping. This was easily accomplished by covering the Silastic tape with a tightly pulled serving of glass tape prior to vulcanization.

The relative abrasion resistance of a section taped with this material compared to organic bonded Fiberglas is well illustrated in Figure 3 In these tests, similar sections were taped with the two materials and subjected to a sandblast for periods of 6 seconds with results as shown.

Further tests were run to determine the effects of continuous immersion in an aqueous solution. Figure 4 shows the effect of immersion in salt water for a period of 40 days on the insulation resistance of this material.

Built-up sections of this tape showed a minimum consistent dielectric strength of 300 volts per mil in the cured condition with two layers of 20-mil tape. Surface resistivity after 24 hours at 50-per cent humidity was in excess of 10^{15} ohms. After 96 hours at 96-per cent relative humidity surface, resistivity was still in excess of 10^{16} ohms. Volume resistivity

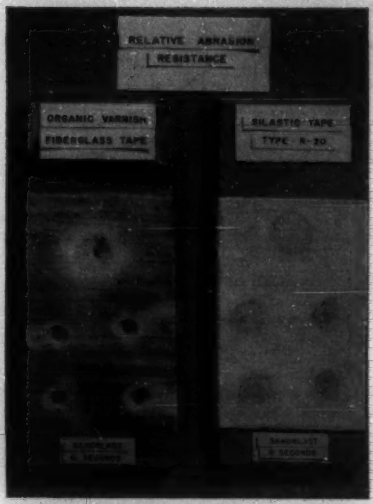

Figure 3 (left). Relative abrasion resistance of Silastic insulation and organic varnish treated Fiberglas tape

Figure 5 (right). Main field coil for traction motor insulated with silicone rubber

after 24 hours at 50-per cent humidity was in excess of 10^{13} ohms-centimeters and was in excess of 10^{10} ohms-centimeters after 96 hours at 96-per cent relative humidity.

Following the development of this tape and the determination of its general characteristics and properties in the laboratory, a number of test coils was insulated. This was done to determine the best methods of application to both new equipment and to equipment which was to be reinsulated after previous service, as well as to give a practical basis for further physical tests and cost estimates. In many applications, particularly on new coils, it is thought that this type of tape can well replace all standard types of insulation. However, the elimination of all mica from standard traction motor field coils seemed too radical to be readily accepted without conclusive tests and operating experience. In addition to this, the reinsulation of field coils where the standard organic bonded turn insulation is not to be disturbed presents another problem. Organic materials, or even uncured silicone varnishes, in contact with Silastic tape will seriously inhibit its vulcanization. Where these materials are inherent in the coils being taped, some sort of a shield must be provided to separate them from the Silastic tape. Silicone bonded Mica-glas tape is well suited for this application and gives an additional dielectric build-up to the total insulation.

Taking into consideration all of the foregoing factors resulted in the following general specifications for reinsulation of a typical traction motor field coil, previously cleaned and stripped of old insulation. The coil first is dipped in silicone varnish and allowed to drain and air-dry until the varnish is tacky. Following this, the coil is taped entirely with a butt-lapped serving of 10-mil glass tape that previously has been treated with silicone varnish for ease of handling. This glass tape serves as a protection between the bare copper and whatever mica is placed next on the coil. For our experiments and subsequent production we have used a one half-lap serving of 7-mil silicone-bonded Mica-glas tape as the next element in our build-up. This is followed with a no-lap serving of 10-mil glass tape to draw the mica down and to reduce the voids.

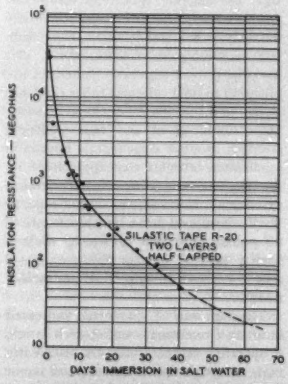

Figure 4. Silastic winding insulation resistance after immersion in salt water

Following these three servings of tape, the coil is heated to 200 degrees Fahrenheit and hot-dipped in silicone varnish for 5 minutes and allowed to drain before baking at 300 degrees Fahrenheit for 3 hours. At this stage of the build-up the insulation is securely bonded with silicone resin and is well compressed into a solid mass relatively free of voids. All volatile solvents have been expelled and the organic materials in the body of the coil have been sealed off effectively so as to preclude any interference with the subsequent vulcanization and cure of the Silastic tape. In addition, there is a solid base over which the Silastic tape may be pulled tightly to give a relatively high pressure between servings.

At this point, pads of silicone rubber are placed on the prospective bearing surfaces to give enough dimensional build-up so that the completed coil will meet specifications in this respect. Silicone rubber paste may be spread on the coil at this stage of the build-up to further fill in any low places and to help strengthen the bond between the silicone-bonded mica and the Silastic tape, which is next applied as a half-lapped serving over the entire coil. It is suggested that a 20-mil tape be used for this purpose and that care be taken to apply it uniformly and with as much tension as is practicable. The thickness and amount of this tape can be varied depending on the amount of resilient material desired in the total build-up. A final serving of 10- or 15-mil glass tape is used half-lapped to increase the pressure between servings of the Silastic tape and to give added mechanical protection to the silicone rubber.

The coil should then be placed in a 300-degree Fahrenheit oven for 1 hour to vulcanize the Silastic tape. It is then hot-dipped in silicone varnish and baked for 12 to 16 hours at 300 to 400 degrees Fahrenheit. The higher temperature is preferable if the materials of which the leads are made will not be injured, although satisfactory cure can be obtained even as low as 300 degrees Fahrenheit. The baking time will vary inversely with the temperature of the cure, which should in any event be higher than the highest operating temperature expected in service.

Coils were insulated to the foregoing general specifications and tested in the laboratory to determine their physical characteristics. A typical coil thus insulated is shown in Figure 5. Dielectric tests were made by clamping metal plates to the surfaces of the coils and applying test voltages while these plates were under pressure. An average breakdown strength of 20,000 volts was determined at room conditions in this manner.

Additional tests were made on this insulation build-up to determine the degree of compression-set that might be expected in service. At a pressure of 40 pounds per square inch, no compression-set could be determined after 2 weeks at 380 degrees Fahrenheit. On a total Silastic build-up of 64 mils thickness, a compression-set of 1.2 mils was produced by a continuous pressure of 75 pounds per square inch for 2 weeks at 380 degrees Fahrenheit. During this time the resiliency of the material was not altered measurably.

Cost estimates at this time indicated that the build-up described would be attained at a figure in a comparable price range to standard class-*B* insulation.

In order to determine the results of actual road service on this type of insulation, one of the larger railroads was approached with the results of the laboratory tests and the cost figures which had been determined. A total of more than 1,300 field coils has been reinsulated in this manner and have been placed in regular service without a single failure of any kind to date. It is not possible at this time to give ultimate life statistics for this type of insulation on the basis of actual service simply because not enough time has elapsed yet for their complete determination. However, from the service indications which we now have, it is confidently expected that loosening of field coils in railroad service and consequent movement on pole pieces will be entirely eliminated.

With this major cause of field coil troubles eliminated, the insulation life expectancy of this class-*H* build-up as compared to other types of insulation for various temperatures should conform to the curves given in Figure 6. Certainly at the temperatures at which traction motor fields are often operated, the life expectancy of this insulation should be many times that of the class-*B* materials now accepted as standard.

Additional tests are being conducted to determine the effect of complete elimination of mica, for example, in new coil construction where there is no need for blocking off the organic materials as there is when old coils are being reinsulated. If this proves feasible, as is indicated at present, there may be some savings over presently-accepted standards of field coil insulation.

On the basis of the tests at the laboratory level and the results of regular production and road service, there seems little doubt that silicone rubber offers a much-needed solution to the problem of keeping traction motor field coils tight over long periods of time at elevated temperatures of operation. In addition to this, it offers all the advantages of class-*H* construction at a cost comparable to that of standard class-*B* construction in a coil which actually will operate at a substantially lower temperature than its class-*B* counterpart under the same conditions of operation.

Figure 6. Life expectancy curves of class-*B* and class-*H* windings at various hot-spot temperatures

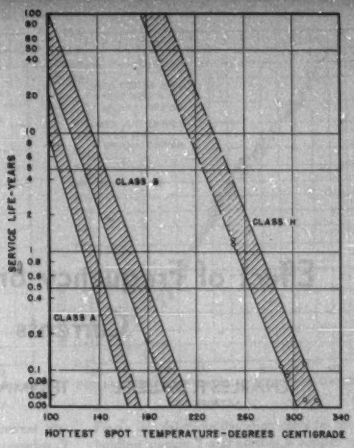

Reference

1. Introduction to AIEE Standards. *AIEE Standard Number 1*, June 1947.

No Discussion

Effect of Frequency on Perception Currents

CHARLES F. DALZIEL
MEMBER AIEE

THOMAS H. MANSFIELD
ASSOCIATE AIEE

Synopsis: The predominating sensation produced by gradually increasing direct current is warmth in the palm of the hand or wrist. Sensations caused by alternating currents below 10,000 cycles are characterized by a tingling or pricking sensation which is localized in the area adjacent to the point of contact, and at very low frequencies the muscles tend to follow the alternations of the current waveform. For frequencies between 10,000 and 100,000 cycles, the sensations are similar to those at the power frequencies, but they are less intense, and perception occurs over larger areas around the point of contact. An abrupt change in the response occurs between 100,000 and 200,000 cycles when the sensation becomes one of internal heating, and heating is believed to be the only sensation produced by currents in excess of 200,000 cycles. The current required for perception increases with increasing frequency, and between about 1,000 and 100,000 cycles the current is nearly proportional to frequency. Approximately 150 men were used in these investigations and it is believed that a sufficient number were used to permit valid statistical predictions to be made, not only for the particular group tested, but also for a normal cross section of the adult male population of the country.

ELECTRIC currents which are just perceptible are important, as it is essential that the user not get the sensation of electric shock when using electric appliances, hand tools, or other electric equipment.[1] Shocks produced by currents near the threshold of perception are generally considered annoying rather than dangerous; however, when such shocks are unexpected, they are startling, and serious accident may result as a secondary effect. For example, an unexpected electric shock, far too feeble to cause injury due to direct effects of the electric current, might produce a sudden movement and cause subsequent contact with a dangerous mechanism, or it might cause loss of balance with an ensuing fall which might cause painful injury.

The investigations reported in this paper were undertaken to expand the knowledge of the effects of electric current on the human body by observing the phenomena of perception under several contact conditions for direct current and for sine-wave alternating currents from 60 to 200,000 cycles per second. The experiments were conducted in the electrical engineering laboratories of the University of California at Berkeley, during the academic years 1940 and 1948–49. Four women and 143 men participated in the investigations.

Only subjects apparently in good physical condition were used in the study, and only those parts of the skin which were free from cuts and abrasions were subjected to quantitative tests. Moist contacts were used in the investigation to minimize the range of contact resistances, and to permit the use of low voltages for safety. As a result of the low voltages employed only minute sparks were produced when the subject interrupted the current. Care was exercised to avoid causing burns at the points of contact with the body, and although burns are extremely important, of necessity this subject was not investigated. It is entirely possible that arcs might occur with commercial apparatus at the higher perception current levels corresponding to the higher frequencies, and these arcs might cause painful burns, especially if sustained for a considerable period of time.

The subject sat in a relaxed position in a chair so located that he was facing away from the test equipment. After the subject was prepared for the test, he was told that the operator would slowly increase the current, and he was asked to report when the first sensation was observed. When the subject perceived the current, the increase in current was stopped, and the magnitude was noted. The current was then decreased to zero in preparation for another run. One or two trial runs allowed the subject to become acquainted with the testing procedure and the sensations resulting from the frequency being investigated. Three or four determinations of the minimum current perceived with slowly-increasing current were then made and the values were recorded. The results of the trial runs were not recorded, as the purpose of these runs was to acquaint the subject with the sensations involved at each frequency. This technique yielded a conservative value, as the current required for perception in the first determination for each subject at any frequency was generally somewhat higher than subsequent values.

Throughout this investigation an individual's threshold of perception at a given frequency is taken as the mean value of current just causing sensation when using a subthreshold approach. The threshold of perception for a group is taken as the mean value of the group. The current likely not to be perceived is taken as that value of current which is detectable by only 0.5 per cent of the group, and the upper limit of perception current is taken as that current perceived by 99.5 per cent of the group.

Aside from physiological factors which were beyond the control of the investigators, five factors are important in determining the current which can just be perceived. These factors are: point of contact; type of contact; rate of increase

Paper 50-184, recommended by the AIEE Safety Committee and approved by the AIEE Technical Program Committee for presentation at the AIEE Summer and Pacific General Meeting, Pasadena, Calif., June 12–16, 1950. Manuscript submitted October 31, 1949; made available for printing April 25, 1950.

CHARLES F. DALZIEL is Professor of Electrical Engineering, University of California, Berkeley, Calif., and THOMAS H. MANSFIELD is Electrical Engineer with Tracerlab Inc., Berkeley, Calif.

Acknowledgment is given Spencer H. Robley who, in 1940, obtained the experimental data for the group of 115 subjects. He was senior student in electrical engineering, University of California, Berkeley, at the time the study was made.

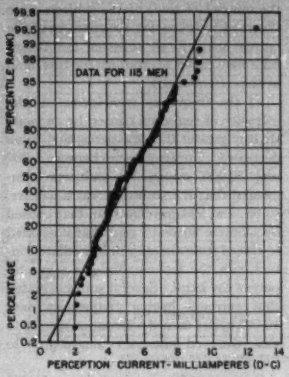

Figure 1. D-c perception distribution curve for hands holding number 7 copper wires

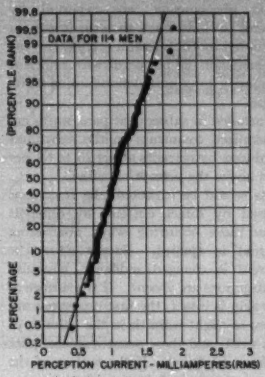

Figure 2. 60-cycle perception current distribution curve for hands holding number 7 copper wires

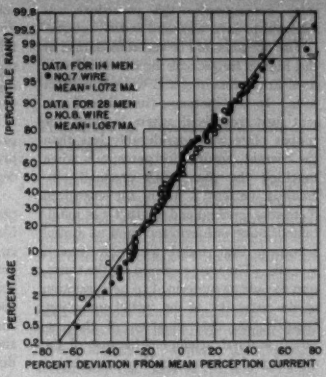

Figure 3. 60-cycle deviation curve for hands holding number 7 and number 8 copper wire electrodes

of current; frequency, and wave form.

Inasmuch as the point of contact with the skin has considerable effect on the level of the current required for perception, it is obvious that a great many different perception thresholds could be investigated. Considerable thought was given to this phase of the problem, and it was decided to concentrate on the hand and fingertips, since contact with the hands is responsible for many of the complaints caused by electric currents near the perception threshold. Preliminary tests were made on the tongue, and although the results of this threshold are of minor practical importance, comparison with the results obtained on the hands emphasizes the range of values for different points of contact on the body.

Three types of contacts were used. These consisted of holding, touching, and tapping test electrodes. In the holding contact tests, a smooth wire or wires were held in the palms of the hands or placed lightly on the tongue. For the touching contact tests, the middle finger was placed lightly on a polished flat copper plate. In the tapping contact test, the middle finger tapped the copper plate at a rate of once to twice a second. Two identical electrodes were used in the first series of tests. In the second series the circuit was completed by an indifferent electrode, consisting of a flexible lead strip wrapped with gauze soaked in salt solution which was clamped around the upper arm.

The magnitude of the current, accommodation effects, and the effect of frequency and wave form on perception will be discussed later in the paper. In the first series, tests were made on 115 men, using direct current obtained from batteries, and commercial 60-cycle alternating current. For subsequent tests, made on 28 men and four women, the a-c power supply consisted of a Hewlett-Packard model *200C* audio-frequency oscillator and a power amplifier. The output was continuously monitored with a Dumont model *208B* cathode-ray oscilloscope, and care was exercised to maintain sinusoidal waveshapes.

General Observations

In addition to the numerical data, certain phenomena were observed relative to the sensations caused by the passage of electric current through the hands. These observations are of assistance in interpreting the quantitative results of the investigation, and will be discussed prior to presentation of the experimental results.

At the outset it was planned to establish the perception current on the hands with both gradually increasing and decreasing currents in anticipation that this procedure would yield an accurate determination of the threshold of perception for a given frequency. However, it was found that when the current was adjusted to a value slightly greater than an individual's threshold of perception, and was then gradually decreased, erratic values were obtained and the subject reported difficulty in determining when the sensation actually ceased. A particular individual might report that he thought the sensation had ceased at current values varying from slightly above his perception value for gradually increasing current to a current of approximately one-half of this magnitude. Results of the tests performed with decreasing current were so variable in comparison with the close agreement of the individual's response at a particular frequency with increasing current that little information of practical importance appears to be gained from this type of test. It was hoped that some observations attributable to aftereffects, or to accommodation processes, might be explained using the intended technique, but the great variation in the reported values prohibits the drawing of worth-while conclusions. The original plan was abandoned, and except for a few preliminary tests, a subthreshold approach was used throughout the investigations.

For tests using frequencies of more than approximately 30,000 cycles, it was observed that the rate at which the current was increased had an appreciable effect on the current level at which perception occurred; in contrast, the perception current at lower frequencies appeared to be independent of the rate at which the current was increased. For higher frequencies, as the current was increased at faster rates the subject reported the presence of sensations at successively lower levels of current. As a result, an attempt was made to approach the higher frequency thresholds at a rate of current increase of approximately 3 to 6 milliamperes per second. Varying the rate at which the current was increased to roughly 75 per cent of the threshold value failed to produce appreciable variations in the threshold provided the remainder of the approach was made at the established

rate; consequently, this procedure was followed to save time and reduce fatigue.

The phenomenon of accommodation at the higher frequencies again manifested itself in the touching and tapping contact tests. In this instance, the value of current just perceived when tapping the copper plate was considerably less than the current required for perception when touching the plate with gradually increasing current. When the energized plate was touched and contact was maintained many subjects reported an initial sensation that faded away in several seconds. The time required for the sensation to fade away seemed to be a function of the intensity of the initial sensation. Quantitative determination of this interval was not attempted because of the difficulty of determining the moment that sensation ceased.

Several subjects reported that they were able to draw slight sparks from the copper plate when the contact was broken during the tapping contact tests at the higher frequencies. The minuteness of the pin-point burns caused by these sparks, which were not visible in a normally lighted room, is attributed to the fact that the voltage used in these tests was sufficient to maintain a spark for only a very short period of time as the finger moved away from the electrode. The open circuit voltages employed varied between about 20 and 100 volts; maximum current was about 112 milliamperes.

Several times during the holding contact investigations the subjects reported a definite sensation when they released the electrodes while a current slightly below the perception level was flowing. The same phenomenon was reported by several subjects when the circuit was interrupted by the operator. However, the phenomenon did not occur with sufficient regularity to permit determination of its cause.

Included in subsequent paragraphs are generalized comments on the sensations produced by currents about 25 to 50 per cent above the perception value.

As would be expected, the sensations caused by direct current are different from those occurring when alternating current is applied. Except when the current is changed suddenly, muscular contractions are absent. If the surface of the skin is intact, the first sensations are those of slight warmth in the palm or in the wrist, and these sensations are quite difficult to detect. If the surface of the skin has minor defects, sharp piercing sensations are produced with very low currents.

The outstanding feature of the sensations in the power frequency range is the sharpness of the sensation when the perception current is exceeded. This sensation is variously described as a tingling or pricking sensation at the point of contact. Many of the subjects also observed this sensation under the indifferent electrode. This effect was not reported at frequencies in excess of 1,000 cycles. The presence of sensation at the indifferent electrode was attributed to the presence of small imperfections in the surface of the skin under this electrode, and was probably due to high-current densities at tender spots, but no explanation is offered for its disappearance at the higher frequencies. At very low frequencies (5 to 20 cycles) the muscles of some of the subjects were observed to follow the alternations of the current wave form, however, insufficient data were taken to establish the threshold at these frequencies.

As the frequency was increased, the intensity of sensation caused by currents slightly greater than the perception value decreased. For frequencies between 1,000 and 10,000 cycles, the subjects commented that the sensation was smoother, softer, and less piercing than that caused by 60-cycle currents, and that it seemed to spread from the area in immediate contact with the test electrode to a greater part of the hand. Several subjects stated that currents having frequencies near 10,000 cycles caused a sensation similar to that observed when the hand "goes to sleep."

Currents of frequencies between 30,000 and 90,000 cycles were reported to give an increasing spread of sensation away from the test electrode, and to cause a sensation of drawing of the skin or of a pressure on the hand. As the frequency increased, the sensation was less intense.

The touching and tapping contact tests using frequencies between 100,000 and 200,000 cycles brought forth the opinion from all subjects that the sensation caused by the higher frequencies was one of heat rather than of the muscle stimulation noted at the lower frequencies. After the subject had reported this change in sensation, an attempt was made to determine the frequency at which the change occurred. A majority of the subjects first became aware of the change in sensation at approximately 100,000 cycles. Several subjects noticed it at about 150,000

Figure 4. Effect of frequency on perception current for hand holding number 8 copper wire

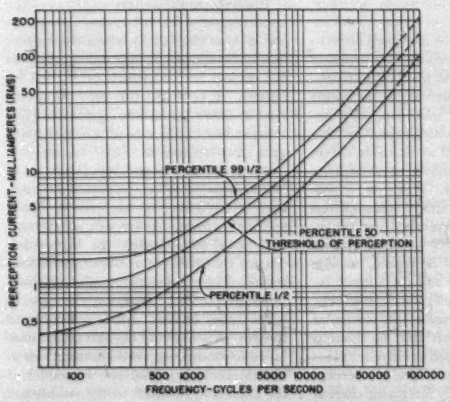

Figure 5. Effect of frequency on perception current with middle finger touching copper block

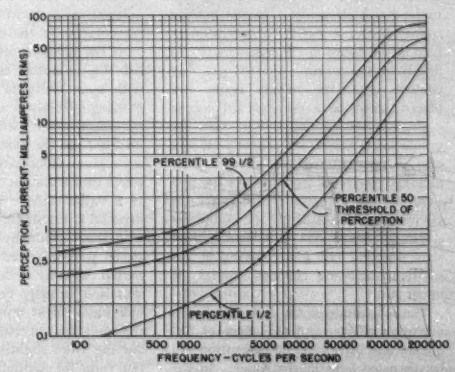

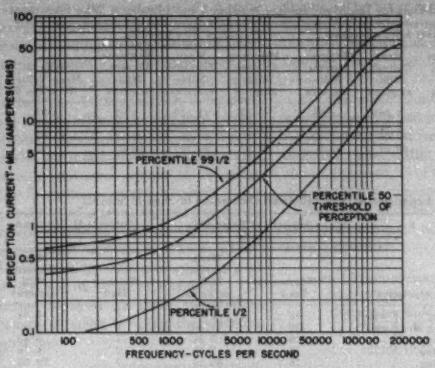

Figure 6. Effect of frequency on perception current with middle finger tapping copper block

cycles, and two subjects failed to observe any material change in sensation until a frequency of 200,000 cycles had been attained. Apparently the change in sensation is a definite change, rather than the gradual changes experienced at frequencies below 100,000 cycles. The sensation of heating at frequencies of 100,000 cycles also was reported by A. E. Kennelly and E. F. W. Alexanderson in their studies on this subject.[2]

The current required for perception at frequencies of 100,000 or more cycles was less dependent upon the rate of increase of the current than at frequencies between 30,000 and 90,000 cycles. A second phenomena was observed that indicates the difference in the nature of perception current in the higher frequency range. When currents of 100,000 or more cycles were adjusted to values slightly less than the perception values and maintained constant, perception was reported after an interval of several seconds. In contrast, for frequencies less than 100,000 cycles, currents of slightly less than the perception value were not perceived after an interval of several minutes.

These changes in perception phenomena with frequency also are apparent from the experimental data. It was observed in this investigation, and also in other investigations involving the response to electric stimulation[4,5,6], that regardless of the current required to initiate a given response, as long as the phenomena are similar, the deviation curves derived from the experimental data will have nearly identical slopes. It was noted that the deviation curves for the touching and tapping contact tests have the same slopes for a frequency range from 1,000 to 70,000 cycles. Similarly the holding contact deviation curves have the same slope for frequencies between 1,000 and 60,000 cycles. At very low frequencies the phenomena are more complicated as the muscles tend to follow the current alternations, and the deviation curves have different slopes. At the very high frequencies stimulation of the heat sensory mechanisms predominate, and again the slopes are different. The transition is completed between 100,000 and 200,000 cycles, and it would seem reasonable to expect that deviation curves for frequencies higher than 200,000 cycles might have slopes similar to those obtained for the 200,000 cycle tests.

Threshold of Perception on the Tongue

The current which can just be perceived with two contacts placed lightly on the tongue was determined using direct current and 60-cycle alternating current. The electrodes consisted of two number 18 wires, 1-inch long, separated by means of a bakelite separator. Platinum wire was used to reduce local galvanic effects. The electrodes were sterilized, washed with water, and dried between tests on different subjects. During the test, the subject held the electrodes lightly on the tip of his tongue and indicated when he first observed sensation as the current was gradually increased. There was considerable variation between successive tests on the same individual, and the average of several trials was taken as the perception value for the individual. The sensation might be described as one of taste, and is distinctly different from the characteristic tingling or warmth usually associated with

Table I. Statistical Data for 28 Men: Effect of Frequency on Perception Current

	Holding Number 8 Wire			Touching Contact			Tapping Contact		
Frequency, Cps	Subjects Used	Percentile 50 Milliamperes	Deviation at 1/2 and 99 1/2, in per cent	Subjects Used	Percentile 50 Milliamperes	Deviation at 1/2 and 99 1/2, in per cent	Subjects Used	Percentile 50 Milliamperes	Deviation at 1/2 and 99 1/2, in per cent
60	28	1.067	63	25	0.36	75	25	0.36	75
300	25	1.234	50						
1,000	25	2.299	40	24	0.65	70	24	0.65	70
3,000	25	4.828	40						
10,000	25	12.13	40	25	3.57	70	25	3.51	70
30,000	25	37.14	40						
40,000	25	53.67	40	24	15.96	70	24	14.04	70
50,000	25	70.10	40						
60,000	25	85.49	40						
70,000	19	101.5*		25	32.20	70	23	25.03	70
100,000				25	43.80	65	25	37.84	65
150,000				25	55.40	50	25	48.51	55
200,000				25	63.63	35	25	55.76	50

*Corrected for size of sample.

Table II. Experimental Data for 28 Men and 4 Women Holding Number 8 Wire Electrode

	Men			Women		
Frequency, Cps	Minimum Current, Milliamperes	Mean Current, Milliamperes	Maximum Current, Milliamperes	Minimum Current, Milliamperes	Mean Current, Milliamperes	Maximum Current, Milliamperes
60	0.47	1.067	1.60	0.85	1.18	1.57
300	0.82	1.234	1.78	1.20	1.27	1.47
1,000	1.67	2.299	2.86	1.70	2.06	2.32
3,000	3.70	4.828	6.55	3.33	4.37	5.03
10,000	8.60	12.13	15.2	9.65	10.96	13.5
30,000	27.1	37.14	48.5	27.9	30.4	31.8
40,000	36.8	53.67	76.3	35.8	42.0	46.5
50,000	48.4	70.10	89.5	52.6	55.0	58.6
60,000	65.0	85.49	112.0	64.6	67.7	70.0
70,000	74.2	94.95	107.8	77.5	80.5	85.1
80,000	89.5	100.3*	106.5	91.0	94.7	100.0
90,000	101.5	104.0†	106.4	100.8	102.7	105.7

*Data for 6 men.
†Data for 2 men.

electric stimulation applied to other parts of the body.

The results using direct current for 115 men were: 44.7 microamperes mean; 16 microamperes median; 0.6 microampere minimum; and 783 microamperes maximum. Results for these men using 60-cycle alternating current were: 45.3 microamperes mean; 30 microamperes median; 4 microamperes minimum; and 315 microamperes maximum. The threshold of perception on the tongue is taken as the mean value and is approximately 45 microamperes for either direct current or 60-cycle alternating current.

It is apparent from these data, and also from a detailed statistical study, that the response did not follow a normal distribution but was skewed positively (toward the higher values). These findings are exceptional as the physiological response of a large group usually follows a normal distribution. A tentative explanation for the skewed response is that the small separation of the electrodes permitted the saliva on the surface of the tongue to shunt part of the current from penetrating to the nerve endings deeper in the tissues. Possibly the response might have more nearly approached a normal distribution had one electrode been placed on the tongue, with the circuit completed by an indifferent electrode located at some remote point, such as an electrode held in the hand.

Threshold of Perception on the Hand

Perception currents for 115 men with electrodes held lightly in the palms of the hands were determined using direct current and commercial 60-cycle alternating current. The results are given in Figures 1 and 2 respectively. The hands were moistened with a saturated salt water solution (NaCl) to reduce and minimize variations in contact resistances, and to permit the use of low voltages for safety. The subjects sat relaxed in a chair and rested the palm of each hand on smooth number 7 copper wires which were supported by the arms of the chair. The current was then gradually increased, and several trials were made to determine the smallest current that could be felt.

The results for 115 men using direct current were: 5.2 milliamperes mean; 5.0 milliamperes median; 2.1 milliamperes minimum; and 12.6 milliamperes maximum. The results using 60-cycle alternating currents were: 1.072 milliamperes mean; 1.05 milliamperes median; 0.44 milliampere minimum and 1.92 milliamperes maximum.

Figures 1 and 2 show that the response closely approximated a normal distribution. The mean and median values are substantially identical, and the mean value is considered to be the threshold. Therefore, the threshold of perception with electrodes held in the hand for direct current is taken as 5.2 milliamperes and 1.07 milliamperes for 60-cycle alternating current. The current likely not to be perceived is taken as the value corresponding to the one-half percentile. For direct current this is approximately 1.0 milliampere, and for 60-cycle alternating current 0.4 milliampere.

Deviation curves are helpful in analyzing the response to electric stimuli, and they were utilized in this investigation in a manner similar to that employed in previous papers in this field.[2,4,5] The solid dots of Figure 3 represent experimental points for the 60-cycle test with both hands holding the number 7 copper wire electrodes. The points are plotted in ascending order to show percentile rank as a function of the per cent deviation from 1.072 milliamperes, the mean of the group. The war period intervened between the completion of the 60-cycle test on the 115 men and similar tests recently completed on an entirely new group of 28 men.[6] Data for this new group are shown by the open dots of Figure 3. Since these data are plotted on probability paper, the straight line of best fit was drawn by eye through the 50th percentile and zero deviation point to establish the deviation curve.

In the latter tests, the 28 subjects grasped a polished number 8 copper wire electrode in the palm of the hand with light pressure and in a steadfast manner. The circuit was completed by an indifferent electrode which was clamped around the upper arm. The indifferent electrode consisted of a $1^1/_2$-inch wide lead strip wrapped with gauze. The strip was sufficiently long to nearly encircle the subject's upper arm, and the arm band was moistened with a saturated salt water solution to insure there being a good electrical contact.

To reduce the electric shock hazard, either the left or right but always the same hand and arm was used to prevent the current from passing across the body. It was found that there was less fatigue when the arm through which the current was passed was allowed to hang loosely at the side, rather than when the arm was allowed to rest upon a surface of a table or on the arm of a chair. For this reason the subject was instructed to let his arm hang free at his side during the tests. Preliminary investigation revealed no significant difference between the perception current obtained when the left or the right hand was used to hold the test electrode, however, the presence of minor cuts on a hand or fingers decreased the amount of current required for perception, and the choice of whether the left or right hand was used depended upon the condition of the skin. The threshold or mean value for this group was 1.067 milliamperes which compares favorably with the value obtained on the larger group eight years before.

The fact that a single line drawn on probability paper accurately represents the response for these two sets of data is significant because the data were obtained from different groups of subjects, at different times, and using different current pathways through the body. It is

Table III. Experimental Data for Ten Men Holding Number 8 and Number 4 Wire Electrodes

Frequency, Cps	Number 8 Wire Electrode: Minimum Current, Milliamperes	Number 8 Wire Electrode: Mean Current, Milliamperes	Number 8 Wire Electrode: Maximum Current, Milliamperes	Number 4 Wire Electrode: Minimum Current, Milliamperes	Number 4 Wire Electrode: Mean Current, Milliamperes	Number 4 Wire Electrode: Maximum Current, Milliamperes	Ratio of Mean Values No. 4/No. 8
60	0.59	1.046	1.38	0.53	1.119	1.52	1.07
1,000	1.29	2.036	2.70	1.25	2.160	3.15	1.06
30,000	21.6	30.03	46.1	21.3	30.90	49.5	1.03
60,000	49.5	65.67	97.4	49.2	69.10	99.0	1.05

Table IV. Experimental Data Tabulated According to Age of Subject

Frequency, Cps	Type of Contact	Subjects 30 Years and Less: Number Used	Subjects 30 Years and Less: Mean Current, Milliamperes	Subjects 31 Years and Over: Number Used	Subjects 31 Years and Over: Mean Current, Milliamperes
60	Holding No. 8 wire	19	0.99	6	1.34
10,000	Holding No. 8 wire	19	11.60	6	13.80
60	Touching	18	0.34	7	0.43
10,000	Touching	18	3.10	7	4.76
200,000	Touching	18	60.25	7	72.33
60	Tapping	18	0.32	7	0.41
10,000	Tapping	18	3.08	7	4.63
200,000	Tapping	18	53.1	7	62.61

evident that the perception of electric current on the hands follows a normal distribution, and that results obtained from groups consisting of approximately 25 subjects are sufficient to permit valid conclusions. Furthermore, it is believed that a sufficient number was used to permit valid statistical predictions, not only for the particular group tested, but also for a normal cross section of the adult male population of the country. The probability of a given current being perceptible is arbitrary and the one-half percentile value was selected as a reasonable criterion for establishing the level of current not likely to be perceived. The current required for other probabilities may be obtained by using the following equation.

Milliamperes = (Mean of Group)(1 + Deviation from Mean corresponding to Percentile Rank Desired)

Perception current tests were made for three different contact conditions over a frequency range from 60 to 200,000 cycles. The contact conditions consisted of holding copper wires, resting the tip of the middle finger on a small copper plate, and tapping the middle finger on the copper plate.

The electrodes used for the holding tests consisted of $4^1/_2$ inch lengths of polished number 8 and number 4 copper wires. For the touching contact test, the tip of the middle finger was allowed to rest upon the copper plate without the exertion of pressure other than that caused by the weight of the finger. In the tapping contact test, the finger was raised from the plate, and then allowed to fall and make contact at a rate of one to two times a second. The test electrode for the touching and tapping tests consisted of a polished copper plate $2^1/_2$ inches by $1^1/_2$ inches by 3/16 inch, which was set on an insulated base and placed on a table in front of the subject.

Deviation curves similar to Figure 3 were established for the holding, touching, and tapping contact tests for the various frequencies. Space limitations prohibit inclusion of deviation curves for each frequency and contact condition. However, the per cent deviation for any percentile rank can be derived from the statistical data given in Table I. The $99^1/_2$-, 50-, and 1/2-percentile points obtained from these deviation curves were entered in Figures 4, 5, and 6, and smooth curves were drawn to show the effects of frequency on perception current for the three contact conditions. The middle curve, which is based on the means or the 50th percentile values, establishes the threshold of perception for the given conditions. The lower curve represents the current likely not to be perceived, while the $99^1/_2$ percentile curve is taken to define the upper limit of perception current.

For the holding contact tests only the most susceptible subjects were able to perceive currents of frequencies in excess of 60,000 cycles within equipment limitations. However, 19 of the group tested at 60,000 cycles reported perception at 70,000 cycles, and the mean value for the group was corrected according to the following equation

$$\text{Corrected Mean of Sample} = \frac{\text{Mean 60,000-cycle Perception Current for 25 Men}}{\text{Mean 60,000-cycle Perception Current for 19 Men}} \times \text{Mean 70,000-Cycle Perception Current for 19 Men}$$

The number of subjects reporting perception for frequencies in excess of 70,000 cycles was too small to justify statistical analysis; however, it is believed that the similarity of the shapes of the curves of Figures 4, 5, and 6 justify extrapolating the holding contact curves to 100,000 cycles. Since the nature of the sensation underwent a noticeable change beginning at about 100,000 cycles the extrapolation was not carried above this frequency.

Experimental results obtained from holding contact tests for the 28 men and four women are given in Table II. Although tests based on only four subjects are not sufficient to warrant more than passing comment, it is significant that the extreme values for the women generally fell within the range of currents perceived by the men. The differences in the mean values for men and women at any frequency are inconsequential.

A series of tests were made on ten male subjects using number 8 and number 4 copper wire electrodes held in the palm of the hand to investigate the effects of contact area. The results of these tests, which are given in Table III, fail to show a significant difference in the current required for perception as a function of electrode diameter. Although the ratio of surface areas of the two electrodes was 1.59, the amount of the surface of each electrode in actual contact with the skin may have been nearly the same due to the folding of the skin around the test electrode. The results reported by H. A. Carter and J. S. Coulter[7] indicate that the current required for perception increases as the contact area is increased, but not in direct proportion to the increase in area. An attempt was made to compare the current required for perception according to different physical characteristics. Inconclusive results were obtained when the subjects were grouped according to complexion and general build (heavy, medium, or slight); however, mean values of perception current for the men segregated into two age groups suggest that the current required for perception is somewhat dependent on age. The results of holding, touching, and tapping contact tests are given in Table IV. A greater number of subjects would be required to definitely establish the relationship between perception current and age.

Although the effects of wave shape were not investigated per se, it is believed that the factors controlling let-go currents[3,4] would also apply to perception currents. There is strong evidence to support the conclusion that the crest and not the rms value is the critical factor in stimulation with low frequency sine waves. The decrease in sensitivity with increasing frequency suggests that the effect of higher harmonics, or repetitive pulses superimposed on low-frequency alternating current, would have less and less effect as the frequency of the superimposed current was increased. Above 100 to 200 kc it might be expected that the sensation of heat would be largely masked out by the muscular stimulation of the lower frequency components.

Sufficient experimental data have been obtained to establish the current required for perception for several contact conditions over the frequency range from 60 to 200,000 cycles, and for direct current. The data follow a normal distribution, which permits valid statistical predictions to be made of the current not likely to be perceived, and that likely to cause perception.

The sensations observed as the frequency is increased fall into four frequency bands. The sensation produced by gradually increasing direct current is predominately one of warmth rather than of the muscular stimulation produced by low-frequency alternating currents. The sensations produced by alternating currents below approximately 10,000 cycles are characterized by a tingling or pricking sensation in the area adjacent to the point of contact, and at very low frequencies the muscles tend to follow the alternations of the current. A clearly defined threshold relatively independent of the rate of increase of current also is present in this range of frequencies. For frequencies between 10,000 and 100,000 cycles, the sensation produced by currents slightly above the perception level is less intense than that produced at the

lower frequencies; it is observed over larger areas around the point of contact, extending even into the wrist, and accommodation processes somewhat obscure the threshold boundary. An abrupt change in phenomena occurs between 100,000 and 200,000 cycles where the sensation becomes one of internal heating, and heating is the principal sensation produced by currents above 200,000 cycles.

The presence of many variables appears to exclude the possibility of any simple relationship between the current required to cause perception and frequency that would hold for the frequency range investigated.

References

1. Limiting Value of Capacitors When Used as Radio Filters on Portable Appliances. *NEMA Publication 105*, National Electrical Manufacturers Association (New York, N. Y.).

2. The Physiological Tolerance of Alternating Current Strengths up to Frequencies of 100,000 Cycles per Second, A. E. Kennelly, E. F. W. Alexanderson. *Electrical World* (New York, N. Y.), volume 56, number 3, July 21, 1910, pages 154–56.

3. Effect of Frequency on Let-go Currents, C. F. Dalziel, E. Ogden, C. E. Abbott. *Electrical Engineering (AIEE Transactions)*, volume 62, December 1943, pages 745–50.

4. Effect of Waveform on Let-go Currents, C. F. Dalziel. *Electrical Engineering (AIEE Transactions)*, volume 62, December 1943, pages 739–44.

5. Dangerous Electric Currents, C. F. Dalziel. *Electrical Engineering (AIEE Transactions)*, volume 65, August-September 1946, pages 579–84.

6. Determination of Perception Currents 30 to 300,000 Cycles, T. H. Mansfield. *Master of Science Thesis*, University of California (Berkeley, Calif.) 1949.

7. Threshold of Stimulation of Alternating Currents, H. A. Carter, J. S. Coulter. *Archives of Physical Therapy*, volume 23, 1942, pages 207–13.

No Discussion

Underground Hydroelectric Power Plants

PAUL E. GISIGER
NONMEMBER AIEE

Synopsis: In recent years a number of underground hydroelectric power stations have been built, mostly in Europe, and many others are under construction. While the last war has undoubtedly had some influence in making substantial protection of generating facilities seem desirable, it is pointed out that underground stations have been built long before the war, and that under certain circumstances there may be valid technical and economical reasons for the choice of this type of construction. Advantages that result from underground locations are discussed, and special emphasis is given to the points which need attention in the design, such as access and safety features, insulation, and ventilation. Several representative underground plants are described in some detail.

THE IDEA of putting hydroelectric power stations under ground is not a recent one. It is perhaps a sad commentary on our time that in any discussion of underground powerhouses in these days, the thought of protection against military attack is one of the main factors. The first sizable underground plant was built, however, at a time when the airplane was still in its infancy and its potentialities as a carrier of military destruction could hardly have been visioned. Progress, if such it be, in the art of carrying destruction to those installations upon which the industrial production of a country depends has now greatly promoted the interest in ways to make generating stations as invulnerable as possible. While under the circumstances this aspect cannot be disregarded, it still is important and interesting to consider the purely economical and technical factors involved. Under certain conditions these may indicate that an underground power house is the most desirable solution to be adopted, quite apart from any consideration of the war risk.

It will be necessary for our purpose to properly define an underground powerhouse. This is not as simple as it might seem. In most hydroelectric powerhouses, a considerable part or the whole installation is below adjacent ground levels. Sometimes turbines have been located in deep pits, connected by long vertical shafts to generators above ground, as for instance in the older Niagara plants. Plants of this type have sometimes been called underground plants. For the purpose of this paper, however, the term is limited to such plants in which the main piece of equipment, that is, the generator stands in a room which is completely submerged below the original natural ground level of the site.

It is fairly obvious that possibilities for the underground arrangement are more frequent for high-head than for low-head plants. Nevertheless, there exists also low-head underground plants. One of the most recent ones, the Lavey development on the Rhone River in Switzerland, has three 24,000-kw units driven by Kaplan wheels under 130 feet of head, see Figure 1.

While the turbine and the generator will of necessity have to be located underground, the transformers may be located

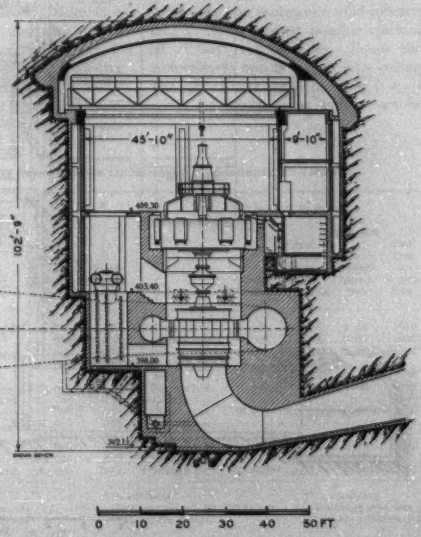

Figure 1. Cross section of Lavey powerhouse

Paper 50-186, recommended by the AIEE Power Generation Committee and approved by the AIEE Technical Program Committee for presentation at the AIEE Summer and Pacific General Meeting, Pasadena, Calif., June 12–16, 1950. Manuscript submitted February 20, 1950; made available for printing May 10, 1950.

PAUL E. GISIGER is with the Companhia Brasileira Administradora de Servicos Tecnicos, Sao Paulo, Brasil.

The author gratefully acknowledges the help received in the preparation of this paper from Hans Marty, Vice President, Bernese Power Company, Berne, Switzerland; J. Baechtold, Chief Engineer, Oberhasli Power Co., Innertkirchen, Switzerland; P. Meystre, Chief Engineer, Power Service of the City of Lausanne, Switzerland; and Dr. Mario Moriara, Managing Director of the Societa Terni, Rome, Italy.

underground or above ground in a separate step-up substation. The first alternative is dependent upon the availability and dependability of high-tension cable and it is, therefore, to be found only in the more recent examples of this type. Among those are the Innertkirchen (1943) and Handeck II (1950) powerhouses in Switzerland (Figures 2 and 3), where power is taken from underground transformers to surface switchyards through 150-kv cables, and the Verbano powerhouse, to be completed 1952, where 220-kv cables will be used.

There also is an important interdependence between the general design and arrangement of a hydroelectric unit and the feasibility of its underground arrangement. It is obvious that with the underground arrangement, economy of space is highly important. Thereby the vertical shaft arrangement is favored, while among the older underground installations, whether they be equipped with Pelton or with Francis wheels, the horizontal shaft arrangement predominates. The more recent installations have, as a rule, vertical-shaft units. This is especially significant for Pelton wheel installations, such as the Innertkirchen, Figure 2, and Handeck II plants which provide recent examples of vertical-shaft single-runner Pelton units.

Advantages of Underground Location

The reasons for which hydroelectric stations have been put underground may be summarized as follows:

1. Under severe climatic conditions, such as in the far North (Porjus) or in the high Alps (Handeck II) construction operations can be continued all year round in an underground cavern, whereas above ground they might have to be interrupted for a considerable part of the year. Therefore, construction time can be saved.

2. The underground arrangement often allows more liberty in the choice of location of the powerhouse. In the high Alps the necessity of keeping away from avalanche paths is avoided; in steep, narrow river canyons there may be no space for a conventional powerhouse and appurtenant works at the point which is indicated by the longitudinal river profile as the most desirable powerhouse location. The length of expensive pressure tunnels may be shortened by providing instead a longer, but less expensive, free-level tailrace tunnel with the location of the powerhouse away from the river inside the mountain. This results in the additional advantage of replacing relatively flat-sloped steel penstocks with a steep or even vertical pressure pit which usually is considerably cheaper. The shorter pressure tunnels and penstocks will furthermore facilitate the speed regulation of the turbines.

3. With an underground location, foundation difficulties which are often present in alluvial river bottoms are completely avoided and the foundations themselves are often less voluminous and, therefore, cheaper than with the conventional type.

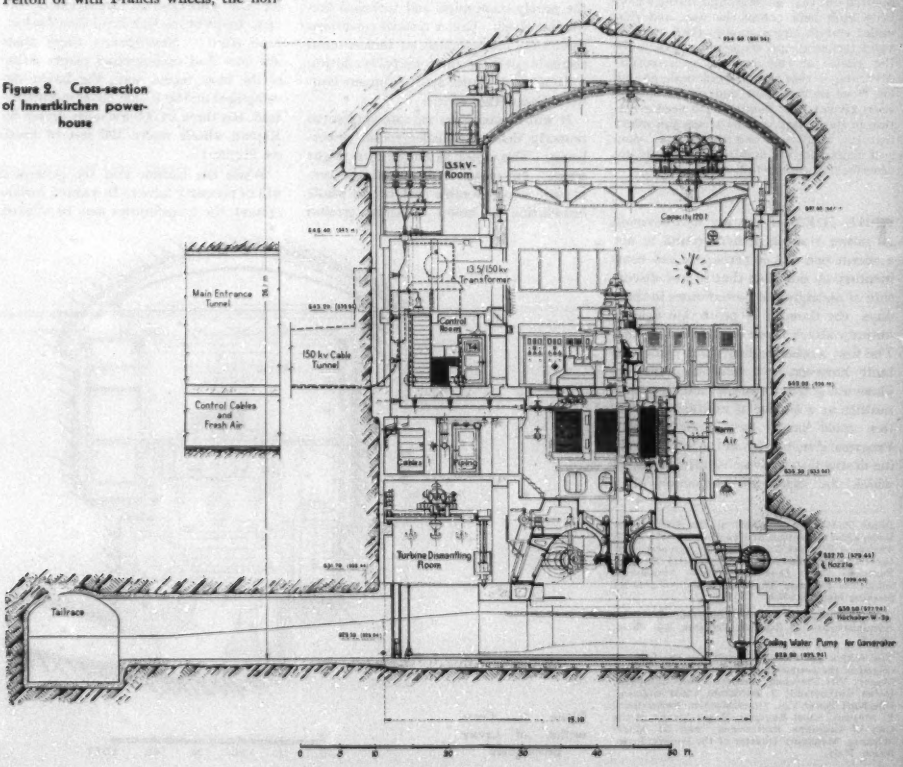

Figure 2. Cross-section of Innertkirchen powerhouse

Figure 3 (left). Handeck II powerhouse, generator erection

Figure 4 (right). Excavation for Handeck II powerhouse after placing of roof arch

Construction Features

The general arrangement of a hydroelectric powerhouse is based on the function and interrelation of its main items of equipment, whether the powerhouse is above or below ground. Plans and cross sections of underground powerhouses follow, in general, the same lines as those of the conventional type. There is perhaps a little more emphasis on economy of space, because the incremental cost of additional space increases more than with the outside type. It is surprising, therefore, that in none of the European underground installations with vertical-shaft units the arrangement with thrust bearing below the generator, which has become so common in America, has been used.

It is axiomatic that the location for a powerhouse cavern should lie in perfectly sound rock because constructive measures to counteract the effect of pressure zones in unstable rock, such as are sometimes unavoidable in railroad or power tunnels, would hardly be economically feasible in case of a powerhouse. A thorough geological investigation is, therefore, still more indispensable in case of a proposed underground powerhouse than for other features of a hydroelectric project.

Construction of the cavern itself is beyond the scope of this paper. It may be mentioned, however, that for Swiss conditions it has proved advantageous to start excavation from several places at once. A good procedure is to drive four headings along the four corners of the cross section. The rock between the two upper headings is then removed, so that the top part of the cross section, between the springing lines of the roof arch, is excavated. It is then possible to concrete the roof arch, using the rock still in place immediately below as a working platform; the headings at the top and bottom of each side wall are connected with a vertical slot, the main rock prism removed, and at the same time the facing of the side walls is placed, see Figures 4 and 5.

Sometimes there is more than one cavern to excavate. In case of the Innertkirchen and Handeck II powerhouses which work under heads of 2,050 and 1,450 feet respectively, there is a valve chamber on the upstream side of the powerhouse proper, see Figure 6. This is a safety measure against flooding of the powerhouse by the possible failure of a valve. The valve chamber is normally closed off against the powerhouse with a heavy bulkhead door and provided with a discharge canal to the [illegible]

As may be seen from Figures 1, 2, and 7 the inside walls and ceilings of all recent underground powerhouses are not in direct contact with the rock. In some cases, the walls are lined with concrete with a thin false wall set in front of the lining; in others, the rock remains unlined, with an independent wall placed in front of the rock. In either case, the resulting air space not only insures against any seepage water getting into the actual building, but is useful as an airduct. The roof is always a solid concrete arch to insure against possible cracking off of any rock particles. Below this arch there is usually a light false ceiling. The space above the false ceiling is again useful for insulation as well as ventilation.

Table I. Some Representative Underground Hydroelectric Powerplants

Plant	Country	Capacity Installed or to be Installed, Kw	Head (Gross) Feet	Turbines	Volume of Powerhouse Cavity Net Cu Yds	Volume of Powerhouse Cavity Incl. Valve Rooms etc. Cu Yds	Volume of Powerhouse Cu Yds/Kw Powerhouse Net	First Year of Operation
Porjus (Original)	Sweden	60,000	183	8 Francis hor.	35,000	41,000	0.58	1910
Brommat	France	186,000	855	6 Francis vert.	60,000	76,000	0.32	1932
Innertkirchen	Switzerland	210,000	2,235	5 Pelton vert.	59,000	79,000	0.28	1942
San Giacomo	Italy	200,000	2,140	3 Twin Pelton hor.	37,000	42,000*	0.19	1948
Provvidenza	Italy	150,000	838	3 Francis hor.	44,000	47,000†	0.29	1949
Lavey	Switzerland	72,000	130	3 Kaplan vert.				1950
Handeck II	Switzerland	114,000	1,518	4 Pelton vert.	39,000		0.34	1950
Harsprunget	Sweden	377,000	346	4 Francis vert.				1951
Santa Massenza	Italy	284,000	1,505					
Monte Argento	Italy	66,000	164	3 Francis vert.	21,000	29,000**	0.32	1952
Montorio	Italy	100,000	845	3 Francis vert.	29,000	30,000	0.29	
Verbano	Switzerland	100,000	973	4 Francis vert.	33,000**		0.33††	1952

*In addition:
Entrance tunnel 54,000 cu yds
Bus shaft 31,000 cu yds
Substation tunnels 67,000 cu yds

†In addition:
Entrance tunnel 29,000 cu yds
††Preliminary design

**In addition:
Entrance and bus tunnels 3,600 cu yds

Figure 3 (left). Handeck II powerhouse during construction

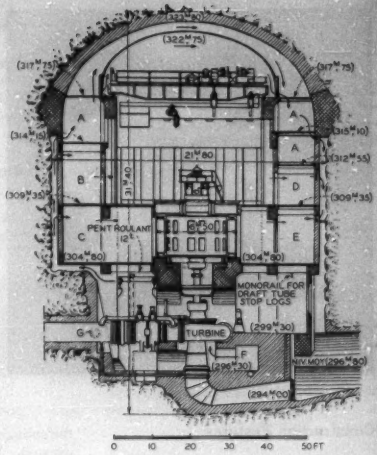

Figure 7 (right). Cross section of Brommat powerhouse

A. Control cables; B. auxiliary services; C. piping; D. rheostats and 15,000-volt apparatus; E. warm air and 15,000-volt cables; F. fresh air tunnel; G. tap for house unit. Dimensions and elevations in meters

Figure 6. Plan of Innertkirchen powerhouse

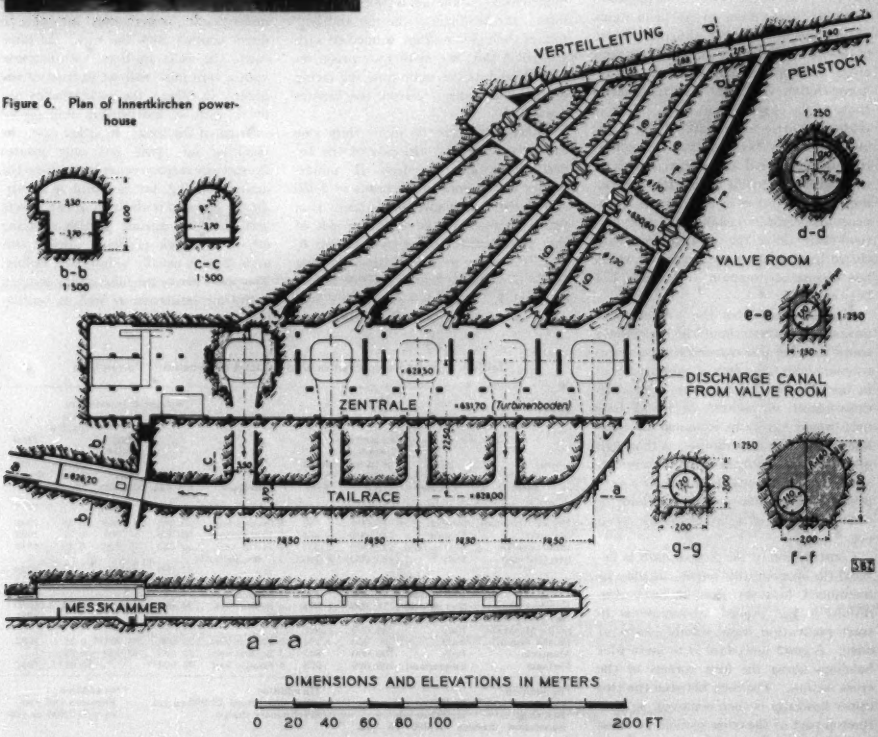

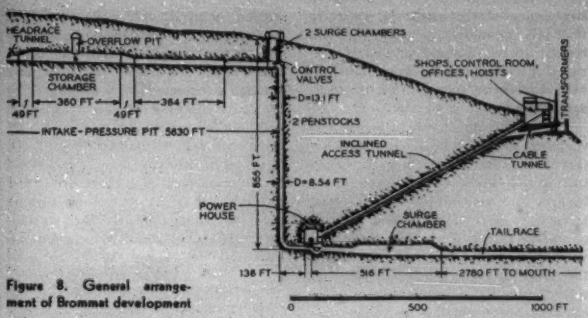

Figure 8. General arrangement of Brommat development

As a matter of curiosity, the Cotilia Powerhouse of the Terni Company in Italy may be mentioned. This has all the characteristics of an underground powerhouse, but has actually been built in an open pit, and covered with a fill about 50 feet high. It nevertheless also is provided with a somewhat modified form of double-wall and ceiling construction.

In Table I are listed some of the more notable recent underground power plants.

Power Take-Off

It is evident that power has to be taken away from an underground powerhouse through cables to an outside starting point for an overhead line. In this respect the underground installations can be clearly divided into two classes: Stations where transformers are located above ground away from the powerhouse, so that the power is carried outside at generator voltage, and stations with transformers located in the powerhouse cavern itself, in which case the power has to be carried outside in high-tension cables. In older plants the outside transformer station was the rule, but now there is a definite trend to have transformers located next to the generators. As soon as vulnerability in war is a consideration, then it is desirable to give the transformers the same degree of protection as the generating equipment. The experience of the last war points to the fact that shell or bomb damage to switching installations is relatively easy to repair, whereas a hit on a transformer may seriously cripple a transmission system.

A low-tension cable installation between an underground powerhouse and an outside step-up and switching station has no different problems than those present at any normal powerhouse with transformers located not directly adjacent to the generators. The cable tunnel is usually combined with the access tunnel, although separate tunnels for outgoing cables also have been used. This holds for high-tension as well as for low-tension cable tunnels. An example for an outside transformer arrangement is the Brommat station in France, built in 1932, Figure 8, where power goes out at the generator voltage of 15,000 volts to a transformer and switchyard. The control room, as well as shops and offices, are located in a service building at this switchyard.

An example for the transformers located alongside the generators is the Innertkirchen plant in Switzerland, completed in 1943, where current is stepped up to 150 kv and then taken to an outside switchyard with high-tension cables located in a tunnel, see Figure 2. The same scheme has been followed for the Handeck II Station, immediately upstream from Innertkirchen, which is under construction and will go into service in the near future. In the Lavey Station on the Rhone River, which has been under construction during the same period, the transformers are located in an outside step-up and switching station.

Ventilation and Lighting

The necessity of providing large tunnels for the access of people and equipment as well as the exit of power and control cables, Figure 9, makes it relatively easy to have an ample turnover of air in an underground powerhouse. The false walls and ceilings which are usually provided to insure dryness of the vital spaces lend themselves to be used as airducts and leave the designer a considerable amount of freedom in arranging for an advantageous circulation of fresh air, and the exhaust of used air. As a rule, fresh air is taken in through the main entrance or cable tunnel and returned through special exhaust ducts located in or near the ceiling. The fans to push or pull the air through may be located at the most convenient point in the circuit. In most of the recent underground installations the generators are cooled with a closed system and, therefore, the amount of heat to be removed is moderate. Depending on climate and season, it may be possible that for considerable periods of time natural ventilation is sufficient and fans do not have to be operated.

With any scheme of ventilation it is essential that there are no rooms or places which are bypassed by the general flow of air. This is especially important for the control room. In most cases it has been found necessary to insure proper working conditions in the control room through a secondary system of ventilation which either pushes fresh air through or exhausts used air from the control room. In a number of instances it has been found satisfactory to introduce the fresh air at the top, and exhaust it near the bottom of the control room because the warm air coming from heat-producing instruments is removed before it has spread out over large parts of the room.

In some underground stations the power is carried outside on open bus bars. In such cases it is preferable to use the bus tunnels for the exhaust rather than for the admission of air, on account of the heat released by the bars.

As might be expected, it has been the general experience that temperatures inside an underground station follow the daily and seasonal variations of the outside temperature only with a greatly reduced amplitude. As a general rule, it appears that working conditions in such a station are in no way inferior to those above ground.

While the lighting of an underground station offers no new problems, it is obvious that for practical as well as psychological reasons it should be given very careful consideration. The advances made in recent years in methods of indirect lighting and the use of fluorescent lamps can be applied to great advantage in a place where daylight is absent 100 per cent of the time. Attention is called to Figures 3 and 10, which show the lighting arrangements in the Innertkirchen and Handeck II Stations.

Some Individual Developments

Porjus Development, Sweden

This development is mentioned briefly because it is the forerunner of all other underground plants. Its construction was begun in 1910 and the initial installation

completed in 1914. It is located north of the arctic circle on the Lulea River. The underground location was indicated by topographic and still more by climatic reasons. The total head of the plant is 183 feet; its general arrangement with individual vertical penstocks recalls somewhat that of the earlier Niagara plants and conveys the thought that the latter could have become underground plants by a relatively small modification. The most significant difference of Porjus against more recent plants is the arrangement whereby the turbines of its horizontal-shaft units are recessed into separate compartments in the rock, while the generators only are located in the continuous, common generator room. Transformers, as well as control room, are located above ground.

Brommat Development, France

This plant, in operation since 1932, has all the features of the modern underground plant. It is located on the Truyere River which originates in the highlands of central France and discharges through the Lot River into the Garonne River. With a static head of 855 feet and a plant discharge of 2,960 cubic feet per second it has a total capacity of 186,000 kw in six units. The reason for locating it underground was lack of space in the narrow river gorge. Water is brought from the Sarrans upstream development through an equalizing basin and then through a pressure tunnel which near its end splits into two conduits leading into separate surge chambers. From each surge chamber a vertical penstock or pressure pit drops to the power house, dividing itself at the bottom into three branches corresponding to the three units fed by each penstock, Figure 8. The steel lining of the penstocks varies in thickness from 1/2 inch to $1^3/_4$ inch, backed up by 12 inches of concrete between steel and rock. Powerhouse as well as pressure tunnels and penstocks are located in compact granite rock.

The powerhouse shown in Figure 7 is equipped with vertical-shaft Francis turbines. Ahead of each spiral casing there is a spherical valve with the usual by-pass and control features. Special precautions were taken against the risk of failure of the cast-steel turbine or valve casings; the quick closing gates at the head of the penstocks are controlled from the powerhouse, any water entering the turbine floor can freely discharge into the tailrace, and the three stairwells between the turbine floor and generator floor can be closed with emergency bulkheads.

The generators are equipped with water coolers for closed-circuit ventilation.

Fresh air for the powerhouse is admitted through a special air tunnel more than 3,000 feet long paralleling the tailrace. A distribution tunnel at draft tube elevation "F" in Figure 7, distributes the fresh air through the length of the powerhouse; it then moves up through the space between rock and side walls into the various powerhouse rooms and is finally evacuated above the false ceiling into the lower section of the inclined access tunnel. A fan at the outside end of this tunnel keeps the air moving.

Access to the powerhouse is provided through an inclined tunnel, Figure 8, 18 feet wide and starting at an outside building in which are located the control room as well as shops, offices, and so forth. This tunnel is equipped with a cable car on a wide gauge track for the transport of heavy as well as light equipment and personnel; along its side walls all control cables are carried from the powerhouse to the control room. Immediately below this tunnel, separated from it only through a concrete slab, is the tunnel for the 15-kv generator cables. This tunnel ends in a low-tension bus room. Step-up transformers are located above this room in the open. The tailrace is again formed by a tunnel in solid rock of more than 3,000 feet length. At its beginning, where the six draft tube discharges are joined together, is a surge chamber to insure uniform free flow.

Innertkirchen Powerhouse, Switzerland

The Innertkirchen Powerhouse is the second step of the Grimsel development on the headwaters of the Aare River. The main feature of this development is a large storage reservoir at an elevation of 6,260 feet at the end of the glaciers on the west flank of the Finsteraarhorn, the highest peak in the Bernese Alps. From this storage reservoir the water goes through Handeck I Powerhouse, completed in 1932, which utilizes a head of 1,790 feet and is of the conventional type. From the discharge of this plant the water is taken through another pressure tunnel and penstock to the Innertkirchen Powerhouse, utilizing a head of 2,200 feet. This second powerhouse was completed in 1942 and is of the underground type. Its construction was decided upon in 1939 and the political situation at the time was making bomb-proof construction desirable; but the underground arrangement had actually been considered several years earlier on account of the economies to be obtained from the embedment of the penstock and its manifold into solid rock, and for safety against rock slides which were a risk at that location.

The pressure tunnel from the upper

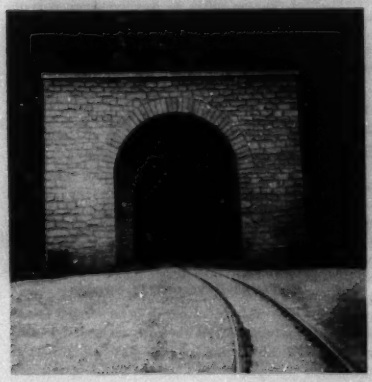

Figure 9 (left). Entrance to Innertkirchen powerhouse

Figure 10 (right). Interior of Innertkirchen powerhouse

Figure 11. View of Innertkirchen Valley

plant to the Innertkirchen surge chamber is 32,700 feet long and dimensioned for a flow of 920 cubic feet per second. From the surge chamber a single inclined pressure pit leads to a manifold where the feeders to the five units branch off, Figures 6 and 11. The pressure pit varies in diameter from 8.54 to 7.88 feet, its steel lining in thickness from 1/2 inch to 13/16 inch.

Pressure pit and powerhouse are located in hard crystalline schist.

From the general plan of the powerhouse, Figure 6, it will be noted that between the branching-off point of the unit feeders and the powerhouse there is located a separate valve room where each conduit can be closed off by spherical service and emergency valves. The special valve room insures against flooding of the powerhouse by failure of a valve casing.

The powerhouse cavity has a minimum vertical rock cover of 130 feet, but the valley flank is so steep that the length of the horizontal access tunnel at generator floor level is only about 130 feet.

The concrete arch above the generator room is not reinforced, but care was taken to fill out all crevices between it and the rock as well as in the rock itself by pressure grouting. The false ceiling underneath is built up of corrugated Transite, Figure 2.

The 42,000-kw units are of the vertical-shaft type with 2-nozzle Pelton wheels, Figures 2 and 10. An innovation is the support of the generator directly on the steel casing of the turbine without an intermediate structural floor. Thereby the foundations were simplified and access to turbine and generator made easier.

Each generating unit is directly connected to a 13/150-kv transformer located in the powerhouse adjacent to generators. From the transformers the current is taken through 150-kv cables in a special cable tunnel to an outside substation.

The powerhouse is reached through a short access tunnel, Figure 9. A 1-meter gauge siding connecting to the railroad line serving the upper Aare Valley enters through this tunnel. Directly underneath is a smaller tunnel for control cables and fresh air. Air is pushed in through a fan at the entrance, flows through the powerhouse upwards into the space above the false ceiling and is exhausted again through one exit tunnel at each end of the cavity. The alignment of the tailrace tunnel could be so chosen that its entire length of 4,240 feet is in solid rock.

The Handeck II Powerhouse, Switzerland

The Handeck II Powerhouse forms a further extension of the Grimsel development and is now under construction. It utilizes water from drainage areas not contributing to the Handeck I Powerhouse and its discharge will increase the flow through the Innertkirchen plant. The Handeck II Powerhouse will contain four 24,000-kw units under 1,450 feet of head and will, in most respects, be similar to the Innertkirchen Powerhouse, see Figures 3, 4, and 5. It will go into operation in 1950.

Lavey Development

This development, belonging to the city of Lausanne and located on the Rhone River, is an example of an underground powerhouse for a low-head installation. Its head of 150 feet is created by cutting off a bend in the river with a pressure tunnel of large dimensions for a plant discharge of 7,000 cubic feet per second. The plant is equipped with three Kaplan units of 24,000 kw each, Figure 1. In its general arrangement the powerhouse is not much different from the preceding ones, except for differences resulting from the different type of turbines and from the outside location of the transformers. This plant also will go into operation in 1950.

Other Underground Developments Under Construction

Underground powerhouses have almost become the rule rather than the exception for new developments in many sections of Europe. A considerable number of them now are under construction. It would be impossible to name all of them. Among the more notable plants may be cited the Harspranget Plant in Sweden, just completed or about to be completed, with an installation of 285,000 kw; the Kilforsen Plant, 240,000 kw, also in Sweden, to be completed in 1954; the Santa Massenza and Provvidenza plants in Italy with installations of 284,000 and 150,000 kw respectively and the Verbano Plant in Switzerland, about to be started, for an installation of 100,000 kw.

References

1. Principal European Hydro-electric Plants with Underground Power Houses and Their Construction Features, Dr. Romagnoli Mosca. *L'Energia Elettrica* (Milano, Italy), volume XII, 1935, pages 85–116.

2. About Underground Power Houses, Giulio E. Dolcetta. *L'Energia Elettrica* (Milano, Italy), volume V, 1928, pages 1407–15.

3. The Hydro-electric Installations on the Truyère River, Jacques Dumas. *Genie Civil* (Paris, France), volume C1, 1932, pages 269–77.

4. The Innertkirchen Power Plant, Second Step of the Oberhasli Development, Kasch, Juillard, Aemmer, Jegher. *Schweizerische Bauzeitung* (Zurich, Switzerland), volume 120, 1942.

5. The Lavey Hydro-electric Development, P. Meystre. *Wasser-und Energiewirtschaft* (Zurich, Switzerland), number 7–8, 1948.

6. Ventilation and Illumination of Underground Power Houses, Dr. Carlo Ritter. *L'Energia Elettrica* (Milano, Italy), volume XXVI, May 1949.

No Discussion

Centralized Control Desirable for Single Boiler-Turbine-Generator Units

J. A. LIND
NONMEMBER AIEE

J. M. GEIGER
MEMBER AIEE

CENTRALIZED control of steam-electric generating units has been a natural and gradual evolution over the years. It has been accelerated by such factors as development of suitable equipment and controls, creation of new plant heat cycles, and rapid growth in the size of the units and of the electrical utility industry. The authors believe that current controversies over centralization of controls are concerned primarily with what shall be included and how centralization is to be accomplished, and not so much with the basic idea of centralization.

In generating stations as well as over-all power systems, the electrical engineers have been able to progress further than the mechanical engineers in this matter of centralization of controls. It is not unusual for power systems with generating plants spread over hundreds of miles to have centralized, and even automatic, control of machine loading from a central load-dispatching and frequency-control station. The purpose of such controls is to co-ordinate the loading of the controlling machines as well as to distribute load among them as required by system conditions. On the Niagara Hudson System, installation of such equipment has resulted in much better control together with less load swing on the machines under control. Previously some of the swings consisted of unnecessary transfer of load among generating stations as a result of unco-ordinated manual control.

Within a single generating station, certain operations need to be co-ordinated with each other. An early problem was the co-ordination of firing in battery many boilers serving a group of turbine generators. With that arrangement, the boilers installed for a particular turbine could serve any other turbine. So long as steam pressure was maintained, it did not especially matter how load was transferred between generating units. With boiler sizes then employed, many more boilers than turbines were required. Control schemes employing large master-pilot steam gauges, steam pressure regulators, and eventually complete combustion control systems seemed to solve a large part of the boiler-room problem. The boiler personnel required constituted a department in itself and it seemed best to let it operate as such. At the same time, the electrical operators were concerned with matters in addition to the generators. They supervised local feeders, tie lines, street lighting, and so forth. Consequently, an over-all plant control scheme developed whereby the electrical group became divorced from the mechanical group and the mechanical group further divided into a turbine-room group and a boiler-room group. This division of responsibility contributed to poor co-operation because of lack of understanding of each others' problems. These conditions laid the groundwork for improvement.

It had become the practice to load machines at a prescribed rate which had been determined by boiler flexibility. It was learned that this rate was not a fixed thing so that sometimes the full capability was not realized and at other times the boiler room was overtaxed. Addition of a steam-header pressure gauge in the electrical control room permitted taking load swings at such rate as the boiler room could stand them at that moment without lowering steam pressure to the point of jeopardizing capacity of steam-driven auxiliaries. Addition of a station load megawatt meter in the boiler room also permitted the boiler operators to do a better job by knowing the magnitude and rate of demands being placed on them. Further co-ordination was attained by use of intercommunication facilities.

When Oswego Steam Station was being designed in the late 1930's a unit system was decided upon, a unit consisting of a boiler, turbine, and generator. No steam, feedwater, or electrical interconnections at generator voltage were provided between units. Merits of the unit system in this case have been described elsewhere.[1] The controls for such a station required an entirely new approach and presented an opportunity for major improvement.

Let us consider such a station with two or more units with no mechanical or electrical interconnections except the transmission system. Suppose now that station load is to be changed. Either unit may assume the whole change or both may share it. On the other hand, suppose the total station output is to remain constant but reapportioned between units. Without steam interconnections, both boilers are subjected to the conditions which accompany a station load change. As the load on one unit is changed, all of the pump outputs must be changed and the firing rate of that unit's boiler must be changed, requiring change in output of pulverizers, feeders, and feedwater regulators. Some of these functions may be automatic and some, such as starting of additional fans and pumps, may be manual. It is valuable, therefore, that the several operators know the magnitude and speed of load change on the unit they are handling as quickly as possible. There are three ways of speeding up this intelligence:

1. Duplicate instrumentation at the several operators' locations.
2. Use a public address system.

Paper 50-187, recommended by the AIEE Power Generation Committee and approved by the AIEE Technical Program Committee for presentation at the AIEE Summer and Pacific General Meeting, Pasadena, Calif., June 12–16, 1950. Manuscript submitted November 17, 1949; made available for printing May 8, 1950.

J. A. LIND and J. M. GEIGER are both with the Niagara Mohawk Power Corporation, Buffalo, N. Y.

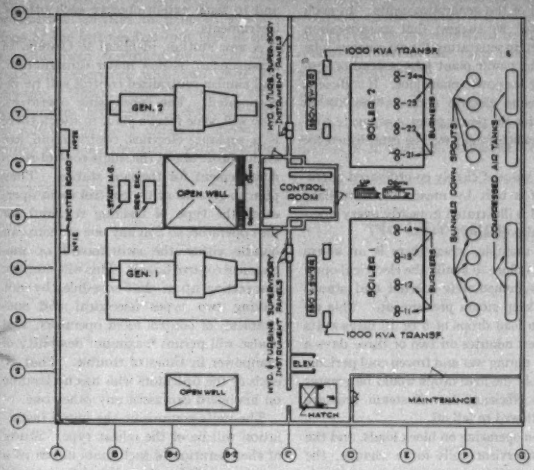

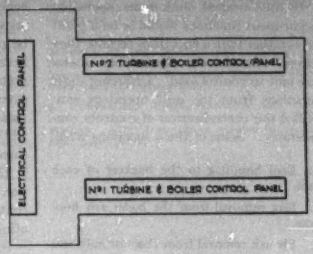

CONTROL ROOM

Figure 1. Arrangement of main operating floor for units 1 and 2 at Oswego steam station showing convenient central location of control room

A similar control center has been provided for unit 3 and future unit 4 which is under construction. Control panel arrangement is shown in enlarged plan of control room

3. Locate all affected operations at one point.

The decision as to which to employ depends on various factors such as:

1. Cost.
2. Suitability and conformity as an extension to an existing station.
3. Allowable time to make necessary changes.
4. Division of responsibility between operators.
5. Expediency.

Studies of loadings for the Oswego Steam Station indicated that it would be largely a bulk power producer. Also, there would be periods of minimum load, stand-by service during heavy run-off to the system's hydro stations, and periods during which it would be regulating. It would be firmly tied into the 115-kv transmission system and there would be few local feeders. These conditions required that each unit be capable of operating over a wide load range and that flexibility of control be provided to meet the variable demands of the system.

A conception, believed to be original, was that of a straight-line organization for each unit, originating with a unit operator who would be in a position to supervise all operations of one boiler-turbine-generator unit. Normally he would control input to suit output, but he also would control output to not exceed the capability of the unit and its associated equipment. In working out details of such a system, including arrangement, cost, and personnel, it appeared more feasible to apply the scheme on a 2-unit basis.

A central control room was located in the building bay between units, and in it were installed an electric switchboard for the two generators, their exciters and related auxiliaries, and a mechanical control board for each of the boiler-turbine units and their auxiliaries. Figure 1 shows the arrangement of the panels in the control room and the orientation of major equipment on the main operating floor. Glass areas in the control room walls permit observation of activities in parts of the boiler room and turbine room. A mirror near a furnace door is used to observe that furnace lighters and burners ignite properly. Other mirror systems afford a view of the bicolor gauge glasses.

Figure 2 shows the control room with the electric control board in the distant center and the two mechanical control boards on the sides. The electric board contains the usual switchboard controls and meters and the mechanical control board contains those instruments, meters, gauges and controls usually found on the boiler-control panel and turbine-control panel. The small size of these main control panels has been accomplished by bringing only essential controls and instruments to this location. Liberal use of telemetering has permitted using smaller instruments on the panels. To illustrate: at each boiler feed pump there is a local panel with flow meter, pressure, gauges push buttons for auxiliary oil pump, recirculation control relays, thermometers, and so forth; in the control room there are only an ammeter, control switch, air control subpanel, and a telemetered flow indicator in a multiple draft gauge type of instrument.

The control room is air-conditioned for the comfort of the operators, and has been arranged for their convenience. They can communicate with the auxiliary operators either by telephone or public address system. Many abnormal operating conditions are called to their attention by an annunciator. Principal auxiliaries of the main units are under their direct control. For the most part this equipment is stopped and started manually, but automatic speed and throttling control is provided. So far as possible, related instruments and controls have been grouped together.

Starting from the boiler-room end, the mechanical panel has a section for soot blowers, then a section for pulverizer and burner controls, followed by the steam pressure and combustion control, including control switches for draft fans. Controls for the turbine and its auxiliaries are at the turbine-room end of the panel. Control of condensate from the condenser to the boiler is located on a section of the panel between the boiler controls and the turbine controls.

The central section of the electric switchboard contains frequency and tie-line loading controls. On either side of center there is a section for instruments and controls associated with one unit, followed by panel sections for auxiliary power boards. Towards the ends are panel sections for local feeders. Station watt-hour meters are on the end wings of the panel.

It was evident that some operating department functions would be on a plant basis rather than a unit basis because they did not immediately affect ability of any one unit to control load. Divorcing these functions from the unit operators simplified the centralization of controls considerably. Some of these functions were:

1. Cool handling to the bunkers of each unit.
2. Slag removal from the boiler ash hoppers.
3. Fly ash removal from the dust collector hoppers.
4. Supervising circulating water screens and gates.
5. Station water and compressed air services.

Most of the functions described were provided with failure or trouble alarms and some of the critical ones were called to the attention of the unit operators.

It seemed unimportant that the unit operators have control of functions related principally to start-up, hence remote control of these items was provided only when convenient. Such items included steam jet air ejectors and sealing water to the turbine. It should be noted that while ejectors may be added or removed from service during operation, they require no adjustment because of machine load changes. The evaporator plant was not placed in the centralized group because the immediate demands of the unit are supplied from condensate storage tanks, and therefore the evaporators need not be co-ordinated with operation of the main units. Control of automatic soot blowers might also have been omitted from centralization, but it was convenient to include them, and since they may operate up to 80 per cent of the time, there is some value in having their program control under surveillance of the operators.[3]

Our purpose, then, has been to centralize control of all those functions which require adjustment for safe and dependable operation over the normal load range of each machine which, in the case of Oswego, represents a load range from about 10 to 100 megawatts. The inclusion of safe operation necessitated provision for emergency shutdown.

There has been advocacy of separation of electric controls,[9] that is, the electric switchboard from the boiler and turbine controls. The authors have no disagreement with such separation in some instances. It is conceivable that some plants, located in load centers, may require more space and personnel in connection with transmission and distribution than in connection with the electric control of the generating units. In such instances, we suggest that consideration be given to separating the extraneous jobs from the power plant jobs instead of separating the power plant jobs. If sufficient extraneous electric controls are to be located in the power plant, a separate control location might well be established for them.

The value of closely co-ordinated operation of a unit by means of centralized control is illustrated in nearly every operating abnormality.

For example, when there is an alarm of coal failure to a mill, the electrical operator is immediately alerted and stands by to keep steam pressure up. This results in load drops of 5 or 10 megawatts for a few minutes on two or three days a month during wet and frozen coal periods. Probably the load drops would be greater due to efficiency loss if steam pressure were allowed to fall off.

When operating on block loads, and the load supervisor calls for a change, the switchboard operator announces what is to be done as he steps to the panel. The mechanical man will advise him if there is reason to make the change in any manner different from normal. If a quick change is required, the rate of change is determined by ability to maintain water level, steam pressure, draft or whatever may be most critical at that moment. If electrical trouble occurs, the boiler operator likewise knows at once the nature of changes necessary to restore order. The two operators watch each others' moves and to some extent observe each others' instruments.

A new station, identical to Oswego in arrangement, is now under construction, and similar centralized control will be incorporated. The supervising operators, who will come from a plant in which there is a separate electrical control room, are enthusiastic about the single control room arrangement for the new station. They plan to give all of the control room operators the type of training required for unit operators so that any one of them can handle either the switchboard or mechanical control boards. This will simplify the setting up of shift schedules by not having two types (electrical and mechanical) of control room operators, and it also will permit maximum flexibility of manpower in times of trouble. That is, each of the operators who has no trouble on his board can assist any other one.

The units comprising the initial installation will be of the reheat type. Study of the operation of such units indicates a greater need for co-ordination between boiler, turbine, and generator controls than is the case with straight-through machines. A joint recommendation of the boiler and turbine manufacturers calls for automatic trip-out of fires in the event of trip-out of the generator or sudden major load loss. It also calls for some of the meters and supervisory devices to be available to both the mechanical and electrical operators. Centralization of controls is an ideal way of doing this.

In conclusion, then, the desirability of

Figure 2. Control panels for units 1 and 2 at Oswego Steam Station

Electric control panel is in background and each of the two panels on the sides contains the instruments and controls for one boiler-turbine unit and its auxiliaries

centralized controls in generating stations of the independent-unit type of design has been confirmed by nearly ten years of experience with two units at Oswego. Observations at Oswego and independent studies have demonstrated its advantages to a different operating group which is experienced with separate electrical control rooms. Even greater benefits can be foreseen when centralization is applied to the new, more complicated heat cycles.

References

1. Advanced Design—Original Features Embodied in New 160,000 Kw Oswego Steam Station, N. R. Gibson, H. M. Cushing. *Transactions*, American Society of Mechanical Engineers (New York, N. Y.), August 1942.

2. Experiences with Automatic Air Soot Blowers at the Oswego and Charles R. Huntley Stations, H. L. Smith. *Transactions*, American Society of Mechanical Engineers (New York, N. Y.), February 1949.

3. Centralized Instrumentation and Controls for Steam Electric Power Stations, B. C. Mallory. *AIEE Transactions*, volume 69, part I, 1950, pages 591–97.

No Discussion

The Determination and Allocation of the Capacity Benefits Resulting from Interconnecting Two or More Generating Systems

C. W. WATCHORN
MEMBER AIEE

THE interconnection of two or more electric generating systems always reduces the amount of generating capacity required to be installed as compared with that which would be required without the interconnection. The amount of such reduction may be large or small, depending on the interrelation of the various factors and characteristics of the interconnecting systems and the desired level of service reliability. The installation of the transmission facilities that are necessary to bring about the interconnection may or may not be justified. This fact can be determined only by a proper economic comparison of the alternate installations.

Having once decided on interconnecting two or more generating systems, some plan or basis is necessary for the allocation of the resulting capacity benefit among the interconnecting systems.

This paper treats generally of the several considerations and factors involved in the determination of the capacity benefit resulting from interconnecting several generating systems as one factor in the determination of the justification of the interconnection, and also as a basis for determining the installed capacity obligations of the interconnecting systems. In addition, the article submits what is believed to be a logical and equitable basis for the determination of such obligations as the result of the allocation of such benefit among the interconnecting systems.

Paper 50-188, recommended by the AIEE Joint Subcommittee on Application of Probability Methods to Power-System Problems and approved by the AIEE Technical Program Committee for presentation at the AIEE Summer and Pacific General Meeting, Pasadena, Calif., June 12–16, 1950. Manuscript submitted July 5, 1949; made available for printing May 1, 1950.

C. W. WATCHORN is with the Pennsylvania Water and Power Company, Baltimore, Md.

Determination of Capacity Benefits

The determination of the capacity benefits resulting from the interconnection of generating systems involves only the evaluation of the composite effect of all the diversities that may exist among them. These diversities, in addition to those resulting from any differences that may exist in the times of occurrence of daily peak loads, include those properly involved in "long-time load-forecasting errors," those resulting from the amount of variation in the magnitude of the daily peak loads, from maintenance requirements, seasonal reductions in the load-carrying capability of both the hydro and steam capacity and from forced outages of generating facilities, including the effect of the number, sizes, pressures, and arrangements of the turbines and boilers. The true composite effect of all these diversities can best and most logically be evaluated by means of probability methods, since such methods automatically give proper weight to each of these factors in accordance with the various conditions relating to the several systems. Various phases of the application of probability methods to this type of problem are discussed in several papers that have been presented during the past several years.[1–6]

Figure 1 illustrates certain of the general results obtained by an application of probability methods to the problem of determining the capacity benefit resulting from the interconnection of two systems. This illustration is developed with respect to Systems B and C treated in the Tables. The curve for the two systems combined, as well as those for the systems separately, are shown on the basis that there are no intra- nor inter-system transmission limitations. If two or more generating systems interconnect, assuming no transmission limitations, they operate, with some given amount of installed generating capacity, at the same level of service reliability regardless of what their separate ideas or desires may be. Thus, when two or more generating systems interconnect, the capacity benefits of the interconnection must be determined on the basis of a mutually agreeable level of service reliability.[7] In other words, regardless of any differences in the reliability that may have existed among the several systems for separate operation, some agreement must be reached as to the capacity requirements of the several systems predicated on a degree of reliability that will be the objective with interconnected operation.

It is believed that a reasonable level of service reliability, when the effect of probable load forecasting errors is included in the evaluation, is a probability of failure to carry the load of in the order of an average rate of one day in from eight to ten years. For the purpose of this illustration, a probability of failure to carry the load one-half the distance between probabilities of 0.001 and 0.0001 was used, which corresponds to the probability of failure to carry the load at the average rate of one day in 8.66 years. The computed capacity benefit resulting from interconnecting Systems B and C, or the reduction in the installed capacity requirements for this degree of reliability, is 170,000 kw with adequate interconnection capacity, which is the difference, along the dotted horizontal line, between the two solid line curves to the right of

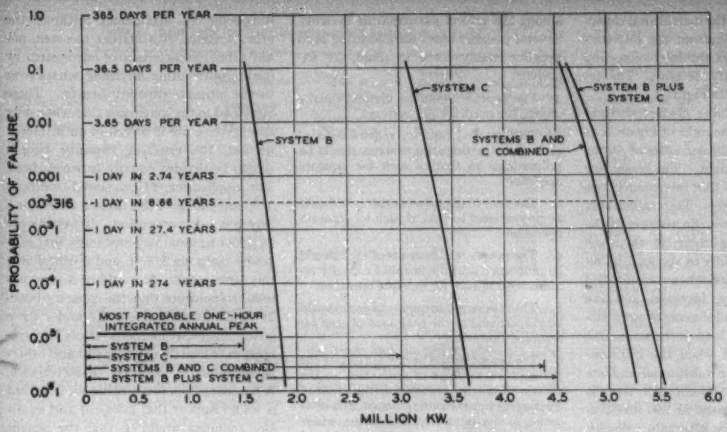

Figure 1. Probability of failure to carry the load versus installed capacity

Figure 1. This is the basic or the indicated maximum capacity benefit, and results when the transmission capacity is equal to at least one-half the amount of such computed deferrable capacity. With interconnecting transmission capacity smaller than one-half the amount of such computed deferrable capacity, the indicated capacity benefit would be reduced to an amount equal to twice that of such smaller transmission capacity.

These results are modified by the fact that the units are of discrete sizes. Because of this fact it would be a remote coincidence if just exactly the desired level of service reliability were obtained. Although a slightly smaller level of service reliability than that selected as standard may be tolerated, what may otherwise appear to be a comparatively small capacity deficiency may result in a grossly inadequate degree of service reliability. This characteristic is indicated by the steepness of the curves in Figure 1. Consequently, as a practical matter the experience probably will be that a greater amount of installed capacity generally will be available than that indicated as being the minimum requirement. This experience would be the case regardless of whether or not the systems are interconnected. The result is that when two or more generating systems are interconnected, additional benefits over those computed in the manner illustrated by Figure 1 are obtainable as the result of staggering the installation of capacity among the interconnecting systems. The amounts of such additional capacity benefits are variable and depend on the differences between the indicated and actual installed capacity requirements, the capacity of the individual units being installed, and the amount of the transmission capacity.

Figure 2 shows the average capacity benefits, over a period of years, resulting from interconnecting Systems B and C with various interconnecting transmission capacities and various capacities of the individual units being installed. The manner in which these results were determined are given in the Appendix.

It will be noted that the curves of Figure 2 are discontinuous for transmission capacity equal to half the capacity of the units being installed, half the capacity benefit computed in the manner illustrated by Figure 1, and transmission capacities equal to the sum of these two latter amounts. The reasons for these characteristics are seen from the Appendix and Figure 4 treated therein. These charac-

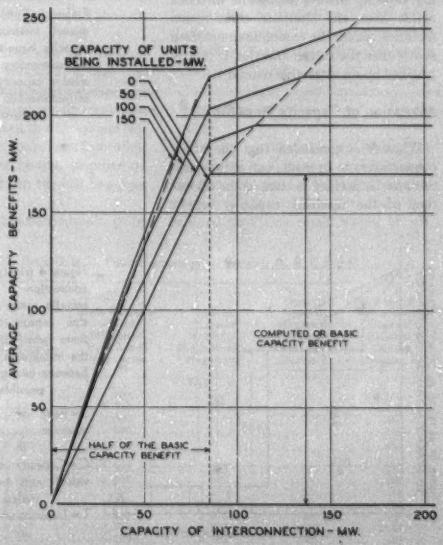

Figure 2. Interconnection capacity benefits versus transmission capacity (Systems B and C)

teristics mean that the incremental capacity benefit resulting from the interconnection decreases as the interconnecting transmission capacity increases. This relationship is shown in Figure 3.

Note the converging characteristic of the two curves to the right of Figure 1, as the service reliability decreases or as the capacity becomes tight. The reason for this characteristic is that interconnections do not create capacity. They rather only make possible greater effective use of the available generating capacity, which use decreases quite rapidly as the load, as related to some specified amount of installed generating capacity, increases and the amount of the installed generating capacity in excess of the load decreases. This is particularly true when the interconnecting facilities are substantial and are not the limitation. By contrast, there is no comparable decrease in the effectiveness with which the alternate capacity may be used as the capacity becomes tight. Thus, for a low level of service reliability, the capacity benefit of an interconnection is greatly reduced. Additional generating facilities are then obviously required to restore a reasonable level of reliability, but such additional generating capacity would be smaller with an interconnection than without. Thus, an interconnection is a substitute for installed generating capacity only where properly backed up. It is believed that a corollary to this characteristic is that the generating capacity always should be installed rather than the alternate transmission facilities, unless the economic comparison shows that the interconnection is clearly justified by an attractive margin.

Allocation of Capacity Benefits

When it is concluded that the interconnection is to be made, one of the questions to be decided is that of the allocation of the resulting capacity benefit among the several participating systems. Several possible bases for allocating such benefits readily come to mind, for example:

1. The benefit should be divided equally among the participating systems.

2. The installed capacity requirements of each of the participating systems should be proportional to that of each for separate operation.

3. The reserve requirements of each should be proportional to that of each for separate operation.

4. The reserve requirements of each should be proportional to the installed capacity requirements of each for separate operation.

5. The reserve requirements of each should be proportional to the peak load of each for separate operation.

6. The benefit should be divided among the participating systems in proportion to the additional benefits obtained as the result of treating each participating system as a newcomer in the interconnected group, which method may be termed "the additional benefits method of allocation."

7. The benefit should be divided among the participating systems in proportion to the benefits for all combinations of two's among them, which may be termed "the mutual benefits method of allocation."

There may be still other bases.

When only two systems participate in an interconnection, the capacity benefit is a mutual benefit to which neither system by itself contributes any more nor less than the other, the benefit thus being impossible of attainment without the other system, with neither the size, nor any other characteristic of one system by itself, contributing anything whatsoever to the ultimate capacity benefit. These facts lead to the conclusion that when only two systems are involved in an interconnection, the resulting capacity benefit should be divided equally between them. The application of suggested methods 1, 6, and 7 all give this desired result for a 2-system interconnection. It would only be under unusual circumstances that suggested methods 2, 3, 4, and 5 would give this same result. It would be a very unusual coincidence that the capacity benefit would be divided equally under these latter suggested methods unless the systems were exactly equal in size and otherwise similar in essential characteristics. When more than two systems are involved it would appear that a logical and equitable requisite would be that the benefit allocated to any one of the participating systems should not be reduced by the addition of any one or more of the other participants into the interconnection. Suggested method 1 generally will not meet this requirement because, if the result with the inclusion of certain of the participating systems in the interconnected group is that small, additional capacity benefits are obtained for all combinations with the other participating systems, while with the similar in-

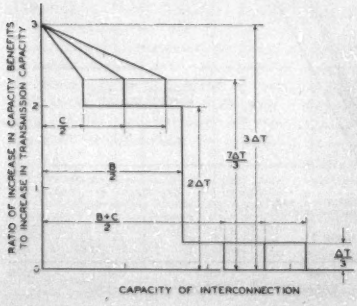

Figure 3 (left). Incremental interconnection capacity benefits versus interconnecting transmission capacity for the interconnection of two systems

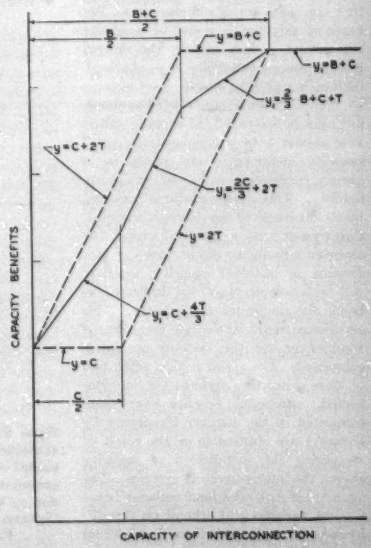

Figure 4 (right). Interconnection capacity benefits versus transmission capacity for the times when staggering the installation of units between two systems is possible

B = Basic or computed maximum capacity benefit

C = Capacity of individual units being installed

T = Transmission capacity

Table I. Basic Data for Three Interconnected Systems A, B and C

Systems and Combinations of Systems	Installed Capacity Requirements, Megawatts	Most Probable 1-Hour Integrated Peak Load, Megawatts	Sum of Separate Capacity Requirements, Megawatts	Capacity Benefits, Megawatts (Column 4 Minus Column 2)	Reserve Requirements, Megawatts (Column 2 Minus Column 3)
A	560	400			160
B	1,725	1,500			225
C	3,360	3,000			360
Total	5,645	4,900			745
A and B	2,220	1,890	2,285	65	330
A and C	3,845	3,385	3,920	75	460
B and C	4,915	4,400	5,085	170	515
A, B, and C	5,395	4,785	5,645	250	610

clusion of other participating systems the additional capacity benefits are large, and the total benefit were allocated equally among all, those systems for which the additional capacity benefits are large would be allocated a smaller amount of capacity benefit when those systems for which the additional capacity benefits are small are included than when such latter systems are not included. Such a result is inequitable to those systems for which the additional capacity benefits are large, and they would have a just basis for objecting to further interconnection that would increase their capacity requirements, even though the making of such interconnection would be justified from an over-all point of view. A somewhat opposite result would be obtained by the use of suggested method 6, "the additional benefits method of allocation," in that, if relatively larger additional benefits are obtained as the result of the inclusion of certain of the participating systems for all combinations with other systems, than with the inclusion of the other systems as additional participants such system would be allocated such a large portion of the total capacity benefit under this method that cases may well result for which other participating systems would be allocated a smaller amount of capacity benefit when such system is included in the interconnection than when it is not included.

These considerations then leave us with only suggested method 7, "the mutual benefits method of allocation," as apparently meeting the two requirements of equal division among the participants when two companies interconnect and of not reducing the allocated benefit to any of the participating parties with the addition of one or more of the other participating systems to the interconnection.

An allocation of the benefit resulting from the interconnection of three systems has been applied to the conditions set forth in Table I, and the results thereof have been tested by the two previously-proposed basic requirements of a proper allocation. The method of making this allocation and the results obtained therefrom are shown in Table II. These calculations are shown with respect to the capacity benefits computed in the general manner illustrated by Figure 1, which we have termed "the basic capacity benefits," without any adjustment for any additional capacity benefits that may result from the staggering of capacity installations. It is believed that this situation is handled satisfactorily by the procedure suggested in the section called Discussion.

In Table I the allocation has been made on the basis that the portion of the total benefit (that is, the 250-megawatt saving shown as the last item of column 5) allocated to each should be proportional to the sum of the benefits for the various combinations of two's among all the participating systems.

Table II illustrates such calculations. Here the benefit allocated on the suggested "mutual benefits method of allocation" meets the stated requirement that the allocated benefits to any system not be reduced by the inclusion of an additional participating system (comparison of the results shown in the last two lines of the table).

This basis of allocation appears to be equally satisfactory with the inclusion of a fourth participating system, System D, the basic data for which conditions are shown in Table III.

Table II. Allocation of Capacity Benefit to Systems A, B and C

Combinations of Systems by Two's	Benefits for Combinations of Two's A	B	C	Total
A and B, megawatts	65	65		130
A and C, megawatts	75		75	150
B and C, megawatts		170	170	340
Total, megawatts	140	235	245	620
Allocation ratios, per cent (from Totals)	22.58	37.90	39.52	100
Allocated benefits, megawatts	56	95	99	250
Minimum allocable benefits, megawatts	37.5	85	85	

The allocation of the total capacity benefits of 350 megawatts resulting from the data of Table III for this group of four interconnected systems, in the same manner as for the group of three interconnected systems as shown on Table II, is shown in Table IV.

Table V shows data not previously shown for combinations of three's among the four systems considered in Tables III and IV, from which, together with prior data, as related to these various conditions, the allocations of capacity benefits for the various combinations of three's were made in the manner shown in Tables II and IV, with the results shown in Table VI.

Discussion

The tables have shown that "the mutual benefits method of allocation" has met the previously stated requirements for all the conditions studied. It is believed that this result would be ob-

Table III. Basic Data for Four Interconnected Systems A, B, C and D

Systems and Combinations of Systems	Installed Capacity Requirements, Megawatts	Most Probable 1-Hour Integrated Peak Load, Megawatts	Sum of Separate Capacity Requirements, Megawatts	Capacity Benefits, Megawatts (Column 4 Minus Column 2)	Reserve Requirements, Megawatts (Column 2 Minus Column 3)
A	560	400			160
B	1,725	1,500			225
C	3,360	3,000			360
D	950	800			150
Total	6,595	5,700			895
A and B	2,220	1,890	2,285	65	330
A and C	3,845	3,385	3,920	75	460
A and D	1,435	1,190	1,510	75	245
B and C	4,915	4,400	5,085	170	515
B and D	2,590	2,285	2,675	85	305
C and D	4,215	3,780	4,310	95	435
A, B, C, and D	6,245	5,565	6,595	350	680

Table IV. Allocation of Capacity Benefit to Systems A, B, C and D

Combinations of Systems by Two's	Benefits for Combinations of Two's A	B	C	D	Total
A and B, megawatts	65	65			130
A and C, megawatts	75		75		150
A and D, megawatts	75			75	150
B and C, megawatts		170	170		340
B and D, megawatts		85		85	170
C and D, megawatts			95	95	190
Total, megawatts	215	320	340	255	1130
Allocation Ratios, per cent (from Totals)	19.02	28.32	30.09	22.57	100
Allocated Benefits, megawatts	67	99	105	79	350
Minimum Allocable Benefits,* megawatts	56	98	102	70	

*From Table VI.

Table V. Capacity Benefits for Combinations of Three's of Systems A, B, C and D

Combinations of Systems	Installed Capacity Requirements, Megawatts	Most Probable 1-Hour Integrated Peak Load, Megawatts	Sum of Separate Capacity Requirements, Megawatts	Capacity Benefits, Megawatts (Column 4 Minus Column 2)	Reserve Requirements, Megawatts (Column 2 Minus Column 3)
A, B, and C	5,395	4,785	5,645	250	610
A, B, and D	3,085	2,675	3,235	150	410
A, C, and D	4,725	4,200	4,870	145	525
B, C, and D	5,765	5,180	6,035	270	585

Table VI. Allocated Capacity Benefits for Combinations of Three's of Systems A, B, C and D

Systems	A	B	C	D	Total
	Megawatts				
Allocated Benefits	56*	95	99		250
Minimum Allocable Benefits	37.5	85	85		
Allocated Benefits	47	50		53	150
Minimum Allocable Benefits	37.5	42.5		42.5	
Allocated Benefits	45		50	50	145
Minimum Allocable Benefits	37.5		47.5	47.5	
Allocated Benefits	98*		102*	70*	270
Minimum Allocable Benefits	85		85	47.5	

*Minimum allocable benefits for the combination of four for these systems (last line of Table IV).

tained for all conditions so long as the installed capacity requirements were determined on the basis of a consistent application of probability methods. Capacity requirements could be assumed or be determined by means other than by an application of probability methods, for which the mutual benefits method might reduce the allocated benefits to one or more of the participating systems with the inclusion of additional systems in the interconnection. If such should occur, it would be the result of inconsistencies of such stated capacity requirements among the various combinations of systems rather than of the method of allocation suggested herein.

It is possible that for certain conditions, particularly those for which there is marked seasonality in the load requirements of some of the participating systems and possibly also with considerable load diversity, that the allocated capacity benefits to one or more of the participating systems may be of such amounts that their resulting capacity requirements would be smaller than their respective most probable annual peak loads. It is not believed that there is anything illogical in such results. Greater reliability would be required of the facilities interconnecting such systems for such conditions than with the other participating systems for which this condition does not obtain.

The same considerations that apply to installed capacity apply also to the allocation of operating capacity benefits. At times the allocation of the operating capacity benefits might also result in the required operation of a smaller amount of capacity by some one or more systems than the amount of their expected loads. Under such circumstance more reliable interconnection facilities would again be required than otherwise.

In practice, the actual capacity installed usually would be greater than that actually required. This would be true of each of the participating systems for separate operation; but for the interconnection as a whole, if the full potential benefits of interconnecting are to be realized, a few of the participating systems and possibly only one would have excess installed capacity and the others would be deficient. This situation requires an adjustment so that the over-all savings may be equitably distributed to all the participating systems. The algebraic sum of these resulting capacity excesses and deficiencies would be equal to the interconnection capacity excess. This interconnection excess should be allocated to each of the participating systems, using the same allocation ratios used to allocate the capacity benefits as shown in Tables II and IV. The deficient capacity systems should be debited with the sum of their respective capacity deficiencies and allocated portions of the interconnection capacity excess, which totals should be credited to the excess capacity systems. Such adjustments could be made either by bookkeeping entries related to capacity or by periodic money settlements. If the latter is to be the practice, a further adjustment would be required to compensate the debit systems where there would be a loss in operating economies because of foregoing the earlier installation of additional economical generating capacity.

Situations may arise where one or more of the participating systems, for various reasons, may desire to install or operate more capacity than that determined as its requirements as a participant. In such case, it alone should be responsible for such additional capacity.

The successful and satisfactory operation of such interconnections require reasonable co-ordination and co-operation among the participating systems, particularly as related to maintenance schedules, which factor is possibly subject to wider control than any of the others that are involved in the determination of the installed capacity requirements. The question as to the loads to be used as a basis for the determination of the installed capacity requirements might present some difficulties. However, these difficulties would be greatly minimized by the use of a mutually agreeable statistical basis for developing the loads to be used for determining the installed capacity requirements. Such a basis would obviate any point of an after-the-fact adjustment for positive load forecasting errors. Such deviations from the forecast loads comprise one of the factors or contingencies for which reserve is provided and consequently their occurrence does not mean

that insufficient capacity was provided any more than if the reduced margin between the available capacity and the load were the result of forced outages of generating facilities. All that is required is that the installed capacity be provided as related to reasonably stable information as related to load forecasts in so far as it is possible to do so, in very much the same general manner as for forced outages of generating facilities.[8] The result is that there would be no more basis or point for hindsight adjustments of the determinations of the capacity requirements after-the-fact with an interconnection than without, which latter is obviously impossible to attain.

There are special situations that may arise that will need to be considered in connection with the actual allocation of capacity benefits that it is not possible to consider in detail in a general paper. For example, the question may arise as to the disposition of the increase, if any, in the firm capacity[4] of the hydro plants that may be available on one or more of the interconnecting systems, that may result from the interconnection. It is believed that such capacity benefits are sufficiently different from the capacity benefits resulting from the interconnection of systems, upon which the installed capacity is all firm, to warrant different treatment to that suggested herein. The same considerations apply to peaking steam capacity. Likewise, after an interconnection is made it is very likely that the participating systems will develop the generating facilities with larger capacity units than if operated separately. This would be more particularly true for the smaller participating systems than the larger. Such a practice would be in line with attaining maximum economy for the interconnecting systems. On the other hand, this practice would tend to result in somewhat higher capacity obligations for the smaller systems than if they continued to install the smaller size units as for separate operation. These increased capacity obligations for the smaller systems, however, are at least largely offset by the greater economies, both as to annual charges per kilowatt of installed capacity and as to operating costs, resulting from the installation of such larger units, which, together with their share of the allocated capacity benefits and of the operating economies resulting from interchange purchases and sales, should, nevertheless, make interconnecting very attractive in many cases, even for the smaller systems.

Likewise, there is the problem as to the allocation among the systems participating in the interconnection of the costs of the interconnecting facilities. This problem is also beyond the scope of this paper, but it would appear that such allocation may well be on approximately the same basis as the allocation of the capacity benefits.

Conclusion

The capacity benefits that result from the interconnection of two or more electric generating systems can best and most logically be evaluated by means of probability methods, and such benefits are most equitably allocated among the systems participating in the interconnection by means of "the mutual benefits method of allocation," since it is based on the benefits mutually contributed by the several systems.

Appendix

After the capacity requirements are adjusted for the allocated computed or basic capacity benefit, two interconnected systems, for which the interconnecting transmission capacity is equal to or greater than half the capacity of the individual units being installed, would require one less unit to be installed 50 per cent of the time, as a matter of chance, as the result of staggering, and still result in the interconnected systems satisfying the combined capacity requirements. This situation results when, without the staggering of the capacity installations, the sum of the installed capacity would be in excess of the indicated combined installed capacity requirements by an amount larger than the capacity of the individual units being installed. The other 50 per cent of the time, the sum of the installed capacity without staggering would be in excess of the indicated combined installed capacity requirements by an amount smaller than the capacity of the individual units being installed, and it is not possible to stagger the capacity installations in such cases.

When staggering is possible, the best results or utilization of the available facilities are obtained when the system with the smaller capacity deficiency continues as the deficient system. In such case the capacity deficiency of the deficient capacity system would range from zero to the smaller of the capacity of the interconnecting transmission facilities and 50 per cent of the capacity of the individual units being installed. The total capacity benefit, for the 50 per cent of the time when staggering is possible, is then equal to the capacity of the individual units being installed and twice the excess of the tie capacity over the capacity deficiency of the deficient capacity system. We then may write

$$y = C + 2(T - x) \tag{1}$$

where

y = the total capacity benefit

C = the capacity of the individual units being installed

T = the capacity of the interconnecting transmission facilities

x = the capacity deficiency of the deficient capacity system

The minimum value of y is C, at which value it remains constant for x equal to T, from T and x equal to zero up to T and x both equal to $C/2$. Since this is the maximum value x can have, y increases thereafter at a 2-to-1 ratio for increasing values of T up to T equal to $(B+C)/2$, where B is the basic capacity benefit with no transmission limitations, determined as discussed in the body of the paper, for which value of T, y is at its maximum value of $(B+C)$. The minimum value x can have is zero, at which value y is again equal to C for T also equal to zero; after which y increases again at a 2-to-1 ratio for increasing value of T, up to T equal to $B/2$, for which y is again at its maximum value of $(B+C)$. These values of y are the boundary values, and they describe a parallelogram as shown by the dash lines of Figure 4. All other values of y for values of x between zero and $C/2$ fall within this parallelogram.

The chances are equal that x will have any value between zero and $C/2$ for T equal to and between $C/2$ and $B/2$. The relative number of occurrences of y for some such value of T is then $(C/2-x)$. We may then weight y with respect to this quantity, as follows

$$y_1 = \frac{\int_0^{C/2}(C/2-x)\{C+2(T-X)\}\,dx}{\int_0^{C/2}(C/2-x)dx} \tag{2}$$

from which we obtain

$$y_1 = \frac{2C}{3} + 2T \tag{3}$$

This means that for values of T equal to and between $C/2$ and $B/2$, the weighted average value of y for the various values of T is two-thirds the distance between the minimum value of $2T$ and the maximum value of $(C+2T)$. For T equal to $C/2$, y_1 is equal to $5C/3$. Then since for T equal to zero, y, and also y_1, are equal to C, we may write for values of T equal to and between zero and $C/2$, assuming a straight line

$$y_1 = C + \frac{4T}{3} \tag{4}$$

This expression also may be obtained in the same general manner as equation 3, as follows, by similarity, for values of T equal to and between zero and $C/2$

$$y_1 = \frac{\int_0^{T}(T-x)\{C+2(T-x)\}\,dx}{\int_0^{T}(T-x)dx} \tag{5}$$

from which we have

$$y_1 = C + \frac{4T}{3} \tag{6}$$

which is identical to equation 4.

Then since for T equal to $B/2$, we have from equation 3 that y_1 is equal to $(2C/3+B)$, and for T equal to $(B+C)/2$, y and y_1 are both equal to $(B+C)$, we may write for values of T equal to and between $B/2$ and $(B+C)/2$, again assuming a straight line

$$y_1=\frac{2}{3}(B+C+T) \tag{7}$$

These values of y_1 of equations 3 and 4 or 6 and 7 are shown by the solid lines of Figure 4.

The weighted average total capacity benefits expressed by equations 3 and 4 or 6 and 7 are available 50 per cent of the time. The other 50 per cent of the time staggering is not possible and for the corresponding conditions for equations 3 and 4 or 6

$$y_1=2T \tag{8}$$

and for the conditions for equation 7, the basic capacity benefit

$$y_1=B \tag{9}$$

For values of T equal to and smaller than $C/2$, the percentage of time the conditions of equations 4 or 6 exist, or for which staggering is possible, is

$$p'=\frac{T}{C} \tag{10}$$

and for which the conditions of equation 8 exist, or for which staggering is not possible, is

$$p''=1-\frac{T}{C} \tag{11}$$

We then may write for the total over-all weighted average capacity benefit, for T equal to and between zero and $C/2$

$$y_2=\frac{T}{C}\left(C+\frac{4T}{3}\right)+\left(1-\frac{T}{C}\right)2T \tag{12A}$$

$$=T\left(3-\frac{2T}{3C}\right) \tag{12}$$

for T equal to and between $C/2$ and $B/2$

$$y_2=0.5\left(\frac{2C}{3}+2T\right)+0.5(2T) \tag{13A}$$

$$=\frac{C}{3}+2T \tag{13}$$

for T equal to and between $B/2$ and $(B+C)/2$

$$y_2=0.5\left(\frac{2}{3}\right)(B+C+T)+0.5B \tag{14A}$$

$$=\frac{5B}{6}+\frac{C}{3}+\frac{T}{3} \tag{14}$$

and for T equal to and greater than $(B+C)/2$

$$y_2=0.5(B+C)+0.5B \tag{15A}$$

$$=B+\frac{C}{2} \tag{15}$$

Equations 12, 13, 14, and 15 are shown plotted on Figure 2, as functions of T, for Systems B and C for which B of the equations is equal to 170,000 kw and for C of the equations equal to zero, 50,000 kw, 100,000 kw, and 150,000 kw.

It is interesting to note that equation 12 is an exponential and that equations 13, 14, and 15 are linear; that equations 12 and 13 are both equal to $4C/3$ for T equal to $C/2$; equations 13 and 14 are both equal to $(B+C)/3$ for T equal to $B/2$; and that equation 14 equals equation 15 for T equal to $(B+C)/2$.

References

1. Determination of Required Reserve Generating Capacity, **W. J. Lyman.** *Electrical World* (New York, N. Y.), volume 127, number 19, May 10, 1947, pages 92–95.

2. Generating Reserve Capacity Determined by the Probability Method, **Guiseppe Calabrese.** *AIEE Transactions*, volume 66, 1947, pages 1439–50.

3. Calculating Probability of Generating Capacity Outages, **W. J. Lyman.** *AIEE Transactions*, volume 66, 1947, pages 1471–77.

4. Outage Expectancy as a Basis for Generator Reserve, **Howard P. Seelye.** *AIEE Transactions*, volume 66, 1947, pages 1483–88.

5. Probability Methods Applied to Generating Capacity Problems of a Combined Hydro and Steam System, **E. S. Lorne, C. W. Watchorn.** *AIEE Transactions*, volume 66, 1947, pages 1645–57.

6. Probability Theory Helps Determine System Reserve Generating Capacity, **G. Calabrese.** *Power* (New York, N. Y.), volume 92, July 1948, pages 423–26.

7. Planning the Development of a Metropolitan Electric System, **M. L. Waring.** *AIEE Transactions*, volume 67, part II, 1948, pages 1467–73.

8. Outage Rates of Steam Turbines and Boilers and of Hydro Units, **AIEE Committee Report.** *AIEE Transactions*, volume 68, part I 1949, pages 450–57.

No Discussion

A Method of Estimating Lightning Performance of Transmission Lines

AIEE COMMITTEE REPORT

SINCE the recognition of the direct lightning stroke as the principal factor in causing outages of high-voltage transmission lines during thunderstorms, engineers have sought to obtain and correlate data on the nature of lightning, and to apply such data toward improvements in the design of transmission systems. Such investigations have been pursued through field and laboratory research accompanied by theoretical studies, and remarkable progress has been made in many directions. Indeed, so much has been learned about lightning protection of electric power systems during the past 20 years one might erroneously conclude that the problem has been solved completely.

Many engineers concerned with the design or operation of high-voltage transmission lines have devised methods of combining the known information on the electrical characteristics of lightning with those of the lines so that their performance might be studied more intelligently and that economical methods for reducing lightning tripouts could be developed.

Notwithstanding the rather general appreciation of the fundamental theoretical considerations underlying all these methods, there have been substantial differences in approach and in the application of engineering judgment among well-informed authors.

It is the purpose of this report to present a method of estimating the lightning performance of transmission lines based on collective evaluation of those factors believed to be of greatest significance and incorporating the results of modern methods of analysis.[1] It is the hope of the Lightning and Insulator Subcommittee that a method so evaluated will prove useful to transmission engineers and that any limitations of the method which remain will stimulate the research needed to remove them. In general, one may classify transmission-line lightning protection measures as those whose function is to prevent the initial insulation sparkover, and those whose function is to avoid a line tripout by preventing sustained fault current following such a flashover. This report is confined essentially to those of the first class, although the application of the method to certain types of construction which fall in both classifications will be evident.

Lines Equipped with Ground Wires

It is impractical to provide a sufficiently high impulse insulation level to withstand the voltage which is developed when a phase conductor is struck by any but the weakest lightning strokes whose currents have been recorded. It is therefore of primary importance to employ shield or ground wires located to intercept direct strokes and to divert the lightning current to earth through the steel towers or conductors provided on wood pole structures for this purpose.

The fundamental objective of line designs employing ground wires is to reduce the impulse voltage impressed across any element of insulation between phase conductors and grounded conductors to a value below the impulse flashover voltage of that element. The first step toward meeting this requirement is the use of properly located ground wires. The next step is to devise means of minimizing the voltage which appears across the insulation as a result of the flow of lightning current to earth. Finally, one may investigate whether it is economically feasible to increase the insulation beyond the levels dictated by consideration of switching surges, either by the addition of insulator units or the use of supplementary wood insulation. It is outside the scope of this paper to discuss design features in detail, but certain basic principles and data will be emphasized in order to indicate the factors believed to be of greatest importance in design.

Factors Affecting Insulation Flashover

The principal factors which determine the impulse voltage impressed across any element of line insulation are now well known and may be listed as follows:

1. The magnitude of the lightning-stroke current.
2. The wave shape of the lightning-stroke current.
3. The inductance and ground resistance of towers.
4. The span length.
5. Electromagnetic coupling as influenced by line configuration, conductor spacing, and height above ground.

Some of these factors are influenced by secondary phenomena whose effects can only be approximated in any method of analyzing line performance which is to be of maximum usefulness to the design engineer. These will be discussed later in order to bring out the character of the engineering approximations involved and to indicate lines of further investigation.

Early theoretical investigations of the nature of lightning were concerned with estimating cloud potentials, and were followed by numerous field studies of the

Paper 50-163, recommended by the AIEE Transmission and Distribution Committee and approved by the AIEE Technical Program Committee for presentation at the AIEE Summer and Pacific General Meeting, Pasadena, Calif., June 12–16, 1950, and represented at the Middle Eastern District Meeting, Baltimore, Md., October 3–5, 1950. Manuscript submitted May 15, 1950; made available for printing May 15, 1950.

This report was prepared by the AIEE Working Group on Methods of Estimating the Lightning Performance of High-Voltage Transmission Lines of the AIEE Lightning and Insulator Subcommittee.

Personnel of the AIEE Working Group on Methods of Estimating the Lightning Performance of High-Voltage Transmission Lines: E. R. Whitehead, *Chairman*, L. V. Bewley, G. D. McCann, Jr., E. L. Harder, S. K. Waldorf, W. W. Lewis.

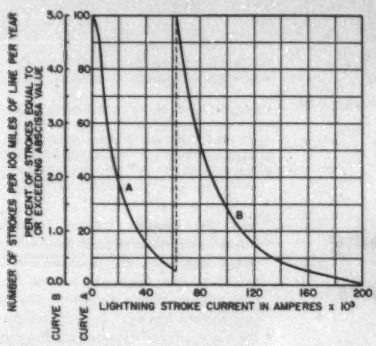

Figure 1 (left). Lightning-stroke current probability curve

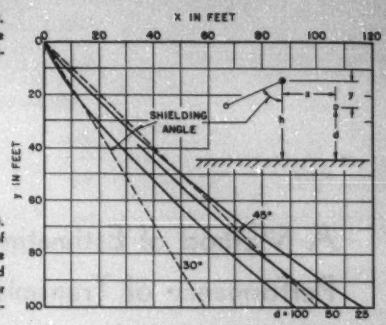

Figure 2 (right). Configuration of shielding wire and protected conductor for 0.1-per cent exposure

surge voltages impressed on transmission lines either directly or through induction by the lightning stroke. Such a development seemed natural since it is the impulse voltage across insulation which results in flashover or breakdown. Rapid development of travelling wave theory led to the concept of a surge impedance for the lightning stroke. With the analytical possibilities thus enlarged, methods of evaluating line performance were developed[2,3,4] which have contributed greatly to progress in line design. The method presented in this report is necessarily an extension and a refinement of these methods made possible by availability of more data and modern methods of engineering analysis.[5] It is based on the concept that the lightning-stroke current is independent of the terminating impedance which is struck.

Relation Between Factors Affecting Flashover

The general relations existing between the factors listed in the preceding section are also well understood. This relation usually takes the form of an equation which permits a computation of the crest magnitude of the lightning-stroke current necessary to cause sparkover of the insulating element involved. Thus, if normal frequency line-to-ground voltage and other minor potentials between conductor and ground are neglected

$$I = \frac{Vk}{(1-C)P} \tag{1}$$

where

I = crest-stroke current required to cause sparkover
V = insulation flashover voltage from standard curves for 1.5x40 microsecond-wave at a specified reference time lag
P = potential from point struck to ground per-unit stroke current
C = coupling factor in per unit
k = a factor converting V to the estimated minimum flashover voltage for the wave shape of the voltage impressed across the insulation

Once the critical value of stroke current required to cause sparkover thus has been obtained, it is only necessary to determine the frequency with which stroke currents have been found to equal or exceed this value in order to obtain the estimated frequency of flashover.

Upon more careful study it becomes apparent that the factors of equation 1 are in fact interrelated to a considerable extent. For example, the coupling factor is affected by corona on the ground wires, which is in turn dependent upon the ground wire voltage. In the case of a stroke to a tower, the potential P must include the effect of tower inductance even if tower capacitance can be neglected. The problem is even more complicated if a distributed grounding system or counterpoise is employed. Finally the insulation flashover voltage Vk should be the value determined for the particular wave shape impressed, which is itself dependent upon the span length and the ground resistance of adjacent structures.

The considerations just outlined require prohibitive labor if even a moderate range of possible design conditions is to be investigated. Through the use of the electric analogue computer it has been found possible to study a suitable range of line conditions with any desired shape of stroke current. The basic assumptions underlying the present approach to the problem are now discussed.

Lightning-Stroke Characteristics

The magnitude and wave shape of the lightning-stroke current have been recognized as factors of primary importance in the determination of impulse sparkover of line insulation. As a result of several years of field investigations, principally with magnetic links, a relatively large number of measurements of stroke current magnitude have been made available in the literature. These have been combined to give the stroke current magnitude frequency curve of Figure 1. Unfortunately there are insufficient data on the wave shape of stroke current to justify any attempt to establish frequency distribution curves with respect to wave shapes, and it has been necessary to exercise the collective judgment of the working group in the selection of a reference wave shape for the purposes of this report. In making such a selection it seemed desirable to choose both a wave front and a duration such that the resulting calculations would be conservative. Accordingly, a 2x40-microsecond wave shape was initially selected. It has been found, however, that only currents in excess of 30 to 40 kiloamperes are of practical importance on the better-designed lines, and for these currents a 4x40-microsecond wave shape has been chosen as more nearly representative for the purpose of this report. Wave shape is undoubtedly one of the most important and fundamental factors upon which fully adequate data are lacking.

Voltage Wave Shape and Insulation Flashover

In equation 1 the factor P represents the crest potential to ground at the point struck, per unit of stroke current. It replaces the tower-footing resistance R formerly used in this type of equation, and depends upon the tower inductance, the effective structure resistance to ground, the span length, and the wave shape of

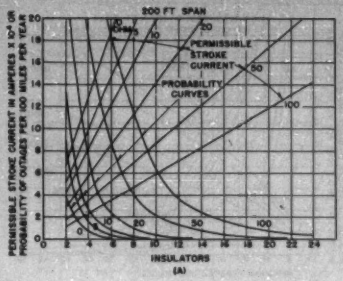

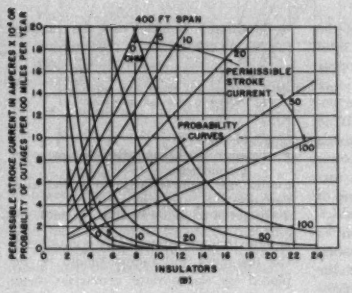

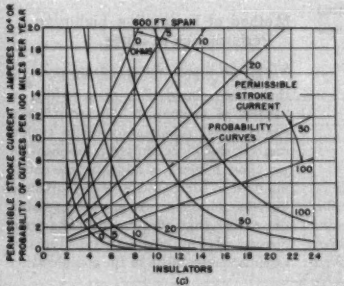

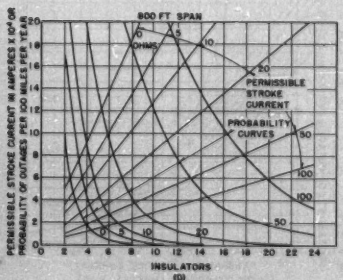

Figure 3. Curves for estimating line performance and insulation

The number of equivalent insulators is based upon 10-inch diameter $5^3/_4$-inch spaced units, and the outage probability is based on an isoceraunic level of 30 thunderstorm days per year

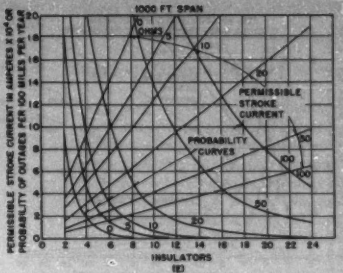

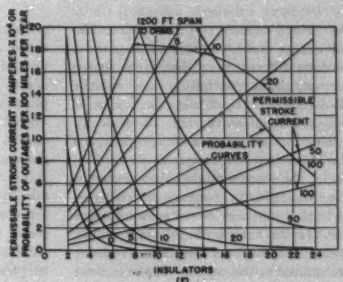

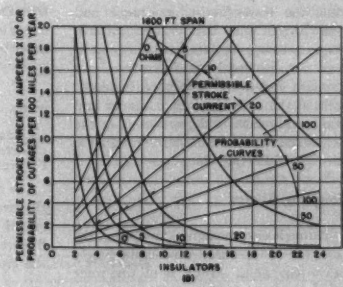

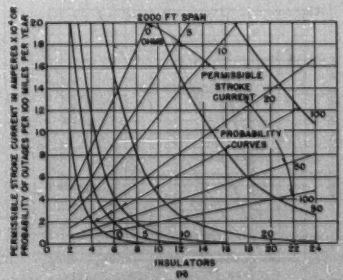

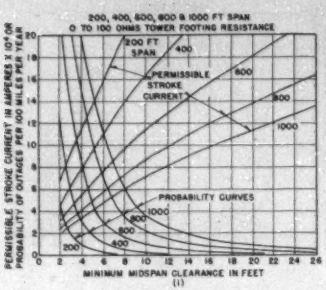

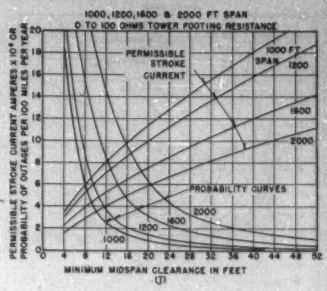

Figure 3 (Continued). Curves for estimating line performance and insulation

The number of equivalent insulators is based upon 10-inch diameter $5^3/_4$-inch spaced units, and the outage probability is based on an isoceraunic level of 30 thunderstorm days per year

the stroke current. Furthermore, the wave shape of this potential will in general be quite different from that of the stroke current, rising and falling more rapidly than the current. While calculations of the potential wave are theoretically straightforward, for practical purposes the labor involved is prohibitive. The use of the electric analogue computer in determining both tower and mid-span potentials has been described by Harder and Clayton,[5] and the results of a similar analysis for the 4-microsecond wave front are utilized in this report. In the present analysis tower or structure inductance has been held constant at 20 microhenrys while the tower-footing resistance and span length were varied over suitable ranges. An appropriate insulation spark-over voltage has been estimated from standard curves for suspension insulator units in the case of tower flashover and from extrapolated rod-gap curves in the case of mid-span flashovers through the selection of an equivalent time lag.

Coupling Factor

Through electromagnetic coupling, the potential of the phase wires immediately below the point struck is of the same polarity and proportional to that of the tower or ground wire. Thus the total ground-wire potential does not appear across the insulation, and the ratio of phase-wire potential to ground-wire potential is the coupling factor, C. If no corona is present, the coupling factor is the same whether computed from electrostatic or magnetic quantities if the surface of the earth is taken as a plane of zero potential and zero resistivity, which seems to be a reasonable assumption for conditions at the point struck. If corona is present, the effective radius of the ground wire is increased, and the electrostatic coupling is increased. It is believed that the best approximation to the actual coupling factor under surge conditions is given by

$$C = \sqrt{C_e C_m} \qquad (2)$$

where

C_m = magnetic coupling factor
C_e = electrostatic coupling factor
C = geometric mean coupling factor

C_m is computed using the actual radii of the ground wires and C_e is computed using effective radii of the ground wires as influenced by corona. The effective radii of the ground wires due to corona are given by McCann.[6] In either case the coupling factors are calculated by the equation

$$C = \frac{\log b/a}{\log 2h/r} \qquad (3)$$

where

$C = C_e$ or C_m
b = distance from conductor to image of ground wire
a = distance from conductor to ground wire
r = radius of ground wire
h = height of ground wire above ground

If more than one ground wire is employed, the distances and radius should be replaced by appropriate geometric mean quantities.

Method of Estimating Lightning Performance of Lines

The preceding discussion outlines the theoretical foundation upon which a method of estimating line performance can be based. To be most useful, such a method should be simple in application yet afford a means of adjusting the entering data to conform closely to individual line characteristics. It has been pointed out earlier that effective shielding from direct strokes to the phase conductor is an essential prerequisite to the consideration

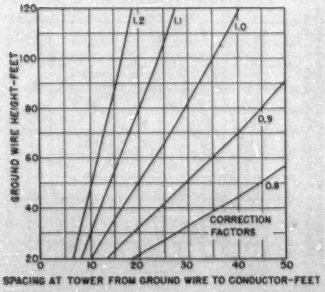

Figure 4 (left). Curve for adjusting the number of insulators when the height and spacing of conductors differ from the reference values. Multiply the actual number of insulators by the correction factor

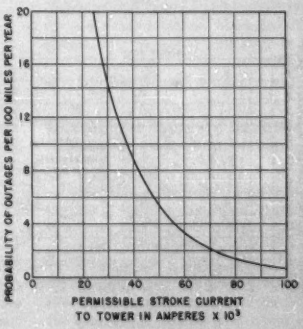

Figure 5 (right). Curve giving total outage probability when the permissible stroke current for mid-span flashover exceeds twice that for tower flashover

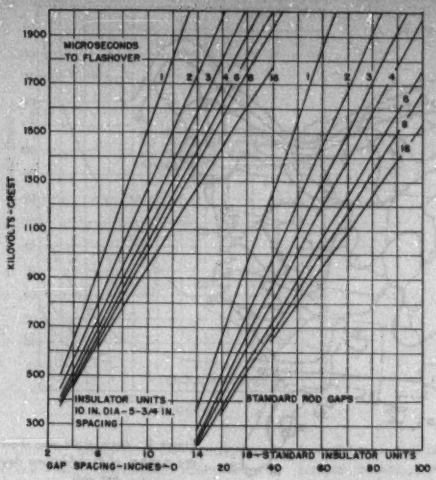

Figure 6. Characteristics of insulators and rod gaps

All values are based on positive waves and corrected to standard atmospheric conditions

of other design factors. Moreover, it is known that not every insulation flashover results in power-follow current and an accompanying tripout. Thus there are three parts to the estimating problem:

1. Number of insulation sparkovers caused by strokes to the phase conductor (shielding failures).
2. Number of insulation sparkovers caused by strokes to the ground wire or tower.
3. Number of tripouts caused by 1 and 2.

Figure 1 shows the configuration of the shielding and the protected phase conductor which permits 0.1 per cent of the strokes to terminate on the phase conductor. Good design practice calls for shielding angles of 30 degrees or less in order to allow for hillside locations and in this case even better average shielding should be expected. Because of the vagaries of natural lightning it seems desirable to allow for 0.1-per cent shielding failures even if perfect shielding is indicated.[7]

Strokes to Ground Wire or Tower

Lightning strokes to the ground wire or tower may cause insulation sparkover at the tower, and allowance must be made for the possibility of mid-span sparkover. The latter are believed to be extremely infrequent, particularly on well-designed high-voltage lines. With the aid of equation 1, the electric analogue computer, and standard impulse flashover curves for insulators and rod gaps, the number of standard insulator units or the minimum mid-span clearance required to withstand sparkover for any assigned crest value of stroke current within the range considered may be determined. The frequency of sparkover in a given case then is given by the frequency with which the assigned current value is equalled or exceeded. Figure 1 shows the magnitude frequency distribution curve which has been used in the present study. It is expressed in terms of strokes per 100 miles per year for an isoceraunic level of 30, and has been derived from 3,214 measurements. It is convenient to establish general curves on the assumption that each insulation sparkover is accompanied by power-follow flashover and a line tripout, and to adjust the results for field experience with particular types of line construction. Accordingly, such curves have been prepared for span lengths from 200 to 2,000 feet, covering the ranges of 0 to 100 ohms structure ground resistance, 2 to 26 insulator units, 2 to 200 kiloamperes stroke current, and 0 to 20 outages per 100 miles per year. Two sets of curves are shown for each span length, one giving the estimated

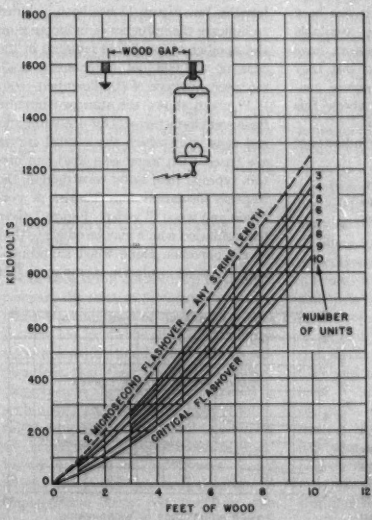

Figure 7 (left). Impulse insulation added to insulator strings by wood

Equivalent insulators to be added may be determined from Figure 6

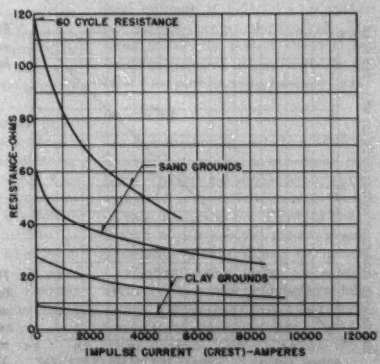

Figure 8 (right). Effect of current on impulse resistance of driven ground rods

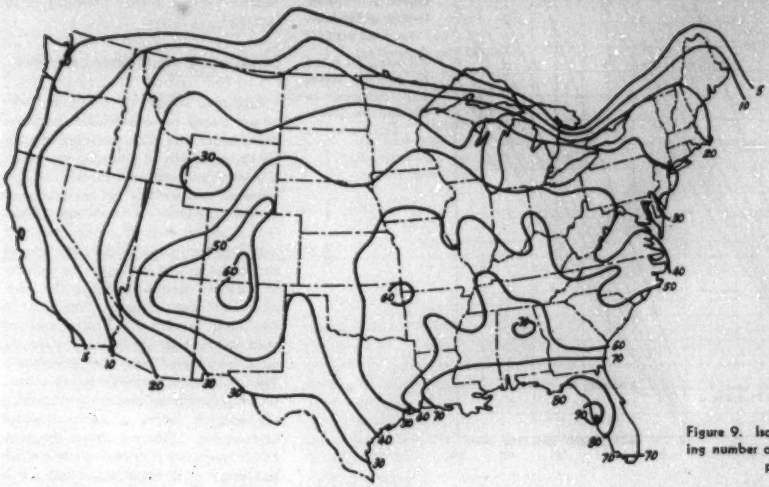

Figure 9. Isoceraunic map showing number of thunderstorm days per year

outages per 100 miles per year as determined by the curve of Figure 1, and the other giving the permissible stroke current for use with more accurate stroke current distribution data which may be available for a particular region under consideration. Curves (A) to (H) of Figure 3 apply for strokes to the tower, while curves (I) and (J) apply for strokes to mid-span.

The outage curves are based on a line configuration which involves a 28-foot separation between a ground wire at a reference height of 75 feet and the most distant phase conductor. If the actual ground wires are at a different height or the geometric mean distance from the ground wires to the most distant phase conductor is other than 28 feet, the actual number of insulators should be multiplied by the correction factor from Figure 4 to obtain the number of insulators with which to enter the curves. The influence of corona on the coupling factor has been included as indicated in equation 2 through the use of effective radii as determined by McCann[8] for the electrostatic coupling factor. In the case of strokes to mid-span, it has been necessary to extrapolate the available data. Increasing coupling factors have been used up to 8 megavolts, but they have been held constant to assure conservative results for voltages above this value.

The reference value of tower inductance has been taken as 20 microhenrys. This is believed to be a conservative value, since it corresponds approximately to a steel tower 100 feet high or to a wood pole 50 feet in height with a ground conductor having an inductance of 0.4 microhenry per foot. It is not possible to give accurate correction factors to modify the indices of Figure 3 for other values of inductance which are applicable to all span lengths, but Figure 11 has been included to indicate the influence of inductance on the number of insulators required in the case of a 1,000-foot span and a 2x40-microsecond wave of 50-kiloampere crest.

Figure 6 shows the standard impulse flashover characteristics for insulators and rod gaps upon which the general curves are based. On wood pole lines and certain types of steel tower construction, the impulse insulation may consist of porcelain and wood in series. Figure 7 gives the insulation which may be added to that of the porcelain alone when supplementary dry wood insulation is employed. It

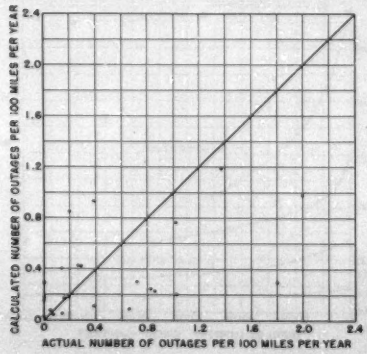

Figure 10 (left). Comparison of estimated performance with experience

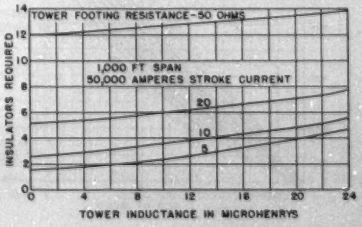

Figure 11 (right). Effect of tower inductance on number of insulators required for a 2x40-microsecond wave of 50-kiloamperes crest

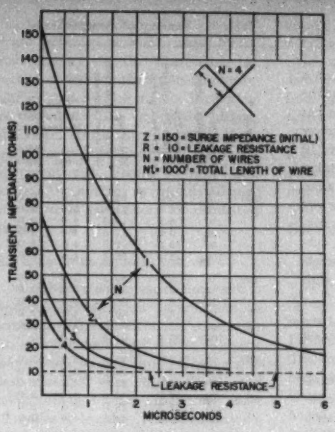

Figure 12. Transient impedance of counterpoise systems

should be noted that the addition decreases with the time to flashover and with the length of the insulator string. Moreover, it has been found that moisture may substantially reduce the impulse insulating value of wood insulation, particularly at the longer time lags.[8] If more accurate data are not available, each foot of wood may be taken as equivalent to one insulator unit if dry, and as equivalent to one-half unit if wet. If the limiting insulation is an air gap, the equivalent number of suspension insulator units may be obtained readily from Figure 6.

Strokes to mid-span may cause tower flashovers if the permissible stroke current for mid-span flashover exceeds twice that of the tower. With small error, the outage probability for such strokes can be combined with that for strokes to the tower to give a single outage probability curve for all strokes to the ground wire. Figure 5 shows the curve to be used in these cases.

Applications of the Estimating Curves

The estimating curves may be used to compare the relative performance of proposed transmission-line designs or to determine the probable effect of modifications to existing lines. It is in such applications that their greatest value lies. Nevertheless, they have been prepared in such a way that, with the help of additional data, they may be used to estimate the actual average performance of lines. Figure 9 shows an isoceraunic map[14] which gives the average number of thunderstorm days per year for the United States and part of Canada. The general outage probability curves are based upon 100 strokes to the line per 100 miles per year for an isoceraunic level of 30.

Three examples will be given illustrating their use.

Example 1

A 138-kv steel tower line, shielded by an overhead ground wire, located in territory with an isoceraunic level of 50, has ten $5^3/_4$-inch spaced insulators per string. The average span is 1,000 feet and the mid-span clearance is 24 feet. The tower-footing resistances are 10 ohms for 20 per cent of the towers and 20 ohms for 80 per cent of the towers. What is the outage probability for this line? From Figure 3(E) for 1,000-foot spans, the outage probability for 10 ohms and 10 insulators is 0.7 outage per 100 miles per year. For 10 insulators and 20 ohms the figure is 2.8. The combined probability for strokes to tower is $(0.7\times0.2)+2.8\times0.8)=2.38$ per 100 miles per year. The permissible stroke currents for the 10 and 20 ohms are 124,000 and 79,000 amperes respectively.

From Figure 3(I) the outage probability is 0.6 per 100 miles per year for 1,000-foot spans with mid-span clearance of 24 feet. The permissible stroke current is 128,000 amperes. The average of 2.38 and 0.6 is 1.49 for an isoceraunic level of 30. The outage probability for the given isoceraunic level of 50 is 50/30 times 1.49 or 2.48 outages per 100 miles per year. This computation assumes perfect shielding and would be increased to approximately 2.65 for 0.1-per cent shielding failures.

Example 2

A 33-kv wood pole line, shielded by ground wire, located in territory with an isoceraunic level of 30 has two $5^3/_4$-inch spaced insulators per string. The minimum flashover path is the porcelain plus four feet of wood. The average span is 200 feet and the mid-span clearance eight feet. The tower-footing resistance is 50 ohms for all poles. The distance between the ground wire and bottom conductor is 10 feet at the tower. What is the outage probability for this line?

From Figure 7 four feet of wood is estimated as adding 450 kv to the insulation strength of the porcelain. Thus the total equivalent insulation is 6.0 units. Since the spacing from ground wire to conductor is considerably less than 28 feet, an adjustment is needed to compensate for increased coupling.

From Figure 4 the correction factor for a 10-foot spacing is 1.2 and the effective insulation becomes $6\times1.2=7.2$ insulators. From Figure 3(A) the outage probability for 7.2 insulators and 50 ohms footing resistance is 5.4 outages per 100 miles per year. The permissible stroke current is 62,000 amperes. From Figure 3(I) the outage probability for strokes to mid-span for a 200-foot span and 8-foot clearance is 0.0 per 100 miles per year and the permissible stroke current is 200,000 amperes.

Since the permissible stroke current for mid-span flashover exceeds twice that for strokes to the tower, the total outage probability should be taken from Figure 5. The permissible stroke current to a tower is 62,000 amperes, for which the total outage probability is read as 3.1 per 100 miles per year. This figure assumes that all insulator flashovers result in tripouts. Experience with such lines indicates that approximately 50 per cent of the flashovers will result in tripouts, so that the final estimate is $0.5\times3.1=1.6$ outages per 100 miles per year for this line. This estimate assumes perfect shielding and would be increased to approximately 1.65 for 0.1-per cent shielding failures.

Example 3

A transmission line is to be constructed in a territory where the isoceraunic level is 30. The line will be shielded by ground wire and it is desirable to insulate the line so that outages due to lightning will be limited to 2.0 per 100 miles per year. Knowledge of existing lines in the territory indicates that tower-footing resistances of 20 ohms can be obtained economically. The choice of towers and conductors calls for an average span of 800 feet. The conductors and ground wire will be

sagged to provide a mid-span clearance of 18 feet. How many insulators are required to effect the desired limitation on outages?

From Figure 3(J) the outage probability for strokes to mid-span is 0.6 outage per 100 miles per year. The outage probability for strokes to tower must be 3.4 if the average is to be 2.0 per year. From Figure 3(D) 8.5 insulators are required for the outage probability of 3.4 if the footing resistance is 20 ohms. Thus nine insulators should limit the outage probability to 2.0 per 100 miles per year.

Outage Estimates and Field Experience

Although the estimating curves are most valuable for comparative purposes, it is believed that they give results consistent with practically all of the published results on actual line performance. In general it is known that 33-kv lines with a basic insulation level of 700 kv and 10 ohms footing resistance result in two or three outages per 100 miles per year. The 132-kv lines designed for good lightning performance will have about one outage, while modern 220-kv lines will have only a small fraction of one outage per 100 miles per year. The latter are often referred to as lightning-proof. Figure 10 shows a comparison of published performance with estimated performance.[13] The estimated performance necessarily is based upon average tower-footing resistance obtained by low voltage measurements. If the distribution of towers having various footing resistances is known, a much more accurate estimate results.

Factors Limiting Accuracy of Estimates

In the evaluation of essential factors affecting the problem, the working group has been fully aware of the uncertainties existing with respect to many of the primary data employed. Moreover, there remain certain points upon which little, if any, research has been conducted. While a few of these have been indicated in appropriate preceding sections, it appears desirable to list the more important ones here. It is quite likely that at least some of these uncertainties tend to offset each other in the end result, and that improvement with respect to one factor would necessitate a corresponding improvement in another. The principal sources of uncertainty with respect to the data employed in constructing the general curves and in the data necessary to use these curves will be discussed.

Variability of Tower Footing Resistance

The estimating curves are based on a constant value of resistance located at the base of the tower. If the resistance has been secured by means close to the tower but is higher than approximately 10 ohms, the resistance to high lightning current may be substantially lower than the 60-cycle value. No correction factors are available for common grounding systems at the significant lightning currents, but Figure 8 shows how the resistance of driven ground rods varies with current.[10]

Effect of Distributed Grounding or Counterpoise Systems

The performance of distributed grounding systems, commonly called counterpoises, has been reported in the literature.[9,10,11,12] Figure 12 shows how the impedance of a counterpoise grounding system varies with time. Since such systems usually extend in both directions from a tower, N may be taken as 2.

For the 4-microsecond wave front of current upon which the general curves are based, it appears satisfactory to use the measured leakage value of the grounding system if this resistance is secured with a total length of buried conductor of 1,000 feet or less per tower. Further comment on this point is made in the section on Current Wave Shape.

Current Wave Shape

Because of the rapid reduction of ground-wire voltage caused by the reflections from adjacent towers, the duration of the tail of the current wave does not greatly influence insulator flashover. However, the wave front of the current wave is of the greatest significance. Unfortunately there are insufficient data upon which to base a really satisfactory distribution curve for wave fronts and in an effort to make the results conservative, a wave front of two microseconds was initially selected for the purpose of the present study. As the investigation proceeded it became apparent that only the higher currents, in excess of 30 kiloamperes, were of especial importance. For these McCann[18] has found that the median value is approximately four microseconds. The use of such a wave front brings the estimated performance more closely into agreement with field experience with respect to mid-span flashovers. The choice of a single wave front, although desirable for simplicity in the development of general curves, cannot be regarded as entirely satisfactory. Occasionally one must expect to have lightning currents whose rate of current rise is sufficiently high to cause flashover either at the tower or at mid-span which would not be indicated from the curves presented.[11]

Table 1. Summary of Anacom Study

Span, Feet	Tower Foot Resistance, Ohms	Tower-Top Voltage Per Ampere of Stroke Current	Mid-Span Voltage Per Ampere of Stroke Current	Time Lag to Insulate Microseconds	
				Tower	Mid-Span
200	0	5.2	14.8	2.0	2.0
	5	6.0	14.8	3.0	2.0
	10	6.9	15.0	4.0	2.0
	20	9.8	15.6	4.0	2.0
	50	16.0	17.3	4.0	2.0
	100	23.4	23.5	4.0	2.0
400	0	6.6	29.5	2.0	2.0
	5	7.4	30.0	3.0	2.0
	10	8.8	30.0	4.0	2.0
	20	13.0	30.7	4.0	2.0
	50	22.2	32.0	4.0	2.0
	100	33.0	34.5	4.0	2.0
600	0	6.8	45.5	2.0	2.0
	5	8.0	46.2	3.0	2.0
	10	9.9	46.2	4.0	2.0
	20	15.0	46.8	4.0	2.0
	50	27.5	48.0	4.0	2.0
	100	40.0	49.5	4.0	2.0
800	0	7.0	62.5	2.0	2.0
	5	8.1	63.0	4.0	2.0
	10	10.5	64.0	4.0	2.0
	20	16.2	64.0	4.0	2.0
	50	30.0	65.0	4.0	2.0
	100	45.0	65.0	4.0	2.0
1,000	0	7.0	74.0	2.0	2.0
	5	8.3	74.0	4.0	2.0
	10	10.9	74.0	4.0	2.0
	20	17.4	75.0	4.0	2.0
	50	33.5	76.5	4.0	2.0
	100	50.5	79.0	4.0	2.0
1,200	0	7.0	86.0	2.0	2.0
	5	8.5	86.0	4.0	2.0
	10	11.2	86.5	4.0	2.0
	20	17.8	88.0	4.0	2.0
	50	35.0	89.0	4.0	2.0
	100	57.0	90.0	4.0	2.0
1,600	0	7.1	112.5	2.0	2.0
	5	8.9	113.4	4.0	2.0
	10	11.5	113.4	4.0	2.0
	20	18.7	114.0	4.0	2.0
	50	37.5	115.0	4.0	2.0
	100	65.0	119.0	4.0	2.0
2,000	0	7.4	130.0	2.0	3.0
	5	9.0	130.0	4.0	3.0
	10	12.0	130.0	4.0	3.0
	20	20.2	130.0	4.0	3.0
	50	41.3	130.0	4.0	3.0
	100	70.0	130.0	4.0	3.0

Stroke Current Magnitude

The magnitude distribution curve of Figure 1 has been derived from 3,214 measurements using magnetic links. The sum of the currents in adjacent towers has been taken as the stroke current. Individual tower currents were determined by addition of currents in all tower legs where such measurements were made, or by multiplication of partial measurements, assuming current distribution in the tower legs.[9] Tower currents so deter-

mined are likely to be too low, since they do not include the current carried by the cross braces. On the other hand, the method of deriving the stroke current results in values which may be in error on the high side to a comparable degree. Moreover, stroke currents which have been directly measured are in quite good agreement with Figure 1. For these reasons the working group has adopted this curve as satisfactory for estimating purposes.

Ratio of Outages to Flashovers

All lightning flashovers do not result in sustained power-follow current and an accompanying line tripout. Performance records on various types of lines give some information on the ratio of outages to flashovers.[16,17] For high-voltage steel tower lines the ratio is 0.85 for lines under 100 miles in length. This ratio may decrease to 0.5 for lines over 200 miles in length. In the case of wood pole lines where the flashover path may include wood members, the ratio of outages to flashovers ranges from 0.35 to 0.50.

If the characteristics of the line and its insulation result in a substantial reduction of the ratio of outages to flashover, this ratio should be included in the final estimate of the outage probability. If, however, the ratio is near unity, it well may be neglected and the general curves used directly to give conservative results.

Other Line Potentials

In the preparation of the general curves, no account has been taken of the normal frequency voltage, nor has consideration been given to any potential which may exist on the phase conductor as a result of electromagnetic induction from the stroke itself. While this uncertainty may represent an area inviting future research or analysis, it is felt that it does not represent a factor which seriously affects the relative usefulness of the method presented.

Conclusions

This report represents the results of a study of various methods of estimating lightning performance which has been made by a working group of the AIEE Lightning and Insulator Subcommittee. The essential factors of the problem have been carefully considered and have been incorporated into a method which, it is hoped, will be of value to those concerned with the design of new lines or the modification of old ones. Various phases of the result involve considerable uncertainty and these have been discussed briefly in order that the character of the approximations adopted may be better understood.

References

1. A Large-Scale General-Purpose Electric Analogue Computer, **E. L. Harder, G. D. McCann.** *AIEE Transactions*, volume 67, part I, 1948, pages 664–73.

2. Electrical Transmission and Distribution Reference Book (book). R. R. Donnelley and Sons Company, Chicago, Ill., 1942. Line Design Based Upon Direct Strokes, A. C. Monteith. Pages 325–48.

3. Protection of Transmission Lines Against Lightning: Theory and Calculations, **L. V. Bewley.** *General Electric Review* (Schenectady, N. Y.), volume 40, April 1937, pages 180–88.

4. *Discussion* by **C. F. Wagner, G. D. McCann** of Experience with Preventive Lightning Protection on Transmission Lines, **S. K. Waldorf.** *AIEE Transactions*, volume 60, 1941, page 702.

5. Transmission Line Design and Performance Based on Direct Lightning Strokes, **E. L. Harder, J. M. Clayton.** *AIEE Transactions*, volume 68, part I, 1949, pages 439–49.

6. The Effect of Corona on Coupling Factors Between Ground Wires and Phase Conductors, **G. D. McCann.** *AIEE Transactions*, volume 62, 1943, pages 818–26.

7. Shielding of Transmission Lines, **C. F. Wagner, G. D. McCann, G. L. MacLane, Jr.** *AIEE Transactions*, volume 60, 1941, pages 313–28.

8. What Wood May Add to Primary Insulation for Withstanding Lightning, **J. T. Lusignan, Jr., C. J. Miller, Jr.** *Electrical Engineering* (*AIEE Transactions*), volume 59, September 1940, pages 534–40.

9. Protection of Transmission Lines Against Lightning (book), **W. W. Lewis.** John Wiley and Sons, Inc., New York, New York, 1950.

10. Impulse and 60-Cycle Characteristics of Driven Grounds—II, **P. L. Bellaschi, R. E. Armington, A. E. Snowdon.** *AIEE Transactions*, volume 61, 1942, pages 349–63.

11. *Discussion* by **J. H. Hagenguth** of Practical Design of Counterpoise for Transmission-Line Lightning Protection, **E. Hansson, S. K. Waldorf.** *AIEE Transactions*, volume 61, 1942, pages 1011–12.

12. Protection of Transmission Lines Against Lightning: Theory and Calculations, **L. V. Bewley.** *General Electric Review* (Schenectady, N. Y.), volume 40, April 1937, pages 180–88; May 1937, pages 236–41.

13. Lightning Performance of Typical Transmission Lines. Ohio Brass Company, Mansfield, Ohio.

14. Hydrometerological Report Number 5—Part II. U. S. Weather Bureau (Washington, D. C.), August 1945.

15. The Measurement of Lightning Currents in Direct Strokes, **G. D. McCann.** *AIEE Transactions*, volume 63, 1944, pages 1157–64.

16. Lightning Surge Effects on Transmission Lines, **G. D. McCann.** *Electric Light and Power* (Chicago, Ill.), May 1945, pages 76–84.

17. An Eight-Year Investigation of Lightning Currents and Preventive Lightning Protection on a Transmission System, **E. Hansson, S. K. Waldorf.** *Electrical Engineering* (*AIEE Transactions*), volume 63, May 1944, pages 251–58.

Discussion

J. H. Hagenguth (General Electric Company, Pittsfield, Mass.): The paper should be of considerable help to the industry in evaluating lightning performance of transmission lines. As pointed out in the paper many of the factors involved in the calculations are known only approximately. One of these is the amplitude of the lightning stroke current and its wave shape.

Measurements of tower current amplitudes by Lewis and Foust, Waldorf, and Grünewald in Germany, result in frequency curves of almost exactly the same shape. A total of 6,377 measurements are involved. It would seem, therefore, that these curves should approach very closely the true frequency distribution of lightning current amplitudes in towers. This curve is considerably below the curve of Figure 1 of the report which gives lightning stroke currents calculated from tower current measurements.

For instance, 5 per cent of the tower currents are 40,000 amperes as compared to 62,000 for the assumed lightning stroke currents. The maximum tower current is of the order of 140,000 amperes as compared to 200,000 amperes lightning stroke current.

Calculations made some time ago[1] indicate that lightning stroke currents are only slightly higher in amplitude than the current in a tower which was struck. This also is substantiated by measurements of the lightning stroke currents in series with transmission towers by means of lightning rods extending beyond the towers. Frequently tower currents and lightning rod currents are alike. Therefore, the frequency curve given in Figure 1 of the report should give pessimistic results. In the case of strokes to midspan, of course, the currents measured on the ground wire should be added up to give total current.

The sparkover characteristic curves shown in Figure 6 do not give the complete story of sparkover in the nonuniform field. It has been shown[2] that sparkover depends greatly on the type of the wave shape applied. For instance, for a 50-inch gap, sparkover may be as low as 1,130 kv for a rectangular wave and as high as 1,630 kv for a straight rising front. The type of voltage wave to be expected at any part of the system depends on the relative values of inductance and resistance in the discharge path. At midspan, the usual case of high inductance and low resistance would produce a rather steep front and very short tail wave corresponding more nearly to the straight rising front condition. For sparkover at 2 microseconds, this would give approximately 330 kv per foot or more to obtain sparkover.

Nevertheless, the examples of Figure 10 show very good correlation between calculated performance and experience.

References

1. *Discussion* by **J. H. Hagenguth** on Lightning Currents and Potentials on Overhead Transmission Lines, **R. H. Golde.** *Proceedings*, Institution of Electrical Engineers (London, England), volume 96, part II, number 49, February 1949, pages 93–94.

2. *Discussion* by **J. H. Hagenguth** on Study of Driven Rods and Counterpoise Wires in High-Resistance Soil on Consumers Power Company

140-Kv System, J. G. Hamstreet, W. W. Lewis, C. M. Foust. *AIEE Transactions*, volume 61, 1942, pages 1001–02.

3. Volt-Time Areas of Impulse Spark-Over, J. H. Hagenguth. *Electrical Engineering* (*AIEE Transactions*), volume 60, July 1941, pages 803–10.

E. R. Whitehead: The points brought out in Mr. Hagenguth's discussion are indeed pertinent and received the careful consideration of the working group in establishing the set of approximations upon which to base the method. The greatest single difficulty is that adequate treatment of these and other factors awaits a degree of knowledge of the wave shape of the lightning current roughly comparable to that concerning the current amplitude.

In its early approach to the problem, the working group recognized two general trends of thought. On the one hand, it appeared desirable to base the method on a very few factors whose influence was firmly established and on which the greatest volume of data was available. On the other hand, it seemed important that the method make the fullest possible use of modern knowledge relating to other factors such as Mr. Hagenguth has mentioned. Study of the latter course soon brought out that the analytical tools and general appreciation of these factors were far ahead of the available data essential for their practical use. Thus, the report of the working group represents its current evaluation of the weight to be accorded the various theoretical considerations in a method which, it is hoped, will be of value to designers of transmission lines.

Theory and Application of Transformer Differential Protection

GEORGE W. McKENNA
ASSOCIATE AIEE

Synopsis: In attempting to use standard percentage differential relays for transformer protection in the most efficient manner for a wide variety of transformer connections and types, several problems have arisen which have resulted in solutions not in the usual repertoire of transformer protection. The scope of this paper is limited to some general remarks on the fundamentals of transformer protection using percentage differential relays, and to a few selected applications of this type of relay which depart somewhat from the usual course of such protection. Certain occasional and independent problems of transformer protection which are superimposed on the basic application requirements to be discussed here, such as relay operation on transient magnetizing inrush current flow, are not included within the scope of this paper.

The Principles of Differential Protection

THE usual statement of Kirchhoff's law concerning current flow found in the standard text books is "The sum of the currents coming toward a junction of conducting branches of an electric circuit is equal to the sum of the currents leaving that same junction." For protective relaying purposes this law can be restated as "If all the currents flowing into and out of the junction or region of an electric circuit through all the legitimate paths are added together and do not equal zero, then there exists one or more improper paths to the junction which represent failures of insulation." The term "failures of insulation" is often replaced by such terms as "faults," "short circuits," or "breakdowns," all of which describe the same electrical misadventures.

Figure 1 depicts the functioning of Kirchhoff's law in differential relaying. Figure 1 (A) represents the general statement of the law. Figure 1(B) places the junction inside a transformer or other device and adds, in relay R, the current flow to and from the junction through current transformers of ratios which match the voltage transformation ratios of the transformer. Figure 1(C) shows that any unorthodox current to the junction, I_z, which is not included in the current summation, would cause a proportionate current to appear in the relay R. Since I_z is fault current relay R can instantly detect a fault in the region bounded by the current transformers, while any such unaccounted-for current beyond the current transformers would have no effect on the summation of the measured currents to zero in the relays as shown in Figure 1(B). This sharp definition of internal faults for which the relay should operate and external faults for which the relay should not operate enables the relay to be made to operate without any intentional time delay (operating time approximately 3 to 6 cycles on a 60-cycle basis).

The Percentage Differential Characteristic

In order to use an unmodified current relay to detect the difference between incoming and outgoing currents in a transformer, two requirements must be met. First, the current transformer ratios must exactly compensate for the transformation ratio of the power transformer so that the secondary currents can be added directly at the relay just as if the transformation ratio were unity. Second, this compensation in ratios must be maintained throughout the entire range of external fault and load currents to prevent the relay from operating incorrectly. Both of these requirements are often difficult, if not impossible, to achieve.

In the general case the necessary current transformer ratios for exact ratio compensation would be anything but standard so that tailor-made current transformers would have to be built for each job at a considerable sacrifice in economy. With transformers with variable ratios, such as those equipped for tap changing under load, the problem of exact compensation is almost practically insuperable.

Generally the current transformers on opposite sides of a transformer must have different turn ratios to match the transformer turn ratio and for this reason the current transformers might behave differently under high external fault currents. Thus, while ratio compensation might be attained completely at low values of current, it might be lacking at the higher values even though the currents in the power transformer leads continued to adhere to the power transformer transformation ratio. Thus an "error" current, which gives the appearance of a fault in the transformer when there is no such fault, will flow through the relay of Figure 2(A) and this current could easily be of such a magnitude as to cause the relay to operate incorrectly.

In order to allow for incomplete compensation and thus permit the use of current transformers of standard ratios and of slightly different behaviour characteristics the percentage differential relay was developed as shown in Figure 2(B). This relay has three coils; current through coil O produces a torque in the contact-closing or operating direction and coil O is thus called the "operating" coil; currents through coils A and B produce a torque in the contact-opening or restraining direction and for this reason these coils are called "restraining" coils.

In order to allow even greater freedom

Paper 50-189, recommended by the AIEE Relays Committee and approved by the AIEE Technical Program Committee for presentation at the AIEE Middle Eastern District Meeting, Baltimore, Md., October 3–5, 1950. Manuscript submitted June 19, 1950; made available for printing September 7, 1950.

GEORGE W. McKENNA is with the Philadelphia Electric Company, Philadelphia, Pa.

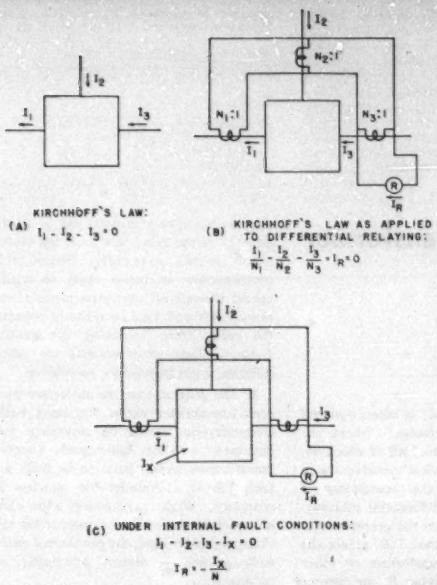

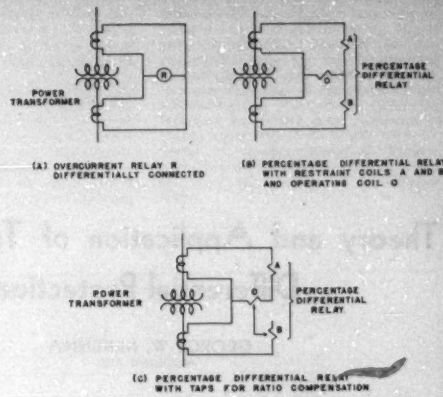

Figure 1 (left). Kirchhoff's law and differential relaying

Figure 2 (above). Differential relays

in the choice of current transformer ratios, taps are provided on the operating coil and one restraining coil so that while an unbalance current might flow through the operating coil circuit due to incomplete ratio compensation, the ampere turns can be balanced to provide compensation on a flux basis rather than on a current basis.

The effect of the restraining coils is to make the operating current for pickup of the relay depend directly on the amount of restraint current, which reflects in turn the current level in the power transformer itself. For low currents in the power transformer the required pickup current in the operating coil is low, while for large currents in the transformer the operating current must be correspondingly higher. The pickup current of such a relay is expressed as a percentage of the smaller restraining current with the term "slope" sometimes used as a synonym for sensitivity. This percentage characteristic, as compared to the single value of pickup current in amperes for the differentially connected overcurrent relay of Figure 2 (A), is primarily designed to allow for variation in current transformer behaviour which produces larger error currents for larger values of primary current.

Figure 3 shows how a 25-per cent slope characteristic takes care of a 10-per cent error in the ratio of a set of 500/5-ampere current transformers in the case of an external fault for which the transformer protective relay should not operate.

Analysis of Differential Relay Operation

In the application of percentage differential relays for transformer protection it is necessary to calculate the behaviour of the relays under external fault conditions for all possible variations in the transformer operation, such as those due to tap changing under load. The percentage characteristic allows a certain deviation from perfect ratio compensation and it is necessary to determine how much of that allowable deviation is used up in order to determine how close the relay is to operation under external fault conditions.

The percentage differential relay for transformer protection has taps as indicated in Figure 2(C) to allow for a wide choice of current transformer ratios and the effect of these taps must be taken into consideration. The tap range usually allows for a variation in current transformer ratios up to at least twice that required for perfect ratio compensation. Figure 4 shows how these taps are used in a 50-per cent slope relay. With the tap associated with the restraint coil A set at 5 amperes and the tap for restraint coil B set at 10 amperes, the compensation at the relay is perfect in spite of the fact that the total operating current in amperes (25 amperes) is 100 per cent of the smaller restraining current and the relay has a 50 per cent characteristic for operation. The perfect compensation is brought about not by balancing amperes but by balancing ampere turns. It appears reasonable, then, that all calculations of differential relay operation should be made in terms of ampere turns rather than in terms of amperes. This procedure becomes imperative in case the phase angle between the currents in coils A and B is neither zero nor 180 degrees.

In Figure 4, with the tap settings previously stated, 50 amperes in coil B and out through the operating coil produce the same ampere turns as 25 amperes in coil A and the operating coil, and with the current flow as shown for an external fault the operating ampere turns cancel exactly producing perfect compensation. This is because the operating coil turns through which the current from the 200/5-ampere current transformer flows are twice as many as those through which the current from the 500/5-ampere current transformer flows.

The difference in turns can be taken care of for calculation purposes by obtaining the equivalent currents on an *equal tap* basis, which can be done by multiplying the current in coil B by the ratio of the tap for coil A divided by the

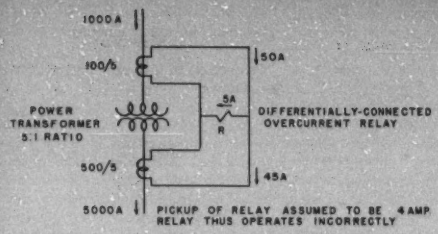

(A) OPERATION OF DIFFERENTIALLY-CONNECTED OVERCURRENT RELAY DUE TO CURRENT TRANSFORMER ERROR

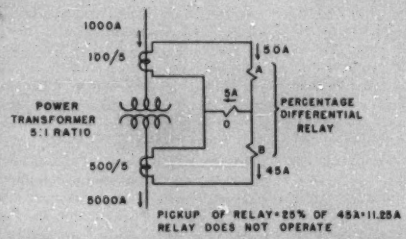

(B) PREVENTION OF INCORRECT RELAY OPERATION BY RESTRAINT COILS

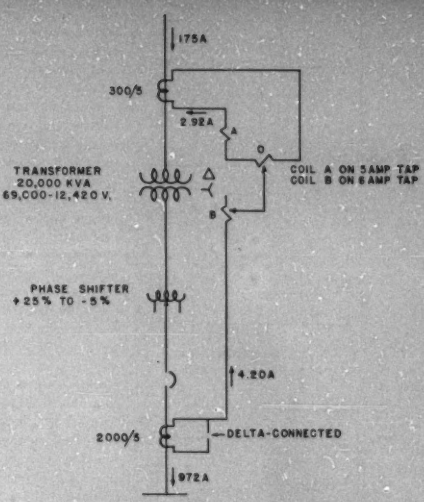

Figure 3 (left). Effect of current transformer ratio error

Figure 5 (above). Over-all protection of transformer and phase shifter

tap for coil B. Expressed as a formula

$$(I_B)\text{equiv} = I_B(T_A/T_B) \qquad (1)$$

where $(I_B)_{\text{equiv}}$ is the equivalent current in coil B for equal tap settings of T_A and T_B; I_B is the actual current in coil B; T_A and T_B are the tap settings associated with coils A and B, respectively.

Once the currents are transformed to an equal tap basis the difference in coil turns is taken care of and the relationships of the transformed currents can be compared directly with the percentage slope of the relay to determine whether the relay will operate correctly with a reasonable safety margin or not. Using this particular method of analysis it is necessary only to remember to base the per cent unbalance under actual fault conditions on the smaller of the two restraint currents after transformation by the tap ratio (T_A/T_B). Other methods are possible but many of these involve two formulas from which the proper choice must be made based on relative current magnitudes. The equivalent current method based on equation 1 is very useful in calculating the margin of safety for a differential relay where the restraint currents are neither in phase nor 180 degrees out of phase.

Protection of Transformer and Phase Shifter

A problem which arose concerning the over-all percentage differential protection of a 20,000-kva 69–13.8-kv transformer and a 13.8-kv phase shifter for load flow control may be of value in pointing out the worth of the equivalent current method. The transformer, the current values involved, and the tap settings used are shown in Figure 5. The phase shifter and the transformer with

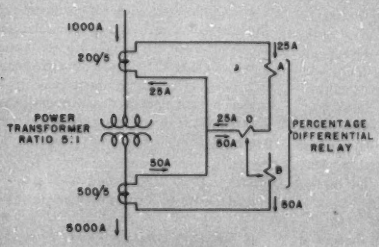

Figure 4 (left). Ratio compensation with aid of relay taps

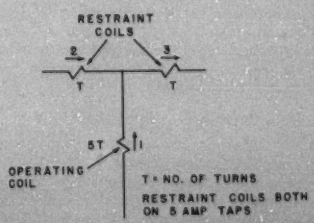

Figure 6 (right). Current distribution for 50 per cent slope differential relay at the pickup point

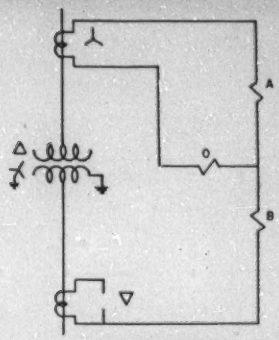

(A) DELTA-WYE GROUNDED TRANSFORMER BANK

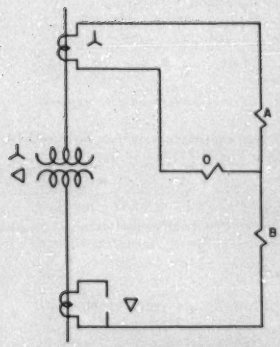

(B) WYE-DELTA UNGROUNDED TRANSFORMER BANK

Figure 7. Protection of Y-delta transformer banks

tap changing under load acted in concert to maintain a constant voltage ratio between the 69-kv line and the 13.8-kv bus regardless of the phase angle between the voltages and currents at those two points. The maximum shift introduced by the phase shifter was approximately 14 degrees.

The first step in the analysis was to get the secondary currents on an equal tap basis. From equation 1

$$(I_B)_{equiv} = I_B(T_A/T_B) = 4.20(5/6) = 3.50 \text{ amperes}$$

Comparing an equivalent $I_B = 3.50$ amperes with an I_A of 2.92 amperes it can be determined that with no shift due to the phase shifter the operating current I_0 would be 0.58 ampere or an unbalance of $0.58/2.92 \times 100 = 19.8$ per cent compared to the pickup unbalance (slope) of 50 per cent, indicating a satisfactory margin of safety.

When the maximum 14-degree phase shift occurs, however, the operating current must be obtained by vector subtraction and the total restraining effect by a vector addition of the restraining currents. It can be deduced from the percentage slope characteristics that for a 50-per cent slope relay the pickup current distribution on an equal tap basis is one unit of current in the operating coil to two units of current in one restraining coil and three units of current in the second restraining coil, as shown in Figure 6. It can be assumed that at pickup the operating ampere turns equal the restraining ampere turns. From this assumption and the current distribution it follows that the operating coil must have five times as many turns as either restraining coil. It also would appear from the design of the relay that the total restraint flux is the sum of the fluxes in the individual restraint coils, or the total effective restraining current is the vector sum of the individual currents in the restraining coils. By comparing this total effective restraining current with five times the operating current (the factor of five takes care of the greater number of turns in the 50-per cent characteristic relay) the tendency toward operation can be evaluated.

In the problem of Figure 5, with the maximum 14-degree phase shift, the restraint currents can be expressed as $2.92 + j0$ amperes for I_A and $3.39 + j0.85$ amperes for $(I_B)_{equiv}$. By subtraction, the operating current is thus $0.47 + j0.85$ amperes. The operating ampere turns are proportional to $5\sqrt{(0.47)^2 + (0.85)^2} = 4.86$. The total effective restraining current is the sum of the two individual restraint currents or $6.31 + j0.85$ amperes and the restraint ampere turns are proportional to $\sqrt{(6.31)^2 + (0.85)^2} = 6.37$. Since an equality between operating and restraining ampere turns represents pickup of the relay, as does the percentage slope figure of 50 per cent, the actual unbalance with the 14-degree phase shift is $4.86/6.37 \times 50$ per cent $= 38.2$ per cent. This unbalance figure of 38.2 per cent with the 14-degree shift compared to the 19.8 per cent unbalance without the shift clearly demonstrates the necessity of the vector treatment of the restraining and operating currents. The 38.2 per cent unbalance leaves a rather small margin of safety under the 50 per cent pickup value but the power transformer taps shown in Figure 5 represent the worse possible combination and will not normally be used.

Protection of Y-Delta Transformer Banks

In the passage of current through a Y-delta transformer bank it is well known that a shift of 30 degrees takes place in the phase angle of the line currents and it is also well known that the proper current transformer connections for differential relays can compensate for this shift. The rule is that current transformers on the Y side of the transformer bank should be connected in delta while those on the delta side should be connected in Y, as shown in Figure 7(A).

A transformer installation as shown in Figure 7(A) was planned and, of course, the foregoing rule was to be followed in the connection of the current transformers feeding the percentage differential relays. Prior to this installation, however, a temporary bank was to be used which had to be connected Y-delta where the permanent bank was to be delta-Y. It was hoped that the change from the temporary bank to the permanent bank could be made without complicated and costly changes in the connections from the current transformers to the relays, which would have been necessitated by a strict adherence to the rule expressed before. It was found that if the Y-connected windings did not have their neutral grounded, the rule could be broken with impunity and the final relay connections could be used without alteration with the temporary bank, as shown in Figure 7(B).

The justification behind this infraction of the rules lay in the fact that the phase angle shift in the line currents could be compensated for by either Y-delta or delta-Y current transformer connections; that the delta connection had to be used on the grounded side of the bank to trap zero sequence currents coming from the ground for external faults, and that if the Y side of the bank were not grounded this trapping effect was unnecessary and the current transformers could be connected Y-delta or delta-Y with complete freedom of choice. A more mathematical justification of the unorthodox connection of Figure 7(B) is given in Appendix I of this paper.

Protection of Paralleled Y-Delta and Delta-Y Transformer Banks

It has been proposed that a pair of paralleled banks, connected delta-Y and Y-delta with common high and low side

circuit breakers, protected by a single set of differential relays, have both Y-connected windings grounded, giving the connections shown in Figure 8(A).

This poses somewhat of a dilemma in that the current transformers must be connected Y-delta to compensate for the 30-degree shift in line currents while the presence of the grounds on both sides of the transformer banks dictates, according to the rule, the use of delta-delta connected current transformers which would make the 30-degree compensation impossible.

Since the Y-connected current transformers are by themselves unable to keep zero sequence operating current out of the differential relays for external ground faults, which trapping effect delta-connected current transformers can produce with ease, some external zero sequence trap must be provided to "suck away," as it were, the disturbing zero sequence current from the relay. This can be done by using the zero sequence current in the neutral itself to cancel out the zero sequence current which emits from the Y-connected current transformers for an external ground fault. All that is needed to accomplish this result is a current transformer in the transformer neutral and one auxiliary current transformer per phase to inject the neutral current into the relay current circuits as outlined in Figure 8(B).

The basis for this additional current circuit lies in the Kirchhoff law requirement for measuring the current in every legitimate path to the transformer, and the neutral connection to ground represents such a path.

Protection of Scott-Connected Transformer Banks

The protection of Scott-connected 3-phase to 2-phase transformer banks is generally accomplished by a relay scheme with connections as shown in Figure 9(A). The reversal of the B-phase current transformer on the 3-phase side should be noted. Because of this reversal there is current flowing under normal load conditions in all three connections from the 3-phase current transformers to the relays, such as at points 1, 2, and 3. If the 3-phase side of the Scott bank is ungrounded a ground overcurrent relay on the 3-phase side can be used to good advantage because it can be set with a maximum of sensitivity since it can get the current it requires for operation only if a ground fault occurs between its current transformers and the bank, or in the 3-phase windings themselves. Such a relay would be insensitive to ground faults on the 3-phase system outside this restricted zone and insensitive also to all 2-phase faults.

However, with the 3-phase current transformer connections of Figure 9(A) there is no place in the current transformer secondary circuit where a ground relay can be introduced, since there is no point where ground current can flow without there also being considerable phase current to confuse the relay.

Using the relay scheme of Figure 9(B)

Figure 8 (below). Protection of paralleled Y-delta banks

Figure 9 (right). Protection of a Scott-connected transformer bank

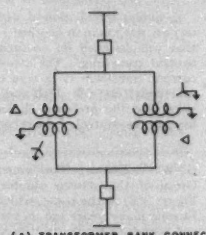

(A) TRANSFORMER BANK CONNECTIONS

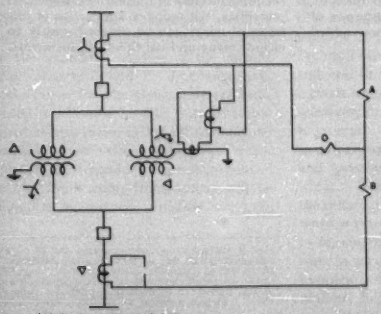

(B) RELAY CONNECTIONS (ONLY ONE PHASE SHOWN)

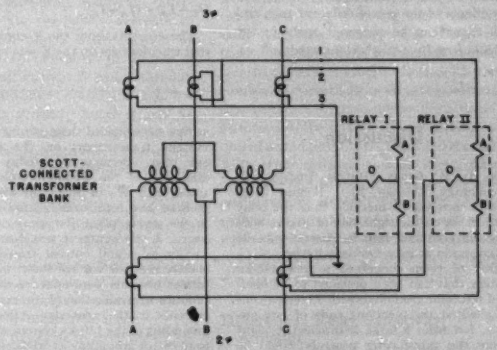

(A) USING REVERSED B-PHASE CURRENT TRANSFORMER

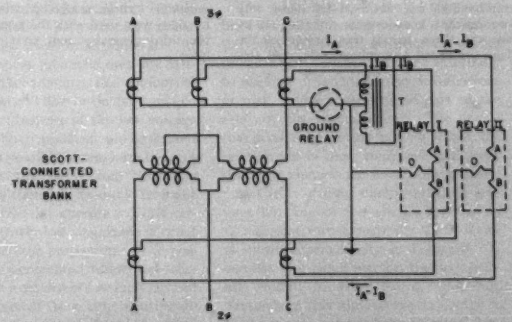

(B) USING MID-TAPPED AUTOTRANSFORMER T

of which the vital element is the mid-tapped autotransformer T, the residual circuit of the 3-phase current transformers is preserved and the ground relay can be introduced into this circuit as shown in Figure 9(B). The autotransformer mixes the currents from phases A and B on the 3-phase side so that the mixture can properly be compared in the differential relay with the current from the current transformer in the A phase on the 2-phase side.

Conclusion

By going back to the basic principles of transformer protection with percentage differential relays the scope of application and the efficiency of protection of such relays can often be increased with little or no sacrifice in economy.

It is suggested in this paper that the mathematical analysis of the operation of percentage differential relays for transformer protection be based on a conversion of the currents involved to an equal tap basis. In this manner the complicating effects of the use of different taps and coil turns can be removed early in the calculations by a straight forward process.

Where the two restraining currents are neither in phase nor 180 degrees out of phase the necessity of the vector determination of both the operating current and the total restraining effect is pointed out.

Appendix I. Protection of a Y-Delta Transformer Bank as in Figure 7(B)

Let I_A, I_B, I_C be the currents in the Y-connected windings of the transformer.

Assuming, for purposes of this demonstration, a power transformer winding ratio of unity, the currents in the delta-connected windings are also I_A, I_B, and I_C, while the line currents on the delta side are I_A-I_C, I_B-I_A, and I_C-I_B.

The current transformers of the delta side are also delta-connected so that the currents fed to the differential relay are proportional to

$$(I_A-I_C)-(I_B-I_A)$$

$$(I_B-I_A)-(I_C-I_B)$$

and

$$(I_C-I_B)-(I_A-I_C)$$

The currents from the Y-connected current transformers on the Y side of the power transformer are proportional to I_A, I_B, and I_C. Connections should be made to feed I_A from the Y-current transformers, denoted as $(I_A)_Y$, to the same relay element to which is fed $(I_A-I_C)_\Delta-(I_B-I_A)_\Delta$ from the delta current transformers, which origin is indicated by the subscript "Δ." For this to be a correct connection it must be proved that

$$n(I_A)_Y=(I_A-I_C)_\Delta-(I_B-I_A)_\Delta$$

where n is a proportionality factor which affects only the current transformer ratios and not their connections.

The proof of the correctness of the foregoing mathematical assertion can be demonstrated as follows

$$n(I_A)_Y=(I_A-I_C-I_B+I_A)_\Delta$$

$$n(I_A)_Y=(2I_A-I_C-I_B)_\Delta$$

$$n(I_A)_Y=(2I_A+I_A-I_A-I_B-I_C)_\Delta$$

Since the Y-connected power transformer winding is ungrounded

$$-I_A-I_B-I_C=0$$

Therefore

$$n(I_A)_Y=3(I_A)_\Delta$$

and thus with the proper current transformer ratios the foregoing connections of Figure 7(B) are correct. It should be noted that the key circumstance is the lack of a neutral ground on the Y-connected side of the power transformer bank.

Discussion

Eric T. B. Gross (Illinois Institute of Technology, Chicago, Ill.): It may be of historic interest to mention that the relay connection on the right side of Figure 8(B) was analyzed and used in Europe some 25 years ago in at least two installations.

One of them concerned a new 110-kv system that had been designed to be operated resonant grounded, with Petersen coils installed at the receiving ends of two circuits, fed from a large hydroelectric plant where the transformer neutrals would be isolated. Differential protection of these transformers was obtained by using only two current transformers on the 110-kv side and three current transformers on the delta-connected low-voltage side, and this saving necessitated delta connection of the current transformers on the low-voltage side also. Because of a delay in the installation of the Petersen coils, however, the system was in operation with the neutrals of two transformers solidly grounded in the power plant for approximately one year. A third current transformer on the 110-kv sides and current transformers (of greatly reduced voltage class) in the transformer neutrals were added temporarily to produce neutralization of the zero sequence currents in the neutrals. After the solid grounding of the 110-kv system was changed to resonant grounding as originally planned, the additional current transformers were removed. Those temporarily on the 110-kv sides were used with the transformer of the third generator unit that was added later.

A similar installation of differential protection was made in another 110-kv system that was designed for operation with solid neutral grounding. The connection of the current transformers in wye and delta respectively on the high-and low-voltage sides, was the preferred choice for reasons beyond the control of the relay engineers.

G. W. McKenna: The description by Dr. Gross of the scheme similar to that of Figure 8(B) in the paper, which was used in Europe many years ago, is very interesting and serves to emphasize the author's basic point that with a thorough familiarity with the fundamentals of transformer differential protection, the scope of application of differential relays can be widened greatly to include many unusual circuit arrangements.

Differential Relay Sensitivity Adjuster

C. L. HEADLEY
MEMBER AIEE

ONE OF the primary difficulties experienced in the protection of a power transformer is false tripping by the differential relays on magnetizing inrush current. The magnitude of inrush current is considerably greater on transformers of modern design, and the use of these transformers, especially in the larger size, has greatly increased the difficulty in the application of differential relays.

The purpose of this paper is to describe a device that has been developed which will prevent the differential relay from tripping on magnetizing inrush. This device is arranged to desensitize the relay during the magnetizing inrush period, and it can be applied to any percentage restraint type differential relay.

The Percentage Differential Relay

Typical differential relay connections using a percentage restraint differential relay for the protection of a transformer are shown in Figure 1. Current transformers are shown installed in the connections to the windings of the power transformer.

The normal load or fault current through the power transformer windings causes currents I_1 and I_2 to flow as shown in the secondary winding of the current transformers, X and Y. For simplicity, connections for one phase only are indicated, see Figure 1. The current transformers have ratios so that for normal load or fault currents through the power transformer, the secondary currents produced in the two current transformers will be equal in magnitude. In this way, the secondary currents produced by the current transformers will flow in the restraint windings, R_1 and R_2, of the differential relay as indicated by the arrows, and no net current will flow in the operating winding, O, of the relay.

In the event of a phase-to-ground fault in either winding of the power transformer or within the zone protected by the differential relay, the secondary currents of transformers X and Y will no longer be equal. This is indicated in Figure 2 where the fault current I_3 passes through current transformer X and through the fault path to ground; hence it has no counterpart in current transformer Y. The fault current I_3 produced by current transformer X passes through the restraint winding R_1 and operating winding, O, of the differential relay and if of sufficient magnitude will cause the relay to operate. It will be noted that the counterpart of the load current, I_1 and I_2, which is produced by current transformers X and Y flows through the restraint windings only of the differential relay.

It is highly desirable to have the differential relay operate on a minimum value of fault current in order to detect a fault of low magnitude. For example, if either winding of the transformer illustrated in Figure 2 becomes grounded near the neutral end of the winding, the amount of current which will flow in the fault will be relatively low because of the low voltage to ground. Such a fault should be cleared as quickly as possible to minimize damage and prevent the fault from becoming worse. It is therefore desirable to make the differential relay operate on fault currents of extremely low magnitude in order to obtain the best protection. It is possible to set a percentage differential relay to operate on a relatively low fault current without danger of the relay operating incorrectly because of slight inaccuracies in the current transformers or slight differences from the ratio of the power transformers. However, there is one difficulty that must be considered when applying differential relaying to a power transformer. This difficulty arises from false tripping on magnetizing inrush current experienced when energizing the transformer. A number of methods have been resorted to in order to overcome this trouble. One of these is to set the relay to operate above the inrush current value. Another method is to adjust the time setting so the relay will function only after a relatively long time (1/2 to 1 second). Still another method is a combination in which the differential relay is given a relatively high current setting and a moderately long time setting. Use of any of these methods results in reduced protection to the transformer. Even with the combination method, overcurrent setting may be above full load rating of the transformers and the minimum time setting required would possibly be about 1/2 second. With relay settings such as these, false operation due to magnetizing inrush currents may be avoided but faults of low magnitude would not be detected and when the fault is of sufficient magnitude to be detected, the time in which the relay will operate is longer than desirable.

Differential Relay Sensitivity Adjuster

The difficulties enumerated previously have led to the development of a differential relay sensitivity adjuster of special design which may be connected externally to existing differential relay installations or may be made an integral part of the relay by the manufacturer. The device functions only during periods when the transformer is being energized, and automatically changes sensitivity of the differential relay during that interval to prevent tripping of the circuit breaker on transformer inrush current. This device is shown schematically in Figure 3. It consists of a small reactor, the magnetizing winding of which has a center tap. The ends of this winding are connected to the terminals 1 and 2 of the differential relay to which the restraint coils are con-

Paper 50-190, recommended by the AIEE Relays Committee and approved by the AIEE Technical Program Committee for presentation at the AIEE Middle Eastern District Meeting, Baltimore, Md., October 3–5, 1950. Manuscript submitted July 5, 1950; made available for printing August 9, 1950.

C. L. HEADLEY is with the Consolidated Gas, Electric Light, and Power Company of Baltimore, Baltimore, Md.

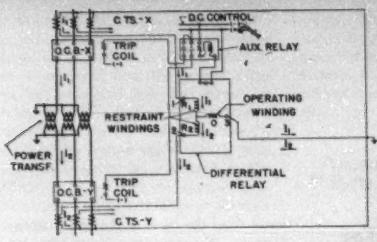

Figure 1 (left). Percentage differential relay connections to one phase of a transformer

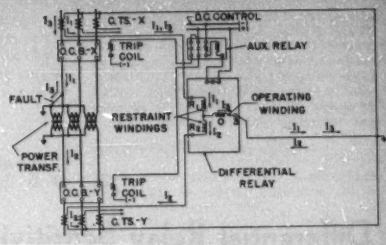

Figure 2 (right). Percentage differential relay operation on faulted transformer

nected. The center tap of the reactor winding is connected to terminal 3 of the differential relay. The circuit between terminal 3 and the reactor mid-point includes a resistor, R, and contacts, C^1, of a time delay relay, C. Terminal 3 of the differential relay is connected to the common connection of current transformers X and Y.

This reactor provides the main control on the amount of desensitization, the adjustable resistor, R, being provided for making finer adjustments if required. The resistor may be eliminated entirely if the reactor is designed for the particular application or if taps for making adjustments are provided at each end of the reactor.

Relay C shown in Figure 3 is energized through a potential transformer connected to one side of the power transformer which is to be protected. When the relay is de-energized, it closes contacts C^1 immediately. However, upon being energized, the relay opens contacts C^1 after a predetermined time delay.

To illustrate the operation of the sensitivity adjuster, we will assume the power transformer to be de-energized and both the oil circuit breakers X and Y open. With this condition, relay C will be de-energized and contacts C^1 will be closed, connecting the center point of the sensitivity adjuster reactor winding through resistance R to the common connection of the current transformers.

Assume that the power transformer is energized by closing oil circuit breaker X and that an inrush current transient occurs which produces a differential current of large magnitude, I_T, between transformers X and Y in the secondary circuit. This differential current may be considered to flow to terminal 1 of the differential relay. At that point, a portion I_a will flow to terminal 1 of the sensitivity adjuster, through one half of the sensitivity adjuster winding to the center tap, through resistance R, through contacts C^1 and back to the common polarity of current transformer X. The other portion I_b of the differential current will flow from terminal 1 of the differential relay, through restraint winding R_1, to the center tap of the relay, where a portion I_c of this current will flow through the operating winding of the relay to terminal 3, and from there to the common polarity of current transformer X. The remaining portion of the differential current, I_d, will flow from the midpoint of the differential relay, through restraint coil R_2, to terminal 2 of the sensitivity adjuster, through the other half of the sensitivity adjuster winding to the center tap, through resistance R, contact C^1, and from there to common polarity of current transformer X.

It will be noted that the currents I_a and I_d flowing from terminals 1 and 2 respectively, of the sensitivity adjuster flow through each half of the reactor winding to the center tap in opposite directions. In this way, the reactance of the coil is neutralized which permits this portion of the current to be shunted around the operating winding of the differential relay, thus desensitizing the relay operation.

The amount of desensitization of the relay is determined by the value of resistance R which is selected to prevent the relay from operating on magnetizing inrush current.

When the power transformer is energized, relay C is also energized and after a time delay, opens its contacts C^1 to disconnect the center tap of the sensitivity adjuster from the differential relay circuit. With contacts C^1 open, current can flow in the adjuster only through the full reactor winding which now has high impedance as compared to the restraint coils R_1 and R_2 of the differential relay so that the sensitivity adjuster no longer affects the operation of the relay. Therefore, opening of contacts C^1 restores the differential relay to normal sensitivity.

If a fault of sufficient magnitude develops during the short period when the auxiliary contacts C^1 are closed, the current I_c in the operating winding of the relay as previously referred to will be increased sufficiently to cause the differential relay to operate to clear the transformer from the system. However, if the fault is not severe enough to cause the differential relay to operate, the transformer will be cleared when the relay contacts C^1 open. The time required to keep the relay contacts closed depends upon the maximum time duration of the magnetizing inrush current; usually 1/2 to 2 seconds is sufficient.

Several different methods of closing contacts C^1 have been used and have proven satisfactory. These methods include response to absence of potential on the power transformer, use of an auxiliary switch on the transformer circuit breakers, and energizing the relay from the closing circuit of the transformer circuit breakers.

The application of the desensitizing circuit to the differential relay has the advantage that the same desensitization is provided regardless of which side of

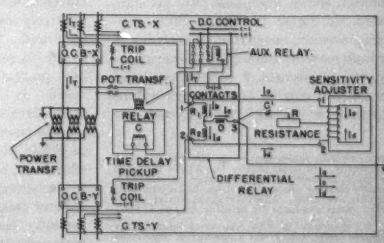

Figure 3. Percentage differential relay equipped with sensitivity adjuster

Table I. Tests without Sensitivity Adjuster

Test Number	Magnetizing Inrush 33-Kv Amperes—RMS Phase A	Phase B	Phase C	Relay Response
1	700	1,160	360	Phase B
2	1,200	500	500	Phase A
3	1,300	1,200	700	Phase A and Phase B

the transformer is energized initially. A further advantage in these arrangements is that the desensitizer may be applied externally to the differential relay and does not require circuit changes within the relay. It also permits setting the relay for maximum sensitivity under normal operating conditions.

In 3-phase applications, one sensitivity adjuster is required for each phase element of the differential relay. The center tap of the reactor winding of each adjuster is connected in series with a resistor and through a pair of contacts on the time delay relay to the operating coil terminal of each differential relay. The outside reactor terminals 1 and 2 are connected to the restraint coil terminals of each differential relay. With the sensitivity adjuster connected as described, no change is made in the differential relay adjustment, nor is the operation of the relay affected so long as the relay contacts C^1 remain open. However, during the interval when the power transformer is being energized, the contacts C^1 are closed to effect desensitizing the differential relay to prevent tripping on magnetizing inrush current.

Performance

The following tests were made by energizing a General Electric 40,000-kva 33/110-kv 3-phase transformer at the Riverside Station of the Consolidated Gas, Electric Light, and Power Company of Baltimore. The transformer was protected by a General Electric type *IJD* differential relay.

Table II. Tests with Sensitivity Adjuster Connected

Test Number	Magnetizing Inrush 33-Kv Amperes—RMS Phase A	Phase B	Phase C	Relay Response
4	350	340	860	None
5	400	1,140	620	None
6	1,200	540	1,200	None
7	700	1,160	400	None
8	1,150	500	400	None

The differential relay was adjusted for the test to operate at approximately 400 amperes at 33 kv with a minimum time for operation of approximately 0.1 second.

The sensitivity adjuster was set to reduce the sensitivity of the differential relay during the magnetizing inrush period from 400 amperes to approximately 1,100 amperes at 33 kv.

The tests were made by energizing the transformer from the 33-kv bus by closing the oil circuit breaker. Tables I and II give the test results with and without the sensitivity adjuster.

Discussion

Eric T. B. Gross (Illinois Institute of Technology, Chicago, Ill.): It appears that the main difficulty experienced with differential protection has been false tripping on transient components of magnetizing currents. Larger inrush currents are being observed on transformers of modern design, not only upon energizing by switching in, but also after through faults upon switching off of the remote short circuit by the circuit breaker next to it. Many solutions have been suggested,[1–4] but the problem of eliminating false tripping of differential relays still seems to exist. I am wondering if the author would show how the sensitivity adjuster described in this paper would eliminate without exceptions false tripping because of magnetizing current transients after through faults, when there was no operation of the transformer circuit breakers, but only of a remote circuit breaker near the far away fault or near a fault in the section next to the transformer installation.

It seems to me that we are still short of a step forward in the direction to higher sensitivity of transformer protection. Surely, we have learned to build better transformers, but we also use larger transformers, and increased sensitivity of protection means reduced damage, and faster and cheaper repair in those few cases of transformer failure that remain. Many kinds of faults are possible, within the tank of transformers, which produce unbalances that are smaller than the permissible lowest setting of any type of differential relay. It may be pointed out that gas and pressure relays provide a solution with greatly increased sensitivity, and without all the troubles produced by inrush currents. Perhaps it is worthwhile to cite here the recommendations of the latest AIEE Committee Report[5] on Transformer Protection which states:

"The value of gas accumulator relays for detecting incipient faults has been underestimated generally in the United States.

"1. Substantial experience in Canada has demonstrated the value of gas accumulator relays to detect conditions such as turn-to-turn faults, core insulation failures, and defective joints.

"2. Objections commonly raised to the gas accumulator method of detecting faults can be overcome largely by suitable application and proper interpretation of relay indications.

"3. The present commercially developed gas detector relays are limited in application to conservator-type transformers. Experimental installations indicate that devices may be developed for extending gas detection principles to other types of transformers.....

"The wider application of pressure protection offers considerable promise. (1) To provide supplemental protection with sensitivity greater than usually obtained with conventional differential schemes alone. (2) For protection, when used with overcurrent relays, where it is not feasible to provide a satisfactory differential scheme. (3) To solve inherently difficult application problems, such as with step regulators and rectifier transformers. (4) For fast low-cost protection and reclosing lockout of feeder voltage regulators."

References

1. Harmonic-Current Restrained Relays for Differential Protection, L. F. Kennedy, C. D. Hayward. *Electrical Engineering* (*AIEE Transactions*), volume 57, May 1938, pages 262–71.

2. Rectifier Relay for Transformer Protection, E. L. Michelson. *Electrical Engineering* (*AIEE Transactions*), volume 64, May 1945, pages 253–54.

3. Enhanced Transformer Protection Through Inrush Proof Ratio Differential Relays, G. Bertola. *Brown Boveri Review* (Baden, Switzerland), volume 32, 1945, pages 129–33.

4. Instantaneous Magnetic Balance Protection for Power Transformers, J. G. Wellings, P. Matthews. *B.T.H. Activities* (Rugby, England), volume 19, 1946, pages 30–32, and *Electrical Review* (London, England), volume 137, 1945, pages 711–12.

5. Relay Protection of Power Transformers, AIEE Committee Report. *AIEE Transactions*, volume 66, 1947, pages 911–17, and *Electrical Engineering*, volume 66, October 1947, pages 964–68.

6. Typical Transformer Faults and Gas Detector Relay Protection, J. T. Madill. *AIEE Transactions*, volume 66, 1947, pages 1052–60.

7. Simplicity in Transformer Protection, Eric T. B. Gross. *Electrical Engineering*, volume 66, June 1947, pages 564–69.

C. L. Headley: In his discussion, Mr. Gross has pointed out that magnetizing inrush currents may be experienced in a transformer immediately following a fault through the transformer that is cleared by a remote circuit breaker, that is, on the secondary side of the transformer. Such a fault would leave the transformer in service. Mr. Gross has asked if the sensitivity adjuster as described will prevent the differential relay from tripping the transformer circuit breaker on this type of magnetizing current transient.

We have never experienced incorrect tripping by the differential relay on magnetizing inrush following a fault current through the transformer. However, the transformer differential relay sensitivity adjuster as described in the paper is controlled by a potential relay which is energized from one side of the transformer that is being protected. Upon being energized, normally closed contacts of the potential relay open after a predetermined time delay to restore the differential to its normal sensitivity. But, upon being de-energized, the potential relay immediately closes its contacts which desensitize the differential relay.

With this arrangement and proper setting of the potential relay to close on reduced voltage, a fault current through the transformer of sufficient magnitude to cause an inrush current great enough to operate the differential relay, will also cause a sufficient drop in voltage at the terminals of the transformer to close the potential relay contacts. This activates the sensitivity adjuster applied to the differential relay circuit and prevents the relay from tripping on the magnetizing inrush transient.

Of course, if the transformer carries load immediately following the clearing of a fault, the load current through the transformer helps to prevent the differential relay from tripping by action of the restraint windings in the relay. Also, the load through the transformer helps to reduce the inrush transient time.

Gas and pressure relays offer a solution for the protection of transformers on faults of low magnitude, particularly on turn-to-turn faults. Also, they are free from troubles produced by inrush currents. However, it is felt that transformers equipped with gas or pressure relays also should be protected by a standard differential relay. One method of protection that we have used successfully where the application of differential relays is difficult, such as induction regulators, step regulators, and phase shifters, is the case ground relay. Such relays are comparatively easy to apply and they can be set with sufficient sensitivity to detect phase-to-case faults of extremely low magnitude. We have experienced several operations of this type of relaying and in each case the trouble was cleared without disturbance to the system and relatively small damage to the equipment.

Resistance Commutation

FRANK D. OLNEY
MEMBER AIEE

Synopsis: Thorburn Reid considered the commutation problem in rotating machines as arising from reactance in the coils being commutated by the varying brush contact resistance. This paper extends Reid's treatment to include the effects of reactance in the coils which are not being commutated, and shows that these noncommutating coils are an important factor in commutation performance. An equivalent circuit for a simplified commutator machine is developed and used as the basis for the analysis given in Appendixes I through VI. By means of this equivalent circuit, the average brush terminal voltage is seen to approach the value of the commutating reactance voltage under severe commutating conditions. Voltage pulses near the end of the commutation period are shown to be produced by a parallel influence of the noncommutating and the commutating coils. A testing device based on the equivalent circuit is described in Appendix VI, and consists of a mechanical inverter connected so as to separate the functions of the brushes in reversing current through the commutating coils, and in passing current through the noncommutating coils. When connected to the armature of a particular machine, the testing device is used to measure the commutating reactance and the brush contact resistance under simulated operating conditions. By means of this device, a correlation between brush electrical wear and severity of commutating conditions is established, which helps to confirm the basic theory.

THE MANY important military, industrial, and domestic applications of commutator machines make it necessary that designers know the commutating ability of these machines. Where commutating poles are used within their range of effectiveness, commutation performance can be predicted with reasonable accuracy. However, where the varying resistances of the brush-to-segment contacts are depended upon to control the commutation, that is, resistance commutation, there is a need for fundamental design information on which may be based calculations of commutation performance from circuit data.

Thorburn Reid[1,2] showed that high voltages appear across the brush-to-segment contact when there is a large reactance in the coils being commutated by the varying brush contact resistance. In a machine connected to a constant line voltage, however, these high voltages can occur only if there is an additional impedance in the circuit across which an opposing voltage may be developed. The present paper shows that the noncommutating coils provide this additional impedance.

The machine selected for analysis is operated from a constant voltage line, and has symmetrical windings in which commutation is accomplished in the neutral zone by means of brushes which span one commutator segment. The magnetic field in the air gap due to armature reaction is considered to be fully compensated. The machine speed is constant, so that the generated voltage due to field excitation of the noncommutating coils and its counterpart in the external line voltage may be omitted. That is, the only external line voltage considered will be that component required to overcome the brush terminal voltage.

The only assumption required under these conditions is that concerning the brush-to-bar contact. Mechanically perfect bearings, commutator, brushes and brushholders are assumed so that electrical contact between the brush and segment is continuous. The contact resistance is assumed to vary inversely with the contact area and to be independent of instantaneous current density under transient conditions. The transient conditions considered are those occurring during the usual commutation period with a duration of the order of one millisecond. No assumption is required as to the condition of the contact film, since the method of analysis utilizes the per-unit system to take into account any relatively slow variations of the film and thus of the contact resistance such as occur with changes in average line current, temperature, wear, atmosphere, and other commutating conditions. This use of the per-unit system, or dimensionless grouping, also will allow test results to be duplicated even though the commutator film changes as a result of load change.

Analysis

Faraday's experiments showed that induced voltages are proportional to the rate of change of flux linkages with the circuit, so that a continuous voltage cannot be induced in an uninterrupted circuit unless the flux increases indefinitely. Therefore, an essential part of every d-c machine, in addition to a provision for generating a voltage, is a means for reducing the flux linkages at intervals by a substitution of circuit[3] in an attempt to avoid generating a voltage, as may be done by the use of a commutator. A commutator may be thought of as a mechanical switch connecting individual armature coils to the power line in such a manner that as a coil is disconnected from the power line, it is short-circuited by the brushes, the polarity is reversed, and it is reconnected to the power line. Complication arises from the fact that the disconnection, short circuit, reversal, and reconnection proceed simultaneously. This complication, together with the fact that outside the range of effectiveness of commutating poles and in all but acyclic machines, the reduction of flux linkages at intervals by a substitution of circuit actually does generate a voltage which appears at the machine terminals, and the additional fact that the brushes are at the same time passing current through the reactance of the remainder of the armature, has led to various opinions as to the

Paper 50-191, recommended by the AIEE Rotating Machinery Committee and approved by the AIEE Technical Program Committee for presentation at the AIEE Middle Eastern District Meeting, Baltimore, Md., October 3–5, 1950. Manuscript submitted March 8, 1950; made available for printing July 31, 1950.

FRANK D. OLNEY is with the General Electric Company, Fort Wayne, Ind.

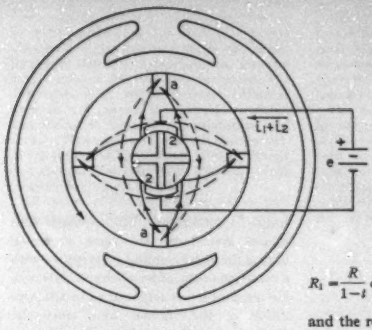

Figure 1 (left). Schematic diagram of commutator machine

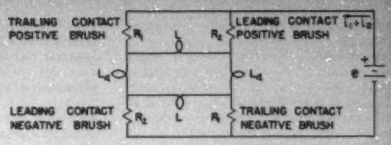

Figure 2 (right). Equivalent circuit of commutator machine

particular factors which give rise to the commutation problem.

The method of analysis used in this paper is to set up an equivalent circuit for a simplified machine as would be seen from reference axes fixed with respect to the commutating coils, to make calculations of commutation performance based on this circuit as given in Appendixes I through V, and then to check the calculations using a test device in which each element entering into the commutation problem may be separately evaluated by suppressing the effects of other elements, as described in Appendix VI. In this way, the basic theory of commutation may be established on a firm footing before some of the more complicated factors met in machines are considered.

Figure 1 is a schematic view of a simplified machine which contains the essential features of more complicated machines. Only two poles and four slots are shown, but of course the analysis is equally valid for any number of slots or poles. The coils in the slots marked (a) are the noncommutating coils, and the edges of the brushes marked (1) are the trailing edges. The commutator bars in contact with the trailing edges of the brushes are termed the trailing bars.

If each brush is separated into leading and trailing contacts, with the insulation between bars as the dividing line, to an observer moving with the armature the circuit of Figure 2 is electrically equivalent to that of Figure 1. The reference axes are fixed in the armature since it is possible for flux to reverse with respect to an armature coil and yet be unchanged with respect to the field, because of rotation. Neukirchen[4] has shown that over 98 per cent of the total brush resistance is in the commutator-to-brush contact and less than 2 per cent is in the brush body of usual brushes, so that the assumed resistance of the trailing contact becomes

$$R_1 = \frac{R}{1-t} \text{ ohms} \tag{1}$$

and the resistance of the leading contact is

$$R_2 = \frac{R}{t} \text{ ohms} \tag{2}$$

Direct analysis of the circuit in Figure 2 is possible, but some of the equations will be redundant because of the symmetry of the circuit. The same voltage will appear across each of the two commutating coils so that they may be combined, but the inductance coefficients should be halved to compensate for the doubling of the current in the combined coils. If this is done, a similar combination of the noncommutating coils will then result in the simplified equivalent circuit of Figure 3.

The simplified equivalent circuit contains the essential geometry of the machine as far as commutation is concerned, and has the general form of a bridge circuit in which the commutating coil carries the unbalance current. Since the arms of the bridge are composed of contact resistances which vary with time, it is possible that the bridge circuit in the path of the line current will act as an impedance which is greater than the net ohmic value of the contact resistances in cases where the commutating inductance is large.

A physical picture of the mechanism by which current is reversed in the commutating coil may be obtained by observing the current paths in the simplified equivalent circuit at the start, mid-point, and end of the commutation period. At the start of the commutation period, the leading contact resistance is open-circuited and the trailing contact resistance is a minimum, so that the line current path is as shown in Figure 4. The brush terminal voltage tends to increase the line current above its initial value, but this increase is opposed by the voltage developed by the reactance of the coils.

At the mid-point of the commutation period, the contact resistances are equal so that the line current divides as it enters the armature, as shown in Figure 5. The current through the commutating coil will be determined by circuit conditions and so is shown dotted.

At the end of the commutation period, the leading contact resistance is a minimum and the trailing contact resistance is open-circuited, so that the line current path is as shown in Figure 6. If the current in the commutating coil has not sufficiently reversed before this time, it can be seen that the line current will be opposed, and that a high voltage may be developed across the noncommutating coils in an attempt to maintain the line current. Commutation is a repeated transient, so that the line current at the end of the period must be the same as at the start of the period. This restriction on the line current gives the boundary conditions to be applied in the analysis, since this means that the commutating coil current must exactly reverse by the end of the period. However, this does not mean that the line current must be constant throughout the commutation period, nor does it place restrictions on the rate of change of line current, nor does it mean that the initial value of the commutating coil current must be equal to the average value of the line current.

Kirchhoff's equations for the circuit of Figure 3 are, where the elapsed time in seconds is written as tT so as to simplify the form of the solutions

$$\frac{L_a}{2T}\frac{d}{dt}(i_1+i_3)+R_1i_1+R_2i_3=e \tag{3}$$

$$i_1=i_2+i_3 \tag{4}$$

$$\frac{L}{2T}\frac{di_3}{dt}+R_1i_1-R_2i_3=0 \tag{5}$$

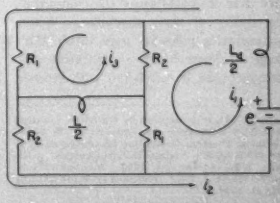

Figure 3. Simplified equivalent circuit

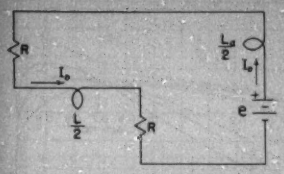

Figure 4. Current path at start of commutation period

Solutions to these equations are given in the appendixes as follows:

Appendix	Ratio of Noncommutating to Commutating Inductance
I	Zero
II	Unity
III	Greater than unity (general case)
IV	Extremely large
V	Zero, but with line resistance

Typical Results

Figure 7 gives the calculated brush terminal voltage for particular values of the commutating and noncommutating inductances, together with test points taken by means of the device described in Appendix VI. The per-unit brush terminal voltage is an index to the severity of the commutating conditions, and has important effects on the short-circuit current of d-c generators, on the sensitivity of amplidynes, on the brush and commutator temperature, and so on. It should be noted that the curves shown are not affected by brush grade, brush temperature, brush spring pressure, type of commutator, speed, average line current, surface film, and so forth, as long as the assumptions are not violated.

Figures 8 and 9 give values for the commutating coil current and line current during the commutation period for typical circuit conditions. The effect of commutating and noncommutating reactance on the line current ripple is shown in Figure 10. The typical saw-tooth shape of the line current is seen to be a result of commutation, and not a result of air-gap permeance variations caused by slots. The significance of line current ripple is that the average commutating coil voltage depends only on the initial line current and is not exactly proportional to the average line current if the brush contact resistance varies with line current, atmosphere, temperature, brush grade, and so forth. Although outside the scope of this paper, this nonlinearity has application to the shape of the black band on certain machines when commutating poles are used, and indicates the reason why a slightly stronger commutating pole field may be needed if low-resistance brushes are replaced by high-resistance brushes.

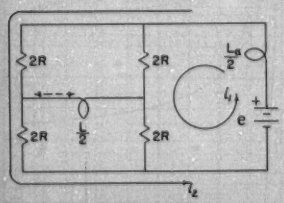

Figure 5. Current paths at mid-point of commutation period

Figures 11, 12, 13, and 14 give values for the circuit voltages during the commutation period for typical commutating conditions. The production of pulse voltages near the end of the commutation period under severe commutating conditions can be seen from these curves. The effect of these pulses on the brushes and bars may be appreciated when it is realized that the square of the trailing brush contact voltage gives the watts per square inch over the trailing contact area, under the assumption that contact resistance is inversely proportional to contact area. That is, if the trailing contact voltage pulse reaches ten times the normal brush drop, the dissipated power density reaches 100 times normal. The effect of the pulses across the noncommutating coils has application to the flashover problem of commutators. In practice, of course, the assumptions made concerning the contact resistance will not hold for the extremely small time interval during which the high-voltage pulse is applied, and this, together with the interturn capacitance, will limit the peak value of the pulse.

Figure 15 is included as an aid to the analysis of Appendix III, and shows average values of the leading brush contact voltage plotted as a ratio to the final leading brush drop instead of in per unit of the base voltage.

Nomenclature

e = Brush terminal voltage for the positive plus the negative brushes
E = Line voltage (appendix V)
I = Average line current, amperes
I_0 = Line current at start or end of commutation period, amperes
i_1 = Trailing brush contact instantaneous current, amperes
i_4 = Leading brush contact instantaneous current, amperes
i_4 = Commutating coil instantaneous current, amperes
L = Commutating coil differential[13] inductance, henrys. This is one-half the sum of the self and mutual inductances of all coils simultaneously commutated by one pair of brushes of opposite polarity

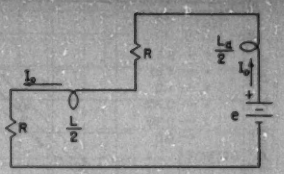

Figure 6. Current path at end of commutation period

L_a = Noncommutating coil differential[13] inductance for one armature circuit, including mutual inductance with other armature circuits, henrys.
R = Brush contact resistance for one full contact area, ohms
R_1 = Trailing brush contact instantaneous resistance, as a function of the trailing contact area, ohms
R_4 = Leading brush contact instantaneous resistance, as a function of the leading contact area, ohms
r = Line resistance, ohms (appendix V)
t = Elapsed time in per unit of commutation period. (t ranges from 0 to 1).
T = Commutation period or time for trailing brush to go from full to zero contact area with respect to one segment, seconds (T is inversely proportional to the speed of rotation)

$$s = \mathrm{Tanh}^{-1}\frac{(1-2t)}{\sqrt{1+\frac{2R}{r}}} \text{ (appendix V)}$$

Per-Unit System[5]

Base Quantities

Unit time = T seconds
Unit resistance = 2 R ohms (positive plus negative brush)
Unit current = I amperes
Unit voltage = (unit ohms) (unit amperes) = 2 IR
Unit inductance = (unit ohms) (unit time) = 2 RT henrys
Unit brush life is explained in Appendix VI

Some Per-Unit Quantities

Per-unit time = t
Per-unit brush terminal voltage = $e/2\,IR$
Per-unit initial line current (line current ripple) = I_0/I
Per-unit reactance voltage = $L/2\,RT$ (in a strict sense, this is the per-unit commutating inductance, but by multiplying numerator and denominator by the average line current, it becomes per-unit reactance voltage, if there is no line current ripple)

Appendix I. Noncommutating Inductance Equal to Zero

Cases in which there is no noncommutating inductance are not ordinarily met in practice, but the analysis is presented be-

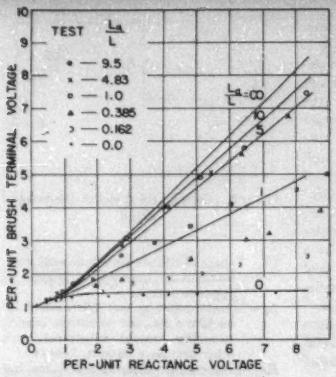

Figure 7 (left). Per-unit brush terminal voltage

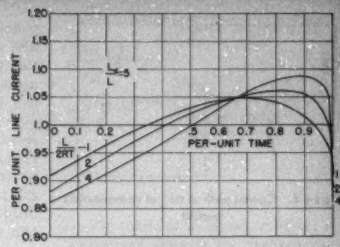

Figure 9 (right). Per-unit line current

cause it completes the range of circuit constants and affords a physical understanding of the commutation process.

If currents i_1 and i_2 are eliminated in equations 3, 4, and 5, there results an equation containing the commutating coil current, when $I_a=0$

$$\frac{L}{2T}\frac{di_3}{dt}+\frac{2R_1R_3}{R_1+R_3}i_3+\frac{R_1-R_3}{R_1+R_3}e=0 \qquad (6)$$

Putting the assumed contact resistances from equations 1 and 2 into 6

$$\frac{L}{2T}\frac{di_3}{dt}+2Ri_3=(1-2t)e \qquad (7)$$

Equation 7 is linear and indicates that with respect to the armature, the commutation circuit contains an applied brush terminal voltage which linearly reverses during the commutation period. The solution to equation 7 is, after the boundary condition that at $t=0$, $i_3=I_0$ is applied

$$\frac{i_3}{I_0}=\epsilon^{-\frac{4RT}{L}t}+\frac{e}{2I_0R}\times\left[\left(1+\frac{L}{2RT}\right)\left(1-\epsilon^{-\frac{4RT}{L}t}\right)-2t\right] \qquad (8)$$

It can be seen from Figure 8 that during the first half of the commutation period the commutating coil current increases rather than decreases, in the absence of any noncommutating inductance. The commutating coil current must reverse by the end of the commutation period, so applying the boundary condition that at $t=1$, $i_3=-I_0$, the value of the brush terminal voltage is

$$\frac{e}{2I_0R}=\frac{1+\epsilon^{-\frac{4RT}{L}}}{2-\left(1+\frac{L}{2RT}\right)\left(1-\epsilon^{-\frac{4RT}{L}}\right)} \qquad (9)$$

The line current is found by substituting the commutating coil current from equation 8 into equations 3 and 4

$$\frac{i_1+i_2}{I_0}=(1-2t)\epsilon^{-\frac{4RT}{L}t}+\frac{e}{2I_0R}\times\left[\left(1+\frac{L}{2RT}\right)(1-2t)\left(1-\epsilon^{-\frac{4RT}{L}t}\right)+2t\right] \qquad (10)$$

When the line current is averaged over a commutation period, the voltages and currents may be plotted in terms of the average line current instead of the initial line current. However, the expressions for voltage and current as explicit functions containing the average line current are complicated, and so the form used in equations 8, 9, and 10 in terms of the initial line current will be continued through the remainder of the mathematical analysis.

The trailing brush contact current is found from equations 3, 4, and 8 as

$$\frac{i_1}{I_0}=(1-t)\epsilon^{-\frac{4RT}{L}t}+\frac{e}{2I_0R}\left(1+\frac{L}{2RT}\right)\left(1-\epsilon^{-\frac{4RT}{L}t}\right)(1-t) \qquad (11)$$

and similarly, the leading brush contact current is

$$\frac{i_2}{I_0}=\frac{e}{I_0R}t-t\epsilon^{-\frac{4RT}{L}t}-\frac{e}{2I_0R}\left(1+\frac{L}{2RT}\right)\left(1-\epsilon^{-\frac{4RT}{L}t}\right) \qquad (12)$$

The remainder of the circuit quantities can be determined directly from equations 1 through 5 without differentiation or integration, and typical values are shown in Figures 11 through 14.

Appendix II. Noncommutating Inductance Equal to Commutating Inductance

For the special case where the noncommutating inductance is equal to the commutating inductance, equations 3, 4, and 5

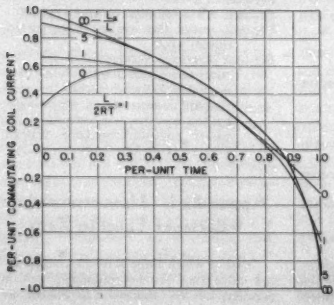

Figure 8 (left). Per-unit commutating coil current

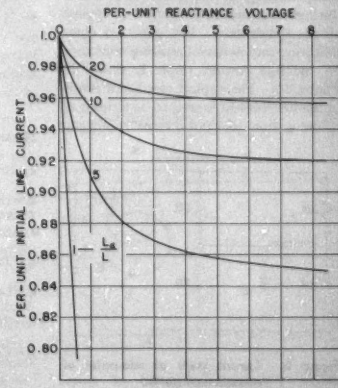

Figure 10 (right). Per-unit initial line current

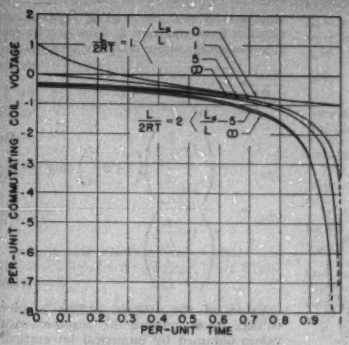

Figure 11 (left). Per-unit commutating coil voltage

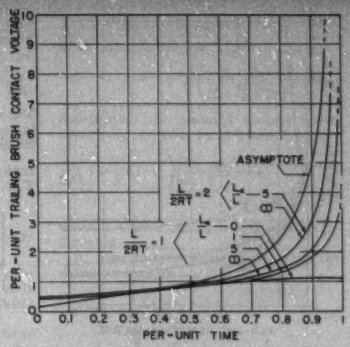

Figure 13 (right). Per-unit trailing brush contact voltage

are solved by eliminating the commutating coil current. If this is done, there results

$$\frac{L}{T}\frac{di_1}{dt}+2R_1i_1=e \tag{13}$$

$$\frac{L}{T}\frac{di_2}{dt}+2R_2i_2=e \tag{14}$$

Putting the assumed contact resistances from equations 1 and 2 into equations 13 and 14 yields

$$\frac{L}{T}\frac{di_1}{dt}+\frac{2R}{1-t}i_1=e \tag{15}$$

$$\frac{L}{T}\frac{di_2}{dt}+\frac{2R}{t}i_2=e \tag{16}$$

The solutions to equations 15 and 16 are, after the initial boundary condition is applied that at $t=0$, $i_1=I_0$, and $i_2=0$.

$$\frac{i_1}{I_0}=(1-t)^{\frac{2RT}{L}}+\frac{e}{2I_0R}\left(\frac{1}{1-\frac{L}{2RT}}\right)\times\left(1-t-(1-t)^{\frac{2RT}{L}}\right) \tag{17}$$

$$\frac{i_2}{I_0}=\frac{e}{2I_0R}\left(\frac{t}{1+\frac{L}{2RT}}\right) \tag{18}$$

Then from equation 4, the commutating coil current is

$$\frac{i_3}{I_0}=(1-t)^{\frac{2RT}{L}}+\frac{e}{2I_0R}\times\left[\frac{1-(1-t)^{\frac{2RT}{L}}}{1-\frac{L}{2RT}}-\frac{2t}{1-\left(\frac{L}{2RT}\right)^2}\right] \tag{19}$$

In order to meet the final boundary condition that at $t=1$, $i_3=-I_0$, the brush terminal voltage becomes

$$\frac{e}{2I_0R}=1+\frac{L}{2RT} \tag{20}$$

The line current is, from equations 17 and 18

$$\frac{i_1+i_2}{I_0}=(1-t)^{\frac{2RT}{L}}+\frac{e}{2I_0R}\times\left[\frac{1-(1-t)^{\frac{2RT}{L}}}{1-\frac{L}{2RT}}-\frac{\frac{L}{RT}}{1-\left(\frac{L}{2RT}\right)^2}t\right] \tag{21}$$

When this line current is averaged over a commutation period as shown in Figure 10, the voltages and currents may be expressed in the per-unit system.

At a value of the per-unit reactance voltage equal to unity, equation 17 for the trailing brush current becomes indeterminate, so that for this point only

$$\left.\frac{i_1}{I_0}\right|_{\frac{L}{2RT}=1}=(1-t)\left[1-\frac{e}{2I_0R}\log(1-t)\right] \tag{22}$$

The remaining circuit quantities may be determined directly from equations 1 through 5, and typical values are given in Figures 11 through 14.

Appendix III. Noncommutating Inductance Greater than Commutating Inductance (General Case)

In general, the noncommutating inductance is larger than the commutating inductance in practical machines. For this case, equations 1 through 5 will be solved by approximating that variations of the leading contact voltage drop from its average value have no effect on the commutation performance. The error due to this approximation can be determined readily, and will be shown to be negligible. Physically, this approximation is equivalent to considering that resistance commutation consists largely in the interruption of current in an inductive circuit by means of contacts in which the contact area decreases at a constant rate.

When the commutating coil current is eliminated in equations 3, 4, and 5, there results

$$\frac{L_s}{2T}\frac{d}{dt}(i_1+i_2)+R_1i_1+R_2i_2=e \tag{23}$$

$$\frac{L}{2T}\frac{d}{dt}(i_1-i_2)+R_1i_1-R_2i_2=0 \tag{24}$$

Multiplying equation 23 by L/L_s

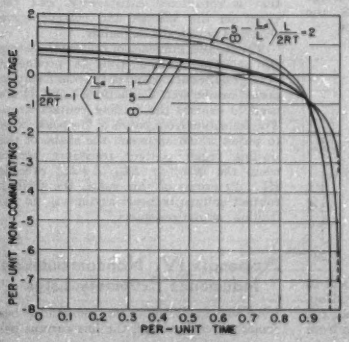

Figure 12 (left). Per-unit noncommutating coil voltage

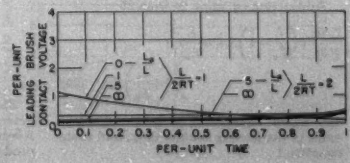

Figure 14 (right). Per-unit leading brush contact voltage

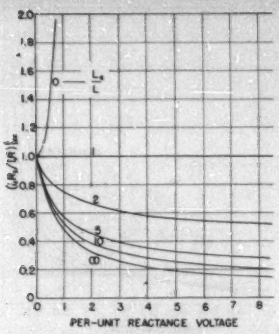

Figure 15. Average leading brush contact voltage

$$\frac{\bar{L}}{2T}\frac{d}{dt}(i_1+i_2)+\frac{\bar{L}}{L_a}R_1i_1+\frac{\bar{L}}{L_a}R_2i_2=\frac{\bar{L}}{L_a}e \qquad (25)$$

and adding equations 24 and 25

$$\frac{L}{T}\frac{di_1}{dt}+\left(1+\frac{L}{L_a}\right)R_1i_1 = \frac{L}{L_a}e+\left(1-\frac{L}{L_a}\right)R_2i_2 \qquad (26)$$

If the leading contact is considered to introduce only a constant voltage, written as $(R_2i_2|\text{av})$, then equation 26 becomes, using equation 1

$$\frac{L}{T}\frac{di_1}{dt}+\left(1+\frac{L}{L_a}\right)\left(\frac{R}{1-t}\right)i_1 = \frac{L}{L_a}e+\left(1-\frac{L}{L_a}\right)(R_2i_2|\text{av}) \qquad (27)$$

The solution to equation 27 is, after the boundary conditions are applied that at $t=0$, $i_1=I_0$, and at $t=1$, $i_1=0$

$$\frac{i_1}{I_0}=\left[1-\frac{\frac{L}{L_a}\left(\frac{e}{I_0R}\right)+\left(1-\frac{L}{L_a}\right)\left(\frac{R_2i_2|\text{av}}{I_0R}\right)}{1+\frac{L}{L_a}-\frac{L}{RT}}\right]\times (1-t)^{\left(1+\frac{L}{L_a}\right)\frac{RT}{L}}+\left[\frac{\frac{L}{L_a}\left(\frac{e}{I_0R}\right)+\left(1-\frac{L}{L_a}\right)\left(\frac{R_2i_2|\text{av}}{I_0R}\right)}{1+\frac{L}{L_a}-\frac{L}{RT}}\right](1-t) \qquad (28)$$

Equation 28 compares exactly with equation 17 in Appendix II for the case where $L_a=L$.

Subtracting equation 24 from 25

$$\frac{L}{T}\frac{di_2}{dt}+\left(\frac{L}{L_a}-1\right)R_1i_1=\frac{L}{L_a}e-\left(1+\frac{L}{L_a}\right)R_2i_2 \qquad (29)$$

and again considering only the average value of the leading contact drop, and using equation 1

$$\frac{L}{T}\frac{di_2}{dt}+\left(\frac{L}{L_a}-1\right)\left(\frac{R}{1-t}\right)i_1=\frac{L}{L_a}e-\left(1+\frac{L}{L_a}\right)(R_2i_2|\text{av}) \qquad (30)$$

The value of trailing contact current found in equation 28 is substituted into equation 30, so that

$$\frac{L}{T}\frac{di_2}{dt}+I_0R\left(\frac{L}{L_a}-1\right)\times\left[1-\frac{\frac{L}{L_a}\left(\frac{e}{I_0R}\right)+\left(1-\frac{L}{L_a}\right)\left(\frac{R_2i_2|\text{av}}{I_0R}\right)}{1+\frac{L}{L_a}-\frac{L}{RT}}\right]\times (1-t)^{\left(1+\frac{L}{L_a}\right)\frac{RT}{L}-1}+I_0R\left(\frac{L}{L_a}-1\right)\times\left[\frac{\frac{L}{L_a}\left(\frac{e}{I_0R}\right)+\left(1-\frac{L}{L_a}\right)\left(\frac{R_2i_2|\text{av}}{I_0R}\right)}{1+\frac{L}{L_a}-\frac{L}{RT}}\right]=\frac{L}{L_a}e-\left(1+\frac{L}{L_a}\right)(R_2i_2|\text{av}) \qquad (31)$$

The solution to equation 31 is, after the boundary conditions are applied that at $t=0$, $i_2=0$, and at $t=1$, $i_2=I_0$

$$\frac{i_2}{I_0}=\left(\frac{L}{L_a}-1\right)\left[\frac{1-\left(\frac{R_2i_2|\text{av}}{I_0R}\right)-\frac{L}{RT}}{1+\frac{L}{L_a}-\frac{L}{RT}}\right]\times\left[(1-t)^{\left(1+\frac{L}{L_a}\right)\frac{RT}{L}}-(1-t)\right]+t \qquad (32)$$

where the brush terminal voltage must satisfy the relation

$$e=\frac{I_0L}{T}+2(R_2i_2|\text{av}) \qquad (33)$$

Equation 33 can be seen by inspection of the equivalent circuit in Figure 3, since physically this states that the brush terminal voltage is equal to the sum of the reactance voltage and twice the average of the leading brush contact voltage drop, if line current ripple is negligible.

Substituting the brush terminal voltage from equation 33 into equation 28, the trailing brush contact current becomes

$$\frac{i_1}{I_0}=\left(1+\frac{L}{L_a}\right)\left[\frac{1-\left(\frac{R_2i_2|\text{av}}{I_0R}\right)-\frac{L}{RT}}{1+\frac{L}{L_a}-\frac{L}{RT}}\right]\times (1-t)^{\left(1+\frac{L}{L_a}\right)\frac{RT}{L}}+\left[\frac{\frac{L}{L_a}\left(\frac{L}{RT}\right)+\left(1+\frac{L}{L_a}\right)\left(\frac{R_2i_2|\text{av}}{I_0R}\right)}{1+\frac{L}{L_a}-\frac{L}{RT}}\right]\times(1-t) \qquad (34)$$

The remaining step in the analysis is to determine the average leading contact drop. Averaging, over a commutation period, the product of the leading contact current from equation 32 and the leading contact resistance from equation 2, there results for the special case where $L/2RT=1+L/L_a$

$$\left.\frac{R_2i_2}{I_0R}\right|_{\text{av}}^{\frac{L}{2RT}=1+\frac{L}{L_a}}=\frac{1-\left(\frac{1-\frac{L}{L_a}}{1+\frac{L}{L_a}}\right)\left(1+2\frac{L}{L_a}\right)(\log 4-1)}{1+\left(\frac{1-\frac{L}{L_a}}{1+\frac{L}{L_a}}\right)(\log 4-1)} \qquad (35)$$

Values of the average leading contact voltage from equation 35, together with values obtained by numerical integration, are plotted in Figure 15. These values enable the commutation performance to be determined from equations 4, 23, 24, 32, and 34 without differentiation or integration. Typical cases are shown in Figures 7–14.

An explicit expression for line current ripple is found by averaging the sum of the leading and trailing brush contact currents from equations 32 and 34

$$\frac{I}{I_0}=\int_0^1\frac{(i_1+i_2)}{I_0}dt=1+\frac{L}{L_a}\left(\frac{\frac{L}{RT}+\frac{R_2i_2|\text{av}}{I_0R}-1}{1+\frac{L}{L_a}+\frac{L}{RT}}\right) \qquad (36)$$

Values from equation 36, after inversion, are shown in Figure 10, and these values are used to express the remaining quantities in the per-unit system.

The error involved in the approximation concerning the effect of variations in the leading contact drop can be found by comparison with exact analysis. For the case where $L_a=L$, equations 32 and 34 become identical with equations 17 and 18 in Appendix II, so there is no error. For the case where L_a is extremely large, at a per-unit reactance voltage equal to 1, the approximate brush terminal voltage is within 2 per cent of the exact value found in Appendix IV. Since these two cases bracket the applicable range of constants, the approximation is considered satisfactory, and the effect on the voltage and current wave shapes is practically negligible.

The parallel influence of the commutating and noncommutating coils in producing voltage pulses at the end of the commutation period can be seen if equations 1 and 34 are used to express the trailing contact drop. The transition from pulses of low peak value to pulses which approach the shape of the trailing brush contact resistance occurs when the quantity $LL_a/(L+L_a)$ exceeds RT. In excess of this value, the trailing contact voltage becomes asymptotic to the trailing contact resistance.

Appendix IV. Noncommutating Inductance Extremely Large

As the noncommutating inductance becomes extremely large, the line current be-

comes constant so that $I_b = I$ (but the instantaneous rate of change of line current may have any value), and equation 5 becomes

$$\frac{L}{2T}\frac{di_2}{dt} + \frac{R_1}{2}(I+i_2) - \frac{R_2}{2}(I-i_2) = 0 \tag{37}$$

where

$$i_1 = \frac{I+i_2}{2} \tag{38}$$

$$i_2 = \frac{I-i_2}{2} \tag{39}$$

Substituting the assumed contact resistance values from equations 1 and 2 into equation 37

$$\frac{L}{T}\frac{di_2}{dt} + \frac{R(I+i_2)}{1-t} - \frac{R(I-i_2)}{t} = 0 \tag{40}$$

Some special solutions to equation 40 have been presented by Thorburn Reid,[1,9] two examples of which are

$$\left.\frac{i_2}{I}\right|_{\frac{L}{2RT}=\frac{1}{2}} = 2\left(1-\frac{1}{t}\right)\log(1-t) - 1 \tag{41}$$

$$\left.\frac{i_2}{I}\right|_{\frac{L}{2RT}=1} = \sqrt{\frac{1}{t}-1}\,[\cos^{-1}(1-2t)] - 1 \tag{42}$$

From equations 1, 38, and 42 the average value of the trailing brush contact voltage for a per-unit reactance voltage of unity is

$$\left.\frac{R_1 i_1}{IR}\right|_{\text{av}\ \frac{L}{2RT}=1} = \int_0^1 \frac{\cos^{-1}(1-2t)}{2\sqrt{t(1-t)}}\,dt = \frac{\pi^2}{4} = 2.467 \tag{43}$$

From the equivalent circuit of Figure 3 it is seen that

$$e = 2(R_1 i_1|\text{av}) - \frac{IL}{T} \tag{44}$$

from which, by dividing by $2IR$, and using equation 43

$$\left.\frac{e}{2IR}\right|_{\frac{L}{2RT}=1} = \frac{R_1 i_1|\text{av}}{IR} - \frac{L}{2RT} = 2.467 - 1 = 1.467 \tag{45}$$

As a comparison with the approximate case given in Appendix III, if the values $L_a = \infty$ and $L/2RT = 1$ are substituted into equations 33 and 35 for the approximate case

$$\left.\frac{e}{2IR}\right|_{\frac{L}{2RT}=1\ \text{(approx.)}} = \frac{2}{\log 4} = 1.443 \tag{46}$$

which compares with the exact value in equation 45.

The voltage appearing across the noncommutating coils is found from equation 3 as

$$\frac{L_a}{2T}\frac{d}{dt}(i_1+i_2) = e - R_1 i_1 - R_2 i_2 \tag{47}$$

and has the instantaneous values given in Figure 12 even though the line current is constant, since the noncommutating inductance is considered to be extremely large.

It will be noted that an extremely large noncommutating inductance in series with the commutation bridge network corresponds physically to an integrating circuit which produces a terminal voltage nearly equal to the average value of reactance voltage.

Appendix V. Line Resistance in Place of Noncommutating Inductance

The voltage pulses calculated in Appendixes II, III, and IV, are contingent on the presence of noncommutating inductance. The question then arises as to whether or not these pulses are produced if the noncommutating inductance is replaced by line resistance. This has application to generators supplying resistance loads, to dynamic braking of motors, and to simulated commutation testing.[11,12]

If line resistance, r, is used in place of the noncommutating inductance in the equivalent circuit of Figure 3, and line voltage, E, is used in place of the brush terminal voltage, equation 3 becomes

$$r(i_1+i_2) + R_1 i_1 + R_2 i_2 = E \tag{48}$$

where

$$E = e + Ir \tag{49}$$

Equations 4 and 5 are unchanged, so that eliminating i_1 and i_2 in these equations

$$\frac{L}{2T}\frac{di_2}{dt} + \left[\frac{2R_1R_2 + (R_1+R_2)r}{R_1+R_2+2r}\right]i_2 = \left(\frac{R_1-R_2}{R_1+R_2+2r}\right)E \tag{50}$$

Substituting the assumed contact resistances from equations 1 and 2 into 50

$$\frac{L}{2T}\left(1+\frac{2r}{R}t(1-t)\right)\frac{di_2}{dt} + (2R+r)i_2 = (1-2t)E \tag{51}$$

which is a linear equation with variable inductance.

In order to solve equation 51, make the change in variable

$$s = \tanh^{-1}\frac{1-2t}{\sqrt{1+\frac{2R}{r}}} \tag{52}$$

so that equation 51 becomes

$$\frac{L}{2T}\frac{di_2}{ds} - R\sqrt{1+\frac{2R}{r}}\,i_2 = -\frac{RE}{r}\tanh s \tag{53}$$

For the special case where $L/2\ RT = \sqrt{1+2R/r}$, the solution to equation 58 is

$$\frac{i_2}{I_0} = -\frac{R}{r\sqrt{1+\frac{2R}{r}}}\left(\frac{E}{I_0R}\right)(1+2s^2\tan^{-1}s^2) + \left(\frac{c}{I_0}\right)s^2 \tag{54}$$

where the line voltage and the constant of integration are evaluated from the boundary conditions that at $t=0$, $i_2 = I_0$, and at $t=1$, $i_2 = -I_0$,

$$\frac{E}{I_0R} = \frac{\frac{r}{R}\sqrt{1+\frac{2R}{r}}\left(1+\frac{s_1^2}{s_0^2}\right)}{1-\frac{s_1^2}{s_0^2}-2s_1^2(\tan^{-1}s_0^2-\tan^{-1}s_1^2)} \tag{55}$$

$$\frac{c}{I_0} = \frac{1+r\frac{R}{\sqrt{1+\frac{2R}{r}}}\left(\frac{E}{I_0R}\right)(1+2s_0^2\tan^{-1}s_0^2)}{s_0^2} \tag{56}$$

in which s_0^2 is the value of s^2 at $t=0$, and s_1^2 is the value of s^2 at $t=1$, so that $s_0^2 s_1^2 = 1$.

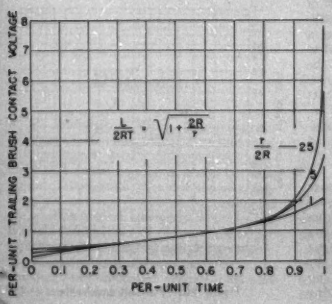

Figure 16 (left). Per-unit trailing brush contact voltage with line resistance in place of of noncommutating inductance

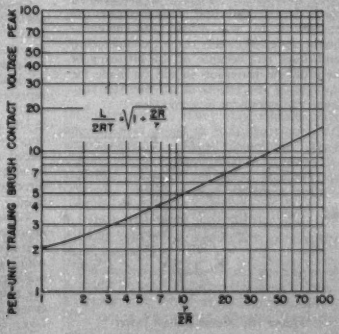

Figure 17 (right). Per-unit peak value of trailing brush contact voltage with line resistance in place of noncommutating inductance

The trailing brush contact voltages for typical values of line resistance for this special case are plotted in Figure 16, and the manner in which the line resistance limits the peak value of the trailing brush contact voltage is shown in Figure 17. For values of per-unit line resistance above 10, the peak value of the trailing brush contact voltage is given by

$$\frac{R_l \hat{i}_l}{2IR}\Big|_{l=1} = \frac{\pi}{2}\sqrt{\frac{r}{2R}} \qquad (57)$$

$$\frac{L}{\delta NT} = \sqrt{1+\frac{\delta R}{r}}$$

where

$$\frac{r}{2R} > 10$$

The line current ripple of course decreases as the line resistance is increased, being equal to 0.55 at a per-unit line resistance of 5, and equal to 0.87 at a per-unit line resistance of 100, for the particular value of reactance voltage being considered. An infinite amount of line resistance would be required to produce constant line current, so that the physical reason for the difficulty in obtaining a general solution to equation 40 in Appendix IV can be appreciated, since constant line current is assumed in this equation without regard to whether inductance or resistance is used to hold the line current constant.

The ability to control the magnitude of the voltage pulses by means of line resistance, as indicated in equation 57, offers interesting possibilities for research as to the threshold of damage to brushes and commutators as commutating conditions become severe. On the other hand, in order to test the commutating ability of brushes under simulated operating conditions,[11,15] no more resistance should be used in the line than occurs in actual machines, if erroneous results are to be avoided.

Appendix VI. Commutation Tester

Since the accuracy of prediction based on mathematical analysis of the commutation performance is limited by the assumptions, it is desirable to find the exact effects of deviations from the idealized conditions by direct measurement on a test machine in which the commutation phenomena can be reproduced at will. The test machine should represent closely the actual operating conditions, but because of the intricacy of the problem, provision should be made for suppressing the effects of all but the particular factors under investigation.

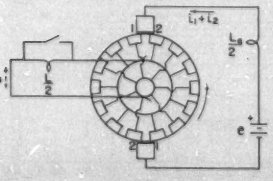

Figure 18. Commutation Tester

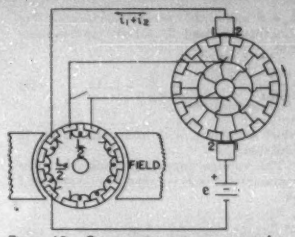

Figure 19. Commutation tester connected so as to measure commutating reactance

The commutation testing device shown schematically in Figure 18 is a counterpart of the equivalent circuit in Figure 3, and the commutating conditions which it can represent are limited to the same degree. Essentially, the commutation tester is a mechanical inverter which consists of a commutator with an even number of bars in which alternate bars are connected to one collector ring, and the remaining bars are connected to another collector ring on the same shaft. The shaft is mounted in bearings and is driven by a motor at the desired speed. The commutator brushes span one bar and are made of the same brush material as those of the machine being investigated. Two silver graphite brushes are used on each collector ring so that the contact voltage drop is negligible even at the highest currents to be carried. An inductor representing the commutating coils is connected between the collector brushes, and another inductor representing the noncommutating coils is connected in series with a low-impedance battery to the commutator brushes.

A short-circuiting switch is provided for the commutating inductor so that after each test reading the switch may be closed and a test measurement made immediately of the brush contact resistance, at the same value of line current. This cancels any error due to changes in the brush film, and allows the test readings to be expressed in the per-unit system. The accuracy of this measurement is good because the readings are direct, and no correction of the readings is needed for counter electromotive force as would occur if field excitation were present in the test machine.

Continuous display of commutation is made possible by the cyclic repetition of initial conditions, so that the effects of changes in circuit conditions are immediately evident. The advantages of using a stationary coil instead of a rotating coil to represent the commutating circuit lie in the ability to change the amount of inductance, in the ease with which direct measurements may be made, and in the separation of induced and generated voltages so that simulated generated voltages may be introduced directly into the commutating coil, if desired.

Values of the brush terminal voltage measured with a d-c voltmeter on a commutation tester are shown in Figure 7, from which it can be seen that this voltage is a nonlinear function of speed. The fact that the brush terminal voltage increases as the speed increases has been pointed out by Gano Dunn,[1] but a method for calculating the amount of the increase and the application of the result to commutation performance has not been presented. This voltage offers a readily measured quantity with which calculations based on circuit data may be compared.

Gano Dunn suggested that the brush terminal voltage be measured on an armature removed from the field and driven at rated speed, with rated current passed through the brushes from an external source. One objection to this method is that an additional voltage is generated by the motion of the commutating coils through the stationary magnetic field of armature reaction set up by the current even with the field poles removed. Another objection is that the absence of the field poles may reduce the inductance of both the commutating and noncommutating coils below their operating values. However, if in order to meet this latter objection, the armature were rotated in its normal position between the field poles with the field unexcited, pole face eddy-current and hysteresis losses due to slot flux pulsations may distort the measurements.

The use of a stationary armature in its normal position between the field poles and connected to a mechanical inverter as shown in Figure 19 overcomes the objections to testing with a rotating armature. Referring to Figure 7, it will be found that for the usual machine, at a per unit brush terminal voltage of 4 or above, the reactance voltage can be read directly, and from this the amount of inductance in the commutating coil can be determined.

Cathode-ray oscilloscope studies with the commutation tester are valuable in obtaining a detailed picture of the brush contact behavior under various commutating conditions. The ordinary oscilloscope is not suitable, however, since the presence of damped radio frequency oscillations introduced by impulse excitation of the interturn capacitance together with low frequency patterns set by the commutation period will result in hash on the normal oscilloscope screen with a re-current sweep. An oscilloscope with an accelerating potential of the order of 10 kv (light output increases as the square of this potential), with a long-persistence screen, and with a trigger circuit to initiate a single sweep of several microseconds duration will provide satisfactory results.

In order to find the relation between brush life and reactance voltage, two com-

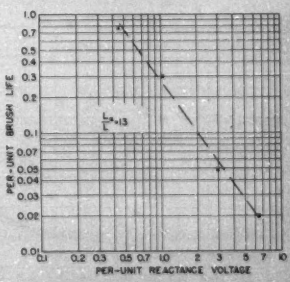

Figure 20. Per-unit brush life

mutation testers were built and operated according to Figure 18 as follows:

Commutator diameter, inches	1.625
Number of bars	24
Brush size, inches	$^7/_{32} \times {}^9/_{16}$
Brush grade	Resin-bonded graphite
Initial brush pressure, pounds per square inch	6
Brushholders	Cartridge type
Commutator runout, inches	Less than 0.0006
Bar-to-Bar runout, inches	Less than 0.0002
Speed, rpm	5,000
Current, amperes	3 (24.4 amperes per square inch)
Ambient humidity, per cent	40 to 60
Brush temperature, degrees centigrade	50 to 70

Inductances (air core coils)

Test Number	L/2 millihenrys	$L_a/2$ millihenrys	L_a/L
1	0.391	5.1	13
2	0.204	2.5	12.3
3	0.086	1.15	13.4
4	0.037	0.53	14.3
		Average	13.2

The brushholders were assembled so that when one brush was in full contact with a bar connected to one ring, the other brush was in full contact with a bar connected to the other ring. Selected ball bearings with tight radial fit were used, and finger-spring axial loading was applied to reduce dynamic commutator runout. The commutators were diamond-turned in their own bearings, then dynamically balanced, and the brushes were sanded and run in until fully seated before each test. A 115-volt, 60-cycle-per-second bar-to-bar test was made every 100 hours to check for short circuits occurring from carbon between bars. The collector ring brush drop was less than 0.05 volt.

The test sequence on one commutator was 100 hours operation with the commutating coil in the circuit, then 100 hours with the commutating coil short-circuited, then with reversed polarity for 100 hours with the commutating coil in the circuit, and then another 100 hours with the commutating coil short-circuited. The test sequence on the other commutator was similar except that the first run was made with the commutating coil short-circuited, and the second with the commutating coil in, and so on. In this way, changes in the condition of the contact film were compensated.

Brush wear measurements were taken after each 100-hour period. Normal brush life was taken as the average of the 16 runs with the commutating coil short-circuited, and was 12,800 hours per quarter-inch. This is typical of life test experience with this brush grade on small commutating-pole machines, but it should be pointed out that there was a substantial decrease in brush life as the noncommutating inductance increased even on the test runs for which the commutating coil was short-circuited. This means that circuit inductance should not be neglected even for brush life testing on collector rings.[13]

Readings of brush terminal voltage were taken every four hours, with the commutating coil both in the circuit and momentarily short-circuited, the current being held constant for both conditions by means of a rheostat adding less than an ohm to the circuit. The brush contact resistance was taken as the average for each test of the readings of brush terminal voltage immediately after the commutating coil was short-circuited, when divided by the line current. A cross-check was maintained on the contact resistance by using the measured per-unit brush terminal voltage in Figure 7 to find the per-unit reactance voltage.

The results of this series of tests are shown in Figure 20. The line drawn through the test points indicates that

$$\text{per-unit brush life} = 0.28/\left(\frac{L}{2RT}\right)^{1.43} \qquad (58)$$

beyond the point where abnormal electrical wear begins. The fact that abnormal electrical wear begins near the value $L\,L_a/L+L_a = RT$ above which high-voltage pulses are predicted, is a strong confirmation of the theory. Other tests with the same conditions except with a copper graphite brush grade have shown the same relation between brush life and reactance voltage as given by equation 58, except of course with a lower base brush life and a lower contact resistance. Although it is too early for general conclusions, this may prove to be a universal brush life correlation, in which case the commutating ability of a particular brush grade could be determined over a wide range of commutating conditions from the results of a minimum of testing.

References

1. Sparking, Its Causes and Effects, Thorburn Reid. *AIEE Transactions*, volume XIV, December 1897, pages 579–606.

2. Limits of Injurious Sparking in Direct-Current Commutation, Thorburn Reid. *AIEE Transactions*, volume XXIV, June 1905, pages 611–48.

3. Flux Linkages and Electromagnetic Induction, L. V. Bewley. *AIEE Transactions*, volume 48, April 1929, pages 327–37.

4. Carbon Brushes (book), J. Neukirchen. Telegraph Press (Harrisburg, Pa.), 1937, page 59.

5. Per-Unit Quantities, Irven Travis. *AIEE Transactions*, volume 56, 1937, pages 22–28 in supplement, and discussion, *Electrical Engineering*, November 1937, pages 1399–1400.

6. Temperature of a Contact and Related Current-Interruption Problems, J. Slepian. *AIEE Journal*, volume 45, October 1926, pages 930–33.

7. Phenomena Connected with the Collection of Current From Commutators and Slip-Rings, H. G. Taylor. *Journal*, Institution of Electrical Engineers (London, England), volume 68, 1930, pages 1356–63.

8. Influence on Commutation of Brush Contact Drop, L. R. Ludwig, R. M. Baker. *AIEE Transactions*, volume 51, December 1932, pages 959–65.

9. Sparking Under Brushes of Commutator Machines, R. E. Hellmund, L. R. Ludwig. *Electrical Engineering* (*AIEE Transactions*), volume 54, March 1935, pages 315–21, and discussion, pages 1109–11.

10. Contact Drop and Wear of Sliding Contacts, R. M. Baker, G. W. Hewitt. *Electrical Engineering* (*AIEE Transactions*), volume 56, January 1937, pages 123–28, and discussion, pages 605–06.

11. Physics of the Sliding Contact, F. Schroter. *Archiv fur Elektrotechnik* (Berlin, Germany), May 1936, pages 338–46.

12. Electrical Brush Wear, V. P. Hessler. *Electrical Engineering* (*AIEE Transactions*), volume 54, October 1935, pages 1050–54, and discussion, volume 55, pages 406–07.

13. Abrasion—A Factor in Electrical Brush Wear, V. P. Hessler. *Electrical Engineering* (*AIEE Transactions*), volume 56, January 1937, pages 8–12, 16, and discussion, pages 601–03.

14. Dynamic Brush Characteristics by the Dynamotor Method, C. J. Herman. *AIEE Transactions*, volume 66, 1947, pages 759–63.

15. Experimental Studies of Commutation in D-C Machines Using a Model, M. F. Karasiov. *Elektrichestvo* (Leningrad, Russia), July 1948, volume 7, pages 37–42.

16. Characteristics of Brush Contacts in D-C Machines, M. F. Karasiov. *Elektrichestvo* (Leningrad, Russia), volume 10, October 1948, pages 36–42.

17. Commutation of D-C Machines and Its Effects on Radio Influence Voltage Generation, D. P. Metter. *AIEE Transactions*, volume 68, part 1, 1949, pages 491–96.

18. Some Aspects of Inductance when Iron Is Present, L. T. Rader, E. C. Litscher, *Electrical Engineering* (*AIEE Transactions*), volume 63, March 1944, pages 133–39.

Discussion

A. F. Puchstein (Jeffrey Manufacturing Company, Columbus, Ohio): The subject of commutation is not simple even if the complete differential equations could be integrated. Historically, the development followed the course: (1) Empirical (examples are, machines spark inherently if core length is made greater than 14 inches, current per brush arm should not exceed 200 amperes). (2) Mathematical. Present paper is an example. They flourished around 1900 and led to such rules as[1]

$$\frac{RT}{L} > 1, \frac{RT}{A} > 1$$

where,[1]

$$A = \frac{L^2 - M^2}{L} \text{ and so forth.}$$

However, some details still remain to be worked out. (3) Semiempirical. These solved the problem for most practical purposes. They go all the way from considering only the effect of local slot and end-leakage fluxes to more elaborate summations of different inductive and speed electromotive forces. They may consider only one coil or a group of coils short circuited simultaneously. Most commonly, they assume sinusoidal or straight line reversals. Dreyfus[2] assumed piecewise straight-line reversals for coil groups. Menges in Holland about 40 years ago proposed a method in which the main part of the armature winding provides a shunt path around the brush contact.

Among contributors we find the names of Arnold,[4] Punga,[5] Hobart, Hawkins,[6] Press,[7] Kennedy,[8] Pichelmayer, Rüdenberg, Bewlay, Lamme,[9] Rezelman, Shenfer, La Tour, Girault, and Rothert.

Mr. Olney's paper is an interesting attempt to extend the theory from the viewpoints of mathematics and physics. From the viewpoint of the practicing engineer, the methods now in use are probably as satisfactory as it will be possible to make any method, considering ease of application, dependability, and the fact that the effects of such factors as the following are exceedingly complex and difficult to evaluate or predict: brush and bar materials; instantaneous current density and direction; instantaneous temperatures; chemical and physical constitution; kind of atmosphere; contact-drops; density of energy concentration and amount to be dissipated; heat dissipative capacity; spark and arc phenomena; vibration; mechanical factors; currents in cross or equalizer connections; dissymmetries of various kinds; brushes not exactly 180 degrees apart, or edges nonparallel, and so forth.

Add to these the fact that Olney's equations omit the effects of speed electromotive forces in the commutation zone, mutual inductances between armature coils, more than one bar under a brush, eddy currents, coupling with field coils, type of winding and possibly capacitance effects, and we have some idea of the difficulties involved in obtaining real precision.

The author does not take up the question of criteria as such or the way in which the information is used. Perhaps, the aim is more to pave the way for the commutation test arrangement given in Figures 18 and 19 of the paper. For criteria, there are available reactance voltage, sparking voltage,[1] volts between bar and brush tips, contact-drop, contact current density, watts and watt-seconds per unit area, volts between bars under a brush, volts across brush tips, and so forth. Their values may be average, effective, instantaneous, or maxima (usually taken at last moment of short circuit when $t = T$).

The idea of an equivalent network is novel. The test arrangement proposed uses two different inductances. It should simulate the commutating conditions quite accurately when the brush covers one bar or less. If the brush covers more than one bar, the simulation may be expected to be less exact, so that the need for further development may be indicated. However, for controlled brush-material life and comparison tests, the arrangement described probably will be as satisfactory as any. Arnold[4] and assistants of Karlsruhe many years ago used another test arrangement.

For most readers, the regular system of units will be more convenient than the per-unit system. Also, it is not certain that idiosyncracies in the physical phenomena can be avoided by changing the system of units.

Appendices I and II of the paper appear to be useful mainly for cross-checking. Presumably, Appendix III can cover Appendix IV approximately but in a broader way if we let L_a become large, so that L/L_a approaches zero in equations (32 and 34). We probably shall not obtain a solution satisfactory from the mathematical standpoint until new approaches to the integration, or machine methods, are developed. Perhaps, since $RT/(T-t)$ and RT/t do not actually go to infinity at $t = T$ and $t = 0$, other forms easier to handle and which represent the physical phenomena with comparable accuracy or even new functions to represent the solution, may be discovered.

For computation the following expressions[7] (with numerical work to illustrate them), which are based on similar assumptions but retain more terms, are quite convenient. At the last moment of short circuit when $t = T$ with $L < RT$, the time rate of change of current is

$$\frac{di}{dt} = I_c \times \frac{2R+2r+w+e}{RT-L}$$

$$= 10 \times \frac{(2\times 0.1+2\times 0+0.002+0.2)}{0.1\times 0.001-0.00005}$$

$$= 80{,}400 \text{ amperes per second}$$

and

$$L\frac{di}{dt} = 0.00005\times 80{,}400 = 4.02 \text{ volts}$$

where R, T, L, and t have the usual meanings. Let their values be 0.1 ohm, 0.001 second, $L = 0.00005$ henry, $t = 0$ to 0.001 second.

a = contact area under a brush = 0.2 inch × 1.0 inch = 0.2 square inch
i = value of current in coil at time t, amperes
r = resistance of lead between coil and commutator bar = 0.0 ohm
w = resistance of an individual armature coil = 0.002 ohm
I_c = current per armature path = 10 amperes
$I_c e$ = electromotive force generated in short-circuited coil by speed action

If coils are full-pitch with brushes in geometrical neutral it is proportional to I_c as indicated, = 0.2 volt per ampere. In the more general case, for any particular load replace $I_c e$ by E, say, where E is the speed electromotive force per coil due to the flux which enters or leaves the armature core and end connections at the commutation zone. This will be positive or negative depending upon which is the stronger, armature or field (or commutation pole if present). Now, let e_s = volts between trailing bar—and brush-tips at the last moment when $t = T$, then

$$e_s = I_c(2R+2r+w+e)\frac{RT}{RT-L} = 10\times(2\times 0.1+2\times 0+0.002+0.2)\times \frac{0.1\times 0.001}{0.00001-0.00005} = 8.04 \text{ volts}$$

This also is equal to

$$I_c(2R+2r+w+e)+L\frac{di}{dt} = 10\times(0.02+0+0.002+0.2)+4.02 = 8.04$$

Average reactance voltage

$$RV = L\left(\frac{di}{dt}\right)_{avg} = L\frac{2I_c}{T} = 0.00005\times\frac{2\times 10}{0.001} = 1.00$$

Energy stored in inductance

$$= \frac{LI_c^2}{2} = \frac{0.00005\times 10^2}{2} = 0.0025 \text{ watt-second}$$

Average contact drop at uniform current density

$$= 2I_c R = 2\times 10\times 0.1 = 2.0 \text{ volts}$$

Current across contact for a voltage drop

$$e_s i_s = \frac{e_s}{R} = \frac{8.04}{0.1} = 80.4 \text{ amperes}$$

Contact current density

$$i_d = \frac{e_s}{R_a} = \frac{8.04}{0.1\times 0.2} = 402 \text{ amperes per square inch}$$

This is also equal to contact current density at the last moment

$$i_d = \frac{T}{a}\frac{di}{dt} = \frac{0.001}{0.2}\times 80{,}400 = 402$$

corresponding contact loss at this density

$$P_d = \frac{e_s^2}{R_a} = \frac{8.04^2}{0.1\times 0.2} = 3{,}225 \text{ watts per square inch}$$

$$= i_d^2 R_a = 402^2\times 0.1\times 0.2 = 3{,}225$$

contact loss for whole area with 402 amperes per square inch would be

$$P_s = \frac{e_s^2}{R} = \frac{8.04^2}{0.1} = 645 \text{ watts}$$

contact loss for uniform current density would be

$$= 2I_c \times \text{volts drop per brush} = 2\times 10\times 2 = 40 \text{ watts}$$

$$= (2I_c)^2 R = (2\times 10)^2\times 0.1 = 40$$

The above equations, of course, do not apply strictly when the brush covers more than one bar. However, if R, L, and other factors are suitably interpreted they are usable and have been so used for many years.[10] For the value of e_s required to produce a spark between commutator and brush, see abstract of an article by Liska[11] written in 1909.

References

1. Theorie der Kommutation, E. Arnold, O. Mie. *Elektrotechnische Zeitschrift* (Berlin, Germany), 1899, page 97.

2. Commutation Theory, F. W. Carter. Electrical World (New York, N. Y.), March 31, 1910, page 804.

3. Die Stromwendung, Grosser Gleichstrommaschinen (book), L. Dreyfus. Julius Springer, Berlin, Germany, 1929.

4. Die Gleichstrommaschine (book), E. Arnold, J. L. La Cour. Julius Springer, Berlin, Germany, volume I, Theory, pages 195–374, and Commutation Test Arrangement, 1919, pages 375–388.

5. Die Wechselstrom Kommutator Motoren (book), F. Punga. Geb. Janecke, Hannover, Germany, 1905. English translation by R. F. Looser, Whittaker and Company, New York, N. Y., 1906.

6. The Apparent Inductance of Armature Coils, C. C. Hawkins. *Electrical World*, (New York, N. Y.), 1903, pages 798, 835, and 1904, pages 871, 913, 961.

7. Commutation Theory, A. Press. *Electrical World* (New York, N. Y.), December 16, 1905.

8. Calculations of Dynamo Sparking Constants, C. L. Kennedy. *Electrical World* (New York, N. Y.), February 16, 1907.

9. A Theory of Commutation and Its Application to Interpole Machines, B. G. Lamme. *AIEE Transactions*, volume 30, part III, pages 2359–2431.

10. Electrical Machine Design (book), A. Gray. McGraw-Hill Book Company, New York, N.Y., 1913 and 1926, page 81.

11. Abstracts of Current Electrical Liter

ATURE, LIEBE. *Electrical World* (New York, N. Y.), February 18, 1909.

Paul W. Franklin (Bendix Aviation Corporation, Teterboro, N. J.): The writer would like to start his discussion with the part of the paper which appears to him of particularly practical importance, namely, a brush testing device.

It is the writer's belief that a testing device, standardized by the AIEE, National Electrical Manufacturers' Association and all major brush companies, with regard to commutation ability and wear, would be of considerable value to everybody concerned. This is particularly the case for the aircraft industry with regard to brush life at high altitudes, where actual environmental tests are expensive. The device suggested by the author appears to be very promising, provided that the experimental conditions are carefully controlled. It is hoped that the paper furnishes the incentive required for such standardization.

It may be of interest to mention here the limitation of the general theory of commutation, as developed by Arnold and advanced by Dreyfus, Trettin, Richter and others, the more, as these limitations have a particular bearing upon a theory based on brush contact resistance.

Arnold, in his book dealing with the d-c machine, mentions the clues indicating these limitations. Discussing certain commutation oscillograms, he notes strong peaks and irregularities in the observed curves, as compared with the calculated values. He also notes, after a very thorough theoretical derivation of the shape of the interpole flux and pole shoe, that practical experience indicates that a narrower interpole shoe, than obtained by theory, will give good commutation.

The first clue, in the writer's opinion, is an indication of the effects of brush vibration, whereas the second may have a bearing on flux fringing, varying zigzag leakage of the commutating slot, and the shape of the actual brush contact area.

Calculations performed on the commutator data presented by the author furnish the following results.

The time required to pass by one commutator bar at the speed of 5,000 rpm is 5.0×10^{-4} seconds. Let us now assume, that the bar-to-bar run out is, as indicated, 2×10^{-6} inches, and let us further assume, that the brush is moved with constant acceleration for this distance during half the time given. During the travel of half a commutator bar, the brush is pushed up or down for the run out of 2×10^{-6} inches. The constant acceleration required for this is of the magnitude of 16 g's* and gives an indication of the severity of the vibrations. Incidentally, these vibrations may cause the designer to consider his brush pressure not so much as pounds per square inch, but rather rate it in pounds per pound brush weight.

Now using the formula given by Dr. Neukirchen in his book[1] (page 3) and assuming the same values for M_1 and M_2 and a difference of 0.001 inch between the commutator and brush radius, we obtain a theoretical contact width of 1/16 inch, as compared with the brush width of 7/32 inch upon which the author's theory is based.

Undoubtedly the author found that the brush surface was uniformly shiny, and therefore either the Hertzian contact equation does not apply or a continuous infinitely small rocking between brush and commutator must take place.

Evidence of such rocking, or rather reseating, can be observed very often on aircraft machines for low voltage, which have a comparatively wide brush and a high number of ampere-conductors per inch. A change of contact will amount essentially to a change of neutral and make itself felt in the amount of required field current for a given condition. It also can be observed, that, if an aircraft generator is run at low speed, then at high speed, and again at low speed, that the field current at low speed after the high speed run has changed from its original value, more than may be accounted for by heating. Definitely, something has changed under the brush; let us call it contact location, shift in neutral, change in film, friction coefficient or eddy current distribution, but a change is evident and also is felt electromagnetically.

Of course, this particular reseating depends upon the stability of the brush holder.

Most of these phenomena are not being noticed on conventional machines, either with low speed, or low design parameters. They are undoubtedly felt however at highly compacted machinery.

In the writer's belief, this goes to show, that the value of a theory of commutation based on steady brush contact is greatly impeded by the erratic nature of this contact. This applies particularly to high-speed high-density machines.

It would have been of interest if the author had shown pictures of his oscillograms and compared these with the calculated current and voltage time curves. Also, it may be of value if the author explains the nature and location of the noncommutating coils interlinked in the commutation process.

The author's experience, that, among other things, brush life is a function of the reactance voltage (in the case of interpole machines, a function of the uncompensated reactance voltage) is fully borne out by the experience of the writer.

The writer feels that Mr. Olney has contributed an interesting and important paper to the art, which again bears out the vast complicity of the commutation problem, and wishes to congratulate him.

REFERENCE

1. See reference 4 of the paper.

Frank D. Olney: Mr. Puchstein describes design methods which have existed for a long time—that is, methods by which commutator machines are designed largely by reference to similar machines and in which there is no general basis for designing from basic dimensions as has been developed for a-c machines. Obviously, a starting point is needed, some benchmark common to all commutator machines on which design formulas may be based with a reasonable expectation that the calculations can be verified by experiment. However, a generalized approach such as this is expected to be of interest mainly to engineers engaged in the development of new and improved machines, and not necessarily at present to those responsible for maintaining an established line of machines.

Improved commutator machines and electric brushes are urgently needed; for example, contrary to a general feeling that brush treatments have solved the altitude problem in aircraft commutator machines, actually trouble has been avoided largely because most flight time has been below 20,000 feet, and for projected aircraft involving long flights of 50,000 feet and above, the brush problem is as serious as it ever was. Again, commercial commutating-pole machines in general cannot be loaded in excess of twice rated load even momentarily without danger of permanent damage to the commutator, even though the operator may not be provided with control over the machine sufficient to prevent overloading. Other serious operating problems which demand a more vigorous analysis are those of flashover, radio noise, and short-circuit currents. The conclusion is inescapable that the commutating pole has not proved to be a complete answer to the commutation problem, and that present electric brushes are not stable enough under actual operating conditions.

All the works mentioned by Mr. Puchstein, and many others including German, Russian, Japanese, and French contributors, were examined during this investigation and were found to comprise largely speculation as to the nature of the brush contact film as for example in Neukirchen's work, or else of assuming the answer concerning the shape of the current reversal in the commutating coil as for example in Dreyfus's work, and all these references are practically devoid of experimental evidence to support any conclusions. For example, in the test arrangement cited by Mr. Puchstein which is shown in Figure 327 on page 375 of "Die Gleichstrommaschine" by E. Arnold, the measured value of commutating reactance is not given, so his data is useless to the practicing engineer. This situation is not unknown to these contributors. Indeed, to quote Arnold, "The longer the problem of commutation is studied the less possible it becomes to investigate this process analytically." However, there is no evidence that any of these writers suspected the existence of a major discrepancy between the circuits described by their mathematics and the circuits used for their tests. For example, Karasiov assumes constant line current during commutation in his calculations, and yet his test arrangement uses a series resistance on a 220-volt line which, as shown in Appendix V of the present paper, does not provide constant current, and will yield erroneous results.

Anyone familiar with the 60-year record of brush and commutation data and the numerous attempts to correlate this data, cannot fail to be impressed with the difficult factors involved. Yet the analysis and tests in this paper show that the inclusion of the measured brush contact resistance under the specific commutating conditions being considered, and the inclusion of the noncommutating inductance as a major factor in the basic magnetic geometry of commutator machines, will enable a general correlation of machine and brush commutating characteristics to be established for design work so as to be applicable to any

*Where g is the acceleration of gravity.

commutator machine. That this is reasonable physically is shown by the analysis in Appendix III where resistance commutation is seen to be very nearly just the interruption of current in an inductive circuit by means of contacts in which the contact area decreases at a constant rate, so that the problem of wear of sliding contacts approaches that of the wear of stationary contacts used in control circuits. The confirmation of this viewpoint has been shown by tests on three widely different brush grades to date—copper graphite, resin-bonded graphite, and electrographitic. These tests were made with simple equipment which can be built by anyone with access to a machine shop.

Further extension of the analysis in Appendix III to the case of commutating pole machines, to brush overlaps different from one segment, and to unsymmetrical windings shows that the form of equations 32 and 34 is unchanged and only the coefficients are different, so that a general correlation of machine and brush characteristics is a reasonable objective. While it is true that the problem is not simple, each factor can be treated as a variation from an idealized machine. And Mr. Puchstein apparently does not actually feel that the problem is impossible of solution because of "exceedingly complex and difficult factors," since he finally states that when these "factors are suitably interpreted they are usable."

Contrary to Mr. Puchstein's statement that the paper does not take up the question of criteria, Figure 20 gives the commutation criteria in the form needed by the designer, that is, at what reactance voltage abnormal electrical brush wear starts, and what magnitude of abnormal wear is expected as that value of reactance voltage is exceeded, as it must be with certain machines. All mention of sparking is deliberately omitted from the paper in order to avoid the pitfalls of unconfirmed speculation.

Regarding the numerical example given by Mr. Puchstein, this example is the same as that given by him in a letter to the AIEE editor in July 1943.[1] The numerical values given for the parameters apparently do not apply to a specific machine since there is no indication as to how the values are calculated or measured. The reactance voltage for this case is 0.5 per unit, so that the commutation would be expected to be almost perfect, and no difficulty will be encountered from the indeterminate expressions which are found above this value of reactance voltage when Mr. Puchstein's method of attack is used. Further, any analysis based on only the last moment of commutation fails to yield the correct value for the average contact drop, which in this case is 2.8 volts instead of the 2.0 volts given by Mr. Puchstein. However, the outstanding thing about this example is that no test results are given to support the calculations, and so while this example might be helpful for explanation, it cannot be used for prediction, since there is no way of knowing whether or not the data is sound.

Mr. Franklin's constructive comments are quite helpful, and the author agrees particularly with his point of view on a standard commutation testing device.

It is true that the calculations apply only to cases where there is a mechanically perfect contact between brush and segment, and while these conditions can be obtained in controlled tests with a diamond-turned commutator using a carefully run-in brush as shown by Figure 7, yet we know that the trailing edges of the brushes are burned back after a short time on life test so that there is not full lateral contact between the brush and segment. We have no way at present of predicting analytically the rate of brush wear under specific commutating conditions—when such information is available, the calculated and test curves of brush wear will probably diverge as a result of this lateral brush wear.

As far as instantaneous irregularities in the brush-to-segment contact are concerned, it seems reasonable to take a statistical view of the situation. For example, in the brush life tests reported in Figure 20, there were 3,200 hours of running time. At 5,000 rpm with 24 segments passing the brushes each revolution, in that period of time there were 23,000,000,000 individual contact separations—certainly enough to average out any deviations. Oscillograms of the commutation process were omitted from the paper because they tend to be confusing unless one is familiar with the techniques involved, and thus they are not of general interest.

Mr. Franklin's question concerning the nature of the noncommutating coils may be clarified by reference to Figure 1 of the paper, where these coils are in the slots marked "a." The noncommutating coils are those with a magnetic axis in quadrature to the main field direct axis, and so they are the working coils of the machine in which the output is generated. Neglecting machine dissymmetry, the ratio of noncommutating to commutating inductance is roughly equal to the ratio of the number of slots under the field poles to the number of slots in the commutation zone.

In regard to brush life as a function of uncompensated reactance voltage in commutating-pole machines; when the brush overlap is equal to one segment it is possible to compensate the reactance voltage by means of commutating poles. With other overlaps a compromise is required, depending on the brush contact resistance, on the ratio of noncommutating to commutating reactance, and on the magnitude of the reactance voltage. That is, the proper commutating-pole voltage for optimum commutation is not in general exactly equal to the reactance voltage. Therefore, it is not strictly correct to say that brush life is a function of the uncompensated reactance voltage in commutating-pole machines—at least until this point has been thoroughly proved by carefully controlled life tests. This point, of course, is outside the scope of the present paper.

Reference

1. Commutation in A-C Motors, A. F. Puchstein. *Electrical Engineering*, volume 62, July 1943, pages 325–26.

Current in Equalizer Connections of D-C Machine Armature Windings

T. M. LINVILLE
FELLOW AIEE

D. P. STRANG
ASSOCIATE AIEE

Synopsis: Equalizer connections are a necessary part of d-c machine armature windings having more than two circuits. Nearly all machines of medium and large sizes and many small machines for special purposes are in this category. These connections cause substantially equal currents to flow in the circuits of the armature winding resulting in minimum losses, minimum temperature rise, and uniform commutation at each brush arm. This paper determines the current which the connections carry when the excitation of the field poles is unbalanced. From the results, the size of the connections to meet a specified temperature rise, under given unbalanced conditions, can be determined. The paper explains the reasons for the use of equalizer connections and describes how they work.

EQUALIZER connections or equipotential connections as described by Arnold[1] have been used for many years but their function has not been fully understood, as pointed out by Moore.[2] A well-known description of them is given in the college textbook by Langsdorf.[3] Their importance for multiplex windings has been emphasized by Nelson.[4] However, a practical analysis of the currents which flow in them has not been found in the literature and only a partial theoretical analysis has been available.

The purpose of the paper is to determine the current carried by the equalizer connections under unbalanced conditions. For example, these conditions might be: (1) that machines are to be built which will not overheat and will continue to commutate in spite of temporary roughness of their commutators; and (2) in case of damage to a field coil, the coil may be removed from the field circuit without affecting the operation of the machine except that operation thereafter will be at reduced voltage as required to avoid overheating of the remaining field coils.

During the war, in the construction of propulsion machinery for naval vessels and machinery for other military purposes, it was vital that operation be undisturbed by failure of a field coil and that repairs be made when convenient rather than as an emergency. In these cases, the equalizer connections and other windings were made to meet the concrete condition of loss of a field coil. These machines also were made to meet the test condition that the brushes of a brush arm could be removed without disturbing commutation. When the current in the equalizer connections is known for such conditions, the required size of conductor for them can be determined. The results of the paper can be applied to determine the current for all conditions of unbalanced field excitation.

In view of the fact that the best conditions are obtained when an equalizer connection is provided for every commutator bar, full or 100-per cent equalization is taken as basic for the paper. Furthermore, the results are expressed for machines having only one turn per armature coil.

The results can be extended readily to cover machines with less than 100-per cent equalization and more than one turn per armature coil.

Results

As shown in the analysis to follow, the maximum current in any equalizer connection for any machine* when excitation is removed from one pole with any excitation of m_f ampere turns on each of the remaining poles, is

$$i_e = (P-2)(4m_f/\pi P)\,(\sin^3(\alpha/2)\cos(\omega t/2) + (1/3)\sin^3(3\alpha/2)\sin(3\omega t/2)) \quad (1)$$

where

$$\alpha = \frac{\pi P}{2S_c} \quad (2)$$

and

P = number of poles
S_c = number of bars in commutator
ω = electrical radians per second

The corresponding rms current* for each equalizer connection and for the whole of the equalizer winding is

$$I_e = \delta(8m_f/\pi)\sqrt{(1/2)\,[\sin^4(\alpha/2) + (1/9)\sin^4(3\alpha/2)]} \quad (3)$$

when the value for δ is taken from Table II.

For practical machines it generally is true that

$$\sin(\alpha/2) = \alpha/2 \quad \text{and} \quad \sin(3\alpha/2) = 3\alpha/2 \quad (4)$$

Therefore, equation 3 becomes

$$I_e = 3.53 m_f P^2/S_c^2 \quad (5)$$

These results are derived by analysis and are substantiated by comparison with test results (limited to one 4-pole machine) and by comparison with analysis of a simplified 4-pole machine, Appendix II.

Assumptions

The current in the equalizer connections is affected by dimensions of the air gap and by the shape and spacing of the main pole tips and by the interpoles. Variation of these dimensions causes the resulting currents in the armature winding, producing armature magnetomotive forces, to be more or less concentrated in the spaces between main poles. Thus the distribution of armature magnetomotive forces is of the nature of a square wave, as shown in Figure 1. With dimensions

* In 4-pole machines where the equalizers do not form a ring, equations 1, 3, and 5 must be multiplied by 2.

Paper 50-192, recommended by the AIEE Rotating Machinery Committee and approved by the AIEE Technical Program Committee for presentation at the AIEE Middle Eastern District Meeting, Baltimore, Md., October 3–5, 1950. Manuscript submitted July 3, 1950; made available for printing August 25, 1950.

T. M. Linville and D. P. Strang are both with the General Electric Company, Schenectady, N. Y.

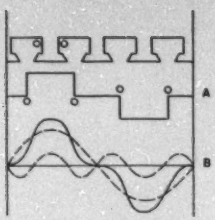

Figure 1. Armature magnetomotive force from equalizer currents when one pole is excited

Curve A: Square wave
Curve B: Corresponding wave from first and third harmonics

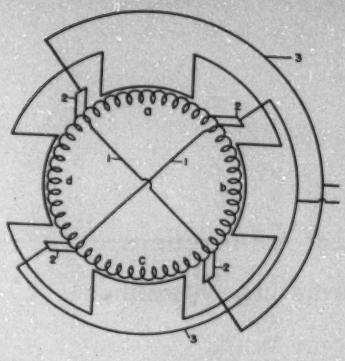

Figure 2. Circuits of d-c machine armature winding

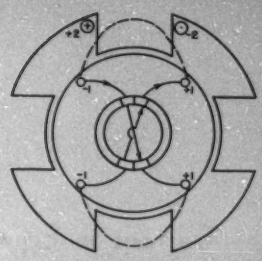

Figure 3. Schematic diagram of 4-pole machine showing two armature coils connected by equalizer connections

found in practice it is considered that the fundamental and third harmonic of the square wave represent the actual magnetomotive force wave. In some cases, this may be optimistic, particularly with respect to the rms, value of current. The influence of saturation is considered negligible.

Discussion of Results and Comparison with Test Results

In Figure 6, curves are shown as obtained by test measurement and as calculated from test data. In Figure 9, these curves are compared directly with calculated curves. The rms value of current in the equalizer connections determined from test is 14.9 amperes (see Appendix I) as compared with 12.0 amperes calculated from equation 5. Comparison of equation 5 with the result of the alternative method of analysis given in Appendix I, equation 20, shows that the two results have common coefficients and numerically give 10.7 amperes for the method of Appendix I compared to 12.0 amperes for equation 5. The method of Appendix I assumes that the equalizing current in the armature coils is distributed symmetrically about the interpole axis in the manner of $i_s = A(1+\cos\phi)$ as shown in Figure 6. Analysis of the test results suggests this assumption.

An additional comparison is afforded by Appendix II, in which a simplified machine with only 12 armature coils is analyzed mathematically. The wave shapes found by this analysis, shown in Figure 8, are similar to the test results, Figure 6, and furthermore, the rms equalizer current agrees well with equation 20 developed in Appendix I. This agreement is shown by comparison of equation 46 with equation 47.

The comparison of test curves (broken lines) with calculated curves (solid lines) shown in Figure 9 illustrates the importance of equalizer connections of low impedance. Harmonics which appear in the current in the armature coils, curve *C*, Figure 9, cause relatively little departure from the calculated current wave. These harmonics cause greater discrepancy between calculated and test currents in the equalizer connections, shown in curve *D*. This illustrates the amplification of harmonic currents in the equalizer connections. There are, of course, many factors in an actual machine to cause these harmonic currents. For example, in our test machine there are three slot openings in each pole face for a compensating winding which was disconnected during the tests. These slot openings in conjunction with the armature slot openings are responsible for the ripple in the test oscillograms, curves *C* and *D*, Figure 5, and for harmonic currents in the equalizer connections, curve *D*, Figure 9.

Function of Equalizers

One way to build the most into a d-c machine, in order to get the most out of it, is to construct it in such a way that every bar in the commutator is connected directly by equalizer connections to every circuit in the armature winding. If this is done, the power current will automatically divide equally between the circuits of the armature winding so that the heating will be minimum and will be uniformly distributed. Then the commutation will be the same at every brush holder arm. Operation can be continued when the commutator becomes rough, causing the brushes to bounce or when a bar is low and fails to contact the brushes, or when a field pole coil has failed and has been removed from the field winding circuit. Moreover, the voltage from bar to bar around the commutator will be minimum and will be distributed in an unchanging pattern.

Figure 2 shows equalizer connections which tie each commutator bar directly to each circuit. A ring winding is shown for illustration having four poles and circuits *a*, *b*, *c*, and *d*, in the armature winding. The brushes 2 contact this winding at four equally spaced points. Theoretically the machine with this armature winding will operate without the equalizer connections, 1. However, without them if the top right-hand one of the brushes 2 should momentarily be lifted out of contact with the winding, the current in branches *a* and *b* will be momentarily zero and will be correspondingly greater in branches *c* and *d*. Likewise, unbalance will be created if the resistance of the contact between this brush and the winding is momentarily greater than for the other brushes because of eccentric movement of the commutator or a spot on the surface or roughness. Such unbalance of current in the branches *a*, *b*, *c*, *d* cannot occur when the connections, 1, are present because the contact of any one of the brushes with the winding is then a 4-way contact. The power current divides between the branches *a*, *b*, *c*, and *d* independently of variations in the brush contacts by flow of current in the connections 1. Because of rotation of the armature, the illustration of Figure 1 holds for only a moment but when all points of contact between the winding and brushes, that is, all of the commutator bars, are connected together by similar connections 1, the conditions at any moment are as shown in Figure 2. Obviously, unless the currents in the branches *a*, *b*, *c*, and *d* are balanced, there will be excessive heating and, because the commutating

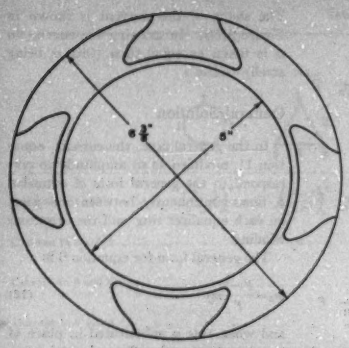

Figure 4 (above). Configuration and approximate dimensions of test machine

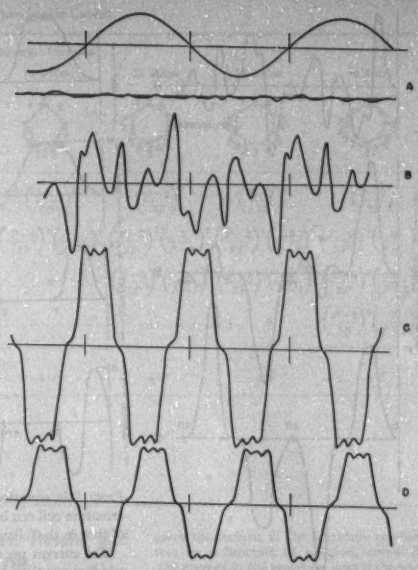

Figure 5 (right). Test oscillograms

Curve A: Current in equalizing connection with all poles excited equally
Curve B: Current in same connection with only one pole excited
Curve C: Bar-to-bar voltage with all poles excited equally
Curve D: Bar-to-bar voltage with only one pole excited
Test Machine: 4 poles; 24 volts; 10,000 rpm; 200/800 amperes; 34 coils; 100 per cent equalization

pole windings will be balanced independently of the currents in the branches, there will be sparking.

Of primary importance also, is the fact that in practice the electromotive force generated in the branches *a*, *b*, *c*, and *d*, without the connections 1, are not equal because the air gaps of the respective poles cannot be made exactly the same. If the electromotive force of branches *c* and *d* are not equal and opposite as they should be, then a current will flow through the bus ring 3 causing sparking. Under certain conditions it is possible that branches *c* and *d* will have harmonics (a ripple) in the electromotive force which will cause a ripple current to flow in bus 3 causing sparking. These currents in bus 3 will not flow when the connections 1 are present because a direct path of relatively low impedance is then provided for them. The flow of the currents sets up a magnetomotive force which "equalizes" the flux for all poles and, therefore, brings the electromotive force of the branches *a*, *b*, *c*, and *d* into balance. Therefore, only a small magnetizing current flows which normally is negligible in comparison with the power current.

It follows that the "equalizer connections" perform three principal functions, namely:

1. Cause the power current to divide between the paths of the armature winding independently of the condition of the brushes or the commutator surface, resulting in minimum heating of the winding and uniform commutation at each brush arm.

2. Cause the flux from each of the poles to be "equal" and allow the necessary magnetizing currents to flow in the armature winding; eliminate current flowing in the bus rings between brush arms; result in minimum core losses, minimum magnetizing current, no sparking from magnetizing current flowing to and from the brushes, and minimum voltage between adjacent commutator bars.

3. "Anchor" the two windings together in the special case of duplex windings and, in addition, to function 1 and 2, cause a fixed voltage between each bar and the bars next to it which in this case belong to a second winding. In this case there is in addition to the winding, *a*, *b*, *c*, *d* of Figure 1, another duplicate parallel winding connected to a set of commutator bars which are interleaved with the bars of the first winding. Study of duplex windings is beyond the scope of the paper.

Analysis

An understanding of the manner in which equalizing current flows in the armature winding and in the equalizer connections can be gained from an analysis built on Figure 3. It is obvious from Figure 3 that two armature coils spaced exactly two pole pitches apart and cross connected by equalizer connections form an elemental circuit in which no current will flow if the armature rotates while the flux from each of the four poles is exactly the same. When the flux from each of the poles is not the same, a current will flow.

In the diagram of Figure 3 consider that the top pole alone is excited. This is equivalent to having all poles excited equally except one which has no excitation, as though one field coil has failed and has been removed from the field circuit. As indicated by the numbers on Figure 3, the ratio of armature magnetomotive force to field magnetomotive force is 1 to 2, that is

$$m_a = 1/2 m_f \tag{6}$$

where m_a is the maximum amplitude of the armature reaction magnetomotive force, see Figure 1, and m_f is the unbalanced magnetomotive force applied to the top pole only. This relation is demonstrated by equation 43, Appendix II. The total armature magnetomotive force, half appearing on one side of the armature and half on the other, is equal to the field magnetomotive force, m_f. Since the elemental circuit rotates rapidly and has very little resistance compared to reactance, its flux linkages must be substantially zero at all times. However, there are a multiplicity of duplicate elemental circuits spaced uniformly around the armature to make the whole winding. Therefore, the linkages which current in

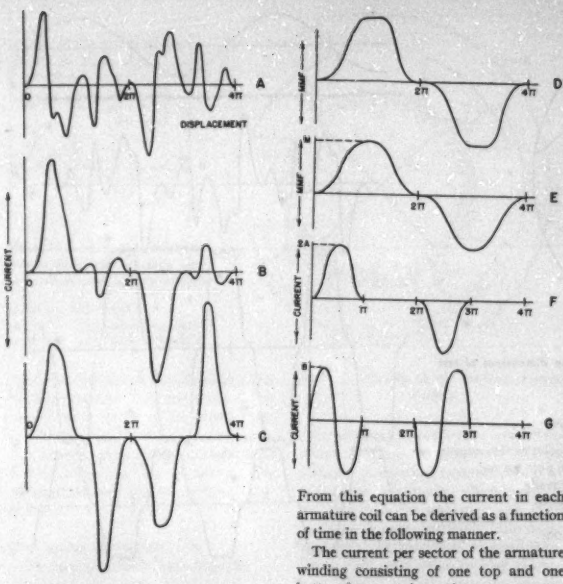

Figure 6. Analysis of test results

Curve A: Equalizer current
Curve B: Current in armature coils
Curve C: Current in armature slot
Curve D: Armature magnetomotive force
Curve E: Idealized armature magnetomotive force
Curve F: Idealized current in armature coils
Curve G: Idealized equalizer current

these coils produces in the elemental circuit of Figure 3 must be included. It follows that the space distribution of the armature magnetomotive force tends to be constant across each pole arc, the same as the distribution of field magnetomotive force, and for a 4-pole machine as illustrated in Figure 1 can be expressed by the Fourier series.

$$m_a = \frac{\sqrt{2}}{\pi} m_f \left(\cos\theta + \frac{1}{3}\cos 3\theta \ldots \right) \qquad (7)$$

where θ is the angle in mechanical radians with respect to the center line of the main pole.

The distribution of current around the periphery of the armature to give the magnetomotive force of equation 7 is obtained by differentiating the magnetomotive force

$$i_a = \frac{d}{d\theta} m_a = \frac{\sqrt{2}}{\pi} m_f (\sin\theta + \sin 3\theta \ldots) \qquad (8)$$

From this equation the current in each armature coil can be derived as a function of time in the following manner.

The current per sector of the armature winding consisting of one top and one bottom layer conductor is

$$i_s = \int_{\frac{\omega t-\alpha}{2}}^{\frac{\omega t+\alpha}{2}} i_a d\theta = (2\sqrt{2} m_f/\pi) \left([\sin(\alpha/2) \sin(\omega t/2) + (1/3) \sin(3\alpha/2) \sin(3\omega t/2) \ldots] \right) \qquad (9)$$

where ω is in electrical radians per second and

$$\alpha = \frac{\pi P}{2S_e}$$

when P is the number of poles and S_e is the number of bars in the commutator.

The harmonic currents in the top conductor are each exactly the same as the current in the bottom conductor except they are in reversed phase quadrature. Hence, the current in every armature coil is

$$i_c = (2m_f/\pi) \left([\sin(\alpha/2) \sin(\omega t/2) - (1/3) \sin(3\alpha/2) \cos(3\omega t/2)] \right) \qquad (10)$$

The current in each equalizer connection is equal to the difference between the currents of two adjacent coils of the winding which with the equalizer connection form a Y junction. The two coils have the same current except for the phase displacement of 2α radians. Therefore, the current in the equalizer connection which is the difference between the two is

$$(i_e = 4m_f/\pi) \left([\sin^2(\alpha/2) \cos(\pi t/2) + (1/3) \sin^2(3\alpha/2) \sin(3\omega t/2)] \right) \qquad (11)$$

The shape of this current is shown in Figure 9(D). In drawing the curve, sin α is taken as equal to α (with α being small).

General Solution

In the general case, the current, equation 11, modified as to amplitude to correspond to the general form of equation 6, flows continuously between one point on each equalizer ring and the armature winding.

The general form for equation 6 is

$$m_a = \frac{P-2}{P} m_f \qquad (12)$$

and when this is substituted in place of equation 6 it has the effect of multiplying equation 11 by $2(P\text{-}2)/P$.

The current divides in each ring, half flowing one way and half the other way around the ring. Accounting for this by dividing by 2, equation 11 becomes true for the general case when multiplied by $(P\text{-}2)/P$ or when

$$i_e = (4m_f/\pi) \; [(P-2)/P] \left([\sin^2(\alpha/2) \cos(\omega t/2) + (1/3) \sin^2(3\alpha/2) \sin(3\omega t/2)] \right) \qquad (13)$$

Equation 13 gives the current in each of two equalizer connections attached to a common commutator segment while the segment is passing through the arc from π radians on one side of the excited pole to π radians on the other side. Other equalizer connections in the same ring carry part of the same current but in diminishing amounts. A given equalizer connection sucessively carries the full current given by equation 13, then a part of it as its location in the ring changes with rotation of the armature. It is important to know the rms current in the ring which will be the same as the rms current in any equalizer connection and also the same as the rms current in the entire equalizer winding. For this rms current and for a given size of the equalizer connections and a given total weight of copper in the equalizer winding, the losses may be calculated. Or the size of conductor may be determined for given allowable losses.

The rms current in the equalizer winding of any machine will be the rms value of equation 13 provided the number of equalizer connections in each equalizer ring is factored into it. This is done by factoring $(P-2)/2P$ out of equation 13 and replacing it with a factor set up from Table I to account for the number of equalizer connections per ring and their respective currents.

In Table I the current in each equalizer connection of a ring is expressed in terms of

Table I. Factor for Mean Square Current

	Squared Currents						
	4 Poles	6 Poles	8 Poles	10 Poles	12 Poles	14 Poles	16 Poles
Current in 1 and 2	$\left(\frac{P-2}{2P}\right)^2$	$\left(\frac{P-2}{2P}\right)^2$	$\left(\frac{P-2}{2P}\right)^2$	$\left(\frac{P-2}{2P}\right)^2$	$\left(\frac{P-2}{2P}\right)^2$	$\left(\frac{P-2}{2P}\right)^2$	$\left(\frac{P-2}{2P}\right)^2$
Current in 3 and 4		0	$\left(\frac{P-2}{2P}\right)^2\left(\frac{2}{P-2}\right)^2$	$\left(\frac{P-2}{2P}\right)^2\left(\frac{4}{P-2}\right)^2$	$\left(\frac{P-2}{2P}\right)^2\left(\frac{6}{P-2}\right)^2$	$\left(\frac{P-2}{2P}\right)^2\left(\frac{10}{P-2}\right)^2$	$\left(\frac{P-2}{2P}\right)^2\left(\frac{10}{P-2}\right)$
Current in 5 and 6				0	$\left(\frac{P-2}{2P}\right)^2\left(\frac{2}{P-2}\right)^2$	$\left(\frac{P-2}{2P}\right)^2\left(\frac{4}{P-2}\right)^2$	$\left(\frac{P-2}{2P}\right)^2\left(\frac{6}{P-2}\right)^2$
Current in 7 and 8						0	$\left(\frac{P-2}{2P}\right)^2\left(\frac{2}{P-2}\right)$
Multiplying factor for mean square	$4/P$	$4/P$	$4/P$	$4/P$	$4/P$	$4/P$	$4/P$

Sum of Each Column Times Factor

$P/2$ even no.: $\left(\frac{P-2}{2P}\right)^2\left(\frac{2}{P-2}\right)^2\frac{4}{P}\left[1+3^2+5^2+----\left(\frac{P-2}{2}\right)^2\right]$

$P/2$ odd no.: $\left(\frac{P-2}{2P}\right)^2\left(\frac{4}{P-2}\right)^2\frac{4}{P}\left[1+2^2+3^2+----\left(\frac{P-2}{4}\right)^2\right]$

the base factor $(P-2)/2P$. Every value is squared so that the sums may be taken to get the mean square. For this purpose the sum of the squares is multiplied by $4/P$ as the number of equalizers carrying equal current is always two and the total number of equalizers which are in a ring is $P/2$.

Therefore, the rms current is the rms value of

$$i_e=(8m_f/\pi)\delta\left([\sin^3(\alpha/2)\cos(\omega t/2)+(1/3)\sin^3(3\alpha/2)\cos(3\omega t/2)]\right) \quad (14)$$

where from Table I, when $P/2$ is an even number

$$\delta^2=\frac{4}{P^2}\left[1+3^2+5^2+\ldots\ldots\left(\frac{P-2}{2}\right)^2\right] \quad (15)$$

and when $P/2$ is an odd number:

$$\delta^2=\frac{16}{P^2}\left[1+2^2+3^2+\ldots\ldots\left(\frac{P-2}{4}\right)^2\right] \quad (16)$$

Numerical values for δ are tabulated in Table II.

Table II. Values for δ

Poles	δ
4	0.250
6	0.273
8	0.280
10	0.283
12	0.285
14	0.286
16	0.287
18	0.287
20	0.288
60	0.289

Appendix I. Test Results and Analysis

The test machine was a 10,000-rpm 24-volt 4-pole 4-circuit-starter motor, shown schematically in Figure 4. It had 34 slots and commutator segments, and 100 per cent equalization. For the tests, one internal equalizer was removed and replaced by one of equal resistance on the outside of the commutator. Pickup wires were connected to each end of the test equalizer, wrapped around it to minimize inductive pickup, and connected to two slip rings. The slip rings were made of brass and fitted over the commutator. On each slip ring was a brush consisting of ten phosphor-bronze strips, to which the oscillograph was connected. The machine was driven at 3,600 rpm by an induction motor, and the d-c brushes were removed from the commutator. The commutating poles were removed from the machine and only the shunt fields were excited. The excitation was kept low to avoid overheating and to prevent saturation.

As a check on the test setup, two tests were made. First, a current of 10 milliamperes through the pickup brushes produced no "hash" from brush contact. Second, with one end of the test equalizer disconnected, no signal could be seen for any magnetic unbalance. Thus there was no inductive pickup.

Oscillogram, Figure 5(A), shows the equalizer current with balanced excitation applied. Oscillogram Figure 5(B), shows the equalizer current with approximately normal excitation on only one pole. This oscillogram is traced on curve A, Figure 6.

In Figure 6, curve A is the current in the equalizer connections as a function of position and, because of the large number of slots and equalizer connections, this current is proportional to the rate of change of armature current. Then the integral of curve A gives the current in the armature conductors as a function of position, curve B. The current in the armature slots is the sum of the current in the top and bottom conductors. Therefore, the slot current as a function of position, curve C, is the sum of the conductor current, curve B, and the negative of conductor current displaced 90 degrees. The integral of curve C gives the armature magnetomotive force curve D.

Before going further with the curves of Figure 6, two more test oscillograms are of interest. Using the same test setup, oscillograms of voltage between two adjacent commutator segments also were taken. Oscillogram Figure 5(C) shows the bar-to-bar voltage with a balanced excitation of 198AT/pole. Oscillogram Figure 5(D) shows the bar-to-bar voltage with 490AT excitation on only one pole. That the voltage of Figure 5(D) is balanced means that armature currents flow to balance the field. Thus one peak of curve D, Figure 6, opposes the applied magnetomotive force, and the other one excites the opposite pole. The amplitude of the armature magnetomotive force must be half of the applied excitation, neglecting leakage. The integration of curve C to obtain armature magnetomotive force of curve D gives a peak of 224AT, which is approximately half of the actual applied excitation.

Now let us analyze the curves, Figure 6. It is clear that the small peaks in armature current, curve B, tend to make the magnetomotive force curve D slightly unsymmetrical. Nevertheless, the armature current curve B, can be idealized as parts of sinusoids, as shown in curve F. This results in a magnetomotive force distribution curve E which is very similar to curve D. The derivative of the armature current curve gives an idealized equalizer current as shown in curve G.

From these idealized curves we can find

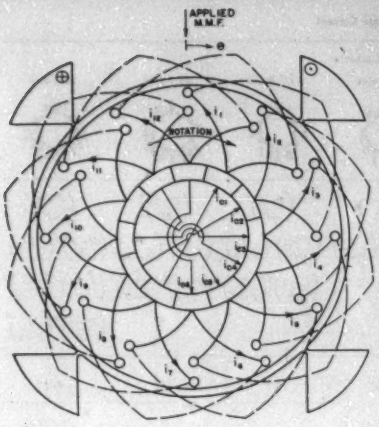

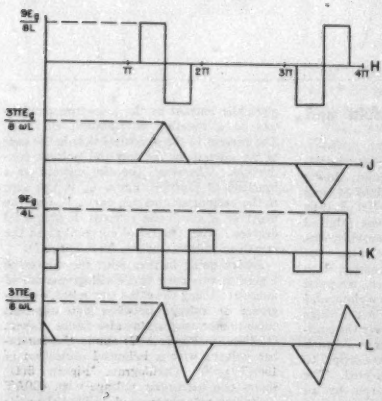

Figure 7 (left). Simple machine for analysis of Appendix II

Figure 8 (lower left). Analysis of simple machine

Curve H: Rate of change of armature current
Curve J: Current in armature coils
Curve K: Rate of change of equalizer current
Curve L: Equalizer current

Figure 9 (right). Comparison of calculated curves with curves from test data

Curve A: Armature magnetomotive force, equation 7 $m_a = 220\ [(\cos\theta + (1/3)\cos 3\theta)]$
Curve B: Current in armature slot, equation 9 $I_s = 41\ (\sin\theta + \sin 3\theta)$
Curve C: Current in armature coil, equation 10 $I_c = 29\ [(\sin(\omega t/2) - \cos(3\omega t/2)]$
Curve D: Current in equalizer connection, equations 11 or 1 $I_e = 5.3\ [(\cos(\omega t/2) + 3\sin(3\omega t/2)]$

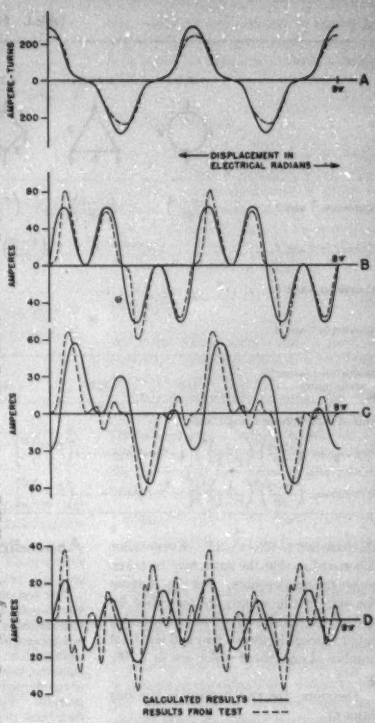

an expression for equalizer current. In Figure 6, the area of one pulse of armature current is πA, and multiplied by the number of armature turns per radian, a, is equal to the peak value of the magnetomotive wave, m_a. Thus

$$A = \frac{m_a}{\pi a} \tag{17}$$

Similarly, the area of one pulse of equalizer current times the number of equalizer connections per radian, b, is the magnitude (B) of the armature current pulse. Thus

$$2A = \frac{2B}{\pi} \times \frac{\pi}{2} \times b$$

or

$$B = \frac{2A}{b} = \frac{2m_a}{\pi ab} \tag{18}$$

The rms value of equalizer current over the complete cycle is

$$I_e = \frac{B}{2} = \frac{m_a}{\pi ab} \tag{19}$$

Now if m_f is the excitation applied to one pole, we have $m_a = m_f/2$ and

$$I_e = \frac{m_f}{2\pi ab} \tag{20}$$

As a check, the excitation to get curve A was 490AT, and for this motor $a = b = 17/2\pi$. Thus,

$$I_e = \frac{2 \times 490 \times \pi}{(17)^2} = 10.7 \text{ amperes} \tag{21}$$

From the actual oscillogram the rms value of equalizer current is 14.9 amperes. Expressed in other terms

$$a = b = \frac{S_s}{\pi P}$$

and equation 20 becomes

$$I_e = \frac{\pi m_f P^2}{2S_s^2} \tag{22}$$

This result, true only for a 4-pole machine, can be compared with equation 5.

Appendix II. Analysis of an Elementary Machine

This analysis is intended to demonstrate, using a simple machine with equalizer connections, that armature currents equalize any unbalance in the applied excitation. Consider the configuration shown in Figure 7, with 12 armature coils, four poles, and six equalizer connections. Assume a uniform air gap, neglect resistance and leakage reactance of the windings, and consider only one pole excited. If the self inductance of one coil is

$$L_{11} = L \tag{23}$$

from the geometry of the machine we have mutual inductances given by

$$L_{14} = L_{15} = L_{16} = L_{17} = L_{18} = L_{19} = L_{1\,10} = -\frac{1}{3}L \tag{24}$$

$$L_{12} = L_{1\,13} = \frac{5}{9}L \tag{25}$$

and

$$L_{12}=L_{1\,11}=\frac{1}{9}L \tag{26}$$

Then taking E_{g1} as the generated voltage in coil 1 due to field excitation, the terminal voltage of coil 1 can be expressed as

$$E_1=E_{g1}-pL\left[i_1+\frac{1}{9}(5i_2+i_3-3i_4-3i_5-3i_6-3i_7-3i_8-3i_9-3i_{10}+i_{11}+5i_{12})\right] \tag{27}$$

Writing similar equations for the other armature coils gives

$$\frac{9}{pL}\begin{array}{lrrrrrrrrrrrr}
 & i_1 & i_2 & i_3 & i_4 & i_5 & i_6 & i_7 & i_8 & i_9 & i_{10} & i_{11} & i_{12} \\
\frac{9}{pL}(E_1-E_{g1})= & -9 & -5 & -1 & 3 & 3 & 3 & 3 & 3 & 3 & 3 & -1 & -5 \\
\frac{9}{pL}(E_2-E_{g2})= & -5 & -9 & -5 & -1 & 3 & 3 & 3 & 3 & 3 & 3 & 3 & -1 \\
\frac{9}{pL}(E_3-E_{g3})= & -1 & -5 & -9 & -5 & -1 & 3 & 3 & 3 & 3 & 3 & 3 & 3 \\
\frac{9}{pL}(E_4-E_{g4})= & 3 & -1 & -5 & -9 & -5 & -1 & 3 & 3 & 3 & 3 & 3 & 3 \\
\frac{9}{pL}(E_5-E_{g5})= & 3 & 3 & -1 & -5 & -9 & -5 & -1 & 3 & 3 & 3 & 3 & 3 \\
\frac{9}{pL}(E_6-E_{g6})= & 3 & 3 & 3 & -1 & -5 & -9 & -5 & -1 & 3 & 3 & 3 & 3 \\
\frac{9}{pL}(E_7-E_{g7})= & 3 & 3 & 3 & 3 & -1 & -5 & -9 & -5 & -1 & 3 & 3 & 3 \\
\frac{9}{pL}(E_8-E_{g8})= & 3 & 3 & 3 & 3 & 3 & -1 & -5 & -9 & -5 & -1 & 3 & 3 \\
\frac{9}{pL}(E_9-E_{g9})= & 3 & 3 & 3 & 3 & 3 & 3 & -1 & -5 & -9 & -5 & -1 & 3 \\
\frac{9}{pL}(E_{10}-E_{g10})= & 3 & 3 & 3 & 3 & 3 & 3 & 3 & -1 & -5 & -9 & -5 & -1 \\
\frac{9}{pL}(E_{11}-E_{g11})= & -1 & 3 & 3 & 3 & 3 & 3 & 3 & 3 & -1 & -5 & -9 & -5 \\
\frac{9}{pL}(E_{12}-E_{g12})= & -5 & -1 & 3 & 3 & 3 & 3 & 3 & 3 & 3 & -1 & -5 & -9
\end{array} \tag{28}$$

Neglecting the impedance of the equalizer connections, the coil terminal voltages are related as

$$\begin{aligned}
E_1-E_7&=0\\
E_2-E_8&=0\\
E_3-E_9&=0\\
E_4-E_{10}&=0\\
E_5-E_{11}&=0\\
E_6-E_{12}&=0
\end{aligned} \tag{29}$$

Thus the 12 equations reduce to

$$\frac{9}{4pL}\begin{array}{lrrrrrrrrrrrr}
 & i_1 & i_2 & i_3 & i_4 & i_5 & i_6 & i_7 & i_8 & i_9 & i_{10} & i_{11} & i_{12} \\
E_{g1}-E_{g7}= & -3 & -2 & -1 & 0 & 1 & 2 & 3 & 2 & 1 & 0 & -1 & -2 \\
E_{g2}-E_{g8}= & -2 & -3 & -2 & -1 & 0 & 1 & 2 & 3 & 2 & 1 & 0 & -1 \\
E_{g3}-E_{g9}= & -1 & -2 & -3 & -2 & -1 & 0 & 1 & 2 & 3 & 2 & 1 & 0 \\
E_{g10}-E_{g4}= & 0 & -1 & -2 & -3 & -2 & -1 & 0 & 1 & 2 & 3 & 2 & 1 \\
E_{g11}-E_{g5}= & 1 & 0 & -1 & -2 & -3 & -2 & -1 & 0 & 1 & 2 & 3 & 2 \\
E_{g12}-E_{g6}= & 2 & 1 & 0 & -1 & -2 & -3 & -2 & -1 & 0 & 1 & 2 & 3
\end{array} \tag{30}$$

In the region of θ between $-\pi/6$ and $+\pi/6$, as shown in Figure 7, the net generated voltages in coils 3, 4, 5, 6, 7, and 8 are zero, and because of the uniform air gap

$$E_{g12}=E_{g1}=E_{g2}=-E_{g8}=-E_{g10}=-E_{g11}=E_g \tag{31}$$

Thus equation 30 becomes

$$\frac{9}{4pL}\begin{array}{lrrrrrrrrrrrr}
 & i_1 & i_2 & i_3 & i_4 & i_5 & i_6 & i_7 & i_8 & i_9 & i_{10} & i_{11} & i_{12} \\
-E_g= & -3 & -2 & 1 & 0 & 1 & 2 & 3 & 2 & 1 & 0 & -1 & -2 \\
-E_g= & -2 & -3 & -2 & 1 & 0 & 1 & 2 & 3 & 2 & 1 & 0 & -1 \\
-E_g= & -1 & -2 & -3 & -2 & 1 & 0 & 1 & 2 & 3 & 2 & 1 & 0 \\
-E_g= & 0 & -1 & -2 & -3 & -2 & 1 & 0 & 1 & 2 & 3 & 2 & 1 \\
-E_g= & 1 & 0 & -1 & -2 & -3 & -2 & 1 & 0 & 1 & 2 & 3 & 2 \\
+E_g= & 2 & 1 & 0 & -1 & -2 & -3 & -2 & 1 & 0 & 1 & 2 & 3
\end{array} \tag{32}$$

The equalizer currents are related to the armature currents as follows in equation 33:

$$\begin{aligned}
i_{e1}&=i_1-i_{12}=i_4-i_7\\
i_{e2}&=i_2-i_1=i_7-i_8\\
i_{e3}&=i_3-i_2=i_8-i_9\\
i_{e4}&=i_4-i_3=i_9-i_{10}\\
i_{e5}&=i_5-i_4=i_{10}-i_{11}\\
i_{e6}&=i_6-i_5=i_{11}-i_{12}
\end{aligned} \tag{33}$$

Thus in terms of equalizer currents equations 32 are:

$$\frac{9}{4pL}\begin{array}{lrrrrrrrrrrrr}
 & i_{e1} & i_{e2} & i_{e3} & i_{e4} & i_{e5} & i_{e6} \\
-E_g= & -3 & 3 & 7 & 9 & 9 & 7 \\
-E_g= & -7 & -3 & 3 & 7 & 9 & 9 \\
-E_g= & -9 & -7 & -3 & 3 & 7 & 9 \\
-E_g= & -9 & -9 & -7 & -3 & 3 & 7 \\
-E_g= & -7 & -9 & -9 & -7 & -3 & 3 \\
+E_g= & -3 & -7 & -9 & -9 & -7 & -3
\end{array} \tag{34}$$

These six equations can be solved, giving

$$i_{e1}=-\frac{18}{16pL}E_g$$

$$i_{e2}=i_{e3}=i_{e4}=0$$

$$i_{e5}=\frac{18}{16pL}E_g$$

$$i_{e6}=\frac{18}{16pL}(-2E_g) \tag{35}$$

Substituting these into the relations between armature and equalizer currents, equation 33 and using the additional condition that the average armature current over a complete revolution must be zero, gives the armature currents as

$$i_1=i_2=i_3=i_4=i_7=i_8=i_9=i_{10}=0 \tag{36}$$

$$i_5=-i_{12}=i_{e1}=-\frac{18}{16pL}E_g \tag{37}$$

$$i_6=-i_{11}=i_{e5}=+\frac{18}{16pL}E_g \tag{38}$$

These equations are valid only in the region of θ between $-\pi/6$ and $+\pi/6$ because this is the region for which the generated voltages were written. Thus in any armature coil the rate of change of current as a function of angular position will be as shown in curve H, Figure 8. Integrating this curve gives the armature current as a function of position, curve J.

The peak value is

$$i_{max}=\frac{9E_g}{8L}\times\frac{\pi}{3\omega}=\frac{3\pi E_g}{8\omega L} \tag{39}$$

Because of the limited number of coils these curves do not represent current distribution. When a coil is at $3\pi/2$ it has maximum current, another at $7\pi/2$ has negative maximum, and all others have no current.

To find the armature magnetomotive force we must find E_g and L. The inductance of a coil is determined by the area and effective length of air gap, and the square of the number of turns.

Thus

$$L=\frac{ld\left(\frac{\pi}{4}\right)n^2}{\frac{4}{3}g}=\frac{3\pi ldn^2}{16g} \tag{40}$$

Nomenclature

a = number of armature turns per electrical radian
b = number of equalizer connections per electrical radian
d = armature diameter
E = terminal voltage of one coil of elementary machine
E_g = generated voltage in one coil of elementary machine
g = air gap length
I_e = equalizer current—rms
i = coil current in elementary machine
i_a = current distribution around armature
i_e = equalizer current
i_s = current per segment of armature winding
l = armature length
L = self-inductance of one coil in elementary machine
m_a = magnitude of armature magnetomotive force
m_f = unbalanced excitation on one pole in ampere turns
n = number of armature turns per segment
P = number of poles
p = operator d/dt
S_c = number of bars in the commutator
t = time—seconds
$\alpha = \pi P/2S_c$
θ = angle with respect to center line of main pole (mechanical radians)
ω = angular armature speed—radians per second (electrical)

The generated voltage depends on the excitation, effective air gap, and the length and speed of conductors.

Thus

$$E_g = \frac{4}{3}\frac{m_f nl}{\frac{4}{3}g} \times \frac{\omega d}{4} = \frac{m_f l d n \omega}{4g} \tag{41}$$

Substituting these into i_{max} gives

$$i_{max} = \frac{3\pi}{8\omega} \times \frac{m_f l d n \omega}{3\pi l d n^2} \times \frac{16g}{4g} \tag{42}$$

$$\frac{m_f}{2n}$$

Thus the armature magnetomotive force when the currents are maximum is

$$n i_{max} = \frac{m_f}{2} \tag{43}$$

exactly half of the applied excitation, and in a direction to oppose the applied magnetomotive force. At another time, such as that shown in Figure 7, the current in coils 11 and 12 will be half of the maximum value, again giving a maximum armature magnetomotive force of half of the applied excitation.

Now let us go back and find the rms value of the equalizer currents. From equation 35 we see that the rate of change of equalizer currents as a function of position is as shown in curve K. Thus integrating gives currents as shown in curve L. The maximum value of this curve is the same as the maximum armature current, that is

$$i_{e(max)} = \frac{m_f}{2n} \tag{44}$$

The rms value of this wave shape is

$$I_e = \frac{m_f}{2n\sqrt{6}} \tag{45}$$

If there is one turn per coil, $n = 1$ and

$$I_e = \frac{m_f}{2\sqrt{6}} = 0.204\ m_f \tag{46}$$

If, as a check, we apply equation 20 developed from the test results to this case we have

$$a = b = \frac{3}{\pi}$$

$$I_e = \frac{m_f}{2\pi ab} = \frac{m_f \pi}{18} = 0.174\ m_f \tag{47}$$

This is a good check considering the entirely different assumptions which were made.

References

1. Die Gleichstrommaschine, **Arnold-la Cour**, Julius Springer, (Berlin, Germany), volume 3, 1919, pages 73–83.

2. Theory of the Action of Equalizer Connections in Lap Windings, **A. D. Moore**. *Electric Journal* (East Pittsburgh, Pa.), 1926, page 624.

3. Principles of D-C Machines (book), **A. S. Langsdorf**. McGraw Hill Book Company, New York, N. Y., 1940.

4. Multiplex Windings for D-C Machines, **Carl C. Nelson**. *AIEE Transactions*, volume 45, June 1926, pages 976–82.

Discussion

Paul W. Franklin (Bendix Aviation Corporation, Teterboro, N. J.): The mathematical treatment of equalizer currents, as given in the paper is very similar to the approximate calculation of synchronous machinery damper winding currents. If we hold a d-c armature stationary, but rotate the stator and the brush gear, passing a current through the brushes, we obtain similar conditions, namely—an armature magnetomotive force (mmf) relatively stationary to the pole wheel. The equalizers superpose a bodily incorporated damper winding upon the normal armature winding, which is short circuited. Since, however, the coil pitch of the new damper winding is equal to double pole pitch, it will be effective only upon subharmonics, that is, harmonics whose integer is below the number of pole pairs, if the first harmonic is assigned to the armature circumference.

The general theory of equalizers could then proceed as follows: Given an irregular stator shunt field mmf, reduced to equal air-gap reluctance (that is, equal shunt coil mmf but unequal air-gap would appear as equal gap but different shunt mmf) said distribution is to be analyzed and the resulting subharmonic mmf's have to be compensated by the equalizer winding. Or, as the authors have done, the mmf of the equalizer winding—now of the nature of a special squirrel cage winding—is equal to the subharmonics, and from this the currents may be computed. This would permit the calculation of currents for moderate unsymmetries, assuming, that the tired and by that time disgusted designer wishes to go so far.

It now would be of interest to speculate upon the influence of resistance and reactance in the equalizers. It should be noted that the equalizing currents caused by differences in pole flux go axially through the armature, whereas equalizing currents, caused by variable brush contact do not enter the armature, if the equalizers are fastened to the commutator. In the first case, a damping factor could be calculated, similar to the treatment published by Richter[1] in 1930, who also states that the equalizer currents are almost 90 degrees out of phase with their voltages. Due to reactance and resistance, the actual equalizer currents will be smaller than resulting by above calculation and this may be the reason why the actual measured rms value of the current was smaller than the sum of the calculated harmonics. There is no doubt, however, that such a refinement is not necessary for ordinary design calculations.

There is, however, one point of interest which should be discussed in connection with this paper. It is generally known that a well equalized lap winding is the best suited for difficult commutation conditions. It has been the experience of friends of the writer, that aircraft generators with well equalized lap windings are occasionally inferior to normal wave windings with regard to commutation. Aircraft generators are characterized by high temperatures, high speeds, high magnetic densities and high electromagnetic loading (ampere conductors per inch).

Whereas equalization for uneven pole flux takes place essentially at pole frequency, equalization for independent voltage polygons takes place at commutator bar frequency, which is at least ten times higher than the pole frequency. It is quite possible that the time constant of the equalizer connection at the high speeds of aircraft machines approaches the magnitude of the time of the commutator bar cycle. In addition to this, increased brush vibration, again at commutator bar frequency, and the ensuing additional need for corrective action from the side of the equalizers, may form a partial explanation for the occasional failure of lap windings in aircraft generators.

The writer wishes to congratulate the authors for their excellent paper, which, to the writer's knowledge, is the first published mathematical treatment of equalizer current.

Reference

1. Electrical Machinery, **Richter**. Julius Springer, Berlin, Germany, volume II, 1930, pages 49–50.

E. P. Smith (General Electric Company, Schenectady, N. Y.): The results of this paper are a definite contribution to the

Table I. Rms Equalizer Currents with One Field Coil Reversed

Item	Kw	Speed	Volts	Poles	Equalizer Current with Rated Field Current, Amperes	Equalizer Current Density, Rated I_f Amps/Sq. In.	Equalizer Current Density, Rated Armature Volts $I_f = I_{fNL}\frac{(P+1)}{(P-1)}$
1	125	3,600	250	4	42	5,160	8,600
2	1,375	1,800	415	6	23.4	835	1,170
3	1,500	514	600	8	13.8	630	810
4	1,750	500	800	12	5.5	408	482
5	4,400	300	750	16	8.2	275	312

All of these machines are fully equalized.

science of d-c machine design. The accuracy with which one can calculate the equalizer current by the formulas presented will determine the true value of these results. The assumptions made in the analysis seem reasonable. However, as stated by the authors, the results are substantiated only by comparison with test of one machine.

In a survey of the d-c machines built by the Large Motor and Generator Engineering Division of the General Electric Company, the only data found that is useful to check the calculations of this paper are that resulting from accident or failure. Obviously, exact numerical results were never taken. Equation 5 of this paper was applied to a number of machines, and the following calculated values of Table I of the discussion were obtained.

The exciter, Item 1 of Table I, had been received in test with one pole reversed. As rated voltage was approached in taking the saturation curve data, the armature smoked severely. The examination of the armature revealed that the equalizer insulation was completely destroyed. The calculated current density would indicate that such results could be expected on a normal equalizer winding which has a very poor heat dissipating ability.

The machine, Item 2 of the table, was a marine propulsion motor. This motor was tested under simulated damaged condition with one field coil removed. It was operated with rated field current and load. The calculated current density for this mode of operation is 417 amperes per square inch. This motor operated with no apparent signs of excessive heating.

The other three items in Table I were calculated for comparison. These machines have never been operated without a field coil excited or with one reversed. However, there have been reports from various mill operators who have operated generators similar to these with one field coil removed from the circuit for extended periods of time with no apparent damage to the equalizer winding. The values given in Table 1 of the discussion, Items 3, 4 and 5 confirm such observations.

In conclusion, this tidbit of evidence supports the results of this paper and makes them seem reasonable. However, further tests on a variety of designs are needed to fully prove its limitations and accuracy.

T. M. Linville and **D. P. Strang:** Mr. Franklin has pointed out correctly the similarity between the flow of currents in a d-c machine armature and the current flow in the amortisseur winding of a synchronous machine. The method of the paper was based upon the presumption that reactance determined the magnitude of the current in the equalizer connections and that resistance was negligible. Speculation on this point as suggested by Mr. Franklin is important. The authors feel that their assumption has been well substantiated by actual experience with d-c machines and by the behavior of similar transient currents in a-c machines. However, more test data showing the flow of equalizer currents is needed and we hope that some of this and further extension of the method for calculation will be done in the colleges. It is a well-known fact that equalizer connections are necessary for the successful operation of all d-c machines except the small ones which can be built with no more than two circuits in the armature winding. Mr. Franklin has pointed out how important it is to know the relative advantages of an equalized lap winding in comparison with a two circuit wave winding for aircraft generators. These matters are of major concern, not only to designers, but to users who depend upon good performance of d-c motors and generators.

We are interested in experiences that motor manufacturers may have had during factory tests when field coils may have accidentally been connected with the wrong polarity. This places an unusual load upon the equalizer connections showing up in overheating. In this connection we are grateful to Mr. Smith for the example cited. He has also given some calculations, based on the paper, showing the current density in the equalizer connections of actual machines when one field coil is reversed. Figures are given for normal field current and also for field current necessary to obtain rated voltage. These figures illustrate the fact that the load on the equalizers is greater the fewer the number of poles.

In the oral discussion, P. L. Alger proposed that the factor δ be calculated by the following relation:

$$\delta = \frac{1}{2P}\sqrt{\frac{P^4-4}{3}}$$

Such a simplification will be helpful. He noted that harmonics in the no-load air gap flux wave higher than the third harmonic were neglected and asked about the influence of including the higher harmonics. Within the limits of our knowledge, it appears that the inclusion of harmonics above the third result only in unnecessary complication for all except the very exceptional machine. We think that the higher harmonics have greater importance in a small machine, such as the aircraft starter used for test results given in the paper. In an industrial motor or generator, the higher harmonics should be of less importance. Mr. Alger pointed out that the reactance of the equalizer connection should be low and we agree that this reactance should be no more than 10 per cent of the slot leakage reactance of a single armature coil. This might be a desirable rule-of-thumb for the maximum value.

A question was raised about the relative merits of a 4-pole armature winding, fully equalized, with single versus double reentrancy. We stated that single reentrancy might be preferable. It must be pointed out, however, that the singly reentrant winding in such a case may result in the flow of equalizer current of higher harmonics, such as at slot frequency. This may result in higher losses such as an increase in the apparent no load core loss. The doubly re-entrant winding may be free of these losses and be entirely satisfactory. The answer to the question should be determined by a calculation of the voltage difference between points which are to be connected by equalizers in the case of each winding under consideration.

We appreciate the mention of B. G. Lamme's work cited by C. G. Veinott.

M. A. Baker asked how the formulas should be modified in case one equalizer connection was used for every other commutator segment rather than an equalizer connection for every segment. In such a case the results given by the paper would need to be doubled. Similarly, if only one-third of the full number of equalizer connections were used, the current calculated by the paper would need to be tripled. This can be seen if the analysis of the paper is considered in terms of increasing the angle α to make it equal to the angle between two adjacent equalizer connections. In case this angle becomes so large that sine α is no longer equal to α (as is necessary if the simple result of the paper is to be valid) equation 3 must be used in place of equation 5.

Measurement and Calculation of D-C Machine Armature Circuit Inductance

H. D. SNIVELY
MEMBER AIEE

PAUL B. ROBINSON
ASSOCIATE AIEE

A PREVIOUS paper[1] discusses the importance of being able to predetermine the transient characteristics of d-c rotating machines, and its lists the papers of several investigators[2,3,4] who have advanced methods for such predetermination. Reference 1 of this paper presents typical d-c machine values for one of the parameters required by the methods of references 2, 3, and 4, namely r_a', the per-unit equivalent resistance. These values were determined by means of the theories[3,4] and were furnished by several manufacturers to the D-C Machinery Subcommittee of the AIEE Rotating Machinery Committee for presentation in reference 1, in which paper it was promised that "as progress is made in the determination of inductances, it is expected that similar analysis and confirmation by test will be forthcoming."

The present paper is a step toward the fulfillment of that promise. Methods will be described for obtaining the inductance by test and for calculating the inductance from design data. Some typical values obtained by these methods will be given, and it is hoped that other investigators will be inspired to use the methods to obtain values of inductance which can then be assembled and presented in a paper which will parallel reference 1. It also is hoped that suggestions will be made toward improving the methods both for test and for calculation.

A-C Impedance Test

The armature circuit inductance may be determined as described in the footnote to Table I of reference 4. This involves the measurement of the a-c impedance between line terminals of the stationary d-c machine by impressing an a-c voltage on these terminals and measuring the resulting alternating current. All brushes are lifted, and copper jumpers of suitable section to carry the expected current are connected between each brush stud and all the commutator leads of the bars which would normally be short circuited by the brushes of that particular stud. This eliminates the brush and brush contact resistance during the test.

For obtaining unsaturated values of inductance, the shunt field winding is left unexcited, either open- or short-circuited, and several readings are taken of a-c volts and a-c amperes with constant line frequency so that a curve of volts versus amperes can be plotted. Usually a curve extending to a current of about one half of the rated line current of the machine will be sufficient to give good results. The slope of this curve is the a-c impedance of the circuit, and if there is any departure from a straight line due to saturation at the higher voltages, the slope of the curve near the origin represents the unsaturated impedance.

For obtaining relatively saturated values of inductance the procedure just described should be repeated with rated d-c field current maintained in the shunt winding.

The principal interest in determining the inductance is to obtain the armature circuit decrement factor σ_a and hence the maximum rate of rise of short-circuit current, equation 3, reference 3. Therefore the transient impedance is desired, and any series windings on compound wound machines should preferably be omitted when conducting the foregoing tests, particularly if the shunt field winding is open circuited. Furthermore, this omission eliminates the tendency to rotate as a series motor.

Experience has shown no perceptible difference in the inductance values obtained by using a-c frequencies ranging from 25 to 60 cycles, and therefore it is suggested that the more convenient frequency, 60 cycles, be used. If this is done it will usually be found that the a-c impedance of the armature circuit may be assumed to be entirely reactance although precautions should be taken to verify this by measuring the resistance of the circuit as tested to see that it is negligible. For a 60-cycle test the per-unit inductance l_a' or the per-unit saturated inductance l_{as}' may be determined from the appropriate test curve as

$$l_a' \text{ (or } l_{as}') = \frac{\text{slope of curve}}{377} \times \frac{I_{a1} \times N_1 \times P}{19.1\, V_1}$$

in which I_{a1} is the rated full-load armature amperes; V_1, the rated armature voltage; N_1, the rated base speed in revolutions per minute; and P, the number of poles. The per-unit inductance l_a' (or l_{as}') is identical with the inductance coefficient C_a referred to in references 3 and 4.

D-C Build-Up Method

Another test method of determining the armature circuit inductance is to measure oscillographically the rate of rise of direct current after sudden application of a low d-c voltage to the terminals of the d-c machine. For this type of test the brush jumpers should be used as in the a-c impedance test; the shunt field should be excited or not depending on whether saturated or unsaturated inductances are desired; and in addition the rotor should be firmly blocked to prevent rotation. The voltage source should be a low-volt-

Paper 50-193, recommended by the AIEE Rotating Machinery Committee and approved by the AIEE Technical Program Committee for presentation at the AIEE Middle Eastern District Meeting, Baltimore, Md., October 3–5, 1950. Manuscript submitted July 5, 1950; made available for printing August 18, 1950.

H. D. Snively and Paul B. Robinson are both with the General Electric Company, Schenectady, N. Y.

The authors wish to thank T. M. Linville for contributions to the Appendix of this paper and to V. C. Strode and W. C. Bachtel for assistance in obtaining test and calculated data.

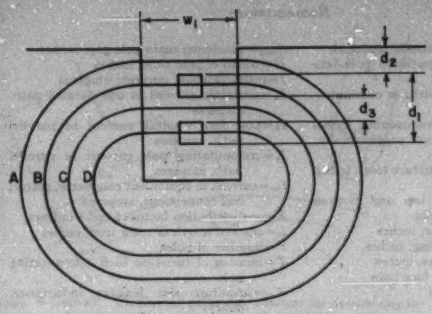

Figure 1. Outline of armature slot showing flux paths

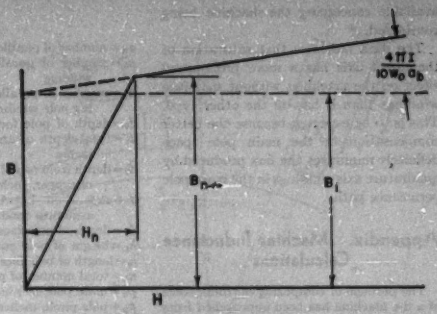

Figure 3. Idealized magnetization curve of pole piece steel

age high-current low-inductance supply capable of maintaining reasonably constant voltage at the machine terminals. The inductance in henrys of the armature circuit can be calculated as the applied terminal voltage divided by the initial rate of rise of current in amperes per second. This inductance multiplied by $(I_{a1}N_1P/19.1\,V_1)$ is the per-unit inductance l_a' (or l_{as}'). Several readings should be taken at different applied voltages resulting in line currents from about 10 per cent up to 50 per cent rated. Care should be exercised not to maintain the current any longer than necessary to obtain the desired data. Terminal resistance should be measured as before so that several points on the build-up curve can be checked in addition to the zero time point.

Due to the somewhat more complicated test set-up and calculations required as well as the need for a stiff voltage source, the d-c build-up method is not as convenient or as cheap as the a-c impedance method. When tests have been made by both methods on the same machine, there has been no indication that either method gives superior results, and hence the a-c impedance test is being used more often than the other method at the present time.

Calculation of Inductance

The calculation of the armature circuit inductance from design data involves the calculation and summation of the inductances associated with each of the various permeance paths of the quadrature axis windings. The series windings are not included for the reasons given previously. The formulas for the various inductances are derived in the Appendix and will not be repeated here. The total inductance calculated from these expressions is in henrys and can be converted to per-unit by multiplying by the factor $(I_{a1}N_1P/19.1\,V_1)$.

It is suggested that these formulas be arranged systematically on a suitable calculation form sheet by anyone who plans to use the method to calculate inductances of a large number of machines.

Comparison of Tests and Calculations

A 900-kw 720-rpm 300-volt 8-pole 40-degree open generator without pole face winding was tested by the a-c impedance method, and the results showed an l_a' of 0.82 with unexcited field and an l_{as}' of 0.371 with excited field. The calculated value of per-unit inductance is based on no saturation and in this case equalled 0.88 which is 7 per cent higher than the test value.

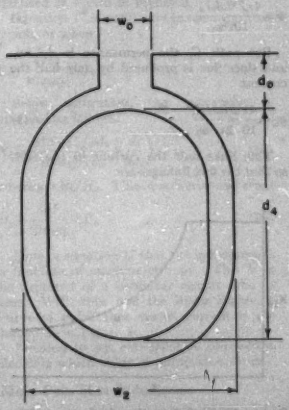

Figure 2. Outline of pole face slot

A 200-kw 3,600-rpm 250-volt 4-pole 40-degree semienclosed generator without pole face winding showed an l_{as}' of 0.42 with excited field. No test was made for unsaturated inductance but calculations gave 0.47 which is not as much higher than l_{as}' as was the previous example.

A 1,500-horsepower 575-rpm 500-volt 8-pole 40-degree open, forced ventilated motor with pole face winding gave an l_a' of 0.15 with unexcited field by the a-c method and 0.16 by the d-c build-up method. For l_{as}' with excited field the results were 0.14 by both methods. The calculated value for l_a' was 0.155.

A 1,500-kw 720-rpm 500-volt 8-pole 40-degree open generator with pole face winding gave an l_a' of 0.26 with unexcited field, while the calculated value was 0.20. The test value of the saturated inductance was not obtained.

A 750-kw 720-rpm 250-volt 6-pole 40-degree open generator with pole face winding gave a test value for l_{as}' of 0.15 with excited field. No test was made for unsaturated inductance. Calculations showed 0.27 for l_a'.

The foregoing data, as well as other results not recorded here, indicate that the method of calculation is reasonably accurate, giving results sometimes higher and sometimes lower than test values for unsaturated inductance. It is the belief of the authors however, that on the average the calculated values are somewhat lower than the tested values.

The data also indicate that the suggested values for C_z in references 3 and 4 of 0.6 for machines without pole face windings and 0.15 for machines with pole face windings, are fairly good approximate figures to use if no better information is

available concerning the machine being considered.

The data indicates that saturation of the direct axis has a more pronounced effect on the machines without pole face windings than it has on the other type. This is to be expected because the better compensation in the main pole space definitely minimizes the flux produced by quadrature axis windings in the main pole permeance paths.

Appendix. Machine Inductance Calculations

The problem of computing the inductance of a d-c machine has been approached from the concept of flux linkages about one electrical path. It is well known that the inductance of a circuit is equal to the flux linkages about it divided by the current in it, and this theorem can be applied to one parallel path in a d-c machine. The total inductance of the machine will be the inductance of one path divided by the number of parallel paths. Thus, the problem is resolved to one of finding the flux linkages about one path of the machine.

The problem is simplified even more by observing that there are many magnetic circuits within the machine which may be treated independently, provided it is assumed that the steel does not saturate. Thus, the various self and mutual inductances within an electrical path can be determined by themselves, then added to get the total inductance of the path.

Because of the symmetry of the machine, all paths are assumed to have equal currents. With this, and the assumption that the steel has infinite permeability, the total magnetomotive force around a particular magnetic circuit can be determined. The magnetomotive force drop will fall entirely across the air paths of the magnetic circuit, and if the permeance of the path can be determined, the total flux can be evaluated. Multiplying this flux by the turns linked in one electrical path gives the flux linkages in that circuit.

The process of calculating inductance, then, follows these steps:

1. Determine the total magnetomotive force existing in the magnetic circuit of interest that affects one electric circuit.
2. Determine the permeance of the magnetic circuit, and multiply by the magnetomotive force, thereby obtaining total flux in the magnetic circuit which affects one electric circuit.
3. Multiply this flux by the number of turns it links in the one electric circuit. This, now, gives the total flux linkages about that electric circuit.
4. Divide these linkages by the current in that one electric circuit to get its inductance.
5. Divide this inductance by the number of paths in parallel to obtain the inductance of the whole machine.

Armature Conductor Leakage Reactance

Consider the leakage reactance of armature conductors embedded in a slot. The magnetomotive force around path A is simply $4\pi/10$ times the total slot current, I_aZ/s. The permeance around path A is Ld_3/w_1. Thus, the flux per slot around path A is, in Figure 1

$$\phi_A = \frac{4\pi}{10}\frac{Z}{s}I_a\frac{Ld_3}{w_1} \tag{1}$$

This flux links all conductors in the slot so that the linkages are

$$\Psi = \frac{4\pi Z^2 L d_3 I_a}{10 s^2 w_1} \tag{2}$$

For path C, the permeance is d_2L/w_1, and since flux is produced by only half the current

$$\phi_C = \frac{4\pi}{10}\frac{ZIa}{2s}\frac{Ld_2}{w_1} \tag{3}$$

This links half the current in the slot, so that the flux linkages are

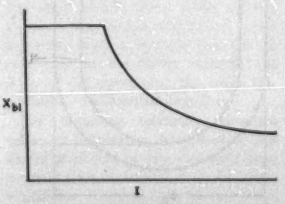

Figure 4. Variation of pole face winding leakage inductance with load current

$$\Psi_C = \frac{4\pi}{10}\frac{Z^2 L d_2 I_a}{4 s^2 w_1} \tag{4}$$

In paths B and D, the magnetomotive force is linear in distance, and the linkages will be parabolic. The average value will be one-third the maximum linkages, because of the parabolic shape. Thus

$$\Psi B,D = \frac{4\pi}{10}\frac{Z^2 L(d_1-d_3)I_a}{3 s^2 w_1} \tag{5}$$

The total of these linkages is

$$\Psi s = \frac{4\pi}{10}\frac{Z^2}{s^2}\frac{L}{w_1}I_a\left(d_2+\frac{d_3}{4}+\frac{d_1-d_3}{3}\right) \tag{6}$$

which is the total linkage per slot. In one parallel circuit, there are s/a_a slots in series, so that the total linkages per circuit may be calculated by

$$\Psi w = \frac{4\pi}{10}\frac{Z^2}{s a_a}\frac{L}{w_1}I_a\left(d_2+\frac{d_3}{4}+\frac{d_1-d_3}{3}\right) \tag{7}$$

The inductance of the circuit is simply $\Psi_w 10^{-8}/I_a$, and the inductance of the a_a parallel circuits is $\Psi_w 10^{-8}/I_a a_a$.

$$X_{al} = \frac{4\pi}{10^8}\frac{Z^2}{s a_a^2}\frac{L}{w_1}\left(\frac{12d_2+4d_1-d_3}{12}\right) \tag{8}$$

For inch units, this must be multiplied by 2.54. Also since d_3 will be quite small with respect to $12d_2$ and $4d_1$, it can be neglected. Thus

$$X_{al} = \frac{31.9}{10^8}\frac{Z^2 L}{s a_a^2 w_1}\left(d_2+\frac{d_1}{3}\right) \text{ henrys} \tag{9}$$

Nomenclature

a_a = number of parallel paths in armature
a_b = number of parallel paths in pole face winding
a_c = number of parallel paths in commutating pole winding
d_0 = depth of pole face slot opening, inches
d_1 = total depth of armature copper in slot, inches
d_2 = depth from top of armature tooth to top of copper, inches
d_3 = separation between top and bottom armature conductors
d_4 = depth of pole face bar, inches
h_p = height of pole punching, inches
l_b = length of pole face bars, inches
n_b = total number of pole face bars
p_a = main pole arc, inches
p_p = pole pitch, inches
s = total number of armature slots
t_c = width of commutating pole tip, inches
w_0 = width of pole face slot opening, inches
w_1 = armature slot width, inches
w_2 = average width of pole face slot, inches
w_c = width of commutating pole body, inches
w_s = width of stator end connection strips, inches
B = width of main pole body, inches
B_i = intrinsic induction of main pole steel, lines/inches^2
B_n = flux density of steel at knee of saturation curve
D = armature diameter, inches
E = height of commutating pole winding, inches
F = height of main pole at tip, inches
G = average main pole gap, inches
G_{max} = maximum main pole gap, inches
H = width of pole shoe, inches
I = rated machine current, amperes
I_a = armature current in one parallel path, amperes
I_b = pole face winding current in parallel path, amperes
I_c = commutating pole current in parallel path, amperes
I_{ss} = current in equivalent conductor, stator, end connections, amperes
K_{dm} = distribution factor of end windings
L = stacked length of rotor iron, inches
P = number of poles
T = number of turns on each commutating pole
X_{al} = armature slot leakage inductance, henrys
X_{bl} = pole face slot leakage inductance, henrys
X_{cl} = commutating pole leakage inductance, henrys
X_G = inductance due to flux under main pole, henrys
X_g = inductance due to flux under commutating pole, henrys
X_{end} = armature end turn inductance, henrys
X_{hend} = stator end connection inductance, henrys
Z = total number of armature conductors
ϕ = angle between armature end turns and core
μ = permeability of steel below saturation—gausses/oersted
Ψ = flux linkage

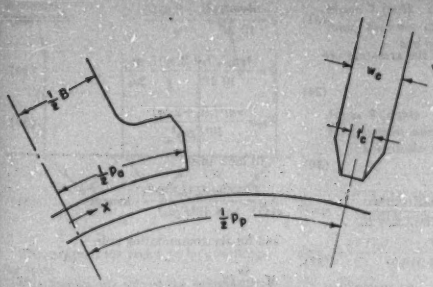

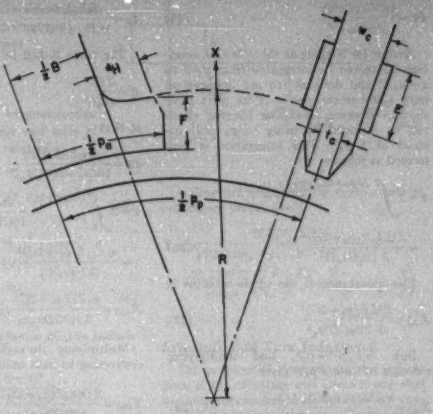

Figure 5 (above). Outline of poles and armature for determining inductance due to flux under main and commutating poles

Figure 6 (right). Outline of poles and armature for determining leakage inductance of commutating pole

Pole Face Bar Leakage

A similar process is used to determine the leakage inductance of the pole face bars. See Figure 2.

Across the gap, the flux linkages are

$$\Psi_A = \frac{4\pi}{10} I_b \frac{d_a L}{w_b}$$

In the slot proper, the same parabolic distribution will occur as in the armature slots, so that

$$\Psi_B = \frac{4\pi}{10} I_b \frac{d_s L}{3w_s} \tag{10}$$

The total linkages per slot are

$$\Psi = \frac{4\pi}{10} I_b L \left(\frac{d_s}{3w_s} + \frac{d_a}{w_b} \right) \tag{11}$$

There are n_b/a_b slots per series circuit, so that the linkages per circuit are

$$\Psi = \frac{4\pi}{10} \frac{I_b n_b L}{a_b} \left(\frac{d_s}{3w_s} + \frac{d_a}{w_b} \right) \tag{12}$$

Dividing this by circuit current I_b and by the number of parallel circuits to get total machine inductances gives

$$X_{bl} = \frac{4\pi}{10^8} \frac{n_b L}{a_b^2} \left(\frac{d_s}{3w_s} + \frac{d_a}{w_b} \right) \tag{13}$$

With inch units

$$X_{bl} = \frac{31.9}{10^9} \frac{n_b L}{a_b^2} \left(\frac{d_s}{3w_s} + \frac{d_a}{w_b} \right) \text{ henrys} \tag{14}$$

If the slot is not open, as is sometimes the case at the edge of a main pole, saturation cannot be neglected around the bar. Assume, however, that saturation occurs in the steel only where the gap would normally be. This being the case, the flux in the saturated steel may be divided into two components: the flux intrinsic with the steel, B_i; and the flux that would exist in spite of the steel, B_a. The B_a, or air flux, is obviously proportional to magnetomotive force. The intrinsic flux, B_i, is a constant once the steel has saturated. The sum of the two gives the well known gently rising characteristic of the flux-density field-intensity curve of steel above its knee.

Thus, the linkage around path A will be, after saturation

$$\Psi_A = \frac{4\pi}{10} I_b \frac{d_a L}{w_b} + B_i d_a L \tag{15}$$

Adding to it the unchanged linkages through the conductor, the total linkages per slot are

$$\Psi = \frac{4\pi}{10} L I_b \left(\frac{d_a}{w_b} + \frac{d_s}{3w_s} \right) + B_i d_a L \tag{16}$$

The total inductance is found as before and is

$$X_{bl} = \frac{31.9 n_b L}{10^9 a_b^2} \left(\frac{d_a}{w_b} + \frac{d_s}{3w_s} \right) + \frac{B_i d_a L n_b}{10^8 I a_b} \text{ henrys} \tag{17}$$

The value of B_i is taken from the flux-density field-intensity curve of the steel, idealized as shown in Figure 3.

Equation 17 is valid only in the saturated region, or when

$$B_i + \frac{4\pi I}{10 w_b a_b} > B_n \tag{18}$$

Below saturation, the expression is modified as follows:

$$X_{bl} = \frac{31.9 n_b L}{10^9 a_b^2} \left(\frac{\mu d_a}{w_b} + \frac{d_s}{3w_s} \right) \tag{19}$$

where $\mu = B_n/H_n$. This equation is valid when

$$B_i + \frac{4\pi I}{10 w_b a_b} < B_n \tag{20}$$

Note in equation 17 that the inductance is a function of machine current. This is to be expected of a nonlinear circuit such as this. With this, and the linear region, a curve of inductance versus current is obtained as in Figure 4.

Needless to say, care must be exercised in deciding which value of inductance to use.

Main Pole Flux Inductance

The next component of inductance to be determined will be that due to armature flux crossing the gap to the main pole. See Figure 5.

The magnetomotive force existing across the gap can be simply expressed in terms of a peripheral distance x from the center of the main pole and the various parameters of the machine, if it is assumed that the armature has a large number of conductors. With this assumption, the current may be considered to flow in a sheet along the armature surface. Considering the conductors in the region $0 < x < \pi D/P$ to be one side of a coil, and those from $\pi D/2P < x < \pi D/P$ to be the other half, the maximum number of turns at $x = \pi D/2P$, with a maximum magnetomotive force of

$$M = \frac{4\pi}{10} \frac{Z}{2P} I_a \tag{21}$$

This magnetomotive force is graded to zero at $x = 0$, so that in the region $0 < x < \pi D/2P$

$$M = \frac{4\pi}{10} \frac{Z x I_a}{\pi D}$$

$$= \frac{4 Z I_a x}{10 D} \tag{22}$$

From $x = 0$ to $x = p_a/2$, the permeance of a differential distance dx is $L dx/G$. Thus, the differential flux is

$$d\phi = \frac{4 Z L I_a x dx}{10 G D} \tag{23}$$

The same magnetomotive forces and fluxes appear under each pole, so that it will be correct to treat the linked conductors of one circuit as if they were all under one pole, provided they are still considered as if in series. Thus the total turns linked will be $Z/2a_a$, and grading this to zero at $x = 0$

$$N = \frac{Z}{2a_a} \frac{2Px}{\pi D}$$

$$= \frac{ZPx}{\pi a_a D} \tag{24}$$

The differential linkage is then

$$d\Psi=\frac{4Z^2LI_aPx^2dx}{10\pi Ga_aD^3} \tag{25}$$

Except for fringing at the pole tips, equation 25 should be integrated from $x=0$ to $x=p_a/2$ and doubled (to get linkages on both sides of the pole). Flux plots have shown, however, that the fringing effect can be included by using $^1/_4(p_a+2G)$ instead of $^1/_2p_a$. This integration is performed as follows

$$\Psi=2\int_0^{^1/_4(p_a+2G)}\frac{4Z^2LI_aPx^2dx}{10\pi Ga_aD^3}$$

$$=\frac{Z^2LI_aP(p_a+2G)^3}{3\ 10\pi Ga_aD^3} \tag{26}$$

The inductance of the whole machine is

$$X_{aG}=\frac{Z^2LP(p_a+2G)^3}{3\ 10^9\pi GD^2a_a^2} \tag{27}$$

But $(\pi D/p)^2=p_p^2$, and multiplying through by $(\pi D/Pp_p)^2$ gives

$$X_{aG}=\frac{\pi Z^2L(p_a+2G)^3}{3\ 10^9GPa_a^2p_p^2} \tag{28}$$

Or, in inch units

$$X_{aG}=\frac{2.66Z^2L(p_a+2G)^3}{10^9GPa_a^2p_p^2}\text{ henrys} \tag{29}$$

The next component of inductance to be determined is that due to flux from the pole face windings that crosses the main gap. Here again it will be assumed that the magnetomotive force is linearly distributed along the face of the main pole. This is not nearly so good an assumption for the pole face windings as for the armature, but at least the depth of the pole face slots tends to smooth out the steps in the magnetomotive force curve.

The same process is used for the pole face windings as for the armature.

$$M=\frac{4\pi n_bI_bx}{10P(p_a+2g)} \tag{30}$$

$$d\phi=\frac{4\pi n_bI_bLxdx}{10P(p_a+2G)G} \tag{31}$$

$$d\Psi=\frac{4\pi n_bLI_bxn_b2xdx}{10P(p_a+2G)G2a_b(p_a+2G)}$$

$$=\frac{4\pi n_b^2LI_bx^2dx}{10PG(p_a+2G)^2a_b} \tag{32}$$

$$\Psi=2\int_0^{^1/_4(p_a+2G)}\frac{4\pi n_b^2LI_bx^2dx}{10PG(p_a+2G)^2a_b}$$

$$=\frac{\pi n_b^2LI_b(p_a+2G)}{3\ 10PGa_b} \tag{33}$$

$$X_{bG}=\frac{\pi n_b^2L(p_a+2G)}{3\ 10^9PGa_b^2} \tag{34}$$

In inch units

$$X_{bG}=\frac{2.66n_b^2L(p_a+2G)}{10^9PGa_b^2}\text{ henrys} \tag{35}$$

The next component will be the mutual inductance between the armature and the pole face windings.

$$M=\frac{4\pi n_bI_bx}{10P(p_a+2G)} \tag{30}$$

$$d\phi=\frac{4\pi n_bI_bLxdx}{10P(p_a+2G)G} \tag{31}$$

The turns linked in the armature are

$$N=\frac{ZPx}{\pi a_aD} \tag{24}$$

so that

$$d\Psi=\frac{4n_bZI_bLx^2dx}{10(p_a+2G)Ga_aD} \tag{36}$$

$$\Psi=2\int_0^{^1/_4(p_a+2G)}\frac{4n_bZI_bLx^2dx}{10GDa_a(p_a+2G)}$$

$$=\frac{n_bZI_bL(p_a+2G)^2}{3\ 10GDa_a} \tag{37}$$

$$X_{abG}=\frac{n_bZL(p_a+2G)^2}{3\ 10^9GDa_aa_b} \tag{38}$$

Multiplying through by $\pi D/Pp_p$, and converting to inch units, gives

$$X_{abG}=\frac{2.66n_bZ(p_a+2G)^2}{10^9GPp_pa_aa_b}\text{ henrys} \tag{39}$$

The sum of the three main gap inductances can be written as follows

$$X_G=X_{aG}-2X_{abG}+X_{bG} \tag{40}$$

The negative sign appears because of the manner of connection between armature and pole face circuits. Inserting equations 29, 35, and 39 into 40, gives

$$X_G=\frac{2.66L(p_a+2G)}{10^9PG}\left(\frac{Z(p_a+2G)}{a_ap_p}-\frac{n_b}{a_b}\right)^2 \tag{41}$$

This equation takes care of all flux under the main pole. Next, one will be derived to account for flux under the commutating pole.

Commutating Pole Flux Inductance

First, that due to armature magnetomotive force. Because of the narrow width of the commutating pole, sufficient accuracy will be obtained by assuming a uniform magnetomotive force under it.

$$M=\frac{4\pi}{10}\frac{Z}{2P}I_a \tag{42}$$

$$\phi=\frac{4\pi}{10}\frac{ZI_a}{2P}\frac{(t_c+2.5g)L}{g} \tag{43}$$

The 2.5g term accounts for fringing, and is based on flux plots.

$$\Psi=\frac{4\pi}{10}\frac{ZI_aL(t_c+2.5g)Z}{2P_g\ \ 2a_a} \tag{44}$$

$$X_{ag}=\frac{\pi Z^2L(t_c+2.5g)}{10Pga_a^2} \tag{45}$$

Or, in inch units

$$X_{ag}=\frac{31.9Z^2L(t_c+2.5g)}{4\ 10^9Pga_a^2} \tag{46}$$

For the pole face windings

$$M=\frac{4\pi}{10}\frac{n_bI_b}{2P} \tag{47}$$

$$\phi=\frac{4\pi}{10}\frac{n_bI_b}{2P}\frac{(t_c+2.5g)L}{g} \tag{48}$$

$$\Psi=\frac{4\pi n_bI_b(t_c+2.5g)L}{10\ 2P\ \ g}\frac{n_b}{2a_b} \tag{49}$$

$$X_{bg}=\frac{\pi n_b^2L(t_c+2.5g)}{10^9Pga_b^2} \tag{50}$$

In inch units

$$X_{bg}=\frac{31.9n_b^2L(t_c+2.5g)}{4\ 10^9Pga_b^2}\text{ henrys} \tag{51}$$

and for the commutating pole

$$M=\frac{4\pi}{10}TI_c \tag{52}$$

$$\phi=\frac{4\pi}{10}TI_c\frac{(t_c+2.5g)L}{g} \tag{53}$$

$$\Psi=\frac{4\pi TI_c(t_c+2.5g)LPT}{10g\ \ a_c} \tag{54}$$

$$X_{cg}=\frac{4\pi T^2PL(t_c+2.5g)}{10^9ga_c^2} \tag{55}$$

In inch units

$$X_{cg}=\frac{31.9T^2PL(t_c+2.5g)}{10^9ga_c^2}\text{ henrys} \tag{56}$$

Just as the self- and mutual-inductances combined into a perfect square for the main pole, they combine into a perfect square for the commutating pole. Therefore, without bothering to derive all the mutual inductances (which can be done easily), the expression for inductance due to commutating pole flux can be written as

$$X_g=\frac{31.9(t_c+2.5g)LP}{10^9g}\times\left(\frac{T}{a_c}+\frac{n_b}{2a_bP}-\frac{Z}{2a_aP}\right)^2 \tag{57}$$

Commutating Pole Leakage Inductance

A very real amount of flux leaks from the commutating pole over to the main pole, and this will represent inductance.

The leakage flux can be divided into two components: that which goes to the tip of the main pole; and that which leaks to the body. Consider first the pole tip components. See Figure 6.

Flux plots show that the flux leaking to the main pole tip comes from near the tip of the commutating pole. This being the case, it will be assumed that the flux links all the turns on the commutating pole.

$$M=\frac{4\pi}{10}TI_c \tag{52}$$

The permeance on one side of the pole tip is given approximately by the following expression

$$P_{cit}=\frac{LF}{\frac{1}{2}\left(p_p-\frac{(p_a+B+2H)}{2}-t_c\right)}$$

$$=\frac{4LF}{2p_p-p_a-B-2H-2t_c} \tag{58}$$

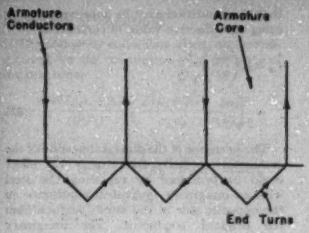

This assumes the region to be a rectangular solid.

The flux on one side of the commutating pole is then

$$\phi_{clt}=\frac{16\pi TI_eLF}{10(2p_p-p_a-B-2H-2t_c)} \tag{59}$$

The total linkages per pole are

$$\Psi_{clt}=2\frac{16\pi T^2I_eLF}{10(2p_p-p_a-B-2H-2t_c)} \tag{60}$$

Since there are P/a_c poles in one series circuit, the total inductance may be written as

$$X_{clt}=\frac{32\pi T^2LFP}{10^9(2p_p-p_a-B-2H-2t_c)a_c^2} \tag{61}$$

Changing to inch units

$$X_{clt}=\frac{255T^2LFP}{10^8a_c^2(2p_p-p_a-B-2H-2t_c)}\text{ henrys} \tag{62}$$

The flux that leaks to the main pole body emanates from along the commutating pole winding. Flux plots show that this flux follows a somewhat curved path, and it will be assumed here that the path is the arc of a circle whose center is the intersection of the extended sides of the main and commutating poles. Also, it will be assumed that the bottom of the commutating pole winding is on the same arc as the top of the main pole tip.

The magnetomotive force along the commutating pole is

$$M=\frac{4\pi TI_e}{10}\frac{(E-x)}{E} \tag{63}$$

The permeance of the path on one side of the pole is given as

$$dP_{clm}=\frac{Ldx}{(R+x)\frac{\pi}{P}} \tag{64}$$

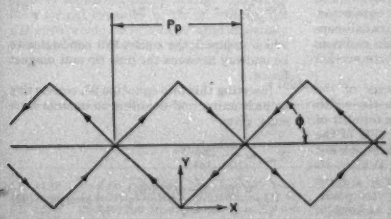

Figure 8 (left). Development of rotor, with core replaced by additional windings

Figure 7 (left). Development of rotor, showing concentration of end turns

Figure 9 (right). Magnetomotive force pattern across end turns at a particular value of y

$$d\phi_{clm}=\frac{4PTI_eL(E-x)dx}{10E(R+x)} \tag{65}$$

$$d\Psi_{clm}=\frac{4PTI_eL(E-x)T(E-x)dx}{10E(R+x)E}$$

$$=\frac{4PT^2LI_e(E-x)^2dx}{10E^2(R+x)} \tag{66}$$

Integrating, with a factor of 2 to include both sides of the pole

$$\Psi_{clm}=\frac{8PT^2LI_e}{10E^2}\int_0^E\frac{(E-x)^2}{R+x}dx$$

$$=\frac{8PT^2LI_e}{10}\left(\left(\frac{E+R}{E}\right)^2\ln\frac{E+R}{R}-\frac{3}{2}-\frac{R}{E}\right) \tag{67}$$

This is still on a per-pole basis. Multiplying by P/a_c, and by the other terms to get total inductances, gives

$$X_{clm}=\frac{8T^2P^2L}{10^9a_c^2}\left(\left(\frac{E+R}{E}\right)^2\ln\frac{E+R}{R}-\frac{3}{2}-\frac{R}{E}\right) \tag{68}$$

Converting to inch units

$$X_{clm}=\frac{21.3T^2P^2L}{10^9a_c^2}\left(\left(\frac{E+R}{E}\right)^2\ln\frac{E+R}{R}-\frac{3}{2}-\frac{E}{R}\right) \tag{69}$$

The radius R can be evaluated in terms of the already-defined quantities. From Figure 6

$$R=\frac{D}{2}-\frac{1}{2}\left(\frac{w_c}{\sin\frac{\pi}{P}}+\frac{B}{\tan\frac{\pi}{P}}\right)+\delta+G_{max} \tag{70}$$

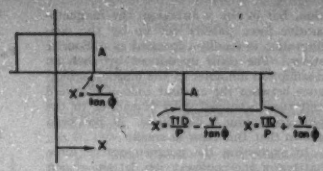

Adding the main and tip components of inductance gives

$$X_{cl}=\frac{255T^2LFP}{10^8a_c^2(2p_p-p_a-B-2H-2t_c)}+\frac{21.3T^2P^2L}{10^9a_c^2}\left(\left(\frac{E+R}{E}\right)^2\ln\frac{E+R}{R}-\frac{3}{2}-\frac{R}{E}\right)\text{ henrys} \tag{71}$$

Armature End Turn Inductance

The problem of determining the inductance of the armature end turns is one that has been approached in almost as many ways as there have been analysts. Each method attempts in its own way to simplify the rather complex physical configuration so that the mathematics involved will not be prohibitive.

The method presented here is used because there exists experimental data to substantiate it, see reference 5. It consists basically of superimposing all the conductors under one pole, treating them as one conductor. The inductance of this one conductor can be found in a fairly straightforward manner. The inductance of the distributed winding is then determined by applying a distribution factor.

The developed armature, with superimposed conductors, is shown in Figure 7.

In any one V-shaped coil, there will be $Z/2P$ individual conductors, each carrying current I_a. Because of commutation, the coils may be considered stationary, while the armature core rotates. The speed of the core, with the resultant eddy currents set up in the steel, means that little flux enters it. This condition may be approximated by replacing the rotor steel with more V-shaped coils, as shown in Figure 8.

If it is assumed that the diamond configuration extends not only in the x direc-

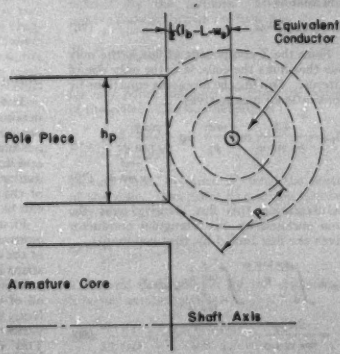

Figure 10 (right). Section through shaft of a machine showing location of equivalent conductor replacing stator end connections

tion, but in the y direction, the magnetomotive force pattern set up by the configuration is readily expressed as a Fourier series. The error introduced by such an assumption amounts to the mutual inductance between the existent coils of Figure 8 and those assumed coils extending in the plus and minus y directions. It has been shown that this error is small.

In expressing the magnetomotive force pattern of the configuration, let the region outside the diamonds in Figure 8 be defined as being at zero electromotive force. For a particular value of y, then, the magnetomotive force is a function of x, see Figure 9.

Fourier analysis of this curve gives for the m-th harmonic of magnetomotive force

$$A_m = \frac{4A}{\pi m} \cos \frac{m\pi x}{p_p} \sin \frac{m\pi y}{p_p \tan \phi} \tag{72}$$

where $m = 1, 3, 5 \ldots$.

This assumes full pitch windings.

The step value of magnetomotive force, A, is determined by the total current in the equivalent conductors of Figure 8. Since $4\pi/10.NI$ represents the magnetomotive force along a closed loop around the conductor, and since Figure 9 represents the magnetomotive force encountered in passing from one side of the conductor to the other, the magnetomotive force along its path must be one half of the total, or $2\pi/10NI$. In this case, I is I_a and N is $Z/2P$.

Therefore

$$A = \frac{\pi Z I_a}{10P} \tag{73}$$

The flux density at any point is determined by applying Maxwell's equations in the current-less region

$$\nabla \times B = 0 \tag{74}$$

Also

$$\nabla \cdot B = 0 \tag{75}$$

which is fundamental to a magnetic field.

Boundary conditions are that at $Z = 0$

$$B_x = -\frac{\partial A_m}{\partial x} \tag{76}$$

$$B_y = -\frac{\partial A_m}{\partial y} \tag{77}$$

and that as

$$B \to 0 \text{ as } Z \to \infty \tag{78}$$

Since the Z component of flux is the only one that links the coils, it is the only one of interest. Solving the foregoing equations by conventional means gives

$$B_{zm} = \frac{4A}{p_p \sin \phi} \cos \frac{m\pi x}{p_p} \sin \frac{m\pi y}{p_p \tan \phi} \times \epsilon^{-\frac{\pi m z}{p_p \sin \phi}} \tag{79}$$

Integrating this flux density over the area enclosed by one triangular conductor gives the flux linked by that conductor.

$$\phi_m = \int_0^{\frac{p_p \tan \phi}{2}} \int_{-\frac{y}{\tan \phi}}^{\frac{y}{\tan \phi}} B_{zm} dx dy$$

$$= \frac{2Ap_p}{m\pi \cos \phi} \tag{80}$$

This links with $Z/2a_a$ conductors, so that

$$\Psi_m = \frac{AZp_p}{m\pi a_a \cos \phi}$$

$$= \frac{Z^2 p_p I_a}{10mPa_a \cos \phi} \tag{81}$$

The uncorrected inductance, then, is

$$X = \sum_{1,3,5\ldots}^{\infty} m \frac{Z^2 p_p}{10^9 m P a_a^2 \cos \phi} \tag{82}$$

for one end of the machine.

The effect of superimposing the end turns can be accounted for by multiplying through by a distribution factor, K_{dm}. This is applicable to each sinusoidal component of inductance, and must be used squared, because of the effect of distribution on not only the production of magnetomotive force but because of the effect on flux linked. The distribution factor for the m-th harmonic is

$$K_{dm} = \frac{P \sin \frac{m\pi}{P}}{s \sin \frac{m\pi}{s}} \tag{83}$$

Thus, the total corrected inductance of the machine due to end turns is

$$X_{a_{end}} = 2 \sum_{1,3,5\ldots}^{\infty} m \frac{Z^2 p_p P^2 \sin^2 \frac{m\pi}{P}}{10^9 m P a_a^2 \cos \phi s^2 \sin^2 \frac{m\pi}{s}} \tag{84}$$

This equation may be simplified by observing that only the first three, say, terms of the series are necessary, and for these, $m\pi/s$ is a very small angle. Therefore, $\sin m\pi/s$ may be replaced by $m\pi/s$ with little loss of accuracy. Also, $p_p = \pi D/P$. Thus

$$X_{a_{end}} = \frac{2Z^2 D}{10^9 \pi a_a^2 \cos \phi} \sum_{1,3,5\ldots} m \frac{\sin^2 \frac{m\pi}{P}}{m^3} \tag{85}$$

Converting to inch units, assuming $\phi = 30°$

$$X_{a_{end}} = \frac{1.87 Z^2 D}{10^9 a_a^2} \sum_{1,3,5\ldots} m \frac{\sin^2 \frac{m\pi}{P}}{m^3} \text{ henrys} \tag{86}$$

Stator End Connection Inductance

The inductance of the stator end connections is likewise elusive in analysis. The connection strips between pole face bars can be lumped into one equivalent conductor, and if the inductance of this equivalent conductor can be determined, a fair estimate of the inductance of the actual connection can be made.

First, assume that the diameter of the equivalent conductor is equal to the width of the connection strips, w_s. The number of strips between two poles on one side of the machine will be $n_b/2P$. Yet they are not all of the same length, meaning that in effect, the equivalent conductor's current varies peripherally from point to point. This variation is near enough sinusoidal that the condition may be approximated by using the effective value of current, or

$$I_{se} = I_b \left(\frac{n_b}{2P}\right) \frac{1}{\sqrt{2}}$$

$$= \frac{I_b n_b}{2\sqrt{2}P} \tag{87}$$

The presence of the steel on one side of the conductor confuses the issue. Its effect could be produced by replacing the steel with an imaginary equivalent conductor on the opposite side of the steel's surface from the original conductor. The imaginary conductor must have equivalent current, I_{se}, in the same direction as in the original conductor in order to properly imitate the effect of the steel. The fact that the currents are in the same direction, with no apparent return path, plus the fact that the currents in the equivalent conductors reverse direction every pole means that an analysis using images is of dubious value.

Another method that seems to give reasonable results is to simply determine the self inductance of the equivalent conductor itself, assuming that the permeance is that of free space close about the conductor, and is zero at a distance greater than from the conductor to a pole tip. See Figure 10.

The conductor is treated as being infinite in length, so that its per-unit length inductance is

$$X_{se} = \frac{2}{10^9}\left(ln \frac{2R}{w_s} + \frac{1}{4}\right) \text{ henrys per centimeter} \tag{88}$$

Using for length $\pi D/a_b$

$$X_{se} = \frac{2\pi D}{10^9 a_b}\left(ln \frac{2R}{w_s} + \frac{1}{4}\right) \text{ henrys} \tag{89}$$

This is still the inductance of the equivalent conductor, which has $I_b n_b/2\sqrt{2}P$ amperes in it. If this conductor is broken up into parallel paths, each of which having I_b amperes, there will be $n_b/2\sqrt{2}P$ such paths, and each will have the same number of linkages as the equivalent conductor. Any one path will have $n_b/2\sqrt{2}P$ times the inductance of the equivalent conductor, and putting all these paths in series, as is the actual case, will give an inductance $n_b^2/8P^2$ times that of the equivalent conductor. Thus, the inductance per machine parallel path for one end can be found, and total machine inductance is that divided by a_b.

$$X_{s_{end}} = \frac{2\pi D n_b^2}{10^9 8 a_b^2 P^2}\left(ln \frac{2R}{w_s} + \frac{1}{4}\right) \tag{90}$$

The constant R is given by

$$R = \frac{1}{2}\sqrt{(l_b - L - w_s)^2 + h_p^2} \tag{91}$$

which assumes the equivalent conductor to be midway between the pole tip and magnet frame.

Inserting this into equation 90, converting to inch units, and doubling to include both ends, gives

$$X_{s_{end}} = \frac{4D n_b^2}{10^9 a_b^2 p^2} \times \left(ln \frac{\sqrt{(l_b - L - w_s)^2 + h_p^2}}{w_s} + \frac{1}{4}\right) \text{ henrys} \tag{92}$$

Summary of Equations

The following equations, then, are recommended for the calculation of inductance of d-c machines

$$X_G=\frac{2.66L(p_a+2G)}{10^8PG}\left(\frac{Z(p_a+2G)}{a_ap_p}-\frac{n_b}{a_b}\right)^2$$

$$X_g=\frac{31.9(t_c+2.5g)LP}{10^8g}\left(\frac{T}{a_c}+\frac{n_b}{2a_bP}-\frac{Z}{2a_aP}\right)^2$$

$$X_{al}=\frac{31.9Z^2L}{10^8a_a^2w_1}\left(d_2+\frac{d_1}{3}\right)$$

$$X_{bl}=\frac{31.9n_bL}{10^8a_b^2}\left(\frac{d_4}{3w_2}+\frac{d_3}{w_3}\right)\text{ (for open slot)}$$

$$X_{bl}=\frac{31.9n_bL}{10^8a_b^2}\left(\frac{d_4}{3w_2}+\frac{d_3}{w_3}\right)+\frac{B_td_6Ln_b}{10^8Ia_b}$$

(for closed slot, saturated)

$$X_{bl}=\frac{31.9n_bL}{10^8a_b^2}\left(\frac{d_4}{3w_2}+\frac{d_3}{w_3}\right)$$

(for closed slot, unsaturated)

$$X_{cl}=\frac{255T^2LFP}{10^8a_c^2(2p_p-p_a-B-2H-2t_c)}$$

$$+\frac{21.3T^2P^2L}{10^8a_c^2}\left[\left(\frac{E+R}{E}\right)^2 ln\frac{E+R}{R}-\frac{3}{2}-\frac{R}{E}\right]$$

$$X_{aend}=\frac{1.87Z^2D}{10^8a_a^2}\sum_{1,3,5}m\frac{\sin^2\frac{m\pi}{P}}{m^2}$$

$$X_{bend}=\frac{4Dn_b^2}{10^8a_b^2P^2}\left(ln\frac{\sqrt{(l_b-L-w_t)^2+h_p^2}}{w_t}+\frac{1}{4}\right)$$

References

1. Maximum Short-Circuit Current of D-C Motors and Generators, AIEE Committee Report. *AIEE Transactions*, volume 69, part I, 1950, pages 146–49.

2. Transient Characteristics of D-C Motors and Generators, A. T. McClinton, E. L. Brancato, Robert Panoff. *AIEE Transactions*, volume 68, part II, 1949, pages 1101–06.

3. Solid Short Circuit of D-C Motors and Generators, T. M. Linville, H. C. Ward, Jr. *AIEE Transactions*, volume 68, part I, 1949, pages 119–24.

4. Current and Torque of D-C Machines on Short Circuit, T. M. Linville. *AIEE Transactions*, volume 65, 1946, pages 956–65.

5. End-Winding Inductance of a Synchronous Machine, B. H. Caldwell, Jr. *Electrical Engineering (AIEE Transactions)*, volume 56, April 1937, pages 455–61.

6. The Calculation of Armature Reactance of Synchronous Machines, P. L. Alger. *AIEE Transactions*, volume 47, April 1928, pages 493–513.

Discussion

M. A. Baker (General Electric Company, Fort Wayne, Ind.): The authors are to be congratulated for an excellent paper on the calculation of d-c machine armature circuit inductance. The formulas derived in the paper are relatively simple and convenient to use. Inductance tests and calculations were made in Fort Wayne on several machines smaller than the examples cited in the paper, and I should like to submit these data to further test and verify the formulas presented.

These tests were made by the a-c impedance method with the fields unexcited. Current values were carried beyond the rated current of the motors, but the inductance was based on the initial slope of the volt-ampere curve. The brushes were not short circuited with jumpers on the machines tested as the authors recommend; this might have reduced the test values very slightly. Both 25- and 60-cycle currents were used, but very little difference was noted in the test values of inductance. The 25-cycle values were slightly higher in all cases. Test values obtained from the 60-cycle test are given in Table I of this discussion. There is no apparent explanation for the difference in accuracy between the first and the last two sets of data. All tests were carefully supervised and the calculations were checked. In Table I the values of C_x for the last two motors are based on the lower horsepower base speed ratings. These motors were conservatively rated for very difficult service and are capable of somewhat higher rating. Based on the thermal capacity of these motors, the *CD-1546* would have a C_x of approximately 0.40, and the *CD-1651* a C_x of 0.35.

R. B. Bross (Massachusetts Institute of Technology, Cambridge, Mass.): It appears that considerable interest has been focused on the determination of d-c machine armature circuit inductance for the purpose of providing the application engineer with information that will assist him in choosing appropriate control and protection equipment to be used with large power motors and generators. Although this is important, the creation of an economical and dependable machine to provide a required electromechanical energy conversion probably is of primary importance. Now in the case of certain small machines, such as those used in servo circuits, the inductance characteristics tend to be of first order importance while the characteristics of electromechanical energy conversion may be of secondary importance. Therefore, it is the hope of this discussor that if ever any standardized procedure is adopted for determining d-c machine armature circuit inductance, some consideration will be given to the needs of the motor designer and instrumentation engineer who must work with servo circuits where inductances and resulting values of characteristic time are very important.

With reference to the formula derived by assuming conditions shown in Figure 1 of the paper, we can note that an open, rectangular slot has been used which is characteristic of large machine design practice. In the case of a small motor, it is quite likely that a semiclosed slot would be used. This merely means that a different permeance would have to be used in this case. With reference to the formula for calculating armature end turn inductance, we can note that the assumption has been made that little flux enters the armature core because of eddy currents in the core due to rotation of the armature. In any case where the armature is not rotating, the desirability of using the formula as derived probably ought to be reconsidered. In general, intelligent use of the formulas presented in the paper probably requires a good understanding of the manner in which the formulas were derived.

John Cybulski (Naval Research Laboratory, Washington, D. C.): The authors have simplified the problem considerably through the assumption of infinite permeability in the iron path, uniform air gaps, linearity and application of the theory of superposition. They have been successful in that purpose, however a question exists as to whether the grading procedure employed in the derivations introduces complexity where there is none. There is a relatively simple approach to obtain the contribution of the conductors beneath the main pole to the armature winding inductance. From Figure 1 of the discussion, representing Figure 22 on page 386 in A. S. Langsdorf's book,[1] the following may be written:

The total number of armature conductors linked by this elementary tube of flux is $Z\,2X/\pi D$. The symbols are the same as defined by the authors. The magnetomotive force acting on the tube p is

$$\frac{4\pi}{10}\frac{Z}{\pi D}2XI_a$$

for any point, distance X, from the center of the pole. The flux density is

$$B=\frac{4}{10}\frac{Z}{D}\frac{2XI_a}{2G}$$

for any point, distance X, from the center of the pole. The total flux in the elementary tube is

$$d\phi=\frac{4}{10}\frac{Z}{GD}I_aXL\,dX$$

The total flux linkages by the elementary tube per parallel path is

$$d\psi=\frac{4}{10}\frac{ZL}{GD}I_a\,dX\frac{Z}{\pi D}\frac{2X}{a_a}$$

Table I

Rating	Inductance Calc.	Inductance 60-Cycle Test	Inductance Ratio Calc/Test	C_x or l'_a (Test)
CD 1136...Four-60 Hp-850/1,750 rpm-230 volt	0.00263	0.0026	1.0	0.435
CD 1546...Four-100/125 Hp-575/1,150 rpm-230 volt	0.00196	0.00156	1.26	0.298
CD 1651...Six-150/200 Hp-500/1,000 rpm-230 volt	0.00093	0.00072	1.29	0.263

An integration is performed to obtain total flux linkages per effective pole arc.

$$\psi = \int_{-1/2(P_a+2G)}^{1/2(P_a+2G)} \frac{Z^2 L\, I_a X^2\, dX}{10\pi G\, a_a\, D^2\pi}$$

$$= \frac{Z^2}{3}\, \frac{L I_a (P_a+2G)^3}{10\pi G\, a_a D^2}$$

The total linkages calculated per parallel path beneath all the poles becomes

$$\frac{Z^2 L\, I_a\, P\, (P_a+2G)^3}{3\, 10 G a_a\, D^2\pi}$$

which corresponds to equation 26 in the paper.

A calculation was made on a 90-horsepower, 1,750-rpm, 250-volt, 298-ampere, 4-pole semienclosed motor without pole face winding using the applicable portions of the authors' equations developed in the paper. The results are given in Table II of this discussion.

The armature and interpole inductances were measured separately at 60-cycle alternating current, giving 1,000 microhenrys and 400 microhenrys respectively, which correspond to items 5 and 8 in Table II of this discussion. A d-c method which employs flux probe coils to obtain the flux distribution in the air gap was also used, giving values for the separate armature and interpole inductances of 900 microhenrys and 2,000 microhenrys, respectively. In the d-c method of calculation the armature slot and end-turn inductance, items 1 and 4 in the table, were not taken into account. The interpole leakage contribution, item 7 in the table, also was neglected.

The explanation for the discrepancy between the measured values and those obtained using the formulas are:

In the armature case the air gap beneath the main pole is not uniform as is assumed by the authors, because of the chamfer at the pole tips. The resulting flux distribution there indicates the necessity to take this factor into account.

The contribution beneath the interpole would be much more accurate if the pole width were not assumed negligible. In that case a calculation can be made for a linear variation of mmf under the pole and, further, there will be a nonuniform air-gap, all of which results in considerably less calculated inductance. A calculation based on these corrections resulted in 810 microhenrys as compared to item 3 in Table II.

In the interpole case the reason essentially is the nonuniform air gap which is an appreciable effect where the interpole shoe width is not considered negligible. The interpoles in the subject machine are not laminated and that probably accounts for the low a-c value obtained.

Figure 1. Calculation of armature flux

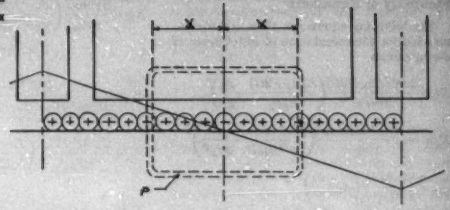

The d-c buildup method of measurement of inductance has never attained an accuracy better than 90 per cent consistently, and generally the errors are as much as 40 per cent because of the difficulty in obtaining an accurate slope. It has been stated by the authors that with the measurement of terminal resistance several points on the buildup curve can be checked. It is presumed that this check will indicate the variation of inductance with current. It would be of interest to learn the result of this check.

It is agreed that a transient value of armature circuit inductance is desirable. Whether the calculated values of armature circuit inductance as determined by formulation, assuming no saturation effects due to initial conditions, will yield the maximum rate of rise of short-circuit current is open to question. The initial value of armature circuit inductance may be adequate for a time shortly after a short circuit in the determination of the maximum rate of rise of current provided the saturation effects are taken into account. However, during any transient change of armature circuit and shunt field currents the coefficients of inductance and mutual inductance as used in any differential equation may not be constant for the following reasons:

1. Saturation effects in the magnetic iron circuit as the inductance is determined by $N\, d\phi/dI$.
2. Flux lag with respect to the magnetomotive force existing in the magnetic circuit because of eddy-current effects.
3. Flux distortion effects in the air-gap which give indication of being the most important.

Summary

1. Variation of the air gap and the width of the interpole should be taken into account in a calculation of inductance.
2. Saturation effects caused by initial armature and shunt field currents should be calculated.
3. The transient behavior of inductance should be further investigated.

Reference

1. Principles of Direct-Current Machines, A. S. Langsdorf. McGraw-Hill Book Company, New York, N. Y., 1940, page 386.

A. M. Harrison (Westinghouse Electric Corporation, East Pittsburgh, Pa.): I would like to congratulate the authors for their interesting paper on this subject.

The methods of calculation are substantially the same as those which we have used, except in the case of the armature end winding flux and stator end connections. As pointed out by the authors, this particular portion of the inductance has been approached in many ways by various people, and the proof of the method is that the results are in close agreement with test results.

The detailed calculation of the inductance of a d-c machine is a tedious process at best, and we have used a method of prorating from representative machines that have been tested which might be of interest. Assuming that a good test of a similar machine is available, it has been found that the inductance is approximately inversely proportional to the square of the speed and directly proportional to the square of the voltage, inversely proportional to the armature length, inversely proportional to the diameter cube and inversely proportional to the pole pitch.

The tests and calculations given in Table

Table II

	Component	Inductance in Microhenrys
1	Armature slot inductance	35
2.	Armature inductance (conductors beneath the main poles)	1,090
3.	Armature inductance (conductors beneath the interpoles)	1,530
4.	Armature end-turn inductance	105
5.	Armature Total	2,760
6.	Interpole inductance (air-gap flux)	4,140
7.	Interpole leakage inductance	
	(a) Main pole tip	90
	(b) Main pole body	25
8.	Interpole Total	4,255

Table III

	1,500 Kw* 250 Volts 514 Rpm	1,500 Kw* 250 Volts 514 Rpm	1,000 Kw 1,500 Volts 514 Rpm	375 Kw 375 Volts 1,200 Rpm
Detailed calculation	3.66×10^{-4}	3.84×10^{-4}	1.30×10^{-4}	8.05×10^{-4}
Detailed calculation (Snively and Robinson	4.76×10^{-4}	4.5×10^{-4}	1.77×10^{-4}	8.99×10^{-4}
Approx. Formula (prorating from similar machine)	4.4×10^{-4}	3.65×10^{-4}	1.58×10^{-4}	
Test (short circuit)	3.8×10^{-4}		1.5×10^{-4}	6.72×10^{-4}
Test, 25 cycle (unsaturated)	3.7×10^{-4}	3.9×10^{-4}		
Test, 25 cycle (saturated)	3.25×10^{-4}			

* These two machines are of exactly the same rating but of somewhat different proportions. The machine in column 2 is a machine which was designed approximately 20 years ago and the machine in the first column is a machine of a relatively modern type of design.

III of this discussion might serve as additional data on this problem.

The machine in the last column is a machine which is noncompensated whereas the other three machines are compensated machines.

The line showing the calculated results in accordance with the author's paper has been added since the discussion was presented. In comparing the various components, we find relatively close agreement in all components except the armature end winding inductance. It is our opinion that the values obtained using the method described by the authors for the armature end winding inductance is too high. As a matter of fact, the discrepancy between the two detail calculation figures shown for the total inductance is very largely accounted for by the variation in the values obtained for the armature end winding inductance.

H. D. Snively and Paul B. Robinson: The authors wish to express their thanks for the very interesting and informative discussions which have been submitted. In particular, the inductance data and the various suggestions for improvements contained in these discussions are indications that the primary objects of the paper as expressed in the introduction will ultimately be fulfilled.

One of our associates has kindly pointed out that a more accurate expression for R in equation 70 is desirable, particularly for machines with small diameters and low numbers of poles, and has suggested the more correct value

$$R=\frac{D}{2}+F+G_{max}-\left[\frac{B^2}{4}+\left(\frac{B}{2\tan\frac{\pi}{P}}+\frac{w_c}{2\sin\frac{\pi}{P}}\right)^2\right]^{1/2}$$

The authors agree that the slight additional calculation necessitated by this use of this expression is justified by its improved accuracy and its more universal applicability to all sizes of machines.

R. B. Bross's point is very well taken that the general viewpoint of our paper is inclined to be that of a large machine designer. However, we hope that the presentation is in sufficient detail so that modifications such as semi-closed armature slots, multiple-turn pole face bars in single slots, and so forth can be taken care of easily.

Measurement of Insulation Resistance on Energized Systems

E. L. BRANCATO
MEMBER AIEE

A. T. McCLINTON
MEMBER AIEE

INSULATION resistance measurement of electric equipment gives an indication of the condition of the electrical insulation through a measurement of the current leakage through and/or over the surface of the insulation. These leakage currents are influenced by the dielectric state of the insulation and by the presence of moisture and other contaminants, therefore a measure of the insulation resistance of electric equipment or of a system assists greatly in determining the safety and reliability of the equipment for operation.

The insulation of electric systems of vessels tends to deteriorate with time, owing to the abundance of moisture and salt that saturates the surrounding atmosphere. This tendency, if not checked, will result in establishing one or more low-resistance paths between system and ground. This condition may endanger the operation of the electric plant, personnel, and possibly the safety of ship when electrically propelled. Thus it is important that the system insulation resistance be continuously observed so that deterioration of insulation resistance can be checked to prevent the establishment of "grounds."

This resistance can be measured easily and directly by a "megger" or other suitable ohmmeters. Their use, however, entails the de-energization of the system during the period of measurements. It is evident that this procedure is not feasible generally and is impossible where continuity of service is necessary.

At present the voltmeter method is employed on energized d-c systems. This consists in measuring with a voltmeter of known internal resistance the system voltages from each line to ground, and across both lines. The three voltage readings and meter resistance are applied to a simple formula which permits calculation of system insulation resistance. This method suffers from a number of shortcomings, namely, involved procedure of multiple measurements and calculations, inaccuracies due to variation in system voltage while obtaining voltmeter readings, and insensitivity of the voltmeter when the insulation resistance is high. It is apparent that this procedure is laborious and indirect, and does not provide the accuracy that can be obtained from measurements on de-energized systems.

Basic Concepts

A consideration of the problems involved with presently employed insulation resistance measuring devices on shipboard, an analysis of operational problems, and a study of insulation characteristics suggest that the requirements for a ground detector be that it shall contain its own source of voltage for stressing the insulation, and that it provides a direct reading with simplicity of operation.

The first requirement is satisfied by an electrically-isolated rectifier-type power supply. The magnitude of its voltage should be approximately equal to the potential of the system to be measured. The importance of proper selection of this voltage has been demonstrated by Evershed[1] and is further illustrated in Figure 1. The influence of voltage, varying from 250 to 800 volts (ohmmeter open circuit voltage), upon observed insulation resistance of electric systems ranging from 0.2 to 20 megohms is depicted. It becomes evident that the application of a voltage stress lower than the system normally experiences would result in an unrealistic measure of insulation resistance whereas the use of a voltage stress higher than system voltage may result in insulation breakdown.[2]

The second requirement can be met through the use of an ohmmeter type of instrument. Such an instrument could utilize a ratio-type meter movement, as employed in a megger, or could consist of a constant potential supply and a microammeter or a milliammeter with a scale calibrated for resistance. In order to employ such a device in a 2-wire ungrounded d-c system it is necessary to be able to select some point at which the potential of the ohm meter circuit can be impressed on the electric system. This point must be selected so that no additional potential is injected into the measuring circuit.

The basic circuit for meeting the foregoing requirement is illustrated in Figure 2. In this circuit R_A and R_B represent the distributed resistance of each line to ground for the associated circuit. The potentiometer connected between points l and m provides a means whereby a point of zero potential, namely that between G and S, can be obtained. This is obtained when the slider of the potentiometer is adjusted to give the relationship

$$\frac{R_x}{R-R_x}=\frac{R_A}{R_B} \tag{1}$$

Thus a point of zero potential has been obtained for insertion of the measuring instrument. However, the presence of the potentiometer will cause an error as given by the equation

$$\text{Error}=\frac{R_x(R-R_x)}{R}\ \text{(ohms)} \tag{2}$$

where R is the total resistance of the potentiometer. It should be noted that this error is dependent only on the poten-

Paper 50-194, recommended by the AIEE Rotating Machinery Committee and approved by the AIEE Technical Program Committee for presentation at the AIEE Middle Eastern District Meeting, Baltimore, Md., October 3-5, 1950. Manuscript submitted July 6, 1950; made available for printing August 31, 1950.

E. L. Brancato and A. T. McClinton are both with the Naval Research Laboratory, Washington, D. C.

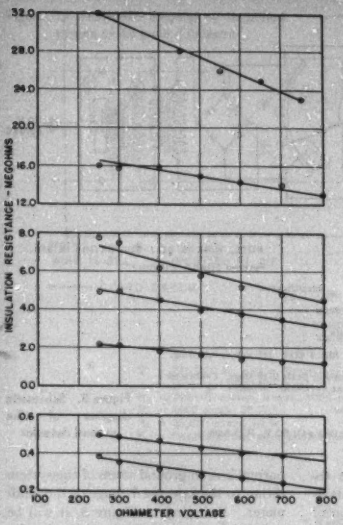

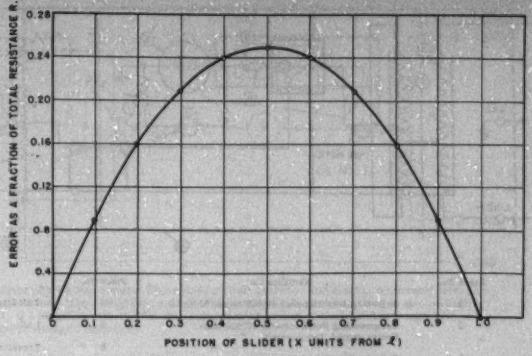

Figure 1 (left). Effect of ohmmeter voltage on insulation

Figure 3 (above). Error produced by balancing potentiometer in basic circuit

tiometer and independent of the insulation resistance. If this error is expressed in terms of the fractional distance, x, of the slider from l it becomes

$$\text{Error} = x(1-x)R \tag{3}$$

The relationship is plotted in Figure 3. (This applies only to a linear potentiometer.) It is evident from equation 3 that the error can be diminished by reducing the resistance value of the potentiometer; however, the reduction of this resistance is limited by the practical consideration of energy dissipation in the potentiometer. For example, on a 700-volt system a 10,000-ohm potentiometer rated 50 watts must be used. Since the reduction of potentiometer resistance to a very low value is impractical, compensation for the error was resorted to. The error, being a variable quantity, was not easily compensated alone. However, putting a second potentiometer in series with the balancing potentiometer produces a total error which is constant; that is, independent of slider position. This error could then be compensated by removing the corresponding amount of resistance from the internal circuit of the measuring instrument.

The resistance at the terminals of the compensating potentiometer, if R_{comp} is allowed to have its minimum possible value, must be given by the equation

$$R_{comp} = [0.25 - x(1-x)]R \tag{4}$$

where R is the total resistance of the balancing potentiometer. A nonlinear potentiometer having this characteristic was connected electrically in series with the balancing potentiometer, with the shafts of the two potentiometers mechanically coupled. The characteristics of the compensating potentiometer and the connections are shown in Figure 4.

Description of the Ground Detector

It becomes evident that operation of a device employing the aforementioned principles requires a circuit to detect the unbalanced voltage between the slider of the balancing potentiometer and ground, and a means of driving the balancing potentiometer to the point of zero potential or null point. Two methods have been developed for performing this operation. The first utilizes a voltmeter and

Figure 2 (below). Basic circuit of ground detector

Figure 4 (right). Characteristics of compensating potentiometer

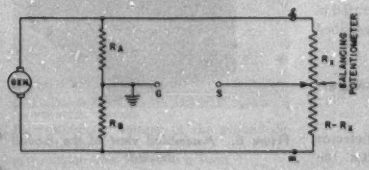

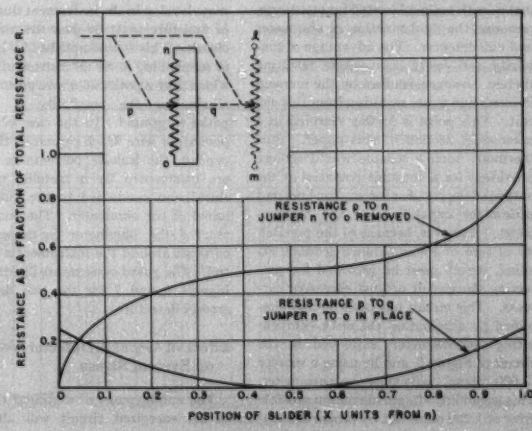

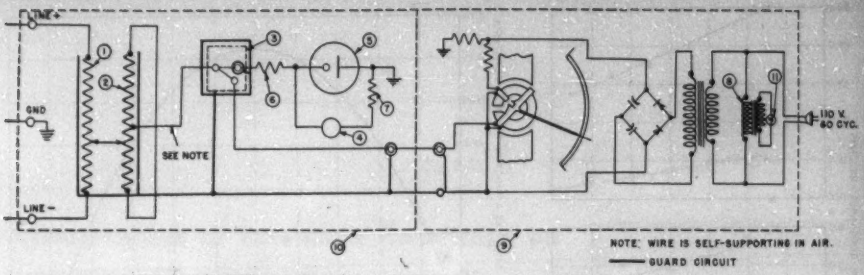

Piece No.	Identification	Piece No.	Identification
1	Balancing Potentiometer 10,000 ohms, 50 watts	6	0.25 Meg., 3 Watts
2	Compensating Potentiometer 10,000 ohms, Center-tapped, taper-wound.	7	1 Meg., 2 Watts
3	Galvanometer Switch Push button type S.P.D.T. Normally closed on ohmmeter circuit.	8	Transformer NRL # 4210 115 V/8 V; 0.15 Amp.
4	Galvanometer Center "O," 50 μA	9	500-Volt Ohmmeter Scale 0-10 Megs. Calibrated with 2500 Ohms in external circuit.
5	Neon Tube 115 V., 2.5 Watts	10	Instrument box
		11	Pilot light MAZDA #47; 6.3 V., 0.15 Amp.

Figure 5. Schematic diagram of the ground detector

manually-controlled potentiometer. This system is illustrated in Figure 5. The detector circuit is designed to allow for observation of voltages as low as 0.25 volt, yet will not be damaged by voltages as high as several hundred volts. The ohmmeter, which is a rectifier-powered device, is normally connected between the compensating potentiometer and ground. By depressing switch 3, the operator can insert the detector, adjust the potentiometer to the null point, and then release the switch for observation of the insulation resistance as measured by the ohmmeter. The developed instrument is illustrated in Figure 6.

Another version of this principle is shown in Figure 7 wherein a d-c milliammeter, with scale calibrated for resistance, performs the dual function of ohmmeter and null detector. The advantage of simplicity and fewer components resulting therein, however, is offset by the increase in insulation stress resulting from this circuit. This point is further clarified in a subsequent section of this paper. Furthermore, such a scheme would require provisions for a constant potential at the output of the rectifier for any load current within the capabilities of the milliammeter. However, because of the possibility of zero or low resistance grounds existing, means must be provided for protecting the circuit against excessive currents. This circuit has been further simplified by eliminating the error compensating potentiometer, employed in the circuit of Figure 5, and by using a smaller (5,000 ohms) balancing potentiometer. This would introduce a maximum possible error of 1,250 ohms but by proper calibration of the milliammeter it can be reduced to ±625 ohms. This potentiometer would necessitate the dissipation of approximately 100 watts for a 700-volt system as compared to 50 watts dissipation of the corresponding potentiometer in the unit of Figure 5. If it is desired to record changes in insulation resistance the balancing operation can be made automatic, servo actuated by the unbalance voltage.

Guard System

It is important that the use of this type of instrument does not influence the value of insulation resistance of the system. Thus all leakage currents which may develop in the instrument due to dirt or moisture must by-pass the measuring circuit. This is accomplished by isolating or suspending in air all instrument wiring which is at a potential above ground, thus eliminating the possibility of leakage paths to ground. In the case of a component, or wire which cannot be thus suspended, the leakage currents to ground are intercepted by a metallic plate or shield and conducted to the guard terminal of the ohmmeter. The guard system of the ohmmeter by-passes these currents around the instrument's current coil. The guard systems are illustrated in Figures 5 and 7 for the two described ground detectors.

Effect of Ground Detector Voltage on System Stress

The employment of a ground detector on an energized circuit will alter the normal line-to-ground stress of the system owing to the injected voltage of the ohmmeter. Referring to Figure 8, it will be noted that the magnitude of the insulation leakage currents to ground, normally i_l for each line, has been modified by currents i_{m1} and i_{m1} induced by the ohmmeter voltage E_M. From inspection it may be observed that the effect of the ohmmeter currents is to raise the voltage of line A to ground and decrease correspondingly the voltage of line B.

In a normal system the line stresses are

$$e_a = \frac{R_A}{R_A + R_B} E_T \tag{5}$$

Figure 6. Assembled view of the ground detector

Figure 7. Schematic diagram of simplified version of the ground detector

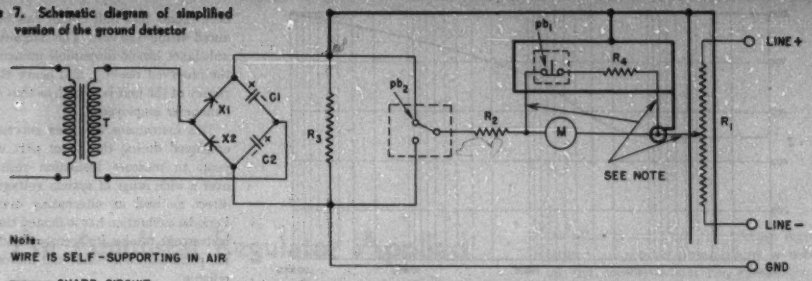

Note:
WIRE IS SELF-SUPPORTING IN AIR

——— GUARD CIRCUIT

M = Milliammeter, 25 Ma full range. To be used as null detector and also as ohmmeter with following calibration: 0 to 1 Megohm, with 35,000-ohm indication at center of scale, on high range; 0 to 0.5 Megohm with 15,000-ohm indication at center of scale on low range (assuming negligible voltage regulation).

T = 115/230 V., 60 Cy. Transformer (constant potential type).
R_1 = Potentiometer, linear, 5000-ohm, 100 W.
R_2 = 5000 ohms, 50 W.
R_3 = 25,000 ohms, 10 W.
R_4 = Shunt to ammeter resistance

x_1 = x_2 = Dry-disc rectifier, 120 Ma, 500 V.
C_1 = C_2 = 100 μfds, 600 V.
Pb_1 = S.P.S.T. Push Button, Normally closed.
Pb_2 = S.P.D.T. Push Button, Normally closed, on ohmmeter circuit.

$$e_b = \frac{R_B}{R_A+R_B}E_T \qquad (6)$$

When a ground detector is connected to a system and properly balanced so that

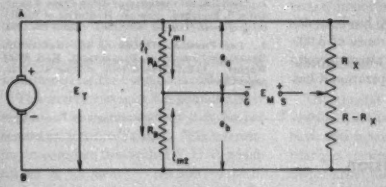

Figure 8. Leakage currents due to components of ground detector and system voltages

$$\frac{R_A}{R_B} = \frac{R_x}{R-R_x} \qquad (7)$$

the corresponding stresses of equations 5 and 6 become

$$e_a = \frac{R_A}{R_A+R_B}E_T + \frac{R_A+R_B}{R+R_A+R_B}E_M \qquad (8)$$

$$e_b = \frac{R_B}{R_A+R_B}E_T - \frac{R_A+R_B}{R+R_A+R_B}E_M \qquad (9)$$

Owing to the fact that the value of R is very small for magnitudes of R_A and R_B greater than one megohm, the above relations may be simplified as follows

$$e_a = \frac{R_A}{R_A+R_B}E_T + E_M \qquad (10)$$

$$e_b = \frac{R_B}{R_A+R_B}E_T - E_M \qquad (11)$$

where

E_T = system voltage
E_M = ohmmeter voltage of the ground detector
e_a = voltage from line A to ground
e_b = voltage from ground to line B
R_A = insulation resistance to ground of line A
R_B = insulation resistance to ground of line B
R = total resistance of balancing potentiometer (10,000 ohms in the subject instruments)
R_x = potentiometer resistance from slider to line at balance

Consideration of equations 10 and 11 reveals that as the insulation resistance of line B is reduced to zero, the voltage to ground of line A approaches in magnitude the sum of the system plus ohmmeter voltages. If the ohmmeter's driving voltage is equal to the system voltage, the insulation stress of line B will approach twice system voltage. This stress could result in breakdown of the insulation. However, this has been averted in the developed ground detector by employing a power supply with voltage regulation characteristics shown in Figure 9. Thus a decrease in voltage accompanies a decrease in resistance below 1 megohm which results in the driving voltage adapting itself to the condition of the insulation. The maximum voltage that can be experienced by a 500-volt system under any condition may be observed in Figure 10. It is to be noted that for the higher values of insulation resistance the system stress can go above 500 volts. However,

Figure 9. Voltage regulation at terminals of ground detector

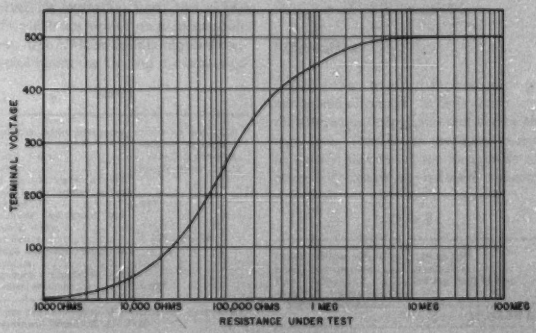

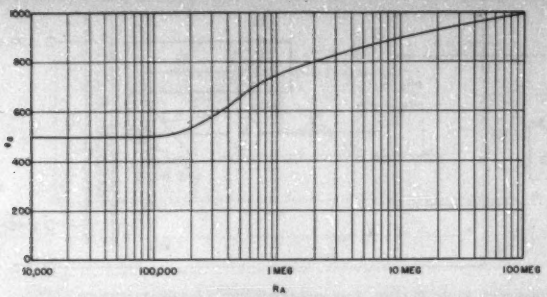

Figure 10. Possible maximum insulation stress on system, due to components of ground detector and system voltages

a consideration of the values of insulation resistance and the required ratios of the resistance for each line to ground reveals that it is highly improbable for the system to experience voltages from 750 to 1,000 volts. Furthermore, when these conditions are established the insulation resistance is sufficiently high that it can withstand the stress.

The ground detector of Figure 7 requires a power supply with no voltage regulation if the calibration of the ohmmeter is to be independent of internal leakage currents through the guard circuit. However, if the power supply is designed with sufficient voltage regulation to avoid overstressing of insulation at low values of resistance, it will result in inaccuracies when measuring in the range of approximately 0.1 megohm and above. This inaccuracy is attributed to guard circuit currents affecting the voltage at the terminals of the ohmmeter.

Results and Conclusions

The instrument, Figure 6, has been developed with a measuring range of 5,000 ohms to 10 megohms and a stressing voltage of 500 volts. During operation it has been found that null circuit can be balanced within 0.25 volt. This magnitude of unbalance has no discernible influence on the observed reading, and hence the accuracy of the unit is as high as that of the ohmmeter employed.

This instrument has been successfully employed during the major part of the year, to measure insulation resistance over a wide range of system voltages, on direct as well as alternating currents. Periodic calibration has indicated that the instrument retains its accuracy and that the performance is stable and thoroughly reliable.

This instrument can be employed to accurately measure the insulation resistance of any ungrounded d-c or a-c system whether energized or nonenergized. It contains its own source of electromotive force for stressing the insulation to its rated voltage but with such regulation as to render the stress proportional to the condition of the insulation. The unit is direct reading and simple to operate.

References

1. The Characteristics of Insulation Resistance, S. Evershed. *Journal*, Institution of Electrical Engineers (London, England), volume 52, 1914.

2. The Physical Nature of the Electrical Breakdown of Solid Dielectrics, Karl Willy Wagner. *AIEE Transactions*, volume 41, 1922, pages 288–99.

No Discussion

An Amplistat Regulator Applied to a 5-Kva 400-Cycle Aircraft Inverter

R. E. MORGAN
MEMBER AIEE

J. A. WALLEY
ASSOCIATE AIEE

A 5-KVA inverter for airborne electric systems has been developed to supply large amounts of 400-cycle power at very close regulation, quick response, high efficiency, and good wave shape. Such features are obtained through the use of an amplistat-type regulator, improved self-ventilation, and newly designed magnetic circuits. Specifically, the inverter has the electrical characteristics shown in Table I.

The regulation shown in Table I is maintained for the conditions of Table II.

This inverter weighs 105 pounds and it regulates the frequency to ±2 cycles per second as noted in Table I. It is interesting to compare this with *AN-3530*, which allows a frequency variation of ±10 cycles per second and maximum weight of 90 pounds. To show what each major component weighs, the 105 pounds may be segregated thus: motor-alternator unit, 68 pounds; regulator, 20 pounds; and other controls, 17 pounds (starting relays, and so forth). This tabulation shows that it is still necessary to pay in weight for a gain in regulation.

Although the close regulation results in some increase in size, the total volume of this inverter is 150 cubic inches less than the 2,600 cubic inches allowed by *AN-3530*. The close frequency regulation permits the use of equipment that cannot operate satisfactorily without added regulating equipment. The operation of much equipment can be improved with close frequency and voltage regulation and fast response of the regulator. Some equipment can be designed lighter and smaller, the closer the regulation of the inverter. Therefore an over-all weight and space saving on the airplane should be obtainable by the use of closer regulation. Figures 1, 2A, and 2B show the inverter, major internal components of the inverter, and the regulator.

Paper 50-195, recommended by the AIEE Air Transportation Committee and approved by the AIEE Technical Program Committee for presentation at the AIEE Middle Eastern District Meeting, Baltimore, Md., October 3–5, 1950. Manuscript submitted July 6, 1950; made available for printing August 21, 1950.

R. E. Morgan is with the General Electric Company, Schenectady, N. Y. and J. A. Walley is with the General Electric Company, Fort Wayne, Ind.

Mechanical Design

The general mechanical design is conventional in that the motor and alternator have two separate magnetic circuits, two bearings support the rotor, and the motor-alternator unit is surmounted by a control box. The inverter is self-cooled with the air brought in at the center and discharged by radial-blade centrifugal fans at each end.

Electrical Design

The output winding on the alternator receives its excitation from two aiding fields which are wound on a salient-pole rotor. One of these fields is supplied continuously from the 115-volt d-c input and the other is fed from the voltage regulator. A similar arrangement is used on the motor, which has cumulative-compound field windings. There are two shunt fields, one of which is supplied from the input and the other fed by the frequency regulator. Two series fields also are provided on the motor. One of these series fields is in the circuit only during starting, and its purpose is to aid in controlling the peak inrush of starting current and its rate of decay. When the unit is started, the starting current does not exceed 1,000 per cent of full load current and it returns to 300 per cent of full load current within 0.2 second after first application of input voltage. The other series field provides extra stability in frequency while the inverter is running.

The continuous fields have important functions. Because of the magnetic amplifier principle, the amplistat must be saturated to some degree before they fire, or supply any output. Therefore, the regulated fields do not receive any appreciable power from the regulator until the output voltage of the alternator increases to a selected value. When the inverter is started, the continuous field on the alternator provides immediate initial excitation, thus insuring a build-up of alternator voltage. When the unit reaches approximately 60 per cent rated speed, the voltage is sufficient to fire the regulator. In addition, the continuous fields have another function pertaining to efficiency which is discussed now.

Efficiencies

The power required by the regulated motor and alternator fields is taken from the alternator output and rectified by the regulator. This feature provides the close regulation desired at the acceptable expense of somewhat reduced regulator

Table I

Frequency, cycles per second	400 ± 1/2 per cent (8,000 rpm nominal)
Voltage, volts	115 ± 2 1/2 per cent
Phase	Single phase
Over-all efficiency at full load (unity power factor), per cent	68*
Maximum individual harmonic, volts	6
Crest factor	1.386 to 1.418
Voltage regulator response, seconds	0.04
Frequency regulator response, seconds	0.025

* 60 per cent minimum allowed by Air Force-Navy Aeronautical Standard *AN-3530*.

Table II

Input voltage, volts d-c	110 to 120
Load, volt-amperes	0 to 5,000
Power factor	0.9 lag to 0.95 lead
Ambient temperatures, degrees centigrade	−55 to +71 (sea level) −55 to −10 (35,000 feet

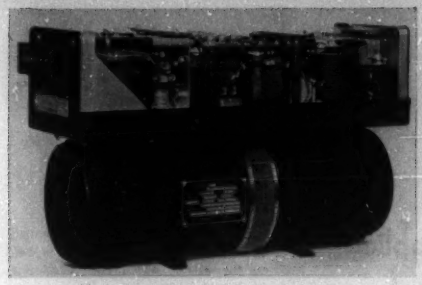

Figure 1. The inverter without control box cover

Figure 2 (B). Major internal components of the motor-alternator

efficiency of the inverter, as compared to other types which obtain the field power directly from the d-c input. However, this reduction is minimized by designing the inverter to have an average of 31 per cent of the field excitation supplied directly to the two continuous fields. The over-all efficiency of the inverter (at full load, unity power factor) without the regulator in the circuit is 71.5 per cent. The over-all efficiency with the regulator is 68 per cent and, therefore, the regulator decreases the efficiency only 3.5 per cent. The regulator itself is approximately 42-per cent efficient.

Overspeed Protection Circuit

Another feature of the design is a circuit which protects the inverter against running away under light-motor-field conditions. Some of the possible circumstances under which the circuit would operate are:

1. Failure of the regulator for any reason to provide field excitation at start.
2. Malfunctioning of any of the regulator components under extraordinary operating conditions.
3. Loss of regulated field through lead breakage or poor connection.

The need for the circuit is increased because of the added complexity of this type of regulator and because of the magnitude of the stored energy in a 30-pound rotor rotating at 8,000 rpm. However, this necessity has been lessened somewhat by designing the regulator to be fail-safe wherever possible.

Two small relays make up the circuit. The explanation of their operation is best understood by referring to Figure 3 and following the sequence of steps at starting:

1. The on-off terminal is connected to the positive side of the input by an external switch.
2. The coil on contactor B is excited through the contact of relay K.
3. Contactor B closes and supplies power to the motor armature and the continuous fields of the motor and the alternator.
4. The inverter starts with both series fields in the circuit.
5. The regulator operates and relay L closes.
6. After the armature voltage increases to a selected value, contactor D closes and shorts out series field number 2.
7. At same time, relay K is actuated and is locked in, through its own contacts and secondary coil.

The inverter is now running under normal conditions with all the contactors and relays (B, D, K, and L) closed. If for some reason the inverter loses its regulated field power, relay L drops out, which de-energizes the coil on line contactor B. The inverter stops and all the components, except relay K, return to the standstill conditions. Since relay K is locked in by its secondary coil, the starting cycle cannot be repeated until the operator opens the external switch. This particular feature prevents the inverter from cycling in the event the protection circuit is called upon to operate.

If the regulator does not operate at

Figure 2 (A). The amplistat regulator (voltage and frequency)

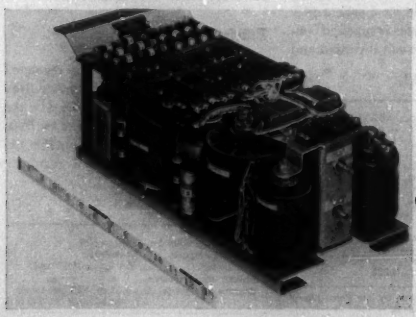

Figure 3. Portion of control circuits pertaining to overspeed protection

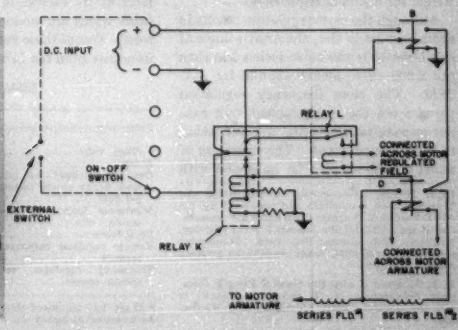

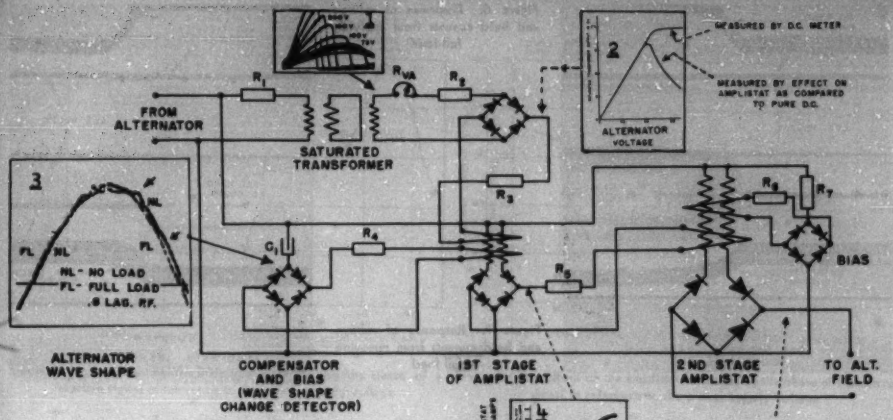

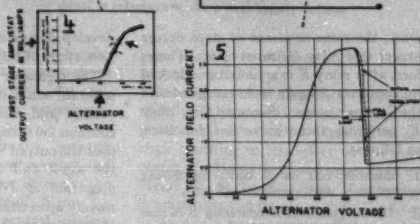

Figure 4 (above). The circuit diagram of the voltage regulator

Amplistat voltage regulator using saturated transformer regulator and compensated by wave shape change

Figure 5 (below). A block diagram of the voltage regulator showing electrical characteristics

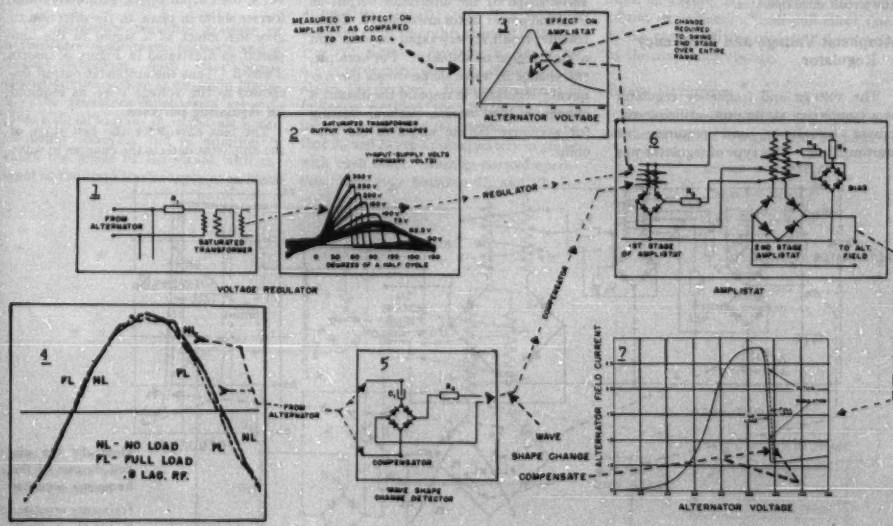

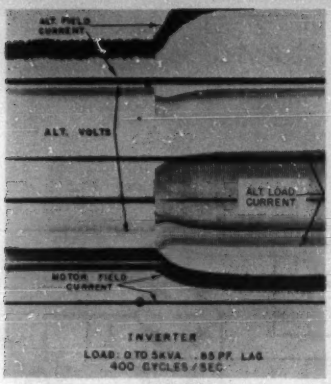

Figure 6. Response of voltage and field currents from applying full load

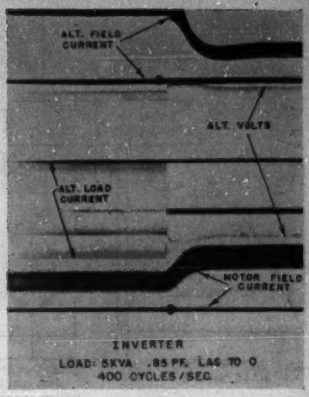

Figure 7. Response of voltage and field currents from removing full load

start, the same sequence of steps occurs except that relay L cannot close. Therefore, after relay K is actuated and locked in, contactor B again is de-energized and the inverter stops. Summarizing, relay K performs three important functions as follows:

1. Controls coil on B contactor during normal start until regulator operates.
2. De-energizes coil on contactor B in case the regulator does not operate.
3. Prevents cycling of the inverter after the circuit once operates.

Amplistat Voltage and Frequency Regulator

The voltage and frequency regulator is a completely static unit, utilizing amplistat techniques, and requiring no warmup time. This type of regulator was developed in an effort to give good regulation, speed of response, and reliability.

The regulator consists actually of two separate amplistat regulators, one for voltage and one for frequency. Each contains two stages of amplification, and uses the output of the alternator as both the signal and the power supply. The operation of both regulators is based mainly upon utilizing differences in phase shift between the signal and the power supply, and also the slight changes in wave shape of the alternator output as load and power factor are changed. These features result in very rapid response and a high degree of stability. For example, the change in wave shape causes the frequency regulator to respond the instant a change in load occurs, without waiting for a change in the speed of the machine.

Voltage Regulator

The voltage regulator circuit is shown in Figure 4. It uses a saturated transformer as the voltage-sensing element, the output of which is applied to the first stage of the amplistat. The output of the amplistat (alternator field current) is determined primarily by the phase of the saturated transformer's output, rather than its amplitude. As the alternator voltage increases above 90 volts, the output of the saturated transformer shifts in phase in the direction to give less effect as a signal to the amplistat as illustrated in Figure 5, inserts 2 and 3. Thus the amplistat output decreases as the voltage rises, as required for regulating purposes.

The bias circuit for the first stage of the amplistat detects the changes in wave

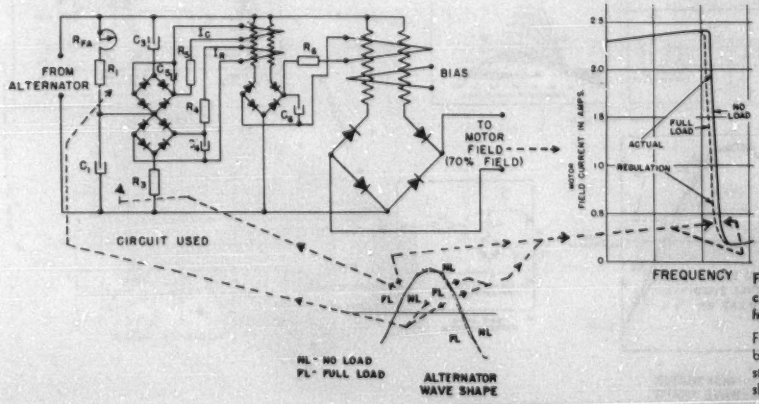

Figure 8. The circuit diagram of the frequency regulator

Frequency regulator by use of an amplistat and a wave shape compensator

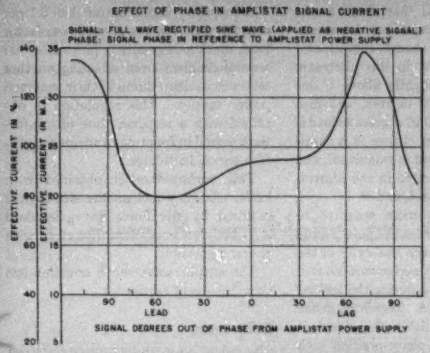

Figure 9 (A). Effect on the amplistat from shifting the phase of a negative signal in reference to the power supply voltage

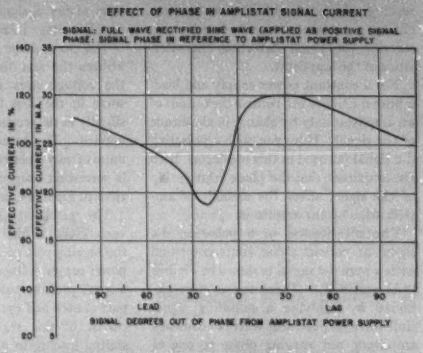

Figure 9 (B). Effect on the amplistat from shifting the phase of a positive signal in reference to the power supply voltage

shape with load, and thus compensates the regulator, so as to give better regulation with less amplification. Less amplification in turn means better speed of response and a higher degree of stability. Flat regulation and even negative regulation have been achieved by such means with complete stability. Figures 6 and 7 illustrate the response time of approximately one-twenty fifth of a second obtained with this regulator.

Frequency Regulator

The frequency regulator consists of a resistance-capacitance network and a 2-stage amplistat, with wave shape change compensation, as shown in Figure 8. The resistance-capacitance network gives a signal varying in amplitude as the frequency changes, and in addition it shifts the phase of the signal with respect to the amplistat's supply to an ideal part of the phase sensitive curves, Figures 9(A), 9(B) and 10. The wave-shape change compensator permits flat frequency regulation with any variation of load at a given power factor.

The resistance-capacitance network consists of two parts: a lead network and a lag network. The former, shown as the upper part of the basic circuit, Figure 10, supplies current I_C to a control winding of the first stage of the amplistat in a direction to decrease the output (that is, a negative signal). The lag network supplies I_R to the other control field as a positive signal. I_R lags in phase by about 60 degrees, whereas I_C is leading by about 120 degrees. However, since it is full-wave rectified, the 120 degrees leading is equivalent to 60 degrees lagging, so that I_C and I_R are approximately in phase with each other. During normal operation, they stay between 45 and 75 degrees lagging in relation to the power supply.

As the inverter frequency decreases slightly, I_C decreases in amplitude and its phase shifts in a leading direction to an angle resulting in less effect on the amplistat, see Figure 9(A) and upper right of Figure 10. At the same time, I_R increases in amplitude and its phase shifts, leading to an angle having more effect on the amplistat, see Figure 9(B) and lower right of Figure 10. Therefore, the amplistat experiences a push-pull effect due to the phase shifting of I_C and I_R as well as the amplitude change.

Phase Detection

Further clarification of the operation of the saturated transformer, frequency

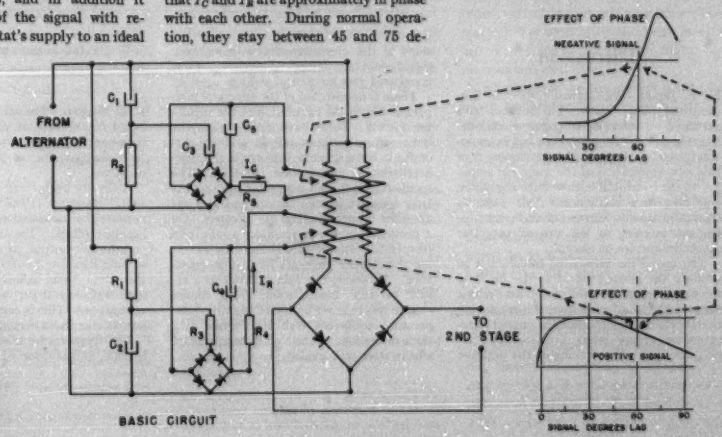

Figure 10. The basic circuit of the frequency regulator

Frequency regulator by use of an amplistat and a wave shape compensator

sensing circuits, and the wave-shape change compensator may be had by considering the phase detection characteristics of the amplistat.

For a constant power supply and load, a pure d-c signal will control the output of an amplistat only by change in amplitude of the signal. However, with a pulsating d-c signal (as used in this regulator), both the amplitude and the phase relationship of the signal affect the amount of amplification by the amplistat.

The effectiveness of a pulsating d-c signal at various phase shifts compared with a pure d-c signal is shown in Figures 9(A) and 9(B). These curves were obtained by applying a pulsating signal (full-wave rectified sine wave) of constant amplitude but varying phase to one of two equal control windings of an amplistat, and a pure d-c signal to the other. As the phase of the first signal was varied, the output of the amplistat was maintained constant by varying the amplitude of the pure d-c signal. The effective-current curve shows the variation of the effect on the amplistat of the pulsating d-c signal as its phase is shifted (not to be confused with an rms value).

In the case of the saturated transformer in the voltage regulator, Figure 5, insert 2 shows that while the peak voltage output increases as the supply voltage increases, the conducting time decreases, so that the average current remains relatively constant. However the phase shift of the trailing edge of the signal shifts away from the most sensitive phase angle, so that increasing alternator voltage decreases the effect of the saturated transformer signal on the first stage amplistat, thus giving a signal that drops as the supply voltage increases and vice versa.

The wave-shape change compensator utilizes the fact that in this alternator the voltage rises slightly above a sine wave in the first 90 degrees, and dips slightly in the second 90 degrees as load is applied. The actual change is a maximum of only 2 per cent in magnitude, and is somewhat exaggerated in the illustrations in Figures 4, and 5, and 8.

The amplistat is more sensitive to variations of a small negative pulse during the lagging part of each half-cycle of the power supply voltage, and to variations of a small positive pulse during the leading part of each half-cycle. Therefore, in one circuit of this regulator the signal is shifted leading to a phase position such that that dip is in the most sensitive phase and the rise in the insensitive phase. This provides a signal that effectively contains mostly the dip and relatively little of the rise. In another circuit, the signal is shifted lagging, and provides a signal that contains mostly the rise and relatively little of the dip. As a result, two signals are developed, one containing the dip and the other containing the rise. The voltage regulator uses the one containing the dip while the frequency regulator uses both.

Conclusions

A 5-kva inverter was developed to supply 400 cycles for aircraft applications where good frequency and voltage regulation are needed. The regulator has over-all regulation of $\pm 1/2$ per cent for frequency and $\pm 2 1/2$ per cent for voltage. The frequency is held better than 0.1 per cent for variation in a given power-factor load, which aids greatly in preventing one servomechanism from affecting another servomechanism through their common power supply. This regulation is obtained with a response time of one-fortieth second in frequency and one-twenty-fifth second in voltage.

This performance is obtained with better efficiency and smaller size than is required by Air Force-Navy Standard *AN-3530* for equivalent inverters with poorer regulation.

The output wave shape contains less than 5 per cent harmonics.

References

1. 400-Cycle Inverters for Military Aircraft, C. P. Hayes, L. L. Ray. *Electrical Engineering (AIEE Transactions)*, volume 64, May 1945, pages 233–37.

2. The Extension of Amplistat Performance by A-C Components, R. E. Morgan, H. M. Ogle, V. J. Wattenberger. *AIEE Transactions*, volume 69, part II, 1950, pages 986–91.

3. The Amplistat—A Magnetic Amplifier, R. E. Morgan. *Electrical Engineering*, volume 68, August 1949, pages 663–67.

4. Self-Saturation in Magnetic Amplifiers, W. J. Dornhoefer. *AIEE Transactions*, volume 68, part II, 1949, pages 835–50.

5. The Transductor, H. B. Rex. *Instruments* (Pittsburgh, Pa.), volume 20, December 1947, pages 1102–09.

6. Saturable Reactors and Magnetic Amplifiers, F. G. Logan. *Electronics* (New York, N. Y.), volume 21, October 1948, pages 104–09.

7. Magnetic Amplifier Circuits, Neutral Type, A. S. Fitzgerald. *Journal*, Franklin Institute (Philadelphia, Pa.), volume 244, October 1947, pages 249–65.

8. Transductor Fundamentals, S. E. Hedstroem, L. F. Borg. *Electronics* (New York, N. Y.), volume 21, September 1948, pages 88–93.

9. A Magnetic Amplifier Frequency Control, L. J. Johnson, H. G. Schafer. *AIEE Transactions*, volume 69, part I, 1950, pages 613–15.

Discussion

H. B. James (Westinghouse Electric Corporation, Lima, Ohio): The authors have prepared an informative paper which adequately covers the work that has been accomplished to date in the development of this new application of the magnetic amplifier to the control of both voltage regulation and frequency regulation. This paper is especially timely because of the recent increased interest in the use of magnetic amplifiers for use on aircraft.

The use of the saturating transformer to produce the correct signal to the input of the first stage of the voltage regulator circuit suggests the use of a bridge circuit employing thyrite elements such that the output characteristic versus input produces an "S" shaped curve. By working on the negative slope of this characteristic the same type signal could be obtained. Have the authors considered this method of voltage sensing?

There is no mention of the effects of temperature upon the calibration of the regulator circuit. Tests have shown that the temperatures encountered in military aircraft can cause a marked change in the characteristics of a magnetic amplifier. The rectifiers used for self-saturation are particularly sensitive in this respect and also the amplifier copper windings are affected. On a particular magnetic amplifier application temperature effects were reduced by shunting the rectifier elements by a high resistance. However, the gain suffered as a result of this modification. The copper change was reduced by use of negative temperature coefficient resistors. Even with these alterations to the circuit, temperature effects were still evident.

Would the authors state how this problem was solved?

R. E. Morgan: The author of the discussion asked if a bridge of thyrite elements had been considered, and what method was used to compensate for temperature effect in the regulator.

A thyrite bridge was tried, and it worked well. However, it was found easier to compensate the saturated transformer for temperature effect. The use of the saturated transformer output, as used for the voltage sensing element, uses the saturation point of the core. Tests indicate this variation was approximately 2 per cent per 100 degrees centigrade. This is compensated by a copper resistor in its output circuit.

The temperature effect on the amplistat is small, and is absorbed in the regulation.

Tracking Radio Noise on Aircraft

T. B. OWEN
ASSOCIATE AIEE

THE SUBJECT of radio noise suppression received a great deal of attention a few years ago, when due to military considerations, large quantities of electronic equipment began to be installed in aircraft. It was found that the shielding of aircraft engine ignition systems which had been reasonably sufficient for the low- and medium-frequency equipment, was entirely insufficient for high- and very high-frequency radio equipment. In addition, quantities of electric equipment were installed: motors, actuators, dynamotors and inverters, all of which added to the problem, as frequently one motor could cause interference sufficient to completely blackout all of the communications equipment.

The problem was attacked from several angles. First, a rigorous program of bonding and shielding all of the electric equipment was initiated, extending all of the way from conduit to junction boxes. Second, line filters were applied to interference producing apparatus. The result was that in most cases it was possible to operate both the electric and radio equipment at the same time, but each airplane was an individual project in interference suppression and as a result no two radio installations were identical. In addition to this additional complexity, the weight increase was considerable, and there was no assurance that the aircraft would remain interference-free in service. Extensive modifications were made in service to correct this, generally adding filtering and shielding at the expense of more weight.

This intolerable situation has been corrected to some extent by a program of specification requirements, so that the electric equipment was made to some limits, and techniques of radio noise suppression were perfected. At this stage, instead of interference suppression being a 100 per cent cut-and-try affair, it became perhaps a 50 per cent cut-and-try.

Since then these techniques have remained relatively static, and while the specification requirements on electric apparatus are very complete and detailed, it is generally not possible to obtain equipment which will meet the specification. Further, very promising leads that had been developed along the lines of producing equipment which was inherently free of radio interference-producing capabilities were allowed to drop.

Even if it were possible to obtain specification equipment, it would still be necessary to operate on a 20 per cent cut-and-try basis, with the optimum perhaps 10 per cent, where the specifications were written on the basis of the best compromise between equipment efficiency and specification workability.

It is evident that even with the best specifications that can be hoped for, the radio engineer will have to make final checks and "fixes" to assure a radio interference-free airplane. This work may be classified as follows:

1. Engine ignition systems (loose magneto covers, loose coupling nuts, faulty shield braid, and so forth).

2. Motors, dynamotors, inverters, and actuators mounted in close proximity to radio apparatus. (Radiation fields produced by this equipment, even though in conformance with the specifications, produces intolerable interference.)

3. Same as (2) above, except mounted within radio apparatus. (Same conditions as above.)

4. Coupling within the airplane to lead-ins. (Open wire lead-ins in proximity to electric equipment or wire bundles, or shielded lead-ins running in strong fields, with radio interference currents flowing in the shield and going to ground in an antenna circuit element.)

Development of an Ignition Test Unit

In a previous publication by the author,[1] a method was briefly noted for locating faulty portions of the aircraft ignition harness. This method consisted of using a commercial VHF (very high frequency) signal generator to inject a modulated signal into the ignition harness of an engine, through a spark-plug lead, at a frequency approximating 150 megacycles, the exact frequency being unimportant. Then, by means of a noisemeter set to the generator frequency, the ignition harness was probed with a shielded loop probe to locate the points where the generator signal could be heard, usually at loose fittings, broken braid on flexible leads, and poorly fitting or loose magneto covers. It was necessary to provide the operator with a pair of headphones to facilitate testing.

Needless to say, this system was very clumsy to set up and use, besides requiring expensive laboratory apparatus out on the flight line where it could be exposed to all types of weather. This method was used with excellent results, but is not too applicable to flight line maintenance activities.

In order to make the system more generally applicable, a portable apparatus was designed and produced. Figure 1 shows the receiver and transmitter as it would be used in the field. Its portability and convenience of operation should be noted. Coupling from the transmitter to the harness at a single point through the triple-shielded lead, as shown, has been found to give sufficient signal to locate faults over the entire ignition system. This includes the magneto-to-ground leads, and so forth, in the accessory section and back of the firewall.

The transmitter is very simple, being a *6J6* dual triode operating at about 150 megacycles, and with a maximum power output of two watts. It is modulated at 1,000 cycles by a *6C4* triode. The oscil-

Paper 50-196, recommended by the AIEE Air Transportation Committee and approved by the AIEE Technical Program Committee for presentation at the AIEE Middle Eastern District Meeting, Baltimore, Md., October 3-5, 1950. Manuscript submitted July 10, 1950; made available for printing August 14, 1950.

T. B. OWEN is with the Hughes Aircraft Company, Culver City, Calif.

Figure 1. Very high frequency signal injection and detection equipment in use on airplane engine

lator and modulator are housed in a completely shielded box, and have external provisions for adjusting the coupling to the load, and a small adjustment of the oscillator frequency. The power is transferred to the load through a constant-impedance coaxial plug, and a meter is provided to read the plate load of the oscillator.

The oscillator-modulator box, with the power supply, is contained in a small case, provided with a handle for ease in carrying. The power supply consists of a 6-volt storage battery, operating a vibrator-rectifier to supply 150 volts of direct current to the oscillator and modulator. Provisions are included for charging the battery directly from commercial frequency a-c lines.

As seen from Figure 1, the receiver is strapped directly on the operator, and while it is designed for both compactness and efficiency it is also very sensitive. There are two tubes, one a *CK556AX* hearing-aid tube operating as a super-regenerative detector, and a *30A* audio amplifier. Two standard flashlight cells provide filament power, and a small $67^1/_2$-volt "B" battery supplies plate power. Plugs for the head-phones and the loop cable are provided, and there is a knob for tuning the receiver over a small range. Since the oscillator frequency varies with loading, some such adjustment is necessary. The loop probe is electrostatically shielded, and for best results should be about 2 inches in diameter; for the location of small leaks a smaller loop is preferable, about 3/4 inch in diameter.

In use, the transmitter is coupled to the ignition harness through one of the spark plug leads, as shown in Figure 1, and the coupling adjusted for minimum output. The receiver is tuned to the transmitter frequency by loosening one of the coupling nuts on the harness, or if the engine already has a number of loose connections, it will be possible to approach the engine and tune the receiver for maximum response as sufficient signal will be present to do so. After this, probing with the loop will show the loose connections. It is only necessary to remember that the loose connection is not always where the probe shows the loudest signal, it may be at the other end of the cable. This is because the shielded loop is responsive to electromagnetic fields, and if the loose joint is voltage-fed, the current nodes that produce electromagnetic fields may be some distance away, but will always be some odd multiple of a quarter-wave at the test frequency. After the more obvious leaks are found and corrected, the power output of the oscillator to the harness is increased, and the process continued until the harness is entirely quiet. If all that is necessary is a general tightening down, an engine can be completely treated in less than a half-hour. More frequently, however, flexible cables must be replaced, or magneto covers tightened down. In any event, the testing is done on a cold engine, and there is no need for recourse to the usual cut-and-try methods of tightening down, running the engine, and so forth, or even finally replacing the entire harness because of an invisible fault in a spark-plug connection. It should be noted that the small drain holes in the distribution ring often emit a definite field that can be located by the 3/4-inch diameter loop. This field, however, has never been found to be capable of producing interference.

Consideration was given to the possibility that better results would be obtained from a square-wave generator. This would mean that the receiver would also have to be tunable over a wide range to get the best results, adding to its complexity. Experiment has shown, however, that the apparatus described gives the desired results without an extensive frequency range, and no useful purpose would be served by the added complication.

In operation, the apparatus has proved very rugged, and is readily used by flight line personnel otherwise untrained in radio-noise work.

During the initial tests of the equipment, considerable time was spent in obtaining a completely shielded oscillator compartment. For these tests, it was found that the receiver, fitted with the 3/4-inch diameter loop, was invaluable. With this loop it was possible to run along a supposedly soldered seam and find the exact spot that was unsoldered. This experience led to an extension of this method for locating radiation field leaks in other electric apparatus, chiefly motors and dynamotors.

Extension of the Signal Injection Test Method to Other Electric Apparatus

The equipment just described was so successful in locating radio interference sources in ignition systems that an extension of the test method was used to locate the radiation fields about an electric motor. Even after an excellent line filter had been applied, the radiation field about the motor in question was so heavy that a 3/4-inch diameter loop could not be brought near the motor without obtaining a full-scale meter reading when on the highest range of a commercial VHF (very high frequency) noisemeter.

A VHF signal generator and noisemeter were set up on a bench as shown in Figure 2. The output of the signal generator fed directly into the power plug on the motor control housing, the coupling lead being well shielded. A frequency of 130 megacycles was used for test.

It was found that by reducing the signal generator output, the exact location of the electromagnetic field sources could be located. In this case, the field laminations, which form a part of the body of the motor, were found to be very "hot." A copper screen was wrapped around the motor and the ends soldered together, with the screen firmly bonded to the motor case. This entirely suppressed the radiation from the field laminations.

The control box was also surrounded by various hot spots, and it was necessary to reduce the signal generator output almost to zero to locate the source. This was found to be the metal tube carrying wires from the motor to the control housing. This tube was firmly bonded to the control box at one end, and to the motor at the other. With this treatment, the radiation field about the motor and control housing completely disappeared, even at full output of the signal generator. When the motor was connected to the line

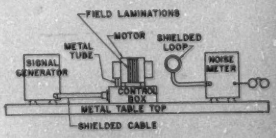

Figure 2. Laboratory setup for field determinations about an electric motor

supply for test, it was found that the radiation field around the assembly was negligible.

This method is very applicable for radiation field tests on small dynamotors and inverters which must be mounted within radio receivers. The test given in current military specifications, where a dipole antenna is mounted in close proximity to the apparatus under test, in a shielded room, is misleading and meaningless for this application. The field absorptions and reflections encountered within a shielded room are liable to give erroneous results. As has been pointed out,[2] the absolute values of the radio-influence voltages are unimportant, the test is whether or not interference is produced in radio apparatus. A piece of electric equipment that passes the radiation test of current military specifications cannot be mounted within or in close proximity to radio apparatus in most cases, as radio engineers well know. The test given here will produce a piece of apparatus that is much more adaptable to such locations.

While the tests were conducted at a frequency of 130 megacycles, the exact frequency is not important. As will be shown in the next section, the higher frequencies are preferable for these tests. The frequency chosen has the advantage that it is near the range of most aircraft VHF receivers, so that radio interference suppression at this frequency will assure that no trouble will occur in practice. For applications where the motor or inverter is to be used in radar work, the frequency used for testing could well be in the range of the equipment in which the test article is to be installed.

Characteristics of Radiation from Openings in Enclosures

As far as the present investigation is concerned, two types of enclosure are of interest: a metallic enclosure in which a strong electromagnetic field exists; and a tubular conduit or pipe containing wires which carry radio-frequency currents.

Metallic Enclosure

The type of enclosure in which we are generally interested will be a motor case, a junction box, or a magneto case.

Due to the type of radio-frequency generator contained in these enclosures, a pulse type of waveform is generated. This type of waveform can be considered as a square wave of very short duration and expansion into a Fourier series gives

$$f(t) = B_1 \sin \omega t + B_3 \sin \omega 3t + B_5 \sin \omega 5t + \ldots.$$

Thus all odd multiples of the basic exciting frequency exist within the enclosure, and fields of all these frequencies exist. Now consider the enclosure as a cavity resonator containing, of course, in the case of the motor and magneto, considerable other material. A cavity resonator of the dimensions of the ordinary motor, magneto, or junction box will have a very high resonant frequency, which will be lowered by the material composing the enclosure, and also by any magnetic material within the enclosure. Frequencies above and below this resonant frequency are attenuated. Since the Q of these enclosures is low due to the material of which they are composed, the frequency range where the fields receive relatively small attenuation is rather wide. The net result is that the lower and higher frequency fields are heavily attenuated, and the only fields of practical significance from an interference radiation standpoint are those which can exist under the conditions of a relatively low Q cavity resonator.

Large currents will flow inside the cavity, particularly at those frequencies around the resonant frequency. Wherever openings in the cavity occur at these large current regions, such as at magneto covers or junction box covers, an interruption to the current path is presented, and the current may actually flow outside the enclosure for a very small distance. At such points, a small electromagnetic field is set up, which may be detected by the loop probe, but which is undetectable by the electrostatic probe. Similarly, in motors, where the field lamination stack forms part of the motor shell, since the laminations are insulated from one another, local fields can occur outside the motor due to current flow there.

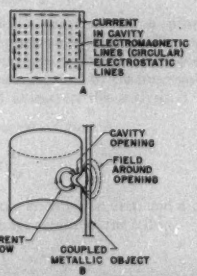

Figure 3. (A) Field configuration inside a resonant cavity. (B) External field about a break in a resonant cavity, showing coupling to proximate metallic objects

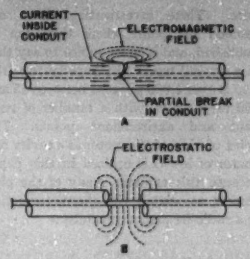

Figure 4. (A) External field about a partial break in conduit. (B) External field about a complete break in conduit

It is to be particularly noted that the fields that occur outside an enclosure which contains a source of radio-frequency energy will be almost entirely electromagnetic, and predominantly at the very-high and the ultra-high frequencies. Since the basic generator is a shock excitation device, any external fields retain this character, and so may in turn shock-excite other metallic objects within a short distance. The frequency of this secondary shock-excitation will depend upon the physical dimensions of the external excited unit, and may bear little relationship to the exciting frequency.

Referring to Figure 3, showing in outline a cavity resonator, large currents flow in the sides of the container, the electromagnetic field is circular, and the electrostatic field is vertical. This field configuration is the very simplest and is for the lowest frequency that can occur within a cylindrical cavity; other field configurations of great complexity and frequency range can also occur. An opening in the cavity in the region where the large currents are flowing permit a local current flow on the outside of the enclosure, setting up a local field, which in turn may excite a control cable, a wiring bundle, or any metallic object. The effects of this excitation may be detected often at a considerable distance from the source of the excitation, appearing as an electrostatic field at voltage nodes, and as an electromagnetic field at current nodes.

It must not be assumed from the foregoing that the only fields that occur within a cavity will be those in the region of the cavity resonant frequency. Tests run on a motor over a wide frequency range indicate that the impedance varies widely, showing that an equally valid conception would be that the motor can be considered as a generator with a multi-sectioned network as the internal imped-

ance. These investigations have not reached the point where they can be published, and it must suffice to say that in a typical motor the impedance variation is over 1,000 per cent between 15 and 150 megacycles, with a number of resonant and antiresonant points. The point of view of the motor as a cavity resonator of low Q is utilized in this paper because this explains many of the phenomena associated with the motor acting as a radio-frequency generator.

Tubular Conduit

The usual form here is a solid wall aluminum conduit, or a flexible braid conduit, in which power or control wiring may run. This wiring and the conduit enclosure may be considered as a form of coaxial cable of relatively high attenuation, since the dielectric is at least partially composed of wire insulation. It must be noted, however, that the attenuation of a coaxial cable decreases with frequency and, therefore, these conduits may form excellent transmission lines for the lower and medium frequencies. Further, these lines are practically never terminated in their characteristic impedance, so a variety of standing waves may exist, and the voltage and current relations that occur at a given point will be very complex, with voltage nodes at some frequencies and current nodes at others. The manner of excitation of these transmission lines will not be discussed except to say that we are considering radio interference generators of any of the types that exist on aircraft.

Take as a first example metallic conduit-carrying wiring which is excited over a wide frequency range. A typical case is shown in Figure 4(A), where a partial break in the conduit is shown. At the frequencies at which appreciable current is flowing on the inner surface of the conduit, a small amount of that current will flow outside the conduit at the break, in a fashion similar to a break in a cavity resonator. No electrostatic field will be detectable at the break, the loop probe must be used to detect the field. At a quarter-wave away from this point an electrostatic field will exist. Since the physical conditions that may exist in an airplane at such a joint or break may be quite varied, the structure will be very complex, and the actual location of the break will be difficult to locate. Such breaks have little significance in aircraft radio interference suppression, except, in magneto grounding circuits or other circuits of high excitation intensity, such as radar video and the trigger cables, or where an open wire lead-in runs close to the conduit. If it is necessary to locate such a break, signal injection into the circuit is about the easiest method.

The second condition that may occur is where a definite and complete break in the conduit is located, see Figure 4(B). At such a point, current nodes cannot occur, and the break will show only with the electrostatic probe. Again, current nodes will occur at a quarter-wave length from the break, and due to the geometry of aircraft structures, the field structure in the vicinity of the break will be very complex. This type of fault will not have any great significance in aircraft radio except as previously noted.

Conclusions

1. The test methods shown are particularly adaptable for the elimination of radio noise from aircraft engine ignition systems.
2. Where it is necessary to provide very close shielding for a piece of electric apparatus, the injection method is both simple and sure.
3. Present specification test methods are inadequate where the apparatus must be mounted in close proximity to, or within, a piece of radio apparatus.

References

1. Very High-Frequency Radio-Noise Elimination, T. B. Owen. *Electrical Engineering* (*AIEE Transactions*), volume 63, December 1944, pages 949–54.

2. Radio-Noise Elimination in All-Metal Aircraft, Fred Foulon. *AIEE Transactions*, volume 62, 1943, pages 877–91.

No Discussion

The Operating Speed of D-C Brake Magnets

J. E. RYAN
MEMBER AIEE

T. M. SPITLER
NONMEMBER AIEE

D-C MAGNETS brakes are used widely in hoist and similar applications where fast and accurate positioning of the load in response to master switch manipulation is very desirable. Ideally, the brake shoes should release instantly when the master switch reaches any operating position and should set in the same way when the controller calls for braking action.

Two principal time delays prevent this ideal from being attained when picking up the shoes; these are: (1) pickup time of the controlling contactor; and (2) time for brake magnet flux to build up to the point where the shoes release. In series brakes, the first is usually the more important despite the fact that eddy currents in the solid parts of the magnet core may appreciably prevent the flux from following the rapidly rising current. For shunt brakes, the second is dominant, and since it depends upon the brake itself, the designer of that device can do something about it.

Delay in setting of the brake is caused by (1) dropout and arcing time of the controlling contactor; (2) time for eddy currents in brake magnet to decay to dropout point; and (3) mechanical travel time of shoes. The travel time of the shoes, once magnetic release has taken place, is quite short. The contactor time is usually the next larger factor, but is less important than the eddy current decay time when a proper contactor is used.

Paper 50-197, recommended by the AIEE Industrial Control Committee and approved by the AIEE Technical Program Committee for presentation at the AIEE Middle Eastern District Meeting, Baltimore, Md., October 3-5, 1950. Manuscript submitted July 5, 1950; made available for printing August 24, 1950.

J. E. Ryan is with the General Electric Company, Lynn, Mass., and T. M. Spitler is with the General Electric Company, Schenectady, N. Y.

The first part of this paper will deal with magnet pickup while the second part will consider dropout.

Pickup of Magnet

In the analysis to follow, the relations between the work required to lift the shoes, the magnet size, and the pickup time are derived. It is applicable to any type of magnet in which saturation is not appreciable in the open-gap position, but only those of one type may be compared at a time. In other words, magnets being compared must be proportional in all important dimensions in order to use the equations and curves.

Although the findings have important application in the design of brake magnets, they apply equally well to any d-c shunt magnet where the load at the initial (open-gap) position is the critical one to overcome.

Derivation

Consider a magnet with a pivoted armature such as is shown in Figure 1. In the open-gap position, the magnetomotive force required by the iron may be neglected, at least for this analysis.

The magnetic torque is

$$T = -aM^2\frac{dP}{d\theta} \tag{1}$$

With the armature at rest, and a constant voltage applied to the coil

$$M = \gamma M_o\left(1-\epsilon^{-\frac{R}{L}t}\right) \tag{2}$$

Further, the permeance P is

$$P = P_W + P_L \tag{3}$$

so that, substituting equations 2 and 3 into 1

$$T = -a\gamma^2 M_o^2\left(1-\epsilon^{-\frac{R}{L}t}\right)^2\frac{dP_W}{d\theta} \tag{4}$$

Let us now express M_o, R, L, and P_W in terms of some characteristic dimensions D. So long as proportions remain the same

$$R = \frac{kr}{D}N^2 \tag{5}$$

Then

$$Q = \frac{M_o^2 R_c}{N^2} = \frac{M_o^2 r}{D} \tag{6}$$

Q is limited by the coil surface area, so that

$$Q = hD^2 \tag{7}$$

Equating equations 6 and 7 and solving for M_o^2

$$M_o^2 = \left(\frac{h}{r}\right)D^3 \tag{8}$$

P_W can be expressed as

$$P_W = kD/\theta \tag{9}$$

so

$$\frac{dP_W}{d\theta} = \frac{-kD}{\theta^2} \tag{10}$$

As for L

$$L = N^2(P_W + P_L) = N^2\left(\frac{kD}{\theta} + lD\right) \tag{11}$$

Then, from equations 5 and 9

$$\frac{R}{L} = \frac{kr}{D^2\left(\frac{k}{\theta}+l\right)} \tag{12}$$

Substituting from the above into equation 4

$$T = \frac{ahk\gamma^2 D^4}{r\theta^2}\left[1-\epsilon^{-\left[\frac{krt}{D^2\left(\frac{k}{\theta}+l\right)}\right]}\right]^2 \tag{13}$$

Now, if γ be taken equal to α, the load torque G will be, from equation 13

$$G = \frac{ahk\alpha^2 D^4}{r\theta^2} \tag{14}$$

When, under higher excitation, $T = G$, pickup will begin. Equating equations

13 and 14 and solving

$$1-\frac{\alpha}{\gamma}=e^{-\left[\frac{\delta r t_1}{D^3\left(\frac{k}{\theta}+l\right)}\right]} \tag{15}$$

whence

$$t_1=\frac{D^3}{\delta r}\left[\frac{k}{\theta}+l\right]\ln\left[\frac{1}{1-\frac{\alpha}{\gamma}}\right] \tag{16}$$

Since W is usually a specified quantity, we can express θ better as

$$\theta=\frac{W}{G}=\frac{Wr\theta^2}{ahk\alpha^2D^4} \tag{17}$$

or

$$\theta=\frac{ahk\alpha^2D^4}{rW} \tag{17}$$

Substituting this into equation 16 and rearranging, there results

$$\frac{\delta r t_1}{lD^3}=\left[\frac{rW}{ahl\alpha^2D^4}+1\right]\ln\left[\frac{1}{1-\frac{\alpha}{\gamma}}\right] \tag{18}$$

In order to make a plot of equation 18 easier to comprehend, let

$$A=\alpha/\gamma \tag{19}$$

$$X=\frac{rW}{ahl\gamma^2D^4} \tag{20}$$

$$Y=\frac{\delta r t_1}{D^3} \tag{21}$$

Then 18 can be written

$$Y=\left[\frac{X}{A^2}+1\right]\ln\left[\frac{1}{1-A}\right] \tag{22}$$

and plotted, for various values of A, in Figure 2.

Interpretation

Note that an envelope curve uv is drawn tangent to the lowest A curve at

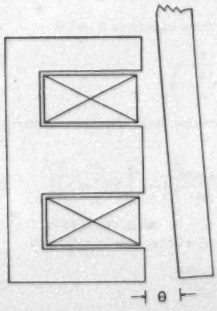

Figure 1. Cross section of magnetic circuit

Nomenclature

a, h, k, l, r = constants dependent only upon the proportions of the magnet type
$f(x)$ = a function of x
i = instantaneous value of current
t = time
x = length of magnetic path
D = characteristic dimension
G = load torque on armature
G_s = conductance of equivalent damping-ring
I_p = steady-state coil current when brake is energized
L = inductance of coil circuit
M = instantaneous magnetomotive force of coil
N = number of turns in coil
P = permeance of entire magnetic circuit
P_w = permeance of working flux paths
P_L = permeance of leakage flux paths
Q = power loss in coil at full rated voltage
R = resistance of coil circuit
T = magnetic torque on armature
W = work required by load
$\alpha = \dfrac{\text{voltage which picks up load in infinite time}}{\text{full rated voltage}}$
$\gamma = \dfrac{\text{voltage applied in a given instance}}{\text{full rated voltage}}$
$\delta = \dfrac{\text{total resistance of coil circuit, including external } R}{\text{coil resistance}}$
θ = armature angle
ρ = resistivity of the magnet material
φ = flux
$\propto$ = is proportional to
Subscripts pertain to:
1 = pickup
2 = dropout
a = arc
c = coil alone
o = steady-state at full rated voltage
p = primary (actual coil)
s = secondary (damping-ring)

each value of X. If W, γ, and the magnet proportions are fixed, and D is tentatively chosen, the X value is established. The minimum possible t then will correspond to the Y of the envelope curve at this X if the A value whose curve touches the envelope at this point is used.

The resultant optimum value of θ

$$\theta=\left(\frac{k}{l}\right)\frac{A}{X} \tag{23}$$

can be obtained from equations 17, 19, and 20. At large values of X, θ becomes relatively small and t increases rapidly. Indeed, if saturation had been considered, the envelope curve would rise even more rapidly toward the right-hand side, so that this always needs to be checked before using the results of Figure 2 blindly.

A study of Figure 2 also will show that, if all factors remain constant except D, and the optimum (envelope line) design is made in every case, t will steadily decrease as D increases.

If D is increased in proportion to $\sqrt[4]{W}$, the X and Y values remain fixed and

$$t_1 \propto \sqrt{W} \tag{24}$$

This appears to be a reasonable balance between size and operating time, but there is nothing uniquely advantageous about it.

An increase in leakage inductance, represented by the constant l, decreases Y less than X and thus gives a longer t, other things being equal. This is confirmed by physical reasoning.

As external series resistance is added to an otherwise fixed system, thereby making $\delta > 1.0$

$$t \propto 1/\delta \tag{25}$$

since Y is constant.

Two Magnets Versus One

Assume that a satisfactory design has been made for a single magnet capable of delivering the work required by the two shoes of a brake. Let W, D, and t_1 apply to this case.

Now design two magnets, each operating one shoe, keeping the same value of X in Figure 2. Since the work per magnet in this case, W', is

$$W'=W/2 \tag{26}$$

X will be held constant only by having

$$D'=\frac{D}{\sqrt[4]{2}} \tag{27}$$

Since Y remains the same

$$Y=\frac{\delta r t_1}{lD^3}=\frac{\delta r t_1'}{l(D')^3}$$

or

$$t_1'=\frac{t_1}{\sqrt{2}} \tag{28}$$

The total volume of the two magnets is 19 per cent greater than in the first case, but the pickup is 41 per cent faster. If the volume of the two were held strictly equal to the one larger magnet, analysis of a number of cases using Figure 2 shows that, even so, a saving of roughly 20 per cent in time is achieved.

Dropout of Magnet

Derivation

The time required for the flux to decay to the dropout point can be found by using a minor variation of a method derived by Pohl.[1] He found it possible to duplicate the effects of distributed eddy currents in the iron through the use of a

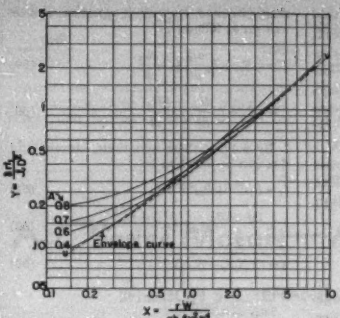

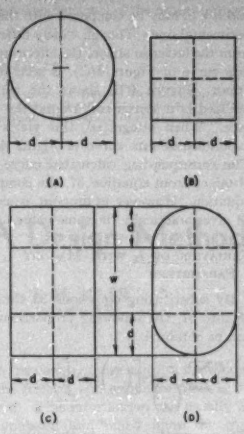

Figure 2 (above). Pick-up characteristics of d-c shunt magnets

Figure 3 (right). Various cross sections of magnetic structures

(A) Circle (B) Square (C) Rectangle (D) Rectangle with semicircular ends

fictitious short-circuited winding (damping-ring) suitably coupled with the actual coil. Although Pohl's solution is for the rise of flux in the presence of eddy currents, the decay of flux can easily be found from the same equations, once a suitable value of contactor arc resistance has been assumed.

The equivalent conductance of the fictitious damping-ring for any particular section of the magnet depends upon the cross-section and length dimensions thereof as well as the resistivity of the iron.

Referring to Figure 3, the equivalent ring conductances for several common cross sections are

Circle:

$$G_s=\frac{s}{8\pi\rho} \tag{29}$$

Square:

$$G_s=\frac{s}{32\rho} \tag{30}$$

Rectangle:

$$G_s=\frac{s}{\rho}\left[\frac{1}{12\left(\frac{w}{2d}-1\right)+32}\right] \tag{31}$$

Rectangle with semicircular ends:

$$G_s=\frac{s}{\rho}\left[\frac{1}{12\left(\frac{w}{2d}-1\right)+8\pi}\right] \tag{32}$$

To find the damping-ring conductance for the entire magnetic circuit, individual conductances for pole and yoke must be combined in the following manner:

$$G_s(\text{total})=G_s(\text{pole})+1/2G_s(\text{yoke}) \tag{33}$$

This method of combining paralle paths gives an indication as to how the damping-ring conductance for a laminated structure can be determined; namely, by finding conductances for individual laminations and combining them in a manner similar to that used in equation 33.

Pohl has also demonstrated that the substitute damping ring should have a leakage flux of 22 per cent to compensate for the fact that the actual eddy currents are distributed rather than concentrated, as in the ring.

The solution for coil current i_p, damping-ring current i_s, and flux φ, following the introduction of the arc resistance, may each be visualized as consisting of two parts: 1. the initial steady-state value; and 2. a transient quantity in the reverse direction which ultimately reaches the same magnitude as part 1. The fictitious reverse voltage V is chosen such that

$$V=I_p(R_a+R_c) \tag{34}$$

Criteria for selecting a suitable constant value of R_a will be given later.

The transformer equations of Appendix I apply, yielding as solutions

$$Ni_p=B_{1e}^{-m_1t}+B_{2e}^{-m_2t} \tag{35}$$

$$i_s=\frac{1+m_1\beta}{\omega}B_{1e}^{-m_1t}+\frac{1+m_2\beta}{\omega}B_{2e}^{-m_2t} \tag{36}$$

$$\varphi=P(Ni_p+i_s) \tag{37}$$

The quantities called for in equations 35, 36, and 37 are found from the basic variables by successive substitution as follows

$$R_s=\frac{1}{G_s} \tag{38}$$

$$n=\frac{R_a+R_c}{N^2R_s}=\frac{R_p}{N^2R_s} \tag{39}$$

$$\omega=\frac{1}{1.22n}=\frac{0.82}{n} \tag{40}$$

$$\beta=\left(\frac{P}{10^8R_s}\right)\frac{0.22}{1.22n}=\frac{0.180P}{10^8R_sn} \tag{41}$$

$$c=\left(\frac{10^8R_s}{P}\right)\frac{1+1.22n}{0.22} \tag{42}$$

$$b=\left(\frac{10^8R_s}{P}\right)^2\frac{n}{0.22} \tag{43}$$

$$m_1=\frac{-c+\sqrt{c^2-4b}}{2} \tag{44}$$

$$m_2=\frac{-c-\sqrt{c^2-4b}}{2} \tag{45}$$

$$K=\frac{1+m_1\beta}{1+m_2\beta} \tag{46}$$

$$B_1=\frac{-1}{K-1}NI_p \tag{47}$$

$$B_2=\frac{K}{K-1}NI_p \tag{48}$$

With all parameters specified, it is now possible to express φ as a function of time only. The φ corresponding to armature

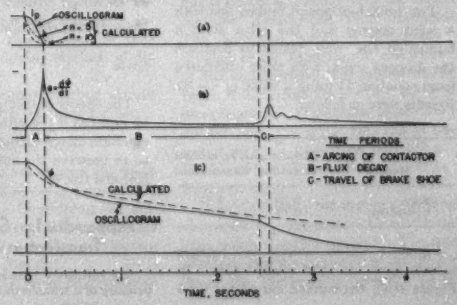

Figure 4. Oscillogram showing drop-out characteristics of an 1,800-foot-pound brake with solid magnet

(A) Coil current
(B) Search coil voltage
(C) Pole face flux

release is known from the mechanical torque applied; hence, the dropout time is determined.

The analysis of Appendix I tacitly assumes constant permeance of the magnetic circuit. Yet most d-c magnets are highly saturated in the closed-gap position. Error due to this assumption can be minimized by using, for the initial ampere-turns NI_1, that value which will make the calculated initial flux φ_0 equal to the actual value

$$(NI_p)=\frac{\varphi_0}{P} \tag{49}$$

As for the assumption of constant arc resistance, this may seem quite unjustifiable. However, it has been found that the exact resistance-time characteristic of the coil circuit is relatively unimportant so long as it is such as to reduce the coil current to a small fraction of its initial value in about the same time that the actual contactor does. This is accomplished in the present analysis by using a suitable value of n, see Figure 4. Any more rigorous method would greatly complicate the mathematics.

Reference to equations 42, 43, 44, and 45 shows that m_1 normally will be considerably smaller than m_2, and therefore will be the controlling time constant. Also, the coefficient B_1 will normally be larger than B_2. Since the latter part of the flux transient is of greatest interest in determining dropout time, one may logically drop the second term of equations 35 and 36 when substituting into 37. Then

$$\varphi=PB_1\left[1+\frac{1+m_1\beta}{\omega}\right]e^{-m_1t} \tag{50}$$

which, when solved for $t=t_2$ and simplified, yields

$$t_2=-\frac{1}{m_1}ln\left[\left(\frac{\varphi_0}{\varphi_2}\right)\left(\frac{B_1}{NI_p}\right)\left(1+\frac{1+m_1\beta}{\omega}\right)\right] \tag{51}$$

Experimental Verification

Two 1,800-foot-pound brakes, one with a solid magnet and the other with a laminated one, were tested to compare the dropout times, with those calculated from equation 51 using a value of $n=10$. Results were as follows

Magnet	Dropout time, t_2, seconds Calculated	Experimental
Solid	0.29	0.24
Laminated	0.09	0.11

Figure 4 shows several oscillograph records from the solid magnet test. In Figure 4(A), the current curves for $n=5$ and $n=10$ may be compared with the experimental one. Though widely different from the latter in shape, the effect on the flux curve of Figure 4(C), is seen to be minor. Figure 4(B) shows the voltage induced in a search coil around the pole face. When integrated, this yields the experimental flux curve of Figure 4(C). The corresponding calculated curve was obtained from equation 37, the complete equation. However, at dropout, equation 51 gives practically the same value.

Variation of t_2 with Magnet Parameters

By substituting equations 32 through 48 into 51, the following proportionality can be obtained

$$t_2\propto\frac{P}{\rho}\sum\frac{z}{f\left(\frac{w}{d}\right)}ln\left[\left(\frac{\varphi_0}{\varphi_2}\right)f(n)\right] \tag{52}$$

The summation refers to the several sections of the magnet iron.

In magnets which are dimensionally similar

$$P\propto D \tag{53}$$

and

$$z\propto D \tag{54}$$

Then, when n and φ_0/φ_2 are substantially independent of magnet size, as they often are, equation 52 reduces to

$$t_2\propto\frac{D^2}{\rho} \tag{55}$$

If D is made proportional to $\sqrt[4]{W}$, as was considered reasonable in the section on Pickup of Magnet, equation 55 becomes

$$t_2\propto\frac{\sqrt{W}}{\rho} \tag{56}$$

Comparison of this with equation 24 shows that both pickup and dropout time tend to vary in the same manner with D or W.

Considering the effect of changing the load torque on a given magnet

$$\varphi_2^2\propto G \tag{57}$$

Using this in equation 52 yields

$$t_2\propto ln\frac{1}{\sqrt{G}} \tag{58}$$

The effects of changes in w/d or n can be explored if the substitutions leading to equation 52 are carried out in such a way as to preserve the actual expressions for $f(n)$ and $f(w/d)$.

Appendix I. Solution of the Transformer Equations

If a voltage V is suddenly applied to the primary of a transformer whose secondary is short-circuited, the circuit equations can be written as follows:

$$V=i_pR_p+L_p\frac{di_p}{dt}+M\frac{di_s}{dt} \tag{59}$$

$$0=i_sR_s+L_s\frac{di_s}{dt}+M\frac{di_p}{dt} \tag{60}$$

By solving these equations, current and flux can be found to be

$$i_p=B_1e^{m_1t}+B_2e^{m_2t}+I_p \tag{61}$$

$$i_s=\frac{1+m_1B}{\omega}B_1e^{m_1t}+\frac{1+m_2B}{\omega}B_2e^{m_2t} \tag{62}$$

$$\varphi=P(N_pi_p+N_si_s) \tag{63}$$

where

$$I_p=\frac{V}{R_p} \tag{64}$$

$$m_1=\frac{-c+\sqrt{c^2-4b}}{2} \tag{65}$$

$$m_2=\frac{-c-\sqrt{c^2-4b}}{2} \tag{66}$$

$$b=\frac{R_pR_s}{L_pL_s-M^2} \tag{67}$$

$$c=\frac{L_pR_s+L_sR_p}{L_pL_s-M^2} \tag{68}$$

$$K=\frac{1+m_1B}{1+m_2B} \tag{69}$$

$$B=\frac{L_pL_s-M^2}{L_sR_p} \tag{70}$$

$$\omega=\frac{MR_p}{L_sR_p} \tag{71}$$

$$B_1=\frac{1}{K-1}I_p \tag{72}$$

$$B_2=-\frac{K}{K-1}I_p \tag{73}$$

Appendix II. Evaluation of Constants a, h, k, l, and r

To evaluate the constants of the section on Pickup of Magnet that are dependent only upon the proportions of the magnet type, we can use equations 5 and 7, respectively, to find that r and h are

$$r=\frac{RD}{\delta N^2} \tag{74}$$

$$h=\frac{Q}{D^2} \tag{75}$$

By manipulating equation 11, we can obtain the following equation of a straight line

$$\frac{L}{N^2D}=l+k\frac{1}{\theta} \tag{76}$$

A plot of L/N^2D as a function of $1/\theta$ therefore results in a straight line of slope k and intercept l.

The remaining constant, a, can be evalu-

ated by solving equation 14. This gives us

$$a = \frac{Gr^2}{hka^3D^4} \tag{77}$$

All of these previously unknown constants are thus now given in terms of other constants that are either known or can be measured on a magnet of the proper proportions.

References

1. Rise of Flux Due to Impact Excitation: Retardation by Eddy Currents in Solid Parts, Robert Pohl. *Proceedings*, Institution of Electrical Engineers (London, England), volume 96, part II, number 49, 1949, pages 57–65.

2. Electromagnetic Devices (book), H. C. Rotors. John Wiley and Sons, Inc., New York, N. Y., 1941.

No Discussion

A-C Series Motors—A Design Method

SHELDON S. L. CHANG
ASSOCIATE AIEE

J. H. KARR
MEMBER AIEE

DESIGN and performance calculations for most common types of motors are well covered in the technical literature. To the uninitiated the agreement between calculated and test results, for example in polyphase motor design, may seem incredibly close. However, there is little recorded evidence of attempts to approach the design of an a-c series motor in the manner that other types of motors are designed. This situation prevails for several reasons. In the first place, almost every series motor has to be tailored to meet the requirements of the application because of the nature of its speed-torque curve. In applying an induction motor to a job, the designer is not ordinarily concerned if he is faced with using a 1/25-horsepower motor where the requirement is for 1/35-horsepower. As a matter of fact, the use of a 1/25-horsepower motor, if this is a standard rating, may be economically sound. It is usually not possible to tolerate this situation in series motor applications because of the marked difference in operating speeds at different outputs. It frequently then becomes necessary to modify motor windings to obtain the required performance on the basis of some such expedient as varying the applied voltage to the motor and proportioning windings from this data. Most series motor manufacturers have accumulated a vast background of motor performance and winding data and the experienced designer can usually select a design which approximates the requirements of the application.

Paper 50-198, recommended by the AIEE Rotating Machinery Committee and approved by the AIEE Technical Program Committee for presentation at the AIEE Middle Eastern District Meeting, Baltimore, Md., October 3–5, 1950. Manuscript submitted October 19, 1949; made available for printing July 31, 1950.

Sheldon S. L. Chang and J. H. Karr are both with Robbins and Myers Incorporated, Springfield, Ohio.

In the design of any motor a knowledge of the friction and windage losses is required. This information can usually be accumulated and relied upon for constant speed motors. The problem is not so simple where series motors are involved. The motor operates over a wide speed range which means that the friction and windage losses change rapidly as the load is changed. Furthermore, a large percentage of the small series motor business involves motor parts, not complete motors. The motor designer in such instances may be required to furnish motor parts, at least in the preliminary stage of development, with very limited data on bearings, air restrictions, and other factors which affect his estimate of friction and windage losses.

All of the foregoing provides some justification for the widespread approach to the design of series motors by the method of proportion, or by the somewhat less elegant method of "cut and try."

Many situations make it desirable and necessary to design series motors by a more direct approach. It is the purpose of this paper to develop and demonstrate such a method for concentrated pole, noncompensated-type motors. The writers believe it is particularly useful in exploratory designs for new frames, to investigate possible ratings, and to contrast effects of modifying mechanical details in laminations.

An acceptable design method should take into account the following factors:

Space Distribution of Flux

At any given instant of time, the space distribution of flux deviates considerably from a sine wave. Considering the ampere turns at different points in the air gap we may visualize the flux distribution about as shown in Figure 1.

The instantaneous speed electromotive force and torque of a single conductor are proportional to the flux density. The total armature electromotive force is the sum of the electromotive forces of individual conductors and is therefore proportional to the total flux which is the integration of flux densities no matter how distributed. Likewise, the torque acting on the armature is proportional to the total flux irrespective of distribution. The nonsinusoidal flux distribution therefore has no appreciable effect on the motor performance.

Wave Forms of Voltage and Current as Functions of Time

The line voltage has a sinusoidal wave form and consists of four parts:

1. Speed voltage of the armature, V_s, which is proportional to the main flux.
2. Transformer voltage of the armature and field, V_t, which is proportional to the time derivative of the main flux.
3. Reactive voltage due to the leakage flux of the armature and field. It is proportional to the time derivative of the leakage flux.
4. Resistance voltage drop in the windings, including brush drop.

The main flux does not have the same wave shape as the current. The leakage flux and the current have about the same wave shapes since the leakage flux path is largely in air. In an ordinary series motor, voltage components (1) and (2) above are much larger than (3) and (4) and as a result the wave form of the main flux is chiefly sinusoidal while the current contains considerable third harmonic. The developed torque is principally a product of the fundamental components of flux and current. The interaction between third harmonics is small, but is always negative. If magnetic saturation is not too high, this interaction can be neglected with the knowledge that the prediction of output and efficiency will be a little optimistic.

It has been observed that in an average motor the amount of third harmonic current is less than 30 per cent. The total effective current is therefore about 1.05 times the fundamental current. In the

proposed design method, it is the effective value of the fundamental component of current to which reference is made. The actual current is then 1.05 I and the copper loss 1.1 I^2R.

Magnetization Curve

The magnetization curve used in this design method is the maximum air gap flux plotted against the effective value of net magnetizing ampere-turns. A d-c magnetization curve would not be useful because it gives the maximum flux versus maximum current. Since there is no simple relationship between peak and effective values of a nonsinusoidal current, such magnetization curves cannot be conveniently applied.

Coil Pitch, Pole Pitch, Brush Lead and Skew

When a fractional pitch winding is used, the conductors in some slots carry opposing currents. The net ampere-turns in each of these slots is zero. A winding development diagram readily shows that slots carrying currents of the same sense occupy a belt equal to the coil pitch, ψ_c, and the coil under commutation is located with its two coil sides at the two ends of this effective belt.

In choosing the angle of brush lead, there are two factors to be considered: all slots under the influence of the pole arc must be within the effective belt in order to fully utilize the gap flux; and the leading coil side of the coil under commutation should be under the influence of the pole arc in order to facilitate commutation.

These two conditions fix the angle of brush lead as

$$\theta_b = 90^\circ\ (\psi_c - \psi) \qquad (1)$$

Rotor skew is intended primarily to improve the starting performance and reduce magnetic noise. It also gives the effect of blurring the edge of the pole arc so that improved commutation results. Skewing does not reduce the torque or speed electromotive force appreciably if the slots containing opposing currents still remain outside the influence of the pole arc.

Brush Short-Circuit Loss

As pointed out by many authors, there are two voltages in time quadrature in the short-circuited coil. The speed voltage can be utilized to assist commutation by properly adjusting the brush position. The transformer voltage always introduces a loss which is inherent in the a-c series motors. There is no way to eliminate the brush loss due to transformer voltage, but an understanding of its basic nature is of some importance in designing a-c series motors. The short-circuit current due to the transformer voltage is limited in general by the brush resistance and the total inductance of the coil under commutation. At the speed and load range for which this type of motors is generally applied, the total inductance is the more important limiting factor, and the brush loss is approximately proportional to

$$\frac{W^2B^2N_a^2}{L \times RPM \times S_c}$$

for a given lamination. L is the total inductance of the short-circuited coil. Since most of the a-c series motors are highly saturated under load, L is approximately proportional to WN_a^2/B, and the brush short-circuit loss is proportional to

$$\frac{WB^3}{RPM \times S_c}$$

This relation indicates that the brush short-circuit loss depends upon the flux density and is independent of the number of armature turns as long as the total inductance L limits the current in the short-circuited turns. It is verified by experiment for higher speeds. However, this cannot be interpreted as an argument in favor of carbon brushes with low resistivity. Though the brush short-circuit current is limited by the inductance, sufficiently high resistivity is still necessary for proper brush life. The magnetic energy stored in the coil under commutation causes uneven distribution of current on the brush face, with higher current density on the trailing edge. In the extreme case such uneven current distribution causes sparking. Other conditions remaining equal, the current distribution is more uniform on a brush with higher resistivity. Thus, the high resistance brush reduces sparking and gives longer life.

Iron Loss

This is treated in another paper by the writers.[1]

Data Required for Design

A manufacturer usually has several standard laminations. He may use a given set of laminations to obtain a number of motor ratings by varying the iron stacking. The following data can be obtained by test or by calculation for each lamination:

1. A-c magnetization curve (maximum air gap flux versus net effective magnetizing ampere-turns).
2. Iron loss curve (iron loss supplied by the stator as a function of flux density and speed).
3. Mechanical load on the rotor due to iron loss and friction and windage losses as a function of flux density and speed.
4. Brush short-circuit loss.

Figure 1 (left). Air gap flux distribution

Figure 2 (below). Vector diagram of series motor

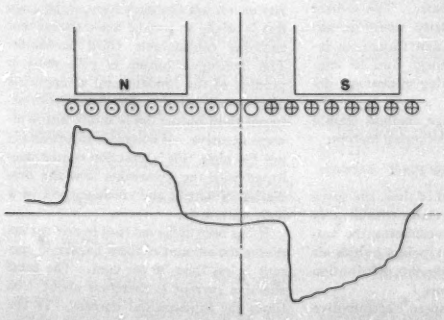

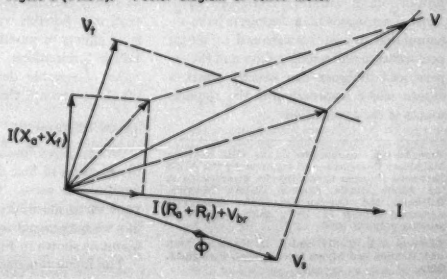

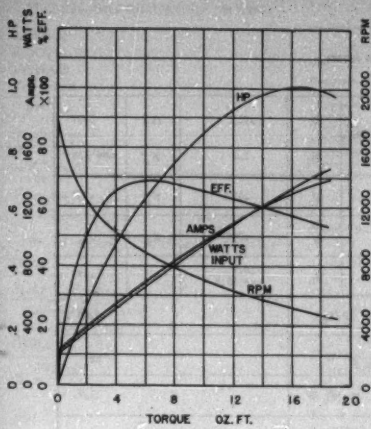

Figure 3. Series motor performance

Ratio of Stator and Rotor Ampere-Turns

The net magnetizing ampere-turns per pole at the center of the pole arc are

$$N_sI = I\left(N_f - \frac{N_aS_c\theta_b}{90\,aP}\right) \tag{2}$$

The net magnetizing ampere-turns at the leading edge of the pole are

$$N_sI - I\,\frac{N_aS_c}{aP}\,\psi$$

In order to prevent a reversal of flux, the foregoing expression must be positive. Therefore

$$N_s > \frac{N_aS_c}{aP}\,\psi \tag{3}$$

Examination of equations 1, 2, and 3 will show that

$$N_f > \frac{N_aS_c}{aP}\,\psi_c \tag{4}$$

In practice it is desirable to have N_f about equal to N_aS_c/aP. If the ratio of field ampere-turns to armature ampere turns is made too high, iron loss and stator copper loss will become excessive. A low value of this ratio results in a motor with good universal characteristics; high values improve commutation. Usual limits are 0.7 to 1.2.

Vector Diagram

The vector diagram of a series motor is shown in Figure 2.

The nature of the four components of voltage has been explained at the beginning of this paper. The gap flux, ϕ, lags the current, I, due to the stator iron loss, rotor iron loss supplied by the stator, and brush short circuit loss due to transformer voltage.

The angle β is determined from

$$\sin\beta = \frac{\text{sum of above losses}}{V_t \times I} \tag{5}$$

Equations for Torques and Voltage

$$\text{Gross torque} = 2.66 \times 10^{-6} P\phi I\,\frac{S_cN_a}{a}\cos\beta \text{ ounce feet} \tag{6}$$

$$V_s = 2.36 \times 10^{-10} P \times RPM \times \phi\,\frac{S_cN_a}{a} = V_s'\,\frac{S_cN_a}{a} \tag{7}$$

Equations 6 and 7 are derived in slightly different forms in Langsdorf's book on Theory of Alternating Current Machinery.[3]

The transformer voltage, V_t, can be written from its usual form as

$$V_t = 4.44 \times 10^{-8}\phi \times PN_t \times f = V_t'(PN_t) \tag{8}$$

In these equations the voltages and current are effective values while the flux per pole is the maximum value. Friction and windage losses and part of the rotor iron loss must be subtracted from the gross torque to obtain the net torque.

From equations 3 and 6 we obtain

$$\phi(N_sI) > \frac{\text{Gross torque} \times 10^{-8} \times \psi}{2.66P^2\cos\beta} \tag{9}$$

This equation gives a convenient starting point in designing an a-c series motor.

Design Procedure

1. Calculate the net torque, T_n, at given speeds.

2. Estimate friction and windage and mechanical load due to rotor iron loss, T_4. These are both in terms of torque. Add these to the net torque to obtain the gross torque, T_g.

3. Calculate $K = T_g \times 10^{-8}/2.66P^2\cos\beta$ In preliminary calculations use $\cos\beta = 0.98$.

4. Choose a point on the magnetization curve so that $\phi \times N_sI$ is slightly larger, say 5 per cent, than $K\psi$.

5. Having selected the operating point in (4) check friction and windage and mechanical load due to rotor iron loss for given speed and flux density. If materially different from estimates in (2), recalculate (3) and (4).

6. Calculate $V_t' = 4.44 \times 10^{-8} \times \phi \times f$.

7. Determine iron loss supplied by stator and brush short-circuit loss.

8. Calculate

$$\sin\beta = \frac{\text{stator iron loss} + \text{brush short-circuit loss}}{V_t'P(N_sI)}$$

9. Using correct values of β and gross torque, recalculate K

10. Calculate

$$\frac{IS_cN_a}{aP} = \frac{K}{\phi} \tag{10}$$

11. Calculate

$$(NI)_f = N_sI + \frac{\theta_b}{90} \times (10) \tag{11}$$

where

$$\theta_b = 90(\psi_c - \psi)$$

12. Calculate $\gamma = (11)/(10)$ and $\gamma_s = N_sI/(10)$.

13. Calculate armature reactive drop constant

$$K_3 = \left[\frac{14.4K_sK_aPW}{S_c} + \frac{1.06\lambda_p\psi^2W}{\Delta K_1 \times S.F.} + 1.8\lambda_pK_s + \frac{3.19W\lambda_p}{\Delta_x}(1-\psi)\psi^2\right]2\pi f \times 10^{-8}$$

14. Calculate field reactive drop constant

$$K_2 = 2\pi f \times 10^{-8}[7.2K_{s,f}W + 3\lambda_p]$$

15. Calculate resistive drop constant

$$K_4 = \frac{\gamma^2 l_{mf}}{CM_f} + \frac{4L_{ca}P}{S_aCM_{sa}}$$

16. Calculate speed voltage per turn

$$V_s' = 2.36 \times 10^{-10} \times P \times RPM \times \phi$$

Table I. Design sheet for series motor

W	$2\frac{1}{4}$	P	2	D	2.063	Δ	.015	Δ_x	.297
F&W	.85	S_s	16	l_{mf}	11.1	K_1	1.2	K_s'	use 1.0
T_n	4.20	S_c	32	l_{ca}	4.75	ψ	.67	K_s	.9
T_d	.24	a	2	CM_f	97500	ψ_c	.875	K_a	.9
T_g	5.29	λ_p	3.27	CM_{sa}	23100	ϕ_b	18.5 use 16.8	K_e	.875
K	$(T_g \times 10^8)/2.62P^2$		5.05×10^7	P_s''	$14.4\ K_s\ K_a\ W\ (P/S_s)$				3.28
ψK	3.38×10^7			P_{sx}''	$1.06\ \frac{\lambda_p \psi^3}{\Delta K_1 \times S.F.}\ W$				68
$N_e I$	258			P_x''	$3.19\ \frac{\lambda_p}{\Delta_x}\ \psi^2\ (1-\psi)\ W$				11.7
ϕ	137500			P_e''	$1.8\ \lambda_p\ K_e$				5.15
$\phi(N_e I)$	3.55×10^7			K_2	$2\pi f \times 10^{-8} \times \sum P''$		3.32×10^{-4}	$\sum P''$	88.13
V_t'	$4.44\ f\phi \times 10^{-8}$		.371	P_s'	$7.2\ K_s'\ W$				16.2
FE_1	11	BSC	11	P_e'	$3\lambda_p$				9.8
$\sin\beta$	$\frac{FE_1 + BSC}{V_t' P\ (N_e I)}$		.115	K_3	$2\pi f \times 10^{-8} \times \sum P'$		$.98 \times 10^{-4}$	$\sum P'$	26
$\cos\beta$	.993	K_{corr}	$\frac{.985K}{\cos\beta}$ 5.01×10^7	R_f'	$\gamma^2 (l_{mf}/CM_f)$		$.91 \times 10^{-4}$		
$(NI)_a$	$\frac{K_{corr}}{\phi}$		365	R_a'	$4\ l_{ca}\ P/S_s\ CM_{sa}$		1.03×10^{-4}		
$(NI)_f$	$(N_e I) + \frac{\phi_b}{90}\ (NI)_a$		326	K_4	$R_f' + R_a'$		1.94×10^{-4}		
γ	$NI_f/(NI)_a$		.893	1	$K_4 (NI)_a$	.0708	4	$(K_2 + \gamma^2 K_3)(NI)_a$	.1496
γ_e	$N_e I/(NI)_a$		.706	2	$V_s' \cos\beta$	.645	5	$-V_s' \sin\beta$	-.0747
V_s'	$2.36\ P\phi \times RPM \times 10^{-10}$		.65	3	$V_t' \gamma_e \sin\beta$	.0302	6	$V_t' \gamma_e \cos\beta$	.260
S.F.			1.92	V_1		.746	V_2		.3349
N	$\frac{V - V_{br}}{V'}$		137	V'	$\sqrt{V_1^2 + V_2^2}$	.818	$V - V_{br}$	112	
N_a	$(aN)/S_c$		8.56 use $8\frac{1}{2}$ #22	I	$1.05\ (P\ NI_a/N)$		5.6		
N_f	$\gamma N/P$		61.2 use 61 #18	W_i	$V_1 P (NI)_a + V_{br} I$		562		
Brush Lead			$1\frac{1}{2}$ Bars	EFF	66.3		P.F.	87.4	

FRAME _____ DRAWING NO. _____ CALC.REF. _____

H.P. $\frac{1}{4}$ RPM 10,000 VOLTS 115 CYCLES 60 SIGNATURE _____ DATE _____

17. Calculate total voltage per turn

In Phase

$K_t \times (10)$

$V_t' \cos \beta$

$V_t' \gamma_t \sin \beta$

$\Sigma = V_1$

Quadrature

$(K_2 + \gamma^2 K_3)\ (10)$

$-V_s' \sin \beta$

$V_t' \gamma_t \cos \beta$

$\Sigma = V_2$

18. Determine number of armature turns

$$\frac{S_c N_a}{a} = \frac{V - V_{br}}{\sqrt{V_1^2 + V_2^2}} \qquad (18)$$

then

$$N_a = \frac{(18)a}{S_c}$$

and

$$N_f = \frac{(18)\gamma}{P}$$

19. Line current, $I = 1.05\ (10)P/(18)$.

Calculated and Test Results

Table 1 shows the design sheet for a 1/2-horsepower 10,000-rpm series motor. Performance of the motor built in accordance with this design is given in Figure 4. Comparative calculated and test results at rated torque are shown in Table II.

Table II

	Calculated	Test
Torque, ounce feet	4.2	4.2
Rpm	10,000	10,200
Horsepower output	0.500	0.510
Amperes	5.6	5.5
Watts input	562	570
Efficiency	66.3	67
Power factor	87.4	90
Armature resistance	0.913	0.875
Field resistance	0.734	0.747

Nomenclature

a = number of parallel paths in armature

B_{sc} = brush short circuit loss

CM_f = copper cross section area of field coil, circular mils

CM_{sa} = copper cross section area per armature slot, circular mils

D = diameter of armature, inches

f = line frequency, cycles per second

FE_1 = iron loss supplied by the stator

F and W = friction and windage loss

K_1 = air gap coefficient, Carter's coefficient

K_a = Adam's pitch factor correction for slot permeance

K_e = Adam's pitch factor correction for end permeance

K_s = slot constant, rotor

K_s' = slot constant, stator

l_{ca} = average length of armature conductor

l_{mf} = average length of field turn

N_a = armature turns per coil

N_f = field turns per coil

$(NI)_a$ = armature ampere-turns per pole

N_eI = effective magnetizing ampere-turns per pole

$(NI)_f$ = field ampere-turns per pole

P = number of poles

P_e' = end leakage permeance of stator

P_s' = slot leakage permeance of stator

P_e'' = end leakage permeance of rotor

P_s'' = slot leakage permeance of rotor

P_x'' = cross axis leakage permeance of rotor

P_{zz}'' = zig-zag leakage permeance of rotor

S_c = number of commutator segments

S_s = number of armature slots

$S.F.$ = saturation factor, defined as ratio of total ampere-turns to air gap ampere-turns for given gap flux

T_n = net torque, ounce feet

T_d = mechanical load on rotor due to iron loss expressed as torque, ounce feet

T_g = gross torque, ounce feet

V = line volts

V_{br} = voltage drop in brush circuit

V_s = speed voltage

V_t = transformer voltage

W = iron stacking, inches

W_i = watts input

Δ = actual air gap, inches

Δ_x = cross axis gap, inches

ψ = pole enclosure as a decimal

ψ_c = coil pitch as a decimal

B = maximum air gap flux per pole

θ_b = angle of brush lead, degrees

γ = ratio of field to armature ampere-turns per pole

γ_t = ratio of effective magnetizing ampere-turns to armature ampere-turns per pole

References

1. Armature Iron Losses in Series Motors, S. S. L. Chang, J. H. Karr. *AIEE Transactions*, volume 68, part 1, 1949, pages 262–65.

2. Theory of Alternating Current Machinery (book), A. S. Langsdorf. McGraw-Hill Book Company, New York, N. Y., pages 533–35.

3. Universal Electric Motors, A. F. Puchstein. *Bulletin* 53, Ohio State Engineering Experiment Station (Columbus, Ohio), 1930.

4. Universal Type Motors, L. C. Packer. *AIEE Transactions*, volume 44, 1925, pages 887–91.

Discussion

L. C. Packer (Westinghouse Electric Corporation, Springfield, Mass.): The authors have made a real contribution to the art of designing noncompensated a-c series motors with their design method. This type of motor is relatively small in size and not of the glamorous type, and is generally looked upon by other motor designers as of no importance in the motor field. However, they are one of the most difficult to design. They are made by the millions every year for some of our most important household and office appliances and portable electrical tools. They are usually designed for high speeds to reduce the size and weight of the product.

The bearing and brush friction and windage will be as much as 15 per cent of the output at high speeds even with ball bearings.

The armature iron loss is relatively high due to the high-frequency and high-flux densities in the armature especially in those teeth on one side of the armature where the cross field adds to the main field flux. The variation also is greater at the high densities because of variations in punching strains and burrs. Annealing the armature laminations will help this situation.

The full load saturation can be troublesome to calculate because of the distortion caused by the cross field and demagnetizing effect. The cross field causes extremely high armature tooth and pole tip densities on the one side. A picture of this may be seen by laying out the field forms of the flux distribution. Fairly accurate full load saturation curves may be layed out from the no-load air gap and armature teeth saturation and the demagnetizing and cross field ampere turns and employing the equal area method. Another method is to take a motor of similar winding ratio and brush shift and obtain a no-load and full-load saturation by test.

Another item that can vary the results is the angle between the current and flux. This is directly proportional to the iron loss and the losses in the coils short circuited by the brush. The speed of the commutator bars under the brush is in the order of tenths of a thousandth of a second allowing very little time for the current to rise very high, therefore this loss cannot be very accurately calculated. However, tests for iron loss and short circuit losses can be taken on similar designs of winding ratio, brush shift, current, speed and flux conditions and those values used for approximating new designs.

The authors method of design is unique in their approach to the problem. My results, when using test constants in their method, were good in some respects and not very good in others. Two different load points of the same motor were tried out as follows:

1. With actual values of flux = 84,000 (max) lines, $K = 3.46 \times 10^7$ and $\psi = 0.62$, the value of N_eI was assumed.

Calculated values, $-N_a = 11.7$, $-N_f = 77.0$, -4.36 amperes, -415 watts.

Actual values, $-N_a = 11$, $N_f = 100$, 4.36 amperes, -410 watts

2. Assuming actual values flux = 84,000 (max), $N_f/N_a = 1.3$, and $I = 4.36$.

Calculated values, $N_a = 10.95$, $N_f = 99.5$, -4.61 amperes, -479 watts.

3. Using another set of actual values, $-$flux = 92,000 (max), $K = 3.78 \times 10^7$, and solving for N_eI.

Calculated values, $N_a = 13$, $N_f = 84.5$, -4.55 amperes, -520 watts.

Actual values $N_a = 11$, $N_f = 100$, -5.18 amperes, -510 watts.

4. Assuming actual values, flux, = 92,000, $N_f = 100$, $N_a = 11$, 5.18 amperes.

Calculated $N_a = 11.5$, $N_f = 105$, -5.18 amperes, 536 watts.

Actual $N_a = 11$, $N_f = 100$, 5.18 amperes, -510 watts.

The motor from which the data was used was very accurately tested, checked, and the vector diagram practically closed. Using actual values in the authors' method checked very close to actual values except the watts in calculation (2).

Calculated values of leakage flux were used which were higher than actual values which would affect the results. The short circuit losses were calculated and they could also vary the results.

The authors' method appears to give good results, except when the value N_aI is obtained from the equation $\phi N_aI = K\psi \times 1.05$. It appears to me that it would be better to solve for S_cN_aI/a in the torque equation. When actual values are substituted in this method the results are very good, but they are not so good when starting with N_aI. At least that is my experience. Maybe some point has been missed and the authors may be able to enlighten me. More use of the method also may help to get the same results obtained with methods more familiar to me.

In the equation for the speed voltage V_s the authors use a constant 2.36. Should not this constant be $2\sqrt{2}$?

The authors consider only the transformer loss in the short circuited coils. Why do they not consider the total loss which includes the rotational loss in quadrature with the transformer loss?

A. F. Puchstein (The Jeffrey Manufacturing Company, Columbus, Ohio): This paper represents a welcome attempt to provide a method of calculation suitable for student and designer. The work is set up on the basis of sinusoidal assumptions. It would have helped to give some evidence to establish the errors resulting from this. See the vector diagram in Figure 2 of the paper. Since a saturation curve is employed, observe that with the brushes on the commutator such curves are different when taken at different speeds and frequencies. As an example, Table I of the discussion gives some figures from tests on a 3/4-horsepower 110-volt 6,500-rpm motor with distributed field winding and brushes on neutral when separately excited and driven at 3,560 rpm by a second motor.

Such saturation curves would be obtained experimentally for each frame (calculation is not very feasible). They may be taken for no-load or load conditions.

For no-load, by driving the armature with an external motor and separately exciting the field with an adjustable low-voltage supply source. Read and record speed, armature volts, field resistance, field amperes, field volts, and field watts. For load conditions, some corrections would be made for armature reaction, commutation effects, and so forth.

For load conditions, connect the motor in the normal way. Provide an adjustable supply voltage and adjustable load. Read and record speed, amperes; line, field and armature volts; line, field, and armature watts. Measure field and armature circuit resistances. If a dynamometer is available, read torque also, make an allowance for rotative loss. Obtain the leakage reactances (ordinarily this means to estimate or calculate). From these, obtain the useful flux per pole (three values; should be alike, but will not be), and its phase position and

Table I

Effective Field Amperes	Effective Armature Volts DC	25 Cycles	60 Cycles
2	21.1	18.3	17.0
4	32.8	28.0	27.0
6	38.7	33.3	32.2
8	42.6	37.0	35.9
10	45.8	39.9	38.8
12	48.1	42.1	41.0

plot as a function of current. However, with small motors, the instrument losses should be corrected for, and the variable nature of brush-contact, brush and motor friction is a problem that must be taken into account in some way, as statistically. All this serves to give a bird's-eye view of the problem. But since the attainable accuracy will be limited anyway, few will have the patience to carry its solution through. The items on the calculation sheet should be numbered in the order in which they are used. A distinction should be made between calculating what a given motor will do and designing one from the ground up. The vector diagram, Figure 2 of the paper, neglects the effects of nonsinusoidal variations in current and flux, and the effects of commutation on the strength and phase of the field flux (see reference by F. Punga) though it does give an approximate method for including the effect of the commutation short-circuit loss. It assumes that the quantities in it are linear and sinusoidal, which, of course, is not true. This means that the lines of the vector diagram will not close if measured experimentally.[2] The derivation of the expressions for leakage resistance is not given.

References

1. Das Funken von Kommutator Motoren, F. Punga. Geb. Janecke, Hannover, Germany, 1905, page 48.

2. Voltage Relations and Losses in Small Universal Motors, A. F. Puchstein, I. S. Campbell. *Bulletin Number 58, The Ohio Engineering Experiment Station*, Columbus, Ohio, 1931.

3. Theory and Calculation of Electrical Apparatus, C. P. Steinmetz. McGraw-Hill Book Company, New York, N. Y., Chapter XX, 1917.

4. Wechselstromtechnik, E. Arnold, J. L. La Cour. Julius Springer, Berlin, Germany, chapter XIII, part II, volume V.

Sheldon S. L. Chang and **J. H. Karr:** The writers appreciate very much Mr. Packer's discussion, from which we realize that one important point in our paper was not made clear. That is probably the cause of discrepancy between calculated and actual values given in Mr. Packer's discussion. Besides the mechanical dimensions, and the specified performance, that is, torque at a given speed, two other factors influence the numbers of field and armature turns, namely: the brush shift θ_b, and the ratio γ. A satisfactory design can be made as long as these two factors are within certain ranges of values. But for different values of θ_b and γ, the numbers of field and armature turns are necessarily different to give the specified torque at the specified speed.

Most of the equations given in this paper are perfectly general. They can be used for both designing new motors and checking the performance of existing motors. In designing new motors, we have to specify θ_b and γ. θ_b is specified with equation 1, and the assumption $\phi N_aI = 1.05k\psi$ automatically determines γ with the ensuing steps in the design sheet. For reasons given in the paper, the choice of values for θ_b and γ this way generally results in good efficiency. The equation $\phi N_aI = 1.05k\psi$ also makes it possible to determine a proper operating point on the magnetization curve.

In checking the performance of existing motors both of the above equations cannot be used. With a motor designed by experience, θ_b and γ generally fall within their respective ranges of acceptable values, but they cannot be expected to equal the specific values given by these equations.

Before we adopted this design method, we made extensive checks on existing motors by a somewhat different procedure. Known quantities were V, I, N_f, N_a, θ_b. The calculated quantities to be compared with actual results are watts, speed, torque, and flux per pole. The procedure is given below:

1. Calculate N_aI from equation 2.

2. Read ϕ from magnetization curve for the calculated value of N_aI.

3. Calculate V_t from equation 8.

4. Calculate γ, γ_d from actual values of N_a and N_f.

5. Calculate K_2, K_3, K_4.

6. Calculate

$$\beta = \sin^{-1} \frac{\text{stator iron loss} + \text{brush short circuit loss}}{V_tI}$$

7. Calculate the resistive and reactive voltage drop:

$$V_x = I\rho\left(\frac{S_cN_a}{a\phi}\right)^2 (K_2 + \gamma^2 K_3)$$

$$V_R = I\rho\left(\frac{S_cN_a}{a\phi}\right)^2 K_4 + V_{b'}$$

8. Calculate the voltage out of phase with V_s:

$$V_1 = V_t + V_x \cos\beta + V_R \sin\beta$$

9. Calculate the voltage in phase with V_s:

$$V_4 = \sqrt{V^2 - V_1^2}$$

10. Calculate

$$V_s = V_4 + V_x \sin\beta - V_R \cos\beta$$

where: V_s is total voltage at right angles to flux, ϕ, and V_4 is total voltage in phase with flux ϕ.

11. Calculate rpm from V_s and ϕ by equation 7.

12. Calculate gross torque from equation 9.

13. Calculate net torque $T_n = T_g - T_d$.

14. Calculate watts input by adding output and losses.

15. Compare actual and calculated values of items 11, 13, and 14.

As the foregoing procedure uses the same basic equations and vector diagram as the design procedure, equally good results can be expected.

Mr. Packer pointed out a number of factors which may introduce some variation from the calculated results. But as all

these factors are taken into account in the design procedure, the variations of these factors from their nominal values do not seem to cause any appreciable discrepancy, insofar as our experience indicates.

The constant 2.36 is an exact constant. Its derivation is given below:

The peak value of speed voltage is

$$2p\phi\times\frac{S_c N_a}{a}\times\frac{\text{rpm}}{60}\times10^{-8}$$

The effective value is

$$\sqrt{2}p\phi\times\frac{S_c N_a}{a}\times\frac{\text{rpm}}{60}\times10^{-8}$$

grouping the constants, we have

$$\frac{\sqrt{2}}{60}\times10^{-8}=2.36\times10^{-10}$$

Generally, both the speed voltage and transformer voltage can cause loss in the short-circuited coils. The loss due to transformer voltage is nearly independent of the brush shift and must be accounted for in a correct design procedure. The quadrature component, or the loss due to speed voltage depends primarily on the brush shift. For a certain value of brush shift, the speed voltage is just enough to reverse the current in the coil during commutation, and the loss is zero. This brush position is about the same for both a-c and d-c operation of the same motor. It is assumed that the actual brush position is close enough to the ideal brush position that this loss is negligible.

The writers also appreciate Mr. Puchstein's discussion. But we do not agree with Mr. Puchstein on two points:

1. That our work is set up on the basis of sinusoidal assumptions.

2. That the calculation of the saturation curve is not very feasible.

For the first point, we do not know how Mr. Puchstein would suggest to analyze a nonsinusoidal problem, other than the following:

1. To distinguish space harmonics from time harmonics.

2. To analyze the nonsinusoidal wave form into a fundamental sine wave and some harmonic sine waves, and to study their interactions.

These are done in the paper. We correct for the effect of the third harmonics wherever correction is necessary. Mr. Puchstein states that the lines of the vector diagram will not close if measured experimentally. But that does not affect the existence of the vector diagram of the fundamental sinusoidal components which does close, nor does it prevent accurate calculation of the machine performance based on the vector diagram of the fundamental waves if the effects of the harmonics are properly studied and corrected for. A close analogy is the vector diagram of a transformer. The vector diagram does not close, but that fact does not prevent the transformer engineers from calculating its performance accurately.

For the second point, most manufacturers calculate the saturation curves of their induction motors. The a-c saturation curve of a series motor can be similarly calculated with slight modification to account for the flux distribution in the armature teeth.

Mr. Puchstein listed some measured values of a saturation curve. His data show considerable difference between a-c and d-c saturation curves while the 25-cycle and 60-cycle data agree within a few per cent.

In the paper, the writers have pointed out that the d-c saturation curve cannot be used in calculating a-c series motors. There is no theoretical basis for a difference of a few per cent between the 60-cycle and 25-cycle magnetization curves, and we doubt if Mr. Puchstein's measurements are accurate enough to establish the difference of a few per cent.

Investigation and Elimination of Unusual Vibration in the Field on a Large Single-Phase Frequency Changer

W. M. H. BALLANTYNE
MEMBER AIEE

J. E. ALLEN
FELLOW AIEE

R. A. BAUDRY
NONMEMBER AIEE

Synopsis: This paper describes the investigation which led to the correction of vibration trouble in the stator and rotor of a large single-phase frequency changer set. The method of correction is described. Measurements taken over a period of eight years show that the cause of vibration has been permanently corrected.

THE electrification program of the Pennsylvania Railroad necessitated a large amount of single-phase 25-cycle power, most of which is supplied by large frequency changers. One of these frequency changers was installed at the Safe Harbor Water Power Corporation's power station in 1934. It consists of two synchronous machines; a 24-pole 3-phase 60-cycle motor rated at 29,000 kva at 90 per cent power and a 10-pole single-phase 25-cycle generator rated at 31,250 kva at 80 per cent power factor. The shafts of both units are solidly coupled. The speed of 300 rpm is the highest at which a 60- to 25-cycle synchronous frequency changer can be made.

Since this frequency changer must operate in parallel with other similar units on the railroad supply system, it is provided with a stator shifting device which permits control of the output. At the Safe Harbor Power Station the frequency changer can transfer power in either direction, that is, from the 60-cycle system to the 25-cycle railroad system or inversely.

The 25-cycle generator stator is supported on springs in order to reduce to a very low value the 50-cycle torque pulsations that are transmitted to the foundation.

The 25-cycle single-phase generator is a large machine having large salient poles and a very deep core subjected to great magnetic and gravity forces which sometimes result in appreciable vibrations, as was found to be the case in this machine.

Stator vibrations were masked by the normal single-phase torque pulsations and were not detected until the machine had been operated for several years and corrective measures had to be taken.

While the stator vibrations were being eliminated, indications of pole vibration were observed. The nature and cause of these vibrations could not be ascertained until vibration measurement could be made on the rotor. As a result of these vibration measurements special wedges were provided for the poles and the vibration practically eliminated.

Investigation and Correction of Stator Vibrations

Stator Construction

The stators of both 25- and 60-cycle machines are of the conventional type used for large a-c machines. The core is made of a number of punchings stacked on cold-rolled steel bars and heavily pressed together by means of rigid end plates. Each stator is built in two sections to permit shipment from the factory to the installation site. The split of the stator is located in the vertical plane, where there is more space to provide liberal flanges which hold the halves of the stator together. This also facilitates inspection and maintenance of the joint in the core. This joint is packed with fishpaper of approximately 1/32-inch thickness in order to provide a good seat at the surface of the core joint and also to prevent short-circuiting the edges of several punchings which could result in excessive eddy current losses and local high temperatures. The split of the frame is provided with a number of steel liners sufficient to provide the desired pressure at the joint of the core, as shown in Figure 1.

The split of the core is subjected to a pulsating pressure of a frequency equal to double the line frequency. In Figure 2 it is seen that when the center line of one pole is in line with the core split, no flux is passing through the surface of the split. When two poles are straddling the split, the flux is a maximum and the unit pressure acting on the surface of the split is equal to $B^2/72$ where B is the flux density in kilolines per square inch. This pulsating force is very strong in machines having a very deep core, such as the 25-cycle generator. This makes it necessary not only to provide ample pressure at the joint but also to ascertain that this pressure is continuously maintained after the machine is placed in service.

On large single-phase machines, such as this 25-cycle unit, it is the practice to support the stator on springs to reduce to a small value the pulsating load transmitted to the foundation. The spring assembly is shown in Figure 3. The springs are arranged so that they still work in compression should the stator be lifted away from the frame foot by the large torques resulting from a short circuit in the system. The flexibility of the springs is such that the natural frequency of the system formed by the stator and the springs ap-

Paper 50-199, recommended by the AIEE Rotating Machinery Committee and approved by the AIEE Technical Program Committee for presentation at the AIEE Middle Eastern District Meeting, Baltimore, Md., October 3-5, 1950. Manuscript submitted July 6, 1950; made available for printing August 18, 1950.

W. M. H. Ballantyne, now deceased, was with the Safe Harbor Water Power Corporation, Baltimore, Md., and J. E. Allen, now deceased, was with the Safe Harbor Water Power Corporation, Lancaster, Pa. R. A. Baudry is with the Westinghouse Electric Corporation, East Pittsburgh, Pa.

The authors wish to acknowledge the co-operation of the Safe Harbor Water Power Corporation and the Westinghouse Electric Corporation, which made it possible to find a very simple and economical solution to a vibration problem which otherwise might have become quite serious.

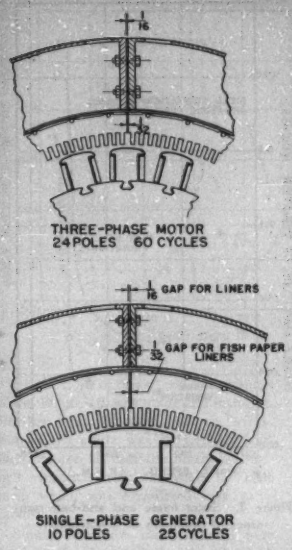

Figure 1. Transversal cross sections of generator and motor showing relative proportions of cores and poles

Figure 2 (below). Magnetic flux pattern in the stator core

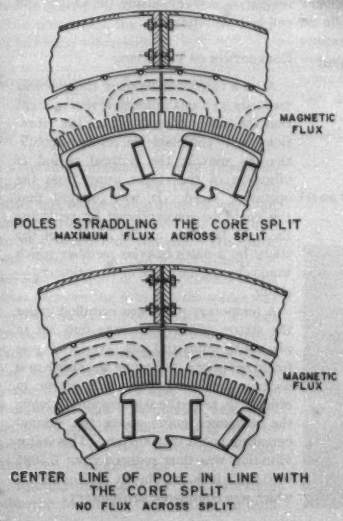

proaches the normal speed frequency of 300 rpm. In order to eliminate the possibility of stator oscillation in the vertical direction, the stator was originally tied to the foundation by means of a vertical flexible plate, shown in Figure 4, which is rigid in the vertical direction and flexible in the tangential direction to permit the free motion of the stator under the single-phase loading or other torque pulsations.

Investigation of Vibration

When initially placed in service in 1934, the machine performed very satisfactorily. There was a small amount of 50-cycle vibration on the stator caused by the single-phase torque, but this was almost entirely absorbed by the spring mounting and not transmitted to the foundation.

In 1937, following an inspection of the machine, it was thought advisable to retighten the split of the core after minute traces of red dust had been found near the split. The machine apparently continued to operate very satisfactorily until a second inspection made in 1939. Then it was found that the parallel winding connection supports had become loose. The vibration was sufficient to have caused one bolt to cut a slot through one of the brass cleats holding the parallel connections, as shown in Figure 5. The stator coils also had become slightly loose in the slot and were retightened by adding a fiber strip under the slot wedges. The weld between the vertical tie plate and the stator was found cracked and it was rewelded.

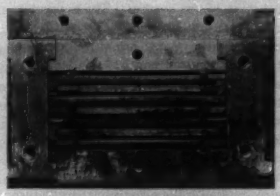

Figure 3 (above). Stator spring mounting

Shortly after the inspection and overhaul of 1939, it was noticed that the vibration of the sheet-steel end bells enclosing the end windings had appreciably increased. At first it was believed that this increased vibration was caused by additional inspection holes which were cut in the end bells in 1939 which could have changed their natural frequency and brought about a condition of resonance. After a further increase in the amplitude of vibration and the occurrence of some cracks in the welded joints of the flange of the end bells, a thorough investigation of the vibration was made.

This investigation showed that the fundamental frequency of vibration was 50 cycles per second, the same as the frequency of the magnetic forces caused by the armature flux. The amplitude of vibration at the horizontal split of the end bells varied from 0.008 to 0.010 inch. Addition of a weight of 150 pounds at the enter of the end bells in order to try to change the natural frequency did not appreciably change the amplitude of vibration.

The amplitude of vibration continued to increase until, in 1940, it reached 0.048 inch at one of the windows. Retightening of the end bell joints and addition of rubber dampers reduced the

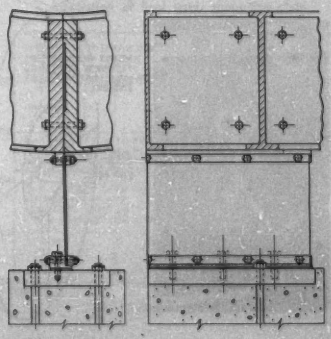

Figure 4 (right). Initial stator vertical supporting plate

vibrations to approximately 0.016 inch.

In the meantime the investigation was continued and showed that:

1. The vibration existed only when the field was on and was nearly proportional to the field current.

2. The amplitude of vibration did not change when the load was increased from 0 to 15,000 kw.

This last observation indicated that although the vibrations were of magnetic origin they were not caused by the leakage flux of the end windings as had been suggested.

A study of vibration measurements which had been made in 1939 indicated that the vibration of the end bells was proportional to the vertical vibration of the stator frame near the vertical plate tying the stator to the foundation. This led to the idea that the end-bell vibration might originate in the stator. The structure of the end bell is shown in Figure 6. The front wall restrains any radial movement of the flanged joint. Any radial motion of the latter near the frame will cause the complete joint to oscillate about the corner of the end bell as a fulcrum. This will cause the vibration of the end bell to be magnified by the ratio of the length of the front wall joint to the length of the axial joint between the front wall and the stator. In order to check this theory, arrangements were made to make a complete series of vibration measurements on both stator and end bell late in 1940.

The results of this investigation are shown in Figures 7, 8, and 9. The frame vibration was measured at the horizontal center line and the end-bell vibration also at the center line near the shaft where both were found to be maximum. In Figure 7 is shown the vibration of the frame and of the end bell as a function of the shaft rpm with an armature temperature of 58 degrees centigrade and a field excitation of 300 amperes. The amplitude of vibration in the stator and the end bell are proportional and reach a very large value at the normal speed of 300 rpm, thus indicating a condition of resonance at this speed. In Figure 8 are given the amplitudes of vibration of the stator at armature temperatures of 30 degrees centigrade and 47 degrees centigrade. The curves show that at 30 degrees centigrade, the resonance point is 275 rpm, and is at exactly 300 rpm at 47 degrees centigrade. As shown in Figure 9, the resonance point also changes with the field current.

These tests showed positively that the end-bell vibrations originated in the stator. The vibration of the stator is caused mainly by the dissymmetry of the splits. The large magnetic force acting on the split causes a small motion which excites the vibration. Changes in pressure at the split and between the core and stator frame cause changes in the elastic constant of the system. These pressure changes can be caused by changes in bolt or shim adjustment, armature temperature, or field strength. Under some operating conditions there was a condition of resonance which caused excessive vibration in the stator and explained the looseness of the stator coils observed and corrected in 1939. The change in the resonance condition with split bolt adjustment and with the armature temperature

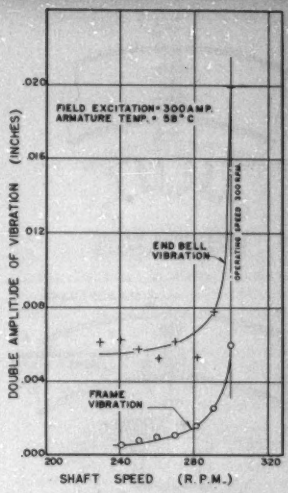

Figure 7. Stator frame and end-bell resonance at beginning of investigation

also explained the freedom from vibration when the machine was placed in service. The split adjustments were first made in 1937 and about 1939 the flow of water in the air coolers was reduced to a minimum, thus increasing the temperature of the armature, bringing the stator closer to resonance, and increasing the stator and end-bell vibrations.

Figure 5 (below). Brass winding clamp. Slot cut as result of stator vibrations

Figure 6 (below). Conversion of stator radial vibration to end-bell axial vibration

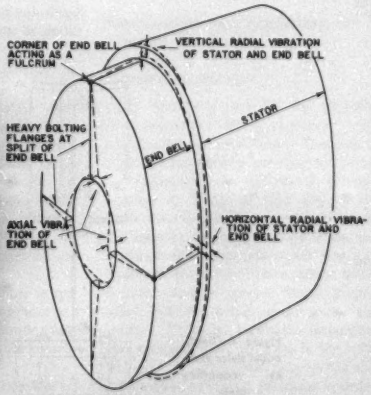

Correction of Vibration

After a further analysis of the problem and tests on a small model, it was thought that the easiest way to reduce the vibration was to eliminate the resonant condition by moving the natural period of vibration of the stator away from the operating speed. It was thought that this could be accomplished by replacing the light tie plate at the bottom of the stator by a much heavier member which would change the mode of vibration of the stator.

A temporary plate was installed under the stator. This plate was first set in place with shims and jack screws. It was found necessary to remove the shims and increase the number of jack screws in order to increase the stiffness and to move the resonance point above the normal operating speed of 300 rpm. The stator vibration was thus reduced from 0.0085 to 0.0015 inch, as shown in Figure 11, which was considered satisfactory.

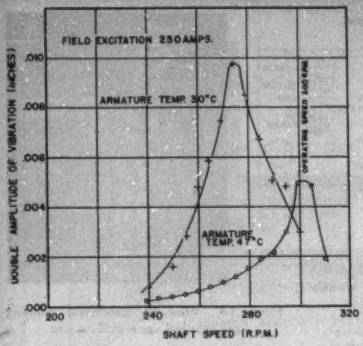

Figure 8 (left). Influence of winding temperature on stator frame resonance

Figure 9 (right). Influence of field current on stator frame resonance

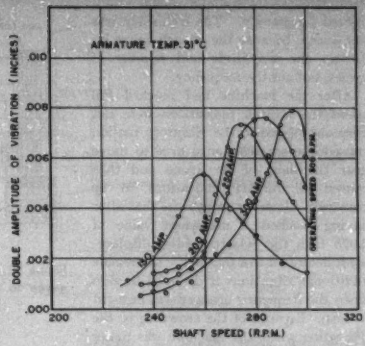

On the basis of these tests a permanent plate, Figure 10, was made and installed. Further tests indicated that the vibration of the stator was reduced to 0.001 inch, Figure 11, and the maximum end-bell vibration near the shaft to 0.006 inch, which was considered very satisfactory.

Similar vibration measurements were made on the 60-cycle end of the set, which is of the same design but has a much smaller radial depth of core, as shown in Figure 1, where both machines are drawn to the same scale. As a result of this smaller core size the total magnetic flux across the split and, therefore, the magnetic forces are much smaller. Furthermore, the stator frame is supported on a cradle securely bolted to the foundation, thus preventing the building up of any appreciable vibrations.

Investigation and Correction of Rotor Vibrations

Study of Rotor Vibrations

The first indication of rotor vibrations was noticed during the 1939 inspection when one of the connections between the collector rings and the field coil was found to be cracked near the coil. The crack was caused by fatigue which usually results from vibration. The presence of red dust between the pole and the spider was another indication of vibration. It was thought that this vibration was resulting from a gradual loosening of the pole dovetail wedges after several years of single-phase operation. These wedges were retightened and a laminated field connector of greater flexibility was used to replace the old one made of a single thickness of copper strap.

Another indication of pole vibration also was found later in 1939 during tests made to determine the overload capacity of the frequency changer. The operating temperature of the stator windings is normally measured by temperature detectors provided with the machine, thus permitting the easy determination of the maximum permissible operating load. The damper windings of a large single-phase machine also are subjected to severe duty, and with high overload their temperature and the resulting thermal stresses increase rapidly. The measurement of temperatures and stresses of rotating parts is much more difficult than on stationary parts, and is usually much less accurate unless very elaborate equipment is used. Several attempts at measuring the temperature of the damper winding under load were made with fusible alloys. These tests indicated that the temperature of the amortisseur ring was very conservative. However, there was some doubt whether with the location of the devices first mentioned the true amortisseur winding temperature was obtained. Then it was thought that it might be possible to measure the radial expansion of the amortisseur end ring with a "de Forest scratch gauge." This gauge, described in Appendix I, can be mounted very easily on rotating parts and indicates displacements which can be measured with an accuracy of 0.0001 inch.

The mounting of this gauge on the amortisseur winding is shown in Figure 12 and is such that the radial displacement of the amortisseur end ring with respect to the upper part of the pole is recorded.

The record of the test is shown in Figure 13 and the results were entirely unexpected. The scratch gauge moving from left to right indicated that the pole first moved outward away from the amortisseur ring. On this radial displacement is superimposed a vibrating motion of 0.003 inch. Since the frequency changer was started from the 60-cycle end, there was no load on the 25-cycle machine during this starting period and the vibrating motion is apparently

Figure 10. Final stator supporting plate

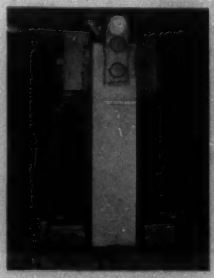

Figure 11. Reduced stator vibration after installation of final stator supporting plate

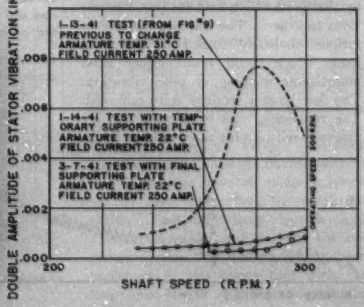

caused by gravity. The frequency was not known because the scratch gauge indicates the amplitude and number of cycles, but not the frequency.

After the machine had reached full speed the scratch indications were not very clear because the vibratory motion caused the scratch gauge arm to move near the limit of its stroke and thus caused all further indications to be crowded. However, it appears that after having reached a maximum value of 0.075 inch the relative radial displacement decreased to 0.045 inch. After some additional vibrations it dropped to zero when the frequency changer was brought to rest. Because of the crowding of the indication when the machine was under load, the radial displacement due to temperature effect was not considered to be of sufficient accuracy to determine the maximum overload which could be carried by the amortisseur winding.

Two significant facts which were not expected were obtained from this test:

1. The upper part of the field coil support attached to the pole was deflecting very appreciably due to centrifugal force.
2. There was a vibratory motion of 0.003 inch between the pole and amortisseur winding.

It was thought that this vibration was caused by the gravity action in the amortisseur winding, thus causing the winding to move with respect to the pole while the machine was rotating.

It was not felt at this time that these two observations had much significance and the machine was continued in service until 1941, when a new inspection was made at the time of the vibration investigation of the stator.

At the first inspection made in January 1941, parts of the pole upper coil support holding the amortisseur bars were found to be cracked. This coil support, as shown in Figure 14, is made of aluminum sheet 1/8-inch in thickness held by the rivets which hold the pole laminations together. The fracture was due to fatigue obviously caused by pulsating loads which could result either from amortisseur winding or pole vibration. The few broken sections were removed. The remaining ones were reinforced by means of self-tapping screws placed in the punching between each two amortisseur bars, as shown in Figure 14.

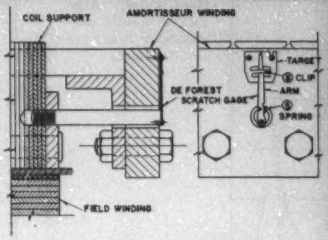

Figure 12. Mounting of de Forest scratch gauge to record radial motion of amortisseur winding

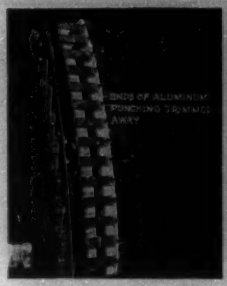

Figure 14. View of amortisseur winding and repaired upper coil support

A few months later at the next shutdown, necessitated by the study of the stator vibration, some cracks were found at the neck of the dovetails of two poles. The material around the cracks was chipped out, and it was found that these cracks were only in the first lamination in one pole and in four laminations in the other. The fractures were caused by fatigue. This indicated the presence of appreciable vibrations because the tensile stress in the neck of the pole at normal speed was very low, less than one-fifth of the yield point or endurance limit of the material.

The following summary of all previous observations and troubles on the pole then was made:

1. Cracked field lead connection.
2. Scratch gauge test indicating vibration in the pole.
3. Presence of red iron oxide dust at the bottom of the pole.
4. Broken amortisseur winding support.
5. Cracked pole dovetail.

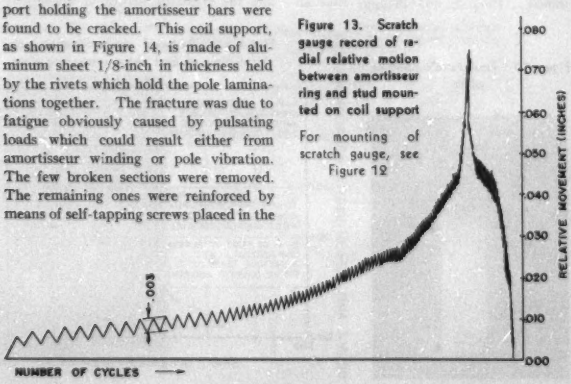

Figure 13. Scratch gauge record of radial relative motion between amortisseur ring and stud mounted on coil support

For mounting of scratch gauge, see Figure 12

Source of Rotor Vibrations

All these observations indicated that the pole itself was vibrating. After the finding of the cracked field connector, the same conclusions already had been reached and the dovetail wedges were retightened in order to eliminate was vibration which, it was then thought, was caused by gradual loosening of the pole dovetail due to the pulsating single phase torque. When considering the fastening of a pole to the spider by means of a dovetail and tapered wedge, it usually is believed that the tension produced by driving the wedges is sufficient to keep the pole tight against the spider under all operating conditions. In this case, with the large width of the pole, it was very difficult to visualize that under these conditions the pole could vibrate relative to the spider. However, by a very simple analysis it can be seen easily that for a pole of the length used in this machine the dovetail key is not of sufficient thickness to overcome the friction forces which would be developed over its complete length if the dovetail was preloaded by a force equal to or larger than the action of the centrifugal force of the pole and coil. Therefore, at normal speed the pole pulls away from the spider and is free to rock about the dovetail neck, the wide pole seat being of no benefit.

A further consideration of the scratch gauge test made in 1939 indicated that this theory was probably correct, and that the large radial displacement of the pole with respect to the amortisseur ring was probably not entirely due to the deformation of the coil support.

It then was decided to install several scratch gauges on the rotor to determine the motion of the pole with respect to the

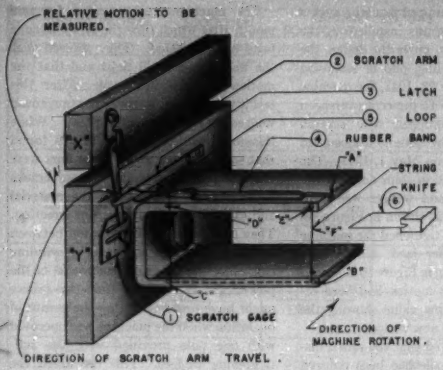

Figure 15. Scratch gauge triggering device

1. Relative motion between parts *x* and *y* is recorded on scratch gauge, 1, by scratch arm, 2
2. Latch, 3, prevents travel of scratch arm while machine is being started and placed under desired operating conditions
3. Rubber band, 4, secured at *A* and held in tension by string secured at *E* and passing through holes *B*, *C*, and *D*. Latch is secured to rubber band by loop, 5
4. Scratch arm is put in normal operation by cutting string at *F*, allowing rubber band to contract and life latch away from scartch arm. String is cut by knife, 6, mounted on stator and moved into path of string

spider. Some consideration was first given to the use of more elaborate devices which could show the motion of the pole over a long period of operation. However, because of its simplicity the use of the scratch gauge was more desirable.

One of the limitations of the scratch gauge shown in the 1939 test was that vibration due to gravity caused the scratch gauge arm to move rapidly to the end of its stroke where all the indications became crowded and before vibrations caused by pulsating torque could be recorded. It then was concluded that the 1939 vibration recordings were caused by gravity, and that the arm had moved to the end of its stroke before the machine could be placed under load. This operation usually takes 20 minutes before all the switching operations are completed. It then was judged desirable to have a triggering device which could prevent operation of the scratch gauge until the frequency changer was placed under a desired load. Such a device was developed and installed on the pole, as shown in Figure 15. The scratch gauges were located on several poles.

A series of tests was made at normal speed under various loads. Typical scratch gauge records made during these tests are shown in Figure 16, which shows the relative motion between the base of the pole and the spider. It is seen that the base of the dovetail moves 0.021 inch away from the spider. The edges of the pole move away a slightly larger amount: 0.029 and 0.022 inch. At these latter points there are also two vibratory motions superimposed on the radial displacement, a high-frequency vibration of 0.003 inch double amplitude and a low-frequency motion of 0.002 inch having a frequency of one-fifth of the former. As previously mentioned, the scratch gauge gives the number of cycles, but having no time scale, does not indicate the frequency. However, there are two large pulsating forces acting on the poles. One force is caused by the single-phase torque of 50 cycles per second, the other resulting from the action of gravity which causes one cycle of vibration per revolution or five per second. The two superimposed vibrating motions of the pole have the same ratio of frequency as the forces just described. It seems very likely, therefore, that the two vibrating motions result from these forces.

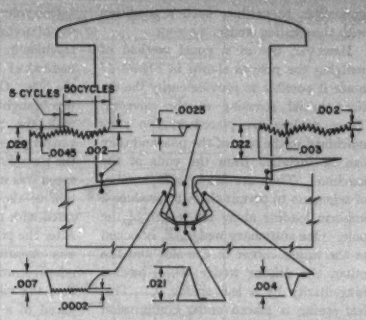

Figure 16. Scratch gauge test: original condition before tangential wedges were driven

Test on pole number 10, May 1, 1941, 30,000-kw load, 300 rpm

The radial displacement of the pole is caused by the elastic deformation resulting from the action of centrifugal force on the dovetail and the spider. This motion is much larger at the end of the pole than at the center, due to the additional weight of the end of the field coil which is concentrated there. However, it was much larger than expected. This motion in itself is not objectionable but by freeing the base of the pole from the spider it permits the pole to oscillate freely about the neck of the dovetail.

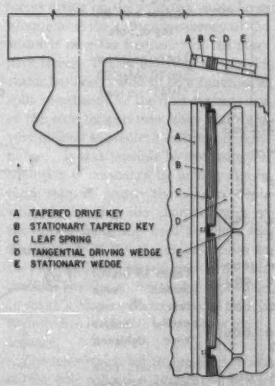

Figure 17. Tangential tightening wedges to prevent rocking of poles

Correction of Rotor Vibrations

As a result of this test it was obvious that a more rigid fastening of the pole to the spider was necessary if the observed vibrations were to be eliminated or reduced to a very low value. This more rigid tie could be obtained on this machine by placing the dovetail under a stress greater than that caused by centrifugal action. This would keep the pole tight against the spider and prevent the observed motion. It has previously been explained in this paper that with the large axial length of this machine it was

impossible to produce such a condition with the existing wedge.

However, use of a novel method of wedging the pole as shown in Figure 17 made it possible to provide easily the desired initial stressing of the dovetail. These wedges are placed in two slots machined in the base of the pole and they can be installed from the ends of the machine. They are made of a number of segments to permit them to produce a uniform loading along the length of the pole. One stationary wedge, *E*, is locked in the upper corner of the slot and the other, the driving wedge, *D*, is pushed tangentially by a leaf spring, *C*. This leaf spring is placed under compression by a tapered key, *AB*, driven axially in the slot from the end of the machine. The force exerted by the spring is sufficient to overcome the tangential frictional force produced between the lower and upper wedges by centrifugal action even at 25-per cent overspeed.

With such an arrangement, as the speed of the machine increases and the pole moves away from the spider, the lower wedge is forced tightly between the spider and the upper wedge. The wedging angle is such that the wedges are self-locking. Thus after the machine has operated at a higher speed than normal (15-per cent overspeed) and after the speed has been reduced to normal, the wedges are compressed very tightly and restrain effectively the vibratory motion of the pole because of the resulting preloading of the dovetail.

One pole was equipped first with such a set of wedges. It was installed on the machine in order to prove the design, the method of assembling, and of removing the pole. On May 23, 1941, the machine was brought up to 15-per cent overspeed with the pole equipped with scratch gauges placed in the same locations as in the preceding test on May 1, 1941. The speed was increased in steps and the motion of the pole and wedges was measured with results as shown in Figure 18. After the pole was tightened the machine was operated under load, and scratch gauge records shown in Figure 19 indicated that the vibratory motion had been reduced to a very low value showing the effectiveness of the new wedges.

This test indicated that the radial displacement of the pole had been reduced from 0.029 and 0.022 inch to 0.012 and 0.018 inch at normal speed. Part of this displacement is due to the gauge support deflection, the other part indicates the additional displacement of the pole at its end. This latter displacement extends over a length of pole smaller than the length of the tangential wedge (6 inches), otherwise it would have been taken up by the tangential displacement of this wedge.

Scratch gauges placed between the upper coil support and the amortisseur ring showed the 5- and 50-cycle motion previously observed on the pole. This motion was caused by the other poles not yet wedged which were transmitting their motion to the amortisseur ring.

The machine was operated for one month after which time the scratch gauge tests were repeated. They showed that the wedges were still tight and that the motion had not increased. After this test it was decided to apply the tangential wedges to the other nine poles. While this work was being done it was found that several of the amortisseur bars were cracked near their ends. These cracks were caused by fatigue of the material and extended in the tangential direction. They resulted from the reaction between the poles and the amortisseur winding caused by the tangential vibration of the pole tips. It was felt that the failure might have occurred during the month of operation when the machine was operated with one pole provided with the self-tightening wedges. This restrained the tangential motion of the amortisseur ring at this pole and resulted in tangential forces acting between the amortisseur winding and the side of the slots in the other poles. Cracked bars were found in several poles around the periphery of the rotor.

Since it was not known if any of the other amortisseur bars which were apparently sound had not begun to develop fatigue cracks, it was felt that in order to avoid the possibility of a later prolonged outage of the machine it was desirable to replace all the amortisseur winding while the poles were in the manufacturer's shop for machining the slots for the tangential self-tightening wedges.

After one year of operation, an inspection of the self-tightening wedges was made and scratch gauges again installed at the leading and trailing edges of all poles. The gauges were locked in order to permit obtaining records while the machine was operated at the desired load.

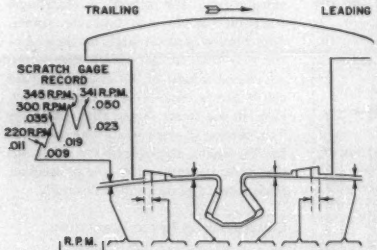

	R.P.M.						
FRONT	0	.000	.000			.000	.000
	85		.008			.005	
	152		.040			.019	
	220	.009	.096	.008	.005	.038	.000
	300	.019	.153	.014	.008	.069	.000
	300		.175			.075	
	345	.023	.221	.021	.012	.092	.000
REAR	0	.000	.000	.000	.000	.000	.000
	85		.038			.017	
	152		.078			.042	
	220	.007	.083	.008	.007	.075	.005
	300	.021	.178	.017	.012	.121	.010
	300		.184			.123	
	345	.022	.220	.022	.017	.160	.014

Figure 18 (left). Tightening of tangential wedges and lifting of pole

Test on pole number 10, May 23, 1941; no load

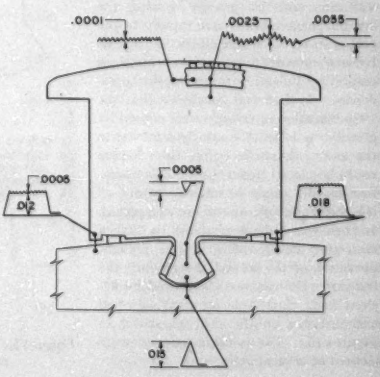

Figure 19 (right). Scratch gauge test; after tangential wedges were tightened

Test on pole number 10, May 23, 1941, 30,000-kw load, 300 rpm

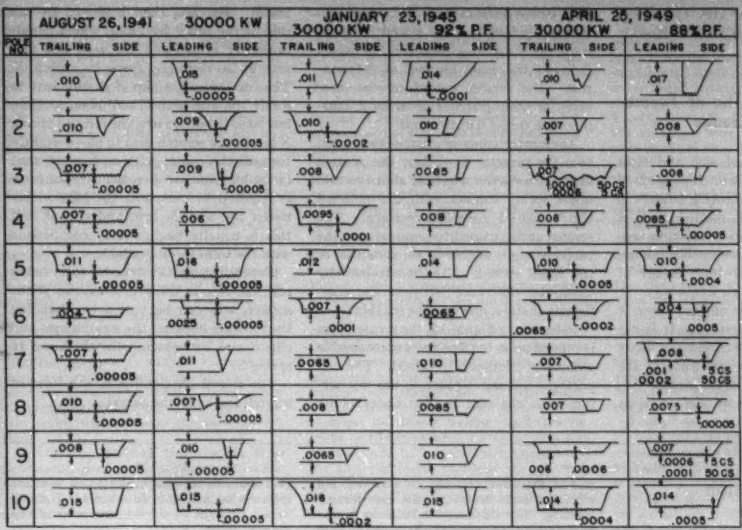

Figure 20. Pole rocking tests

One set of tangential wedges and the springs were removed. They were found in good condition. These wedges were reinstalled and retightened by running the machine at 15 per cent overspeed.

Scratch gauge tests were repeated in 1943, 1945, and 1949 to determine the tightness of the assembly. The scratch gauge records of the 1945 and 1949 tests are shown in Figure 20, along with the initial readings taken in 1941. They show that in 1945 after four years of operation no appreciable vibration could be observed. However, in 1949 after seven years of operation a very small 5-cycle vibration could be detected on one pole.

When appreciable pole vibrations reappear, it will be a simple matter to run the machine at 15 per cent overspeed to bring all the wedges into the initial state of tightness and eliminate the vibration.

Scratch gauges mounted on the poles of the 60-cycle machine indicated a radial motion of the pole varying from 0.003 to 0.006 inch. At maximum load on the machine there was a very small vibration, of the order of 0.0001 inch which could hardly be detected. This is due to the fact that there is little or no single-phase torque acting on the poles of this machine; furthermore the gravity forces are much smaller, thus reducing the pulsating forces to a very small value. These measurements conformed the operating experience which shows that no maintenance from the standpoint of vibration has been required on this machine.

Conclusion

Large 300-rpm single-phase 25-cycle generators are huge machines subjected to pulsating forces acting on both the stator and the rotor.

The stator of this machine is split to permit shipment. The large magnetic forces acting on the split can cause large vibrations if the natural frequency of the stator is near the frequency of the magnetic forces. The natural frequency of the stator has been found to be a function of split adjustment, of the field current, and of the core temperature, thus making it very difficult to predict conditions of resonance. It was possible to eliminate the condition of resonance by adding a very rigid support under the stator; this, without changing the characteristics of the spring mounting used to limit the transmission of the torque pulsations to the foundation. Experience with this machine has also shown that it is possible to make a large split stator core that is entirely free of trouble with proper maintenance.

The tests which led to the elimination of the pole vibration brought a better understanding of the behavior of dovetail fastening for long large single-phase machines. Although the self-tightening wedges developed for the present machine were a very satisfactory solution, their application to a new machine is unnecessary. The same effect can be obtained by using a wider dovetail or a double dovetail, depending on the proportions of the pole. The conventional salient-pole machine usually has a pole of the same proportions as used on the 60-cycle end of the set, where the gravity and pulsating torques did not cause any vibrations which could be detected with the scratch gauge.

The development of methods of measuring stresses and vibrations in rotating machines is of invaluable help to the mechanical engineer. Without the use of such a device it would have been very difficult to determine the cause of the pole vibration and to develop a satisfactory method of eliminating it. The scratch gauge is a very accurate device which can easily be mounted on rotating parts and even without a time base can give very valuable information.

Large, slow-speed machines usually cannot be assembled in the manufacturer's plant or be operated there under normal operating conditions. Therefore, minor adjustments which are common to most new apparatus have to be solved and corrected in the field. The design of these machines is usually very sound and liberal. When vibrations occur, if the fundamental cause can be de-

termined, the cure is very often very simple, as it was in the case described in this paper.

Appendix I. The de Forest Scratch Gauge

Because of its small size and light weight, the de Forest scratch gauge is of particular value in measuring stresses in inaccessible locations in rotating parts of machines under conditions of high centrifugal or inertia forces. The gauge, however, records only the number of stress cycles and not their frequency.

With this gauge it is not necessary to have any collector rings; also, it is not subject to stray electric currents or fluxes in electric machines as are some of the more accurate electric strain gauges.

The gauge can record deformations from 0.0001 inch to 0.050 inch over a 2-inch gauge length. The record obtained is in the form of a fine scratch which indicates the exact amount of deformation. The scratch record can be measured or photographed at suitable magnification under a microscope.

The scratch gauge consists of two parts: one, the target; the other, the scratch arm which carries a special abrasive held under spring contact with the polished chrome-plated recording surface. The scratch arm is caused to progress over the target at right angles to the direction of the strain record. This is obtained by using the difference between the coefficients of static and moving friction.

Referring to Figure 12, the scratch arm is pressed upon by clip B so a considerable amount of friction is obtained. The two parts are secured in place on the test surface with the arm in the center of its travel. The arm then is moved to one side or the other by hand, which simultaneously established the zero line and sets up a restoring force in spring S. The friction under clip B is sufficient to retain the arm while there is no motion, but when strain occurs, the force of spring S causes the scratch arm to move slightly towards the center with each movement in the longitudinal direction. Some force is required to overcome the friction between the scratch arm and clip B, but this is usually negligible in comparison with the total force available.

Depending on the type of tests being run, the rate of transverse motion of the scratch arm can be varied by changing the pressure between the scratch arm and clip B and by reducing the thickness of spring S.

The record obtained is in the form of scratch marks on the target.

Discussion

J. W. Jones (Philadelphia Electric Company, Philadelphia Pa.): This paper is a valuable addition to the limited available information on operating experience with large single-phase frequency changers. Such machines present difficult design problems because of their large physical size combined with the pulsating torque and continuous heavy losses in the amortisseur windings. Much credit is due the authors for their thorough investigation of the troubles and the development of very ingenious and successful means of correction.

Troubles due to vibration have been experienced on large single-phase frequency changers of the Philadelphia Electric Company, some of which operate in parallel with the Safe Harbor machine through common supply to the Pennsylvania Railroad System. Since these troubles have some similarity to the Safe Harbor experience, it might be of interest to mention them briefly.

After several years service, fatigue fractures developed in some parts of the amortisseur windings of two 42,860-kva single-phase frequency changers. These parts were replaced with new designs to better withstand vibration but the failures continued. The thought was advanced that the trouble might be due to a combination of mechanical and thermal stresses since the machines were subject to occasional overload swings. To check this, temperature measurements were made using Tempil pellets attached to various parts of the winding. The color of the pellets changes when certain temperatures are exceeded and this showed some parts above the original design temperature limit. As a consequence new amortisseur bars were installed made of special oxygen-free silver bearing copper which has better fatigue characteristics at high temperatures.

While the performance since installing the new bars has been much improved there have been two additional broken bars and it was therefore decided to measure the vibration and strains in the amortisseur winding. For this purpose Baldwin Southwark resistance wire strain gauges were installed connected to an oscillograph through temporary slip rings. This provided time curves of the axial, radial, and tangential forces on the windings showing a very definite 5-cycle component due to the effect of gravity as observed at Safe Harbor. It was concluded that flexure of the generator shaft was the principal cause of a 5-cycle reversal of stresses which resulted in the amortisseur bar failures. These machines have multiple dovetails supporting each pole and there was no observable pole rocking. As a consequence of this test some additional improvements have been indicated and new parts have been ordered to be ready for installation if any further trouble develops.

A few vibration troubles developed on two 21,400-kva single-phase frequency changers. One involved fatigue fracture of a bolt which supports the connection between field coils. This has been corrected by replacement with alloy steel bolts of improved design. There were a few cases of severely worn brass winding clamps used for supporting the stator winding paralleling bars such as experienced at Safe Harbor. These are believed due to insufficient tightening at the time of assembly. Excessive vibration in the end bells at certain temperatures was corrected by installation of additional reinforcing ribs.

C. T. Pearce (Westinghouse Electric Corporation, Philadelphia, Pa.): This is an unusual paper in that it is devoted entirely to describing the correction of vibration on a piece of electric equipment in the field. It is obvious that the solution of this problem involved the same high degree of engineering ability as any of the subjects covered by the more usual type of AIEE technical paper. The authors are to be commended for their ability and ingenuity in the solution of this problem, and also for making this valuable information available to other AIEE members. Perhaps we should have more of this type of paper.

This paper also brings out the fact that field difficulties with large rotating machines cannot always be foreseen during design and manufacture, in addition to which complete operating tests may not be possible in the factory before shipment. The Safe Harbor Water Power Corporation deserve a great deal of credit for their co-operation with the manufacturer in carrying out this correction program on their property.

B. Van Ness, Jr. (Safe Harbor Water Power Corporation, Baltimore, Md.): This paper records the results of a 3-year battle against vibration trouble in the 25-cycle unit of a large single-phase frequency changer set. It is the record of the discovery and cure of what seemed to be a continuous series of difficulties; until we really were able to get at the root of the trouble, that is, movement from the single-phase double-frequency vibration, it appeared as though we were working on an endless task. It is also the record of a job on which hard work, persistence, ingenuity, and the courage to resort to novel designs produced a satisfactory solution to a tough problem.

As mentioned in the paper, we had indication of our troubles (Figure 13) two years before they appeared, but at that time the pressure was not sufficiently severe to force us to recognize them. When the severe field failures did appear, we tried every means within our knowledge to locate and determine the source of the difficulty. At that time vibration failures in turbine blades were being studied through a complicated series of mirrors and lights developed by Mr. Kroon and we first gave consideration to the adoption of this method. It was too costly and Mr. Baudry conceived the idea of the scratch gauge triggering device (Figure 15) which turned the scratch gauge into a usable device and thus was the key to the

discovery of our real difficulties. The scratch gauge triggering device and the novel system of tangential wedges conceived by Mr. Baudry and installed and tested by Mr. Ballantyne and Mr. Allen and their associates were so unusual and looked so much like a "Rube Goldberg" that real courage was required to put them into operation on a machine of this size and importance.

We suspect that radial pole movement is responsible for many more difficulties in salient pole machines than is generally realized. As a result of this work we believe that there has been developed a method which will be useful in many fields; certainly it has earned its salt in this case and it is still being used effectively to check the continued effectiveness of the system adopted.

While the paper rightfully points out that the application of the self-tightening wedge will not necessarily be required for a new machine, I personally feel that these wedges have been so successful in this machine that were another to be installed, I should prefer to reproduce the self-tightening wedge system rather than change the dovetail designs.

The manufacturer of this machine is to be congratulated on his willingness to make available to the industry this story of troubles, a story which should be of real value to other users.

John Parmakian (United States Bureau of Reclamation, Denver, Colo.): This paper presents an interesting account of the difficulties encountered in ascertaining the specific cause of failures due to vibration in large rotating machines. The method adopted by the authors in the solution of their problem should be found helpful by other investigators in the solution of similar vibration problems. Through analysis the engineer can often produce many probable causes for failures, but he often has to rely on measured quantities to establish the actual cause. In this particular case the authors could not use a wide choice of instruments because of the presence of stray currents within the unit. No doubt this limitation extended the time required to find the solution.

At the present time the United States Bureau of Reclamation is conducting a test program of the vibration phenomena associated with the formation of extensive fatigue cracks in the blading of large, slow speed turbines. The problem is being attacked by methods similar to those described in the paper. First, the probable causes of the cracking are determined from analysis and second, attempts are being made to isolate the actual cause from data representing measured quantities. In this particular instance the data consists of strains, accelerations, and pressures measured at locations on the turbine runner while the unit is in operation. The transmitters or pickup instruments used for these measurements have resistance-sensitive elements. Signals produced by these gauges on the rotating runner are transmitted through silver-plated collector rings and silver-graphite brushes to direct writing oscillographs. Most of the equipment for these tests was designed and built to suit the requirements for this particular problem. It is hoped that the results of these studies can be made available to the profession at a later date.

Even with good recorded data it is often very difficult to filter out the primary cause of the trouble. The ordinary methods of harmonic analysis are laborious unless special equipment designed for the purpose is available. Moreover, the solution to the vibration problem will not always result in a simple inexpensive modification as obtained by the authors. In some cases a major redesign of the faulty member or adjoining members may be required before a satisfactory solution can be found.

R. A. Baudry: The interest shown in this paper and the contributions made by the discussers are very much appreciated.

The reference made by Mr. Jones to the application of "resistance wire strain gauges" for the investigation of vibrations on two large single-phase frequency changers is noted with interest. This type of strain gauge came into wide use after the investigation at Safe Harbor was concluded. The resistance wire strain gauge is much more sensitive than the scratch gauge and also permits the measurement of the vibration frequency. With the scratch gauge the time base is lacking and the frequency of vibrations has to be assumed. However, the scratch gauge is not affected by electrostatic or magnetic fields as is the resistance wire strain gauge which on rotors of electric machines require very complete shielding. The effectiveness of this shielding is very difficult to ascertain when the strains which are being measured are caused by and have the same frequency as the above fields.

Such shielding usually requires much time and effort and in cases where the frequency of vibrations is known or can be determined by other means the scratch gauge therefore offers many advantages.

As observed by Mr. Parmakian, the use of the resistance wire strain gauge to determine the cause of vibration on a slow speed hydraulic turbine is not limited by problems of shielding. The use of collector rings permitting an accessible location of the recording equipment offers distinct advantages over the scratch gauge and permits obtaining much more complete data.

The Safe Harbor Power Company conducted similar tests on one of their turbines several years ago.

Modern gauging practice has made possible the successful investigation of many difficulties on rotating parts and has resulted in a distinct progress in the art of designing and operating large rotating equipment. As pointed out by B. Van Ness and C. T. Pearce, this type of investigation is of great value and it is hoped that the interest shown by users will lead to the publication of similar subjects.

Design Calculations for A-C Generators

DAVID GINSBERG
MEMBER AIEE

Synopsis: This paper presents simplified formulas and curves for rapid and accurate evaluation of steady-state and transient performance of a-c generators. The calculations provide for the determination of no-load, zero-power-factor and full-load field current, short-circuit ratio, leakage reactance, synchronous reactance, transient reactance, subtransient reactance, transient open-circuit and short-circuit time constants, and d-c time constant. A simple formula is proposed for rough approximation of no-load core loss. These formulas and curves apply to very small machines with semi-enclosed slots, very short air gaps and high flux densities in the iron, as well as to the larger machines covered by previous papers on this subject.

THE expanding use of electric equipment by the armed forces has created a demand for lightweight generators having exceptionally good wave form and transient performance. The greatest demand is for generators from 0.15 kw to 150 kw. It was found that many designers of a-c generators within this range of sizes completely ignored transient characteristics because of the absence of criteria for these characteristics and because they did not have the time to formulate a systematic design procedure from the various papers on the subject published over a period of more than 30 years. These papers agree with each other in principle, but differ from each other in terminology, in simplifying assumptions and in calculating methods. The difficulty of applying the results of the papers to the machines in question is that they apply predominantly to synchronous generators having open-slot stators and air gaps with a length of more than 3/4 per cent of the pole pitch. It also was found that the conventional methods of calculating the magnetomotive force required by the steel were quite inaccurate. For generators having small air gaps and highly saturated iron, the calculated and test values could differ from each other by more than 100 per cent. Such inaccuracies obscure the opportunities for design improvement which can be realized by better machine proportions, by full utilization of new materials, and by taking advantage of recent developments in automatic regulators. It is the purpose of this paper to extend and simplify the results of the published literature on the subject and to formulate a systematic design procedure which can be applied with accuracy to the machines in question.

Paper 50-201, recommended by the AIEE Rotating Machinery Committee and approved by the AIEE Technical Program Committee for presentation at the AIEE Middle Eastern District Meeting, Baltimore, Md., October 3–5, 1950. Manuscript submitted September 16, 1949; made available for printing August 7, 1950.

DAVID GINSBERG is with the United States Army Engineer Research and Development Laboratories, Fort Belvoir, Va.

The author wishes to express his appreciation to Leo J. Misenheimer and R. Powers for their assistance in preparing this paper.

A-C Generator Design Sheets

This procedure follows Kilgore's[1] methods and terminology, where applicable. It is incorporated in a 2-page design sheet, Figures 1 and 2, in which an actual generator design is worked out as an example. The calculation of all but seven quantities can be completed from information directly available on the design sheets and without reference to any other curves or formulas. The seven quantities which require supplementary data for their determination are C_1, C_p, steel magnetization curves, core-loss factors, slot constant K_1, and chording leakage factor K_2. The factor Z on the bottom of Figure 2 represents the effect of the pole embrace on the tooth-tip and zig-zag leakages and the derivation was based on considerations presented in a 1918 paper by Doherty and Shirley.[2]

Fundamental of the Field Form C_1

This constant (denoted by Wieseman[3] as A_1) is the ratio of the peak fundamental flux density of the no-load field form to the peak actual flux density of the field form. Values of C_1 are given on Figure 3 in terms of the pole embrace and the ratio of maximum air gap to minimum air gap. The ratio of air gap to pole pitch has been ignored and, in this respect these curves differ from those of Wieseman.[3] The values were derived by ignoring the flux in the interpolar spaces, assuming that the flux density at any point under the pole shoe is inversely proportional to the air gap length at that point, and applying the Fourier integral to obtain the magnitude of the fundamental. Although the flux in the interpolar space is large enough to have a slight effect on some design constants, it has a negligible effect on C_1 because it is far removed from the pole axis and its main contribution is to the harmonic content of the flux wave. Although this assumption may not be justified for machines with very large ratios of air gap to pole pitch having very small values of pole embrace, it is justified by tests and calculations of all machines within the writer's experience. A comparison of calculated and test results for various machines is listed in Table I. Full test data is not available for all machines, since the tests were made by various agencies and were not, in general, intended for use in design studies. Further experimental verification has been obtained by the use of exploring coils to make oscillograms of the no-load field forms of a number of generators. These field forms were then analyzed to compare the actual values of C_1 (and C_p) with the calculated values.

The elimination of the ratio of air gap to pole pitch as a parameter makes it possible to express the values of C_1 by means of a single family of curves and to apply these curves to machines whose dimensions are outside the range of Wieseman's[3] curves. These curves, like Wieseman's, were calculated for pole faces which form a continuous arc of a

Figure 1. A-c generator design sheet number 1

ELECTRICAL ENGINEERING BRANCH, M.B.E.E. DEPARTMENT ENGINEER RESEARCH & DEVELOPMENT LABORATORIES, FT. BELVOIR, VA.

A.C. GENERATOR DESIGN SHEET Cont. No. W44 - 009 eng - 468 SHEET I OF 2.

KW 5 PF 0.80 VOLTS 120 PHASES 1 FREQ 60 RPM 3600 INS A MFG EM Co AMPS 52

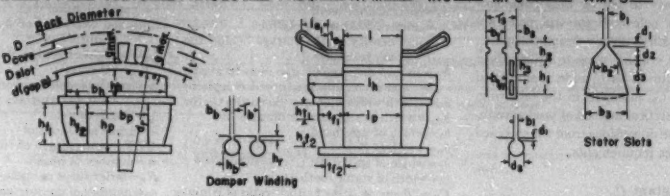

	Armature	Field
No. slots	27 (18 used)	2 Poles
Connection	1 Circ. Y	Series
Series turns/coil	4	822
Slot throw	1- 11	
K_p = sin 90 (pitch)	0.218	
$K_d = \frac{P \sin 90 \left(\frac{s_g}{\tau_p}\right)}{BS_g \sin 90 \left(\frac{P}{BS_t}\right)}$	0.829	
Conductor cu.	8- #17	#17
Conductor insul.	HF	HF
Coil length	31.4	18.3
Resist./term @ 75° C	0.147	15.6
Total series cond., W	144	1644
Amps/sq. inch	4088	1366

Damper Data	
End ring: Thck. 0.125 Area 0.31	No. of Bars
OD ID	

d	7.02	τ_s	0.817	b_s or b_1	0.10
d_r	6.92	τ_r	10.87	h_2 or d_1	0.063
gmin	0.05	l	6.875	d_2	0.131
gmax	0.05	l_{e_1}	1.75	b_2	0.452
d_e	0.053	l_{e_2}	0.5	h_1, d_3 or d_s	0.420
b_h	5.49	l_b	3.875	b_3	0.60
t_p	2.5	l_p	4.375	h_3	—
h_p	2.06	h_b	0.26	τ_b	0.906
h_{f_1}	2.00	b_b	0.63	h_r	0.095
h_{f_2}	0.06	h_h	1.40	D	11.00
h_{t_1}	0.50	t_{f_1}	1.45	D_{slot}	8.248
h_{t_2}	1.50	t_{f_2}	1.11	D_{core}	9.624
l_t	0.614	b_{t_m}	0.41	C_1	1.00
Slot skew	13.3°			C_p	0.58
Useful slot area				n_e	132

$\alpha = \frac{\text{Parc sin}\left(\frac{b_h}{d}\right)}{180} = 0.58$ K_pK_d 0.781

$C_w = \frac{E_T}{E_p} \frac{C_1K_d}{\sqrt{2}\ (\text{Phases})} = 0.568$

$\phi_T = \frac{8000 \times 10^8 E_T}{C_1 n_e\ (\text{RPM})} = K_2 \times 10^3 = 2272 \times 10^3$

$\phi_p = \frac{C_p \phi_T}{2}\left[1 + x_p^2\right] = 785 \times 10^3$

$\phi_{core} = \frac{\phi_T C_p}{2_p} = 374 \times 10^3$

$A_g = \pi d l$ 84.9

$A_t = l b_{t_m}$ (No. slots) (0.93) = 40.0

$A_{core} = l \frac{D - D_{slot}}{2}$ (0.93) = 4.96

$A_p = l_p b_p$ (0.93) = 10.4

A_{spider} 15.1

TEETH	CORE LENGTH	POLE	SPIDER
l_p	$\frac{\pi(D+D_{slot})}{4P}$	h_p	$\frac{\pi(d_{sc}+d_{sl})}{4P}$
0.614	7.56	2.06	1.4

$\frac{d_e}{g} = \frac{\tau_s(4.4g + 0.75b_1)}{\tau_s(4.4g + 0.75b_1) - b_1^2 g}$ or $\left(\frac{\tau_s(5.5g + b_s)}{\tau_s(5.5g + b_s) - b_s^2}\right) =$ $d_e = 0.05\left[\frac{0.817(0.22 + 0.075)}{0.244 - 0.01}\right] = 0.053$

	Lgth.	Area	B	STEEL Gade	STEEL Grade	NI/inch	ΣNI	B^1	NI/inch	ΣNI	WATTS lb.	Pounds	Watts
Gap (F_g)	0.053	84.9	30,000			9500	503	33,500	10800	573			
Teeth	0.614	40.0	64,300	29	0.72 WL	3.8	2.3	71,000	7	4.3	1.49	6.9	10.3
Core	7.56	4.96	75,400	29	0.72 WL	9.8	74.1	83,500	15	114	2.06	42	86.5
Subtotal													
Pole	2.06	10.4	75,300	24	1.1 WL	9.4	19.4	83,400	15	31			
Spider	1.4	15.1	51,600	24	1.1 WL	3.65	5.1	57,400	4	5.6			
Total ($\frac{F}{P}$)							604			721			

A = effective series ampere-conductors = $WIK_p = n_e I_p h$ = 6975

$C_m = \frac{\alpha\pi + \sin\alpha\pi}{4 \sin\left(\frac{\alpha\pi}{2}\right)}$ = 0.863

F_{d_m} = armature reaction = $\frac{0.45 n_e I p h \alpha K d}{P}$ = 1133

F.S.C. = $F_{dm} + X_1 F_g$ = 1198 S.C.R. = $\frac{F_o}{F.S.C.}$ = 0.504

X_d = (A.S.) = $\frac{F.S.C.}{F_g} = \frac{1}{S.C.R.} \times \frac{F_o}{F_g}$ = 2.38

FIELD HEATING

$MLT = 2(l_p + b_p) + \pi\left[\frac{t_{f1} h_{t1}}{h_{f1}} + \frac{(t_{f1} + t_{f2}) h_{t2}}{2h_{f1}}\right]$ = 18.3

Radiating Sfc. = MLT $(2h_{f1} + t_{f1} + t_{f2})$ = 120

F.L. $\frac{I^2R}{\text{Pole}}$ = 40

SQ. IN / WATT = $\frac{120}{40}$ = 3.0

Zero P.F. rated volt exc. = $(F_o' + F_{dm})(1 + X_d')$ = (721 + 1133) (1.09) = 2020

F_{FL} (AT 0.80 P.F.) = $\left[F_g \frac{1 + 0.6(X_s + X_d) + X_s X_d}{\sqrt{1 + 1.2 X_q + X_q^2}} + F_o' - F_g\right]\left[1 + X_d'\right]$ = (1530 + 155) (1.09) = 1680

F_{FL} (EM Approximation) = $1.05 \frac{\sqrt{1 + 1.3\ SCR + 1.2(SCR)^2}}{SCR} F_o$ =

Date:

By

single circle whose radius is located on a radial line through the center of the pole embrace.

The simplification of the curves for C_1 make it easy to tell by inspection how changes of pole embrace and pole face shape will affect certain design constants. Work now is being done to utilize these simplified curves for C_1 and the simplified curves for C_p, discussed in the following, into an analytical method of predetermining machine dimensions from the specified performance requirements.

Pole Constant C_p

Curves for the determination of C_p are included in Figure 3, which also contains the curves for C_1 discussed previously. The curves for the portion of the flux under the pole, were derived analytically using the simplifying assumptions previously discussed in connection with the C_1 curves except, of course, that a direct integration of flux density over the pole embrace was substituted for the Fourier integral. In order to take account of the flux in the interpolar spaces a correction factor for C_p also is plotted in Figure 3. The correction factor was obtained by plotting Wieseman's[3] values of K_ϕ against the ratio of air gap to pole pitch and averaging the results for various ratios of maximum gap to minimum gap. The values of C_p, which represents the ratio of the average flux density to the actual peak flux density of the field form, can not be obtained directly from Wieseman's paper. They can be derived from Wieseman's curves for K_ϕ by means of the following formula

$$C_p = 0.636 C_1 K_\phi$$

From Figure 3, it is seen that the affect of the ratio of air gap to pole pitch, though finite, is not large and, for machines with relatively small air gaps, can be disregarded.

The simplicity of the single family of curves for C_p facilitates its use for design analysis and calculation. Comparison of calculations and test data indicates that the curves have a high degree of accuracy for the types of machines considered.

Steel Magnetizing Curves

The magnetizing force for the air gap is calculated by dividing 3.19 (the permeability of air) into the peak actual flux density of the air gap. This peak actual flux density is the value obtained by following the procedure of the design sheet and equals the ratio ϕ_r/A_g.

The magnetizing force for the teeth and core is plotted against flux density on Figure 4. These curves differ radically from the published d-c curves for the same steel because the latter do not take into account the unequal distribution of flux densities that exist in the teeth and core of an a-c generator. The usual textbook method of calculating ampere-turns is to calculate the maximum flux density in a part, determine from the published d-c

Symbols Used in Figures 1 and 2

A = effective series ampere conductors
A_g = total area of air gap
A_p = area of pole body
A_t = total area of teeth
A' = ampere conductors per inch
B' = flux density at the voltage behind the potier reactance
B_g = air gap density (air gap density at the pole center averaged over tooth pitch)
b_{tm} = tooth width half way down the teeth
b_{bar} = width of rectangular damper bar
b_h = width of pole head
b_p = width of pole
b_s = width of stator slot
b_t = width of stator tooth at tip
C_m = "demagnetizing factor" ratio of equivalent field ampere turns to maximum sine wave armature ampere turns (ratio of field to armature ampere turns for same fundamental flux)
C_p = "pole constant" ratio of average to maximum field form
C_w = winding constant
C_1 = "fundamental of field form" the ratio of the maximum fundamental to the actual maximum value of field form (figured with no saturation)
Connection = number of parallel paths, type of circuit (for example, 2-circuit Y)
D = frame bore (outer diameter of punchings)
d = stator bore
d_r = rotor diameter
d_{so} = outside spider diameter
d_{si} = inside spider diameter
E_t = rated terminal voltage
E_p = rated phase voltage
F = total no-load ampere turns
F_{dm} = demagnetizing ampere turns per pole
F_{FL} = field ampere turns at full load
F_g = air gap ampere turns per pole at rated voltage
F_g' = air gap ampere turns at $(1+X_l)\times$rated voltage
F_o = no-load ampere turns per pole
F_o' = total no-load field ampere turns at $(1+Xl)\times$rated voltage
FSC = field ampere-turns for symmetrical steady-state short circuit at rated armature current
f = rated frequency
g = single air gap
g_e = effective air gap
g_{max} = single air gap at pole tip
g_{min} = single air gap at center of pole face
h_{bar} = depth of rectangular damper bar
h_h = depth of pole head
h_p = depth of pole body
h_1 = depth of copper in slot (including insulation)
h_2 = depth of slot to the copper
I_p or I_{ph} = rated phase current
K_d = distribution factor
K_p = chord factor = sine 90 (pitch)
K_T = total flux, kilolines, in the machines the value of which would exist if density were uniform and equal to the maximum
K_z = lot chording, leakage factor
K_{1d} = damper slot reactance factor
K_1 = slot reactance factor
L_f = total field circuit inductance
l = length of stator core (including vents)
l_{et} = axial extension of diamond portion of stator winding
l_{et} = straight extension of stator and winding (average)
l_h = length of pole head including any magnetic coil supports
l_p = length of pole
l_t = depth of stator slot
MLT = mean length of turn
m = number of phases
N_p = series turns per pole on the field
n_b = number of damper bars per pole
n_e = total effective conductors
P = number of poles
q = slots per phase per pole
R_F = total field circuit resistance
r_a = armature resistance per phase
S_t = total number of stator slots (including empty)
S_ϕ = number of slots per phase
S_1 = number of stator slots used
SCR = short-circuit ratio
T_a = d-c time constant
T_d' = short-circuit transient time constant
T_{do}' = open circuit transient time constant
W = total series conductors
X = true armature leakage reactance
X_{ad} = direct axis armature magnetizing reactance
X_{aq} = quadrature-axis armature magnetizing reactance
X_d = direct-axis synchronous reactance
X_{du}' = unsaturated transient reactance
X_F' = field leakage reactance
X_l = armature leakage reactance
X_q = quadrature-axis synchronous reactance
y = number of slots spanned by the coil
Z = zig-zag leakage correction factor
α = ratio of pole arc to pole pitch
β = minimum number of poles having an integral number of slots
θ = slot skew in electrical degrees
ϕ_l = pole leakage flux
ϕ_p = total flux per pole
ϕ_r = total flux in the machine the value of which would exist if density were uniform and equal to the maximum
τ = pole pitch measured at the stator bore
τ_b = damper bar pitch (average if not uniform)
τ_r = pole pitch on rotor diameter
τ_s = stator slot pitch
λ_a = armature magnetizing permeance
λ_B = phase belt permeance
λ_b = damper bar winding permeance
λ_{Dq} = quadrature-axis damper winding permeance
λ_{Dd} = direct-axis subtransient winding permeance
λ_e = end connection permeance
λ_F = field leakage permeance
λ_{Fe} = field and leakage permeance
λ_{Fz} = field side leakage permeance
λ_l = slot permeance
λ_{pl} = pole tip damper winding

Figure 2. A-c generator design sheet number 2

ELECTRICAL ENGINEERING BRANCH, M.&E.E. DEPARTMENT ENGINEER RESEARCH & DEVELOPMENT LABORATORIES, FT. BELVOIR, VA.

A.C. GENERATOR DESIGN SHEET Cont. No. W44 - 009 eng - 488 SHEET 2 OF 2.

KW 5 PF 0.80 VOLTS 120 PHASES 1 FREQ 60 RPM 3600 INS A MFG EM Co AMPS 52

$$X = \left(\frac{A}{mi}\ \frac{E_g}{\sqrt{2}\,C_1 B_g}\right) = \frac{I_2}{E_p}\left(\frac{\pi n_s^2 X_d^2}{mp \times 10^8}\right) = \frac{I_2}{E_p}\left(\frac{E_p X_1}{4.44\ C_1 B_g d}\right) = \frac{52}{120}\left[\frac{60\times3.875\times138^2\times0.800^2}{2}\right] = 0.006$$

LEAKAGE REACTANCE $X_1 = X\left(\lambda_1 + \lambda_2 + \lambda_3\right) = .006\times18.98 = 0.114$

m = number of phases.
q = slots per phase per pole.

$$\lambda_1 \begin{cases} \text{For open slots} \\ \text{For semi-enclosed Slots} \end{cases} = \frac{5}{mq}\left(\frac{3 \times \text{slots spanned}}{\text{Total slots/pole}} + 1\right)\frac{I}{X_p n_s^2}\left[\frac{h_2}{b_s} + \frac{h_1}{3b_s} + 0.2 + \frac{b_t^2}{16\tau_{s\phi_s}}\right] = \underline{\qquad}$$

$$= \frac{20\ PK_x}{X_p n_s^2 S_1}\left[K_1 + \frac{{}^*\overline{\lambda}_d}{S_1 \phi_s}\right] + 24\,\lambda_s\left[\frac{\theta}{1000}\right]^2 = 3.06(1.41+2.68)+1.81\times14.20$$

K_x = chording leakage factor = 0.80

K_1 = slot reactance factor = 1.41

θ = slot skew in electrical degrees = 13.2°

NOTE: For 3 phases, $\lambda_3 = 0$ (negligible)

$$\lambda_s = \frac{4}{1}(21e_2 + 1e_1) = \frac{4}{3.875}(1.0 + 2.75) = 3.87$$

$$\lambda_3 = 0.028\left(\frac{d}{p\phi_s}\right)\left(\frac{\sin\frac{3\pi}{2mq}}{E_p}\right)^2 = 6.30\times0.14 = 0.88$$

18.98

MAGNETIZING REACTANCE (X_{md}, X_{mq})

$$X_{md} = X\,(C_m C_1)\,\lambda_a = 2.27 \times 0.980 \times 1.0 = 2.27$$

$$X_{mq} = X\,C_{q1}\,\lambda_a = 2.27 \times 0.398 = 0.906$$

$$\lambda_a = \frac{0.383}{p\phi_s} = \underline{426}$$

$$C_{q1} = \frac{4\alpha + 1}{5}\ \frac{\sin\alpha\pi}{\pi} = \underline{0.398}$$

EFFECTIVE FIELD LEAKAGE $X_f^1 = 0.091$

$$X_f^1 = X_{md}\left[1 - \frac{\frac{C_1}{m}}{2\,C_p + \frac{4}{\pi}\frac{\lambda_f}{\lambda_a}}\right] = 2.27 \times 0.94 = 0.091$$

$$\lambda_f = \lambda_{f_s} + \lambda_{f_e} = 5.6$$

$$\lambda_{f_s} = 4.25\left[\frac{3(h_h + \phi - 0.058\tau_r)}{\tau_r - b_h}\right] + \frac{h_{f_1} + \frac{\tau_r}{10}\left(\frac{p-10}{p}\right) + 3h_{f2}}{\frac{\pi}{p}\,(d_r - 2h_h - 0.4h_{f_1}) - b_p}$$

$$\lambda_{f_s} = 4.25\left[\frac{3(1.46 - 0.8)}{5.4}\right] = 2.0$$

$$\lambda_{f_e} = 3.19\left[\frac{4(1h - 1) + 2h_{f_1} + 0.5\,b_p}{1}\right] = 3.6$$

DIRECT-AXIS DAMPER LEAKAGE $X_{fd}^1 = 0.0183$

(For direct-axis use dimensions of end bar near pole)

$$X_{fd}^1 = X\ \lambda_{fd} = 0.006 \times 3.04 = 0.0183$$

$$\lambda_{fd} = \left[\cos\frac{(n_h - 1)}{\tau_r}\frac{\tau_1}{2}\frac{\pi}{2}\right]\left[\frac{(h_h + h_{pt})\lambda_p}{\lambda_b + h_{pt} + h_r}\right] = \left[\cos 45\right]4.2 = 3.04$$

$$\lambda_{pt} = 6.38\left[\frac{b_h - \tau_h\,(n_h - 1)}{3d_e}\right] = 6.38\left[\frac{5.49 - 0.54}{3 \times 0.053}\right] = 2$$

$$\lambda_b = 6.38\,(X_{1d} + 0.5) = 6.38\left[\frac{.088}{.0\overline{70}} + 0.625 + 0.5\right] = 18.7$$

X_{1d} = damper slot reactance factor

QUADRATURE-AXIS DAMPER LEAKAGE $X_{fq}^1 = 0.0246$

(Use dimensions of center bars)

$$X_{fq}^1 = X\ \lambda_{fq} = 0.006 \times 4.1 = 0.0246$$

$$\lambda_{fq} = \frac{20\ \tau_b}{\tau_r}\left[\frac{h_r}{b_b} + \frac{h_{bar}}{3b_{bar}} + 0.5 + \frac{\phi}{\tau_b}\right] = \frac{18.1}{10.9} \times 2.68 = 4.1$$

$$^*\overline{\lambda} = 0.75\,\alpha^2\left[1 + \frac{98}{\lambda_a}\left(\frac{1}{\alpha^2} - 1.1\right)\right] = 0.250 \times 1.432 = 0.36$$

REACTANCES

Direct-axis synch. $X_d = X_1 + X_{md} = 0.114+2.27=2.38$

Quadrature-axis syn. $X_q = X_1 + X_{mq} = 0.114+0.906=1.12$

Unsaturated trans. $X_{1u} = X_1 + X_f^1 = 0.114+0.091=0.205$

Saturated trans. $X_1^1 = 0.68\,X_{1u} = \underline{0.18}$

Subtransient direct-axis: w/dampers. $X_d'' = X_1 + X_{fd}' = \underline{0.138}$; w/o dampers. $X_d'' = X_1' = \underline{\qquad}$

Subtransient quadrat. axis: w/ dampers. $X_q'' = X_1 + X_{fq}' = \underline{0.139}$; w/o dampers. $X_q'' = X_q = \underline{\qquad}$

Negative sequence. $X_2 = 1/2\,(X_d'' + X_q'') = \underline{0.138}$

Zero-sequence = X_0

w/dampers $\lambda_{20} = \left(\frac{Kxo}{Kx}\right)\lambda_{D1} =$ Not applicable

w/o dampers $\lambda_{20} = \frac{Kxo}{K_p^2}\,(0.7\,\lambda_a) =$ " "

$$X_0 = X\left[\left(\frac{Kxo}{Kx}\right)\lambda_1 + \lambda_{20} + \frac{2C(h_1 + 2h_2)}{mq(K_p^2 K_d^2)12b_s}\right] = \text{" "}$$

$$Kxo = \left(\frac{3\pi}{mq} - 2\right);\quad Kx = \frac{3\pi}{4mq} + \frac{1}{4} = \text{" "}$$

TIME CONSTANTS (Seconds)

Open-circ. trans.: $T_{do}' = \frac{L_f}{R_f} = \underline{1.85}$

$$L_f = \frac{N_f^2 pl}{10^8}\left(C_p\frac{\pi}{2}\lambda_a + \lambda_f\right) = \frac{600^2 \times 2 \times 3.66(4.02)}{10^8} = 21$$

S.C. transient: $T_d' = \frac{X_d'}{X_d}\,T_{do}' = \underline{0.10}$

Armature (or DC): $T_a = \frac{X_2}{2\pi f r_a} = \frac{0.138}{3.77 \times .073} = .006$

DATE

BY

Table I

Generator Number	1		2		3		4		5		6		7		8	
Phase	1		1 and 3		1 and 3		3		3		3		3		3	
Kw	5		5		5		25		60		60		100		100	
Power factor	0.80		0.80		0.80		0.90		0.80		0.80		0.80		0.80	
Volts	120		208/120		208/120		208/120		208/416		450		450		450	
Frequency	60		60		400		60		60		60		60		60	
Rpm	3,600		3,600		3,420		1,200		1,800		1,200		1,200		1,200	
d	7.02		6.5		9.0		17.0		13.0		17.0		17.0		20.37	
g	0.05		0.08		0.02		0.175		0.110		0.099		0.09		0.115	
	Calc	Test	Calc	Test	Calc	Test	Calc	Test	Calc	Test	Calc	Test	Calc	Test	Calc	Test
F_g	503	503	1,000	1,000	308	310	2,340	2,360	2,600	2,600	1,800	1,860	1,940	1,900	1,800	1,850
F_{f1}	1,860						3,500	3,480	6,850	6,950*	4,400	4,420			4,650	4,600
SCR	0.504	0.505	0.848	0.850	1.84	1.90	2.04	2.16	0.83	0.83	1.46	1.42	1.37	1.32	1.10	1.11
X_d	2.38	2.38	1.29	1.29	0.56	0.52	0.518	0.48	1.45	1.44	0.96	0.98	1.07	1.02	1.09	1.10
X_d'	0.18	0.19	0.17		0.085	0.080	0.10		0.184	0.19	0.135	0.132	0.127	0.133	0.152	0.164
X_d''	0.132		0.115		0.07	0.05					0.115	0.113	0.09	0.10		
T_{do}'	1.35	1.32	1.30		0.078	0.083					1.51		1.40			
T_d'	0.10	0.11	0.18		0.012	0.02					0.2	0.18	0.167	0.172		

* Test value at 211 volts, 0.792 power factor.

steel curves, the corresponding magnetizing force in ampere-turns per inch, and to multiply this magnetizing force by the length of the magnetic path in inches. In applying this method to such a part as the core, where the flux density varies nearly sinusoidally along the length of the magnetic path, the actual magnetomotive force is the sum of the products of the magnetizing forces of each increment of the path by the length of the corresponding increment. The magnetizing force for each increment can be obtained from the d-c steel curves for the flux density prevailing in that increment.

The curves of Figure 4 were obtained for different values of maximum flux density by an averaging process. The flux densities were assumed to vary sinusoidally in accordance with the formula $B = B_{max} \sin X$, where X was increased from zero to 90 degrees in equal 5-degree increments. For each increment, the value of magnetizing current was determined from the published d-c magnetization curves for the steel and the sum was divided by the number of terms. The use of these curves has made accurate prediction of saturation curves possible where the conventional method sometimes led to ridiculous results.

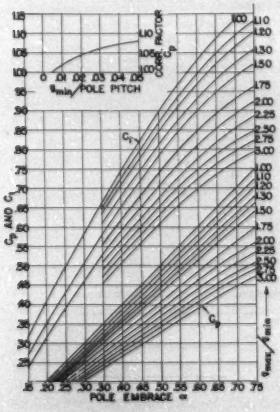

Figure 3. Peak fundamental and average of no-load flux wave

Core Loss

A rough estimate of the no-load iron losses for teeth and core can be obtained from the following equation

$$\text{Core loss in watts} = 5W(WL)\left(\frac{B}{100}\right)^2\left(\frac{f}{60}\right)^{1.4}$$

where

W = weight of part (core or teeth)
B = maximum flux density in part (kilolines per square inch)
f = fundamental frequency in part (cycles per second)
(WL) = watts per pound guaranteed by the manufacturer at 10,000 gauss, 60 cycles per second, for the grade and thickness of the steel laminations used

For a more accurate calculation, Spooner's method[4,5,6] can be used.

Slot Factor K_1

The slot factor K_1 is the permeance of the slot leakage path and the formulas are given in numerous text books and technical papers. Using the nomenclature of the design sheet, the value can be obtained for a rectangular semienclosed slot by the formula

$$K_1 = \frac{d_1}{b_1} + \frac{2d_2}{b_1+b_2} + \frac{d_3}{3b_2}$$

The permeance of a circular slot with an opening of normal size at the top is

$$K_1 = \frac{d_1}{b_1} + 0.625$$

The permeance of a semicircular slot bottom is equal to 0.14, so that for a semienclosed rectangular slot with semicircular bottom

$$K_1 = \frac{d_1}{b_1} + \frac{2d_2}{b_1+b_2} + \frac{d_3}{3b_2} + 0.14$$

Chording Leakage Factor, K_2

The chording leakage factor is given in Figure 1 of Kilgore's[1] article, Figure 2 of Alger's[7] article, and in Figure 143, page 219 of Kuhlmann's design text.[8]

Discussion

The design method outlined takes into account only the performance characteristics of the machine but does not attempt to evaluate losses or heat dissipation factors accurately. This was done partly because of the fact that no method is known for the accurate predetermination of temperature rises and partly because for the generators under consideration, the design will usually be dictated by performance rather than by temperature rise. This condition will become increasingly true as the use of high-temperature insulation becomes more prevalent. For the present, some indication of reasonable temperature rises is afforded by using such criteria as d^2l, current densities, ampere-conductors per inch of periphery, and cooling air velocities. For the machines in question, the values of d^2l, can be assumed to be proportional to $(kw/rpm)^{0.64}$.

In basing the design on transient performance, suitable criteria had to be established. An important criterion was the ability of the generator to start and accelerate motors. To prevent stalling of motors and opening of contactors during the accelerating period, it is necessary that the minimum rms voltage of the

generator, as determined by oscillograph, should not drop to less than 70 per cent of rated voltage. It also is necessary that during the accelerating period, after the automatic voltage regulator action has stabilized, the generator voltage should be at least 80 per cent of rated voltage. These values are based on drop-out voltage of 65 per cent for magnetic contactors and a pull-out torque of 200 per cent for induction motors. At 70 per cent voltage the pull-out torque is 128 per cent, leaving some margin for acceleration when driving a load having constant torque characteristics.

The following equation is used for determining the minimum transient rms voltage in per unit

$$E_{min} = \frac{Z_L}{Z_L + X_d} + \left(\frac{Z_L}{Z_L + X_d'} - \frac{Z_L}{Z_L + X_d}\right) e^{-t/T'_{d1}}$$

where

Z_L = impedance of starting motor in per unit
X_d = direct axis synchronous reactance
X_d' = transient reactance of generator in per unit
t = response time for regulator (0.1 second for most mechanical regulators)
T_{d1}' = generator time constant for load Z_L
T_{do}' = generator open-circuit time constant

$$T_{d1}' = T_{do}' \frac{Z_L + X_d'}{Z_L + X_d}$$

Further work is necessary in order to generalize the effects of machine dimensions on the flux in the interpolar spaces. This would make it possible to calculate field harmonics accurately without resorting to laborious flux plotting for each new generator design.

The leakage factor X_p', used in Figures 1 and 2 is calculated in accordance with the formulas of Kilgore.[1] It is correct only for the determination of transient reactance since it evaluates the linkages of the leakage flux with the field winding rather than the total leakage flux. However, the value X_p' has been used in the design sheets to calculate total leakage flux. The results obtained so far do not appear to require a separate calculation for total leakage flux.

In calculating full-load and zero-power-factor ampere-turns the factor $(1+X_p')$, was used to make some allowance for the increase in ampere-turns of the field pole because of the increase of leakage flux resulting from the component of field required to neutralize the armature demagnetizing action.

Appendix I. Derivation of Equations for C_1

The field form at no load has no even harmonics, it is symmetrical with respect to the origin of co-ordinates, and the fundamental component can therefore be expressed by: (Refer to Figure 5)

$$C_1 = \frac{B_1}{B_m} = \frac{g_n}{3.19\ NI} \times \frac{4}{\pi} \times 3.19\ NI \int_0^{\pi/2} \frac{\cos\phi\, d\phi}{g} = \frac{4g_n}{\pi} \int_0^{\pi/2} \frac{\cos\phi\, d\phi}{g}$$

Assuming the effect of flux in the interpolar spaces to be negligible

$$\int_0^{\pi/2} \frac{\cos\phi\, d\phi}{g} = \int_0^{\alpha\pi/2} \frac{\cos\phi\, d\phi}{g}$$

For a uniform air gap

$$C_1 = \frac{4g_n}{\pi}\left[\frac{\sin\phi}{g}\right]_0^{\alpha\pi/2} = 1.27 \sin\frac{\alpha\pi}{2}$$

For the air gap shown in Figure 5

$$C_1 = \frac{4g_n}{\pi} \int_0^{\alpha\pi/2} \frac{\cos\phi\, d\phi}{g} = \frac{4g_n}{\pi} \times \int_0^{\alpha\pi/2} \frac{\cos\phi\, d\phi}{g_n + \left(\frac{g_x - g_n}{\sin^2\frac{\alpha\pi}{2}}\right)\sin^2\phi}$$

$$C_1 = 1.27 \int_0^{\alpha\pi/2} \times \frac{\cos\phi\, d\phi}{1 + \left(\frac{g_x}{g_n} - 1\right)\left(\frac{1}{\sin^2\frac{\alpha\pi}{2}}\right)\sin^2\phi}$$

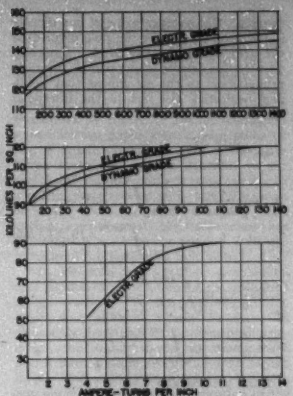

Figure 4. Magnetizing curves for steel, showing the effect of sinusoidal distribution of flux density

$$C_1 = 1.27\left[\sqrt{\left(\frac{g_x}{g_n} - 1\right)\left(\frac{1}{\sin^2\frac{\alpha\pi}{2}}\right)}\right] \times \tan^{-1}\left[\sin\frac{\alpha\pi}{2}\sqrt{\frac{\frac{g_x}{g_n} - 1}{\sin^2\frac{\alpha\pi}{2}}}\right]$$

$$C_1 = 1.27 \sin\frac{\alpha\pi}{2} \frac{\tan^{-1}\sqrt{\frac{g_x}{g_n} - 1}}{\sqrt{\frac{g_x}{g_n} - 1}}$$

Appendix II. Derivation of Equation for C_p

C_p is the average value of flux density divided by the maximum value of flux

Figure 5. Length of air gap as a function of pole shape and angular displacement from pole center

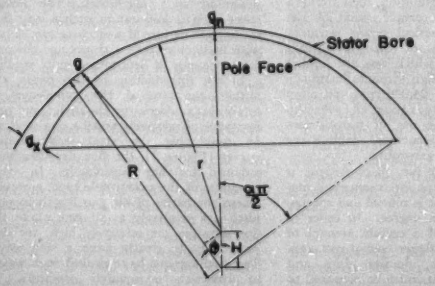

g_n = Minimum gap
g_x = Maximum gap
g = gap at any point
R = Radius of stator bore
r = Radius of pole face
H = Offset of center of pole face arc from center of stator circle
α = Pole embrace
ϕ = Angular position of point with gap "g" with respect to center of pole

$$g = R - H\cos\phi - \sqrt{r^2 - H^2\sin^2\phi}$$
$$g_n = R - H - r$$
$$A = R - r - g_n$$
$$g_x = R - H\cos\frac{\alpha\pi}{2} - \sqrt{r^2 - H^2\sin^2\frac{\alpha\pi}{2}}$$
$$\sqrt{r^2 - H^2\sin^2\phi} \approx r\left(1 - \frac{H^2\sin^2\phi}{2r^2}\right)$$
$$H\cos\phi - H\sqrt{1 - \sin^2\phi} = H\left(1 - \frac{1}{2}\sin^2\phi\right)$$
$$g \approx (R - H - r) + \frac{1}{2r}(H^2 + HI)\sin^2\phi$$
$$g \approx g_n + \frac{1}{2r}(H^2 + HI)\sin^2\phi$$
$$g_x \approx g_n + \frac{1}{2r}(H^2 + HI)\sin^2\frac{\alpha\pi}{2}$$
$$\frac{1}{2r}(H^2 + HI) = \frac{g_x - g_n}{\sin^2\frac{\alpha\pi}{2}}$$

density. The average value of flux density is the total flux under the pole divided by the area under the pole pitch. Assuming that the flux density at any point is inversely proportional to the air gap at that point, and neglecting the flux in the interpolar spaces: (See Figure 5)

$$B_{max} = \frac{3.19\ NI}{g_n}$$

$$B_{av} = \frac{\phi_p}{\text{pole area}} = \frac{2}{1R\pi}\int_0^{\pi/2} BdA = \frac{2}{1R\pi}\times \int_0^{\alpha\pi/2} \frac{3.19\ NI\ 1Rd\phi}{g}$$

$$B_{av} = \frac{2}{\pi}\times 3.19\int_0^{\alpha\pi/2}\frac{d\phi}{g}$$

$$C_p = \frac{B_{av}}{B_{max}} = \frac{2}{\pi}\frac{g_n}{}\int_0^{\alpha\pi/2}\frac{d\phi}{g}$$

For a uniform gap

$$C_p = \frac{2}{\pi}\frac{g_n}{}\frac{\frac{\pi}{2}\alpha}{g_n} = \alpha$$

For the gap shown on Figure 5

$$C_p = \frac{2}{\pi}\int_0^{\alpha\pi/2}\frac{d\phi}{1+\left(\frac{g_x}{g_n}-1\right)\frac{1}{\sin^2\frac{\alpha\pi}{2}}\sin^2\phi}$$

The integral is of the form

$$\frac{1}{2}\int\frac{d(2\phi)}{\left(1+\frac{a^2}{2}\right)-\frac{a^2}{2}\cos 2\phi}$$

$$C_p = \frac{0.636\sin\frac{\alpha\pi}{2}}{\sqrt{\frac{g_x}{g_n}-1+\sin^2\frac{\alpha\pi}{2}}}\times \tan^{-1}\left[\frac{\frac{g_x}{g_n}-1+\sin^2\frac{\alpha\pi}{2}\left(\tan\frac{\alpha\pi}{2}\right)}{\sin\frac{\alpha\pi}{2}}\right]$$

$$C_p = 0.636\tan\frac{\alpha\pi}{2}\times \frac{\tan^{-1}\sqrt{\frac{g_x/g_n}{\cos^2\frac{\alpha\pi}{2}}-1}}{\sqrt{\frac{g_x/g_n}{\cos^2\frac{\alpha\pi}{2}}-1}}$$

References

1. Calculation of Synchronous Machine Constants, **L. A. Kilgore.** *AIEE Transactions*, volume 50, December 1931, pages 1201–14.

2. Reactance of Synchronous Machines and Its Application, **R. E. Doherty, O. E. Shirley.** *AIEE Transactions*, volume 37, part 2, 1918, pages 1209–1340.

3. Graphical Determination of Magnetic Fields, **R. W. Wieseman.** *AIEE Transactions*, volume 46, February 1927, pages 141–54.

4. Tooth Pulsation in Rotating Machines, **T. Spooner.** *AIEE Transactions*, volume 43, February 1924, pages 252–61.

5. Surface Iron Losses with References to Laminated Materials, **T. Spooner, I. F. Kinnard.** *AIEE Transactions*, volume 43, February 1924, pages 262–81.

6. No-Load Induction Motor Core Losses, **T. Spooner, C. W. Kincaid.** *AIEE Transactions*, volume 48, April 1929, pages 645–55.

7. The Calculation of the Armature Reactance of Synchronous Machines, **F. L. Alger.** *AIEE Transactions*, volume 47, February 1928, pages 493–513.

8. Design of Electrical Apparatus, **John H. Kuhlman.** John Wiley and Sons, New York, N. Y., second edition, 1946.

9. Mapping Magnetic and Electrostatic Fields, **A. D. Moore.** *Electric Journal* (East Pittsburgh, Pa.), volume 23, July 1926, pages 355–62.

10. The Interpolar Fields of Saturated Magnetic Circuits, **Th. Lehmann.** *AIEE Journal*, volume 46, December 1927, pages 1411–14.

11. The Reactances of Synchronous Machines, **R. H. Park, B. L. Robertson.** *AIEE Transactions*, volume 47, February 1928, pages 514–36.

12. Determination of Synchronous Machine Constants by Test, **S. H. Wright.** *AIEE Transactions*, volume 40, December 1931, pages 1331–1.

Discussion

Paul W. Franklin (Bendix Aviation Corporation, Teterboro, N. J.): Mr. Ginsberg is to be congratulated for his publication, which regrettably is one of the few papers dealing with actual design calculations. Whereas there is no lack in the number of theoretical papers, actual design methods are rarely published and thus the average designer cannot always benefit from the advances of theory.

Mr. Ginsberg developed his paper for the design of light-weight minimum-size machinery for the Armed Forces. It is of interest to note that for aircraft this type of equipment was required and produced years ago. The specifications as to weight, bulk, and performance are difficult to attain. This led to the development of a special line of rotating equipment, the performance of which indicates that sooner or later the principles and procedure employed will be adopted by manufacturers, wherever light-weight minimum size equipment is essential.

The design of minimum size equipment was made possible by the use of Silicone varnish, inorganic insulation, high strength materials, and to a certain extent by the development of practical power selenium rectifiers. The use of Silicone varnish permitted a design which was not limited by temperature. High strength materials permitted speeds of 24,000 rpm and more for comparatively large ratings and selenium rectifiers permit the use of transductors and may, to a certain extent, replace the commutator on d-c generators.

The theory, used for these designs is of course the same as for commercial machines, except that it is refined and specialized to a very high degree. In order to get the most out of a certain amount of material, a good designer cannot use commercial proportions, density data and empirical curves, but must be prepared to rederive and modify his formulas, for example, leakage flux and reactance formulas, as his design proceeds.

Mr. Ginsberg states that the customary methods to calculate the saturation curves are insufficient. In minimum size machines, the actual physical flux, that is, air gap flux plus local leakage flux, must be calculated closely to permit the use of high magnetic densities without resulting oversaturation. Local saturation around slots carrying high currents should be checked. Depression of the originally sinusoidal air gap flux due to tooth saturation occurs, but can be approximated. The ampere turns required to drive the flux through the yoke are usually much less than obtained by commercial formulas and may be obtained either as Mr. Ginsberg indicates, or by using the results of investigations published. In the same way, the pole-to-pole leakage flux formulas for commercial design must be disregarded and each case should be calculated on its own merits. Direct and quadrature axis coefficients become a function of the saturation in the vicinity of the air gap and a field weakening occurs, due to flux distortion under load, similar to the uncompensated d-c machine.

All these points of consideration complicate the design work to a great extent, but on the other hand permit the design of a light-weight machine where each dimension is reduced to the minimum and where each component carries just as much as it can and not more. The result of this is that today 400-cycle machines can be built, with magnetic densities determined entirely by saturation and not by temperature, and that often with a 100 per cent overload capacity. Copper densities have been increased two to four times that of commercial machines without detriment to a reasonable lifetime.

It appears to the writer, that the designer of such equipment must be well versed in theory and rather unprejudiced by commercial design methods. He should discard empirical curves and semiempirical formulas and take nothing for granted. Under these conditions a design sheet serves only as a neat record for final design data, but by no means as a method.

R. C. Powers (Electric Machinery Manufacturing Company, Minneapolis, Minn.): Although Mr. Ginsberg's paper presents no new concepts in the design of a-c generators, it does present a simplified procedure for designing such machinery. The design sheet itself is laid out in such a way that a complete picture of a machine can be had with little more than a glance and the performance can be determined quite readily.

In the introduction of this paper, the author has stressed the importance of establishing criteria for the design and performance of relatively small a-c generators. In developing the steel magnetization curves (Figure 4), the flux densities were assumed to vary sinusoidally. In small machines of the salient-pole type, however, where the ratios of air gap length to pole pitch are relatively small and where the flux densities are relatively high, the flux wave departs greatly from a sine wave. Test oscillograms have proved such waves to approach a squared condition. In

$$\left[\frac{1+0.6(X_{ag}+X_{ad})+X_{ag}X_{ad}}{\sqrt{1+1.2\,X_{ag}+X_{ag}^2}}-1\right]\left[1+X_F'\right]F_g$$

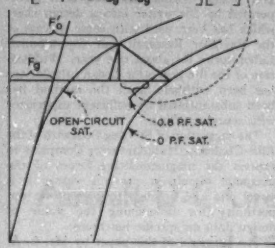

Figure 1

determining the constants C_1 and C_p from these oscillograms, however, they, too, differed from those obtained from curves included in this paper (Figure 3). Tests indicate that these differences occur in such a way that, if C_1 and C_p are determined from Figure 3 and a sine wave of flux is assumed in obtaining the flux density–field intensity curves, the end results (magnetizing forces) are substantially the same as when C_1, C_p, and the flux wave form are obtained from oscillograms.

About the time the material was being prepared for this paper, an independent investigation was being conducted for the purpose of obtaining reliable stator magnetization curves. The flux wave was analyzed by the same method as Mr. Ginsberg describes in this paper with the exception that an oscillogram of an actual air gap flux wave was used for analysis instead of a pure sine wave of flux. The flux density–field intensity curves resulting from this investigation were effectively identical with those of Figure 4 of the paper. However, these curves proved to be too optimistic when applied to analyses of machines already in existence and tested; that is, the curves indicated excessively high effective iron permeabilities.

Therefore, a new approach was used to determine reliable magnetization curves. The total magnetomotive forces at various inductions were determined by test for several machines using 29 gauge, 0.72 watt-loss steel. The air gap magnetomotive forces were calculated, and the pole and spider magnetomotive forces determined from manufacturer's d-c magnetization curves at these inductions. The tooth and core flux densities were calculated at the corresponding inductions. Tooth and core magnetization curves were then plotted in such a way as to provide stator magnetomotive forces so that the total calculated machine magnetomotive forces met the test values of total magnetomotive force at all inductions. These flux density–field intensity curves for all machines effectively coincided with one another to result in a single curve for 29 gauge, 0.72 watt-loss steel. Test results of additional machines designed in accordance with the design sheets (Figures 1 and 2) of this paper and by the use of this curve met the calculated performance estimates very closely in all cases. This curve indicates lower effective permeabilities than those indicated by Figure 4 of this paper but higher effective permeabilities than those indicated by manufacturers' d-c magnetization curves at corresponding inductions. Stator flux density–field intensity curves for grades of steel other than 29 gauge, 0.72 watt-loss can be interpolated from this curve and the proper manufacturers' d-c magnetization curve.

As expressed in this paper, there is a present demand for small light-weight a-c generators. The trend is toward higher flux densities, and, in order to maintain optimum electric and magnetic balances, the current densities become correspondingly higher. Recent developments in high temperature materials and high permeability electric steels have made such machines more practical from an economy standpoint. In high temperature a-c generators having good transient performance, armature resistance becomes increasingly effective; it may become as much as 250 per cent and more of the armature leakage reactance. In calculating the short-circuit ratio, reactances, and load excitations of a machine (refer to Figures 1 and 2), therefore, armature resistance cannot be ignored.

The author's expression for full load excitation at 0.8 power factor (Figure 1) should be modified slightly:

$$F_{FL}=\left[\frac{1+0.6(X_{ag}+X_{ad})+X_{ag}X_{ad}}{\sqrt{1+1.2X_{ag}+X_{ag}^2}}-1\right]\times[1+X_F']F_g+F_o'[1\times X_F']$$

This expression is evident from test results, and from Figure 1 of this discussion.

E. R. Martin (University of Michigan, Ann Arbor, Mich.): The importance of transient factors on a small single-phase generator would appear to be relatively unimportant, and it is unfortunate that a 3-phase design was not used to illustrate the calculations.

The design itself is not according to usual practice. The stator has 27 slots which makes the winding unsymmetrical. A lap winding is used while a concentric winding would give better wave shape and use about 14 per cent less copper. The rotor is evidently of special construction, since the pole dimensions leave no room for a shaft, so the revolving field must be supported between nonmagnetic rings with stub shafts attached, which is expensive construction and not very satisfactory. In this case there is no spider, contrary to calculations shown. The core density is higher than the tooth density while the reverse is generally used. The teeth are tapered, being wider near the air gap which makes it appear that a slot die was used which was made for another machine. The test value of core loss was not given in Table I, and that is one item that is difficult to calculate.

A good 3-phase design would have made a much better foundation for the calculations.

David Ginsberg: Mr. Franklin's discussion emphasizes the importance of returning to fundamental principles of design and discourages the use of empirical formulas. The author heartily agrees with this philosophy and hopes that he will find the opportunity to describe these methods more fully. It would be interesting to compare the calculation of one of Mr. Franklin's generators by means of the methods presented in this paper with a calculation by Mr. Franklin's method. The need for a better knowledge of flux densities in the useful and leakage paths is recognized. In a recent conversation with Mr. Wieseman of the General Electric Company, the author learned that Mr. Wieseman has developed a machine for making 2-dimensional and 3-dimensional flux plots.

Mr. Franklin seems to have overlooked one important application of the proposed design method. To the extent that the paper has adhered closely to formulas rigorously derived from fundamental principles, the design sheets are much more useful than a mere record for final design data. The orderly array of the formulas and curves provide a clear indication of the effect of the various design parameters on generator performance and facilitate the selection of these parameters in accordance with actual limitations rather than average practice.

Mr. Powers makes a number of significant points which call for specific answers. As he correctly points out, the stator magnetization curves were based on a sinusoidal distribution of flux density, although a discontinuous linear distribution (for a perfectly flat flux wave) would be more nearly correct for many generators. While the theoretical validity of this argument has been realized, it is pointed out that the exact equation of flux distribution is relatively unimportant providing the differences between actual and sine wave flux densities are confined mainly to the unsaturated portion of magnetic circuit where the differences in the required magnetomotive forces are negligibly small. In the saturated portions of the magnetic circuit, the sine wave approximation is quite close and results on actual machines have borne this out. The experimental investigation of stator magnetization curves and field form coefficients referred to by Mr. Powers was made at the writer's suggestion in the course of a Government development contract with the Electric Machinery Manufacturing Company. At that time stator magnetization curves had been calculated for electrical grade steel only and it is not surprising that the ampere-turn values were optimistic compared to Mr. Powers' test data made with 0.72 watt-loss steel. A theoretical stator magnetization curve for 0.72 watt-loss steel has since been calculated and is compared in the following table with Mr. Powers' curve embodied in a report to the Engineer Research and Development Laboratories.

Flux density (kilolines)	.95	.105	.115	.120	.125	
Mmf by Powers' test data	.36	.64	.118	.168	.240	
Mmf from calculated curve	.25	.60	.118	.165	.250	

As Mr. Powers points out, his data were obtained for machines with an almost rectangular flux wave and for a very small pole embrace, yet the agreement between

test and calculated curves is well within the limit of experimental error. The alternative implied by Mr. Powers' discussion is to have separate magnetization curves for every conceivable pole-shoe and air gap configuration. The writer believes that this would be a step backward.

Mr. Powers is correct in stating that the voltage drop due to armature resistance cannot be ignored in concentrated machines operated at high temperatures. This factor has been taken into account in the formula for full-load field excitation by basing it on the stator flux required to generate the arithmetic sum of the terminal voltage plus the leakage reactance drop instead of the vector sum of these two quantities. Assuming the stator resistance to be of the same order of magnitude as the leakage reactance, this takes the resistance into account and simplifies the calculation.

Mr. Powers implies that his proposed equation corrects a theoretical mathematical error in the writer's formula. It appears that his proposed formula contains typographical errors. For example, the subscript "ag" should be "aq" and the factor "$1 + F'''$" should apparently be a leakage drop factor such as "$1 + X_1$." Taking these obvious corrections for granted, Mr. Powers' formula would be theoretically more correct than that in the paper if he had not overlooked a very important physical phenomenon. This phenomenon involves the effect of armature reaction on the pole leakage flux. At a no-load per-unit voltage of $1 + X_1$ the pole body flux density is the corresponding value of B' in the design sheet. However, at full load the pole leakage increases in proportion to the following quotient: stator plus gap plus armature reaction ampere-turns divided by stator plus gap ampere-turns. This increases the pole-body flux density and magnetomotive force. It is a very large factor where the pole bodies are highly saturated. By rigorous mathematical standards the writer's formula for full-load 0.80 power factor is incorrect but it is relatively simple and contains compensating errors which take account of the increased pole leakage under load. Its accuracy may be estimated by reference to Table I of the paper. Since the paper was written, the writer has applied his method to the design of a number of 50-cycle, 60-cycle, and 400-cycle machines which have since been built and tested. The accuracy of the full-load and no-load field currents have been within 4 per cent of the predicted values even though the designs covered a wide range of ratings and extreme differences in magnetic saturation. It also has been found by mathematical analysis that the expression for field excitation can be still further simplified with negligible loss of accuracy. The simplified formula is:

$$F_{FL} = [0.90F_g(1+X_d)+F_a'-F_g'][1+X_F']$$

Mr. Martin questions the importance of transient factors on small single-phase generators and raises several questions concerning the construction of the machine used as an illustrative example of the design method.

Transient response is very important for small generators since they are frequently called upon to start and accelerate motors whose locked-rotor current may be more than twice the rated current of the generator. The need for good transient response has been borne out by military experience. It also should be noted that some of the transient characteristics are used for the accurate calculation of steady-state values. This is particularly true of single-phase machines in which negative-sequence impedance determines steady-state characteristics. The 27-slot winding is not unsymmetrical but is a typical fractional slot winding so chosen as to permit the elimination of multiples of the third harmonic. The rotor of this machine actually does have a shaft and the term "spider," used in the calculations, refers to that portion of the magnetic circuit of the rotor which is located between the poles. The fact that the pole density is greater than the tooth density and that "the reverse is generally used" is of minor importance compared with the attainment of design goals. Mr. Franklin's discussion has clearly explained the fallacy of blind adherence to custom. Slot dies are normally used for a large number of machines and are not usually allocated to any specific machine. The slot die used on the generator calculated in the design sheets is one of the standard dies used by a prominent manufacturer and was selected as being the most suitable available die. The actual open-circuit core loss on this generator was 105 watts at rated volts.

A small single-phase generator was deliberately chosen for illustrative purposes to show that the proposed design method applies even to these machines which have been ignored by the literature.

Several oral discussions also were made at the meeting, and the author takes this opportunity to answer them.

Mr. W. R. Hough of the Reliance Electric and Manufacturing Company expressed an interest in d-c generator design calculations similar to those for a-c generators presented in this paper. Such d-c generator design calculations have been incorporated by the writer into a design sheet which has been used with some success at the Engineer Research and Development Laboratories for about one year. Publication of the d-c generator design calculations has been withheld until the method has been substantiated by sufficient experience with actual machines.

The suggestion of Sterling Beckwith of the Allis-Chalmers Manufacturing Company to express the magnetomotive forces of the magnetic circuit in per-unit values is a novel one and appears to present an opportunity for broadening the value of design data on specific machines.

The approval of this paper by Mr. L. A. Kilgore of the Westinghouse Electric Corporation is particularly gratifying since his paper of 1931[1] furnished much of the background for the present paper. His comments concerning the need for a synthetic design method are encouraging. As stated in my paper, considerable work has already been done toward this goal. The initial equations are set up to solve for generator dimensions in terms of desired values of generator weight, electrical output, transient reactance, and square inches per watt of heat dissipating surface. A number of simplified analytical expressions have been derived to make this approach practical. For example, the constant C_1 can be calculated from the formula:

$$C_1 = 1.27\left(\frac{g_2}{g_n}\right)^{-0.35} \text{Sin } (90\times\text{pole embrace})$$

Certain attitudes toward accurate equations expressed in the paper and in the foregoing discussions may seem contradictory but they are actually consistent. In striving toward a synthetic design method which could be used for development, no attempt was made to simplify the equations by assuming factors based on customary design procedure or by ignoring factors which are negligible only in conventional machines. A high degree of accuracy even for unconventional designs is necessary if safety factors are to be reduced to a bare minimum. On the other hand, every effort was made to eliminate complicated expressions whose only justification was their mathematical rigor.

Reference

1. Calculation of Synchronous Machine Constants—Reactances and Time Constants Affecting Transient Characteristics, L. A. Kilgore. *AIEE Transactions*, volume 50, December 1931, pages 1201–14.

Aircraft D-C Circuit Breakers for 28 and 120 Volts

B. S. BEALL, III
ASSOCIATE AIEE

P. J. REIFSCHNEIDER
ASSOCIATE AIEE

Synopsis: The electric systems of many modern airplanes, particularly the generator circuits of multiengined airplanes, are being operated without adequate electrical operation. This practice is quite different from that usually followed in other electric systems. To provide the necessary protection, new aircraft circuit breakers have been developed with ratings of 300 and 600 amperes at 28 volts and 250 amperes at 120 volts. The interrupting ratings, over a range of altitude from sea level to 50,000 feet, are 12,000 amperes and 5,000 amperes for the 28- and 120-volt circuit breakers respectively. A compact and efficient interrupter makes the 120-volt rating possible. For generator circuit applications, an inverse time-delay reverse-current trip device has been designed for the circuit breakers. For other applications, nondirectional time delay and directional and nondirectional instantaneous trip devices have been designed. Trip-free mechanisms for both the manually and electrically closed circuit breakers and antipump control for the closing solenoid add to the protection provided by these circuit breakers. The operation of these circuit breakers is satisfactory under conditions of vibration, shock, sand and dust, and extremes of temperature and humidity, incident to aircraft.

THE electric systems of airplanes, both commercial and military, are increasing continually in size, complexity, and importance to the over-all operation. To insure the safety of persons in flight and to safeguard equipment, generators and their associated circuits, feeder circuits and load circuits should all be protected. Circuit breakers with adequate continuous current and interrupting capacity, trip-free mechanisms, manually and electrically closed, and with suitable fault sensing elements, offer the best means of protection.

A circuit breaker is primarily a protective device and to be reliable must be free from contact welding, provide fast fault interruption, and have positive and accurate time-current tripping characteristics. Recently, new single-pole d-c aircraft circuit breakers have been developed which meet present and anticipated future requirements. The ratings, size, and weights of these circuit breakers are shown in Table I.

Either directional or nondirectional trip devices with instantaneous or inverse time characteristics can be incorporated in these circuit breakers. The selection of the type of trip device and its setting depends upon the application of the circuit breaker in the electric system.

Application

The most important application for the recently developed circuit breakers is in generator circuits of multiengined airplanes. In the electric system of a 4-engined airplane, as many as six generator circuits may be connected in parallel to the bus.

A typical generator circuit, including a reverse-current circuit breaker and a generator relay, is shown in Figure 1(A). The generator relay consists of a contactor and a pilot relay. When the generator voltage exceeds the bus voltage, indicating that the generator can supply current to the bus, the contactor closes. When the generator voltage falls below the bus voltage, the reverse flow of current from the bus to the generator causes the contactor to open. For these normal switching operations, the generator relay is adequate. However, under fault conditions in the generator circuit, the generator relay may not be able to clear the circuit because of its limited interrupting capacity. A circuit breaker with adequate interrupting capacity is required to quickly and safely remove the faulted generator circuit from the bus. System tests and operating experience indicate that only circuit breakers with suitable tripping elements provide the needed protection.

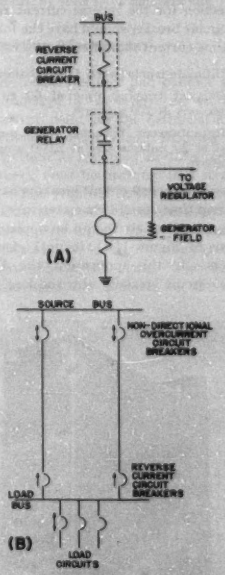

Figure 1. Typical applications of aircraft circuit breakers

A. Generator circuit
B. Dual channel feeder circuit

Paper 50-202, recommended by the AIEE Air Transportation Committee and approved by the AIEE Technical Program Committee for presentation at the AIEE Middle Eastern District Meeting, Baltimore, Md., October 3-5, 1950. Manuscript submitted June 21, 1949; made available for printing August 14, 1950.

B. S. BEALL, III and P. J. REIFSCHNEIDER are both with the General Electric Company, Philadelphia, Pa.

The authors wish to acknowledge the assistance of their associates in the General Electric Company and to members of the Power System Group of the Air Materiel Command during the development of this circuit breaker.

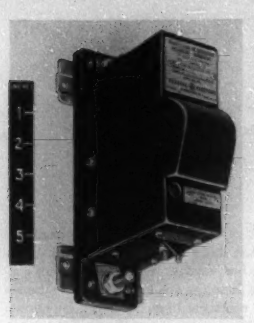

Figure 2. Manually-closed single-pole aircraft circuit breaker

Left. Front oblique view, cover on
Right. Front oblique view with cover removed, and transparent side frame for illustration

1. Mounting plate
2. Molded base
3. Bus terminal
4. Control terminals
5. Auxiliary contacts
6. Indicator
7. Opening springs
8. Closing lever
9. Shunt trip armature
10. Shunt trip coil
11. Reverse current trip device
12. Escapement mechanism
13. Generator terminal

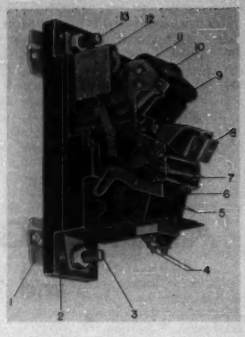

Table I. Ratings, Size, and Weights

Voltage Rating, Volts D-C	Continuous Current Rating, Amperes	Interrupting Rating, Amperes (Sea Level to 50,000-foot Altitude)	Size: Width, Depth, and Height, Inches	Weight, Pounds
28	300	12,000	$2^1/_2$ by $4^{27}/_{32}$ by $8^1/_2$	4.5
28	600	12,000	$2^1/_2$ by $4^{27}/_{32}$ by $8^1/_2$	5
120	250	5,000	$2^1/_2$ by $4^{27}/_{32}$ by $8^1/_2$	4.5

To properly protect the generator circuit and to provide adequate back-up protection for the reverse current relay, the circuit breaker should have the following time-current characteristics:

1. Ultimate trip between 150–200 amperes.
2. Delayed tripping time of 60 to 100 milliseconds at 700 amperes.
3. Instantaneous tripping time not in excess of 20 milliseconds at 2,000 amperes and above.

Reverse-current circuit breakers having different time-current characteristics from those described above can be applied, as shown in Figure 1(B), in dual channel feeders. In this application, the directional circuit breakers near the load trip instantly when current flows from the load bus into the feeder. The circuit breakers located at the source bus are equipped with nondirectional overcurrent trip devices.

For other applications such as bus sectionalizing, single feeder circuits and load circuits, the circuit breakers are equipped with nondirectional overcurrent trips in place of the reverse current devices. For remote tripping in any application, the shunt device may be energized by a relay or other means.

General Description

Figure 2 shows a manually-closed circuit breaker and Figure 3, an electrically-closed circuit breaker. All ratings of the manually-closed circuit breaker are identical in size and outward appearance. The weight of the 600-ampere rating is slightly greater than that of the two lower current ratings because of the greater cross section of the current carrying parts. The addition of the closing solenoid increases the weight of the circuit breaker by two pounds and the depth by two inches.

The general arrangement of the circuit breaker is shown on the right in Figure 2. For the purpose of illustration, one side frame of the mechanism has been made of transparent material. The trip devices (9, 10, 11, and 12) are located at the top of the circuit breaker above the operating mechanism. The circuit breaker contacts are completely enclosed in the interrupting chamber in the base and therefore are not visible in this figure.

Interrupter

The interrupter of the 28-volt circuit breaker contains a simple bridge contact structure shown in Figure 4. The moving contact is made of two parallel copper bridge members. When the circuit breaker is closed, this contact completes the circuit between the two stationary copper connecting bars. The contact tips, both moving and stationary, are made of arc-resistant silver tungsten carbide material. Experience has shown that this material provides long contact life

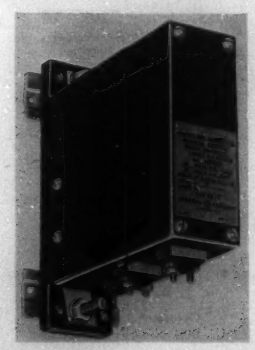

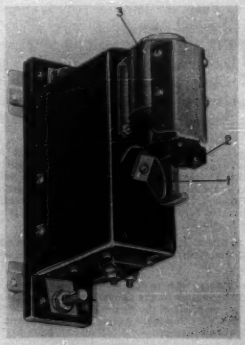

Figure 3. Electrically-closed single-pole aircraft circuit breaker

Left. Front oblique view—cover on
Right. Front oblique view—cover off

1. Closing lever extension
2. Short-circuiting switch
3. Solenoid

Figure 6 (right). Contacts and interrupter for 120-volt circuit breakers

1. Steel half tube
2. Fiber tube
3. Copper bridge
4. Valve
5. Operating rod

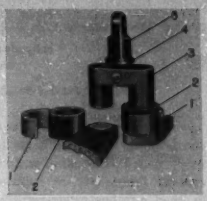

Figure 4. Contacts for 28-volt circuit breakers, 300 and 600 amperes

1. Parallel bridges 2. Operating rod

and is free from welding. The contacts are assembled in the interrupting chamber in the circuit breaker base which is closed by an insulating sheet. This sheet and the base are made of highly arc-resistant material.

A pressure of about seven pounds per pair of contact tips, provided by the contact spring, is ample to maintain the temperature rise of the contacts within desired limits. The two parallel bridge members provide sufficient conducting cross-sectional area for the maximum rating of 600 amperes.

Two advantages are gained in using a bridge-type contact instead of a hinge construction: flexible connections are unnecessary, and considerable blowout effect is obtained without coils or permanent magnets. The current path through the contact structure is such as to cause the arc to loop outward from each end of the bridge member when the contacts part. The arc is extinguished quickly due to the voltage drops in the lengthened arc path and the two cathodes in the double break interrupter. In a 28 volt interrupter, the two cathode drops constitute a large percentage of the total system voltage, making interruption relatively easy. The performance of this 28-volt interrupter is virtually unaffected by altitudes as high as 50,000 feet, up to its interrupting rating of 12,000 amperes.

The problems of developing a d-c interrupter for high altitude duty are much more difficult at 120 volts than at 28 volts. It is likely that this difficulty has delayed the development of the 120-volt aircraft electric system. Although interruption is not entirely a function of the dielectric strength of the medium surrounding the contacts, it is in some measure proportional to it. The curve of the dielectric strength of air at various absolute pressures shown in Figure 5 extends over a range from 1.7 pounds per square inch, which represents an altitude of 50,000 feet, to 100 pounds per square inch. This curve shows that air is a relatively poor insulator at high altitudes and that its insulating properties improve rapidly with increasing pressure. This characteristic suggests that interruption can be accomplished quickly by allowing the arc to generate its own pressure and raise the dielectric strength of the gas surrounding the contacts.

Experience has shown that hard white vulcanized fiber, specially prepared for interrupters, is an excellent material for producing gas and does not deposit sufficient carbon to cause tracking. The interrupter which was designed for the 120-volt circuit breakers, contains this type of fiber. The gases evolved are permitted to build up the pressure in a tight enclosure, helping considerably to extinguish the arc and withstand the recovery voltage.

A skeleton view of the essential parts of the 120-volt interrupter is shown in Figure 6. These parts are supported in a recess in the phenolic asbestos base which forms the enclosure for the interrupter. The bridging contact provides a double break, total of three-quarters of an inch, and like the contact structure in the 28-volt interrupter, eliminates the necessity for flexible braids. Closely surrounding the movable and stationary contact tips, and extending upward for slightly more than the length of the breaks, are two fiber tubes. At current levels above approximately 1,000 amperes, there is sufficient blowout effect from the contact configuration to drive the arcs against the inner surfaces of the tubes. Below 1,000 amperes, the steel half tubes around the fiber tubes help to draw the arcs against the fiber. As the contacts reach the fully open position, a valve (4) on the operating rod (5) closes against a valve seat molded in the base to seal the top of the interrupter enclosure. The bottom of the enclosure is effectively sealed.

The performance of this compact and efficient interrupter is shown graphically in Figure 7. The family of arcing time versus current curves at altitudes up to 50,000 feet shows that over a range of currents up to 5,000 amperes, the maximum arcing time is 32 milliseconds.

Operating Mechanism

The break distance and contact pressure required by the interrupter establish a starting point for the design of a circuit-breaker mechanism. Bridging contacts, such as are used in these circuit breakers, must be operated in a straight line. The required motion and contact pressure are obtained from a conventional latched, over-center toggle mechanism. The mechanism is tripped when the trip devices release the latch. Two strong springs snap the contacts to the open position.

To close the mechanism manually, pressure is exerted on the closing lever

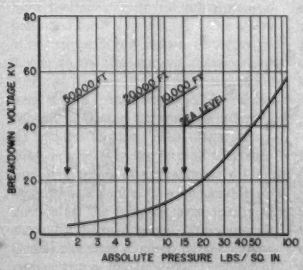

Figure 5 (left). Breakdown voltage—absolute pressure for air with 3/8 inch diameter, electrodes 3/8 inch apart

Figure 7 (right). Arcing time versus current at altitudes from sea level to 50,000 feet for the 120-volt interrupter

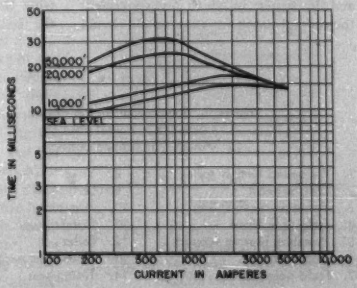

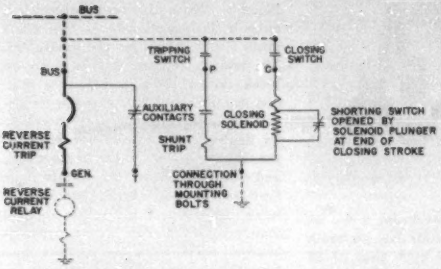

Figure 8. Control circuit for electrically-closed circuit breaker

of the circuit breaker toward the base. The required pressure may easily be applied with the heel of the hand. In the electrically-operated circuit breaker, the solenoid exerts the required force on the closing lever extension, (1) in Figure 3.

One of the outstanding features of this mechanism and one that makes it different from earlier aircraft circuit-breaker mechanisms is that it is trip free. By trip free it is meant that the contacts are able to open fully and quickly if the circuit breaker is tripped while the mechanism is in the process of being closed or while the mechanism is held in the closed position. With this type of mechanism, it is impossible for the operator to maintain power flow into a fault.

Closing Solenoid

In order to conserve space, circuit-breaker closing solenoids usually are designed with a very short time rating and must be energized only momentarily. To protect the coil against overheating, some automatic means should be provided of de-energizing the coil after the solenoid has closed the circuit breaker. It is not good practice to rely on momentary contact control switches which depend entirely on the judgment of the operator to determine the length of time the coil should be energized.

For the protection of the circuit breaker and the system to which it is connected, the control circuit for the solenoid should be antipump. Antipump signifies that the closing solenoid will make but one attempt to close the circuit breaker each time the solenoid is energized.

To keep the size and weight to a minimum and to produce an antipump control circuit, a 2-winding coil is used in the solenoid. The two windings are connected in series with a short-circuiting switch across the high-resistance winding, as shown in the schematic circuit diagram, Figure 8. When the solenoid plunger comes to the end of its stroke, the short-circuiting switch, (2) in Figure 3, is opened and both windings are placed in series. The plunger is held in this position at the end of its stroke until the closing switch is opened. Should the circuit breaker trip while the solenoid is energized, it can not reclose until the operator intentionally opens and recloses the closing switch.

Trip Devices

For generator circuit applications two trip devices ordinarily are used, the shunt trip and the time-delay reverse-current trip. The shunt trip device makes possible remote tripping over a wide range of system voltage. To protect the coil against overheating, one of the auxiliary switches, (5) shown in Figure 2, is connected in series with the shunt trip coil as shown in Figure 8. As the circuit breaker trips, this switch opens and de-energizes the coil. Closing the circuit breaker closes the auxiliary switch and automatically sets up the trip circuit.

The time-delay reverse-current trip device consists of two elements, the time-delay escapement mechanism, 1, 2, and 11 through 14 in Figure 9(A), and the magnetic circuit comprising the field and moving armature. These elements are shown separated from each other in Figure 9(A), and in their normal assembled positions in Figure 9(B). The armature, (10), the center position of which is a permanent magnet, is supported in pivots between the pole pieces, (4) and (7) of the field structure. The single-turn series coil, (9), loops through the yoke, (8), and passes over the top of the armature.

With forward direction current or no current in the series coil, the armature seeks the normal position of Figure 9(A). When the current in the series coil reverses, the armature moves to the tripped position of Figure 9(B). As it moves, the armature releases the latch of the circuit breaker mechanism. These actions of the armature, in response to either forward or reverse direction current, occur because the armature at all times seeks the position that offers the path of least reluctance for its flux. A reset lever actuated by the opening of the circuit breaker mechanism returns the armature from the tripped position back to the normal position.

In either the normal position with forward current in the series coil, or the tripped position with reverse current in the coil, the armature is in a magnetizing field. However, when the armature is in the normal position and the current builds up with a very high rate of rise in the reverse direction, unless proper precautions have been taken in the design, demagnetization can occur. A succession of reverse currents of fault magnitude with high rates of rise in the order of 3 to 4 million amperes per second may completely demagnetize the armature unless some means are employed to prevent the series coil flux from bucking down the armature flux.

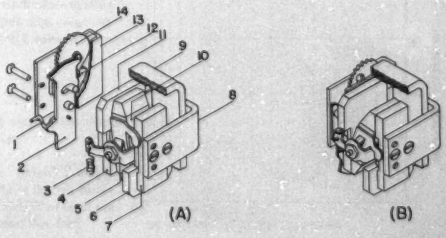

Figure 9. Reverse current trip device
A. Armature in normal position
B. Armature in tripped position

1. Preloaded torsion spring
2. Gear segment
3. Armature return spring
4. Field pole piece
5. Armature bearing support
6. Copper slug
7. Field pole piece
8. Yoke
9. Series coil
10. Armature
11. Copper slug
12. Pallet
13. Escapement mechanism frame
14. Timing gear

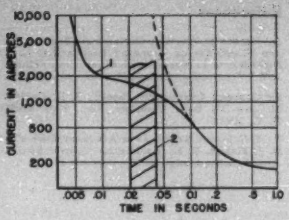

Figure 10. Time current tripping characteristics of reverse current device

1. Trip device characteristic
2. Relay operating time 0.02–0.04 second

In this design, the copper slugs (6, 11) in and around the forward current air gaps are used to prevent demagnetization. The copper slugs oppose a sudden decrease or possible reversal of flux in the pole pieces which they cover. Since these slugs are in two diagonally opposite air gaps, they have no effect on the flux in the other pair of air gaps. The armature has an opportunity to move toward the tripped position without being demagnetized because the sudden reversal of flux is choked in one pair of the air gaps by the copper slugs. Tests made with reverse currents rising at the rate of 3 to 4 million amperes per second up to 13,500 amperes show that the armature is not demagnetized.

For application to generator circuits, the tripping of the circuit breaker must be delayed as described in earlier paragraphs. The time-delay escapement mechanism, 1, 2, and 11 through 14 in Figure 9(A), delays the rotation of the armature as it moves to the tripped position. This escapement is so arranged that it delays the armature only during the first half of its rotation. Thereafter, the armature rotates freely and delivers an impact to release the latch of the circuit-breaker mechanism.

The connection between the escapement mechanism and the armature is a preloaded torsion spring, (1). The action of this spring is best demonstrated by referring to the time-current characteristic curve of Figure 10. If this connection were a rigid member, the time-delay tripping characteristic would be indicated by the dotted line. The series spring, however, yields to the force of the armature at currents of approximately 1,500 amperes and above. A considerable reduction in the tripping time results as shown by the solid curve. This curve indicates the time required by the reverse current trip device to release the latch of the circuit-breaker mechanism at various currents.

Performance Characteristics

The co-ordination between generator relays and one of the new reverse current circuit breakers is shown in Figure 10 by the intersection of the circuit breaker tripping characteristic and the band of opening time of the generator relays. The operating time of most generator relays falls within this band, extending from 0.02 to 0.04 second. Above the intersection of the curve and the band, the circuit breaker trips before the relays open, viding the much-needed backup protection for the relay. This protection is required because of the limited interrupt-ng capacity of the relay.

Below the intersection of the curve and the band, the relay normally opens before the circuit breaker. If, however, the relay fails to open, due to welding of its contacts or improper functioning of the pilot relay, the circuit breaker will open the circuit on reverse currents of 200 amperes or more. The inverse time-current characteristic of the trip device prevents the circuit breaker from tripping falsely on transient reversals. This tripping characteristic is very desirable for generator circuit applications because of the protection which is provided throughout the entire range of currents.

A family of arcing time curves of various altitudes for the 120-volt interrupter is shown in Figure 7. These indicate that over the range of currents up to the interrupting rating and altitude from sea level to 50,000 feet, a maximum arcing time of 32 milliseconds occurs at 600 amperes and 50,000 feet. At lower altitudes and at currents above and below this value, the arcing time is considerably less. The arcing time of the 28-volt interrupter is approximately 1.5 milliseconds and is essentially constant through the entire range of current and altitude. Typical oscillograms of interrupting tests made on 28- and 120-volt circuit breakers are shown in Figure 11.

It is sometimes desirable to know the over-all interrupting time of the circuit breaker to determine the heating effect in other connected devices. This can be obtained at any current by adding the tripping time, the arcing time, and the mechanism operating time. The circuit-breaker mechanism operating time, which is the time from the release of the latch until the contacts start to part, is 5 milliseconds for all values of current. For example, the over-all interrupting time at 5,000 amperes and 50,000-foot altitude for the 120-volt circuit breaker is 24 milliseconds; for the 28-volt circuit breaker at 12,000 amperes and 50,000 feet it is 16 milliseconds.

Auxiliary Contacts

Faults in the generator circuit are isolated from the bus by the opening of the circuit breaker. To stop the flow of power into the fault from the generator, the generator field should be de-energized as the circuit breaker opens. A field switch can be provided in the circuit breaker to do this directly, or the second auxiliary contact, (5) shown in Figure 2(B), can be used to control a relay in the field circuit. The rating of the auxiliary contacts is 10 amperes at 28 volts and 0.3 ampere at 120 volts.

Conclusions

The new aircraft circuit breakers described in this paper meet the requirements of the present-day aircraft electric systems. The continuous current carrying ability and the interrupting capacity of these circuit breakers are adequate for present and proposed 28-volt d-c systems and for proposed 120-volt d-c systems.

Proper co-ordination is obtained between these circuit breakers and generator relays of various types in generator circuits under all conditions. The long time-delay reverse-current trip device developed for these circuit breakers eliminates nuisance trips of circuit breakers in generator circuits. These conclusions are borne out by the results of system tests presented in a conference paper of the

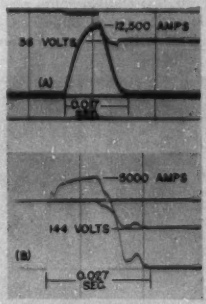

Figure 11. Typical oscillograms of interrupting tests

A. Test at 36 volts, 12,000 amperes and 50,000 foot altitude
B. Test at 144 volts, 5,000 amperes and 50,000 foot altitude

AIEE Pacific General Meeting, San Francisco, Calif., August 23–26, 1949 on A New Aircraft D-C Generator Control System, by Mr. G. A. Phillips.

With instantaneous reverse current and nondirectional trips, these circuit breakers are applicable for bus sectionalizing and in dual- and single-channel feeder circuits and load circuits.

It is believed that the difficulty of obtaining adequate interrupting ability at high altitude has been one of the major problems in the development of 120-volt d-c systems. The development of these circuit breakers and the information now available on interruption performance at altitudes should help further the development of these systems.

References

1. Effect of Altitude on Electric Breakdown and Flashover of Aircraft Insulation, L. J. Berberich, G. L. Moses, A. M. Stiles, C. G. Veinott. *AIEE Transactions*, volume 63, 1944, pages 345–54.

2. Gaseous Conduction (book), J. D. Cobine. McGraw-Hill Book Company, Inc., New York, N. Y., 1941.

3. D-C Power Systems for Aircraft, Part VII, H. J. Finison, R. H. Kaufmann. *General Electric Review* (Schenectady, N. Y.), August, 1948.

No Discussion

An Environment-Free 120-Volt D-C High-Performance Limit Switch

THOMAS R. STUELPNAGEL
ASSOCIATE AIEE

THE *H420A* switch is a newly developed, high performance, hermetically sealed, 120-volt d-c aircraft limit switch. This switch was specifically designed to carry $3^1/_2$ kw and to interrupt a 1.8 kw motor load, 15 times a second, for duty cycles of 15 seconds each.

The development of the *H420A* switch was undertaken because no existing switch would meet these particular requirements and because present 120-volt d-c aircraft electric systems have need for a limit switch capable of interrupting up to 30 amperes of motor current. Electric loads of this nature are now being controlled with switch and sealed-relay combinations which are inherently larger, heavier, and more unreliable than a corresponding switch. This limit switch weighs 1/2 pound and was designed to replace a $2^1/_2$-pound sealed relay.

The purpose of this paper is to discuss, through the medium of a specific design problem, the factors which complicate a seemingly simple device like a 120-volt d-c limit switch, and to emphasize several features of the *H420A* switch that are considered essential though not available in any aircraft limit switch. These features include: positive contact separation in addition to snap action; 8-ounce contact pressures; high-temperature glass-fused mica insulation; a contact assembly capable of interrupting a 1.8 kw motor load one million times without failure; hermetic sealing, and double-break magnetic arc suppression.

Basic objectives in this switch development were first to design a simple long-life mechanism capable of positively opening the switch contacts, and second to obtain environmental-free operation by hermetically sealing the mechanism and contact assembly. Unfortunately, in available aircraft limit switches, the emphasis has been placed on the snap-action contact separation—little effort has been expended in providing positive mechanical follow-up on these snap-action mechanisms which could, in an emergency, open the contacts with the many pounds of force available in the typical operating device instead of the few ounces of force available in the typical snap-action mechanism.

Summary of the H420A Switch Characteristics

Primary considerations in the switch design were a positive break, snap-action mechanism and adequate electrical capacity. Secondary considerations were operating force, differential plunger travel and accuracy of the snap-action trip point. The prototype switch is shown in Figure 1.

Mechanical Features

The switch mechanism incorporates four mechanical features considered essential in an aircraft limit switch.

1. Positive mechanical operation of the contacts as a follow-up to normal snap-action of the switch mechanism.

2. Eight ounces of contact pressure per contact.

3. No detectible contact bounce during switch closure.

4. A magnetic snap-action which maintains substantial contact pressure until after the mechanism trips. In the closed position each contact is mechanically preloaded to 8 ounces by a contact arm deflection of 0.020 inch; therefore, actual contact separation occurs at an interval after the contact armature has been accelerated to a high velocity.

Simplicity

The foregoing mechanical features are obtained without using the complicated lever and spring assemblies common to this type of switch. Such complication is eliminated by using a 1-ounce Alnico V magnet for producing the detent and snap-action. Phenomenal cyclic rate is obtained by combining ample thermal capacity in the contact assembly with magnetic arc suppression. Rapid mechanical operation necessary for such high cyclic rate is secured by applying the operating force directly to the contact armature.

Electrical Capacity

The *H420A* switch is capable of interrupting up to 3.5 kw of 120-volt d-c motor load and was designed specifically to interrupt a 1.8-kw motor load 15 times a second for a 15-second duty cycle. Tests with this switch indicate that the peak voltages resulting from inductive circuit interruption never exceed 1,000 volts be-

Figure 1. The *H420A* 120-volt d-c aircraft limit switch (prototype)

Paper 50-203, recommended by the AIEE Air Transportation Committee and approved by the AIEE Technical Program Committee for presentation at the AIEE Middle Eastern District Meeting, Baltimore, Md., October 3–5, 1950. Manuscript submitted July 6, 1950; made available for printing August 22, 1950.

THOMAS R. STUELPNAGEL is a research engineer residing in Los Angeles, Calif.

Table I

Current carrying capacity	30 amperes
Interrupting capacity (inductive)	30 amperes 120 direct volts (10 operations per minute, L/R of 0.013)
	15 amperes 120 direct volts (900 operations per minute, L/R of 0.003, 15-second duty cycle)
Altitude (hermetically sealed)	100,000 feet
Weight	1/2 pound
Dimensions	1 1/4 × 1 × 3 inches
Plunger force	7 pounds (sea level)
	12 pounds (50,000 feet)
Plunger travel	0.070 inch
Differential travel	0.020 inch
Overtravel	0.100 inch
Mechanical cyclic rate	in excess of 1,000 operations per minute

cause the arc time increases directly with load energy.

Materials

The switch is constructed entirely of metal and a very high quality dielectric composed of fused mica and glass which will stand exceptionally high temperatures and will not track under repeated arcing.

Life

Tests indicate a mechanical and electrical switch life in excess of 50,000 cycles at rated loads.

Hermetic Sealing

Environmental-free electrical operation can be obtained by hermetically sealing the switch at one atmosphere of pressure in dry air. At the design motor load of 15 amperes, 120 direct volts, a hermetic seal is required for operation above 30,000 feet altitude.

H420A Switch Specifications

The specifications for the switch are given in Table I.

Details of the H420A Switch Design

A successful electrical switching operation involves two factors: first, the energy of the electric load, usually inductive, must be thermally absorbed by the switch in the form of arc energy; second, the separation of the switch contacts must introduce enough impedance into the electrical circuit to extinguish this arc after the load energy has been dissipated.

The interrelation of these two factors, coupled with the lack of published data on the variations introduced by different contact materials, rates of contact separation, and atmospheric conditions, makes the job of switch design and switch rating largely experimental.

Test Equipment and Procedures

The test set-up and procedure used in designing the contact arrangement for the *H420A* switch was geared to eliminate much of the time delay and inconvenience associated with the collection of transient switch data. Application of a dual-beam oscilloscope provided simultaneous presentation of switch current and voltage from which measurements of peak voltage, arc current, arc time, and arc energy were readily obtained. A continuous presentation of the switching transient was obtained on the oscilloscope by cycling the test switch at a frequency of 10 to 15 cycles per second. The use of this rapid cycling process for switch investigation is dependent upon the rate of contact temperature rise. However, if a test switch can be rapidly cycled, even in 1-second bursts, a great deal of information can be obtained without the need for a long persistence oscilloscope tube or an oscilloscope camera. The observation of a repeated switching transient insures a typical result and makes the adjustment of synchronization circuits less critical.

Permanent records of switching phenomenon were photographed with a special oscilloscope camera which exposes, develops, and prints each oscillogram in a 1-step 60-second process.

Contact Arrangement

The design of compact, high-capacity 120-volt d-c switchgear is complicated by the fact that the voltage drop across a stable arc remains almost constant with an increase in arc current past 3 amperes, and that this voltage drop even for a one centimeter arc length is less than 40 volts. Theoretical relationships derived by Aytron and Windred[1,2] show that a stable arc is composed of three series voltage drops; an anode drop in the immediate vicinity of the positive contact, a cathode drop at the negative contact, and a column drop between the two. The values of these arc potentials can be calculated from the following equations:[1]

$$\text{Anode drop, } (e_a) = \frac{4a}{5} + \frac{b}{I} \text{ (volts)} \qquad (1)$$

$$\text{Cathode drop, } (e_c) = \frac{a}{5} \text{ (volts)} \qquad (2)$$

$$\text{Column drop, } (e_l) = c + \frac{d}{I} \text{ (volts/centimeter)} \qquad (3)$$

For silver contacts, the values of the constants are $a=19$; $b=11.4$; $c=14.2$; $d=3.6$; I = arc current in amperes.

The theoretical anode voltage drop for a current of three amperes is 19 volts, the cathode drop is 3.8 volts and the column drop is 15.4 volts per centimeter; the total voltage drop across a 1-centimeter arc is, therefore, 38.2 volts. Because of the varying degrees of arc stability which can occur in actual switching operations, it would be difficult to predict the break capacity of a particular switch from the foregoing equations. However, these equations do establish the relative magnitude of each arc characteristic and demonstrate the effectiveness in compact 120-volt d-c switchgear of splitting the arc into a number of series anode and cathode voltage drops with multiple break contacts or deion grids and the ineffectiveness of merely increasing the contact separation.

From the theoretical equations alone, it appears necessary to use four series breaks of 0.1-inch each in a reliable 120-volt d-c switch capable of interrupting the specified 15 amperes. Such an arrangement is impractical, however, because of the mechanical problems involved in supplying adequate contact pressure, operating force, and adjustments to four series contacts in a small snap-action limit switch. In addition to these problems, test results indicated that such a switch would have to be hermetically sealed for reliable, 15-cycle-per-second operation at 50,000 feet.

Magnetic Arc Suppression

The use of magnetic arc suppression, rather than multiple-break contacts, as a means of quenching the arc in a her-

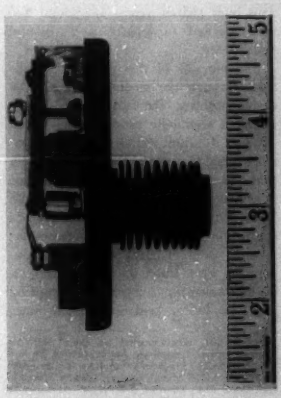

Figure 2. The permanent magnet switch mechanism

metically-sealed 0.1-inch gap snap-action limit switch has several advantages. The increased break capacity and minimum arc energy obtainable with blowout magnets permit the design of a simpler, more compact, 2-break switch capable of interrupting higher energy inductive loads at a given cyclic rate.

Although complete agreement has not been reached in the literature on the theoretical aspects of magnetic blowout, it is generally believed that:[1,3,5]

1. The increased arc path caused by the magnetic field contributes to arc suppression.

2. The rapid movement of the arc across the contact surfaces retards the formation of the molten anode and cathode spots necessary for sustaining an arc.

3. Altitude reduces the effectiveness of magnetic arc suppression until at a critical level the blow out forces have no effect on the arc. At altitudes higher than the critical level, the direction of the arc appears to reverse and the switch break-capacity will then increase.

Were it not for the reduced effectiveness of magnetic arc suppression with altitude, this form of arc quenching would adequately solve the majority of 120-volt d-c switching problems, and in this particular switch there would then be no necessity for hermetic sealing.

Experimentation with the 1/6-ounce blowout magnets used in the subject switch resulted in the location pictured in Figure 1. For the particular conditions of the test (double break contacts with 0.1-inch gaps, silver cadmium-oxide contacts and a 15-ampere aircraft motor load having a buildup time constant of 0.003 second) it was found that the best compromise between altitude and sea level break-capacity could be obtained by supplying a uniform magnetic field between the contacts. Such a field was obtained by locating the blowout magnets in front of the contacts, thereby drawing the arc directly into the magnets. This arrangement affords maximum arc stability, contributes to cooling of the arc gas, and simplifies the magnet mounting problem.

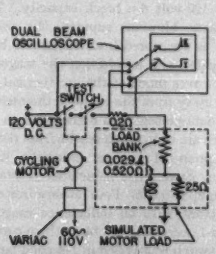

Figure 3. A typical switch testing circuit

The Alnico II magnets used to supply the blowout fields were found to be exceedingly stable when demagnetized to about one half of their maximum flux density. Further tests demonstrated that drawing an arc directly into such blowout magnets had no appreciable effect on their magnetic stability, and that variations of 50 per cent in field strength of the blowout magnets did not measurably alter the switch break-capacity. During life tests 2,000,000 15-ampere 1.5-joule arcs were drawn into the blowout magnets at a continuous rate of 15 cycles per second without affecting their field strength. The emergency overload capacity of the switch was demonstrated in a second test when 75-ampere 70-joule arcs were interrupted 10 times a second for 100 1-second duty cycles without altering the blowout field.

Contact Materials

The selection of suitable contact materials was found to be of fundamental importance in the design of a high cyclic rate, high-capacity switch. Preliminary tests indicated that arc energy, and consequently the contact temperature and life were intimately associated with the contact material used. In addition the high contact temperatures encountered even with materials demonstrating low arc energy required that the contact be riveted rather than brazed or resistance welded to the contact arm.

A silver cadmium-oxide contact material was found to give the best results of several materials tested because it exhibited superior qualities of low arc energy, long life, and high electrical conductivity; and is ductile enough to be riveted directly to the contact arm. As a result the contacts can be overloaded to a red heat without apparent damage.

The importance of selecting suitable contact materials was demonstrated by life tests conducted with the circuit shown in Figure 3. In these tests a 15-ampere simulated motor load was interrupted continuously 15 times a second with a double-break magnetic blowout switch; the switch contacts were not externally cooled. Two life tests were conducted with $^1/_4$-inch diameter silver-cadmium-oxide contacts riveted to beryllium copper arms. Each set of these contacts went 1,000,000 consecutive cycles without failure and a maximum contact temperature of 400 degrees Fahrenheit resulted from the 1.5-joule arc energy.

When the identical test was attempted with silver tungsten-carbide contacts, brazed to similar contact arms, failure occurred after 4,500 cycles of operation because tripled arc energies resulted which in turn caused contact temperatures in excess of 1,000 degrees Fahrenheit. The high temperature caused these contacts to erode rapidly and eventually fall off.

Transient thermal capacity was provided in the *H420A* switch by riveting the stationary silver-cadmium-oxide contacts to solid copper blocks having 20 times the mass of each contact.

Switch Mechanism

The permanent-magnet detent mechanism provides the essential limit switch features of adequate contact pressures, snap-action "make" and "break", no detectible contact bounce and a positive mechanical contact separation. In addition, the mechanism is rugged, simple, and extremely rapid.

Operation of this mechanism, shown in Figure 2, results from the difference in shape of the force-distance curves of a magnet and a spring. During the plunger pretravel the plunger spring is compressed against the contact armature which in turn is held against the detent magnet with ten pounds of magnetic pull. When the plunger spring is compressed to a force sufficient to overcome the difference force between the detent magnet and the contact preload, the armature is suddenly released by the magnet and driven to the full open position by the energy stored in the spring. During opening, the armature driving force is the difference force between the opposing spring and magnet. A mechanical opening speed of about 2 milliseconds results because this force of more than a pound is applied directly to the contact armature. If, after the switch has been opened, the plunger position is reduced 0.020 inch from the trip point, the slope of the magnetic force curve becomes greater than that of the spring curve and the armature snaps shut.

Should gross electrical overloads weld the contacts, the switch overtravel causes the plunger to bottom directly on the contact armature. Extensions of the contact armature, not shown in Figure 1, then open the contacts with a force transmitted directly from the operating device.

Eight-ounce contact pressure is provided in the *H420A* switch. In view of the vibration, contact bounce, and surface oxidation problems encountered with switches and relays having contact pressures less than 4 ounces, it appears very desirable on a series break device using silver base semirefractory contact materials to have 8 ounces of contact pressure per contact.

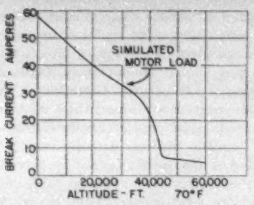

Figure 4. Altitude characteristics of an unsealed double-break magnetic blowout switch. The electrical circuit constants are given in Figure 3

Contact gap: 0.1 inch, contact material: silver cadmium-oxide

Substantial contact pressure is maintained until after the switch mechanism trips. With the perfect magnetic detent device, constant contact pressure would be maintained until the contact armature was suddenly snapped open. In the actual device, mechanical tolerances contribute to a reduction of contact pressure from 8 ounces to 6 ounces as the plunger trippoint is approached.

Contact bounce during switch closure has been minimized by combining the magnetic snap-action mechanism with a low inertia spring loaded contact assembly. Minimum contact bounce is especially important when such a switch is used for d-c motor control because motor surge currents several times greater than the running current build up in a few milliseconds after contact closure.

Hermetic sealing in a high permeability case increases the reliability of the permanent magnet mechanism by excluding foreign matter and effectively shielding the detent magnet from external fields.

Hermetic Seal

The reduced effectiveness of magnetic arc suppression with altitude requires that the *H420A* switch, when interrupting the specified 15-ampere motor load, be hermetically sealed for reliable operation above 30,000 feet.

Some of the more obvious problems involved in such an hermetic seal are:

1. Transmission of mechanical movement and electrical energy through the seal.
2. Selection of proper sealing atmosphere.
3. Effect of altitude and temperature on switch operation force.
4. Prevention of excessive temperature rises near the soldered joints of the case.

The hermetic seal has not yet been tested; however, a brief discussion of this seal has been provided for completeness of the switch report. Glass to metal terminals capable of handling 30 amperes were selected for the electric connections. A bellows rather than a diaphragm has been used for transmission of mechanical movement because of the large travel obtainable (0.3 inch maximum in the specified bellows), ruggedness, reproducibility and a life expectancy in excess of 50,000 operations. The switch case is 1/32-inch steel, silver soldered at all joints except the top and electrical terminals. The sealing atmosphere is dry air.

Insulation

There is no easy solution to the problem of insulating an electrical arc. Unfortunately, the insulators that can withstand the intermittent arc temperatures of several thousand degrees without breaking down or carbon tracking are of a ceramic nature. Ceramics meeting the requirements were brittle, difficult to machine and expensive to assemble.

If these mechanical problems associated with the use of ceramics are accepted as the price to pay for excellent arc insulation the rewards are gratifying. All of the insulation in the *H420A* switch is glass-bonded mica, a material which has excellent high temperature characteristics, will not carbon track, is reasonably machinable, and can be bonded to itself or metal with a special high-temperature ceramic cement. For arc insulation, this material proved far superior to glass-silicone laminates, melamine or Bakelite.

The insulation problem of a low production switch, where quality rather than cost is the controlling factor, can be effectively solved by surrounding the switch mechanism with 1/16-inch thick pieces of glass-bonded mica which are mechanically interlocked and then bonded to the metal switch case with the ceramic cement.

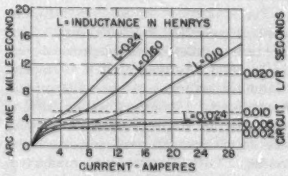

Figure 5. Break-capacity of a hermetically sealed *H420A* 120-volt d-c aircraft limit switch

These curves were obtained with an unsealed switch operating at sea level pressure and 10 cycles per second for 1-second intervals. Inductance ratings are based on current rise time

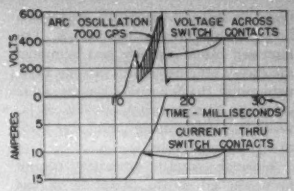

Figure 6. Typical oscillogram of the *H420A* switch interrupting a 15-ampere inductive load. Electrical load L/R ratio = 0.012

The switch shown in Figure 1 contains insulation of this type.

Altitude Characteristics of an Unsealed Switch

The break-capacity of an unsealed *H420A* switch at altitudes up to 60,000 feet has been presented in Figure 4. The break capacity of the unsealed switch when interrupting the simulated motor load described in Figure 3 is 58 amperes at sea level, linearily reduces to 22 amperes at 40,000 feet, and then suddenly drops to 6 amperes at 45,000 feet. Arc reversal phenomenon was observed at altitudes.

Break capacity was based on maintaining a constant 10-milliseconds arc time. Further testing and data reported in the literature indicate that the altitude at which the blowout forces disappear or in some instances reverse in direction, depends upon the variables of switch gap, contact materials, contact temperature, blowout field strength and location, load current, and possibly the speed of contact separation. Because of the large number of variables involved in a particular switching operation the altitude characteristics shown in Figure 4 cannot necessarily be extrapolated to higher inductive loads.

Switch Break Capacity

Hermetically sealed at one atmosphere of pressure, this switch has an unusually high 120-volt d-c break capacity. The magnetic blowouts suppress the arc as soon as the stored load energy has been dissipated and in addition the magnetic field drives much of the arc thermal energy away from the contacts themselves. The data presented in Figure 5 shows the switch arc time which results from the interruption of various inductive loads having current rise inductance-resistance ratios up to 0.025. Four low-loss iron core inductors, with an inductance range of 10-to-1, were used to obtain these curves. The switch was cycled in 1-second bursts at 10 cycles per second.

For all practical purposes the switch arc time was found to have a constant value for a given circuit time constant or inductance-resistance ratio. For example: the interruption of inductive loads having a current rise inductance-resistance ratio of 10 milliseconds resulted in an arc time of 5 milliseconds; the interruption of a 20-millisecond inductance-resistance ratio resulted in a 11 milliseconds arc time. This characteristic provides a convenient basis for rating the *H420A* switch.

Peak voltages resulting from interruption of the inductive loads described in Figure 5 never exceed 1,000 volts. This characteristic is of particular importance because it is not unusual for d-c aircraft switches to cause peak voltages over 5,000 volts.[4] In most instances the peak voltages measured across the *H420A* switch decreased with an increase in arc time past 3 milliseconds. An arc modulation frequency of several kilocycles was observed in arcs lasting longer than 5 milliseconds. A typical oscillogram of the transient switch current and voltage resulting from the interruption of a 15-ampere inductive load has been reproduced in Figure 6.

References

1. Electrical Contacts Data Book. P. R. Mallory and Company, 1945.

2. Electrical Contacts (book), G. Windred. MacMillan and Company, Limited, London, England, 1940.

3. D-C Arc Interruption for Aircraft, L. T. Rader, J. S. Quill. *Electrical Engineering* (*AIEE Transactions*) volume 63, December 1944, pages 883–88.

4. Peak Voltages with D-C Arc Interruption for Aircraft, V. E. Phillips, W. P. Mitchel. *Electrical Engineering* (*AIEE Transactions*), volume 63, December 1944, pages 944–49.

5. Immobility Phenomena and Reverse Driving Phenomena of the Electric Arc, S. Yamashita. *Journal of Applied Physics* (New York, N. Y.), volume 21, March 1950, pages 193–96.

No Discussion

The Design of Reactors for Radio Interference Filters

L. I. KNUDSON
NONMEMBER AIEE

RADIO noise filters in their simplest form may consist of a capacitor inserted between the interference source and that portion of the circuit that is to be isolated. The attenuation of such a filter is limited by the inherent impedance of the leads between the noise generator and the capacitor. It is economical to provide additional impedance at this point in the form of a reactor. Figures 1(A) and 1(B) show the two conditions.

The load or output voltage E_0 neglecting Z_g and taking Z_L as the impedance of the capacitor in parallel with the load is evidently given by

$$E_0 = \left(\frac{Z_L}{Z_S + Z_L}\right) E_g \tag{1}$$

and in general, it is desirable from an attenuation standpoint to have Z_g as large as possible and Z_L as small as possible. Resonant conditions which eventually occur as the frequency is increased are a serious limitation on a single section filter. Additional high-frequency sections may be added to provide attenuation where the above section becomes ineffective. The problem of particular interest in this paper, however, is the consideration that may be given to the reactor.

Closer inspection of Z_s reveals that Figure 2 is representative of an equivalent circuit for an inductor containing a high-loss magnetic material where L_x is the inductance, R_x is the shunting effect due to iron losses, R_w is the actual winding resistance taking into account the skin effect, and C_d is the distributed capacity. The distributed capacitance may have losses, but these are generally swamped by those already stated. For direct current and low-frequency alternating currents R_x becomes very high while R_w approaches the d-c value of the winding. From a radio-interference-filter standpoint and the expression of equation 1, R_x, L_x, and R_w may be large, while C_d should be as small as possible so that antiresonance of L_x and C_d may occur at as high a frequency as possible. Low values of R_x are desirable as a means of preventing unwanted drop in power currents which also is true of L_x for alternating currents. The desirability of high L_x and R_w for attenuation against radio-influence currents as against low L_x and R_w for low attenuation against power currents is a designer's compromise.

A factor occasionally overlooked is that relatively low values of R_x may be tolerated in radio-interference filters, as the filter operates well beyond cut off where rapid transition from pass to stop is not generally required. Consider that R_x is primarily responsible for limiting the Q factor of the coil. Figure 3(A) is the circuit and Figure 3(B) is a plot of the absolute value of normalized impedance versus Q, where Q is taken as $R_x/\omega L_x$. Note that values of Q as low as three reduce the impedance to only 0.707 of the unloaded value.

As the reactor is examined at increasingly greater frequencies, it will be observed that R_x reduces, as the iron losses will increase with frequency and reactance of the distributed capacity becomes appreciably low. R_w of Figure 2 may generally be neglected so that Figure 4 is the equivalent circuit.

Equation 2 expresses the impedance of this circuit but R_x should be considered as being a complex function of frequency.

$$Z_s = \frac{\dfrac{1}{R_x} - j\left(\omega C_d - \dfrac{1}{\omega L_x}\right)}{\left(\dfrac{1}{R_x}\right)^2 + \left(\omega C_d - \dfrac{1}{\omega L_x}\right)^2} \tag{2}$$

At the natural frequency of the coil the impedance becomes simply R_x which may or may not be a high value. For frequencies greater than the natural frequency, Z_s becomes less and less. It is well to reduce C_d as much as possible and this may be done by obtaining the inductance by connecting in series a multiplicity of coils the antiresonant or natural frequency of any one coil being the limiting factor. π windings and even straight solenoidal windings are examples of such arrangements. Space-wound solenoids are still more effective in this respect and should the spacing be increased without limit a straight wire results. The anti-

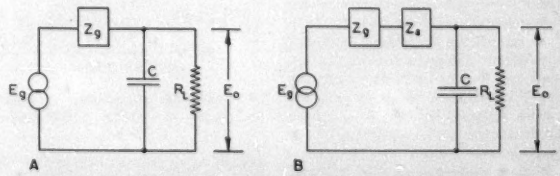

Figure 1(A). Equivalent noise generator and load resistance isolated by a capacitor

Figure 1(B). Equivalent noise generator and load resistance isolated by Z_s and capacitor

Paper 50-204, recommended by the AIEE Air Transportation Committee and approved by the AIEE Technical Program Committee for presentation at the AIEE Middle Eastern District Meeting, Baltimore, Md., October 3-5, 1950. Manuscript submitted July 7, 1950; made available for printing August 23, 1950.

L. I. Knudson is with General Laboratory Associates, Inc., Norwich, N. Y.

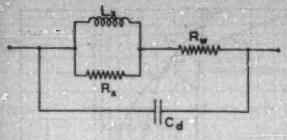

Figure 2. Equivalent circuit of inductor

resonant frequency for the straight wire occurs when it becomes electrically a half wave length long.

Suitable coils may take many forms. Figure 5(A) represents one arrangement whose greatest merit is ease of manufacture. Figure 5(B) represents an improvement over Figure 5(A) as a return flux path is provided. Figure 5(C) is quite similar except that somewhat higher distributed capacity may offset the increased inductance value.

Figure 6 is still better and makes good use of available space, allows a very close fitting shield to be used, and has a relatively low value of distributed capacity.

The saturation effects of load currents should be checked although the large airgap provided by Figure 5(A) plus the intrinsic airgap of powdered iron due to the interstices between the iron particles generally prevents saturation. Figure 6, however, should be carefully checked as saturation may easily occur. This becomes particularly so should end caps of magnetic material be added forming a familiar cup core.

The foregoing remarks are doubly applicable to the toroid and variations of the toroid. The toroid provides a satisfactory filter reactor as the external magnetic flux is almost nil, the distributed capacity may be satisfactorily low and for a given space requirement provides a good value of inductance. As only single-layer windings generally prove practical the difficulty of winding such a coil is considerably relieved. The toroid may utilize 0.001–0.003 inch laminations of ferrous material as parallel rings or as a continuous wound strip. Alternatively the core may be molded from the ferrites or from the more conventional powdered irons. All such cores require an airgap whose value may be for the ferrous and ferrite materials computed from the method of Hanna,[4] while for the powdered irons an intrinsic airgap is effected by the interstices between the iron particles. In both cases it is the incremental inductance that is of interest as the load currents are much greater than the radio-influence currents.

Computations on closed toroids of rectangular cross section which may or may not have an intrinsic airgap may be made rather easily from the following relations. The total F is given by

$$F=\frac{4\pi NI}{10} \quad \text{gilberts} \tag{3}$$

$$H=\frac{4\pi NI}{2\times 10\pi r}=\frac{2NI}{10r} \quad \text{oersteds} \tag{4}$$

$$B_\Delta=\frac{2NI}{10r}\mu_\Delta \quad \text{gausses} \tag{5}$$

where μ_Δ is a function of H for saturable materials.

$I=I_0+I_\Delta$

b = core width

R_2 = outer radius

R_1 = inner radius

and as by definition

$$L_\Delta=\frac{N\phi_\Delta}{I_\Delta}\times 10^{-8} \text{ henrys} \tag{6}$$

together with equation 5 gives

$$L_\Delta=\frac{2N^2b}{10}\int_{R_1}^{R_2}\mu_\Delta\frac{dr}{r}\times 10^{-8} \quad \text{henrys} \tag{7A}$$

The μ_Δ may be held constant to an average value of $1/2\ (\mu_{\Delta_2}+\mu_{\Delta_1})$ as an approximation whose error becomes nil as $R_2-R_1\rightarrow 0$.

Values of μ^Δ are taken from curves relating μ_Δ versus H. Where R_2-R_1 is appreciable the integration may be done

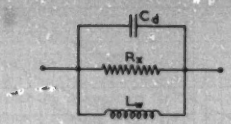

Figure 4. Equivalent circuit of inductor neglecting series resistance only

in parts using different values of average μ_Δ. Equation 7(B) expresses this relation and in addition is applicable to the simultaneous use of different core materials arranged in annular fashion where μ_Δ under a particular integral may be taken as an average value between the limits of integration or as an exact value taken as a complex function of r from the μ_Δ versus H curves.[1]

$$L=\frac{2N^2b}{10}\left[\int_{R_1}^{R_2}\frac{\mu_{\Delta_2}dr}{r}+\int_{R_2}^{R_3}\frac{\mu_{\Delta_3}dr}{r}\times\int_{R_{\mu-1}}^{R_\mu}\mu_\Delta dr\right]\times 10^{-8}H \tag{7B}$$

For toroids with round cross sections, equation 8 of reference 2 is included where r_1 is radius of core section.

$$L=\frac{4\pi N^2}{10}\left[R-\sqrt{R^2-r_1^2}\right]\mu_\Delta\times 10^{-8}H \tag{8}$$

Equations 7 and 8 may be written as

$$L=N^2\rho \tag{9}$$

where ρ is the permeance of the magnetic circuit. In general, when the turns occupy substantially the same space in any coil ρ remains constant except for saturation effects.

This equation may be plotted and the parallel lines with a slope of two of Figure 7(A) are loci for different values of ρ. Figure 7(B) is a plot on log–log paper of ampere turns versus ρ for a given toroid. Use of Figures 7(A) and (B) allows rapid calculation of incremental inductance for various values of d-c load current. The bending to the right of the ampere turns versus ρ curve is due to saturation while the extreme left vertical line is the curve

Figure 3 (below) (A). Equivalent circuit of inductor neglecting series resistance and shunt capacity
(B). Plot of normalized impedance versus Q

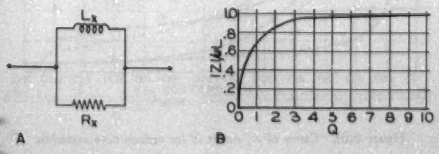

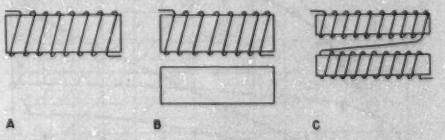

Figure 5 (above). Inductor

(A) With no return path; (B) With return path; and (C) Alternate form with return path

Figure 6. An inductor with symmetrical flux return path

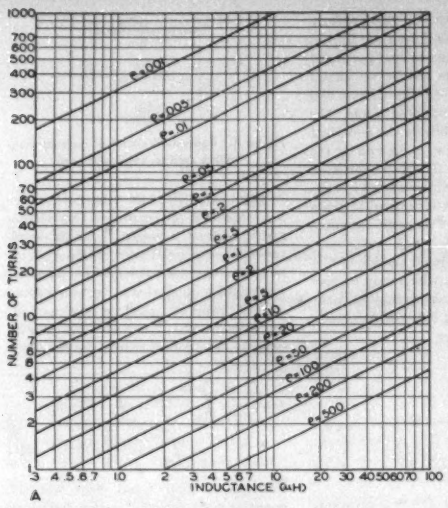

Figure 7(A). Curve providing relations between ρ, L, and N

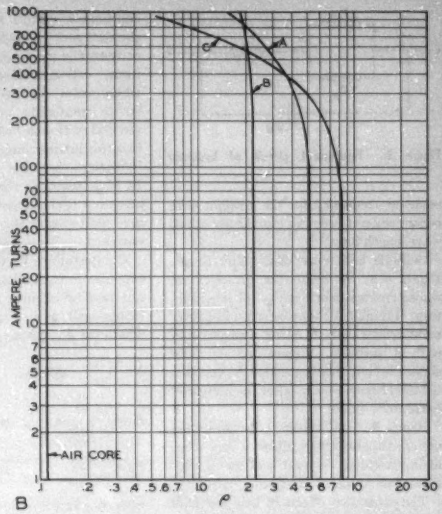

Figure 7(B). Curve providing relations between ρ and ampere turns

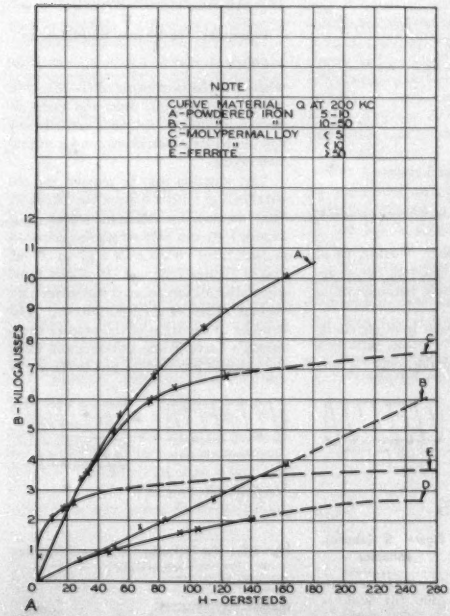

Figure 8(A). Normal B versus H curve for cores suitable for radio noise inductors

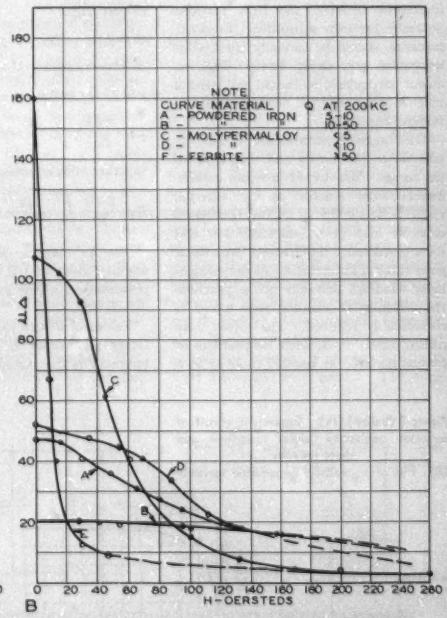

Figure 8(B). Curve of μ_Δ versus H for various core materials

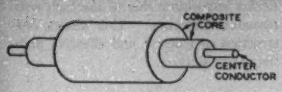

Figure 9. High-frequency inductor with composite core

for an air-core toroid. The μ_Δ for identical size cores is given by the ratio of the permeance for an iron core to the permeance of an air core.

Figures 7(A) and (B) provides rapid determination of the inductance for a coil with a given number of turns and d-c load current. Figures 7(A) and (B) are most applicable for evaluating existent cores operating under various conditions. Intersection of the ampere turns versus ρ curves indicates that point at which one core becomes more suitable than another. Figure 8(A) is a B versus H curve and Figure 8(B) is a μ_Δ versus H curve for five different magnetic materials. The crossing points on these curves indicate where one material provides greater μ_Δ than another for a given magnetizing force.

One type of toroid which is of particular interest for construction of high-current filters passing several hundreds of amperes and/or for high-frequency sections, consists of a straight round conductor surrounded by a suitable annular core. It will be shown that this is very nearly equivalent to a single turn toroid and for practical purposes the same formulas are used except that N^2 becomes unity. The package-ability, low d-c drop and high antiresonant frequency combine to affect a low value of inductance. Equation 7(B) is directly applicable to the arrangement of Figure 8(B), where several different magnetic materials are arranged annularly.

In argument for the foregoing statements, consider a long, straight, round very small diameter wire carrying current I. The magnetic intensity at a point p external to the wire is given by equation 10 of reference 3

$$H=\frac{I}{10r}(\cos\alpha_1+\cos\alpha_2)\text{ oersteds} \tag{10}$$

In equation 10 and Figure 10, H is in oersteds, I is in amperes, and r is in centimeters. Should point p be symmetrically located so that $\alpha_1=\alpha_2=\alpha$ and the wire length is large compared to r the expression reduces to

$$H=\frac{2I}{10R} \tag{11}$$

From Figure 10(B) the total flux is given by

$$\phi=b\int_{R_1}^{R_2}\frac{2I}{10r}dr\mu_\Delta \tag{12}$$

provided μ_Δ is sufficiently large to render that flux between wire center and R_1 and R_2 and $R_=$ insignificant which is generally the case. The inductance by definition being:

$$L=\frac{N\phi}{I}\times10^{-8}$$

becomes for this case of $N=1$

$$L=\int_{R_1}^{R_2}\frac{2I}{10r}dr\mu_\Delta\times10^{-8}\text{ henrys} \tag{13}$$

Additional terms may be added if required so that equation 7(B) will result. Should μ_Δ be constant for the magnetic intensity varying from R_1 and R_2, equation 13 reduces to

$$L=\frac{b2I}{10}\mu_\Delta\ \ln\frac{R_2}{R_1}\times10^{-8}\text{ henrys} \tag{14}$$

Dividing equations 13 and 14 by b gives inductance per unit length for a long wire but in actual practice where μ_Δ is substantial the equation holds quite well for finite values of b.

Another point to emphasize is that the magnetic intensity at a point P is independent of conductor size provided P is external from the concentric conductor. This follows by recalling that the total F acting around the conductor may be computed as the line integral of magnetic intensity through P Figure 10(A). The integration taken over a concentric circle through P gives from equation 11

$$F=\frac{2\pi r2I}{10r}=\frac{4\pi I}{10}\text{ gilberts} \tag{15}$$

which is the total magnetomotive force. Note that the radius has dropped out indicating that any path of integration in a

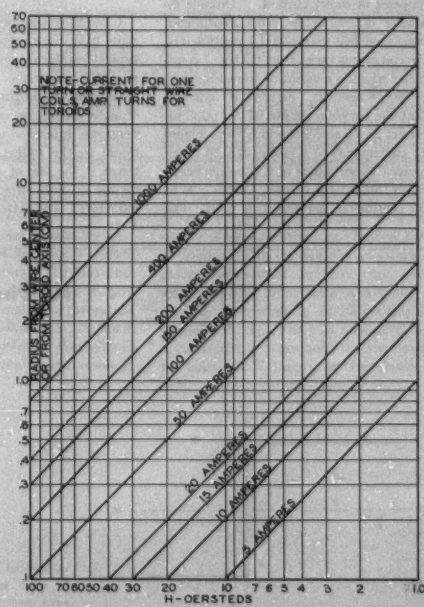

Figure 10(A) (below). Conductor carrying current I producing magnetic intensity at point P as given by equation 10

Figure 10(B) (below). Section of conductor carrying current I surrounded by annular magnetic material with inner radius R_1 and outer radius R_2 used to derive equation 12

Figure 11 (right). Curve providing relations between current for single conductor, ampere turns for multiple conductors, radius to a point, and field intensity at that point

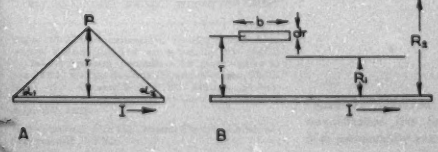

panel perpendicular to the wire could have been followed. Although Figures 10(A) and (B) together with equations 11, 12, 13, and 14 were postulated around a thin round conductor, from equation 15 it follows therefore that any conductor of symmetrical shape will produce an F equal to $0.4\,\pi\,I$.

As magnetic intensity is F per unit length, one may divide by the flux path length $2\pi R$ and arrive again to equation 11. As the magnetic force at that point is independent of conductor size and mediums between the conductor and point provided the medium does not conduct electrically or dielectrically due to very high dielectric constant, but does depend on distance r from conductor axis and on current, the plot of Figure 11 showing H versus r for values of current is useful. This curve provides rapid determination of magnetic intensity for a given coil and allows one to check the degree of saturation that may exist from the μ_Δ versus H curves. It should be apparent that the diagonal lines are in reality ampere turns and may be used to rapidly determine the magnetic force at a point in a toroid as well.

An example of a composite design is given by first stating the problem. Determine the optimum unit inductance of a conductor carrying intermittently 100 amperes of direct current. Outside diameter of conductor $=0.4$ centimeter, maximum coil diameter 1.4 centimeters, the coil radius varies from 0.2 to 0.7 centimeter which is a variation from Figure 11 of 100–28 oersteds. Figure 8(B) indicates that the curves for material A and C intersect at 75 oersteds which from Figure 11 corresponds to a radius of 0.26 centimeter. From radius of 0.2 to 0.26 centimeter, material A is used. From 0.26 to 0.7 centimeter, material C is used. The inductance per-unit length is determined from equation 7(A). Using average values of $\mu_{\Delta A}=25.75$ and $\mu_{\Delta c}=61.25$ and $N=1$ and $b=1$ centimeter for materials A and C respectively integrating equation 7(B) gives

$$L_\Delta=2\left[\mu_{\Delta A}\ln\frac{r_a}{r}+\mu_{\Delta c}\ln\frac{r_c}{r_a}\right]10^{-9}$$

$$=0.135\,\mu H/\text{cm}$$

In another case a high-frequency section is desirable. About 7 amperes of direct current is carried continuously, indicating that number 16 wire would be suitable. Allowing a hole of 0.080-inch diameter for this wire and a maximum diameter of 0.375 inch, what is the best material and what is the unit inductance? Figure 11 shows that for a radius of $0.04 \times 2.54=0.102$ centimeter a magnetic intensity of 13.5 oersteds will exist. The greatest average permeability taken between the outside diameter and inside diameter specified above, from Figure 8 (B) is 87.25, and is given by material E. Again from equation 7(B) the inductance becomes

$$L_\Delta=2\mu_\Delta\ln\frac{r_3}{r_2}\,10^{-9}\text{ henrys}$$

$$=0.27\mu H/\text{cm}$$

Conclusions

Interesting possibilities of inductor designs have been presented together with typical graphical information for various available materials. It is shown to a reasonable approximation that for a straight conductor or a toroid that the magnetic intensity is inversely proportional to the radius. Of particular interest is the use of composite materials for use in both toroids and straight-wire inductors. The latter group are of particular importance due to the high antiresonant frequency. This allows construction of efficient and effective high-frequency sections.

Symbols

E_g = equivalent noise voltage of interference source
Z_g = effective impedance of interference source
E_0 = load voltage
R_L = equivalent load resistance
Z_s = impedance
R_g = shunting effect due to iron losses
Z_L = load impedance
L_x = inductance
R_w = winding resistance
C_d = distributed capacity
$Q=R_x/\omega L_x$
H = magnetic intensity
B_Δ = incremental magnetic flux density
μ_Δ = incremental permeability
ϕ_Δ = incremental flux
ρ = permeance
F = magnetomotive force
b = width
R_1 = inner radius
R_3 = outer radius
r = radius
I_0 = direct current
I_Δ = incremental current
I = total current
L_Δ = incremental inductance
N = number of turns

References

1. Electrical Engineering (book), **Clarence V. Christie.** McGraw-Hill Book Company, Inc. New York, N. Y., 1931, pages 70–75.

2. Electrical Measurements and Measuring Instruments (book), **Sir E. W. Golding.** Isaac Pitman and Sons, Ltd., London, England, equation 8, pages 164–190.

3. Lessons and Problems in Electricity (book), **Newell C. Page,** Massachusetts Institute of Technology, Cambridge, Mass., 1934, equation 10, page 120.

4. Design of Reactances and Transformers Which Carry Direct Current, **C. R. Hanna.** *AIEE Transactions*, volume 46, February 1927, pages 155–60.

No Discussion

Series-Connected Saturable Reactor with Control Source of Comparatively High Impedance

H. F. STORM
MEMBER AIEE

Synopsis: The object of this analysis is to form a clear picture of the function of the saturable reactor with resistive load, and to derive simple, and yet reasonably accurate equations. Four modes of operation are analyzed for normal and underexcitation and one mode of operation for overexcitation. The results of the mathematical derivations are condensed into graphs in normalized form. With the aid of these graphs the effect of any circuit parameter can be readily understood. A numerical example is included to demonstrate the usefulness of the normalized graphs for the quick calculation of the saturable reactor.

SATURABLE reactors may be classified as series-connected or parallel-connected, depending upon the respective connection of the load windings. The function of the saturable reactor is further determined by the relative magnitude of currents induced into the control windings from the load windings. These induced currents become larger as the outer control-circuit impedance decreases and therefore are largest when the outer control-circuit impedance is zero; conversely, for very high outer circuit impedance the induced currents become practically zero. Consequently, each class of saturable reactor may be subdivided into one category where the outer control-circuit impedance is comparatively small and another where the outer control-circuit impedance is relatively high. In order to accentuate the differences between these two categories, one may assume extremes for the outer control circuit impedance; namely, zero for the first category and infinity for the second. In the following pages only the latter category will be analyzed. Reactors approaching this case have many applications, including the measurement of large direct currents[1] and the production of constant direct currents and voltages.

A rigorous analysis of saturable reactor circuits become quite difficult due to the presence of nonlinear and multivalued functions. The following analysis relinquishes some rigor in return for a quicker and clearer understanding of the fundamentals of reactor circuits. In addition, it permits one to calculate performance simply and yet with a reasonable degree of accuracy. To this end, simplifications are made in such a manner as to obtain good agreement of theoretical calculations and actual results. It should be kept in mind, however, that simplifications, by their very nature, result in derived solutions which are accurate only as long as the simplifications closely approximate actual conditions. This reservation should be remembered when interpreting the results of this paper.

One approximation consists in reducing the hysteresis loop to a single-valued function; this is permissible because core losses are not considered in this analysis. The wide present-day use of grain-oriented steels and other square-loop materials permits a further simplification of the magnetization line. Because such materials are characterized by a high differential permeability (over 50,000 gauss per oersted) and a sharp knee of the B-H curve, the latter is assumed of rectangular form, see Figure 1. Leakage reactance of the load windings is considered negligible in comparison with the load resistance, and the resistance of the load windings is lumped with the load resistance R_L. Operation is considered for steady state only.

The saturable reactor described in the following consists of two magnetic circuits, Figure 2, arranged in such a manner that they cancel voltages of fundamental frequency and odd harmonics in the control circuit.[2] The two magnetic circuits may consist of two separate units A and B as shown, or they may be embodied in a 3- or 4-legged construction, without change of basic performance. Each of the two units exhibits the essentials of a single-phase transformer: an iron core, one winding $X1$-$X2$ connected as a load winding, the other winding $Y1$-$Y2$ used as a control winding. The load resistance R_L is connected in series with the two load windings ($X1$-$X2$) and a rectifier instru-

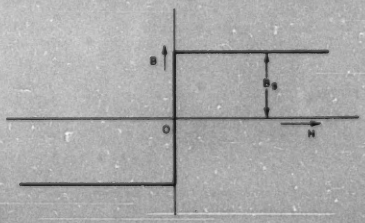

Figure 1. Idealized rectangular magnetization line for cores of high permeability and sharp knee

Paper 50-205, recommended by the AIEE Electronics Committee and approved by the AIEE Technical Program Committee for presentation at the AIEE Middle Eastern District Meeting, Baltimore, Md., October 3–5, 1950. Manuscript submitted May 4, 1950; made available for printing August 7, 1950.

H. F. STORM is with the General Electric Company, Schenectady, N. Y.

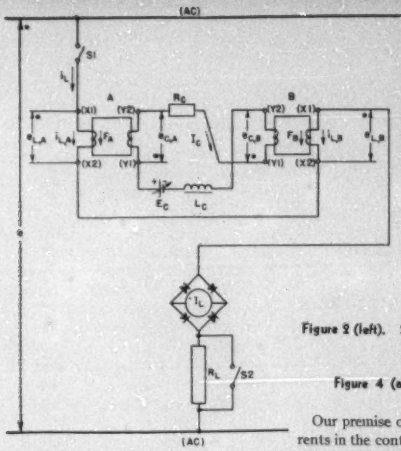

Figure 2 (left). Schematic diagram of saturable reactor circuit, consisting of two single-phase transformers *A* and *B*

Figure 4 (above). Permanent magnet current standard, maximum burden 10 watts

ment, reading the average value I_L of the rectified load current. Increasing the control voltage E_C will strengthen the control current I_C and result in a larger load current I_L. As will be shown later, control current and load current are proportional over a wide range; hence this circuit can be used for measurement purposes. This proportionality is obtained despite variations of line voltage, frequency, and load resistance (burden).

The dots in Figure 2 signify winding polarities. A current is called positive when it flows through the winding in a direction away from the dot. The magnetomotive force is called positive when derived from a positive current and the positive direction is indicated by the arrows near F_A and F_B. A voltage across a winding is defined positive when the terminal with the dot is more positive than the other terminal. A-c supply voltage e is counted positive when the a-c bus with the dot is the more positive one.

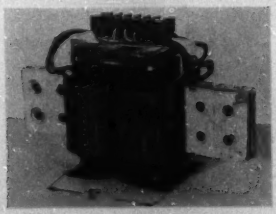

Figure 3. D-c transformer 3,000/5 amperes, approximate weight 50 pounds

Our premise of negligible, induced currents in the control windings is schematically indicated in Figure 2 by the insertion of an inductance L_C; a resistance or a combination of resistance and inductance would serve as well. This condition of negligible, induced currents occurs naturally in d-c meter transformers for large currents, such as the 3,000-ampere model shown in Figure 3, where the control winding consists simply of the d-c bus whose current is to be measured.

The condition of no induced control currents also occurs in the permanent magnet current standard, Figure 4, where the d-c magnetomotive force is obtained from a permanent magnet. The effect of the permanent magnet is in the circuit shown in Figure 5 is similar to a constant control current in the circuit of Figure 2. Remembering that load current and control current are proportional, it follows that with a permanent magnet, the load current will remain constant. This constancy holds despite considerable variations in line voltage, frequency, and burden.

The Normal- and Underexcited Saturable Reactor

Zero Load Resistance

In order to win a toehold on the problem, let us assume that the load resistor R_L in Figure 2 has been shorted by switch *S2*, while switch *S1* was still open. The control voltage source E_C drives the control current I_C through the two control windings. As with other a-c circuits containing resistance and inductance, a switching transient should be expected when switch *S1* is closed at a random time. However, if the switch is closed at the instant at which the steady-state value of the alternating current would be zero, no switching transient will result.[8] In linear, purely inductive circuits the alternating current becomes zero when the voltage reaches its crest value and it suggests itself to close switch *S1* in our nonlinear circuit also at this instant ($\theta = \pi/2$, Figure 6)

Let

$$\theta = \omega t \tag{1}$$

and the supply voltage

$$e = E_m \sin \omega t \tag{2}$$

Before closing switch *S1*, the magneto-

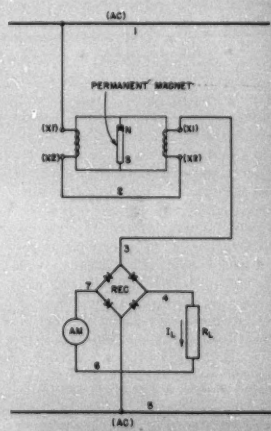

Figure 5. Schematic diagram of permanent magnet standard, using 3-legged core structure

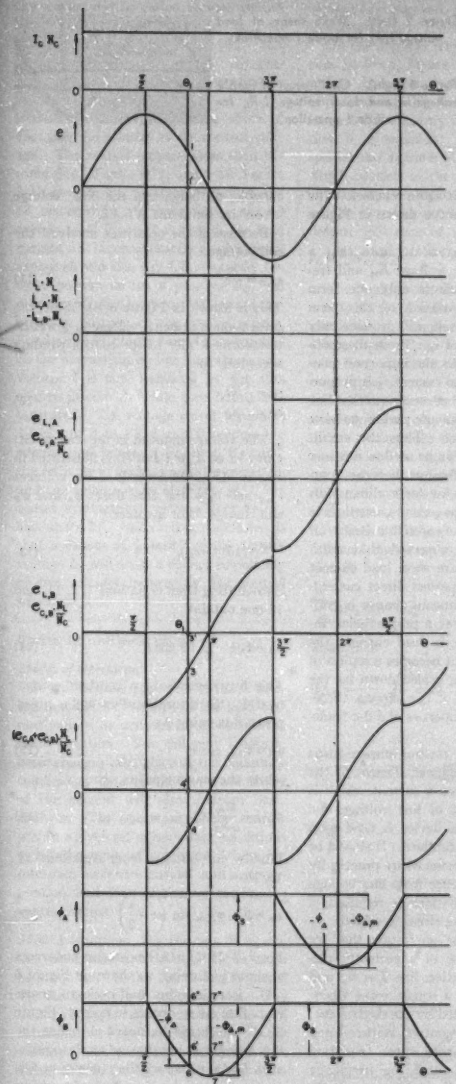

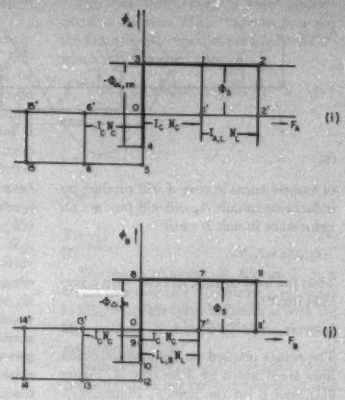

TABLE I

POINTS ON FLUX GRAPHS OF FIGS. 6 I, J AS FUNCTION OF θ

θ	0	$\frac{\pi}{2}$	$\frac{\pi}{2}+0$	$\frac{\pi}{2}+\theta$	π	$\frac{3\pi}{2}-0$	$\frac{3\pi}{2}+0$	2π	$\frac{5\pi}{2}-0$	$\frac{5\pi}{2}+0$
ϕ_A	1	1	2	2	2	2	3	4	3	2
ϕ_B	7	7	8	9	10	8	11	11	11	8

Figure 6. Wave shapes in various parts of the circuit of Figure 2, for load resistance $R_L=0$

motive forces in the cores are due to the control ampere-turns only. The resultant flux is obtained from the magnetization lines of the cores shown again in Figure 6(I) for core A and in Figure 6(J) for core B. For $\theta<\pi/2$ the magnetomotive forces are 0 to 1′ and 0 to 7′, and the core fluxes are 1 to 1′ and 7 to 7′. The operating points 1 and 7 are located on the saturation branches of the magnetization lines and hence the fluxes ϕ_A and ϕ_B equal the saturation flux Φ_s. If the magnetomotive force in the core is changed, for instance, by a current flowing in the load winding, such current will not cause a change in the fluxes ϕ_A or ϕ_B when the load current is positive, nor will it produce a change of flux when the load current is negative, qualifying the latter case for load ampere-turns not exceeding control ampere-turns. This means that the flux linkages remain constant and therefore no inductance will be exhibited by the reactor for the circumstances just mentioned.

Suppose switch $S1$ is closed at $\theta=\pi/2$, impressing a voltage e, Figure 6(B), on the circuit which at this moment has no inductance and which according to a previous assumption has no resistance. Under the effect of the line voltage e the load current will rise with a vertical front, Figure 6(C). The directions of the load current i_L and the driving voltage e are the same. Because of the polarities observed.

$$i_{L,A}=i_L \tag{3}$$

$$i_{L,B}=-i_L \tag{4}$$

The load ampere-turns are positive in core A and negative in core B. As previously pointed out, a positive increase

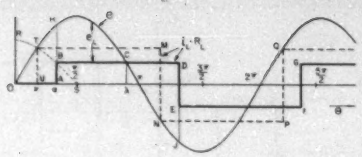

Figure 7 (left). Wave shape of load voltage $I_L R_L$ for mode 1 operation

Figure 8 (right). Oscillogram of supply voltage e and load voltage $I_L R_L$ for mode 1 operation

of ampere-turns in core A will produce no inductance in unit A, and will produce no inductance in unit B until

$$-i_{L,B}N_L = I_C N_C \tag{5}$$

Thus the load current will rise with a vertical front to

$$i_L = -i_{L,B} = I_C N_C / N_L \tag{6}$$

The points reached on the magnetization lines are denoted by *2* for core A, Figure 6(I), and *8* for the core B, Figure 6(J). At this instant, which is designated by $\theta = \pi/2 + 0$, the steep region 12 to 8 in core B is reached and thence unit B will exhibit an inductance L. The current i_L follows from

$$e = L\frac{di_L}{dt} = \omega L \frac{di_L}{d\theta} \tag{7}$$

and

$$i_L = \frac{1}{\omega L}\int_{\pi/2}^{\theta} e \, d\theta + C \tag{8}$$

At the starting instant $\theta = \pi/2$ the integral of equation 8 is zero and hence

$$C = I_L \tag{9}$$

Substituting from equations 2 and 9 into equation 8

$$i_L = I_L\left[1 + \frac{E_m \pi}{\omega L I_L}\sin\left(\theta - \frac{\pi}{2}\right)\right] \tag{10}$$

where

$$\pi/2 < \theta < 3\pi/2$$

It follows that the load current consists of a constant component I_L on which a sinusoid is superposed. In practical cases $E_m/\omega L I_L$ is a small quantity because the high permeability in the core produces a large L. The term I_L of the load current is proportional to the control current I_C equation (6).

For $\pi/2 < \theta < \pi$ electric energy is received from the line and is returned to the line over an interval of equal length. Therefore at $\theta = 3\pi/2$ all energy has been returned and current i_L can no longer be maintained against the opposing line voltage e. The current collapses at $\theta = 3\pi/2$ and then assumes the same direction as the instantaneous line voltage. The current now flows in its new direction for π radians until it again reverses. The result is a square wave shown in Figure 6(C).

It is also important to note that a variation in supply voltage E_m and frequency $f = \omega/2\pi$ affects only the term $E_m/\omega L I_L$. Any variation of this term which is small in itself, will produce only a minor variation of i_L. From these observations one draws the important conclusion that the load current i_L is proportional to the control current, and that line voltage or line frequency variations have only a minor effect. Thus the circuit shown in Figure 2 can be used to measure current. This technique becomes particularly practical for large direct currents, where cost, space, and power loss in shunts become an appreciable item. It should further be observed that rectification of the square wave load current produces a nearly perfect direct current. Because an instantaneous change in control current produces a proportional, instantaneous change in load current, the rectified load current becomes a replica of the control current, scaled down by the turn ratio N_C/N_L. The circuit therefore exhibits the properties of a d-c transformer.

By replacing the control ampere-turns by a permanent magnet, Figure 5, the circuit now produces a current which is nearly independent of line voltage and frequency. Such a device is used as a voltage or current standard. It should be mentioned that in cases where practically complete independence from line voltage and frequency variations is required, a simple compensating circuit is added.

Summarizing, one may state that for the theoretical case of a perfectly rectangular magnetization line $L = \infty$, and the load current is a square wave whose height is so controlled by the control current I_C that the control ampere-turns equal the load ampere turns (equation (6). Line-voltage and line-frequency variations have no effect on the magnitude of the load current for normal and underexcitation as defined later.

Because of the saturation of core A during $\pi/2 < \theta < 3\pi/2$, no voltage appears across the terminals of unit A, (Figure 6 (D). However, during the same interval core B is unsaturated and therefore capable of balancing the line voltage across its terminals *X1-X2*.

Because of the polarities involved the coil voltage

$$e_{L,B} = -e \tag{11}$$

This is shown in Figure 6(E). Since no saturation is present, voltage $e_{L,B}$ will be transformed fully to the control winding according to

$$\frac{e_{L,B}}{e_{C,B}} = \frac{N_L}{N_C} \tag{12}$$

The voltage induced in the control circuit (*Y1* of A to *Y2* of B) is illustrated in Figure 6(F). As a result of the voltages $e_{L,A}$ and $e_{L,B}$, the core fluxes ϕ_A and ϕ_B will change. For instance

$$\frac{d\phi_B}{dt} N_L 10^{-8} = e_{L,B} \tag{13}$$

Substituting from equations 1, 2, 11, and 13 one obtains

$$\phi_B = \Phi_s + \frac{E_m}{\omega N_L} 10^8 \cos\theta \tag{14}$$

This flux consists of a constant component Φ_s, the saturation flux, and a superposed flux swing ϕ_Δ

$$\phi_\Delta = \Phi_{\Delta,m} \cos\theta \tag{15}$$

where the maximum flux swing

$$\Phi_{\Delta,m} = \frac{E_m}{\omega N_L} 10^8 \tag{16}$$

Finally one obtains from equations 14 15, 16

$$\phi_B = \Phi_s - \Phi_{\Delta,m} \sin\left(\theta - \frac{\pi}{2}\right) \tag{17}$$

For $\pi/2 < \theta < 3\pi/2$ the core flux undergoes a sinusoidal swing as shown in Figure 6 (H). For the other half-cycle an analogous flux swing occurs in core A, Figure 6(G). It should be noted also that the flux swing does not depend on the inductance L of the load winding (equation 16). It also is apparent that if the flux swing should exceed twice the saturation flux Φ_s, core B would become newly saturated along branch 12 to 14, and hence unit B will lose its inductance. When this happens a different mode of operation results. It therefore becomes necessary to further subdivide the reactor operation;

the reactor will be called normal excited when the maximum flux swing, $\Phi_{\Delta,m}=2\Phi_s$, overexcited when $\Phi_{m\Delta,}>2\Phi_s$, and underexcited when $\Phi_{\Delta,m}<2\Phi_s$. All previous equations hold only for normal or underexcited reactors.

Next, let us investigate the effect of changing the polarity of the control voltage. The control ampere-turns then become 0–6′, Figure 6(I), and 0–13′ Figure 6(J), and the flux positions become 6 and 13, respectively. If again for $\theta=\pi/2+0$ switch *S1* of Figure 2 is closed, the load current will increase exactly as previously explained and also will follow exactly the same pattern as for a positive E_C. In other words, the load current cannot discern the polarity of the control source. For $\theta=\pi/2+0$ points 5 and 14 are reached on the magnetization line, and the supply voltage e is now balanced by the flux change in core A, while core B becomes saturated. The voltage across terminals *Y1* of unit A to *Y2* of unit B become the symmetrical image of Figure 6(E) using the ordinate at $\theta=\pi$ as axis of symmetry, and the voltage wave of Figure 6(D) becomes symmetrical with respect to an axis at $\theta=2\pi$. One further conclusion is that a change in polarity of the control voltage E_C will cause a change in polarity of the voltages induced in the control windings.

Finite Load Resistance

Modes of Operation

It will become apparent in the following that the wave shape of the load current cannot be derived from one and the same equation. For different loadings, basic changes take place in the boundary conditions; as a result, the wave shape of the current will also undergo basic changes. The operation of the reactor within a given set of boundary conditions is called a mode of operation; there are four such modes for normal- and underexcitation and four analogous modes for overexcitation.

Mode 1 operation: For the case of $R_L=0$, the maximum flux swing follows from equation 16. If the flux swing is just 2 Φ_s, the excitation is called normal. The voltage $E_{s,o,m}$ is called the critical no-load saturation voltage and is defined as the voltage which produces a maximum flux swing of 2 Φ_s for $R_L=0$. From equation 16 for $\Phi_{\Delta,m}=2\Phi_s$

$$E_{s,o,m}=2\Phi_s\omega N_L 10^{-8} \tag{18}$$

In the following the load resistance R_L is introduced in the circuit by opening switch *S2* in Figure 2. Similar to linear *R-L* circuits, the steady-state value of the current becomes zero at a point ahead of the crest value of the voltage.

Let the angle at which zero current occurs be $\theta=\alpha$, Figure 7. As in the preceding discussion, the reactors have no impedance at this instant and the load current will abruptly increase until equation 5 is satisfied. One recognizes a spectacular feature of mode 1 operation which consists in the equality of control current ampere-turns and load current ampere-turns as expressed by equation 6 despite existence of load resistance R_L.

$$I_L=I_C N_C/N_L \tag{6}$$

The angle α can be determined by the steady-state premise which requires all quantities to resume their original values after a lapse of 2π radians. Applied to the core flux, it means that the downswing must equal the upswing. The downswing is caused by the voltage e_L across the load winding terminals *X1-X2* shown as the difference between the supply voltage e and the load voltage $I_L R_L$; in the following analysis it is irrelevant whether this difference voltage occurs on unit A or B, and therefore the notations $e_{L,A}$, $e_{L,B}$, have been simplified to e_L. The flux swing follows from an equation similar to equation 13

$$\frac{d\phi_\Delta}{d\theta}\omega N_L\, 10^{-8}=e_L \tag{19}$$

and hence

$$\Phi_{\Delta,m}=\frac{10^8}{\omega N_L}\int_\alpha^\lambda e_L d\theta \tag{20}$$

The flux downswing is seen proportional to the area HCB. In order to make the flux upswing equal, areas $CDJ=HCB$, which relation determines α

$$\int_\alpha^{\alpha+\pi}(E_m \sin\theta - I_L R_L)d\theta=0 \tag{21}$$

and

$$\alpha=\text{arc}\cos\frac{I_L R_L}{E} \tag{22}$$

where

$$E=\frac{2}{\pi E_m} \tag{23}$$

The locus of point B, Figure 7, is a cosine function ($RTBS$) whose crest value is $2E_m/\pi$. This value is identical with the line voltage E measured by a rectifier instrument.

With the ratio $I_L R_L/E$ increasing, point B moves to the left on its cosine locus, and will finally reach the intersection T with the supply voltage e for $\theta=\nu$. A further increase of $I_L R_L/E$ will not cause point B to continue along section T-R of the cosine function because for $\alpha<\nu$ the line voltage is not large enough to produce the load voltage $I_L R_L$. The logical conclusion is that the previously described mode of operation comes to an end at T. For larger values of the ratio $I_L R_L/E$ a different mode of operation occurs and will be discussed later.

The boundary angle ν for the first mode of operation follows from equations 2 and 22

$$e=I_L R_L=E_m \sin\nu=E\cos\nu \tag{24}$$

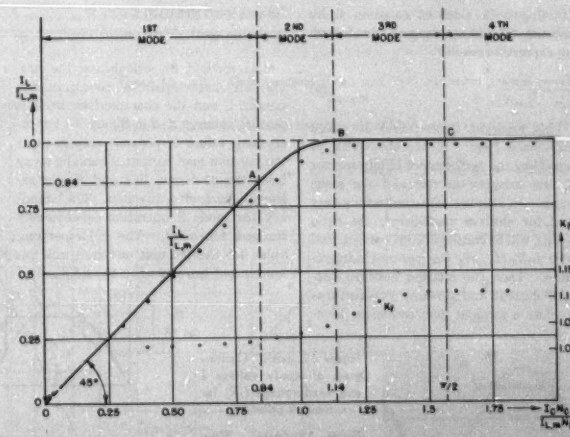

Figure 9. Normalized characteristic of per-unit load current and load current form factor k_f versus per-unit control ampere-turns; measured values shown by dots

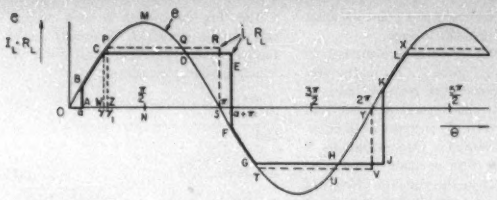

Figure 10 (above). Wave shape of load voltage $I_L R_L$ for mode 2 operation

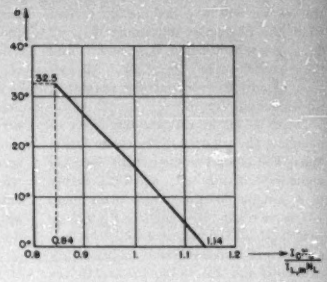

Figure 12 (right). Angle of retard α versus per-unit control current for mode 2 operation

$$\nu = \text{arc tan } \frac{2}{\pi} = 32.5° \left(\frac{\pi}{180}\right) \tag{25}$$

and

$$\cos \nu = 1/\sqrt{1+\left(\frac{2}{\pi}\right)^2} = 0.844 \tag{26}$$

The boundary condition for mode 1 operation is therefore

$$0 < \frac{I_L R_L}{E} \leq 0.844 \tag{27}$$

The wave shape for the boundary case is shown in Figure 7 by *UTMNPQ*.

In order to express equation 6 more generally, the maximum load current $I_{L,m}$ is introduced. It is that current which flows when the saturable reactor loses all its inductance and therefore is limited by the load circuit resistance R_L only

$$I_{L,m} = E/R_L \tag{28}$$

Dividing both sides of equation 6 by equation 28 and rearranging, the following expression results

$$\frac{I_L}{I_{L,m}} = \frac{I_C N_C}{I_{L,m} N_L} \tag{29}$$

This form of presentation is called normalized form. It has the virtue of describing the performance of any reactor of this category in one and the same graph. In keeping with the terminology used for electric machinery[4], the ratio $I_L/I_{L,m}$ will be called per-unit current, and ratio $I_C N_C / I_{L,m} N_L$ the per-unit ampere-turns. Then the relation between per-unit current and per-unit ampere-turns becomes a straight line, which for identical scales subtends an angle of 45 degrees with the axes. See Figure 9.

Due to air-core reactance, actual measurement will give slightly lower results in the upper part of the range, and somewhat higher values are measured in the lower range because of the finite magnitude of iron-core reactance.

Figure 8 shows an oscillogram of the supply voltage e and the voltage $I_L R_L$ across the load resistance. The per-unit ampere-turns are 0.552 as calculated from $I_C = 0.25$ ampere, $N_C = 200$ turns, $I_{L,m} = 0.153$ ampere, $N_L = 592$ turns. The angle $\alpha = \text{arc cos } 0.552 = 56.5$ degrees $(\pi/180)$. Actual measurement of α, from the oscillogram of Figure 8, is within one degree of the calculated value.

Mode 2 operation: For $I_C N_C / I_{L,m} N_L >$ 0.84 a new mode of operation is obtained as shown in Figure 10. The load voltage $i_L R_L = e$ for $\alpha < \theta < \nu$. Between $\nu < \theta < \alpha + \pi$ the current i_L is constant and follows from equation 6

$$i_L = I_C N_C / N_L \tag{6}$$

The method for calculating the normalized characteristic is shown in Appendix I, and the characteristic itself is plotted as curve *A-B* in Figure 9. For increasing values of per-unit ampere-turns the per-unit load current is bending away from the 45-degree line and finally assumes a horizontal direction. The boundary for mode 2 operation is obviously reached for $\alpha = 0$. The corresponding value for the per-unit ampere-turns follows from Figure 12 as 1.14, and $\nu_1 = 46.4$ degrees. The wave shape at this boundary is shown in Figure 10 by *OBPQRSF-TUVYKX*.

An oscillogram of mode 2 is shown in Figure 11. The circuit constants are the same as for Figure 8, except $I_C = 0.45$ ampere. The per-unit current becomes 0.994 and $\alpha = 16.5$ degrees from Figure 12. A check with the oscillogram will disclose practically the same value for α.

Mode 3 operation: Increasing the per-unit ampere-turns over 1.14, angle α remains zero. The current wave shape is shown in Figure 13 by *OBCDEFGHJK-LMN*, and $I_L R_L$ is the average of area *OBCDEFO*. As in the preceding, areas *BCP* = *CDE* and therefore $I_L R_L$ also equals *OBPCEFO*

$$I_L R_L = E \tag{35}$$

It follows from equation 28 that $I_L = I_{L,m}$ and although the current is changing its wave shape, the average value remains constant. The value of i_L in its flat region is still determined by equation 6. Increasing the control current will bring i_L to its boundary

$$\frac{I_C N_C}{N_L} = i_L = \frac{E_m}{R_L} \tag{36}$$

The maximum per-unit control ampere-turns for mode 3 operation therefore are

$$\frac{I_C N_C}{I_{L,m} N_L} = \frac{\pi}{2} \tag{37}$$

which is the upper boundary for mode 3

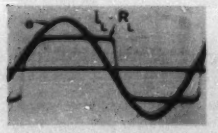

Figure 11 (left). Oscillogram of supply voltage e and load voltage $I_L R_L$ for mode 2 operation

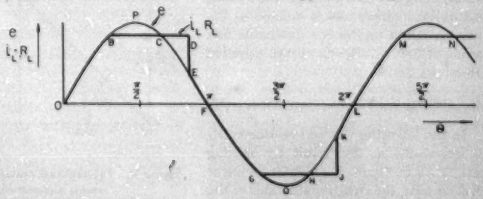

Figure 13 (right). Wave shape of load voltage $I_L R_L$ for mode 3 operation

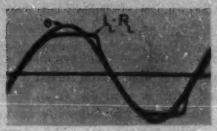

Figure 14. Oscillogram of supply voltage e and load voltage I_LR_L for mode 3 operation

operation. While the average value of the load current remains constant (*B-C*, Figure 9) during mode 3 operation, the rms value of the load current changes.

An oscillogram of mode 3 operation is shown in Figure 14. The per-unit control ampere-turns are 1.32. The current I_L is measured as 0.153 ampere which is identical with the measured value of $I_{L,m}$.

Mode 4 operation: By increasing the per-unit ampere-turns over $\pi/2$, the circuit acts as though no iron were present in the reactor. The load current is sinusoidal and its value remains $I_{L,m}$. Its representation in the normalized characteristic of Figure 9 is a horizontal line to the right of *C* at the level of unity. In contrast to mode 3 operation, where the rms value of the load current is changeable, the rms value of the load current during mode 4 operation is constant.

Conclusion From Normalized Curves

Power gain: The normalized characteristics can be written in the following form

$$y=f(x) \tag{38}$$

where

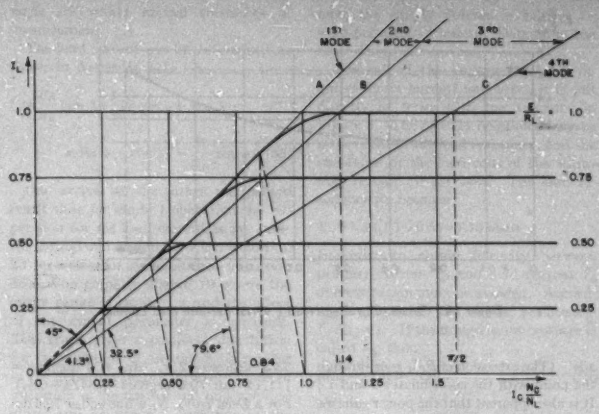

Figure 16. General characteristic of load current I_L versus referred control current I_CN_C/N_L

$$y=\frac{I_L}{E/R_L} \tag{39}$$

and

$$x=\frac{I_CN_C}{I_{L,m}N_L} \tag{40}$$

The power gain G_p is defined as the ratio of output power P_o divided by input power P_i

$$G_p=\frac{I_L^2R_L}{I_C^2R_C}k^2{}_f \tag{41}$$

where k_f is the form factor of the load current. Substituting for I_L from equation 39 for I_C from equation, 40, and using equation 28 one obtains

$$G_p=\left[\frac{f(x)}{x}\right]^2\frac{R_L}{R_C}\frac{N_C^2}{N_L^2}k^2{}_f \tag{42}$$

The function $(f(x)/x)^2$ can be calculated from the normalized characteristic (Figure 9) and is plotted on double logarithmic scales (Figure 15). The form factor k_f has been plotted in Figure 9 from experimental data. Thus, one notes that the power gain is constant for per-unit ampere-turns up to 0.844 (point *A*), then drops to B_2 $(1/1.14^2=0.77)$, and finally declines at the rate of 40 decibels per dec-

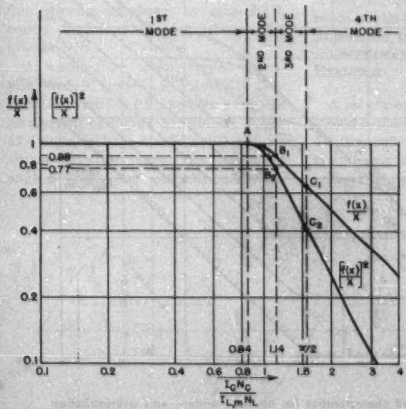

Figure 15 (left). Gain functions $f(x)/x$ and $[f(x)/x]^2$ versus per-unit control current

Figure 17 (below). General characteristic of load current I_L versus ratio E/R_L

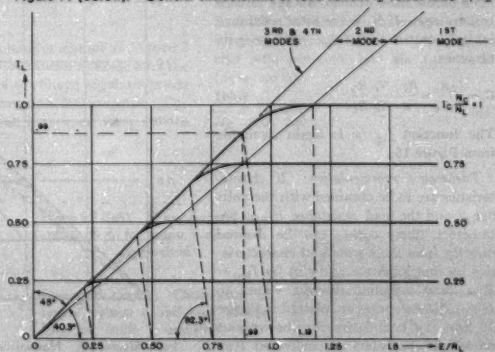

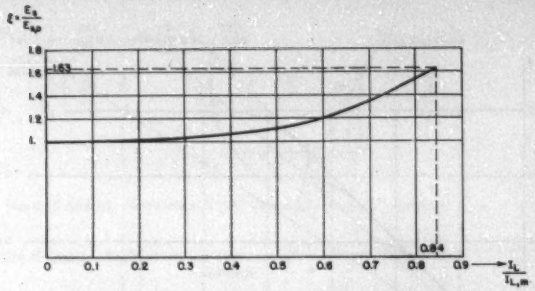

Figure 18. Saturation voltage ratio ξ versus per-unit load current

ade. (The extension of B_1C_1 goes through the point with the co-ordinates 1 and 1.) It is also apparent that the power gain for mode 1 operation is equal to the ratio of load resistance R_L to control circuit resistance R_C when referred to the load winding. It is furthermore important to note from equation 42 that the permeability of the core material does not affect the power gain. A typical value for power gain is 100.

Current gain: The current gain G_i is defined as the ratio of the load current I_L over the control current I_C

$$G_i = \frac{I_L}{I_C} = \frac{f(x)}{x} \frac{E/R_L}{I_{L,m}N_L/N_C} = \frac{f(x)}{x} \frac{N_C}{N_L} \qquad (43)$$

The function $f(x)/x$ also is plotted in Figure 15. It can be seen that the current gain is constant for mode 1 operation and equals the turn ratio N_C/N_L. For higher modes of operation the current gain falls off to $1/1.14 = 0.88$ at point B_1 and then drops at the rate of 20 decibels per decade.

Voltage gain: The voltage gain G_e is defined as the ratio of load voltage to control voltage. If R_C is the total resistance in the control circuit the voltage gain becomes

$$G_e = \frac{I_L R_L}{I_C R_C} = \frac{f(x)}{x} \frac{N_C}{N_L} \frac{R_L}{R_C} \qquad (44)$$

The function $f(x)/x$ is again available from Figure 15.

Parametric representation: If characteristics are to be obtained with the voltage E and the load resistance R_L as parameters, these curves can be derived directly from the normalized characteristics by multiplying x and $f(x)$ by $I_{L,m} = E/R_L$ and assigning discreet values to E/R_L. These curves are plotted in Figure 16 and the boundaries for the various modes of operations are indicated (tan 32.5 degrees $= 2/\pi$, tan 41.3 degrees $= 1/1.14$, tan 79.6 degrees $= 0.84/1-0.84$). For a given $I_C N_C/N_L$ a line under 79.6 degrees intersects the 45-degree line OA at the boundary between mode 1 and 2 operation. Lines OB and OC are boundaries between mode 2 and 3, and mode 3 and 4 operation. It should be observed that no dimensions are assigned to the axes and parameters, because any dimension derived from a consistent system is suitable. Furthermore, scaling up and down both axes and the parameters by the same factor is permissible. Therefore Figure 16 represents the characteristics of any saturable reactor of the category in question.

For the control current as a parameter, one obtains the characteristics shown in Figure 17. From equations 38, 39, and 40, one obtains

$$I_L = \frac{E}{R_L} f(x) \qquad x = \frac{I_C N_C}{E/R_L N_L}$$

With $I_C N_C/N_L$ as parameter and E/R_L as variable, the new characteristics can be plotted; $f(x)$ is available from Figure 9. The lines under the following angles indicate boundaries: tan 32.5 degrees $= 2/\pi$, tan 40.3 degrees $= 0.84$, tan 82.3 degrees $= 1/(1.14-1)$. Here too, consistent systems of units and their multiples can be assigned to the axes and parameters. These curves represent the operation of any saturable reactor of the specified category within the limits previously stated.

The Overexcited Saturable Reactor Example

Boundary

All previous calculations and conclusions were based on the assumption of normal- or underexcited operation as previously defined. For zero load resistance, the critical no-load saturation voltage $E_{s,o}$ (equation 18 for $E_{s,o,m}$) will just produce a flux swing equal to $2\Phi_s$. An increase of line voltage over $E_{s,o}$ will result in a second zone of saturation along the lower branch of the magnetization line with subsequent change of wave shape and hence change in the mode of operation. With the introduction of load resistance R_L some of the line voltage is now taken up by the load resistance and only the remainder is left for a flux swing. Consequently, an increase of line voltage over $E_{s,o}$ can be permitted until the flux swing reaches $2\Phi_s$. The voltage at which this

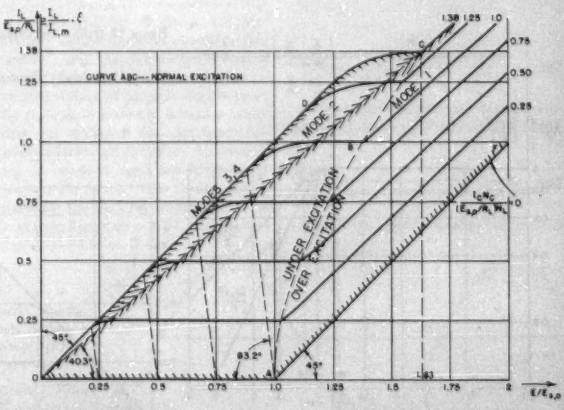

Figure 19. Normalized characteristics for normal-, under-, and overexcitation

flux swing is obtained is designated by E_s and is called the critical saturation voltage in the presence of load resistance. It is determined in Appendix II; the ratio $E_s/E_{s,o}$ as function unit load current is shown in Figure 18.

The full significance $E_s/E_{s,o}$ becomes apparent when the axes and parameters of the graph in Figure 17 are multiplied by $R_L/E_{s,o}$. This new graph is shown in Figure 19. It can be seen that the ratio $E/E_{s,o}$ can be increased over unity for increasing control ampere-turns (namely up to the dashed curve ABC) without change of mode of operation. The points on the dashed curve ABC signify ratios $E_s/E_{s,o}$ which satisfy equation 48 and therefore indicate normal excitation. The area to the left of ABC includes underexcited operation, the area to the right overexcited operation.

Overexcited Operation, Mode 1

The current will start at α, as shown in Figure 20, so that equation 6 is satisfied

$$i_L = I_C N_C / N_L \tag{6}$$

For $\alpha < \theta < \vartheta$ the voltage e_L causes a flux swing which is proportional to the area between the sine wave and the load voltage $i_L R_L$. In the case shown in Figure 20, the maximum flux swing is reached at $\theta = \vartheta$. For $\theta > \vartheta$ the lower branch of the magnetization line is reached and the reactor loses all inductance. The load resistance then finds itself exposed to the full line voltage and the load current increases accordingly. For $\vartheta < \theta < \lambda$ the load voltage is equal to the line voltage. At $\theta = \lambda$ the vertical part of the magnetization line is reached and hence the reactor again exhibits inductance. The load current again follows equation 6 until the flux upswing as shown by area EFR, equals the flux downswing indicated by area $BCDQ$.

An oscillogram of overexcited operation, mode 1, is shown in Figure 21. The control current is 0.25 ampere as in the oscillogram of Figure 8. Voltage $E_{s,o} = 42.8$ volts, voltage $E = 54$ volts, and resistance $R_L = 280$ ohms. The calculated angle (67 degrees) and the measured-angle are within normal tolerances of measurement.

The load current can be determined as shown in Appendix III

$$I_L = \frac{E_m}{R_L}\left[\sin\lambda + \frac{1}{\pi}(2\cos\alpha + \cos\lambda - \pi\sin\lambda - \cos\lambda)\right] = \frac{E}{R_L}\cos\alpha \tag{55}$$

One arrives at the rather unexpected result that for mode 1 operation the expression for the load current is the same for normal and underexcitation (equation 22), as well as for overexcitation (equation 55). The graph in Figure 19 covers the entire range of excitation and the effect of any circuit parameter is apparent. This graph gives a complete description for the operation of any saturable reactor of the defined category for every mode of operation in the normal and underexcited state, and for mode 1 operation in the overexcited state. Higher modes of operation in the overexcited state have hardly any practical significance and are not shown in Figure 19.

Mode 1 operation occurs in the area between the straight lines OC and AF. The area is subdivided by the curve ABC in the left-hand section corresponding to normal- and underexcitation, and the right-hand, overexcited part. Mode 2 operation occurs between lines OC and OD, while modes 3 and 4 operation occurs along line OD. The underexcited range for modes 2, 3, and 4 is limited by the characteristic with the parameter 1.38.

The overexcited characteristic for the parameter O is a straight line under 45 degrees; for higher parameters the characteristics are slightly curved. The intersection OD with a line subtending an angle of 83.2 degrees gives the border point between modes 3 and 4 operation and mode 2 operation, for a given $E/E_{s,o}$.

Example

A saturable reactor similar to Figure 2 should deliver 2 amperes average into the 5.5-ohm coil of a voltage regulator when the primary current is 500 amperes. The primary current may vary from 500 to zero, the supply voltage is subject to ±25-per cent variation. Determine the basic design parameters.

The coil of the voltage regulator requires direct current and hence it is put directly in series with the ammeter in Figure 2. The rectifier resistance may be 20 per cent of the load resistance, and the resistance of the load coils of the saturable reactor 10 per cent. The load resistance R_L becomes

$$R_L = 5.5 + 1.1 + 0.55 = 7.15 \text{ ohms}$$

In order to obtain linearity between primary current I_C and load current I_L overexcitation must be avoided. According to Figure 19 the highest permissible $E/E_{s,o} = 1$. If the design center voltage is called E_d, then

$$E_{min} = 0.75 E_d \tag{56}$$

and

$$E_{max} = 1.25 E_d \tag{57}$$

The minimum voltage ratio $E_{min}/E_{s,o}$

$$\frac{E_{min}}{E_{s,o}} = \frac{E_{min}}{E_{max}} = \frac{0.75}{1.25} = 0.6 \tag{58}$$

The parameter for the curves of Figure 19 has to be determined so as to provide a horizontal characteristic over the whole range of voltage fluctuation. The limiting line OC has a slope of 1/1.18 as shown in Figure 17. The intersection of line OC Figure 19 with the ordinate $E_{min}/E_{s,o} = 0.6$ (equation 58) occurs at $0.6/1.18 = 0.508$. Hence

$$E_{s,o} = E_{max} = \frac{I_L R_L}{0.6/1.18} = \frac{2 \times 7.15}{0.508} = 28.1 \text{ volts} \tag{59}$$

and from equation 57

$$E_d = \frac{E_{max}}{1.25} = 22.4 \text{ volts} \tag{60}$$

It follows that the core design has to aim at a no-load saturation voltage of $28.1/0.9 = 31$ volts rms, the supply voltage for the load circuit is $22.4/0.9 = 24.9$ volts rms ±25 per cent, and the turn ratio (equation 6)

$$\frac{N_L}{N_C} = \frac{2}{500} = \frac{1}{250} \tag{61}$$

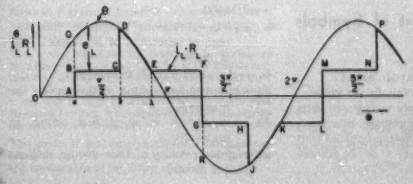

Figure 20 (left). Wave shape of load voltage $I_L R_L$ for mode 1 operation, overexcited

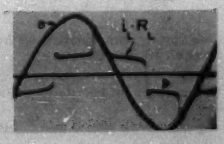

Figure 21 (right). Oscillogram of supply voltage e and load voltage $I_L R_L$ for mode 1 operation, overexcited

With this basic data, the reactors may be calculated in much the same manner as any ordinary transformer.

Appendix I

The average load current I_L follows from

$$I_L=\frac{1}{\pi}\int_{\alpha}^{\alpha+\pi} i_L d\theta=\frac{1}{\pi}\left[\int_{\alpha}^{\gamma} i_L d\theta+\frac{I_C N_C}{N_L}(\alpha+\pi-\gamma)\right]$$

$$=\frac{E}{R_L}\frac{\cos\alpha-\cos\gamma}{2}+\frac{I_C N_C}{N_L}\left(1-\frac{\gamma-\alpha}{\pi}\right) \quad (30)$$

In per-unit notation

$$\frac{I_L}{I_{L,m}}=\frac{\cos\alpha-\cos\gamma}{2}+\frac{I_C N_C}{I_{L,m} N_L}\left(1-\frac{\gamma-\alpha}{\pi}\right) \quad (31)$$

Next, γ is determined

$$\sin\gamma=\frac{CW}{MN}=\frac{\frac{I_C N_C}{N_L}R_L}{E_m}=\frac{2}{\pi}\frac{I_C N_C}{I_{L,m} N_L} \quad (32)$$

As in the preceding paragraphs the flux swing is proportional to area *CMD*. For steady-state operation areas *CMD* and *DEF* are equal, hence

$$\int_{\gamma}^{\alpha+\pi}\sin\theta d\theta-(\alpha+\pi-\gamma)\sin\gamma=0 \quad (33)$$

and

$$\cos\alpha+\cos\gamma-(\alpha+\pi-\gamma)\sin\gamma=0 \quad (34)$$

This is a transcendental equation which is graphically solved, using γ from equation 32. The solution as function of the per-unit load current is shown in Figure 12. The per-unit load current now is obtainable from equation 31 and the normalized characteristic plotted in Figure 9.

Appendix II

The criterion for normal excitation is

$$\Phi_{\Delta,m}=2\Phi_s \quad (45)$$

Let

$$\xi=E_s/E_{s,o} \quad (46)$$

The flux swing follows from equation 20. The voltage e_L is seen in Figure 7

$$\Phi_{\Delta,m}=\frac{10^8}{\omega N_L}\int_{\alpha}^{\lambda}(e_L-I_L R_L)d\theta$$

$$=\frac{10^8}{\omega N_L}[E_m(\cos\alpha-\cos\lambda)-I_L R_L(\lambda-\alpha)] \quad (47)$$

Substituting into equation 45 from equations 47, 18, and 46

$$1/\xi=\cos\alpha-\cos\lambda-\frac{2}{\pi}\left[\frac{I_L R_L}{E}(\lambda-\alpha)\right] \quad (48)$$

ξ can now be plotted as a function of the per-unit load current, since α follows from equation 22, and is shown in Figure 18.

Appendix III

First, angle α will be determined. The flux swing which is represented by the area *EFR* equals $2\Phi_s$, therefore equals the area of a quarter sine wave with the amplitude $E_{s,o,m}$.

$$\text{area } EFR=i_L R_L(\pi+\alpha-\lambda)-\int_{\lambda}^{\alpha+\pi}\sin\theta d\theta=i_L R_L(\pi+\alpha-\lambda)-E_m(\cos\alpha+\cos\lambda) \quad (49)$$

and

$$i_L R_L=E_m\sin\lambda \quad (50)$$

Substituting equation 50 in 49 one obtains

$$\text{area } EFR=E_m[(\pi+\alpha-\lambda)\sin\lambda-\cos\alpha-\cos\lambda]=E_{s,o,m}\int_0^{\pi/2}\sin\theta d\theta=E_{s,o,m} \quad (51)$$

The angle α now can be determined graphically for any voltage ratio $E/E_{s,o}$.

Next the load current is calculated; it can be seen to consist of a constant part *B-F* and a sinusoidal part *CDE*

$$I_L=\frac{E_m}{R_L}\left[\sin\lambda+\frac{1}{\pi}\int_{\vartheta}^{\lambda}\sin\theta d\theta-\frac{1}{\pi}(\lambda-\vartheta)\sin\lambda\right]=\frac{E_m}{R_L}\left\{\sin\lambda+\frac{1}{\pi}[(\cos\vartheta-\cos\lambda+(\vartheta-\lambda)\sin\lambda)]\right\} \quad (52)$$

In order to solve this equation, one remembers that the flux upswing equals the flux downswing, hence areas $EFR=BCDQ$

$$\text{area } BCDQ=E_m\int_{\alpha}^{\vartheta}\sin\theta d\theta-i_L R_L(\vartheta-\alpha)=E_m(\cos\alpha-\cos\vartheta)-i_L R_L(\vartheta-\alpha) \quad (53)$$

Equating equations 49, 50, and 53, one obtains

$$\cos\vartheta+(\vartheta-\alpha)\sin\lambda=2\cos\alpha+\cos\lambda-\pi\sin\lambda \quad (54)$$

Substituting equation 54 in equation 52

$$I_L=\frac{E_m}{R_L}[\sin\lambda+\lambda(2\cos\alpha+\cos\lambda-\pi\sin\lambda-\cos\lambda)]=\frac{E}{R_L}\cos\alpha \quad (55)$$

α is obtainable from equation 51.

Appendix IV. List of Symbols

B = flux density in gauss
B_s = saturation flux density, in gauss
e = instantaneous supply voltage, in volts
E = average rectified supply voltage, in volts
E_m = amplitude of supply voltage, in volts
$e_{L,A}, e_{L,B}$ = instantaneous voltage across load winding of reactor *A* or *B*, respectively, in volts
e_L = instantaneous voltage across both load windings, in volts
E_C = voltage of control source, in volts
$e_{C,A}$, $e_{C,B}$ = instantaneous voltage across control winding of reactor *A* or *B* respectively, in volts
$E_{s,o,m}$ = amplitude of no-load saturation voltage, in volts
$E_{s,o}$ = average rectified no-load saturation voltage, in volts
E_s = average rectified saturation voltage, in volts
E_d = design center voltage, rectified average, in volts
E_{max} = highest permissible overvoltage, rectified average, in volts
E_{min} = lowest permissible undervoltage, rectified average, in volts
f = frequency, cycles per second
$f(x)$ = ordinates of normalized characteristic of Figure 9, unity
F_A, F_B = magnetomotive force in core *A* or *B* respectively, in gilberts
G_e = voltage gain, unity
G_i = current gain, unity
G_p = power gain, unity
H = magnetic intensity, oersted
i_L = instantaneous current in load resistor R_L, in amperes
I_L = average rectified load current, amperes
$I_{L,m}$ = average rectified maximum load current (equation 28), in amperes
$i_{L,A}$, $i_{L,B}$ = instantaneous current in load winding of reactor *A* or *B*, respectively in amperes
I_C = average value of control current, in amperes
k_f = form factor of load current, unity
L = inductance of load winding, in henrys
L_C = fictitious inductance of the outer control circuit, in henrys
N_C, N_L = number of turns of one control winding or one load winding, respectively
P_i = power supplied to control circuit, in watts
P_o = power delivered to load resistor R_L, in watts
R_C = resistance of the entire control circuit, in ohms
R_L = load resistance, in ohms
t = time, seconds
x = per-unit control ampere-turns
y = per-unit load current
α = angle of retard, in degrees or radians
γ = phase angle shown in Figure 10, in degrees or radians
γ_1 = boundary angle between mode 2 and 3, in degrees or radians
ϑ = phase angle at which saturation occurs (Figure 20), in degrees or radians
θ = phase angle, degrees or radians
λ = phase angle in Figure 7, in degrees or radians
ν = angle of retard at boundary between mode 1 and 2, in degrees or radians
ξ = saturation voltage ratio (equation 46), units
π = 3.14159
ϕ_A, ϕ_B = instantaneous magnetic flux in core of reactor *A* or *B*, respectively, in maxwells
Φ_s = saturation flux, in maxwells
ϕ_Δ = instantaneous value of flux swing, in maxwells
$\Phi_{\Delta,m}$ = maximum value of flux swing, in maxwells
ω = angular velocity of time vector, radians per second

References

1. Current Responsive Arrangement, W. Krämer. *United States Patent Number 2,153,378*, April 4, 1939.

2. Some Fundamentals of D-C Controlled Reactors with Resistive Load, H. F. Storm. *AIEE Transactions*, volume 68, part 1, 1949, pages 188–94.

3. Electric Circuits (book), Massachusetts Institute of Technology Staff. John Wiley and Sons, Inc., New York, N. Y., 1943, page 341.

4. Magnetic Circuits and Transformers (book), Massachusetts Institute of Technology Staff. John Wiley and Sons, Inc., New York, N. Y., 1945, page 380–88.

No Discussion

Determination of Steady-State Performance of Self-Saturating Magnetic Amplifiers

EDWARD J. SMITH
ASSOCIATE AIEE

Synopsis: The performance of the half-wave circuit under the conditions of high external control-circuit impedance and no rectifier leakage is taken as the basis for the steady-state analysis of the self-saturating magnetic amplifiers. Transfer curves for the basic circuit are determined by a combination of idealized and no-load methods, each applied in the appropriate region of operation, and the results extended to the full-wave and doubler circuits. Rectifier leakage and control-circuit impedance effects are computed for each type of circuit. Transfer curves for all three circuits under practical operating conditions are obtained by correcting the basic curves for these effects. Satisfactory results are obtained on test amplifiers containing orthonik and hypersil cores.

THE purpose of this paper is to describe a method for determining the steady-state performance of the basic self-saturating magnetic amplifier circuits. Consideration of magnetic core loop width, rectifier forward resistance, and rectifier reverse (or leakage) current flow is essential to the investigation of all self-saturating amplifier circuits. The latter factors have been generally neglected in recent papers.

This paper considers the performance of the half-wave circuit, with no rectifier leakage and constrained magnetization (no circulating alternating current in the control winding), as basic for all self-saturating circuits. To determine the actual transfer curve for each type of circuit, half-wave, full-wave, and doubler, when rectifier leakage and control alternating currents are present, corrections are applied to the curve of the basic circuit. The term transfer curve, as used in this paper, refers to the plot of average load current versus d-c control current with fixed resistive load and a-c supply voltage.

Magnetic Core Characteristics

When a magnetic material is magnetized in a cyclic and symmetrical manner, the relationship between flux density and field intensity is defined by a family of symmetrical loops. For many purposes the locus of the end points, which essentially coincides with the d-c magnetization curve, may be taken as a satisfactory approximation to the actual relationship between flux density and field intensity. When the magnetization process is asymmetrical, no single magnetization curve can be defined.

In the case of the more sensitive magnetic materials, when the maximum core flux approaches saturation value during cyclic operation, the upper branch of the asymmetrical loop traversed coincides with the upper branch of a large symmetrical loop. The situation is illustrated in Figure 1(A). Since both the upper and lower end points of the asymmetrical loops lie on this curve, the upper branch of a large symmetrical loop can be taken as an equivalent magnetization curve when the core saturates during the cycle. When the flux variation is symmetrical, or nearly symmetrical without large cyclic saturation, the d-c magnetization curve can be used, Figure 1(C). In computing the transfer curves for the self-saturating amplifiers, the magnetic characteristics of the core are assumed to be represented by the upper branch of a large symmetrical loop when the cyclic core saturation is large, and by the d-c magnetization curve when the flux variation is nearly symmetrical (in the region of minimum load current). In the intermediate region, illustrated in Figure 1(B), an additional assumption is made.

In computing amplifier performance, a knowledge of the relationship between core flux and ampere turns is required. The core-flux density is not uniform across its sectional area, and the total core flux, corresponding to a given number of impressed ampere turns, is not readily determinable. It is, therefore, necessary to

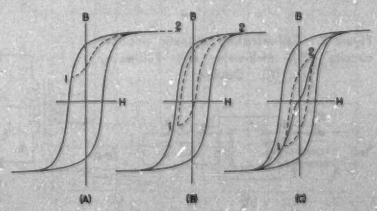

Figure 1. Flux variations in various regions of hysteresis loop

Paper 50-206, recommended by the AIEE Electronics Committee and approved by the AIEE Technical Program Committee for presentation at the AIEE Middle Eastern District Meeting, Baltimore, Md., October 2–5, 1950. Manuscript submitted May 11, 1950; made available for printing August 7, 1950.

Edward J. Smith is Research Fellow at the Microwave Research Institute, Polytechnic Institute of Brooklyn, Brooklyn, N. Y.

The author expresses his gratitude to Professors M. Liwschitz-Garik and E. Weber of the Polytechnic Institute of Brooklyn for their generous guidance and encouragement in all phases of the research work, and to Mr. A. Schwartz of the Microwave Research Institute who obtained much of the experimental data for this paper.

The study of magnetic amplifiers is being undertaken at the Microwave Research Institute under the sponsorship of the Office of Naval Research.

have available magnetic data which give the relationship between an equivalent uniform flux density and a field intensity based upon the mean length of the core. That is, it is necessary to have magnetic data which apply for the particular material and core shape.

Rectifier Forward Resistance

The forward resistance of dry-disk rectifiers (resistance when current flows in the forward direction), as used in magnetic amplifiers, decreases as the forward current increases. Consideration of the variable nature of the forward resistance during a cycle greatly complicates the already difficult problem, and is not really necessary in practical circuits. Then it is assumed that the rectifier has an equivalent constant forward resistance over a cycle. Furthermore, it has been found possible to assume a constant forward resistance for operation over the entire transfer curve.

For a particular transfer curve in regions of large positive control current, each load mesh consists essentially of the load resistance in series with the rectifier and applied alternating voltage. (The self-saturating circuits are shown in Figure 2.) The effect of forward rectifier resistance upon average load current is therefore maximum in this region. As long as operation continues above the knee of the transfer curve, the change in average load current is relatively small and the change in rectifier forward resistance is even smaller. Below the knee of the transfer curve, the inductance of the reactor dominates and relatively large changes in circuit resistance have little affect upon average load current. Consequently, it seems very reasonable to expect that, if the equivalent rectifier forward resistance is selected under conditions similar to the region of its maximum importance, good results will be obtained over the entire transfer curve.

The previous considerations suggest the direct measurement of the rectifier equivalent forward volt-ampere characteristic by an a-c method. Figure 3 shows the test circuit arrangement and measured characteristic for a particular selenium disc rectifier. Briefly, a sinusoidal voltage is applied to the rectifier, and the average current (direct) is measured for varying values of alternating voltage. Under these conditions, the operation of the rectifier in an actual amplifier circuit above the knee of the transfer curve is very closely duplicated. The characteristic curve is plotted as average applied voltage (over a half-cycle) versus average rectifier current. For prescribed values of applied alternating voltage and load resistance, the ultimate average load current (per mesh) is determined by constructing a load line in the conventional manner and observing its intersection with the measured curve. The equivalent forward resistance then is given by

$$R_f = \frac{V_{avg}}{I_{avg}} \tag{1}$$

in which the values of V_{avg} and I_{avg} are obtained from the intersection. A curve of equivalent rectifier resistance as a function of average current is shown in Figure 4. The duplication of measured points in certain regions is the result of remeasurements at later dates. Their somewhat scattered disposition gives an idea

Nomenclature

A = Core cross-sectional area, square inches
B = Flux density, lines per square inch
B_c = Premagnetization flux density, lines per square inch
B_m = Maximum value of flux density variation, lines per square inch
B_m' = Equivalent maximum value of flux density variation, lines per square inch
B_s = Saturation flux density, lines per square inch
D_m = Deviation from linearity of H_m, ampere turns per inch
E = Reactor voltage, volts
E_f = Reactor voltage during forward conduction, volts
E_r = Reactor voltage during reverse conduction, volts
H, $(\boldsymbol{H})$ = Core magnetization (period average), ampere turns per inch
H_c = D-c control magnetization, ampere turns per inch
H_L, $(\boldsymbol{H}_L)$ = Load magnetization (period average), ampere turns per inch
H_m = Magnetization corresponding to B_m, ampere turns per inch
i = Load current, amperes
i_c = Control current, amperes
I = Average load current in basic half-wave circuit, amperes
I_{cl} = Control current equivalent of leakage demagnetization, amperes
I_{EX} = Control current equivalent of control coupling demagnetization, amperes
I_f = Average forward load current, amperes
I_{Ll} = Load current equivalent of leakage demagnetization, amperes
I_{MC} = Control current equivalent of resistance magnetizing effect in half-wave circuit, amperes
I_{po} = Postsaturation load current, amperes
I_{pr} = Presaturation load current, amperes
I_r, (I_{rh}) = Average reverse load current (half period), amperes
I_s = Ultimate average forward load current, amperes
I_T = Total average load current, amperes
l_m = Mean path length of magnetic flux, inches
N = Turns on load winding
N_c = Turns on control winding
r = Load winding resistance, ohms
r_c = Control circuit resistance, ohms
r_c' = Control circuit resistance referred to load circuit, ohms
R = Load mesh resistance, ohms
R_f = Forward rectifier resistance, ohms
R_L = Load resistance, ohms
R_r = Reverse rectifier resistance, ohms
R_T = Forward load mesh resistance, ohms
t = Time, seconds
t_0 = Time of start of forward current flow, seconds
t_1 = Time of end of forward current flow, seconds
t_s = Time of core saturation, seconds
$V_{D\text{-}C}$ = D-c control circuit voltage, volts
V_m = Maximum value of a-c applied voltage, volts
V_m' = Maximum value of effective a-c applied voltage, volts
V_r, (V_r) = Reverse rectifier voltage (average), volts
Φ = Core flux, lines
Φ_c = Premagnetization flux, lines
Φ_c' = Premagnetization flux in presence of rectifier leakage, lines
Φ_m = Maximum value of flux variation, lines
Φ_s = Saturation flux, lines
σ = Ratio of Φ_s to Φ_m
ω = Angular frequency of supply, radians per second

Subscripts 1 and 2 used in combination with certain of the above symbols refer to meshes 1 and 2, respectively.

Figure 2. Self-saturating magnetic amplifier circuits: (A). Half-wave; (B). Full-wave; (C). Doubler

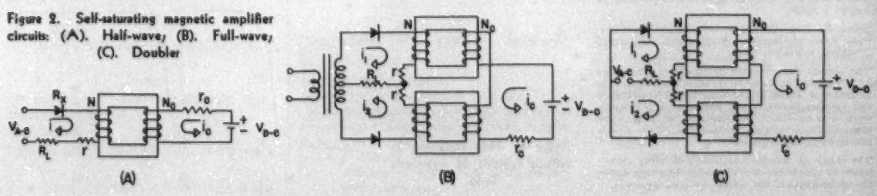

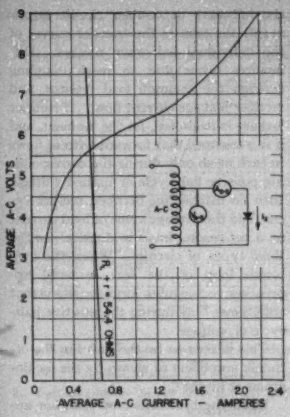

Figure 3. Rectifier forward a-c volt-ampere characteristic (10-disk selenium rectifier)

as to the constancy of rectifier properties which may be expected. From measured transfer curves of experimental hypersil and orthonik amplifiers, values of equivalent rectifier forward resistance necessary to produce the observed values of ultimate average load current were computed. These points, shown as circles in Figure 4, indicate reasonable agreement with the measured characteristic.

Basic Half-Wave Circuit

Under conditions of constrained magnetization and no rectifier reverse current flow, the initial cyclic (presaturation) flux density is determined solely by the d-c control current and the hysteresis loop. Above the knee of the transfer curve the presaturation flux density B_e is assumed to be specified by the upper branch of a large symmetrical loop. For more sensitive materials a saturation flux density B_s can be defined. The mesh equations are

$$V_m \sin \omega t = Ri + NA\frac{dB}{dt} \tag{2}$$

$$V_{D-C} = r_d i_e \tag{3}$$

The presaturation flux density is determined by control circuit magnetization

$$H_e = \frac{N_d i_e}{l_m} \tag{4}$$

The problem is simplified further by assuming that the actual cyclic process can be approximated by initial change in flux without load current flow (up to saturation B_s), followed by current flow with no further change in flux.[1] The actual current wave is replaced by one having zero value until saturation is reached at time t_s, and then having sinusoidal form until time $(1/2)T$. Thereafter, the load current remains at zero value during the negative half-cycle of applied voltage. The saturation angle is given by

$$\omega t_s = \cos^{-1}\left[1-\left(\frac{B_s-B_e}{B_m}\right)\right] \tag{5}$$

and the average load current is

$$I = I_s\left[1-\left(\frac{B_s-B_e}{2B_m}\right)\right] \tag{6}$$

in which

$$B_m = \frac{V_m}{\omega NA}, \quad I_s = \frac{V_m}{\pi R_T}$$

The results given by such an idealized method are generally satisfactory above the knee of the transfer curve; below the knee of the transfer curve, the calculated curve is too steep. In the latter region the presaturation current flow cannot be neglected, nor can the presaturation flux be obtained from the upper branch of the large symmetrical loop. Results for a hypersil half-wave amplifier are shown in Figure 5.

When the core saturation is small, the inductance of the reactor predominates and the load current is essentially independent of load resistance. The rms voltage drop across the load at the minimum point is usually less than 5 per cent of the supply voltage in practical amplifiers. The assumption of zero circuit resistance simplifies the mathematics and permits solution for load current by direct graphic integration or by analytical methods. The d-c or normal magnetization curve can be used in this region. Such procedures undoubtedly lead to satisfactory results, but are somewhat tedious and special. A more general and rapid method is sought. In particular, it is the aim to focus attention upon the most critical regions of the transfer curve, and to accept less accuracy for the less important regions. The region of minimum load current is such a critical region; the region to the left does not represent a usual operating region, and is not of great importance. With zero forward mesh resistance, the current flows in a positive direction over the entire cycle and becomes zero at the start of each positive half-cycle of applied voltage. The average value of load winding magnetizing force is

$$H_L = H - H_e \tag{7}$$

in which H is the average value of total core magnetization. When the flux variation is symmetrical.

$$H = 0, \text{ and } H_L = -H_e \tag{8}$$

independent of the shape of the magnetization curve. When the minimum current region of the transfer curve corresponds to operation along a portion

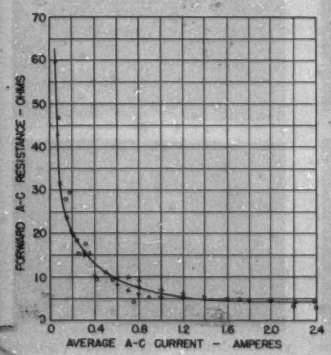

Figure 4 (left). Rectifier forward a-c resistance characteristic (10-disk selenium rectifier). The crosses denote measured values; the circles denote values computed from measured transfer curves

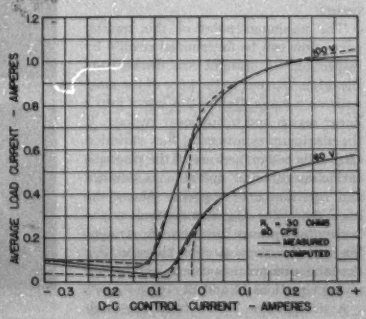

Figure 5 (right). Comparison of measured and computed transfer curves for a half-wave circuit (hypersil cores with constrained magnetization)

of the magnetization curve which is essentially linear, symmetrical flux variation occurs at the point of minimum load current, and

$$H_{L\,(min)} = |H_c| = H_m \tag{9}$$

H_m is the magnetizing force corresponding to B_m.

When symmetrical flux variation does not occur in a linear region of the transfer curve, the minimum point occurs when the flux variation is shifted in the positive B direction. Since operation near the minimum point does not involve large core saturation, the magnetization curve can usually be represented in this region by

$$H = k_1 B + k_3 B^3$$

For this representation there obtains[2]

$$H_L = H_m + D_m S_1(\sigma) \tag{10}$$

where

$$\sigma = \frac{B_c}{B_m}, \text{ and } S_1(\sigma) = 3(\sigma^3 + 1.5\sigma + 0.5)$$

and D_m is the deviation of the magnetization curve from linearity at B_m. The minimum average value of load current is found to occur for $\sigma = -3/4$; from equation 10

$$H_{L(min)} = H_m - \frac{3}{16} D_m \tag{11}$$

and the corresponding control direct current required is found from the magnetization curve from

$$|B_c| = \frac{3}{4} B_m \tag{12}$$

This should be compared with

$$|B_c| = B_m$$

in the case of linear operation. Higher power terms could be added to the curve representation, but usually are not necessary because large saturation does not occur.

The minimum point of the transfer curve now can be determined readily by inspection. A straight line drawn from the origin tangent to the knee of the magnetization curve divides this curve into a linear region and a nonlinear region. If the maximum symmetrical flux variation (B_m) falls below the knee of the magnetization curve, linear operation is assumed and equation 9 is applied. Above the knee the value D_m is measured as the horizontal distance between the straight line and the magnetization curve at B_m; the minimum point is determined by applying equations 11 and 12.

A straight line drawn from the minimum point tangent to the knee of the transfer curve, computed by the aforementioned idealized method, closely approximates the steep portion of the transfer curve. To the left of the minimum point the transfer curve is computed from equation 10. When the hysteresis loop of the material approaches a rectangular shape, the relation[3]

$$H_L = |H_c| \tag{13}$$

more closely describes the behavior in this region. Computed transfer curves for a test hypersil amplifier, shown in Figure 5, agree closely with measured curves. Discrepancies in the region of the knee of the upper curve are due primarily to rectifier leakage and will be considered later. Similar agreement was found for a test orthonik amplifier.

Full-Wave and Doubler Circuits

For the case of constrained magnetization, the steady-state transfer curve for the full-wave or doubler circuit is primarily the sum of the transfer curves of the individual half-wave meshes. Differences occur due to mesh coupling through the common load resistor, and rectifier leakage current flow. If rectifier leakage is neglected, for the moment, and if it is assumed that forward current flows in each mesh only during the corresponding positive half-cycle of applied voltage, then no interaction between meshes occurs and the average value of load current on a per-reactor basis is identical for the three types of circuits. When the hysteresis loop of the core material approaches rectangular form, mesh current truly flows only during the positive half-cycle of voltage.

This is seen to be the case for the orthonik amplifiers as shown by the oscillograms of Figure 6.

When the hysteresis loop does not approach this rectangular form, the forward mesh current continues to flow after the applied voltage becomes zero. For such

Figure 6. Comparison of load voltage wave forms (orthonik cores): (A). Half-wave; (B). Full-wave; (C). Doubler

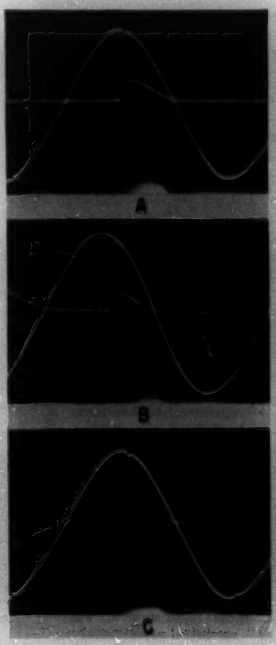

Figure 7. Comparison of load voltage wave forms (hypersil cores): (A). Half-wave; (B). Full-wave; (C). Doubler

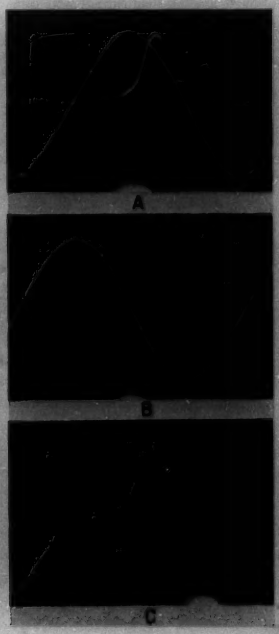

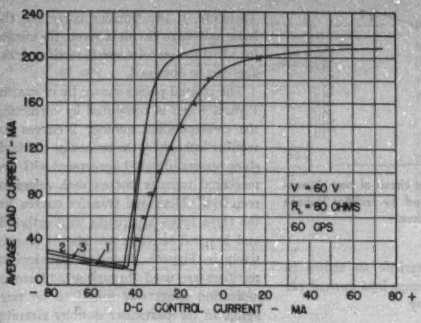

Figure 8. Transfer curves with and without rectifier leakage

(Orthonik cores and constrained magnetization)

1. Sum of transfer curves of individual meshes with *5R4YG* vacuum tube rectifiers
2. Full-wave circuit with *5R4YG* vacuum tube rectifiers
3. Full-wave circuit with selenium rectifiers

Crosses are values obtained by correcting curve number 2 for rectifier leakage

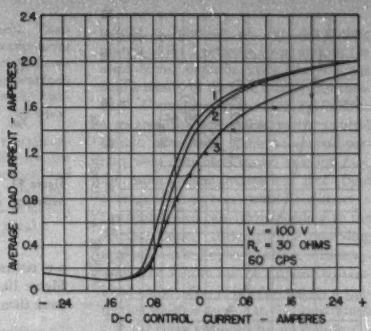

Figure 9. Transfer curves with and without rectifier leakage

(Hypersil cores and constrained magnetization)

1. Sum of transfer curves of individual meshes with *872A* mercury tube rectifiers
2. Full-wave circuit with *872A* mercury tube rectifiers
3. Full-wave circuit with selenium rectifiers

Crosses are values obtained by correcting curve number 2 for rectifier leakage

materials there exists the possibility, in the case of the full-wave and doubler circuits, of simultaneous forward current flow in two meshes over a portion of the cycle. Interaction occurs, and the average load current per reactor is not exactly the same for all three circuits. Although the forward current in one mesh may continue flowing well into the negative half-cycle, the effect of this current overshoot upon average load current is only in proportion to the ratio of overshoot area under the load voltage wave to the area under the applied voltage wave from the start of a positive cycle to saturation.[3] The overshoot area is the area under the load voltage wave of the half-wave mesh from time $(1/2)T$ until the load voltage becomes zero. The saturation point is arbitrarily defined as the point at which the mesh current increases with maximum rate. Oscillograms of load current for hypersil amplifiers for an intermediate value of core presaturation are given in Figure 7. Reference to the oscillogram for the half-wave circuit shows the positive load voltage to persist for approximately 60 degrees into the next half-cycle; nevertheless, the overshoot area under this curve is small as compared with the area under the applied voltage wave before saturation.

In order to measure the effect of mesh interaction without the additional complication of rectifier leakage, the dry-disc rectifiers were replaced by vacuum or mercury vapor tubes. Transfer curves for the individual half-wave meshes were measured and their sum determined by adding individual mesh load currents corresponding to various values of control current; transfer curves for the composite full-wave circuits then were measured and compared with the previous curves. The results for the orthonik amplifiers, given in Figure 8, show the effect of mesh interaction to be negligible. The results for the hypersil amplifiers, given in Figure 9, show a small and approximately uniform shift of the curve for the composite amplifier to the right. This may be due partially to unbalance in the individual meshes. The shape of this transfer curve does not differ appreciably from the shape of the curve of the half-wave meshes; the shape of the curve is, above all, the more important feature.

A corresponding curve for the full-wave circuit using selenium disc rectifiers also is shown in each case. (Total forward mesh resistance at ultimate saturation and load resistance were maintained fixed for each material by adjusting resistors in series with the reactors.) In each case, this curve deviates from the previous two curves by a large amount, especially in the region of the knee, and illustrates very clearly the large effect of rectifier leakage. Therefore, it is concluded that mesh interaction is of negligible importance as compared with rectifier leakage effects when resistive loads and reasonably sensitive (but by no means ideal) materials are employed.

Rectifier Leakage Effects

Rectifier leakage current flow modifies the operation by contributing directly to the average load current, and by demagnetizing the core. The first effect is small and usually negligible, but the demagnetizing effect can not generally be neglected. Only the effect of rectifier leakage on the shape of the transfer curve will be considered.

In the steady-state case the flux is periodic and the time integral of reactor inductive voltage drop over a period of applied voltage is zero. If E_f and E_r denote respectively the inductive voltage across the reactor load winding during the intervals of forward (t_0 to t_1) and reverse (t_1 to t_0+T) rectifier current flow, then

$$\int_{t_0}^{t_1} E_f dt + \int_{t_1}^{t_0+T} E_r dt = 0 \tag{14}$$

For the half-wave circuit

$$\left.\begin{aligned} E_f &= V_m \sin \omega t - I_f(R_L + r + R_f) \\ E_r &= V_m \sin \omega t - I_r(R_L + r + R_r) \\ E_r &\approx V_m \sin \omega t - V_g \end{aligned}\right\} \tag{15}$$

where R_L, r, R_f, and R_r are the load, reactor winding, rectifier forward, and rectifier reverse resistances respectively. (R_r is not assumed constant.) I_f and I_r denote the forward and reverse instantaneous values of mesh current, and V_g is the instantaneous reverse rectifier voltage. From equations 14 and 15 there obtains the result

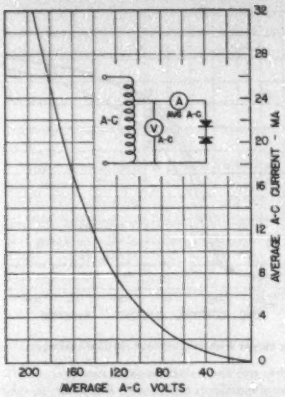

Figure 10. Rectifier reverse a-c volt-ampere characteristic (10-disk selenium rectifier)

$$V_z = I_f(R_L + r + R_f)$$

where V_z and I_f are average values taken over a complete period, t_0 to t_0+T. If the assumption of equal periods of forward and reverse rectifier current flow is made, then

$$V_{zh} = 2I_f(R_L + r + R_f) \tag{16}$$

V_{zh} is the half-period average or d-c value of reverse rectifier voltage over the interval of reverse current flow. The periods of forward and reverse current flow are nearly equal in actual circuits, except possibly in the region of minimum load current where rectifier leakage effects are unimportant. This is not the same as assuming zero current overshoot, and applies even when the overshoot is appreciable. Following the same line of reasoning, for the full-wave and doubler circuits, one correspondingly obtains for full-wave

$$V_{zh} = 2I_f(2R_L + r + R_f) \tag{17}$$

for doubler

$$V_{zh} = 2I_f(r + R_f) \tag{18}$$

where I_f is the average forward current per mesh. From equations 16 to 18 it is seen that the leakage effects are smallest in the doubler, intermediate in the half-wave, and largest in the full-wave circuits.

The determination of rectifier reverse current flow requires a knowledge of the wave form of V_z. For the purpose of evaluating the contribution of reverse current (a small effect) to the average load value, V_z may be assumed half sinusoidal in shape. The corresponding half-period average current I_{rh} is obtained from the

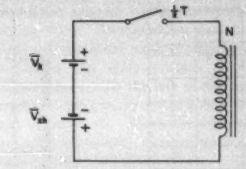

Figure 11. Equivalent circuit of core demagnetization effect caused by rectifier leakage current

a-c reverse characteristic as shown in Figure 10. The average load current per mesh then is given by

$$I_L = I_f \pm I_r, \text{ where } I_r = \frac{1}{2} I_{rh} \tag{19}$$

The minus sign applies to the half and full-wave circuits, and the plus sign to the doubler circuit.

The determination of rectifier leakage demagnetization effect requires a somewhat different approach. Integration of the reactor inductive voltage drop over the interval of reverse current flow yields the relation

$$2\frac{N}{T}(\Phi_a - \Phi_c') = E_{rh} = V_k - V_{zh} \tag{20}$$

where

$$V_k = \frac{V_m}{\pi}(\cos \omega t_0 - \cos \omega t_1) + \begin{Bmatrix} 0 \\ -1 \\ +1 \end{Bmatrix} 2I_f R_L$$

E_{rh} is the d-c value over the interval t_1 to t_0+T. The $(0, -1, +1)$ refer to the half-wave, full-wave, and doubler circuits respectively. Equal intervals of forward and reverse rectifier current flow are assumed. $(\Phi_c - \Phi_c')$ is the core demagnetization equivalent of rectifier leakage current. If it is assumed that the effect on average load current is contained completely in the reduction of core premagnetization, then the same effect results from applying two series d-c batteries, having voltages V_{zh} and V_k, across the load winding of the reactor for a half-period $1/2T$ as results under actual operating conditions. The equivalent circuit is shown in Figure 11. The constant reverse rectifier current I_{Ld} required to produce the fixed voltage V_{zh} is obtained directly from the rectifier d-c reverse volt-ampere characteristic (not shown). When referred to the control circuit

$$I_{cd} = \frac{N}{N_c} I_{Ld} \tag{21}$$

I_{cd} is the equivalent d-c control current which must be added to the original value (without leakage) in order to maintain the same average value of load current. Therefore, if the transfer curve for the basic half-wave circuit is given, the curves for all three circuits, with rectifier leakage, can be obtained.

The plotted points shown by crosses in Figures 8 and 9, computed by correcting the corresponding number 2 curves for rectifier leakage by the preceding method, show reasonably good agreement with the measured transfer curves with selenium rectifiers. Measured transfer curves for the three types of circuits with orthonik and hypersil reactors are shown respectively in Figures 12 and 13. Selenium rectifiers are used throughout. Demagnetization effect was found to be negligible in the particular doubler circuits. It was assumed that the doubler curves were free from leakage effects, and, therefore, essentially identical with the curves of the corresponding basic half-wave circuits (without leakage). Corrections then were computed for the half and full-wave circuits and these points are shown in the figures. The method proposed for evaluating leakage effects, although not analytically exact, has a firm theoretical basis and yields results which are useful and accurate enough to give a good appreciation of these effects.

Control-Circuit Resistance Effect

When the control circuit contains finite resistance and no external choke, transformer action between load and control meshes results in the half-wave circuit, and coupling between the two load meshes results in the full-wave and

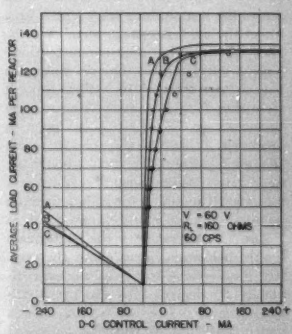

Figure 12. Comparison of transfer curves (orthonik cores and constrained magnetization): A. Doubler; B. Half-wave; C. Full-wave

The crosses are computed points for the half-wave circuit, and the circles are computed points for the full-wave circuit

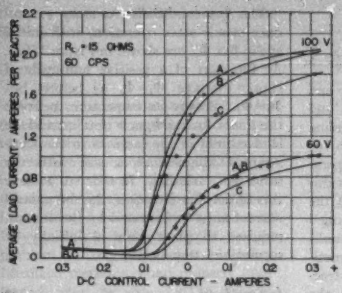

Figure 13 (left). Comparison of transfer curves (hyperbolic cores and constrained magnetization): A. Doubler, B. Half-wave, C. Full-wave

The crosses are computed points for the half-wave circuit, and the circles are computed points for the full-wave circuit

doubler circuits. The two effects are basically different and require separate consideration.

Half-Wave Circuit

The control mesh voltage equation becomes

$$V_{D-C}=r_e i_c+N_c A\frac{dB}{dt} \tag{22}$$

If the idealized approach is followed as in the basic half-wave circuit, then from equations 2 and 22, the presaturation load current is given by

$$i=\frac{V_m}{R_T+r_e'}\sin\omega t \tag{23}$$

and

$$V_m'\sin\omega t=NA\frac{dB}{dt} \tag{24}$$

where

$$r_e'=\frac{N^2}{N_c^2}r_c,\quad V_m'=\frac{r_c'}{R_T+r_e'}V_m,\quad B_m'=\frac{V_m'}{\omega NA}$$

The flux builds up as in the constrained case but with reduced voltage V_m'. The saturation angle is found from equation 5 by substituting B_m' for B_m. The saturation angle is seen to be increased over the constrained case. The presaturation average load current is found from equation 23 to be

$$I_{pr}=I_s\frac{R_T}{r_c'}\left(\frac{B_s-B_c}{2B_m}\right) \tag{25}$$

After saturation, the current flows as in the constrained case, and the average value obtained from B_m' and equation 6 reduces to

$$I_{po}=I-I_s\frac{R_T}{r_c'}\left(\frac{B_s-B_c}{2B_m}\right) \tag{26}$$

The total average load current is

$$I_T=I_{pr}+I_{po}=I \tag{27}$$

This rather surprising result states that, under idealized conditions, the value of average load current corresponding to a particular presaturation flux density B_c is independent of control circuit resistance. The increase due to presaturation current is exactly compensated by the decrease in postsaturation current. The value of d-c control circuit current required to produce a given B_c does, however, depend upon control circuit resistance.

During the presaturation period, alternating current flows in the control circuit by transformer action; after saturation and until time $(1/2)T$, $dB/dt=0$, and the control current remains constant at its d-c value. The average control current over the positive half-cycle is

$$I_c=\frac{V_{D-C}}{r_c}-I_{MC} \tag{28}$$

where

$$I_{MC}=2\frac{N}{N_c}I_{pr}=2\frac{N_c}{N}\frac{R_T}{r_c}(I_s-I) \tag{29}$$

The average value of control current over an entire period must equal the d-c impressed value. Therefore, the d-c value of control current during the negative half-cycle is

$$I_{c-}=-\frac{V_{D-C}}{r_c}+I_{MC} \tag{30}$$

The presaturation flux density is primarily a function of the descending branch of the hysteresis loop[4] and, in the ideal sense, depends upon the average field intensity of the core during unsaturation. Consequently, the term I_{MC} acts as a magnetizing component in the control circuit. Therefore, if the d-c control current were decreased by an amount I_{MC}, the same premagnetization flux (and average load current) would result as in the constrained case corresponding to the original value. Although the preceding analysis is based upon idealized considerations, the results can be applied to nonideal cases. I_{MC} is interpreted as a correction which is applied to the constrained transfer curve obtained by previously described methods. It is shown readily that the average reverse rectifier voltage is the same as in the constrained case, and the effect of rectifier leakage may be assumed the same as in this case.

Measured transfer curves for the orthonik amplifiers, for several values of control-circuit resistance, are given in Figure 14. Computed points show good agreement with the measured curves to the right of the minimum point in each case. To the left of the minimum point the idealized considerations, which neglect magnetizing currents, do not apply. However, it is possible to estimate the transfer curve for the case of finite control resistance by correcting the constrained curve down to the point of intersection with the left-hand branch of the constrained curve. To the left the constrained curve may be used.

Full-Wave and Doubler Circuits

The full-wave and doubler circuits with finite control-circuit resistance are not amenable to simple analytic methods; only the limiting cases of constrained and natural (zero control-circuit resistance and no external choke) magnetization are considered. The basic mesh voltage equations for Natural Magnetization are

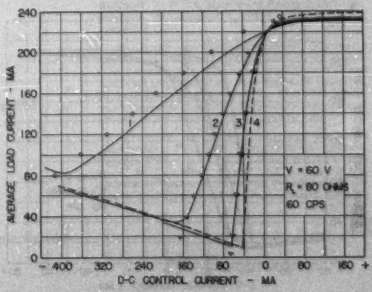

Figure 14 (right). Effect of control-circuit resistance on transfer curves of a half-wave circuit (orthonik cores)

1. Control-circuit resistance, 24 ohms; 2. 100 ohms; 3. 600 ohms; 4. large choke in control circuit. Plotted points are computed values

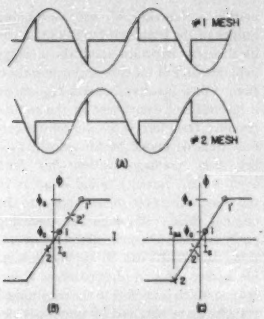

Figure 15. Semi-ideal behavior of full-wave circuit with natural magnetization

(A). Reactor voltages with ideal core materials; (B). Flux conditions during first cycle of applied voltage; (C). Steady-state flux conditions with initial flux value Φ_c

$$\left.\begin{aligned} V_m \sin \omega t &= R_1 i_1 \pm R_L i_2 + N\frac{d\Phi_1}{dt} \\ -V_m \sin \omega t &= \pm R_L i_1 + R_2 i_2 + N\frac{d\Phi_2}{dt} \\ 0 &= \frac{d\Phi_1}{dt} + \frac{d\Phi_2}{dt} \end{aligned}\right\} \tag{31}$$

By substitution, the equations for meshes 1 and 2 may be put in the form

$$\left.\begin{aligned} V_m \sin \omega t &= R_1' i_1 + N\frac{d\Phi_1}{dt} \\ -V_m \sin \omega t &= R_2' i_2 + N\frac{d\Phi_2}{dt} \end{aligned}\right\} \tag{32}$$

Figure 16. Transfer curves with constrained and natural magnetization (orthonik full-wave circuit)

1. Constrained magnetization with *5R4YG* rectifiers; 2. Natural magnetization with *5R4YG* rectifiers; 3. Constrained magnetization with selenium rectifiers; 4. Natural magnetization with selenium rectifiers

where

$$R_1' = \frac{R_1 R_2 - R_L^2}{R_2 \pm R_L}, \quad R_2' = \frac{R_1 R_2 - R_L^2}{R_1 + R_L}$$

The $\pm$ sign applies for the full-wave and doubler circuits, respectively. R_1' and R_2' assume different values depending upon the direction of current flow in the individual meshes.[4] If idealized operation is approached, then the presaturation mesh current is negligible, and the flux build-up in one mesh (accompanied by flux decay in the adjoining mesh) proceeds as in the Constrained Magnetization case. For ideal operation (rectangular hysteresis loop materials) the Natural Magnetization and Constrained Magnetization cases are identical. It is therefore evident that differences in performance which occur are due essentially to deviation of the magnetic core hysteresis loop from the ideal shape. A very simple nonideal shape will be considered.

The characteristic curve will be assumed to have a large linear slope in the unsaturated region, and zero slope in regions of positive and negative saturation. In the absence of alternating voltage, a d-c control current I_c would produce a value of flux Φ_c in each core, as shown in Figure 15(B). The solid circle and cross (1 and 2 in the figure) denote initial values of flux in reactors number 1 and 2. If the alternating voltage now is applied, the flux in reactor number 1 builds up to saturation (Φ_s) sinusoidally, and, from equation 31, the flux in reactor number 2 decreases by an equal amount. As core number 1 unsaturates (starting at time 1/2T) Φ_1 decreases from 1′ to 1, and Φ_2 increases from 2′ to 2. It was stated before that core number 2 should saturate as number 1 unsaturates, but the above description has left the second reactor unsaturated at the time at which the first reactor has returned to its premagnetization flux value. The circuit must finally settle down to steady-state operation at a reduced effective premagnetization flux.

The flux conditions necessary to produce steady-state operation, with initial cyclic flux Φ_c, are shown in Figure 15(C). At the start of a positive half-cycle of supply voltage $\Phi_1 = \Phi_c$ as before, but $\Phi_2 = \Phi_s$. Steady-state operation between the limits Φ_c and Φ_s now obtains, and the load current is the same as in the Constrained Magnetization case with the same flux variation. In order to achieve this initial flux situation, the d-c control current must be increased by the amount required to place point 2 initially at saturation; that is

$$I_{BX} = \frac{1}{2}(I_{SA} - I_c) \tag{33}$$

The maximum value of I_{BX} occurs at minimum load current, or at $I_c = -I_{SA}$. Therefore,

$$I_{BX(\max)} = I_{SA} \tag{34}$$

The results of the preceding analysis may be used to estimate the deviation between Natural Magnetization and Constrained Magnetization transfer curves. An approximate value of I_{SA} can be obtained for nonideal materials by extending a line, drawn tangent to the upper branch of the hysteresis loop at the axis of the field intensity, to saturation flux value. The deviation of the line at saturation from the ideal rectangular shape loop specifies an approximately equivalent I_{SA}. For orthonik and hypersil the values, referred to the control winding, are 11.6 and 29.8 milliamperes, respectively. Reference to measured transfer curves in Figures 16 and 17, for full-wave amplifiers using the two materials, reveals the maximum deviation between the Natural Magnetization and Constrained Magnetization curves to be about 11 and 28 milliamperes for orthonik and hypersil, respectively.

Average values of reverse rectifier voltage for corresponding Natural Magnetization and Constrained Magnetization circuits are equal, and it may be assumed

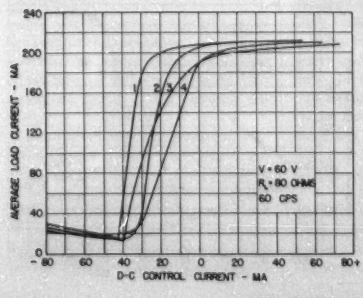

Figure 17 (right). Transfer curves with constrained and natural magnetization (hypersil full-wave circuit

1. Constrained magnetization with *872A* rectifiers; 2. Natural magnetization with *872A* rectifiers; 3. Constrained magnetization with selenium rectifiers; 4. Natural magnetization with selenium rectifiers

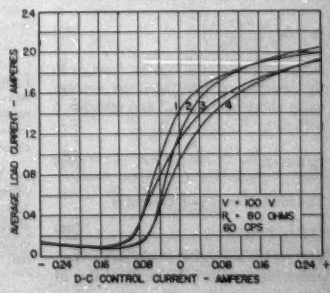

that the effect of rectifier leakage is the same in both cases.

Conclusions

A direct mathematical approach to the determination of magnetic amplifier performance invariably leads to abridgment or omission of very significant characteristics of the circuit elements. By considering the circuit operation on a regional basis, these characteristics may be more fully considered without complicating the problem to the point of insolvability. Idealized methods, when properly interpreted, may be extended to nonideal situations with useful results. In particular, it is possible to estimate the effect of finite control-circuit resistance in the half-wave circuit, the corresponding effect of mesh coupling through the control circuit in the full-wave and doubler circuits, and rectifier leakage effects in all three circuits by application of these methods.

Appendix I. Sample Calculation of Transfer Curve for a Basic Half-Wave Circuit

Amplifier Data

Hypersil toroidal wound core, 0.005-inch strip

$l_m = 11.5$ inches

$A = 1.64$ square inches

$N = 276$

$N_c = 100$

$R_L = 30$ ohms

$r = 1.40$ ohms

$V = 100$ volts rms, 60 cycles per second

$B_s = 120$ kilolines per square inch

$$B_m = \frac{V_m}{\omega NA} = \frac{\sqrt{2}\times 100\times 10^8}{120\pi\times 276\times 1.64} = 82.8 \text{ kilolines per square inch}$$

$R_L + r = 30 + 1.40 = 31.4$ ohms

From Figure 3 and the appropriate load line

$I_s = 1.23$ amperes

and from Figure 4

$R_f = 5.5$ ohms

In the region of large core presaturation, equation 6 applies

$$I = I_s\left[1-\left(\frac{B_s - B_c}{2B_m}\right)\right]$$

$$I = 1.23\left[1-\left(\frac{120 - B_c}{165.6}\right)\right]$$

Also

$$I_c = \frac{l_m H_c}{N_c}$$

For various values of B_c, values obtained for I_c and I are given in Table I.

In the region of small load current the maximum symmetrical flux variation falls above the knee of the magnetization curve; equation 10 applies here. Corresponding to $B_m = 82.8$ kilolines per square inch, there is observed

$H_m = 2.58$ ampere turns per inch

$D_m = 1.55$ ampere turns per inch

From equation 10

$$H_L = H_m + D_m S_1(\sigma)$$

$$= 2.58 + 1.55 S_1(\sigma)$$

Table II gives values of the transfer curve for a basic half-wave circuit using the equations developed in Appendix I.

The plotted results are shown in Figure 5. The linear region of the transfer curve is approximated by a straight line drawn from I_{min} tangent to the computed upper branch as previously explained.

Table I

B_c, Kilolines Per Square Inch	I_c, Amperes	I, Amperes
99	+0.46	1.075
90	0.23	1.005
80	0.115	0.933
70	0.046	0.859
57.5	0	0.766
40	−0.0173	0.636
25	−0.023	0.524
0	−0.0299	0.341
−27.5	−0.046	0.138
−45.4	−0.069	0.015

Table III

I_f, Milliamperes	V_{sh}, Volts	I_{Ld}, Milliamperes	I_{sd}, Milliamperes
130	94.2	25.0	100.
120	87.0	18.5	74.0
110	80.0	14.0	56.0
100	72.6	10.3	41.2
90	65.2	7.50	30.0
80	58.0	5.70	22.8
70	50.8	4.50	18.0
60	43.6	3.20	13.2
50	36.2	2.30	9.2
40	29.0	1.50	6.0
30	21.8	1.00	4.0

Table II

σ	$S_1(\sigma)$	H_L, Ampere Turns Per Inch	I, Amperes	B_c, Kilolines Per Square Inch	H_c, Ampere Turns Per Inch	I_c, Amperes
−0.75*	−0.189	2.29	0.0953	−62.1	−1.04	−0.120
−0.80	−0.180	2.30	0.0958	−66.2	−1.25	−0.144
−0.90	−0.123	2.39	0.0995	−74.5	−1.60	−0.184
−1.00	0	2.58	0.1075	−82.8	−2.58	−0.295
−1.10	+0.180	2.86	0.1190	−91.2	−3.10	−0.357

* Minimum I.

Appendix II. Sample Calculation of Rectifier Leakage Effect

Amplifier Data

Full-Wave Circuit, Orthonik Toroidal Wound Core, 0.001-inch strip

$l_m = 7.7$ inches

$A = 1.0$ square inch

$N = 400$

$N_c = 100$

$R_L = 160$ ohms

$r = 14.4$ ohms

$V = 60$ volts rms, 60 cycles per second

$R_f = 28.6$ ohms

$R_T = R_L + r + R_f = 203$ ohms

From equation 17

$$V_{sh} = 2(R_L + R_T)I_f$$

$$= 2(160 + 203)I_f$$

$$= 726 I_f$$

The control current is corrected by adding the component I_{cd}

$$I_c' = I_c + I_{cd}$$

where

$$I_{cd} = \frac{N}{N_c} I_{Ld} = 4 I_{Ld}$$

The reverse current I_r is not considered.

To avoid simultaneous comparison of several computed results, the measured constrained transfer curve for the doubler circuit is assumed to be identical with ideal curve of the basic half-wave circuit. The full-wave transfer curve then is obtained by correcting the doubler curve for leakage. (It is readily demonstrated that this particular doubler circuit is essentially free of rectifier leakage effect.)

Table III gives values for the full-wave transfer curve, taking the rectifier leakage effect into account.

The computed values for the full-wave circuit are plotted for comparison with the measured curve in Figure 12.

References

1. Self-Saturation in Magnetic Amplifiers, W. J. Dornhoefer. *AIEE Transactions*, volume 68, part II, 1949, pages 835–50.

2. A Study of Self-Saturating Magnetic Amplifiers. Part I: Steady-State Response of Half-Wave Circuit, E. J. Smith. *Report R-229-49, PIB-174*, Microwave Research Institute, Polytechnic Institute of Brooklyn, Brooklyn, N. Y., December 1949.

3. A Study of Self-Saturating Magnetic Amplifiers. Part II: Investigation of Rectifier Reverse Current Flow, and Steady-State Analysis of Full-Wave and Doubler Circuits, E. J. Smith. *Report R-230-50, PIB-175*, Microwave Research Institute, Polytechnic Institute of Brooklyn, Brooklyn, N. Y., February 1950.

4. A Study of Self-Saturating Magnetic Amplifiers. Part III: Influence of Control Circuit Resistance on Steady-State Performance, E. J. Smith. *Report R-231-50, PIB-176*, Microwave Research Institute, Polytechnic Institute of Brooklyn, Brooklyn, N. Y., March 1950.

No Discussion

Transient Analysis of a Voltage-Regulated Aircraft D-C System

DONALD G. SCORGIE
ASSOCIATE AIEE

IN PRESENT-DAY aircraft d-c systems some form of automatic voltage regulator is always necessary. Most commonly used is the carbon-pile type which has been analyzed in detail.[1,2] This paper includes a study of the transient characteristics of a d-c generator and of the combined regulator-generator system. Two objectives are in mind, the first to express qualitatively the stability and speed-of-recovery characteristics of the system, and the second to express exactly the terminal voltage transient upon removal of load as a function of the parameters of the regulator and generator. The latter problem is of interest to designers of circuit breaker equipment.

Basic principles of the theory of servomechanisms and feedback amplifiers have been utilized in this study. The great usefulness of servomechanism theory is due in part to the fact that a complex system may be broken into smaller components, and the characteristics of each analyzed and measured separately. This advantage is lost in analyzing by the usual approach[3] a system containing a carbon pile voltage regulator. The d-c reference voltage for the system is furnished by a critical balance of forces within the carbon pile regulator. If one allows this reference voltage to enter the study, the several transfer functions and the feedback loop within the regulator must be analyzed. This analysis is quite difficult, and cannot be checked empirically. Therefore, in this paper, the entire regulator is treated as a single component in a closed control loop.

The resulting analysis is not without disadvantages. The disadvantages, however, lie in the need for initial clarity and understanding rather than in the use of the results. In this paper the inputs to the generator-regulator system are considered to be perfect equivalent-voltage generators introduced in the generator armature and field circuits because of external disturbances such as the removal of generator load. The variable, $E_o(t)$, corresponding to servomechanism output is defined as the contribution to the generator terminal voltage due to field resistance changes and other inputs to the field. To conform with standard terminology, this quantity is called the output. However, it is the algebraic sum of this output and the armature input which actually appears at the generator terminals and directly affects the voltage regulator. This sum is the error, $\mathcal{E}_1(t)$, which is the variable to be controlled, and it becomes convenient later to define and utilize the error transfer function.

Both the generator and the regulator are highly nonlinear components, and the latter introduces the feature of a purposely variable parameter, namely carbon pile resistance. However, linearizing assumptions have been made, and consequently it has been possible to derive the transfer functions of both regulator and generator. The utility of these approximations is illustrated by the close agreement between calculated and measured terminal voltage transients which are presented in this paper.

By means of the frequency spectrum analysis technique discussed briefly in a later section, qualitative predictions of system performance can be made from an inspection of the transfer function of the control loop. The loop transfer function is determined easily from the derived transfer functions of the individual components. In turn, the effect of a single parameter change upon a component of the loop can be easily seen. The method, therefore, provides a swift, convenient tool with which to investigate methods of improving voltage regulation.

The Regulator Transfer Function

The system which will be analyzed consists of a shunt wound d-c generator and a carbon pile voltage regulator connected as shown in Figure 1. Each of these components is highly nonlinear. It was pointed out in an earlier paper[1] that the carbon pile regulator remained linear for small changes from some arbitrary reference condition in the operating range. The transfer function of a stable linear component was defined there as the complex ratio (a function of frequency) of a sinusoidal output variation to the sinusoidal input which produced it. (An alternative definition is the ratio of the Laplace transforms of output to input, the input being an arbitrary function of time.) In the case of the carbon pile regulator, the input quantity is a voltage disturbance at the operating coil terminals, and the output is a variation of the resistance of the carbon pile. Each is measured with respect to some arbitrary

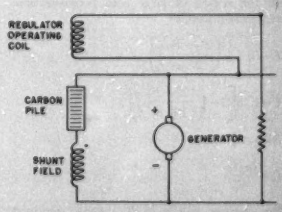

Figure 1. Regulated aircraft d-c generator

Paper 50-208, recommended by the AIEE Air Transportation Committee and approved by the AIEE Technical Program Committee for presentation at the AIEE Middle Eastern District Meeting, Baltimore, Md., October 3–5, 1950. Manuscript submitted July 5, 1950; made available for printing August 16, 1950.

DONALD G. SCORGIE is with the Naval Research Laboratory, Washington, D. C.

The author wishes to express his appreciation to N. W. Matthews, R. L. Mills, and D. H. Schaefer for their valuable suggestions and criticisms.

reference point taken as zero in the operating range. The transfer function of the regulator was derived as

$$T_r = \frac{UP}{R_cK - \omega^2 R_c M + j\omega(LK + U^2 - \omega^2 LM)} \quad (1)$$

where

U = coupling coefficient equal to the rate of change of magnet force per change of operating coil current
P = carbon pile resistance change per-unit change of carbon pile length
R_c = resistance of the operating coil circuit
K = difference in rates of change of force with deflection between the magnet curve and the carbon pile curve
M = effective mass of the armature
L = incremental inductance of the operating coil

The transfer function given in equation 1 is unwieldy, but can be simplified for use in analyzing the system under study. The simplification relies upon the fact that, for frequencies above a certain low band, the characteristics of the regulator contribute very little to the system performance. If the assumption is made that the top of the band is considerably below the frequency for which the regulator phase shift is 90 degrees (that is, $\omega^2 \ll K/M$) then equation 1 can be approximated by

$$T_r = K_r\left(\frac{\alpha_r}{j\omega + \alpha_r}\right) \quad (2)$$

where

$$K_r = \frac{UP}{KR_c}$$

and

$$\alpha_r = \frac{R_cK}{U^2 + KL}$$

The Generator Transfer Function with No Load

The generator no-load transfer function will be first defined assuming that the output of the regulator is the sole input to the generator. That is to say—the generator will be disturbed by a variation, $R(t)$, of shunt field resistance.

Suppose for the purpose of this derivation that the generator is operating in its normal no-load condition, but with no regulator. If the field resistance is suddenly changed by a small step, $\Delta R = (R_2 - R_1)$, the resulting terminal voltage transient is $E_o(t)$. The generator transfer function T_g', is the ratio of the Laplace transforms of these time functions,*

$$T_g' = \frac{E_o}{R}(s)$$

In order to derive the transfer function, we assume that no-load saturation curve of the generator is a straight line with slope K_s at the operating point. The following differential equation would be exact throughout the transient

$$E_o(t) = L_f\frac{di(t)}{dt} + R_s i(t) + I_1\Delta R \quad (3)$$

where

i = change of field current from the initial value
I_1 = initial shunt field current
L_f = incremental self inductance of the field circuit

But the saturation curve was assumed to be

$$E_1(t) = K_1 + K_s I_f(t) \quad (4)$$

so that

$$E_o(t) = K_s i(t) \quad (5)$$

From equations 3 and 5

$$-I_1\Delta R = \frac{L_f}{K_s}\frac{dE_o(t)}{dt} + \frac{E_o(t)}{K_s}(R_s - K_s) \quad (6)$$

* The same symbols will be used for time functions and their Laplace transforms with the appropriate variable (t or s) indicated at all times.

the Laplace transform of equation 6 is

$$-K_s\frac{I_1\Delta R}{s} = E_o(s)[sL_f + R_s - K_s] \quad (7)$$

or

$$E_o(s) = -\frac{\Delta R}{s}\left[\left(\frac{K_sI_1}{R_s - K_s}\right)\left(\frac{\frac{R_s - K_s}{L_f}}{s + \frac{R_s - K_s}{L_f}}\right)\right] \quad (8)$$

If ΔR is very small relative to $R_1 - K_s$, equation 8 becomes

$$E_o(s) = -\frac{\Delta R}{s}\left[\left(\frac{K_sI_1}{R_1 - K_s}\right)\left(\frac{\frac{R_1 - K_s}{L_f}}{s + \frac{(R_1 - K_s)}{L_f}}\right)\right] \quad (9)$$

This is the product of a driving function, $\Delta R/s$ and the transfer function of the generator, which can be written

$$T_g' = -K_g'\left(\frac{\alpha_g}{s + \alpha_g}\right) \quad (10)$$

where

$$\alpha_g = \frac{R_1 - K_s}{L_f}$$

and

$$K_g' = \frac{K_sI_1}{R_1 - K_s}$$

The transfer function given in equation 10 is, of course, independent of the input function provided it remains small.

It will be more convenient to consider the input to the generator as a voltage instead of a resistance. Rearranging equation 3, assuming

$\Delta R \ll R_1$

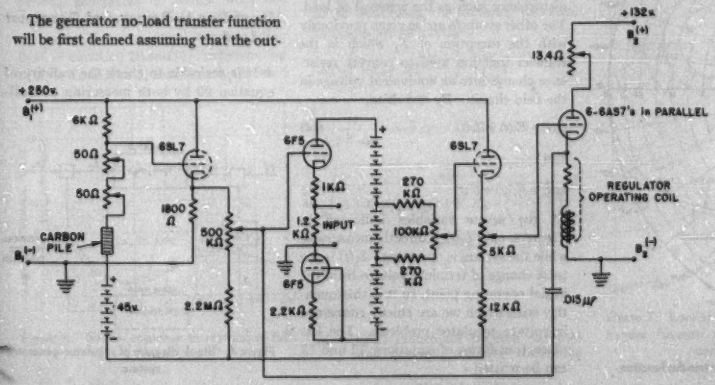

Figure 2. Schematic diagram of regulator test circuit

$$E_s(t) - I_1 \Delta R = L_f \frac{di(t)}{dt} + R_f i(t) \tag{3}$$

Then evidently $-I_1 \Delta R$ is equivalent to a voltage, $\mathcal{E}'$, impressed upon the field circuit of the generator. The second form of the transfer function is given by

$$T_g = \frac{E_o}{\mathcal{E}'}(s) = +K_g\left(\frac{\alpha_g}{s+\alpha_g}\right) \tag{11}$$

where

$$K_g = \frac{K_s}{R_1 - K_s}$$

E_o also affects the shunt field directly. This constitutes a minor feedback loop within the generator, but in no way invalidates the over-all transfer function.

Measurement of Generator Transfer Function

If the generator were truly a linear device, the measurement of its transfer function would be quite simple. It would only be necessary to introduce a step function change of resistance into the field circuit and measure the time constant of the resulting exponential rise of terminal voltage. Unfortunately, even small hysteresis in the magnetic circuit of the generator introduces large errors in the results obtained by such a test. In its place a method has been devised for introducing a sinusoidally varying resistance into the generator field circuit and for measuring the sinusoidal terminal voltage response. In a previous paper[1] an electronic circuit was described for measuring the transfer function of a carbon pile regulator. This circuit is reproduced in Figure 2. The same circuit may be utilized in the analysis here, but in addition, a special carbon pile regulator is required. A regulator was obtained in which the armature compresses two carbon piles instead of one. The two piles are electrically isolated from each other, and one is used in the electronic circuit as shown in Figure 2. When a sinusoidal signal is introduced into the electronic circuit both piles respond. The second may be used to introduce the sinusoidal resistance variation into the field of the d-c generator, and the transfer function is thus obtained easily by measuring the relative magnitude and phase of the voltages at the generator terminals and the grid of the first *6SL7* triode, Figure 2.

A typical result is shown in Figure 3. The transfer function is measured with constant generator output variation at all frequencies in order to assure that the iron in the magnetic circuit is operating around the same minor hysteresis loop for all measurements. The second curve, which is offered for comparison, is the transfer function of a simple time lag with inverse time constant $\alpha_g = 5.7$ and amplification $K_g = 1.5$.

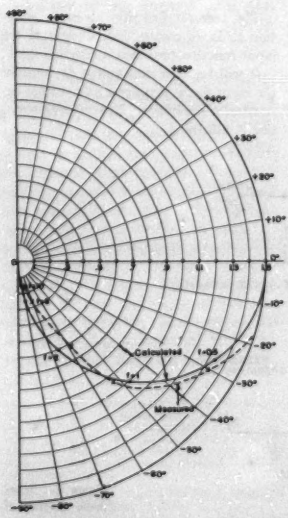

Figure 3. Generator transfer function

Analytical System Response

The system under study can be represented schematically by the block diagram of Figure 4. E_i and E_i' are voltages introduced into the generator armature and field circuit, respectively, due to some disturbance such as the removal of load. The other symbols are as given previously with the exception of T_f which is the transfer function used to convert resistance change into an equivalent voltage in the field circuit. By definition

$$\mathcal{E}_1(t) = E_i(t) + E_o(t) \tag{12}$$

and

$$\mathcal{E}_2(t) = E_i'(t) + \mathcal{E}'(t) \tag{13}$$

Of the seven variables indicated in Figure 4, only $\mathcal{E}_1(t)$ is directly measurable while the system is operating. $\mathcal{E}_1(t)$ is the total change of terminal voltage from the initial operating point, so it is this quantity with which we are chiefly concerned in voltage regulator problems. The Laplace transforms of equations 12 and 13 can be written

$$\mathcal{E}_1(s) = E_i(s) + E_o(s) \tag{14}$$

and

$$\mathcal{E}_2(s) = E_i'(s) + \mathcal{E}'(s) \tag{15}$$

Suppose for the moment that $E'_i = 0$. We get the additional equation

$$E_o(s) = \mathcal{E}_i(s).T_r.T_g.T_f \tag{16}$$

or

$$T_r.T_g.T_f = \frac{E_o}{\mathcal{E}_i}(s) \tag{17}$$

where $E_o/\mathcal{E}_1(s)$ is known as the loop transfer function. From equations 14, 16, and 17 we get the contribution to the terminal voltage variation due to E_i as the inverse transform of

$$E_i(s)\left(\frac{1}{1-\frac{E_o}{\mathcal{E}_i}(s)}\right)$$

Now suppose that $E_i = 0$ and E_i' is not zero. We know that

$$E_o(s) = T_g.\mathcal{E}_2(s) \tag{18}$$

$$\mathcal{E}'(s) = \mathcal{E}_i.T_r.T_f \tag{19}$$

From equations 14, 15, 18, and 19 we find that the contribution to the terminal voltage transient due to E_i' is given by the inverse transform of

$$E_i'(s)\left(\frac{T_g}{1-\frac{E_o}{\mathcal{E}_i}(s)}\right)$$

The transform of the total terminal voltage transient is

$$\mathcal{E}_1(s) = E_i'(s)\left(\frac{T_g}{1-\frac{E_o}{\mathcal{E}_i}(s)}\right) + E_i(s)\left(\frac{1}{1-\frac{E_o}{\mathcal{E}_i}(s)}\right) \tag{20}$$

Input Due to Removal of Generator Load

It is desirable to check the validity of equation 20 by both measuring and cal-

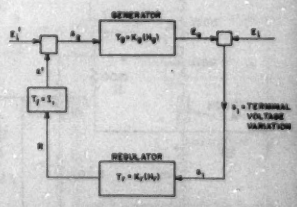

Figure 4. Block diagram of regulator-generator system

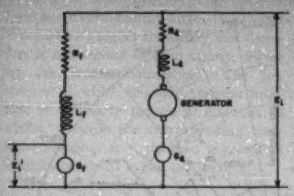

Figure 5. Voltages equivalent to removal of load

culating a transient response to a known input. Unfortunately, the input disturbances which can be applied to a system are not readily controlled independent variables. The simplest common input is the removal of load from the generator. If a good circuit breaker is used, the load drops linearly to zero. Nevertheless the equivalent input is complicated and consists of several superimposed voltages as follows:

1. The change of IR_a voltage drop which is linear with time while current is decreasing (R_a = armature resistance).

2. A step function voltage which is introduced in the armature circuit as a result of armature circuit self-inductance and mutual inductance with the shunt field. An equal but opposite step function occurs as the load current reaches zero.

3. A voltage due to the change of direct armature reaction and cross magnetizing of the pole face. This demagnetizing voltage is assumed to change linearly with load current and constitutes an input disturbance to the armature circuit.

4. A step function voltage is introduced into the field circuit due to the mutual inductance between the armature and field windings. When the load current reaches zero an equal but opposite step function results.

These voltages can be considered as perfect generators in series with the armature and shunt field circuits, (1), (2), and (3) being inputs corresponding to E_t of equation 20 and (4) corresponding to E_t'. In Figure 5, these are represented by G_a and G_f respectively. Figure 5 also indicates the quantities E_t and E_t' which correspond to those of Figure 4. By definition the voltage of G_f is E_t', but we must assume that the armature inductance and resistance are negligibly small with respect to the shunt field inductance and resistance before it is obvious that the voltage of G_a is E_t. In Appendix I a discussion is presented showing that the input voltages (3) and (4) above lead to equal and opposite terminal voltage responses and hence will be neglected.

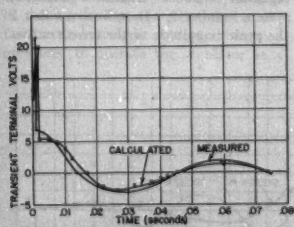

Figure 6. System response to removal of full load

Calculated and Measured Transients Compared

It was pointed out previously that the generator is nonlinear and that both amplification and time constant depend upon the incremental permeability of the magnetic circuit, hence upon the magnitude of the output signal. The transfer function of the generator is measured for a number of signal amplitudes and at a number of initial operating points it is seen that K_g and α_g vary between upper and lower limits. For an arbitrarily chosen generator which was tested, K_g varied between 1.50 and 2.00 and α_g varied between 4 and 9. The mean values then were $K_g = 1.75$ and $\alpha_g = 6.5$. The same condition existed when measuring the regulator transfer function, and an average yielded $K_r = 15$ and $\alpha_r = 65$.

Using these four constants, calculations have been made of the terminal voltage response to the removal of full load from the generator. It was assumed that a 75-ampere load was reduced linearly to zero in 0.002 second. The mean inductance and resistance of the generator armature were measured as 0.000373 henry and 0.1 ohm respectively. Using the inputs (1) and (2) discussed previously, and taking the inverse Laplace transform of equation 20 for both cases, the following two time functions are determined:

$$f_1(t) = \left[-L_a + M\left(\frac{M+L_a}{M+L_f}\right)\right]\frac{di_a}{dt} \times$$

$$\left[\frac{1}{1+K_rK_g} - K_rK_g \times \right.$$

$$\left. \frac{\alpha_r\alpha_g}{\sqrt{(1+K_rK_g)\alpha_r\alpha_g(1+K_rK_g) - \left(\frac{\alpha_r+\alpha_g}{2}\right)^2}} \times e^{-\alpha t}\sin(\beta t+\psi)\right] \quad (21)$$

where

M = mutual inductance between the field and armature circuits, where the armature circuit is taken to include compensating and commutating windings

L_a = armature inductance

i_a = load current

$$\alpha = \frac{\alpha_r+\alpha_g}{2}$$

$$\beta = \sqrt{\alpha_r\alpha_g(1+K_rK_g) - \left(\frac{\alpha_r+\alpha_g}{2}\right)^2}$$

$$\psi = \tan^{-1}\left(\frac{\beta}{\alpha}\right)$$

and

$$f_2(t) = -R_a\frac{di_a}{dt}\left\{\frac{K_rK_g(\alpha_r\alpha_g)}{\alpha_r\alpha_g(1+K_rK_g)^2} + \frac{t}{1+K_rK_g} - \frac{K_rK_g}{\beta(1+K_rK_g)}e^{-\alpha t}\sin(\beta t+2\psi)\right\} \quad (22)$$

The sum of two time functions is easily plotted. At time $t = 0.002$ when the load current reaches zero, the same quantity but with opposite sign is again introduced. The total value is shown plotted in Figure 6, and is seen to be substantially in agreement with the measured transient.

Frequency Spectrum Analysis

The function $\varepsilon_t/E_t(s)$ is called the error transfer function, and from it predictions

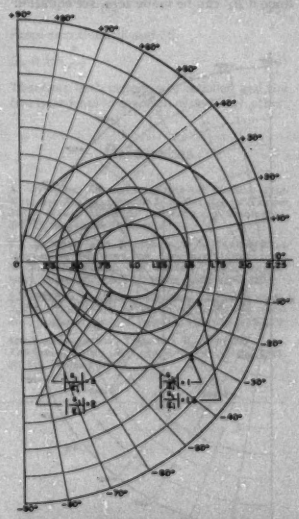

Figure 7. Loci of constant magnitude of error transfer function on loop transfer function complex plane

of system performance can be made qualitatively without laborious calculations. The absolute magnitude of the ideal error transfer function would of course equal zero for all frequencies, but this is never even approximately realized in practice. Typically, the magnitude of the error transfer function is very small at zero frequency, then rises to a resonance peak. At higher frequencies it then drops asymptotically to 1.0. In general, the error response to a transient disturbance will take the form of a damped sinusoid of frequency near that of the error transfer function resonance peak. The oscillation will be damped to a lesser degree the larger the magnitude of the resonance peak, so every effort is made to keep this peak as small as possible. In addition, however, the error transient depends upon the predominant frequencies in the input disturbance. The common inputs such as step functions and ramp functions have frequency components which drop off at least at $1/\omega$ or faster. It is therefore better in general to have a resonance peak occur at higher frequencies. Special considerations must be taken into account individually. For instance, mechanical vibration of frequency near the resonance peak must be avoided.

The error transfer function must be expressed in terms of the loop transfer function to be of great use. This can be done if E_t' can be made zero, see equation 20. However, E_t' and E_t are not truly independent of each other because of the mutual coupling between the armature and field circuits. We have previously shown a specific instance where the response due to E_t' was cancelled by the response due to that portion of E_t arising from the demagnetizing effect of armature current. These two transient responses virtually cancel each other even when $I_a(t)$ has a more general form, since equation 20 will always have a multiplying term $[s/(s+\alpha_p)-1]$ which is zero for all but extremely low frequencies. The steady-state values do not cancel each other of course. If E_t includes only those inputs due to $i_a r_a$ drops and self induction in the armature circuit, it is then seen that $\mathcal{E}_1/E_t(s)$ can be expressed in terms of the loop transfer function alone. The loop transfer function in turn is determined easily from the characteristics of the individual components of the control loop. Once the relationship between loop and error transfer functions is established it is no longer necessary to plot the error transfer function in order to analyze the system.

We therefore plot the loop transfer function on the complex plane which indicates its magnitude and phase shift at each frequency, Figure 9. Using equation 20, a magnitude and phase shift, Figures 7 and 8 respectively, of the error transfer function can be determined corresponding to every point on the loop transfer function complex plane. Typical constant magnitude loci are shown to be circles concentric about the $1+j0$ point. The radii of these circles are given by

$$r = \frac{1}{\left|\frac{\mathcal{E}_1}{E_t}\right|}$$

Typical constant phase shift loci are shown to be radii emanating from the $1+j0$ point. If Nyquist's[4] stability criterion is satisfied then the resonance peak of the error transfer function is determined solely by the point at which the loop transfer function approaches closest to the $1+j0$ point. Figure 9 shows the loop transfer function of two generator-regulator systems. These functions were calculated using equation 16 and experimental values of T_r and T_g. System number 1 in the figure is the generator-regulator system which was used for the preceding transient analysis. The frequency for which the curve most nearly approaches the critical point is 19 cycles. Noting the co-ordinates of this point and referring to Figure 7 this corresponds to an error transfer function magnitude of slightly less than 2.0. The transient response shown in Figure 6 is a damped sinusoid whose period is approximately 0.058 second. The reciprocal of the period is a frequency of about 17 cycles per second as would be expected. In Figure 9 and Figure 10 this system is compared with another which employed the same regulator with a different generator, system number 2. In system number 2 the peak magnitude of the error transfer

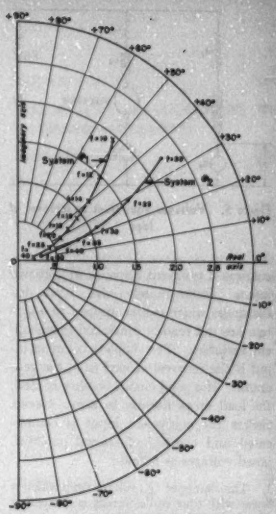

Figure 9. Loop transfer functions of generator-regulator systems

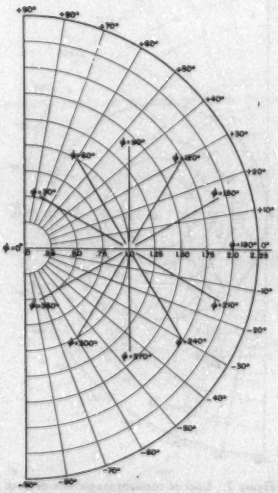

Figure 8 (left). Loci of constant phase of error transfer function on loop transfer function plane

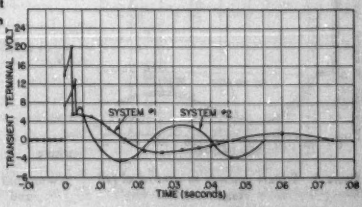

Figure 10 (right). Terminal voltage transients due to removal of load

function is considerably larger (2.87), but it occurs at a higher frequency and therefore is not excited to such a large degree by the input disturbance. The frequency at which the loop transfer function is closest to the $1+j0$ is about 34 cycles, whereas the corresponding transient response is a damped sinusoid of approximately 31 cycles per second.

Summary

The system consisting of a single generator and a carbon pile voltage regulator is a closed-loop regulating system of the proportional type. As such, its stability and dynamic characteristics can be analyzed by the standard theory of servomechanisms. It is, however, necessary to define the variable quantities very carefully as they are not easily recognizable or measurable. For this system it is convenient to utilize the concept of an error transfer function (defined in this paper) rather than to use the system transfer function common in servomechanism literature. When this is done the criteria for frequency spectrum analysis are altered somewhat, as discussed before.

The purpose of the foregoing analysis has been to simplify the problem of improving an existing regulator-generator system. A complete loop transfer function can be written in terms of the regulator and generator parameters. From this it can be seen by inspection whether a given system will be stable. For stable systems the effect of changing parameters can easily be determined by examining equations 2, 10, 21, and 22.

It is clear that the regulator characteristics alone do not determine the stability of the system. The generator and regulator characteristics must be considered together instead of separately. When the same regulator is used with two different generators, one system may be stable while the other is not. This can be due to the difference of the generator characteristics alone. However, it may be due to the fact that, in order to obtain the desired direct voltage, it has been necessary to operate the regulator at a different starting point. Hence, with a second generator the parameters of the regulator itself may have been effectively changed. Therefore, even though the d-c terminal voltage has been ignored in the foregoing analysis, it is important that it be considered in relation to the restrictions which it places upon a free choice of regulator and generator parameters.

The generator transfer function derived in this paper was for no load only. However, the extension to the case of load is possible by means of standard circuit analysis.

Appendix. Neglected Input Disturbances

In the calculation of transient response to the removal of full generator load two voltage inputs were neglected. These were (3) and (4) under the general discussion of inputs. The first of these is a ramp function, $E_a = K't$, impressed upon the armature circuit, and the time response is the corresponding inverse Laplace transform of equation 20. The second input is a step function introduced in the shunt field of the generator due to mutual inductance between armature and field windings; the corresponding time function is the inverse Laplace transform of equation 20.

The two terminal voltage transients will be equal and opposite if equations 23 and 24 are satisfied

$$\tan^{-1}\left(\frac{2\beta}{\alpha_r-\alpha_g}\right)+\tan^{-1}\left(\frac{2\beta}{\alpha_r+\alpha_g}\right)=2\tan^{-1}\left(\frac{2\beta}{\alpha_r+\alpha_g}\right) \quad (23)$$

where

$$\beta=\alpha_r\alpha_g(1+K_rK_p)-\left(\frac{\alpha_r+\alpha_g}{2}\right)^2$$

$$D_a=K_p\alpha_gM \quad (24)$$

where D_a is the rate of change of terminal voltage with armature current due to demagnetization effects, and M is the mutual inductance between armature and shunt field circuits.

Every effort is made to satisfy the criterion of equation 23 in the manufacture of voltage regulators; that is α_r is made much larger than α_g. In practical systems approximation, equation 23 is true to within about 4 degrees, which is negligible. Equation 24 can be shown to be true. Let us consider ϕ as a change from an initial reference value. Let e, i_f, and i_a be the corresponding changes from the initial values of terminal voltage, shunt field current, and load current, respectively. From equation 5 we can write

$$K_f=\frac{\partial e}{\partial i_f} \quad (25)$$

By definition

$$D_a=\frac{\partial e}{\partial i_a} \quad (26)$$

Therefore

$$D_a=K_p\frac{S\partial\phi}{\partial i_a} \quad (27)$$

where K_p = a constant of the generator and S is a constant generator speed.

But

$$\frac{\partial\phi}{\partial i_a}=\frac{M}{kN_f}=\frac{M}{L_f}\frac{\partial\phi}{\partial i_f} \quad (28)$$

where

N_f = number of turns in the field winding

k = a constant of proportionality between the field pole flux and the flux responsible for generated voltage

From equations 27 and 28

$$D_a=K_pS\frac{M}{L_f}\frac{\partial\phi}{\partial i_f} \quad (29)$$

Using equation 29 and the definitions of K_s and α_g given with equations 10 and 11,

$$D_a=MK_p\alpha_g\frac{K_pS\frac{\partial\phi}{\partial i_f}}{K_s} \quad (30)$$

From equations 25 and 30

$$D_a=MK_p\alpha_g \quad (24)$$

Therefore both criteria are satisfied and the two transients in question cancel each other.

References

1. Dynamic Characteristics of Carbon Pile Voltage Regulators, R. L. Mill. *Report Number* 3519, Naval Research Laboratory (Washington, D. C.), September 10, 1949.

2. Analysis and Redesign of a Carbon Pile Voltage Regulator for Aircraft Generators, W. B. Kouwenhoven, G. J. Thaler. *AIEE Transactions*, volume 67, part II, 1948, pages 1197–1203.

3. Theory of Servo Systems, A. L. Whiteley. *Journal*, Institution of Electrical Engineers (London, England), part II, August 1946, pages 353–73.

4. Regeneration Theory, H. Nyquist. *Bell Telephone System Monograph B-642* (New York, N. Y.), January 1932.

No Discussion

Electrical Instrumentation in Medical Research

J. MALVERN BENJAMIN, Jr.
ASSOCIATE AIEE

JOHN HALE
NONMEMBER AIEE

EDWIN L. CARSTENSEN
NONMEMBER AIEE

HOWARD E. TOMPKINS
ASSOCIATE AIEE

RECENTLY there has been a heartening trend in biological research toward closer collaboration between the physical and the biological sciences. This paper is a résumé of a collaborative program of this type which is being pursued at the University of Pennsylvania. In order that such a program be well balanced, research, education, and instrumentation are all required.

Work done in the field of electrocardiography may be cited as one example of research. (This work was carried out with the Robinette Foundation of the Hospital of the University of Pennsylvania.) In explanation of the distribution of potentials on the body surface, arising from heart action, an ingenious theory has evolved which is widely accepted. However, some of the fundamental postulates on which this theory is based are open to question. Chief among these is the assumption that for electrocardiographic purposes, the body behaves as a homogenous volume conductor. Through the years numerous attempts have been made to check this assumption both by measuring directly the resistivities of the various tissues within the body and by more indirect means. Investigators have reached widely-differing conclusions from their experiments so that there is still no definitive answer to the question. This past work has been reviewed and evaluated[1] and at present a series of experiments is underway which, it is hoped, will further clarify the subject.

The educational phase of the program has been conducted at both the formal and the informal levels. Courses have been given in radiologic physics, physics applied to physical medicine, electrical instrumentation for research workers in the biologic sciences, electricity applied to electrocardiography, and lectures on the physical aspects of radioactivity applied to medicine. So far, the education of the engineering personnel has been informal in nature, although formal courses for physical scientists interested in the biologic sciences are being contemplated. It is felt, however, that the informal type of education for both engineers and medical men has been of considerable value, and it is considered that one of the important justifications for the entire collaborative effort lies in the opportunity provided for education of this type.

The third phase of the program consists of the development of instruments for physiological measurements. These instruments are tools for basic research in the medical field; therefore the engineering which goes into their development is considered an integral part of the medical research program. The remainder of this paper will concern itself with a description of specific instruments which have been devised for this purpose.

In order to study experimentally the functioning of a complex electric circuit, it is necessary to measure certain of its basic quantities, such as voltage, current, and impedance. Similarly, in any physiological system there also are certain basic parameters whose behavior must be studied to gain an understanding of the over-all functioning of the system. In this connection, temperature, blood pressure, and volume rate of flow of blood are regarded as particularly important. Much time has therefore been spent on the development of devices to measure these quantities.

In developing any measuring device, it is of prime importance that introduction of the device into the system shall not excessively alter the quantity to be measured. In biological work, this requirement is much harder to meet than in most of our physical instrumentation because the variables are very closely interrelated. Thus it is extremely difficult not to alter the normal behavior of the system when the measuring device is introduced. Furthermore, this complexity makes it difficult to trace the effect of altering one of the variables. For example, suppose the temperature of the skin is to be measured by means of a thermocouple. The direct approach would be to fasten the thermocouple securely to the skin. The fastening however, may exert pressure on the blood capillaries under the skin, interfere with blood flow, and so disturb the skin temperature. The fastening is also likely to interfere with sweating by stopping air circulation over the area covered leading once again to an alteration of the skin temperature it is desired to measure.

Temperature Measurement*

In measurement of body and skin temperature both thermistors and thermocouples have been used. Electrically, the thermistor is more convenient than the thermocouple for the following reasons:

1. A thermistor has a much higher impedance than a thermocouple (usually several thousand ohms as compared to a few ohms). Hence lead resistances and

Paper 50-209, recommended by the AIEE Therapeutics Committee and approved by the AIEE Technical Program Committee for presentation at the AIEE Middle Eastern District Meeting, Baltimore, Md., October 3–5, 1950. Manuscript submitted February 23, 1950; made available for printing August 14, 1950.

J. MALVERN BENJAMIN, JR. is with the Franklin X-Ray Company, Philadelphia, Pa., and JOHN HALE, EDWIN L. CARSTENSEN and HOWARD E. TOMPKINS are all staff members with the Moore School of Electrical Engineering, University of Pennsylvania, Philadelphia, Pa.

The authors would like to express their appreciation to Dr. Stephen M. Horvath, Dr. H. C. Bazett, and Dr. L. H. Peterson of the School of Medicine of the University of Pennsylvania and to Dr. S. Reid Warren, Jr., and Mr. Ralph Saunders of the Moore School of Electrical Engineering for their continuous help, interest, and suggestions.

* This work was aided by a grant from the National Foundation for Infantile Paralysis.

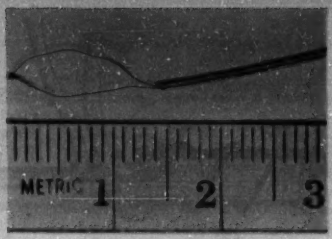

Figure 1 (left). Bottom view of skin temperature measuring device with thermistor mounted at apex of lucite cone

Figure 2 (right). Thermistor assembly for use in measurement of deep tissue temperatures. To complete the assembly the wires are pulled back through the tubing until only the thermistor head protrudes

switch contact resistances are unimportant and it is not necessary to take special precautions in the wiring of associated circuits.

2. Because of its high temperature coefficient (−3 per cent per degree centigrade), a thermistor is approximately ten times as sensitive as a thermocouple when circuits with indicating devices of the same sensitivity are used for the comparison.

3. In a thermistor circuit it is not necessary to maintain a constant reference temperature.

4. Since the thermistor detects a change in temperature as a change in resistance, it may be incorporated in an a-c bridge whose unbalance may be amplified with an a-c amplifier before measurements. The thermocouple, however can produce only a direct voltage, and the d-c amplification required is difficult to achieve.

The thermocouple, however, has two distinct advantages over the thermistor:

1. It can be made smaller.

2. Its output voltage is approximately a linear function of temperature, whereas the thermistor is quite nonlinear.

In skin temperature measurement, the problems mentioned earlier have been considered in the design of the device shown in Figure 1. This particular unit contains a thermistor as the active element although the housing* is equally adaptable to a thermocouple. Because the thermistor itself is very small, 0.016 inch (Western Electric Company, type *V597*) it causes a minimum of interference with sweating when placed in contact with the skin. The housing is supported by the skin approximately one inch from the point at which temperature is to be measured. By adjusting the springs that hold the core to the outside ring, any desired degree of pressure may be obtained.

In another instrument using a radiation thermopile the influence of the measuring device on skin temperature has been reduced further. Such a unit has been combined with a direct-reading self-calibrating potentiometer to form an instrument that is capable of close measurements of skin temperature but which eliminates the necessity of physical contact with the body.

The thermistor also has been adapted to the measurement of temperature within the body.[3] Figure 2 shows a fine tube of polyvinyl chloride (outside diameter, 0.020 inch) with a *V597* thermistor mounted at its end. This tube is fine enough to be slid into a reasonably small (number 19) hypodermic needle. In use, the needle with the thermistor inside it is first introduced into the desired position. The needle is then withdrawn over the thermistor tubing leaving the thermistor exposed to the tissue.

A thermistor has also been incorporated in a device used to measure rectal temperature. If only a single determination of rectal temperature is required, a thermometer is the simplest solution to the problem. However, it is often required to continuously record rectal as well as other temperatures over a period of time and for this purpose both the thermocouple and the thermistor seem well suited.

The thermistor is thus seen to afford a simple and convenient means of measuring temperatures wherever it can be used. However, there are still some situations in which it cannot be used because of its size. For example, as a possible aid in the diagnosis and study of arthritis it would be useful to know the temperature of finger joints. For this purpose one must use the smallest clinically acceptable hypodermic needle to introduce the measuring device into the joint space. A number 25 hypodermic needle is considered to be the best compromise between size and mechanical strength. This has an inside diameter of approximately 0.009 inch, while the smallest commercially available thermistor, it will be recalled, has a diameter of about 0.016 inch, not including the necessary insulation and protective housing. So for this application a thermocouple is required.

A diagrammatic explanation of the thermocouple that was developed for this work is shown in Figure 3. It has been possible to make a thermocouple approximately 0.0037 inch diameter (one and a half times the diameter of a human hair) by use of a concentric layer construction. Its core consists of a 0.001-inch diameter enameled constantan wire from which the enamel is removed at one end leaving an exposed tip of constantan about 1/32-inch long. A thin layer of silver is deposited over the front half of the wire, making contact with the bare constantan at the end. This contact forms the measuring junction. Other constructional details are indicated in Figure 3. The reference junction at the back end of the thermocouple is placed in a small bottle filled with ice and water to form the cold junction, and finally two copper lead wires are brought out from the assembly to be connected to a recording potentiometer.

Since the thermocouple is very fine it is quite fragile and the special arrangement required to hold the ice bottle and the insertion needle in the proper positions with respect to the couple, is shown in Figure 4.

For possible use in measuring the temperature of the blood in capillaries, a unit of similar construction to the one just described, but having an over-all outside diameter of 0.0015 inch instead of 0.0037 inch, has also been constructed. However, this unit is extremely fragile.

Blood-Pressure Measurement

Blood pressure is conventionally measured by wrapping a rubber cuff around the arm and determining the minimum pressure required to stop flow. This indirect procedure yields information of considerable clinical value. However, much more detailed information may be obtained concerning the functioning of various parts of the blood circulating system by directly measuring the pressure

* The housing is a refinement of a commercial unit developed by the Revere Corporation of America, Wallingford, Conn.

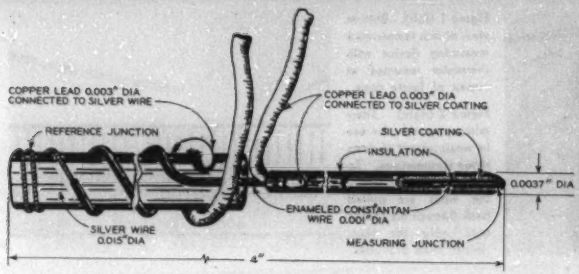

Figure 3. Diagrammatic explanation of construction of fine wire silver-constantan thermocouple

of the blood within the heart and the blood vessels. An instrument[3,4] to perform this measurement was recently developed at the University of Pennsylvania through the joint efforts of the Johnson Foundation for Medical Physics, the Department of Physiology of the Medical School, and the Moore School of Electrical Engineering. This work was performed under a contract with the Office of Naval Research.

A plastic tube, called a catheter, is introduced through a hypodermic needle into the vessel under study. The instrument end of the catheter is led to a small chamber, one wall of which is a thin metal membrane. This movable membrane is spaced a short distance from a fixed metal plate, thus forming a capacitance. Small movements of the membrane, with respect to the fixed plate, are measured electrically as changes in this capacitance. The chamber and tube are filled with saline solution so that blood will not clot in the system. Pressure changes at the end of the tube in the blood vessel are transmitted by the liquid back to the movable membrane. The varying membrane capacitance is part of one leg of a high-frequency bridge whose degree of unbalance is a measure of change in capacitance, hence of change in pressure. This unbalance voltage, after amplification and detection, drives a Brush recording oscillograph, thus producing a graphical record of blood pressure against time.

The sensitivity of the device may be expressed in various ways. At maximum sensitivity a pressure change of 1 millimeter of mercury causes an output voltage change of 0.6 volt across a 1,500-ohm load.

An alternative expression of sensitivity is in terms of the volume of the fluid which must be supplied to produce a given output. The stiffness of the diaphragm is such that 10^{-7} milliliters of fluid enters the chamber for a pressure change of one millimeter of mercury. Hence the overall volume sensitivity is about 1.7×10^{-6} milliliters per volt. This small volume displacement results in good reproduction of fast transient wave shapes even when very small tubing is used between the source of pressure and the capacitance chamber.

Finally, the sensitivity may be expressed in terms of the capacitance variation. A figure of approximately 0.02 micromicrofarad per volt of output is typical.

Blood-Flow Measurement*

Blood flow is conventionally measured by one of two possible procedures. One is to measure the flow through a single vessel. The other approach, applicable to measurements on extremities, is to measure the total volume of blood flowing through a complete body member. This latter technique is known as plethysmography.

Let us suppose it is desired to measure the rate of blood flow into the hand. The hand is sealed into an air-tight chamber. A rubber cuff similar to the type used for measuring blood pressure is wrapped around the wrist. The cuff is inflated just enough to stop the blood flow through the veins leaving the hand, but not enough to retard arterial blood flow into the hand. The resultant rate of swelling will also increase the pressure inside the air-tight chamber to which a pressure recording device is connected. Thus, the rate of blood flow into the hand can be indirectly measured. The device is calibrated by introducing a known amount of liquid into the air-tight chamber.

A number of theoretical and practical objections to the technique of plethysmography can be raised.

The temperature change resulting from the introduction of the hand into the air-tight chamber causes a pressure change which may be of the same order of magnitude as the blood-flow pressure change to be measured. Also conventional plethysmographs are made of metal, and there may be measurable heat transfer through the walls of the device.

The air-tight chamber is usually connected to the pressure measuring device through a long rubber tube in which air is employed as the transmitting fluid. This introduces an unnecessarily long and possibly variable time constant into the system. Furthermore, the pressure is measured with a lever system actuated by a stretched rubber diaphragm. The power from the diaphragm is used directly to drive a pen across a piece of smoked paper or to cause a mirror deflection. Either system introduces mechanical uncertainty into the system and the pen drive takes appreciable power as well.

The sealing of the hand into the air-tight chamber is conventionally effected by passing the hand through a slit in a small rubber sheet. The sheet is then glued to the wrist. However, the pressure of the rubber on the arm restricts blood flow by an unknown and uncontrollable amount. It is difficult to make this seal truly air-tight. And, finally, because of the flexibility of the rubber, slight movements of the arm can be transmitted through the membrane to cause false readings.

Nevertheless, medical research men feel that information of clinical value can

Figure 4. Complete fine wire thermocouple assembly with insertion needle and ice water bath

Hypodermic needle is attached to sliding crossbar with semicircular cutout. The crossbar is locked in forward position for insertion, then withdrawn to allow fine thermocouple to contact surrounding tissue. A double exposure has been made to show the crossbar and needle in forward and withdrawn positions

* This work was aided by a grant from the National Foundation for Infantile Paralysis.

be obtained by plethysmography. Therefore, a plethysmograph was designed to eliminate as many of these objections as possible.

Temperature drift is compensated for by placing a thermistor in the chamber and using its output to buck out a portion of the signal from the pressure measuring transducer. The device is built of Plexiglass, with low heat conductivity to minimize heat transfer through the walls, and it incorporates large removable ground glass plugs so that the hand may have normal air circulation around it until immediately before the test.

Pressure change is measured by a differential transformer used as an electromechanical transducer. The movable iron slug of the transformer is connected directly to a diaphragm placed in a wall of the air-tight chamber. The electrical signal is amplified to drive a Brush recorder. This arrangement has the advantages of ruggedness, high sensitivity, and a small time constant.

Finally, the rubber arm seal is replaced by a cloth impregnated with paraffin. This seal can be made air-tight more easily; it is easy to attach; applies minimum constricting force to the wrist, and when hard it becomes stiff enough to keep small body motions from being transmitted to the measuring chamber.

In addition to the instruments just described, several others have been designed to perform more highly specialized functions. For example, a device has been developed to aid in the diagnosis of certain anatomical abnormalities occurring in the cardiovascular system. A part of the diagnostic procedure in such cases consists of taking X-ray pictures of the affected area. In order to show the contour of the heart or vessel wall, a small amount of a dye opaque to X-rays is injected into the blood stream. When the blood containing the dye reaches the general region to be studied, a series of pictures is taken to show the blood at successive points as it flows through the blood vessels in the area. The vessels then show up in sharp contrast to the surrounding tissue. If, for example, there should be an abnormal opening between two chambers of the heart, it will be made apparent in the X-ray film by the shadow of the opaque blood flowing through it.

To make use of this technique a device is necessary which will rapidly move an X-ray plate (cassette) into place, take a picture, move the exposed cassette out of the way, and move another unexposed cassette into position. The device developed for this purpose will handle seven cassettes, changing them at the rate of two per second. A timing device, however, allows exposures to be made with any desired interval of time between each successive exposure from one second to 30 seconds. This feature is necessary to allow the blood to reach the regions under investigation before any pictures are taken.

Work on several other interesting problems in this field is in progress but, unfortunately, none are yet at a stage that warrants description. However, the few devices discussed seem to bear witness to a heartening new trend in science; the drawing together of the physical and biological sciences for collaborative investigation of the enormously complex mechanisms of the body in the hope that these sciences working together may be able to unravel mysteries that have thus far withstood the attacks of each science working alone.

References

1. The Electrical Conductivity of Living Tissues, J. M. Benjamin, Jr. H. Schwan, C. F. Kay, J. H. Hafkenschiel. *Circulation*, (New York, N. Y.), September 1950, page 321.

2. Temperature Measurement Inside the Body Using a Thermistor, J. M. Benjamin, Jr., S. M. Horvath. *Science* (Washington, D. C.), June 10, 1949, page 592.

3. A New Capacitance-Blood-Pressure-Manometer Amplifier, H. E. Tompkins. *American Heart Journal*, (St. Louis, Mo.) April 1949, page 783.

4. A Variable Capacitor for Measurements of Pressure and Mechanical Displacements: A Theoretical Analysis and Its Experimental Evaluation. J. G. Lilly, V. Legallais, R. Cherry. *Journal of Applied Physics* (Lancaster, Pa.) July 1947, pages 613–28.

No Discussion

Automatic Feathering—To Reduce the Hazard of Aircraft Engine Failure at Take-off

WILFRED L. KERSHAW
ASSOCIATE AIEE

FAILURE of an aircraft engine in flight changes the propeller of that engine from a source of thrust to a parasitic source of drag. Present-day propellers, selected for the efficiency with which they convert tremendous horsepower into thrust with comparatively small blade area, absorb proportionately high horsepower when windmilling the engine. The propeller used on the Martin model 202 airplanes converts a maximum of 2 400 horsepower into thrust at take-off. The same engine and propeller combination exerts a drag equivalent to approximately 220 horsepower when being windmilled at take-off airspeed. In contrast, the drag of the propeller feathered is equivalent to 12 horsepower. Thus, it is evident that in the event of an engine failure, in addition to the immediate loss of half the thrust, a windmilling propeller steals approximately 10 per cent of the horsepower available from the remaining engine, reducing the net thrust to approximately 45 per cent of normal. With one propeller producing drag and the other producing thrust, a turning moment exists, tending to turn the airplane in the direction of the faulty engine.

Take-off is in some ways the most critical part of a normal flight. With most of the runway used, the airplane is normally gaining both speed and altitude, but has too little of either to permit any immediate landing maneuver. It is at this time that the pilot depends most on an uninterrupted flow of power from the engines. Of the multiplicity of instruments which confront the pilot, there may be none which will immediately and reliably tell him that one engine has ceased to deliver its share of thrust. Changes in directional and lateral trim are often the best indication of the trouble. Well-trained pilots generally diagnose the meager symptoms correctly, but the possibility of human error is definitely aggravated by the atmosphere of emergency resulting from engine failure during take-off. The proximity of the ground leaves no opportunity for recovery if the pilot feathers the propeller of the good engine. Such mistakes have occurred with disastrous results.

The automatic propeller feathering system described in this paper was designed to initiate the propeller feathering cycle soon enough after engine failure to limit propeller drag to that of a feathered propeller, thus providing the maximum possible thrust for the remainder of the take-off and the landing approach to follow. Automatic feathering allows the pilot to devote his full attention to trimming the airplane, completing the take-off, and planning the best approach procedure. Electrically, the automatic feathering system prevents the pilot from feathering the propeller of the good engine. The system to be described was designed for a 2-engine airplane and is based on 2-engine premises. Although the critical need for automatic feathering decreases as the number of engines increases, the device is capable of improving the reliability of all multiengine aircraft.

Performance

If, after an engine power failure, the propeller feathering sequence is started while the propeller is rotating faster than windmilling speed, and the propeller pitch is advanced rapidly enough so that actual rpm is maintained above windmilling rpm throughout the feathering cycle, part of the kinetic energy of the whirling engine and propeller can be converted into thrust to reduce the propeller drag during the feathering cycle to less than that of a feathered propeller. It has been determined experimentally on the Martin model 202 airplane that, if the feathering cycle is initiated within 2 seconds after an abrupt loss of power, the propeller drag during the complete feathering cycle, starting at the instant of engine failure, will be less than that of a feathered propeller. If feathering is delayed, 2.4 seconds after an abrupt engine failure, the windmilling propeller will start to produce drag, which will rapidly increase to full windmilling drag. Under the stress created by an engine failure during take-off, an average pilot requires 5 seconds or longer to initiate propeller feathering manually. After feathering has been initiated belatedly, the propeller will continue to produce a drag greater than that of a feathered propeller until the windmilling rpm corresponding to the changing propeller pitch is sufficiently less than actual rpm. Automatic feathering completely eliminates the time span during which the propeller drag exceeds that of a feathered propeller. This advantage of automatic over-manual feathering may well determine whether or not the take-off will be successfully completed.

Figure 1 shows a time history of an automatic feathering cycle recorded in flight at an indicated air speed of 120 miles per hour, at 100 feet altitude. One plot shows propeller rpm versus time.

Paper 50-210, recommended by the AIEE Air Transportation Committee and approved by the AIEE Technical Program Committee for presentation at the AIEE Middle Eastern District Meeting, Baltimore, Md., October 3–5, 1950. Manuscript submitted July 3, 1950; made available for printing August 17, 1950.

WILFRED L. KERSHAW is with The Glenn L. Martin Company, Baltimore, Md.

The author gratefully acknowledges the assistance of R. A. Engelhardt and other associates during the preparation of this paper. The views expressed in this paper are those of the author and not of The Glenn L. Martin Company.

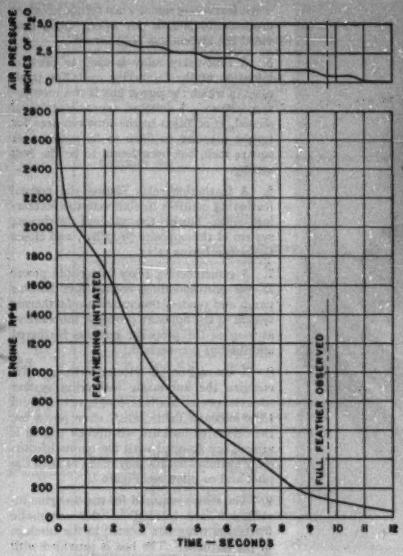

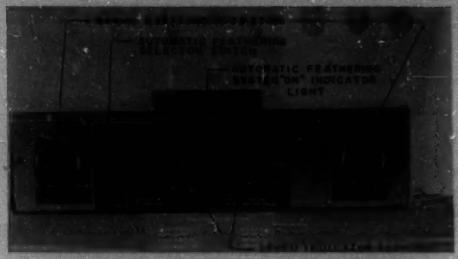

Figure 1 (left). Time history of an automatic feathering operation in flight. Indicated airspeed 120 miles per hour, altitude 100 feet. The air-pressure curve shows the impact pressure in excess of that due to airspeed, measured aft of the feathering propeller

Figure 3 (above). Propeller control panel, showing the manual feathering switches, the automatic feathering selector switch, and indicator lights

The time required to feather the propeller was 9.7 seconds, including 1.7 seconds before initiation of the feathering cycle. The feathering initiation and full feather indications were obtained electrically. The second plot shows the impact pressure in excess of that caused by airspeed measured by a pressure rake installed just aft of the propeller. The latter curve shows that the propeller did not create drag while it was being feathered.

Sensing Engine Failure

Engine torque is used as the means of determining the need to feather a propeller. This method is applicable to any engine equipped with a torque nose; that is, where the propeller gearing is so arranged that the full engine torque is transmitted through a ring gear which is prevented from rotating by a series of pistons working in oil-filled cylinders. The oil pressure thus developed, called torque pressure, can be measured at an outlet provided on the propeller gear case at the forward end of the engine. The automatic feathering system is so arranged that when it is turned on and when normal take-off engine torque is expected, the propeller will be feathered if engine torque drops below a preset value.

Engine rpm cannot be used to indicate failure, because the windmilling rpm of the engine at take-off airspeed is within the range of rpm which might be obtained with a faulty propeller governor. Even though engine rpm is lowered by a faulty propeller governor, the engine would continue to deliver power and feathering would be undesirable.

Manifold pressure is likewise of no use as a failure sensing means, since it is proportional to engine rpm and throttle setting, and does not depend on the actual firing of the cylinders and development of power.

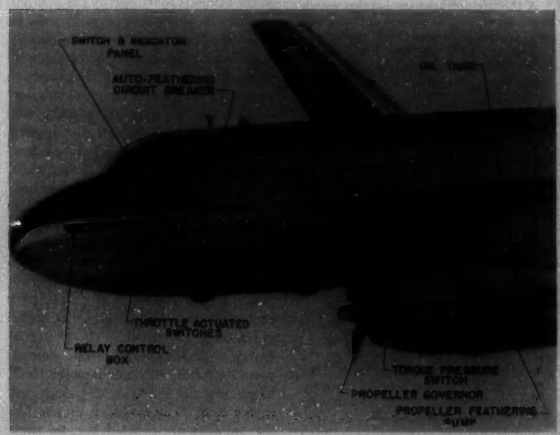

Figure 2. Phantom view of the airplane with the location of the major components of the automatic feathering system shown

Automatic Feathering System Design

The automatic feathering system used on the Martin model 202 airplanes was designed on the following premises:

1. The propeller of the engine should be feathered if, after an indication has been obtained that the engine is operating at

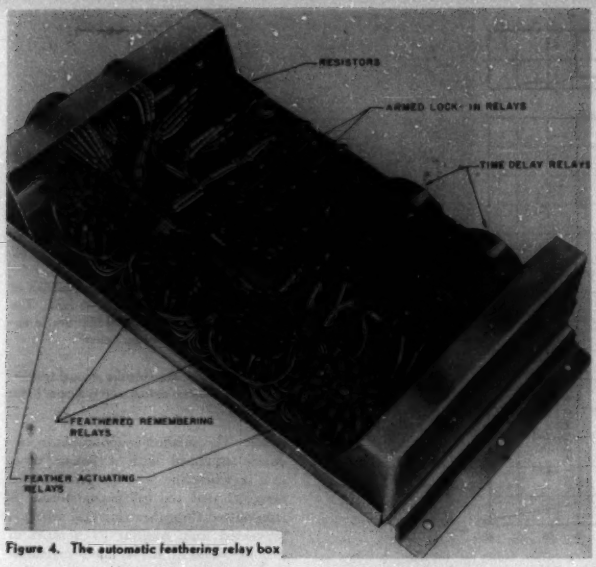

Figure 4. The automatic feathering relay box

take-off power and no change in engine controls has been made which would reduce engine power, it is determined that engine power has dropped below some prescribed minimum value and has remained below that minimum value longer than would be caused by a momentary engine cough or sputter.

2. The manual feathering system of one propeller should be rendered inoperative while the other propeller is being feathered automatically in order to eliminate the possibility of pilot error.

3. The automatic feature should be so designed that no component of the normal propeller feathering system need be redesigned.

4. A failure of the automatic feathering system should not interfere with the operation of the normal feathering system.

5. The pilot should be able to override the automatic system to unfeather the propeller if power is regained after feathering has started.

6. The automatic feathering system of the second propeller should be rendered inoperative after one propeller has been feathered either manually or automatically.

7. The automatic feathering system must not create any hazard or limitation during any feathering operation.

The following description of components of the automatic feathering system applies to the Martin model *202* airplane with Pratt and Whitney *R-2800* series engines and Hamilton standard propellers. In general, the system is applicable to any multiengine airplane equipped with engines each having a torque nose and propellers capable of being feathered.

The automatic feathering system, shown schematically in Figure 2, has four functions: arming, initiating, feathering, and remembering. They are performed as follows:

1. A throttle-operated snap-action switch, located in the engine control pedestal, provided to accomplish part of the arming function, indicates that the throttle is advanced to a position corresponding to low take-off power.

2. A high torque pressure switch, mounted directly on the engine, completes the arming signal when engine torque pressure exceeds 80 pounds per square inch (corresponding to 1,130 horsepower at 2,220 rpm), indicating the engine has achieved take-off power. The purpose of this switch is to preclude the possibility of inadvertent feathering during a throttle burst or during engine starting, at which time the throttle switch might be closed while torque pressure would be less than the setting of the low-torque pressure switch to be described later.

3. An arming relay is provided to maintain the armed signal as long as the throttle switch is closed, regardless of later torque pressure decrease below the initial arming value of 80 pounds per square inch. The system can be disarmed only by retarding the throttle to open the throttle switch or by turning automatic feathering off.

4. A low-torque pressure switch, mounted with the high-torque pressure switch on the engine torque nose, completes the automatic feathering signal when torque pressure drops to 30 pounds per square inch, provided the system has been armed.

5. A time-delay relay is used to prevent initiation of the feathering cycle for those cases in which the power loss is of a momentary nature. A delay of approximately 0.2 second, in addition to the time required for torque pressure to drop to 30 pounds per square inch, has been found to be the best setting.

6. A feathering relay shunts the normal feathering controls to complete the feathering cycle, blocks the manual feathering system of the opposite propeller, and closes the remembering relay.

7. A remembering relay interrupts power to the corresponding engine fuel booster pump and renders the automatic feathering system of the opposite propeller inoperative as long as the propeller remains feathered and the bus is energized.

8. A manual on-off selector switch, to deenergize the automatic feathering system when its protection is no longer needed, and three indicator lights, one to show power on, the others to indicate when each engine is armed, are grouped with the manual feathering switches within easy reach of both the pilot and co-pilot, see Figure 3.

9. The relays required for the 2-engine installation are located in the automatic feathering relay box located in the fuselage of the airplane. The box is provided with Cannon-type quick disconnects to facilitate testing and replacement, see Figure 4.

The Automatic Feathering Circuit

Figure 5 shows the complete automatic feathering circuit and the manual feathering and unfeathering circuits of the Hamilton Standard hydromatic propeller. In this variable pitch propeller, the pitch of the blades is controlled by the position of a piston, within the propeller hub, to which the blades are geared. In normal operation the position of the piston, and hence the propeller pitch, is controlled by a governor and valving arrangement using oil at moderate pressure provided by an engine-driven, small capacity pump, which is an integral part of the governor. To produce rapid pitch change while feathering and unfeathering the propeller, an electric motor driven pump of greater capacity, working at much higher pressure, is used, and the normal governor operation is by-passed.

The legend of Figure 5 will be used to designate the various relays and relay contacts in the following description of the operation of the circuit. The circuit is drawn with the propellers in normal operating pitch, throttles retarded, and torque pressure less than 30 pounds per square inch. The reversing circuits for the propeller are omitted because they have no effect on the operation of the automatic feathering system. The opera-

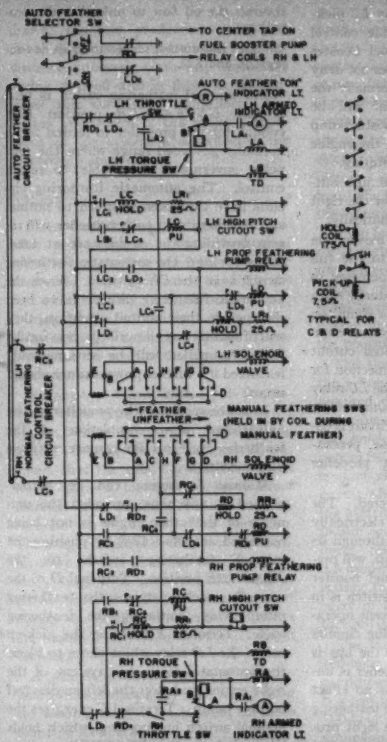

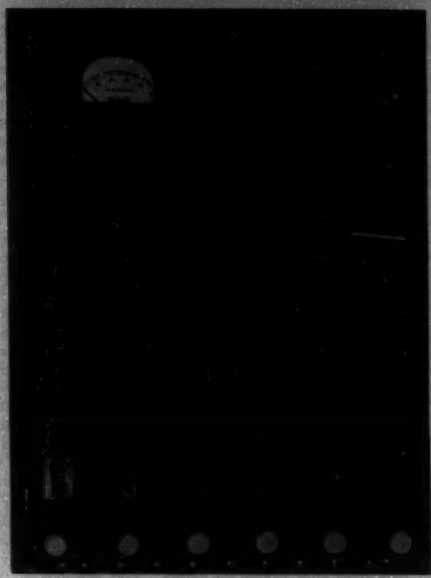

Figure 5 (left). The automatic feathering circuit showing connections to the manual feathering and unfeathering circuits

LA, RA—left or right arming relay. *LB, RB*—left or right time delay relay. *LC, RC*—left or right feathering relay. *LD, RD*—left or right remembering relay. *PU*—pick-up coil. *TD*—time delay coil. LR_1—left resistor number one (typical)

Figure 7 (above). Bench test panel to simulate flight operation of the automatic feathering relay panel

tion of the left engine circuits will be described.

With the selector switch off, all connections from the bus to the automatic feathering system are open and the engine fuel booster pump control relays are grounded through the selector switch. When the selector switch is placed in the *ON* position, the left fuel booster relay is grounded through normally-closed relay

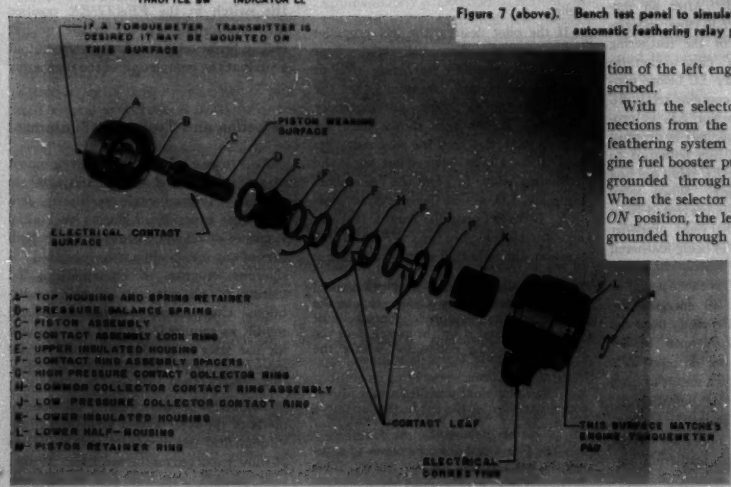

Figure 6. Exploded view of the piston-type torque pressure switch

contacts LD_3, and power is available to the left throttle switch.

When the left throttle is advanced to a position corresponding to low take-off power, the left throttle switch closes, completing the circuit to contact *C* on the torque pressure switch. Note that even though the torque pressure switch is in the low-pressure position, no circuit is available to close the time delay relay *LB* to initiate the feathering cycle. As torque pressure rises to 80 pounds per square inch, the torque pressure switch closes on contacts *A* and *C*. The arming relay, *LA*, closes and is electrically locked in by its own contacts. This condition is indicated by the left armed indicator light. The purpose of the LA_1 relay contacts is to prevent an improper armed indication if some circuit element should present a resistance high enough to prevent relay *LA* from closing. The circuit is now armed and will feather the propeller if torque pressure should drop below 30 pounds per square inch. The circuit can be disarmed by opening the left throttle switch (by retarding the throttle) or by switching the selector switch to *OFF*.

Assuming the circuit is armed, if torque pressure drops to 50 pounds per square inch, the torque pressure switch will assume some intermediate position, opening the connection between its contacts *A* and *C*, but the circuit will remain in the armed condition. If torque pressure drops to 30 pounds per square inch, the torque pressure switch will close on contacts *A* and *B*, energizing the coil of the time delay relay, *LB*. After an 0.2-second delay, contacts LB_1 close, energizing the pick-up coil of the feathering relay, *LC*. Contacts LC_1 close to energize the holding coil of relay *LC* before contacts LC_4 open to de-energize relay *LC* pick-up coil. The resistor LR_1 is provided so that the *LC* relay may be dropped out by application of bus potential to the ground side of the *LC* relay holding coil during unfeathering. When relay *LC* picks up, the pilot is prevented from manually feathering the right propeller while the left propeller is being feathered automatically, and the pick-up coil of the remembering relay, *LD*, is energized.

Contacts LD_1 close to energize the holding coil of relay *LD* directly from the bus before contacts LD_4 open to de-energize the pick-up coil of relay *LD*. The resistor LR_2 provides a means to drop out the *LD* relay during unfeathering. Operation of relay *LD* starts the feathering pump, blocks the operation of the right engine automatic feathering circuits, de-energizes the arming circuit of the left propeller and the relay *LC* pick-up coil circuit, and opens the control circuit to the left engine fuel booster pump. This last operation does not deny fuel to the left engine since normally the left engine-driven fuel pump will be operating. Rather, the fuel booster pump is stopped to prevent loading the engine with fuel as the engine stops rotating.

With the circuit conditions just outlined, it is impossible to feather the right propeller manually or automatically.

As the feathering pump moves the blades of the left propeller to the full feathered stop, oil pressure increases to the value necessary to momentarily open the high pitch cutout switch (a Hamilton Standard manual feathering system component). While the high pitch cutout switch is open, the ground connection for the *LC* relay is removed and the *LC* relay drops out. The feathering pump stops, and the *LD* relay pick-up coil circuit is de-energized. Contacts LC_3 close, permitting operation of the right propeller *manual* feathering circuit.

The left propeller is feathered. The left remembering relay, *LD*, electrically locked in by the connection through its own contacts directly to the bus, will prevent operation of the left fuel booster pump as long as the selector switch is in the *ON* position, and will prevent operation of the automatic feathering circuits of either propeller as long as the bus is energized, unless the left propeller is unfeathered. The *LD* relay has no effect on the operation of the manual feathering or unfeathering circuits of the right propeller.

If the pilot desires, the left propeller can be unfeathered manually at any time during the automatic feathering cycle or after its completion. Assuming that the left propeller is being automatically feathered, it has been shown that the arming relay, *LA*, and the time delay relay, *LB*, have been dropped out, while the feathering relay, *LC*, and the remembering relay, *LD*, are in the energized position. If the left propeller manual feathering switch is pulled to the *UNFEATHER* position, the following events take place:

1. Terminals *D*, *G*, and *H* of the manual switch are energized by a connection to the bus through the left propeller control circuit breaker, terminal *A* on the switch, and the common switching connection within the manual switch.

2. The *D* terminal provides a new, direct source of power for the left feathering pump relay.

3. The *G* terminal provides power to actuate the left propeller solenoid valve. This valve, located on the propeller governor, reverses the oil flow to unfeather the propeller.

4. The *H* terminal serves to drop out relays *LC* and *LD*.

The manual feathering switch is held in the *UNFEATHER* position long enough for the propeller to return to its normally governed range where the propeller governor is then able to regain control. The automatic feathering circuits have thus been returned to normal and the circuits for each propeller will rearm providing the engines are at take-off power and the automatic feathering switch is in the *ON* position. Since the automatic feathering circuits have been returned to their normal condition, they will function as described previously. Either propeller will be automatically feathered if a further power failure should occur.

It can be seen that the propeller can be unfeathered after completion of the feathering cycle in a like manner, with the same results.

Manual feathering can be accomplished at any time, provided the propeller of the other engine is not being feathered automatically, by pushing the manual feathering switch to the *FEATHER* position. Terminal *D* of the manual switch energizes the feathering pump relay, initiating the feathering cycle. Terminal *F* energizes the pick-up coil of the *LD* relay which closes to block the automatic feathering system of the right engine and stop the left engine fuel booster pump. Terminal *C* energizes the manual switch holding coil, which holds the switch in the *FEATHER* position until the ground circuit to the holding coil is broken by the high pitch cutout switch at the completion of the feathering cycle.

Selection and Testing of Equipment

As is to be expected in the development of any new control system subjected to extreme environmental conditions, failures were experienced during the initial stages of development and testing. Failures of any sort could not be tolerated. A rigorous program of examination and testing of all components was undertaken. Components were redesigned and rebuilt as required; testing rigs suitable for use later in production and service were developed to aid in trouble shooting, and after suitable operation was obtained in flight and on the ground, all components of the system were subjected to environmental requirements well in excess of those expected on the airplane. Within four months after the first circuit was

drawn, the first production units had flown 75 hours and had completed hundreds of automatic feathering operations during take-off and in flight at all altitudes from sea level to 6,000 feet. The testing and design of the major components in the system is described in the following paragraphs.

Relays

A standard air dash-pot type time delay relay proved adequate since the limited altitude range within which the automatic feathering system operates has little affect on the timing function of the relay. During the initial testing a drift in the delay setting was found. This drift was prevented by sealing the time delay adjustment screw.

Rotary-type relays, with 5-pole double-throw wafer-type contacts, were selected for feathering relays and remembering relays. During the test program it was found that the relays would hold-in on coil voltages as low as 0.5 volts of direct current. This condition was not tolerable because of the unfeathering operation. The magnetic parts of the rotor of the relay were chrome plated to raise the drop-out voltage to a minimum of 5 volts of direct current. To prevent dropout during bus voltage transients, the relays are required to hold-in at 12 volts direct current.

A standard aircraft quality, double-pole double-throw relay was selected for the arming relay. No trouble has been found in its operation.

The complete automatic feathering relay box, Figure 4, was subjected to a 50-hour vibration test at normal and elevated temperatures. While being vibrated at a frequency of 2,500 cycles per minute and a total amplitude of 0.031 inch, the automatic feathering circuits were cycled every two minutes with simulated normal load at the output terminals. The first 40 hours of the test were conducted at room temperature, while the last ten hours were conducted in an ambient of 165 degrees Fahrenheit. The test was completed without failure in two days and two hours.

Torque Pressure Switches

After a careful study of the available pressure switches, the piston-type torque pressure switch now used was designed. The construction of the piston switch is illustrated in Figure 6. A piston made of an insulating material is balanced between oil at engine torque pressure and a calibrated balance spring. The piston carries a brass, bridging contact ring, which makes contact with (1) the common contact leaf at all times, (2) the low-pressure contact leaf below 32, ± 2 pounds per square inch oil pressure, and (3) the high-pressure contact leaf above 75, ±5 pounds per square inch. The piston and spring, the various contact leaves, and the electric connector and wiring are assembled in a split shell aluminum alloy housing. The bottom face of the housing fits the standard engine torquemeter pad. The top face is made similar to the engine torquemeter pad for the installation of a torquemeter transmitter if desired. The housing is drilled with suitable oil passages to permit oil flow to and from the piston and the torquemeter pad atop the housing.

The slow-moving, sliding contacts of the piston switch are well suited for their required duty. The high pressure contact closes the circuit to the arming relay coil which draws approximately 0.1 ampere at 28 direct volts. The low pressure contact closes the time delay relay coil circuit whenever the automatic feathering system is tested or whenever engine failure occurs during take-off. The time delay relay coil draws approximately 0.3 ampere at 28 direct volts. After initiating the circuit, the contacts do not carry or break any current. Long contact life is expected.

The piston switch was subjected to a 100-hour vibration test under the same conditions described in the relay control box test previously outlined. During the 100-hour period, the switch was cycled approximately 9,200 times at normal electric load. The high and low pressure settings varied over a maximum range of 2.5 pounds per square inch. No contact pitting or wear was visible after completion of the test. The switch is not affected by vibration or high ambient temperature and exhibits no tendency to chatter.

After soaking at a temperature of −40 degrees Fahrenheit for a period of 4 hours at a pressure of 80 pounds per square inch, the low-pressure switch contact closed 1.1 seconds after releasing the oil pressure. The results of the test were deemed satisfactory, since the test was conducted without the benefit of vibration and it is unlikely that the oil temperature in the torque nose would be as low as that tested after engine warm-up, even in extreme ambient conditions.

During the test program it was found that an improperly-bled fluid-type torquemeter transmitter can cause a low-pressure switch closing delay of as long as 15 seconds. The use of an electric transmitter is recommended on aircraft employing the automatic feathering system if a torquemeter is required.

Propeller Feathering Components

No change of design of any of the components furnished with the propeller was required.

Some minor troubles in the manual feathering equipment, of little consequence when feathering manually, were found during the automatic feathering test program. Hamilton Standard Propeller Division engineers and service representatives gave willingly of their time and experience to isolate and correct the difficulties.

Flight Testing and Service Performance

Two complete sets of automatic feathering system components were built for the initial flight test program. The components were flown alternately, one set of equipment being flight tested, while the second set was being reworked or equipped with redesigned parts to eliminate troubles isolated on previous flights.

To facilitate trouble shooting, a test box was developed for observation of the progress of the feathering cycle in flight. Two groups of indicator lights, one for each propeller, were arranged so that the lights came on in sequence during normal operation of the automatic feathering system. Improper light sequence isolated the source of system trouble. The test box was connected to the circuits to be observed by inserting a short length of cable between the automatic feathering relay control box disconnect receptacle and the airplane wiring disconnect plug. Thus the test box could be installed or removed readily.

Bench test arrangements were built for ground checking all major components of the system before flight. The bench test panel, developed to facilitate ground testing of the automatic feathering relay panel, was later used as a production test fixture. The test panel, shown in Figure 7, simulated the operation of all other components of the manual and automatic feathering systems.

After all deficiencies had been eliminated, the design was standardized and the final evaluation was begun. During the final evaluation program the system was subjected to a cycling test and an accelerated service test. During the cycling test, repeated engine failures were simulated in flight. The system successfully completed 100 automatic feather operations in succession in one day's flying. During the accelerated

service test, a 75-hour cross-country airplane service performance test without maintenance, engine failures were simulated 11 times.

During the final flight test evaluation and the more than two years of commercial airline service to date, there is no known instance of the automatic feathering system failing to feather a propeller when such action was indicated or inadvertently feathering the propeller of an engine when such action was not required.

Conclusions

Automatic propeller feathering after engine failure is one of a series of electromechanical devices which are providing increased safety of flight. It automatically detects an engine failure, selects the faulty engine, and corrects the deficiency, eliminating windmilling drag and its detrimental effects during take-off. It prevents the fatal error of feathering the wrong propeller. It allows the pilot to devote his full attention to maintain his flight pattern, and to plan his proper approach procedure. It allows improved airplane operating economy by increasing the safe gross weight at take-off.

The automatic feathering system used on Martin model *202* airplanes was designed to give trouble-free performance with a limited amount of maintenance. Much thought was given to make the system easy to service, free of periodic failures, and to provide a fail-safe design which would not interfere with the normal feathering system.

Aircraft operators, both civil and military, look askance at each new electromechanical device. Their confidence can be gained only by consistently faultless performance. The automatic feathering system used on the Martin *202* airplane achieved faultless performance after a development period of less than a year. The success of the system is due to careful evaluation during the early design stages, followed by thorough testing before production. Such a program is essential before the designers of aircraft electric equipment can win and maintain a reputation for providing equipment which works the first time, every time.

No Discussion

Aluminum Conductors from an Aircraft Manufacturer's Viewpoint

W. W. SCHUMACHER
NONMEMBER AIEE

WEIGHT is one of the major factors in aircraft design and any reliable means of weight reduction must be thoroughly exploited. Since substitution of aluminum for copper conductors offers appreciable weight savings, especially in view of the continuing increase in the size and power of aircraft electrical systems, the development of reliable means for using this material has received considerable attention in the past few years.

The designer of aircraft electrical systems is very limited in the amount of weight that he can save. Aside from choosing the lightest components, the only other weight economy that he can control is the cable weight of his system. Since the cable weight of recent military and commercial aircraft is approximately 32 per cent of the total electrical system weight, weight reductions of 40 to 100 pounds may be readily realized by the use of aluminum cable and bus bars.

Aluminum cables and bus bars have been used successfully for the past 50 years and have been thoroughly proved in regard to their electrical and mechanical characteristics.[1] However, these installations have been primarily in the fields of high voltage power distribution, electric railways, and heavy industrial loads. Use of insulated aluminum cable on aircraft in lower voltage distribution systems is comparatively new and has required considerable development and testing to obtain reliable means for termination and joining.

Comparison of Aluminum to Copper Conductors

In comparison to standard annealed copper wire of the same size, the hard drawn wire of aluminum electrical conductor material suffers from a somewhat lower tensile strength: 23,000 to 32,000 pounds per square inch for aluminum versus 30,000 to 35,000 pounds per square inch for copper. However, the conductivity of aluminum is only 61 per cent that of copper and to obtain equivalent resistance, in general, two American Wire Gauge sizes larger aluminum cable must be used. Experimental data and service experience have shown that hard-drawn aluminum cable compares favorably in all respects to annealed copper cable of the equivalent current carrying capacity. This is true in regard to breaking strength, flexibility, and vibration.

The weight of electrical conductor aluminum is only 30.2 per cent that of copper. For equal resistance, an aluminum cable must be 62 per cent larger in cross-sectional area than the corresponding copper cable. Even with this increase in size, the aluminum conductor will have only 49.4 per cent the weight of an equivalent copper conductor. Thus, when considerable lengths of cable are used, especially in the larger sizes, a very worth-while saving in weight can be obtained. The data just mentioned is based on a bare conductor. Because of the larger size of aluminum cable required, the weight of insulation will be somewhat more than for a comparable copper cable. Thus, in the smaller size cables the weight which can be saved is considerably reduced because the insulation comprises a larger percentage of the cable weight. Table I compares typical aluminum and copper cables, showing the weight actually saved per 1,000 feet and the percentage of copper cable weight saved. In aircraft applications, the use of aluminum cable smaller than number 8 is currently not considered advantageous.

Rectangular bar, rod, tubular, and structural shape aluminum conductors have demonstrated satisfactory performance for many years as bus bars in high-voltage transmission and heavy industrial installations. The bus-bar requirements in aircraft electrical systems are for the most part rectangular bars of the smaller sizes. As with cable, an aluminum bar will be 62 per cent larger in cross section but will weigh only 49.4 per cent as much as a copper bar of the same electrical resistance. Figure 1 shows the standard

Table I. Comparison of Typical Aluminum and Copper Cables

Cable Size		Weight, Pounds Per 1,000 Feet		Weight Saved, Pounds Per 1,000 Feet	Saving, Per Cent
Aluminum	Copper	Aluminum*	Copper†		
8	10	30.3	42.5	12.2	28.7
6	8	46.1	66.4	20.3	30.5
4	6	64.8	101.0	36.2	35.8
2	4	93.1	154	60.9	39.5
1/0	2	154.4	246	91.6	37.2
2/0	1	175	299	124	41.5
3/0	1/0	210	378	168	44.4
4/0	2/0	270	480	210	43.7

* Packard cable, specification *A N-C-161*.

† Packard cable, specification *A N-J-C-49a*.

Paper 50-211, recommended by the AIEE Air Transportation Committee and approved by the AIEE Technical Program Committee for presentation at the AIEE Middle Eastern District Meeting, Baltimore, Md., October 3-5, 1950. Manuscript submitted July 5, 1950; made available for printing August 14, 1950.

W. W. Schumacher is with the Glenn L. Martin Company, Baltimore, Md.

The author gratefully acknowledges the assistance of Erle P. Barlow, Thomas E. Lyon, and other individuals of the Glenn L. Martin Company, Electro-Mechanical Department, in preparing this paper. The views expressed in the paper are those of the author and not of the Glenn L. Martin Company.

sizes of aluminum bus bars used in one manufacturer's aircraft and the comparable standard sizes of copper bus bar for equivalent current carrying capacity.

Weight Saved by Use of Aluminum Conductor

Obviously the total amount of weight which can be saved by the use of aluminum conductors depends on the size, the voltage, and the extent of the system in which it is used. The larger the airplane and the more extensive its electrical system, the greater will be the saving in weight. In the past the high-voltage a-c power employed in airplane systems was comparatively small and could be handled by the smaller size wires not justifying substitution of aluminum. Therefore aluminum cable has been used mostly in the low-voltage d-c systems. Recent increases in the high-voltage a-c power requirements for radio, radar, fire control, and other special equipment now make it desirable to use aluminum in the a-c as well as in the d-c circuits. Table II shows the actual weight saving accomplished by use of aluminum conductors in the design of several recent types of aircraft.

Problems Encountered in Use of Aluminum Conductor

Aluminum cable is so similar to the copper cable of equivalent current carrying capacity in mechanical characteristics, method of manufacture, and insulation that no change is required in the design of installation of electrical systems. The problems which have required considerable development and testing have been in obtaining terminal connections with satisfactory resistance and temperature-rise characteristics. These problems arise primarily because of the rapid oxidation and susceptibility of aluminum to corrosion by contact with copper in a damp, or salt, atmosphere.

Table II. Aircraft Weight Savings by Use of Aluminum Conductor

Aircraft Type	Total Weight of Electric Equipment and Cable (All Copper), Pounds	Weight of Cable (All Copper), Pounds	Weight of Copper Cable that may be Converted to Aluminum, Pounds	Weight of Aluminum Cable, Pounds	Weight Saved by Using Aluminum Cable, Pounds
2-Motor Commercial Transport	1,183	351	89	52	37
Light Bomber	1,102	343	131	68	63
Patrol Plane, Primary System 30 volts direct current	1,861	684	312	180	132
Patrol Plane, Primary System 120/208 volts alternating current	2,240	668	202	134	68

When exposed to air, aluminum quickly becomes coated with a thin film of oxide which acts as an insulator. In stranded cable this oxide forms not only on the cable surface but on all of the strands as well. This causes a transverse resistance between the inner strands and the cable surface which must be overcome if satisfactory joining and termination of cables is to be accomplished. Because of this transverse resistance, the breaking of a few strands at the cable surface, which come in contact with the terminal barrel, may be considerably more serious than with copper cable. Therefore greater care is being used to avoid cutting or nicking the strands when stripping insulation for terminal application.

The corrosion encountered is of two types: first, the building up of oxides or salts at the cable to terminal contact surface; and second, the electrolytic corrosion which occurs where aluminum terminals contact other metals, such as the brass nuts or studs frequently used on electrical equipment. These corrosive effects must be minimized if low resistance connections are to be maintained over a satisfactory period of time. The use of silver-plated aluminum bus bars on tin-plated copper bus bars, together with cadmium-plated steel bolts, nuts, and washers in contact with tin-plated aluminum terminals, has given excellent performance.

In early postwar efforts to adapt aluminum cables and terminals to aircraft use, difficulty was experienced with high-resistance terminals and terminals in which the resistance increased excessively with age or corrosion. Extensive development and tests have been devoted to overcoming these troubles. It now appears that the early failures were due primarily to the use of soft aluminum cable, inadequate terminal installation procedures, and faulty plating of the terminals.

Development of Satisfactory Terminals

Types of Terminal

Terminals for aircraft cable must be small in size, light in weight, easy to attach, and possess good mechanical strength. Most terminals fall under the classifications of welded, soldered, clamped, or pressure-applied fittings. Although welding terminals to cables provides a good permanent joint, problems of expense, convenience and burning of insulation must be overcome. In spite of the use of special solders and fluxes, soldering of terminals to cables has not proved satisfactory. In particular, difficulty has been experienced with soldered terminals in overcoming the transverse resistance and obtaining sound connections to the inner strands. Clamped fittings providing the surface area and pressure necessary for satisfactory joints suffer from disadvantages of size, weight, and atmos-

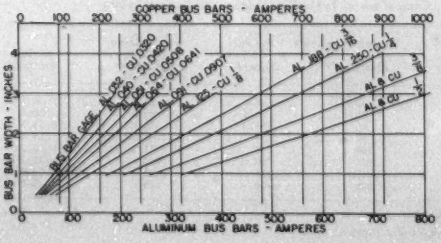

Figure 1 (left). Maximum allowable current capacity for various aluminum and copper bus bars

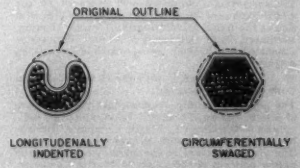

Figure 2 (right). Types of aluminum terminals

pheric exposure at the connection with subsequent oxidation.

Of the pressure-applied terminals the two general types are the longitudinally indented and the circumferentially swaged, cross-section views which are shown in Figure 2. Either of these, when properly applied, will provide a satisfactory connection. The longitudinal indent permits a wide latitude in acceptable cable cross-section for a given maximum and minimum pull-out force. In the longitudinal indent the strands are drastically reshaped wiping off the oxide coating. The U-shaped cross section of the longitudinal indent appears to maintain its shape against relaxation of pressure and springback and provides a mechanically strong terminal, thus contributing to satisfactory operation in service. Less pressure, and therefore lighter equipment, is required to install the longitudinally-indented terminal. Pressure-applied type terminals should be made of electrical conductor grade aluminum so the lug and cable will have the same coefficient of expansion and rate of recovery after compression.[3] This minimizes creep of the cable and loosening of the joint which results in high-resistance connections. However, aluminum is malleable and cold flow of the terminal tongue must be considered. The tongue may be distorted on installation and may continue to flow with consequent reduction in contact pressure and increase in resistance. The longitudinally-indented type terminals are manufactured from aluminum tubing which becomes work-hardened during its forming stages. This work-hardening renders the terminal less susceptible to cold flow when subjected to the pressure of installation hardware. The use of aluminum terminals having the largest practical contact areas, fastened with steel bolts, nuts, washers, and heavy split-type lock washers, has overcome these difficulties satisfactorily.

Special tin-plated connectors are available for connection of aluminum to copper cable and for connection of aluminum cable to Army-Navy type plugs and receptacles. The former consists of a copper cylinder with an aluminum barrel attached at one end for indentation on the aluminum cable and a copper barrel of the correct size attached at the opposite end for indentation on the equivalent copper cable. The latter consists of an aluminum barrel for indentation on the aluminum cable with an integral aluminum pin for soldering into the Army-Navy connector. While worthy of further development, these adaptors have not yet met the stringent requirements for aircraft use. A recommended procedure is to carry copper cable from Army-Navy connectors, or other equipment requiring its use, to the nearest terminal block where it can be connected to the aluminum cable using standard terminal lugs.

Use of Joint Sealing Compounds

Although the wiping action from rearrangement of strands in the longitudinally indented terminal helps reduce the transverse resistance of aluminum cable, it was found that further means were required to obtain completely satisfactory and reliable terminal installations. Investigation indicated that use of a joint sealing compound, such as a petrolatum jelly containing zinc dust, would reduce the transverse resistance.[3] This compound is used to coat the inside of the terminal barrel and is forced up between the strands of the cable. When the terminal is indented onto the end of the cable, the particles of metallic zinc break through the oxide coating and form low-resistance current paths from strand to strand and from cable to terminal. The petrolatum jelly acts to prevent reformation of the oxide which would increase the terminal resistance with age.

Plating of Terminals and Bus Bars

Plating of aluminum terminals prevents the formation of oxide on the terminal and reduces the effect of electrolytic corrosion between the terminal and other metals to which it may be attached. Early tests of unplated, copper-plated, and zinc-plated terminals indicated that zinc plating of the aluminum terminals provided the most satisfactory results, as shown in Glenn L. Martin Company laboratory tests. Although these tests indicated the superiority of zinc-plated terminals, it was found that in use the contact surfaces turned black and high-resistance connections occasionally resulted. At a later time, tin-plated terminals became available and have been shown both by test and experience to give satisfactory performance without these aging characteristics.[4] At first, considerable trouble was encountered with peeling of the tin plating. However, improved plating methods have overcome this difficulty.

Aluminum bus bars for aircraft use also require protection from the effects of

Figure 3(A) (left). Cross section of an improperly indented terminal

Figure 3(B) (right). Cross section of a properly indented terminal

Figure 4(A) (left). Proper position of terminal indent

Figure 4(B) (right). Improper position of terminal indent

Table III. Indents for Longitudinally-Indented Terminals on Hard Aluminum Cable

Cable Size	Indent		
	Optimum	Maximum	Minimum
8	0.153	0.168	0.138
6	0.140	0.154	0.124
4	0.155	0.175	0.135
2	0.210	0.240	0.180
1	0.250	0.290	0.220
1/0	0.306	0.346	0.286
2/0	0.366	0.396	0.336

The above dimensions apply to indentors and nests of a given contour.

oxidation and corrosion. It has been found that silver plating affords very satisfactory service in this respect. Silver-plated aluminum bus bars have been used in one manufacturer's aircraft for five years without any reports of trouble. Silver-plated bus bars are used because the facilities for the process were available and perfected before the advent of tin-plated terminals. Tin-plated bus bars would undoubtedly also offer good service. Bare aluminum bus bars are not recommended unless special precautions are used to remove the oxide from the area in contact with the terminal, and coating this surface with a compound which will prevent reoxidation. The bus-bar material that offers the highest conductivity is electrical conductor grade aluminum.

Other materials such as $2SO$, $2S^1/_2H$, and $2SF$ may be used but their lower conductivity should be taken into consideration.

Terminal Installation

In practice, terminal lugs are cleaned of oxide, plated, filled with compound, and the barrels are sealed by the manufacturer. On installation the seal is removed and the cable is pressed into the barrel, forcing the compound in between the strands of the cable. Improved performance resulting from better distribution and deeper penetration can be obtained by forcing the compound into the cable with a grease gun just prior to terminal installation. Portable hydraulic tools and pneumatic bench tools are available for indenting the terminal barrels.

Taping Cable to Terminal Joint

Another practice which has proved to be beneficial is taping of the cable to terminal junction. After installation, the joint is tightly wrapped with vinyl electrical tape, covering a good area of the cable insulation and all of the terminal barrel. By sealing in the compound and sealing out the air, the tape prevents reoxidation of the aluminum and corrosion at the cable-to-terminal junction.

Standards of Acceptability

The accepted method of determining the reliability of a cable-to-terminal connection is by measuring the voltage drop across the terminal and the temperature rise of the terminal when subjected to the rated current of the cable. To determine the effects of aging and corrosion, samples are subjected to these measurements immediately after terminal installation, after an aging period, and at intervals during exposure to corrosive atmospheres or liquids. A maximum voltage drop of 20 millivolts and a maximum temperature rise of 70 degrees Fahrenheit have been used arbitrarily as standards of acceptability after careful consideration of the requirements of aircraft electrical systems. While the optimum voltage drop and temperature rise will vary for different sizes of cable and terminals, these values were adopted for all sizes used in order to simplify inspection procedure (Laboratory tests, Glenn L. Martin Company).

Development and Tests

It appeared that in attaching compression-type terminals, the depth of indent used would be the criterion of connection quality, since it determines the amount of pressure and wiping effect on the strands. Figure 3(A), the cross section of an improperly indented terminal, shows the poor contact between strands resulting from low indenting pressures. Figure 3(B) shows the cross section of a properly indented terminal for comparison. Figures 4(A) and 4(B) illustrate samples of good and poor indentation in regard to position of the indent. Work curves have been prepared similar to Figure 5, for longitudinally-indented terminals applied to various sizes of aluminum cable (Laboratory tests of the Burndy Engi-

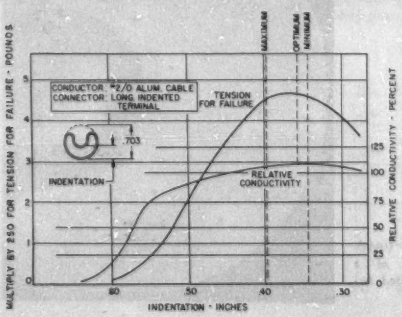

Figure 5 (left). Work curve indentation versus relative conductivity and tension for failure

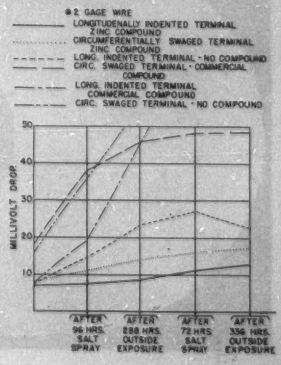

Figure 6 (right). Effect of joint sealing compound

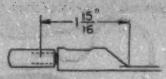

Figure 7. Location of needle point probes for voltage-drop measurement

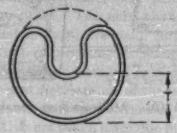

Figure 8. Depth of indent measurements

neering Company, Inc.). The tension for failure increases with depth of indent to a maximum and then decreases. To the left of the peak, the connection fails because the cable pulls out of the terminal. To the right, the cable strands are damaged by excessive pressure and break under tension. In general, the relative conductivity (ratio of terminal conductivity to conductivity of an equal length of cable) reaches a maximum in the vicinity of the maximum tension for failure and is better than 100 per cent in this region. These data have been of great value in standardizing the depth of indent for optimum terminal installation on the various sizes of cable and for specifying the maximum and minimum acceptable indentations listed in Table III.

To determine the effects of joint sealing compounds a test was run in 1946 using pressure-applied terminals of number 1/0, number 2 and number 4 gauge cables (Glenn L. Martin Company Laboratory tests). Measurements were made after alternate periods of salt spray and outdoor exposure of various samples using zinc compound, commercial compound, and no compound. The increase in voltage drop throughout the corrosion tests was smallest for the combination of longitudinally-indented terminals and zinc compound and was well within the acceptable limit of 20 millivolts. The curves for the number 2 gauge cable are shown in Figure 6. It is of interest to note that this performance was achieved with annealed cable, zinc-plated terminals, and no protective taping.

To determine the effect of taping the cable-to-terminal joint, tests were made of two samples each of number 4 cable from five manufacturers. The terminals of one sample of each type were taped with vinyl electrical tape. Millivolt drop and temperature rise data were taken and the ends of each sample were then submerged in a saturated sodium chloride solution for three weeks. After thorough drying, the readings were repeated. In general the results showed somewhat better performance for the taped terminals.

Voltage-drop measurements may be made by pressing two needle point probes at a predetermined separation, one into the terminal tongue and the other through the insulation into the conductor as shown in Figure 7. This method has the disadvantage of the conductor being damaged if the probes are not carefully inserted. The use of a tool which limits the depth of probe penetration eliminates this danger and assures consistent millivolt readings.

Complete test records of depth of indent and voltage drop have been kept on all aluminum cable for 19 ships of one type of airplane. Table IV shows samples of this data picked at random from the test reports. For ease and accuracy of measurement, depth of indent is taken as the thickness remaining at the bottom of the indent, as shown in Figure 8, rather than the depth from the original outline to the bottom of the indent.

The material and installation improvements that have been made in the past five years have added considerably to the reliability of aluminum cables and terminals to the point where their use should not create any skepticism. In fact, soft aluminum cables with zinc-plated terminals which were installed five years ago in aircraft are still giving reliable service.

Standard Procedure for Cable Assembly

As the result of many tests, only a few of which have been discussed, the following procedures have been developed by one manufacturer for the use of aluminum cable in aircraft. For all cable sizes number 8 and larger, aluminum cable may be used except in the following service, for which the use of aluminum cable is not recommended. In nacelles forward of the engine fire walls, as connections to shock-mounted equipment; and as connections to equipment subject to frequent service or replacement. These are applications where frequent bending or large vibrations may occur and complete reliability of aluminum cable and terminals for such use has not been fully proved to their satisfaction.

Hard-drawn electrical conductor aluminum cable complying with government specification *AN-C-161*, and meeting additional requirement that no absorbent wrapping be used next to the conductor, is recommended. This is done to prevent moisture from being carried back under the insulation and corroding the conductor. To simplify cable inspection a 10-inch sample, stripped of insulation,

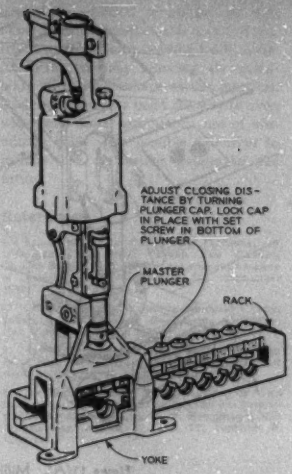

Figure 10(A). Pneumatic-indenting bench tool

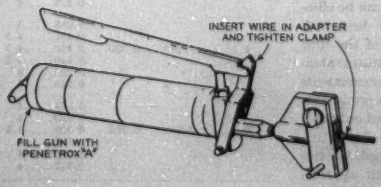

Figure 9 (left). Cable-impregnating gun and adapter

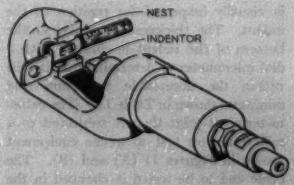

Figure 10(B) (right). Hydraulic-indenting portable tool

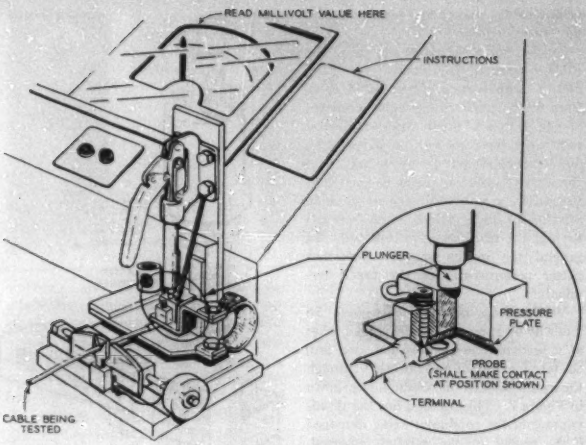

Figure 11(A). Millivolt-drop bench tester

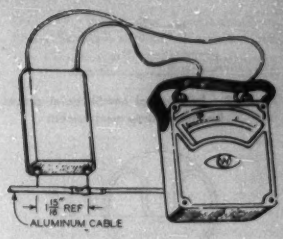

Figure 11(B). Millivolt-drop portable tester

may be weighed to insure that sufficient metal is present to carry the specified current. The sample weight is checked against a minimum acceptable weight which has been established for each size cable. Several strands then are taken from the cable and their tensile strengths are measured to insure compliance with specifications.

Cables may be cut to the desired lengths using a swing-type power saw, which minimizes possibilities of burring or displacing the strands. The cable end is placed in a clamp and zinc petrolatum compound forced into the cable by means of the grease gun shown in Figure 9. The proper length of insulation then is removed, using a hot blade cable stripper which removes insulation cleanly without danger of cutting or nicking the strands.

The cable is inserted in a terminal holding a finger over the inspection hole to prevent escape of compound from the barrel. The assembly is placed in the pneumatic bench tool (or portable hydraulic tool) shown in Figures 10 (A) and (B), and indented, using the proper die and closing distance. The terminal then is visually inspected for position of the indent. The thickness remaining at the bottom of the indent is checked with a dial micrometer to determine that it falls within the acceptable maximum and minimum shown in Table III. The cable-to-terminal joint then is subjected to a millivolt drop test with the equipment shown in Figures 11 (A) and (B). The cable end to be tested is clamped in the machine, which insures good contact of the cable and needle point probes at the specified separation. The other end is clamped to a power supply and the current is adjusted to the rated value for the cable size. The voltage drop then is read from the meter, and if it exceeds 20 millivolts the terminal is rejected. This inspection procedure is recommended because the use of aluminum cable on aircraft is relatively new to most electricians. After a reasonable indoctrination period when successful assembly procedures have been definitely established, the millivolt-drop measurement may be discontinued. However, a terminal depth of indent measurement should be made on each assembly to assure that the proper indenting dies have been used.

Temperature-rise measurements can be made with relatively simple equipment. Cable samples to be tested are connected in series and thermocouples are clamped to the terminals. Terminal temperatures are measured and rated current then is applied to the cables until the temperature stabilizes. Terminals showing more than a 70 degrees Fahrenheit rise are rejected. The effects of drafts can be eliminated by surrounding the test rack with an enclosure. Because of the time required for setup and temperature stabilization, temperature-rise measurements are not made on all cables of a production run. This test is recommended only as a quality control sampling procedure.

After the tests just mentioned, the terminal barrels are taped with approximately $2^1/_2$ turns of 3/4 inch by 0.010 vinyl adhesive tape, making sure to seal the gap between the insulation and terminal barrel at one end and the inspection hole at the other. The needle probe holes in the cable insulation adjacent to the terminal are self-sealing and are not detrimental in any manner. Electrical leakage is either nonexistent or insignificant at the voltage levels currently used in aircraft power systems.

Portable indenting and voltage drop measuring instruments are used when the installation must be made in an airplane. "Go" and "No-Go" type gauges some-

Table IV. Typical Test Data, Production Assembly of Aluminum Cable

Aluminum Cable Size	Specified Indent: Maximum	Specified Indent: Minimum	Measured Indent	Millivolt Drop
			0.158	9
			0.162	8.5
8	0.168	0.138	0.160	8.5
			0.155	8.5
			0.152	8
			0.158	9
			0.150	7
			0.136	8
6	0.154	0.124	0.150	8
			0.146	7
			0.148	6
			0.145	8
			0.150	6.5
			0.164	6.5
4	0.175	0.135	0.151	6.5
			0.152	7
			0.150	6
			0.146	7
			0.221	6
			0.217	6
2	0.240	0.180	0.225	6
			0.222	6.5
			0.207	6
			0.225	6
			0.258	5
			0.251	4.5
1	0.280	0.220	0.260	4.5
			0.240	4.5
			0.252	4
			0.258	5
			0.323	4
			0.320	4
0	0.346	0.286	0.325	3.5
			0.318	4
			0.330	4
			0.322	4

times are used in place of the micrometer for checking depth of indent.

Maintenance

Because of the similarity of installations, maintenance procedures established for copper cable will suffice for aluminum cable. The only change recommended is more frequent inspection of terminal connections to assure that bolted connections have not become loose and that heat discoloration of the terminal or the cable insulation adjacent to the terminal has not taken place due to a poor connection. With more actual operating data on types of installation, specific inspection periods can be established.

Future Developments

While satisfactory methods of applying aluminum cable to aircraft electrical systems have been demonstrated and such cable is being used as standard equipment in aircraft, efforts are continuing to improve the reliability and useability of this material. With more experience as to the effect of vibration, it is felt that it will be safe to specify aluminum cable in a few locations noted previously where it is not now being used. Further development of techniques for welding terminals to aluminum cable could make this method practical for production use. The good correlation between voltage-drop and depth of indent in the process presently standardized indicates that it may be possible to eliminate the voltage-drop test and control manufacturing quality from the depth of indent alone. Another improvement now under development is an insulation sealing terminal. The barrel of this terminal is extended in a larger diameter to cover the end of the insulation. This extension is crimped onto the insulation at the same time the terminal is indented into the cable. In addition to sealing the terminal to cable junction, this terminal distributes vibration or bending loads to the insulation, thereby reducing the possibility of cable breakage at the junction. Such developments point the way to even wider and more satisfactory use of aluminum cable with possible extension to include use of smaller gauges in the future.

References

1. Aluminum as a Conductor Material in Insulated Electrical Wires and Cables, Charles Braglio, R. R. Cope. Aluminum Company of America, New Kensington, Pa., September 1947.

2. Connectors for Aluminum Aircraft Cable, Julius Rogoff. Burndy Engineering Company, New York, N. Y., April 1945.

3. Application of Insulated Aluminum Wire and Cable, C. W. Sage, E. E. McIlwee. *Electrical World* (New York, N. Y.), September 1947.

4. An Experimental Investigation of the Electrical Performance of Bolted Aluminum-to-Copper Connections, W. F. Bewwitt. *AIEE Transactions*, volume 67, part II, 1948, pages 1206–10.

No Discussion

Analogue Techniques for Turbojet Thrust Instrumentation

E. S. VAN VALKENBURG
NONMEMBER AIEE

N. W. MATTHEWS
MEMBER AIEE

THE THRUST of a turbojet engine is the primary parameter indicating engine performance, but it is not directly measurable during flight. By simplification of the thermodynamic function of momentum thrust, gross thrust can be determined during flight by simple automatic metering and computing techniques. A prototype model of this computer has been constructed and evaluated at the Naval Research Laboratory.

In contrast to the large scale computers functioning in many of the nation's laboratories, a great number of surprisingly compact, light weight, special purpose computers are being designed and used for control or instrumentation computations. The large scale computer is inherently large physically in order to perform a multitude of mathematical operations, and thus is applicable to an infinite variety of problems. Special purpose computers are usually of the analogue type in which as many parameters as possible are held fixed permitting only certain specified solutions.

Analogue computing principles are readily adaptable in control systems by transforming physical measurements into the required input variables by appropriate transducers. Likewise, the output of the computer can operate an actuator in a control system or automatically record the specified solutions. Thus, one envisions a completely automatic system of measurements, calculations, and actuation.

A recent application of such a special purpose computer, which has been developed at the Naval Research Laboratory, is a thrust computer for turbojet engines. This device is rather simple as compared to many other applications. However, this simplicity is due largely to the analysis of the function which was to be solved. It will be shown that the theoretical function involved in this application is quite complex, but simplification of this function without sacrificing accuracy, resulted accordingly in simpler, more compact, and comparatively inexpensive equipment. The purpose of this paper is to present the formulation of the thrust functions and analogue techniques utilized in this special computer.

Requirements of a Thrust Computer

Effective operation of military aircraft requires instrumentation which includes an indication of engine performance. With the introduction of turbojet aircraft came the demand for instrumentation which includes a means for determining the engine's thrust. Thrust is the primary parameter indicating turbojet performance, but the components of thrust are not directly measurable during flight. Therefore, thrust must be computed according to the thermodynamic properties of the engine.

Those thermodynamic functions are unavoidably complex. Thus, the pilot of a turbojet aircraft is not capable of accurate interpretation of engine performance when provided only with instruments indicating the parameters from which thrust can be computed. As a result, it is necessary to apply automatic computing techniques to thrust determination during flight. Such an automatic computer based on analogue principles can instantaneously and continuously solve the thermodynamic equation for thrust and thus indicate the thrust of a turbojet engine directly with a single instrument reading. This will facilitate flight test programs and enable a pilot to determine engine performance with a degree of precision not presently possible.

The net thrust, F_n, developed by a turbojet engine is the resultant of the gross thrust, F_g, measured at the exhaust nozzle and the ram-drag, F_r, occurring at the air intake.

$$F_n = F_g - F_r \tag{1}$$

Net thrust is directly measurable only for engines at rest. Thus, when a jet aircraft is in motion net thrust must be computed from equation 1 where gross thrust and ram-drag are thermodynamic functions. The principal component of net thrust indicating turbojet performance is gross thrust. Gross thrust instrumentation for test of turbojet aircraft has involved lengthy computations from data recorded upon a photo panel during test flights. Naval establishments concerned with flight test programs have found it desirable to record and/or indicate the instantaneous gross thrust continuously during flight evaluation operations. The analogue computer which has been designed for this purpose meets weight and space requirements for jet aircraft installation and could be adapted easily as a gross thrust indicator for operational aircraft. A prototype model, hereafter called the jet thrust computer, has been constructed and evaluated under controlled laboratory conditions.

Gross Thrust Measurements

The gross thrust of a turbojet engine can be expressed as a function of total, P_{tj}, and static, P_{sj}, pressures at the exhaust nozzle and the ambient pressure, P_a. Let the effective area of the exhaust nozzle in the region of pressure measurements be A_j, and let the ratio of specific heats at the exhaust be γ_j. The deriva-

Paper 50-212, recommended by the AIEE Air Transportation and Computing Devices Committees and approved by the AIEE Technical Program Committee for presentation at the AIEE Middle Eastern District Meeting, Baltimore, Md., October 3–5, 1950. Manuscript submitted June 26, 1950; made available for printing August 29, 1950.

E. S. Van Valkenburg and N. W. Matthews are both with the Naval Research Laboratory, Washington, D. C.

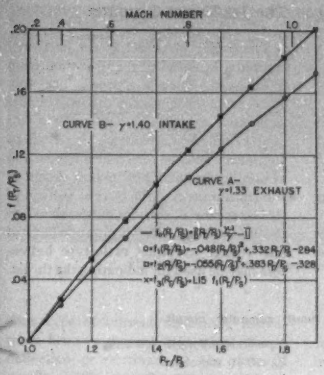

Figure 1 (left). Determination of empirical constants for exhaust and intake gases

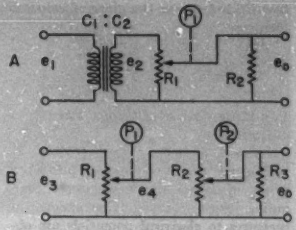

Figure 2 (right). Multiplication operators

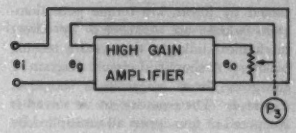

Figure 3 (right). A division operator

tion of gross thrust from the thermodynamics of ideal adiabatic expansion of the exhaust gases gives

$$F_g = A_j P_{sj} \frac{2\gamma_j}{\gamma_j - 1}\left[\left(\frac{P_{tj}}{P_{sj}}\right)^{\frac{\gamma_j - 1}{\gamma_j}} - 1\right] +$$

Momentum Thrust Term

$$A_j(P_{sj} - P_a) \qquad (2)$$

Pressure Thrust Term

These pressures can be measured through pressure probes in the form of a rake across the exhaust or by single total and static probes critically located in the exhaust nozzle to give close approximations to integrated values of pressure.

Equation 2 can be simplified for the purpose of designing an analogue computer without sacrificing accuracy by expanding the bracketed portion of the momentum thrust term into an infinite power series of P_{tj}/P_{sj}. This is possible since γ_j remains nearly constant over usual operating conditions. This expansion gives

$$\left(\frac{P_{tj}}{P_{sj}}\right)^{\frac{\gamma_j - 1}{\gamma_j}} - 1 = \sum_{n=0}^{\infty} K_n \left(\frac{P_{tj}}{P_{sj}}\right)^n \qquad (3)$$

where K_n' is the coefficient of the nth term. A satisfactory empirical representation can be obtained using the first three terms of such a power series as is evident from Figure 1, curve "A". The maximum deviation of the empirical curve from the theoretical curve within the range of Mach numbers 0 to 1 is ± 0.3 per cent. Substituting these first three terms of the series in equation 2 and multiplying each K_n' by $2\gamma_j/(\gamma_j - 1)$ to become K_n gives the simplified equation for gross thrust.

$$F_g = A_j\left[K_1 P_{sj} + K_2 P_{tj} + K_3 \frac{P_{tj}^2}{P_{sj}} + K_4(P_{sj} - P_a)\right] \qquad (4)$$

where K_4 is equal to the unity coefficient of the pressure thrust term.

Pressure-Potential Analogue

An analogue computer has been designed to provide continuous solution of equation 4 for gross thrust. This is accomplished by establishing analogues between pressures and electrical potentials in such a way that voltages proportional to each of the four terms of equation 4 are developed for any conditions of pressure parameters. The sum of these four voltages, which are connected in series, is then proportional to the gross thrust.

The methods of multiplication used in this computer are flux linkages (transformers) and mechanical displacements applied to potentiometers. Consider the simple circuit shown in Figure 2(A) as a multiplication operator. The input voltage e_1 is applied to a potentiometer (R_1) through a transformer whose secondary-to-primary turns ratio is $C_2/C_1 = C' = a$ constant. The wiper arm of this potentiometer is displaced linearly with pressure P_1. If the impedance R_2 is much greater than R_1, then $e_0 = e_1 C' k P_1 = e_1 C P_1$ where k relates pressure and wiper arm displacement. Therefore, this circuit performs two multiplication operations in series.

Any function e_1 is multiplied by a constant and a variable.

This analogue can be expanded to perform multiplication of a function by two variables by employing R_2 as a second potentiometer as shown in Figure 2(B) and controlling the displacement of this second potentiometer by a pressure P_2. Then

$$e_0 = e_3 k P_1 k P_2 = e_3 k^2 P_1 P_2 \text{ provided that } R_3 >> R_2 >> R_1$$

The operation of division is accomplished using a negative feedback amplifier similar to the circuit shown in Figure 3. This amplifier has a large amplification (G). Then $e_0 = -e_g G$. Let the displacement of the wiper arm on the potentiometer across the output of the amplifier be D then $D = kP_3$. Then $e_g = e_i + De_o$. Eliminating e_g gives $e_o = -e_i G/(1 + DG)$. If G is sufficiently large

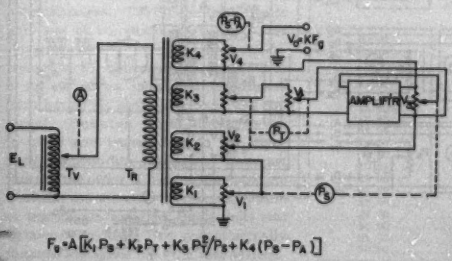

Figure 4. Schematic diagram of a gross thrust computer

that $DG >> 1$ over the range of values D then

$$e_o = \frac{-e_i}{D} = \frac{-e_i}{kP_3}$$

Fundamentals of a Gross Thrust Computer

The jet thrust computer utilizes a system of the foregoing analogues for computing gross thrust. Conversions of pressures to electrical potentials are obtained by linear, low-torque potentiometers which are connected by direct mechanical linkages to pressure sensing bellows. A simplified circuit diagram of the gross thrust computer is shown in Figure 4. The equation to be solved is composed of four terms all multiplied by the area, A_j. An analogue of A_j is obtained by an autotransformer, T_v, which is adjusted so that the line voltage of the aircraft E_L, is converted to a voltage proportional to A_j. This voltage is applied to a special transformer T_R designed to introduce the required constants K_1, K_2, K_3, and K_4 by proper turn ratios between each of its secondary windings. The outputs of these secondaries are applied to a system of pressure transducers indicated in the diagram by the pressure actuated potentiometers. Then the voltage appearing between ground and the lowest sliding contact is

$$V_1 = A_j K_1 k P_{tj} \tag{5}$$

The second term is obtained in the same manner as the first except that this transducer is controlled by P_{tj}.

$$V_2 = A_j K_2 k P_{tj} \tag{6}$$

The third is a more complex function and requires a combination of operations. The total pressure is squared by using two potentiometers in series, Figures 2(B), with both wiper arms being driven by P_{tj}.

$$V_i = A_j K_3 k^2 P_{tj}^2$$

This voltage, V_i is applied to the feedback amplifier circuit, Figure 3, which divides V_i by $k\ P_{sj}$ or

$$V_3 = A_j K_3 k \frac{P_{tj}^2}{P_{sj}} \tag{7}$$

The final term is generated by use of a differential pressure transducer. The wiper arm displacement in such a transducer is proportional to the difference of two applied pressures. This displacement is $k\ (P_{sj} - P_a)$, and

$$V_4 = A_j K_4 k (P_{sj} - P_a) \tag{8}$$

Adding these four voltages in series produces a voltage between ground and output lead of

$$V_o = kA_j\left[K_1 P_{tj} + K_2 P_{tj} + K_3 \frac{P_{tj}^2}{P_{sj}} + K_4 (P_{sj} - P_a)\right] \tag{9}$$

or

$$V_o = kF_g \tag{10}$$

A voltage indicator measuring V_o can be calibrated linearly in units of gross thrust.

The Jet Thrust Computer

The prototype model of the jet thrust computer is designed for operation from a 115-volt 400-cycle source. The 400-cycle supply was chosen for this model since that frequency is normally available in military aircraft. This type of computer could be designed for operation at another frequency by proper design of the transformers. The output voltage of the computer is directly proportional to the line voltage. To eliminate effects of line voltage variation ratio-type indicators may be used for indicating the thrust.

Figure 5. Jet thrust computer circuit

P_1 = 10,000 ohms*
P_2 = 10,000 ohms†
P_3 = 20,000 ohms†
P_4 = 2,000 ohms**
P_5 = 20,000 ohms**
P_6 = 10,000 ohms**
R_1 = 10,000 ohms, 0.5 watt
R_2 = 22,000 ohms, 0.5 watt
R_3 = 160,000 ohms, 0.5 watt
R_4 = 280,000 ohms, 0.5 watt
R_5 = 390,000 ohms, 0.5 watt
R_6 = 56,000 ohms, 0.5 watt
R_7 = 560 ohms, 0.5 watt
R_8 = 10,000 ohms, 10 watts
R_9 = 1 megohm, 0.25 watt
R_{10} = 1,000-ohm rheostat
R_{11} = 1,000-ohm rheostat
R_{12} = 1,000-ohm rheostat
C_1 = 0.05 microfarad
C_2 = 10 microfarads, 25 volts
C_3 = 0.10 microfarad
C_4 = 20 microfarads, 600 volts
C_5 = 0.0012 microfarad
C_6 = 10 microfarads, 25 volts
C_7 = 20 microfarads, 600 volts
C_8 = 20 microfarads, 600 volts
C_9 = 0.10 microfarad
L_1 = 15 henrys, 70 milliamperes
L_2 = 15 henrys, 70 milliamperes
V_1 = type 9001, voltage amplifier
V_2 = type 6AK6, power amplifier
V_3 = type 6X4, rectifier
T_R = ratio transformer, NRL Number 3423, primary 115 volts, 400 cycles; secondary K_2 = 71.4 v., K_3 = 10.0 v., K_1 = 61.1 v., K_4 = 9.5 v.
T_P = power transformer NRL Number 3425, primary 115 volts, 400 cycles; secondary 6.3 v. and 350-0-350 v.
T_O = output transformer, Thordson type T72558
T_V = autotransformer, Variac type 2008
S = double-pole double-throw switch
F_1 = fuse 1a
F_2 = fuse 3a
X = Type 1N35 crystal rectifier

* Linear potentiometer of differential pressure transducer (0–10) psi.
† Linear potentiometers of static pressure transducers (0–30) psi.
** Linear potentiometers of total pressure transducers (0–30) psi.

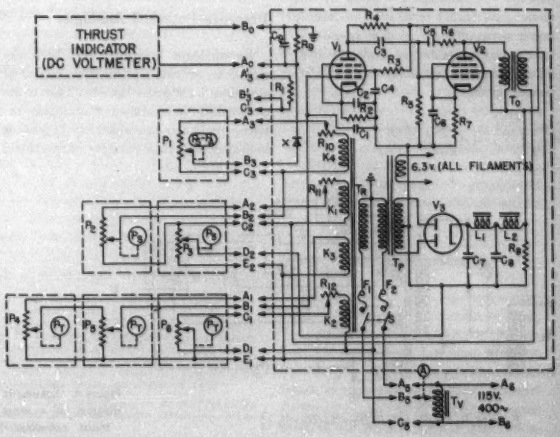

Figure 6. Gross thrust computer

Figure 7. Experimental apparatus to determine computer accuracy

This type of current measuring instrument has two current coils which give a deflection proportional to the ratio of currents. The current sensing movement of megger instruments is of this type. The computer output current is rectified by a half-wave crystal detector and applied to one of these current coils. A portion of the line current is applied through a matched crystal to the other coil of the ratio instrument, a variation of ±50 per cent in the line voltage was not detectable on such a thrust indicator. Simultaneous recording of computer output and line voltage could be used for a continuous recording of thrust without a ratio-type indicator.

A complete circuit diagram of the jet thrust computer is shown in Figure 5. The system of pressure transducers is shown at the left in the diagram. Six pressure measurements are necessary. These include two static pressure measurements, three total pressure measurements, and one differential pressure measurement. Two systems of transducers were investigated. The first system, purchased from a private contractor, used only three pressure sensing units. A static pressure unit was designed such that a single set of pressure sensing bellows produced sufficient torque to drive two potentiometers connected in tandem. The total pressure unit was similar in that one set of bellows operated three potentiometers. The differential pressure unit was of conventional design. This system was employed in an attempt to decrease space requirements as compared to a system of six individual transducers each having its own pressure sensing elements. However, recent developments in small size transducers do not make such compounding necessary. Compact units of the order of 2-inch cubes now are available commercially. A second system of transducers using six single units was obtained recently. This system actually requires less space than the first system.

Rheostats are connected in series with three of the secondaries of the ratio transformer to compensate for a slight nonuniformity among the transducers. The amplifier for the dividing circuit is composed of a high-μ pentode resistance-capacitance coupled to a power pentode. These electron tubes and the power supply rectifier are miniature types. The gain is approximately 300 with no external feedback. The internal feedback path across the power stage through R_4 and C_4 was found necessary for stabilization throughout the external feedback range.

The autotransformer for introducing the effective area of the exhaust nozzle could be eliminated if the computer were designed for a specific type of turbojet engine having a fixed effective area. The constant A_j could then be included in the design of the ratio transformer or instrument calibration. For those turbojet engines having variable exhaust area, the movable arm of the autotransformer could be automatically controlled through a mechanical linkage to this area control.

Figure 6 shows the complete analogue computer for computing gross thrust. The amplifier and ratio transformer are mounted on the 7-inch square chassis. This chassis is larger than necessary to facilitate work upon circuitry during tests. The 6-unit transducer system is shown mounted compactly in a 4-inch square box. This computer equipment weighs about 16 pounds, exclusive of the weight of connecting cables and plumbing which depends on the actual aircraft installation. The weight of the computer could be decreased to less than ten pounds for operational aircraft instrumentation. After the computer has been initially adjusted for a particular type engine, no further adjustments should be required.

Laboratory Evaluation of the Jet Thrust Computer

The prototype model has been evaluated by controlled laboratory measurements. This evaluation was conducted in two phases. First, it was desirable to determine the limits of accuracy of the complete analogue computer without including errors due to transducer characteristics. The results of these measurements indicated an actual evaluation of the analog principles used in the thrust computer. This was accomplished by use of calibrated potentiometers which could be adjusted manually for feeding equivalent pressure data into the computer. These potentiometers were assembled in ganged units similar to the 3-unit trans-

Table I. Jet Thrust Computer Accuracy Tests

Total Pressure, Psi	Static Pressure, Psi	Measured Thrust, Pounds	Actual Calculated Thrust, Pounds	Deviation, Per cent of Max. Thrust
13.80	13.80	20	0	+0.61
15.20	14.30	260	257	+0.09
15.65	14.35	350	358	−0.06
16.40	14.40	545	538	+0.21
17.95	14.50	755	760	−0.15
18.10	14.60	935	938	−0.09
18.80	14.65	1,070	1,090	−0.61
19.35	14.70	1,195	1,205	−0.30
19.85	14.80	1,295	1,305	−0.30
21.30	15.05	1,570	1,580	−0.30
22.00	15.10	1,720	1,720	0.00
24.00	15.20	2,130	2,120	+0.30
26.00	15.30	2,520	2,505	+0.45
28.00	15.40	2,860	2,860	0.00
30.00	15.50	3,180	3,180	0.00

Table II. Jet Thrust Measurements Using Assimilated Exhaust Pressures and the Jet Thrust Computer with the 6-Unit Transducer System

Altitude, Feet	Rpm	Total Pressure, in. Hg	Static Pressure, in. Hg	Measured Thrust, Pounds Min.	Measured Thrust, Pounds Max.	Actual Calculated Thrust, Pounds	Maximum Deviation, Per cent of Maximum Thrust
5,000	11,800	31.4	27.9	500	560	500	3.3
	12,800	33.2	28.9	580	670	630	2.3
	13,800	36.4	30.3	820	920	860	3.3
	15,500	40.7	32.9	1,100	1,200	1,130	3.9
	16,700	45.7	36.3	1,320	1,460	1,370	5.0
	16,800	49.7	38.8	1,590	1,720	1,680	5.0
10,000	11,800	26.7	22.7	480	520	500	1.1
	13,800	30.6	25.1	700	780	760	3.3
	15,500	36.1	28.4	1,100	1,160	1,100	3.3
	16,800	42.0	32.2	1,370	1,500	1,470	5.5
15,000	12,800	23.3	19.8	510	510	460	2.8
	13,800	25.2	20.8	620	680	610	3.9
	15,500	29.5	23.1	890	960	910	2.8
	16,800	33.1	25.2	1,100	1,210	1,130	4.4
20,000	13,800	20.7	17.1	550	590	510	4.4
	15,600	24.6	19.2	740	800	780	2.2
	16,900	27.9	21.4	960	1,000	980	1.1

ducer system. Figure 7 shows this equipment as assembled for momentum thrust computations. Typical momentum thrusts, as computed by this equipment, are shown in Table I. The maximum errors introduced by the empirical representation of thrust and analogues are ±0.61 per cent. Therefore, the accuracy of the jet thrust computer should be largely a function of the accuracy of the transducers.

Measurements of the transducer characteristics (pressure versus displacement) for each potentiometer indicated a linearity to within ±2 per cent. There also exists an error of ±0.5 per cent maximum due to a hysteresis effect observable between increasing and decreasing pressure variations.

The complete transducer system was connected through a series of manually-controlled needle valves to a source of compressed air. In this manner controlled constant pressures could be applied to the jet thrust computer simulating independent total and static pressures. Ambient pressure was simulated for various altitudes by a controlled vacuum line. These pressures were measured with aircraft manifold pressure gauges which were calibrated against a mercury manometer. Gross thrusts as calculated according to the original thermodynamic equation for steady-state conditions of total, static, and ambient pressures were compared with the computer outputs. Table II shows typical results for the six single-unit system. The simulated exhaust pressures indicated in Table II are values taken from data recorded on a *FH-1* during flight. The two columns of measured thrusts in Table II indicate the minimum and maximum thrusts observed for any given set of conditions during repeated measurements. Therefore, the column of errors shown are the maximum errors observed during a series of tests. The average error observed was of the order of ±3.5 per cent. The average error using the ganged system was about ±2.5 per cent. These errors may be reducible in the future through improved design of low-torque potentiometers.

A study of the operation of the jet thrust computer in a turbojet installation has not been completed to date. The prototype model will be installed on a turbojet engine mounted on strain gauges in a test cell for evaluation of the thrust computer against strain-gauge indicated gross thrust.

Ram-Drag Measurements

An analysis of ram-drag at the air intake of a moving turbojet engine is incomplete at the present time. Several theories, varying in basic concepts, have been proposed, yet no particular theory is generally accepted. However, the jet thrust computer has certain properties that makes it applicable to certain types of ram-drag measurement. These possibilities will now be presented.

The jet thrust computer is adaptable to investigating ram-drag when it is assumed that ram-drag is a function of the gas velocities at the entrance of the air intake and that these gases behave adiabatically. Under these conditions it can be shown that the relationship between total and static pressures at the intake and ram-drag is similar to momentum thrust of the exhaust gases. Explicitly

$$F_r = A_4 P_{si} \frac{2\gamma_i}{\gamma_i - 1}\left[\left(\frac{P_{ti}}{P_{si}}\right)^{\frac{\gamma_i - 1}{\gamma_i}} - 1\right] \qquad (11)$$

This equation is the same as for the representation of momentum thrust except that the exhaust parameters are replaced by intake parameters. γ_i varies only to a second order with ambient temperature and can be assumed constant. If P_{ti}/P_{si} is plotted against

$$\left[\left(\frac{P_{ti}}{P_{si}}\right)^{\frac{\gamma_i - 1}{\gamma_i}} - 1\right]$$

for $\gamma_i = 1.40$, one obtains curve "B" in Figure 1. A determination of empirical constants for the power series representation of this function yields a characteristic which is within ±0.5 per cent of the original function within the range of gas velocities between Mach numbers 0 and 1. It was found that the ratios between these empirical constants and those determined for momentum thrust can be considered constant for all practical purposes, that is, $K_1'' = CK_1'$, $K_2'' = CK_2'$ and so forth, where $C = 1.15$.

Thus it may become possible to compute ram-drag on the basis of gas velocities at the air intake with the jet thrust computer. This is accomplished by using a jumper to by-pass the pressure thrust components and introducing the constant ratio (C) by the autotransformer. Figure 5 shows the simple circuitry for bypassing the pressure thrust components. The bypass cable is connected from $A_1B_2C_2$ to $A_1'B_2'C_2'$ instead of to the terminals of the differential transducer The resistor R_1 has the same resistance as the potentiometer P_1 for maintaining a balanced load on the ratio transformer.

If it is established in the future that ram-drag can be measured in the manner discussed, then net thrust can be measured during flight by connecting two jet thrust computers (gross thrust and ram-drag) in series opposition. The voltage developed across this combination should be proportional to net thrust.

No Discussion

Dynamic Characteristics of Carbon Pile Voltage Regulators

ROBERT L. MILLS
MEMBER AIEE

THE dynamic characteristics of voltage-regulated d-c electric systems are generally determined by empirical tests. By these tests one learns how the particular generator-regulator combination tested behaves, but the questions of how the regulator might work with another generator and how the regulator might be changed to improve the system operation are unanswered. In order to find an analytical method of answering these and other questions concerning the system operation a detailed study of the system was inaugurated at the Naval Research Laboratory in Washington, D.C.

Early in the study an opinion was formed that since the automatically-regulated electric system comprises ac losed loop it should be subject to analysis by the frequency spectrum method which had been devised for and advantageously applied to the analysis of servomechanisms and other obviously closed-loop systems. To realize the advantages of using this method it was found that a transfer function had to be defined for each system component and that the definition was not arbitrary. A transfer function is simply the ratio of an output variable to an input variable, but the input and output quantities of a particular system component must be those variables which are related to each other in this way: the output quantity must depend solely on the input quantity which in turn must be completely independent of the output except through the operation of the other components in the closed loop. The complete dependence of a component output quantity on the input variation makes it possible to study a component independently of the rest of the system and to determine a unique transfer function for the component. A transfer function defined as the ratio of the two quantities which satisfy the discussed criterion is a description of the behavior of a component regardless of the system in which the component is used. Simple graphical or analytical methods can be used to determine the operation of any system when all the component transfer functions are known.

Considering the variables involved in the operation of an electric system regulated by a carbon pile voltage regulator led to the conclusion that a proper transfer function for the regulator would have to be defined as the ratio of carbon pile resistance variations to regulator operating coil voltage variations. Resistance variation as an output quantity was recognized as an unconventional consideration to say the least, but a necessary one also. What other variable quantity which might be considered to be the regulator output would be unaffected by whether or not the carbon pile was connected into the field of a generator? And what other quantity would be unaffected by whether the generator with which the regulator is used is a low or high field current machine?

Having accepted this definition of regulator transfer function as a proper one, the next step was to obtain an expression for the function in terms of the constants of the regulator. This expression was derived from a regulator analysis which is described in detail in the body of this paper. It is based on the assumptions that deviations of the regulator variables from average values are small enough that the regulator can be considered linear and that variable frequency sinusoidal voltages are applied to the regulator operating coil. The regulator transfer function is therefore a function of frequency. Curves of amplitude and phase of the function versus frequency are presented in Figures 5 and 6.

In order to verify the validity of the transfer function expression it was necessary to measure a regulator transfer function. Doing this was by no means a simple matter. It was soon found that, in the neighborhood of the normal operating voltage, pile resistance is so sensitive to changes in voltage it is impractical to attempt to operate the regulator in its normal range in any situation in which feedback is not employed to make the operating coil voltage depend on pile resistance. The standard voltage regulated electric system is one in which the regulator can be operated normally, but use of this system for making transfer function measurements was prohibited by the difficulties involved in causing variable frequency sinusoidal voltages to occur across the regulator operating coil, and in measuring the amplitude and relative phase of the resulting pile resistance variations. Since there was no record of anyone's previously designing a system for making measurements similar to those we wanted to make, our only alternative was to design and build a system for the purpose. The system which finally operated as desired is described in detail in this paper. Electronic amplifiers are used to provide the feedback necessary to cause the regulator to operate normally and provisions were made in the design of the circuit so that a desired input signal can be easily impressed and so that resistance variations can be easily measured.

A plot of a regulator transfer function measured while the regulator was operated in this system is presented for comparison with the predicted curves in

Paper 50-213, recommended by the AIEE Air Transportation Committee and approved by the AIEE Technical Program Committee for presentation at the AIEE Middle Eastern District Meeting, Baltimore, Md., October 3–5, 1950. Manuscript submitted July 5, 1950; made available for printing August 23, 1950.

ROBERT L. MILLS is with the Magnolia Petroleum Company, Dallas, Texas.

This paper was prepared while the author was at the Naval Research Laboratory, Washington, D. C. and portions were done in partial fulfillment of the requirements for the degree of Master of Science at the University of Maryland.

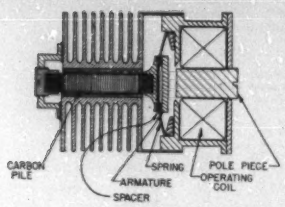

Figure 1. Section view of typical carbon pile regulator

Figures 5 and 6. The general agreement of the curves substantiates the validity of the analysis of the regulator from which the transfer function expression was derived. The disagreement of the two curves is attributed partially to the fact that, as yet, no method of determining the effective values of all the regulator constants has been devised.

The regulator analysis and the transfer function measuring system presented in this paper constitute the work done by the author on the "regulator section" of the study of the entire voltage regulated electrical system. Further studies of the regulator, a study of the generator transfer function, and methods of combining the transfer functions of the regulator and generator to obtain the system operating characteristics is continuing at the Naval Research Laboratory. Some of the progress made along these other lines is presented in a paper by Donald G. Scorgie entitled Transient Analysis of a Voltage-Regulated Aircraft D-C System.[1]

The order of presentation of the regulator analysis and the measuring circuit description is the reverse of the order in which they were mentioned in this introduction. The description of the measuring circuit is presented first to spare those who are just interested in a method of finding how a particular regulator works from a description of a mathematical argument to show why the regulator behaves as it does. Those interested in the mathematics of the situation will be pleased to note that the description of the circuit, though first, is brief.

General Description of Carbon Pile Regulator

Before discussing either the method of measuring the carbon pile regulator transfer function or the regulator analysis let us make sure everyone knows just what the carbon pile voltage regulator is. It is an electromagnetic device employing magnetic coupling between the electrical and mechanical parts. The most important parts are a stack or pile of carbon disks, a spring which has a soft iron armature attached to its movable end, and an electromagnet. Figure 1 is a diagram showing the arrangement of these parts in a typical regulator.

Here is how the regulator works. The spring exerts a force on the armature to compress the pile of carbon disks and reduce the pile resistance. The electromagnet and the reactive force of the pile oppose the force of the spring. The motion of the armature depends on an unbalance of these forces and the armature is stationary only when the force of the spring in one direction equals the forces of the pile and the magnet in the other direction. The spring and magnet are designed so that there is only a very small range of forces for which the spring force and the magnet force even approximately balance. This range corresponds to the small range of operating coil voltages in the vicinity of the desired regulating value and over this range of voltages the pile resistance varies from its maximum to its minimum useful values. For lower applied voltages (hence lower magnet forces) the balance of forces on the armature is attained with high pressure on the carbon pile and hence extremely low pile resistance. Figure 2 shows the type of carbon pile resistance versus electromagnet or operating coil voltage characteristic to be anticipated from a regulator designed in this manner. When the regulator is used to control the terminal voltage of a generator, the carbon pile is connected in series with the shunt field of the generator and the generator terminal voltage is applied to the regulator operating coil. It can be seen that if stability criteria are satisfied, the generator voltage will build up when the machine is first started to approximately the desired voltage and will then be stopped by the sudden increase in pile resistance. A desirable characteristic of the regulator is that it have high resistance sensitivity to voltage variations in the vicinity of the desired voltage. A particular advantage of a regulator that operates like the carbon pile regulator does is that the regulating action is made independent of the source of disturbance to the system.

Measurement of Regulator Transfer Function

High sensitivity of pile resistance to voltage variation which is necessary for most desirable regulating action was mentioned previously in this paper as the regulator characteristic which makes operating the regulator for study in some sort of feedback arrangement necessary. Figure 3 is the schematic diagram of an electronic feedback circuit that was devised for use with a 28-volt regulator. When the regulator is operated in this system its operation about any desired operating point in its normal operating range can be studied. You can see from the circuit diagram that once the regulator is operating at a desired resistance value that value of resistance will be automatically maintained. If the pile resistance tends to increase, for example, the electronic amplifier will make the regulator operating coil current increase and by the action of the regulator the resistance will be returned to its initial value. The initial desired value of pile resistance is set by means of one or both of the 50-ohm potentiometers shown in series with the carbon pile.

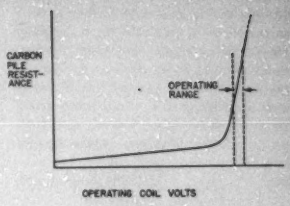

Figure 2. Idealized d-c characteristic of regulator

The principal advantages of measuring the regulator transfer function and otherwise studying the regulator operation while the regulator is operated in this system are the ease with which variable frequency sinusoidal voltages can be applied to the regulator operating coil and the ease and accuracy with which pile resistance variations can be measured. By applying the output of an audio or low-frequency oscillator to the input terminals noted on the diagram of Figure 3, a disturbance of any desired frequency or amplitude can be applied to the regulator operating coil. The magnitude of the disturbance to the regulator can be measured at the operating coil. The resistance in series with the carbon pile was made so large that the current through the carbon pile remains practically constant. The voltage across the carbon pile is proportional to the carbon pile resistance. The regulator output can then be simply found by dividing the alternating voltage measured right across the carbon pile by the current through the pile. The voltage variations across the pile are in

phase with the pile resistance variations, so the phase angle of the regulator transfer function which is the phase of the resistance variations relative to the a-c voltage across the operating coil can be measured by finding the phase angle of the a-c pile voltage relative to the a-c operating coil voltage. Measuring the same quantities while the regulator is operated with a standard generator would certainly not be this simple.

Figures 5 and 6 are plots of transfer function amplitude and phase versus frequency. The data for one curve in each figure were obtained while the regulator being tested was operated in the circuit of Figure 3. Voltage amplitudes were measured at the specified locations by standard methods and phase angles were calculated from measurements of Lissajous figures displayed on an oscilloscope. To make sure that the incremental inductance of the regulator operating coil did not vary with frequency, a measurement of total flux change was made at each frequency and maintained at a constant value. This measurement was effectively made by measuring the open circuit voltage induced in a coil wound concentrically with the operating coil. Since the voltage induced in this coil should vary linearly with frequency if the total flux change through the coil is constant, it was possible to insure constant flux change by adjusting the magnitude of the disturbance to the regulator at each frequency so that the auxiliary coil voltage varied linearly with frequency. This auxiliary coil, incidentally, is standard equipment on most carbon pile regulators. It is the coil which is ordinarily used for adjusting the division of load between two or more regulated generators operated in parallel.

During the tests of the regulator it was found that the transfer function depended on the average operating point to which the regulator is set for making measurements and on the input magnitude for small magnitudes. Dependence of the transfer function on the operating point can be attributed to changes in the incremental values of the regulator constants with operating point. The other dependence of the transfer function is probably due to changes in the incremental inductance of the operating coil. This inductance depends on the average slope of the minor hysteresis loop in the iron circuit. In typical regulators the inductance appears to reach a maximum value when an output of roughly 5 rms ohms is obtained and the transfer function is constant for greater disturbances.

The linearity of the regulator operation was criticized only by observing the wave shape of the output quantity on the oscilloscope, but surprisingly little distortion was noted over what was considered to be very wide deviations of the regulator variables from their average values. No distortion was noted while the data plotted in Figures 5 and 6 were being obtained as rms input voltages as high as 0.75 volt were used at the higher frequencies and rms resistance variations as high as 5.35 ohms occurred at the lower frequencies.

The shape of the transfer function curves shown in Figures 5 and 6 might have been surprising to those taking the data had the analysis of the regulator in which we had some slight confidence not been conducted previously. Is it not somewhat surprising, though, to notice that at one frequency (the frequency at which the phase shift is 180 degrees) as the regulator operating coil voltage increases decreasing pile resistance indicates that the armature moves away from the electromagnet? Obtaining reasonable explanations of how situations like this can come about is what makes analysis interesting.

Determining the Transfer Function by Analysis

The fact was pointed out in the general description of the regulator and illustrated in Figure 2 that the pile resistance versus operating coil voltage curve was characterized by a rather sharp break at some voltage below the normal operating voltage range. This break is necessary for achieving a very high sensitivity in the desired voltage range and adjustment of its location on the voltage axis is a convenient method of setting the voltage at which the regulated system operates. This break, however, must be disregarded if we are to analyze the regulator on the assumption that it is a linear device. In order to do this all d-c components of variables must be eliminated and only variations about arbitrary reference values considered. When only these variations are considered the assumption is tacitly made that the reference values are attainable. In other words the analysis we are conducting will be useful in determining the behavior of a regulated aircraft electric system which is disturbed by something such as the removal or application of load after it has first reached a stable condition. If the system never reaches the first stable condition, its dynamic behavior after a certain disturbance is of little interest anyway, so, by considering only variations about reference values, only knowledge of interesting systems which have once been stable will be obtained. A further linearizing assumption, that all deviations

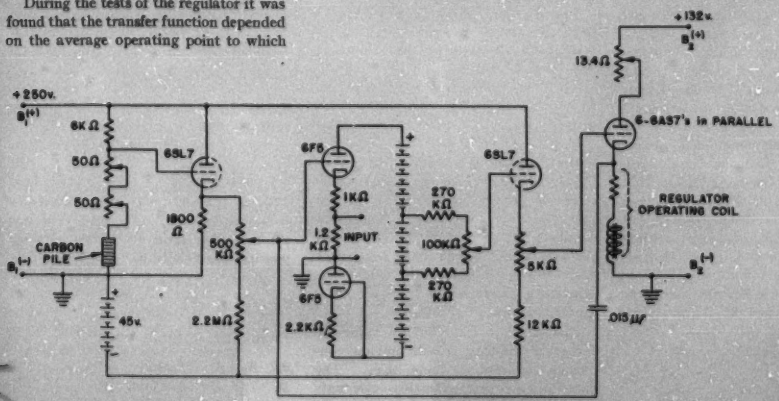

Figure 3. Schematic diagram of measuring circuit

from reference values are small enough that they are proportional to the quantity which caused them, will be made.

The correlation between the frequency characteristics and the transient behavior of linear systems has received sufficient publicity that it need not be repeated here, but because it does exist sufficient information to determine the regulator behavior when subjected to any disturbance will be at hand when its frequency characteristics are known. For this reason the object of the regulator analysis might be stated to be the determination of the regulator frequency characteristics. Whether the result of the analysis be called the frequency characteristics or the transfer function is actually unimportant, since hairs have to be split to distinguish between the two terms. What is important, since analytic results can be checked by comparatively easy tests, is that the regulator can be analyzed on the assumption that the input quantity is sinusoidal. Under this assumption, and according to the definition of transfer function given in the introduction, the transfer function, symbolized by T_r, is

$$T_r = \frac{R}{\epsilon}(\omega)$$

where R and ϵ are sinusoidal variations of carbon pile resistance and operating coil voltage, respectively, and ω is the angular frequency of the sinusoidal applied voltage.

To obtain the desired expression in terms of the regulator constants a solution to the differential equations describing the behavior of the regulator must be obtained. The regulator has already been described as a device involving motion of mechanical parts and current in an electrical circuit. For this reason two equations are necessary to describe the regulator behavior; one dealing with the electrical elements, the other with the mechanical elements. The one dealing with the electrical circuit can be an expression of the fact that the sum of the voltage drops equals the applied voltage. The one dealing with the mechanical parts can be an expression of the fact that the sum of the forces applied to a mass equals the inertia force. Noting that voltage drops are due to the resistance and rate of change of flux linkages of the operating coil and that forces are applied to the armature by the electromagnet, the spring, and the carbon pile, the two equations can be written

$$E_o + \epsilon = R_c(I_o + i) + N\frac{d\phi}{dt} \tag{1}$$

$$F_M + F_s + F_p = M\frac{d^2x}{dt^2} \tag{2}$$

where

$E_o + \epsilon$ = applied voltage
E_o = desired reference operating coil voltage
ϵ = instantaneous variation in operating coil voltage
$(I_o + i)$ = operating coil current I_o and i having definitions analogous to E_o and ϵ, respectively
R_c = resistance of the operating coil circuit
N = number of effective turns in the operating coil
ϕ = total flux crossing the air gap and linking the operating coil, expressed in webers
F_m = force of the electromagnet
F_s = force of the spring
F_p = force of the carbon pile
M = effective mass of the moving armature
x = instantaneous deviation of the armature from its reference position
t = time

Viscous damping of the armature due to air is disregarded in equation 2. That it was negligible was verified by measuring the transfer function of a regulator operated in an evacuated chamber.

The signs of the forces of the magnet, the spring, and the pile can be determined only after an arbitrary decision has been made concerning positive displacement of the armature. So, let displacement toward the magnet be positive. Then by reference to the regulator diagram of Figure 1 it can be seen that forces of the magnet and the carbon pile are positive while the force of the spring is negative. All of these forces are functions of armature position. The force of the magnet, however, is also a function of the operating coil current and cannot be written in an expression as simple as those for the spring and the carbon pile. A detailed expression for the magnet force is presented later.

The regulator has been assumed to be a linear device so the expressions for the spring and pile forces can be assumed to be

$$F_s = -F_{0s} - K_s x \tag{3}$$

$$F_p = F_{0p} - K_p x \tag{4}$$

where F is used as a symbol for force, x for displacement of the armature from its reference position as above, and K for proportionality constants. The subscripts, s and p, refer to the spring and the pile, respectively, and the zero before the subscripts indicates the value of the quantity represented when the displacement (x) is zero.

The signs of the reference values of forces are seen to agree with previous conclusions concerning these signs. The signs of the proportionality constants were determined by simple reasoning. The negative force of the spring increases with positive armature displacement so the sign of the proportionality constant must be negative. The positive force of the pile decreases with positive armature displacement so the sign of the constant must be negative.

Substitution of these expressions for the spring and pile force in equation 2 gives

$$F_M + (F_{0p} - F_{0s}) - x(K_s + K_p) = M\frac{dx^2}{dt^2} \tag{5}$$

Equations 1 and 5 apply to the regulator simultaneously, but they cannot be solved until the total number of variables is reduced still further. The number of dependent variables can be reduced to two by first expressing the flux as a function of operating coil current and armature position and then expressing the magnet force as a function of the expression for flux.

If the assumption is made that the reluctance of the iron in the flux path is negligible in comparison to the reluctance of the air gap, the flux can be expressed as a function of the operating coil current and the air gap reluctance

$$\phi = N(I_o + i)/Rel_{AG} \tag{6}$$

where Rel_{AG} is the air gap reluctance in meter-kilogram-second units. The air-gap reluctance is proportional to the air-gap length and can be expressed as

$$Rel_{AG} = 2(s - x)/\mu A \tag{7}$$

where

s = distance from the pole face to the surface of the armature when $x = 0$
A = effective area of the air gap (in practice very nearly the pole piece area), and
μ = permeability of the air gap, and equals $4\pi \times 10^{-7}$ in meter-kilogram-second units

From equations 6 and 7

$$\phi = N(I_o + i)\mu A/2(s - x) \tag{8}$$

Letting i and x equal zero, we obtain the reference flux

$$\phi_0 = \frac{NI_oA\mu}{2s} \tag{9}$$

The flux is a continuous function of i and x, and can be expressed approximately by the first three terms of the Taylor's expansion about the point (I_o, s).

$$\phi = \phi_0 + i\frac{N\mu A}{2s} + x\frac{NI_o\mu A}{2s^2} \tag{10}$$

From equation 10 we obtain

$$\frac{d\phi}{dt} = \frac{N\mu A}{2s}\frac{di}{dt} + \frac{NI_o\mu A}{2s^2}\frac{dx}{dt} \tag{11}$$

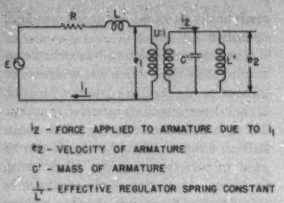

Figure 4. Equivalent circuit of carbon pile regulator

The force due to the magnet can be expressed as a function of flux. By following the same procedure as above, a reference force value can be found and the force for different values of coil current and armature displacement found by means of an expansion.

The force due to the magnet is proportional to the square of the total flux (2ϕ) between the surfaces, and inversely proportional to the total area (approximately twice the A previously defined) through which this flux passes. Using the previously-defined symbols the force is

$$F_m = \frac{\phi^2}{\mu A} \simeq \frac{N^2(I_o+i)^2 A\mu}{4(s-x)^2} \tag{12}$$

and the reference value of the force is

$$F_{0m} = \frac{N^2 I_o^2 A\mu}{4s^2} \tag{13}$$

Then expanding equation 12 and neglecting second order terms

$$F_m = F_{0m} + i\frac{I_o N^2 A\mu}{2s^2} + x\frac{N^2 I_o^2 A\mu}{2s^3} \tag{14}$$

By substituting the expression 11 for $d\phi/dt$ in equation 1 and expression 14 for F_m in equation 5 the following equations are obtained

$$E_o + e = R_c(I_o+i) + \mu\frac{N^2 A}{2s}\frac{di}{dt} + \frac{N^2 A I_o \mu}{2s^2}\frac{dx}{dt} \tag{15}$$

$$F_{0m} - F_{0s} + F_{0p} + i\frac{I_o N^2 \mu A}{2s^2} + x\left[\frac{N^2 I_o^2 A\mu}{2s^3} - K_s - K_p\right] = M\frac{d^2x}{dt^2} \tag{16}$$

The two equations describing the regulator now have only two dependent variables, x and i, and can be solved for either one when the applied voltage $E_o + e$ is known.

To simplify the equations: eliminate $F_{0m} - F_{0s} + F_{0p}$ from equation 16 because the sum of the forces on the armature is zero when it is stationary in its reference position, eliminate the steady-state voltage and current, E_o and I_o, from equation 15 for reasons discussed previously, and let

$$L = \frac{N^2\mu A}{2s},\ U = \frac{N^2\mu A I_o}{2s^2},\ \text{and}\ K = K_s + K_p - \frac{N^2 I_o^2 \mu A}{2s^3}$$

The equations then become

$$e = R_c i + L\frac{di}{dt} + U\frac{dx}{dt} \tag{17}$$

$$Ui = M\frac{d^2x}{dt^2} + Kx \tag{18}$$

Now, since we are interested in a steady-state solution when e is sinusoidal, replace the symbol, d/dt, indicating differentiation with respect to time, with the imaginary quantity $j\omega$ where ω is the angular frequency of the applied voltage. Use bold face italic letters to symbolize variable quantities which can be interpreted as vectors and equations 17 and 18 become

$$\boldsymbol{E} = \boldsymbol{I}(R_c + j\omega L) + j\omega U\boldsymbol{X} \tag{19}$$

$$U\boldsymbol{I} = \boldsymbol{X}(K - \omega^2 M) \tag{20}$$

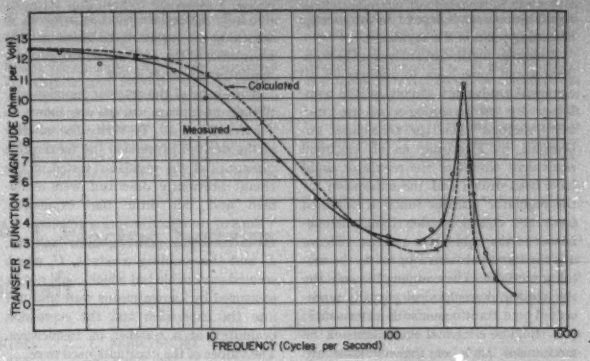

Figure 5. Transfer function magnitude

Only algebraic manipulation is now necessary to solve the equations for the ratio of $\boldsymbol{X}$ to $\boldsymbol{E}$. If we now multiply this ratio by P, where P is defined to be the proportionality constant between carbon pile resistance and armature displacement, we have arrived. The result is an expression for the carbon pile voltage regulator transfer function.

$$T_r = \frac{UP}{KR_c - \omega^2 R_c M + j\omega(KL + U^2 - \omega^2 LM)} \tag{21}$$

The constants of this expression are what have been referred to throughout this paper as the regulator constants. The expressions defining these constants show how they are affected by the factors entering into the design of the regulators. The defining expressions are also of value in indicating approximately how the

Figure 6. Transfer function phase

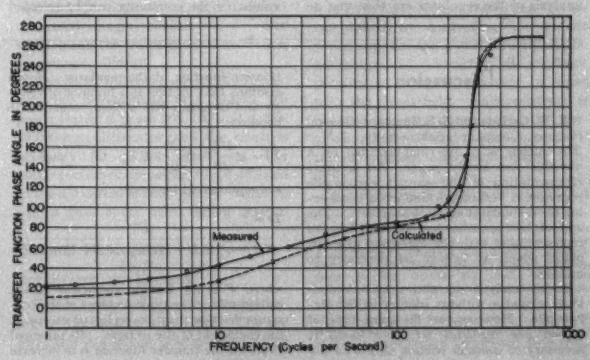

regulator constants depend on the average operating point of the regulator.

A simpler method of analyzing the regulator would have been to analyze an all electrical equivalent circuit of the regulator. By using analogies of the "mobility method" and the procedures authorized by Firestone[2] an all electrical equivalent circuit of the regulator could have been drawn and the expression for the regulator transfer function obtained from the equations describing the behavior of the equivalent system. Figure 4 is the circuit obtained by using the mobility method. The coupling between the electrical and mechanical parts is represented by a transformer with a turns ratio of U:1. The electrical equivalents of the mechanical parts of the regulator are shown to the right of the transformer in the figure. Those interested are welcome to verify the fact that the equations describing this circuit are identical to those describing the regulator when the analogies listed in Figure 4 are used. In attempting to derive the regulator transfer function expression from the equations of the electric system notice that the voltage e_2 is analogous to the velocity and not the displacement of the armature. To handle this difficulty go ahead and find the ratio of e_2 to E, then divide the result by $j\omega$ to obtain an expression for the ratio of displacement to applied voltage.

The principal usefulness of this equivalent circuit is that those familiar with electrical circuits can readily determine the qualitative effect of a proposed change in the value of a regulator constant by noting the change that would occur in the equivalent electrical circuit element. The effect of this change on the operation of the all electrical circuit can then be determined and interpreted in terms of regulator operation. The disadvantages of using the equivalent circuit for a detailed analysis of the regulator are that you do not fully appreciate what is involved in assuming the system to be linear and the usefulness of the expressions defining the regulator constants is lost.

The shape of the transfer function amplitude and phase curves are shown in Figures 5 and 6. To verify the validity of the derived expression the measurable constants of the regulator tested in the circuit previously described were evaluated and put into the expression. Values of the effective spring constant, K, the incremental operating coil inductance, L, and the coupling constant, U, which seemed reasonable but which could not be measured by known means were also put into the expression and the expression evaluated at a number of frequencies. The values of the constants used were

$R_c = 39$ ohms
$P = 327{,}000$ ohms per meter
$M = 0.059$ kilogram
$K = 76{,}600$ newtons per meter
$L = 0.145$ henry
$U = 114$ newtons per ampere

The plot of the calculated value of amplitude and phase are shown for comparison on the same figure with the corresponding measured curves.

Conclusions

The most important conclusion that can be reached from the work described in this paper is that the derived expression for the carbon pile regulator transfer function is a true expression to a high degree of accuracy. This conclusion is supported by the agreement obtained between measured and calculated values of the function. The implications of this conclusion are that the expression can be used to determine the effect on the dynamic behavior of the regulator of proposed regulator design changes and that values of the constants can be selected analytically to cause improved regulator operation.

The only conclusion to be reached concerning the circuit which was designed for measuring the regulator transfer function is that it performed its intended function. There is little doubt in the mind of the author, however, that the circuit can be used to perform numerous other useful functions. Operation of the regulator in this circuit will certainly simplify making direct studies of the effects on regulator operation of varying regulator parameters, changing the adjustment of the regulator, operating the regulator over wide ranges of temperature, pressure, and humidity conditions, and operating the regulator while it is being subjected to vibration.

Of course, the effects of the regulator operating characteristics on the dynamic characteristics of the entire voltage regulated electric system must be determined before evaluation of the factors affecting regulator operation is worthwhile. This becomes a relatively simple matter, though, when the analytical method involving the use of transfer functions, which was mentioned earlier in this paper, is used. The author therefore suspects that the most significant contribution of this paper to the field of analyzing electric systems regulated by variable resistance devices may turn out to be the pointing out of the fact that the "figure of merit" of the regulator, its transfer function, should be defined as the ratio of resistance variation to operating voltage variation.

References

1. Transient Analysis of a Voltage-Regulated Aircraft D-C System, **Donald G. Scorgie.** *AIEE Transactions*, volume 69, part II, 1950, pages 1318–23.

2. Mechanical-Electrical Analogies, **F. A. Firestone.** *Journal of Applied Physics* (New York, N. Y.), June 1939, pages 373–87.

Discussion

K. W. Carlson and **E. S. Sherrard** (General Electric Company, Schenectady, N.Y.): The author is to be complimented on a valuable and timely paper. An accurate representation of the aircraft carbon-pile regulator is very important when considering the stability of an electric system. The analysis by the author has resulted in a good representation with the exception of a few points which we believe are necessary to include.

In his analysis the author considers an ideal regulator without friction in the carbon pile. However, on the same type of carbon pile regulator we have found it necessary to consider friction effects on the transfer function of the regulator. If one assumes that friction is a function of velocity and linearizes the system, equation 18 becomes:

$$Ui = M\frac{d^2X}{dt^2} + F\frac{dX}{dt} + KX$$

and equation 21 becomes:

$$Tr = \frac{UP}{KR_c - \omega^2(R_cM + FL) + j\omega(KL + U^2 + R_cF - \omega^2LM)}$$

where F is the friction coefficient of the carbon pile. For typical values of the constants friction may be neglected except in the coefficient of the ω^2 term. Its principal effect on the transfer function is to increase the phase shift at low frequencies, decrease the slope of the phase shift curve in the region of resonant frequency, and lower the peak of the transfer function magnitude at the same resonant frequency.

Another departure from an ideal regulator involves the iron losses of the regulator. A plot of the ratio of voltage to current of the regulator coil versus frequency will show that the ideal equations do not accurately represent the regulator. This effect possibly may be approximated by the introduction of a shorted turn linked magnetically with the voltage coil.

R. L. Mills: I am grateful for the comments of Mr. Carlson and Mr. Sherrard on my paper and I find their opinions concern-

ing pile friction particularly interesting. I regret that they did not go into more detail on how they came to the conclusion that the term needed for improving the accuracy of the transfer function expression appears when pile friction is considered. In trying to picture pile friction in my mind I visualize particles on the surfaces of adjacent carbon disks sliding against one another as pile pressure is varied. I am skeptical of forces resulting from such friction being proportional to velocity and of them being of appreciable magnitude. Therefore I wonder if an equivalent term might not appear in the expression if some other factors neglected in the analysis were considered. Iron losses, for example, which were mentioned by Carlson and Sherrard unquestionably exist and proper consideration of their effect may also give rise to the desired term. In this case the existence of appreciable pile friction would certainly be open to question.

These discussions serve to emphasize the point that much is still to be learned and explained about the behavior of the carbon pile regulator. I admit that many factors affecting the operation of the device were neglected in this first reported study of the dynamic characteristics. It is to be hoped that these other factors will be considered in future studies so that regulator design can be more easily improved, but I feel that further refinements in the regulator analysis are unnecessary for reasonably accurate analyses of the systems in which the regulator is used.

Wide Speed Range A-C Electric Systems for Aircraft

H. B. JAMES
ASSOCIATE AIEE

R. P. JUDKINS
ASSOCIATE AIEE

C. L. MERSHON
ASSOCIATE AIEE

Synopsis: The increased demand for variable-frequency a-c generating systems on present-day aircraft calls for the development of adequate generators and their controls in order that the advantages of these systems may be fully realized. The requirements are good voltage regulation, exciter stability over the required speed range, and general reliability in operation under the various environmental conditions experienced in military aircraft service. Several such generators and their controls have been developed and tested.

WITHIN the past few years there has been a noticeable movement on the part of the military services and the aircraft manufacturers toward the use of variable-frequency electric power for use on newer airplanes. This movement has resulted in the need for a-c generators which can be mounted directly on an engine accessory pad and be driven at speeds proportional to those of the main engines. This has meant that speed changes of as much as 2-to-1 must be covered in the rated speed range of the alternator.

Extensive work has been done in the past on the development of constant-frequency generating systems for aircraft use and is adequately covered by other authors.[1,2,3] The main incentive for the use of the variable-frequency system over the constant-frequency system is the elimination of the variable-ratio, constant-speed drive between the main engine and the power take-off to the generator shaft. Constant speed drives are not highly efficient and their weights approach that of the alternators which they are to drive.

The higher efficiency and lower weight of the variable-frequency generating system is especially attractive to the military aircraft industry and within the past few years more and more applications have been made of this type of electric power supply. It has long been recognized[4] that such a system has an inherent disadvantage in that it is not suitable for induction motor loads. Electronic, lighting, and heating loads can be served adequately, but the torque and speed of induction motors changes with frequency. However, the majority of the applications for this type of electric power are radar and other electronic loads, deicing equipment, and various heaters of all types.

Actually, the use of variable-frequency power on aircraft is not an entirely new idea, but in the past most of these systems were either bus-excited from the conventional 28-volt d-c system or were self-excited by means of electronic exciters.[5] The important change to be considered here is the use of an integral exciter, mounted on the same shaft as the rotating field of the alternator. In the past the design and development of such a direct-connected integral exciter was a factor which made the use of such an excitation system very difficult.

This paper will cover specifically the design and development of a 30-kva, 0.9 power factor, 3-phase 208/120-volt 4,000-/8,000-rpm alternator and the controls necessary for proper operation. The major portion of the paper will be devoted to the discussion of this system. Mention will be made of one other similar system.

General Description

Alternator and Exciter

Figure 1 shows a cross-sectional drawing of the 30-kva alternator. The a-c generator is a salient pole machine which provides a frequency of 600 cycles per second at the nominal speed of 6,000 rpm. A rotating field is used with damper windings to improve the wave form and limit the degree of phase voltage unbalance for unbalanced loads.

The exciter is a 6-pole machine with pole-face winding and a full set of interpoles. Compensation against armature reaction is essential to obtain good commutation and to reduce compounding effects from the conductors undergoing commutation.

The a-c generator and exciter are mounted on the same shaft which is supported between two bearings. The rotor is built to withstand an overspeed of 11,000 rpm giving a peripheral velocity of 20,800 feet per minute. To withstand the high centrifugal forces, the rotating field magnetic structure was made by stacking punchings on a tubular shaft. Each punching is an incremental part of the 12 salient poles and the yoke. This construction necessitated winding the coils directly upon the punchings since individual poles are not removable.

An internal fan attached to the rotor provides ventilating air while the airplane is on the ground and there is no ram air pressure. This gives sufficient cooling for the alternator to deliver 25 per cent rated load. Figure 2 illustrates the unit.

Voltage Regulator

Alternator voltage regulation is accomplished by controlling the exciter which supplies the power directly to the alternator field. A carbon-pile regulator provides a variable resistance in series with the shunt field. This resistance is changed in accordance with the particular speed and load conditions to maintain a constant alternator output voltage.

A conventional voltage sensing circuit

Paper 50-276, recommended by the AIEE Air Transportation Committee and approved by the AIEE Technical Program Committee for presentation at the AIEE Middle Eastern District Meeting, Baltimore, Md., October 3-5, 1950. Manuscript submitted July 11, 1950; made available for printing August 30, 1950.

H. B. James, R. P. Judkins, and C. L. Mershon are all with the Aviation Engineering Department of Westinghouse Electric Corporation, Lima, Ohio.

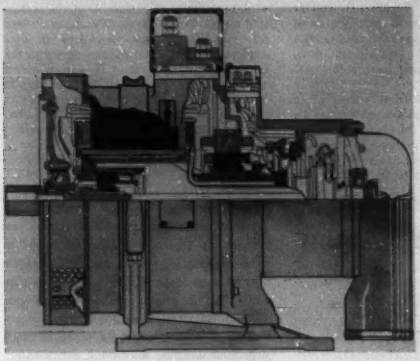

Figure 1 (left). Cross-sectional view of 30-kva 3-phase 208/120-volt wide-speed-range aircraft alternator and exciter

Figure 2 (right). Side view of 30-kva aircraft alternator and exciter

is used as shown in Figure 3. Open-delta-connected transformers and a 3-phase full-wave bridge rectifier supply the signal to the regulator coil circuit. This particular transformer connection is lighter and less bulky than a 3-phase delta or Y connection. The signal is an average of the three line voltages, and has the advantage of holding all line voltages near an average value, when unbalanced loads are imposed upon the alternator; then the third harmonics and others which exist when sensing a single line to neutral voltage, are cancelled. The open-delta-connected transformers are designed for the minimum frequency encountered, because the maximum flux density in the core and the maximum core losses occur at this frequency for a constant voltage input.[6] Tests have shown that the effect of frequency over the range involved is negligible so far as it concerns the sensing circuit of the regulator.

The carbon-pile regulator is similar to conventional d-c generator voltage regulators.[7,8] It is a self-contained unit which, when properly adjusted, will operate to maintain the generator output voltage within 2 to 3 per cent if the operating range for which the system is designed is not exceeded. Alternator speed and load changes, result in momentary changes in the generated voltage, which are received as signals at the regulating coil of the carbon-pile regulator. This produces a change in the coil magnetizing force which, in turn, ~~acts on the~~ armature of the magnet to oppose the force exerted on the carbon pile by the armature spring. The pressure change on the carbon pile is sufficient to change its resistance so that the exciter field current will assume the required value to allow the alternator to again generate the desired voltage.

In order to co-ordinate the design of an alternator and a regulator certain factors concerning the limitations of the carbon pile must be considered.

The particular force-deflection characteristic of the carbon pile and its relationship to the magnet pull curves and armature spring characteristic[9] demand that the ratio of maximum to minimum external exciter shunt field resistance should not exceed approximately 30-to-1. If a resistance ratio greater than 30-to-1 is required, due to the particular exciter de-

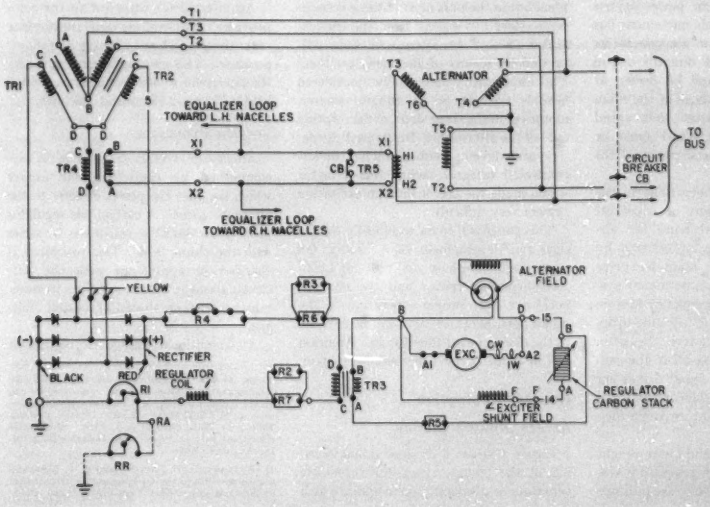

Figure 3. Schematic wiring diagram of aircraft a-c electric system

TR1—line transformer (step-down)
TR2—line transformer (step-down)
TR3—stabilizing transformer
TR4—mutual reactor transformer
TR5—current transformer
R1—voltage adjusting rheostat
RR—remote voltage adjusting rheostat
R4—ballast resistor
R5—feedback adjustment resistor
R2, R3, R6, and *R7*—temperature compensating resistors

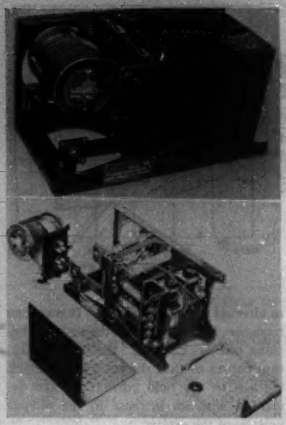

Figure 4. 30-kva aircraft alternator voltage regulator

Top—side view, completely assembled
Bottom—carbon-pile regulating element, cover and end plate removed

sign and load demand, difficulty is likely to be encountered at either or both ends of the resistance range.

For example, at the lower end of the resistance range an increasingly greater droop in voltage may be required to produce the force necessary on the carbon pile to obtain this resistance. At the higher end of the resistance range the force required may be so small that the regulator is susceptible to vibration and acceleration.

Experience indicates that for most applications the average voltage per carbon disk in the pile should not exceed a maximum of one-half volt. If this value is exceeded an arcing condition results which is much like that encountered in instability of mechanical vibration conditions. This maximum value of voltage per disk can be exceeded slightly but only at the expense of the resistance range.

The maximum wattage dissipated in the carbon pile is another important consideration. The designer of the alternator and exciter should bear in mind that any regulator has definite maximum heat dissipating capacity and this value should not be exceeded, except for possible short time intervals. The maximum power in the regulator at any output voltage of a shunt exciter is expressed as.[10]

$$P_{max} = \frac{V^2}{4R_F}$$

where

P_{max} = maximum power, watts
V = exciter output volts
R_F = exciter field resistance, ohms

Consideration also should be given to altitude conditions particularly with respect to the possibility of the regulator overheating. Higher wattage capacity has been obtained by using more than one standard regulator, but this adds to the problem of adjustment and maintenance, both of which are important factors to the successful design of any electric power system.

An anticipating transformer is used to stabilize the excitation system under transient load conditions. This transformer introduces a signal into the regulator coil circuit in series with the signal from the main voltage sensing rectifier. This feedback signal is of such a polarity as to oppose the original change and is proportional to the rate of change of the exciter output voltage. The effect of this stabilization tends to prevent over or under shooting the correct value of the excitation for the new load condition. Theoretically, the direct current flowing in the primary and secondary windings of the transformer should cancel each other preventing saturation in the transformer core. Actually this condition cannot be obtained except for a particular exciter output voltage, because the primary of the transformer is directly connected across the exciter, while the secondary is in series in the regulator coil circuit which carries essentially constant current. For this reason an air gap is purposely introduced into the magnetic core in order to obtain the maximum possible incremental permeability over the range of operation of the system.

The regulator circuit is temperature compensated by means of the inverse-temperature-resistance characteristic of two special carbon resistors and the selenium rectifier cells. Tests have demonstrated that the voltage regulation is between 3 and 4 per cent over the temperature range of −55 and +71 degrees centigrade.

Figure 4 shows a view of the regulator completely assembled, and also shows the same regulator with the carbon pile element removed and the cover and end plate removed from the box assembly.

General Theory

An excitation system for a constant-frequency alternator will be discussed first since the scheme to be discussed later has many points in common with this system. Figure 3 indicates the essential parts of the system under consideration.

The operation of the exciter and its required regulator resistance range can be studied by the aid of curves given in Figure 5.

The shunt field line, voltage versus current, can be drawn in as a straight line assuming that its resistance is constant at a particular temperature condition. On the load saturation curve "OD" at any particular value of exciter output voltage, V, there is a corresponding field current, I_F, a voltage across the regulator stack,

Figure 6 (below). Curves of separately-excited exciter and various amounts of external resistance. See schematic diagram Figure 10

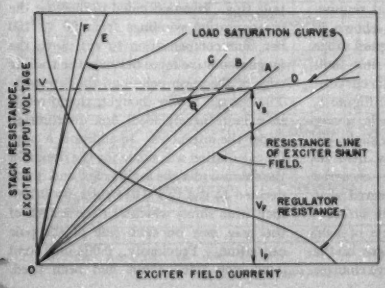

Figure 5 (left). Load saturation curves at maximum and minimum speed of a shunt exciter with resistance lines for the shunt field and various amounts of external resistance

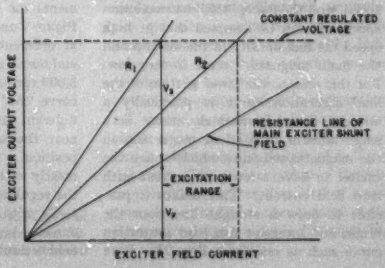

V_S, and a voltage across the field, V_F. The stack resistance is then simply V_S/I_F. Different values of stack resistance can be readily calculated and plotted as indicated by the resistance curve in Figure 5. It is apparent that if the resistance curve should have zero slope or positive slope at any point there could exist more than one value of output voltage for a given regulator stack resistance. This will cause the exciter to be very unstable and result in the output voltage of the alternator being modulated at a frequency corresponding to the regulator stack movements.

Another way of arriving at the stack resistance, amounting to the same thing but somewhat more explicit, is to draw in a number of resistance lines intersecting the load saturation curve at various points such as the lines *OA*, *OB*, and *OC*. Each of these lines represents the shunt-field plus a certain amount of stack resistance. In regard to stability with this method of analysis, the saturation curve resistance must not coincide with any resistance line of the exciter, nor can there be any resistance line that intersects the load saturation curve at more than one point if the exciter is to be stable.

The degree of stability of the exciter is indicated by the magnitude of the angle between a resistance line and the saturation curve.[11] This is apparent by observing that as this angle becomes small, a very small change in stack resistance produces a great change in the exciter output voltage. Restating this principle in other words, the intersection angle between the two lines must always be greater than zero.[12]

Considering a wide-speed-range alternator of 2-to-1 speed range, such as the 30-kva alternator described, the problem is greatly complicated in attempting to fulfill the requirements previously mentioned. The same remarks must apply for all speeds within the rating of the machine, or an infinite number of saturation curves. For instance, the saturation curve, "OD," may be for minimum speed, and the curve "OE" for maximum speed. It can be assumed that at high speed the flux density in the air gap and the main magnetic circuit is very low. For this reason, the lower portion of the load saturation curve is practically a straight line. Fortunately, there is a small amount of residual magnetism in the magnetic structure which causes the exciter to have a few volts output with zero field current. This makes it possible to draw a straight line from the origin and intersect this load saturation curve such as resistance line *OF*. Here

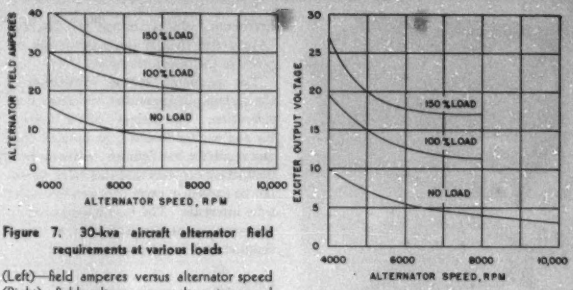

Figure 7. 30-kva aircraft alternator field requirements at various loads

(Left)—field amperes versus alternator speed
(Right)—field voltage versus alternator speed
(includes slip ring brush drop)

the angle of intersection becomes very small, and if it were not for excellent performance from the carbon pile regulator and the stabilizing circuit, very likely the speed range would have to be reduced for satisfactory operation.

When a separately-excited exciter is used, the problem is simplified in several respects. Here the regulator stack resistance is not influenced by the exciter output voltage, see Figure 6. As before, the stack resistance is equal to the value of the resistance line, such as R_1 or R_3, less the field resistance for any particular values of field current. For any desired value of the exciter output voltage, a set of load saturation curves will be required.

The time constants of the exciter field, the alternator field and the exciter armature are important considerations in a study of the stability of an a-c generating system. It is beyond the scope of this paper to discuss these constants and reference is made to R. E. Doherty's authoritative paper Exciter Instability.[11] This paper also deals with exciter polarity reversals, a difficulty which is encountered on aircraft application of exciters.

Test Results

Curves of the voltage-current requirements for this alternator are shown in Figure 7 and cover the entire speed range at different loads. The first unit built and tested gave a load saturation curve at 5,000 rpm as roughly shown in Figure 8, curve "A." For different speeds, giving different saturation curves, the slight dip near the origin approximately held its position. Since the trouble occurred mostly at high speeds, it appeared that the regulator could not operate satisfactorily with such small amounts of field current, because minute changes in the field current resulted in very large changes in alternator output voltage. It was then recognized, however, that the problem became one of "shaping" the load saturation curves so that the ratio of the stack voltage to the field current always decreased with an increase in the output voltage of the exciter.

It was theorized that the dip in curve "A," near the origin was a result of the compounding effect from the conductors undergoing commutation. This was not enough, however, to account for the dip in the curve. Changing of the interpole face and adjusting the interpole ampere-turn strength resulted only in a slight shifting of the position of the dip.

Realizing the difficulty in correcting the compounding effect, the problem was approached by placing shims under the main poles, the thought being that the shims would begin to saturate at the point of dip in the curve. Above that point the thickness of the shim would be virtually the equivalent to an air gap added to the magnetic circuit of a length equal to the thickness of the shims. Results were somewhat encouraging, but the dip still remained to the extent that the machine would not regulate with the carbon pile regulator.

Since the air gap between the pole tips was relatively small, the leakage flux from the tips of the interpoles to the main poles was blamed for saturating the interpole tips. It was decided to increase the compensating windings from 50 to 100 per cent compensation to cut down the magnetomotive force between the trailing edge of the main poles and the interpole. The change, it was thought, would result in a more nearly ideal flux distribution under the interpoles. In addition, a careful calculation was made for the design of the shims under the main poles, and it was decided to use two 0.014-thick by 0.100-inch wide shims which ran the length of the pole, one on each side of the pole centerline. Previously, 0.002-inch and 0.005-inch thick shims had been used.

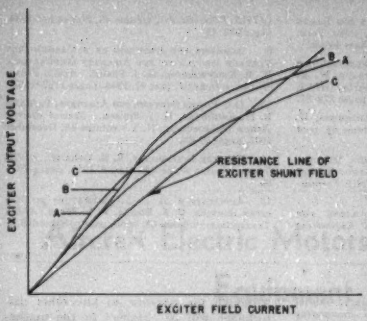

Figure 8 (left). Typical curves of shunt exciter showing effect of modifications in design

A—Original design
B—Compensation increased to 100 per cent and shims added to magnetic circuit
C—Main pole tips ground to decrease leakage to the interpoles

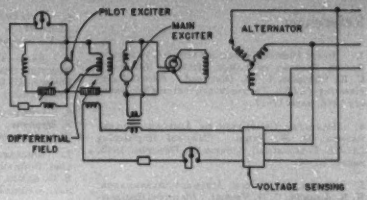

Figure 10 (above). Schematic diagram of 60-kva aircraft a-c electric system showing separately-excited exciter

The material selected was carbon steel shim stock.

Test results gave a curve as shown in Figure 8, curve "B." This was an improvement over previous attempts, but there was still a slight dip in the curve. The regulator worked to a degree at all speeds but there was a slight modulation of the output voltage when the exciter was operating on the dip part of the curve at some speeds. At most speeds it was satisfactory, but when the conditions of load and speed were reached such that the ratio of the stack voltage to the exciter field current was a constant, the trouble occurred.

The last trial gave satisfactory results. The output of the exciter was more than ample to supply the alternator, so it was decided that the output could be lowered a slight amount and permit grinding off the main pole tips to further decrease the leakage to the interpoles. The pole arc was reduced from approximately 67 per cent of the pole pitch to 60 per cent. Tests on this unit gave data which resulted in a curve shaped as shown in Figure 8, curve "C." There were no dips or straight portions on any part of the curve except at the very low voltages below minimum operating point. The regulator controlled the voltage over the speed range from no-load to full-load with the allowed $2^1/_2$ per cent regulation.

Curves for the final exciter as described are given in Figure 9. Resistance lines are drawn in to readily give the regulator stack resistance values. It is to be noted that the maximum resistance of the field circuit is 18 ohms at 10,000 rpm, no-load, and the minimum is 5.5 ohms at 4,000 rpm, 150 per cent load. A requirement of the applicable government specification was that the voltage should be controlled from 8,000 to 10,000 rpm at no load. Subtracting the field resistance of 4 ohms gives a regulator stack resistance of 14 ohms and 1.5 ohms for the two conditions which are well within the required 30-to-1 resistance ratio.

Other Systems for Wide Speed Application

There is a program of development at the present time on a 60-kva a-c generator and control system which incorporates the use of a pilot exciter to supply the main exciter field, thus eliminating the trouble encountered in "shaping" the main exciter load saturation curve. This additional exciter is regulated to a constant voltage of 35 volts by a separate carbon pile regulator. This constant voltage provides excitation to the main exciter field. A second carbon pile regulator serves to adjust the main exciter field current, by means of a circuit the same as that described for the 30-kva machine. Figure 10 shows this system. An additional feature which contributes to the stability of the system is the differential field on the main exciter. This field, excited from the constant voltage of the pilot exciter, gives a magnetizing force which opposes that of the main exciter field windings. Thus, the zero-output voltage point of the main exciter is at some field current value which provides just sufficient ampere turns to balance those of the differential field. This effectively lowers the resistance range required of the main regulator stack by reducing maximum required resistance.

Conclusions

The self-excited exciter electric power system appears to be the most advantageous from the point of simplicity and weight, because there is a minimum of auxiliary controls necessary for its proper operation. However, there is considerable difficulty in properly adjusting the exciter to provide the suitable type of load saturation curve desired. Differences in commutator films and commutation qualities, coupled with unavoidable brush movements at high speeds, indicates that some other solution to the problem is to be desired.

The pilot exciter and main exciter electric power system is inherently more stable than one without a pilot exciter, and it eliminates the danger of polarity reversals. The recovery time of the system would be shorter than that of a system without a pilot exciter because of the constant voltage available for supplying the main exciter field.

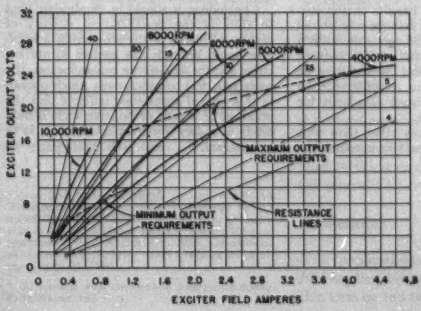

Figure 9. Curves of final exciter for 30-kva aircraft alternator

References

1. Basic Design Principles for A-C Electric-Power Systems in Large Military Aircraft, **C. K. Chappius, L. M. Olmstead.** *Electrical Engineering (AIEE Transactions)*, volume 65, January 1946, pages 12–17.

2. Parallel Operation of Airplane Alternators, **D. W. Exner.** *Electrical Engineering (AIEE Transactions)*, volume 62, December 1943, pages 755–60.

3. 40-kva 400 Cycle Aircraft Alternator, **H. E. Keneipp, C. G. Veinott.** *Electrical Engineering (AIEE Transactions)*, volume 63, November 1944, pages 816–21.

4. Alternating-Current Systems for Large Aircraft, **J. D. Miner,** *Aero Digest*, (New York, N. Y.) volume 55, September 1947, pages 40–42.

5. Basic Considerations in Selection of Electric Systems for Large Aircraft, **W. K. Boice, L. G. Leroy.** *Electrical Engineering (AIEE Transactions)*, volume 63, June 1944, pages 279–87.

6. Lightweight Aircraft Transformers, **D. S. Stephens,** *AIEE Transactions*, volume 68, part II, 1949, pages 1073–78.

7. Aircraft Carbon-Pile Voltage Regulators, Fundamentals, and Design Improvements, **B. O. Austin, H. H. C. Richards.** *AIEE Transactions*, volume 68, part II, pages 983–87.

8. Carbon-Pile Voltage Regulators for Aircraft, **W. G. Nield.** *Electrical Engineering (AIEE Transactions)*, volume 63, November 1944, pages 839–43.

9. Analysis and Redesign of a Carbon-Pile Voltage Regulator for Aircraft Generators, **W. B. Kouwenhoven, G. J. Thaler.** *AIEE Transactions*, volume 67, part II, 1948, pages 1197–1203.

10. D-C Power Systems for Aircraft, Part III, **R. H. Kaufmann, H. J. Finison.** *General Electric Review* (Schenectady, N. Y.) volume 48, December 1945, pages 56–59.

11. Exciter Instability, **R. E. Doherty.** *AIEE Transactions*, volume 41, August 1922, pages 767–80.

12. Application of D-C Generators to Exciter Service, **C. A. Boodie, F. L. Moon,** *AIEE Transactions*, volume 39, 1920, pages 1595–1616.

Discussion

K. W. Carlson and **E. S. Sherrard** (General Electric Company, Schenectady, N. Y.): The authors are to be complimented on their lucid description of an a-c aircraft electric system. However, several points of the sections on General Theory and Conclusions need discussion.

In the section on general theory the statement is made that if the system is to be stable the angle θ must be positive. θ is the angle at the operating point between the slope of the exciter saturation curve and the field circuit resistance line. A method is described for insuring the positive value of θ by shaping the exciter saturation curve.

It should be noted that an AIEE paper[1] in 1939 conclusively shows that systems of this type may be stable even when θ is negative. In particular, a large margin of stability may be obtained for $\theta = 0$ or slightly negative.

If the saturation curve is shaped the weight of the machine is normally increased and regulator sensitivity also must be increased to maintain the same system performance. The shaped saturation curve may change with commutator film, brush wear, and overhauls by users.

We suggest that a stability analysis would show that stability can be obtained by more reliable methods than the shaping of exciter characteristics.

In the conclusions a pilot exciter system is suggested for future systems. This will introduce into the system a third machine, a third set of brushes, and a second carbon pile regulator. The resultant system could be expected to be heavier and also would afford more opportunities for failure or malfunctioning of the system. We believe a pilot exciter system could be less reliable than a simpler single exciter system. Reliable methods of stabilizing these simpler systems can be determined by stability analyses.

Reference

1. The Direct-Acting Generator Voltage Regulator, **W. H. Boice, S. B. Crary, Gabriel Kron, L. W. Thompson.** *Electrical Engineering (AIEE Transactions)* volume 59, March 1940, pages 149–57.

H. B. James, R. P. Judkins, and **C. L. Mershon:** Mr. Carlson and Mr. Sherrard refer the authors to an AIEE Paper, published in 1940 which covers the case of a "negative angle" between the exciter saturation curve and the field circuit resistance line.

The stability boundary, in this paper, is found by applying Routh's criterion. It is shown that Routh's criterion may be satisfied if the slope of the exciter saturation curve is greater than the slope of the resistance line, both being taken at the operating point, provided that there is a suitable feedback transformer. If Routh's criterion is in fact met then the system response to either a unit step or a unit impulse in alternator output voltage will consist of decaying oscillations or exponentials, or combinations of these. Since the response to any other disturbance may be found by a simple integration the system is considered stable.

Should the angle θ discussed in the paper be negative, and if the regulator stack resistance starts to increase say according to $R(t) = R_o + Kt$, then it is readily shown by elementary mathematics that the shunt field current (and with it the exciter output voltage) begins to increase. If now a sufficiently large rate signal is applied to the regulator, its stack resistance will increase so rapidly that the shunt field current transient is arrested, and the system is stable.

In the case of a unit impulse or unit step in alternator output voltage, the initial rate signal applied to the regulator coil is a well-defined number, and the subsequent oscillations in shunt field current may be calculated. The system response may be compared with established standards for acceptable performance.

However, disturbances other than unit steps or unit impulses may be encountered. Although the response to any other disturbance will be "stable" in the mathematical sense, that is, the oscillations or exponentials in the response will decay, this does not guarantee that the changes in the system variables will remain within the range of linearity. For example, if the regulator stack resistance should increase slowly, with θ negative, the amount of rate signal is much reduced. The shunt field current is then free to increase to a high value before adequate regulator action takes place. Whether the regulator is able to regain control depends upon the degree of nonlinearity and the amount of rate signal. Situations of this kind, which tend toward instability, may be eliminated if θ is made greater than or equal to zero.

The particular system under consideration operates over a wide speed range, resulting in excitation changes over the full range of approximately 8 to 1 (see Figure 9). In order to provide stable operation of the system under this variable voltage condition, air gaps are placed in the magnetic circuit of the anticipating transformer which result in an increase in weight of this component to provide the proper amount of mutual inductance for stable operation. If the additional condition of a negative angle, θ, be imposed, this adds further to the weight of the transformer, and as pointed out before even this may not be adequate to provide a stable system due to deviation from the idealized case of linearity of the various system parameters. This deviation of parameters is always much more severe in the case of aircraft applications due to ambient conditions and operating characteristics far more severe than those encountered in central station practice.

Concluding, it should be emphasized that in spite of the mathematical validity of stable conditions in the presence of a negative angle between the exciter saturation curve and the field circuit resistance line, the more practical considerations which prevail in this type of application indicate that the criterion of a zero or positive angle is definitely necessary if a practical solution is to be attained.

Aircraft Electric Motors Need Test Equipment

I. E. ROSS
MEMBER AIEE

ALERT manufacturers of electric devices for aircraft must continually analyze their ability to conceive, evaluate, and produce in adequate quantities new equipment to meet the everchanging performance needs of civil and military aviation. This statement is especially true of companies which may feel the major manufacturing impact of various X-group Air Force programs authorized by Congress.

An important segment of the large problem is the matter of equipment performance evaluation. In recent months this phase of designing for aircraft has been rendered increasingly difficult both by the complexity of current environmental requirements and tests, and by continued assault upon the limits of the operating arena. Test equipment, painstakingly and ingeniously designed to simulate specified operating conditions, may often become obsolete in the time consumed by the drafting, development procurement, and installation cycle.

This paper is a discussion of one manufacturer's program to provide a test facility for evaluating rotating electric equipment not exceeding 100 pounds in weight, and over-all dimensions of 30 by 10 by 15 inches, and having d-c or a-c power dissipation of 5 kw.

The program required two years to complete at an actual expenditure in excess of $160,000 for only the four types of equipment discussed. When equipment to administer specified tests for humidity, fungus, explosion-resistance, sand and dust, salt spray, and sea level cold must also be purchased, the outlay in time and money is appreciably greater.

Analysis of this manufacturer's problem revealed that equipment was needed to meet existing specifications of acceleration, altitude, low temperature, mechanical shock, and vibration. In some cases, equipment already available was obsolete, failing to meet revised requirements. In other instances it was of inadequate physical or thermal capacity. Engineers were assigned the responsibility of obtaining, either by purchase or by manufacture, a group of indicative testing machines. The project was subdivided into several phases as follows:

1. Analysis of currently applicable military specifications to establish immediate testing goals.
2. Selection, through discussion with official aeronautical groups, of goals sufficiently beyond existing requirements to insure utility of the equipment when actually put into service. Final decision on this point was a compromise between the fruits and the costs of foresight.
3. Examination of appropriate equipment both within and without the company, on the premises of other industrial organizations or among the laboratories of the Armed Forces.
4. Choice between purchasing or building the desired machines.

Discussion of the program as it was applied to the several pieces of equipment will generally follow this outline.

Acceleration

In specifications *AN-M-40*[1] and *AN-I-10b*[2] are found requirements for acceleration tests on two types of rotating equipment, d-c motors and inverters. Motors must "start and run satisfactorily" while "mounted on a centrifuge" "operated at a speed that will produce an acceleration of ten gravitational units." The test is made for six positions of the motor. Inverters are required to withstand the force, in each of six axial directions, of five gravitational units. Under this test, a maximum deviation of 3 per cent in controlled voltage and frequency is allowed at full load and at no load. An earlier United States Air Force-32590,[3] requires a test of 12 gravitational units.

The United States Air Force General Specification for Environmental Test of Equipment, Number 41005-B,[4] stipulates that test equipment must be capable of administering steady accelerations up to 20 *g*'s.*

It is significant that acceleration requirements are not encountered in all specifications. The indication is that the test is not of universal importance. Investigation of this point with representatives of one of the Services, however, revealed an opinion that acceleration performance to them is more important than operation through short-duration shocks. At the recommendation of this group, a design bogey of 100 g was established for a new centrifuge.

No equipment suitable for the testing of rotating machines was discovered within the company or within the laboratories at Wright Field or the Naval Research Laboratory. Accordingly, it was necessary to develop a new device.

Centrifuge Design

The new centrifuge, Figure 1, is designed to carry a load of 400 pounds distributed thus:

	Pounds
Test piece	100
Mounting	100
Counterbalance†	200

† May be a second test piece and mounting.

Maximum acceleration of 103 *g* is obtained at 450 rpm and a radius of 18 inches. In construction, the centrifuge is a 4-foot diameter steel table out of which

* *g*—acceleration of 32.2 feet per second per second.

Paper 50-277, recommended by the AIEE Air Transportation Committee and approved by the AIEE Technical Program Committee for presentation at the AIEE Middle Eastern District Meeting, Baltimore, Md., October 3–5, 1950. Manuscript submitted July 14, 1950; made available for printing August 28, 1950.

I. E. Ross is with the General Electric Company, Fort Wayne, Ind.

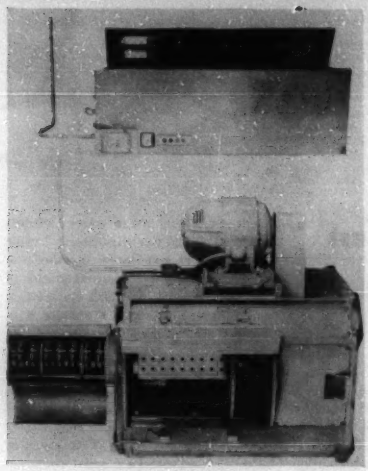

Figure 1 (left). 100-g centrifuge

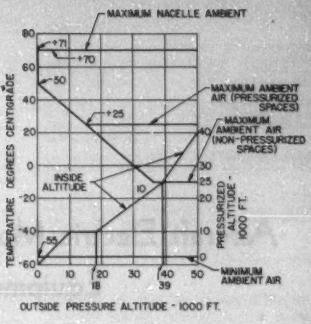

Figure 2 (right). Standard temperature-altitude chart, Specification AN-M-40

rises a 12-inch square shaft. Provision is made for mounting test pieces on the flange and on the sides of the shaft, if desired.

The drive is a 15-horsepower d-c motor utilizing automatic speed control. Interlocks are provided to prevent accidental operation of the machine when test motors are being assembled or removed. The control circuits can be arranged for dynamic braking or plugging to obtain rapid stopping. Preliminary tests indicate that the plugging circuit will not be necessary. The motor will bring the fully loaded centrifuge up to 450 rpm in approximately 10 seconds.

Power to operate the units under test is provided through 14 slip rings located at the top of the machine. That number is considered adequate not only for power but for instrument or thermocouple leads as well.

The entire machine is surrounded by a shell of 3/4-inch steel plate to protect operating personnel in case of a failure of mounting or motor.

Altitude and Low Temperature

Applicable Air Force-Navy specifications in effect at the opening of this program require operation up to 50,000 feet at a temperature of −55 degrees centigrade. The generally accepted temperature-altitude combination is as shown in Figure 2, taken directly from specification *AN-M-40*.[1]

United States Air Force specification 41065B[4] suggests that apparatus for altitude testing should be capable of holding 85,000 feet and an internal ambient temperature of −65 degrees centigrade. It further requires that the dew point of internal air be controllable between zero and −80 degrees centigrade. A warning is added that no grease, oil, or other impurities shall be present within the evacuated space. Another reference to quality of the air is found in an earlier specification, AN-M-10a,[5] where a dew point of −50 to −80 degrees centigrade is specified.

The careful design and construction of a good altitude chamber can take 12 to 18 months. In these days, with ceilings continually rising and unexpectedly low temperatures being recorded, it is difficult to decide what performance will be needed two years hence. Altitudes of 60,000 and 80,000 feet are already being specified. Horizons of 200,000 feet are mentioned for sustained flight. Temperatures of −85 degrees centigrade in conjunction with high altitude are being reported.

Furthermore, the difficulty of design and the cost in time and money of chamber construction increase cumulatively as altitudes become higher and colder. Even at altitudes under 100,000 feet, heat dissipation by convection is practically nil, and refrigerating plate areas increase by leaps and bounds. At the same time, the lower temperature levels tax the capabilities of simple refrigerating systems using normal refrigerants.

Under these circumstances the problem of setting practicable design parameters was a difficult one.

Figure 3 shows the predicted performance of the chamber which became the final design after most of the elements of compromise had been considered. For light thermal loads, an ambient temperature of −45 degrees centigrade will be available at 100,000 feet. The chamber was designed to dissipate 3 kw plus internal fan and lighting losses at −65 degrees centigrade and 60,000 feet. Minimum cold temperature at low altitudes of −75 degrees centigrade is predicted.

Investigation of numerous altitude chambers throughout the eastern part of the country revealed none which was completely suitable. A 90,000-foot chamber at Wright Field had no refrigeration. An 80,000-foot chamber in the Lynn River Works of the General Electric Company was too large, having been designed for engine testing. Another 80,000-foot tank at Wright Field was without humidity control. The chamber most closely resembling the needs of the program was located in the Naval Research Laboratory in Anacostia, Md. Rated at 70,000 feet, −60 degrees centigrade and equipped for

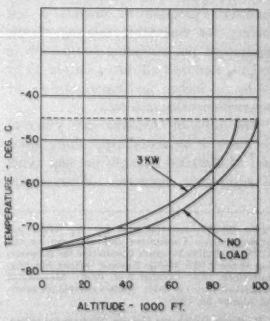

Figure 3. Altitude chamber performance

admitting clean dry air, it included humidity control down to −60 degrees centigrade dew point.

It was decided to design a new chamber. The parts would be purchased wherever approved components could be found, and the entire chamber and auxiliary devices would be assembled on the manufacturer's premises.

Altitude Chamber Design

Mechanical

The structural backbone of the chamber is a 10-foot diameter reinforced steel horizontal cylinder 3/8-inch thick, and about 15 feet long. Centrally fixed within this piece is a second cylinder made of stainless steel and having an inside diameter and length of 8 feet by 13 feet 6 inches, Figure 4. The 7 feet to the rear of this space, separated by a bulkhead, enclose cooling coils and internal circulating fan. The remainder is arranged to provide 50 square feet of workspace. A rectangular door 74 inches by 30 inches, mounted on the front end of the tank provides physical access to the interior.

The space between the two cylinders contains reflector-type insulation of stainless steel. There are 17 layers of 0.005-inch sheets located on 1/2-inch centers provided with breather holes between layers to permit evacuation of the entire assembly without distortion of the insulation structure. A window is provided on each side of the chamber, enabling operators to observe tests in progress.

It is an almost universally accepted fact that the keynote in reliable altitude chamber performance is cleanliness and dryness of the ambient air. This characteristic of chamber operation reflects itself in design at least at five points.

1. The interior must be free from materials which retain moisture vapor or other contaminants. Finishes or materials having a vapor pressure of their own must be avoided.

2. The evacuation and through ventilation system must handle only dry clean air.

3. There must be provision for purging the chamber with quantities of dry clean air at the beginning of tests.

4. Interior ventilating and refrigerating systems must remove dust and vapor contaminants from circulating air.

5. Leakage of all kinds must be kept to an absolute minimum.

Vacuum System

Evacuation of the new chamber is accomplished by a 750-cubic-feet-per-minute vacuum pump driven by a 40-horsepower motor. Specified pull-down time to an interior pressure of 8 millimeters of mercury (100,000 feet altitude) is six minutes. An altitude condition of 60,000 feet can be obtained in 3 minutes. Bleed-in air is taken from the factory compressed air line at 25 degrees centigrade, 90 pounds per square inch, Figure 5. It is passed through filters and refrigerated to +5 degrees centigrade to remove contamination and much of the moisture vapor. An activated alumina drier removes most of the remaining water vapor and delivers approximately 90 pound-per-square-inch air having a dew point of −80 degrees centigrade and a temperature of +10 degrees centigrade to an expansion valve located just outside the chamber. At this point provision is made for sampling the air and measuring the dew point. The cooled, cleaned air is allowed to expand through a second cooling coil, located in the internal refrigerated circulating air stream, into the front section of the chamber. A flexible tube is provided so that incoming air can be directed to any desired spot within the work area.

At sea level pressures, 300 cubic feet of prepared air per minute can be drawn in and circulated through the tank for purging purposes. This value represents about one complete air change every two minutes in the inner tank. At an altitude of 60,000 feet the vacuum pump capacity of 750 cubic feet per minute will draw about 75 cubic feet of purified sea level air into the chamber each minute. At 100,000 feet the per-minute bleed-in volume is nearly 10 cubic feet of atmospheric air. Both of these conditions represent a complete air change every minute within the tank.

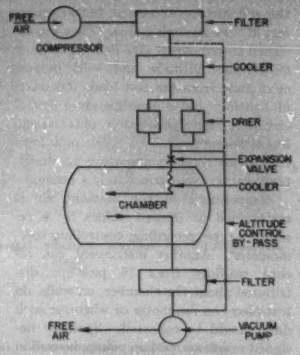

Figure 5. Altitude chamber ventilation system including preparation in-bled air

The suction pipe to the vacuum pump draws air directly from the work space. Like the bleed-in line, the exhaust can be fitted with a flexible tube if it is desired to withdraw air from any specific portion of the test area. The low-pressure air is filtered before reaching the pump to prevent damage to that component from excessive contamination and carbon dust. Automatic altitude control is provided by means of by-passing clean air from the outlet of the alumina drier (or the high-pressure filter) to the inlet of the continuously running vacuum pump. The device which controls this operation also records the internal pressure.

Refrigeration

Low temperatures inside the chamber are developed by a 2-stage mechanical refrigeration system using Freon-22 gas. Three 40-horsepower 1,750-rpm motors drive 8-cylinder 600-rpm compressors of which two cylinders each are high pressure, or second stage, and six cylinders are low pressure. Part of the refrigerant is delivered, through a heat exchanger and a supercooler, to the low-temperature coils in the rear section of the chamber. The remainder is directed through coils on the walls of the inner cylinder to provide a cold-wall barrier to thermal leakage through the insulation. The walls and

Figure 4. Altitude chamber layout

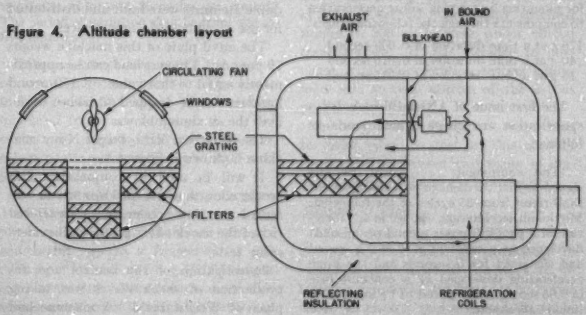

the coil surfaces represent 10,000 square feet of heat-absorbing area. They are designed to remove 47,000 Btu per hour at 60,000 feet altitude and −55 degrees centigrade from the test load, 100 watts of lighting, and approximately 2 kw of circulating fan motor power, plus thermal leakage losses. At sea level, pull-down time from room temperature to design temperature is approximately 4 hours.

Temperature of the ambient air is maintained at desired values by a resistance-type, recording, controlling thermometer. Another instrument can record readings from 16 pick-ups distributed about the chamber, on walls, on test piece, on fan motor or wherever such data should be collected. Specially designed resistance pickup points, housed in small stainless steel bulbs and shielded from radiation, are used as sensing elements.

Of interest in connection with the low-temperature tests is the provision inside the chamber of electric heating elements. These units are to be used at the conclusion of a cold test to return the chamber to room temperature before it is opened to a moist warm atmosphere. This step will prevent the voluminous condensation of water which would otherwise take place.

Recirculation

The treatment of circulating air is carefully worked out to limit cumulative contamination as tests of long duration progress. Inside air is drawn along the walls, over the refrigerating coils, and past the inbled air cooler by a 36-inch vane-axial fan mounted in the top half of the top half of the bulkhead which divides the chamber. The output is delivered directly to the front section above the work. The table tops and the floor are plated steel gratings which provide for easy mounting of test units and allow the circulating air to pass down to its return area below the floor level. Directly beneath the steel gratings are 300 activated charcoal filters, arranged to pass all the circulating air. Mounted in sections, and on racks, they can be removed easily for cleaning or replacement. It is felt that the filters, plus the cold coils, will render recirculated air satisfactorily free from contamination.

The circulating fan is powered by a 3-phase 60-cycle 4-pole motor rated three horsepower. It is of totally-enclosed ball-bearing construction and draws power from a variable-voltage variable-frequency motor-generator set. The rating of the fan is 25,000 cubic feet per minute at 1,660 rpm of air having 0.097 specific gravity (approximately 80,000 feet) and dissipates at that point 2.2 horsepower. At sea level, the fan is rated 5,000 cubic feet per minute and draws 0.4 horsepower at 400 rpm. The motor-generator delivers power over a frequency range of 13 to 60 cycles to match the fan requirements.

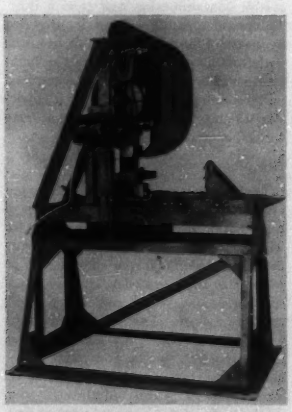

Figure 6. Standard "light-weight" Navy impact machine

Mechanical Shock

Specifications *AN-M-40*[1] and *AN-I-10b*[3] require d-c motors and inverters to withstand 60 shocks, ten in each direction along the three axes. The value of the shock is specified as "10 g". An earlier United States Air Force specification 71-854[6] called for 10 shocks of 25 g intensity.

United States Air Force specification 41065B[4] reads:

"The apparatus shall consist of a device.... for mounting and giving linear acceleration to components through the following ranges:

175 g at a time duration of 0.003 second
40 g at a time duration of 0.010 second
15 g at a time duration of 0.015 second

The first issue of AN-E-19[7] included a specification for shock which reads as follows:

"The equipment.....shall be designed so that no damage or maladjustment shall result from 25 cycles of the following: Maximum acceleration, applied in any direction of 8 g (257 feet per second per second) developed at a constant rate in 0.1 second and sustained for 3 seconds and the same acceleration developed at a constant rate in 0.05 second and reduced to 1 g in an additional 0.05 second."

Few engineers understood it and the Armed Forces admitted not being able to reproduce it. Amendment 1 substituted this requirement:

"The equipment shall not suffer damage .....when it is subjected to 30 impact shocks of 30 g, each shock impulse having a time duration of 11, ± 1 millisecond."

This specification is interpreted as meaning that the time for acceleration from 1 g to a maximum of 30 g and return to 1 g shall equal 11 ±1 millisecond.

Discussion of shock testing techniques and equipment brought out many points of view but no prediction as to what the future might hold for aircraft components in this area of performance. It was concluded that a worthy objective was to understand the specifications and attempt to meet them in their current form. If new requirements arose, new equipment could be developed as needed.

The quotation marks around "10 g" were taken directly from the text of the specification. The reason for them, and for the numerous ways of specifying shock test, became more evident as the search for equipment developed. The impossibility of defining a shock independent of time had led to the use of "10 g" as a symbol without meaning. As had happened in other fields of application, the solution of this problem had assumed two phases: first, the definition of "standard" machines to describe the means of administering the shock; second, an investigation into methods of recording and repeating definite acceleration-time curves.

The "standard" machine which appeared to match best the requirements of the program was observed in operation both at Wright Field and at the Naval Research Laboratory. It is known as the "light weight" or "electronic" shock machine and was developed by the Boston Naval District in conjunction with a manufacturer in Rhode Island. Several duplicate units were built and distributed for use as calibrated shock devices.

The anvil plate of this machine weighs 70 pounds. The test load can be approximately equal to that value. A 150-pound hammer can be dropped 36 inches to deliver the maximum blow.

The standard light-weight Navy machine is shown in Figure 6.

It will be used in conjunction with acceleration-sensitive pickups which will record the time-acceleration characteristics of the shock effect on the unit undergoing tests.

Investigation of the control and reproduction of shock waves was taking place at Wright Field. A machine had

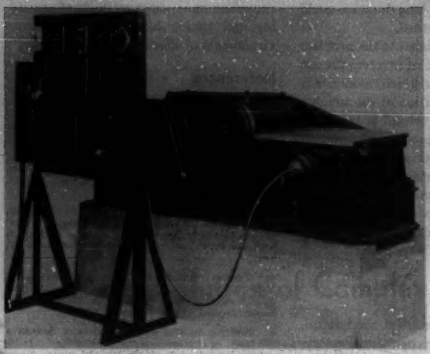

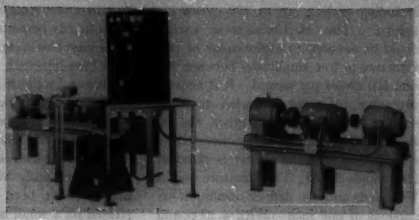

Figure 7 (left). Mechanical vibration machine for 0-to-100-cycle range

Figure 8 (above). Electromagnetic vibration exciter

been developed there which delivered the shock by dropping into a sand pit a platform carrying the test piece. Magnitude of accelerations and time of duration could be controlled by height of fall and configuration of blocks placed on the under side of the platform. Stopping times up to 100-milliseconds duration had been recorded on an oscillograph by pickups attached to the device under test.

It was concluded that the Navy machine would satisfy current specification requirements and that a different machine could be obtained if and when specifications reflected new approaches to the defining and generation of shock waves.

Vibration

Most official specifications define vibration tests in terms similar to the following excerpt from AN-M-10a[3]:

"The motor shall be subjected to vibration consisting of simple harmonic motion, having an amplitude of approximately 0.03 inch (maximum total excursion of 0.06 inch), and a frequency varied uniformly between the limits of 10 and 55 cycles per second. The period of variation shall be from one to five minutes."

Other specifications confine the period of variation to one minute. The latest motor specification AN-M-40[1] calls for an increased frequency range of 10 to 100 cycles per second. Inverters, on the other hand, need meet only 0.03-inch total excursion.

United States Air Force Specification 41065B[4] paves the way for examination of vibration characteristics of aircraft components up to a frequency of 500 cycles per second at 20 *g* (0.00152-inch total excursion). This document also describes a method of test which is gathering increased usage. The test piece is vibrated at low amplitude through a given range of frequency. Resonant points are determined by observation and the piece is given extended test at each such point.

Other specifications, written for components designed for specific applications, include long periods of vibration at single frequencies. A propeller pitch motor for instance, must pass a 60-hour test at 240 cycles per second. Other devices are vibrated at 135 cycles per second.

Search for a design goal in the matter of vibration testing brought out the fact that knowledge about vibrations present in aircraft exceeded the ability of available test equipment to reproduce these conditions. For tests at single frequencies and small excursions, tailor-made exciters and resonant beam devices had been used with success. However the problem of exploring a range of frequencies above 100 cycles per second, either in short steps or continuously, had not been solved. Although frequencies as high as 10,000 cycles per second had been recorded in operating aircraft, few applicable specifications actually involved range testing above 100 cycles per second. Increasing specified ranges to 200 cycles were under official consideration. It was decided to purchase available vibration testing equipment and to keep abreast of the art as progress developed.

Investigation of equipment being used to make vibration test on this class of equipment discovered two types of machine, mechanical and electromagnetic.

Mechanical Vibrators

Mechanical vibrators, Figure 7 are equipped with a table approximately 18 inches square on which the work to be tested is mounted. By means of belts and cams, an electric motor drives the table linearly or circularly at a specified excursion and frequency. Cam adjustments control excursion, while motor speed determines frequency. Early machines were developed to match the 0.06-inch 10-55 cycle specification in AN-M-10a[3]. They were equipped with a control which automatically produced the range cycling within the required 1 to 5 minutes. This "brute force" approach to vibration generation was rough on the testing machines and maintenance was fairly high. Even at 55 cycles, the life of the early machines was limited. A new improved design was developed. It was of sufficient size to carry the weights involved, and could be used to 100 cycles per second. An improved lubrication system and modified mounting of auxiliary equipment had rendered it a more acceptable device. It was decided to purchase one of these machines for this phase of the vibration testing program.

Electromagnetic Vibrators

Electromagnetic vibrators of the loudspeaker type were finding extensive use as exciters of resonant beams to obtain tests at fixed frequencies, Figure 8. Power supplies to drive the exciters up to 500 cycles per second were available, and point-to-point explorations of vibration resistance in that range could be made. The control problem involved in automatically testing at constant "g" and variable amplitude over a range of frequencies is a complex one. So, too, is the constant amplitude–variable-"g" test. To date no such automatic control is available, but the exciter can be a useful tool under manual control.

For the purposes of satisfying immediate testing problems, it was concluded that the mechanical machine could be used for exploration and extended tests,

including cycling, up to 100 cycles per second. The electromagnetic exciter could be devoted to explorations of performance at low amplitudes between 100 and 500 cycles per second. If it became necessary to make extended tests at specific frequencies in the range, the exciter could be used in conjunction with a resonant beam. The exciter is rated at 200 pounds thrust. The armature weighs 10 pounds and can deliver maximum excursions of one inch. With a 10-pound load, the 10-pound armature can produce maximum accelerations of 10 *g*. For higher accelerations or appreciably larger loads, the use of resonant beams is mandatory.

This phase of the test equipment program emphasized the urgent need for a heavy duty, adjustable or continuously variable resonant beam system. Used in conjunction with an electronically powered exciter and controlled by feed back from the operating bar, the combination would be useful as a cycling device in the region above 100 cycles per second. Furthermore, tests of long duration could more readily be performed.

At least two approaches to the problem have been initiated. One involves the use of bars and weights in which resonance is controlled by the position of the weights along the bar. The second is based on providing a variable-pressure compressed air cushion which acts as a controllable and continuously variable spring. The principle has been successfully demonstrated on a small model and some plans are under way to adapt it to systems involving test loads of 100 pounds.

Conclusion

Already complex electrical, mechanical, and environmental performance requirements for electric rotating machinery designed for aircraft are continually becoming more involved. Only through the expenditure of many man-hours and much money can a manufacturer equip himself to evaluate completely his designs. Additional work is needed toward providing more exact methods of specifying and testing for the mechanical environments of shock and vibration.

References

1. 24-Volt System Direct Current Aircraft Motors. *Air Force—Navy Aeronautical Specification Number AN-M-40*, United States Naval Air Station (Johnsville, Pa.), July 26, 1948.

2. Rotary Inverters. *Air Force—Navy Aeronautical Specification Number AN-I-109*, United States Naval Air Station (Johnsville, Pa.), July 12, 1948.

3. General Specification for Alternating Current 400-Cycle Induction Motors. *United States Air Force Specification Number 32590*, Air Materiel Command (Dayton, Ohio), December 17, 1947.

4. General Specification for Environmental Test of Equipment. *United States Air Force Specification Number 41065 B*, Air Materiel Command (Dayton, Ohio), March 31, 1949.

5. 28-Volt System Direct Current Aircraft Motors. *Air Force—Navy Aeronautical Specification Number AN-M-10a*, United States Naval Air Station (Johnsville, Pa.), November 5, 1945.

6. General Specification for Aircraft Electronic Equipment. *United States Air Force Specification Number 71-854a*, Air Materiel Command (Dayton, Ohio), April 19, 1945.

7. General Specification for Electronic Equipment. *Air Force—Navy Aeronautical Specification Number AN-E-16*, United States Naval Air Station (Johnsville, Pa.), March 30, 1949.

No Discussion

Special Devices Aid Differential Analyzer Solution of Complex Problems

A. C. COOK
ASSOCIATE AIEE

L. K. KIRCHMAYER
ASSOCIATE AIEE

C. N. WEYGANDT
ASSOCIATE AIEE

A PAPER by Kuehni and Peterson[1] described the differential analyzer which was placed in service at the General Electric Company shortly after the beginning of World War II. The paper described the basic analyzer and the then new servo amplifiers for use with the integrators. The original amplifiers have been replaced by modified amplifiers of the type developed by the General Electric Company for the analyzer built for the University of California.

Several papers have been written[2,3,4] describing the analyzer and the variety of complex problems which can be studied effectively with this machine.

The range of the analyzer is being continuously extended by the development of special devices which will generate auxiliary functions and assist in the representing of physical detail, thus, in effect, increasing the number of integrators available for the solution of a given problem.

The initial installation of the analyzer included provisions for generating many functions without the aid of integrators. These functions are discussed in the following sections: Curve Input; Vector Summation; Generation of Sinusoids on the Polar Input Table; Multiplication of Two Variables; and Phase Angle Determination. These functions in general required operators to track a curve or follow a template by turning a crank which was geared to an indicator. The development of an automatic follower has led to the possibility of performing all of these functions automatically. The automatic follower and applications of this follower will now be described.

Paper 50-215, recommended by the AIEE Computing Devices Committee and approved by the AIEE Technical Program Committee for presentation at the AIEE Fall General Meeting, Oklahoma City, Okla., October 23–27, 1950. Manuscript submitted March 14, 1950; made available for printing August 8, 1950.

A. C. Cook and L. K. Kirchmayer are with the General Electric Company, Schenectady, N. Y., and C. N. Weygandt is with the University of Pennsylvania, Philadelphia, Pa.

The Automatic Follower

A sectional sketch of the follower is shown in Figure 1. It will be noted that there is a light source A and two paths for the light. One path is through the window W to phototube B. This is a reference amount of light which can be adjusted. The other path is through the lens L to the viewing aperture O and by reflection to phototube C. It is possible to adjust the window W so that the light on phototube B is equal to the reflected light at C when the viewing aperture of the follower scans a surface which is half black and half white, Figure 2. The follower can be adjusted to follow the edge of a template.

The phototubes form part of a bridge circuit which serves as the input to a preamplifier. The preamplifier provides a signal to the main amplifier, which controls an amplidyne-motor drive geared to the follower head. The servo loop is shown in Figure 3.

Automatic Operation

The application of the automatic follower to the functions mentioned previously is now discussed.

The Automatic Curve Follower

Functions of the form of equation 1 can be generated by means of the input tables of the analyzer

$$y=f(x) \tag{1}$$

In earlier applications, an operator tracked a plotted input curve by hand, turning a crank which fed $f(x)$ to the problem. Application of the automatic follower to the task of curve following has eliminated the necessity for additional man power for manual operation and also has reduced the error considerably.

The curves to be followed are ordinarily prepared with black ink against a white background. As Figure 2 shows, the curve must be colored solidly for a depth of about one inch along one side. Templates also can be prepared for various functions. The follower has been used to follow templates (usually moving templates) in applications to be discussed later.

Figure 4 shows the automatic follower arranged for following a function such as equation 1.

The Vector Mechanism

There are many problems where the vector sum of the x and y components is needed. The summation of these rectangular components is accomplished by means of the vector mechanism shown schematically in Figure 5. S is the input shaft which drives the lead screw and positions the target which is a bakelite template (although it is not shown by Figure 5, S must actually be supplied through corrective gearing to compensate for the error caused by rotation of vector arm). There is a protruding surface on the follower head which slides freely in the channel-like body of the vector mechanism and provides the angular relationship for the vector arm. If the motion x and y is supplied by the analyzer, the automatic follower can supply the motion S so that the target is always

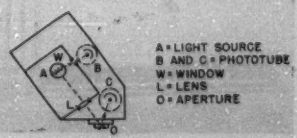

Figure 1. Sectional view of follower head

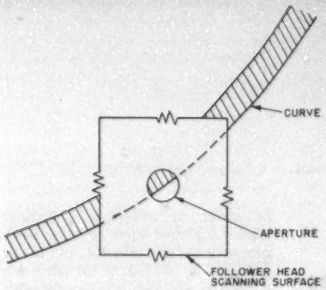

Figure 2 (left). Portion of curve viewed by follower head

Figure 3 (right). Servo loop for the automatic follower

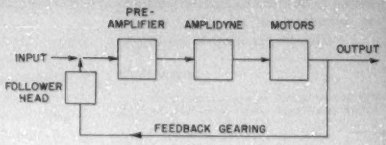

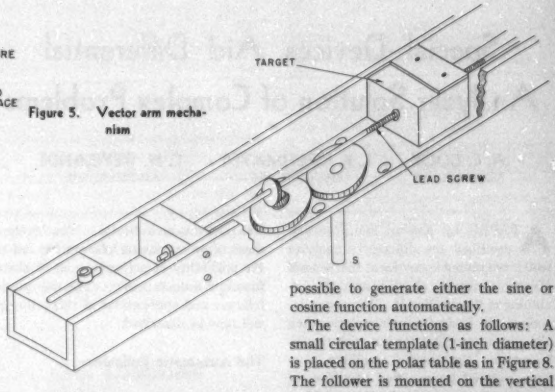

Figure 5. Vector arm mechanism

beneath the indicator and equation 2 is the relationship which results

$$S=\sqrt{x^2+y^2} \qquad (2)$$

The vector mechanism with the automatic follower is shown in Figure 6.

Provision has been made also to supply the phase angle of the vector sum. In Figure 6 there is a large protractor beneath the vector mechanism and a pointer attached to the heel of the vector arm. An operator can read the angle of the vector sum and manually supply the variable θ to the problem by causing the counter in Figure 7 to agree with the angle read from the protractor. This operation is not automatic, but it can be made so (see the section on Phase Angle) if one is willing to supply the vector magnitude manually.

The Generation of Sinusoids by Polar Input Table

The sine or cosine function can be generated by two integrators solving the equation

$$\frac{d^2x}{dt^2}=-x \qquad (3)$$

but frequently a means of obtaining the sine or cosine, without the need for integrators, is sought. If a dot or mark is placed near the outer end of a radius of the polar table and the polar table given a motion θ, the sine θ may be generated by an operator turning the vertical lead screw so that an indicator is always aligned with the dot. Simultaneously the motion $\cos\theta$ must be applied to the horizontal lead screw by the same, or by another, operator.

The automatic follower has made it possible to generate either the sine or cosine function automatically.

The device functions as follows: A small circular template (1-inch diameter) is placed on the polar table as in Figure 8. The follower is mounted on the vertical lead screw and the servo motor drives the follower so that it always aligns with the bottom edge of the small circular template.

It is necessary that an external means provide $\cos\theta$ to the horizontal lead screw. If two polar tables are available, $\sin\theta$ can be generated on one and $\cos\theta$ on the other, so that the whole operation is automatic.

A further valuable application of this device is obtained when $\sin\theta$ and $\cos\theta$ are given, and the angle θ is desired. The angle θ can be obtained automatically from this device by attaching the servo

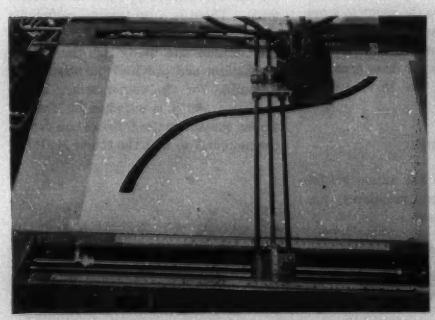

Figure 4. Input table arranged for automatic curve follower

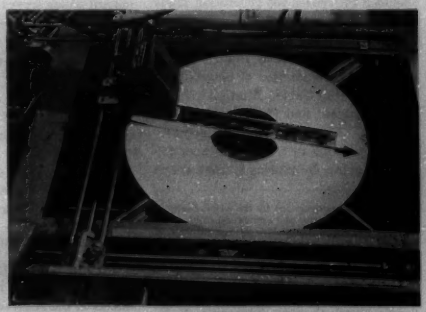

Figure 6. Input table arranged for automatic vector solving operation

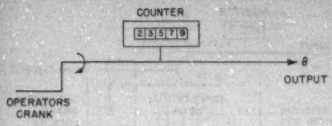

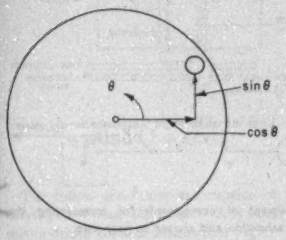

Figure 7 (upper left). Crank and counter assembly for an auxiliary manual input

Figure 8 (lower left). Polar table with 1-inch circular template

Figure 10 (right). Polar table with straight line template

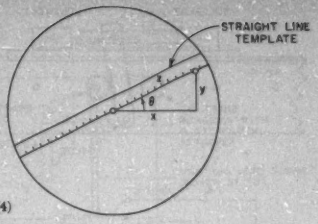

motor to the polar table, or θ drive. The magnitude of θ is not limited.

The Automatic Multiplication of Two Variables

It is a well-known fact that the product of two variables can be obtained from a 2-integrator setup solving equation 4

$$uv = \int u\,dv + \int v\,du \tag{4}$$

A device which will multiply directly without the use of integrators has been in use for many years.

This device is obtained by modifying the polar table mechanism so that a diametral line across the polar table is moved through an angle θ by a tangent bar so as to satisfy equation 5.

$$\tan\theta = z/k \tag{5}$$

where z is the input variable to the tangent bar lead screw and k is a constant associated with the geometry of the system.

Early applications required an operator to keep the index on the vertical lead screw aligned with the straight line (diameter of polar table) and by so doing produced a relationship of equation 6

$$\tan\theta = y/x \tag{6}$$

where y was the motion of the horizontal lead screw and x the hand-cranked motion of the vertical lead screw.

Combining equations 5 and 6, it can be seen that

$$y = zx/k \tag{7}$$

This operation has been made automatic by replacing the straight line with a template and using the automatic follower. The servo motor then positions the vertical lead screw to satisfy equation 7. The automatic multiplier is shown in Figure 9.

It will be observed that this scheme can be used to obtain the quotient of two variables by solving equation 7 for x, using the servo motor to drive the horizontal lead screw

$$x = ky/z \tag{8}$$

However, the denominator must not be allowed to approach zero.

Figure 9. Polar table arranged for automatic multiplying operation

Phase Angle

A new application arises by using the straight line template of the section preceding to determine the phase angle between the vector sum and one of its components. This phase angle is obtained automatically by supplying the two components x and y in Figure 10 as horizontal and vertical drives respectively and gearing the servo motor to the polar table to drive θ. The follower head mounted on the vertical lead screw provides the signal to the motor.

The vector magnitude can be obtained simultaneously from this application by having an operator interpolate the vector magnitude from the graduations provided on the template. This is the inverse of the operation in the section on The Vector Mechanism where the vector magnitude was obtained automatically and the angle was obtained by means of an operator reading a scale.

Other Devices

Numerous other devices have been developed for use on the analyzer either to make the operation more nearly auto-

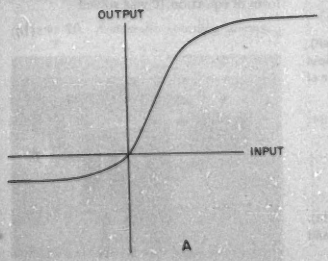

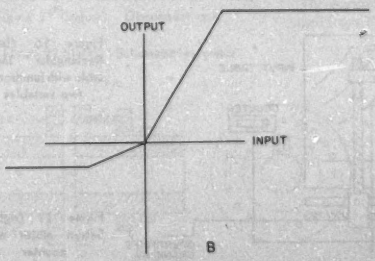

Figure 11(A). Actual amplifier characteristic. (B). Approximate amplifier characteristic

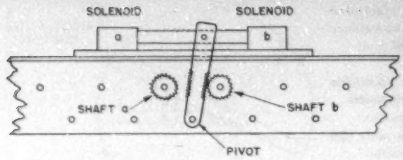

Figure 12 (left). Schematic drawing of the automatic shaft locking device

Figure 13 (right). Schematic arrangement of components for representing saturation

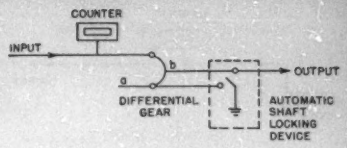

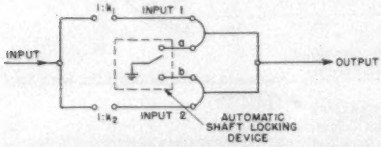

Figure 14 (above). Schematic arrangement of components for representing change of gear ratio

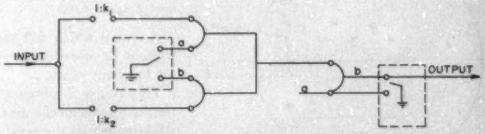

Figure 15. Schematic arrangement of components for representing the combined effect of saturation and change in gear ratio

matic or to enable a more accurate representation of physical systems. Some of these devices are: Gear Ratio Selector; Remote Indicator; Transportation Lag Device; Recording Counter; Deadband Units; and Disconnect Units.

Gear Ratio Selector

The representation of control systems on the differential analyzer brings about the need to represent amplifiers whose gain for positive signal is different from the gain for negative signal. Also, the need for representing saturation arises with these problems. Figure 11(A) shows an amplifier characteristic in which both conditions exist.

The actual curve of Figure 11(A) could be represented on an input table and the function could be fed into the analyzer automatically by using an automatic follower. Frequently, though, input tables are needed for other functions, and when an input table is not available an automatic shaft-locking device can be used to produce a function such as Figure 11(B) which is an approximation to Figure 11(A). Differential gears must be used in conjunction with the automatic shaft-locking device.

This automatic shaft-locking device is shown schematically in Figure 12. A braking bar (with gear teeth to insure positive grip) is pivoted on a lower shaft of the pillow block. When solenoid *a* is energized, the braking bar locks shaft *a*; when solenoid *b* is energized, the braking bar locks shaft *b*.

To represent saturation only, the shaft-locking device is used as in Figure 13.

When the output is proportional to the input, shaft *a* must be locked; when the output is saturated, shaft *b* must be locked.

To represent the change in gear ratio corresponding to the change in amplification factor, two differential gears are required with the shaft-locking device. Figure 14 shows that when the output is to be driven by input *1*, shaft *a* must be locked and when the output is to be driven by input *2*, shaft *b* must be locked.

These operations can be made automatic by including a lead screw-operated microswitch which energizes either solenoid *a* or solenoid *b*.

To represent the function of Figure 11(B) both saturation and gear-ratio change must be represented. This requires a connection such as Figure 15.

Remote Indicators

Many problems require inputs which are functions of more than one variable. Such inputs can be generated as long as the progress of all variables can be observed readily by an operator. The functions are prepared as in Figure 16 for use on the input tables in the form of a family of curves. The analyzer provides the vertical drive y and the progress of z is given by the counter. In the past the counter was driven by a flexible shaft, but some difficulty arose because of the backlash in the flexible shaft drive. Hence a system of selsyn motors driven by selsyn generators has been adopted.

Since the progress of z is known, an operator can position the horizontal lead-screw so that the indicator aligns with the proper magnitude of z and y. This solves equation 9 for x

$$x = f(y, z) \tag{9}$$

The process is one of the interpolation which is not difficult, since ordinarily the variables involved are not moving rapidly. As a matter of fact, functions of three variables have been generated by this means, so that an equation of the form of equation 10 was solved

$$x = f(y, z, w) \tag{10}$$

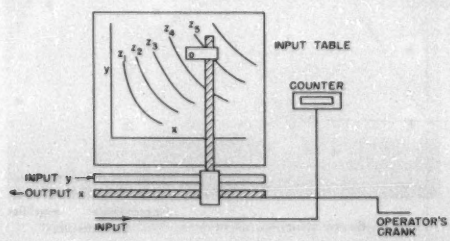

Figure 16 (left). Rectangular input table with function of two variables

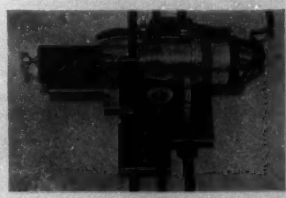

Figure 17 (right). Selsyn motor and counter

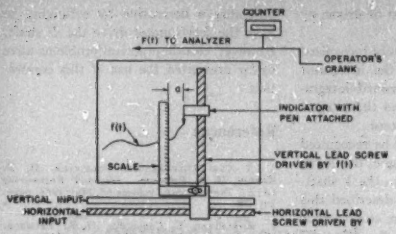

Figure 18. Rectangular input table arranged to generate $F(t) = f(t\text{-}a)$

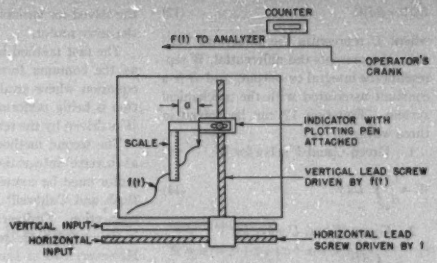

Figure 19. Rectangular input table arranged for generating $F(t) = f(t) - f(t\text{-}a)$

The selsyn generators are capable of driving more than one motor. A typical selsyn-driven counter is shown in Figure 17.

Transportation Lag Device

Problems have been encountered where the magnitude of a function $f(t)$ as it was at some previous time $(t-a)$ was desired as an input. This requires a form of memory.

The function is generated on the analyzer by plotting the function $f(t)$ and arranging a scale on the vertical carriage as shown in Figure 18. An operator is required to read the magnitude of the function a units behind the plotting pen. The operator cranks the counter to agree with the scale reading and produces the function

$$F(t) = f(t-a) \tag{11}$$

The distance a is adjustable.

In certain color register control problems it has been necessary to generate the function $F(t) = f(t) - f(t-a)$. For this application the scale is attached to the plotting pen, as shown in Figure 19. An operator provides $F(t) = f(t) - f(t-a)$ directly by cranking the counter to agree with the scale. Here also the distance a is adjustable.

Recording Counter

Four quantities can be plotted on the output tables, and for cases where the input tables are not in use, four more output plots may be obtained. However, the input tables are seldom idle and the need for more output information than the four curve plots had led to the use of a recording counter (this recording counter is a modified version of the one developed by Massachusetts Institute of Technology for their original analyzer). The recording counter is shown in Figure 20.

There are two features of the recording counter which are sometimes of advantage: one, the numerical results from the counter preserve a higher degree of accuracy than a plot; and two, facilitate any arithmetic manipulations of the results which may be required. For example, a derivative can be obtained by preparing a table of first differences from the recorded numerical data. This first difference method has been of value in machine studies where only the integral of the torque was conveniently available and the torque itself was desired. Ordinarily, however, it is more convenient to have results in curve form.

Deadband Units

Kuehni and Peterson[1] have described the deadband units. These units are used to represent discontinuities, such as backlash in control systems.

Disconnect Units

In control problems the need for representing overriding signals is simplified by using a unit called a disconnect unit. A sectional view and an end view of the disconnect unit are shown in Figure 21. The disconnect unit is used in place of a normal coupling and when the drive is to be open-circuited the ring is moved to the right so that the pin disengages from the hole in Figure 21. To re-engage the drive, the ring must be moved to the left so that the pin enters one of the holes.

To accommodate a complex system of input signals, all possible signals are provided with a complete path to the input point and one disconnect is included in the drive of each signal. As the driving signals must be changed, combinations are quickly selected by means of the disconnect units. It is a simple matter to open the disconnect unit of unwanted drives and to close the unit of the desired drives. The chief gain is in the speed of connecting and disconnecting the driving shafts.

The automatic shaft-locking device described previously provides a means of manipulating overriding signals automatically.

Inverse Integration

The normal integrator equation is obtained from Figure 22

Figure 20. Automatic recording counter

Figure 21 (below). Disconnect unit

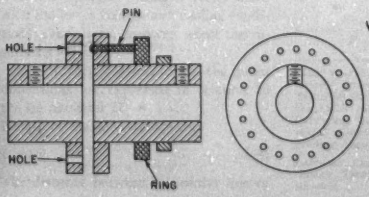

Figure 22 (right). Schematic integrator

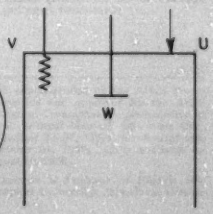

$$UdV = BdW \tag{12}$$

where U represents the integrand variable, V represents the differential, W represents the integral or output, and B is a constant associated with the mechanical system. Equation 12 can be solved in three ways:

1. Given U and V solve for W

$$W = \frac{1}{B}\int UdV \tag{13}$$

2. Given W and U solve for V

$$V = B\int \frac{dW}{U} \tag{14}$$

3. Given W and V solve for U

$$U = B\frac{dW}{dV} \tag{15}$$

It will be observed that for each method the solved-for variable must be driven by the servo motor.

The first method is quickly recognized as the common form of the integrator equation where straightforward integration is being performed and the integral W is driven by the servo motor.

The second method will be recognized as inverse integration where the servo motor must be connected to the V shaft. Bush and Caldwell[5] have described this connection. Ordinarily the servo motor is permanently geared to the W shaft. However, two of the integrators on the General Electric Analyzer have been provided with external servo motors which can be geared to any shaft. This makes inverse integration easily possible and has been found to be a valuable feature.

The third method suggests a means of obtaining a derivative by arranging to have the servo motor drive the U shaft. However, certain practical problems have so far prevented the use of this connection.

References

1. A New Differential Analyzer, H. P. Kushni, H. A. Peterson. *Electrical Engineering (AIEE Transactions)*, volume 63, May 1944, pages 221–28.

2. Analyzers, C. Concordia, H. A. Peterson. *General Electric Review*, September 1945, pages 29–37.

3. Differential Analyzer Applications, F. J. Maginniss. *General Electric Review*, May 1945, pages 54–59.

4. More Differential Analyzer Applications, A. C. Cook, F. J. Maginniss, *General Electric Review*, August 1949, pages 14–20.

5. A New Type of Differential Analyzer, V. Bush, S. H. Caldwell. *Journal*, Franklin Institute, volume 240, October 1945, pages 255–326.

Discussion

D. Lebell (University of California, Los Angeles, Calif.): This paper is of particular interest to those of us who have been operating the University of California differential analyzer. As would be expected, several of the limitations and special problems which the authors have encountered in operating the General Electric differential analyzer have occurred in our work also. It may be of interest to point out differences in our respective solutions to these difficulties.

The Automatic Follower

The University of California automatic curve follower differs from General Electric's in that it is designed to follow an inked line rather than the boundary between a dark and light region. This is achieved by utilizing the reflection of two light beams which straddle the line to be followed. Two photocells arranged in a bridge circuit convert any difference in the intensity of the reflected light beams to an electrical error signal. This error signal after suitable amplification is made to control the servo motor in much the same manner as is described in the paper. It is interesting to note that the automatic follower employed in the differential analyzer described by Walther and Dreyer,[1] is similar to General Electric's in that it employs a 1-hole aperture. The aperture diameter appears to be sufficiently small to permit following of one edge of the line describing the function.

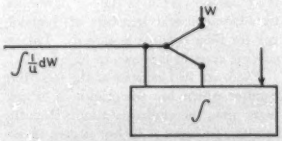

Figure 1. Alternate method for performing inverse integration

Inverse Integration

An alternate method for performing inverse integration which requires no special modification of equipment is shown in Figure 1 of this discussion. It has proved quite satisfactory except, of course, in the neighborhood where $1/u \rightarrow \pm\infty$.

Reference

1. Walther, Dreyer. *Die Naturwissenschaften* (Berlin, Germany), volume 36, 1949, pages 199–206.

A. C. Cook: The authors wish to express their appreciation for Mr. Lebell's discussion and for the benefit of the readers wish to say that the analyzers at the University of California, the University of Pennsylvania, and at the General Electric Company are similar analyzers. With these analyzers the integrators, the interconnection system, and the functional inputs are all mechanical, while the integrator follow-up systems and the automatic followers have electronic amplifiers to control their servo motors.

We were pleased to learn that a line follower had been built for the California analyzer. We recognize definite advantages to the automatic line follower. The General Electric Company has available such a follower which at present is being applied to industrial applications for contour following on automatic machine tools.[1]

Mr. Lebell indicates an alternative method for performing inverse integration. This method is similar to the regenerative connection proposed by Amble.[2] There are a number of functions which can be accomplished by the regenerative technique and Michel[3] gives a method for synthesizing these connections. Several of the regenerative schemes work very well, but most of them require extra precautions to avoid unstable conditions.

References

1. Optical Contour Follower, T. M. Berry. *General Electric Review* (Schenectady, N. Y.), volume 53, June 1950, page 44.

2. On a Principle of Conversion for the Bush Integrator, O. Amble. *Journal of Scientific Instruments* (London, England), volume 23, 1946, page 284.

3. Extensions in Differential Analyzer Technique, J. G. L. Michel. *Journal of Scientific Instruments* (London, England), volume 25, 1948, page 357.

Economical Design of a 3-Phase Transformer

LADISLAV CIGANEK
MEMBER AIEE

A TRANSFORMER of a given output P, frequency f, and voltage ratio U_1/U_2 can be designed to perform its duties at a lowest possible production price. Choice of main dimensions, however, is very limited by the complicated mutual relations which result from economic and performance requirements.

The following considerations prove that exact values of core loss P_{Fe}, copper loss P_{Cu}, impedance voltage e_z, and no-load current I_0, as prescribed by the national standards of different countries, limit the design so much that only one set of dimensions conforms to all requirements. Sometimes even an exact solution is impossible. The most economical design can be derived from the exact solution by varying prescribed performance data within allowances. Considerations are restricted to the 3-phase core-type transformer with concentric windings and natural oil cooling. Similar method applies to other types of transformers.

It is advantageous that, unlike rotating machinery, both core and windings of the transformer can be so widely subdivided to provide for necessary cooling ducts and surfaces, that preliminary design can be performed regardless of the cooling requirements.

Core loss of the transformer

$$P_{Fe}=Q_{Fe}w_B \tag{1}$$

Q_{Fe} = core weight, w_B = per-unit weight loss of the assembled core at a maximum flux density B and frequency f. In Figure 1, w_B plotted against B corresponds to page 150 of reference 1 for 29-gauge 4.2 per cent silicon steel at 60 cycles with 10 per cent increase due to stamping burrs.

The no-load current is practically only magnetising current. Assuming equal density in legs and yokes, the per cent no load current

$$I_0=\frac{100Q_{Fe}v_B}{3U_1I_1} \tag{2}$$

v_B is the reactive power input needed to magnetise a unit weight of laminations to the maximum density B at a frequency f. In Figure 1, v_B plotted against B is for the same material as the plot of w_B (page 192 of reference 1).

Using equations 1 and 2 the following ratio is obtained

$$\frac{v_B}{w_B}=\frac{PI_0}{P_{Fe}100} \tag{3}$$

The ratio v_B/w_B plotted against B in Figure 1 determines only the flux density conforming to both core-loss and no-load requirements.

Main dimensions of the transformer core and windings are represented by Figure 2. Insulation clearances b, c, and d, according to present practice (references 2, 3, 4), are plotted against higher voltage. Thickness of both coils a_1+a_2 as well as low-voltage coil-core clearance e are plotted against diameter D of the leg-section circumscribing circle. Coil thicknesses vary very little with a transformer of a given output[2] in concord with Schwartz,[5] who proved that the window width is constant for a given output and voltage. Value e varies more with the lower voltage and cooling conditions; variations, however, affect the results very little.

For further considerations the main dimensions are expressed in relation to the leg diameter D.

Length of the high-voltage coil

$$L_c=\lambda D \tag{4}$$

The distance between the center line of neighboring coils

$$M=\mu D=D+2(e+b+a_1+a_2)+c \tag{5}$$

Mean diameter of windings for reactance calculation

$$D_m=\delta D=D+2e+b+a_1+a_2 \tag{6}$$

Net section of core leg

$$S_c=\alpha D^2 \tag{7}$$

For three steps of the core section (Figure 2) and 0.9 stacking factor α equals 0.61. It grows up to 0.65 with a 5-step core section. Cooling passages and clamping devices reduce α a little.

Equivalent length of the core with constant section S_c according to Figure 2

$$l_{Fe}=\zeta D=3L_c+4M+6d+1.5D=\left(3\lambda+4\mu+6\frac{d}{D}+1.5\right)D \tag{8}$$

The core weight

$$Q_{Fe}=\alpha\zeta\gamma_{Fe}D^3 \tag{9}$$

γ_{Fe} = per-unit weight of laminations (7.6×10^{-3} kilograms/cubic centimeter). ζ varies between 14 and 20 with an average of 17. Assuming $\alpha=0.61$ and taking Q_{Fe} from equation 1, the preliminary diameter

$$D_p=2.34\sqrt[3]{Q_{Fe}} \tag{10}$$

With help of this value and of dimensions given by Figure 2, μ and δ are computed from equations 5 and 6. They are practically constant for a given transformer output and voltage.[3]

Relative coil length λ is determined chiefly by the necessary reactance. The per cent reactance

$$e_x=\sqrt{e_z^2-e_r^2} \tag{11}$$

where the per cent resistance

$$e_r=100\frac{P_{Cu}}{P} \tag{12}$$

Paper 50-216, recommended by the AIEE Transformers Committee and approved by the AIEE Technical Program Committee for presentation at the AIEE Fall General Meeting, Oklahoma City, Oklahoma, October 23–27, 1950; manuscript submitted November 21, 1949; made available for printing August 10, 1950.

LADISLAV CIGANEK is Professor of Electric Machinery, Technical University, Bratislava, Czechoslovakia.

With dimensions in centimeter, neglecting minor factors, the per cent reactance

$$e_x = \frac{4.25\times10^8 P b_e \delta}{\alpha^2 f \lambda B^2 D^4} \tag{13}$$

where equivalent clearance between coils

$$b_e = b + \frac{a_1 + a_2}{3} \tag{14}$$

D corresponding simultaneously to equations 9 and 13 offers simple relation

$$\lambda = (3\lambda + K)^{4/3} A \tag{15}$$

with constants

$$K = 4\mu + 6d/D + 1.5 \tag{16}$$

and

$$A = \frac{6.3\times10^6 P b_e \delta}{\alpha^{3/2} Q_{Fe}{}^{1/2} f e_x B^2} \tag{17}$$

Solution of equation 15 gives the only possible set of dimensions of the transformer core. The function $\lambda = f(A)$ for constant K is represented by Figure 3. Two values of λ conform to every A up to A_{max}. The higher value is economically unsound, because it results in very high transformer price. Solution

$$\frac{dA}{d\lambda} = 0$$

determines that

$$A_{max} = 0.156\lambda^{-1/3} \tag{18}$$

for $\lambda = K$.

Equation 15 is solved graphically by the chart system of Figure 4 with $K = 7 - 12 = 12$ as parameters. Should the computed A fall above A_{max} no set of dimensions conforms to all requirements. Reduction of A can be achieved, according to equation 17 solely by increase of P_{Fe}, giving higher Q_{Fe}, or higher B, or both.

Design procedure according to offered method is represented by the example of a 200-kva transformer, operating at 22 kv, 60 cycles. American practice gives (page 916 of reference 6.)

$P_{Fe} = 985$ watts

$P_{Cu} = 2830$ watts

$e_x = 5.2$ per cent

I_0 is not prescribed, Czechoslovak standards require for this type that I_0 equal 6.2 per cent with ±30-per cent allowance.

$$\frac{v_B}{w_B} = \frac{200\times10^3\times6.2}{985\times10^3} = 12.6 \text{ volt-amperes per watt} \tag{3}$$

From Figure 1

$B = 14350$ gauss

$w_B = 2.84$ watts per kilogram

$$Q_{Fe} = \frac{985}{2.84} = 348 \text{ kilograms} \tag{1}$$

$$D_p = 2.34\sqrt[3]{348} = 16.5 \text{ centimeters} \tag{10}$$

From Figure 2

$b = 1.5$ centimeters

$c = 2$ centimeters

$d = 2.8$ centimeters

$e = 0.6$ centimeter

$a_1 + a_2 = 4.3$ centimeters

$$M = 16.5 + 2(0.6 + 1.5 + 4.3) + 2 = 31.3 \text{ centimeters} \tag{5}$$

Therefore

$$\mu = \frac{31.3}{16.5} = 1.9$$

$$D_m = 16.5 + 2\times0.6 + 1.5 + 4.3 = 23.5 \text{ centimeters}$$

Therefore

$$\delta = \frac{23.5}{16.5} = 1.43 \tag{12}$$

$$e_r = \frac{100\times2830}{200\times10^3} = 1.415 \text{ per cent}$$

$$e_x = \sqrt{5.2^2 - 1.415^2} = 5 \text{ per cent} \tag{11}$$

$$b_e = 1.5 + \frac{4.3}{3} = 2.93 \text{ centimeters} \tag{14}$$

$$K = 4\times1.9 + 6\times\frac{2.8}{16.5} + 1.5 = 10.1 \tag{16}$$

$$A = \frac{6.3\times10^6\times200\times10^3\times2.93\times1.43}{(0.61)^{3/2}(348)^{4/3}\times60\times5(14350)^2} = 0.0497 \tag{17}$$

From Figure 4

$\lambda = 2$

$$\zeta = 3\times2 + 10.1 = 16.1 \tag{8}$$

$$D = \sqrt{\frac{348\times10^3}{7.6\times0.61\times16.1}} = 16.8 \text{ centimeters} \tag{9}$$

$$L_c = 2\times16.8 = 33.6 \text{ centimeters} \tag{4}$$

From Figure 2

$L = 33.6 + 2\times2.8 = 39.2$ centimeters

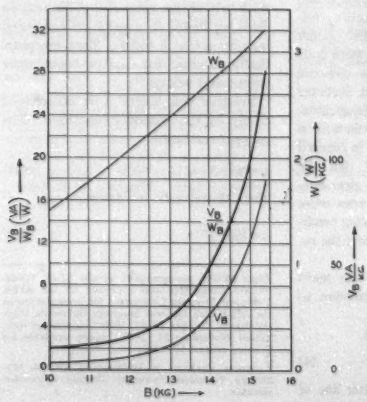

Figure 1 (left). Per-unit loss and magnetising input of the 29-gauge 4.2 per cent silicon steel at 60 cycles

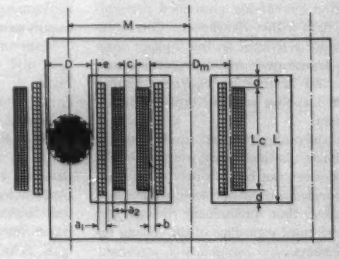

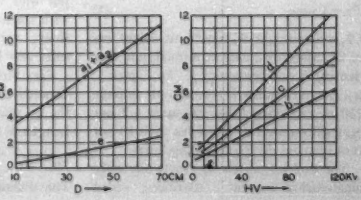

Figure 2 (right). Main dimensions of the 3-phase core transformer

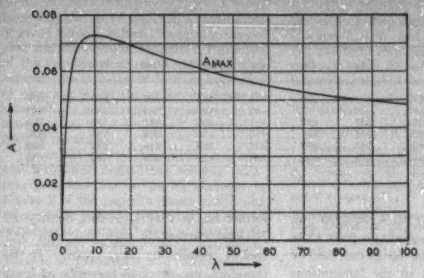

Figure 3. Function $\lambda = f(A)$ for $K=10$

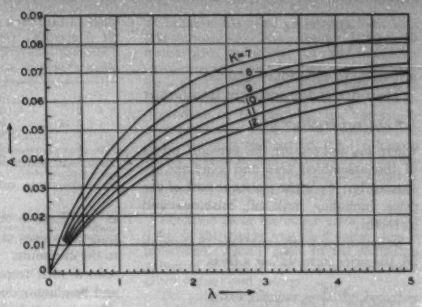

Figure 4. Solution of equation 15

$$M = 16.8 + 2(0.6 + 1.5 + 4.3) + 2 = 31.6 \text{ centimeters} \quad (5)$$

It is interesting to note that very wide variations of I_0 affect A and therefore the dimensions of the core vary little. In fact, a variation of B between 13 and 16 kilogausses gives practically no change in core dimensions. An increase of B is compensated by the reduction of Q_{Fe} and vice versa.

A slight deviation from the performance standards may result in more economical design. I_0 having widest allowances of all values, it is advisable to keep other values unchanged and proceed to the optimum solution as follows.

Using equations 15, 8, 17, and 1 to obtain values of λ_0, ξ_0, A_0 and Q_{Fe0} respectively. New value of λ gives new

$$A = \frac{\lambda}{(3\lambda + K)^{1/2}}$$

Corresponding core weight

$$Q_{Fe} = Q_{Fe0}\left(\frac{A_0}{A}\right)^{3/4} \quad (19)$$

With B and w_p unchanged, the loss in legs and yokes respectively are

$$P_l = Q_{Fe} w_p \frac{3\lambda + 6d/D}{3\lambda + K} \quad (20)$$

$$P_y = Q_{Fe} w_p \frac{4\mu + 1.5}{3\lambda + K} \quad (21)$$

With $\lambda < \lambda_0$, the resulting core loss is higher than the prescribed P_{Fe}. Increase can be compensated for by increasing the yoke section and thereby reducing flux density. In narrow limits of B, unit loss increases with B^2. Therefore, an increase of yoke section results in a linear decrease of yoke loss. The new yoke weight necessary to keep prescribed core loss with leg loss unchanged is then

$$Q_y = Q_{Fe} \frac{4\mu + 1.5}{3\lambda + K} \frac{P_y}{P_{Fe} - P_l} \quad (22)$$

The new core weight

$$Q_{Fe2} = \frac{Q_{Fe}}{3\lambda + K}\left[3\lambda + 6d/D + \frac{P_y}{P_{Fe} - P_l}(4\mu + 1.5)\right] \quad (23)$$

The corresponding no-load current will be lower than prescribed. With $\lambda > \lambda_0$, the yoke section should be reduced to keep core loss the same, and I_0 is higher than required.

Assuming equal ampere loading of both low- and high-voltage windings, the weight of all windings

$$Q_{Cu} = 6\pi\delta D N_1 s_1 \gamma_{Cu}$$

where N_1 is the primary turns per phase and s_1 is the section of primary conductor. Taking $\gamma_{Cu} = 8.9 \times 10^{-3}$ kilogram per cubic centimeter and the specific resistance $\rho = 2.2 \times 10^{-4}$ ohm centimeter for copper at 70 degrees centigrade

$$Q_{Cu} = \frac{4 \times 10^3}{P_{Cu}}\left(\frac{P\delta}{B\alpha Df}\right)^2 \quad (24)$$

With the low-voltage winding in zigzag, the weight increases by 7.5 per cent. Allowance for stray losses is to be taken for heavy conductors.

Changing λ_0 in λ, the original copper weight Q_{Cu0} changes in

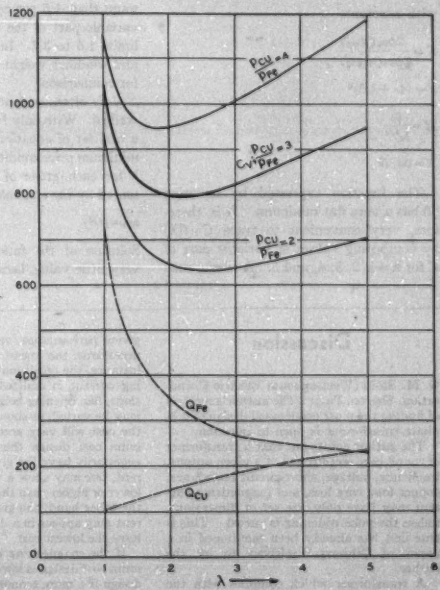

Figure 5. Price function of the 200-kva transformer

$$Q_{Cu} = Q_{Cu0}\left(\frac{\lambda}{\lambda_0}\right)^{1/2} \tag{25}$$

according to equations 9 and 24.

The price of the complete transformer

$$C = p_{Fe}Q_{Fe} + p_{Cu}Q_{Cu} + C_k$$

where p_{Fe} and p_{Cu} are the per-unit prices of the assembled core and windings respectively. C_k is the constant part of the price, including tank, oil, bushings, and so forth.

Substituting from equations 18 through 25, the price formula has a form

$$C = p_{Fe}Q_{Fe0}\frac{\lambda_0^{3/4}}{\xi_0}\left[3\lambda^{1/4} + 6\frac{d}{D}\lambda^{-3/4} + \frac{(4\mu+1.5)^2}{\frac{\xi_0}{\lambda_0^{3/4}}\lambda^{3/4} - 3\lambda^{1/4} - 6\frac{d}{D}\lambda^{3/4}}\right] + p_{Cu0}Q_{Cu0}\left(\frac{\lambda}{\lambda_0}\right)^{1/2} + C_k \tag{26}$$

A minimum price results from

$$\frac{dC}{d\lambda} = 0$$

where λ conforms to the following equation

$$X\lambda^{1/4} + \frac{\lambda - N}{\lambda} = Y\frac{2M\lambda^{-1/4} - 7 - N\lambda^{-1}}{(M\lambda^{3/4} - 3\lambda - N)^2} \tag{27}$$

with constants

$$X = \frac{2p_{Cu}Q_{Cu0}\xi_0}{3p_{Fe}Q_{Fe0}\lambda_0^{3/4}}$$

$$Y = (4\mu + 1.5)^2$$

$$M = \frac{\xi_0}{\lambda_0^{3/4}}$$

$$N = 6d/D$$

The function expressed by equation 26 has a very flat minimum. It is, therefore, very convenient to trace $C = f(\lambda)$ by computing values of variable part of C for $\lambda = 1, 2, 3, 4$, and 5. A curve, such as in Figure 5 offers to a designer full range of values of λ, giving a price close to the minimum. The design can then be refined with respect to the laminations and conductor dimensions, as well as to other items which up to now were not taken into consideration. Variable part of the price

$$C_v = Q_{Fe2} + \frac{p_{Cu}}{p_{Fe}}Q_{Cu} \tag{28}$$

is computed with help of equations 19 through 24. For the transformer of the preceding example values are given in Table I.

Table I

λ	A	Q_{Fe}	P_l	P_y	$P_{Fe}-P_l$	Q_{Fe2}	Q_{Cu}	C_v
1	0.0322	484	420	955	565	718	107	1,039
2	0.0497					348	151	901
2.15	0.0524	337	430	527	555	327	156	795
3	0.0576	301	450	410	535	268	185	823
4	0.0646	237	480	338	505	249	213	888
5	0.0685	273	494	282	491	231	239	948

The optimum design corresponds to $\lambda = 2.15$ obtained from equation 27. Results are represented by Figure 5. The ratio p_{Cu}/p_{Fe} was assumed to be 3. Additional curves for p_{Cu}/p_{Fe} equal to 2 and 4 show that the minimum slides towards higher λ with the reduction of p_{Cu}/p_{Fe}. The price function has such a flat minimum that +5 per cent allowance in the variable part of the price gives λ in the limits 1.5 to 3.2. In Figure 5 both core and windings weight is plotted against λ for comparison.

Very often, no-load current is not prescribed. With only P_{Fe}, P_{Cu} and ε_z given, a new set of equations together with the minimum price condition determine a new λ for each grade of laminations, represented by the equivalent function.

$$w_B = f(B)$$

Solution of the function, however, has very little value, because resulting transformer has a very high flux density B. No-load current is then too high and cooling conditions very poor. It is, therefore, necessary to prescribe at least limits of I_0 to achieve to an economically sound design.

Summary

A method of preliminary design of a 3-phase core transformer is offered, giving lowest priced transformer conforming to performance requirements of core loss, copper loss, per cent impedance and no-load current. A flat minimum of the resulting price function allows further refinements of the design. The only empirical values used in the procedure are the insulation clearances and coil thicknesses given by Figure 2. Technological improvements are introduced in the design by corresponding corrections of the charts of Figure 2.

References

1. Magnetic Circuits and Transformers (book), *Massachusetts Institute of Technology Electrical Engineering Staff*. John Wiley and Sons, New York, N. Y., 1946.

2. Transformer Design, **Pesak**. ESC, Prague, Czechoslovakia, 1948.

3. Praktische Transformatorenbau, **Kohse**. Enke, Stuttgart, Germany, 1934.

4. Elektrische Maschinen III, **Richter**. Springer, Berlin, Germany, 1932.

5. Der Wirtschaftliche Entwurf Des Transformators, **Benno Schwartz**. *Elektrotechnik und Maschinenbau* (Vienna, Austria), 1931, page 973, pages 873–81.

6. American Electrician's Handbook (book), **Terrell Croft**. McGraw-Hill Publishing Company, New York, N. Y., 1942.

Discussion

G. M. Stein (Westinghouse Electric Corporation, Sharon, Pa.): The author's method of finding the most economical design of a 3-phase transformer is open to question.

The author points out that a transformer of round core section and of a given output, frequency, voltage, short-circuit impedance, copper loss, core loss, and magnetizing current may have only one set of dimensions, unless the yoke widening is varied. This is true and has already been mentioned in a paper of Schwartz[1] referred to by the author.

A transformer which complies with the given performance values exactly is not necessarily the lowest cost design. If, for instance, the condition of a given magnetizing current is omitted, one set of dimensions, like opening height and leg diameter, may be varied, as shown by Schwartz,[1] and the cost will vary accordingly. The minimum cost design thus obtained does not necessarily have the given magnetizing current, but may show a value which is either lower or higher than the required limit. On the other hand, the given magnetizing current may appear in a design which does not have the lowest cost.

If the magnetizing current in the minimum cost design is lower than required, this design is a more economical choice than the one with the given magnetizing current. If, however, the magnetizing current turns out to be too large at the minimum cost, the design with the given current, but of higher cost has to be considered. Again it can be shown that this design may not have the lowest cost. For this purpose the condition of a given core loss is replaced by that of a fixed magnetizing current or of a fixed flux density which practically furnishes the same result. If the core loss in the corresponding minimum cost design is lower than the required limit, this design, and not the one with the given loss, will represent the most economical choice.

As shown by Schwartz, the thickness of the windings and the opening width can

have only one set of values in a transformer of given output, voltage, frequency, copper loss, and short-circuit impedance, regardless of the required core loss and magnetizing current. As a matter of fact, an inspection of equation 9a in the paper by Schwartz shows that a given ratio of resistance to reactance fixes the opening width regardless even of the output.

The author ignores this limiting condition and introduces instead the winding thickness as a function of the leg diameter in Figure 2 of the paper, without mentioning where these values come from. Then he computes his opening height so that the design complies with a given impedance. There is no reason for it, and the author does not show why this design should accommodate the copper weight corresponding to the given copper loss according to his equation 24.

In order to co-ordinate this copper weight with the design, the author would have to introduce winding space factors and current densities, as done by Schwartz, but ignored in the paper discussed.

The author uses a linear relationship between an increase in yoke section and a corresponding decrease in core loss in order to compute the cost as a function of the yoke height. The same assumption was made by Schwartz, but is not true, since the loss in the corners of the core increases with the yoke height. As a result, and as shown by the writer in two papers published in 1933[3] (Figures 3, 4, 5) and 1947[2] (Figures 7, 13, 14), the total core loss decreases towards a constant value if the yoke section is made larger than that of the leg.

References

1. See reference 5 of the paper.

2. Berechnung der Eisenverluste von Transformatoren aus ihren Potentialfeldern. **E. Biharri, G. M. Stein.** *Elektrotechnik und Maschinenbau* (Vienna, Austria), 1933, numbers 7 and 8, 8 pages.

3. Influence of the Core Form Upon the Iron Losses of Transformers. **G. M. Stein.** *AIEE Transactions*, volume 67, part 1, 1948, pages 95–105.

Ladislav Ciganek: The purpose of the paper was to show the shortest possible procedure leading to a minimum-priced transformer with P_{Fe}, P_{Cu}, ϵ_z, and I_0 prescribed within fixed limits. Omitting prescription of the magnetizing current, the minimum price condition leads to the design with the flux density high above 20 kilogaus.

This design is useless. It is better to prescribe I_0, than to check afterward to see if the resulting value complies with the requirements.

Values of coil thicknesses in Figure 2 of the paper were taken from practice. It is possible to relate them to the leg diameter D, because this value varies very little with transformers of a given output. This conforms with Schwartz, as the insulation clearances and filling factors vary very little for a fixed output. Schwartz's equation 9a does not prove that the opening width is independent of the output, because resistance–reactance ratio is a characteristic value for only one output. All values in Figure 2 used in further considerations are only in form of relative numbers δ and μ, the results are not affected by possible differences.

Equation 24 of the paper gives the exact value of the copper weight, if copper loss is prescribed. Flux is given by the computed values of B and D and δ is constant for a given output and voltage.

The author is familiar with the fact that core losses in corners and knots are higher than in the linear part of the yoke. The ratio of the yoke section to the core section, however, is never far from 1, and in this case the error is not great. The price function given in Figure 5 of the paper is affected but little thereby.

It was the aim of the author to present a clear concept of mutual relations of different parameters of the transformer, primarily for educational purposes. The majority of the relations is very well known to the transformer designers but some, such as given by Figures 1, 3, 5, are new and author hopes that they will improve design methods.

Control Circuit Transformers

JEROME M. FRANK
MEMBER AIEE

A. J. HAUCK
ASSOCIATE AIEE

CONTROL circuit transformers perform a vital function in many electrical applications. In order to use a control circuit transformer to best advantage, this paper will discuss the electrical design features involved and present a method for obtaining accurate regulation data.

Control circuit transformers are divided into two classes, namely high reactance and low reactance.

High-reactance control transformers are transformers of limited power input, capable of withstanding the short circuiting of the secondary terminals without burnout or excessive heating, and are capable of delivering a greater power output than a doorbell transformer. Examples of this type are chime and furnace damper control transformers.

Low-reactance control transformers are dry-type transformers, designed to limit the terminal voltage drop on overloads to a minimum and to isolate the low-voltage control circuit from the high-voltage power circuit. This paper will limit itself to the low-reactance type and will cover the factors involved in designing and testing control transformers 1/4 kva and larger.

A transformer with a dual voltage primary of 230/460 volts, rated for 60/50 cycles and with a secondary voltage compensated to give 115 volts at rated load at 100 per cent power factor would meet 90 per cent of the applications involved. This transformer would be of the open-type construction for panel mounting and would have either screw-type terminals mounted on the coil or a terminal board.

The two most important factors in the design of a control transformer are the temperature rise and the regulation.

The copper loss, the iron loss, the proportionality between the copper loss and the iron loss, the surface area of the coil and core, and the type of enclosure are the dominent factors in predetermining the temperature rise. The number of watts that can be dissipated from a given surface varies with the frame size and is an experimentally determined constant. The transformers are designed for a 55 degree rise by resistance in accordance with National Electrical Manufacturers Association standards. This rise plus a 40-degree ambient and a 10-degree allowance for hot spots equals 105 degrees, the permissible ultimate temperature for class *A* Insulation. In mounting this transformer in an enclosure, enough surface area and space must be allowed to dissipate the losses of the transformer.

The resistance and reactance of a transformer are usually expressed as a per cent of the rated voltage drop, in order that the regulation of transformers of different voltages and kilovolt-ampere ratings can be directly compared. The per cent of voltage drop through the resistance, *IR*, for example, is found by multiplying the total effective resistance referred to the secondary by the secondary rated current times 100 and then dividing by the rated secondary voltage.

The per cent *IR* is dependent upon the wire size, the number of turns, the length of mean turn, and the temperature rise. For a given temperature rise there is very little that can be done in changing the per cent *IR*, provided the core is proportioned so that the mean length of turn is at a minimum.

The per cent of voltage drop through the reactance, *IX*, varies with the square of the number of turns, the thickness and length of the coils, and the spacing of the windings. The turns for an economical flux density and for a reasonable magnetizing current are fixed. However, the reactance can be greatly reduced by interleaving the windings. The noninterleaved transformer has approximately three times the reactance of the interleaved winding. In addition, interleaving assures the equal division of current in dual winding primaries operating in parallel. Another method to improve the regulation is to use a larger core than is required to meet the temperature requirements. This results in a lower reactance as the turns can be reduced in proportion to the increase in area.

The factors affecting the size of the transformer are the continuous load current required, the inrush current required, the power factor of the inrush current, and the minimum voltage required for the attached devices to operate.

When the time that the inrush current exists is less than 20 per cent of the total time, the full load current will determine the heating of the transformer. The continuous load current should not exceed the rated full load current of a transformer, as shown in Table I. Where the inrush time is an appreciable part of the total time, the equivalent full load current should be calculated by the following formula

$$\text{Equivalent full load amperes} = \sqrt{\frac{(\text{amperes inrush})^2 \times \text{time} + (\text{load amperes})^2 \times \text{time}}{\text{time for 1 cycle}}}$$

As a general rule, the temperature rise is not the limiting factor in choosing a transformer. The limiting factor is the minimum secondary voltage acceptable during the inrush period. The poorest regulation occurs at the point where the load power factor equals the impedance power factor of the transformer. For a well-designed interleaved transformer, the impedance power factor is nearly unity. As a result, a regulation curve drawn for a 100 per cent power factor load is very pessimistic. As a matter of fact, it has little significance, inasmuch as a 100 per cent power factor load, being of a resistive nature, has no inrush current other

Paper 50-217, recommended by the AIEE Transformers Committee and approved by the AIEE Technical Program Committee for presentation at the AIEE Fall General Meeting, Oklahoma City, Oklahoma, October 23–27, 1950. Manuscript submitted September 30, 1948; made available for printing August 11, 1950.

JEROME M. FRANK and A. J. HAUCK are both with Hevi Duty Electric Company, Milwaukee, Wis.

Table I. Primary Voltage 600 or Lower Secondary Voltage 115

Kva	Rated Full Load Amperes at 115 Volts	60 Cycles %IR at 75° C	60 Cycles %IX	50 Cycles %IR at 75° C	50 Cycles %IX	Remarks
1/4	2.17	7.0	3.0	7.0	2.5	Not interleaved
1/3	4.35	3.3	0.6	3.3	0.5	Interleaved
3/4	6.52	2.8	0.6	2.8	0.5	Interleaved
1	8.70	2.8	0.7	2.8	0.6	Interleaved
1 1/2	13.05	2.0	0.6	2.0	0.5	Interleaved
2	17.40	2.2	0.7	2.2	0.6	Interleaved

than the steady-state value. The 100 per cent power factor curve is shown on Figures 1 and 2, inasmuch as it has been a practice among transformer manufacturers to show this curve. The most common power factor encountered, where control circuit transformers are used, is approximately 20 per cent. As a result, the curves of Figure 1 and Figure 2 show the regulation for 20 per cent power factor, for both 60 and 50 cycles. In all cases the 50-cycle curve indicates better regulation than the 60-cycle curve because of the decrease in reactance on 50 cycles. With the exception of the 1/4 kva, where space limitations make it very difficult to interleave, the per cent IX is approximately one-third the per cent IR. As a result, the regulation at low power factors is very good. The regulation at any power factor can be found by the equation given in the Standard Handbook for Electrical Engineers[1] as follows:

"Regulation in per cent

$$=\left[mr+nx+\frac{(mx-nr)^2}{200}\right] \text{ at rated load}$$

where

m = power factor of load ($\cos\theta$)
n = reactive factor of load ($\sin\theta$)
θ = angle of lag
r = per cent IR at 75 degrees centigrade
x = per cent IX."

Where the inrush current is six times rated current, the per cent regulation is approximately six times as great.

The fact that the regulation curves are drawn to 1,000 per cent load in some cases, does not indicate that the transformer can carry more than rated load continuously.

In order to use the regulation curves, the maximum sealed and inrush current that exists at any one time must be found and the approximate load power factor calculated. Choosing a regulation curve where the rated full load current is slightly larger than the required continuous current, the intersection of a line drawn at the value of maximum current encountered at any instant and the curve gives the value of the transformer secondary voltage at the time the maximum current occurs.

Since good regulation is the prime requisite for a control transformer, the methods of measurement to secure the data required for the regulation curves is of interest. The impedance of the transformer is effectively in series with the load and, therefore, reduces the current flow through it. The measurement of impedance is quite simple if a quantitative knowledge of its components is not required. A rms responsive voltmeter and ammeter will suffice to measure it. To determine the regulation at any power factor, we must know the value of its components, namely the reactance and the effective resistance.

The method generally employed for determining the reactance and resistance components of an impedance makes use of a wattmeter, voltmeter, and ammeter. The circuit is shown in Figure 3. It is generally agreed that the determination of the circuit parameters in low power factor circuits by this method is complicated by corrections due to phase angle errors in the current transformer and in the potential circuit of the wattmeter. What is not generally appreciated is the limitation of this method in determining the reactance in high power factor circuits. An example will illustrate this shortcoming.

1. Assume a 10-kva 1,000-volt transformer and an ammeter reading of 10 amperes, a voltmeter reading of 30.5 volts, a wattmeter reading of 300 watts. Neglecting losses in the potential circuits: volt amperes = 305; watts = 300; reactive volt-amperes = $\sqrt{305^2-300^2}=55$; per cent $IR=3.0$; per cent $IX=0.55$.

2. If the losses in the potential circuits are taken into account corrected ammeter reading = 9.98 amperes; volts = 30.5 volts; corrected wattmeter reading = 299.4 watts; volt amperes = 304.39; reactive volt-amperes = 54.9; per cent $IR=2.99$ per cent; per cent $IX=0.549$.

For the foregoing set of conditions the potential circuit errors may be neglected without appreciably affecting the results.

3. Now assume that in (1) the ammeter reads 1/4 per cent high, voltmeter reads 1/4 per cent high, wattmeter reads 1/4 per cent low, then: actual volt-amperes = 303.475; actual watts = 300.75; volt-amperes = 40.5; per cent $IR=3.01$; per cent $IX=0.405$; and error in IX from (1) = 35 per cent.

The example shown assumes impedances having a low reactance-to-resistance ratio. Control Transformers have been furnished in which the reactance-to-resistance ratio is even lower than the case cited. One remedy for the shortcoming cited involves the use of a reactive-volt-ampere meter instead of a wattmeter, so that the reactance component can be measured directly. One aspect of the case cited is favorable to the use of wattmeters and varmeters, namely the 30.5 volts drop across the impedance. Many control transformers have a high-voltage rating of 220 volts. The voltage drop across this winding would not exceed 6 or 7 volts for an impedance test. This voltage is too low to produce a reasonable scale deflection on commercially available wattmeters and varmeters. We have so far avoided mention of reading errors and the difficulty of reading three instruments under fluctuating voltage supply conditions. When these additional factors are taken into account, the results obtained are of doubtful accuracy.

Several null methods have been devised for determining the reactance and resistance components of an impedance. Most of these methods permit balance in spite of supply voltage fluctuations. Some of these methods permit the use of phase selective detectors so that independent balance of reactance and resistance com-

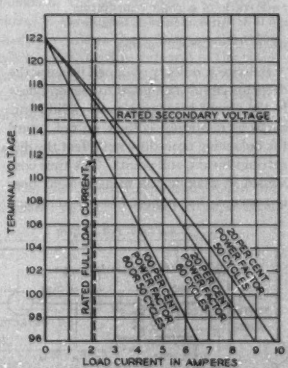

Figure 1. Regulation curve for 0.25 kva single-phase transformer, winding not interleaved

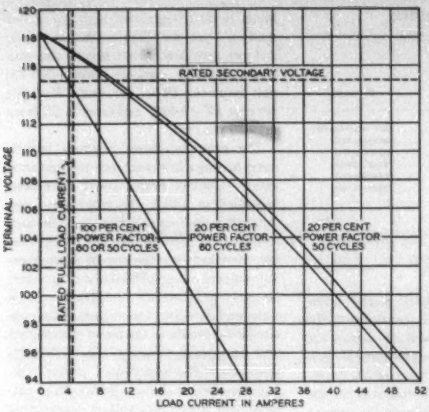

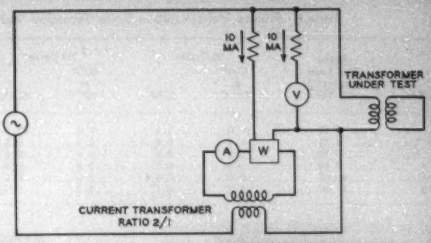

Figure 2 (left). Regulation curve for 0.5 kva single-phase transformer, winding interleaved

Figure 3 (above). Impedance measurement with wattmeter

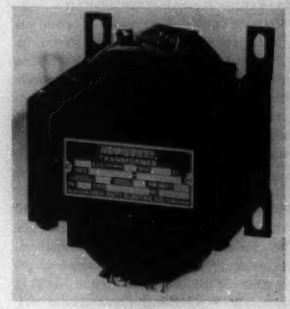

Figure 5. 0.5 kva transformer

ponents is possible. The circuit employed to measure the characteristics of the control transformers has both of these valuable features.

Referring to Figure 4, a current I_1 flows through the primary of current transformer T and impedance $\boldsymbol{Z}=r+jx$, causing a voltage drop $\boldsymbol{E}_z=E_r+jE_x$ across this impedance. A current I_2 flows through the secondary of the current transformer, the primary of the mutual inductor M and the adjustable resistor R. By adjustment of M and R, voltages E_z and E_r can be made equal in magnitude and phase. This condition, indicated by zero response of the detector, results when $jE_m=jE_x$ and $E_R=E_r$. Knowing the ratio of the current transformer, we can write

$r=$ R/ratio of current transformer
$x=WM$/ratio of current transformer

where $W=6.28\times$frequency

Balance is quickly obtained because the detector circuit is phased to respond only to the circuit being adjusted. Wide fluctuations in supply voltage do not retard the balancing procedure nor affect the dial settings for the null points. The time consumed in making the measurement does not exceed that required for conventional methods. A single operator can determine the circuit parameters with an accuracy of approximately 1 per cent and can compute the results in a fraction of the time required for methods involving square roots.

This circuit is useful for measuring linear impedances ranging from $0.0001+j0.003$ to $0.1+j0.08$ ohms without drawing any current from the impedance under test. A potential divider interposed between the impedance and the detector circuit increases the range to $30+j24$ ohms. The maximum error introduced by the shunting effect of the potential divider is 1/10 per cent. It is apparent that this circuit is more suitable than the standard ammeter-voltmeter-wattmeter method for measuring the components of a linear impedance.

Adoption of this null method for determining the impedance characteristics of control transformers has made it possible to furnish reliable regulation curves. The accuracy obtained in the measurement of the reactance is especially important since the regulation at low power factor loads depends largely on this component of transformer impedance.

The factors affecting the cost of a transformer are the kilovolt-ampere rating, the quantity involved, the number of additional taps involved, the primary voltage, and the insulation required. High-voltage primaries (above 600 volts) require special insulation and are not interleaved as a rule, due to the necessity of maintaining a high insulation level between the primary winding and the secondary and core. Special insulation for tropical service or high ambient conditions requires special impregnation and wire.

Several groups are trying, at the present time, to standardize control transformer ratings, performance, and size but due to many diversified load and size requirements the attempt has not as yet been successful.

In choosing a control transformer, consideration must be given to the continuous full load current required and the regulation required. Choosing a transformer with interleaved windings insures good regulation at power factors in the operating range.

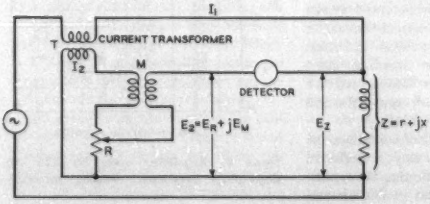

Figure 4. Impedance measurement with bridge

Reference

1. Standard Handbook for Electrical Engineers (book), Archer E. Knowlton. McGraw-Hill Book Company, Inc., New York, N. Y., eighth edition, section 6, 1949, page 561.

No Discussion

Integral Controller for Use in Carrier-Type Servomechanisms

R. L. COSGRIFF
ASSOCIATE AIEE

Synopsis: This paper presents an analysis and characteristics of a 2-phase induction motor system which may be used as an a-c integral controller in servomechanism designs or as an a-c integrator. The control phase winding of the motor is excited by a nonlinear amplifier in such a manner that the rotor acceleration is nearly proportional to the input voltage, and the output voltage, derived from the output of an a-c tachometer driven by the motor, is nearly proportional to the time integral of the input voltage. The inherent range and accuracy of the motor-tachometer combination as an integrator are substantially increased by the use of the nonlinear amplifier which linearizes the speed-torque characteristics of the 2-phase induction motor.

THE purpose of an integral controller in a servo system is to reduce the steady-state error of the system without greatly impairing the transient response.[1,2] An integral controller for the d-c systems fulfilling the above requirements usually consists of a simple resistance-capacitance network; however, integral controllers for a-c systems are more complex and are usually a source of trouble. One well-known type of a-c integral controller consists of a very narrow bandpass filter, tuned to the carrier frequency, which usually occurs in the form of a bridged-T or parallel-T network in the feedback circuit of an amplifier.[2,3,4] Unfortunately, a small change in carrier frequency renders this type of controller useless. Another method often used is to convert the a-c signal voltage into a direct voltage, allowing a d-c network to perform the integral operation, and then to reconvert the resulting d-c signal to the carrier frequency level.[5,7] This latter type, although insensitive to carrier frequency changes, is far from ideal due to the drift of the phase-sensitive detector and modulator, and the filtering problem in the output of the detector.

Because of the limitations of the conventional a-c integral controllers now in use, an investigation was made of several electromechanical devices which might be used as integral controllers. One of the more successful types studied was the 2-phase inertia motor controller described herein.

In this particular type controller or integrator, the rotors of a 2-phase motor and tachometer, together with two steel inertia disks, are mounted on a common shaft, the entire assembly being supported by an air bearing formed by introducing air flow in the motor airgap. Since the surfaces between the rotor and rotor housing are separated by a layer of air, the friction of the rotor assembly is small and for all practical purposes entirely viscous in nature. This allows the rotor to go through zero speed without the error caused by static and Coulomb friction.

The block diagram showing the method used to excite the motor is given in Figure 1. The current in the fixed phase of the motor is held constant at all times by the fixed-phase amplifier. The current in the control phase of the motor is proportional to the sum of the input signal which is to be integrated and the compensating signal which overcomes the effects of the viscous friction and nonlinearities of the motor. This compensating signal is derived from the output of the nonlinear amplifier which amplifies the output voltage of the tachometer. The gain of the nonlinear amplifier is controlled by the absolute magnitude of the current in the control winding.

When the system described is in operation, the effects of the viscous friction between the rotor and rotor housing and the effects of the nonlinear speed-torque characteristics are minimized, and the acceleration of the rotor is then nearly proportional to the input voltage. The voltage developed at the output terminals of the a-c tachometer is proportional to the angular velocity of the rotor assembly. Since the velocity of the rotor assembly is the time integral of the rotor acceleration, the voltage developed by the tachometer is proportional to the time integral of the input voltage.

Analysis

The exact speed-torque equation of the 2-phase motor is rather complicated.

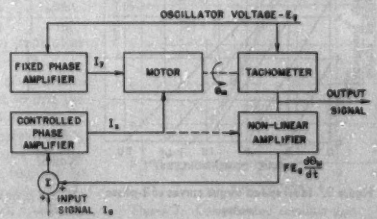

Figure 1. Basic controller system

Paper 50-219, recommended by the AIEE Feedback Control Systems Committee and approved by the AIEE Technical Program Committee for presentation at the AIEE Fall General Meeting, Oklahoma City, Okla., October 23–27, 1950. Manuscript submitted June 5, 1950; made available for printing August 21, 1950.

R. L. COSGRIFF is with the Curtiss-Wright Corporation, Columbus, Ohio.

This paper is based on work done at the Airplane Division of the Curtiss-Wright Corporation for the Air Forces. This material was also used by the author as a Master's Thesis at the Ohio State University. The author is indebted to Dr. E. H. Gamble, J. R. Campbell, R. Geiger, and W. Horton of the Curtiss-Wright Corporation and Prof. C. E. Warren of the Ohio State University for their helpful guidance and assistance.

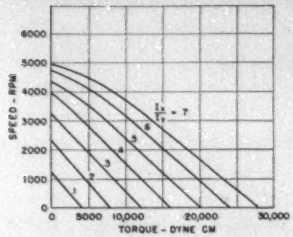

Figure 2. Speed torque curves of 2-phase drag cup motor

However, when the effective rotor resistance is ten or more times larger than the sum of the effective rotor leakage reactance and the mutual impedance representing the coupling between the stator winding and rotor conductors, the relationship between the torque T and speed $d\theta_m/dt$ may be simply expressed by (see Appendix I)

$$T = K\left(\omega_0 I_x I_y - \frac{I_x^2 + I_y^2}{2}\frac{d\theta_m}{dt}\right) \tag{1}$$

where

K = a function of the impedance elements and is constant for a given carrier frequency
ω_0 = synchronous speed of motor
I_x = current in the control winding of motor
I_y = current in the fixed-excited winding of motor

In equation 1 it is assumed that I_x and I_y are in time quadrature.

The speed-torque curves for the actual motor used in the present investigation are shown in Figure 2, while ideal curves are shown in Figure 3.

The developed torque, as given by equation 1, accelerates the rotor assembly and opposes the reaction torque due to the friction between the rotor assembly and the rotor housing. If the moment of inertia of this rotor assembly is represented by J and the coefficient of viscous friction by f, then the equation of motion of the rotor assembly may be written

$$J\frac{d^2\theta_m}{dt^2} + \left[f + \frac{K}{2}(I_x^2 + I_y^2)\right]\frac{d\theta_m}{dt} = KI_xI_y\omega_0 \tag{2}$$

The fixed phase current I_y is equal to the product of the oscillator voltage E_y and the gain G_2 of the fixed phase amplifier, that is

$$I_y = G_2E_y \tag{3}$$

The control-phase signal I_x consists of two components: the input signal I_a which is to be integrated and the velocity feedback component $FE_v d\theta_m/dt$. The function F is not a constant, but is a function which must be generated in a manner presently to be explained to overcome the nonlinearity of the motor damping. Let G_0 be the gain of the control-phase amplifier. Then

$$I_x = G_0\left(I_a + FE_v\frac{d\theta_m}{dt}\right) \tag{4}$$

Assume that the function F is

$$F = G_1(1 + \beta I_x^2) \tag{5}$$

where G_1 and β are constants. It now will be shown that a proper choice of G_1 and β will make the system linear within certain limits. It is to be noted that the gain of the nonlinear feedback amplifier is determined by $|I_x|$.

To simplify the computations, let

$$A_1 = G_1E_v\frac{d\theta_m}{dt}G_0 \tag{6}$$

Substituting equation 5 into equation 4 and using equation 6 yields

$$\beta A_1 I_x^3 - I_x + A_1 + G_0I_a = 0 \tag{7}$$

from which

$$I_x = \frac{1 - \sqrt{1 - 4(I_aG_0 + A_1)\beta A_1}}{2A_1\beta} \tag{8}$$

By substituting the values of I_x and I_y, expressed by equations 3 and 8 respectively, into the system equation 2, the equation of motion becomes

$$J\frac{d^2\theta_m}{dt^2} + \left[f + \frac{K}{2}\left(G_2^2E_y^2 - \frac{1}{\beta}\right)\right]\frac{d\theta_m}{dt} = \frac{I_aK}{2G_1E_y\beta} + K\left[\frac{1 - \sqrt{1 - 4(I_aG_0 + A_1)A_1\beta}}{2G_1E_y\frac{d\theta_m}{dt}G_0\beta}\right]\left[\omega_0G_2E_y - \frac{1}{2\beta G_1E_yG_0}\right] \tag{9}$$

Now if

$$\frac{1}{\beta} = \frac{2f}{K} + G_2^2E_y^2 \tag{10}$$

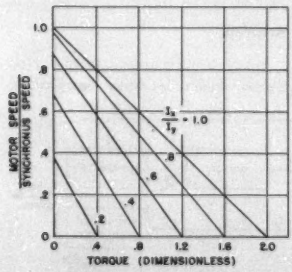

Figure 3. Ideal speed torque curves of 2-phase motor

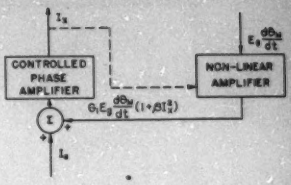

Figure 4. Nonlinear feedback circuit

and

$$\omega_0G_2E_y = \frac{1}{2G_1E_y\beta G_0} \tag{11}$$

then equation 9 simplifies to

$$J\frac{d^2\theta_m}{dt^2} = \frac{I_aK}{2G_1E_y\beta} \tag{12}$$

which is the equation desired, since both the angular velocity of the rotor and the voltage output of the tachometer are proportional to the time integral of the input signal I_a. It should be noted that any desired linear coefficient of viscous friction, positive or negative, may be effectively obtained by a proper choice of β.

The values of I_x, I_a, and $d\theta_m/dt$ all have upper limits which may not be exceeded for proper operation. The upper limit of $d\theta_m/dt$ is ω_0, the synchronous speed of the motor, and cannot of course be exceeded. However, it is physically possible for both I_x and I_a to exceed their limits. If the value of I_a exceeds its limit, then the value of I_x expressed by equation 8 becomes a complex quantity. The maximum real value of I_x as obtained from equation 8 is

$$I_{x\max} = \frac{1}{2A_1\beta} \tag{13}$$

Substituting the values for A_1 and β obtained from equations 6 and 11, respectively, and replacing G_2E_y by I_y, equation 13 reduces to

$$\frac{I_{x\max}}{I_y} = \frac{\omega_0}{d\theta_m/dt} \tag{14}$$

If the maximum value of I_x is exceeded, the nonlinear amplifier becomes unstable. The unstable nature of the feedback amplifier is evident from an inspection of Figure 4. As I_x becomes large the gain of nonlinear amplifier also becomes large and the amplifier under such condition is similar to a regenerative feedback amplifier. The point of instability as given by equation 14 may also be obtained by taking the partial derivative of I_x with respect to I_a and solving for I_x when this partial derivative is infinite.

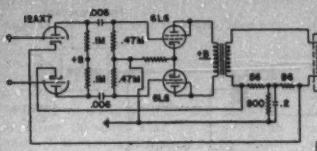

Figure 5. Controlled phase feedback amplifier

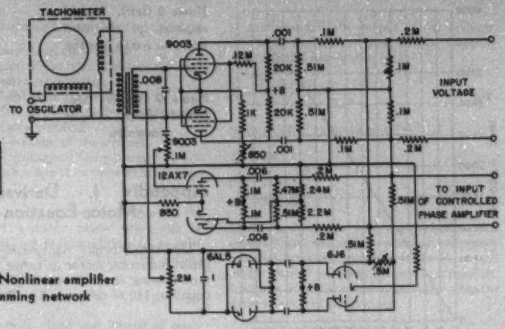

Figure 6. Nonlinear amplifier and summing network

Tachometer

The a-c tachometer used is quite as important to the operation of the system as the motor itself.[6] A drag-cup type tachometer is used which has a very low output voltage level when the rotor is stationary. If the tachometer is to be linear, it is necessary that the leakage reactance and the resistance of the excited stator winding be made as small as possible in comparison with the value of the rotor resistance. The design parameters governing tachometer performance are discussed in Appendix II.

Electronic Equipment

The two amplifiers used to drive the two phases of the motor are conventional amplifiers with a large amount of current feedback, so that the current in each phase of the motor is proportional to the input voltage to the amplifier, see Figure 5.

As shown in Figure 6, the tachometer amplifier actually consists of two amplifiers, the outputs of which are added in a summing network. One amplifier has a fixed gain. The second amplifier consists of two pentodes both biased by a voltage proportional to the absolute value of I_x. This voltage is obtained from a rectifier which converts the absolute value of an alternating voltage proportional to I_x into a positive direct voltage. If this d-c bias is denoted by e, then the following power series for the gain G of the pentode stage may be written,

$$G = g_0 + g_1 e + g_2 e^2 + g_3 e^3 \ldots \tag{15}$$

By proper adjustment of the cathode resistance and the plate and screen voltages it is possible for the value of G to become approximately

$$G \approx g_0 + g_2 e^2 \tag{16}$$

A plot of $G - g_0$ versus e is shown in Figure 7, together with an ideal curve.

If equation 16 holds, then the gain of the tachometer amplifier will consist of two components. One component of the gain will be constant while the second component will be proportional to e^2 and consequently I_x^2. By adjusting the magnitude of these two components the gain of the tachometer amplifier can be made to approach the value of F required by equation 5.

Operation of the Controller

The operating characteristics of the controller are better in many respects than the conventional a-c integral controllers. For example, the equivalent bandpass filter used as an integral controller would have a Q of over a 10^6 at 400 cycles. This corresponds to a pass band of less than one cycle per hour. The ratio of maximum velocity to minimum velocity of the described controller is over 8×10^3 and may be increased by balancing the rotor mechanically. The velocity range is greater if the region of improper compensation is also considered. A typical response of the system to a step function is shown in Figure 8.

It is very difficult to adjust the amplifier to obtain the accuracy mentioned, and changes in the frequency of the oscillator voltage necessitates readjustment of the amplifier. The effect of the frequency change is to introduce a friction term in equation 12. However, it has been found possible to eliminate this source of trouble by allowing the gain of the tachometer amplifier to decrease at a rate of 6 decibels per octave in the region of operation.

Simplified Motor Integral Controller

The rotor resistance of a 2-phase induction motor may be adjusted so that the speed-torque curves, plotted in a manner similar to those shown in Figures 2 and 3, are nearly vertical as the rotor velocity approaches zero. At speeds less than 30 per cent of synchronous speed the acceleration of the rotor of such a motor is nearly proportional to the input signal. Since the back electromotive force is nearly proportional to the velocity of the rotor, this voltage may be used for the output signal. This may be done by arranging the motor in a bridge circuit as shown in Figure 9.

The input impedance of the motor with a blocked rotor may be made real by adding a condenser in series or in parallel with the motor. By adjusting R until it is equal to this blocked rotor input impedance the output voltage at standstill will be zero, and the developed voltage at this output terminal will be nearly proportional to the angular velocity of the rotor. Likewise the driving voltage at the output of the amplifier will be proportional to the amplifier input voltage plus a component proportional to the rotor velocity. Thus the integral control signal may be obtained directly from the output terminals of the amplifier if desired. The characteristics of this controller may be

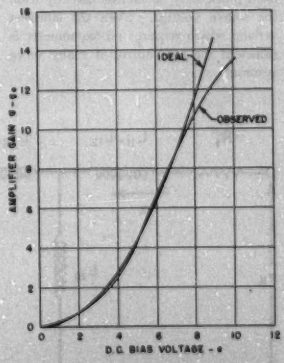

Figure 7. Compensated amplifier gain

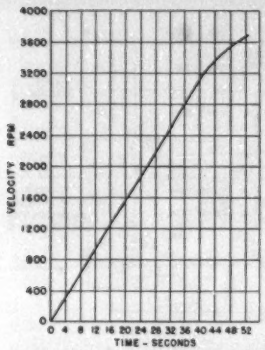

Figure 8 (left). Typical response of the controller to a step function

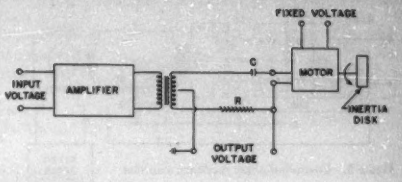

Figure 9 (right). Simplified motor integral controller

changed by the use of voltage and current feedback in the amplifier.

Conclusions

The performance of the compensated integral controller described is very much better than is usually required for most servo systems. In fact, as has been pointed out, the controller is actually an excellent integrator. Since the effects of oscillator frequency shift, originally a limitation of the controller, may be largely eliminated, it appears that the ultimate limitation of the device depends upon the accuracy with which the gain as required by equation 11 may be approximated, and upon the drift of the amplifier used to obtain this gain.

The controller may be simplified in several ways for practical applications. For example, a good mechanical bearing of conventional design can be substituted for the air bearing. Furthermore, the fixed phase may be excited directly from the source voltage. Even the simplest version which requires no tachometer is sufficient for the control of many servo systems.

Appendix I. Derivation of Motor Equation

The speed-torque relationship for a 2 phase induction motor in terms of the current flowing in each winding is given by equation 110 of reference 5. This equation is

$$T' = (I_x^2 + a^2 I_y^2)(R_f - R_b) + 2aI_xI_y(R_f + R_b) \sin\phi \quad (17)$$

where

T' = average developed torque in synchronous watts

I_x = rms current flowing in the controlled phase

I_y = rms current flowing in the fixed phase

a = turns ratio of the x and y stator windings

ϕ = phase shift between I_x and I_y

If $\phi = \pi/2$ and $a = 1$, equation 17 becomes

$$T' = (I_x^2 + I_y^2)(R_f - R_b) + 2I_xI_y(R_f + R_b) \quad (18)$$

The values of R_f and R_b are given by equations 54 and 57 of reference 5 and are

$$R_f = \frac{X_m^2 R_2 S}{R_2^2 + S^2(X_2 + X_m)^2}$$

$$R_b = \frac{X_m^2 R_2 (2-S)}{R_2^2 + (2-S)^2(X_2 + X_m)^2} \quad (19)$$

where

X_m = coupling reactance between the stator winding and the rotor conductor

R_2 = effective rotor resistance referred to the stator winding

X_2 = effective rotor leakage reactance referred to the stator winding

S = slip of the motor

When a 2-phase motor is used for control purposes it is convenient to use α, the ratio of motor speed to synchronous speed, as the variable instead of the slip S. The value of S in terms of α is simply

$$S = 1 - \alpha \quad (20)$$

Let

$$\xi = \frac{X_2 + X_m}{R_2} \quad (21)$$

Then equations 19 may be written

$$R_f = \frac{X_m^2}{R_2}\left[\frac{1-\alpha}{1+(1-\alpha)^2\xi^2}\right]$$

$$R_b = \frac{X_m^2}{R_2}\left[\frac{1+\alpha}{1+(1+\alpha)^2\xi^2}\right] \quad (22)$$

Using equations 22 the values of $R_f + R_b$ and $R_f - R_b$ may be easily shown to be

$$R_f + R_b = \frac{2X_m^2}{R_2} \cdot \frac{1+(1-\alpha^2)\xi^2}{[1+(1-\alpha)^2\xi^2][1+(1+\alpha)^2\xi^2]}$$

$$R_f - R_b = -\frac{2X_m^2}{R_2} \cdot \frac{\alpha[1-(1-\alpha^2)\xi^2]}{[1+(1-\alpha)^2\xi^2][1+(1+\alpha)^2\xi^2]} \quad (23)$$

Putting equations 23 in equation 18 yields

$$T' = \frac{2X_m^2}{R_2} \cdot \frac{-\alpha(I_x^2 + I_y^2)[1-(1-\alpha^2)\xi^2] + 2I_xI_y[1+(1-\alpha^2)\xi^2]}{[1+(1-\alpha)^2\xi^2][1+(1+\alpha)^2\xi^2]} \quad (24)$$

Now

$$\lim_{\xi \to 0} T' = \frac{2X_m^2}{R_2}[-\alpha(I_x^2 + I_y^2) + 2IxIy] = T \quad (25)$$

When I_x is equal to I_y the error ratio de-

Figure 10. Equivalent circuit of 2-phase motor with nonlinear elements

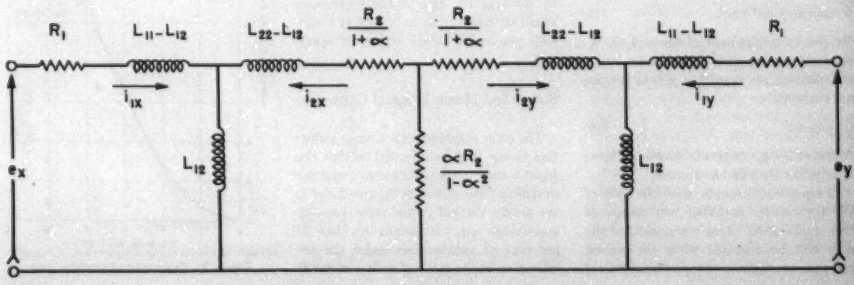

fined as $(T'-T)/T$ may be readily shown to be

$$\frac{T'-T}{T}=-\xi^2(1-\alpha)^2 \tag{26}$$

in which terms in ξ^4 have been neglected. Equation 26 shows that the approximate value T is very nearly equal to the actual torque T' when $\xi \leq 0.1$. For small values of ξ then, the developed torque becomes

$$T=K\left[-\frac{d\theta_m}{dt}\frac{(I_x^2+I_y^2)}{2}+\omega_0 I_x I_y\right] \tag{27}$$

which is equation 1.

Appendix II. A-C Tachometer Characteristics

The equivalent circuit of a 2-phase motor shown in Figure 10 may be found in reference 7. From this equivalent circuit the following set of equations may be derived.

$$\begin{aligned}
e_x &= Z_{11}i_{1x}+Z_{13}i_{2x}\\
e_y &= Z_{11}i_{1y}+Z_{13}i_{2y}\\
0 &= Z_{13}i_{1x}+Z_{22}i_{2x}-\alpha[Z_{13}i_{1y}+(Z_{22}-R_2)i_{2y}]\\
0 &= Z_{13}i_{1y}+Z_{22}i_{2y}-\alpha[Z_{13}i_{1x}+(Z_{22}-R_2)i_{2x}]
\end{aligned} \tag{28}$$

In these equations the impedances are defined as

$$\begin{aligned}
Z_{11} &= R_1+j\omega L_{11}\\
Z_{13} &= j\omega L_{13}\\
Z_{22} &= R_2+j\omega L_{22}
\end{aligned} \tag{29}$$

where

R_1 = resistance of each stator winding
L_{11} = sum of the stator leakage reactance and L_{13}
L_{13} = mutual reactance coupling the stator winding to rotor conductors
L_{22} = sum of the rotor leakage reactance and L_{13}
R_2 = equivalent rotor resistance referred to the stator winding

and the voltages and currents are defined as

i_{1x} = stator current in the x-phase
i_{2x} = rotor current in the x-phase referred to the stator winding
i_{1y} = stator current in the y-phase
i_{2y} = rotor current in the y-phase referred to the stator winding
e_x = terminal voltage of the x-phase
e_y = terminal voltage of the y-phase
α = ratio of rotor speed to rotor synchronous speed

The open-circuit voltage developed at the terminals of y-stator phase now will be found. Since for this condition i_{1y} is zero, the value of e_y becomes from the second of equations 28

$$e_y=Z_{13}i_{2y} \tag{30}$$

Solving the first, third and fourth of equations 28 simultaneously for i_{2y} yields

$$i_{2y}=\frac{\begin{vmatrix} Z_{11} & Z_{13} & ex\\ Z_{13} & Z_{22} & 0\\ -\alpha Z_{13} & -\alpha(Z_{22}-R_2) & 0\end{vmatrix}}{\begin{vmatrix} Z_{11} & Z_{13} & 0\\ Z_{13} & Z_{22} & -\alpha(Z_{22}-R_2)\\ -\alpha Z_{13} & -\alpha(Z_{22}-R_2) & Z_{22}\end{vmatrix}} \tag{31}$$

which when expanded and substituted in equation 30 gives

$$e_y=\frac{-\alpha Z_{13}^2R_2e_x}{\alpha^2[Z_{13}^2-Z_{11}(Z_{22}-R_2)](Z_{22}-R_2)+Z_{22}(Z_{11}Z_{22}-Z_{13}^2)} \tag{32}$$

Since in the derivation of the equivalent circuit all voltages and currents having a "y" subscript lead the actual values by $\pi/2$ radians, the voltage e_y is leading the actual voltage at the output of the tachometer by $\pi/2$ radians.

The effects of α^3 in the denominator must be minimized if the output of the tachometer is to be linear. This can be done by reducing the impedance ratio

$$R_a=\frac{Z_{11}Z_{22}-Z_{13}^2-R_2Z_{11}}{Z_{11}Z_{22}-Z_{13}^2} \tag{33}$$

to as small a value as possible. If

$$Z_{11}=Z_{13}$$

and

$$Z_{22}=R_2+Z_{13}$$

then R_a becomes zero as desired. This means that the stator winding resistance and the leakage reactance of the rotor and stator should be made as small as possible. Likewise if R_2 is much larger than Z_{13}, the same effect will be obtained.

References

1. Principles of Servomechanisms (book), **G. S. Brown, D. P. Campbell.** John Wiley and Sons, Inc., New York, N. Y., 1948, pages 204–16.

2. The Analysis and Synthesis of Linear Servomechanisms (book), **A. C. Hall.** The Technology Press, Massachusetts Institute of Technology (Cambridge, Mass.), 1943, pages 63–88 and 189–91.

3. Parallel "T" Stabilizing Networks for A-C Servos, **A. Sobczyk.** *Radiation Laboratory Report Number 811*, Massachusetts Institute of Technology (Cambridge, Mass.), March 7, 1946.

4. Theory of Servomechanisms (book), **H. M. James, N. B. Nichols, R. S. Phillips.** McGraw-Hill Book Company, Inc., New York, N. Y., 1947, pages 117–23.

5. Revolving Field Theory of the Capacitor Motor, **Wayne Morrill.** *AIEE Transactions*, volume 48, April Section, 1929, pages 614–32.

6. Components Handbook (book), **J. F. Blackburn.** McGraw-Hill Book Company, Inc., New York, N. Y., 1949, page 384.

7. The Equivalent Circuit of the Capacitor Motor, **Sheldon S. L. Chang.** *AIEE Transactions*, volume 66, 1947, pages 631–40.

8. Servomechanism Fundamentals (book), **H. Lauer, R. Lesnick, L. E. Matson.** McGraw-Hill Book Company, Inc., New York, N. Y., 1947, pages 204–09.

No Discussion

Single-Phase Power Transformer Formed Cores

T. D. GORDY
MEMBER AIEE

G. G. SOMERVILLE
MEMBER AIEE

Synopsis: For many years power and distribution transformer cores were built of hot-rolled laminations assembled into a core structure. When cold-rolled, oriented strip steel was introduced into transformers, new types of distribution transformer cores were developed. These cores were of the wound type and utilized the magnetic properties of oriented steel very efficiently. Recently, a new type of single-phase power transformer core using oriented steel has been developed and put into production. A description of the design, manufacture, and characteristics of this new core is given. Power transformers with this type of core built by the General Electric Company are designated Spirakore transformers.

STEELS FOR magnetic circuits have been improved in many ways during the years of transformer improvement. Lower core loss, lower exciting current, improved mechanical properties, and non-aging characteristics are but a few of the improvements that have been made on the steel. However, until the introduction of highly oriented, cold-rolled steel, essentially all distribution and power transformer cores were built by stacking rectangular, L-shaped, or E- and I-shaped laminations into a core structure.

In order to utilize better the improved magnetic characteristics of this new steel, a wound core was developed for distribution transformers.[1] Even though this type of core had good magnetic characteristics, it was limited to distribution transformer sizes. Weight, size, and mechanical requirements of cores used in power transformers prevented its use in these sizes. In order to obtain characteristics similar to the wound-core distribution transformer, a new type of precut-preformed, single-phase core for use in power transformers has been developed and put into production in sizes up to and including 3,333 kva. This paper discusses the characteristics of oriented cold-rolled steel and the development of the Spirakore for use in power transformers.

Properties of Material

Nonlinearity between flux density and magnetizing force is a characteristic of all steels used in power transformer cores. In addition, highly oriented, cold-rolled steel has more important characteristics that must be considered if it is to be used efficiently in power transformer cores.

Directional Characteristics

Cold-rolled steel is produced in continuous strips or bandwidths, while hot-rolled material is produced in sheet form. With certain composition, working, and processing, highly directional magnetic properties may be obtained. A large proportion of the crystals are oriented so that an easy direction of magnetization is parallel to the rolling direction. In such material, when the flux passes through the lamination in a direction parallel to the direction of rolling, low core loss is obtained, and a low magnetizing force is required. If flux is caused to pass through such steel in directions other than one parallel to the rolling direction, core loss and magnetizing force are increased. The amounts which these quantities increase depend upon the flux density. Figure 1 illustrates the variation of core loss with the direction in which flux passes through such steel for three different flux densities. Figure 2 illustrates the variation of magnetizing force with the direction in which flux passes through the steel for three different flux densities.

Magnetic characteristic variations, shown in Figures 1 and 2, show why it is important to use oriented cold-rolled steel in transformer cores so that flux passes through the steel in the direction of rolling. Not only may the lowest possible core loss and exciting current be obtained, but also minimum flux distortion will result.

Strain Effects

Oriented cold-rolled transformer core steel is much more sensitive to mechanical strain than is hot-rolled core steel. Both core loss and magnetizing force are increased as strain is increased. Because of this strain-loss relation, strain in the core structure must be seriously considered and minimized.

Core steel may be strained and formed into any desired shape before final anneal; but after anneal, the steel should be maintained in its annealed form for minimum core loss and magnetizing force. Therefore, in a core structure, core steel should be supported and clamped such that it is kept in the same form in which it was annealed.

General Design of Core Structure

Aside from using oriented cold-rolled steel such that flux passes through it in a direction parallel to the rolling direction, other fundamental functions of the core must be achieved. In designs using cylindrical windings, core cross section inside the winding circle should approach a circle. Heat generated in the magnetic circuit must be efficiently transmitted to the cooling liquid. Lifting, shipping, and short-circuit forces must be transmitted or withstood by the core and clamp structure. These requirements are fulfilled by this type of core.

Paper 50-220, recommended by the AIEE Transformers Committee and approved by the AIEE Technical Program Committee for presentation at the AIEE Fall General Meeting, Oklahoma City, Okla., October 23–27, 1950. Manuscript submitted July 24, 1950; made available for printing August 21, 1950.

T. D. Gordy and G. G. Somerville are both with the General Electric Company, Pittsfield, Mass.

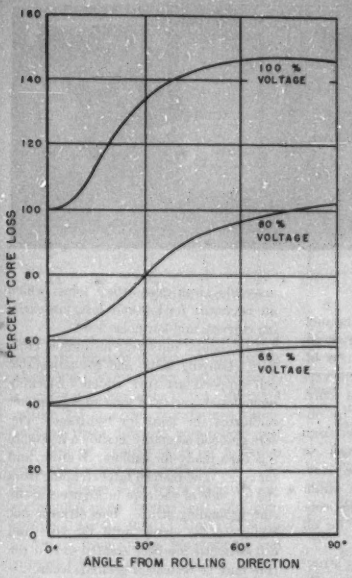

Figure 1 (left). Variation of core loss with angle from rolling direction of steel

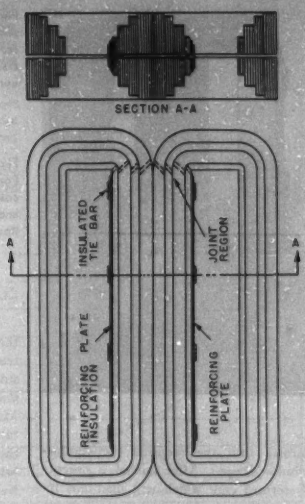

Figure 3 (right). General arrangement of core quarter-sections and cross sections

Core Cross Section

It has been shown that for a given number of widths of steel to be built into a core cross section approaching a circle, certain widths and builds of packets will give a maximum cross-sectional area.[1,3] Theoretical optimum cross-section dimensions are first determined. These dimensions may be modified slightly to permit use of stocked steel widths on a line of core sizes and to allow for bolts, tie-bars, and tie-plates. These modifications do not reduce the cross-sectional area appreciably from the theoretical optimum area. Some form of bolting, bonding, or tie-barring is required if a high space factor of iron is to be obtained. Several widths of steel are used in any one core design, depending on the rating. The core has been divided into four quarters; quarters have been clamped in the center leg by insulated tie-plates and tie-bars, as shown in Figure 3. Outside legs are secured by angled plates which are a part of the clamp.

Not only does this arrangement afford efficient utilization of the available iron space, but it gives step-backs in the yokes at the tops and bottoms of the windows into which adjustable coil support brackets may be fitted.

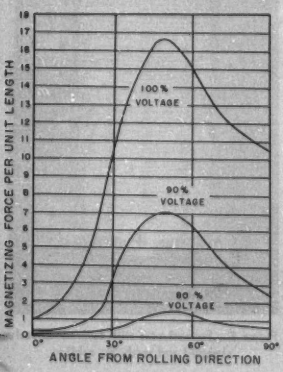

Figure 2 (left). Variation of magnetizing force per-unit length with angle from rolling direction of steel

Core Form

To maintain the desirable magnetic characteristics of the wound-type, cold-rolled steel core, the precut-preformed method was developed. This core, as applied in most Spirakore power transformers up to 3,333 kva, has one joint per lamination convolution. Joints are staggered in the joint region of Figure 3 such that a stepped joint having small overlap is obtained.

Starting with the lamination convolution forming one of the windows and progressing outward through the build of the core, lengths of the strips will increase linearly. Hence, if the core be developed horizontally into straight laminations, stacked with one end of the laminations at a vertical reference, the laminations would appear as a trapezoid with a rectangular end. Such laminations are progressively cut by an automatic indexing shear. As sheets leave the shear, they are coated with a material which acts as a separator during annealing of the core and remains as an insulation coating to limit eddy currents between laminations during transformer operation.

As laminations leave the coating machine, they are stacked into a ring, then

Figure 4 (right). One-quarter of a single-phase Spirakore power transformer core

Figure 5 (left). Assembly of quarter cores into bottom clamps of a Spirakore power transformer

Figure 7 (right). Formed core with coils on center leg and part of laminations reassembled around coils

formed into the required rectangular-window shape. After anneal, a precut-preformed core which will maintain its formed shape is obtained. Figure 4 shows one-quarter of a Spirakore power transformer at this stage of its processing and demonstrates how the joints may be staggered and maintained in proper position in the magnetic circuit. All of the steel is utilized in the rolling direction, and no corner effects are introduced. Four such quarter cores are assembled into clamps as shown in Figure 5. In this figure, top clamps and clamp insulation are removed.

Figure 6. Assembly of core and clamps of power transformer; top clamps in place but not completely bolted

Clamps

The clamping structure should be such that little if any strain on the core is introduced. Also, the core must be insulated from the clamps so that the core may be grounded at one point only. Multiple grounds which would be obtained if the core were not insulated from the clamps would result in partial- or total-turn short circuits on the core. Even though clamps should not strain the core, they should secure the core firmly and leave space for ducts for oil flow to cool the core.

For this type of core, a clamping structure has been designed which will cradle the core and permit lifting. Figure 6 shows the core of Figure 5 with top clamps in place. Outer legs of the core are supported by the insulated outer vertical members of the clamping structure and insulated cross bars. The core is supported from the bottom by bottom cross bars auxiliary cradling straps, and blocks. Coil supports on the bottom clamps support the windings, and lifting and short-circuit forces are sustained by the clamping structure, not by the core. It will be shown later how adjustable top coil supports are attached to top clamps to maintain a tight coil stack.

Coil Assembly

Coils are placed on the center leg of the core by removing the top clamps, opening the joint, folding back the laminations, and then lowering the coil stacks into place. The laminations that are folded back must be supported in the folded-back position such that the elastic limit of the core steel is not exceeded; exceeding the elastic limit would increase core loss and exciting magnetomotive force.

Laminations are put back into place until all of the laminations are back in the position in which they were annealed. Bands around each quarter core help maintain closed joints and reduce noise level. This method of core building and assembly gives close-fitting joints which are necessary for low core loss, low exciting current, and low noise level.

Top clamps, top clamp insulation, cross bars, clamping bolts, and the adjustable coil supports are then added. Blocking immediately over the joint region further reinforces the joint for tightness. The core and coil assembly as shown in Figure 8 is then ready for cabling, treating, and tanking. The pierced tab extending from the left side of the core in Figure 8 is the core grounding strap. This strap is not bolted to the clamp until the core and coil structure has been treated so that the core may be tested for grounds when it is ready for final tanking.

Characteristics of Transformer

Effective utilization of oriented cold-rolled steel in the formed core is best measured by the characteristics of the com-

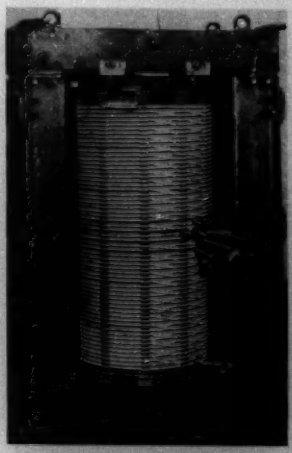

Figure 8. Formed core with coils completely clamped and ready for cabling

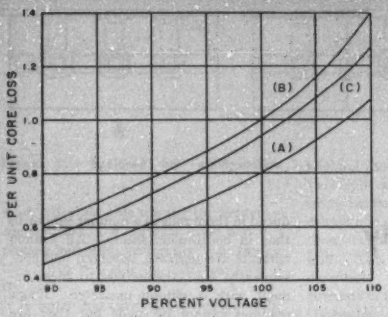

Figure 9 (left). Curves showing variation of core loss with per cent voltage

A. Formed core
B. Plate core with lapped joints
C. Plate core with mitered joints

pleted transformer built on this type of core. In Figures 9 and 10 are curves which show 60-cycle core loss and exciting current as functions of per cent rated voltage for a given transformer rating built on three different cold-rolled steel core designs. Curve A is for a design using the formed core as described in this paper. Curve B is for a design using rectangular-plate laminations and conventional lapped joints. Curve C is for a design using plate laminations and mitered joints.

The improvement in core characteristics resulting from the Spirakore construction is quite obvious. The core loss is reduced to 80 per cent, and the exciting current to 35 per cent of the values obtained with a core using plate laminations and lapped joints. The improvement from the use of mitered joints is appreciable but not as great as from the use of Spirakore construction.

Several factors account for these improvements in core loss and exciting current:

1. Flux passes through the core steel and joints in a direction parallel to the rolling direction of the steel.

2. Joint regions are a small part of the total magnetic circuit; thus, introduce very little reluctance in the magnetic circuit.

3. Strain effects on the core are reduced by cradling clamps around the core and not loading the core with coil weights and supporting forces.

4. Joints are closed and maintained tight by the clamping structure.

5. The core is annealed in its final form so that no assembly, piercing, forming, or shearing strains remain in the core.

Figure 10 (right). Curves showing variation of exciting current with per cent voltage

A. Formed core
B. Plate core with lapped joints
C. Plate core with mitered joints

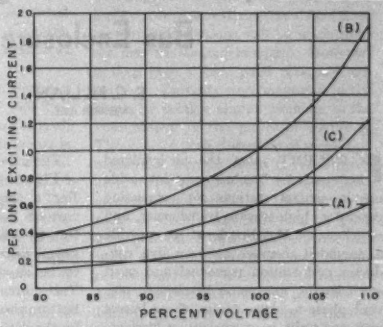

Although the 3-leg 4-section, single-phase core has been described in this paper, similar 2-leg 2-section designs have been made and built. These designs may be built with either two or four joints per convolution, depending upon the particular design requirements.

Conclusions

Efficient and economical utilization of oriented cold-rolled steel requires that:

1. The magnetic flux traverses the steel in the rolling direction.

2. The effect of joints be reduced.

3. The strains in the finished core be minimized.

These requirements are fulfilled by the Spirakore design described in this paper. Reductions in core loss, exciting current, and noise level have been obtained and demonstrated; they are being realized in routine production units of this type.

References

1. The Wound-Core Distribution Transformer, E. D. Treanor. *Electrical Engineering* (*AIEE Transactions*), volume 57, November 1938, pages 622–25.

2. The Cross Section of Transformer Cores, H. B. Dwight. *General Electric Review* (Schenectady, N. Y.), volume 38, No. 2, February, 1935, pages 92–93.

3. Stepped Core Sections for Power Transformers, A. L. Morris. *The Engineer* (London, England), December 9, 1947, pages 581–83.

No Discussion

Induced Currents in High-Capacity Bus Enclosures

S. C. KILLIAN
MEMBER AIEE

IN RECENT years the air-insulated high-capacity bus has come into wide use in central stations for connecting generator, high-tension transformer, and switchgear. Metal-enclosed to provide a grounded member between live conductor and station personnel and most often having interphase barriers to prevent phase-to-phase faults, these busses now are built in a variety of designs. Each has features to recommend it when considered from an economic, mechanical, structural, or electrical viewpoint. The electrical problem, much less evident than the others, centers about the enclosure rather than the conductor and involves the question of circulating currents in the enclosure.

These currents may be allowed to flow as in the unsegregated phase enclosure, Figure 1(A) and the segregated phase enclosure, Figure 1(B) where they will heat the enclosure but protect adjacent building steel from inductive and magnetic heating. In the isolated phase enclosure, Figure 1(C), it will be readily seen that enclosure currents cannot flow between phases. The individual phase ducts are also broken into sections by insulating strips which further reduce these currents. Heating in these enclosures will be small but adjacent steel will not be protected from inductive and magnetic heating. Other external means must then be used to keep the temperature of this steel at reasonable values.

Where circulating currents are allowed to flow in the enclosure, a careful choice of enclosure material must be made as this will determine the losses in the enclosure and the voltage drop in the main bus. This paper will discuss in the main those enclosures in which circulating currents are allowed to flow.

The induced currents in the enclosures of Figures 1(A) and 1(B) will be similar. For a simplified diagram of induced current flow in such an enclosure refer to Figure 2. Consider instantaneous current flow in the conductors to be as shown by the heavy arrows. The currents induced in the top and bottom sheets will then appear as shown by the dotted lines, and will flow so as to generate fields whose flux will oppose the field of the main conductor through as much duct length as possible. This requires the closing of these circuits in the very edges of the sheets as shown by the double-dotted lines. This end effect with its high current concentration produces a comparatively high temperature rise. It occurs in the laboratory when a heat run is made as shown in Figure 3 but not very often in practice. In almost all instances the bus duct will terminate on a generator casing, a transformer, or switchgear housing. In these cases the closing circulating current will flow in these various housings. Since these housings have a comparatively large mass, this current will produce a small temperature rise. On the other hand, the bus duct may terminate at a wall and the conductors continue through and then the higher rise due to end effect appears.

Current Distribution in the Duct and the Effects of Duct Length

In order to study the effects of current distribution and duct length, a mock duct was built of rods as shown in Figure 4. The network above and below the main conductors represents the top and bottom sheets of the duct while those beside the conductors represent the side walls and barriers. Circulating currents will be induced in these rods in a manner similar to that in continuous sheets. All branch currents are separate, however, and consequently lend themselves to measurement with a clip-on ammeter. Exact readings cannot be made but they are amply accurate for an investigation of this kind.

The current distribution in one of the ends of a mock duct test is shown in Figure 5. The over-all length of the grid was 10 feet 6 inches. Rods were 3/4-inch diameter copper. Other dimensions are shown in the figure. The current in the mains which were placed in the centers of the three sections was 2,500 amperes. The figures marked on the various network members are induced currents in amperes. Note how the currents distribute and close in rods "T" and "B" representing the bottom and top sheets of the duct. Although no near rods were used in this network parallel to bars "B" and "T", Figure 6 will show that even if close-by parallel paths are available, the greatest percentage of the current will still flow in the end conductors because of end effect.

All readings are given exactly as made. While care was taken to make up all joints in an identical manner, their resistances did vary somewhat. This accounts for the apparent small discrepancies in the diagram when it is analyzed. Note how the currents in rods "L", "M", "N", and "O", Figure 5, representing the side walls and barriers, divide almost perfectly; half of the current flowing into the bottom network and half into the top. The 100 amperes flowing up in the rod at the extreme left are joined by the 80 in the rod representing the corner of the duct. Their sum, 180, closely checks the 190 read. This 190 is joined by the 160 in the rod immediately above the conductor to produce 350, close to the 370

Paper 50-222, recommended by the AIEE Power Generation Committee and approved by the AIEE Technical Program Committee for presentation at the AIEE Fall General Meeting, Oklahoma City, Okla., October 23-27, 1950. Manuscript submitted March 13, 1950; made available for printing August 21, 1950.

S. C. KILLIAN is with the Delta-Star Electric Company, Chicago, Ill.

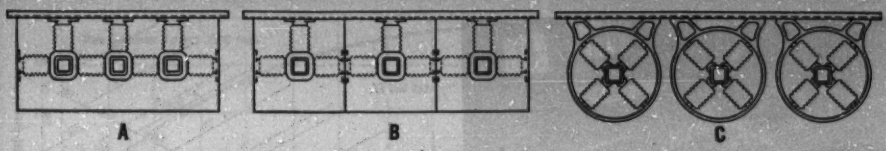

Figure 1. Enclosed bus configurations

read. Beyond this toward the center of the network, the currents close between phases and add vectorially. A similar check can be made on other sections of the grid.

In order that current distribution in the duct ends could be compared to all other points, the covers on top of the duct shown in Figure 3 were removed and replaced with the closely spaced network of rods shown in Figure 6. This network was insulated from the duct. Results would not, of course, be directly comparable to the grid shown in Figure 4 but do indicate what the relative current distribution would be. Furthermore, the time required to build a closely spaced grid completely around the main conductors, as in Figure 4, would be prohibitive. The current in the mains was 4,500 amperes. Grid currents are marked in amperes. The long rods were placed directly above the main conductors and parallel to them. Note that the current in these rods is consistent for the entire length of the grid. Note how quickly the current density falls off in the cross rods from the ends toward the center. Variations in joint resistivity account for the unequal current distribution in the "r" and "s" branches across the grid.

Another factor influencing current distribution to a small degree was the presence of the duct under the grid. Although the grid was insulated from the duct, the circulating currents in the duct affected those in the grid. Duct sections were split as shown in Figure 6 and entirely insulated from one another. This caused end effect currents in the duct and these in turn affected currents in the grid. This accounts for the somewhat disorderly progression from maximum currents in the grid ends to a minimum at the center.

The graph above the grid in Figure 6 plots average values read on rods "r" and "s" for each position across the grid. The curve plotted through these points is an average which would appear if all grid joint resistances were equal and the duct was not present under the grid. The actual readings and the curve are not far apart as can be noted from the figure. The curve forcefully pictures the large currents carried in the end members as compared to other members.

Figure 7 is a correlation of data in graph form for various lengths of networks similar to Figure 4. Maximum currents in rods "A", "B", and "C" as marked in Figure 4 are shown. It will be noted that for short lengths the circulating current increases rapidly with an increase in duct length. With further increases in duct length, this current increases much more slowly. The current in rod "B" was approximately the same as that in the other rods directly above and below the main conductors. Also the current in rod "C" was about the same as that in the other rods at the same elevation between phases.

As a further check on the relationship between duct length and maximum current and temperature rise, a setup as shown in Figure 8 was made. Here the duct is represented by a single sheet. The length of this sheet was varied. This is not a true picture of the actual duct since current contributions will be made from the side sheets and barriers. However, it does give a very good relative comparison. Currents were measured in the sheets by using a clip-on ammeter in the holes shown in the plates of Figure 8. This is not a perfect method of measuring maximum current but is sufficiently accurate for our purposes. Note the same general characteristic as obtained with rods—a steeply ascending curve, gradually flattening out. Temperature rises in the sheets also were taken on this series of tests and it is interesting to compare them with currents and note that they go hand-in-hand as would be expected. Temperature rises taken in the middle of the sheets at line C–C, as shown by the lower curve, were much lower than in the ends.

As still another check to determine what effect the bus duct length might have on temperature rise, an actual section of bus was tested. After temperature readings were taken on the 18-foot section of duct shown in Figure 3, the duct itself was divided electrically into three sections, 10-feet, 2-feet, and 6-feet long. Maximum rises in the ends of each section were close to one another and also to the maximum rise in the 18-foot section. This is about what would be expected from

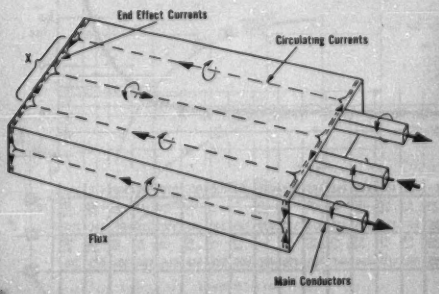

Figure 2. Simplified diagram of induced current flow in enclosure

Figure 3. 5,000-ampere bus on test

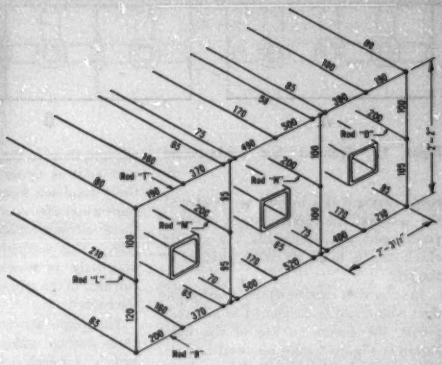

Figure 4 (above). Study induced currents by means of mock duct

Figure 5 (right). Induced current flow in end section of mock duct

Figures 7 and 8 and from proximity effect in the adjacent sheet ends which is discussed in the following section.

This variety of tests definitely proves the desirability of connecting duct sections together electrically in order to avoid the appearance of end effects over and over at every joint. This is done by means of annular rings which protrude through holes in the gaskets where the sections join each other and are bolted together. Field tests on duct installations in powerhouses have verified the proficiency of this method and the absence of hot spots.

Comparative tests and values on an actual duct would likely be of interest. Figure 3 shows a 5,000-ampere dust-tight bus under test. Double-phase barriers are used and the entire duct structure is constructed of aluminum. The duct is 18 feet long. At 5,000 amperes the maximum rise in the duct ends was 42 degrees centigrade. This temperature was recorded at the end of the duct in the area marked with an "X" in Figure 2 and is concentrated in the end of the sheet. A very large temperature differential can be obtained if readings are taken only 2 inches from the end of the duct. All other points on the duct ran much cooler, rises of 19 to 23 degrees centigrade being in the big majority. Readings taken on this bus after it was installed in the powerhouse produced lower maximum rises. This is true because end effect currents close on switchgear of low resistance, producing smaller losses.

At 4,000 amperes the laboratory test of Figure 3 produced a maximum end rise of 31 degrees centigrade. At 3,000 amperes this rise was 17 degrees centigrade. A rise of 17 degrees centigrade is not high enough to cause concern and the electrical bonding between duct sections can

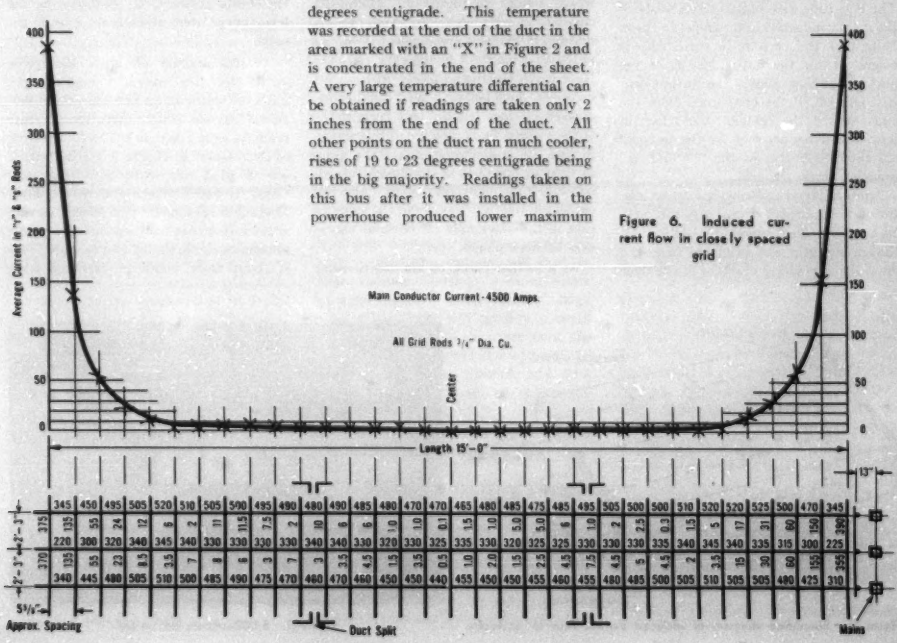

Figure 6. Induced current flow in closely spaced grid

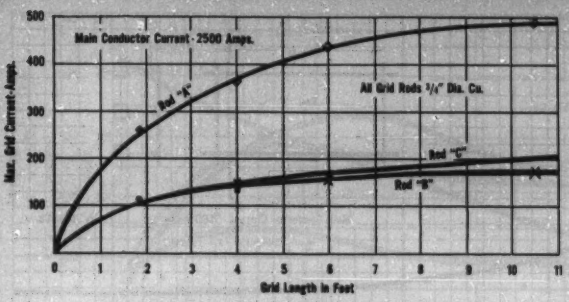

Figure 7. Influence of grid length on induced current

be eliminated if so desired. Above 4,000 amperes, duct sections should be bonded.

Proximity Effect in Adjacent Bus Duct Sections

It would be expected that proximity effect has a bearing on the end effect when duct sections are insulated one from another, as in Figure 3. In order to test this directly, the setup of Figure 9 was constructed. The two sheets were separated or insulated from each other by 1/8 inch. From the grid test illustrated in Figure 6, we know that even in an isolated grid or sheet, the closing currents will concentrate to a very great extent in the ends of the grid or sheet. This condition is even further intensified by the proximity effect. Closing currents at lines A and B, Figure 9, will oppose one another. These opposition currents will generate fluxes which will oppose one another, and shift the fields of the two currents to points of maximum possible separation. This in turn locates maximum reactance at a maximum distance and maximum current at a minimum distance.

The values marked on the aluminum sheets of Figure 9 are temperature rises in the sheets with 5,000 amperes in the mains. Note that the maximum rise at line "C" closely checks the maximum rise for the 3 foot 6 inch sheet of Figure 8 and that the maximum rise at line "D" closely checks with the maximum rise for the 24-inch sheet of the same figure. The rise at line "A" however is 35 degrees as compared to 24 degrees at line "C", and 31 degrees at "B" compared to 24 degrees at "D". In all previous tests mentioned, sheets were tested alone or isolated from adjacent sheets by several feet and rises in both ends of the sheet were identical. This discrepancy, 11 degrees and 7 degrees, is due to proximity effect where the sheets almost touch each other. This shows that duct sections insulated from each other by thin material will heat more than sections tested alone and much more than sections bonded together electrically.

This also explains why the various sections of Figure 3—10 feet, 2 feet and 6 feet

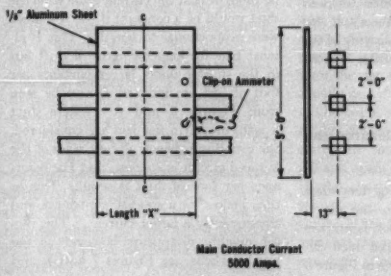

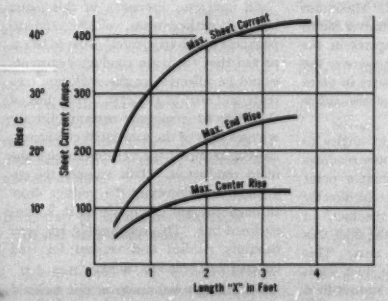

Figure 8. Influence of sheet length on induced current

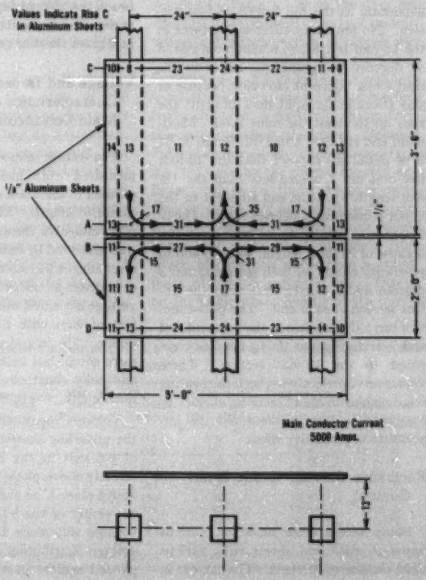

Figure 9. Influence of proximity effect on induced current

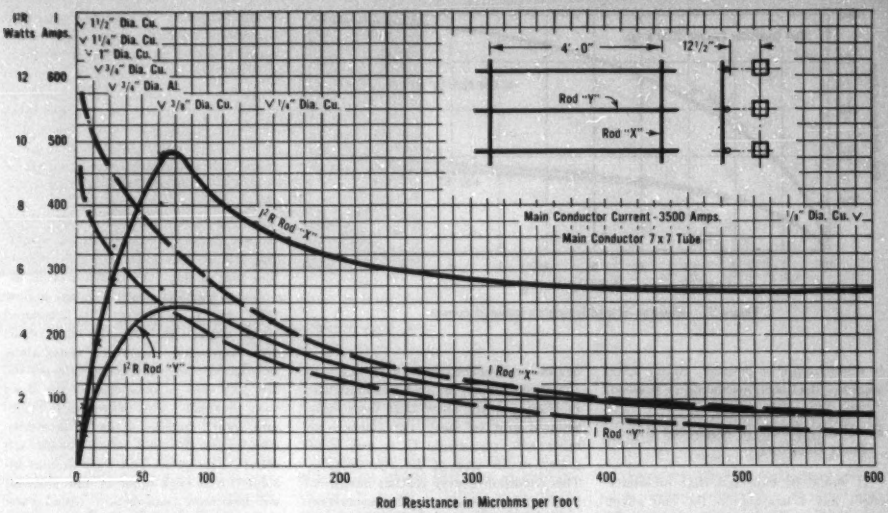

Figure 10. Influence of grid resistance on induced current

long—all insulated from each other, heated at their ends to about the same maximum as the full length 18-foot section. No proximity effect was present in the 18-foot test where a maximum rise of 42 degrees centigrade was found in the duct ends. Current crowding because of this effect in the split duct brought the rises up to about the same level. Maximum end rises are noted on Figure 3. It is of detail significance that the 10-foot free end ran 1 degree less than the 18-foot length while the end adjacent to the 2-foot section ran 2 degrees more. The 2-foot section, which should heat much less because of its short length, was exposed to proximity effects on both sides and ran 3 degrees and 6 degrees less than the 18-foot section at each end. The 6-foot section ran 2 degrees less at the adjacent end and 5 degrees less at the free end as compared to the 18-foot section. These values serve perfectly to check the heating relationships of short sections of duct as compared to long sections and the importance of proximity effect.

Enclosure Current versus Main Current

Many setups were made on various forms of grids and sheets with various main-conductor currents. The current in the grids or sheets was measured and it was found that, as would be expected, this induced current was in direct proportion to the main current for a given setup.

Phase spacings of main conductors also were varied. As taught by theory, it was found that decreasing phase spacing of the mains decreased the circulating current in a given sheet or grid.

Voltage and Impedance Characteristics of Enclosures and Main Conductors

The voltage induced in a bus duct when measured from one end to the other, parallel to the main conductor, is proportional to length. The induced open circuit voltage for the duct shown in Figure 3 was measured by removing the covers and stretching wires above each of the main conductors at the cover level. Maximum voltage measured was 1.3 volts over the 18 feet of duct with 5,000 amperes in the mains. The largest voltage read over the same setup, but with the covers in place and fully short circuited for the entire duct length, was 0.26 volt.

Voltages measured at right angles to the preceding showed maximum readings of 0.8 volt in the covers from a point directly above phase A to a point directly above phase C at the end of the duct. In the center of the length of the duct this voltage difference became zero. This voltage distribution over the duct when plotted against duct length results in a curve similar to Figure 6.

Since voltages induced in the duct are proportional to length and duct resistances are proportional to length, it would be thought that the current induced in the duct would be a constant if the reactance were proportional to length. This is almost true for longer lengths of duct but in the shorter ducts larger currents per foot of bus are induced as can be seen from Figures 7 and 8. Where duct lengths of only a few feet are considered, the coupling between all four sides of the induced circuit is so close that the reactance per foot of duct is small. This in turn makes for a smaller impedance and consequently a larger current. This factor quickly disappears however as the bus lengthens, see Figures 7 and 8, and the current almost becomes a constant, and independent of bus length.

All foregoing discussion in this paper has dealt with currents, voltages, and impedances of the enclosures. It is to be expected that the main conductor currents would be affected by the enclosure currents and such is the case. The flux of the induced enclosure current directly opposes that of the associated conductor, thereby reducing the net flux linking the main conductors. This reduces the reactance and decreases the voltage drop through the bus as compared to an unenclosed bus. This relationship has been carefully studied and verified for lead covered and armored cables.[1]

No attempt was made on this series of enclosure tests to determine by repeated

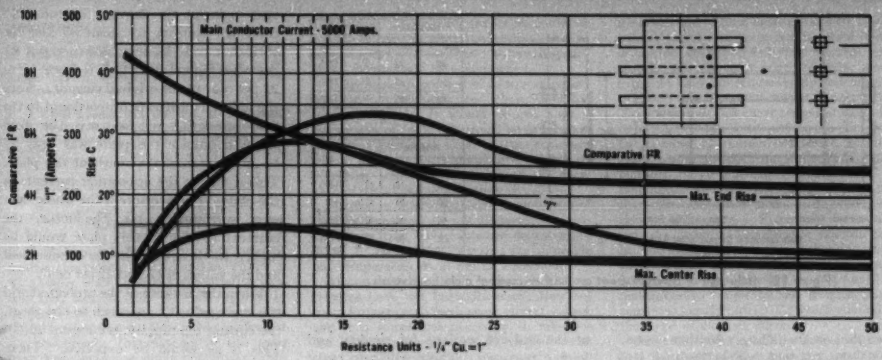

Figure 11. Influence of sheet resistance on induced current

runs what effect the enclosure had on voltage drop. One test was made however on isolated bus sections, Figure 1(C), each phase 17 feet 3 inches long. Each phase enclosure was entirely independent electrically of other phases and separated into four 4 feet $3^3/_4$ inch sections electrically insulated from each other. The current in the mains was 4,500 amperes, the phases arranged in flat configuration, and enclosures were 1/8-inch copper. If the current in the mains with no enclosure is taken as 100 per cent, it was found that the enclosure just described permitted a current of 110 per cent to pass with an identical impressed voltage. Short circuiting the insulation between each of the four 4 foot $3^3/_4$ inch long sections permitted 115 per cent current. Removing these short circuits, and short circuiting between phases, so that four 4 foot $3^3/_4$ inch long 3-phase loops were available for circulating current, permitted 113 per cent current. Leaving these shorts and restoring those between 4 foot $3^3/_4$ inch sections so that all three phases were shorted on each other and the entire phase length was shorted on itself, permitted 133 per cent current. The latter approximates the segregated phase bus which is dealt with in most of this paper. This conclusively points out that the reactance of the system is reduced as more and more circulating currents are allowed to flow.

Selection of Enclosure Material Based on Power Loss

It is well known that if the resistance of a duct or sheath around a conductor is plotted against the loss in the duct, that is, I^2R, the curve will originate at 0-0, since $I^2R=0$ when $R=0$. It returns again to 0 at $R=$infinity since $I^2R=0$ when $I=0$ as it must when $R=$infinity. In order to study the shape of this curve a grid made of only five rods as shown in Figure 10 was constructed. Different diameter copper and aluminum rods were used in order to vary R. Because the grid structure of Figure 4 was too difficult to construct each time a rod size was changed, the simplified grid of Figure 10 was used. While the current in the closing rods "X" would be larger with a complete grid, this simplified grid does show the shape and character of the curve equally as well.

The curve shape of Figure 10 conclusively demonstrates the truth of the statement that the curve originates at 0-0 and again returns to 0 at $R=$infinity. It also sharply points up the fact that some type of enclosure (at the top of the curve) is the poorest that could be used and that this condition should be carefully avoided. Currents are also plotted in the figure and it is interesting to note the orderly decrease of I as R is increased. I decreases slowly, however, for large increases of R, showing the reactance of the circuit is large compared to the resistance.

In order to further study this curve characteristic and to link it directly to duct material and thickness, the setup shown in Figure 8 was again used, varying the sheet material and thickness to obtain complete curves. All sheets tested were 2-feet long. This single plate again does not give correct readings for a complete duct but does give a true indication of the character of the curve. Results of these tests are plotted in Figure 11 and detailed in Table I. Since the data are intended to be qualitative and not quantitative, a 1/4-inch section of copper was given a resistance value of 1, a 1/8-inch section a value of 2, and so on. Aluminum and stainless steel were tested for conductivity and given a resistivity rating from this and the sheet thickness. Relative I^2R values were then found by multiplying this value by the current squared and basing values on the 1/4-inch copper. Copper sheets 1/4-inch thick and stainless steel sheets 1/16-inch thick would apparently make ideal materials from which to construct ducts from a standpoint of low temperature rises. One is on the rising characteristic of the curve,

Table I. Rises and Induced Currents in 2'-0"×5'-0" Sheets—Main Conductor Current 5,000 Amperes

Material, Inches	Max. End Rise, °C	Max. Center Rise, °C	Current, Amperes	Conductivity, Per Cent (Cu = 100%)	Comparative Resistance (1/4" Cu = 1)	Comparative I^2R Loss,*
1/4†	9.0	8.0	415	100	1.0	1.00 H
1/8†	12.0	9.0	400	100	2.0	1.86 H
1/8**	21.5	12.5	350	40	5.0	3.54 H
1/8**	21.0	12.5	370	31	6.4	5.08 H
0.064**	26.5	15.0	360	57	6.8	5.13 H
0.032**	26.0	12.0	280	58	13.5	6.17 H
0.040**	26.5	12.5	260	35	17.8	7.00 H
0.020**	23.0	9.5	180	48	25.0	4.90 H
1/16‡	12.0	9.0	51	1.4	286.0	4.33 H

* I^2R loss obtained by squaring column 4, multiplying by column 6, and equating to 1.00 H unit for 1/4-inch copper. Values for other materials are obtained in a like manner and appear as multiples of 1.00 H unit.

† Copper. ** Aluminum. ‡ Stainless steel.

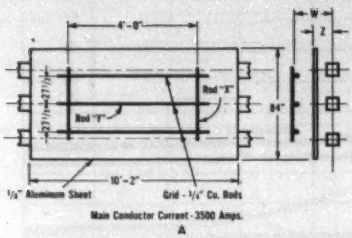

Amperes		Z	W
Rod "X"	Rod "Y"		
80	78	3 1/4	12 1/2
85	82	6 1/4	12 1/2
88	83	7 1/8	12 1/2

B

Amperes		Z	W
Rod "X"	Rod "Y"		
76	70	12 1/2	14 1/8
60	54	12 1/2	16
48	42	12 1/2	18 1/2
38	29	12 1/2	21 1/8

C

Figure 12. Influence of inserted sheet on field strength of main conductors

the other on the falling. Neither is practical—the 1/4-inch copper because it is too heavy and expensive and the 1/16-inch stainless because it is too thin. Furthermore the circulating current in the stainless is so small that only a small opposition flux would be generated and adjacent steel given less protection. Aluminum sheets of 1/8-inch to 1/4-inch thickness and of good conductivity are the best practical choice. It should be noted that the peak of this curve will move slightly to the right or to the left if phase spacings of the mains are enlarged or reduced.[1] It also should be noted that in all I^2R calculations the d-c value of R is used. Skin effect and proximity effect are neglected since they are of little consequence on these conductors.

This method of testing also allows for the making of qualitative heat runs on the sheets. All sheets were covered with an identical paint so that emissivities were equal and temperature rises could be compared directly. It is interesting to note the small difference in temperature rises between the copper sheets and the 1/8-inch aluminum sheets. In an actual duct this difference would be somewhat accentuated because of the larger closing currents. However, the heat from the main conductor would have to be conducted through these sheets and would be the same in all cases, so the rises in the various ducts would tend to draw together. Note the orderly progression of the various currents and the large differential in temperature rises between the ends of the sheets and the center of the sheets. Readings on the sheet centers were taken along line C-C, Figure 8. This large differential is present even though the sheet is only 2-feet long and the center tends to heat from the end effect by conduction. In long sheets this differential would of course be greater.

It must be kept in mind that in actual ducts, structural members must appear at the ends of sections for rigidity and joining purposes. These will help carry end effect currents, thereby reducing I^2R losses and temperature rises.

It is interesting to compare the power losses in a segregated-phase duct itself and in the main conductor in an approximate manner. Exact comparisons are difficult, if not impossible, because of the problem of measuring induced currents in the housings. From Figure 5, however, we can total the induced current in the rods about one conductor. By comparing the resistance of this group of rods and that of one phase of the duct enclosure shown in Figure 3, a close estimate of the current which would flow in the duct can be found. The I^2R loss can then be calculated for one phase of duct. It is found that this is approximately half the loss in the conductor itself.

Ferrous Sections and Current Loops Outside Enclosure

In Figure 3 note the steel sections laid on top of the duct. These steel members were arranged in a closed loop so that circulating current might flow and of course the steel would heat in itself because of magnetic effects. A maximum rise of 10 degrees centigrade was found at 5,000 amperes which is much lower than the rise would have been had the duct sheet not been interposed between the main conductor and the steel.

In order to study this effect more closely an arrangement as shown in Figure 12 was constructed. When "W" was set equal to 12 1/2 inches the circulating current in the grid could be compared to other readings. When "Z" was set equal to 12 1/2 inches the protection of the duct was demonstrated on outside grids at varying distances. In Figure 12 (B) note that the position of the aluminum sheet made little difference in the current flowing in the grid but its presence reduced the current in rod "X" from 490 amperes to about 85 and the current in rod "Y" from 350 to about 80. See also Figure 10. This is from 17 to 22 per cent of the original current. Since the induced current is proportional to the field strength, we can say the field strength outside the plate was only 17 to 22 per cent of that without the plate. This is due to the opposition currents in the plate. Furthermore if the whole duct were surrounding the conductor, the currents flowing in this plate would be higher, further reducing the outside field and the values of 17 and 22 per cent.

When the distance of the protected grid was changed with reference to the sheet, the current fell rapidly, see Figure 12(C). This is as would be expected. These tests demonstrate conclusively the protecting effect of the sheet metal duct on building steel, conduits, reinforcing rods, and other structural members. Magnetic heating in steel also is dependent on field strength, so that it too is reduced when the net field strength is reduced.

The protection of exterior ferrous members has been studied by others[2] and also can be accomplished by short circuiting loops.

Conclusion

On the basis of this paper and basic electrical theory the following axioms can be formulated for segregated and nonsegregated phase busses:

1. Induced currents in enclosures are proportional to main currents.
2. Decreasing phase spacing of the mains decreases induced currents.
3. Voltages induced are proportional to enclosure length and to the current in the mains.
4. Circulating currents flowing in enclosures reduced the reactances between the main conductors.
5. Circulating currents in enclosures do not increase with the lengthening of the bus after a length of, say, 10 to 20 feet is exceeded.
6. Large end effect currents will flow at the end of each enclosure section and to avoid heating from these currents at every enclosure joint, all sections should be electrically bonded together.
7. Proximity effect in enclosures insulated from each other must be considered since this produces additional heating.
8. On basis of power loss, an enclosure material can be selected which will provide minimum loss consistent with necessary structural strength and economic requirements.
9. Induced currents in enclosures reduce the field strength outside the enclosure to about 10 per cent of that without enclosures.

References

1. Armored Single Conductor Lead Covered A-C Cables, O. R. Schurig, H. P. Kuehni, F. H. Buller. *AIEE Transactions*, volume 48, April 1929, pages 417–35.

2. A 7,000 Ampere Station Bus, H. L. Unland, W. B. Morton, V. R. Bacon. *Electrical Engineering* (*AIEE Transactions*), volume 53, June 1934, pages 994–1004.

Discussion

L. H. Ruhlen and **F. D. Morgan** (Commonwealth Services Inc., Jackson, Mich.): This paper is an excellent contribution in a field that has not been too well explored in the past, and there are still unknown quantities where induced currents in bus enclosures are concerned. Installations of this type have been made applying certain assumptions, and corrections applied as required. By applying the information made available in this paper, it will be possible to obtain greater accuracy of design in the future. The method of approach is reasonable, and the results indicate the upward trend of induced current as the bus current is increased. Observations and temperature recordings made of actual installations tend to verify the results obtained in these experiments.

While the paper discusses current ratings only up to 5,000 amperes, it would seem logical to assume that higher current ratings may be considered on the same basis providing the I^2R of the bus structures are kept at a safe value. It appears that this could be done by increasing the cross sectional area of parts of the bus structure where high induced current will be encountered.

There is no discussion of means of reducing hot-spot temperatures where they become excessive. It would appear that a simple way of doing this would be to increase the cross sectional area of the structure where the hot spots occur by welding or otherwise attaching a section of the same kind of metal as the structure.

Maximum safe operating temperatures of the bus enclosures are not discussed, but it is important that the maximum temperature of these structures be such that the allowable bus temperatures will not be exceeded.

Although short circuit stresses on the enclosures have not been discussed, they become important at high short circuit values, and it is sometimes necessary to reinforce the enclosure to prevent distortion under short circuit conditions.

S. C. Killian: Mr. Ruhlen and Mr. Morgan have raised several good points which probably should have been stressed to a greater degree in the paper. A rating of 5,000 amperes has been designated as a top value for this type of bus by our company because of large end effect heating. It is true that heating due to end effect is reduced by increasing the section of the duct carrying these currents. This was verified by comparing the mock duct which was built of sheet only with actual ducts which carried structural members at the ends These structural members did reduce heating because of the reduced total resistance but the gain is not of major consequence. The current still crowds into the very edges of these members and they consequently do not provide as much advantage as might be expected. These hot spot end effect temperatures have to be more or less lived with at the duct ends but it must be remembered that, as mentioned in the paper, the duct usually terminates on a generator, transformer, or switchgear and the rises here will be less than shown because of the large sections in these equipments. Economic facts also must be faced. Considerable expense may be encountered in reducing heating from these end effect currents above 5,000 amperes. It is then possible that it would be preferable to resort to the isolated phase construction of Figure 1(C) which eliminates this type of induced current.

Bus temperatures are limited in all cases to a maximum of 45 degrees centigrade over outside ambient as prescribed by the various standards. Discounting end effect temperatures, all other points on the duct itself will be below the 30-degree centigrade rise prescribed by the standards for locations which may readily be touched by personnel.

The question of short circuits inducing high currents in the enclosure is a good one. These currents will attain considerable magnitude and the forces they will create are provided for by rigidly bracing the entire duct with structural members and forming the side sheets for additional stiffness in the higher capacities.

Centralized Control Board for Steam-Electric Generating Plants

H. L. LOWE
FELLOW AIEE

R. L. HODGKINS
MEMBER AIEE

THE centralization of boiler, turbine, generator, and auxiliary electrical control functions has had considerable attention during the past decade in plans and designs of new steam-electric generating plants. The result accomplished is basically a grouping of the several conventional control boards, formerly placed at scattered locations, into a specific area. The plan of such a typical control room is shown in Figure 1, from which it is seen readily that a considerable area of valuable station space is required and that simplicity of operation has not been wholly attained.

In the design of the new Morgan Creek Plant for the Texas Electric Service Company, a new approach to centralized control for all combustion, steam, and electrical power facilities has been taken. Of greatest importance is the opportunity afforded for one man to have a comprehensive knowledge of the entire plant performance, and for all important operating functions to be under the control of one operator. Another major advantage is that the new design resulted in approximately a 50 per cent decrease in the control-room area and a substantially larger reduction in linear footage of the control panels.

This new and compact centralized control board is of the duplex-type bench-board construction and is shown in Figures 2 and 3 for front and rear areas respectively. Each of the two boiler-turbine-generator sections is 7-feet long. The entire control board, which includes a 4-foot long transmission line control and relay section, is 18-feet long. The structure is 7-feet 6-inches high and 5-feet deep between the vertical panels. The bench section protrudes 1 foot 9 inches beyond the face of the vertical panels. This station consists of 2-unit type boiler-turbine generators. Each boiler is suitable for gas or oil firing, and is rated 220,000 pounds per hour, 925 pounds psi gauge and 905 degrees Fahrenheit. The turbine-generator is rated 20,000 kw, 850 pounds psi gauge, 900 degrees Fahrenheit, 3600 rpm, 13,200 volts. The generator is hydrogen cooled and is equipped with a direct-connected exciter. This plant began operation in June 1950.

Designs are completed, plant construction has begun, and manufacture of the centralized control boards is underway for several other new plants having a combined capacity of more than 700,000 kw.

Centralized control boards now are being furnished for new boiler-turbine-generator units rated 75,000 kw, and it is anticipated that such boards can readily be applied, with only minor modifications to the basic design, to units rated up to 125,000 kw.

Figure 4 shows the operating floor plan of a new 2-unit 132,000-kw plant employing the new type centralized control board. This plant is arranged so that it may be enlarged in the future for the installation of a similar additional centralized control board for the ultimate control of four large units from one central area. Although this may be considered a rather bold step in furthering centralized control to an extent not previously attempted, it is considered logical and reasonable, particularly for the single boiler-turbine type of plant design.

One of the disadvantages of the conventional central control area is the substantial amount of valuable space it requires in the most congested part of the plant. Obviously, to obtain an appreciable reduction in the size of this area, the various boiler, turbine, generator, and auxiliary control panels must be made smaller. In planning and working along these lines, the new and compact centralized control board evolved and has demonstrated its worth in effectively reducing space requirements. In its final design, other economies in plant construction, installation, and operating facilities are being realized.

Compact Design

The compactness of the centralized control board was achieved in various ways. First, careful consideration was given to include only those indications and controls that the central control room operator will require for easy and efficient adjustment of the various boiler, turbine, and generator auxiliaries during normal and emergency operating conditions. Secondly, all front-of-panel instruments, gauges, and control devices were selected to secure minimum size consistent with required readability and accuracy and for ease and convenience of manipulation. Particularly, for the boiler and turbine sections of the board, instruments are of miniature proportions as compared with conventional instruments ordinarily used on boiler-turbine gauge boards. These smaller instruments utilize the principle of retransmission of indications, with low-pressure compressed air as a medium, controlled by transmitters integral with normal full-sized instruments located remotely. This principle of retransmission results in the total elimination of high-pressure piping to the control board, thereby further contributing to compactness of design as well as to installation economies. Finally, the duplex type of construction of the centralized control

Paper 50-223, recommended by the AIEE Power Generation Committee and approved by the AIEE Technical Program Committee for presentation at the AIEE Fall General Meeting, Oklahoma City, Okla., October 23–27, 1950. Manuscript submitted July 20, 1950; made available for printing August 21, 1950.

H. L. Lowe is with Ebasco Services, Inc., New York, N. Y. and R. L. Hodgkins is with the General Electric Company, Philadelphia, Pa.

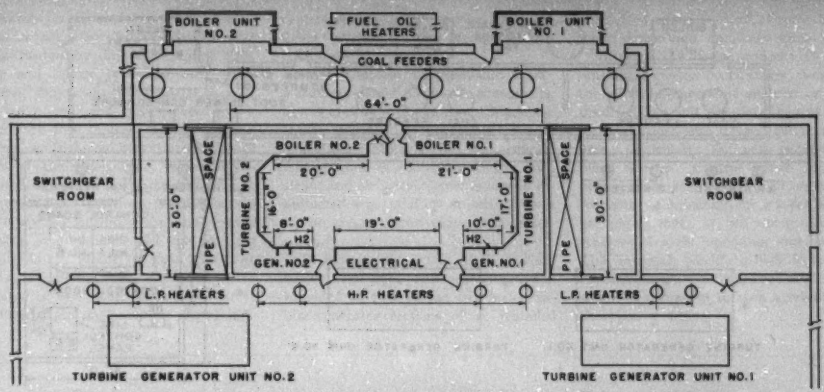

Figure 1. Operating floor plan of a recent 88,000-kw steam-electric station showing conventional control room with individual boiler, turbine, and electrical control boards

board facilitates the efficient use of space and provides sufficient area on the rear panels for all recording instruments, watthour meters, relays, and automatic station oscillographs, if required.

Safety

With the elimination of all high-pressure control and instrument piping from the central control board, any possible damage to the equipment or injury to operating personnel from the dangers of live steam, water, oil, gas, or similar hazards is removed. No barriers or compartmentation is required for protection of electrical connection against steam, water or mercury leaks, or spillage. This further contributes to simple and economical control-board construction.

Figure 5 shows the compactness and simplicity of installation of low-pressure piping to a group of gauges.

The control board is of dead-front construction throughout, with no exposed electrical connections on the outside surfaces, which further contributes to safe operation.

Design Advantages

The new centralized control board is flexible in application to various operating requirements and conditions, as space is initially provided for the maximum number of instruments and controls for which need may reasonably be anticipated. For the various control boards already built or now under construction, the only major differences among them are the number of fans per boiler, number of boiler feed pumps, and the differences in fuel usage and in the combustion control systems.

The basic design of the board provides instruments and controls for AIEE and American Society of Mechanical Engineers preferred standard and handbook turbine-generators. It can readily be modified to accommodate central control requirements for the more complicated installations, such as those employing reheat cycles.

Of major importance is the opportunity afforded for saving in operating personnel. Except for the starting of the plant, essential normal operations can be controlled entirely from the control board by one man. In starting up cold, the opening and closing of drains, the starting of miscellaneous motors, and various other local manual operations are required. These are not necessarily simultaneous, but, in general, can be handled by a man who, at other times, attends to routine plant duties.

The compactness and the arrangement of the control board offer the advantage of making it possible for one man to have a comprehensive grasp of the entire plant performance. Meters and gauges are easily read and controls are within convenient reach from the central operating position for one unit. As a result, it is expected that one man can observe instruments and adjust controls for all normal operations in a 2-unit plant. The extent to which this can be done for unusual or emergency conditions will depend upon the capabilities of the operator, and the complexities of the plant and the electrical system to which it is connected.

Another advantage is the reduction in

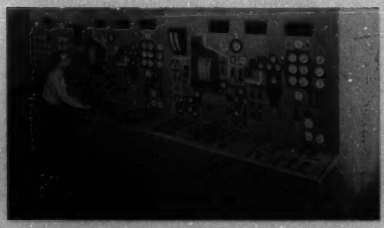

Figure 2 (left). Front elevation of the new 2-unit centralized control board recently installed at the Morgan Creek Steam-Electric Station of Texas Electric Service Company

Figure 3. Rear elevation of centralized-control board

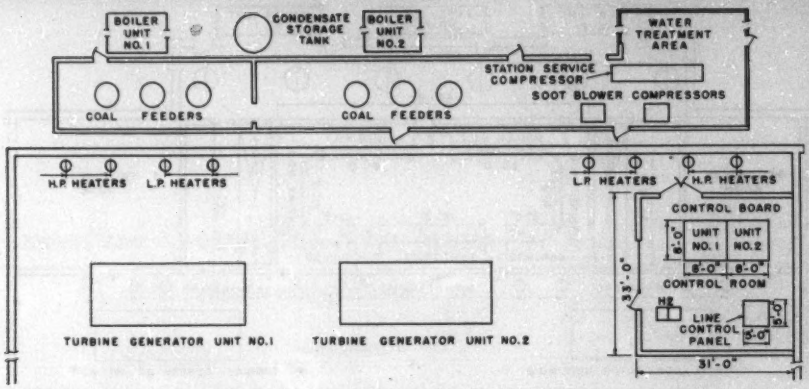

Figure 4. Operating floor plan of a new 132,000-kw 2-unit steam-electric station showing reduced control room area requirements by using the new 2-unit centralized-control-board design with separate transmission line control unit

size of the room required to house the control equipment. This represents a very sizable saving in structure, lighting, ventilation, and air conditioning costs. Although additional costs for retransmission facilities are involved, the net savings in capital investment by the use of the combined board are substantial.

Functional

A mimic delineation of major units of apparatus such as the boiler and accessories, induced and forced draft fans, turbine, condenser, generator, and shaft exciter, is outlined on the face of the control board. Their arrangement is in a logical manner so that the power production process from fuel to generator output can be readily followed. The various instruments and gauges associated with a specific piece of apparatus are confined within its mimic area as far as practicable. To present to the operator a clear picture of the function he is observing or controlling, the principal runs of piping and electrical circuits are likewise shown in mimic form, and are identified by distinctive colors for the various functions.

Many of the control devices, indicating lamps, and gauges are incorporated directly in the mimic system. Where

Figure 5. Back view of control panel showing partially installed low-pressure piping to a group of gauges

Figure 6. Control and instrument section for one boiler-turbine-generator unit. Numbered sections outline basic indication and control grouping

1. Boiler feed pumps and feedwater regulator controls and gauges. 2. Boiler draft and air heater controls and gauges. 3. Boiler gauges. 4. Combustion control. 5. Fuel (gas and oil) controls and gauges. 6. Steam temperature controls. 7. Main steam and throttle valve controls and gauges. 8. Turbine and condenser gauges. 9. Condenser circulating water and condensate control. 10. A-c generator and main transformer controls and instruments. 11. D-c exciter controls and instruments. 12. Station service transformer controls and instruments. 13. Boiler annunciator (15 indications). 14. Turbine annunciator (21 indications). 15. Generator and transformer annunciator (17 indications)

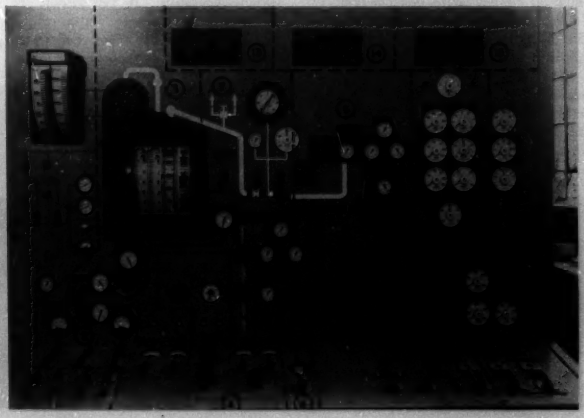

indicators for similar functions are located close to each other, further identification is facilitated by different colored dials. Safe and unsafe operating ranges are visually shown on pressure-gauge dials by the use of red- and green-colored zones. The green zone represents safe operating ranges, while the red zones, on one or both sides of the green zone, represent abnormal or unsafe operating ranges. To represent valve positions, rectangular signal lamps are located in the mimic piping system, one parallel and one at right angles to the piping, so that both color and position will indicate whether or not a piece of equipment is in use. Green lights at right angles to the piping indicate equipment out of service, while red lights parallel to the piping indicate equipment in use.

Such complete diagrammatic representation should facilitate acquainting new operators with equipment functions. It also should aid in the interpretation of indications and enable fast and accurate manipulation of controls involving both steam and electrical elements in well-coordinated sequential operations. This is of the greatest importance in an emergency.

To indicate the extent of the various control functions and instrumentation provided at each of the two boiler-turbine-generator sections of an installed centralized control board, Figure 6 is shown divided into numbered zones.

Although the design concept of the centralized control board is new, none of the applied components are new or untried. As a result, the development has met with widespread interest and acceptance, particularly for new generating plant designs. Control boards of the new type are now installed, or on order for factory fabrication, for a total of 13 generating units in ten steam-electric stations of eight operating companies. This has made possible a high degree of standardization usually not achieved with a new development in such a relatively short period of time.

Discussion

K. S. Garrett (Philadelphia Electric Company, Philadelphia, Pa.): The modern unit type generating stations of two units or possibly four are particularly well suited for centralized control as described by H. L. Lowe and R. L. Hodgkins. In general, the fundamentals discussed are sound, and it is evident that at Morgan Creek Plant a compact economic safe centralized control room has been constructed.

The use of oil or gas as a fuel, a minimum number of pumps and fans, and a system of combustion control utilizing little board space, appears to have contributed greatly to the high quality of this installation. A change in any of these characteristics might be expected to add considerably to the space required for centralized control. This could be a serious difficulty in connection with small units, but as units become larger, as in the 100-megawatt class and above, it is more likely that sufficient space can be found without adding to the plant dimensions. This was borne out recently when it was necessary to determine the space required to control two pulverized coal fired boilers of 850,000 pounds of steam per hour each and two 125-megawatt turbo generators. Because no detailed plan of control had been decided on, space was allowed for the use of standard size mechanical instruments and the type of combustion control which would require the most panel space. In spite of this, little difficulty was experienced in arranging the panels in an enclosure 36 by 40 feet. This was accomplished in such a manner that very little congestion resulted and well-defined lines of demarkation existed between different control function zones.

The authors state in their conclusion that centralized control has received widespread acceptance, particularly in connection with new generating plant designs. In connection with this acceptance, it is felt that a word of caution should be offered and that each new installation, whether in an established plant or on a new site, should be studied carefully, paying particular attention to the following points: Will the station in its ultimate be of the unit design? Will the full control of the plant be within the reasonable ability of one man to handle? Will the transmission associated with the plant be a very minor part? Can sufficient space be made available at a suitable location for full control of the unit without adding to the building dimensions?

If the answer is not yes to all of these questions, it is possible that centralization of control should be modified or limited.

C. P. West (Westinghouse Electric Corporation, East Pittsburgh, Pa.): Centralized control boards, as described by the authors are a valuable contribution to the control of central station steam and electric generators.

They show a definite trend toward co-ordinating the size and appearance of instruments and gauges. These devices are viewed in the same room by the same people at the same distances. It is obvious that the same sizes, shapes, and dial markings are desirable for both. Circular scales approximately four inches in diameter appear well suited for this application. Larger diameters do not seem justified.

Retransmission by low pressure air has made possible the safe intermingling of boiler room and electrical indications. Further changes to bring more boiler indicating devices into round cases are still desirable.

Manufacturing problems on centralized control boards are somewhat different but, in general, combine the techniques required for gauge board and switchboard construction.

Mimic bus layouts of main electric circuits have been considered helpful in central station operation for years. Extending this reasoning to the complete plant seems entirely logical.

Completely centralized control boards for unit type boiler, turbine, and generator combinations, with their associated auxiliaries, are just going into service. Operating experience is yet to be obtained. Reports on the functioning of these combinations during system or plant disturbances will furnish the final answer as to the part they will ultimately play in station design. A future paper on operating experience would be of great interest. It is hoped that the expected benefits of these new centralized control boards will be fully realized.

H. L. Lowe: A few impressions have been gained in review of various oral and written statements offered by discussers of this paper, which seem to justify further comment by the authors.

Apparently, the opinions of utility engineers vary concerning the extent to which centralized control is feasible. Some would limit the centralization of instrumentation and controls in a single control area to one or possibly two boiler units. Others would group instrumentation and control facilities of one or two boiler-turbine units, but would not install generator controls in the same area. A few consider it feasible to install boiler gauge boards, turbine gauge boards and the generator and electrical auxiliary control boards for one or two boiler-turbine generator units in the same room, however, in general, there has been little or no attempt to arrange the boards so that one operator could observe instruments and manipulate all controls from one location. Control of one or more complete boiler-turbine-generator units from one location and by one operator has been limited, as far as is known to installations employing the type of combined boiler-turbine-generator control board described in this paper. The number authorized, however, now exceeds 25 boards.

The combined boiler-turbine-generator control board does not impose the necessity that full control of a plant or unit be under one man. On the contrary, it provides a means by which all instrumentation can be observed and all or any part of the operation can be controlled by an individual, if this is desired. The extent to which the responsibilities for full operation of one or more boiler-turbine-generating units are imposed in one man is a matter of choice in interpretation of the philosophy of proper plant operation. The important advantage of the combined board is that it permits any degree of centralization of operation, from separate responsibility for one boiler, one turbine, or one generator, to consolidation of the responsibilities for all of these, and, if desired, additional elements of similar units in the same power plant.

Mr. Garrett states that "use of oil or gas as fuel, a minimum number of pumps and fans, and a system of combustion control utilizing little board space, appears to have contributed greatly to the high quality" of

the Morgan Creek installation. Actually, our basic design of this combined board provides sufficient panel space for instrumentation and controls for any or all of the common fuels used in power plants, including oil, gas, and pulverized coal; for various combinations and numbers of forced and induced draft fans; and for various types of modern electric and pneumatic combustion control systems for units up to and including 60/75 megawatt capacity. This is provided on a combined board for one boiler-turbine-generator panel with over-all length of eight feet. Space is provided on the board for up to four pulverizer-feeder groups for coal firing, two induced and two forced draft fan groups, and three condensate-three boiler feed pump groups.

In a recent adaptation of this board for 100/125 megawatt unit installations, using oil, gas, and pulverized bituminous coal for fuel, it was necessary to extend the length of the board by only eight inches to provide sufficient space for layout of instruments and controls for the unit combined board.

Several questions have been raised in connection with employment of centralized control for new generating plant designs, particularly where boiler-turbine-generator unit design is not employed. It is recognized that the maximum advantages of centralized control are realized in the boiler-turbine-generator unit design. However, most of the principles employed in the design of the combined board described in this paper are applicable to any type of plant design—for greater economy, greater compactness, and improved safety of installation. Referring to the unit design, it is anticipated that most future installations will be of this type, so that the advantages in economy and simplicity of operation of this system will be more fully utilized.

Mr. Garrett questions use of centralized control in plants where full control of the plant may not be within the reasonable ability of one man to handle. The combined boiler-turbine-generator control board does not require that only one man be assigned to handle the controls. The combined board merely makes it possible for this to be done if considered desirable. The relative amount of transmission and distribution associated with the plant should have no influence upon whether or not the combined boiler-turbine-generator control board is employed. If transmission and distribution controls are brought to a central location, the facilities for combined supervision are provided, but this does not require that controls be operated by one man. On the other hand, if controls are not brought to a central location, it would be impossible to institute centralized control later without expenditure of a relatively large amount of money—and what seems of even greater importance, the pattern of operation having once been established could not be as readily changed at a later date, because of the psychological aspects.

The combined board is not a development which has established the use of centralized control; it is, instead, a development which has provided the possibilities for realizing more fully the many advantages of this arrangement of controls.

A question has been raised about space requirements for centralized control. The combined board described in this paper requires less space than a boiler gauge board of the conventional type, so that it is likely that sufficient space for a centralized control room housing a combined unit board could be found without necessitating additions to power plant building dimensions.

Mr. West comments on the lack of operating experience with the combined control boards. We concur that it is unfortunate that more experience could not be obtained before it was necessary to employ them in such relatively large numbers. On the other hand, no single element of the board involves any new or untried principle, and nothing done in connection with the layout and arrangement of the boards and the rooms in which they are installed will preclude reverting to decentralized operation, if this is determined to be necessary. The Morgan Creek boards have been in operation approximately six months at this writing and the centralized operation is meeting every expectation.

Practical Experiences with Resonant Grounding in a Large 34.5-Kv System

HAROLD H. BROWN
MEMBER AIEE

ERIC T. B. GROSS
FELLOW AIEE

Synopsis: A large 34.5-kv system was operated ungrounded until early in 1946, at which time resonant grounding was installed, since it promised to be the most effective and most economical method of improving reliability of service. The layout of the system and a description of tests with the ground-fault neutralizer installed are given. Records of operation indicate that the improvements gained by resonant neutral grounding are considerable and fully in line with expectations.

IT IS well known that most faults in transmission and distribution systems are single line-to-ground faults or start as such. Anyone concerned with the problem of improving service on such systems should give serious consideration to the application of resonant neutral grounding, because this method of protection eliminates most ground faults as a source of line outages.

Resonant neutral grounding[1] is effected by grounding the neutral of the power system through a reactor, the inductive reactance of which is within broad margins nearly equal to the magnitude of the capacitive reactance-to-ground of the system.[2] This reactor is called a ground-fault neutralizer or Petersen coil, and is essentially an iron core reactor which is adjustable by means of taps on the winding. Taps at not less than 10 per cent apart are satisfactory, and a current ratio of approximately 1.5-to-1 can be obtained on regular designs without deviating from the required degree of saturation.

Resonant grounding is effective in clearing both transient and sustained single line-to-ground faults. Such faults represent 60 to 85 per cent of the troubles in most systems; they are due to lightning, wind, tree limbs, sleet, birds, small animals, and any other causes which ground one of the phase wires. Since interphase faults develop frequently from arcing grounds, such faults and the consequent outages can be avoided through the arc-extinguishing effect of Petersen coils. Ground faults do not affect the operation of the consumers' equipment, because the line-to-line voltages are not influenced by the occurrence of a ground fault, transient or otherwise, and voltage dips do not occur.

Description of System and Equipment

In 1944, when the greatly increased mileage of the 34.5-kv system of the Wisconsin Michigan Power Company was recognized to be responsible for a relatively large number of faults, various protective measures were investigated. The system was operated ungrounded as a delta system; its mileage of 252 miles of overhead lines could be increased to a total of 353 miles whenever up to 101 miles of a neighboring utility system were connected near Clintonville. Figure 1 shows the 34.5-kv system, which comprises 252 miles. Interconnection at higher voltages with such lines and with lines of neighboring companies takes place at Appleton, Stiles, and at a transformer station between New London and Clintonville. The type of overhead line construction used is shown in Figures 2, 3, and 4. It is the type of tower and pole which has been in general use in systems of this voltage. Figure 4 is of particular interest because of the 50-pair telephone cable installed below the 34.5-kv line. This installation was added in 1948 after resonant neutral grounding had been applied, and no difficulty was experienced by this telephone cable in spite of the fact that many permanent ground faults were on the system for a number of hours each.

In the investigation of means for reducing outages, several possible schemes were considered. One was the installation of static wires, which was found too costly, since ground wires over nearly the entire system would have been necessary. Another was the installation of protector tubes; however, tubes would require solid neutral grounding, and consequently all single line-to-ground faults would produce severe shocks to the system. It should be mentioned here that the system is directly or indirectly connected to twelve paper mills to which power is entirely or partially supplied. Voltage dips or momentary outages are extremely objectionable to such customers because they result in a costly loss of production. Such a voltage dip can interrupt production for at least one hour, and often longer.

Resonant neutral grounding proved to be the least costly solution, and yet it accomplished all the desired features of

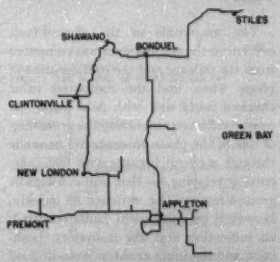

Figure 1. 34.5-kv system, Wisconsin Michigan Power Company

Paper 50-224, recommended by the AIEE Protective Devices Committee and approved by the AIEE Technical Program Committee for presentation at the AIEE Fall General Meeting, Oklahoma City, Okla., October 23–27, 1950. Manuscript submitted July 24, 1950; made available for printing August 31, 1950.

HAROLD H. BROWN is with the Wisconsin Michigan Power Company, Appleton, Wis., and ERIC T. B. GROSS is with the Illinois Institute of Technology, Chicago, Ill.

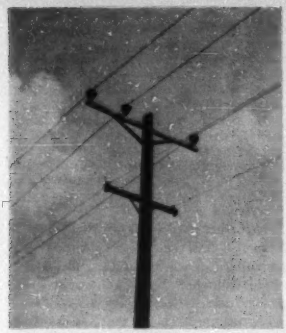

Figure 2. Overhead lines 34.5 kv on wood poles

service improvements. The system lent itself readily to this grounding method since all lightning arresters are rated for full line-to-line voltage, autotransformers are not in use, and the line sections are well balanced electrostatically; no long single-phase tap-feeders existed.

Ninety per cent of the system consists of flat-type wood poles without ground wires, Figures 2 and 4. Ten per cent are steel tower lines, Figure 3. The smallest size of conductor is number 1/0 stranded copper, which is supported generally on pin-type insulators. Many of the poles also carry 4-kv primary lines and secondary supply circuits. A ground-fault neutralizer with extended time rating, for 80 amperes maximum current and with 15 taps from 80 to 40 amperes, was purchased in 1945 for installation at Appleton. This size provides for a reasonable growth of the network. The cost of resonant neutral grounding of the 252 miles of system was about $51.50 per mile.

Tests

The magnitude of the ground-fault current in the delta system was computed from the mileage and the configuration of phase wires, and the computed value checked fairly well with field tests. Of course, such tests involving the grounding of one of the phase wires should be made through a circuit breaker with fast overcurrent relaying, so that any consequent ground fault will be switched off quickly. However, no consequent faults occurred, an indication that the insulators, bushings, and lightning arresters were in good condition and able to operate at full system voltage to ground. These tests were made with all three phases and the results differed but slightly, indicating that the system was fairly well balanced to ground electrostatically and that no additional transpositions were necessary.

Early in 1946, after the equipment was installed, tuning tests were made on the system during regular operation by measuring the current through the Petersen coil for a number of taps and finding the tap for maximum coil current. This is a simple test that is based on the existence of a small capacitive unbalance-to-ground of the delta system, which unbalance produces the voltage $\boldsymbol{E}_0$ between neutral and ground. Any resonant

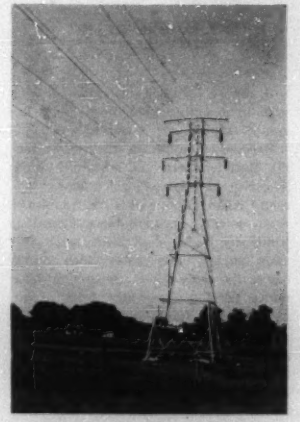

Figure 3. Overhead lines 34.5 kv on steel towers

grounded 3-phase system, Figure 5, can be replaced (see Appendix), as far as its zero sequence is concerned, by Figure 6(A), in which R_G, X_G is the ground impedance of the system, that is, the impedance equivalent to the parallel connection of $\boldsymbol{Z}_{AG}$, $\boldsymbol{Z}_{BG}$, and $\boldsymbol{Z}_{CG}$ in Figure 5. If the ground impedance is replaced by a series connection X_G', r, Figure 6(B), a circuit results which will resonate when X_P is equal to X_G'. The current through X_P will be near its maximum for this condition. This method leads to somewhat too large currents as far as compensation for actual ground-fault conditions is concerned, since a properly designed ground-fault neutralizer will saturate at or near phase voltage. However, the maximum voltage $\boldsymbol{E}_N$ across the coil will be only a fraction of phase voltage during this test so that the reactance will be larger than its saturated value. A resonance curve on which I_P is plotted versus the tap position, expressed by the rated current for each tap, does not readily show with which tap, or between which taps, optimum conditions were reached.

Greater accuracy in selecting the proper tap in this test,[8] which is easily made during normal operation of the system, can be reached by drawing the circle diagram of neutral displacement $\boldsymbol{E}_N$. Since $\boldsymbol{E}_0$, Figures 6(A) and (B), is a constant voltage impressed on two impedances in series, one of which, $\boldsymbol{Z}_G(=r-jX_G')$, is constant, while the other, $\boldsymbol{Z}_P$, is linearly variable, the locus of $\boldsymbol{E}_N$ for various settings of $\boldsymbol{Z}_P$ will be the circle shown in Figure 7. Perhaps the simplest method of obtaining the data for such a circle diagram is to measure, for each tap setting on the Petersen coil, the three voltages to ground $\boldsymbol{E}_{AG}$, $\boldsymbol{E}_{BG}$, and $\boldsymbol{E}_{CG}$, together with the line voltages by means of a 3-phase potential transformer with grounded neutral, Figure 6(C).

The results of such tests, made in 1948, are given in Figure 8, where the small circle indicates magnitude and phase of $\boldsymbol{E}_N$ for all possible values of $\boldsymbol{Z}_P$. This system is well balanced and $\boldsymbol{E}_0$ is quite small. However, an increase of unbalance will increase both $\boldsymbol{E}_0$ and the size of the circle, as shown in the same figure. The numbers next to the test points of the larger circle indicate the respective taps 10, 11, and 12. It is easy to see that resonance would exist on a tap between 10 and 11. Because of saturation, tap 11 with the lower rated current should be

Figure 4. Telephone cable under overhead lines 34.5 kv

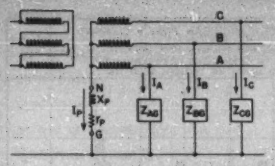

Z_{AG}, Z_{BG}, Z_{CG}: GROUND IMPEDANCES OF PHASES
$Z_P = r_P + jX_P$: IMPEDANCE OF PETERSON COIL

Figure 5. Resonant grounded system without fault

used, since saturation at full voltage on an actual ground fault reduces X_P and improves tuning. The increased unbalance was produced during these tests by switching off two of the three phases of a short section; this is the simplest way of producing such unbalance for test purposes. It may be mentioned that the same selection of the "best" tap was made from the results of the test which led to the small circle, but the points are so near to each other that the scale to which the figure is drawn does not permit an indication in Figure 8. The average ground-fault current of the system is 0.2 ampere per mile.

Another method of tuning, which is recommended as the best acceptance test and which should include arcing ground tests to show the effectiveness of resonant neutral grounding and the small effect of deviations from resonant tuning by over- and undercompensation, is the grounding of one phase, Figure 9, as staged fault. The equipment used and the instruments needed are indicated in Figure 10 The results are shown in Figure 11, which is self-explanatory. These tests, Figure 11, were made in 1948, in order to find the loss or in-phase component of the residual fault current which is important for the setting of sensitive ground relays.[4] It should be noted that at least two (better three) wattmeter readings are necessary, each with a different line-to-line voltage, in order to resolve the fault current I_F into its in-phase and quadrature components. Practical

Figure 7 (right). Neutral displacement with resonant grounding

experience has shown that ±20 per cent off resonance tuning has practically no effect on the self-extinction of an arcing ground. For this reason the taps on the Petersen coil rarely are changed when line sections are added or switched off. The taps 12 through 15 have never been used.

Performance Experiences

Since resonant neutral grounding was put in service early in 1946 it has never been out of service. It has functioned properly without any repair or maintenance expense. During severe storm periods previous to 1946 it was necessary to dispatch several crews to repair the 34.5-kv transmission lines and substation equipment. Now very little transmission-line trouble is experienced during storms. Since the installation of the ground-fault neutralizer, maintenance crews devote their efforts almost exclusively to rural and distribution circuits. Resonant grounding has made the decided difference.

When a permanent ground fault develops along the 252 miles or more of transmission system, an alarm indicates that a ground fault is on the system and a crew then is dispatched to the trouble and corrective measures are taken.

Resonant grounding has greatly reduced the number and length of outages. For example, there was an average reduction of 40 per cent in the number of outages per year in the 2-year period following this installation. However, the decided gain during the first two years with resonant grounding in service was 81 per cent less in outage time on a mile-hour basis.

Figure 12 shows that the number of operations has continued to reduce each

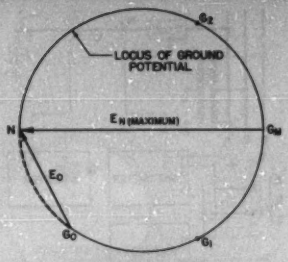

G_0: Δ-SYSTEM (E_0)
G_1: UNDER-COMPENSATED (E_{N1})
G_M: TUNED TO RESONANCE ($E_{N\,MAX.}$)
G_2: OVER-COMPENSATED (E_{N2})

year since. The reduction in the number of operations of the ground-fault neutralizer in general can be attributed to the gradual elimination of old conductor burns and old insulator damages that prevailed when the system was operated ungrounded. Previous to the ground-fault neutralizer installation, any arcing ground that occurred continued with all its fury until the relays tripped out the line in trouble. Such arcs severely burnt the conductors and the intense heat cracked off skirts from otherwise good insulators. The ground-fault neutralizer prevents the development of high values of arc current, since the arc is wiped out

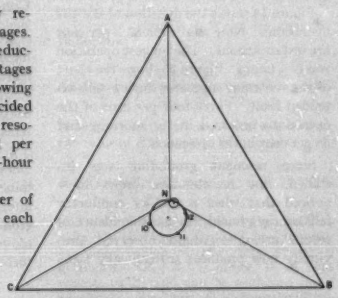

SMALL CIRCLE: FULL SYSTEM
LARGE CIRCLE: TWO PHASES OF SHORT SECTION OFF

Figure 8 (right). Resonant grounding with electrostatic unbalance

Figure 6 (below). Neutral displacement with resonant grounding

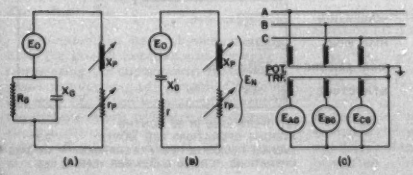

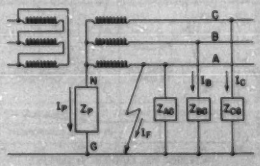

Z_{AG}, Z_{BG}, Z_{CG}: GROUND IMPEDANCES OF PHASES
Z_P : IMPEDANCE OF PETERSEN COIL

Figure 9 (right). Single line-to-ground fault in resonant grounded system

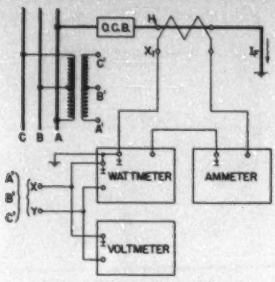

Figure 10 (left). Single line-to-ground fault test

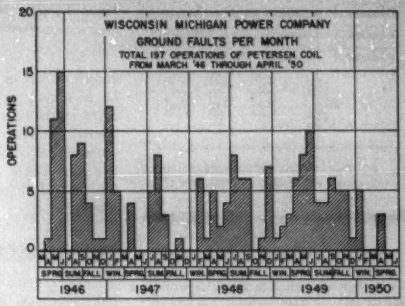

Figure 12 (right). Record of operations, 1946–1950

in a few cycles, at least, if caused by a flashover produced by lightning or other overvoltages. Also, for sustained ground faults the fault current is reduced to relatively small values.

Figure 13 shows in graphical representation an analysis of the causes of ground faults. Note that 46.2 per cent occurred during lightning storms. The operations because of unknown causes are relatively high, since the Petersen coil quenches the transient trouble quickly, so that damage is limited and not readily detected by the operating and maintenance personnel. Figure 13 covers 197 operations over a period of more than 4 years of experience. A recording ammeter, which measures the current in the Petersen coil, and an automatic oscillograph furnish records of the operations.

Figure 14 shows the duration of the 197 operations. Note that over 83.3 per cent are instantaneous. The longest operation was $6^1/_2$ hours. Figure 15 shows the chart of the recording ammeter during this extended fault. Forty-four per cent of the operations occurred in the morning and 56 per cent in the afternoon.

Since resonant grounding was installed, line maintenance crews have noticed that when a 34.5-kv conductor falls on the ground, the usual evidence of severe arcing-to-ground observed previously now produces scarcely any signs of trouble. The ground-fault neutralizer quenched all severe arcing. There have been no unsatisfactory conditions reported for this power system from communication companies because of permanent ground faults or of ground-fault neutralizer operations.

The great improvements brought about by the introduction of resonant neutral grounding are evident from a comparison of outages before and after the installation of the Petersen coil. The number of disconnected mile-hours per year because of faults during the year previous to the installation of the ground-fault neutralizer was 381.87. The mile-hours per year for the first two years after installation was 72.55, or a reduction of 81 per cent.

Conclusions

1. Resonant neutral grounding is a highly effective and most economical method of improving substantially the continuity and reliability of service in subtransmission and distribution systems.

2. Resonant neutral grounding provides protection for transient and sustained ground faults. The number of interphase short circuits is reduced and ground faults are eliminated as a source of voltage dips and other system disturbances.

3. Ground-fault neutralizers require practically no maintenance. Changes of tap settings are rarely necessary since operation is satisfactory on out-of-tune ratios of ±20 per cent and more, whenever lines are switched off or added. Therefore, taps are quite satisfactory if they are 10 per cent or more apart. A current ratio of about 1.5 to 1.0 (currents on maximum and minimum taps) will serve the needs of most systems, and will result in a smaller ground-fault neutralizer with proper saturation characteristics.

4. Reduction of ground-fault currents results in reduced line maintenance since severe damage to conductors and insulators is eliminated. Reduction in circuit-breaker operation consequently minimizes oil and contact maintenance.

5. Residual ground-fault current reductions make possible operation with permanent ground fault for many hours. Maximum duration in this system was more than six hours.

6. A sensitive relaying system to simplify indications of ground-fault locations is desirable.

7. Equipment, including lightning arresters, must be designed for full (line-to-line) insulation to ground.

8. Ground-fault neutralizers designed for extended time rating provide many advantages compared to short time rated equipment.

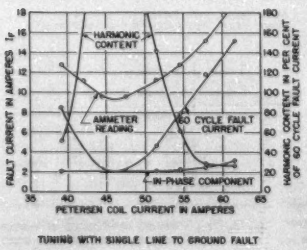

Figure 11 (left). Tuning with single line-to-ground fault

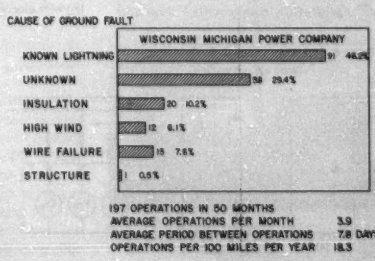

Figure 13 (right). Causes of single line-to-ground faults, March 1946 through April 1950

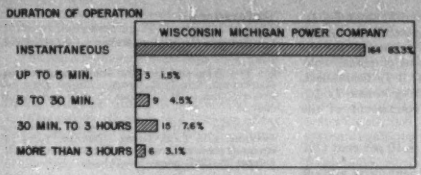

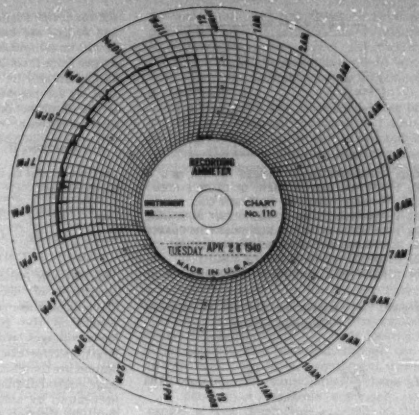

Figure 14 (above). Durations of single line-to-ground faults, March 1946 through April 1950

Figure 15 (right). Chart of recording ammeter, indicating sustained ground fault of 6½ hours duration

Appendix. Derivation of Equivalent Circuits

Delta System (Ungrounded System)

Using the notations of Figure 5, eliminating Z_P, since an ungrounded system is considered, and applying Kirchhoff's law leads to the phasor equation

$$I_A+I_B+I_C=0 \tag{1}$$

Loads, as well as capacitances between conductors, are omitted since they do not influence currents and voltages-to-ground directly.[8] If E_A, E_B, E_C denote voltages to ground, equation 1 may be written

$$\frac{E_A}{Z_{AG}}+\frac{E_B}{Z_{BG}}+\frac{E_C}{Z_{CG}}=0 \tag{2}$$

If we call E_{NG} the voltage from neutral to ground, and E_{AN}, E_{BN}, E_{CN} the three phase voltages, the relations

$$E_A=E_{AN}+E_{NG}$$

$$E_B=E_{BN}+E_{NG}$$

$$E_C=E_{CN}+E_{NG} \tag{3}$$

change equation 2 into

$$\frac{E_{AN}}{Z_{AG}}+\frac{E_{BN}}{Z_{BG}}+\frac{E_{CN}}{Z_{CG}}+E_{NG}\left(\frac{1}{Z_A}+\frac{1}{Z_B}+\frac{1}{Z_C}\right)=0 \tag{4}$$

In this phasor equation the following substitution can be made

$$\frac{1}{Z_{AG}}+\frac{1}{Z_{BG}}+\frac{1}{Z_{CG}}=\frac{1}{Z_G} \tag{5}$$

and

$$\frac{E_{AN}}{Z_{AG}}+\frac{E_{BN}}{Z_{BG}}+\frac{E_{CN}}{Z_{CG}}=I_u \tag{6}$$

Both quantities have physical meaning: Z_G is the ground impedance of the system representing the capacitances of the three phase conductors to ground (including leakage). I_u is the unbalanced current of the system, which indicates the degree of electrostatic unbalance.

Since $E_{AN}+E_{BN}+E_{CN}=0$, by definition of the phase voltages, $I_u=0$ if $Z_{AG}=Z_{BG}=Z_{CG}$, because the system is balanced under this special condition. Using the symbols introduced in equations 5 and 6 changes 4 into the form

$$E_{NG}=-I_uZ_G \tag{7A}$$

which equation determines the neutral displacement of the ungrounded system from the two characteristic quantities I_u and Z_G.

This value $(-I_uZ_G)$ is an important quantity which enters into many relations in the following where resonant grounding is considered. Since this voltage is the neutral displacement of the delta system, which may be measured as the voltage between a free neutral (the star point of a large power transformer) and ground, the symbol E_0 will be used, so that equation (7A) takes on the form

$$E_0=-I_uZ_G \tag{7B}$$

Resonant Grounded System without Fault

From Figure 5, Kirchhoff's equation now is

$$I_A+I_B+I_C+I_P=0 \tag{8}$$

or

$$\frac{E_A}{Z_{AG}}+\frac{E_B}{Z_{BG}}+\frac{E_C}{Z_{CG}}+\frac{E_{NG}}{Z_P}=0 \tag{9}$$

Using equations 3, 5, and 6, equation 9 becomes

$$-I_u+\frac{E_{NG}}{Z_G}+\frac{E_{NG}}{Z_P}=0 \tag{10}$$

or if the subscript G in E_{NG} is dropped and equation 7B is used

$$-\frac{E_0}{Z_G}+\frac{E_N}{Z_G}+\frac{E_N}{Z_P}=0 \tag{11}$$

E_N indicates the voltage from neutral to ground in the resonant grounded system, for any degree of tuning. Equation 11 also may be written

$$E_N=\frac{E_0}{Z_G+Z_P}Z_P \tag{12}$$

which equation is represented by the equivalent circuits of Figures 6(A) or 6(B).

Resonant Grounded System with Ground Fault

From Figure 9, Kirchhoff's equation now is

$$\frac{E_A}{Z_{AG}}+\frac{E_B}{Z_{BG}}+\frac{E_C}{Z_{CG}}+\frac{E_{NG}}{Z_P}+\frac{E_A}{R}=0 \tag{13}$$

if R is the resistance of the path of the fault current I_R.

Using equations 3, 5, 6, and 7B, equation 13 becomes

$$E_{NG}\left(\frac{1}{Z_G}+\frac{1}{Z_P}+\frac{1}{R}\right)+\frac{E_{AN}}{R}-\frac{E_0}{Z_G}=0 \tag{14}$$

If symmetrical component analysis is used, the value of R is found to be more accurately

$$R=R_F+\frac{1}{3}(Z_1+Z_2) \tag{15}$$

and the equivalent circuit of Figure 16 results. In this figure $X=A$, B, or C depending upon which of the three phases is grounded. (Z_1+Z_2) is always small with respect to Z_G and can be neglected in all practical applications, E_0 is always small relative to the phase voltage E_{XN}, and may also be neglected under fault conditions. If the ground fault is a solid ground, $R_F=0$, and the residual current in the fault will be, assuming also $Z_1+Z_2=0$, and $E_0=0$

$$I_R=-E_{XN}\frac{Z_G+Z_P}{Z_G\ Z_P} \tag{16}$$

Using equation 12, equation 16 becomes

$$E_N=-\frac{E_0E_{XN}}{I_RZ_G}=E_0\frac{I_G}{I_R} \tag{17}$$

where

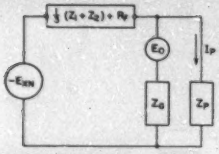

E_{XN} : PHASE VOLTAGE OF PHASES X = A, B, OR C
E_0 : NEUTRAL DISPLACEMENT OF DELTA SYSTEM
I_P : CURRENT THROUGH PETERSEN COIL
Z_1 : POSITIVE SEQUENCE EQUIVALENT IMPEDANCE
Z_2 : NEGATIVE SEQUENCE EQUIVALENT IMPEDANCE
Z_0 : GROUND IMPEDANCE OF DELTA SYSTEM
Z_P : IMPEDANCE OF PETERSEN COIL
R_F : RESISTANCE AT POINT OF GROUND FAULT

Figure 16. Equivalent diagram of resonant grounded system

$$I_G = -\frac{E_{XN}}{Z_G} \tag{18}$$

is the ground-fault current of the delta system. Equation 17 may be written

$$\frac{E_N}{E_0} = \frac{I_G}{I_R} \tag{19}$$

which is often referred to as Jonas' equation.[9] It now is possible to predict the diameter of the circles in Figures 7 and 8, since E_0, I_G, and $I_{R(min)}$ are known quantities. E_0 and I_G can be computed and I_R may be approximated from tests in systems of similar voltages. E_N will be largest, if I_R is smallest, that is, for resonant tuning, when $I_{R(min)}$ is the in-phase or loss component of the residual current.

For example, if $\frac{I_{R(min)}}{I_G}$ is 10 per cent (0.1 per unit) and if E_0 is 3 per cent phase voltage E_N becomes

$$\frac{E_N}{E_{XN}} = \frac{E_0}{E_{XN}}\frac{I_G}{I_R} = \frac{3\%}{0.1} = 30 \text{ per cent of phase voltage}$$

This example indicates that the permissible magnitude of electrostatic unbalance (E_0) depends on the magnitude of the loss component of the ground-fault current. At lower voltages, when the losses are larger, larger electrostatic unbalances of the delta system are therefore tolerable. Undesirably large neutral displacements, $E_{N(max)}$, may be prevented: by small values of E_0, by self-detuning through saturation (E_{V2} in Figure 7), by detuned setting,[8] or by increased losses (r_p in Figure 6). Transpositions in substations are nearly always possible and the most economical way of decreasing E_0. Saturation is valuable as protection against neutral displacements under unusual system conditions.

References

1. Neutral Grounding Devices. *AIEE Standard Number 32*, May 1947.

2. The Why and How of Resonant Neutral Grounding, **Eric T. B. Gross.** *Electric Light and Power* (Chicago, Ill.), volume 25, July and August 1947.

3. Tuning Tests in Resonant Grounded Systems, **Eric T. B. Gross.** *Bulletin*, Swiss Institute of Electrical Engineers (Zurich, Switzerland), volume 28, 1937, pages 165–71.

4. Sensitive Ground Protection for Transmission Lines and Distribution Feeders, **Eric T. B. Gross.** *Electrical Engineering* (*AIEE Transactions*), volume 60, November 1941, pages 968–71.

5. Sensitive Ground Protection, **AIEE Relay Committee.** *AIEE Transactions*, volume 69, part I, 1950, pages 473–76.

6. Transient Performance of Electric Power Systems (book), **R. Rudenberg.** McGraw-Hill Book Company, Inc., New York, N. Y., 1950, pages 340–54.

7. Ground Faults in High Voltage Systems (book), **R. Willheim.** Julius Springer, Berlin, Germany, 1936.

8. The Protection of Transmission Systems Against Lightning (book), **W. W. Lewis.** John Wiley and Sons, Inc., New York, N. Y., 1950.

9. Protection of High Voltage Systems Which Are Electrostatically Unbalanced with Respect to Ground, **J. Jonas.** *Elektrotechnik und Maschinenbau* (Wien, Austria), volume 38, 1920, pages 453–60.

10. Resonant Grounding of Distribution Systems, **E. Herzog.** *Proceedings*, Midwest Power Conference (Chicago, Ill.), volume 11, 1939, pages 237–40.

Discussion

Carl Sutter and **W. A. Wolfe** (Kansas Gas and Electric Company, Wichita, Kan.): We have operated with a Petersen coil since February 1947, on a 24-kv system with approximately 69 miles of line. This system was operated for many years with an isolated neutral, followed by one year with solidly grounded neutral prior to installation of the Petersen coil. The number of line trip-outs with the Petersen coil in service runs at about the same rate as with an isolated neutral, but considerably less than during the year with solidly grounded neutral. The extended outage record has been materially improved.

There is some electrostatic unbalance which requires that the coil be operated about two steps off resonance. We have been operating the coil two steps below resonance (at lower reactance) as recommended by the manufacturer. We note in reading the paper by Brown and Gross that where the point of exact resonance was found to be between two tap positions, the higher tap was chosen as the preferred tap. We would appreciate the authors' opinion as to whether the performance of our coil might be improved by operating above resonance rather than below.

We are in agreement with the authors' choice of a coil with extended time rating. We have experienced several instances in which permanent ground faults have been on the line for a considerable time and have been found and cleared without interruption to the circuit.

On the other hand, although line outage time has been greatly reduced following the installation of the Petersen coil, there have been several instances of crossarm fires following indication of permanent-line-to-ground faults. When the coil was installed, it was not believed that the small residual current (calculated to be approximately 1 ampere) flowing into a permanent ground fault would be of sufficient magnitude to cause a pole or crossarm fire. Neither was it thought that the theoretically calculated current of approximately 1.5 amperes resulting from off tune operation would be sufficient to cause a pole to be ignited. However, three cases have occurred in which crossarms were set on fire following a permanent ground fault in which the insulator was cracked or the conductor was lying on the crossarm. If the 1.5 amperes flowing into a ground fault under present operating conditions is capable of producing pole fires, then it is probable that even with a coil operating exactly in tune that the residual current of approximately 1 ampere could be expected to initiate a pole fire under some conditions. Of course it should be remembered that without the Petersen coil, and with the system operating with the neutral isolated, the ground fault current was approximately 8 amperes. Therefore, the likelihood of pole fires has been greatly reduced, but has not been eliminated as was anticipated when the coil was installed.

The authors state that 90 per cent of the system described consists of flat-type wood poles without ground wires. Assuming that this means no ground wire on the poles, we are surprised at the excellent results reported. It would seem that practically all faults with this construction would of necessity be phase-to-phase which would, of course, trip out the circuit. Our line is of similar construction, but there is a ground wire on each pole.

Harold H. Brown (Iowa Electric Light and Power Company, Cedar Rapids, Iowa): Our experience up to now has been with short-time rated coils. Also, we converted from a grounded neutral system instead of from an isolated neutral system. With these differences in application and experience, I cannot, of course, say that I concur exactly with the conclusions expressed in this paper. In general, however, I do agree that our experience largely confirms its conclusions.

We have approximately 1,600 miles of a 34.5-kv system and now have five ground-fault neutralizers in service. The last of these to go in service is a continuous rated coil, but as yet we have not isolated its section of the system from the rest and, therefore, have not had the benefit of the operation of a continuous rated coil. We would be interested in experience and practices in locating and isolating permanent ground faults when they occur as this is the problem which we have to solve before we do isolate this section of our system.

Lawrence M. Robertson (Public Service Company of Colorado, Denver, Colo.): We have one 100-kv Petersen coil in service since 1937 and two 13.8-kv coils since 1944. The 100-kv line is in the Rocky Mountains at high altitudes with a maximum of 13,500 feet and average of 10,000 feet and normally operates with corona loss. The length was originally 225 miles and now 285 miles. The main portion was a pioneer line built in 1909 and operating records indicated a need for improvement. The Petersen coil installation cost was about one-tenth the cost of other schemes such as overhead ground wires.

The 13.8-kv coils are operating on the

Denver system with about 1,500 equivalent miles of line made up of overhead and cable circuits. The coils have continuous ratings.

The authors have presented a very valuable paper on the tests and operation of the 34.5-kv coil. Our experience agrees with theirs, that the tuning is not critical and sections can be disconnected without effect on arc extinction. Our experience has shown that the coils will clear faults where they are of the type which are possible to be cleared. Our experience record is similar to that of the authors.

The continuous rating of the coils is usually justified as the cost is not much more and many faults can remain until they can be cleared later. This is in agreement with the authors.

What sensitive relaying is used by the authors to simplify ground fault locations and do they trip circuit breakers on faults and if so what relaying is used?

C. B. Hinton (General Electric Company, Schenectady, N. Y.): The operating experience on an extensive subtransmission system as described in this paper is an excellent example of the high degree of service reliability which can be obtained through the use of ground-fault neutralizers.

Methods of initial tuning of ground-fault neutralizers have received considerable attention and as a result it is possible to arrive at the correct tap position without conducting line-to-ground fault tests, and without the use of the instruments and potential transformers mentioned in the paper. Thus tuning can be accomplished in a very short time with a minimum number of workers. This method consists simply of tuning for maximum current in the neutralizer and then compensating for the effect of saturation when the data are plotted. It has been used on several systems and the results obtained in this manner have been identical to those obtained from line-to-ground fault tests on the same systems. A complete description of the method is given in the reference listed at the end of this discussion.

The authors' reference to the proper current range of ground-fault neutralizers does not seem to have the same importance as other comments relating more directly to operating experience. The matter of current range must be determined independently for every individual system, most of which require a greater range than 1.5 to 1. The application of ground-fault neutralizers in this country has not followed the same pattern as it has in Europe, where low current ranges are common. In general, our 23- through 69-kv systems were operated for many years with the neutral isolated. When they became too extensive for this type of operation the ground-fault neutralizer offered an effective, inexpensive way of improving service reliability. The ratio of maximum to minimum miles of connected line on such systems is usually greater than 1.5 to 1, thereby requiring neutralizers with correspondingly higher current ranges. In contrast to this, European practice has been to include Petersen coils, as ground-fault neutralizers are called there, as an essential element in the initial system design. As the systems grew larger, neutralizers were added with each new section, thus giving a pattern of several neutralizers with low current range.

American experience on systems equipped with ground-fault neutralizers having current ranges up to 4 to 1 has been entirely satisfactory. It is recognized that if several neutralizers are used on a system the current range need not be as great as 4 to 1. A 2-to-1 range is usually adequate for such a system and also is satisfactory for many systems equipped with only one neutralizer.

REFERENCE

1. TUNING OF GROUND-FAULT NEUTRALIZERS, N. E. Dillow, J. R. Burkhart. *General Electric Review* (Schenectady, N. Y.), December 1949.

Harold H. Brown and **Eric T. B. Gross:** It is indeed gratifying to learn that the experience in other systems has been similar to ours; the interest in this paper shown by many discussers is greatly appreciated and acknowledged with thanks.

Mr. Sutter and Mr. Wolfe point out the improvement in outage record after the change from solid to resonant grounding. This should be of particular interest to many who have not yet considered the merits of resonant grounding. Electrostatic unbalance requires off-tune setting in order to limit neutral displacement voltages during operation without ground faults. Since a properly designed coil will reduce its reactance with increasing voltage because of saturation of its iron core section, the tap with higher reactance will provide the desirable undercompensated "off-tune" setting at normal system condition. However, saturation will reduce this out-of-tune ratio and improve automatically the performance of the Petersen coil during ground faults.

As for pole fires, there have been a few cases in this system where the crossarm was charred and set on fire. However, in some cases a 34.5-kv phase wire has remained in continuous contact with a wooden arm without producing a fire, despite the fact that the residual current on this system is 9 amperes and over. It appears that crossarm fires occurring during single-line-to-ground faults can be prevented or greatly reduced by eliminating cracked or even only hairline cracked insulators. It is advisable to check all insulators regularly in the spring before the lightning season and if possible, once each year, early on a Sunday morning, during tests with one phase after the other solidly grounded and the other phases held for some time at full line to line voltage to ground. These tests have revealed weak spots, helped eliminate the occurrence of subsequent ground faults, and made possible the undisturbed operation of the system during sustained ground faults.

The data given in the paper may be supplemented by the following:

1. None of the cross arms are grounded on the wood poles. Wood V braces are used with the cross arms. None of the hardware is grounded. Wood strain insulators are inserted in the guys from the poles to ground.

2. Most of the steel towers are provided with extra insulation, in many cases with a basic impulse insulation level corresponding to the 69-kv class. It is difficult to discern from operating results any difference between wood poles and steel towers relative to flashovers to ground.

3. The ground-fault neutralizer at Appleton is composed of a 3-phase zig-zag grounding unit and a single-phase Petersen coil in one tank. Had there been available a 34.5-kv neutral of a power transformer, the cost of resonant grounding would have been only about half the amount mentioned in the paper.

Mr. Brown and Mr. Robertson bring up the question of finding the location of a sustained ground fault. The 34.5-kv system is fed from the power plant at Appleton and through step-down transformers at various other points. Therefore, it is possible to locate faults by sectionalizing. For example, if the circuit breaker at Bonduel in the line to Stiles is opened, power will still be supplied from Stiles, but the elimination of this line from the remaining system will help indicate whether or not the fault is still on the Appleton part. In the densely populated areas, trouble is almost always quickly identified and reported. Sensitive ground relays (for indication of the fault location) have not yet been installed, though consideration is given to such equipment which is in use abroad in many similar systems.

A number of engineers expressed approval of the conclusions reached in this paper in discussion and in letters to the authors. Pertinent parts of two of these may be quoted here: "I was pleased to learn that someone in this country is using coils with extended time rating. The large number of automatically switched grounding points involved when using short time rated coils is an expense which might better be invested in extended time rating. It is surprising that only one coil was used on such a large loop with several high-voltage supply points", and "The conclusions reached in this paper are in agreement with our experience with ground fault neutralizers and coincide with my personal opinions."

Mr. Hinton seems to prefer the least accurate method of finding the best setting, a method which is due to Petersen and which was used by him more than 30 years ago during tests with the first installation of a ground fault coil, as Petersen coils[1] are called in most countries abroad. It can hardly be assumed that it is more difficult to read voltmeters than ammeters; however, there is no doubt that an accurate test is generally considered preferable even if it is less simple. We feel that every acceptance test should include arcing grounds. Valuable by-products of such tests are the resolution of the residual current into its fundamental and harmonic components and information about the saturation characteristic of the ground fault neutralizer. Petersen's tuning method referred to by Mr. Hinton does not provide these system data.

The matter of the current range to be selected is certainly dependent upon the individual system, but it is hardly practical to consider only one ground fault neutralizer for a system in which the circuit miles vary by more than the ratio 1 to 1.5. A ratio such as suggested by Mr. Hinton does not mean a wide range coil must be used, but implies separation of the system into two sections which are operated separately. Therefore, the need for two ground-fault neutralizers is indicated, one for each of the two sections for protection which will be independent of switching conditions at all times. The ground-fault neutralizer used in this system has 15 taps. Neither taps 13 through 15 nor the taps near the upper cur-

rent region have ever been used. The minimum current to be considered in this system is 46 amperes, the maximum current 65 amperes, that is, a range of 1 to 1.4. The advantages of a small range are mentioned in the paper. As for the 1 to 4 ratio, from a paper by E. Herzog[2] may be quoted: "Improvements suggested by experience." . . . . . "The higher than normal range (1 to 4) of coil reactance has never been used, and large decreases in system capacity are unusual. It would have been a better design to put existing needs near the upper limit and use most of a smaller range for future expansion."

A recent survey[3] concerning the application of resonant grounding in the United States has indicated that taps are never being changed in as many as 27 per cent of all the systems so grounded in this country. It is evident that these systems do not need ground-fault neutralizers with a 1-to-2 range; much less than the 1-to-1.5 range suggested in this paper would do excellently. Future designs should consider this experience gained by many operators.

The same survey[4] also shows that other data referred to by Mr. Hinton are not based on facts. For example, of all systems in this country above 22-kv now resonant grounded, only 33 per cent were previously ungrounded, 52 per cent were changed from some other grounding method (35 per cent from solid grounding) to resonant grounding, and 15 per cent were new systems designed to be resonant grounded. We happen to know from first-hand experience that the European practice has been exactly what Mr. Hinton describes as the practice in this country. In general, systems operating at voltages below 66 kv were ungrounded until they became so extensive that resonant grounding (and hardly any other grounding method) was introduced to provide reliability of service. The European systems in this voltage range grew very much like those in this country. The reasons discussed above and the problem of saturation[1] were responsible for the selection of current ranges of less than 1 to 2 in all but a few exceptional cases.[1] The name Petersen coil has been in common use in this country with American operating engineers. It is even used in the titles of nine papers dealing with operating experience[4] published in this country, whereas three papers refer in their titles to resonant grounding, one paper to Bauch transformer and only two to ground-fault neutralizer.

References

1. See reference 7 of the paper.
2. See reference 10 of the paper, page 177.
3. Application of Resonant Grounding in Power Systems in the United States, Eric T. B. Gross, Edward W. Atherton. *AIEE Transactions*, volume 70, part I, 1951 (*Proceedings T1-64*).
4. Ibid., Bibliography.

Transformer Noise and Its Confinement

CORBETT McLEAN
MEMBER AIEE

RAPID INCREASES in population and load density necessitating the installation of larger transformers, the scarcity of suitable substation property, the noise consciousness of the general public, and the practice of working the new oriented or cold-rolled core steel to a high flux density, have recreated a major problem which must be considered and solved by all electrical utilities operating in well-developed residential areas. Low-frequency transformer hum is apparently a noise to which the average resident has not been accustomed. It differs from the routine traffic disturbances contributing to the general din which all modern city dwellers casually accept but which would have driven our forefathers from the confines of the city. The awareness of the utilities to the problem of transformer noise is demonstrated by the numerous papers presented at engineering and operating meetings and the experiments in wall and building construction.

This paper concerns the noise problems encountered after the energization of a newly installed unit substation in a residential area. It describes the attempts made, under pressure to relieve adjacent substations of severe overloading, to secure immediate temporary reduction of noise level by drapes and noise cancellation devices, to readily accumulate sufficient data from other utilities and from technical papers to permit an engineering approach to the problem, and to make tests on various building materials locally available for insurance of an adequate permanent reduction in noise level at reasonable cost. A 4-walled enclosure consisting of sand-filled hollow pumice block with partial tile roof was finally designed and built with satisfactory results.

Conclusions and recommendations include: (1) insistence to manufacturers for more consideration in design of noise free transformers; (2) procurement of sufficient substation property; (3) comparison of costs between excessive premium for reduction of innate transformer noise level below National Electrical Manufacturers Association (NEMA) Standards and sound insulating enclosures; (4) selection of material for enclosures plus desirability for energization of transformer before completion of sound attenuating device; and (5) improvement in appearance of the substation.

Installation of Substation and Complaints

In the fall of 1949 the Pacific Power and Light Company completed installation of a 15,000/25,000-kva 110/66–11-kv unit type substation with four feeder positions in a residential district in the southeast section of Portland, Oreg. Factors entering into the selection of the site included: (1) close proximity to the load center; (2) size of ground area; (3) availability of property; (4) zoning code restrictions; and (5) ease of entrance of transmission tap line and egress of distribution feeders.

A site measuring approximately 70 by 95 feet was the largest area which could be secured to satisfy requirements. This property was located on an arterial thoroughfare flanked by a medium class residential district. Owing to the somewhat limited size of the property acquired and the advisability of leaving space for future duplexing of the station, the transformer section of the initial unit was placed at the east end of the property which was relatively close to an adjacent frame dwelling, Figure 1.

When the unit substation was energized for service, residents in the area adjoining the substation vigorously complained of disturbing noise. The distribution of dwellings in this vicinity and the location of residents voicing these strenuous complaints are shown in Figure 2. Reflections from buildings created a crazy-quilt pattern of noise intensity.

An investigation which included sound level tests based upon NEMA Standards was made. Briefly these tests consisted of averaging the readings taken at a number of points around the transformer at specified heights and at a distance of one foot from the major sound producing surfaces. Since the switchgear cubicles were in place, all NEMA recommendations for tests could not be fully complied with. The performance standards prescribe that for a 15,000-kva 115-kv oil-immersed self-cooled (class *OA*) transformer the average sound level shall not exceed 75 decibels without fans and 79 decibels with fans when energized at normal voltage and frequency with no-load. Tests indicated average sound levels of 71 decibels and 73.5 decibels respectively on the *A* or 40-decibel frequency weighted scale with a maximum of 81.5 decibels without fans. All readings subsequently used in this paper are without operation of fans.

To further aggravate conditions, the daytime average ambient noise level was approximately 40 decibels; but because of almost continuous heavy daytime traffic on Division Street the intermittent sound level rose at times to 100 decibels. This condition made the transformer noise at night seem more intense. To maintain good public relations and avoid statute violations of a zoning ordinance, a means of reducing the noise level of the substation became imperative.

Preliminary Experiments

To suitably attack the problem and provide temporary relief it was necessary to explore the proportion of earthborne

Paper 50-225, recommended by the AIEE Transformers Committee and approved by the AIEE Technical Program Committee for presentation at the AIEE Fall General Meeting, Oklahoma City, Okla., October 23–27, 1950. Manuscript submitted July 17, 1950; made available for printing August 21, 1950.

CORBETT McLEAN is with the Pacific Power and Light Company, Portland, Oreg.

Figure 1 (left). Unit substation before construction started on the pumice block enclosure

Figure 2 (right). Buildings in vicinity of substation

Hatched areas indicate dwellings where disturbance was most noticeable

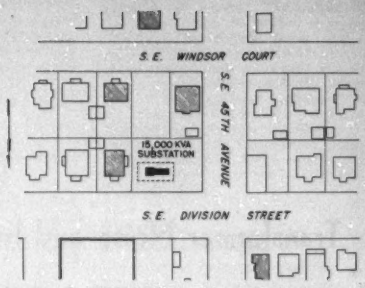

and airborne noise and to determine if the predominating frequency was that of magnetostriction, 120 cycles per second. Physically very little vibration could be felt on the substation pad and none could be noticed in the surrounding earth.

By the use of available equipment including contact and crystal microphones, Ballantine vacuum tube voltmeter, and cathode-ray oscillograph, it appeared that the resonant frequency of the concrete pad was 600 cycles and that of the transformer shell was 720 cycles. The contact microphone was utilized to measure this vibration. The contribution through the surrounding earth was apparently negligible. With a crystal microphone accurate from 50 to 10,000 cycles per second it appeared that the major airborne frequency was 240 cycles. Later information included in this paper showed that the frequency varied with the test location.

A quantity of burlap was purchased and a double layer approximately 20 feet by 20 feet was suspended between the transformer and the nearest residence. Even with many folds in this form of drape and with the burlap later saturated with water, no improvement could be observed. A better understanding of the distinction between sound absorption and sound insulation would have eliminated this test.

Noise cancellation was then attempted as another temporary expedient. A high-fidelity crystal microphone was used in conjunction with a very linear audio amplifier to drive two 12-inch cone-type speakers 180 degrees out-of-phase with the noise source and pointed in the direction of the desired noise reduction. The speakers were positioned about the transformer without accomplishing any successful improvement. The sound wave lengths of the various frequency components later determined to be present, ranged from approximately 10 inches to 9 feet.

Because the microphone could not be located at the same spot as the speakers on account of feedback and because of the multiplicity of sound generating sources on the transformer, the cancellation of noise from one source was offset by the reinforcement of noise from another source. However, additional thought is being given to this idea for possible future installations requiring temporary immediate relief. Perhaps some solution may be found for effective unidirectional cancellation for local areas perpendicular to a major transformer surface.

Compilation of Available Information

An accumulation of data through correspondence, review of technical papers, and inspection of installations of other utilities confronted with similar problems, resulted in a collection of information concerning intercepting walls on one or more sides of the transformers, resilient pads under transformer bases, inner liners in compartments, heavy plantings of shrubbery, enclosures, and complete masonry buildings. All emphasized the severity of the problem and the impossibility of an exact analysis with specific improvement per dollar expended. In addition to the uncertainties of proper evaluation of noise measurements, the equation of ear response versus human reaction was most disturbing.

Figure 3. Equipment and samples employed in making sound insulation tests

The following excerpts adduced from a recent technical paper by C. E. Baugh[1] were extremely pertinent:

1. Units of the same design show a wide variation—as high as 12.5 decibels—in sound level.

2. Units with cold-rolled steel cores have an average sound level about 7.5 decibels higher than that of earlier units built to the same specifications.

3. The housing of unit substations is contrary to the philosophy under which this type of apparatus was developed.

The study of information led to the conviction that the only solution for a substation of such a high noise level was the construction of a suitable wall or barrier around the unit that would effect the reduction of the noise level at the locations of the complainants without interference with necessary ventilation and operation.

Some thought was given to the use of sound metal panels in place of a masonry enclosure. The panels, as manufactured, were constructed of a heavy steel frame faced with perforated metal, and where exposed to the weather, the outside sheet was of solid metal. Separators were placed in between the steel sheets and a

Figure 4. Sound attenuation tests through building blocks

A = concrete B = pumice C = concrete-sawdust. Open columns indicate hollow building blocks. Hatched columns indicate building blocks filled with dry sand

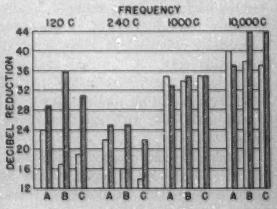

Figure 5 (left). Start of construction on pumice block enclosure

Figure 6 (right). Enclosure before roof section was added

high-grade spun mineral felt packed within. This resulted in a meritorious product having high absorption coefficients at the lower as well as the higher frequencies. The cost of a complete enclosure of the substation with sound metal panels was estimated to be considerably more than masonry construction. No data were available on the efficiency of these panels as sound insulation.

It is important at this point to note that there are two distinct problems encountered when dealing with sound. These are sound absorption and sound insulation. Sound absorption deals with the dissipation of sound incident upon a surface. In other words, a material having a high absorption coefficient will permit minimum reflection and reduce reverberation. Sound insulation applies to the reduction of sound intensity level when transmitted through a structural wall. It is the problem of sound insulation with which one is confronted in attempting to reduce transformer noise by the erection of walled enclosures. Practically all acoustical information on hand dealt with sound absorption.

Lacking definite information on the sound insulating qualities of the various acoustical materials, a series of tests were conducted on those thought to be most suitable for exterior application. Experiments were made on various acoustical wood fiber, cork, Fiberglas, and asbestos boards but it was soon evident that these lighter materials were not efficient sound insulators. The attenuation of noise passing through these substances was insignificant. No suitable practical method was evolved to satisfactorily check published data on the sound absorption coefficients of these materials. Differences in reflection (and absorption) between panels of fiber board, pressed shavings, plywood, and polished marble could not be detected with existing equipment.

These tests and previously published information on the efficiency of sound insulating walled enclosures, indicated that materials having large masses were required for efficient noise attenuation. This explains why tests by this company and other utilities using burlap or canvas walls as sound insulators produced negligible improvement. Particular attention was therefore given to the various types of masonry blocks available in the area.

The test procedure consisted of providing a directional noise source, a wall of the material under test, and a sound measuring device. As illustrated in Figure 3, the noise source was provided by enclosing a speaker in a heavy plywood box open on one side and lined on all inner surfaces with acoustical board. The speaker was driven by an audio signal generator and a very linear audio amplifier which permitted control of both the sound intensity and frequency. The material under test formed the remaining wall. A General Radio Company sound level meter was used to measure the sound intensity before and after the wall was in place—the difference between the two readings being an indication of the sound insulating efficiency of the wall material under test.

Figure 4 illustrates the sound reduction obtained for frequencies from 120 cycles per second to 10,000 cycles per second by the use of walls built of concrete, pumice, and concrete sawdust blocks with and without sand filling. A very noticeable increase in sound insulation at the lower frequencies was obtained in each case by filling the hollow blocks with dry sand, an average of 12 decibels at 120 cycles per second for the three types under discussion. Possibly because pumice blocks were good sound absorbers as well as good sound insulators, the sand-filled pumice block construction appeared the best and was chosen for the construction of the substation enclosure. In contrast to these findings, one of the manufacturers repeatedly expressed an opinion that even though the sand would add to the mass of the walls it was doubtful if it would have any beneficial effect external to the enclosure. Although blocks were immersed in water to measure its absorption, no tests were made to determine the characteristics of wet sand. However, sound

Figure 7. Interior of enclosure showing roof construction

Figure 8. Rear of completed enclosure showing tile roof, service entrance, and closed vents

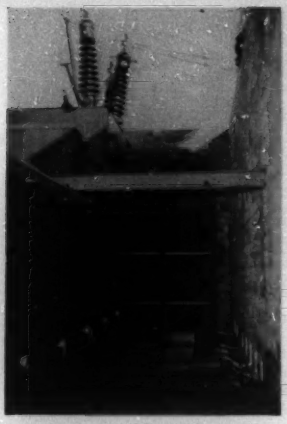

Figure 9. Interior of enclosure showing I-beam support for baffle wall

dampening qualities of sand were believed to be better when dry and provision was later made to keep the sand in this dry condition.

Following considerable study of sound absorbent materials, 2-inch thick pressed Fiberglas panels of the type used for roof insulation were selected as an inner liner

Figure 10. Interior baffle wall and I-beam support

to provide the most suitable means of additional sound absorption if such were found necessary upon completion of the building. By using pumice-block construction these panels could be nailed directly to the inside of the wall.

Design of Structure to Confine Noise

With hollow pumice blocks filled with sand showing superior qualities as a wall material, the task of designing an enclosure that would produce the expected results at a minimum of cost and with an appearance that would be in keeping with the buildings surrounding the substation location was undertaken.

In addition to strenuous objections of residents whose locations are illustrated in Figure 2, there were many complaints from customers at random locations about the substation. The noise pattern observed led to the conclusion that a 2-sided enclosure would probably cause sufficient reflections to create hot spots of even higher than original intensity on the unprotected sides. The exposure of the substation to the public in the adjacent main traffic artery also was a potent argument for an acceptable appearance. Although a complete roof did not seem practical on account of the high-voltage leads, a partial roof seemed necessary to eliminate line of sight noise transmission and to reduce spill-over.

The enclosure finally adopted consisted of four closed walls 24-feet wide, 46-feet 8-inches long, and 16-feet 6-inches high built of pumice block masonry, using 8 by 8 by 16-inch units erected on a reinforced concrete footing poured independent of all other station foundations, Figures 5 and 6. The height including partial roof was 21 feet 8 inches.

The cavities in the individual blocks were filled with sand after every six or eight courses of block were placed. Clean dry sand was used, well rodded to insure complete filling. The 4-inch thick glass block panels, which were added for decorative purposes only, measured 6 by 8 feet and were backed with 4 by 8 by 16-inch pumice block also sand-filled to provide full wall thickness at all points. Corner columns were built up of standard block units, concrete filled to provide additional strength and to comply with the city building code.

Pumice sand was used in the mortar to provide a material having nearly the same expansion coefficient as the blocks themselves. Placed longitudinally in the mortar joint between every third course of blocks were steel reinforcing rods which served to reinforce the wall structurally

Figure 11. Interior of structure

Note small wall of uncemented pumice blocks originally installed to reduce sound transmission through ventilating openings

and provide a method of stopping expansion cracks which might develop. The walls were capped with a partial roof consisting of a poured reinforced concrete slab covered with clay roofing tile, Figures 7 and 8. The contractor was given the option of constructing the roof by use of the conventional wood forms or by the "Hy Rib" method which employed metal lath and cement plaster. He elected to use the wood-form method.

The internal baffle wall mounted on an I-beam shown in Figure 9 and extending from a height of approximately 9 feet

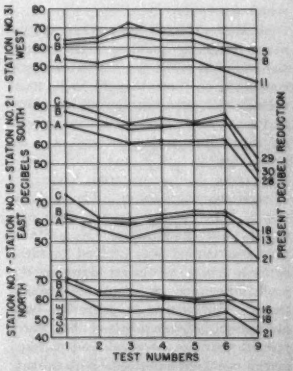

Figure 12. Progressive sound level tests of pumice block enclosure during construction

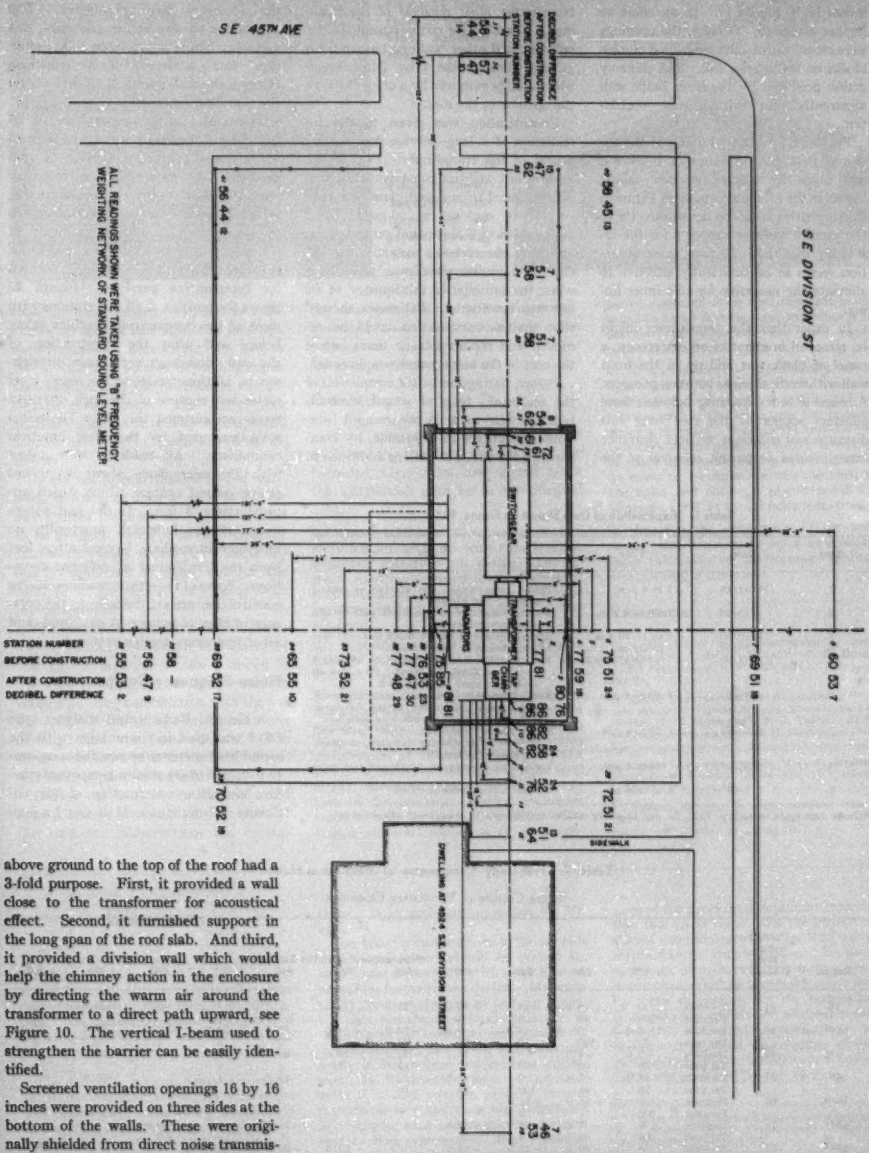

above ground to the top of the roof had a 3-fold purpose. First, it provided a wall close to the transformer for acoustical effect. Second, it furnished support in the long span of the roof slab. And third, it provided a division wall which would help the chimney action in the enclosure by directing the warm air around the transformer to a direct path upward, see Figure 10. The vertical I-beam used to strengthen the barrier can be easily identified.

Screened ventilation openings 16 by 16 inches were provided on three sides at the bottom of the walls. These were originally shielded from direct noise transmission to the outside by a low baffle wall approximately 18 inches from the inside of the main wall and approximately 36

Figure 13. Comparative sound level tests showing effectiveness of enclosure

inches high, Figure 11. In an effort to further attenuate the noise, the openings were closed with 4-inch sand-filled pumice blocks on the interior side. The chimney action produced by the inner baffle wall apparently provided adequate ventilation.

Provision for internal lining of the enclosure roof with the Fiberglas insulation was made by placing wooden nailing blocks in the concrete as poured, Figure 7. Furring strips could be nailed directly to the pumice walls as supports for the insulating material. To date, noise reduction seems to be sufficiently effective to alleviate the necessity for this inner lining.

In order that the transformer might be removed in event of an emergency, a panel of block was laid up in the front wall with vertical joints between pilasters. A concrete beam spanning between these pilasters supported the roof over this distance and sufficient vertical clearance was provided to permit removal of the transformer after removal of the bushings. Tap changer compartment, feeder cubicles, and other portions too large for passage through the 4 by 7-foot metal door could be removed by a crane through the opening in the roof.

Consideration was given to the installation of a large service door for removal of the transformer. One of the midwestern utilities constructed such a door or panel from 2-inch glass fiber bats completely enclosed in 20-gauge sheet steel. Although this panel proved to be almost as effective as a masonry wall the cost of a similar panel was prohibitive when the anticipated infrequency of its use was considered. Estimates showed that the masonry section could be removed and replaced three times before the cost of the metal panel was exceeded.

Before, during, and after completion of the enclosure, tests of sound level intensities were made at prearranged locations or stations to determine, by comparison, the effect as various additions to the enclosure were completed. The completion of the entire enclosure was necessary before appreciable noise reduction was achieved. This reduction through the wall averaged 23 decibels on the *B* or 70-decibel scale.

Attenuation at the property line on all four sides of the substation varied from 15 to 24 decibels with an average of 18.5 decibels. As expected, the intensity level increased inside the enclosure because of reflections. Results of these tests are shown graphically by Figure 12 for specific locations on all four sides of substation (described in Table I), selected for comparative purposes. Figure 13 shows the position of all test stations with most of the comparative readings taken before and after the construction of the wall. Readings were taken throughout on all three scales of the sound level meter but because of the high intensity levels encountered the *B* or 70-decibel scale was used for the most practical comparison. All readings were taken with the microphone about 12 inches above ground contour which varied approximately 3 feet. Initial and subsequent checks indicated practically no difference in readings beyond a few feet from the transformer at different elevations. Some of the erratic readings during construction are attributable to the presence of piles of pumice blocks, sand, and other temporary foreign material.

Table I. Explanation of Data Shown on Figure 12*

Test	Date	Time	Notes
1	10/31/49	1 to 4 p.m.	Before construction was started on sound barrier. See Figure 1
2	2/13/50	1:30 to 3 p.m.	Average height of pumice block wall—5 feet above ground level
3	2/16/50	9 to 11:30 a.m.	Average height of pumice block wall—11 feet
4	2/25/50	1 to 4 p.m.	Average height of wall—15 feet
5	2/27/50	3:30 to 4:30 p.m.	Wall completed to full height of 16 feet 6 inches and filled with sand. Door and all ventilators open. See Figure 6
6	4/3/50	1:30 to 4 p.m.	Roof completed. Door in place. All ventilators open. Complete except for inner baffle wall in front of ventilator openings
7	4/10/50	1:30 to 4 p.m.	Sound barrier completed. Inner baffle wall in front of ventilating openings, in place. See Figures 11 and 15
8	6/30/50	1:30 to 4 p.m.	Ventilating openings on north and east sides closed
9	7/6/50	1 to 4:30 a.m.	All ventilating openings closed

* Tests were made at stations 7, 15, 21, and 13 where maximum difference in sound level was indicated.

Noise Frequency Components

A General Radio sound analyzer type *760A* was used in conjunction with the sound level meter to secure the comparative values of frequency components before and after construction of the enclosure. From Table II it can be seen

Table II. Frequency Components of Transformer Noise

Before Closure of Ventilating Openings

Station	Decibel Sound Level, C Scale		Frequency—Cycles Per Second 120	240	360	480	600	720	840	960	1,080	1,320	1,560
1*	81	Decibels	0	−16.0	−22.0	−30.0	−21.0					−22.0	
		Per cent	100	16	8	3	9					7	
1**	86	Decibels	−5.2	0	−6.0	−9.0	−13.0	−24.0	−20.0	−26.0	−27.0	−27.0	30.0
		Per cent	55	100	50	35	23	6	10	5	4.5	4.5	3
9**	88	Decibels	−2.0	−4.0	0	−12.5	−22.0	−26.0	−28.0	−28.0		−24.0	
		Per cent	80	62	100	19	8	5	4	4		6	
15*	74	Decibels	−3.0	−7.0	0	−12.0	−20.0		−25.0			−30.0	
		Per cent	70	45	100	25	10		6			3	
15**	62	Decibels	0	−14.0	−21.0								
		Per cent	100	16	9								
20**	74	Decibels	0	−1.0	−22.0	−15.5			−26.0		−30.0		
		Per cent	100	90	8	12			5		3		
29**	73	Decibels	0	−10.5	−12.0	−18.0		−20.0	−30.0	−30.0			
		Per cent	100	30	20	13		10	3	3			

* Readings before construction of enclosure.

** Readings after construction of enclosure but before bottom ventilating openings were closed.

Figure 14 (left). Front of pumice block enclosure after completion

Figure 15 (right). Substation transformer and adjacent dwelling after completion of enclosure

that the noise ranged from 120 to 1,560 cycles per second and that the predominate frequencies were either 120, 240, or 360 cycles per second depending upon test location and the progress of the enclosure construction. The transformer auxiliary equipment provided local sound sources of varying frequency and intensity.

It did not appear that effects of variation in ambient noise level were less for any specific frequencies. There seemed to be as much variation in the frequency analyzer readings at any given frequency due to ambients as there was for the total of all frequencies emanating from the transformer.

The completed structure before planting of shrubbery is shown in Figures 14 and 15. A sage green color included in the waterproofing for the outside surface made a pleasing combination with the red tile roof. A sprinkling system later was installed and the lawn planted. The shrubbery, some of which is fairly large, will be transplanted in early fall.

During the assembly of materials and approximately two weeks before start of the enclosure construction, the substation was energized and left in this condition until it was necessary to remove the voltage on the high-tension leads because of progress on the walls.

Conclusions

From experience gained in the attempt to reduce the transformer noise level, the following suggestions are offered when the installation must be in a residential area:

1. Continue to press the manufacturers for more uniform assembly with noise level an important feature in the design. The extreme variation in sound levels of identical unit substations included under the same purchase order is a strong factor in this argument.

2. If possible, procure enough property so that the transformers can be placed at least 100 feet from the nearest dwelling.

3. Compare the additional cost of a more quiet transformer with the construction of a sound confining enclosure. There exists a 25 per cent increase in price for designing transformers at 10 decibels below NEMA levels. A 20-decibel decrease in noise level might therefore increase the transformer cost by 50 per cent. Several enclosures could be built for this high premium. The almost universal consensus of those contacted appeared to be that this cost is unwarranted and that the best procedure is to energize the substation and then apply remedial measures if required.

4. If an enclosure is economically advisable, select for its construction the available material that provides the best sound insulation and at the same time the greatest sound absorption. Energize the transformer two weeks before construction is started and as much as possible during construction in an effort to accustom the neighborhood to the noise and obtain a psychological advantage as well as actual noise reduction.

5. Improve the appearance of the substation and property as much as economically justifiable by landscaping, lighting, and painting of structures.

References

1. Audio Noise in Transformers in Residential and Commercial Areas, C. B. Baugh. *AIEE Transactions*, volume 69, part I, 1950, pages 121–28.

2. Quiet Transformer Installations—a Problem for Both Equipment and Substation Designers, I. S. Mendenhall, F. L. Taylor. *AIEE Transactions*, volume 69, part II, 1950, pages 1148–53.

3. Sound and the Human Ear, S. Bennon. *Westinghouse Engineer* (Pittsburgh, Pa.), volume 9, March 1949, page 60.

4. Theory and Use of Architectural Acoustical Materials. *Bulletin*, Acoustical Materials Association (Chicago, Ill.), page 18.

Discussion

T. D. Gordy (General Electric Company, Pittsfield, Mass.): Mr. McLean has presented an excellent paper covering the reduction of transformer noise level at an installation. The author's complete description of the procedure should be very worthwhile to other operators confronted with similar problems.

The difference between sound absorption and sound insulation is one that often is not fully appreciated. The author's comments on this difference are most timely; realization of what is the difference between absorption and insulation will eliminate many failing attempts of various noise reduction methods for particular cases. This applies to noise suppression within the transformer as well as to enclosures described by Mr. McLean.

The first conclusion drawn in the paper is that manufacturers should be pressed for more uniform assembly, with noise level an important feature in the design. Manufacturers are more desirous of uniform assembly than are the operators; variations in assembly and construction require large design tolerances, and these tolerances are costly in design time and material utilization. In its simplest form, transformer noise is a very complex problem for the manufacturer,[1,2] and variations introduced in processing and assembling transformers lead to more complexity. That manufacturers consider noise level an important feature in design is demonstrated by technical papers of the past year.[1,2,3]

Related to the third and fourth conclusions of the paper is an important contribution that must come from the operator—that of determining what noise level will be satisfactory for the installation. Economic appraisals of noise reduction methods cannot be made until an acceptable noise level has been determined for the installation. Some data are available on acceptable noise levels,[4,5,6] but more investigations are needed. It is hoped that findings of such investigations will be reported as completely as the one presented by Mr. McLean.

References

1. Transformer Sound Level Considerations, A. J. Maslin. *AIEE Transactions*, volume 69, part II, 1950, pages 1142–47.

2. Audible Noise of Power Transformers, T. D. Gordy. *AIEE Transactions*, volume 69, part I, 1950, pages 45–50.

3. Harmonic Index—A Tool for Trans-

former Audio Noise Investigation, W. H. Mutschler, Jr., T. F. Madden. *AIEE Transactions*, volume 69, part I, 1950, pages 115–18.

4. Transformer Audio Noise Problems on An Electric Power System, C. S. Murray. *AIEE Transactions*, volume 68, part I, 1949, pages 740–47.

5. Reference 1 of the paper.

6. Reference 2 of the paper.

T. R. Specht (Westinghouse Electric Corporation, Sharon, Pa.): This is a timely paper that gives quite well the problems involved in installing a large transformer in a residential district. The problem of transformer noise is becoming more serious as the size of residential loads increase and consequently the size of the transformers increase. Even a transformer as small as 1,000 kva may cause complaints if it is in a quiet location and is installed near a residence.

The tests given in this paper bring out a point that should be emphasized. Although the sound attenuation near the wall due to the wall is relatively large, the paper gives 23 decibels, at greater distances the attenuation decreases. The average attenuation due to the wall, from the tests for distances over 40 feet, is 9 decibels. A wall gives more attenuation near to the wall than farther from the wall. This represents about the average results that can be expected with a wall.

In the paper, they stated that they filled the pumice blocks with sand as their tests indicated that the sand increased the attenuation at the lower frequency. Pumice block must be quite porous, for one reference[1] gives an attenuation of 8 decibels at 128 cycles for 4-inch thick pumice block and with the same block with one side plastered the attenuation was 31 decibels. The paper gives an attenuation of 17 decibels for a plain 8-inch pumice block, and 36 decibels for a sand filled block. The amount of sound insulation which will be useful in the wall will depend on the attenuation secured with a perfect wall at the desired point. For the case in this paper, the transformer was practically on the property line, and the measured attenuation was about 23 decibels. The wall attenuation should be appreciably higher than this figure so it would be justified in this case to use a wall with 36-decibel attenuation. If the point at which it is desired to reduce the sound level is 40 feet out from the transformer, the attenuation secured was only 9 decibels. At this distance considerable sound bends over the wall back to the ground, and the wall could have less than 36-decibel attenuation and not increase the sound level at the point of measurement to any extent.

The paper quotes from a paper by C. E. Baugh that units with cold rolled steel cores have an average sound level about $7^1/_2$ decibels higher than that of earlier units built to the same specifications. It is presumed that this means the same electrical specifications which means smaller size and weight. It may be true the sound levels are higher, but it also is true that if the same transformer has cold rolled steel substituted for older hot rolled steel, it will be quieter. The tendency has been, though, to use the new cold rolled steels at higher inductions than the old steels because the losses are much lower for the new steels. This makes a less expensive transformer for the customer and for the majority of locations is quite acceptable.

The past practice of a certain percentage price increase for a certain decibel reduction for all sizes of transformers has not been in agreement with the actual costs. A recent paper by A. J. Maslin[2] has shown that a small transformer will cost a much higher percentage for the same decibel reduction from the NEMA standard[3] than a large transformer. From the curves in Mr. Maslin's paper, a 25,000-kva transformer designed to a NEMA level of 76 decibels would weigh 35 per cent more if the sound level were to be 67 decibels instead. The cost increase would not be as much, but would probably be around 20 per cent. Some manufacturers now are pricing more in line with actual costs, which for the smaller transformers, means the premium for quieter transformers is quite high.

In general, the procedures outlined in the paper for installations in residential areas are to be recommended. For the very large transformers, though, it may be necessary to have a special quiet transformer in addition to the use of a sound barrier around the transformer.

References

1. Acoustical Designing in Architecture, V. O. Knudsen, C. M. Harris. John Wiley and Sons, New York, N. Y., 1950, page 434.

2. Transformer Sound Level Considerations, A. J. Maslin. *AIEE Transactions*, volume 69, part II, 1950, pages 1142–47.

3. Standards for Transformers, Publication Number 48-132, National Electrical Manufacturers Association (New York, N. Y.), September 1948, pages 33–34.

Corbett McLean: The discussions by T. D. Gordy and T. R. Specht are indeed pertinent and lend a voice of authority to the paper. Their comments amplify certain factors, apparently insufficiently emphasized by the author, and are greatly appreciated.

Simplified Subscriber Toll Dialing for Low-Rate Low-Density Toll Circuits Between Community Dial Offices

ERIC BROOKE
MEMBER AIEE

J. M. BLACKHALL
MEMBER AIEE

W. H. BLASHFIELD
ASSOCIATE AIEE

WITH the installation of more and more dial telephones and the replacement of operators with automatic switching equipment, increasingly difficult problems appear as the simpler installations are completed. One of the problems is the handling of short-haul toll calls between dial exchanges. If it is necessary to retain an operator to handle only toll calls, the small exchange dial conversion cannot be justified, as the same operator also can handle the local switching.

This situation has been met with various partial solutions involving special trunking arrangements and special circuits to permit operators at distant points to complete toll calls. With increasing costs of operating and of line construction, this procedure has become awkward and expensive, so that the need for some different solution has become apparent.

Some of the present accepted methods of establishing toll calls between automatic exchanges are:

1. With dial-back operation a call is established from one automatic exchange to an operator office. The operator then dials back over the trunk on which the call was received, completing the connection to the second automatic exchange. This is illustrated by Figure 1(A). This procedure is expensive in toll line mileage, as it holds a circuit to the operator office in addition to the one between dial exchanges. A modification which has been used to reduce circuit usage is to permit the operator to release the trunk to her office, leaving the connection established only between the two dial exchanges. With the operator released, it is not possible to time the call; subscribers recognizing this condition tend to carry on unnecessarily long conversations from which no corresponding revenue is derived. As a correction, automatic time disconnect has been provided in some instances, interrupting the call after a predetermined time. Time disconnect, however, often meets with adverse customer reaction.

2. Complete the connection through a third office at which an operator is available. This method is also wasteful of toll line mileage, as the route through the manual office may be considerably longer than the direct route between the two dial exchanges. Figure 1(B) illustrates such a situation. Furthermore, the services of an operator on short-haul calls may cost more than the revenue derived from the calls.

3. A third practice is to abandon the toll charge between automatic exchanges, permitting subscribers to dial nearby exchanges on what is known as a "free-service" basis. It must be realized, however, that the term "free-service" is misleading, for the cost of providing this service must be spread among all the subscribers at both exchanges, with the result that subscribers who make little use of the so-called "free" service are helping to pay for those who do use it. Furthermore, offering free-service increases the traffic so that the operating company may be faced with the necessity of providing more circuits between exchanges. It usually is not easy to obtain increased exchange rates to pay for the increased investment.

Development

The period from 1930 to 1940 saw the start of widespread conversion of small exchanges to dial operation. During the latter part of this period, the need for some better solution to the short-haul toll problem became obvious. The war years, however, interfered with normal development, so that it is only since 1945 that our company has been giving intensive thought to a different solution. Some form of automatic ticketing appeared desirable, permitting the toll call to be completed in a manner similar to a local automatic connection. In other words, a subscriber in one exchange would be able to dial numbers in other exchanges, with trunk equipment automatically producing a record of calling and called numbers and duration of conversation.

It is realized that an automatic ticketing system will not completely handle all toll requirements, as person-to-person, collect, and paystation calls still must be supervised manually. With short-haul traffic, however, the percentage of person-to-person and collect calls is small. It is probable that the introduction of automatic ticketing will tend to reduce the types of call that cannot be handled over it. The appeal of easily dialing a number in a distant office is expected to encourage the placing of station-to-station calls in preference to person-to-person calls via an operator, particularly in the low-rate situations for which this system is intended.

Simplicity and economy of equipment are of utmost importance in a ticketing system for low-rate low-volume traffic. In the first place, the revenue to be derived from this class of traffic will not support a large investment or skilled maintenance on highly complex apparatus. Secondly, the expansion of large urban areas to the surrounding countryside and the tendency of some state commissions to advocate county-wide service on a flat rate basis is causing the free-service situation to become more and more prevalent; therefore the possibility of obsolescence limits the prudent investment in ticketing equipment. Design of the apparatus also should contemplate more or less ready removal from one location to another, to make maximum usage of the investment.

Low cost has necessitated thinking

Paper 50-227, recommended by the AIEE Communication Switching Systems Committee and approved by the AIEE Technical Program Committee, for presentation at the AIEE Fall General Meeting, Oklahoma City, Okla., October 23–27, 1950. Manuscript submitted July 24, 1950; made available for printing August 22, 1950.

ERIC BROOKE, J. M. BLACKHALL, and W. H. BLASHFIELD are all with the North Electric Manufacturing Company, Galion, Ohio.

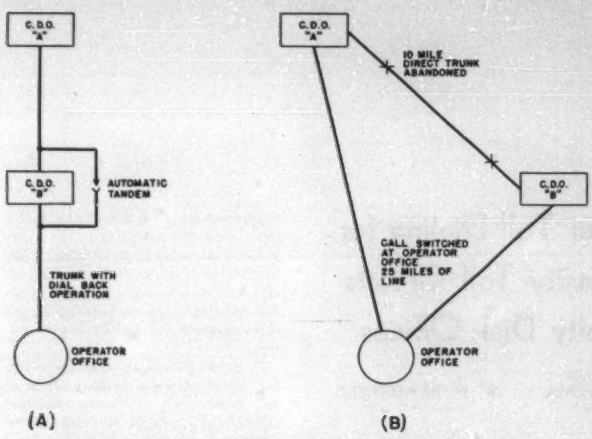

Figure 1. Methods of providing for toll connections between dial offices

(A) Dial-back method (B) Switching through third offices

along different lines from other automatic ticketing systems which have been designed for large urban areas. Salient points of these other systems are:

1. Automatic identification of the calling number.
2. A recorder which registers information in printed form or in the form of complex markings or punchings intended for direct handling by automatic sorting and accounting machines.
3. Translating equipment to convert information derived from the trunk into suitable signals for actuating the recorder.
4. Storage and switching circuits to permit the use of a common recorder for a number of trunks.

In contrast, distinguishing features of the system to be described are:

1. The calling station is identified by the subscriber dialing his own number.
2. The recorder consists of a simple punch mechanism perforating a single row of holes in a tape. The punch is actuated directly by dial pulses.
3. No translating equipment.
4. Each trunk has its own recorder. This is permitted by the simplicity of the recorder, and eliminates the cost of storage and connecting circuits required by a common recorder.

When subscriber toll dialing was first contemplated more than 25 years ago the method of requesting the subscriber to identify himself by first dialing his own number was given consideration. It may seem strange at this late date to revert back to that system as it was originally conceived. Nevertheless, abandonment of the original method in favor of automatic calling number identification builds the equipment up to such a point that it is practical for use only in the larger urban areas where the high density of traffic can support the necessary investment. We, therefore, do not feel that it is a retrograde step to propose an operating method of this kind at this time. Contacts with operating companies have substantiated this belief, the decision being based on the fact that with manual operation the customer is verbally asked to identify his telephone number, hence there should be no adverse reaction to asking him to identify himself by dialing a number instead of giving it verbally to an operator.

A means of checking that the subscriber correctly identifies himself is essential if the equipment is to be completely automatic. Such a check is provided by a check link which responds to the number dialed and verifies that the dialing was received from the line indicated. The equipment at present does not check the party on the line, it being thought that if the incorrect party digit has been dialed, the range of inquiry for locating origination of the call has been reduced to the point where little trouble should be encountered. Although it would be entirely possible to verify the party on the line, the cost of special equipment at each subscriber's telephone would tend to defeat the low-cost objec-

Figure 2. Tape recorder with and without cover

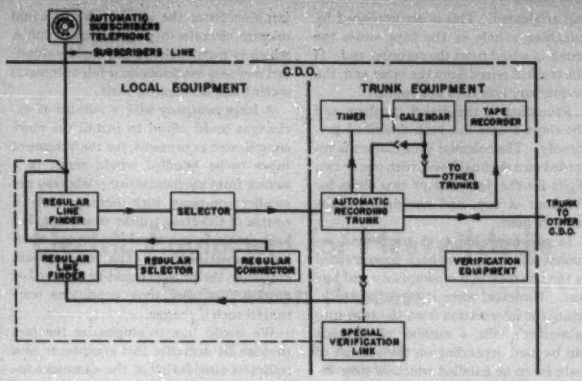

Figure 3. Block diagram of automatic ticketing trunk and checking link

tive of the system. The matter has been discussed with several operating companies, who are inclined to agree with this reasoning.

The method of recording information must be of the simplest in order to keep costs within reason. As the trunk receives both calling and called numbers in the form of dial pulses, the direct recording of these pulses with no intervening translating equipment provides a simple, reliable, and ready solution. Each digit can be represented as a line of holes perforated along a narrow tape, with a space between digits, wider spacing between groups of information, and a still wider space between calls. Duration of conversation can be registered by punching a hole once each minute, and date and time of day can be recorded digitally from a "calendar" as will be described later.

As such a recorder is simple and can be manufactured at low cost, a recorder per trunk is the logical arrangement, eliminating the more complicated universal recorder and associated storage and switching circuits.

The recorder is illustrated in Figure 2. It consists basically of a punch magnet to perforate the tape and a step magnet to feed the tape through the recorder. The step magnet operates each time the punch magnet is energized, and also can be operated independently to provide additional spaces between series of perforations.

Operation

The equipment involved in the automatic ticketing system is shown in the block diagram of Figure 3. The tape recorder, timer, and calendar appear only at one end of the trunk, the other end being the same except for omission of these items.

The timer and calendar are common to a group of trunks or entire office. The timer consists of a clock which transmits an impulse once a minute to any trunk that has been answered, thereby recording as perforations the duration of conversation in minutes. The calendar comprises relay counting circuits, or rotary switches, or mechanically geared contacts, which are driven from the clock to register the time of day and date. When a trunk is connected to the calendar, the calendar transmits impulses to the recorder representing the date and time of day as digits.

The trunk termination consists of relay circuits involving relatively few relays above those required for normal trunk operation, the termination at the non-recorder end being simpler than the one at the end with recorder. The circuits are adaptable for any of the common types of trunk signaling, such as loop dial, composite or carrier, and can be applied to any conventional dial switchboard.

To place a call, the subscriber first dials the single-digit trunk code, then dials his own number, then dials the desired number in the distant exchange. Ringing, answering, talking, and release follow exactly as on a local exchange call.

Assuming the call originated from the recording end, the dialing of the trunk code completes a circuit from the subscriber's telephone through a regular exchange link to the trunk. The trunk immediately seizes a check link.

When the subscriber dials his own number, the impulses are registered on the recorder and also are transmitted to the check link, creating a connection through that link back to the calling line.

At this time, the trunk circuit momentarily "flashes" (answers and unanswers) the regular link. The calling line receives answer supervision in the normal manner, which supervision is picked up by the check link and carried back to the trunk. If the flash received by the trunk over this local loop circuit coincides with the one transmitted, the identity of the calling line is verified. If the subscriber has dialed a line number other than his own, the loop back through the check link is not complete and the flash not received, in which case the trunk returns busy signal and blocks further dialing. As soon as the check has been made, the check link is automatically released and is available for other calls.

The check links can consist of regular exchange links modified to transmit supervision back through the link in the necessary manner. In exchanges with sleeve supervision or having a fourth wire available, the modifications are simple and maximum economy is obtained by using regular links for checking. In exchanges with other types of supervision, the modifications might be more difficult and under certain conditions it may be preferable to install special verification links. Figure 3 has a solid line to show the path verifying with a regular link, and a dotted line if a special link has to be used.

When the subscriber dials the called number, assuming that his own number has been checked satisfactorily, the digits are registered on the recorder and are transmitted over the trunk to the distant office, where the connection is completed in the normal manner. When the call is answered, the trunk engages the common timer, which punches a hole on answer and one each minute thereafter, so that the total number of holes represents the total chargeable minutes for the call.

Figure 4. Completed call registered on tape

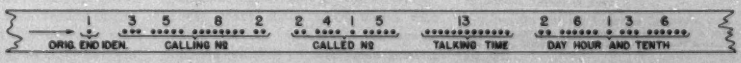

When either party hangs up, the local exchange link is released so that the local line is immediately available for other calls. The trunk is held, however, until it receives date and time of day from the calendar. If the calendar is busy transmitting information to some other trunk at that time, the trunk is held until the calendar is free. If several trunks are waiting for the calendar, the calendar transmits to all simultaneously.

If the subscriber encounters a busy line or all trunks or all links busy, he receives the usual busy signal and hangs up. In this case, or in case the called number does not answer, the call is registered as incomplete, no elapsed time nor calendar information being punched on the tape for that call.

A call originating at the distant (non-recorder) end of the trunk proceeds in the same manner as described before, except, that in this case the dialing of the subscriber's own number is transmitted over the trunk so that it may be received by the recorder.

Tape Information

Figure 4 illustrates the appearance of a completed call as it appears on the tape. Information shown consists of:

1. Originating end indication.
2. Calling number.
3. Called number.
4. Duration of conversation.
5. Date and time of day.

As one recorder is used for calls in either direction over the trunk, it is necessary to indicate at which exchange the call originated. This is accomplished by punching a hole in the tape when the trunk is seized from the recorder end. If the trunk is seized from the other end, the preliminary hole does not appear.

Recording of the dialed numbers and the elapsed time has been described previously. The calendar information is recorded on a decimal basis, with one or two digits for the date, one or two digits for the hour of day, and one digit for the tenth of hour.

In the final design of trunk and recorder, all efforts have been concentrated in the one direction of simplicity and low cost. However, when it comes to translating the information from the tape into subscriber's bills, a number of methods can be used depending on the volume of material to be handled which in turn determines the revenue available for mechanization of tape reading and billing.

The simplest way would be to count numerically the perforations on the tape and write out a toll ticket from that information. This would be feasible only when the volume of work was extremely small, though it could be facilitated by a simple indicator to show the number of perforations without requiring counting of each hole.

Another method would be to feed the tape through a simple mechanical or photoelectric sensing device, from which would be derived impulses to actuate counters giving a display of numbers on a panel. Information from the panel then could be transcribed on tickets. A further refinement would be to arrange for automatically photographing the display, to gain speedier operation and eliminate errors in transcribing. To go still further, impulses from the sensing device could operate circuits to prepare punch cards, which in turn could be handled by standard business machines on a full automatic sorting and accounting basis.

A large company with a number of exchanges could afford to install the more complicated equipment, for the volume of tapes to be handled would result in a saving from mechanization; whereas the smaller company with perhaps only a couple of ticketing trunks would not find it desirable to use anything beyond manual transcribing of the information. However, the process could be changed or amplified at any time conditions warranted such a change.

We would like to emphasize the fact that we do not offer this equipment as a complete cure for all of the situations involving automatic toll trunks between community dial offices, but we do believe that it has possibilities of considerably relieving this situation and permitting conversion of manual exchanges which at the present time would not be considered for conversion because of the necessity of maintaining operators at these points. While realizing the method of operation departs considerably from previously accepted subscriber toll dialing practices, this has been done in the interest of economy, as this type of service is never a very profitable operation and any additional costs are difficult to justify. We believe that it will find an application where conditions are such that toll charges over certain routes must be maintained for some time in the future, and it is undesirable to continue with an operator office at these locations for this small amount of service.

No Discussion

Electric Equipment for Heavy-Media Separation Process

J. J. BEAN
NONMEMBER AIEE

K. A. BLIND
MEMBER AIEE

BECAUSE of the depletion of the so-called high grade ores, most of the nonferrous metals, such as copper and lead, are produced today from low grade ores of surprising low gross value. Similarly more and more of our so-called "nonmetallic" minerals like fluorspar, magnesite, and glass sand must be treated in some manner for the removal of impurities to bring them to the high standards previously set when virtually pure minerals could be mined, and on which the consuming industries have been built up.

Due to new labor conditions, the coal mining industry, both bituminous and anthracite, is turning more and more to mechanized mining, which because of its very nature results in the production of coal with increasingly larger amounts of ash, since the machine cannot be operated to mine selectively, choosing only the good coal and leaving behind the waste.

This trend toward lower grade mining products has been met by the introduction of milling methods such as froth flotation and cyanidation in the metal mining field, and better washing practices in coal mining.

Among the newest developments in beneficiation of ores and coal are the heavy-media separation processes, which separate the desired mineral from its accompanying waste by the difference in specific gravity between the two components.

The heavy-media separation process was introduced to the metal mining industry in the mill of the American Zinc Lead and Smelting Company at Mascot, Tennessee in 1938, and its use has grown rapidly until now a wide variety of materials including lead-zinc, and zinc ores, iron ore, fluorspar, magnesite, garnet, and tin ore are being commercially beneficiated through its use.

The process is a practical application of the old laboratory technique of heavy liquid separation, wherein a mixture of solids of different specific gravities is immersed in a liquid having a specific gravity intermediate between the high and low gravity components of the mixture. The portion of lower specific gravity than the liquid floats while that of higher specific gravity sinks and thus a separation is made. A very simple example would be the separation of a mixture of sand and sawdust by shoveling it into a bucket of water.

Although heavy liquids having the correct specific gravity to make separations of some materials, notably coal from slate, are available, their use in a commercial plant is difficult if not impossible from both the economic and the handling standpoints for they are expensive, generally toxic, and hard to recover. In plant practice great care would be required to prepare the raw feed to prevent the penetration of the liquids which would make their subsequent recovery difficult, and to provide vaportight systems to prevent losses by vaporization and hazards to health.

The heavy-media separation method utilizes the same general principle, but employs a suspension of a finely ground (90 per cent-200 mesh) heavy solid in water. Such suspensions have some of the properties of a true liquid, one being the ability to float materials of lighter gravity than that of the suspension. Suitably heavy materials for such suspensions are galena, barite, ferrosilicon, and magnetite. These heavy solids when mixed with water provide a cheap, recoverable medium, which is nontoxic, noncorrosive, and may be used in a system open to the atmosphere.

However, since they are suspensions and not liquids, they present some problems from the standpoint of settling rate, viscosity, particularly toward the upper limit possible with a given solid which may be roughly stated as half that of the specific gravity of the solid, and viscosity due to the introduction of fine lighter material from the ore itself.

Originally the problem of removing contaminants from the medium suspension was met by recovering the medium solid from the dirty suspension by means of froth flotation. This method is entirely practical and gives excellent results on certain ores; however, it has some disadvantages which are inherent with any flotation operation. Principal of these is the fact that a froth flotation operation must have steady conditions with respect to feed rate, dilution, reagents, and character of material to be floated. These limitations of the flotation process mean that the heavy-media plant operator must operate with the flotation plant limitations in mind, and is not entirely free to adjust the amount of medium cleaning to the needs of the heavy-media plant. Furthermore, the soft nature of galena, which is the most common nonmagnetic solid used for this type of medium, results in its degradation in use, and the very fine galena resulting is hard to float. It oxidizes readily and becomes increasingly hard to recover by froth flotation.

When the heavy-media separation process was first tried on iron ores, these limitations of froth flotation cleaning were so great that a new medium had to be developed, and the use of a magnetic solid was conceived. Ferrosilicon containing 15 per cent silicon was selected as the most suitable since it was hard, rela-

Paper 50-230, recommended by the AIEE Mining and Metal Industry Committee and approved by the AIEE Technical Program Committee for presentation at the AIEE Fall General Meeting, Oklahoma City, Okla., October 23–27, 1950. Manuscript submitted August 19, 1948; made available for printing August 23, 1950.

J. J. Bean is with the American Cyanamid Company, Stamford, Conn., and K. A. Blind is with the Dings Magnetic Separator Company, Milwaukee, Wis.

Figure 1. American Cyanamid Company heavy-media separation standard flow sheet

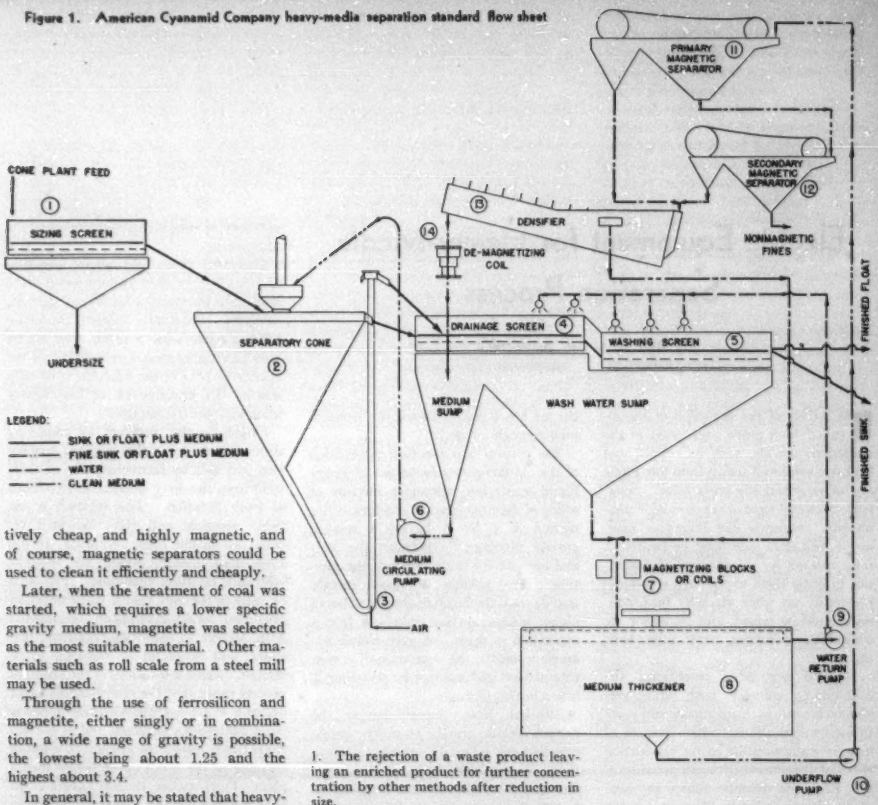

tively cheap, and highly magnetic, and of course, magnetic separators could be used to clean it efficiently and cheaply.

Later, when the treatment of coal was started, which requires a lower specific gravity medium, magnetite was selected as the most suitable material. Other materials such as roll scale from a steel mill may be used.

Through the use of ferrosilicon and magnetite, either singly or in combination, a wide range of gravity is possible, the lowest being about 1.25 and the highest about 3.4.

In general, it may be stated that heavy-media separation processes will treat any ore in which the valuable mineral constituents have an appreciable difference in specific gravity from that of the worthless gangue. This difference in specific gravity can be less than that required for efficient separations by jigging or tabling.

In general, three types of ore are amenable to heavy-media separation processes:

1. Ores whose valuable constituents are liberated from unwanted mineral at a grind of 48-mesh or coarser.

2. Ores containing valuable minerals in the form of lenses or veins separated from each other by barren gangue.

3. Ores containing barren gangue which can be rejected after coarse crushing.

The heavy-media separation processes are capable of performing three main functions:

1. The rejection of a waste product leaving an enriched product for further concentration by other methods after reduction in size.

2. The production of a finished concentrate and a rejectable waste in one operation.

3. The production of a finished concentrate and a low grade reject for additional treatment.

Heavy-media separation processes have a wide field of usefulness as preconcentration methods for removing gangue, at low cost, after coarse crushing. They, therefore, offer a cheap and effective means for making ore out of sub-ore, waste dumps, and tailings, by concentrating the valuable constituents into a smaller product of sufficiently high grade to warrant treatment by more expensive methods such as flotation or cyanidation.

The application of heavy-media separation processes is closely related to the type of mining practiced or contemplated. It is, therefore, necessary to study the geological structure of the deposit to determine whether high cost selective mining methods may be eliminated through use of these processes to reject waste rock mined over greater widths. Similarly, by locating the heavy-media plant underground a hoisting bottle neck may be eliminated, at far less expenditure of time and money than would be required to sink and equip a new shaft. Installation underground, moreover, provides a waste product for back filling at no additional cost.

Of particular importance to established operations are the opportunities through heavy-media separation processes for increased profits by lowering of costs, for increases in production, and for reduction in over-all labor requirements per ton of metal or mineral produced. An existing flotation mill, for instance, may greatly increase its metal

Figure 2. Flow sheet heavy-media separation-full-size range treatment

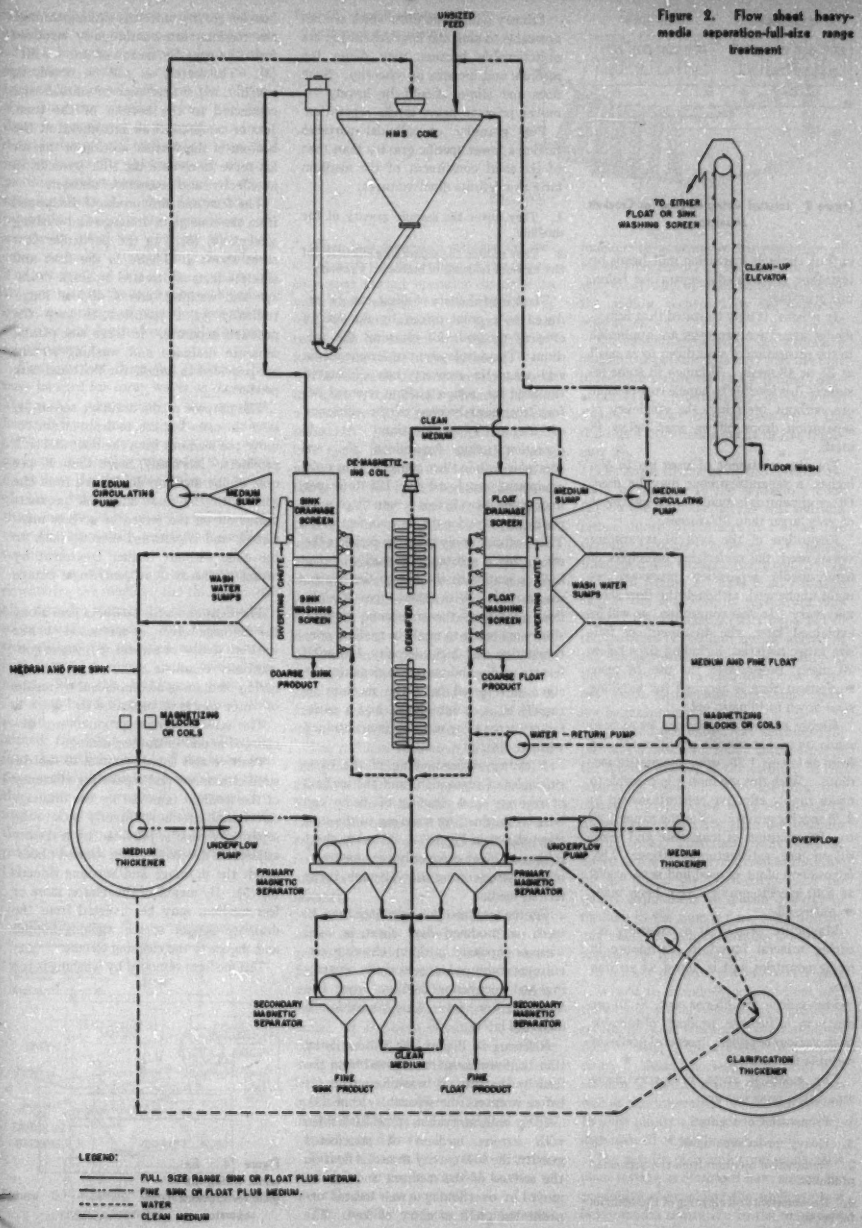

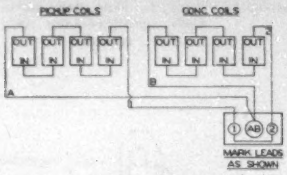

Figure 3. Internal wiring diagram for Crockett separator

output through increasing mill heads by installing heavy-media separation before fine grinding.

In general, it may be stated that heavy-media separation processes are applicable to the separation of sizes down to as small as 35 or 48 mesh. Although in some instances it is feasible to handle run-of-mine ore without presizing, the efficiency of separation drops off on sizes below 48 mesh.

For the treatment of sizes up to $3^1/_4$ inches, a separatory cone may be used. Other apparatus is available for treatment of sizes larger than $3^1/_4$ inches.

Regardless of the type of separatory vessel used, the underlying principles of heavy-media separation processes remain unchanged, although the flow sheet may vary. In this connection, as will be explained later, the treatment of full-size range material, including sizes below 10 mesh, necessitates the use of more equipment than is required for handling sizes down to 10 mesh only.

Highly efficient separations have been made on coal at specific gravities ranging from as low as 1.25, using magnetite medium. With this medium it is possible to make highly effective separations up to 2.20 specific gravity. For the range 2.20 to 2.90, mixtures of magnetite and ferrosilicon are satisfactory. Above 2.85, ferrosilicon alone is used and separations at 3.40 specific gravity have been made commercially.

Magnetite (Fe_3O_4) is a naturally occuring mineral found in abundance in many countries and is mined as an iron ore.

Ferrosilicon (Fe 85 per cent, Si 15 per cent) is a furnace product obtainable from various suppliers in several grades of suitable fineness.

The essential steps in heavy-media separation processes are:

1. Preparation of the feed.
2. Heavy media separation.
3. Removal of medium from the separated products.
4. Reclamation and cleaning of the medium for reuse.

Primary slimes and fines which are not amenable to sink and float separation are objectionable because they dilute the medium and increase its viscosity. Such fines and slimes should be largely removed prior to heavy-media separation.

Fine granular or colloidal particles having a lower specific gravity than that of the solid constituent of the medium have two definite disadvantages:

1. They lower the specific gravity of the medium.
2. They reduce the separating efficiency of the medium because of increased viscosity.

The harmful effect of slime can be reduced to a great extent by the use of efficient methods for cleaning the medium. The development of ferrous media and magnetic recovery has eliminated the need for complete slime removal before treatment because of the efficiency of magnetic concentration. At one operation using ferrosilicon the ore treated is high in slime content. The only equipment employed for 125 tons per hour is one 4 by 12 foot screen fitted with washing sprays for the first six feet only. This treatment only partially deslimes the ore, in fact a substantial quantity of clay balls is sent with the ore to the heavy-media cone. With other types of sink-float processes, the treatment of such slimey ore tends to result in medium contamination and high viscosity, but with ferrous media and magnetic cleaning, the slime is rejected from the medium as rapidly as it is introduced and a satisfactory separating medium is maintained without difficulty.

A clearer understanding of the basic principles of separation, and the method of recovery and cleaning of media can best be obtained by referring to the flow sheet shown in Figure 1. This flow sheet is the one most commonly used for treatment of sizes coarser than 10 mesh, using ferrous media.

For the treatment of sizes finer than 10 mesh, a modified flow sheet is used wherein separate medium cleaning circuits are employed for selectively separating and recovering medium from fine float and fine sink. This innovation is discussed later.

Referring to Figure 1, it will be noted that the finer sizes are removed from the feed by the primary washing screen (1) before it enters the separatory cone (2).

In the separatory cone (2) which is filled with ferrous medium of preselected gravity, the low gravity minerals float on the surface of the medium and are removed by overflowing a weir located opposite the point of entry of feed. The heavier gravity minerals sinking through the medium are continuously removed from the cone by means of an "air-lift" (3). The latter, as will be noted, is, roughly, a J-shaped pipe of suitable size connected to the bottom of the cone. Jets of compressed air introduced at the bottom of the vertical section of this air lift serve to elevate the sink particles in an effective and economical manner.

The float and sink products discharged from the cone go to drainage and washing screens (4) (5). In the particular flow sheet shown in Figure 1, the float and sink products are treated on single drainage and washing screens divided longitudinally by a partition to keep the products separate. In large size plants, separate drainage and washing screens are provided to handle the float and sink products.

The purpose of the drainage screen (4) is, as the name implies, to drain off and remove the medium from the float and sink products. Normally, more than 90 per cent of the medium discharged from the cone with the float and sink products drains off on the screen or screens mentioned, and is returned directly back to the cone without further treatment by means of one or more centrifugal pumps (6).

The float and sink products pass along the drainage screen, or screens (4) to the washing screen, or screens (5), where substantially complete removal of the adhering medium is accomplished by means of water sprays as indicated in Figure 1.

The screen oversize products are discharged as concentrate or tailing.

Positive and simple control of the desired cleanliness and separating efficiency of the medium removed by the drainage screens and circulated directly back to the separatory cone is provided by a readily adjustable diverting chute located underneath the drainage and washing screens (4) (5). By means of this chute, more or less medium may be diverted from the drainage hopper to the washing hopper and thence to the cleaning circuit.

The medium removed by washing is too

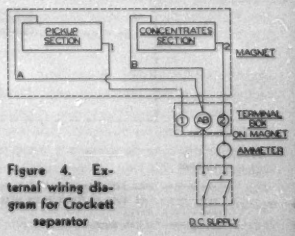

Figure 4. External wiring diagram for Crockett separator

dilute and, in many instances, too contaminated with fine impurities to permit of its being returned directly back to the separatory vessel. Accordingly, it is treated in a novel manner: the undersize from the washing screen (5) first flows by gravity or is pumped to a medium reclamation thickener (8). Just before it enters the thickener, the diluted medium passes between a set of magnetizing blocks (7). These latter serve to magnetize the discrete ferrosilicon or magnetite particles whereby they become mutually attracted and flocculate. The net result of this is faster settling of the particles in the thickener with consequent advantage of requiring less thickener area and depth than would otherwise be necessary.

The overflow from the thickener (8) may be used for spray water as shown in Figure 1. Alternatively, the overflow from this unit may be sent to another thickener which may serve as water-storage and clarification means for the entire operation. In the latter event, a portion of the overflow from this secondary thickener would be used for spray water over the previously mentioned washing screen (5).

In addition to serving as a means for dewatering the medium, the thickener (8) also provides storage for medium during off-operating periods. For this reason, this thickener is provided with a motorized device for raising and lowering the rakes. When the plant is shut down, the rakes are lifted to some point above the settled solids. When operations are resumed, the rakes are gradually lowered into the settled solids and the latter are then rendered sufficiently mobile so that they may be eventually removed by means of a centrifugal pump (10) and thereby sent to the cleaning circuit comprising at least two magnetic separators (11) (12).

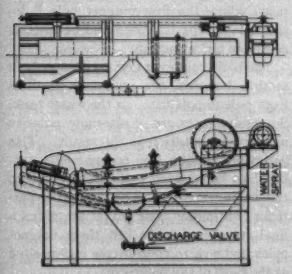

Figure 5. Outline drawing of Crockett separator

Figure 6. Longitudinal section through magnet bank

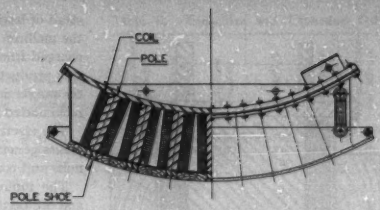

When it is desired to increase the specific gravity of the medium in the separatory cone during operation in order to meet some change in characteristics of feed, an extra amount of medium can readily be introduced into the circuit by lowering the rakes in the thickener.

The magnetic cleaning circuit, as shown in Figure 1, comprises a primary (11) and a secondary (12) Crockett-type magnetic separator. These separators are of the belt type, the magnet assembly being mounted just above the lower section of the belt. Feed is added under the belt as shown and the fines not immediately picked up by the action of the magnets and carried by the rubber belt, are dropped and eliminated through the hopper, as shown. This tailing, or reject, goes by gravity to the secondary magnetic separator (12) for additional treatment in order to recover any traces of medium not picked up in the primary separator. The tailing from the secondary separator (12) goes to waste; or if sufficiently valuable, may be sent to some other form of cleaning such as froth flotation.

The medium recovered on the belt of the primary magnetic separator (11) is discharged into the hopper, as shown in Figure 1 after the belt passes the influence of the magnetic field. This recovered medium is too diluted with water to return directly to the separatory cone (2) and it is therefore treated in the following manner.

As shown in Figure 1, the primary magnetic separator concentrate flows by gravity, or it may be pumped, to a densifier (13). The densifier is essentially a screw-type classifier, but acts as a thickener and storage reservoir for clean medium. It is not a classifier in the accepted sense of the term. The machine must be fed at the end by means of a feed box, and overflows at the sides—just the opposite of a classifier. The screw is a double-helix flight and is equipped with a variable-speed drive.

Either a manually operated or motorized-lifting device is provided to raise or lower the screw as required.

The densifier performs the important function of assisting in the regulation of the specific gravity of the medium in the separatory cone in addition to dewatering the medium recovered by the magnetic separators.

The medium removed by the secondary magnetic separator (12) may join the flow of medium recovered by the primary separator (11). Alternatively, as shown in Figure 1, it may join the overflow of the densifier (13) which returns to the thickener (8).

The screw discharge of the densifier returns by gravity to the separatory cone (2) via the drainage hopper and medium return pump (6). Before it reaches the drainage hopper, however, it passes through an a-c demagnetizing coil (14) as shown in Figure 1. This is an essential step in the heavy-media separation flow sheet. The dispersing effect imparted to the particles of medium by the action of the demagnetizing coils gives fluidity to the medium in the separatory cone without which satisfactory operation could not be maintained.

As stated previously, the densifier (13) provides a means for ready adjustment of the specific gravity of the medium in the separatory cone. The medium discharged by the screw is of considerably higher specific gravity than the medium in the cone. Therefore, water may be added to the medium returned to the cone by the pump (6). Ordinarily, any required adjustment of specific gravity of medium in the cone is done most quickly and easily by simply turning a valve to regulate the flow of water.

A bucket elevator, not shown in Figure 1, is used to introduce new medium into the circuit, and also is used as a means of returning any clean-up material from floor washing to the system. When necessary to dump the separatory unit, this elevator is used to return the medium, as well as the intermixed ore, to the circuit. In some plants a pump is used to advantage instead of an elevator.

The results of recent continuous pilot plant testing at Stamford have shown the possibility of extending the application of heavy-media separation to the treatment

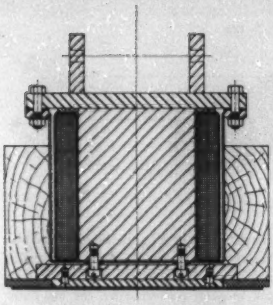

Figure 7. Transverse section through magnet

of material as fine as 28 mesh to 48 mesh.

For the treatment of sizes below 10 mesh, a modified flow scheme has been developed. Essentially, this flow scheme involves the use of dual magnetic cleaning circuits wherein the undersize float and the underize sink products from the screens are separately subjected to magnetic separation. The magnetic separators recover the medium for reuse and the tailings from these separations are either a finished float or a finished sink product as the case may be.

The flow sheet shown in Figure 2 describes the equipment used and the flow of products and medium through the circuit.

It will be noted that, just as in the case of the flow sheet shown in Figure 1, a certain portion of the medium removed on the drainage screens is returned directly back to the separatory cone. The amount thus returned is controlled by the position of the diverting chute and is dependent upon the quantity of undersize float and sink in the original feed. It will be apparent that when treating a feed containing a large proportion of undersize material, it becomes necessary to divert a greater amount of drainage medium to the cleaning circuit than would be the case when the cone feed contains a smaller proportion of fines. In other words, the amount of fine material that can be recirculated back to the cone with the medium depends on just how much can be tolerated in the cone without interfering with the separatory efficiency of the medium.

Eventually, of course, all of the fine material in the separatory cone circuit reports as finished float or finished sink. The advantage of recirculating a portion of the fines with the drainage medium is that a saving in the size of magnetic separator units is thereby effected. Instead of having to clean at one time all of the medium and accompanying fines discharged from the cone with the float and sink products, only a portion of it goes to the magnetic separators, the remainder is recirculated back to the cone.

The electric equipment in heavy-media plants generally is similar to that used in mills and coal washers.

The motors should all be splashproof and in certain places, for instance the pump motors, they should be totally enclosed fan-cooled so that the plant can be washed down readily without fear of injuring the motors.

Usually magnetic across the line starters are used so that the various pieces of equipment can be readily interlocked to prevent burying of the units with feed in the case of the failure of one unit. This interlocking is similar to that used in conveying systems.

Since demagnetizing and magnetizing of the medium are vital to the proper operation of the plant, audible signals are provided to indicate unit failure.

The tailing discharge of the final magnetic separators is provided with a magnetic trip which operates when the direct power fails and diverts the contents of the magnetic separator to the thickener or to a sump to prevent its loss.

Electrically the most important devices are the magnetic separators, the demagnetizing coil, and the magnetizing blocks. These are described in detail later in this paper, but it might be well to outline briefly their requirements here.

The magnetic separators must recover virtually 100 per cent of the magnetics going to them in a reasonably clean product. They must handle widely varying loads without loss of efficiency and with a minimum of adjustment or attention.

The demagnetizing coil must be rugged, do a thorough job of demagnetizing the cleaned medium, and have a large capacity.

The magnetizing blocks must be rugged, waterproof, and of such strength that the medium is magnetized even when flowing at a rapid rate. For this purpose, both permanent magnets and electromagnets are used. There are advantages to both types and the final choice is largely one of personal perference.

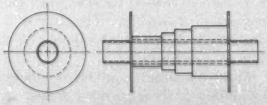

Figure 8. Outline drawing of demagnetizing coil

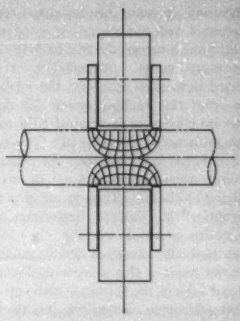

Figure 9. Magnetizing blocks field distribution in passage way of feed

Crockett Magnetic Separator

The Dings high intensity Crockett-type submerged belt magnetic separator is designed for wet separation. The separator consists of a stationary curved bank of eight magnets, partly submerged in water under which passes the conveyor belt. The pole shoes are located outside the magnet casing and are in close contact with the traveling belt, being separated from it only by a lubricating film of water.

The magnet is suspended from the main structure of the separator, the belt is supported by a head and tail pulley. The driving power is supplied by a motor with gear reducer or gearhead motor. The feed to the separator must be wet and is fed to the separator on a rubber-lined feed launder at from 5 to 60 per cent solids. The launder feeds the material below the first and second magnetic poles which lift the magnetic particles from the pulp.

The launder is so designed that the material enters the water tank just at the point where the first magnet pole is located, retarding its speed and permitting complete pickup action.

The main conveyor belt continuously in motion transfers the magnetic particles from pole to pole through the water tank. Successive poles are of alternate polarity and severe agitation is the result. This agitation permits the nonmagnetic material to be released and discharged into the tailing section. The magnetic particles continuing their travel are given a final spray under the last three magnet poles and a clean concentrate is deposited at the head of the separator.

It is important that the pulp passing down the feed launder approaches the

Table I. Recovery Data on 36-Inch Wide Type-SF Crockett Separator

2 Magnetic Separators in Tandem
(Primary and Secondary Crockett)

	Primary Feed	Primary Overflow	Primary** Tailings	Secondary Overflow	Secondary Tailings
Gallons per minute	300	150	150	50	100
Per cent solids by weight	8.02	4.01	9.64	3.11	11.62
Pounds per hour	12,250*	3,060	7,370	790	5,940
Magnetic Analysis					
Per cent magnetic on tube tester	34.49	2.93	4.46	0.75	0.2
Pounds per hour magnetic	4220	90.0	328.0	6.0	12.0
Per cent loss referred to primary feed		2.1	7.8	0.14	0.28
Per cent loss referred to secondary feed				1.28	3.7
Pounds of Magnetic Loss per Ton of Feed to the Plant†					
	16.9	0.36	1.3	0.024	0.048

Efficiency of Magnetic Separators

	Magnetite in Feed	Magnetite Not Recovered	Magnetite Recovered
Pounds per hour	4,220	12	4,208
Per cent	100	0.28	99.72

* The weight of solids was calculated by using a constant of 8.5 pounds per gallon of feed.
** Primary tailings are equivalent to the secondary feed.
† Capacity of plant, 250 tons per hour.

water level in the tank at the first pole of the magnet.

The weirs located on either side of the tailings section are a convenient means for adjustment of the water level and provide an overflow channel for the slimes.

The magnet bank consists of two subdivisions, the pickup and concentrate sections which are treated as individual circuits and are connected in parallel. The internal electric connections are shown in Figure 3 and the external connections in Figure 4. Most of the heavy-media installations can tolerate a certain amount of carry-over of nonmagnetic material into the concentrate. The poles of the concentrate section remain fully excited and the water sprays under the concentrate section, Figure 5, are kept inoperative.

For installations where a clean magnetic concentrate is required, a rheostat is inserted in series with the electrical circuit of the concentrate section and the magnetic strength of the last four poles can be varied. The decreased intensity permits particles of smaller size or lower susceptibility to be dropped or discharged into the tailings compartment. The water sprays extend transversely across the belt and can be controlled individually. They consist of pipes with a large number of fine openings or a continuous fine slot through which the water is directed against the burden of the belt. The final adjustment is made during initial operation to obtain a clean magnetic concentrate without loss of ferrosilicon or magnetite in the tailings discharge. The opening in the discharge gate at the lower end of the tailings tank is adjusted to obtain the proper amount of overflow on the weirs located on the lateral sides of the tailings tank.

The arrangement of the magnetic circuit is shown in Figure 6. The housing of the magnet bank is made of nonmagnetic steel and entirely waterproof. The interspace between the pole shoes lying external to the magnet housing are filled with wooden blocks properly fitted and treated for continuous exposure to water.

Figure 7 shows a transverse section through the magnet bank. This separator is entirely automatic and continuous in operation, produces a sharp separation and maximum recovery of the magnetic solids in the pulp. Operating results obtained in actual installation are recorded in Table I.

The Crockett separator requires a small amount of d-c excitation, the power requirements for the drive are very nominal despite the magnetic force between magnet and magnetic particles to which the belt is subjected. The friction between belt and magnet is considerably reduced through the introduction of water between belt and magnet bank. Capacities and operating data are given in Table II.

Although the Crockett separator operates within a small fraction of 100 per cent as shown in Table I, it is advisable to install a secondary Crockett which is fed by the tailings from the first machine as a precautionary measure in case the primary Crockett should become inoperative and large amounts of ferrosilicon would be lost permanently.

The secondary Crockett in addition will recover a small amount of magnetic material which is not recovered by the first separator.

Table II. Capacities and Operating Data

Magnet, Width in Inches	Bulk, Width in Inches	Capacity, Gal/Hr.	Watts, D.C.	Mechanical Horsepower	Water, Gallons Per Minute
12	17	80	600	1	30
24	29	160	1,300	1 1/2	50
36	41	240	1,700	2	70

Demagnetizing Coil

The purpose of the demagnetizing coil is to disperse the highly magnetized particles of the medium magnetite or ferrosilicon and is placed in the flow sheet following the classifier.

Ferromagnetic substances when exposed to the influence of magnetic fields retain a certain amount of magnetism defined as coercive force and residual flux. Each particle has become a miniature magnet and the implied coercive force must be removed.

Ordinary magnets of small dimensions can be placed between the poles of a rotating magnet and slowly removed from their original position or they can be placed within a solenoid. Gradual reduction of the exciting current decreases the existing magnetism following the characteristic of the Hysteresis curve to zero or near zero.

The demagnetizing coil is a solenoid of 3 to 6 inches in diameter and of 16 to 18 inches in length with a decreasing number of turns from one end to the other briefly called tapered winding. Constant excitation of commercial voltage and frequency is applied to the solenoid and the material passes through the coil in the direction of decreasing taper. A solenoid of this type consists of a tubing and end plates of nonmagnetic material such as stainless steel or bakelite with a coil of the proper number of turns depending on voltage and frequency with a resultant average magnetizing force of 300–400 oersteds. A typical demagnetizing coil is shown in Figure 8.

Magnetizing Blocks

The magnetite or ferrosilicon particles are of extremely fine size and settle very slowly in the thickener. The product coming from the washing screens is therefore magnetized before being fed to thickener.

The rubber hose conveying the material is passed through a magnetic field created by the magnetizing blocks.

The operating principle is shown in Figure 9. A magnetic field originating from two horseshoe-shaped magnets passes

through the rubber hose. Polarity and direction of the two separate halves of the field are shown in the same figure. While the pulp is passing through the rubber hose, the fine particles of magnetite or ferrosilicon are magnetized resulting in flocculation of the solids. The average intensity of the field is approximately 800 oersteds.

Figure 10 shows the actual build up of the magnetizing blocks with waterproof windings and watertight conduit and fittings.

Tractive Force on Particles in a Magnetic Field

A magnet is defined as a body which produces a magnetic field external to itself. The field represents a form of potential energy which is located primarily in the air gap between magnet and keeper. This energy stored in the magnetic field is available to do external work.

The field can be described by subdividing it into a number of channels or flux tubes which are obtained through the method of field mapping. The boundary lines of each flux tube are drawn tentatively and the field area is subdivided transversely to the flux tubes through equipotential lines which intersect the flux lines at right angles. Each small area, which must be approximately a square, then represents the same permeance. A field map typical for the described magnetic separator is shown in Figure 11.

The induction or flux density can be calculated in air from the available magnetomotive force in the winding and the permeance of flux tube in accordance with Maxwell's equations of the magnetic field. Flux density is usually designated by the letter B and measured in lines per square centimeter in the centimeter-gram-second system. The magnetizing force, H, measured in oersteds in the centimeter-gram-second system can be calculated from the magnetomotive force and the dimensional constants of the field.

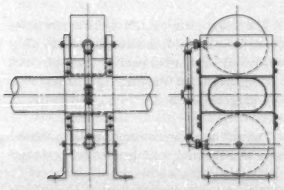

Figure 10. Outline drawing of magnetizing blocks

The energy in a unit volume or density in a uniform field is represented by the equation

$$\sigma = \frac{H \times B}{8\pi} \text{ ergs/cm}^3 \tag{1}$$

This equation also applies to nonuniform fields where the field is subdivided into a large number of regions of uniform density. For many applications it is sufficient to consider a cross section of the field in order to reduce and solve the problem in two dimensions. Magnetic separation is accomplished in media of the permeability $\mu = 1$ such as air or water and equation 1 can be written as

$$\sigma = \frac{B^2}{8\pi} \text{ ergs/cm}^3 \tag{2}$$

The force available at a certain point of the field is equal to the change of energy which can be stated in this form

$$F = \frac{B^2}{8\pi} \text{ dynes/cm}^3 \tag{3}$$

By substitution the following practical formula can be developed

$$F = \left(\frac{B}{5{,}000}\right)^2 \text{ kg/cm}^3 \tag{4}$$

This formula furnishes acceptable results for the calculation of attractive force in the design of magnets but erroneous results for particles of low susceptibility in a magnetic field.

Feebly magnetic materials do not become magnets themselves and the induction B must be replaced by the intrinsic induction B_1.

Intrinsic induction for a given value of magnetizing force is the excess of the normal induction over the induction in vacuum.

$$B_1 = B - \mu_v H \tag{5}$$

In the centimeter-gram-second system $\mu_v = 1$ therefore

$$B_1 = B - H \tag{6}$$

The relation between intensity of magnetization I, flux density, and magnetizing force is expressed in the formula

$$B = H + 4\pi I \tag{7}$$

or

$$I = \frac{B - H}{4\pi} = \frac{B_1}{4\pi} \tag{8}$$

$$B_1 = 4\pi I \tag{9}$$

Introducing $B_1 = 4\pi I$ in equation 1, we obtain

$$\sigma_1 = \frac{H \times I}{2} \text{ ergs/cm}^3 \tag{10}$$

The intensity of magnetization I depends on the susceptibility k and the magnetizing force H, therefore

$$I = kH \tag{11}$$

and substituted in equation 10

$$\sigma_1 = kH^2/_2 \text{ ergs/cm}^3 \tag{12}$$

The attractive force on the particle is therefore

$$F = \frac{d}{dx}\sigma_1 = kH\frac{dH}{dx} \tag{13}$$

where H is the magnetizing force and dH/dx the gradient of the field at the location of the particle.

The attractive force depends on several other factors besides those expressed in equation 12.

The introduction of the particle in the field distorts the original field. The shape of the particle as well as other forces acting on the particles especially in wet separation must be taken in consideration.

The susceptibility of materials varies with the applied magnetizing force and has different values for various materials. The attractive force to the face of a magnet has been calculated for several minerals and illustrated in Figure 12 based on the formula $F = kH^2/_2$ dynes.

Tractive force for particles exists only in a nonuniform or convergent field. For paramagnetic particles $\mu > 1$ the particle will move in the direction of higher field concentration that is on the separator described it will move towards the edges of the pole. It is evident that if the tractive force on the particle is great enough to attract it to the belt, the holding force is considerably greater and will permit thorough spraying and washing before the particles can be removed forcibly from the belt and dispersed in the surrounding medium.

Figure 11 shows the lines of force and equipotential lines of the magnetic field between two poles. The magnetic system must be designed to provide sufficient magnetic strength at a reasonable dis-

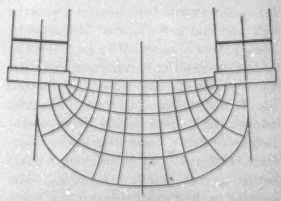

Figure 11. Typical field distribution from pole to pole

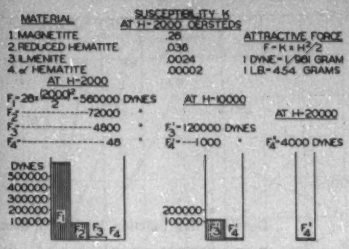

Figure 12 (left). Magnetic attraction of materials of low susceptibility

Figure 13 (right). Flux densities in gausses from pole to pole

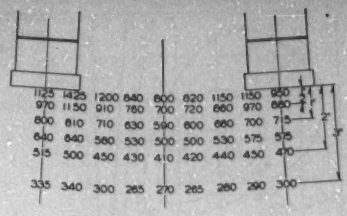

tance from the belt which in turn determines the pole pitch or pole spacing of the individual poles.

Figure 13 illustrates the flux density in gausses at various locations of the field between two poles. The figures shown represent readings taken with the General Electric Company gaussmeter.

References

1. Magnetic Separation of Ores. *Bulletin 425*, United States Department of the Interior, Bureau of Mines, (Washington, D. C.), 1941.

2. American Standard of Definitions of Electrical Terms. AIEE, 1941.

No Discussion

Stability of Voltage Regulators

FRANK E. BOTHWELL
MEMBER AIEE

THE theory of Liapounoff on the stability[1] of dynamical systems under small displacements from equilibrium, together with the Routh-Hurwitz stability criterion, is applied to an n-stage d-c generator employing a 3-terminal nonlinear regulator, such as the vacuum tube or a step resistor, the resistance value of which varies in steps with the control voltage. A graphical method for locating the stability boundary for a general control element with empirically given characteristic is presented. The method is exemplified by a 3-stage generator and a nonlinear vacuum tube as control element. Analytical treatments of the linear control element and of the nonlinear controlled resistance are made, and equations are derived for the stability boundary as a function of the time constants of the generator system and the open loop gain of the complete system. The difference between the stability boundaries of the linear and nonlinear control elements is forcefully expressed by these two examples. It is shown that whereas a raise in the open loop gain produces instability in the circuit employing the linear control element, in the case of the controlled resistance, the opposite effect occurs, and a raise in gain insures stability. A method for the determination of the maximum time constant of a dynamical system subjected to small displacements from equilibrium is derived from a variation of the Routh-Hurwitz criterion, and is applied to the voltage regulation problem.

Inasmuch as the current trend in voltage regulator circuits is toward the use of nonlinear control elements, no sufficient mathematical investigation of the behavior of these circuits has as yet been made. However, as Liapounoff[1] has shown that the stability of nonlinear systems under small displacements from equilibrium is completely determined by the linear perturbation terms, the problem of stability is a linear one, and the location of stability boundaries may be effected by an application of the Nyquist criterion[3] or by means of the powerful methods of Routh[3,4] and Hurwitz.[5]

The fact that stability depends upon linear terms only has led to the misconception that for stability analyses, the behavior of the nonlinear control element is the same as the behavior of the linear one.[6] However, the shift of the operating point of the characteristic of the control element with loop gain and the corresponding change in the slope of the characteristic at the operating point are important in the location of stability boundaries. In fact, in the case of the controlled resistance, a raise in loop gain has an effect on stability just opposite to that for a linear control element.

Analysis of the Network

The generator circuit with its generalized control element is shown schematically in Figure 1. The voltage developed across the control element C is assumed to be a function (with negligible time lag) of its current I_1 and the control voltage V. Denoting this function by $f(I_1, V)$, then

$$E = E_1 + f(I_1, V) \tag{1}$$

Inasmuch as the voltage E_j developed at the jth stage is proportional to its corresponding field current I_{j-1}, a steady-state gain K_j may be defined by the expression

$$E_{j+1} = K_j R_j I_j \tag{2}$$

The Kirchhoff relations

$$E_j = L_j \frac{dI_j}{dt} + R_j I_j \tag{3}$$

together with equations 1 and 2 yield the set of $n+1$ equations

$$\begin{aligned} E &= E_1 + f(E_2/K_1R_1, V) \\ \frac{dE_2}{dt} &= (R_1/L_1)(K_1E_1 - E_2) \\ \frac{dE_3}{dt} &= (R_2/L_2)(K_2E_2 - E_3) \\ &\cdots\cdots\cdots\cdots \\ \frac{dE_n}{dt} &= (R_{n-1}/L_{n-1})(K_{n-1}E_{n-1} - E_n) \\ \frac{dV}{dt} &= (R_n/L_n)(K_0K_nE_n - V) \end{aligned} \tag{4}$$

in the $n+1$ voltages, $E_1, E_2, \ldots, E_n, V$.

The system is in equilibrium when all voltages have reached constant values, that is, when $dE_2/dt = dE_3/dt = \cdots = dV/dt = 0$. These equilibrium values are found by setting all derivatives equal to zero in equation 4. Denoting the equilibrium values of the voltages by subscript 0, one finds

$$\begin{aligned} E_{20} &= K_1E_{10} \\ E_{30} &= K_1K_2E_{10} \\ &\cdots\cdots\cdots\cdots \\ E_{n0} &= K_1K_2\ldots K_{n-1}E_{10} \\ V_0 &= K_0K_1K_2\ldots K_nE_{10} \end{aligned} \tag{5}$$

in which E_{10} is given by the equation (in general nonlinear)

$$E = E_{10} + f(E_{10}/R_1,\ K_2K_1\ldots K_nE_{10}) \tag{6}$$

Small transient motions in the vicinity

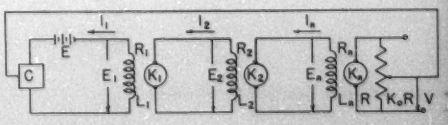

Figure 1. Voltage regulated N stage d-c generator

Paper 50-231, recommended by the AIEE Feedback Control Systems Committee and approved by the AIEE Technical Program Committee for presentation at the AIEE Fall General Meeting, Oklahoma City, Oklahoma, October 23–27, 1950. Manuscript submitted June 6, 1950; made available for printing August 23, 1950.

FRANK E. BOTHWELL is with Northwestern University, Evanston, Ill.

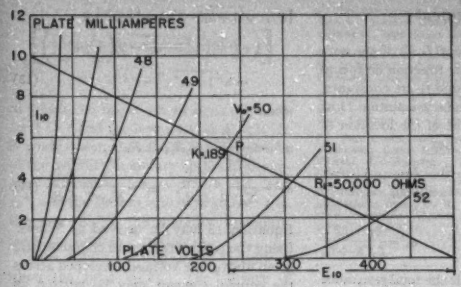

Figure 2. Nonlinear control characteristic

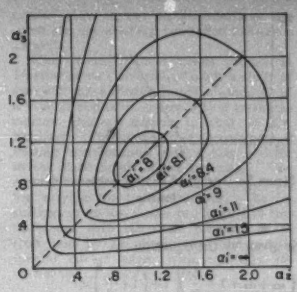

Figure 4. Stability boundary for linear control element

of the equilibrium point may be investigated by forming the first variation of equations 4. Setting $E_j=E_{j0}+e_j$ and $V=V_0+v$, one finds the set of linear perturbation equations

$$
\begin{aligned}
&e_1+(f_{I_1}/K_1R_1)e_2+f_Vv=0\\
&\frac{de_2}{dt}+(R_1/L_1)e_2-(K_1R_1/L_2)e_1=0\\
&\cdots\cdots\cdots\cdots\cdots\cdots\\
&\frac{de_n}{dt}+(R_{n-1}/L_{n-1})e_n-(K_{n-1}R_{n-1}/K_{n-1})e_{n-1}=0\\
&\frac{dv}{dt}+(R_n/L_n)v-(K_nK_nR_n/L_n)e_n=0
\end{aligned}
\tag{7}
$$

in which f_{I_1} and f_V denote the partial derivatives of f with respect to I_1 and V, evaluated at the equilibrium point. These two derivatives are of utmost importance in the determination of stability boundaries.

Liapounoff's Theorem

The theorem of Liapounoff states that the stability of a continuous periodic solution of a system of nonlinear differential equations is determined by the linear perturbation equations of the first variation of the system of differential equations. The only cases in which the method fails are those in which either all linear perturbation terms vanish or the system is subjected to large disturbances. Our concern here is the special case in which the periodic solution is the equilibrium point $E_{10}, E_{20}, \ldots, E_{n0}, V_0$.

According to Liapounoff[1] the stability of the original system 4, and hence the stability of the circuit of Figure 1, is governed by the stability of the set of linear equations 7. However the stability of the latter is determined by the location of the roots of the characteristic equation

$$
\left(p+\frac{R_n}{L_n}\right)\left(p+\frac{R_{n-1}}{L_{n-1}}\right)\cdots\left(p+\frac{R_2}{L_2}\right)\times\left[p+\frac{R_1}{L_1}\left(1+\frac{f_{I_1}}{R_1}\right)\right]+K\frac{R_1R_2\ldots R_n}{L_1L_2\ldots L_n}f_V=0 \tag{8}
$$

in which $K=K_0K_1\ldots K_n$. In fact the necessary and sufficient condition that the circuit of Figure 1 be stable is that all roots of the algebraic equation 8 have negative real parts.

Routh-Hurwitz Stability Criterion

Inasmuch as the problem of the stability of the circuit of Figure 1 is reduced to the location of the roots of the polynomial 8, a criterion of stability such as Nyquist's[3] may be employed. However, the Nyquist method is numerical, and at least for this simple network, it is not as profitable as the analytical method of Routh and Hurwitz. This latter criterion is in the form of a relation among the coefficients of the polynomial, and for our purposes, takes the following form: If a_0 and a_n are of like sign, the stability boundary of the equation

$$a_0p^n+a_1p^{n-1}+\ldots+a_n=0 \tag{9}$$

consists of certain branches of the following equation

$$
\begin{vmatrix}
a_1 & a_0 & a_{-1} & -a_{3-n}\\
a_3 & a_2 & a_1 & -a_{5-n}\\
a_5 & a_4 & a_3 & -a_{7-n}\\
\cdots & \cdots & \cdots & \cdots\\
a_{2n-3} & a_{2n-4} & a_{2n-5} & -a_{n-1}
\end{vmatrix}=0 \tag{10}
$$

in which every element with subscript greater that n or less than zero is to be replaced by zero. For example, for second, third, and fourth degree polynomials, the conditions are respectively

$$a_1=0$$

$$\begin{vmatrix} a_1 & a_0\\ a_3 & a_2 \end{vmatrix}=a_1a_2-a_0a_3=0$$

$$\begin{vmatrix} a_1 & a_0 & 0\\ a_3 & a_2 & a_1\\ 0 & a_4 & a_3 \end{vmatrix}=(a_1a_2-a_0a_3)a_3-a_1^2a_4=0$$

Equation 10 will separate the a_0-a_n space into certain finite or infinite regions. To test a given region for stability, it is only necessary to test a single point in the region, for the stability can change only by a crossing of the boundary curve, equation 10. However not all branches of equation 10 are necessarily boundary curves, so that one point in each region must be checked. However this checking can usually be accomplished by inspection.

Returning to the characteristic equation 8 for the voltage regulated generator circuit, one may observe the essential features of stability by consideration of a 3-stage system. In this case

$$a_0=1$$

$$a_1=\frac{R_3}{L_3}+\frac{R_2}{L_2}+\frac{R_1}{L_1}\left(1+\frac{f_{I_1}}{R_1}\right)$$

$$a_2=\frac{R_2R_3}{L_2L_3}+\left(\frac{R_3}{L_3}+\frac{R_2}{L_2}\right)\frac{R_1}{L_1}\left(1+\frac{f_{I_1}}{R_1}\right)$$

$$a_3=\frac{R_2R_3R_1}{L_2L_3L_1}\left(1+\frac{f_{I_1}}{R_1}+Kf_V\right)$$

The coefficient a_0 is greater than zero, and since f_{I_1} and f_V must each be positive for proper regulation, a_3 also is greater than zero. Therefore the stability boundary

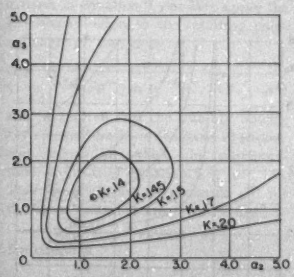

Figure 3. Stability boundary for control element characteristic of Figure 2

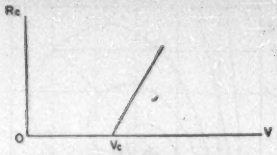

Figure 5. Idealized control resistance characteristic

is given by the equation

$$\left(\alpha_2+\alpha_3+1+\frac{f_{I1}}{R_1}\right)\left[1+\left(1+\frac{f_{I1}}{R_1}\right)\times\left(\frac{1}{\alpha_2}+\frac{1}{\alpha_3}\right)\right]=1+\frac{f_{I1}}{R_1}+Kf_V \quad (11)$$

in which

$$\alpha_2=\frac{R_2L_1}{L_2R_1},\quad \alpha_3=\frac{R_3L_1}{L_3R_1}$$

Graphical Method

Consider a control element with characteristic as shown in Figure 2. The equilibrium, or operating, point P is determined by the plate battery voltage E, the slope of the load line, R_1, and the gain K of the open loop circuit of Figure 1 defined by the relation

$$K-V_0/E_{10}$$

As the gain is varied, the operating point moves along the load line. One may tabulate the values of the derivatives f_{I_1} and f_V (the instantaneous plate resistance and amplification) as functions of gain K for the given choice of E and R_1. These values, coupled with equation 11 yield the stability boundary shown in Figure 3. The region of stability lies below the surface shown in the form of a contour map.

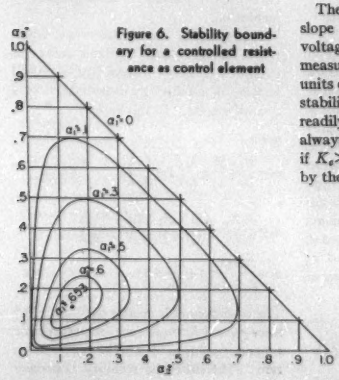

Figure 6. Stability boundary for a controlled resistance as control element

Linear Control Element

If the characteristic $f(I_1,V)$ of the control element is a linear function of I_1 and V, the derivatives f_{I_1} and f_V are constants, and the stability boundary, equation 11 is, of course, independent of the location of the operating point. Let

$$\alpha_1'=K\frac{f_V}{1+\frac{f_{I1}}{R_1}},\quad \alpha_2'=\frac{R_2}{L_2}\frac{L_1}{R_1+f_{I1}},$$

$$\alpha_3'=\frac{R_3}{L_3}\frac{L_1}{R_1+f_{I1}}$$

and note that $R_1+f_{I_1}$ is the total resistance of the first loop of the circuit of Figure 1, and that α_1' is the gain around the complete closed loop. Equation 11 becomes

$$(1+\alpha_2'+\alpha_3')\left(1+\frac{1}{\alpha_2'}+\frac{1}{\alpha_3'}\right)=1+\alpha_1' \quad (12)$$

and the surface is shown in the form of a contour map in Figure 4. Again the region of stability lies below the surface.

Controlled Resistance

A common control element for high-voltage generators is the controlled resistance. It is a step resistor the resistance value of which varies in steps with the control voltage V. The essential features of its stability in connection with Figure 1 may be observed by assuming that the resistance varies linearly and continuously with control voltage when the latter exceeds a critical value, V_c. Any time lag in the operation of the resistor must either be negligible or must form one of the stages of the generator circuit itself. Thus the control resistance R_c takes the form of Figure 5, or

$$R_c=0 \qquad \text{if } V<V_c$$
$$R_c=K_c(R_1/V_c)(V-V_c) \qquad \text{if } V>V_c$$

The dimensionless constant K_c, the slope of the control resistance, control voltage characteristic when the former is measured in units of R_1 and the latter in units of V_c, plays an important role in the stability of the circuit. In fact, it is readily shown that if $K_c<1$, the system is always stable, regardless of gain, whereas if $K_c>1$, the stability boundary is given by the expression

$$[(1/2)\sqrt{1+\alpha_1''}-1)+\alpha_2''+\alpha_3'']\times\left[1+(1/2)(\sqrt{1+\alpha_1''}-1)\left(\frac{1}{\alpha_2''}+\frac{1}{\alpha_3''}\right)\right]=\sqrt{1+\alpha_1''} \quad (13)$$

where

$$\alpha_1''=4\frac{K_c}{(K_c-1)^2}K_0K_1\ldots K_n\frac{E}{V_c},$$

$$\alpha_2''=\frac{1}{K_c-1}\frac{R_2L_1}{L_2R_1},\quad \alpha_3''=\frac{1}{K_c-1}\frac{R_3L_1}{L_3R_1} \quad (14)$$

Equation 13 may be derived as follows. Using the control resistance characteristic given above, the voltage developed across the control element may be written as

$$f(I_1,V)=0 \qquad \text{if } V<V_c$$

$$f(I_1,V)=K_c\frac{R_1}{V_c}(V-V_c)I_1 \qquad \text{if } V>V_c$$

The operating (equilibrium) values of the various circuit voltages E_{i0} are given by equations 5 and 6. Thus

$$I_{10}=\frac{E_{10}}{R_1}=\frac{2E}{(K_c-1)R_1\alpha_1''}(1\pm\sqrt{1+\alpha_1''})$$

$$V_0=\frac{K_c-1}{2K_c}V_c(1\pm\sqrt{1+\alpha_1''})$$

There are two possible operating points. However in order that the control element have a regulating effect upon the system, it is necessary that $V_0>V_c$. Thus if $K_c<1$, the negative signs must be used, whereas if $K_c>1$, the positive signs are used.

The partial derivatives of the control function $f(I_1,V)$ are now readily found. They are found to satisfy the following relations

$$1+\frac{f_{I1}}{R_1}=-\frac{1}{2}(K_c-1)(1\mp\sqrt{1+\alpha_1''})$$

$$Kf_V=\frac{1}{2}(K_c-1)(1\pm\sqrt{1+\alpha_1''})$$

Using these relations in equation 11, it follows that the stability boundary is given by the equation

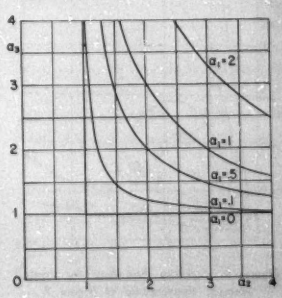

Figure 7. Locus of parameter values for which maximum time constant of circuit of Figure 1 with linear control element is $L_1/(R_1+f_{I_1})$

$R_1+f_{I_1}$ is total resistance of first loop in Figure 1

$$[(^1/_2)(\sqrt{1+\alpha_1''}\mp 1)+\alpha_2''+\alpha_3'']\times$$
$$\left[1+(^1/_2)(\sqrt{1+\alpha_1''}\mp 1)\left(\frac{1}{\alpha_2''}+\frac{1}{\alpha_3''}\right)\right]$$
$$=\pm\sqrt{1+\alpha_1''}$$

in which the upper set of signs are used for $K_e>1$ and the lower set for $K_e<1$. It is readily seen that for $K_e<1$ no portion of the stability boundary occurs in the region of positive values of α_1'', α_2'', and α_3'', and the system is always stable. For the case $K_e>1$ the stability boundary takes the form of equation 13.

Thus stability in this case is dependent upon the ratio E/V_c. The surface is shown in contour form in Figure 6. In this case the region of stability lies above the surface. That is to say, the region of instability lies inside the mound enclosed by the surface and the co-ordinate plane $\alpha_1''=0$.

For the stability boundaries of the linear control element and of the nonlinear controlled resistance element, the variable α_1'' is in each case proportional to the circuit loop gain. However the boundaries differ greatly, and in fact the region of stability for the linear control element lies below the boundary, whereas the corresponding region for the controlled resistance lies above the boundary.

Maximum Time Constant

In many applications it is necessary not only to insure stability of the over-all circuit but to insure a degree of stability. That is to say, every root of the characteristic equation must not only have negative real part, but the real part must be larger in absolute value than some given value, b. This, of course, is a way of saying that the maximum time constant of the system for small transients about the equilibrium point must be less than $1/b$. If the substitution

$$p=p'-b$$

is made in equation 9, one may apply the Hurwitz criterion to the resulting polynomial in p', that is, to

$$a_0(p'-b)^n+a_1(p'-b)^{n-1}+\ldots+a_n$$
$$=a_0'p'^n+a_1'p'^{n-1}+\ldots+a_n' \quad (15)$$

and be assured that the stability boundary of equation 15 is the locus of parameter values for which the maximum time constant of equation 9 is just $1/b$. This procedure has been carried out for the linear control element, see Figure 7.

References

1. The General Problem of Stability of Motion (book), M. A. Liapounoff. Princeton University, Princeton, N. J., 1947.

2. Regeneration Theory, H. Nyquist. *Bell System Technical Journal* (New York, N. Y.), volume 11, 1932, pages 126–47.

3. Stability of a Given State of Motion, E. J. Routh. Adams Price Essay, MacMillan Company, London, England, 1877.

4. Dynamics of a System of Rigid Bodies (book), E. J. Routh. MacMillan Company, London, England, part 2, chapter 6, 1905.

5. The Conditions for Which an Equation Possesses Only Roots with Negative Real Parts, A. Hurwitz. *Mathematische Annalen*, (Berlin, Germany), volume 46, 1895, pages 273–84.

6. Recent Developments in Generator Voltage Regulation, C. R. Hanna, K. A. Oplinger, C. E. Valentine. *AIEE Transactions*, volume 58, 1939, pages 838–45.

Discussion

Hugh M. Taylor, Jr. (Mississippi State College, State College, Miss.): Dr. Bothwell has written an interesting paper on the generator voltage regulator system. There are some points, however, on which his paper is somewhat confusing. The most important of these is the use of the terms "open loop gain," "loop gain," "gain K of the open loop circuit," "circuit loop gain," and "gain around the complete closed loop." All of these terms except the last are used in variance with the normal nomenclature to mean the gain from the field of generator 1 to the return voltage V without regard to the control element C. Thus, as an example, the statement in the section of the controlled resistance that "For the stability boundaries the variable α_1' is in each case proportional to the circuit loop gain" refers, not to the gain from one point, through the circuit, and back to that point, but only to a portion of this loop.

Equation 12 and the stability boundaries of Figure 4 are more universal than Dr. Bothwell has brought out. Although they are given for the case of the linear control element, no assumptions of linearity were actually made. Thus, these curves apply not only to the circuit containing the linear control element, but to the nonlinear element and the idealized controlled resistance as well.

While working on a thesis project at Northwestern University, I made a study of an electronic-feedback-amplifier analogue of a voltage regulator system with a nonlinear control element similar to that of Dr. Bothwell. This consisted of three stages of voltage amplification with a load resistor in the plate circuit of the last stage. The circuit included three variable capacitors for varying the time constants. The resulting curves are shown in Figure 1 of this discussion with the same terminology as that used by Dr. Bothwell. The experimental curves agree with equation 12, within the accuracy expected.

Frank E. Bothwell: I wish to thank Mr. Taylor for his comments and for the presentation of his experimental results which so well verify the general stability boundary, equation 12.

I should like to point out that equation 11 (or equation 12 if you wish) is merely a partial answer to the question of stability for nonlinear systems, in that it relates the stability boundary to basic parameters in a very implicit manner. Each co-ordinate α_1', α_2', α_3', is a function of the partial derivatives f_{I_1} and f_e evaluated at the equilibrium point. In order to use the boundary in this form, it is necessary for each choice of circuit parameters to calculate the operating point of the system and certain partial derivatives evaluated at the operating point.

In order to avoid this difficulty, equation 13 and Figure 6 were derived for the case of the controlled resistance. They present the stability boundary in terms of the time constant ratios of the generator stages, the gain of each stage, the gain of the feedback path, the applied voltage, the critical control voltage, and the slope of the control resistance curve. Such expressions for stability in terms of circuit parameters have been formalized by the Russians under the name of "Vysnegradskii diagrams".

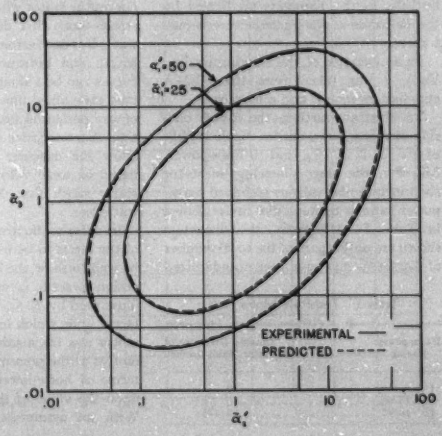

Figure 1. Experimental and theoretical stability boundaries for an analogue of a voltage regulator system

A Method of Total Design as Applied to Polyphase Induction Motors

C. H. CROUSE
ASSOCIATE AIEE

IN recent years standardization, both within the organizations involved with motor manufacturing and with the various motor manufacturers represented by the National Electrical Manufacturers Association (NEMA) has caused the design and manufacture of various ratings of motors to be restricted to the smallest possible number of stator and rotor punching combinations. Each motor manufacturer, who has been or intends to supply the machine tool industry with motor parts, that is, wound stators and rotors without the shaft bearings, or frame, soon finds the necessity of setting up the various ratings in as few punching combinations as is found necessary to adequately supply the various customer's demands. These punching combinations generally fall not only in the standardized punching diameters as outlined by NEMA but also in the diameters predicated by the demands of the manufacturer's customers.

As an example of the standardization, Table I was taken from the NEMA standard on motors and generators.[1]

To illustrate further, the 8-inch outside diameter series carries 2-pole ratings of $1^1/_2$, 2, 3, 5, $7^1/_2$, and 10 horsepower. Likewise, the other diameters of stator shell include the various standard horsepower ratings between the limits shown in Table I. Obviously, the diameters shown are only a part of the total number of diameters that have been standardized by NEMA or the individual motor manufacturer.

Table I. Two-Pole Motor Parts

Horsepower Rating	Outside Diameter of Stator Shell, Inches
$1^1/_2$ to 10	8
$7^1/_2$ to 20	10
15 to 25	12.375

To anyone faced with the task of providing designs for ratings, which are to be changed over to new or different punching combinations, it is apparent that the amount of calculation necessary would be enormous. The process of standardization often entails considerable amount of calculation in order to observe the over-all picture of the changeover so that intelligent decisions can be made as to what combinations of punchings result in the best performance. The purpose of this paper is to relieve the designer of as much detailed calculation as possible.

It will be shown how the salient points of any particular design can be observed from a set of curves, which are characteristics of any particular stator and rotor punching combination. From these curves the stator winding current density, stator tooth flux density, and full load watts loss can be found for any given core length and horsepower output. These curves can be valuable to the designer in that they allow him to follow the trends of any design as some of the various design characteristics change. The curves allow the designer to choose a design based on some value of current density, stator tooth flux density, or full load watts loss.

In order to illustrate the origin of some of the terms to be used later on, it would be well to show the basis upon which the design process is established. As was illustrated by T. C. Lloyd,[2] the desirable factor upon which to base the design of a motor was the maximum torque. Many motors at the present time are defined, in terms of horsepower, by NEMA solely upon the value of the maximum torque. With an assumed value of maximum torque, the necessary curves for design purposes can then be made.

By the use of the approximate equivalent circuit for a polyphase induction motor the maximum torque equation is:

$$T_m = \frac{7.05}{\text{Syn rpm}} \times \frac{nE^2}{2\,(R_1+\sqrt{R_1^2+X^2})}$$

pound feet

This equation can be modified by use of the ratio R_1/X, into the following form:

$$T_m = \frac{3.53nE^2}{(\text{Syn rpm})\,(X)}\left[\frac{1}{\frac{R_1}{X}+\sqrt{\left(\frac{R_1}{X}\right)^2+1}}\right]$$

If the exact equivalent circuit is used, two additional terms will be introduced. One term is K_r, which is the flux factor made up of K_s and K_p. K_s and K_p are defined as follows:

$$K_s = \frac{X_m}{X_1+X_m}$$

$$K_p = \frac{X_m}{X_1+X_m}, \text{ and } K_r = K_s \times K_p$$

The other term, which can be called τ, is the correction applied to the terminal voltage to take care of the stator impedance drop. This same term appeared as $(OE/ZE)^2$ in a paper by W. J. Branson.[3]

$$\tau = \frac{\text{Tan}\,\frac{\theta}{2}}{1+(1-K_r)\left(\frac{R_1}{X}\right)^2}$$

where

$$\theta = \cot^{-1} K_r \frac{R_1}{X}\left[\frac{1}{1+(1-K_r)\left(\frac{R_1}{X}\right)^2}\right]$$

Paper 50-232, recommended by the AIEE Rotating Machinery Committee and approved by the AIEE Technical Program Committee for presentation at the AIEE Fall General Meeting, Oklahoma City, Oklahoma, October 23–27, 1950. Manuscript submitted October 31, 1949; made available for printing August 22, 1950.

C. H. CROUSE is with Robbins and Myers, Inc., Springfield, Ohio.

The writer wishes to acknowledge the work of Dr. S. S. L. Chang in originating the theory of total design as applied to polyphase induction motors. Dr. Chang's development of the original theory made the present paper possible. The writer also is indebted to T. C. Lloyd for his very helpful suggestions during the preparation of this paper.

Table II. Necessary Design Constants From Which Figures 2 and 3 Were Plotted

W	σ_L	$\sigma_0 E_w^3$	$\frac{R_1}{X}$	K_r	τ^3	a	b	(ac)	Horsepower 300 cm/amp	Horsepower 500 cm/amp	Horsepower 700 cm/amp	Primary Copper Loss 300 cm/amp	Primary Copper Loss 500 cm/amp	Primary Copper Loss 700 cm/amp	θ w 300 cm/amp	θ w 500 cm/amp	θ w 700 cm/amp	Total Losses 300 cm/amp	Total Losses 500 cm/amp	Total Losses 700 cm/amp
1	2.315	25.1	0.787	0.85	0.512	0.0935	0.161	0.347	0.651	0.235	0.12	213	76.5	39.1	11,800	7,100	5,060	310	166	129
2	3.33	49.5	0.613	0.9	0.575	0.072	0.13	0.511	1.79	0.645	0.326	245	88	45	11,000	6,600	4,700	428	230	164
3.0	4.34	73.8	0.532	0.93	0.615	0.0795	0.121	0.69	2.82	1.01	0.518	277	99.5	52.8	10,500	6,300	4,500	521	240	164
4.0	5.36	122.6	0.445	0.93	0.663	0.0856	0.12	0.858	4.25	1.48	0.819	311	122.5	62.5	8,750	5,200	3,750	674	300	193
5.0	6.38	171.3	0.402	0.94	0.695	0.0897	0.119	0.996	6.45	2.32	1.18	405	145	74.3	8,370	5,000	3,570	825	365	225
7	8.41																			

With the two additional terms, the maximum torque equation becomes:

$$T_m = \frac{E^2 \times 3.53 \times K_r \times \tau \times n}{\text{Syn rpm} \times X}$$

A curve for τ for various values of R_1/X and K_r is shown in Figure 1.

In addition to the equation for maximum torque, three other constants should be derived. These constants are defined as follows:

$$a = \frac{\text{rotor input per phase}}{E^2/X}$$

$$b = \frac{\text{primary current}}{E/X}$$

and

$$c = \frac{\text{secondary current (in primary terms)}}{E/X}$$

With the exact equivalent circuit, a, b, and c are determined from constants available in the equivalent circuit.

$$A_1 = \frac{K_r}{1+(1-K_r)^2(R_1/X)^2}$$

$$B = 1 + A(1-K_r)(R_1/X)^2$$

$$D = R_2/sX$$

$$c = \sqrt{\frac{A_1}{\left(A_1\frac{R_1}{X}+D\right)^2+B^2}}$$

$$a = c^2 D$$

$$b = \frac{c}{\sqrt{K_r}}\sqrt{1+(1-K_r)^2D^2}$$

Since K_r and R_1/X are known for any particular design, A_1 and B can be calculated. Arbitrary values of D must then be assumed for the particular value of slip for which the performance is desired. With A_1, B, and D known a, b, and c can be calculated.

Derivation of Total Design Curves

It has been shown[4] that any stator lamination has a certain inherent volt-ampere rating. The volt-ampere formula can be combined with the maximum torque equation to produce the basis upon which the total design curves can be plotted. The flux per pole in kilolines is:

$$\phi = \frac{E \times 45 \times 10^3}{C \times f \times K_w}$$

$$\frac{E}{C} = \frac{\phi \times f \times K_w}{45 \times 10^3} \qquad (1)$$

If F is the ratio of the total bare conductor area to the total slot area and A is equal to the slot area in square inches

$$I = \frac{A}{C} \times \frac{S_p}{n} \times 12{,}730 \times F \times \frac{1}{D_c}$$

Where D_c is equal to the current density in 100 circular mils per ampere

$$V-A \text{ rating} = nEI = \frac{AS_p\phi f K_w F}{D_c} \times \frac{12{,}730}{45{,}000}$$

$$V-A \text{ rating} = 0.283 F f A S_p K_w \frac{\phi}{D_c} \qquad (2)$$

The maximum torque, as shown before, is

$$T_m = \frac{E^2 \times 3.53 K_r \tau n}{\text{Syn rpm} \times X}$$

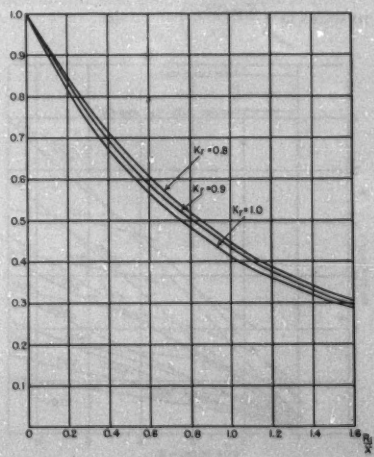

Figure 1. τ versus R_1/X for various values of K_r

Nomenclature

$a = \dfrac{\text{rotor input per phase}}{E^2/X}$

A = slot area in square inches

$b = \dfrac{\text{primary current}}{E/X}$

$c = \dfrac{\text{secondary current (in primary terms)}}{E/X}$

C = total series conductors per phase

D_c = current density in 100 circular mils per ampere

E = terminal volts per phase, Y assumed

F = slot space factor, ratio of total bare-conductor area to total slot area

F_L = friction loss per horsepower

$F_w = \dfrac{F_L}{746+F_L}$

FLT = full load torque, pound feet

f = line frequency

I = primary current

K_p = primary leakage coefficient, $K_p = \dfrac{X_m}{X_1+X_m}$

K_s = secondary leakage coefficient, $K_s = \dfrac{X_m}{X_2+X_m}$

$K_r = K_s \times K_p$

K_w = winding factor = distribution factor × pitch coefficient

l_c = one-half average length of conductor, in inches

n = number of phases

$\mathcal{P}_L$ = total leakage permeance

$\mathcal{P}_O$ = open circuit permeance

R_1 = primary resistance, ohms

s = slip = 1 − (rpm/Syn rpm)

S_p = primary slots

W = core width, in inches

X_1 = primary leakage reactance

X_2 = secondary leakage reactance

$X = X_1 + X_2$ = total leakage reactance, where $X_1 = X_2$

X_m = magnetizing reactance, ohms

ae = apparent efficiency = watts input/$3EI$

ϕ = total flux per pole, Maxwells

τ = correction applied to terminal voltage to account for stator impedance drop

$$\theta = \cot^{-1} K_r \frac{R_1}{X}\left[\frac{1}{1+(1-K_r)\left(\frac{R_1}{X}\right)^2}\right]$$

$$T_m = \frac{3.53E^2K_r\tau n}{\text{Syn rpm} \times 2\pi f C^2 \mathcal{P}_L \times 10^{-8}}$$

Eliminating E/C with equation 1 it follows that

$$T_m \times \text{Syn rpm} = \frac{3.53K_r\tau n\phi^2 f^2 K_w^2}{2\pi f\,\mathcal{P}_L(45\times10^8)^2\times10^{-8}} = \frac{0.0277K_r\tau n\phi^2 f K_w^2}{\mathcal{P}_L} \qquad (3)$$

Let $\gamma = T_m/FLT$ and assume slip, $s = 4$ per cent at full load

$$\text{HP} = \frac{\text{Syn rpm} \times T_m}{\gamma}(1-0.04)\frac{1}{7.04\times746}$$

$$\text{HP} = \frac{\text{Syn rpm} \times T_m}{\gamma} \times 1.83\times10^{-4}$$

$$\text{HP} = 5.06\times10^{-6}\left(\frac{K_r\tau n\phi^2 f K_w^2}{\mathcal{P}_L\gamma}\right) \qquad (4)$$

If ae denotes apparent efficiency, equation 2 becomes

$$\text{HP} = \frac{V-A \text{ rating} \times ae}{746}$$

$$\text{HP} = 3.80\times10^{-4}\times FfAS_pK_w(ae)\frac{\phi}{D_c} \qquad (5)$$

Eliminating ϕ between equations 4 and 5, it follows that

$$\text{HP} = 0.0285F^3\left(\frac{AS_p}{D_c}\right)^2\frac{\gamma f}{n}\times\frac{(ae)^2\mathcal{P}_L}{K_r\tau} \qquad (6)$$

When $n = 3$ and $F = 0.27$

$$\text{HP} = 0.000693\left(\frac{AS_p}{D_c}\right)^2\gamma f\frac{(ae)^2\mathcal{P}_L}{K_r\tau} \qquad (6a)$$

With the introduction of $\gamma = T_m/FLT$ the maximum torque equation can be rearranged.

$$\text{Syn rpm} \times T_m = \frac{E^2\times3.53\times K_r\tau\times3}{X}$$

$$\text{Syn rpm} \times FLT = \frac{E^2\times3.53\times K_r\tau\times3}{3.75X}$$

when $\gamma = 3.75$.

If the average friction loss per horsepower is obtained, the following ratio results:

$$F_w = \frac{F_L}{746+F_L}$$

With the preceding equations available, the important relations can then be set down.

$$\text{Rotor input} = \frac{\text{Syn rpm} \times FLT}{7.04}(1+F_w)$$

$$a = \frac{\text{rotor input}}{\dfrac{3E^2}{X}}$$

$$a = (1+F_w)\frac{\text{Syn rpm} \times FLT}{7.04}\times\frac{X}{3E^2}$$

$$a = (1+F_w)\times\frac{\text{Syn rpm} \times FLT \times E^2\times3.53\times K_r\tau\times3}{7.04\times3.75\times\text{Syn rpm} \times FLT\times3E^2}$$

$$a = 0.1338(1+F_w)K_r\tau$$

$$\text{Primary current} = \frac{E}{X}b$$

$$\text{Apparent watts} = \frac{3E^2b}{X}$$

$$\text{Output watts} = \frac{3E^2a}{X}\frac{(1-s)}{(1+F_w)}$$

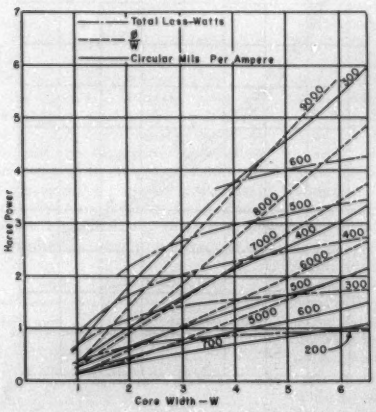

Figure 2 (left). Total design curves for a 4-pole, 60-cycle, 3-phase induction motor with the ratio $T_m/FLT = 3.0$

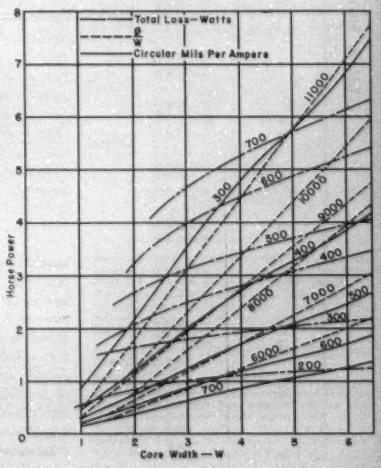

Figure 3 (right). Total design curves for a 4-pole 60-cycle 3-phase induction motor with the ratio $T_m/FLT = 3.75$

$$\text{Apparent efficiency} = \frac{(1-s)}{(1+F_w)}\frac{a}{b} \tag{7}$$

Primary copper loss $= Fl_eAS_p$ watts per cubic inches

where

$$\frac{\text{watts}}{\text{cu. in.}} = \frac{(1{,}273{,}000)^2}{\left(\frac{\text{CM}}{\text{amp}}\right)^2}\times\text{resistivity}$$

$$= \frac{1}{D_e^2}\times 12.73^2\times\frac{1.724\times 1.13}{2.54}$$

$$= \frac{124}{D_e^2}$$

$$\text{Primary copper loss} = Fl_eAS_p\frac{124}{D_e^2} \tag{8}$$

Equation 5 can be rearranged to produce ϕ/W

$$\frac{\phi}{W} = \frac{\text{HP}\times D_e}{3.80\times 10^{-4}FfAS_pK_w(ae)W} \tag{9}$$

Example

From equations 6, 7, 8, and 9, it now is possible to tabulate the various points necessary from which total design curves may be drawn. Table II illustrates the form in which the calculations can be made. The quantities σ_L, σ_O, K_w, R_1/X, and K, have been defined previously and are redefined in the nomenclature.

Figures 1, 2, and 3 show the manner in which design trends can be observed. After the designer has chosen the stator and rotor punching combination as well as the rotor winding, curves similar to those illustrated allow the designer to choose a core width and horsepower combination and observe at a glance the trends which may be expected. Should the full load current density be a prerequisite, then immediately the stator tooth flux density and the full load watts loss can be observed. Likewise, any of the other factors can be established, while the trends of the remaining quantities can be observed. It is hoped that the present process can be of help to designers faced with either changes in existing lines of motors, or the necessity of designing a complete new line of motors.

References

1. Standards for Motors and Generators, *MG-1 1949*, National Electrical Manufacturers Association (New York, N. Y.), part 7, MG1-7.216. October 1949.

2. Some Aspects of Electric Motor Design—Polyphase Induction Motor Design to Meet Fixed Specifications, T. C. Lloyd. *Electrical Engineering* (*AIEE Transactions*), volume 63, January 1944, pages 14–20.

3. Polyphase Induction Motors, W. J. Branson. *AIEE Transactions*, volume 49, January 1930, pages 319–32.

4. Some Aspects of Polyphase Motor Design—The Design and Properties of the Magnetic Circuit, T. C. Lloyd, Howard E. Stone. *Electrical Engineering* (*AIEE Transactions*), volume 65, December 1946, pages 812–18.

No Discussion

A Study of Directional Element Connections for Phase Relays

W. K. SONNEMANN
MEMBER AIEE

THE subject of the performance of single-phase directional relay elements for phase fault protection has never been completely analyzed with consideration given to all the possible variables. The analyses which have been made have been limited in scope when intended to be general in nature, or have been slanted toward specific problems. It is the purpose of this paper to extend the boundaries of the generalities of the analysis in the hope that the results will be beneficial to the industry through making answers available which have heretofore been difficult to obtain.

Scope

The relay directional elements to be studied in this paper are single-phase elements only as normally applied for the purpose of making directional discriminations for interphase faults. Polyphase directional relays are excluded on the basis that the method of approach used here is not adaptable to predicting their performance. Ground relays are excluded on the basis that they may be more conveniently studied as a separate problem, free of many of the complications that enter into a consideration of phase relays. The single-phase directional elements that are to be studied are used widely and thus form a conveniently separable bloc in the over-all problem of directional discrimination. This bloc is characterized by certain conditions that may be grouped into the two classifications of (1) fixed, and (2) variable considerations. These are as follows:

Fixed Considerations

There are three relay directional elements for a 3-phase system, one for each phase. There are four types of faults, which are phase-to-phase, single-phase-to-ground, 2-phase-to-ground, and three phase. There are four types of connections which are commonly used, these being the 90-degree, two forms of 60-degree, and the 30-degree connections. (These will be further described.) There is also the consideration of the location of the relays in the power system relative to delta star (or star delta) connected transformer banks, parallel feeds, and zero sequence sources. The author believes that the variables of location in the system can be reduced to three as typified by Figures 1, 2, and 3, and this will be discussed. Multiplying together the numbers involved in the above groups yields a product of 144, indicating that there are 144 facets to the problem to be borne in mind while studying the variable considerations. These are actually reduced to 86 in number, however, by virtue of the facts that: it is only necessary to study one relay out of three for 3-phase faults; some of the relays are not affected by some of the faults; and, the system of Figure 2 is a duplicate of that of Figure 1 insofar as phase-to-phase and 3-phase faults are concerned. These 86 facets are involved in the interpretation of the effects of the variable considerations.

Variable Considerations

The impedances of the power system are conveniently broken down into two single equivalent impedances for each sequence network, which are the impedance of the source up to the relay location, and the impedance of the transmission line from the relay to the point of fault. The impedance of the line may vary from zero representing a close in solid fault, to a relatively large value representing either a fault far removed from the relay location, or else a fault involving an arc of very considerable length. For any given line impedance to the point of fault, the source impedance may be relatively small, large, or in between. The impedance angle of the line may be different from that of the source. The author has considered that the line angle may vary from zero degrees (arcing fault) to 90 degrees lagging, and that the source impedance angle may vary between the limits of 60 to 90 degrees lagging. The zero sequence impedances for the source and line may differ in relative magnitude and impedance angle with respect to each other and quite independently of the positive and negative sequence network impedances. The 86 facets of the problem are interpreted in the light of these variable considerations.

There are other variables which are not covered in this study. These are concerned with the effects of load current and synchronizing current during faults, and the variations possible between the positive and negative sequence networks. This study is limited to the effects of short circuit current only, and is based on the assumption that the positive and negative sequence impedances are identical. In certain special cases, it may be necessary to consider the effect of load current, but it is believed that such cases will be relatively infrequent.

The Four Commonly Used Connections

Directional element connections are conveniently and popularly described in terms of the angle by which unity power factor balanced load current flowing in the tripping direction leads the voltage applied to the relay potential coil with due

Paper 50-233, recommended by the AIEE Relay Committee and approved by the AIEE Technical Program Committee for presentation at the AIEE Fall General Meeting, Oklahoma City, Okla., October 23–27, 1950. Manuscript submitted July 26, 1950; made available for printing August 23, 1950.

W. K. Sonnemann is with the Westinghouse Electric Corporation, Newark, New Jersey.

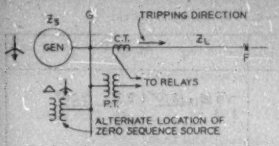

Figure 1. System diagram showing relay location and system constants

consideration given to the polarity of the relay coils. In order that no confusion will exist with regard to what is meant by the terminology used in describing the four commonly used connections, Table IV identifies these connections in terms of the voltage and current used on each relay. In this table, as well as throughout this paper, the double subscript voltage notation used is in accordance with the concept recently recommended to the AIEE Standards Committee for consideration as a recommended standard practice, the sense of which is that when the vector quantity so represented is to be considered as being in the positive half cycle, there is a drop in potential from the terminal of the first subscript to the terminal of the second subscript. Similarly, the single subscript notation used with the currents identify them by phases and in the sense that the vector quantities (currents) so represented are to be considered positive when actually flowing through the line in the tripping direction.

Method of Approach

In the great majority of cases, a sufficient answer is obtained if it is determined whether the torque on the directional element is contact opening or contact closing. This might be termed a qualitative analysis, and is determined purely by the relative phase angle between the current and the voltage applied to the relay and a consideration of the phase-angle characteristics of the relay. In a quantitative analysis, it would be necessary to multiply together the magnitudes of the voltage and current and some function of the phase angle between them as modified by the angle by which the maximum torque line of the relay leads the reference voltage vector, thus determining the magnitude of the torque as well as its direction. The qualitative analysis method serves the purpose, remembering that if the voltage is zero, the directional element will not operate anyway, and this method greatly simplifies the problem. The question then becomes that of determining the relative phase angle between the current and voltage applied to the various relays for the various connections for the various faults. To illustrate the method used, consider relay A operating with the 90-degree connection. It is actuated by the voltage V_{bc} and the current I_a. We may arbitrarily write

$$Z_D = \frac{V_{bc}}{I_a} \tag{1}$$

in which Z_D represents an artificial impedance value obtained by dividing V_{bc} by I_a. Recalling the principles of vector algebra, it is remembered that when the operation is done in polar form, the characteristic angle of the quotient (Z_D) is obtained by subtracting the angle of the denominator (I_a) from the angle of the numerator (V_{bc}). Using the mathematicians' concept for positive angle, it is clear that when this is done, the resulting angle characteristic of Z_D will be that angle by which V_{bc} leads I_a, or, conversely, the angle by which I_a lags V_{bc}. This is exactly the kind of answer that is wanted to determine directional element operation.

It was found through making a general analysis by the method of symmetrical components that the relay voltage and relay current could be reduced to terms involving only the source voltage and the system impedance constants such that when one is divided by the other, the source voltage cancels out and the remaining expression consists of one or more system impedance values together with complex operators. With the expression for Z_D thus being reduced to a function of impedance, it is possible to substitute the appropriate values for the impedances involved for any particular system location and determine the characteristic angle for Z_D for that particular condition, and thereby determine the angle by which the relay current lags the relay voltage. The work of deriving the Z_D formulas for the 86 facets of the problem is given in the Appendixes. All quantities are kept in primary terms, neglecting the instrument transformer ratios.

Tabulation of Results

Tables I, II, and III show the final form of the Z_D formulas. These formulas are applicable to any system which can be reduced to a simplified equivalent represented by Figures 1, 2, or 3, respectively. These three figures are believed to be adequate to represent the portion of interest of any system. While it is possible to make specific applications of the formulas to fit particular conditions, it is desirable to study the formulas in general

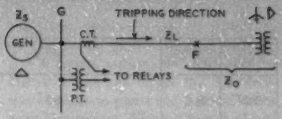

Figure 2. System with zero sequence source concentrated at opposite end of transmission line

terms on the basis of determining the maximum possible spread of possibilities. This has been done and the results are shown in Tables V, VI, and VII, corresponding respectively to Tables I, II, and III, and Figures 1, 2, and 3. In Tables V, VI, and VII the relay voltage vector is shown as the reference vector in each case, extending along the x-axis, and the maximum spread of angular position of the current with respect to it, either leading or lagging or both, is shown by the shaded area and with symbolic notation that will be explained.

Systems Studied

Figure 1 represents the simplest system layout wherein the relays at bus G protect the line from G to the fault at F. In general terms, Z_L represents the impedance of the line to the point of fault and includes the arc resistance, if any. The source is represented schematically by the generator having an impedance Z_S. The positive and negative sequence source circuit may or may not include the zero sequence source circuit, so that an alternate location is shown for the latter, illustrating the freedom of variation of sequence source impedances. This figure is adaptable to a section of any system not otherwise bound to be considered in line with Figures 2 or 3. For example, a system section (not shown) feeding the fault from the right-hand side and having similar sequence current distribution factors will not affect the section shown other than through increasing the apparent magnitude of the arc resistance. This contingency is taken care of by the freedom of variation of the line impedance Z_L in the formulas. Again, other ties be-

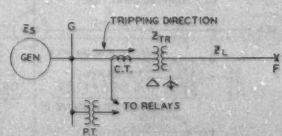

Figure 3. System with transformer bank located between the relay and the fault

Table I. System Figure 1—Z_D Values

CONNECTIONS	PHASES FAULTED	RELAY A	RELAY B	RELAY C
90°	BC	∞	$\sqrt{3}\,Z_{1S}\angle 270^\circ + 2Z_{1L}\angle 240^\circ$	$\sqrt{3}\,Z_{1S}\angle 270^\circ + 2Z_{1L}\angle 300^\circ$
	A-G	$\frac{1}{\sqrt{3}}\left[2Z_{1S}+Z_{0S}+2Z_{1L}+Z_{0L}\right]\angle 270^\circ$	∞	∞
	BC-G	∞	$\frac{\sqrt{3}\,AZ_{1S}\angle 330^\circ + (1+2A)Z_{1L}\angle 300^\circ}{1+A\angle 60^\circ}$	$\frac{\sqrt{3}\,AZ_{1S}\angle 210^\circ + (1+2A)Z_{1L}\angle 240^\circ}{1+A\angle 300^\circ}$
	ABC	$\sqrt{3}\,Z_{1L}\angle 270^\circ$		
60°•1	BC	$\sqrt{3}\,Z_{1S}\angle 270^\circ + 2Z_{1L}\angle 240^\circ$	$\frac{\sqrt{3}}{2}Z_{1S}\angle 270^\circ + Z_{1L}\angle 300^\circ$	$2Z_{1L}$
	A-G	$\frac{1}{\sqrt{3}}\left[Z_{1S}\angle 270^\circ + (Z_{0S}+2Z_{1L}+Z_{0L})\angle 330^\circ\right]$	∞	$\frac{1}{\sqrt{3}}\left[2Z_{1S}+Z_{0S}+2Z_{1L}+Z_{0L}\right]\angle 270^\circ$
	BC-G	$\frac{\sqrt{3}\,AZ_{1S}\angle 330^\circ + (1+2A)Z_{1L}\angle 300^\circ}{1+A\angle 60^\circ}$	$\frac{\sqrt{3}\,AZ_{1S}\angle 270^\circ + (1+2A)Z_{1L}\angle 300^\circ}{1+2A}$	$\frac{(1+2A)Z_{1L}\angle 300^\circ}{1+A\angle 300^\circ}$
	ABC	$Z_{1L}\angle 300^\circ$		
60°•2	BC	∞	$\frac{2}{\sqrt{3}}\left[Z_{1S}+Z_{1L}\right]\angle 270^\circ$	$\frac{1}{\sqrt{3}}\left[Z_{1S}\angle 270^\circ + 2Z_{1L}\angle 330^\circ\right]$
	A-G	$\frac{1}{\sqrt{3}}\left[Z_{1S}\angle 270^\circ + Z_{0S}\angle 330^\circ\right] + \frac{1}{3}\left[2Z_{1L}+Z_{0L}\right]\angle 300^\circ$	∞	∞
	BC-G	∞	$\frac{1}{\sqrt{3}}\left[\frac{2AZ_{1S}+Z_{0S}+(1+2A)Z_{1L}}{1+A\angle 60^\circ}\right]\angle 330^\circ$	$\frac{1}{\sqrt{3}}\left[\frac{AZ_{1S}\angle 210^\circ + Z_{0S}\angle 300^\circ + (1+2A)Z_{1L}\angle 270^\circ}{1+A\angle 300^\circ}\right]$
	ABC	$Z_{1L}\angle 300^\circ$		
30°	BC	∞	$\sqrt{3}\,Z_{1S}\angle 270^\circ + 2Z_{1L}\angle 300^\circ$	$2Z_{1L}$
	A-G	$\frac{1}{\sqrt{3}}\left[Z_{1S}\angle 270^\circ + (Z_{0S}+2Z_{1L}+Z_{0L})\angle 330^\circ\right]$	∞	∞
	BC-G	∞	$\frac{\sqrt{3}\,AZ_{1S}\angle 330^\circ + (1+2A)Z_{1L}}{1+A\angle 60^\circ}$	$\frac{(1+2A)Z_{1L}\angle 300^\circ}{1+A\angle 300^\circ}$
	ABC	$\sqrt{3}\,Z_{1L}\angle 330^\circ$		

tween a system section to the right of the fault and the bus G have the effect of changing the value of the source impedance Z_g to use in the formulas as the fault is moved down the line.

There is one effect of a source circuit to the right of the fault which is not adequately represented in Figure 1 and the formulas pertaining thereto, as follows. With a relatively low zero sequence impedance in the grounding source connected to bus G, there tends to be a preponderance of zero sequence current in the line compared to positive and negative sequence currents as faults involving ground are moved closer to the bus G, and to a degree depending upon the magnitude of the positive and negative sequence source impedances to the right of the fault compared with those to the left of the relay. This is illustrated in more detail in Figure 4, fault location 1. With a preponderance of zero sequence current from the left, the effect will be to produce fault current in B and C phases for a phase-A-to-ground fault, and in A phase for a phase-B-to-C-to-ground fault. The formulas in this paper do not take care of this situation. It is dismissed from analysis in this paper in view of the fact that such an analysis does not appear to be strictly necessary for the following reasons:

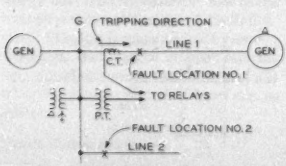

Figure 4. System showing alternate fault locations

First, it is the prime function of a protective relay to operate when the fault lies in its protected section. Single-phase-to-ground faults are to be cleared by ground relays and they may be eliminated from further consideration because this paper is concerned with directional elements for phase relays. Two-phase-to-ground faults, however, do lie within the domain of phase relays but generally more so when the system is grounded through an impedance. In this illustration the zero sequence impedance connected to bus G is low, no additional impedance being used in the neutral, or else the effect under discussion would exist only to a limited extent. Under these conditions, it may be properly expected that for the more aggravated conditions, even the 2-phase-to-ground fault may or should be properly cleared by the ground relay because of the magnitude of the zero sequence current. With all of this shifting the responsibility to the ground relay, however, it is believed as a result of a separate vector analysis not included here that the preponderance of zero sequence current for a close in fault involving ground would not prevent the correct phase relay directional element from operating.

Secondly, it is a function of protective relays not to trip when the fault is in some other location. If one of the 3-phase relays gives an incorrect directional indication for fault location 1 in Figure 4, it is of no consequence as long as tripping is obtained by another relay. The question then arises if the incorrect

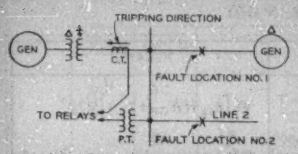

Figure 5. System diagram showing relay location requiring special consideration

indication can cause false tripping if the fault is back of the relay, as in fault location 2. There are two answers to this question. The answer for the relay location as shown in Figure 4 is that the conditions affecting the relays at bus G on line 1 are completely changed by a fault at location 2 on line 2. The preponderance of zero sequence current disappears from all parts of line 1, and the analysis of relay action for this case is made by considering the relays of Figure 2 in reverse.

The second answer is involved when the relay location is as shown in Figure 5, and connected for the tripping direction as shown. In this case, with fault location 1 or 2, and with a heavy preponderance of zero sequence current from the left, it appears quite likely that false tripping might result with three of the commonly used connections, which are the 90 degree, the 60 degree number 2, and the 30 degree. This is because of the tendency of the large zero sequence components to draw the three line currents together in phase position, and since these are used with three different voltages in the three different elements, it appears that at least one is likely to operate incorrectly. If the connection identified as 60 degree number 1 is used, however, the difficulties are removed inasmuch as the relay is then not sensitive to zero sequence components, either current or voltage.

Figure 2 represents the opposite condition to that discussed for Figures 1, 4, and 5 in that all of the zero sequence comes from the far end of the line so that the relays are operable from positive and negative sequence currents only. Since the result of this study can be applied in reverse to cover fault location 2 in Figure 4, it is important that all directional elements associated with fault detecting elements (such as overcurrent elements, impedance elements, and so forth) receiving enough current to operate should give a correct indication. The study of Figure 2 does not repeat the consideration of phase-to-phase and 3-phase faults, as in this respect, Figure 2 is a duplicate of Figure 1.

Figure 3 represents a typical condition wherein a delta star connected transformer bank is interposed between the relay location and the fault. Here again, it is important that all directional elements associated with fault detecting elements receiving enough current to operate should give a correct indication inasmuch as the conditions affecting the relays of Figure 3 may be applied in reverse to other relays at bus G protecting source circuits feeding into bus G.

The study of Figure 3 has been based on the connections as shown schematically in that the star side of the bank is connected to the line. Further, the line voltages X, Y, Z, lead the bus voltages A, B, C by 30 degrees in accordance with American Standards Association standard practice based on the line having the higher voltage. Other combinations were

Table II. System Figure 2—Z_D Values

CONNECTIONS	PHASES FAULTED	RELAY A	RELAY B	RELAY C
90°	A-G BC-G	$\frac{\sqrt{3}}{2} Z_T \angle 270^\circ$ $\sqrt{3}(1+2A) Z_{1L} \angle 270^\circ$	$\frac{\sqrt{3}\left[Z_{1S}\angle 270^\circ + (Z_0 + 2Z_{1L})\angle 330^\circ\right]}{1+\sqrt{3}A\angle 30^\circ}$ $\frac{3A Z_{1S}\angle 300^\circ + \sqrt{3}(1+2A) Z_{1L}\angle 270^\circ}{1+\sqrt{3}A\angle 30^\circ}$	$\frac{\sqrt{3}\left[Z_{1S}\angle 270^\circ + (Z_0 + 2Z_{1L})\angle 210^\circ\right]}{1+\sqrt{3}A\angle 330^\circ}$ $\frac{3A Z_{1S}\angle 240^\circ + \sqrt{3}(1+2A) Z_{1L}\angle 270^\circ}{1+\sqrt{3}A\angle 330^\circ}$
60° #1	A G BC-G	$\frac{\frac{1}{\sqrt{3}}\left[Z_{1S}\angle 270^\circ + (Z_0 + 2Z_{1L})\angle 330^\circ\right]}{1+A\angle 60^\circ}$ $\frac{\sqrt{3}A Z_{1S}\angle 330^\circ + (1+2A) Z_{1L}\angle 300^\circ}{1+A\angle 60^\circ}$	∞ $\frac{\sqrt{3}A Z_{1S}\angle 270^\circ + (1+2A) Z_{1L}\angle 300^\circ}{1+2A}$	$\frac{\frac{1}{\sqrt{3}} Z_T \angle 270^\circ}{1+A\angle 300^\circ}$ $\frac{(1+2A) Z_{1L}\angle 300^\circ}{1+A\angle 300^\circ}$
60° #2	A-G BC-G	$\frac{1}{2}\left[\sqrt{3} Z_{1S}\angle 270^\circ + \sqrt{3} Z_0\angle 330^\circ + 2Z_{1L}\angle 300^\circ\right]$ $(1+\sqrt{3}A\angle 330^\circ) Z_{1L}\angle 300^\circ$	$2 Z_{1L}$ $\frac{\sqrt{3}A Z_{1S}\angle 300^\circ + (1+3A) Z_{1L}\angle 300^\circ}{1+\sqrt{3}A\angle 30^\circ}$	$\sqrt{3} Z_{1S}\angle 270^\circ + \sqrt{3} Z_0\angle 210^\circ + 2Z_{1L}\angle 240^\circ$ $(1+\sqrt{3}A\angle 30^\circ) Z_{1L}\angle 300^\circ$
30°	A-G BC-G	$\frac{\sqrt{3}}{2}\left[Z_{1S}\angle 270^\circ + (Z_0 + 2Z_{1L})\angle 330^\circ\right]$ $3A Z_{1S} + \sqrt{3}(1+2A) Z_{1L}\angle 330^\circ$	$\frac{\sqrt{3}\left[Z_{1S}\angle 90^\circ + (Z_0 + 2Z_{1L})\angle 30^\circ\right]}{1+\sqrt{3}A\angle 30^\circ}$ $\frac{3A Z_{1S}\angle 300^\circ + \sqrt{3}(1+2A) Z_{1L}\angle 330^\circ}{1+\sqrt{3}A\angle 30^\circ}$	$\sqrt{3} Z_T \angle 270^\circ$ $\frac{\sqrt{3}(1+2A) Z_{1L}\angle 330^\circ}{1+\sqrt{3}A\angle 330^\circ}$

Table III. System Figure 3—Z_D Values

CONNECTIONS	PHASES FAULTED	RELAY A	RELAY B	RELAY C
90°	YZ	$\sqrt{3}\left[Z_{1S}\angle 270^\circ + 2(Z_{1TR}+Z_{1L})\angle 330^\circ\right]$	$\sqrt{3}\left[Z_{1S}\angle 270^\circ + 2(Z_{1TR}+Z_{1L})\angle 210^\circ\right]$	$\sqrt{3}\left[Z_{1S}+(Z_{1TR}+Z_{1L})\right]\angle 270^\circ$
	X-G	$\sqrt{3}Z_{1S}\angle 270^\circ + \left[2Z_{1TR}+2Z_{1L}+Z_0\right]\angle 240^\circ$	$\sqrt{3}Z_{1S}\angle 270^\circ + \left[2Z_{1TR}+2Z_{1L}+Z_0\right]\angle 300^\circ$	∞
	YZ-G	$\dfrac{\sqrt{3}\left[AZ_{1S}\angle 210^\circ + (1+2A)(Z_{1TR}+Z_{1L})\angle 270^\circ\right]}{1+A\angle 300^\circ}$	$\dfrac{\sqrt{3}\left[AZ_{1S}\angle 330^\circ + (1+2A)(Z_{1TR}+Z_{1L})\angle 270^\circ\right]}{1+A\angle 60^\circ}$	$\dfrac{\sqrt{3}\left[2AZ_{1S}+(1+2A)(Z_{1TR}+Z_{1L})\right]\angle 270^\circ}{1+2A}$
	XYZ	$\sqrt{3}(Z_{1TR}+Z_{1L})\angle 270^\circ$		
60°#1	YZ	∞	$\frac{2}{\sqrt{3}}\left[Z_{1S}+(Z_{1TR}+Z_{1L})\right]\angle 270^\circ$	$\frac{1}{\sqrt{3}}\left[Z_{1S}\angle 270^\circ + 2(Z_{1TR}+Z_{1L})\angle 330^\circ\right]$
	X-G	$\frac{1}{2}\left[\sqrt{3}Z_{1S}\angle 270^\circ + (2Z_{1TR}+2Z_{1L}+Z_0)\angle 300^\circ\right]$	$2Z_{1TR}+2Z_{1L}+Z_0$	$\sqrt{3}Z_{1S}\angle 270^\circ + \left[2Z_{1TR}+2Z_{1L}+Z_0\right]\angle 240^\circ$
	YZ-G	$AZ_{1S}+(1+2A)(Z_{1TR}+Z_{1L})\angle 300^\circ$	$\dfrac{\left[2AZ_{1S}+(1+2A)(Z_{1TR}+Z_{1L})\right]\angle 300^\circ}{1+\sqrt{3}A\angle 30^\circ}$	$\dfrac{AZ_{1S}\angle 240^\circ + (1+2A)(Z_{1TR}+Z_{1L})\angle 300^\circ}{1+\sqrt{3}A\angle 330^\circ}$
	XYZ	$(Z_{1TR}+Z_{1L})\angle 300^\circ$		
60°#2	YZ	$2(Z_{1TR}+Z_{1L})$	$\sqrt{3}Z_{1S}\angle 270^\circ + 2(Z_{1TR}+Z_{1L})\angle 240^\circ$	$\frac{\sqrt{3}}{2}Z_{1S}\angle 270^\circ + (Z_{1TR}+Z_{1L})\angle 300^\circ$
	X-G	$\frac{2}{\sqrt{3}}\left[Z_{1S}+Z_{1TR}+Z_{1L}+\frac{1}{2}Z_0\right]\angle 270^\circ$	$\frac{1}{\sqrt{3}}\left[Z_{1S}\angle 270^\circ + (2Z_{1TR}+2Z_{1L}+Z_0)\angle 330^\circ\right]$	∞
	YZ-G	$\dfrac{(1+2A)(Z_{1TR}+Z_{1L})\angle 300^\circ}{1+A\angle 300^\circ}$	$\dfrac{\sqrt{3}AZ_{1S}\angle 330^\circ + (1+2A)(Z_{1TR}+Z_{1L})\angle 300^\circ}{1+A\angle 60^\circ}$	$\dfrac{\sqrt{3}AZ_{1S}\angle 270^\circ + (1+2A)(Z_{1TR}+Z_{1L})\angle 300^\circ}{1+2A}$
	XYZ	$(Z_{1TR}+Z_{1L})\angle 300^\circ$		
30°	YZ	$\sqrt{3}\left[Z_{1S}\angle 90^\circ + 2(Z_{1TR}+Z_{1L})\angle 30^\circ\right]$	$2\sqrt{3}\left[Z_{1S}+(Z_{1TR}+Z_{1L})\right]\angle 270^\circ$	$\sqrt{3}\left[Z_{1S}\angle 270^\circ + (Z_{1TR}+Z_{1L})\angle 330^\circ\right]$
	X-G	$\sqrt{3}Z_{1S}\angle 270^\circ + (2Z_{1TR}+2Z_{1L}+Z_0)\angle 300^\circ$	$2Z_{1TR}+2Z_{1L}+Z_0$	∞
	YZ-G	$\dfrac{\sqrt{3}\left[AZ_{1S}\angle 30^\circ + (1+2A)(Z_{1TR}+Z_{1L})\angle 330^\circ\right]}{1+A\angle 300^\circ}$	$\dfrac{\sqrt{3}\left[2AZ_{1S}\angle 330^\circ + (1+2A)(Z_{1TR}+Z_{1L})\angle 330^\circ\right]}{1+A\angle 60^\circ}$	$\dfrac{\sqrt{3}\left[AZ_{1S}\angle 270^\circ + (1+2A)(Z_{1TR}+Z_{1L})\angle 330^\circ\right]}{1+2A}$
	XYZ	$\sqrt{3}(Z_{1TR}+Z_{1L})\angle 330^\circ$		

considered, such as star (low-voltage) to delta (high-voltage), and with the non-standard condition of the 30-degree lagging relationship. It was found that the same results were obtained, the only difference being that when the 30 degree lagging connections were used, the formulas became associated with relays for different phases. Hence it follows that what is the best connection for Figure 3 also is the best for the other possible transformer connections.

The Search for Limits

With the formulas derived as shown in Tables I, II, and III it became desirable to analyze these formulas to determine the maximum spread in phase angle between the current and the voltage. The results of this study are shown in Tables V, VI, and VII. Several of the vector diagrams in these tables will now be discussed in order to clarify the method of analysis used as well as the peculiar notation used with the diagrams. Dash lines in the table mean that that particular relay received no current for the fault in question. Blank spaces in the B and C relay columns for the 3-phase fault, ABC, indicate that the consideration given one relay, relay A, is sufficient.

Remembering that Table V is associated with Table I and Figure 1, it is determined that the diagram for relay B, line 1 (90-degree connection, phase-B-to-C fault) comes from the formula

$$Z_D = \sqrt{3}Z_{1S}\angle 270^\circ + 2Z_{1L}\angle 240^\circ \qquad (2)$$

The angle of Z_D is the angle by which the current lags the voltage, so that the current vector will be plotted clockwise from the reference voltage vector by whatever positive angle results from evaluating equation 2. The impedance terms Z_{1S} and Z_{1L} are the positive sequence impedances of the source and the line, respectively. The expressions $\angle 270^\circ$ and $\angle 240^\circ$ are mathematical operators producing a positive angular rotation of the amount indicated. In this particular formula, $-j$ could have been used for $\angle 270^\circ$ and the a^2 operator of symmetrical components could have been used for $\angle 240^\circ$. These two substitutions were not made, however, because so many of the other formulas contain operators in steps of 30 degrees that is was considered preferable to keep all of the operators in this form.

Equation 2 is to be studied for limits. One limit is apparent immediately in that if the fault is close enough, Z_{1L} becomes zero and all that is left is $\sqrt{3}Z_{1S}\angle 270^\circ$.

Table IV. Table of Connections

CONNECTIONS	RELAY A		RELAY B		RELAY C	
	VOLTAGE	CURRENT	VOLTAGE	CURRENT	VOLTAGE	CURRENT
90°	V_{bc}	I_a	V_{ca}	I_b	V_{ab}	I_c
60° NO.1	V_{ac}	I_a-I_b	V_{ba}	I_b-I_c	V_{cb}	I_c-I_a
60° NO.2	$-V_{cn}$	I_a	$-V_{an}$	I_b	$-V_{bn}$	I_c
30°	V_{ac}	I_a	V_{ba}	I_b	V_{cb}	I_c

Table V. System Figure 1

CONNECTIONS	PHASES FAULTED	RELAY A	RELAY B	RELAY C
90°	BC	—		
	AG		—	—
	BC-G	—		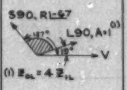
	ABC			
60°*1	BC	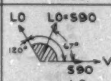		
	AG		—	
	BC-G	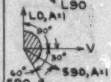		
	ABC			
60°*2	BC	—		
	A-G		—	—
	BC-G	—		
	ABC			
30°	BC	—		
	A-G		—	—
	BC-G	—		
	ABC			

The source cannot have an angle greater than 90 degrees, so if we take 90 degrees for the angle of the source impedance and rotate it by $\underline{/270°}$, the answer comes out at an angle of 360 or zero degrees. This is the characteristic angle of Z_D and thus means that the current and voltage are in phase. Referring to the vector diagram in Table V, it will be seen that a current vector has been drawn in phase with the voltage vector, and the notation for it is *S*90. This notation means that the source impedance (*S* for source) governs for this limit, and that it has an angle of 90 degrees.

Assume that the source impedance has an angle of 60 degrees. Adding 60 to 270 degrees yields 330 degrees, meaning that the current lags the voltage by 330 degrees (leads by 30 degrees) and such a current vector would fall in the shaded area, not establishing a limit, and hence was not plotted.

For this case, equation 2, the maximum possible angular position was found by assuming that the fault is close in and involves an arc of great length so that the impedance of the line is not only at 0 degrees, but also so large that the impedance of the source becomes negligible. In this case, through neglecting Z_{1S}, the expression for Z_D is evaluated by considering the second term of equation 2, or $2Z_{1L}\underline{/240°}$, and with Z_{1L} having its own angle of zero degrees, it follows that the current leads the voltage by 120 degrees.

Another current vector is shown accordingly in the vector diagram, and wherein the notation *LO* signifies that the line impedance governs and that it has an angle of zero degrees. It was felt that it was a bit pessimistic to lean too heavily on the limit thus established because this calls for the arcing fault to absorb the entire system voltage, even though arcs on horizontally spaced lines approaching full system voltage have been reported. Consequently, a compromise condition was evaluated as shown by the current vector at 67 degrees leading, wherein the notation $LO = S90$ means that the line impedance at zero degrees (all arc) was taken numerically equal to the source impedance at 90 degrees and Z_D evaluated accordingly, giving due attention to the $\sqrt{3}$ and 2 factors. This would account for the arc absorbing somewhat more than half of the available voltage. Other intermediate vectors representing alternate conditions are occasionally used in other diagrams throughout these tables.

The method of analyzing the formulas is thus established as a study to determine what possible impedance values, both in

angle and in magnitude, can be utilized to yield the maximum angle and the minimum angle in either direction, and anything of a more reasonable nature as a limit in between.

As might be expected, the 2-phase-to-ground fault condition was more difficult to handle, both in derivation and analysis, than the other three combined. The only practical way which could be found was to introduce a factor A, a real or complex number, letting

$$A = \frac{Z_0}{Z_1} \tag{3}$$

in which Z_0 and Z_1 represents the final equivalent single impedances for the entire zero and positive sequence networks, respectively, as used in calculating the fault current components. The factor A is thus a ratio, and may vary from slightly more than zero to a very large number. In general, however, its possibilities were considered on the basis of it being either 0+ or 1. Large values of A make the 2-phase-to-ground fault approach the conditions of a phase-to-phase fault, as may be verified by comparing the formulas. (The one case where this does not hold true is for the 60°, number 2 connection, Figures 1 and 2, which received the necessary special attention.)

Typical of a case where A is taken at 0+, consider Relay B, line 3, Table V. The formula is

$$Z_D = \frac{\sqrt{3}AZ_{1S}\underline{/330^\circ} + (1+2A)Z_{1L}\underline{/300^\circ}}{1+A\underline{/60^\circ}} \tag{4}$$

Consider the limiting condition when the line impedance is zero so that the second term of the numerator drops out. Now assume that A is very small, and a real number (meaning that Z_0 and Z_1 have the same angle). The denominator is then practically unity and may be neglected. This leaves the angle to be determined by $Z_{1S}\underline{/330^\circ}$, and with a 90-degree source circuit, this yields 60 degrees for current lagging voltage. A current vector is accordingly shown at this angle in the vector diagram with the notation $S90$, $A=0+$.

It is of importance of note that the magnitude of Z_D, heretofore not discussed, is a measure of the ratio of the voltage to the current. If this ratio becomes low enough, the relay will not operate. The condition just discussed approaches this condition, where $A=0+$. An auxiliary condition was calculated for $A=1$, a real number, yielding an angle of 30 degrees lagging, which has been shown.

A value of $A=1$ can be obtained three ways. First, at zero line impedance, the ratio of source impedances can be unity.

Table VI. System Figure 2

CONNECTIONS	PHASES FAULTED	RELAY A	RELAY B	RELAY C
90°	A-G	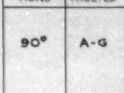	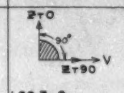	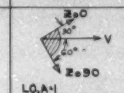
	BC-G	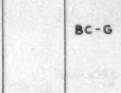	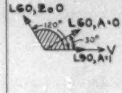	
60° #1	A-G	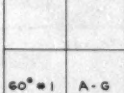	—	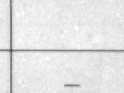
	BC-G	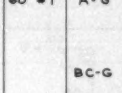		
60° #2	A-G	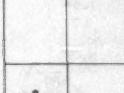	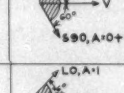	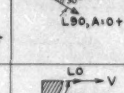
	BC-G	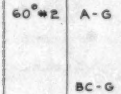	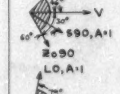	
30°	A-G	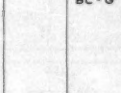	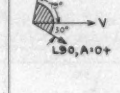	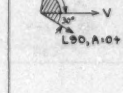
	BC-G	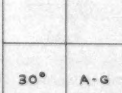	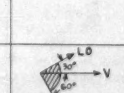	

Secondly, if the line impedance is represented by a high value of arc resistance, A automatically becomes one. Such a condition forms the 90-degree current leading limit for the diagram under discussion. Thirdly, an assumption has been made that, for the sake of even figures, the zero sequence impedance of the line is equal to four times the positive sequence impedance, hence if the fault is appropriately located a sufficient distance down the line, A becomes unity, even with a low zero sequence source impedance.

Transferring attention to the diagram for Relay C, line 3, Table V, a new symbol $R\underline{/-67^\circ}$ is discovered. It represents the maximum angular rotating effect of -67 degrees which could be discovered by trial calculations for the portion $A/1+A\underline{/300^\circ}$ of the formula for this relay as applied to the Z_{1S} term with $Z_{1L}=0$ and in which A is a complex number occasioned by the existence of a resistance to ground in the fault affecting the zero sequence network only, as illustrated by R_g in Figure 6. The R factor appears again at different points in these tables representing the same type of operation with

Table VII. System Figure 3

CONNECTIONS	PHASES FAULTED	RELAY A	RELAY B	RELAY C
90°	YZ			
	X-G			—
	YZ-G			
	XYZ			
60°#1	YZ	—		
	X-G			
	YZ-G			
	XYZ			
60°#2	YZ			
	X-G			—
	YZ-G			
	XYZ			
30°	YZ			
	X-G			—
	YZ-G			
	XYZ			

angular values appropriate to the occasion. In all cases where the R factor was used, it was evaluated on the basis that the source impedances were at angles of 90 degrees lag and that $Z_{0S}=0.05Z_{1S}$. In the same vector diagram (Relay C, line 3, Table V) the factor A is used equal to 1 based on $Z_{0L}=4Z_{1L}$.

The 2-phase-to-ground fault condition is particularly tricky to handle for the 60°, number 2 connection by virtue of the fact that the fault condition in itself is complicated enough, and with the relay using phase-to-ground voltage for polarization, the analysis becomes tedious. In this case, the R_f value Figure 6 is likely to become quite important, as may be seen by the 150-degree angle shown for Relay C, Table V, line 11. This diagram also shows a case where it was desirable to consider values for A of 1, 4, and infinity.

Other symbolic notation used in these tables is explained as follows:

$L=0$ means that the line has no impedance, contrasting with the symbol LO described previously.

Z_{0S} denotes the zero sequence impedance in the source up to the relay, while Z_0 denotes the total zero sequence network.

Z_T represents the total of all impedances used in making the initial fault current calculation, as for example, in calculating a single-phase-to-ground fault $Z_T=Z_1+Z_2+Z_0$.

Z_{TR} represents the impedance of the transformer in Figure 3.

In preparing Table VII for Figure 3, it was necessary in some cases to assume a very low limit for the impedance of the transformer, but not zero. In such cases, it was assumed equal to 5 per cent of the positive sequence source impedance and is so indicated.

Summary of Results

The vector diagrams now may be studied in the light of directional element phase angle characteristics either as they are, or as they should be.

Considering the 90-degree connection first, it will be recalled that when this connection is used, the relay is usually equipped with phase shifting means to put the zero torque line at 45 degrees lagging—135 degrees leading, and the directional element therefore has maximum torque when the current leads the voltage by 45 degrees. A study of the vector diagrams reveals three cases where the current falls in the contact opening zone by being either more than 45 degrees lagging or more than 135 degrees leading. These

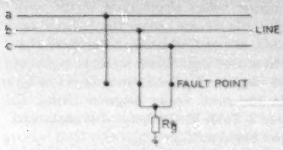

Figure 6. Location of fault resistance affecting zero sequence network only

are (1) Relay *B*, *BC-G* fault, System Figure 1; (2) Relay *C*, *A-G* fault, System Figure 2; and (3) Relay *B*, *YZ* fault, System Figure 3. The last two cases may be dismissed as nontroublesome on the basis that the conditions assumed for these limits are associated with such low current values that the fault detecting element can hardly be expected to operate. In case of doubt, the formulas may be used to investigate particular conditions short of the limits shown here. In the first case, however, a hazard of possible false operation does exist when the relay location is as shown in Figure 5 and with the fault back of the relay as in location 1 or 2. It will be remembered that for this location, a previous discussion gave the 60-degree, number 1 connection a preference for other reasons

The 60-degree, number 1 connection is generally used with an element having a watt-type characteristic, which means that the zero torque line falls at 90 degrees leading and lagging the reference voltage, with a maximum contact closing torque produced when the current and voltage are in phase. With this type of characteristic, the only possibilities of trouble are for Relay *A*, *BC* fault, System Figure 1, and for Relay *C*, *X-G* fault, System Figure 3. In each of these cases it is doubtful if the fault detecting element will receive enough current to operate.

In the case of the 60-degree, number 2 connection, if a watt-type element is used, the first possibility of trouble is encountered in connection with System Figure 1, *BC-G* fault, Relay *C*, for the condition of $R_g=0+$, $A=0+$, $L=0$, where an incorrect directional indication would obtain. This fault would be cleared by relay *B* acting alone. The problem of the incorrect indication of relay *C* causing a false trip out is, once again, limited to a location as shown by Figure 5. Other cases where the current leads the voltage by more than 90 degrees are discovered for System Figure 2, *A-G* fault, Relay *C*, and System Figure 3, *YZ* fault, Relay *B*. The possibility of causing a false trip out by approaching these limits depends on the magnitude of current involved as it affects the fault detecting element.

The 30-degree connection remains free of trouble only as long as the application is described by System Figure 1. If applied as shown by Figures 2 or 3, it is easily seen that erroneous directional indications will result with probable current magnitudes within the range of operation of the fault detecting element, thus leading to false tripping.

Conclusions

1. The general practice of shifting the angle of maximum torque to approximately 45 degrees leading for the 90-degree connection appears to give the best characteristic to fit the spread of possible phase angles.
2. A watt-type element appears to be best suited to the three remaining types of connections.
3. Each connection theoretically involves possibility of trouble in certain extreme cases.
4. The 30-degree connection is not suited to systems as shown by Figures 2 and 3.

General Notes on Derivation of Formulas

The following appendixes I, II, and III, cover the calculation of the necessary fault currents and voltages for the four types of faults, following which the Z_D formulas appropriate to the several relay connections are derived for enough cases to illustrate the method. The sequence network connections for the various fault calculations are not shown as it is taken for granted that those who check this work will be familiar with the method of symmetrical components.

The following remarks, however, are appropriate.

V_a' represents the generated voltage which causes the fault current to flow.

Subscripts 1, 2, and 0 denote positive, negative, and zero sequence, respectively, as applied to current, voltage, or impedance.

Subscripts *S* and *L* denote source and line, respectively.

Impedance symbols with 1, 2, or 0 subscripts only denote the total impedance of the respective positive, negative, or zero sequence network to the point of fault.

The relay voltages are calculated for the bus *G*.

A is the ratio Z_0/Z_1.

For simplicity, phase-to-ground voltages at bus *G* are written without the second subscript, V_a instead of V_{ag}.

Appendix I. System Figure 1

$Z_1=Z_{1S}+Z_{1L}$
$Z_2=Z_1$
$Z_0=Z_{0S}+Z_{0L}$

Phase-to-Phase Fault on Phases BC

Calculate currents and voltages

$$I_{a1}=-I_{a2}=\frac{V_a'}{Z_T}=\frac{V_a'}{Z_1+Z_2} \tag{5}$$

$$I_a=I_{a1}+I_{a2}=0 \tag{6}$$

$$I_b=a^2I_{a1}+aI_{a2}=\frac{V_a'}{Z_T}(\underline{/240^\circ}+\underline{/300^\circ})=\frac{V_a'}{Z_T}\sqrt{3}\,\underline{/270^\circ} \tag{7}$$

$$I_c=aI_{a1}+a^2I_{a2}=\frac{V_a'}{Z_T}(\underline{/120^\circ}+\underline{/60^\circ})=\frac{V_a'}{Z_T}\sqrt{3}\underline{/90^\circ} \tag{8}$$

$$I_a-I_b=\frac{V_a'}{Z_T}\sqrt{3}\underline{/90^\circ} \tag{9}$$

$$I_b-I_c=\frac{V_a'}{Z_T}2\sqrt{3}\underline{/270^\circ} \tag{10}$$

$$I_c-I_a=\frac{V_a'}{Z_T}\sqrt{3}\underline{/90^\circ} \tag{11}$$

Voltages at relay location, bus *G*

$$V_{a1}=V_a'-I_{a1}Z_{1S}=V_a'-\frac{V_a'}{Z_T}Z_{1S}=\frac{V_a'}{Z_T}(Z_T-Z_{1S})=\frac{V_a'}{Z_T}(Z_{1S}+2Z_{1L}) \tag{12}$$

$$V_{a2}=-I_{a2}Z_{2S}=\frac{V_a'}{Z_T}Z_{1S} \tag{13}$$

$$V_a=V_{a1}+V_{a2}=\frac{V_a'}{Z_T}(2Z_{1S}+2Z_{1L}) \tag{14}$$

$$V_b=a^2V_{a1}+aV_{a2}=\frac{V_a'}{Z_T}(a^2Z_{1S}+2a^2Z_{1L}+aZ_{1S})=\frac{V_a'}{Z_T}(Z_{1S}\underline{/180^\circ}+2Z_{1L}\underline{/240^\circ}) \tag{15}$$

$$V_c=aV_{a1}+a^2V_{a2}=\frac{V_a'}{Z_T}(aZ_{1S}+2aZ_{1L}+a^2Z_{1S})=\frac{V_a'}{Z_T}(Z_{1S}\underline{/180^\circ}+2Z_{1L}\underline{/120^\circ}) \tag{16}$$

$$V_{ab}=V_a-V_b=\frac{V_a'}{Z_T}(3Z_{1S}+2\sqrt{3}Z_{1L}\underline{/30^\circ}) \tag{17}$$

$$V_{bc}=V_b-V_c=\frac{V_a'}{Z_T}(2\sqrt{3}Z_{1L}\underline{/270^\circ}) \tag{18}$$

$$V_{ca}=V_c-V_a=\frac{V_a'}{Z_T}(3Z_{1S}\underline{/180^\circ}+2\sqrt{3}Z_{1L}\underline{/150^\circ}) \tag{19}$$

Derive the Z_D formulas

90° Connection

$$\text{Relay A: } Z_D=\frac{V_{bc}}{I_a}=\infty \text{ (no current)} \tag{20}$$

Relay B: $Z_D = \frac{V_{ca}}{I_b} =$

$$\frac{3Z_{1S}\angle 180^\circ + 2\sqrt{3}Z_{1L}\angle 150^\circ}{\sqrt{3}\angle 270^\circ} \times \frac{\angle 90^\circ}{\angle 90^\circ}$$

The term V_a'/Z_T is not shown because it appears in both numerator and denominator and therefore cancels out. The multiplication by $\angle 90^\circ/\angle 90^\circ$ is to convert the denominator to a real term.

$$Z_D = \sqrt{3}Z_{1S}\angle 270^\circ + 2Z_{1L}\angle 240^\circ \tag{21}$$

Relay C: $Z_D = \frac{V_{ab}}{I_c} =$

$$\frac{3Z_{1S} + 2\sqrt{3}Z_{1L}\angle 30^\circ}{\sqrt{3}\angle 90^\circ} \times \frac{\angle 270^\circ}{\angle 270^\circ}$$

$$= \sqrt{3}Z_{1S}\angle 270^\circ + 2Z_{1L}\angle 300^\circ \tag{22}$$

60° Connection
Number 1

Relay A: $Z_D = \frac{V_{ac}}{I_a - I_b} = \frac{-V_{ca}}{I_a - I_b} =$

$$\frac{3Z_{1S} + 2\sqrt{3}Z_{1L}\angle 330^\circ}{\sqrt{3}\angle 90^\circ} \times \frac{\angle 270^\circ}{\angle 270^\circ}$$

$$= \sqrt{3}Z_{1S}\angle 270^\circ + 2Z_{1L}\angle 240^\circ \tag{23}$$

Relay B: $Z_D = \frac{V_{bc}}{I_b - I_c} \quad \frac{-V_{ab}}{I_b - I_c} =$

$$\frac{3Z_{1S}\angle 180^\circ + 2\sqrt{3}Z_{1L}\angle 210^\circ}{2\sqrt{3}\angle 270^\circ} \times \frac{\angle 90^\circ}{\angle 90^\circ}$$

$$= \frac{\sqrt{3}}{2}Z_{1S}\angle 270^\circ + 2Z_{1L}\angle 300^\circ \tag{24}$$

Relay C: $Z_D = \frac{V_{cb}}{I_c - I_a} = \frac{-V_{bc}}{I_c - I_a} =$

$$\frac{2\sqrt{3}Z_{1L}\angle 90^\circ}{\sqrt{3}\angle 90^\circ} = 2Z_{1L} \tag{25}$$

60° Connection
Number 2

Relay A: $Z_D = \frac{-V_c}{I_a} = \infty$ (26)

Relay B: $Z_D = \frac{-V_a}{I_b} =$

$$\frac{2Z_{1S}\angle 180^\circ + 2Z_{1L}\angle 180^\circ}{\sqrt{3}\angle 270^\circ} \times \frac{\angle 90^\circ}{\angle 90^\circ}$$

$$= \frac{2}{\sqrt{3}}(Z_{1S}\angle 270^\circ + Z_{1L}\angle 270^\circ) \tag{27}$$

Relay C: $Z_D = \frac{-V_b}{I_c} =$

$$\frac{Z_{1S} + 2Z_{1L}\angle 60^\circ}{\sqrt{3}\angle 90^\circ} \times \frac{\angle 270^\circ}{\angle 270^\circ}$$

$$= \frac{1}{\sqrt{3}}(Z_{1S}\angle 270^\circ + 2Z_{1L}\angle 330^\circ) \tag{28}$$

30° Connection

Relay A: $Z_D = \frac{V_{ac}}{I_a} = \infty$ (29)

Relay B: $Z_D = \frac{V_{ba}}{I_b}$

$$= \frac{3Z_{1S}\angle 180^\circ + 2\sqrt{3}Z_{1L}\angle 210^\circ}{\sqrt{3}\angle 270^\circ} \times \frac{\angle 90^\circ}{\angle 90^\circ}$$

$$= \sqrt{3}Z_{1S}\angle 270^\circ + 2Z_{1L}\angle 300^\circ \tag{30}$$

Relay C: $Z_D = \frac{V_{cb}}{I_c} = \frac{2\sqrt{3}Z_{1L}\angle 90^\circ}{\sqrt{3}\angle 90^\circ} = 2Z_{1L}$ (31)

Phase A-to-Ground Fault

Calculate currents, and voltages at bus G

$$I_{a1} = I_{a2} = I_{a0} = \frac{V_a'}{Z_1 + Z_2 + Z_0} = \frac{V_a'}{Z_T} \tag{32}$$

$$I_a = 3I_{a1} = 3\frac{V_a'}{Z_T} \tag{33}$$

$$I_b = I_c = 0 \tag{34}$$

$$I_a - I_b = 3\frac{V_a'}{Z_T} \tag{35}$$

$$I_b - I_c = 0 \tag{36}$$

$$I_c - I_a = 3\frac{V_a'}{Z_T}\angle 180^\circ \tag{37}$$

$$V_{a1} = V_a' - I_{a1}Z_{1S} = V_a' - \frac{V_a'}{Z_T}Z_{1S}$$

$$= \frac{V_a}{Z_T}(Z_T + Z_{1S}\angle 180^\circ) \tag{38}$$

$$V_{a2} = -I_{a2}Z_{2S} = \frac{V_a'}{Z_T}Z_{2S}\angle 180^\circ \tag{39}$$

$$V_{a0} = -I_{a0}Z_{0S} = \frac{V_a'}{Z_T}Z_{0S}\angle 180^\circ \tag{40}$$

$$V_a = V_{a1} + V_{a2} + V_{a0} =$$

$$\frac{V_a'}{Z_T}(Z_T + 2Z_{1S}\angle 180^\circ + Z_{0S}\angle 180^\circ) \tag{41}$$

But $Z_T = 2Z_{1S} + 2Z_{1L} + Z_{0S} + Z_{0L}$ (42)

$$V_a = \frac{V_a'}{Z_T}(2Z_{1L} + Z_{0L}) \tag{43}$$

$$V_b = a^2V_{a1} + aV_{a2} + V_{a0}$$

$$= \frac{V_a'}{Z_T}(Z_T\angle 240^\circ + Z_{1S}\angle 60^\circ + Z_{1S}\angle 300^\circ + Z_{0S}\angle 180^\circ)$$

$$= \frac{V_a'}{Z_T}(\sqrt{3}Z_{1S}\angle 270^\circ + \sqrt{3}Z_{0S}\angle 210^\circ + 2Z_{1L}\angle 240^\circ + Z_{0L}\angle 240^\circ) \tag{44}$$

$$V_c = aV_{a1} + a^2V_{a2} + V_{a0}$$

$$= \frac{V_a'}{Z_T}(Z_T\angle 120^\circ + Z_{1S}\angle 300^\circ + Z_{1S}\angle 60^\circ + Z_{0S}\angle 180^\circ)$$

$$= \frac{V_a'}{Z_T}(\sqrt{3}Z_{1S}\angle 90^\circ + \sqrt{3}Z_{0S}\angle 150^\circ + 2Z_{1L}\angle 120^\circ + Z_{0L}\angle 120^\circ) \tag{45}$$

The phase-to-phase voltages are derived as in a preceding section by taking the difference between the appropriate phase-to-ground voltages, above. Substitutions are made within the parenthesis for Z_T in accordance with equation 42 in order to separate the source and line impedance terms so that the end results are:

$$V_{ab} = \frac{V_a'}{Z_T}(\sqrt{3}Z_{1S}\angle 90^\circ + \sqrt{3}Z_{0S}\angle 30^\circ + 2\sqrt{3}Z_{1L}\angle 30^\circ + \sqrt{3}Z_{0L}\angle 30^\circ) \tag{46}$$

$$V_{bc} = \frac{V_a'}{Z_T}(2\sqrt{3}Z_{1S}\angle 270^\circ + \sqrt{3}Z_{0S}\angle 270^\circ + 2\sqrt{3}Z_{1L}\angle 270^\circ + \sqrt{3}Z_{0L}\angle 270^\circ) \tag{47}$$

$$V_{ca} = \frac{V_a'}{Z_T}(\sqrt{3}Z_{1S}\angle 90^\circ + \sqrt{3}Z_{0S}\angle 150^\circ + 2\sqrt{3}Z_{1L}\angle 150^\circ + \sqrt{3}Z_{0L}\angle 150^\circ) \tag{48}$$

The relay formulas are derived in the same manner as in a preceding section. The expression for current in each case is so simple that performing the necessary division of current into voltage is done in one step, yielding at once the formulas which are already tabulated in Table I for phase-A-to-ground fault, hence there is no point in repeating them here.

Two-Phase-to-Ground Fault on Phases B and C

The sequence networks are, of course, connected in parallel, and from this consideration

$$Z_T = Z_1 + \frac{Z_2Z_0}{Z_2 + Z_0}$$

Letting

$$A = \frac{Z_0}{Z_1} \tag{49}$$

and since $Z_1 = Z_2$ is assumed

$$Z_T = Z_1\left(\frac{1+2A}{1+A}\right) \tag{50}$$

Calculate the currents, and voltages at bus G

$$I_{a1} = \frac{V_a'}{Z_T}$$

$$I_{a2} = -I_{a1}\frac{Z_0}{Z_2 + Z_0} = -I_{a1}\frac{AZ_1}{Z_1(1+A)} = \frac{A}{1+A} \times I_{a1}\angle 180^\circ \tag{51}$$

$$I_{a0} = -I_{a1}\frac{Z_2}{Z_2 + Z_0} = -I_{a1}\frac{Z_1}{Z_1(1+A)}$$

$$= \frac{1}{1+A}I_{a1}\angle 180^\circ \tag{52}$$

$$I_a = I_{a1} + I_{a2} + I_{a0} = 0 \tag{53}$$

$$I_b = a^2I_{a1} + aI_{a2} + I_{a0} =$$

$$I_{a1}\left(\angle 240^\circ + \frac{A}{1+A}\angle 300^\circ + \frac{1}{1+A}\angle 180^\circ\right)$$

$$= \frac{V_a'}{Z_T(1+A)}(\sqrt{3}\angle 210^\circ + \sqrt{3}A\angle 270^\circ) \tag{54}$$

Similarly,

$$I_c=\frac{V_a'}{Z_T(1+A)}(\sqrt{3}\underline{/150^\circ}+\sqrt{3}A\underline{/90^\circ}) \quad (55)$$

$$I_a-I_b=\frac{V_a'}{Z_T(1+A)}(\sqrt{3}\underline{/30^\circ}+\sqrt{3}A\underline{/90^\circ}) \quad (56)$$

$$I_b-I_c=\frac{V_a'}{Z_T(1+A)}(\sqrt{3}\underline{/270^\circ}+2\sqrt{3}A\underline{/270^\circ}) \quad (57)$$

$$I_c-I_a=\frac{V_a'}{Z_T(1+A)}(\sqrt{3}\underline{/150^\circ}+\sqrt{3}A\underline{/90^\circ}) \quad (58)$$

$$V_{a1}=V_a'-I_{a1}Z_{1S}=V_a'-\frac{V_a'}{Z_T}Z_{1S}$$

$$=\frac{V_a'}{Z_T}(Z_T-Z_{1S}) \quad (59)$$

$$V_{a2}=-I_{a2}Z_{1S}=\frac{A}{1+A}I_{a1}Z_{1S}$$

$$=\frac{V_a'}{Z_T}\left(\frac{A}{1+A}Z_{1S}\right) \quad (60)$$

$$V_{a0}=-I_{a0}Z_{0S}=\frac{1}{1+A}I_{a1}Z_{0S}$$

$$=\frac{V_a'}{Z_T}\left(\frac{1}{1+A}Z_{0S}\right) \quad (61)$$

$$V_a=V_{a1}+V_{a2}+V_{a0}$$

$$=\frac{V_a'}{Z_T}\left(Z_T+Z_{1S}\left(-1+\frac{A}{1+A}\right)+\frac{Z_{0S}}{1+A}\right)$$

$$=\frac{V_a'}{Z_T(1+A)}(2AZ_{1S}+Z_{0S}+Z_{1L}(1+2A)) \quad (62)$$

$$V_b=a^2V_{a1}+aV_{a2}+V_{a0}=$$

$$\frac{V_a'}{Z_T}\left((Z_T-Z_{1S})a^2+\frac{A}{1+A}aZ_{1S}+\frac{1}{1+A}Z_{0S}\right)$$

$$=\frac{Va'}{Z_T(1+A)}(AZ_{1S}\underline{/180^\circ}+Z_{0S}+(1+2A)Z_{1L}\underline{/240^\circ}) \quad (63)$$

$$V=aV_{a1}+a^2V_{a2}+V_{a0}$$

$$=\frac{V_a'}{Z_T}\left((Z_T-Z_{1S})a+\frac{A}{1+A}a^2Z_{1S}+\frac{Z_{0S}}{1+A}\right)$$

$$=\frac{V_a'}{Z_T(1+A)}(AZ_{1S}\underline{/180^\circ}+Z_{0S}+(1+2A)Z_{1L}\underline{/120^\circ}) \quad (64)$$

The phase-to-phase voltages are derived as before, and separating source and line impedances, they are found to be

$$V_{ab}=\frac{V_a'}{Z_T(1+A)}(3AZ_{1S}+\sqrt{3}(1+2A)Z_{1L}\times\underline{/30^\circ}) \quad (65)$$

$$V_{bc}=\frac{V_a'}{Z_T(1+A)}(\sqrt{3}(1+2A)Z_{1L}\underline{/270^\circ}) \quad (66)$$

$$V_{ca}=\frac{V_a'}{Z_T(1+A)}(3AZ_{1S}\underline{/180^\circ}+\sqrt{3}(1+2A)\times Z_{1L}\underline{/150^\circ}) \quad (67)$$

With the expressions of voltage and current now available, the relay formulas are derived in a manner similar to those in the two preceding sections. The algebra of the operations is a bit more complicated in this case, however, because of the greater complexity of the current expressions, hence the derivations will be given here for the "90° Connection," to illustrate the method.

90° Connection

Relay A: $Z_D=\frac{V_{bc}}{I_a}=\infty$ (68)

Relay B: $Z_D=\frac{V_{ca}}{I_b}=$

$$\frac{3AZ_{1S}\underline{/180^\circ}+\sqrt{3}(1+2A)Z_{1L}\underline{/150^\circ}}{\sqrt{3}\underline{/210^\circ}+\sqrt{3}A\underline{/270^\circ}} \quad (69)$$

There are two different angular operators in the denominator so that it is impossible to reduce each of them to a real number in the same way that the denominators in previous illustrations were reduced. The best that can be done is to reduce one of the factors to a real term, and the factor chosen is the one not involving A. Inspection shows that if an angle of 150° is added, this will be done, hence multiply both numerator and denominator by $\underline{/150^\circ}$, and cancel out $\sqrt{3}$ from each.

$$Z_D=\frac{\sqrt{3}AZ_{1S}\underline{/330^\circ}+(1+2A)Z_{1L}\underline{/300^\circ}}{1+A\underline{/60^\circ}} \quad (70)$$

Relay C: Z_D

$$=\frac{3AZ_{1S}+\sqrt{3}(1+2A)Z_{1L}\underline{/30^\circ}}{\sqrt{3}\underline{/150^\circ}+\sqrt{3}A\underline{/90^\circ}}\times\frac{\underline{/210^\circ}}{\underline{/210^\circ}}$$

$$=\frac{\sqrt{3}AZ_{1S}\underline{/210^\circ}+(1+2A)Z_{1L}\underline{/240^\circ}}{1+A\underline{/300^\circ}} \quad (71)$$

Utilizing the above method of derivation yields the formulas for the remaining relay connections, and these are listed in Table I.

Three-Phase Fault

Calculate the currents, and voltages at bus G

$$I_{a1}=\frac{V_a'}{Z_{1S}+Z_{1L}}=\frac{V_a'}{Z_T} \quad (72)$$

$$I_{a2}=I_{a0}=0 \quad (73)$$

$$I_a=I_{a1}=\frac{V_a'}{Z_T} \quad (74)$$

$$I_b=a^2I_{a1}=a^2\frac{V_a'}{Z_T} \quad (75)$$

$$I_c=aI_{a1}=a\frac{V_a'}{Z_T} \quad (76)$$

$$I_a-I_b=\sqrt{3}\frac{V_a'}{Z_T}\underline{/30^\circ} \quad (77)$$

$$I_b-I_c=\sqrt{3}\frac{V_a'}{Z_T}\underline{/270^\circ} \quad (78)$$

$$I_c-I_a=\sqrt{3}\frac{V_a'}{Z_T}\underline{/150^\circ} \quad (79)$$

$$V_a=I_{a1}Z_{1L}=\frac{V_a'}{Z_T}Z_{1L} \quad (80)$$

$$V_b=a^2V_a=\frac{V_a'}{Z_T}Z_{1L}\underline{/240^\circ} \quad (81)$$

$$V_c=aV_a=\frac{V_a'}{Z_T}Z_{1L}\underline{/120^\circ} \quad (82)$$

$$V_{ab}=V_a-V_b=\sqrt{3}\frac{V_a'}{Z_T}Z_{1L}\underline{/30^\circ} \quad (83)$$

$$V_{bc}=V_b-V_c=\sqrt{3}\frac{V_a'}{Z_T}Z_{1L}\underline{/270^\circ} \quad (84)$$

$$V_{ca}=V_c-V_a=\sqrt{3}\frac{V_a'}{Z_T}Z_{1L}\underline{/150^\circ} \quad (85)$$

Because of the symmetry of the 3-phase fault, only one relay formula is needed per connection. These are derived as before, and are listed in Table I.

Appendix II. System Figure 2

Inasmuch as Appendix I has shown the method of derivation of the Z_D formulas for the relay directional elements as well as the method of deriving the currents and voltages this appendix will merely list for reference the currents and voltages involved. This will only be necessary for faults involving ground, because for phase-to-phase and 3-phase faults, Figure 2 is a duplicate of Figure 1. The Z_D formulas are given in Table II.

Phase-A-to-Ground Fault

$$Z_T=Z_1+Z_2+Z_0=2Z_1+Z_0 \quad (86)$$

$$I_{a1}=I_{a2}=I_{a0}=\frac{V_a'}{Z_T} \quad (87)$$

$$I_a=2\frac{V_a'}{Z_T} \quad (88)$$

$$I_b=\frac{V_a'}{Z_T}\underline{/180^\circ} \quad (89)$$

$$I_c=\frac{V_a'}{Z_T}\underline{/180^\circ} \quad (90)$$

$$I_a-I_b=3\frac{V_a'}{Z_T} \quad (91)$$

$$I_b-I_c=0 \quad (92)$$

$$I_c-I_a=3\frac{V_a'}{Z_T}\underline{/180^\circ} \quad (93)$$

$$V_{a1}=\frac{V_a'}{Z_T}(Z_T+Z_{1S}\underline{/180^\circ}) \quad (94)$$

$$V_{a2}=\frac{V_a'}{Z_T}Z_{1S}\underline{/180^\circ} \quad (95)$$

$$V_{a0}=\frac{V_a'}{Z_T}Z_0\underline{/180^\circ} \quad (96)$$

$$V_a=\frac{V_a'}{Z_T}2Z_{1L} \quad (97)$$

$$V_b=\frac{V_a'}{Z_T}(\sqrt{3}Z_{1S}\underline{/270^\circ}+\sqrt{3}Z_0\underline{/210^\circ}+2Z_{1L}\underline{/240^\circ}) \quad (98)$$

$$V_c=\frac{V_a'}{Z_T}(\sqrt{3}Z_{1S}\underline{/90^\circ}+\sqrt{3}Z_0\underline{/150^\circ}+2Z_{1L}\underline{/120^\circ} \quad (99)$$

$$V_{ab}=\frac{V_a'}{Z_T}(\sqrt{3}Z_{1S}\underline{/90^\circ}+\sqrt{3}Z_0\underline{/30^\circ}+2\sqrt{3}Z_{1L}\underline{/30^\circ}) \quad (100)$$

$$V_{bc}=\frac{V_a'}{Z_T}(2\sqrt{3}Z_{1S}\underline{/270^\circ}+\sqrt{3}Z_0\underline{/270^\circ}+2\sqrt{3}Z_{1L}\underline{/270^\circ}) \quad (101)$$

$$V_{ca}=\frac{V_a'}{Z_T}(\sqrt{3}Z_{1S}\underline{/90^\circ}+\sqrt{3}Z_0\underline{/150^\circ}+2\sqrt{3}Z_{1L}\underline{/150^\circ}) \quad (102)$$

Two-Phase-to-Ground Fault on Phases B and C

$$Z_T=Z_1+\frac{Z_0Z_2}{Z_0+Z_2}=Z_1\frac{1+2A}{1+A} \quad (103)$$

$$A=\frac{Z_0}{Z_1} \text{ and } Z_1=Z_2 \quad (104)$$

$$I_{a1}=\frac{V_a'}{Z_T} \quad (105)$$

$$I_{a2}=\frac{A}{1+A}\frac{V_a'}{Z_T}\underline{/180^\circ} \quad (106)$$

$$I_{a0}=\frac{1}{1+A}\frac{V_a'}{Z_T}\underline{/180^\circ} \quad (107)$$

Currents at relay location, bus G, do not involve zero sequence.

Therefore

$$I_a=I_{a1}+I_{a2}=\frac{V_a'}{Z_T}\frac{1}{1+A} \quad (108)$$

$$I_b=\frac{V_a'}{Z_T}\frac{1}{1+A}(1\underline{/240^\circ}+\sqrt{3}A\underline{/270^\circ}) \quad (109)$$

$$I_c=\frac{V_a'}{Z_T}\frac{1}{1+A}(1\underline{/120^\circ}+\sqrt{3}A\underline{/90^\circ}) \quad (110)$$

$$I_a-I_b=\frac{Va'}{Z_T\ (1+A)}(\sqrt{3}\underline{/30^\circ}+\sqrt{3}A\underline{/90^\circ}) \quad (111)$$

$$I_b-I_c=\frac{V_a'}{Z_T\ (1+A)}(\sqrt{3}\underline{/270^\circ}+2\sqrt{3}A\underline{/270^\circ}) \quad (112)$$

$$I_c-I_a=\frac{Va'}{Z_T(1+A)}(\sqrt{3}\underline{/150^\circ}+\sqrt{3}A\underline{/90^\circ}) \quad (113)$$

$$V_{a1}=\frac{V_a'}{Z_T}(Z_T-Z_{1S}) \quad (114)$$

$$V_{a2}=\frac{A}{1+A}\frac{V_a'}{Z_T}Z_{1S} \quad (115)$$

$$V_{a0}=\frac{1}{1+A}\frac{V_a'}{Z_T}Z_0=\frac{A}{1+A}\frac{V_a'}{Z_T}Z_1 \quad (116)$$

$$V_a=\frac{Va'}{Z_T(1+A)}(3AZ_{1S}+Z_{1L}(1+3A)) \quad (117)$$

$$V_b=\frac{V_a'}{Z_T(1+A)}(Z_{1L}(1\underline{/240^\circ}+\sqrt{3}A\underline{/270^\circ})) \quad (118)$$

$$V_c=\frac{V_a'}{Z_T(1+A)}(Z_{1L}(1\underline{/120^\circ}+\sqrt{3}A\underline{/90^\circ})) \quad (119)$$

$$V_{ab}=\frac{V_a'}{Z_T(1+A)}(3AZ_{1S}+\sqrt{3}(1+2A)Z_{1L}\underline{/30^\circ}) \quad (120)$$

$$V_{bc}=\frac{V_a'}{Z_T(1+A)}(\sqrt{3}(1+2A)Z_{1L}\underline{/270^\circ}) \quad (121)$$

$$V_{ca}=\frac{V_a'}{Z_T(1+A)}(3AZ_{1S}\underline{/180^\circ}+\sqrt{3}(1+2A)Z_{1L}\underline{/150^\circ}) \quad (122)$$

Appendix III. System Figure 3

In this case, a delta star connected transformer bank is interposed between the relay location and the fault. The phase relationships assumed are that the star side voltages x, y, z, (high voltage assumed) are 30° leading the delta voltages a, b, c (low voltage assumed). Calculations are made initially from the star connected side, but it must be remembered that in passing through the transformer bank to the relay location, the positive sequence currents and voltages are rotated 30° lagging, the similar negative sequence components are rotated 30° leading, and the zero sequence current and voltage disappear.

In line with the policy established in Appendix II, only the expressions for the necessary currents and voltages will be shown here, remembering that the Z_D formulas are given in Table 3. Also, V_x' is used for the source voltage in this case rather than V_a' because of the different phase terminology used to identify the side of the transformer bank away from the relay.

Phase-to-Phase Fault on Phases YZ

$$Z_1=Z_{1S}+Z_{1TR}+Z_{1L}=Z_2 \quad (123)$$

$$Z_T=Z_1+Z_2=2Z_1 \quad (124)$$

$$I_{a1}=\frac{V_x'}{2Z_1}\underline{/330^\circ} \quad (125)$$

$$I_{a2}=\frac{V_x'}{2Z_1}\underline{/210^\circ} \quad (126)$$

$$I_a=\frac{V_x'}{2Z_1}\underline{/270^\circ} \quad (127)$$

$$I_b=\frac{V_x'}{2Z_1}\underline{/270^\circ} \quad (128)$$

$$I_c=\frac{V_x'}{Z_1}\underline{/90^\circ} \quad (129)$$

$$I_a-I_b=0 \quad (130)$$

$$I_b-I_c=\frac{3V_x'}{2Z_1}\underline{/270^\circ} \quad (131)$$

$$I_c-I_a=\frac{3V_x'}{2Z_1}\underline{/90^\circ} \quad (132)$$

$$V_{a1}=\frac{V_x'}{2Z_1}(2Z_1\underline{/330^\circ}+Z_{1S}\underline{/150^\circ}) \quad (133)$$

$$V_{a2}=\frac{V_x'}{2Z_1}Z_{1S}\underline{/30^\circ} \quad (134)$$

$$V_a=\frac{V_x'}{2Z_1}(2Z_1\underline{/330^\circ}+Z_{1S}\underline{/90^\circ}) \quad (135)$$

$$V_b=\frac{V_x}{2Z_1}(2Z_1\underline{/210^\circ}+Z_{1S}\underline{/90^\circ}) \quad (136)$$

$$V_c=\frac{V_x'}{2Z_1}(2Z_1\underline{/90^\circ}+2Z_{1S}\underline{/270^\circ}) \quad (137)$$

$$V_{ab}=\sqrt{3}Vx' \quad (138)$$

$$V_{bc}=\frac{\sqrt{3}V_x'}{2Z_1}(2Z_1\underline{/240^\circ}+\sqrt{3}Z_{1S}\underline{/90^\circ}) \quad (139)$$

$$V_{ca}=\frac{\sqrt{3}V_x'}{2Z_1}(2Z_1\underline{/120^\circ}+\sqrt{3}Z_{1S}\underline{/270^\circ}) \quad (140)$$

Phase-to-Ground Fault on Phase X

$$Z_T=Z_1+Z_2+Z_0=2Z_1+Z_0 \quad (141)$$

$$Z_1=Z_{1S}+Z_{1TR}+Z_{1L} \quad (142)$$

$$Z_0=Z_{0TR}+Z_{0L} \quad (143)$$

$$I_{a1}=\frac{V_x'}{Z_T}\underline{/330^\circ} \quad (144)$$

$$I_{a2}=\frac{V_x'}{Z_T}\underline{/30^\circ} \quad (145)$$

$$I_{a0}=0 \quad (146)$$

$$I_a=\sqrt{3}\frac{V_x'}{Z_T} \quad (147)$$

$$I_b=\sqrt{3}\frac{V_x'}{Z_T}\underline{/180^\circ} \quad (148)$$

$$a_0=0 \quad (149)$$

$$I_a-I_b=2\sqrt{3}\frac{V_x'}{Z_T} \quad (150)$$

$$I_b-I_c=\sqrt{3}\frac{V_x'}{Z_T}\underline{/180^\circ} \quad (151)$$

$$I_c-I_a=\sqrt{3}\frac{V_x'}{Z_T}\underline{/180^\circ} \quad (152)$$

$$V_{a1}=\frac{V_x'}{Z_T}(Z_T\underline{/330^\circ}+Z_{1S}\underline{/150^\circ}) \quad (153)$$

$$V_{a2}=\frac{V_x'}{Z_T}Z_{1S}\underline{/210^\circ} \quad (154)$$

$$V_a=\frac{V_x'}{Z_T}(Z_T\underline{/330^\circ}+\sqrt{3}Z_{1S}\underline{/180^\circ}) \quad (155)$$

$$V_b=\frac{V_x'}{Z_T}(Z_T\underline{/210^\circ}+\sqrt{3}Z_{1S}) \quad (156)$$

$$V_c=\frac{V_x'}{Z_T}Z_T\underline{/90^\circ} \quad (157)$$

$$V_{ab}=\frac{V_x'}{Z_T}(\sqrt{3}Z_T+2\sqrt{3}Z_{1S}\underline{/180^\circ}) \quad (158)$$

$$V_{bc}=\frac{V_x'}{Z_T}(\sqrt{3}Z_T\underline{/240^\circ}+\sqrt{3}Z_{1S}) \quad (159)$$

$$V_{ca}=\frac{V_x'}{Z_T}(\sqrt{3}Z_T\underline{/120^\circ}+\sqrt{3}Z_{1S}) \quad (160)$$

Two-Phase-to-Ground Fault on Phases YZ

$$Z_1=Z_{1S}+Z_{1TR}+Z_{1L}=Z_2 \quad (161)$$

$$Z_0=Z_{0TR}+Z_{0L}=AZ_1 \quad (162)$$

$$Z_T = Z_1 + \frac{Z_0 Z_2}{Z_0 + Z_2} = Z_1 \frac{1+2A}{1+A} \quad (163)$$

$$I_{a1} = \frac{V_x'}{Z_T} \underline{/330^\circ} \quad (164)$$

$$I_{a2} = \frac{V_x'}{Z_T} \frac{A}{1+A} \underline{/210^\circ} \quad (165)$$

$$I_{a0} = 0 \quad (166)$$

$$I_a = \frac{V_x'}{Z_T(1+A)} (1\underline{/330^\circ} + A\underline{/270^\circ}) \quad (167)$$

$$I_b = \frac{V_x'}{Z_T(1+A)} (1\underline{/210^\circ} + A\underline{/270^\circ}) \quad (168)$$

$$I_c = \frac{V_x'}{Z_T(1+A)} (1\underline{/90^\circ} + 2A\underline{/90^\circ}) \quad (169)$$

$$I_a - I_b = \sqrt{3} \frac{V_x'}{Z_T(1+A)} \quad (170)$$

$$I_b - I_c = \frac{V_x'}{Z_T(1+A)} (\sqrt{3}\underline{/240^\circ} + 3A\underline{/270^\circ}) \quad (171)$$

$$I_c - I_a = \frac{V_x'}{Z_T(1+A)} (\sqrt{3}\underline{/120^\circ} + 3A\underline{/90^\circ}) \quad (172)$$

$$V_{a1} = \frac{V_x'}{Z_T} (Z_T\underline{/330^\circ} + Z_{1S}\underline{/150^\circ}) \quad (173)$$

$$V_{a2} = \frac{V_x'}{Z_T} \left(\frac{A}{1+A} Z_{1S}\underline{/30^\circ} \right) \quad (174)$$

$$V_a = \frac{V_x'}{Z_T(1+A)} (\sqrt{3} A Z_{1S} + (1+2A)(Z_{1TR} + Z_{1L})\underline{/330^\circ}) \quad (175)$$

$$V_b = \frac{V_x'}{Z_T(1+A)} (\sqrt{3} A Z_{1S}\underline{/180^\circ} + (1+2A)(Z_{1TR} + Z_{1L})\underline{/210^\circ}) \quad (176)$$

$$V_c = \frac{V_x'}{Z_T(1+A)} ((1+2A)(Z_{1TR} + Z_{1L})\underline{/90^\circ}) \quad (177)$$

$$V_{ab} = \frac{V_x'\sqrt{3}}{Z_T(1+A)} (2A Z_{1S} + (1+2A)(Z_{1TR} + Z_{1L})) \quad (178)$$

$$V_{bc} = \frac{V_x'\sqrt{3}}{Z_T(1+A)} (A Z_{1S}\underline{/180^\circ} + (1+2A)(Z_{1TR} + Z_{1L})\underline{/240^\circ}) \quad (179)$$

$$V_{ca} = \frac{V_x'\sqrt{3}}{Z_T(1+A)} (A Z_{1S}\underline{/180^\circ} + (1+2A)(Z_{1TR} + Z_{1L})\underline{/120^\circ}) \quad (180)$$

Three-Phase Fault

$$Z_T = Z_1 = Z_{1S} + Z_{1TR} + Z_{1L} \quad (181)$$

$$I_{a1} = \frac{V_x'}{Z_1} \underline{/330^\circ} \quad (182)$$

$$I_{a2} = I_{a0} = 0 \quad (183)$$

$$I_a = I_{a1} = \frac{V_x'}{Z_1} \underline{/330^\circ} \quad (184)$$

$$I_b = \frac{V_x'}{Z_1} \underline{/210^\circ} \quad (185)$$

$$I_c = \frac{V_x'}{Z_1} \underline{/90^\circ} \quad (186)$$

$$I_a - I_b = \frac{V_x'}{Z_1} \sqrt{3} \quad (187)$$

No other "delta" currents are needed.

$$V_a = I_a(Z_{1TR} + Z_{1L}) = \frac{V_x'}{Z_1} (Z_{1TR} + Z_{1L})\underline{/330^\circ} \quad (188)$$

$$V_b = \frac{V_x'}{Z_1} (Z_{1TR} + Z_{1L})\underline{/210^\circ} \quad (189)$$

$$V_c = \frac{V_x'}{Z_1} (Z_{1TR} + Z_{1L})\underline{/90^\circ} \quad (190)$$

$$V_{ac} = V_a - V_c = \frac{V_x'}{Z_1} (Z_{1TR} + Z_{1L})\sqrt{3}\underline{/300^\circ} \quad (191)$$

$$V_{bc} = V_b - V_c = \frac{V_x'}{Z_1} (Z_{1TR} + Z_{1L})\sqrt{3}\underline{/240^\circ} \quad (192)$$

No other voltages are needed.

Discussion

Myron A. Bostwick (Portland General Electric Company, Portland, Oreg.): I wish to compliment Mr. Sonnemann for his excellent analysis of single-phase directional element connections. He has used a simple, readily understood approach to the problem, and provides more definite limits for successful operation than have been published previously. A glance at the many pages of calculations provides an indication of the thoroughness of his investigation.

Fortunately it is not necessary to dig through these voluminous calculations to use the information that has been provided. The vector diagrams tell the whole story, when considered in terms of the particular relay characteristics and connections. It also is essential to consider details of the power circuit as Mr. Sonnemann has indicated.

The need of this is emphasized by consideration of the diagrams, as described in the section on Summary of Results. The author has indicated that there are "three cases where the current falls in the contact opening zone by being either more than 45 degrees lagging or more than 135 degrees leading." He then discusses three conditions that may cause undesirable operation. In this discussion he fails to mention two conditions (the *B* relay, 90-degree connection, for a phase A-to-ground fault on system Figure 2, in table VI and the phase *A* relay, 90-degree connection, in Table VII for a *Y-Z* fault in system Figure 3) that also cause contact opening torque. Discussion of these was apparently omitted because the relays will not trip incorrectly on the reversed flow of current to an external fault. I think it desirable to have consideration of these relays included in the discussion for future reference and suggest that it be added to the paper.

The analysis has clinched my opinion that the 90-degree connection should be used generally in all applications, except those noted as being subject to incorrect operation. Individual study of those installations may then be required. In closing these remarks, I wish to thank Mr. Sonnemann for his clear analysis of the problem, and the tremendous amount of work that was required to present it.

W. K. Sonnemann: Mr. Bostwick has picked out two conditions which should have been discussed in the original paper. In the fourth paragraph preceding the "Conclusions," the reference should be to five cases where the current falls in the contact opening zone rather than just three. As a matter of fact, all of the vector diagrams were studied individually for their implications at the time of their original derivation, including these two. At the time of sifting and sorting all of the work which had been done in order to prepare the paper, however, these two were missed. The author regrets that they were missed, and thanks Mr Bostwick for calling attention to them.

In the first case, relay *B*, 90-degree connection, phase-*A*-to-ground fault, system Figure 2, there is the possibility of incorrect tripout for relays located at certain other points than that illustrated in Figure 2. For example, relays in the source circuit at bus *G*, as well as relays on the left-hand side of any bus interposed between the bus *G* and the fault, will "see" the vector relationships of Table VI line 1 in reverse, hence it is apparent that the possibility of erroneous tripout for relay *B* should be examined further. It is in cases such as this that it is well to bear in mind that the vector diagrams show extreme conditions which may be more theoretical than practical, and that an examination of the system constants may show the trouble to be nonexistent for a particular system. The formula for relay *B* under discussion is:

$$Z_D = \sqrt{3}[Z_{1S}\underline{/270^\circ} + (Z_0 + 2Z_{1L})\underline{/330^\circ}]$$

The limit condition of the current lagging by 60 degrees was obtained in this case by assuming that the zero sequence impedance is the governing factor through being large enough to make the other factors negligible, and that it has an angle of 90 degrees. The 90-degree angle is not too bad an assumption if the fault occurs at the far end of the line at the grounding bank location provided that the bank is not grounded through a resistor. If the fault is at the far end of the line, however, the impedance of the line is not necessarily negligible, and whether or not the source impedance is negligible by comparison depends upon the system. Assume, for example, that the line impedance is negligible, and take Z_0 at 1.00 $\underline{/90^\circ}$ for reference. If Z_{1S} is assumed at 90 degrees, it is found that it requires a scalar value of only 0.366 to bring the Z_D value to a 45-degree angle, the border line condition. Thus, if Z_{1S} exceeds 36.6 per cent of Z_0, the problem disappears for relays having a 45-degree characteristic. If Z_{1S} has a smaller angle than 90 degrees, a slightly greater

value will be required. If the transformer is grounded through a resistor, the characteristic angle of Z_0 approaches zero degrees, and the current approaches the 30-degree leading position.

The second case mentioned by Mr. Bostwick covering relay A, 90-degree connection, YZ fault, system Figure 3 is similar to the first in that relays in source circuits at bus G require scrutiny. The most severe condition occurs when the fault is right at the line terminals of the transformer so that Z_{1L}, assumed to have a smaller angle than 90 degrees, is zero. The angle of the transformer impedance Z_{1TR} is near 90 degrees, however, and dependence must be placed on the source impedance being relatively large in order to reduce the angle of Z_D to less than 45 degrees. If there are several source circuits connected to the bus, the condition will be materially aggravated for the relays on these source circuits by virtue of the multiplying effect of the current from the other sources on the apparent value of Z_{1TR} as seen, in reverse, by any one set of relays on a source circuit. It is conceivable that there will be systems wherein the 90-degree connection, with the 45-degree phase shifter, will be unsatisfactory. In such cases, the solution is to modify the 45-degree phase shifter if this does not cause trouble from one of the other limits, or else use one of the two 60-degree connections.

Local Wire Video Television Networks

C. N. NEBEL
NONMEMBER AIEE

A satisfactory local video distribution system is necessary to interconnect television studios, transmitters, and pick-up points within a city and to connect them to the coaxial cable and microwave intercity television networks.[1,2] Wire extension circuits also are necessary to distribute video signals from local microwave circuits which are used to pick up remote program material. This is necessary because space on a broadcaster's premise is often unavailable and undesirable from a system maintenance point of view for the operation of remote microwave equipments. A local video distribution system has been developed for the Bell Telephone System utilizing existing telephone facilities as much as practicable. Backbone routes in local areas use newly developed low loss shielded video cable pairs. In many cases these are supplemented by end links of existing paper pair cables.

Equipment is provided for the equalization and amplification of the video signals transmitted over wire circuits. This equipment consists of a transmitting terminal, an intermediate repeater with cable equalizers, and a receiving terminal. Video repeating coils (line transformers) are sometimes used at the terminals for direct connections to the cable pairs. A clamper also is used at the receiving terminal as a stabilizing element for low-frequency circuit noise and for restoring the low-frequency signal components which are removed by the terminal repeating coils.

The intermediate repeater contains four blocks of gain in the form of input and output amplifiers and two amplifier gain networks. The equalization for the cable loss is obtained by utilizing the gain-frequency characteristics of the two amplifier gain networks and of the equalizers which are connected between the two amplifiers. The equalization and gain is distributed throughout the system so as to obtain a reduction in cable and amplifier noise. Increased high-frequency noise suppression is obtained by means of signal predistortion, that is by transmitting the low-level high-frequency signal components over the system at a higher than normal level and restoring them to normal level at the receiving end of the circuit.

It is the purpose of this paper to describe these video transmission facilities more fully and to show the results obtained with some typical circuit applications.

Characteristics of Cable Plant

The cable plant in the local exchange areas available for video transmission consists of coaxial cables, existing interoffice trunk and subscriber paper insulated cables, and shielded polyethylene string and tape insulated cables.

Coaxial Cables

The first 4-megacycle video transmission circuits were used for relatively short studio-transmitter connections. Special installations of 0.268-inch coaxial cables with specially designed equalizers were provided to care for these cases. These were very special cases where the 4-megacycle loss was less than 20 decibels requiring no intermediate gain in the cables. Although they were short circuits, they had the disadvantage that ground currents induced into the outer coaxial conductor by neighboring power circuits caused serious interference. Although it could be balanced out by special means on short circuits, it was found impracticable to employ long unbalanced coaxial circuits in a large video transmission plant. Balanced pair cables provide a natural balance of 75 decibels or more to these interfering power frequencies and are, therefore, much more suitable for use in the development of a large video plant facility.

Existing Cable Plant

A wide variety of balanced circuits are to be found in the existing plant in the form of paper-insulated interoffice trunks and subscriber cable pairs. These existing facilities were fairly extensively used in the initial stages of this video plant development. It will be interesting at this point to examine the limitations of these circuits for video transmission.

There are four principal sources of noise interference on balanced transmission circuits. First are the voltages induced between the line conductors and ground from neighboring power systems. These act upon unbalances between the line conductors and ground to produce components in the metallic circuit. Second are impulse-type noises arising from cross-induction from message-circuit pairs in the cable. These originate in the many switching operations occurring in

Table I. Attenuation of Line Facilities for Video Transmission

Paper Pair Cables, Gauge	Attenuation in Decibels at 4 Megacycles 1,000 Feet	Per Mile
10	4.7	25.0
13	5.7	30.0
16	6.9	36.0
19 CNB	10.0	53.0
22	13.0	68.0
24	16.0	84.0
26	18.0	95.0
Shielded Video Cables		
Number 16 *PSV* spiral shield	3.41	18.0
Number 16 *PSV* longitudinal shield	3.22	17.0
754C double braid	5.0	27.5
Coaxial Carrier Cables		
0.268-inch longitudinal shield		10.9
0.375-inch longitudinal shield		7.7
Office Cabling		
Paired—754B	5.2	
Coaxial—794	4.63	

Paper 50-234, recommended by the AIEE Wire Communication Systems Committee and approved by the AIEE Technical Program Committee for presentation at the AIEE Fall General Meeting, Oklahoma City, Okla., October 23–27, 1950. Manuscript submitted July 31, 1950; made available for printing August 29, 1950.

C. N. Nebel is with the Bell Telephone Laboratories Inc., Murray Hill, N. J.

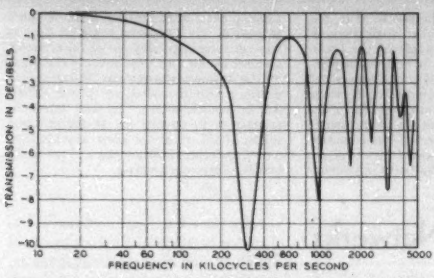

Figure 1. Transmission variations caused by a 500-foot open-ended bridged tap on a number 22CSA equalized paper pair video circuit

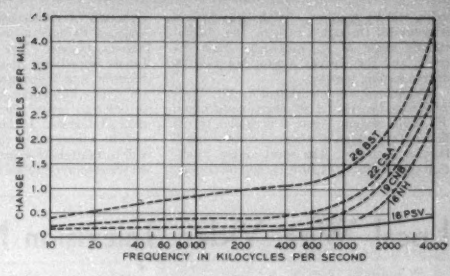

Figure 3. Change in attenuation of typical paper cables at video frequencies for a total seasonal temperature change of 26 degrees Fahrenheit

the message plant, for example from switchhooks, dialing, ringing, teletypewriter, and so forth. Third are disturbing components arising by induction from other video in the same cable. Fourth is the noise due to thermal agitation in the cable conductors and shot noise in the vacuum tubes, usually referred to as amplifier input noise.

In general, protection from the first three types of noise is obtained by cable pair balance. A certain amount of impulse noise and amplifier input noise reduction is obtainable by pre-equalization and predistortion of the signal. Otherwise, increased shielding or separation of circuits must be provided to further reduce both impulse noise and video circuit crosstalk. Amplifier input noise at present is not limiting since it is kept to within about 15 decibels of the irreducible minimum which is cable thermal noise. The maximum repeater spacing is determined by one or more of these factors, that is, the repeater spacing or line loss may be increased until the signal becomes so small that a certain margin or difference exists between the signal level and the noise level. This level margin is the tolerable or acceptable viewing signal-to-noise ratio.

In the case of paper pair circuits, impulse noise limits the maximum repeater spacings to a 4-megacycle line loss of approximately 65 decibels with signal predistortion. When the input and output circuits to a repeater are in the same cable, interaction crosstalk[3] around the repeater limits the 4-megacycle loss of the line preceding the repeater to approximately 40 decibels If the input and output circuits to the repeater are in different cables, interaction crosstalk loss is usually so high that it is not a limitation. If two circuits operate in opposite directions within a cable, near end crosstalk limits the maximum 4-megacycle loss in both circuits to 40 decibels. If two circuits operate in the same direction within a cable, far end crosstalk limits the maximum 4-megacycle loss in both circuits to approximately 40 decibels. It can readily be seen from Table I on cable attenuation that crosstalk in paper pair circuits results in either very short repeater spacings or limits the number of circuits to one per cable. The average office spacing even in such high-density areas as metropolitan New York exceeds 40 decibels for paper pair. An office spacing of even 65 decibel is often difficult to obtain where only the impulse noise limitation is controlling. In these cases recourse to interoffice repeater locations on private property is necessary.

Subscriber pairs are provided with bridged taps or multiple outlets at various locations along the length of the pairs to make them more useful or available for assignment purposes. The presence of these taps introduce reflections or echoes from their open ended condition when such subscriber circuits are used for video transmission. The effect of such a tap upon the transmission characteristic is illustrated in Figure 1. The only satisfactory way to avoid this tap distortion in the video band is to remove the taps from the line. Since most taps are located within lead cable splices in man-

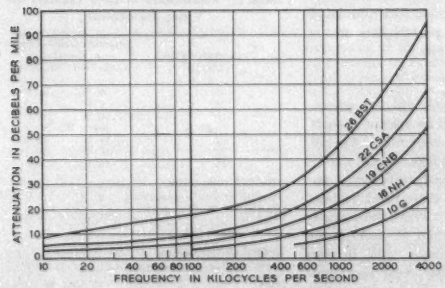

Figure 2. Attenuation of typical paper pair cables at video frequencies

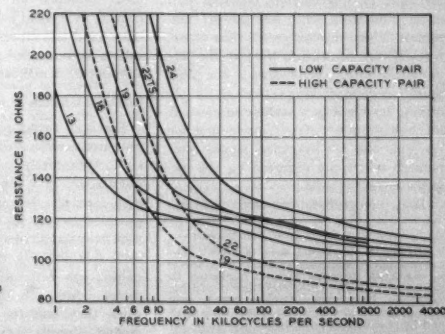

Figure 4. Resistance component of typical paper pair cable impedance

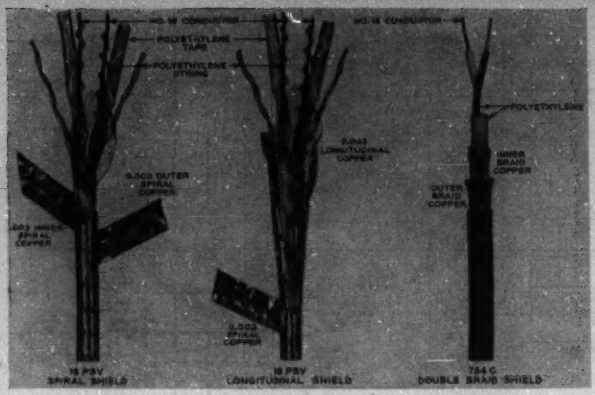

Figure 5. Newly developed shielded video cables for use in the telephone plant

holes, their removal results in considerable expense and lengthy operations in preparing a pair for video use.

There is a wide variety of paper pair circuits available in the telephone plant. The transmission characteristics of these circuits have a large bearing upon their usefulness for video transmission purposes.

The attenuation of representative paper pairs throughout the 4-megacycle video band is shown in Figure 2. The bulk of the available pairs is confined to smaller gauges of 19 to 26 where the 4-megacycle loss ranges from 53 to 95 per mile. With the limitation of about 65-decibel repeater spacings imposed by impulse noise the maximum repeater spacings are then 1.23 miles for 19 gauge, and 0.685 mile for the 26-gauge-per-cable sheath. Due to existing office spacings these repeater spacings would make necessary a large number of off premise or private property repeater locations. Also a large number of repeaters would be required for the longer circuits encountered. These longer circuits may be from 10 to 20 miles in length. In these cases seasonal temperature variations become important, necessitating frequent circuit re-equalization. Temperature measurements in underground cable ducts in lower New York City were made throughout 1948. They gave a seasonal range of 26 degrees Fahrenheit. Figure 3 gives the attenuation-temperature variation throughout the 4-megacycle band in decibels per mile for a seasonal change of 26 degrees Fahrenheit for paper pair circuits. It will be seen that the 4-megacycle seasonal loss change for the average 22 gauge pair is 34 decibels for a 10-mile circuit having a total 4-megacycle loss of 680 decibels. This circuit would probably have 13 repeaters each of which would have to be re-equalized at least monthly to minimize the temperature effect upon circuit attenuation.

A given paper pair circuit is usually a composite of the various gauges available between two repeaters. The characteristic impedance of the various gauges varies considerably from one to another. The impedance mismatch at the junction of unlike gauges and especially between the smaller gauges and the repeater termination creates reflection losses. These reflection losses depend upon the particular gauges involved making it difficult to predetermine the necessary equalizer shapes to use. The resistance component of the characteristic impedance $(R+JX)$ of some paper pairs is given in Figure 4.

All of the enumerated characteristics of paper pair cables militate against their widespread use in a large and complex video plant. A more stable and lower cable loss is needed for the backbone circuits including broadcaster terminal and studio-transmitter circuits. The paper pair cables are then used mainly for short radial pickup circuit connections to the backbone route.

Shielded Video Cable Pairs

A new video cable pair has been developed to meet the demands of the backbone circuits. The high-frequency loss has been kept low by the use of large conductors and polyethylene insulation. The impulse noise and crosstalk have been

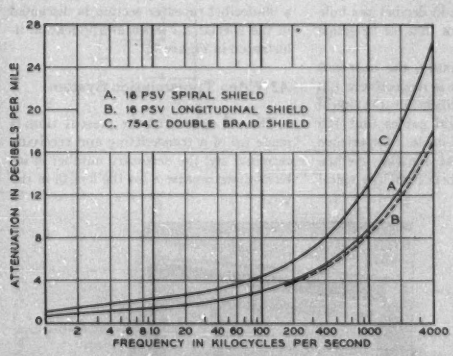

Figure 6. Attenuation of newly developed shielded video cables for use in the telephone plant

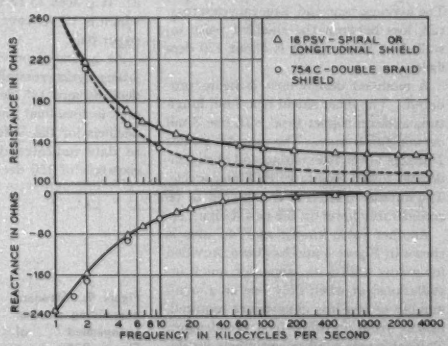

Figure 7. Impedance of newly developed shielded video cables for use in the telephone plant

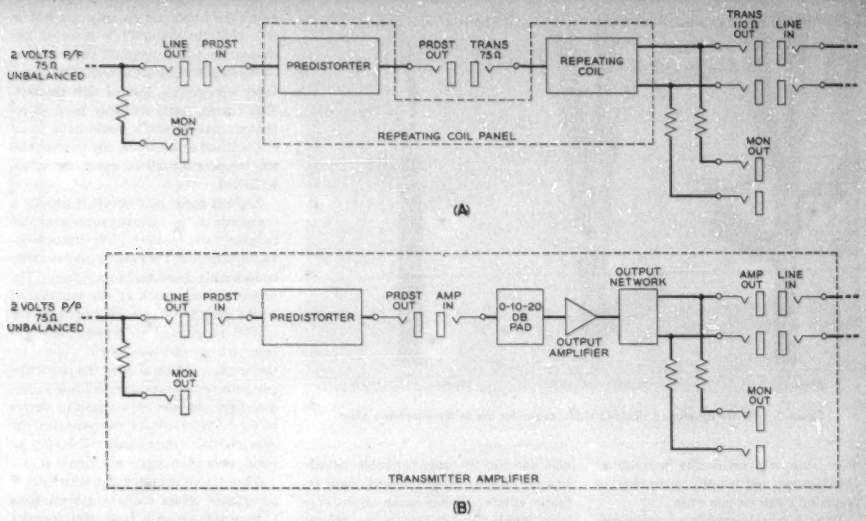

Figure 8. Transmitting terminal of the *A2* video transmission system

reduced by shielding the balanced pairs. It is known as number 16 *PSV* (polyethylene shielded video). As shown in Figure 5 each number 16 American Wire Gauge copper conductor is insulated with a spirally wound polyethylene string and tape. Two spirally-wound 3-mil copper tapes with opposite lay are then placed around a pair of the insulated conductors to form the shielded pair. The 16 *PSV* shielded pairs are then placed in their own lead sheath or in with other paper pairs in large interoffice trunk cables. The average near end 4-megacycle crosstalk loss between the shielded pairs installed in this manner is about 120 decibels.

A modified design now is being produced. The inner shield is a 3-mil longitudinal seam copper tape with one 3-mil outside spiral tape. The new design has 1-decibel lower attenuation and about 25-decibel lower crosstalk at 4 megacycle. The impulse noise also is expected to be considerably lower on the new design.

Another cable known as *754C* also is shown in Figure 5 and has been provided for wiring within an office, for quick installations, or when only one or a small number of low loss circuits are required, usually from an office to a broadcaster. This cable uses solid polyethylene insulation covered with a double-braided copper shield with an outside jacket of grey polyvinyl chloride. The near end 4-megacycle crosstalk loss between two adjacent *754C* shielded cables is approximately 150 decibels. It is moisture resistant and may be pulled into underground cable ducts.

Representative attenuation and impedance characteristics of the shielded video pairs are given in Figures 6 and 7. The 4-megacycle loss of the number 16 *PSV* spiral shield and longitudinal shield cable is seen to be 18 decibels and 17 decibels per mile respectively. The attenuation-temperature change for a seasonal temperature range of 26 degrees Fahrenheit is given by the lower curve on Figure 3. It is seen to be 0.45 decibel per mile which is 13 per cent of that for 22-gauge paper pair.

As indicated previously, the near end 4-megacycle crosstalk is respectively 120 decibels and 145 decibels for the spiral and longitudinal shield cables and 150 decibels for the *754C* cable. Experience to date indicates that for the average crosstalk of 120 decibels from the spiral shield cable, 10 tandem repeater links of about 85 decibels each at 4 megacycles should result in substantially no impairment in picture quality due to crosstalk and office impulse noise. This assumes that the gain and equalization in each repeater is sufficient to make up for the preceding length of cable. However, office spacings and especially repeater spacings of such great lengths and numbers are not expected to occur frequently. Therefore, it should be satisfactory to operate occasional repeater spacings of 5 to 10 decibels longer if repeaters are provided with sufficient gain, equalization, and shielding for the purpose. An example of a 90-decibel repeater section is discussed in the special *A2* repeater application illustrated in Figure 22.

A2 Video Transmission System

The *A2* system at the present time is made up of a transmitting and receiving terminal and the necessary number of intermediate repeaters for the length of the

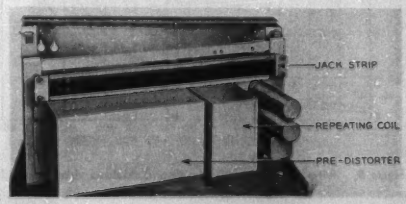

Figure 9. Standard transmitting terminal arrangement of Figure 8(A) in a wall mounted bracket

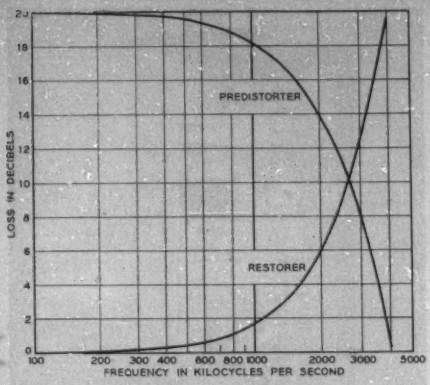

Figure 10. Loss characteristics of predistorter and restorer networks used for noise protection

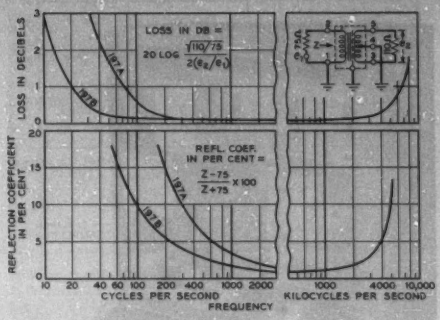

Figure 11. Transmission characteristics of video repeating coils (line transformers)

cable circuit in use. The line equalization and most of the circuit gain is furnished by the repeater except in special cases.

Transmitting Terminal

The transmitting terminal arrangements are shown in Figure 8. It is common practice to use the repeating coil arrangement in Figure 8(A) to avoid the operation of the off premise transmitting amplifier in Figure 8(B). Figure 9 shows a standard transmitting terminal in a wall mounted cabinet. It has been normal practice for the broadcaster to deliver a 2-volt peak-to-peak signal from a 75-ohm unbalanced generator impedance to the transmitting terminal. The predistorter is used as shown if noise protection is needed in the circuit due to one or more long repeater links. The predistorter is an unbalanced 75 ohm constant resistance equalizer having the characteristic shown in Figure 10. The low-frequency loss below 1 megacycle is 20 decibels. This loss is great enough to isolate the customer's line monitor jacks from any impedance irregularity which may exist due to the repeating coil or the video cable pair. The predistorter is connected to the video cable pair with the 75: 110-ohm repeating coil as shown. The monitor jacks at the repeating coil output are for continuity monitoring.

The frequency characteristics of the *197A* and *197B* repeating coils are shown in Figure 11. The *197B* is a later design with a low-frequency cut off at 10 cycles per second The use of repeating coils

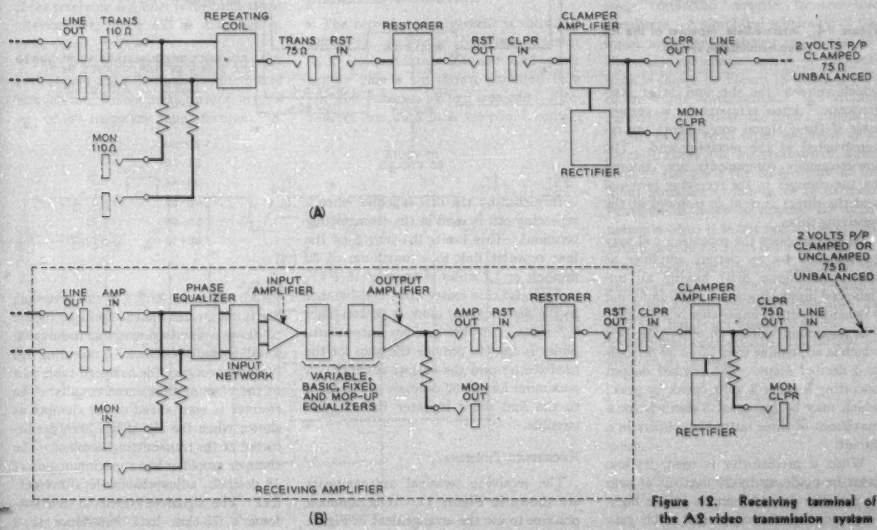

Figure 12. Receiving terminal of the A2 video transmission system

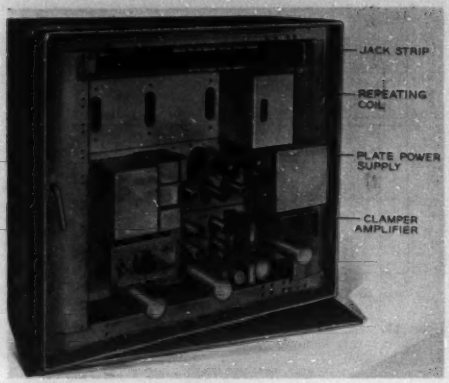

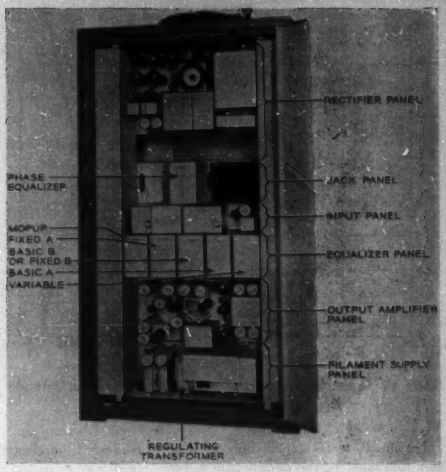

Figure 13 (above). Standard receiving terminal arrangement of Figure 12(A) in a wall mounted bracket

Figure 15 (right). Intermediate repeater of Figure 14 mounted in a portable cabinet

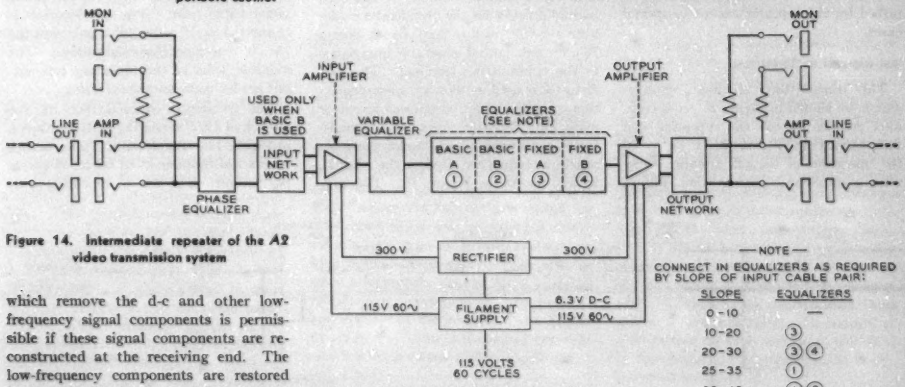

—NOTE—
CONNECT IN EQUALIZERS AS REQUIRED BY SLOPE OF INPUT CABLE PAIR:

SLOPE	EQUALIZERS
0-10	—
10-20	3
20-30	3 4
25-35	1
35-45	1 3
45-55	1 3 4
50-60	1 2
60-70	1 2 3

Figure 14. Intermediate repeater of the A2 video transmission system

which remove the d-c and other low-frequency signal components is permissible if these signal components are reconstructed at the receiving end. The low-frequency components are restored by the clamper in the receiving terminal and the direct current is restored at the receiving tube.

In special cases the repeating coil may be replaced by an output amplifier as shown in Figure 8(B) having an unbalanced input impedance of 75 ohms and a balanced output impedance of 110 ohms. The maximum voltage gain is 30 decibels which is adjustable from 20 to 30 decibels in 2-decibel steps. The normal output operating level is 2 volts (peak to peak) which may be increased 3 decibels for a maximum of three output amplifiers in a circuit.

When a predistorter is used, its loss must be made up by 20 decibels of gain to give the desired increase in the high-frequency signal components. This gain is furnished by the first repeater when a repeating coil is used in the transmitting terminal. This limits the length of the first repeater link to a maximum of 30 decibels or 1.7 miles of number 16 *PSV*.

A special case exists when the distance to the first repeater office is greater than 1.7 miles. In this case an output amplifier is used to provide the gain for the predistorter and the output network. A maximum loss of 63 decibels or 3.5 miles to the first office repeater then is permissible.

Receiving Terminal

The receiving terminal arrangements are shown in Figure 12. It is common practice to use the arrangement in Figure 12(A), when the length of the preceding line is not greater than 27 decibels. Figure 13 shows a standard receiving terminal in a wall mounted cabinet. A repeating coil is used to connect the balanced cable pair to the 75-ohm unbalanced circuits. The restorer is used ahead of the clamper as shown when the signal has been predistorted at the transmitting terminal. The clamper amplifier has a maximum gain of 18 decibels, adjustable in steps of 1 decibel. The signal delivered to the customer's 75-ohm load impedance is 2

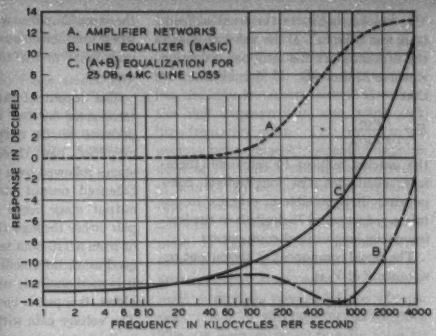

Figure 16 (left). An installation of intermediate repeaters in a telephone office

Figure 18 (above). Characteristics of cable equalizers

(A) Amplifier networks (B) Basic number 16 *P5V* cable equalizer (C) Sum of amplifier network and basic equalizer for 4-megacycle cable loss of 25-decibels

volts (peak to peak) and it is clamped.

When the length of the preceding link is greater than 27 decibels a repeater also is used as a receiving amplifier as shown in Figure 12(B). The signal is clamped and a 2-volt (peak to peak) decibel signal is provided the customer as in the previous receiving terminal. In this case the maximum length of the preceding link is 90 decibels with the extra gain provided by the clamper amplifier. The operation of the receiving amplifier is the same as an intermediate, which will be described in more detail.

The *1B* clamper amplifier provides 18-decibel gain and a 31-decibel reduction of 60-cycle interference and a correction for a loss of low-frequency signal components. It is used in the receiving terminal for gain and to restore the low-frequency signal components after transmission through video repeating coils or over circuits whose length is such that increased low-frequency amplitude or phase distortions may result. The theory of design and the operation of this and other clampers has been presented[4,5] elsewhere and will not be described here.

Intermediate Repeater

The repeater arrangement is shown in Figure 14. In Figure 15 a single repeater with its regulated filament and plate supply panels are shown mounted in a portable cabinet. When a number of repeaters are used in a telephone central office, they are mounted three on an 11 foot relay rack with the necessary cable terminals and interconnecting jack panels as shown in Figure 16. The repeater consists of three principal elements, the input amplifier, the cable equalizers, and the output amplifier as shown in the block diagram of Figure 14.

The input amplifier consists of an input amplifier network, a balanced input stage of gain followed by a cathode output stage connected directly to the line equalizers. A simplified schematic of the input amplifier is shown in Figure 17. The response characteristic of the network is shown on Figure 18 which is part of the cable equalization. The voltage gain of 13 decibels at the high frequencies is part of the total input amplifier gain. Since it raises the high-frequency signal level at the grids the noise figure of the input amplifier is improved 13 decibels. Provision is made to remove the input network when it is not needed as equalization or gain for short cable lengths.

The input longitudinal balance of the amplifier to keep down 60-cycle pickup is provided by the feedback resistance R_K and the balancing adjustment R_1. The longitudinal component at the output resistance R_L of V_3 is

$$e_L = \frac{e_1+e_2}{2} R G_m \left[\frac{K(1+R_K G_m) - R_K G_m}{1+2R_K G_m} \right]$$

where

$$K = \frac{R_2}{R_1+R_2},\ R_2 = 2{,}000 \text{ ohms},\ G_m = 10{,}000 \times 10^{-6}$$

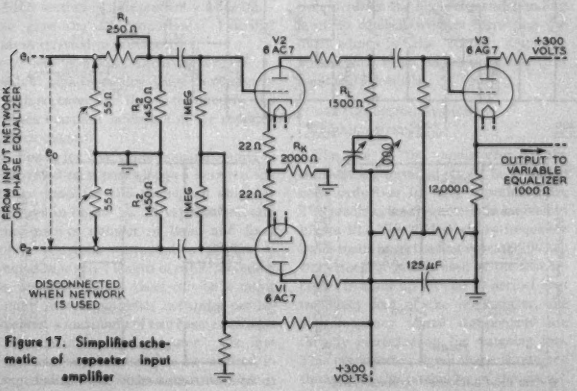

Figure 17. Simplified schematic of repeater input amplifier

The bracket indicates the total of feedback and balance. If the value of $R_1=0$, the bracket gives the feedback reduction which is 32 decibels. If R_1 is adjusted so that

$$K=\frac{R_2G_m}{1+R_2G_m}$$

the bracket reduces to zero and, therefore, eliminates the longitudinal component. It is possible in practice to obtain a reduction of 75 decibels in the low-frequency longitudinal components.

The signal component at the output resistance R of V_2 is

$$e_s=eRG_m{}^1/_2\left[\frac{K(1+R_2G_m)+R_2G_m}{1+2R_2G_m}\right]$$

The loss of the balance circuit is indicated by one half the bracket. If $R_1=0$ the loss reduces to 1/2. If R_1 is adjusted for maximum longitudinal balance as above, the total balance circuit signal loss becomes

$$\frac{R_2G_m}{1+2R_2G_m}$$

which reduces to 20/41 or still approximately 1/2 for the previous circuit conditions. The well-known methods of shunt peaking of the interstage plate resistance R_L is used to obtain a 6-megacycle band which has flat amplitude response and very small phase distortion out to 4 megacycles. The voltage gain of the input amplifier without the input network and terminated in the 1,000-ohm impedance of the cable equalizers is 14 decibels.

The output of the cable equalizers is terminated by the 1,000-ohm input impedance of the output amplifier. This amplifier has three unbalanced gain stages followed by a phase inverter and a balanced output stage. The balanced output stage feeds the balanced cable pair either through the amplifier network or from a 110-ohm termination when it is used as an intermediate repeater. When it is used similarly as a transmitting amplifier its input is terminated in 75 ohms. The voltage gain without the output network, but terminated in 110 ohms is 30 decibels. The normal output operating level is 2 volts (peak to peak) which may be increased 3 decibels for a maximum of three output amplifiers in a circuit. When it is to be used in a receiving amplifier to feed a 75-ohm unbalanced circuit the output is taken from only one of the output tubes terminated in 75 ohms. A simplified schematic is shown in Figure 19. The amplifier network is the same as the one used in the input amplifier having the response characteristic shown in Figure 18. Shunt peaking of the interstage plate resistances is used to obtain a 6-megacycle band which has flat amplitude response and very small phase distortion out to 4 megacycles. Plate load decoupling is used in individual stages to obtain good transient response at the very low frequencies.

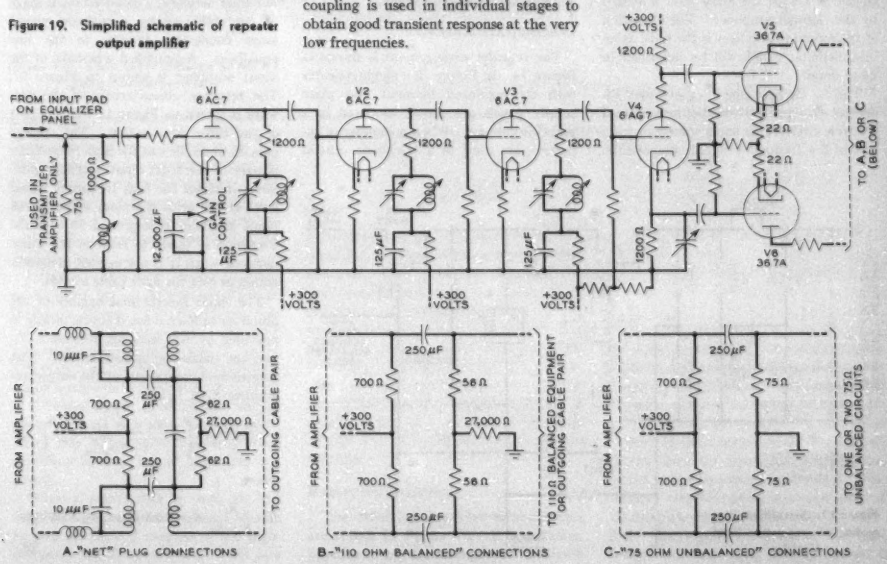

Figure 19. Simplified schematic of repeater output amplifier

Over-all Repeater

The tandem operation of many repeaters requires that systematic irregularities be kept to very small limits. Therefore, the response below 4 megacycles is capable of adjustment to ±0.05 decibel in manufacture or subsequent maintenance work if sufficient care is exercised. The greatest part of this irregularity occurs above 2 megacycles and it is practically zero in the more critical region of the band below 500 kc.

The common operating procedure is to receive a 2-volt (peak to peak) signal from the customer, to operate each repeater output at 2 volts (peak to peak) and to return to the customer at the receiving end of the circuit 2 volts (peak to peak) into a 75-ohm load. The low-frequency loss of the cable pair may be anything from near zero for very short circuits to 5 decibels for a 3.5-mile circuit of number 16 *PSV*. Since the input amplifier operates directly from the line its overload at low frequencies is important. The overload in the input amplifier and the output amplifier of a repeater has been kept low so that compression at operating signal levels is negligible with ten repeaters used in tandem.

Equalization of Cable Characteristic

The equalization of the cable characteristic is accomplished by using multiples

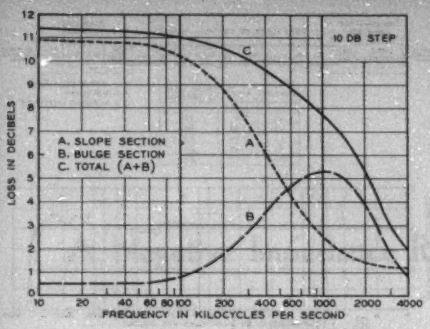

Figure 20. Characteristics of variable and fixed cable equalizer units

(A) Slope section (B) Bulge section (C) Sum of both sections each of which are adjustable in the variable equalizer

of three constant resistance equalizer units located between the input and output amplifiers. These equalizers are referred to as basic, fixed, and variable.

The basic is always associated with an amplifier network. Referring to Figure 18 it will be seen that the sum of the characteristics of the amplifier network and the basic equalizer gives curve *C* which is the inverse characteristic of number 16 *PSV* cable loss. It has been plotted as response instead of loss so it may be recognized easily as proportional to the number 16 *PSV* cable characteristic shown on Figure 6. This combination of units will equalize 25 decibels of 4-megacycle number 16 *PSV* cable loss.

The fixed unit will equalize 10 decibels of 4-megacycle number 16 *PSV* loss. The 10-decibel step of the variable unit has the same characteristic as the fixed unit. The variable unit is adjustable in 12 proportional 1-decibel steps. It consists of two sections in tandem. The sum of these two sections gives the desired loss characteristic *C* as shown in Figure 20. Each section is independently adjustable to give the 12 proportional 1-decibel steps referred to previously.

There is a very small amount of residual high-frequency phase deviation in each repeater link that is removed by the phase equalizer indicated in the repeater block diagram.

Space for five cable equalizer units is provided on a panel located between the input amplifier and the output amplifier as seen in Figure 15. A variable unit and the correct number of basic and fixed units are thus connected in tandem to equalize a given length of cable preceding a repeater. Since there can be a maximum of two amplifier networks per repeater, a maximum of two basic equalizers may be utilized per repeater. The first of these two networks to be utilized in equalizing a line is the output network at the preceding repeater. If the 4-megacycle line loss is 50 decibels or greater the repeater input network is added. Fixed and variable equalizers are then added as needed for longer lengths of cable. The gain of the amplifiers with the equalization that is provided allows for a maximum repeater spacing of about 3.5 miles of spirally shielded number 16 *PSV* or 63-decibel line loss at 4 megacycles.

The general result of the equalizer loss is to attenuate low frequencies more than high frequencies and in the proper amount so that over-all response of the line and equalizer is uniform to a transmitted signal. The impulse noise, originating at the receiving end of the cable, with the cable and amplifier input noise become attenuated with the low-frequency signal components. Therefore, there is a noise reduction in the low-frequency region. There is, also, a reduction in the interfering effect of the noise due to its concentration in the high-frequency band. The use of the output network at the preceding repeater as part of line equalization increases the high-frequency sending level 13 decibels without increasing the overloading in the output amplifier. This results in an added noise improvement of 13 decibels.

Noise Reduction by Signal Predistortion

The use of the predistorter at the transmitting terminal results in an added noise reduction for long repeater links. The predistorter characteristic is given in Figure 10. The 20-decibel low-frequency loss is made up at the first repeater. When 20 decibels of gain is used at the first repeater to make up for the 20-decibel low-frequency loss of the predistorter, the high-frequency signal components are thereby increased on the outgoing line. This predistorted signal shape is retained throughout the remainder of the circuit. It is finally restored to its original shape at the receiving terminal, by the use of a complementary equalizer characteristic shown in Figure 10. Since this restorer has the high loss characteristic shown at the high frequencies it, also, attenuates high-frequency noise. This results in an average improvement in signal-to-impulse noise of 16 decibels and an improvement of almost 20 decibels in the signal-to-random noise from the cable and input amplifier. However, this reduction of noise is not obtained without some penalty. The load capacity of the repeater output stage must be increased some 4 decibels because of the adverse peak factor of the pre-equalized signal. The net gain in signal-to-noise ratio is, therefore, 4 decibels less than the values just given.

Circuit Application

The application of this video transmission system can best be shown by the use of two typical number 16 *PSV* circuit cases.

The simplest circuit case is the one where a central office repeater is located between the transmitting and receiving terminals as shown in Figure 21. In this case the circuits are short and noise protection is not needed. The maximum cable slope characteristic that can be equalized in this case is $L_1+L_4=69$ decibels, with the restriction that $L_4 \leq 27$ decibels. This restriction is necessary to prevent the output amplifier from overloading on the high peaked signals resulting from the pre-equalization for the final link. In the case shown in Figure 21 the loss of L_1 and L_4 are 32 decibels and 20 decibels respectively. The transmission response of the circuit is as shown in the figure.

A more complex circuit application is illustrated in Figure 22. The total length of the five video lines is 11.72 miles having a total 4-megacycle loss of 211 decibels. Also, it will be observed that line L_3 is 5 miles in length with a 4-megacycle loss of 90 decibels and the normal operating procedures must be modified to accommodate this special case.

There is not enough gain or equalization in repeater R_3 to operate a 90-decibel line. However, it is accomplished in this case by altering the operating procedure in three ways. First, it is permissible to operate the output of repeater R_1 at a level which is 3.5 decibels higher than normal. Second, since line L_3 is short the output network in repeater R_3 can be used in the equalization of line L_4. This equalization occurs in the form of 13 dec-

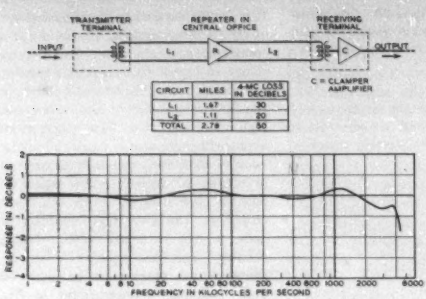

CIRCUIT	MILES	4-MC LOSS IN DECIBELS
L_1	1.67	30
L_2	1.11	20
TOTAL	2.78	50

Figure 21. Simple circuit application of *A2* video transmission system

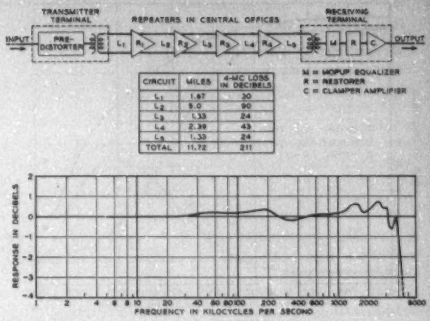

CIRCUIT	MILES	4-MC LOSS IN DECIBELS
L_1	1.67	30
L_2	9.0	90
L_3	1.33	24
L_4	2.39	43
L_5	1.30	24
TOTAL	11.72	211

Figure 22. More complex circuit application of *A2* video transmission system

ibels of high-frequency gain instead of low-frequency loss. Third, since line L_4 is short there is no noise protection problem at repeater R_4 so that the output level of repeater R_4 can be operated the necessary 10 decibels lower than normal. The signal arrives at repeater R_5 10 decibels lower than normal and is raised to normal by use of excess gain in repeater R_5. In this manner the 27 decibels of gain has been obtained to increase the normal repeater spacing of 63 decibels to 90 decibels. This cannot always be done and it is seldom desirable to deviate from a standard operating procedure but in this case it made the operation of an off premise extra repeater unnecessary.

The remainder of the circuit follows normal operating procedure. A final mop-up equalizer is located at the receiving terminal to reduce the amplitude of the residual transmission distortion characteristic. The over-all transmission characteristic is given in Figure 22.

Conclusion

The *A2* video system just described makes use of new repeating coils and new low-loss cables. The new clamping techniques are utilized to restore low-frequency components that may be lost in transmission, reduce low-frequency interference, and improve the low-frequency stability in general of long video circuits.

The video transmission system is ordinarily applied according to a standard operating procedure. However, it has been shown by a complex circuit application that it can be flexibly applied to care for difficult nonstandard operating conditions.

References

1. Television Transmission over Wire Lines, **M. E. Strieby, F. Wentz,** *Bell System Technical Journal* (New York, N. Y.), volume XX, January, 1941.

2. Television Transmission, **M. E. Strieby C. L. Weis.** *Proceedings*, Institute of Radio Engineers (New York, N. Y.) volume 29, July 1941, pages 371–81.

3. Cross Talk and Noise Features of Carrier Telephone System, **M. A. Weaver, R. S. Tucker, P. S. Darnell.** *Bell System Technical Journal* (New York, N. Y.), volume 17, January 1938.

4. The Clamp Circuit (part I and part II), **C. L. Townsend.** *The Broadcast Engineer's Journal* (New York, N. Y.), January 1947, pages 7–9, April 1947, pages 6–9.

5. Clampers in Video Transmission, **S. Deba, Jr., J. W. Rieke.** *AIEE Transactions*, volume 69, part I, 1950, pages 477–87.

No Discussion

A Negative Impedance Repeater

J. L. MERRILL, JR.
NONMEMBER AIEE

IN SPITE of the increasingly widespread use of carrier, coaxial and radio in the long distance plant of the Bell Telephone System, the basic transmission medium for distances in the order of 20 miles or less, is the 2-wire circuit operating at voice frequencies. Such lines serve to link a subscriber's telephone set to its associated central office and to interconnect the various central offices within an area covering a city or a group of towns, known as an exchange area. To improve transmission on these exchange-area lines a new type of device, the negative impedance repeater, has been developed.

As the nation has grown, the exchange area plant has been continually extended and rearranged to meet the changing conditions of the times. Shifts in population or demands for new or special telephone services have required either that some additional device be developed to improve transmission over existing lines or that new facilities having a lower transmission loss per-unit length be installed. One of the first devices developed to lower the loss per-unit length of a copper wire line was the loading coil; and loading coils have found application in the exchange area as well as in the toll plant. Another device developed to reduce circuit loss was the voice frequency repeater, which made the first transcontinental line feasible. However, because of the amount of equipment necessary for 2-wire application, this type of vacuum tube repeater did not prove generally to be an economical answer to the problem of reducing line attenuation in the exchange area.

The negative impedance repeater described herein, designated the *E1* telephone repeater, has been designed specifically for application in exchange area circuits. While it has few parts, it is complete in that it does contain all the equipment necessary for direct insertion in a 2-wire line. Its "package" nature simplifies the equipment and engineering aspects of installation. There are no external jacks, coils, or networks to be associated with it.

The principal field of use of the *E1* repeater appears to be on tandem trunks, toll connecting trunks, and special service lines. In an exchange area some central offices are connected directly with each other by means of direct trunks while others are connected together through an intermediate switching point known as a tandem office. As compared to direct trunking of all calls, tandem switching results in a smaller number of and more efficient trunk groups. However, tandem trunking involves greater distances than direct trunking and hence can require a lower loss per-unit length of line. *E1* repeaters may provide an economical means of reducing transmission losses on trunks from a distant office to tandem. Similarly, they may be used to lower the loss of a trunk connecting a local central office to a toll switching point. Also they may find important application where a subscriber requests a special telephone service and the use of existing line facilities alone would result in poor transmission.

Features

The *E1* repeater consists of three basic parts, Figure 1, a transformer, an amplifier, and a network. The transformer couples the amplifier to the telephone line through two balanced windings, one inserted in each line conductor. The amplifier is a feedback arrangement referred to as a negative impedance converter because, in effect, it transforms the impedance of the network into a negative impedance. This negative impedance is inserted in series with the line by means of the transformer. The network is adjustable. Its impedance determines the voice frequency gain introduced by the repeater, and no other gain control is provided.

No gain is provided for low-frequency signaling current. Direct current can pass through the line windings of the transformer with but slight impairment to d-c supervision (about 40 ohms). Ringing currents, 20 cycles per second, and dial pulses pass through with moderate loss.

The Western Electric Company *407A* vacuum tube used in the amplifier is a twin triode of the miniature type. The two heaters of the *407A* connected in parallel draw 100 milliamperes from a 24-volt central office supply, or connected in series draw 50 milliamperes from the 48-volt supply (power drain in either case 2.4 watts). The plates operate at 130 volts and each one of the two draws 5.5 milliamperes (power drain for the two plates is 1.5 watts). For special applications with an a-c operated power supply a *2C51* vacuum tube can be operated with 6.3 volts on the heater and 130 volts on the plates.

The network contains a number of inductors, capacitors, and resistors which are brought out to terminals on a block under a can cover. Various impedance combinations are available depending

Paper 50-235, recommended by the AIEE Wire Communication Systems Committee and approved by the AIEE Technical Program Committee for presentation at the AIEE Fall General Meeting, Oklahoma City, Okla., October 23–27, 1950. Manuscript submitted July 25, 1950; made available for printing August 29, 1950.

J. L. Merrill, Jr. is with the Bell Telephone Laboratories, Inc., New York, N. Y.

The writer acknowledges the help of K. S. Johnson, P. B. Llewellyn, R. C. Mathes, G. C. Reier, and K. O. Van Wynen, all of the Bell Telephone Laboratories, in evolving the concept of negative impedance expressed herein. He also acknowledges the contributions of W. J. Kopp and J. A. Weller, also of the Bell Telephone Laboratories, to the theory and practical design outlined herein of the negative impedance converter of the *E1* type.

upon the pattern in which these terminals are interconnected or "strapped." The strapping is determined by the type of line facility with which the repeater is to be associated and by the amount of gain required. Two typical network configurations are shown in Figure 2. Both the gain obtainable and the power handling capability of the *E*1 repeater are ample. The maximum usable gain (integrated over a voice frequency range of about 300 to 3,500 cycles per second) is about 10 decibels. The gain at any one frequency may differ somewhat from this integrated value. Because of the impedance relationships found in the exchange plant greater gain than 10 decibels would seldom be usable from any 2-wire repeater. The gain of the *E*1 is the same for both directions of transmission. The repeater will handle without noticeable distortion speech volumes of +10 volume units, and can be located at any point in a circuit since, with present telephone instruments at least, overloading is not a factor.

Method of Application

For most telephone applications the *E*1 repeater can be considered as a negative impedance connected in series with a line. The action of the amplifier can be thought of as converting the impedance of the network to a negative impedance which is coupled in series with the line by means of the line transformer.

In general, a negative impedance inserted at random in a line will provide a transmission gain by increasing the flow of current. It also will produce reflection effects. These reflection effects can be reduced to tolerable proportions by the expedient of limiting the amount of negative impedance allowed under various circumstances, which means limiting the repeater gain. When inserted in a cable circuit a single *E*1 repeater can reduce the loss of a line to about one half of that of the nonrepeatered line without producing noticeable reflection effects. However, more gain can be obtained from a repeater when connected at about the middle of the line than can be had from the repeater when located at or near one end. Where a line consists of a nonloaded section of cable joined to a coil-loaded section maximum permissible gain will be obtained, in general, when the repeater is located at the junction of these two line facilities.

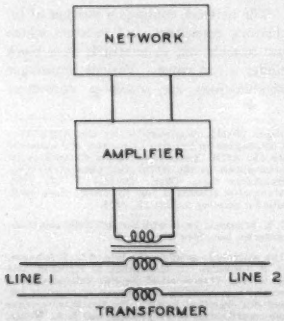

Figure 1. Block diagram of *E*1 telephone repeater

When any lumped impedance, positive or negative, is inserted in a smooth transmission line reflection effects will result unless these effects are phased out in a way similar to that used with coil loading. In general, the term "loading" implies the methodical addition to a uniform transmission line of some impedance or impedances for the purpose of changing the transmission characteristics of the line. For the most part loading is applied for the purpose of reducing line attenuation. It also will change the velocity of propagation and the characteristic impedance of the line. Loading sections need not be of the same length as long as they have about the same impedance where they are joined together, preferably at midsection. Loading with coils adds inductance and thereby reduces the attenuation of a line, decreases the speed of propagation along it and increases the magnitude of the characteristic impedance seen at midsection. Loading with negative impedance adds negative resistance and inductance. This type of loading can be made to reduce line attenuation, increase the speed of propagation, at least at the lower frequencies, and decrease the value of the mid-section characteristic impedance with reference to the characteristic impedance of the nonloaded line. In general, the speed of propagation on lines loaded with negative impedance will materially exceed that of coil-loaded lines. Because of the greater speed of propagation the distance between loading points can be greater with negative impedance loading than it can be for coil loading for the same band of frequencies transmitted. Furthermore, negative impedance loading can reduce line attenuation below that possible with coil loading because the negative resistance element supplies additional power to a line. At present, negative impedance loading appears to be a side issue to the main application of *E*1 repeaters which consists of connecting a single repeater in a coil-loaded or a nonloaded line. These repeaters will be located in convenient central offices.

As mentioned, an *E*1 repeater can be applied on the basis that it is a 2-terminal negative impedance and as such can be inserted in series with a telephone line or other impedances. Thus the repeater may be considered as containing two fundamental elements rather than the three parts shown in Figure 1. The repeater can be considered as consisting of a positive impedance network and a converter whose function is to multiply the impedance of the network by a factor which transforms this positive impedance into a negative impedance. The amplifier and transformer of Figure 1 are both part of this negative impedance converter.

The Negative Impedance Converter

The idea of negative impedance originated over 30 years ago, and was associated with the concept of resistance neutralization. This concept was based on the fact that a 2-terminal device containing a feedback amplifier, an electric arc, or some semiconductor inserted in series with a single mesh circuit could produce the same current flow as would flow otherwise were a resistance R removed from this mesh. Thus, in effect, the device could neutralize[1] an amount of resistance equal to R. Within certain frequency limits such a device could be treated as a negative resistance equal in magnitude to $-R$. However, negative resistance cannot be completely dissociated from reactance at many of the frequencies in the band which must be studied in order to make certain of stability. Consequently, the term negative impedance is used herein to designate the effect produced by a 2-terminal device which has the property of negative re-

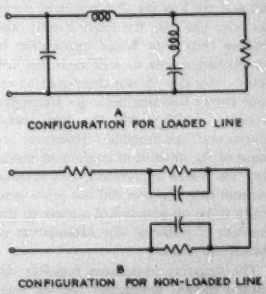

Figure 2. *E*1 repeater network

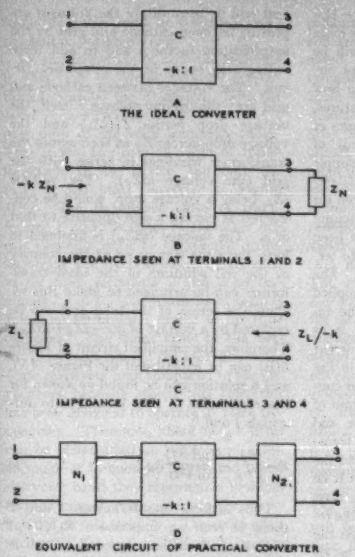

Figure 4 (right). The E1 converter

Figure 3 (above). The negative impedance converter

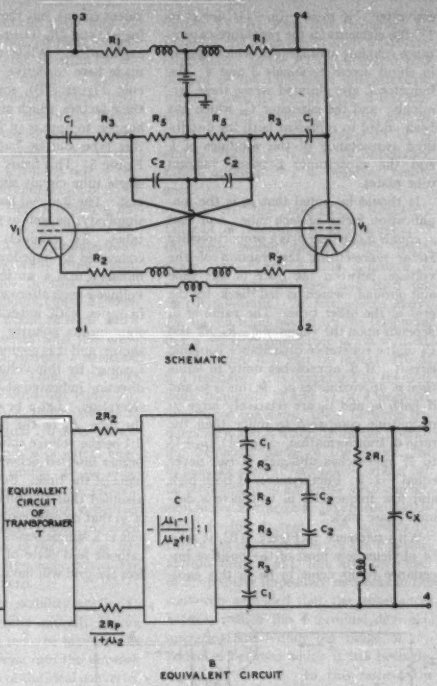

sistance at some frequencies, negative resistance plus reactance at other frequencies, and positive impedance at still other frequencies.

Heretofore, a number of feedback amplifier circuits have been devised for producing negative impedance. These circuits can be described as converting positive impedance into negative impedance. In general, they can be reduced to an electrically equivalent, 4-terminal network consisting of a combination of positive impedance elements together with an approximately ideal negative impedance converter.

An ideal negative impedance converter, Figure 3(A), resembles a form of transformer: it has a ratio of transformation of $-k:1$, can have four terminals and is capable of bilateral transmission. Assume that a positive impedance Z_N is connected to terminals 3 and 4 and $-kZ_N$ is seen at terminals 1 and 2, Figure 3(B). Then it must follow from the theory described herein that if a positive impedance Z_L is connected to terminals 1 and 2, a negative impedance $Z_L/-k$ will be seen at terminals 3 and 4, Figure 3(C).

George Crisson stated[2] that there are two types of negative impedance which he defined as the series type and the shunt type respectively. His series type is the reversed voltage type of negative impedance $-kZ_N$ equivalent to $-E/I$; and his shunt type is the reversed current type $Z_L/-k$ equivalent to $E/-I$. This is a logical development considering that impedance Z equals E/I, and therefore negative impedance $(-Z)$ equals either $-E/I$ or $E/-I$ where E is the voltage measured across the impedance and I is current flowing through it.

A practical converter circuit can be represented by Figure 3(D). A vacuum tube circuit contains positive impedance elements. Some of these will show up in the equivalent circuit on the left-hand side of the ideal converter; others will show up on the right-hand side of the ideal converter. This will be clarified in the discussion of the E1 circuit which follows. The equivalent circuit of any practical negative impedance converter of this type can be represented by the equivalent circuit of Figure 3(D) which shows the positive impedance elements associated with the vacuum tube in the form of two equivalent networks (N_1 and N_2) arranged one on each side of the ideal converter (C) having a transformation ratio of $-k:1$.

The circuit of the negative impedance converter used in the E1 telephone repeater is a new converter circuit. It consists of a transformer, two triode tubes, a resistance-capacitance network and an inductor, Figure 4(A). The transformer T couples the cathodes of the two tubes to terminals 1 and 2. The tubes work in push-pull and are biased for class-A operation. The resistance-capacitance network couples the plate of each tube to the grid of the other. The inductor L supplies plate current.

By the application of circuit theory, an equivalent circuit for Figure 4(A) can be found, Figure 4(B). In obtaining this equivalent circuit the two tubes have been assumed to be identical. Thus the converter used with the E1 repeater can be reduced to a 4-terminal network consisting of (reading from left to right): the equivalent circuit of the line transformer T; the two biasing resistances R_3; the two plate resistances R_p divided by $(1+\mu_2)$; the ideal negative impedance

converter C of ratio $-(\mu_1-1)/(\mu_2+1)$ to 1; the elements in the resistance-capacitance coupling arrangement which appear in shunt across terminals 3 and 4; the inductor L also shunted across these terminals; and the capacitor C_X which has been added to represent both the distributed capacitance of the windings of L and the capacitance between vacuum tube plates.

It should be noted that μ_2 is the amplification factor of each tube; and that μ_1 equals $\beta_1\mu_2$ where β_1 is a proportionality factor representing the fraction of the voltage, between the plate of one tube and ground, which is fed back to the grid of the other tube. The value of β_1 depends upon the values of C_1, R_3, R_5, and C_2 of the resistance-capacitance coupling circuit. If β_1 approaches unity in value then μ_1 approximates μ_2. If this is so and if both μ_1 and μ_2 are relatively large in magnitude compared to unity then the ratio of transformation, $-(\mu_1-1)/(\mu_2+1)$ to 1, approaches although it can never equal $-1:1$. Furthermore, at both high and low frequencies μ_1 will have a definite phase angle.

With reference to Figure 4(B), it may be obvious how most of the positive impedance terms come to be in this equivalent circuit, but the factors $-(\mu_1-1)/(\mu_2+1)$ and $2R_p/(1+\mu_2)$ may require more explanation. While no attempt will be made here to derive the equivalent circuit, Figure 4(B), some idea as to how these factors, which are essential features, happen to appear in feedback circuits of this type can be had from a study of Figure 5. This figure represents a simple single tube circuit similar to the $E1$ circuit. The line coil has been removed for simplicity, as well as one of the vacuum tubes. To terminals 1 and 2 has been connected an impedance Z_L; and to terminals 3 and 4, an impedance Z_N. The voltage e is an alternating voltage applied in series with impedance Z_L. The instantaneous polarity of voltage e is as shown, and it is assumed that the current i caused by this voltage will flow in the direction indicated at the time under consideration. Let μ be the voltage gain of the tube, R_p be the plate resistance, and β:1 be the voltage ratio of the ideal transformer inserted between the grid and the plate of the tube. Furthermore, let it be assumed that the tube is operating class A so that no grid current flows and the result is a simple series circuit through the cathode and plate of the tube. The effect the grid will have on this flow of current will be to multiply the voltages appearing between cathode and grid by the amplification factor μ and to add these voltages in series in the simplified circuit. The voltages between cathode and grid are: the driving voltage e itself, the voltage drop across $Z_L(iZ_L)$ and the voltage drop across Z_N as seen across the transformer windings in series with the grid (the voltage $i\beta Z_N$). The voltage iZ_L, being a voltage drop, would be considered as having a sign opposite to that of e. The voltage $(i\beta Z_N)$ is assumed to have the same sign as e and the polarity of the coil windings of the ideal transformer can be arranged to make this so. Thus the action of the tube grid can be replaced by a voltage of $\mu(e-iZ_L+i\beta Z_N)$. Therefore, the simplified circuit of Figure 5(B) can be substituted for Figure 5(A), and a solution can be found as shown for the impedance Z seen looking into terminals 1 and 2.

$$Z=\frac{R_p}{1+\mu}-\frac{(\mu\beta-1)}{(\mu+1)}Z_N \qquad (1)$$

Thus looking into terminals 1 and 2 there is seen an impedance $R_p/(1+\mu)$ in series with an impedance Z_N which is multiplied by $-(\mu\beta-1)/(\mu+1)$, the transformation ratio of an ideal converter. The transformation ratio can be expressed as $-(\mu_1-1)/(\mu_2+1)$ to 1. In one sense this transformation ratio represents the action of both positive and negative feedback. If μ_1 approximates μ_2 in both magnitude and phase, and if this magnitude is large compared to unity then the trans-

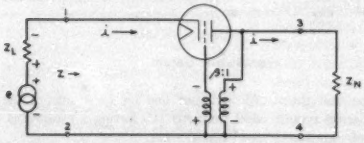

WHERE:
e = AC APPLIED VOLTAGE
i = CURRENT FLOW RESULTING FROM e
β = VOLTAGE RATIO OF TRANSFORMER
Z_L = LINE IMPEDANCE
Z_N = NETWORK IMPEDANCE

A
SCHEMATIC

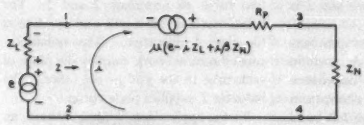

WHERE:
μ = VOLTAGE GAIN OF TUBE
R_P = PLATE RESISTANCE OF TUBE
AND:
NEITHER GRID NOR TRANSFORMER DRAWS CURRENT

$$e+\mu\left[e-iZ_L+i\beta Z_N\right]=i\left(Z_L+R_P+Z_N\right)$$

$$\left[e-iZ_L\right]\left[\mu+1\right]=i\left[R_P+Z_N\left(1-\mu\beta\right)\right]$$

$$Z=\frac{e-iZ_L}{i}=\frac{R_P}{1+\mu}-\frac{Z_N\left(\mu\beta-1\right)}{\mu+1}$$

B
SIMPLIFIED CIRCUIT OF A

Figure 5 (left). Operation of the E1 converter

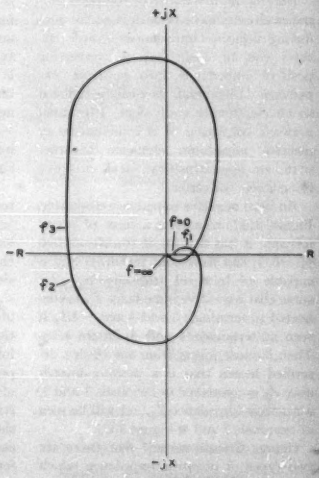

Figure 6 (right). Impedance locus of E1 repeater with resistance network

formation ratio would be relatively independent of variations in μ.

As an illustration of how the elements in this type of circuit may be proportioned, consider the $E1$ design. Here the ratio $-(\mu_1-1)/(\mu_3+1)$ to 1 is $-0.9:1$ over most of the voice frequency range. This is not the over-all ratio of transformation of the device, but only the ratio of the ideal converter C, Figure 4(B). The impedance ratio of transformer T and the effect of the other circuit elements must be considered in determining the over-all effect of the converter from terminals 1 and 2 to terminals 3 and 4. The transformer ratio is 1:9 from terminals 1 and 2 to the tube cathodes. The shunt arms of the networks on both sides of the ideal converter C are relatively high compared to the impedances between which this converter has been designed to operate at voice frequencies. Therefore, these shunt arms can be disregarded at voice frequencies, although at frequencies above and below the voice band they represent a problem for the circuit designer from the viewpoint of circuit stability. The series arms such as $2R_p/(1+\mu_3)$ and $2R_3$ could be cancelled out by adding in series on the right-hand side of the ideal converter a resistance of 1,800 ohms (not shown in Figure 4). The final result is that the impedance seen looking into terminals 1 and 2 of the $E1$ converter when 1,800 ohms plus a network Z_N is connected to terminals 3 and 4 equals $-0.1\ Z_N$ within a reasonable percentage of error over the frequency range from about 300 to 3,500 cycles per second for values of negative impedance from about 100 to 2,000 ohms. Actually this multiplying factor of -0.1 has a slight phase angle at frequencies other than about 1,000 cycles per second which must be taken into account for detailed design work.

In the $E1$ design two line windings instead of the one shown connected between terminals 1 and 2 in Figure 4(A) are provided on transformer T. In practice one of these windings is inserted in each side of the telephone line in a balanced arrangement. Terminals 1 and 2 are thus effectively connected in series with the line, and the $E1$ repeater inserts in the telephone line a reversed voltage type of negative impedance $(-E/I)$, which is the means of introducing additional power in the line, thereby providing a transmission gain.

Stability

Like any amplifier whose output connects back to its input, the negative impedance converter can run away with itself and oscillate if not properly terminated. Fortunately, the criterion for determining stability is simple. Consider again the ideal converter, Figure 3(B). Assume that Z_L, not shown on Figure 3(B), is an impedance connected to terminals 1 and 2. Consider the circuit mesh formed on the left-hand side of the ideal converter by the connection of Z_L to terminals 1 and 2. Here a negative impedance $(-kZ_N)$ is seen looking into terminals 1 and 2, and a positive impedance (Z_L) is seen looking away from them. The total impedance in this mesh is Z_L-kZ_N. If kZ_N should equal Z_L then the total impedance would be zero; and a voltage inserted in series with this mesh would call for infinite current, a situation obviously impossible. Thus it becomes evident that kZ_N should not equal Z_L; or, what is the same thing, the ratio kZ_N/Z_L should not equal 1/0 if the system is to be stable. From a practical engineering viewpoint, a simple rule for judging stability can be stated as follows: The ideal negative impedance converter will be unconditionally stable provided that the magnitude of kZ_N/Z_L is less than unity at any frequency where the angle of this ratio is zero.

This same rule for stability applies to any practical converter circuit, Figure 3(D). However, Z_L must be taken as the impedance seen looking into the network N_1 from the position of the ideal converter C, and Z_N must be taken as the impedance seen looking into network N_2 from the ideal converter C. In other words, the effect of N_1 must be included in Z_L and the effect of N_2 must be included in Z_N.

Actually, the proper handling of N_1 and N_2 to insure inherent stability of a negative impedance converter is the job of the circuit designer just as the elimination of parasitic oscillations of any kind is his concern. The engineer who applies these devices in the field does not have to bother with such details.

Impedance Characteristics

Figure 6 presents an example of an impedance characteristic of the $E1$ repeater, Figure 4(A), as viewed from terminals 1 and 2 with a resistance connected to terminals 3 and 4. The impedance locus is plotted on the resistance-reactance plane. Frequency is taken as the "running" parameter and the impedance is presented for the frequency range from zero to infinity. At zero frequency this impedance would be a small positive resistance equal to the d-c resistance of the primary windings of transformer T. At some low frequency f_1, Figure 6, the locus would show a positive impedance. In the $E1$ repeater it is this portion of the impedance characteristic which is used for the passage of low frequencies such as ringing, dialing, and so forth. Between the frequencies of f_2 and f_3, Figure 6, is seen an impedance which approximates a negative resistance.

This is the operating frequency range of the repeater. At high frequencies the locus would approach the origin again. In Figure 6 this approach is shown through the first and then the fourth quadrant. At frequencies above the speech band passed by the telephone line a negative impedance is not wanted. From Figure 6 it can be observed that if a resistance R is connected to the network terminals (3 and 4) of a negative impedance converter, then, between frequencies f_2 and f_3 which define the operating frequency range of the device, the impedance seen at terminals 1 and 2 can be represented by kR where k is a conversion factor having an angle approximately equal to 180 degrees. The factor k includes not only the effect of the transformation ratio $-k:1$, but also the effect of the positive impedance networks in the converter provided that the impedances between which this 4-terminal device is operating are within the range of impedances between which it has been designed to operate. In this respect the negative impedance converter is like a transformer. Furthermore, if a network having an impedance Z_N is connected to terminals 3 and 4 then at terminals 1 and 2 will be seen an impedance equal to kZ_N which will be a negative impedance between frequencies f_2 and f_3.

The question of stability becomes a relatively easy problem in the application of a properly designed negative impedance of the reversed voltage type. If the network used with the converter is designed to have an impedance characteristic similar to the sum of the two line impedances (line 1 and line 2 of Figure 1) and if the magnitude of the sum of these two impedances is greater than kZ_N at all frequencies the system will be stable. It should be noted that k is the conversion factor only for the band of frequencies between f_2 and f_3. However, in a properly designed converter the magnitude of the negative real component of k will be greater within this band of frequencies than it will be outside this band. Hence, any error in the assumption that k applies at frequencies outside the band defined by f_2 and f_3, in most cases, will be on the side of increased stability.

Conclusion

A repeater having the properties of a negative impedance converter can be used in a telephone line for the following purposes:

1. To decrease the transmission loss of a line by the application of a single repeater. This is accomplished with negative impedance by cancelling, in effect, part of the line impedance thus causing an increase in current flow. Of course, the magnitude of the negative impedance should be kept below the value where reflection effects become noticeable. It is expected that most applications will be of this kind where a single *E*1 repeater is used on a tandem trunk, a toll connecting trunk or a special service line.

2. To load a line with negative impedance. By this means it is possible to produce a low loss line without reflection effects.

3. To eliminate a lumped impedance irregularity equal to Z by the series addition to it of a negative impedance equal to $-Z$.

References

1. Theory of Thermionic Vacuum Tube Circuits (book), L. J. Peters. McGraw-Hill Book Company, New York, N. Y., 1927.

2. Negative Impedance and the Twin 21-Type Repeater, G. Crisson. *Bell System Technical Journal* (New York, N. Y.), July 1931.

3. Regeneration Theory, H. Nyquist. *Bell System Technical Journal* (New York, N. Y.), January 1932.

4. Stabilized Negative Impedances, E. L. Ginzton. *Electronics* (New York, N. Y.), July 1945.

5. Network Analysis and Feedback Amplifier Design (book), H. W. Bode. D. Van Nostrand Company, Inc., New York, N. Y., 1945.

No Discussion

Effect of Three-Phase Motor Loads on Voltage Changes Produced by Single-Phase Loads

M. A. FAUCETT
MEMBER AIEE

M. FISHER, JR.
ASSOCIATE AIEE

M. S. HELM
ASSOCIATE AIEE

THE problem of determining the voltage changes produced by single-phase loads has increased during the past several years. One of the principal reasons for this increase is the application of single-phase resistance welding to many new processes. The usual type of single-phase resistance welder requires for its operation large intermittent values of kilovolt-amperes at a low power factor. This type of load will, of course, produce voltage fluctuations on the power system adjacent to the welder. If these variations are severe enough, they may cause objectionable lighting flicker to the other customers served from the same portion of the power system. The usual range of permissible voltage variation is from 0.5 to 1.5 volts on a 120-volt base. The actual value is dependent upon the type of welder load, whether cyclic or noncyclic, and if cyclic upon the frequency of the load application.

Since such variations are objectionable, it is necessary that the power company engineer be able to determine accurately what the variation in voltage will be in order to provide adequate service at the lowest cost. In general these problems have been handled satisfactorily with considerable ingenuity in devising schemes to keep the cost of service reasonable. However, in some cases voltage drops measured after a welder was installed were appreciably lower than had been calculated. It was reasoned by many power company engineers that this was caused by motor loads adjacent to the welder. In the calculations any possible effect of these motor loads in reducing the voltage changes had been neglected.

It is shown in this paper that there is definitely an improvement in the voltage regulation as a result of motor loads adjacent to a single-phase load. Methods of determining this improvement are given together with the results of some typical calculations. These calculations show that the improvements are large enough to warrant consideration in an accurate analysis of the voltage change produced by a single-phase load.

Analytical Development

General Method of Analysis

In this paper the analysis of voltage changes produced by a single-phase load is made by the method of symmetrical components. The method used is similar to that employed for nonsymmetrical fault calculations.

It is assumed that the single-phase load is the only unbalance on an otherwise symmetrical system. It also is assumed that all currents and voltages are sinusoidal.

In Figure 1, I_a, I_b, and I_c represent the currents flowing to the single-phase load. V_a, V_b, and V_c are the neutral-to-line voltage rises of the respective phases after the load is connected.

Sequence Network Relations

In this analysis ABC is taken as the positive phase sequence and the subscripts 1, 2, and 0 refer to the positive, negative, and zero sequences respectively. The general sequence networks are shown in Figure 2. In this figure F_1, F_2, and F_0 indicate the point of unbalance in the respective networks. V_{a_1} is the neutral-to-line voltage rise of phase A at F_1 in the positive-sequence network. I_{a_1} is the current of phase A flowing from the positive-sequence network into the unbalanced load. V_{a_2}, V_{a_0}, I_{a_2}, and I_{a_0} are similarly defined.

Let V_{F_A} be the positive-sequence neutral-to-line voltage rise of phase A at F before the load is connected. Then by the principle of superposition

$$V_{a_1} = V_{F_A} - I_{a_1} Z_1 \tag{1}$$

where Z_1 is the positive-sequence impedance from F_1 to the neutral bus (generated electromotive forces considered zero). Likewise

$$V_{a_2} = -I_{a_2} Z_2 \tag{2}$$

$$V_{a_0} = -I_{a_0} Z_0 \tag{3}$$

where Z_2 and Z_0 are defined in a manner similar to Z_1. Since the system was balanced originally, there would be no negative- or zero-sequence voltages existing before the single-phase load was connected.

General Equivalent Circuit

Referring to Figure 1, the conditions at the point F are:

$$I_a = 0 \qquad I_b = -I_c \qquad V_b - I_b Z_F = V_c \tag{4}$$

The symmetrical components of the single-phase load currents are:

$$I_{a_0} = {}^1/_3(I_a + I_b + I_c) = {}^1/_3(0 + I_b - I_b) = 0$$

$$I_{a_1} = {}^1/_3(I_a + aI_b + a^2 I_c) = {}^1/_3(0 + aI_b - a^2 I_b) = \frac{a - a^2}{3} I_b$$

$$I_{a_2} = {}^1/_3(I_a + a^2 I_b + aI_c) = {}^1/_3(0 + a^2 I_b - aI_b) = -\left[\frac{a - a^2}{3}\right] I_b$$

$$I_{a_2} = -I_{a_1} \tag{5}$$

The voltage rises at the point F in

Paper 50-236, recommended by the AIEE Electric Welding and Transmission and Distribution Committees and approved by the AIEE Technical Program Committee for presentation at the AIEE Fall General Meeting, Oklahoma City, Okla., October 23–27, 1950. Manuscript submitted July 17, 1950; made available for printing August 25, 1950.

M. A. Faucett, M. Fisher, Jr., and M. S. Helm are all with the University of Illinois, Urbana, Ill. The problem discussed in this paper was studied in co-operation with the Utilities Research Commission, Chicago, Ill.

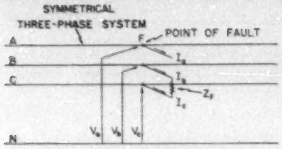

Figure 1. Single-phase load considered as a line-to-line fault on a symmetrical 3-phase system

terms of their symmetrical components are:

$$\begin{aligned} V_a &= V_{a_1}+V_{a_2}+V_{a_0}=V_{a_1}+V_{a_2} \\ V_b &= V_{b_1}+V_{b_2}+V_{b_0}=a^2V_{a_1}+aV_{a_2} \\ V_c &= V_{c_1}+V_{c_2}+V_{c_0}=aV_{a_1}+a^2V_{a_2} \end{aligned} \tag{6}$$

Since $I_{a_0}=0$, V_{a_0} must also equal zero.

Using the relations expressed in equations 4 and 6 it can be seen that

$$V_b-V_c=(a^2-a)V_{a_1}-(a^2-a)V_{a_2}=I_bZ_F$$

since

$$I_b=I_{b_1}+I_{b_2}+I_{b_0}=a^2I_{a_1}+aI_{a_2}=(a^2-a)I_{a_1}$$

the preceding equation becomes

$$V_b-V_c=(a^2-a)V_{a_1}-(a^2-a)V_{a_2}=(a^2-a)I_{a_1}Z_F$$

or

$$V_{a_1}=V_{a_2}+I_{a_1}Z_F \tag{7}$$

In order to satisfy the conditions given in equations 5 and 7, the sequence networks must be connected as shown in Figure 3.

I_{a_1} can be found in terms of the sequence network impedances and the voltage existing before the single-phase load is connected. Solving equation 1 for V_{F_A} and making use of equations 2, 5, and 7

$$V_{F_A}=V_{a_1}+I_{a_1}Z_1=V_{a_2}+I_{a_1}Z_F+I_{a_1}Z_1=I_{a_1}Z_2+I_{a_1}Z_F+I_{a_1}Z_1$$

or

$$I_{a_1}=\frac{V_{F_A}}{Z_1+Z_2+Z_F} \tag{8}$$

V_{a_1} and V_{a_2} also can be determined in terms of the sequence network impedances and the voltage existing before the fault. From equations 1 and 8

$$V_{a_1}=V_{F_A}-I_{a_1}Z_1=V_{F_A}\left[1-\frac{Z_1}{Z_1+Z_2+Z_F}\right] \tag{9}$$

and from equations 2, 5, and 8

$$V_{a_2}=-I_{a_2}Z_2=V_{F_A}\left[\frac{Z_2}{Z_1+Z_2+Z_F}\right] \tag{10}$$

Equations for Voltage Changes at the Primaries of the Transformer Bank Supplying the Single-Phase Load

The preceding general relations and equivalent circuit can be used to determine equations for finding the voltages at a given point in a specific circuit. In this section, these general relations are used to determine the voltage changes for the particular circuit shown in Figure 4. This circuit is typical of many single-phase welder supply systems. The voltage changes at the primaries of the supply transformers are of interest to the utility engineer since it is the primary voltage changes which affect adjacent customers. The following analysis will also show the general method of analyzing other circuit configurations.

For the system of Figure 4, let:

E_{S_A} = excitation voltage rise of the source, neutral-to-line (phase A)
Z_{S_1} = impedance of supply (source and line) to positive sequence
Z_{S_2} = impedance of supply to negative sequence
Z_{MP_1} = impedance of motor load and associated transformer bank at P to positive sequence (equivalent Y-Y)
Z_{MP_2} = impedance of motor load and associated transformer bank at P to negative sequence (equivalent Y-Y)
Z_{T_1} = impedance of supply transformer to positive sequence (equivalent Y-Y)
Z_{T_2} = impedance of supply transformer to negative sequence (equivalent Y-Y)
Z_{MF_1} = impedance of motor load at F to positive sequence (Y value)
Z_{MF_2} = impedance of motor load at F to negative sequence (Y value)
Z_F = impedance of single-phase load
V_{Pa1}, V_{Pb1}, and V_{Pc1} = the positive-sequence neutral-to-line voltage rises at the point P after the single-phase load is connected
V_{Pa2}, V_{Pb2}, and V_{Pc2} = the negative-sequence neutral-to-line voltage rises at the point P after the single-phase load is connected
V_{Pab}, V_{Pbc}, and V_{Pca} = the line-to-line voltage rises at the point P after the single-phase load is connected
V_{PAB}, V_{PBC}, and V_{PCA} = the line-to-line voltage rises at the point P before the single-phase load is connected
V_{PA}, V_{PB}, and V_{PC} = the neutral-to-line voltage rises at the point P before the single-phase load is connected

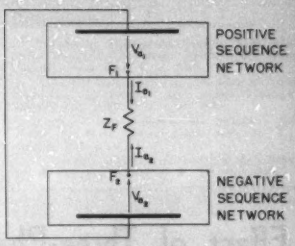

Figure 3. Connection of sequence networks for a line-to-line single-phase load

Using the preceding definitions, the equivalent circuit for the system of Figure 4 is given in Figure 5. The motors in this equivalent circuit have been shown only as impedances and therefore strictly speaking represent induction motors. Synchronous motors in such a circuit must be shown in the same manner as the source, that is, as an excitation voltage in series with an impedance. However, this does not affect the analysis of conditions after the single-phase load is connected since the impedances Z_1 and Z_2 which appear in the solution are defined as the impedances viewed from the point F in the respective networks with all generated electromotive forces considered zero. These definitions can be made as a result of the principle of superposition.

The circuit of Figure 5 is applicable after the single-phase load is connected. In accordance with equations 5 and 8

$$I_{a_1}=\frac{V_{F_A}}{Z_1+Z_2+Z_F} \tag{11}$$

and

$$I_{a_2}=-I_{a_1} \tag{12}$$

where

$$Z_1=\frac{\left[\dfrac{Z_{S_1}Z_{MP_1}}{Z_{S_1}+Z_{MP_1}}+Z_{T_1}\right]Z_{MF_1}}{\dfrac{Z_{S_1}Z_{MF_1}}{Z_{S_1}+Z_{MP_1}}+Z_{T_1}+Z_{MF_1}} \tag{13}$$

Figure 4. A typical system for supplying a single-phase welder load

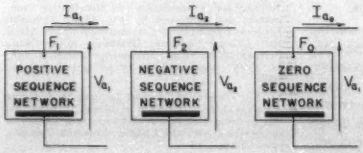

Figure 2 (left). General sequence networks

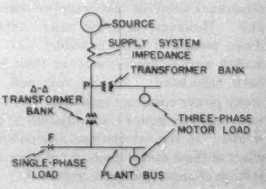

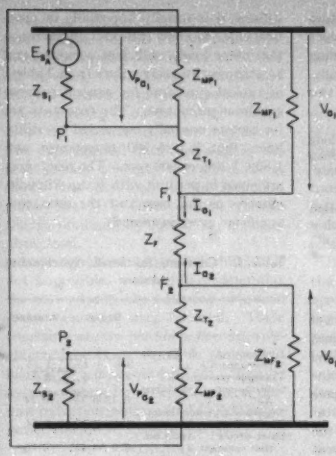

Figure 5 (left). Equivalent circuit for the system shown in Figure 4, after the single-phase load is connected

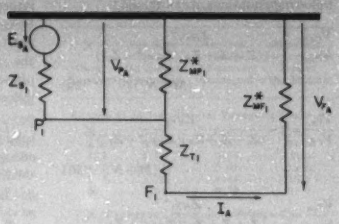

Figure 6 (right). Equivalent circuit for the system shown in Figure 4, before the single-phase load is connected

$$Z_2 = \frac{\left[\dfrac{Z_{S_2}Z_{MP_2}}{Z_{S_2}+Z_{MP_2}} + Z_{T_2}\right] Z_{MF_2}}{\dfrac{Z_{S_2}Z_{MP_2}}{Z_{S_2}+Z_{MP_2}} + Z_{T_2} + Z_{MF_2}} \tag{14}$$

The component of current in Z_{S_1}, due to the single-phase load is

$$I_{P_{a1}} = I_{a_1} \frac{Z_{MF_1}}{Z_{T_1} + \dfrac{Z_{S_1}Z_{MP_1}}{Z_{S_1}+Z_{MP_1}} + Z_{MF}} \times \frac{Z_{MP_1}}{Z_{S_1}+Z_{MP_1}}$$

$$= I_{a_1} \frac{Z_{MF_1}Z_{MP_1}}{Z_{S_1}Z_{MP_1} + Z_{T_1}Z_{S_1} + Z_{T_1}Z_{MP_1} + Z_{MF_1}Z_{S_1} + Z_{MF_1}Z_{MP_1}} \tag{15}$$

Likewise

$$I_{P_{a2}} = I_{a_2} \frac{Z_{MF_2}}{Z_{T_2} + \dfrac{Z_{S_2}Z_{MP_2}}{Z_{S_2}+Z_{MP_2}} + Z_{MF_2}} \times \frac{Z_{MP_2}}{Z_{S_2}+Z_{MP_2}}$$

$$= I_{a_2} \frac{Z_{MP_2}Z_{MP_2}}{Z_{S_2}Z_{MP_2} + Z_{T_2}Z_{S_2} + Z_{T_2}Z_{MP_2} + Z_{MP_2}Z_{S_2} + Z_{MP_2}Z_{MP}} \tag{16}$$

Before the single-phase load is connected, the equivalent circuit is the positive-sequence network shown in Figure 6. In this figure I_A is the load current to the motors at F and V_{PA} is the voltage rise (neutral-to-line) at point P before the load is connected. $Z_{MP_1}{}^*$ is the impedance of the motor load at F as determined from the voltage, current, and power of the motor load before the single-phase load is connected. $Z_{MP_1}{}^*$ is similarly defined. In the case of an induction motor, such an impedance is the same as the impedance determined from the usual equivalent circuit. An impedance determined from the impressed voltage, current, and power factor of a synchronous motor gives a completely fictitious impedance since the equivalent circuit is usually an excitation voltage in series with the synchronous impedance. All other quantities in Figure 6 are as previously defined.

From Figure 6 it is seen that

$$V_{PA} = V_{PA} + I_A Z_{T_1} = V_{PA} + \frac{V_{PA}}{Z_{MP_1}{}^*} Z_{T_1} \tag{17}$$

V_{PA} is the positive-sequence voltage rise at P before connecting the single-phase load. V_{Pa1} is the positive-sequence voltage rise at P after connecting the single-phase load. I_{Pa1} is the component current in Z_{S_1} due to the single-phase load. Therefore by the principle of superposition

$$V_{Pa_1} = V_{PA} - I_{Pa1} Z_{S_1} \tag{18}$$

Likewise

$$V_{Pa_2} = 0 - I_{Pa_2} Z_{S_2} = -I_{Pa2} Z_{S_2} \tag{19}$$

since there was no negative-sequence voltage at P previous to connecting the single-phase load.

Substituting V_{PA} from equation 17, I_{Pa1} from equation 15, and I_{a1} from equation 11 into equation 18

$$V_{Pa_1} = V_{PA}\left[1 + \frac{Z_{T_1}}{Z_{MP_1}{}^*} - \frac{1}{Z_1+Z_2+Z_F} M\right] \tag{20}$$

where

$$M = \frac{Z_{MP_1}Z_{MP_1}Z_{S_1}}{Z_{S_1}Z_{MP_1} + Z_{T_1}Z_{S_1} + Z_{T_1}Z_{MP_1} + Z_{MF_1}Z_{S_1} + Z_{MF_1}Z_{MP_1}} \tag{21}$$

Similarly

$$V_{Pa_2} = V_{PA}\left[\frac{1}{Z_1+Z_2+Z_F} N\right] \tag{22}$$

where

$$N = \frac{Z_{MP_2}Z_{MP_2}Z_{S_2}}{Z_{S_2}Z_{MP_2} + Z_{T_2}Z_{S_2} + Z_{T_2}Z_{MP_2} + Z_{MP_2}Z_{S_2} + Z_{MP_2}Z_{MP_2}} \tag{23}$$

It can be shown by the use of equations similar to equation 6 that

$$V_{Pab} = V_{Pb} - V_{Pa} = a^2 V_{Pa_1} + a V_{Pa_2} - V_{Pa_1} - V_{Pa_2}$$
$$= \sqrt{3}\angle 210^\circ \quad V_{Pa_1} + \sqrt{3}\angle 150^\circ V_{Pa_2} \tag{24}$$

Also

$$V_{PAB} = V_{PB} - V_{PA} = (a^2 - 1) V_{PA}$$
$$= \sqrt{3}\angle 210^\circ \; V_{PA} \tag{25}$$

and

$$\frac{V_{Pab}}{V_{PAB}} = \frac{V_{Pa_1} - V_{Pa_2}\angle 120^\circ}{V_{PA}} \tag{26}$$

In a similar manner

$$\frac{V_{Pbc}}{V_{PBC}} = \frac{V_{Pa_1} - V_{Pa_2}}{V_{PA}} \tag{27}$$

$$\frac{V_{Pca}}{V_{PCA}} = \frac{V_{Pa_1} - V_{Pa_2}\angle 240^\circ}{V_{PA}} \tag{28}$$

Putting the values of V_{PA}, V_{Pa_1}, and V_{Pa_2} from equations 17, 20, and 22 respectively into the preceding relations the

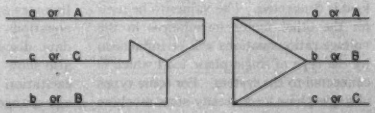

Figure 7. Lettering convention used for a Y-delta transformer bank

following equations are obtained

$$\frac{V_{Pab}}{V_{PAB}}=\left|1-\frac{Z_{MF_1}^*}{(Z_1+Z_2+Z_F)(Z_{MF_1}^*+Z_{T_1})}\times(M+N/\underline{120^\circ})\right| \quad (29)$$

$$\frac{V_{Pbc}}{V_{PBC}}=\left|1-\frac{Z_{MF_1}^*}{(Z_1+Z_2+Z_F)(Z_{MF_1}^*+Z_{T_1})}\times(M+N)\right| \quad (30)$$

$$\frac{V_{Pca}}{V_{PCA}}=\left|1-\frac{Z_{MF_1}^*}{(Z_1+Z_2+Z_F)(Z_{MF_1}^*+Z_{T_1})}\times(M+N/\underline{240^\circ})\right| \quad (31)$$

The voltage ratios given by equations 29, 30, and 31 are given in the form of the absolute value of a complex quantity since usually only the magnitude of the voltage changes are of importance. The results are expressed as a ratio of the voltage existing after and before the single-phase load is connected since usually the actual voltages at a given point would not be known. If, for example, a ratio of 0.985 were obtained, it would indicate that the single-phase load would reduce the voltage in question to 0.985 times its former value or a voltage drop of 1.5 per cent.

Y-Delta Transformer Bank

The equations just given for the primary line-to-line voltages apply only to a delta-delta connected transformer bank. For a Y-delta transformer bank it can be shown that equations 29, 30, and 31 still give the primary line-to-line voltage ratios provided the plus sign between the M and N terms is replaced by a minus sign.

If the ratios of the line-to-neutral voltages of the Y-delta bank are desired, equations 29, 30, and 31 can be used as follows: equation 29 for the ratio V_{Pc}/V_{PC} equation 30 for the ratio V_{Pa}/V_{PA}, and equation 31 for the ratio V_{Pb}/V_{PB}. This is based on the lettering convention for the Y-delta bank shown in Figure 7.

Motor Impedances to Be Used in Voltage Ratio Equations

The impedance $Z_{MF_1}^*$ which appears in some of the voltage ratio equations is always determined from the voltage, current, and power factor of the motor load connected at F before the single-phase load is connected. The values to be used for the other motor impedances in the voltage ratio equations will be influenced by the type of single-phase load which is connected to the system. For some types of single-phase loads steady-state machine impedances can be used while in other cases subtransient or transient values must be used. To help in determining the proper motor impedances, single-phase loads will be divided into the two following types:

1. Loads connected for an indefinitely long time or connected with an "on" period long enough for the system to reach a steady-state condition.

2. Loads connected with an "on" period so short that the system does not reach a steady-state condition before the "off" period occurs.

Synchronous Motors

For most practical problems of voltage changes involving synchronous machines it is sufficiently accurate to neglect the armature resistance and to use cylindrical rotor theory for both nonsalient pole and salient-pole machines. In the latter case, the direct-axis reactance X_d of the salient-pole machine is used as the synchronous reactance X_s of the equivalent cylindrical-rotor machine.

For type (1) single-phase loads, the synchronous reactance $X_s=X_d$ is used for the positive-sequence motor impedance and the synchronous machine negative-sequence reactance X_2 is used for the negative-sequence motor impedance. For type (2) single-phase loads, the synchronous machine subtransient reactance X_d'' should be used for the positive-sequence motor impedance with loads having "on" periods of 2 or 3 cycles or less and the transient reactance X_d' should be used for the longer "on" periods. The negative-sequence reactance X_2 is used for the negative-sequence motor impedance for type (2) single-phase loads since this value is by its very nature a transient value.

Synchronous machine impedances are affected some by saturation, in other words, by the load on the machine and the amount of field excitation. However, this refinement does not need to be considered in this investigation since the negative-sequence motor impedance, which has the most effect of the voltage change, is nearly independent on saturation due to the damper windings used with synchronous motors. The negative-sequence motor impedance has more effect on the voltage change than the positive-sequence motor impedance since it is the smaller of the two. This effect becomes apparent when the voltage ratio equations are used. The experimental data discussed in the following section also show that the magnitude of the field excitation has a minor effect on the voltage change.

Since it is usually impossible in practical cases to know the exact character of the motor loads, sufficient accuracy can be obtained by using values from Table I of typical constants for general purpose synchronous motors. The constants are for motors normally connected to utility lines, that is, 25–500 horsepower and 1,800, 1,200, or 900 rpm. The reactances are given in per unit with stator kilovolt-amperes as the base and the time constants are given in seconds.

Table I. Constants for Small Synchronous Motors

	Range	Average
Unsaturated direct-axis reactance X_d	0.6 –1.45	1.15
Transient reactance X_d'	0.2 –0.5	0.37
Subtransient reactance X_d''	0.13–0.35	0.24
Negative-sequence reactance X_2	0.13–0.35	0.24
Short-circuit transient time constant T_d'	0.5 –0.65	0.58
Short-circuit subtransient time constant T_d''	0.01–0.02	0.015

Induction Motors

The positive-sequence impedance of an induction motor is the impedance determined from the usual equivalent circuit. This impedance depends on the slip S, that is, on the load carried by the motor. The negative-sequence impedance can be determined by substituting a slip of (2-S) for the S of the usual equivalent circuit. This will show that the negative-sequence impedance is for all practical purposes equal to the blocked-rotor impedance. For transient studies involving induction motors an impedance equal to the blocked rotor impedance is used for the positive-sequence impedance. This impedance might be compared to the subtransient impedance of a synchronous machine. Since there is no field winding, there is no impedance of an induction motor which is comparable to the transient impedance of a synchronous machine.

For type (1) single-phase loads, the usual positive-sequence and negative-sequence impedances are used for the motor impedances in the voltage ratio equations. For type (2) single-phase loads, the blocked-rotor impedance should be used as the positive-sequence motor impedance with loads having "on" periods of 1 or 2 cycles; for "on" periods longer than this the usual positive-sequence impedance should be used. For all type (2) loads, the blocked-rotor impedance is used as the negative-sequence motor impedance.

The usual positive-sequence imped-

ance of an induction motor varies with load. In general, this will not need to be taken into account and the full-load value can be used. This follows from the fact that the negative-sequence impedance has much more effect on the voltage change than the positive-sequence impedance. The experimental data discussed in the next section confirms the above as it shows that the load on an induction motor has little effect on the voltage change produced by connecting a single-phase load.

In practical cases where it is difficult, if not impossible, to accurately determine the motor loads, the following induction motor constants may be used. These constants are in per-unit, the kilovolt-ampere base being equal to the output kilowatts (horsepower x 0.746). They are average values for 60-cycle, general purpose induction motors rated 10–500 horsepower and 1,800, 1,200 or 900 rpm.

Full-load impedance	$0.8\angle 27°$
Blocked-rotor impedance	$0.135\angle 70°$

Experimental Data

Several specific cases were investigated in the laboratory to verify the equations that are given in this paper. As a matter of convenience the supply transformer bank was considered to be connected delta-delta in each case that was investigated. In the laboratory this permitted the use of series impedances in place of the actual transformer bank. Tests were made in which the single-phase welder load was connected for both long and short "on" periods, that is, for some of the tests the single-phase load was connected long enough for the system to reach steady-state conditions and for other tests the "on" period was so short that the system did not have a chance to reach steady state.

In each of the cases that were investigated one or both of the ratios $V_{bc}/V_{F_{BC}}$ and $V_{F_{bc}}/V_{F_{BC}}$ were determined from measured voltages and by calculation. The equations for the voltage ratio at the point F, although not given in this paper, are similar to those for the point P. Phase BC, the one supplying the single-phase load, was used for the check between the experimental and calculated values of the voltage ratio. This phase has the greatest voltage change when the transformer bank is connected delta-delta and therefore the calculation of the voltage change on this phase is usually the most important.

In each of the cases the measured and the calculated values of voltage ratio agreed very closely with a maximum difference of less than 1 per cent. This experimental data definitely showed that both induction and synchronous motors cause a reduction in the voltage change produced by a single-phase load and that this change is not appreciably influenced by the load on the motor or by the excitation in the case of a synchronous machine.

Range of the Motor Effect

In order to provide an indication of the improvement that might be expected in a practical case, calculations were made for six actual single-phase welder installations which are served by the Commonwealth Edison Company of Chicago. The voltage changes produced by these welder loads were computed both with and without the benefit of adjacent motor loads.

The results, given in Table III, of the calculations for these six cases show that reductions in the voltage changes of the order of 25 per cent may reasonably be expected. The actual improvements ranged from 12.5 to 27.0 per cent. In each case the improvement on the phase having the maximum voltage drop is of most interest, since it is the maximum voltage change which will determine if the load is to produce objectionable voltage variations. For this reason, the fact that the motor load causes an increase in the change in the line-to-line voltage CA for case number 4 is not objectionable since the line-to-line voltage AB has a greater voltage change.

Table III. Calculated Results

Case Number	Per Cent Change No motors Connected	Per Cent Change All motors Connected	Per Cent Improvement Due to the Motors
Change in Line-to-Neutral Voltage of Phase A			
1	0.77	0.62	19.5
2	0.81	0.61	24.6
3	1.17	0.86	26.5
4	1.04	0.91	12.5
5	1.76	1.44	18.2
6	1.05	0.78	25.7
Change in Line-to-Line Voltage AB			
1	0.54	0.50	7.4
2	0.48	0.42	12.5
3	1.09	0.83	23.9
4	1.14	0.98	14.0
5	1.04	1.02	2.0
6	0.73	0.59	19.2
Change in Line-to-Line Voltage CA			
1	0.61	0.46	24.5
2	0.74	0.54	27.0
3	0.66	0.55	16.7
4	0.41	0.44	−7.3
5	1.60	1.21	24.4
6	0.84	0.64	23.8

As can be seen from the results of these calculations the effect of the motors may be appreciable and should be taken into account in determining whether a single-phase load will produce objectionable voltage fluctuations.

The calculated results given in Table III are expressed in terms of the lettering convention of Figure 7. The voltage changes are all given for the point P, the primary of the transformer bank supplying the welder.

Field Tests

Field tests were conducted at two plants having single-phase welder installations, one plant being supplied at 4 kv and the other at 34.5 kv. These tests were performed to determine how measured voltage drops would compare with those calculated by the method given in this paper using field data. The results checked well within the accuracy normally expected in field tests.

Table II. Circuit* and System Data

Case No.	Welder Load, Kva	Line Voltage, Volts	Welder Power Factor, Per Cent	Duration of Weld in Cycles	Transformer Bank Supplying Welder, Kva	Impedance of Transformers in Per Cent	Resistance of Supply System in Ohms	Reactance** of Supply System in Ohms	Motor HP at P	Motor HP at F
1	72	232	67	30	3–75	2.4	0.538	0.484	2,200	0
2	95	230	40	10	3–50	3.25	0.424	0.451	1,900	125
3	147	223	89	10	3–25	3.25	0.310	0.481	3,300	55
4	140	226	98	12	3–50	3.4	0.361	0.403	750	160
5	58	221	60	15	3–25	2.4	1.678	1.151	650	45
6	94	218	47	24	3–37½	2.4	0.380	0.571	2,000	120

* The circuit to which these data apply is shown in Figure 8.

** Reactance of transformers supplying motor load at $P = 4$ per cent (on motor base)

Summary

1. The effect of the motor loads adjacent to a single-phase load is to reduce the maximum voltage variations produced by the single-phase load. In many cases this effect may be appreciable and should therefore be included in an accurate analysis of the voltage changes produced by the single-phase load.

2. The voltage change produced by a single-phase load with the effect of the motor loads included can be calculated on the basis of the method and equations given in this paper.

3. The amount of load on the motor and the excitation in the case of a synchronous machine have little effect on the voltage change.

4. In practical cases it is found that the exact character of the motor load adjacent to the single-phase load cannot usually be determined. It is also found that the motor loads are usually induction motors. Because of this and the foregoing statement concerning the effect of the load on the motor, most practical cases involving single-phase loads with "on" periods longer than two cycles may be handled with sufficient accuracy by using the average full-load and blocked-rotor impedances for induction motors as the positive and negative-sequence motor impedances respectively. For those cases involving an appreciable amount of synchronous motor load it is necessary to use the impedances given previously for synchronous machines. For those few cases involving single-phase loads with an "on" period of two cycles or less the impedances suggested for type (2) single-phase loads should be used.

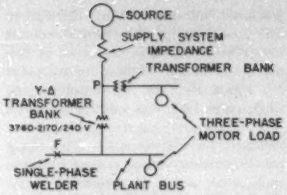

Figure 8. Welder supply system used in the determination of the voltage changes produced in practical cases

5. Balanced 3-phase loads other than motors have not been considered for two reasons. The first is that the usual industrial load is largely motor load. The second reason is that the positive- and negative-sequence impedances of the other balanced 3-phase loads are equal and therefore they do not affect the voltage change caused by the welder nearly as much as the same kilovolt-amperes of 3-phase motor load. In cases where there are appreciable balanced 3-phase loads other than motors connected to the system, they can be taken into account by including their impedances when setting up the positive and negative-sequence networks.

6. All of the equations given in this paper are based upon sinusoidal currents and voltages. However, there are single-phase welders which have phase-shift heat control and do not draw sinusoidal currents except at the 100 per cent heat setting. There are two types of phase-controlled welders that need consideration. The first is the type which does not use series capacitors for power factor correction. For this type it is recommended that the voltage drop be determined for the 100 per cent current setting since the maximum drop occurs under this condition.[6]

For the second type which uses series capacitors to correct the power factor to approximately unity, the maximum drop in the line-to-line voltage for a delta-delta transformer bank or the line-to-neutral voltage for a Y-delta bank does not occur at 100 per cent current but at a current reduced by phase control.[6] Therefore the maximum voltage drop cannot be determined by the method in this paper since the current would be nonsinusoidal. The solution of this problem was not included in the preceding investigation and remains a problem for further study.

References

1. Circuit Analysis of A-C Power Systems (book), **Edith Clarke.** John Wiley and Sons, Inc., New York, N. Y., 1943.

2. Electrical Transmission and Distribution Reference Book. Westinghouse Electric and Manufacturing Company, East Pittsburgh, Pa., 1944.

3. Symmetrical Components (book), **C. F. Wagner, R. D. Evans.** McGraw-Hill Book Company, Inc., New York, N. Y., 1933.

4. Applications of the Method of Symmetrical Components (book), **W. V. Lyon.** McGraw-Hill Book Company, Inc., New York, N. Y., 1937.

5. Electric Circuits, Theory and Applications (book), **O. G. C. Dahl.** McGraw-Hill Book Company, Inc., New York, N. Y., 1928.

6. Voltage Changes Caused by Resistance Welding Loads, **I. B. Johnson, H. A. Peterson, C. M. Rhoades, Jr.** *AIEE Transactions*, volume 66, 1947, pages 664–75.

No Discussion

Vibration and Fatigue Life of Steel Strand

J. C. LITTLE
ASSOCIATE AIEE

D. G. MACMILLAN
ASSOCIATE AIEE

J. V. MAJERCAK
ASSOCIATE AIEE

AEOLIAN vibration and vibration fatigue failure occurring therefrom have been a recognized limiting factor in nonferrous conductor life for many years. During this time, much work has been done in the study of its nature and of protective and preventive measures (see references at end of this paper). In addition, the high-amplitude low-frequency types of vibration, more commonly known as "galloping", have received considerable attention.[1,2,3] This type of vibration, however, will not be discussed here.

Little recognition appears to have been given the problem of steel strand vibration failures, perhaps because of the better fatigue properties inherent in this material. In recent years, failures in steel strand used for shield wires have been reported, seemingly in increasing numbers, particularly in installations utilizing the higher strength types of strand. These failures have not been confined to any one region or to the materials of any one manufacturer.

Since the nature of the failures indicated that the materials were being worked beyond their endurance limits, it appeared desirable to evaluate the appropriate mechanical properties, construction practices, and other factors which might be affecting performance.

Little of the experience gained in the past seems to have been applied to shield wires in spite of the fact that, as early as 1928, samples of vibration failure in ground strands were cited.[4] The remedial measures accruing from the experience with conductors resulted in measurably increased conductor life but the lack of application of this experience to ground strands has been, we believe, a definite contributing factor toward the current situation.

Nature of Stresses

As previous investigators have pointed out,[5] the total stress governing the life of a multiple wire cable is composed of four stress components:

1. Stress due to initial static tension.
2. Bending stress due to static sag.
3. Bending stress due to curvature of the loops in vibration.
4. Increased tensile stress due to the necessary increase in length of cable in a vibrating loop.

Obviously, to insure maximum cable life, the sum of the constituent stresses must not exceed the endurance limit of the material. (Endurance limit is defined as the maximum stress that a metal will withstand without failure during a specified large number of cycles of stress.) This value of working stress may be exceeded when vibration occurs either because of high static tension or because of the occurrence of temperature appreciably below that for which the installation was designed. The thought has been expressed that the endurance limit also might be adversely affected by extremely low operating temperatures.

Object and Scope

A study of the wire and strand properties was instituted to determine:

1. The endurance limit and endurance ratio of the various materials used in overhead ground strands.
2. The effect of operating temperature on the endurance limit of each material.
3. The extent to which the change in elastic modulus caused by temperature changes affected the calculated stresses.
4. The extent to which operating stresses were affected by thermal expansion coefficients of ground strand materials.
5. The effect of working tension on the vibration fatigue life of clamped Extra High Strength galvanized strand.
6. Consideration of possible measures for promoting improved operating performance of ground strands.

Paper 50-237, recommended by the AIEE Transmission and Distribution Committee and approved by the AIEE Technical Program Committee for presentation at the AIEE Fall General Meeting, Oklahoma City, Okla., October 23–27, 1950. Manuscript submitted July 25, 1950; made available for printing August 29, 1950.

J. C. Little and J. V. Majercak are both with the American Steel and Wire Company at Cleveland, Ohio, and D. G. MacMillan is with the American Steel and Wire Company at Worcester, Mass.

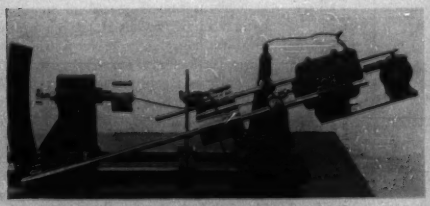

Figure 1. Rotating-strut type wire fatigue testing machine

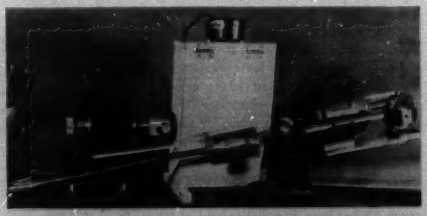

Figure 2. Rotating-strut type wire fatigue testing machine with insulated box for specimen

Figure 3. General view of vibration fatigue testing equipment

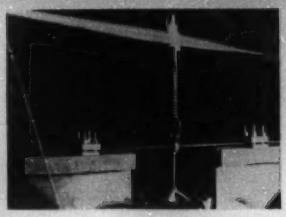

Figure 4. Detail of coupling spring arrangement

Figure 5. Typical vibration failure of strand in suspension clamp (shoe and bolts removed)

Apparatus and Testing Procedure

A brief description of the various kinds of testing apparatus used will promote better understanding of the results referred to later. For obtaining endurance data on the component wires of the various strands, the rotating-strut type fatigue testing machine (a modification of the Haigh-Robertson testing machine) was used as shown in Figure 1. For sub-zero temperature tests and for the elevated temperature tests, an insulated box enclosed the specimen, as shown in Figure 2. Cold temperatures were obtained by cooling the air inside the box with "dry ice" while the warmer temperatures were obtained by thermostatically controlled electric heaters.

The thermal expansion and elastic modulus data at various temperatures were obtained in a specially constructed "thermo-extensometer." It is, essentially, a tubular frame having a lever mechanism for applying tension to a specimen which passes through an insulated pipe, also containing an agitated coolant or heating fluid, whichever the test requires. The specimen motion due to temperature change or due to load application, is measured on a dial indicator actuated by the differential motion of two gauge points on the specimen, 100 inches apart.

Vibration fatigue testing at resonant frequencies of the strands was done on special equipment described in an earlier paper.[8] Shown in Figure 3, it consists of a heavy frame and a lever system for tensioning a specimen. In the center is an electromagnetic type vibration transducer, coupled to the specimen by means of a spring. Careful choice of the spring characteristics minimizes the effect of the coupled mass at the center vibrating loop as shown in Figure 4. The specimen, about 35 feet long, is suitably held at the ends in strain clamps and is rigidly supported in suspension clamps, each secured to the machine frame 20 feet apart. Vibration amplitude, one of the most critical factors affecting strand vibration life, is observed by means of a cathetometer focused at the center of a vibrating loop. An automatic shutoff control circuit, sensitive to small amplitude variation, stops the apparatus when a specimen failure occurs. A typical "failed" specimen is shown in Figure 5. In all tests, the clamp bolts were tightened to 50 foot pounds torque. To produce one curve or envelope of amplitude versus life cycles requires testing many separate specimens, each at a different level of vibration amplitude. In the course of these tests, some 3,000 feet of strand was consumed.

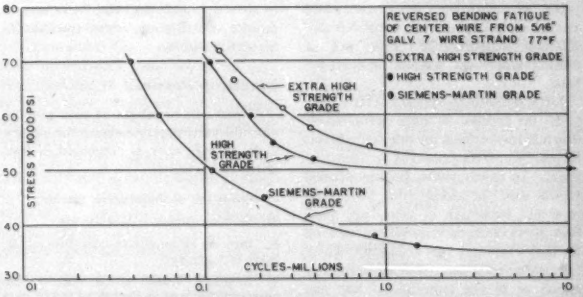

Figure 6. Reversed bending fatigue of center wire from 5/16-inch galvanized 7-wire strands (77°F) various grades

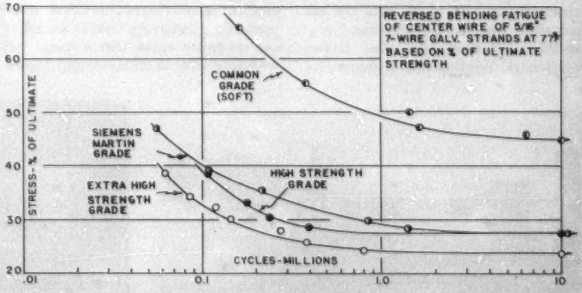

Figure 7. Reversed bending fatigue of center wire of 5/16-inch 7-wire strands. Based on per cent of ultimate strength

Experimental Results

To eliminate the extraneous effects due to gripping, clamping or abrasion, wires were first tested in reversed bending endurance, thus reflecting the inherent resistance to fatigue of each material. Test specimens were prepared by unstranding lengths of 7-wire strand, removing the core wire which was then hand straightened. These tests were followed by vibration fatigue tests on the complete strands held in conventional line hardware and under tension.

Endurance Limit Versus Grade

Fatigue curves shown in Figure 6 are the results of samples taken at random from mill production of hot-dipped galvanized strand in Siemens-Martin, High Strength, and Extra High Strength grades. As expected, the endurance limit level of the wire increases as the tensile strength is increased. This relationship, however, is not linear, since the effect of galvanizing tends to limit the endurance limit stress at the higher wire strength levels. This effect is more clearly indicated in Figure 7 showing the wire life as a function of the stress in percentage of ultimate strength. It will be noted that the Extra High Strength wire has the lowest endurance ratio (endurance limit divided by ultimate strength) although it possesses the highest endurance limit.

The graph in Figure 8 shows a comparison of the reversed bending fatigue characteristics at room temperature of hot-dipped galvanized Extra High Strength carbon steel and type *302* stainless steel wire samples. Inherently, the smooth hard drawn surface and the homogeneous nature of stainless steel provide it with improved resistance to fatigue (63,000 pounds per square inch) as compared to the galvanized carbon steel whose (52,300 pounds per square inch) reversed bending endurance limit is influenced by the layer of metallic zinc.

Endurance Limit versus Temperature

Shown in Figure 9 is the effect of stressing Extra High Strength galvanized wire in reversed bending at temperatures from −55 to +200 degrees Fahrenheit. When proper corrections are made for elastic modulus at each temperature, less than 3 per cent change of endurance limit due to temperature was found as indicated by the points within the envelope. The endurance limits were 53,500, 52,300, and 52,000 pounds per square inch for −55, +77, and +200 degrees Fahrenheit, respectively.

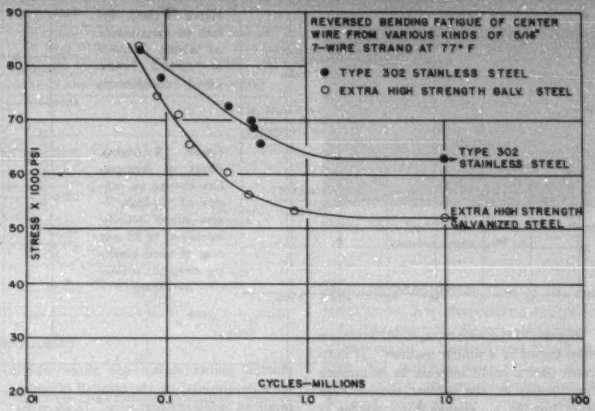

Figure 8. Reversed bending fatigue of center wire from various kinds of $^5/_{16}$-inch wire strand (77°F)

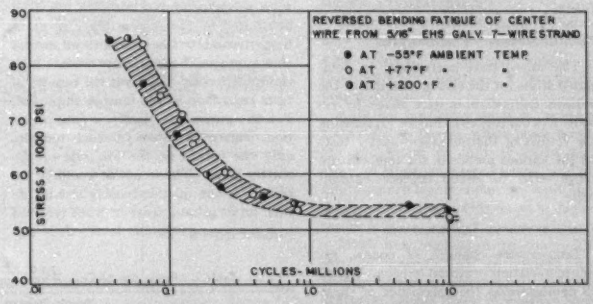

Figure 9. Reversed bending fatigue of center wire from $^5/_{16}$-inch Extra High Strength galvanized 7-wire strand at −55°F, +77°F, and +200°F

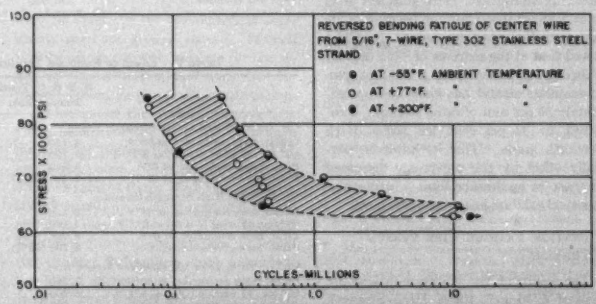

Figure 10. Reversed bending fatigue of center wire from $^5/_{16}$-inch 7-wire, type 302 stainless steel strand at −55°F, +77°F, and +200°F

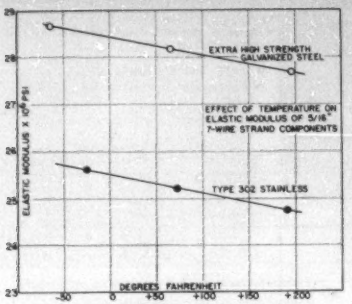

Figure 11 (left). Effect of temperature on elastic modulus of $^5/_{16}$-inch 7-wire strand components

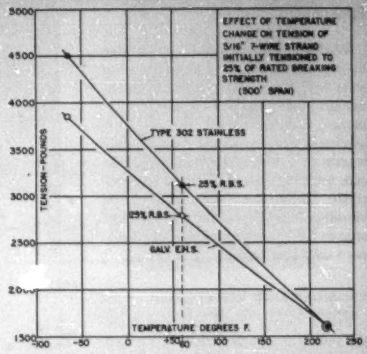

Figure 12 (right). Effect of temperature change on tension of $^5/_{16}$-inch, 7-wire strand initially tensioned to 25 per cent of rated breaking strength. (500-foot span)

Figure 10 represents type *302* stainless steel tested in a similar manner. It indicates that a small increase in endurance limit exists at the coldest temperature level, but that no change is in evidence at temperatures above normal. At −55, +77, and +200 degrees Fahrenheit, the endurance limits were 65,000, 63,000, and 63,000 pounds per square inch respectively.

Modulus versus Temperature

The appropriate corrections in computed stress for the elastic modulus at the various temperatures were made by referring to the curves in Figure 11, showing the results of thermo-extensometer tests on the various metals in the temperature range −55 to +200 degrees Fahrenheit.

Tension versus Temperature

Temperature changes, of course, result in variation in strand tension. Figure 12 demonstrates the magnitude of these changes for Extra High Strength steel strand and for type *302* stainless steel strand, both strung to normal (60 degrees Fahrenheit) tensions of 25% of their rated breaking strengths. Here stainless steel is at a slight disadvantage because of its higher coefficient of expansion. It will be noted that at the extreme of −65 degrees Fahrenheit, the tension in a 500-foot span of stainless strand has risen to approximately 36 per cent of rated strength, compared to 34 per cent for Extra High Strength grade. This is, however, partially offset by the previously discussed increase in endurance limit which stainless steel exhibits at low temperatures.

Vibration Fatigue Life versus Tension

The results of the vibration fatigue life tests of 5/16-inch Extra High Strength galvanized strand under various static tensions are shown in Figure 13. The plotted points shown are those which were determined by the number of cycles required to fail the first wire. In all cases, the failures occurred in the strand at a point within the clamp on the top side where the clamp shoe first made full contact. A great amount of scatter in results was experienced and this has been attributed to the susceptibility of extra high strength grade strand to an erratic characteristic performance under high clamping forces. This was the case in all tests regardless of the tension employed. For the purpose of clarity in interpretation, Figure 13 shows for each tension, only the points on the low side of the scatter band. The trend, as would be expected, is one of a decreasing strand life with an increasing tension, when referred to a common amplitude level. It is significant to note that the 2,800-pound tension, amounting to 25 per cent of the ultimate strand strength, is approximately 1 per cent higher than the endurance limit stress of the core wire tested in reversed bending. Obviously, any decrease in tension from this value could be expected to greatly promote strand fatigue life, since it is then more probable that the working stress will not exceed the endurance limit. Increasing tension, on the other hand, only serves to elevate the stress further into the danger zone.

Effect of Armoring

It was found by vibration fatigue testing of 5/16-inch Extra High Strength galvanized strand that the application of galvanized steel preformed armor rods was effective in extending the strand

Table I. Properties of Core Wire Components from $^5/_{16}$-Inch 7-Wire Strands

Material	Tensile Strength, Psi	Endurance Limit, Psi (77°F)	Endurance Ratio, Per Cent
Common galvanized	75,000	35,000	46.3
Siemens-Martin, galvanized	127,000	35,000	27.6
High Strength, galvanized	180,000	50,000	27.8
Extra High Strength, galvanized	220,000	53,300	23.8
Type 302 stainless	236,000	63,000	26.8

Table II. Effect of Reduced Tension Limitations in an 800-Foot Span

	N. E. S. C. Tension Limitations		Suggested Reduced Limitations	
	Tension Lbs.	Sag Ft.	Tension Lbs.	Sag Ft.
$^3/_{16}$" (7-Wire) Extra High Strength Strand				
Initial, bare conductor, at 60°F	3,150	5.5	2,030	8.2
$^1/_2$" ice, 4# wind +0.29, at 0°F.*	5,100	17.7	4,480	20.3
Final, bare conductor, at 0°F	3,250	5.1	2,240 (20%)	7.6
Final, bare conductor, at 60°F	2,800 (25%)	5.9	1,830	8.8
$^1/_2$" (7-Wire) High Strength Strand				
Initial, bare conductor, at 60°F	3,150	7.0	2,740	8.0
$^1/_2$" ice, 4# wind +0.29, at 0°F.*	5,470	17.9	5,160	18.9
Final, bare conductor, at 0°F	3,290	6.7	2,700 (25%)	8.1
Final, bare conductor, at 60°F	2,700 (25%)	8.1	2,250	9.8
$^5/_{16}$" (7-Wire) Type 302 Stainless Strand				
Initial, bare conductor, at 60°F	3,380	5.0	2,720	6.2
$^1/_2$" ice, 4# wind +0.29, at 0°F.*	5,300	17.0	4,890	18.5
Final, bare conductor, at 0°F	3,750	4.5	3,125 (25%)	5.5
Final, bare conductor, at 60°F	3,125 (25%)	5.5	2,520	6.8

* Rule 251, Fifth Edition, National Electrical Safety Code.

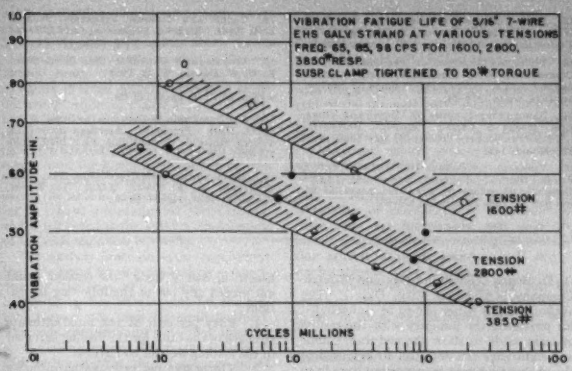

Figure 13. Vibration fatigue life of 5/16-inch 7-wire Extra High Strength galvanized strand at various tensions, frequency 65, 85, 98 cycles per second for 1,600, 2,800, and 3,850 pounds respectively. Suspension clamps tightened to 50 foot pounds

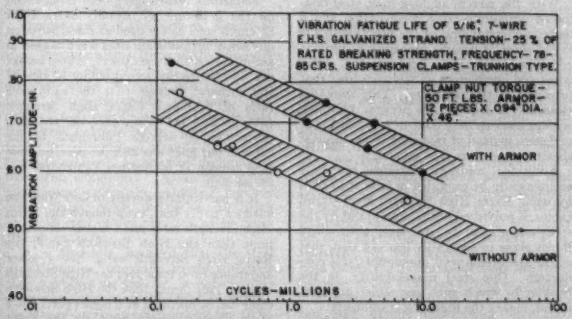

Figure 14. Vibration fatigue life of 5/16-inch 7-wire Extra High Strength galvanized strand, tension 25 per cent of rated breaking strength, with and without armor, frequency 78–85 cycles per second, suspension clamps—trunnion type

vibration life many times. This is shown in Figure 14 where tests made on both the unarmored and on armored strand secured in suspension clamps tightened to 50 foot pounds indicated that by the application of armor there was less strand abrasion and chafing, that clamping forces were more evenly distributed, and that a considerable amount of vibration damping was in evidence. Referred to any amplitude level, the life of the armored strand was greater by approximately ten times than that of unarmored strand. Figure 15 shows an armor assembly clamped for testing.

Experimental data appear to confirm the reported field experience that usual tension limitations as specified by the current National Electrical Safety Code[7] may be excessive for the materials commonly used for ground strand. Several possibilities present themselves for the relief of this situation, and may be employed either singly or in combination.

Reduction of the working tension to a value commensurate with the endurance limit of the material would appear to be one logical step. For example, the endurance ratio of Extra High Strength wire is approximately 23.8 per cent of ultimate strength (see Table I). The National Electrical Safety Code specifies a normal (60 degrees Fahrenheit final unloaded) tension of 25 per cent of rated strength. It is felt that a more appropriate limitation for this material would be 20 per cent of rated strength at 0 degrees Fahrenheit. There would then be less likelihood of exceeding the endurance limit of the material under low temperature operation.

Figure 15. Section of test span at clamp having armor applied

In like manner, Siemens-Martin and High Strength galvanized steel strand and type *302* stainless steel strand, all of which exhibit endurance limits near 28 per cent might well be limited to 25 per cent at 0 degrees Fahrenheit, rather than at 60 degrees Fahrenheit. Table II shows the effect that these reduced limitations would have on sags and tensions in a typical span.

Additional insurance against failure may be obtained by the practice of using armor rods at all points of support in locations where vibration is known to be a potential hazard.

A further possibility exists in the use of stainless steel strand, which has a tensile strength equal to that of extra high strength grade galvanized strand, and exhibits a much higher endurance limit, thus safely permitting operation at a higher tensile level.

Much work remains to be done. The relative susceptibility of various materials to clamping stresses may be of importance. Some types of existing hardware leave much to be desired. It is the hope of the authors that the work reported herein will serve to stimulate further investigation and improvement of practice.

References

1. Dancing Conductors, A. E. Davison. *AIEE Transactions*, volume 49, October 1930, pages 1944–49.

2. Transmission Line Vibration Due to Sleet, J. P. DenHartog. *AIEE Transactions*, volume 51, December 1932, pages 1074–78.

3. Galloping Conductors and a Method for Studying Them, E. L. Tornquist, C. Becker. *AIEE Transactions*, volume 66, 1947, pages 1154–61.

4. Vibration of Transmission Line Conductors, T. Varney. *AIEE Transactions*, volume 47, July 1928, pages 799–807.

5. Vibration of Overhead Transmission Lines, R. A. Monroe, R. L. Templin. *AIEE Transactions*, volume 51, December 1932, pages 1059–73.

6. Conductor Vibration, L. C. Peakin. *Bulletin*, Edison Electric Institute (New York, N. Y.), August 1939, pages 404–14.

7. National Electrical Safety Code. *Handbook B32*, National Bureau of Standards (Washington, D. C.), 1941.

8. The Singing of Circular and Streamline Wires, E. L. Relf, E. Ower. *Report Number 825*, Aeronautical Research Committee. (London, England), March, 1921.

9. Notes on the Vibration of Transmission Line Conductors, T. Varney. *AIEE Transactions*, volume XLV, 1926, pages 791–95.

10. Conductor Vibration, P. J. Ryle. *Journal*, Institution of Electrical Engineers (London, England), volume 69, 1931, page 811.

11. Vibration and Fatigue in Electrical Conductors, A. E. Davison, J. A. Ingles, V. M. Martinoff. *AIEE Transactions*, volume 51, December 1932, pages 1047–51.

12. Field Tests on Conductor Vibration, E. M. Wright, J. Mini. *Electrical Engineering* (*AIEE Transactions*), vol. 53, July 1934, pages 1123–27.

13. Vibration Analysis of Transmission Line Conductors, W. B. Buchanan. *Electrical Engineering* (*AIEE Transactions*), volume 53, November 1934, pages 1478–84.

14. Laboratory Studies of Conductor Vibration, Joseph S. Carroll. *Electrical Engineering* (*AIEE Transactions*), volume 55, May 1936, pages 543–47 and 1148.

15. Vibration of Cables and Dampers, part I, R. G. Sturm. *Electrical Engineering* (*AIEE Transactions*), volume 55, May 1936, pages 455–65, and part II, June 1936, pages 673–88.

16. Cable and Damper Vibration Studies, L. A. Pipes. *Electrical Engineering* (*AIEE Transactions*), volume 55, June 1936, pages 600–14.

17. Vibration of Overhead Line Conductors, E. W. W. Double, W. D. Tuck. *Journal*, Institution of Electrical Engineers (London, England), volume 86, 1940, pages 129–60.

18. Fatigue Tests on Zinc Coated Steel Wire, D. G. Watt. *Proceedings*, American Society for Testing Materials (Philadelphia, Pa.), 1940, pages 717–32.

19. Measurement and Control of Conductor Vibration, G. E. Tebo. *AIEE Transactions*, volume 60, 1941, pages 1188–93.

Discussion

H. D. Fischer, Jr. (Southern California Edison Company, Los Angeles, Calif.): In connection with the aeolian vibration study being conducted by the Southern California Edison Company, fatigue tests were run on several samples of stranded cable in an effort to determine the effect of the properties on the life of the cable.

The first tests were set up to simulate as nearly as possible the loop lengths and amplitudes which were measured in the field.

Under these conditions failures were not obtained within 10,000,000 cycles and an examination of the cable indicated it would endure indefinitely. The conditions were then exaggerated (the tension being held at 7,000 pounds which is normal line tension) until failure occurred within 1,000,000 cycles for all types of cable being tested. These conditions, 1/8-inch displacement and half loop length of $3^3/_4$ inches with the end connection and center connection being rigidly supported so that bending stresses occurred at both ends, produced the results shown in Table I of this discussion. The physical characteristics of each specimen as determined in the tests also are shown.

The results obtained here indicate a different trend in the endurance limit than those presented in the paper. However, these tests were made on complete 7-strand cable and the connections were of the compression type.

These tests were made in an effort to find some reason for the better performance experienced on one line than that experienced on another, both of which traverse similar terrain and are subject to similar weather conditions. Another point that may be brought out along these lines is that from a vibration standpoint, the performance of lines which are supported by towers with latticed-pyramid type steel footings seems to be better than that of lines supported on towers with rigid cast in place concrete footings.

O. D. Evans (Oklahoma Gas and Electric Company, Oklahoma City, Okla.): The authors of this paper are to be commended for providing the industry with the results of tests made to show the endurance limit and endurance ratio of steel strand used to shield electric power transmission lines from lightning strokes. This information has long been needed and will, no doubt, result in a revision of the steel manufacturing companies' published sag charts and tables to show a reduction in working tensions.

With the advent of long-span steel-reinforced aluminum-cable construction and a better understanding of the function of the shield wires, it became necessary to provide additional clearances between the shield wires and conductors at midspan over that provided at the structure. This increased clearance is required to prevent lightning strokes from spilling over to a conductor at midspan, instead of traveling to the nearest structure and thence to ground.

Additional midspan clearance can most economically be provided in long span lines by using Extra High Strength steel strand cables, if published sag tables put out by the steel manufacturers are used, since these tables show considerably less sag than that of the steel-reinforced aluminum-cable conductors. One steel manufacturer, in the booklet in which such sag tables are published, makes the following statements:

"1. Steel has greater strength and, therefore, can be pulled to less sag than any of the nonferrous conductor materials, thus creating more midspan clearance. Also, steel has better fatigue strength than the other conductor materials, thereby causing less trouble from vibration fatigue failures.

"2. Armor rods are not ordinarily required for use on steel."

The published sag tables of two major steel companies were, therefore, used for stringing steel shield cables on our newer transmission lines so as to realize the benefit of the additional clearance provided at midspan. These sags were calculated by the manufacturers such that under the assumed loading of rule *251* of the current National Electrical Safety Code,[1] the tension would not exceed any one of the following limitations:

1. Fifty per cent of the rated ultimate strength of the cable for the loading specified in the loading district concerned.

2. Thirty-five per cent of the ultimate strength of the cable at 60 degrees Fahrenheit stringing sag without external load.

3. Twenty-five per cent of the ultimate strength of the cable at 60 degrees Fahrenheit final sag without external load.

Numerous breaks have been experienced on the 5/16-inch (7 strand) Extra High Strength steel cables used as shield wires on our newer transmission lines when sagged in accordance with these tables. These breaks can now be readily accounted for in view of the authors' findings that the endurance ratio of 5/16-inch Extra High Strength cable is 23.8 per cent, since the stringing tension at 60 degrees Fahrenheit of the cable in our lines was 28.2 per cent, and the final tension at 60 degrees Fahrenheit was 25 per cent.

It is particularly worthy of note from the authors' paper that, even though the Extra High Strength cable has a higher endurance limit than the High Strength cable, the Extra High Strength cable has a lower endurance ratio than does the High Strength cable. This means that the High Strength cable can be operated at a higher percentage of its ultimate tension than can the Extra High Strength cable without experiencing strand breaks. For example, the endurance ratio tension of 5/16-inch Extra High Strength cable (11,200 pounds ultimate strength) would be 2,665 pounds, whereas the endurance ratio tension of 3/8-inch High Strength cable which has slightly less ultimate strength (10,800 pounds) would be 3,002 pounds, some 337 pounds more than the Extra High Strength cable.

Table II of the paper illustrates the effect of reducing the tension in 5/16-inch Extra High Strength cable and 3/8-inch High Strength cable to obtain tension values at all probable temperatures below their respective endurance ratio tensions. It will be noted from this table that even though the ultimate strength of these two cables is approximately the same, the allowable tensions in the High Strength cable are, at all temperatures, in excess of those in the Extra High Strength cable. Nevertheless, the 5/16-inch Extra High Strength cable has less final sag at 60 degrees Fahrenheit (although the initial sags at 60 degrees Fahrenheit are about the same) and since the 5/16-inch Extra High Strength cable is slightly lower in cost than the 3/8-inch High Strength cable, the 5/16-inch Extra High Strength

Table I

Type of Cable	Per Cent of Rated Ult. Tension	Average Cycles to Failure	Av. Yield Strength, Pounds per Sq. Inch	Av. Ult. Strength, Pounds per Sq. Inch	Average Elongation, Per Cent per 2 In.
1/2-inch 7-strand HS	37.2	563,000	117,000	147,000	14.5
1/2-inch 7-strand EHS	26.0	289,000	167,000	213,000	9.0
1/2-inch 19-strand HS	36.6	892,000	119,000	139,000	14.2
1/2-inch 19-strand EHS	26.2	436,000	150,000	198,000	10.0

HS—high strength. EHS—extra high strength.

cable must still be considered as being more economical for shielding purposes than the 3/8-inch High Strength cable.

According to my understanding of Figures 13 and 14, the "2,800-pound tension" curve of Figure 13 is the same curve as the "without armor" curve of Figure 14, yet, at 0.50-inch vibration amplitude, Figure 13 indicates 3,000,000 cycles whereas Figure 14 indicates 8,000,000 cycles, with both values taken from the lower limits of the scatter band. Since the frequency and clamp pressure is the same in both curves, I am wondering if I have misinterpreted these curves, and if not, what is the authors' explanation of the wide variation in results.

The authors state in their conclusions that the usual tension limitations as specified by the current National Electrical Safety Code may be excessive for the materials commonly used for ground strand. The code requirements state that the tensions shall not exceed the amounts specified, and, in my opinion, do not attempt to set the tensions used. The Aluminum Company of America uses 0 degree Fahrenheit for determining their limiting tensions of $33^1/_3$ per cent initial tension and 25 per cent final tension, instead of 60 degrees Fahrenheit as specified by National Electrical Safety Code rule *261F4*.

The discussion of the National Electrical Safety Code states that operating experience, together with a study of the observed mechanical characteristics of conductor materials under operating and test conditions, should determine the sags. The authors' tests results strongly indicate that the steel manufacturers published sag tables for 5/16-inch (7 strand) Extra High Strength cable will cause strand failures due to aeolian vibrations. The authors' paper also indicates that the published sags for other Extra High Strength and High Strength steel cables are such as to cause strand breakage.

It is, therefore, believed that the steel manufacturing companies should withdraw their published sag data for these steel cables to prevent other companies from encountering strand breaks experienced by the Oklahoma Gas and Electric Company and other companies. Vibration difficulties will be experienced sooner in windy places like Oklahoma but, in my opinion, will be experienced eventually in less windy places if these sag data are used. Sags, in accordance with the authors' conclusions (using 20 per cent of the ultimate cable strength at 0 degree Fahrenheit final tension for Extra High Strength cables and 25 per cent for High Strength cables) seem to be the answer to preventing fatigue failures.

The use of armor rods as additional insurance, as recommended by the authors, also is worthy of consideration, inasmuch as these rods are inexpensive and easy to install, and they provide mechanical protection against clamping stress as well as reducing the effects of vibration.

It is doubtful if the additional cost of stainless steel cables could ever be justified except in those regions where corrosion is a factor.

Reference

1. See reference 7 of the paper.

J. C. Little, D. G. MacMillan, and **J. V. Majercak:** The authors wish to thank both Mr. Fischer and Mr. Evans for their discussion on results of related tests and on power utility viewpoints.

Mr. Fischer shows that High Strength grade strand either of 7-wire or 19-wire construction, had approximately two times greater vibration life than Extra High Strength grade strand when each was initially tensioned to the same load. This apparently occurred in spite of a lesser percentage of rated ultimate strength being used for the Extra High Strength grade strand. It should be noted, however, that all of the initial tensioned stresses employed in the discussor's tests are in excess of the endurance ratio values shown in our paper for each particular grade of strand. It is, therefore, not too surprising to see isolated data indicating a reversal of finite life trend because, in our vibration testing experience, a life variation as great as eight to ten times can exist despite maintaining amplitude variation to less than 5 per cent. Such admittedly erratic performance has been attributed to high and variable stress concentrations produced in the wires of strands held in fitting types exerting high compression forces. The data on which Mr. Fischer bases his discussion supports our belief that were a larger quantity of testing done, the result would be a scatter band with the High Strength test points falling somewhat below the Extra High Strength test points.

The discussor's data showing longer life for the 19-wire strands than the 7-wire strands is in alignment with the lower expected bending stresses developed in strands having smaller wire sizes.

Mr. Evans questions a difference between the location of the 2,800-pound tension curve in Figure 13 and the "without armor" curve in Figure 14. The authors attribute the displacement between the two curves to the use of two different clamp types since no other known variable existed. The difference was not pointed out in our paper since it was not our original intent to condemn or promote any one clamp. In Figure 13 a conventional suspension clamp was used and indicated as "susp. clamp", whereas in Figure 14, the caption bears "trunnion type." Both type clamps were, however clamped rigidly; thus the tests do not reflect either clamp's ability to follow line vibration. The differences in life indicated are probably due to a variation in keeper curvatures and in the different distribution of clamping pressures of the two clamp types.

Since making the original tests, further incompleted testing on stainless steel strand indicates that while the reversed bending endurance limit of its wires ranks highest of the kinds tested, the strand is somewhat more susceptible to the vibration-type stresses than is Extra High Strength grade galvanized strand. It would, therefore, appear that the original suggested limitation on this material (25 per cent of rated strength at 0 degree Fahrenheit for final tension of bare conductor) is excessive, and that it should not be worked at a greater tension than that specified for Extra High Strength galvanized strand.

An Improved Reclosing Relay

L. E. GOFF
ASSOCIATE AIEE

Synopsis: This paper describes a new reclosing relay which offers several features not included in available automatic, reclosing relays. Among the features included are: reset of the relay a short interval after any successful reclosure, to eliminate needless delay in subsequent reclosures and reduce unnecessary lockouts; a simple internal means of blocking the instantaneous trip circuit after the initial circuit breaker trip-out, to facilitate system sectionalizing; immediate first reclosure through an initially closed contact in the relay to reduce first-reclosure time. Operation of the relay and circuit is completely described with emphasis on the operating conditions creating a demand for and the advantages offered by the several improvements. Possible settings and adjustments are discussed which provide a wide degree of versatility in application.

Historical Background

THE desire on the part of operating companies to improve customer service has resulted in the now nearly universal use of automatic reclosing on transmission lines and distribution feeders. The general application of automatic reclosing relays can be traced back for more than 30 years and the history of their development during this period is interesting.

Early schemes for reclosing service assumed many forms and usually involved some combination of timing and auxiliary relays. One form for example made use of a simple plunger-type time delay relay to initiate reclosures and a notching relay to determine the number of reclosures. Since the successive reclosing of a circuit breaker involves essentially a timing operation these early schemes were soon discarded in favor of various forms of motor driven timers with their operation initiated by the opening of the associated circuit breaker. The initial attempt to reclose the circuit breaker occurred after a considerable delay and was followed at intervals by one or more additional attempts to reclose. If the circuit breaker remained closed after the final reclosure attempt the reclosing relay operated to its reset position and was again ready to respond to a circuit breaker outage. If, however, the circuit breaker remained open after the final attempt the reclosing relay stopped in a locked-out position or operated a lockout relay, sounded an alarm, and remained in this condition until steps were taken to reclose the circuit breaker manually.

Operating experience soon indicated that a large portion of the outages on overhead lines were of a transient nature and hence were cleared immediately when the circuit breaker opened. This knowledge led some operating companies to attempt reclosure of the circuit breaker as soon as possible following the initial occurrence of a fault, a step which proved extremely successful and resulted in the modification of then existing reclosing relays by the manufacturers to provide an immediate initial reclosure. From these early designs the present forms of motor-driven reclosing relays, commonly referred to as "multishot" reclosing relays, have evolved with provision for either immediate or delayed initial reclosure, followed by two or more delayed reclosures.

Records made during these early investigations[1] indicated reclosing relay performance as shown in Table I for delayed initial reclosure and for immediate initial reclosure. These figures caused many operating companies to question the need in attended stations for reclosing relays having provision for more than one automatic reclosure, when manual reclosure could produce roughly the same results as the second and third automatic reclosures, and led to the development of the "single-shot" reclosing relays now on the market. Such reclosing relays have more recently seen extensive application on the higher voltage transmission lines where, because of multiple feed, delayed reclosing is not always possible without dead-line or automatic synchronizing and synchronism-check relays. The same figures, however, also indicated a real need for several automatic reclosures in unattended stations. The figures in Table I indicate that there would have been three times as many permanent service interruptions if the immediate initial reclosure had not been followed by a second and third delayed reclosure. Although more up-to-date information[2] now is available on the application and performance of automatic reclosing equipment, when all types of loads are considered it is found that the information in Table I is still remarkably accurate. More extensive experience has indicated, however, that on circuits consisting mainly of residential load the immediate initial reclosure may be successful as much as 90 per cent of the time.

Need for Improved Relay

Since the early addition of the immediate initial reclosure feature there have been no basic changes in the motor-driven reclosing relays offered by manufacturers. In evaluating the improvements which are needed it would be well to first consider some of the requirements which should be met by a modern reclosing relay:

1. Either immediate or delayed initial reclosure should be available, the change from one to the other to be as simple as possible.

2. If immediate the reclosure should be initiated as soon as possible, preferably through a normally closed or "preclosed" contact in the reclosing relay.

3. The reclosing relay should be able to reset automatically a definite time after any successful reclosure.

Paper 50-238, recommended by the AIEE Relays Committee and approved by the AIEE Technical Program Committee for presentation at the AIEE Fall General Meeting, Oklahoma City, Okla., October 23–27, 1950. Manuscript submitted July 25, 1950; made available for printing August 25, 1950.

L. E. Goff is with the General Electric Company, Philadelphia, Pa.

Table I. Reclosing Relay Performance With Delayed and With Immediate Initial Reclosure

Reclosure	Successful Reclosures Delayed Initial Reclosure, Per Cent	Successful Reclosures Immediate Initial Reclosure, Per Cent
First	85	75
Second	5	15
Third	1	2
Lockout	9	8

4. At least three delayed reclosures should be available, adjustable up to a maximum of three minutes.

5. The reclosing relay must provide pump-free circuit breaker operation.

6. If all reclosure attempts are unsuccessful, the reclosing relay should lock out and remain locked out until the circuit breaker has been successfully reclosed manually.

7. A means should be included in the reclosing relay for blocking the instantaneous trip circuit after the initial circuit breaker outage and prior to the initial reclosure.

While available motor-driven reclosing relays with provision for several reclosures meet most of these requirements, none conform with all of them. Items 2, 3, and 7 are conspicuously absent although they can be of great importance in meeting today's high standards of service reliability.

The use of a preclosed contact in the circuit for immediate initial reclosure places the responsibility of initiating this reclosure on the circuit breaker auxiliary contact which closes when the circuit breaker trips. This results in a reduction in the initial reclosing time by the interval required to operate an auxiliary relay unit, on the order of two or three cycles. While this seems insignificant in itself, it assumes greater importance when total circuit breaker reclosing times in the range of 10 to 20 cycles are considered.

A definite-time reset feature following a successful reclosure also is of great importance. A glance at the column in Table I headed "Immediate Initial Reclosure" shows that operating experience indicates successful circuit breaker reclosure at least 75 per cent of the time on the immediate first reclosure. With available types of motor-driven reclosing relays the relay must time through the entire cycle, or as much as three minutes, before the reset position is reached even though the initial reclosure is successful. If a second transient fault entirely independent of the first occurs within this interval, reclosure of the circuit breaker will be needlessly delayed until the next delayed-reclosure position is reached; or if the second fault should occur during the interval between the final-reclosure position and lockout an unnecessary lockout will result with accompanying lengthy interruption in service. Since the attendant has no way of knowing that the lockout resulted from two entirely independent faults of a transient nature he may, depending upon operating practice of the system concerned, waste additional time in trying to locate a permanent fault which never existed.

It is interesting to note that definite-time reset following a successful circuit breaker reclosure was a feature of the time delay and notching relay combination mentioned in the introductory paragraphs, but was omitted from the more modern motor-driven reclosing relays. Many operating companies have recently indicated that such a feature is now needed, and at least one has developed a reclosing relay using standard relay components[3] which provides quick resetting of the reclosing relay following a successful circuit breaker reclosure.

The use of sectionalizing fuses on branch feeders, described later in detail, depends upon the blocking of instantaneous tripping on first and subsequent reclosures. This has been accomplished previously by an auxiliary unit, either included in the relay or external to it, but can be handled more advantageously by a single contact in the reclosing relay.

A New Reclosing Relay

This paper describes a new circuit breaker reclosing relay and circuit which combines these needed features with those long associated with automatic reclosing relays, and offers a degree of versatility previously unobtainable. The new relay is shown in Figure 1 in its case with cover in place. It should be noted that the case size will represent a reduction of approximately 50 per cent when compared with previously available "multishot", motor-driven reclosing relays. The relay consists essentially of a synchronous driving motor, a gear train and cam shaft with reset spring driven through a crown-gear clutch, a magnetic clutch release, and a series of cam-operated switches for initiating the reclosures and reset attempts and performing the various auxiliary functions essential to the operation of the relay and circuit. A 2-position interlocking relay unit, necessary to obtain the advantage of the preclosed contact on immediate reclosure, and an auxiliary unit which can be used as an antipump relay, also are included in the reclosing relay. All cam-operated contacts are of an enclosed construction

Figure 1. The type *ACR* reclosing relay

with high contact pressure and are of a type used extensively on aircraft where reliability is vital, even at low operating voltages. All components including the motor are insulated to withstand normal switchgear high-potential tests.

The mechanical features of the relay when in the reset position are clearly illustrated by the schematic mechanical diagram in Figure 2. Nomenclature used in the figure and the following description agrees also with designations in the circuit diagram described later. The driving torque is transmitted from the small synchronous motor through a crown-gear clutch consisting of a driving member pinned to the motor shaft, and an idler member. The idler member, which includes a star cam and pinion, is free to slide back and forth on the motor shaft and is normally held in engagement with the stationary member by a compression spring which is a part of the clutch release seal-in switch. The pinion on the idler member drives gear "*A*" pinned to the auxiliary cam shaft causing windup of the reset spring. The auxiliary shaft, which turns through slightly less than 360 degrees during a complete reclosing cycle, carries depressions in its body which operate the roller-actuated snap-action switches "*GH*", "*DE*", and "*JK-KL*" performing auxiliary functions which will be described later. An adjustable cam segment can be set to operate switch "*RS*" at any point in the reclosing cycle. The front dial hub is in turn driven through the gear pair "*B*" and "*C*" and makes slightly less than a half revolution during the complete reclosing cycle.

The dial hub carries a set of double-ended adjustable cams "*D*" which operate switch "*AB-BC*" to initiate delayed reclosures, and switch "*MN*" to reset the relay in the event of a successful reclosure.

These cams consist of round flat plates with diametrically opposite projections which operate the roller actuators. The interval between a delayed reclosure, initiated by the operation of "*AB-BC*", and a subsequent reset attempt, initiated by the operation of "*MN*", is determined by the location of switch "*MN*" in relation to the reclosing switch "*AB-BC*" and thus is the same for all delayed reclosures. The interval between immediate initial reclosure and resetting of the relay if the reclosure is successful is determined by the setting of cam "*E*". This cam actually consists of three separate plates each with a single projection. For the normal adjustment of the relay indicated in Figure 2 these plates are arranged so that the projections are back-to-back, providing in effect a single cam projection. The contribution of these single-ended cams to the versatility of the relay is described in a later section.

Resetting of the relay is accomplished by energizing the clutch release magnet which attracts the release armature and draws the idler member of the clutch away from the fixed member. This permits the gear train, cam shaft, and dial hub to return to their reset position under the influence of the charged reset spring. During the reset cycle the escapement follower retards the motion of the star cam reducing the reset speed to a point where there will be no rebound when the reset position is reached. The clutch release unit is equipped with a seal-in contact to shunt the reset contact "*MN*" during the reset cycle. A manual release rod is provided to permit releasing the clutch from the front of the relay so that the gear train can be turned by hand.

The Reclosing Circuit

The functions of the various components described previously are illustrated by Figure 3 which shows an elementary diagram of a typical circuit utilizing the new reclosing relay. The diagram shows the connections for an immediate initial reclosure followed by one or more delayed reclosures, with all contacts in the reclosing relay, identified by the device function number *179*, shown with the relay in its reset position. With these connections a total of six leads, including control power leads, will normally be required between the circuit breaker and the relay panel.

Immediate Reclosing Circuit

When the circuit breaker trips, the circuit to the closing relay is completed by the "*b1*" and "*LC*" switches of the circuit breaker *152* through the "preclosed" contact *179E1* in the reclosing relay and the *8-8C* contact of the control switch 101. Thus the initial reclosing time is determined solely by the tripping time of the circuit breaker, and the operating times of the closing relay *152X* and the closing mechanism. Operation of the auxiliary contact of the closing relay *152X* energizes the trip winding of the interlocking relay *179E*, which opens the "preclosed" contact *179E1* prior to the initial reclosure of the circuit breaker contacts, starts the timing motor through *179E3*, and sets up the reset circuit by means of *179E2*.

Reset Circuit

A short time after the start of the cycle, contact "*MN*" of *179* is operated by the single-ended cam "*E*" as described previously. If the immediate reclosure was successful, which will be true in the majority of the cases, contact "*a*" of *152* will be closed and the clutch release unit *179R* will be energized, through the *5-5C* contact of *101* and contact *179E2*. The reclosing of contact "*DE*" of *179* when the reset position is reached energizes the *179E* reset coil and the interlocking relay returns to its reset position. The reclosing relay now is ready to initiate an immediate reclosure in the event of a subsequent opening of the circuit breaker.

Delayed Reclosure Circuit

If the circuit breaker had tripped again after the initial reclosure the open "*a*" contact of *152* prevents reset of the reclosing relay, which will then continue to operate until the first delayed-reclosure point is reached as determined by the adjustments of the double-ended cams "*D*" on the front dial hub. The antipump relay, *179Z*, is picked up when the *b2* contact of *152* is closed so a subsequent operation of the "*AB-BC*" contact combination of *179* by one of the cam projections "*D*" completes the delayed reclosing circuit operating the closing relay *152X*. The antipump feature results from the response of the *179Z* relay to the opening of the *b2* contact when circuit breaker *152* recloses. Even a momentary opening of the *b2* contact causes *179Z* to drop out, breaking the seal-in circuit around the "*BC*" contact of *179* and opening the delayed-reclosure circuit. Thus only one reclosure of the circuit breaker is possible for each cam-operation of the "*AB-BC*" contacts of *179*. Since the control circuit involving the closing relay *152X* is frequently inherently pump-free, the *179Z* unit will usually be available for use in other capacities as desired.

A definite time interval after the operation of "*AB-BC*" by a cam projec-

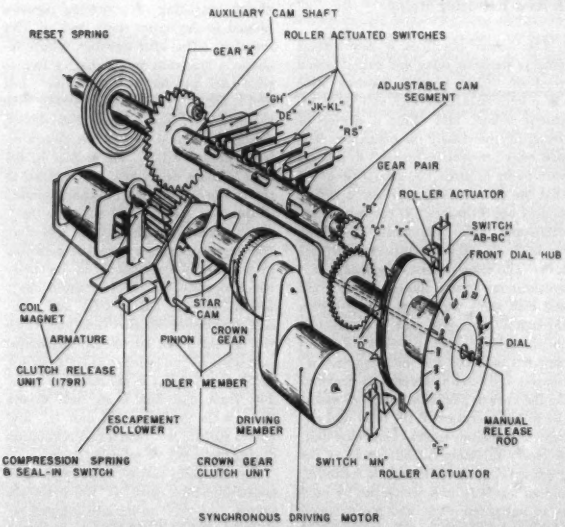

Figure 2. Schematic representation of the operating mechanism in the new reclosing relay

tion "*D*", the opposite end of the same cam plate operates the "*MN*" contact of *179*. If the *a* contact of *152* is closed the circuit responds as described previously and the relay resets. Otherwise the relay continues through its cycle until the next delayed reclosure point is reached and the operations described previously are repeated.

Lockout

If none of the attempts to reclose the circuit breaker is successful the relay continues to operate until the lockout position is reached. This is indicated by the operation of contact "*GH*" of *179* by the auxiliary cam shaft, opening the motor circuit. This condition of the relay is indicated by the simultaneous operation of alarm contact "*JK-KL*" of *179*. In the lockout position contact "*NM*" of *179* is held closed by the projection of fixed cam plate "*F*", which is keyed to the dial hub, providing for reset of the reclosing relay after a successful manual reclosure of the circuit breaker.

Functions of Control Switch

The control switch designated as master element *101* continues to play an important part in the control circuit for the new reclosing relay. For example, with the relay in the locked-out position as described before, subsequent reclosure of the circuit breaker must be initiated by operation of switch *101* to the "close" position. The switch contact tabulation shown in Figure 3 indicates that when switch *101* is operated to the "close" position the circuit breaker is reclosed through contact *1-1C* but that the reset circuit of the reclosing relay is kept open by the *5-5C* contact until the switch is released and returns to the "normal after close" position. Thus reset of the reclosing relay is prevented if the circuit breaker is manually reclosed on a sustained fault.

The contacts of the control switch as connected in the elementary diagram prevent needless duty on the circuit breaker during a manual reclosure following servicing of the circuit breaker or line repair. For example if a circuit breaker is removed from service and grounded, and the grounding chains inadvertently left in position, the circuit breaker will be manually reclosed on a severe fault. It is desirable, if possible, to prevent the relay from initiating an immediate reclosure under these conditions. With the circuit shown, operation of the closing relay *152X* on manual reclosure trips the interlocking relay *179E*, blocking the immediate reclosing circuit before the circuit

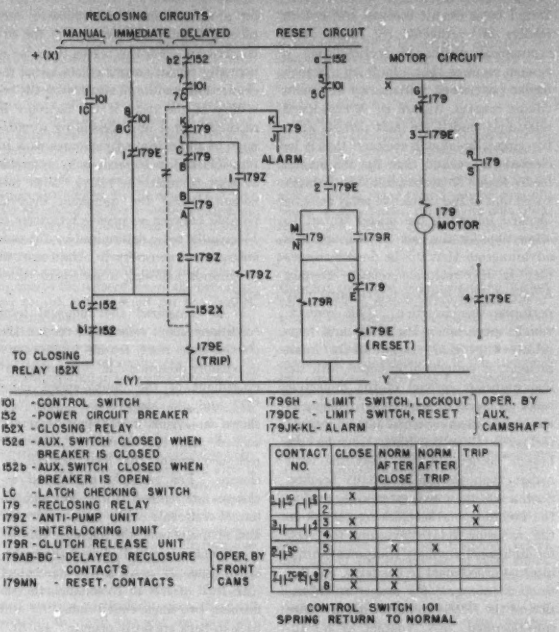

Figure 3. Elementary diagram showing a typical application of the new reclosing relay

breaker can reopen, and starting the timing motor. The time interval before the first delayed reclosure provides ample time for the operator to react to the situation and return switch *101* to the "normal after trip" position. A successful manual reclosure following circuit breaker servicing or line repair will be followed after a brief interval by reset of reclosing relay.

Adjustment of Initial Reclosure

The new relay offers a degree of versatility in adjustment and application heretofore unavailable in motor-driven reclosing relays. The first requirement for a modern reclosing relay is that the initial reclosure shall be either immediate or delayed with the change from one to the other to be as simple as possible. In the new relay the type of initial reclosure is determined solely by the position of the preclosed contact *179E* in the reclosing circuit. This contact is shown in Figure 3 connected for immediate initial reclosure and its function has been described. For delayed initial reclosure the "preclosed" contact is connected in the position shown by the dotted lines. The closure of the *b2* contact of *152* following a circuit breaker outage will now energize the interlocking unit trip coil immediately, starting the timing motor and setting up the reset circuit. When the relay is first installed the position of the "preclosed" contact can be determined easily by the external wiring to the relay. A subsequent change from immediate to delayed initial reclosure can be accomplished either by a change in the external wiring of the "preclosed" contact or, as is usually more convenient, by removing the relay from its case and reconnecting the two leads from the *179E1* contact to a different pair of terminals. The contact leads are marked plainly and the terminals involved in the change are adjacent. No mechanical change is required in the relay unless different delayed reclosure intervals are desired, in which case a simple change in the setting of the cam plates carried on the dial hub suffices.

Co-ordination with Branch Circuit Fuses

On some systems involving multishot reclosing relays the main feeder is pro-

tected by a circuit breaker and branch feeders are protected by fuses. This economical means of sectionalizing a system requires that a fault on a branch feeder be cleared initially by the main circuit breaker tripped by a high-speed relay unit, and if the fault persists when the circuit breaker is reclosed that it be cleared the second time by the branch feeder fuse. To accomplish this the high-speed unit of the protective relay must be blocked following the initial tripout to allow time for the fuse to clear and it is advantageous that this be done by a contact in the reclosing relay. Contact *179E4* of the 2-position interlocking relay performs this function. This contact, which opens when the *179E* unit trips prior to the initial reclosure of the circuit breaker, is connected in series with the instantaneous contact of the protective relay to block instantaneous tripping of the circuit breaker on first and subsequent reclosures thus providing time for the branch feeder fuse to clear the fault rather than the main circuit breaker. Such a scheme now is extensively used so the inclusion of the blocking contact in the reclosing relay obviating the need for additional auxiliary equipment, either internal or external to the relay, is a distinct advantage. By proper co-ordination of the *179E4* contact with the spare cam-operated "*RS*" contact of *179* instantaneous tripping also can be blocked at other points in the reclosing cycle.

Reclosure Intervals

Opinion on the proper settings of a multishot reclosing relay is quite diversified, being influenced by the type of system and the condition of equipment involved, local meteorological conditions, and previous experience of the operating company. The design of the new reclosing relay is such that it can be adapted to meet the many different requirements for reclosing cycles. One object of the new design is to meet industry demand for a definite-time reset following any successful automatic reclosure of the circuit breaker. For this reason the relay is normally set for an immediate initial reclosure followed in 10 seconds by the resetting of the relay if the reclosure is successful, or if unsuccessful by a maximum of three delayed reclosures each in turn followed in 10 seconds by a similar attempt to reset the relay. With this normal setting the minimum interval possible between successive reclosures is 15 seconds, being determined by the cam arrangement necessary to obtain reset in 10 seconds following a successful reclosure.

It is recognized that unusual local conditions may sometimes render the definite-time reset feature unnecessary or possibly objectionable. By proper arrangement of the double-ended cams "*D*" and the single-ended cams "*E*" shown in Figure 2 and previously described, reset can be omitted after any reclosure except the final delayed reclosure. For example if delayed reclosures are desired at 15-, 30-, and 30-second intervals with reset after the final reclosure only, the following cam arrangement is required: One of the single-ended cams "*E*" is set to operate contact "*AB-BC*" of *179* at 15 seconds, the remaining two single-ended cams "*E*" still back-to-back are set to operate "*AB-BC*" 30 seconds later, and finally the three double-ended cams "*D*" with their projections back-to-back are set to operate "*AB-BC*" after another 30-second interval. Since the single-ended cam plates "*E*" do not operate contact "*MN*" there will be no possibility of the relay resetting until 10 seconds after the final reclosure.

By proper use of the single-ended cams to omit the definite-time reset after certain of the reclosures, intervals of less than 15 seconds can be obtained. It is in fact possible to set the relay for immediate reclosure followed by delayed reclosures at intervals of 5, 5, and 5 seconds, with reset of the relay 10 seconds after the final reclosure if any of the reclosures was successful. The definite-time reset which always follows the final delayed reclosure obviates the necessity for total reclosing cycles of less than three minutes.

Conclusions

The new relay includes several features previously not available in multishot, motor-driven reclosing relays. The definite-time reset feature following a successful reclosure will improve service by eliminating many unnecessary lockouts or delays in reclosure, and will allow more freedom in the selection of reclosure intervals. The preclosed contact for immediate initial reclosure will materially reduce the reclosing time and will be of value where ultrahigh speed reclosing is contemplated. An internal means of blocking instantaneous tripping on first and subsequent reclosures will simplify relaying of systems including branch feeders with sectionalizing fuses.

Apart from these material improvements the new relay will offer many advantages from the standpoint of versatility and ease of adjustment. The facility in selecting either immediate or delayed initial reclosure, involving no mechanical changes in the relay, will be especially valuable. The wide range of reclosing cycles now possible will permit universal application of the relay, combining in effect the advantages of the "single-shot" reclosing relay with the versatility of the multishot reclosing relay.

References

1. Automatic Reclosing of Oil Circuit Breakers, **A. E. Anderson.** *Electrical Engineering (AIEE Transactions)*, volume 53, January 1934, pages 48–53.

2. Interim Report on Application and Operation of Automatic Reclosing Equipment on Stub Feeders, **AIEE Committee Report.** *Electrical Engineering (AIEE Transactions)*, volume 62, August 1943, pages 536–40.

3. A Novel Reclosing Relay, **P. O. Bobo.** *Electrical Engineering (AIEE Transactions)*, volume 60, December 1941, pages 1041–45.

Discussion

R. J. Cooper (Georgia Power Company, Atlanta, Ga.): In order to supply good service economically, reclosing circuit breakers, co-ordinated into automatic control schemes, are a necessity. Operating companies are seeking improvements continually and are interested in the development of new equipment that is reliable.

As switchboard space is becoming more valuable, the size of the new recloser is very attractive. Blocking of instantaneous trip devices in protective relays after initial operation is being used extensively and we are glad to find consideration being given this feature by making it accessible if desired.

We now have in operation a number of reclosing relays which have the feature of resetting in a definite time (about 15 seconds) after a successful reclosure. Although some may be inclined to think it unwise to use such a circuit we have had no disastrous results in our experience which covers about 75 reclosers of this type over a period of 15 years.

Lower initial time for reclosing and elimination of lockouts due to second faults after the last time interval, are desirable. There are methods of accomplishing both of them with the present reclosing relays. Our experience with successful reclosing operations follows very closely the tabulation given by Mr. Goff. If the complete timing interval of the present relay is 90 seconds and the reclosing intervals 0-15-60 seconds, there is not much danger of lockout due to second faults after the last operation.

It is hoped that the designers have not sacrificed too much power in changing to the synchronous-type motor. Surplus power is essential to reliable operation under adverse conditions.

In our fast growing industry it is soon realized that the majority of our installations change so fast that they may be considered to be of a temporary nature. Any scheme that requires some special type of associated equipment for its operation is not desirable. Control switches with the contact arrangement shown in Figure 3 are very unusual in our estimation. In shifting equipment from one location to another this one requirement could cause considerable confusion on occasions.

We have in operation on our system approximately 750 reclosing circuit breakers. Of these circuit breakers approximately 325, mostly on the transmission system, are controlled by d-c operated reclosing relays. Our automatic substations require d-c reclosing relays in order to function after bus differential relay operation, or in some cases, transformer differential relay operation. The schemes always provide for one attempt to restore service from a preferred source after such an operation and our experience justifies the practice. Pneumatic circuit breaker operators, carriers for relaying or telemetering, or communication and control have all contributed to the necessity of station batteries. We tried a-c control schemes in an effort to economize and now are convinced that a light duty battery is the most reliable and economical source for automatic control. If it could be justified, all our principal reclosing schemes would be d-c operated and we are very concerned that the indications are that no d-c reclosing relay will be available. We prefer not to complicate a reclosing scheme or decrease its reliability by using inverters or vibrators or similar devices in order to use an a-c reclosing relay. Neither should it be necessary to add a "1-shot" type recloser in order to accomplish what we now do with one relay.

A survey of the users of the largest numbers of reclosing relays in our area indicates an increasing demand for d-c reclosing relays. We recognize the fact that there are improvements and advantages in this new relay but cannot help but feel that it is limited in its application whereas the present relay is universal.

H. C. Barnes (American Gas and Electric Service Corporation, New York, N. Y.): The announcement of the new reclosing relay described by Mr. Goff was welcome news to us since it came just as we had decided to try a single reclosure on distribution feeders of 13.2 kv and below.

Unless experience dictates otherwise it is planned to use instantaneous first trip, immediate reclose and subsequent time delay trip to lockout. This policy was predicated by observations that most faults which do not clear on the initial trip are permanent faults. These should be isolated by branch fuses after the immediate reclosure when the instantaneous trip relays are cut out. Further tripping and reclosing to clear the few remaining faults which may not be permanent does not seem justifiable when the increased damage in closing into permanent faults is considered. The ideal reclosing circuit for this arrangement would be one which permitted one immediate reclosure plus a realization of savings from eliminating the reclosing timer, yet readily adaptable to changing from immediate to time delay reclosure or additional reclosures if required. Relays previously available could be utilized to provide immediate reclosing at some economy but made the addition of time delay or additional reclosures cumbersome and expensive. The new relay will provide all of the versatility required plus the desirable feature of a definite short time reset after any successful reclosure. Since facilities for cutting out and restoring the instantaneous trip are incorporated in it, a reduction in cost should be realized by the elimination of the external relays previously used for this purpose. If the new relay is comparable in cost to the older *AC-1*, the over-all cost of the new reclosing equipment will be very little more than that of a single immediate reclosing scheme with subsequent time delay trip. Further economy may be realized by reduction in panel size and wiring due to the reduced size of the new relay and to the instantaneous cut out feature being internal.

Like most new devices this one may require modification to meet the rigors of operation. A great many distribution relays are installed in unheated outdoor cabinets mounted on the oil circuit breakers. The driving motor provided must be a much lower power device than the previous motor to permit the reduction in over-all size. Whether it will have enough torque to operate at temperatures well below zero after it has been subject to wear and atmospheric corrosion remains to be seen. Our experience with micro and miniature switches on such outdoor installations as transformer alarms has not been too good. Performance of the telephone relay contacts in the instantaneous trip circuit where heavy auxiliary relay contacts were previously used will need proving particularly since they will normally be closed and may not have had the benefit of recent wiping action.

The driving motor being synchronous apparently this relay is designed only for operation on alternating current. This should not be an insurmountable objection since there is not much point in closing a circuit breaker if no power is available. Distribution circuit breakers are usually closed from transformers and therefore have supply for the relay available. Where additions are being made to existing stations having battery closing, supply for the relay can be obtained from the potential transformers. This may occasionally require an additional potential transformer or throw-over devices. High-voltage transmission stations may require operation from bushing and capacitor potential devices when closing from a line after a complete station outage. Probably the extra burden can be handled by the bushing potential device but the volt-ampere and wattage requirements will need to be known to determine this. We assume that the component parts have sufficient insulation to withstand the fluctuations of the voltage output of these devices. Normally the relays could be supplied from the bus potential transformers, with throw-over to the line potential devices when the bus is dead.

Since we do not use the timer in high-speed reclosing of high-voltage lines the two or three cycles gained by the preset immediate reclosing feature does not at the present appear to be too beneficial. A similar reduction in the tripping time of low-voltage circuit breakers would do much more towards successful reclosing since conductor damage would be reduced, particularly when weatherproof insulation is required. The connection of the antipump relay *179Z* shown in Figure 3 is certainly desirable in that it operates on a drop out principle and assures antipump action even when closing into severe faults which cause the station control voltage to dip.

Occasionally a 6-minute timer is required to permit a complete testing sequence for a line having a series of automatic sectionalizing air break switches. We would be interested in knowing if gear pairs will be available to obtain other than 3-minute over-all time. It may be that the definite time reset feature will permit circuit changes which eliminate the need for the 6-minute timer requirement.

In conclusion we believe the developers of this relay should be congratulated on having taken a step in reducing the size and cost of control relaying and in applying telephone relays to combine several functions in one case. We have endeavored for some time to get around to developments in this direction but pressure of other work has prevented it. While passing of the old standbys like the HFA and HGA would be regrettable, considerable savings might be realized by packaging several telephone relays in one case with a flexible arrangement of connections and coil ratings to provide the hot line or bus indication, circuit breaker positioning indication, sequential relaying, and other auxiliary functions required in most automatic control circuits. Savings should result not only from the lower cost telephone relays but also in the elimination of relay cases, reduction of external wiring, and decreased switchboard space requirements. Circuit changes would not be as costly since they would mean mostly internal relay changes, thereby eliminating the need for panel rearrangement.

G. E. Brooks (Oklahoma Gas and Electric Company, Oklahoma City, Okla.): Announcement of a multishot reclosing relay with quick-reset features should be welcomed by many operating companies. The Oklahoma Gas and Electric Company has had in use on its system for more than ten years[1] a number of assembled reclosing relays in which are incorporated selective quick-reset features. There are now 32 circuit breakers controlled by these relays and there has never been an experience which would disfavor the quick-reset operation.

The new relay has, in addition to the fast-reset provision, a number of commendable features, such as compactness, relative simplicity and flexibility. Separate external terminals for the various elements of the relay, such as immediate reclosure, delayed reclosures, reset and motor circuits, permit flexibility for special applications. Perhaps as a result of compromise between simplicity and flexibility, certain operating disadvantages appear and are here briefly discussed.

Pump-free Circuit Breaker Operation

The new relay uses an antipump unit (*179Z*) to insure pump-free operation on delayed reclosures. This is a conventional scheme depending on sequential operation of timer-operated contacts, released by opening of circuit breaker auxiliary switch, *b2-152*. Pump-free operation on immediate

reclosure depends upon the action of an interlocking unit, *179E*, which is shown to be energized by a contact of the closing relay, *152 X*. This circuit will require some modification when applied to pneumatically operated circuit breakers having no closing relay contacts. Referring to Figure 3, operation of the timer motor for delayed reclosures is entirely dependent upon the action of the interlocking unit, *179 E*, during the interval in which the closing relay, *152 X*, is closed. For this reason and the one stated for pneumatically operated circuit breakers, it would appear desirable to use a contact of the mechanism pump-free relay, *152 Y*, to operate interlocking unit.

Experience has shown that a latch check switch, connected as shown in Figure 3, will defeat the purpose of the antipump relay, *152 Y*, in the mechanism in the event of latch failure. This fact is mentioned here only to emphasize the need for pump-free features in both the mechanism and reclosing relay. It would appear that the scheme employed here for delayed reclosing could be applied for pump-free immediate reclosing at an increase of two cycles in reclosing time. In many cases, additional delay would be permissible, and in some instances necessary, for successful immediate reclosing.

Selective Control of Immediate Reclosure

For reduction of hazard to personnel during hot-line work, it is often desirable to eliminate the immediate reclosure for a limited period. Unless a convenient means is provided for removing this feature (preferably by means of a panel-mounted control switch) the circuit breaker must be placed on manual control and an attendant provided during these periods, with instructions to close the circuit breaker on a "1-minute hold" schedule. To save the cost of such standby operators, the Oklahoma Gas and Electric Company has equipped several installations with switches for making the first or immediate reclosure inoperative. In some instances, this requires a major modification of the reclosing relay. Referring to Figure 3, such a choice of reclosing schedules may be made by selecting the solid or dotted connections for contact, 1-179E. This selection should be made external to the relay itself.

Control of Instantaneous Trip

Selective co-ordination of feeder relays with branch fuses, that is, co-ordination of fuses with relays for temporary faults and co-ordination of relays with fuses for permanent faults, has proved practicable and economical on many urban and suburban feeders. The effectiveness of the scheme in saving fuses during transient faults depends in part upon how low a setting can be applied to the instantaneous relays. Should the instantaneous relays be set too close to the feeder load current, operations may be expected when the circuit is energized following outages of more than a few seconds. This inrush and abnormal current, due to temporary loss of diversity of cyclic loads, can cause repeated operations or lockout of the feeder circuit breaker by the instantaneous relays.

On the Oklahoma Gas and Electric Company system these undesirable lockouts are prevented by modification of the instantaneous trip controlling relay.[3] This modification, which was made following the publication of the reference paper, is a scheme to provide supervision of the controlling relay by the instantaneous relays. By a series connection of normally closed contacts on the instantaneous relays the controlling relay, after having opened the tripping circuit, is prevented from timing out until all instantaneous relays have returned to normal. Normal position must be retained throughout the controlling relay's timing period before the tripping circuit for the instantaneous relays can be re-established. Thus, a load current of tripping magnitude upon circuit breaker reclosure will hold the instantaneous relays inoperative for the period of abnormalcy plus the timing period of the controlling relay. With this "super control" of instantaneous relays, momentary load currents may be allowed to exceed the relay setting without causing lockout of the feeder.

The new relay represents the first major improvement in manufactured reclosing relays in many years. As with other new designs, some modifications may be necessary to permit wider application. Any changes resulting in increased flexibility are certain to multiply its usefulness and defer its obsolescence.

References

1. A Novel Reclosing Relay, P. O. Bobo. *Electrical Engineering (AIEE Transactions)*, volume 60, December 1941, pages 1041–45.

2. A New Electronic Timing Relay for Reducing Outages of Power Circuits, Frank S. Dlouhy. *Electrical Engineering (AIEE Transactions)*, volume 65, July 1946, pages 407–11.

C. A. Streifus (Ebasco Services Incorporated, New York, N. Y.): The relay described by Mr. Goff appears to be the most complete relay of its type for controlled immediate and delayed reclosing of circuit breakers as it has the required functional characteristics as well as being small, compact, and assembled in one case of conventional design.

Five years ago during proposed application of reclosing relays and observation of installed relays, our company reviewed the characteristics of available reclosing relays and wrote a series of desired operating specifications. None of the relays could meet these specifications without being modified or without addition of supplementary relays and timing circuits requiring considerable space. It is gratifying to note on comparing the specifications written at that time with those in the paper that this new relay meets them as well as having other desirable characteristics.

A most important feature of this new relay is its fast reset feature, similar to that in certain "1-shot" relays, except that there is provision for adjusting the time of reset. Fast reset prevents the circuit breaker from remaining open when a second temporary or arcing type fault occurs a few seconds after a successful immediate reclosure. This feature should raise further the percentage of successful immediate reclosures. On a number of occasions, the writer observed temporary type of faults occurring during the long reset period on installations where the reclosing relays did not have the fast reset feature. This caused the circuit breakers to remain open, thus the advantage of the first immediate reclosure was negated.

The feature of blocking the instantaneous trip circuit after initial circuit breaker tripout should be helpful in co-ordinating system relaying.

Circuit breaker duty and capacity should be reviewed for each application of relays with immediate reclosure and fast reset because of the relatively short interval possible between circuit breaker openings and resulting increase in duty caused by rapid occurrence of faults.

This new relay takes an important place in the series of developments pioneered by such men as E. E. George and J. T. Logan in the field of instantaneous reclosing of circuit breakers which is related to power system stability, reduction in length of outages of transmission and distribution lines, and broad problems associated with maintaining service to important loads.

L. E. Goff: The new reclosing relay described in this paper was developed to meet an indicated demand for a relay having features not provided in available multishot reclosing relays. It is gratifying to note from the comments of Messrs. Streifus, Barnes, Cooper, and Brooks that in general the goal has been achieved.

Cooper has pointed out that the choice of a synchronous motor makes the new relay unattractive for applications using d-c control voltage. The decision to use an a-c motor in the new relay was based on several factors. Small synchronous motors with relatively high operating torque and with insulation levels meeting switchgear standards are available. Universal types of motors with governors, providing comparable operating torque and insulation, are much larger and would not have permitted the desirable reduction in relay size. From all indications a dependable source of a-c control voltage is available on a large majority of circuit breaker installations. Where two or more sources of a-c control voltage are involved a simple throw-over scheme insures operation of the reclosing relays following a circuit breaker outage if voltage is available from any one of the sources. If all sources are dead nothing is gained by reclosing the circuit breaker. There is a distinct possibility that where station batteries are involved a throwover scheme would be required anyway to insure a dependable voltage source for the battery charging equipment. It should be noted that the low burden of the synchronous motor permits its operation from bushing potential devices.

Cooper suggests that the danger of unnecessary lockouts can be practically eliminated with available relays by using a short total time cycle and setting the final delayed reclosure close to lockout. While this is a possible solution, it does not prevent needless delay in initiating reclosure when two transient faults occur during the operating cycle of the relay. Furthermore, it places a limitation on the reclosing intervals possible for a given relay.

It should be emphasized that the new relay is not limited to application with the control switch shown in Figure 3. The control switch now considered conventional for automatic reclosing applications can be used, but because of the need for controlling the reset circuit of the new relay an additional

lead between the circuit breaker and relay panel is required. The new switch eliminates the need for this extra lead. The sequence of operation is the same in the new switch and it could be used if necessary as a substitute for the present one.

Barnes' proposed application of the new reclosing relay on distribution feeders illustrates very well its usefulness where it is desired to block instantaneous tripping after the initial tripout and prior to the first reclosure. The relay lends itself well to such applications where it may subsequently be desired to include several delayed reclosures, in addition to the immediate reclosure, at a later date, which is not possible with available single-shot reclosers.

The relay has been designed and has passed tests for starting and operation over the temperature range specified in the American Standards Association standards for switchgear relays, that is −20 to +40 degrees centigrade. Where temperatures lower than −20 degrees are encountered it is expected that heaters will be installed in the relay compartment.

The small switches used in this relay were originally designed for use in military aircraft and consequently met rigorous requirements, including satisfactory operation at temperatures well below those normally encountered on outdoor circuit breaker installations. It is interesting to note that the contact force of these switches is approximately 90 grams, or much higher than that of the usual auxiliary relay. It is felt that the telephone-type relay has already proved itself worthy of use in protective relays. In line with Barnes suggestion, groups of telephone-type relays in a single case have for a number of years been used in conjunction with standard carrier relaying equipment to perform various auxiliary functions, and their service record has been excellent.

As Brooks points out the circuit shown in Figure 3 depends upon an interlock contact of closing relay *152 X* to energize the *179E* "trip" winding and provide pump-free operation following immediate initial reclosure. On pneumatically operated circuit breakers there is of course no such contact available, so other means must be found for energizing the *179 E* coil. This question has already been considered and a circuit worked out for applying the relay on pneumatically operated circuit breakers, employing the *179Z* unit in conjunction with a seal-in resistor.

It is true that starting of the timing motor to initiate delayed reclosures is dependent upon the successful operation of interlocking unit *179E* during the interval in which closing relay *152 X* is closed. However, the operating time of *179E* is less than one cycle, whereas the *152 X* relay will remain picked up for from 10 to 15 cycles, so there is a wide margin favoring successful operation of the unit.

Over-simplification of the schematic diagram in Figure 3 has evidently caused confusion as to the intended connections of the seal-in contact of *152 Y*. This contact will seal-in around the "*LC*" and "*b*" switches of the circuit breaker and hence will provide satisfactory pump-free operation.

Brooks also has pointed out a potential difficulty in blocking the instantaneous trip circuit when the reclosing relay has the quick reset feature. If high-dropout instantaneous relays are used to permit a setting close to normal load current, they will probably pick up on inrush following a successful delayed reclosure and may still be closed when the reclosing relay resets. This would cause an unnecessary tripout since the instantaneous trip circuit would be restored when the reclosing relay reset.

The trouble can be avoided by either of two methods. A normally closed contact of the instantaneous relay for each phase could be connected in series in the reclosing relay motor circuit. Thus the reclosing relay will not run following a successful reclosure until inrush current in each phase has fallen below the dropout point of the respective phase relay. This scheme will not prevent an unnecessary tripout if the circuit breaker is successfully reclosed manually with the reclosing relay in the locked out position, since the relay would then reset as soon as the manual switch was released, reinstating the instantaneous trip circuit. An alternate scheme using a simple hinge-type auxiliary relay in conjunction with normally open contacts of the high-dropout instantaneous relays will prevent this trouble also. The normally open contacts of the three instantaneous relays would be connected in parallel to operate the auxiliary relay if any of the instantaneous relays were picked up. A normally closed contact of the auxiliary would be connected in the motor circuit and another in the reset circuit of the reclosing relay. This will prevent the timing motor from operating following a successful circuit breaker reclosure until the instantaneous relays have all reset, and will also prevent reset of the relay from its locked out position until the same relays have dropped out following a successful manual reclosure. Of course if the motor and reset circuits of the reclosing relay are both operated from the same a-c supply, the same thing could be accomplished by connecting series normally closed contacts of the instantaneous relays in the common lead.

Ice Testing of Outdoor Disconnecting Switches to Simulate Field Conditions

J. B. OWENS
ASSOCIATE AIEE

THE "ice storm" is one of the major difficulties encountered in the operation of electric power systems. Under certain atmospheric conditions a deposit of hard clear ice can build up in a few hours to a thickness which causes overhead lines to fail, and which renders the operation of outdoor switching equipment very difficult. To overcome operating difficulties under these conditions, many ingenious outdoor switches which employ some auxiliary blade motion to break ice have been developed. This blade motion has been accomplished by a great variety of mechanisms, and doubtless many others will follow.

The testing of these outdoor switches to determine the effectiveness of their ice breaking mechanisms has long been a problem to both switch manufacturers and power system engineers. In most locations, severe ice storms occur infrequently so that testing under natural conditions becomes impractical. Thus the problem arises of producing artificially the thickness and density of ice coating which occurs in nature. If any outdoor switch were frozen in a giant ice cube large enough to contain the entire switch, obviously it would be inoperable. Therefore, testing must be done with an ice thickness comparable to that actually encountered in service. Also the strength and tenacity of an ice coating varies considerably with variations in the air temperature, water temperature, and rate of application. These factors must be controlled carefully to obtain proper results. It is the purpose of this paper to describe an ice test which produces conditions comparable to those obtained in the field, and to describe the design features of a switch which can be operated easily under severe icing conditions.

Formation of Ice

The weather conditions which most often produce severe ice storms are those which prevail when a warm air mass has overrun a cold air mass so that rain is falling through air which is slightly below freezing. Such warm fronts usually extend over a considerable area producing wide precipitation belts, and these fronts are slow moving compared to cold fronts so that the rain may persist for a number of hours.

Under the conditions described, the falling water is cooled by evaporation and by its travel through the cool air mass so that it freezes almost instantly upon contact with objects on the earth. When the temperature of the air near the ground is only a few degrees below freezing, the ice which is formed is hard and clear and free from the inclusion of air bubbles. This is the kind of coating which creates the greatest difficulty in switch operation.

In general, ice which is formed at very low temperature (below 15 degrees Fahrenheit), and ice which is formed from moisture condensing from the air onto cold surfaces has a very porous and weak structure. Such ice is called rime ice, and is characterized by a white rather than clear appearance. This appearance is a result of the many small air spaces included in the structure. A good example of rime ice is the formation on the cooling coils of a home refrigerator.

It has been found that if switches are cooled to temperatures below 15 degrees Fahrenheit and are sprayed with a fine mist, a coating of rime ice is deposited. This coating is broken very easily even when the thickness is great, and such a test is not a real measure of the ice breaking ability of the mechanism.

A test which has been found to give consistently a clear hard ice deposit is as follows:

1. Assemble all poles and mechanism of the switch on a structure to permit normal operation. The operating pipes may be shortened to suit space requirements.

2. Clean all traces of oil or grease from all outside switch surfaces. Even thin films of oil or grease prevent ice from adhering to the switch and greatly change test results.

3. With the switch blade in the desired position, lower the air temperature to 35 degrees Fahrenheit, and then spray the switch with water which has been cooled to approximately 35 degrees Fahrenheit. This spray should be arranged to simulate a general rain and not a fog or mist. The water should fall from above and at an angle not exceeding 45 degrees from vertical. The location of the spray should be such that the pole units and entire operating mechanism are covered with a uniform rainfall.

4. After the rain is started, the air temperature should be lowered at the rate of approximately 3 degrees Fahrenheit per hour to a final temperature of 25 degrees Fahrenheit. This causes the switch to be sprayed for an hour before freezing temperature is reached, and the switch is thoroughly wet when freezing begins. The amount of water supplied should be such that ice forms at the rate of about 1/4 inch per hour.

5. Continue the spraying while holding the air temperature between 25 and 30 degrees Fahrenheit until a deposit of ice one inch thick has formed.

6. After the ice has been deposited, the switch may be operated and the operating effort noted.

Typical Test Arrangement

A laboratory setup to make the test just described is shown in Figure 1. The switches which were tested were two 15-kv 400-ampere 3-pole manually gang

Paper 30-239, recommended by the AIEE Switchgear Committee and approved by the AIEE Technical Program Committee for presentation at the AIEE Fall General Meeting, Oklahoma City, Okla., October 23–27, 1950. Manuscript submitted July 6, 1950; made available for printing August 31, 1950.

J. B. Owens is with the Westinghouse Electric Corporation, East Pittsburgh, Pa.

The author wishes to acknowledge the contributions to these tests made by W. R. Smith, George Lambert, and other engineers of the Pennsylvania Power and Light Company.

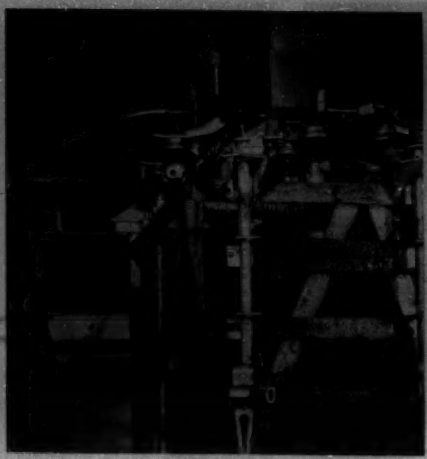

Figure 1 (left). Ice test setup for two 15-kv 400-ampere air switches

Figure 3 (above). Close-up view of final ice coating showing the exceptionally heavy clear ice coating

operated air switches with offset torsional mechanisms.

Figure 1 also shows the pipes which comprised the spraying system to create the rain on the switches. These pipes were located at the level of the switch bases, and were supplied with water cooled to 35 degrees Fahrenheit by being circulated through a coil embedded in dry ice. The pipes were 1/2-inch thin-wall brass tubing and were drilled with 0.028-inch diameter holes on 9-inch centers to release the spray. The water pressure was adjusted to cause the streams to rise about six feet into the air before falling onto the switches. With this particular arrangement $1^1/_2$ gallons of precooled water were sprayed per hour per square foot of area sprayed to cause the ice to form at the desired rate. An air blower in the cold chamber served to agitate the rainfall to assist in uniform distribution over the switch.

Figure 2 shows the arrangement used to precool the water for the rain. Tap water was used, and it was cooled by being passed through 120 feet of 1/2-inch copper tubing wound into a coil surrounded with dry ice. The coil was placed in a micarta tube approximately 16 inches in diameter and 30 inches long. Dry ice chips were packed in the center of the coil. The output water temperature was controlled by varying the amount of dry ice used, and by varying how closely the chips were packed.

Figure 3 shows the clarity of the coating on the test switches after ice has been deposited. After the switches were operated, they were placed in an intermediate position between open and closed, and the photograph of Figure 4 was taken. This shows how the blade twisting motion, and the flexing of the jaws have cleared the ice from the contacts.

Measurement of Ice Thickness

One of the chief problems in making tests of this kind is that of knowing when the right quantity of ice has been deposited. Many utility company specifications have been studied, and "one inch of radial ice" is most commonly specified for testing of this kind. A final thickness of one inch is suggested as a standard for testing since this amount is rarely exceeded in service in the continental United States. However, ice does not form with uniform thickness over all switch surfaces, and the further problem arises of determining the correct place to measure the ice.

Figure 2. Dry ice chamber for precooling water to spray switches

On a power transmission or distribution system which has been blanketed with an ice storm, the ice of greatest interest, and that which has the most nearly uniform thickness, is that formed on horizontal overhead conductors. Around these circular conductors ice is formed with approximately uniform thickness. A measure of the radial thickness of the coating on a horizontal conductor is a fair measure of the severity of the storm.

On outdoor air switches, ice forms much more rapidly on some surfaces than others. Therefore, a measurement of the ice at any one place on the switch will probably not give a fair measure of the severity of the coating. One method which has given good results is to mount a piece of copper cable so that it is horizontal and receives the same rainfall as the switch. A measurement of the ice thickness at the top side of this conductor can be taken as an index of the thickness of the ice coating.

Many of the outdoor air switches now on the market have a single blade of circular section. A measure of the ice on the top side of the blade of such a switch in the closed position compares closely with ice on a circular conductor, and can be used as a measure of ice severity.

Figure 4. Close-up view of switch pole units with each switch in an intermediate position after being operated

Design Features of an Ice Breaking Switch

In developing the ice tests described in this paper, a great number of tests were made on a variety of switches, and certain desirable features of design for ice breaking switches were determined.

An ideal design for an air switch to operate when covered with ice, is one in which all moving parts are totally enclosed and cannot accumulate ice. Obviously, a practical design cannot enclose the blade and break jaw, and there is a need for auxiliary blade motion to break ice on the jaw. Many such motions have been devised; one of the most popular being a blade twisting motion that takes place before blade rise begins. In general, this motion is very effective in clearing the jaw of ice, provided the mechanism used to obtain the blade motion does not itself become fouled with ice It is possible to design a mechanism which is itself entirely enclosed and protected from icing; such a mechanism has been described by H. W. Graybill and J. S. Ferguson.[1] This mechanism is employed in the switch described here. Thus the first feature of switches designed to work under ice conditions should be an enclosed blade actuating mechanism.

The tests which have been described revealed further that the hinge-end contact was another source of difficulty under ice conditions. Switches were tested which had jaw contacts at the hinge, similar to those used at the break end. These hinge jaws gathered ice and increased the initial effort required to start the switch moving. Switches with totally enclosed hinge contacts showed a considerable reduction in operating effort under ice conditions.

It also was made apparent during the testing of these switches that adjacent switch parts with relative motion should be widely spaced. Any flat surface which was required to move with respect to a closely-adjacent parallel stationary surface was particularly troublesome. Ice bridging between these surfaces was very difficult to break. Therefore, a third feature of ice breaking switches is the freedom from closely spaced parallel surfaces which have relative motion during switch operation.

Figure 6 shows a pole unit of a switch which was designed to operate under severe ice coatings, and which incorporates all of the features found desirable in the testing program.

Summary

At the present time, there is no standardized method of testing outdoor air switches to evaluate their performance when covered with ice. A careful study has been made of the problem of produc-

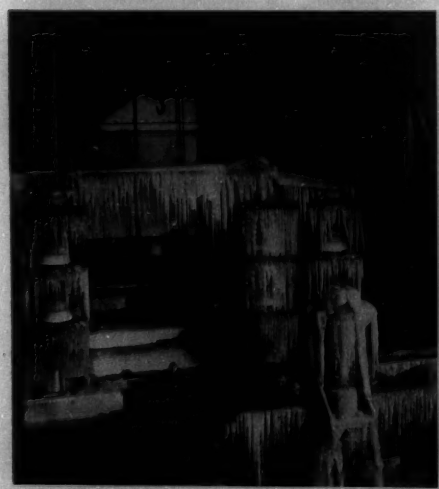

Figure 5 (left). Test setup for 115-kv 1,200-ampere switches

Figure 6 (below). Pole unit of a switch especially designed to have good performance under heavy ice coatings

ing ice in artificially cooled rooms which corresponds in density, and strength of bonding with that encountered in service. The essential elements of a testing procedure to give the desired results are as follows:

1. Assemble a complete switch for normal operation, and clean all traces of oil or grease from switch surfaces.

2. Lower the air temperature to 35 degrees Fahrenheit and start a general rain of water which has been precooled to 35 degrees Fahrenheit.

3. After the rain has been started, lower the air temperature approximately 3 degrees Fahrenheit per hour until a final temperature of 25 degrees Fahrenheit has been reached.

4. Continue the rain with the air temperature at 25 degrees until an ice thickness of one inch has been reached on the top of the switch blade or on a horizontal conductor receiving the same rain as the switch.

5. Operate the switch and note the operating effort.

During the testing of many switches using these specifications, certain important features of design for ice breaking switches were determined. These features are as follows:

1. An auxiliary ice breaking motion should be imparted to the blade before blade rise begins. The mechanism which imparts this motion to the blade should be enclosed and protected from ice accumulations in both open and closed positions.

2. The hinge-end electrical contacts should be protected from ice accumulation.

3. Closely spaced parallel parts with relative motion during switch operation should be avoided.

It is suggested that the testing method developed be considered as a standard procedure for outdoor switch testing.

References

1. A New Outdoor Air Switch and the Principles Involved in Its Design, H. W. Graybill, J. S. Ferguson. *Electrical Engineering (AIEE Transactions)*, volume 64, August 1945, pages 583–86.

2. Meteorology, Theoretical and Applied (book), E. W. Hewson, R. W. Longley. John Wiley and Sons, New York, N. Y., 1945.

Discussion

C. S. Beattie and **S. C. Killian** (Delta-Star Electric Company, Chicago, Ill.): The ice tests described in the paper are interesting and a big step toward a possible standard for testing which might be used for comparing the ice breaking ability of the many types of outdoor switches now offered by various manufacturers.

Laboratory setups without the exact control described in the author's paper have been used for a good number of years and have served the purpose of securing valuable design data in connection with outdoor disconnecting switches. The test specifications proposed will produce ice and sleet of certain characteristics but operating experience indicates it is extremely difficult if not impossible to duplicate the work of nature during certain sleet storms. It also has been proved that the thickness of the ice or sleet coating bears no definite relation to the operating effort required to break a switch loose under certain sleet conditions. Very thin coatings under some conditions appear to be much more troublesome than ice coatings several inches thick.

Laboratory tests although valuable for comparative purposes are no insurance that the equipment will be sleet- and ice-proof over long years of service and under all conditions of corrosion, type of operating mechanism, and method of mounting. The tests described are not difficult to pass using a modern corrosion-free switch with a simple short operating mechanism.

The author stresses the importance of enclosed hinge contacts. The introduction of hinge contacts on rotating insulator vertical break disconnects is a direct result of the trend to eliminate flexible shunts on outdoor switches.

Assuming that the break contact is the best design possible, it is only good sense to attempt to use this design at the hinge contact also. If the over-all switch design does not lend itself to this, some other contact must be used at the hinge. Since this is an entirely different contact design it can be so constructed as to be covered. However, by putting it into a limited space, the rugged and reliable break contact design is lost and a multiplicity of small contact springs, small bridging members and current carrying pins must be used. Current interchange surfaces also are needlessly increased. Furthermore, this design does not lend itself to use in high capacity switches such as 4,000 and 5,000 ampere.

Too often the cover over the hinge contact creates much more of a hazard than the contact itself. This large cover area must move in relation to the remainder of the switch and under ice this will increase the possibility of immobility.

There is small difficulty in making a switch ice and sleet proof in a design using identical break and hinge contacts since inherently greater mechanical advantage is available at the hinge because of the shorter lever arm from the blade driving mechanism to the hinge contact as compared to the lever arm required at the jaw end. The ease of inspecting or replacing either blades or contacts is a decided operating advantage, best realized by the use of a properly designed open hinge contact combined with a powerful factory-sealed blade driving mechanism.

R. M. Smith (Railway and Industrial Engineering Company, Greensburg, Pa.): We wish to congratulate Mr. Owens for his work in bringing before the Institute a subject which needs additional attention and discussion. While the matter of ice testing of switches has received consideration throughout the past years, there has been no concerted effort to standardize laboratory tests in order to obtain a comparison of results and to more nearly simulate actual conditions met with in service.

We note that as a result of the testing of switches under icing conditions, Mr. Owens concludes that the switch should have an "auxiliary ice breaking motion" before the blade rise begins. We are glad that Mr. Owens concurs with our findings, for C. G. Koppitz of the Railway and Industrial Engineering Company first developed a switch of this nature about 25 years ago, and this construction, popularly known as the tail-twister design, is now practically a standard for the industry.

We concur with Mr. Owens' conclusions regarding the generous spacing of parts in relative motion during switch operation. Also, our present switch construction encloses the hinge end contacts, and we consider this most important for a good ice breaking switch. In fact, our tests indicate that the effort required to move the various bearings on the switch can become a major portion of the total effort and requires special attention. For example, in our construction, the blade itself has only one exposed bearing where ice must be sheared, whereas some constructions current today have two exposed bearings, and, in some cases, even four.

In the same manner, the bearings carrying the rotating insulator stack may add considerably to the operating effort, when they are heavily coated with hard ice. We have always used the construction shown in Figure 1 of this discussion in which a sealed, dry, ball-bearing construction is used. The sealing consists of a neoprene gasket, running on a bronze machined race, so as to give a weatherproof seal. Tests indicate that this bearing, under dry conditions, requires about 25-inch pounds to cause it to rotate. When fully sealed and dry but covered with 5/8-inch of hard ice, it requires 136-inch pounds to shear the ice. However, when

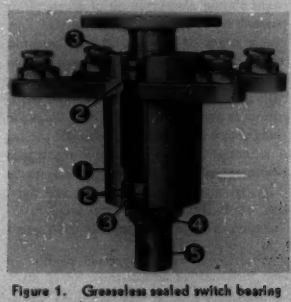

Figure 1. Grease-less sealed switch bearing

1. Heat treated aluminum housing
2. Stationary and take-up ball races
3. Synthetic rubber gasket for weather seal
4. Adjusting and take-up nut
5. Galvanized forged steel rotor

$1^3/_4$ ounces of water are deliberately introduced inside the bearing and frozen, with no external ice, it requires from 600- to 1,000-inch pounds to rotate a single bearing. This illustrates the advantage of the dry, sealed, ball bearing, and also shows that a good ice breaking switch must have attention directed to all of the components and not only to the current carrying path.

Mr. Owens describes a hood or cover over the hinge and rear electrical contact, which appears to keep the water out of the inside when mounted in the upright position. We would assume, however, that with the switch mounted in the inverted position, it would be most difficult to keep water from entering this cover since it would then be mounted in the opposite position and water would tend to run into this pan around the bearing of the rotating insulator.

W. B. Morton (Pennsylvania Power and Light Company, Allentown, Pa.): The tests and procedures covered by this paper were promoted at the instigation of engineers of the Pennsylvania Power and Light Company, as a result of years of investigation into the vagaries of sleet formation, and much experimentation with various kinds of sleet-melting devices on a transmission system covering 9,500 square miles of territory that is highly vulnerable to sleet formation. It was discovered in these investigations that no disconnecting switches on the Pennsylvania Power and Light Company system, of any manufacturer, were entirely immune to freezing fast and becoming inoperable in service, despite elaborate ice testing by the manufacturers' laboratories.

This experience led to one obvious conclusion that current practices were inadequate to produce the conditions of ice formation actually experienced under field conditions. Thus a new concept of ice freezing technique was developed and promoted by Pennsylvania Power and Light Company engineers with results outlined in the paper.

The paper should lay more emphasis on the important fact that this new concept of ice testing differs from all previous ones in that it is based on a high-temperature slow-freeze, in contrast to the previous universally accepted, but erroneous, thinking that low temperature quick freezing is a true criterion of field conditions. Moreover, an important consideration early discovered in the Pennsylvania Power and Light Company investigations, that is not pointed out by the author, is the necessity for thoroughly spraying the equipment for at least an hour prior to the test, as a sleet storm is usually preceded by rain before reaching the sleet stage, to insure that water has penetrated all crevices and interstices, which penetration under field conditions is one of the major causes of some switch failures that are not detected in the obsolete laboratory "quick freeze—low temperature testing."

The paper also should emphasize that the needed revisions to the AIEE standards for disconnecting switches should require that they be ice tested in both open and closed positions.

J. B. Owens: The testing program which provided the information for this paper revealed that in general a switch which was frozen in the closed position required a higher operating effort than the same switch frozen in the open position. This was a result of ice on the break jaw and arcing horns interfering with starting the switch toward the open position. With a well designed switch the closing operation could be started easily and the inertia of the parts provided enough impact to shatter ice on the jaw to allow full closing. In the evaluation of a new design, however, it should certainly be tested in both the open and closed positions.

This paper has not attempted to describe all the details of design which are required to make a good ice-breaking switch. It has only pointed out salient features which contribute to a good ice-breaking performance. To produce an outdoor switch to operate satisfactorily under all conditions requires careful attention to many details such as proper bearing design, complete sealing of ball bearings, and proper design of switch parts to prevent water accumulation with any switch mounting position. These details have all received proper attention in the switch shown in the paper.

The interest which has been shown in the development of these tests indicates a real desire for standardization of ice testing procedures.

It is hoped, therefore, that this paper will provide a starting point from which procedures can be devised which will be satisfactory to all concerned.

A Simplified 48-Channel Carrier Telephone System

L. G. ERICKSON
MEMBER AIEE

Synopsis: This paper describes a 48-channel single side band carrier system which provides toll quality telephone transmission bands with exceptional simplicity and dependability of equipment. Through the use of a novel frequency translation pattern, speech bands covering the range from 200 cycles to 3,500 cycles are secured at 4-kc channel separation without resort to crystal filters. In this system, improved translating modulator techniques and other advanced features reduce the number of vacuum tubes to a minimum while achieving exceptionally high performance standards, stability, and ease of maintenance.

Prior Art

THE single-side band suppressed carrier method of deriving multiple communication channels from a common transmission medium is now almost 40 years old. The solutions to the basic transmission problems were set forth by E. H. Colpitts and O. B. Blackwell in a paper, now classic, which appeared in 1921.[1] The first systems to provide good telephone circuits by this method came into widespread use about 1927. From this point on, advances in the art were rapid with large scale installations of 3-channel systems coming to be a factor in trunkline telephony about 1933. By 1938 the 12-channel systems for open wire and cable, those recognized by communication engineers as the *J* and *K* systems, had attained a high degree of development.[2,3,4] Relatively soon thereafter the coaxial carrier system, designated as type *L*, was developed to provide really large numbers of channels on a common transmission circuit.[5] Further developments in multiple-channel communication, both delayed and accelerated by World War II, are the present-day introduction of radio relaying, and long strides in the direction of simplification and reduction in carrier equipment cost.

The same general pattern is traceable through the history of progress of many technological advances in all fields. First, the invention is shown to be of utility, though exhibiting perhaps no marked operational or economic advantages. Next, its performance is improved, sometimes at inordinate cost, creating a demand for the higher standard. Then comes the protracted period of simplifying designs while at the same time improving dependability and reducing maintenance cost, finally realizing the full advantages which the early inventor had dreamed for the new method. The advent of a multiple-channel telephone carrier economically applicable to circuits as short as 20 miles realizes an ambition set many years back.

The Present Contribution

The communication industry now is reasonably well standardized on 4,000-cycle separation for telephone channels having the transmission quality attendant to a bandwidth of at least 3,000 cycles. To achieve such spectrum economy and performance in systems having many bands translated to positions above one another, relatively costly crystal filters were brought into being. These are widely used in many systems currently being installed. The design of a system which affords 3,400 cycles of bandwidth per channel while employing relatively simple and inexpensive inductance-capacity filters marks a definite advance, particularly for short-haul wire line and radio applications. It is noteworthy too that while earlier multiple channel systems employed on the average 12 electron tubes per 2-way conversation circuit derived, the latest technologies reduce the tubes to approximately five per 2-way circuit.

General Description and Theory

Communication literature discloses the single side band suppressed carrier principle so well, both in theory and application, that a detailed explanation here is undesirable. However, in the interest of making this paper self-sufficient, a very basic concept of the end result of single side band modulation is justifiable. The intelligence frequencies essential to the reproduction of good telephone conversation may be regarded as a heterogeneous, though, of course, a discrete mixture of sinusoidal components within the range from 200 cycles to 3,500 cycles. A balanced modulator which suppresses both the original intelligence frequencies and the carrier frequency, followed by an appropriate filter which passes only one complete set of beat notes between those intelligence frequencies and the carrier frequency, is in fact a frequency translating system.

A plot of the currents resulting from two tandem stages of single-side-band modulation, as shown in Figure 1 serves to illustrate in an extremely simple manner. Graph "A" presumes the instantaneous speech current to be a sinusoidal wave of 1,000 cycles. The upper side band after modulation by 8,000 cycles is the 9,000-cycle current of "B." If "B" is passed through a second stage of modulation, the carrier of which is still higher, the single-side-band current again is a sinusoidal wave 9,000 cycles removed from the new carrier as shown by "C." Two quite reciprocal translations will bring back the original input intelligence

Paper 50-240, recommended by the AIEE Wire Communication Systems Committee and approved by the AIEE Technical Program Committee for presentation at the AIEE Fall General Meeting, Oklahoma City, Okla., October 23-27, 1950. Manuscript submitted July 26, 1950; made available for printing September 27, 1950.

L. G. Erickson is with the Leakurt Electric Company, San Carlos, Calif.

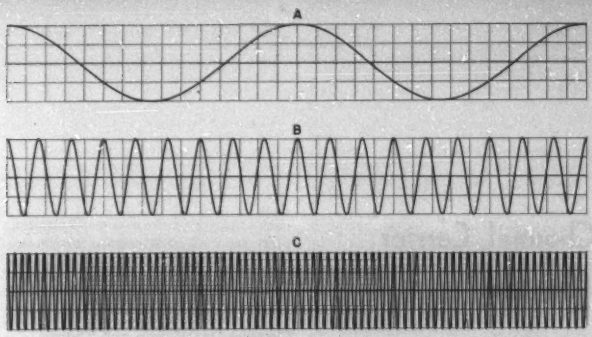

Figure 1. Translation of speech currents

frequency, in this case the 1,000-cycle sine wave. If the original speech wave is a frequency other than 1,000 cycles, the location of the frequency which represents it after each translation is different by an exactly corresponding amount. If the original wave is of a different amplitude, then the side-band wave which represents it has a corresponding different amplitude.

Fidelity of reproduction of the complex wave of speech depends upon the degree of amplitude linearity of the translating device, and upon the absence of extraneous currents introduced by the process. Thanks to current communication engineering practices, these translations now are accomplished in almost any desired number, with little, if any, detectable distortion of the original intelligence wave form. Of great practical significance, these translations are accomplished in the equipment being described largely by inert devices having a very high degree of stability and indefinite life.

The prime requirement of the filter employed to separate the desired group of side bands from the undesired group is that it shall adequately suppress the latter group. The secondary requirement, though still an important one, is that it shall pass those frequencies representing that side band which is to be used with a minimum of difference in attenuation and a minimum of relative phase shift. "Adequately," of course, is a matter of degree, but if the unwanted group is allowed to go over the transmission circuit, the result is interference to some other channel of the system, the magnitude of which is directly proportional to the unsuppressed voltage. High-grade telephone circuit operation, then, requires that the unwanted "image" be suppressed at least 55 to 60 decibels with respect to the wanted group.

When we consider the first translation from the speech frequency it becomes evident that the filter employed to select the wanted side band must offer a high degree of attenuation to the lowest frequency of the unwanted side band. The "guard" band, or the interval in which the filter characteristics must change from very low attenuation to very high attenuation is then twice the lowest frequency in cycles to be transmitted over the channel. Since we are going to stack channels later at 4-kc intervals, it also is necessary that frequencies beyond the high end of the pass band be attenuated greatly since otherwise they would be detected as low frequencies in an adjacent channel. This means that if we are to transmit frequencies of 3,600 cycles over a particular channel, the characteristics of the band pass filter we are considering also must change from very low attenuation to very high attenuation for a change of frequency equivalent to 3,600 cycles in one channel to a frequency of 200 cycles in the channel immediately above. This would correspond to a guard band required on the "high" side of 600 cycles. This performance is attainable at reasonable cost only at relatively low carrier frequencies.

Translation System of the Type 42

This new 48-channel carrier telephone system employs two successive stages of modulation to accomplish frequency translations for each channel. With this method the first stage of modulation utilizes an 8-kc carrier frequency, and the upper side band is selected for transmission. Regardless of its future frequency allocation, each channel is positioned initially at an intermediate frequency band between 8 and 12 kc. Filters having very

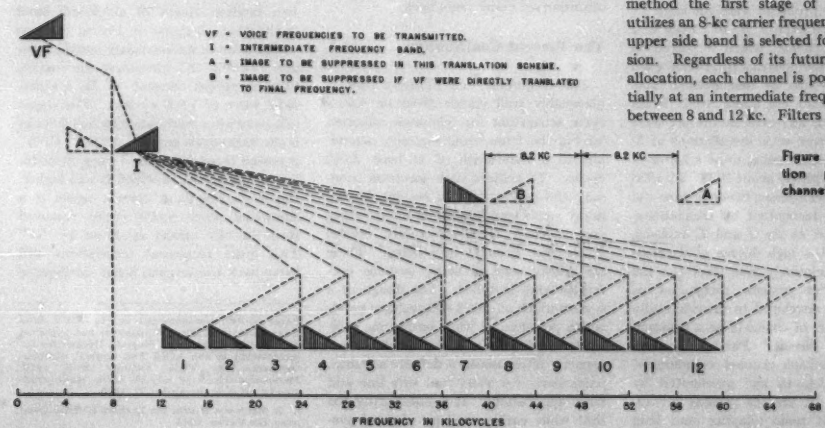

Figure 2. Translation pattern and channel allocation chart

Figure 3. Functional diagram of typical channel

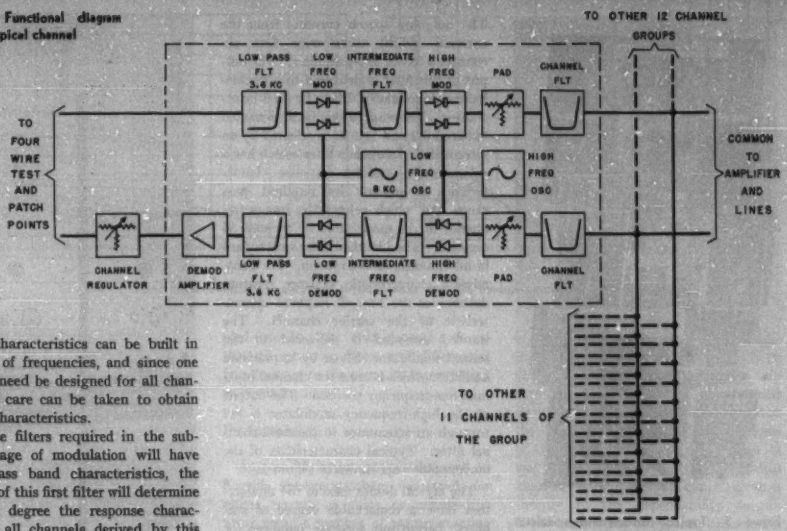

desirable characteristics can be built in this range of frequencies, and since one filter only need be designed for all channels, great care can be taken to obtain optimum characteristics.

Since the filters required in the subsequent stage of modulation will have broader pass band characteristics, the pass band of this first filter will determine to a large degree the response characteristic of all channels derived by this method, and this response characteristic is remarkably uniform from channel to channel.

Subsequent to this initial modulation, higher frequency modulators are used to accomplish frequency translations between the intermediate frequency band and the final line frequencies of 12 to 204 kc. In this way up to 48 channels may be assembled on 4-kc spacing with guard bands of only 600 cycles between channels; yet the high frequency modulators and filters only need to meet the design requirements for a system having a guard band of 16 kc between channels.

The translation pattern of the type 42 system is easiest explained with reference to Figure 2, the channel allocation chart. The first two channels are moved upward to their line frequency location by a conventional single stage of translation which

Figure 4. Transmission characteristics of intermediate filter and typical channel filter

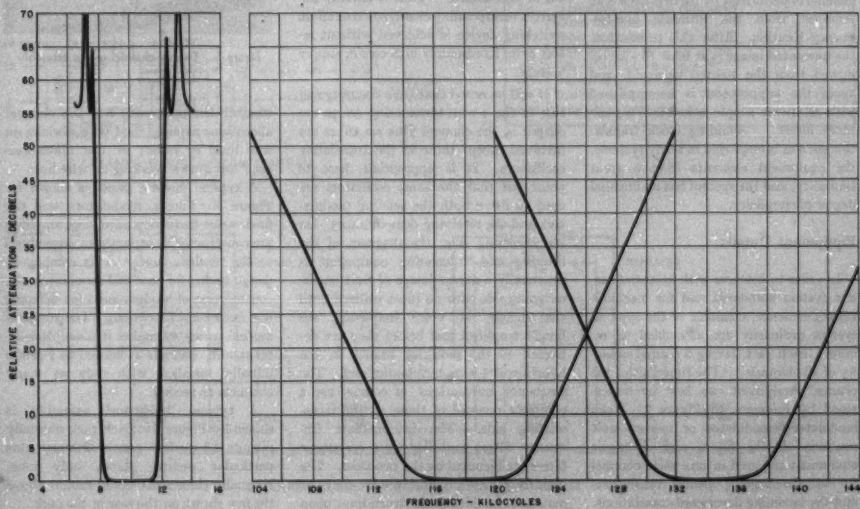

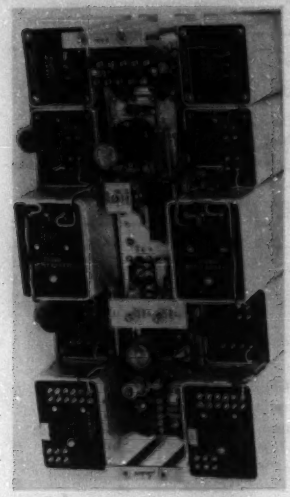

Figure 5. Typical modulator-demodulator (modem) panel

needs no further explanation. Excepting these first two channels, each voice band is first modulated to an intermediate position between 8.2 to 11.5 kc. At this location, the unwanted image is easily suppressed without resort to crystal filters. A second translation for each channel is performed by carriers each 8 kc removed from the ultimate line-frequency location. After this translation, the unwanted image is at least 16.4 kc removed from the wanted sideband, and again the suppression is accomplished with relatively simple inductance-capacitance filters. Avoiding block translation such as is employed in many systems, the equipment elements have a great similarity, and the system has an unusual degree of simplicity.

Equipment Details

In order to conform with accepted carrier system standards and for mechanical convenience, channels of the type 42 system ordinarily are assembled as required, each rack having a normal capacity of 12 channels. The functions of the channel equipment can best be understood by reference to Figure 3. Each modulator-demodulator or modem unit contains all the filters and electronic equipment required in one voice channel for both the outgoing upward-translations and the incoming downward-translations. The outgoing speech currents from the external hybrid transformer first encounter a 3.6-kc low-pass filter. The output of this filter is delivered to a double-balanced modulator driven by an 8-kc oscillator. The wanted side band, included between 8.2 and 11.6 kc is selected by an intermediate frequency filter which has a substantially uniform response characteristic throughout its required pass range and which rejects the image frequency of the modulation by at least 55 decibels. The identical filter is standard in all channels of the system. Its transmission characteristic in large measure determines the over-all response characteristic of the carrier channel. The wanted sideband is delivered to the second modulator driven by a precision oscillator which locates the channel in its final line-frequency position. The output of the high-frequency modulator is fed through an attenuator to the final channel filter. Typical characteristics of the modem filters are shown in Figure 4.

The crystal diodes used in the modulators have a remarkable degree of stability, permitting accurate balances for the suppression of both the carrier and the original voice-frequency input signal. Their freedom from noise allows both translations to be accomplished without the amplifiers customarily employed to recover power level between successive stages. The modulator circuit is so arranged as to minimize the effect of the back-voltage-versus-current characteristic of the diodes. Thus a current linearity corresponding closely to a true off-on switching device is achieved without resort to an inordinately high carrier supply voltage.

It will be noted that from the outgoing side of the 4-wire terminating set to the output of the channel filter no tubes are involved except those in the translating oscillators. It is appropriate here to point out that the same oscillators are used to drive both the sending modulators and the receiving demodulators. On the incoming side, the diagram of the filtering and translating equipment is practically a mirror image of that on the outgoing side with no tubes utilized until the signals, at voice frequency, are finally amplified just before they are delivered to the receiving branch of the hybrid-coil 4-wire terminating set. The frequency translations, of course, are a complete reversal of those on the transmitting side. The intermediate frequency filters and the voice frequency filters are identical on the two sides. The high-frequency channel filters may or may not be identical, depending upon

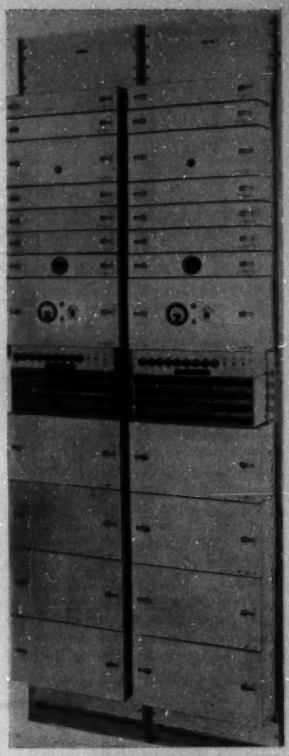

Figure 6. Twelve-channel group assembly

whether the equipment has the channel allocations required for 4-wire working on wire lines or radio, or the allocations used for 2-wire working on wire lines.

A typical modem panel is shown by Figure 5. Filters, modulators, and the final voice-frequency receiving amplifier are constructed as separate subassemblies to the modem panel. This component design makes for ease and economy in the construction of modem units for different line frequency allocations. The compact modem assembly makes it a simple matter to add channels as needed to a group initially installed with only as many channels as needed.

A typical 24-channel assembly is shown by Figure 6. Each rack normally mounts 12 modem panels although this particular picture shows only nine. Normally three more would mount above the five shown on the rear of the rack.

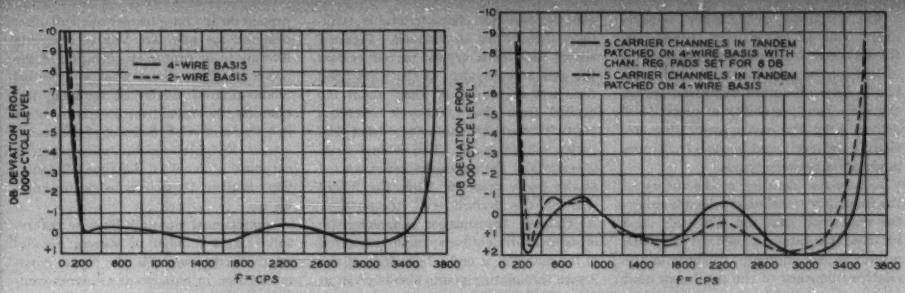

Figure 7. Transmission characteristic of typical single channel and five tandem patched channels

A channel level-adjustor on the incoming side is located adjacent to a master jackfield for the 12-channel bay assembly. This jackfield gives access to the 2-wire side of the 4-wire terminating set and to the sending and receiving loops of the 4-wire side. The 4-wire terminating sets, the fuses, terminal blocks and other common equipment are mounted at the top of the 12-channel assembly. Shown above the jackfields are the pilot regulators incorporated when 2-wire operation of a 12-channel system is required.

Each rack is provided with a transmitting and receiving amplifier for the group of 12 channels, which, in turn, are multipled into 24-, 36-, or 48-channel systems through grouping filters and differential transformers to the common transmitting or receiving lines.

Performance

Any multiplexing system designed to provide a large number of channels for either record or voice communication must meet a number of rather exacting performance requirements. In the first place, it must be thoroughly dependable. Modern-day standards require that lost time due to equipment failures shall be an exceedingly small per cent of total operating time. Causes for such system interruptions due to equipment must easily be determined and located. Apparatus failures which can interrupt all channels simultaneously must be reduced almost to the vanishing point. The independence of the 12 channel groups of the type 42 and the independence of the individual channels within a group contribute materially to the dependability sought. With the number of electron tubes in the equipment held to a minimum, interruptions due to tube failures are correspondingly reduced.

Figure 8. Interconnection of 12-channel groups

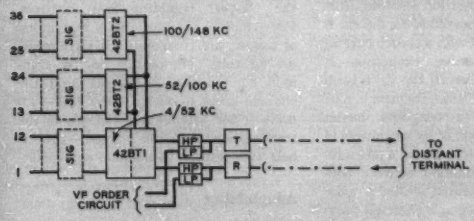

36 CHANNEL RADIO SYSTEM DIAGRAM

LEGEND	
42BT1	12 CHANNEL TERMINAL WITH CARRIER LINE EQUIPMENT
42BT2	12 CHANNEL TERMINAL LESS CARRIER LINE EQUIPMENT
SIG	12 CHANNEL SIGNALING EQUIPMENT
T	RADIO TRANSMITTER
R	RADIO RECEIVER
HG	HIGH GROUP FILTER – 96/144 KC
LG	LOW GROUP FILTER – 36/84 KC
HP	HIGH PASS LINE FILTER
LP	LOW PASS LINE FILTER
42BR	12 CHANNEL REPEATER

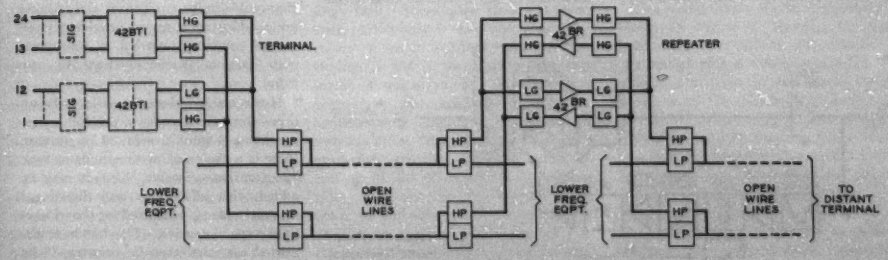

24 CHANNEL OPEN WIRE LINE SYSTEM DIAGRAM

The electrical performance requirements can be listed very briefly as: freedom from frequency shift; uniformity of attenuation within the derived voice band; low wave-form distortion within the voice band; stability of power level delivered by the voice band; low residual noise level; and freedom from cross modulation between bands.

A little consideration of the theory of the frequency translation principle brings the realization that the oscillators used for those translations should not drift with respect to one another. Changes in the relative frequency of the oscillators used to step the audio signal up to its intermediate frequency position at the sending end and back again from the intermediate frequency position to the final audio at the receiving end produces a corresponding change in the frequency of the audio signal, cycle for cycle. Likewise, changes in the relative frequencies of the oscillators driving the modulators which perform the high-frequency translations both upward and downward cause a corresponding frequency difference between the audio input, and the audio output of the channel. To the ear, these changes are imperceptible unless they exceed about 20 cycles. If carrier system bands are connected together end on end in tandem, the frequency stability of all translating devices must be such that the over-all frequency drifts do not exceed the allowable tolerance. If certain bands are used for the transmission of dialing tones, or more particularly, if they are used for telegraphy, frequency changes between the two terminals must be held even closer. High-stability inductance-capacitance oscillators are used for all frequencies below 50 kc; above 50 kc the oscillators are crystal controlled. Over-all characteristics of all channels are such that frequency changes from input audio to output audio do not exceed about 10 cycles over long periods of time.

Since the intermediate frequency filters determine almost exclusively the attenuation characteristic within the voice band, this performance characteristic is strikingly uniform for all channels. Figure 7 shows that for a typical carrier system the over-all equivalent of the voice band does not deviate more than about 0.5 decibel from the 1,000-cycle reference point throughout the range from 200 cycles to 3,500 cycles. This characteristic is essentially the same whether measured at the 4-wire point or from the 2-wire side of the hybrid coil termination. A channel transmission characteristic measured through five systems connected in tandem end on end by patching at the 2-wire terminating points also is given in Figure 7. This shows less than −1 decibel and +2 decibels deviation from the 1,000-cycle equivalent.

Wave form distortion within a voice band of a carrier system may arise from a great variety of causes among which are nonlinearity of modulators, overloading of core materials in transformers and filters, and overloading of tubes both in individual channel amplifiers and common amplifiers. Good design keeps harmonics and cross-modulation products at such a low level that it is undetectable by the telephone user. It has recently become recognized that harmonics contribute but very little to wave form distortion unless the equipment design is extremely bad. Cross modulation between frequencies simultaneously transmitted within the band is far more likely to be offensive. Again, distortion resulting from this cause, while discernible to the ear is not easily measured with a speech current load. A quantitative evaluation is readily made, however, if the voice band load is a group of voice-frequency tone channels such as a telegraph carrier group. An indication of its magnitude in the type 42 system is given by a measurement of cross modulation between telegraph channels operated within a voice band. With 15 telegraph channels operating simultaneously within a band, a signal-noise ratio measurement on the 16th band shows a 35-decibel margin.

Common causes of residual noise (noise present on any one channel when all other channels are idle) are lack of adequate filtering in or proper stabilization of the power supplies, direct leakage or intermodulation of carrier or signaling frequencies, thermionic or microphonic noise in tubes, and noise in diodes of the modulators. Weighted residual noise power in a typical channel of the type 42 equipment is about 75 decibels below one milliwatt.

Interchannel crosstalk likewise can result from a number of sources: inadequate discrimination in the filters, cross-modulation in equipment elements common to all channels, or generally poor engineering design in the construction, shielding and wiring of the apparatus. In this system the long-time average interchannel crosstalk resulting from normal loads on the various channels does not exceed a weighted power level of about −67 decibels below 1 milliwatt.

Commercially available industrial vacuum tubes are used throughout. The modem oscillators have been so designed that their drift due to tube aging is inconsequential. Some drop in over-all system and in individual channel levels inevitably does result from undetected tube decay, even though reasonably good preventive maintenance tube inspection is realized. Over-all channel equivalents, however, can be maintained within very narrow limits by occasional adjustment of the channel regulator level controls. Pilot channel automatic level regulators, of course, will compensate in large measure for tube deterioration in the common equipment. Regulators hold the channel levels to within +0.5 and −1.0 decibels for attenuation changes in the transmission medium of +5 and −10 decibels with respect to nominal equivalent.

Adaptability

With a complete range of channel allocations from 12 kc to 208 kc available through the use of small compact interchangeable units, equipment assemblages are readily made up to provide all the groups commonly needed to coordinate with existing carrier systems of any type.

If the transmission circuit is to be an open-wire pair already in use for a conventional 6-band 2-wire 30-kc system, there is a choice of two methods of type 42 operation. Twelve channels may be added with allocations and directional separation as standardized for the widely-used type *J* carrier. The bands transmitted eastward then lie between 36 kc and 84 kc; and those transmitted west-

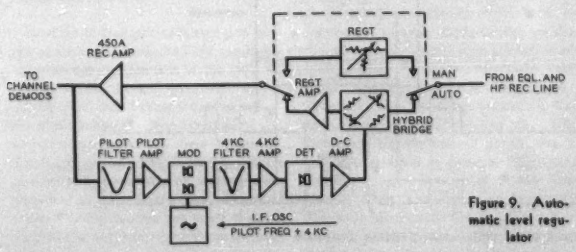

Figure 9. Automatic level regulator

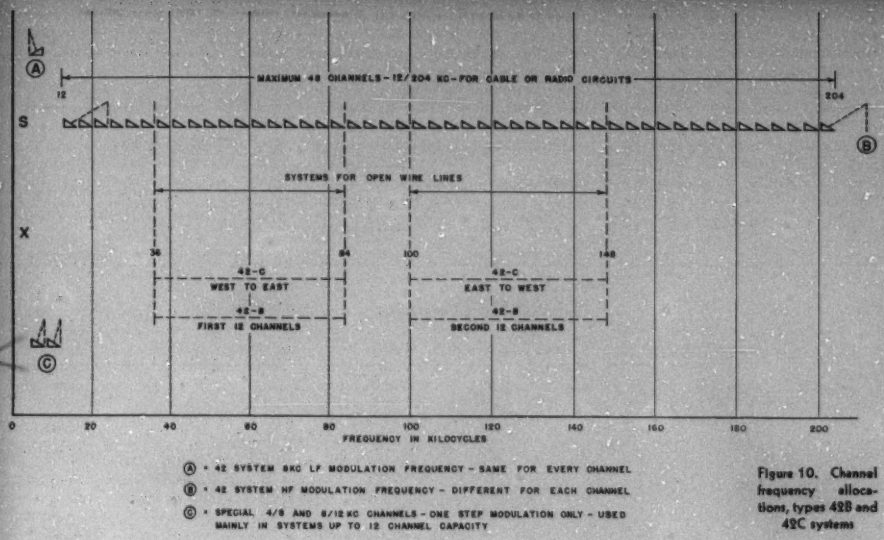

Figure 10. Channel frequency allocations, types 42B and 42C systems

ward between 100 kc and 148 kc.

When more than one *J* system is applied to a lead, it is frequently very desirable to minimize crosstalk between systems by inverting and/or displacing the side band frequencies for the higher frequency direction of transmission, which is the east-west direction. This arrangement shifts the relative allocations of the principal energy-bearing components of the translated speech carrier and renders the remaining crosstalk interference unintelligible. This is commonly referred to as the "staggering advantage" of the frequency allocation.

With the type 42 system, inversion of the side bands for one direction of transmission is accomplished by selection of the upper rather than the lower side band in the second stage of modulation. Displacement of the side band is accomplished by correct choice of the carrier oscillator frequency for the second stage of modulation. These highly desirable alternate allocations for the higher frequency direction of transmission can then be accomplished without sacrificing any of the features which provide economies in the production of modem units.

Where line conditions permit noncoordinating 4-wire installations and where 24 or more 2-way channels are needed there may be economic advantages to a 4-wrie method of operation with 24 or more channels operating eastward on one pair and the same allocations used for westward transmission on another pair. With the same carrier line frequencies for each channel used for opposite directions of transmission, coupling between the two line pairs results only in "sidetone" interference but not in interchannel crosstalk.

On cable circuits where effectively isolated transmission paths are available, two 12-channel groups may readily be operated, the first using the allocations from 12 kc to 60 kc, and the second those between 72 and 120 kc. With selected cable pairs, several systems may be installed on a cable.

For radio working, any desired grouping of channels is readily assembled. If the linearity of the radio system permits, up to 48 channels would be possible on a single link. More often than not, however, particularly if the radio system involves repeater stations, marked advantage is had by keeping the channels within a single octave. This situation arises from the proclivity of presently available radio equipment to produce intermodulation distortion. Depending upon the particular design of the radio equipment, the advantage in signal-noise ratio of confining the used "audio" spectrum to one octave may vary from 6 decibels to as much as 16 decibels. If this restriction is imposed, channel allocations between 00 and 108 kc, 12 channels, or between 100 and 196 kc, 24 channels, are commonly chosen, depending upon the load capacity and modulation frequency limitations of the radio equipment.

Twelve channel groups of whatever allocation needed are easily assembled. System assemblies of 12 channel groups are facilitated, and repeater regulation and flat and "twist" equalization problems are simplified by handling each group more or less independently from terminal to terminal. This is accomplished by interconnecting the carrier frequency lines of the groups through group filters and hybrid transformers as shown in Figure 8. At repeaters and at terminals, each group is amplified and equalized separately. If automatic gain regulation is used, a pilot control frequency is assigned to each group.

The wholly electronic level regulator is shown by Figure 9. Briefly, the pilot frequency is separated out, amplified, and mixed with a locally generated frequency 4 kc removed. A second simple filter selects the difference frequency resulting. This is amplified and rectified. The direct current thus obtained is made to adjust the transhybrid loss of a hybrid transformer type of bridge, one arm of which is a current sensitive resistor.

Type 42 equipment is engineered on the building-block basis, now virtually a standard for carrier systems. Basic terminal assemblies provide only moderate

transmitting and receiving gains which permit the installation of low-cost systems for short circuits. Optional booster amplifiers can be installed when needed to convert the equipment to long-haul use. Inexpensive pilot regulator equipment suitable for short-haul systems or systems installed on leads which are not exposed to weather extremes can be replaced where required by more complex regulators.

The over-all design permits application of type 42 equipment to a wide range of open wire line, cable or radio link applications, yet component assemblies are standardized to make possible volume of manufacture and the resultant economies. A high degree of stability and ease of maintenance has been accomplished by careful attention to detail.

References

1. Carrier Current Telephony and Telegraphy, E. H. Colpitts, O. B. Blackwell. *AIEE Transactions*, volume 40, 1921, pages 205–300.

2. A 12-Channel Carrier Telephone System for Open-Wire Lines, B. W. Kendall, H. A. Affel. *Electrical Engineering* (*AIEE Transactions*), volume 58, July 1939, pages 351–60.

3. Cable Carrier Telephone Terminals, R. W. Chestnut, L. M. Ilgenfritz, A. Konner. *Electrical Engineering* (*AIEE Transactions*), volume 57, May 1938, pages 237–44.

4. An Improved Cable Carrier System, H. S. Black, F. A. Brooks, A. J. Wier, L. O. Wilson. *AIEE Transactions*, volume 66, 1947, pages 741–46.

5. Frequency Division Techniques for a Coaxial Cable Network, R. E. Crane, J. T. Dixon, G. H. Huber. *AIEE Transactions*, volume 66, 1947, pages 1451–59.

No Discussion

An Improved Transmitted Carrier System for Telephone Lines of Short or Medium Length

G. H. BRODIE
NONMEMBER AIEE

Synopsis: This paper describes a stackable 1-, 2-, or 3-channel short-to-medium haul telephone carrier system, which has been developed primarily to meet the needs of the independent telephone field. Features of this type number 5 carrier system are transmitted carrier frequencies in harmonic relationship, ringdown signaling by carrier interruption, dial signaling by carrier frequency shift, excellent transmission capabilities, particularly in the second and third channels, and simple installation, testing, and maintenance procedure. Partial suppression of the transmitted carrier frequencies is available, for the occasional application in which the normally higher carrier level on the line might prove objectionable. Through particular attention to the engineering design, the significant objections to transmitted carrier have been overcome, while its greater convenience to the user has been employed to good advantage. The feasibility and desirability of this system have been amply proved by hundreds of successful installations, some of which are on difficult lines where other carrier systems previously failed.

TRANSMISSION of the carrier frequency on telephone lines is as old as carrier telephony itself, but, in the first successful use of carrier circuits on multiple long lines applications, this practice fell into disfavor for the reasons set forth by Colpitts and Blackwell[1] in 1921. Several of the important advantages associated with transmitted carrier were recognized at that time but they were held to be outweighed by its disadvantages. Considering the nature of typical long lines applications and the state of the art in those early days, suppression of the carrier appears to have been the only logical choice. But the use of telephone carrier circuits no longer is confined to long lines and the state of the art had advanced a great deal.

There are 6,106 independent telephone companies in the United States and possessions[2] which are operating, for the most part, over lines of short-to-medium electrical lengths. Bell Telephone companies serving rural areas, many railroads, oil companies, and other organizations own and operate additional lines of similar characteristics. Since World War II the use of carrier circuits on such lines has become widespread and is increasing rapidly. Here the requirements and operating conditions usually differ materially from those found on long lines applications. For these reasons, it does not follow that the type of carrier system most suitable for one field must also be best for the other.

Contemporaneously with the increased use of carrier systems on the shorter independent lines, several makes of equipment have been presented to fill the need in this field.[3–8] These differ from each other in details, but all carry over into this newer field the old "long lines-suppressed carrier" approach.

Where technical personnel is available to make the necessary measurements and adjustments, suppressed carrier systems generally are satisfactory. They do, however, impose unnecessary hardship on the small company where suitably trained technicians are not always available. Furthermore, the desirable characteristics of suppressed carrier systems are of less importance in the independent field than in multiple long lines applications. Conversely, the increased simplicity of adjustment and maintenance possible with a transmitted carrier system becomes of relatively greater importance.

It was our conviction that a transmitted carrier system, if a suitable one could be developed, would be of great advantage to most independent operators. This conviction resulted in the production, early in 1947, of a single-channel carrier system operating on the transmitted carrier principle. The first model was readily accepted in the independent field and almost immediately proved its worth. From this beginning the stackable 1-, 2-, or 3-channel type Number 5 carrier system, as described in this paper, came into being.

It is interesting to note that, while this development was in process, an increased interest also was shown in transmitted carrier systems in Australia.[9] As the advantages possible with equipment of this type become more generally appreciated, it seems likely that its use in the independent field will become more general.

Description and General Considerations

Figure 1 shows the general appearance and arrangement of the various panel-mounted units making up a complete 3-channel terminal for the type Number 5 carrier system. The arrangement shown is for ringdown signaling over the first channel and dial signaling over the second and third, with power obtained from two Number 105 power supplies. A single heavier duty power supply can be used to save rack space, and signaling units can be of the dial or the ringdown type on any of the channels. Standard 19-inch rack space required for a single-channel terminal is $22^3/_4$ inches. For two channels

Paper 50-241 recommended by the AIEE Wire Communication Systems Committee and approved by the AIEE Technical Program Committee for presentation at the AIEE Fall General Meeting, Oklahoma City, Okla., October 23–27, 1950. Manuscript submitted July 24, 1950; made available for printing September 1, 1950.

G. H. Brodie is Chief Research Engineer with the Kellogg Switchboard and Supply Company, Chicago, Ill.

The author is indebted to the engineers who developed and tested the Number 5 carrier system, particularly C. E. Wood, O. Blyholder, B. E. Swanson, and O. S. Ostberg.

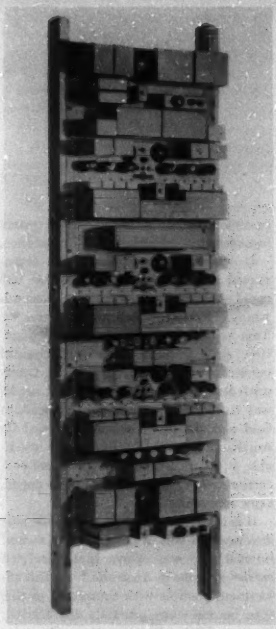

Figure 1. General appearance of a 3-channel carrier system terminal

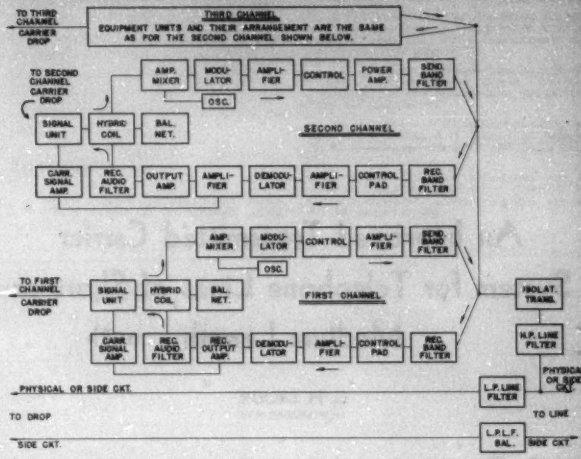

Figure 3. Block diagram of 3-channel terminal

this becomes 35 inches; and for three channels with one power supply, $47^1/_4$ inches. With two power supplies the figure is increased by 7 inches.

Considering the panel-mounted units from top to bottom, the first is a conventional power supply delivering 200 volts of direct current and 6.3 volts of alternating current. The second is the line unit consisting of high and low pass line filters, a carrier frequency repeating coil, and a simple balancing network to be inserted in the other pair of a phantom group when no carrier is installed thereon. The third unit is the first channel carrier terminal and the fourth is its associated ringdown signaling unit. Number five is the second channel carrier terminal and six is its associated dial signaling unit. Numbers seven and eight are the third channel units corresponding to five and six respectively, while Number nine is the second power supply.

The frequency allocations for this carrier system and, for comparison, the Association of American Railroad's carrier frequency agreement,[18] are shown by Figure 2. It may be noted that the carrier frequencies are in such harmonic relationship that they can generate no beat frequency falling in either the audio or in one of the carrier bands. Thus one of the disadvantages sometimes associated with transmitted carriers is circumvented.

The over-all layout and sequence of operations in this system are illustrated in block diagram form by Figure 3.

While the carrier terminal panels for each of the three channels are similar in size and general appearance, the first channel uses no power amplifier tube and transmits at a maximum level of 10 decibels above one milliwatt. The second and third channels employ power amplification and transmit at a maximum level of 20 decibels above one milliwatt. The available transmitting and receiving gain is approximately 23 decibels for the first channel and 35 decibels for the second and third channels. With this arrangement, performance measured in miles of typical line is approximately equal for the first and second channels, with the third channel dropping from $12^1/_2$ to 30 per cent.

Since the elimination of objectionable intermodulation products is a serious problem, particularly in a multichannel carrier system employing transmitted carrier at relatively high levels, very careful consideration has been given to the design of the filters and other circuit elements. The inductance of certain coils in the band-pass and other carrier frequency filters must remain constant from the lowest to the highest signal level. This means that large powered metal or oxide cores of low permeability, or air cores, are required.

In the case of the carrier frequency repeating coils, a Mu metal core is used which provides a high initial permeability and also holds its permeability reasonably constant throughout the range of the magnetizing force encountered. Thus,

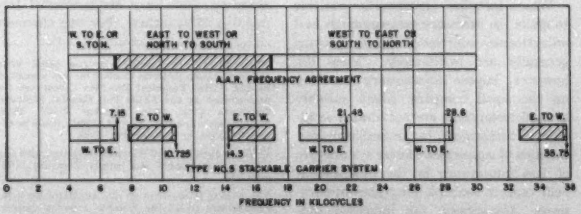

Figure 2. Type Number 5 and American Association of Railroads frequency assignments

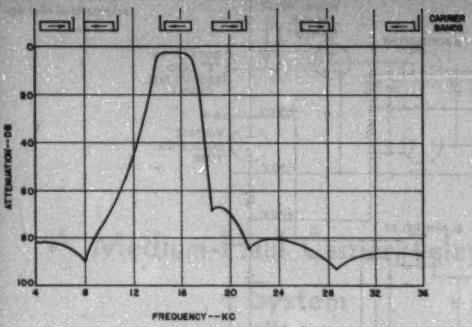

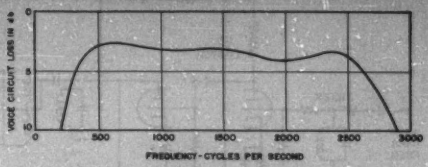

Figure 4 (left). Frequency response of filter for east-west band of second channel

Figure 5 (above). Voice frequency response through a 25-decibel line

by using an adequate cross section, thin laminations, and a large number of turns, intermodulation products from this source are kept very low.

Excellent frequency stability over a wide temperature range is attained through the use of stabilized toroidal inductors and a special type of ceramic capacitor, with air dielectric variable capacitors for making the final adjustments.

Band filter requirements are fairly severe in a carrier system of this type, since the other high level carriers, as well as their associated sidebands, must be excluded from a given channel. This applies most forcefully with respect to the carriers transmitted in the opposite direction. Very high attenuation outside of the pass band, with rejection notches where they are most helpful, keep interchannel cross talk well below the generally accepted one millivolt level. The frequency response of a typical bandpass filter is shown by Figure 4.

When the carrier is transmitted at full strength, a small amount of low-frequency signal from the rejected sideband unavoidably is included. Suitable equalization is built into the receiving circuits to correct for the increased low-frequency audio signal which otherwise would result. Actually, the over-all response is uniform within 3 to 4 decibels from 250 to 2,750 cycles approximately (Figure 5).

Another disadvantage commonly associated with transmitted carrier systems is that one (or more) of the carrier frequencies present on the line, at levels several decibels higher than that of the sidebands, is likely to be picked up by other makes of carrier systems on the same pole line and be demodulated in the receiving terminal. There it would appear as a steady audio tone. It has been our experience that such conditions are only seldom encountered in the independent telephone field. An inexpensive provision has been made, however, to partially suppress the carrier frequencies on the type Number 5 system when it is necessary or desirable to do so. These frequencies then appear on the line at levels no higher than the sidebands and are selectively amplified to the desired extent in the receiving terminals.

In the early days of telephone carrier practice the vacuum tubes then available limited the power which could be handled conveniently to rather low levels. Today it is entirely practicable to handle powers in excess of one watt in the final amplifier, so the former objection that transmitted carrier would overload the amplifier tubes is no longer very significant.

Principles of Operation

Except as the processes are modified by the characteristic features mentioned elsewhere in this paper, voice frequency signals are transmitted and received in the conventional manner.

The extreme simplicity of the ringdown method of signaling is easily understood from a short study of Figure 6. Ringing voltage, when applied across the carrier circuit drop, interrupts the transmitted carrier. At the distant terminal the interruption of the carrier places ringing voltage from a local source across the carrier circuit drop, causing operation of a switchboard signal, or a telephone ringer, in the normal manner.

The dial signaling unit, as shown schematically by Figure 7, provides means for accepting d-c pulses at the local carrier terminal and for delivering duplicate pulses to a suitable circuit associated with the distant terminal. Full supervision is available at all times as will be shown. The required signaling functions are performed by causing the carrier frequency to shift slightly each time battery voltage is applied to or removed from the "M" lead. The amount of shift is not enough to interfere with voice frequency transmission, but is enough to cause the discriminator and biased triode amplifier at the receiving end to operate a relay. The discriminator and signaling relay faithfully reproduce the dial pulses just as they come into the carrier system.

Considering a call from a toll operator to an automatic telephone office, the operation of the carrier shift principle is as follows. With the carrier channel idle, each carrier stands shifted to its off-normal frequency. When the operator at the east terminal plugs into the drop circuit, battery voltage is placed on the "M" lead. This operates the dialing relay and shifts the westbound carrier back to normal frequency. The change in frequency operates the signal relay con-

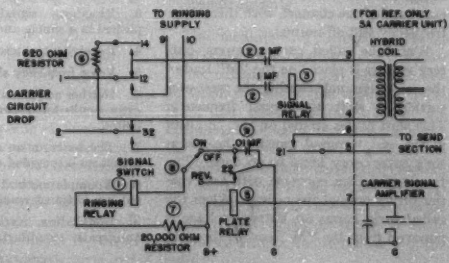

Figure 6. Circuit schematic of ring-down signal unit

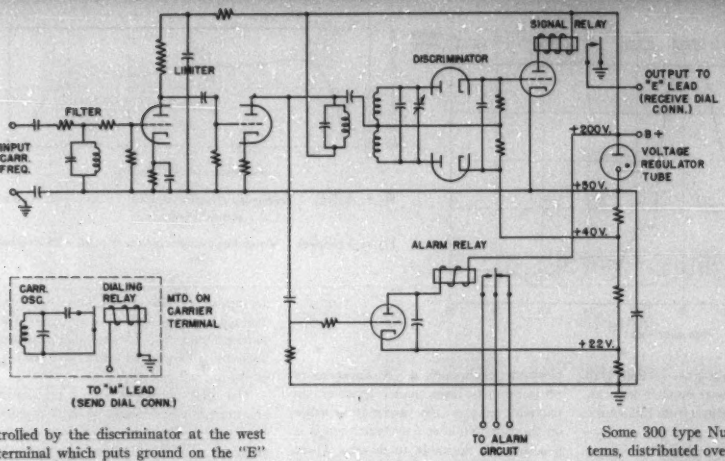

Figure 7. Circuit schematic of dial signal unit

trolled by the discriminator at the west terminal which puts ground on the "E" lead. This permits battery current to flow in the trunk entering the automatic switching equipment in the west central office. The trunk is seized and dial tone is passed back into the west terminal carrier circuit drop to indicate to the operator that the switching mechanism is ready to receive dial pulses.

The west-to-east carrier is still on its off-normal frequency but the circuit is capable of perfect audio transmission and reception. The east operator hears the dial tone and proceeds to dial the required digits. Each pulse temporarily shifts the frequency of the east-west carrier to off-normal. The normal frequency corresponds to the makes and the off-normal frequency to the breaks at the calling dial or sender. The signaling relay at the west terminal reproduces these dial pulses and passes them along on the "E" lead to the west central office. After the dialing operations are completed the east-west carrier remains on normal frequency. The mechanism in the west office connects the incoming trunk to the called line and revertive ringing tone (or busy signal) comes back to the caller over the west-east band of the channel, with this carrier frequency still off-normal.

When the called party answers, battery voltage is placed on the "M" lead of the west terminal, causing the west-east carrier to shift to normal frequency. This shift places ground on the "E" lead at the east terminal, causing the operator's supervisory lamp to go dark. The two parties then converse with each carrier on its normal frequency. When the called party hangs up, battery voltage is removed from the "M" lead at the west terminal, allowing the west-east carrier to shift to its off-normal frequency. This shift takes ground off the "E" lead at the east terminal, allowing the operator's supervisory light to glow. The operator then withdraws the cord, removing battery from the "M" lead at the east terminal, and restoring the east-west carrier to off-normal frequency. This last frequency shift takes ground from the "E" lead at the west terminal, which in turn releases the circuits in the automatic switchboard. The carrier channel is then in its standby position, ready for another call.

Advantages

This type of transmitted carrier system enjoys the following advantages, as compared with suppressed carrier equipment:

1. Neither synchronization of local and distant oscillators nor critical carrier leak adjustments are required.
2. The carrier frequency signal can be traced through the entire system and measured easily when the channel is either in use or idle.
3. Ringdown signaling can be accomplished in a simple and inexpensive manner.
4. Receiving oscillators are not required.
5. Voice frequency shift is eliminated.
6. Neither additional pilot frequencies nor extra bands for dialing or signaling are required.
7. The basis for an automatic circuit failure alarm is provided.
8. A simple method of modulation, without use of transformers is made possible.
9. Installation, testing, and maintenance are greatly simplified.

Some 300 type Number 5 carrier systems, distributed over nearly all sections of this country, now are operating satisfactorily with a minimum of maintenance. Although some of these installations are on difficult lines where, previously, other carrier systems failed, very few troubles of any sort have been encountered. This indicates that a transmitted carrier system, designed and constructed as described, is particularly suitable for use on lines such as those most frequently employed in independent telephone field.

References

1. Carrier Current Telephony and Telegraphy, E. H. Colpitts, O. B. Blackwell. *AIEE Transactions*, volume XL, 1921, pages 205–300.

2. Telephony's Directory of the Telephone Industry. *Telephony* (Chicago, Ill.), 1950, page 180.

3. Adler Carrier System as Used by Stromberg-Carlson, Dr. Arthur W. Melloh. *Telephony* (Chicago, Ill.), April 19, 1947, pages 30–34.

4. Kellogg Telephone Carrier Systems, Dr. G. H. Brodie. *Telephony* (Chicago, Ill.), June 28, 1947, pages 28–30.

5. Lenkurt Carrier Equipment for Toll and Rural Lines, J. N. Petrie. *Telephony* (Chicago, Ill.), August 9, 1947, pages 16–18 and 30.

6. The Application of Carrier, H. R. Hunkins. *Telephony* (Chicago, Ill.), October 23, 1948, pages 58–61.

7. Multi-Channel Carrier for the Independent Company, B. L. Arnold. *Fortnightly Telephone Engineer* (Chicago, Ill.), September 1949, pages 13–14 and 30–32.

8. Stackable Carrier with All-Electric Pilot Regulation, D. G. Clifford. *Railway Signaling and Communication* (New York, N. Y.), March 1950, pages 158–62 and 169.

9. Carrier on Junction Cables, T. S. Skillman. *Communications Review* (Sydney, Australia), volume 1, March 1948, pages 1–33.

10. Manual of the Association of American Railroads. Association of American Railroads (Washington, D. C.), Communications Section 2-J-46, 1946.

No Discussion

A Medium-Haul Carrier Telephone System

HOWARD H. SMITH
NONMEMBER AIEE

CARRIER TELEPHONE equipment has been in use for about 30 years, and its place in providing economical long-range circuits has become well understood and widely accepted. However, the recent amazing growth in demand for more communication channels on the part of both private communication operators and common carrier telephone companies has been accompanied by a change in requirements which has begun to make many present carrier systems obsolescent. We now find carrier telephone channels serving to multiplex broad-band radio links as well as providing circuit relief in relatively short trunk groups in the local or medium-range toll wire plant. The great rise in toll and long distance dialing requirements has forced reconsideration of the provisions for signaling. Space is becoming a serious problem in many offices. As carrier is adopted by more of the smaller companies because of its attractive low initial cost, new problems involving maintenance by personnel with little electronic background must be faced.

Telephone circuits are now sometimes required to handle one or more voice-frequency channels in place of, or in addition to the speech, which may be used for telegraphy, telemetering, supervisory control, pilot relaying and many other purposes limited only by the ingenuity of the users. As part of radio systems, they help provide remote control and alarm features. It is the purpose of this paper to analyze these functions and to describe a new carrier telephone system which has been designed specifically to meet a majority of these requirements.

Paper 50-242, recommended by the AIEE Wire Communication Systems Committee and approved by the AIEE Technical Program Committee for presentation at the AIEE Fall General Meeting, Oklahoma City, Okla., October 23–27, 1950. Manuscript submitted August 2, 1950; made available for printing September 11, 1950.

HOWARD H. SMITH is with the Federal Telephone and Radio Corporation, Clifton, N. J.

General

When the earlier carrier telephone systems were introduced, the need was principally for relatively long-haul channels, with simple signaling on a 2-way ringdown basis between operators. Some systems employed an audible-frequency signal somewhere in the speech band, with various provisions to hinder speech sounds from causing a false signal, others made use of methods in which the entire speech channel was made inoperative during ringing intervals. The former arrangement was very difficult to adapt for dialing, while the latter made it impossible to use speech-plus or simultaneous speech and voice-frequency or control systems. To eliminate these limitations in existing systems is generally costly. With these and other similar factors in mind, it is clear that the communications engineer must avoid investment in obsolescent types of equipment by anticipating the trends in signaling, as well as the requirements for speech transmission.

Long-, Short- and Medium-Haul Systems

Long-haul systems are generally understood to be those capable of placing carrier currents on open-wire lines at levels up to +15 to +18 dbm (decibels referred to 1 milliwatt in 600 ohms) and capable of receiving signals down to about −18 dbm, with provision for extending the range more or less indefinitely by use of carrier repeaters. Automatic level regulation is a practical necessity for such systems. Attempts were made to answer the need for relatively short circuits by what were termed short-haul carrier systems, of one or more channels. These generally had only sufficient amplification to operate over lines with carrier-frequency attenuations up to 10 to 18 decibels maximum. While short-haul systems operated successfully within these limitations, it was found that they could not be used on a considerable number of short wire lines because of entrance cable losses.

Much wire plant was installed before inexpensive carrier equipment became available, and it often turns out that one or two miles of 19, 22, or even in some cases, 24-gauge (American wire gauge) nonloaded cable pairs must be included in the circuit unless expensive alterations are to be made. The losses introduced at carrier frequencies by such pieces of cable often exceeded the total available gain of a short-haul carrier system, although the total geographical length of the circuit might be 10 or 15 miles, or less. It thus became apparent that for such service, a carrier system with gains and levels approaching those of long-haul systems was required, but that some long-haul features such as line-slope equalization, and automatic level regulation could be omitted. Such systems are designated as medium-haul systems. Depending on conditions, they may be from 5 to 200 miles in actual length.

Medium-Haul Transmission Requirements

The medium-haul category includes most of the intrastate toll and trunk telephone circuits up to 200 miles, as well as longer circuits of the railroads, pipelines, and power utilities. Many are operated at net losses as low as 2 decibels, the average being 4 to 6 decibels. A reasonably flat audio bandwidth between 300 and 2,700 cycles per second is acceptable, while the upper limit may be lowered to about 2,200 cycles per second in many interoffice trunks and terminal toll circuits.

Choice of Carrier Frequencies and Levels

Where carrier channels are to be added to lines already equipped with some carrier systems, it is desirable to observe proper co-ordination of frequencies and power levels of the various systems. Any new system should be capable of transmitting levels of at least +12 dbm, and receiving levels as low as −15 dbm. The side bands transmitted should lie in the frequency bands conventionally accepted for east-to-west and west-to-east transmissions.

Carrier Frequency Stability

Since efficient use of the available carrier-frequency spectrum practically dictates use of single side band, suppressed-carrier transmission, the question of how close the frequency of the demodulator oscillator must be kept to that of the oscillator at the transmitting terminal, is imposed when the telephone channel is used for one or more subcarrier channels of amplitude-modulated or frequency-shift telegraphy or telemetering. Under these conditions, the maximum tolerable departure from synchronization is of the order of 10 cycles per second. Otherwise, however, it can be demonstrated that a deviation of 20 cycles alone will cause no noticeable distortion in speech. But if it is combined with excessive carrier leak, low line losses, and poor hybrid balances, very weird sounds may be heard, and the circuit may be made quite unacceptable. A beating effect is sometimes very prominent, and since the other effects tend to disappear when zero beat is attained, a natural reaction is to concentrate upon maintaining absolute carrier synchronization. However, if proper steps are taken to reduce carrier leak by improving modulator balance, or to correct the poor hybrid balance, or to align system levels properly, the synchronization problem promptly vanishes. Therefore we may conclude that if the carrier oscillators are themselves constant to within 2 or 3 cycles per second, further synchronization is not ordinarily justified economically. This figure thus represents a rational design requirement for the stability of a carrier oscillator for a carrier telephone system.

Signaling Requirements

Since practically all telephone circuits are used intermittently, it is necessary to provide for signaling in both directions between opposite ends. Manual and automatic switchboards use d-c signals and impulses, and a-c signals with frequencies below 100 cycles per second, for such purposes as dialing, supervision, and ringing. Obviously these signals cannot be sent as such over a telephone channel which passes only frequencies between 300 and 2,700 cycles, with power of the order of one milliwatt. Equivalent results must be obtained by transmitting some other kind of signal either in the carrier-frequency band used by the speech, or adjacent to it, and establishing a relation between it and the a-c or d-c signal paths at the terminals. Such a signaling system must:

1. Provide a separate signaling path in each direction.
2. Create no interference with the normal functioning of the speech channel.
3. It must be immune from false operation by speech currents.
4. Should be capable of transmitting all types of signaling, such as 20-cycle ringing, telephone dialing and supervision, railway selector impulses at a $3\frac{1}{2}$-cycle rate, and the like.

Each 1-way signaling channel is similar to a 1-way telegraph channel, and will usually require a transmitting relay and a receiving relay. The transmitting relay may be required to operate on a-c ringing current for ringdown service, or on d-c dial or supervisory or other control signals, depending on its application, so that it is desirable to be able to change the relay type readily. The receiving relay may be required to apply ringing current to the talking conductors toward the switchboard drop, or to repeat various d-c impulses over separate conductors. It is therefore preferable that the signaling circuits be flexible so that by a minimum of adjustment and strapping, a terminal may be set up for any of the common ringdown or dialing circuit arrangements. In dial operation signaling circuits are required to perform perfectly under a wide variety of circuit conditions where the impulses transmitted may be badly distorted at their source. Under these circumstances, it is imperative that the signaling circuit contain means for adjusting the dial pulse ratio, since the additional relays in the circuits between the carrier and the exchanges may produce additional distortion.

In ringdown operation, difficulty is sometimes experienced due to transient discharges from capacitance in switchboard circuits causing a false ring to be transmitted in the opposite direction at the end of a ringing signal. It is highly desirable for the carrier equipment to be able to suppress such false operation.

Sometimes it may be required that a carrier telephone channel be connected permanently to a common battery telephone subscriber set, at a location where telephone office battery and ringing current are not available. For such cases, it is desirable to be able to supply direct current from the carrier set for talking battery, through the windings of the signaling transmitting relay. The latter thus serves as a line relay, and can repeat hook-switch indications and dialing impulses to the central office. The ringers of most telephone sets can be adjusted to ring fairly well on 50- or 60-cycle alternating current, or ringers of harmonic ringing types can be substituted, so that provision of a suitable winding on the carrier power-supply transformer will take care of the ringing requirements in most cases. The circuit of the receiving relay should be adaptable by some means to permit setting up the ringing circuit.

Carrier Channel Line Circuit Arrangements

The most flexible arrangement of carrier channels is that which provides stackable channels connected to the line or radio system through common line filters, separate from the channel equipment. In such an arrangement, it is convenient to mount a pair of line filters together, which will serve an open-wire phantom group, or a radio-link transmitter and receiver. In the latter case, addition of a hybrid coil circuit facilitates derivation of a 2-wire audio channel over the radio link. The transmitting filters for all channels are connected in parallel, as are the receiving filters, and connected to their respective transmitting and receiving line filters for a radio link. For 2-wire physical lines, the transmitting and receiving filters are all connected together and to the line filter.

In wire line applications, especially in 1- or 2-channel systems, some compactness may be gained by including the line filter on the terminal panel for the first or lowest frequency channel.

Separate line filters are required to provide transfer sets to by-pass obstacles and for balancing line filters for line-balancing networks of 2-wire telephone repeaters. In a stackable system, a line filter should be provided with a cutoff frequency just below each channel, to permit superposition of higher frequency channels over lower frequency systems of different type, and to permit separating channels at various points where one or more are dropped, or where they must diverge.

Carrier Channel Drop Circuit Arrangements

It is desirable to be able to terminate the voice-frequency side of a carrier channel on either a 2-wire or a 4-wire basis. For use when the channel is connected to a 2-wire switchboard, a compromise network should be provided capable of giving a moderate balance against the various types of terminations which may be connected. Provision should be made to permit substitution of an external balancing network when a more precise balance is required, as when the carrier circuit is extended by a permanent connection to a line. When it is required to operate the channel on a 4-wire drop basis, as for back-to-back connection to another channel, or for other reasons, it is desirable to be able to convert the hybrid coil circuit into separate input and output circuits operable with 600-ohm circuits, either balanced or unbalanced with respect to ground.

Requirements for drop transmitting and receiving levels usually are different for 2-wire and 4-wire operation. While the level transmitted from 2-wire drop into the hybrid is normally considered to be at a test power level of 0 dbm (1 milliwatt), the modulator input on a 4-wire basis is commonly desired to be at a −13 dbm level. Likewise, the output from the hybrid into the 2-wire drop may be at a −2 dbm level, down to −8 dbm or lower, but it is commonly required that the demodulator branch output be +4 dbm on a 4-wire basis. Suitable pads or level controls should be provided to permit meeting the required 2-wire and 4-wire levels, preferably without having to do soldering or substitution of removable elements.

Installation and Maintenance Requirements

In an extensive toll plant employing many telephone repeaters and carrier systems, it may be necessary to line up levels and net losses of circuits to within a few tenths of a decibel, and to maintain them within such limits. For this purpose it is practicable to install relatively expensive oscillators and transmission measuring equipment, and to train people to use it properly. In such a situation, controls may be adjusted and readjusted according to meter readings, and there is little need to mark or record the physical settings.

However, many users are purchasing carrier for the first time, and the carrier may be the first electronic equipment in the plant, with possibilities of growth limited. In such cases it is desirable that the installation and maintenance of a medium-haul carrier system should not require highly trained personnel and elaborate measuring equipment. A medium-haul carrier telephone system should be designed so that a workable circuit adjustment could be obtained with approximately the following test equipment:

1. A-c–d-c volt-ohmmeter with decibel scale reading down to about −15 dbm.
2. Oscillator giving 1,000-cycle test tone a 0-dbm level, with 600-o hm-output impedance.
3. Telephone dial in good adjustment, when dialing is involved.

The oscillator and decibel meter may be used to adjust the net loss of the talking circuit, on an audio-to-audio basis, relying on the factory-set carrier transmitting level. The performance of the dialing channel in terms of dial pulse ratio may be measured with the dial and ohmmeter, the latter serving as a pulse ratio meter. Often such work must be done by a single technical man, with a relatively unskilled helper. If all line-up and routine maintenance adjustments may be made by means of controls having knobs and closely graduated dials or scales, the assistant may be directed to make adjustments and report settings by telephone, thereby greatly expediting the work. Provision of clearly marked test points, and places where the circuit may be cut for testing, by jacks or removable test links, is of additional assistance.

Compactness

Where only one or two carrier terminals are installed in an office, physical size is relatively unimportant. However, when dozens of terminals must be given space, a floor space problem is frequently encountered. With the rising costs of building, and in some cases limitations of space available to extend the building, it becomes highly important to make carrier equipment as compact as may be consistent with convenient maintenance accessibility.

Description of Federal 9-H-2 Medium-Haul Carrier Telephone System

A 3-channel system was developed, capable of being installed one channel at a time, with the same equipment interchangeably used to provide a 6-channel system operating on a 4-wire basis over broad-band radio links of suitable characteristics. Thus the same voice-frequency and signaling features are available for wire and radio systems, so that the resulting circuits appear in terminating offices on exactly the same basis. While retaining the accessibility of parts for adjustment and maintenance, a relatively compact physical design was achieved, whereby each channel is completely contained on a single panel, from line filter to power supply, ready to plug in. Additional channels including their own power supplies, not requiring line filters, are stacked physically and electrically up to the maximum number.

Frequency Allocation

This system uses single-side band, carrier-suppressed transmission, with separate carrier frequencies for each direction of transmission. The signaling frequencies lie outside the utilized speech side bands, being 3.4 kc away from the carrier frequency on the same side as the speech band. It was arranged that the transmitted energy from the various channels would co-ordinate with a scheme of frequency allocation which is generally recognized, in which the long-haul systems use frequencies below about 17 kc for east-to-west (or north-to-south) transmission, and frequencies from about 17 kc up to about 30 kc for west-to-east (or south-to-north) transmission. This scheme also permits use of the band be-

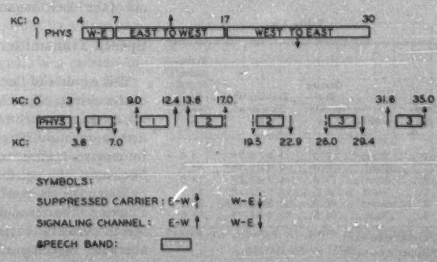

Figure 1. Frequency allocation, 9-H-2 carrier telephone system.

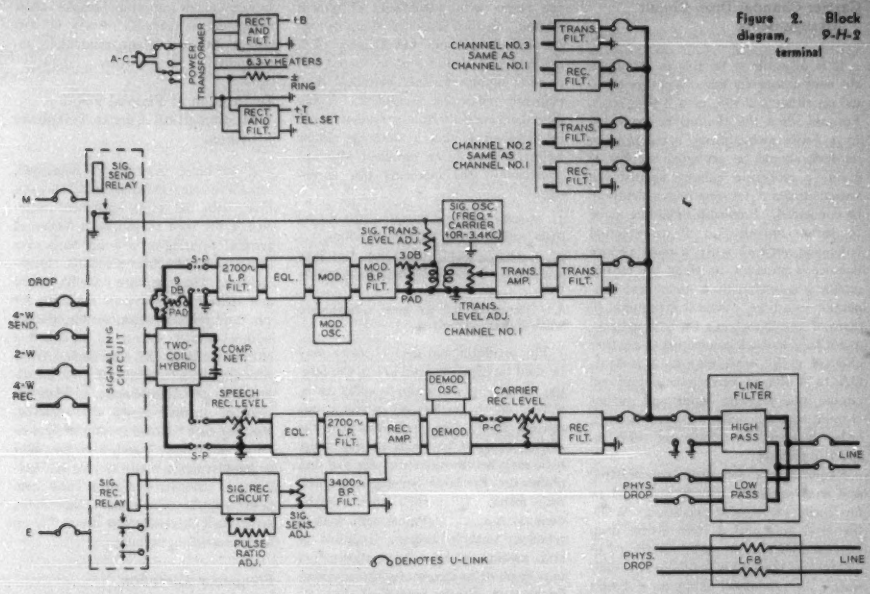

Figure 2. Block diagram, 9-H-2 terminal

tween approximately 3 kc and 7 kc for west-to-east transmission, which is used for the return side of single-channel systems.

This frequency allocation is shown in Figure 1, along with the actual assignments selected. Channel 1 uses the bands for single-channel systems. Channel 2 straddles the 17-kc break of the 3-channel allocation, while channel 3 uses the top part of the 3-channel allocation for west-to-east transmission, and a return band lying above 30 kc which is outside the normally used 3-channel allocation.

For the record, the frequencies of carrier, transmitted side band and signaling channels are as shown in Table I.

The spacing of the channels is increased slightly and progressively at the higher frequencies partly as a matter of filter economy, and partly to fit into the standard frequency-band allocation.

Table I

Channel	Terminal	Carrier Frequency, Kc	Transmitted Side Band, Kc	Transmitted Signal Frequency, Kc
1	West	7.0	4.3– 6.7*	3.6
1	East	9.0	9.3–11.7**	12.4
2	East	17.0	14.3–16.7*	13.6
2	West	19.5	19.8–22.2**	22.9
3	West	26.0	26.3–28.7**	29.4
3	East	35.0	32.3–34.7*	31.6

*Lower side band.

**Upper side band.

Analysis of Circuits

Functionally the circuits of a complete channel terminal may be broken into seven parts, which are as follows:

1. Speech transmitter circuit.
2. Speech receiver circuit.
3. Signaling transmitter circuit.
4. Signaling receiver circuit.
5. Voice-frequency terminating circuits.
6. Carrier-frequency terminating circuits.
7. Power supply circuits.

These will next be discussed with the aid of the block diagram, Figure 2.

Speech Transmitter Circuit

This consists of the upper main branch of the circuit. Speech arriving from the left through the hybrid coil circuit passes first through a 2,700-cycle low-pass filter to remove speech currents above that frequency. An equalizer is inserted next to flatten the channel frequency response. Entering the modulator circuit, the speech currents are transformed by the alternate blocking and unblocking of germanium diodes at carrier frequency into upper and lower side bands, only one of which is to be utilized. In this type of modulator, the carrier frequency is suppressed, appearing in the output circuit only due to unbalances in the modulator. An adjustable resistor is provided to facilitate the adjustment of carrier leak to at least 20 decibels below the test power level. The modulator also suppresses the original speech frequencies.

The modulator band-pass filter selects the upper or lower side band as required by the frequency allocation, permitting it to pass through a 3-decibel matching pad to the transmitting amplifier input transformer. At this point the transmitting signaling current is introduced, as described later. The transmitting level-adjustment control is thus common to the speech side band and the signaling channel, permitting their simultaneous adjustment to meet transmitting level requirements without disturbing the ratio between them. The 2-stage transmitting amplifier is followed by a filter which has two purposes. One is to reduce further undesired frequencies from the channel output. The other purpose is to prevent the output resistance of the amplifier from being shunted across the filters of the other channels, by providing impedance

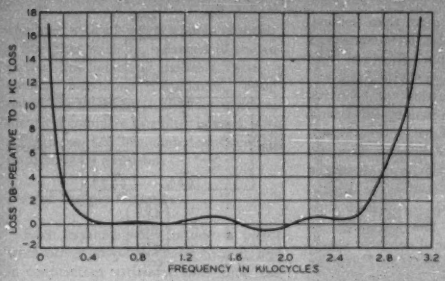

Figure 3. Typical channel loss-frequency characteristic, 9-H-2 carrier telephone system

matching only in its transmitted band. The output of the transmitting filter is applied to the high-pass part of the line filter in parallel with the other channels.

Speech Receiver Circuit

Carrier-frequency side band currents arriving from the distant speech transmitter circuit from the right are separated from those of other channels by the receiving band filter. This is followed by a carrier receive-level attenuator control which is adjusted to bring signals to a nominal level before application to the demodulator. The demodulator is substantially identical to the modulator, and its output consists of the unwanted high carrier frequencies resulting from interaction between the side band and the carrier, and the desired low frequencies which reproduce the original speech. Both groups are amplified by a fixed gain amplifier, and applied to a 2,700-cycle low-pass filter which eliminates the undesired frequencies from the output. Following the equalizer of the receiving channel is a second level control, affecting only the speech receive level. The received signaling current is also demodulated, producing a 3,400-cycle current which is picked off by a filter, described later. A typical over-all channel loss versus frequency characteristic is given in Figure 3.

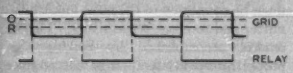

Figure 4. Pulse ratio control circuit operation, no correction of pulse length

Figure 5. Pulse ratio control circuit operation, adjustment to lengthen pulses

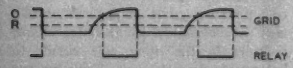

Figure 6. Pulse ratio control circuit operation, adjustment to shorten pulses

Signaling Transmitter Circuit

The signaling oscillator is in operation continuously, but its output is short-circuited by contacts of a relay as a means of keying it. The oscillator generates a signal 3.4 kc away from the carrier, on the same side as the speech side band to be used. It is thus equivalent to use of a 3,400-cycle signaling tone originating on the speech side of the modulator. However, by not passing the signal through the modulator, certain interaction products are thereby avoided. The level of the signaling current relative to the speech side band may be adjusted in steps which are usually preset at the factory. The sending or transmitting relay is either an a-c relay for operation on nominal 20-cycle or other low-frequency ringing current, or a 2-winding d-c relay for operation as a line relay or as controlled over a signaling or dialing lead by associated equipment. Relays are conventional telephone type, mounted on plug-in bases for ease of interchange or for convenience of adjustment. The circuit may be wired to permit transmission of the signaling tone when the transmitting relay is operated, or when it is idle, by a strapping change.

Although the signal lies outside of the speech side band, all things being equal, it is desirable to have the signal cut off during the time the circuit is in use for speech. For ringdown operation, therefore, the relay normally short circuits the tone, whereas in dialing operation, it is usually arranged to leave the tone on the line until the circuit is seized for a call. Dial impulses at speeds up to about 14 per second may be transmitted.

Signaling Receiver Circuit

The 3,400-cycle signals which appear in the output of the receiving amplifier are selected by a 3,400-cycle band-pass filter and applied to the input of the signal receiving circuit through a gain control. The signal receiving circuit consists of vacuum tube circuits which both amplify and limit the signal, the output being delivered by means of a telephone-type receiving relay in the anode circuit of the last tube. The operation of the circuit is such that in the absence of received tone, the relay is operated. Received tone applies negative bias to the last grid, causing the relay to release. A feature of considerable utility in dialing service is a pulse-ratio control circuit. This may be adjusted so as to vary the length of the output pulses relative to those delivered by the associated circuits at the distant transmitting office, which is of value in dialing operation as a means of correcting a certain amount of distortion which might otherwise exist due to repetition through a number of pulsing relays in tandem. Figures 4, 5, and 6 indicate the forms of voltage impulses applied to the last grid, and the resulting relay output impulses for no pulse ratio correction, for lengthening and for shortening the impulse, respectively. Figure 7 is a curve representing the effect of changes in the level of the received signal on the output pulse ratio, for a given setting of the control.

The pulse-ratio control circuit also is useful in some ringdown applications in which a kick-back occurs at the end of a received ringing signal, causing a false signal to be transmitted back to the other terminal. This transient disturbance is frequently caused by capacitance in the switchboard circuits. In some cases, circuit engineers have added slow-releasing relay circuits to such switchboard circuits to delay the restoration of the circuit to normal until these charges have had time to leak off. These measures are rendered unnecessary if the false ringing signal can

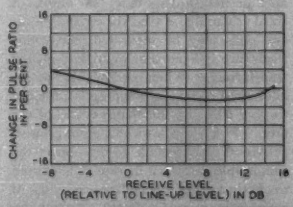

Figure 7. Change in pulse ratio versus received signal level

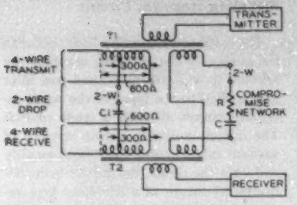

Figure 8. Two-coil hybrid circuit for 2-wire or 4-wire operation

be prevented from reaching the switchboard. By increasing the time-constant of the pulse-ratio control circuit by a factor of 20, sufficient delay may be introduced to keep a momentary false ringing signal from operating the receiving relay. The length of delay is adjustable by use of the same control used for dial pulse-ratio adjustment.

The receiving relay is a single-winding d-c telephone relay, of a type adaptable for either connecting ringing current to the switchboard or other drop in ring-down operation, or for repeating dialing or other d-c signals. It is mounted on a plug-in base.

Voice-Frequency Terminating Circuits

For most applications, it is necessary to connect the transmitting and receiving speech channels to an ordinary 2-wire telephone circuit. This is done by use of a conventional 2-coil hybrid or 4-wire terminating circuit, equipped with a compromise network for operation under average switchboard or subscriber set conditions. The 2-coil hybrid circuit used has several advantages over the frequently-used single-coil circuit, which utilizes line and network windings which have common junction points. One advantage is that the line, network, modulator, and demodulator circuits are all insulated from one another. A second is that the circuits may all be any impedance desired, in this case, 600 ohms. A third advantage is that the circuits of the two coils may be separated, converting them into independent input and output transformers. When used in this way, an additional section of winding is provided to give 600-ohm impedances toward the drop. Figure 8 shows this arrangement. Provision also is made to disconnect the compromise network in case it is desired to obtain a more precise balance by use of a separate external network, as when the drop side of the carrier terminal is permanently connected to a 2-wire cable or open-wire circuit of more than nominal length. Figures 9 and 10 indicate how this 2-coil hybrid circuit functions with speech currents from and to the drop.

The signal transmitting and receiving relays may be connected to the hybrid circuit and the associated external equipment in a number of different ways, by means of wiring between terminals on the main panel terminal strip. The separation filters required for speech-plus-duplex telegraph or tone signaling systems may be introduced on either the 2-wire or 4-wire side of the hybrid circuit, as required by the application. The filters for 4-wire application are inserted between the terminals marked *S-P*.

A 9-decibel pad is provided adjacent to the hybrid winding leading to the modulator circuit, controlled by a U-link which may be moved between its IN and OUT positions as desired. In the 4-wire drop arrangement of the hybrid coil circuit, this pad may be cut out, so that speech signals corresponding to −13 dbm test power level may be applied to the 4-wire sending circuit from the drop. In the 2-wire drop arrangement, this pad is cut in, so that the modulator will operate at its proper levels with speech signals corresponding to 0-dbm test power level received from the 2-wire drop.

Carrier Frequency Terminating Circuits

In operation over 2-wire line facilities, the transmitting and receiving filters of all channels are connected in parallel to the high-pass portion of the line filter. The latter passes all frequencies above about 3 kc, including the 3.6-kc signal of the lower half of the first channel. Only one line filter is required in this case for all three channels. This filter is commonly provided on the panel of the first channel in wire applications, as a measure of compactness, although for maximum flexibility it is sometimes supplied on a separate panel, with appropriate test U-links. The high-pass line filter and all of the channel filters are designed to have one side grounded for compactness and economy of manufacture. The low-pass line filter, however, is required to operate in a balanced circuit, and is normally inserted between the d-c composite equipment or bare line, and the voice-frequency line or simplex repeating coil or other drop equipment. The passage of independent composite dialing signals up to about 70 milliamperes through the two sides of the low-pass line filter does not affect carrier performance, however, so that in telephone offices having combined repeating coil and composite set equipments, used with dialing, the line filter may be located on the line side of the d-c composite set. When the carrier equipment is used to multiplex a broad-band radio link, it is necessary to separate the transmitting filters from the receiving filters, as they must be connected to the radio link transmitter and receiver, respectively. This is readily accomplished by making the proper interpanel strappings. It is generally desirable to be able to use the basic voice band beneath the first carrier channel as a telephone circuit, and for this purpose, two line filters are required, with a hybrid or 4-wire terminating circuit to provide for 2-wire operation. This equipment is provided on a separate filter panel, which is equipped with test U-links at convenient points. In 2-wire applications, if a line filter is inserted in one side of a phantom group only, phantom balance is maintained by inserting simple resistors in the other side circuit to balance the d-c resistance. These are designated line filter balance (*LFB*) resistors. However, if the voice circuit is

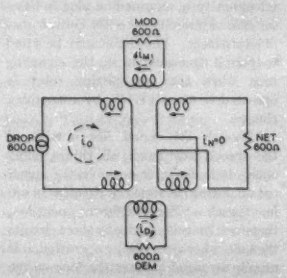

Figure 9. Operation of 2-coil hybrid: speech signal coming from drop circuit, resulting in no current in network when balanced

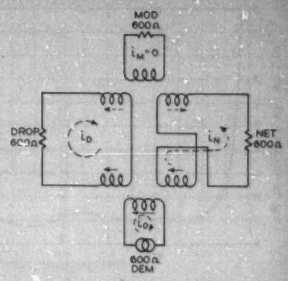

Figure 10. Operation of 2-coil hybrid: speech signal coming from demodulator circuit, resulting in no current in modulator when balanced

equipped with a 2-wire telephone repeater, a line filter must be balanced in the repeater line-balancing network with a similar 4-terminal impedance, designated line filter net (LFN), for which an identical complete line filter is used, with its high-pass side terminated in its normal impedance by a resistor.

Power Supply Circuits

Each terminal panel includes a power transformer providing heater current, and in conjunction with a rectifier tube and filter, providing plate current. Another winding of this transformer provides about 70 volts at a-c mains frequency for use in operating bells of associated subscriber sets, or other equipment, when it is not practicable to secure the usual low-frequency ringing current from an external source. This winding also provides current through a rectifier-filter circuit for transmission battery and dialing loop current for a manual or automatic telephone subscriber set. Each terminal consumes about 45 watts of a-c power.

Controls and Adjustments

Five variable controls with knobs and closely graduated dials provide all necessary adjustments required for normal lineup. These are indicated on the block diagram, Figure 2.

Transmitting Level. A grid potentiometer in the transmitting amplifier, for simultaneous adjustment of the output of speech side band and signaling channel. This permits maintaining their ratio while meeting levels other than normal required by co-ordination with other carrier systems. Normally a +12-dbm level for the speech side band test power level is transmitted to the line.

Carrier Receive Level. A control with a range of 40 db, for reducing the demodulator input to a predetermined level, therefore acting to compensate for differences between the losses of different lines.

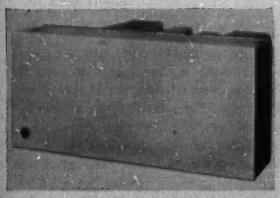

Figure 11. Terminal for 1 channel, 9-H-2 medium-haul carrier telephone system

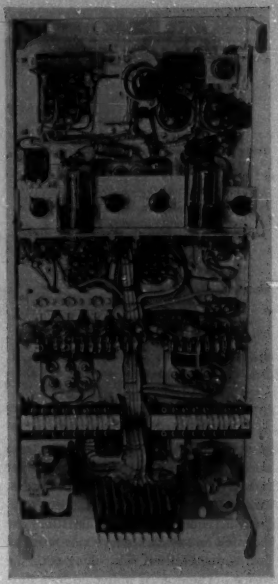

Figure 12. Carrier channel terminal, front cover removed to show accessibility for adjustment and maintenance

Speech Receive Level. A control with a range of 40 decibels, for adjusting the over-all circuit net loss without affecting the signaling receiver.

Signal Sensitivity. A grid potentiometer for the first tube of the signal receiving circuit, changed when required to place the received signal level at an optimum point.

Pulse Ratio. A potentiometer in the d-c portion of the signal receiving circuit, for increasing or decreasing the per cent make of the dialing impulses transmitted to the associated dial telephone switchboard equipment, to compensate for cumulative characteristic distortion resulting from pulsing relays in tandem.

In some cases it may be required to operate the signaling channel at a lower level than normal relative to the speech test power level; a tapped adjustment is provided for this, designated in Figure 2 as "SIG TRANS LEVEL ADJ".

The carrier and signaling oscillators are provided with variable-capacitance trimmers for adjusting their frequencies slightly. Modulator and demodulator circuits have low-resistance potentiometers for adjusting carrier leak to a minimum.

Test U-Links

While it is desirable to be able to break into the voice-frequency and carrier-frequency circuits to make tests and isolate sections of the equipment for trouble shooting, convenient facilities for the purpose have sometimes been skimped or omitted in an effort to keep the cost low, due to the relatively high cost of conventional telephone jacks. Inexpensive removable U-links are provided in the system described, located in the following circuits:

1. In the voice-frequency circuits between carrier and drop, for both 2-wire and 4-wire connections.
2. In the d-c leads between signaling transmitting and receiving relay circuits and the associated drop equipment, when such leads are used.
3. In the carrier-frequency circuits between the transmitting and receiving channel filters and the common bus where they are connected in parallel.
4. In the line filter circuits, between the filters and the line, carrier equipment and physical drop circuits.
5. In the modulator input circuit, where a single link may be moved between IN and OUT positions to control a 9-decibel pad.

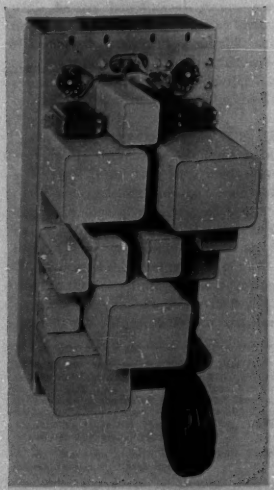

Figure 13. Carrier channel terminal, rear view showing inert components

This pad is normally used in 2-wire drop operation, and cut out for −13 dbm 4-wire operation.

6. One pair of U-link pin jacks is provided with both jacks connected to ground, for convenience in making measurements of voltages and levels where one side of the circuit is at ground potential.

The U-link jacks will accept standard cord tips, facilitating the use of portable servicing equipment. Bridging measurements may be made without removing the U-links, by clipping to the links.

Performance Characteristics

The levels and gains shown in Table II represent limits recommended for normal use to obtain best performance. The levels are based upon a 0 dbm (1 milliwatt into 600 ohms) level applied to the 2-wire drop.

Physical Design

A relatively compact terminal assembly was designed on a single panel 19 inches wide, $8^3/_4$ inches high, containing all of the equipment for a single-channel terminal, including power supply and line filter. Thus a complete 3-channel terminal group occupies only $26^1/_4$ inches of standard rack space. On the rear side of the panel are mounted the larger components, such as filters, transformers, and potted capacitors. Smaller components, controls and vacuum tubes are mounted on vertical brackets or terminal boards on the front side, along with the wiring. The front is protected by a dust cover. An auxiliary panel is provided when it is desired to mount line filters separately, either in conjunction with a wire line or radio terminal, or at intermediate points to transfer the carrier-currents around obstacles. This panel has two forms: one mounting two line filters with related U-links, with provision for adding a 4-wire terminating hybrid set when used with a radio link; the other mounting four line filters only, used for transfer sets and telephone repeater line filter net units. This panel is 19 inches wide and $3^1/_2$ inches high.

The appearance of a single channel terminal panel is shown in the illustrations. Figure 11 is a front view with cover. The cover is removed in Figure 12, revealing the components. At the left end are the transmitting relay, terminal strip, and receiving relay, in order from the top. Adjacent are the two test U-link assemblies. On a vertical bracket are the tubes and four of the adjustable controls. A fifth control is mounted just to the left of this bracket. The power supply equipment occupies the right end of the panel. The rear of an unmounted panel is seen in Figure 13. Except for the relay socket wiring, there are no wires or cable forms on the back of the panel.

Table II

Carrier Levels	
Speech sideband transmitting level to line	+12 dbm
Signaling channel transmitting level to line	+10 dbm ±2 db
Receiving level from line, minimum	−18 dbm
Two-wire drop operation	
Net gain, drop to line	12 db
Net gain, line to drop	14 db
Total loop gain	26 db
Four-wire drop operation	
Net gain, drop to line, −13 dbm modulator input level	25 db
Net gain, line to drop, +4 dbm output level to drop	18 db
Total loop gain	43 db
Signaling Channel	
Signal receive range beyond line-up level	10 db
Range of pulse-ratio control	±10 per cent
Dial speed, pulses per second	14
Speech Channel	
Over-all channel width to 2-db rise above 1,000-cycle point: 300 to 2,700 cps; to 10 db rise: 100 to 3,000 cps.	

No Discussion

Light Steel Tower Line Design

A. A. OSIPOVICH
ASSOCIATE AIEE

THE problem of mounting costs of constructing high-voltage transmission lines has been of considerable concern to the Bonneville Power Administration. This problem assumed especial significance during the early postwar period, see Table I, when demands for many products entering into construction of high-voltage lines, and especially for steel, have kept pace with war-time demands, and in many cases exceeded it.

It was necessary, therefore, to develop a practical method to combat high cost of transmission line construction without sacrificing reliability of service. As a result, tangent-suspension and dead-end structures of the "light steel" design have been developed to carry large size conductors for 230 kv and possibly higher voltage applications.

This paper reviews the statistical and design background, as well as the physical performance of the Bonneville Power Administration's system of high-voltage transmission lines built from its inception in 1938 to date. It describes design ideas used in developing light steel structures and their application in "light steel tower lines." Results so far obtained are presented and limitations inherent in the design are discussed.

Steel Towers Form Large Component of Line Costs

The cost of steel towers in place comprises a considerable portion of the overall cost of a high-voltage transmission line. This is particularly true, percentagewise, in fairly level or rolling type of open country where right-of-way clearing and access road construction, which are also large components of line costs, are not a serious factor.

Since 1938, when construction of first lines began, the Bonneville Power Administration (BPA) has designed and built nearly 2,000 miles of steel tower lines (over 2,300 circuit miles). This total given in Table II includes lines at present under construction or ready to be contracted, as well as lines designed to the point where contracts for their steel towers have already been issued. It embraces steel tower lines of 115 kv and 230 kv, as well as of single- and double-circuit construction. It includes lines traversing all types of terrain in the states of Oregon, Washington, Idaho, and Montana.

The total cost of BPA steel tower lines, including the cost of right-of-way and clearing, represents an estimated initial investment of nearly $68,000,000. Of this amount, the cost of steel structures in place approximates $29,000,000, or 43 per cent of the total. The amount of steel in towers and foundations adds up to the impressive total of over 84,000 tons, see Table II.

It is obvious from the foregoing that any new approach to steel tower design which would result in measurable savings of dollars and tonnage would constitute a worth-while step toward achieving over-all economy of initial system investment. This is especially important in view of the fact that costs of materials and construction are still on the rise.

Conventional Designs Used by BPA in the Past

In search of ways to combat high postwar costs, BPA engineers have been constantly and critically reviewing their design practices. These practices in the past largely followed standards of design established by the electric power industry over a period of years. Single circuit structures used in BPA lines were predominantly of the so-called "rotated," self-supporting type having conductors in horizontal configuration. Double circuit towers were of the conventional, 3-crossarm type (middle crossarm extended) placing each of the circuits into a nearly vertical configuration. Both types have been developed for a variety of conductor sizes used in 115-kv and 230-kv applications. They have been designed to withstand, under actual tests, the various combinations of transverse, vertical, and longitudinal forces prescribed by the National Electrical Safety Code[1] and applicable State codes.

Tangent-Suspension Towers Predominate in a Line

As designers well know, the predominating type of a transmission line structure is the so-called "tangent-suspension" tower. This structure is used, as its name implies, in tangent or very small angle positions in the line; it usually employs a single string "suspension" type of conductor attachment which is inherently a very flexible support. Except in cases of a broken conductor or overhead ground wire, serious longitudinal strains are rarely imposed upon this type of tower. Nevertheless, standards generally accepted at the present require that suspension towers be designed and tested for broken conductor or ground wire conditions.

The tangent-suspension tower is, by its very nature, the most economical type of structure; it is, therefore, used to a maximum consistent with the terrain and alignment of a given line. BPA experience indicates that on the average this type of tower represents approximately 70 per cent of the total number of structures in the line. In open, flat, or rolling country, this percentage is even higher, more in the nature of 90 per cent, see

Paper 50-243, recommended by the AIEE Transmission and Distribution Committee and approved by the AIEE Technical Program Committee for presentation at the AIEE Fall General Meeting, Oklahoma City, Okla., October 23–27, 1950. Manuscript submitted March 15, 1950; made available for printing September 5, 1950.

A. A. Osipovich is with the Bonneville Power Administration, Portland, Oreg.

The author acknowledges the assistance given by F. W. Farr who originated the light steel tower designs, and others in the BPA who helped in developing the idea and in compiling the statistical data included in this paper.

Table I. In-Place Cost of Towers and Foundations, BPA Steel Tower Lines*

Fiscal Years Inclusive	Line Miles	Tons of Steel	Costs in Cents per Pound	Remarks
1938–1945	1191.1	51,947	11.6	Indicative of low and steady costs of material and labor prevalent before and during the war. Costs are based on capital records
1946–1950	769.6	32,132	26.7	Reflecting increased costs of the postwar period. Costs are based on capital records and estimates
1938–1950			17.3	Gross average over the period of 12 years
1938–1950	1987.7	84,079		Totals

* Includes all material and labor for foundations (excavation, reinforcing steel, concrete) and towers complete in place.

Table II. It should be obvious, therefore, that any attack upon economy in the cost of steel structures in a transmission line is to be directed first of all toward this type of tower.

Dead-End Towers Are Very Costly

Another important type of structure in a line is the so-called "dead-end" or "strain" tower. This structure is ordinarily used in terminal positions, at important sectionalizing points in the line, at heavy angles, or at important crossings. Prevailing standards require that this type of structure be designed for the full effect of longitudinal tensions resulting from all conductors and overhead ground wires being broken on one side of the tower in combination with other transverse and vertical loadings resulting from standard design conditions generally accepted in a given area. By its very nature, this is a very expensive structure, especially because it requires, in order to be self-supporting, heavily designed, and expensive foundations.

This type of tower constitutes, therefore, the second focal point of attack in any attempt at economy of line construction. Quite naturally, then, BPA designers directed their next effort toward developing more economical, yet fully dependable, designs for the "dead-end" structures.

Table II. Summary of Data on BPA Steel Tower Lines

Item Number	Item	Data
1	Total line miles of steel tower construction	1987.7
	Total circuit miles of steel tower lines	2316.0
2	Total cost of lines (including clearing, roads, material and labor)	$67,688,369
	Cost of steel in place, including foundations	$28,943,465
	Cost of steel in place in per cent of total cost	43%
	Total tons of steel	84,079
3	Gross average per cent of tangent structures in all lines	70%
	Average estimated per cent of tangent structures in flat country lines	90%
4	Circuit mile years of operation of all BPA steel tower lines	25,470
5	Estimated tons of steel saved by use of light steel to date	12,840
	Estimated saving of federal funds to date	$4,168,460

Table III. Light Steel Transmission Lines Construction and Cost Data

Line	ACSR Conductor MCM Copper Equiv.	Length Miles	Tons per Mile	Total Number Structures	Date Bids Opened	Number Bidders	Labor* Cost/Mile	Al-L Structures, Per Cent	Lattice Pole Structures, Per Cent	Other Standard Structures, Per Cent
A	500	34.0	23.98	210	2-28-49	4	$10,719	83	4	13
B	500	22.9	28.53	117	4-22-49	6	9,356	84	8	8
C	500	16.8	27.06	83		**	6,681	77	4	19
D	500	59.9	30.52	290	2-15-50	11	7,340	53	11	36
E	500	34.0	23.98	210	5-1-50	9	6,576	83	4	13
F	500	39.0	35.98	164	5-18-50	8	7,950	55	11	34
G	500	75.7	31.81	353				70	4	25
H	500	105.0	31.81	504				69	3	28
I	800	75.7	33.24	359	6-7-49	6	10,852	71	5	24
J	800	101.9	29.47	483				76	5	19
K	800	28.9	29.74	129				53	6	41
L	800	34.4	28.54	249				74	6	20
Totals		628.2		3151						

* Based on costs, as contracted; does not include material costs.

** Constructed by BPA forces 1949.

War-Time Experience Leads to New Design Ideas

The basic approach of BPA designers in their effort to effect economy in steel tower construction, without sacrificing reliability, resulted from an early wartime experience. The problem at hand was to design a 230-kv circuit paralleling on the same right-of-way a "standard" steel tower line previously built between Grand Coulee Dam and the Covington Substation, located in the Seattle load area. Because of the scarcity of steel and the insistence of the War Production Board that its use be brought to a minimum, it was decided to place upon wood structures those portions of this line (110 miles out of a total of 183) which were located in open, easily accessible and fairly flat terrain of low elevation.[2,3] Naturally, it was not economically practicable to design the 230-kv wood structures of the "tangent-suspension" type for the "broken-conductor" loading conditions for which the initial "standard" steel tower line was constructed. Hence, these structures were designed primarily for the usual standard transverse and vertical loadings, but only for limited longitudinal loads. Experience with this line, in operation since 1944, and with a total to date of nearly 1,900 mile-years of operating 230-kv wood lines built since then, indicates nearly a perfect record of mechanical performance. This fact, and the parallel record of nearly 25,500 mile-years, Table II, of operating the entire BPA system with only one or two physical failures (at that not entirely attributable to loading) proved the reliability and safety of using "flexible" structures and, thus, formed the basis for the theory of our light steel tower line designs.

"Light Steel Tower Line" Defined

A light steel tower line is defined, in BPA usage, as a line in which the predominating "tangent-suspension" structures have been designed for conditions analogous to those used in designing wood pole lines. In other words, these structures in a light steel tower line are designed primarily for transverse and vertical loads resulting from the ice, wind,

Figure 1. Typical light steel tangent-suspension towers, rotated type
230-kv design for 500,000 circular mil copper equivalent steel-reinforced aluminum cable conductors

Figure 2. Typical light steel dead end structures, lattice-pole type
230-kv design for 500,000-circular-mil copper equivalent steel-reinforced aluminum cable conductors

and temperature conditions usually prevailing in the Pacific Northwest. As an inherent consequence of steel design, these structures also are capable, under certain conditions which will be discussed later, of resisting fairly large longitudinal unbalanced loads.

The light-steel tangent-suspension towers, as designed by BPA, are of the rotated type; they do not differ in outward appearances from the "rotated," single circuit towers of the standard design. Like their standard protypes, they are fitted to the topography of the tower site and to varying heights required in a transmission line by a system of body- and tower-leg extensions, see Figure 1.

The analogy with wood pole lines also is carried in a light steel tower line to the design of "dead-end" and "heavy angle" structures. To effect economy, these structures in a light steel tower line are no longer self-supporting towers. They are designed as steel lattice pole frames capable of withstanding the columnar action resulting from all prescribed design loads imposed upon them. To meet the full longitudinal and transverse strains resulting from maximum design loading conditions, these steel poles are adequately guyed much in the same manner as their wood pole counterparts would be, see Figure 2. In this design, the amount of steel in the structures and the quantities of material in their foundations are reduced considerably, as is also, the amount of labor and the total cost required to erect these structures, Table II.

Intermediate types of towers, such as double-suspension and medium- to large-angle structures, employed in a light steel tower line are of the same standard type as used in all other BPA lines. In other words, where long spans are required, or power line, railroad, highway, and similar important crossings occur, the heavier standard types of towers are used.

Consequently, while differing outwardly from the BPA standard steel tower lines only in the appearance of dead-end, heavy-angle and transposition structures, the light steel tower line provides the economy of initial construction approaching that of wood pole lines, yet affords the advantages of minimum maintenance and longer life usually associated with steel tower construction.

It may be in order at this time to underscore a point which is probably self-evident by now; namely, that the light steel tower line idea has been applied to date only to single circuit designs. However, light steel tower lines using steel reinforced aluminum-cable conductors of both the 500,000 circular mil and the 800,000 circular mil copper equivalent have been designed and constructed at the present time. Designs of structures for each conductor size are naturally associated with a maximum working tension which is considered to be most economical for the conditions under which the given conductor is used. Therefore, the 500,000 circular mil and the 800,000 circular mil conductors each require their own set of light steel structures.

It should be pointed out also that a light steel tower line is not a constant, but a fluctuating concept in that the per-mile tonnage of any given line is naturally dependent on terrain, alignment, and other factors characteristic of the area which it traverses. Hence, the percentage of light steel tangent-suspension and lattice-pole dead-end structures, as well as the total per-mile tonnage for every light steel tower line, are variables, see Table III.

Economy Studies Made in 1946

Early studies which ultimately resulted in the acceptance of the idea of light steel tower line designs date back to 1946.[4,5] At that time comparisons were made of initial construction costs, as well as of average annual costs over a 50-year life period for different types of line construction.

In these studies, each one of the structure types under consideration was applied to actual profiles of lines with somewhat similar terrain but differing in density of population and development of

Table IV. General Data on BPA Transmission Lines; Fiscal Years 1939–1950, Inclusive

Item Number	Remarks	Data	Remarks
1	Line miles in operation	3738.8	All types and voltages; wood and steel lines
	Circuit miles in operation	4036.9	
2	Total number of steel towers	8,305	All BPA steel lines
3	Per cent of tangent-suspension structures	70%	Gross average for all types and voltages of steel tower lines
	Per cent of dead-end structures	8%	
	Per cent of other structures	22%	

roads, utilities, and so forth. Results indicated that the initial cost of light steel tower lines is not much higher than that of the most economical wood pole lines. Yet, on the basis of average annual costs for a 50 year-life period, the light steel tower lines are indicated to be the more economical, Table V. It is admitted, of course, that this relation may be upset by differing cost trends in the steel and wood industries. This, however, has not been proved the case to date; at least not to the point of upsetting the basic conclusion.

New Designs Subjected to Full Size Tests

Basic designs and preparation of detail plans for the various types of structures usually employed in a line proceeded apace after the conclusion was reached to adopt the new light steel design for future BPA lines where conditions would warrant its application. These designs were made for "heavy" loading conditions, namely: 1/2 inch radial ice, 8 pounds wind at 0 degree Fahrenheit.

The first contract for light steel was placed with the American Bridge Company in 1948. A full scale test of a "tangent-suspension" tower designed for the 500,000 circular-mil copper equivalent steel-reinforced aluminum-cable conductor was performed under this contract in November of that year. This test has proved the following to the complete satisfaction of both the BPA designers and the steel fabricators:

1. That this light steel structure will carry all transverse design loads with a minimum safety factor of 1.5.
2. That it will carry all vertical design

Table V. Study Estimates for Various Types of BPA Transmission Line 230-Kv Designs for 500,000-Circular-Mil Copper Equivalent Steel-Reinforced Aluminum-Cable Conductors

		SPECIMEN LINES STUDIED											
		LINE M			LINE N			LINE O			LINE P		
		STD STEEL TOWERS	LIGHT STEEL TOWERS	WOOD POLES SPAR X-ARMS	STD STEEL TOWERS	LIGHT STEEL TOWERS	WOOD POLES SPAR X-ARMS	STD STEEL TOWERS	LIGHT STEEL TOWERS	WOOD POLES SPAR X-ARMS	STD STEEL TOWERS	LIGHT STEEL TOWERS	WOOD POLES SPAR X-ARMS
TONS/MILE		37.1	22.8		39.5	25.2		39.6	30.8		39.6	26.6	
INITIAL COST PER MILE	* RATIO A	119.2%	91.8%	72.4%	126.2%	100.0%	76.2%	130.3%	110.0%	82.3%	124.2%	97.7%	82.0%
	** RATIO B	1.30	1.00	0.79	1.28	1.00	0.76	1.18	1.00	0.75	1.27	1.00	0.84
ANNUAL COST PER MILE	* RATIO A	116.5%	92.9%	106.7%	124.4%	100.0%	111.8%	126.2%	108.6%	119.3%	121.0%	98.0%	119.0%
	** RATIO B	1.27	1.00	1.16	1.26	1.00	1.10	1.19	1.00	1.01	1.27	1.00	1.12

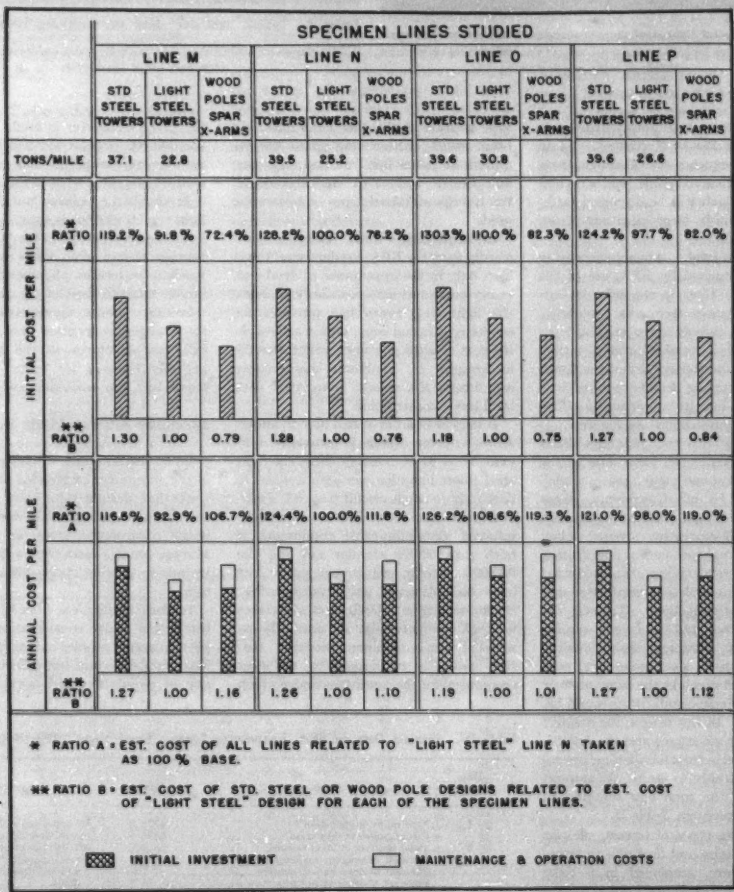

* RATIO A = EST. COST OF ALL LINES RELATED TO "LIGHT STEEL" LINE N TAKEN AS 100% BASE.

** RATIO B = EST. COST OF STD. STEEL OR WOOD POLE DESIGNS RELATED TO EST. COST OF "LIGHT STEEL" DESIGN FOR EACH OF THE SPECIMEN LINES.

INITIAL INVESTMENT — MAINTENANCE & OPERATION COSTS

loads with a minimum safety factor of 2.0.

3. That, when otherwise not subjected to appreciable wind and ice loads, it will resist an unbalanced longitudinal load at one of the outside conductors in excess of 6 kips.

A few improvements which were indicated by the results of the full scale tests, as well as some minor changes which resulted from field experiences in erecting the structures, were incorporated into the final designs of the initial series of structures (using 500,000 circular-mil conductors).

Since that time, a full series of light steel structures have been designed for use with 800,000 circular-mil copper equivalent conductors. These structures are so designed that they will accommodate insulation and clearance requirements for future operation at 287 kv.

Light Steel Tower Lines Savings Appraised

A number of light steel tower lines have been designed by BPA engineers during the last three years. Some of these have been constructed and are in operation. Others are at present under construction; and major materials have been ordered for a few more; see Table III.

It now is estimated that for the lines shown in Table III, a total saving of over 12,800 tons of steel has been effected directly attributable to the use of light steel instead of the standard steel designs. This saving in tonnage, coupled with related savings in costs of transporting, handling in the yards, and erecting in the field, would result in an estimated saving of nearly $4,170,000. These savings in material and funds are, of course, considerable by any standards.

To these savings must be added others which have not, or cannot be accurately evaluated. Under this heading would come:

1. Savings to contractors due to greater use of mechanized equipment in erecting light steel structures because of their reduced total weights, which in turn makes possible assembly of larger structure sections on the ground and smaller number of lifts per structure; hence, greater productivity in terms of structures erected per day or week for a given crew.

2. Faster erection permits shorter construction periods; this, in turn, makes possible earlier energization and the advancement of the time when a line begins to return revenue.

A word of caution seems in order at this point. Light steel tower line designs should be applied judiciously with respect to both terrain and climatic conditions prevailing in an area. These designs should not be used at high elevations, in places inaccessible through a considerable portion of the year, or in areas known to be subject to heavy ice and sleet storms. Also, they should not be used where future plans call for installation of overhead ground wires, as they are not designed for this purpose.

Studies Continue for Perfecting Structural and Mechanical Designs

As indicated previously, future lines of the Bonneville Power Administration through areas free from severe icing and lightning will be predominantly of the light steel design. This does not mean that BPA studies and explorations in the field of structural and mechanical design, as related to high-voltage lines, will not continue. Studies now are oriented toward further perfection of the light steel designs for conductor sizes mentioned in this paper and, perhaps, larger ones. Studies also are in progress for lines of higher voltages than 287 kv, both in standard steel and light steel designs, as well as for single and "bundle" conductors. Investigations have been started toward development of steel structures which would permit a practical combination of the light steel idea, with the need for overhead ground wire protection in areas of high lightning frequency.

Use of structural aluminum in transmission line applications is being studied co-operatively with manufacturers and fabricators. Efforts also are under way toward establishing a more logical correlation between structural designs and hardware development for larger conductors and higher voltage applications.

Conclusion: No Troubles Anticipated in Operating Light Steel Lines

It is, of course, too early to draw upon operating experience with our newly designed light steel tower lines. However, we have been careful to apply this design only in those portions of our various lines where conditions for its use are appropriate. Therefore, we do anticipate the same nearly trouble-free mechanical performance of light steel tower lines as we had with operating and maintaining the BPA system since its inception.

References

1. National Electrical Safety Code. National Bureau of Standards (Washington, D. C.).

2. 230-Kv Wood Pole Structure Design and Tests, A. A. Osipovich. *Electrical World* (New York, N. Y.), May 26, 1945.

3. H-Frame 230-Kv Wood Pole Lines, Crossarm Design Practice, A. A. Osipovich. *Electrical World* (New York, N. Y.), September 25, 1948.

4. Light Steel Tower Design May Save One-Tenth over Wood Pole Lines, F. W. Fritz. *Electrical World* (New York, N. Y.), April 23, 1949.

5. Editorial. *Electrical West* (San Francisco, Calif.), November 1949.

Discussion

O. D. Evans (Oklahoma Gas and Electric Company, Oklahoma City, Okla.): This paper raises again the long and much-discussed question of whether or not to design steel tower transmission lines for one, or more, conductors or shield wires broken. A perusal of technical literature on the subject of steel tower design leads to the conclusion that nearly all companies design steel tower lines for at least one, and in many cases two, conductors or shield wires broken. The fact that wood pole tangent structures are not designed for broken cables is one of the reasons they are considerably less in initial cost than are steel tower lines.

A cost estimate, made by us for a short section of 66-kv double circuit line in 1948, indicated that we could expect to pay over twice as much for a steel tower line as for a wood pole line if we were to consider two conductors (or one conductor and one shield wire) broken, which we deemed necessary for this particular line. A saving could have resulted in the steel tower design had we eliminated the broken conductor (or shield wire) requirement, but the steel tower design could never have been made competitive in initial cost with the wood pole line; however, consideration of rights-of-way procurement, appearance, and permanency of the standard steel tower design dictated its use and this line was recently constructed and placed in operation. It is recognized, however, that the differential between steel-tower and wood-pole designs would tend to decrease as the voltage ascended to 287 kv which the paper discusses.

The author is careful to point out that his light steel tower designs should not be used in areas subject to heavy ice and sleet storms. This, in itself, would eliminate a large portion of this country from using light steel tower designs; yet, wood pole lines have been used in these areas for years. A conductor or shield wire break in a well-designed modern transmission line is not likely to occur, and future breaks should be even less likely as our knowledge of conductor and shield wire vibrations and the phenomena of "galloping" conductors is enhanced. Airplanes will tend to present a constantly increasing menace, but it is not believed economically feasible to design for airplanes hitting electric power transmission

lines. It is extremely unlikely that an airplane will ever hit a line in open country and, if one does, it will probably break more than two cables.

Suppose one or two cables are broken on one of the light steel tangent tower designs—what would happen? There would be an initial impact on the tower after which the cable would probably slip through the suspension clamp. One way to lessen this impact would be to use "J-bolt" type suspension clamps and not to tighten the nuts on these clamps too securely. The clamp is required merely to support the cable and any changes in longitudinal tension, other than a conductor break, would probably be taken care of by a deflection of an insulator string in the case of a conductor or by the shield wire attachment if a sufficiently flexible assembly is used. The impact, if sufficiently heavy, might deform the steel crossarm member without further damage to the tower; in such cases, wood crossarm members could be used for temporary repairs until steel members had been fabricated.

Should a cable break seriously damage one or more towers, which seems unlikely considering the inherent longitudinal strength that would result from a satisfactory transverse and vertical load design, temporary wood pole structures could be hurriedly erected to provide service. This could be done in such a way as to leave the towers free for maintenance work.

As indicated in the author's paper, the light steel tower design will inherently withstand fairly large longitudinal loads, much more so than will wood pole lines. It seems to me, therefore, that the question boils down as to why the designer is using the steel tower design. If it is to obtain longitudinal strength for broken cables, and this consideration outweighs everything else, then the so-called standard steel towers must be used. If a tower line is being used for any other reason, then careful consideration should be given to the light steel tower designs. In the tower line recently constructed by our company, mentioned earlier in this discussion, a large part of the line was in the city limits of Oklahoma City and a tower collapse would entail heavy property damage and possible loss of life.

The lattice-pole type angle and dead-end structures used in the light steel tower design particularly fascinates me. This design has all the advantages of the standard steel tower design and at approximately half the cost. I can see no reason why this design should not be used in all designs except in (or near) towns where rights-of-way for guying are too expensive or cannot be obtained.

In designing lightning-resistant lines, the effect of wood as an insulator for lightning strokes must be taken into consideration when comparing costs. The lowered ground resistance that the steel tower will have over the wood pole structure will partially offset this difference in lightning impulse strength of the structure.

Finally, the structure life also enters into the cost analysis. From one of the author's references it was ascertained that 25 years was used as the expected life of a wood pole line and 50 years as the expected life of a steel tower line. Many conditions, particularly soil conditions, enter into the life of a particular line. Fifty years seems to be the accepted life value of a steel tower line, but many companies use 30 years expected life for a creosoted pine wood pole, and some even use 40 years.

The engineer must be ever alert to new ideas and improvements. It is predicted that the light steel tower designs discussed by the author will become rather common in the years to come as our knowledge of conductor failures is advanced and as the depletion of our supply of wood poles increases the cost of wood pole lines.

Jordan Lummis (Southern California Edison Company, Los Angeles, Calif.): A transmission tower is so much a creature of its designers assumptions that any attempt to compare the structures of two engineers runs squarely against this subjective difficulty. Mr. Osipovich has made a definite study of his own structures which have yielded him economic results but other designers should be warned that the results can be applied to their own structures only with caution. The assumptions used in tower engineering may be divided into two broad groups; those pertaining to design and those pertaining to loadings. None of them are completely sound and many are wide of the truth.

In the case of design assumptions, the first are those defining the maximum tension and compression limits and these are strictly a matter of personal opinion. Limiting tensions used in tower design vary from 18,000 to 25,000 pounds per square inch. In the case of compression we have a wide choice of column formulas, and we must also assume end conditions, minimum slenderness, and minimum thickness. One column formula in common use permits a compressive stress of 7,000 pounds per square inch under the same conditions that an equally common formula permits 12,000 pounds per square inch. Again, one common specification limits slenderness-ratio in redundant members to 200 while another permits 275. In one case increasing minimum thickness from 1/8 inch to 3/16 inch increased the weight of a tower more than 16 per cent.

In the case of the common type of tower Mr. Osipovich is concerned with, the distribution of torsion becomes a very important factor because this style of structure is statically indeterminate in a high degree. An out-and-out assumption of the amount of torsion carried by each face of the tower can be, and often is, made. More exact analyses can be based on the principle of virtual force, least work, or limit design but even these are approximate approaches.

Loading assumptions also can vary greatly and this condition is made more complex by lack of agreement on wire tension. However, assume tension fixed for the moment and consider the other assumptions that must be made; the line angle, the span length, the vertical load, the wind velocity, the number of broken wires, the reduction in tension caused by broken wire, the effect of impact, and any special conditions required for safe construction. Now note that most of these assumptions are permutations of maximum tension which is commonly assumed anywhere in the range of 25 to 50 per cent of wire strength.

Another very important assumption which does not fall into either of the preceding classifications will involve the nature of the steel itself. Steel companies now commonly furnish tower steel in "structural" and "high elastic" grades. The greater strength of the "high elastic" steel usually results in economies when used for legs, cross arms, and other highly stressed members. Yet many fabricators roll, but will not guarantee, "structural" grade steel exceeding the requirements of the higher grade. In any case, the assumption of limiting basic stress will be an important one.

Mr. Osipovich's "light" tower results from a reduction in loading assumptions. It is probably possible to arrive at the same result by changing design assumptions. In a recent case an old 66-kv tower was compared to a new tower based on less conservative design assumptions. The duty of each tower was nominally the same but the more conservative tower weighed 3,000 pounds while the less conservative weighed 1,800 pounds.

While many assumptions have been noted, many more could be. The effect of these assumptions have only been hinted, yet they are far reaching and sometimes surprising as may be seen in the case where the minimum allowable size of members was reduced from 3/16 inch to 1/8 inch. This structure performed admirably in test but in service many of the thin members broke from vibration and the reduction of thickness meant failure within six months of members that would otherwise last indefinitely.

B. R. Murphy (The Hydro-Electric Power Commission of Ontario, Toronto, Ontario, Canada): If the chief purpose for considering light steel tower designs is to reduce transmission line costs, this must be proved by operating experience in any given system.

Transmission engineers should, however, give serious consideration to the suggestion that the loading introduced by the assumption of a broken conductor be disposed of. Elimination of this loading as well as the omission of ground cables are basic differences between light steel tower designs and so-called conventional designs. Developments and operating experience which affect the suggested trend to less steel are:

1. Should a broken conductor occur, suspension insulators swing to relieve considerably the unbalanced pull on the tower.

2. Experience indicates that conductors, especially steel-reinforced aluminum cable with fast switching, simply do not break or burn off. In a hurricane, nine 230-kv conductors and six ground wires did not break when either one or two towers in three parallel 230-kv single-circuit lines were twisted and flattened practically always on their own foundations. One of about five towers lay somewhat along the line. During the winter of 1949–50, a rather severe sleet storm moved across Michigan and Ontario. In Ontario most of the copper, and like conductors, at the rural distribution level and lower voltages came to ground. Steel-reinforced aluminum-cable conductors seldom, if ever, broke. They did hold up trees in some cases and poles were broken in other cases.

3. Very short spans between dead ends and at a 90-degree corner using two 45-degree angles with conductors dead ended can result in high unbalances in tension

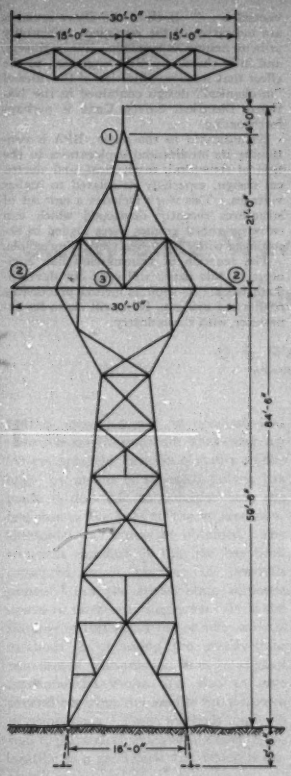

Figure 1. 110-kv 1939 type single-circuit suspension tower

Conductors, 3-477,000 circular mil steel reinforced aluminum cable; ground cable, $1^3/_{16}$-inch galvanized steel; normal span, 1,000 feet; maximum tangent span, 1,350 feet; maximum angle in line, 3 degrees; voltage, 110,000

Loads: I. Vertical, 1,200 pounds at point 1 and 2,200 pounds at each of three points 2 and 3. II. Horizontal-transverse, 1,500 pounds at point 1 and 2,200 pounds at each of three points 2 and 3. III. Horizontal-longitudinal, 4,000 pounds at point 1 or 3,750 pounds at one point 2 or 7,500 pounds at point 3. IV. Dead load. Combine I and IV with II or III or use twice I alone. Load II contains allowance for wind on tower and 3-degree turn in line

which may affect closely designed light steel towers.

4. If ground cables can be eliminated in a design for light steel towers, then use of these towers becomes territorial and depends on the climatic conditions.

5. A fabricated structure and one assembled in part in the field differs from a wood pole structure or steel structure, welded into large units as used in Sweden. Changes in factors of safety will tend to make their use and comparative reliability possible. The cost of failure in closely designed structures should be accounted.

Designers and operators in Ontario have been using light steel towers widely in the 120-kv field since 1939, see Figure 1 of this discussion. It has since been found from experience that the connection between horizontal members of the footing and the leg were not properly detailed and, secondly, that the uplift characteristics were not entirely satisfactory in clay. This structure, with minor modifications, is still being used.

Wood structures have not been used yet in Ontario for 230-kv construction, but their use has been considered.

Policy is involved in reducing the amount of steel used in transmission lines towards some light steel tower design. Some policy makers may say that the end cost of a kilowatt-hour is not importantly involved in an even fairly long high-voltage transmission line. It would be interesting to know the actual weight of a light steel tower design and of a heavier modern alternative design.

Would Mr. Osipovich use guyed dead-end towers at the entrance to a transformer station?

Some engineers might class "A" frame towers as light steel towers. Both structurally and operationally the reasons now are available why such types should be avoided. It is true that an "A" frame can be designed with considerable resistance to loads along the line; however, it is necessary to give rather careful attention to the details of stringing the first two ground wires on such lines. After that it is possible to erect three or more conductors successfully.

Summarizing, it appears that the advantages in using light steel tower designs will be territorial and will be governed by climatic conditions.

While there are still some fairly obvious reasons why twin wood poles seem to stand up well under extraordinary wind loads, nevertheless, there is no attempt in this discussion to explain why twin poles should not be used.

A. A. Osipovich: The author appreciates the interest shown and the effort expended by O. D. Evans, J. Lummis, and B. R. Murphy in preparation of their written discussion and by Dr. E. L. Kanouse who restricted his comment to oral remarks at the session.

It appears to the author that all the discussors have agreed upon one important point. This point is that the long existing problem of correlating practicability and economy still remains a very important one for the industry in relation to design of transmission line structures. These discussors also underscore a related fact that no solution proposed for this problem can escape the danger of being regarded as controversial.

The author agrees with Mr. Lummis that designing a set of transmission line structures is a highly "individualistic" endeavor. It is so because no two engineers will think alike with respect to basic design assumptions, or will apply the same criteria in the use of basic materials. It is so, also, because no two important transmission systems ever present an identical combination of the numerous factors (such as terrain, climate, load, voltage, and so forth) which enter prominently into determination of the type of design to be employed in any given case.

It is true, as Mr. Murphy suggests, that the degree to which a given design idea accomplishes the objective of combining practicability with economy is usually determined through the long test of years of performance. However, the author feels that in a young system such as that of the Bonneville Power Administration, a synthesis of design experience and line performance, related to a substantial number of mile-years, can and should be logically relied upon for the establishment of a set of design assumptions, such as were arrived at in the economic studies which preceded the adoption of the "light steel" design by BPA.

Table I of this discussion combines information contained in the slides shown during the presentation of the paper to give the comparison in weight and costs between several comparable types of "light" and "standard" structures placed side by side as part of two parallel circuits on the same right-of-way.

The weight and cost information shown in this table is based on unit prices taken from contracts which covered both "light" and "standard" structures. These unit prices were contained in low bids of February 3, 1949, for materials, and February 2, 1950, for construction of the Chehalis-Covington 230-kv line. The tabulation shows in all cases a considerable advantage in favor of "light" over "standard" structures.

The author wishes to underscore again the point made in the paper that the "light steel" designs have their limitations and, therefore, are not applicable under conditions encountered in those parts of the country where icing and lightning conditions are severe. However, where these designs are properly applicable, they result not only in the immediate savings of the initial investment, when compared with "standard steel" designs, but also in the long range economy based on annual costs when compared with functionally equivalent wood

Table I

Tower Type	Conductor Height Above Ground, Feet	Total Weight of Steel in Structure and Grillage Foundation: Light, Pounds	Total Weight of Steel in Structure and Grillage Foundation: Standard, Pounds	Total Cost Erected: Light	Total Cost Erected: Standard
Tangent-suspension	62	7,828	13,331	$1,864.80	$2,796.15
Medium-angle	63/65	14,041	21,287	3,892.35	4,610.60
Dead end	72	17,548	36,625	5,872.50	7,641.00

pole lines for which the initial investment may be smaller.

There is one more important factor, which was not mentioned in the original paper, favoring the use of "light" steel designs in a large transmission system such as that of the Bonneville Power Administration. This may be designated as the "diversity" factor. When a transmission system has a number of high capacity circuits paralleling each other between important generation and load centers; when such a system is also interconnected with a number of other systems in the area to form a regional pool of power; and when the most important load and distribution centers in the region are provided with at least a 2-way feed; —then the elements of "risk" involved in losing a circuit is reduced to a minimum and such a "risk" becomes economically justifiable. Hence, the decision to use "light steel" designs for circuits paralleling the initial "standard steel" circuits (or "back-bone" circuits as they are called in BPA) in areas where past performance of the initial lines has shown a high degree of reliability. That such a calculated "risk" is justified, especially in the light of resulting economies both as far as material and costs are concerned, is one of the points which was intended to be brought out by the author in his paper.

Finally, the author finds encouragement in the statement of Mr. Murphy that "transmission engineers should give serious consideration to the suggestion that the loading introduced by the assumption of a broken conductor be disposed of." Also encouraging is the prediction made by Mr. Evans that "the light steel tower designs . . . will become rather common in years to come, as our knowledge of conductor failures is advanced. . . ." Both of the above remarks are indicative of the sentiment evidentally present among transmission line engineers, and fully shared by BPA engineers, to the effect that some modification of the rules of "mechanical" design contained in the National Electrical Safety Code is perhaps forthcoming.

As indicated in the paper, BPA is continuing its studies and explorations in the field of structural, mechanical, and electrical design, especially as related to higher voltages. This work includes a new set of structures recently developed which can carry overhead ground wires loaded in accordance with "light steel design" principle.

The reaction of transmission line engineers to this paper will spur our development work. As soon as further practicable results are evident, BPA will share its experience with the industry.

Steady-State Waves on Transmission Lines

D. L. WAIDELICH
MEMBER AIEE

THE increased use of nonsinusoidal waves on transmission lines such as, for example, the location of faults on the lines[1] by means of repeated pulses, has made it desirable to consider how the response of the lines to the applied nonsinusoidal waves may be obtained. The transient response of the line has been presented in a number of previous papers[2,3] but the steady-state response seems to have been neglected. It is the purpose of this paper to consider various methods of obtaining the steady-state response of transmission lines to applied nonsinusoidal waves and also to give several experimental results for purposes of comparison. These methods apply as well to plane electromagnetic waves propagating in a good dielectric which is isotropic.

In making the mathematical analysis it is assumed that the frequencies are sufficiently high so that certain simplifications may be made. For example, in the operational expression for the characteristic impedance Z_0 of the transmission line

$$Z_0=\sqrt{(R+Lp)/(G+Cp)}$$
$$=\sqrt{\frac{L}{C}}\left[1+\frac{1}{p}\left(\frac{R}{2L}-\frac{G}{2C}\right)+\ldots\right] \quad (1)$$

where R, L, G, C are the resistance, the inductance, the conductance, and the capacitance of the line for a unit length, it is assumed that only the first term in the series is necessary. From this point on it will then be assumed that $Z_0=\sqrt{L/C}$. Similarly for the propagation constant γ the operational expression is

$$\gamma=\sqrt{(R+Lp)(G+Cp)}$$
$$=p\sqrt{LC}\left[1+\frac{1}{p}\left(\frac{R}{2L}-\frac{G}{2C}\right)-\frac{1}{8p^2}\left(\frac{R}{L}-\frac{G}{C}\right)^2+\ldots\right] \quad (2)$$

and only the first two terms in the series will be used so that

$$\gamma=(p/V)+a \quad (3)$$

where $V=1/\sqrt{LC}$ = velocity of propagation of the waves and

$$a=\frac{R}{2}\sqrt{\frac{C}{L}}+\frac{G}{2}\sqrt{\frac{L}{C}}=\text{attenuation constant}$$

To show how the various methods may be used to determine the steady-state waves appearing on a transmission line, a particular example will be employed. This example is that of a line with a square-wave generator connected to one end while the other end is open-circuited. The voltage e_R at the open end is to be determined. The generator is assumed to have zero internal impedance, and the generated voltage e_g is shown in Figure 1. The steady-state transform[4] E_g of the generated voltage is

$$E_g=\frac{E}{p}(1-\epsilon^{-pT/2})^2 \quad (4)$$

The steady-state transform E_R of the voltage at the open end of the line is

$$E_R=\frac{E_g}{\cosh \gamma l} \quad (5)$$

where l is the length of the line. The voltage is then

$$e_R=\frac{1}{2\pi j}\int_W \frac{\epsilon^{pt}E(1-\epsilon)^{-pT/2}dp}{p(1-\epsilon^{-pT})\cosh\left[(pl/V)+al\right]} \quad (6)$$

where W is a certain path of integration[4] in the p-plane. If the substitutions $p'=pT$, $\beta=(l/VT)$, $\alpha=al$ and $\theta=(t/T)$ are made in equation 6,

$$\frac{e_R}{E}=\frac{1}{2\pi j}\int_W \frac{\epsilon^{p'\theta}(1-\epsilon^{-p'/2})^2dp'}{p'(1-\epsilon^{-p'})\cosh(p'\beta+\alpha)} \quad (7)$$

The primes now will be omitted.

The first method of evaluating the integral of equation 7 uses the poles within the path W, sometimes called the driving function or "voltage" poles, and leads to the usual Fourier series for the voltage e_R. These poles are $p=\pm j2\pi n$ where n is a positive integer or zero. When the residues at each one of these poles are added, the result is

$$\frac{e_R}{E}=\sum_{n=1}^{\infty} Y_n \sin(2n\pi\theta-\delta) \quad (8)$$

which is summed over all odd integral values of n and in which

$$Y_n=4/n\pi\sqrt{\sinh^2 a+\cos^2 2n\pi\beta}$$

and

$$\delta=\tan^{-1}\left[(\tanh a)(\tan 2n\pi\beta)\right]$$

The even harmonic voltages are absent in e_R since there are none in the applied square wave of voltage. The result of equation 8 is useful in determining the amount of harmonic voltages present, but is of very little use in determining the actual waveforms present except in some very special cases. One such special case is that for $\alpha=0$ and $\beta=1/6$ which means that the losses in the transmission line are zero and that a wave on the line travels the length of the line in one-sixth of the period of the applied square wave. From equation 8 the open end voltage is

$$\frac{e_R}{E}=2\left[\frac{4}{\pi}\sum_{n=}^{\infty}\frac{\sin 2n\pi\theta}{n}\right]-\left[\frac{4}{\pi}\sum_{n=1}^{\infty}\frac{\sin 6n\pi\theta}{n}\right] \quad (9)$$

Paper 50-244, recommended by the AIEE Basic Sciences Committee and approved by the AIEE Technical Program Committee for presentation at the AIEE Fall General Meeting, Oklahoma City, Okla., October 23-27, 1950. Manuscript submitted March 13, 1950; made available for printing August 30, 1950.

D. L. WAIDELICH is with the University of Missouri, Columbia, Mo.

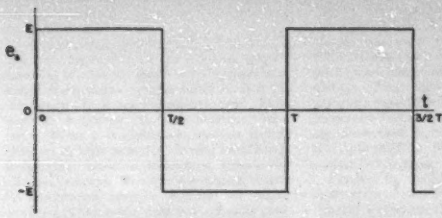

Figure 1. The square-wave voltage e_S of the generator

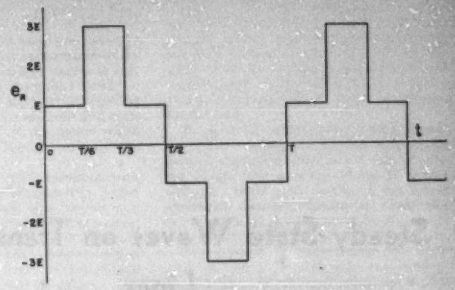

Figure 2. The open-end voltage e_R of the transmission line with no attenuation ($\alpha=0$)

which are summed over all odd integral values of n. The first series of equation 9 is a square wave of amplitude $2E$ and period T, while the second is a square wave of amplitude E and period $(T/3)$. The resulting wave is shown in Figure 2, and this may be called the sum function of the series of equation 9.

For circuits with concentrated parameters the sum function of the Fourier series may be obtained without difficulty by using the poles outside the path W, sometimes called the system-function or "impedance" poles. In most circuits these poles are finite in number and thus lead to an expression with a finite number of terms. This approach was tried as the second method of evaluating the integral of equation 7. The poles are $-(\alpha/\beta)\pm j(m\pi/2\beta)$, where m is an odd positive integer. Since there are again an infinite number of poles, the resulting expression[4] is an infinite series somewhat resembling a Fourier series. When $0<\theta<1/2$, the voltage at the open-circuited end is

$$\frac{e_R}{E}=\frac{1}{\cosh\alpha}+\sum_{m=1}^{\infty}\frac{(-1)^{\frac{m+1}{2}}4\epsilon^{-\sigma\theta}}{\beta(\sigma^2+\mu^2)}A_m \quad (10)$$

in which

m = an odd positive integer

$$A_m=\frac{\sigma[\sin\mu\theta+\epsilon^{-\sigma/2}\sin\mu(\theta-1/2)]+\mu[\cos\mu\theta+\epsilon^{-\sigma/2}\cos\mu(\theta-1/2)]}{[1+2\epsilon^{-\sigma/2}\cos(\mu/2)+\epsilon^{-\sigma}]}$$

$\sigma=\alpha/\beta$

$\mu=m\pi/2\beta$

Again this is useful in determining waveforms only in some special cases such as the one used in the preceding paragraph. If $\alpha=0$ and $\beta=1/6$, the result is a Fourier series similar to equation 9 but not the same series.

$$\frac{e_R}{E}=1+\frac{4}{\pi}\sum_{m=1}^{\infty}\frac{\sin 3\pi m\theta}{m}-\frac{4}{\pi}\sum_{m=1}^{\infty}(-1)^{\frac{m-1}{2}}\frac{\cos 3\pi m\theta}{m} \quad (11)$$

in which m is an odd positive integer. The second term of equation 11 is a square wave of amplitude E and period $(2T/3)$, while the third term is a square wave of the same amplitude and period but shifted in phase by $(T/6)$. When the three terms of equation 11 are added, the result is again the wave of Figure 2.

The third method involves the use of steady-state convolution or "faltung" integrals.[5] Let $A(t)$ be the voltage at the open end of the line when a unit voltage is suddenly applied[3] to the generator end of the line, and $A(t)=A(\infty)+R(t)$ where $A(\infty)$ is a constant approached by $A(t)$ as t becomes very large and then $R(t)$ approaches zero as t becomes large. The form of the steady-state convolution integral to be used is:

$$e_R=A(\infty)e_s(t)+\frac{d}{dt}\int_0^T e_s(t-\tau)P(\tau)d\tau \quad (12)$$

where

$$P(t)=\sum_{n=0}^{\infty}R(t+nT)$$

and n is a positive integer or zero. In the example at hand, from $\theta=0$ to $\theta=\beta$, $A(t)=0$, and from $\theta=m\beta$ to $(m+2)\beta$, where m is an odd positive integer,

$$A(t)=2\epsilon^{-\alpha}\left[\frac{1+(-1)^{\frac{m-1}{2}}\epsilon^{-(m+1)\alpha}}{1+\epsilon^{-2\alpha}}\right] \quad (13)$$

Then

$$A(\infty)=2\epsilon^{-\alpha}/(1+\epsilon^{-2\alpha}) \quad (14)$$

and also from $\theta=0$ to $\theta=\beta$, $R(t)=-2\epsilon^{-\alpha}/(1+\epsilon^{-2\alpha})$, and from $\theta=m\beta$ to $\theta=(m+2)\beta$, where m is an odd positive integer

$$R(t)=(-1)^{\frac{m-1}{2}}\frac{2\epsilon^{-(m+1)\alpha}}{1+\epsilon^{-2\alpha}} \quad (15)$$

Then for the special case of $\beta=1/6$, from $\theta=0$ to $\theta=1/6$,

$$P(t)=\frac{-2\epsilon^{-\alpha}}{(1+\epsilon^{-3\alpha})(1+\epsilon^{-4\alpha})}$$

and from $\theta=m/6$ to $\theta=(m+2)/6$ where m is an odd positive integer

$$P(t)=(-1)^{\frac{m-1}{2}}\frac{2\epsilon^{-(m+1)\alpha}}{(1+\epsilon^{-3\alpha})(1+\epsilon^{-4\alpha})} \quad (16)$$

With the aid of equations 12, 14, and 16 and in the interval from $\theta=0$ to $\theta=1/6$:

$$e_R=\frac{2E(-\epsilon^{-\alpha}+\epsilon^{-3\alpha}+\epsilon^{-5\alpha})}{(1+\epsilon^{-4\alpha})}$$

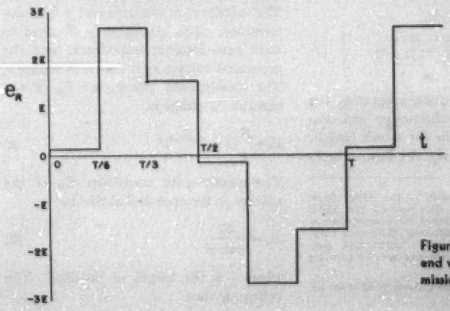

Figure 3 (left). The open-end voltage e_R of the transmission line with attenuation ($\alpha=0.2$)

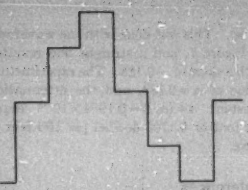

Figure 4. The calculated output voltage of the line for an applied square wave

from $\theta=1/6$ to $\theta=1/3$

$$e_R=\frac{2E(e^{-\alpha}+e^{-3\alpha}+e^{-5\alpha})}{(1+e^{-6\alpha})} \tag{17}$$

and from $\theta=1/3$ to $\theta=1/2$

$$e_R=\frac{2E(e^{-\alpha}+e^{-3\alpha}-e^{-5\alpha})}{(1+e^{-6\alpha})}$$

The values of e_R for the second half cycle from $\theta=1/2$ to $\theta=1$ are the negatives of those given in equation 17. When $\alpha=0$, the receiving end voltage as calculated from equation 17 is again the wave of Figure 2. For a line with losses the wave is not quite so symmetrical as is shown in Figure 3 for the case of $\alpha=0.2$.

The fourth method depends upon an extension and summation of the various waves obtained from the response $A(t)$ to a unit voltage. Consider

$$A(t)=\frac{1}{2\pi j}\int_{W_1}\frac{e^{p\theta}(1-e^{-p/2})^2dp}{p(1-e^{-p})\cosh(p\beta+\alpha)} \tag{18}$$

where W_1 is the usual path of integration for the inverse Laplacian transform and is to the right and parallel to the imaginary axis. Equation 18 should be compared with equation 7. By use of the series:

$$\frac{(1-e^{-p/2})^2}{1-e^{-p}}=1-2e^{-p/2}+2e^{-p}-2e^{-3p/2}+\ldots.$$

and

$$\frac{1}{\cosh(p\beta+\alpha)}=2e^{-(p\beta+\alpha)}-2e^{-3(p\beta+\alpha)}+2e^{-5(p\beta+\alpha)}-\ldots.$$

the response to the unit voltage is

$$A(t)=\sum_{m=1}^{\infty}A_m(t) \tag{19}$$

where m is an odd integer and

$$A_m(t)=\frac{1}{2\pi j}\int_{W_1}(-1^{\frac{m-1}{2}}2e^{-m(p\beta+\alpha)})\times[1-2e^{-p/2}+2e^{-p}-2e^{-3p/2}+\ldots.]\times\frac{e^{-p\theta}}{p}dp$$

In the problem used as an example $\beta=1/6$. Consider one of the terms in the series for $A(t)$, say

$$A_3(t)=(-2)\frac{1}{2\pi j}\int_{W_1}e^{-3(p/3+\alpha)}\times[1-2e^{-p/2}+2e^{-p}-\cdots]\frac{e^{p\theta}}{p}dp$$

which represents a square wave beginning at $\theta=1/2$ and with an amplitude of $2e^{-3\alpha}$. This square wave should be continued or extended back to $\theta=0$. Each one of the square waves for each of the A_m's should be extended back in a like manner to $\theta=0$. All of the square waves may then be summed to give the required steady-state output voltage e_R. The result is for $0<\theta<1/6$.

$$\frac{e_R}{E}=-2e^{-\alpha}+2e^{-3\alpha}+2e^{-5\alpha}+2e^{-7\alpha}-2e^{-9\alpha}-2e^{-11\alpha}-2e^{-13\alpha}+\ldots.$$

$$=\frac{-2e^{-\alpha}+2e^{-3\alpha}+2e^{-5\alpha}}{1+e^{-6\alpha}}$$

for $1/6<\theta<1/3$

$$\frac{e_R}{E}=\frac{2e^{-\alpha}+2e^{-3\alpha}+2e^{-5\alpha}}{1+e^{-6\alpha}} \tag{20}$$

for $1/3<\theta<1/2$

$$\frac{e_R}{E}=\frac{2e^{-\alpha}+2e^{-3\alpha}-2e^{-5\alpha}}{1+e^{-6\alpha}}$$

These results are identical with equation 17 and will thus give the waves of Figures 2 and 3.

Experimental Results

In the experimental work a square-wave generator with a high output impedance was used with a length of *RG-8/U* coaxial cable, and the voltage across the other end of the cable was observed with a high-impedance cathode-ray oscilloscope. For this purpose then both ends of the cable were effectively open circuited. Under these conditions the operational voltage at the receiving end is

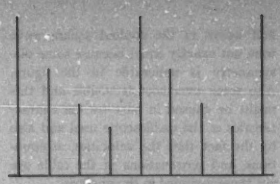

Figure 6. The calculated output voltage of the line for an applied pulse wave

$$E_R=\frac{Z_0V_g}{R_g\sinh\gamma l} \tag{21}$$

where V_g is the transform of the generator voltage and R_g is the output impedance (considered a pure resistance) of the generator. By the use of the fourth method given in the analysis section for $\beta=1/12$, it is found that for

$$0<\theta<1/12,\quad \frac{e_R}{E}=\frac{Z_0}{R_g}\left[\frac{-2e^{-\alpha}-2e^{-3\alpha}-2e^{-5\alpha}}{1+e^{-6\alpha}}\right]$$

for $1/12<\theta<1/4$

$$\frac{e_R}{E}=\frac{Z_0}{R_g}\left[\frac{2e^{-\alpha}-2e^{-3\alpha}-2e^{-5\alpha}}{1+e^{-6\alpha}}\right]$$

for $1/4<\theta<5/12$

$$\frac{e_R}{E}=\frac{Z_0}{R_g}\left[\frac{2e^{-\alpha}+2e^{-3\alpha}-2e^{-5\alpha}}{1+e^{-6\alpha}}\right] \tag{22}$$

for $5/12<\theta<1/2$

$$\frac{e_R}{E}=\frac{Z_0}{R_g}\left[\frac{2e^{-\alpha}+2e^{-3\alpha}+2e^{-5\alpha}}{1+e^{-6\alpha}}\right]$$

where E is the peak value of the applied square wave.

The calculated receiving end voltage e_R for $\alpha=0.2$ and $\beta=1/12$ is shown in Figure 4, and the experimental wave form is that of Figure 5. Evidently the two

Figure 5 (left). The experimental output voltage of the line for an applied square wave

Figure 7 (right). The experimental output voltage of the line for an applied pulse wave

half waves of the applied square wave were not exactly equal because some dissymmetry is noticeable in the figure. Also some overshoot is visible and this might be caused in part by the characteristics of the oscilloscope used and also by the fact that the velocities, attenuations, and terminations of the cable are not those assumed in the analysis.

The action of repeated pulses[4] on a transmission line also was studied. If E is the transform of the applied repeated pulses, the output voltage e_R will be calculated for a transmission line effectively open circuited at both ends. Again using the fourth method given in the analysis section for $\beta=1/8$, it is found that

at $\theta=1/8$

$$e_R=\frac{Z_0E}{R_gT}\left(\frac{2\epsilon^{-\alpha}}{1-\epsilon^{-2\alpha}}\right)$$

at $\theta=3/8$

$$e_R=\frac{Z_0E}{R_gT}\left(\frac{2\epsilon^{-3\alpha}}{1-\epsilon^{-2\alpha}}\right) \tag{23}$$

at $\theta=5/8$

$$e_R=\frac{Z_0E}{R_gT}\left(\frac{2\epsilon^{-5\alpha}}{1-\epsilon^{-2\alpha}}\right)$$

at $\theta=7/8$

$$e_R=\frac{Z_0E}{R_gT}\left(\frac{2\epsilon^{-7\alpha}}{1-\epsilon^{-2\alpha}}\right)$$

The output voltage would then be four pulses per period as shown in Figure 6 which was calculated for $\alpha=0.2$. The experimental wave form is shown in Figure 7, and it was obtained using a pulse length of 0.5 microsecond and a pulse repetition rate of 84.3 kc per second on a 957-foot length of *RG 8/U* coaxial cable. The velocity of propagation may be obtained from

$$V=l/\beta T=1.97\times10^8 \text{ meters per second} \tag{24}$$

and the velocity factor, that is, the ratio of the velocity of the pulses on the line and the velocity of light in space, is 65.7 per cent. From equation 24, at $\theta=n/8$ where n is 1, 3, 5, or 7, e_R is proportional to $\epsilon^{-n\alpha}$. If $\ln e_R$ is plotted versus n, the result should be a straight line of slope $(-\alpha)$. This was done with the waveform of Figure 7, and a straight line resulted with a slope of -0.188. The experimental value of $\alpha=0.188$, and the attenuation constant $a=(\alpha/l)=0.1964\times10^{-3}$ neper per foot or 0.1703 decibel per 100 feet of cable.

References

1. Pulse Echo Measurements on Telephone and Television Facilities, L. G. Abraham, A. W. Lebert, J. B. Maggio, J. T. Schott. *AIEE Transactions*, volume 66, 1947, pages 541–48.

2. Transformation Calculus and Electrical Transients (book), S. Goldman. Prentice-Hall, Inc., New York, N. Y., 1949, pages 256–318.

3. Modern Operational Calculus (book), N. W. McLachlan. The MacMillan Company, New York, N. Y., 1948, pages 78–99.

4. The Steady-State Operational Calculus, D. L. Waidelich. *Proceedings*, Institute of Radio Engineers (New York, N. Y.), volume 34, 1946, pages 78–83.

5. Steady State Currents of Electrical Networks, D. L. Waidelich. *Journal of Applied Physics* (New York, N. Y.), volume 13, 1942, pages 706–12.

6. Response of Circuits to Steady-State Pulses, D. L. Waidelich. *Proceedings*, Institute of Radio Engineers (New York, N. Y.), volume 37, 1949, pages 1396–1401.

No Discussion

Transients in Coupled Inductance-Capacitance Circuits Analyzed in Terms of a Rolling-Ball Analogue

P. C. MAGNUSSON
MEMBER AIEE

AN ELECTRIC system consisting of two inductance-capacitance loops with negligible resistance, and inductively coupled together, has a dynamical analogue in the form of a freely rolling ball on an elevated surface. The time integrals of the loop currents are used as the co-ordinates, with the loop currents themselves analogous to the velocity of the ball along those co-ordinates. The magnetic field energy becomes analogous to the kinetic energy of the ball if the scales of the co-ordinates are made proportional to the square roots of the corresponding self inductances, and are inclined with respect to each other at the angle whose cosine is the coefficient of coupling.

The height of the surface, and hence the potential energy of the ball, is made proportional to the dielectric field energy at each co-ordinate position. Contours of dielectric field energy are concentric ellipses, the axes of which also are known as the normal co-ordinates. General motion of the ball on the surface may be resolved into two independent component motions parallel to those axes.

Geometrical representation of the ball path and of mathematical quantities associated with it aids in the interpretation of transients in systems with two degrees of freedom. By suitable choice of vertical and horizontal scales, a physical model may be designed with a known ratio between its time scale and that of the original circuit.

Advances of the last two to four decades in the study of linear transients have been primarily in the refinement and extension of mathematical procedures, notably operational calculus and the Laplace transform. Energy is not dealt with directly in applying those techniques, and its encompassing role in relating physically a particular set of initial conditions to the corresponding response tends to be neglected. The rolling-ball analogue, which emphasizes the significance of energy in the physical problem, gives a geometrical presentation which unifies the transient behavior of a lumped-constant system.

Two inductance-capacitance loops inductively coupled together will be used as the basic example. Two degrees of freedom make a system considerably more complicated than one with a single degree of freedom, and are sufficient to give a good insight into multiple degree of freedom cases in general.

Derivation of Analogue

Two physical systems are said to be analogous if they give rise to mathematically similar equations of motion. The analogue developed here is that of a freely rolling ball on a curved surface, wherein the path followed by the ball corresponds, in terms of appropriately oriented and scaled co-ordinates in the base plane, to the response of the original system.

Since the equations of motion are derivable by Lagrange's method[1] from the potential and kinetic energies, the parallel nature of analogous systems appears in those quantities. With comparison of expressions for energy in the two systems as the plan of attack, the analogue may be conveniently derived.

Let the quantity of electricity or charge q be chosen as the dynamical co-ordinate of an inductance-capacitance (L-C) circuit; the energy stored in the capacitor may be readily expressed in terms of q, and the energy stored in the magnetic field is proportional to the square of the current, which is the time rate of change of q, or dq/dt.

The potential energy of the ball is proportional to the height of the surface, which is a function of location in the base-plane co-ordinates. Kinetic energy, on the other hand, is proportional to the square of the velocity, or time derivative of position along the co-ordinates. It follows that analogies should be sought between kinetic energy and magnetic field energy, and between potential energy and dielectric field energy.

It is assumed that the vertical component of the ball velocity in the analogue is small compared with the horizontal component, so that the latter may be considered equal in magnitude to the total velocity. A further assumption is that gyroscopic effects in the ball are negligible.

Generalized co-ordinates which are directly proportional to linear displacement will be used as measures in the base plane of the analogue in this discussion. Determination of the correct vertical and horizontal scales in a physical model to obtain a prescribed ratio of time scales

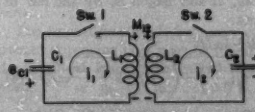

Figure 1. Circuit for which analogue is derived

Paper 50-245, recommended by the AIEE Basic Sciences Committee and approved by the AIEE Technical Program Committee for presentation at the AIEE Fall General Meeting, Oklahoma City, Okla., October 23-27, 1950. Manuscript submitted March 7, 1950; made available for printing August 29, 1950.

P. C. MAGNUSSON is Assistant Professor of Electrical Engineering, Oregon State College, Corvallis, Oreg.

Part of the study and research for this paper was sponsored by the Engineering Experiment Station at Oregon State College.

between the model and the electric circuit is discussed in the Appendix.

Magnetic Field and Kinetic Energies

The energy stored in the magnetic field at any instant in the circuit shown in Figure 1 is:

$$W_L = (^1/_2)(L_1 i_1^2 + L_2 i_2^2 - 2M_{12} i_1 i_2) = (^1/_2)\left[L_1\left(\frac{dq_1}{dt}\right)^2 + L_2\left(\frac{dq_2}{dt}\right)^2 - 2M_{12} \times \frac{dq_1}{dt}\frac{dq_2}{dt}\right] \quad (1)$$

Kinetic energy is independent of the direction of the velocity vector, hence the generalized co-ordinates representing q_1 and q_2 in the analogue should be scaled with respect to those quantities so that a given magnitude of velocity will always correspond to the same amount of magnetic field energy. The first step towards obtaining this correspondence is to define the generalized co-ordinates x_1 and x_2 as follows:

$$\left.\begin{aligned} x_1 &= q_1\sqrt{L_1} \\ x_2 &= q_2\sqrt{L_2} \end{aligned}\right\} \quad (2)$$

Differentiation of equations 2 yields:

$$\left.\begin{aligned} \frac{dx_1}{dt} &= \frac{dq_1}{dt}\sqrt{L_1} \\ \frac{dx_2}{dt} &= \frac{dq_2}{dt}\sqrt{L_2} \end{aligned}\right\} \quad (3)$$

Substitution of equations 3 into equation 1 gives the following:

$$W_L = (^1/_2)\left[\left(\frac{dx_1}{dt}\right)^2 + \left(\frac{dx_2}{dt}\right)^2 - 2\left(M_{12}/\sqrt{L_1L_2}\right)\frac{dx_1}{dt}\frac{dx_2}{dt}\right] \quad (4)$$

The coefficient of coupling k may be substituted here.

$$k_{12} = M_{12}/\sqrt{L_1L_2} \quad (5)$$

$$W_L = (^1/_2)\left[\left(\frac{dx_1}{dt}\right)^2 + \left(\frac{dx_2}{dt}\right)^2 - 2k_{12}\frac{dx_1}{dt}\frac{dx_2}{dt}\right] \quad (6)$$

The generalized velocities dx_1/dt and dx^2/dt are vectors in the co-ordinate plane, and will be assumed to be separated by angle β, defined as follows:

$$\cos\beta = -k_{12} \quad (7)$$

This situation is sketched in Figure 2; the vector sum of the component velocities dx_1/dt and dx_2/dt is, by the law of cosines:

$$|dx_1/dt + dx_2/dt| = \sqrt{\left(\frac{dx_1}{dt}\right)^2 + \left(\frac{dx_2}{dt}\right)^2 + 2\frac{dx_1}{dt}\frac{dx_2}{dt}\cos\beta} \quad (8)$$

Hence

$$W_L = (^1/_2)|dx_1/dt + dx_2/dt|^2 \quad (9)$$

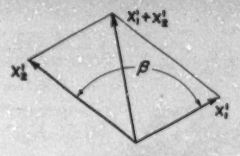

Figure 2. Vector addition of velocity components

Thus if the co-ordinates representing q_1 and q_2 in the analogue are laid out at angle β with respect to each other, and with scales (in terms of coulombs) proportioned in accordance with equations 2, the kinetic energy of the ball will be analogous to the total magnetic field energy of the coupled L-C circuits.

Dielectric Field and Potential Energies

The energy stored in the dielectric form in capacitors C_1 and C_2 is:

$$W_C = (^1/_2)(C_1e_1^2 + C_2e_2^2) \quad (10)$$

$$= (^1/_2)[(q_1^2/C_1) + (q_2^2/C_2)] \quad (11)$$

Substitution of the generalized co-ordinates defined in equations 2 gives the following expression:

$$W_C = (^1/_2)[(x_1^2/L_1C_1) + (x_2^2/L_2C_2)] \quad (12)$$

The potential energy of the ball in the analogue is proportional to the height h of the surface, hence h is proportional to the right-hand side of equation 12.

Transformation to Normal Co-ordinates

When the motion is analyzed in terms of the oblique co-ordinates used thus far (x_1,x_2), a set of two simultaneous equations results, both of which involve two dependent variables. With W_C a quadratic function of the x_1,x_2 co-ordinates, it is possible to select a set of rectangular co-ordinates in terms of which each equation of motion contains only one dependent variable. These are known as the normal co-ordinates,[1] and will be designated by y_1, y_2.

Orientation of Normal Co-ordinates

Contours of the W_C surface, or loci of constant values of W_C, prove to be ellipses and, as will be seen, the normal co-ordinates are parallel to the axes of these ellipses. Co-ordinate y_1 will be considered as displaced by angle α from x_1, as shown in Figure 3, and angle α will next be evaluated.

$$\left.\begin{aligned} y_1 &= x_1\cos\alpha + x_2\cos(\beta-\alpha) \\ y_2 &= -x_1\sin\alpha + x_2\sin(\beta-\alpha) \end{aligned}\right\} \quad (13)$$

Equations 13 are solved for x_1 and x_2.

$$\left.\begin{aligned} x_1\sin\beta &= y_1\sin(\beta-\alpha) - y_2\cos(\beta-\alpha) \\ x_2\sin\beta &= y_1\sin\alpha + y_2\cos\alpha \end{aligned}\right\} \quad (14)$$

Equations 14 are substituted into equation 12.

$$W_C = [1/(2\sin^2\beta)]\{(1/L_1C_1)[y_1^2 \times \sin^2(\beta-\alpha) - 2y_1y_2\sin(\beta-\alpha) \times \cos(\beta-\alpha) + y_2^2\cos^2(\beta-\alpha)] + (1/L_2C_2)[y_1^2\sin^2\alpha + 2y_1y_2 \times \sin\alpha\cos\alpha + y_2^2\cos^2\alpha]\} \quad (15)$$

If y_1 and y_2 are to be parallel to the axes of the ellipse, the sum of the terms involving the product y_1y_2 must be zero, hence:

$$-(1/L_1C_1)\sin(\beta-\alpha)\cos(\beta-\alpha) + (1/L_2C_2)\sin\alpha\cos\alpha = 0 \quad (16)$$

This reduces as follows:

$$-\sin 2(\beta-\alpha) + [(L_1C_1)/(L_2C_2)]\sin 2\alpha = 0$$

$$-\sin 2\beta\cos 2\alpha + \cos 2\beta\sin 2\alpha + [(L_1C_1)/(L_2C_2)]\sin 2\alpha = 0$$

$$\tan 2\alpha = (\sin 2\beta)/\{[(L_1C_1)/(L_2C_2)] + \cos 2\beta\} \quad (17)$$

Equations of Motion

Expressions for W_C and W_L in terms of the normal co-ordinates may be substituted into Lagrange's equation[1] to obtain the equations of motion.

$$\left.\begin{aligned} &\partial(W_C - W_L)/\partial y_1 - d[\partial(W_C - W_L)/\partial dy_1/dt]/dt = 0 \\ &\partial(W_C - W_L)/\partial y_2 - d[\partial(W_C - W_L)/\partial dy_2/dt]/dt = 0 \end{aligned}\right\} \quad (18)$$

Equation 15 states W_C in terms of the normal co-ordinates, but it may be simplified by subtracting equation 16.

$$W_C = [1/(2\sin^2\beta)]\{(1/L_1C_1)[y_1^2 \times \sin^2(\beta-\alpha) + y_2^2\cos^2(\beta-\alpha)] + (1/L_2C_2)[y_1^2\sin^2\alpha + y_2^2\cos^2\alpha]\} \quad (19)$$

An expression for W_L in terms of dy_1/dt and dy_2/dt, the generalized velocities along y_1 and y_2, may be obtained by substituting equations 14 (with velocities dx_1/dt, dx_2/dt, dy_1/dt and dy_2/dt substituted for co-ordinates x_1, x_2, y_1, and y_2) into equation 6. After simplification of the trigonometric forms, the following is obtained:

$$W_L = (^1/_2)\left[\left(\frac{dy_1}{dt}\right)^2 + \left(\frac{dy_2}{dt}\right)^2\right] \quad (20)$$

Upon substituting equations 19 and 20 into equations 18, these equations of motion result:

$$\left.\begin{aligned} &(1/\sin^2\beta)[(1/L_1C_1)\sin^2(\beta-\alpha) + (1/L_2C_2)\sin^2\alpha]y_1 + d^2y_1/dt^2 = 0 \\ &(1/\sin^2\beta)[(1/L_1C_1)\cos^2(\beta-\alpha) + (1/L_2C_2)\cos^2\alpha]y_2 + d^2y_2/dt^2 = 0 \end{aligned}\right\} \quad (21)$$

Equations 21 may be solved by the following substitutions:

$$\left.\begin{aligned} y_1 &= A_1\sin\omega_1 t + B_1\cos\omega_1 t \\ y_2 &= A_2\sin\omega_2 t + B_2\cos\omega_2 t \end{aligned}\right\} \quad (22)$$

These values are found for ω_1 and ω_2:

$$\left.\begin{aligned}\omega_1 &= (1/\sin\beta)\times\\ &\sqrt{(1/L_1C_1)\sin^2(\beta-\alpha)+(1/L_2C_2)\sin^2\alpha}\\ \omega_2 &= (1/\sin\beta)\times\\ &\sqrt{(1/L_1C_1)\cos^2(\beta-\alpha)+(1/L_2C_2)\cos^2\alpha}\end{aligned}\right\} \quad (23)$$

The quantities A_1, A_2, B_1, and B_2 in equations 23 are arbitrary constants; they are found to be the following in terms of the initial values of y_1, y_2, dy_1/dt and dy_2/dt:

$$\left.\begin{aligned}y_1(0) &= B_1\\ y_1'(0) &= \omega_1 A_1\\ y_2(0) &= B_2\\ y_2'(0) &= \omega_2 A_2\end{aligned}\right\} \quad (24)$$

In terms of the initial voltages on the capacitors and the initial currents in the coils, these initial conditions are (substituting equations 2 into 13):

$$\left.\begin{aligned}y_1(0) &= e_1(0)C_1\sqrt{L_1}\cos\alpha+\\ &\quad e_2(0)C_2\sqrt{L_2}\cos(\beta-\alpha)\\ \frac{dy_1}{dt}(0) &= i_1(0)\sqrt{L_1}\cos\alpha+\\ &\quad i_2(0)\sqrt{L_2}\cos(\beta-\alpha)\\ y_2(0) &= -e_1(0)C_1\sqrt{L_1}\sin\alpha+\\ &\quad e_2(0)C_2\sqrt{L_2}\sin(\beta-\alpha)\\ \frac{dy_2}{dt}(0) &= -i_1(0)\sqrt{L_1}\sin\alpha+\\ &\quad i_2(0)\sqrt{L_2}\sin(\beta-\alpha)\end{aligned}\right\} \quad (25)$$

The voltages across the capacitors may be found as functions of time by substituting equations 22 into 14, and the latter into equations 2.

$$\left.\begin{aligned}e_1 &= [1/(C_1\sqrt{L_1}\sin\beta)][\sin(\beta-\alpha)\times\\ &\quad (A_1\sin\omega_1 t+B_1\cos\omega_1 t)-\\ &\quad \cos(\beta-\alpha)(A_2\sin\omega_2 t+\\ &\quad B_2\cos\omega_2 t)]\\ e_2 &= [1/(C_2\sqrt{L_2}\sin\beta)][\sin\alpha(A_1\times\\ &\quad \sin\omega_1 t+B_1\cos\omega_1 t)+\cos\alpha(A_2\\ &\quad \sin\omega_2 t+B_2\cos\omega_2 t)]\end{aligned}\right\} \quad (26)$$

These results agree with those obtained by operational solution of the loop circuital equations, and are in a form adapted to graphical interpretation.

Analysis of Analogue

An isometric projection of part of a typical analogue surface is shown in Figure 4. (Data are listed in Table I.) The surface, which has been proportioned in accordance with the theory just developed, is a paraboloid with elliptical cross-section, and extends upwards indefinitely on all sides. The path followed by a freely rolling ball on this surface will have projections on the oblique base co-ordinates x_1,x_2 which will correspond identically, except for change in time scale, to the oscillations of the respective parts of the circuit. These co-ordinates have been scaled in terms of charge; corresponding capacitor voltages may be found by dividing the charge by the respective capacitance.

Paths of motion projected onto the base plane may be described, in the terminology of mathematical physics, as paths of the representative point of configuration space (2-dimensional here); such paths are sketched in Figures 3 and 6 for two particular sets of initial conditions. Capacitors C_1 and C_2 are charged to some initial voltage; switches 1 and 2 (Figure 1) are closed simultaneously in the first case, while in the second example, switch 1 is closed shortly before switch 2. Since the circuit is nondissipative, the total energy of the system remains constant at the initial value, and the W_C contour corresponding to this initial energy (the same in both examples) is shown in Figures 3, 4, and 6. The axes of this elliptical contour are colinear with the normal co-ordinate axes.

Example with Initial Charges but No Initial Current

The geometric framework within which the ball path is plotted in Figure 3 may be constructed in this manner: The co-ordinate axes x_1 and x_2 are laid out at angle β (equation 7) with respect to each other, and angle α is found from equation 17, after which the axes of the normal co-ordinates may be drawn. The initial charges are scaled on the x_1 and x_2 axes, with oa equal to $q_1(0)\sqrt{L_1}$, (or $e_1(0)\ C_1\sqrt{L_1}$), and ob equal to $q_2(0)\sqrt{L_2}$ (or $e_2(0)\ C_2\sqrt{L_2}$). A parallelogram is formed by drawing bc parallel to oa, and ac parallel to ob. The value of W_C at point c represents the initial energy, and the contour previously mentioned therefore passes through point c. (Drawing of the contour is not an essential part of this graphical construction, however.) Line cd is drawn perpendicular to normal co-ordinate y_1, and ce, perpendicular to y_2. Comparison with the first and third of equations 25 indicates that od is $y_1(0)$, and equal to B_1, the amplitude of the cosine oscillatory motion in the analogue with frequency of $\omega_1/2\pi$, and that oe is $y_2(0)$, equal to B_2, the amplitude of the cosine motion with frequency of $\omega_2/2\pi$. Because there are no initial currents in this example, the coefficients of the sine terms, A_1 and A_2, are zero.

The amplitude of each frequency component appearing in e_1 may be found by drawing lines df and eg parallel to the x_1 axis.

$$e_1 = [of/(C_1\sqrt{L_1})]\cos\omega_1 t+ [og/(C_1\sqrt{L_2})]\cos\omega_2 t \quad (27)$$

Table I. Parameters, Initial Conditions and Derived Quantities for Numerical Examples

Item	Value	Reference
L_1	0.08 henry	Figure 1 (assumed)
L_2	0.10 henry	Figure 1 (assumed)
C_1	75 microfarads	Figure 1 (assumed)
C_2	100 microfarads	Figure 1 (assumed)
k_{12}	0.4	Equation 5 (assumed)
β	113 degrees 35 minutes	Equation 7
α	41 degrees 58 minutes	Equation 17
ω_1	481 radians per second	Equation 23
ω_2	392 radians per second	Equation 23
Example A: At Simultaneous Closing of Switches at t Equals Zero		
$e_1(0)$	240 volts	Figure 1 (assumed)
$e_2(0)$	250 volts	Figure 1 (assumed)
$i_1(0)$	0 ampere	Figure 1 (assumed)
$i_2(0)$	0 ampere	Figure 1 (assumed)
$q_1(0)$	1.8×10^{-3} coulombs	$C_1e_1(0)$
$q_2(0)$	2.5×10^{-3} coulombs	$C_2e_2(0)$
$W_C(0)$	5.28 joules	Equation 11
$z_1(0)$	5.09×10^{-3} coulomb $\sqrt{\text{henry}}$	Equation 2; Figure 3 oa
$z_2(0)$	7.90×10^{-3} coulomb $\sqrt{\text{henry}}$	Equation 2; Figure 3 ob
$y_1(0)$	6.27×10^{-3} coulomb $\sqrt{\text{henry}}$	Equations 13, 25; Figure 3 od
$y_2(0)$	4.09×10^{-3} coulomb $\sqrt{\text{henry}}$	Equations 13, 25; Figure 3 oe
Example B: Switch 1 Closed at t Equals —0.003 Second; Switch 2 Closed at t Equals Zero		
$e_1(-0.003)$	240 volts	Figure 1 (assumed)
$1/\sqrt{L_1C_1}$	408 radians per second	Equations 29
$e_1(0)$	81.1 volts	Equations 29
$i_1(0)$	—6.90 amperes	Equations 29
$e_2(0)$	250 volts	Figure 1 (assumed)
$i_2(0)$	0 ampere	Figure 1 (assumed)
$W_C(-0.003)$	5.28 joules	Equation 11
$q_1(0)$	0.61×10^{-3} coulombs	$C_1e_1(0)$
$q_2(0)$	2.50×10^{-3} coulombs	$C_2e_2(0)$
$z_1(0)$	1.72×10^{-3} coulomb $\sqrt{\text{henry}}$	Equations 2, 29; Figure 6 bf
$dz_1/dt(0)$	—1.95 ampere $\sqrt{\text{henry}}$	Equations 3, 29
$z_2(0)$	7.90×10^{-3} coulomb $\sqrt{\text{henry}}$	Equations 2; Figure 6 ob
$y_1(0)$	3.77×10^{-3} coulomb $\sqrt{\text{henry}}$	Equations 13, 25; Figure 6 ov
$dy_1/dt(0)$	—1.45 ampere $\sqrt{\text{henry}}$	Equations 13, 25
$y_2(0)$	6.35×10^{-3} coulomb $\sqrt{\text{henry}}$	Equations 13, 25; Figure 6 oz
$dy_2/dt(0)$	1.30 ampere $\sqrt{\text{henry}}$	Equations 13, 25

Similarly, the amplitudes of the two components in e_3 may be found by drawing dj and ek parallel to the x_1 axis.

$$e_3 = [oj/(C_3\sqrt{L_3})]\cos\omega_1 t + [ok/(C_3\sqrt{L_3})]\cos\omega_2 t \quad (28)$$

Comparison may be made with equations 26; the correctness of the corresponding terms may be readily checked by applying the sine law to Figure 3. Plots of e_1 and e_3 as functions of time are given in Figure 5.

The range of the path of motion was initially limited by the W_C contour corresponding to the initial energy of the system, but by equations 22, with the values now found for the arbitrary constants, the range is further limited to the rectangle $ckmn$. This rectangle is symmetric about both the y_1 and y_2 axes. If the ratio ω_1/ω_2 is irrational, the path of motion will eventually pass infinitesimally close to every point within this rectangle; should the frequency ratio be rational, the path will assume a repetitive pattern.

It should be noted that for a given value of W_C, an infinite number of inscribed rectangles is possible, one corresponding to each point x_1, x_2 along the contour. Thus any ratio between the amplitudes of the two components may be obtained by appropriate selection of the initial conditions, and if the "starting point" is on one of the normal co-ordinate axes, the amplitude of one frequency component is reduced to zero.

Example with Initial Charges and One Initial Current

The initial current in this example will be obtained by closing switch 1 a short time τ before zero time, but leaving switch 2 open until t equals zero. Then the L_1C_1 portion of the circuit will act as an independent circuit during that period, and the current and voltage will vary as follows:

$$\left.\begin{aligned} e_1 &= e_1(-\tau)\cos[(t+\tau)/\sqrt{L_1C_1}] \\ i_1 &= -e_1(-\tau)\sqrt{C_1/L_1}\sin[(t+\tau)/\sqrt{L_1C_1}] \end{aligned}\right\} \quad -\tau \leq t \leq 0 \quad (29)$$

In terms of the analogue, this amounts to motion constrained to a path parallel to the x_1 axis, and is shown in Figure 6 by cp, where the co-ordinate system and point c were located as in the preceding example. At t equals zero, and switch 2 closes, the constraint is removed, and motion is characterized by two degrees of freedom. The projection of point p onto the normal co-ordinate axes yields, as before, the amplitudes of the cosine oscillations, that is, or equals B_1 and os equals B_2. Substituting the second of equations 29 into 25 and 24, with t equal to zero, yields:

$$\left.\begin{aligned} A_1 &= -e_1(-\tau)[\sqrt{C_1}/\omega_1]\sin(\tau/\sqrt{L_1C_1})\cos\alpha \\ A_2 &= e_1(-\tau)[\sqrt{C_1}/\omega_2]\sin(\tau/\sqrt{L_1C_1})\sin\alpha \end{aligned}\right\} \quad (30)$$

The resultant magnitudes D_1 and D_2 of the sine and cosine waves of the same frequencies are:

$$\left.\begin{aligned} D_1 &= \sqrt{A_1^2+B_1^2} \\ D_2 &= \sqrt{A_2^2+B_2^2} \end{aligned}\right\} \quad (31)$$

In Figure 6, D_1 is represented by od', and D_2 by oe'. The complete rectangle $c'k'm'n'$ may then be drawn. This rectangle proves to be one inscribed within contour W_C.

The magnitudes of the cosine components appearing in e_1 and e_2 may be found, as in the preceding example, by projecting points r and s parallel to the x_1 or x_2 axis until the other axis is intersected. Similarly, if A_1 and A_2 are plotted along the y_1 and y_2 axes, projections may be made to determine the magnitudes of the sine components in e_1 and e_2.

Effect of Resistance

Resistance in an electric circuit produces a voltage instantaneously proportional to the current. The analogous effect in the rolling-ball system, with two degrees of freedom, is a force which is a function of the velocity. In general, however, the force vector is not colinear with the velocity vector, nor are the magnitudes proportional. Exact analysis of the resistance force field is complicated, and its physical realization in a rolling-ball analogue would be difficult if not impossible.

From the standpoint of the complete solution as a function of time, the presence of resistance in a single-loop resistance-inductance-capacitance circuit attenuates the oscillation exponentially and lengthens the period of oscillation beyond what it would be if the resistance were zero. The latter effect is significant only when the resistance is high enough to cause rather heavy attenuation. Still greater resistance will cause the period of oscillation to become imaginary, and the transient currents or voltages become sums of two real exponential functions. Qualitatively it may be said that results in a coupled 2-loop circuit are similar.

Extension to Other Systems

The general principle developed in this paper was that of deriving a co-ordinate system and an elevated surface in terms of which the kinetic and potential energies of a rolling ball will correspond rigorously to the magnetic and dielectric field energies of an electric circuit. This plan should be applicable to any dynamically conservative electrical or mechanical system with two degrees of freedom. In some instances it may be more advantageous to make the magnetic field energy analogous to the potential energy, and the dielectric field energy analogous to kinetic energy. This interchange of the quantities which are to correspond to each other, as compared to the arrangement used in the body of this paper, is similar to the concept of "dual" circuits.

If the potential energy is considered as associated simply with a contour on the co-ordinate plane, and gravity and the elevated surface are dispensed with, generalization to three degrees of freedom is possible; then potential energy contours would be surfaces (concentric ellipsoids, in the case of a strictly linear system) rather than lines.

Although the example treated in this paper was a linear system, this is not essential for the representation of a system by a rolling-ball analogue. Solutions in closed form for nonlinear systems with two degrees of freedom are usually out of the question, but the potential energy surface and the contour of total system energy for specified initial conditions can still be of considerable aid in determining the nature of the motion. Trajectories plotted on the surface from numerical solutions of the equations of motion will further clarify the situation. Instability will occur in some nonlinear systems if the energy associated with the initial conditions exceeds a certain critical value, and the analogue surface and initial energy contour depict this situation.

Conclusions

The rolling-ball analogue, a concept which should prove helpful in gaining insight into the transient behavior of two degree of freedom systems generally, has been derived for a system of two inductance-capacitance loops inductively coupled together. This analogue consists of a curved surface, elevated above a co-ordinate plane, on which a spherical ball may roll freely.

The dielectric field energy stored in the capacitors is made analogous to the potential energy of the ball, which is propor-

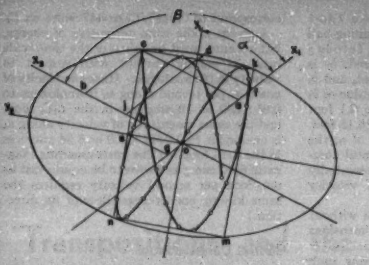

Figure 3. Ball path analogous to circuit behavior when switches are closed simultaneously. Circled points correspond to intervals of 0.001 second in circuit response

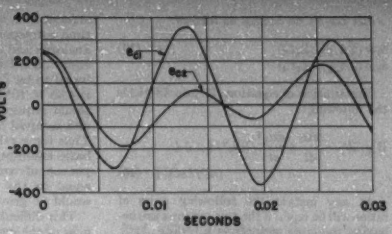

Figure 5 (right). Capacitor voltages (Figure 1) as functions of time when switches are closed simultaneously

tional to the height of the surface above a reference plane. The magnetic field energy of the coupled circuit is made analogous to the kinetic energy of the rolling ball. Velocity of the ball is therefore analogous to current, and the co-ordinates represent the time integral of current (or charge) in each loop. These must be scaled in proportion to the square roots of the respective self inductances if the kinetic-magnetic energy equivalence is to be valid. The presence of mutual inductance further requires that these co-ordinates be oblique rather than perpendicular to each other, and the angle separating them is the inverse cosine of the coefficient of coupling.

Contours of the analogue surface are concentric ellipses, and motion may be resolved into two characteristic components of motion parallel to the axes of those ellipses, which also are known as the normal co-ordinates. Various initial conditions may be plotted in the co-ordinate field, and the relative magnitudes of the component harmonic motions visualized.

Physical models may be built in a convenient size, with a known ratio of time scale relative to the original system. Such models, used in conjunction with "top view" plots of ball paths, would probably furnish the best educational means of applying the theory developed in this paper.

Appendix. Scaling of a Physical Model

It is of interest to know the scales of various dependent variables in a physical model in relation to the analogous quantities in the actual circuit, and to note the effect of making the two time scales different. This information will aid in actually designing such a model, which would be of assistance in demonstrating the transient behavior of two degree of freedom systems.

Analogue Proportions for Unity Time Scale Ratio

The problem of determining the proportions which a physical model should have will be attacked by comparing the expressions for energy in the two systems. The kinetic energy of the ball is given by the following:

$$W_K = (1/2)\left[(w/g)v^2 + J(v/r)^2\right] \tag{32}$$

Here w is the weight of the ball, r the radius, and J, the moment of inertia. For a solid spherical ball, (moment of inertia equals $(2/5)(w/g)r^2$), this reduces to:

$$W_K = (1/2)(1.4w/g)v^2 \tag{33}$$

Velocity v may be replaced by the vector sum of du_1/dt and du_2/dt, component velocities separated by angle β.

$$W_K = (1/2)(1.4w/g)\left|\frac{du_1}{dt} + \frac{du_2}{dt}\right|^2 \tag{34}$$

The corresponding term in the analogue, magnetic field energy stated in terms of generalized co-ordinates, is:

$$W_L = (1/2)\left|\frac{dx_1}{dt} + \frac{dx_2}{dt}\right|^2 \tag{9}$$

Let the height h of the elevated surface be defined as follows:

$$h = (1/2)(b_1u_1^2 + b_2u_2^2) \tag{35}$$

Here b_1 and b_2 are constants which will be evaluated later. The potential energy W_P is:

$$W_P = wh = w(1/2)(b_1u_1^2 + b_2u_2^2) \tag{36}$$

The analogous quantity, dielectric field energy, is:

$$W_C = (1/2)\left[(x_1^2/L_1C_1) + (x_2^2/L_4C_4)\right] \tag{12}$$

Both the potential and kinetic energies in the model are directly proportional to the weight of the ball, yet the period of oscillation of such a system is independent of that weight, hence it is not essential that the potential and kinetic energies of one system equal numerically the corresponding energies in the other for them to have identical responses as functions of time. Comparing the ratio of W_L/W_C to W_K/W_P will suffice to determine the constants b_1 and b_2 in terms of the circuit parameters.

$$W_L/W_C = \left|\frac{dx_1}{dt} + \frac{dx_2}{dt}\right|^2 / \left[(x_1^2/L_1C_1) + (x_2^2/L_4C_4)\right] \tag{37}$$

$$W_K/W_P = (1.4w/g)\left|\frac{du_1}{dt} + \frac{du_2}{dt}\right|^2 / \left[w(b_1u_1^2 + b_2u_2^2)\right]$$

$$= (1.4/g)\left|\frac{du_1}{dt} + \frac{du_2}{dt}\right|^2 / (b_1u_1^2 + b_2u_2^2) \tag{38}$$

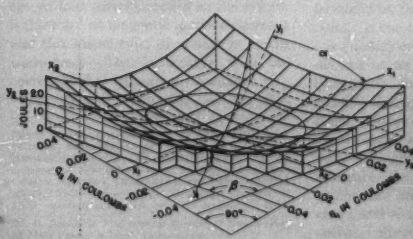

Figure 4. Isometric projection of part of analogue surface

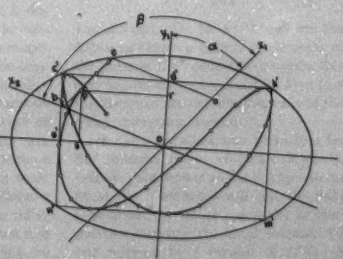

Figure 6 (right). Ball path analogous to circuit behavior when switch 1 is closed 0.003 second before switch 2. Circled points correspond to intervals of 0.001 second

Let the b's be defined as follows:

$$b_1 = (1.4/g)/(L_1C_1) \tag{39}$$
$$b_2 = (1.4/g)/(L_2C_2)$$

Substitution of equations 39 into 38 yields the following:

$$W_K/W_P = \left|\frac{du_1}{dt} + \frac{du_2}{dt}\right|^2 / [(u_1^2/L_1C_1) + (u_2^2/L_2C_2)] \tag{40}$$

At any instant the following pairs of ratios will be equal if the two systems are behaving the same with respect to time:

$$\left.\begin{aligned} x_2/x_1 &= u_2/u_1 \\ \frac{dx_1}{dt}/x_1 &= \frac{du_1}{dt}/u_1 \\ \frac{dx_1}{dt}/x_1 &= \frac{du_2}{dt}/u_1 \end{aligned}\right\} \tag{41}$$

Under these circumstances, the right-hand sides of equations 37 and 40 will equal each other, but they would not do so if b_1 and b_2 had not been defined as stated in equation 39.

Since g has the dimensions of $(length)/(time)^2$, and the product LC has the dimensions of $(time)^2$, the b's have the dimensions of $(length)^{-1}$, and are measures of the curvatures of the surface along the u_1 and u_2 axes.

Use of Nonunity Time Scale Ratio

Application of the foregoing to a numerical example, the data for which are given in Table I, will demonstrate that in many instances it is impractical to obtain a 1-to-1 time correspondence between a rolling-ball analogue and the original circuit. Letting g equal 32.2 feet per second squared, b_1 is found to be 7.23×10^4 inverse feet, and b_2 is 4.35×10^4 inverse feet. This value of b_1 would require that at u_1 equal to 0.1 foot and u_2 equal to zero, h would be 36.15 feet. Thus for a relatively small value of u_1 the basic assumption that the horizontal component of velocity be always essentially equal to the total magnitude of velocity would be grossly violated.

This difficulty may be overcome without making the model of microscopic dimensions by having a time scale of the model longer than that of the circuit. Increasing each LC product by the factor of 10^4 would, according to the theory of vibrations, increase the periods of oscillation by the square root of that factor, or 10^2; diminishing the b's by the factor of 10^{-4} will have the same effect. In this case a time scale ratio of 200 (multiply the b's by 2.5×10^{-4}) would be suitable, for at u_1 equal to one foot and u_2 equal to zero, h would be 0.0905 foot, and at u_1 equal to zero and u_2 equal to one foot, h would be 0.0544 foot.

Relative scales of u_1 and u_2 are indicated by equations 2. For the values of L_1 and L_2 given in Table I, if one foot along u_1 is to be equivalent to 0.05 coulomb, the same distance along u_2 would be equivalent to $0.05 \sqrt{L_1/L_2}$ or 0.0447 coulombs. In terms of the capacitor voltages which would result from those charges, for the values of C_1 and C_2 given in the same table, one foot along u_1 would correspond to $0.05/C_1$ or 667 volts on C_1, and one foot along u_2 would correspond to $0.0447/C_2$ or 447 volts on C_2.

Current is the time derivative of charge, but account must be taken of the time scale ratio in scaling current with respect to velocity in the analogue. Hence a velocity of one foot per second along u_1 is analogous to 0.05×200 or 10 amperes in the L_1C_1 loop, and the same magnitude of velocity along u_2 is analogous to 0.0447×200 or 8.94 amperes in the L_2C_2 loop. (The corresponding magnetic field energies prove to be equal, just as one foot per second velocity requires the same kinetic energy regardless of its direction.)

Model Construction

To construct a model on which the rolling ball would follow a path which would correspond closely to the calculated circuit behavior for several cycles would, of course, necessitate great care in shaping the analogue surface, a degree of care perhaps comparable to that taken in grinding lenses or telescope reflectors. It is doubtful if such precise construction would be justified, and in fact, as much educational value could probably be gained from a relatively crude model. It is suggested that the techniques for making relief maps be used as a guide if such construction is undertaken.

Reference

1. Introduction to Theoretical Physics (book), J. C. Slater, N. H. Frank. McGraw-Hill Book Co., Inc., New York, N. Y., 1933, pages 39–46, 55–60, 107–118.

No Discussion

Transpositions and the Calculation of Inductance from Geometric Mean Distances

W. B. BOAST
MEMBER AIEE

Synopsis: The calculation of the inductance of power transmission lines by the method of geometric mean distances is discussed in most transmission line textbooks. The assumption is usually made therein that the single-phase case for which the return currents are established uniformly equal to $-I/n$ in the return n conductors may be expanded automatically to encompass also the transposed 3-phase case even though the return currents of the other two phases obviously do not satisfy the $-I/n$ condition. This paper demonstrates with mathematical rigour that the inductance per phase can be calculated by the geometric-mean-distance method, and further, it shows the necessary and sufficient conditions for the system of transpositions that must be satisfied for the general 3-phase case. For special 3-phase systems, possessing symmetry among certain spacing distances some of these transpositions, however, may then be unnecessary.

THE total inductance of a circuit expressed in henrys is defined as the derivative of the meter-kilogram-second flux linkages with respect to the total current of the circuit in amperes. In transmission line systems the components of flux linkage are linearly proportional to the various currents acting in the system if there are no magnetic materials present and this linear type of system is herein considered. The inductance then becomes the flux linkages per ampere.

The general expression for the flux linkages per unit of circuit length for one conductor due to N parallel solid cylindrical conductors is

$$\lambda_1 = 2\times 10^{-7}\left[I_1\left(\frac{1}{4}+\ln\frac{1}{r_1}\right)+\sum_{k=2}^{k=N} I_k \ln\frac{1}{D_{1k}}\right] \quad (1)$$

where

λ_1 = meter-kilogram-second flux linkages per meter of conductor 1
I_1 = current of the number 1 conductor in amperes
I_k = current of each of the other conductors in amperes and designated in the same direction as is I_1
r_1 = radius of conductor 1, in any unit of length
D_{1k} = distances from the center of conductor 1 to the center of the respective conductors, measured in the same unit of length as r

The derivation of this or similar expressions may be found in several textbooks[1-6] dealing with magnetic fields or with transmission lines.

The vector or scalor nature of λ_1 is determined by the similar nature of the currents. If the currents are the instantaneous (scalar) currents existing in the conductors at an instant of time, the flux linkage is likewise the instantaneous (scalar) linkage at that same instant of time. However, if the currents are steady-state harmonic currents with a vector designation with respect to some reference, the flux linkage is likewise a vector flux linkage with the same reference; and as such may be converted to a vector voltage drop by multiplying by $j2\pi f$. This latter designation is quite convenient in handling some untransposed line problems which cannot be treated rigorously by the method of geometric mean distances and the concept of a real self-inductance.

Linkage Relationships for $N+n$ Conductors

Figure 1 represents the cross-sectional view of two or more parallel nonmagnetic cylindrical conductors. The conductors carrying the total current $+I$ (those on the left in the figure) will be numbered from 1 to N and each carries a current of $+I/N$. Only two areas are shown in the figure, that is, N is equal to 2.

The conductor or conductors carrying the total return current will be designated by letters from a to n. In the case of polyphase circuits this return current will flow in all of the conductors of all the other phases where attention has already been directed to a particular phase in the designation of the N parts. Only two conductors are shown in the figure, that is n is equal to b (or 2). No restriction is made that each conductor carries a current of $-I/n$.

If all the $N+n$ currents of the system are designated in the same direction, the linkages about element 1 per meter are

$$\lambda_1 = 2\times 10^{-7}\left[\frac{I}{N}\left(\frac{1}{4}+\ln\frac{1}{r_1}+\sum_{k=2}^{k=N}\ln\frac{1}{D_{1k}}\right)+\sum_{k=a}^{k=n} I_k \ln\frac{1}{D_{1k}}\right] \quad (2)$$

The distances D_{1k} for $k=2$ to N are the distances between centers of elements of the parts of the conductor or conductors carrying the current $+I$ and for $k=a$ to n the distances are between elements of the going and return currents.

Similar expressions may be written for the linkages about elements 2, 3, 4, —to N. The sum of all the linkages about all of the N elements will give the linkages about the entire conductor or conductors carrying the total current $+I$ but referred to a current of I/N. A

Paper 50-246, recommended by the AIEE Basic Sciences, Transmission and Distribution Committees and approved by the AIEE Technical Program Committee for presentation at the AIEE Fall General Meeting, Oklahoma City, Okla., October 23-27, 1950. Manuscript submitted March 8, 1950; made available for printing August 25, 1950.

W. B. Boast is Professor of Electrical Engineering at Iowa State College, Ames, Iowa.

linkage has been defined in a manner that makes it depend upon the current to which it is referred, and one linkage about one of N equal elements of a conductor system should contribute only $1/N$ of a linkage with respect to the entire conductor system. Consequently the sum of the linkages about elements 1 to N must be divided by N to preserve the total conductor linkages with respect to the entire conductor system.

Then

$$\lambda=\frac{1}{N}\sum_{k=1}^{k=N}\lambda_k$$

$$=\frac{2\times10^{-7}I}{N^2}\left[\frac{1}{4}+\ln\frac{1}{r_1}+\sum_{k=2}^{k=N}\ln\frac{1}{D_{1k}}\right.$$

$$+\frac{1}{4}+\ln\frac{1}{D_{21}}+\ln\frac{1}{r_2}+\sum_{k=1}^{k=N}\ln\frac{1}{D_{2k}}$$

$$+\frac{1}{4}+\sum_{k=1}^{k=2}\ln\frac{1}{D_{3k}}+\ln\frac{1}{r_3}+\sum_{k=4}^{k=N}\ln\frac{1}{D_{3k}}$$

$$+\ldots\ldots\ldots\ldots\ldots\ldots\ldots\ldots$$

$$\left.+\frac{1}{4}+\sum_{k=1}^{k=N-1}\ln\frac{1}{D_{Nk}}+\ln\frac{1}{r_N}\right]$$

$$+\frac{2\times10^{-7}}{N}\left[\sum_{k=a}^{k=n}I_k\ln\frac{1}{D_{1k}}+\right.$$

$$\sum_{k=a}^{k=n}I_k\ln\frac{1}{D_{2k}}+\ldots+$$

$$\left.\sum_{k=a}^{k=n}I_k\ln\frac{1}{D_{Nk}}\right] \quad (3)$$

Combining like terms in the first group gives

$$\lambda=\frac{2\times10^{-7}I}{N^2}\left[\frac{N}{4}+\sum_{k=1}^{k=N}\ln\frac{1}{r_k}+\right.$$

$$2\sum_{k=2}^{k=N}\ln\frac{1}{D_{1k}}+2\sum_{k=3}^{k=N}\ln\frac{1}{D_{2k}}$$

$$+\ldots+2\sum_{k=N-1}^{k=N}\ln\frac{1}{D_{(N-2)k}}+$$

$$\left.2\ln\frac{1}{D_{(N-1)N}}\right]+\frac{2\times10^{-7}}{N}\times$$

$$\left[\sum_{k=a}^{k=n}I_k\left(\frac{1}{D_{1k}}+\ln\frac{1}{D_{2k}}+\ldots+\ln\frac{1}{D_{Nk}}\right)\right] \quad (3A)$$

Several approaches to this equation can be made. Several slightly different approaches may be found in the transmission textbooks mentioned previously.[2,3,4,5] However, in no case is the result rigorously proved for polyphase systems inasmuch as all approaches assume that each of the n currents of the return system are equal.

Single-Phase Systems

Although the principal purpose of this discussion is a consideration of the necessary and sufficient conditions for transpositions in the polyphase case, the results for the single-phase case are included here for completeness. If the mathematical restriction that each current in the n group is equal to $-I/n$ is applied to equation 3A, then

$$\lambda=\frac{2\times10^{-7}I}{N^2}\left[\frac{N}{4}+\sum_{k=1}^{k=N}\ln\frac{1}{r_k}+\right.$$

$$2\sum_{k=2}^{k=N}\ln\frac{1}{D_{1k}}+2\sum_{k=3}^{k=N}\ln\frac{1}{D_{2k}}$$

$$+\ldots+2\sum_{k=N-1}^{k=N}\ln\frac{1}{D_{(N-2)k}}+$$

$$\left.2\ln\frac{1}{D_{(N-1)N}}\right]$$

$$-\frac{2\times10^{-7}I}{nN}\left[\sum_{k=a}^{k=n}\left(\ln\frac{1}{D_{1k}}+\right.\right.$$

$$\left.\left.\ln\frac{1}{D_{2k}}+\ldots+\ln\frac{1}{D_{Nk}}\right)\right] \quad (4)$$

Combining the various logarithmic terms and writing out the summations, which now become products, give

$$\lambda=2\times10^{-7}I\left[\frac{1}{4N}+\right.$$

$$\left.\ln\frac{\sqrt[nN]{[D_{1a}D_{1b}\ldots D_{1n}][D_{2a}D_{2b}\ldots D_{2n}]\ldots\ldots[D_{Na}D_{Nb}\ldots D_{Nn}]}}{N^2\sqrt{[r_1r_2\ldots r_N][D_{12}D_{13}\ldots D_{1N}]^2[D_{23}D_{24}\ldots D_{2N}]^2\ldots[D_{(N-2)(N-1)}D_{(N-1)N}]^2}}\right] \quad (5)$$

The $1/4\ N$ term is derived from the internal portion of the linkages of the system of N conductors and hence is associated with the denominator term involving the self dimensions.

Inasmuch as

Figure 1. A system of $N+n$ conductors

$$\frac{1}{4N}=\ln\frac{1}{N^2\sqrt{e^{-N/4}}} \quad (6)$$

equation 5 may be rewritten as

$$\lambda=2\times10^{-7}I\ln\frac{\sqrt[nN]{[D_{1a}D_{1b}\ldots D_{1n}][D_{2a}D_{2b}\ldots D_{2n}]\ldots\ldots[D_{Na}D_{Nb}\ldots D_{Nn}]}}{N^2\sqrt{e^{-N/4}[r_1r_2\ldots r_N][D_{12}D_{13}\ldots D_{1N}]^2[D_{23}D_{24}\ldots D_{2N}]^2\ldots[D_{(N-2)(N-1)}D_{(N-1)N}]^2[D_{(N-2)N}]^2[D_{(N-1)N}]^2}} \quad (6A)$$

The numerator of the logarithm involves all the mutual distances between elements of the two sides of the single-phase system and is defined as the *mutual geometric mean distance* between the total current $+I$ and its return. The symbol D_m is commonly employed as an abbreviation.

The denominator of the logarithm involves the distances among the N elements of the total current $+I$ and is defined as the *self-geometric mean distance* of the N group of conductors. The symbol D_{SN} is commonly employed as an abbreviation.

The self-inductance per unit of circuit length of the N group of conductors is $d\lambda/dI$, or with no nonlinear magnetic materials present, simply λ/I, and

$$L_N=2\times10^{-7}\ln\frac{D_m}{D_{SN}}\ \text{henrys/meter} \quad (7)$$

The self-inductance of the n group of conductors (the return) is obtained in the same manner by interchanging the n and the N. The mutual geometric mean distance is not changed by this procedure. If the symbol D_{Sn} is used for the self-geometric mean distance of the n group

$$L_n=2\times10^{-7}\ln\frac{D_m}{D_{Sn}}\ \text{henrys/meter} \quad (8)$$

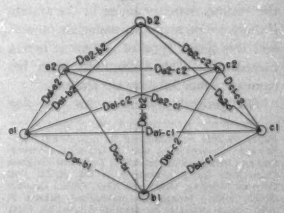

Figure 2. A system of 3N conductors for N=2

The total inductance per unit of circuit length of the single-phase system is

$$L = L_N + L_n = 2\times10^{-7} \ln \frac{D_m^2}{D_{SN} D_{Sn}} \quad \text{henrys/meter} \tag{9}$$

Transpositions in Single-Phase Systems

The preceding relationships assumed that each current in the N group of conductors was the same, and also that each of the n currents of the return also were identical to each other.

Several conditions are necessary and sufficient in order that these equalities of currents exist. Each of the N conductors must possess the same resistance and also be so oriented with respect to the return and to each other that over the length of the line the induced voltage in each conductor is the same as in every other conductor of the N group. Similar conditions must apply to each of the n group.

Usually each of the N conductors of a system will be the same as every other of that group as regards configuration and materials. Likewise the n conductors will usually be the same within that group. Hence the only physical requirement of the line is that the necessary transpositions be effected unless symmetry of mutual dimensions has already established the sufficient conditions for balanced inductive effects.

The most general type of transposition, where the N conductors are assigned to N positions and likewise the n conductors are assigned to a different set of n positions and no interchange of conductors is permitted between these two group positions, requires Nn transposition sections.

Table I illustrates the schedule of positions needed for the general case where no symmetry exists among any parts. The original positions of conductors 1 and a are used for reference positions for other sections. Thus section $1b$ indicates that conductors of the N group have not moved but that b lies where a did in section $1a$, and the others in the n group have moved in a similar cyclic order.

Very often symmetry may obviate the need for many sections of transpositions which might otherwise be necessary.

The transpositions do not influence the calculations of the inductance in the single-phase case where the N-group and the n-group of conductors are each assigned to their own respective positions, but are necessary (except for symmetrical combinations) and sufficient for the use of I/N and I/n as common factors for the establishment of equation 4.

Polyphase Systems and Their Transpositions

A restricted type of polyphase system will be discussed, consisting of three phases, each of which contains N identical conductors. A general discussion for p phases each containing a different number of conductors is possible but becomes very involved and tedious in specifications. The use of an equal number of identical phase conductors is common in most multicircuit power transmission lines. Likewise 3-phase transmission lines are almost universal. For certain applications which may not be covered by this discussion with these restrictions, a solution for the particular case can be developed from the fundamental linkage equations perhaps as quickly as attempting to interpret a very involved derived result.

The n conductors of the return (where attention has been directed to one phase of N conductors) for the 3-phase system consists of $2N$ conductors. Rather than continue with this notation, a more direct system of symbols will be used. The letters of the alphabet will be used as phase designators (which is a common notation) and numbers will be used to indicate the conductor number of that phase. Thus conductor $b2$ indicates conductor number 2 of the b phase and conductor cN indicates the Nth conductor of the c phase. These double symbols will be used as subscripts for distance designations. Thus D_{b2-cN} indicates the distance from the center of conductor $b2$ to that of cN. Figure 2 illustrates a system for $N=2$.

The linkages per meter of the a phase, if the N currents of each phase are the same, are

$$\lambda = \frac{2\times10^{-7}}{N^2}\left\{ I_a\left[\frac{N}{4} + N\ln\frac{1}{r} + 2\sum_{k}^{k=N}\ln\frac{1}{D_{a1-ak}} + 2\sum_{k=2}^{k=N}\ln\frac{1}{D_{a2-ak}} + \ldots + 2\sum_{k=N-1}^{k=N}\ln\frac{1}{D_{a(N-1)-ak}} + 2\ln\frac{1}{D_{a(N-1)-aN}}\right] + \sum_{k=1}^{k=N} I_b\left(\ln\frac{1}{D_{a1-bk}} + \ln\frac{1}{D_{a2-bk}} + \ldots + \ln\frac{1}{D_{aN-bk}}\right) + I_c\left(\ln\frac{1}{D_{a1-ck}} + \ln\frac{1}{D_{a2-ck}} + \ldots + \ln\frac{1}{D_{aN-ak}}\right)\right\} \tag{10}$$

The equality of the N currents in the N identical conductors of each phase is desirable to maintain minimum losses for a fixed amount of conductor material and total current. A cyclic order of simultaneous transpositions within each group of phase conductors is both necessary and sufficient to accomplish this balance for the general case where no symmetry exists.

Furthermore, balanced inductive voltage drops are desirable among phases under balanced current conditions so that each phase may possess the same voltage regulation as every other phase. Transpositions among phases are necessary and sufficient to accomplish this balance for the general case where no symmetry exists.

Table II illustrates the schedule of positions needed for the general case of no symmetry. The reference system for transposition sections follows the same plan as was used in the single-phase case. The linkage equation 10 is the same for section $a1$, $a2$, $a3$, ... aN since interchanging equal components of phase currents in the assigned phase positions does not influence this equation.

However, the linkages of phase a for the transposition sections of the b group and also of the c group are different and must be considered. If the linkages of equation 10 are called λ_{ak}, then λ_{bk} will mean the linkages of phase a when phase b conductors have been transferred to the original phase a positions. If the distance notation for the first (ak) section is used throughout, then

$$\lambda_{bk} = \frac{2\times10^{-7}}{N^2}\left\{ I_a\left[\frac{N}{4} + N\ln\frac{1}{r} + 2\sum_{k=2}^{k=N}\ln\frac{1}{D_{a1-ak}} + 2\sum_{k=3}^{k=N}\ln\frac{1}{D_{a2-ak}} + \ldots + 2\sum_{k=N-1}^{k=N}\ln\frac{1}{D_{a1-ak}} + 2\ln\frac{1}{D_{a(n-1)-an}}\right] + \sum_{k=1}^{k=N}\left[I_b\left(\ln\frac{1}{D_{a1-ak}} + \ln\frac{1}{D_{a2-ak}} + \ldots + \ln\frac{1}{D_{aN-ak}}\right) + I_c\left(\ln\frac{1}{D_{a1-bk}} + \ln\frac{1}{D_{a2-bk}} + \ldots + \ln\frac{1}{D_{aN-bk}}\right)\right]\right\} \tag{11}$$

Table I. Single-phase Transposition Schedule

Transposition Section	N-Group Positions					n-Group Positions			
1a	1	2	...	N		a	b	...	n
1b	1	2	...	N		b	c	...	a
⋮	⋮	⋮	⋮			⋮	⋮	⋮	
1n	1	2	...	N		n	a	...	(n−1)
2a	2	3	...	1		a	b	...	n
2b	2	3	...	1		b	c	...	a
⋮	⋮	⋮	⋮			⋮	⋮	⋮	
2n	2	3	...	1		n	a	...	(n−1)
⋮	⋮	⋮	⋮			⋮	⋮	⋮	
Na	N	1	...	(N−1)		a	b	...	n
Nb	N	1	...	(N−1)		b	c	...	a
⋮	⋮	⋮	⋮			⋮	⋮	⋮	
Nn	N	1	...	(N−1)		n	a	...	(n−1)

and

$$\lambda_{ck}=\frac{2\times10^{-7}}{N^2}\left\{I_a\left[\frac{N}{4}+N\ln\frac{1}{r}+\right.\right.$$

$$2\sum_{k=2}^{k=N}\ln\frac{1}{D_{b1-bk}}+2\sum_{k=1}^{k=N}\ln\frac{1}{D_{b2-bk}}$$

$$+\ldots+2\sum_{k=N-1}^{k=N}\ln\frac{1}{D_{b(N-2)-bk}}+$$

$$\left.2\ln\frac{1}{D_{b(N-1)-bN}}\right]$$

$$+\sum_{k=1}^{k=N}\left[I_b\left(\ln\frac{1}{D_{b1-ck}}+\ln\frac{1}{D_{b2-ck}}+\right.\right.$$

$$\left.\ldots+\ln\frac{1}{D_{bN-ck}}\right)+I_c\left(\ln\frac{1}{D_{b1-ak}}+\right.$$

$$\left.\left.\left.\ln\frac{1}{D_{b2-ak}}+\ldots+\ln\frac{1}{D_{bN-ak}}\right)\right]\right\}\quad(12)$$

The average linkage per meter of the transposed system then will be the sum of the three equations 10, 11, and 12 divided by three. This yields the equation

$$\text{Average }\lambda\text{ of phase }a=\frac{2\times10^{-7}}{3N^2}\times$$

$$\left\{I_a\left[\frac{3N}{4}+3N\ln\frac{1}{r}+2\sum_{k=2}^{k=N}\times\right.\right.$$

$$\left(\ln\frac{1}{D_{a1-ak}}+\ln\frac{1}{D_{b1-bk}}+\ln\frac{1}{D_{c1-ck}}\right)+$$

$$2\sum_{k=3}^{k=N}\left(\ln\frac{1}{D_{a2-ak}}+\ln\frac{1}{D_{b2-bk}}\ln\frac{1}{D_{c2-ck}}\right)$$

$$+\ldots\ldots\ldots\ldots$$

$$+2\sum_{k=N-1}^{k=N}\left(\ln\frac{1}{D_{a(N-2)-ak}}+\right.$$

$$\left.\ln\frac{1}{D_{b(N-2)-bk}}+\ln\frac{1}{D_{c(N-2)-ck}}\right)+$$

Table II. Three-Phase Transposition Schedule

Transposition Section	Conductor Pattern							
a1	a1	a2	...	aN	b1	b2	...	bN	c1	c2	...	cN
a2	a2	a3	...	a1	b2	b3	...	b1	c2	c3	...	c1
⋮	⋮	⋮	⋮		⋮	⋮	⋮		⋮	⋮	⋮	
aN	aN	a1	...	a(N−1)	bN	b1	...	b(N−1)	cN	c1	...	c(N−1)
b1	b1	b2	...	bN	c1	c2	...	cN	a1	a2	...	aN
b2	b2	b3	...	b1	c2	c3	...	c1	a2	a3	...	a1
⋮	⋮	⋮	⋮		⋮	⋮	⋮		⋮	⋮	⋮	
bN	bN	b1	...	b(N−1)	cN	c1	...	c(N−1)	aN	a1	...	a(N−1)
c1	c1	c2	...	cN	a1	a2	...	aN	b1	b2	...	bN
c2	c2	c3	...	c1	a2	a3	...	a1	b2	b3	...	b1
⋮	⋮	⋮	⋮		⋮	⋮	⋮		⋮	⋮	⋮	
cN	cN	c1	...	c(N−1)	aN	a1	...	a(N−1)	bN	b1	...	b(N−1)

$$2\left(\ln\frac{1}{D_{a(N-1)-an}}+\ln\frac{1}{D_{b(N-1)-bn}}+\right.$$

$$\left.\ln\frac{1}{D_{c(N-1)-cN}}\right)\Bigg]+\sum_{k=1}^{k=N}\left[I_b\left(\ln\frac{1}{D_{a1-bk}}+\right.\right.$$

$$\ln\frac{1}{D_{a2-bk}}+\ldots+\ln\frac{1}{D_{aN-bk}}+$$

$$\ln\frac{1}{D_{b1-ck}}+\ln\frac{1}{D_{b2-ck}}+\ldots+\ln\frac{1}{D_{bN-ck}}$$

$$+\ln\frac{1}{D_{c1-ak}}+\ln\frac{1}{D_{c2-ak}}+\ldots+$$

$$\left.\ln\frac{1}{D_{cN-ak}}\right)+I_c\left(\ln\frac{1}{D_{a1-ck}}+\ln\frac{1}{D_{a2-ck}}\right.$$

$$+\ldots+\ln\frac{1}{D_{aN-ck}}+\ln\frac{1}{D_{b1-ak}}+$$

$$\ln\frac{1}{D_{b2-ak}}+\ldots+\ln\frac{1}{D_{bN-ak}}+\ln\frac{1}{D_{c1-bk}}+$$

$$\left.\left.\ln\frac{1}{D_{c2-bk}}+\ln\frac{1}{D_{cN-bk}}\right)\right]\Bigg\}\quad(13)$$

The multipliers upon the I_b and the I_c are identical. Inasmuch as I_b+I_c is equal to $-I_a$, equation 13 may be rewritten (following similar reasoning regarding the (1/4) N term as was explained in the single-phase case) as

$$\text{Average }\lambda\text{ of phase }a=2\times10^{-7}I_a\times$$

$$\ln\frac{\dfrac{3N^2\left|\begin{array}{l}[D_{a1-b1}D_{a1-b2}\ldots D_{a1-bN}]\\[D_{a2-b1}D_{a2-b2}\ldots D_{a2-bN}]\\\ldots\ldots[D_{aN-b1}D_{aN-b2}\ldots D_{aN-bN}]\\[D_{b1-c1}D_{b1-c2}\ldots D_{b1-cN}]\\[D_{b2-c1}D_{b2-c2}\ldots D_{b2-cN}]\\\ldots\ldots[D_{bN-c1}D_{bN-c2}\ldots D_{bN-cN}]\\[D_{c1-a1}D_{c1-a2}\ldots D_{c1-aN}]\\[D_{c2-a1}D_{c2-a2}\ldots D_{c2-aN}]\\\ldots\ldots[D_{cN-a1}D_{cN-a2}\ldots D_{cN-aN}]\end{array}\right|}{\sqrt{\begin{array}{l}3N^2e^{-3N/4\mu_r}[D_{a1-a1}D_{a1-a2}\ldots D_{a1-aN}]^2\\[D_{b1-b1}D_{b1-b2}\ldots D_{b1-bN}]^2\\[D_{c1-c1}D_{c1-c2}\ldots D_{c1-cN}]^2\\[D_{a2-a1}D_{a2-a}\ldots D_{a2-aN}]^2\\[D_{b2-b1}D_{b2-b1}\ldots D_{b2-bN}]^2\\[D_{c2-c1}D_{c2-c1}\ldots D_{c2-cN}]^2\\\ldots\ldots[D_{a(N-2)-a(N-1)}D_{a(N-2)-aN}]^2\\[D_{b(N-2)-b(N-1)}D_{b(N-2)-bN}]^2\\[D_{c(N-2)-c(N-1)}D_{c(N-2)-cN}]^2\\[D_{(aN-1)-cN}]^2[D_{b(N-1)-bN}]^2\\[D_{c(N-1-cN}]^2\end{array}}}\quad(14)$$

The numerator of the logarithm involves all of the mutual distances taken in all combinations of the transposed line and is defined as the *mutual geometric mean distance* between the current I_a and its return. The same symbol D_m may be used as for the single-phase case but it represents the equivalent value for the transposed system of phase positions.

The denominator of the logarithm involves the various combinations of distances among the conductors of the same phase and is defined as the *self-geometric mean distance* of the phase conductors. The symbol D_s may be employed as an abbreviation.

Attention has been directed in the derivation of equation 14 at phase a of the polyphase system. The complete system of transpositions, however, has made each phase equivalent to every other in so far as geometric conditions are concerned. Hence D_m and D_s are the same for phases b and c as for phase a. Therefore no phase subscripts are used on the symbols. The average inductance per unit of circuit length of any phase of the transposed system then is

$$L=2\times10^{-7}\ln\frac{D_m}{D_s}\text{ henrys/meter}\quad(15)$$

References

1. Principles of Electric and Magnetic Fields (book), W. B. Boast. Harper and Brothers, New York, N. Y., chapter 13, 1948.

2. Electrical Transmission of Power and Signals (book), E. W. Kimbark. John Wiley and Sons, Inc., New York, N. Y., chapters 3 and 4, 1949.

3. Introduction to Electric Power Systems (book), J. G. Tarboux. International Textbook Company, Scranton, Pa., chapter 4, 1944.

4. Electric Power Transmission (book), M. P. Weinbach. Macmillan Company, New York, N. Y., chapter 1, 1948.

5. Principles of Electric Power Transmission (book), L. F. Woodruff. John Wiley and Sons, Inc., New York, N. Y., chapter 2, 1938.

No Discussion

Dial Telephone Central Office Buildings for Small Communities

F. D. REESE
ASSOCIATE AIEE

E. C. ROYS
NONMEMBER AIEE

BECAUSE of increasing costs, the design of dial telephone central office buildings for small communities is being scrutinized closely by most telephone operating companies, with the object of specifying the most economical type of construction consistent with the rather special requirements. In examining this problem, it is necessary first to review the requirements, after which the elements of the problem can be identified, and proposed solutions for the several elements can be discussed separately. The general building design features are determined chiefly by the type of community and the climate, while the detailed design is governed by the housing requirements of the equipment. These factors are examined in detail and solutions to the various problems encountered are discussed in some detail.

Type of Central Office Under Consideration

The type of central office under consideration is that generally referred to in the industry as a community dial office. This is defined as a small telephone central office arranged to complete calls within a community by machine switching, and having facilities to enable users to pass all calls, such as toll calls or service calls, requiring handling by operators to a nearby central office having operators in attendance.

Paper 50-248, recommended by the AIEE Communication Switching Systems Committee and approved by the AIEE Technical Program Committee for presentation at the AIEE Fall General Meeting, Oklahoma City, Okla., October 23–27, 1950. Manuscript submitted July 25, 1950; made available for printing August 31, 1950.

F. D. Reese and E. C. Roys are both with the Pennsylvania Telephone Corporation, Erie, Pa.

General Building Design Features

The considerations which control the general design are:

Range of Sizes

The maximum size required, while not inflexibly fixed, may be taken as that required for a machine switching apparatus having a capacity of 1,000 subscriber lines. The floor dimensions usually employed fall into the size divisions given in Table I which are for a single story building with no basement.

The maximum sizes indicated provide additional floor space where required for trunk terminations, carrier terminals or telephone repeaters, and in general are for offices having a greater than average number of toll or trunk lines to adjacent offices.

Table I

Subscriber Lines Accommodated	Floor Dimensions Maximum, Feet	Minimum, Feet
100	12 by 14	8 by 12
200	14 by 18	12 by 14
400	16 by 20	14 by 18
600	18 by 22	18 by 18
1,000	25 by 28	25 by 25

Location

The general design will be influenced by such factors as the type of community (whether rural or suburban); the prominence of the site in the community (whether on a main street or on a side street or alley); and the climatic conditions anticipated. The exact location of the site within the community will be determined by reference to the ultimate center of wire distribution, with consideration given to avoiding flood or fire hazards, or excessive vibration from trains or heavy machinery. Since the machine switching equipment will not require an attendant, all features of the building should be so designed as to permit satisfactory nonattended operation.

Consideration of these factors may indicate the need for inclusion in the general design of certain features, even though these add to the cost, such as:

1. Architectural decorative treatment or styling in harmony with neighboring structures, where a prominent site is chosen. Figure 1 illustrates such treatment.

2. A roof designed to support heavy snow loading, or to shed snow where winters are severe.

3. Fully fireproof construction, such as solid masonry, if hazard of fire cannot be avoided. Note concrete block walls, metal covered door and concrete base of the building illustrated in Figure 2.

4. Vibration-proof construction, such as a reinforced concrete floor slab if excessive vibration is foreseen.

Figure 1. Mayville, N. Y. central office

Figure 2. Jourdanton, Tex. central office

The control of cost through a choice of a less expensive design, such as frame construction, or through the elimination of architectural decorative effects, is therefore limited in certain instances.

Special Building Design Features

There should be considered as a basis for the detailed design those factors having an influence on the operation of the equipment to be housed. A discussion of these factors follows:

Resistance to Fire

Having in mind protection of the communication service, full consideration should be given fire risks. It has already been indicated that where the fire hazard is excessive, full fireproof construction should be considered. At locations where the risk of fire is a normal one, such as might be offered by a grass fire on the site, or by windborne sparks from a more remote fire, the exterior siding and roof covering should be of fire resistant material such as metal, asbestos siding or asphalt shingles.

Floor Loading

The load which will be imposed on the floor structure by the telephone equipment must be taken into account. Floor load varies from 125 to 150 pounds per square foot, depending on the type of equipment to be installed. The usual floor consists of a 5-inch slab of reinforced concrete which is amply strong and ordinarily not susceptible to vibration.

Figure 3. Brookings, Oreg. central office

Temperature Control

Insulation will be required in the ceiling or under the roof to prevent inside temperatures rising excessively in summer with resultant damage to potted apparatus or variation in relay or switch adjustments due to the unequal expansion of dissimilar metals. For example, in a building located in the Sacramento Valley in California, an interior temperature of 128 degrees Fahrenheit has been recorded. In buildings which are not to be heated, no wall or floor insulation is necessary, except in the case of buildings constructed of metal which require insulation to prevent condensation of moisture on the metal inside surfaces. Insulating board such as Celotex or asbestos sheets is the usual choice. If a fibrous material such as Celotex is used, it should be treated with a sealer on the inside surfaces to avoid any possibility of wear releasing fibrous particles which would interfere with the operation of the equipment by fouling the electrical contacts of relays or switches.

Heat is required in nonattended dial offices principally to provide some degree of comfort for maintenance personnel during short periodic visits made for the purpose of inspecting or routining the equipment. An exception would be the case of an office located in an extremely cold climate. Here it may be necessary to provide heaters, usually electric, arranged to prevent the temperature dropping to a very low level, with resultant possibility of variation in relay or switch adjustments through unequal contraction of dissimilar metals in spring assemblies.

Some use has been made in buildings of up to 400 lines capacity of portable electric heaters comprised of a 2- or 3-kw heating element with an associated blower. These are carried from office to office by the maintenance personnel and used either as spot heaters directed toward the piece of equipment being routined, or as a unit heater placed in operation long enough to warm the building sufficiently to permit work to proceed. They seem to be unsatisfactory to the maintenance people when so used, because they are not adequate to provide quickly any considerable temperature increase and because the floors are not warmed. Further, intermittent heating, with consequent variation of the dew point of the air within the building, makes control of moisture condensation difficult. In cases where heating is proposed, usually it is advisable to consider fixed heater installations.

Figure 4. Seven Corners, N. D. central office

The building being nonattended, automatic heater operation under control of a thermostat is essential. An electric heater, oil burner or gas-fired heater meets this requirement. Because of the higher cost of operating the conventional electric convection heater, oil- or gas-fired heaters are quite frequently used, but these offer serious disadvantages, the principal ones being:

1. Small oil heaters, which ordinarily are of the wick or pot type, give rise to fumes which are an explosion hazard, unless very well maintained. In addition, there is a possibility of a backfire (caused by faulty draft) spreading soot which would foul the equipment with resultant disruption of service.

2. Gas-fired heaters, while cleaner than oil heaters, may present a greater explosion hazard. In a nonattended building, there would be no opportunity for detection of a gas leak. Any slight leak might result in the accumulation of gas sufficient to form an explosive mixture with the air.

3. The minimum length of flue required to insure good draft is seldom if ever attained in these small buildings. Since one of the products of combustion is water vapor, any deficiency in draft might result in introducing moisture into the building. It therefore appears that neither gas nor oil is entirely satisfactory as a fuel.

Fixed electric heaters, because of the high cost of operation, are used more at present for the prevention of equipment trouble due to very low temperatures, than for heating sufficiently to contribute to the efficiency of the maintenance personnel. For example, in North Dakota,

Figure 5. Cooperstown, Pa. central office

the Northwestern Bell Telephone Company uses electric heaters of three kw capacity to prevent the temperature dropping below 10 to 15 degrees above 0 degrees Fahrenheit. The Northern Ohio Telephone Company uses similar heaters to hold the temperature between 15 and 20 degrees Fahrenheit.

A possible solution to the heating problem is seen in the electric radiant heaters now available. Preliminary investigation of one type seems to indicate considerable promise of successful operation at a reasonable cost. The type under investigation is comprised of panels arranged for mounting on the ceiling, each containing a layer of electrically conductive rubber sandwiched between layers of paper impregnated with phenolic resin. The principle involved is that heat is radiated from the ceiling panels to the walls, floor and other solid objects, including the equipment frames and cabinets, without directly heating the air. The effect noticed by personnel is a sensation of warmth which results from a reduction in the rate of heat transfer from body surfaces. This effect is in a considerable degree independent of the air temperature.

Estimates of annual operating costs have been prepared by the manufacturer for average Chicago weather. These estimates are based on a 400-line building of concrete block construction built on a 5-inch concrete slab and having a frame roof covered with asphalt shingles. The proposal is to maintain a minimum temperature of 40 degrees Fahrenheit during the winter. With four inches of insulation in the ceiling, but without wall or floor insulation, the annual power consumption is estimated at 1,480 kilowatt hours representing a cost of $44.40 annually at a power rate of three cents per kilowatt hour. Adding two inches of insulation to the walls and between the floor slab and its footings would reduce the power consumed to 1,030 kilowatt hours representing a cost of $30.90 annually. These costs will be increased materially if workmen raise the thermostat setting during periods when they occupy the building. The installed cost of the panels required to meet these conditions will be less than $300.

Figure 6. Vintondale, Pa. central office

Control of Moisture

The effect of moisture condensation or absorption on central office equipment is to lower the insulation resistance of wiring or cables, and of apparatus assembled on spacer blocks of insulating materials. The result can readily be failure of the functioning of the apparatus affected. Any absorption of moisture in the insulating covering of conductors in cables may result in a virtual short circuit. The cables carry 48-volt d-c potentials, and under such a condition it is possible that a severe electrical burn may occur with consequent interruption of service and serious damage to the equipment. Means of preventing accumulation of moisture within the building are therefore of great importance.

Seepage of moisture through concrete floors can be eliminated either by supporting the floor slab on footings above the ground level, or by pouring the concrete on a waterproof membrane such as impregnated building paper laid on a fill of cinders or gravel. Where an extremely dry soil is encountered, such as well-drained pure sand, no particular precaution may be necessary.

Condensation of moisture within the building results from the exposure of cold surfaces to warmer air which has a high relative humidity, or from admitting warm humid air to the building which will later become cooled below the dew point. Probably because of varying climates in different sections of the country, there is a diversity of opinion among engineers as to the measures necessary to control condensation.

Ventilation seems to be effective at some locations, but less so at others. The theory applied where ventilation is employed seems to be that vents should have movable louvers which can be opened during warm weather, permitting equalization of the temperature of the air within the building with the temperature of the air outside. However, many engineers believe that hermetic sealing during humid weather is more effective, on the theory that the less air is admitted, the less moisture may accumulate. Ventilation does offer one disadvantage, in that dust may be introduced into the building, with resultant possible fouling of relay or switch contacts. This may be partially overcome by locating the vents on the same wall rather than on opposite walls. The Telephone Service Company of Ohio provides vents equipped with movable louvers which are normally open but close under control of a thermostat when the temperature falls to 32 degrees Fahrenheit inside the building.

Electric dehumidifying equipment can be applied to remove moisture. Such equipment removes moisture from the air by cooling at the point of intake. When operated under control of a humidistat, these devices are efficient, but because first cost and operating cost would be fairly high, their employment would be limited to locations, such as tropical locations, where long periods of very high humidity might be anticipated. Another practical disadvantage is that during hot weather, employees may be influenced to seek relief from the heat through unnecessary visits to the building so equipped.

At humid locations, chemical dehydrators, employing a hygroscopic compound, would be effective. However, these usually result in the accumulation of a highly corrosive residue, raising a problem of disposal, and are not widely recommended.

The covering of interior surfaces with an insulating material will be found necessary in the case of buildings sheathed with steel, or built of ordinary glazed building tile. However, some areas report the successful use of hollow tile for wall construction, where the tiles are so formed as to provide drainage within the wall to a drainage vent at or near the foundation, and where a choice of interior glazes can be made which will eliminate condensation on the interior wall surfaces.

Where heaters are provided, they may be turned on during extremely humid weather so as to raise the air temperature and consequently the dew point, thus preventing condensation of moisture.

Other Special Features

There are certain other features which, while not requiring detailed discussion, should be mentioned. These are:

1. The door should be of sufficient size to

Figure 7. Waldo, Ohio central office

provide for entrance of the switching equipment to be housed.

2. Fixtures requiring plumbing should be avoided because of the cost of providing water and waste connections. Further, the introduction of water piping would make it necessary to heat sufficiently to avoid freezing, at the least.

3. While the telephone storage batteries ordinarily have a considerable reserve capacity, it might be necessary, in case of a protracted failure of the commercial power supply, to introduce a portable emergency engine-generator set. At slight cost, an electric receptacle can be provided to facilitate plugging in such portable equipment. The receptacle should preferably be provided for an alternating voltage source, since a-c operated equipment, such as telephone repeaters or carrier terminals, may be in service.

4. To minimize interruptions on the a-c circuits supplying battery chargers, such circuits should be fused separately from circuits provided for lighting or convenience outlets.

Typical Building Designs

From the foregoing it is apparent that no one design will be applicable to all locations and all conditions. Instead, various companies operating in various parts of the country have developed designs which best meet the conditions encountered locally.

For example, the West Coast Telephone Company, having low first cost and portability in view, employs a wood frame building covered with asbestos cement shingles. In areas where heavy snow is expected, a hip roof of frame construction, covered with asbestos or asphalt shingles is used. In other areas a flat roof built up of roofing felt is used. A concrete floor slab provides a foundation. In some cases the building is constructed with an additional wood floor which sets on the concrete slab. This company has on occasion moved a building, complete with the equipment, a distance of 50 miles, at a reported cost, including the new concrete foundation, of $400. Figure 3 illustrates one of these frame buildings.

The Illinois Commercial Telephone Company constructs buildings of glazed hollow tile on a reinforced concrete floor slab. The slab is raised above the ground level to insure a dry floor. The roof is of frame construction and covered with asbestos or asphalt shingles. A ceiling of sheet asbestos is provided. There is no provision for heating. The same building design is used by Commonwealth Telephone Company in Wisconsin.[7]

The Northwestern Bell Telephone Company employs frame construction in portable buildings for its operations in North Dakota. The walls are covered with asbestos shingles, and both walls and ceiling are insulated with four inches of rock wool, and covered inside with Transite sheets. The wood floor is insulated with eight inches of rock wool. The roof is of frame construction, covered with asphalt shingles. The temperature is held to a minimum of 10 to 15 degrees Fahrenheit by a thermostatically controlled electric heater of the blower type. These buildings are assembled and the equipment installed at Fargo, N. D. and then transported to the site of operation where they are set on posts to raise them about one foot off the ground. When set, the soil on the site is treated chemically to prevent growth of brush or weeds, and a surrounding fill of crushed stone is put in to guard against brush fires. The building illustrated in Figure 4 was built in Fargo, N. D., the equipment installed and the completed structure was then moved to Seven Corners, N. D.

Pennsylvania Telephone Corporation constructs masonry buildings on a reinforced concrete slab, using a concrete block made of a lightweight aggregate waterproofed with Portland cement paint, with an asphalt shingle roof. Small glass block windows are installed to provide some natural light without risking condensation of moisture such as occurs with single glass panes. A ceiling of sound absorbent material provides insulation. Electric receptacles are provided for portable electric heaters. In rural communities, the exterior walls are given a waterproof cement finish. In suburban communities, brick veneer is added to improve the appearance of the exterior. Ventilation is provided for by installing two small openings in one wall, with movable copper louvers, see Figures 5 and 6.

A similar building of the Ohio Associated Telephone Company is shown in Figure 7.

The San Joaquin Associated Telephone Company employs concrete framing in a brick building set on a 4-inch concrete slab. Glass block windows are placed in two walls to give some natural lighting. The roof is of frame and asbestos shingle construction. A plaster ceiling is employed and the attic space is vented by a rotary wind motor ventilator. The attic is vented into the room below, which in turn is vented through fixed louvers in the door.

General Telephone Corporation is investigating the feasibility of designing a prefabricated building which might either be assembled at the site, or transported there after assembly at a convenient central point. Preliminary investigation is under way of a metal building constructed of galvanized steel, aluminum, or stainless steel sheets stretched on a steel frame. The sheets would be stretched tight between the frame members by being wedged into supporting channels on all four sides. Either a flat or hip-type metal roof could be obtained. At least two inches of insulation would be required, and if electric heat were provided, at least twice that amount would be required to control heating cost. No ventilation would be required. This building, set on a concrete slab, would probably cost less than $1,200 in the 400-line size or well under one-half the cost of a masonry building of the same size.

Conclusion

Rising building costs are focusing attention on the need for an economical building design. An analysis of the cost of recently constructed masonry buildings has indicated to the authors that wood-frame construction should be specified for small offices in which limited operating revenues make control of plant investment a paramount consideration. For example, the bill of materials for a rather plain 200-line masonry building built this year was about $1,200, or about one-third the cost of the completed building. In the construction of this building, carpenters, masons, tile setters, electricians, bricklayers and truck drivers, with their helpers were necessary, and these craftsmen travelled daily to the site from neighboring cities. A low-cost building is not attainable under these conditions.

A building comprised of prefabricated metal or wood sections, which could be erected on the site by two or three workmen might offer a solution, but at this time, a suitable prefabricated design does not seem to be available.

A building of conventional wood-frame construction could in most cases be built in the small town by local craftsmen, and seems to offer the most promise for control of cost in such small communities. The recommendation of the authors for the design features of such a building are as follows:

1. The site should be on a secondary street rather than on a main street, to obviate the necessity for architectural ornamentation. A rear-lot site with alley access would be suitable if the neighboring structures do not offer fire hazards.

2. A reinforced concrete base poured over a waterproof membrane, laid on a gravel fill, should be specified to prevent moisture seeping through the floor.

3. The walls and roof should be covered

with asbestos shingles laid over 3/4-inch wood or composition sheathing to provide a degree of resistance to fire. Two inches of insulation in the form of strips laid between the studs and joists should be supplied. The interior should be finished with gypsum board or similar material nailed to the studs and ceiling joists thus avoiding the necessity for employing plasterers.

4. A wood floor of 3/4-inch plywood laid on wood joists and covered with linoleum or similar floor covering should be specified. Such a floor will be warmer than a concrete floor.

5. The space between ceiling and roof should be vented to prevent excessively high summer temperatures. No other ventilation is required. A gable rather than a hip roof may be specified for better ventilation. Storm water drains from the roof should be omitted to reduce costs.

6. A fire-resistant metal sheathed wood door should be specified. Metal weather stripping should be employed to eliminate entry of dust or rain.

7. Outlets should be provided for a thermostatically controlled electric heater of the blower type, and for a portable a-c engine-generator, for use in the event of a commercial power failure.

8. A 4-inch gravel fill should be placed around the building foundation for a distance of four feet, to prevent the walls being splashed by drainage from the roof and thereby stained. This fill should be sprayed to prevent growth of weeds.

9. In localities where termite infestation is prevalent, a sheet-metal shield should be installed along the upper edge of the foundation to prevent termite colonies reaching the wood floor or wall members.

No Discussion

General Aspects of Community Dial Office Equipment

ALBERT BURKETT
MEMBER AIEE

COMMUNITY dial central office equipment is used presently as central office equipment serving exchanges which vary in size from a few lines to several hundred lines. The equipment is usually located at a point some distance from traffic and plant department personnel and therefore must operate satisfactorily on an unattended basis, except for routine visits. The equipment should adequately provide all the necessary services required in its service area. It should be reasonable in first cost and low in maintenance. It should be compact in size so as to require a minimum building space, yet it should be easily accessible for maintenance. It is desirable that it be readily expandable to care for growth and for the addition of service features.

Community dial offices are telephone central offices of the dial-switching type that are designed particularly for small communities. They are distinguished by relatively small size, by a preponderance of multiparty lines, by equipment assemblies designed for quick installation at remote points, and by maintenance features to facilitate unattended operation with a high grade of service.

Low cost is an important objective in the design of community dial offices because they frequently serve sparsely settled areas where it is difficult to furnish adequate telephone service at reasonable costs. However, these offices are designed for providing all service features that may be desired by the customers at a reasonable cost.

Many community dial offices serve less than 100 subscriber lines. Other offices serve several hundred up to a thousand or more lines. Larger offices are generally considered outside of the community dial category, although their features may in many cases be essentially the same.

Service Features

General

The service features required for community dial offices vary from location to location, depending upon size of the office and its proximity to larger centers of population. However, these service features may be divided into two general classifications: those required in all offices; and those required for the particular installation in question.

Multiparty Lines

Provision must be made in all cases for serving lines on a multiparty basis and, in general, equipment capable of serving lines having eight or ten parties per line will be adequate. However, in certain areas it may be necessary that the equipment be arranged to handle lines serving up to 20 parties each. In smaller community dial offices individual, 2-party, and 4-party lines are handled as unfilled multiparty lines. Provision also may be made for handling a small group of lines on a consecutive line hunting basis. In addition to these lines which are arranged for flat rate service, it is usually necessary to serve coin stations. In a very large percentage of community dial offices these lines are served on a post payment coin basis, that is, deposit of coins after answer of the called party or upon request by the operator.

Uniform Audible Signals

In order that telephone users throughout the country may be able to dial calls in a uniform manner, it is necessary that any audible signals that they may encounter in making a call be uniform. The first of these audible signals which the user will encounter is dial tone, which tells him the equipment is ready for him to begin dialing. The time interval between removing the receiver from the telephone to application of dial tone should be as short as possible, to reduce to a minimum the probability of mutilated dialing. When the calling party has been connected to another line or to a trunk to an operator, he should receive an audible ringing indication to satisfy him that the called party or operator is being signaled. If the user encounters a busy condition, he should receive busy tone. Busy tone is a tone of the same fundamental frequency as dial tone but interrupted 60 times per minute. The length of the tone intervals and silent intervals being 0.5 second each.

Reverting Call Arrangements

Reverting call arrangements must be provided to enable stations on the same line to call each other. Where the exchange is equipped for bridged or divided code ringing, reverting calls may be made by the calling subscriber dialing the listed directory number of the desired station on his line. Upon completion of dialing busy tone will be returned. The calling subscriber then hangs up and the central office equipment tests to determine if the calling and called lines are the same. If so, the called code is rung. If the line is arranged for divided ringing, a reverting ring one half second in length should be rung on the opposite side of the line during each half of the ringing cycle. When ringing is tripped due to answer of the called party, the calling party lifts his receiver and the conversation may begin.

Paper 50-249, recommended by the AIEE Communication Switching Systems Committee and approved by the AIEE Technical Program Committee for presentation at the AIEE Fall General Meeting, Oklahoma City, Okla., October 23-27, 1950. Manuscript submitted July 25, 1950; made available for printing August 25, 1950.

Albert Burkett is with the Bell Telephone Laboratories, Inc., New York, N. Y.

In offices arranged to serve multiparty lines on a semiselective or full selective basis, reverting call selector circuits must be provided. These circuits are usually reached from a selector level of first selectors or their equivalent. In offices equipped with reverting call selectors, the calling party must dial an arbitrary number rather than the listed directory number to reach another station on his line. Otherwise the method of operation by the subscriber is essentially the same as for the directory number method.

Operator Office Trunks

Trunks for handling traffic to the operator office are reached by dialing "0" and are usually arranged for 2-way operation. In order that the trunks may be used with various types of outside plant facilities it is necessary that they be available for loop, composite, or simplex signaling operation. Since they are used in common by flat rate and coin subscribers, facilities are provided so that the operator may know when coin stations originate the calls, so she may request deposit of coins. This is usually done by applying a short spurt of dial tone at the time the operator answers. It is desirable that the arrangement should be such that the operator may check for this tone by pulling down the cord and replugging.

Under some conditions it may be desirable to route traffic from a community dial office through another community dial office used as a tandem center. For this arrangement, the trunks from a tandem center to the operator office are as previously described. The trunks between the end community dial office and the tandem point may be arranged for access to the operator office only, as shown in Figure 1, or for dual use as trunks to the operator office and as dial trunks for completing calls between subscribers at the end office and the tandem office, as shown in Figure 2. In either case, subscribers at the end community dial office should reach the operator by dialing a single digit "0". When the trunk is arranged to reach the operator office only, the dialing of the digit "0" causes the community dial office equipment to select a trunk to tandem. At the tandem office the trunk is automatically connected to one of the common groups of operator trunks, without the need of extra digits. If the trunk is arranged for traffic both to the operator and to the tandem office, the community dial office equipment selects the trunks to tandem when the subscriber dials "0" and then the trunk automatically sends a digit "1" to the tandem equipment. This digit causes a trunk to be selected to the operator office. If the trunk is used for a call terminating in the tandem office, a digit other than "0" is used to select the trunk, and then the regular listed directory number is dialed for completing the call.

In areas served by several community dial offices which reach the operator office through a tandem point, and where there is a toll charge for calls between offices, as shown in Figure 1, it is sometimes desirable to use dial-back type operator office trunks between the tandem office and the operator office. Dial back operator office trunks are trunks over which an operator may receive an incoming call from a community dial office and complete it by dialing back over the same trunk to subscribers in the community dial office where the trunk terminates, or via that community dial office to subscribers in a dial exchange beyond. This type of trunk may be desirable where excessive backhaul would otherwise be involved. In general, trunks of this type have disadvantages from an operating viewpoint for use with an operator office employing a large toll board because the supervision is different from that on regular operator office trunks. However, there may be cases where avoidance of long backhaul would result in appreciable savings.

There are two general types of dial back trunks:

1. Simple dial back, where the calling subscriber holds the line while the operator dials back over the same trunk to reach the called party.

2. Dual dial back, which functions similarly to (1) but also allows the operator to complete calls on a delayed basis. To complete a delayed call the operator first dials the calling party and upon answer she then proceeds to dial the called party over the same trunk. These trunks require circuits at the operator office which permit dialing back against either on-hook or off-hook supervision.

Stop-Dial Signals

Trunks from operators which terminate on line circuits or for other reasons are not prepared to receive dial pulses upon seizure should be arranged to give a stop-dial signal. This signal consists of an off-hook condition which should persist from immediately after seizure to the time the trunk is in condition to receive pulses. The stop-dial signal functions to stop operators or mechanical senders from pulsing to trunks before the circuits have conditioned themselves to receive pulses.

Figure 1. Tandem trunking arrangement for access by subscribers to operator only

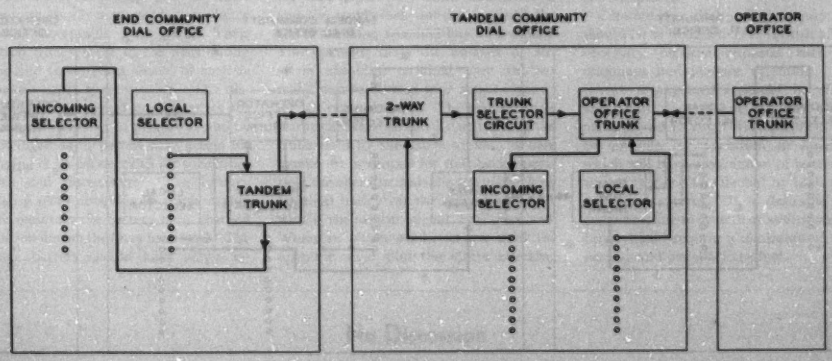

Flashing Supervision to Operators

All circuits which complete calls from toll operators should be arranged to give the originating operator flashing supervision when a line busy or trunk busy condition is encountered. The speed of flashing for line busy is 60 interruptions per minute with tone and for trunks busy is 120 interruptions per minute without tone.

Control of the Connection

On calls between subscribers in the same exchange, the calling party usually has control of the connection. On calls from a subscriber to an operator, the connection should be jointly controlled by both subscriber and operator after answer by the operator. This arrangement permits the subscriber to flash the operator and also allows the operator to change cords, if necessary, without losing the connection. On calls from the operator to a community dial office subscriber the operator usually controls the connection. This arrangement allows the subscriber to flash but prevents him from holding a trunk out of service due to failure to hang up.

Traffic Registers

Traffic registers are provided to determine the amount of traffic handled by the office and also to determine if calls are being lost due to an insufficient amount of equipment. The following registers are usually provided:

1. Peg count register per finder group.
2. All finders busy register per finder group.
3. Peg count register per incoming selector group.
4. All trunks busy register per trunk group.
5. All trunks busy register for reverting call selectors.
6. Peg count register per connector or final group.

Terminal Per Line versus Terminal Per Station Service

Smaller community dial offices in rural areas are nearly always arranged to serve subscribers on a terminal per-line basis. This makes for economy in amounts of terminating equipment. However, some flexibility is sacrificed and the problem of providing intercept service, if required, is made more difficult and costly. In areas where these features may be required, it is desirable to serve subscribers on a terminal per-station basis. This is usually the case in offices exceeding roughly 500 lines in ultimate size and in all offices, regardless of size, which are located near metropolitan areas.

Transmission Balance

At the present time, with the expanding use of electric services in the rural areas, it is essential that transmission circuits be as carefully balanced as possible to avoid noise due to inductive interference. It is necessary to have the subscriber lines balanced as well as possible, but it also is necessary that all central office terminations which may be connected to these lines be carefully balanced.

Community dial offices frequently have to be arranged to give services that are not uniformly required in all offices. The most commonly encountered of these services are verification, intercepting, and message rate line circuits.

Verification

It is desirable that verification arrangements be provided where possible, particularly in offices near metropolitan centers, in order that emergency calls may be completed to busy lines. These facilities also permit verification of a line busy condition. In community dial offices verification calls are usually completed through the regular switch train by the operator dialing a preliminary or supplementary code in addition to the subscriber's number. The arrangement most generally used is to dial a code followed by the number to be verified. Verification facilities should be available to operators only. Wherever verification facilities are provided they should be of such a type as to permit a uniform method of operation with all the community dial offices involved.

Intercepting Service

Intercepting facilities are not ordinarily provided in offices of less than 500 lines unless the offices are adjacent to metropolitan areas, due to the cost of this type of equipment. In offices not equipped with intercept facilities, final terminals should not be made busy nor return the audible ringing signal to calling subscribers or operators, since these signals would be false indications. If intercept facilities are not used, it is desirable that the equipment be arranged so that no signal is returned on the call.

Message Rate Service

In some cases it may be necessary to serve a few lines on an individual line message rate basis. This is usually accomplished by the addition of an auxiliary circuit ahead of the regular line circuit. The auxiliary circuit operates the subscriber message register upon answer of

Figure 2. Tandem trunking arrangement with dual use trunks

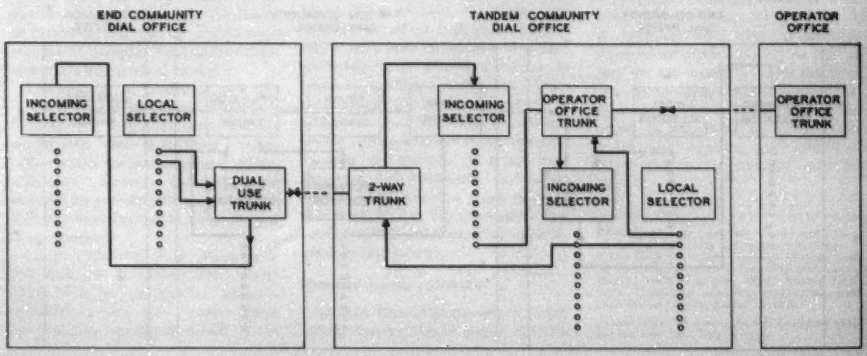

the called party. To prevent improper operation of the circuit due to surges, a delay interval of 2 to 4 seconds is usually provided between the answer of the called party and the actual application of the charge condition.

Equipment Features

Simplified Installation

It is desirable that community dial equipment be designed in such a manner as to permit the maximum amount of wiring and cabling at the factory. This tends to reduce installation time on the job. The equipment may be arranged in unitized packages; these packages to be of such dimension and weight as to be handled easily in shipment and permit entrance through standard sized doors. For the very small sized offices, it may be possible to have the equipment for the entire office mounted on one such frame. For larger offices several frames may be required. Although it is desirable to have the equipment frames as small and compact as possible, care should be exercised to prevent crowding of apparatus and difficult access for maintenance. The total weight of the frame should not exceed reasonable permissible floor loading limits.

Adequate Traffic Capacity

The design of the frames should allow for an adequate number of switching paths to care for expected growth in lines and traffic. Although the initial installation may not require the frame or frames to be fully equipped, the ability to add circuit units as required as economically as possible is desirable. This may be accomplished in many cases by the use of "jacked-in" units.

Standard Floor Plan

Installations requiring two or more frames are usually arranged in accordance with an acceptable floor plan. Their location with respect to the distributing frame and power plant should be such as to permit short runs of cable. The distributing frame should provide space for an adequate number of protectors and be so arranged as to permit easy access for changing cross connections for subscriber moves and disconnects. The battery charging plant should have ample capacity to maintain the battery in a charged condition during the busy hour load. The storage battery should have ample reserve capacity to protect against office failure during times of commercial power stoppages. The necessary reserve for any particular office is usually determined by an estimate of the reliability of the commercial power service, and will vary in different areas.

Table I

	Alarm Transmitted after Delay of:	Signal on Checking Terminal
Major Alarms		
Main and common fuses blown	0	No tone
Ringing failure	1–4 minutes	No tone
Low or high voltage	1–4 minutes	No tone
Master charge control relay failure	1–4 minutes	No tone
Line finders blocked	1–4 minutes	No tone
Excessive Number of Permanents	0	Dial tone
Minor Alarms		
Individual fuses blown	0	Busy tone
Ringing transfer	1–4 minutes	Busy tone
Release magnet failure	1–4 minutes	Busy tone
Permanent signals less than excess number	20–60 minutes	1-ring code
No trouble		2-ring code

Maintenance Facilities

Alarms

Since community dial office equipment is unattended, means may be provided to supervise the operating condition of the office. This is accomplished by providing a final terminal as an alarm checking terminal. Whenever this terminal is dialed by the distant operator or maintenance man, the presence of tones or lack of tone indicates the condition of the office. In addition to the alarm checking terminal, an alarm sender is usually provided. When a trouble condition occurs at the community dial office the alarm sender seizes a regular trunk to the operator office. When the operator answers, no special indication of the trouble is given. It appears to be an abandoned call except the cord supervisory lamp remains dark and the trunk does not release until the alarm checking terminal has been dialed. The operator dials the number of the alarm checking terminal over another trunk and receives a tone signal indicating the class of alarm. The dialing of the alarm checking terminal also releases the trunk used by the alarm sender. Where trunks are arranged for dial back operation, the operator dials the alarm checking terminal back over the same trunk over which the alarm signal was received. When an alarm sender is not used the operator must dial the alarm checking terminal periodically to determine if a trouble condition exists. When an operator receives an alarm indication she refers it to proper channels for action.

The signals given in Table I are usually used to indicate the class of alarm when the alarm checking terminal is called.

General Maintenance Facilities

As stated before, easy access to all apparatus greatly facilitates maintenance. In many cases most routine tests and maintenance operations will be performed by personnel who spend only a part of their time working with central office equipment. Therefore, it is important that testing procedures be as simple and straightforward as possible. Most of these tests can be in the nature of operational tests. The circuits employed in community dial offices should be simple and the use of marginal operating arrangements avoided where possible. Simple make-busy arrangements should be provided to hold circuits which are in trouble out of service. In general, fewer common circuits and relatively simple circuit design will result in easier maintenance of the equipment.

Community dial office equipment should be so designed as to furnish all the necessary services required with the minimum maintenance attention. The circuit arrangements should be simple and easily understandable. The equipment should be rugged in design so as to be suitable for operation in buildings which will have a minimum of heating in winter, yet not be affected by high summer temperatures. It is desirable that expansion due to growth or additional features should require a minimum of engineering and installation effort.

No Discussion

Some Aspects of Lightning Surges on Power Systems and Their Suppression

S. KANEFF
ASSOCIATE AIEE

Synopsis: The paper points out that lightning surges contain an infinite band of frequency components and for this reason, the behavior of a system to surges depends on its impedance characteristics over a wide range of frequencies.

A capacitive-inductive suppression device is suggested and design details and test results given. This device is most effective for short-duration steep-sided surges. At present, it seems practicable for lower voltage circuits but if cheaper capacitors can be constructed, it also could be used for higher voltages.

An aspect of power systems not usually considered by power engineers is that of behavior at frequencies well above the generated frequency.

Although not of interest during normal conditions, this behavior becomes important when surges, especially due to lightning, impinge on the system. Lightning surges contain (as indicated in the following section) an infinite band of frequencies, and it is clear that impedance characteristics should be known over a wide range of frequencies in order that a clear picture be obtained of system behavior when subjected to surges.

Considering lightning surges in terms of frequency components suggests suppression devices similar to communication-type low-pass filters and consisting of capacitors and inductances.

At present such protection seems to be practicable for low-voltage circuits, where it should find many applications, but an obvious objection for high voltages is the cost of capacitors. However, high-voltage capacitors are being used more extensively (for example, for power-factor correction, carrier-system coupling units, potential dividers, and so forth) and it is possible that with improvements in techniques, capacitors may be economically available for the higher-voltage systems also.

Amplitude-Frequency Spectrum Analysis

As is well known, lightning surges can be expressed mathematically by the relation

$$f(t) = E(e^{-at} - e^{-bt}) \tag{1}$$

Surges can be represented with sufficient accuracy by equation 1 by suitably choosing the parameters a, b, and E, Figure 1.

It is proved in mathematical texts that if a function in time, $f(t)$, can be represented as

$$f(t) = \int_{-\infty}^{\infty} g(\omega) d\omega e^{j\omega t} \tag{2}$$

then it can be converted into a frequency function

$$g(\omega) = \frac{1}{2\pi} \int_{-\infty}^{\infty} f(t) dt e^{-j\omega t} \tag{2}$$

subject to certain restrictions which are, however, fulfilled by any practical function, see the appendix and reference 1.

The frequency function for a lightning surge represented by equation 1 is then given by

$$g(\omega) = \frac{E}{2\pi} \left\{ \left(\frac{1}{a+j\omega} - \frac{1}{b+j\omega} \right) \right\}$$

and the amplitude-frequency spectrum is

$$|g(\omega)| = \frac{E(b-a)}{2\pi\sqrt{a^2b^2+\omega^4+\omega^2(a^2+b^2)}} \tag{3}$$

see Appendix.

Figure 2(B) shows amplitude-frequency spectra for four typical surges, the ordinate at any abscissa value gives the actual amplitude of the sinusoidal component of that frequency.

From equation 3 and from Figure 2 it is evident that:

1. All frequencies from zero to infinity are present in the surge.
2. As the duration of the loop of the surge increases, the spectrum height increases for the lower frequencies and decreases for the higher—more of the energy being concentrated in the lower-frequency components—and conversely, the shorter the loop, the more is the energy concentrated in high frequencies.
3. In general, the most destructive surges have a comparatively short loop and steep sides, these have most of their energy in the higher frequencies.

It follows then, that if a clear physical picture is to be obtained of the behavior of a system subjected to lightning surges, it is necessary to know its impedance-frequency characteristic from power-frequencies up to quite high frequencies. If this characteristic is known, then a better understanding will be reached as to the

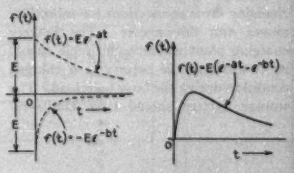

Figure 1. Typical lightning surge

Paper 50-250, recommended by the AIEE Transmission and Distribution Committee and approved by the AIEE Technical Program Committee for presentation at the AIEE Fall General Meeting, Oklahoma City, Okla., October 23-27, 1950. Manuscript submitted May 15, 1950; made available for printing September 5, 1950.

S. Kaneff is with the Electrical Engineering Department of The University of Adelaide, Adelaide, Australia.

The author wishes to express his appreciation for the co-operation shown by the Electricity Trust of South Australia in allowing him the use of equipment and personnel for his tests. Thanks are due to R. E. Vowels and E. Heider for valuable suggestions, while special acknowledgment is due to Professor E. O. Willoughby who suggested the research and under whose direction it was conducted. The author also wishes to acknowledge the assistance received from the Electricity Supply Association of Australia, by the provision of funds through the Electrical Research Board.

type and characteristics of protection devices required.

Requirements of a Suppression Device

From the previous section it is seen that the complete suppression of a surge involves the elimination of a band of frequencies from zero to infinity.

Practically, complete suppression is unnecessary; it is sufficient that the amplitude and steepness of a surge be reduced to values permitted by the strength of protected apparatus.

In terms of the amplitude-frequency spectrum, for effective suppression, as many of the frequency components as is practicable, should be eliminated.

T, π, L Networks as Surge Suppressors

The problem of suppressing a band of frequencies above the transmitted (power) frequency is solved in communication circuits by low-pass filters—T, π, or L networks in the simplest form, see Figure 3(A).

Such networks should, therefore, suppress lightning surges.

Theory

The method of connecting the network in a power circuit is indicated in Figure 4(A) and (B). Figure 3(B) shows the well-known attenuation characteristic of a low-pass filter. For the present discussion, it is convenient to consider this in a slightly different form as in Figure 3(C), where ordinate values represent the quantity:

$$\frac{\text{Output Voltage from Filter}}{\text{Input Voltage to Filter}}$$

at each frequency. At any given frequency, this curve shows what fraction of the amplitude of that particular frequency component is transmitted by the suppression network, and what fraction is suppressed.

Applying the curve in Figure 3(C) to the amplitude-frequency spectrum of an incident surge will give the amplitude-frequency spectrum of the surge emerging from the suppression network. In Figure 2(B), this has been done for the surges of Figure 2(A). The full lines represent the amplitude-frequency spectrum of the incident surge and the dotted lines that of the transmitted surge.

It will be noted that the network has eliminated the higher frequencies, leaving low-frequency components only. This indicates that the surge transmitted by the suppression network has been reduced in amplitude and steepness and lengthened in time. This is confirmed by the output surges as calculated in the Appendix and recorded in Figure 2(C).

The effect of the T, π, or L network is, therefore, to reduce the surge in amplitude and steepness and to lengthen it in time; that is, to render it less harmful. The network acts for surges of any magnitude (unlike spark-gap devices, which act only after the voltage has attained a certain amplitude.)

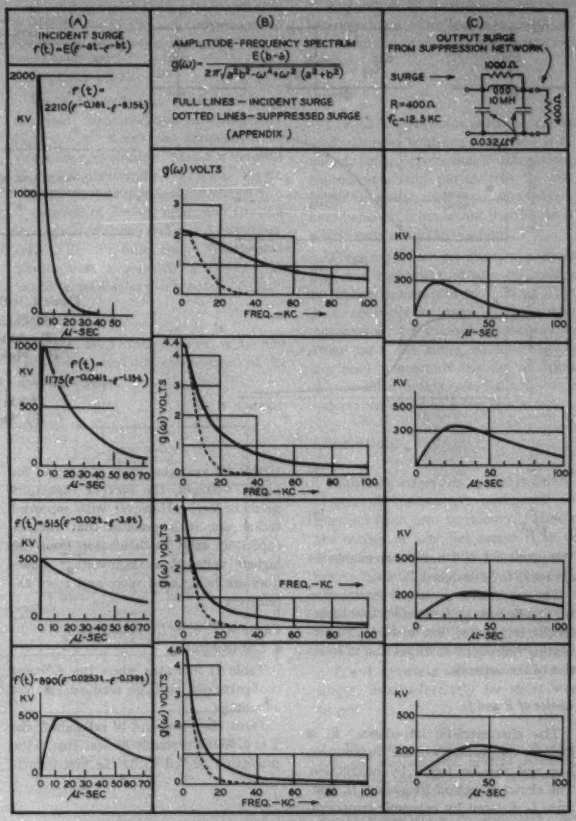

Figure 2. Amplitude-frequency spectra and network suppression

(A) Incident surge
(B) Amplitude-frequency spectrum
(C) Output surge from suppression network

Design

The following sections indicate the manner of designing a T, π, or L network for a practical setup.

Equations

The algebraic relations for low-pass filters (as given in any elementary text) are:

$$R = \sqrt{\frac{L_1}{C_1}} = \text{characteristic impedance, line to earth} \quad (4)$$

$$f_c = \frac{1}{\pi\sqrt{L_1 C_1}} = \text{cut-off frequency of the filter} \quad (5)$$

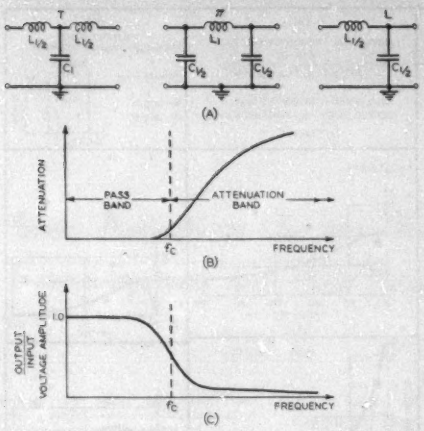

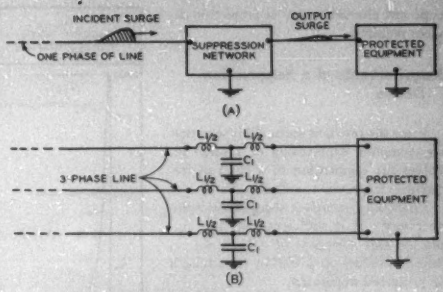

Figure 3 (left). Low-pass filters—T, π, L networks
(A) Circuit arrangement
(B) Attenuation characteristic
(C) New form of attenuation characteristic

Figure 4 (above). Method of connecting suppression network
(A) In general
(B) Using T network in 3-phase line

$$L_1 = \frac{R}{\pi f_c} \tag{6}$$

$$C_1 = \frac{1}{\pi f_c R} \tag{7}$$

Equations 4, 5, 6, and 7 then enable the networks to be designed.

The suppression network is matched to the line by making R of network = characteristic impedance, line to earth, so preventing reflections of surges due to insertion of the network.

Choice of R and f_c

The characteristic impedance, R, is fixed by the geometry of the transmission line and can be found by calculation. The choice of cut-off frequency, f_c, however, is dictated by economic considerations.

Table I shows size of components for various cut-off frequencies for characteristic impedances of 400 ohms and 600 ohms, most lines having values of this order.

Practical tests have indicated that f_c need not be below 10 kc for effective suppression. At present, such a cut-off frequency appears to be economically practicable for voltages below 66 kv, but for higher voltages, the cost of capacitors would be large. However, with improved techniques, it is possible that cheaper capacitors may be made for even the highest voltages, as high-voltage capacitors are being used more and more extensively.

Table I. Network Constants

Cut-off Frequency, f_c, cycles	R = 400 Ohms L_1, Millihenrys	R = 400 Ohms C_1, Microfarads	R = 600 Ohms L_1, Millihenrys	R = 600 Ohms C_1, Microfarads
5,000	25.5	0.16	38.2	0.107
10,000	12.75	0.08	19.1	0.053
20,000	6.38	0.04	9.55	0.0265

Choice of T, π, or L—Impedance Considerations

Table II indicates where the different configurations may be used to greatest advantage.

From the viewpoint of reliability, the T or L would probably be best, due to the protection offered C_1 by the first inductance.

A knowledge of the impedance frequency characteristics of protected equipment is desirable, as this allows a proper design of protection to be made. Figure 5 shows the impedance frequency properties of a small substation, Figure 5(A), and also a large switchyard, Figure 5(B). In the first case, the terminal impedance is mainly high and π suppression would be recommended, while in the second, the impedance is low and T suppression would be best. (L suppression could be used for either case.)

Suppression of Ringing

To prevent ringing of the suppression networks due to steep-sided surges, the

Table II

Network	Remarks	Recommended for Following Terminations	Examples of Where Beneficial
Surge T 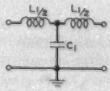	C_1 is protected from full surge by $L_{1/2}$. T presents high impedance in either direction	Low impedance capacitive and inductive	Large substations and large transformers
Surge π 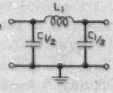	First $C_{1/2}$ unprotected from full surge. π presents low impedance either way	Inductive or capacitive. High impedance	Small substations and small transformers. Rotating machines
Surge L 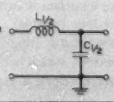	For given f_c, suppression not as good as T or π, but cheaper	Capacitive or inductive.	Substations, transformers, and rotating machines

inductances must be damped by resistors. If resistive ohms = numerically reactive ohms of inductance at f_c, then volt amperes/watt ratio for the resistive inductive branch will be equal to, or less than, unity for frequencies at and below f_c, and no ringing will occur.

The capacitors should be protected against exceedingly high voltages (in excess of maximum capacitor strength) by spark gaps—necessary for the π network, but not so important for T and L, as the capacitor is connected to a low-voltage point in the latter cases.

Effect of Suppression Device on Power-Frequency Operation

A practical suppression network will have negligible effect on the operation at power frequencies. For example, the network used in Figure 6(A) corresponds to a length of line of the order of two miles (as far as reactance is concerned).

Results of Tests

Figure 6 records tests carried out using recurrent surge oscilloscope equipment. Figure 6(A) shows the suppression of various surges obtained from a π network of $R = 400$ ohms and $f_c = 12.5$ kc. Figure 6(B) shows the suppression produced by a T network of $R = 600$ ohms and $f_c = 12.5$ kc connected at the end of a 33-kv transmission line $2^1/_4$ miles long. This demonstrates that a network of $f_c = 12.5$ kc would be satisfactory in practice.

Effectiveness

Figure 2(C) and Figures 6(A) and (B) indicate that the effectiveness of the T, π, L networks decreases as the surge becomes longer and less steep, and increases as the surge becomes steeper and shorter.

Uses

T, π, or L suppression networks can be used wherever lightning protection is required, for the protection of substations, transformers, and particularly for machines connected directly to transmission lines (where it is important that no steep-sided surges enter the machine).

Where capacitors are already in use on lines and equipment, it may be possible by adding inductances to build up T, π, or L networks for more effective surge suppression; for example, capacitors are often used for surge modification on machines connected directly to transmission lines, in this case, the addition of inductance would be a simple matter.

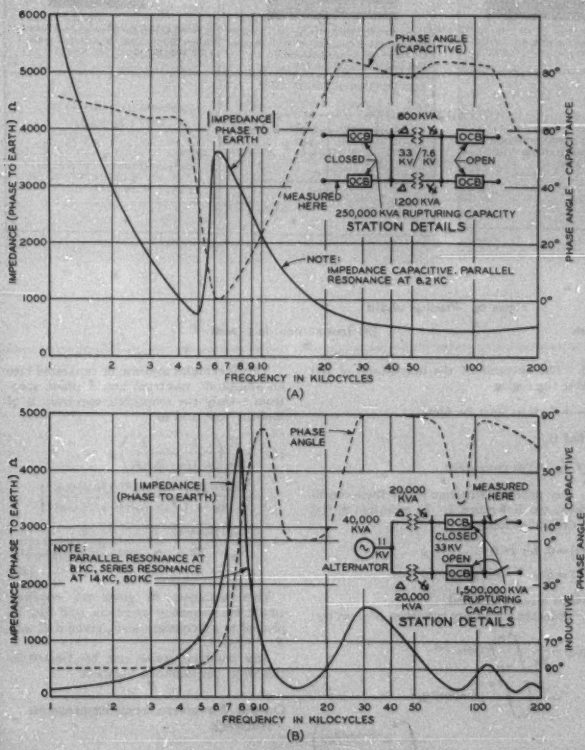

Figure 5. Impedance-frequency characteristics

(A) Small substation (B) Section of power station switchyard

Conclusions

Lightning surges can be analysed into a system of components having all frequencies from zero to infinity. Most of the energy of long flat surges is in the lower frequencies, while for short steep surges (generally the most destructive), the energy is mainly in the higher frequencies. A knowledge of impedance-frequency characteristics of systems over a wide range of frequencies is desirable.

T, π, L networks will suppress lightning surges, most effectively for short steep surges.

1. The networks reduce a surge in amplitude and steepness and prevent oscillations in terminal equipment. The networks act for surges of any amplitude.

2. They can cause no reflections (since they are matched to the line) and voltage cannot build up between themselves and protected equipment due to reflection.

3. For given cut-off frequency, a T network is best; L is most economical but not as good a suppressor.

4. T, π, L networks have negligible effect on the power-frequency operation of a system.

5. Where capacitors are already used, it may be possible by adding inductances to form T, π, or L networks for better suppression.

6. T, π, L networks will suppress the frequency components above f_c of any surge, switching, and so forth.

7. At present, these networks appear to be practicable for voltages below 66 kv. With improved techniques in capacitor manufacture, it may be possible that the networks also will be feasible for much higher voltages.

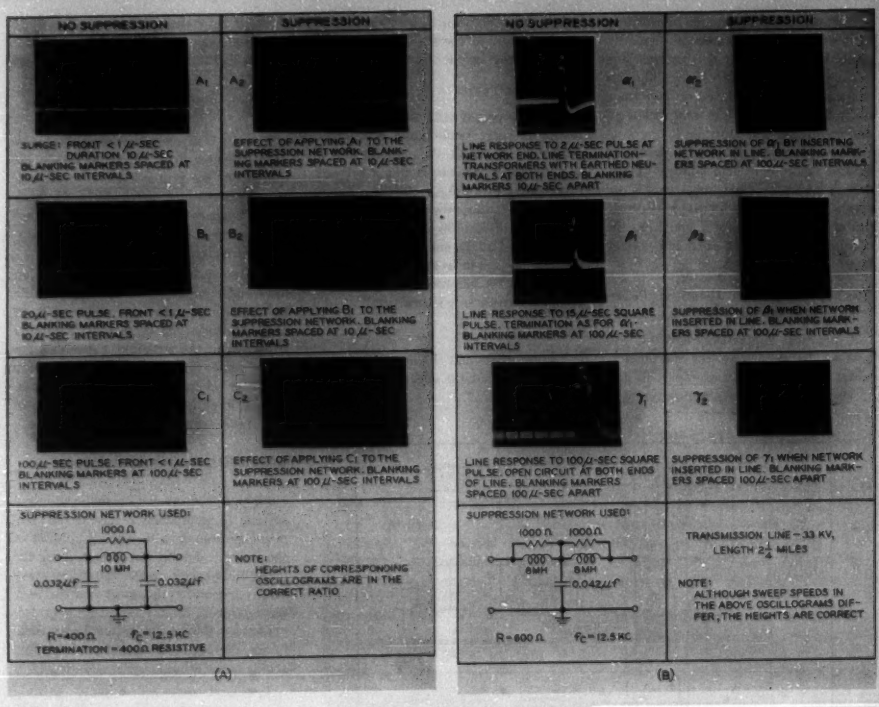

Figure 6. Practical results

(A) Network tests **(B) Transmission line tests**

Appendix

Frequency Spectrum of Surges

$$f(t) = E(e^{-at} - e^{-bt}) \tag{8}$$

It is proved in textbooks of mathematics that, if a function in time, $f(t)$ can be represented as

$$f(t) = \int_{-\infty}^{\infty} g(\omega)\, d\omega\, e^{j\omega t} \tag{9}$$

then it can be converted into a frequency function

$$g(\omega) = \frac{1}{2\pi}\int_{-\infty}^{\infty} f(t)\, dt\, e^{-j\omega t} \tag{9}$$

This is the Fourier Integral in a general form.

The restrictions on $f(t)$ are:

1. $f(t)$ must be continuous over intervals of finite length. At points of discontinuity, say at $t = a$, the value of the function shall be understood to be the arithmetical mean; that is

$$f(a) = {}^1/_2\{f(a-0) + f(a+0)\}$$

2. The integral of the magnitude of $f(t)$ over the region

$-\infty < t < \infty$ must be finite

that is,

$\int_{-\infty}^{\infty} |f(t)|\, dt$ must exist

Any practical function fulfils these conditions, see Reference 1. In equation 8, $f(t)$ is defined as follows:

$f(t) = 0$, for $t < 0$

$f(t) = E(e^{-at} - e^{-bt})$ for $t > 0$

where a and b are real.

Then the frequency spectrum is given by:

$$g(\omega) = \frac{1}{2\pi}\int_{-\infty}^{\infty} f(t)\, dt\, e^{-j\omega t}$$

$$= \frac{E}{2\pi}\left(\int_{0}^{\infty} e^{-(a+j\omega)t}\, dt - \int_{0}^{\infty} e^{-(b+j\omega)t}\, dt\right)$$

$$= \frac{E}{2\pi}\left(\frac{1}{a+j\omega} - \frac{1}{b+j\omega}\right)$$

This is complex and can be separated into an amplitude spectrum and a phase spectrum. Only the amplitude spectrum is of interest here, and so

$$g(\omega) = \frac{E}{2\pi}\left(\frac{1}{a+j\omega} - \frac{1}{b+j\omega}\right)$$

$$= \frac{E(b-a)}{2\pi}\left\{\frac{(ab-\omega^2) - j\omega(b+a)}{(ab-\omega^2)^2 + \omega^2(b+a)^2}\right\}$$

$$\therefore |g(\omega)| = \frac{E(b-a)}{2\pi}\cdot\frac{1}{\sqrt{a^2b^2 + \omega^4 + \omega^2(a^2+b^2)}} \tag{10}$$

Then equation 10 gives the required amplitude-frequency spectrum and can be plotted to a frequency scale, given a, b, and E.

Any practical wave can be treated in this way; for example, Figure 2.

Output Waveform from Suppression Network

As the network cannot be considered alone, some terminating impedance (z), must be specified. For simplicity, let it be

resistive and equal to R_1, Figure 7.

It is required to find the voltage v, across R_1, when a surge V is applied to the π-type suppression network.

Using the Laplace Transform method of solution, let $v(p)$ represent the transform of output voltage, and let $V(p)$ represent the transform of input voltage.

Then,

$$v(p) = \frac{V(p)\dfrac{2}{Cp}R_1}{\dfrac{2}{Cp}+R_1} \times \left(\frac{R_2Lp}{R_2+Lp} + \frac{\dfrac{2}{Cp}R_1}{\dfrac{2}{Cp}+R_1}\right) = V(p)\frac{2}{R_2C}\times \left\{\frac{\left(p+\dfrac{R_2}{L}\right)}{\left[p+\left(\dfrac{1}{CR_1}+\dfrac{1}{CR_2}\right)\right]^2+\dfrac{2}{LC}-\left(\dfrac{1}{CR_1}+\dfrac{1}{CR_2}\right)^2}\right\}$$

$$= V(p)\frac{2}{R_2C}\left\{\frac{(p+a_4)}{(p+\alpha)^2+\beta^2}\right\} \quad (11)$$

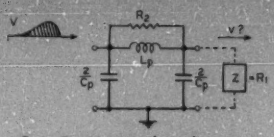

Figure 7. π section subjected to a surge

where $a_4 = R_2/L$ and $\alpha = \left(\dfrac{1}{CR_1}+\dfrac{1}{CR_2}\right)$

$$\beta^2 = \left[\frac{2}{LC} - \left(\frac{1}{CR_1}+\frac{1}{CR_2}\right)^2\right]$$

If

$$V = f(t) = E(\epsilon^{-at} - \epsilon^{-bt})$$

is applied to the network, then

$$V(p) = E\left(\frac{1}{(p+a)} - \frac{1}{(p+b)}\right)$$

$$\therefore v(p) = \frac{2E}{R_2C}\left(\frac{1}{p+a} - \frac{1}{p+b}\right)\cdot\left(\frac{(p+a_4)}{(p+\alpha)^2+\beta^2}\right)$$

from equation 11. This gives

$$v = \frac{2E}{R_2C}\left\{\left[\frac{a_4-a}{(\alpha-a)^2+\beta^2}\right]\cdot\epsilon^{-at} + \frac{1}{\beta}\left[\frac{(a_4-a)^2+\beta^2}{(a-\alpha)^2+\beta^2}\right]^{1/2}\cdot\epsilon^{-\alpha t}\sin(\beta t+\psi_1) - \left[\frac{a_4-b}{(\alpha-b)^2+\beta^2}\right]\cdot\epsilon^{-bt} - \frac{1}{\beta}\left[\frac{(a_4-\alpha)^2+\beta^2}{(b-\alpha)^2+\beta^2}\right]^{1/2}\cdot\epsilon^{-\alpha t}\sin(\beta t+\psi_2)\right\} \quad (12)$$

where

$$\left[\left(\psi_1 = \arctan\frac{\beta}{a_4-\alpha} - \arctan\frac{\beta}{a-\alpha}\right.\right.$$

$$\left.\left.\psi_2 = \arctan\frac{\beta}{a_4-\alpha} - \arctan\frac{\beta}{b-\alpha}\right)\right]$$

Equation 12 gives the output wave from the network. This has been used in Figure 2(C) to obtain the output waves shown.

Reference

1. Communication Networks, E. A. Guillemin. John Wiley and Sons, New York, N. Y., volume II, September 1949, pages 461–70.

No Discussion

Synchronous Machine Damping Torque at Low Speeds

CHARLES CONCORDIA
FELLOW AIEE

IN connection with the problem of starting two electrically connected synchronous machines from rest,[1] damping torque is one of the important factors. This has been indicated by the results of the approximate starting performance calculations neglecting rotor resistances presented in reference 1, which show in some cases amplifying oscillations after synchronizing sufficiently severe to cause loss of synchronism. The object of this paper is to show the magnitudes and characteristics of the damping torque as affected by the various system parameters, including the rotor circuits.

The observed tendency toward negative damping may be explained qualitatively by noting that operation at low speed is roughly equivalent to operation with high armature resistance, and it has been known[2] for a long time that high armature resistance tends to produce a component of negative damping in a synchronous motor or generator operating in parallel with other synchronous machines. On the other hand, if the armature resistance becomes extremely high, its contribution is a component of positive damping torque.[3] Both of these previous conclusions are found to be in accord with the results obtained in the present study.

Two Round Rotor Machines—Rotor Circuits Neglected

As an approximation to the actual conditions, small oscillations, at a prescribed frequency, about a constant average synchronous speed have been assumed. Then if rotor windings are neglected and $x_d = x_q$ for both machines, the system equations are:[4]

$$(px+r)i_{d1} - xi_{q1}p\theta_1 = E_2 \sin(\theta_2-\theta_1)p\theta_2$$
$$xi_{d1}p\theta_1 + (px+r)i_{q1} = E_1 p\theta_1 - E_2\cos(\theta_2-\theta_1)p\theta_2 \quad (1)$$

$$M_1 p^2\theta_1 = -E_1 i_{q1} - T_{L1}$$
$$M_2 p^2\theta_2 = E_2[i_{q1}\cos(\theta_2-\theta_1) - i_{d1}\sin(\theta_2-\theta_1)] - T_{L2} \quad (2)$$

where

$M = 4\pi fH$ = rotor inertia
r = total armature circuit resistance
x = total armature circuit reactance
θ = machine angle
i_d = direct-axis component of armature current
i_q = quadrature-axis component of armature current
E = equivalent rotor excitation
T = prime mover or load torque
Subscripts 1 and 2 refer to the two interconnected machines

For small oscillations about an average speed ω, equations 1 become, on dropping the current subscripts and letting $\theta_1 - \theta_2 = \delta$

$$(px+r)\Delta i_d - (\omega x)\Delta i_q = (xi_{q0}p - E_2\omega\cos\delta_0)\Delta\theta_1 + (-E_2\sin\delta_0 p + E_2\omega\cos\delta_0)\Delta\theta_2$$
$$(\omega x)\Delta i_d + (px+r)\Delta i_q = (E_1 p - xi_{d0}p + E_2\omega\sin\delta_0)\Delta\theta_1 - (E_2\cos\delta_0 p + E_2\omega\sin\delta_0)\Delta\theta_2 \quad (3)$$

Solving for Δi_d, Δi_q,

$$D\Delta i_d = [(\omega x)(-xi_{d0}p + E_1 p + E_2\omega\sin\delta_0) + (px+r)(xi_{q0}p - E_2\omega\cos\delta_0)]\Delta\theta_1 + [(px+r)(-E_2\sin\delta_0 p + E_2\omega\cos\delta_0) - (\omega x)(E_2\cos\delta_0 p + E_2\omega\sin\delta_0)]\Delta\theta_2 \quad (4)$$
$$D\Delta i_q = [(px+r)(-xi_{d0}p + E_1 p + E_2\omega\sin\delta_0) - (\omega x)(xi_{q0}p - E_2\omega\cos\delta_0)]\Delta\theta_1 - [(\omega x)(-E_2\sin\delta_0 p + E_2\omega\cos\delta_0) + (px+r)(E_2\cos\delta_0 p + E_2\omega\sin\delta_0)]\Delta\theta_2$$

where

$$D = (\omega^2+p^2)x^2 + r^2 + 2xrp$$

From equations 1, the required steady-state currents are:

$$Di_{d0} = -\omega r E_2\sin\delta_0 + \omega^2 x(E_1 - E_2\cos\delta_0)$$
$$Di_{q0} = \omega r(E_1 - E_2\cos\delta_0) + \omega^2 x E_2\sin\delta_0 \quad (5)$$

where

$$D_0 = r^2 + \omega^2 x^2$$

It also is evident from equations 4 that the relative magnitudes of $\Delta\theta_1$ and $\Delta\theta_2$ affect the torque. The amplitudes of the natural-frequency components of the machine oscillations (which are the principal components during the starting periods considered here) will be very nearly in the ratio

$$\frac{\Delta\theta_1}{\Delta\theta_2} = -\frac{M_2}{M_1} \quad (6)$$

The cases studied have involved machines of unequal inertias, the generator inertia being roughly twice the motor inertia and the total effective inertia being such as to make the per-unit natural frequency s about 0.02. For example, in the work reported in reference 1, $H_1 = 5.0$ and $H_2 = 2.55$ in most of the cases. The natural frequency is approximately given by the formula:

$$s^2 \cong \frac{T_s\ (\text{avg})}{M}$$

where

$$M = \frac{M_1 M_2}{M_1 + M_2}$$

CASE 1, $E_1 = E_2 = 1.0$, $\delta = 0$

With no steady load and equal (unit) excitations, there is:

$$E_1 = E_2 = 1.0$$
$$\delta_0 = 0$$
$$i_{d0} = i_{q0} = 0$$

Equation 4 for Δi_q is then reduced to

$$\Delta i_q = \frac{[(px+r)p + \omega^3 x]}{(p^2+\omega^2)x^2 + r^2 + 2xrp}\Delta\delta = \Delta T_1 \quad (7)$$

where $\Delta\delta = \Delta\theta_1 - \Delta\theta_2$ and T_1 = electrical torque on machine 1.

Equation 7 is valid for either machine. For an oscillation frequency s, $p = js$, and[4]

$$\frac{\Delta T_1}{\Delta\delta} = \frac{(\omega^2 - s^2)x + jrs}{(\omega^2 - s^2)x^2 + r^2 + j2xrs} = T_s + jsT_d \quad (8)$$

Paper 50-252, recommended by the AIEE Rotating Machinery Committee and approved by the AIEE Technical Program Committee for presentation at the AIEE Fall General Meeting, Oklahoma City, Okla., October 23–27, 1950. Manuscript submitted June 19, 1950; made available for printing August 30, 1950.

CHARLES CONCORDIA is in the Analytical Division of the General Electric Company, Schenectady, N. Y.

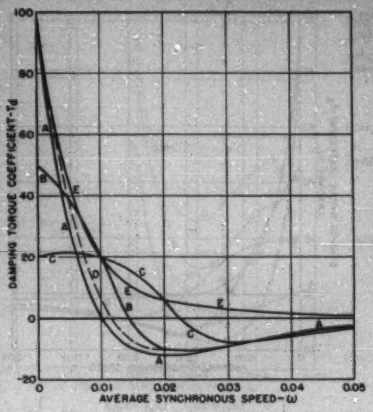

Figure 1 (left). Damping torque coefficient for oscillations at frequency s, of two synchronous machines running at low speed ω

$E_1=E_2=1.0$; $\delta=0$; $x=1.0$; $r=0.01$
Curve A, $s=0$; B, 0.01; C, 0.02; D, 0.5ω; E, ω

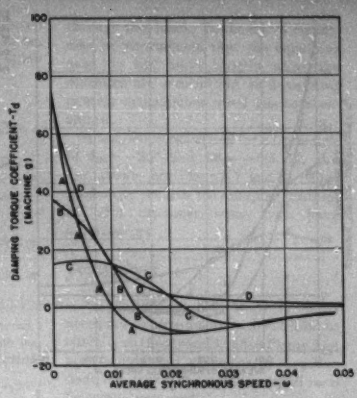

Figure 3 (right). Damping torque coefficient for oscillations at frequency s, of two synchronous machines running at low speed ω

Effect of Unequal Excitations

$E_g=1.0$; $E_m=0.5$; $\delta=0$; $x=1.0$; $r=0.01$
Curve A, $s=0$; B, 0.01; C, 0.02; D, ω

Then the damping torque coefficient T_d is

$$T_d=\frac{[r^2-(\omega^2-s^2)x^2]r}{[(\omega^2-s^2)x^2+r^2]^2+(2xrs)^2} \tag{9}$$

T_d is therefore negative, and the oscillations consequently unstable, for

$$r^2-(\omega^2-s^2)x^2<0 \tag{10A}$$

or

$$\omega^2>\frac{r^2}{x^2}+s^2 \tag{10B}$$

or

$$s^2<\omega^2-\frac{r^2}{x^2} \tag{10C}$$

Note that equation 10A may be regarded as related to conclusion 2 of reference 3, in that for $s=0$, r must be greater than ωx for stable operation.

If $r=0$, equations 10 are invalid and $T_d=0$. The synchronizing torque coefficient T_s is

$$T_s=\frac{[(\omega^2-s^2)^2x^2+(\omega^2+s^2)r^2]x}{[(\omega^2-s^2)x^2+r^2]^2+(2xrs)^2} \tag{11}$$

Figures 1 and 2 show the damping and synchronizing torque coefficients respectively for the five cases,

$s=0, 0.01, 0.02, 0.5\omega, \omega$
$E_1=E_2=1$, $\delta=0$
$x=1.0$, $r=0.01$
$0<\omega<0.04$

From Figure 1 it is seen that, for all cases except $s=\omega$, the damping torque is first positive at very low speeds, then becomes negative and reaches a maximum negative value at $\omega\geqslant 0.02$, then decreases again and finally approaches zero at infinite speed. It is to be noted that the criteria developed by Nickle and Pierce[2] show this system to be unstable at normal speed, and, therefore, lead to correct results except for $s=\omega$, which is outside of the range of oscillation frequencies considered in their work. In Figure 2 the interesting feature is the marked dip in the synchronizing torque at constant oscillation frequency near the point $s=\omega$.

Case 2. $E_1\neq E_2$, $\delta=0$

Next the effect of unequal excitations is studied. With $\delta=0$ and $\Delta\theta_2=-\Delta\theta_1$, equations 4 and 5 yield for the damping torque coefficient of machine 1:

$$T_d=\frac{[r^2-(\omega^2-s^2)x^2]rE_1(E_1+E_2)}{2\{[(\omega^2-s^2)x^2+r^2]^2+(2xrs)^2\}} \tag{12}$$

By comparing equations 12 and 9, it is seen that with $\Delta\theta_2=-\Delta\theta_1$, the form of T_d as a function of ω and s is unchanged, and the only effect of unequal excitations is to make T_d proportional to the product of the excitation (E_1) on machine 1 and the average excitation $1/2\ (E_1+E_2)$. Equations 10 are thus still valid.

Figures 3 and 4 show the damping torque coefficients of both machines, when the ratio of excitations is one half, for the four cases,

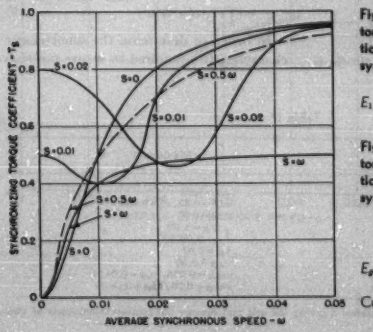

Figure 2 (left). Synchronizing torque coefficient for oscillations at frequency s, of two synchronous machines running at low speed ω

$E_1=E_2=1.0$; $\delta=0$; $x=1.0$; $r=0.01$

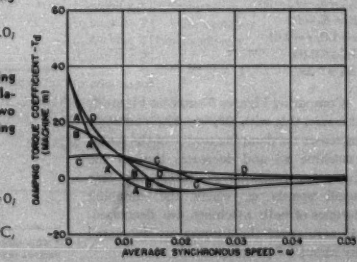

Figure 4 (right). Damping torque coefficient for oscillations at frequency s, of two synchronous machines running at low speed ω

Effect of Unequal Excitations

$E_g=1.0$; $E_m=0.5$; $\delta=0$; $x=1.0$; $r=0.01$
Curve A, $s=0$; B, 0.01; C, 0.02; D, ω

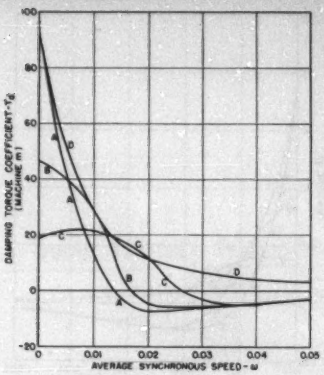

Figure 5 (left), Figure 6 (right). Damping torque coefficient for oscillations at frequency s, of two synchronous machines running at low speed ω

Effect of Load Angle
$E_1 = E_2 = 1.0$; $\delta_{2m} = \theta_g - \theta_m = 30°$; $x = 1.0$; $r = 0.01$
Curve A, $s = 0$; B, 0.01; C, 0.02; D, ω

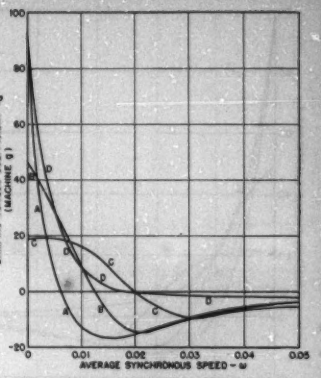

$s = 0, 0.01, 0.02, \omega$
$\delta = 0$
$E_g = 1.0$; $E_m = 0.5$; $g, m = 1,2$
$x = 1.0$, $r = 0.01$
$0 < \omega < 0.04$
$\Delta\theta_2 = -\Delta\theta_1$

From the last condition,

$$\frac{\Delta\theta_1}{\Delta\delta} = 0.5; \quad \frac{\Delta\theta_2}{\Delta\delta} = -0.5$$

From Figures 3 and 4 or equation 12 the damping torque coefficient for the machine with unit excitation is three quarters of that for the case of unit excitation on both machines, while the damping torque coefficient for the machine with 0.5 excitation is only three eighths of that for the case of unit excitation on both machines.

CASE 3. $E_1 = E_2 = 1.0$, $\delta \neq 0$

As the next step, the effect of load angle is studied. (Consideration of a load angle may be expected to indicate in some degree the effects of acceleration.) Figures 5 and 6 show the results for the four cases

$s = 0, 0.01, 0.02, \omega$
$\delta_{2m} = \theta_g - \theta_m = 30°$
$E_1 = E_2 = 1.0$
$x = 1.0$, $r = 0.01$
$0 < \omega < 0.04$
$\Delta\theta_2 = -\Delta\theta_1$

Comparing Figures 5 and 6 to Figure 1, it is seen that with $\Delta\theta_2 = -\Delta\theta_1$, load angle increases the damping torque of the motor (machine m) and decreases that of the generator (machine g), except for very small speeds ω, where the damping torques of both machines are decreased. At zero speed the torques are decreased by about 6.7 per cent.

Effect of Rotor Circuits

If the effects of rotor circuits are included, equations 3 may be shown to become:[4]

$$[\cos\delta_{120}(z_{d1}(p)+z_{d2}(p)) - \omega\sin\delta_{120}(x_{d1}(p)+x_{q1}(p))]\Delta i_{d1} - [\sin\delta_{120}(z_{q1}(p)+z_{q2}(p)) + \omega\cos\delta_{120}(x_{q1}(p)+x_{q2}(p))]\Delta i_{q1} = -[e_{d20} + i_{q20}\omega x_{q2}(p) + i_{q20}z_{q2}(p) + \sin\delta_{120}\psi_{d10}p + \cos\delta_{120}\psi_{q10}p]\Delta\delta_1 + [e_{q20} + i_{d20}\omega x_{q2}(p) + i_{q20}z_{q2}(p) + \psi_{q20}p]\Delta\delta_1 = -[e_{q20} + i_{q20}\omega x_{q2}(p) + i_{q20}z_{q2}(p) + \psi_{q20}p]\Delta\delta_{12} + [(\psi_{q20} - \psi_{d10}\sin\delta_{120} - \psi_{q10}\cos\delta_{120})p]\Delta\delta_1 \quad (13A)$$

$$[\sin\delta_{120}(z_{d1}(p)+z_{q2}(p)) + \omega\cos\delta_{120}(x_{d1}(p)+x_{d2}(p))]\Delta i_{d1} + [\cos\delta_{120}(z_{q1}(p)+z_{q2}(p)) - \omega\sin\delta_{120}(x_{q1}(p)+x_{d2}(p))]\Delta i_{q1} = [e_{d20} + i_{d20}z_{q1}(p) - i_{q20}\omega x_{d2}(p) + \cos\delta_{120}\psi_{d10}p - \sin\delta_{120}\psi_{q10}p]\Delta\delta_1 - [e_{d20} + i_{d20}z_{q2}(p) - i_{q20}\omega x_{d2}(p) + \psi_{d20}p]\Delta\delta_2 = [e_{d20} + i_{d20}z_{q2}(p) - i_{q20}\omega x_{d2}(p) + \psi_{d20}p]\Delta\delta_{12} + [(\psi_{d10}\cos\delta_{120} - \psi_{q10}\sin\delta_{120} - \psi_{d20})p]\Delta\delta_1 \quad (13B)$$

where $z(p) = px(p) + r$.

The required steady-state quantities are given by

$$D_0 i_{d20} = \left[r - \frac{\omega}{2}(x_{q1} - x_{d1})\sin 2\delta_{120}\right] \times \omega E_1 \sin\delta_{120} + \left[x_{q1} + \frac{(x_{q1}+x_{d1})}{2} + \frac{(x_{q1}-x_{d1})}{2}\cos 2\delta_{120}\right] \times \omega^2(E_2 - E_1\cos\delta_{120}) \quad (14)$$

$$D_0 i_{q20} = \left[r + \frac{\omega}{2}(x_{q1} - x_{d1})\sin 2\delta_{120}\right] \times \omega(E_2 - E_1\cos\delta_{120}) - \left[x_{d1} + \frac{(x_{q1}+x_{d1})}{2} - \frac{(x_{q1}-x_{d1})}{2}\cos 2\delta_{120}\right] \times \omega^2 E_1 \sin\delta_{120}$$

where

$$D_0 = r^2 + \omega^2[x_{q1}x_{d1} + x_{q2}x_{d2} + 0.5(x_{q1}+x_{d1})(x_{q2}+x_{d2}) - 0.5(x_{q1}-x_{d1})(x_{q2}-x_{d2})\cos 2\delta_{120}]$$

$$\psi_{d20} = E_2 - x_{d2}i_{d20}$$
$$\psi_{q20} = -x_{q2}i_{q20} \quad (15)$$

$$e_{d20} = -r_2 i_{d20} - \omega\psi_{q20}$$
$$e_{q20} = -r_2 i_{q20} + \omega\psi_{d20} \quad (16)$$

$$i_{d10} = -i_{d20}\cos\delta_{120} - i_{q20}\sin\delta_{120}$$
$$i_{q10} = +i_{d20}\sin\delta_{120} - i_{q20}\cos\delta_{120} \quad (17)$$

$$\psi_{d10} = E_1 - x_{d1}i_{d10}$$
$$\psi_{q10} = -x_{q1}i_{q10} \quad (18)$$

The torque is now

$$\Delta T_1 = (\psi_{d10} + i_{d10}x_{q1}(p))\Delta i_{q1} - (\psi_{q10} + i_{q10}x_{d1}(p))\Delta i_{d1} = (T_s + jsT_d)\Delta\delta_{12} \quad (19)$$

In order to determine the amortisseur characteristics required to insure positive

Table I*

Machine 1	Machine 2
$x_{ad} = 1.70$	$x_{ad} = 1.00$
$x_{ad}' = 0.53$, $r_1 = 0.005$	$x_{ad}' = 0.33$, $r_2 = 0.005$
$x_{aD} = 1.41$	$x_{aD} = 0.83$
$x/r_a = 1.70$	$x/r_a = 1.03$
$r/r_a = 0.00066$	$r/r_a = 0.00033$
$x_{qa} = 1.18$	$x_{qa} = 0.67$
$x_{aQ} = 0.89$	$x_{aQ} = 0.50$
$x_{kkh} = 1.591$, $r_{kh} = 0.0190$	$x_{kkh} = 0.975$, $r_{kh} = 0.0152$
$x_{kkq} = 1.203$, $r_{kq} = 0.0524$	$x_{kkq} = 0.75$, $r_{kq} = 0.0420$

* This table follows the notation of reference 5 giving the self and mutual inductance coefficients of the various machine windings.

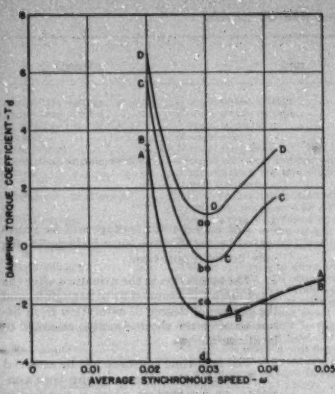

Figure 7. Damping torque coefficient of oscillations at frequency s, of two synchronous machines running at low speed ω

Effect of Amortisseur

Points ⊙ are for $\delta_{120} = -30°$, $\Delta\theta_2 = -0.5\Delta\theta_1$

Point a, machine 1 } Amortisseur in
b, machine 2 } both machines
c, machine 1 } No amortisseur
d, machine 2 }

Curve A, No amortisseur, field resistance = 0
B, No amortisseur, field resistance considered
C, amortisseur, in machine 1—field resistance considered
C, amortisseur. In both machines, field resistance considered

$E_1 = E_2 = 1.0$, $\delta_{120} = 0$, $s = 0.02$

damping, equations 13 through 19 have been applied to a system with constants as shown in Table I.

First, with $E_1 = E_2 = 1.0$ and $\delta_{120} = 0$, equations 13 reduce to

$$D\Delta i_{d1} = -\omega(r_1 + r_2)\Delta\delta_{12}$$
$$D\Delta i_{q1} = [(\omega^2 + p^2)(x_{d1}(p) + x_{db}(p))]\Delta\delta_{12} \tag{20}$$

where

$$D = (\omega^2 + p^2)(x_{q1}(p) + x_{db}(p))(x_{q1}(p) + x_{q2}(p)) + r^2 + rp(x_{d1}(p) + x_{db}(p) + x_{q1}(p) + x_{q2}(p))$$

and

$$\Delta T_1 = \Delta i_{q1} \tag{21}$$

Figures 7 and 8 show the damping and synchronizing torque coefficients respectively calculated by equation 20 with $s = 0.02$ for the cases:

1. No amortisseurs, $r_{f1} = r_{f2} = 0$.
2. No amortisseurs, $r_{f1} = 0.00066$, $r_{f2} = 0.00033$.
3. Amortisseur in machine 1, $r_{f1} = 0.00066$, $r_{f2} = 0.00033$.
4. Amortisseurs in both machines, $r_{f1} = 0.00066$, $r_{f2} = 0.00033$.

Even with zero field resistances the damping torque is smaller in absolute magnitude than that of curve C, Figure 1, since now the effect of saliency is included and the machine reactances are different. Field resistance increases the absolute magnitude of the damping torque very slightly, while amortisseur windings make the torque more positive. With an amortisseur in only one machine the damping torque is negative for a very narrow speed band (approximately $0.027 < \omega < 0.034$), so that if the machines are accelerating from zero speed they may not have sufficient time to drop out of step in the interval required to pass through this band. It should, of course, also be remembered that the equations used do not apply strictly when the machines are accelerating, as a constant average synchronous speed has been assumed.

A few points calculated for a load angle of $\delta_{120} = -30°$ and $\Delta\theta_2 = -0.5\ \Delta\theta_1$ also are shown on Figures 7 and 8. This load angle reduces the damping torques of both machines, when both have amortisseurs.

Conclusions

As a result of this study it seems necessary to have amortisseurs at least as effective as those considered in Figure 7 on both motor and generator, if negative damping during the starting period is to be surely prevented.

If the system is accelerating it may, of course, not be necessary to have positive damping at all speeds, as the two machines may stay in step for a sufficient length of time even with some negative damping.

References

1. Synchronous Starting of Generator and Motor, C. Concordia, S. B. Crary, C. E. Kilbourne, C. N. Weygandt, Jr. *Electrical Engineering (AIEE Transactions)*, volume 64, September 1945, pages 629–34.

2. Stability of Synchronous Machines—Effect of Armature Circuit Resistance, C. A. Nickle, C. A. Pierce. *AIEE Transactions*, volume 49, January 1930, pages 338–50.

3. Damping and Synchronizing Torques of Power Selsyns, C. Concordia, G. Kron. *AIEE Transactions*, volume 64, 1945, pages 366–71.

4. Two Reaction Theory of Synchronous Machines, R. H. Park. *AIEE Transactions*, part I, volume 49, July 1929, pages 716–27; part II, volume 52, June 1933, pages 352–54.

5. Operational Impedances of a Synchronous Machine, S. B. Crary, M. L. Waring. *General Electric Review* (Schenectady, N. Y.), volume 34, November 1932, pages 578–82.

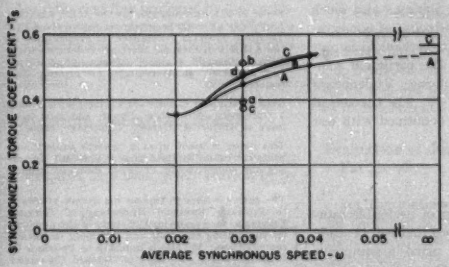

Figure 8. Synchronizing torque coefficient for oscillations at frequency s, of two synchronous machines running at low speed ω

Effect of Amortisseur

Points ⊙ are for $\delta_{120} = -30°$, $\Delta\theta_2 = -0.5\ \Delta\theta_1$

Point a, machine 1 } Amortisseur in
b, machine 2 } both machines
c, machine 1 } No amortisseur
d, machine 2 }

Curve A, No amortisseur
B, Amortisseur in machine 1
C, Amortisseur in both machines

$E_1 = E_2 = 1.0$, $\delta_{120} = 0$, $s = 0.02$

No Discussion

Symmetrical Short Circuits on Saturated Alternators

SAAD L. MIKHAIL
ASSOCIATE AIEE

THE investigation of the performance of the synchronous machine under transient conditions initiated by sudden short circuits is not a new problem. For the unsaturated machine, the problem was first investigated by Punga[1] in 1906, followed by a number of authors. Karapetoff[2] and Doherty and Nickle[3] give an excellent bibliography of the subject up to 1930. Since then several applications and extensions of Park's theory[4] have appeared.

On the other hand, the study of the saturated machine under steady-state conditions was under way. The saturation in the direct-axis was taken care of either by adding to the field excitation diagram, a saturation magnetomotive force obtained from a magnetization curve corresponding to the direct-axis current considered, as followed by Doherty and Nickle,[5] and by Robertson, Rogers and Dalziel,[6] or by the use of the no-load magnetization curve in conjunction with either Potier triangle[7,8] or Rüdenberg lines.[9–12]

However, as far as short-circuit transients on the saturated machine and with the exception of the contributions of Rüdenberg,[9–12] the literature has been satisfied with the shading of the unsaturated machine constants with empirical coefficients such as given by Wright[13] and Kilgore.[14] Rüdenberg's method consists in extending the construction used for the treatment of the steady-state direct-axis loading of the saturated machine, to give the symmetrical component of the current in the saturated machine under transients arising from switching of direct-axis loads.

It is the object of this paper to present the complete solution to the transients occurring in a saturated salient-pole synchronous machine due to a sudden 3-phase short circuit through an external inductance. The solution for a terminal short circuit is obtained by setting the value of the external inductance equal to zero. The case considered will be that with a constant excitation voltage and with the short circuit occurring from no-load. The machine will be assumed to have only one rotor circuit, namely, the field winding.

Starting with Park's equations,[4] and with the differential equation of the field winding, the classical method for their solution will be used. Obtained first will be the free transient which is the solution of the differential equations after the omission of all the stimulants in the circuits which in this case is the exciter voltage. Secondly, integration constants are evaluated from initial conditions; among which the initial current is evaluated using the principle of conservation of flux linkage in the field winding as used first by Doherty and Shirley,[15] and which is analogous to the principle of conservation of momentum in mechanical impact problems. Thirdly, the particular solution is obtained using Rüdenberg's method of analysis.[9–12] The theoretical results obtained are confirmed with test results.

Assumptions

With the exception of negligible saturation, the assumptions that will be made are essentially the usual assumptions made by previous authors:

1. Small stator and rotor resistances will be assumed.
2. The flux in the air-gap will be assumed the same as that effective in producing saturation in the armature.
3. The actual rotor leakage will be represented by an effective rotor leakage flowing only between pole tips.
4. The saturation in the armature after the short circuit is assumed to be negligible, and the change of degree of saturation from before to after the short circuit is assumed to be instantaneous.
5. The field time constant will be assumed much greater than the armature time constant; an assumption which is justified in big machines.

System of Notation

A nonreciprocal system of notation similar to that used by Doherty and Nickle[5] and by Park,[4] will be used. The units for magnetomotive force, flux, and reluctance will be different as they will be defined according to the field circuit. Table I gives the definitions for the various units used and their values for the machine tested.

Before attacking the main problem the subsequent definitions and relations will be introduced.

Equivalence Factor Between Rotor and Stator Currents

The equivalence factor γ between rotor and stator currents will be defined as the ratio of rotor to stator currents

Paper 50-253, recommended by the AIEE Rotating Machinery Committee and approved by the AIEE Technical Program Committee for presentation at the AIEE Fall General Meeting, Oklahoma City, Okla., October 23–27, 1950. Manuscript submitted July 20, 1950; made available for printing September 5, 1950.

SAAD L. MIKHAIL is Assistant Lecturer with Faroukh I University, Alexandria, Egypt, and now is on leave at Harvard University, Cambridge, Mass.

This paper is based upon a research project now being carried on by the author at Harvard University and supervised by Professor Reinhold Rüdenberg.

The author wishes to express his sincere gratitude to Professor Reinhold Rüdenberg of Harvard University for suggesting the study of the problem, for supervising the work and for many important contributions. He also is indebted to Professor C. L. Dawes and R. T. Gibbs of Harvard University for valuable help and interest. Credit is also given to F. Grotjohan and H. Baxter for their outstanding work in the manufacture of the necessary equipment and to the General Electric Company for supplying the requested design data for the machine tested. The author owes a great deal to the class notes on electrical machinery given by Professor C. A. Keener, of the University of Illinois and to his encouragement and interest.

Table I. Per-Unit System Used

Quantity	Unit	Value Corresponding to Machine Tested
Armature voltage	Normal phase voltage	120 volts
Armature current	Normal phase current	283 amperes
Armature impedance	Normal impedance	0.424 ohm
Speed	Normal speed	1,200 rpm
Frequency	Normal frequency	60 cycles
Electrical angular velocity	Normal electrical angular velocity	377 radians/second
Time	Time required for one electrical radian at unit frequency	1/377 second
Armature flux linkage	Armature flux linkage that when changes at unit rate produces unit voltage	0.318 volt sec
Field current	Field current corresponding to unit armature voltage of the air-gap line	3.946 amperes
Field impedance	Resistance of the field winding at the temperature of the test	8.46 ohms
Field voltage	Voltage necessary to drive unit field current through unit field impedance	33.382 volts
Flux	Total air-gap flux produced by the field winding, whose fundamental produces unit voltage at unit speed	1.96 megalines
Magnetomotive force	Field magnetomotive force per pole corresponding to unit field current	1,425 ampere turns
Reluctance	Reluctance that if a unit flux passes through it, the magnetic potential across it will be unit magnetomotive force	726 ampere turns/megaline
Field flux linkage	No-load field flux linkage	7.75 volt sec

that if each was acting alone, the same area for the air-gap flux density curve will be produced in each case.

However, if these two currents were acting simultaneously with their magnetomotive forces in opposition, the resultant air-gap flux density curve (Figure 8E), will have zero average value by definition, yet its fundamental will have a value. Since linkage with the field winding is proportional to the average value of the flux density wave, while linkage with the armature is proportional to its fundamental, such flux as of Figure 8(E), is a flux that links the armature and leaks with respect to the field, and thus it could be counted as an armature leakage flux. This flux will be called the difference leakage flux to distinguish it from the differential leakage flux, a term already used for the harmonic leakage flux.[18] The value of the armature linkage due to the difference flux produced by unit armature current is defined as the difference reactance and will be given the symbol x_Δ. In Appendix I, the value of x_Δ will be derived.

Armature Leakage Reactance

A definition for the armature leakage reactance has been given previously by Doherty and Nickle[5] and followed by Alger[16] and Kilgore[17] in its calculation and by March and Crary[18] and by Rogers[19] in its measurement. This definition being that the armature leakage reactance is the difference between the synchronous reactance and the armature reaction reactance in either the direct- or quadrature-axis. The armature reaction reactance being defined as that due to the space fundamental of armature magnetomotive force. This definition is a very useful one especially in the calculation of the machine constants. However, it is evident that it is not the only possible one, and a different definition will be used here. To the previous definition x_l, will be added the difference reactance x_Δ and the sum will be called the stator leakage reactance x_s, thus:

$$x_s = x_l + x_\Delta \tag{1}$$

It was advisable to use this definition, since dealing with saturation and with field flux linkage, the field magnetic circuit is affected by the average value of the air-gap flux density wave rather than by its fundamental.

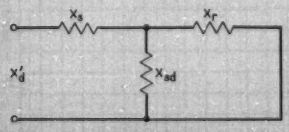

Figure 1. An equivalent circuit for direct-axis transient reactance

Evaluation of the Equivalence Factor γ

Let the machine be considered under the condition of a 3-phase short circuit, the rotor and stator currents being I and i respectively. Thus through the main magnetic circuit of the machine is acting a magnetomotive force of $I-\gamma i$ which drives a flux of ix_s through the air-gap; the iron being unsaturated, thus:

$$I-\gamma i = ix_s \tag{2}$$

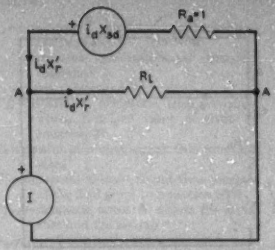

Figure 2. The main magnetic circuit of the machine when a direct-axis current is fed to the armature with the field winding short circuited

but

$$I = ix_d \tag{3}$$

from equations 2 and 3:

$$\gamma = x_d - x_s \tag{4}$$

$$= x_{sd} \tag{5}$$

where x_{sd} is the excess of the unsaturated direct-axis synchronous reactance over the stator leakage reactance.

Transient Reactance of the Unsaturated Machine

If a direct-axis current is supplied to the armature, with the field short circuited on itself, the reactance seen from the armature is the direct-axis transient reactance x_d'. This is generally decomposed into armature leakage reactance x_l and an effective field leakage reactance x_f'. Having used a different definition for the armature leakage reactance, x_d' will be decomposed into stator leakage reactance x_s and an effective rotor leakage reactance x_r', thus:

$$x_d' = x_s + x_r' \tag{6}$$

x_r' is then decomposed into x_{sd} in parallel with the rotor leakage reactance x_r. In

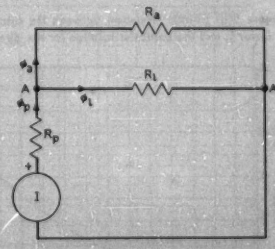

Figure 3. The main magnetic circuit of the machine at no-load

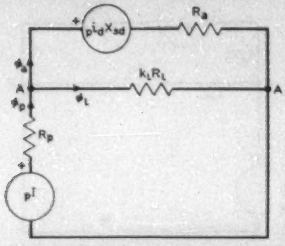

Figure 4. The main magnetic circuit of the machine after the occurrence of the short circuit

Figure 1, is shown the equivalent circuit for x_d' just described. It is obvious that:

$$x_r' = \frac{x_r x_{sd}}{x_r + x_{sd}} \tag{7}$$

In Figure 2 is shown the main magnetic circuit of the unsaturated machine with direct-axis current fed to the armature while the field winding being short circuited. The magnetomotive force of the armature is $i_d x_{sd}$; the total flux is $i_d x_d'$, the part $i_d x_r$ is a stator leakage and only $i_d x_r'$ crosses the air-gap. However, no part of it can link the field winding since it is short circuited on itself with an induced current I in it to drive all the flux $i_d x_r'$ in the rotor leakage paths.

Writing the circuital law equation for the outer circuit of Figure 2, there is:

$$i_d x_{sd} - I = i_d x_r' \tag{8}$$

or

$$I = i_d(x_d - x_d') \tag{9}$$

Writing the circuital law equation for the upper circuit of Figure 2, there is:

$$i_d x_{sd} = i_d x_r'(1 + R_l) \tag{10}$$

or

$$R_l = \frac{x_{sd}}{x_r'} - 1 \tag{11}$$

From equations (7) and (11); there is:

$$R_l = \frac{x_{sd}}{x_r} \tag{12}$$

Relation Between Per-Unit Pole Flux ϕ_p and Per-Unit Field Linkage Ψ

A linear relation always exists between Ψ and ϕ_p whether the machine is saturated or not, thus this relation will be obtained for the unsaturated machine and the results will be used for the saturated machine. In Figure 3 is shown the main magnetic circuit of the machine at no-load. Since the machine is unsaturated, then $R_a = 1$ and $R_p = 0$. Taking $\phi_a = 1$, thus:

$$\phi_l = 1/R_l \tag{13}$$

and

$$\phi_p = \phi_a + \phi_l = 1 + 1/R_l \tag{14}$$

This corresponds to unit flux linkage Ψ, thus:

$$\Psi = \frac{R_l}{R_l + 1}\phi_p \tag{15}$$

Substituting equations 7 and 12 in equation 16, there is:

$$\Psi = \phi_p \frac{x_r'}{x_r} \tag{16}$$

Having derived the necessary relations, the main problem now will be treated.

Differential Equations of the Machine

In order to solve the short-circuit problem, any investigator has to start by writing the differential equations in one form or another for each closed winding either on the stator or on the rotor. Any of these differential equations is of the form, $e = p\psi - ir$, where e is the terminal voltage, $p = d/dt$, ψ is the flux linking the winding, r is its resistance and i is the current through it considered positive when flowing from the induced to the terminal voltage. The solution of all these differential equations under the specified initial conditions gives the desired result. However, the difficulty in their solution arises from their nonlinearity. In fact there exist here two kinds of nonlinearity. The first is due to the change of coupling coefficients between the different windings due to the rotation of the rotor.

This nonlinearity could be removed by using the transform from phase to direct and quadrature components as used previously by Park.[4] The second nonlinearity is due to the saturation in the magnetic circuits and this nonlinearity could be treated by separating the solution into a free transient which meets linear though not unsaturated conditions, and a particular solution which meets saturated conditions and could be obtained by Rüdenberg's method.[9–13] The initial current being obtained by the principle of conservation of flux linkage in the field winding.[15]

Park's Equations

The differential equations of the stator windings as transformed to direct, quadrature, and zero components, has been used previously by Park[4] as:

$$e_d = p\psi_d - ri_d - \psi_q p\theta \tag{17}$$

$$e_q = p\psi_q - ri_q + \psi_d p\theta \tag{18}$$

$$e_0 = p\psi_0 - ri_0 \tag{19}$$

The differential equation for the field winding, using the opposite convention for the sign of the current is:

$$E = T_0 p\Psi + I \tag{20}$$

Figure 5(A) (below). Relation between pole reluctance R_p and particular solution for field flux linkage $_p\Psi$

Figure 5(B) (right). Relation between the rotor leakage saturation factor k, and the particular solution for the direct-axis current $_pi_d$

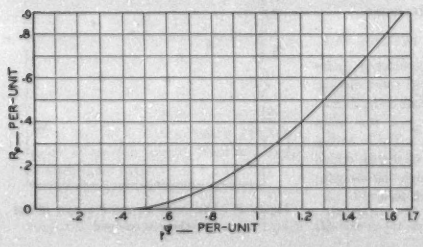

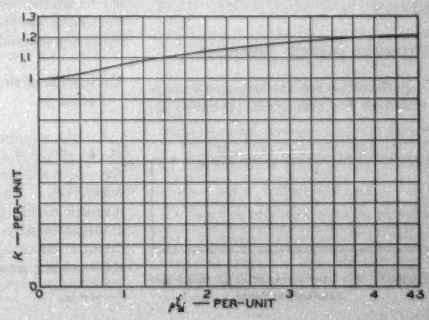

Equations 17 to 20 are applicable to both the saturated and the unsaturated machines and their solutions give the desired result. Since in a 3-phase short circuit, $i_0=0$, equation 19 will be omitted.

The Free Solution

As in the case of simple transients solved by the classical method, the complementary function gives the free transient. Thus if the stimulant E is omitted, the problem reduces to a machine having its field winding short circuited, running at synchronous speed, and carrying an armature current through an external inductance. In this case:

$$_f\psi_{ds}=-{}_fi_d(x_{ds}'+x_a) \tag{21}$$

and

$$_f\psi_{qs}=-{}_fi_q(x_{qs}'+x_a) \tag{22}$$

where the left-hand subscript f indicates the free solution, the subscript s indicates the saturated value and the subscript t indicates the totalized quantity of the machine and the load. The values of x_{ds}' and x_{qs} will remain constant all through the duration of the free transient. The reason for this will now be explained. Having assumed that the field time constant is much bigger than the armature time constant, the field leakage due to the particular solution keeps the pole tips very highly saturated, so that they are on the upper linear part of their characteristic all through the small duration of the free transient. Flux paths for the free solution involve the unsaturated armature, the very highly saturated pole tips and air paths; thus it is justifiable to write the linear though not unsaturated relations 21 and 22. The values of x_{ds}' and x_{qs}' will be discussed later.

Substituting equations 21 and 22 in equations 17 and 18 and using totalized values for the terminal voltage, flux linkage, and the resistance, and putting $e_{dt}=0=e_{qt}$, the condition for a symmetrical short circuit after the external reactance, there is:

$$0=-[r_t+p(x_{ds}'+x_a)]{}_fi_d+(x_{qs}'+x_a){}_fi_q \tag{23}$$

and

$$0=(x_{ds}'+x_a){}_fi_d+[r_t+p(x_{qs}'+x_a)]{}_fi_q \tag{24}$$

Equations 23 and 24 are two simultaneous equations in ${}_fi_d$ and ${}_fi_q$. Eliminating ${}_fi_d$, there is:

$$0=\left[p^2+r_t\left(\frac{1}{x_{ds}'+x_a}+\frac{1}{x_{qs}'+x_a}\right)p+1+\frac{r_t^2}{(x_{ds}'+x_a)(x_{qs}'+x_a)}\right]{}_fi_q \tag{25}$$

This is a second order differential

Nomenclature

All quantities are in the per-unit system given in Table I.

e = stator phase voltage
e_d,e_q,e_0 = direct, quadrature, and zero components of stator phase voltages respectively
E = field voltage
i = stator phase current
i_a,i_b,i_c = currents of phases a, b, c respectively
i_d,i_q,i_0 = direct, quadrature, and zero components of stator phase currents respectively
I = field current
r = armature resistance
x_d = unsaturated direct-axis synchronous reactance
x_{ad} = unsaturated armature reaction reactance
x_l = armature leakage reactance defined by Doherty and Nickle[5]
x_Δ = difference reactance derived in Appendix I
$x_s=x_l+x_\Delta$ a stator leakage reactance
$x_{sd}=x_d-x_s$
x_d' = unsaturated direct-axis transient reactance
$x_f'=x_d'-x_l$ effective field leakage reactance
$x_f=\frac{x_{ad}x_f'}{x_{ad}-x_f'}$ field leakage reactance
$x_r'=x_d'-x_s$ effective rotor leakage reactance
$x_r=\frac{x_{sd}x_r'}{x_{sd}-x_r'}$ rotor leakage reactance
x_b = armature leakage reactance with the rotor removed
$\alpha=x_r/x_{sd}$
x_{ds}' = saturated direct-axis transient reactance offered to the free transient
X_{ds}' = saturated direct-axis transient reactance offered to the particular solution
x_q = unsaturated quadrature-axis synchronous reactance
x_{qs}' = saturated quadrature-axis transient reactance
x_a = external reactance
T_{ds} = saturated armature time constant whose totalized value is given by equation 27
T_0 = unsaturated open-circuit field time constant
T' = unsaturated short circuit time constant of the field given by equation 50 B
$M_{\Delta\Delta}$ = magnetic potential across the armature and the air-gap
ϕ_a,ϕ_l,ϕ_p = fluxes in the armature, rotor leakage paths, and pole body respectively
R_a,R_l,R_p = reluctances of the armature and the air gap, that of the rotor leakage paths, and that of the pole body respectively
k = saturation factor for the rotor leakage paths at any instant and is greater than 1.
k_1 = value of k immediately after the occurrence of the short circuit
$B_1,B_{an},B_{ln},B_{11},C_1,C_{ln},C_p,C_{p1}$ = defined in Appendix 1
ψ_d,ψ_q,ψ_0 = direct, quadrature, and zero components of armature phase flux linkages respectively
Ψ = field flux linkage
ν = frequency of free transient given by equation 28
θ = angle by which the direct-axis leads the axis of phase a at any time
θ_0 = value of θ at the time of occurrence of the short circuit
$p=d/dt$
t = time
"t" added to the subscripts of a quantity indicates the totalized quantity of the machine and the external load.

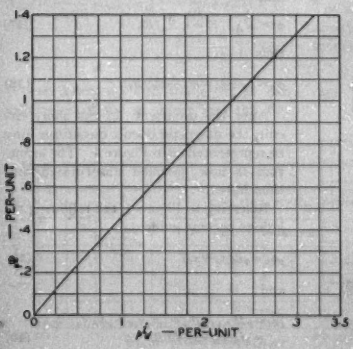

Figure 5(C) (left). Relation between the particular solutions for field flux linkage $_p\Psi$ and direct-axis current $_pi_d$

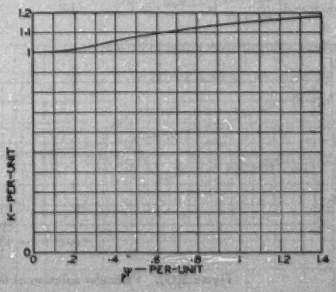

Figure 5(D) (right). Relation between rotor leakage saturation factor k, and the particular solution for field flux linkage $_p\Psi$

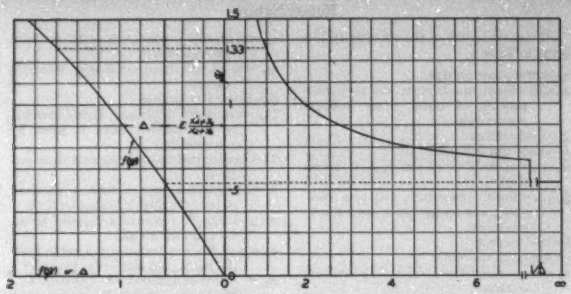

Figure 5(E)(left), Figure 5(F)(right). Graphical solution of equation 51

equation whose solution is:

$$_f i_q = A\epsilon^{-t/T_{a1s}} \sin(\nu t+\beta) \tag{26}$$

where

$$T_{a1s} = \frac{2(x_{ds}'+x_a)(x_{qs}'+x_a)}{r_1[(x_{ds}'+x_a)+(x_{qs}'+x_a)]} \tag{27}$$

and

$$\nu^2 = 1+\frac{r_1^2}{(x_{ds}'+x_a)(x_{qs}'+x_a)} - \frac{1}{T_{a1s}^2} \tag{28}$$

and where A and β are integration constants.

The assumption of small resistance in the armature circuit allows ν to be taken equal to unity. Also at time $t=0$, $_f i_q = A \sin \beta$. Since the short circuit is occurring from no-load, this value must be equal to minus the value at time equal to zero of the particular solution of i_q which will be shown afterwards to be equal to zero, thus $\beta=0$, giving:

$$_f i_q = A\epsilon^{-t/T_{a1s}} \sin t \tag{29}$$

The value of A will be evaluated later.

Substituting equation 29 in either equations 23 or 24, and keeping in mind the assumption of small totalized armature resistance, the free solution for i_d is given by:

$$_f i_d = -A\left(\frac{x_{qs}'+x_a}{x_d'+x_a}\right)\epsilon^{-t/T_{a1s}} \cos t \tag{30}$$

whose value at time equal to zero is

$$-A\left(\frac{x_{qs}'+x_a}{x_{ds}'+x_a}\right)$$

This must be equal to minus the value at time equal to zero of the particular solution. The latter will be defined as equal to e/X_{d1s}', where X_{d1s}', is the totalized transient reactance and whose value will soon be derived. From the above discussion, the value of A is given by:

$$A = \frac{e}{X_{d1s}'}\left(\frac{x_{ds}'+x_a}{x_{qs}'+x_a}\right) \tag{31}$$

Thus the free solutions of the direct and quadrature currents are given by:

$$_f i_d = -\frac{e}{X_{d1s}'}\epsilon^{-t/T_{a1s}} \cos t \tag{32}$$

and

$$_f i_q = \frac{e}{X_{d1s}'}\frac{x_{ds}'+x_a}{x_{qs}'+x_a}\epsilon^{-t/T_{a1s}} \sin t \tag{33}$$

Substituting equations 32 and 33 in equations 13 of Park's paper,[4] and setting $\theta=\theta_0+t$, the free solution for the phase currents is given by:

$$_f i_a = -\frac{e}{2X_{d1s}'}\epsilon^{-t/T_{a1s}} \times \left[\frac{(x_{ds}'+x_a)+(x_{qs}'+x_a)}{x_{qs}'+x_a}\cos\theta_0 + \frac{x_{qs}'-x_{ds}'}{x_{qs}'+x_a}\cos(2t+\theta_0)\right] \tag{34}$$

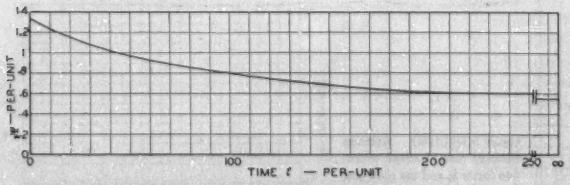

Figure 5(G). Particular solution of the field flux linkage $_f\Psi$

For a terminal short circuit, putting $x_a=0$ and replacing X_{d1s}' by X_{ds}', the free solution for i_a is then given by:

$$_f i_a = -\frac{e}{2X_{ds}'}\epsilon^{-t/T_{a1s}}\left[\frac{x_{ds}'+x_{qs}'}{x_{qs}'}\cos\theta_0 + \frac{x_{qs}'-x_{ds}'}{x_{qs}'}\cos(2t+\theta_0)\right] \tag{34B}$$

Expression for $_f i_b$ could be obtained by replacing θ_0 by $\theta_0-2\pi/3$ in equations 34.

Expression for $_f i_c$ could be obtained by replacing θ_0 by $\theta_0+2\pi/3$ in equations 34.

The free solution for the field current could be obtained by substituting equation 32 in equation 9 and replacing x_d' by x_{ds}', giving:

$$_f I = -\frac{e}{X_{d1s}'}(x_d-x_{ds}')\epsilon^{-t/T_{a1s}} \cos t \tag{35}$$

For a terminal short circuit, the free solution for the field current is given by:

$$_f I = -\frac{e}{X_{ds}'}(x_d-x_{ds}')\epsilon^{-t/T_{a1s}} \cos t \tag{35B}$$

Totalized Direct-Axis Saturated Transient Reactance X_{d1s}'

This reactance has been defined as the ratio of the voltage before the occurrence of the short circuit to the particular solution of the armature current immediately after its occurrence, and will be calculated by finding the flux linkage in the field winding at no-load, then after the short circuit and equating these two flux linkages thus utilizing the principle of conservation of flux linkage.[15]

To obtain the pole flux before the short circuit, reference is made to Figure 3.

$$\phi_a = e \tag{36}$$

and

$$\phi_1 = M_{AA}/R_1 = e\ R_a/R_1 \tag{37}$$

thus

$$\phi_p = \phi_a+\phi_1 = e(1+R_a/R_1) \tag{38}$$

After the occurrence of the short circuit, the magnetic circuit quantities may be represented as in Figure 4. The armature is now assumed unsaturated and thus $R_a=1$.

Referring to Figure 4, the following relations become evident:

$$_p\phi_a = {}_p i_d(x_l+x_a) \tag{39}$$

and

$$_p\phi_1 = {}_p M_{AA}/k_1R_1 = ({}_p i_d x_{ld} + {}_p\phi_a R_a)/k_1R_1 = {}_p i_d(x_d+x_l)/k_1R_1 \tag{40}$$

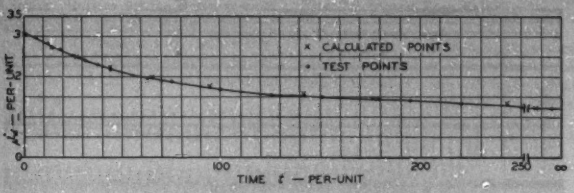

Figure 5(H). Particular solution for the direct-axis current $_pi_d$

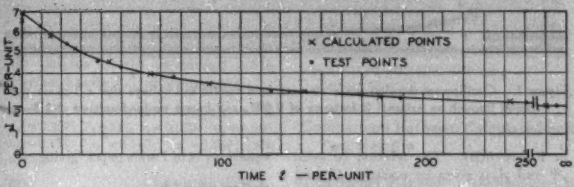

Figure 5(I). Particular solution for the field current $_pi$

thus

$$_p\phi_p = \phi_a + \phi_1 = {}_pi_d\left[x_s + \frac{x_d}{k_1R_1} + x_e(1+1/k_1R_1)\right] \quad (41)$$

where the left-hand subscript p indicates the particular solution of the quantity.

Let $_pi_d(0)$ be the value of the particular solution of i_d immediately after the occurrence of the short circuit. By the principle of conservation of flux linkage, and since the free transient does not produce any field flux linkage at any time during its whole duration, and since the field flux linkage is proportional to the pole flux, equations 38 and 41 are equated, and substituting for R_1 from equation 12, there is:

$$X_{ds}' = \frac{e}{_pi_d(0)} = (x_s + x_e)\frac{1+\alpha/k_1}{1+\alpha R_a} + x_r'\frac{1}{k_1}\times\left(\frac{1+\alpha}{1+\alpha R_a}\right) \quad (42)$$

Where $\alpha = x_r/x_{1d}$ and where R_a is the reluctance of the armature and the air-gap before the occurrence of the short circuit.

For a terminal short circuit, substituting $x_e = 0$, there is:

$$X_{ds}' = x_s\frac{1+\alpha/k_1}{1+\alpha R_a} + x_r'\frac{1}{k_1}\left(\frac{1+\alpha}{1+\alpha R_a}\right) \quad (42B)$$

Equations 42 and 42B show two important points, the first is that the saturation of the pole body plays no role in the determination of the initial short-circuit current.

The second point is that although the stator leakage reactance x_s or the external reactance x_e do not saturate, yet their sum appears multiplied by a saturation factor. This is because although they do not saturate, yet the voltage behind their sum, constitutes a part of the magnetic potential that stimulates field leakage through the saturated pole tips. The appearance of the saturation of the armature in the expression is because it influences the field leakage before the short circuit which is a part of the flux linking the field winding then.

Values of x_{ds}' and x_{qs}'

x_{ds}' is the reactance offered to a direct-axis armature current when the field winding is short circuited and when the pole tips are saturated. Its value is thus given by:

$$x_{ds}' = x_s + \frac{1}{k_1}x_r' \quad (43)$$

The value of x_{qs}' varies from the unsaturated quadrature-axis synchronous reactance x_q when the machine is unsaturated to the reactance of the armature with the rotor removed x_{lb} when the machine is very highly saturated. The exact variation between these two limits will not be discussed here, and only an intermediate value will be taken. The value of x_{lb} could be calculated as shown by Schenkel.[20]

The Particular Solution

In order that the solution of the differential equations may be complete, to equations 32, 33, and 35, must be added any other solution due to the introduction of the stimulant E, previously omitted.

Since the resistance in the armature circuit has been assumed small, hence the steady-state armature current is a direct-axis current, implying that $_pi_q(\infty) = 0$, and hence, i_q is a current whose steady-state value vanishes, and thus its complete solution is the free transient, and only i_d and I have particular solutions.

Rüdenberg's Method

The particular solution for i_d and I, has been given previously by Rüdenberg.[9–12] Rüdenberg's method now will be rewritten, slightly modified.

The pole flux at any instant is given by equation 41. Substituting equation 12 in

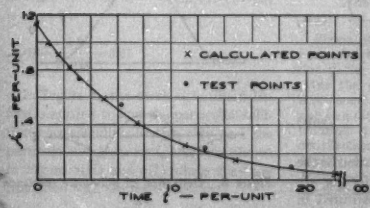

Figure 6(A)(left). Free solution for the current, $_fi_{a1}$, in phase a

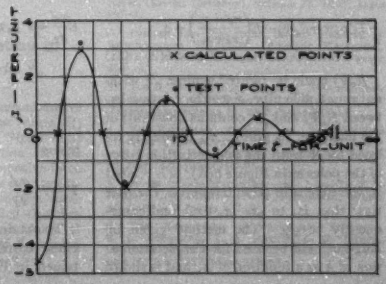

Figure 6(B) right. Free solution for the field current $_fi$

equation 41, there is:

$$_{s}\phi_{p} = {}_{s}i_{d}\left[\frac{x_r}{x_r'}x_d' - (1-1/k)\alpha x_d + x_s(1+\alpha/k)\right] \tag{44}$$

Substituting equation 16 in equation 45, there is:

$$_{p}\Psi = {}_{s}i_{d}\left[x_d' - (1-1/k)\frac{x_d}{x_{sd}}x_r' + x_s\frac{1+\alpha/k}{1+\alpha}\right] \tag{45}$$

Writing the circuital law equation for the outer circuit of Figure 4, there is:

$$_{p}I = {}_{s}i_{d}(x_d + x_s + {}_{s}\phi_{p}R_p) \tag{46}$$

Substituting equation 44 in equation 46, there is:

$$_{p}I = {}_{s}i_{d}\left[x_d + x_s + R_p\left\{\frac{x_r}{x_r'}x_d' - (1-1/k)\alpha x_d + x_s(1+\alpha/k)\right\}\right] \tag{47}$$

Substituting equations 46 and 47 in equation 20, there is:

$$E = T_0 p_p \Psi + {}_{p}\Psi \times \frac{x_d + x_s + R_p\left[\frac{x_r}{x_r'}x_d' - (1-1/k)\alpha x_d + x_s(1+\alpha/k)\right]}{x_d' + x_s - (1-1/k)\frac{x_d}{x_{sd}}x_r' - x_s\frac{(1-1/k)\alpha}{1+\alpha}} \tag{48}$$

or

$$E\frac{x_d'+x_s}{x_d+x_s} = T_t' p_p \Psi + {}_{p}\Psi \times \frac{1 + R_p\left[\frac{x_r}{x_r'}\frac{x_d'}{x_d+x_s} - (1-1/k)\alpha \times \frac{x_d}{x_d+x_s} + \frac{x_s}{x_d+x_s}(1+\alpha/k)\right]}{1-(1-1/k)\frac{x_d}{x_{sd}}\frac{x_r'}{x_d'+x_s} - \frac{x_s(1-1/k)\alpha}{(x_d'+x_s)(1+\alpha)}} \tag{49}$$

where

$$T_t' = T_0\frac{x_d'+x_s}{x_d+x_s} \tag{50}$$

Equation 49 can be written as:

$$-T_t' p_p \Psi = f({}_{p}\Psi) - E\left(\frac{x_d'+x_s}{x_d+x_s}\right) = \Delta, \tag{51}$$

Figure 5(E)

$f({}_{p}\Psi)$ could be plotted against ${}_{p}\Psi$ without much difficulty, since the relation between $f({}_{p}\Psi)$ and ${}_{p}\Psi$ contains constants of the machine, R_p and k. R_p is directly related to ${}_{p}\Psi$ from the magnetization curve of the poles as in Figure 5(A); k is related to the magnetic potential across the pole tips, that is, to ${}_{s}i_d\ (x_d+x_s)$ and consequently to ${}_{s}i_d$. The method given by Kilgore[14] will be used for the determination of k as a function of ${}_{s}i_d$ and is shown in Figure 5(B). The relation between ${}_{p}\Psi$ and ${}_{s}i_d$ is given by equation 45, and can thus be represented by Figure 5(C). From Figure 5(B) and Figure 5(C), the relation between ${}_{p}\Psi$ and k can be obtained and is shown in Figure 5(D). From Figure 5(A), Figure 5(D), the constants of the machine, and equation 49, Figure 5(E) could be obtained giving Δ against ${}_{p}\Psi$. From which $1/\Delta$ against ${}_{p}\Psi$ could be obtained as in Figure 5(F).

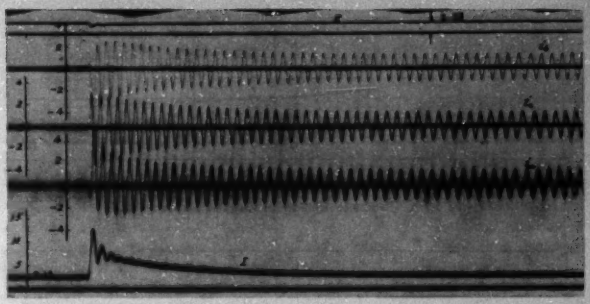

Figure 7. Oscillogram showing phase currents, field current and voltage after a 3-phase short circuit through an external inductance of 0.095, and from a no-load voltage of 1.3

From equation 49, there is:

$$\int dt = -T_t' \int \frac{1}{\Delta} d_p\Psi \tag{52}$$

For any value of ${}_{p}\Psi$, the value of $\int 1/\Delta \cdot d_p\Psi$ could be obtained by graphical integration from Figure 5(F), and thus the variation of ${}_{p}\Psi$ with time could be obtained as in Figure 5(G). From Figure 5(G), and Figure 5(C), the variation of ${}_{s}i_d$ with time could be obtained as is shown in Figure 5(H). From equations 46 and 16, Figure 5(A), Figure 5(G), and Figure 5(H), the variation of ${}_{p}I$ with time could be obtained as in Figure 5(I).

To get the particular solution for a terminal short circuit, x_s is equated to zero in the foregoing analysis. Equation 49 then becomes:

$$E\frac{x_d'}{x_d} = T' p_p \Psi + {}_{p}\Psi \times \frac{1 + \left(\frac{x_r}{x_r'}\frac{x_d'}{x_d} - \alpha(1-1/k)\right)}{1-(1-1/k)\frac{x_d}{x_{sd}}\frac{x_r'}{x_d}} \tag{49B}$$

where

$$T' = T_0\frac{x_d'}{x_d} \tag{50B}$$

To obtain the particular solution of the phase currents, the solution for ${}_{s}i_d$ obtained in Figure 5(H) is substituted in equations 14 of Park's paper[4] giving:

$$_{s}i_a = {}_{s}i_d \cos(l+\theta_0) \tag{53}$$

$$_{s}i_b = {}_{s}i_d \cos(l+\theta_0-2\pi/3) \tag{54}$$

$$_{s}i_c = {}_{s}i_d \cos(l+\theta_0+2\pi/3) \tag{55}$$

which means that the particular solution of the phase currents is the symmetrical component of the total solution and is a 60-cycle wave modulated according to the solution for ${}_{s}i_d$. These par-

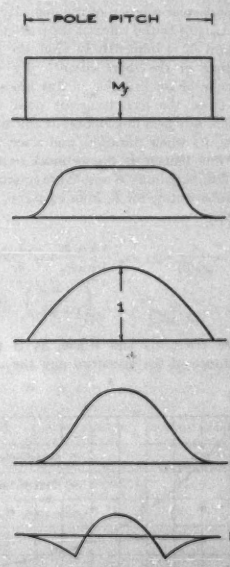

Figure 8. Derivation of difference reactance x_Δ

ticular solutions for the stator currents and that of the rotor current shown in Figure 5(I), together with the free solution obtained before in equations 34 and 35, constitute the complete solution of the problem.

Application and Test Results

Only final results will be given here, intermediate steps will be omitted to save space.

The machine tested is 100 horsepower, 208 volts, 283 amperes, 60 cycles, General Electric synchronous motor. The damper bars of the machine were taken out for the purpose of the experiment. The machine has the following constants:

$x_d=1.83$; $x_1=0.093$; $x_r=0.224$; $x_{ad}=1.606$; $x_d'=0.367$; $T_0=412$; $r_1=0.0599$; $x_q=1.056$; $x_{1b}=0.174$; $x_r'=0.143$; $x_r=0.157$; $\alpha=0.0978$

T_0 was determined oscillographically, the leakages were calculated, the rest of the constants were both calculated and measured giving differences of less than 3 per cent. With the exception of T_0, the foregoing values are the calculated values.

With the exception of the constants introduced in this paper, Kilgore's paper[17] was followed in the calculations of the constants.

The machine was short circuited at no-load at a voltage of 1.3, a field current of 2.38, and through an external reactance $x_e=0.095$ at $\theta_0=1.955$.

The Calculated Particular Solution

Figure 5(A) to 5(I) corresponds to this case. From Figure 5(D), $k_1=1.177$, thus

$$x_{ds}'=0.244+\frac{1}{1.177}0.143=0.346$$

$$X_{dis}'=(0.224+0.095)\frac{1+0.0978/1.177}{1+1.28\times0.0978}+0.143\times\frac{1}{1.177}\times\frac{1+0.0978}{1+1.28\times0.0978}=0.4255$$

Where 1.28 is the value of R_a before the short circuit, thus the initial symmetrical component of armature current is given by:

$${}_pi_d(0)=\frac{1.3}{0.4255}=3.05$$

In Figure 5, the method outlined before is applied to find the particular solution corresponding to this case and the particular solutions for i_a and I are shown in Figure 5(H) and 5(I) where they are compared with the tested results.

The Calculated Free Solution

No attempt was made to find the exact value of x_{qs}' and since the value of the second harmonic observed in the armature current was negligible, x_{qs}' was taken equal to x_{ds}' thus

$$T_{ds}'=\frac{0.346+0.095}{0.0599}=7.37$$

thus

$$_fi_a=-3.05(\cos 1.955)\epsilon^{-t/7.37}=1.14\epsilon^{-t/7.37}$$

and

$$_fI=3.05(1.83-0.346)\epsilon^{-t/7.37}\cos t=4.52\epsilon^{-t/7.37}\cos t$$

Comparison Between Calculated and Test Results

In Figure 7 is shown the oscillogram taken from the machine corresponding to this case. In Figure 5(H) is shown the envelope to the symmetrical component for i_a both calculated and tested results. In Figure 5(I), is shown the particular solution for the field current I, both calculated and tested. The deviation near zero time is due to assumption 4 that the drop of saturation in the armature is instantaneous; actually it decays approximately with the armature time constant. Otherwise the agreement between calculated and test results is within 4 per cent. In Figure 6(A) and 6(B) is shown the free solutions for i_a and I both calculated and measured. Since x_{qs} was not calculated but assumed on the basis of the oscillogram, and since the angle θ_0 was also estimated from the oscillogram, no real check could be claimed for the free solution.

In the oscillogram is observed that the field voltage is not constant but there is a small fluctuation which is due to the drop of the free solution of the field current through the inductance of the exciter armature. Since it is small and lasts for a small duration, it is ignored.

Appendix I. Evaluation of Difference Reactance X_Δ

Figure 8(A) gives the magnetomotive force distribution of maximum value M_f due to the field current only. Figure 8(B) gives the permeance distribution for the zero component of the magnetomotive force and to a different scale, the flux density distribution due to the magnetomotive force distribution of Figure 8(A). Let this flux density wave have a maximum value of M_fB_m, an average value of M_fB_{av} and a fundamental of M_fB_1.

Following Kilgore's nomenclature,[17] let:

$$C_1=B_1/B_m \tag{56}$$

and

$$C_p=B_{av}/B_m \tag{57}$$

In Figure 8(C), is shown the distribution of the space fundamental of magnetomotive force of unit magnitude due to stator currents. Neglecting the small variation of the permeance distribution from the zero harmonic of magnetomotive force to the fundamental,[4] the multiplication of Figures 8(B) and 8(C) gives the air-gap flux density distribution due to the stator magnetomotive force only and is given in Figure 8(D). Let the fundamental of Figure 8(D) be B_{11} and let C_{d1} and C_m be defined such that:

$$C_{d1}=C_1C_m=B_{11}/B_m \tag{58}$$

The condition for the definition of the difference reactance is that the curve of Figure 8(D) and that of Figure 8(B) have the same area. The difference between the former and the latter is the wave shown in Figure 8(E) which must have zero area, thus:

$$\frac{1}{2}C_1B_m=M_fC_pB_m \tag{59}$$

or

$$M_f=C_1/2C_p \tag{60}$$

The difference reactance, by definition is proportional to the fundamental of the curve of Figure 8(E), or to the difference between the fundamentals of Figures 8(D) and 8(B)

$$x_\Delta=\lambda(C_{d1}-C_1M_f) \tag{61}$$

Where λ is a constant of proportionality. Substituting equation 60 in equation 61, there is:

$$x_\Delta=\lambda(C_{d1}-C_1^2/2C_p) \tag{62}$$

But the armature reaction reactance x_{ad} is proportional to C_{d1}, thus:

$$x_{ad}=\lambda C_{d1} \tag{63}$$

Substituting equation 63 in equation 62 there is:

$$x_\Delta=x_{ad}(1-C_1/2C_mC_p) \tag{64}$$

References

1. The Sudden Short Circuiting of Polyphase Generators, F. Punga. *Elektrotechnische Zeitschrift* (Berlin, Germany), volume 27, 1906, pages 827–31.

2. Initial and Sustained Short Circuits in Synchronous Machines, Vladimir Karapetoff. *AIEE Transactions*, volume 44, April 1925, pages 403–19.

3. Three-Phase Short Circuit Synchronous Machines—V, R. E. Doherty, C. A. Nickle. *AIEE Transactions*, volume 49, 1930, pages 700–14.

4. Two-Reaction Theory of Synchronous Machines, Generalized Method of Analysis—Part I, R. H. Park. *AIEE Transactions*, volume 48, July 1929, pages 716–30.

5. Synchronous Machines—Part I and II, R. E. Doherty, C. A. Nickle. *AIEE Transactions*, volume 45, June 1926, pages 912–42.

6. The Saturated Synchronous Machine, B. L. Robertson, T. A. Rogers, C. F. Dalziel. *Electrical Engineering* (*AIEE Transactions*), volume 56, July 1937, pages 858–63.

7. Armature Reaction of Alternators, **A. Potier.** *L'Eclairage Electrique* (Paris, France), volume 24, 1900, pages 133–41.

8. Potier Reactance for Salient-Pole Synchronous Machines, **Saad L. Mikhail.** *AIEE Transactions*, volume 69, part i, 1950, pages 235–38.

9. Switching Processes in Operation of Saturated Synchronous Machines, **Reinhold Rüdenberg.** *Wissenschaftliche Veröffentlichungen aus dem Siemens-Konzern* (Berlin, Germany), volume 10, 1931, pages 1–23.

10. Saturated Synchronous Machines Under Transient Conditions in the Pole Axis, **Reinhold Rüdenberg.** *Electrical Engineering* (*AIEE Transactions*), volume 61, June 1942, pages 297–306.

11. Damper Circuits and Rotor Leakage in the Transient Performance of Saturated Synchronous Machines, **R. Rüdenberg.** *Journal*, Franklin Institute (Philadelphia, Pa.), volume 234, 1942, pages 40–61.

12. Transient Performance of Electric Power Systems (book), **Reinhold Rüdenberg.** McGraw-Hill Book Company, New York, N. Y., 1950, chapters 53, 54, 55.

13. Determination of Synchronous Machine Constants by Test, **S. H. Wright.** *AIEE Transactions*, volume 50, December 1931, pages 1331–50.

14. Effects of Saturation on Machine Reactances, **L. A. Kilgore.** *Electrical Engineering* (*AIEE Transactions*), volume 54, May 1935, pages 545–50.

15. Reactances of Synchronous Machines and Its Applications, **R. E. Doherty, O. E. Shirley.** *AIEE Transactions*, volume 37, part 2, 1918, page 1251.

16. Calculation of the Armature Reactance of Synchronous Machines, **P. L. Alger.** *AIEE Transactions*, volume 47, April 1928, pages 493–513.

17. Calculation of Synchronous Machine Constants, **L. A. Kilgore.** *AIEE Transactions*, volume 50, December 1931, pages 1201–13.

18. Armature Leakage Reactance of Synchronous Machines, **L. A. March, S. B. Crary.** *Electrical Engineering* (*AIEE Transactions*), volume 54, April 1935, pages 378–81.

19. Test Values of Armature Leakage Reactance, **T. A. Rogers.** *Electrical Engineering* (*AIEE Transactions*), volume 54, July 1935, pages 700–5.

20. The Determination of Stray Flux in Alternating Current Windings, **M. Schenkel.** *Elektrotechnik und Maschinenbau* (Berlin, Germany), volume 27, 1909, pages 201–8.

No Discussion

An Experimental and Analytical Study of Turbine Generator Rotor Ventilation

CARL J. FECHHEIMER
FELLOW AIEE

THERE is no way known whereby the volume and pressure distribution of the gas flowing in the rotor of a completed turbine generator can be measured, nor can copper temperatures at selected points be measured readily. Surface temperatures taken after shutdown either by thermometer or contact thermocouple are none too good, owing to lapse of time, and they convey no information about localized copper temperatures. The only dependable method is temperature by resistance of the winding; this gives only the average temperature, and the engineer still lacks test data on copper temperature distribution. Recognizing the importance of the knowledge of the latter, the researches described herein were undertaken as a first step in the solution. It is still another step to calculate the temperature distribution of the steel and copper, after the ventilation pattern has been obtained. The Peck[1] and Soderberg[2] methods involve tedious calculations, and with the violent disturbances in the gas streams, the heat transfer coefficients should be determined from tests on models, if such data had not been obtained, before proceeding with the temperature calculations.

The experimental work described herein was undertaken some years ago at the Westinghouse Electric Corporation, but was not published. Experiments were made on a stationary as well as on a rotating model. The stationary model simulated the construction of a 4-pole plate rotor which was manufactured by them then; and the rotating model tests were made in combination with a model of part of a stator having the multiple path radial ventilation system.[3] As a few details of the two models differ from most present-day constructions, experiments on another relatively simple stationary model could be made; perhaps added tests on another rotating model, would not be needed.

Some of the experimental data and methods of approach and calculation may prove to be useful to engineers engaged in the design of gas-cooled turbine generators. So far as is known, nothing of a similar nature has been published. Also, there were some unexpected phenomena which may be of scientific interest to engineers engaged in fluid flow studies. No claim is made as to the means of calculation for a generator rotor being precise, and they are herewith presented as reasonably close approximations. The results from the rotating model may be helpful in a study of other rotor ventilation problems. Attention also is called to the application of the model experiments to an actual rotor and the plot of the results in Figure 13. The ventilation system studied is the one in which there are longitudinal ducts below the winding slots, and the gas emerges from radial ducts in the teeth. Inasmuch as engineers are familiar with that system, a schematic illustration is not included. The experiments were made with air, but the results can be applied readily to similar rotors cooled with hydrogen.

From the data secured from the stationary model, the volume* distribution was obtained, and discharge coefficients were evaluated. Such information, although valuable, was insufficient. From the rotating model the following were determined:

1. Pressure volume curves of the rotor acting as a fan, and their equations.
2. The influence of the axial components of the gas velocities in the air gap upon the gas that passed through the rotor vents.
3. The influence of the velocities of the gas streams from the stator vents discharging into the air gap, in the same, or not in the same plane as the rotor vents.

Data obtained from the stationary and the rotating models were then used in the calculation of an actual rotor's ventilation. Then the back pressure in the air gap arising from the stator ventilation is also allowed for.

The Stationary Model

The stationary model is shown in Figure 1, and is built of hardwood, in which one axial channel and 34 radial vents are reproduced. It simulated the full size vent system of one slot and tooth in half of a rotor whose body length would be 215 inches. A suitable centrifugal fan supplies air through a thermal volume meter whose inside sectional dimensions are $3^1/_2$ by $3^1/_2$ inches. There is comparatively little loss of head where the air turned a right angle corner before entering the axial channel in the model, as the velocities in those parts were low. The air then flowed through the 18-inch axial channel whose rectangular section is the same as the channel below the slots. This corresponds to the distance for flow through an end forging. One of the 34 blocks that followed is shown in detail at the left in Figure 1. Each block imitates a plate with a 3/8-inch radial vent at each plate. Soft rubber plugs could be driven into the outlets of the vents to close them as might be desired for a particular test.

* For simplicity, "volume" is used in this paper to denote the volume of gas flow per unit of time.

Paper 50-254, recommended by the AIEE Rotating Machinery Committee and approved by the AIEE Technical Program Committee for presentation at the AIEE Fall General Meeting, Oklahoma City, Okla., October 23–27, 1950. Manuscript submitted July 26, 1950; made available for printing August 31, 1950.

CARL J. FECHHEIMER is a consulting engineer, Milwaukee, Wis.

The author wishes to express his appreciation to the Westinghouse Electric Corporation for having given him the opportunity to conduct the research, and for permission to publish the results after a considerable lapse of time following the experiments. He also wishes to thank G. W. Penney and H. B. Holroyd, who assisted ably in the investigations.

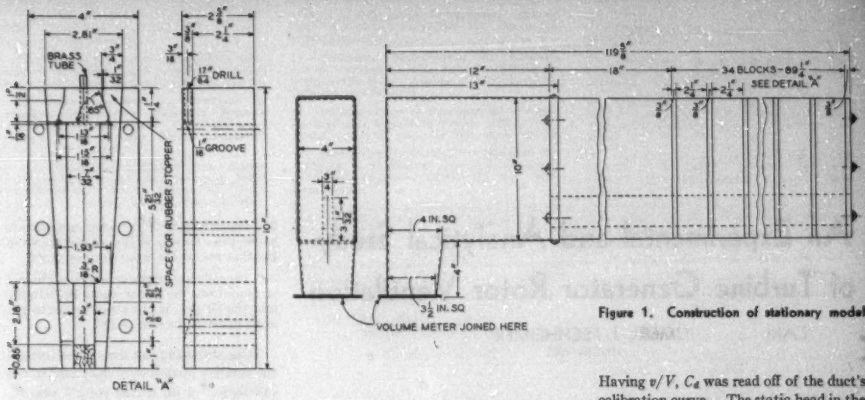

Figure 1. Construction of stationary model

The brass tubes at the tops of the wedges are connected through rubber tubing to a manifold provided with a large number of cocks, one for each tube, and the manifold is connected to a manometer. The 1/16-inch diameter holes just below the wedges connect the tooth ducts with the holes into which the brass tubes have been driven. When an outlet is closed with a soft rubber plug, no air flows in that duct, and consequently only axial duct static pressure is read. When an outlet is open, and air flows in the vent, there is a loss of head from the bottom of the wedge to atmosphere, and its measurement affords the means of determining the volume of flow in the duct, when suitably calibrated. For calibration, the ducts before and after the one being calibrated are closed, they being used for pressure measurement. The pressure at the duct through which air flowed is taken to be the arithmetical mean of the pressures at the closed ducts.

A dimensionless coefficient is defined by:

$$C_d = \frac{P/\gamma}{V^2/2g} \qquad (1)$$

where V is the radial velocity in the tooth duct at its minimum section, g is the acceleration of gravity, P is the pressure, and γ is the fluid's weight density. P/γ is the head required to drive the air through the vent. (Wherever $V^2/2g$ is used for air having a density γ of 0.074 pound per cubic foot, it may be written as $(V/4030)^2$, and V is then in feet per minute, and P/γ is in inches of water column.) It was found that C_d is far from being a constant, but is dependent upon the axial duct velocity. Generally about the same values of C_d were obtained for given values of v/V (axial velocity/radial velocity). The axial velocity is taken just ahead of the radial duct. A plot of C_d for the average duct is shown in Figure 2.

No satisfactory explanation has been given for this curve's peculiar shape. The points around the hump were taken very close together and with great care, and there is no doubt regarding its existence. There is a much smaller hump at higher values, which was noticeable when plotted to a larger scale. Also, why is the range of values of C_d so large? Curves for C_d were taken for many ducts, and the points obtained were not always coincident. The model was then dismantled, and the areas at the minimum sections were measured, and were found to differ appreciably. A calibration was required for each duct. Tests made previously on a model for C_d for stator vents also showed a rise of C_d with axial duct velocities, but the high values were not so great as for the rotor ducts, and no hump was observed. This was pointed out in a previous paper.[8]

Distribution curves were subsequently taken with many radial ducts open. In Figure 3 are typical curves, with 24 radial vents open, the first eight, tenth, and last ducts being closed. The radial volumes were obtained from manometer readings of the pressure at the bottom of the wedges, in combination with the previously obtained calibrations, and from the measured minimum areas for individual ducts the radial velocities V were calculated. The axial volume is that from the volume meter readings minus the sum of the volumes discharged from previous radial ducts. This divided by the axial duct section gives the axial velocity v. Having v/V, C_d was read off of the duct's calibration curve. The static head in the axial duct, P/γ, was then calculated from equation 1. Values of $P/\gamma + v^2/2g$ are plotted in Figure 3. The general shape of the radial duct volume curve is somewhat similar to those found for turbostator and salient-pole alternator radial duct discharge. The volume in duct 33 is about 4.6 times that near the entrance.

The Rotating Model

For the rotating model, the parts that simulated the rotor were built of two plates, shown in Figure 4, there being but one vent duct axially. It was made one third the size of a 51-inch diameter rotor, the width of the vent being 0.125 inch instead of 0.375 inch. Metal bars were placed in the slots and wedges in the wedge grooves after assembling. Figure

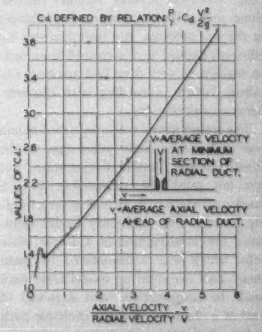

Figure 2. Coefficients of discharge in a rotor vent duct, plate construction

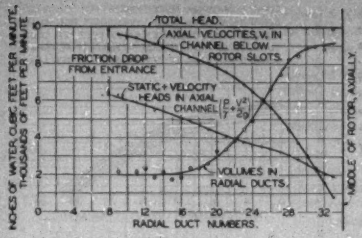

Figure 3 (left). Stationary model test results

Figure 5 (right). Cross-section of rotating model

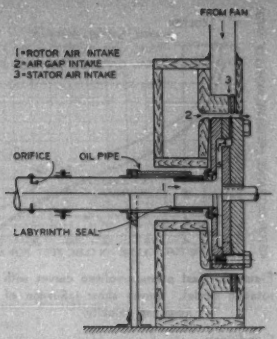

5 shows a cross-section and conveys a picture of the paths for air flow. Attention is called to the following:

1. The rotor, acting as a fan, caused air to flow from the atmosphere into the air gap (passages 1, 5, 4 and so forth), the volume being controlled by throttling in the stationary duct ahead of the entrance to the rotor.

2. A separate fan supplied air for axial flow in the air gap, entering the gap at 2.

3. Another separate fan supplied air for inward radial flow from the stator, entering the stator vents at 3.

4. The stator, provided with two vents, could be moved axially, so that tests could be made with the stator and rotor vents in line, and with the rotor vent midway between the stator vents.

By adjusting the speeds of the separate fans, their volumes were controlled. The effects were studied separately and in combination.

The labyrinth seal almost eliminated air leakage. However, tests were made with the aid of a vacuum cleaner fan which blew air into the clearance in the seal, with a rubber stopper closing the entrance to the rotor inlet, and the leakage volumes were measured with an orifice for various pressures. Allowances for leakages were made in subsequent tests, the corrected data only being given on the curve sheets.

The air volumes and pressures were measured as follows:

1. For the flow into the rotor, an orifice was placed in the intake pipe. A vacuum cleaner fan was placed in series so as to compensate for the drops in the orifice and pipes up to the rotor entrance. A thermal volume meter was used for calibration. A manometer connected to the entrance read the static head for the rotor air, below atmospheric pressure.

2. For the flow into the air gap, a manometer was connected to an impact tube placed at the entrance of the separate fan discharging into the air gap. After calibration with an impact tube held at the air gap, this afforded a means of measuring the air gap volume. This was sufficiently accurate, although not of the same degree as the other measurements.

3. For the flow to the stator vents an orifice was used. The pressure measured beyond the orifice was taken as the "stator pressure."

Notches were cut into the stator's surface adjacent to its inner periphery to imitate sunk stator slots. The stator was made of wood. The air gap in the model was 0.50 inch radially.

Results of Tests with the Rotating Model

In an actual machine most of the rotor pressures are positive, that is, above atmospheric pressure. In the model tests they were negative. Neglecting small differences due to departures in air density, the pressure volume curve should not be affected thereby.

Effect of Axial Flow in the Air Gap

Typical pressure-volume curves are like those in Figure 6. No air was supplied to the stator, and the fan for axial gap air was either stationary or driven at

Figure 4. The two plates of rotating model

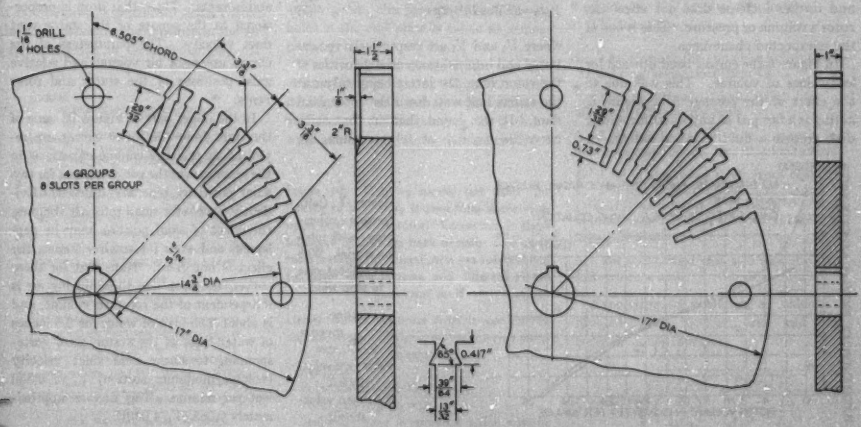

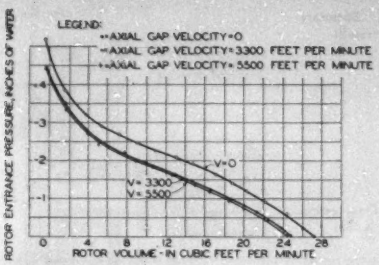

Figure 6. Test pressure-volume curves with rotating model. Curves show influence of axial gap velocity

Conditions:
Rotor speed = 2,000 rpm
Stator vent duct velocity = 0
No vane to stop whirl

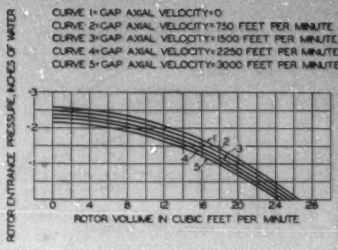

Figure 8 (right). Calculated pressure volume curves for rotating model. All curves are parabolas, and show influences of axial gap velocity

Conditions:
Rotor speed = 2,000 rpm
Stator vent duct velocity = 0

such speeds that the axial gap velocity was 3,300 or 5,500 feet per minute, the rotor running at constant speed of 2,000 rpm. The difference in pressures between any two curves is substantially constant for all values of volume. Thus, the effect of gap axial flow is to produce the equivalent of a constant pressure drop for a given axial gap velocity. Although this pressure difference is appreciable, the difference is small from 3,300 to 5,500 feet per minute. (The values of axial gap velocities should be taken as relative to the peripheral velocity, in this case 8,900 feet per minute.) An explanation is that the moving axial stream cleans off the rotor surface, thereby making the egress from the radial vents more difficult. After a particular relative gap velocity is attained, the surface is completely cleaned and further increase does not affect the rotor's volume or pressure. This is one of the unexpected phenomena.

In Figure 6 the curves bend upward for low values of volume. This was due to the effect of the passage 5 in Figure 5, acting as a fan just as any smooth rotating disk propels a fluid to some extent. A stationary vane was placed in that passage which almost eliminated the whirling of the air therein, which then became negligible, except for small volumes. A plot in Figure 7 is of tests made with and without the vane. The dotted curve is that of a parabola, which coincides substantially with the major and important part of the curve. In Figure 8 the curves are calculated parabolas for various axial gap velocities, the pressure differences between any two curves being independent of the volume.

Equation of the curves in Figure 8 is

$$P/\gamma = P_0/\gamma[1-(Q/Q_0)^2] \qquad (2)$$

P/γ is the entrance head at volume Q, (P_0/γ) is the rotor entrance head at zero volume, and Q_0 is the volume at zero pressure. For the calculated curve in Figure 7, which is the top curve in Figure 8, the equation is

$$P/\gamma = 2.63[1-(Q/_{26.6})^2]$$

For zero axial velocity in the air gap, and zero volumes in the stator and rotor vents,

$$P_0/\gamma = (U_2^2 - U_1^2)/2g \qquad (3)$$

where U_2 and U_1 are respectively the external and internal tangential velocities of the rotor vent, the latter being taken at the radius half way down the rotor axial duct. It was found that on that same curve the volume at zero pressure, Q_0, could also be calculated within a few per cent, the resistances to air flow having been estimated, and the assumption was made that all the generated head, P_0/γ, was consumed in resistance drop.

To allow for the effect of the axial velocity in the air gap, the curve in Figure 9 may be used. The fraction of peripheral velocity head $(U_2^2/2g)$ to deduct from the generated head is plotted against: (axial gap velocity)/(rotor peripheral velocity).

Effect of Gas Impinging from the Stator Vents

The air flowing radially inward from the stator vents creates disturbances in the air gap which make the egress of air from the rotor vents more difficult. In the lower part of Figure 10 the curves from tests are of the rotor net pressure for various stator pressures back of the core, with inward air flow, and zero axial flow in the gap. The six curves are straight lines, showing that the drop in rotor pressure due to the disturbance is proportional to the pressure drop through the stator vents. Thus, that drop is proportional to the square of the stator vent duct velocity. The parameters of the curves are rotor air volume and relative axial positions of the stator and rotor vents.

In the upper part of Figure 10 some of the data from the lower curves are replotted as pressure-volume curves, as in the lower curves the rotor volumes for two axial positions generally differed. Evidently, except for small rotor air volumes, the effect of axial position may be neglected, and even for small volumes, the effect is not great. Note that for these curves, the drop due to impinging air is independent of the rotor air volume, and is about 0.35 inch of water for 2.5 inches of water back of the stator core, corresponding to stator vent duct velocity (volume/minimum section) V_s of 9,350 feet per minute. This drop is approximately $0.065\ (V_s/4{,}030)^2$.

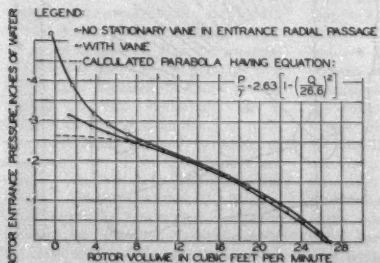

Figure 7 (left). Pressure - volume curves with rotating model. With and without vane to stop whirl

Conditions:
Rotor speed = 2,000 rpm
Stator vent velocity = 0
Axial gap velocity = 0

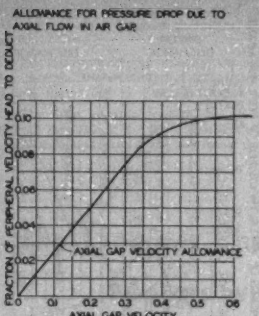

Figure 9 (left). Allowance for pressure drop due to axial flow in air gap

Figure 11 (right). Test pressure-volume curves. These curves show influence of axial gap velocity and of flow from stator vents

Conditions:
Rotor speed = 2,000 rpm
Stationary vane in entrance radial passage

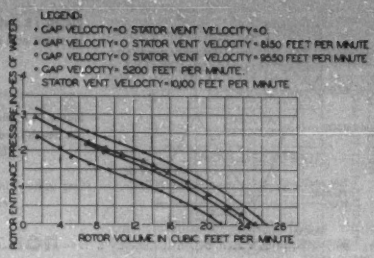

Combined Effects

In Figure 11 the test curves show the influence of axial gap velocity and of inward flow from the stator vents. In Table I calculated and test pressures are compared for 14 cubic feet per minute.

Table I

Gap Velocity	Vent Velocity	Net Head Calc.	Net Head Test
0	0		1.88
0	8,150	1.62	1.60
0	9,550	1.52	1.47
5,200	10,100	0.94	0.98

Although no experiments were made to determine the influence of outward flow in the stator ducts upon the rotor pressure or volume, it seems evident that since little, if any, disturbance is produced in the air gap thereby, no allowance need be made. It is, of course, essential to deduct from the rotor pressure, the pressure in the air gap in addition to these deductions. It also seems that since the rotor volumes are small compared with those needed for stator cooling, the influence of the air flowing through the rotor vents upon the volumes and pressures for the stator may be neglected.

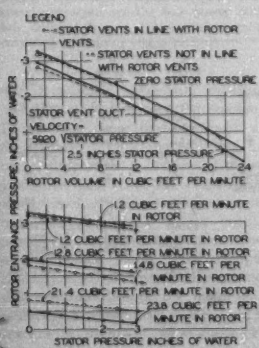

Figure 10. Rotating model test data. Influence of impinging streams from stator vents upon flow through rotor. Lower curves show influence of pressure back of stator core upon rotor pressure for several rotor gas volumes and for stator vents in same and different planes from rotor vents

Upper curves obtained from lower curves, and are pressure-volume curves for two stator pressures

Conditions:
Rotor speed = 2,000 rpm
Axial gap velocity = 0
Stationary vane in entrance radial passage

Calculations for a Turbogenerator Rotor

The calculations are for a generator which was rated 62,500 kva, 60 cycles, 1,800 rpm. It had a plate rotor, and was built some years ago, before turbos were cooled with hydrogen, and before the advent of large 2-pole 60-cycle rotors. With internal centrifugal fans, there is a decrease in pressure in the region of the rotor end plates where the gas enters, and such pressure must then be deducted from the rotor generated pressure. Allowance for this negative pressure may be made with the aid of Figures 29 and 30, of the paper on Centrifugal Fans for Electrical Machinery.[4] With propeller fans, their delivered pressure should be added to the rotor generated pressure. For the example given, the pressure ahead of the holes in the end plate is taken as atmospheric pressure.

The ventilation of the stator was calculated, and plotted in Figure 12. This includes gap and radial vent velocities, and pressures in the air gap, for both inward and outward flow. The methods for these calculations are given in a previous paper.[3]

When there is atmospheric pressure at entrance, the general equation, from Bernoulli's theorem, is:

$$P_0/\gamma = 1/\gamma(P_g + P_{ax} + P_s) + v^2/2g + \Sigma \text{ losses} \quad (4)$$

where

P_0 = generated pressure from equation 3
P_g = gap back pressure from Figure 12
P_{ax} = drop due to axial flow in gap from Figures 9 and 12
P_s = drop due to impinging air from stator
$v^2/2g$ = velocity head in axial duct

Since C_d depends upon the velocities, and consequently upon the volume of gas flow, it is first necessary to estimate roughly that volume. P_0/γ from equation 3 was found to be 23.5 inches of water. From Figure 12, rough averages of P_g/γ and gap axial velocities are about 6.5 inches and 4,200 feet per minute respectively, the latter 0.162 times the rotor peripheral velocity. With the aid of Figure 9, $P_{ax}/\gamma = 1.7$ inches. P_s will be neglected in this first approximation.

The losses are:

1. Loss through the end plate holes of area A_b and contraction coefficient C_b.

2. Loss at entrance to the axial ducts of area $A_a = 1/2$ velocity head.

3. Loss due to friction drop. Assume for first approximation to be 1/2 velocity head.

4. Loss in the radial ducts from equation 1. For first approximation take C_d and V $(= Q/A_d)$ as constants, Q being the total volume from one end, and Ad the area at minimum section.

5. For $v^2/2g$, treat this as a loss also, and 1/2 velocity head.

Expressing all velocities as volume Q divided by the sectional area, and pressures in inches of water

$$Q = 4{,}030\sqrt{\frac{P_0 - P_g - P_{ax} - P_s}{\left(\frac{1}{A_b C_b}\right)^2 + \frac{1.5}{(A_a)^2} + \frac{C_d}{(A_d)^2}}} \quad (5)$$

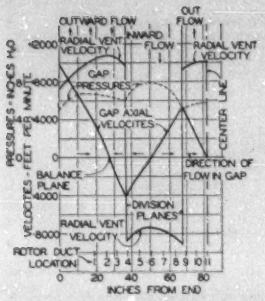

Figure 12 (left). Velocities and pressures in stator and air gap in a turbine generator

Figure 13 (right). Calculated air velocities, net heads, and discharge coefficients in a turbine generator rotor

Gas volume in rotor body = 3,350 cubic feet per minute at each end

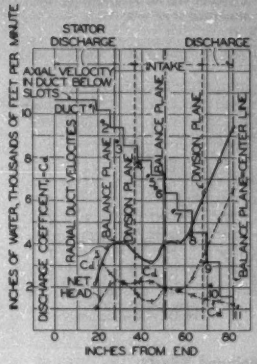

For $A_b = 1.04$, $A_a = 0.315$, $A_d = 0.68$ (all in square feet), and for $C_b = 0.80$, and $C_d = 1.80$, the numerical values of other quantities having been given previously, $Q = 3{,}450$ cubic feet per minute at each end.

For the second approximation this volume was used, and checked step by step, without the radical assumptions of the first approximation. The volume of 3,450 was found to be slightly high, as it did not give zero axial duct velocity at the middle of the rotor. As a third approximation, 3,350 cubic feet per minute was used, giving velocity at entrance to axial ducts of 10,620 feet per minute (see item 3, duct number 1, Table II). The air through the retaining ring vent holes of about 800 cubic feet per minute is added, giving 4,150 cubic feet per minute, as the air through the end plate holes.

The total drop up to the first radial vent is the sum of the following drops: end plate, 1.54 inches; entrance to axial ducts, 3.46 inches; friction drop through 18.875 inches of axial duct with coefficient of 0.0054, 2.48 inches; velocity head, 6.92, giving 14.40 inches of water drop, see item 4, duct number 1, Table II.

In Table II, results of calculations are entered for only three ducts. The drops are entered as pressures, P, and are given in inches of water. The methods for determining each quantity are given in the table. Items 11 and 12 were determined by cut and try, but it was not burdensome after a few attempts. Item 15 takes account of the gain in static head in the axial duct due to the abstraction of air in the radial duct, from which the loss of head due to reduction in axial velocity was deducted. For item 16 the coefficient of friction was taken to be the same throughout (0.0054), although it rises slightly with declining Reynolds numbers. (With small Reynolds numbers this loss is nearly negligible, because the velocity is low.)

There were a total of 21 ducts in the rotor, with number 11 at the center. Half of the air for that duct came from each end. There is a small residue of 198 cubic feet per minute, and had the chosen volume been just right, there would have been no residue. Considering that there are always some uncertainties in such calculations, it is not worthwhile to recalculate.

As a check on the arithmetic, the total volume is given by the sum of the volumes in the radial ducts, (item 13) plus the residue.

The results for one-half of the rotor are plotted in Figure 13. The axial velocity is shown as a stepped curve; the discharge at each radial duct decreases the velocity in the axial duct, and for simplicity, the axial velocity is shown as of constant value between adjacent radial ducts, since the shape of the curve over the width of, and adjacent to, a radial duct is unknown. The steps in the axial velocity curve do not change at a definite rate, as the discharges in the radial ducts change at an irregular rate. The radial duct velocity is 4,030 $\sqrt{\text{net head}/C_d}$, and both quantities under the radical change. They also are plotted in Figure 13, and should help to clarify the picture. The net head is item 10 in Table II, and is dependent upon the axial duct pressure minus the three drops in the air gap. In Figure 13 it appears as an irregular curve, and the radial duct velocity curve is of somewhat similar shape. The decrease in axial velocity from duct 10 to 11 would have been twice as great if there had been 22 ducts, and then no air for duct 11 would have come from the other end.

The unexpected phenomena which were observed in the experiments may be enumerated as follows:

1. The hump in the curve for C_d and the large increase with increasing ratios of axial to radial velocities, Figure 2.
2. The comparatively large decrease in ef-

Table II. Calculations of Turbo Rotor Ventilation 3,350 Cubic Feet Per Minute Each End

Item No.			
1	Duct number	1	6	11
2	Distance from end, inches	18.875	50 7/16	82.0
3	$V_a = V_a + 1$ (item 14) from previous duct	10,620	7,186	1590
4	$P_a' = P_a' + 1$ (item 17) from previous duct (inches water)	−14.4	−13.40	−11.27
5	Gap velocity from Figure 12 (feet/minute)	3,600	200	00
6	Gap velocity loss from item 5 and Figure 9	1.46	0.08	00
7	Gap back pressure from Figure 12	6.60	7.90	5.7
8	Stator duct velocity from Figure 12, V_s	Outgoing	Ingoing	Outgoing
			7,400	
9	Loss due to incoming air from stator = 0.065 $(V_s/4030)^2$	0.00	0.22	0.00
10	Net head = $P_s + P_n' -$ drops = 23.5 + item 4 − (items 6+7+9)	1.04	1.90	6.53
11	C_d from Figure 2	3.61	1.90	1.20
12	$V_a = 4{,}030\sqrt{\text{net head}/Cd}$	2,160	4,030	9,400
13	Q_n = radial duct volume = 0.0646 V_n	140	260	304
14	$v_{a+1} = v_a - Q_n/$axial area $= v_a - Q_n/0.315$	10,176	6,361	630
15	$P_{a+1}'' = P_a' + \left[\frac{(v_a)^2 - (v_{a+1})^2}{(4{,}030)^2}\right] - \left[\frac{v_n - v_{a+1}}{4{,}030}\right]^2$	−13.84	−12.75	−11.2
16	Friction drop between adjacent ducts = $f\left(\frac{\text{Length between ducts} \times \text{perimeter}}{\text{area}}\right)\left(\frac{v_{a+1}}{4030}\right)^2$	0.75	0.30	Negligible
17	$P_{a+1}' = P_{a+1}'' -$ friction drop	−14.59	−13.05	−11.2

fective pressure up to a certain axial gap velocity and small decrease thereafter, Figure 6.

3. For a given axial gap velocity, the drop is substantially independent of rotor volume of flow, Figure 6.

4. The drop in rotor pressure due to impinging streams of air from the stator is nearly independent of rotor volume of flow, Figure 11.

5. The relative axial positions of the stator and rotor radial vents have nearly negligible effect upon the rotor volume of flow.

References

1. Heat Flow in Turbine Generator Rotors, C. E. Peck. *Electrical Engineering* (*AIEE Transactions*), October, 1934, pages 1359–65.

2. Steady Flow of Heat in Large Turbine-Generators, C. Richard Soderberg. *AIEE Transactions*, June 1931, pages 782–802.

3. Ventilation of Turbo Alternators—Concluding Study, C. J. Fechheimer, G. W. Penney. *AIEE Transactions*, February 1926, pages 253–67.

4. Performance of Centrifugal Fans for Electrical Machinery, C. J. Fechheimer. *Transactions*, American Society of Mechanical Engineers (New York, N. Y.), 1924, pages 287–347.

No Discussion

The Goerges Phenomenon—Induction Motors with Unbalanced Rotor Impedances

HAROLD L. GARBARINO
ASSOCIATE AIEE

ERIC T. B. GROSS
FELLOW AIEE

Synopsis: The Goerges phenomenon is the operation of a 3-phase wound-rotor induction motor at half of synchronous speed, and it is obtained by unbalancing the rotor circuit. If the motor is started with one rotor phase opened or with rotor impedances greatly unbalanced, it will accelerate to half speed and operate stably as a motor or generator. Several investigators have made tests and analyses to find the characteristics of a motor operated in this way. In the present work a physical explanation and an equivalent circuit are given. Results of tests and calculations for a 5-horsepower motor are compared and found to be in good agreement. The unbalanced rotor impedances cause unbalanced rotor currents of slip frequency, and balanced stator currents of two frequencies, the fundamental and a subharmonic, the frequency of which depends on the speed. The motor may be operated stably at half or full speed. The torque at half speed is greater than at full speed, and may be almost as great as the rated torque for a balanced rotor. It may be desirable to operate an induction motor at half speed intermittently or as a temporary measure. Disadvantages of half speed operation are the low power factor, low pull-out torque, the subfrequency line currents, and motor vibrations.

THE induction motor with unbalanced rotor resistances was first studied by H. Goerges[1] more than 50 years ago. Since then several investigators have contributed to the knowledge of the subject with theoretical and experimental work. Early studies were concerned with one particular phase of the problem, namely, the 3-phase induction motor with a single-phase rotor. The operating characteristics of this machine are quite different from those of the motor with a balanced 3-phase rotor. The singular feature of operation with single-phase rotor is acceleration to only half synchronous speed upon starting, and stable operation in this speed region. The maximum torque for motor operation with this connection is greater at half speed than at full speed.

H. Goerges published[1] the first paper describing these characteristics in 1896, and others have since referred to the half-speed characteristic as "Goerges Phenomenon."[2,3] Goerges pointed out that at one-half of synchronous speed the motor torque is zero. In certain tests, the motor was used to operate a lift. At about half speed the motor was first used to raise the load, and then to act as a brake during the lowering of the load. Goerges stated that a 3-phase motor with a single-phase rotor could be operated at this reduced speed with less losses than the corresponding 3-phase rotor machine. He found that the efficiency for the single-phase connection was about 60 per cent at half speed, compared to 40 per cent for balanced 3-phase rotor at this same speed. Three-phase motors with single-phase rotors have been studied by others, and expressions derived for input current, torque, power, and other operating characteristics. Early studies were made in Europe,[4,5] in this country, B. G. Lamme[6] appears to be the first to have introduced the problem. Analyses, tests, and calculations based on an equivalent circuit confirmed some of the early observations of Goerges.

A problem closely related to that of the single-phase or unbalanced rotor is the starting from the line of a salient pole synchronous machine, or one with short-circuited field. With no damper winding this machine effectively has a single-phase rotor. When started, the machine may "crawl" at half speed.

A principal motive for the investigation of the unbalanced rotor circuit has been the search for a simple method of speed control. One important but inefficient method of speed control has been achieved by the use of variable resistances in the rotor circuit. Efficiency with this type of operation is reduced approximately in proportion to the speed; the electrical efficiency can never exceed the per cent speed at which the machine is operating. These resistances, which are also used for increasing starting torque and reducing starting current are often so constructed that they are unbalanced at many of the stepped positions at which they may be set. Studies were made to investigate the effect of this unbalance on input current, torque, and the losses in the motor. Gazda[7] and Jones[8] made tests to find the extent to which the rotor resistance may be unbalanced without deviating too much from normal performance. Other more recent contributions to the theory of the problem are contained in papers by Fourmarier,[9] Lyon,[10] Mauduit,[11] and Wagner and Evans.[12]

Analysis

An analytical approach to obtain a physical picture of the unbalanced rotor circuit phenomena, and to provide a basis for calculating the operating characteristics of such a machine, is based on the method of symmetrical components. This technique is suited for solving many 3-phase problems in which the electrical quantities are partially unbalanced. In

Paper 50-235, recommended by the AIEE Rotating Machinery Committee and approved by the AIEE Technical Program Committee for presentation at the AIEE Fall General Meeting, Oklahoma City, Okla., October 25–27, 1950, also presented as a conference paper at the AIEE Great Lakes District Meeting, May 11–12, 1950. Manuscript submitted May 10, 1950; made available for printing August 31, 1950.

Harold L. Garbarino was Instructor in Electrical Engineering at the Illinois Institute of Technology when this investigation was made. He now is with the General Electric Company, Pittsfield, Mass. Eric T. B. Gross is Professor of Power System Engineering with the Illinois Institute of Technology, Chicago, Ill.

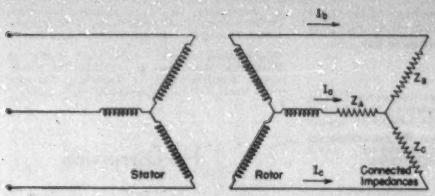

Figure 1. The induction motor with unbalanced rotor impedances

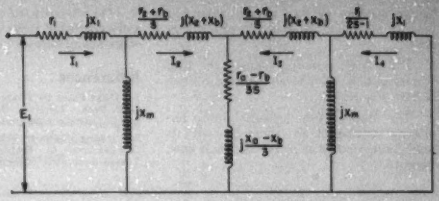

Figure 2. Complete equivalent circuit for two equal impedances in the rotor circuit

the problem at hand, the impedances of the three phases are the same, and the applied voltage is assumed balanced. The only unbalance is introduced by the connection of unbalanced resistances at the rotor slip rings. Resistance may be inserted between two phases, while leaving one line open, or resistances of different finite values may be inserted in all three phases, as shown in Figure 1. In this last case the characteristics of the motor approach those of the balanced rotor as the degree of unbalance is decreased. In symmetrical component analysis, the unbalanced quantities are resolved into balanced sets, and then treated separately in the calculations. This method has been the most common attack for the problem of the balanced 3-phase motor with unbalanced applied voltages which has been studied more frequently.

A description of the component motor fields which result in the unusual performance will be given here but for the derivation of equations for motor torque, losses, and currents, reference is made to previous authors.[12] It is well known that 3-phase voltages applied to the stator of a machine result in a magnetic field revolving at synchronous speed. When the rotor is at standstill, the field will induce voltages in the rotor of the same frequency as applied to the stator. When the rotor is rotating, the frequency of the induced rotor voltages and currents will depend on the relative velocity between the stator field and the speed of the rotor. This frequency will be greater if the rotor is rotating against the revolving field, and less if both are rotating in the same direction. The rotor quantities will be of a frequency equal to the product of the slip and the applied stator frequency (slip in per cent).

Any arrangement of unbalanced impedances connected externally in the rotor circuit, will cause unbalanced voltages of slip frequency to appear at the rotor terminals. These unbalanced voltages may be resolved into two symmetrical sets of phasors, the positive and negative sequence voltage components. Looking into the motor from the rotor terminals, the circuit will appear as a balanced network with unbalanced applied voltages, a problem of limited unbalance, and therefore suited for the application of symmetrical components.

The two symmetrical sets of rotor voltages and currents will be associated with two rotating fields revolving in opposite directions at slip speed with respect to the rotor, and may be arbitrarily identified as clockwise and counterclockwise. For the single-phase rotor, only a pulsating field will exist due to rotor currents, and this field may be resolved into equal components revolving in opposite directions. When the unbalance in the external circuit is small, the counterclockwise or negative sequence field will be rel-

Figure 3 (below). Equivalent circuit for the motor with single-phase rotor, or for two identical motors in concatenation

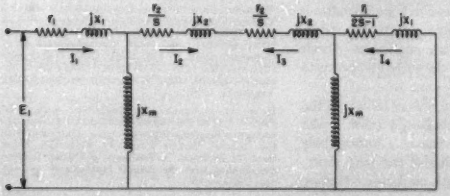

Figure 4 (right). Exact positive sequence stator current locus for single-phase rotor. External resistance, R is zero

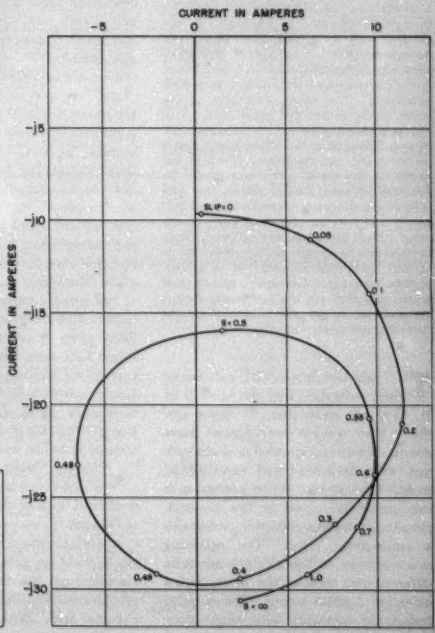

atively small. If all speeds are taken as fractions of the synchronous speed, the per-unit slip is s, and the rotor speed is $(1-s)$, defined as moving in the clockwise direction. The rotor field then is moving with respect to the stator at a speed of s plus $(1-s)$, or at the same speed as the field set up by the balanced applied stator voltages. The applied voltages and positive sequence rotor terminal voltages, together with the appropriate impedances between, constitute the positive sequence network. Since this network is balanced, only one phase need be analyzed. The field arising from the negative sequence rotor terminal voltage rotates at a speed $(-s)$ with respect to the clockwise direction of the rotor, or at a speed $(-s)$ plus $(1-s)$ equal to $(1-2s)$ with respect to the stator. Therefore, this field will induce voltages of frequency $(1-2s)$ in the stator. The circuit for the currents of this frequency is through the impedances of the stator winding and the power lines supplying the induction motor. In general the impedance of the stator will be much greater than that of the power supply so that these currents may be considered as short circuited through the stator impedance with negligible error. An inspection of the frequency, $(1-2s)$, shows that it becomes zero for s equal 0.5, or at one-half of synchronous speed. Evidently, then, at this speed, the negative sequence rotor field is stationary with respect to the stator, and no current due to this component will flow in the stator.

The next question is: what are the directions of torque due to these component fields, and will the machine start? We may deduce a rule that a rotating field caused by stator currents produces torque in the same direction as that of field rotation, and that a rotating field caused by motor currents produces torque in the direction opposite to that of the rotating field. The torque in each case is in such direction as to decrease the relative speed of the rotating field and the conductors which it crosses on the opposite winding. The positive sequence circuit is similar to that of a balanced motor in the unbalanced machine, and will give a clockwise torque for most speeds. Considering next the negative sequence rotor field, it is apparent that at speeds less than half, the field is moving counterclockwise with respect to the stator conductors, and a clockwise torque is developed. Conversely, when the rotor is moving at greater than half speed, a counterclockwise torque is developed by the negative sequence component. For some conditions of unbalance the positive sequence torque will be counterclockwise at some speeds because of a change in the direction of positive sequence rotor currents, but over most speeds the torque will be clockwise. Therefore, the negative sequence torque will generally aid that of the positive up to half speed, and oppose it above half speed. At exactly synchronous speed, the relative velocity of the rotor and stator field is zero, and no rotor current will flow.

In a manner similar to that for the balanced induction motor, equivalent circuits can be derived for the positive and negative sequence networks of the machine with unbalanced rotor. Under certain conditions one complete network can be found, which will yield all sequence components of current in the machine. It is possible to connect the positive and negative sequence networks through a third network, representing the external rotor impedances, if two of the external impedances are equal. If this condition is not fulfilled, two equivalent circuits and in addition some relating equations must be used to solve the problem. An equivalent circuit for the conditions Z_b equal Z_c is shown in Figure 2. Here I_1 is the positive sequence stator

Table I. Test and Calculated Data for the Unbalanced Rotor Circuit

Calc. or Test Conditions	External Resistance Referred to Stator	Per Cent Speed	Stator Power Factor	Stator Current, Amperes	Torque, Lb-Ft.	Elec. Effic., Per Cent
Figure 6	0	95	0.51		17	90
	0	90	0.55		27	87
	0	52	−0.27		−33*	65
	0	45	0.42		40	75
	1.6	80	0.53		21	84
	1.6	45	0.53		38	72
	4.1	70	0.48		18	79
	4.1	45	0.35		21	71
Figure 7	0	95	0.48	11.1	9	69
	0	91	0.53	15.5	16	78
	0	87.2	0.57	19.5	22	75
	0	52.2	−0.43	20.5	−32*	18
	0	47.6	0.41	19.9	28	74
	0	44.8	0.42	24.3	34	69
	1.97	79.7	0.49	13.8	13	69
	1.97	52.8	0.06	21.6	−30	0
	1.97	38.9	0.43	22.2	26	47
	9.44	68.8	0.40	10.3	7	44
	9.44	48.2	0.41	11.3	11	51
	1.97	92.5	0.61	14.2	19	90
Figure 8	1.97	85.5	0.61	21.6	29	83
	1.97	55.6	0.57	33.1	33	43
	9.44	86.6	0.55	21.4	25	87
	9.44	47.3	0.64	26.4	44	57
	22.8	88.8	0.58	19.1	22	81
	22.8	46.7	0.53	24.5	41	63
Figure 9	0.618	76.6	0.70	26.8	42	76
	0.618	58.3	0.58	36.2	42	50
	1.97	76.5	0.71	19.1	29	75
	1.97	54.8	0.64	27.1	34	48

* Generator operation.

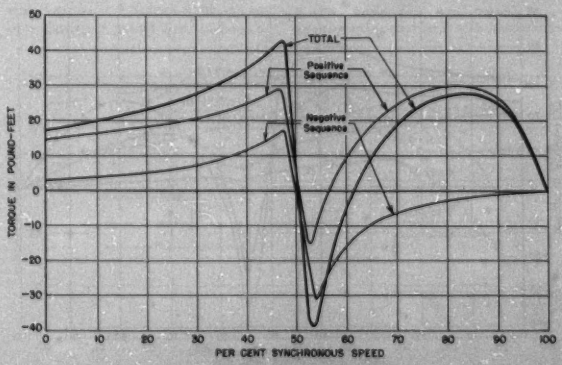

Figure 5. Calculated sequence components and total torque of induction motor with single-phase rotor and zero external resistance

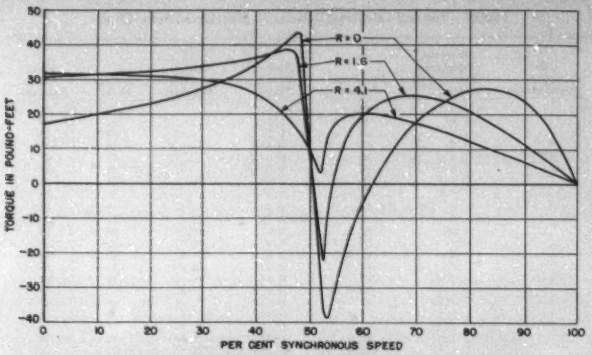

Figure 6. Calculated torque-speed characteristics of induction motor with single-phase rotor. (R is external rotor resistance referred to stator)

current of applied frequency, I_2 is the positive sequence rotor current of slip frequency, I_3 is the negative sequence rotor current of slip frequency, and I_4 is the negative sequence stator current of frequency $(1-2s)$. The impedances shown are the supply frequency equivalents which enable the actual values of component currents to be found for any rotor speed. Assumptions on which the circuit is based are: the impedances are constant, iron losses are negligible, and the electromagnetic fields are sinusoidally distributed in space. From the equivalent circuit the currents may first be found, and these then used to calculate the motor performance. For the single-phase rotor with zero external impedance between two rotor terminals, and with the third terminal open, the equivalent circuit reduces to that shown in Figure 3. It has been of interest to several writers[12] on the subject that this also is the equivalent circuit for two identical induction motors in concatenation, that is, connected in direct cascade, with the rotors connected together electrically and mechanically. In fact, Lamme calls the single-phase rotor a poor form of internal cascade, as compared to machines which are built with internal cascade connections for more flexible speed control.

Calculations and Tests

For calculation and test of an actual motor, a 5-horsepower 220-volt 8-pole 60-cycle wound rotor induction motor was used. The machine was rated at 18.2 amperes stator current and 845 rpm. Coupled to the motor was a d-c generator of about the same rating. Because of this it was impossible to conduct some desirable tests. By common test procedure the stator and rotor resistances and reactances, and the transformation ratio were found. The 60-cycle resistance was used as the stator resistance, although this is admittedly too high for the subfundamental frequency currents impressed from the rotor. For the rotor, the d-c resistance was used as the best approximation. Calculations were made of several electrical characteristics for the motor with single-phase rotor. One of these was the positive sequence stator current as shown in Figure 4, where the power component of current is in the direction of the abscissa, and the quadrature component in the direction of the ordinate. It is acting as a generator. Also calculated were the positive and negative sequence components and total torque as functions of speed, as shown in Figure 5, for the single-phase rotor. The maximum torque developed at approximately half-speed as generator is almost as great as the torque for the machine acting as motor, and these quantities are both greater than the maximum torque near the synchronous speed. Other calculated speed-torque characteristics are given in Figure 6, which shows the effect of inserting resistance between two rotor terminals. For an increase in resistance the torque curve tends to flatten out, and the dip near half speed becomes less until negative torque is no longer developed in this speed region. If the mechanical load on the motor is not too great, it will accelerate from standstill to speeds approaching synchronous.

Tests were made for several conditions of unbalanced external rotor resistance, and measurements taken of all electrical quantities, speed, and shaft torque. The applied motor voltage was about half of rated value, and the test results were corrected to values for rated voltage. Because of the small capacity of the coupled machine, it was impossible to make measurements in one unstable speed region, and characteristic curves in this region have been approximated. Four tests were performed on the motor with a single-phase rotor for different resistances between the two rotor phases. The resultant torque-speed characteristics are given in Figure 7. The value of torque in these curves is the total electrical torque, that is, the measured shaft torque plus the torque required to overcome friction and windage in the motor. This addition was made to give a better

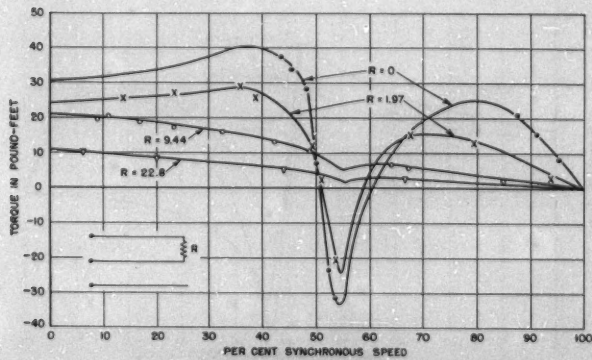

Figure 7. Torque-speed characteristics obtained from tests of the single-phase rotor. (R is external equivalent resistance referred to stator)

comparison of test results with calculated electrical torque, although this component was at most 1.1 pound-feet.

Comparison of the test and calculated curves for zero external rotor resistance shows reasonable agreement. The torque at very low speeds was found to be higher than the calculated value, a result which was probably caused by a decrease of the leakage reactance with saturation at high currents.

Calculated efficiencies also agree fairly well with test results. Again from the test results, it is seen that the maximum negative torque in the half speed region decreases as the resistance is increased, and the positive torque at other speeds is decreased. If the motor is started with a sufficiently small load, and with enough resistance between the rotor terminals, it will accelerate past the half-speed region. When operating near synchronous speed, too high an increase in the load will cause the motor to lose stability, and slow down to the half-speed region, where the pull-out torque is higher. This maxmium torque at half speed is considerably less than the calculated maximum torque of the balanced motor, which is about 57 per cent higher than that of the single-phase rotor at half speed, and about 150 per cent higher than that of the single-phase rotor operating near synchronous speed.

Another series of tests was performed with a resistance inserted in one phase, and zero resistance in the other two, Figure 8. As expected, a reduction of resistance R causes the curve to approach the condition for balanced rotor. The curve for the single-phase rotor, or infinite resistance in one phase, is given again for comparison. Other tests were conducted with equal resistances in two phases and zero resistance in the third, Figure 9. The irregularity of the speed-torque curve is here less pronounced. An increase in the resistances decreases the torque near synchronous speed, and increases the torque at low speeds. These curves are more qualitatively similar to the performance of the balanced motor than those for the previous tests. Other test data for stable operating conditions are summarized in Table I, where the figure references give the test condition or calculation.

Considering that the rated current for the motor is 18.2 amperes, it can be seen from the data, Table I, that there exist several rotor connections at several speeds where the motor might be operated without exceeding this rating very much. For example, using the single-phase rotor connection with zero external resistance,

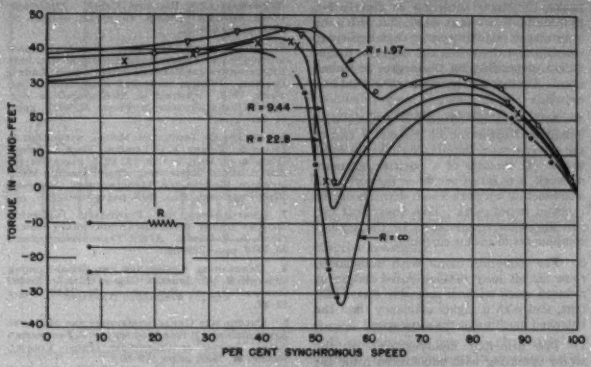

Figure 8. Torque-speed characteristics obtained from tests with external resistance in one rotor phase. (R is referred to stator)

a torque of 28 pound-feet can be developed with a current of 19.9 amperes at 47.6 per cent of synchronous speed. The rated full-load torque of the balanced machine is calculated to be 31 pound-feet, so that almost rated torque can be carried at the reduced speed without unreasonable stator current. This is done at an efficiency of 74 per cent, a much higher value than could be realized with the balanced machine.[1] Similar results can be observed in the data for some of the other rotor connections.

The data also show that the motor having greatly unbalanced connections has quite a low power factor; for the example above being only 41 per cent. Another disadvantage of the single-phase rotor is the vibration caused by pulsating torque, which has not been discussed here. These vibrations, in general undesirable or possibly damaging, would have to be considered in the design of the machine if it were built for such operation.

Conclusions

1. The performance of the induction motor with unbalanced rotor impedances is analyzed by the method of symmetrical components. Sequence components of the currents, the voltages, and the fields in the machine are treated separately, and the results superposed.

2. An unbalance in the rotor circuit causes unbalanced currents of slip frequency in the rotor phases, and balanced components of current in the stator at two frequencies, one of fundamental frequency and the other a subharmonic, the frequency of which depends on the speed.

3. The motor with single-phase rotor is similar in operation to two identical motors connected in concatenation.

4. The unbalanced rotor results in a torque-speed characteristic with two positive

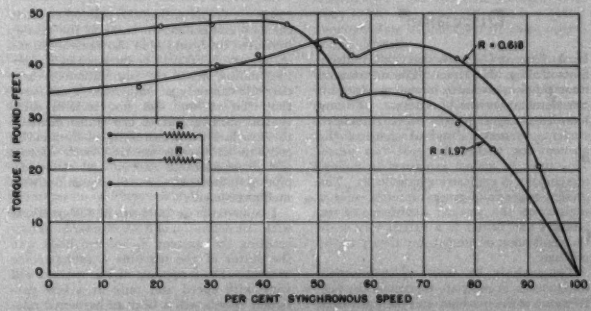

Figure 9. Torque-speed characteristics obtained from tests with external resistance in two rotor phases. (R is referred to stator)

peaks, the larger occurring at slightly less than half synchronous speed, and with a dip occurring at slightly greater than half-speed which may extend into the negative torque region, depending on the degree of unbalance. The motor may operate stably at two speeds.

5. An equivalent circuit for a motor with unbalanced rotor can be derived if two of the external rotor impedances have the same value. It consists of a positive sequence network, a negative sequence network, and a connecting network which depends on the external impedances. This equivalent circuit simplifies computation of the various components of motor currents.

6. The induction motor with unbalanced rotor circuit may develop rated torque at reduced speed without excessive stator current, and with a higher efficiency than the balanced machine at the same speed.

7. The principal disadvantages of the motor operating with unbalanced rotor are the low power factor, the decreased maximum torque, the subharmonic frequency current impressed into the power supply lines, and the vibrations present when the rotor circuit is greatly unbalanced.

8. There may be instances where it is desirable to operate an induction motor at half speed as a temporary measure, or intermittently, and the results of this investigation help in predicting the motor performance.

Bibliography

1. Ueber Drehstrommotoren mit verminderter Tourenzahl, **Hans Goerges**. *Elektrotechnische Zeitschrift* (Berlin, Germany), volume 17, 1896, pages 517–18; also in *Electrical Review* (London, England), volume 39, 1896, pages 689–90.

2. Die Kaskadenschaltung zweier Asynchronmotoren, von denen einer einem Einphasenrotor besitzt, **C. Schenfer**. *Elektrotechnische Zeitschrift* (Berlin, Germany), volume 46, 1925, pages 801–04; also *Elektrotechnik und Maschinenbau*, (Vienna, Austria), volume 43, 1925, pages 525–31.

3. Current Loops of Induction Motors Under Some Unbalanced Conditions, **Y. Hasumi**. *Journal*, Institute of Electrical Engineers, Tokyo, Japan, volume 54, 1934, pages 813–18. English abstract pages 96–98.

4. Ueber Drehstrommotoren mit Einphasiger Ankerwicklung, **Hermann Cahen**. *Elektrotechnische Zeitschrift* (Berlin, Germany), volume 19, 1898, pages 819–21.

5. Die Theorie des Drehstrom-Asynchronmotors in Der Einachsigen-Schaltung und Ihre Experimentelle Nachprüfung, Thesis, **Ludwig Dreyfus**. Wilhelm Ernst und Sohn, Berlin, Germany, 1910; Abstract in *Elektrotechnische Zeitschrift* (Berlin, Germany), volume 33, 1912, pages 91–92.

6. Polyphase Induction Motor with Single-Phase Secondary, **B. G. Lamme**. *Electric Journal*, (Pittsburgh, Pa.), volume 12, 1915, pages 394–96; also *Electrical Engineering Papers* (book), Westinghouse Electric and Manufacturing Company, (East Pittsburgh, Pa.), 1919, pages 519–24.

7. Performance of Polyphase Induction Motors Under Unbalanced Secondary Conditions, **A. A. Gazda**. *AIEE Transactions*, volume 36, 1917, pages 339–59.

8. Unbalanced Resistance and Speed-Torque Curves, **B. W. Jones**. *General Electric Review* (Schenectady, N. Y.), volume 51, 1948, pages 32–37.

9. Calcul des Caracteristiques des Moteurs Asynchrones a Rotor Monophase, **P. Fourmarier**. *Revue Generale de l'Electricite* (Paris, France), volume 31, 1932, pages 376–80.

10. Applications of the Method of Symmetrical Components (book), **W. V. Lyon**. McGraw-Hill Book Company, Inc., New York, N. Y., 1937.

11. Theorie du Moteur a Induction a Rotor Monophase, **A. Maudult**. *Revue Generale de l'Electricite* (Paris, France), volume 26, 1929, pages 5–15.

12. Symmetrical Components (book), **C. F. Wagner, R. D. Evans**. McGraw-Hill Book Company, Inc., New York, N. Y., 1933.

13. Theory and Calculation of Electrical Apparatus (book), **C. P. Steinmetz**. McGraw-Hill Book Company, Inc., New York, N. Y., 1917.

14. Die Wechselstromtechnik (book), **E. Arnold, J. L. LaCour**. Julius Springer, Berlin, Germany, volume 5, Die Asynchronen Wechselstrommaschinen: part I, Die Induktionsmaschinen, 1909.

15. Theorie der Wechselstrommaschinen (book), **O. S. Bragstad, R. S. Skancke**. Julius Springer, Berlin, Germany, 1932.

16. Graphische Behandlung der Kaskadenschaltung von Drehstrommotoren, **Max Breslauer**. *Elektrotechnische Zeitschrift* (Berlin, Germany), volume 24, 1903, pages 1–6.

17. The Operation of Induction Motors in Cascade, **H. Cotton**. *Journal*, Institution of Electrical Engineers (London, England), volume 61, 1923, pages 384–93.

18. Theory and Design of Electrical Machines (book), **F. Creedy**. Pitman and Sons, London, England, 1929.

19. Das Drehmoment des Asynchronmotors beim Anlassen mit Unsymmetrischen Laufterwiderstanden, **A. Drehmann**. *Elektrotechnik und Maschinenbau* (Vienna, Austria), volume 57, 1939, pages 509–21.

20. Induction Motors on Unbalanced Circuits, **A. M. Dudley**. *Electric Journal* (East Pittsburgh), volume 21, 1924, pages 339–43.

21. Controllers for Wound-Rotor Motors, **P. B. Harwood**. *Electrical Contracting* (Chicago, Ill.), volume 43, 1944, pages 117–20, 139–42.

22. The Cascade Induction Motor, **L. J. Hunt**. *Electrician* (London, England), volume 73, 1914, pages 603–05.

23. Unbalanced Secondary Resistances of Three-Phase Induction Motors, **Huzita-Ibatiro**. *Shibaura Review* (Yokohama, Japan), volume 18, 1939, pages 73–87.

24. Experimental Electrical Engineering (book), **V. Karapetoff**. John Wiley and Sons, Inc., New York, N. Y., volume 2, third edition, 1927.

25. Application of Tensors to Rotating Electrical Machinery, **G. Kron**. *General Electric Review* (Schenectady, N. Y.), series of articles, volumes 38–41, 1935–1938.

26. Principles of Alternating-Current Machinery (book), **R. R. Lawrence**. McGraw-Hill Book Company, New York, N. Y., 1940.

27. Induction Motors Under Unbalanced Conditions, **E. O. Lunn**. *Electrical Engineering* (*AIEE Transactions*), volume 55, April 1936, pages 387–93.

28. An Extension of the Method of Symmetrical Components Using Ladder Networks, **W. V. Lyon**. *AIEE Transactions*, volume 59, 1940, pages 1025–30.

29. Overvoltages in Polyphase Induction Motors During Single-Phase Operation, **C. MacMillan, G. K. Carter**. *Electrical Engineering* (*AIEE Transactions*), volume 60, August 1941, pages 819–23.

30. A Propos de la Theorie du Moteur a Induction a Rotor Monophase, **A. Maudult**. *Revue Generale de l'Electricite* (Paris, France), volume 31, 1932, pages 662–64.

31. The Secondary Circuits of Synchronous Induction Motors, **G. H. Rawcliffe**. *Journal*, Institution of Electrical Engineers (London, England), volume 87, 1940, pages 283–98, 693–694; and volume 88, 1941, part 2, page 162.

32. Induction Motors for Multisfeed Service with Particular References to Cascade Operation, **H. C. Specht**. *AIEE Transactions*, volume 27, 1908, pages 1177–95.

33. Speed Control of Slip Ring Motors Using Unbalanced Rotor Circuits, **T. Timpson**. *Metropolitan Vickers Gazette* (Manchester, England), volume 22, 1948, pages 270–74.

34. The Three-Phase Induction Motor with Unbalanced Rotor Impedances, **H. L. Garbarino**. Thesis, Illinois Institute of Technology, Chicago, Ill., 1949.

Discussion

M. A. Thomas (New Mexico State College, State College, N. Mex.): The unbalanced rotor problem seems to have experienced a considerable revival of interest. To my knowledge three schools have persuaded students to make a special study of the phenomenon within the past two years. This topic is seldom explained in college textbooks or in engineering handbooks. The present paper is of general interest since it summarizes the previous knowledge of the problem and brings to a satisfactory state the application of present-day theory to the problem.

The analysis, by means of symmetrical components, is adequate to explain the performance of the machine, and the equivalent circuits which have been developed permit the prediction of the characteristics in many cases. It should perhaps be pointed out that the two component currents in the stator, indicated by I_1 and I_4 in the equivalent circuits, are of different frequencies in the actual motor, hence the summation of these currents can only be indicated. I am sorry that the authors did not include some typical oscillograms of the stator currents to show how these two different frequencies combine at various speeds. Such records are of considerable interest and often surprising to those who are not acquainted with such phenomena.

I believe the authors are in disagreement with the definition of ASA standards in designating the current I_4 induced back into the stator of the machine a subharmonic current. The frequency of this current will vary with speed and only at a few particular speeds will it bear an harmonic relation to the line frequency. The usual situation will result in the two currents swinging in-phase and out-of-phase at a rate depending upon the difference of the two frequencies. This produces fluctuations in the magnitude of the resultant current which are quite noticeable on an ordinary ammeter. At standstill the two component currents are of the same frequency. They will then result in unbalanced effective values in the three lines. The particular condition of unbalance will depend upon the relative position of rotor and stator.

The power system lines and load may receive an appreciable effect from the odd frequency currents which flow in the stator as the result of this phenomenon. Several years ago the community in which I live was troubled intermittently by flickering of incandescent lamps over a residential and rural area of several square miles. This difficulty was similar to, but more pronounced than, that caused by operation of lamps on 25-cycle power. The cause of the

trouble was finally traced to a 100-horsepower wound-rotor motor which was driving a cotton gin. After careful inspection of all parts of the motor a poor connection was finally discovered in the rotor controller. It can be assumed that the flickering of the lights was caused by the occasional single-phase operation of the rotor of this motor. Had the power company engineers been familiar with the phenomenon described in this paper they would have been able to analyze the trouble and to locate the defective circuit much more quickly.

Stephen Freeman, Jr. (Purdue University, Lafayette Ind.): It may be worthwhile calling attention to the very real effects which the Goerges Phenomenon may have where low capacity power supplies feed motors whose capacity approaches the same order of magnitude as the transformer, lines, and other nearby parts of the power supply network. Faulty operation of these motors caused by accidental impedance unbalances can be readily detected in noticeable voltage flicker in the power supply system, affecting all customers in the general vicinity of the motor. Recognition of the existence of the Goerges Phenomenon has led, in several cases in my experience as engineer with a power company, to solution of the flicker problem in the power lines as well as helped to speed correction of faulty motor operation.

G. W. Heumann (General Electric Company, Schenectady, N. Y.): The Goerges Effect as such is a very interesting phenomenon, but it has not found practical application for the speed control of induction motors. The analysis presented by the authors leads, however, to a more thorough understanding of the phenomena which may occur when a wound-rotor induction motor is started or speed-controlled with unbalanced resistance in the rotor circuit.

Many drum controllers for the secondary control of wound rotor motors use a circuit on the first step which is the equivalent of the one shown in Figure 7 of the paper. The advantage of this circuit is that a smaller secondary resistor is required to obtain a certain reduction in starting torque, than would be required with a symmetrical 3-phase resistor. Referring to Figure 1(A) of this discussion, a resistance R in each rotor phase would produce a starting torque of one half of that obtained with all three rotor phases connected to the Y point. Expressed differently, with all three phases connected to the Y point, a resistance of $2R$ would be required to obtain the same starting torque. On the second step of a drum controller, the third rotor phase is connected to the Y point, thereby doubling the starting torque and permitting the motor to accelerate on a symmetrical and balanced rotor circuit. Since the single-phased starting connection results, as the authors have pointed out, in possible severe vibration of the motor at half speed, the unbalanced starting connection should not be used for large motors, and its application is generally restricted to motors of 75 horsepower or less.

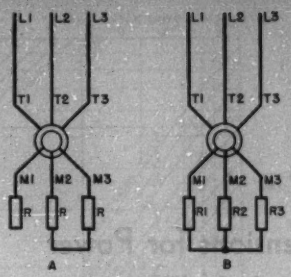

Figure 1. Wound rotor motor with unbalanced secondary resistor

Referring to Figure 7 of the paper, the rated torque of the 5-horsepower test motor (with a synchronous speed of 900 rpm) is approximately 30 pound-feet. Thus, the curves marked $R=9.44$ and $R=22.8$ (which would correspond to $R=4.72$ and $R=11.4$ in Figure 1 of this discussion) would produce starting torques of approximately 0.7 and 0.35 per unit respectively. This is the order of magnitude for which starting resistors are designed for material handling equipments, movable bridges, and similar applications. Examination of Figure 7 of the paper indicates that the dip in torque at one half synchronous speed is not very pronounced and will permit a lightly loaded motor to accelerate past that speed.

When the drum controller is advanced toward the full-speed position, resistance may be cut out in unequal steps, making every other controller point balanced and in-between points unbalanced. Figure 1(B) of this discussion shows the rotor circuit in a generalized manner. The degree of unbalance is generally moderate, hardly exceeding a 1 to 2 ratio between resistor phases. Speed-torque curves would be similar to those shown in Figure 9 of the paper, with the torque dip at one half speed of minor proportions. On the next-to-the-last point of the drum controller, a connection similar to the one shown in Figure 8 of the paper is used, where resistance in two rotor phases is short circuited and resistance left in the third phase. In order to avoid rough acceleration on the final controller point, resistance R will hardly be higher than 0.2 per unit of normal (where normal ohms is that resistance in each balanced rotor phase which would obtain unity starting torque) or, in terms of the authors' test motor, R will not exceed approximately 1.8. Examination of Figure 8 indicates again a moderate torque dip at one half speed.

Referring to Figure 1(B) of this discussion, the control designer is interested in knowing what motor performance he may expect from his motor for certain values of secondary resistance. Experience has shown that the following approximations obtain reasonably good results. If the variation in speed due to load changes is to be determined (which will occur at speeds above one half), an effective resistance

$$R_{eff}=\frac{R_1+R_2+R_3}{3}$$

may be used. If it is desired to determine the starting torque, calculation with an effective resistance

$$R_{eff}=\frac{R_1R_2+R_2R_3+R_3R_1}{R_1+R_2+R_3}$$

obtains better results.

In conclusion it may be stated that the findings of the authors are in agreement with practical experience gained over many years with unbalanced drum controllers. The Goerges effect need not be feared in connection with the design of resistors used with such drum controllers, provided the degree of unbalance between phases is moderate.

Harold L. Garbarino and **Eric T. B. Gross:** M. A. Thomas is quite correct in pointing out that a subharmonic is defined[1] as an integral submultiple of the fundamental. The subfrequency currents in the stator vary with the rotor speed and cover a whole frequency band; we are very grateful for this correction, however, we hope that the explanation in the text brought out the real character of the subfrequency currents.

It is very interesting that both Mr. Freeman and Mr. Thomas had the opportunity to observe some of the practical consequences of the Goerges phenomenon. Perhaps our textbooks should mention the effects of unbalanced rotor impedances, and some time may be devoted to such motor operation in college courses on a-c machinery. We know that Professor Harry Baum at the School of Technology of City College of New York included the Goerges phenomenon in his course for many years, and at Illinois Institute of Technology one full laboratory period has been devoted to it since 1946. The students' gain is a better understanding of induction machine operation in general.

Some other important practical applications are pointed out by Mr. Heumann, whose discussion is a valuable supplement to our investigation. We wish to thank the discussors for the interest they have shown in this paper, and for their comments.

REFERENCE

1. AMERICAN STANDARD DEFINITIONS OF ELECTRICAL TERMS. AIEE, section 65.10.035, 1941, page 201.

Critical Inside Dimensions for Power Cable Manholes

EDWARD S. HALFMANN
ASSOCIATE AIEE

THE THREE basic approaches to manhole design are: duplication of existing design; modification of existing design to eliminate certain known defects or inadequacies; and new design based on recently developed methods of predicting cable sheath life. This paper deals primarily with the latter, but it is well to keep in mind that existing design has been given a field test, whether formal or informal, and that the lessons learned from experience are extremely valuable. Since manholes and allied underground structures are of so many different sizes and shapes depending on the purpose which they serve, it has been necessary to limit the scope of this paper to power cable manholes and in particular, to the manholes along the route of transmission or express circuit cable lines.

The useful life of a modern paper-insulated lead-covered cable is essentially equal to the life of its sheath. Cable failures today can rarely be attributed to natural aging of the insulation. Almost every cable failure can be traced to a break of some kind in the lead sheath which has allowed moisture to enter the cable and cause insulation deterioration. Adjacent to the bends of a cable in a manhole, circumferential cracks caused by mechanical fatigue of the lead develop in the sheath. These cracks are produced by the repeated flexing of the cable which is necessary to accommodate the longitudinal movement of the cable at the duct mouths. The cable movement in turn is produced by changes in load on the cable causing it to expand and contract longitudinally in the duct between manholes. The rate of development of the cracks is dependent on the movement of the cable at the duct mouth and on the dimensions of the cable offset in the manhole. Cable movement cannot readily be controlled but the length and the width of the offset can be so chosen to produce the desired cable life.

Halperin[1,2] pioneered in the study of cable movement and its relationship to sheath life. Schifreen[3,4,5] obtained actual charts of cable movement at the duct mouth as a function of time and load current. Through a stress-strain analysis of the sheath at bends in the manhole, Schifreen developed a method of calculating the life of a cable for a given length and width of offset in the manhole. By making certain assumptions, Schifreen's method can be reduced to the single composite graph shown in Figure 1. By using this chart, the relationships between load, life, and offset dimensions for a given cable can readily be obtained.

Use of the Chart

The chart in Figure 1 may be used: to find offset dimensions which will produce the desired life of a cable under given load conditions; to find the life of a cable under given conditions of load and offset dimensions; or to find the load which will produce the desired cable life in a given manhole. It is necessary to know or to assume the conductor size and voltage rating of a cable before the chart can be used. The voltage rating of the cable is set by the system in which the cable will operate and the conductor size is usually determined by the normal and emergency current carrying requirements.[6] Tables I, II, and III have been prepared so that the factor (K) for frequently used cables would be readily available. K is equal to the a-c resistance of one conductor in ohms per foot multiplied by the thermal resistance from one conductor to the duct in degrees centigrade per watt for one foot of cable.

To find the length and width of offset which will produce the desired life for a given cable, proceed as follows:

1. Determine the minimum 4-hour average current and the maximum 4-hour average current for a representative working day. Divide the former by the latter and express the quotient in per cent.
2. Enter Section I of Figure 1 at the maximum 4-hour average current.
3. From the intersection of the maximum 4-hour average current and the per cent minimum-maximum determined in step 1 trace horizontally across the chart to the proper value of K in Section II, from which the daily conductor temperature range may be found if desired.
4. Trace vertically upward to the proper cable outside radius in Section III, from which the daily cable movement at each duct mouth may be obtained if desired.
5. From the intersection in Section III, trace horizontally to the desired cable sheath life line in Section IV and then vertically downward into Section V.
6. In Section V, a number of combinations of offset length (L) and offset width (F) along the vertical trace and above the minimum allowable bending radius (R) will satisfy the sheath life requirement. Select the combination most suitable for the particular location concerned. The minimum allowable bending radius for a cable may be taken as 12 times its outside diameter.

To find the expected life for a given cable in a given manhole, the procedure is the same as for finding offset dimensions as far as entering Section IV of the chart with a horizontal trace. Then a vertical trace is drawn from the intersection of the known width and length of offset in Section V. The intersection of this vertical

Paper 50-256, recommended by the AIEE Insulated Conductors Committee and approved by the AIEE Technical Program Committee for presentation at the AIEE Fall General Meeting, October 23–27, 1950. Manuscript submitted May 31, 1950; made available for printing August 25, 1950.

EDWARD S. HALFMANN is with the Philadelphia Electric Company, Philadelphia, Pa.

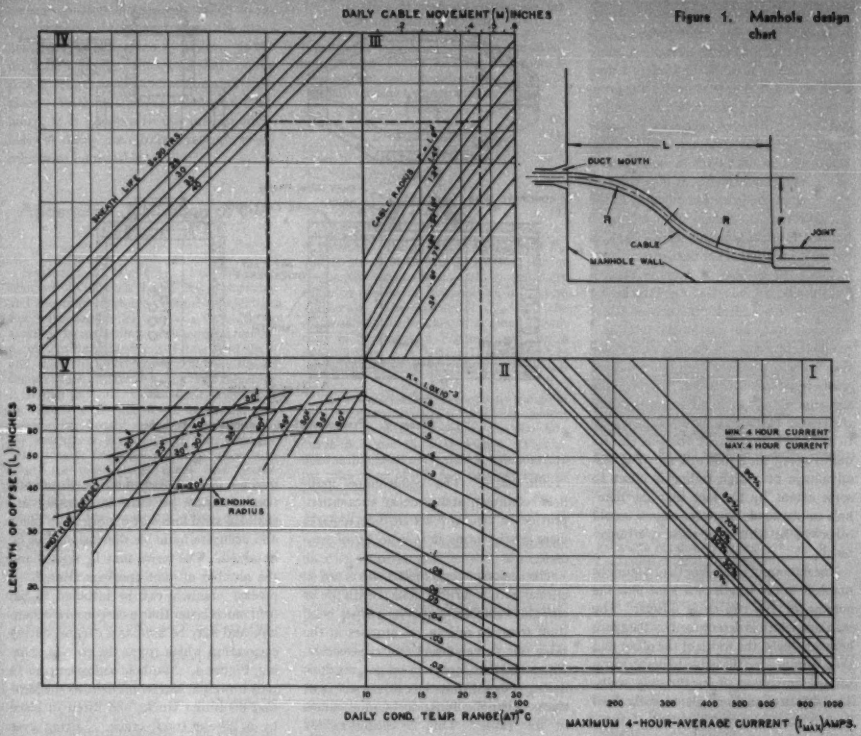

Figure 1. Manhole design chart

trace with the horizontal trace indicates the expected sheath life.

To find the loading of a cable which will produce the desired sheath life in a given manhole, start at the intersection of known width and length of offset in Section V and trace back through Sections IV, III, II, and I. In Section I, it will be found that a number of combinations of maximum 4-hour average current and per cent minimum-maximum along the horizontal trace will produce the desired sheath life.

Manhole Dimensions

In general, the only dimensions affecting the life of a cable in a manhole are the length and width of offset which can be determined from Figure 1. The remaining dimensions must be determined by the space required for working in the manhole and for equipment to be installed. The number and arrangement of ducts entering the manhole are important. The ideal arrangement for a straight manhole is two ducts wide at each end of the manhole as shown in Figure 2. This permits racking the cables in single tiers along each side wall which provides excellent accessibility to the joints. It also eliminates the necessity of moving one cable to work on another. The "2-wide" arrangement may be further improved by staggering the vertical position of the ducts as shown in Figure 2. This permits a cable entering at one side to be

Table I. Constant K for Single-Conductor Solid-Type Paper-Insulated Lead-Covered Cables

(Multiply Values Below by 10^{-9})

Conductor Size, Circular Mils	Line-to-Line Voltage Rating 7.5 Kv	15 Kv	23 Kv	34.5 Kv	46 Kv	69 Kv
250,000	0.288	0.288	0.308	0.316	0.326	
300,000	0.231	0.299	0.248	0.254	0.260	
350,000	0.190	0.189	0.207	0.210	0.214	0.225
400,000	0.162	0.160	0.167	0.180	0.183	0.192
500,000	0.122	0.122	0.131	0.137	0.140	0.147
600,000	0.099	0.098	0.105	0.108	0.109	0.117
700,000	0.081	0.083	0.087	0.089	0.090	0.097
750,000	0.079	0.076	0.080	0.082	0.083	0.089
800,000	0.069	0.070	0.074	0.076	0.077	0.083
1,000,000	0.054	0.055	0.056	0.057	0.058	0.063
1,250,000	0.041	0.042	0.043	0.044	0.045	0.049
1,500,000	0.033	0.033	0.035	0.036	0.036	0.040
1,750,000	0.028	0.028	0.029	0.030	0.031	0.034
2,000,000	0.023	0.024	0.025	0.026	0.027	0.029

Values of K were determined from Table 20, page 35 of reference 6.

racked on the opposite side wall without interfering with any other cable. A 2-wide duct arrangement permits a minimum width of manhole and offers a duct bank with excellent heat dissipating properties. Every duct can be fully utilized but the cost of such a duct bank is usually higher than other configurations. If this added cost of duct bank is not justified by thermal requirements, it is possible to change duct configuration adjacent to the manhole that is, change from a 2 by 6 bank at the manhole to a 4 by 3 bank in the major portion of the duct run.

When the number of ducts is large, a 2-duct-wide manhole may need too high a ceiling to be practical. It has been found advisable to locate the lowest joint in a manhole at least 18 inches above the floor so that a splicer may make a good joint even if the floor is wet. Likewise the top joint should be at least 2 feet below the ceiling to afford good working conditions. For a 2 by 6 duct manhole this requires about an 8-foot ceiling. The disadvantage of a high ceiling is offset to some extent by the fact that the manhole can be made narrower than it would otherwise be with other racking arrangements.

The minimum inside length of a straight manhole is the length of a joint plus the lengths of the two cable offsets. The manhole width is determined by the space between ducts, the width of the offset and the allowance for the cable joints to move toward and away from the side walls. The sideways motion due to daily load cycle is small but over a period of time, movement is considerable at some locations due to the tendency of the cable to gradually creep into one manhole from another. In general a distance of 8 to 12 inches from the wall to the axis of the cable and joint is ample.

There are two general shapes of straight manholes; rectangular and the so-called "coffin shape." The "coffin shape" manhole requires a little smaller excavation, provides a stronger design, but requires more costly forms if it is to be of concrete.

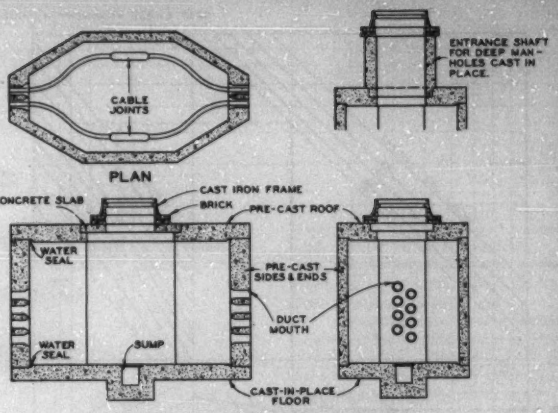

Figure 2. Precast straight transmission manhole

The design of corner manholes is not so critical with regard to cable sheath life as straight manholes since the corner bend itself tends to relieve the stresses in the cable due to expansion and contraction. The important factor in corner manhole design is to see that the cable is not bent sharper than the minimum bending radius of the cable. This is conservatively given as 12 times the outside diameter. It is, however, advisable to provide a cable offset at one end of the manhole as shown in Figure 3. It also is important to provide for ample sideways movement of the cable on the racks in this type of manhole.

Precast manholes have recently come into use in a number of cities. A precast manhole may be cast in carefully assembled steel forms at a fabricating plant and accurate manhole dimensions can be obtained. The forms may be reused and the number of duct openings altered. A precast manhole can be installed in the field much faster than a cast-in-place manhole and may be used as a caisson during excavation which saves the cost of shoring, Figure 4. Manhole sections up to 14 tons in weight can be brought to the location on trailer trucks and lifted in place by a 20-ton truck crane. Lifting eyes must be provided to facilitate handling with a crane. The wall section is reinforced so that it will be self-supporting when lifted and that it will withstand the maximum pressure which may be exerted from the outside. When this wall section is in position, a sufficient number of building blocks are placed under the walls to support it and then a concrete floor is poured in place. A water sealing compound is placed at the joint between the walls and the floor. A sump is cast into the floor so that water on the floor will drain into the sump and may readily be pumped out.

The roof slab, Figure 5, is precast and lifted in place by the crane. It is designed to be not only self-supporting but also to be able to support a wheel load of 25,000 pounds. A step around the edge of the casting, Figure 2, locks the roof in place on the walls and a water seal is installed to prevent leaking. In order to permit the same manhole to be used at different depths, an adjustable opening is provided. If the roof is close to the surface,

Table II. Constant K for Three Conductor Belted Solid-Type Paper-Insulated Lead-Covered Cables

(Multiply Values Below by 10^{-3})

Conductor Size, Circular Mils	Line-to-Line Voltage Rating 4.5 Kv	7.5 Kv	15 Kv
250,000	0.619	0.619	0.600
300,000	0.492	0.488	0.482
350,000	0.402	0.403	0.393
400,000	0.340	0.344	0.337
500,000	0.257	0.262	0.250
600,000	0.205	0.206	0.204
700,000	0.170	0.172	0.169
750,000	0.158	0.158	0.156

Values of K were determined from Table 21, page 36 of reference 6.

Table III. Constant K for Three Conductor Shielded Solid-Type Paper-Insulated Lead-Covered Cables

(Multiply Values Below by 10^{-3})

Conductor Size, Circular Mils	Line-to-Line Voltage Rating 15 Kv	23 Kv	34.5 Kv
250,000	0.482	0.477	0.468
300,000	0.387	0.385	0.372
350,000	0.322	0.322	0.312
400,000	0.275	0.276	0.272
500,000	0.213	0.215	0.208
600,000	0.173	0.175	0.169
700,000	0.145	0.155	0.141
750,000	0.136	0.134	0.131

Values of K were determined from Table 22, page 37 of reference 6.

precast concrete slabs are installed to reduce the size of the opening and the manhole frame is supported by bricks. If the manhole is deeper, an access shaft of the proper length is cast after the roof is in place. With this added feature of flexibility, it is possible to use precast manholes at many more locations than would otherwise be possible.

Appendix. Derivation of the Chart

Sections I and II of Figure 1 establish the relationship between the loading of the cable and the daily conductor temperature range. For purposes of this analysis it has been assumed that the duct bank temperature remains constant during any one load cycle and that the cable will reach its ultimate temperature change in four hours following a change in load. It has been found that by using the average of the maximum four consecutive hourly ammeter readings and the average of the minimum four consecutive hourly ammeter readings, the daily conductor temperature range can be obtained with reasonable accuracy.

For a constant load on a cable, the temperature of the conductor above the temperature of the duct bank can be expressed as follows:

$$T_c - T_d = I^2 r_{cond} R_{th} \qquad (1)$$

where

T_c = conductor temperature in degrees centigrade
T_d = duct bank temperature in degrees centigrade
I = phase current in amperes
r_{cond} = a-c resistance of one conductor in ohms per foot
R_{th} = thermal resistance from one conductor to duct in degrees centigrade per watt for one foot of cable

Equation 1 may be written for the maximum 4-hour current and the minimum 4-hour current and the difference will then be the daily conductor temperature range.

$$T_{c_{max}} - T_d = I_{max}^2 r_{cond} R_{th} \qquad (2)$$

$$T_{c_{min}} - T_d = I_{min}^2 r_{cond} R_{th} \qquad (3)$$

$$T_{c_{max}} - T_{c_{min}} = (I_{max}^2 - I_{min}^2) r_{cond} R_{th}$$

$$\Delta T_c = (I_{max}^2 - I_{min}^2) K$$

$$\Delta T_c = I_{max}^2 \left[1 - \left(\frac{I_{min}}{I_{max}} \right)^2 \right] K \qquad (4)$$

K represents the product of r_{cond} and R_{th} and is given in Tables I, II, and III for frequently used cables. ΔT_c is the daily range of conductor temperature in degrees centigrade. The product of I_{max}^2 and the expression in the bracket is obtained graphically in Section I of Figure 1 and this is multiplied by K in Section II of Figure 1 to obtain daily range of conductor temperature.

The relationship between daily range of conductor temperature and cable movement at a duct mouth is based on the test data curve in Figure 15 of reference 5. This indicates that cable movement at a duct mouth for cable runs of 300 feet or more may be expressed as follows:

$$M = (\Delta T_c - 5) 0.03 \text{ inch} \qquad (5)$$

More recent studies taking into account duct irregularities indicate that 80 per cent of this value is more nearly correct for relatively long duct runs, hence the relationship used in Figure 1 in obtaining the movement scale of Section III is:

$$M = (\Delta T_c - 5) 0.024 \text{ inch} \qquad (6)$$

The relationship between cable movement, strain in the sheath and offset dimensions is based on the per cent strain equation developed in Appendix A of reference 3.

$$\epsilon = \frac{850 r \sqrt{F^2 + LM} - F\sqrt{F^2 + 2LM - M^2}}{L^2 + F^2} \qquad (7)$$

Figure 4. Precast manhole partially installed

where

ϵ = per cent strain in the sheath
r = outside radius of the sheath in inches
F = width of offset in inches
L = length of offset in inches
M = cable movement in inches

This equation may be expressed as

$$\epsilon = 850 r f(F, L, M) \qquad (8)$$

When $f(F, L, M)$ is evaluated for a number of values of F, L, and M, it is found that, for the range of values applicable to manhole design, this function is directly proportional to M. The expression may, therefore, be rewritten

$$\epsilon = 850 r M f(F, L) \qquad (9)$$

The relationship between sheath life in load cycles and maximum per cent strain of the lead is obtained from Figure 11 of reference 5. This curve may be converted to years life by assuming 275 load cycles per year

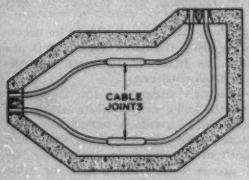

PLAN

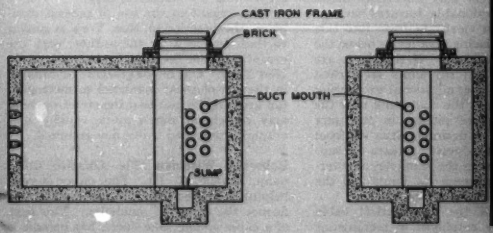

Figure 3 (left). Cast-in-place corner transmission manhole

Figure 5 (right, below). Precast manhole roof

and may then be expressed by the equation

$$S = 1.6e^{-1.44} \tag{10}$$

where S is sheath life in years and e is maximum per cent strain in the sheath. This can be rewritten:

$$e = 1.39S^{-0.7} \tag{11}$$

Combining equations 9 and 11 we have

$$1.39S^{-0.7} = 850rMf(F, L) \tag{12}$$

or

$$\frac{1.39S^{-0.7}}{Mr} = 850f(F, L) \tag{13}$$

The product of $M \times r$ is obtained in Section III of Figure 1. The term $1.39\ S^{-0.7}$ is divided by $M \times r$ in Section IV of Figure 1 and equated to $850\ f(F, L)$ which is evaluated in Section V.

The bending radius lines superimposed in Section V are obtained from the equation

$$R = \frac{L^2 + F^2}{4F} \tag{14}$$

The bending radius lines merely serve as a guide in selecting offset dimensions and do not enter directly into the solution of the problem.

References

1. Load Ratings of Cables—I, Herman Halperin. *Electrical Engineering* (*AIEE Transactions*), volume 58, October 1939, pages 535–55.

2. Load Ratings of Cables—II, Herman Halperin. *AIEE Transactions*, volume 61, 1942, pages 930–42.

3. Cyclic Movement of Cables—Its Causes and Effects on Cable-Sheath Life, Clement S. Schifreen. *AIEE Transactions*, volume 63, 1944, pages 1121–30.

4. Oil-Filled Cable Forms Link in 66-Kv Philadelphia Loop—I, Clement S. Schifreen. *Electric Light and Power*, (Chicago, Ill.), July 1948, pages 45–49.

5. Oil Filled Cable Forms Link in 66-Kv Philadelphia Loop—II, Clement S. Schifreen. *Electric Light and Power* (Chicago, Ill.), August 1948, pages 64–69.

6. Current Carrying Capacity of Impregnated Paper, Rubber and Varnished Cambric Insulated Cables. Insulated Power Cable Engineers Association (New York, N. Y.), first edition, December 1943.

Discussion

H. A. Adler and **K. H. Wadleigh** (Commonwealth Edison Company, Chicago, Ill.): This paper is a convenient and condensed presentation of the method of calculating sheath life as proposed by C. S. Schifreen (see references 3, 4, and 5 of the paper). Instead of having to refer to several graphs and formulas, Figure 1 of the paper makes it possible to solve the problem in one continuous process.

This graph is satisfactory if Schifreen's method is accepted as the basis of sheath life calculations. However, some of its limitations should have been made clear in order to avoid misleading conclusions. Figure 1 applies only to copper bearing lead sheath and not to alloy sheath. It applies to a sheath temperature of 40 degrees centigrade. The amount of cable movement is based on data for 1,500,000 circular mil, 66-kv oil-filled cable with a diameter of 2.44 inches. Other cables may be much more flexible and may have less movement. Furthermore, differences in friction and variations in duct profile may produce different movements. The movement given in Figure 1 is the average movement per duct mouth. Schifreen has presented statistical diagrams which indicate that due to unequal movement on the ends of a length, the movement may be considerably more than average at one duct mouth. Similar data were presented in Figure 10 of a paper by Herman Halperin.[1]

Figure 1 applies specifically to standard straight-type manholes with free moving joints. There are several simplifying assumptions to facilitate the graph, but they appear acceptable within the accuracy of this method. With these qualifications, we consider this method a very convenient procedure for determining sheath life.

Reference

1. See reference 2 of the paper.

W. A. Del Mar (Phelps Dodge Copper Products Corporation, Yonkers, N. Y.): The author assumes that cables in ducts will attain their maximum temperature in four hours. Is this assumption based on observations under operating conditions?

I take exception to the author's assumption that his values of K, derived from Insulated Power Cable Engineers Association's tables of carrying capacity in free air, are applicable to cables in ducts. This assumption is so far from being correct that it throws considerable doubt on the accuracy of his method.

C. T. Hatcher (Consolidated Edison Company of New York, Inc., New York, N. Y.): Mr. Halfmann has presented in a practical and useful form the results of a very detailed investigation of cable manhole sizes as related to cable life.

The maintenance of the integrity of the cable sheath has been a continuing problem in utility companies having underground systems and the situation has been aggravated in many companies by the tendency toward greater feeder loading, producing increased cable movement, and by the installation of larger cables in old duct and manhole systems.

When building new duct systems, particularly those intended for important tie feeders, the installation of manholes sufficiently large to permit adequate offsets for optimum cable life may be justifiable on an economic basis. The straightforward solution of installing wide manholes so as to permit horizontal offsets may not be possible of attainment in many cases since the manhole would become an intolerable obstruction of lanes assigned to other subsurface utilities such as gas, steam and water mains, sewers, and telephone ducts.

An alternative would be the building of manholes of normal width, but of greater than usual depth to permit offsets to be made in a vertical or sloping plane. This alternative solution may sometimes introduce other objectionable features such as bringing the floor elevation down into tide water levels or placing floor levels below the sewer system elevation. If the ducts are brought in low and the joints are racked high in the manhole, additional excavation is required to lower the duct bank near the manholes and these pitches in the duct bank produce a less desirable situation from a cable-pulling standpoint. Means for supporting the cables in the manholes at intermediate points between the joints and the duct mouths are also complicated.

A variation of the symmetrical cable racking normally employed in rectangular manholes would be to have the duct entrance location at one end of the manhole near one side wall and at the other end, near the opposite side wall. Each cable passing through the manhole would have a full wide offset at one end of the manhole and almost none at the other end.

Experience with 138-kv oil-filled cables in manholes of this type has been good and that design was recently employed in a 69-kv oil-filled cable installation. It would be of interest to compare the expected life of cables racked in this way in a given manhole to the life anticipated in the same size manhole if the duct entrances were centered and two complete, although small, offsets are employed. It would also be of interest to determine the advantages of having wide offsets at both ends of the manhole as compared with having a wide offset at one end only.

The "unsymmetrical" scheme just described, embodying an offset at only one end of each manhole on any particular cable, would make it seem desirable to install left and right manholes so that the duct entrances of adjacent manholes would be properly positioned with respect to each other.

If this were not done, it would be necessary to deflect the duct bank as it approached the manhole to meet the off-center point of entrance.

The author's suggestion for staggering duct mouths and crossing cables within the manholes does provide a means for gaining greater cable offsets without increasing the width of the manholes materially, although access to the duct mouth for cable pulling and for installation of fairleaders, duct sealing, installation of bond ties, and arcproofing are made less easy.

With regard to the use of precast manholes, the practice in New York is similar to that described by the author, with the exception that floors are also precast in New York. One of the greatest advantages in the use of these manholes in metropolitan areas is the fact that the street opening may be closed much more rapidly and normal unimpeded traffic flow resumed.

Robert J. Wiseman (The Okonite Company, Passaic, N. J.): This paper is very helpful in appreciating the factors that influence the design of manholes. This part of a cable system, like ducts, has become a

highly technical and engineering problem. If it had been appreciated years ago that the life of a cable depends on how it is installed in a manhole, many cables would have had a longer life. Reading this paper explains why manholes must be increased in dimensions to take care of present day cables.

The author has presented a very fine method for determining the dimensions of a manhole for a given cable or what the life of a cable may be knowing the manhole dimensions. This will be very helpful to a design engineer. I would like to ask the author if there is an optimum value of "R" the width of offset of the center of the cable in the duct from the center of the joint and "L" the length of offset from the edge of the duct wall to the end of the joint. Figure 1 of the paper shows how both vary but is there some particular value that would be preferred, say as a function of the diameter of the cable. The author suggests as a value of "R" the radius of bending of the cable as 12 times the over-all diameter. It seems to me as if this is too high as it would mean large manholes. We have used a value of ten times the outside diameter and even as low as eight times on small cables.

The chart as set up in Figure 1 is based on using copper bearing lead. Could the author estimate what changes he would make if an alloyed lead such as the arsenical types were used? As a first guess could we say the life would be doubled?

Can the author give an idea of the relative cost of manholes today as compared to pre-World-War II?

E. S. Halfmann: The comments and questions of the discussors are greatly appreciated by the author and indicate a genuine interest in a simplified approach to manhole design.

As pointed out by H. A. Adler and K. H. Wadleigh, the chart in Figure 1 may be used for cable having commercially pure or copper bearing lead sheath and is not applicable to cables with alloy sheaths. The relationship between daily cable movement and daily copper temperature range was obtained by taking the test curve for 1,500,000 circular mil, 69-kv oil-filled cable shown in Figure 15 of reference 5 of the paper and modifying it in accordance with field experience on all sizes of cable. Equation 6 in the Appendix which was used in setting up the chart is therefore representative for movement of all large single- and 3-conductor cables and is in keeping with the field observations reported by Mr. Halperin in reference 2 of the paper. The daily cable movement as indicated in Figure 1 is, of course, the average movement which may be expected. The actual movement at a specific location may vary from 0 to 200 per cent of this value as illustrated in Figure 14 of reference 5.

Mr. Del Mar has questioned the propriety of using a 4-hour time constant for cable in underground duct. A duct bank in which cables have the same load cycles day after day remains at nearly constant temperature. Tests have indicated that the variation in temperature under these conditions may be a degree or less during any 24-hour period. It is therefore reasonable to assume that the duct bank temperature is constant. The long thermal time constant of a duct bank observed when a cold duct bank is first loaded has no bearing on the daily cable movement problem.

Tests on 3 × 250,000 circular mil and 3 × 500,000 circular mil 5-kv cable in duct indicated that the cables attained 80 to 86 per cent of their ultimate temperature rise above duct in four hours. This value will vary somewhat with different types of conduit and with cable size. Most cables, however, have an attainment above 80 per cent in four hours. A complete determination of daily temperature range could only be made by the use of a specifically designed temperature rise indicator[1] or by an hour-by-hour transient calculation of temperature variation with load. A short cut to this laborious calculation is to use the average of the four maximum hourly ammeter readings and the average of the four minimum hourly ammeter readings, and assume 100 per cent attainment. It has been found that for most load cycles and cable types, this method will give a remarkably close approximation.

The values of K in Tables I, II, and III are based on the Insulated Power Cable Engineers Association values of thermal surface resistivity as defined in reference 6. Studies by J. H. Neher,[2] have shown that cable-to-duct thermal resistance for cable in concrete inclosed fiber duct is very nearly equal to the values obtained by this method. The thermal resistance in concrete duct or concrete-inclosed transite or terra cotta duct is slightly lower. Accordingly the values of K vary slightly with different types of duct construction but these variations are small and may be neglected.

Mr. Hatcher has pointed out that in some manholes the cable is brought in straight at one end and the entire cable movement must be taken up by the offset at the opposite end. This method of racking would require provision to be made for the joint to move longitudinally as well as laterally. The mathematical analysis of the strains in the sheath would be different in this case than in the case of the symmetrical manhole and hence Figure 1 may not be used directly for this type of construction.

In reply to Dr. Wiseman, there does not appear to be any mathematical optimum ratio of length of offset to width of offset provided the bending radius of the cable is greater than its minimum allowable bending radius. This ratio should be determined by practical considerations in the manhole. Dr. Wiseman has pointed out that alloy lead sheaths will outlast copper bearing lead sheaths on fatigue tests. This is true, but adequate information on alloy lead sheathed cable is not available in order to predict sheath life by the method used in Figure 1.

In conclusion it should be pointed out that certain limitations must be observed. However, for nonalloy sheathed cable in symmetrical manholes, this method can be relied upon to determine the appropriate manhole dimensions and to predict cable sheath life.

References

1. Thermal Circuit Gives Remote Hot-Spot Temperature, A. H. Kidder. *Electrical World* (New York, N. Y.), volume 134, number 1, July 3, 1950, page 89.

2. Temperature Rise of Cables in a Duct Bank, J. H. Neher, *AIEE Transactions*, volume 68, part I, 1949, pages 540–549.

Underground Conduit for Electric Power Systems—Fundamentals and Basic Design Considerations

E. G. WATKINS
NONMEMBER AIEE

THE intent of this presentation is to discuss the fundamentals and basic considerations involved in the design of conduit systems for transmission and distribution of electric power. The design of other distribution structures, such as manholes and boxes, is not included and only the influence of those structures on the design of conduits will be considered herein.

General Considerations

Fundamentally, a conduit system is good or bad depending upon its suitability for the installation, operation, protection, and maintenance of the cables which it is to contain. Fundamentals and basic considerations for conduit design and the construction of conduit systems are not essentially different now than they have been in the past but progress in the art frequently adds or detracts emphasis. For example, the growing tendency to install cables of greater capacity and to carry higher loads in existing systems adds emphasis to thermal requirements. Probably, the only new development in recent years involving conduit construction is the installation of high-voltage transmission cable in steel pipe with gas or oil under high pressure. This type of construction is much closer to oil and gas line construction than to conventional conduit construction and has been discussed in detail in recent articles in trade and engineering journals. The cost and lack of flexibility usually restricts this system to transmission uses.

It is presupposed that other electric transmission and distribution systems have been considered before undertaking the design and installation of an underground system. Installation of cables in an underground conduit system is usually the most expensive method of distributing electricity except in congested city areas where load densities make an overhead system impractical. Buried cable, without the use of conduit, is economically attractive in some instances. Aerial cable also may provide a less expensive system than conduit. The use of combination overhead and underground construction is frequently economical, particularly in suburban areas where there are civic or political objections to overhead services. One combination gas and electric company finds such a system to be practical.

In some suburban sections of their territory, the secondary electrical distribution ducts are installed in a common trench with the gas main while primary feeders and transformers are carried on poles and feed the secondary system by means of pole risers. Compared to an overhead system, the initial cost of a conduit system is high. There is some compensation, however, in the fact that the maintenance cost on a percentage basis is less than for an overhead system.

The complexity of the design problems pertaining to an underground conduit system will depend on whether it is intended as a new system in which there will be a greater flexibility of choice with respect to materials and methods or whether it is intended to extend or modify an existing underground conduit system, in which case the design must be made to accommodate certain features of the existing system. In any event, the basic principles of design, whether for a new system or for the extension and modification of an existing system, are the same. Co-ordination and compromise are usually necessary to attain the most satisfactory electrical, mechanical, and economical arrangement.

A standard underground conduit system can usually be adopted by a utility company which has or is planning to install its electrical transmission and distribution facilities underground. In order to standardize, conduit material and the design installation must be made to conform with general conditions. Special methods should be reserved for locations where, because of either cost or physical conditions, standard procedures would not be satisfactory. The ideal design for a particular set of circumstances can be more closely approached in the case of a conduit installation for industrial usage or as a through route for feeders between electric switching or generating stations.

Design Considerations

Fundamentals and basic considerations involved in the design of conduit systems include such known factors as:

1. General route.
2. Number and size of cables.
3. Purpose for which the system is to be used.
4. Thermal requirements.
5. Physical obstructions.
6. Character of soil.
7. Number of spare ducts for future extension.
8. Other limitations, such as municipal regulations.

The following items permit a wide variety of choice and the decision of selecting the most satisfactory choice to

Paper 50-257, recommended by the AIEE Insulated Conductors Committee and approved by the AIEE Technical Program Committee for presentation at the AIEE Fall General Meeting, Oklahoma City, Okla., October 23–27, 1950. Manuscript submitted June 6, 1950; made available for printing August 25, 1950.

E. G. WATKINS is with the Consolidated Edison Company of New York, Inc., New York, N. Y.

suit any particular situation becomes a problem of the design:

1. Layout in street.
2. Kind of conduit material.
3. Size of conduits.
4. Arrangement of conduits.
5. Construction details.

Layout in Street

The location of conduit systems in streets is influenced by such factors as existing street facilities, subsurface structures, width of street, type of pavement, sidewalk arrangements, type of conduit and manhole installation, number and character of services, manhole locations, cover, probability of damage from street excavations, municipal regulations, and possibly some others. Interference with other subsurface structures probably represents the most difficult problem. It usually requires considerable planning to keep a conduit line reasonably straight and avoid water mains and services, surface water drains, sewers, gas mains, telephone conduits and manholes, and sometimes underground steam mains. Both in the interest of straight conduits and future maintenance, a street lane at a standard distance from the building or curb line is usually desirable.

For an express run, the location in the street may not be important, but where services must be supplied, the width of the street will probably determine the economics of whether conduits should be installed on one or both sides of the street or in the middle. The middle of the street is usually reserved for sewer construction. Since manholes and service boxes generally require more lane space than conduits, it is usually desirable to locate those structures first and then readjust them later, if necessary, to achieve the best over-all location for the complete underground system. When more than one electrical feeder is to be installed along the same general route, it is considered desirable practice to install them on separate streets if economically feasible.

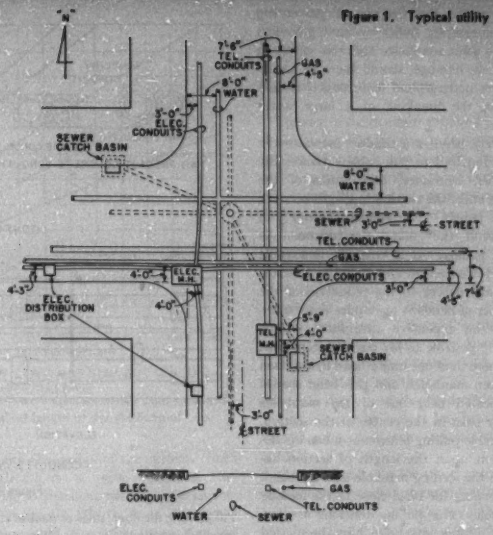

Figure 1. Typical utility lanes

Table I. Conduit Material and Characteristics

	Steel		Fiber		Concrete		Tile Duct		Transite		
							Encased in Concrete				
	Bare	Encased in Concrete	Standard Encased in Concrete	Heavy No Concrete	Square	Round	Single Duct	Multiple 2, 3, 4, 6, and 9 Ducts	Standard No Concrete	Korduct Encased in Concrete	Wood Creosoted
Weight-pounds per foot—4" dia. (bare)	11.0	11.0	1.9	4.1	20.0	13.0	9.0	.....	4.1	2.3	8.5
Usual section length, feet	10	10	8	8	4	5	1.5	2 and 3	10	10	6
Common sizes available, inches	2, 2½, 3, 3½, 4, 5, 6	2, 2½, 3, 3½, 4, 5, 6	2, 3, 4, 4½, 5, 6	2, 3, 4	2, 3, 4, 5	2, 4, 5	3½, 3½, 4, 4½, 5½	3½, 3½, 4½	2, 3, 4, 5, 6	2, 3, 4, 4½, 5, 6	3, 4
Strength in bending—4" Dia. (bare) Concentrated load on 24" span-pounds	High	High	1,500	3,000	3,000	3,000	.....	.....	3,000	1,500	3,000
Friction factors—ungreased—approx.	0.50	0.50	0.45	0.45	0.60	0.60	0.50	0.50	0.55	0.55	0.45
Resistance to corrosion	Good	Good	Good	Good	Excellent	Excellent	Excellent	Excellent	Excellent	Excellent	Good
Heat dissipation	Good	Good	Fair	Fair	Good	Good	Good	Good	Fair	Fair	Fair
Relative material cost—4" dia. (bare)	3 unit	3 unit	0.6 unit	Unit	Unit	Unit	Unit	.....	Unit	0.6 unit	0.7 unit
Relative construction cost—4" dia.											
Single duct	1.3 unit	1.8 unit	1.4 unit	Unit	Unit	Unit	1.4 unit	.....	Unit	1.4 unit	Unit
Two duct	1.5 unit	2.0 unit	1.4 unit	Unit	Unit	Unit	1.4 unit	.....	Unit	1.4 unit	Unit
Four duct	1.5 unit	2.0 unit	1.3 unit	Unit	Unit	Unit	1.4 unit	1.2 unit	Unit	1.4 unit	Unit
Relative maintenance cost—4" dia.	Average	Low	Low	Average	Low	Low	Average	Average	Average	Low	Average
Principal advantage	Flexibility	Strength	Light-weight	Light-weight	Ease of installation	Durable	Durable	Durable	Light-weight	Durable	Light-weight
Principal disadvantage	Magnetic	Magnetic	Envelope expensive	Effect of water	Heavy	Difficulty of stacking	Brittle	Communication of electrical faults	Difficulty of stacking	Envelope expensive	Decay

This serves the purpose of preventing communicating faults by having feeders in the same manholes and also serves to limit the damage, should there be an extensive underground disturbance, for example, the breaking of a large water main.

Every bend in a conduit increases the force required to pull cable. Hence, the number, character, and radius of the bends affect the maximum length between splice points. The greater the angle of the bend, the greater the resistance to cable pulling. It is virtually impossible to install a conduit system without bends. The alternative to the reduction of the number of bends is to require more manholes—an expensive alternative. It is usually possible to lay out a system with not more than one major bend in a section between manholes, and this bend should be located near one of the manholes rather than in the center of the section. The cable-pulling tension at a bend is dependent upon the length of section between the feeding manhole and the bend. By keeping the bend close to the feeding manhole, cable-pulling tensions are lessened. Angle manholes have been used in some instances to avoid conduit bends. The effect of vertical bends to avoid obstructions also must be considered. Most frequently, these bends are of such slight angles and of such large radii that their effect is not appreciable.

A radius of curvature exceeding 300 feet adds so little to the pulling strain that such a curve can be neglected. Radii of curvature of less than eight times the duct diameter should not be permitted. In the design of a conduit system, bends of varying degree may be expressed as equivalent length of straight conduit; thus, for example, if it has been determined that the maximum length of straight pull should be 600 feet and a section contained a bend which was equivalent to 50 feet of straight conduit, the straight portion of this section should not

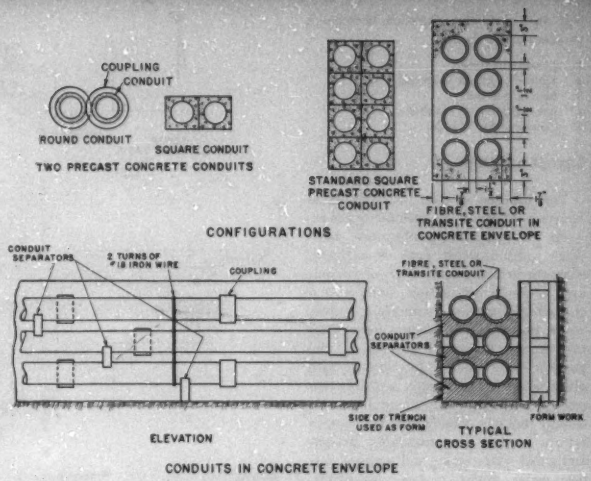

Figure 2. Conduit formations

All joints in the fiber, steel or transite conduits shall be staggered. Conduit separators shall be installed every eight feet for fiber conduit and every ten feet for steel and transite conduits. After conduits have been assembled with couplings and separators the assembly shall be fastened rigidly with two turns of number 18 iron wire every ten feet. When the side of the trench is compact, trench wall may be used as the form for the concrete envelope. Minimum cover on distributor conduits shall be 18 inches, on trunk conduits one foot 10 inches

Figure 3 (left). Comparative qualifications of standard duct formations

CONDUIT FORMATIONS	COST OF CONDUIT CONSTRUCTION	ABILITY TO RADIATE HEAT	CABLE SUPPORT AND RACKING IN MANHOLES
	EXPENSIVE	BEST	BEST
	MODERATE +	GOOD	GOOD
	MODERATE	GOOD	GOOD
	LEAST EXPENSIVE	POOR	POOR

⊗ UNDESIRABLE FOR CABLE INSTALLATION

Figure 4 (below). Characteristic dissipation of live loads at various depths

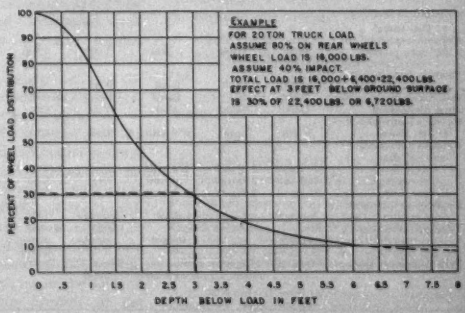

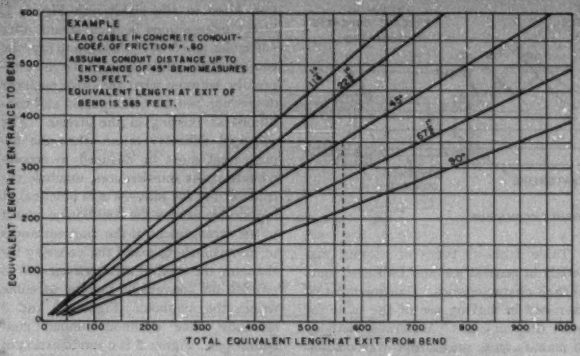

Figure 5. Effect of bends expressed as equivalent length of straight conduit

exceed 550 feet. An example of a method of determining equivalent lengths is shown in Figure 5. Factors entering this problem are conduit material, permissible pulling stresses of the cable to be used, and the type and kind of cable to be installed.

The length of the sections of conduit may be determined by the need for manholes and boxes dictated by local service conditions. Where there is no need for splicing chambers because of local distribution considerations, the length of the conduit sections is determined by the pulling stresses required for the introduction of cable into the conduit system.

Conduit Materials

Any material appropriate for fabrication into a pipe or duct may be considered as a possibility for a conduit. The materials in general use today—not necessarily in order of use—are steel, laminated materials or homogeneous mixtures such as fiber and transite, ceramic materials such as vitreous tile, concrete–reinforced and unreinforced–round and square, wood and plastics. The most common are steel, fiber, concrete, transite, and tile.

The ideal conduit or duct material is one which is least expensive, is smooth to lessen cable-pulling stresses and minimize damage to cable being pulled, readily dissipates heat, has no objectionable magnetic effects, is free from properties deleterious to the cable covering, can be economically installed, will not deteriorate, and, if damaged, can be repaired readily. All of these factors must be balanced to obtain a most satisfactory compromise material.

The type of conduit material used will influence the design of the system. Such considerations as size, flexibility, resistance to corrosion, methods of construction, magnetic effects, heat dissipation characteristics, formation for racking and splicing in manholes, all enter into the selection of types of conduits and likewise affect the over-all design of the system.

Conduit Size and Shape

The size of the conduits required for the cables to be contained is a controversial subject because it involves the stresses cable engineers are willing to use in pulling cable and the thermal performance of various combinations. The answer to the question of the size of conduit to accommodate cable or vice versa, the number and kind of cable that can be installed in a conduit of a given size, depends upon the permissible pulling tensions. A frequently used "rule of thumb" is that the conduit diameter should be at least 1/2-inch greater than the diameter of a circle which would enclose the cables. A large diameter single lead sheathed cable ordinarily will require a duct having a diameter as much as 1 inch greater than the cable.

Conduits suitable for underground installation are generally available in almost any size desired. Single conduits are usually manufactured with a round bore. This shape is considered preferable for cable pulling since the cables are of round

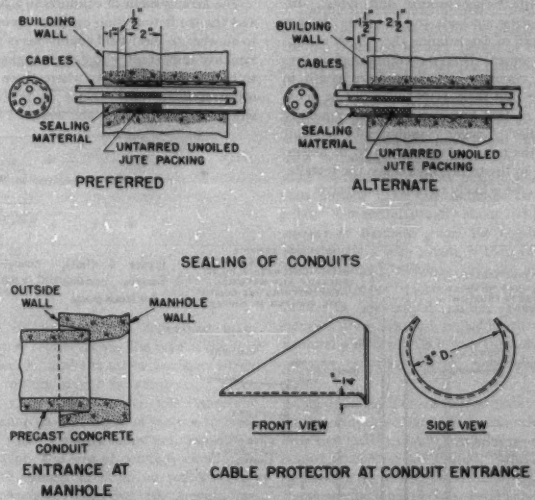

Figure 6. Conduit entrances or terminations

Conduit seals shall be applied to the following

1. At the transformer manhole end of all conduits entering transformer manholes
2. At both ends of all conduits entering a transformer vault from a street or private property conduit system
3. At both ends of conduits between network vaults
4. At both ends of underground service conduits

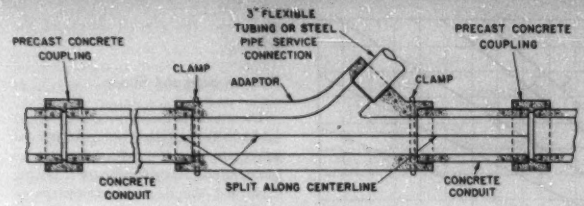

Figure 7. Adaptor for service connection

cross section. A circular cross section is also the most efficient from a standpoint of strength and economy of material. The external cross section or shape of the conduit is of minor significance in single or double conduit construction. Square external cross-section conduits are advantageous when laid in bank formation of three or more. The outside square cross section readily permits the stacking of the conduits either in vertical or horizontal formation and avoids the necessity of using special shape separators. Banks of conduits made up of square outside cross section are quite stable and usually do not require concrete encasement.

The length of individual conduit pieces is usually determined by the particular manufacturing process and costs. Installation methods and handling also are factors in determining the length of conduit pieces. Heavy conduits, such as precast concrete, are limited in length in order that their weight may not be in excess of that which a man can ordinarily handle. Longer individual conduit lengths require fewer joints to be assembled in the trench and hence the installation cost is likely to be less expensive.

Table I shows types of conduit materials in general use and indicates some of their characteristics. Caution must be exercised in making use of the table for other than an index. Materials, methods of manufacture, prices, and even characteristics of materials are subject to change or modifications. Also because equal weight cannot be given to each item in the table and because local conditions may add or detract from the importance of the items, it is submitted only as an index and guide. For items where absolute values cannot be given, materials are compared relatively.

Configurations

The arrangement of conduits in a bank and the transition from one arrangement to another to meet field conditions is particularly important where duct banks are to be installed in streets where there are other facilities and where, as in large cities, certain utilities are assigned certain lanes in the street, see Figure 1. Street intersections in such streets offer particular problems. Needless to say, the configuration must usually be a compromise between what the cable engineer desires for best heat dissipation and conditions as existing in the streets. The principal difficulty arises when the arrangement must be changed to accommodate street interferences, manhole entrances, and the like. Where practical, it is desirable to have the duct bank conform to the arrangement of the duct entrances to the manhole to avoid the necessity for changing the conduit arrangement and to provide for convenient racking of cable within the manhole. Figures 2 and 3 illustrate some common conduit configurations. Figure 3 is a modification of a similar figure which appeared in the Underground Reference Book.[1]

Construction Methods

The method of installation of conduits depends upon more than the least expensive method of installing a given number of conduits in a trench of least expensive dimensions. The arrangement of conduits must meet the demands of cable engineers for satisfactory heat dissipation and minimum clearances must be maintained between conduits and other substructures. Heat dissipation requirements will influence both the arrangement of the conduits and the required cover. Sufficient clearance must be provided to provide working space around

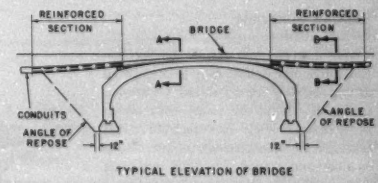

Figure 8 (left). Service conduit for lamp posts

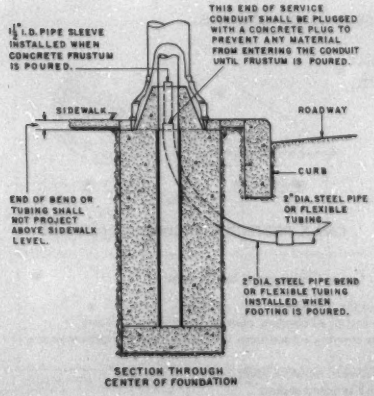

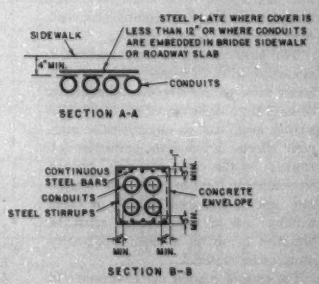

Figure 9 (right). Conduit construction at bridge abutment

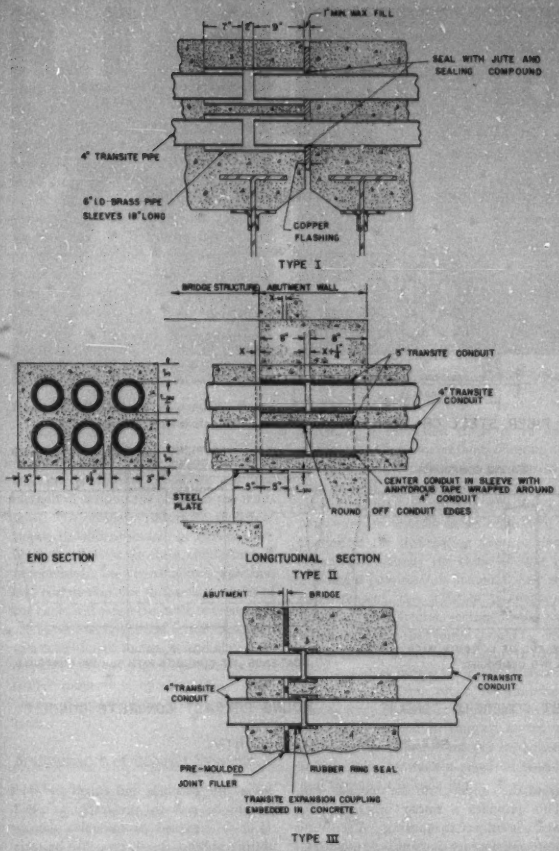

Figure 10. Expansion joints at bridges

the conduits and adjoining substructures. A clearance of 12 inches is frequently specified. Within the limitations of heat dissipation and clearance requirements, the most satisfactory trench size must then be determined. Where pavement is a factor, it is frequently advantageous to arrange the conduits so as to make a trench deeper to save width. Where mechanical excavation is practical, the size and dimensions of the trench may be influenced by the trench dimensions most economically excavated by the digging equipment available. The amount and character of work to be actually performed in the trench must be considered.

The minimum cover required on a conduit or duct bank is dependent upon thermal requirements, the type of conduit materials, and the street loads to which the system might be subjected. Since live street loads become less important a factor as the depth of cover increases and earth loadings alone are not serious for pipes the size of conduit, excavation depth usually involves no problems except possibly sheeting the trench, see Figure 4. A cover of 18 inches is safe for most conduit construction and most street loads, and usually satisfies thermal requirements. Where less than 18 inches is obtained and surface loads are a factor, some provision should be made for protecting the conduit system from the street loading. Shallow cover also exposes conduit systems to damage when the street is excavated for installing other subsurface structures. Protection is frequently obtained by the use of steel plates or creosoted wooden planks. Either affords protection against damage from foreign street excavations; steel plate is more suitable for protection against street loading.

The bottom of trenches should be graded uniformly for proper alignment of the conduit. Where grading is difficult, for example in rock areas, a graded soil bed should be provided. It is usually advantageous to slope the conduits to drain to a manhole. Backfill placed around the conduits should be uniformly and firmly tamped to prevent future settlement. Compacting of the backfill by flushing with water should not be used because of the possibility of infiltration of fine soil into conduits. Precast concrete conduits and other conduits not in a concrete envelope usually are not sealed at the joints.

Bends of large radius, 100 feet or greater, can frequently be made by deflecting the joints. Smaller bends should be made with the use of manufactured conduit bends.

During the progress of installation, the ends of the conduits should be plugged if the job is halted for any period of time, such as overnight. After the installation is complete, the individual conduits must be cleared and their identity in adjoining manholes must be established especially where transposition has taken place. This is usually accomplished by "rodding"—insertion of short flexible jointed rods pushed from one manhole to the other. A mandrel, usually about 1/4-inch smaller in diameter than the conduits, preceded by a wire brush, is then pulled from manhole to manhole. Finally, if the conduits are to be occupied in the near future, a galvanized pulling wire of number 10 or 12 gauge, pulled in with the mandrel and brush, is left in the conduit for the convenience of cable-pulling crews.

There is equipment in use today for mechanically installing single conduits in a trench but usually conduits are installed in the trench by hand. Steel pipe and materials having fixed couplings can frequently be joined in long lengths before dropping or pulling into a trench in order to avoid the more inconvenient and usually more expensive coupling in the trench. Conduit materials such as precast concrete and tile must be assembled in the trench. In unpaved areas, single conduits have been successfully ploughed

Figure 11. Installation of conduits in unstable soils

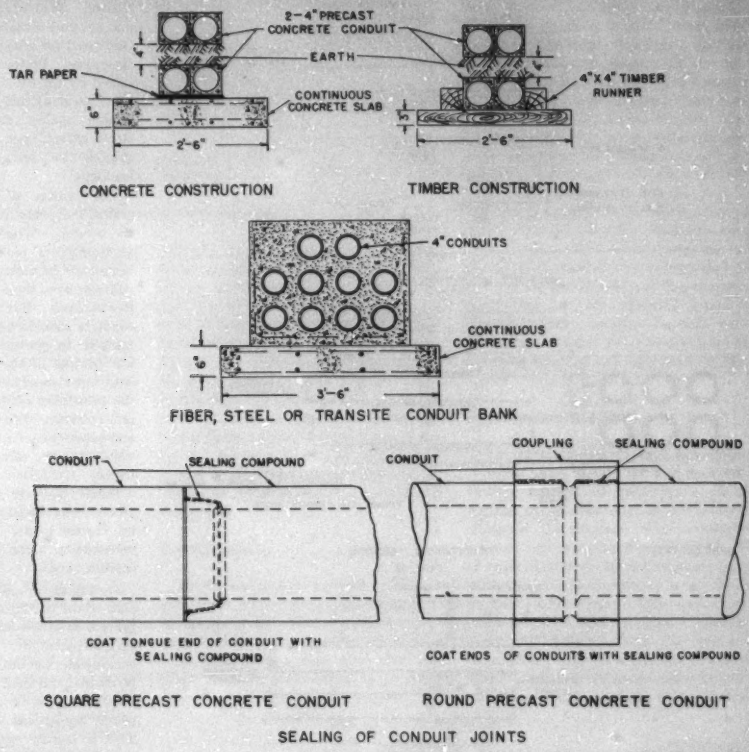

into the ground, eliminating the necessity for an excavated trench.

Concrete envelope or monolithic construction is required for thin-wall nonmetallic conduits, such as fiber, transite and, in some instances, vitreous tile. This type of construction is necessary in the case of thin-wall nonmetallic conduits since they have limited structural strength and the concrete envelope furnishes the strength and protection for lasting qualities. The heavier types of conduit, such as precast concrete, steel pipe, and so forth are not usually built with an envelope. Monolithic reinforced concrete construction also is used in exceptionally poor soil or other unusual conditions where the conduit bank must have considerable strength.

If a watertight seal is required between the manhole and the conduit bank, there are several methods and materials available for making a satisfactory mechanical joint. The most common is probably to grout the conduit into the manhole wall. This provides a rather inflexible joint which is subject to cracking. A generally more satisfactory method is to use a sealing compound which adheres well to the materials involved and which does not harden to brittleness with age.

The conduit entrance or termination also should be designed so that the cable is not damaged by contact with the manhole wall or the conduit edge during pulling operations. Provision should be made to permit cable movement resulting from expansion or contraction of the cable without scraping the manhole wall.

Figure 6 indicates a method of sealing conduit entrances. The method used may depend on local conditions. If the manhole is in a normally dry location, watertightness may not be of particular importance. If the conduit section between manholes is short, expansion or contraction may not be too important. At any rate, the window for the cable as it leaves the manhole and enters the duct should be smooth, preferably bevelled. If it is designed to minimize damage during pulling, it will probably be satisfactory in so far as expansion or contraction of the cable is concerned. There are various devices on the market to make the conduit edge smooth. Most commonly used are precast duct bells of concrete or porcelain and conduit shields made of zinc or galvanized steel as illustrated by Figure 6.

Lubrication has the effect of nullifying to a large extent the difference in friction factors of various materials. It is general practice, however, to lubricate the cable sheath during the pulling operation rather than to attempt to lubricate the conduit system. Care must be exercised in the selection of lubricants for rubber or synthetic coated cables because of the deleterious effect of some oils and greases on these coatings.

The movement of the cables in the

Figure 12. Precast concrete conduit—change in elevation at manhole

Figure 13. Precast concrete conduit—offset at manhole

Figure 14. Single duct tile conduit encased in concrete

conduits caused by expansion and contraction is usually absorbed by the method of racking the cables in the manholes. In ordinary runs with moderate slopes, no difficulties will be experienced. However, if the slope of the conduit run is pronounced, the continuous expansion and contraction due to the heat cycles of the cable will cause the cable to creep into the lower manhole because the expansion of a cable due to its weight will always be downhill. Movement of the cable is generally prevented by installing grade clamps around the cable in the upper manhole.

Maintenance of Conduit Systems

In the design of a system, the possibility of future maintenance must of necessity be considered. This is particularly important in areas where damage might be reasonably expected as, for example, in a congested street or in unstable soil. Common methods of repair to conduits usually include the use of some type of split sleeve or adaptor for minor repairs without disturbing the cables. Major repairs usually mean rebuilding a portion of the installation and the construction is usually the same as that in building a new conduit system. Any repairs present the difficult problem of matching the repaired section to the existing section in that joints should be perfectly aligned to prevent damage to cable by sharp edges during their installation or withdrawal. Care must be exercised during a repair to be certain that backfill is properly placed in tamped layers to avoid the likelihood of uneven settlement taking place between a repaired section and the initial installation.

Services

Service conduits require the same considerations in selecting the material, size, and method of installation as does the main conduit system. In cases of large customers, the service conduits are often the same size, material and number as the distribution conduit system in the street. Residences, small customers, and street lamps, however, are usually supplied through one conduit. This single conduit may be of any material but it is not economical to install a conduit for this purpose that requires a concrete envelope. When selecting the conduit material, in addition to the usual considerations, thought must be given to the connections to the main conduit system and to the entrance of the conduit in the building or street lamp.

Connections to the main conduit system are usually made by diverting a conduit of the main system to a small manhole and running several conduits from this manhole to the buildings to be served. In isolated cases, adaptors are used to

Figure 15 (left). Multiple duct tile conduit

Figure 16 (right). Precast concrete conduit, distribution box, steel service pipe, and gas main

break into and tee off a main conduit in order to obtain a branch for a service connection. Figure 7 shows a typical adaptor. Where the building is set back from the property line, a small concrete box is installed at the property line for splicing the cable. The conduit into the building must be sealed or grouted around its outside surface to prevent water from seeping through the walls. The space around the cables inside the conduit also must be sealed for the same reason. Figure 6 shows a method of sealing the conduit.

Special Construction

Frequently such problems as unstable soils and bridge crossings necessitate modification of standard conduit design. In the case of bridge crossings, the usual difficulty is that there may be some movement of the bridge with respect to the roadway approaches or vice versa. This is likely to cause a failure of a conduit bank at the street junction with the bridge structure. The usual design in this case is to construct either a reinforced concrete conduit bank or to utilize steel pipe conduits to span the section from the bridge structure to firm soil off the bridge approaches, see Figure 9. The method of attachment of the conduits to the bridge structure obviously depends upon the type of the bridge. In some cases, it is possible to install conduits in the roadway or the sidewalk by spreading in a horizontal formation. In other instances, it is possible to support the conduits on hangers either beneath or on the side of the bridge. If a bridge is a steel structure and subject to appreciable expansion or contraction, the expansion joints such as shown in Figure 10 may be required.

When conduits are to be installed in unstable soil, the ideal design would be to have the conduit structure so built that it would accommodate itself readily to any soil movement. This frequently is not desirable from a point of view of maintaining cables. It may be necessary, in some instances, to support the conduit bank on pile bents. This requires the construction of a reinforced concrete slab of sufficient strength to carry the weight of the conduits and the superimposed live and dead loads for the span between the bents. Other methods utilized in poor soil conditions include the construction of either a reinforced concrete spread footing or a timber plank mat, see Figure 11. The purpose of this type of foundation is to reduce the unit load on the soil to a minimum and to insure if any settlement should occur that it would be of a uniform nature for the entire length of the conduit bank.

For installation beneath railroad embankments, busy highways or extensive lawns where open trenching might be inadvisable or impractical, conduits can frequently be installed by drilling methods.

Equipment is commercially available for drilling holes in excess of 100 feet in length and for diameters ranging from 2 inches to 24 inches.

Conclusion

The designer of a conduit system must be intimately familiar with both the electrical and structural problems involved. The time spent by competent personnel in planning is invariably repaid many times over by savings in construction, operation, and maintenance costs.

Reference

1. Underground Systems Reference Book. National Electric Light Association (now Edison Electric Institute), New York, N. Y.

Discussion

E. J. Dawson (Commonwealth Edison Company, Chicago, Ill.): In this paper, Mr. Watkins has assembled general design considerations for the arrangement, location, and installation of conduit runs. The information presented will be of considerable interest to utility engineers embarking on a new underground program; also to underground engineers for comparison or review of their existing policies.

With this view in mind, the following comments are offered.

1. The length of a main conduit run may be maintained at a maximum, and intermediate service tap locations provided by the installation of a so-called service-type manhole. This is a narrow structure built to include the conduit along one wall. The top horizontal row of ducts, which by policy contain the secondary main cables, are omitted or broken out, permitting the main cables to be exposed in the manhole for service tap connections.

2. Although longer lengths of individual conduit pieces are desirable for more economical handling and better alignment of ducts, their limitations in congested areas should be recognized. Shorter conduit lengths are of value in obtaining large radius sweeps in the run and for splitting layers of ducts above and below service pipes of other utilities. When such curvature is included in a run, the cumulative angular displacement should be limited to an amount consistent with permissible cable pulling tensions.

3. Conduit capable of being split longitudinally on the job is of value for use in swinging an existing conduit run containing cables into a new manhole, for enclosing new lengths of cable that are field duct spliced to existing cables, or for piecing out a conduit run through a manhole that is being abandoned. A precast concrete conduit which can be split along two longitudinal V-shaped grooves on opposite sides is manufactured for this purpose.

4. Under the subcaption of Figure 6 was the statement that both ends of conduits between manholes or vaults should be sealed. This practice may cause serious corrosion of the lead sheath of cables if the conduit is encased in concrete. Ground water seeping through the concrete will react with the uncombined free lime in the cement to form calcium hydroxide. With the conduit sealed at both ends, the alkalinity of the solution will increase to the strength where the lead will be attacked. To reduce this action, only one end of the run should be sealed, preferably at the building or vault wall, and the conduit sloped from this end to the line manhole. In this way, sewering of the manhole or occasional pumping for construction work will drain the ducts, thus preventing trapping of seepage water.

5. As mentioned by Mr. Watkins, it is usually advantageous to slope conduit runs to drain to a manhole. However, existing underground equipment may sometimes necessitate installation of a new conduit run below such equipment. To avoid excessive cost of continuing at a low elevation to the next manhole, the conduit may be brought up to normal elevation, and the corrosive possibilities of the resulting sump eliminated by either one of two methods: Neoprene jacketed lead covered cables may be installed in this run; or a drainage gap, employing fiber or transite conduit having drilled drainage holes is installed across a gap left in the concrete sheathing at the low point in the run. Drainage may be obtained to either a gravel basin or municipal sewer.

6. One method of installing conduit not mentioned in the paper is that of pushing steel conduit through the ground by means of a hydraulic jack. This method has been successfully employed at street or railroad crossings to eliminate traffic problems or costly box tunnel construction work. This procedure is, of course, limited to 1-, 2- or 3-duct installations in earth where the presence of boulders or the equipment of other utilities is not anticipated.

W. A. Del Mar (Phelps Dodge Copper Products Corporation, Yonkers, N. Y.): Figure 5 does not take into account the radius of curvature of bends, an important factor in determining the equivalent length to be added for friction at bends. The friction coefficient of 0.6 seems to be extraordinarily high. Values around 0.4 are more usually found for duct lines.

E. G. Driscoll (Phelps Dodge Copper Products Corporation, Yonkers, N. Y.): Figure 5 of the paper contains an error which may or may not be of much consequence, depending on the dimensions of the bend in relation to the straight run. It represents the equiv-

alent length at the exit from the bend as a straight line function of the length at the entrance to the bend. No consideration is given to the length of the bend itself and this omission introduces an error.

The general equation for the condition under consideration, based on belt slippage on a pulley, is:

$$L_1 = e^{Ka}(L + Ra)$$

a = angle subtended by curve in radians
e = base of Naperian logarithm
K = coefficient of friction
L = equivalent length at entrance to bend in feet
L_1 = equivalent length at exit from bend in feet
R = radius of curve in feet

In order to represent this relation as a straight line it is necessary to plot the equivalent exit length against the quantity $L+Ra$, not against L alone. The present error can be eliminated by stating the ordinate to be "Equivalent Length at Entrance to Bend Plus Length of Bend."

Robert J. Wiseman (The Okonite Company, Passaic, N. J.): This paper presents in a clear yet brief manner the various factors that must be considered when designing duct systems for the transmission and distribution of electric power. One readily notes that it is not a haphazard, hit or miss proposition, but a highly technical engineering problem involving many factors as listed under the section on Design Considerations. With the increase in the use of the streets, a design of a duct line becomes quite a problem and costly. Therefore, everything possible that can reduce costs yet maintain high efficiency must be done. Table I of the paper shows how the various materials that may be used affect the design. Figure 3 shows how the shape of the duct structure influences heat dissipation, yet we do not consider it when we calculate the thermal resistance of the duct bank and surroundings. We take the same duct heating constant whether the ducts are laid up to give the best ability to radiate heat or the poorest. With the desire today to get every ampere of load possible out of a cable it appears that we will have to abandon the use of the present duct heating constants and set up new ones which take into consideration the duct formation. This can be done as we already have had a paper on heat dissipation from underground systems.[1]

We all know the importance of cable movement on the life of a cable and how necessary it is to properly train the cables in the manhole to prevent sheath cracking. Snaking of a cable in a duct bank also is helpful. Where the duct has curves in it, it helps snaking. Has the author ever considered actually putting a wave in a duct run even though it could have been installed straight to help out the snaking?

Costs of duct systems are constantly rising which makes it necessary to consider direct buried cables, although in some instances the flexibility of the latter is not good. Could the author give us an idea of what costs might be today as compared to pre-World-War II?

C. S. Schifreen (Philadelphia Electric Company, Philadelphia, Pa.): This paper contains a good qualitative check list of fundamental design considerations, but we believe it is inadequate in the author's treatment of pulling friction and of the corrosion characteristics of conduit materials.

The derivation of his Figure 5 uses a coefficient of friction so high that it could be representative only of cable installations made without the use of any lubricants whatever. We also infer that the 600-foot maximum length suggested in his discussion of this figure is based upon a disregard of the advantages of pulling lubricants. We think that the use of such lubricants is a fundamental design consideration which has not been evaluated by the author. Our laboratory tests on 100-foot lengths of 69-kv single-conductor 1,500,000 circular mil and 15-kv 3-conductor 350,000 circular mil paper and lead cables in straight $4^1/_4$-inch tile ducts developed an average friction coefficient of 0.27 when using customary cable pulling lubricants. The averages were 0.30 for starting and 0.24 for sliding friction. The author's failure to account for lubrication therefore unreasonably reduces the maximum allowable pulling length. Present standard practices in the Philadelphia Electric Company authorize 1,000-foot maximum lengths in conduit sections having bends of not less than 500-foot radius. Our maximum pulls to date have been upwards to 800 feet of 69-kv single-conductor 1,500,000 circular mil and 15-kv triplexed 500,000 circular mil paper and lead cables in typical runs of $4^1/_2$-inch fiber and $4^1/_4$-inch tile ducts and have been accomplished with no difficulties.

The corrosion problem was very carefully reviewed before authorizing the use of fiber conduit in Philadelphia, and does not support the author's evident conclusion, Table I, that tile duct is preferable to fiber from the corrosion point of view. Field surveys of corrosion exposures have shown consistently that fiber conduit encased in a concrete envelope interposes a much higher coupling resistance between the lead sheath and its environment than is found in comparable installations of concrete-encased tile. In our evaluation of the relative merits of conduit materials we have given weight to this quality of fiber conduit only in situations where other things were equal. For the purpose of this discussion, however, it is sufficient only to point out that the corrosion characteristics of fiber conduit are at least equal and, under average conditions, superior to those of any other conduit material.

E. G. Watkins: It was intended and hoped that this paper would present the fundamentals and basic principles which might serve as a basis for the design of an underground electric conduit system. No attempt was made to discuss construction practices in detail. Obviously, there are many such practices in common use of which no mention was made.

The author's company has had experience in obtaining friction coefficients as low as those mentioned by Mr. Schifreen. Figure 5 was presented as an illustration of a tool for determining the length of conduit sections. The curves do take into consideration the lengths of the bends; they are specific for radii between 3 feet and 20 feet. Since our data indicate that within limits the angle of the bend is the most important factor rather than the radius of the bend, the curves are useful for radii exceeding 20 feet. The equation for these curves, as developed by the engineers of the Consolidated Edison Company, is:

$$L_2 = L_1 \cosh F\alpha + \sqrt{L_1^2 + \left[\frac{R}{F}\right]^2} \times \sinh F\alpha$$

where

L_1 = the equivalent length at the entrance to the bend
L_2 = the equivalent length at the exit from the bend, including the length of the bend itself
F = the pulling coefficient of friction
α = the angle of the bend in radians
R = radius of bend

Reference

1. The Thermal Resistance between Cables and a Surrounding Pipe or Duct Wall, F. H. Buller, J. H. Neher. *AIEE Transactions*, volume 69, part 1, 1950, pages 342-349.

Terminal Risers for Solid-Type Impregnated Paper Cables

W. A. DEL MAR
FELLOW AIEE

TERMINAL risers for impregnated paper cables have long presented a problem to utility engineers because of the diverse operating results reported. In one place trouble would be reported on risers about 15 feet high, and yet in another place risers three or four times that height gave no trouble.

The Insulated Power Conductors Committee undertook a study of this situation, and the present paper presents the views of the Subcommittee* charged with this task. The scope of this study is confined to pole, terminal tower and station risers, and is not intended to include distribution risers in tall buildings, mine cables, or other extreme cases. It covers only solid-type paper-insulated cables. No attempt has been made to cover varnished cambric or rubber-insulated riser cables, although these are used occasionally.

The problem stated in terms of physics, is to maintain intact a group of parallel capillary columns of viscous oil. These columns, in a new cable, lie in the interstitial edge spaces of paper and metallic tapes, in the interstrand spaces of conductors, in the irregular spaces in the fillers, to a less extent in the flat spaces between tapes, and to an almost negligible extent between the fibers of paper. In a cable which has been subjected to severe load cycles, the most important columns of oil are in the spaces directly under the lead sheath. Each of these columns of oil may be likened to a modified barometric mercury column. Consider a closed-top glass tube, say 40 inches high, standing in a trough of mercury. If the tube had been filled with mercury before it was inverted over the trough, the mercury in the tube would drop to, say 30 inches above that in the trough, leaving a vacuum above. If, however, instead of an open trough, we had a closed metallic vessel completely filled by the mercury, atmospheric pressure could no longer balance part of the mercury column, and the sides of the closed vessel would be subjected to an internal pressure due to the entire 40 inches of mercury. Let us now consider a third case, where the trough is replaced by a closed rubber vessel. Here we have three evident forces at work; the weight of 40 inches of mercury is opposed both by the weight of the atmosphere and by the elastic tension of the rubber vessel as it is stretched by the weight of mercury. In this case the mercury will not sink to the 30-inch level, but to some higher level, depending on the stress in the rubber walls. The last case is analogous to the capillary oil columns in a vertical cable, the lead sheath acting somewhat like the rubber walls of the vessel in our imaginary model.

Let us first consider the case of an unloaded or lightly loaded cable. The forces at play are the weight of the oil column opposed by the hoop stress in the lead. There also is a small force assisting these two, due to the surface tension at the top of the column of oil, but we may neglect this, for the present. The hoop stress in the lead is proportional to the difference between the hoop pressure due to the atmosphere and the hoop tension due to the weight of the oil column. These are equal and opposite when the oil column is about 35 feet high; but when it is over 35 feet, the hoop stress becomes a tension corresponding to the excess of the height over 35 feet.

A normal sheath of copper-bearing lead is able to carry a hoop stress corresponding to an internal gauge pressure of about one atmosphere. This is the principle upon which low gas pressure cables operate. Therefore, under ideal conditions, such a sheath should support a riser of twice the barometric height, that is, 70 feet.

If absolute reliance could be placed on the gas-tightness of every pothead, and if other conditions were ideal, including light current loading, there would be no riser problem for heights up to 70 feet, but experience has shown that with the best control of workmanship, absolute gas tightness cannot be relied upon where large numbers of potheads are involved. It is, therefore, customary to assume the possibility of slow leaks and design accordingly. The unpredictability of slow leaks accounts for some of the operating discrepancies noted. Such leaks are not necessarily the result of poor workmanship by linesmen, but may be due to porosity of materials used. However, in special cases, such as station risers, where particular care can be given to making the potheads tight, design may be based on the assumption that the hydrostatic pressure results only from the head of oil in excess of the barometric height. This is subject to the limiting condition that the pressure due to head is not augmented by expansive pressure of the oil sufficiently to exceed the permissible hoop stress in the lead.

Some of the early troubles with short risers were traced to the use of a type of pothead which did not terminate the

Paper 50-258, recommended by the AIEE Insulated Conductors Committee and approved by the AIEE Technical Program Committee for presentation at the AIEE Fall General Meeting, Oklahoma City, Okla., October 23–27, 1950. Manuscript submitted July 27, 1950; made available for printing September 12, 1950.

W. A. Del Mar is with Phelps Dodge Copper Products Corporation, Yonkers, N. Y.

*The Subcommittee, over the several years this subject was studied, included the following members: Wm. A. Del Mar, Chairman, E. D. Best, C. T. Hatcher, M. H. McGrath, J. H. Neher, G. B. Shanklin, F. V. Smith, R. J. Wiseman, M. Ghen, R. K. Woodson, and D. M. Farnham. Many paragraphs of this paper, as well as the appendixes, are due to one or other of these committee members. Mr. Homer Martin also contributed useful data. Appendix I was written by M. Ghen; Appendix II by R. K. Woodson; Appendix III by D. M. Farnham; Appendix IV by W. A. Del Mar; Appendix V by C. T. Hatcher; and Appendix VI by Homer Martin.

cable conductors but carried the bare or insulated conductors through the top. Air and moisture penetrated into the cable through the strand spaces and led to failure. Other trouble occurred when thinner insulation was introduced, giving rise to higher stresses and more intense ionization where the level of oil had fallen due to stretching of the lead by oil expansion.

Considering the case where absolute gas-tightness of the pothead cannot be relied upon, the critical height due to head of oil may be calculated from equation 1.

$$\text{Critical height, feet} = \frac{5PT}{D} \qquad (1)$$

where

P = permissible hoop stress, usually taken as 125 pounds per square inch for plain lead, 150 pounds per square inch for copper-bearing lead, and 175 pounds per square inch for arsenic-alloy lead
T = thickness of sheath, inches
D = internal diameter of sheath, inches

For heights below the critical value thus established, no special precautions are ordinarily required in northern climates, for lightly loaded cables, but for greater heights, or heavily loaded cables, one or other of the expedients subsequently described is ordinarily adopted. Experience indicates that in the South, the critical height of risers is, in general, less than 35 feet. The comparison of a cable to a modified barometer would be substantially true for an oil-filled cable, that is, with sizable oil channels and oil of low viscosity, provided that the loading of the cable is light.

When a completely impregnated solid-type cable is first installed, it can be conceived of as an oil-filled cable without voids but with longitudinal oil feed channels of extremely high flow resistance. Due to the high viscosity of the oil and the extremely small feed channels, the restriction to longitudinal flow of oil is thousands of times higher than that in an oil-filled cable. The surplus oil in those small channel spaces is not held back completely by capillary attraction, as is the useful oil in the compact insulation, but responds very gradually to gravity. Head pressure will eventually be built up at the base of the riser, after which a ratcheting effect will occur if temperature is suddenly raised by load or otherwise. Longitudinal restriction to flow is so great that the expansion pressure cannot be fully relieved by a return of compound towards the top. This means that the transient expansion pressures are superimposed on the slow, steady build-up of gravity head pressure, and if the total pressure at the base exceeds the creep strength of the sheath, stretching will occur and it will be cumulative unless this condition is relieved. Obviously, any lead sleeve joint near the base of the riser must be reinforced or a more rapid and concentrated swelling will occur at this point.

Compound migration in solid-type cable is primarily due to a pressure differential along the length of the cable, whether caused by gravity or other agency. A striking illustration of this is the behavior of nonreinforced lead sleeve joints on grades. When such solid-type cable lines are heavily loaded, there is a tendency for swelling or collapsing of these lead sleeves simply because they are the weakest link in the chain. A study of such happenings shows that the sleeve swelling is rarely related to profile and gravity drainage. Sleeve swelling can occur on level ground or at the tops of grades just about as often as at the bottom of grades. This is primarily due to two factors. First, the joints are far apart and gravity drainage through the highly restricted longitudinal "feed channels" is so slow that it cannot respond in any great length of cable and is only pronounced on extremely steep and short slopes or in vertical risers. Second, a pressure increase uphill must mean a pressure differential in this direction, tending to push the compound uphill, and this is due to a difference in temperature and compound expansion (or shrinkage) along the length of the line, caused by thermal variations along the length. If the line is hotter downhill, pressure builds up and tends to push the compound uphill towards the cooler portion, or towards a portion that has previously drained and has low pressure.

In short vertical risers, gravity drainage is a more important factor, but reverse pressure differential also can occur in vertical risers due to the fact that there is a much wider temperature variation in the exposed vertical length as compared with a horizontal underground length. However, even with a sunlight temperature of 50 degrees centigrade, riser cables are usually 5 to 10 degrees cooler than duct cables. Night and day temperature variations, wind, rain, snow, and seasonal variations all tend to set up such differential pressures and make the behavior somewhat unpredictable. This does not occur in oil-filled cable because the response to gravity drainage is too quick. The net result is that under some conditions excessive pressure can be built up at the base of the riser, and under other conditions it can be built up at the top of the riser, tending to start leakage in the potheads.

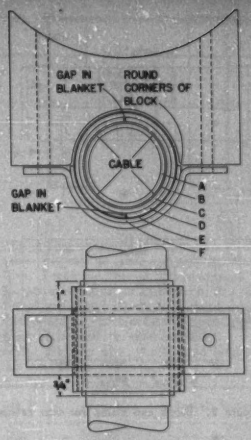

Figure 1. Cable clamp cushion. Clamp size is cable size + 1/2 + 0.5 inch

A—Cable sheath
B—Two layers friction tape
C—One-eighth inch rubber blanket
D—One-eighth inch rubber blanket
E—Two layers friction tape covered with P & B paint
F—Lead shim to make clamp circular

Heights Above Critical

For heights above the critical, or where loading adds appreciably to the pressure, three classes of measures have been used to overcome migration.

1. Where Measures Are Directed to Preventing Vacuum Formation Above the Critical Height

(a). A highly viscous oil is used in the pothead which can seep into the vacuous space below the pothead, but is so viscous and has such high adhesion or surface tension that it adds little to the head of oil.

(b). This type of construction has operated successfully on a 22-kv system for eight years, the risers of an average height of 50 feet. A number of them operate at full load even during the hot summer months, but the average load on the risers is 50 to 80 per cent of the cable rating. A simple semistop joint is used in the manhole at the base of the riser, see Appendix I.

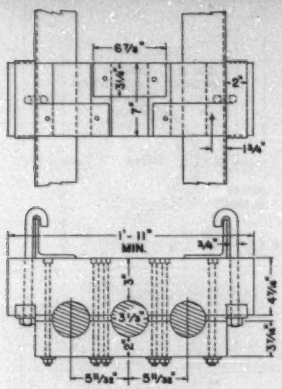

Figure 2. Block and clamp for riser cables

2. Where Measures Are Directed to Preventing Excessive Strain of the Lead

(a). Reinforcement of the lead sheath by bronze or coated glass tapes. An installation of seven solid-type 66-kv riser cables 75 feet high on steel poles has been operating for 19 years. The riser cables have double lead sheath with bronze reinforcement, gravity feed reservoirs at the top and stop joints at the bottom. Wooden supporting clamps (without cushions) are credited with stopping migration between sheath and insulation, see Appendix III.

(b). Use of clamps with rubber cushions to prevent oil migration between sheath and underlying layer. Risers approximately 30 feet high, with plain lead sheaths on wooden poles, were originally supported by galvanized iron straps with 1/8-inch lead lining. Vibration led to intercrystalline fracture of the lead. These clamps were replaced by wooden clamps with rubber cushions which have proved satisfactory, see Appendix II.

3. Where Measures Are Directed Both to Preventing Vacuum Formation Above and Excessive Head Below

(a). Reservoir of cable oil at base of pothead and reservoir at joint nearest to base of riser, the oil which has dripped into the lower reservoir being periodically restored to the top reservoir, see Appendices III and IV.

(b). Use of a partially drained cable with 12-pounds-per-square-inch nitrogen gas pressure applied to the cable near the top. This also requires a reservoir to receive oil which may subsequently drain, see Appendix V.

When Each Type of Construction Is Advisable

Constructions described under section 1 should not be used without due consideration to the possibility of sheath stretch and bursting of joint sleeves below the riser, especially when high operating temperatures are attained.

Construction described under section 2 should not be used without due consideration to the possibility of vacuum or air pocket formation at or below the base of the pothead and, where necessary, providing protection against this possibility either by the means described under section 1 or by using thin oil in the pothead and a reservoir of thin oil attached thereto. Ordinary clamps should not be used, however, where the structure to which the cable is attached is subject to much vibration. Wood poles with aerial wires are subject to severe vibration. A special cushioned clamp, described in Appendix II, overcomes this difficulty. See also Appendix III.

Constructions described under section 3 are the most reliable, although the most expensive. They are particularly desirable in the Southern states where long periods of high temperature aggravate conditions.

Types of Cables

Due to the smaller diameter and consequently greater critical height of single-conductor cables, as compared with 3-conductor cables, it is desirable to trifurcate at the base of the riser, using a trifurcating joint and to rise to the potheads with single-conductor cables. While this is usually practicable for station risers, it is not always practicable for pole risers in streets.

Drainage is more severe with shielded than with belted cables. However, if the usual bronze binder is replaced by a belt of paper, shielded cables suffer less disadvantage.

Joints

The joint at the base of a riser should be more or less of a stop-joint. A practical construction has blocked connectors covered with oil-silk sealed with oil-insoluble material, such as Harvel oil-stop, Vinsol resin, or Minerallac and castor oil, varnished cambric insulating tape, and oil-insoluble solid-type compound where a reservoir is not to be attached. If a reservoir is to be attached, a fluid oil compound must be used. In either case, the joint should be shielded throughout, if the cable is shielded.

Cables with Viscous Compounds

Some utilities have used riser cables impregnated either with petrolatum or a viscous stringy compound containing a highly polymerized oil derivative. Petrolatum has a melting point of about 55 degrees centigrade, and above that temperature is less viscous than ordinary oil impregnants. If, therefore, viscosity is the desired characteristic, it is attainable with petrolatum only if the operating temperature of the cable is kept very low. Viscosity, however, does not inhibit migration of compound; merely makes it slower. A more desirable characteristic would be high surface tension, but the available range is quite limited. A stringy adhesive cable impregnant has more merit for delaying migration, but it is not a cure and is open to the objection that it requires special cable which does not have the best electrical characteristics, yet is apt to be very expensive due to unusual manufacturing requirements.

In view of the complications and the varied behavior involved, it is not possible to be guided by calculated head pressure alone, as is the case with oil-filled cable. Such calculations throw some light on the problem and help in reaching a clearer understanding, but the ultimate answer must be based on actual field experience in different localities and climates and under different conditions of loading. Due, however, to the many factors entering into the problem, records of field experience are contradictory and confusing. The data required for a complete study of a riser cable are listed in Appendix VII. Therefore, we end our study with the unsatisfactory conclusions that both theory and recorded experience are unreliable guides and this paper is, therefore, not an effort at standardization, but a presentation of the subject as known to us, and an invitation to bring broader experience to bear on the problem.

Appendix I. 22-Kv Cable Terminals—Viscous Compound Filled*

The Duquesne Light Company, Pittsburgh, Pa., has successfully operated viscous compound filled cable terminals on its cable system for the past eight years.

Ten years ago their terminal pole construction was changed to a 3-way multiple

* Example of case cited in section 1(b).

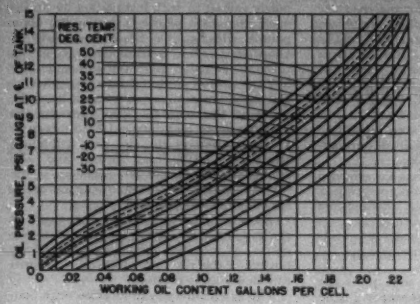

Figure 3 (left). AC reservoirs. Characteristic curves at various temperatures

Res. Size Gallons	No. of Cells	Res. Size Gallons	No. of Cells
2	10	8	36
3	14	9	41
4	18	10	46
5	23	11	51
6	28	12	55
7	32	13	60
		14	65

joint in the manhole with single-conductor cables from manhole to the cable terminals instead of 3-conductor pole risers with the "Y" joint on the terminal pole, but no change was made in the method of installing the cable terminal. Cable failures on terminal poles began to occur more frequently, and in most cases the cause could be assigned to cable impregnating compound migration, because of the lighter oils used in new cables. To overcome this problem of loss of cable impregnating oils in the cable insulation, the filling compound for cable terminals was changed to a mineral oil compound similar to that used in impregnating the cable insulation.

Several failures were soon experienced in the new construction; therefore, it was necessary to conduct special tests to determine construction standards for cable terminals. These tests and results were discussed in a paper made by W. P. Cook before the Thirty-first Meeting of the Transmission and Distribution Committee of the Edison Electric Institute on May 10, 1943. Our present standard is practically the same as shown in the above-mentioned paper, the only major change being in the compound. During the past five years, we have experimented with various compounds and at present our standard is 80 per cent cable oil and 20 per cent polyisobutylene.

The Duquesne Light Company has approximately 400 22-kv risers on their system of which approximately 300 (900 potheads) are now viscous compound filled. They are installed on both single-conductor and 3-conductor cable, with single-conductor as their present standard, and have operated successfully at 22 kv over a period of eight years. The maximum height of any riser on the system is 80 feet, with the average being approximately 50 feet. (The 80-foot riser has a special tacky oil.)

Sheath bulges were expected at the bottom of the risers originally, but operating experience to date has shown none. However, present standard construction is an oil stop joint in manhole at the base of the riser: three layers of silk tape, each layer basted with an oil-insoluble compound, are applied to each conductor prior to the application of the varnish cambric insulation and the joint is filled with a hard, oil-insoluble compound. A barrier-type connector is used to prevent compound migration through the strands. The riser cables are not clamped to stop migration between the sheath and core; so far it has not been found necessary.

No checks were made on the actual operating temperature of these risers; however, a number of them operate at times at full load rating even during the hot summer months. A large per cent of risers feed the overhead system in comparatively lightly loaded areas where the emergency load ratings automatically limit maximum daily loads. The average load of the risers is 50 to 80 per cent of the cable rating.

An inspection of terminals is made approximately once each 3-year period. In most instances, the compound dropped on an average of one pint in the terminal at the first inspection; the second inspection usually shows a decrease in the loss of compound. In no instances have more than two inspections been made to date. Internal flashover due to a vacuum in the terminal is not feared inasmuch as the use of a 46-kv terminal on the 22-kv system due to external contamination, and the over-all length of the porcelain is sufficient to prevent such an occurrence.

There are two essentials which we feel are necessary for successful operation of oil-filled cable terminals:

1. Absolutely tight seals on gaskets and wipes. Glyptal lacquer is used to cover joints.
2. Proper lightning protection by installing the lightning arrester on the same arm with the cable terminal.

To sum up the problem, it is not believed feasible to operate oil impregnated cables as pole risers without provision for keeping the cable saturated throughout its entire length. This applies especially to the portion of the cable within the base of the terminal. Even though this type of system appears to operate successfully in Pittsburgh, Pa., the author would be reluctant to recommend such a system for localities subjected to much higher summer temperatures.

The viscosity of the compound used on this installation was as follows:

Deg. F	Saybolt, Seconds
100	7,200
140	2,030
212	397

Appendix II. Operation of Cables on Wooden Poles—Kansas City Power and Light Company

Paper-insulated lead-covered cables are used as pole risers on the 13.2-kv and 4-kv system in this company. The majority of the 13.2-kv risers are of 400,000-circular-mil shielded type, while the 4-kv risers, as discussed here, have been mostly of 3/0-4-conductor belted construction.

Iron lateral pipes are installed from ground level up to the height specified in the National Electric Safety Code.[1] These are attached to the pole with perforated pipe strap and spike nails. A wooden block, bored to the cable size, is used on top of this pipe. The cable is attached to the pole at 3-foot intervals above the pipe to directly below the bend leading to the multiconductor "Y" shape pothead.

Prior to 1941 considerable trouble was encountered with crystallization of the lead sheath at the pole blocks which were galvanized iron straps with only a 1/8-inch lining of lead between strap and cable. This was definitely traced to vibration of the poles.

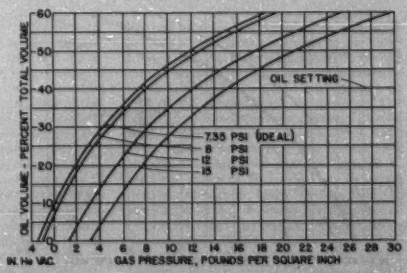

Figure 4. Constant volume oil reservoirs for cable joints

1—Oil setting 40 per cent

2—Gas pressure indicated on each curve as at specified oil setting

At that time a cushion type of clamp, shown in Figure 1, was developed and has eliminated all trouble from that source.

The most effective example of the value of this cushion is a pair of cable replacements on *1527-2* terminal pole. This cable of 400,000-circular mil 3-conductor 15-kv belted construction was installed on the pole in 1936. This pole was one of the two pole structures carrying a lightning arrester rack, platform disconnects, and so forth. The pothead is approximately 30 feet above ground. The structure is dead end one way and no side guys are used. On April 28, 1935, the sheath was found to be crystallized at three clamps and the cable was replaced. Again, on October 30, 1940, the same condition was found, a new section of cable was again installed. Rubber cushions were used in the blocks on this installation, and no further trouble has developed.

The system contains approximately 261 cables terminating on wood poles. Between 1929 and 1942 ten sections of cable are known to have been replaced due to "crystallized" lead, while eight other sections *may* have been replaced due to this trouble from 1920 through 1923, and in the year 1939. The records are not too good on this point. Since the advent of the rubber cushions, no further trouble has developed.

Appendix III. Risers with Wooden Clamps—Quebec Hydroelectric Commission

There are 13 66-kv cables, each approximately 4,000 feet long, running from steel poles at the foot of St. Lawrence Boulevard to Vallee Substation. The cables are all single-conductor, 750,000 circular mil stranded copper, paper-insulated, 0.003 metallized paper tape and 9/64-inch lead sheath.

Seven of the cables are nonhollow core and have an insulation thickness of 28/32 inch. The other six are hollow core and have an insulation thickness of 30/32 inch; these six were impregnated with rosin-bearing compound, in general of the type used in 1926.

The end lengths of the cables from the end manholes to the substation and the steel poles are specially reinforced. For the nonhollow-core cables the reinforcing over the insulation consists of: 0.008 metallized paper tape, 0.125-inch plain lead, 0.005 phosphor bronze tape, one layer of paper and 0.100 plain lead over-all. For the hollow-core cables, the reinforcing is obtained by using lead with 0.5 per cent antimony instead of plain lead.

At the steel poles and at Vallee Substation the cables terminate in oil-filled outdoor-type terminals rated at 110 kv.

The joints in the cable lines are oil-filled and connected to oil reservoirs to maintain positive oil pressure. The hollow-core cable terminals have their own glass reservoirs mounted on the terminal tops, while the nonhollow-core cable terminals are fed from gravity-type reservoirs.

The cable risers on the steel poles are mounted and supported as shown in Figure 2, and while the wood block clamps were originally placed there to adequately support the cable, it is felt that they have served as sheath clamps to prevent the migration of oil or compound between the lead sheath and the cable insulation.

Experience from 1926 to date has been extremely satisfactory as far as the riser cables are concerned and, in the main, this is attributed to the fact that there has been very little compound migration. The nonhollow-core risers were manufactured in 1931, and the compound in these is the cylinder oil class. When they were installed, transformer oil was fed into the strand of the cable at the upper end of the riser and allowed to run through to the lower end, thus washing all compound out of the strand to permit the free passage of oil. The end lengths were then connected to the horizontal runs through stop joints. The height of these risers is about 75 feet.

Appendix IV. Reservoir Systems for Impregnated Paper Insulated Riser Cables

General

The reservoir system for impregnated paper-insulated riser cables provides a method for eliminating the troubles ordinarily caused in such installation by downward migration of the impregnating compound. Briefly, the method consists of allowing a slow continuous flow of oil through the cable, from top to bottom, by feeding viscous cable oil into the splice at the top of the rise and draining it from the splice at the bottom. This prevents the building up of high internal head pressures at the bottom of the rise with attendant stretching of the lead sheath, and also avoids desaturation of the insulation at the top of the rise with accompanying loss of desirable electrical properties.

The arrangement requires a reservoir at the top of the rise which supplies oil to the system as required, and a reservoir at the bottom of the rise into which oil is drained to relieve excess pressure.

This system may be used either with constant volume reservoirs in which the oil is in contact with nitrogen gas or with bellows or cell type reservoirs in which the oil and gaseous pressure medium are separated by metal partitions. In the former case, identical reservoirs are used at top and bottom of the rise. In the latter case two different types of reservoirs are used, as described below. The operations are identical for the two types of reservoirs except that the constant volume reservoir at the top is maintained at a minimum of 1 pound per square inch and preferably several pounds per square inch nitrogen gas pressure, whereas the top bellows type reservoir, type *CC*, remains at atmospheric pressure.

A type *CC* reservoir contains cable oil in a stack of collapsible cells immersed in transformer oil. The amount of oil in the cells is indicated by the sight-glass level of the transformer oil outside the cells. Type *AC* reservoirs, which are used at the foot of riser, also contain collapsible cells, but these cells are filled with gas under pressure and sealed at the factory. The cable oil is contained in the tank *exterior* to the cells. Characteristic pressure curves for these reservoirs are shown in Figure 3.

Viscous cable oil is used in the system. If thin oil were used, it would soon wash out the original oil of the cable and require an excessive frequency of servicing to keep the pressure in the *AC* reservoir below the safe limit. With the viscous oil, the frequency of servicing will be high at first, but will soon

Figure 5. Constant volume oil reservoirs for cable joints

1—Oil setting 50 per cent
2—Gas pressure indicated on each curve as at specified oil setting

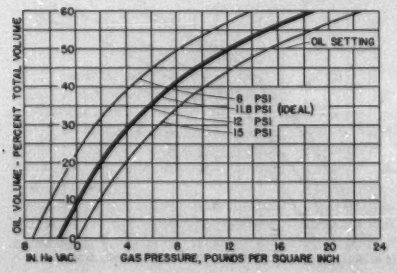

Figure 6. Constant volume oil reservoirs for cable joints

1—Oil setting 70 per cent
2—Gas pressure indicated on each curve as at specified oil setting

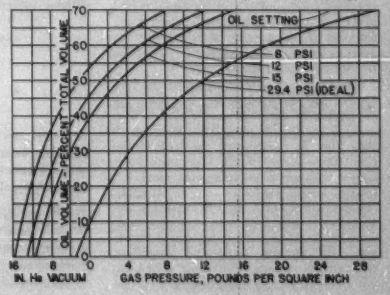

settle down to a practical value. During the first few weeks after installation, therefore, the system should be watched carefully, but after the oil flow has reached a steady state, servicing will be required probably but once or twice a year. Servicing involves the operations described below.

Reservoir at Bottom of Rise

The oil pressure at the center line of the lowest joint at the bottom of the rise should not be allowed to exceed 10 pounds per square inch. This pressure may be determined by the gauge on the manifold by using the following formula:

Pressure, pounds per square inch at center line of joint = gauge reading $+0.4B$

where

B = difference in elevation in feet between gauge and center line of joint

When the pressure approaches 10 pounds per square inch, oil should be drained from the reservoir until the pressure at the center line of the highest point fed by the reservoir is 0.5 pound per square inch. This pressure may be determined from the gauge reading by means of the following formula:

Pressure, pounds per square inch at highest point = gauge reading $+0.4A$

where

A = difference in elevation in feet between highest point and gauge

If necessary, add cable oil to bring the pressure up to at least 1 pound per square inch, using a hand-operated pump in the case of an *AC* reservoir or a cylinder of nitrogen gas in the case of the constant volume reservoir.

Reservoir at Top of Rise

In the case of the *CC* reservoir, the oil level as shown by the sight glass on the reservoir should not be allowed to fall below 0.5 gallon. When this limit is approached, it is necessary to add oil. Using the hand-pressure pump, add cable oil until the sight glass shows the reservoir to be filled to one gallon less than its rated capacity. In the case of the constant volume reservoir, two outlets are provided and a measuring rod is provided which is inserted in the lower outlet. Here again the level should not fall below 0.5 gallon.

Appendix V. Gas Pressure and Oil Tank Method*

The use of this method was decided upon in connection with attempting to reduce the migration of the joint filling oil in the street cables adjacent to river tunnel crossings. This joint filling oil was found to be migrating down the vertical riser cables and into the tunnel portion of the cable, creating an excessive pressure and consequent bursting of the joint sleeves. These vertical riser cables have a drop of approximately 50 feet. It was decided to experiment with the use of nitrogen gas pressure at the upper end of the riser cable on one particular feeder. This riser cable was installed in 1931 and is a 3-conductor, 350,000-circular-mil shielded-type construction with 345 mils paper and 125 mils lead. The diameter under the lead sheath is approximately 2.85 inches. This cable operates on a 27,000-volt neutral-grounded system.

A 10-gallon reservoir was connected to a stop joint at the top of this riser and filled with nitrogen gas at a pressure of 8 pounds per square inch. A stop joint also was installed at the lower end of this cable, with similar oil reservoir attached. This installation was made in 1938, and the reservoirs have been inspected approximately twice a year since this time. The pressure in the upper reservoirs has been found to have dropped to as low as 3 pounds per square inch at some inspections. The pressure was raised to 8 pounds per square inch at every inspection.

Appendix VI. Servicing of Constant Volume Reservoirs

In using constant volume gas pressure reservoirs (Appendix V) particular attention must be paid to initial and servicing settings of oil and gas and also to the amount of oil returned in relation to "built-up" pressure resulting from such quantities of oil flowing back into the reservoir.

The curves listed in Table I were developed to facilitate both the instructions for the setting of this oil line and gas pressure, and also in selecting the proper positions of the various fittings in the shell of the horizontal reservoir.

*Method given in section 3(b).

Table I

Curve	Oil Setting (Levelling Fitting Location)	Setting
Fig. 4	40% level* (tank cap.)	40% oil, 8#
		10% oil, zero #
		30% working oil
Fig. 5	50% level	50% oil, 8#
		22% oil, zero #
		28% working oil
Fig. 6	70% level	70% oil, 8#
		53% oil, zero #
		17% working oil

*The 40% level will permit the quoted range of usefulness for riser cable application.

Appendix VII. Schedule of Data Required for Complete Evaluation of Experience with a Riser

1. Height of riser from base of pothead to lowest part of cable.
2. Distance (along cable) from base of riser to nearest joint.
3. Description of cable.
   Conductor compact or uncrushed.
   Number and size of conductors.
   Thickness of individual tapes.
   Total thickness of insulation.
   Shielded or belted.
   Type of binder tape.
   Thickness and type of lead.
   Cable diameter under lead.
   Viscosity of impregnant over operating range or year and name of maker.
   Reinforcement, if any, over sheath.
4. Type of supporting clamp, if any.
5. Range of ambient temperature.
6. Range of load.
7. Type of pothead and opinion of its gas tightness.
8. Type of pothead compound.
9. Pertinent conditions noted.

Reference

1. National Electrical Safety Code. Department of Commerce (Washington, D. C.), 1949.

Discussion

E. W. Greenfield (Anaconda Wire and Cable Company, Hastings-on-Hudson, N. Y.): The analogy of a lead-sheathed cable to a rigid tube having an expansible rubber membrane at the bottom probably is an over-simplification of the case. Instead, it seems reasonable that a riser cable is more likely a tube closed at both top and bottom with rigid sections, the tube walls being of a relatively high-strength elastic material.

The two analogies operate quite differently. In the first, as long as the top of the column is tight, the tube at its base will be compensated in pressure to the extent of that exerted by the atmosphere; namely, 15 pounds per square inch, or a total height of oil of about 35 feet. This does not agree with known facts. Actually, when pressure is applied externally to a tube, a considerable drop occurs across the circular rigidity of the tube. When sufficient pressure is applied, it is found that the sheath tends to crumple rather than to compress inward uniformly. For example, in a gas compression cable, when 200-pound-per-square-inch pressure is applied externally, a pressure drop through the lead diaphragm of 30 to 40 pounds per square inch may occur. On the other hand, pressure applied internally subjects a round sheath to continuous motion in the form of creep once the critical value is exceeded. For common lead, this critical value is quite low. Another factor preventing the cable from operating in accordance with the assumed analogy is that no impregnation is absolutely perfect; accordingly, some oil always will be displaced downwards. The net result is that a riser installation with perfectly tight potheads can still exert sufficient pressure at the base of a 15-foot riser to cause sheath deformation. Added to this, the effect of load cycling is to immediately create more space between core and sheath for further drainage in these areas.

I believe that the author underestimates the forces of adhesion in his analysis of the migration problem. Whereas the surface tension forces in capillarity action operate

only at the top of the column, the forces of adhesion are active throughout the column. These forces have to do with the molecules in the liquid and in the column walls and also are dependent upon temperature. For small columns, adhesion can overcome completely the effects of gravity. The degree to which this occurs, however, must be related to the temperature.

We agree with the author that, in a low-pressure gas-filled cable, the oil can migrate. Unfortunately this is not universally appreciated in the industry.

The author indicates that drainage in a belted cable is less severe than in a shielded cable and refers to the improvement in the latter by substitution of paper for metal binder tapes. In our carbon-black (resilient binder) construction, this advantage is obtained without sacrifice to shield-to-ground continuity required for safe operation.

In Appendix I of the paper, the author refers to the satisfactory use of a viscous compound for filling terminals, consisting of a blend of cable oil and polyisobutylene (Vistanex). However, the viscosity is reported to be only 397 seconds Saybolt at 212 degrees Fahrenheit. In view of this low value, we would be interested to know the molecular weight of the polyisobutylene used in the blend.

L. F. Hickernell (Anaconda Wire and Cable Company, Hastings-on-Hudson, N. Y.): While presenting no universal panacea, this paper is valuable in focusing attention on the troublesome problem of terminal risers and attempting to reconcile some conflicting reports which have arisen from various interpretations of so-called operating experience.

Certain statements in the paper prompt the following observations:

For 15-kv cable, the following critical heights are calculated from equation 1: 3-conductor, 750,000 circular mils, compact sector = 15 feet; and, 1-conductor, 4/0 American wire gauge, compact round = 70 feet. Practical experience would indicate that the former is very conservative, while the latter is excessive with modern standard insulation thicknesses.

Our creep data on tubes show that arsenic-lead (*F-3*) alloy can be operated as safely at 250 pounds per square inch as copper-lead at 150 pounds per square inch. It is possible that even this value may be increased in the future by further refinements in the improved extrusion methods recently introduced.

When fluid materials are used in potheads, care should be exercised to select oil (or blends) which are compatible dielectrically with the cable impregnant.

Literally speaking, the statement that "a stringy adhesive cable impregnant . . . requires a special cable which does not have the best electrical characteristics . . .," is true. Cables impregnated with our blend of mineral oil and Vistanex have very slightly higher losses than those impregnated with unblended mineral oil. However, the difference is insignificant and losses of both cables are considerably below the maximum permitted by the Association of Edison Illuminating Companies specifications. Also, the difference in cable price is negligible.

In Appendix VII under the section on Description of Cable, the author should have included "Grade of lead" or "Type of alloy" since the creep rate under pressure varies with the sheathing material.

Until further information is available, we have been suggesting the following construction:

CONDUCTOR

Compact strand—to reduce volume of oil to a minimum.

INSULATION

Type CB, shielded—to retard deterioration of oil and reduce maximum stress.

Above-standard thickness, if feasible to use special cable—to further reduce stresses on drained paper should migration occur.

BINDER

Carbon-black paper—to obtain most of the mechanical benefits, if any, of belted cable and all the superior electrical performance of shielded cable.

SHEATH

Arsenic-lead (F-3) alloy—to increase bursting strength and reduce creep under internal pressure; thereby reducing volume of channel between core and sheath in which oil can migrate.

For those who desire a *viscous impregnant*, we furnish a blend of mineral oil and Vistanex.

Wayne A. Parker (Oklahoma Gas and Electric Company, Oklahoma City, Okla.): We have not had trouble on our risers due to migration, however we have very few risers above 30 feet, the highest being approximately 50 feet. Our only trouble with these higher risers is the pressure at the top of the riser. This pressure has been so great that it has pulled the heads of the pothead body bolts through the insulator spacers. We use "Ozite B" compound in the pothead and also have some difficulty of it forcing its way out of the cap-nut gasket. The load cycle is very severe. Ambient temperature varies from 110 degrees Fahrenheit in the daytime to 70 degrees Fahrenheit at night with a load cycle of 50 amperes to 300 amperes. The cable is on a 13.8-kv circuit and rated 15 kv, 500,000 circular mils, one conductor, paper insulated, lead covered. The distance from the base of the pole to the first splice is 105 feet. The conductor is uncrushed. Insulation thickness is 0.195 inch unshielded with 0.095 inch of lead sheath and no reinforcement. It is supported at the top of the riser with a flexible copper braid wrapped around the three conductors so as to give a gripping distance of approximately 10 inches along the sheath. The type of pothead is a 23-kv G&W single conductor pothead with the mounting bracket insulated from the cable sheath. We have been able to maintain gas tightness except when the pressure has been enough to open a part of the pothead as mentioned previously.

We use only single-conductor potheads and single-conductor cable. Where it is necessary to trifucate we go to the first manhole away from the riser. We are eliminating all multiconductor potheads as rapidly as possible. Our operating experience with multiconductor potheads has been very poor. This is due mostly to the inability to obtain enough pressure on the gaskets. We feel that even on the single-conductor potheads now on the market a need for more unit pressure on the gaskets is necessary.

We have several oil-filled potheads with the reservoir under approximately ten pounds nitrogen pressure. These are only used on important circuits, such as generator leads but our operating experience with this type has been 100 per cent perfect.

Robert J. Wiseman (The Okonite Company, Passaic, N. J.): This paper should be read by everyone interested in cable risers as it explains very nicely the conditions under which cable risers operate. Cable manufacturers are asked frequently why risers do not operate as well as cable operating in a horizontal position. When the migration of the oil is referred to, then we are asked to furnish a nonmigrating compound, yet we know that none exists unless it is almost solid such as a petrolatum and the cable is below 50 degrees centigrade. Even here there will be a slow migration.

The author's suggestions for meeting the problem are possible solutions but one must not expect them to be 100 per cent proof as every case has peculiarities that can offset what is desired. A positively sealed pothead is one of the best ways of meeting the situation. It at least will delay migration and at the same time prevent entrance of moisture which is one of the major causes of terminal trouble.

Wm. A. Del Mar: Dr. Greenfield is undoubtedly correct in his view that our analogy of a sheath to a rubber pipe is not an exact one. However, in citing the forces acting on a lead sheath, external atmospheric pressure is one of them, and is certain; whereas elastic forces in lead, especially when long periods are involved, are very questionable.

Moreover, Dr. Greenfield's cylinder does not adequately represent an actual cable, especially after it has been reeled, unreeled, and pulled into a duct. Such a cable is far from having the outline of a perfect cylinder, and experience shows that it is slowly susceptible to external pressure without "crumbling."

Dr. Greenfield confirms the statement that a stringy adhesive impregnant has merit for delaying migration, but apparently gives it more merit than our Committee was willing to concede. He says that its efficacy "must be related to the temperature." In plain language, it doesn't work so well when the cable gets hot.

Both Mr. Hickernell and Dr. Greenfield claim merit for a carbon-black paper binder because it gives shield-to-ground continuity. Such continuity is not necessary, as shown by the fine operating record of the Commonwealth Edison 13,200-volt cables with a binder consisting of four insulating papers, the shields being grounded to the sheath at the joints.

Fear might be expressed that, with this arrangement, a cable failure might result in burning the shielding tapes between the point of failure and the joints and thus making the remainder of the cable unavailable for use on shorter runs or with a duct splice.

The facts are that with or without the

insulating paper between shield and sheath, the two paths are in parallel and the current in the shield will be the same in either case as it depends only on the shield impedance and the voltage, both of which are the same in the two cases.

The charging current in the shields is, of course, quite negligible. For example, the charging current of each phase of a 3-conductor 350,000 circular mil 34.5-kv shielded cable, 500 feet long, with shields grounded at both ends, would be less than 0.2 ampere at each end, and the voltage drop of the order of 1 volt.

However, if such continuity is desired, it is better attainable with metallized paper tapes, better because where there is any sheath swelling, as there is likely to be at the base of risers, the contact between binder tape and sheath becomes imperfect and much better continuity is obtainable with the low resistance film of aluminum on metallized paper than with a material like carbon-black paper, which is only semi-conducting.

With regard to Mr. Hickernell's suggested construction, compact stranding probably has some advantage. Above-standard thickness of insulation is also advantageous for the higher voltages. Carbon-black paper as a binder has been discussed above. Arsenic-lead is helpful, as indicated in the paper, although the Committee prefers to design on the basis of a hoop stress of 175 pounds per square inch rather than the 250 pounds per square inch suggested by Mr. Hickernell, at least until more experience is available. One reason for this is the relative inferiority of arsenic-lead at press-stops and in the vicinity of joint wipes.

Wayne Parker works on the safe side in trifurcating at the manhole, and his observation that multiconductor potheads are unreliable because they are difficult to seal, is an important contribution.

His difficulty is pressure at the top of the riser. The view expressed in the paper is that this occurs when the cable is hotter below than above, and therefore there is a tendency for the compound to be pushed upward toward the cooler portion. This may be because the three cables are huddled together in a steel pipe below and open to the breezes above.

Automatic Control of Metal-Clad Switchgear Serving Oil Refinery Motors During Power System Disturbances

R. T. HORSFALL
MEMBER AIEE

K. N. THOMPSON
NONMEMBER AIEE

R. W. MILLS
MEMBER AIEE

P. O. BOBO
MEMBER AIEE

IN a previous paper[1] by one of the co-authors, a picture of a procedure followed in planning and carrying out electrification of power drives in a petroleum refinery was presented. This paper pointed out that the use of large scale electric power in petroleum refining is relatively new. This is primarily the result of process developments requiring more mechanical energy and the industry's gradual change of viewpoint with regard to reliability of electric power versus that of steam. It is the purpose of this paper to describe some of the controls incorporated in the metal-clad switch-gear serving the Sohio Refinery at Lima, Ohio. These controls afford reliable service to this refinery during power disturbances from a system subject to lightning flashovers and similar upsets.

Refinery Use of Electric Power

The oil refiner's use of electric drive for blowers, pumps, fans, and compressors is increasing rapidly owing to several basic causes. First it is possible to generate his steam requirements at high pressure and to top the process steam through noncondensing turbine generators, thereby producing electric energy with about 4,500 Btu per kilowatt-hour. Second, it is possible to purchase electric energy for around 6 to 10 mils per kilowatt-hour in many refinery locations. Table I shows approximate comparative costs per brake-horsepower of 9 mil electric power drive with other types of drives. Electric power drive compares very favorably when the factors of labor, maintenance, supervision, and return on investment, not included in the table, are considered. Rapid process developments utilizing new drives, continuously present opportunities to improve efficiency in the use of energy.

Also in many locations, it is necessary to minimize the use of water, either because it is not available in large quantities and of suitable analysis, or because the problem of disposing of waste water thoroughly separated from oil and other contaminants is costly. This was the case at the Lima refinery. By maximum use of electric energy, the plant capacity was increased from 20,000 to 40,000 barrels per day of crude run, and a solvent lubricating oil plant was installed. Induced draft cooling towers having a total capacity of 40,500 gallons per minute were installed, and the complete expansion is being operated without materially increasing either the quantity of water taken from the ground or the capacity of the boiler house.

Reliability Required

Electrical service for petroleum plants must be dependable. It must compare with refinery steam plants where one failure in approximately 20 years is the normal case. A 4-minute outage on a delayed coking unit at a Toledo refinery means a 3-day shutdown, and a 10-minute outage at the Lima refinery would cost about $30,000.[1] Of first importance therefore, is the primary source of power. It should be chosen with a sufficient number of firm feeders to give the degree of reliability desired. Reliability, however, does not necessarily mean absolute continuity of station power. For example loss of power up to four seconds at the Lima refinery is not serious because of the complete controls incorporated in the switchgear. Here reliability becomes a function of the probability of a sustained total outage to the refinery.

Reliable electric service for the Lima refinery is derived from a duplex design all the way from 132-kv source down to 480 volts at the motors. Duplex stations were chosen over a low-voltage network because of the large distances between load centers over a 200-acre area. The duplex substation of Figure 1 is supplied from two firm feeders of a 34-kv network which is served from two separate 132-kv substations. The two 3,000-horsepower synchronous motors which drive the blowers for the catalytic cracking unit, are the largest in the refinery and are served from separate busses of the dual 4.16-kv switchgear unit. All other important motor loads are served from dual low-voltage switchgear. Originally in 1949 only the two 5,000-kva transformers shown in the center of Figure 1 were installed. The third 5,000-kva transformer was added about a year later

Table I. Approximate Utilities Costs Per Brake Horsepower Hour*

	Costs
Gas engine (30¢ gas)	0.46
Electric motor (9 mils/kwhr)	.80
Diesel engine (14¢ gal.)	.87
Gasoline engine (18¢ gal.)	2.08
Steam turbine—condensing (over 200 hp)	.88
Steam turbine—mechanical drive	2.75
Steam pump—reciprocating (small)	8.25
Steam valued @ 55¢/1,000 pounds	

*No labor, maintenance, supervision, or return on investment included.

Paper 50-261, recommended by the AIEE Switchgear Committee and approved by the AIEE Technical Program Committee for presentation at the AIEE Fall General Meeting, Oklahoma City, Okla., October 23–27, 1950. Manuscript submitted July 26, 1950; made available for printing August 28, 1950.

R. T. Horsfall is with the Dingle Clark Company, Cleveland, Ohio, K. N. Thompson and R. W. Mills are both with the Standard Oil Company of Ohio, Cleveland, Ohio, and P. O. Bobo is with the Westinghouse Electric Corporation, East Pittsburgh, Pa.

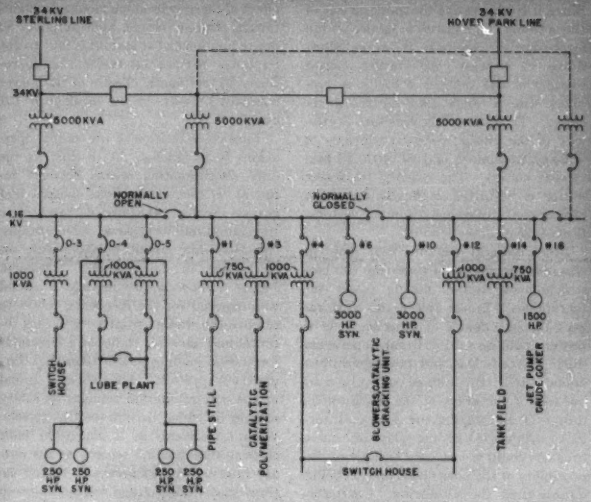

Figure 1. One-line diagram of refinery circuits

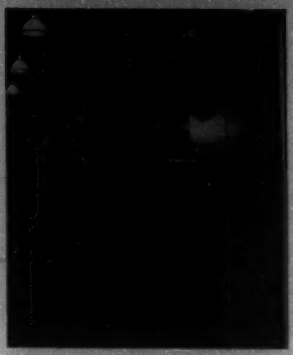

Figure 2. Front view, 4.16-kv metal clad switchgear showing control and protective relays

to serve the lube plant expansion. Distribution from the 4.16-kv and 480-volt switchgear busses to the catalytic cracking unit is underground. Overhead 4.16-kv radial circuits connect to the duplex low-voltage substations serving the three solvent lube units, the lube oil tankage and shipping areas, the crude distillation unit, the main tank field, and gas plant areas. The 150-megavolt-ampere 4.16-kv switchgear, houses all of the service control and protective relays for the feeders and motors served by its air circuit breakers. It also houses the field contactor and associated controls of two 3,000-horsepower synchronous motors, see Figure 2.

The feeder circuit breakers have induction inverse-time and instantaneous overcurrent protective relays. The circuit breakers of the more important circuits have single-shot reclosing relays for automatic restoration of feeder service.

The protection afforded each of the large blower motors is complete. It consists of ratio differential relays for sensitive detection of winding faults, inverse-time overcurrent relays for overload protection, instantaneous overcurrent relays for heavy short circuit protection, undervoltage relays for sustained undervoltage protection, thermal relays for protection against overheating, a damper winding relay located in the field discharge circuit for damper winding protection under near-locked rotor conditions, air-flow controls on the blower to limit motor output current to 110 per cent of rating, and a sequence timing relay for limiting the duration of the starting cycle.

Service Problems and Controls for Their Solution

Like most medium voltage lines the 34-kv network lines of the power company are overhead and are subjected to flashovers by lightning and other causes. Likewise, the refinery overhead circuits, served from the 4.16-kv switchgear, are subjected to the same types of faults. Such faults create voltage disturbances on the refinery for the duration of the fault clearing times. One of the 34-kv incoming lines is equipped with pilot wire protection and the other incoming circuit together with other lines of the network are protected by the conventional induction disk time delay and instantaneous overcurrent relays. Over-all clearing times range from under 0.2 second to approximately 1.5 seconds, most of them, however, being under 1 second.

All important induction motors are equipped with time delay undervoltage protection to ride over these disturbances.

In order to hold down the initial costs of the electric power supply, very little reserve in transformer capacity above immediate load requirements was installed. Following momentary power interruptions or severe voltage disturbances, it was found necessary to break up the reapplication of load, because the heavy inrush currents cause excessive voltage drops through these transformers. The means of segregating these loads and restoring them constituted the major control problem at Lima and is explained in subsequent paragraphs.

The 3,000-horsepower synchronous blower motors were selected for across-the-line starting and with a limited inrush of 9,330 kva. The limiting pull-in torque is 40 per cent of rating. It is, therefore, necessary to tie in the air-load control of the blowers with the electrical control of their synchronous motors in order to synchronize or pull them into step. This is done by interlocking the circuit breaker closing (motor starting) circuit with the closed position of the blower dampers so that the motors are started with the blowers unloaded. The starting circuit of each motor is interlocked with the starting sequence-timing relay of the alternate motor so that the two motors cannot be placed in the starting cycle simultaneously. Other interlocks in the closing circuit of each circuit breaker are: a phase-sequence voltage relay, a frequency relay, and an exciter voltage relay to insure alternating voltage of the proper sequence, magnitude, and frequency and good exciter voltage prior to starting. One additional interlock of a tripping relay prevents starting following tripouts by certain protective relays such as the differential relays. Upon completion of the motor starting cycles electrical interlocks cause the respective blower dampers to open and apply air load to the blowers.

Application of field to these motors for synchronizing is accomplished by a syn-

chronizing relay in the motor field discharge circuit which operates the field contactor on a slip-frequency of about 1 cycle per second and at a time when the poles of the motor are in a favorable relationship for synchronizing.

The most difficult control problems result from momentary outages to the refinery rather than from system voltage disturbances. The controls for the two conditions are slightly different and are described in the following paragraphs.

Momentary Outages to Refinery

Ordinarily, service restoration following a complete station outage can be accomplished in well under 1 second by immediate reclosure of a circuit breaker or circuit breakers. This cannot be done here because even a reclosure within 15 cycles may find the 3,000-horsepower synchronous blower motors 180 degrees out of phase with the incoming source. Such an occurrence might possibly cause mechanical damage to these motors which are coupled to high inertia gear boxes of 1,200 rpm to 5,087 rpm to drive the high speed blowers. An alternative would be to remove the motor fields prior to reclosure, but this would incur time—long enough to permit deceleration of plant motors to the extent that high inrush currents and resulting high-voltage drops would occur.

Since the 4.16-kv bus voltage under these conditions of re-energization would be less than 80 per cent normal, it becomes necessary to break-up restoration of service to the refinery. The decision, therefore, was to trip both blower motors so that upon re-energization of the station, sufficient bus voltage would be present for reaccelerating the induction motors. Re-energization of the station is accomplished through automatic reclosure of the power company's 34-kv line circuit breakers. Since it is imperative that at least one of these blowers be replaced in service within approximately 1 minute, to prevent slowdown of process, the master circuit breaker of the number 6 motor is provided with a single shot automatic recloser. This automatic reclosure is subject to the closing circuit conditions of voltage, frequency, and so forth, as previously stated. The number 10 blower motor is restarted manually from the blower room following automatic restoration of the number 6 motor.

Much thought and time were spent in choosing the means of removing the two synchronous motors during power interruptions. Power factor and watt relays though capable of detecting loss of power would be subject to false operation during certain load and fault conditions encountered. Bus voltage cannot be used because of the effect of the synchronous motors on maintaining the voltage. Interlocks with the 34-kv line relays or circuit breakers could not be used because of the possibility of the power interruption being remote from the substation. Computations of speed reduction of the refinery system on separation indicated that an under-frequency relay could be used. With a setting of approximately 58¾ cycles per second, which is considered below the minimum frequency to which the power system would ever be expected to drop, the blowers even at light load can be tripped off the line in less than 1.5 seconds.

Figure 3 shows the variation of both frequency and voltage for a staged interruption test. Note here that both motors were tripped within 1 second. The decay in motor frequency compared with that of the reference voltage, approximately 29 cycles in 0.5 second, 57 cycles in 1 second, and 83 cycles in 1.5 seconds from instant of outage, and the effect of the synchronous motors on maintaining station voltage, approximately 80 per cent of normal at instant of first motor tripping. Service was restored to the refinery by automatic closure of the power company's 34-kv circuit breaker in 157 cycles.

Time co-ordination of the control operations is as follows. With time as the only discriminating means between removal of the synchronous motors and circuit breaker reclosure to re-energize the station following power interruptions, the 34-kv line circuit breakers were set to reclose in 2.5 seconds. Although Figure 3 shows approximately 1 second was required for the frequency relays to remove the motors from service, this interval may increase to about 1.5 seconds for station loading lighter than that during the staged test. Thus about 1 second of the outage interval remains as safety margin in which to remove the motors. With 1.5 seconds as a maximum fault clearing time and 2.5 seconds as the outage interval, it was necessary to set the time-delay-undervoltage release units up to 4 seconds. Although this may seem to give a rather small margin of safety, the effect of the synchronous motors on maintaining bus voltage gives a large margin of safety in holding in the release coils.

Out-of-Step Conditions Caused by Voltage Disturbances

To take care of out-of-step conditions of these synchronous motors which may occur during system voltage disturbances, pull-out relays are installed in series with the field circuit of each motor. The relays respond to the alternating voltage induced into the field circuit when the machines slip a pole. The pull out relay of number 6 motor is connected to trip its masters circuit breaker while that of number 10 is connected to remove its

Figure 3. Oscillogram of a staged interruption test on refinery showing decay of voltage and frequency and tripping times of the 3,000-horsepower motor circuit breakers by under-frequency relays

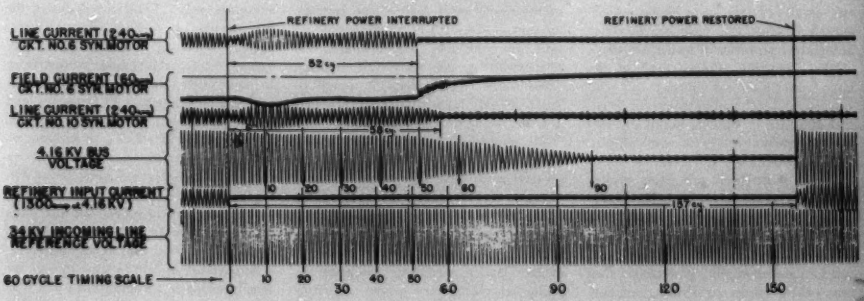

motor field and thus place this motor in its starting cycle to be re-accelerated and resynchronized. If the duration of the voltage disturbance is not excessive following the out-of-step condition, the number 10 motor will continue in its starting cycle and resynchronize when the blower dampers automatically close to unload the motors below pull-in requirements, otherwise the starting-sequence-timing relay, set for 30 seconds, will shut the machine down. The pull-out relays of both motors are not connected for resynchronizing because of the possibility of placing both in starting cycle simultaneously, a condition which would result in less than 80 per cent bus voltage. Upon restoration of normal voltage and frequency following the completion of the starting cycle of number 10 motor, the reclosing relay of the number 6 circuit breaker will restart the number 6 motor and place it on the line.

Operating Experiences

Since the new substation and switchgear have been in service, October 1949 to July 1950, there have been 12 voltage disturbances from the power company system which caused the synchronous blower motor to drop out of step. The blower motors resynchronized successfully on ten of these disturbances. One of the failures to synchronize can be attributed to placement of the two motors in their starting cycle together following a very severe voltage disturbance. Because of low bus voltage, insufficient torque was developed to permit the motors pulling back into step. This has since been remedied by interlocking their starting cycles as described previously. The other failure was due to the oil pump motor for the blower hydraulic air control system dropping off on undervoltage. This, likewise, has since been remedied by blocking its starting circuit pushbutton in the closed position.

On July 19, 1950, Lima was struck by a tornado which severely damaged the power company's lines. It was the most devastating thing that had ever happened to their lines in that area. One 34-kv feeder remained firm, but multiple voltage dips were experienced. Both blower motors pulled out of step. One dropped into its starting cycle and resynchronized and was followed by the second upon closure of its master circuit breaker. Then on a subsequent voltage disturbance the motors again pulled out of step. One resynchronized as before but the circuit breaker of the second motor locked out because the second disturbance occurred before the reclosing relay had reset. The one motor maintained the refining process in operation.

There have been no complete power outages to the refinery from the power company system over this period from October 1949 to July 1950. A total of five fault clearing operations have occurred on the 4.16-kv feeders during that period. These were cleared sufficiently fast as not to effect the stability of the synchronous motors.

While several difficulties have been experienced and since corrected, it is felt that all major electrical problems have been overcome and it is now possible to keep important equipment on the line during any power system disturbance where complete extended interruptions are not involved.

The installation of counters on circuit breakers and field contactors, annunciator drops on important relays without built-in targets and, of course, relay targets have proved their value in analyzing the operating experiences of this automatic equipment.

Conclusions

1. The use of electric drive in refinery service is increasing rapidly for economy and other reasons.

2. At Lima, electric drive is especially valuable in that it permitted a much larger expansion of the refinery than otherwise would have been practicable with the known quantity of water available.

3. Electric power to refineries must be and can be reliable.

4. With proper controls incorporated in switchgear, reliability becomes not a function of absolute service continuity, but a function of service without sustained station outages. Controls can be provided which will permit refinery motors to ride over power system voltage-disturbances, or be quickly restored to service following momentary station outages in a manner not causing interruption to the refinery processes.

5. Operating experience with such controls at the Lima refinery is showing that the very high degree of service required for petroleum refining can be obtained by electric equipment with power supplied from a power company.

Reference

1. Engineering an Oil Refinery Distribution System, K. N. Thompson. AIEE Special Publication S-38, August 1950, pages 223–35.

Discussion

H. M. Stewart (Humble Oil and Refining Company, Baytown, Tex.): The authors are to be complimented on this very interesting and timely presentation. The statistics given on operating experience give rather convincing evidence of the effectiveness of this control application, and add materially to the value of the paper. The excellent results attest to the effectiveness of the installation.

It is evident that the problem faced at the outset was of sufficient magnitude and importance to warrant a sizable expenditure of study, effort, and money, in view of the large debits to be expected in case of interruptions to process plant operations. The application is considered to represent a significant step toward keeping pace electrically with the strides being made by modern industrial production and manufacturing processes. Developments in the near future are likely to call for a degree of ingenuity of the order that has been demonstrated in this instance.

The design and functional aspects of the several protective features have been set forth with such clearness that there are only a few questions that might be raised regarding the application as a whole and the means devised to accomplish the desired results. Processwise, it is supposed that the timely restoration of one of the 3,000-horsepower blowers is a practically certain safeguard against a plant outage, allowing ample time for the other 3,000-horsepower unit and associated 480-volt equipment to be restored to normal operation either automatically or manually, as determined by circumstances. As the 480-volt induction motor drives are equipped with time delay undervoltage devices, they would be expected successfully to ride through most disturbances of the type described. Although there might be a fairly large number of such drives in the plant, it is assumed that their process functions are such that the time required for restarting them is not a major factor in the over-all scheme of things, even after a severe disturbance requiring re-energization of the 4.16-kv busses.

It is beyond the scope of the paper to go into the matter of transformer capacity, but the question arises as to whether plant operations might not be penalized heavily in case of an extended outage of one of the 5,000-kva stepdown transformers. It would be interesting to know whether any provisions were made to take care of such a contingency.

It is noted that one of the tie circuit breakers in the 4.16-kv bus is normally open. It is probably advisable to do this to limit the duty imposed on the feeder circuit breakers. If there are other reasons, it would be interesting to know them.

It would appear the number 6 motor might be prevented from restarting by its reclosing relay if number 10 is in trouble. Must number 10 complete its starting cycle before number 6 can be reclosed? It is likely that a winding failure in number 10 motor would be cleared so quickly by differential relay action that number 6 would continue to operate without going through a restarting cycle, but if number 6 were called upon to restart under this circumstance, is there anything inherent in the scheme that would keep number 6 from restarting, without the necessity of resetting some device interlocked with its closing circuit?

It is noted that there were five fault-clearing operations on the 4.16-kv feeders during the same period from October 1949 to July 1950, when there were 12 disturbances from the power company system. Offhand, the ratio of five disturbances on the 4.16-kv feeders to the 12 on the power company system appears to be high, as it seems certain that this ratio is out of proportion to exposure, particularly since the 4.16-kv system extends over a relatively small area and some of its feeders are underground and not vulnerable to lightning. It is suggested that future data regarding the outages on the overhead and underground portions of the plant distribution system would be interesting and might point toward opportunities of improvement, if operating experience indicates an economic justification for bettering the record.

In view of its history of success up to now, the automatic control application described by the authors seems certain of having a good record in the future, and it is believed that many engineers will be interested in any supplemental statistics that may be published in the future.

L. M. Goldsmith (The Atlantic Refining Company, Philadelphia, Pa.): The paper is an excellent one, and indicates that considerable thought was given to the selection and installation of equipment to prevent or reduce to an absolute minimum of time the power outages on the 3,000-horsepower motors on the number 6 and number 10 blowers.

We are particularly interested in this installation since we have a similar installation in the Point Breeze Refinery in Philadelphia, except that our blower motors are rated 2,500 horsepower and our operators will not permit an unplanned shut down of even one minute.

We have made no attempt to automatically restart either of these motors since the period of time during which they may be shut down is so small that even a 1-shot recloser, such as is used on the author's number 6 motor will not prevent disruption of our cycle. Although we have given this matter of keeping the blowers on the line considerable thought, we have been unable to arrive at a relay protective scheme that can be justified.

However, we do have considerable protection from power failure since we have approximately 7,000 kw generating capacity at 60 cycles in this plant as well as seven separate feeders from the local power company which assures us continuity of service under practically all but the most adverse conditions.

In the detailed description of the various types of protection described in the paper, there is no mention made of that provided for the transformer banks and the transformer busses. In our opinion, it is as important to protect these pieces of equipment, particularly by differential relays, if continuity of service and equipment protection is desired.

We agree wholeheartedly with the conclusions arrived at in the paper, particularly, since we have been interested for a great number of years in the promotion of electric drive in refinery service and have advanced it and promoted it at every opportunity. The excellent results which we have received in our own refinery agree with the conclusion the author has given concerning the reliability and high grade of service to be expected from electric drives in refineries.

G. E. Brooks (Oklahoma Gas and Electric Company, Oklahoma City, Okla.): Requirements of service reliability and the hazards and expense of shutdowns to refinery loads are well known. These, together with the economic restrictions imposed by a competitive rate for electric power, present serious problems in equipment protection and control. In this particular location, where transient outages and voltage disturbances could not be avoided, the effects of such interruptions have been minimized by careful analysis and judicious application of load segregating equipment. Automatic devices are employed to keep the loading within system capability during recovery periods without jeopardizing the various plant processes. While some problems may not yield to a sequential-restoration solution such as this one, the only course for the control engineer is to take advantage of all possible "breaks" and favor the critical elements.

Several forms of service restoration and outage-sustaining equipment have been applied to large induction and synchronous motor loads served from Oklahoma Gas and Electric Company system. Most prevalent are mechanically delayed under-voltage releases for compensator-start and across-the-line start induction motors. Field removal and restoration equipment is used where single large synchronous motors drive flour mills or pump stations. In one flour mill, where wound-rotor induction motors are controlled by sequence contactors operating in the rotor circuit, power for the contactor coils is supplied from a motor-generator set. Inertia of the motor-generator holds the contactor coils energized during transient outage, with little reduction in motor speed. A delay of five seconds in service restoration causes the equipment to return to starting position for reduced power input.

On the Oklahoma Gas and Electric Company system, the most critical problems associated with service restoration and voltage disturbances to refinery loads are where plant generators operate in parallel with the system. Various schemes, employing frequency relays, power directional and overcurrent relays, have been used to effect necessary separation.

Each installation supplying critical loads calls for consideration of the special requirements and hazards involved. Discerning and fortunate is the engineer who can solve his problem by temporarily eliminating or removing the major cause of difficulty, as was done in this instance at Lima, Ohio.

J. H. Kinghorn (American Gas and Electric Service Corporation, New York, N. Y.): The picture this paper presents of a large industrial operation which has found electric drive advantageous is an old one for many industries, but a newer one for the refinery industry. It is particularly gratifying to us in the electric utility business to note that purchased power in this case meets the requirements of economy and reliability.

Absolute assurance of power supply from any source, either purchased or locally generated is, of course, impossible to obtain. The requirement here is to obtain an overhead transmission system which although subject to lightning and other natural hazards will equal or exceed the reliability of a local generating system.

Lima is supplied by four 132-kv transmission lines, two of which interconnect with the Indiana and Michigan Electric Company system at Fort Wayne. The remaining two connect to The Ohio Power Company main transmission network. The voltage is stepped down to 33 kv for distribution in the local area. The principal substation, where all four 132-kv lines terminate, has duplicate 25,000-kva transformer banks and duplicate 132-kv and 33-kv busses. A 33-kv network is fed from this station and in addition, a single 132-kv line feeds the Sterling Substation where there is a 25,000-kva transformer bank stepping down to 33 kv and also connecting into the 33-kv network. Lima Refinery is supplied by two 33-kv lines. One is 2.13 miles long and comes directly from the Sterling Substation. The other is 0.17-mile long and comes from a sectionalizing station in the main 33-kv network. The fact that both lines are quite short and of good construction makes it unlikely that both will be out of service simultaneously. The shorter line is protected with pilot wire relays which will clear short circuits in 0.15 second including circuit breaker time. The longer line has instantaneous and induction overcurrent relays which will clear short circuits in from 0.15 to 1.4 seconds depending on their location. Ninety per cent of the line length is covered by the 0.15-second clearing time. With this short time, it is unlikely that temporary flashovers will cause enough damage to prevent successfully re-energizing the line immediately after a tripout. There have been no tripouts on these lines between January 1 and September 1, 1950. The tornado referred to in the paper damaged the other 33-kv lines supplying the network but left Sterling Substation feeding the refinery and the remaining sound portion of the network.

The requirement that after a power interruption the incoming circuit be reclosed after the synchronous blower motors have been removed but before the time delay undervoltage devices have shut down the various induction motors is a severe one and leaves little leeway for inaccuracy in the devices employed. For instance, if the pilot wire protected circuit were open and a severe short circuit should occur on the line from Sterling, the voltage at the refinery would immediately dip and the

undervoltage devices start timing. Under the worst condition, the circuit breaker at Sterling would open in 1.4 seconds. It would reclose about 2.5 seconds later or only 0.1 second before the undervoltage releases operate. Under the best condition, the circuit breaker at Sterling would trip by instantaneous relays and the reclosure would occur 1.35 seconds before the undervoltage releases operate approximately as shown in Figure 3 of the paper.

The margin of safety for the worst condition might be increased by reclosing more quickly but this would reduce the time between synchronous motor opening and power restoration. Because of the uncertainties of the tripping time of the underfrequency relays, this does not seem advisable. It is to be expected that this occurrence will be quite rare. It is evident that to insure correct action on those occasions, periodic checks will have to be made on the timing of undervoltage releases and circuit breaker reclosing timers to make sure they remain in proper operating condition.

P. O. Bobo: Mr. Stewart is correct in that the restoration of one 3,000 horsepower synchronous blower motor to service following a momentary station outage is sufficient, providing also that the important induction motor loads are maintained on the line. These motors, as Mr. Stewart says, are expected to ride over disturbances of this type. He also is correct in his assumption that the reacceleration time of the motors after such disturbances is not a major factor in the over-all scheme of things, but the element of time does require automatic equipment to prevent loss of processes; the time required for manual restoration of the many individual drives would be excessive and result in serious loss of production. The time-sequence in restoring electric drives at Lima largely determined the amount of automatic equipment required. Of course, all drives cannot be simultaneously restored because of the limited transformer capacity. Fortunately the two 3,000-horsepower motors can be dumped, if one is subsequently restored to service within one minute. This permits the use of the simple time-delay undervoltage release to as much induction load as transformer capacity can safely restart and a minimum of automatic controls to restart the dumped load upon subsequent voltage recovery.

Only one bus-tie circuit breaker is normally closed in order to limit the duty imposed on feeder circuit breakers.

The starting of the two 3,000-horsepower motors are electrically interlocked so that they can not be started together, either manually or automatically. However, the controls of the two motors function differently for operations resulting from momentary power interruptions to the station, than they do for those resulting from out-of-step conditions. For power interruptions, both are tripped by their underfrequency relays. One is restarted by automatic circuit breaker reclosure upon restoration of good voltage and frequency and the other is left off to be manually restarted.

For the out-of-step conditions, the two motors are interlocked so that if both pullout together, they will not both restart together and cause a low-voltage condition. One motor is placed in its starting cycle by removal of its field while the other motor is tripped—to be restarted automatically upon completion of the starting cycle of the first.

The high ratio of feeder faults to power company line faults as noted by Mr. Stewart is due to man-made faults within the refinery during a construction period. The ratio undoubtedly will drop in the future.

To answer the inquiries of Mr. Stewart and Mr. Goldsmith, the three 5,000-kva transformers are individually protected by ratio differential and overcurrent relays. In the event of an emergency loss of one transformer, the refinery load can be carried for extended periods on any two of the three transformers. Figure 1 of the paper shows how connections can be made through bus-tie circuit breakers.

It is interesting to note that the degree of reliability desired for the plant referred to by Mr. Goldsmith requires seven incoming feeders from the local power company plus generation of their own. Mr. Brooks pretty well sums up problems of this type in his statement "While some problems may not yield to a sequential-restoration solution, the only course for the control engineer is to take advantage of all possible breaks and favor the critical elements." At first sight at Lima, there appeared to be no "breaks," but when faced with the facts, and the costly results of a shutdown or preventative alternatives, round table discussions with process men and electrical men of the refinery company, with the power company engineers, the contractor and equipment supplier, it was found that certain equipments could be disturbed for short periods without serious loss of process. The result was the subject control system, which to date has proved its reliability.

Mr. Kinghorn's picture of the 132-kv and 34-kv lines to Lima, and his analysis of the close timing requirements show what can be accomplished by automatic controls on a system subject to several transient interruptions, but to date no extended outages.

In conclusion, two general statements are here given:

First, many cases of either severe damage or loss of production can be prevented by utilizing equipment automatized to perform certain functions in which the "what-to-do thinking" has been done beforehand instead of afterwards. Second, the probability of permanent faults to feeders serving important loads—either main lines serving a station or feeders therefrom—can be greatly reduced by high speed clearing of faults such as by pilot wire, carrier-current, or distance relays.

The authors wish to thank these gentlemen for the important contributions they have made to this subject.

An Electric Analogue Computer Using the Photo Cell as a Nonlinear Element

ELDO C. KOENIG
ASSOCIATE AIEE

THE electric analogue computer was built primarily for the purpose of analyzing magnetic circuits; however, its application can be extended to cover the solutions of many other nonlinear systems in the fields of fluid flow, aerodynamics, and mechanics. During the past 12 months of operation, the computer has been used extensively to analyze the magnetic circuit of salient pole and cylindrical rotor synchronous machines for the purpose of investigating iron losses, effect of saturation of the component parts on the characteristic saturation curves, and for determining the normal field excitation. Not only is the amount of labor greatly reduced in solving magnetic saturation problems with the computer but more accurate solutions are obtained. Without a computer it is often necessary to arrive at solutions by empirical methods which sometimes give erroneous and unreliable results.

The photo cell was used in the basic element because its features make the computer relatively simple in design and operation. The current through an element, of which the photo cell is a component part, is a single valued function of the voltage across the element. The computer then is a direct electric analogue of the system being analyzed, and the effects of changing the value of a component of the system can be observed readily by making the corresponding change on the analogue. The purpose of this paper is to describe the electric analogue computer as a device for solving problems involving single valued nonlinear parameters and to describe in general its design features.

Paper 50-263, recommended by the AIEE Computing Devices Committee and approved by the AIEE Technical Program Committee for presentation at the AIEE Fall General Meeting, Oklahoma City, Okla., October 23–27, 1950. Manuscript submitted March 15, 1950; made available for printing September 12, 1950.

ELDO C. KOENIG is with Allis-Chalmers Manufacturing Company, Milwaukee, Wis.

The author is indebted to Dr. Sterling Beckwith for suggestions in the preparation of this paper, and for his valuable aid in the development of the analogue computer and in applying its use to the analysis of magnetic circuits; to Walther Richter for his suggestions in the design and building of the computer; and to John Borsk and staff for the splendid co-operation and assistance in carrying out the laboratory work. All are of the Allis-Chalmers Manufacturing Company.

Photo Cell Characteristics and Features

The vacuum photo cell has unique advantages for use as a nonlinear parameter. Representative characteristic curves of a silver-cesium oxide-cesium cell are shown in Figure 1 as curves A, B, and C. The light intensity was the parameter for obtaining the three curves. The important feature here is that when the light excitation is changed from one value to another, the per-cent change in current is essentially the same at all voltages. Therefore, a family of curves is obtainable by varying the amount of excitation.

These curves in the upper region have essentially a constant slope. This suggests the photo cell to have the characteristics of an inherent constant and a variable resistance in parallel. Curves A_1, B_1, and C_1 of Figure 1, which are the characteristic curves of a constant resistance, are drawn through the origin with slopes equal to the constant slopes of curves A, B, and C, respectively. When the ordinates of each of the curves A_1, B_1, and C_1 are subtracted from the corresponding ordinates of each of the respective curves A, B, and C, the curves A_2, B_2, and C_2 result. Each of these resultant curves is the characteristic curve of the inherent variable resistance for a particular excitation value. When setting up the analogue of a magnetic circuit, the inherent variable resistance of the photo cell is made to represent the inherent variable reluctance of the magnetic material of that circuit.

If a group of cells is excited from a single light source and the cells for a given light intensity are adjusted to give equal current outputs for a given voltage, then for an increase of light excitation, the current output of each of the cells will increase an equal amount. Therefore, cells to represent equal nonlinear parameters can be conveniently excited from the same source of light and their current outputs varied a like amount, simultaneously, by changing the light output of the exciting lamp.

Since the light excitation circuit and the photo cell circuits are completely isolated from each other, there is no problem of circulating currents through metallic connections between circuits. This feature is not possible with other electronic tubes requiring bias.

After the photo cells of the silver-cesium oxide-cesium type have been properly aged (see Appendix I for aging method), the characteristic curves of the majority of the cells show close agreement. Approximately 70 per cent of the cells of this type used in the computer were selected as having current-voltage characteristics near enough alike to give the desired accuracy. In Figure 2, curves U and L and curves U' and L' are the limits within which the characteristics of the inherent variable resistance and constant resistance of the cells had to be contained for maximum allowable error. Curves A and A' are the average characteristics of 60 cells which fell within the limits.

The Basic Elements

One or more photo cells in combination with one or more constant resistances in series or parallel, and in some instances voltages within the element network, form

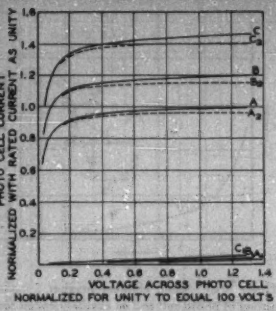

Figure 1 (left). Characteristics of a single photo cell showing family of curves possible by varying the amount of light excitation

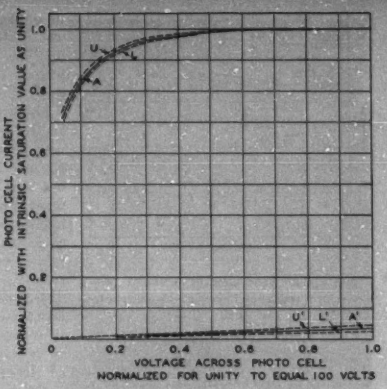

Figure 2 (right). Limits of the photo cell characteristics for selecting cells

several basic elements which may be used to represent the nonlinear parameters of systems.

Figure 3(A) shows the characteristic current-voltage curve for a basic element number 1 consisting of a constant resistance in series with the photo cell. The characteristic curve of the photo cell now approaches the characteristic curve of the series resistance instead of the current axis as the voltage approaches zero.

A second basic element consists of an aiding or an opposing voltage in series with the photo cell in order to shift the characteristic curve of the cell to the left or to the right with respect to the current axis as is shown in Figure 3(B). Since the cell current is very small, around ten microamperes, the voltage drop through the voltage sources used in the circuit will be relatively small. Therefore, the amount of shift will be essentially equal for all values of current flowing through the circuit.

Figure 3(C) shows a third basic element which consists of a photo cell and an auxiliary circuit for inverting the characteristic curve of the cell. The plotted current I is equal to the current I_S through the auxiliary circuit minus the current I_C through the cell.

A fourth basic element is shown in Figure 3(D). The effect of the resistance in parallel with the cell is an increase in the total current through the basic element which results in an increase in the slope of the characteristic current-voltage curve.

In addition to the examples just given using the photo cell and only one other component in the basic element, the cell and any combination of two or more components may be used. Still another parameter, the light excitation, can be changed to produce the effect described in the previous section. Also, instead of one photo cell in its branch circuit, two or more may be used to increase the current capacity, which is controlled by the cell rating.

With a single fixed relationship between the analogue and the represented system, it may not be possible to represent the nonlinear parameter for an infinite number of values of the function. However, when such is the case, results of sufficient accuracy may be obtained by matching the characteristics only over the range of values expected to be involved in the solution for that given set of conditions.

Representation of the Inherent Variable Resistance Characteristic of the Photo Cell by a Mathematical Expression

To determine what type of nonlinear parameters could best be represented by the current-voltage characteristic of the photo cell a number of equations, each representing one or more family of curves, was analyzed. The following equation describes most accurately the functional relationship between current and voltage of the cell and is of the form found by Gokhale[1] to be the law which more nearly represents the magnetization curve near saturation:

$$I = S - e^{-[a(E \pm H) + c]}$$

where

I = current through the inherent variable resistance of the photo cell
S = intrinsic saturation value of current
E = electromotive force across the cell and any opposing or aiding voltage in series
$+H$ = aiding voltage in series with the cell
$-H$ = opposing voltage in series with the cell
a,c = arbitrary constants

The current-voltage characteristic curve of the inherent variable resistance of the cell which was used for comparison with the equation was the average of those which fell within the limits shown in Figure 2 and is the curve A of that figure.

A particular equation resulted from the general equation by assigning a value of H equal to 0.015 (normalized for unity to equal 100 volts) opposing the voltage E. The constants a and c were calculated from the values at the points on curve A corresponding to E equal to 0.20 and 0.40 and found to equal 6.15 and 1.45, respectively. The resulting particular equation is:

$$I = 1 - e^{-[6.15(E - 0.015) + 1.45]}.$$

Curve A of Figure 4 shows the per-cent error in representing curve A of Figure 3 by the equation. Curves B and C of Figure 4 are the per-cent error limits for selecting the photo cells. From E equal to 0.2 to 1.0 the equation represented the average characteristic curve exactly for the points checked and did not exceed the allowable error for selecting the cell between the values for E equal to 0.13 and 1.0

Fundamentals in Setting Up the Analogue of Magnetic Circuits

To establish the relationship between flux and current, and magnetomotive force and electromotive force the characteristic curve of the inherent variable resistance of the photo cell is made to match as nearly as possible the characteristic curve of the inherent variable reluctance of one cubic inch of magnetic material. Figure 5 shows curve P', the average characteristics of the inherent variable

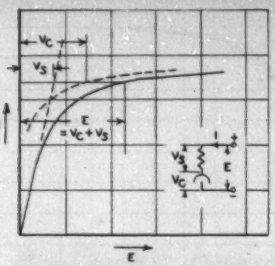

Figure 3(A). Basic element number 1 consisting of a resistance in series with the photo cell

resistance of the cells of Figure 2, matched as closely as possible with the curve M', the characteristics of the inherent variable reluctance of silicon steel. However, in order to match the two curves, the current axis had to be displaced to the left of the flux axis by 1.5 volts, as is shown in the figure. To consider this displacement in the analogue circuit, the basic element number 2 of Figure 3(B) can be used. The voltage V in series with the cell must aid the voltage applied across the element.

After the two characteristic curves of the inherent variable resistance and reluctance are matched, it is usually found that the value of the inherent constant resistance of the cell is too great in representing the inherent constant reluctance of the magnetic material. Consequently, curve P of Figure 5, which is the current-voltage characteristics of the cell, will be too low in matching the curve M, which is the magnetization curve of the one cubic inch of silicon steel. By the addition of an external resistance of proper value in parallel with the cell, curve

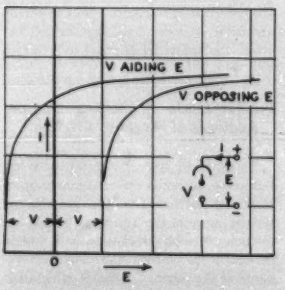

Figure 3(B). Basic element number 2 consisting of a photo cell with either an opposing or an aiding voltage in the cell circuit

M will be matched as closely as possible. The basic element number 4 of Figure 3(D) has an external resistance in parallel with the cell and can be used to make this correction.

From the foregoing discussion, when an analogue circuit is to represent a magnetic circuit, a combination of the components of the basic elements numbers 2 and 4 of Figures 3(B) and 3(D), respectively, must be used to represent accurately the magnetization curve of one cubic inch of magnetic material. The resulting new basic element would then consist of an external resistance in parallel with a photo cell and an aiding voltage of 1.5 volts in series with the cell. For simplifying purposes, the magnetization curve could be represented almost as accurately by using basic element number 4 in series with the aiding voltage of 1.5 volts, but the aiding voltage need not be a separate source in series with each of the number 4 elements used in the analogue circuit. Instead, an additional voltage equal to 1.5 volts multiplied by the number of elements in series can be added to the true voltage to be applied across that group of number 4 elements in series. This method is used on the computer for setting up analogues of magnetic circuits.

Since nonmagnetic material has linear flux–magnetomotive-force characteristics, any nonmagnetic material in series with magnetic material in a magnetic circuit can be represented by a constant resistor in the analogue. The relationship between reluctance and resistance is established from the relationship between magnetomotive force and electromotive force, and flux and current.

For conditions of magnetic and nonmagnetic material in parallel in a magnetic circuit, the flux that passes through the nonmagnetic material is represented by additional current through the external parallel resistor of the basic element. Therefore, to meet this condition in the analogue circuit, an adjustment of the parallel resistor of the basic element is all that is required.

Description of the Computer

There are 60 basic nonlinear elements and a number of electromotive forces and separate linear resistors used in the computer. A cell and an adjustable constant resistor in parallel make up the basic element which is number 4 of Figure 3(D). The elements are not permanently connected to form a particular network but can be readily connected in any fashion. The electromotive forces

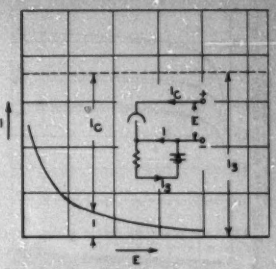

Figure 3(C). Basic element number 3 consisting of photo cell and an auxiliary circuit for inverting the characteristic curve of the cell

and adjustable linear resistors are available for inserting between the basic elements wherever required. The computer is shown in Figure 6.

An example of how the basic elements, resistors, and electromotive forces can be connected on the computer to represent a magnetic circuit is shown in Figure 7. The magnetic circuit represented is that of a salient pole synchronous machine for the conditions of open circuit and zero power factor lagging or leading. It is assumed the teeth and pole head saturate and the remaining magnetic material of the circuit has infinite permeability.

Five basic elements in series represent the reluctance along each tooth. The reluctance of each pole tip is represented by three elements in series. The resistors R_S and R_G represent the reluctance across the slots and air gap, respectively. The electromotive forces, E_S, represent the magnetomotive-forces in the stator slots resulting from current flow in the stator conductors. The sum of the electromotive forces, E_G and $(1/2)E_T$, equal the voltage representing the resulting magnetomotive force acting at the

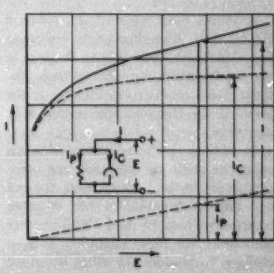

Figure 3(D). Basic element number 4 consisting of a photo cell in parallel with a resistance

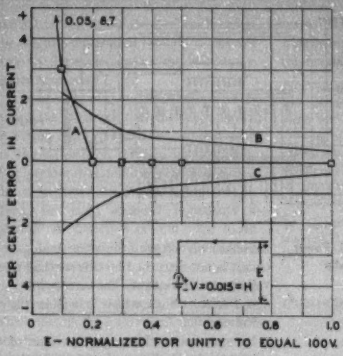

Figure 4 (left). Error in representing the characteristics of inherent variable resistance of photo cells by an exponential law

Figure 6 (right). Electric analogue computer

point under consideration across the pole plus the product of the number of elements in series and 1.5 volts. For example, E_a nearest the quadrature axis plus $(1/2)E_T$ equals the true voltage plus the product of 8 and 1.5 volts. As discussed in the preceding section, the 1.5 volts is a correction factor required for the matching of the photo cell characteristics with the magnetization characteristics of one cubic inch of magnetic material. When open circuit conditions are considered, E_s and E_a are zero and the only electromotive force acting is E_T.

The photo cells of the elements of the computer are excited from six separate incandescent light sources with ten cells excited from each source. The excitation of each cell is adjusted initially by a shutter on the opening through which the light passes to the cell. The excitation of the ten cells in each group can be varied simultaneously by changing the voltage across the exciting lamp. A master control is used for changing the voltage across all the exciting lamps and thereby can be used to adjust the excitation of all 60 of the cells simultaneously.

The example circuit of Figure 7 illustrates the convenience of the system of simultaneous control of the excitation of a group of cells. Since each of the ten cells of a row represents the reluctance of magnetic material of the same cross-section, all ten of the cells in each of the five rows are excited from a single light source. Therefore, to adjust the analogue circuit for a change in tooth paper the voltage across the exciting lamp for each row of cells is changed. When the tooth area is changed with the taper held constant, an accompanying change of voltage across all five of the exciting lamps is made with the master control.

The voltages and currents in the analogue circuit are unidirectional and are not amplified. The values of current in different parts of the network system may cover a range from zero to approximately

Figure 5. Matching of magnetization characteristics of silicon steel with the characteristics of a basic element

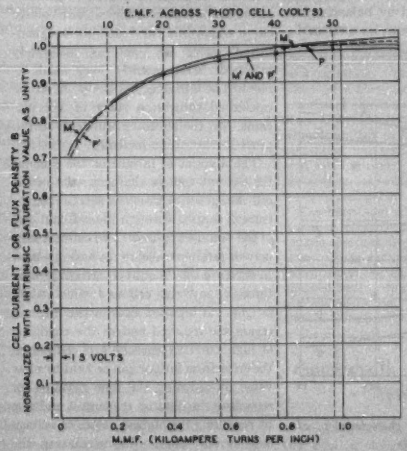

Figure 7. Analogue block diagram of the magnetic circuit of a salient pole synchronous machine assuming only the teeth and pole head saturate

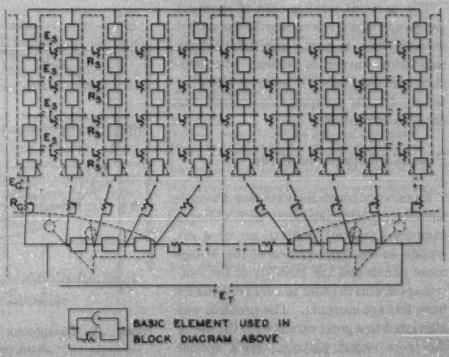

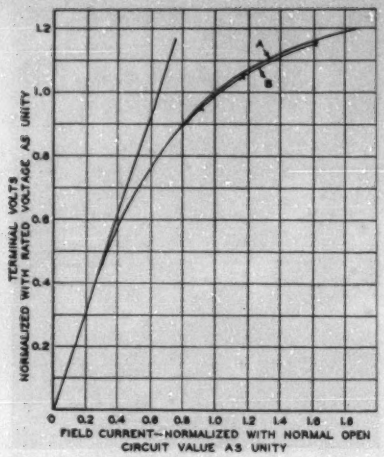

Figure 8 (left). Comparison of an open circuit saturation curve of a salient pole synchronous machine obtained from test with the curve calculated on the analogue computer

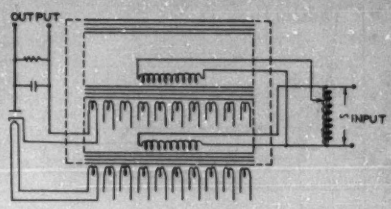

Figure 10 (upper right). Power supply of computer

125 microamperes; however, the current through individual photo cells seldom exceeds 15 microamperes.

The unidirectional electromotive forces are supplied by half-wave rectifiers. The values of electromotive forces can be varied from zero to as high as 2,000 volts in some cases. As many as ten separate and isolated voltages can be varied simultaneously. A description of the method used is given in Appendix II.

The circuit of Figure 7 employs the method of simultaneous variation of a number of isolated voltages. Each of the nine electromotive forces E_S in each of the four rows and also each of the ten electromotive forces E_G can be varied simultaneously by a single control to adjust for a change in current flowing in the stator conductors.

The network arrangement of elements shown in Figure 7 is similar to the actual network used in part for calculating the saturation curves of salient pole synchronous machines. A separate circuit is set up on the computer for calculating the pole saturation.

Possible Sources of Error

Since very small currents flow through the circuits with relatively high voltages impressed, special precautions were exercised in the construction of the instrument panels and the building of the control apparatus in order to avoid difficulties from leakage currents. The problem was alleviated to a great extent with the use of the more recent plastics. As a special precaution in guarding against future leakage currents, the computer apparatus was completely enclosed and air conditioned. With these precautions exercised there have been no leakage difficulties.

The error involved in the measurement of current and voltage of the analogue circuit is primarily that which is normal for the measuring instruments. Since the resistance of any element of the circuit is large, in the order of megohms, a microammeter with an internal resistance of approximately 100 ohms will introduce an insignificant error in addition to the normal error of the meter. Voltages of the circuit are measured by balancing a variable voltage, which can be measured with a conventional voltmeter, against the unknown voltage. Since the analogue circuit is not disturbed by this method of voltage measurement, the error introduced here is that which is within the voltmeter.

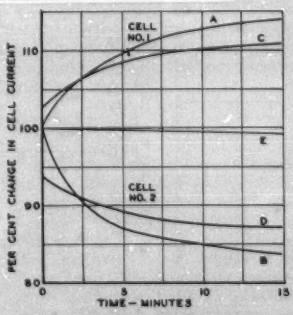

Figure 9. Current-time characteristics of photo cells

In representing the magnetic circuit of a salient pole synchronous machine by the analogue circuit shown in Figure 7, the following are likely sources of error in the solution:

1. The current-voltage characteristics of the basic element not matching exactly the flux–magnetomotive-force characteristics of the magnetic material.
2. The current-voltage characteristics not remaining constant with respect to time.
3. Too small a number of elements arbitrarily chosen to be connected in series.
4. Too small a number of series groups of elements arbitrarily chosen to be connected in parallel.
5. The assumed direction of flow of flux not the true direction, and the direction changing with increased saturation.
6. Neglecting certain parts of the magnetic circuit in setting up the analogue for simplifying purposes.

There nearly always will be some elements of the circuit of Figure 7 operating at the lower region of the current-voltage curve where this curve and the magnetization curve are not as accurately matched. Consequently, very small errors will be introduced at any point on the calculated saturation curve of the machine, but the accuracy will tend to improve as saturation increases.

The amount of fatigue or the amount the current-voltage characteristics of the cell changes with time is a function of the current flowing through the cell and also of the voltage applied. Two or more cells may be put in parallel in the basic element to decrease the amount of current flowing through any one cell and thus reduce fatigue. If high voltages in the intrinsic region are required and/or the condition of high currents through the cells exist, the error from fatigue can be held to a low value by reducing the time required for recording the data on the circuit and also by recording the highest values of voltage and current first. In calculating the

saturation curves of electric machines at the highly saturated region, a current drop of 2 per cent after ten minutes is seldom exceeded.

The number of elements in series to represent the saturation of the teeth shown in Figure 7 is typical of the number used in the saturation studies of machines. The greater the number, the more true the representation of the actual conditions, for each element represents a parallel sided section of tooth, the width being the mean width of the actual tapered tooth section.

For the circuit of Figure 7 the number of groups of series elements is equal to ten which means the equivalent machine has ten teeth per pole. If the number arbitrarily chosen is small, the principal inaccuracies resulting will be in connecting the elements representing pole head saturation in the circuit, for it may become a choice whether to connect an air gap resistance on one end of an element or the other. In the saturation studies of machines it was found that an equivalent ten teeth per pole meet the requirements for most machines.

An assumed direction of the flow of flux is required in determining the values and locations of some of the components of the analogue circuit. If the assumed direction is correct for one condition of saturation, it may be in a different direction for other conditions. The direction of the flow of flux in the pole head must be assumed in order to divide it into sections to be represented by the basic elements. The direction of flow of flux is assumed for unsaturated conditions. If the direction changes for saturated conditions, the resulting error in calculating the machine saturation curve will not be large.

In setting up the analogue circuit of an electric machine, certain parts of the actual magnetic circuit are neglected for simplifying purposes since their affects on the final results are negligible. An example is that of pole and stator end leakage.

The accuracy obtained in calculating the open circuit saturation curve on a typical machine is shown in Figure 8 by comparing the test curve A with the calculated curve B. Results of calculations of the saturation curves of rotating machines indicate an accuracy of $\pm$ 2 per cent in magnetomotive force.

Conclusion and Summary

The Electric Analogue Computer using the photo cell as a nonlinear element shows promise as a useful device for solving many types of problems involving single valued nonlinear parameters. This is deduced from the following summary of important points of the paper:

1. The photo cell as a nonlinear element has distinctive merits with respect to flexibility and simplicity.

2. The basic element consisting of the photo cell in combination with one or more resistors and electromotive forces is general in application as a nonlinear function of a dependent variable.

3. Operation of the computer has proved successful in the analyzing of magnetic circuits.

Appendix I. Method of Aging Photo Cells

It was found that most photo cells are unstable and require some light aging before they are suitable for use in the computer. When first put into operation, the cells have either a rising or falling current output characteristic with respect to time. This instability in part appears to be the result of a gas sealed within the cell as discussed in detail in reference 1. By subjecting the "gassy" cells to cyclic periods of excitation and zero excitation at the higher voltages with outputs of current of relatively high values during the excitation period, they can be made to approach stable conditions.

Curves A and B of Figure 9 show the current-time characteristics of two photo cells, numbers 1 and 2, respectively, taken when the cells were first put in operation and representing the two extreme cases of rising and falling current characteristics. Curves C and D of the same figure were taken following curves A and B after a 2-hour rest period and represent the characteristics of cells numbers 1 and 2, respectively. Curve E shows the current-time characteristics after the aging period is completed. The improvement in stability, which results from aging, is evident by the comparison of the curves.

Most cells can be stabilized after about 25 cycles; each cycle is made up of a 5-minute excitation period followed by ten minutes of zero excitation. The cells in the computer which have been aged by this method show less than 1 per cent drop in current output after a period of 20 minutes of operation when operating in the region near intrinsic saturation, and with approximately 150 per cent rated current. The cells regain the 1 per cent current output after approximately a 1-hour rest period.

The functional relationship between current and voltage of the photo cell appears to remain constant after long periods of operation. Characteristic curves have been taken after the cells have stabilized and checked again after long periods of intermittent operation. The results show that there is no apparent change.

Appendix II. Description of a Power Supply

Figure 10 shows a diagram of a power supply used in the computer. Ten separate unidirectional electromotive forces are obtained from the outputs of half-wave rectifiers supplied by ten windings on the center leg of the 3-legged core transformer. The single winding on the low-voltage side is connected to a source of a-c supply through an autotransformer, which is used to vary all of the ten unidirectional electromotive forces simultaneously.

A second group of ten separate windings on an outer leg of the transformer supplies current to the heater filaments of the rectifiers. The single winding on the low-voltage side is connected directly to the a-c source.

All windings are insulated carefully from one another to hold the current leakage to a minimum.

References

1. Law of Magnetization, S. L. Gokhale. *AIEE Transactions*, volume 45, June 1926, pages 1013–35.

2. Phototube Characteristics as Influenced by Small Amounts of Gas, A. H. Taylor. *General Electric Review* (Schenectady, N. Y.), June 1949, page 43.

3. Frolich. *Elektrotechnische Zeitschrift* (Berlin, Germany), 1886, page 164.

4. Rational and Empirical Formulas Showing the Relation Between the Magnetomotive Force (H) and the Resulting Magnetization (B), Charles E. Ronay. *AIEE Transactions*, volume 9, 1892, pages 193–222.

5. Empirical Equations for the Magnetization Curve, James P. Barton. *AIEE Transactions*, volume 52, June 1933, pages 659–66.

6. Magnetic Analysis, Raymond L. Sanford. *AIEE Transactions*, volume 49, July 1929, pages 731–36.

7. A Large-Scale General Purpose Electric Analog Computer, E. L. Harder, G. D. McCann. *AIEE Transactions*, volume 67, part I, 1949, pages 664–73.

8. Solution of the General Voltage Regulator Problem by Electrical Analogy, E. L. Harder. *AIEE Transactions*, volume 66, 1947 pages 815–26.

9. A New Device for the Solution of Transient Vibration Problems by the Method of Electrical-Mechanical Analogy, H. E. Criner, G. D. McCann, D. E. Warren. *Journal of Applied Mechanics* (New York, N. Y.), volume 12, September 1945, page 135.

10. Solving Complex Problems by Electrical Analogy, part I, G. D. McCann, H. E. Criner, *Machine Design* (Cleveland, Ohio), December 1945; part II, February 1946.

11. Magnetic Amplifier Studies on the Analog Computer, E. L. Harder, W. H. Hamilton, D. F. Aldrich, J. T. Carleton, F. H. McClure. *Proceedings*, National Electronics Conference (Chicago, Ill.), volume 5, 1949.

12. Photoelectric Wave Form Generator, David E. Sunstine. *Electronics* (New York, N. Y.) February 1949, pages 100–03.

13. Application of the California Institute of Technology Electric Analog Computer to Nonlinear Mechanics and Servo Mechanics, G. D. McCann, C. H. Wilts, B. N. Locanthi. *AIEE Transactions*, volume 68, part I, 1949, pages 652–60.

14. New Techniques on the Anacom-Electric Analog Computer, E. L. Harder, J. T. Carleton. *AIEE Transactions*, volume 69, part I, 1950, pages 547–55.

15. Photo Electricity and Its Application (book), V. K. Zworykin, E. G. Ramberg. John Wiley and Sons, Inc., New York, N. Y., 1949.

No Discussion

Information Theory Applied to System Design

W. G. TULLER
NONMEMBER AIEE

A DISCUSSION of general principles of the application of information theory to system design is followed by a specific example of its use in studying the private line air traffic control communication system.

The statistical theory of communications, developed over the past few years and often called information theory, can be of real assistance in the design of communication systems. Although very little can be obtained in system performance by the use of this theory that could not have been predicted by earlier methods, the theory provides a logical and straightforward method of evaluating a communications problem and gives a direct answer as to the effect of necessary compromises from the ideal in bandwidth, power, rate of transmission of information, and so forth. In this paper a short general discussion of the method will be followed by a practical example of a communication system that has been designed, on paper, in accordance with the method. This is the interim "private line" communication link between the airport traffic controller and the aircraft under his surveillance.

Design Principles

A preliminary statement of the method of system design is deceptively simple. One merely computes the maximum rate at which information must be transmitted in units of bits or Hartleys* per second. The available bandwidth and carrier to noise ratio are then used to determine the maximum rate at which information may be transmitted over the facilities available. If the second quantity is greater than the first, the system designer is indeed fortunate, the information may be transmitted over the transmission link, and the problem is reduced to one of inserting a controlled redundancy into the message to improve transmission clarity. If the facilities are inadequate to the task, then the designer must strive either to obtain more facilities, that is, bandwidth, power, sensitivity, or he must wring some redundancy from his message if he does not give up entirely. In either event a straightforward calculation yields an immediate answer as to the possibility of accomplishing the desired task with the available equipment and spectrum. If by any chance either transmitter power, receiver sensitivity, or transmission bandwidth are under the complete control of the system designer, then he may choose one of these to allow transmission of his information at the required rate. Usually, however, this is not the case.

The equations used to determine the information content of the set of possible messages and the information handling capacity of the system are well known[2,3] but will be repeated here for completeness.

To find the information content of the set of messages that may be transmitted, use the expression.

$$H_1' = n' \log_{10} s \tag{1}$$

Where H_1' is the rate of information output of the message source in Hartleys per second, and s is the number of possible equally likely significant values (the case where the values are not equally probable was taken up by C. E. Shannon,[1] but is of practical use only when complex coding is permissible), which the message may have at any given time, and n' is the number of times per second a value must be chosen in order not to lose information. If our message is in the form of an electrical signal, and has no redundancy, that is, its future may not be guessed with significant accuracy from a priori knowledge or from the past history of the message, we have

$$s = 1 + \frac{S}{N} \tag{2}$$

where S/N is the signal to error (noise) ratio at the input to the modulator in the generalized communication system shown in Figure 1. S/N must also be the signal to error (noise) ratio at the output of the demodulator in this system if no information is to be lost.

Said in another way, from the viewpoint of the information source, s is the number of symbols that could have been emitted at any instant of time. Of this ensemble, one will be emitted n' times per second. This relation defines n' in equation 1. In electrical terms we have

$$n' = 2f_e \tag{3}$$

where f_e is the premodulation and postdemodulation bandwidth of the system shown in Figure 1. The coder and decoder of Figure 1 may be used to remove and/or insert redundancy into the message as desired.

To determine if our facilities are adequate for the information source we use

$$H_2' = 2B \log_{10}\left(1 + \frac{C}{N}\right) \tag{4}$$

* Bit is defined as a unit of information capacity, equal to one binary decision, or the designation of one of two possible values or states of anything used to store or convey information.

Hartley is defined as a unit of information capacity, equal to one decimal decision or the designation of one of ten possible values or states of anything used to store or convey information.

Paper 50-266, recommended by the AIEE Electronics Committee and approved by the AIEE Technical Program Committee for presentation at the AIEE Fall General Meeting, Oklahoma City, Okla., October 23–27, 1950. Manuscript submitted July 27, 1950; made available for printing September 6, 1950.

W. G. TULLER is with Melpar Incorporated, Alexandria, Va.

Although the writer served on Special Committee 41 of the Radio Technical Committee for Aeronautics the material in this paper is primarily the work of a large group on this committee, too numerous to name individually. The evaluation was a group effort under the guidance of Vernon C. Weihe, and should be acknowledged as such. A complete report is given in RTCA Paper 116-49/DO-30.[1]

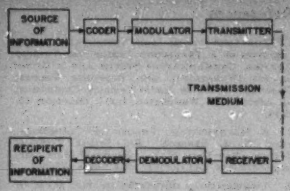

Figure 1. Generalized communications systems

Here H_2' is the information handling capacity of the transmission link, B is the bandwidth of the elements between modulator and demodulator, and C/N the carrier-to-noise ratio at the input to the demodulator.

If H_2' is greater than H_1' the system is adequate to handle the demands of the source of information. If not, as has been mentioned before, something must be done to either the information or the communication equipment.

Application of Theory to Air Traffic Control Problem

To go now to a practical example, Special Committee 41 of the Radio Technical Committee for Aeronautics had as its task an operational and technical evaluation of a "transition period air traffic control communication system," a private line between the air traffic controller and each aircraft under his control. The purpose of such a system is to provide more rapid exchange of messages between a ground station and each aircraft on an individual communication link than can be done by radio telephone. The evaluation was done by Special Committee 41 using information theory, and the techniques used in the evaluation of the ground-air link are given in the following paragraphs.

Available for this communication system is the band of audio frequencies between 5,000 and 7,000 cycles. This band lies between the voice channel and the subcarrier used in the very high frequency omnidirectional radio range (VOR) equipment. It is available on VOR, VHF (very high frequency) localizers, and VHF tower and VHF enroute communication transmitters. It also is available in the standard VHF navigation receiver. Thus, if this audio band could be used, no new radio equipment would have to be added on the aircraft or on the ground to perform the private line function. Only terminal equipment would be required. Inasmuch as the radio frequency carriers may be modulated by other subcarriers, only 15 per cent modulation is available for private line. This means the system must operate well with a minimum carrier to noise ratio.

Substituting bandwidth and minimum carrier to noise ratio in equation 4 we have

$$H_2' = (2)(2{,}000)\log(1+1) \tag{5}$$

Since C/N must be assumed a minimum of unity (actually rms carrier to noise ratio must be 8 decibels to obtain a peak carrier to noise ratio of unity) it is convenient to take H_2' in bits per second and use a logarithm to the base 2. This gives

$$H_2' = 4{,}000 \text{ bits per second} \tag{6}$$

as the capacity of the equipment. The remainder of the system design comprised an attempt to force the information source to fit this mold. By the use of visual presentation to the pilot, and automatic or key punch message selection, a predetermined group of messages may be used and one chosen and presented efficiently.

As a result of considerable work by the operational group, the messages to be presented, and their display, were chosen as shown in Figure 2. In this figure the possible messages that may appear in each position are shown in tabular form beneath the rectangle depicting the slot through which the message appears. Circles indicate buttons to be pressed by the pilot to tell the controller that he is acting on instructions (corresponding to "WILCO").

From Figure 2 it may be seen that a complete ground-to-air message comprises seven "words" and that each word has a maximum of ten possible choices or values. This sets s in equation 1 as ten. Since transmission must be in binary code to operate at minimum carrier to noise ratio, s was fixed at 16, the nearest larger power of two, or 2^4, with a resultant possibility of an increased number of messages or a safety code (one employing redundancy) should it be desired. From Figure 2 we also obtain n as seven words per unit of time in which an aircraft must be contacted.

Operationally it was determined that each of at least 15 aircraft should be contacted every 5 seconds, and that at least 60 assignable aircraft identities should be available. The aircraft identity, which makes the private line private, therefore requires two more words.

Summing up, nine words per aircraft must be transmitted in 5/15 or 1/3 second. This means a rate of 27 words per second. Each word has a content of four bits, since 16 choices are available. The information handling capacity required of the system is therefore 108 bits per second.

Comparing the required capacity of 108 bits per second with the available capacity of 4,000 bits per second, we see that ample system information handling capacity is available. Since equation 4 is based on the use of ideal filters, a conservative design would only attempt to obtain 2,000 bits per second.

Efficient Use of Excess Channel Capacity

Since the available channel capacity is so much greater than required, it was recommended that controlled redundancy be introduced in the form of a self-checking code. If a word is sent once in the marks and once in the spaces of a code group, it is immediately apparent if an error has been made. This safety coding requires a capacity of 162 bits per second. The additional capacity still available may be used to obtain improved operation at low carrier to noise ratios or to contact more aircraft per second. In practice, some capacity also must be used up in this particular system to allow for transmission lag through the link and to allow for a "screen lift" signal, not previously mentioned, that assures the pilot his instructions have been checked on the ground, after retransmission from plane to ground, and found accurate. Inasmuch as the private line is to be operated in conjunction with the phase and inter-

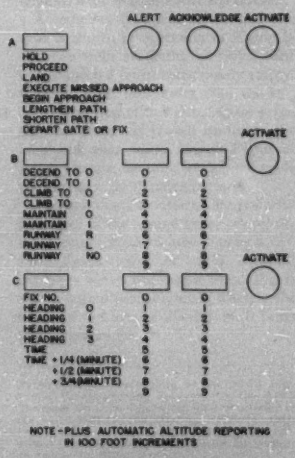

Figure 2. Information to be presented by cockpit display

ference sensitive VOR circuits, it was thought that the remaining additional capacity would best be used in protecting these circuits and in obtaining improved performance at low-signal levels.

Results of Analysis

The preliminary analysis given above ensured that a conservative system design could be obtained, and that the necessary equipment design would be a relatively straight-forward problem. It was then possible to proceed with confidence to a consideration of specific equipment.

The example given illustrates certain basic principles worthy of special note. These are the calculation of system information handling capacity and information source output, the use of a coding scheme exactly fitted to the limited information to be transmitted, and controlled redundancy to obtain improved system reliability.

References

1. The Operational and Technical Characteristics of a Transition Period Air Traffic Control Communication System and a Study of Its Operational and Economic Values. *Paper 116-49/DO-30*, Radio Technical Commission for Aeronautics (Washington, D.C.), December 15, 1949.

2. A Mathematical Theory of Communication, C. E. Shannon. *Bell System Technical Journal* (New York, N. Y.), volume 27, July 1948, pages 379–424, and October 1948, pages 623–657.

3. Theoretical Limitations on the Rate of Transmission of Information, W. G. Tuller. *Proceedings*, Institute of Radio Engineers (New York, N. Y.), volume 37, May 1949, pages 468–78.

No Discussion

The Further Development of Fluid Mappers

A. D. MOORE
FELLOW AIEE

Synopsis: Fluid mappers can be built to simulate, and lead to the solution of a great many field situations in electrostatics, electromagnetics, eddy currents, heat conduction, and other analogous cases. Distributed sources, as well as ordinary sources, may be represented. Fluid mapper techniques are well enough developed so that many fields now can be simulated with sufficient accuracy, by applying tested routines to building and operating the mappers. But like all other devices, fluid mappers have their own special problems, troubles, and limitations. Also, they will be called upon to go beyond the limits within which the writer's work has been carried out. Further invention, research, and development of additional techniques are called for. By pointing out the problems and limitations, the paper does two things. First, those who are building fluid mappers for teaching, research, or application, are assisted in understanding the limitations and in minimizing inherent effects tending to reduce accuracy. Second, the numerous problems and needs described should invite interested workers, graduate students especially, to tackle the tasks that will lead to more and bettered techniques, a broadening of the range of work to which mappers may be applied, and an increase in the knowledge required for designing fluid mappers for particular jobs. Two phenomena occurring within certain distributed sources are described and named. It can at least be said that both are relatively unknown; and one of them may be new.

FLUID mappers may be described as fluid flow devices for visually simulating electrostatic, electromagnetic, heat conduction, and other analogous situations. This description is incomplete, but it will serve in an introductory way. The writer has described fluid mappers in detail in his first paper[1] on the subject, and it will be called the "first paper" herein.

Before Hele-Shaw did his work a half century ago, it was recognized that an ideal fluid (nonviscous) flowing in a thin flow space with suitable boundaries could theoretically simulate electrostatic and other fields. At any one location, the ideal fluid's velocities, taken across the flow space, would be constant. Whereas, with a real (viscous) fluid flowing in streamline or laminar fashion, the velocity at any one location would have a parabolic distribution. Hele-Shaw was the pioneer who showed, by his remarkable work, that a viscous fluid, with its parabolic velocity distribution across the space, would also yield an analogy. Hele-Shaw's methods were not carried on. His techniques, though admirably accurate, were costly and inflexible.

In fluid mappers developed by the writer, the upper plate (a piece of plate glass) is retained. But Hele-Shaw's lower plate is replaced by a slab made of artificial stone (dental stone), cast on plate glass to give it a flat surface. Thus great flexibility as to sources and sinks and as to slab boundary shape is attained, and with a medium offering cheapness and high accuracy. Also, the writer's invention of the sandbed as a distributed source or sink carries the fluid mapper into the extremely complicated realm of distributed source phenomena.

Dental stone powder costs only 15 to 20 cents a pound. Thin little slabs a few inches across take about a pound; larger slabs, one foot square and 5/8-inch thick, may take around four pounds. By spending a few dollars for some plate glass; a tray; some rubber tubing; two or three tanks; some brass pieces for molds, cores and barriers; some potassium permanganate; some dental stone powder; and a few other knickknacks–for a small expenditure, anyone can set up a fluid mapper laboratory for demonstrating a great variety of cases. With a further small investment in screen material and shotted metal, sandbed types of mappers become available.

Fluid mappers as now developed fall into three main types, all being represented in Figures 1 and 2.

The first type, shown at the right in both figures, is a slab without a sandbed. The sources amount to one or more simple wells of any shape or size. The bottom-up view, Figure 1, shows the plaster feet added to the plaster slab, the celluloid well bottom plastered on, and the connector tubes plastered into the well bottom.

The second type, at the left in Figures 1 and 2, is to operate as a slab with a sandbed. A suitable screen is mounted horizontally across the well, to support a sandbed above it, and having a plenum chamber below it. The plenum chamber has an aluminum bottom (it could just as well be celluloid).

The third type, at the top in both figures, is the isolated sandbed, a sandbed without a slab. Between the bottom and the screen is the plenum chamber. The sandbed is to be built above the screen.

A complete fluid mapper of the first type is shown in operation in Figure 3. The two wells are acting as sinks, their two connected tanks being nearly empty, with the right tank lower than the left. In the top view of this slab, Figure 4, the singular point has moved nearer to the large sink than where it is in Figure 3: this is because the tank levels were made the same, for the Figure 4 pattern.

Figure 5 shows a pattern obtained with a mapper of the second type. Here, the entire round sandbed area acts as a uniform distributed sink. The sandbed margin is not an isopressure line. This is very different from Figure 4, wherein the edge of a well acts as a boundary, it being an isopressure line.

Paper 50-267, recommended by the AIEE Electronics Committee and approved by the AIEE Technical Program Committee for presentation at the AIEE Fall General Meeting, Oklahoma City, Okla., October 23–27, 1950. Manuscript submitted July 20, 1950; made available for printing September 15, 1950.

A. D. Moore is Professor of Electrical Engineering, University of Michigan, Ann Arbor, Mich.

Figure 1 (left). The lower members of the three types of fluid mappers, shown bottom up. The upper member, the plate, is always plate glass

Figure 3 (right). A complete fluid mapper of the first type, in operation

The third type, an isolated sandbed, occurs in Figure 6. Here, the boundary of the sandbed is an isopressure line, it being open to the tray water.

For those who have not seen the first paper,[1] the foregoing will serve to describe the general nature of fluid mappers; and modifications not mentioned in the foregoing will receive attention further on. But space is not available here to set forth the numerous techniques needed for making and operating mappers in routine fashion. Many of these are covered in the first paper. Since that paper has appeared, the writer has continued intensive development work; many of the earlier techniques have been improved, some have been replaced, and a number of new techniques have been perfected. These will be included in a manual on fluid mappers and field mapping, now in preparation. And again, very little can be said here about the various analogous field phenomena that fluid mappers can be made to simulate. For this, the reader can consult the first paper; also the second paper[2] on soap film and sandbed techniques; and the third paper[3] in which fluid mappers are used to verify certain electromagnetic propositions.

Purpose of the Paper

The techniques already developed by the writer will serve for making and operating fluid mappers for portraying a great variety of the more ordinary situations. But looking ahead, the versatility of these devices indicates their wide adoption for a large range of diversified work. It appears inevitable that mappers will be built that will go beyond the limits within which the writer has worked. Others are adopting mappers, and others should join in contributing ideas.

The inherent errors, defects, and limitations of fluid mappers should be described; and where further invention, research, and development are needed on fluid mappers, the problems should be stated so that work can be started in proper directions. Plenty remains to be done. This paper will address itself to some of these problems.

Slab Permeability

Slabs made of dental stone are very slightly permeable. Since pressure differences must occur within the flow space, there is always a slight fluid leakage through the slab. The effect of this leakage would appear to be completely negligible whenever the slab has an open edge, with the flow space terminating directly in the tray water. In closed-edge mappers having an all-around barrier confining the flow to the slab face, it is possible to build up a considerable positive or negative pressure in the flow space, by having the general levels of the tanks much above or much below the tray. With a large, thin slab, it is barely possible that slab permeability might have to be guarded against, or taken into account. Slab permeability should be measured, and operating rules (if found to be needed) should be provided to insure operation within safe limits.

Slab Erosion

This is not mechanical erosion. It is disappearance of slab face material, due to its going into solution. Calcium sulphate, the main ingredient in dental stone, is slightly soluble in cold water, roughly in ratio of 2:1000. The rate of slab erosion in a fluid mapper has not been measured. The writer's experience indicates that erosion is irregular: the regions of higher flow space velocities erode fastest, which is to be expected.

For accurate fluid mapper work with plaster slabs, erosion trouble can be avoided by using a fresh-cast (or resurfaced) slab before erosion becomes serious. The thinner the flow space used, the more will flow space accuracy be altered by a given amount of erosion. The spacing-cubed law must be kept in mind here. As an illustration of the law: if a mapper is operated, first with a given flow space, then with a flow space of twice as much, the rate of fluid flow for the same pressure drop will be increased eight times.

Figure 2 (left). The lower members of the three types of fluid mappers

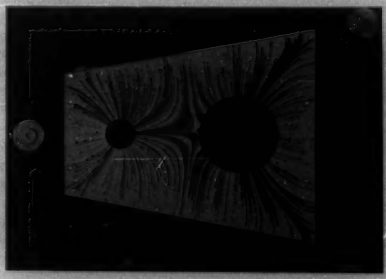

Figure 4 (right). Direct view of flow pattern. To produce this pattern, the tank levels were made equal

If erosion rates become known, we would know more as to how long a new slab could be operated without fear of it having become inaccurate.

A different attack is to stop erosion. There are at least three possibilities to look into. First, let the water used be made a saturated solution of calcium sulphate. Second, change the slab's surface from calcium sulphate to calcium stearate, which is nearly insoluble. Treating the slab with stearic acid might do it; or an application of any soft soap has been suggested. Third, the slab surface might be treated by painting it with a waterproofing material.

The writer has tried only the third expedient, and that in a limited way only. A synthetic rubber emulsion paint, Spred Satin, was used. If applied to a dry slab, it is a failure. When the slab is immersed, the water enters all surfaces except the painted surface; pushes the entrapped air out through pores in the paint; and, with build-up of capillary pressure, soon blisters the paint.

Spred Satin can be put on a wet slab, and will remain intact if the slab is kept wet. It should stop erosion. However, it takes a permanent pattern record, as is brought out later on. If a slab is to be used for a series of different operations, a confusion of recorded patterns would soon appear on the painted surface.

A fourth possibility might be worth a trial: dry the slab, then metallize the surface by metal spraying.

Slab Resurfacing

The writer has often reclaimed eroded slabs by a simple resurfacing technique. A large sheet of waterproof silicon carbide cloth, grit number 100 (Minnesota Mining and Manufacturing Company) is placed, face up, on plate glass. A little water is put on it. The wet slab, placed face down, is skated around with a random motion. When done, the loose plaster is washed off, excess water is wiped off, and a piece of plate glass is pressed against the slab face for testing. Where good contact is made here and there, a water film appears. A good distribution of such water films appears to indicate a high degree of flatness, and numerous operations of reclaimed slabs seem to indicate very good accuracy. However, all this should be looked into, and checked.

Slab Materials

Plaster, so far, is the prime material for slab-making; and the writer's guess is that it will remain so for most purposes. Patching plaster from the hardware store was used in the writer's early slabs. Plaster of Paris would do. These products, along with dental stone (artificial stone) are all basically calcined gypsum, calcium sulphate with two molecules of water. The writer usually calls all of these materials "plaster", even though the dental product is called "stone." When water is mixed with the powder, crystallization proceeds. Of all these, dental stone is the most highly developed, being hard, strong, smooth. Duroc, the latest dental stone powder, has a setting expansion of only one-half of one tenth of one per cent. With all of the numerous things that can be done in the casting process to alter shapes, plus the high workability of dental stone as to drilling or machining, plaster is most attractive. However, the tendency to erode may eliminate the plaster slab for some mappers; and then there is the tendency to stain.

Plastics, especially thermoplastics, should be given experimental attention. Plastics are priced high; but if a suitable thermoplastic that could be remolded many times could be found, that objection would be eliminated.

Metal slabs, such as aluminum, cast and machined, are attractive for purposes of high and continued accuracy. When a slab must be machined down to give a varying flow space (as mentioned later) it may be unwise to put machining time into a plaster slab which may erode seriously before the operation is finally completed.

Some metal slab techniques deserve attention.

Very Large Slabs

The writer's largest slabs are one foot square. These slabs are feasible in every respect, and are turned out and operated in routine fashion. The same routines ought to handle slabs up to 18 inches square, and perhaps 7/8-inch thick. But there is ample reason to think that still larger slabs will sometimes be needed. With increase in size, a point will be reached where the 1/4-inch plate glass on which a slab is cast may become distorted, unless it rests on a flat surface, or on supports that are in a plane and are at frequent enough intervals.

Next, how thick must a very large slab be, to be self-supporting in the tray, on its own feet, without distortion?

Another prospect is to cast slab sections, in rather accurate square or rectangular fence molds; then fit these sections together, edge to edge. This should be entirely feasible. It means placing accurate feet on the sections, so that the thickness from foot plane to slab surface is uniform. In the tray, a bottom piece of plate glass is placed first. The single slabs of Figures 1 and 2 are so prepared, and are so operated (with the off-slab spacer technique) in Figures 3, 4, and 5. Here again, with several sections making up a very large slab, problems of distortion of the bottom plate and the top plate would begin to enter. This problem calls for investigation.

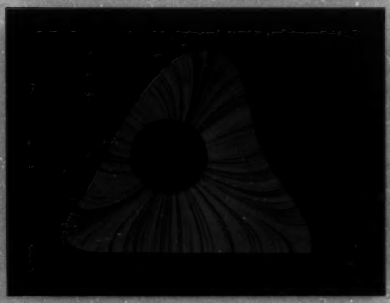

Figure 5 (left). A mapper of the second type, a sandbed within a slab. The sandbed here acts as a uniformly distributed sink. Note the kernel

Figure 6 (right). An isolated sandbed: a fluid mapper of the third type. Note the kernel and the ridgeline

Figure 7 (left). A record slab

Figure 8 (right). With velocities high to get sharp pattern lines, inertia effects moved the break-away point nearly to the wing tip

Record Slabs

When a slab is sprinkled with potassium permanganate crystals to make the flow pattern visible, it is a "floor pattern." The colored streamlines are on or close to the floor of the flow, which is the slab surface. Slab staining follows, whereby a fairly good temporary pattern record appears on the slab face. Pink at first, and fairly definite, it soon diffuses when the slab is removed. Also, it changes to brown as manganese dioxide replaces the permanganate.

Excellent permanent record slabs are made by one of the writer's more recent techniques. Spred Satin 3400 White (The Glidden Company, Cleveland, Ohio) a synthetic rubber emulsion, is painted onto the wet slab face, after excess surface water is mopped off. A few minutes after painting, the paint is set well enough to permit operation. Whereupon, the permanganate of the colored flow lines chemically unites with the paint, and a record slab is produced. The record slab, Figure 7, was made on December 9, 1949. At this writing, just six months later, the record is as clear as ever.

The problem here is to change the painting job from an art to a science. Brush painting is somewhat tricky, and will at times cause enough irregularity of paint thickness, to affect the flow pattern by altering the flow spacing. For example, spray painting of Spred Satin has not been tried. It might be the answer.

Record slabs are very beautiful as well as useful. As to utility, they make fine classroom teaching aids. Also, making a record slab can often eliminate photographic steps, for the record slab pattern can be traced directly.

Fluids

Air, being free, perhaps deserves first mention in discussing fluids for fluid mappers. The writer has used air. Smoke streams are made by dotting the plate with hydrochloric acid, and loading the air with ammonia fumes. Results are not good. It is impossible to keep velocities down to within the streamline range, and not encounter high diffusion of the smoke streamers.

Tap water holds first place for most demonstration work with mappers, and will serve for accurate work when the conditions are right. In the quantities needed, water costs nothing; and when colored, is discarded. But flow space velocities must be made high enough to keep dye diffusion down so that a good pattern is achieved. In certain cases, this can mean that in going around corners or through narrow channels, local velocities can be great enough to bring in inertia effect, which spoils the laminar (streamline) flow in that region.

To point up the problem, refer to Figures 8 and 9 for flow around a Clark-Y airfoil section. In Figure 8, there is a good pattern with sharp lines; but the break-away point is very close to the wing tip. In Figure 9, velocities have been reduced; inertia effect has been greatly reduced; the break-away point has moved forward from the tip, and now is at, or close to, the singular point that would occur in a corresponding field of, say, heat conduction devoid of inertia. Thus, if we are solving for heat conduction or similar fields, we want the Figure 9 laminar flow; but it is bought at the expense of sharpness of line—the dye lines have more time for lateral diffusion.

A way out of the difficulty is to use a high-viscosity fluid such as glycerol, which Hele-Shaw used to get his beautiful lines. However, glycerol, (glycerine) is too costly for most fluid mapper work. Instead, Methocel (a Dow Chemical Company product) in water can be used to make a cheap high-viscosity fluid. Stanley Seltzer was the first to apply Methocel to fluid mapper work, when using mappers on an Air Forces heat transfer project in the Engineering Research Institute at the University of Michigan in 1950.

Methocel, a cellulose ether, is a colloid and is nontoxic. Of the several viscosity types available, the writer has used Methocel 1500 centipoises. Two per cent by weight of this, in water, gives a viscosity about 1,500 times that of water. It is then diluted to get any desired lower viscosity. (The company will send a booklet on Methocel.)

To see clearly why such a material as Methocel will get results, think of operating any such case as Figure 8, with water going fast enough to get a good pattern, but with undesired inertia effect at the corner. Then replace the water with Methocel solution having, say, four times the viscosity of water. Operate with the same head. Then the over-all flow rate will be one-fourth as much, thereby greatly reducing inertia effect. At first thought, it seems that we are as bad off as ever, for now a dye line has four times as much time in which to diffuse and become broad. But next, diffusion rate is inversely related to viscosity; and in theory, the pattern would have the same sharpness of line as when water was used. Anyone doing fluid mapper work should be fully aware of the possibilities of Methocel.

Investigation with a variety of mappers should be carried out, varying the shapes, the flow space, and the fluid viscosity. From this, rules might be written by which, in a given mapper, the viscosity needed to eliminate inertia effect could be known in advance.

Pattern Levels

Dye added to water increases the density, hence, dye lines tend to sink. When crystals are sprinkled on the slab

surface, the pattern starts out from the crystals at levels near the floor of the flow, and remains at such levels. This gives what we will call a floor pattern. Floor velocities being low, floor pattern lines move slowly, and tend to become broad due to lateral diffusion.

Dye crystals glued to the plate with Cutex form dye lines at high levels near the flow ceiling. They thus start out to form a ceiling pattern. Ceiling velocities being low, these lines tend to sink. But in sinking slightly, they get into higher-velocity levels in the flow space, and may be carried along as thin, sharp lines. Ceiling patterns are good patterns.

Dyes differ. The writer has tested methylene blue and permanganate crystals side by side, glued to the plate. In one straight-flow test, the permanganate line was heavy enough to sink to the floor within a quarter inch of travel; whereas, the blue lines remained as a sharp ceiling pattern for 8 inches, and would have gone much farther.

Methylene blue, made years ago in crystal form, is apparently quite unobtainable in that form today. Other dye crystals should be investigated with the hope of finding something better than permanganate for forming ceiling patterns.

Ideally, the middle pattern, half-way down across the flow space, would be the best from the standpoint of sharpness of line; for here, in the parabolic velocity distribution, velocities are greatest. We have now, no simple techniques for forming middle patterns.

Dyes and Dye Effects

Potassium permanganate is the best all-around material for most demonstrations, and for many applications of fluid mappers requiring good accuracy. It is cheap, and safe to work with. Its staining effect on slabs is easily cleared up,[1] and sodium bisulphite solution removes stains from the hands.

Methylene blue gives sharper lines, and the crystals last much longer. The hunt for a supply of these crystals must go on. It is safe, but it does permanently stain slabs, and the stain on the hands may last for some days. Still other dyes should be investigated for their good and bad properties.

One effect of the dye, still uninvestigated, is the effect on viscosity. No visual evidence has turned up, tending to show that this effect is ever serious. Nevertheless, it should receive attention.

Advancing Dye Front

Let a fluid mapper be operated without crystals, the flow being invisible. If permanganate dust is stirred into a tank feeding a source, the precolored water entering the flow space from the source will spread out over the slab with an advancing dye front. In the case of a long narrow sandbed in the middle of a large slab, the front has an approximately elliptical boundary. It is a very striking effect. No formal interpretation of this effect has yet been made. The effect undoubtedly has a meaning, possibly in terms of electromagnetic radiation. Someone should look into this effect.

Flow and Potential Control

When two or more tanks are used, connected to two or more wells, the problem of control of fluid flow or of potential (pressure) arises. The fluid mapper pattern must be made to conform to the conditions of the problem being solved. In many symmetrical cases, tank elevations need merely be adjusted until pattern symmetry prevails; but in more general cases, this expedient will not serve.

In many electromagnetic cases, for example, the rates of flow for the several wells must be proportioned to the corresponding currents which are setting up the magnetic field. Approximate determination of such fluid sources and sinks can be effected by making the long rubber tube connectors from tanks to wells equal in length and nominally equal in inside diameter; fixing tank levels to give the proper heads above or below tray water level will then fix the flows as desired. But rubber tubing is undependable for accurate work. Techniques should be worked out whereby the main resistance from tank to well mouth resides in a calibrated flow tube unit, having enough flow resistance so that all resistances outside it (including resistance offered in the flow space) can be largely or wholly ignored.

The other type of problem occurs when, say, the electrostatic field is being simulated, and isopressure lines bounding the several well edges must correspond to electrical potentials of charged bodies. The complete equipment that would enable the right setup to be made by a direct, or nearly direct approach, would seem to call for having a series of manometer tubes, with each tube connected to its well: tank levels could then be adjusted until the heads indicated at the manometer tubes would be as desired. Such additions are not attractive; for, unless thin and very accurate flow spaces are used (or a high viscosity fluid is adopted) the heads would be quite small. An alternative is to do without the manometer tubes, and approach the achievement of the desired relative pressures indirectly, by steps. This would be feasible if only two wells, connected to their own tanks, are present. Fixing one tank level throughout, set the second tank level arbitrarily, and get a pattern; then set at a new level, get another pattern; then repeat once more. Analyze each pattern locally, just far enough to deter-

Figure 9 (left). With lowered velocities, the inertia effects drop out and laminar flow prevails. Lines are more diffuse

Figure 10 (right). A semiobstacle case with flow spacings 2:1, representing permeability or conductivity ratio of 8:1

mine relative pressures of each. Plot relative pressure against tank level, to find the level needed to produce the pressure required.

In another form, a flow control problem occurs, as to flow equality, when a number of nominally equal sources are fed from a common plenum chamber. If the sources are small round holes, for example, what variations in diameter and depth are permissible?

Edge Effects at Isopressure Boundaries

In most fluid mapper work, the edge or boundary of a well, or the open edge of the slab, may be taken as the location of a boundary isopressure line. But in strict accuracy, pressure drop is not entirely confined to the flow space: a slight additional drop occurs where the space flow opens out into tray water or well water. The limiting isopressure line should therefore be taken as slightly beyond the flow space limit, at such locations. When is it necessary to do this and under what conditions, and where, exactly, should it be located, in terms of flow space thickness?

The problem is accentuated when a well must be used that is small in diameter, compared to the flow space thickness. In the general area over such a source or sink, there will be a large vertical component of flow. Where, in a given case, is the effective center of such a well, what is the well's effective diameter, and will these matters depend on whether a floor pattern or a ceiling pattern is used?

Edge Effect Along Barriers and Obstacles

To repeat, an ideal (nonviscous) fluid, having perfect slip at the fluid-solid interface, would give perfect simulations. A real, or viscous fluid, having no slip at floor and ceiling, and with its parabolic velocity distribution, also gives perfect simulations, as Hele-Shaw showed. However, when the flow is bound by barriers or obstacles, the perfection is marred by the fact that there is also no slip at these surfaces. Hele-Shaw used very thin flow spaces, and he does not appear to have discussed the edge effect that barriers and obstacles have on the flow pattern.

In the first paper[1] it is suggested that when necessary, this edge effect be allowed for approximately by cutting back the edges by one-fourth of the flow spacing. This is based on a velocity distribution analysis obtained by use of a sandbed mapper. This rule must be taken as an approximation, and as a means of getting a general pattern that is reasonably accurate. It cannot be taken as a cure for the difficulty, as far as flow very near to the edge itself is concerned. This edge effect needs thorough study. It may help to see into the problem if we note that, close to an edge, the flow patterns will be different at different levels.

Using an edge cutback, and a plain, or vertical edge on barrier or obstacle, would a floor pattern, or a ceiling pattern, or a middle pattern give the most accurate representation?

And then, there is another possibility. A study might show that if the edge is rounded with some curve, concave or convex to the flow, this, with a floor, or ceiling, or middle pattern, might give the best representation.

Stability

The necessity for using a thin flow space has been repeatedly emphasized. One reason, already covered, is to minimize edge effects. Another is to secure stability. With too great a spacing, the fluid wanders: upper-level patterns fail to coincide with lower-level patterns, when viewed from above. At this writing, no one knows the upper limit of the flow space thickness, for a given case, in terms of stability: we can only try it and see.

If we classify swirl effect[1] under stability, we can point to entry velocities from a connecting tube being so high in a large well, that the well edge is not an isopressure line: the flow pattern in the area near the well is spoiled. This can often be cured by crowding gauze into the lower half of the well.[1] The writer proposes trying a possibly more convenient cure: to drop fine, flexible metal chain into the well to cover the inlet tube and kill off unwanted inertia effect. A very small well acting as a source offers a stiffer problem: the smaller the source, the higher are the velocities near it, and the greater the tendency to ruin the desired streamline pattern. It is suggested that rounding the edge of the mouth of such a source might be beneficial.

The previous discussion of inertia effects, and their elimination by going to a fluid of higher viscosity, might just as well have been brought in here under the heading of stability.

Disturbing Influences

A dye crystal disturbs the flow. The flow may still be laminar around the crystal, but the crystal is a disturbing influence nonetheless. Can sprinkling of crystals ever be heavy enough to affect the general pattern seriously? We do not know.

A similar problem arises when spacers are laid on the slab to support the plate. How far does their disturbing influence reach, when a given degree of accuracy is desired?

A quite different kind of disturbing influence comes in if slabs of finite size must be used, when an infinite slab is in theory called for. Depending on the problem, the slab edge may be open, or it may be closed by a barrier, or it may be partly the one and partly the other. How close in can slab boundaries be brought, without unduly disturbing the central phenomena? This is a serious problem, and it needs attention.

Barriers

Barriers may be loose, or fixed. The loose barrier is laid on the slab, in location; and the plate is placed on it with care, so as not to shift it out of place.

The rubber barrier, cut from rubber sheet, is a very attractive loose barrier, in that complicated shapes are easily cut out. It should continue to receive consideration, even though the faults are serious. Rubber, or rubber-like sheet, is strictly unobtainable commercially, in a uniform thickness. Thus, the uniformity of flow space yielded by using the barrier as a spacer is somewhat untrustworthy, and must be checked for accurate work. Next, and especially in closed-edge cases (a complete barrier) flow space pressures are enough to cause very serious barrier leakage, unless plenty of *DC4* silicone grease is used for sealing.

Several-piece brass barriers, made from rolled brass strip and flattened by hand, are very convenient loose barriers for making up flow space areas of rectangular shapes, when an edge of the slab is open to tray water. Such an open edge insures low pressures across the barrier and leakage is often negligible even without sealant. The writer's experience has been confined to strips 1/16-inch thick. Such barriers are seen in Figures 8 and 9. Experience should be gained with 1/32-inch thickness, or even thinner, to learn about precautions needed, accuracy secured, and so on.

To insure accuracy and no leakage, even with large pressure heads on a complete barrier case, the writer has developed the fixed barrier. The slab is cast flat, as usual, but is made an inch larger all around, than the flow space area

needed. Thin plaster is laid down on the inch-wide barrier space. Spacers are laid on the flow space area. A piece of plate glass is then put down, with shifting movements, to squeeze the barrier plaster down to where the plate rests on the spacers. One must learn how to lay the plaster so that it squeezes in over the flow area somewhat. If the first attempt is a failure, simply wash off the added plaster and start right over again. As soon as possible, the plate is removed, and the trespassing plaster is trimmed back by narrow cuts, to the proper flow area border. This is done while the plaster is still soft. A little silicone sealant brushed onto the plate where it will rest on the barrier prevents all leakage. If positive pressure is put on the flow space, the plate may have to be weighted. With negative pressure (tank levels below tray level) a self-sealing job is secured. All this needs further experimentation, to make sure the process is invariably reliable as to spacing accuracy. Also, it is conceivable that careless spreading of sealant might have an effect on the spacing; and this should be investigated. In Figure 10, the slab has a fixed plaster barrier on three of its four edges.

Depressions

To simulate two media having differing dielectric constants, differing thermal conductivities, and so forth, a depression in the slab may be needed. One way to make a depression is to cast the slab flat; make it, with its feet, to accurate thickness; put it on the milling machine; and end-mill the depression into the slab face. Another way, suggested here but not yet tried, is to sweep it in: core a well in the slab when casting it, of the shape desired for the depression. With the slab face up, fill the well with plaster mix; then sweep the plaster as it sets with a sweeping tool, the blade of which extends down into the well to the right depth, and the extensions of which slide on the slab face. Any such technique has to be proved in before it can be trusted.

Metal slabs would be milled in any case; and depressions are then merely an extension of the milling job.

Semiobstacles

The airfoil section in Figures 8 and 9 is a complete obstacle, which we may simply call an obstacle: all flow goes around it. When a semiobstacle is present, Figure 10, some flow goes over or under it, depending on whether it is placed on the floor or ceiling. The effect is the inverse of that obtained by using a depression; but again, the two different flow spacings are used to represent two media.

Simple, reliable, and accurate techniques for making semiobstacles are much needed. Most of the ideas that will occur to one will be rejected. For example, it is a waste of time to cut a semiobstacle from rubber sheet, and lay it on the slab since it will not be flat; likewise for metal pieces, unless the area is quite small. Moreover, if an on-the-slab semiobstacle is reliably developed, then a ceiling pattern must be used: dye lines forming a floor pattern will be in that part of the flow that goes around, rather than over, the semiobstacle.

A floor pattern is used in Figure 10, in which the semiobstacle of celluloid is attached to the plate with acetone. Here, the two flow-spacings are 1:2, thus giving thermal conductivity ratios (for example) of 1:8. A larger view is shown in Figure 11. The celluloid attached to the plate is of one thickness. Spacers, made of two thicknesses of celluloid, were used in forming the fixed plaster barrier, thus achieving the 1:2 spacings mentioned.

These are simple techniques, but one of them is unreliable. The celluloid semiobstacle thus cemented to the plate might be quite uniform in thickness (after cementing) in one case, but not in the next. Let us hope that someone will work out something like this: dust the plate with a very thin coating of a thermoplastic in powder form; lay down the transparent semiobstacle; press it, with moderate heat; and get a waterproof bond of good transparency and negligible thickness.

Change of Flow Space More Generally Considered

The depression or the semiobstacle will often occur singly, and often in a small area surrounded by a much larger area of flow. Techniques suitable for making up such mappers may be too troublesome to apply to the more general case, in which there might be two (or more) spacings used, each occupying a considerable fraction of the area. For example, think of the magnetic problem offered by a motor pole piece, the air in gap and slots, and the teeth and core of the armature. The writer has made up a slab for such a case by greasing pieces cut from white 3 by 5 cards, with silicone *DC4* grease; sticking the pieces to the plate with the grease itself; laminating the cards to desired numbers of layers; casting the slab onto the plate thus built up; slipping the slab off when plaster is set; and then removing the card pieces. The slipping job is slow, and calls for use of a good deal of force, the grease being quite stiff. Results are crude. Such a slab is only a demonstrator rather than an accurate simulator, since uniform flow spaces are not to be achieved so easily.

Another way to alter the face of a flat-cast slab is, of course, to mill it down. Still another way is to add plaster to it in stages, using the technique described before for making fixed barriers.

It is to be hoped that when more workers apply their thinking to these problems, simple and accurate techniques for making any desired shapes of different flow spacings will be forthcoming.

Axial Symmetry Cases

A 3-dimensional field having an axis of symmetry may be said, in brief, to have axial symmetry. As shown in the first paper, some of these cases can be solved by fluid mappers. The type of mapper to be built depends on which of the two orthogonal systems is to be represented by the fluid flow. In the cross-axis type, where fluid crosses the axis, the flow spacing must be varied inversely with the cube root of the radius from the axis; in the pro-axis type, it must vary directly with the cube root of the radius.

In the writer's work so far, he has cast the slabs flat; then end-milled by steps or

Figure 11. A closer view of the semiobstacle pattern

Figure 12. Shotted metal samples. Left to right: tin, bronze, copper, nickel. Tin and bronze not suitable for sandbeds because of angularity

passes; then smoothed out the steps by hand-scraping the slab.

Two other possibilities should be given attention. First, if the steps or terraces left by end-milling are narrow enough, the flow space might be left terraced; and hand-scraping would drop out. How narrow should the steps be? Second, it is inviting to think of making metal molds, accurately finished, one of each type; and then casting the slabs on the curved mold surface. That part of it is simple enough. The difficulty comes in devising techniques for accurately adding barriers, wells, sandbeds, depressions, semi-obstacles, and so on. Here again, we need more ideas from interested and ingenious workers.

Quasi-3-Dimensional Cases

The preceding section dealt with axially symmetric three-dimensionals. The discussion prior to that can all be taken as bearing on 2-dimensional cases. We now come to cases that are neither of these. For example, think of current flowing in a reasonably flat metal sheet having constant resistivity, but with the sheet varying in thickness; or, think of oil flowing through a permeable underground bed, the permeability being uniform but the bed varying in thickness. In either case, the third dimension comes in. However, in both cases, it does not "get out of bounds": it is limited rather than unlimited. Fluid mappers, built to take the spacing-cubed law into account, can simulate such cases. We here call them quasi-3-dimensional cases.

If the thickness is smoothly varying, then a smoothly-varying flow space is called for. However, it would seem that if contour lines were laid out on a flat-cast slab (or metal slab) so that the slab could be milled down to terraced form in narrow enough steps and left that way, the uncertainties of hand-scraping could be eliminated.

Of course, such mappers would also apply to cases where the thickness of the actual case is uniform, but the property (such as resistivity, permeability, and so forth) varies; and further, they also could apply where both sorts of variations come in.

Sandbed Materials

The material used in the writer's first sandbeds was Standard Ottawa sand. It was so troublesome that it had to be given up. Glass beads must be mentioned here, tiny beads now available, and much used in Scotchlite. They deserve mention because others frequently suggest their use to the writer. But like sand, their specific gravity is such that a very slight water movement would serve to wash them out of place, when building the bed or when placing the plate.

Shotted metal was adopted to get away from the above difficulty. Plenty of Aerosol OT must be used as a wetting agent, to keep the metal granules from causing trouble by floating on the tray water. The metal granules should be heavy, round, bright, stable, and of uniform size. The ideal shotted metal for sandbeds has not yet been found.

We are talking here of loose sandbeds, each made up as needed. In the writer's opinion, the fixed sandbed of permanent type is just as unattractive, for practical reasons, as when the first paper was written.

Shotted Metal Sandbed Problems

Samples of four kinds of metal granules are shown in Figure 12. Tin, at the left, is very angular, and could not be trusted to pack uniformly. The bronze shot, next in line, is also too angular to be suitable. Third comes copper; and fourth, at the right, is nickel.

The nickel shot, being very round, smooth, and highly uniform, is almost self-packing. Under water, it flows into place with very little urging. Although it is darker than freshly cleaned copper, it is lighter than copper after the permanganate has had a chance to oxidize the copper. Nickel is much the best material yet found, and it is regrettable that it is not commercially available.

Shotted copper is none too round; not very smooth; lacks size uniformity; and has quite a few nonspheroidal particles. This at once raises the question of segregation. The threat of segregation should be avoidable by careful sifting to get size uniformity. If this is not done, very serious nonuniformity of the bed might at times occur because of segregation. Someone should look into the segregation problem, both to find the conditions of handling that may bring it on, and also those that will eliminate it. Along with this investigation, it would be desirable if a universal test for sandbed uniformity could be devised.

Making a good sandbed inherently brings in the packing problem. One phase of it pertains to arching that may occur next to the sandbed vertical walls, and in corners. This refers to the formation of large voids. Angular shot would be especially bad in this respect.

With reasonably uniform, round, smooth shot, major voids would not occur. But a localized packing problem remains, as an edge effect, where granules make contact with the sandbed wall. There are two possibilities. First, packing against the wall may very well give a relative absence of small local voids, thus cutting down on the vertical flow through the sandbed next to its margin. But second, the bed formation here might go the other way, creating an excess of voids next to the wall, and inducing extra and unwanted flow at the sandbed area margin. In the chemical field, a good deal of research has been done on the packing of various materials; but it appears that this particular problem has not been touched. It is important in sandbed work, and should be investigated.

In narrow sandbeds, a critical problem is to determine the minimum width in terms of number of grain diameters, that will still permit uniform packing. Obviously, a narrow sandbed only two or three grain diameters wide would result in irregular jamming of granules rather than uniform packing. What is the limit? In some cases, this limit will dictate the size of granule that must not be exceeded.

Sandbed—Flow Space Relationships

When a sandbed occurs within a slab, and a 2-dimensional field in one uniform

medium is being simulated, the flow space everywhere should be constant. If the sandbed is filled until the tops of the top granules just touch a plate placed directly on the slab face, then the flow space over the sandbed will be, in effect, slightly greater than the flow space over the slab: this is because of the presence of top voids. The thinner the spacing, or the larger the granules, the greater this effect becomes. The practical absence of flow refraction at the sandbed margin will indicate that the effect is negligible. However, this effect should be investigated, so that limits could be set in advance. Or again, in cases where the effect might be unavoidable and enough to worry about, the sandbed might be built high, by some fraction of a grain diameter, by using thin spacers on the slab when finishing off the sandbed. What fraction should this be?

The resistance to vertical flow up through the sandbed should, in theory, be infinite compared to the flow space resistance over the sandbed. The practice so far is empirical. Make a setup, as in Figure 5, and operate. Then cut the flow space, say, in half, and operate again.

If the previous pattern is duplicated, then all is well, and either flow space could be used, or any spacing in between. But looking ahead, we need to have work done on this problem of relationship, so that fluid mappers, even when pushed to extremes, can be designed with confidence. A theoretical-plus-experimental research on these flow resistance relationships should be carried out.

Another sandbed problem is to determine the minimum sandbed thickness, as related to grain size, that will give a uniform bed.

Still another arises from the fact that since fluid appears (or disappears) all over the sandbed area, there is a vertical component of flow in this part of the flow space. This component is foreign to the fields being simulated. Its effect in possibly distorting the pattern theoretically desired should be thoroughly investigated. In regions considerably removed from the kernel, or from the "ridgeline" to be mentioned further on, the horizontal flow component would be large compared to the vertical, and the effect should be very small. But near the kernel, the vertical component becomes relatively large; and at the kernel, it is relatively very great. Again, an empirical check like that mentioned above (halving the flow space and checking for pattern duplication) serves as a practical measure to lend assurance. But theoretical or experimental attacks should be used to look into this problem, going beyond the empirical stage.

Nonuniform Sandbeds

Up to now, only uniform sandbeds (constant in depth) have been discussed. Such sandbeds simulate uniformly distributed sources or sinks. But distributions of space charges, currents in conductor sections, and so on, may be nonuniform. Fluid source distributions over the sandbed should be varied accordingly. At this writing, no one has carried out any such work. However, it is easy to suggest three possibilities.

First, the continuous sandbed can be retained, but its depth can be varied at will by varying the screen depth. If sandbed depth is kept low compared to area, and if depth is not varied sharply, fluid flow density will vary nearly inversely as the depth.

Second, the sandbed can be compartmented, or divided into vertical and adjacent cells, all fed from a common plenum chamber. Using the same grain size, screen depths can be varied; or, using the same screen depths, grain sizes (using previously calibrated granules) could be varied.

The third prospect is to use the compartmentation idea, but with separate tanks connected to each cell, and with rate of feed adjustable by adjusting tank levels. All of the practical features of the techniques involved have yet to be worked out.

Sandbed Plenum Chamber

Ideally, the bottom of a sandbed (screen level) should be an isopressure surface; and this would be achieved by having a plenum chamber so large that pressure drops in it are negligible. Practically, the depth of a sufficiently good plenum chamber is far less than most would suspect. An easy practical test of a chamber is to have two connectors going to it, separated as far as possible. If, in switching the plenum chamber feed from one connection to the other, no pattern change is observed, the chamber is deep enough. However, looking ahead to possibly extreme conditions that may be required of some fluid mappers, the problem should receive experimental attention, at least.

The Kernel, and Lines of No Work

An apparent center within a distributed source or sink, where the lines seem to coverge, is clearly seen in Figure 5 or Figure 6. This is a well-known phenomenon. The name "kernel" has been applied to such a "center" or point, and the name is recognized.

Next, consider the flow lines of Figure 5. Interpret the pattern electromagnetically: then the sandbed area represents a conductor section with uniform current density. The lines of Figure 5, outside the conductor section, represent equipotential lines. But inside the current, the lines are not equipotentials. However, a point pole moved along any one line would require no work to be done upon it. Such lines—within a distributed source—have been distinctively called "lines of no work." This is also a well-known phenomenon, and the term is accepted. It may help to make the distinction between equipotential lines, and lines of no work, if we return to the fluid flow of Figure 5, and make the corresponding fluid flow distinction. Outside the sandbed area, the flow tubes are ordinary flow tubes, unaugmented. But within the sandbed area, we have what the writer calls augmented flow tubes. In a tube, the further we go out from the kernel, the greater is the flow in a tube section, due to the sandbed acting as a distributed source.

These two known phenomena within the distributed source are cited here, in order to lead up to two others, not so well known.

The Ridgeline Phenomenon

Distributed source fields are so extremely difficult to deal with theoretically, that very few solutions have ever been made, and very few good maps within such sources have been available. Also, until sandbed types of mappers came into existence, we had no way of setting up distributed source cases so as to look directly at the complete field representation. Thus, distributed source phenomena are quite unfamiliar to most, including most experts. Thus it happens that the writer has had the privilege of having an exceptional opportunity for

Figure 13. The point of inection, shown in the bar of the dumbbell. Nickel shot used in the sandbed

observing these phenomena, in operating numerous sandbed mappers.

One of the phenomena appears under certain conditions. It is a distinctive line, with the kernel located on this line. Such a line occurs in Figure 6, and it might be thought of as a "distributed kernel." In fact, a number of experts to whom the writer has shown such sandbed patterns have independently suggested this as a name. But another name will be proposed. The line under discussion is by no means well recognized; and a check with mathematicians and physicists indicates that it has not been named.

To lead to a name choice, think of having drawn the orthogonal system in Figure 6. The new lines would be isopressure lines. They would look like contour lines on a topographic map. Much to the point is the fact that if a soap film, stretched on the lip of this (emptied) sandbed ring is mildly inflated, its contour lines (as shown in the second paper) would correspond to the sandbed's isopressure lines. Whenever the sandbed has a line of the kind we are discussing, the corresponding soap film would have a ridge to correspond. Therefore, it is here proposed to call the line a "ridgeline."

The Point of Inaction Phenomenon

There is still another phenomenon. The writer has built sandbeds in which flow from one region tends to meet flow from another, the meeting place being also over the sandbed rather than outside it. A point of stagnation, or of no action, occurs. The "dumbbell" case, Figure 13, was especially built to illustrate this phenomenon. This isolated sandbed has a kernel in each lobe. The point of no action occurs in the middle of the connecting area.

There is the temptation to call this a "singular point within a distributed source." But to use "singular point" at all is to run the risk of implying that the field in this region is like the field about an ordinary singular point; whereas, it is very different.

This phenomenon, discovered in observing the operation of sandbed mappers, appears not to have been recognized; in fact, the possibility of its existence does not seem to have been suspected. To give it its own distinctive name, the writer proposes that it be called "point of inaction." Mathematicians are invited to the task of trying to work out the formal theory of this phenomenon.

Investigative Sandbed Work

With the foregoing instances as examples; with the recognition that probably, theory alone may never yield much insight into phenomena occurring within the distributed source except in the very simplest cases; and recognizing that sandbed fluid mappers offer a way of visually simulating these exceedingly complex phenomena, it may follow that some fruitful experimental work might be done with sandbeds, to gain insight, and possibly to discover additional phenomena.

References

1. Fields from Fluid Flow Mappers, A. D. Moore. *Journal of Applied Physics* (New York, N. Y.), volume 20, August 1949, pages 790–804.

2. Soap Film and Sandbed Mapper Techniques, A. D. Moore. *Journal of Applied Mechanics* (New York, N. Y.) volume 17, number 3, September 1950, pages 291–98.

3. Four Electromagnetic Propositions, With Fluid Mapper Verification, A. D. Moore. *Electrical Engineering*, July 1950, pages 607–10.

No Discussion

Continuous Scavenging System for Hydrogen-Cooled Generators

D. S. SNELL
MEMBER AIEE

L. P. GROBEL
ASSOCIATE AIEE

Synopsis: This paper describes a new method for the operation of the hydrogen system of hydrogen-cooled generators which permits the use of untreated oil for supplying the shaft seals, thereby eliminating the need for the vacuum treating equipment formerly supplied with these generators. The new method provides for the removal of most of the air and moisture brought into the generator through the shaft seals by a system of continuous scavenging, through which the purity and relative humidity of the hydrogen in the generator are maintained at substantially the same values as are obtained with the vacuum treating system, and with a hydrogen consumption not significantly greater. Operating experience over a 4-year period with 24 generators of small and medium size, has demonstrated the reliability of the new system, and this system now is being applied quite generally to generators in all sizes except the very largest.

WITH the first hydrogen-cooled generators that were placed in commercial service, a system for vacuum treating the oil supplied to the shaft seals was provided. Vacuum treatment removes both gases and moisture from the sealing oil so that both the purity and dryness of the hydrogen in the generator are automatically maintained at high values. While this system has proved entirely successful, and is in current use with a large number of generators, the vacuum treating equipment is somewhat complicated, and also requires the operation and maintenance of a number of auxiliaries; hence, a study was early begun by the General Electric Company to simplify and improve the hydrogen system without sacrificing the many advantages of vacuum treatment.

The first approach to this problem was to develop a shaft seal having very low oil flow to the hydrogen side, so that the amount of air carried into the generator with the oil, using untreated oil for the seals, would be so small that a low rate of gas scavenging from the generator casing would permit the maintenance of the desired high value of hydrogen purity. However, even with the low rates of oil flow that were obtained with the type of shaft seal developed, the hydrogen consumption was several times that obtained with the vacuum system. This required either that a radically different type of shaft seal be used, or a different method of scavenging. Since the seal developed possessed several advantages over other types that would have a lower oil flow, it was decided to retain the seal and improve the method of scavenging. The method developed has been designated as the "continuous scavenging system"[1] and differs from the usual method of scavenging employed with hydrogen-cooled generators in that the gas is scavenged from the small annular space between the oil deflectors and the shaft seals, instead of from the much larger generator casing itself. This system was first applied to generators in 1946, and is described briefly in reference 2. Since the first installation, 24 generators using this system have been placed in operation (as of April 1950), and the scavenging system now is being applied quite generally to all hydrogen-cooled generators, except the very largest, built by the General Electric Company.

Operating Principle and Characteristic Curves

Fundamental Relations

If a hydrogen-cooled generator is operating with untreated oil supplied to the shaft seals, some of the air dissolved in this oil will be released to the hydrogen atmosphere, Figure 1. In order to maintain the hydrogen purity in the generator at a value satisfactory for safe and economical operation under these conditions, a certain amount of the impure hydrogen in the generator must be continuously discharged to atmosphere and sufficient fresh hydrogen must be added to maintain a constant gas pressure, this process being known as "scavenging." Considering first the conventional method of scavenging, in which gas is discharged from the generator itself, let it be required to determine the amount of fresh hydrogen q_0 cubic foot per hour of purity S_0 continuously required to maintain a generator hydrogen purity of S, for an air inflow of (a) cubic foot per hour. Since for the condition of constant gas pressure in the generator, the amount of hydrogen and air entering the generator must equal the amount of hydrogen and air leaving, the purity of the mixture entering the generator must equal S, as given by the equation

$$S = \frac{S_0 q_0}{q_0 + a} \tag{1}$$

from which

$$q_0 = \frac{Sa}{S_0 - S} \tag{2}$$

The above derivation, which was obtained from reference 3, is not strictly accurate, since it neglects the loss of gas by absorption in the sealing oil; however, as shown in Appendix I, the resulting equations are sufficiently accurate for most practical purposes.

Considering a generator operating with untreated oil supplied to the shaft seals,

Paper 50-268, recommended by the AIEE Power Generation Committee and approved by the AIEE Technical Program Committee for presentation at the AIEE Fall General Meeting, Oklahoma City, Okla., October 23-27, 1950. Manuscript submitted July 17, 1950; made available for printing September 20, 1950.

D. S. Snell and L. P. Grobel are both with the General Electric Company, Schenectady, N. Y.

The authors gratefully acknowledge the assistance of R. E. Gorman and F. T. Horan in connection with the development and design of the system herein described, and the assistance of Dr. Saul Dushman and Dr. Ferd E. Williams in the development of the equations given in Appendix II.

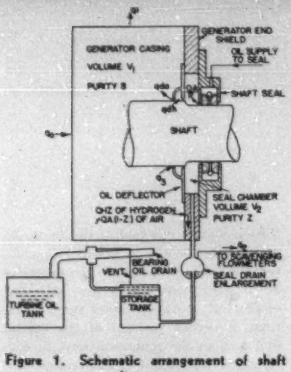

Figure 1. Schematic arrangement of shaft sealing system

resulting in an inflow of air with the oil of $a=0.4$ cubic foot per hour, let it be required to determine the amount of hydrogen of purity $S_0=1$ continuously required in order to maintain a purity of $S=0.97$ in the generator, by scavenging hydrogen from the generator itself. This amount from equation 2, would be

$$q_0=\frac{0.97\times 0.4}{1-0.97}=13 \text{ cubic feet per hour, or } 310 \text{ cubic feet per day}$$

Such an amount of hydrogen would usually be considered too large for economical operation.

If, however, the hydrogen purity in the generator is maintained by discharging to atmosphere impure hydrogen from the space between the shaft seals and the oil deflectors, (as in the arrangement shown in Figure 1), rather than from the generator casing, the term S in equation 2 will be replaced by Z, the hydrogen purity in the above space, and the amount of hydrogen required for scavenging will be appreciably less than that given by equation 2 since Z is significantly less than S. For a typical generator, operating at 0.5 pound per square inch hydrogen pressure, the purity difference $S-Z$ may be assumed as about 0.12. For the conditions of the above example, the amount of fresh hydrogen required to maintain a generator hydrogen purity of $S=0.97$, with gas at purity $Z=0.85$ discharged to atmosphere from the space between the shaft seals and the oil deflectors would be, from equation 2, with S replaced by Z,

$$q_0=\frac{0.85\times 0.4}{1-0.85}=2.27 \text{ cubic feet per hour, or } 55 \text{ cubic feet per day}$$

This amount is about one-sixth of that calculated for the same generator if scavenged by discharging gas from the generator casing, and is sufficiently low to make operation with this type of scavenging economical.

The large reduction in the amount of hydrogen required for scavenging by use of the above method in place of the conventional method of scavenging is the result of the generator construction; the provision of oil deflectors for preventing the entrance of oil and oil vapor into the generator, resulting in the separation of the space adjacent to the shaft seals from the generator itself by a partition acting to limit the diffusion of gases between the two sections, so that an appreciable difference in the hydrogen purities in the two sections can be maintained. (Although offering resistance to diffusion, the oil deflectors do not, however, materially restrict the flow of hydrogen from the generator into the seal chambers that is required for scavenging the impure hydrogen from the latter; the low rate of scavenging required causing negligible pressure drop across the annular space between the deflectors and the shaft. For a typical generator, a gas velocity of only about 10 feet per minute through this space is obtained.) By discharging impure hydrogen from the seal chambers to atmosphere, most of the air carried into the seal chambers with the sealing oil is removed before it can diffuse into the generator; hence, the amount of fresh hydrogen required to maintain a given hydrogen purity in the generator will be less than if scavenging were done from the generator itself.

Factors Influencing the Operation of the Scavenging System

In Appendix II, equations are derived for calculating the hydrogen consumption of a generator using the system here described, under various conditions of operation. It is shown that the gas consumption depends principally upon the following factors:

1. Rate of oil flow to hydrogen side of shaft seals. (F) or (Q)
2. The "apparent" solubilities of air and hydrogen in the sealing oil. (A) and (H)
3. The purity of the hydrogen in the generator. (S)
4. The "diffusion constant." (K)
5. The generator hydrogen pressure. (p)
6. The purity of the supply hydrogen. (S_0)

The apparent solubility of air in the sealing oil (A) represents the percentage of air by volume that is released from the oil as the latter enters the hydrogen atmosphere. This quantity is always somewhat less than the actual solubility of air in the oil which is the percentage of air by volume dissolved in the oil as would be determined from laboratory tests. Figure 2 shows values of air and hydrogen solubilities in a typical turbine oil at different temperatures, as determined from such tests. For oil at 45 degrees centigrade (representing the usual temperature of oil supplied to the shaft seals) Figure 2 indicates an actual solubility of 10 per cent for air and 6.4 per cent for hydrogen. In Figure 3 values of apparent solubility of air in the sealing oil as estimated from tests on a number of generators using the continuous scavenging system are shown. These values were calculated from equation 19 in Appendix II, the value of q_2 in this equation being estimated from the measured hydrogen consumption, an assumed loss of hydrogen by absorption in the oil, and an assumed value of generator hydrogen leakage. The values thus calculated range from 6 to 10 per cent, and are doubtless higher than the true apparent solubilities due to the nature of the assumptions made in their calculation. From tests on a 100,000-kva generator, in which fairly accurate measurements of the scavenging rate q_2 were obtained, apparent solubilities of air in the oil of between 4 and 6 per cent were calculated, see Figure 11. It is probable, therefore, that the apparent solubility of air in the sealing oil is between 50 and 75 per cent of the actual solubility.

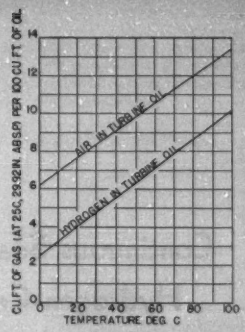

Figure 2. Solubilities of air and hydrogen in light turbine oil as determined from laboratory tests. Oil viscosity 150 Saybolt universal seconds at 100 degrees Fahrenheit. Specific gravity 0.863

The apparent solubility of hydrogen in the sealing oil (H), (which represents the percentage of hydrogen by volume absorbed by the oil leaving the generator) is of minor importance in determining the

characteristics of the scavenging system, since this quantity affects only the amount of hydrogen lost by absorption in the oil, which is always small in comparison with the amount lost by scavenging. Tests on the 100,000-kva generator mentioned indicated an apparent solubility for hydrogen in the oil of 4.8 per cent, or 75 per cent of the actual solubility, which is a reasonable proportion, considering that about this same proportion of the air dissolved in the oil was found to be released to the hydrogen atmosphere.

The "diffusion constant" (K) is a factor representing the relative ease with which air may diffuse from the seal chambers into the generator casing through the clearance space between the oil deflectors and the shaft. It has the dimensions of cubic feet per hour and is determined by the effective axial length of one oil deflector (L), the area of the annular space between the deflectors and the shaft (for the two ends) (B), and the diffusion coefficient for air into a hydrogen-air mixture (K_a); the constant being expressed by the equation

$$K = K_a B/L \tag{3}$$

For an average gas temperature of 40 degrees centigrade, the coefficient of diffusion for hydrogen into itself, or into a hydrogen-air mixture containing more than about 75 per cent hydrogen (K_h), is 6.06 square feet per hour. From equation 28 in Appendix II,

$$K_a = K_h/3.8 = 6.06/3.8 = 1.6 \text{ square feet per hour}$$

hence

$$K = 1.6B/L \text{ cubic feet per hour} \tag{4}$$

From equation 4, using values of B and L obtained from the oil deflector drawings, the diffusion constant K has been calculated for a number of generators using the continuous scavenging system, giving the values shown in Figure 3. From equation 31 in Appendix II, values of K also have been calculated for these generators from readings of hydrogen purity and from the measured hydrogen consumption as obtained in tests. These values are shown in Figure 3 for comparison with values calculated from equation 4, and are observed to check the latter reasonably well, the differences obtained between the test and theoretical values being readily explainable by differences between the actual deflector dimensions and the drawing dimensions, due to wear or to slight inaccuracies in machining or assembly.

The relation between total hydrogen consumption q_0 and the diffusion constant K is obtained from equation 31 as

$$q_0 = \frac{K(S-Z)(3.8-2.85)}{(S_0-S)} \text{ cubic feet per hour} \tag{5}$$

For a specified value of generator hydrogen purity S, the hydrogen consumption is shown by equation 5 to be proportional to the product of the diffusion constant (K) and the purity difference ($S-Z$).

Calculated Operating Characteristics

From the equations derived in Appendix II, a number of characteristic curves illustrating the performance of generators using the continuous scavenging system have been prepared, which are given in Figures 4 to 10 inclusive. These curves show the calculated hydrogen requirements, also the purity of the scavenged hydrogen and the amount of hydrogen lost by scavenging, for different values of the generator hydrogen purity and pressure and for different rates of oil flow to the gas side of the shaft seals. Also, the influence of the value of the diffusion constant (K) and of the apparent solubility of air in the sealing oil (A) on the hydrogen requirements are shown. In the calculation of the various curves, hydrogen leakage from the generator casing has been neglected, the influence of this leakage on the generator hydrogen purity being shown by the equations of Appendix II to be small; also, a value of $S_0 = 0.996$ has been assumed.

In Figures 4, 5, and 6, the calculated hydrogen consumption is given for different values of generator hydrogen purity, gas pressure, and diffusion constant, at different rates of seal oil flow. Values of $H = 0.05$ and of $A = 0.10$ respectively for the apparent solubilities of hydrogen and air in the sealing oil have been assumed, a maximum value for the air solubility being used in order to obtain maximum values of hydrogen consumption. (These values for the solubilities were also used in preparing the curves of Figures 7, 8, and 10.)

To illustrate the use of the foregoing characteristic curves, a generator having an oil flow to the hydrogen side of the shaft seals of 0.5 gallons per minute ($F = 0.5$) will be considered, and the hydrogen consumption for hydrogen purities of 95 and 97 per cent will be determined for various conditions. Referring

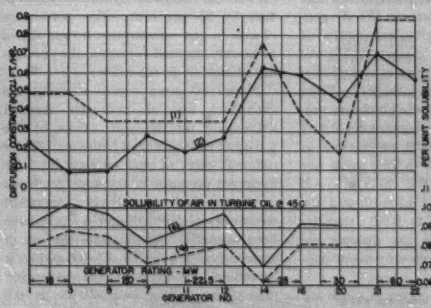

Figure 3. Calculated values of diffusion constant K and apparent solubility of air in sealing oil for several generators

Curves (1) Diffusion constant calculated from dimensions of oil deflectors, (equation 4). (2) Diffusion constant calculated from test data, using equation 31. (3) Apparent solubility calculated from test data assuming zero hydrogen leakage using equation 19. (4) Same as curve 3 except leakage of 5 cubic feet per day assumed

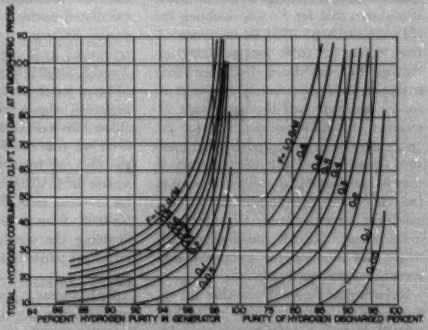

Figure 4. Calculated values of hydrogen consumption in operation at 0.5 pound per square inch hydrogen pressure for different values of generator hydrogen purity, and different purities of hydrogen discharged from seal chambers, at several rates of oil flow to gas side of shaft seals. For diffusion constant $K = 0.4$ cubic foot per hour and gas solubilities $A = 0.10$, $H = 0.05$

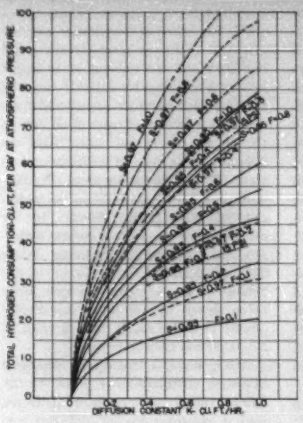

Figure 5 (left). Calculated hydrogen consumption of a generator for different values of the diffusion constant (K), for several assumed rates of oil flow to gas side of shaft seals (F) and for two values of generator hydrogen purity (S). For gas solubilities in oil of $A=0.10$, $H=0.05$. Operation at 0.5 pound per square inch hydrogen pressure assumed, except as noted

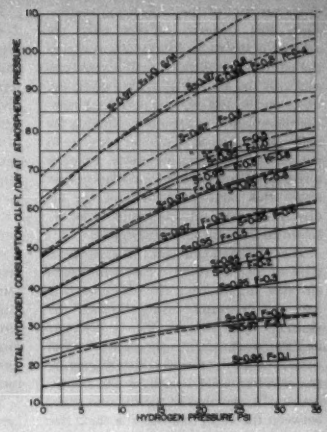

Figure 6 (right). Calculated hydrogen consumption of a generator at different hydrogen pressures, for several assumed rates of oil flow to gas side of shaft seals (F) and for two values of generator hydrogen purity (S). For gas solubilities in oil of $A=0.10$, $H=0.05$. For a diffusion constant of $K=0.4$ except as noted

to Figure 4, the curves of which have been calculated for a diffusion constant of $K=0.4$ cubic foot per hour and for a hydrogen pressure of 0.5 pound per square inch, the hydrogen consumption for the above seal oil flow is given as 36 cubic feet per day at 95 per cent purity and 50 cubic feet per day at 97 per cent purity. The corresponding purities of the scavenged hydrogen Z are given as 80.5 and 85 per cent, respectively.

Referring to Figure 5, which shows the influence of the value of the diffusion constant (K) on the calculated hydrogen requirements, for various rates of seal oil flow and for two different values of generator hydrogen purity and gas pressure, it is shown that for $F=0.5$, doubling the diffusion constant (that is, increasing K from 0.4 to 0.8 cubic foot per hour) increases the calculated hydrogen consumption by approximately 40 per cent, (or by less than half the percentage increase in the diffusion constant) for the two values of hydrogen purity and pressure considered. From this analysis, it may be concluded that a slight increase in the oil deflector clearances in service, causing a correspondingly slight increase in the value of the diffusion constant (K), would not increase the hydrogen consumption significantly.

Referring to Figure 6, showing the influence of hydrogen pressure on the calculated hydrogen consumption for different rates of seal oil flow and for two values of hydrogen purity and diffusion constant, it is shown that for $F=0.5$, doubling the absolute hydrogen pressure (that is, increasing the gauge pressure from 0.5 to 15 pounds per square inch) increases the hydrogen consumption by between 34 and 38 per cent, or by nearly the same amount as was shown in Figure 5 for a similar increase in the value of the diffusion constant K. The percentage increases in hydrogen consumption with increasing gas pressure shown in Figure 6 for generators using the continuous scavenging system, are much less than are obtained with generators using the vacuum system, if leakage is neglected; since with the latter system, the gas consumption (which is due only to absorption in the sealing oil, for no leakage) is proportional to the absolute gas pressure.

The influence of hydrogen pressure and diffusion constant, respectively, on the calculated purity difference ($S-Z$)–generator hydrogen purity less purity of scavenged hydrogen– is shown in Figures 7 and 8, for different rates of seal oil flow (F) and for $S=0.95$ and $S=0.97$. From Figure 7, the curves of which are calculated for a diffusion constant $K=0.4$, it is shown that for $F=0.5$, an increase in gas pressure from 0.5 to 15 pounds per square inch reduces the value of $S-Z$ for $S=0.95$ from 0.15 to 0.10, and for $S=0.97$, from 0.125 to 0.08; that is, doubling the absolute gas pressure reduces the purity difference by about one-third.

From Figure 8, the curves of which are calculated for a hydrogen pressure of 0.5 pounds per square inch, it is shown that for $F=0.5$, increasing the diffusion constant from 0.4 to 0.8 (that is, doubling it) reduces the calculated purity difference for $S=0.95$ from 0.15 to 0.105 and for $S=0.97$ from 0.125 to 0.088, or by about the same amounts as were obtained from Figure 7 for a similar percentage increase in the absolute hydrogen pressure.

The influence of the apparent solubility of air in the sealing oil on the calculated hydrogen consumption is shown by the curves in Figure 9, which are calculated for different values of seal oil flow, hydrogen purity and pressure, and diffusion constant K. An apparent solubility for hydrogen in the sealing oil of $H=0.05$ has been assumed. It is shown, for example, that in operation at 0.5 pound per square inch hydrogen pressure for $F=0.5$, $S=0.95$, and $K=0.4$, a 50 per cent reduction in the air solubility (that is, a reduction from $A=0.10$ to $A=0.05$) reduces the calculated hydrogen consumption by 25 per cent. The percentage change in gas consumption is thus shown to be only one-half as large as the percentage change in air solubility.

Figure 10 gives curves showing the calculated loss of hydrogen through scavenging for different values of the purity of the scavenged hydrogen (Z), for different rates of seal oil flow, and for hydrogen pressures of 0.5 and 15 pounds per square inch respectively. Apparent solubilities of $H=0.05$ and $A=0.10$ have been assumed. To illustrate the use of these curves, let $F=0.5$, $K=0.6$ and let it be required to determine the scavenging rate corresponding to $S=0.95$ at 0.5 pounds per square inch hydrogen pressure. Referring to Figure 8, the purity difference $S-Z$ for these conditions is 0.12, hence $Z=0.95-12=0.83$. Referring to Figure 10 for $F=0.5$, $Z=0.83$ at 0.5 pounds per square inch hydrogen pressure, the calculated hydrogen loss by scavenging is 39.6 cubic feet per

day. From Figure 5, the calculated total hydrogen consumption for the above conditions is 43.8 cubic feet per day, hence, the difference 43.8−39.6 =4.2 cubic feet per day must represent the loss by absorption in the sealing oil. From equation 12 in Appendix II, the latter loss is QHZ at casing pressure; hence, for the values of Q, H, and Z in the example, the absorption loss should be

$$0.5\times0.05\times0.83\times1.03\times1{,}440/7.5\times0.996 = 4.2 \text{ cubic feet per day}$$

which checks the value estimated from the curves.

Time Variation of Hydrogen Purity

When a generator employing the continuous scavenging system is first placed in operation, a considerable period of time is usually required for the generator hydrogen purity and the purity of the scavenged hydrogen to reach their final values. This is due to the large volume of the generator casing and the relatively slow rate of air inflow with the sealing oil. Figure 11 shows the time variation of the hydrogen purity values for a 100,000-kva 1,800-rpm generator operating with the scavenging system, during the first few weeks of operation, as obtained from tests. Since the scavenging rate was changed several times during this period, a considerable variation in the purity of the scavenged hydrogen was obtained; however, due to the large volume of the generator casing as compared with the volume of the seal chambers, this variation is shown to have had little effect on the generator hydrogen purity.

Equations have been derived for calculating the time variation of the hydrogen purity in the generator and in the seal chambers, respectively, during periods when these purities are changing. The equations and their derivation have not been included in the present paper. To check the accuracy of these equations, the purity values were calculated for the above generator for the initial period of operation for an assumed constant scavenging rate equal to the average rate actually maintained during this period. The calculated values are shown in Figure 11 and indicate a somewhat slower variation with time than was actually obtained. Considering, however, the considerable variation in the scavenging rate obtained in the test, the agreement between the test values of hydrogen purity and the values calculated for the assumption of a constant scavenging rate may be considered reasonable.

Design and Operation

Shaft Seals

The construction of the shaft seals used with most of the generators in service provided with the continuous scavenging system is illustrated in Figure 12. Each seal consists of a housing, supported on the outer end shield of the generator, in which are contained a pair of annular bronze sealing rings, made in segments, and having internal diameters slightly larger than the shaft diameter. The rings are held together radially and apart axially by a pair of coil springs attached to the upper and lower sections of the seal housing. Oil is supplied to the chamber containing the rings at a pressure about 4 pounds per square inch above the hydrogen pressure in the generator. This pressure creates an oil film between the rings and the shaft which prevents the outward leakage of hydrogen along the shaft.

The radial clearance on the shaft of the hydrogen-side seal ring is made considerably smaller than that of the air-side ring, this difference in clearances permitting a small oil flow to the hydrogen side of the seal, and a relatively large flow to the air side. The high air-side flow provides cooling for the rings so that their radial expansion is retarded and a low clearance on the hydrogen side, and, thereby a low oil flow to this side, can be maintained.

With some of the larger generators using the continuous scavenging system, a type of shaft seal having a single ring in place of a pair of rings, is supplied. The single ring is provided with a number of radial holes around the circumference, on the center line, through which oil from the seal housing is supplied to the inside bore surface of the ring, to provide a seal and supply cooling.

Shaft Sealing System

The arrangement of the shaft sealing system is illustrated diagrammatically in Figure 13. In normal operation, oil is supplied to the shaft seals from the bearing oil header, the flow being regulated by one of two differential pressure regulating valves arranged in parallel, one valve serving as a spare. At hydrogen pressures below about 10 pounds per square inch the bearing header pressure is adequate for supplying the seals directly,

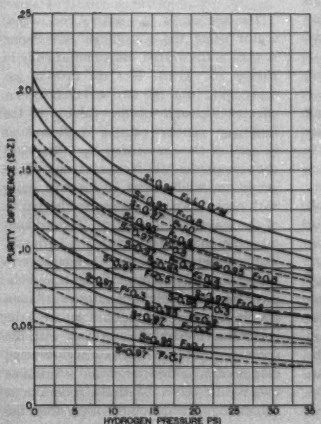

Figure 7 (left). Calculated difference between generator hydrogen purity (S) and purity of the hydrogen discharged from seal chambers (Z) at different hydrogen pressures, for several assumed rates of oil flow to gas side of shaft seals (F), and for two values of generator hydrogen purity (S). For a diffusion constant of $K=0.4$ and for gas solubilities in oil of $A=0.10$, $H=0.05$

Figure 8 (right). Calculated difference between generator hydrogen purity (S) and purity of the hydrogen discharged from seal chambers (Z) for different values of the diffusion constant (K) for several assumed rates of oil flow to gas side of shaft seals (F), and for two values of generator hydrogen purity (S). For operation at 0.5 pound per square inch hydrogen pressure and for gas solubilities in oil of $A=0.10$, $H=0.05$

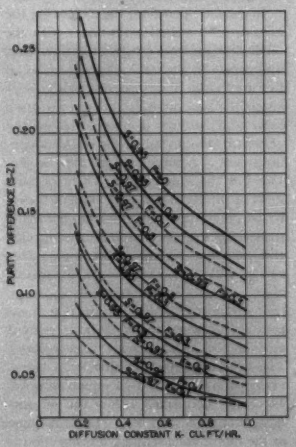

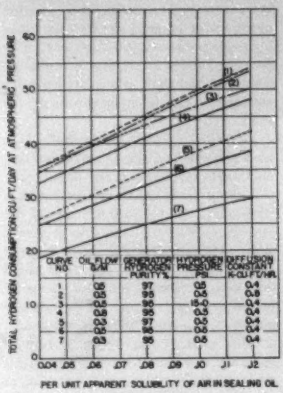

Figure 9 (left). Calculated hydrogen consumption of a generator for different values of apparent solubility of air in the sealing oil (A), for different values of gas-side seal oil flow (F), generator hydrogen purity (S) and pressure (P), and diffusion constant (K). Assumed solubility of hydrogen in oil $H=0.05$

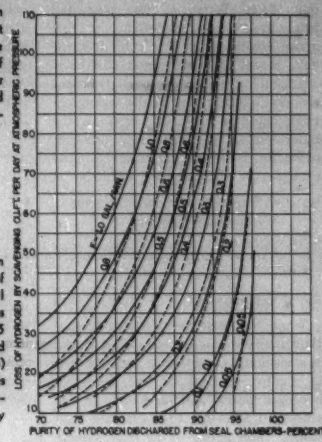

Figure 10 (right). Calculated hydrogen loss by scavenging for different values of purity of hydrogen discharged from seal chambers (Z), for different rates of gas side seal oil flow (F). For operation at 0.5 pound per square inch (solid curves) and 15 pounds per square inch (dashed curves) hydrogen pressure. For gas solubilities in oil of $A=0.10$, $H=0.05$. Hydrogen loss calculated at purity of supply hydrogen $S_0=0.996$

through the regulating valves. Above this pressure, however, the seal oil pressure must be maintained through the operation of one of two seal oil pumps, acting as "boosters" for the bearing oil pressure. One pump is driven by an a-c motor and cuts in automatically if the hydrogen pressure exceeds about 10 pounds per square inch; the other pump is driven by a d-c motor and is arranged to cut in if the a-c supply is unavailable. In standby operation, the seal oil pumps are started automatically on loss of bearing oil pressure, which can occur if the turning gear oil pump is shut down. In such operation, the pumps are supplied from the storage tank of the sealing system, which in turn receives the oil discharged from the shaft seals.

In normal operation, the oil leaving the air side of the shaft seals mixes with the oil discharged from the generator bearings and passes to the main oil tank. The oil flowing to the hydrogen side of the seals enters the seal oil drain and passes into a horizontal section of piping below the generator designated as the seal drain enlargement. A large surface area is provided in the enlargement which permits most of the hydrogen entrained in the oil to be given up; the released hydrogen passing back to the seal chambers through the seal drain piping (as this piping does not run full of oil, ample space is available above the oil for the passage of gas, so that separate pipes for equalization of gas pressure between the drain enlargement and the seal chambers are unnecessary). The enlargement is divided by a transverse partition into two equal sections, which are connected below the oil surface through a loop seal. From a dome in the top of each section, a connection is made to atmosphere for scavenging gas from the generator. From the seal drain enlargement, the hydrogen-side seal oil passes to a float trap, which discharges the oil into the storage tank, from which it passes in normal operation to the bearing drain header. (In standby operation with no oil pressure in the bearing oil header, the gas side oil is returned to the seals by operation of the seal oil pumps, as previously explained.)

The storage tank, float trap, regulating valves, and seal oil pumps are mounted on a common base as shown in Figure 14. A panel on the side of the assembly carries gauges for reading the seal-oil and hydrogen pressures, the pressure switches for starting the seal oil pumps, and an alarm pressure switch for low differential seal oil pressure.

It will be observed from the foregoing description that the hydrogen-contaminated oil leaving the shaft seals does not become evacuated, as with the vacuum treating system, but normally passes into the bearing drain header. No operating hazard is thereby created, however, since the hydrogen-side oil flow from the shaft seals is so small in comparison with the total oil flow from the bearings of the turbine-generator set, that the dilution of the hydrogen in the sealing oil with air through mixing with the bearing oil results in a negligible percentage of hydrogen being present in the free air space in the bearing oil system. As shown in the section on Operating Principle and Characteristic Curves, the amount of hydrogen absorbed by the sealing oil of a generator is of the order of 4 or 5 cubic feet per day. Considering that the vapor extractor circulates many thousand cubic feet of air per day through the bearing drain system, it is evident that the creation of an appreciable concentration of hydrogen in this system is normally impossible. Tests made on a number of generators using the continuous scavenging system, with the vapor extractor shut down, have indicated a maximum concentration of hydrogen in the air atmosphere in the main oil tank of 0.3 per cent hydrogen in air, which is less than 10 per cent of the lower explosive limit of hydrogen in air.

Gas System

The system of gas control for a generator using the continuous scavenging system is illustrated diagrammatically in Figure 15. Control of the rate of gas scavenging from the two seal chambers is effected through needle valves at the hydrogen control panel. A flowmeter in each of the scavenging lines measures the scavenging rate from each end of the generator, while a gas analyzer in series with each flowmeter measures the purity of the scavenged hydrogen. A third analyzer measures the purity of the hydrogen in the generator casing. Connections to the latter analyzer from the high and low pressure zones of the generator ventilation circuit permit a circulation of gas from the generator through the analyzer with the generator operative, the rate of flow being measured on a flowmeter and adjustable by a needle valve. With the generator at standstill, a small amount of gas from the generator is continuously bled to atmos-

phere through the analyzer. The gas analyzers operate on the well-known thermal conductivity principle.

Other instruments on the control panel include: a fan pressure gauge, which, with the generator operative, gives a reading proportional to the density, and therefore to the purity, of the hydrogen in the generator; a dial thermometer reading the generator cold gas temperature; and two pressure gauges for reading the hydrogen pressure in the generator in operation at both 0.5 pound per square inch and at elevated pressures. A typical hydrogen control panel is shown in Figure 16.

Since the continuous scavenging system does not completely remove from the generator any moisture that may enter with the sealing oil, a gas dryer is provided. The dryer is connected into the high- and low-pressure zones of the generator ventilation circuit which permits gas from the generator to be continuously circulated through it. The dryer contains a quantity of activated alumina drying agent, which may be reactivated when moist, by energizing a heating coil in the dryer and operating a small blower to circulate air through it, the dryer being first isolated from the generator through the operation of shut-off valves.

A liquid detector is connected to the bottom of the generator casing which operates an alarm to indicate the presence of water or oil in the generator.

Alarm Signal System

An annunciator is provided at the hydrogen control panel which gives a visual and audible indication of any abnormal condition in the hydrogen system. The following alarm conditions are indicated by the signal system:

1. Machine gas temperature—high.
2. Machine gas pressure—low or high.
3. Hydrogen manifold pressure—low.
4. Hydrogen purity—low, or analyzer failure.
5. Differential seal oil pressure—low.
6. Liquid detector—full.
7. Seal oil drain—high oil level.

For a generator provided with a vacuum treating system for the sealing oil, a total of 12 alarm conditions are indicated by the alarm signal system as compared with seven for the system here described. This considerable reduction in the number of alarm conditions requiring supervision, obtained by the use of the new system in place of the vacuum system well illustrates the greater simplicity of the scavenging system.

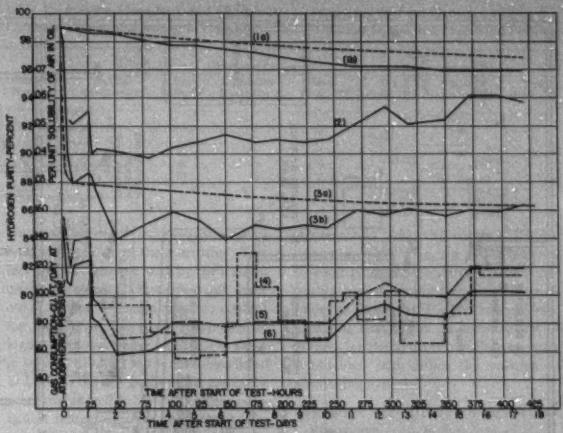

Figure 11. Data from tests on 100,000-kva 1,800-rpm generator showing variation of generator hydrogen purity and purity of scavenged hydrogen with time, following placing of generator in service, with calculated purity values shown for comparison. Also measured rates of hydrogen consumption and loss by scavenging

Curves (1a and 1b) Generator hydrogen purity, calculated and test values, respectively. (2) Apparent solubility of air in sealing oil, calculated from test data. (3a and 3b) Purity of hydrogen discharged from seal chambers (Z) calculated and test values, respectively. (4) Average hydrogen consumption from daily records. (5) Measured loss of hydrogen of purity (Z) through scavenging from seal chambers. (6) Loss of hydrogen of supply purity (S_h) through scavenging from seal chambers as estimated from curves (3b) and (5)

Operating Experience

Hydrogen Consumption and Scavenging Rate

Data on operation of 22 generators using the continuous scavenging system are summarized in Figure 17. The hydrogen consumption for these generators at 0.5 pound pressure is shown to range from 32 to 90 cubic feet per day, the average consumption being about 50 cubic feet per day, which compares favorably with the consumption for generators using the vacuum treating system. The gas-side oil flow for the shaft seals of these generators is between 0.2 gallons per minute for the smaller sizes, and 0.7 gallons per minute for the largest 3,600-rpm generators. For the two 60,000-kw, 1,800-rpm units, the gas side seal oil flow is about 0.4 gallons per minute. Figure 17 also shows the reported average scavenging rates for the different generators as read on the flowmeters at the two ends of the generator, which are observed to range from 200 to 1,000 cubic centimeters per minute.

Many of these readings, however, especially the very high or very low values, cannot be regarded as accurate, giving values of hydrogen loss by scavenging either unreasonably low or high. Some of the readings, however, are apparently quite accurate. For example, generator number 5 had a reported average scavenging rate of 560 cubic centimeters per

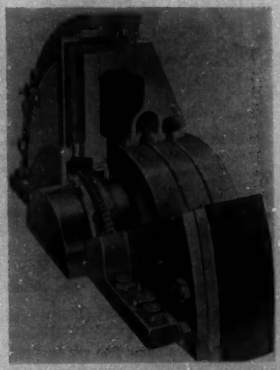

Figure 12. Shaft seal for hydrogen cooled generator

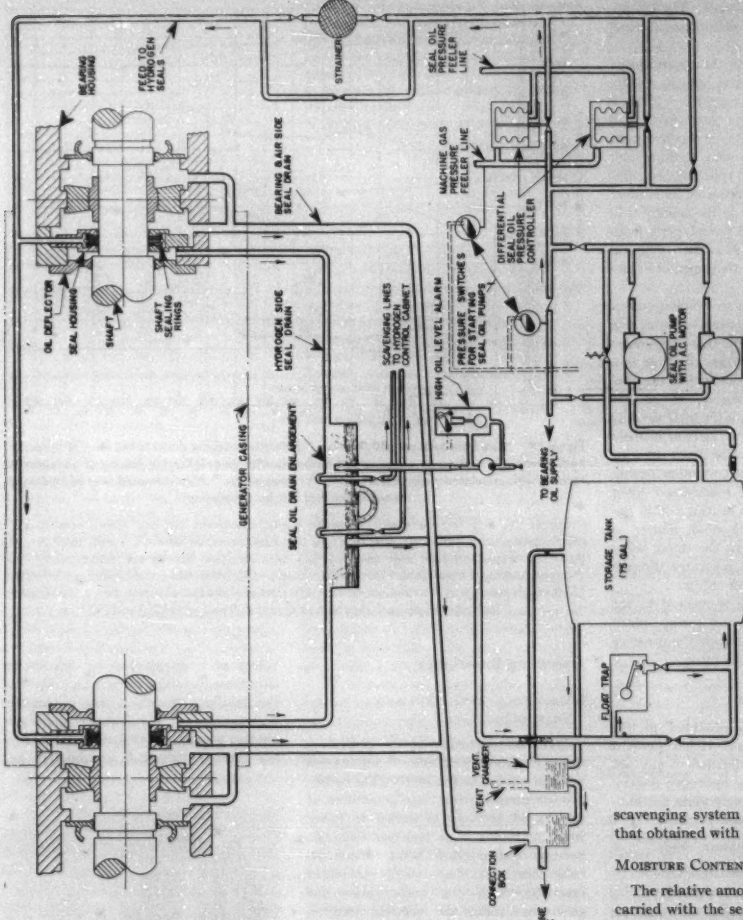

Figure 13. Arrangement of shaft sealing system

minute at 86.4 per cent purity and a total hydrogen consumption of 41 cubic feet per day. For a flowmeter correction factor of 0.72, the hydrogen loss by scavenging, assuming hydrogen at 99.6 per cent purity, would be

$$2\times\frac{0.72\times0.864\times560\times0.051}{0.996}=35.6 \text{ cubic feet per day}$$

The difference between total hydrogen loss and the estimated loss by scavenging is $41-35.6=5.4$ cubic feet per day, representing the loss by absorption in the sealing oil and by leakage, which is a reasonable amount.

The hydrogen purity in the various generators is shown in Figure 17 to range from 95 to 99 per cent, the average value being about 97 per cent. The percentage of hydrogen in the scavenged gas is shown to range from 80 to 91 per cent, the average value being about 86 per cent. For generators using the vacuum-treating system, a machine hydrogen purity of 98 per cent or higher is usually maintained; hence, the average purity held with the scavenging system is slightly lower than that obtained with the vacuum system.

Moisture Content of Gas

The relative amounts of moisture being carried with the sealing oil into the various generators included in the above survey, are indicated approximately by the frequency of regeneration of the gas dryer, given in Figure 17. For generators 17 and 18, an appreciable amount of moisture was present in the turbine oil, due to abnormal operating conditions, which was reflected in having to regenerate the dryers daily. For the other generators, however, the dryers required regeneration at intervals ranging from 1 to 12 times per month, the average frequency being once a week.

Readings of relative humidity and dew point for the gas in four of the generators listed in Figure 17 are given in

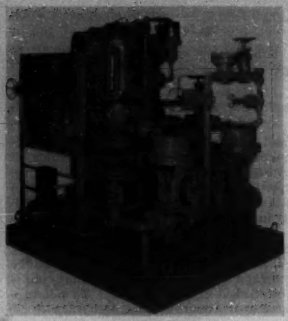

Figure 14. Seal oil supply unit

Table I. Relative Humidities and Dew Points of Hydrogen in Four Generators Using the Continuous Scavenging System in Operation at 0.5 Pound Per Square Inch Hydrogen Pressure

Generator Number	Rating, Megawatts	Generator Casing: Dry Bulb, °F	Generator Casing: Relative Humidity, %	Generator Casing: Dew Point, °F	Scavenged Gas: Dry Bulb, °F	Scavenged Gas: Relative Humidity, %	Scavenged Gas: Dew Point, °F
2	15	81	33	49	84	50	62
17	30	93	17	39	77	83	72
20	30	84	21	37	85	36	54
21	60	68	5	0	Not Taken		
21*	60	74	5	2.5	Not Taken		

*Dryer out of service.

quite as effective in removing moisture as in removing air from the generator. This fact also was demonstrated by the tests on generator number 21 which, with dryer out of service, indicated moisture content for the gas in the casing only slightly higher than was obtained with the dryer in service. For all of the machines listed in Table I, the dew point of the gas in the generator is well below the coldest practicable temperature for the water to the gas coolers, so that no possibility of moisture condensation is present.

Measurements of the relative humidity of the hydrogen atmosphere in a number of generators using the vacuum-treating system have indicated dew points between zero and 40 degrees Fahrenheit, which represents approximately the same range of values as shown in Table I. It is evident, therefore, that about the same degree of dryness for the hydrogen in the generator is obtained with either the vacuum or scavenging systems.

Operation at Elevated Hydrogen Pressures

A few of the generators using the continuous scavenging system have been operated at hydrogen pressures up to 15

Figure 15. Arrangement of gas control system

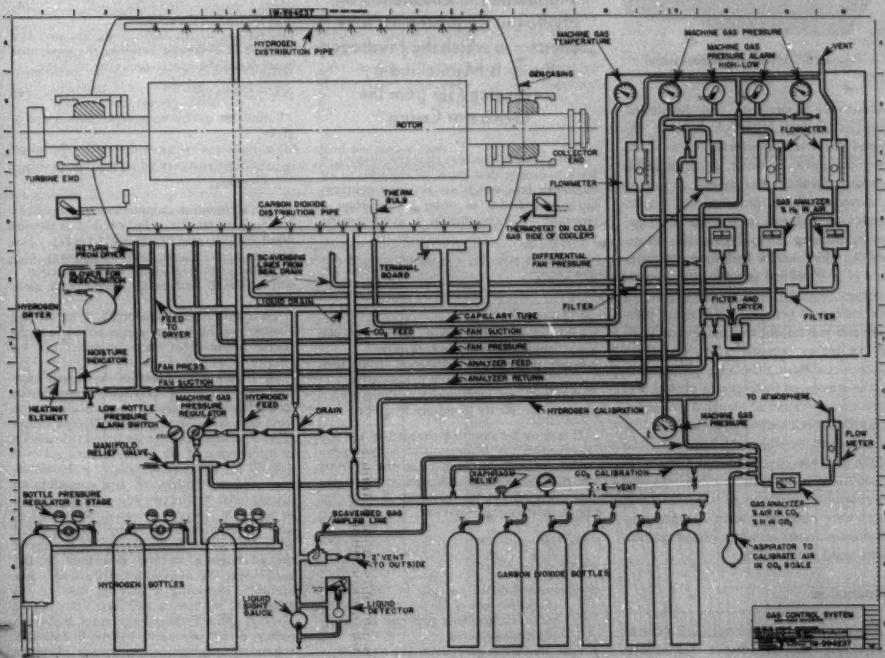

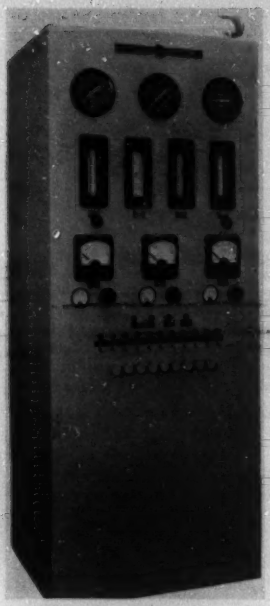

Figure 16. Hydrogen control panel

pounds per square inch, and the characteristics for such operation as given previously have been approximately realized. In most cases, however, an appreciable amount of leakage was present, so that an accurate check on the calculated characteristics could not be obtained. Generator number 20 in Figure 17, for example, which had a hydrogen consumption of 54 cubic feet per day at 0.5-pound pressure, operated with a consumption of 150 cubic feet per day at 15-pound pressure and was known to have several leaks at the higher pressure which could not be corrected during the tests. The purity of the scavenged hydrogen as obtained in tests on generators at elevated pressures, has always been somewhat higher than the values given by Figure 6; however, none of the tests was continued long enough for equilibrium values to be obtained and considerable variations in the scavenging rates were obtained, hence definite conclusions as to the accuracy of the calculations could not be made.

Conclusion

Operating experience with 24 generators using the continuous scavenging system, in place of the system of vacuum treatment of the sealing oil formerly used, has demonstrated that the scavenging system maintains the purity and relative humidity of the hydrogen within the generator at approximately the same values as are obtained with the vacuum treating system, and with a hydrogen consumption not significantly greater. Satisfactory performance of the scavenging system is shown to depend chiefly on the maintenance of the minimum practicable oil flow to the gas side of the shaft seals. The solubility of air in the sealing oil and the oil deflector dimensions and construction, also are shown to influence the operating characteristics of the system. The greater simplicity of the continuous scavenging system and its lower maintenance and operating costs, as compared with the vacuum treating system, are believed to compensate for a slightly greater hydrogen consumption, and to warrant the application of this system to generators in sizes considerably larger than those on which operating experience has been gained.

Appendix I. Calculation of Hydrogen Requirements for a Generator in which the Hydrogen Purity Is Maintained by Scavenging Gas from the Generator Casing

It is shown in the text that the amount of fresh hydrogen that must be supplied to an enclosure into which air is being continuously introduced, in order to maintain a constant hydrogen purity, is given by the equation

$$q_0 = \frac{Sa}{S_0 - S} \tag{2}$$

where

a = rate of inward air flow, cubic feet per hour at pressure in enclosure
q_0 = rate of hydrogen admission, cubic feet per hour at pressure in enclosure
S = per-unit hydrogen purity in enclosure
S_0 = per-unit purity of supply hydrogen

If it may be assumed that all of the air dissolved in the sealing oil of a hydrogen-cooled generator is given up as the oil from the seals enters the hydrogen atmosphere, the value of (a) in equation 2 may be approximately expressed as

$$a = QA/p \tag{6}$$

where

A = per-unit solubility of air in the sealing oil (cubic feet of air per cubic foot of oil at atmospheric pressure and supply temperature)
p = gas pressure in generator, atmospheres
Q = oil flow to gas side of shaft seals, cubic feet per hour

Substituting equation 6 in equation 2 gives the equation

$$q_0 = \frac{SQA}{p(S_0 - S)} \tag{7}$$

from which the amount of hydrogen required to maintain a specified value of hydrogen purity in a generator may be approximately determined, from the rate of seal oil flow and the value of the air solubility in the oil.

Equation 7 does not, however, take account of the loss of hydrogen in the sealing oil, and the fact that the air leaving the generator casing with the sealing oil is absorbed at casing pressure. To obtain a more exact equation for q_0, let

q_x = rate of discharge of hydrogen from generator through scavenging, including leakage, cubic feet per hour at casing pressure
H = per-unit solubility of hydrogen in sealing oil (cubic feet of hydrogen per cubic foot of oil at atmospheric pressure and supply temperature)

Also, it will be assumed that both hydrogen and air will be absorbed in the oil leaving the generator in proportion to the hydrogen and air solubilities. Then, for the condition that a constant gas pressure is maintained in the generator we have,

$$q_0 + QA/p = q_x + QHS + QA(1-S) \tag{8}$$

and for the steady-state condition that the amount of hydrogen entering the generator must equal the amount leaving we have,

$$q_0 S_0 = q_x S + QHS \tag{9}$$

Eliminating q_x between equations 8 and 9 gives

$$q_0 = \frac{SQ}{S_0 - S}[A/p - (1-S)(A-H)] \tag{10}$$

Which is the same as equation 7 except that in equation 10 the value of A/p is diminished by the quantity $(1-S)(A-H)$. For high values of casing purity, however, this term becomes negligible, hence equation 7 will be found sufficiently accurate in most cases.

To obtain from equations 2, 7, or 10, the amount of hydrogen required at atmospheric pressure, q_0 must be multiplied by (p).

In Figure 18, values of hydrogen consumption for different values of generator hydrogen purity are shown, as calculated from equations 7 and 10, for different values of seal oil flow and for assumed solubilities of hydrogen and air in the sealing oil of 5 and 10 per cent, respectively. The differences in the values of gas consumption calculated from the two equations are shown to be small. A comparison of the values of gas consumption as given by Figures 6 and 18, respectively, illustrates the advantage of the scavenging method described in the paper over the conventional method. For example, assuming a seal oil flow of 0.5 gallon per minute, a diffusion constant of $K = 0.4$, and a required generator hydrogen purity of 97 per cent, Figure 6 indicates values of hydrogen consumption obtained

with the new method of scavenging of 50 and 68 cubic feet per day at 0.5 and 15 pounds per square inch hydrogen pressure, respectively; while with the conventional method of scavenging, for the same conditions of oil flow and hydrogen purity, Figure 18 indicates a hydrogen consumption of 350 cubic feet per day at either 0.5 or 15 pounds per square inch hydrogen pressure, which is 7 and 5.2 times the amounts estimated to be required by the new method at 0.5 and 15 pounds per square inch pressure, respectively.

Appendix II. Calculation of Hydrogen Requirements for a Generator Using the Continuous Scavenging System

Referring to Figure 1, representing schematically the arrangement of the shaft seal at one end of a hydrogen-cooled generator, let

A, H, p, Q, and S_0 be as defined in Appendix I

S = per-unit hydrogen purity in generator casing

Z = per-unit purity of hydrogen in seal chambers (purity of scavenged hydrogen)

q_0 = rate of hydrogen admission to generator casing

q_1 = rate of gas leakage from generator casing

q_2 = rate of gas scavenging from the two seal chambers, including any leakage from these sections

q_3 = amount of gas from generator casing entering seal chambers, apart from amount entering by diffusion

qd_b = amount of hydrogen passing into seal chambers from generator casing by diffusion through clearance space between oil deflectors and shaft

qd_a = amount of air passing into generator casing from seal chambers by diffusion

The quantities q_0, q_1, and so forth are expressed in cubic feet per hour at casing pressure. The quantities q_2, q_3, qd_b, and qd_a represent the combined gas flows for both ends of the generator; also, the oil flow Q represents the combined gas-side flow from the two seals. To obtain cubic feet per hour at atmospheric pressure, the values of q_0, q_1, and so forth must be multiplied by (p).

It will be assumed, as in Appendix I, that all of the air dissolved in the sealing oil is given up as the oil enters the hydrogen atmosphere, and that both hydrogen and air are absorbed in the oil leaving the generator in proportion to the solubilities of these gases. (This assumption is pessimistic, giving higher values of hydrogen consumption than are actually obtained. However, any error in the assumption can be corrected for by proper choice of the values of A and H in the resulting equations.) For the condition of constant gas pressure in the generator we have*

$$q_0 + QA/p = q_1 + q_2 + QHZ + QA(1-Z) \quad (11)$$

Also, since under steady state conditions, the amount of hydrogen entering the generator must equal the amount leaving, we have

$$q_0 S_0 = q_1 S + q_2 Z + QHZ \quad (12)$$

Solving equation 12 for q_2 gives

$$q_2 = (q_0 S_0 - q_1 S - QHZ)/Z \quad (13)$$

*Actually, the gas pressure in the seal chambers must be slightly less than that in the generator casing, in order to have an outward gas flow q_3. However, the difference in pressures is too small to be considered here.

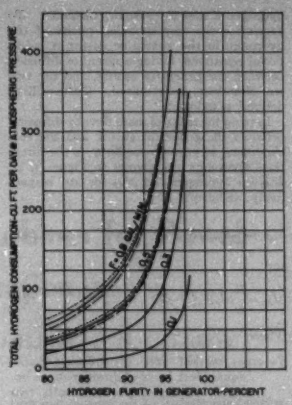

Figure 18. Calculated hydrogen consumption of a generator for which the hydrogen purity is maintained by scavenging from the generator itself (instead of from the seal chambers) for different values of the purity held. For several rates of oil flow to gas side of shaft seals (F). For gas solubilities in oil of $A=0.10$, $H=0.05$

Solid curves—calculated by exact equation 10 for 0.5 pound per square inch hydrogen pressure. Dashed curves—calculated by equation 10 for 15 pound per square inch hydrogen pressure. Dotted curves—calculated by approximate equation 7 for any hydrogen pressure

Figure 17. Data obtained in operation at 0.5 pound per square inch hydrogen pressure of 22 generators provided with continuous scavenging system

Curves (1) Generator hydrogen purity. (2) Purity of hydrogen discharged from seal chambers. (3) Average reading of scavenging flowmeters (right-hand scale). (4) Average daily hydrogen consumption (left-hand scale). (5) Frequency of reactivation of gas dryer (right-hand scale)

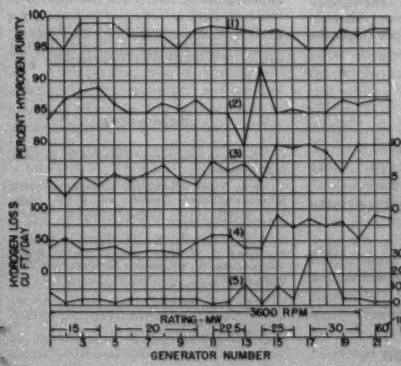

Figure 19. Calculated purity of hydrogen discharged from seal chambers (Z) for different values of the ratio of hydrogen consumption (q_0) to diffusion constant (K), and for different values of generator hydrogen purity (S) from equation 32, assuming $S_0=0.996$

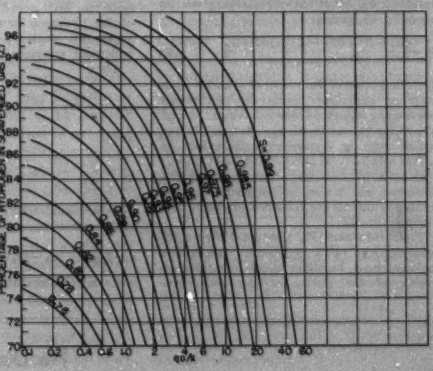

Substituting equation 13 in equation 11 gives

$$q_9 = \frac{Z}{S_9 - Z}\left[QA(Z+1/p-1) + q_1\frac{(S-Z)}{Z} + QH(1-Z)\right] \quad (14)$$

For zero casing leakage equation 14 becomes

$$q_9 = \frac{ZQ}{S_9 - Z}[A/p - (1-Z)(A-H)] \quad (15)$$

Which is the same as equation 10 in Appendix I except that S is replaced by Z. Eliminating q_9 between equations 11 and equation 13 gives

$$Z = \frac{q_2 S_9 + QAS_9(1-1/p) + q_1(S_9 - S)}{q_1 + Q(H(1-S_9) + AS_9)} \quad (16)$$

from which the purity of the scavenged hydrogen may be determined from the scavenging rate q_2 if the casing leakage q_1 is neglected. Equation 16 also may be written

$$q_2 = \frac{S_9}{S_9 - Z}\left[QA(Z+1/p-1) - \frac{q_1}{S_9}(S_9 - S) + \frac{QHZ}{S_9}(1-S_9)\right] \quad (17)$$

from which the scavenging rate q_2 may be determined for a given purity of the scavenged hydrogen Z, if the casing leakage q_1 is neglected.

In deriving the foregoing equations, it has been assumed that all of the air dissolved in the sealing oil is given up as the oil enters the hydrogen atmosphere, and that hydrogen and air are absorbed by the oil leaving the generator through the seal drain lines in proportion to the hydrogen and air solubilities. The correctness of these assumptions may be checked by calculating the values of A and H from tests on an actual hydrogen-cooled generator, by the use of equations 11 and 13. For convenience in making such calculations, equation 13 may be solved for H, giving

$$H = \frac{q_9 S_9 - q_1 S - q_2 Z}{QZ} \quad (18)$$

and equation 11 may be solved for A, first substituting for H the expression given by equation 18, giving

$$A = \frac{q_1(1-S) + q_2(1-Z) - q_9(1-S_9)}{Q(Z-(1-1/p))} \quad (19)$$

Determination of the values of H and A from tests on generators using the continuous scavenging system, from equations 18 and 19, will give values of apparent solubility, which may be compared with values of actual solubility as determined from laboratory tests to show the extent to which the dissolved air in the oil is given up and hydrogen and air are absorbed by the oil in a given generator.

From equation 15, the total hydrogen consumption of a generator, neglecting leakage, may be determined for different values of the purity of the scavenged hydrogen Z and the system constants. To determine the corresponding purity of the hydrogen in the generator casing S, additional equations, taking account of diffusion between the generator casing, and the two seal chambers, are required. These will be derived as follows:

Letting the rates of mass flow by diffusion between the generator casing and the seal chambers, in pounds per hour, in the directions shown by the arrows in Figure 1, be M_{dh} for hydrogen and M_{da} for air, respectively, we have

$$M_{dh} = \frac{B}{L}\rho d_h K_h(S-Z) \quad (20)$$

and

$$M_{da} = \frac{B}{L}\rho d_a K_a(S-Z) \quad (21)$$

Where

B = cross section area of diffusion path, square feet (area of annular space between oil deflectors and shaft, two ends)

L = length of diffusion path, feet (axial length of one oil deflector)

d_h = density of pure hydrogen at atmospheric pressure, pounds per cubic foot

d_a = density of air at atmospheric pressure, pounds per cubic foot

K_h = diffusion constant for hydrogen, square feet per hour

K_a = diffusion constant for air, square feet per hour

(The constants K_h and K_a are assumed to be determined for the condition that both hydrogen and air are diffusing into a mixture that is predominately hydrogen, for example, 75 per cent or higher. For this condition, the value of K_h will be approximately the same as for pure hydrogen diffusing into itself, while the value of K_a will bear a fixed relation to K_h depending on the ratio of the molecular weights of hydrogen and air. Also, it will be assumed that the diffusion rate is uninfluenced either by the peripheral speed of the shaft or by the axial gas velocity in the clearance space between the oil deflectors and the shaft due to the flow of hydrogen to the seal chambers to make up the loss of impure hydrogen by scavenging. This assumption is based on the fact that both the shaft speed and the axial velocity of the hydrogen in the deflector clearance space are small in comparison with the molecular velocities of gases.)

Then

$$q_{dh} = \frac{M_{dh}}{\rho d_h} = \frac{B}{L}K_h(S-Z) \quad (22)$$

and

$$q_{da} = \frac{M_{da}}{\rho d_h} = \frac{B}{L}K_a(S-Z) \quad (23)$$

For the condition of constant gas pressure in the generator casing, we have

$$q_9 = q_1 + q_2 + q_{dh} - q_{da} \quad (24)$$

while for the condition that the amounts of hydrogen entering and leaving the casing are equal,

$$q_9 S_9 = (q_1 + q_2)S + q_{dh} \quad (25)$$

Eliminating $q_1 + q_2$ between equations 24 and 25 gives

$$q_9 S_9 = S(q_9 - q_{dh} + q_{da}) + q_{dh} \quad (26)$$

Substituting in equation 26 the values of q_{dh} and q_{da} from equations 22 and 23 gives

$$q_9(S_9 - S) = \frac{B}{L}(S-Z)[K_h(1-S) + K_a S] \quad (27)$$

Since the diffusion constants of two different gases with respect to a third gas are related to each other by the square root of the ratio of their molecular weights, we may write

$$K_h = \sqrt{14.4}K_a = 3.8K_a \quad (28)$$

Substituting equation 28 in equation 27 gives

$$q_9(S_9 - S) = K(S-Z)(3.8 - 2.8S) \quad (29)$$

Where

$$K = \frac{K_a B}{L} \quad (30)$$

This quantity is designated as the "diffusion constant" of the generator. Then from equation 29

$$K = \frac{q_9(S_9 - S)}{(S-Z)(3.8 - 2.8S)} \quad (31)$$

From this equation, the value of the constant K for a given generator may be calculated from tests from measurements of q_9, S, S_9 and Z.

Also, from equation 31

$$q_9/K = \frac{(S-Z)(3.8 - 2.8S)}{S_9 - S} \quad (32)$$

In Figure 19 curves of Z versus q_9/K, as determined from equation 32 are drawn for several assumed values of S. From these curves, it is possible to determine, for any value of S, the corresponding values of q_9/K and Z. Then with K known, values of Q may be determined from equations 14 or 15 for known values of A, H, and q_1. Or, assuming the oil flow Q and the value of K are known, and it is required to find q_9 for a given value of S, equations 14 or 15 may be used in conjunction with Figure 19 by a process of cut and trial, to determine q_9.

References

1. United States Patent 2,454,979, D. S. Snell, L. P. Grobel.

2. Nine Years Operating Experience with Hydrogen-Cooled Generators, D. S. Snell, L. P. Grobel. *Power Plant Engineering* (Chicago, Ill.), May–June, 1947.

3. Liquid Film Seal for Hydrogen-Cooled Machines, C. W. Rice. *General Electric Review* (Schenectady, N. Y.), volume 30, November 1927, pages 516–30.

No Discussion

Control of Gas Turbines for Power Generation

D. C. HOFFMANN
MEMBER AIEE

A. G. MELLOR
ASSOCIATE AIEE

N. E. STARKEY
NONMEMBER AIEE

THE DEVELOPMENT of the combustion gas turbine as a new type of prime mover for power generation[1] has required the parallel development of suitable controls. The control scheme at present being used provides for semiautomatic starting and stopping of the unit, for speed and load control, and for prosection of the unit under abnormal operating conditions or in the event of malfunctioning of any component part. This paper describes the main components used in the control of General Electric gas turbines and how these components are combined to accomplish the above functions.

Characteristics of Gas Turbines

Several characteristics of gas turbines make the control problem different from that encountered with other types of prime movers. For instance, gas turbines are not self-starting and do not become self-sustaining until they reach about 50 per cent speed. A means must therefore be provided to crank the unit to firing speed and to assist acceleration after firing. A temperature control must be provided to limit the maximum and the rate of change of turbine inlet temperature to prevent damage to the turbine. Turbines that normally operate on bunker C oil must be started on diesel oil and transferred to bunker C at or above idle speed.

The starting sequence required, consists of several steps outlined briefly as follows:

1. Cranking the unit to approximately ten per cent speed to establish air flow through the combustion chambers.
2. Admitting the correct amount of fuel to the combustion chambers and applying ignition and booster air to initiate combustion.
3. Accelerating the unit after firing assisted by the starting motor.
4. Disengaging the starting motor when the gas turbine reaches self-sustaining speed.
5. Transferring from diesel oil to bunker C.

The stopping sequence required consists of the following steps:

1. Transferring from bunker C to diesel oil and operating on diesel oil for sufficient length of time to remove the heavy bunker C from the fuel pump, fuel lines, and fuel nozzles.
2. Shutting off the fuel supplied to the combustion chambers.
3. Rotating the unit after shutdown to allow proper cooling of all parts.

The unique characteristics of the gas turbine as outlined previously, made it desirable to provide partial automatic control on the first commercial gas turbines. In the first design of gas turbine control,[2] the various steps in the starting and stopping sequences were accomplished by manual operation of a control switch through six positions in sequence. Later designs, evolving from the first control, have retained the same basic control scheme but have been made more automatic. Operation of a master switch initiates the starting or stopping sequence which then proceeds automatically through the various steps required. Certain other changes have been made to improve reliability, to prevent possible damage by operational errors and to provide additional protection for the gas turbine under some abnormal conditions.

The first application of the automatic control has been to a 3,500-kw oil-fired unit.[3] The same basic control can, however, be applied to other sizes of gas turbines and also to natural gas fired units.

Control Components and Accessories

The following main components of the control system are mounted on the gas turbine:

Fuel Pump. Speed and load control of the gas turbine is obtained by varying the fuel flow to the combustion chambers. The required range of fuel flow is obtained by controlling the displacement of a variable displacement, piston type pump which is driven through gears from the gas turbine, Figure 1. The displacement or stroke of the pump determines the flow and this is directly proportional to a control oil pressure which is supplied by the fuel regulator. This control pressure will be referred to later as variable control oil (VCO). The fuel pump has six outlets with each outlet being supplied by three pistons 120 degrees apart in time phase and thus the pump splits the fuel flow among the six combustion chambers as well as setting the total flow.

Fuel Regulator and Electric Governor. The fuel regulator, Figure 2, is an electro-hydraulic servo-mechanism into which are fed a speed signal, an adjustable fuel limit and an exhaust temperature signal. The output of the fuel regulator is a VCO pressure in accordance with whichever of the above signals requires the least fuel flow.

The speed control is an electro-hydraulic governor similar to that used on Alco-General Electric diesel-electric locomotives.[4] The speed signal for the governor is obtained from a 3-phase tachometer generator with a permanent magnet rotor driven from the turbine shaft. The output of this generator is rectified to give a direct voltage which is essentially proportional to speed in the operating range. This direct voltage is applied to a circuit

Paper 50-269 recommended by the AIEE Power Generation Committee and approved by the AIEE Technical Program Committee for presentation at the AIEE Fall General Meeting, Oklahoma City, Okla., October 23–27, 1950. Manuscript submitted July 18, 1950; made available for printing September 7, 1950.

D. C. HOFFMANN is with the General Electric Company, Philadelphia, Pa., and A. G. MELLOR and N. E. STARKEY are both with the General Electric Company, Schenectady, N. Y.

consisting of a solenoid operated pilot valve and a speed setting rheostat. The governor, as used in this application, has approximately a 2-to-1 speed range with speed being adjustable by varying the resistance of the speed setting rheostat by means of a split series field d-c motor mounted on the regulator. This motor also positions the adjustable fuel limit.

The adjustable fuel limit is used to set the correct VCO for starting and for acceleration. Above about 40 per cent speed the unit is under the control of either the speed governor or the exhaust temperature control and the adjustable limit is no longer effective.

The turbine exhaust temperature signal is obtained from a gas-filled bellows and tube assembly, mounted on the turbine exhaust hood and connected to the regulator by a capillary and bellows. This signal limits the VCO output of the regulator (and consequently the flow from the fuel pump) to prevent the turbine exhaust temperature exceeding a set limit. The exhaust temperature control also limits the rate of change of exhaust temperature by limiting the rate of change of VCO pressure. No control of the rate of decrease of exhaust temperature is possible under emergency conditions since it is necessary to shut off the flow of fuel as rapidly as possible.

Stop Valve. The stop valve is a solenoid operated valve located in the inlet line to the fuel pump.

Overspeed Governor. This is a flyball type governor, Figure 3, which operates a valve to reduce VCO pressure in the event of overspeeding of the unit. It also incorporates a switch, set to operate at 110 per cent speed which will act to close the stop valve and shut down the unit.

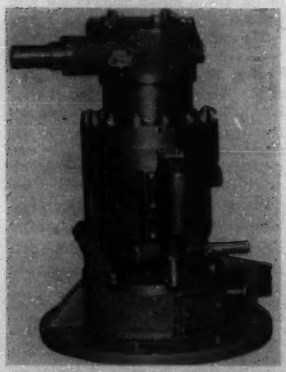

Figure 1. Variable displacement fuel pump

Fuel Transfer Valve. This is a motor operated, 3-way valve used to transfer from diesel oil to bunker C and vice versa. Since the diesel oil used is approximately at room temperature while the bunker C is at approximately 225 degrees Fahrenheit, the transfer from one fuel to another must be made gradually to avoid rapid temperature changes in the fuel pump.

Flame Detector. The flame detector consists of a thermopile which has several thermocouples exposed to the radiation from the flame in the combustion chambers and an equal number of thermocouples exposed to compressor discharge air temperature. The output from this thermopile is amplified and used to actuate certain relays in the turbine control panel.

Ignition System. Two 60-cycle 110/-15,000-volt ignition transformers and two spark plugs are used to initiate combustion. Fuel in the other four combustion chambers is ignited through cross-fire tubes between adjacent combustion chambers. The spark plugs used are of a retractable type which are extended into the combustion chambers by springs when the gas turbine is at rest or operating at low speeds. As the turbine accelerates to idle speed, the increased air pressure in the combustion chambers forces the spark plugs to a retracted position away from the flame.

Atomizing Air Compressors. This is a 2-stage centrifugal compressor driven from the gas turbine. Air, extracted from the main compressor discharge, is cooled, compressed in the atomizing air compressor and supplied to the fuel nozzles for fuel atomization.

A booster air compressor is used to increase the atomizing air flow during starting of the gas turbine. This is an induction motor-driven compressor which is shut down when the main atomizing air pressure is sufficient.

Lubricating Oil Pumps. This is a centrifugal type pump driven from the gas turbine. This pump is capable of supplying all the lubricating oil required above about 75 per cent speed of the gas turbine.

An a-c motor-driven auxiliary lubricating oil pump is provided to supply lubricating oil for starting and also is started automatically in case of failure of the main lubricating oil pump.

A d-c motor-driven emergency lubricating oil pump is provided as a backup in case of failure of both the main and auxiliary lubricating oil pumps.

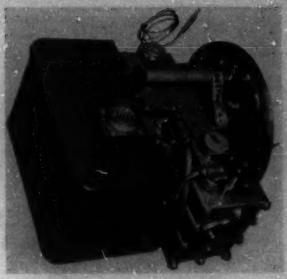

Figure 2. Fuel regulator

Starting Equipment. A 2-hp a-c motor-driven turning gear is used to start the gas turbine from rest in order to establish an oil film in the bearings before starting the main cranking motor. The turning gear is also used to rotate the unit to insure proper cooling. The turning gear drives the turbine shaft through gears and is engaged by means of a solenoid.

The main cranking motor is an 1,800-rpm wound rotor induction motor which drives the turbine through a step-up gear and clutch. Switching of the secondary resistors of this motor gives the correct torque characteristic for cranking the unit up to firing speed and for assisting acceleration to idle speed after firing.

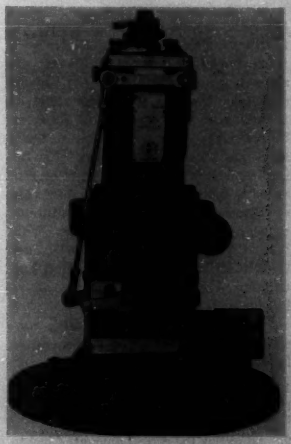

Figure 3. Overspeed governor

Figure 4. Turbine control board, front view

MISCELLANEOUS EQUIPMENT

A gas-filled tube mounted in the turbine exhaust hood protects the turbine against excessive temperatures.

Several pressure and temperature switches are provided in the lubricating oil, fuel oil, and atomizing air systems to indicate abnormal conditions.

Electric pressure transmitters are used to give an indication of lubricating-oil pressure and fuel-oil pressure at the turbine control panel.

A high-low level indicator with alarm contacts is provided in the lubricating-oil tank.

Turbine Control Board

The turbine is controlled from the main duplex control board located on the turbine room floor. The board consists of stationary front and rear panels with top plates and an end enclosure with hinged door, all bolted together to form a rigid self-supporting structure. The control board is bolted to and forms part of the a-c switchgear for the generator. Instruments, recorders, annunicator, and control switches are mounted on the front panels, Figure 4. Sequence and protective relays are mounted on the rear panels, Figure 5.

In an installation of this type, many conditions must be checked before the turbine can be started safely. Starting and stopping the unit includes steps that must be performed in correct sequence and at proper time intervals. Automatic control is provided to relieve the operator of most of the routine and responsibility of performing and checking each step in the starting and stopping sequences. The indications to start and stop the unit normally are given by a master control switch on the duplex control board.

In designing the control and protective circuits, principles well established in other applications of automatic control were used to full advantage. Such principles include the use of a station battery, selective fusing of control and trip circuits, and interlocking of sequence and timing functions to obtain maximum reliability, safety, and continuity of service.

Protective devices are grouped so that they are selective in regard to the manner in which the unit is shut down, as will be detailed later.

Automatic Starting Sequence

All automatic control functions are directed by a master relay that must be energized by the master control circuit before the unit can be started. This master circuit includes contacts of protective relays and other devices that check that normal operating conditions exist before the starting sequence can begin. If normal conditions exist, the operator may start the unit by means of the master control switch.

While the actual starting sequence is automatic, there are a number of operations and checks that the operator must make before starting and during the starting sequence. If it is assumed that control and auxiliary power are available and that all protective devices and annunciator drops are in their normal reset positions, the following are the specific steps that the operator must take to put the unit on the line:

1. Check that the operation selector switch is in the automatic position to permit the starting sequence to take place without interruption. Other positions of this switch are used for test purposes, as will be described later.

2. Check that the fuel selector switch is in the desired position. With the switch in the bunker C position, the turbine is started on diesel fuel and transferred to bunker C fuel automatically at the proper time in the sequence. The switch may be put in the diesel fuel position for continuous operation on diesel fuel.

3. Start any required cooling water and fuel oil pumps and check temperature and pressure of fuel oil. The diesel fuel oil must be at proper operating pressure before the turbine can be started. In an emergency, the turbine can be started and run on diesel oil until bunker C oil at proper temperature and pressure is available.

4. Start the auxiliary lubricating oil pump to provide oil pressure during starting. After the turbine has come up to speed, the direct connected oil pump will supply lubricating oil at the required pressure, and the auxiliary oil pump can be shut down.

5. Close the circuit breaker feeding the d-c emergency lubricating oil pump so that the pump will be ready to start at any time upon failure of normal pressure, whether supplied by the direct connected pump or by the auxiliary pump.

6. Operate the master control switch to the start position. This causes the turbine to start automatically (see subsequent details).

7. Stop the auxiliary lubricating oil pump when the turbine is up to approximately full speed.

8. Synchronize the generator to the bus and pickup load.

When the operator turns the master control switch to the start position in step

Figure 5 (left). Turbine control board, rear view

Figure 6 (right). 3,500-kw gas turbine-generator set

Table I

Nature of Trouble	Type of Device	Group I Prevent Starting	Group II Alarm	Group III Immediate Shut Down
High exhaust temperature	Temperature switch (low set)		X	
High exhaust temperature	Temperature switch (high set)	X		X
High exhaust temperature	Temperature recorder		X	
High lube oil temperature	Temperature switch (low set)		X	
High lube oil temperature	Temperature switch (high set)	X		X
High bearing temperature	Temperature recorder		X	
High atomizing air temperature	Temperature switch (low set)		X	
High atomizing air temperature	Temperature switch (high set)	X		X
Low fuel temperature (bunker C)	Temperature switch		X*	
Hot auxiliary lube, pump motor	Thermal overload relay		X	
Hot d-c emergency lube pump motor	Thermal overload relay		X	
Hot turning gear motor	Thermal overload relay		X	
Hot cranking motor	Thermal overload relay		X	
Low lube oil pressure	Pressure switch (high set)		X	
Low lube oil pressure	Pressure switch (low set)	X		X
Low fuel pressure (bunker C)	Pressure switch		X*	
Low fuel pressure (diesel)	Pressure switch	X		X
Low lube oil level	Float switch		X	
High lube oil level	Float switch		X	
D-c emergency oil pump running	Contact on starter		X	
Low d-c voltage for emergency lube pump	Undervoltage relay	X	X	
Excessive vibration	Vibration recorder		X	
Overspeed	Centrifugal switch	X	X	X
Failure to fire	Definite time relay		X	X
Incomplete starting sequence	Definite time relay		X	X
Loss of governor voltage	Undervoltage relay		X	X
Loss of flame	Flame detector		X	X
Fuel transfer valve not in diesel position	Position switch	X		
Generator protective devices	Lockout relay	X		X
Automatic tripping of generator breaker	Breaker interlock		X	
Station service transformer trouble	Lockout relay	X		X
Abnormal voltage on auxiliary power bus	Reverse phase and undervoltage relay	X	X	
Emergency of any kind	Emergency stop buttons			X

* Also automatically transfers fuel supply from bunker C to diesel oil.

6 above, the following operations take place automatically and in the sequence indicated:

1. The green lamp above the switch is extinguished and the yellow lamp is lighted. The green lamp indicates that conditions are proper for starting the unit (see Protective Operation). The yellow lamp indicates that the unit is in the process of starting.

2. The turning gear motor starts and turns the turbine shaft at 2 rpm.

3. The cranking motor starts and accelerates the turbine to about ten per cent speed. The cranking motor is connected to the turbine shaft by a solenoid engaged overrunning clutch that is energized before the motor is started.

4. The combustion chambers are purged of possible explosive mixtures by allowing the cranking motor to drive the turbine at about ten per cent speed for several minutes.

5. The regulator positioning motor is adjusted to provide a fuel setting proper for firing.

6. The fuel valve opens, the booster air compressor starts, and ignition is turned on. Booster air pressure is used to insure complete atomization of the fuel at the low speed at which the turbine is running.

7. When the turbine fires, the flame detector operates to cause the sequence to proceed. If the turbine does not fire within a predetermined time, the ignition, fuel, and booster air are cut off. The turbine runs at 10 per cent speed for a definite time to purge the combustion chambers, after which the ignition, fuel, and booster air are turned on again. If the turbine does not fire after the second such attempt, it is shut down completely and locked out (see Protective Operation).

8. When the flame detector indicates that the turbine has fired, the speed of the cranking motor is gradually increased by shunting out secondary resistance and the turbine is accelerated by the cranking motor and by its own power. The ignition is cut off.

9. Fuel is increased and as the turbine comes up to self-sustaining speed, the cranking motor disengages and shuts down. The booster air compressor also is shut down.

10. When the turbine reaches about 80 per cent speed, the fuel transfer valve gradually changes the fuel supply from diesel to bunker C. The yellow lamp is extinguished and the red lamp is lighted to indicate the end of the starting sequence.

When the end of the starting sequence is indicated by the red lamp, the operator should shut down the auxiliary lubricating oil pump, as the direct connected pump is capable of supplying sufficient pressure. The operator may now synchronize the generator, connect it to the bus, and load it in the usual manner.

Normal Shutdown Sequence

The normal shutdown sequence of the unit is almost entirely automatic. The definite steps to be taken by the operator are:

1. Decrease load to zero and disconnect the generator from the bus in the usual manner.

2. Operate the master control switch to the stop position. This initiates the automatic stopping sequence (see subsequent details).

3. Stop the motor-driven fuel supply pumps.

4. At the end of the automatic stopping sequence, open the circuit breaker to the d-c emergency lubricating oil pump so that the pump will not start when step 5 is taken.

5. Stop the auxiliary lubricating oil pump and cooling water pumps.

When the operator turns the master control switch to the stop position in step 2 above, the following operations take place automatically in the sequence indicated:

1. The red lamp is extinguished and the yellow and green lamps are lighted. The yellow lamp indicates that the stopping sequence is in progress. The turbine can be restarted any time that the green lamp is on and during cooldown.

2. The diesel-fuel supply pump starts and the fuel transfer valve gradually changes the fuel supply from bunker C to diesel oil.

3. The turbine runs for several minutes on diesel oil to purge the lines of the heavier bunker C oil. At the completion of this run, the green lamp goes out.

4. The fuel supply is gradually reduced until the flame goes out. The fuel valve then closes completely.

5. The turbine coasts to a stop.

6. The turning gear motor starts and the turbine is rotated for several minutes to allow proper cooling of all parts.

7. The turning gear motor stops and the turbine coasts to a stop. The yellow lamp is extinguished and the green lamp is lighted to indicate the end of the stopping sequence.

Test Operation

An operation selector switch is provided for interrupting the starting sequence at several selected points for test purposes, or to facilitate calibration of protective and control devices. The switch has the following positions: manual; turning gear; crank; fire; speed control; and automatic.

During normal operation, the selector switch is in the automatic position and the sequence is not interrupted. In the manual position, various turbine accessories that ordinarily start automatically can be started and stopped only by individual control switches. The devices that can be so operated are: turning gear motor (jogging only); booster air compressor motor; governor positioning motor; ignition transformers; and fuel transfer valve.

The other positions of the selector switch indicate points at which the sequence can be stopped. For example, in crank position, the automatic starting

sequence progresses only to the point where the turbine is cranked at 10 per cent speed by the cranking motor. The operator can set the switch in any of the four positions and the starting sequence will proceed to that point, or the operator can progress from point to point.

Protective Operation

The turbine and its accessories are protected against damage due to any abnormal condition likely to occur in an installation of this kind. The turbine is prevented from starting unless all conditions affecting its operation are normal. Contacts of the devices that check these conditions are connected in series with the master control relay. Other protective devices shut down the turbine if any trouble develops while it is in operation. In order to obtain maximum continuity of service, which means not shutting down the turbine unless necessary, the protective devices are grouped according to the seriousness of the abnormal condition.

Group I includes devices that prevent the turbine from starting.

Group II includes devices that detect trouble of relatively minor nature. These devices operate an annunciator and sound an alarm so that the operator can take the necessary steps to correct the trouble before a shutdown becomes necessary.

Group III includes devices that detect serious trouble that requires immediate shutdown of the turbine. In an emergency such as this the fuel is shut off immediately. The normal shutdown sequence is not used, that is, the fuel lines are not purged and the turbine is not cranked for cooling. The operator must take appropriate action, depending upon circumstances.

There may be some differences of opinion among operators and gas turbine engineers as to the grouping of the various protective devices. Operating experience will eventually determine the best practice. Table I is the grouping used at the present time.

Control of Auxiliary Motors

Conventional motor control equipment is used for the various auxiliary motors referred to in the description of the turbine control. Additional interlocks are provided as required to enable these motors to be started and stopped at the correct points in the sequences. Thermal overload relays in the motor circuits are used to give a warning in case of overheating of a motor.

In addition to the motors directly associated with the operation and control of the gas turbine, a complete gas turbine generating station requires motor-driven cooling water pumps, diesel-oil supply pumps, bunker C oil supply pumps and bunker C centrifuges. This equipment and its control is all of conventional design.

Modification of Control for Gas Fired Units

The turbine control described is designed for a liquid fuel-fired gas turbine unit. The modifications required to adapt the control for a gas-fired unit are minor and result in some simplification. Fuel flow for a gas-fired unit is determined by the opening of a gas control valve. The same fuel regulator is used but the VCO output of the regulator controls the position of the gas control valve instead of the displacement of the fuel pump. No atomizing air compressors are required on gas-fired units and the control for transfer of fuel from diesel oil to bunker C is eliminated. No fuel supply pumps or centrifuges are required, but, in cases where the available gas pressure is too low, a fuel gas compressor is required.

Automatic Gas Turbine Stations

The possibility of building completely automatic, unattended gas turbine generating stations was taken into consideration in the design of this control system. The modifications and additions required for an unattended gas-fired station are minor but an unattended oil-fired station presents some additional complications mainly in the fuel handling, heating and centrifuging equipment required for the bunker C oil.

Conventional supervisory equipment can be used for remote control and telemetering of any number of quantities desired.

References

1. Two Gas Turbines for Power Generation, **Alan Howard.** *AIEE Transactions*, volume 68, 1949, part I, pages 461–6.

2. Huby Gas Turbine Ticks Off 3,400 Hours, **J. W. Blake, R. W. Tuby.** *Power* (New York, N. Y.), February 1950.

3. Gas-Turbine Electric Generating Unit Installed at Farmingdale, Maine. *Power Engineering* (Chicago, Ill.), June 1950, pages 72–73.

4. Electro-Hydraulic Control of Diesel Electric Drives, **C. B. Lewis, M. A. Edwards.** *Mechanical Engineering* (New York, N. Y.), November 1946.

Discussion

Joel W. Blake (Oklahoma Gas and Electric Company, Oklahoma City, Okla.): The authors have presented a very complete outline of the control of gas turbines with particular reference to a system for starting and governing as used on General Electric Company gas turbines burning either liquid or gaseous fuel.

The control for a gas turbine is quite complex. The starting phase involves many variables such as purging; control of exhaust temperature (both rate of change and top limit) acceleration; supervision of flame; and so forth. When up to speed and on the line, all of the features of steam turbine governing must be covered, with the addition of exhaust temperature control and supervision of flame.

My discussion will be limited to the control as applies to the simple cycle unit installed at Belle Isle Station burning natural gas only.

At our insistence, particular consideration was given to protection against any possibility of explosion occurring during the starting phase. Originally, a purging blower was included to remove any gas fuel which might pass the closed control valve while the unit was shut down. After a few starts, it was apparent that this device was unnecessary and it was removed. The present practice is the same as is followed on our gas fired boilers, namely, when the unit is down a lubricated cock in the gas supply to the unit is closed and the vent down-stream from this valve is opened to atmosphere.

Another precautionary step in the starting cycle was the inclusion of a purge period. It was felt that if such a step were included, the exhaust duct system and recuperator would be entirely scavenged and when the unit did fire, there would be no possibility for an explosion to occur. The duration of this purging period is six minutes and we have seen no occasion to alter the length of time.

The governing of the unit has been very good. Being steam turbine minded, we were quite skeptical of the electro-hydraulic governor used. It was felt that any type of turbine should have a governor which could be "worked on" with a wrench and screw driver rather than an electrical analyzer set and turning of rheostats or changing condensers. We must admit though, that the governor is a good one and our concern was unfounded. This device, being one with which our men were unfamiliar, required a complete set of instructions which we now have. We still have the self-satisfaction, however, that the last line of defense, the emergency governor, is of the fly-ball type.

Protective devices have functioned as intended, with a minimum of trouble. One unit, the dual flame detector, originally was of rather short life, however, improvements in mounting have greatly prolonged their life. The unit functions only if both the detectors go bad. This has happened only once to date and since they are the "fail-safe" type, it merely caused a shutdown.

The quality of the entire starting and gov-

erning system is demonstrated by pointing out that it has functioned perfectly through over 100 starts and almost 9,000 hours of operation. It also should be pointed out that the maintenance on the entire control equipment is work for a high type electrical technician rather than an unskilled man.

Our unit can be called a semiautomatic job with complete supervision and protection of all important points. It is easy for us to foresee that little added equipment would be necessary to make it fully automatic. As such, there is no reason why the unit should not function entirely by remote control.

Thrust Bearing Problems and Their Solution on Turbine-Generator Units and Auxiliaries of the Consolidated Edison System

JOHN M. DRISCOLL
NONMEMBER AIEE

H. C. OTTEN
MEMBER AIEE

IT HAS BEEN our purpose in preparing this paper to describe a few of the thrust bearing failures which have occurred in the plants of the Consolidated Edison Company of New York, Inc., and its affiliate, The Yonkers Electric Light and Power Company.

The failures selected for this presentation were chosen because their causes have been reasonably well-established, and the necessary corrective alterations have now been made to prevent recurrence. In some other instances it was difficult to determine the reasons for the thrust bearing failures, because of the almost total destruction which ensued. Without clues there is little chance of making an accurate appraisal of the factors contributing to the failure.

Still, it can be stated with some degree of certainty that, in our system, very rarely if ever, have the thrust bearing failures been the result of outright lubrication stoppage. Therefore, the failures that we have had on horizontal shaft units must be attributed to some temporary upset which boosted the thrust load to values several times higher than the calculated carrying capacity of the bearing, or else to the end result of gradual and slow wear of the thrusting surfaces.

Case 1

In horizontal auxiliary machines having little or no axial load, the thrust bearing consists of shaft shoulders, or equivalent arrangement, thrusting against parallel babbitted surfaces at each end of a journal bearing. This is a simple construction which is satisfactory in these cases because, in the absence of axial load, the function of the bearing is limited to the maintenance of the correct relationship between revolving and stationary elements.

Our systems have many auxiliaries provided with that type of thrust bearing and, in the main, they have given satisfactory service. There are, however, exceptions and among them the most outstanding are three identical General Electric turbines driving three 2,000 gallons per minute boiler feed pumps through reduction gears. These impulse turbines which revolve at 7,664 rpm are rated at 1,000 horsepower and transmit their power through Falk flexible couplings to reduction gear pinions so that no axial load is transmitted from the gears to the turbine shaft. All the bearings are forced lubricated by a shaft-driven gear oil pump which is part of the installation.

Since initial operations, some 25 years ago, the thrust bearings of these turbines have failed intermittently, sometimes in rapid succession and at other times taking several months of operation. After repeated investigations with negative results, efforts to reach a solution were abandoned and every one concerned arrived at the conclusion that these particular turbine thrust bearings were mechanical oddities.

This feeling had prevailed for a long time until recently when a new approach was initiated. The new study was precipitated by a series of thrust bearing failures which nearly crippled the Station.

As a first step in the new investigation, thermocouples were embedded in the thrust plate and their readings indicated metal temperatures as high as 190 degrees Fahrenheit. This was attributed to lubrication deficiency and the oil passages were enlarged so as to double the oil flow to the thrust bearing, but no improvement resulted. This led to the assumption that the axial thrust load was higher than computed and that a better type of thrust bearing was required to absorb it. Accordingly, the manufacturer advised us to substitute their standard tapered land thrust bearing plate for the old single plane stationary plate. Bearings of this newer type have their thrusting surfaces so designed that they can withstand loadings resulting in pressures of 175 to 250 pounds per square inch and are able for short intervals, to sustain pressures as high as 1,500 pounds per square inch with impunity. As this was several times greater than the load-carrying capacity of the old thrust bearing, it was hoped that there would be no need for increasing the thrusting surfaces, and this surface was kept to 11.77 square inches, as in the old type.

After the substitution, failures occurred again but it was observed that very often the temperature of the thrust plate was highest during starting operations. This observation led to the conclusion that damage originated during starting periods and that, once started, this damage progressed with more or less rapidity until total failure occurred. It was then decided to supply more oil during starting by introducing high pressure oil from the independent station system, and maintaining that pressure until the turbine had reached sufficient speed to insure hydrodynamic lubrication by the self-pumping effect in the thrust bearing.

As a result of these innovations, the life of the thrust bearing was extended,

Paper 50-270, recommended by the AIEE Power Generation Committee and approved by the AIEE Technical Program Committee for presentation at the AIEE Fall General Meeting, Oklahoma City, Okla., October 23-27, 1950. Manuscript submitted July 25, 1950; made available for printing September 19, 1950.

JOHN M. DRISCOLL is with the Consolidated Edison Company of New York, Inc., New York, N. Y., and H. C. OTTEN is with The Yonkers Electric Light and Power Company, Yonkers, N. Y.

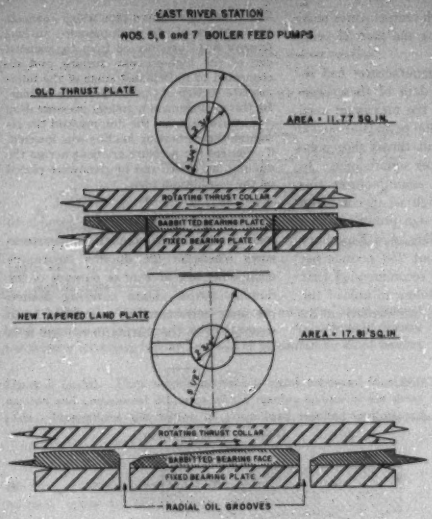

Figure 1. Sketch illustrating changes in form and dimensions of thrust bearing elements to obtain satisfactory performance

but thermocouple temperatures gradually increased over a period of months to the point of failure of the bearing. It was then decided to increase the bearing surface from 11.77 square inches to 17.81 square inches, that is, by about 50 per cent. At the same time the oil piping was rearranged so that the turbine admission valves could not be opened unless the station central oil system was cut in and the thrust bearing supplied with high-pressure oil. Figure 1 shows the developed surfaces of the old and new thrust plates.

Since these last changes a few months ago, the thrust bearing metal temperature has not exceeded 140 degrees Fahrenheit which is the lowest temperature recorded for this bearing, and we now have confidence that the problem has finally been solved.

Case 2

No matter how disturbing to the operation of a power plant a thrust bearing failure of an auxiliary can be, it does not compare with the havoc which can be wrought by the loss of the thrust bearing of a turbine generator. For this reason, the balance of this paper will be devoted to failures of this latter type.

In the same station where the boiler feed pump mentioned previously is located, there is a General Electric 60,000 kw turbine generator which developed cracks in the high-pressure section of the turbine shell. At the appropriate time, it was decided to ship this turbine shell to the manufacturer for repair, and at the same time modernize the unit. Included in the alterations was the replacement of the turbine multicollar marine type thrust bearing by a tapered land thrust bearing.

After repairs and renovation the unit was tested, and the thrust bearing failed when full load was reached. Fortunately, the slender stub shaft carrying the thrust collar and overspeed governor vibrated so violently when the failure occurred that the overspeed governor operated and tripped the machine. Measurements taken afterwards indicated a turbine spindle shift of 0.140 inch toward the generator. As this was less than the smallest axial clearance, no internal damage resulted.

Upon inspection, the babbitted surface of the thrust ring was found to be completely wiped and the corresponding steel face of the thrust collar was badly scored for a width of about 2 inches near its outer rim. After rebabbitting the ring and grinding the collar, the thrust bearing was reassembled.

Hardly had the machine been restored to service when another thrust bearing failure developed. This time the machine did not trip itself but was tripped by the engineer hurriedly summoned, after smoke and oil temperature rise were first noticed. Less than one minute elapsed between the discovery of the trouble and the tripping of the machine. Measurements indicated a turbine spindle shift of 0.167 inch with serious damage to the packing strips.

A more detailed inspection of the component parts of the thrust bearing was made, and it was then found that the vertical wall of the thrust cage upon which the damaged thrust plate was bearing was relatively thin and was permanently dished out. After this finding, the cause for the failure became evident and was easily explained as follows:

Under the total thrust load, this wall of insufficient thickness deflected, and as the wall was receding from the thrust collar near the shaft, the load shifted radially and concentrated at the outer periphery of the thrust ring thus creating, at that location, enormous unit pressures and, ultimately, causing the failure of the ring and scoring of the thrust runner.

Temporary repairs were made, and pending receipt of a new, larger, and stronger thrust bearing, the machine was operated at a load which resulted in a thrust plate thermocouple temperature of 185 degrees Fahrenheit. In time the new thrust bearing was received and installed, and the load restriction was lifted. Figures 2 and 3 illustrate the preceding discussion.

The deflected position of the thrust plate as shown by the dotted line on Figure 2 is greatly exaggerated. Actually this deflection amounted to only a few mils but was nevertheless sufficiently large to cause the thrust bearing failure. And, although the thrusting surface which failed was enlarged in the new thrust bearing, the real cause was not in the faulty design of this surface proper but in an error in the structural computation of the thrust bearing cage.

Case 3

Of a different nature were the two thrust bearing failures which occurred in another unit. This other machine is a 50,000-kw tandem compound Westinghouse unit which had been in operation, at the time of the first failure, for 22 years. Besides this unit, we had two other identical ones, and when these machines misbehaved upon occasion, their Kingsbury thrust bearings were never involved.

Then one day, and for no apparent reason, the thrust bearing of this unit failed with severe damage to the blading. The thrust bearing destruction of course was complete and not much was left to establish the origin of the failure. However, during the inspection which followed it was found that a vent hole, which should have been provided at the top of the thrust cage did not exist. As no such omission was found in the two

other sister units, it was concluded that an air pocket had built up at the top of the thrust cage and had depressed the oil level in the cage to a point where parts of one or two top shoes did not bathe any longer in oil. The result of such a happening would be to overload the other shoes.

As mentioned earlier in this paper, complete certainty as to the causes of a failure is almost impossible to attain, and not everyone was in agreement with the above deduction, the main objection being one to which we could not find the answer, namely, why had this failure not occurred during the preceding 22 years.

The damaged rows of blades were cut out, the thrust collar was resurfaced, and the thrust shoes were rebabbitted. The unit was then restored to service, but with its maximum load limited to 30,000 kw because of the missing rows of blades.

The unit was operated under these conditions for about eight months without any further indication of thrust bearing trouble. It was finally taken out of service to reblade the high-pressure turbine and, at the same time modernize the whole unit. This work required approximately four months.

Shortly after the unit had been recommissioned, the thrust bearing failed again, and in the process many of the newly installed blades were either broken or so badly bent that they had to be renewed. Once more the thrust collar was resurfaced and the thrust shoes rebabbitted, but this time thermocouples were embedded in the thrust shoes on either side of the thrust collar, and as soon as the blading damage was repaired, some two months after the failure, the unit was returned to service.

To the general alarm of everyone concerned, it was found that the metal temperature of the loaded thrust shoes, as indicated by the thermocouples, was directly proportional to the kilowatt load and had already reached 185 degrees Fahrenheit when that load was only 40 megawatts, with every indication that the temperature would have continued to climb had the load been increased. Rather than risk a third failure, the load on the machine was limited to 40 megawatts and the problem referred to the manufacturer.

While awaiting the manufacturer's recommendations, the second identical unit in the station was taken out of service to install thermocouples in its thrust shoes for comparison purposes and it was found that under load their metal temperature was likewise running close to 180 degrees Fahrenheit. It was then assumed that these high temperatures must have prevailed during the past 23 years on both units.

Meanwhile, the manufacturer had reviewed the original data of these units and had found that the maximum axial thrust force was 63,300 pounds at 50,000 kw, resulting in a unit thrust shoe pressure of 443 pounds per square inch. In the opinion of the manufacturer this pressure was too high when compared with present-day design practice which limits the shoe loading of a Kingsbury type bearing to about 250 pounds per square inch, and he recommended that immediate steps be taken to unload the thrust bearing. This was carried out by the following method:

The 7-inch equilibrium pipe which connects the exhaust of the high-pressure turbine dummy was disconnected from the exhaust end of the high-pressure turbine and reconnected to the exhaust stage of the intermediate section of the low-pressure turbine. By this arrangement a greater pressure drop was attained across the dummy and the resultant thrust bearing loading was lowered. To control the pressure gradient across the dummy, an orifice and by-pass were placed on the equilibrium pipe.

With the by-pass, it also is possible to maintain the same exhaust dummy pressures whenever the dummy clearances change because of wear or damage of the dummy strips. Data covering desired pressures corresponding to definite loads were given to the station force, and it is

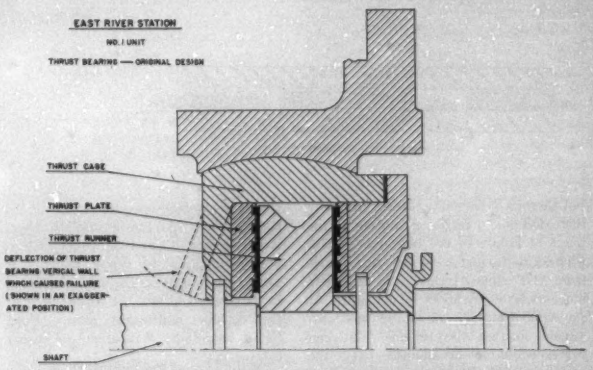

Figure 2. Inadequate stiffness of thrust bearing cage permitted slight deflection under load. Resulting local loading of thrust plate caused overheating and failure

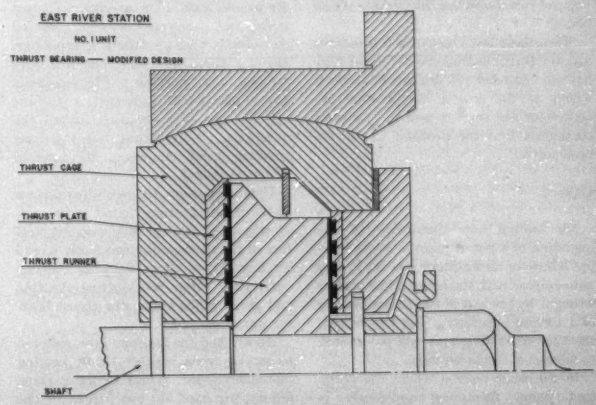

Figure 3. Modified design of thrust bearing provided greater stiffness of cage wall and increased area of bearing surface

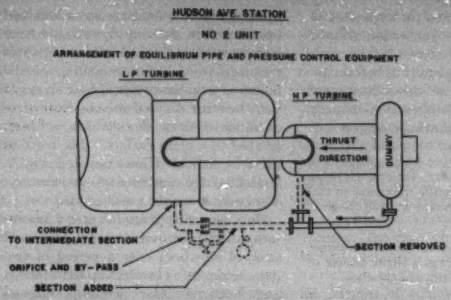

Figure 4 (above). Change in arrangement of piping introduced steam at lower pressures on low-pressure side of dummy. Axial thrust of dummy was thereby increased, leaving less load to be carried by thrust bearing

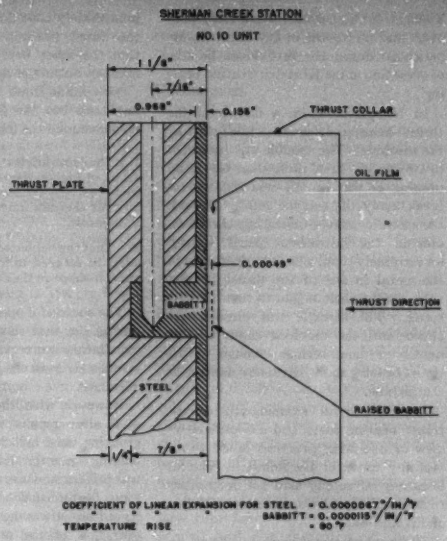

Figure 5 (right). Thick section of babbitt metal produced local expansion and consequent distortion of the running surface of the thrust plate. Nonuniform distribution of thrust load resulted and caused overheating of the metal

the duty of the operator to manipulate the by-pass valve to obtain these recommended dummy exhaust pressures as the load changes.

Figure 4 shows the piping alterations made to reduce the thrust load.

Case 4

From the experience derived from the cases previously reported, it is now the practice of the Consolidated Edison Company to install thermocouples in the metal of turbine generator thrust bearing plates or shoes. This job is done whenever the units are taken out in turn for overhaul, or in new units specified during contract negotiations.

Recently, one of these newly purchased units was commissioned with thermocouples installed in the thrust bearing plates by the manufacturer. However, our original request was for the thermocouples to be embedded in the steel section of the thrust plate as close to the root of the babbitt metal as possible without touching it. Instead, and because he considered such a method would not give true babbitt metal temperature, the manufacturer designed babbitt wells, or plugs, contiguous to the babbitt surface, as shown in Figure 5, which were intended to transmit the true babbitt metal temperature to the thermocouples without endangering the load surface of the babbitt by local pressure from the thermocouples.

After a few months of operation, the thermocouples began to show erratic readings and soon thereafter registered alarming high temperatures. As no corresponding increase in thrust bearing return oil temperatures was indicated, it was assumed that the recording instrument was at fault, but this was quickly dispelled by a test, and the machine was removed from service to inspect the thrust bearing.

At first no damage was noted but a closer observation showed two well-defined sections about 2 inches in diameter, slightly raised on the surface of one of the thrust plates. As they were in line with the two thermocouples embedded in the plate, it was immediately suspected that they were in some way responsible for the trouble. This led to an inquiry which revealed the existence of the construction related above.

In possession of this knowledge, an investigation was made of all possible causes which might force the babbitt plug to protrude, and the conclusion was drawn that the trouble was due to the difference in the thermal coefficient of expansion between steel and babbitt.

In Figure 5, the pertinent dimensions and results are given. They show that for an increase of 80 degrees Fahrenheit. above the shop temperature at which the plate was machined, the differential expansion of the plug was about 0.5 mil. As small as this dimension appears, it is a large percentage of the thickness of the oil film existing between runner and stationary plate, and the high temperatures indicated by the thermocouples reflected the local heating resulting from the extra load imposed upon the raised surfaces.

This type of construction now has been eliminated and the thermocouples are embedded in th thrust plates as originally specified.

Case 5

A 20,000-kw Curtis-type vertical shaft turbine generator was removed from one of the generating stations of the Consolidated Edison Company and was installed in 1947 in the Glenwood Station of The Yonkers Electric Light and Power Company. The machine was built in 1911 and was originally equipped with a thrust bearing of the step type requiring a continuous supply of oil at high pressure during operation. Because of the high cost of reconditioning and installing the large high-pressure pumps and accumulator, it was decided to equip the turbine generator at its new location with a Kingsbury thrust bearing. This decision was influenced by a record of some eight years of successful operation of a Kingsbury thrust bearing on a vertical shaft 15,000-kw Curtis turbine-generator at one of the stations of the Philadelphia Electric Company.

Operation of the 20,000-kw machine at the Glenwood Station in the city of

Yonkers, N. Y., commenced in December 1947, and no trouble of any kind was experienced during the first eleven months of operation of the Kingsbury thrust bearing.

In November 1948, a failure of the thrust bearing occurred while starting the machine. The trouble was indicated in two ways: first, more than the usual opening of the throttle was required to break away the turbine rotor. Second, the electric remote-indicating thermometer on the instrument panel showed an extremely rapid rise in temperature of the metal in one of the thrust bearing shoes as the shaft began to turn at slow speed. The throttle was immediately closed and the machine came to rest quickly without serious damage to the thrust bearing and without any damage to the turbine.

A very careful examination of the thrust bearing parts and a complete review of operating practices failed to reveal any cause for the failure. The lubricating oil supply had not been interrupted and the oil was exceptionally free of dirt and water.

The babbitt metal surfaces of the six pivoted segmental shoes of the thrust bearing were found to be undamaged except for scoring in a narrow band about $2^1/_2$-inches wide directly above the center of the pivot plug on the under side of each shoe. Looking down upon the assembled shoes the scored areas presented the shape of an annulus. The width of the babbitted surface of each shoe is about $9^1/_4$ inches in a radial direction.

The nickel alloy cast iron runner which is fastened to the bottom end of the vertical shaft of the machine and constitutes the upper element of the thrust bearing was also found to be discolored but not scored, in a ring-shaped area to match the scoring of the shoes.

Repairs were made by hand-stoning the under surface of the runner, in place, to remove visible particles of babbitt and a spare set of thrust shoes was installed.

Upon restoration to service, the thrust bearing operation appeared to be normal for four days. On the fifth day a groaning noise was noticed as the machine came to rest in shutting down. The noise was thought to come from the thrust bearing. The machine was started twice the next day and no abnormal temperatures of the thrust bearing shoe or of the oil were observed. The noise at shutdown persisted, however. At the next attempt to start the machine on the following day a rapid rise in indicated shoe temperature from 76 degrees Fahrenheit to 110 degrees Fahrenheit occurred and the machine was immediately shut down for inspection of the thrust bearing. Inspection showed that the shoes were scored in the same manner, but not as severely as before.

No specific cause for this failure could be found but the Kingsbury Company recommended the following changes:

1. That the lubricating oil be changed to an oil of higher viscosity, the change being from 140 Saybolt seconds universal to 220 Saybolt seconds universal at 100 degrees Fahrenheit.

2. That the babbitted surfaces of the thrust shoes be scraped to form a slight hollow of circular shape in the center of the shoe.

The successful operation of the bearing during the first eleven months after its installation was regarded as an indication that the over-all design of the bearing was adequate.

However, when the machine was operated after repairs were completed the groaning noise associated with the thrust bearing when the shaft came to standstill was present and was more severe than before. No unusual temperatures were observed but it was decided not to continue operation of the machine under these conditions. Accordingly the thrust bearing was once more opened for inspection.

No additional scoring was found but the babbitt metal showed many bright spots in the area outside of the central depressed area. It was the manufacturer's opinion that the louder noise which had been heard in shutting down could have been caused by the higher unit pressures resulting from the introduction of the hollow area in the center of each shoe. It was therefore decided to substitute a reconditioned set of shoes which had been scraped to a plane surface. The truth of the runner surface was checked with a straight edge and found satisfactory. The bearing was then reassembled.

Following the manufacturer's recommendation, the unit was started and stopped six times over a period of two days before being brought up to full speed and loaded. Regular operation continued for about two weeks during which the noise on shutdown persisted but no abnormal rise in temperature occurred until one day at the end of the period, when another failure was evidenced by a rapid rise in indicated temperature of the bearing shoe.

Upon the occurrence of this failure which was considered to be the fourth, it was decided to dismantle the entire thrust bearing and to return all of the parts to the factory for more thorough inspection and checks than were possible with the runner in place on the turbine shaft.

Inspection at the factory revealed two conditions which had not been found previously during field inspections conducted under difficult conditions. The cast-iron runner was found to have small particles

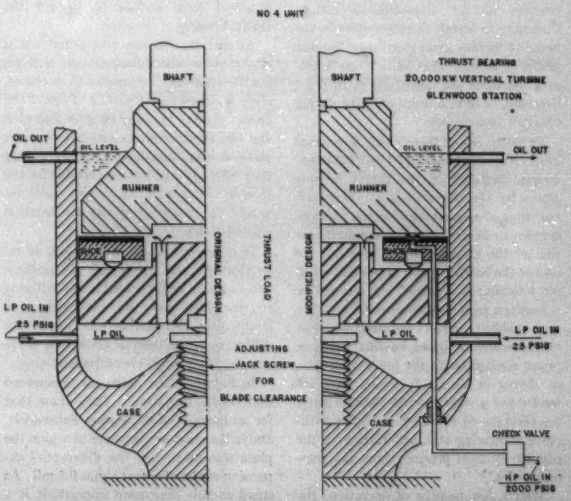

Figure 6. Simplified sketch showing the method used for introducing oil at high pressure to the active surfaces of a thrust bearing required to start and stop while subjected to heavy loading

of babbitt metal embedded in its surface. These were thought to be the result of the first failure of the bearing and the probable cause of the second, third and fourth failures. Hand-stoning would not remove the babbitt particles so the runner was reground and then lapped to a fine finish.

The runner surface also had been found to be very slightly convex instead of being in a true plane. When refinished the surface was left very slightly concave which was regarded as a more favorable condition.

It was the manufacturer's opinion at this stage of the investigation that the second, third and fourth failures might have been prevented had it been possible to observe the embedded particles of babbitt in the surface of the runner after the first failure.

It was decided at this time to make another change of lubricating oil to one of still higher viscosity, 415 Saybolt seconds universal at 100 degrees Fahrenheit, in an attempt to reduce metal-to-metal friction during the critical starting period. It was also decided to use the thrust shoes having a hollow depression in the center.

When the bearing was restored to service this time several months of successful operation were obtained but considerable apprehension was felt because of the continuance of the distinct groaning noise heard each time the unit was approaching standstill in shutting down. The noise occurred only while the shaft was making the last fraction of a turn to standstill. Over a period of several months this groaning noise was kept under close observation and seemed to be gradually becoming louder.

Another failure occurred in July 1949, this being the fifth failure. The manufacturer was then asked to consider design changes in the thrust bearing to make it adequate for the service required. The most obvious remedy, that of reducing the unit loading on the shoes, could not be applied since the load to be supported was fixed and the available space for the thrust bearing was limited by the existing dimensions of the turbine condenser and foundation.

Because of the fact that the bearing showed no sign of distress while operating at full speed it was decided to modify the design to provide for high-pressure forced lubrication of each of the pivoted shoes during starting and stopping periods only.

A method of applying high-pressure forced lubrication to the shoes of a Kingsbury type bearing was first employed in 1929 on two vertical shaft outdoor synchronous condensers of 25,000-kva rating at the Leaside Transformer Station in Toronto, Province of Ontario, Canada.[1] In that installation, high-pressure forced lubrication of the shoes was applied for the purpose of achieving a low-starting torque requirement.

Figure 6 is a simplified cross section of the Kingsbury thrust bearing applied to the 20,000-kw Curtis turbine at the Glenwood Generating Station. On the left side of the shaft center line is shown the original design of the bearing. On the right side of the center line is shown the method by which the high-pressure oil for supplementary lubrication was introduced at the center of the babbitted surface of each pivoted segmental shoe.

The modified thrust bearing was restored to service in October 1949, and has operated satisfactorily since that time. In the period from that date to June 30, 1950, there have been 169 starts of this turbine and 1,265 hours of operation.

It is our practice to start the high-pressure oil pump which has a capacity of 3 gallons per minute at 2,000 pounds per square inch gauge, at the same time that the low-pressure pump for normal lubrication of the turbine-generator is started.

The shaft of the turbine carrying a total weight of about 111 tons, lifts about $3^1/_2$ mils when the pressure at the face of the shoes is about 1,200 pounds per square inch gauge.

The turbine is then started and after full speed of 720 rpm is reached, the high-pressure oil pump is shut down.

When shutting down the main turbine the high-pressure oil pump is started when the turbine speed drops to about 100 rpm and is kept in operation until after the turbine shaft has come to a dead standstill.

It is believed that this procedure will result in continued satisfactory operation of the thrust bearing.

Conclusions

It should be made clear that, with one exception, the thrust bearing failures which are reported in this paper refer to old machines which were built when unit pressures adopted for thrust bearing design were nearly twice as large as the more conservative ones used today. Therefore, in new units trouble of this kind ought not to be encountered.

It has been our intention to show the important role played by the metal temperature-detecting-elements embedded in the thrust shoes or plates. With their help it has been possible to diagnose the trouble and follow the improvement resulting from successive alterations to thrust bearings. Also, as a temporary expedient, it has been possible to continue operation of important units at reduced loads by use of these devices as a guide.

These embedded temperature devices have been found capable of very fast response, and give indication of an abnormal temperature rise much more effectively than the conventional thermometer readings of the bearing oil return temperature. Under steady and normal conditions, the temperature differential between metal and oil was found to be 30 degrees Fahrenheit or more.

The favorable experience that we have had thus far with metal temperature-detecting-devices, has resulted in the decision of the Consolidated Edison Company to specify for new turbine generators on order, automatic alarm and tripping devices actuated by thermocouples embedded in the thrust bearing shoes or plates.

These devices now are expected to provide greater assurance of safety while permitting a minimum of attention from turbine room attendants.

References

1. Vertical Shaft 25,000-Kva Synchronous Condensers, H. A. Ricker, J. R. Dunbar, R. R. Day. *AIEE Transactions*, volume 49, October 1930, pages 1616–27.

Discussion

R. Sheppard (General Electric Company, Schenectady, N. Y.): There certainly can be no question that a thermocouple is one type of indicator that may be used to study progressive improvements in thrust bearing performance in steam turbines. When connected to a recording instrument, a permanent record may thus be kept. Increased temperature of the thrust plates gradually occurring over a period of time may indicate increased loading on the bearing due to formation of deposits upon the buckets or other abnormal change within the turbine.

Until about five years ago, it was the practice in thrust bearing design to combine the discharge oil flows from both the unloaded thrust plate and the loaded plate into a single drain line having one thermometer to register the outlet oil temperature. This practice originated in the old multirunner thrust bearings because it was difficult, if not impossible to separate the oil flows. With the development and introduction to steam turbine practice of the single collar

taper land bearings with two separate thrust plates, the old method of combining the outlet oil flows of the two plates was continued for many years. With a generous size oil supply line from the bearing oil header open right up to the oil grooves of the loaded and unloaded plates, the metered oil flow was regulated by the restriction of the 10 to 12 mils end clearance. The temperature of the combined outlet oil flows after mixing did not rise as a function of greatly increased thrust load.

It is well-known to all thrust bearing designers and experimenters that the power loss of a babbitted thrust plate increases rapidly as thrust load increases. The principal reason for the apparently negligible rise in oil temperature of a single collar thrust with combined discharges is explained in the next paragraph.

Division of oil flow through the two plates when there is no thrust on the bearing is approximately equal because the collar floats between the plates with about equal film thickness. As thrust increases in one direction, the film thickness decreases and somewhat less oil quantity will flow past this loaded plate. However, the clearance increases on the unloaded plate and a greater quantity of cool oil is drawn through it. The two oil streams combining on the discharge side thus exhibit only a negligible rise in temperature with wide changes in the thrust. It is, therefore, not surprising that operators gradually came to feel that the outlet oil temperature was a poor medium by which to judge thrust bearing performance.

Many of the thrust bearings in the turbine generator sets of the Consolidated Edison System have this combined discharge line with the single thermometer as described before. Thermocouples installed in the babbitted plates of these bearings are desirable, if there is any uncertainty, since a properly located thermocouple in the plate will indicate a much larger temperature change with wide variation in thrust load than would a thermocouple placed in the combined discharge oil line.

More recently, the single collar taper land thrust bearings for large turbine generators have all been designed with separate discharge oil passages with individual thermometers in the two oil flow lines. Figure 1 of this discussion represents actual observed temperature readings of the two thermometers as a function of turbine-generator load. The thrust in this particular turbine increased greatly with load and is in one direction throughout the load range. This arrangement of separated discharge oil flows very clearly indicates the direction of the

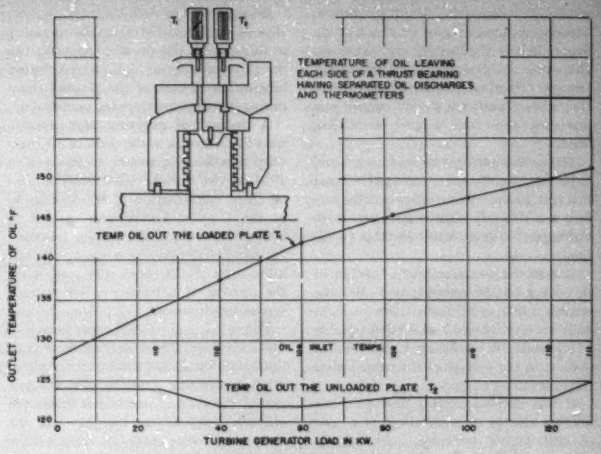

Figure 1. Temperature of oil leaving each side of a thrust bearing having separated oil discharges and thermometers

thrust in a unit, and the temperature rise of the loaded plate is appreciable and easily measured either with thermometers or with recording thermocouples. The outlet oil temperature varies as a function of the load on the turbine-generator through a wide enough range of temperatures that is practical to measure and to clearly indicate abnormal increases in turbine thrust.

The writer believes that the design of single collar thrust bearing with separately measurable oil discharge temperatures will permit satisfactory operator supervision of the turbine thrust bearing equal to that of a thermocouple inserted loosely in a hole in the steel thrust plate about 3/8 inch from the surface of the babbit.

Thrust bearings with embedded thermocouples in the thrust shoes or plates can be made on production units; however, to do so presents practical difficulties in threading them down through heavy bearing caps and housings in such a way that they can be removed easily when rolling out the heavy bearing parts during disassembly and inspections of the turbine. It would appear that a more rugged and lasting arrangement can be obtained if the thermocouples are permanently installed in the drain oil lines of the bearing pedestal where they do not have to be disturbed. They can be installed in the drain oil lines with much less complication to the manufacturers.

The authors make it clear in their conclusions that the thrust failures reported in this paper refer to older machines which were built with design margins far less conservative than present-day practice. This is certainly true considering the prevalence of thrust bearing failures 15 to 20 years ago. In this connection, it may be of interest to know that about 15 years ago the General Electric Company began a program of replacement of low margin thrust bearings in large units of older vintage. Hundreds of such modernizations have been accomplished so that today the industry is relatively free of disturbing thrust bearing failures.

It is the opinion of the writer that the adaptation of signaling and tripping devices that automatically shut down large essential prime movers upon indication of high thrust bearing temperature is justifiable only as a temporary measure on a particular machine whose thrust bearing is of marginal design, until such time as a stronger, more rugged thrust bearing can be installed.

An Air Delayed Selective Overcurrent Tripping Device for Low-Voltage Air Circuit Breakers

B. G. TREMBLAY
NONMEMBER AIEE

M. E. HORN
MEMBER AIEE

ECONOMICS of modern power distribution demand more than ever before that service on low-voltage systems be continuous and that unfaulted portions of the system receive a minimum of interference as a result of faults elsewhere on the system.

This requirement has popularized the use of selective tripping arrangement which, in turn, has imposed new requirements on both air circuit breakers and the tripping devices used with them. Because of the simplicity afforded by direct acting series tripping devices, attention has been focused on this type of device and its time-current characteristics.

The time-current requirement of a tripping device varies considerably with the position of the circuit breaker in a selective system and therefore a device providing a wide range of adjustment is essential for general application. To achieve the main objective, the device must function repeatedly as an accurate timer under variable temperature and atmospheric conditions, it must also possess the all-important feature of resetability which enables the device to respond to an overcurrent impulse but halt tripping action and automatically reset to its initial condition if the overcurrent condition is removed by some other protective device.

Paper 50-271, recommended by the AIEE Switchgear Committee and approved by the AIEE Technical Program Committee for presentation at the AIEE Fall General Meeting, Oklahoma City, Okla., October 23–27, 1950. Manuscript submitted June 29, 1950; made available for printing September 15, 1950.

B. G. Tremblay and M. E. Horn are both with the Westinghouse Electric Corporation, East Pittsburgh, Pa.

A series device has been developed which provides a high degree of adjustability together with a delaying element which is virtually immune to temperature or other atmospheric changes for use with a new line of circuit breakers.

Design Features

This series overcurrent tripping device is air delayed with all of its elements completely adjustable. It is particularly well adapted for use in selective tripping systems. Such a device ready for mounting to a circuit breaker pole unit by means of two or four bolts, depending on coil rating, is shown in Figure 1. The unit shown has a 1,000-ampere coil rating. The maximum coil rating used with the 1,600-ampere frame size circuit breaker is 1,600 amperes. The same unit with the suitable coil can be used on the 225- and 600-ampere frame size circuit breakers.

The device consists of the two main subassemblies, namely:

1. The magnetic frame and coil assembly as shown in Figure 2(A).

2. The delay elements assembly as shown in Figure 2(B).

These two assemblies bolted together form the complete unit.

The magnetic frame and coil assembly, as can be seen from Figures 3, 4, 5, and 6, is always of the same construction and consists of the magnetic frame A, and the stationary core B around which is the series coil D. The magnetic circuit is completed by the moving core C which is part of the delay elements assembly.

The delay elements assembly contains the air chamber and the diaphragm as well as all of the elements to produce the adjustable long-time delay short-time delay, and instantaneous characteristics of the circuit breaker tripping curve. These three elements can be included singly or collectively in any combination.

All parts of these two subassemblies other than the magnetic circuit are made from nonferrous or noncorrosive materials. The diaphragm is molded integrally from silicone rubber and a synthetic fabric which has heat-resisting properties many times greater than that of cotton. A diaphragm made from these materials has been subjected to 4,000,000 operations at 175 degrees Fahrenheit over a period of four months, after which the diaphragm was still in good operating condition. The aging characteristics of silicone rubber are very good over a wide range of temperatures (approximately from −60 to 200 degrees centigrade.) Contrary to the behavior of natural or neoprene rubber, the tensile strength, hardness, and elongation of silicone rubber remain essentially constant with time over this wide range of temperatures.

An overload or short circuit current through the series coil D will cause the

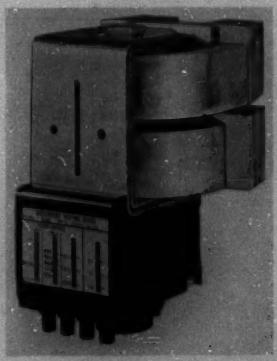

Figure 1. Air delayed overcurrent tripping device with all its adjustable features

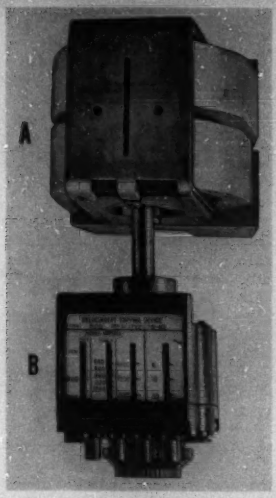

Figure 2. Air delayed overcurrent tripping device showing (A) the magnetic frame and coil assembly and (B) the delay elements assembly

moving core C to be attracted and move toward the stationary core B. At low currents, the moving core C will carry the tripping stem F along with it, immediately closing valve G, after which motion is retarded by the diaphragm E. The rate of travel of the diaphragm is determined by the rate at which air is permitted to enter chamber T by the various valves, H, J, and K. At higher currents when the attraction between the moving core C and the stationary core B is greater than the load on the spring inside the moving core, the moving core will compress the spring and travel independently of the tripping stem F. This spring ensures a constant maximum force pattern acting on diaphragm E. Up to the time the circuit breaker is tripped, this force must always be less than $A(p_a - p_t)$ where

A = area of diaphragm
p_a = atmospheric pressure
p_t = pressure inside air chamber T

By limiting in this way, the maximum force transmitted to the delaying element, the motion of the tripping plunger is dependent only on the rate at which air is admitted to chamber T through the long delay, short delay, and instantaneous valves.

Long-Time Delay Element

The long-time element purposely delays tripping of the breaker on motor starting, overload, and high impedance fault currents. As mentioned previously, Figure 3 shows how the tapered valve H controls the rate at which air is permitted to enter chamber T. For any given setting valve H remains fixed, but a wide variation of settings can be obtained by merely turning the long-time calibration dial S. The pickup current setting of the long delay element can be adjusted over a wide range by means of the adjusting screw P which controls the load on a spring. This spring, in turn, puts a restraining force on the moving core C through lever V.

Short-Time Delay Element

The short-time element intentionally delays tripping of the circuit breaker on fault currents. As in the long delay element, the short delay is controlled by the rate at which air is permitted to enter chamber T. Figure 4 shows how a second tapered valve J also working on the air chamber produces these short delays. Normally valve J is held closed by the adjustable spring Q through the armature M. On overcurrents, it is held closed by the pressure differential between the outside and inside of the air chamber in addition to the spring. The amount of delay is determined by the extent to which valve J is opened which in turn is controlled by the adjustable stop R. Since short delays are of the order of 4 to 30 cycles, this valve must therefore open a comparatively larger orifice than the valve controlling the long-time delay which produces delays of the order of seconds. The pickup current setting is determined when armature M is attracted to the magnetic frame A thereby opening valve J. This setting can be varied by means of the adjustable spring Q which loads the armature M and closes valve J in normal operation.

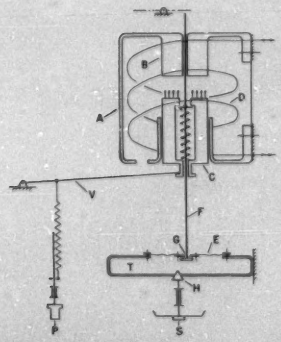

Figure 3. Schematic diagram of the long-time delay element

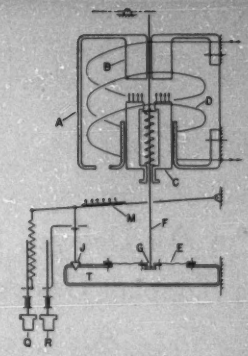

Figure 4. Schematic diagram of the short-time delay elements

Instantaneous Element

The instantaneous element provides no intentional delayed tripping of the circuit breaker, consequently, it is the fastest operating element. From Figure 5, it can be seen that its pickup is obtained by an armature L which is attracted to the magnetic frame A just as with the short-time pickup. The motion of this armature opens a valve K as wide and as fast

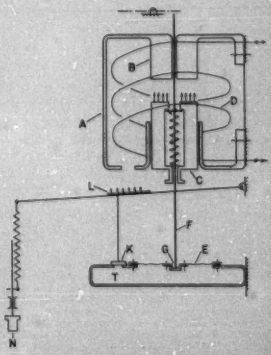

Figure 5. Schematic diagram of the instantaneous element

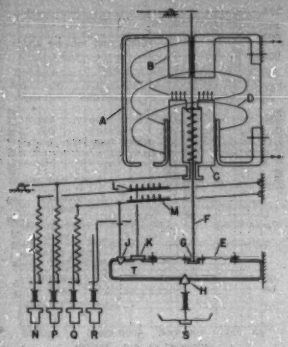

Figure 6. Schematic diagram of long-time delay, short-time delay, and instantaneous elements all on one unit

as possible so that the over-all circuit breaker clearing time may be as short as possible. The magnitude of current at which the pickup will take place can be varied by means of the adjustable spring N which also keeps the valve K closed during normal operation.

Finally in Figure 6, all of the elements that appear in Figures 3, 4, and 5 are combined into a single unit. The elements all perform their individual functions independently. Any or all of the three elements, namely the long delay, the short delay, and/or the instantaneous element may be made inoperative by replacing their easily accessible valves with a plug. In addition, the adjustable features of all the elements providing ranges of adjustment are still present. Reviewing again, these will give:

Calibration dial S—range of long-time delay.

Calibration knob P—range of long-time delay pickup.

Calibration knob R—range of short-time delay.

Calibration knob Q—range of short-time pickup

Calibration knob N—range of instantaneous pickup

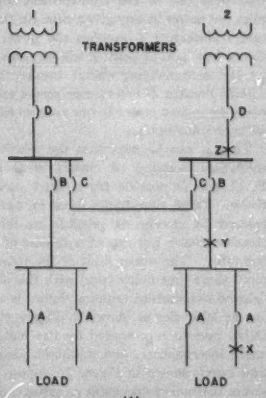

Figure 7(A). Schematic diagram of a typical distribution system

Time Current Characteristics

The time-current curve of this air delayed device has an inverse time characteristic up to approximately 500 per cent of coil rating in the long-time range as seen in curve "A" of Figure 7(B). Within this range, the moving core and tripping stem move as a unit, that is, the magnetic pull has not increased sufficiently to overcome the loaded spring inside of the moving core. Above 500 per cent, the tripping time is constant with increase in current. Within this region, the magnetic force is sufficient to overcome the spring inside the moving core at the outset, thereby subjecting the diaphragm to the constant force pattern of the spring. The transition between the vertical and horizontal portions of the tripping curve have an inherently generous curvature due to the fact that the pickup points are obtained by overcoming spring loaded armatures. The effect of the pickup becomes noticeable toward the outer end of the time delay portion of the curve. In this region, the forces on the armatures as well as on the valve approach and pass through zero. And since this takes place in a finite time, it must reflect on the curvature at the transition point. Outside the transition region, the short-time delay also is constant for increasing currents.

It should be noted that the tripping characteristics are given as band curves, the top part of which represents the total clearing time. This is the duration of fault current flow, including arcing time. The lower limit of the band represents the resettable delay. This is the duration of fault current flow after which the circuit breaker may trip even though the fault current may subside to a value less than 80 per cent of the circuit breaker rating. However, if the fault current subsides in less than the resettable delay, the circuit breaker will not trip and the delaying device will reset. With this air delayed device, it is possible to maintain the band width at a minimum. Its complete ad-

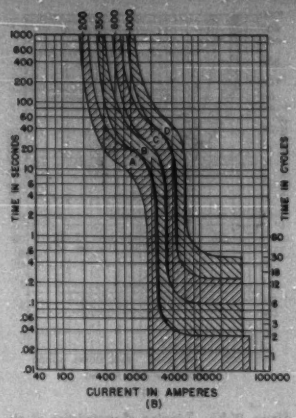

Figure 7(B). Time-current characteristics of air delayed overcurrent tripping device for motor starting and selective operation

Curve A—200-ampere load circuit breaker with long-time delay and instantaneous trip

Curve B—350-ampere feeder circuit breaker with long-time delay and minimum short-time delay

Curve C—600-ampere sectionalizing-circuit breaker with long-time delay and intermediate short-time delay

Curve D—1,000-ampere transformer-circuit breaker with long-time delay and maximum short-time delay

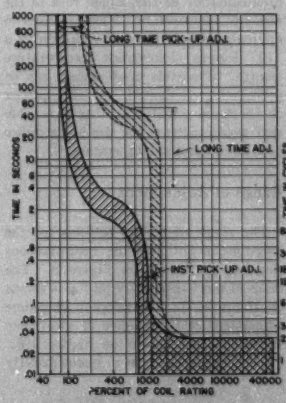

Figure 8. Tripping characteristics of air delayed overcurrent tripping device with long-time and instantaneous elements

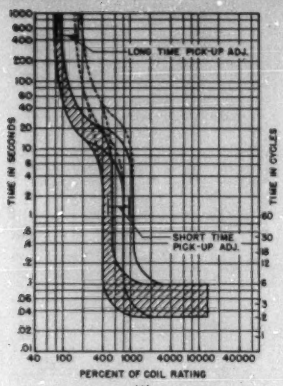

Figure 9(A). Tripping characteristics of air delayed overcurrent tripping device showing range of pickup settings

justability eliminates the necessity of increasing the bandwidth to compensate for manufacturing variations and different coil ratings. The variation of tripping time due to temperature change has been almost completely eliminated from the bandwidth. This is possible with air as the delaying medium. The tripping time depends on the mean velocity with which the air flows through the orifice and it is not affected by changes in air density. It is, however, affected slightly by changes in viscosity. The viscosity of air varies approximately as the square root of the absolute temperature. This amounts to approximately 15 per cent variation for a 110 degrees Fahrenheit temperature change. Even this small change can be practically eliminated by the proper choice of valve materials, that is, a value that would increase the size of its orifice with an increase in temperature.

Range of Adjustment

The range of pickup settings for the long-time delay and the instantaneous elements are shown on Figure 8. The range of short-time delay pickup is shown on Figure 9(A). The range of long-time adjustment and the range of short-time adjustment are shown on Figure 9(B). These ranges are given quantitatively below:

Long-time pickup—from 80 to 160 per cent of coil rating.

Long-time delay—from 4 to 90 seconds (at 600 per cent of pickup).

Short-time pickup—from 500 to 1,000 per cent of coil rating.

Short-time delay—from 4 to 30 cycles.

Instantaneous pickup—from 1,000 to 1,500 per cent of coil rating.

Settings may be made at any value within these ranges by merely turning an adjusting knob as described previously in connection with the construction. The adjustments are independent of one another, that is, the long-time pickup can be changed without affecting the short-time pickup, or the long-time delay can be changed with a negligible change in the short-time delay. All of the possible combinations of adjustment and their effects on the tripping curve are illustrated in Figures 8 and 9.

Application of Air Displacement Device to a Selective System

Figure 7 shows the curves for a typical selectivity application together with a schematic diagram of the system. Curve "A" shows the characteristics for a 200 ampere-load circuit breaker *A* which is provided with long-time delay to permit motor starting and instantaneous tripping on currents above the motor starting range. Curve "B" shows the characteristics for a 350-ampere feeder circuit breaker *B* which is provided with long-time delay and short-time delay elements. The delay setting is such that a load fault at *X*, Figure 7(A), will be cleared by circuit breaker *A* while circuit breaker *B* remains closed and continues to feed

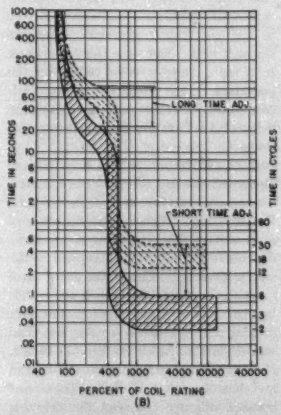

Figure 9(B). Tripping characteristics of air delayed overcurrent tripping device showing range of delay settings

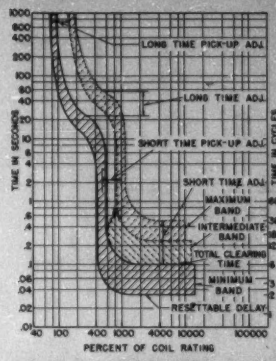

Figure 10. Tripping characteristics of air delayed overcurrent tripping device with long-time and short-time elements

other load circuits. Curve "C" shows the characteristics for a 600-ampere sectionalizing circuit breaker *C* which also is provided with long-time delay and short-time delay elements. The delay setting in this case is longer than for circuit breaker *B* so that a feeder fault at point *Y*, Figure 7(A), will be cleared by circuit breaker *B*, thus permitting service on other feeders to continue uninterrupted. Curve "D" shows the characteristics for a 1,000-ampere transformer circuit breaker which is likewise provided with long-time delay and short-time delay elements. The short-time delay for any short circuit current is longer for circuit breaker *D* than for circuit breaker *C*. Assuming that only one of the transformers supplies the power at any given time (in this case transformer 1 supplies the power), then a bus fault at point *Z* will be cleared by the sectionalizing circuit breaker *C*. Circuit breaker *D* will remain closed and continue to feed power to bus number one without interruption.

Thus it can be seen that the relative short-time settings of circuit breakers *B*, *C*, and *D* provide the desired selectivity. These time bands must be compressed as closely as possible so that clearing time is not excessive in case of a bus fault. The upper limit of the maximum short-time delay band with this air delayed overcurrent tripping device is as low as 30 cycles as shown in Figure 10. Delay periods represented by the maximum, intermediate, and minimum short time bands shown in Figure 10 impose a severe thermal requirement on series coils of lower rating. Consequently, some limitation in application must be recognized. Table I shows the time bands to

Table I. Coil Ratings

Interrupting Rating in Rms Total Amperes	Range of Coil Rating—Amperes		
	Minimum Band	Intermediate Band	Maximum Band
15,000	100–225	125–225	150–225
25,000	175–600	200–600	250–600
50,000	350–1,600	400–1,600	500–1,600

which each coil is applicable. Coils having ratings less than those listed are applicable only where tripping is instantaneous for overcurrents above the motor starting range.

Conclusions

A series tripping device has been developed which provides all the basic delay characteristics required for either motor circuit protection or for use in selective tripping systems. By the use of filtered air as the escapement medium and by incorporating adjustable features to all pickup and delay settings, a tripping device has been provided which is both versatile in application and precise in operation over a wide range of operating temperature.

References

1. Improved Selective Tripping of Low-Voltage Air Circuit Breakers, C. F. West. *Electrical Engineering* (*AIEE Transactions*), volume 63, August, 1944, pages 508–10.

2. Fault Protection on Shipboard A-C Power Distribution Systems, H. G. Rickover, F. N. Ross. *AIEE Transactions*, volume 63, 1944, pages 1109–20.

3. An Improved Overcurrent Tripping Device for Low-Voltage Circuit Breakers, H. L. Rawlins, J. Sandin. *AIEE Transactions*, volume 66, 1947, pages 1149–53.

4. New Low-Voltage Air Circuit Breaker with 50,000 Amperes Interrupting Capacity at 600 Volts A-C, M. E. Horn, J. J. Mikos. *AIEE Transactions*, volume 69, Part II, 1950, pages 1653–56.

No Discussion

New Low-Voltage Air Circuit Breaker with 50,000 Ampere Interrupting Capacity at 600 Volts A-C

M. E. HORN
MEMBER AIEE

J. J. MIKOS
MEMBER AIEE

CONTINUED development during the last two decades has given to the art air circuit breakers of the low-voltage class with high interrupting capacities.[1] Arc chambers employing deionizing principles and arcing contacts made from metals instead of carbon have been major contributing factors in obtaining excellent performance in protecting distribution circuits.

The recent war saw these circuit breakers, with shock-proofing features added, protect main power and auxiliary power circuits in various military electric systems, particularly those on naval combat vessels.

The ability of low-voltage circuit breakers to meet extraordinary demands in performance during the war period, established the feasibility of raising the interrupting capacity and current carrying ability per-unit volume or unit mass of material used to produce the circuit breaker. The acceptable temperature rise measured at the terminal of a circuit breaker now has increased to 40 degrees centigrade. For enclosed circuit breakers the allowable rise is 55 degrees centigrade.

Many of the circuit breakers for naval use were equipped with series tripping arrangements which delayed the tripping to effect a measure of selective operation of circuit breakers on vital circuits. However, the circuit breaker contacts and closing arrangement had limited short-time rating which in turn greatly limited the range of fault current over which selective tripping could be offered.

The new low-voltage air circuit breaker discussed in this paper, offers not only a short-time rating equal to the interrupting rating, but includes an electrically operated closing means for closing and latching on this current. With these basic features, the new circuit breaker may be equipped with tripping devices of either the direct acting or relay type to provide full selective tripping performance over the complete range of fault current.

Principles of Design

Pole units on this circuit breaker have the current parts divided into a main current circuit and an arcing circuit. The main current carrying circuit consists of two upper bridging members on the moving contact arm and four lower bridging members associated with the upper terminal of the series coil as is indicated in Figure 1. This arrangement provides for making use of magnetic forces caused by short-circuit currents. By employing blow-on type of main contacts, it becomes possible to carry fault current for an appreciable length of time without excessive damage to the main contacts. As the lower bridges move away from the circuit breaker panel because of magnetic forces, the lower contacts of the upper bridges are subjected to this magnetic force causing the upper bridge to rotate against the upper stationary contact and exert pressure which tends to keep all the contact members tightly together during the period of high fault current. Contact springs need be only strong enough to provide the proper force per lineal inch of contact surface necessary to meet the allowable temperature rise. The upper main contacts are faced with a hard silver-nickel alloy to withstand the impact caused by electric closing and to maintain low contact drop.

The arcing circuit also is divided into two sections, namely, the secondary and primary contacts. Above the main contacts at the upper stud are the secondary contacts which also are constructed to be blow-on contacts. In the stationary portion of the arcing details is a flexible conductor which is so situated that when short-circuited current flows, the magnetic forces tend to increase pressure at the secondary contacts. This same flexible conductor has its loop placed in a manner to enhance the transfer of current from the path through the secondary contacts to the path through the primary or uppermost arcing contacts. An insulating barrier is provided between the secondary contacts and the upper main contacts to prevent hot gases generated by the arc at the primary arc tip from descending to the opening between the mains and causing a breakdown. A silver-tungsten alloy of such conductivity as to provide adequate protection for the main contacts when they are allowed to open, is placed on each secondary contact. The hardness of these secondary contacts must be sufficient to withstand considerable impact forces when closing the circuit breaker electrically.

Wide bearings at each moving contact arm hinge are provided to minimize any sidewise motion caused by interphase attractions and repulsions. Shunts around the moving contact arm hinge are provided to insure minimum friction in the hinges by the elimination of pitting. The primary arcing contacts are faced with a silver-tungsten alloy of lower conductivity and a greater hardness than the secondary contacts in order to withstand the impact caused by closing and latching against short-circuit currents and

Paper 50-272, recommended by the AIEE Switchgear Committee and approved by the AIEE Technical Program Committee for presentation at the AIEE Fall General Meeting, Oklahoma City, Okla., October 23–27, 1950. Manuscript submitted June 29, 1950; made available for printing September 15, 1950.

M. E. Horn and J. J. Mikos are with the Westinghouse Electric Corporation, East Pittsburgh, Pa.

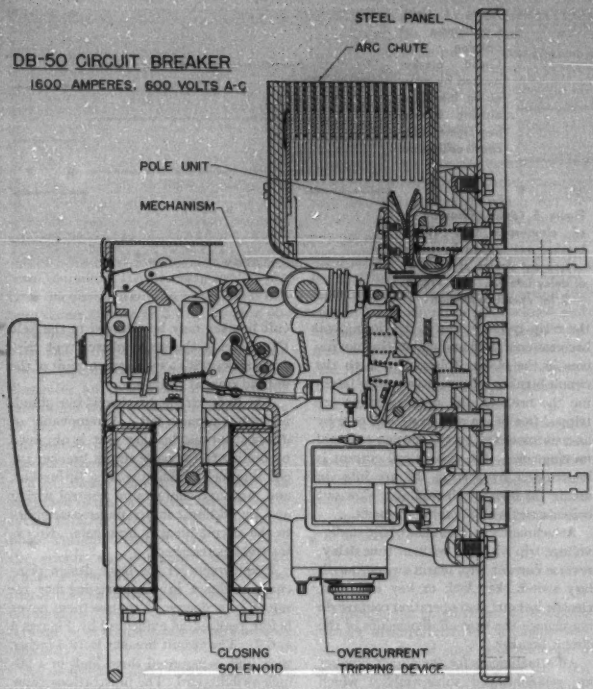

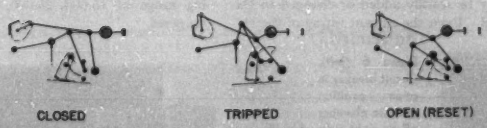

Figure 1 (above). Cross-sectional view of new low-voltage air circuit breaker in closed position

Figure 2 (below). Oscillogram of circuit calibration obtained by measuring the current through a bolted fault

to better withstand the erosion caused by arcing.

Extensive tests indicated that the contact materials selected perform better than any other known materials.

Arc extinction is obtained by employing the Deion principle[1,2,3] in an arc chamber consisting of steel plates[4] with V notches at the lower portion of the plate where the arc enters the arc chamber. These plates are interposed in the arc path at right angles to the arc. Above the steel plates are plates made from arc resisting insulating material to keep the arc confined in the arc chamber and to further cool the hot gases caused by the arc. The steel and the insulating plates are fitted into ceramic arcing shields in each side of the arc chamber.

The steel plates provide the necessary magnetic action to pull the arc into the chamber and against the plates causing the formation of a number of short arcs. Ionized gases give up great amounts of energy to the steel plates and to the ceramic shields which are so shaped that a throat is formed providing a Venturi effect to speed the gases upward. Proportions are such that the back pressure is kept to a minimum. Some turbulence is caused by the discontinuity between the steel and the insulating plates thus further cooling the exit gases.

Interruption tests were conducted on this circuit breaker, mounted in a cubicle which had a steel partition mounted $4^3/_8$ inches above the arc chambers and grounded to the circuit breaker frame and cubicle. Excellent interruptions were obtained with no failures.

The conventional insulating base was replaced with a strong steel framework on which individual pole units were mounted. Phase-to-ground insulation is provided by the base mold for the individual pole assemblies. By this arrangement, longer and more effective creep distances have been introduced which provide greater safety and conform to insulating standards associated with a maximum design alternating voltage of 625 volts.

The circuit breaker frame, vertical panel, and operating mechanism are all at ground potential, thus providing the greatest possible protection to personnel.

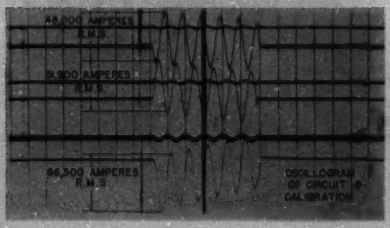

Figure 3 (right). Oscillogram of momentary test obtained by measuring the current through a closed circuit breaker. See Figure 2 for circuit calibration

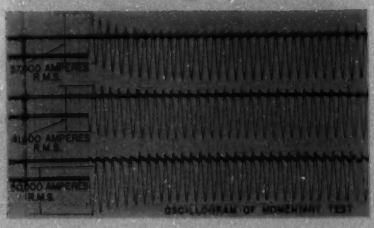

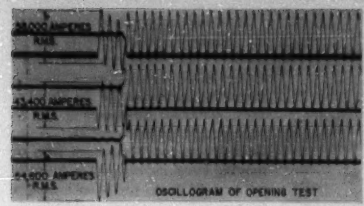

Figure 4 (left). Oscillogram of opening test. Circuit breaker opened by energizing the shunt tripping device. See Figure 2 for circuit calibration

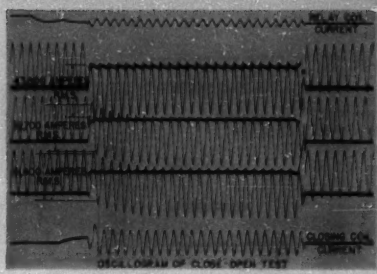

Figure 5 (right). Oscillogram of close-open test. Circuit breaker was tripped by series overcurrent device at the end of delay interval. See Figure 2 for circuit calibration

The operating mechanism for this circuit breaker is of the trip-free type designed for low mass and consequent high-speed tripping. Manual closing is provided for testing only. Molded insulating links on each pole unit provide the necessary dielectric between the operating mechanism and current carrying parts.

Low mass in the operating mechanism has been made possible by the use of fabricated stainless steel parts which have been heat treated. To insure long trouble-free life in this mechanism, corrosion-resistant metals have been employed.

A d-c closing solenoid has been chosen as the means for electrically operating this circuit breaker against short-circuit currents. High-speed closing is made possible with a simple device of small dimensions and weight. This solenoid is controlled by a relay designed for this particular duty. When the operating coil of the control relay is energized, a pair of contacts in series with the closing coil is closed by the movement of a magnetic core which is latched to an insulated arm containing the contacts. As soon as the relay contacts touch, the closing coil becomes energized and causes the moving core in the closing solenoid to latch the circuit breaker. Immediately after latching the breaker, the relay contacts are tripped free of the relay magnetic core by an arm mounted on the closing solenoid moving core. The closing coil current is interrupted by driving the arc into an arcing chamber by the aid of a blow-out coil in series with the relay contacts.

Attachments such as shunt trip, undervoltage trip with and without time delay, reverse current trip, alarm switch, auxiliary switch, key lock or key interlock, electric lockout, and operation counter do not change the over-all dimensions of the circuit breaker.

All attachments for the circuit breaker are self-contained subassemblies which may be mounted to the circuit breaker frame as required. These attachments may be readily added or changed in the field. Even the current rating of the circuit breaker may be changed in the field by replacing the series overcurrent tripping device with a replacement unit of the desired current rating.

The basic circuit breaker is free standing when unmounted. A removable or drawout circuit breaker unit is obtained by bolting to the basic circuit breaker the cell interlock, guiding rollers, lifting bar, and auxiliary contacts for control wiring and by adding contact finger assemblies to the circuit breaker terminals. No extra truck is required.

Employment of the basic design principles outlined in the foregoing has resulted in a degree of compactness never before realized as evidenced by Figures 6 and 7. The circuit breaker is 19.5-inches wide and is mounted three high in a 90-inch switchboard. The illustrations show the extension of a line of air circuit breakers which cover a current interrupting range of 15,000, 25,000, and 50,000 amperes.

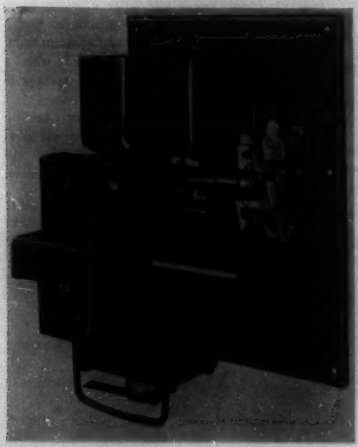

Figure 6 (left). Circuit breaker in open position with arc chamber off on right pole unit

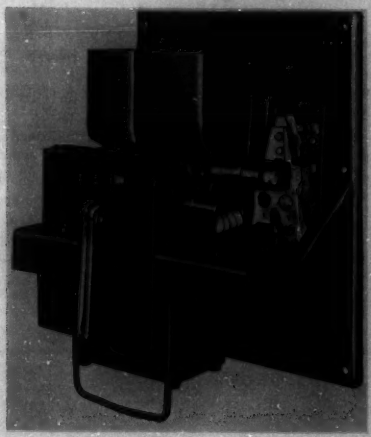

Figure 7 (right). Circuit breaker in closed position with arc chamber off on right pole unit

Test Results

Many tests have been performed to establish the characteristics of this circuit breaker. Some of the results are recorded to illustrate the successful operation of the design principles employed in this circuit breaker.

Electric closing time measured from the time the control relay is energized to the time the circuit breaker is latched is seven cycles on a 60-cycle basis as shown in Figure 5.

Shunt tripping time measured from the time the shunt trip is energized to the time the circuit has been interrupted has been determined to be 3.4 cycles on a 60-cycle basis.

In line with existing practice of rating low-voltage air circuit breakers, Figure 2 illustrates an oscillogram of the circuit calibration with no circuit breaker in the circuit. An average of 55,400 amperes rms measured 1/2 cycle after the circuit was energized was obtained.

While closed, the circuit breaker was subjected to a short-circuit current for 33 cycles or 0.55 second. The average 3-phase current measured 1/2 cycle after the circuit was energized, was 49,530 amperes rms and was 36,600 amperes rms at the end of the 32nd cycle, Figure 3. No welding of contacts or appreciable deterioration of contacts was experienced in this test.

An oscillogram of an opening operation initiated by the shunt trip device is shown in Figure 4. An average 3-phase current of 53,000 amperes rms measured 1/2 cycle after the start of current flow through the circuit breaker was obtained. This opening operation was a clean interruption with a minimum amount of disturbance. Two minutes after the record shown in Figure 4 was taken, the oscillogram shown in Figure 5 was obtained. In this test the circuit breaker was electrically closed and latched against the short-circuit current which was allowed to flow through the circuit breaker for 24 cycles or 0.4 second. After this delay interval, the series overcurrent trip device tripped the circuit breaker and allowed the circuit breaker to interrupt the circuit. The circuit breaker closed and latched against 49,460 amperes rms measured 1/2 cycle after the start of current flow through the circuit breaker. At the 23rd cycle the average 3-phase current was 39,000 amperes rms.

These recorded results serve to indicate that the design principles discussed in this paper do make possible a circuit breaker which can close and latch against currents and have a 0.5-second rating equal to the interrupting rating of the air circuit breaker.

Conclusion

Through the employment of a unique contact arrangement and a highly discriminating use of space and material, a new low voltage circuit breaker has been provided which offers greater performance with a reduction in space and weight. The short time rating has been raised to equal the interrupting rating of 50,000 amperes.

The added ability to close and latch on this current permits tripping to be delayed throughout the entire range of fault current which, in turn, facilitates application to obtain the ultimate in selective tripping performance. A high degree of flexibility has been achieved in adapting the circuit breaker for drawout mounting and in adding or changing tripping devices or attachments in the field.

References

1. Extinction of an A-C Arc, J. Slepian. *AIEE Transactions*, volume 47, October 1928, pages 1398–1408.

2. Theory of the Deion Circuit Breaker, J. Slepian. *AIEE Transactions*, volume 48, April 1929, pages 523–527.

3. Extinction of a Long A-C Arc, J. Slepian. *AIEE Transactions*, volume 49, April 1930, pages 421–430.

4. Enclosed Low-Voltage Deion Air Circuit Breaker of High Interrupting Capacity, Jerome Sandin. *Electrical Engineering* (*AIEE Transactions*), volume 57, November 1938, pages 657–661.

5. A New High-Capacity Air Breaker, L. R. Ludwig, G. G. Grissinger. *Electrical Engineering* (*AIEE Transactions*), volume 58, August 1939, pages 414–420.

6. A Brief Review of Switchgear and Circuit Breaker Practice in the United States, M. H. Hobbs. *AIEE Transactions*, volume 67, part II, 1948, pages 893–898.

7. An Air Delayed Selective Overcurrent Tripping Device for Low Voltage Air Circuit Breakers, M. E. Horn, R. G. Tremblay. *AIEE Transactions*, volume 69, part II, 1950, pages 1048–52.

Discussion

Robert H. Nau (University of Illinois, Urbana, Ill.): The new low-voltage magnetic deion circuit breaker has certainly been perfected from the prototype of 1939.[1] Controlled engineering design has made this progress possible. Indeed, the unison of the mechanical and electrical features introduces a new acme for magnetic circuit breakers.

The several features are aptly described in the paper. The development and use of the molded insulation material for the base, the insulating links of the operating mechanism, and the arc chamber housings and internal barriers have done much in making possible the indicated compactness and the small unit mass. The new arrangement of main contact bridges utilizes the forces of current-loops to provide the necessary contact pressures and to eliminate contact chatter on short circuit.

The interrupting principles of the arc chamber have not been altered from the prototype. In the present paper, in the reiteration of the action of the arc chamber, it is stated that "the steel plates provide the necessary magnetic action to pull the arc into the chamber and against the plates, causing the formation of a number of short arcs." It does not seem that short arcs are truly formed. Such a transfer would mean a series of hot cathodes, which, in turn, would supply a terrific display of pyrotechnics at the currents of higher short circuits. Yet, it is known that no display is evident!

To be sure, I am indeed gratified to see that the mechanical development has been so completely extended from that which we had in 1938 and 1939.

Reference

1. See reference 5 of the paper.

M. E. Horn and J. J. Mikos: With reference to questions raised concerning the exact behavior of the arc inside the arc chamber during interruption the authors wish to direct attention to the following:

The slot shape in the magnetic splitter plates, shape of insulating shields, provisions for venting and so forth, are all arranged so that the arc is forcibly maneuvered into a position where arc voltage is substantially increased.

Therefore all of the mechanisms necessary for causing transfer into a number of shorter arcs are present. Conceivably transfer can take place at one place in the arc chute without a complete transfer throughout the entire length. Actually upon dissassembly of test samples the telltale marking produced by a cathode spot is present on some of the plates.

In conclusion, due to the relatively short arcing time required in a-c interruption, whether or not one or more additional cathode is formed, is of little significance as long as the required arc voltage is obtained.

Contributing Factors in Determining the Ratings of Power Transformers for Use on the Systems of The Hydro-Electric Power Commission of Ontario

D. B. FLEMING
MEMBER AIEE

J. S. LOTIMER
NONMEMBER AIEE

Synopsis: Transformers like most other commodities change in style from time to time as the years pass. It is the intent of this paper to delve back 40 years into the history of the Hydro-Electric Power Commission of Ontario and, in regard to transformers, compare the mode of thinking then with that of the present time, and to follow the changes that have occurred in four decades and the governing factors that have influenced these changes. Today a transformer can be considered to be one of the most reliable pieces of equipment in operation. It has been developed partially from operating experience and partially to satisfy conditions and circumstances that presented themselves. Tappings in a transformer can be extremely hazardous and therefore should be kept to a minimum. The indoor transformer has given place to the outdoor. Water cooling has been largely superseded by self-cooling, then forced-air cooling, finally augmented with forced-oil. Single-phase transformers once used exclusively are not now preferred to 3-phase units. Capacities have been stepped up from 750-kva to 100,000-kva units. Autotransformers are used to advantage whenever they can be applied. Both manually operated off-load and automatically controlled under-load tap changing equipment has been developed. Refinements have been made to temperature indicating devices. Current transformers used for relaying and control are now economically located on the bushings within the transformer tanks. Interchangeability of the various manufacturers' bushings has become a reality and is of great advantage to the operating companies. The gas detector relay is no longer an experiment but a sure telltale of trouble in transformers. The new features that have been added to transformers have appeared so gradually that unless one takes time out to compare notes they are not fully appreciated.

DURING its 40 years of operation the Hydro-Electric Power Commission of Ontario has purchased over 840 transformers for its 115,000- and 230,000-volt stations, totalling in capacity over 8,300,000-kva. The types and characteristics of the transformers purchased and installed have varied from time to time to best satisfy system conditions as they developed and to take advantage of new and improved features as they were introduced by the designers.

Over 98 per cent of the total kilovolt-ampere capacity of the transformers purchased are still in service, those disposed of being some of the original water-cooled indoor units.

1909–1920

The specification under which the Commission first purchased transformers for its 115,000-volt step-down stations called for:

750-, 1,250-, and 2,500-kva indoor transformers, 63,500/110,000Y—13,200-volts, 25 cycles, 40-degree-centigrade rise, 1-phase, water-cooled, with four $2^1/_2$ per cent under-voltage taps in the high-voltage and eight $2^1/_2$ per cent taps in the low-voltage winding (four above and four below normal voltage).

These transformers were installed in the ten original step-down stations strategically located in the more or less concentrated heavily industrialized centers of southern Ontario. In 1913 the section of the foregoing specification pertaining to the low-voltage windings was revised to provide for 26,400/13,200-volt windings on transformers to be installed in three additional stations which were then being constructed in areas where the load centers were widely distributed and from which long feeders would radiate.

With the limited experience at that time in the operation of 115,000-volt transformers, information was not available as to their reliability in the type of service contemplated. Accordingly, a spare unit was provided at each station. In the initial stages prospective load growth was rather uncertain and the possibility of having to install a second or replacement bank of larger unit capacity at the various stations, had to be kept in mind. Very few of the stations were conveniently located in respect to railway facilities, necessitating the skidding of the transformers from the railway sidings to station sites. With all the foregoing problems in mind single-phase transformers were considered to have an advantage over the heavier 3-phase units.

Forty years ago there were few, if any, 115,000-volt transformers of 750-kva capacity or larger, other than the water-cooled type. The water-cooled was cheaper than the self-cooled type and could be readily installed indoors on considerably less floor space, thereby greatly reducing the cost of installation, and avoiding station ventilating problems.

In the initial stages outdoor installations were not given very serious consideration by the Commission's engineers and not until 1921 was the first outdoor station erected at Hamilton.

Ratings of all transformers at this time were based on 40-degree-centigrade temperature rise with a 125 per cent capacity rating for two hours at 55 degrees centigrade. This method of rating was considered a reasonable attempt to provide the correct capacity in keeping with the daily load curve and was found to work out exceptionally well with water-cooled transformers. No great difficulty was experienced in keeping the ambient temperature within proper bounds. Cooling coils required little or no maintenance and

Paper 50-273, recommended by the AIEE Transformers Committee and approved by the AIEE Technical Program Committee for presentation at the AIEE Fall General Meeting, Oklahoma City, Okla., October 23–27, 1950. Manuscript submitted July 12, 1950; made available for printing September 18, 1950.

D. B. Fleming and J. S. Lotimer are both with The Hydro-Electric Power Commission of Ontario, Toronto, Ontario, Canada.

the insulation was always in a healthy state.

The range of taps provided, in both the high-voltage and low-voltage windings, was considered necessary to take care of line regulation along the 115,000-volt transmission circuits from Niagara to Windsor, a distance of some 250 miles.

In 1916, fifteen 5,000-kva transformers were purchased to the same specifications to replace a group of 2,500-kva units, the former being the largest capacity transformers that could be accommodated in the original pockets. It may be of interest to note that all these 5,000-kva transformers are still in service at this location and no failures have occurred in their 34 years of operation.

1920–1930

In 1920 load growth on the system rapidly increased beyond the rated capacity of the installed transformers. Tests carried out on transformers in the manufacturers' plants at loadings simulating a normal daily load curve revealed that peak loads of over 140 per cent of rated capacity of the transformers could be carried without exceeding safe temperature limits. Increased loading of the existing transformers was authorized accordingly.

To provide for further load increase additional transformers were required. Consideration was given to outdoor installations. However, such installations did not appear to be warranted at stations where the existing indoor transformers could be replaced with larger capacity units. It was finally decided to purchase outdoor transformers and install them either indoor or outdoor as circumstances might dictate.

The specifications for new transformers called for:

Outdoor transformers, 63,500/110000Y—28,400/14,200-volts, 25 cycles, 55-degree-centigrade rise, 1-phase, water-cooled with two 5 per cent taps above and two 5 per cent taps below rated voltage in the high-voltage windings only.

The water-cooled type was retained with a view to keeping the size of the transformers within the existing pocket limitations. The rated capacity of these transformers was based on a temperature rise of 55 degrees centigrade to conform with the AIEE standard. However, as it was considered the existing cooling ponds might not altogether adequate, the transformers were to be rated 5,000-kva with 35-degree centigrade ambient. In order to keep within permissible temperature limits, the transformers had of necessity to be designed for larger capacity, their final rating being established at 6,000-kva.

Taps were eliminated from the low-voltage windings in view of the frequent mechanical failures experienced with many of the earlier transformers. These failures were considered directly attributable to the large range of taps with which the low-voltage windings had been equipped. In order to provide for the required range of tap positions, the taps on the high-voltage windings were increased to a range of 20 per cent, which unfortunately proved to be another weakness. The voltage rating of the low-voltage windings was raised sufficiently to compensate for regulation at full load 80 per cent power factor. Over 100 transformers normally rated 5,000 and 10,000-kva were purchased to the foregoing specifications.

In 1927 when considering equipment for the first 230,000-volt station to be erected at Leaside on a site immediately adjacent to the north-east boundary of the city of Toronto, it was decided to use water-cooled in preference to self-cooled transformers partially because of the restricted area of the site. Shortly after this station was placed in service, the load demand greatly exceeded the rated capacity of the transformers, necessitating their operation over long periods at hottest spot temperatures of 95 degrees centigrade. These 230,000-volt, and most of the foregoing 115,000-volt transformers were furnished with hottest-spot temperature indicating equipment and crude as it was, every effort was made to use it and operate the transformers on a temperature basis. It was soon realized that the cooling ponds were inadequate to take care of the extra losses resulting from this method of operation. Spray towers had to be erected, make-up water requirements were found to be excessive and the cooling coils also require frequent acid cleaning. As the result of this experience it was concluded that water-cooled transformers should not be used in future installations for other than generating stations where the water supply would be plentiful and pass through the cooling coils only once.

1930–1940

During the depression years of the 1930's very few transformers were purchased. However, those that were purchased were either self-cooled or forced-air-cooled. Forced-air cooling also was added to a number of the self-cooled units. Operation on a temperature basis was practiced to a greater degree and every effort was made to improve the temperature indicating equipment.

Just prior to the war, nearing the end of the depression period, the rapid load growth necessitated the formulation of a decided policy in regard to future transformers. Operating experience with the more modern transformers (those built subsequent to 1926) indicated that they were very reliable pieces of equipment. No failures were experienced on any of the 115,000-volt units. However, there were two failures on the 230,000-volt units, each of which was traceable to the inclusion of a 156,000-volt tap in the high-voltage winding. This tap was originally specified as a precautionary measure, should the 230,000-volt rating prove to be too high as an operating voltage. It reduced the impulse strength of the transformers, resulting in the failure of both of these units during heavy lightning storms. This tap was subsequently removed from all the transformers and no further electrical failures have occurred. No lightning arresters were in service at the time of the failures.

1940–1950

By 1939 confidence in the modern transformer had increased to such a degree that it was decided to install 3-phase transformers wherever possible. Specifications prepared for purchase of 115,000-volt transformers called for:

Outdoor transformers, 110,000-28,400/-14,200-volts, 25 cycles, 55-degree-centigrade rise, 3-phase, forced-air cooled, with four $2^1/_2$ per cent over-voltage taps in the high-voltage winding and equipped with hottest-spot temperature indicating equipment.

During the 10-year period 22 transformers of 25,000-kva capacity were purchased to this specification.

As long radial feeders emanating from a number of stepdown stations became heavily loaded, regulation became a serious problem. Accordingly, it was decided to erect small ancillary stations at strategic points to relieve this condition. At these stations, 8,000-kva transformers built to the foregoing specification and equipped with underload tap changers for automatic voltage regulation were used.

Modern station design makes no provision for the maintenance or rebuilding of transformers on the site. In all cases where major overhaul or repairs are required, it is the intent that the transformers will be returned either to the manufacturer's factory or to the Commission's central repair depot. A 135-ton depressed center car was procured for this

purpose to avoid the delay often experienced in obtaining suitable railway equipment. To provide for necessary spare capacity in the case of failure of an operating unit, provision is made for sufficient load transfer between adjacent stations to permit the removal and replacement of any unit that may become defective, the original practice of providing a spare unit at every station being discontinued.

In 1941 the Commission's second 230,000-volt station was brought into service at Burlington, located approximately five miles to the north of Hamilton. Transformers for the initial installation consisted of ten units (one spare) built to the following specifications:

25,000-kva outdoor transformers, 204,000 ground Y/118,000-68,250/118,000Y-13,200-volts, 25 cycles, 50-degree-centigrade rise, 1-phase, forced-air-cooled, with two 5 per cent taps in the high-voltage winding (one above and one below normal voltage).

The radiators were banked in A-frame structures, equipped with blowers and with conservator tanks mounted above, the cooling units being located to the rear of the transformers. The banked radiators greatly facilitate the installation of the units and simplify the separation of the transformer proper from its cooling equipment when removal is necessitated for maintenance or replacement purposes. The governing factor in determining the capacity of these transformers and the choice of 1-phase instead of 3-phase was the limitation in weights and dimensions that could be transported by rail.

Prior to the establishment of basic insulation levels by the AIEE, Edison Electric Institute, National Electrical Manufacturers Association Insulation Coordination Committee, the Commission's specifications called for insulation tests on all 115,000-volt transformers to be twice the highest tap voltage, that is, 242,000-volts. When insulation levels were established a choice had to be made between the 115,000- and 138,000-volt insulation classes. The choice was 115,000-volts for step-down transformers and 138,000-volts for generating-station transformers. It was felt that the higher factor of safety in the latter case was good insurance and the specifications were revised accordingly.

When forced-oil, forced-air cooling was first introduced by the manufacturers it was given very serious consideration by the Commission for installation on existing water-cooled transformers, the purpose being to eliminate cooling ponds, pumps and cooling coils, all of which were items of expense in the maintenance of water-cooled equipment. The transformers under consideration at the time however, were units of relatively small capacity and would each require one cooler only, necessitating the oil pump being in continuous operation while the transformer was in service. Accordingly, the failure of any one of three pumps would result in the loss of a complete transformer bank. This hazard was considered to rule out the contemplated replacements at single bank stations where means of load transfer was nonexistent. It also resulted in the deferment of the decision to use this equipment until some experience had been gained on the performance of the oil pumps.

In 1946 experimental tests were conducted on forced-oil forced-air cooling units in co-operation with one of the transformer manufacturers. These units were temporarily fitted to a 25,000-kva 3-phase transformer in operation at one of the Commission's stations. On completion of the experiments and final approval of the design by the manufacturer, the Commission purchased a number of 6,000-kva 1-phase transformers to be equipped with the new forced-oil forced-air coolers. These transformers were for installation in an extension to an existing station equipped with several banks of water-cooled units of similar capacity, where the pocket space and runway clearances had previously been established.

For service in stations with multiple transformer banks in operation, where the loss of any one bank would not be considered a hazard, due to the ready absorption of the rejected load by the banks remaining in service, the installation of unit coolers, one per transformer, was considered to be satisfactory, hence the purchase of the foregoing 6,000-kva units so equipped.

When considering the transformers for Kipling, the third 230,000-volt station, located immediately adjacent to the south-westerly limits of the city of Toronto, a bank of three transformers (plus one spare unit) was purchased to the same specifications as the Burlington transformers, with the exception that the new transformers were equipped with forced-oil forced-air coolers. By adopting this modification it was found possible to slightly lower the cost and appreciably reduce the space requirements.

Frequency Standardization

Frequency standardization introduced a new problem in the future purchase of transformers for the 25-cycle system. During the investigation stage it was considered expedient to provide for the efficient use of such equipment for either 25-or 60-cycle service, and require all transformers to be designed for dual frequency, that is, to be supplied for 25-cycle service with adequate provision made for ready reconnection for 60-cycle service in a minimum of outage time.

In regard to the existing installations it was decided that where the transformer reactance is relatively low, they would be operated at 60 cycles without any change in the windings. However, in the vast majority of cases, the transformers will have to be brought in for reconnection or replacement of a considerable portion of the windings. In the case of water-cooled transformers consideration will be given to the replacement of the cooling coils with forced-oil, forced-air cooling equipment.

A new 230,000-volt 60-cycle supply is being brought in to three of the Commission's latest step-down stations, namely: Kipling to the south-west of Toronto; Burlington to the north of Hamilton; and Westminster adjacent to London. Eight transformers are presently being installed at these stations: three at Kipling, two at Burlington and three at Westminster. All were purchased to the following specifications:

100,000-kva outdoor autotransformers, 228,800/116,900 ground Y-12,750-volts, 60 cycles, 55-degree-centigrade rise, 3-phase, forced-oil, forced-air cooled, with four taps in the high-voltage winding-223,300/217,850/212,650/207,450-volts.

When considering the transformers for these stations thought was first given to 2-winding 1-phase units, to provide a bank capacity equivalent to the capacity of the line. Network calculator studies however, showed that it was necessary to keep the reactance as low as possible in order to obtain a satisfactory margin of stability. Autotransformers appeared to be the answer to this problem. As they would materially reduce the physical size of the units required, 3-phase autotransformers were investigated. On advice from the manufacturers that 3-phase forced-oil forced-air cooled autotransformers of the capacity stated could be built and shipped and that no insurmountable problem existed in the design of such autotransformers, this type of unit was specified. The voltage ratings of these transformers appear as odd values. This is the result of trying for something different after the transformer design is well advanced and the coils are partially wound. Each 12,750-volt tertiary is associated with a 48,000-kva

13,800-volt hydrogen-cooled, synchronous condenser and permits over-excited operation without exceeding rated voltage on the condenser, thus reducing field heating.

In addition to the 100,000-kva autotransformers, four 60,000-kva autotransformers of similar voltage rating were purchased and are being installed at two line stations one adjacent to Peterborough and the other at Essa, adjacent to Barrie. It may be interesting to note that as a result of a subsequent change in plans, additional capacity for emergency use will be required in the 60,000-kva transformers and even though the designs were completed it was found possible to provide for the attachment to each transformer of two additional unit-type forced-oil forced-air coolers and thereby increase by 30 per cent, the rating of each transformer. These additional cooling units may be installed separately from the transformers and arranged to be automatically brought into service by thermal control on either one of the two transformers if the other becomes defective or is otherwise removed from service.

Conclusions

In the original 115,000-volt stations both high-voltage and low-voltage lightning arresters were used. Also in the first 230,000-volt station at Leaside lightning arresters were used for the protection of the first six banks of transformers. It is not now the Commission's standard practice to use lightning arresters at any high-voltage station and only a few of the older stations retain this equipment. However, all such stations are protected with overhead shielding and co-ordinating gaps. All the 115,000-volt transformers are fully insulated and only one electrical failure has occurred on any unit built since 1926. The Niagara 25-cycle system is operated with the high-voltage grounded at points through water resistors, approximating 250 ohms each. The other systems have solidly grounded neutral.

This paper would not be complete without mentioning the effort that has been made in Canada, for the past 25 years to bring about a certain measure of standardization of transformer bushings whereby those supplied by any one bushing manufacturer may be replaced by any other Canadian-made bushing of the same voltage rating. This is now in effect.

The efforts that the Commission has put forward in developing hottest-spot temperature indicating equipment that can be readily calibrated and maintained also has given results and such equipment is shortly to be placed in service.

For the protection of transformers, the Commission has experimented with the gas detector relay and has co-operated with the manufacturer in overcoming a number of short-comings in the original equipment.

The gas detector relay has never failed to operate in case of trouble in the transformers where installed.

The original transformers purchased were simple pieces of equipment in spite of their many taps, requiring large connecting boards, also the now obsolete chloride breathers. They were equipped with only the bare essentials for their operation. The transformers of today have many accessories, notably the large number of current transformers on all bushings. The 100,000-kva autotransformers previously referred to, each has a total of 26 current transformers mounted on the bushings inside the tank with all the secondary leads brought down to a common terminal box on the side of the case. Under-load tap changers, oil pumps, and blowers all require their controls with the interconnecting wires and conduit runs. Temperature equipment, oil conservators, relief vents, trucks and jack-steps, all make for a piece of equipment vastly different from the 1910 vintage, but each improvement was developed as conditions and circumstances demanded.

Discussion

D. W. Callander (Canadian Westinghouse Company, Limited, Hamilton, Ontario, Canada): Within the last 20 years many notable and important developments incorporated in the design of power transformers have greatly increased their reliability at the same time allowing for decreased weight and physical size per kilovolt-ampere in capacity output.

The intensive studies made in the late 1920's on lightning protection and insulation co-ordination have resulted in transformers with greatly improved impulse strength to withstand lightning and switching surges. In many instances the more economic arrangement of this improved insulation has resulted in reduction in the weight and the physical size of large high-voltage power transformers below those for transformers previously built for corresponding kilovolt-ampere capacities and voltages.

The use of the better grades of sheet steel recently made available (such as oriented cold rolled hipersil) has made possible transformers of reduced weight with improved magnetic performance.

In the manufacture of large power transformers, Westinghouse has always sponsored the use of the shell-type construction. Form-fit tanks now are standard for these transformers, their main advantages being further reduction in weight and physical dimensions, together with great reduction in oil content. This construction lends itself advantageously to the application of the various combinatjons of forced-oil and forced-air cooling. It also is advantageous in the application of transformers located at generating stations. Such transformers due to their comparatively small plan dimensions have made an appreciable saving in the concrete foundation required in the tail race of such power developments as Des Joachims and La Cave on the Ottawa River.

Altogether these developments involving reductions in weights and dimensions have allowed for the economic manufacture and ready shipments of transformers completely assembled (less accessories) of much larger ratings than were previously possible. It is interesting to note that the Hydro Electric Power Commission has always been in the forefront in taking full advantage of such developments in order to furnish economic and reliable service.

Stability of Servomechanisms with Linearly Varying Elements

M. J. KIRBY
MEMBER AIEE

As control technology progresses, more and more situations arise in which the variation of one or more elements with time cannot be ignored. The mass of a rocket decreases as its fuel is consumed. The inertia of a roll of strip steel in a mill changes as the steel is rolled or unrolled. In some cases, variation may be purposely introduced into the control system, for example so that a controlled process may proceed rapidly at first, then more slowly and smoothly during the final critical stages.

This paper presents a method for determining the stability of servosystems in which one or more elements vary linearly with time, that is, systems which can be described by a differential equation relating the output, θ_o, to the input, θ_i, and time, t, of the form

$$(a_n+b_nt)\frac{d^n\theta_o}{dt^n}+\ldots+(a_j+b_jt)\frac{d^j\theta_o}{dt^j}+\ldots+(a_0+b_0t)\theta_o=F(t) \quad (1)$$

The stability of such systems has sometimes been predicted by taking "snapshots" or sets of values of the coefficients at several discreet instants of time, and assuming that at each instant the system acts as a constant coefficient system having the appropriate coefficients. The present method is more rigorous since it is based on the actual solution rather than an assumed solution to equation 1. This solution is not always a simple exponential, as is shown for example by the case in which the damping remains constant but the inertia and gain vary. Furthermore, the method is simple to apply; determination of the absolute stability of a system described by equation 1 requires slightly less work than a single "snapshot" in the constant-coefficient-approximation method.

Equation 1 may be obtained, for example, by combining one equation relating motor torque to the error $(\theta_i-\theta_o)$ through the control network, with another equation relating motor torque to output, θ_o, through the load inertia, J, and damping, D. The right side, $F(t)$, is a known function of time, composed of θ_i, its derivatives, and products of these by t.

Stability is defined as Nyquist[1] defined it: a stable system is one in which an impressed small disturbance (which itself dies out) results in a response that dies out. More precisely, equation 1 is a linear equation; two or more solutions can be added and their sum will be a solution. Furthermore, the solution can be separated into a particular integral which is a function of $F(t)$ and is usually considered the steady-state solution, and a complimentary function dependent only upon the physical system and the energy stored in it initially. The complimentary function will be referred to henceforth as the transient response, and is the solution to equation 2,

$$(a_n+b_nt)\frac{d^n\theta_o}{dt^n}+\ldots+(a_j+b_jt)\frac{d^j\theta_o}{dt^j}+\ldots+(a_0+b_0t)\theta_o=0 \quad (2)$$

A system will be defined to be stable if the transient response, θ_o, when excited dies out completely as $t\rightarrow\infty$. If any part of the transient response persists or increases indefinitely, the system will be considered unstable.

The method of determining stability is based on the fact that the transient response can be expressed as a definite integral in the complex plane of an arbitrary complex variable herein called s. As $t\rightarrow\infty$, this integral approaches an exponential type of function in which the exponents are easily found from the rates of variation of the elements—the b coefficients in equation 1.

The Stability Criterion

It is not necessary to write this integral in order to apply the criterion. Stability is determined by the exponents, and a polar plot similar to a Nyquist plot is all that is needed. The specific steps in determining the stability of a system are:

1. Form the polynomial, $P(s)$ from the coefficients of the variable terms in equation 1, thus:

$$P(s)=b_ns^n+b_{n-1}s^{n-1}+\ldots+b_1s+b_0 \quad (3)$$

2. Plot $P(s)$ as s traverses a contour consisting of the imaginary axis from $-j\infty$ to $+j\infty$, and a semicircle of arbitrarily large radius, R, enclosing the right half plane. The plot will start from b_0 and will approach infinity at an angle of $+n\pi/2$ as s takes on purely imaginary values from zero to $+j\infty$. As s follows the semicircle of radius R, the b_n term overpowers all the others, and $P(s)$ follows a circular arc of radius b_nR^n from $+n\pi/2$ through zero to $-n\pi/2$. For purely imaginary values of s between zero and $-j\infty$, the plot of $P(s)$ is the reflection in the real axis of the plot for positive imaginary values of s.

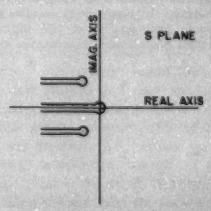

Figure 1. Typical contour for equation 5 consisting of lines parallel to the real axis and small circles around the roots of P(s)

Paper 50-274, recommended by the AIEE Feedback Control Systems Committee and approved by the AIEE Technical Program Committee for presentation at the AIEE Fall General Meeting, Oklahoma City, Okla., October 23–27, 1950. Manuscript submitted June 12, 1950; made available for printing September 11, 1950.

M. J. Kirby is with the Sperry Gyroscope Company, Great Neck, N. Y.

The writer wishes to acknowledge the assistance of Mrs. Ellen J. Adler, who planned and executed much of the electronic analogue computer work.

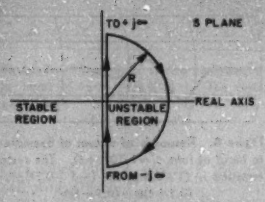

Figure 2. $P(s)$ is plotted as s traverses this contour, which encloses the right half (unstable region) of the s-plane. R is arbitrarily large

3. If the plot of $P(s)$ does not encircle the origins, the system is stable; if it encircles the origin, the system is unstable.

4. If the plot of $P(s)$ passes through the origin for finite, imaginary values of s, a type of response is indicated which has no counterpart in the performance of a constant coefficient system. The transient increases or decays as a power of t, which is slower than the familiar exponential rise or attenuation. In such a case, determine the numerical value of s for which $P(s)$ passes through the origin. For each such value, s_k, find the corresponding coefficient, λ_k, in the partial fractions expansion of $Q(s)/P(s)$ where $Q(s)$ is defined by equation 9 and

$$\lambda_k = \left.\frac{Q(s)}{\dfrac{dP(s)}{ds}}\right|_{s=s_k} \tag{4}$$

If the real part of each pertinent $(-\lambda_k-1)$ is negative, the system is stable. If any $(-\lambda_k-1)$ corresponding to a value of s_k for which $P(s)$ is zero, is positive, the system is unstable.

This method involves two restrictions. The elements of the servo must vary so that the coefficients of the differential equation describing the system have the form $(a+bt)$. This is often not too serious since practical variations can frequently be represented fairly well by a straight line throughout a reasonable time interval. A further restriction is that the coefficient of the highest order derivative term must vary; that is, b_n must exist. The remaining a subscript; and b subscript; coefficients may be either finite or zero.

The Transient Response Expressed as an Integral

The solution to equation 2 by means of definite integrals is discussed by a number of authors, including Forsyth,[2] Goursat,[3] and Ince.[4] The treatment given here follows Ince, chapter 18. It is pointed out there that the solution to equation 2 can be written as a contour integral

$$\theta_o(t) = \int e^{st} V(s) ds \tag{5}$$

Nomenclature

$a_1, a_2 \ldots a_j, a_n$ = constant parts of the coefficients of the differential equation describing the servo performance
$b_1, b_2 \ldots b_j, b_n$ = variable parts of the same coefficients
D = damping of servomotor and load
J = inertia of servomotor and load
$j = \sqrt{-1}$, also used as a subscript
J_0 = Bessel function, first kind, zero order
K = constant; in Figure 3 the gain of the servo
n = order of the differential equation describing the servo
$P(s)$ = polynomial in s defined by equation 6
$Q(s)$ = polynomial in s defined by equation 7
R = arbitrarily large radius in s-plane
r = arbitrarily small radius in s-plane
s = complex variable of integration
t = time
t_d = developed torque of servomotor
$V(s)$ = function of s, in contour integral expression for servo response
α_j = real part of γ_j
γ_n = j'th zero of $P(s)$
λ_1, λ_n = constant coefficients in the partial fractions expansion of $Q(s)/P(s)$
μ = complex constant, equation 10
θ_i = servo input
θ_o = servo output; usually denotes the transient part of the output
$\theta_1, \theta_r - \theta_j \theta_n$ = terms making up θ_o
ω_j = imaginary part of γ_j

when the function $V(s)$ and the contour C in the s-plane are properly chosen.

The conditions which $V(s)$ and C must satisfy can be determined by substituting the assumed solution (equation 5) into the equation 2.

$$\begin{aligned}(a_n+b_nt)\int_C s^n e^{st} V(s)ds + \ldots + \\ (a_j+b_jt)\int s^j e^{st} V(s)ds + \ldots + \\ (a_1+b_1t)\int_C se^{st} V(s)ds + \ldots + \\ (a_0+b_0t)\int_C e^{st} V(s)ds = 0\end{aligned} \tag{6}$$

Integration of the b terms by parts will remove t as a multiplying factor. When this is done, the equation becomes:

$$[(b_ns^n+\ldots+b_js^j+b_1s+b_0)e^{st}V(s)]_C + \int_C \left\{ \begin{aligned} &(a_ns^n+\ldots+a_js^j+\ldots+a_1s+a_0)V(s) \\ &\left[-\frac{d}{ds}(b_ds^n+\ldots+b_js^j+\ldots+b_1s+b_0)\right]V(s) \\ &-(b_ns^n+\ldots+b_js^j+\ldots+b_1s+b_0)\frac{dV(s)}{ds} \end{aligned} \right\} e^{st}ds = 0 \tag{7}$$

This will be satisfied if the contour C is chosen so that the term (in brackets) outside the integral sign is zero independent of t, and if $(V)s$ makes the differential expression inside the integral sign identically zero.

The function $V(s)$ must therefore satisfy the differential equation

$$P(s)\frac{dv}{ds} - Q(s)V = 0 \tag{8}$$

where

$$P(s) = b_ns^n+\ldots+b_js^j+\ldots+b_1s+b_0 \tag{3}$$

and

$$Q(s) = a_ns^n+\ldots+a_js^j+\ldots+a_1s+a_0 - [nb_ns^{n-1}+(n-1)b_{n-1}s^{n-2}+\ldots+2b_2s+b_1] \tag{9}$$

A useful form of the solution can be obtained by writing equation 8 as

$$\frac{1}{V}\frac{dv}{ds} = \mu + \frac{\lambda_1}{s-\gamma_1} + \frac{\lambda_2}{s-\gamma_2} + \ldots + \frac{\lambda_n}{s-\gamma_n} \tag{10}$$

where $\gamma_1, \gamma_2, \ldots \gamma_n$ are the zeros of $P(s)$ and the λ's are the constant coefficients in the partial fractions expansion of $Q(s)/P(s)$. μ is a constant which like $\lambda_1, \ldots, \lambda_n$ may be complex.

The solution is

$$V(s) = e^{\mu s}(s-\gamma_1)^{\lambda_1}(s-\gamma_2)^{\lambda_2}\ldots(s-\gamma_n)^{\lambda_n} \tag{11}$$

which has n singularities at the points $\gamma_1, \gamma_2, \ldots, \gamma_n$ in the s-plane.

It can be shown that a fundamental set of solutions to equation 2 can be obtained by using $V(s)$ given by equation 11, and a set of n contours, each of which follows a line parallel to the real axis and passing through a different one of the γ's, say γ_j. The representative point on each such contour starts at $-\infty$, moves along the line toward the particular γ_j until it is a small distance, r, from γ_j then encircles γ_j in the negative direction and retraces its linear path to $-\infty$. (See Figure 1).

This outline of the conditions which $V(s)$ and the contour C must satisfy is very sketchy. Further information and proofs are given in Chapters 5 and 8 in Ince.[4]

It might be noted in passing that equation 8 can be obtained formally by

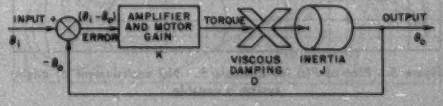

Figure 3. Block diagram of second order servomechanism of Examples 1, 2, and 3

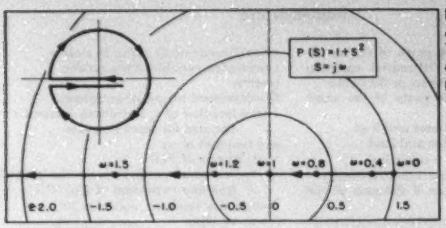

Figure 4 (left). Plot of $P(s)$ for Example 1. The plot starts and ends at $P(s)=1+j0$ and passes through the origin twice, for $s=\pm j$

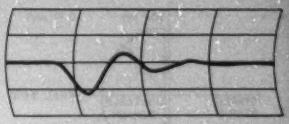

Figure 6. Response of system of Example 2 to input of form $\theta_i=1/(0.1+t)$. The system equation is: $(1+0.4t)p^2\theta_o+(-1+0.5t)p\theta_o+(0.1+t)\theta_o=(0.1+t)\theta_i$

applying LaPlace transform techniques as explained, for example, by Churchill.[5] The present derivation, however, is especially adapted to the study of solutions to equation 2 which increase without limit as $t\rightarrow\infty$.

Form of the Transient as $t \rightarrow \infty$

Upon substituting expression 11 for $V(s)$, the integral becomes:

$$\theta_o=\int_c(s-\gamma_1)^{\lambda_1}(s-\gamma_2)^{\lambda_2}\ldots(s-\gamma_n)^{\lambda_n}e^{(s+1)t}ds \tag{12}$$

where the contour C, as shown in Figure 1, consists of three integrals, two along the line parallel to the real axis from $-\infty$ to (γ_j-r) and from (γ_j-r) to $-\infty$, and the third around the small circle of radius r with center at γ_j.

As $t\rightarrow\infty$, the first two integrals approach zero, and the third integral approaches the limit

$$\theta_j\rightarrow\frac{K_j e^{\gamma_j t}}{t^{\lambda+\lambda_j}} \tag{13}$$

where K_j is an arbitrary constant, and γ_j may have a real part α_j and an imaginary part ω_j.

The complete solution for θ_o therefore approaches the limit

$$\theta_o=\frac{K_1e^{\gamma_1 t}}{t^{\lambda+\lambda_1}}+\frac{\gamma^{\gamma t}}{t^{\lambda+\lambda_2}}+\ldots+\frac{K_ne^{\gamma_n t}}{t^{\lambda+\lambda_n}} \tag{14}$$

Equations 13 and 14 bring out the interesting fact that the transient response of a system described by equation 1 approaches a function in which the dominant part of each term is the exponential $e^{\alpha_j t}$ $(\cos\omega_j t+j\sin\omega_j t)$. Since the α's and ω's are the real and imaginary parts of the roots (γ's) of $P(s)$, the coefficients of the time-varying terms, $b_n\ldots b_0$, in equation 2 determine whether or not the solution is oscillatory, the frequency if it is oscillatory, and the damping. In so doing, the b's play much the same role as do the coefficients in the characteristic equation corresponding to a differential equation with constant coefficients.

Each exponential function is multiplied by $t^{-\lambda_j-1}$, but this is overpowered by $e^{\alpha_j t}$ whenever α_j is not zero. Thus the eventual rate of rise or decay of the transient, the stability of the system, is determined by the coefficients of the time-varying terms; if all the α's are negative the system is stable, if any α is positive the system is unstable.

If no α is positive, but one or more are zero, the $1/t^{\lambda+1}$ factors for these terms will determine the system stability. The transient response is oscillatory with frequency ω_j but rises or decays as $1/t^{\lambda+1}$ which will frequently be a fractional power of t. The response has no counterpart of the performance of constant coefficient system; the increase or decay of the transient is much slower than the familiar exponential rise or decay. Bessel functions of zero order are functions of this type (see the first example which follows).

The problem of determining stability now is reduced to the problem of investigating the location, in the s-plane, of the γ's which are the roots of $P(s)$. There are three possible cases:

1. If all the γ's lie in the left half of the s-plane, the system is stable.

2. If any γ lies in the right half of the s-plane, the system is unstable.

3. If any γ lies in the imaginary axis of the s-plane, the stability of the system must be determined from the $t^{-\lambda-1}$ factor for each such term. If each pertinent $(-\lambda-1)$ is negative, the system is stable. If any $(-\lambda-1)$, corresponding to a γ lying on the axis, is positive, the system is unstable.

A convenient means of determining how many γ's lie on the imaginary axis or in the right half of the s-plane is to plot the function $P(s)$ as the representative point describes a contour which encloses the right half of the s-plane. A theorem (see Copson,[6] or James, Nichols, and Phillips,[7]) sometimes referred to as "The Principle of the Argument" states that as the representative point traverses the contour once the plot of the function $P(s)$ will encircle the origin once in the positive direction for each γ which lies inside the contour, that is, in the right half or unstable region of the s-plane.

The contour used here consists of the imaginary axis from $s=-j\infty$ to $+j\infty$, together with a semicircle whose radius

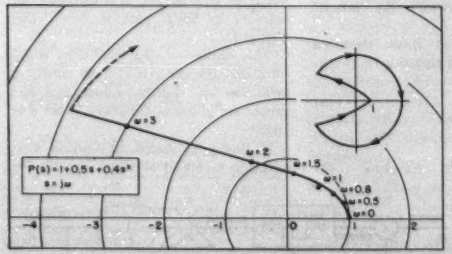

Figure 5. Plot of $P(s)$ for Example 2. No encirclement of origin; system is unstable

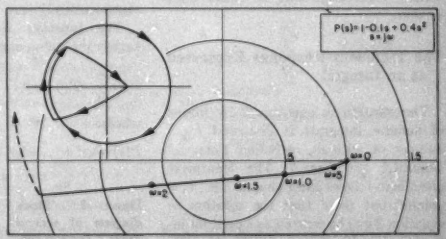

Figure 7. Plot of $(P)s$ for Example 3. Two encirclements of origin; system is unstable

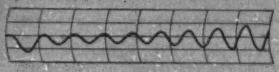

Figure 8. Response of system of Example 3 to input of form $\theta_i = 1/(1+t)$. The system equation is: $(1+0.4t)p^2\theta_o + (1-0.1t)p\theta_o + (1+t)\theta_o = (1+t)\theta_i$

approaches infinity, enclosing the right half plane, (Figure 2).

The plot of $P(s)$ begins at b_0 for $s=0$, and approaches infinity as $s \to +j\infty$; the angle of $P(s)$ approaches $\doteq \pi/2$ if the highest power of s in $P(s)$ is unity, $\doteq \pi$ if the highest power is s^2, and in general $\doteq n\pi/2$ where $P(s)$ is of the order n.

In order to avoid confusion as to the number of encirclements, $P(s)$ should be plotted for values of s on the semicircular part of the contour as well as along the imaginary axis. This can be easily accomplished by letting the radius of the semicircle be an arbitrary value, R, large enough so that all possible roots of $P(s)$ are inside the semicircle, and large enough so that all terms of $P(s)$ except $b_n s^n$ can be neglected. As the representative point in the s-plane travels clockwise around the semicircle from $s=+jR$ to $s=-jR$, the plot of $P(s)$ follows a circular arc of radius $b_n R^n$ from $+n\pi/2$ through zero to $-n\pi/2$. Figures 4, 5, 7, and 9 illustrate this.

The labor of plotting $P(s)$ is lessened by the fact that for pure imaginary values of s the real part of $P(s)$ is an even function and the imaginary part of $P(s)$ is an odd function. The plot of $P(s)$ for negative imaginary values of s is the reflection in the real axis of the plot for positive imaginary values of s.

If any of the γ's have zero real parts, the plot of $P(s)$ will pass through the origin of the $P(s)$ plane for the corresponding finite imaginary values of s. This is case 3 mentioned previously, and the following procedure (see, for example, Churchill[9]), can be used to determine whether $(-\lambda-1)$ is positive or negative for each lying on the imaginary axis.

Find the numerical value of s at which the zero of $P(s)$ occurs. This is the value of s for which the plot of $P(s)$ passes through the origin. Call this s_k. The value of λ_k, the coefficient of the $1/s-s_k$ term in the partial fractions expansion of $Q(s)/P(s)$ is

$$\lambda_k = \left.\frac{Q(s)}{\dfrac{dP(s)}{ds}}\right|_{s=s_k} \tag{4}$$

where $Q(s)$ is defined by equation 9.

It is not necessary, of course, to find the value of λ corresponding to any γ which has a nonzero real part.

It might be noted that the stability criterion could be stated in terms of a plot of $1/P(s)$ as well as $P(s)$. A plot of $1/P(s)$ would start at $1/b_0$ and approach the origin, describing a small circular arc of radius $1/b_n R^n$ as s follows the semicircle. Encirclement of the origin would determine stability, in a manner similar to the present criterion. If any of the zeros of $P(s)$ lie on the imaginary axis, the plot of $1/P(s)$ would be infinite for the corresponding values of s.

The stability criterion can be modified and extended to apply to servomechanisms in which the elements vary as powers of t higher than the first. Space does not permit this in the present paper, but will be the subject of a future paper.

Examples

In the interest of brevity, the number of examples which follow is held to the minimum. The plots of the response to typical test inputs, θ_i, which are included in examples 2 to 4 were obtained with the aid of an electronic analogue computer. The number of computing elements available limited the examples to second and third order systems. The amount of noise inherent in certain of the elements

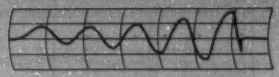

Figure 10. Response of system of Example 4 to an input of form $\theta_i = 1/(1+0.4t)$. The system equation is: $(1+0.4t)p^3\theta_o + (1+0.3t)p^2\theta_o + (1+0.4t)p\theta_o + (1+0.4t)\theta_o = (1+0.4t)\theta_i$

limited the gains which could be used, particularly the variable part of the coefficient of the highest order derivative. These limitations are not serious, but explain what may appear to be arbitrary choices of the numerical values of a_0, b_2, a_3, b_3, and so forth.

Example 1

In order to provide a familiar starting point, this example concerns a system whose transient response is a Bessel Function of order zero.

Consider a servo consisting of a motor driving an inertia load with viscous damping. The amount of damping does not vary, but the inertia J and the gain, K, increase linearly with time, and are so small as to be negligible at $t=0$, Figure 3. For convenience assume the numerical values of the fixed damping and the rates of increase of inertia and gain are all unity.

The differential equation for the system is

$$t\frac{d^2\theta_o}{dt^2} + \frac{d\theta_o}{dt} + t\theta_o = t\theta_i \tag{15}$$

since

$$b_2 = 1,\ b_1 = 0,\ b_0 = 1$$
$$P(s) = s^2 + 1 \tag{16}$$

The plot of $P(s)$, Figure 4, shows poles on the imaginary axis, at $s=\pm j$; the stability must be determined from the values of λ associated with the $1/(s+j)$

Figure 9. Plot of P(s) for Example 4. Two encirclements of the origin; the system is unstable

Figure 11. Comparison of polar plots for four third-order systems having the system equations shown. To compare plots, adjust scales so that all start from the same point at $\omega=0$. Thus, plot A is actually farthest from the origin

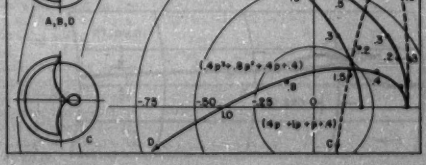

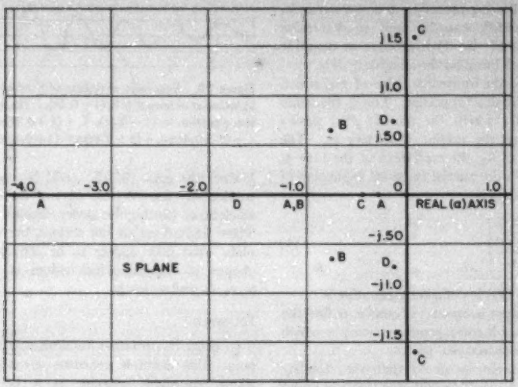

Figure 12. Location of zeros of $P(s)$ for the four systems of Figure 11

term in the partial-fraction expansion of $Q(s)/P(s)$

$$\lambda = \left.\frac{Q(s)}{\dfrac{dP(s)}{ds}}\right|_{s=j} \tag{4}$$

where

$$Q(s) = -s \qquad \frac{dP}{ds} = 2s$$

$$\lambda_j = -\frac{1}{2} \qquad -\lambda_j - 1 = -\frac{1}{2}$$

This indicates that the transient response of the servo approaches $(1/\sqrt{t})\cdot(e^{jt}+e^{-jt})$ times a suitable constant; hence is stable, although it approaches zero quite slowly as $t \to \infty$.

The stability of this servo can be verified analytically, since its transient response is a tabulated function. If θ_i is a unit step, for example, and $\theta_o = 0$ initially, the solution to equation 16 is

$$\theta_o = 1 - J_0(t) \tag{17}$$

The transient, $J_0(t)$ approaches zero as $t \to \infty$; furthermore, at large values of t,

$$J_0(t) \to \frac{K \cos t - \frac{\pi}{4}}{\sqrt{t}} \tag{18}$$

where K is a constant (see, for example, McLachlan[9]). McLachlan[10] discusses the derivation of asymptotic expansions for Bessel function using contour integrals wherein the contours consist of lines parallel to the real axis, and encirclements of singular points, similar to Figure 1.

Example 2

Consider a second-order servo like that of Figure 1, but in which the inertia and gain are not zero initially. Assume that the damping is initially negative but increases with time, so that the differential equation is

$$(1+0.4t)\frac{d^2\theta_o}{dt^2} + (-1+0.5t)\frac{d\theta_o}{dt} + (0.1+t)\theta_o = (0.1+t)\theta_i \tag{19}$$

If stability depended on the constant coefficients a_2, a_1, a_0, the system would be violently unstable because of the negative damping, a_1. However, for this system

$$P(s) = 0.4s^2 + 0.5s + 1 \tag{20}$$

and the plot of $P(s)$, Figure 5, indicates stability because there is no encirclement of the origin.

Figure 6 is a plot of the response of this system to an input of the form

$$\theta_i = \frac{1}{0.1+t} \tag{21}$$

and shows that the servo is indeed stable. Its transient decays more rapidly than that of the previous example, because of the presence of the damping term, b_1, in $P(s)$.

Example 3

A servo similar to the previous one but in which the damping is initially large and positive and changes slowly in the negative direction is considered next. Assume the numerical values are such as to give the differential equation:

$$(1+0.4t)\frac{d^2\theta_o}{dt^2} + (1-0.1t)\frac{d\theta_o}{dt} + (1+t)\theta_o = (1+t)\theta_i \tag{22}$$

Figure 7 is a plot of $P(s)$, which is:

$$P(s) = 0.4s^2 - 0.1s + 1 \tag{23}$$

This encircles the origin, indicating instability. The response of the servo to the input

$$\theta_i = \frac{1}{1+t} \tag{24}$$

is given in Figure 8 and verifies the instability. (The solution was not continued for a longer time because of overloading of some of the elements of the computer). If the constant coefficients, a_2, a_1, a_0 alone were effective in determining stability, the system would be stable, whereas it is actually unstable owing to the negative value of b_1. Increasing the amount of positive constant damping, a_1, would postpone but never eliminate the eventual instability of this system.

Example 4

Assume that in some manner a servo has been obtained which is described by

Figure 13(A). Response of system *A*, Figure 11, to input $\theta_i = 40/(1+0.2t)$. The system equation is: $(1+0.2t)p^2\theta_o + (0.5+t)p^2\theta_o + (0.5+t)p\theta_o + (1+0.2t)\theta_o = (1+0.2t)\theta_i$. Broken line is approximate steady-state response

Figure 13(B). Response of system *B*, Figure 11, to input $\theta_i = 40/(1+0.4t)$. The system equation is: $(1+0.4t)p^2\theta_o + (1+t)p^2\theta_o + (1+t)p\theta_o + (1+0.4t)\theta_o = (1+0.4t)\theta_i$

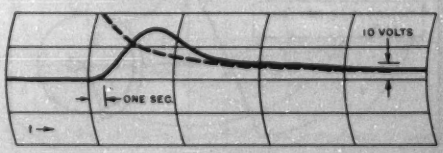

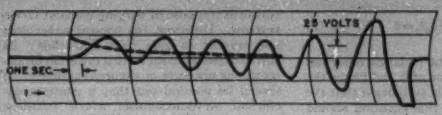

Figure 13(C). Response of system C, Figure 11, to input $\theta_i=40/(1+0.4t)$. The system equation is: $(1+0.4t)p^3\theta_o+(0.5+0.1t)p^2\theta_o+(0.5+t)p\theta_o+(1+0.4t)\theta_o=(1+0.4t)\theta_i$. Broken line is approximate steady-state response

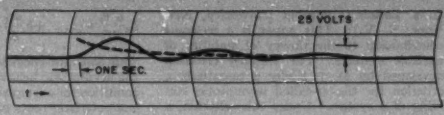

Figure 13(D). Response of system D, Figure 11, to an input $\theta_i=40/(1+0.4t)$. The system equation is: $(1+0.4t)p^3\theta_o+(1+0.8t)p^2\theta_o+(1+0.4t)p\theta_o+(1+0.4t)\theta_o=(1+0.4t)\theta_i$. Broken line is approximate steady-state response

the differential equation:

$$(1+0.4t)\frac{d^3\theta_o}{dt^3}+(1+0.3t)\frac{d^2\theta_o}{dt^2}+(1+0.4t)\frac{d\theta_o}{dt}+(1+0.4t)\theta_o=(1+0.4t)\theta_i \quad (25)$$

The function $P(s)$ is plotted in Figure 9.

$$P(s)=0.4s^3+0.3s^2+0.4s+0.4 \quad (26)$$

and indicates instability by encircling the origin, Figure 13, which is the response to an input:

$$\theta_i=\frac{1}{1+0.4t} \quad (27)$$

illustrates the instability.

Relative Stability

A polar plot of $P(s)$, in addition to indicating absolute stability, gives information about the form of the servo response at large values of time. Since the main parts of the terms in the response are exponentials whose exponents are the zeros of $P(s)$, the locations of these zeros in the complex s-plane determine the response. The distance of each zero from the real axis determines the frequency of oscillation; the distance from the imaginary axis determines the rapidity of damping; the farther from the real axis, the higher the frequency of oscillation; the closer to the imaginary axis, the longer the "tail", the slower the decay.

The closeness with which the polar plot approaches the critical point in the $P(s)$ plane indicates the closeness of the zeros to the imaginary axis in the s-plane. The frequency (ω) at which the polar plot most closely approaches the critical point is the predominant frequency of the oscillation.

These properties of the polar plot are illustrated by Figures 11, 12, and 13. Figure 11 contains polar plots of four third-order systems, Figure 12 shows the locations of the zeros of $P(s)$ in the s-plane for these servomechanisms, and Figure 13 displays their responses to an input of the form $\theta_i=1/(1+t)$. In order to correctly compare the closeness of the polar plots to the origin of the $P(s)$ plane, their respective scales must be adjusted so that all plots start from the same point at zero frequency. When this is done, it can be seen that as the polar plots approach progressively closer to the origin, the transient response decays more slowly. (The decaying steady state response, which is approximately $1/(1+t)$, should not be confused with the transient.)

It must be remembered that $P(s)$ is not a "transfer function" but rather has the properties of a characteristic equation. While a plot of $P(s)$ can indicate the frequency and relative damping of the terms in the transient response, it cannot indicate the magnitudes of the terms, hence cannot indicate overshoot.

References

1. Regeneration Theory, H. Nyquist. *Bell System Technical Journal* (New York, N. Y.), volume XI, January 1932.

2. A Treatise on Differential Equations (book), A. R. Forsyth. The MacMillan Company, New York, N. Y., sixth edition, chapter 7.

3. A Course in Mathematical Analysis, Edouard Goursat. Translated by E. R. Hedrick, O. Dunkel, Ginn and Company, Boston, Mass., part II, volume II, 1917, 300 pages.

4. Ordinary Differential Equations (book), E. T. Ince. Dover Publishing Company, New York, N. Y., 1944, 558 pages.

5. Modern Operational Mathematics in Engineering (book), R. V. Churchill. McGraw-Hill Book Company, New York, N. Y., 1944, 306 pages.

6. An Introduction to the Theory of Functions of a Complex Variable (book), E. T. Copson. Oxford University Press, London, England, 1946, 448 pages.

7. Theory of Servomechanisms (book), H. M. James, N. B. Nichols, R. S. Phillips. McGraw-Hill Book Company, New York, N. Y., section 2.35, 1947, 373 pages.

8. Ibid., R. V. Churchill. Section 16.

9. Bessel Functions for Engineers (book), N. W. McLachlan. Clarendon Press (Oxford, England), 1934, 192 pages.

10. Complex Variable and Operational Calculus (book), N. W. McLachlan. University Press, Cambridge, England, 1939, articles 4.2-1 and 14.6, 355 pages.

11. Servomechanisms, Charts for Verifying Their Stability and Finding the Roots of Their Third and Fourth Degree Characteristic Equations, Y. L. Lin. Massachusetts Institute of Technology (Cambridge, Mass.), 1941, pages 55–74.

Discussion

G. M. Anderson and **William Caywood, Jr.** (Carnegie Institute of Technology, Pittsburgh, Pa.): Dr. Kirby is to be congratulated for an elegant treatment of the stability problem of servomechanisms defined by a differential equation with linearly time varying coefficients. The analysis extends the usual stability criterion applicable to linear differential equations with constant coefficients in a logical, simple manner.

It is felt that perhaps some emphasis should be placed on the result that there is one simple condition, which can be determined by inspection, which is an indication of instability. As is suspected by analogy with the constant coefficient system all of the b coefficients must be of the same algebraic sign, otherwise there are zeros of $P(s)$ to the right of the imaginary axis and the system cannot be stable. Mere fulfillment of this condition is not sufficient in itself to insure stability but it is necessary.

There is another simple requirement for stability that is applicable to systems with constant coefficients, that all of the lower order terms must exist. The analogous conclusion can not be so simply drawn with the $P(s)$ function as missing terms also may be due to zeros on the imaginary axis, resulting in a critical case as is discussed in the paper.

The following errors were noted in the text. The character μ as defined by equation 10 is a real number since $\mu=a_n/b_n$. It is not complex as claimed.

Stability condition (3) following equation 14 should be corrected, in part, to read: ...If "the real part of" each pertinent $(-\lambda-1)$ is negative, the system is stable. If "the real part of" any $(-\lambda-1)$, corresponding to a γ lying on the axis is positive the system is unstable.

The reason for the insertion of "the real part of" is that λ will in general be complex. Consider the system defined by

$$t\frac{d^2\theta_o}{dt^2}+\frac{d\theta_o}{dt}+(1+t)\theta_o=0$$

which is identical with Example 1 given in the paper, except for the addition of $a_0=1$. In this case

$$P(s)=s^2+1$$
$$Q(s)=s+1-[2s]=1-s$$
$$\lambda_j=\left.\frac{Q(s)}{\frac{dP}{ds}}\right|_{s=j}=\left.\frac{1-s}{2s}\right|_{s=j}=\frac{-1}{2}[1+j]$$

and

$$-\lambda_j-1=-\frac{1}{2}[1-j]$$

L. A. Zadeh (Columbia University, New York, N. Y.): This paper is a welcome contribution to the theory of stability of variable systems. The stability criterion developed by M. J. Kirby is essentially a criterion for the so-called asymptotic stability of a system. Under this criterion, a system is stable if the transient response or, more precisely, any solution of equation 7 of the paper, dies out as $t \to \infty$. Thus, on the basis of this criterion a system whose response to an input exhibits violent overshoots over the period of observation, but is such that the response eventually dies out as $t \to \infty$, would be classified as a stable system. It is evident, however, that in most practical cases it would not be justifiable to classify a system as stable or unstable solely on the basis of the behavior of the system for very large t, particularly since this phase of the behavior is frequently of little practical interest. The fact that the author's criterion does not provide any information whatsoever regarding the magnitude of the overshoots, constitutes in my opinion a serious shortcoming of this criterion.

It should be noted that in general it is easiest to investigate the location of the zeros of $P(s)$ by using Hurwitz's criterion,[1] which eliminates the necessity for plotting $P(s)$. In particular, in Example 3, the instability of the system follows immediately from the fact that one of the coefficients in $P(s)$ is negative. Any polynomial having one or more negative coefficients is certain to have some zeros in the right half of the s-plane.

For the case where none of the coefficients b_j is zero, Mr. Kirby's criterion can readily be obtained by noting that for large values of t the terms a_j become negligible versus $b_j t$ and hence the differential equation becomes

$$b_n t \frac{d^n \theta_0}{dt^n} + \ldots + b_1 t \frac{d\theta_0}{dt} + b_0 \theta_0 = 0 \qquad (1)$$

or

$$b_n \frac{d^n \theta_0}{dt^n} + \ldots + b_1 \frac{d\theta_0}{dt} + b_0 \theta_0 = 0 \qquad (2)$$

This constant-coefficient equation describes the asymptotic behavior of θ_0 and hence the condition for asymptotic stability is that the characteristic roots of this equation should have negative real parts. This is essentially the criterion given by the author.

The above derivation fails when some of the b_j's are zero. For this case it is necessary to use the rigorous procedure described by Mr. Kirby.

The criterion under discussion would unquestionably be very useful in some practical cases. An extension of this criterion to systems in which the coefficients involve powers of t higher than the first would be of great value.

REFERENCE

1. THE MATHEMATICS OF CIRCUIT ANALYSIS, E. A. Guillemin. John Wiley and Sons, Inc., New York, N. Y., 1949.

M. J. Kirby: Both discussions emphasize a very worthwhile point; a Nyquist plot is by no means the only method for determining the signs of the real parts of the roots of $P(s)$. Because Nyquist's method is used in many well-known American texts on servomechanisms, it was used in this paper. However, inspection of $P(s)$, or the use of a simple rule such as the one stated by Drs. Anderson and Caywood will suffice in many cases. In more complicated situations the Routh-Hurwitz criterion, as pointed out by Dr. Zadeh, and also by Dr. F. E. Bothwell[1] is more useful than a Nyquist diagram.

The comment that μ is real is correct Likewise, condition (3) should be corrected to agree with the main statement of the stability criterion in the paper, "...the real part of each pertinent $(-\lambda-1)$..."

There is definite need, as Dr. Zadeh points out, for a method of predicting relative stability, or the initial size of the transient response of varying-element servosystems. However, the present paper does not purport to give such a method; its stated object is to set forth a criterion for determining absolute or eventual stability. It should be pointed out that a constant coefficient servomechanism whose transient response exhibits violent overshoots initially but eventually dies out, would be classed as stable by the commonly used criteria of Nyquist or Routh-Hurwitz. The definition of stability used in the paper is parallel to that customarily used for constant-element systems.

Furthermore, it is not necessarily true that the asymptotic response of a system is of little practical interest. The transient responses of the systems of the examples of the paper, and many practical systems reach their eventual or asymptotic forms in a comparatively small number of time constants. The unstable examples (Figures 8, 10, and 13C) in particular illustrate this.

The advantage of dividing the original differential equation by t and letting t approach infinity, as suggested, in order to obtain the stability criterion is not clear. Obtaining a criterion is not an operation which must be repeated for each determination of stability; it need be performed only once and has been accomplished rigorously in the paper. Applying a limit process to a differential equation, in the manner suggested, before solving it, is not usually a rigorous procedure. This amounts to the limiting case of the constant coefficient approximation or "snapshot" procedure mentioned in the introduction. It does not give the complete asymptotic form of the solution (the $t^{-\lambda-1}$ factors are omitted) and it does not have any obvious warning within itself as to when its results are unreliable; as when some of the b_j terms are zero.

REFERENCE

1. NYQUIST DIAGRAMS AND THE ROUTH-HURWITZ STABILITY CRITERION, F. E. Bothwell. *Proceedings*, Institute of Radio Engineers (New York, N. Y.), volume 38 November 1950, page 1345.

Variations of Tank Pressure with Transformer Loading in Sealed Transformers

E. W. TIPTON
MEMBER AIEE

IN A modern power transformer only the insulation consisting of oil and fibrous materials shows appreciable deterioration under normal operating conditions. It is, consequently, only natural that much effort has been applied to the problem of preventing or retarding this deterioration. Many schemes for this purpose have been devised; open air breathers, dehydrating breathers, conservators, gas-oil seals, sealed tanks, inert gas atmospheres, and thermosiphon clay filters, to name a few. These devices have one or two objectives which are: to prevent the entrance or to minimize the effects of moisture, or to exclude oxygen and minimize the effects of oxidation. The simplest method is to seal the transformer tank and, as is often the case, the simplest also is the equal in effectiveness of any of the methods. This has been demonstrated by direct comparison on life test.[1]

First applied to submersible network transformers, the practice of tightly sealing power transformers has been proposed as an industry standard for small and moderate sized transformers; those up to about 10,000 kva in rating. As a parallel development has come the welding on of covers to eliminate the main gasket. A definite trend toward solder sealed or welded bushings is another step toward the elimination of gaskets to better insure a tight tank.

When a transformer is tightly sealed with a gas space over the top of the oil surface, it is subject to variation in internal pressure during its operating cycle. Changes in temperature due to ambient changes and to heating from excitation and load losses cause the oil to expand, and produce heating of the gas. Both effects result in an increase in internal tank pressure. The variation of pressure as a function of load and ambient temperature is of interest, both to transformer designers and to transformer operators.

The calculation of pressure as a function of load is not a simple one. The principal factors involved are:

1. Oil expansion due to heating.
2. Pressure temperature effects on the gas.
3. Tank wall deflection.
4. Solubility of the gas in transformer oil.
5. Chemical reactions between the gas and transformer oil.

The effects of the first two of these factors may be easily and accurately calculated. Tank wall deflection is a relatively minor, though appreciable factor and it can be estimated empirically from test results with fair accuracy. Gas solubility and reaction with transformer oil are complex and difficult to calculate, but they play the major role in determining transformer pressure.

Effect of Oil Expansion and Gas Heating

The change in pressure due to oil expansion and gas heating may be calculated easily using the temperature coefficient of expansion of the oil and the gas laws.

If we let:

P = absolute pressure in the gas space, pounds per square inch
V = volume of gas space, cubic inches
T = gas temperature, degrees Kelvin
θ = average oil temperature, degrees Kelvin
v = volume of oil, cubic inches

These apply to conditions at some load which is being investigated.

P_0, V_0, T_0, θ_0, and v_0 have the same meaning as above, but apply to conditions at the time the transformer is sealed.

K = volumetric coefficient of expansion of oil per degrees centigrade
$R = V_0/v_0$ ratio of gas volume to total oil volume at sealing temperature, $T_0 = \theta_0$

By the gas law:

$$\frac{P_0V_0}{T_0} = \frac{PV}{T} \text{ or } P = P_0\frac{V_0}{V}\frac{T}{T_0} \text{ pounds per square inch}$$

The increase in oil volume due to its thermal expansion will be equal to the decrease in the gas volume and:

$$V = V_0 - K(\theta - \theta_0)v_0$$

$$P = P_0\frac{T}{T_0}\frac{V_0}{[V_0 - K(\theta - \theta_0)v_0]} \text{ or } P = P_0\frac{T}{T_0}\frac{R}{[R - K(\theta - \theta_0)]} \text{ pounds per square inch} \quad (1)$$

Based on the gas laws, the maximum pressure to be expected under normal operating conditions can be determined from the following considerations:

1. By the standards of the American Standards Association the maximum permissible oil rise at rated load is 50 degrees centigrade, and the average copper rise is 55 degrees centigrade.

2. For a given hot oil rise, the oil will have the highest average temperature in a transformer having the lowest hot spot gradient. If we assume the gradient to be 8 degrees centigrade, then the transformer hot spot rise will be 63 degrees centigrade.

3. The difference between hot copper and average copper is essentially the same as the difference between hot oil and average oil. If top oil rise is 50 degrees centigrade, this gives an average oil rise of $50 - 8 = 42$ degrees centigrade.

Paper 50-275, recommended by the AIEE Transformers Committee and approved by the AIEE Technical Program Committee for presentation at the AIEE Fall General Meeting, Oklahoma City, Okla., October 23–27, 1950. Manuscript submitted July 26, 1950; made available for printing September 11, 1950.

E. W. TIPTON is with Westinghouse Electric Corporation, Sharon, Pa.

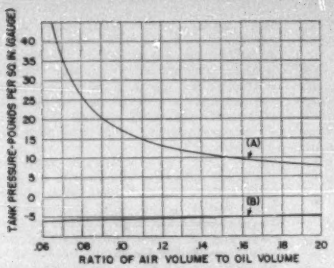

Figure 1. Minimum and maximum tank pressures as a function of the ratio of air volume to oil volume

(A) Maximum pressures
(B) Minimum pressures

4. Maximum ambient for full load operation is 40 degrees centigrade.

5. Assume ambient at the time the transformer is sealed to be 20 degrees centigrade.

6. The thermal drop from the top oil to outside air is made up of three drops in series; from the oil to the gas in the top of the transformer, from this gas to the cover, and from the cover to the outside air. These three drops involve approximately the same surface areas and are approximately equal. On this basis, the air temperature rise will be two thirds that of the hot oil.

7. Transformer will be sealed at atmospheric pressure with the gas and oil at ambient temperature.

If these conditions hold:

$P_0 = 14.7$ pounds per square inch
T = two thirds hot oil rise plus ambient plus 273 = 346 degrees Kelvin
θ = average oil rise plus ambient plus 273 = 355 degrees Kelvin
T_0 = sealing ambient plus 273 = 293 degrees Kelvin
$\theta_0 = T_0 = 293$ degrees Kelvin
$K = 0.00074$ (approximately)
$P_{max.} = 17.4R/(R-0.046)$ pounds per square inch (absolute)

By a similar process of reasoning, the minimum pressure to be expected might be taken to apply to an idle transformer, such as an unexcited spare unit, in an ambient of −30 degrees Centigrade. For these conditions:

$P_0 = 14.7$ pounds per square inch
T = ambient plus 273 = 243 degrees Kelvin
$\theta = T = 243$ degrees Kelvin
T_0 = sealing ambient plus 273 = 293 degrees Kelvin
$P_{min.} = 12.2R/(R-0.037)$ pounds per square inch (absolute)

In Figure 1, the values of the minimum and maximum internal pressures are plotted as a function of the ratio of gas volume to oil volume in the transformer tank.

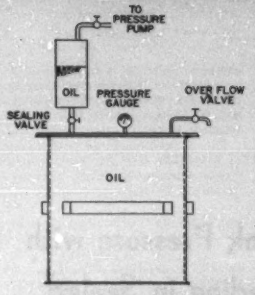

Figure 2. Test setup to determine effect of tank wall deflection

Effect of Tank Wall Deflection

Many power transformers of small and moderate rating are built in rectangular tanks. Flat sides of such tanks are braced to enable the tank to withstand test and operating pressures. Under pressure or vacuum, the flat unbraced portions of the tank wall are permitted to deflect within the elastic limit of the material. Deflection of the tank walls under pressure has the effect of increasing the tank volume and decreasing the observed pressure below what would be calculated by the methods discussed previously.

To determine experimentally the quantitative effect on pressure of tank wall deflection, a number of transformer tanks were tested with the simple test setup shown in Figure 2. A small reservoir was connected through a valve into the top of the sealed transformer tank. In the main tank cover were an overflow valve and a vacuum pressure gauge. Then with the main tank completely full of oil and a reserve supply of oil in the reservoir, the system was pumped up to a predetermined pressure after which the valve between reservoir and main tank was closed. The overflow valve is then opened and the amount of oil which flows out as the pressure returns to zero is a measure of the increase in volume of the tank due to pressure.

Rectangular tanks for transformers ranging from 150 kva to 1,500 kva were tested. These tanks had inside dimensions varying from 25 by 36 inches to 32 by 68 inches and heights from 64 to 126 inches. They were designed for a test pressure of eight pounds per square inch and had horizontal channel braces. In addition, one similar tank designed for complete vacuum was tested. The results of the tests are shown in curve form in Figure 3, curve B.

For tanks designed for an 8-pound test, the experimental data are very closely approximated by assuming that the increase in volume varies linearly from 0 to 1.4 per cent of the tank volume as the internal pressure varies from 0 to 8 pounds per square inch.

$$V_1 = V_0 + 0.00175(P-14.7)v_0$$

Letting $R = V_0/v_0$, then

$$V_1 = V_0\left(1 + 0.00175\frac{P-14.7}{R}\right)$$

where

V_1 = gas volume at absolute pressure P
V_0 = gas volume at atmospheric pressure
v_0 = oil volume

When designed for full vacuum, the tanks are more rigid and for the tank which tested as shown in Figure 3:

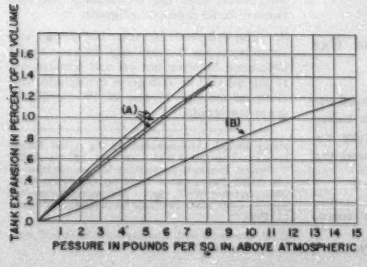

Figure 3 (left). Increase in tank volume due to pressure

(A) Tanks designed for 8 pounds per square inch test pressure
(B) Tank designed for 15 pounds per square inch test pressure

Figure 4 (right). Time-pressure curve for Test 1. Transformer oil filled at atmospheric pressure then sealed

(A) Calculated gas pressure
(B) Tested gas pressure

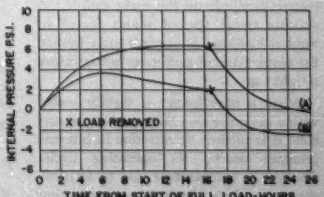

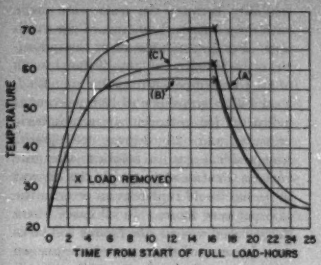

Figure 5. Time-temperature curve for Test 1. Transformer oil filled at atmospheric pressure then sealed

(A) Hot oil temperature
(B) Air temperature in gas space
(C) Average oil temperature

$$V_1 = V_0\left(1+0.0008\frac{P-14.7}{R}\right)$$

These figures are for a particular type of transformer tank and have no general application. They are of interest in that they apply to typical braced rectangular tanks which probably show the maximum to be expected for this effect. The tests show that the maximum increase in volume due to pressure is about 1.5 per cent of the oil volume. Normally the gas space in sealed transformers is about 10 per cent of the oil volume. The maximum tank volume expansion expressed in per cent of the gas volume is 15 per cent. From this, we can conclude that the measured gas pressure at a given load may be reduced a maximum of 15 per cent below the calculated value, due to tank wall deflection.

Figure 6. Time pressure curves for Tests 1 to 4, 9 and 10. All tests with air in gas space

(A) Oil filled at atmospheric pressure, then sealed
(B) Oil filled under vacuum, sealed at atmospheric pressure
(C) Oil filled under vacuum. Air space open for 24 hours, then sealed at atmospheric pressure
(D) Oil filled under vacuum. Run at normal load for 24 hours with air space open, then sealed at atmospheric pressure
(E) Oil filled at atmospheric pressure. Sealed at a pressure of 3 pounds per square inch
(F) Oil filled under vacuum. Sealed at a pressure of 6 pounds per square inch

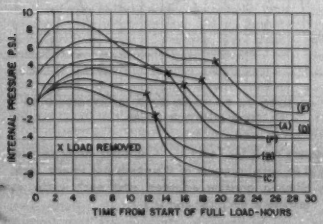

Figure 7. Time pressure curves for Tests 5, 6, 7, and 8. All tests with nitrogen in gas space

(A) Oil filled at atmospheric pressure. Blown out with dry nitrogen and sealed at atmospheric pressure
(B) Oil filled under vacuum. Blown out with dry nitrogen and sealed at atmospheric pressure
(C) Oil filled under vacuum. Blown out with nitrogen, allowed to stand for 24 hours with low pressure nitrogen blanket, then sealed at atmospheric pressure
(D) Oil filled under vacuum, blown out with nitrogen, operated for 24 hours at normal load with low pressure nitrogen blanket, then sealed

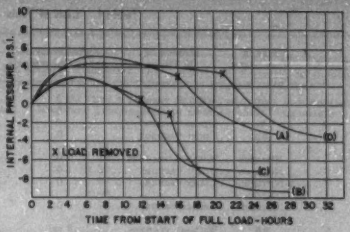

Effects of Gas Solution in Transformer Oil

Test Apparatus

To determine the effects of gas solubility on the internal pressure of sealed transformers, a series of load tests were run on a 500-kva transformer. A round case with heavy walls was used to eliminate the effects of tank wall deflection. Six thermocouples were installed; five in the oil, distributed from the top to the bottom of the case, and the sixth in the gas space above the hot oil. By assuming straight line temperature variation between adjacent thermocouples at different levels, the average oil temperature could be determined. For taking data, the test transformer was equipped with a vacuum pressure gauge and a visual oil level indicator. When filled with oil to the normal oil level at 20-degree centigrade temperature, the transformer case contained 212 gallons of oil and 29.1 gallons of gas.

Method of Testing

A total of 13 tests were made with certain procedures maintained constant for all. In each case, the core and coils assembly of the transformer was placed in a large tank and vacuum impregnated with oil. It was then placed in its own tank and filled with new oil and sealed, following which a pressure test was made to determine that the case was tight. After this preparation, a standard short circuit temperature run was made. At the start and at half-hour intervals throughout the test, measurements were made of gas space temperature, oil temperature at five different levels, and gas pressure. Measurements were continued during the heating period, while constant temperature was held for two hours, and after the load was removed until the transformer returned to ambient temperature. Tests were made under 13 different conditions of filling and initial gas pressure as shown in Table I.

Test Results

The test data are given in graphical form in Figures 4 to 10. Figure 4 shows the measured values of internal pressure during the test and the corresponding values calculated by equation 1, which neglects the solubility of the gas. Data are taken for test number 1 in which the

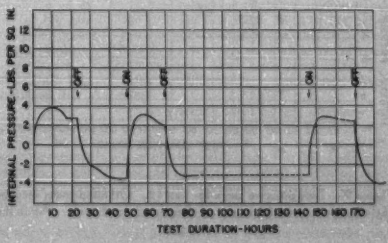

Figure 8. Time pressure curve for Test 11. Oil filled and sealed at atmospheric pressure. Repeated load cycles. Air in the gas space

Table I. Lists of Tests

Test No.	Gas In Gas Space	Method of Oil Filling	Initial Pressure Above Atmospheric	Time of Sealing After Filling
1	Air	Without vacuum	0	Immediately
2	Air	Under vacuum	0	Immediately
3	Air	Under vacuum	0	After standing open 24 hours
4	Air	Under vacuum	0	After standing open for 24 hours operation at full load
5	Nitrogen	Without vacuum	0	Immediately
6	Nitrogen	Under vacuum	0	Immediately
7	Nitrogen	Under vacuum	0	After standing open to low pressure nitrogen 24 hours
8	Nitrogen	Under vacuum	0	After 24-hour operation at full load exposed to low pressure nitrogen
9	Air	Without vacuum	3 psi	Immediately
10	Air	Under vacuum	6 psi	Immediately
11	Air	Without vacuum	0	Immediately
	Three temperature runs made without breaking transformer seal with 24-hour interval between runs			
12	Air	Under vacuum	0	Immediately
	Three temperature runs made without breaking transformer seal with 24-hour interval between runs			
13	Nitrogen	Under vacuum	8 psi	Immediately
	After the first temperature run, additional nitrogen was added to bring pressure up to 3 psi and then three more temperature runs were made			

transformer was not vacuum filled and was sealed at atmospheric pressure. Values of hot oil, average oil, and gas temperature for this test are plotted in Figure 5. These curves are typical of those obtained on all the tests.

In Figure 6 the measured pressure curves are plotted for all the single run tests made with air in the gas space. The corresponding pressure curves for those tests with nitrogen in the gas space are given in Figure 7.

Figures 8 to 10 give the pressure time curves for the three repeated cycle tests. They apply respectively to the tests with air in the gas space when the transformer was not vacuum filled, when it was vacuum filled, and to the test with nitrogen in the gas space in which nitrogen was supplied until the oil was saturated.

Results Calculated From Test Data

In each of the tests the volume, temperature, and pressure of the gas in the gas space were known at the start of the test cycle. At each point in the test cycle the gas pressure and temperature were known by direct measurement. The corresponding volume can be calculated by subtracting from the original volume the calculated oil expansion based on the measured oil temperatures. If the gas volume at any point in the test is corrected to the same pressure and temperature which held at the start of the test, then the difference is the amount which went into solution. This volume can then be corrected to atmospheric pressure and a temperature of 25 degrees centigrade and expressed as a per cent of the oil volume at 25 degrees centigrade. Such calculations have been made for each of the tests for three conditions in the test cycle:

1. At the time of maximum pressure.
2. At the time of maximum temperature.
3. At the time where the transformer has again cooled to ambient temperature.

These results are shown in Table II. Except for the final test, test number 13, these figures do not represent the total solubility because the tests were made with only a limited amount of gas available. For test number 13, if the quantities of gas which went into solution in each of the four temperature cycles are added, a solubility by volume of 12.5 per cent is indicated for nitrogen at atmospheric pressure and 25 degrees centigrade. Any residual gas in solution after the vacuum treatment to which the oil was subjected would represent an error in the 12.5 per cent figure. In all cases where the gas used was air, the figures will be in error because of that part of the oxygen which reacted chemically with the oil. In practice, all of the oxygen will eventually be used up in this manner. Also, there is some error because an ordinary commercial vacuum pressure gauge was used and the figures are obtained by routine commercial test procedure rather than by laboratory measurements.

Conclusions

1. With commercial methods of processing, due mainly to the solubility of gas in transformer in oil, a transformer as delivered for use will have a load pressure characteristic greatly different from that calculated by means of the gas laws. This is true whether the transformer is or is not filled under vacuum. The maximum pressure under load will be reached before constant temperature is attained, and the maximum pressure will be lower than that calculated by the gas laws. After cooling to ambient, the pressure will be less than the sealing pressure.

2. If vacuum filled, then allowed to stand open for 24 hours before sealing, the results are about the same as when the transformer is sealed immediately. The gas does not quickly go into solution at ambient temperature with nonagitated oil. If, however, a vacuum filled transformer is given a standard temperature

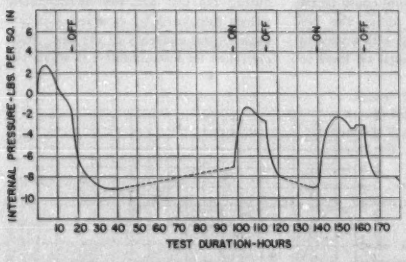

Figure 9. Time pressure curve for Test 12. Oil filled under vacuum and sealed at atmospheric pressure. Repeated load cycle. Air in the gas space

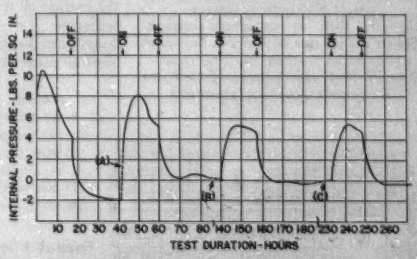

Figure 10. Time pressure curve for Test 13. Oil filled under vacuum Sealed with nitrogen at an initial pressure of 8 pounds per square inch. Repeated tests with nitrogen pressure adjusted after each cycle, as marked at (A), (B) and (C)

run while open to the air, and then is sealed, it thereafter acts like a transformer which is not vacuum filled.

3. As illustrated by Figures 8 and 9, the pressure load characteristic of sealed transformers stabilizes after about one full load temperature test cycle. When not vacuum filled in the test transformer, which had a gas-to-oil ratio of 0.1375, the pressure ranged after stabilization between limits of −4 pounds per square inch and +3 pounds per square inch with the average oil temperature between limits of 20 and 65 degrees centigrade. When vacuum filled, the pressure ranged from −9 to −2 pounds per square inch for the same temperature limits.

4. After a transformer is vacuum filled, a considerable amount of gas must be added under pressure while the oil is hot before it becomes saturated with gas. In test number 13, Figure 10, the oil dissolved 12.5 per cent of nitrogen by volume corrected to 25 degrees centigrade and atmospheric pressure. Afterwards, on a temperature run load cycle, the pressure started at atmospheric and returned to atmospheric when again cooled to ambient temperature. Even in this case, the maximum pressure was reached before constant temperature was attained and the measured pressure was less than that calculated by the gas laws by approximately 18 per cent.

5. If negative pressures are to be avoided in sealed transformers, it is necessary to restore gas which is removed by vacuum filling of the transformer. This gas is not easily restored. A complete temperature run cycle with the gas space open will do it but this is not a practicable method. One suggested method is to charge the transformer with dry nitrogen to a positive pressure of from 6 to 8 pounds per square inch before it is placed in operation. This charge should then be repeated once or twice after the transformer has undergone a load cycle This practice is safe if the tank is protected with a relief valve set to operate at a pressure a little lower than the tank test pressure.

6. Another and simpler method of restoring gas to the oil is to provide the transformer with a relief valve to relieve excess external pressure. During normal operation after a few temperature extremes, sufficient air is admitted to saturate the oil to the extent that thereafter, no further adjustment will take place. The amount of oxygen admitted is too small to adversely affect the oil properties.

Table II. Gas in Solution as a Per Cent of Oil Volume

Test No.	Temp. Cycle No.	Volume of Gas (25 Degrees Centigrade and Atmospheric Pressure) in Solution Expressed in Per Cent of the Oil Volume at 25 Degrees Centigrade: At Time of Maximum Pressure	At Time of Maximum Temperature	When Transformer Has Returned to Ambient Temperature
1		0.75	2.74	2.5
2		1.65	4.72	5.5
3		1.18	8.30	8.5
4		0.75	2.88	3.5
5		0.52	2.40	3.16
6		1.08	4.53	8.65
7		0.99	3.26	6.65
8		0.94	2.12	3.4
9		1.65	4.31	4.4
10		2.12	7.50	9.4
11	1	1.37	2.60	3.3
	2	2.31	2.92	2.63
	3	2.17	2.60	3.78
12	1	1.63	5.76	8.4
	2	4.85	6.00	8.4
	3	5.33	6.10	7.9
13	1	0.73	7.3	8.26
	2	1.87	3.75	3.24
	3	0.33	1.11	0.24
	4	0.66	1.51	0.83

Reference

1. Controlled Temperature and Insulation Protection in the Operation of Power Transformers, W. W. Satterlee, R. D. Reed. *AIEE Transactions*, volume 68, part 1, 1949, pages 753–60.

Discussion

F. J. Vogel (Illinois Institute of Technology, Chicago, Ill.): Mr. Tipton's paper is very interesting in showing the great effect of gas solubility in oil. Many small transformers for fairly high voltage, relatively speaking, are used for radar and other electronic device applications. They must be definitely free from corona under operating conditions, and large variations in temperature. Great difficulty was once experienced in their manufacture.

To obtain high dielectric strength, some thought it necessary to seal them as soon as they were filled, under extremely high vacuum. To allow for expansion, complicated devices, such as bellows, were used, and marbles were sometimes added to reduce the oil volume subject to expansion. An answer was actually much simpler. After filling under vacuum, if air was not allowed to go into solution in the oil, the dielectric strength was low and corona was found. So, a few-hours exposure to air was found necessary. Also, it was found that the amount of gas space could be absurdly small and still the actual pressure variations were small. In this connection, it is of interest that the dielectric strength of oil is very much a function of the gas in solution, and that after filling a transformer with oil under vacuum, some time allowance and exposure to air is necessary to develop full dielectric strength. Data regarding these effects have already been published in the past.

H. H. Wagner (Pennsylvania Transformer Company, Canonsburg, Pa.): This paper introduces a subject which is of interest to both manufacturers and operators of transformers. The author discusses primarily the effects on tank pressures of the oil expansion due to heating and of the pressure-temperature effects on the gas. It appears however, that the chief problem presented is that of negative pressures occurring on new transformers, and this effect, of course, is caused by the gas solubility in transformer oil.

The chemical reaction of nitrogen with transformer oil is negligible, but the gas solubility in oil is of great importance. Fortunately, the laws of solubility of gas, especially nitrogen in oil, while not so generally known, can be determined by practical methods.

Tests on the temperature effect of gas solubility show that with nitrogen over the oil at a pressure of one atmosphere at 25 degrees centigrade oil temperature, the solubility of the gas in the oil at the equilibrium is 9 per cent. At 80-degree centigrade oil temperature at the same pressure, the nitrogen in solution in the oil increases to 10 per cent. These values of gas volume are corrected to 25 degrees centigrade. It is noted that the increase in gas solubility is not due to increased volume of oil at the higher temperature since the increase in oil volume is 4 per cent for the same temperature range while the increase in volume of dissolved gas is 11 per cent.

These values for solubility are lower than the $12^1/_2$ per cent value given in the paper, probably due to the fact that these values are based on laboratory tests while the $12^1/_2$ per cent value is based upon commercial tests using commercial type gauges and equipment.

The pressure effect on gas solubility follows Henry's Law in that a linear relation applies from absolute zero pressure all the way up through pressures below and above one atmosphere. In other words, at absolute zero pressure (complete vacuum) the nitrogen solubility in oil is zero. At one atmosphere pressure, the nitrogen solubility is 9 per cent at 25 degrees centigrade. At 10 pounds per square inch gas pressure, the

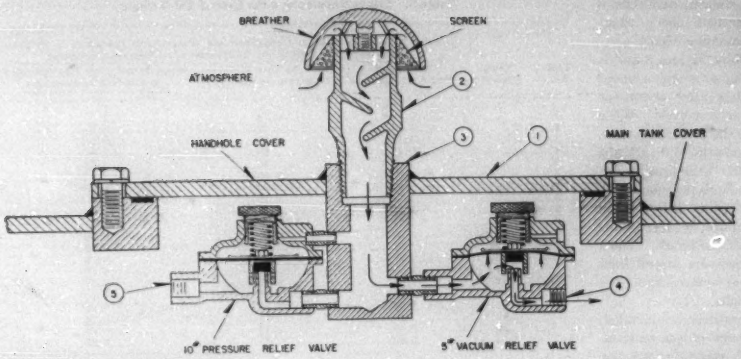

Figure 1. Assembly of diaphragm relief device showing operation of vacuum relief valve

solubility is approximately 15 per cent at 25 degrees centigrade. Thus, the effect of pressure change is much greater than that of temperature on the solubility of gas in transformer oil.

The author's conclusion number 6 states that after a few temperature cycles with breathing the oil becomes saturated with air, and thereafter no further adjustments will take place. This depends upon the amount of gas space in the design of the transformer at the normal 25 degrees centigrade oil level and on the settings of the relief valves. Figure 1 of the paper shows that for the normal gas volume of 10 per cent, the pressure range is from —5.5 pounds per square inch to +17 pounds per square inch, which will occur if the tank is so well braced as to prevent tank wall expansion.

We prefer to use 15 per cent gas space which limits the maximum pressure to less than 10 pounds per square inch under the same conditions of operation, and, therefore, the pressure relief valve can be set at 10 pounds without permitting breathing.

The data in the paper show that the only appreciable reduction in the maximum positive pressure to be expected below the calculated value would be due to tank wall deflection, which is obviously a variable dependent upon the safety factor used in design of the tank. Therefore, an important and additional conclusion is that the tank must be designed for the maximum and not the final pressure during load cycles. Analysis of the data shows that the drop in pressure after the peak of the pressure curves during the heating cycle is due only to the gradual increase in the solubility of the gas in the oil at the higher pressures and temperatures.

For a complete analysis of this subject, we have found three very useful principles, which have been confirmed at least in part by other investigators.[1,2]

1. Expansion of transformer oil with temperature change is substantially the same whether or not it contains dissolved nitrogen.
2. Transformer oil at a given temperature has the same volume whether or not it is saturated with nitrogen.
3. The change in transformer oil volume as a result of changing gas pressure is negligible over the range in pressure encountered.

It might appear to be somewhat of a paradox that in filling the transformer with oil we use a vacuum process which in our factory removes over 99½ per cent of the air; and then we find that we want to reintroduce gas into the oil during operation. The reason for this is that, first of all, there are two purposes in removing all the air from the oil:

1. Air removal during filling is necessary as part of the process of removing the air from the spaces in and between the solid insulation in the transformer and thus to prevent air pockets in the insulation, which would greatly reduce the dielectric strength.
2. Vacuum filling also removes the suspended gas bubbles in the oil which lower the dielectric strength of the oil.

On the other hand, the air or gas which later enters the de-aerated oil through solution remains as dissolved gas which does not appreciably affect the dielectric strength of the oil, but is necessary for preventing excessive negative pressures during operation.

In any system for transformer oil preservation employing a sealed tank system, a certain amount of maintenance attention will be required to assure that proper sealing is maintained and that excessive posi-

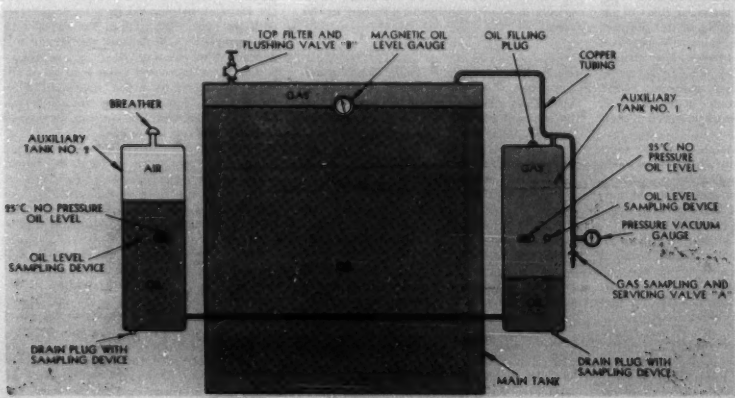

Figure 2. Diagrammatic drawing of inert gas-oil seal system

tive or negative pressures do not develop. It would usually be impractical to frequently recharge the transformer with nitrogen, and therefore some type of a pressure-vacuum limiting device should be used. This requirement can be met by either a mechanical relief device, such as shown in Figure 1 of this discussion, which operates at fairly high pressure limits, or by a manometer principle system employing auxiliary tanks arranged as shown in Figure 2 of this discussion which not only provides an extremely simple and reliable pressure-vacuum relief in case of extreme temperature range of operation, but also considerably reduces the pressure range obtained in operation. Due to the much lower operating pressures obtained in the manometer type system, which is commonly known as the "gas-oil seal system," the maintenance problems of proper sealing and accessories are reduced to a minimum.

References

1. Absorption of Air by Mineral Oils, A. Gemant. *Transactions*, Faraday Society (London, England), volume 32, 1936, page 694.

2. The Effect of Gases in Transformer Oil, *Transactions*, Electrochemical Society (New York, N. Y.), volume 47, 1925, pages 71–92.

E. W. Tipton: The discussions by Mr. Vogel and Mr. Wagner bring up a number of interesting points and are very much appreciated. Both discussions, Mr. Wagner's in some detail, bring out the important consideration that restoring the gas to solution does not defeat the purpose of vacuum filling. It should also be emphasized, I believe, that vacuum filling is very necessary if the full strength of the transformer insulation is to be developed.

Mr. Wagner is of the opinion that the chief problem presented is that of negative pressures. The data given in the paper cover the principal factors affecting the pressure in sealed transformers, as these factors affect both positive and negative pressures. The effect of the thermal expansion of the oil and gas is to increase the internal pressure. Gas solubility in the oil and tank wall deflection decrease the pressure. Practically, the effects on the maximum pressure are more important than the negative pressures.

Also in Mr. Wagner's discussion it is stated, "The data in the paper show that the only appreciable reduction in the maximum positive pressure to be expected below the calculated value would be due to tank wall deflection, —". The test data actually show, as stated in conclusion number 6 of the paper, that even with oil saturated with gas, the maximum internal pressure is less than that calculated by about 18 per cent. The maximum reduction to be expected due to tank wall deflection is about 15 per cent which is in addition to the reduction due to solubility of the gas.

The author did not intend to make a comparison of methods of sealing, a subject not properly within the scope of the paper, but since the point is raised in the discussion, it should be pointed out that simply sealing transformers tightly eliminates the necessity for auxiliary tanks which add to the size of the transformers and in some cases, blanket surfaces needed for cooling. Also, sealed transformers do not require frequent recharging with nitrogen but at most, only the addition of gas during the first load cycle. As shown in the paper, a single temperature run cycle with gas supplied restores the gas removed by vacuum filling. The oil and insulation protection afforded with this simple system has been shown to be unexcelled.[1]

Reference

1. See reference 1 of the paper.

Use of Techniques from Electrical Analogues in the Study of Transmission Line Vibration

J. LUMMIS
MEMBER AIEE

A. KLOPFENSTEIN
ASSOCIATE AIEE

THE PHYSICAL components of a span of transmission line cable and its end supports can be studied by comparing it with an equivalent network of electrical components. An equivalent network for the cable span consists of distributed inductance and capacitance representing the electrical transmission line shown in Figure 5. The equivalent terminating network is determined by the mass of the insulators and the flexibility and friction in the supporting structure. The impedance to motion at supports generally does not equal the impedance of the span so that vibrational wave energy is reflected by these terminations. When waves of energy are trapped between two reflection points, energy will build up to destructive levels in standing waves from only a small input source. Similar conditions of reflection cause standing waves in radio transmission lines. Damage occurs at reflection points where direction and polarity of waves are changed in a restricted region. Electrical standing waves are undesirable in radio transmission lines and have been prevented with proper terminations, see reference 8(c). Techniques used in this field have been found applicable to the field of mechanical vibration. Mechanical impedance matching devices can be used, equivalent measuring techniques can be followed, and the design of tower, insulator string, and clamp system can be made with the idea of matching the impedance of the span and to stabilizing it against vibration. Using electrical techniques, work on a full scale test span has shown promising results in finding solutions to problems of mechanical vibration of transmission line spans.

A span of cable is excited into transverse motion by the wind. Its motional frequency is determined by its diameter and the wind velocity. Waves of transverse motion excited in the span, travel at a definite velocity determined by the mass per-unit length and tension in the span.[134] An electric transmission line is likewise excited so that waves of electric energy travel down the line. If there is negligible resistive loss and leakage in the line, velocity of wave travel is determined by distributed capacitance and inductance of the line, see reference 8(b). Linear density is analogous to distributed inductance and tension to the reciprocal of distributed capacitance. It can be shown that friction and resistance, transverse deflection and charge, transverse velocity and current, transverse force and voltage, potential energy stored in elastic deflection and electrostatic field energy and, also, kinetic energy stored in moving mass and electromagnetic field energy are analogous in the mechanical and electric systems, see reference 8(d).

Techniques of physical measurement are difficult in the light flexible system of vibrating span without disturbing the system. From the development of radio transmission lines and their terminations there has evolved means of measurement which show many phenomena existing in the electrical analogy.

The tendency toward oscillation of a terminated radio transmission line usually is expressed in terms of a voltage standing wave ratio. The more closely this ratio

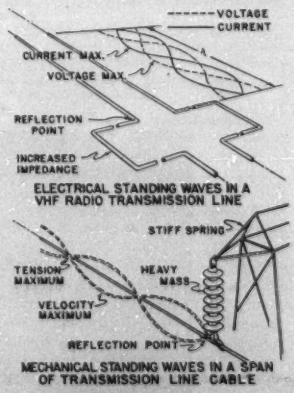

Figure 1. Analogous standing waves in electrical and mechanical systems

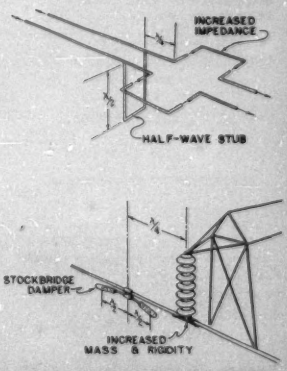

Figure 2. Tuned devices to prevent standing waves

Paper 50-276, recommended by the AIEE Transmission and Distribution Committee and approved by the AIEE Technical Program Committee for presentation at the AIEE Fall General Meeting, Oklahoma City, Okla., October 23–27, 1950. Manuscript submitted July 31, 1950; made available for printing September 1, 1950.

J. LUMMIS and A. KLOPFENSTEIN are both with the Southern California Edison Co., Los Angeles, Calif.

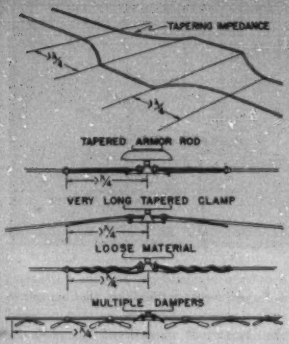

Figure 3 (left). Untuned devices to prevent standing waves

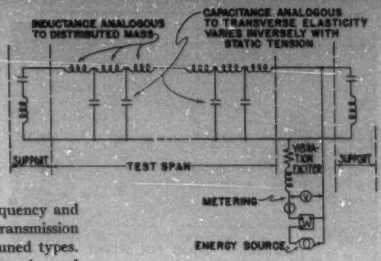

Figure 5 (right). An equivalent electric network for a span of transmission cable

approaches unity, the more nearly perfect the radio transmission line has been terminated. Tendency toward oscillation also can be expressed in terms of the Q of the terminated system which is found by dividing the input impedance measured at resonance by input impedance measured at antiresonance. The Q ratio of a network is the total impedance looking into a network divided by the resistance seen at this point. The Q of a properly terminated transmission line is near unity. Impedance measured at resonance is the total impedance while antiresonant impedance is only the resistance, see references 8(a), 8(b), and 9. The Q of a mechanical system also can be found.

Tuned Impedance Matching Devices

Impedance matching devices to prevent electrical standing waves of voltage and current on very high frequency and ultra high frequency radio transmission lines fall into tuned and untuned types. The tuned type is most commonly used where matching need only be done for one frequency or narrow frequency band. These consist of tuning stubs, matching quarter wave length sections, re-entrant sections, and so forth.[9] There is very little energy dissipated in these devices. While adding resistance reduces their efficiency it also increases the width of the frequency band in which the devices are effective.

The Stockbridge damper is a device of this type. Its frictional losses reduce its resonant efficiency but increase its band of effectiveness. Den Hartog analyzes this effect in describing dynamic vibration absorbers, see reference 7(a).

These devices introduce a reflected wave into the system at a point one-quarter wave length from troublesome reflection points so that the introduced wave is diametrically out-of-phase with the unwanted reflected wave and has the proper amplitude to completely cancel the unwanted reflected wave.

Untuned Matching Devices

Electrical impedance matching devices of the untuned type are used where a large band of frequencies must be carried by a radio transmission line. They operate above a minimum cutoff frequency which is determined by the maximum physical dimensions of the device. Those that do not dissipate energy are usually sections of line where impedance is exponentially tapered along a length gradually changing from the impedance of the line to the impedance of the terminal device. Open wire radio transmission lines are often tapered in this fashion to match the impedance of untuned types of antennas. Tapered horns are often used to match the impedance of a microwave guide to the impedance of free space or match two types of wave guides, see references 5, 6, 9(d). Reflection occurs from all points in the taper because the impedance is continually changing. The action of reflection changes the phase of a wave 180 degrees and two waves which have been reflected from points 90 degrees apart on the taper will be 180 degrees out-of-phase, since one has travelled 180 degrees farther than the other, and cancellation will take place between these two waves. If the taper is of the correct exponential nature, it makes the amplitude of all reflected waves equal so that cancellation will be complete. Since cancellation is only complete between waves which are reflected from points 90 degrees apart, the cutoff frequency is one which makes the taper one-quarter wave length long.

Tapered armor rods and tapered-mouthed suspension clamps reduce standing waves in cables by the action described for the exponentially tapered electrical section. Since these devices are generally not designed with this action in mind, complete impedance matching is not obtained. However, any device which causes reflections to occur from points in a region near a troublesome reflection point will reduce standing wave ratios and the effective Q of the system. For the best

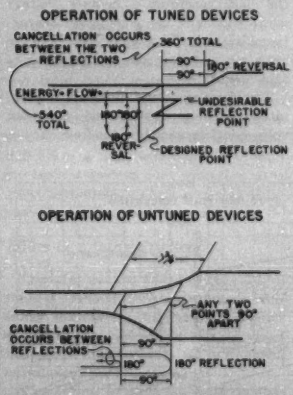

Figure 4. Operation of devices designed to set up waves for cancelling undesirable reflections

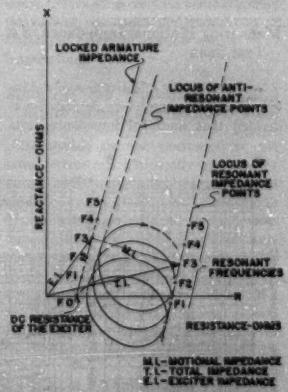

Figure 6. Resistance - reactance locus for vibration exciter and test span

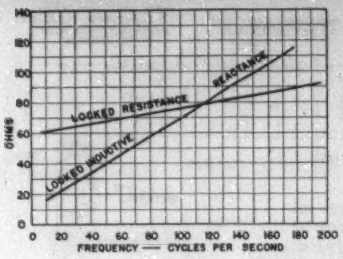

Figure 7 (left). Graph of locked armature resistance and reactance of vibration exciter

Figure 8 (right). Loci of test span resonant and anti-resonant motional impedance

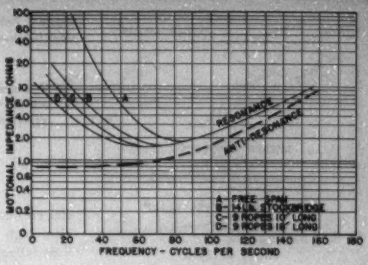

results, the length of this region must be more than a quarter wave length at the lowest frequency at which the device is to be effective. As frequency is increased above the cutoff frequency the taper increases in angular length and as the taper length approaches infinity, the device will approach a perfect impedance match.

Festoon Type Matching Devices

Loose cables hung or festooned on transmission line cables near terminations have been successful in reducing standing waves in the span. Waves enter the festoon from the span, travel at slow speed and then are reintroduced into the span at the next point of attachment. If there are enough contact points along a region so that cancellation between these many reflected waves can occur, then standing waves will be prevented. It has been found that the festoon works best if tension in the loose material is negligible. This allows the festoon to be the most flexible and reduces the wave velocity in the festoon to a minimum.

Measuring Motional Impedance of a Test Span

To compare the effectiveness of damping or impedance matching devices it was decided that motional impedance tests should be made on a test span. This was done in the same manner that a communication or transmission line is tested to find how it acts when excited with the band of frequencies which it will transmit when in use. Measurements of input impedance variations were made electrically at the exciting source with changing frequency while deflection standing wave ratios were measured at the remote termination.

Description of the Vibration Exciter

In studying the vibration of transmission line conductors, a test span was vibrated with an electrical exciter to simulate wind induced vibration. This machine is similar to a dynamic loud speaker with the diaphragm removed and consists of a d-c excited electromagnet, and an armature coil which is flexibly mounted in its magnetic field and mechanically connected to the device to be vibrated. The vibration exciter was driven by applying a-c energy to the armature coil. Voltage, current, and power were measured with an electronic instrument which was accurate over the range of frequencies excited, and had no effect on the electrical source or load.

Before making measurements with the machine coupled to the cable, the armature was locked and low currents and voltages were applied to the armature over a range of frequencies that covered the expected vibrational frequencies. In this way the components of impedance due to the inductance and resistance of the machine were found so they could be separated from the effects of motion.

Information concerning the ease in which the span of cable could be set into resonance at different harmonic frequencies and with different damping devices was desired. The vibration exciter was coupled to the span of cable at a point which became a point of maximum motion when the cable was excited at a resonant frequency.

When current was made to flow through the armature coil, force was applied through a coupling rod to the cable, causing it to move. The applied force was approximately proportional to the current.

Voltage Generated by the Vibration Exciter

Motion of the armature coil through the field generates a counter voltage which will be in phase with and proportional to the instantaneous velocity of the armature and the cable at the point of attachment.

The phase angle and difference in magnitude between applied and generated voltage is determined by the frequency of

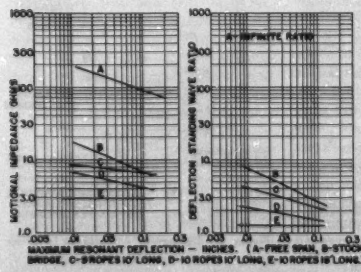

Figure 9 (left). Loci of test span 29 cycles per second resonant motional impedance with changing amplitude of deflection

Figure 10 (right). Loci of test span resonant impedance and deflection standing wave ratio with fixed maximum deflection

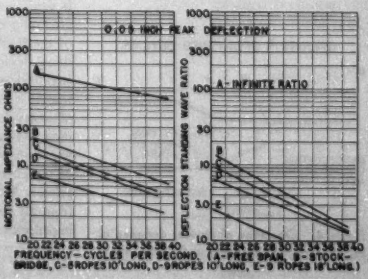

Figure 11 (left). Test span showing west dead end test support and instrument house

Figure 12 (right). Vibration exciter and tensioning lever and weight

excitation and the mechanical impedance of the system being vibrated. The electrical impedance of the armature also has an effect on the angular and amplitude difference between applied and generated voltage.

Cable Span Equivalent Circuit

An electrical equivalent circuit of the cable span, as measured through the exciter, is shown in Figure 5. Such a device has multiple resonance characteristics. The supports also resonate at high frequencies. The electrical impedance of the vibration exciter affects the resonant characteristics of the system at certain frequencies. Mechanical impedances are coupled mechanically into the exciter and appear in the electrical driving circuit where they can be measured. The total impedance of machine and cable varies with frequency, as shown in locus form, see reference 8(d).

Generated Voltage Forms Motional Impedance

The voltage generated by motion of the coil acts as an impedance to the flow of current which is called motional impedance. It is the difference between locked and total input impedance. The motional impedance locus alone without machine impedance is a circle. The diameter of a motional impedance circle is an indication of the power required to set a mechanical system into vibration at a given amplitude. The larger this diameter, the smaller the power needs.

Effect of Adding Friction

Damping devices added to the cable of the test span reduced the diameter of this circle. An effective measure of this circle diameter is the ratio of the total motional impedance at resonance to the motional impedance at antiresonance.

The friction in a mechanically oscillating system limits the maximum and the minimum impedances that occur at resonance and antiresonance respectively. When the oscillating system is modified so that more power is required to drive the system, this indicates an increase in mechanical friction which is similar to a decrease in electrical parallel resonant impedance or an increase in series resonant impedance.

Q Ratio of a Resonant Electrical Circuit

A measure of the quality of an electrically resonant circuit is the ratio of its impedance at resonance to its impedance at antiresonance. This quality ratio is called the Q of the circuit. The larger the value of Q, the less energy required to cause a given amplitude of oscillation.

The object in most studies of mechanical vibration is to determine how to reduce the amplitude of vibration for a given energy input. This would mean that the Q of a mechanically multiresonant oscillating system should be reduced toward unity. The effect of reducing the Q of a mechanical system can be measured through a vibration exciter so that the effectiveness of a damping or detuning device can be studied.

Figure 13. Vibration exciter on dolly coupled to test span

Reduction of Apparent Q Without Adding Resistance

An electric transmission line several wave lengths long is multiresonant if it is not terminated properly at load and source. If the line is to be used over a wide range of frequencies, the terminating devices must not be resonant. Terminations have been designed which prevent the transmission line from being a resonant length by designing a terminating section so that the impedance of the section exponentially tapers with length becoming equal to the impedance of the terminating equipment. Waves of energy are reflected at all points of changing impedance in the tapered section. These points are infinite in number and should extend over a minimum of a quarter wave length. There will be waves of energy of opposite polarity reflected by points which are one-quarter wave length apart causing cancellation of reflected energy to take place. This effectively prevents standing waves and resonance for frequencies at which the tapered section is several wave lengths long.

Reducing the Equivalent Q of a Multiresonant Mechanical System

Resonance can be prevented in the same manner mechanically by causing many points which reflect equal amounts of energy over at least a half wave length of a multiresonant system. Such devices were qualitatively tested on a small scale model span of string and then quantitatively tested by measuring the resonant and antiresonant motional resistance of a test span of actual transmission line material. Graphs and charts of some of these results follow in this paper.

Results of a Typical Test

Tests were made to study the vibrational stability of a test span of steel re-

inforced aluminum cable. Descriptions will follow of various graphs that present the data collected.

Locked Armature Test (Figure 7)

The armature of the vibration exciter was locked, as securely as possible, to the field structure. Power, current, and voltage were measured as the armature was excited over a range of frequencies. From these values the resistance and reactance were calculated.

The reactance curve is nearly a straight line. An extension of this line passes close to, but not through, zero ohms at zero frequency. The resistance increases almost linearly above 60 cycles. Below 60 cycles, the resistance curve falls away from the straight line. The increase in resistance with frequency is caused by increasing iron losses. The knee in the resistance curve may be due to incomplete locking of the armature which would allow more mechanical friction loss at the lower frequencies where inertia has a lower restraining effect.

Maximum and Minimum Motional Impedance (Figure 8)

These curves are a loci of maximum and minimum motional impedance points that occur at span resonance and antiresonant frequencies. This graph plots motional impedance versus frequency over a fairly wide range of frequency. Vibration amplitude could not be held constant over this wide range of frequencies.

Below 60 cycles the nearly parallel lines indicate motional impedance of the span with various devices added. The lower the maximum resistance that occurs at resonance, the more stable the span. Different devices reduce maximum impedance by different amounts. Above 60 cycles per second the impedance loci tend to join, and above 90 cycles per second, they all begin to increase to approximately the same value. For frequencies above 90 cycles per second the supports, over which the cable is strung, seem to be in resonance and to move nearly as much as the cable.

The minimum motional impedance occurs at antiresonance. Since almost no motion of the cable occurs at antiresonance, the motional impedance is nearly the same as locked impedance. Metering errors sometimes are as large as the small quantities being measured, so there is a wide variation in the data for minimum motional impedance. As frequency increases, minimum and maximum motional impedance approach each other, becoming nearly coincident above 150 cycles.

The increase in minimum impedance at antiresonance with increasing frequency is due to the increased rate of energy absorption due to hysteresis losses of bending and stretching. This same effect reduces maximum impedance at resonance. The reduction of maximum impedance is limited by the antiresonant minimum impedance. When these two limits are close together, the cable becomes very stable.

When the supporting structures are resonant they receive energy from the cable and are damaged. There actually have been reports of tower damage where bolt holes and bolts have been worn, members broken and nuts worked loose due to vibration. These were in locations where high velocity winds have excited vibrations and set parts of the tower in resonance.

If the tower receives energy from the span and is set into motion, it does prevent span resonance.

Impedance with Changing Amplitude (Figure 9)

This graph shows loci of maximum impedance occurring at resonance near 29 cycles per second in which the maximum amplitude was varied by controlling the power supplied to the span. This graph shows how motional impedance varies with amplitude on the free span and the damped span. The standing wave ratio is the ratio of maximum to minimum deflection measured at loop center and at nodes.

A graph such as this was plotted for each of several frequencies between 20 and 40 cycles per second to determine data for graphs of Figures 10.

The resistance of most of the devices decreased with amplitude. If the opposite were true, very destructive amplitudes would build up. The horizontal line for the 18-foot ropes indicates little change of resistance with amplitude. The lower the impedance locus, the more nearly its slope approaches zero while remaining negative, the more effective the device.

Fixed Amplitude—Variable Frequency Impedances (Figure 10)

The graph is similar to Figure 8, except that data is plotted for 0.05-inch maximum deflection at loop centers for a smaller range of frequencies. In this region most of the data tends to fall in a straight line.

Analysis of Graphs

The purpose of the test was to explore this method of investigation of vibrational stability and to test the stabilizing effect of terminating a test span of steel reinforced aluminum cable in a section loosely covered with small wire rope.

The rope covered section acts as a region of reflection instead of the point of reflection that occurs at the mouth of a suspension clamp. The loose rope tends to move out-of-phase with the cable. These motions cause impacts between the two which set up reflections at all the points of contact. Graphs indicate the effectiveness of the loose rope stabilizer. These data show that the longer the section and the greater loose mass added, the more effective the device.

Conclusion

Electrical analogues are being used to study many vibration problems and can also be applied to the study of transmission line vibration. A very high frequency or ultra high frequency radio transmission line is analogous to a span of transmission line cable and the tendency toward oscillation often found in a radio transmission line is due to the low rate of energy dissipation in the line and incorrect impedance at terminations. This is also true for a span of cable. Suppression of the electrical standing waves has been accomplished with electrical devices whose theory of operation has been tested with electrical techniques. This theory for electrical devices also fits analogous mechanical devices which have been used to reduce vibration in transmission line spans. Impedance matching better describes the operation of these mechanical vibration reducers than the term damper. Electrical theory shows that transmission line dampers do not operate primarily by dissipating energy. Friction in these devices reduces their maximum resonant effectiveness although it widens their effective frequency spectrum. Electrical testing techniques can be carried out mechanically to find the mechanical standing wave ratio and Q of a span. Finally, it has been shown that improved vibration reducing devices can be designed and tested using methods analogous to proved electrical techniques.

References

1. Vibration of Overhead Transmission Lines, **R. A. Monroe, R. L. Templin.** *AIEE Transactions*, volume 51, December 1932, pages 1059–73.

2. Vibrational Analysis-Transmission Line Conductors, **W. B. Buchanan.** *Electrical Engineering (AIEE Transactions)*, volume 53, November 1934, pages 1478–85.

3. Vibration of Cables and Dampers, **R. G. Sturm.** *Electrical Engineering (AIEE Transactions)*, volume 55, May 1936, pages 455–65, and June 1936, pages 673–87.

4. Cable and Damper Vibration Studies, **L. A. Pipes.** *Electrical Engineering (AIEE Transactions)*, volume 55, June 1936, pages 600–14.

5. Exponential Transmission Lines, **Charles R. Burrows.** *Bell System Technical Journal* (New York, N. Y.), volume 17, number 4, October 4, 1938.

6. Transmission Lines with Exponential Taper, **Harold A. Wheeler.** *Proceedings*, Institute of Radio Engineers (New York, N. Y.), volume 27, January 1939, page 65.

7. Mechanical Vibrations (book), **J. P. Den Hartog.** McGraw Hill Book Company, Inc., New York, N. Y., 1947, (a) Dynamic Vibration Absorber, pages 112–130; (b) Vibrating Strings, and Beams, pages 170–93.

8. Communication Engineering (book), **W. L. Everitt.** McGraw Hill Book Company, Inc., New York, N. Y., 1937, (a) Multiple Resonance, pages 86–93; (b) Infinite Line, pages 95–123; (c) Reflection, pages 128–78; (d) Electromechanical Coupling, pages 672–709.

9. Radio Engineer's Handbook, **F. E. Terman.** McGraw Hill Book Company, Inc., New York, N. Y., 1943, (a) Transmission Lines, pages 172–97; (b) Impedance Matching, page 187; (c) Irregularities, page 196; (d) Exponentially Tapered Lines, page 197.

No Discussion

Determination of Reserve Capacity by the Probability Method

G. CALABRESE
MEMBER AIEE

THE probability method of determining generating reserve capacity has received a great deal of attention in the past few years. A number of papers, by different authors, have been published during the same period, attacking the problem from different angles and describing different general methods of calculation. In a paper[1] presented at the AIEE Midwest general meeting in Chicago in 1947, the author described a method for determining the reserve capacity of a system taking into consideration the shape of the load duration curve. This permitted to check, in a rational manner, the variation of the reserve requirements of a system with the changing character of the load. The method given in that paper is general, and applies regardless of shape of load duration curve.

Since calculations usually are laborious, it was suggested at that time to replace the actual load duration curve with a straight line or portions of straight lines. By doing so, calculations are greatly simplified. However, great as the simplifications may be, calculations still remain laborious, particularly in the general case of a system composed of units of diverse sizes and outage rates. In the practical application of the method, there are cases when it is possible to replace the actual system with a system composed of units all of the same size and outage rate, without great sacrifice in the accuracy of the results. This replacement further simplifies calculations and, in addition, permits to precalculate a set of key curves from which the reserve requirements of a system can readily be determined. In those cases where the system cannot be replaced by one composed of units of the same size and outage rate the curves can be used to obtain a quick preliminary answer to a reserve problem, an answer which can be checked later on when more time is available.

It is one of the purposes of this paper to further develop the exact expressions given in the previous paper[1] for the accurate determination of the reserve requirements of a system, and to give curves for the quick determination of the same reserve under the above-mentioned assumption that all units are of the same size and outage rate. The mathematical development for both the exact expressions and the curves is given in the Appendix.

In the application of the probability method to reserve problems, it is essential to establish some indexes for measuring the level of service reliability corresponding to a given reserve. A number of different indexes have been proposed or used for this purpose. The question then arises: what are the merits and disadvantages of each?

It also is the purpose of this paper to give a comparative discussion of three indexes of service reliability, namely:

A. *Probability of loss of load.* This is defined as the fraction of any period of time during which loss of load may be expected to occur due to forced capacity outages in excess of reserve. It can also be expressed as an expectancy of one day's loss of load every so many years. Expressions for calculating it are given in the Appendix.

B. *Expected energy loss per kilowatt of maximum load per year.* This is defined as the expected kilowatt-hours per kilowatt of maximum load per year, that cannot be supplied to the load because of forced capacity outages in excess of reserve. Expressions for calculating it are given in the Appendix.

C. *Expected energy loss per kilowatt of installed capacity per year.* The definition of this index is similar to (b), and expressions for calculating it also are given in the Appendix.

As a result of the discussion it is recommended that the probability of loss of load, introduced at the 1947 meeting, be retained and given preference.

The Load Duration Curve

The load duration curve referred to in this paper is the one obtained on the basis of the daily maximum loads having 365 points per year. The curve may be based on the actual daily maximum loads, in which case, more appropriately, it may be

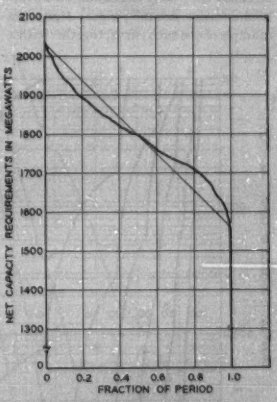

Figure 1. Example of daily maximum load overhaul duration curve and straight line approximation

Duration curve of 1-hour peak requirements

Paper 50-280, recommended by the AIEE Power Generation and System Engineering Committees and approved by the AIEE Technical Program Committee for presentation at the AIEE Fall General Meeting, Oklahoma City, Okla., October 23–27, 1950. Manuscript submitted November 3, 1949; made available for printing September 25, 1950.

G. CALABRESE is Professor of Electrical Engineering at New York University, New York, N. Y.

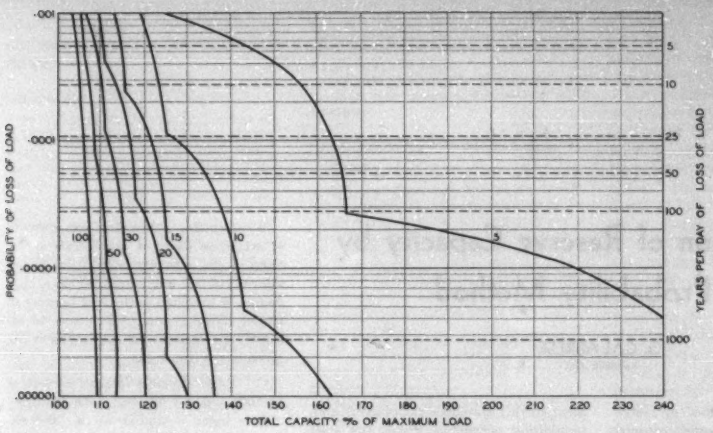

Figure 2. Probability of loss of load for various numbers of units all of the same capacity assuming a straight line load duration-curve, an outage rate of $q = 0.02$, and a daily maximum load ratio $l = 0.5$

called the "daily maximum load duration curve." If this curve is used it will be necessary, after the contingency reserve has been determined, to check its adequacy for overhaul requirements, taking into consideration the cycle and duration of the overhauling period of the units involved.

For most practical cases, however, it will be sufficient and simpler to use a load duration curve based on the actual maximum daily loads plus requirements for overhaul.

The curve that is thus obtained may be called the "daily maximum load-overhaul duration curve." Figure 1 gives an example of one such curve, together with a straight line which may be used to replace it. It should be clearly understood that the use of the daily maximum load-overhaul duration curve introduces some duplications and errors in the results. It is believed that in most cases these errors are not serious. However, in doubtful cases, the reserve of a system should be determined on the basis of the daily maximum load duration curve.

Corresponding to the daily maximum load duration curve is the daily maximum load ratio given by:

$$\frac{\text{Sum of all daily maximum loads}}{365 \times \text{yearly maximum load}}$$

Similarly, the ratio corresponding to the daily maximum load-overhaul duration curve, which may be called the daily maximum load-overhaul ratio, will be defined by:

$$\frac{\text{Sum of all daily maximum loads plus overhaul requirements}}{365 \times \text{yearly maximum load plus overhaul at peak time}}$$

In the following discussion, for simplicity, reference will be made only to the daily maximum load duration curve and to the daily maximum load ratio "l", it being understood that the conclusions apply both to duration curves and ratios, exclusive or inclusive of overhaul requirements.

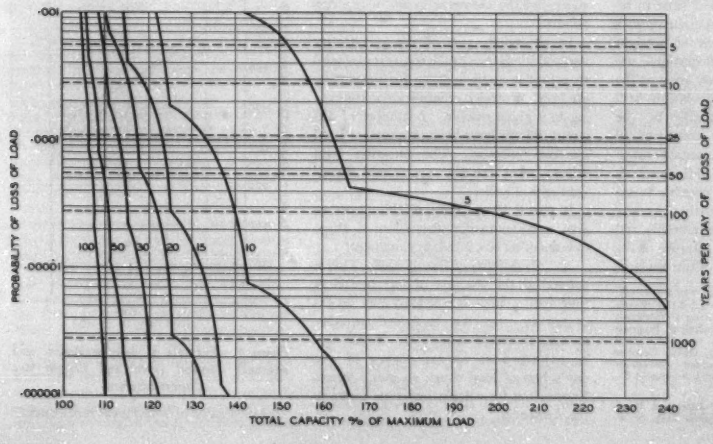

Figure 3. Probability of loss of load as for Figure 2, excepting that $l = 0.7$

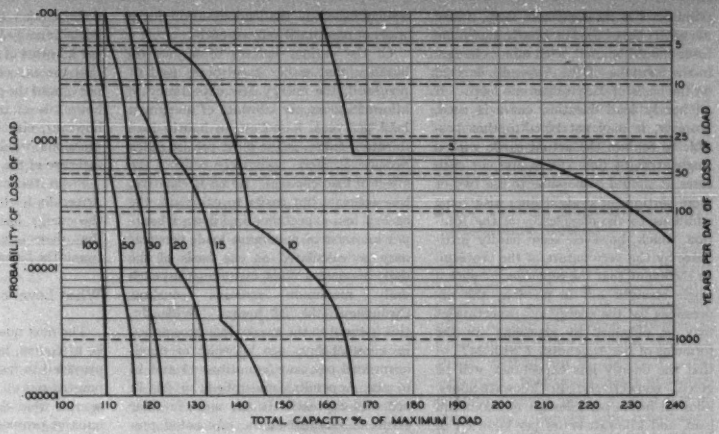

Figure 4. Probability of loss of load as for Figure 2, excepting that $l=0.9$

Curves of Probability of Loss of Load and Energy Loss Requirements

The curves of Figures 2, 3, 4 have been plotted, using the methods outlined in the Appendix. Based on an outage rate, $q=0.02$, these curves give the probability of loss of load in function of the total capacity as a fraction of maximum load for 5, 10, 15, 20, 30, 50, and 100 units, all of the same capacity, and for values of the daily maximum load ratio equal to 0.5, 0.7, 0.9, respectively. If the daily maximum load ratio is equal to 1.0, the probability of loss of load coincides with the probability of outage in excess of reserve given in Table I of the 1947 paper.[1] Figure 5 gives the energy loss expectancies for 10, 15, 20, 30, 50, and 100 units, all of the same capacity, outage rate $q=0.02$, and daily maximum load ratio $l=0.5$ and 0.9, respectively. For intermediate values of l, the energy loss expectancies within the range of Figure 5 are proportional to $1/1-l$.

The curves of Figures 2 and 5, inclusive may be considered as key curves for an outage rate $q=0.02$, since from them, by appropriate replotting, it should be possible to obtain loss of load probabilities and energy loss expectancies for any practical value of n, the number of units, and l, as illustrated in Figure 6.

Limitations

The use of a load duration curve, based on daily maximum loads for the determination of indexes of level reliability, ignores the hourly fluctuation of the load. The various indexes thus obtained implicitly assume that each maximum daily load lasts throughout the day. For these reasons, strictly speaking, for systems having hourly load curves of radically different character, the indexes of service reliability thus calculated are not com-

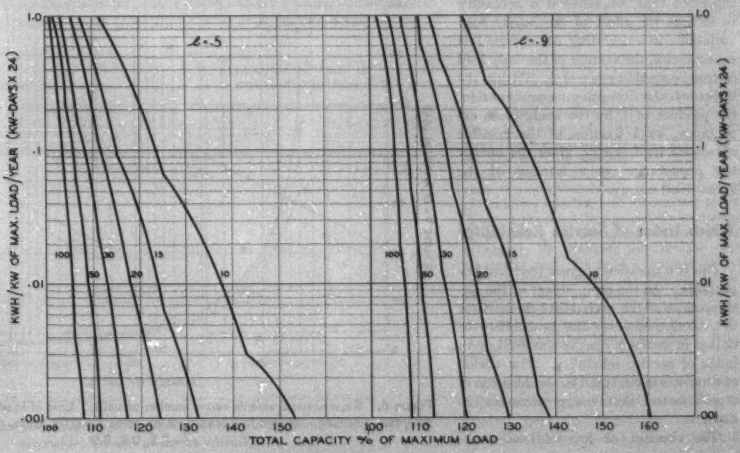

Figure 5. Energy loss expectancy for 10, 15, 20, 30, 50, and 100 units all of the same capacity, straight line daily maximum duration curve, outage rate $q=0.02$, and daily maximum load ratio $l=0.5$ and 0.9

parable. For these extreme cases, a load duration curve based on hourly maximum loads should be used, with minor changes in the formulas of the Appendix derived on the basis of daily maximum loads. If an hourly load duration curve is used, however, it may not be altogether possible to replace the actual curve with a single straight line. Of course, in such cases, it should be possible to use two or more portions of straight lines with some additions to the complexity of the solution, which, however, seem hardly justifiable by the very nature of the problem. In the event that the replacement with a single straight line is possible, the expressions for the energy loss expectancies may be obtained by replacing (in the formulas of the Appendix) T with $24T$, so that the energy loss expectancy will be given, respectively, in kilowatt-hours, kilowatt-hours per kilowatt of maximum load, and kilowatt-hours per kilowatt of installed capacity.

Otherwise, an approximation to the energy loss expectancy in kilowatt-hours, kilowatt-hours per kilowatt of maximum load, and kilowatt-hours per kilowatt of installed capacity, respectively can be obtained from the expressions obtained on the basis of the daily maximum load curve, Sections 4 and 5 of the Appendix, by replacing T with $24TL$. Here L should be the ratio between the sum of the kilowatt-hours loss, taking into consideration the hourly variation of the load, and the kilowatt-hours loss assuming each daily peak constant throughout the day. The calculation of this factor would involve difficulties hardly justifiable by the nature of the problem. It is therefore suggested that, whenever it is necessary to include the effect of the hourly load variations in calculating the energy loss expectancies, the average of the daily load factors be used in place of L. Within the limits of the foregoing approximation, the product of L by the energy loss expectancy, as a fraction of the possible maximum load energy, gives the energy loss expectancy, as a fraction of the actual load energy.

Which Index of Service Reliability?

This is a question of great practical importance. In the early stages of the development of the probability method for determining reserve, the probability of outage in excess of reserve was used as an index of service reliability. The period of time was taken equal to the duration of a peak season, that is, approximately 100 days.

The concept of loss of load probability based on the load duration curve was not used until very recently.

Of the various indexes of service reliability that either have been used or proposed, the energy loss expectancy in kilowatt-hours per kilowatt of maximum load per year, based on an hourly load duration curve, is the most precise index because it more accurately reflects the effect of load changes. As an alternative, less accurate but easier to calculate, the energy loss expectancy in kilowatt-hours per kilowatt of maximum load, per year may be calculated on the basis of the daily maximum loads, assuming that each daily maximum remains constant throughout the 24 hours. Evidently, this is equal to the energy loss expectancy in kilowatt-days per kilowatt of maximum load per year (equations 11 and 15 of the Appendix) multiplied by 24, in order to express it in the more familiar terms of kilowatt-hours. As noted previously, the latter approximate index of service reliability can be multiplied by the average of the daily load factors in order to obtain a more accurate approximation.

The probability of loss of load as an index of service reliability is not as accurate a measure of service reliability as the kilowatt-hours per kilowatt per year, or the kilowatt-days per kilowatt per year. However it has the advantage of being easier to calculate and, for the problem under discussion, should give entirely satisfactory results. To state that the expectancy of loss of load is, say, one day in 25 years seems to carry a more definite idea than to say that the expected energy loss is 0.018 kilowatt-hours per kilowatt of maximum load per year, or that the expected energy loss is 0.000206 per cent of the possible maximum kilowatt hours use of the load. Unquestionably, however, either one of the last two expressions would give a more accurate measure of the expectancy.

From the expressions derived in the Appendix for loss of load probability and the energy loss expectancy it is evident that there is no definite relationship between the former and the latter.

What Level of Service Reliability?

The next question in line of importance is, of course, how much reserve must be provided to insure adequate service? As pointed out on other occasions, the question of what degree of service reliability must be provided in a particular situation depends entirely on local conditions and personal judgment. Under emergency conditions the corrective measure is available of lowering the voltage which, within certain limits and if not used too often, may be relied upon to relieve the situation. Generally speaking, it seems altogether reasonable to assume that a reserve giving a loss of load expectancy of 1 day in, say, 50 years or a probability of loss of load of 0.0000548, after reduction of voltage, should be satisfactory.

Published information indicates that voltage can be safely lowered by 5 per cent and that approximately a 1 per cent drop in load is obtained for every 1 per

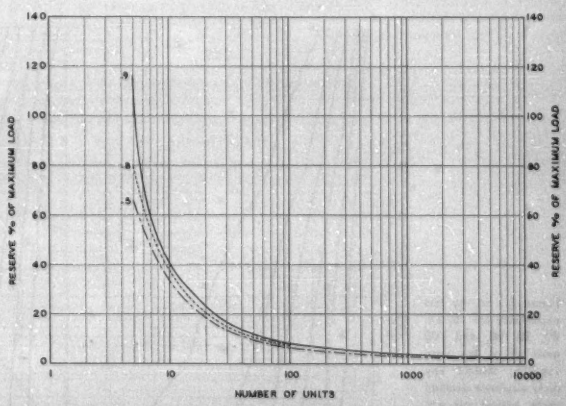

Figure 6. Reserve requirements versus number of units. Loss of load expectancy of 1 day in 50 years, assuming a straight line load duration curve $q = 0.02$, and a daily maximum load ratio $l = 0.5, 0.8, 0.9$

cent drop in voltage, assuming that voltage regulators, where used, have been made inactive. If voltage is reduced, to alleviate the situation under emergency, two pertinent questions arise which require full consideration, namely: with a given reserve, what is the expected frequency of voltage reduction, and what is the effect on this frequency of the number of units of the system? In order to answer these two questions, it will be noted that, as shown in Figure 7, a reserve R_0', as a fraction of the maximum load *Lam* without voltage reduction, is equivalent to a reserve of

$$R_0'' = \frac{0.05 + R_0'}{0.95}$$

as a fraction of the maximum load 0.95 *Lam*, obtaining with a 5 per cent voltage reduction. It follows that, in order to obtain a reserve R_0'' with 5 per cent voltage reduction, it will suffice to provide a reserve $R_0' = 0.95R_0'' - 0.05$ without voltage reduction. Thus, a system of 20 units having an outage rate $q = 0.02$ and a daily maximum load ratio $l = 0.8$ requires a reserve of approximately 0.21 times the maximum load in order to provide the stated level of service reliability of 1-day loss of load expectancy for every 50 years. If advantage is taken of the 5 per cent voltage and load reduction, the reserve to be provided as a fraction of the maximum load without voltage reduction is, from the above relation: $0.20 - 0.05 = 0.15$. This is the required installed reserve as a fraction of the maximum load *Lam* without voltage reduction. To it corresponds a probability of loss of load of 0.00049, or a loss of load expectancy of 1 day for every 5.6 years. This means that, with 20 units and an installed reserve equal to 0.15 the maximum load, the expectancy of having to drop voltage up to 5 per cent is 1 day for every 5.6 years.

If, on the other hand, the system has five units—assuming the same outage rate $q = 0.02$ and maximum load ratio $l = 0.8$—the required reserve is 0.80 the maximum load. By taking advantage of the 5 per cent voltage reduction as before, the installed reserve is reduced to 0.71 the maximum load. To this reserve corresponds a probability of loss of load of 0.000061 or a loss of load expectancy of 1 day for every 45 years, a value altogether different from the value obtaining with 20 units.

From this comparison it is seen that, starting with the same level of reliability after the 5 per cent voltage reduction, the probability of voltage drop within the 5 per cent limit depends on the number of units, being smaller the smaller the number of units. Tentatively a drop of voltage expectancy, within the 5 per cent limit, of 1 day for every 5 years in general seems altogether satisfactory. With a large number of units, however, the probability of voltage drop may become unduly large. In such cases it may become necessary to increase the reserve in order to increase the number of years per day of load to the level stated before. For instance, with a system of 50 units, $q = 0.02$ and $l = 0.8$, the reserve required with no voltage reduction is 0.11 the maximum load. With 5 per cent voltage reduction the installed reserve reduces to 0.0545 the maximum load without voltage reduction. The corresponding probability of voltage reduction within the 5 per cent limit is 0.0014, an expectancy of 1 day for every 2 years. This value in itself is not excessive; however, local factors, such as the degree of automatic voltage regulation used, may make it necessary to increase the reserve to something of the order of 0.075 in order to decrease the above expectancy to 1 day for every 5 years. The actual value should be determined after evaluating all local factors involved, making use of the information available from past experience.

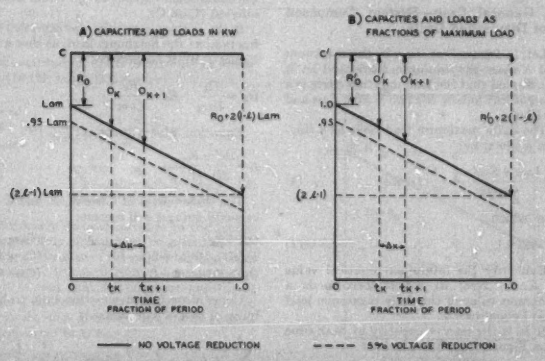

Figure 7. Straight line daily maximum load duration curve used in deriving the expressions of the various indexes of service reliability

Other Possible Applications of the Probability Method

It is true, as stated previously, that the probability method has received recently a great deal of attention yet there are still a number of possible problems to which, in the author's opinion, the probability method can be applied to great advantage: reserve and water utilization of hydro-systems, proper allocation of reserve savings derived from interconnections, rationalization of feeder reserve practices, and economic evaluation of alternative schemes of supply. The author is of the opinion that hydro-systems are ideally suited to the application of the probability method in so far as their reserve and water utilization are concerned. Perhaps this is already done. However, as far as the author has been able to learn, very little use is made in this field, at present, of the probability method.

How consistent are the feeder reserve practices followed by the various companies? The probability method should prove a powerful tool in answering this question. In regard to the economic evaluation of alternative schemes of supply, the author likes to close this paper by repeating a statement made in the paper presented at the 1947 meeting:[1]

"Apart from the application of the probability theory to the determination of an appropriate absolute level of service reliability for a group of units connected to the same bus, there is another class of problems for the solution of which the probability theory seems especially well suited. This class of problems concerns the evaluation of the relative reliability of alternative plans. What is the reliability gained by increasing or decreasing the reserve capacity of a group of units? By changing the size and connection of ties? By using a common header for a group of boilers? To the analysis of problems such as these, the probability theory is well adapted. It places, so to say, the alternative schemes in their proper relative positions from the standpoint of reliability."

The essence of this statement has been repeated on other occasions and is repeated here to emphasize one fact, namely: the immense economic value of

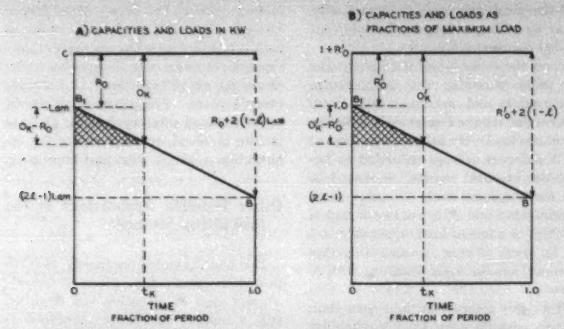

Figure 8. Energy loss caused by a capacity outage $O_k \leqslant R_0+2(1-l)Lam$

the probability method in comparing alternative schemes. It is rather strange that we should have started by using, and should continue to use, this method mostly for the determination of reserve capacity, requiring the setting of absolute values of indexes of service reliability, the most difficult to establish and interpret, and should at the same time fail to apply it in comparing alternative schemes involving only relative values of indexes of service reliability of much easier interpretation.

Conclusions

These may be summarized as follows:

1. It is recommended that loss of load probability be used as an index of service reliability.

2. Curves are given for the quick determination of the reserve requirements of a system for any given value of the daily maximum load ratio and any desired level of service reliability.

3. It is suggested that a level service reliability, corresponding to a loss of load expectancy of 1 day in 50 years after reduction of voltage, be used for general purposes.

4. Expressions are given in the Appendix for the accurate calculation of the reserve of a system assuming a straight line daily maximum load duration curve.

5. The two terms "daily maximum load ratio" and "daily maximum load-overhaul ratio" are defined and suggested for use in determining reserve capacity by the probability method.

In closing, the author wishes to point out the fact that this paper deals exclusively with installed reserve.

Appendix

In the 1947 paper,[1] it was shown that the contribution of a capacity outage O_k to the system probability loss of load in given by either $P_k\Delta_k$ or p_kt_k. Here P_k is the probability of capacity outages in excess of O_k, p_k is the probability of a capacity outage exactly equal to O_k.

$$\Delta_k=(t_{k+1}-t_k)$$

is the interval of time, as a fraction of the period, between the two successive capacity outages, O_k and O_{k+1}, and is obtained from Figure 7 where C is the total capacity of the system, t_k is the fraction of the period during which loss of load occurs with a capacity outage O_k. As shown also in the 1947 paper, the system probability of loss of load, P_s, is obtained by adding the products $P_k\Delta_k$ or p_kt_k for all possible values of O_k, that is, by:

$$p_s=\Sigma P_k\Delta_k \text{ or } P_s=\Sigma p_kt_k$$

When a straight line load duration curve is used, both expressions are susceptible of simplification. However, only the second expression will be fully developed here for two cases, namely: the general case when the system is composed of diversified units; and the special case when the units of the system are of the same size and outage rate.

1. General Case—System Composed of Diversified Units

Let, in Figure 7(*a*), *Lam* be the maximum and *KaLam* the minimum loads and let it be assumed that the load duration curve is a straight line joining the two points, *Lam* and *KaLam:*

The daily maximum load ratio as a fraction is given by:

$$l=\frac{Lam+KaLam}{2Lam}=\frac{1}{2}(1+Ka) \tag{1}$$

from which

$$Ka=2l-1 \tag{2}$$

Evidently the minimum practical value of *Ka* is zero, to which corresponds a minimum value of the daily maximum load ratio l equal to 0.5.

If R_0 is the reserve capacity at peak time from Figure (7A), it is obtained:

$$t_k=\frac{O_k-R_0}{(1-Ka)Lam}=\frac{O_k-R_0}{2(1-l)Lam} \tag{3}$$

The magnitude of O_k may fall in one of the following three cases:

$O_k \leqslant R_0$ (Case A)
$R_0<O_k\leqslant R_0+2(1-l)Lam$ (Case B)
$O_k>R_0+2(1-l)Lam$ (Case C)

Evidently, if $O_k \leqslant R_0$, Case (A), no loss of load will occur. Under Cases B and C loss of load occurs. The system loss of load probability is then the sum of the two probabilities of loss of load obtaining for all values of O_k falling in the limits of Cases B and C and is calculated as follows:

Capacity outages O_k such that $R_0<O_k\leqslant R_0+2(1-l)Lam$ (Case B)

These cause loss of load during the time t_k. Let p_k be the probability of losing exactly the capacity O_k. Their contribution to the system loss of load probability is:

$$\sum^{b} p_kt_k=\frac{1}{2(1-l)Lam}\sum^{b} p_kO_k-\frac{R_0}{2(1-l)Lam}\sum^{b} p_k \tag{4}$$

It will be noted that $\sum^{b} p_kO_k$ is the expectancy in the interval R_0, $R_0+2(1-l)Lam$. It can be calculated by subtracting from the total expectancy, the sum of the expectancies corresponding to outages outside of the interval.

Similarly $\sum^{b} p_k$ is the total probability of capacity outages in the same interval. It can be calculated by subtracting from 1 the total probability of capacity outages outside of the interval.

Capacity outages O_k such that $O_k>R_0+2(1-l)Lam$ (Case C)

The contribution of these capacity outages to the system loss of load probability is $\sum^{c} p_k$.

In the foregoing expressions, $\sum^{b}$ indicates that the summation extends to all values in the interval (Case B), and $\sum^{c}$ indicates that the summation extends to all values in the interval (Case C).

If the various capacities are expressed as fractions of the maximum load, as shown in Figure 7(B), it is obtained:

$$O_k'=\frac{O_k}{Lam}\ ;\ R_0'=\frac{R_0}{Lam}$$

Equation 3 for t_k becomes:

$$t_k=\frac{O_k'-R_0'}{2(1-l)} \tag{5}$$

The three ranges of Cases A, B, and C of capacity outages will become:

$O_k' \leqslant R_0'$ (Case A)
$R_0'<O_k'\leqslant R_0'+2(1-l)$ (Case B)
$O_k'>R_0'+2(1-l)$ (Case C)

Under Case B from equation 4 the probability of loss of load becomes

$$\sum^{b} p_kt_k=\frac{1}{2(1-l)}\left\{\sum^{b} p_kO_k'-R_0'\sum^{b} p_k\right\} \tag{6}$$

Under Case C the probability of loss of load becomes $\sum^{c} p_k$.

2. All Units Are Similar and of the Same Capacity

Under these conditions let C be the total capacity of the system of n units all of the same capacity C_1. It is:

$$C = nC_1 = R_0 + Lam = \left(1 + \frac{R_0}{Lam}\right) Lam = (1 + R_0')\,Lam$$

The total capacity C and the capacity of each unit, expressed as a fraction of the system maximum load Lam, are:

$$C' = \frac{C}{Lam} = 1 + R_0'; \quad C_1' = \frac{C'}{n} = \frac{1 + R_0'}{n}$$

An outage of k units causes a capacity outage, $O_k = kC_1$. Thus:

$$O_k' = \frac{kC_1}{Lam} = \frac{k}{n}(1 + R_0')$$

and equation 5 becomes:

$$t = \frac{1}{2(1-l)} \left\{ \frac{k}{n}(1 + R_0') - R_0' \right\} = \frac{1}{2(1-l)} \left\{ \frac{k}{n} - R_0'\left(1 - \frac{k}{n}\right) \right\} \quad (7)$$

The three ranges of Cases A, B, and C will become:

$$k \leq \frac{R_0'}{1 + R_0'} n \quad \text{(Case A)}$$

An outage of k units, where k is any integer from 0 to the maximum value satisfying the above relation, causes no loss of load.

$$\frac{R_0'}{1 + R_0'} n < k \leq \left\{ 1 - \frac{(2l-1)}{1 + R_0'} \right\} n \quad \text{(Case B)}$$

That is, the range (Case B) includes all outages of k units larger than

$$\frac{R_0'}{1 + R_0'} n$$

and equal to, or smaller than,

$$\left\{ n - \frac{(2l-1)}{1 + R_0'} n \right\}$$

The contribution to the probability of loss of load in this range is given by:

$$\sum^{b} p_k t_k \frac{1}{2(1-l)} \left\{ \frac{1 + R_0'}{n} \times \sum^{b} p_k k - R_0' \sum^{b} p_k \right\} \quad (8)$$

Evidently this contribution to the probability of loss of load can be calculated directly as the sum of the products $p_k t_k$, using equation 7 to calculate t_k. From equation 8, it is seen that for constant number of units n and reserve R_0' the contribution to the probability of loss of load in this range is proportional to $1/2(1-l)$.

$$k > \left[1 - \frac{(2l-1)}{1 + R_0'} \right] n \quad \text{(Case C)}$$

The contribution to the loss of load probability due to capacity outages of a number of units k satisfying the above relation is $\sum^{c} p_k$.

As the number of units increases, and for values of l not close to 1.0, say, between 0.5 and 0.9, the contribution to the loss of load probability due to capacity outages in the range (Case C) decreases and for a sufficiently large number of units becomes negligible. Under these conditions, as seen from equation 8, the total probability of loss of load is proportional to $1/2(1-l)$.

If the maximum load ratio is equal to 1, the interval, Case B, reduces to zero and the probability of loss of load reduces to that computed as under Case C.

The loss of load probability curves, such as those shown in Figures 2, 3, 4, obtained by plotting probability of loss of load versus total installed capacity as a fraction of maximum load, for constant number of units n and daily maximum load ratio l, will be continuous curves with discontinuity points in their slope taking place whenever either the lower limit

$$\frac{nR_0'}{1 + R_0'}$$

or the upper limit

$$\left\{ 1 - \frac{(2l-1)}{1 + R_0'} \right\} n$$

of the range (Case B) is equal to an integer. Thus, for increasing values of R_0', a break in the continuity of the slope of the curve for a specified n, regardless of the value of l, will occur when

$$\frac{nR_0'}{1 + R'} = n_1, \text{ or } R_0' = \frac{n_1}{n - n_1}$$

for all values of $n_1 = 1, 2, 3, \ldots (n-1)$. Other breaks, due to a change in the upper limit of the range (Case B), occur for all values of R_0' satisfying the relation:

$$n \left\{ 1 - \frac{2l-1}{1 + R_0'} \right\} = n_2, \text{ or } R_0' = \frac{n_2 - 2n(1-l)}{n_2}$$

where n_2 is a positive integer smaller than n. In using these formulas only the value of n_1 and n_2, corresponding to significant outage probabilities, need be considered.

3. Limiting Case When the Number of Units Becomes Very Large

Units are all similar and of the same capacity. As the number of units, n, becomes large approaching infinity, the probability of having continuously a number of units qn out approaches unity, at the same time as $n \to \infty$, the probability of larger outages than nq, approaches zero. The value qn, therefore, represents the very minimum theoretical reserve of the group, attainable only when $n = \infty$. If the reserve is nq units, the maximum load will be pn units, so that the reserve as a fraction of the load is:

$$R_0' = \frac{q}{p}$$

This is, then, the minimum theoretical reserve of a group of units n as n approaches infinity. If $q = 0.02$, $R_0' = 0.0204$.

4. Energy Loss Expectancy Assuming a Straight Line Load Duration Curve

The straight line daily maximum load duration curve, used to calculate loss of load probabilities, now will be used to calculate energy loss expectancies. The energy loss with a given capacity outage depends on such factors as the nature of the load, the magnitude of the outage, and the method of voltage regulation. For the purpose of this discussion let it be assumed that with a capacity outage O_k in excess of reserve the load is decreased, say, by lowering the voltage, until equality between capacity available and load is re-established. On this basis, the energy loss with the outage O_k will be proportional to the area of the shaded triangle in Figure 8(A). The area of this triangle from equation 3 is:

$$\frac{1}{2} t_k (O_k - R_0) = (1-l) t_k^2 Lam$$

Let us assume that capacities are expressed in kilowatts. The energy loss expectancy in kilowatt-days during a period of T days, due to the outage O_k in the range (Case B),

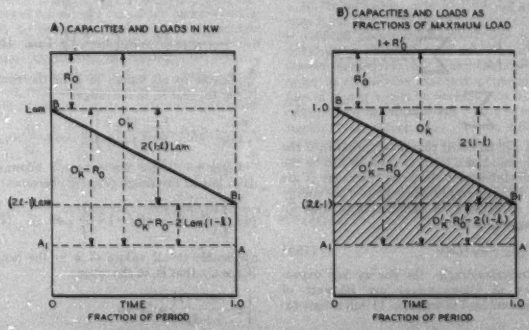

Figure 9. Assumed energy loss caused by a capacity outage $O_k > R_0 + 2(1-l)Lam$

will be given by the following equation:

$$p_k T(1-l)t_k^2 Lam$$

$$= p_k T \frac{(O_k - R_0)^2}{4(1-l)Lam} = \frac{p_k T(O_k' - R_0')^2 Lam}{4(1-l)} \quad (9)$$

This expression is correct only if O_k is in the range (Case B), that is, if:

$$R_0 < O^k \leqslant R_0 + 2(1-l)Lam$$
$$R_0' < O_k' \leqslant R_0' + 2(1-l)$$

For values of O_k in the range (Case C) point "A," Figure 9, that is, in the range:

$$R_0 + 2(1-l)Lam < O_k \leqslant R_0 + Lam$$
$$R_0' + 2(1-l) < O_k' \leqslant 1 + R_0'$$

the expected kilowatt-days lost with the outage O_k will be proportional to the area $AA_1\ BB_1$ (Figure 9) or to:

$$\{O_k - R_0 - (1-l)Lam\}$$

The expected kilowatt-days loss will be:

$$p_k\{O_k - R_0 - (1-l)Lam\}T$$
$$= p_k\{O_k' - R_0' - 1 + l\}Lam\ T \quad (10)$$

The total energy loss expectancy in kilowatt-days will be given by the sum of: all terms as equation 9 for values of O_k' in Case B, plus all terms as equation 10 for values of O_k' in the range (Case B).

The energy loss expectancy in kilowatt-days per kilowatt of maximum load will thus be given by

$$T\{(1-l)\sum^{b} p_k l_k^2 + \sum^{c} p_k(O_k' - R_0' - 1 + l)\}$$
$$= T\left\{\frac{1}{4(1-l)}\sum^{b} p_k(O_k - R_0')^2 + \sum^{c} p_k(O_k' - R_0' - 1 + l)\right\} \quad (11)$$

Where, as previously stated, $\sum^{b}$ indicates that the summation is extended to all values of O_k' in the range $R_0' < O_k' \leqslant R_0' + 2(1-l)$ and $\sum^{c}$ indicates that the summation is extended to all values of O_k' in the range $R_0' + 2(1-l) < O_k' \leqslant 1 + R_0'$.

The energy loss expectancy in kilowatt-days per kilowatt of total capacity will be given by:

$$\frac{T}{1+R_0'}\left\{\frac{1}{4(1-l)}\sum^{b} p_k(O_k' - R_0')^2 + \sum^{c} p_k(O_k' - R_0' - 1 + l)\right\} \quad (12)$$

It will be noted that if $l = 1$, that is, if the daily maximum loads are assumed to be the same throughout the year, the range (Case B) disappears and equation 10 for the energy loss expectancy in kilowatt-days, with an outage O_k, becomes:

$$p_k T(O_k' - R_0')Lam \quad (10A)$$

Correspondingly, the energy loss expectancy in kilowatt-days per kilowatt of maximum load of equation 11 will reduce to:

$$T\{\sum p_k O_k' - R_0' \sum^{c} p_k\} \quad (11A)$$

It will be noted that both the energy loss expectancy in kilowatt-days per kilowatt of maximum load (equation 11), and in kilowatt-days per kilowatt of total capacity (equation 12), are proportional to the quantity:

$$(1-l)\sum^{b} p_k l_k^2 + \sum^{c} p_k(O_k' - R_0' - 1 + l) \quad (11\text{-}1A)$$

or its equivalent:

$$\frac{1}{4(1-l)}\sum^{b} p_k(O_k' - R_0')^2 + \sum^{c} p_k(O_k' - R_0' - 1 + l) \quad (11\text{-}1B)$$

Either one of these two expressions represents the energy loss expectancy expressed as a fraction of the possible maximum load energy, during a period T, that is, as a fraction of $T\ Lam$.

It will also be noted that equations 11-1A and 11-1B represent the sum of the products of the probabilities p_k by the shaded areas shown in Figures 8(B) and 9(B). If the energy loss expectancy as a fraction of the possible maximum load energy (equations 11-1A or 11-1B) is known, the energy loss expectancy per kilowatt of maximum load, during a period T, is obtained by multiplying these equations by T. Similarly, the energy loss expectancy, during T, per kilowatt of total capacity is obtained by multiplying equations 11-1A or 11-1B by $T/1+R_0'$.

5. Energy Loss Expectancy Assuming a Straight Line Load Duration Curve and All Units Similar and of the Same Capacity

Let us assume again, as under section 2 of this Appendix, that the system has n units all of the same capacity C_1. In this case:

$$O_k' = \frac{k}{n}(1 + R_0')$$

where k is the number of units out causing the outage O_k. Equation 9 for the expected energy loss in kilowatt-days in the range (Case B) becomes:

$$\frac{T}{4(1-l)} p_k \left\{\frac{k}{n}(1+R_0') - R_0'\right\}^2 Lam =$$
$$\frac{T}{4(1-l)} p_k \left\{\frac{k}{n} - R_0'\left(1 - \frac{k}{n}\right)\right\}^2 Lam \quad (13)$$

applicable to all values of k in the range (Case B), that is, in the range:

$$\frac{nR_0'}{1+R'} < k \leqslant \left\{1 - \frac{2l-1}{1+R'}\right\}n$$

Equation 10 for the expected kilowatt-days loss in the range (Case C) becomes:

$$p_k T\left\{\frac{k}{n}(1+R_0') - R_0' - 1 + l\right\} Lam \quad (14)$$

applicable to all values of k in the range (Case C), that is, in the range:

$$\left\{1 - \frac{(2l-1)}{1+R_0'}\right\}n < k \leqslant n$$

The energy loss expectancy in kilowatt-days per kilowatt of maximum load during the period T will be given by the equivalent of equation 11, that is, by:

$$T\left[\frac{1}{4(l-1)}\sum^{b} p_k\left\{\frac{k}{n}(1+R_0') - R_0'\right\}^2 + \sum^{c} p_k\left\{\frac{k}{n}(1+R_0') - R_0' - 1 + l\right\}\right] \quad (15)$$

The energy loss expectancy in kilowatt-days per kilowatt of total capacity is obtained from equation 15 by dividing by $(1+R_0')$.

Again it will be noted that if $l = 1$, equation 15 reduces to:

$$T\sum^{c} p_k\left\{\frac{k}{n}(1+R_0') - R_0'\right\} \quad (15\text{-}1)$$

Evidently, the expressions for the energy loss expectancy as a fraction of the possible maximum load energy in this case, from equation 15, is given by:

$$\frac{1}{4(1-l)}\sum^{b} p_k\left\{\frac{k}{n}(1+R_0') - R_0'\right\}^2 + \sum^{c} p_k\left\{\frac{k}{n}(1+R_0') - R_0' - 1 + l\right\} \quad (15\text{-}2)$$

or by:

$$(1-l)\sum^{b} p_k l_k^2 + \sum^{c} p_k\left\{\frac{k}{n}(1+R_0') - R_0' - 1 + l\right\} \quad (15\text{-}3)$$

Bibliography

1. Generating Reserve Capacity Determined by the Probability Method, G. Calabrese. *AIEE Transactions*, volume 66, 1947, pages 1439–50.

2. Outages Rates of Steam Turbines and Boilers and of Hydro Units, AIEE Committee Report. *AIEE Transactions*, volume 68, part I, 1949, pages 450–57.

3. Probability Theory Helps Determine System Reserve Operating Capacity, G. Calabrese. *Power* (New York, N. Y.), volume 92, July 1948, pages 423–26.

4. Emergency Control of System Loads, J. M. Comly, C. B. Kelley, J. E. McCormack, H. W. Phillips, T. W. Schroeder. *AIEE Transactions*, volume 67, part II, 1948, pages 1474–82.

5. Calculating Probability of Generating Capacity Outages, W. J. Lyman. *AIEE Transactions*, volume 66, 1947, pages 1471–77.

Discussion

C. W. Watchorn (Pennsylvania Water and Power Company, Baltimore, Md.): The author has presented a very interesting method for determining various characteristics related to the application of probability methods to power system problems, including the effect of load characteristics, which latter factor has been neglected too often in generalized papers presented on this subject. However, it is desired to emphasize the author's admonition that the pro-

posed simplified method of calculation should be used for practical purposes only to obtain quick preliminary answers to problems involving the determination of installed capacity requirements. This caution is being emphasized because there are probably very few systems for which the load duration characteristics approach a straight line sufficiently to be so represented and result in reasonably reliable answers; and also, because there are probably very few systems for which their units, boilers and turbines in combination and interconnected variously, may be reasonably represented as being of average size without distorting the answers too greatly to be considered as other than being merely preliminary.

As the author points out, probability methods provide a very powerful tool for the solution of problems involving the relative advantages of alternative facilities. However, such relative advantages cannot be determined, at the present time, with sufficient accuracy other than by means of the longer more accurate application of probability methods, particularly as related, in most cases, to at least the alternative installations.

The discussor agrees fully with the author's recommendation that the probability of loss of load is the most practical and significant measure of service reliability and that it should be used as the index therefor. However, the "shedding" of load that results from a voltage reduction is in itself a loss of load and certainly should be so treated, and considered for what it actually is, an emergency measure for the rationing of service, rather than treating it as capacity, which it definitely is not. In addition, the variability of the general load level or the "load forecasting error" is a necessary factor in the rational determination of the level of service reliability. Consideration of the effect of these two elements in the evaluation of system capacity requirements leads to the conclusion that the level of service reliability of a loss of load expectancy of in the order of at the average rate of one day in ten years in both reasonable and adequate. The discussor has already so recommended or indicated on several occasions.[1,2,3]

REFERENCES

1. PROBABILITY METHODS APPLIED TO GENERATING CAPACITY PROBLEMS OF A COMBINED HYDRO AND STEAM SYSTEM, E. S. Lorne, C. W. Watchorn. *AIEE Transactions*, volume 66, 1947, pages 1645–54.

2. ELEMENTS OF SYSTEM CAPACITY REQUIREMENTS, C. W. Watchorn. AIEE Special Publication S-38, August 1950, pages 5–42.

3. THE DETERMINATION AND ALLOCATION OF THE CAPACITY BENEFITS RESULTING FROM INTERCONNECTING TWO OR MORE GENERATING SYSTEMS, C. W. Watchorn. *AIEE Transactions*, volume 69, part II, 1950, pages 1180–86.

G. Calabrese: I agree with Mr. Watchorn that the lowering of the voltage in order to reduce the load is an emergency measure. For this reason, it should not be used too often. How often it can and should be used depends on the type of service rendered and the composition of the system.

I also am in agreement with Mr. Watchorn's statement that the load forecasting error should be taken into consideration in determining the level of service reliability of a system.

Mr. Watchorn states that there are few systems for which the daily maximum load duration curve approaches a straight line. While this is undoubtedly true, I believe that in most cases it should be possible to replace the actual curve with a straight line, particularly if this is drawn to fit the portion of the actual curve corresponding to the higher loads, the most significant from the standpoint of the problem in hand. In extreme cases, when this is not considered satisfactory, the actual curve can be replaced with segments of straight lines.

Mr. Watchorn suggests a loss of load expectancy of one day in ten years. He does not state whether this level should be before or after voltage reduction.

Before closing this discussion, mention should be made of another point, namely, how often can loss of load be expected to occur? In other words, what is the expected frequency of loss of load expressed in terms of one loss of load occurrence every so many years. To the probability of loss of load, discussed in the paper, corresponds an expectancy of loss of load of one day every so many years. This expectancy, however, represents an average value which may obtain as a result of a large number of short loss of load occurrences or through a small number of long ones. The loss of load expectancy yields no information in this respect excepting that, on the average, loss of load will occur one day every so many years, or D days per year, in general D being a fraction of one day.

In order to answer the above question relative to the expected frequency of occurrence of loss of load, it is necessary to introduce the concept of continuance probabilities for simultaneous outages of units. Briefly, these are the probabilities that outages involving simultaneously a given number of units, say k, should last 1, 2, or 3 days once they have occurred. From past records, continuance probabilities for outages of k units are calculated as follows: let N_k be the total number of k-unit outages that have occurred in a past period. Of these N_k outages $n_{k1}, n_{k2}, n_{k3}, \ldots\ldots$, have lasted respectively 1, 2, 3, . . . days. From these recorded values, the continuance probabilities $\pi_{k1}, \pi_{k2}, \pi_{k3}, \ldots\ldots$ are now calculated.

$\pi_{k1} = \dfrac{n_{k1}}{N_k}$ = continuance probability that a k-unit outage shall last 1 day once it has occurred.

$\pi_{k2} = \dfrac{n_{k2}}{N_k}$ = continuance probability that a k-unit outage shall last 2 days once it has occurred.

Let $d_k = n_{k1} + 2n_{k2} + 3n_{k3} + \ldots\ldots$ be the total number of k-unit outage days involved. It is easily seen that

$$n_{k1} = \frac{\pi_{k1} d_k}{\pi_{k1} + 2\pi_{k2} + 3\pi_{k3} + \ldots}$$

$$n_{k2} = \frac{\pi_{k2} d_k}{\pi_{k1} + 2\pi_{k2} + 3\pi_{k3} + \ldots} \qquad (1)$$

that is, once the continuance probabilities for k-unit outages are obtained from past records, the number of k-unit outages lasting respectively 1, 2, 3 . . . . days, that can be expected to occur during a reasonably long period, can be calculated if the expected total number of k-unit outage days is known.

The continuance probabilities $\pi_{k1}, \pi_{k2} \ldots\ldots$ should be calculated for as many values of k as necessary and should be checked for stability, following the same general method outlined in reference 2 of the paper.

In order to determine the expected frequency of loss of load from the expected number of D days of loss of load, it is first necessary to determine the number of units k of the outages causing loss of load, for instance as shown in column 2 of the lower part of Table VI of reference 2. In this particular case, it is seen that loss of load is caused almost entirely by 3-unit outages. In the more general case, loss of load will be caused by outages of 1, 2, 3 . . . . units. In such a case, a complete analysis would require the fractionalization of D into portions $D_1, D_2, D_3 \ldots\ldots D_k \ldots\ldots$ according to the number of units involved. For each class of outages of k-units, the number of outages $n_{k1}, n_{k2}, \ldots\ldots$, lasting 1, 2 . . . . days, respectively, that may be expected during a sufficiently long period of years T, may now be calculated by replacing d_k with TD_k in equation 1 above. Sufficiency of the length of T for each value of k should be determined by the number of k-unit outage days necessary to obtain stable values of the continuance probabilities $\pi_{k1}, \pi_{k2}, \ldots\ldots$

Values of continuance probabilities for boilers and turbines, disregarding the number of units out simultaneously, may be obtained from Figures 5, 6, 7, and 8 of reference 1 of the paper.

In the particular case of Table VI reference 2, the calculated loss of load probability is 0.00162 corresponding to 1 day every 6,200 days. Since loss of load is caused almost exclusively by 3-unit outages, in order to obtain the expected frequency of loss of load it would be necessary to have a continuance probability for 3-unit outages. Lacking this information, for the sake of discussion let it be assumed that the average duration of a unit outage is four days. If it is assumed that this figure is applicable to 3-unit outages, the expected frequency of loss of load would be once every 24,800 days.

Report of the Board of Directors

THE BOARD OF DIRECTORS of the American Institute of Electrical Engineers presents to the membership its 66th annual report, covering the fiscal year ending April 30, 1950. It contains a brief summary of the principal activities of the Institute during the year, a general balance sheet showing the financial condition of the Institute at the close of the fiscal year, a statement of cash receipts and disbursements, and a schedule of securities owned. Much additional information regarding the activities appeared in various issues of *Electrical Engineering*.

BOARD OF DIRECTORS' MEETINGS

Five meetings of the Board of Directors were held during the year, two in New York, N.Y., one in Swampscott, Mass., one in Cincinnati, Ohio, and one in Providence, R.I.

Information regarding many of the more important matters which were considered by the Board of Directors appeared in various issues of *Electrical Engineering*.

INSTITUTE POLICY

As a result of many discussions, in meetings of the Board of Directors and other groups, regarding proposals that the Institute participate in various activities of the broader, nontechnical types, a resolution intended to define the Institute as "strictly a scientific and educational organization" was discussed for several hours in the April 1949 meeting of the Board of Directors.

The resolution was referred to a special committee whose assignment was to stimulate discussion and consideration of the subject both in the next meeting of the Section Delegates and in the Sections, and to report to the Board of Directors not later than the time of the Board meeting at the 1950 Winter General Meeting.

All Sections were requested to urge their members to vote upon the following two courses:

1. I favor adhering to the technical field.

2. I favor expanding in nontechnical field with increased dues.

The vote was 7,245 in favor of proposition 1, and 2,063 in favor of proposition 2.

The special committee presented to the Board of Directors, on February 2, the following proposals of policy:

1. The Board of Directors will work continually for the unification of the profession.

2. The Board of Directors recognizes the fact that the Institute finds its chief reason for existence in the technical field.

3. The Board of Directors will handle questions on nontechnical affairs as necessary and as they arise, on an emergency basis until through unification they can be handled on a general professional basis.

The Board of Directors approved the recommendation that these three proposals be published in *Electrical Engineering* for March, with a report on the vote conducted by the Sections, and a return postal card, on which each member was requested to approve or disapprove each of the three proposals.

At the meeting of the Board of Directors in Providence, on April 27, the following results, to April 14, were reported:

Proposal	Number 1	Number 2	Number 3
Approved	3,391	3,386	3,331
Disapproved	252	290	312

The time for conclusion of the ballot was extended to May 15.

INSTITUTE VISITS BY PRESIDENT FAIRMAN

California
Pacific General Meeting, San Francisco; Summer and Pacific General Meeting, Pasadena

Florida
Florida Section, Gainesville

Georgia
Georgia Section, Atlanta

Illinois
Urbana Section; Illinois Valley Section, Peoria

Indiana
Fort Wayne Section

Iowa
Iowa Section and Iowa State College Branch, Des Moines

Kentucky
Louisville Section

Louisiana
Shreveport Section; New Orleans Section

Maryland
Maryland Section, Baltimore

Michigan
Great Lakes District Meeting, Jackson; University of Michigan Branch, Ann Arbor

Minnesota
Minnesota Section, Minneapolis

Nebraska
Nebraska Section and University of Nebraska Branch, Omaha

New York
Winter General Meeting, New York; New York Section; Niagara Frontier Section, Buffalo

North Carolina
North Carolina Section, Winston-Salem

Ohio
Columbus Section; Fall General Meeting, Cincinnati; Cleveland Section

Oklahoma
Oklahoma City Section; Tulsa Section

Oregon
Portland Section

Pennsylvania
Pittsburgh Section and Carnegie Institute of Technology, Pennsylvania State College, University of Pittsburgh, and University of West Virginia Branches, Pittsburgh; Philadelphia Section; Lehigh Valley Section, Sunbury

Rhode Island
North Eastern District Meeting, Providence

South Carolina
South Carolina Section, Columbia

Tennessee
East Tennessee Section, Chattanooga

Texas
Panhandle Plains Section, Amarillo; South Texas Section, San Antonio; Houston Section; Beaumont Section

Utah
Utah Section, Salt Lake City

Virginia
Virginia Section, Richmond; Western Virginia Section Roanoke

Washington
Seattle Section; Spokane Section

West Virginia
West Virginia Section, Charleston

Wisconsin
Madison Section; Milwaukee Section

ANNUAL MEETING

The 66th annual business meeting of the Institute was held in Swampscott, Mass., June 22, 1949. The annual report of the Board of Directors for the fiscal year which ended April 30, 1949, was presented in abstract by Secretary H. H. Henline, who also presented a report of the Committee of Tellers on the vote of the membership on the election of officers whose terms were to begin on August 1, 1949. In the absence of Treasurer W. I. Slichter, his report on Institute finances was presented by Secretary Henline. President-elect James F. Fairman was introduced, and responded with a brief address.

The Lamme Medal for 1948 was presented to Dr. V. K. Zworykin, Vice-President and Technical Consultant, Radio Corporation of America Laboratories Division, Princeton, N. J.

An address, "The Expanding Horizons in Engineering Education," was given by William F. Ryan, Engineering Manager, Stone and Webster Engineering Corporation. Preceding his address, Mr. Ryan, as Vice-President of the Northeastern Section of the National Society of Professional Engineers, presented to Mr. Fairman a tribute of esteem from his friends in many parts of the United States, a richly bound volume of congratulatory letters from officers of the NSPE and the presidents of many of the state societies.

The last item on the program was an inspiring address entitled "Open Doors," by President Everett S. Lee.

GENERAL MEETINGS

Four general meetings were held during the year, and a brief report on each follows:

Summer General Meeting. The 65th Summer General Meeting was held in Swampscott, Mass., June 20–24, 1949, with a registration of 1,650. The program included 30 technical sessions and conferences, the official annual business meeting of the Institute, 50 committee meetings, Section Delegates conferences, and a meeting of the Board of Directors. Social and entertainment features included a barn-dance, President's reception and banquet, New England entertainment, and special events for the ladies. Various types of inspection trips were available.

Pacific General Meeting. The Pacific General Meeting was held in San Francisco, Calif., August 23–26, 1949, with a registration of 878. There were a general session ad-

dressed by W. C. Mullendore, President, Southern California Edison Company, Ltd.; a luncheon meeting addressed by President Fairman; 15 technical sessions and conferences; two student sessions; a meeting of District, Section, and national officers, and Branch Counselors; a meeting of Branch officers and Counselors; a banquet; a student dinner and meeting; inspection trips; golf tournament; and ladies' events.

Fall General Meeting. The third Fall General Meeting was held in Cincinnati, Ohio, October 17–21, 1949. The registration was 1,045. The program included a general session with three addresses, by President Fairman, Dr. Raymond Walters, President of the University of Cincinnati, and Robert S. Peare, Vice-President in charge of Public Relations, General Electric Company; 31 technical sessions and conferences; a luncheon and session at the University of Cincinnati for discussion of intersociety relationships in Cincinnati; inspection trips; a dinner-dance; and an extensive ladies' program. Also, a meeting of the Board of Directors, a District Executive Committee meeting, and about 40 committee meetings were held.

Winter General Meeting. The Winter General Meeting was held in the Hotel Statler, New York, N. Y., January 30–February 3, 1950, with a registration of 3,213, and a record program of 58 technical sessions and conferences, and presentation of 243 papers. In a general session, addresses were given by Harold E. Stassen, President, University of Pennsylvania, and Sir Ernest Benn of London, England (in absentia), and an Honorary Member certificate was presented to Dr. Vannevar Bush, President, Carnegie Institution of Washington. Approximately 90 meetings of technical and administrative committees and a meeting of the Board of Directors were held. In addition, there were inspection trips, a smoker, a dinner-dance, and ladies' entertainment events.

DISTRICT MEETING

North Eastern District Meeting. A North Eastern District Meeting was held in Providence, R.I., April 26–28, 1950, with headquarters at the Sheraton-Biltmore Hotel. The registration was 502. The meeting consisted of eight technical sessions, two student technical sessions, a luncheon meeting of Branch Chairmen and Counselors, inspection trips, two banquets, and ladies' events. A meeting of the Board of Directors, a conference of Vice-Presidents, and a meeting of the District Executive Committee were held.

SPECIAL TECHNICAL CONFERENCES

"Special Technical Conferences" were inaugurated in 1948, and have proved so successful that the number being planned and held has increased rapidly. The conferences are intended to be national in interest, technical in character, and concentrated as to subject matter toward one particular industry or objective. This type of meeting is designed to explore thoroughly a limited field and to afford specialists in that field an opportunity to discuss mutual technical problems. The conferences may be defined as a program of panel discussions, technical papers, or exhibits under the auspices of a national technical committee, in co-operation with an AIEE local Section, which might act as host to the conference. Operating under the policy and procedure which has been set up, the following conferences were held during the past fiscal year.

Conferences on the Textile Industry. Electrical engineering problems in the textile industry was the subject of two technical conferences held in May 1949. The first was in Boston, Mass., May 3, and was sponsored by the Textile Industry Subcommittee of the Committee on General Industry Applications, in co-operation with the Boston Section. Seven papers and two moving pictures were presented during the two sessions of the conference. Subjects covered by the papers ranged from cloth production in the loom to cloth finishing. The attendance was 65. Approximately 95 persons attended the conference at the Georgia Institute of Technology, Atlanta, Ga., May 27–28, which was sponsored also by the Textile Industry Subcommittee, in co-operation with the Engineering Extension Division of the Georgia Institute of Technology and the Georgia Section. Among the many interesting subjects discussed were electric equipment for textile machines, loom research, fire hazards, electrostatic air cleaning, and so forth. Proceedings of these conferences have not been published, but some digests of the papers presented appear in the September 1949 issue of *Electrical Engineering*.

Conference on Electric Equipment for Materials Handling Bridges was held in Cleveland, Ohio, May 13, 1949, sponsored by the Materials Handling Subcommittee of the Committee on General Industry Applications and the Cleveland Section. The topic of "Electric Equipment for Materials Handling Bridges" was considered in several prepared papers, followed by round-table discussion. The attendance was 85.

Conference on Electronic Instrumentation in Medicine and Nucleonics was held in New York, N. Y., October 31, November 1–2, 1949, sponsored jointly by committees of AIEE and the Institute of Radio Engineers. The sponsoring committees included:

For AIEE: Committee on Nucleonics, Committee on Electronics, Committee on Instruments and Measurements, Joint Subcommittee on Nucleonic Instrumentation, Joint Subcommittee on Electronic Aids to Medicine

For IRE: Professional Group on Nuclear Science, Nuclear Studies Committee

The first day of the 3-day gathering was devoted to the nonnucleonic phases of electronics in medicine. The second day's sessions dealt with nucleonics in medicine. A round-table discussion on "Evaluation of Radiation Hazards" was held during the evening of the second day. The last day's sessions were concerned with nucleonic developments in industry and government. Six sessions provided for the presentation of 21 papers, in addition to the discussions and address which were a part of the round-table discussion panel held in the evening. More than 800 persons attended the conference, and an interesting and very popular feature was an exhibit of commercially available nucleonic equipment. Complete proceedings of the conference have been printed in book form and are available at a price of $3.50.

Conference on Electric Welding was held at the Rackham Memorial Building, Detroit, Mich., April 5–7, 1950, sponsored by the Committee on Electric Welding, in co-operation with the American Welding Society and the Industrial Electrical Engineers' Society in Detroit. The conference, which was the second Welding Conference, provided an opportunity for the presentation in six sessions of 24 papers on arc and resistance welding. Two of the evenings were devoted to demonstrations of electric welding techniques and equipment. These included several inert gas welding processes, stud welding, submerged arc welding, a 3-phase rectifier-type d-c arc welder, portable gun welding, and resistance welding controls. The total attendance at the conference was 420. The papers and discussions will be published in a bound volume at a price of $3.50.

Conference on Electric Space Heating was held at the Rogue Valley Country Club, Medford, Oreg., on April 12, 1950, sponsored by the Committee on Domestic and Commercial Applications. This was a 1-day meeting with a general session in the evening. No prepared papers were presented, but for those wishing to present technical data there was a preliminary meeting in the afternoon to make arrangements so that everyone who was interested could be heard. Subjects discussed were domestic heating, domestic load control, and heat pump performance. The attendance was 34.

The Second Southern Conference on Electrical Application for the Textile Industry was held at the Georgia Institute of Technology, Atlanta, Ga., April 13–14, 1950, sponsored by the AIEE Textile Industry Subcommittee of the Committee on General Industry Applications, and the Georgia Institute of Technology. Three sessions at this conference provided for the presentation of nine papers, which were arranged to keep the persons in the textile field informed on new scientific and engineering developments which are in progress. The subjects covered packaged drives, power wiring, lighting, electronics, and air conditioning. The attendance was 210. A Conference on Textiles for New England was incorporated as a session, on April 27, of the North Eastern District Meeting, which was held in Providence, R. I. Four papers were presented at this session, and an inspection was made on the same day of the Owens-Corning Fiberglas Corporation plant at Ashton, R. I. The attendance at the session was 126.

Power Conference. The Pittsburgh Section was host to a 2-day Power Conference in Pittsburgh, Pa., April 19–20, 1950, sponsored by the Committees on Industrial Power Systems, Power Generation, and System Engineering. A well diversified program was planned to attract as large an attendance as possible and ensure active discussion. This resulted in the presentation of 18 papers in four sessions, and all proved of practical interest to central-station and industrial plant designers and operators. This was the first technical conference to be sponsored by a committee within the Power Group, but was most successful, with an attendance of 300. Published proceedings of this conference will be available at a price of $2.50.

General Committees

BOARD OF EXAMINERS

The Board of Examiners, for the first time in many years, has been able to conduct its business at the regularly scheduled monthly meetings, without having to hold extra sessions.

Table I. Applications for Admission and Transfer, 1949–1950

Applications for Admission		
Recommended for grade of Associate	3,792	
Re-elected to the grade of Associate	90	
Not recommended	8	
		3,890
Recommended for grade of Member	324	
Re-elected to the grade of Member	19	
Not recommended	73	
		416
Recommended for grade of Fellow	4	
Not recommended	0	
		4
Applications for Transfer		
Recommended for grade of Member	560	
Not recommended	45	
		605
Recommended for grade of Fellow	115	
Not recommended	1	
		116
Students		
Recommended for enrollment as Students		7,733
Total		12,764

Statistics relating to the number of cases handled by the Board are given in Table I. The current total, excluding "enrolled Students," is four per cent less than for 1948–49. This is largely due to a decrease in Associate applications, which have dropped seven per cent. Student enrollments have dropped 12 per cent. The decrease in Associate applications and in Students' enrollments was not unexpected, both being largely affected by enrollments in colleges under the "GI Bill o Rights."

COMMITTEE ON CODE OF PRINCIPLES OF PROFESSIONAL CONDUCT

Two matters were carried over from the preceding year. The first was the case of the Southwestern Power Administration in advertising for competitive bids for professional electrical engineering services. Formally, that matter was closed two years ago with this committee's report to the Board of Directors (in which it was found that there had been no violation of the Canons of Ethics of the Engineers' Council for Professional Development, or of the Institute Code. The committee's belief was reported that such practices should not be encouraged and that necessity for them by such a governmental agency should be removed by legislative or executive action). This matter has been before the committee this year only through copies received of correspondence of the Institute President and the Southwestern Power Authority aimed to find out if the prior technical difficulties had been removed. However, the question of competitive bidding is a live matter, being discussed by regional engineering associations, and this subject could well be continued by this committee.

The second matter carried over was the projected "Statement of Principles of Professional Conduct" combining the Canons of Ethics of the Engineers' Council for Professional Development, verbatim, with certain rules of practice contained in the old Code of the Institute. It was thought that a draft had been agreed upon for submission when a new matter arose which led to a recommendation to change the Institute Bylaws. That change suggested a change or addition to the pending "Statement of Principles" which has held up the presentation. It is expected that this whole matter can be closed during the current administrative year.

One new matter arose during the year. A case was reported to the Institute, and referred to the committee, where an electrical contractor who was an Associate did business under a corporation name, and carried insignia of the Institute on corporation letterhead and advertising. The committee believed that the Associate in question had merely not appreciated the distinction between the Institute and contractors' associations by which such practices are approved. It was emphasized that membership in the Institute is a wholly personal and professional matter, that insignia are to be displayed only on Institute letters and publications, except of course in the wearing of membership badges and use of personal membership statements on stationary, and so forth. A change in the Bylaws clarifying this whole situation was recommended to the Directors and adopted by them. It now rests with the Committee on Constitution and Bylaws. A corresponding addition to the projected "Statement of Principles of Professional Conduct" is being considered.

COMMITTEE ON CONSTITUTION AND BYLAWS

This committee submitted certain recommendations to the Board of Directors in advance of three meetings, and the Bylaws were amended as outlined in the following.

June 23, 1949. A change was made in Section 19 to clarify the time of notification of Members for Life.

A change was made in Section 26 regarding the general meetings, identifying them as Winter General Meeting, Summer General Meeting, Pacific General Meeting, and Fall General Meeting.

Section 64 was amended to include certain new committees and rearrangement of the technical committees.

October 20, 1949. Sections 6 and 7 were amended so as not to require the publication in *Electrical Engineering* of the names of applicants for admission to the Institute as Associates.

February 2, 1950. Sections 10 and 17 were amended to clarify the requirements of notice regarding members in arrears.

The printing on the annual dues bill and each of the quarterly notices sent to those remaining in arrears of Sections 16, 17, 18, and 12 of the Bylaws, covering the billing of annual dues, delinquencies, and reinstatement, is now required by Section 17.

COMMITTEE ON EDUCATION

The committee sponsored three conference sessions as reported in the following paragraphs.

At the Summer General Meeting, the conference theme "Accrediting of Engineering Curricula" was dealt with in two talks, one on the accrediting program from the point of view of those administrating it, and the other on what the visitor sees. The purpose of the session was to provide an opportunity for Institute members to become acquainted with what the committee thinks is a powerful, but not very well known, influence in electrical engineering education.

At the Fall General Meeting, the conference subject was "Problem and Thesis Subjects From Industry." In three excellent papers presented by six engineers in industry, typical problems were presented, by example, from the fields of application, design, and industrial electronics. Such problems are of value to the teacher and student especially in bringing the point of view of the classroom closer to that of industry.

At the Winter General Meeting, the theme was "Post-College Development of Engineers." The five papers, resulting from studies made by the ECPD Committee on Professional Training, covered the various aspects of the subject: the orientation and training of the young engineer in industry, his continued education, methods for appraising himself, professional registration, and integrating him into his community. These were the basis of a spirited discussion, and should be of particular significance to the Institute, whose life and growth are in a large measure dependent upon the quality and attitudes of the young men from whose ranks it recruits its new members.

Four of the five papers of the first two conferences were published in *Electrical Engineering*, and a summary of the third conference is in prospect for publication.

The conference scheduled for the Summer and Pacific General Meeting deals with the planning of new electrical engineering laboratory facilities for colleges. Quite a number of new laboratories have been built in recent years, and others are in the planning stages; hence, the conference should serve as a medium for the exchange of ideas.

Future work of the committee is expected to include studies through subcommittees, of the following subjects: objectives of the electrical engineering curriculum, graduate programs, measuring the effectiveness of educational programs, and accrediting. It is expected that these topics will be the subjects of future conferences.

FINANCE COMMITTEE

For the budget year October 1, 1949, to September 30, 1950, the Board of Directors adopted a balanced budget, and the financial performance for the first six months of that period has been approximately in line with the budget provisions. Due to the fact that expenditures occur fairly evenly from month to month, but receipts are much greater after May 1 then they are prior to that time, it is necessary to engage in temporary transfers or borrowings during the later winter. This year is no exception, and $40,000 was transferred from the Reserve Capital Fund to the General Fund, which will be repaid from dues receipts after May 1.

The remedial factors mentioned in last year's report which are designed to ease the Institute's financial situation are in operation:

1. Increased advertising rates in *Electrical Engineering*.
2. Registration fees for general and District meetings.
3. More adequate price scales for Institute publications.
4. Excellent co-operation by committees responsible for sizable expenditures in the effort to live within budget limitations.

The results of these measures and others effective in the same direction were such as to remove the apparent immediate necessity for an increase in dues, so the Special Committee on Institute Dues was discharged with thanks.

It is recognized, however, that the financial picture can change radically with great speed, due both to substantial decreases in income

and to a sustained upward trend in expenditures, so the necessity for continued vigilance in financial matters is just as important now as it has been. So far, income is holding up very well, but items tending to enlarge the size of expenditures are constantly appearing. Publication costs, both for material and production, are still going up; appropriations to other organizations, maintained in part by the Institute, are increasing; a study has been made of the Institute traveling allowances, with the view of making them more adequately compensatory under present conditions; to mention only a few such influences.

The Reserve Capital Fund is the Institute's "anchor to windward," and it is available to permit the maintenance unimpaired of our present activities during any probable necessary period for the adjustment of our financial requirements to a new situation.

HEADQUARTERS COMMITTEE

The chief activity of this committee concerned the study and application of air-conditioning equipment for all office space at Headquarters. In accordance with a recommendation to the Board of Directors, a special grant was authorized and an order placed for the installation of 21 units. At the time of this report, the installation is practically complete, and it is expected that considerable increase in office efficiency will result during the summer months.

The committee also continued the program of modernization of lighting fixtures with the installation of additional fluorescent units in several offices. Replacement of the fixtures in the Board of Directors' room with units of more modern design is under consideration, and will be accomplished in the near future.

The table in the Board of Directors Room was polished and provided with a new felt cover.

Other matters on the agenda concern the cleaning of rugs, shampooing of upholstered furniture, addition of identifying lettering on office doors, and a new bulletin board for the reception area.

COMMITTEE ON MANAGEMENT

The major question before the Committee on Management during the year was to decide whether such an activity fitted into the scope of the AIEE. To this end, a very complete questionnaire was circulated to the members of the committee, and a meeting was held in New York during the Winter General Meeting. As a result of this work, the committee had a part-session at the North Eastern District Meeting, and is organizing a session for the 1951 Winter General Meeting, with a view to finding out the interest of the membership in such meetings.

It is believed that, as a result of these two sessions, the committee will be in a much better position to judge whether or not management should be a part of AIEE activities.

MEMBERSHIP COMMITTEE

Membership in the Institute increased by 3,407 members in the year ending April 30, 1949. This was a 40-per cent greater growth than 1949, and the largest on record. Previous to this period, the maximum annual increase had been 2,018 in 1946. Table II of membership statistics shows the nature of the changes in membership during the year. The substantial growth reflects both the heavy graduation of electrical engineering students from the universities and the stepped-up activity of the Membership Committee itself. Of the total applications amounting to 6,450 received during the year, 4,033 were from students, and 2,417 from others. The total applications received include those of graduates who applied last June and who were not elected to Associate membership until April 1950. There were a total of 3,347 former Student members approved at this meeting. Apparently the new plan has stimulated interest among the graduating Student members.

A further stimulation to transfer has come from the accelerated activity of the Membership Committees among the college graduates during their first year out of school.

Members in arrears for dues for the fiscal year ending April 30, 1950, reached a total of 1,510 compared with 1,376 last year. This represents a delinquency of 0.442 per cent compared with 0.448 per cent a year ago, showing slight improvement. During the year, there were 682 members dropped compared with 685 for the previous year. On the other hand, the number resigning increased from 277 to 343, but this loss of membership is to be expected due to the larger number of members.

During the year, the Membership Committee completed work on a revised "Membership Information" pamphlet, under the subcommittee chairmanship of Walter Bloomquist. The new booklet was designed for wide distribution. It gives short statements on the value of membership in the Institute and eligibility requirements. It is thought that this will be a valuable tool for Membership Committees in the future.

The Subcommittee on Survey of Student Branches under the chairmanship of J. C. Woods, co-operating with the Committee on Student Branches, submitted its final report. The purpose of this committee was to organize and undertake a survey of Student Branch membership as a function of maximum potential membership at each school, and to investigate the policies surrounding and reasons for the acceptance of local members. Since

Table III. Number of Applications Received From Student Members and From All Others

Year Ending April 30	Students	All Others	Total
1950	4,033	2,417	6,450
1949	2,286	2,192	4,478
1948	1,481	2,272	3,753
1947	938	2,331	3,269
1946	308	2,453	2,761
1945	249	2,179	2,428
1944	466	1,908	2,374
1943	783	1,431	2,214

Table IV. Number of Student Members as of April 30

Year	New Applications	Renewals	Total
1950	7,876	12,792	20,668
1949	9,967	9,461	19,428
1948	7,876	6,041	13,917
1947	5,092	3,929	9,021
1946	2,574	2,513	5,087
1945	2,326	2,287	4,613
1944	2,242	2,656	4,898
1943	2,512	3,200	5,712

Table II. Membership Statistics for Fiscal Year Ending April 30, 1950

	Honorary Members	Fellows	Members	6-Year Associates	Associates	Subtotals	Total
Membership April 30, 1949	8	1,172	8,669	8,637	12,305		30,791
Additions							
New members qualified		3	261		4,078	4,342	
Former members reinstated or re-elected			86	74	113	273	
Subtotals		3	347	74	4,191	4,615	
Transfers	1	110	491	1,575		2,177	
Totals	1	113	838	1,649	4,191	6,792	
Deductions							
Died	1	27	84	49	22	183	
Resigned			45	163	135	343	
Dropped		2	84	230	366	682	
Subtotals	1	29	213	442	523	1,208	
Transfers		1	108	411	1,657	2,177	
Totals	1	30	321	853	2,180	3,385	
Net Changes		83	517	796	2,011	3,407	
Membership April 30, 1950	8	1,255	9,186	9,433	14,316		34,198

Table V. Record of AIEE Membership

Year	Total May 1	Year	Total May 1	Year	Total May 1
1884	71	1907	4,521	1929	18,133
1885	209	1908	5,674	1930	18,003
1886	250	1909	6,400	1931	18,334
1887	314	1910	6,681	1932	18,003
1889	333	1911	7,117	1933	17,010
1890	427	1912	7,459	1934	15,230
1891	541	1913	7,654	1935	14,269
1892	615	1914	7,876	1936	14,400
1893	673	1915	8,054	1937	15,308
1894	800	1916	8,202	1938	16,078
1895	944	1917	8,710	1939	16,605
1896	1,035	1918	9,282	1940	17,213
1897	1,073	1919	10,352	1941	17,886
1898	1,098	1920	11,345	1942	18,944
1899	1,133	1921	13,215	1943	20,161
1900	1,183	1922	14,263	1944	21,407
1901	1,260	1923	15,298	1945	23,072
1902	1,549	1924	16,455	1946	25,090
1903	2,229	1925	17,319	1947	26,470
1904	3,027	1926	18,158	1948	28,408
1905	3,460	1927	18,344	1949	30,791
1906	3,870	1928	18,265	1950	34,198

the Student members are the most important source of new Institute members, it was thought that maximum effort should be exerted in this field. It has been recommended that the Committee on Student Branches take an active interest in this subject and develop a uniform method of membership practices in the universities, which will stimulate student activities.

The committee wishes to commend the excellent co-operation and sincere efforts of the Section Membership Chairmen throughout the year. The increase in applications from other than Student members attests to the fact that they have been extremely active. The District Vice-Chairmen have increased their contact with the local Section Chairmen substantially, and this new method is also proving highly effective. The tremendous growth of the Institute indicates that sights should be raised above those of the past and serious consideration given to the day not far ahead when a membership of 50,000 will be reached.

COMMITTEE ON PLANNING AND CO-ORDINATION

The committee held its usual number of meetings during the year, each preceding by a few days a Board of Directors meeting.

Scheduling of Future Meetings. The future general and District meetings of the Institute have been scheduled up to and including 1952. The attempt to obtain spacing between District meetings, even though these are held in widely separated parts of the United States, has been continued. Consideration was given to respacing the general meetings with particular attention to the Fall and Winter General Meetings. After thorough study, however, the committee was convinced that the present procedure provides the best general schedule. With the assistance of the Technical Program Committee, an attempt is being made to swing papers from both the Summer and Winter General Meetings into the Fall General Meeting. A growing number of technical conferences is being arranged for and co-ordinated through the proper technical committees.

Registration Fees. The matter of registration fees to be charged at general and District meetings has been subjected to continuing review. There has been general acceptance of the present method and no change is contemplated.

Technical Activities. With the recommendation for the establishment of the Technical Advisory Committee, the Technical Activities Subcommittee, active since Dr. Wickenden's administration, will be discestablished.

Ex Officio Assignments. After a study of the large number of ex officio assignments which have grown up under the existing Bylaws, the committee has recommended the dropping of all such assignments in the Bylaws. This will tend to relieve the burden on some of the key committee positions and to distribute in more balanced fashion and to a greater number of members the administrative work of the Institute. As an instance, the Committee on Award of Institute Prizes, whose chairman in the past had been the Chairman of the Technical Program Committee, has been divorced completely from this ex officio relationship, and in the coming year will operate with a group of members who, while appointed from the technical committees, are not rigidly held to an ex officio group. Many other similar simplifications are in the process of being made.

Changes in District Setup. The study of redistricting done by the committee four years ago was brought out and re-examined with a recommendation for no change in the immediate future.

Emblem. Various suggestions as to special emblems to recognize specific offices and for change in design of the present emblem were reviewed, with the recommendation that the emblem design and procedure remain as at present.

PUBLICATION COMMITTEE

The publication services of the Institute can be divided into five broad classifications: *Electrical Engineering, Transactions, Proceedings,* Advance Pamphlet Copies of papers to be presented at meetings, and Special Publications. Provision for these publications was made in the policy which became effective January 1, 1947. The number of pages of published material for the calendar year

Table VI. Deaths of AIEE Members Reported in Electrical Engineering

Name	Date of Election	Date of Death	Grade at Death	Obituary Notice in Electrical Engineering
Appleyard, Arthur E.	A '96		M	June '49, p. 553
Atkins, David F.	A '07	Jan. 8, '49	M	Dec. '49, p. 1108
Austin, Eugene H.	M '42	Sept. 13, '49	M	Feb. '50, p. 177
Avery, Morton B.	M '24	Jan. 26, '50	M	May '50, p. 473
Bacon, Frank R.	A '10	Oct. 6, '49	M	Dec. '49, p. 1108
Ballantyne, William M.	A '21	Aug. 29, '49	M	Nov. '49, p. 1009
Barron, Jacob T.	A '07	Mar. 12, '50	F	May '50, p. 472
Bascom, Henry M.	M '19	Mar. 14, '50	F	May '50, p. 472
Berthold, Martin	A '08	Oct. 16, '49	M	Dec. '49, p. 1109
Blake, Samuel H.	A '03	Aug. 24, '48	F	Jan. '50, p. 87
Bogan, Louis E.	A '99	Dec. 3, '49	F	Feb. '50, p. 176
Bollaert, Remi	A '38	Dec. 2, '49	M	Feb. '50, p. 176
Borch, Frederik	A '08	Aug. 15, '49	F	Nov. '49, p. 1009
Brinckerhoff, Henry M.	A '96	Oct. 12, '49	M	Dec. '49, p. 1108
Brown, Jr., Charles E.	A '40	Nov. 8, '49	A	Jan. '50, p. 87
Burton, Paul G.	A '95	Nov. 14, '49	F	Mar. '50, p. 282
Clausen, Henry P.	A '03	Dec. 20, '49	M	Mar. '50, p. 283
Cluff, T. Walker	M '37	Nov. 6, '49	M	Jan. '50, p. 87
Collett, Charles O.	A '07	Oct. 15, '49	M	Jan. '50, p. 87
Creaghead, Thomas J.	A '93	Mar. 4, '50	A	May '50, p. 472
Dann, Norman L.	A '17	Oct. 27, '49	A	Jan. '50, p. 88
Dean, Samuel M.	A '25	May 31, '49	F	Aug. '49, p. 708
DeForest, Cornelius W.	A '07	Nov. 17, '49	F	Feb. '50, p. 176
Dickinson, William N.	F '35	Jan. 26, '50	F	Mar. '50, p. 379
Diederich, Peter	A '24	Nov. 1, '49	F	Jan. '50, p. 88
Doonan, Joseph J.	M '33	May 21, '49	M	Aug. '49, p. 709
Dutland, Rudolph	A '23	Nov. 8, '49	M	Feb. '50, p. 176
Dunn, John F.	A '07	Jan. 12, '50	M	May '50, p. 472
Ekern, Emil A.	A '04	Jan. 3, '50	M	May '50, p. 472
Ely, Robert B.	A '41	July 6, '49	A	Dec. '49, p. 1108
Ferguson, James W.	A '40	Jan. 3, '50	A	Mar. '50, p. 283
Ferguson, Samuel	A '02	Feb. 10, '50	A	May '50, p. 472
Finkle, Frederick C.	A '08	Apr. 7, '49	A	July '49, p. 638
Finlaw, John	A '35	Nov. 8, '49	A	Feb. '50, p. 177
Fish, Fred A.	A '00	May 20, '49	F	Sept. '49, p. 820
Flanders, Charles K.	A '19	Jan. 11, '50	M	May '50, p. 473
Goodman, Lynn S.	A '11	July 27, '49	M	Oct. '49, p. 903
Gustink, Norman J.	A '28	Mar. 21, '49	A	July '49, p. 638
Hall, Harry C.	A '01	June 20, '49	M	Oct. '49, p. 903
Hallenbeck, Charles S.	A '21	Jan. 2, '50	M	May '50, p. 473
Hodgkinson, Francis	A '02	Nov. 4, '49	A	Jan. '50, p. 86
Hoffman, William L.	M '41	Feb. 7, '49	M	June '49, p. 553
Jewett, Frank B.	A '03	Nov. 18, '49	F	Jan. '50, p. 86
Kearney, Sr., James R.	M '25	Oct. 4, '49	M	Jan. '50, p. 88
Kifer, Edwin H.	A '09	Apr. 14, '49	F	July '49, p. 638
Kuester, Albert J.	A '46	Feb. 22, '49	A	June '49, p. 553
Lawrence, William H.	A '99	Aug. 8, '49	M	Nov. '49, p. 1009
Lee, Jr., Addison W.	A '08	May 1, '49	M	July '49, p. 638
Leland, Cyrus A.	M '27	May 25, '49	F	Aug. '49, p. 708
Magraw, Lester A.	A '07	Mar. 25, '49	M	June '49, p. 553
Matthews, Howard D.	M '42	Feb. 28, '50	F	May '50, p. 472
Meyer, Grover C.	M '44	June 2, '49	M	Sept. '49, p. 820
Millar, Preston S.	A '03	June 17, '49	M	Sept. '49, p. 819
Morse, George H.	F '22	June 1, '49	F	Sept. '49, p. 819
Munor, Cecil M.	A '16	July 6, '49	A	Oct. '49, p. 904
Murphy, John	A '00	Sept. 23, '49	F	Dec. '49, p. 1108
McAfferty, Herbert G.	A '36	Nov. 16, '49	A	Feb. '50, p. 177
McDermott, Franklin P.	A '07	Oct. 31, '49	A	Jan. '50, p. 88
McKenzie, Daniel A.	A '15		M	Feb. '50, p. 177
Price, Harold W.	A '03	Feb. 14, '50	M	May '50, p. 473
Rea, Norman L.	A '02	May 10, '49	A	Sept. '49, p. 819
Rice, Ivan S.	A '27	Aug. 11, '49	M	Dec. '49, p. 1109
Rogers, Fred A.	A '06	Mar. 18, '49	M	July '49, p. 638
Roper, Denny W.	A '93	Oct. 5, '49	F	Jan. '50, p. 86
Ross, William E.	M '38	May 5, '49	M	Aug. '49, p. 708
Ryan, John J.	M '23	Jan. 29, '50	M	Mar. '50, p. 282
Scarlett, Farrell M.	A '47	May 6, '49	A	July '49, p. 639
Schweitzer, E. O.	A '99	Sept. 22, '49	F	Dec. '49, p. 1108
Sisson, Charles E.	A '19		F	Feb. '50, p. 176
Smith, Walter E.	A '00	Apr. 21, '49	A	July '49, p. 639
Stearns, William G.	A '35	Jan. 3, '50	A	Mar. '50, p. 283
Stoddard, Raymond R.	A '38	June 16, '49	A	Sept. '49, p. 820
Stubbs, Walter W.	A '26	Apr. 12, '49	M	July '49, p. 638
Thorpe, John E. S.	A '06	Feb. 24, '50	M	May '50, p. 472
Tracy, Joseph H.	A '08	Mar. 15, '49	M	June '49, p. 553
Val Davies, Arthur E.	A '21	July 6, '49	A	Oct. '49, p. 903
Vaughan, Eleaser A.	M '22	July 10, '49	M	Oct. '49, p. 904
Wallace, Ross S.	A '44	Aug. 28, '49	A	Nov. '49, p. 1009
Walsh, Frank	A '26	Jan. 27, '50	M	Mar. '50, p. 282
Ware, John S.	M '21	Apr. 23, '49	F	July '49, p. 638
Washington, Lee S.	A '19	Apr. 9, '49	A	Aug. '49, p. 708
Watson, Frank C.	M '23	Sept. 2, '49	M	Nov. '49, p. 1009
Woods, Joseph E.	M '48	Sept. 18, '49	M	Dec. '49, p. 1108
Woodward, Clifford D.	A '09	Oct. 26, '49	A	Jan. '50, p. 88
Wotherspoon, Henry H.	A '28	Apr. 5, '49	M	July '49, p. 638
Yarnall, Joseph H.	M '19	June 5, '49	F	Sept. '49, p. 820
Young, James W.	A '03	Feb. 1, '50	M	Mar. '50, p. 283
Zimmer, Albert R.	A '12	Nov. 11, '49	M	Feb. '50, p. 177

1950 is shown in Table VII, together with the number of pages published in preceding years for ready comparison.

Electrical Engineering. Efforts have been made to keep the quality of publication on a high standard by not republishing material which has been published previously elsewhere. In Table VIII, a classification of articles in seven broad fields is presented. The tabulation shows a substantial increase in the number of general interest articles, as well as the number of communication articles. In the future, attempts will be made to increase the number of articles in the fields of industry and general applications to bring these fields more nearly in proportion to the interests of the members.

The practice of publishing a series of essays by well-known authorities, which present a statement of a problem one month, followed by the solution the succeeding month, has met with popular response. The activity has met with favor particularly in the field of education.

The circulation of *Electrical Engineering* has steadily increased with the growth in membership and number of Student members with an all-time high of 58,000 copies of the December issue and an average circulation of 53,825 copies for the year 1949, as compared with 47,800 copies for the year 1948.

Advertising. The number of pages of advertising is about the same as it was a year ago. By the end of the appropriation year, the gross revenue and the net revenue will be larger than they were for the preceding year because all contracts will have been in effect for the entire year at the increased rates which became effective February 1, 1948.

Transactions. Volume 68 of the 1949 *Transactions* has been made available in two parts. Part 1, which contains the papers presented during the first half of the year consisting of 800 pages, was made available for distribution November 15. Part 2, including the papers which were presented during the last half of the year, the Board of Directors' Report, and a complete index comprising 644 pages, was made available for distribution on March 27. This is a month and two months sooner than the corresponding parts were made available for the previous year.

AIEE Proceedings. During the year there has been a substantial increase in the number of *Proceedings* papers ordered and distributed. A total of 7,709 orders were received as compared with 6,295 orders during the preceding year. This represents a $22^1/_2$-per cent increase in the total number of orders received and represents a distribution of 55,826 copies of papers. When it is considered that there were 202 papers available this year as compared with 247 during the preceding year, the percentage increase on the basis of the number of orders received per paper is even greater, or 47.6-per cent. The increase is attributed to the publication of a reference on the cover of *Electrical Engineering* to the location of the *Proceedings* order form in the advertising section. Most of the copies ordered are for the 10-per cent free allowance and the total receipts were $945.70 as compared with $644.00 during the preceding year.

The *Proceedings* are an interim service to members and Student members only who fill out order forms published in *Electrical Engineering* every few months. In the case of members, there is a 10-per cent free allowance; but in the case of Student members, there is no free allowance.

Table VII. Numbers of Pages of Published Material

Year	Electrical Engineering: Technical Articles	Electrical Engineering: News	Electrical Engineering: Transactions Sections	Transactions Only: Technical Papers	Transactions Only: Discussions	Transactions Only: Total
1941	337	281	600	542	268	2,028
1944	246	214	738	493	231	1,922
1945	255	225	736	121	143	1,480
1946	285	315	832	254	120	1,806
1947	806	474		1,600*	153*	3,033
1948	832	395		1,643†	172†	3,042
1949	796	320		1,275‡	167‡	2,558

* Preprinted in 227 sections of *AIEE Proceedings*, except for a 17-page technical paper in *Electrical Engineering*.

† Preprinted in 247 sections of *AIEE Proceedings* requiring a total of 2,090 pages.

‡ Preprinted in 202 sections of *AIEE Proceedings* requiring a total of 1,795 pages.

Table VIII. Classification of Articles in Electrical Engineering in Seven Broad Fields

	May	June	July	Aug.	Sept.	Oct.	Nov.	Dec.	Jan.	Feb.	Mar.	April	Total
General interest	1		1	2	2	3	2	2	1	2	4	2	22
Educational	1	1	1	1			1	1	1	1	1		9
Science and electronics	2	2	1	1	1	1	4	3	3	2	2	3	25
Communication	3	2	1	1	2	1	1	2		3	3	1	20
Power	2	2	1	2	2	3	3	1	2	3	3	4	28
Industry			3	1	1		1	1		1		2	10
General applications		1	2			1	1						5
	9	8	10	8	8	9	13	10	7	12	13	12	119

Special Publications. During the year, the following ten special publications have been made available and ten more are in prospect. The editorial staff has been enlarged to handle the increased number of these publications. They fill a specialized need and some are used for educational purposes. The special publications are on a self-supporting basis and they are made available to members at cost and in general to nonmembers at double cost through order forms published in *Electrical Engineering* from time to time. In the future, sale prices are to include the cost of editorial time.

1. Electric Arc Resistance Welding* (5/49).
2. Mathematics for Engineers (7/49).
3. Industrial Application of Electron Tubes* (9/49).
4. Interior Wiring Design for Commercial Buildings (10/49).
5. Automatic Contouring Control of Machine Tools (10/49).
6. Electrical Engineering Problems in the Rubber and Plastics Industries* (12/49).
7. Bibliography on Rotating Machinery (1/50).
8. Symposium on Electrical Properties of Semiconductors and the Transistor (1/50).
9. Bibliography on Electronic Power Converters (1/50).
10. Electronic Instrumentation in Nucleonics and Medicine* (4/50).

Advance Copies of Papers. The practice of making technical papers approved for presentation at meetings available in advance copy pamphlet form by a photolithographic process has been continued. The few of the papers which are not of permanent record value have been made available as miscellaneous papers known as (ACO) "Advance Copy Only." Advance copies of papers are intended primarily for discussion purposes with a free allowance of ten copies to authors and 50 copies to the sponsoring committee. The other copies are sold to members at a price of 30 cents each and to nonmembers at a price of 60 cents each. The activity is nearly on a self-supporting basis.

* AIEE Conference Report.

Cumulative Index, 1939–1949. Work is well under way on an 11-year cumulative index to the *Transactions*, thus completing the series of cumulative indexes to the *Transactions* since the founding of the Institute in 1884. The index is expected to be made available the latter part of June or early in the summer and it is estimated that it will sell at a price of $2.50 per copy.

Special Subcommittee. A Special Subcommittee has been appointed to consider publication policy in relation to the following suggestions received: The view was expressed that the present publication policy was inadequate to command the loyalty of young but brilliant men electrically trained who are doing frontier work in the electrical sciences in the newer phases of electrical engineering closely related to electronics. Another suggestion received was to the effect that the publication policy to publish 1-page digests of all technical papers in *Electrical Engineering* should be abandoned in favor of briefer abstracts of eight or ten lines, to permit more space to be devoted to the treatment of papers in full. These suggestions are being given thorough consideration and study.

COMMITTEE ON PUBLIC RELATIONS

This year has marked the beginning of a strengthened public relations program for the Institute. Following authorization by the Board of Directors of a modest budget for this purpose, the committee on September 1, 1949, engaged the services of Raymond C.

Mayer to serve as Public Relations Counsel. The Mayer organization is thoroughly familiar with Institute affairs, having publicized several Winter General Meetings in New York and prepared the "publicity kit" which was distributed to Section officers in the spring of 1949, and has since been augmented.

It is the aim of the committee and of its counsel to treat the Institute's public relations as a continuing and integrated program rather than as a series of sporadic efforts centered about the Winter General Meeting. So far as is possible, all important Institute meetings are being given complete news coverage on papers, awards, and other items that show any promise of interesting the general public.

For the Fall General Meeting, 72 papers were examined, and 19 press releases issued. The releases were prepared by the Mayer organization and issued in the Cincinnati area through the AIEE publicity chairman. Releases to national periodicals, press services, trade papers, and others are sent out directly from New York. The same procedure was followed for the North Eastern District Meeting and will be continued for the meetings in Pasadena, Baltimore, Oklahoma City, and elsewhere. Institute technical conferences and a number of the Section meetings are also being systematically publicized.

The publicity kit, giving a large amount of instruction and sample material for local use, supplied to Section Chairmen and publicity officers, has been favorably received. New material for the kit is being distributed on a continuing basis; it includes sample radio programs and general instructions for conducting radio and television programs.

At the Winter General Meeting, a fully equipped and well staffed press room was maintained at the Hotel Statler. A large number of newspaper writers and photographers were given assistance, and 54 releases on technical papers and special addresses and awards were issued. At the suggestion of the committee, the general session was held on the opening day. This aroused an immediate interest in the meeting on the part of newspaper men, an interest which continued throughout the week. The committee also assisted in the preparation of a television exhibit which formed an attractive feature of the meeting.

Assistance has been given to several Sections and to other Institute groups confronted with special problems in their local fields or dealing with special areas of work.

In general the year's activities represent considerable progress in carrying forward the public relations policy established by the Board of Directors. The committee thinks this is on the right track and further progress is to be expected. This program will aid materially in promoting adequate recognition of the work of the Institute and of engineers.

COMMITTEE ON REGISTRATION OF ENGINEERS

The committee has continued its efforts to advise the AIEE membership on the problems of registration.

The committee held a meeting at the Winter General Meeting, with practically the entire membership in attendance.

Previously this committee had arranged for the publication of a paper entitled "Registered Professional Engineers," by R. W. Sorensen and A. H. Lovell. This paper appeared in the August 1949 issue of *Electrical Engineering*. This committee has advised the Student Branches and Sections that this paper is available at headquarters for their use, and has further suggested that it be used as a basis for discussion at local meetings.

It is planned to follow the Sorensen–Lovell paper with two other papers, each covering a particular phase of registration. These are to be published in *Electrical Engineering* in the near future. Reprints of these papers will also be made available at Headquarters.

At the request of the committee, the Board of Directors approved the plan of indicating in the Year Book the AIEE members who are registered professional engineers. This will start with the 1950 edition.

COMMITTEE ON RESEARCH

The Committee on Research sponsored jointly with the Committee on Basic Sciences a symposium on dielectrics. Seven speakers presented various phases of the subject very effectively. Attendance at each of the two sessions exceeded 200.

Plans for sponsoring a symposium on a new and interesting subject are now being formulated for the 1951 Winter General Meeting.

SECTIONS COMMITTEE

Section Activities. Two new Sections, Oak Ridge and Northeastern Michigan, were formed, and applications for two more, Sacramento and Saginaw Valley, are pending.

New Subsections were formed as follows: Eastern Shore, Maryland Section; Mobile-Pensacola, Alabama Section; Ridgway, Erie Section; St. Lawrence International, Syracuse Section; Savannah, Georgia Section; Tacoma, Seattle Section; West Michigan, Michigan Section.

The following additional Subsections are pending: Columbus, Ga.; Boise, Idaho; Alaska; Evansville, Ind.; Grand Rapids, Mich.; Sioux City, Iowa; Finley, Ohio; and Youngstown, Ohio.

Section, Subsection, and membership development has been very active and healthy, as noted above and as shown in Table IX.

The Vancouver Section which has been a part of District 10 has been transferred to District 9, but provision has been made for a yearly visit by the Vice-President of District 10.

Prize Award Rules. A revision of the Institute Prize Paper Rules was prepared by a subcommittee of the Sections Committee, and approved by the Board of Directors, and is now in effect.

Meetings of the Sections Committee. A meeting of the Sections Committee was held during the Winter General Meeting. Two meetings are scheduled for Section delegates during the Summer and Pacific General Meeting.

Section Finances. A subcommittee of the Sections Committee, under the chairmanship of G. W. Bower, has made a progress report on its survey and study of the problem of Section finances for the next 5-year period, which indicates that in general the Sections are getting along fairly well with their present allotments, and should be able to get along for the next few years without an increase. This subcommittee will continue the study and co-operate with the Sections in an endeavor to make this possible.

Survey of Membership Opinion on Institute Policies. At the request of M. D. Hooven, Chairman of a special committee appointed by the Board of Directors to obtain the opinion of the members on the Institute's future policy, a very thorough survey was conducted by the Sections. On the basis of some 9,000 votes, the Board of Directors came to the following conclusions:

1. To work continually for the unification of the profession.
2. To recognize the fact that the Institute finds its chief reason for existence in the technical field.
3. To handle questions on nontechnical affairs as necessary, and as they arise, on an emergency basis, until through unification they can be handled on a general professional basis.

Special Activities. A subcommittee has been appointed to revise the present suggested Bylaws for Sections, not only to bring them up to date to incorporate operation of Subsections, but also to emphasize the desirability of training officers by giving them a sequence of positions, and also simplifying the method of nominating candidates so as to obtain the best officer material.

Possible District boundary changes of one or two Districts are also under present consideration.

General Conclusions. The rate of membership growth is probably the best indication of active and effective Section operation. The recent change in the method of contacting graduating students should show a higher percentage of new members from that source. In general, the rate of growth in members for the next year is expected to be even higher than during 1949–50.

STANDARDS COMMITTEE

During the year, a number of steps in reorganizing Standards Committee activities have been accomplished.

The Standards Manual was revised and approved by the Board of Directors; the President of the Canadian National Committee of the International Electrotechnical Commission was made an ex-officio member of the Standards Committee; a liaison representative from Mexico was appointed to the Standards Committee; and a successful and satisfactory year has been enjoyed under the services of the new committee Secretary, J. J. Anderson, Jr., for whom the current year marks the first full year under his very capable surveillance.

In the field of Standards and Codes, the following were completed or revised during the year: AIEE *550*, "Master Test Code for Resistance Measurement"; *C37.1*, "Relays Associated With Electric Power Apparatus"; AIEE *43*, "Recommended Practice for Testing Insulation Resistance of Rotating Machinery"; *C57.15*, "Step Voltage and Induction Voltage Regulators"; a "Recommended Practice for Minimization of Interference From Radio-Frequency Heating Equipment"; AIEE *22*, "Air Switches, Insulator Units, and Bus Supports"; AIEE *57*, "Guiding Principles for Dielectric Tests"; AIEE *18*, "Capacitors"; AIEE *50*, "Automatic Circuit Reclosers for A-C Distribution Systems." The following were submitted to the Standards Committee and have been approved subject

to certain minor revisions which were referred back to their respective committees: AIEE *16*, "Electric Control Apparatus for Land Transportation Vehicles;" "Test Code for Aircraft Circuit Interrupting Devices."

Further action in connection with two other Standards has become necessary. For Standard *C55*, "Capacitors," for which AIEE is sponsor, a new ASA sectional committee is being organized to permit accomplishing adoption of this Standard as an American Standard. For Standard *C62.1*, "Valve and Expulsion-Type Lightning Arresters," Sectional Committee *C62*, for which AIEE is also sponsor, is being reactivated.

Another responsibility delegated to the Standards Committee by the Board of Directors this year is that of appointing representatives to the Electrical Section of the National Fire Protection Association. This step became a logical one since the AIEE interest in the Electrical Section of the NFPA is principally that occasioned by its responsibility for the National Electrical Code.

Co-operating with the ASA in a very appropriate effort to bring magnet wire into one sectional committee of ASA and all other wire—copper and aluminum alike—into one sectional committee, the Standards Committee withdrew AIEE sponsorship of the *C11* Sectional Committee on Hard Drawn Aluminum Conductors, in order that its scope might be combined with the Sectional Committee *H4* on Specifications for Copper Wire in a new sectional committee, *C7*, having for its scope: specifications for metallic conductors made of wire, whether for use in uninsulated form or for subsequent use in making insulated or covered cable.

The AIEE is, of course, represented on both the *C9* and *C7* sectional committees of ASA.

Recognition should be extended to the retirement of a number of AIEE representatives on various ASA sectional committees where noteworthy service had been rendered for many years in behalf of the Institute and the cause of voluntary standardization in the United States.

Special mention should be made noting the retirement of C. A. Powel, Past President of the Institute and Chairman of Standards Co-ordinating Committee Number 2, and of V. M. Montsinger, Chairman of Standards Co-ordinating Committee Number 3, past Chairman of the Standards Committee, and for many years past a most ardent worker in behalf of standardization both within the Institute and in ASA.

UNITED STATES NATIONAL COMMITTEE OF INTERNATIONAL ELECTROTECHNICAL COMMISSION

Dr. H. S. Osborne, Chief Engineer of the American Telephone and Telegraph Company, and heretofore, Senior Vice-President of the United States National Committee of the International Electrotechnical Commission, was elected President of the United States National Committee to succeed the late L. F. Adams. Dr. Osborne began his term of office in May 1949.

The year was an active one for the IEC, meetings of advisory committees being held as follows:

Advisory Committee 1—Nomenclature, Stresa, Italy, June.

Subcommittee 5A of Advisory Committee 5—Turbo-Alternator Sets, Brussels, September.

Advisory Committee 8—Standard Voltages and Currents, Stresa, June.

Advisory Committee 10—Insulating Oils, Stresa, June.

Advisory Committee 17—Switchgear, Stresa, June.

Advisory Committee 22—Electronic Devices, Stresa, June.

A.C. 28—Co-ordination of Insulation, Stresa, June.

A.C. 31—Flameproof Enclosures, Paris, November.

Subcommittee 34A of Advisory Committee 34—Lamps, London, July, and Paris, November.

Experts Preparatory Committee on Subcommittee 34B of Advisory Committee 34—Lamp Caps and Holders, Paris, November.

Advisory Committee 32—Fuses, Paris, May.

Committee of Action, Stresa, June.

Council, Stresa, June.

The group of meetings at Stresa was attended by 168 representatives of 14 countries, including a delegation of six from the United States, headed by Dr. Osborne.

At the meeting of the Council, Dr. Max Schiesser, Managing Director of the Brown-Boveri Company, was elected President of the International Electrotechnical Commission in place of E. M. Uytborck of Belgium, whose term had expired. Also at the Council meeting the revision of the Statutes and Rules of Procedure, which had been worked on for several years, was approved and declared in effect as of June 1949. These statutes and rules of procedure bring up to date fundamental documents of the IEC so that they should be a better guide to the orderly and systematic conduct of the work. At the meeting of the Council, attention was also given to the finances of the IEC by a Subcommittee on Finances which came to agreements which should place the finances on a sounder basis.

Technical progress was made in the committees which met during the year. A "Recommendation on Lamp Caps and Holders Together With Gauges for the Control of Interchangeability of Lamps" is approaching completion as an international recommendation.

During 1949, the United States National Committee initiated a review of all of the 35 technical projects of the IEC to determine whether or not those in the United States who are most directly concerned with the subject matter of each project are interested in continued participation of the United States in the work. In the past, the USNC has been represented on all these committees. In the review thus far, it has been decided that the USNC will continue participation in 20 projects, and discontinue participation in two projects. It is also concluded that the United States should relinquish one secretariat, though keeping membership on the committee. Thirteen projects remain to be studied to arrive at a decision on continued participation.

A group of 13 technical committee meetings and the Committee of Action will be held in Paris and London in July 1950. These meetings are as follows:

Advisory Committee 3—Graphical Symbols, Paris, July.

Advisory Committee 5—Steam Turbines, London, July.

Advisory Committee 12—Radio Communication, Paris, July.

Advisory Committee 17—Switchgear, Paris, July.

Advisory Committee 23—Electrical Accessories, Paris, July.

Advisory Committee 24—Electric and Magnetic Magnitudes, and Units, Paris, July.

Advisory Committee 25—Letter Symbols, Paris, July.

Advisory Committee 28—Co-ordination of Insulation, Paris, July.

Advisory Committee 32—Fuses, Paris, July.

Advisory Committee 33—Power Capacitors, Paris, July.

Advisory Committee 34A—Lamps, Paris, July.

Advisory Committee 35—Dry Cells and Batteries, Paris, July.

Committee of Action, Paris, July.

International Special Committee on Radio Interference (CISPR), July.

A strong delegation of American representatives will attend this group of meetings.

The work of the IEC continues to expand in scope and in interest to the electrical industry in the United States.

UNITED STATES NATIONAL COMMITTEE OF THE INTERNATIONAL COMMISSION OF ILLUMINATION

The ICI is an international organization of those interested in illumination. It is composed of national committees, representing most of the important countries of the world. Each nation may organize its own committee in any way that it sees fit, so long as it is truly representative of the country. The United States National Committee consists of some 40 persons from the following groups:

AIEE
Association of Edison Illuminating Companies
Illuminating Engineering Society
Optical Society of America
Society of Automotive Engineers
Society of Motion Picture Engineers
Members at large
Delegates to previous conventions

Most of the work of the ICI is carried on through some 25 committees to which the national committee appoints a representative. So far as possible, the work of these committees is handled by correspondence, and they report at the ICI meetings which are normally held once in three years. The next meeting will be in Stockholm in June 1951. At present, the secretariats for four of these committees are in the United States. They are: Colorimetry; Lighting of Public Ways; Lighting Practice (Interior); and Television Lighting. The United States National Committee also has a representative on each of the other 21 committees, and in addition the committee is also planning to offer four technical papers for the next conference.

At the general meeting held in Paris in 1948, the Central Bureau of the ICI previously located in England was moved to the United States. Carl A. Atherton, Member AIEE, is the Honorary Secretary. There is a fair possibility that the 1954 conference will be held in America. If this does take place, the work of arranging for it will fall largely on the United States National Committee. The attendance at Paris in 1948 consisted of approximately 200 delegates plus guests.

The work of the committees and of the Triennial Conference ICI are deemed to be very worth while, furnishing as they do an opportunity for experts from various countries to exchange data and views, and thereby promote the science and art of illumination. The International Commission on Illumination is the only international lighting organization.

COMMITTEE ON STUDENT BRANCHES

The Committee on Student Branches has studied and recommended to the Committee on Constitution and Bylaws changes in several sections of the Bylaws relating to Student

members, Student Branches and Joint Student Branches, Branch Counselors, the District Committees on Student Activities, and the Committee on Student Branches. The proposed changes are intended to clarify certain points regarding Student membership and to include the Chairmen of the District Committees on Student Activities as appointed members of the Committee on Student Branches, and also adjust the times for nominating and appointing Counselors and electing the Chairmen of the District Committees on Student Activities. The latter will enable the President-elect to appoint the members of the Committee on Student Branches at the same time other committee appointments are made. The proposal regarding the membership of the committee was approved in principle by the Board of Directors on June 23, 1949.

A subcommittee of the Committee on Student Branches has investigated the desirability of making an annual Branch award for outstanding student activity and has made the following recommendations:

1. That the AIEE make available a certificate of award to be given annually to one member of each Student Branch.

2. The certificate shall be awarded to the Branch member who has demonstrated the most outstanding Branch activities, particularly in the preparation or presentation of Branch, Section, or District papers, but with due consideration given to committee work, news publications of the Branch, co-operation with local Section, and so forth.

3. The recipient shall be selected by a committee of three consisting of the Counselor of the Branch and two Branch members appointed by the Chairman of the Branch.

4. The certificate shall be signed by national officers only—the President and the Secretary.

The committee recommended that the report be accepted as a progress report, and circulated to the full Committee on Student Branches for study and comments. Action will be taken on the subcommittee's recommendation at the June meeting of the committee.

With the authorization of the Board of Directors, the Chairman participated in two meetings of an "Inter-Society Conference on Engineering Student Chapters" on September 12, 1949, and January 27, 1950. These conferences were sponsored by the American Society of Civil Engineers, and were participated in by the following societies: American Road Builders' Association, American Institute of Chemical Engineers, AIEE, American Institute of Mining and Metallurgical Engineers, American Society of Civil Engineers, American Society for Engineering Education, American Society of Mechanical Engineers, National Society of Professional Engineers, and Society of Automotive Engineers. The purpose of these conferences was to obtain an exchange of ideas and views regarding the operation and objectives of Student Branches and Chapters. The first meeting was exploratory, and the second meeting took the action and made the recommendations that follow:

Action Taken

Recommendations of this conference upon release shall be referred to the respective societies for consideration by their committees on student activities or student chapters.

Recommendations of this conference shall be presented to the Engineers' Joint Council for the information of the Committee on Unity of the Engineering Profession, with the request that a new committee of EJC be set up for special consideration of problems of student organization.

Table IX. Section and Branch Statistics

	For Fiscal Year Ending April 30					
	1945	1946	1947	1948	1949	1950
Sections						
Number of Sections	73	75	75	81	84	87
Number of meetings held	884	1,210	1,333	1,340	1,561	1,605
Total attendance	96,346	113,531	155,649	109,637	128,025	135,847
Branches						
Number of Branches	125	125	126	127	129	130
Number of meetings held	547	716	1,018	1,172	1,350	1,298
Total attendance	17,132	22,844	40,669	77,040	103,828	80,672

Recommendations Agreed Upon

1. That student engineering organizations should be utilized to promote unity and professional consciousness among the students.

2. That at each college which does not have some organized co-ordination of engineering student groups there be formed a council or local society to advise and co-ordinate such groups.

3. That new engineering student activities be carried on by expansion and co-ordination within existing groups so far as practicable.

4. That there be prepared a set of general recommended principles regarding operation of engineering student societies for the guidance of college administrators.

5. That there be formulated a program of typical desirable activities for student engineering groups.

6. That student members of all approved student engineering groups be considered eligible upon graduation for membership in the national engineering organizations, without payment of an admission fee.

The report of the surveys of Student Branch membership as a function of maximum potential membership in each school has been transmitted to the Counselors of all Branches for their information and guidance. This report was prepared by the joint subcommittee of the Membership, Sections, and Student Branches Committees organized last year.

The committee held two meetings, one in Swampscott, Mass., on June 20, 1949, and the other in New York, N. Y., on January 30, 1950.

The Student Branches now number 130, of which 30 are Joint Branches with the Institute of Radio Engineers. The Student membership as of March 27, 1950, was 20,050.

TECHNICAL PROGRAM COMMITTEE

Technical activity in the AIEE, as evidenced by the presentation and publication of technical papers, has continued at a very high level, just under the record set by the previous year. This intense activity has occasioned some congestion, especially at the Winter General Meeting, where there were 58 technical sessions. There has also been a considerable increase in conference-type papers.

The Technical Program Committee has adopted a plan of operation through an Executive Committee composed of the Division Advisors and the appointed members of the Technical Program Committee. This Executive Committee is giving careful consideration to the trend toward conference papers and crowding at some general meetings. It is hoped that a better distribution of technical papers and sessions among the general meetings may be attained.

The effort to plan the program activities on an annual basis has succeeded very well through the co-operation of the technical committee chairmen and the Division Advisors. The preliminary estimates of sessions and papers have been surprisingly accurate, and are very helpful in guiding the Technical Program Committee.

Table X gives a summary of the programs for the year.

COMMITTEE ON TRANSFERS

Activities of the past two years have culminated this year in the preparation of an Operations Guide called "Transfers" and a Publicity Pamphlet entitled "Why Transfer?" both for use by Section Committees on Transfers. As of April 30, these pamphlets were in the final draft form ready for submission to the Board of Examiners and the Board of Directors for approval, following which they will be published.

The recommended Operations Guide officially presents a new conception of Section transfers work, including the development of uniform methods of procedure for guidance of the Section committees. The Publicity Pamphlet as recommended presents reasons why advancement to the higher grades should be of interest to members.

A report on results of the questionnaire sent to Section Committees on Transfers under date of March 18, 1949, consolidated with returns from the questionnaire dated March 22, 1948, was presented to the Committee on Transfers at its meeting in Swampscott, Mass., on June 22, 1949.

The main purpose of issuing the 1949 questionnaire was: to secure information for use in developing a manual of recommended

Table X. Number of Papers Presented During the Year Ending April 30, 1950

Meeting	District	Advance Copy Only	Conference Papers	Transactions	Total	Attendance
Summer, Swampscott	10	60	63	133	1,650
Pacific, San Francisco	10	36	17	63	878
Fall, Cincinnati	22	52	50	124	1,045
Winter, New York	14	137	92	243	3,218
North Eastern, Providence	18	2	14	34	502
Total	18	58	285	236	597	7,293

over-all transfers procedure; to reveal the present extent and nature of Section transfers activities throughout the Institute.

Replies to the 1949 questionnaire were received from 57 per cent of the Sections, representing 56 per cent of the total Institute membership. This volume compares with 33 per cent of returns in reply to the 1948 questionnaire; an increase of 73 per cent which it would seem is indicative of a substantially increased interest in transfers work throughout the Institute. A total of 53 Sections out of 84 (63 per cent) were heard from in reply to the 1948–49 questionnaires. Results submitted would therefore appear to be reliably representative of conditions throughout the Institute.

The questionnaire returns revealed the following information:

1. As of June 1949, 62 per cent of all Sections were engaged in transfers work.

2. Section committees used 16 different names for their respective committees. It has since been recommended, for purposes of uniformity, that all Section committees use the same name as the Institute committee, namely, "Committee on Transfers."

3. Of all Sections reporting, 43 per cent have standing Committees on Transfers, as compared with 57 per cent which do not. However, there does appear to be progress in amending Section Bylaws to provide for Committees on Transfers as standing committees, as initially recommended by the Committee on Transfers in its letter of December 30, 1946, to all Sections. It is hoped that all Sections will adopt this recommendation.

4. In the 48 Sections reporting, 216 members are in transfers work. The average number of Section members per committee men was found to be 72.

5. Regarding methods and policy used in handling transfers work, about 40 per cent of the Sections reporting appear to follow a procedure approaching that recommended in the 1946 letter to all Sections from the Institute Committee on Transfers characterized by complete coverage of Section membership; about 40 per cent engaged in moderate activities on transfers work by various methods; about 20 per cent engaged in little or no transfers activities.

6. About 75 per cent of all Sections apparently are afflicted with a condition of apathy relative to attaining higher grades of membership. How can AIEE grades be held in esteem by those outside the Institute if those within regard them so disinterestedly? Correction of this unhealthy condition is the aim of the method proposed in the Operations Guide.

7. When the Sections were asked for reasons for the foregoing conditions, the majority opinion was that the higher grades did not involve sufficient recognition benefit to induce members to seek advancement. The Publicity Pamphlet "Why Transfer?" and publicity in *Electrical Engineering* are expected to clear this point.

8. When asked how the apathy situation could best be corrected, the majority of replies confirmed the opinion of the Institute Committee on Transfers that the condition can best be overcome through encouragement of the Section committees by: provision of a manual of transfer procedure; and encouraging and assisting in publicizing the significance and advantages of the higher grades.

9. Many suggestions and criticisms were received concerning the over-all subject of transfers. These comments were reviewed and discussed at the June meeting in Swampscott, Mass.

The committee met a second time at the Winter General Meeting. Most of the time at this meeting was spent reviewing the first draft of the Operations Guide.

At the Winter General Meeting, the Chairman of the Committee on Transfers, by invitation, spoke at meetings of the Sections Committee on January 31, and the Membership Committee on February 1. The belief was expressed at these meetings that a milestone in AIEE progress is being reached through introduction of the Board of Review method of Section transfers work; that, when this system has been adopted by the majority of the Sections, rapid progress can be made toward the objective: "Each Member in the Highest Grade for Which He Is Qualified"; that when this objective is reached or closely approached the professional strength, prestige, and vitality of AIEE will have been greatly improved. It was pointed out that a situation such as presently exists with only 32 per cent of the membership in the directly professional grade (Member and Fellow) is not healthy. What this percentage would be if all members were in the highest grades for which qualified is not known, but it is believed that it would be in the neighborhood of 50 per cent.

Other projects completed by the Committee on Transfers during the subject fiscal year are as follows: outline of a publicity article for publication in *Electrical Engineering*; headquarters contacted relative to improvement of Year Book data and prompt notification of approved transfers; Committee on Constitution and Bylaws requested to amend Section 86 of the Bylaws to give the Committee on Transfers representation on District Executive Committees similar to the representation of the Membership Committee, as approved by the Committee on Transfers at its meeting on February 2, 1949; recommendations prepared for improvement of "Proposal" and "Application for Transfer" forms.

On April 7, 1950, a letter was sent to all Chairmen of Section Committees on Transfers outlining to them results of the 1949 questionnaire, informing them of the status of the proposed Operations Guide and Publicity Pamphlet, requesting a report on their transfer activities for the year ending May 13, 1950, and asking their opinion relative to the present requirement of five signers of the "Proposal for Fellow" form number 216 as compared with the former requirement of five Fellow or Member signers.

It is the considered opinion of the Committee on Transfers that the interest and activities of the Sections in this work was greater during the past year than in any other year.

Technical Committees

Co-ordinating Committees

COMMUNICATION, GENERAL APPLICATIONS, INDUSTRY, POWER, SCIENCE AND ELECTRONICS

It has been unnecessary to change the organization or scope of any technical committee. Some problems of overlapping jurisdiction have arisen, but these have been settled within the co-ordinating committees.

A difference of opinion exists on the matter of administrative jurisdiction of joint subcommittees. An opinion poll is under way, which will serve as the basis of action during the next administrative year.

The Communication Co-ordinating Committee, after functioning for one year, and based on the experience during that year, has recommended that the Committee on Aural Broadcasting Systems and the Committee on Television Broadcasting Systems be consolidated to form a new committee to be known as "Committee on Television and Aural Broadcasting Systems." The scope will be established before the end of the current administrative year.

With expansion of technical activities, it is desirable that the members of the Institute be kept informed of the programs of the various technical committees, their scopes, and general organization. This has been accomplished by continuation of the policy instituted last year of devoting a section in *Electrical Engineering* to news items concerning current activities of the technical committees. In addition, the 1949 Year Book for the first time includes a complete publication of organization and scopes for technical committees, subcommittees, joint subcommittees, and working, or project, committees. This information also will be included in future issues of the Year Book as a permanent policy.

In recognition of the fact that the title of the Committee on Servomechanisms does not properly define the scope of this committee, the Board of Directors approved the change in designation to "Committee on Feedback Control Systems."

The Board of Directors has approved the following changes, effective as of August 1, 1950:

1. Change in name of "Co-ordinating Committee" to "Division Advisory Committee."

2. Designation of the Chairman of the Division Advisory Committee as "Division Advisor."

3. Appointment of a new standing committee of ten members to be called "Technical Advisory Committee," which will replace the present Technical Activities Subcommittee of the Committee on Planning and Co-ordination.

4. Membership of the new Technical Advisory Committee to consist of the five Division Advisors, formerly called Co-ordinating Committee Chairmen, namely,

(a). Communication Division Advisor.
(b). General Applications Division Advisor.
(c). Industry Division Advisor.
(d). Power Division Advisor.
(e). Science and Electronics Division Advisor.

and

Chairman of the Technical Program Committee.
Chairman of the Standards Committee.

Three members-at-large to be appointed by the President, one of whom to be designated chairman of the committee.

5. The scope of the new Technical Advisory Committee is "to stimulate, promote, and encourage technical activities and specifically to be concerned with:

(a). All scopes of technical committees.
(b). Special events which may involve committees in more than one Division, such as special technical conferences, symposia, and general procedure.
(c). Joint subcommittees and other technical committee organization.
(d). Assistance to the Technical Program Committee, the Standards Committee, and the Committee on Planning and Co-ordination, when solicited.
(e). Consideration of problems brought up by any Technical Division."

6. The Chairman of the Technical Advisory Committee to be a member of the Committee on Planning and Co-ordination.

7. The several Division Advisors no longer to be members of the Committee on Planning and Co-ordination, or Committee on Award of Institute Prizes.

After the approval of the foregoing items, the Board of Directors voted to eliminate from the Bylaws provisions for ex officio memberships of committees.

The foregoing changes give recognition to the previously stated policy that the grouping of technical committees into Divisions, formerly Co-ordinating Committees, does not deprive the chairman of a technical committee of any prerogatives which he had prior to such grouping; the success of the Institute technical activities will continue to depend upon the degree of voluntary co-operation by each technical committee chairman; the Division Advisor will represent the committees within his Division; the creation

of a Technical Advisory Committee will provide the long-needed medium for the exchange of views among Division Representatives and the formulation of recommendations relating to technical committee activities.

During the year, a manual of instructions for technical committee chairmen was completed, and it will be distributed to incoming chairmen. It is intended as a source of information to new chairmen for their general guidance in the performance of their duties.

Technical conferences on specialized subjects continued in popularity during the year, as evidenced by the large attendance at each conference. The success of these conferences is due in part to the willingness of local Sections to act as sponsoring hosts and to arrange for the necessary meeting facilities and publicity. Some technical committees are now sponsoring annual and semiannual conferences under a continuing program. Conferences are scheduled also with societies outside of the Institute—Instrument Society of America, Institute of Radio Engineers, National Telemetering Forum, Radio Manufacturers Association, and so forth. Reports on the conferences held during the past year are given under the heading "Special Technical Conferences."

Technical activities in general continued at a strong pace during the year, taxing the facilities available for parallel sessions during the general meetings. The problem of accommodating the number of papers requiring preprinting and publication in *Transactions* was not too great, due to the combining of the 1950 Summer and Pacific General Meetings, and the co-operation of committee chairmen in estimating their requirements at least one year in advance. Although these matters are primarily the responsibility of the Technical Program Committee, successful operation must depend upon the co-operation of the individual technical committee chairmen, which has been accomplished through the assistance of the Division Advisors.

Communication Group

COMMITTEE ON AURAL BROADCASTING SYSTEMS

The activities of this committee were devoted to the procurement and review of technical papers, and minor participation in review of several Standards referred to it by the Standards Committee. The committee covers a field that is relatively stabilized and at present inactive because of the shift of interest to television. Therefore, on August 1, this committee and the Committee on Television Broadcasting Systems will be combined, and the new committee will be known as "Committee on Television and Aural Broadcasting Systems." During the year, the committee furnished, upon request, some material on the outstanding developments in the field of aural broadcasting for inclusion in an article for *Electrical Engineering*.

COMMITTEE ON COMMUNICATION SWITCHING SYSTEMS

The committee held one well-attended meeting in New York on September 15, 1949, for the purpose of discussing committee work plans for the year. At this meeting, specific papers to be sponsored for the Winter General Meeting were discussed and plans for this meeting were crystallized. Also, tentative plans for the next two general meetings were discussed.

The committee sponsored three formal papers at the Winter General Meeting. The session was well-attended, and each of these papers was followed by stimulating discussion.

The committee is sponsoring three papers at the Summer and Pacific General Meeting. The papers chosen are on closely related subjects, and are particularly appropriate for this meeting, since they are concerned with telephone switching equipment now in service on the Pacific Coast in both Bell and independent operating companies.

Special consideration has been given to plans for the Fall General Meeting, in view of the expressed need to build up interest in this meeting. The committee considered that, while this location is not best suited for papers on the large city switching systems, it would be quite an appropriate location for a symposium of papers on the small community dial office systems. Also, the committee thought it very desirable to obtain participation by both Bell System and independent fields in the meeting.

COMMITTEE ON RADIO COMMUNICATION SYSTEMS

This committee held one formal meeting, on February 1, 1950. Most of the committee activities were conducted by mail and by telephone. The chairman of the committee attended several meetings of the Technical Program Committee.

The committee reviewed a number of technical papers, most of which have been presented at AIEE meetings and some recommended for publication. This effort is being continued to arrange for papers for presentation at future meetings. The committee is co-operating with the Committee on Carrier Current in arranging for the presentation of papers concerning the use of microwave radio equipment for relaying, telemetering, and supervisory control for electric power distribution systems.

The committee sponsored one session with three papers at the Fall General Meeting, and two sessions with six papers at the Winter General Meeting.

The Mobile Radio Subcommittee has undertaken the study of the protection of base stations in mobile radio service against damage by lightning, in co-operation with certain members of the Lightning and Insulator Subcommittee.

COMMITTEE ON SPECIAL COMMUNICATION APPLICATIONS

During the past year, the committee held one full committee meeting and sponsored one technical session. This committee's work is largely devoted to subjects which do not logically fall within the scope of the other communication committees.

A full technical session was sponsored at the Fall General Meeting, on railroad communication, which proved to be of considerable interest. Much of the work in arranging this session had been done by the committee when it was a subcommittee of the Committee on Communication.

In expanding to full committee status, some members were added to the original subcommittee, and it is expected some growth will occur in the first few terms of the committee. At the meeting held during the Winter General Meeting, much time was devoted to searching for areas that are not covered by the other committees. Three subcommittees have been organized, and they are endeavoring to find sources of technical papers on subjects of train control, centralized traffic control, caboose power supplies, communication, and train entertainment. In the field of electroacoustics, material on public address systems and recording schemes are highlighted as the most logical for investigation. The Subcommittee on Special Activities expects to get into the subjects of ceramics, ferrites, and materials with high dielectric constants.

COMMITTEE ON TELEGRAPH SYSTEMS

One meeting of the entire committee was held during the year, at the Winter General Meeting. The committee reviewed its program in furtherance of which it had presented a paper on an electronic regenerative repeater and one on a submarine cable carrier at the Winter General Meeting. There was consensus of opinion that the application of electronic distributors to multiplex telegraph and radiotelegraph circuits is of interest to the profession, and that a symposium of papers should be developed for the Fall General Meeting. Subsequent developments have thrown doubt upon the advisability of presenting such a symposium where the prospective audience would be too small to support the papers with adequate discussion, there being a considerable concentration of telegraph engineers in New York and Chicago.

There was also consensus of opinion that a comprehensive paper on American and possibly foreign telegraph printers should be developed. Substitution of aluminum for copper in certain line applications also will be watched for developments. In the submarine cable field, it is expected that submerged repeaters will soon command attention.

The Subcommittee on Facsimile reported on the conference session on its subject held at the Winter General Meeting. The conference itself proved to be an attraction to every segment of the facsimile industry. Particularly stimulating was an address by the officer heading the Armed Forces' development and procurement activities, who emphasized the essential nature of facsimile to military operations and the unity of effort now being applied to the solution of outstanding problems.

COMMITTEE ON TELEVISION BROADCASTING SYSTEMS

This committee was newly formed this year, and devoted all of its activity to initiation of technical programs, solicitation and review of timely papers, and the conduct of sponsored sessions. The field of activity is divided between transmission systems and receiving systems, each being covered by a separate subcommittee. During the year, the committee sponsored two complete technical sessions, at which eight papers of interest to the membership in the field of television were presented. One of these sessions was at the Fall General Meeting; the other at the Winter General Meeting.

While no specific standardizing activities were undertaken during this first year of the committee, a number of proposals before the Standards Committee were reviewed and comments submitted, where necessary. A

brief statement on television developments in 1949 was prepared for publication in *Electrical Engineering*. Particular effort is being directed toward obtaining papers on the more general aspects of television systems which are of interest to the over-all membership, and effort is being directed toward arranging for additional sessions at future meetings.

COMMITTEE ON WIRE COMMUNICATION SYSTEMS

This committee was formed as a full committee at the time the Communication Group was split from the Communication and Science Group. Meetings were held in September 1949 and in February 1950. One serious problem faced by this committee is that the members are so widely spaced geographically it is very rare for some of them to be able to attend meetings held in the East. Such wide geographical spacing is desirable, of course, to cover the field as thoroughly as possible. To alleviate this situation, it is proposed to hold committee meetings at all general meetings so that each member will be able to attend at least some meetings. This procedure should stimulate interest, make new members available, and, perhaps, increase the number of papers from the western part of the country.

A complete session was sponsored at the Fall General Meeting. A joint session at the Winter General Meeting was sponsored with the Committee on Telegraph Systems. A joint session at the Summer and Pacific General Meeting is planned, and a complete session is planned for the Fall General Meeting. Some papers are already scheduled for the Winter General Meeting and for the 1951 Summer General Meeting.

General Applications Group

COMMITTEE ON AIR TRANSPORTATION

The committee held one meeting of the entire committee, in San Francisco, on August 22, preceding the Pacific General Meeting. Approval was voiced of the plan to concentrate technical sessions at one principal meeting during the year, alternating between the eastern and western sections of the country. It was further decided that areas in which aircraft activities are located should be chosen for the meetings. In view of this, the committee decided to concentrate on technical papers to be presented at the Middle Eastern District Meeting, Baltimore, October 3–5, 1950. A meeting of the committee has been scheduled for October 2, in Baltimore.

Aircraft Electric Rotating Machinery Subcommittee. The subcommittee activities have been concentrated on rewriting Test Code No. 800 for reissue. A subcommittee meeting was held in New York on February 2 to review the material on hand. Most of the work has been completed, and it is expected that a draft of the code will be circulated to the committee for review and approval. It is further expected that the revised Test Code No. 800 will be submitted to the Institute during the summer.

Aircraft Electric Control, Protective Devices, and Cable Subcommittee. The "Test Code for Aircraft Interrupting Devices" that was submitted to the Standards Committee in July 1949 was acted on by letter-ballot. As a result of the ballot several criticisms were received that the Standards Committee believed should be considered before publication of the test code. These criticisms were referred to the subcommittee.

A similar Code for Carbon Pile Regulators is in the process of being prepared for submission to the Standards Committee.

Basic Principles of Altitude Rating Subcommittee. This subcommittee has experienced considerable difficulty in obtaining and compiling data on which to base a Standard on the Basic Principles of Altitude Rating of Electric Machinery. It is continuing its efforts to complete present data, and will extend them from 50,000 feet to 60,000 feet and further if practicable.

Aircraft Electric Systems Subcommittee. This committee is engaged in preparing new material for inclusion in the "Report on Aircraft Electric System Guide," AIEE *750*, issued in July 1947. This will be a continual process as data become available for new sections or revision of existing sections.

COMMITTEE ON DOMESTIC AND COMMERCIAL APPLICATIONS

The subject of domestic and commercial applications is one in which general interest by AIEE members is only awakening. It exists, but has been dormant. In the preparation of meetings and technical conferences, it has often been necessary to solicit papers from outside the Institute membership. The time has not arrived where the committee receives many voluntarily submitted papers. Hence, the time factor in arranging a session is vital, and it is difficult to get papers prepared long enough in advance for the usual review. Time and continued committee activity and enthusiasm will help correct this situation. Meanwhile, the need of continuity is evident, as papers may have to be started during one administrative year for presentation during another.

The subject of electric heating of houses, whether by full conversion of electric power input by resistance heating, or by partial conversion of electric power input to extract heat from earth, air, or water by a pump, is of widespread interest not only to home owners, but also to public utilities, and the committee thinks it important to keep the Institute informed on developments in the field by appropriate meetings in the future.

The manufacture of domestic appliances is a substantial segment of American industry. The energy to operate electric appliances in the home makes up a substantial part of the load on power systems. A great deal of high-class engineering is involved in this field. An unusual opportunity exists for service to the people of the nation. It is worth while for the Institute to recognize the magnitude and opportunity of engineering in this area, and to take steps to attract into its membership those who are already active in its engineering phases.

The committee held a meeting in New York, on February 3, at which ten members were in attendance. Notices of the activities of the committee have appeared from time to time in *Electrical Engineering*, in the section devoted to "Committee Activities."

L. R. Emmert has been appointed the committee's delegate to the National Farm Electrification Conference, with L. N. Roberson as alternate.

The committee has organized three subcommittees to carry out its objectives.

Subcommittee on Electric Heating of Houses, and Heat Pumps, for the West Coast. This subcommittee organized and held a special technical conference in its field in Medford, Oreg., on April 12.

Subcommittee on Electric Heating of Houses, and Heat Pumps, for the East. This subcommittee sponsored a session at the Winter General Meeting. Five papers were presented, three on heat pumps, and two on electric resistance heating, and 155 persons attended the session.

Subcommittee on Domestic Appliances. This subcommittee has arranged a special technical conference to be held in Cleveland, Ohio, on June 20, in co-operation with the Cleveland Section.

COMMITTEE ON LAND TRANSPORTATION

This committee has continued to keep in active touch with the developments in the field of electric transportation. The outstanding developments during the past year have been the development of the gas-turbine electric locomotive, and the application of ignitrons to railroad motive power to enable the advantages of high-voltage a-c power transmission to be combined with the advantages of the d-c traction motor for train propulsion. Papers on both of these developments were presented at the Winter General Meeting, and these subjects will be actively followed by further papers and reports. The continuing development and application of diesel-electric motive power has been reported in the form of various papers covering the details of improvement to this type of motive power for the Winter General Meeting, and the 1950 Summer and Pacific General Meeting.

The developments in urban transportation equipment are being followed, and papers are being prepared for presentation at future meetings of the Institute in connection with this particular application. Subcommittee activity continues in connection with the review of AIEE Standards applicable to this committee assignment, and to the continuing collection of data relative to the existing railroad electrification development, both in this country and abroad.

One committee meeting was held in connection with the Winter General Meeting, at which 17 members of the committee were present, and further meetings are planned for during the year as opportunity permits.

COMMITTEE ON PRODUCTION AND APPLICATION OF LIGHT

A very lively conference session on long tube fluorescent lighting was held as a part of the Winter General Meeting. As has been the custom, a meeting of this committee was held at that time. Attendance was unusually good, due to consideration that was being given to a recommendation to Standards Committee on approval of Illuminating Engineering Society "Recommended Practice for Office Lighting" as a possible American Standard.

Discussion of committee activities during the year led to a decision to hold one lighting session each year, with preference being given to the Winter General Meeting. A list of possible subjects for next year's session

was suggested. A plea was made for papers on related subjects which might be published in *Electrical Engineering*. Subcommittees were inactive during the year.

COMMITTEE ON MARINE TRANSPORTATION

The committee held one well-attended meeting at Institute headquarters on April 14, 1949. The committee has been working on revisions to "Recommended Practices for Electrical Installation on Shipboard," as issued in December 1948. The committee also has been working on the international standardization of electric installations on shipboard.

Subcommittee Activities. The subcommittees have been quite active, each reviewing the sections of Standard *45* under its cognizance, and making reports to the main committee.

Industry Group

COMMITTEE ON CHEMICAL, ELECTROCHEMICAL, AND ELECTROTHERMAL APPLICATIONS

The committee held one session at the Summer General Meeting, and two sessions during the Winter General Meeting.

During the past year, the work has followed the pattern set during the preceding year. In the past year, the Metallic Rectifier Subcommittee was elevated to full committee status in the Institute and removed from the jurisdiction of this committee.

The activity of the subcommittees is outlined in the following:

1. *Arc Furnaces and Electrothermal Processes.* This subcommittee continues to study the problems of arc furnace application. The problems of surging and regulation are again coming to the fore, and are being actively studied. A session is planned for the 1950–51 season.

2. *Electrolytic Processes.* This subcommittee is continuing its work on subcommittee report on influence of cell line characteristics on the selection of electric power and conversion equipment.

3. *Cathodic Protection.* This subcommittee has been inactive during 1949–50, due to the resignation of the chairman and inability to obtain a new chairman. A new chairman has now been appointed, and full activity is expected next year. The committee is planning a session on corrosion.

4. *Petroleum Refining and Production.* This subcommittee has been relatively inactive during the current year. However, activity is planned for the 1950–51 season.

5. *Batteries, Battery Forming and Charging.* This subcommittee has been very active this year. An excellent conference session was sponsored at the Summer General Meeting, and additional meetings are planned for 1950–51. The committee is continuing its work on the inconsistencies in the Storage Battery Standards and is making every effort to have these problems resolved in the near future.

6. *Chemical Industries.* This subcommittee sponsored two sessions at the Winter General Meeting, on the application of power cables in chemical plants. There continues to be great interest in this subject, and further sessions are planned for the next Winter General Meeting to attack the installation problem. The subcommittee is continuing its study of the application of equipment to this industry.

COMMITTEE ON ELECTRIC HEATING

The committee has generally agreed that it will emphasize the Winter General Meeting as a time for general paper presentation, with an investigation going on as to the prospects for a Conference on Electric Heating in the midwest area, similar to the biannual Welding Conference. This plan was decided on at the committee meeting in New York on January 30, 1950. Meanwhile, the work of the subcommittees is going on as follows.

Subcommittee on Induction and Dielectric Heating is co-operating actively with the Federal Communications Commission on reports of radio interference from heating equipment. Members are working on assigned sections of proposed equipment Standards and performance tests. Some sections have been received and are being edited and reviewed. Work on definitions is being co-ordinated with the Institute of Radio Engineers.

Subcommittee on Radiation Measurements Above 200 Megacycles is working actively on preliminary Standards in this field. With several FCC personnel included in its membership, co-operation and field tests are progressing satisfactorily. Various sections are to be submitted at the next meeting for editing and review.

Radiant Heating Subcommittee has been working with the Ovens and Furnaces Committee of the National Fire Protection Association to extend and clarify Standards for electric equipment for Class *A* ovens and furnaces. These proposed Standards presumably will become effective on June 1, 1950. Meetings are continuing to sponsor investigation of controversial questions regarding various sources of infrared radiation.

Subcommittee on Resistance Heating and Electric Furnaces is planning to recommend that its title and scope be limited to resistance heating. A working group is being organized to collect, edit, and disseminate information on various resistance heating applications, probably in a loose-leaf handbook form.

COMMITTEE ON ELECTRIC WELDING

The activities of this committee have been directed toward fostering interest in electric welding, organizing subcommittees for study and research on this subject, and sponsoring a "Special Technical Conference on Electric Welding." A special technical conference was conducted in co-operation with the American Welding Society and the Industrial Electrical Engineers Society in Detroit. The purpose was to bring industrial electrical engineers together in a conference on subjects in which all were primarily interested. The committee plans to hold a similar Electric Welding Conference every other year.

The committee conducted a session during the Winter General Meeting, and held a number of committee meetings during the year for planning its activities, including the work necessary for the conference.

Subcommittee on Power Supply for Resistance Welding is continuing its work on a special report, and, during the February 2 meeting of the main committee, two working groups were recommended for addition to the Power Supply Subcommittee, namely, Working Group on Probability and Working Group on Proposed Protection Devices in Welding. However, during a meeting of the subcommittee, it was decided that this work, because of its nature, should be included with that of the Users Working Group instead of in a separate group. The subcommittee, in order to cover all interests in power supply for welders, has a Users Working Group, a Manufacturers Working Group, and a Utilities Working Group, with each preparing a section of the special report. The special report of this Power Supply Subcommittee should be available in the near future.

Subcommittee on Welding Research was organized during the year. This subcommittee hopes to increase the efficiency and usefulness of the electric arc research by: the interchange of information on past, present, and planned future research activities; the co-ordination of active research projects through mutual co-operation; the definition of basic electric-arc problems which need further study and research; the stimulation of technical papers and sessions on electric arcs; encouraging the education of graduate students for electric-arc research; and bringing the needs and advantages of electric-arc research to the attention of industrial and other potential sponsors for research. It plans to initiate this program by: preparing a reasonably complete bibliography of past research in the field of high-pressure electric arcs; preparing a summary of nonconfidential electric-arc research projects in effect at present; and defining the basic electric arc problems which must be studied now. Should the subcommittee be successful in carrying out the three initial phases outlined, the material it has collected and organized may serve as a basis for significant technical papers and for sessions or conferences on high-pressure electric arcs. Publication of such information and indication of useful research projects for the future might lead to increased interest on the part of industry and other potential sponsors of fundamental research.

COMMITTEE ON FEEDBACK CONTROL SYSTEMS

Last fall, the committee was formed to take over the duties previously delegated to the Joint Subcommittee on Servomechanisms. While this action necessitated no drastic change in the objectives of the group, the change to full-committee status appreciably enhanced the opportunities for effective operation. The committee had 32 members at the close of the year.

The scope of the committee covers the treatment of matters in which the dominant factors are the terminology, requirements, design, construction, and operation of equipment, and the circuits pertaining to control systems involving feedback, such as servomechanisms, regulators, and governors, excluding measuring and recording instruments. This committee co-operates by means of liaison membership with other technical committees within the Institute interested in servomechanisms, regulators, or other control systems, as well as with related committee work in associated societies.

Participation in two Institute general meetings during the year consisted of the sponsorship of ten papers, of which one was a subcommittee report on terminology. The two prize-paper awards in the Industry Group announced at the Winter General Meeting were for papers sponsored by this committee. At the Summer General Meeting, a joint session was held with the Committee on Industrial Control, and at the Winter General Meeting a joint session with that committee and a session on feedback control were held.

Subcommittee on Terminology and Definitions. Because of the rapid growth of professional activity in the field of feedback control, the problems regarding unified terminology and definitions pertaining to such devices as servomechanisms, regulators, and amplifiers are many. This subcommittee was appointed to work on the subject in co-operation with subcommittees of other Institute technical committees. During the year, three subcommittee meetings were held. At the Winter General Meeting, a conference paper report on the work of this subcommittee in collaboration with similar committees in ASME, ASA, and AIEE was given. Future activity is expected to define basic terms, and prepare a glossary of symbols, terminology, and specifications for performance.

Related Activity. One of the important functions performed by the committee has been to advise the editorial staff of *Electrical Engineering* on the suitability of manuscripts. Formal AIEE activity in the field of feedback control systems has stimulated many manuscripts in this field. Codifying these manuscripts and recommending their allocation either to *Electrical Engineering* or the Technical Program Committee has been a large activity. At the close of this year, a backlog of manuscripts was under review for the *Transactions*.

Future Activity. Consideration has been given to the feasibility of scheduling an AIEE conference on feedback control systems late in 1951.

Because of the wide geographical distribution of the interest in feedback control systems, this committee has appointed subcommittee groups on the West Coast and in the Middle West.

COMMITTEE ON GENERAL INDUSTRY APPLICATIONS

The activities of this committee have been directed toward fostering interest and coordinating activities within the various subcommittees, and sponsoring "special technical conferences," where industrial electrical engineers can meet others in the same or allied fields and discuss electrical applications. Industrial processes in a mass production age offer numerous and diversified opportunities for the application of equipment utilizing electric power. The use of electric power in industry has increased 118 per cent (from 79.0 to 171.5 billion kilowatt-hours) in the last ten years (1939 to 1949) and accounts for 57 per cent of all the power used in the United States. Programs of the special technical conference type are ideally suited for discussing problems associated with an industry or a group of related industries.

The committee held two general meetings during the year, one in Cincinnati, in October 1949, and the second in New York, in February 1950. At both of these meetings, plans for future activities were discussed. The committee sponsored a technical session at the Winter General Meeting, on the subject of "Explosion Hazards in Industry and Their Relation to Electrical Installations." A second session on this general theme is being planned for the 1951 Winter General Meeting. A technical session is also being planned for the Fall General Meeting.

The activities of subcommittees covering specific assignments are summarized in the following.

Subcommittee on Machine Tools. This subcommittee organized three sessions on machine tools for the Fall General Meeting. Ten papers discussing machine tool applications and problems were presented at the three sessions, which were well attended. This subcommittee is planning on holding a special technical conference in New England next fall.

Subcommittee on Rubber and Plastics Industry. This group has arranged to hold, jointly with the Akron Section, an annual special technical conference in Akron. The program this year was an all-day session on May 5.

Subcommittee on Textile Industry. A conference was held in Atlanta on April 13 and 14, and a session was held at the North Eastern District Meeting.

Subcommittee on Pulp and Paper Industry. In connection with the West Coast Subcommittee, this group is planning a technical session at the Summer and Pacific General Meeting, the theme being "Lumber and Paper Mills." It will feature papers on the application of electric equipment to saw mills, paper machine drives, and pulp mills.

Subcommittee on Materials Handling. A technical session on factory elevators and hoists is being planned for presentation at the 1951 Winter General Meeting. Freight elevators form a vital part of the material-handling system in multifloor factories, warehouses, garages, and other types of buildings. Each freight elevator installation usually involves a special engineering study, and the session will be of interest to engineers who have the problem of determining elevator requirements and types of equipment for industrial plants.

The subcommittee work discussed does not cover, by any means, all the industries which come within the scope of the committee. One of the problems discussed at the February 2 meeting was the organization of additional subcommittees to cover other industries, such as food processing, and the ceramic and cement industries, where the electrical engineering problems of general interest to these industries may be discussed.

This committee thinks there is no better way to further engineering knowledge and bring the AIEE close to engineers working on industrial problems than to bring together in technical sessions and conferences a group of these engineers. The committee has met with some degree of success in this task. Effort will be made to make the work more effective in the future through a long-term planning program.

COMMITTEE ON INDUSTRIAL CONTROL

The committee held two meetings, and sponsored five technical sessions, three of which were held in conjunction with other committees of the Industry Group. The following projects have been worked on by the various subcommittees.

Subcommittee on Standards has completed work on a proposal to revise the Industrial Control Section of ASA Standard *C42*, "Definition of Electrical Terms," which is sponsored by AIEE. The proposal is now in the hands of ASA Sectional Committee *C42*, to be considered for the final revision of that Standard. Another AIEE sponsored Standard is ASA *Z32.12*, dealing with graphical symbols for electric apparatus. This Standard has been in use for several years, and its acceptance by industry has been very satisfactory in general. However, certain criticisms have been raised in some industries claiming inadequacy of certain symbols. For this reason, the committee has started a study of the basic symbols with the aim of resolving difficulties.

Subcommittee on Electronic Control, through its working groups, has been active in discussing definitions of terms. This work is approaching completion, and it is expected that, during the ensuing year, proposals for definitions will be presented to the proper ASA channels.

Subcommittee on Bibliography has completed the draft of a comprehensive bibliography on industrial control, which includes brief abstracts on all important American and foreign literature on the subject. The final draft of the manuscript is being prepared for printing as an AIEE publication.

Subcommittee on Regulators and Feedback Control Systems has been newly formed. The subcommittee will provide liaison with other committees operating in related fields, and special emphasis is laid on the importance of such systems for industrial applications. The first project of the subcommittee is the development of system classifications and definitions.

COMMITTEE ON INDUSTRIAL POWER SYSTEMS

The committee has been quite active this year, starting with two sessions at the Fall General Meeting, one of which was sponsored jointly with the Committee on Industrial Control. Three committee meetings were held.

On April 19–20, a Power Conference was held in Pittsburgh under the joint sponsorship of the Pittsburgh Section, the Committee on Power Generation, the Committee on Industrial Power Systems, and the Committee on System Engineering. This first Power Conference was very well received, and the sponsoring committees have been strongly urged to present another in the near future.

For the Summer and Pacific General Meeting, the committee is sponsoring a session, jointly with the Committee on Chemical, Electrochemical, and Electrothermal Applications, on problems in the petroleum field.

Subcommittee on Revision of "Electric Power Distribution for Industrial Plants." This subcommittee has been working actively to prepare a revised and improved edition

of the report. This work has not reached the publication state as early as anticipated, but should be ready early next year.

Subcommittee on Wiring Design for Commercial Buildings. This subcommittee prepared its report in published form in time for announcement at the Fall General Meeting. The report contains a wealth of information, including quick-estimating charts and valuable check lists, which will be helpful to anyone interested in the wiring design for large commercial buildings.

COMMITTEE ON MINING AND METAL INDUSTRY

This committee is continuing its program of presenting papers of interest to the electrical engineers in the fields of mining and metal. There are two active subcommittees. The Mining Subcommittee includes members interested in bituminous coal, anthracite coal, potash, copper, and other ores. The Metal Subcommittee includes members in the fields of steel, copper, aluminum, and other nonferrous metals. The committee sponsored two sessions on mining and one session on metal at the Fall General Meeting, and has arranged for two sessions on mining and one session on metal at the Summer and Pacific General Meeting.

The present program of the committee includes the development of Standards, co-operation with the American Mining Congress and the Association of Iron and Steel Engineers, and the sponsoring of sessions which will interest primarily the electrical engineers working for the mining and metal industries. In addition to having many members on the committee who are also members of the Association of Iron and Steel Engineers and the American Mining Congress, the committee has one member each assigned as liaison between it and these organizations. The committee hopes to develop technical conferences which can be scheduled in such locations and at such times that the co-operation of the other two organizations can be obtained.

One item of special interest is that a representative of *Coal Age*, a publication for the mining industry, covered the mining sessions at the Fall General Meeting, and gave a good write-up with favorable publicity for AIEE in an issue immediately following the meeting. Arrangements have been made to have the *Engineering and Mining Journal*, a publication for the hard rock mining industry, cover the two mining sessions at Pasadena in the same manner.

Power Group

COMMITTEE ON CARRIER CURRENT

During the year, the committee held four meetings, and sponsored one conference-type session on microwave applications at the Summer General Meeting. Much of the work is carried on by subcommittees.

Subcommittee for Preparation of a General Interest Paper on Carrier Current is approaching the end of its work, and it is expected to go out of existence.

Subcommittee to Report on Application Guidances for Carrier Current is also completing its assignment, which has been carried on essentially by one man, and will cease to exist.

Subcommittee on Methods of Measurement is checking its report against field observations, and modifying the report from time to time in minor details to promote simpler or more accurate methods of field testing.

Subcommittee on High-Frequency Characteristics of Power Equipment originally planned to carry out factory tests. However, it develops that in most plants this would cause undue interference with the routine of production. It thus appears that such data will be derived from tests of equipment in the field.

Subcommittee on Carrier Current Characteristics of Transmission Lines and Systems has obtained excellent response to some 130 copies of a questionnaire, but unfortunately very little of the information is in such form as to be useful for comparison with other field observations. Up to the present time, field tests were conducted on a random basis, in general, observing only relative values.

Subcommittee on Standard Terminology for Carrier Current has completed its report, and will go out of existence as soon as co-ordination with the Standards Committee is completed.

Subcommittee on Long Life Tubes is assembling information from both manufacturer and user sources, and will draw up a report with recommendations.

Subcommittee on Use of Microwave Equipment for Relaying, Telemetering, and Supervisory Control has been most active. It provided material for a conference session at the Summer General Meeting, and is presently assembling papers for a full technical session at the Summer and Pacific General Meeting.

Subcommittee on Operating Experience With Carrier Current Relaying Channels has sent questionnaires to at least the major users o carrier equipment, and is assembling and tabulating the replies.

Plans for the coming year include a technical session on microwaves and a conference session on carrier current during the Summer and Pacific General Meeting. At the same time, it is planned to call a meeting of the entire committee, and invite all interested parties to attend. The subcommittee seeks an expansion in membership, especially on the West Coast, and plans to establish a West Coast Division, possibly under a second vice-chairman. The general objectives remain about the same, but will be adjusted, as required, to cope with new factors as they arise.

One new element is Federal Communication Commission Docket Number 9288 in which it is proposed to expand the low power rule so that power-line carrier would be specifically included. Many interested organizations are co-operating with the FCC in making field observations. The committee is interested in the academic factors, and will assemble field data from all possible sources to expand knowledge of propagation from practical lines in clear areas, as well as those in which the field will be distorted by foreign objects.

COMMITTEE ON INSULATED CONDUCTORS

Organization. The committee has 48 members and, in addition, 46 special members who serve only on subcommittees. The initial organization of this new committee into 12 subcommittees has continued. This arrangement has facilitated carrying out one of the main reasons for forming this committee, that is, to form avenues for considering all types of projects relating to research, design, installation, and operation of various types of insulated wires and cables.

Committee Meetings. The committee is pursuing the policy of having two meetings during each administrative year. The first is for one day, and is held in the fall in the East (has been New York). The second is for two days, in order to allow ample time for subcommittee meetings and for general informal discussions, and this meeting is held in the Middle West (to be held in Chicago in May this year). The average attendance at the committee meetings has been about 60. In addition, the Administration Subcommittee has had two meetings at the time of AIEE general meetings.

Projects. The subcommittees have over 90 projects under consideration. In addition, informal reports on various items of general interest are being presented at the meetings. The discussions of these projects and of the reports, and the records thereof in the minutes, are helping make the activities of considerable value to the members and special members.

Standards. Recently, the work on revising the definitions for wires and cables was completed and forwarded to the ASA Sectional Committee *C-42* for its use in the revision of "Definitions of Electrical Terms." Work on other Standards and test codes is under way by the committee.

Technical Papers. Twelve papers obtained by the committee were presented at three technical meetings of the AIEE. It is to be noted that a good share of these pertain to subjects such as design of cable accessories, which were not given the attention that they might have had under the AIEE committee organization that obtained several years ago. In addition, a summary of information and conclusions drawn from a survey conducted by the committee on practices relating to protective coverings for lead-sheathed power cables was published in *Electrical Engineering*.

COMMITTEE ON POWER GENERATION

The committee held three meetings during the year, the first at the Summer General Meeting, the second at the Fall General Meeting, and the third at the Winter General Meeting. The activities of the committee, as reported by the various subcommittees, are as follows.

Prime Mover. Preliminary talks with The American Society of Mechanical Engineers representatives have indicated their willingness to discuss the feasibility of setting up Standards for turbines rated at 7,500 kw and smaller.

Station Design. Through the efforts of this subcommittee, a session was organized on "centralized control," at which papers and discussions were presented in favor of and against centralized control. The subcommittee is sponsoring two sessions for the 1951 Winter General Meeting, one on the co-ordination of station design and analysis of plant operating troubles, and another on safety and fire-fighting equipment.

Speed Governing. A session was held at the Fall General Meeting. Specifications for governing of steam turbines 500 kw and up were completed by the joint AIEE-ASME Committee on Speed Governing Specifica-

tions. Progress was made on specifications for hydraulic turbine governors. Work also was started on speed governing specifications for internal combustion engines.

Excitation Systems. This subcommittee completed the revision of definitions of terms relating to excitation. It organized a session for the Winter General Meeting, and is sponsoring a session for the Summer and Pacific General Meeting.

Application of Probability Methods. This subcommittee organized a session for the Fall General Meeting, and sponsored the collection of outage data on high-pressure units and boilers, which are being collected by the Edison Electric Institute and analyzed by the Consolidated Edison Company of New York, Inc. The subcommittee is planning a symposium for the 1951 Winter General Meeting, on the reserve practices of hydroelectric companies. The objective of this symposium is that of divulging these practices and of stimulating the use of probability methods in hydro systems.

Hydroelectric Systems. The activities of this subcommittee during the year covered the study of outstanding developments in the field. Along these lines, the subcommittee is sponsoring a session for the Summer and Pacific General Meeting, which will include papers on underground hydroelectric plants and on factors determining the electrical design of power systems with large hydroelectric stations.

Pacific Coast. This subcommittee held two meetings during the year, one in San Francisco and one in Los Angeles, at which various problems of general interest were discussed.

Other activities of the Committee on Power Generation were:

AIEE Pittsburgh Power Conference was organized jointly with the Committees on Industrial Power Systems and System Engineering for presentation of 18 papers. Subjects ranged from general power-plant administration topics to central-station and industrial-station design and operating problems.

1950 Fall General Meeting. Three sessions are planned for this meeting on the subjects of: supervisory instruments; enclosed motor applications in power plants; gas turbines; and quick-starting of steam turbines.

Economic Evaluation of Alternate Central Station Layouts. This project will be carried by the System Economics Subcommittee as a joint project with the Committee on System Engineering.

COMMITTEE ON PROTECTIVE DEVICES

Three meetings were held by the committee, at which time the subcommittees reported on their activities and reviewed their plans for future work. The activities of the committee are carried on largely by three subcommittees.

Fault Limiting Devices Subcommittee. Application guides covering the grounding of synchronous generating systems, the methods of grounding transmission systems, and the application of ground fault neutralizers were completed during the year. These guides were presented as ACO (advance copy only) papers, and issued on a trial basis with the expectation that they would be reviewed by the AIEE membership. The working groups that prepared these guides are anxious to receive comments from anyone interested in making suggestions for their improvement. Early next year, the working groups will proceed to make final revisions.

The "Bibliography on Resonant Neutral Grounding," containing references to articles on resonant neutral grounding in the American and foreign press, was completed through the year 1938 and presented at the Fall General Meeting by title only. The bibliography covering the period 1938 to 1947 has been assembled and is scheduled for presentation by title only at the Fall General Meeting.

The Working Group on Power System Fault Limitation completed its report on methods of limiting fault currents on expanding systems, and presented it as a conference paper at the Winter General Meeting. After comments have been received, it will be brought up to date and presented formally at an AIEE meeting, and also published in the *Transactions.*

A report entitled "Field Survey of Unbalanced Charging Currents" was presented at the Fall General Meeting. This report covered the results of the survey, and indicated that the requirement that ground fault neutralizers be capable of continuously carrying 30 per cent circulating current is adequate.

One of the projects now under consideration is a survey to determine present grounding practices on industrial systems. This survey will determine if there is any accepted practice or agreement in the connection of the neutral, that is, whether the power system neutral should be grounded through a resistor, a reactor, potential transformer, ground fault neutralizer, or a combination distribution transformer and resistor. This survey will cover plants with independent generating systems as well as those which are tied in with utilities. Later, if the survey indicates that there is a need for an application guide on industrial systems grounding, a suitable group will be organized to prepare this guide. It is expected that this project will be joint with the Committee on Industrial Power Systems.

A report is also being prepared outlining the factors which determine the size and rating of grounding transformers.

Lightning Protective Devices Subcommittee. The activities of the Lightning Protective Devices Subcommittee during the past several years have been directed toward the co-ordination and unification of information relating to: performance characteristics; testing Standards; and applications of various types of lightning protective devices. Formerly, this information was incomplete, contained inconsistencies, and was scattered through several publications.

1. Performance characteristics of various types of lightning protective devices was issued for the first time under one cover in September 1949, AIEE 49-286.

2. The difficult and extensive work, particularly in the co-ordination of fundamental definitions and terminology, carried on by working groups within the subcommittee has resulted in the publication of a new and much-needed combined Protective Devices Standard *28A*, February 1950. The Standard was issued in report form and as a proposed revision to ASA *C-62* to avoid overriding an existing ASA Standard. It will be reviewed by the *C-62* Committee in the revision of the ASA Standard.

3. The subcommittee is now directing its efforts toward the completion of the "Application Guide for Lightning Protection of Substations." This guide, while it is directed particularly to the problems of substation protection, will treat important application problems of a general nature relating to the various types of protective devices. It will supplement the Performance Report and Combined Standards to provide essential lightning protection information in convenient, compact form. The Application Guide is scheduled for publication and presentation at the Fall General Meeting.

The studies which have been under way on recovery voltage characteristics of distribution systems in collaboration with the Committee on Transmission and Distribution are nearing completion. When this information becomes available, the subcommittee will reconsider the recommendation of specific recovery voltage conditions to apply during standard tests. The addition of the recovery voltage data will complete the present Lightning Protective Devices technical information program. The agenda of the subcommittee include new items relating to the protection of aerial cable, dry-type transformers, rod gap characteristics in the short-time region, and evaluation of the effects of rate of rise of surge current with respect to arrester performance.

Co-ordination of Insulation Subcommittee. This subcommittee was set up to deal with problems of insulation co-ordination which come within the scope of the Committee on Protective Devices. To date, its function has been to keep the members of the committee informed on the activities on insulation co-ordination in other Institute and ASA committees which are dealing with this subject. There are no plans for active project groups in this subcommittee at present.

COMMITTEE ON RELAYS

The committee held three meetings, and sponsored three technical sessions, at which 11 technical papers and two conference papers were presented. The technical activities of this committee were carried on through a number of project committees which are appointed to fulfill specific assignments. During the past year, four new project committees were organized. Following are the reports of the various project committees.

Generator Protection. This committee is investigating various methods of generator protection, and expects to publish a report of its findings. In May 1948, a draft of an AIEE Committee Report on Generator Protection was prepared and distributed to members of the project committee for comment. Discussion of the material in this report indicated the need for obtaining more data on present practices, and a decision was made to issue a questionnaire. A draft of the proposed questionnaire was prepared and distributed to the committee members for comment in September 1949. This draft has been revised to include the suggestions that were received, and is about ready to be issued in final form to a representative list of utility companies. The data from the replies will be summarized and used as a basis for preparing the final committee report.

Bibliography of Relay Literature. An interim report has been prepared from the relay papers presented in 1949. It is planned that

another formal report covering the past three years will be available in 1950.

Co-ordination of Construction and Protection of Distribution Circuits. This joint working group of the Committee on Relays, the Distribution Subcommittee, and the Edison Electric Institute Transmission and Distribution Committee is continuing its study of correlation of construction and protection practices on the performance of distribution circuits with regard to number of faults occurring and percentage of faults which are permanent. Thirty-eight operating companies have supplied the working group with information regarding faults on 209 circuits for the year 1949. Items being investigated include effects of type of system, size and covering of wire, configuration and spacing, and insulator and cross brace material on the number of faults occurring; and the effects of speed of clearing of faults on the percentage of faults which become permanent. It is expected that a report will be presented at the 1951 Winter General Meeting.

Standards for Power Relays. This committee completed, in 1949, a proposed revision of the ASA Standard *C-37*, American Standard for Relays Associated With Electric Power Apparatus. The Standard was approved by letter-ballot of the Committee on Relays early in 1949. It was sent to the AIEE Standards Committee in May, and was sent to the ASA *C-37* Committee on August 4. The ASA *C-37* Committee approved the Standard with minor editorial changes. The committee is in the process of gathering material on performance requirements of relays so that on the next revision a section on "Performance Standards" can be added to the existing Standard.

Insulation Levels for Relay and Control Circuits. This project committee completed its work, and a report was presented at the Fall General Meeting. The committee found that a value of 1,500 volts a-c is an adequate test voltage for the current, potential, and trip circuits of relays and associated circuits. An investigation of the standard recommended contact spacings for various types of high-speed relays showed that all of these are adequate to withstand a test of at least 1,500 volts a-c across contacts.

Sensitive Ground Protection. This committee presented its final report in the form of a technical paper at the Winter General Meeting. The report summarizes available methods for sensitive ground protection of 3-wire systems and outlines the limitations of presently available methods for the protection of systems with multigrounded neutrals.

Transmission-Line Protection. This committee sponsored three papers on transmission-line protection at the Winter General Meeting. These papers describe methods of protecting a hypothetical transmission system which involves many of the problems that are of current interest.

Electronic Relay Applications. This project committee is continuing to watch developments in the field of electronic protective relays, and is continuing its study of the application of microwave channels to protective relaying.

Relaying of Interconnections Between Industrial and Utility Generating Systems. This committee has obtained information from 32 electrical utility systems with respect to their practice of relaying interconnections with their industrial customers. Replies showed no specific trend nor recommended practice. Protective devices are applied in accordance with the individual economic or operating situation. The committee is pursuing its analysis of the problem, and plans to complete its work in 1950, with a summary of basic considerations and of suggested solutions.

Relaying Performance of Current Transformers. The activity of this committee consisted of the following: In connection with the proposal to eliminate the 2.5-accuracy classification of current transformers for relaying services, a letter was sent to members of the Committee on Relays requesting comments; only two replies were received. Information published by the Westinghouse Electric Corporation on a new line of auxiliary current transformers was reported at a meeting of the Committee on Relays.

The following are reports of the four new project committees formed this year.

Pilot Wires. The objective of this committee is to bring up to date operating experience with pilot-wire circuits used for protective relaying and transferred tripping. It is the intent that operating experience for both leased and privately owned lines will be gathered for the years 1942–49, inclusive. It is also intended to compile information relative to new or unusual pilot-wire relay schemes.

Remote Tripping Schemes. It is the objective of this committee to collect all possible information on the engineering features of all types of existing remote tripping schemes and a statement of operating experience with each. It is hoped that an analysis of these data will enable the committee to ascertain what primary difficulties are being experienced with this type of relay protection and to determine the direction in which further research is required to eliminate fundamental difficulties. A questionnaire will be circulated shortly to request data from various operating companies which have such equipment installed. It is hoped that the data will be in such form that a conference session will be possible some time in the next 12 months.

Effect of Vibration and Shock on Relays. At the request of the Committee on Relays, the project committee was formed late in 1949 to study the effect of vibration and shock on relays. The first meeting was held during the Winter General Meeting, and another is scheduled to be held during the Great Lakes District Meeting. The committee plans to study the effect of vibration and shock on relays used on electric power systems and industrial applications. It is proposed to make a survey of the industry to determine what work has been done on vibration and shock in the past, and to use such information as may be available in this study. It is proposed to make laboratory tests on various types of switchboard panels and relay mountings to determine the range of both frequency and amplitude which is most critical. This will be supplemented by a number of field tests of vibration and shock in generating plants and substations. From this information, the committee proposes to prepare a paper offering a suggested guide, which should be useful to the industry in designing and applying protective relays to avoid difficulty from shock and vibration.

Project Committee on Relay Test Methods. This committee held one meeting, at which it was decided that the committee would attempt to collect data from all available sources on portable field testing equipment suitable for testing the majority of the more complicated types of relays. The data will then be reviewed by the project committee and one or two of the most efficient sets of equipment selected, possibly improved by suggestions, and this information will be presented to the Committee on Relays. Along with the description of any test equipment, there will be submitted general instructions on its applications and use. Some data have been furnished by committee members. However, since some very efficient equipment may not otherwise come to their knowledge, all members of the Committee on Relays will be asked to submit their ideas and recommendations.

Joint and Associated Projects. Through representation, the committee participates in the activities of the Instrument Transformer Subcommittee of the Committee on Transformers, with special attention to the relaying performance of current transformers and the transient performance of capacitance potential devices. Close co-ordination has been maintained with activities of the Committee on Carrier Current on items of joint interest.

COMMITTEE ON ROTATING MACHINERY

A report on the activities of each subcommittee is given in the following.

Single-Phase and Fractional-Horsepower Subcommittee. Review is in process of the test code for single-phase motors, and an attempt will be made to correlate with the Master Test Codes, AIEE *550* and *557*. Since small d-c motors are now officially within the scope of the committee, activity will be pushed along this line. A technical conference is planned for applications of fractional-horsepower motors, and may be held in Dayton in the spring of 1951.

D-C Subcommittee. Culminating more than two years of concentrated activity, including two committee papers on the subject, the subcommittee has now submitted a definite proposal for revision of Table I of ASA *C-50*, covering limiting observable temperature rise of d-c rotating machines. The proposal is based on data amassed from commercial testing and from a group of co-operative research tests, and features expansion of use of the resistance method as an alternate to a thermometer, as well as inclusion of Standards for short-time rated machines. The subcommittee is now active on the matter of d-c machine short-circuit currents.

Synchronous Machinery Subcommittee. An active technical paper program is bearing fruit. A review is being made of telephone influence factor and deviation factor.

Induction Machinery Subcommittee. A test code revision is being completed. An active program is being followed on technical papers.

Insulation Subcommittee. The subcommittee has concluded and the Standards Committee has accepted a revision of AIEE Standard *43* on insulation resistance testing. The subcommittee is being expanded to cover insulation practices as well as insulation resistance.

Test Code Co-ordinating Subcommittee. The subcommittee is working with other subcommittees and with ASA on revision and co-ordination of test codes, the dominant theme being proper use of the Master Test Codes *550* and *551* where possible to avoid duplication and mass of information.

Future Meetings. A symposium on induction, and possibly synchronous, machinery for oil well applications is being considered for the Fall General Meeting.

COMMITTEE ON SUBSTATIONS

The status of the projects on which work is in progress in the subcommittees and working groups of this committee is as follows.

Automatic and Supervisory Control Subcommittee. Besides collecting material for use in the next revision of American Standard *C37.2*—1945 for Automatic Station Control, Supervisory, and Telemetering Equipments, this subcommittee is studying rectifier reclosing control problems, standardization of annunicator systems, and the relative merits of insulating versus grounding d-c switching structures.

Distribution and Conversion Substations Subcommittee's study of the relative merits of bus voltage regulation versus feeder voltage regulation has resulted in the preparation of a paper by one of its members for the Middle Eastern District Meeting, in October, with a group of related papers to follow at a later meeting. Comparative studies of circuit breaker versus reclosing fuse application will shortly result in the preparation of a paper by another member of this subcommittee. Those working on the outdoor substation lighting problem have been in touch with the IES committee that is engaged in similar activities.

Transmission Substation Subcommittee met at the end of January to review progress made in the study of its assigned problems, including the basic structural design of substation structures for 110 kv and above, and safety considerations in substations.

Working Group on Basic 1-Line Diagrams was recently formed from personnel from both the Distribution and the Transmission Substation Subcommittees to review existing practices and classify current opinions regarding suitability of various fundamental connection schemes for substations. The work of this group will serve as the basis of further activity on the part of its two parent subcommittees.

Working Group on Device Function Numbers has been requested to recommend what minor changes in the present device function numbers should be made, after the returns from their nationally circulated questionnaire showed 78 per cent favored no changes.

Working Group on Rectifier Switchgear is devoting some attention to the formulation of equivalent constants for rectifiers, for use in calculating board studies, and to a study of the voltage surge problem.

Working Group on Substation Grounding Practice has prepared a 3-page questionnaire for widespread circulation, and has submitted this to all the main committee members for comments by mail.

Committee Meetings. In addition to subcommittee and working group meetings, meetings of the main committee were held on June 20, in Swampscott, on October 21, in Cincinnati, and on February 1, in New York. A meeting of the main committee was also tentatively scheduled for June 14, in Pasadena.

COMMITTEE ON SWITCHGEAR

AIEE Standard *20A*, which was published for trial use, is still on a trial basis. Further action on it is held up because of controversy over temperature rise clauses. It is hoped that data will be available shortly so that this point can be cleared up.

The proposed Standard *22A* was published in November 1949, and covers "Air Switches, Insulator Units, and Bus Supports, Combined With Air Interrupter Switches." It is now on a trial basis.

Subcommittee on Switches, Fuses and Insulators is actively working on a revision of Standard *25* for fuses above 600 volts.

Standard *27*, covering "Switchgear Assemblies," which had been recommended to the Standards Committee during the previous year, was returned last summer to the Committee on Switchgear, which, in turn, referred it back to the Subcommittee on Switchgear Assemblies. Objections from a number of sources to the temperature rise clauses have held up this Standard until the point can be clarified. During this waiting period, the subcommittee has been actively making minor revisions.

Proposed Standard *50* for "Automatic Circuit Reclosers for A-C Distribution Systems" was published in September of 1949 for a 1-year trial.

Circuit Breaker Subcommittee is actively working on the "Test Code for Power Circuit Breakers," and good progress has been made on the "Code for Low-Voltage Air Circuit Breakers." The "Guide for Application of Low-Voltage Air Circuit Breakers," which was prepared last year and presented at the Summer General Meeting, was published in *Electrical Engineering* and in pamphlet form during the summer. The subcommittee is also very active on the revision of the Standards for "A-C Power Circuit Breakers," "Methods for Determining the RMS Value of a Sinusoidal Current Wave and a Normal Frequency Recovery Voltage," and "Rated Control Voltages."

The Joint Subcommittee on Out-of-Phase High-Voltage Switching rendered its report, which was submitted by mail to the members of the Switchgear Committee. The Switchgear Committee, by letter-ballot, approved the report, recommended the discharge of the subcommittee, and recommended that the report be printed.

The committee sponsored a session at the Summer General Meeting, and also one at the Winter General Meeting.

COMMITTEE ON SYSTEM ENGINEERING

This committee was active at all three general meetings. The same subcommittee setups were continued into what is now the third year since this committee was formed. There was a realignment of personnel at the start of the year, with about one-fourth of the membership new members to stimulate the thinking in the committee and to give additional representation in several of the cities in the central west and southwest areas of the country.

It continues to be the policy of this committee to confine its program to one topic at each technical session and develop it fully as material is available. Because of the broad-gauged nature of the work, this has proved a more satisfactory approach than that normally followed in talking about detailed apparatus problems and their utilization which would fall to more specialized committees. A total of five normal papers and 13 conference papers were presented.

There were two committee meetings during the year, one each at the Fall and Winter General Meetings, and a full 1-day meeting in Chicago during May. The meetings held in connection with the general meetings were largely devoted to a review of the program to be followed at subsequent meetings. The meeting in Chicago covers a more adequate discussion of engineering aspects of the problems in addition to the review of the committee programs for future meetings. The success of this meeting will be weighed in determining whether it should be the annual policy of this committee.

System Planning Subcommittee. This subcommittee is sponsoring a group of five companion papers at the Summer and Pacific General Meeting, which will discuss design features and long-range planning of the systems in the Pacific Southwest. The extensive use of high voltage transmission and the co-ordination of hydro and steam plants in that area will stimulate discussion of better planning practices. This subcommittee also sponsored several papers dealing with the use of the calculating board. This well-established tool for assistance in system planning is universally used, but new techniques for simplifying the application were described at the Fall General Meeting, with extensive interest as a companion to an earlier presentation the previous winter.

System Economics Subcommittee. This subcommittee considers both the economics of system operation and economics of over-all system engineering. In the first category, it has sponsored a paper which described the use of the calculating board as an operating tool in determining most economical loading of generating stations. The committee is now actively investigating problems associated with economics of interconnections, economics of high-cost high-efficiency generating capacity versus lower cost and lower efficiency capacity, rehabilitation of old plants, use of gas turbines for peak load, and economical sizes of units and power plants. Evaluation of system losses as a component of system capacity requirement is being studied also.

System Operations Subcommittee. This subcommittee sponsored a conference session at the Winter General Meeting, devoted to the subject "Operation of Systems at Leading Power Factor." The high power factor of systems now being experienced during light load periods due to installation of high-voltage underground and overhead transmission systems and extensive use of static capacitors has forced a review of the original concept of system operation requiring operation at substantial lagging power factor. Conference papers were presented by both generator manufacturers and power-system representatives, discussing the theory of operation at leading power factor and of a few cases of practical experience cited. The desirability of using automatic voltage regulators extensively in this operation was pointed out. A few companies had considered the necessity for loss of field relays in this connection to pre-

vent the sustained reactive demand and low voltage which results from loss of field. It was the opinion of the subcommittee that the conference did not develop any papers which could be presented on a formal basis, but the conclusion was reached by the speakers that leading power factor operation could be entered into on a moderate scale as the necessary safeguards are provided.

This subcommittee is studying the problem of adequate station electric auxiliaries in power stations during periods of system trouble. Several recent shutdowns of power systems have pointed out the need for studying this problem and reviewing operating procedures.

System Control Subcommittee. Although this subcommittee has not been active during the year, it is now studying two basic problems: the use of automatic load control on high-efficiency versus low-efficiency capacity; and the most desirable rate of load change on different types of generating equipment.

Joint Subcommittees. The subcommittee on out-of-phase high-voltage switching completed its study and presented a report which was accepted.

The Probability Subcommittee is active. It presented a second report at the Fall General Meeting, and now is extending its study to include more recent data on outages of turbine generator units operating at 700-pound or higher and hydro units.

The Committee on System Engineering was one of the sponsors of the Power Conference in Pittsburgh, Pa. It co-operated with the Committee on Industrial Power Systems in the program for April 20, and it presented two papers discussing problems associated with utility power-system supply to industrial plants.

COMMITTEE ON TRANSFORMERS

This committee consists of 33 members operating 15 working groups. In addition, 42, mostly members of the Institute, assist in the working group activities.

The following report gives changes in the status from that reported in last year's activities.

Co-ordinated Study of Life of Transformer Insulation Working Group. Apparatus and technique for this subject is all well developed, but some difficulty has arisen in obtaining satisfactory test samples. All of this work is limited to the pilot tests, which will form the basis for the final aging program.

Joint Subcommittee on Instrument Transformers. The subcommittee has a number of active subjects under discussion. "Application Guide for Grounding of Instrument Transformer Secondary Circuits and Cases" has been issued as ACO paper 50-65.

Subcommittee on Papers. This subcommittee has been responsible for obtaining, so far this year, 20 technical papers, and three conference papers. For the Summer and Pacific General Meeting, two sessions have been arranged.

Operating Guides for Regulators Working Group. Technical paper 49-228 has been referred to the Standards Committee for approval as a revision of ASA *C57.35*, dated 1948.

Short-Circuit Thermal Ratings of Induction and Step Regulators Working Group. The work on this assignment is progressing, but, at the present moment, is not ready for final decision. This subject deals primarily with the revision of ASA *C57.35*, and includes an explanation of paragraph 15.050 in connection with reclosing devices.

Magnetization Characteristics of Transformers Working Group. The scope of this assignment remains unchanged, and all the committee can report is progress.

Revision of Dielectric Tests Working Group. The same problems confront this working group as outlined in last year's report. Additional pressure is being exerted to bring up to date all impulse testing technique.

Guides for Operation and Maintenance of Dry-Type Transformers With Class-B Insulation Working Group. A report on the activities of this subcommittee has been submitted to both the Edison Electric Institute and the National Electrical Manufacturers Association for comment and review. The committee now awaits final comments of the National Electrical Manufacturers Association's Standards Committee before proceeding with any further changes to the Guides.

Co-ordination of Insulation Working Group. The work of this committee is progressing satisfactorily. Additional requests for information have been received.

Electronic Power Converters Working Group. This is a 1-man committee acting as liaison representative between the Committee on Electric Power Converters and the Committee on Transformers.

Methods of Making Temperature Tests on Transformers Working Group. Technical paper 50-99 has been issued as a preliminary report dealing with temperature tests. The committee is completing a report which will be a revision of ASA *C57.22.100*.

Power Factor Measurements Working Group. This originally was a 1-man committee, but has now been augmented with an additional member. The committee expects to complete this report by the end of the term.

Audible Noise in Transformers Working Group. A number of technical papers have appeared due to the activities of this group. Work has not been completed to a point where a report can be issued.

Hot-Spot Temperature Rise of Class-B Reactors Working Group. This is a new group and will cover Class-*B* reactors not now included in Table *C57.11.021*.

Permissible Maximum Oil Temperature in Service Working Group. This committee is working on the permissible maximum oil temperature of transformers in service. This subject is a study to determine whether it is permissible to operate sealed-type transformers in excess of the 100-degree-centigrade limitation in the present Guide *C57.32*.

COMMITTEE ON TRANSMISSION AND DISTRIBUTION

The general plan of operating the committee during the past year has been to continue the five subcommittees dealing with subjects within the scope of the main committee, and assign to them additional subjects of interest and importance in the transmission and distribution field as they arise, either from suggestions of committee members or others outside the committee. It has been the aim of the committee to clear all valuable and important information to Institute members by technical or conference papers, when any work has progressed to a point where it is of significant value. No attempt has been made to enhance the committee prestige by soliciting papers merely to get volume, but rather an effort has been made to obtain high-grade well-digested material for technical papers to record the progress of the art, promote constructive thinking, and study and investigate engineering features within the committee scope.

In the distribution field, a study is being made jointly with the Edison Electric Institute to obtain records of operating experience on distribution lines. This project, mentioned last year, is still in progress. The subject of distribution system economics is also being given attention.

In the lightning field, a laboratory study on the lightning strength of wood-pole lines in the subtransmission range is progressing. It is expected co-ordination of this work with field experience will be of value.

The predetermination of the lightning performance of transmission lines, which has been studied from a theoretical point of view, is reaching fruition in a committee report planned for the Summer and Pacific General Meeting. The Lightning Bibliography, which takes the place of the proposed second volume of the Lightning Reference Book, has been completed, and is expected to be published and made available for distribution in the summer of 1950. Two projects affecting transmission-line operation are progressing satisfactorily. One relates to a general survey of the causes of all transmission-line outages, and the other is a study of system recovery voltage.

After the co-ordinated technical session on capacitors at the Fall General Meeting, where an extensive discussion developed on capacitor operation, further study has been undertaken, mainly directed to capacitor temperature, tank corrosion, and short-time capacitor voltage ratings. A bibliography on this subject is in the course of preparation. Further public presentation on this subject is tentatively planned for 1951.

The series capacitor has been given some consideration, with regard to its application on high-voltage lines, as well as on low-voltage lines, to prevent voltage flicker.

In the conductor field, a study is being made on higher permissible conductor current loading, damage to conductors from vibration, and means of alleviating the trouble. A symposium on this latter subject is being planned for the Fall General Meeting.

A number of other subjects being dealt with in subcommittees have not yet reached the stage where present publicity would serve any useful purpose. During the year, the committee sponsored papers, solely or jointly with other committees, at general meetings, and at one District Meeting. It has offered papers within its field for the Middle Eastern District Meeting. For the Winter General Meeting, a session on technical features of high-voltage transmission is being arranged.

During the past year, technical papers passing through committee review have included those on power capacitors, recovery rates of voltage on distribution systems, arc extinction characteristics of gaps, insulator contamination and corrective measures, primary network systems, corona and radio-influence effects, distribution system planning, and operational characteristics.

For the 1950 Great Lakes District Meeting, three papers were offered, dealing with plan-

ning subtransmission and distribution systems, right-of-way brush control, and protection against conductor burndown.

For the Summer and Pacific General Meeting the committee is sponsoring papers on corona features, economics and lightning performance of high-voltage transmission lines, as well as other papers dealing with insulation co-ordination and interrupting ability of horn gaps.

COMMITTEE ON BASIC SCIENCES

The committee sponsored one session each at the Summer General Meeting, and the North Eastern District Meeting; a total of eight papers were presented at these meetings. It also sponsored a session on voltage induction during the Fall General Meeting, in the course of which five conference-type papers were presented. The committee had meetings at the Summer General Meeting and the Winter General Meeting, the prime object of which was the review of the activities and plans of the six subcommittees of the Committee on Basic Sciences, as well as discussion of items of general interest, such as the standardization of voltage and current notation and the nomenclature pertaining to sinusoidally varying alternating values.

Perhaps the most valuable service rendered to the members of the Institute by the committee is through the co-ordination and sponsorship of the work of its six subcommittees, all of which were very active during the past year; the symposia arranged by several of these subcommittees enjoyed a surprisingly large attendance, proving that the subject matter was of great interest to electrical engineers.

Reports on the activities of the subcommittees follow.

Subcommittee on Electrical Properties of Solids and Liquids. Because of the rapidly increasing use of semiconductor devices in electrical engineering, this subcommittee has been unusually active in the past year. A symposium on electrical properties of semiconductors and the transistor was held at the Summer General Meeting. Four articles covering the subject matter of the symposium appeared in *Electrical Engineering*, and have been assembled in a pamphlet. A second symposium of seven papers on "dielectrics" was held at the Winter General Meeting. These additional symposia were intended primarily for the nonspecialist engineer. For engineers who are specializing in semiconductor devices, a Conference on Electron Devices is to be held at the University of Michigan in June. This is jointly sponsored by the IRE and several AIEE committees.

Subcommittee on Energy Sources. The subcommittee sponsored its fourth Conference on Energy Sources at the Winter General Meeting. Three papers, dealing with recent developments in the field of electric batteries, were presented. The subcommittee is arranging for publication, in pamphlet form, of the first 14 papers presented since the formation of the subcommittee in 1946.

Subcommittee on Electric Circuit Theory. This subcommittee sponsored a conference on applications of conformal mapping in electric circuit analyses at the Fall General Meeting. Three papers were presented. Members of the subcommittee have been generous in devoting time to review the unusually large number of papers in electric circuit theory submitted to the Institute in recent months.

Subcommittee on Applied Mathematics. The subcommittee sponsored two conferences on applied mathematics, one at the Summer General Meeting and another at the Winter General Meeting. The subcommittee also expects to participate in the International Conference of Mathematicians, to be held in Boston, Mass., August 30 to September 6, 1950. The subcommittee has proposed to the Committee on Basic Sciences a new plan of activity, a full description of which was published in the May issue of *Electrical Engineering* under "Committee Activities." Briefly, the plan consists of inviting prominent mathematicians to become members of this subcommittee and enlisting their co-operation in solving engineering problems which would be submitted by the members of the Institute. Approximately ten prominent mathematicians have already signified their willingness to participate in this venture. The co-operation of the membership of the Institute in this project will determine to what extent the plan will be successful. The subcommittee is corresponding with the chairmen of various technical committees in the hope that it can stimulate interest in this project and obtain the problems in the fields of these committees, which lend themselves to mathematical treatment.

Subcommittee on Electrical Properties of Gases. This newly formed subcommittee held two meetings in 1949, one in April and one in November, both of which were attended by the full membership. Both of these meetings were concerned primarily with plans for a session on the electrical properties of gases at the 1950 Winter General Meeting. This session, the first organized and sponsored by this subcommittee, was held as scheduled; papers by four outstanding speakers were presented, and the attendance was very gratifying. The papers are scheduled for publication in *Electrical Engineering* as a series in succeeding issues. The members of the subcommittee held another meeting during the Winter General Meeting. Encouraged by the interest shown in the subject as shown by the large attendance, a similar session on the electrical properties of gases during the 1951 Winter General Meeting is planned.

Subcommittee on Magnetics. The subcommittee arranged for a symposium for the Winter General Meeting, consisting of seven papers on various subjects connected with magnetics, and a moving picture showing the movement of domain boundaries during magnetization. The attendance was exceedingly good, reaching 400 on Tuesday afternoon. This indicated a continuing interest in the subject, and another symposium is planned for the 1951 Winter General Meeting.

COMMITTEE ON COMPUTING DEVICES

The intense activity in the field of large-scale computing devices which arose following the end of the war is showing results in a steadily increasing number of papers in this field. There is intense competition among large laboratories in a development race which remains largely under cover. However, a tremendous range of applications is being investigated, and the possibility of using electronic computers in place of, or in addition to, present business machines seems attractive. There have been investigations of the possibility of using large-scale computers in place of a-c calculating boards and at the same time there have been improvements in the use of a-c calculating boards which have increased their efficiency appreciably.

In the field of large-scale computing itself, problems continue to grow in proportion as the ability to solve them grows, and there appears pressure for types of work which only a few years ago would not have been contemplated. The realization of the power of computing devices and the ease with which they can be manipulated has led to the growth of many special-purpose devices. As the principles become better known, it seems that the field of large-scale computers will be a well-defined engineering field, and a large part of the technical work will fall within electrical engineering.

Not much has been said with regard to continuous variable computers, but these are widely used and are being continuously improved. One reason for less information concerning them is that many applications are in the military field.

The Committee on Computing Devices held one session at the Winter General Meeting and at that time laid plans for the remainder of the year. These are resulting in two sessions at the Summer and Pacific General Meeting, one of which is on the application of large-scale computers in aircraft development, a possible session at the Fall General Meeting on applications of large computers to the petroleum industry, a session at the North Eastern District Meeting, a session at the coming Middle Eastern District Meeting, in October, and at least two sessions at the 1951 Winter General Meeting.

A special activity of the committee is the preparation of a bibliography covering the field of computers. This work is to be done in co-operation with a corresponding IRE committee, and it is hoped that a publication will result.

The committee has two subcommittees, one on continuous variable computers and one on digital computers. The work of these subcommittees has been devoted largely to the procurement of papers and the organization of those sessions which have been held or are contemplated.

There is an interesting side line in the field of the committee, in that many basic problems in the field are associated with others in the fields of communications, switching, control, and so forth. In this connection, not many persons realize that what is practically an entirely separate system of algebra has been built up especially for use in the computing device and associated fields. The committee is endeavoring to obtain an authoritative paper on this aspect of its work to see whether there is sufficient interest among electrical engineers to warrant presenting new developments of this type before the AIEE.

COMMITTEE ON ELECTRONIC POWER DEVICES

The activities of the committee during the year consisted mainly in completing projects previously initiated and encouraging papers on new developments and applications. Some new projects are also under consideration. Plans for the year were outlined at a meeting of the Administrative Subcommittee held September 12, 1949, in Pittsburgh, Pa. A meeting of the full committee was held on February 1, 1950, in New York. Meetings were held also by some of the subcommittees during the year.

The progress on the various projects is summarized in the following reports.

"*Survey on Operation of Mercury-Arc Rectifiers.*" The Subcommittee on Electronic Converter Applications has been making a survey on operation of mercury-arc rectifier installations. Questionnaires requesting operational data have been sent to rectifier users. A preliminary report on the results of the survey was presented at the Fall General Meeting. The final report will be presented at the Summer and Pacific General Meeting.

"*Report on Inductive Co-ordination on the D-C Side of Rectifier Installations.*" A working group of the Subcommittee on Applications is preparing a report on inductive co-ordination aspects relating to the d-c side of rectifier installations. A second draft of the report has been written and it is now expected to have the report completed in time for presentation at the Winter General Meeting.

"*Protection of Electronic Power Converters.*" A working group consisting of members of the Subcommittee on Electronic Power Converter Circuits and representatives of the Committee on Substations have been engaged in the preparation of a report on "Protection of Electronic Power Converters." This report is devoted primarily to the problem of protection of power rectifiers of the sizes and types usually encountered in railway, electrochemical, and general industrial applications. The report was presented in two parts at meetings in January and October 1949. These have been revised and combined into a single report for final presentation at the Summer and Pacific General Meeting and publication in the *Transactions*.

"*Bibliography on Electronic Power Converters.*" A bibliography covering the years from 1903 to the end of 1947 has been published by AIEE. The Subcommittee on Papers and Speakers reported no other activity.

"*Standards for Hot-Cathode Power Converters.*" The Subcommittee on Hot-Cathode Power Converters has been transferred from the Committee on Electronics to the Committee on Electronic Power Converters, in order to facilitate co-ordination with the pool cathode group. This subcommittee is engaged in the preparation of Standards for hot-cathode power converters. A set of definitions has been adopted by the subcommittee, and is being circulated in the main committee for comments.

The activities of the subcommittees and working groups, other than those reported on the foregoing projects, were carried on as follows.

Subcommittee on Electronic Power Converter Circuits is soliciting papers on surges, fault currents, protective gear, and rectifier power factor.

Subcommittee on Rectifier Transformers is soliciting papers on transformer noise and surge protection.

Subcommittee on Rectifying Devices is co-operating with other committees working on Standards for pool tubes, and is keeping the members of the main committee informed on such activities.

West Coast Subcommittee is co-ordinating AIEE activities relating to electronic power converters in that region.

Rectifier Standards. A working group has been organized to review the development of world standards on rectifiers, and to keep the members of the main committee informed on such activities.

Conference on Rectifier Cooling Systems. The committee is planning to hold a conference on cooling and corrosion problems relating to rectifier cooling systems during the fall in 1950.

COMMITTEE ON ELECTRONICS

The sponsorship of 2- or 3-day conferences relative to specific work areas in electronics has been one of the important continuing contributions of the committee for the past several years. Thus, the Second Annual Joint Conference on Electronic Instrumentation in Nucleonics and Medicine was held in New York, October 31, November 1–2, 1949. This was sponsored jointly by the Committees on Electronics, Nucleonics, and Instruments and Measurements within the AIEE, and the Nucleonics Studies Committee of the IRE. The conference was fully as successful as its predecessors, and plans have been formulated for a similar conference in the fall of 1950.

A 3-day Symposium on Improved Quality Electronic Components will be held in Washington early in May 1950, under the sponsorship of the AIEE Joint Subcommittee on Electronic Instruments, the Institute of Radio Engineers, and the Radio Manufacturers' Association. This is the third annual spring conference in a general series dealing with various aspects of engineering problems involved in the industrial applications of electronics.

The Subcommittee on Electron Tubes is sharing with the IRE Committee on Electron Tubes and Solid State Devices the sponsorship of the annual Conference on Electron Devices, to be held at the University of Michigan, Ann Arbor, Mich., June 22–23, 1950. This conference deals, on a completely informal basis, with new discoveries and projected methods and techniques in research and early development work on electron tubes and semiconductor devices.

Meetings of the committee were held in Swampscott in June 1949, at the National Electronics Conference in Chicago in September 1949, and at the Winter General Meeting.

The National Electronics Conference, held annually in the fall, in Chicago, is a very large middle-western forum for the presentation of papers of electronic interest, incorporating an extensive manufacturer's display of electronic instruments and new products; the *Proceedings* of the National Electronics Conference, published annually, contains in complete form the papers presented at the NEC.

It has become the policy of the Committee on Electronics to give substantial support to the NEC. Thus, during the past year, the chairman of the committee has served actively as the AIEE representative on the NEC Board of Directors, and various members of this and other AIEE committees have assisted in building greater strength into the industrial electronics part of the annual NEC program.

As a part of the continuing effort to bring to AIEE membership early reports on new electronic developments, various specific areas of work have been emphasized by holding three conference sessions at the Summer General Meeting and four at the Winter General Meeting.

A full program of papers of electronic interest is assured for the Summer and Pacific General Meeting, and for the Fall General Meeting.

The changes in the technical subcommittee structure during the year have been: the addition of Subcommittees on Electronic Systems Engineering and on Liaison With Electronic Heating, the transfer of the Subcommittee on Hot-Cathode Electronic Power Converters to the jurisdiction of the Committee on Electronic Power Converters, and the transfer of the Subcommittee on Electronic Aids to Medicine to the status of a joint subcommittee, sponsored also by the Instruments and Measurements Committee. At present, there are 19 subcommittees and two joint subcommittees.

With active advice and counsel from the chairman of the Subcommittee on Electronic Standards, there has been substantial progress towards Standards formulation in the following areas: X-Ray Tubes, Apparatus, and Applications; Electron Tubes, particularly High-Vacuum Tubes, Cathode-Ray Tubes, Gas-Filled Tubes, Phototubes, and Mercury-Pool Tubes.

COMMITTEE ON INSTRUMENTS AND MEASUREMENTS

The committee had a very interesting and active season. The personnel was changed so that 38 members were carried over from last year's roster, and 18 new members replaced 14 retiring members of last year's committee. Two vice-chairmen were named to assist in the operation of the committee, one for the East, and one for the West. The duties of the vice-chairman for the East were to procure and process papers originating in cities bordering on the Mississippi River and east of that river for technical sessions, and to arrange all technical programs sponsored by the committee at general or District meetings held in the afore-mentioned area. The duties of the vice-chairman for the West were similar except that he covered the area west of the Mississippi. The purpose of this arrangement was to ensure that instruments and measurements activities will be ably represented at all general and District meetings.

A committee meeting was held on September 19 to plan the year's program. A luncheon meeting was held January 31 to further the committee activities. This meeting was attended by 35 committee members and nine guests, including President Fairman, who spoke on joint activity of AIEE with other societies. A meeting is planned for May, in Philadelphia, and one will be held at the Summer and Pacific General Meeting.

The changes in the committee structure and the activities of the continuing subcommittees are reported as follows.

Changes

1. *Subcommittee for Revision of ASA's C-39* has been discontinued, since this work has been completed.

2. *Subcommittee on a Master Test Code for Resistance Measurements* has been discontinued, since the test code has been completed.

3. *Joint Subcommittee on Servomechanisms* has been promoted to full committee status.

4. *Subcommittee on Co-operation With the Instrument Society of America* has been named a standing subcommittee, since it is expected that the AIEE will continue to participate in the yearly instrument conference of the ISA.

Two interesting technical sessions were

arranged by this committee at the September 1949 conference held in St. Louis.

5. *Subcommittee on Electrical Aids to Medicine* has broadened its scope and is now a Joint Subcommittee of the Committees on Instruments and Measurements, Electronics, and Therapeutics.

6. *Subcommittee on Organization* was set up to study the relationship of the Committee on Instruments and Measurements to other technical committees and to make recommendations for future activities of the Committee on Instruments and Measurements.

7. *Joint AIEE–IRE Committee on High-Frequency Measurements* has been set up to handle jointly technical conferences, Standards, and definitions in this particular field. The AIEE representatives on this committee will form the Subcommittee on High-Frequency Measurements to act on matters pertinent to the AIEE.

8. *Subcommittee on Industrial Spectroscopy* has been formed, and will handle matters relating to design and characteristics of instruments and measurements pertinent to the field of industrial spectroscopy. It will promote technical sessions covering new or improved practices and determine Standards and definitions for this particular field. The final scope will be determined when the subcommittee becomes better organized and has its first meeting. One of its first activities was to schedule an informal conference session at the Winter General Meeting.

9. *Subcommittee on Master Test Code for Power Measurements* has been formed, and will draft a master code as required throughout the field of electrical engineering. It will be similar in construction to the Master Test Code for Resistance Measurements and the Master Test Code for Temperature Measurements which have been completed recently by the Committee on Instruments and Measurements.

Continuing Subcommittees

1. *Subcommittee on the Revision of Standard 4* (Measurement of Test Voltage in Dielectric Tests) is currently awaiting the prosecution of further tests and test data formulation from several commercial, industrial, and government laboratories. Completion of this work, particularly in the field of short-time impulse measurement, is awaited to assist the resulting work of standardization projected by this subcommittee.

2. *Subcommittee on Watt-hour Meters* issued a report entitled "Errors in Watt-hour Meter and Electrical Indicating Instrument Readings Caused by Harmonics in the Wave Form of the Supply Voltage," on January 24, 1950, for informal release to the New England Power Service Company and others technically interested. The subcommittee has tentatively established for itself the following fields of activity:

(a). Preparation of a bibliography on the subject of watt-hour meters and associated fields such as demand meters.

(b). The study of metering of loads of very short duration such as welders.

(c). A study of the performance of watt-hour meters on high frequencies, 400 cycles and above.

(d). A study of the testing of calibrating techniques for the watt-hour meter.

(e). The effect of temperature and the resulting errors when testing watt-hour meters out of doors at light loads.

Item *a* will be actively processed. Concurrently, the suitability of the other items will be appraised.

3. *Subcommittee on Definitions* still has under consideration the second draft of the definitions of Group 30, Instruments, Meters, and Meter Testing, which are being prepared by the *C42* Subcommittee, Number 6. Final approval of the second draft should be completed shortly.

4. *Subcommittee on Electrical Tests on Dielectric Measurements in the Field* is making a survey to determine current practices in field testing of dielectrics. A conference session on insulating oils was sponsored by this subcommittee during the Winter General Meeting.

5. *Subcommittee on a Master Test Code for Temperature Measurements* is revising Section 2 of the test code, AIEE *551*, in accordance with a request of the Standards Committee to make it identical with the corresponding section of AIEE Number *1*.

6. *Subcommittee on High-Frequency Measurements* sponsored a technical session at the Winter General Meeting.

7. *Subcommittee on Marking Varmeters and Related Instruments* has completed its survey with regard to practices in marking varmeters, and a report is in progress.

Joint Subcommittees

1. *Joint Subcommittee on Instrument Transformers* has been assisting actively in preparation of Standards and held a very successful technical session at the Winter General Meeting.

2. *Joint Subcommittee on Telemetering* has continued active collaboration with the National Telemetering Forum through attendance at NTF meetings and an increasing cross-membership. This subcommittee has accepted the responsibility of completing a "Glossary of Radio Telemetering Terms," which had been started by the Instrument Research Division of NACA. This joint subcommittee held a Technical Conference on Telemetering, jointly sponsored by the NTF in Philadelphia, May 24–26.

3. *Joint Subcommittee on Electronic Instruments* arranged a technical session on miscellaneous electronic instruments for the Winter General Meeting, and, with the assistance of the Joint Subcommittee on Telemetering, a technical session on radio telemetering for the 1949 Summer General Meeting. This joint subcommittee represented the AIEE in sponsoring jointly with IRE and the Radio Manufacturer's Association a Conference on Improved Quality Electronic Components, May 9–11, 1950, in Washington, D. C. Work has continued on the formulation of standardized forms for the specification of vacuum-tube voltmeters and for cathode-ray instruments, including a glossary of pertinent terminology.

4. *Joint Subcommittee on Nucleonic Instruments*, working with the Joint Subcommittee on Electrical Aids to Medicine and the IRE, sponsored the Second Annual Joint AIEE–IRE Conference on Electronic Instrumentation in Nucleonics and Medicine, held in New York, October 31, November 1–2, 1949. Plans already are under way for a 1950 conference. This subcommittee also sponsored a session on nucleonic instruments for the Winter General Meeting.

The Committee on Instruments and Measurements has been active in other fields through its representation on other committees of the AIEE, American Standards Association, and The American Society of Mechanical Engineers. In addition to the previously mentioned nine technical sessions, which were sponsored by its subcommittees, the committee also sponsored two sessions at the Summer General Meeting, one session at the Fall General Meeting, one session at the Winter General Meeting, and one session at the North Eastern District Meeting. This makes a total of 14 technical sessions for the 1949–50 season.

COMMITTEE ON METALLIC RECTIFIERS

During the past year, full meetings of this committee were held on June 24, in Swampscott, and on January 31, in New York.

The chief accomplishment of the year has been the preparation of Standards for Metallic Rectifiers, which include standard definitions and testing standards. The last revision of these Standards is in practically its final form.

At the January meeting, a new Subcommittee on Miniature Rectifiers was organized to take care of the special requirements of this type of equipment. At the same meeting, another subcommittee was set up for the purpose of developing necessary technical information which will be useful to users of metallic rectifiers and which will standardize many of the commonly used circuit ratings and other design or application factors.

Plans are being made for a conference session on metallic rectifiers at the Summer General Meeting in 1951.

COMMITTEE ON NUCLEONICS

The committee held two meetings during the year, one in connection with the Summer General Meeting, and the other during the Winter General Meeting.

The Subcommittee on Safety and Health Protection Against Radiation has been dissolved, and its functions transferred to the Joint Subcommittee on Nucleonic Instruments. A new Subcommittee on Nuclear Machines is in the process of being set up. Four subcommittees of this committee are now as follows: Joint Subcommittee on Nucleonic Instruments (Joint with the Committee on Instruments and Measurements), Subcommittee on Isotopic Tracers, Subcommittee on Nuclear Physics, and Subcommittee on Nuclear Machines.

The committee activities were directed toward bringing nucleonic information to the Institute membership. The committee sponsored or will sponsor conference sessions on nucleonics at the following meetings:

Summer General Meeting, four papers covering nucleonic instrumentation, sponsored by Subcommittee on Nucleonic Instruments.

Winter General Meeting, five papers covering nucleonic instrumentation, sponsored by Subcommittee on Nucleonic Instruments.

Joint AIEE/IRE Special Technical Conference on Electronic Instrumentation in Nucleonics and Medicine, New York, October 31, November 1 and 2, 1949, with 27 papers. A joint committee is preparing for a similar conference in October 1950.

The committee will be a joint sponsor of two sessions at the Summer and Pacific General Meeting, one with the Committee on Electronics and the other with the Committee on Electronic Power Converters.

A meeting of the Atomic Energy Commis-

sion Ad Hoc Committee on Technological Information for Industry was attended. This work is now being carried on by C. S. Rich, Editor, *Electrical Engineering*.

The committee has also co-operated in the review of the various nucleonics glossaries now nearing completion under the auspices of the National Research Council.

COMMITTEE ON THERAPEUTICS

Activity of this committee has consisted of review and approval for publication of a technical paper entitled "Electrical Instrumentation in Medical Research" by J. Malvern Benjamin, Jr., John Hale, Edwin L. Carstensen, and Howard E. Tompkins. Presentation of the paper is presently being scheduled.

Awards

COMMITTEE ON AWARD OF INSTITUTE PRIZES

The award of technical paper prizes was made on a Division basis for the first time during the current administrative year. The committee thinks the selection of the prize papers for the Divisions and also for the student prize paper contest can be handled most effectively by one committee, the Committee on Award of Institute Prizes, which should be composed of working groups in the several fields of interest, corresponding to the Divisions. This method of operation will assure that the prizes will continue to be Institute prizes and that the responsibility for selection will be definitely placed and recognized.

CHARLES LEGEYT FORTESCUE FELLOWSHIP COMMITTEE

The committee held one meeting, in New York, at which time business affairs were discussed and selection of recipients for the academic year 1950–51 was accomplished. Two fellowships, each carrying a stipend of $1,000, were granted. One recipient was Robert R. Johnson, of the University of Wisconsin, who will undertake graduate study in electrical engineering at Yale University. The other winner was Robert E. Horn, of Washington University in St. Louis, who will enter the graduate school of that university for study in electrical engineering. Both of these men had undergraduate records that approached perfection, and are well-balanced personalities as well.

The committee wishes to report a very encouraging response to the fellowship competition last winter. A record number of applications, 23, were received, and nearly all were from well-qualified young men. The committee believes that the fellowship continues to be a very worth-while project.

JOHN FRITZ MEDAL

The John Fritz Medal may be awarded annually for notable scientific or industrial achievements, by a board of award composed of representatives of the American Society of Civil Engineers, The American Society of Mechanical Engineers, American Institute of Mining and Metallurgical Engineers, and AIEE. The 1950 medal was awarded to Walter Hull Aldridge, President of the Texas Gulf Sulphur Company, with the following citation: "As Engineer of mines and statesman of industry who, by his rare technical and administrative skills, has importantly augmented the mineral production of our country and Canada, and who, by giving unselfishly of his wisdom and vision, has guided his professional colleagues to higher achievements."

The medal was presented to him on November 16, 1949, at a dinner at the University Club.

MARSTON MEDAL

The Marston Gold Medal is awarded to an alumnus of Iowa State College, of at least 30 years' standing, for achievement in engineering in a broad field. The board of award includes representatives of the college, and five engineering societies: ASCE, AIME, ASME, AIEE, and American Institute of Chemical Engineers.

WASHINGTON AWARD

The Washington Award for 1950 was made to Wilfred Sykes, President, Inland Steel Company, Chicago, Ill., and was presented at a dinner meeting on February 27. The award is made annually to an outstanding engineer, a citizen or resident of the United States, who ably has served human needs, and is administered by a commission representing the Western Society of Engineers, ASCE, AIME, ASME, and AIEE.

EDISON MEDAL

The Edison Medal for 1949 was awarded to Dr. K. B. McEachron, Manager of Engineering, Transformer and Allied Products Division, General Electric Company, Pittsfield, Mass., "for his contributions to the advancement of electrical science in the field of lightning and other high-voltage phenomena and for the application of this knowledge to the design and production of electric apparatus and systems," and was presented to him on February 1, 1950, in an evening session of the Winter General Meeting.

The medal may be awarded annually for meritorious achievement in electrical science, electrical engineering, or the electrical arts. Awards are made by a committee of 24 members of the Institute.

LAMME MEDAL

The Lamme Medal for 1949 was awarded to C. M. Laffoon, Manager of A-C Engineering Department, Westinghouse Electric Corporation, East Pittsburgh, Pa., "for outstanding contributions to the design of electrical machines, particularly large turbine generators and high-frequency generators." The medal will be presented to him on June 12, 1950, during the Summer and Pacific General Meeting.

The medal may be awarded annually by a committee of nine members to a member of the AIEE for "meritorious achievement in the development of electrical apparatus or machinery."

ALFRED NOBLE PRIZE

The Alfred Noble Prize award is made to a member of any grade of the ASCE, AIME, ASME, AIEE, or WSE for a technical paper of exceptional merit officially accepted for publication in any of their technical publications, provided the author has not passed his 31st birthday at the time the paper is submitted to the society in practically its final form. The prize award carries a handsome certificate and $350 cash. It is an important award, and greater publicity should be given to it by each of the participating societies in order that it will more fully stimulate the writing of papers by young members.

Ten AIEE papers were eligible, and from this group the paper "Relative Surface Voltage Gradients of Grouped Conductors" by M. Temoshok, Associate AIEE, was chosen as most worthy of the award.

After due consideration by the committee, the award was given to J. C. Fisher, ASME, for the paper "Anisotropic Plastic Flow."

It is interesting to note that Mr. Fisher is Research Associate, General Electric Research Laboratory, and that his paper is of the research type with related papers having been previously published in the *Journal of Applied Physics*. The AIEE paper "Relative Surface Voltage Gradients of Grouped Conductors" by Mr. Temoshok was of a different type, being a practical engineering type of paper of great value to the important development of long-distance power transmission at higher voltages than are in current use. It is very difficult when the committee is called upon to judge an engineering paper in comparison with a fundamental research paper.

The Alfred Noble Prize has been awarded each year since 1931, with the exception of 1934, 1935, and 1940, for a total of 16 times. It has been awarded to authors of AIEE papers eight times. However, there has been no award for an AIEE paper for the last five years.

HOOVER MEDAL

In September the Board of Award for the Hoover Medal awarded this distinguished honor to Dr. Frank B. Jewett, past-President of the AIEE. The Hoover Medal is awarded by a board representing the ASCE, AIME, ASME, and AIEE "for outstanding civic or humanitarian activities constituting distinguished public service." The citation accompanying this award is as follows:

FRANK B. JEWETT

> Great pioneer of industrial research, leader in molding scientific and engineering work to the needs of humanity, distinguished organizer of scientific effort for the service of the nation in war and peace.

The Institute suffered a great loss in the death of Dr. Jewett in November last. Accordingly, the medal was presented posthumously with appropriate ceremonies on Wednesday evening, February 1, during the Winter General Meeting of the Institute. Dr. Gano Dunn presented a statement of the achievements of the Medalist. The medal was presented by Dr. Scott Turner, Chairman of the Hoover Medal Board of Award, and it was received on behalf of his father by Harrison L. Jewett, Dr. Jewett's elder son, and himself a member of the Institute.

Joint Activities

UNITED ENGINEERING TRUSTEES, INC.

The funds and property held jointly by the four Founder Societies, including the Engineering Societies Building, the Engineering Societies Library, and the endowment funds of the Engineering Foundation, are administered by the United Engineering

Trustees, Inc., which also serves as treasurer of the Engineers' Council for Professional Development.

The building is fully occupied, and two of the Founder Societies have substantial amounts of space in other buildings.

The corporation is making studies of the possibility of securing a more modern building for the engineering societies.

ENGINEERING FOUNDATION

The Engineering Foundation is a department of the United Engineering Trustees, Inc., and its general objective is "the furtherance of research in science and engineering."

With the income from its endowment funds, it supports a broad range of research projects, now numbering about 15. Some of its most effective contributions are those supporting studies and analyses necessary in the early stages of organizing projects on such bases that financial support from other sources becomes available. A special study is being devoted to the future employment of foundation funds in advancing research.

ENGINEERING SOCIETIES LIBRARY

The library is a department of the United Engineering Trustees, Inc., and was formed by combining the separate libraries of the ACSE, AIME, ASME, and AIEE, and is conducted as a free public reference library.

In addition to affording the use of a large collection of engineering books and periodicals, the library renders special services such as bibliographies, translations, photostats, searches, and book loans by mail.

A broad survey has been made for the purpose of reorienting the library with other technical libraries in the United States and for improving its services.

Many valuable gifts of books and periodicals were received during the past year.

ENGINEERS' COUNCIL FOR PROFESSIONAL DEVELOPMENT

The principal activities of ECPD include programs for the guidance of young persons thinking of entering the engineering field, the accrediting of curricula of engineering schools, and encouragement and assistance to individuals in their engineering and cultural studies during several years following graduation. The council represents ASCE, AIME, ASME, AIEE, AIChE, the Engineering Institute of Canada, the American Society for Engineering Education, and the National Council of State Boards of Engineering Examiners.

ECPD approved and referred to the constituent societies the report of the Committee on Professional Recognition recommending the adoption of uniform grades of membership. The AIEE Board of Directors has approved the uniform grades for submission to the membership by letter ballot after they are approved by at least two other societies.

THE NATIONAL FIRE WASTE COUNCIL

A meeting of the National Fire Waste Council was held in Washington, D. C., Friday, March 31. The meeting was well attended, 55 of the 58 members having been present.

It was pointed out that the fire loss in 1949 amounted to 700 million dollars. This is equivalent to a $5 per capita loss. The association is attempting to reduce this loss which is enormous, particularly when it is compared with the figures for Britain, where the loss is 50 cents per capita, and with Germany, where it is 12 cents per capita. The majority of fires are due to carelessness; matches and smoking are responsible for the largest number. The next most common cause is defective wiring. The AIEE and its affiliates might well consider means of reducing this. The council is extremely anxious to reduce the fire loss, and it was pointed out by the speakers that the first step in any locality is the adoption of a fire prevention code; the second, the enforcement of this code. The National Board of Fire Underwriters has available a sample code. The council works through the Chambers of Commerce in the various localities and through these local Chambers attempts to educate the citizens and school children in fire protection. The council's plan is to organize in each Chamber a fire prevention committee to handle the problem in the locality.

In addition, the council is carrying on a hospital inspection program. This inspection is made available to hospitals, but no legal pressure is brought to bear. The committee reported that the larger hospitals welcome the inspection. They also stated that it was only the small hospitals that do not wish to be inspected. It was thought that the communities should be informed of the program; that they should assume the responsibility of seeing that it is carried out.

The Red Cross pointed out that there were 317 disasters (a disaster occurs when five or more families are involved) in 1949, of which 170 were caused by fires. It was stated that well over half of the disasters in this country are due to fires. The Red Cross is active in providing literature on fire prevention.

REPRESENTATIVES

A complete list of about 40 joint bodies upon which the Institute is represented appears in the Year Book and in the October issue of *Electrical Engineering* each year.

Appreciation

The Board of Directors notes with much satisfaction the continuing rapid increase in the membership and the substantial expansion in the activities of the general and technical committees, and the District, Section, and Branch officers and committees.

The Board of Directors expresses its deepest appreciation of the splendid co-operation received from all of these groups and from the membership in general.

Respectfully submitted for the Board of Directors.

H. H. HENLINE
Secretary

HASKINS & SELLS
CERTIFIED PUBLIC ACCOUNTANTS

250 PARK AVENUE
NEW YORK 17

ACCOUNTANTS' CERTIFICATE

American Institute of Electrical Engineers:

We have examined the balance sheet of American Institute of Electrical Engineers, and schedule of securities owned, as of April 30, 1950, and the related statements of income and operating fund reserve and of restricted fund reserves for the year then ended. Our examination was made in accordance with generally accepted auditing standards, and accordingly included such tests of the accounting records and such other auditing procedures as we considered necessary in the circumstances.

In our opinion, the accompanying balance sheet, schedule of securities owned, and statements of income and operating fund reserve and of restricted fund reserves, respectively, present fairly the financial position of, and securities owned by, the Institute at April 30, 1950, and the results of its operations for the year then ended, in conformity with generally accepted accounting principles applied on a basis consistent with that of the preceding year.

(*Signed*) HASKINS & SELLS

New York,
May 17, 1950

AMERICAN INSTITUTE OF ELECTRICAL ENGINEERS

Balance Sheet, April 30, 1950

Exhibit A

ASSETS

Property Fund Assets:		
One-fourth interest in physical properties of United Engineering Trustees, Inc.:		
Land, buildings, and equipment (less depreciation and renewal reserve)	$320,525.41	
Funded depreciation and renewal reserve	177,923.07	
Total	$498,448.48	
Equipment:		
Library (volumes and fixtures)—estimated value	36,366.37	
Office furniture and fixtures (less reserve for depreciation, $33,849.74)	26,070.65	
Works of art, etc.	3,001.35	
Total property fund assets		$ 563,886.85
Restricted Fund Assets:		
Securities—at cost (quoted market value, $633,201.43)—Schedule 1	$572,455.35	
Cash (including $12,626.78 Canadian funds):		
Reserve capital fund	9,266.71	
Life Membership fund	2,409.81	
Member-for-Life fund	6,236.86	
International Electrical Congress of St. Louis Library fund	873.69	
Lamme Medal fund	160.00	
Mailloux fund	1,021.38	
Volta Memorial fund	401.48	
Retired employees insurance fund	2,000.00	
Accrued interest receivable	319.98	
Total restricted fund assets		595,145.26
Operating Fund Assets:		
Cash (not including $1,655.69 for Federal taxes withheld from employees)	$ 12,977.22	
Accounts receivable:		
Members—for dues (less reserve, $6,300.00)	12,849.68	
Advertisers	2,218.70	
Miscellaneous	4,388.71	
Technical Conference loans	650.00	
Accrued interest receivable	2,360.83	
Inventories:		
Transactions, etc.	1,764.00	
Text and cover paper	15,511.21	
Badges	12,336.24	
Deferred charges—Production charges for May issue of *Electrical Engineering*	16,089.81	
Total operating fund assets		81,146.40
Total		$1,240,178.51

LIABILITIES

Property Fund Reserve		$ 563,886.85
Restricted Fund Reserves (Exhibit *C*):		
Reserve capital fund	$543,295.65	
Life Membership fund	7,610.88	
Member-for-Life fund	11,288.94	
International Electrical Congress of St. Louis Library fund	6,382.33	
Lamme Medal fund	4,440.44	
Mailloux fund	1,021.38	
Volta Memorial fund	19,105.64	
Retired employees insurance fund	2,000.00	
Tota restricted fund reserves		595,145.26
Operating Fund Reserves, Liabilities, etc.:		
Accounts payable	$ 40,122.69	
Deferred income:		
Dues received in advance	4,155.75	
Entrance fees and dues advanced by applicants for membership	1,815.75	
Subscriptions to publications received in advance	21,501.00	
Miscellaneous (including unallocated receipts)	1,493.48	
Operating fund reserve (Exhibit *B*)	12,057.73	
Total operating fund reserves, liabilities, etc.		81,146.40
Total		$1,240,178.51

AMERICAN INSTITUTE OF ELECTRICAL ENGINEERS

Exhibit B — **Statement of Income and Operating Fund Reserve for the Year Ended April 30, 1950**

Income:		
Dues (including $187,998.00 allocated to *Electrical Engineering* subscriptions)	$410,958.61	
Advertising in *Electrical Engineering*	197,221.72	
Transactions subscriptions	11,208.56	
Electrical Engineering subscriptions	31,070.83	
Miscellaneous publications (preprints, Standards, and other publications)	53,097.10	
Students' fees	39,747.75	
Entrance fees	23,634.10	
Registration fees—Institute Meetings and Technical Conferences	19,365.62	
Membership badges	5,018.20	
Transfer fees	3,015.00	
Interest and dividends on investments of Reserve Capital Fund	24,700.69	
Total income		$819,038.18
Expenses:		
Publications expense:		
Electrical Engineering text $185,497.50		
Electrical Engineering advertising 102,816.89	$288,314.39	
Transactions	23,378.64	
Proceedings	32,834.51	
"Year Book"	17,771.06	
Miscellaneous publications (preprints, Standards, and other publications)	40,680.50	
Institute meetings	28,996.56	
Institute Sections	85,234.65	
Institute Branches, including paper prizes, etc.	8,366.65	
Finance Committee	1,088.88	
Headquarters Committee	946.14	
Membership Committee	22,364.67	
Standards Committee	17,229.69	
Technical Committees	16,195.48	
Committee on Public Relations	5,387.88	
Committee on Registration of Engineers	16.34	
Edison Medal Committee	277.02	
Forward	$589,083.06	$819,038.18

Income (forward)		$819,038.18
Expenses (forward)	$589,083.06	
Traveling expenses:		
Geographical Districts:		
Executive Committees	6,614.62	
Vice-Presidents	2,487.94	
Conferences on Student activities	9,901.28	
Board of Directors	10,114.00	
Nominating Committee	1,682.79	
President's appropriation	305.13	
Institute representatives	484.44	
Administrative expenses	105,836.71	
Geographical Districts—Branch paper prizes	280.63	
Institute prizes	626.25	
Retirement system AIEE—normal contribution	8,646.21	
American Standards Association	1,500.00	
Canadian Radio Technical Planning Board	10.00	
Canadian Council of Professional Engineers and Scientists	161.55	
Engineers' Council for Professional Development	2,008.50	
Engineering Foundation Project—Welding Research	250.00	
Engineers Joint Council	701.80	
Hoover Medal	234.26	
National Council of State Boards of Engineering Examiners	500.00	
United States National Committee—International Commission on Illumination (two years' appropriations)	600.00	
National Fire Protection Association (two years' dues)	200.00	
United Engineering Trustees, Inc.:		
Building assessments	19,547.72	
Library assessments	14,369.65	
Library retirement plan	3,123.20	
Lamme Medal Committee	155.51	
Membership badges	4,929.59	
Legal services	250.00	
Inventory adjustment—"Electrical Definitions"	537.00	
Rent, etc.—Editorial office, 500 Fifth Avenue	6,928.67	
Exchange allowances	5,581.32	
Provision for doubtful accounts	7,559.81	
Transfer to Retired Employees Insurance Fund (Exhibit *C*)	2,000.00	
Transfer to Property Fund Reserve for furniture and fixtures expenditures	12,587.16	
Total expenses		$819,798.80
Excess of expenses over income for the year		$ 760.62
Operating fund reserve, May 1, 1949		22,818.35
Total		$ 22,057.73
Less—Repayment of advances from Reserve Capital Fund (net)		10,000.00
Operating fund reserve, April 30, 1950		$ 12,057.73

Exhibit C — **Statement of Restricted Fund Reserves for the Year Ended April 30, 1950**

	Total	Reserve Capital Fund	Member-for-Life Fund	Life Membership Fund	International Electrical Congress of St. Louis Library Fund	Lamme Medal Fund	Mailloux Fund	Volta Memorial Fund	Retired Employees Insurance Fund
Balance, May 1, 1949	$580,409.03	$531,660.79	$ 9,632.17	$8,312.51	$6,442.30	$4,440.44	$1,012.15	$18,908.67	
Additions:									
Income from bonds	$ 744.81		$ 125.00	$ 127.56	$ 135.28	$ 160.00		$ 196.97	
Interest on bank balances	73.80			53.57			$ 20.23		
Operating fund loan repayments:									
1948–1949	40,000.00	$ 40,000.00							
1949–1950	9,190.84	9,190.84							
Transfer from operating fund	4,043.55		2,043.55						$2,000.00
Supplementary fee	66.28			66.28					
Profit on sale of securities, etc.	1,634.86	1,634.86							
Total additions	$ 55,754.14	$ 50,825.70	$ 2,168.55	$ 247.41	$ 135.28	$ 160.00	$ 20.23	$ 196.97	$2,000.00
Total	$636,163.17	$582,486.49	$11,800.72	$8,559.92	$6,577.58	$4,600.44	$1,032.38	$19,105.64	$2,000.00
Deductions:									
Operating fund loan—1949–1950	$ 39,190.84	$ 39,190.84							
Authorized withdrawal from Life Membership fund	949.04			$ 949.04					
Purchase of medal, cost of engraving, etc. (exclusive of $99.30 paid from operating fund)	160.00					$ 160.00			
Library purchases	206.25				$ 195.25		$ 11.00		
Traveling expenses—District Branch prize winners	511.78		$ 511.78						
Total deductions	$ 41,017.91	$ 39,190.84	$ 511.78	$ 949.04	$ 195.25	$ 160.00	$ 11.00		
Balance, April 30, 1950 (Exhibit *A*)	$595,145.26	$543,295.65	$11,288.94	$7,610.88	$6,382.33	$4,440.44	$1,021.38	$19,105.64	$2,000.00

AMERICAN INSTITUTE OF ELECTRICAL ENGINEERS

Securities Owned, April 30, 1950

Schedule 1

	Principal Amount of Bonds or Number of Shares of Stock	Restricted Funds						
		Reserve Capital Fund	Life Membership Fund	Member-for-Life Fund	International Electrical Congress of St. Louis Library Fund	Lamme Medal Fund	Volta Memorial Fund	Total
Railroad Bonds:								
Atlantic Coast Line first consolidated 4%, due 1952	$ 4,000.00					$4,253.78		$ 4,253.78
Baltimore & Ohio, Pittsburgh, Lake Erie & West Virginia System refunding 4%, due 1980	10,000.00	$ 6,450.00						6,450.00
New York Central Railroad Company 4% series A consolidated mortgage, due 1998	15,000.00	9,812.50						9,812.50
Northern Pacific Railway Company 4½% collateral trust, due 1975	15,000.00	15,307.50						15,307.50
Total railroad bonds		$ 31,570.00				$4,253.78		$ 35,823.78
Public Utility Bonds:								
American Telephone & Telegraph Company 2¾% convertible debentures, due 1961	$40,000.00	$ 33,154.75	$5,153.12		$5,457.85			$ 43,765.72
Consolidated Edison Company of New York, Incorporated 3% convertible debentures, due 1963	20,000.00	21,825.00						21,825.00
Total public utility bonds		$ 54,979.75	$5,153.12		$5,457.85			$ 65,590.72
United States Government Bonds:								
Treasury bonds, 2%, due March 15, 1952/50	$ 3,000.00	$ 3,074.22						$ 3,074.22
Treasury bonds 3%, due September 15, 1955/51	2,000.00						$ 2,081.66	2,081.66
Defense bonds series G 2¼%, due December 1, 1954	18,000.00	13,000.00		$5,000.00				18,000.00
Treasury savings bonds series G 2¼%, due September 1, 1955	40,000.00	40,000.00						40,000.00
Treasury savings bonds series G 2¼%, due November 1, 1956	17,000.00	17,000.00						17,000.00
Treasury savings bonds series G 2¼%, due May 1, 1957	20,000.00	20,000.00						20,000.00
Treasury savings bonds series G 2¼%, due October 1, 1957	30,000.00	30,000.00						30,000.00
Treasury savings bonds series G 2¼%, due May 1, 1961	30,000.00	30,000.00						30,000.00
Treasury savings bonds series G 2¼%, due July 1, 1961	15,000.00	15,000.00						15,000.00
Treasury bonds 2¼%, due December 15, 1962/59	16,000.00						16,480.00	16,480.00
Total United States Government bonds		$168,074.22		$5,000.00			$18,561.66	$191,635.88
Total bonds		$254,623.97	$5,153.12	$5,000.00	$5,457.85	$4,253.78	$18,561.66	$293,050.38
Capital Stocks:								
American Can Company	60 shares	$ 4,988.40						$ 4,988.40
American Gas & Electric Company	400 shares	15,079.38						15,079.38
Atchison, Topeka & Santa Fe Railway Company preferred	200 shares	19,174.71						19,174.71
Boston Edison Company	200 shares	4,927.50						4,927.50
Commonwealth Edison Company	200 shares	7,580.68						7,580.68
Consolidated Natural Gas Company	100 shares	4,428.80						4,428.80
Dow Chemical Company $4 cumulative preferred, series A	100 shares	11,547.50						11,547.50
Eastman Kodak Company	300 shares	9,699.90						9,699.90
E. I. du Pont de Nemours & Company	300 shares	12,278.14						12,278.14
General Electric Company	200 shares	7,748.66						7,748.66
General Motors Corporation $5 preferred	200 shares	25,820.00						25,820.00
General Motors Corporation	100 shares	4,235.53						4,235.53
Gulf Oil Corporation	200 shares	12,264.20						12,264.20
Insurance Company of North America	120 shares	10,847.50						10,847.50
International Harvester Company	300 shares	5,030.50						5,030.50
Louisville & Nashville Railroad Company	100 shares	6,278.13						6,278.13
Ohio Edison Company 4.40% preferred	200 shares	21,279.25						21,279.25
Pacific Gas and Electric Company	200 shares	8,345.12						8,345.12
Public Service Electric and Gas Company $1.40 dividend preference common stock	300 shares	9,040.55						9,040.55
Scoville Manufacturing Company 3.65% cumulative preferred	100 shares	10,111.25						10,111.25
Sears, Roebuck and Co.	400 shares	6,014.97						6,014.97
Socony Vacuum Oil Company	400 shares	8,216.87						8,216.87
Standard Oil Company of Indiana	200 shares	8,170.32						8,170.32
Standard Oil Company of New Jersey	250 shares	12,049.69						12,049.69
Swedish Match Company class B	18 shares	100.00						100.00
Union Carbide & Carbon Corporation	300 shares	7,277.42						7,277.42
United Fruit Company	300 shares	11,985.00						11,985.00
United States Steel Corporation 7% cumulative preferred	100 shares	14,885.00						14,885.00
Total capital stocks		$279,404.97						$279,404.97
Total		$534,028.94	$5,153.12	$5,000.00	$5,457.85	$4,253.78	$18,561.66	$572,455.35

Officers of A.I.E.E. for 1950–1951

PRESIDENT

TITUS G. LECLAIR
Chicago, Ill.
(Term expires July 31, 1951)

PAST PRESIDENTS

EVERETT S. LEE, Schenectady, N. Y.
(Term expires July 31, 1951)

JAMES F. FAIRMAN, New York, N. Y.
(Term expires July 31, 1952)

VICE-PRESIDENTS

District
2 C. G. VEINOTT, Lima, Ohio
4 Walter J. SEELEY, Durham, N. C.
6 W. C. DUVALL, Boulder, Colo.
8 RALPH A. HOPKINS, Los Angeles, Calif.
10 A. H. FRAMPTON, St. Catharines, Ont.
(Terms expire July 31, 1951)

District
1 J. G. TARBOUX, Ithaca, N. Y.
3 C. S. PURNELL, New York, N. Y.
5 J. R. NORTH, Jackson, Mich.
7 H. R. FRITZ, St. Louis, Mo.
9 J. A. McDONALD, Salt Lake City, Utah
(Terms expire July 31, 1952)

DIRECTORS

W. L. EVERITT, Urbana, Ill.
A. C. MONTEITH, Pittsburgh, Pa.
ELGIN B. ROBERTSON, Dallas, Tex.
(Terms expire July 31, 1951)

C. W. FICK, Cleveland, Ohio
M. D. HOOVEN, Newark, N. J.
F. O. McMILLAN, Corvallis, Oreg.
(Terms expire July 31, 1952)

Ernest W. DAVIS, Cambridge, Mass.
N. B. HINSON, Los Angeles, Calif.
H. J. SCHOLZ, Birmingham, Ala.
(Terms expire July 31, 1953)

Walter J. BARRETT, Newark, N. J.
Allen G. DEWARS, Minneapolis, Minn.
VICTOR SIEGFRIED, Worcester, Mass.
(Terms expire July 31, 1954)

TREASURER

W. I. SLICHTER, New York, N. Y.
(Term expires July 31, 1951)

SECRETARY

H. H. HENLINE, New York, N. Y.
(Term expires July 31, 1951)

LOCAL HONORARY SECRETARIES

AUSTRALIA—V. J. F. Brain, Electricity Authority of N.S.W., Box 2600 G.P.O., Sydney, New South Wales

BRAZIL—Richard H. Bowles, Sao Paulo Tramway Light and Power Company, Caixa Postal 26-B, Sao Paulo

ENGLAND—Sir A. P. M. Fleming, Metropolitan Vickers Electric Company, Trafford Park, Manchester 17

INDIA, NORTHERN, S. S. Kumar, P.W.D. Electricity Secretariat, Ellerslie, Simla-E, East Punjab

INDIA, SOUTHERN—M. S. Thacker, India Institute of Science, Bangalore

NEW ZEALAND—R. D. Neale, School of Engineering, Canterbury University College, Christchurch G.1

PAKISTAN—(Vacancy)

SWEDEN—Edy Velander, Box 5073, Stockholm 5

TRANSVAAL—Francis E. Ingham, Box 6067, Johannesburg, Transvaal, South Africa

PAST PRESIDENTS—*1884–1950*

*NORVIN GREEN 1884–85–86
*FRANKLIN L. POPE 1886–87
*T. COMMERFORD MARTIN 1887–88
*EDWARD WESTON 1888–89
*ELIHU THOMSON 1889–90
*WILLIAM A. ANTHONY 1890–91
*ALEXANDER GRAHAM BELL 1891–92
*FRANK JULIAN SPRAGUE 1892–93
*EDWIN J. HOUSTON 1893–94–95
*LOUIS DUNCAN 1895–96–97
*FRANCIS BACON CROCKER 1897–98
*A. E. KENNELLY 1898–1900
*CARL HERING 1900–01
*CHARLES P. STEINMETZ 1901–02
*CHARLES F. SCOTT 1902–03
*BION J. ARNOLD 1903–04
*JOHN W. LIEB 1904–05
*SCHUYLER SKAATS WHEELER 1905–06
*SAMUEL SHELDON 1906–07
*HENRY G. STOTT 1907–08
*LOUIS A. FERGUSON 1908–09
*LEWIS B. STILLWELL 1909–10
DUGALD C. JACKSON 1910–11
GANO DUNN 1911–12
RALPH D. MERSHON 1912–13
*C. O. MAILLOUX 1913–14
*PAUL M. LINCOLN 1914–15
*JOHN J. CARTY 1915–16
H. W. BUCK 1916–17
*B. W. RICE, JR. 1917–18
COMFORT A. ADAMS 1918–19
*CALVERT TOWNLEY 1919–20
*A. W. BERRESFORD 1920–21
*WILLIAM McCLELLAN 1921–22
*FRANK B. JEWETT 1922–23
*HARRIS J. RYAN 1923–24
*FARLEY OSGOOD 1924–25
*M. I. PUPIN 1925–26
*C. C. CHESNEY 1926–27
*BANCROFT GHERARDI 1927–28
*R. F. SCHUCHARDT 1928–29
*HAROLD B. SMITH 1929–30
*WILLIAM S. LEE 1930–31
*C. E. SKINNER 1931–32
H. P. CHARLESWORTH 1932–33
J. B. WHITEHEAD 1933–34
*J. ALLEN JOHNSON 1934–35
*H. B. MEYER 1935–36
A. M. MACCUTCHEON 1936–37
W. H. HARRISON 1937–38
JOHN CASTLEBREAGH PARKER 1938–39
F. MALCOLM FARMER 1939–40
R. W. SORENSEN 1940–41
DAVID C. PRINCE 1941–42
HAROLD S. OSBORNE 1942–43
NEVIN E. FUNK 1943–44
C. A. POWEL 1944–45
*W. E. WICKENDEN 1945–46
J. ELMER HOUSLEY 1946–47
B. D. HULL 1947–48
EVERETT S. LEE 1948–49
JAMES F. FAIRMAN 1949–50

* Deceased.

Past and Present Officers of the Institute

Abbott, Arthur V., *V-P.* 1900–02.
Adams, Comfort A., *M.*, 1912–13; *V-P.*, 1915–17; *P.*, 1918–19.
*Adsit, C. G., *V-P.*, 1921–23.
Alger, P. L., *D.*, 1944–48.
*Anthony, Wm. A., *V-P.*, 1886–89; *P.*, 1890–91; *V-P.*, 1894–96.
*Armstrong, A. H., *M.*, 1903–06; *V-P.*, 1906–08.
*Arnold, Bion J., *M.*, 1895–98; *V-P.*, 1902–03; *P.*, 1903–04.
Auty, K. A., *V-P.*, 1932–34.

*Babcock, A. H., *V-P.*, 1918–19.
Barker, J. W., *V-P.*, 1940–42.
Barnes, H. H., Jr., *M.*, 1910–13; *V-P.*, 1913–15.
Barrett, Walter J., *D.*, 1949–54.
*Barstow, W. S., *M.*, 1900–03; *V-P.*, 1903–05.
Barton, T. P., *V-P.*, 1939–40; *D.*, 1940–44.
Bates, D. H., *V-P.*, 1885–87.
*Baum, Frank G., *V-P.*, 1906–08.
Beardsley, C. R., *D.*, 1937–41.
Beaver, J. L., *V-P.*, 1927–29.
Bedell, Frederick, *M.*, 1914–17; *V-P.*, 1917–18.
*Behrend, B. A., *M.*, 1913–16; *V-P.*, 1916–18.
*Bell, Alexander G., *V-P.*, 1884–85; *P.*, 1891–92.
*Bell, Louis, *M.*, 1891–94.
Bennett, Edward, *V-P.*, 1924–26.
*Berresford, A. W., *M.*, 1909–12; *V-P.*, 1912–14; *P.*, 1920–21.
Berry, J. H., *V-P.*, 1947–49.
Bettis, A. E., *V-P.*, 1926–28; *D.*, 1928–32.
Bickelhaupt, C. O., *V-P.*, 1927–29.
Bingham, L. A., *V-P.*, 1943–45.
Black, R. G., *M.*, 1910–13.
Blackwell, O. B., *V-P.*, 1936–38.
Blaisdell, L. T., *V-P.*, 1936–38.
Bolton, P. C., *V-P.*, 1938–40.
Bonney, R. B., *V-P.*, 1933–35.
Bower, G. W., *V-P.*, 1947–49.
*Brackett, Cyrus F., *M.*, 1886–89.
*Bradley, Chas. S., *M.*, 1894–97; *V-P.*, 1897–99, 1899–1902.
*Brooks, David M., *M.*, 1885–88.
*Brooks, Morgan, *M.*, 1907–10; *V-P.*, 1910–12.
*Brush, Chas. F., *M.*, 1884–87.
Bryant, J. M., *M.*, 1924–28.
Buck, Harold W., *M.*, 1907–10; *V-P.*, 1910–12; *P.*, 1916–17.
*Buckingham, Chas. L., *M.*, 1885–88.
Buckley, O. E., *V-P.*, 1946–48.
Bush, Vannevar, *D.*, 1937–41.
Bussey, H. E., *V-P.*, 1923–25.

Callahan, J. L., *V-P.*, 1948–50.
Carle, N. A., *M.*, 1916–19; *V-P.*, 1919–20.
*Carlton, W. G., *M.*, 1908–11; *V-P.*, 1911–13.
Carpenter, C. B., *V-P.*, 1944–46.
*Carpenter, H. V., *V-P.*, 1930–32.
*Carty, John J., *M.*, 1893–95, 1900–03, 1903–04, 1906–08; *V-P.*, 1904–06, 1908–11; *P.*, 1915–16.
*Chamberlain, J. C., *M.*, 1890–93.
Charlesworth, H. P., *M.*, 1923–27; *V-P.*, 1930–32; *P.*, 1932–33.
*Chesney, C. C., *M.*, 1905–08; *V-P.*, 1908–10; *P.*, 1926–27.
Chesterman, F. J., *D.*, 1926–30.
Christie, C. V., *V-P.*, 1935–37.
Chubb, L. W., *D.*, 1931–35.
Chubbuck, L. B., *V-P.*, 1931–33.
Church, W. Lee, *M.*, 1887–88.
*Clarke, Chas. L., *M.*, 1904–05.
Clifford, H. E., *M.*, 1908–11.
Coldwell, O. B., *V-P.*, 1921–22.
*Compton, Alfred G., *M.*, 1891–94.
Cone, D. L., *V-P.*, 1947–49.
Cooper, A. B., *V-P.*, 1927–29; *D.*, 1930–34.
Coover, M. S., *D.*, 1940–44; *V-P.*, 1944–46.
Copley, A. W., *V-P.*, 1931–33.
*Craft, E. B., *M.*, 1920–24.
Craft, F. M., *V-P.*, 1933–35.
*Crocker, Francis B., *M.*, 1888–90; *V-P.*, 1890–92, 1894–96; *P.*, 1897–98.
*Crosby, Oscar T., *V-P.*, 1892–94.
*Cross, Chas. R., *V-P.*, 1884–85.
*Cuttrias, Chas., *M.*, 1888–91.

Danner, R. F., *V-P.*, 1946–48.
Davis, Ernest W., *V-P.*, 1946–48; *D.*, 1949–53.
Dawes, Chester L., *V-P.*, 1938–40.
*Delany, Patrick B., *M.*, 1890–93; *V-P.*, 1893–95.
Del Mar, Wm. A., *M.*, 1917–21; *V-P.*, 1921–22.
Dewars, A. G., *V-P.*, 1942–44; *D.*, 1950–54.
Dobson, W. P., *V-P.*, 1925–27.
*Dolbear, A. E., *V-P.*, 1885–87.
*Don Carlos, H. C., *D.*, 1926–30.
*Downing, F. M., *V-P.*, 1925–27.
*Duncan, Louis, *P.*, 1895–97.
Dunn, Gano, *M.*, 1897–1900; *V-P.*, 1900–02; *M.*, 1902–05; *V-P.*, 1905–07; *P.*, 1911–12.
DuVall, W. C., *V-P.*, 1949–51.

Eales, H. W., *V-P.*, 1921–26.
*Eckert, J. W., *M.*, 1884–85.
*Edgar, Chas. L., *M.*, 1905–08.
*Edison, Thos. A., *V-P.*, 1884–85.
*Eglin, W. C. L., *M.*, 1903–06; *V-P.*, 1907–09.
Eldredge, M. B., *V-P.*, 1933–37; *D.*, 1939–43.
Ellestad, I. M., *V-P.*, 1947–49.
*Emmet, W. L. R., *V-P.*, 1900–02.
Evans, Herbert S., *V-P.*, 1929–31.
Evenson, W. E., *V-P.*, 1945–47.
Everitt, W. L., *D.*, 1947–51.
Ewart, F. R., *V-P.*, 1921–23.

*Faccioli, G., *M.*, 1918–22; *V-P.*, 1922–24.
Fair, R. H., *V-P.* 1935–37.
Fairman, J. F., *V-P.*, 1944–46; *D.*, 1946–49; *P.*, 1949–50.
Farmer, F. M., *D.*, 1934–38; *V-P.*, 1938–39; *P.*, 1939–40.
*Ferguson, Louis A., *M.*, 1904–07; *V-P.*, 1907–08; *P.*, 1908–09.
Ferguson, O. J., *V-P.*, 1927–29.
Fick, C. W., *D.*, 1948–52.
*Field, Stephen D., *M.*, 1884–86.
Fields, E. S., *V-P.*, 1945–47.
*Finney, John H., *M.*, 1914–17; *V-P.*, 1917–18.
*Fisken, John B., *M.*, 1916–19; *V-P.*, 1919–20.
Flanigen, J. M., *D.*, 1945–49.
Fleager, C. E., *V-P.*, 1929–31.
*Foster, Horatio A., *M.*, 1890–93.
*Fowle, F. F., *M.*, 1919–23.
*Fowler, A. C., *M.*, 1887.
Fowler, M. M., *D.*, 1925–29.
Frampton, A. H., *V-P.*, 1949–51.
*Freeman, W. E., *V-P.*, 1931–33.
Fritz, H. E., *V-P.*, 1950–52.
Funk, N. E., *D.*, 1934–38; *P.*, 1943–44.

Gamble, Lester R., *V-P.*, 1938–40; *D.*, 1941–45.
Gaylord, J. M., *V-P.*, 1943–45.
Gear, H. B., *D.*, 1934–38.
Geiger, D. G., *V-P.*, 1947–49.
*Geyer, Wm. E., *M.*, 1888–92.
*Gherardi, Bancroft, *M.*, 1905–08; 1914–17; *V-P.*, 1908–10; *P.*, 1927–28.
Gilson, Walter J., *V-P.*, 1943–45.
Goldsborough, W. E., *M.*, 1901–04; *V-P.*, 1904–06.
*Gray, Elisha, *M.*, 1884–86.
*Green, Norvin, *P.*, 1884–86; *V-P.*, 1886–88.
*Greene, S. Dana, *M.*, 1899.

Hall, Walter A., *M.*, 1917–21; *V-P.*, 1921–22.
*Hamilton, Jas., *M.*, 1891–94; *V-P.*, 1894–96.
*Hamilton, George A., *V-P.*, 1884–86; *Natl. Treas.*, 1895–1930.
Hamilton, J. L., *V-P.*, 1940–42.
*Hammer, William J., *V-P.*, 1901–03; *M.*, 1893–96.
Hanker, F. C., *D.*, 1927–31.
Hansen, K. L., *V-P.*, 1940–42; *D.*, 1942–46.
*Harding, C. F., *V-P.*, 1936–38.
*Harisberger, John, *V-P.*, 1924–26.
Harrison, W. H., *V-P.*, 1935–37; *P.*, 1937–38.
*Haskins, Chas. H., *V-P.*, 1884–86.
*Hasson, W. F. C., *V-P.*, 1895–97; *M.*, 1897–1900.
*Hazard, Rowland R., *Treas.*, 1884–86; *V-P.*, 1887–89.
*Hellings, M. L., *M.*, 1884–85.
*Hellmund, R. E., *D.*, 1939–42.
*Henderson, S. E. M., *V-P.*, 1923–25.
Henline, H. H., *Act. Secy.*, 1932; *Secy.*, 1933–.
Henry, R. T., *V-P.*, 1944–46; *D.*, 1946–50.
*Hering, Carl, *V-P.*, 1891–93; 1895–98, *P.*, 1900–01.
*Herzog, F. Benedict, *M.*, 1887–92.
Hewitt, Chas., *M.*, 1893–96.
Hibbard, Augus S., *M.*, 1892–95; *V-P.*, 1895–97.
Hibshman, N. S., *V-P.*, 1941–43.
*Higson, C. R., *V-P.*, 1932–34.
Hinson, N. B., *V-P.*, 1935–37; *D.*, 1949–53.
Hitchcock, H. W., *V-P.* 1939–41.
*Hobart, H. M., *M.*, 1922–26; *V-P.*, 1926–28.
Hooven, M. D., *D.*, 1948–52.
Hopkins, Ralph A., *V-P.*, 1949–51.
Housley, J. R., *V-P.*, 1941–43; *P.*, 1946–47.
*Houston, Edwin J., *M.*, 1884–87; *P.*, 1893–95.
*Howell, John W., *M.*, 1888–90.
Hull, A. H., *V-P.*, 1933–35.
Hull, B. D., *V-P.*, 1928–30; *D.*, 1931–35; *P.*, 1947–48.
*Humphrey, H. H., *V-P.*, 1906–08.
Hunting, F. S., *M.*, 1911–14; *V-P.*, 1914–16.
*Hutchinson, Cary T., *M.*, 1895–98; *V-P.*, 1898–1900.
*Hutchinson, F. L., *Natl. Secy.*, 1912–32.

*Imlay, L. E., *M.*, 1919–23.

Jackson, Dugald C., *V-P.*, 1897–99; *P.*, 1910–11.
*Jackson, W. B., *M.*, 1912–13; *V-P.*, 1918–19.
James, Wm. F., *V-P.*, 1923–25.
Jamieson, B. G., *V-P.*, 1926–28.
*Jewett, F. B., *M.*, 1915–18; *V-P.*, 1918–19; *P.*, 1922–23.
Johnson, F. Ellis, *D.*, 1936–39.
*Johnson, J. Allen, *D.*, 1928–32; *V-P.*, 1932–34; *P.*, 1934–35.
Jollyman, J. P., *V-P.*, 1937–39.
Jones, A. L., *V-P.*, 1941–43.
Jones, C. R., *D.*, 1935–39; *V-P.*, 1942–44.
*Jones, Francis W., *M.*, 1884–85; *V-P.*, 1885–87.
*Jorgensen, I. R., *V-P.*, 1919–20.
Juhnke, P. B., *D.*, 1933–37.
*Junkersfeld, P., *M.*, 1913–16; *V-P.*, 1916–18.

Kearns, J. E., *D.*, 1929–33.
*Keith, Nathaniel S., *Secy.*, 1884–85.
*Kelsch, Raymond S., *V-P.*, 1918–19.
*Kennelly, Arthur E., *V-P.*, 1892–94; *M.*, 1894–97; *V-P.*, 1897–98; *P.*, 1898–1900.
Kidder, H. A., *M.*, 1925–28; *V-P.*, 1928–30.
*Knight, G. L., *M.*, 1922–26; *V-P.*, 1926–28.
Knowlton, A. E., *D.*, 1930–34.
Konitzky, G. A., *D.*, 1932–36.
Kouwenhoven, W. B., *V-P.*, 1931–33; *D.*, 1935–39.

Lacy, T. N., *V-P.*, 1930–32.
Laffoon, C. M., *D.*, 1942–47.

*Lamme, Benj. G., *M.*, 1907–10.
Lane, F. H., *D.*, 1937–41.
Lardner, H. A., *M.*, 1913–16.
Lawton, F. L., *V-P.*, 1945–47.
LeClair, T. G., *D.*, 1941–45; *V-P.*, 1946–48; *P.*, 1950–51.
Lee, Everett S., *D.*, 1933–37; *V-P.*, 1940–42; *P.*, 1948–49.
*Lee, William S., *M.*, 1911–14; *D.*, 1929–30; *P.*, 1930–31.
*Leonard H. Ward, *M.*, 1890–93; *V-P.*, 1893–95.
*Lieb, John W., *M.*, 1896–99; *V-P.*, 1899–1901; *M.*, 1901–03; *V-P.*, 1903–04; *P.*, 1904–05.
*Lighthipe, J. A., *V-P.*, 1913–15.
Lincoln, J. F., *M.*, 1920–24.
*Lincoln, Paul M., *M.*, 1906–09; *V-P.*, 1909–11; *P.*, 1914–15.
Liversidge, H. P., *D.*, 1927–31.
*Lloyd, Herbert, *M.*, 1898–1901.
*Lockwood, Thos. D., *V-P.*, 1886–87; *M.*, 1888–90; *V-P.*, 1891–93.
Lovell, A. H., *D.*, 1932–36; *V-P.*, 1938–40.
*Lozier, R. T., *M.*, 1902–04.
Lunn, Ernest, *M.*, 1922–26.

MacCutcheon, A. M., *D.*, 1928–32; *P.*, 1936–37.
*Macdonald, E., *V-P.*, 1923–25.
*Macfarlane, Alexander, *M.*, 1897–1900.
Machachlan, Willis, *V-P.*, 1919–20.
*Magnusson, C. E., *V-P.*, 1920–21.
Mahood, E. T., *V-P.*, 1942–44.
*Maillour, C. O., *M.*, 1886–89; *V-P.*, 1898–99; *M.*, 1899–1902; *V-P.*, 1902–04; *M.*, 1905–07; *P.*, 1913–14.
*Mapes, L. R., *D.*, 1938–42.
*Martin, T. Commerford, *Act. Secy.*, 1884–85; *M.*, 1885–87; *P.*, 1887–88; *V-P.*, 1888–90.
Martindale, E. H., *M.*, 1917–20; *V-P.*, 1920–21.
*Maver, Wm., Jr., *M.*, 1888–91.
Maxwell, Fred R., Jr., *V-P.*, 1939–41; *D.*, 1941–45.
*Maynard, Geo. C., *V-P.*, 1886–88.
*McAllister, A. S., *M.*, 1914–17; *V-P.*, 1917–18.
McClellan, L. N., *V-P.*, 1937–39.
*McClellan, William *M.*, 1912–15; *V-P.*, 1915–17 *P.*, 1921–22.
McConahey, W. M., *M.*, 1923–27.
McDonald, A., *V-P.*, 1950–52.
McDowell, C. S., *V-P.*, 1920–21.
McEachron, K. B., *D.*, 1930–40; *V-P.*, 1942–44.
McHenry, M. J., *V-P.*, 1937–39; *D.*, 1944–48.
McKay, Richard, *V-P.*, 1948–50.
McMillan, F. O., *V-P.*, 1934–36; *D.*, 1948–52.
*Merriam, E. B., *M.*, 1924–28; *V-P.*, 1928–30.
Mershon, Ralph D., *M.*, 1909–03; *V-P.*, 1903–05; *P.*, 1912–13.
*Meyer, E. B., *D.*, 1927–31; *V-P.*, 1932–34; *P.*, 1935–36.
Meyer, F. J., *V-P.*, 1934–36; *D.*, 1939–43.
*Michaelis, O. E., *M.*, 1886–89; *V-P.*, 1889–90.
Mier, C. W., *D.*, 1943–47.
Mills, C. A., *V-P.*, Aug.–Oct. 1932.
Mitchell, W. E., *V-P.*, 1925–27.
Montieth, A. C., *D.*, 1947–51.
*Morehouse, L. F., *M.*, 1919–23; *V-P.*, 1924–26.
*Morrow, L. W. W., *D.*, 1933–37.
Mortensen, S. H., *D.*, 1943–47.
Morton, W. B., *D.*, 1941–46.
Moultrop, I. E., *D.*, 1926–30; *V-P.*, 1930–32.
*Mullin, E. H., *M.*, 1902–04.
*Murray, Wm. S., *M.*, 1908–09; 1909–12; *V-P.*, 1912–14.

Newbury, F. D., *M.*, 1918–22.
*Nichols, E. L., *V-P.*, 1889–91.
*Norris, H. H., *M.*, 1909–12.
North, J. R., *D.*, 1945–49; *V-P.*, 1950–52.
Northmore, B. R., *V-P.*, 1927–29.

Osborne, H. S., *D.*, 1938–42; *P.*, 1942–43.
*Osgood, Farley, *M.*, 1911–14; *V-P.*, 1914–16; *P.*, 1924–25.
Owens, R. B., *V-P.*, 1898–1900.

Parker, John Castlereagh, *V-P.*, 1921–22; *P.*, 1938–39.
Patton, P. H., *V-P.*, 1931–33.
*Peek, F. W., Jr., *D.*, 1930–33.
Pender, Harold, *M.*, 1915–18; *V-P.*, 1918–19.
*Perrine, Frederick A. C., *M.*, 1898–1900.
*Phelps, Geo. M., Jr., *M.*, 1885–87; *Treas.*, 1886–95.
*Pickernell, F. A., *M.*, 1896–99.
Pierce, A. G., *M.*, 1921–25; *V-P.*, 1925–27.
Pingree, G. N., *V-P.*, 1948–50.
Plumb, H. T., *V-P.*, 1922–24.
*Pope, Franklin L., *V-P.*, 1884–85; *P.*, 1886–87; *V-P.*, 1887–89.
*Pope, Ralph W., *Secy.*, 1885–1911; *Hon. Secy.*, 1911–29.
Post, G. G., *V-P.*, 1934–36.
Powel, C. A., *D.*, 1936–40; *V-P.*, 1942–43; *P.*, 1944–45.
Pratt, H. A., *M.*, 1921–25.
*Prescott, Geo. B., *M.*, 1884.
*Prescott, G. B., Jr., *M.*, 1888–91.
*Price, C. A., *V-P.*, 1941–43.
Prince, D. C., *D.*, 1938–41; *P.*, 1941–42.
*Puffer, Wm. L., *M.*, 1896–99.
*Pupin, Michael I., *M.*, 1892–95; *V-P.*, 1895–97; 1901–03; *P.*, 1925–26.
Purnell, C. S., *V-P.*, 1950–52.

Quarles, D. A., *D.*, 1944–48.
Quinan, G. E., *V-P.*, 1928–30.

*Reber, Samuel, *M.*, 1901–04; *V-P.*, 1904–06.
*Rice Calvin W., *M.*, 1900–03; *V-P.*, 1903–05.
*Rice, E. W., Jr., *P.*, 1917–18.
Ricker, Claire W., *V-P.*, 1943–45.
Robbins, Chas., *M.*, 1916–20; *V-P.*, 1920–21.
Robertson, Elgin B., *D.*, 1947–51.
Robertson, L. M., *V-P.*, 1945–47.
*Robinton, L. T., *M.*, 1913–16; *V-P.*, 1916–18, 1920–21.
*Rodman, W. S., *V-P.*, 1929–31.
Rogers, C. E., *V-P.*, 1936–38.
*Ruffner, Chas. S., *M.*, 1916–20; *V-P.*, 1920–21.
*Rugg, W. S., *M.*, 1910–13.
*Rushmore, D. B., *M.*, 1908–11; *V-P.*, 1911–13.
*Ryan, Harris J., *M.*, 1893–96; *V-P.*, 1896–98; *P.*, 1923–24.
*Ryan, W. T., *V-P.*, 1928–30.

*Sands, Herbert S., *V-P.*, 1923–27
*Sargent, W. D., *M.*, 1885–86.
Schilling, E. W., *V-P.*, 1942–44.
*Schoen, A. M., *M.*, 1906–09; *V-P.*, 1919–20.
Scholz, H. J., *D.*, 1949–53.
Schoolfield, H. H., *V-P.*, 1926–28.
*Schuchardt, R. F., *V-P.*, 1922–24; *P.*, 1928–29.
*Scott, Chas. F., *M.*, 1895–98; *V-P.*, 1899–1901; *P.*, 1902–03.
*Scribner, Chas. S., *M.*, 1910–13; *V-P.*, 1913–15.
Seeger, R. W., *V-P.*, 1949–50.
Seeley, W. J., *V-P.*, 1949–51.
Sever, Geo. F., *M.*, 1898–1901; *V-P.*, 1901–03; *M.*, 1903–06.
*Shaad, G. C., *V-P.*, 1930–32; *D.*, 1935–36.
*Shelbourne, Sidney, F., *M.*, 1886–87.
*Sheldon, Samuel, *M.*, 1898–1901; *V-P.*, 1901–03; *M.*, 1903–06; *P.*, 1906–07.
Sibley, R., *V-P.*, 1921–23.
Siegfried, Victor, *V-P.*, 1948–50; *D.*, 1950–54.
Sinclair, C. T., *V-P.*, 1939–41.
*Sisson, C. H., *V-P.*, 1929–31.
*Skinner, C. E., *M.*, 1915–19; *V-P.*, 1919–20; *P.*, 1931–32.
Slichter, Walter I., *M.*, 1918–22; *V-P.*, 1922–24; *Treas.*, 1930–.
*Smith, H. B., *M.*, 1920–24; *V-P.*, 1924–26; *P.*, 1929–30.
Smith, Walter Charles, *V-P.*, 1941–43; *D.*, 1945–49.
Smith, W. R., *D.*, 1942–46.
*Smith, W. W., *M.*, 1884–85.
Sorensen, R. W., *V-P.*, 1933–35; *D.*, 1936–40; *P.*, 1940–41.
*Spencer, Paul, *M.*, 1906–09; *V-P.*, 1909–11.
*Sprague, Frank J., *V-P.*, 1890–92; *P.*, 1892–93.
*Springer, F. W., *V-P.*, 1921–23.
*Sprong, S. D., *M.*, 1909–12; *V-P.*, 1912–14.
*Stanley, Wm., *V-P.*, 1898–1900.
Stein, I. Melville, *V-P.*, 1937–39.
*Steinmetz, Chas. P., *M.*, 1892–95; *V-P.*, 1896–98; *M.*, 1898–1901; *P.*, 1901–02.
*Stephens, C. E., *D.*, 1923–33.
Stevens, A. C., *D.*, 1932–36; *V-P.*, 1936–38.
*Stevens, J. Franklin, *M.*, 1912–15; *V-P.*, 1915–17.
*Stillwell, Lewis B., *M.*, 1896–99; *V-P.*, 1899–1901; *P.*, 1909–10.
Stine, Wilbur M., *V-P.*, 1896–98.
Stokes, Stanley, *V-P.*, 1932–34.
*Stone, Chas. W., *M.*, 1908–11; *V-P.*, 1911–13.
Stone, E. C., *D.*, 1925–29; *V-P.*, 1929–31.
*Storer, Norman W., *M.*, 1911–14; *V-P.*, 1914–16 1921–23.
*Stott, Henry G., *M.*, 1904–07; *P.*, 1907–08.
Sykes, Wilfred., *M.*, 1917–21.

Tapscott, R. H., *D.*, 1930–34; *V-P.*, 1934–36.
Tarboux, J. G., *V-P.*, 1950–52.
Taylor, A. LeRoy, *V-P.*, 1940–42.
Taylor, John B., *M.*, 1915–18; *V-P.*, 1918–19.
Terrell, C. F., *V-P.*, 1946–48.
*Terry, Chas. A., *M.*, 1902–05; *V-P.*, 1905–07.
Terry, I. A., *V-P.*, 1948.
*Tesla, Nikola, *V-P.*, 1892–94.
*Thomas, B. F., *M.*, 1885–87.
Thomas, Percy H., *M.*, 1907–10; *V-P.*, 1910–12.
Thompson, Edward P., *M.*, 1887–88.
*Thomson, Elihu, *V-P.*, 1887–89; *P.*, 1889–90.
Thomson, J. M., *V-P.*, 1939–41.
Timbie, W. H., *V-P.*, 1934–36.
*Townley, Calvert, *M.*, 1905–08; *V-P.*, 1908–10; *P.*, 1919–20.
*Townsend, Henry C., *M.*, 1899–1902.
*Trowbridge, Wm. P., *M.*, 1884–86.
Turner, A. L., *V-P.*, 1939–41.

*Upton, Francis R., *V-P.*, 1889–90; *M.* 1890–92.

*Vail, Theo. N., *M.*, 1884–86.
*Vanderpool, W. K., *M.*, 1923–27.
*Van Hoevenbergh, H., *M.*, 1888–90.
Veinott, C. G., *V-P.*, 1949–51.
*Vonnlae, W. B., *M.*, 1894–97.

*Wallace, Wm., *V-P.*, 1893–95.
Warner, R. G., *D.*, 1940–44.
Warner, R. W., *V-P.*, 1944–46.
*Weaver, W. D., *M.*, 1894–97; 1899–1902.
Webb, Herbert L., *M.*, 1891–94; 1897–1900.
*Weston, Edward, *M.*, 1884–87; *P.*, 1888–89; *V-P.* 1889–91.
*Wetzler, Jos., *M.*, 1888–90; *V-P.*, 1890–92.
*Wheeler, Schuyler S., *M.*, 1887–90; *V-P.*, 1890–91; 1902–04; *M.*, 1904–05; *P.*, 1905–06.
*White, Jas. G., *M.*, 1904–07; *V-P.*, 1907–09.
Whitehead, John B., *M.*, 1924–28; *P.*, 1933–34.
*Wickenden, W. E., *V-P.*, 1943–45; *P.*, 1945–48.
*Williamson, R. B., *M.*, 1921–25.
*Wilson, A. M., *V-P.*, 1933–35.
*Wirt, Chas., *M.*, 1892–95.
*Wolcott, Townsend, *M.*, 1902–05; *V-P.*, 1905–07.
Wolf, H. B., *V-P.*, 1945–47.
*Wood, Edwin D., *V-P.*, 1937–39.
*Woodrow, H. R., *D.*, 1931–35.

Yerkes, E. P., *D.*, 1946–50.

Abbreviations: *P.*, President; *V-P.*, Vice-President; *M.*, Manager; *D.*, Director; *Natl. Secy.*, National Secretary; *Secy.*, Secretary; *Hon. Secy.*, Honorary Secretary; *Natl. Treas.*, National Treasurer; *Treas.*, Treasurer.

*Deceased.

Honorary Members, 1884–1950

*Sir William Preece.....1884
*Norvin Green.....1889
*Moses G. Farmer.....1890
*Lord Kelvin.....1892
*Cyrus Field.....1892
*E. W. von Siemens.....1892
*Andre E. Blondel.....1912
*C. E. L. Brown.....1912
*Emil A. Budde.....1912
*S. Z. de Ferranti.....1912
*Antonio Pacinotti.....1912
*S. P. Thompson.....1914
*Guglielmo Marconi.....1917
*Oliver Heaviside.....1918
*Ferdinand Foch.....1921
*Thomas A. Edison.....1928
*John J. Carty.....1928
*M. I. Pupin.....1928
*Ambrose Swasey.....1928
*Elihu Thomson.....1928
Herbert Hoover.....1929
*Charles F. Scott.....1929
*Charles F. Brush.....1929
Motoji Shibusawa.....1929
*Frank J. Sprague.....1932
*W. L. R. Emmet.....1933
*G. A. Hamilton.....1933
*Arthur E. Kennelly.....1933
R. A. Millikan.....1933
*E. W. Rice, Jr.....1933
*Edward Weston.....1933
*Bion J. Arnold.....1937
*Alex Dow.....1937
*Cummings C. Chesney.....1938
Andrew G. L. McNaughton.....1942
Dugald C. Jackson.....1944
*Charles E. Skinner.....1945
Gano Dunn.....1945
*Frank B. Jewett.....1945
Vannevar Bush.....1949

* Deceased.

See page 120 for information concerning living Honorary Members.

Headquarters Staff

33 West 39th Street, New York 18

Secretary.....H. H. Henline
Office Manager and Business Manager of Publications.....F. A. Norris
Editor.....C. S. Rich
Associate Editor.....G. C. Baxter Rowe
Secretary, Technical Program Committee.....Edward C. Day
Secretary, Board of Examiners and Standards Committee.....J. J. Anderson, Jr.
Technical Committee Activities.....R. S. Gardner
Advertising Manager.....J. S. Lopes

General Counsel

Simon Presant.....55 Liberty St., New York 5

Sections

Name	District	Organized	Chairman	Secretary	Secretary's Address
Akron	2	Aug. 12, '20	J. R. Dorney	J. C. Hall	1374 Roslyn Ave., Akron 20, Ohio
Alabama	4	May 22, '29	M. M. Collins	J. F. Webb	Alabama Power Co., 600 No. 18th St., Birmingham 2, Ala.
Arizona	8	Mar. 22, '41	Americo Lazzari	J. E. Redmond	Drawer 869, Phoenix, Ariz.
Arkansas	7	Apr. 23, '47	M. E. Crippen	C. E. Hutchison	707 Boyle Building, Little Rock, Ark.
Arrowhead	5	Apr. 23, '47	Jennings Johnson	Harvey Sargent	Superior Water, Light & Power Co., Superior, Wis.
Beaumont	7	June 27, '45	H. E. Mortimer	W. T. Evans	1070 Central Drive, Beaumont, Tex.
Boston	1	Feb. 13, '03	L. F. Cleveland	L. J. Weed	Boston Edison Co., 182 Tremont St., Boston 11, Mass.
Canton	2	Nov. 5, '47	R. V. Reich	D. L. Westhoefer	Hilscher-Clarke Elec. Co., 519—4th St., N. W., Canton 3, Ohio
Central Indiana	5	Jan. 12, '12	J. W. Sears	C. A. Wilson	3541 No. Wallace St., Indianapolis 18, Ind.
Chicago	5	1893	E. L. Michelson	W. M. Ballenger	General Electric Co., 840 So. Canal St., Chicago 80, Ill.
Cincinnati	2	June 30, '20	W. H. McNutt	W. W. Gulden	3272 Daytona Ave., Cincinnati 11, Ohio
Cleveland	2	Sept. 27, '07	W. H. Chase	L. E. Knapp	Westinghouse Electric Corp., 1370 Ontario St., Cleveland, Ohio
Columbus	2	Mar. 17, '22	R. L. Merrill	Floyd Knapp	Ohio Bell Tel. Co., 42 East Gay St., Columbus 15, Ohio
Connecticut	1	Apr. 16, '21	H. M. Turner	F. W. Buck	United Illuminating Co., 80 Temple St., New Haven 6, Conn.
Dayton	2	June 9, '43	J. M. Rodgers	R. L. Dingle	4315 Corlinth Blvd., Dayton 10, Ohio
Denver	6	May 18, '15	W. A. Morgan	H. F. Gidlund	Pub. Serv. Co. of Colo., P.O. Box 840, Denver 1, Colo.
East Tennessee	4	Sept. 2, '36	R. M. Alspaugh	J. W. Crabtree	626 South Gay St., Knoxville 11, Tenn.
Erie	2	Jan. 11, '18	K. H. Ishler	G. H. Ramandanes	103 East 35th St., Erie, Pa.
Florida	4	Jan. 28, '31	Fred H. Pumphrey	John W. Wilson	Box 2155, University Station, Gainesville, Fla.
Fort Wayne	5	Aug. 14, '08	R. E. Trovinger	M. A. Baker	General Electric Co., 1635 Broadway, Fort Wayne, Ind.
Georgia	4	Jan. 14, '04	J. R. Raney	H. P. Peters	Georgia Inst. of Tech., Engg. Experiment Sta., Atlanta 3, Ga.
Houston	7	Aug. 7, '28	E. G. Westheimer	C. R. Wischmeyer	Rice Institute, P. O. Box 1892, Houston 1, Tex.
Illinois Valley	5	June 30, '45	R. P. Pfeiffer	M. V. Meyer	911 So. 17th St., Pekin, Ill.
Iowa	5	June 29, '29	F. E. Keith	A. V. Donnelly	State Univ. of Iowa, 340 Ellis Ave., Iowa City, Iowa
Ithaca	1	Oct. 15, '02	E. M. Guyer	G. E. Dana	N. Y. State Elec. & Gas Corp., 62 Henry St., Binghamton, N. Y.
Kansas City	7	Apr. 14, '16	H. V. Rathbun	M. L. Perry, Jr.	Black & Veatch, 4706 Broadway, Kansas City 2, Mo.
Lehigh Valley	2	Apr. 16, '21	G. M. Keenan	A. L. Price	Pennsylvania Power & Light Co., Hazleton, Pa.
Los Angeles	8	May 19, '08	J. H. Vivian	E. W. Rockwell	Metropolitan Water District of So. Calif., 306 West 3d St., Los Angeles 13, Calif.
Louisville	4	Oct. 15, '26	H. T. Smith	W. G. Adair	Southern Bell Tel. & Tel. Co., Louisville, Ky.
Lynn	1	Aug. 22, '11	R. E. Franck	T. C. Sargent	Sylvania Elec. Prod., Inc., 60 Boston St., Salem, Mass.
Madison	5	Jan. 8, '09	H. A. Peterson	T. J. Higgins	University of Wisconsin, Madison 6, Wis.
Mansfield	2	Mar. 6, '39	H. R. Delahooke	J. M. Blackhall	North Electric Mfg. Co., Galion, Ohio
Maryland	2	Dec. 16, '04	J. W. Gore	F. Hamburger	Johns Hopkins Univ., Homewood, Baltimore, Md.
Memphis	4	May 22, '30	J. R. Owens	W. J. Fransioli, Jr.	Memphis Light, Gas & Water Div., 179 Madison Ave., Memphis, Tenn.
Mexico	7	June 29, '22	F. Aubert	G. Fortoul	Mexican Light & Power Co., Ltd., Gante No. 20, Mexico D.F., Mexico
Miami	4	Feb. 3, '49	J. Bronaugh	S. G. Kent	W. Killian Drive, P. O. Box 27, Kendall, Fla.
Michigan	5	Jan. 13, '11	O. B. Bowles	I. B. Bacon	Michigan State College, East Lansing, Mich.
Milwaukee	5	Feb. 11, '10	E. H. Frederick	R. C. Ball	Cutler-Hammer, Inc., 315 No. 12th St., Milwaukee 1, Wis.
Minnesota	5	Apr. 7, '02	A. J. Hendry	G. B. Germain	Westinghouse Electric Corp., 2303 Kennedy St., N. E. Minneapolis 13, Minn.
Montana	9	June 24, '31	Harry Murphy	C. E. Beardslee	3041 State St., Butte, Mont.
Montreal	10	Apr. 16, '43	A. Malkin	L. K. Hart	Square D Co. of Canada Ltd., 5012 Western Ave., Montreal 28, Que., Canada
Nebraska	6	Jan. 21, '25	C. S. Roadhouse	C. N. Allen	Allis-Chalmers Mfg. Co., 9th & Farnam Sts., Omaha 8, Nebr.
New Mexico-West Texas	7	Mar. 7, '40	J. Armstrong	C. C. Homan, Jr.	El Paso Natural Gas Co., P. O. Box 1492, El Paso, Texas
New Orleans	4	Dec. 8, '33	F. Hollins	H. E. Pritchard, Jr.	5836 General Haig St., New Orleans 19, La.
New York	3	Dec. 10, '19	J. D. Tebo	J. A. Parrott	American Tel. & Tel. Co., 195 Broadway, New York 7, N. Y.
Niagara Frontier	1	Feb. 10, '25	B. S. Rice	C. J. Brumbaugh	129 Hunt Ave., Hamburg, N. Y.
Niagara International	10	Aug. 5, '48	B. A. Bovee	Walter Turecki	The Carborundum Co., Niagara Falls, N. Y.
North Carolina	4	Mar. 21, '29	F. C. De Weese	N. H. Erlandson	Carolina Power & Light Co., Raleigh, N. C.
Northeastern Michigan	5	Feb. 2, '50	F. H. Justin	A. E. Stevens	504 No. Van Buren St., Bay City, Mich.
North Texas	7	May 18, '28	R. L. Biesele, Jr.	E. W. Rogers	Dallas Power & Light Co., Dallas, Tex.
Oak Ridge	4	Feb. 1950	W. J. Pollock, Jr.	G. A. Holt	105 South Tampa Lane, Oak Ridge, Tenn.
Oklahoma City	7	Feb. 16, '22	R. E. Thornton	J. C. Turner	Southwestern Bell Tel. Co., 1004 Telephone Bldg., Oklahoma City 2, Okla.
Ottawa	10	June 23, '49	W. G. Hoyle	A. M. Pedersen	Hydro-Electric Comm. of Ont., 620 University Ave., Toronto 2, Ont., Canada
Panhandle Plains	7	June 12, '47	G. R. Bunton	D. H. Buck	General Electric Co., 300 So. Polk, Amarillo, Tex.
Philadelphia	2	Feb. 18, '03	S. R. Warren, Jr.	W. K. Denkhaus	Bell Telephone Co. of Pa., 1401 Arch St., Philadelphia, Pa.
Pittsburgh	2	Oct. 13, '02	L. N. Grier	A. A. Johnson	Westinghouse Electric Corp., East Pittsburgh, Pa.
Pittsfield	1	Mar. 25, '04	M. I. Alimansky	E. A. Raney	General Electric Co., 100 Woodlawn Ave., Pittsfield, Mass.
Portland	9	May 18, '09	Howard Arnett	J. D. Frantz	Pacific Pr. & Lt. Co., 920 S. W. 6th Ave., Portland 4, Oreg.
Providence	1	Mar. 12, '20	J. E. Hall	C. B. Leathers	General Electric Co., 111 Westminster St., Providence, R. I.
Richland	9	Apr. 23, '48	F. J. Mollerus	G. M. Clifton	523 North 9th, Pasco, Wash.
Rochester	1	Oct. 9, '14	E. M. Morecock	J. A. Gienger	17 Flower City Park, Rochester 13, N. Y.
Rock River Valley	5	Apr. 23, '47	W. C. Busch	C. F. Vinci	Mattison Machine Works, Rockford, Ill.
Sacramento	8	June 15, '50	G. A. Fleming	A. B. Johnson	Westinghouse Electric Corp., 1720—14th St., Sacramento 14, Calif.
St. Louis	7	Jan. 14, '03	C. W. Schemm	D. M. Allison	Westinghouse Electric Corp., 411 No. 7th St., St. Louis 1, Mo.
San Diego	8	Jan. 18, '39	J. P. Conner	A. H. Keith	3827 Polk Ave., San Diego 5, Calif.
San Francisco	8	Dec. 23, '04	W. L. Carter	J. C. Beckett	Wesik Electric Heater Co., 390 First St., San Francisco 5, Calif.
Schenectady	1	Jan. 26, '03	D. E. Garr	C. C. Herskind	General Electric Co., Schenectady 5, N. Y.
Seattle	9	Jan. 19, '04	W. S. Gordon, Jr.	L. D. Barter	Westinghouse Elec. Corp., 3451 East Marginal Way, Seattle 4, Wash.
Sharon	2	Dec. 11, '25	A. J. Maslin	M. M. Morisuye	84 Buhl Court, Sharon, Pa.
Shreveport	4	June 12, '47	C. M. L. Pons	E. D. Nuttall	Box 1407, Shreveport, La.
South Bend	5	Feb. 26, '41	C. O. Moyer	A. W. Fraps	1260 Longfellow Ave., South Bend 15, Ind.
South Carolina	4	Mar. 2, '40	W. E. Dent, Jr.	S. A. Ferguson	3608 Wheat St., Columbia 5, S. C.
South Texas	7	May 23, '50	A. C. Alberti	R. A. Nicholson, Jr.	City Public Service Board, Box 1771, San Antonio 6, Tex.
Spokane	9	Feb. 14, '13	S. J. Pope	W. T. Connolly	Washington Water Pr. Co., 825 W. Trent Ave., Spokane 6, Wash.
Springfield	1	June 29, '22	W. L. Vest, Jr.	S. H. Magruder	1387 Main St., Springfield 3, Mass.
Syracuse	1	Aug. 12, '20	H. H. Graley	N. W. Landis	302 Empire Bldg., Syracuse 2, N. Y.
Toledo	2	June 3, '07	D. L. Rexford	L. H. Fox	3433 Aldringham Road, Toledo 6, Ohio
Toronto	10	Sept. 30, '03	J. T. Thwaites	D. N. Culver	Bell Tele. Co. of Canada, 76 Adelaide St. West, Toronto 1, Ont., Canada
Tulsa	7	Oct. 1, '37	G. R. Van Burkleo	V. J. Sittel	Service Pipe Line Co., Box 1979, Tulsa 2, Okla.
Urbana	5	Nov. 25, '02	D. F. Hang	J. A. Barkson	1002 West Oregon, Urbana, Ill.
Utah	9	Mar. 9, '17	P. W. Worthen	L. Dale Harris	1738 Logan Ave., Salt Lake City, Utah
Vancouver	9	Aug. 22, '11	F. O. Wollaston	F. Noakes	University of British Columbia, Vancouver, B. C., Canada
Virginia	4	May 19, '22	P. R. Spracher	R. B. Liverman	348—54th St. Newport News, Va.
Washington	2	Apr. 9, '03	F. B. Crider	D. S. Bender	Bell Tele. Labs., Inc., 725—13th St., N. W., Washington 5, D. C.
West Virginia	2	Apr. 9, '40	J. J. FitzGibbon	H. L. Lindsey	Charleston Elec. Supply Co., 914 Kanawha Blvd., Charleston 29, W. Va.
Western Virginia	4	June 23, '49	B. H. Adkins	H. E. Rothwell	2307 Dennston Ave., Roanoke 15, Va.
Wichita	7	Sept. 16, '37	Charles Yoe	O. R. Hantla	Kansas Gas & Electric Co., Box 208, Wichita, Kans.
Worcester	1	Feb. 18, '20	R. E. Pfeif	W. G. Coleman	General Electric Co., 507 Main St., Worcester 8, Mass.
Total Sections	88				

Subsections

Name	Chairman	Secretary	Secretary's Address
Albuquerque (New Mexico-West Texas Section)	L. C. Trunler	A. D. Taylor	3306—43rd Place, Sandia Base, Albuquerque, N. Mex.
Baton Rouge (New Orleans Section)	L. V. McLean	W. S. Syrett	1366 Stephens Ave., Baton Rouge 15, La.
Billings (Montana Section)	H. A. Black	L. R. Stickelberger	502 5th Ave., Laurel, Mont.
Binghamton Area (Ithaca Section)	W. J. Rider	L. F. McGowan	North Chenango St., Greene, N. Y.
Black Hills (Denver Section)	J. O. Kammerman	Robert G. Aehrim	Black Hills Power and Light Co., Rapid City, S. D.
Boulder City (Los Angeles Section)	W. M. Doak	L. J. Hudlow	U. S. Bureau of Reclamation, 315 Utah St., Boulder City, Nev.
Casper, Wyo. (Denver Section)	A. Braitman	E. Krupotich	740 South Grant St., Casper, Wyo.
Central Texas (North Texas Section)	J. R. Moore, Jr.	Earl Hinson, Jr.	3024 Wenz Ave., Waco, Tex.
Centre County (Pittsburgh Section)	H. I. Tarpley	J. A. Wensel	Ordnance Research Lab., Box 30, State College, Pa.
Charleston (South Carolina Section)	C. T. Razor	T. C. R. Legare	103 Pine St., Ashley Forest, Charleston, S. C.
Charlotte (North Carolina Section)	I. G. Wallace, Jr.	W. C. Burnett	Box 240, Charlotte 1, N. C.
Columbia (South Carolina Section)	Orem Long	J. T. Steppe, Jr.	3950 Live Oak St., Columbia, S. C.
Corpus Christi (South Texas Section)	M. D. Jester	J. E. Dean	Texas College of Arts & Industries, Kingsville, Tex.
Eastern Shore (Maryland Section)	C. D. Appleby	C. M. Mullican, Jr.	Salisbury C & P Telephone Co. of D. C., 208 East Church St., Salisbury, Md.
Eureka (San Francisco Section)	A. E. Gleisberg	M. D. McLellan	Pacific Tel. & Tel. Co., Eureka, Calif.
Fort Worth (North Texas Section)	C. K. Beyette	Harold Farrington	Texas Electric Service Co., P. O. Box 970, Fort Worth 1, Tex.
Fox River Valley (Milwaukee Section)	J. J. Rock	W. W. Lund	Kurz & Root Co., Appleton, Wis.
Freeport (Houston Section)	W. D. Coar	R. T. Windecker	P. O. Box 33, Lake Jackson, Tex.
Fresno Division (San Francisco Section)	W. M. Green	G. W. Hayden	4325 Iowa Ave., Fresno 2, Calif.
Great Falls (Montana Section)	W. Lowe	J. Radcliffe	2805 First Ave., N., Great Falls, Mont.
Hamilton (Toronto Section)	J. P. Skillen	C. V. Ryder	396 Main St. E., Hamilton, Ont., Canada
Hampton Roads (Virginia Section)	S. H. Fletcher	L. E. Rhinesmith	1119 East Warwick Road, R. D. 1, Box 35, Hilton Village, Va.
Hudson Valley Division (New York Section)	M. F. Clement	A. V. Platter	International Business Machines, Poughkeepsie, N. Y.
Jackson (Miss.) (New Orleans Section)	A. N. Saxon	W. L. Harp	Southern Bell Tel. & Tel. Co., P. O. Box 811, Jackson 106, Miss.
Jacksonville (Florida Section)			
Johnstown (Pittsburgh Section)	B. H. Drum	R. S. Baum	University of Pittsburgh, 325 Cypress Ave., Johnstown, Pa.
Lake Charles (New Orleans Section)	J. J. Alleman	C. Valdes	738 Kirkby St., Lake Charles, La.
Lancaster-York (Maryland Section)	F. C. Sieber	G. E. Cons, Jr.	Allis-Chalmers Mfg. Co., 42 East King St., York, Pa.
Lima (Dayton Section)	O. M. Swain	E. S. Reed	Westinghouse Electric Corp., Lima, Ohio
Mid-State (North Carolina Section)	H. G. Taylor	S. M. Sprowl, Jr.	P. O. Drawer K-1, Greensboro, N. C.
Mobile-Pensacola (Alabama Section)	R. L. Pulley	A. M. Quarterman	Yonge & Hart, 611 Blount Bldg., Pensacola, Fla.
Muscle Shoals (East Tennessee Section)			
Nashville (Memphis Section)	J. L. Simpson, Jr.	W. Criley	Vanderbilt Univ., Nashville 4, Tenn.
New Hampshire (Boston Section)	W. C. Tallman	P. W. Buxton	Public Service Co. of N. H., 205 Main St., Nashua, N. H.
New Jersey Division (New York Section)	F. Seely	E. H. Shimp	Pub. Serv. Elec. & Gas Co., 938 Clinton Ave., Irvington 11, N. J.
Northwest Arkansas (Arkansas Section)	V. V. Fletcher	F. M. Hinkle	411 Rebecca St., Fayetteville, Ark.
Quad-Cities (Iowa Section)	M. P. Roller	A. W. Kremer	Allis-Chalmers Mfg. Co., 901 Kahl Bldg., Davenport, Iowa
Red River Valley Division (Minnesota Section)	B. H. Barnard	R. Faiman	North Dakota Agri. College, Fargo, N. Dak.
Richmond (Virginia Section)	L. D. Johnson, III	C. E. McMurdo	3523 Patrick Ave., Richmond 22, Va.
Ridgway (Erie Section)	R. F. Edwards	J. H. Schneider	217 Little Ave., Ridgway, Pa.
St. Lawrence International (Syracuse Section)	P. F. Mengel	L. F. Pries	New York State Agric. & Tech. Inst., 8 College St., Canton, N. Y.
St. Maurice Valley (Montreal Section)	D. King	G. Auger	Aluminum Co. of Canada, Shawinigan Falls, P. Q., Canada
San Jose (San Francisco Section)	W. Raab	A. F. Lowe	Pacific Tel. & Tel. Co., 1199 Lennon Way, San Jose, Calif.
Sangamon (Illinois Valley Section)	C. P. Hafel	F. C. Blythe	P. O. Box 37, Springfield, Ill.
Savannah (Georgia Section)	E. H. Overby	E. B. Dawson	Savannah Armature Works, Inc., 126 West Bay St., Savannah, Ga.
Shasta Division (San Francisco Section)	Roy Greer	A. A. Craig	220 West St., Willows, Calif.
Tacoma (Seattle Section)	H. M. Manning	H. A. Brenner	General Electric Co., P. O. Box 1485, Tacoma 1, Wash.
Tri-State Division (West Virginia Section)			
Vancouver Island (Vancouver Section)	A. Bradfield	J. B. Hedley	The B. C. Power Commission, Victoria, B. C., Canada
West Central Texas Division (North Texas Section)	C. V. Herbert	J. G. McKeown	880 Ross Ave., Abilene, Tex.
West Coast (Florida Section)			
West Michigan (Michigan Section)	P. R. Coffman	L. A. Zaborsky	127 Colfax, N. E., Grand Rapids, Mich.
Wilmington (Philadelphia Section)	W. J. Mearns	M. G. Young	Univ. of Delaware, Newark, Del.
Zanesville (Columbus Section)	A. Wurdack	F. Nikel	743 Convers Ave., Zanesville, Ohio

Geographical District Executive Committees

District	Chairman (Vice-President, AIEE)	Secretary (District Secretary)	Chairman, District Committee on Student Activities
1 North Eastern	J. G. Tarboux, Cornell University, Ithaca, N. Y.	E. B. Alexander, New York State Elec. & Gas Corp., 62 Henry St., Binghamton, N. Y.	H. F. Cooke, University of Syracuse, Syracuse 10, N. Y.
2 Middle Eastern	C. G. Veinott, Westinghouse Electric Corp., Lima, Ohio	W. A. Dynes, 312 Lonsdale Ave., Dayton 9, Ohio	J. S. Antel, Jr., George Washington University, Washington 7, D. C.
3 New York City	C. S. Purnell, Westinghouse Electric Corp., 40 Wall St., New York 5, N. Y.	D. W. Taylor, Public Service Elec. & Gas Co., 80 Park Place, Newark 1, N. J.	R. T. Weil, Manhattan College, New York 63, N. Y.
4 Southern	W. J. Seeley, Duke University, Durham, N. C.	Russell Ranson, 116½ East Fourth St., Charlotte 2, N. C.	P. H. Nelson, University of Florida, Gainesville, Fla.
5 Great Lakes	J. R. North, Commonwealth Services, Inc., 212 W. Michigan Ave., Jackson, Mich.	G. M. Chute, General Electric Co., 700 Antoinette St., Detroit 2, Mich.	H. S. Dixon, North Dakota Agri. College, State College Sta., Fargo, N. Dak.
6 North Central	W. C. DuVall, University of Colorado, Boulder, Colo.	G. E. Gless, Jr., University of Colorado, Boulder, Colo.	E. J. Ballard, Jr., University of Nebraska, Lincoln 8, Nebr.
7 South West	H. R. Fritz, Southwestern Bell Tel. Co., 2502 Telephone Bldg., St. Louis 1, Mo.	R. C. Meyerand, Union Elec. Co. of Missouri, 315 No. 12th Blvd., St. Louis 1, Mo.	A. J. McCrocklin, Jr., University of Texas, Engg. Bldg. 145, Austin 18, Tex.
8 Pacific	R. A. Hopkins, Westinghouse Electric Corp., 600 St. Paul Ave., Los Angeles 14, Calif.	T. M. Blakeslee, Dept. of Water & Power, Box 3669 Terminal Annex, Los Angeles 54, Calif.	R. M. Saunders, University of Calif., Berkeley 4, Calif.
9 North West	J. A. McDonald, General Electric Co., 200 So. Main St., Salt Lake City, Utah	F. O. Wald, Utah Power & Light Co., P. O. Box 899, Salt Lake City 10, Utah	O. C. Haycock, University of Utah, Salt Lake City Utah
10 Canada	A. H. Frampton, English Elec. Co. of Canada, Ltd., St. Catharines, Ont., Canada	John I. Gram, Hydro-Electric Power Comm. of Ont., Box 237, Niagara Falls, Ont., Canada	

NOTE: Each District Executive Committee includes also the Chairmen and Secretaries of all Sections within the District, the District Vice-Chairman of the AIEE Membership Committee, and a member of the Sections Committee who is resident in the District.

Student Branches

Name and Location	District	Counselor (Member of Faculty)
*Akron, University of, Akron, Ohio	2	K. F. Sibila
Alabama Polytechnic Institute, Auburn	4	James Chadwick
Alabama, University of, University	4	W. F. Gray
*Alberta, University of, Edmonton, Canada	10	R. E. Phillips
*Arizona, University of, Tucson	8	J. G. Clark
Arkansas, University of, Fayetteville	7	D. D. Lingelbach
British Columbia, University of, Vancouver, Canada	9	W. B. Coulthard
Brooklyn, Polytechnic Institute of, Brooklyn, N. Y., (Day)	3	F. A. Wahlers
Brooklyn, Polytechnic Institute of, Brooklyn, N. Y., (Evening)	3	Anthony B. Giordano
Brown University, Providence, R. I.	1	F. N. Tompkins
*Bucknell University, Lewisburg, Pa.	2	Ralph C. Walker
California Institute of Technology, Pasadena	8	Gilbert D. McCann
*California, University of, Berkeley	8	R. M. Saunders
*Carnegie Institute of Technology, Pittsburgh, Pa.	2	George M. Anderson
Case Institute of Technology, Cleveland, Ohio	2	Carl F. Schuneman
Catholic University of America, Washington, D. C.	2	Joseph C. Michalowicz
Cincinnati, University of, Cincinnati, Ohio	2	A. C. Herweh
Clarkson College of Technology, Potsdam, N. Y.	1	George W. Reed
Clemson A & M College, Clemson, S. C.	4	F. T. Tingley
Colorado A & M College, Fort Collins	6	C. H. Chinburg
*Colorado, University of, Boulder	6	S. I. Pearson
*Columbia University, New York, N. Y.	3	Walter A. LaPierre
*Connecticut, University of, Storrs	1	Clarence W. Schultz
Cooper Union, New York, N. Y.	3	E. W. Starr
*Cornell University, Ithaca, N. Y.	1	W. H. Erickson
Delaware, University of, Newark	2	H. S. Bueche
*Denver, University of, Denver, Colo.	6	A. M. Stiles
*Detroit, University of, Detroit, Mich.	5	Guido Ferrara
Drexel Institute of Technology, Philadelphia, Pa.	2	F. C. Powell
Duke University, Durham, N. C.	4	Otto Meier, Jr.
Fenn College, Cleveland, Ohio	2	R. W. Schindler
*Florida, University of, Gainesville	4	Paul H. Nelson
George Washington University, Washington, D. C.	2	J. S. Antel, Jr.
Georgia Institute of Technology, Atlanta, Ga.	4	H. B. Duling
Harvard University, Cambridge, Mass.	1	John C. Fisher
Howard University, Washington, D. C.	2	E. R. Welch
Idaho, University of, Moscow	9	J. H. Johnson
Illinois Institute of Technology, Chicago	5	E. T. B. Gross
*Illinois, University of, Urbana, and Chicago Division, Chicago	5	E. A. Reid
*Iowa State College, Ames	5	G. A. Richardson
Iowa, University of, Iowa City	5	E. B. Kurtz
Johns Hopkins University, Baltimore, Md.	2	C. F. Miller
Kansas State College, Manhattan	7	Earl L. Sitz
*Kansas, University of, Lawrence	7	E. B. Phillips
Kentucky, University of, Lexington	4	H. Alex Romanowitz
*Lafayette College, Easton, Pa.	2	J. G. Reifsnyder
Lehigh University, Bethlehem, Pa.	2	W. Lyle Donaldson
Louisiana Polytechnic Institute, Ruston	4	S. P. Gullatt, Jr.
Louisiana State University, Baton Rouge	4	A. K. Ramsey
Louisville, University of, Louisville, Ky.	4	Thomas R. Bailey
*Maine, University of Orono	1	P. M. Seal
Manhattan College, New York, N. Y.	3	Robert T. Weil
*Marquette University, Milwaukee, Wis.	5	E. W. Kane
*Maryland, University of, College Park	2	L. J. Hodgins
*Massachusetts Institute of Technology, Cambridge	1	E. W. Boehne
*Michigan College of Mining and Technology, Houghton	5	G. W. Swenson
Michigan State College, East Lansing	5	M. D. Rogers
*Michigan, University of, Ann Arbor	5	John J. Carey
Milwaukee School of Engineering, Milwaukee, Wis.	5	R. J. Ungrodt
*Minnesota, University of, Minneapolis	5	Paul A. Cartwright
Mississippi State College, State College	4	Paul B. Jacobs, Jr.
*Missouri School of Mines and Metallurgy, Rolla	7	J. W. Rittenhouse
*Missouri, University of, Columbia	7	G. V. Lago
Montana State College, Bozeman	9	R. C. Seibel
*Nebraska, University of, Lincoln	6	E. J. Ballard, Jr.
Nevada, University of, Reno	8	Harold J. Hendriks
Newark College of Engineering, Newark, N. J.	3	Robert E. Anderson
*New Hampshire, University of, Durham	1	A. J. Merlini
*New Mexico College of A & M Arts, State College	7	M. A. Thomas
New Mexico, University of, Albuquerque	7	Ralph W. Tapy
New York, College of the City of, New York	3	Harold Wolf
*New York University, New York	3	B. James Ley
North Carolina State College, Raleigh	4	Arthur R. Eckels
North Dakota Agricultural College, Fargo	5	Harry S. Dixon
*North Dakota, University of, Grand Forks	5	Robert G. Brown
*Northeastern University, Boston, Mass.	1	R. G. Porter
*Northwestern University, Evanston, Ill.	5	A. H. Wing
Norwich University, Northfield, Vt.	1	D. B. Staake
*Notre Dame, University of, Notre Dame, Ind.	5	L. F. Stauder
Ohio Northern University, Ada	2	J. L. Klingenberger
*Ohio State University, Columbus	2	Edmund D. Ayres
*Ohio University, Athens	2	D. B. Green
Oklahoma A & M College, Stillwater	7	David L. Johnson
*Oklahoma, University of, Norman	7	William B. Lewis
*Oregon State College, Corvallis	9	L. N. Stone
*Pennsylvania State College, State College	2	A. P. Powell
*Pennsylvania, University of, Philadelphia	2	Kenneth A. Fegley
Pittsburgh, University of, Pittsburgh	2	R. C. Gorham
Pratt Institute, Brooklyn, N. Y.	3	R. B. Morgan
*Princeton University, Princeton, N. J.	2	W. H. Surber
Puerto Rico, University of, Mayaguez	3	Jose Luis de Quevedo
Purdue University, Lafayette, Ind.	5	Stephen Freeman, Jr.
*Rensselaer Polytechnic Institute, Troy, N. Y.	1	E. D. Broadwell
*Rhode Island State College, Kingston	1	Robert S. Haas
Rice Institute, Houston, Texas	7	J. S. Waters
Rose Polytechnic Institute, Terre Haute, Ind.	5	C. C. Knipmeyer
*Rutgers University, New Brunswick, N. J.	3	H. T. Rights
Santa Clara, University of, Santa Clara, Calif.	8	Henry P. Netteheim
South Carolina, University of, Columbia	4	S. A. Ferguson
South Dakota School of Mines and Technology, Rapid City	6	J. O. Kammerman
South Dakota State College, Brookings	5	John N. Cheadle
*Southern California, University of, Los Angeles	8	Rodney C. Lewis
*Southern Methodist University, Dallas, Texas	7	F. W. Tatum
*Stanford University, Stanford, Calif.	8	Wm. G. Hoover
Stevens Institute of Technology, Hoboken, N. J.	3	W. L. Sullivan
Swarthmore College, Swarthmore, Pa.	2	R. W. Merriam
*Syracuse University, Syracuse, N. Y.	1	Henry F. Cooke
Tennessee, University of, Knoxville	4	W. O. Leffell
*Texas, A & M College of, College Station	7	N. F. Rode
*Texas Technological College, Lubbock	7	V. D. Wade
*Texas, University of, Austin, and Texas Western College Sub-Branch, El Paso	7	A. J. McCrocklin, Jr.
Toronto, University of, Toronto, Ont., Canada	10	
*Tufts College, Medford, Mass.	1	G. H. Hammond
*Tulane University, New Orleans, La.	4	Daniel H. Vliet
Union College, Schenectady, N. Y.	1	Owen G. Owens
*Utah, University of, Salt Lake City	9	O. C. Haycock
Vanderbilt University, Nashville, Tenn.	4	Walter Criley
Vermont, University of, Burlington	1	Howard M. Smith, Jr.
Villanova College, Villanova, Pa.	2	J. B. Clothier
Virginia Military Institute, Lexington	4	J. S. Jamison
Virginia Polytechnic Institute, Blacksburg	4	Claudius Lee
Virginia, University of, Charlottesville	4	Gordon K. Carter
Washington, State College of, Pullman	9	O. E. Osburn
*Washington, University of, Seattle	9	H. M. Rustebakke
Washington University, St. Louis, Mo.	7	Pierre M. Honnell
*Wayne University, Detroit, Mich.	5	Edward L. Fairchild
West Virginia University, Morgantown	2	Everette C. Dubbe
Wisconsin, University of, Madison	5	John Baird
*Worcester Polytechnic Institute, Worcester, Mass.	1	Donald C. Alexander
*Wyoming, University of, Laramie	6	R. K. Beach
*Yale University, New Haven, Conn.	1	R. R. Shank
Total Branches	131	

* Joint AIEE-IRE Branches.

Committees and Representatives for 1950–51

General Committees

Executive

Titus G. LeClair, *Chairman;* Commonwealth Edison Company, 72 West Adams St., Chicago 90, Ill.
W. J. Barrett — Newark, N. J.
W. L. Everitt — Urbana, Ill.
J. F. Fairman — New York, N. Y.
Everett S. Lee — Schenectady, N. Y.
A. C. Monteith — Pittsburgh, Pa.
W. I. Slichter — New York, N. Y.

Board of Examiners

P. H. Adams, *Chairman;* Public Service Electric and Gas Company, 80 Park Place, Newark 1, N. J.
Sidney Withington *Vice-Chairman* — New Haven, Conn.
John J. Anderson, Jr., *Secretary* — AIEE Headquarters
A. E. Anderson — Philadelphia, Pa.
R. W. Atkinson — Bayonne, N. J.
R. H. Barclay — New York, N. Y.
C. R. Beardsley — New York, N. Y.
C. A. Butcher — Ampere, N. J.
J. L. Callahan — New York, N. Y.
H. A. Dambly — Philadelphia, Pa.
E. W. Davis — Cambridge, Mass.
G. W. Douglass — Newark, N. J.
E. D. Doyle — Philadelphia, Pa.
C. W. Franklin — New York, N. Y.
W. N. Goodwin, Jr. — Newark, N. J.
S. B. Grisdom — East Pittsburgh, Pa.
N. S. Hibshman — Brooklyn, N. Y.
L. F. Hickernell — Hastings-on-Hudson, N. Y.
J. W. Horton — New London, Conn.
A. E. Knowlton — Short Beach, Conn.
Henry Logan — New York, N. Y.
Lee M. Moore — Columbus, Ohio
L. G. Pacini — New York, N. Y.
F. O. Runyon — Newark, N. J.
F. J. Scudder — Manhasset, N. Y.
B. E. Shackelford — New York, N. Y.
H. W. Tenney — Jersey City, N. J.
Gordon Thompson — New York, N. Y.
Robert Treat — Schenectady, N. Y.
H. M. Trueblood — Dobbs Ferry, N. Y.
B. Van Ness, Jr. — Baltimore, Md.
R. G. Warner — New Haven, Conn.
S. S. Watkins — New York, N. Y.
Roland Whitehurst — Philadelphia, Pa.

Constitution and Bylaws

N. B. Hinson, *Chairman;* Southern California Edison Company, Ltd., Edison Building, Los Angeles 53, Calif.
F. M. Farmer — New York, N. Y.
W. Scott Hill — Pittsfield, Mass.
B. D. Hull — Dallas, Tex.
W. W. Lewis — Schenectady, N. Y.
W. S. Peterson — Los Angeles, Calif.
Walter C. Smith — Palo Alto, Calif.
E. P. Yerkes — Philadelphia, Pa.

Finance

W. J. Barrett, *Chairman;* New Jersey Bell Telephone Company, Engineering Department, Room 1405, 540 Broad Street, Newark 2, N. J.
M. D. Hooven — Newark, N. J.
C. S. Purnell — New York, N. Y.

Headquarters

D. W. Taylor, *Chairman;* Public Service Electric and Gas Company, 80 Park Place, Newark 1, N. J.
W. J. Barrett — Newark, N. J.
H. H. Henline — New York, N. Y.

Members-for-Life Fund

N. E. Funk, *Chairman;* 1520 Spruce Street, Philadelphia 2, Pa.
T. F. Barton — New York, N. Y.
C. R. Beardsley — New York, N. Y.
Mark Eldredge — Washington, D. C.
A. H. Hull — Toronto, Ontario, Canada
B. D. Hull — Dallas, Tex.

(Continued in next column)

E. H. Martindale — Cleveland, Ohio
W. I. Slichter — New York, N. Y.
R. W. Sorensen — Pasadena, Calif.
J. F. Tritle — Erie, Pa.
E. P. Yerkes — Philadelphia, Pa.

Membership

J. C. Woods, *Chairman;* Commonwealth Edison Company, 72 West Adams Street, Chicago 90, Ill.
Charles Clos, *Vice-Chairman* — New York, N. Y.
F. A. Norris, *Secretary* — AIEE Headquarters
E. W. Allen — Oklahoma City, Okla.
F. S. Black — New York, N. Y.
W. C. Bloomquist — Schenectady, N. Y.
C. W. Fick — Cleveland, Ohio
Thomas Ingledow — Vancouver, British Columbia, Canada
C. R. Kingsbury — Seattle, Wash.
W. S. Leake — New Orleans, La.
E. W. Morris — Los Angeles, Calif.
C. G. Rumohr — Denver, Colo.
P. L. Savage — Los Angeles, Calif.
W. E. Scholz — Philadelphia, Pa.

District Vice-Chairman

1 T. M. Linville — Schenectady, N. Y.
2 M. L. Lehman — Philadelphia, Pa.
3 M. A. Jones — Newark, N. J.
4 J. D. Harper — Alcoa, Tenn.
5 H. R. Heckendorn — Chicago, Ill.
6 J. L. McKinley — Denver, Colo.
7 R. G. Kloeffler — Manhattan, Kans.
8 B. L. Robertson — Berkeley, Calif.
9 H. B. Hodgins — Salt Lake City, Utah
10 C. L. Roach — Montreal, Quebec, Canada

Planning and Co-ordination

M. D. Hooven, *Chairman;* Public Service Electric and Gas Company, 80 Park Place, Newark 1, N. J.
W. J. Barrett — Newark, N. J.
J. L. Callahan — New York, N. Y.
F. E. Harrell — Cleveland, Ohio
H. H. Henline — New York, N. Y.
W. Scott Hill — Pittsfield, Mass.
A. E. Knowlton — Short Beach, Conn.
Elgin B. Robertson — Dallas, Tex.
M. J. Steinberg — New York, N. Y.
C. H. Willis — Princeton, N. J.

Publication

K. B. McEachron, *Chairman;* General Electric Company, 100 Woodlawn Avenue, Pittsfield, Mass.
F. R. Benedict — East Pittsburgh, Pa.
P. B. Garrett — Chicago, Ill.
R. K. Honaman — New York, N. Y.
F. O. McMillan — Corvallis, Oreg.
T. A. O'Halloran — Washington, D. C.
G. C. Quinn — Milwaukee, Wis.
C. S. Rich — New York, N. Y.
G. C. Tenney — San Francisco, Calif.
C. H. Willis — Princeton, N. J.

Public Relations

G. T. Minasian, *Chairman;* Consolidated Edison Company of New York, Inc., 4 Irving Place, New York 3, N. Y.
Guy Bartlett — Schenectady, N. Y.
G. W. Bower — Haddonfield, N. J.
V. A. Diggs — Cleveland, Ohio
R. T. Ferris — Philadelphia, Pa.
H. H. Henline — New York, N. Y.
R. K. Honaman — New York, N. Y.
J. T. Kimball — Phoenix, Ariz.
A. E. Knowlton — Short Beach, Conn.
G. J. Lowell — New York, N. Y.
H. W. Marquardt — New York, N. Y.
K. B. McEachron — Pittsfield, Mass.
J. P. Neubauer — New York, N. Y.
H. J. Schols — Birmingham, Ala.
W. B. Stephenson — Oklahoma City, Okla.
O. W. Titus — Toronto, Ontario, Canada
C. H. Willis — Princeton, N. J.

Research

M. J. Kelly, *Chairman;* Bell Telephone Laboratories, Inc., 463 West Street, New York 14, N. Y.
J. A. Hutcheson, *Vice-Chairman* — East Pittsburgh, Pa.
M. B. Long, *Secretary* — New York, N. Y.
B. G. Ballard — Ottawa, Ontario, Canada
J. W. Barker — New York, N. Y.
R. D. Bennett — Silver Spring, Md.
L. V. Berkner — Washington, D. C.
E. W. Boehne — Cambridge, Mass.
Cledo Brunetti — Stanford, Calif.
C. R. Burrows — Ithaca, N. Y.
A. G. Conrad — New Haven, Conn.
H. P. Corwith — New York, N. Y.
H. E. Edgerton — Cambridge, Mass.
M. A. Edwards — Schenectady, N. Y.
W. L. Everitt — Urbana, Ill.
R. S. Glasgow — Annapolis, Md.
T. J. Killian — Washington, D. C.
J. T. Littleton — Corning, N. Y.
A. D. Moore — Ann Arbor, Mich.
B. K. Northrop — Ithaca, N. Y.
W. H. Pickering — Pasadena, Calif.
C. S. Schifreen — Philadelphia, Pa.
E. F. Seaman — Washington, D. C.
C. G. Suits — Schenectady, N. Y.
J. B. Thomas — Fort Worth, Tex.
E. A. Walker — Arlington, Va.
V. K. Zworykin — Princeton, N. J.

Safety

W. B. Kouwenhoven, *Chairman;* The Johns Hopkins University, Baltimore 18, Md.
M. M. Brandon, *Vice-Chairman and Secretary,* — New York, N. Y.
Robin Beach — Brooklyn, N. Y.
J. H. Berry — Norfolk, Va.
Handley Blackmon — Pittsburgh, Pa.
W. B. Buchanan — Toronto, Ontario, Canada
C. F. Dalziel — Berkeley, Calif.
G. S. Diehl — Lancaster, Pa.
W. P. Dobson — Toronto, Ontario, Canada
J. P. Ferguson — Brooklyn, N. Y.
J. M. Flanigen — Atlanta, Ga.
C. E. Ganther — Cleveland, Ohio
J. A. Gienger — Rochester, N. Y.
M. C. Goodspeed — Harborcreek, Pa.
Floyd Goss — Los Angeles, Calif.
N. B. Hinson — Los Angeles, Calif.
O. S. Hockaday — Fort Worth, Tex.
J. O. Leslie — Reading, Pa.
R. L. Lloyd — Washington, D. C.
Albrecht Naeter — Stillwater, Okla.
G. R. Radley — Milwaukee, Wis.
P. X. Rice — State College, Pa.
W. T. Rogers — New York, N. Y.
A. H. Schirmer — New York, N. Y.
J. C. Strasbourger — Cleveland, Ohio
E. E. Turkington — Boston, Mass.
H. H. Watson — Bridgeport, Conn.
H. B. Williams — New York, N. Y.
Wm. R. Wood — Windber, Pa.

Sections

D. I. Anzini, *Chairman;* General Electric Company, 806 Russ Building, San Francisco 6, Calif.
C. S. Purnell, *Vice-Chairman* (East) — New York, N. Y.
Walter C. Smith, *Vice-Chairman* (West) — Palo Alto, Calif.
F. S. Benson, *Secretary* — San Francisco, Calif.
F. S. Black — New York, N. Y.
G. W. Bower — Newark, N. J.
T. C. D. Churchill — Toronto, Ontario, Canada
Bradley Coazens — Los Angeles, Calif.
H. A. Dambly — Philadelphia, Pa.
O. R. Enriquez — Mexico, Federal District, Mexico
C. W. Fick — Cleveland, Ohio
D. E. Garr — Schenectady, N. Y.
R. C. Horn — St. Louis, Mo.
C. W. Keller — Denver, Colo.
R. E. Kistler — Seattle, Wash.
C. P. Knost — New Orleans, La.

(Continued in next column)

A. L. O'Banion — Boston, Mass.
F. H. Pumphrey — Gainesville, Fla.
E. T. Sherwood — Milwaukee, Wis.
D. W. Taylor — Newark, N. J.
H. H. Wagner — Canonsburg, Pa.

Standards

E. B. Paxton, *Chairman;* General Electric Company, 1 River Road, Schenectady 5, N. Y.
C. M. Gilt, *Vice-Chairman* — New York, N. Y.
John J. Anderson, Jr., *Secretary* — AIEE Headquarters
Joseph Wm. Allen — Teterboro, N. J.
R. W. Atkinson — Bayonne, N. J.
R. L. Bailey — Highland Park, Mich.
Sterling Beckwith — Milwaukee, Wis.
F. R. Benedict — East Pittsburgh, Pa.
R. C. Bergvall — East Pittsburgh, Pa.
M. M. Brandon — New York, N. Y.
J. E. Clem — Schenectady, N. Y.
C. L. Dawes — Cambridge, Mass.
R. D. de Kay — New York, N. Y.
W. P. Dobson — Toronto, Ontario, Canada
I. W. Gross — New York, N. Y.
F. E. Harrell — Cleveland, Ohio
R. T. Henry — Buffalo, N. Y.
F. C. Holtz — Springfield, Ill.
W. R. Hough — Cleveland, Ohio
H. R. Huntley — New York, N. Y.
H. E. Kent — New York, N. Y.
A. C. Muir — Philadelphia, Pa.
J. R. North — Jackson, Mich.
J. E. O'Brien — Washington, D. C.
G. H. O'Sullivan — New York, N. Y.
R. W. Sherwood — Beaumont, Tex.
F. B. Silsbee — Washington, D. C.

Technical Advisory

M. J. Steinberg, *Chairman;* Consolidated Edison Company of New York, Inc., 4 Irving Place, New York 3, N. Y.
R. S. Gardner, *Secretary* — AIEE Headquarters
H. C. Coleman — East Pittsburgh, Pa.
E. I. Green — Murray Hill, N. J.
L. F. Hickernell — Hastings-on-Hudson, N. Y.
J. J. Orr — New York, N. Y.
T. R. Rhea — Schenectady, N. Y.
H. I. Romnes — Chicago, Ill.
J. D. Tebo — New York, N. Y.
C. C. Whipple — Brooklyn, N. Y.

Technical Program

C. H. Willis, *Chairman;* Princeton University, Princeton, N. J.
M. M. Brandon, *Vice-Chairman* — New York, N. Y.
Edward C. Day, *Secretary* — AIEE Headquarters
H. Blackmon — East Pittsburgh, Pa.
F. B. Bramhall — New York, N. Y.
W. R. Brownlee — Jackson, Mich.
J. L. Callahan — New York, N. Y.
W. G. Dow — Ann Arbor, Mich.
J. D. Leitch — Cleveland, Ohio
G. S. Lunge — Schenectady, N. Y.
Walther Richter — West Allis, Wis.
O. A. Wilde — Chester, Pa.

Transfers

C. W. Fick, *Chairman;* General Electric Company, 4966 Woodland Avenue, Cleveland 4, Ohio
W. C. Bloomquist — Schenectady, N. Y.
Charles Clos — New York, N. Y.
F. A. Cooper — St. Louis, Mo.
J. D. Harper — Alcoa, Tenn.
F. S. Himebrook — Dayton, Ohio
M. R. Horne — Dearborn, Mich.
W. R. Hough — Cleveland, Ohio
L. F. Hunt — Los Angeles, Calif.
M. M. Moore — Washington, D. C.
L. R. Patterson — Denver, Colo.
John Wm. Robinson — San Francisco, Calif.
E. W. Stone — Peoria, Ill.
J. J. Tesar — Cleveland, Ohio
W. W. Walters — Chicago, Ill.
F. W. Willcutt — Washington, D. C.
H. R. Wood — Boston, Mass.

Professional Division Committees

Professional Division Advisory

W. Scott Hill, *Chairman;* Commercial Engineering Division, General Electric Company, 100 Woodlawn Avenue, Pittsfield, Mass.
F. S. Black, *Vice-Chairman* New York, N. Y.
A. G. Conrad New Haven, Conn.
A. H. Kehoe New York, N. Y.
J. B. MacNeill East Pittsburgh, Pa.
F. O. McMillan Corvallis, Oreg.
A. C. Monteith Pittsburgh, Pa.
H. N. Muller, Jr. East Pittsburgh, Pa.
J. J. Orr New York, N. Y.
Elgin B. Robertson Dallas, Tex.
R. W. Sorensen Pasadena, Calif.

Charles LeGeyt Fortescue Fellowship

J. W. Barker New York, N. Y.
R. I. Wilkinson New York, N. Y.
(Terms expire July 31, 1951)
F. W. Bush Milwaukee, Wis.
A. G. Conrad, *Chairman* New Haven, Conn.
(Terms expire July 31, 1952)
Guy Klein East Pittsburgh, Pa.
F. E. Sanford Jackson, Mich.
(Terms expire July 31, 1953)

Code of Principles of Professional Conduct

R. W. Sorensen, *Chairman;* 384 South Holliston Ave., Pasadena 5, Calif.
Dugald C. Jackson, *Honorary Chairman* Cambridge, Mass.
R. E. Argersinger Boston, Mass.
Harry Barker New York, N. Y.
Edith Clarke Austin, Tex.
F. F. Evenson San Diego, Calif.
E. S. Fields Cincinnati, Ohio
C. A. Heinze Los Angeles, Calif.
W. B. Kouwenhoven Baltimore, Md.
R. D. Maxson Chicago, Ill.
E. L. Moreland Boston, Mass.
J. S. Waters Houston, Tex.

Edison Medal

Appointed by the President for term of five years

C. A. Corney Boston, Mass.
J. R. North Jackson, Mich.
I. M. Stein Philadelphia, Pa.
(Terms expire July 31, 1951)
Marvin W. Smith Philadelphia, Pa.
H. S. Osborne New York, N. Y.
H. A. Winne Schenectady, N. Y.
(Terms expire July 31, 1952)
D. I. Cone San Francisco, Calif.
J. B. MacNeill, *Chairman* East Pittsburgh, Pa.
Philip Sporn New York, N. Y.
(Terms expire July 31, 1953)
J. L. Callahan New York, N. Y.
J. M. Flanigen Atlanta, Ga.
R. I. Wilkinson New York, N. Y.
(Terms expire July 31, 1954)
J. F. Calvert Evanston, Ill.
B. A. Case Swampscott, Mass.
John Grotzinger Akron, Ohio
(Terms expire July 31, 1955)

Members of Board of Directors elected by the Board for term of two years

W. L. Everitt Urbana, Ill.
A. H. Frampton St. Catharines, Ontario, Canada
A. C. Monteith Pittsburgh, Pa.
(Terms expire July 31, 1951)
M. D. Hooven Newark, N. J.
F. O. McMillan Corvallis, Oreg.
C. S. Purnell New York, N. Y.
(Terms expire July 31, 1952)

Education

H. N. Muller, Jr., *Chairman;* Westinghouse Electric Corporation, East Pittsburgh, Pa.
J. D. Ryder, *Vice-Chairman* Urbana, Ill.
M. L. Waring, *Secretary* New York, N. Y.
E. B. Alexander Binghamton, N. Y.
(Continued in next column)
E. D. Ayres Columbus, Ohio
R. D. Bennett Silver Spring, Md.
R. L. Biesele Dallas, Tex.
E. W. Boehne Cambridge, Mass.
D. S. Bridgman New York, N. Y.
M. S. Coover Ames, Iowa
W. C. DuVall Boulder, Colo.
A. W. Friend Princeton, N. J.
H. E. Hartig Minneapolis, Minn.
A. R. Hellwarth Detroit, Mich.
T. C. Lloyd Springfield, Ohio
K. B. McEachron, Jr. Schenectady, N. Y.
E. W. Morris Los Angeles, Calif.
H. A. Peterson Madison, Wis.
Walther Richter West Allis, Wis.
E. M. Strong Ithaca, N. Y.
B. R. Teare, Jr. Pittsburgh, Pa.
G. F. Tracy Toronto, Ontario, Canada
E. A. Walker Arlington, Va.
S. Reid Warren Philadelphia, Pa.

Lamme Medal

J. H. Berry Norfolk, Va.
T. H. Morgan Worcester, Mass.
L. A. Umansky Schenectady, N. Y.
(Terms expire July 31, 1951)
C. B. Jolliffe Princeton, N. J.
A. H. Kehoe, *Chairman* New York, N. Y.
J. B. MacNeill East Pittsburgh, Pa.
(Terms expire July 31, 1952)
W. J. Barrett Newark, N. J.
L. L. Bosch Boston, Mass.
Walther Richter West Allis, Wis.
(Terms expire July 31, 1953)

Management

A. C. Monteith, *Chairman;* Westinghouse Electric Corporation, 306 Fourth Avenue, Pittsburgh, Pa.
C. J. Beller, *Vice-Chairman,* Cleveland Electric Illuminating Company, 75 Public Square, Cleveland 13, Ohio
P. L. Alger Schenectady, N. Y.
K. P. Applegate Hartford, Conn.
R. D. Bennett Silver Spring, Md.
F. W. Bush Milwaukee, Wis.
W. L. Cisler Detroit, Mich.
E. E. Hill New York, N. Y.
E. L. Moreland Boston, Mass.
H. A. Peterson New York, N. Y.
D. A. Quarles New York, N. Y.
F. M. Roberts Schenectady, N. Y.
D. D. Smalley San Francisco, Calif.

Prizes, Award of Institute

J. J. Orr, *Chairman;* United States Rubber Company, 1230 Avenue of the Americas, New York 20, N. Y.
Edward C. Day, *Secretary* AIEE Headquarters
H. A. Affel Murray Hill, N. J.
J. C. Aydelott Erie, Pa.
Gordon S. Brown Cambridge, Mass.
W. R. Brownlee Jackson, Mich.
M. J. Kelly New York, N. Y.
A. E. Knowlton New York, N. Y.
K. B. McEachron Pittsfield, Mass.
G. W. Scott, Jr. Lancaster, Pa.
Arthur Bessey Smith Chicago, Ill.
S. D. Summers Washington, D. C.
H. M. Turner New Haven, Conn.
L. A. Umansky Schenectady, N. Y.
C. H. Willis Princeton, N. J.
Harold Winograd Milwaukee, Wis.

Registration of Engineers

Elgin B. Robertson, *Chairman;* P. O. Box 745, Dallas 1, Tex.
S. W. Anderson Lexington, Va.
J. M. Flanigen Atlanta, Ga.
J. H. Foote Jackson, Mich.
N. L. Freeman Schenectady, N. Y.
Ward Harrison Cleveland, Ohio
J. E. Hobson Stanford, Calif.
J. T. Hood Tacoma, Wash.
C. C. Knipmeyer Terre Haute, Ind.
K. B. McEachron Pittsfield, Mass.
E. W. Oesterreich Pittsburgh, Pa.
L. M. Robertson Denver, Colo.
E. W. Seeger Milwaukee, Wis.
R. W. Sorensen Pasadena, Calif.
P. G. Wallace Dallas, Tex.
R. G. Warner New Haven, Conn.
E. R. Whitehead Chicago, Ill.

Student Branches

F. O. McMillan, *Chairman;* Oregon State College, Corvallis, Oreg.
J. S. Antel, Jr. Washington, D. C.
E. J. Ballard, Jr. Lincoln, Neb.
Sterling Beckwith Milwaukee, Wis.
H. F. Cooke Syracuse, N. Y.
H. S. Dixon Fargo, N. D.
A. G. Ennis Washington, D. C.
R. A. Galbraithe Syracuse, N. Y.
O. C. Haycock Salt Lake City, Utah
Oswald N. Jones Cleveland, Ohio
Rodney C. Lewis Los Angeles, Calif.
A. J. McCrocklin, Jr. Austin, Tex.
H. N. Muller, Jr. East Pittsburgh, Pa.
P. H. Nelson Gainesville, Fla.
R. G. Porter Boston, Mass.
Fred H. Pumphrey Gainesville, Fla.
E. A. Reid Urbana, Ill.
R. M. Saunders Berkeley, Calif.
E. W. Spring Detroit, Mich.
F. W. Tatum Dallas, Tex.
R. T. Weil New York, N. Y.

Volta Scholarship Trustees

W. L. Everitt Urbana, Ill.
(Term expires July 31, 1951)
C. A. Powel Boston, Mass.
(Term expires July 31, 1953)
H. S. Osborne, *Chairman* New York, N. Y.
(Term expires July 31, 1955)
R. S. Gardner, *Secretary* AIEE Headquarters

Technical Committees

Communication Division

Communication Division Committee

H. I. Romnes, *Chairman;* Illinois Bell Telephone Company, 212 West Washington Street, Chicago 6, Ill.
F. B. Bramhall, *Vice-Chairman* New York, N. Y.
R. R. O'Connor, *Secretary* Chicago, Ill.
L. G. Abraham Murray Hill, N. J.
W. J. Barrett *(Representing Board of Directors)* Newark, N. J.
J. L. Callahan New York, N. Y.
I. S. Coggeshall New York, N. Y.
J. B. Coleman Camden, N. J.
R. C. Davis New York, N. Y.
E. W. Kenefake Syracuse, N. Y.
G. T. Royden New York, N. Y.

Committee on Communication Switching Systems

R. C. Davis, *Chairman;* Bell Telephone Laboratories, Inc., 463 West Street, New York 14, N. Y.
John Meszar, *Vice-Chairman* New York, N. Y.
A. E. Frost, *Secretary* New York, N. Y.
Eric Brooke Galion, Ohio
L. L. Burns Dallas, Texas
D. G. Geiger Toronto, Ontario, Canada
G. H. Gray New York, N. Y.
C. F. Lynch Poughkeepsie, N. Y.
R. S. Neikirk Washington, D.C.
H. V. Schofield New York, N. Y.
J. O'D. Shepherd Atlanta, Ga.
A. B. Smith Chicago, Ill.
D. L. Solomon Rochester, N. Y.
W. G. Storey Chicago, Ill.
C. M. Tomlinson Philadelphia, Pa.

Committee on Radio Communications Systems

G. T. Royden, *Chairman;* Mackay Radio and Telegraph Company, 67 Broad Street, New York 4, N. Y.
E. D. Becken, *Vice-Chairman* New York, N. Y.
A. C. Dickieson, *Secretary* New York, N. Y.
C. M. Backer Clifton, N. J.
I. F. Byrnes New York, N. Y.
R. D. Campbell New York, N. Y.
H. P. Corwith New York, N. Y.
Edward Daskam, Jr. New York, N. Y.
(Continued in next column)
G. E. Dodrill Washington, D. C.
L. W. Gregory Baltimore, Md.
D. D. Grieg Nutley, N. J.
J. W. Kearney Mineola, N. Y.
S. C. Leyland Newark, N. J.
L. P. Morris Chicago, Ill.
David Talley New York, N. Y.

Committee on Special Communications Applications

E. W. Kenefake, *Chairman;* General Electric Company, Electronics Department, Syracuse, N. Y.
L. A. Smith, *Vice-Chairman* New York, N. Y.
L. C. Holmes, *Secretary* Rochester, N. Y.
S. C. Bartlett New York, N. Y.
G. W. Baughman Swissvale, Pa.
I. F. Byrnes New York, N. Y.
Melville Eastham Cambridge, Mass.
W. D. Hailes Rochester, N. Y.
R. H. Kline Baltimore, Md.
Newton Monk New York, N. Y.
W. A. Ready Malden, Mass.
H. H. Spencer Camden, N. J.
R. B. Valle, Jr. Stanford, Calif.
A. J. Warner Nutley, N. J.

Committee on Telegraph Systems

I. S. Coggeshall, *Chairman;* Western Union Telegraph Company, 60 Hudson Street, New York 13, N. Y.
J. A. Duncan, Jr., *Vice-Chairman* New York, N. Y.
E. C. Chamberlin, Jr., *Secretary* New York, N. Y.
E. P. Bancroft New York, N. Y.
A. S. Benjamin Chicago, Ill.
A. G. Cooley New York, N. Y.
L. G. Erickson San Carlos, Calif.
W. G. H. Finch Washington, D. C.
H. H. Haglund New York, N. Y.
J. V. L. Hogan New York, N. Y.
Grosvenor Hotchkiss New York, N. Y.
Alfred Kahn New York, N. Y.
R. E. Mathes Hartford, Conn.
R. E. Pierce New York, N. Y.
R. B. Shanck New York, N. Y.
R. B. Steele Toronto, Ontario, Canada
E. F. Watson New York, N. Y.

Committee on Television and Aural Broadcasting Systems

J. B. Coleman, *Chairman;* Radio Corporation of America, R.C.A. Victor Division, Camden, N. J.
I. J. Kaar, *Vice-Chairman* Syracuse, N. Y.
W. L. Lawrence, *Secretary* Camden, N. J.
T. J. Boerner Camden, N. J.
G. H. Brown Princeton, N. J.
G. E. Dean Little Neck, L. I., N. Y.
D. G. Fink New York, N. Y.
J. C. Gaudio Chicago, Ill.
P. C. Goldmark New York, N. Y.
W. H. Heiser Patterson, N. J.
W. R. Hewlett Palo Alto, Calif.
M. A. Honnell Atlanta, Ga.
R. M. Johnson New York, N. Y.
D. G. Little Baltimore, Md.
F. H. McIntosh Washington, D. C.
C. B. Plummer Washington, D. C.
E. G. Porta Clifton, N. J.
L. M. Rodgers Philadelphia, Pa.
R. E. Shelby New York, N. Y.
S. C. Spielman Philadelphia, Pa.

Committee on Wire Communications Systems

L. G. Abraham, *Chairman;* Bell Telephone Laboratories, Inc., Murray Hill, N. J.
G. B. Ransom, *Vice-Chairman* New York, N. Y.
P. G. Edwards, *Secretary* Murray Hill, N. J.
H. A. Affel Murray Hill, N. J.
A. L. Albert Corvallis, Oreg.
W. M. Allen Portland, Oreg.
E. Dale Bacus Los Angeles, Calif.
Hezzie Clark Houston, Texas
A. B. Credle Ithaca, N. Y.
F. C. Dodds Phoenix, Ariz.
G. E. Dodrill Washington, D. C.
H. E. Ellithorn Notre Dame, Ind.
L. G. Erickson San Carlos, Calif.
(Continued on page 1725)

G. H. Gray New York, N. Y.
W. D. Hailes Rochester, N. Y.
E. B. Hansen Seattle, Wash.
E. B. Harmon Denver, Colo.
L. M. Hartwell Dallas, Tex.
H. R. Hunkins Clifton, N. J.
H. R. Huntley New York, N. Y.
R. R. O'Connor Chicago, Ill.
A. L. Rumsey Albany, N. Y.
L. J. Shafler Cleveland, Ohio
Arthur Bessey Smith Chicago, Ill.
L. A. Smith New York, N. Y.

General Applications Division

General Applications Division Committee

C. C. Whipple, *Chairman;* Polytechnic Institute of Brooklyn, 85 Livingston Street, Brooklyn 2, N. Y.
O. A. Wilde, *Vice-Chairman* Chester, Pa.
W. H. Reed, *Secretary* New York, N. Y.
W. V. Boughton So. Pasadena, Calif.
H. F. Brown New Haven, Conn.
E. B. Robertson (*representing Board of Directors*) Dallas, Tex.
E. H. Salter New York, N. Y.
Carl F. Scott Bridgeport, Conn.
S. D. Summers Washington, D. C.

Committee on Air Transportation

W. V. Boughton, *Chairman;* Phaostron Company, 151 Pasadena Avenue, South Pasadena, Calif.
D. E. Fritz, *Vice-Chairman* Cleveland, Ohio
W. L. Berry, *Secretary* Culver City, Calif.
J. W. Allen Teterboro, N. J.
G. W. Almassy Los Angeles, Calif.
J. H. Blankenbuehler Troy, Ohio
W. C. Bryant Burbank, Calif.
J. P. Dallas Culver City, Calif.
Peter Duyan, Jr. Santa Monica, Calif.
D. W. Exner Seattle, Wash.
Elio Fuoyo Miami, Fla.
C. E. Gagnier Los Angeles, Calif.
S. H. Hanville, Jr. Washington, D. C.
W. T. Harding Dayton, Ohio
R. D. Jones Fort Wayne, Ind.
W. B. Keller Cleveland, Ohio
Paul Lebenbaum, Jr. Lynn, Mass.
R. J. Lusk East Pittsburgh, Pa.
Karl Martinez Seattle, Wash.
C. F. McCabe San Diego, Calif.
R. E. McDonald St. Paul, Minn.
R. S. Mead Kansas City, Mo.
R. A. Millermaster Milwaukee, Wis.
J. D. Miner Lima, Ohio
W. F. Moore Schenectady, N. Y.
Joseph Nader Chicago, Ill.
H. F. Rempt Burbank, Calif.
R. A. Rugge Grand Rapids, Mich.
K. R. Smythe Johnsville, Pa.
G. E. Sylvester Fort Worth, Tex.
F. H. Walker Farmingdale, N. Y.
S. H. Webster Burbank, Calif.

Committee on Domestic and Commercial Applications

Carl F. Scott, *Chairman;* General Electric Company, 1285 Boston Avenue, Bridgeport, Conn.
T. H. Cline, *Vice-Chairman* Newark, Ohio
J. C. Beckett San Francisco, Calif.
M. M. Brandon New York, N. Y.
C. T. Brasfield, Jr. Birmingham, Ala.
W. B. Buchanan Toronto, Ontario, Canada
O. K. Buck Los Angeles, Calif.
L. R. Emmert East Pittsburgh, Pa.
R. W. Fleming South Bend, Ind.
R. R. Herrmann Minneapolis, Minn.
T. C. Johnson Bloomfield, N. J.
B. H. Martin Chattanooga, Tenn.
L. W. McCullough New York, N. Y.
W. G. Meese Detroit, Mich.
B. F. Parr Mansfield, Ohio
C. R. Reid North Canton, Ohio
L. N. Roberson Seattle, Wash.
G. S. Smith Seattle, Wash.
G. C. Tenney San Francisco, Calif.
T. T. Woodson Bridgeport, Conn.
R. F. Zimmerman Dayton, Ohio

Committee on Land Transportation

H. F. Brown, *Chairman;* New York, New Haven, and Hartford Railroad, Railroad Station, New Haven 6, Conn.
L. W. Birch, *Vice-Chairman* Mansfield, Ohio
R. L. Kimball, *Secretary* New York, N. Y.
J. C. Aydelott Erie, Pa.
L. S. Billau Baltimore, Md.
H. R. Blomquist Providence, R. I.
W. A. Brecht East Pittsburgh, Pa.
D. M. Burckett Boston, Mass.
C. N. Chase Brooklyn, N. Y.
Andrew Costic Hoboken, N. J.
Llewellyn Evans Chattanooga, Tenn.
A. P. Frey Baltimore, Md.
J. E. Gardner Chicago, Ill.
K. H. Gordon Philadelphia, Pa.
P. H. Hatch New Haven, Conn.
G. L. Hoard Seattle, Wash.
J. G. Inglis Toronto, Ontario, Canada
Charles Kerr, Jr. East Pittsburgh, Pa.
S. B. Lent Boston, Mass.
T. M. C. Martin Portland, Oreg.
P. A. McGee New York, N. Y.
E. B. Meissner St. Louis, Mo.
S. R. Negley Philadelphia, Pa.
I. S. Nippes Ridgway, Pa.
A. G. Oehler New York, N. Y.
W. R. Simmons Montreal, Quebec, Canada
Dwight L. Smith Highwood, Ill.
Jacob Stair, Jr. Philadelphia, Pa.
M. C. Swanson Schenectady, N. Y.
R. G. Thring Washington, D. C.
J. P. Tretton Indianapolis, Ind.
R. S. Warren Elkhart, Ind.
R. A. Williamson Erie, Pa.
G. M. Woods East Pittsburgh, Pa.
H. P. Wright Baltimore, Md.
Lawrence Wylie Seattle, Wash.

Committee on Production and Application of Light

Ernest H. Salter, *Chairman;* Electrical Testing Laboratories, Inc., 2 East End Avenue, New York 21, N. Y.
R. C. Putnam, *Vice-Chairman* Cleveland, Ohio
R. L. Oetting, *Secretary* Cleveland, Ohio
J. F. Angler Washington, D. C.
L. H. Brown Stanford, Calif.
S. W. Bruun New York, N. Y.
H. S. Bull Ann Arbor, Mich.
J. F. Dickerhoff Mineola, N. Y.
M. J. Dring South Bend, Ind.
G. C. Harvey Fort Wayne, Ind.
O. W. Holden Los Angeles, Calif.
H. E. Mahan West Lynn, Mass.
F. H. Murphy Portland, Oreg.
Harris Reinhardt New York, N. Y.
D. W. Rowten Cleveland, Ohio
T. C. Sargent Salem, Mass.
E. M. Strong Ithaca, N. Y.
J. D. Thomas Jacksonville, Fla.
H. F. Wall Detroit, Mich.
M. N. Waterman Bloomfield, N. J.
C. C. Whipple Brooklyn, N. Y.

Committee on Marine Transportation

Oscar A. Wilde, *Chairman;* Sun Shipbuilding and Dry Dock Company, Chester, Pa.
J. B. Feder, *Vice-Chairman* Washington, D. C.
W. N. Zippler, *Secretary* New York, N. Y.
W. B. Armstrong Washington, D. C.
H. C. Coleman East Pittsburgh, Pa.
P. J. DuMont New York, N. Y.
R. W. Frost Amesbury, Mass.
A. R. Gatewood New York, N. Y.
E. A. Geary Camden, N. J.
L. M. Goldsmith Philadelphia, Pa.
P. A. Guise New York, N. Y.
H. F. Harvey, Jr. Newport News, Va.
W. E. Jacobsen Schenectady, N. Y.
J. E. Jones Milwaukee, Wis.
Cornelius Krommenhock Brooklyn, N. Y.
Clarence Lynn East Pittsburgh, Pa.
V. W. Mayer Washington, D. C.
S. N. Mead Amesbury, Mass.
W. H. Reed New York, N. Y.
E. M. Rothen New York, N. Y.
J. D. Shuster Quincy, Mass.
C. W. Souder Great Neck, N. Y.
E. H. Stivender Milwaukee, Wis.
G. O. Watson London, England

Industry Division

Industry Division Committee

T. R. Rhea, *Chairman;* General Electric Company, Room 410, Building 2, Schenectady 5, N. Y.
J. D. Leitch, *Vice-Chairman* Cleveland, Ohio
R. S. Gardner, *Secretary* New York, N. Y.
J. S. Gault Ann Arbor, Mich.
J. C. Handy Baltimore, Md.
S. W. Herwald Pittsburgh, Pa.
G. W. Heumann Schenectady, N. Y.
T. B. Montgomery Milwaukee, Wis.
J. J. Orr New York, N. Y.
Kennard Pinder Wilmington, Del.
Leroy W. Roush South Charleston, W. Va.
Victor Siegfried (*Representing Board of Directors*) Worcester, Mass.
Myron Zucker Royal Oak, Mich.

Committee on Chemical, Electrochemical and Electrothermal Applications

Leroy W. Roush, *Chairman;* Union Carbide and Carbon Corporation, South Charleston 3, W. Va.
M. A. Hyde, Jr., *Secretary* Pittsburgh, Pa.
F. V. Andrese Chattanooga, Tenn.
F. M. Baxandall Midland, Mich.
F. R. Benedict East Pittsburgh, Pa.
E. C. Benjamin New York, N. Y.
F. T. Bowditch Cleveland, Ohio
E. H. Browning East Pittsburgh, Pa.
A. B. Campbell Houston, Tex.
W. H. Dickinson Linden, N. J.
W. C. Dreyer Houston, Tex.
F. S. Glass Freeport, Tex.
L. M. Goldsmith Philadelphia, Pa.
W. E. Gutzwiller Milwaukee, Wis.
E. A. Hanff Pittsburgh, Pa.
J. D. Harper Alcoa, Tenn.
T. G. Hieronymus Kansas City, Mo.
J. E. Hobson Stanford, Calif.
H. E. Houck Wilmington, Del.
J. D. Hunnberger Trenton, N. J.
F. L. Kaestle Schenectady, N. Y.
Rollin Kennard Butte, Mont.
R. J. Kuhn New Orleans, La.
D. H. Levy Dallas, Texas
J. Z. Linsenmeyer East Pittsburgh, Pa.
J. J. Loustaunau Boston, Mass.
J. A. McLellan Linden, N. J.
F. J. Mollerus Richland, Wash.
Waldo Porter Vancouver, Wash.
R. L. Rayner Detroit, Mich.
H. C. Riggs Philadelphia, Pa.
G. B. Scheer Oakland, Calif.
E. H. Schick New York, N. Y.
E. O. Scott Welland, Ontario, Canada
H. P. Sherer Cleveland, Ohio
Joel Tompkins Massena, N. Y.
J. J. Unger Cleveland, Ohio
H. W. Wahlquist New York, N. Y.
R. M. Wainwright Urbana, Ill.
H. H. Zielinski Schenectady, N. Y.

Committee on Electric Heating

J. C. Handy, *Chairman;* Consolidated Gas, Electric Light and Power Company, Lexington Building, Baltimore, Md.
P. H. Goodell, *Vice-Chairman* Detroit, Mich.
Harold Bunte, *Secretary* Chicago, Ill.
E. L. Bailey Highland Park, Mich.
R. M. Baker Baltimore, Md.
I. J. Barber Fostoria, Ohio
E. J. Bates Dayton, Ohio
A. H. Cannada Schenectady, N. Y.
F. T. Chesnut Trenton, N. J.
L. M. Duryee Waterbury, Conn.
R. H. Ellis Pittsburgh, Pa.
M. M. Greer Pittsburgh, Pa.
E. M. Guyer Corning, N. Y.
L. F. Hynes Haddonfield, N. J.
J. E. Johansen St. Louis, Mo.
T. P. Kinn Baltimore, Md.
G. F. Leland Schenectady, N. Y.
R. C. Machler Philadelphia, Pa.
C. E. Peck Meadville, Pa.
Kennard Pinder Wilmington, Del.
L. N. Roberson Seattle, Wash.
W. C. Rudd Larchmont, N. Y.
E. H. Schick New York, N. Y.
G. W. Scott, Jr. Lancaster, Pa.
T. H. Story Camden, N. J.
J. T. Thwaites Hamilton, Ontario, Canada
G. E. Walters Peoria, Ill.
H. R. Winemiller Chicago, Ill.

(*Continued in next column*)

Committee on Electric Welding

Myron Zucker, *Chairman;* Myron Zucker Engineering Co., 1708 Crooks Road, Royal Oak, Mich.
R. C. McMaster, *Vice-Chairman* Columbus, Ohio
C. N. Clark, *Secretary* Pittsburgh, Pa.
J. H. Blankenbuehler Troy, N. Y.
W. G. Bostwick Cincinnati, Ohio
J. F. Deffenbaugh Warren, Ohio
D. D. Douglass Oakland, Calif.
R. G. Freeman Fitchburg, Mass.
G. W. Garman Detroit, Mich.
J. W. Gore Baltimore, Md.
E. M. Guyer Corning, N. Y.
W. B. Kouwenhoven Baltimore, Md.
E. J. Lampel Milwaukee, Wis.
S. W. Lather Detroit, Mich.
R. S. Phair Philadelphia, Pa.
C. M. Rhoades, Jr. Schenectady, N. Y.
M. S. Shane Cleveland, Ohio
C. E. Smith Warren, Ohio
H. W. Snyder Beaseman, Mont.
C. B. Stadum Buffalo, N. Y.
H. I. Stanback Milwaukee, Wis.
R. F. Steinert Buffalo, N. Y.
G. I. F. Theriault Dayton, Ohio
H. W. Tietze Newark, N. J.
R. M. Wheeler Flint, Mich.
L. P. Winsor Troy, N. Y.
B. L. Wise Bay City, Mich.
R. E. Young Kankakee, Ill.

Committee on Feedback Control Systems

S. W. Herwald, *Chairman;* Westinghouse Electric Corporation, 1844 Ardmore Boulevard, Pittsburgh 21, Pa.
F. E. Crever, *Vice-Chairman* Schenectady, N. Y.
A. G. Kegel, *Secretary* Pittsburgh, Pa.
W. R. Ahrendt College Park, Md.
E. R. Behn New York, N. Y.
W. W. Bender Baltimore, Md.
G. S. Brown Cambridge, Mass.
H. W. Cory Milwaukee, Wis.
F. H. Ferguson Washington, D. C.
R. W. Jones Evanston, Ill.
O. W. Livingston Schenectady, N. Y.
J. R. MacIntyre West Lynn, Mass.
H. T. Maxcy Jersey City, N. J.
G. D. McCann Pasadena, Calif.
R. C. McMaster Columbus, Ohio
Arthur Porter Toronto, Ontario, Canada
O. H. Schuck Minneapolis, Minn.
W. H. Surber Princeton, N. J.
H. I. Tarpley State College, Pa.
C. N. Weygandt Philadelphia, Pa.
Gifford E. White Beverly Hills, Calif.
A. J. Williams, Jr. Philadelphia, Pa.

Committee on General Industry Applications

Kennard Pinder, *Chairman;* E. I. duPont de Nemours and Company, 10th and Market Streets, Wilmington, Del.
J. C. Fink, *Vice-Chairman* Pittsburgh, Pa.
V. O. Johnson, *Secretary* New York, N. Y.
B. T. Anderson Rockford, Ill.
A. T. Bacheler Buffalo, N. Y.
V. B. Baker East Pittsburgh, Pa.
L. B. Blalock Dallas, Tex.
E. L. Blankenbeker Pittsburgh, Pa.
S. A. Bobo Atlanta, Ga.
M. A. deFerranti Schenectady, N. Y.
J. M. Delfs Schenectady, N. Y.
R. J. Demartini Schenectady, N. Y.
A. W. Frankenfeld Wilmington, Del.
E. L. Happ Pisgah Forest, N. C.
E. M. Hays Pittsburgh, Pa.
L. W. Herchenroeder Pittsburgh, Pa.
L. T. Jester, Jr. Boston, Mass.
K. W. John Detroit, Mich.
T. A. Kauppi Midland, Mich.
G. W. Knapp Schenectady, N. Y.
R. E. Koontz Niles, Mich.
A. F. Luhan Lynn, Mass.
H. B. Mathieu Lubbock, Tex.
E. F. Mekelburg Milwaukee, Wis.
J. F. Moore Toronto, Ontario, Canada

(*Continued on page 1726*)

E. K. Murphy New York, N. Y.
D. R. Percival Worcester, Mass.
G. E. Plaisted San Francisco, Calif.
H. A. Rose Seattle, Wash.
R. G. Rudrow Wilmington, Del.
A. G. Scifried Akron, Ohio
H. L. Smith New York, N. Y.
R. H. Smith Cleveland, Ohio
F. D. Snyder Boston, Mass.
R. F. Snyder Akron, Ohio
R. E. Stroppel Cincinnati, Ohio
J. A. Tudor Portland, Oreg.
H. C. Uhl Sylacauga, Ala.
L. A. Umansky Schenectady, N. Y.
R. H. Zacherle Philadelphia, Pa.

Committee on Industrial Control

G. W. Heumann, *Chairman;* Control Engineering Divisions, General Electric Company, Schenectady 5, N. Y.
J. A. Cortelli, *Vice-Chairman* Cleveland, Ohio
H. L. Palmer, *Secretary* Schenectady, N. Y.
E. H. Alexander Schenectady, N. Y.
H. H. Angel Bethlehem, Pa.
E. L. Bailey Detroit, Mich.
T. H. Bloodworth Milwaukee, Wis.
G. S. Brown Cambridge, Mass.
W. H. Elliot Milwaukee, Wis.
C. T. Evans Milwaukee, Wis.
H. G. Frostick East Pittsburgh, Pa.
J. E. Gahagan Binghamton, N. Y.
J. A. Giesger Rochester, N. Y.
F. Y. Grepe Toronto, Ontario, Canada
Walter Hansen Boston, Mass.
R. W. Jones Evanston, Ill.
R. W. Kowitz Dearborn, Mich.
J. D. Leitch Cleveland, Ohio
O. W. Livingston Schenectady, N. Y.
L. H. Matthias Milwaukee, Wis.
E. F. Mekelburg Milwaukee, Wis.
E. E. Moyer Troy, N. Y.
A. H. Mylea Cleveland, Ohio
J. J. O'Connor New York, N. Y.
J. W. Picking Cleveland, Ohio
C. C. Sawyer Phoenix, Ariz.
W. Schaelchlin East Pittsburgh, Pa.
F. E. Strauss Oakland, Calif.
E. H. Vedder Buffalo, N. Y.

Committee on Industrial Power Systems

J. S. Gault, *Chairman;* Electrical Engineering Department, University of Michigan, Ann Arbor, Mich.
H. G. Barnett, *Vice-Chairman* East Pittsburgh, Pa.
S. A. Warner, *Secretary* New York, N. Y.
H. H. Angel Bethlehem, Pa.
J. E. Arberry Pittsburgh, Pa.
D. L. Beeman Schenectady, N. Y.
Y. T. Chaney Plainville, Conn.
E. S. Dibble Los Angeles, Calif.
V. E. Dodson Seattle, Wash.
Leo Dolkart Chicago, Ill.
D. D. Douglass Oakland, Calif.
E. F. Drake Port Townsend, Wash.
W. J. Ellenberger Washington, D.C.
K. K. Falk South Bend, Ind.
J. E. Gahagan Binghamton, N. Y.
F. S. Glass Freeport, Tex.
W. S. Gordon, Jr. Tacoma, Wash.
J. D. Harper Alcoa, Tenn.
E. H. Hulse San Francisco, Calif.
C. R. Johnson New York, N. Y.
R. E. Johnson Rockford, Ill.
C. M. Lathrop Linden, N. J.
D. H. Levy Dallas, Tex.
R. W. Luther Detroit, Mich.
M. C. Mapes New Haven, Conn.
A. E. Marshall St. Louis, Mo.
J. L. McKeever Peterboro, Ontario, Canada
T. Y. Merrell Phoenix, Ariz.
J. S. Morgan Milwaukee, Wis.
W. A. Moseller Detroit, Mich.
A. L. Nelson Blanco, Tex.
Waldo Porter Vancouver, Wash.
W. H. Rollman Dallas, Tex.
G. C. Saunders Wilmington, Del.
G. W. Schemm St. Louis, Mo.
W. J. Secrest Akron, Ohio
W. D. Stevenson, Jr. Raleigh, N. C.
T. O. Sweatt New York, N. Y.
H. T. Theis Bristol, Pa.
B. F. Thomas, Jr. New York, N. Y.
F. A. Wahlers Brooklyn, N. Y.

(*Continued in next column*)

R. C. Waldron Passaic, N. J.
R. H. Whaley Indianapolis, Ind.
R. T. Woodruff St. Louis, Mo.
William Zelley Roebling, N. J.
T. O. Zittel Lackawanna, N. Y.

Committee on Mining and Metal Industry

T. B. Montgomery, *Chairman;* Allis-Chalmers Manufacturing Company, Box 512, Milwaukee 1, Wis.
A. C. Muir, *Vice-Chairman* Philadelphia, Pa.
L. N. Grier, *Secretary* Pittsburgh, Pa.
J. E. Arberry Pittsburgh, Pa.
H. W. Bikerborn Newark, Ohio
J. E. Breth Bessemer, Ala.
Graham Bright Pittsburgh, Pa.
A. B. Chafetz Carlsbad, N. Mex.
R. J. Corfield Garfield, Utah
F. W. Cramer Pittsburgh, Pa.
E. W. Davis Cambridge, Mass.
J. M. Downie Erie, Pa.
J. H. Edwards New York, N. Y.
Sam Ein Chicago, Ill.
R. H. Ellis Pittsburgh, Pa.
Cecil Farrow Cleveland, Ohio
J. J. Fitzgibbon Charleston, W. Va.
Lanier Greer Cleveland, Ohio
C. L. Gust Lead, S. Dak.
W. R. Harris East Pittsburgh, Pa.
L. H. Harrison Birmingham, Ala.
J. G. Ivy Chicago, Ill.
L. H. James Scranton, Pa.
G. F. Johnson Michigan City, Ind.
J. Z. Listenmeyer East Pittsburgh, Pa.
R. C. McMaster Columbus, Ohio
W. E. Miller Schenectady, N. Y.
H. P. Musser Charleston, W. Va.
M. G. Myers, *Jr.* Boston, Mass.
F. C. Nicholson Wilkes-Barre, Pa.
C. A. Poppino Phoenix, Ariz.
B. E. Price New York, N. Y.
D. E. Renshaw Chicago, Ill.
L. W. Roush South Charleston, W. Va.
E. G. Schlup Middletown, Ohio
F. O. Schnure Sparrows Point, Md.
Victor Siegfried Worcester, Mass.
H. I. Stanback Milwaukee, Wis.
O. J. Swanson Gary, W. Va.
C. L. Tyler Irwin, Pa.
T. R. Weichel Wilkes-Barre, Pa.
J. R. Wickey Cleveland, Ohio
W. G. Wilson Phoenix, Ariz.
C. O. Wood Chicago, Ill.

Power Division

Power Division Committee

L. F. Hickernell, *Chairman;* Anaconda Wire and Cable Company, Hastings-on-Hudson 6, N. Y.
W. R. Brownlee, *Vice-Chairman* Jackson, Mich.
R. S. Gardner, *Secretary* New York, N. Y.
S. C. Bartlett New York, N. Y.
Robert Brandt Boston, Mass.
R. C. Ericson Hammond, Ind.
I. W. Gross New York, N. Y.
Herman Halperin Chicago, Ill.
J. R. Hodtum Pittsburgh, Pa.
W. R. Hough Cleveland, Ohio
L. F. Kennedy Schenectady, N. Y.
A. E. Knowlton New York, N. Y.
E. L. Michelson Chicago, Ill.
H. V. Nye West Allis, Wis.
W. J. Rudge Pittsfield, Mass.
H. J. Schols (*Representing Board of Directors*) Birmingham, Ala.
R. G. A. Skrotzki New York, N. Y.
C. F. Wagner East Pittsburgh, Pa.

Carrier Current Committee

S. C. Bartlett, *Chairman;* American Gas and Electric Service Corporation, 30 Church Street, New York 8, N. Y.
C. W. Boadway, *Vice-Chairman (East)* Toronto, Ontario, Canada
R. H. Miller, *Vice-Chairman (West)* San Francisco, Calif.
E. W. Kenefake, *Secretary* Syracuse, N. Y.
T. M. Blakeslee Los Angeles, Calif.
W. H. Blankmeyer Butte, Mont.
R. C. Cheek East Pittsburgh, Pa.
J. M. Dunham New York, N. Y.
L. G. Eaton Boston, Mass.

(*Continued in next column*)

J. R. Ellison Oklahoma City, Okla.
G. E. Farmer Chattanooga, Tenn.
L. F. Kennedy Schenectady, N. Y.
S. C. Leyland Newark, N. J.
Samuel Lubin Washington, D. C.
L. E. Ludekens Los Angeles, Calif.
D. M. MacGregor New York, N. Y.
T. W. MacLean Spokane, Wash.
O. K. Mangum Parker Dam, Calif.
T. T. Smith Vancouver, Wash.
O. A. Starcke Kansas City, Mo.
B. W. Storer Chicago, Ill.
H. J. Sutton Beaumont, Tex.
T. DeWitt Talmage Chicago, Ill.
Mead Warren, Jr. Alcoa, Tenn.
M. H. Wood Baltimore, Md.

Committee on Insulated Conductors

Herman Halperin, *Chairman;* Commonwealth Edison Company, 72 West Adams Street, Chicago 90, Ill.
V. A. Sheals, *Vice-Chairman* Schenectady, N. Y.
C. T. Hatcher, *Secretary* New York, N. Y.
G. W. Acock Trenton, N. J.
C. F. Avila Boston, Mass.
H. G. Barnett East Pittsburgh, Pa.
C. E. Baugh San Francisco, Calif.
E. D. Bent Montreal, Quebec, Canada
Andrew Bodicky St. Louis, Mo.
A. S. Brookes Newark, N. J.
W. R. Bullard New York, N. Y.
H. W. Clark Washington, D. C.
E. W. Davis Cambridge, Mass.
W. A. Del Mar Yonkers, N. Y.
D. M. Farnham Montreal, Que., Canada
G. H. Fiedler Rochester, N. Y.
L. E. Fogg Phillipsdale, R. I.
J. D. Frantz Portland, Oreg.
M. W. Ghen Pittsburgh, Pa.
L. F. Hickernell Hastings-on-Hudson, N. Y.
R. A. Hopkins Knoxville, Tenn.
A. H. Kidder Philadelphia, Pa.
R. H. Kolks Cincinnati, Ohio
L. I. Komives Detroit, Mich.
M. J. Lowenberg Boston, Mass.
C. G. Mansfield Los Angeles, Calif.
R. E. Morse New York, N. Y
C. T. Nicholson Buffalo, N. Y
Lawrence Palmer Seattle, Wash.
W. T. Peirce Worcester, Mass.
R. S. Peterson Chicago, Ill.
A. D. Pettee Perth Amboy, N. J.
R. A. Schatzel Rome, N. Y.
G. B. Shanklin Schenectady, N. Y.
H. D. Short Toronto, Ontario, Canada
F. V. Smith Chicago, Ill.
L. G. Smith Baltimore, Md.
G. M. L. Sommerman Evanston, Ill.
E. G. Sturdevant Bristol, R. I.
Gordon Thompson New York, N. Y.
H. H. Watson Bridgeport, Conn.
R. J. Wiseman Passaic, N. J.
R. K. Woodson Kansas City, Mo.
K. S. Wyatt Yonkers, N. Y.
C. W. Zimmerer New York, N. Y.
W. N. Zippler New York, N. Y.

Committee on Power Generation

B. G. A. Skrotzki, *Chairman;* Associate Editor, *Power,* 330 West 42d Street, New York 18, N. Y. *
J. A. Brooks, *Vice-Chairman* New York, N. Y.
G. Calabrese, *Secretary* New York, N. Y.
R. E. Appleyard Milwaukee, Wis.
J. E. Barkle, Jr. East Pittsburgh, Pa.
E. P. Bryant Los Angeles, Calif.
A. D. Caskey Chicago, Ill.
H. E. Deardorff Dayton, Ohio
S. M. Denton Denver, Colo.
E. F. Dismeyer Jackson, Mich.
Alex. Dovjikov Portland, Oreg.
C. B. Fontaine Lynn, Mass.
G. A. Harrington Cleveland, Ohio
H. R. Harris Detroit, Mich.
A. P. Hayward Pittsburgh, Pa.
A. J. Krupy Chicago, Ill.
F. L. Lawton Montreal, Quebec, Canada
J. T. Madill Arvida, Quebec, Canada
E. F. Maryatt San Francisco, Calif.
J. B. McClure Schenectady, N. Y.
I. E. Moultrop Belmont, Mass.
D. R. Pattison Johnstown, Pa.
W. W. Perry Binghamton, N. Y.
A. L. Pollard Seattle, Wash.

(*Continued in next column*)

Michael Pope New York, N. Y.
C. S. Randall Washington, D. C.
C. W. Watchorn Baltimore, Md.
W. F. Wetmore Detroit, Mich.
R. R. Wiener Boston, Mass.
G. R. Woodman Los Angeles, Calif.

Committee on Protective Devices

W. J. Rudge, *Chairman;* General Electric Company, 100 Woodlawn Avenue, Pittsfield, Mass.
H. R. Stewart, *Vice-Chairman* Boston, Mass.
A. A. Johnson, *Secretary* East Pittsburgh, Pa.
J. P. Barron Dallas, Tex.
V. J. Cissna Chattanooga, Tenn.
J. E. Clem Schenectady, N. Y.
J. O. Coleman Boston, Mass.
L. M. Connors Toronto, Ontario, Canada
H. A. Cornelius Chicago, Ill.
F. M. Defandorf Washington, D. C.
G. K. Ditlow Washington, D. C.
G. B. Dodds Pittsburgh, Pa.
J. R. Eaton Lafayette, Ind.
R. H. Earle Milwaukee, Wis.
T. I. Eldridge Philadelphia, Pa.
W. D. Hardaway Denver, Colo.
E. M. Hunter Schenectady, N. Y.
P. A. Jeanne New York, N. Y.
W. A. Lewis, Jr. Chicago, Ill.
F. R. Longley Springfield, Mass.
Cort Lowerison Los Angeles, Calif.
Corbett McLean Portland, Oreg.
W. A. McMorris Pittsfield, Mass.
R. H. Mertz Detroit, Mich.
E. G. Norell Chicago, Ill.
A. M. Opsahl East Pittsburgh, Pa.
H. L. Rorden Portland, Oreg.
H. D. Ruger Sparrows Point, Md.
O. L. Sidenfaden Los Angeles, Calif.
W. T. Smith Arlington, Va.
J. M. Towner Baltimore, Md.
S. S. Watkins New York, N. Y.
E. H. Yonkers Chicago, Ill.

Committee on Relays

E. L. Michelson, *Chairman;* Commonwealth Edison Company, 72 West Adams Street, Chicago 90, Ill.
A. J. McConnell, *Vice-Chairman* Schenectady, N. Y.
J. R. Linders, *Secretary* Cleveland, Ohio
C. E. Asbury Jackson, Mich.
J. E. Barkle, Jr. East Pittsburgh, Pa.
M. A. Bostwick Portland, Oreg.
J. W. Bowman Fort Wayne, Ind.
R. J. Cooper Atlanta, Ga.
R. E. Cordray Philadelphia, Pa.
G. E. Dana Binghamton, N. Y.
L. L. Draper Los Angeles, Calif.
M. A. Faucett Urbana, Ill.
F. S. Fehr Reading, Pa.
L. L. Fountain East Pittsburgh, Pa.
Sidney Goldsmith Cincinnati, Ohio
E. T. B. Gross Chicago, Ill.
T. R. Halman Detroit, Mich.
V. J. Hayes Waterbury, Conn.
B. C. Hicks Montreal, Quebec, Canada
R. O. Hopkins Beaumont, Tex.
J. H. Kinghorn New York, N. Y.
R. A. Larner Fort Worth, Tex.
S. C. Leyland Newark, N. J.
H. F. Lindemuth New York, N. Y.
Cort Lowerison Los Angeles, Calif.
W. E. Marter Pittsburgh, Pa.
H. A. McLaughlin Poughkeepsie, N. Y.
W. A. Morgan Denver, Colo.
C. E. Parks Indianapolis, Ind.
H. R. Paxson Philadelphia, Pa.
E. G. Ratz Hamilton, Ontario, Canada
H. P. Sleeper Newark, N. J.
W. K. Sonnemann Newark, N. J.
George Steeb Buffalo, N. Y.
Frank Von Roeschlaub New York, N. Y.

Committee on Rotating Machinery

W. R. Hough, *Chairman;* Reliance Electric and Engineering Company, 1088 Ivanhoe Road, Cleveland, Ohio
C. G. Veinott, *Vice-Chairman* Lima, Ohio
J. L. Fuller, *Secretary* Cleveland, Ohio
W. R. Appleman Dayton, Ohio
R. E. Arnold Lynn, Mass.
E. L. Bailey Detroit, Mich.
M. A. Baker Fort Wayne, Ind.

(*Continued on page 1727*)

Sterling Beckwith Milwaukee, Wis.
B. H. Caldwell, Jr. Schenectady, N. Y.
C. F. Cameron Stillwater, Okla.
James DeKiep Minneapolis, Minn.
E. F. Dismeyer Jackson, Mich.
L. O. Dorfman New York, N. Y.
W. H. Fifer Washington, D. C.
D. E. Fritz Cleveland, Ohio
J. S. Gault Ann Arbor, Mich.
C. B. Hathaway Buffalo, N. Y.
V. P. Hessler Urbana, Ill.
J. W. Jones Philadelphia, Pa.
Richard Lanborn Erie, Pa.
I. M. Levy Dayton, Ohio
M. R. Lory East Pittsburgh, Pa.
Clarence Lynn East Pittsburgh, Pa.
H. C. Marcroft Lancaster, Pa.
W. E. Meserve Ithaca, N. Y.
C. Frank Miller Baltimore, Md.
R. C. Moore Milwaukee, Wis.
J. G. Noest New York, N. Y.
E. I. Pollard Ridgway, Pa.
C. P. Potter St. Louis, Mo.
F. C. Rushing Buffalo, N. Y.
V. E. Schlosberg East Chicago, Ind.
M. L. Schmidt Fort Wayne, Ind.
J. F. Sellers Milwaukee, Wis.
P. H. Trickey St. Louis, Mo.
J. H. Vivian Los Angeles, Calif.
R. W. Wieseman Schenectady, N. Y.
W. W. Wishard Chicago, Ill.
S. S. Wolff St. Louis, Mo.

Committee on Substations

R. C. Ericson, *Chairman;* North Indiana Public Service Company, 5265 Hohman Avenue, Hammond, Ind.
K. L. Wheeler, *Vice-Chairman* Cleveland, Ohio
N. G. Larson, *Secretary* Chicago, Ill.
T. J. Allen Atlanta, Ga.
Herman Bany Philadelphia, Pa.
Harris Barber Boston, Mass.
R. O. Bell Milwaukee, Wis.
F. J. Berger Philadelphia, Pa.
C. C. Crane Madison, Wis.
B. D. Dexter San Francisco, Calif.
M. V. Eardley Los Angeles, Calif.
G. P. Fallon Baltimore, Md.
Marino Fraresso Toronto, Ontario, Canada
H. F. Gidlund Denver, Colo.
E. M. Hunter Schenectady, N. Y.
S. C. Killian Chicago, Ill.
W. M. Larson Minneapolis, Minn.
R. F. Lawrence East Pittsburgh, Pa.
G. S. Lunge Schenectady, N. Y.
W. M. McCauley Greensburg, Pa.
J. L. McKee New York, N. Y.
S. P. Melville Boston, Mass.
I. S. Mendenhall Detroit, Mich.
D. C. Millard Denver, Colo.
K. E. Personius Elmira, N. Y.
P. R. Pierson East Pittsburgh, Pa.
M. E. Reagan East Pittsburgh, Pa.
J. H. Rixse, Jr. Alexandria, Va.
W. S. Scheering Springfield, Mass.
C. H. Smoke Portsmouth, Va.
R. F. Stevens Portland, Oreg.
R. S. Sullivan Phoenix, Ariz.

Committee on Switchgear

H. V. Nye, *Chairman;* Allis-Chalmers Manufacturing Company, West Allis, Wis.
R. L. Webb, *Vice-Chairman* New York, N. Y.
J. M. Geiger, *Secretary* Buffalo, N. Y.
F. S. Benson San Francisco, Calif.
C. K. Beyette Fort Worth, Tex.
H. F. Brown New Haven, Conn.
J. S. Brown Pittsburgh, Pa.
E. A. Childerhose Boston, Mass.
H. W. Codding Newark, N. J.
V. L. Cox Philadelphia, Pa.
G. K. Ditlow Washington, D. C.
G. H. Doan Detroit, Mich.
J. A. Elzi Jackson, Mich.
W. E. Enns Portland, Oreg.
K. J. C. Falck Philadelphia, Pa.
R. M. Ferrill Chattanooga, Tenn.
W. J. Gilson Toronto, Ontario, Canada
J. W. Graff Birmingham, Ala.
C. W. Gragg Amarillo, Tex.
W. D. Hardaway Denver, Colo.
V. J. Hayes Waterbury, Conn.
M. H. Hobbs East Pittsburgh, Pa.
L. M. Hovey Winnipeg, Manitoba, Canada
C. L. Killgore Denver, Colo.

(*Continued in next column*)

I. T. Knight Kansas City, Mo.
F. A. Lane New York, N. Y.
H. A. P. Langsiaff Pittsburgh, Pa.
F. W. McCloskey Chicago, Ill.
W. J. McLachlan Schenectady, N. Y.
R. G. Meyerand St. Louis, Mo.
E. F. Miller Davenport, Iowa
V. G. Munsway Schenectady, N. Y.
H. H. Rudd Greensburg, Pa.
E. K. Sadler Los Angeles, Calif.
A. W. Shelhorse Atlanta, Ga.
O. L. Sidenfaden Los Angeles, Calif.
J. F. Sinnott San Diego, Calif.
Garland Stamper Dayton, Ohio
E. A. Stroberg Boston, Mass.
Anthony Van Ryan South Milwaukee, Wis.
J. H. Vivian Los Angeles, Calif.
C. P. West East Pittsburgh, Pa.
C. E. Winegartner Cleveland, Ohio
J. D. Wood Philadelphia, Pa.
J. C. Woods Chicago, Ill.
S. W. Zimmerman Ithaca, N. Y.

Committee on System Engineering

Robert Brandt, *Chairman;* New England Power Company, 441 Stuart Street, Boston 16, Mass.
H. L. Harrington, *Vice-Chairman* Buffalo, N. Y.
O. W. Manz, Jr., *Secretary* New York, N. Y.
C. G. Adams Schenectady, N. Y.
C. P. Almon, Jr. Chattanooga, Tenn.
E. C. Brown Hartford, Conn.
W. R. Brownlee Jackson, Mich.
D. H. Cameron Kansas City, Mo.
O. E. Charlton Birmingham, Ala.
O. A. Demuth Portland, Oreg.
A. G. Dewars Minneapolis, Minn.
W. B. Fisk New York, N. Y.
G. D. Floyd Toronto, Ontario, Canada
A. P. Fugill Detroit, Mich.
E. E. George New York, N. Y.
S. M. Hamill, Jr. Cincinnati, Ohio
A. P. Hayward Pittsburgh, Pa.
R. G. Hooke Newark, N. J.
L. R. Janes Chicago, Ill.
W. R. Johnson San Francisco, Calif.
J. C. Jones Portland, Oreg.
C. B. Kelley Des Moines, Iowa
C. L. Killgore Denver, Colo.
H. J. Klumb Rochester, N. Y.
R. F. Lawrence East Pittsburgh, Pa.
H. A. Lott Los Angeles, Calif.
M. H. Lovelady Corpus Christi, Tex.
N. M. Lovell Tucson, Ariz.
C. W. Mayott Hartford, Conn.
G. H. McDaniel New York, N. Y.
W. E. Montgomery Los Angeles, Calif.
S. B. Morehouse Philadelphia, Pa.
W. H. Osterle Pittsburgh, Pa.
H. P. Peters Atlanta, Ga.
H. W. Phillips Philadelphia, Pa.
R. T. Purdy Chicago, Ill.
G. F. Switzer Indianapolis, Ind.
G. M. Tatum Richmond, Va.
J. J. Tésar Cleveland, Ohio
D. G. Vaughan Washington, D. C.
R. M. Walker El Paso, Tex.
J. B. Ward Lafayette, Ind.
C. W. Watchorn Baltimore, Md.
G. S. Whitlow St. Louis, Mo.
A. L. Williams Los Angeles, Calif.

Committee on Transformers

J. B. Hodtum, *Chairman;* Allis-Chalmers Manufacturing Company, N. S. Station, Pittsburgh 33, Pa.
F. J. Vogel, *Vice-Chairman* Chicago, Ill.
M. K. Brown, *Secretary* Buffalo, N. Y.
J. A. Adams Philadelphia, Pa.
H. E. Bonheimer Cleveland, Ohio
F. S. Brown Pittsburgh, Pa.
R. J. Brown Toronto, Ontario, Canada
J. L. Cantwell Pittsfield, Mass.
J. H. Chiles Sharon, Pa.
J. E. Clem Schenectady, N. Y.
G. W. Cloubter Milwaukee, Wis.
Merrill De Merit Chattanooga, Tenn.
W. M. Edmunds Washington, D. C.
J. A. Elzi Jackson, Mich.
H. W. Evans Alexandria, Va.
I. W. Gross New York, N. Y.
A. V. Hughes Columbus, Ohio
W. G. James Sharon, Pa.
A. A. Johnson East Pittsburgh, Pa.
H. B. Keath St. Louis, Mo.
D. L. Levine Chicago, Ill.

(*Continued in next column*)

C. M. Lovell St. Louis, Mo.
J. R. Meador Pittsfield, Mass.
V. M. Montsinger Pittsfield, Mass.
H. R. Osborne Toronto, Ontario, Canada
M. H. Pratt Syracuse, N. Y.
T. D. Reimers New York, N. Y.
S. E. Schultz Portland, Oreg.
W. C. Sealey Milwaukee, Wis.
F. L. Snyder Sharon, Pa.
K. M. Stevens Alhambra, Calif.
J. M. Towner Baltimore, Md.
H. H. Wagner Canonsburg, Pa.
P. L. Weir Washington, D. C.
Harry Wells Phoenix, Ariz.
W. C. Whitman Boston, Mass.

Committee on Transmission and Distribution

I. W. Gross, *Chairman;* American Gas and Electric Service Corporation, 30 Church Street, New York 8, N. Y.
S. B. Crary, *Vice-Chairman* Schenectady, N. Y.
R. E. Pierce, *Secretary* New York, N. Y.
C. E. Baugh San Francisco, Calif.
H. C. Bingham Cleveland, Ohio
D. K. Blake Schenectady, N. Y.
P. W. Blye New York, N. Y.
C. A. Booker Boston, Mass.
Bryce Brady Oklahoma City, Okla.
T. J. Brosnan Buffalo, N. Y.
Harold Cole Detroit, Mich.
E. R. Coulbourn Birmingham, Ala.
A. E. Curtis Montreal, Quebec, Canada
H. L. Davis, Jr. Philadelphia, Pa.
A. E. Davison Toronto, Ontario, Canada
T. C. Duncan New York, N. Y.
H. A. Frey Baltimore, Md.
J. H. Hagenguth Pittsfield, Mass.
K. E. Hapgood Chattanooga, Tenn.
E. R. Hendrickson Maywood, Ill.
E. K. Huntington Rochester, N. Y.
E. L. Kanouse Los Angeles, Calif.
C. H. Kraft St. Louis, Mo.
J. T. Lusignan Mansfield, Ohio
D. W. Nethercut Jackson, Mich.
J. E. O'Brien Washington, D. C.
E. W. Oesterreich Pittsburgh, Pa.
A. A. Osipovich Portland, Oreg.
C. K. Poarch New York, N. Y.
L. M. Robertson Denver, Colo.
E. V. Sayles Jackson, Mich.
A. N. Shealy Baltimore, Md.
D. M. Simmons New York, N. Y.
F. V. Smith Chicago, Ill.
H. B. Thacker East Pittsburgh, Pa.
C. F. Wagner East Pittsburgh, Pa.
P. G. Wallace Dallas, Tex.
R. L. Witzke East Pittsburgh, Pa.

Science and Electronics Division

Science and Electronics Division Committee

E. I. Green, *Chairman;* Bell Telephone Laboratories, Inc., Murray Hill, N. J.
W. G. Dow, *Vice-Chairman* Ann Arbor, Mich.
W. F. Davidson, *Secretary* New York, N. Y.
J. G. Brainerd Philadelphia, Pa.
W. R. Clark Philadelphia, Pa.
C. C. Herskind Schenectady, N. Y.
M. G. Malti Ithaca, N. Y.
H. D. Moreland Baltimore, Md.
I. R. Smith Buffalo, N. Y.
I. Melville Stein Philadelphia, Pa.
J. G. Tarboux (*representing Board of Directors*) Ithaca, N. Y.
J. D. Tebo New York, N. Y.

Committee on Basic Sciences

Michel G. Malti, *Chairman;* School of Electrical Engineering, Cornell University, Ithaca, N. Y.
Dimiter Ramadanoff, *Vice-Chairman* Cleveland, Ohio
W. G. Johnson, *Secretary* Princeton, N. J.
J. A. Becker Murray Hill, N. J.
L. V. Bewley Bethlehem, Pa.
R. M. Bozorth Murray Hill, N. J.
J. G. Brainerd Philadelphia, Pa.
C. B. Brown White Oak, Md.

(*Continued in next column*)

C. R. Burrows Ithaca, N. Y.
H. J. Carlin Brooklyn, N. Y.
F. M. Clark Schenectady, N. Y.
Charles Concordia Schenectady, N. Y.
P. C. Cromwell Knoxville, Tenn.
L. A. Finzi Pittsburgh, Pa.
M. F. Gardner Cambridge, Mass.
E. A. Guillemin Cambridge, Mass.
C. W. Hansell Rocky Point, N. Y.
F. K. Harris Washington, D. C.
V. P. Hessler Urbana, Ill.
N. S. Hibshman Brooklyn, N. Y.
T. J. Higgins Madison, Wis.
G. B. Hoadley Raleigh, N. C.
T. B. Jones Baltimore, Md.
R. M. Kalb St. Paul, Minn.
E. W. Kimbark Evanston, Ill.
W. R. LePage Syracuse, N. Y.
W. H. MacWilliams, Jr. Whippany, N. J.
F. C. Magnuson Corvallis, Oreg.
L. W. Matsch Chicago, Ill.
G. D. McCann Pasadena, Calif.
W. E. Phillips Philadelphia, Pa.
H. J. Plumley Silver Spring, Md.
Walther Richter West Allis, Wis.
H. H. Skilling Stanford, Calif.
Joseph Slepian East Pittsburgh, Pa.
J. J. Smith Schenectady, N. Y.
V. G. Smith Toronto, Ontario, Canada
W. L. Sullivan Hoboken, N. J.
G. S. Timoshenko Storrs, Conn.
J. S. Waters Houston, Tex.
A. H. Waynick State College, Pa.
W. M. Young Fort Monmouth, N. J.

Committee on Computing Devices

J. G. Brainerd, *Chairman;* Moore School of Electrical Engineering, University of Pennsylvania, Philadelphia 4, Pa.
W. H. MacWilliams, Jr., *Vice-Chairman* Whippany, N. J.
F. J. Maginnis, *Secretary* Schenectady, N. Y.
S. N. Alexander Washington, D. C.
S. W. Caldwell Cambridge, Mass.
J. M. Coombs St. Paul, Minn.
W. G. Dow Ann Arbor, Mich.
E. L. Harder East Pittsburgh, Pa.
J. W. Mauchly Philadelphia, Pa.
G. D. McCann Pasadena, Calif.
M. S. McIlroy Ithaca, N. Y.
J. C. McPherson New York, N. Y.
P. L. Morton Berkeley, Calif.

Committee on Electronic Power Converters

C. C. Herskind, *Chairman;* Power Electronics Division, General Electric Company, Schenectady 5, N. Y.
W. N. Farquhar, *Vice-Chairman* Pittsburgh, Pa.
C. R. Marcum, *Secretary* East Pittsburgh, Pa.
B. D. Bedford Schenectady, N. Y.
H. R. Blomquist Providence, R. I.
W. F. Bonner Clifton, N. J.
J. L. Boyer East Pittsburgh, Pa.
A. G. Dickinson Trail, British Columbia, Canada
J. B. Donnelly Philadelphia, Pa.
I. K. Dortort Philadelphia, Pa.
W. J. Gilson Toronto, Ontario, Canada
W. E. Gutzwiller Milwaukee, Wis.
G. N. Hughes Alcoa, Tenn.
Otto Jensen Philadelphia, Pa.
F. D. Kalser Sharon, Pa.
Armin Leuthold Montreal, Quebec, Canada
D. E. Marshall Bloomfield, N. J.
A. J. Maslin Sharon, Pa.
L. W. Morton Schenectady, N. Y.
R. A. Nelson Pittsfield, Mass.
F. O. Nottingham, Jr. Atlanta, Ga.
Waldo Porter Vancouver, Wash.
M. E. Reagan East Pittsburgh, Pa.
August Schmidt, Jr. Schenectady, N. Y.
W. C. Sealey Milwaukee, Wis.
F. W. Smith Easton, Pa.
S. L. Smith Philadelphia, Pa.
H. C. Steiner Schenectady, N. Y.
O. J. Swanson Gary, West Va.
J. T. Thwaites Hamilton, Ontario, Canada
D. E. Truckess New York, N. Y.
J. C. Walter Camden, N. J.
C. H. Willis Princeton, N. J.
Harold Winograd Milwaukee, Wis.

Committee on Electronics

W. G. Dow, *Chairman;* Department of Electrical Engineering, University of Michigan, Ann Arbor, Mich.
J. T. Thwaites, *Vice-Chairman (East)* Hamilton, Ontario, Canada
A. M. Zarem, *Vice-Chairman (West)* Los Angeles, Calif.
E. M. Boone, *Secretary* Columbus, Ohio
W. R. G. Baker Syracuse, N. Y.
R. W. Barker Pittsfield, Mass.
C. J. Breitwieser San Diego, Calif.
C. B. Brown White Oak, Md.
R. S. Burnap Harrison, N. J.
J. M. Cage Lafayette, Ind.
A. H. Canada Schenectady, N. Y.
W. R. Clark Philadelphia, Pa.
L. G. Cowles Houston, Tex.
G. J. Crowden Cambridge, Mass.
A. V. Eastman Seattle, Wash.
G. V. Elgroth Philadelphia, Pa.
W. T. Evans Beaumont, Tex.
Rudolf Feldt Clifton, N. J.
G. H. Fett Urbana, Ill.
W. J. Field St. Paul, Minn.
D. G. Fink New York, N. Y.
H. L. Flowers Akron, Ohio
W. A. Geohegan New York, N. Y.
R. E. Haberland Silver Spring, Md.
E. L. Harder East Pittsburgh, Pa.
G. W. Hewitt East Pittsburgh, Pa.
J. E. Hobson Stanford, Calif.
J. R. Hyneman New York, N. Y.
T. P. Kinn Baltimore, Md.
K. S. Koon Endicott, N. Y.
O. W. Livingston Schenectady, N. Y.
D. E. Marshall Bloomfield, N. J.
H. R. Meahl Schenectady, N. Y.
H. R. Mimno Cambridge, Mass.
T. H. Morrin Stanford, Calif.
G. A. Morton Princeton, N. J.
R. E. Mumma Dayton, Ohio
R. A. Nielsen Los Angeles, Calif.
B. K. Northrop Ithaca, N. Y.
David Packard Palo Alto, Calif.
G. W. Penney Pittsburgh, Pa.
W. H. Pickering Pasadena, Calif.
A. J. Quigley Notre Dame, Ind.
Simon Ramo Culver City, Calif.
J. G. Reid, Jr. Washington, D. C.
L. E. Reukema Berkeley, Calif.
R. W. Reynolds Wilmington, Del.
J. D. Ryder Urbana, Ill.
M. R. Shaw Corning, N. Y.
E. T. Sherwood Milwaukee, Wis.
S. W. Smith Washington, D. C.
E. P. Spandau Dayton, Ohio
C. F. Spitzer New Haven, Conn.
H. C. Steiner Schenectady, N. Y.
C. M. Summers Fort Wayne, Ind.
E. R. Thomas New York, N. Y.
F. N. Tompkins Providence, R. I.
Irven Travis Philadelphia, Pa.
D. E. Trucksess New York, N. Y.
D. C. Ulrey Lancaster, Pa.
W. C. White Schenectady, N. Y.
C. H. Willis Princeton, N. J.
D. G. Wilson Lawrence, Kans.
Harold Winograd Milwaukee, Wis.

Committee on Instruments and Measurements

W. R. Clark, *Chairman;* Leeds and Northrup Company, 4901 Stenton Avenue, Philadelphia 44, Pa.
J. E. Hobson, *Vice-Chairman (West)* Stanford, Calif.
J. H. Miller, *Vice-Chairman (East)* Newark, N. J.
J. G. Reid, Jr., *Secretary* Washington, D. C.
W. S. Pritchett *Secretary (West)* Berkeley, Calif.
N. M. Albert Emeryville, Calif.
P. L. Bellaschi Portland, Oreg.
H. W. Berry Camden, N. J.
P. A. Borden Waterbury, Conn.
D. L. Brown Portland, Oreg.
A. L. Brownlee Chicago, Ill.
L. A. Burckmyer, Jr. Ithaca, N. Y.
D. T. Canfield Lafayette, Ind.
J. H. Chiles, Jr. Sharon, Pa.
J. E. Clem Schenectady, N. Y.
Nelle Coda Erie, Pa.
A. B. Craig Boston, Mass.
C. L. Dawes Cambridge, Mass.
F. C. Doble Belmont, Mass.
G. W. Downs Pasadena, Calif.
C. K. Duff Toronto, Ontario, Canada

(*Continued in next column*)

G. W. Dunlap Schenectady, N. Y.
I. G. Easton Cambridge, Mass.
W. N. Eddy Cambridge, Mass.
G. V. Elgroth Philadelphia, Pa.
J. H. Enns Ann Arbor, Mich.
Rudolf Feldt Clifton, N. J.
John G. Ferguson Murray Hill, N. J.
F. J. Gaffney Brooklyn, N. Y.
W. A. Geohegan New York, N. Y.
T. S. Gray Cambridge, Mass.
Kendrick Hare Buffalo, N. Y.
A. J. Hornfeck Cleveland, Ohio
W. S. Hunt Boulder City, Nev.
W. G. Knickerbocker Detroit, Mich.
A. E. Knowlton New York, N. Y.
H. C. Koenig New York, N. Y.
G. L. Lane Spokane, Wash.
E. S. Lee Schenectady, N. Y.
B. E. Lenehan Newark, N. J.
W. N. Lindblad Emeryville, Calif.
J. T. Lusignan, Jr. Mansfield, Ohio
Harold Lyons Washington, D. C.
C. G. Mansfield Los Angeles, Calif.
L. W. Matsch Chicago, Ill.
N. W. Matthews Washington, D. C.
W. J. Mayo-Wells Silver Spring, Md.
G. A. Morton Princeton, N. J.
David Packard Palo Alto, Calif.
H. J. Plumley White Oak, Md.
F. A. Redding Alhambra, Calif.
L. M. Rodgers Philadelphia, Pa.
C. F. Savage, Jr. West Lynn, Mass.
J. P. Scott St. Louis, Mo.
F. B. Silsbee Washington, D. C.
G. S. Smith Seattle, Wash.
Harry Sohon Philadelphia, Pa.
K. M. Stevens Alhambra, Calif.
L. N. Stone Corvallis, Oreg.
J. M. Vanderleck Toronto, Ontario, Canada
Ernst Weber Brooklyn, N. Y.
A. H. Wing, Jr. Evanston, Ill.
C. J. Zeller New York, N. Y.

Committee on Metallic Rectifiers

I. R. Smith, *Chairman;* Motor Engineering Division, Westinghouse Electric Corporation, Buffalo 5, N. Y.
W. F. Bonner, *Vice-Chairman* Clifton, N. J.
E. A. Harty, *Secretary* West Lynn, Mass.
L. W. Burton Lynn, Mass.
J. T. Cataldo Fort Monmouth, N. J.
P. G. Cobb Newark, N. J.
M. E. Gamble Indianapolis, Ind.
K. S. Geiges New York, N. Y.
E. A. Groeteke St. Louis, Mo.
C. E. Hamann Lynn, Mass.
C. W. Hansell Rocky Point, N. Y.
L. K. Hedding Pittsburgh, Pa.
C. C. Herskind Schenectady, N. Y.
W. E. Phillips Philadelphia, Pa.
Glen Ramsey North Chicago, Ill.
J. T. Thwaites Hamilton, Ontario, Canada
D. E. Trucksess New York, N. Y.
J. L. Wagner Endicott, N. Y.

Committee on Nucleonics

W. F. Davidson, *Chairman;* Consolidated Edison Company of New York, Inc., 4 Irving Place, New York 3, N. Y.
G. W. Dunlap, *Vice-Chairman* Schenectady, N. Y.
W. E. Barbour, Jr., *Secretary* Boston, Mass.
H. W. Bibber Schenectady, N. Y.
H. W. Brackney Washington, D. C.
D. W. Cardwell Oak Ridge, Tenn.
J. O'R. Coleman Boston, Mass.
J. M. Cork Ann Arbor, Mich.
J. R. Dunning New York, N. Y.
I. A. Getting Cambridge, Mass.
T. S. Gray Cambridge, Mass.
H. L. Hull Chicago, Ill.
T. R. Kohler Irvington-on-Hudson, N. Y.
C. V. Larrick Richland, Wash.
R. G. Lorraine Schenectady, N. Y.
L. C. Marshall Berkeley, Calif
H. B. Marvin Syracuse, N. Y.
M. S. Oldacre Chicago, Ill.
J. K. Pickard Washington, D. C.
Walther Richter Milwaukee, Wis.
P. N. Ross Pittsburgh, Pa.
W. E. Shoupp Pittsburgh, Pa.
J. J. Smith Schenectady, N. Y.
Abe Tilles San Francisco, Calif.
John G. Trump Cambridge, Mass.
R. E. Watson Philadelphia, Pa.

Committee on Therapeutics

H. D. Moreland, *Chairman;* Westinghouse Electric Corporation, 2519 Wilkens Avenue, Baltimore 3, Md.
S. Reid Warren, Jr., *Vice-Chairman* Philadelphia, Pa.
Scott W. Smith, *Secretary* Washington, D. C.
L. F. Ehrke Bloomfield, N. J.
T. H. Rogers Springdale, Conn.
W. R. Smith Sweet Briar, Va.
H. I. Trenary Milwaukee, Wis.
R. E. Watson Philadelphia, Pa.

AIEE Representatives

Appointed by the Board of Directors

Alfred Noble Prize Committee, ASCE
T. M. Linville Schenectady, N. Y.

American Association for the Advancement of Science, Council
J. W. Barker New York, N. Y.
I. Melville Stein Philadelphia, Pa.

American Research Committee on Grounding
C. T. Sinclair Pittsburgh, Pa.

American Standards Association, Standards Council
F. E. Harrell Cleveland, Ohio
Charles Rufus Harte New Haven, Conn.
R. T. Henry Buffalo, N. Y.
Alternates
R. C. Bergvall East Pittsburgh, Pa.
J. R. North Jackson, Mich.
E. B. Paxton Schenectady, N. Y.

American Year Book, Advisory Board
H. H. Henline New York, N. Y.

Conference of Representatives From Engineering Societies of Western Europe and USA
T. G. LeClair Chicago, Ill.

Construction Industry Advisory Council
Henry A. Lardner New York, N. Y.

Engineering Foundation Board
J. W. Barker New York, N. Y.
C. G. Suits Schenectady, N. Y.

Engineering Societies Monographs Committee
W. F. Davidson New York, N. Y.
W. I. Slichter New York, N. Y.

Engineers' Council for Professional Development
R. H. Barclay New York, N. Y.
M. S. Coover Ames, Iowa
M. D. Hooven Newark, N. J.

Engineers Joint Council
J. F. Fairman New York, N. Y.
H. H. Henline New York, N. Y.
T. G. LeClair Chicago, Ill.
Everett S. Lee Schenectady, N. Y.
Alternates
W. J. Barrett Newark, N. J.
J. L. Callahan New York, N. Y.

General Electric Educational Fund Fellowship Committee
J. F. Fairman New York, N. Y.

Herts Award Committee
M. S. Coover Ames, Iowa

Hoover Medal Board of Award
H. S. Osborne New York, N. Y.
D. C. Prince Schenectady, N. Y.
J. G. Tarboux Ithaca, N. Y.

John Fritz Medal Board of Award
J. F. Fairman New York, N. Y.
J. Elmer Housley Alcoa, Tenn.
B. D. Hull Dallas, Tex.
Everett S. Lee Schenectady, N. Y.

Joint AIEE-IRE Co-ordination Committee
J. L. Callahan New York, N. Y.
Everett S. Lee Schenectady, N. Y.

Library Board, United Engineering Trustees, Inc.
N. S. Hibshman Brooklyn, N. Y.
W. G. Vieth New York, N. Y.

Marston Medal Board of Award
Harry B. Gear Chicago, Ill.

National Association of Corrosion Engineers, Inter-Society Committee on Corrosion
L. J. Gorman New York, N. Y.
H. M. Trueblood Dobbs Ferry, N. Y.

National Bureau of Engineering Registration, Advisory Board
Elgin B. Robertson Dallas, Tex.

National Electronics Conference, Board of Directors
W. G. Dow Ann Arbor, Mich.

National Engineering Advisory Committee
A. H. Kehoe New York, N. Y.

National Fire Waste Council
Robin Beach Brooklyn, N. Y.
W. B. Kouwenhoven Baltimore, Md.

National Research Council, Division of Engineering and Industrial Research
W. B. Kouwenhoven Baltimore, Md.

Quarterly of Applied Mathematics
M. G. Malti Ithaca, N. Y.

United Engineering Trustees, Inc.
J. F. Fairman New York, N. Y.
A. G. Oehler New York, N. Y.
D. A. Quarles New York, N. Y.

United States National Committee of the International Commission on Illumination
Ward Harrison Cleveland, Ohio
Harris Reinhardt Flushing, N. Y.
E. H. Salter New York, N. Y.

United States National Committee of the International Electrotechnical Commission
F. E. Harrell Cleveland, Ohio
J. J. Pilliod New York, N. Y.
Alternates
H. E. Farrer New York, N. Y.
I. W. Gross New York, N. Y.
E. B. Paxton Schenectady, N. Y.

Washington Award Commission
W. A. Lewis, Jr. Chicago, Ill.
Frank V. Smith Chicago, Ill.

World Power Conference, Executive Committee of United States National Committee
T. G. LeClair Chicago, Ill.

Appointed by Standards Committee

Aeronautical Electrical Equipment Standardization
W. V. Boughton, liaison with NASC and SAE South Pasadena, Calif.

Electrical Standards Committee, ASA
F. E. Harrell Cleveland, Ohio
E. B. Paxton Schenectady, N. Y.
J. J. Pilliod New York, N. Y.
Alternates
H. E. Farrer New York, N. Y.
I. W. Gross New York, N. Y.
Division Assignment
Division on Communication and Electronics
H. E. Farrer New York, N. Y.
F. E. Harrell Cleveland, Ohio
J. J. Pilliod New York, N. Y.
Division on Power
I. W. Gross New York, N. Y.
E. B. Paxton Schenectady, N. Y.

Industry Committee on Interior Wiring Design
M. M. Brandon New York, N. Y.
L. C. Peterman New York, N. Y.

Joint Committee for Development of Statistical Applications in Engineering and Manufacturing
W. P. Dobson Toronto, Ontario, Canada

National Fire Protection Association, Electrical Section
Robin Beach Brooklyn, N. Y.
W. B. Kouwenhoven Baltimore, Md.

AIEE Technical Subcommittees—1950–51

Communication Division

Communication Switching Systems

No subcommittees

Radio Communications Systems

Mobile Radio Subcommittee

A. C. Dickieson, *Chairman;* Bell Telephone Laboratories, Inc., 463 West Street, New York 14, N. Y.
C. M. Backer — Clifton, N. J.
I. F. Byrnes — New York, N. Y.
G. E. Dodrill — Washington, D. C.
J. W. Kearney — Mineola, N. Y.
L. P. Morris — Chicago, Ill.
David Talley — New York, N. Y.

Point-to-Point Radio Subcommittee

E. D. Becken, *Chairman;* R.C.A. Communications, Inc., 66 Broad Street, New York 4, N. Y.
R. D. Campbell — New York, N. Y.
H. P. Corwith — New York, N. Y.
Edward Daskam, Jr. — New York, N. Y.
G. E. Dodrill — Washington, D. C.
L. W. Gregory — Baltimore, Md.
D. D. Grieg — Nutley, N. J.
S. C. Leyland — Newark, N. J.

Special Communications Applications

Electro-Acoustics Subcommittee

R. B. Vaile, Jr., *Chairman;* Standard University, Stanford Research Institute, Stanford, Calif.
I. F. Byrnes — New York, N. Y.
L. C. Holmes — Rochester, N. Y.
H. H. Spencer — Camden, N. J.

Railroad Communications Subcommittee

W. D. Hailes, *Chairman;* General Railway Signal Company, 801 West Avenue, Rochester 11, N. Y.
G. W. Baughman — Swissvale, Pa.
L. E. Kearney — New York, N. Y.
R. H. Kline — Baltimore, Md.
Newton Monk — New York, N. Y.

Special Activities Subcommittee

A. J. Warner, *Chairman;* Federal Telecommunication Laboratories, 500 Washington Avenue, Nutley 10, N. J.
Melville Eastham — Cambridge, Mass.
R. H. Kline — Baltimore, Md.
Newton Monk — New York, N. Y.
H. H. Spencer — Camden, N. J.

Telegraph Systems

Facsimile Subcommittee

R. E. Mathes, *Chairman;* Gray Research and Development Company, Inc., 16–30 Arbor Street, Hartford 1, Conn.
A. G. Cooley — New York, N. Y.
W. G. H. Finch — Washington, D. C.
J. V. L. Hogan — New York, N. Y.
Grosvenor Hotchkiss — New York, N. Y.
J. R. Krock — Washington, D. C.

Television and Aural Broadcasting Systems

No subcommittees

Wire Communications Systems

No subcommittees

General Applications Division

Air Transportation

Aircraft Electrical Rotating Machinery Subcommittee

L. R. Larson, *Chairman;* Naval Research Laboratory, Washington, D. C.
J. W. Allen — Teterboro, N. J.
J. B. Crockford — Lima, Ohio
William Fell — Cleveland, Ohio
S. H. Hanville, Jr. — Washington, D. C.
R. D. Jones — Fort Wayne, Ind.
Paul Lebenbaum, Jr. — Lynn, Mass.
G. W. Sherman — Dayton, Ohio
R. R. Smith — Baltimore, Md.

Aircraft Electrical Systems Subcommittee

G. W. Almassy, *Chairman;* General Electric Company, 6900 South Stanford Avenue, Los Angeles 1, Calif.
J. W. Allen — Teterboro, N. J.
Phil. Binderman — Washington, D. C.
H. B. Bunce — East Pittsburgh, Pa.
L. M. Cobb — Johnsville, Pa.
D. W. Exner — Seattle, Wash.
H. L. Hildebrandt — Dayton, Ohio
C. S. Milliken — Burbank, Calif.
W. F. Moore — Schenectady, N. Y.
G. A. Phillips — Schenectady, N. Y.
V. O. Ray — Los Angeles, Calif.
D. H. Scott — Washington, D. C.
A. J. Snyder — Tulsa, Okla.
A. F. Trumbull — Santa Monica, Calif.

Principles of Altitude Rating of Electrical Apparatus Subcommittee

Karl Martinez, *Chairman;* Boeing Airplane Company, Plant 1, Seattle, Wash.
J. W. Allen — Teterboro, N. J.
S. H. Hanville, Jr. — Washington, D. C.
V. C. Holloway — Washington, D. C.
J. G. Hutton — Schenectady, N. Y.
C. A. Maple — Dayton, Ohio
R. A. Rugge — Grand Rapids, Mich.

Aircraft Electrical Control, Protective Devices and Cable Subcommittee

B. O. Austin, *Chairman;* Aviation Engineering Department, Westinghouse Electric Corporation, Lima, Ohio
Earl Barlow — Baltimore, Md.
E. E. Magee — Dayton, Ohio
R. A. Millermaster — Milwaukee, Wis.
H. S. Moore — New Haven, Conn.
W. F. Moore — Schenectady, N. Y.
J. Ottmar — Attleboro, Mass.
Milton Schach — Washington, D. C.
Omar Wally — Cleveland, Ohio
W. W. West — New York, N. Y.

Domestic and Commercial Applications

Electric Heating of Homes and Heat Pumps Subcommittee

J. C. Beckett, *Chairman* (West); Westx Electric Heater Company, 390 First Street, San Francisco 5, Calif.
T. C. Johnson, *Chairman* (East); General Electric Company, 5 Lawrence Street, Bloomfield, N. J.

Domestic Appliances Subcommittee

C. R. Reid, *Chairman;* Engineering Laboratories, The Hoover Company, North Canton, Ohio

Land Transportation

Heavy Traction Electrification Data Subcommittee

L. W. Birch, *Chairman;* Ohio Brass Company, Mansfield, Ohio
H. F. Brown — New Haven, Conn.
A. G. Oehler — New York, N. Y.
R. A. Williamson — Erie, Pa.
G. M. Woods — East Pittsburgh, Pa.

Projects:
(1). Catenary overhead systems
(2). Third rail systems
(3). Electric locomotives
(4). Substations
(5). Power supply

The personnel of the projects is as follows: (1) and (2). L. W. Birch, *Chairman,* Ohio Brass Company, Mansfield, Ohio; H. F. Brown, New Haven, Conn.
(3), (4), and (5). A. G. Oehler, New York, N. Y.; R. A. Williamson, Erie, Pa.; G. M. Woods, East Pittsburgh, Pa.

Heavy Traction Papers and Plans Subcommittee

H. F. Brown, *Chairman;* New York, New Haven, and Hartford Railroad, Railroad Station, New Haven, Conn.
W. A. Brecht — East Pittsburgh, Pa.
R. L. Kimball — New York, N. Y.

Light Traction Papers and Plans Subcommittee

G. M. Woods, *Chairman;* Industry Engineering Department, Westinghouse Electric Corporation, East Pittsburgh, Pa.
H. R. Blomquist — Providence, R. I.
D. L. Smith — Highwood, Ill.

Subcommittee on Revision of AIEE Standard Number 16 (Electric Railway Control Apparatus) ASA C48

R. A. Williamson, *Chairman;* Railroad Rolling Stock Division of Locomotive and Car Equipments Divisions, General Electric Company, Erie, Pa.
P. H. Hatch — New Haven, Conn.
J. G. Inglis — Toronto, Ontario, Canada
G. M. Woods — East Pittsburgh, Pa.

Marine Transportation

Power Generation Subcommittee

Clarence Lynn, *Chairman;* Westinghouse Electric Corporation, East Pittsburgh, Pa.
W. B. Armstrong — Washington, D. C.
H. C. Coleman — East Pittsburgh, Pa.
L. M. Goldsmith — Philadelphia, Pa.
W. E. Jacobsen — Schenectady, N. Y.
E. H. Stivender — Milwaukee, Wis.
O. A. Wilde — Chester, Pa.

Power Application Subcommittee

L. M. Goldsmith, *Chairman;* Atlantic Refining Company, 260 South Broad Street, Philadelphia, Pa.
W. B. Armstrong — Washington, D. C.
H. C. Coleman — East Pittsburgh, Pa.
W. E. Jacobsen — Schenectady, N. Y.
J. E. Jones — Milwaukee, Wis.
Clarence Lynn — East Pittsburgh, Pa.
E. H. Stivender — Milwaukee, Wis.

Wires and Cables Subcommittee

W. N. Zippler, *Chairman;* Gibbs and Cox, Inc., 1 Broadway, New York 4, N. Y.
P. J. DuMont — New York, N. Y.
J. B. Feder — Washington, D. C.
A. R. Gatewood — New York, N. Y.
W. E. Jacobsen — Schenectady, N. Y.
V. W. Mayer — Washington, D. C.
W. H. Reed — New York, N. Y.

Switchboards and Control Subcommittee

H. C. Coleman, *Chairman;* Westinghouse Electric Corporation, East Pittsburgh, Pa.
P. J. DuMont — New York, N. Y.
H. F. Harvey, Jr. — Newport News, Va.
J. E. Jones — Milwaukee, Wis.
C. Krommenhock — Brooklyn, N. Y.
J. D. Shuster — Quincy, Mass.
E. H. Stivender — Milwaukee, Wis.

Distribution Subcommittee

H. F. Harvey, Jr., *Chairman;* Newport News Shipbuilding and Dry Dock Company, Newport News, Va.
W. B. Armstrong — Washington, D. C.
A. R. Gatewood — New York, N. Y.
E. A. Geary — Camden, N. J.
L. M. Goldsmith — Philadelphia, Pa.
P. A. Guise — New York, N. Y.
V. W. Mayer — Washington, D. C.
W. N. Zippler — New York, N. Y.

Fittings and Appliances Subcommittee

V. W. Mayer, *Chairman;* United States Maritime Commission, Technical Division, United States Department of Commerce Building, Washington, D. C.
P. J. DuMont — New York, N. Y.
J. B. Feder — Washington, D. C.
R. W. Frost — Amesbury, Mass.
E. A. Geary — Camden, N. J.
P. A. Guise — New York, N. Y.
H. F. Harvey, Jr. — Newport News, Va.
E. M. Rothen — New York, N. Y.
J. D. Shuster — Quincy, Mass.
O. A. Wilde — Chester, Pa.

Communications and Alarm Subcommittee

W. H. Reed, *Chairman;* Bruce Electric Company, 196 West Houston Street, New York 14, N. Y.
R. W. Frost — Amesbury, Mass.
A. R. Gatewood — New York, N. Y.
E. A. Geary — Camden, N. J.
C. Krommenhock — Brooklyn, N. Y.
S. N. Mead — Amesbury, Mass.
E. M. Rothen — New York, N. Y.
J. D. Shuster — Quincy, Mass.
C. W. Souder — Great Neck, N. Y.

Navigation Equipment Subcommittee

S. N. Mead, *Chairman;* Sig-Trans, Inc., Haverhill Road, Amesbury, Mass.
R. W. Frost — Amesbury, Mass.
P. A. Guise — New York, N. Y.
C. Krommenhock — Brooklyn, N. Y.
E. M. Rothen — New York, N. Y.
G. W. Souder — Great Neck, N. Y.

Publicity, Personnel, and History Subcommittee

W. H. Reed, *Chairman;* Bruce Electric Company, 196 West Houston Street, New York 14, N. Y.
H. F. Harvey, Jr. — Newport News, Va.

Editing Subcommittee

W. N. Zippler, *Chairman;* Gibbs and Cox, Inc., 1 Broadway, New York 4, N. Y.
J. B. Feder — Washington, D. C.
H. F. Harvey, Jr. — Newport News, Va.
W. H. Reed — New York, N. Y.

International Standardization Subcommittee

A. R. Gatewood, *Chairman;* American Bureau of Shipping, 45 Broad Street, New York 4, N. Y.
H. C. Coleman — East Pittsburgh, Pa.
H. F. Harvey, Jr. — Newport News, Va.
W. N. Zippler — New York, N. Y.

Production and Application of Light

Nomenclature of Electronic Lamps Subcommittee

R. C. Putnam, *Chairman;* Case Institute of Technology, Cleveland, Ohio
G. S. Evans — Bloomfield, N. J.
L. R. Keiffer — Cleveland, Ohio
T. C. Sargent — Salem, Mass.

Industry Division

Chemical, Electrochemical and Electrothermal Applications

Arc Furnaces and Electrothermal Processes Subcommittee

E. H. Browning, Jr., *Chairman;* Industry Engineering Department 10-L, Westinghouse Electric Corporation, East Pittsburgh, Pa.
F. V. Andreae — Chattanooga, Tenn.
W. L. Bundy — Wilson Dam, Ala.
R. A. Geiselman — East Pittsburgh, Pa.
E. A. Hanff — Pittsburgh, Pa.
A. R. Olzrogge — Schenectady, N. Y.
E. Scheick — New York, N. Y.
H. H. Zielinski — Schenectady, N. Y.

Cathodic Protection Subcommittee

R. M. Wainwright, *Chairman;* College of

Engineering, University of Illinois, Urbana, Ill.
A. E. Archambault New York, N. Y.
J. D. Brance Houston, Tex.
A. S. Brooks Newark, N. J.
Guy Corfield Los Angeles, Calif.
G. C. Cox Charleston, W. Va.
I. A. Dennison Washington, D. C.
I. C. Dietze Los Angeles, Calif.
L. J. Gorman New York, N. Y.
T. G. Hieronymus Kansas City, Mo.
R. J. Kuhn New Orleans, La.
D. H. Levy Dallas, Tex.
R. W. Linney Oklahoma City, Okla.
F. J. Mollerus Richland, Wash.
R. L. Rayner Detroit, Mich.
H. W. Wahlquist New York, N. Y.

ELECTROLYTIC PROCESSES SUBCOMMITTEE

W. E. Gutzwiller, *Chairman;* Allis-Chalmers Manufacturing Company, Milwaukee, Wis.
Felix Glass Freeport, Tex.
J. D. Harper Alcoa, Tenn.
H. E. Houck Wilmington, Del.
F. L. Kaestle Schenectady, N. Y.
Rollin Kennard Butte, Mont.
F. L. Lawton Montreal, Quebec, Canada
G. H. Orcutt Wyandotte, Mich.
Waldo Porter Vancouver, Wash.
G. B. Scherer Oakland, Calif.
Joel Tompkins Massena, N. Y.

PETROLEUM REFINING AND PRODUCTION SUBCOMMITTEE

Lester Goldsmith, *Chairman;* Atlantic Refining Company, 260 South Broad Street, Philadelphia 1, Pa.
H. J. Appel New York, N. Y.
E. C. Benjamin New York, N. Y.
W. H. Dickinson Elizabeth, N. J.
J. B. Glasby Philadelphia, Pa.
E. L. Hoyle East Chicago, Ind.
D. H. Levy Dallas, Tex.
E. L. Nopper Philadelphia, Pa.

STORAGE BATTERIES SUBCOMMITTEE

H. C. Riggs, *Chairman;* Electric Storage Battery Company, 19th and Allegheny Avenue, Philadelphia 32, Pa.
J. D. Hunnsberger Trenton, N. J.
L. A. Murray Providence, R. I.
E. T. Rummel Cleveland, Ohio
J. J. Unger Cleveland, Ohio
K. A. Vaughn Depew, N. Y.
H. H. Zielinski Schenectady, N. Y.

CHEMICAL INDUSTRIES SUBCOMMITTEE

L. W. Roush, *Chairman;* Union Carbide and Carbon Corporation, South Charleston, W. Va.
Felix Glass Freeport, Tex.
E. M. Hansford Montgomery, W. Va.
J. A. Horacek Fairport Harbor, Ohio
H. E. Houck Wilmington, Del.
M. A. Hyde East Pittsburgh, Pa.
S. J. Rosch Hastings-on-Hudson, N. Y.

Electric Heating

RADIANT HEATING SUBCOMMITTEE

I. J. Barber, *Chairman;* Fostoria Pressed Steel Corporation, 1945 Bradner Street, Fostoria, Ohio
E. J. Bates Dayton, Ohio
Earl Benson Boston, Mass.
P. O. Blackmore Newark, N. J.
P. H. Bowman Chicago, Ill.
A. H. Canada Schenectady, N. Y.
C. S. Cogger Nutley, N. J.
P. H. Goodell Detroit, Mich.
J. C. Handy Baltimore, Md.
S. G. Hibben Bloomfield, N. J.
W. F. Hickes Foxboro, Mass.
J. E. Johanson St. Louis, Mo.
J. E. Kolb Pittsburgh, Pa.
E. A. Linsday Cleveland, Ohio
R. C. Machler Philadelphia, Pa.
C. L. Raylor Detroit, Mich.
C. E. Russell Philadelphia, Pa.
Lawrence Stout St. Louis, Mo.
W. H. Wannamaker Philadelphia, Pa.

INDUCTION AND DIELECTRIC HEATING SUBCOMMITTEE

W. C. Rudd, *Chairman;* 68 Lansdowne Drive, Larchmont, N. Y.
R. M. Baker Baltimore, Md.
G. P. Bosomworth Akron, Ohio
E. W. Chapin Laurel, Md.
F. T. Chesnut Trenton, N. J.
L. M. Duryee Waterbury, Conn.
J. E. Eiselein Camden, N. J.
C. W. Frick Schenectady, N. Y.
W. H. Hickok Louisville, Ky.
R. J. Hunn Wilmington, Del.
T. P. Kinn Baltimore, Md.
G. W. Klingaman Camden, N. J.
Eugene Mittleman Chicago, Ill.
William Paulin Toronto, Ont., Canada
G. W. Scott, Jr. Lancaster, Pa.
R. S. Tucker New York, N. Y.
J. T. Vaughan Cleveland, Ohio
D. E. Watts Syracuse, N. Y.
Otto Weitmann New York, N. Y.

RADIATION MEASUREMENTS ABOVE 200 MEGACYCLES SUBCOMMITTEE

R. M. Baker, *Chairman;* Westinghouse Electric Corporation, 2519 Wilkens Avenue, Baltimore 3, Md.
H. H. Beiser Fort Monmouth, N. J.
Marvin Bock Waltham, Mass.
E. W. Chapin Laurel, Md.
H. E. Disger Washington, D. C.
J. E. Eiselein Camden, N. J.
C. W. Frick Schenectady, N. Y.
J. C. Handy Baltimore, Md.
Paul Hines Newton, Mass.
W. L. Roberts East Pittsburgh, Pa.
Ralph M. Showers Philadelphia, Pa.
H. E. Sorrows Wheaton, Md.
A. J. Vadasz Syracuse, N. Y.

Electric Welding

POWER SUPPLY FOR RESISTANCE WELDING MACHINES SUBCOMMITTEE

C. N. Clark, *Chairman;* Duquesne Light Company, 435 Sixth Avenue, Pittsburgh, Pa.
N. A. Kieb, *Vice-Chairman;* Detroit, Mich.
E. L. Bailey Highland Park, Mich.
W. K. Boice Schenectady, N. Y.
W. G. Bostwick Cincinnati, Ohio
W. W. Brumby Toronto, Ontario, Canada
J. F. Deffenbaugh Warren, Ohio
S. W. Luther Detroit, Mich.
R. S. Phair Philadelphia, Pa.
C. E. Smith Warren, Ohio
J. L. Solomon Chicago, Ill.
C. B. Stadum Buffalo, N. Y.
H. W. Tietze Newark, N. J.
H. R. Wall Jackson, Mich.
Myron Zucker Royal Oak, Mich.

FUNDAMENTAL ELECTRIC ARC RESEARCH SUBCOMMITTEE

R. C. McMaster, *Chairman;* Battelle Memorial Institute, 505 King Avenue, Columbus 1, Ohio
J. H. Chyle Milwaukee, Wis.
J. D. Cobine Schenectady, N. Y.
Wolfgang Finkelnburg Fort Belvoir, Va.
W. J. Greene Murray Hill, N. J.
Julius Heuschkel East Pittsburgh, Pa.
W. B. Kouwenhoven Baltimore, Md.
Robert Krieger Columbus, Ohio
J. M. Parks Chicago, Ill.
S. F. Radtke Newport, Del.
R. E. Somers Bethlehem, Pa.
E. H. Wilhelm Annapolis, Md.
L. P. Winsor Troy, N. Y.

Feedback Control Systems

TERMINOLOGY AND NOMENCLATURE SUBCOMMITTEE

F. E. Crever, *Chairman;* Atomic Power Division, General Electric Company, Schenectady, N. Y.
W. R. Ahrendt College Park, Md.
H. W. Cory Milwaukee, Wis.
Paul Travers Cambridge, Mass.
A. J. Williams, Jr. Philadelphia, Pa.

General Industry Applications

MACHINE TOOLS SUBCOMMITTEE

D. R. Percival, *Chairman;* Machinery Electrification Inc., 98 Union Street, Worcester, Mass.
B. T. Anderson Rockford, Ill.
R. W. Brown Windsor, Vt.
J. M. Delfs Schenectady, N. Y.
R. T. Fenn Springfield, Vt.
L. W. Herchenroeder Pittsburgh, Pa.
J. J. Jaeger West Hartford, Conn.
E. F. Mekelburg Milwaukee, Wis.
W. J. Piper Springfield, Vt.
S. Rice Worcester, Mass.
E. J. Rivoire Cincinnati, Ohio
R. E. Stroppel Cincinnati, Ohio
W. B. Wigton Cincinnati, Ohio
T. A. Wetzel Milwaukee, Wis.

MATERIALS HANDLING SUBCOMMITTEE

S. P. Blakeman, *Chairman;* Haughton Elevator Company, 1725 Fairmount Avenue, Philadelphia, Pa.
F. W. Ate Philadelphia, Pa.
E. L. Blankenbeker Pittsburgh, Pa.
A. R. Dunne Port Hope, Ontario, Canada
D. C. Gray St. Paul, Minn.
C. P. Hamilton Schenectady, N. Y.
E. M. Hays Pittsburgh, Pa.
W. O. Land Philadelphia, Pa.
G. N. Meyers Philadelphia, Pa.
Fred A. Miller Wilmington, Del.

PULP AND PAPER INDUSTRY SUBCOMMITTEE

W. B. Baker, *Chairman;* Westinghouse Electric Corporation, Industrial Engineering Division, East Pittsburgh, Pa.
H. B. Barrow Atlanta, Ga.
G. C. Ehemann Rittman, Ohio
G. W. Knapp Schenectady, N. Y.
E. K. Murphy New York, N. Y.
E. H. Overby Savannah, Ga.
H. A. Rose Seattle, Wash.
J. L. Van Nort Cleveland, Ohio

RUBBER AND PLASTICS INDUSTRIES SUBCOMMITTEE

H. F. Snyder, *Chairman;* Goodyear Tire and Rubber Company, 1144 East Market Street, Akron, Ohio
A. T. Bacheler Buffalo, N. Y.
L. T. Blalock Dallas, Texas
B. J. Dalton Schenectady, N. Y.
K. W. John Detroit, Mich
G. V. Kulligren Akron, Ohio
J. F. Moore Toronto, Ontario, Canada
H. R. Neighbours Mishawaka, Ind.
R. G. Rudrow Wilmington, Del.
W. J. Secrest Akron, Ohio
R. E. Seddon Wilmington, Del.
A. G. Seifried Akron, Ohio
H. L. Smith New York, N. Y.
W. S. Watkins Willoughby, Ohio
B. H. Zacherle Philadelphia, Pa.

TEXTILE INDUSTRY SUBCOMMITTEE

R. J. Demartini, *Chairman,* General Electric Company, Industry Engineering Division, Schenectady 5, N. Y.
A. T. Bacheler Buffalo, N. Y.
S. A. Bobe Atlanta, Ga.
Swaffield Cowan Charlotte, N. C.
R. B. Flowers Atlanta, Ga.
A. W. Frankenfield Wilmington, Del.
H. Haley Philadelphia, Pa.
L. T. Jester Boston, Mass.
A. F. Lukens West Lynn, Mass.
V. P. Sepavich Worcester, Mass.
F. D. Snyder Boston, Mass.
H. C. Uhl Sylacauga, Alabama

Industrial Control

BIBLIOGRAPHY SUBCOMMITTEE

R. W. Jones, *Chairman;* Department of Electrical Engineering, Northwestern University, Evanston, Ill.
W. H. Elliott Milwaukee, Wis.
E. E. Moyer Troy, N. Y.
J. W. Picking Cleveland, Ohio
Walter Schaelchlin East Pittsburgh, Pa.

ELECTRONIC CONTROL SUBCOMMITTEE

H. L. Palmer, *Chairman;* General Electric Company, 1 River Road, Schenectady 5, N. Y.
F. T. Bailey Buffalo, N. Y.
H. B. Black Ampere, N. J.
L. H. Dee Schenectady, N. Y.
W. H. Elliot Milwaukee, Wis.
William Few Cleveland, Ohio
E. W. Hutton Schenectady, N. Y.
L. U. G. Kelling Schenectady, N. Y.
M. H. A. Lindsay New York, N. Y.
E. B. McDowell Schenectady, N. Y.
F. O. Nottingham Lafayette, Ind.
J. W. Picking Cleveland, Ohio
L. C. Poole Detroit, Mich.
V. J. Porter Philadelphia, Pa.
K. P. Puchlowski Pittsburgh, Pa.
W. G. Roman Buffalo, N. Y.
C. A. Schurr Cleveland, Ohio
H. I. Stanback Milwaukee, Wis.
G. F. Stark Baltimore, Md.
B. B. Stuart Waltham, Mass.
C. M. Summers Fort Wayne, Ind.
B. F. Tellkamp Milwaukee, Wis.

Working Groups:

(1). Electronic Control of D-C Motors
J. W. Picking, *Chairman;* Reliance Electric and Engineering Company, 1049–1088 Ivanhoe Road, Cleveland 10, Ohio
H. B. Black Ampere, N. J.
L. H. Dee Schenectady, N. Y.
W. H. Elliot Milwaukee, Wis.
William Few Cleveland, Ohio
L. C. Poole Detroit, Mich.
W. G. Roman Buffalo, N. Y.
H. I. Stanback Milwaukee, Wis.
B. B. Stuart Waltham, Mass.
B. F. Tellkamp Milwaukee, Wis.

(2). Photoelectric Pickup Systems
L. U. G. Kelling, *Chairman;* General Electric Company, 1 River Road, Schenectady 5, N. Y.
F. T. Bailey Buffalo, N. Y.
M. H. A. Lindsay New York, N. Y.
E. M. Pritchard Boston, Mass.
L. L. Worner Rankin, Ill.

(3). Electronic Relaying Devices
E. B. McDowell, *Chairman;* General Electric Company, 1 River Road, Schenectady 5, N. Y.
C. A. Schurr Cleveland, Ohio
B. F. Tellkamp Milwaukee, Wis.

(4). Electronic Control of A-C Power
E. W. Hutton, *Chairman;* General Electric Company, 1 River Road, Schenectady 5, N. Y.
H. B. Black Ampere, N. J.
W. H. Elliot Milwaukee, Wis.
W. G. Roman Buffalo, N. Y.
G. F. Stark Baltimore, Md.
B. F. Tellkamp Milwaukee, Wis.

REGULATORS AND FEEDBACK SYSTEMS SUBCOMMITTEE

O. W. Livingston, *Chairman;* Electronics and Regulator Control Engineering Division, General Electric Company, 1 River Road, Schenectady 5, N. Y.
H. B. Black Ampere, N. J.
S. L. Burgwin Buffalo, N. Y.
E. T. Davis Philadelphia, Pa.
W. H. Elliot Milwaukee, Wis.
William Few Cleveland, Ohio
J. W. Picking Cleveland, Ohio
B. F. Tellkamp Milwaukee, Wis.

STANDARDS SUBCOMMITTEE

J. O'Connor, *Chairman;* Associate Editor, *Power,* McGraw-Hill Publishing Company, 330 West 42nd Street, New York 18, N. Y.
E. L. Bailey Detroit, Mich.
J. E. Gahagan Binghamton, N. Y.
J. A. Gienger Rochester, N. Y.
F. Y. Grepe Toronto, Ontario, Canada
R. W. Kowitz Dearborn, Mich.
L. H. Matthias Milwaukee, Wis.
F. E. Strauss Oakland, Calif.

TEST CODES SUBCOMMITTEE

C. T. Evans, *Chairman;* Cutler-Hammer, Inc., 315 North 12th Street, Milwaukee, Wis.
D. K. Frost Rockford, Ill.
B. W. Jones Schenectady, N. Y.
H. E. Nason Chicago, Ill.
W. E. Pakala East Pittsburgh, Pa.
H. E. Rhoads Schenectady, N. Y.
C. A. Schaefer Milwaukee, Wis.

Industrial Power Systems

EXECUTIVE SUBCOMMITTEE

Main Committee Officers:
J. S. Gault, *Chairman;* Electrical Engineering Department, University of Michigan, Ann Arbor, Mich.
H. G. Barnett, *Vice-Chairman* East Pittsburgh, Pa.
S. A. Warner, *Secretary* New York, N. Y.

Subcommittee Chairmen:
H. G. Barnett East Pittsburgh, Pa.
D. I. Beeman Schenectady, N. Y.
C. R. Johnson New York, N. Y.
A. E. Marshall St. Louis, Mo.
T. O. Sweatt New York, N. Y.
B. F. Thomas, Jr. New York, N. Y.

POWER SUPPLY SUBCOMMITTEE

A. E. Marshall, *Chairman;* Monsanto Chemical Company, 1700 South 2nd Street, St. Louis 4, Mo.
A. J. Claes East St. Louis, Ill.
R. T. Woodruff St. Louis, Mo.

Distribution Systems for Industrial Plants Subcommittee

H. G. Barnett, *Chairman;* Westinghouse Electric Corporation, East Pittsburgh, Pa.
J.P.E. Arberry Pittsburgh, Pa.
D. L. Beeman Schenectady, N. Y.
D. D. Douglass Oakland, Calif.
W. S. Gordon, Jr. Tacoma, Wash.
C. R. Johnson New York, N. Y.
C. M. Lathrop Elizabeth, N. J.
S. W. Luther Detroit, Mich.
J. E. Mellett Atlanta, Ga.
Dick Ray Tulsa, Okla.
C. C. Saunders Wilmington, Del.
R. C. Waldron Passaic, N. J.
R. M. Wilson, Jr. Schenectady, N. Y.
T. O. Zittel Lackawanna, N. Y.

Distribution Systems for Commercial Buildings Subcommittee

B. F. Thomas, Jr., *Chairman;* N. A. Lougee and Company, 120 Broadway, New York 5, N. Y.
Allan Coggeshall New York, N. Y.
L. C. McCullough New York, N. Y.
A. C. Youngson New York, N. Y.

Characteristics of Loads Subcommittee

T. O. Sweatt, *Chairman;* Wearn, Vreeland, Carlson and Sweatt, Inc., 43 Exchange Place, New York 5, N. Y.
V. E. Dodson Seattle, Wash.
K. K. Falk South Bend, Ind.
J. D. Harper Alcoa, Tenn.
C. M. Lathrop Elizabeth, N. J.
C. C. Saunders Wilmington, Del.
W. J. Secrest Akron, Ohio
T. O. Zittel Lackawanna, N. Y.

Industrial Grounding Subcommittee

D. L. Beeman, *Chairman;* General Electric Company, Schenectady 5, N. Y.
H. H. Angel Bethlehem, Pa.
J. E. Arberry Pittsburgh, Pa.
K. M. Bausch San Francisco, Calif.
Fred Heller New York, N. Y.
E. M. Hunter Schenectady, N. Y.
L. W. Roush South Charleston, W. Va.
C. C. Saunders Wilmington, Del.
J. M. Schmidt Baytown, Texas
T. O. Sweatt New York, N. Y.
H. B. Thacker East Pittsburgh, Pa.
B. F. Thomas, Jr. New York, N. Y.
S. A. Warner New York, N. Y.

Codes and Standards Subcommittee

C. R. Johnson, *Chairman;* The Port of New York Authority, Engineering Department, 111 Eighth Avenue, New York 11, N. Y.
L. W. McCullough New York, N. Y.

Mining and Metal Industry

Metal Industries Subcommittee

W. R. Harris, *Chairman;* Westinghouse Electric Corporation, Department 10-L, East Pittsburgh, Pa.
J. E. Arberry Pittsburgh, Pa.
H. W. Bakeborn Newark, Ohio
F. W. Cramer Pittsburgh, Pa.
Sam Ein Chicago, Ill.
R. H. Ellis Pittsburgh, Pa.
Cecil Farrow Cleveland, Ohio
Lanier Greer Cleveland, Ohio
L. N. Grier Pittsburgh, Pa.
W. E. Miller Schenectady, N. Y.
B. E. Price New York, N. Y.
E. G. Schlup Middletown, Ohio
F. O. Schnure Sparrows Point, Md.
Victor Siegfried Worcester, Mass.
H. I. Stanback Milwaukee, Wis.
J. R. Wickey Cleveland, Ohio

Mining Subcommittee

J. J. Fitzgibbon, *Chairman;* General Electric Company, 306 MacCorkle Avenue, Charleston 28, W. Va.
J. E. Breth Bessemer, Ala.
Graham Bright Pittsburgh, Pa.
A. B. Chafets Carlsbad, N. Mex.
R. J. Corfield Garfield, Utah
E. W. Davis Cambridge, Mass.
J. M. Downie Erie, Pa.
J. H. Edwards New York, N. Y.
C. L. Gust Lead, S. Dak.
L. H. Harrison Birmingham, Ala.
J. G. Ivy Chicago, Ill.
L. H. James Scranton, Pa.
G. F. Johnson Michigan City, Ind.
J. Z. Linsenmeyer East Pittsburgh, Pa.
R. C. McMaster Columbus, Ohio
A. C. Muir Philadelphia, Pa.
H. P. Musser Charleston, W. Va.
M. G. Myers, Jr. Boston, Mass.
F. C. Nicholson Wilkes-Barre, Pa.
C. A. Poppino Phoenix, Arizona
B. E. Rector East Pittsburgh, Pa.
D. E. Renshaw Chicago, Ill.
L. W. Roush South Charleston, W. Va.
O. J. Swanson Gary, W. Va.
C. L. Tyler Irwin, Pa.
T. R. Weichel Wilkes-Barre, Pa.
W. G. Willson Phoenix, Arizona
C. O. Wood Chicago, Ill.

Power Division

Carrier Current

Subcommittee for Preparation of a General Interest Paper on Carrier Current

M. H. Wood, *Chairman;* Westinghouse Electric Corporation, Electronics and X-Ray Division, 2519 Wilkens Avenue, Baltimore 3, Md.
S. C. Bartlett New York, N. Y.
J. D. Booth Baltimore, Md.
L. F. Kennedy Schenectady, N. Y.

Subcommittee to Report on Application Guidance for Carrier Current

D. M. MacGregor, *Chairman;* Ebasco Services, Inc., 2 Rector Street, New York 6, N. Y.
C. W. Boadway Toronto, Ontario, Canada
T. D. Talmage Chattanooga, Tenn.

Methods of Measurement Subcommittee

E. W. Kenefake, *Chairman;* General Electric Company, Electronics Department, Syracuse, N. Y.
S. C. Bartlett New York, N. Y.
C. W. Boadway Toronto, Ontario, Canada
M. H. Wood Baltimore, Md.

High-Frequency Characteristics of Power Equipment Subcommittee

S. C. Leyland, *Chairman;* Westinghouse Electric Corporation, 95 Orange Street, Newark 2, N. J.
T. A. Cramer Schenectady, N. Y.

Carrier Current Characteristics of Transmission Lines and Systems Subcommittee

T. D. Talmage, *Chairman;* Kellogg Switchboard and Supply Company, 6650 Cicero Avenue, Chicago 38, Ill.
W. H. Blankmeyer Butte, Mont.
R. C. Ericson Hammond, Ind.
W. J. Googe Shreveport, La.
L. E. Ludekens Los Angeles, Calif.

Long Life Tubes Subcommittee

L. G. Eaton, *Chairman;* New England Power Service Company, 441 Stuart Street, Boston 16, Mass.
R. W. Beckwith Syracuse, N. Y.
L. F. Ferri Elyria, Ohio
Samuel Lubin Washington, D. C.
M. H. Wood Baltimore, Md.

Use of Microwave Equipment for Relaying, Telemetering, and Supervisory Control Subcommittee

S. C. Leyland, *Chairman;* Westinghouse Electric Corporation, 95 Orange Street, Newark 2, N. J.

Operating Experience With Carrier Current Relaying Channels Subcommittee

O. A. Starcke, *Chairman;* Kansas City Power and Light Company, Box 679, Kansas City, Mo.
T. A. Cramer Schenectady, N. Y.
J. R. Curtin Portland, Oreg.
W. J. Googe Shreveport, La.
V. J. Hayes Waterbury, Conn.
H. W. Lenzner Newark, N. J.
L. E. Ludekens Los Angeles, Calif.
B. W. Storer Chicago, Ill.
Mead Warren, Jr. Alcoa, Tenn.

Insulated Conductors

Administration Subcommittee

Herman Halperin, *Chairman;* Commonwealth Edison Company, 72 West Adams Street, Chicago 90, Ill.
V. A. Sheals, *Vice-Chairman* Schenectady, N. Y.
C. T. Hatcher, *Secretary* New York, N. Y.
L. F. Hickernell Hastings-on-Hudson, N. Y.

Subcommittee Chairmen:
H. W. Acock Trenton, N. J.
W. A. Del Mar Yonkers, N. Y.
G. H. Fiedler Rochester, N. Y.
L. E. Fogg Phillipsdale, R. I.
M. W. Ghen Pittsburgh, Pa.
L. I. Komives Detroit, Mich.
W. T. Peirce Worcester, Mass.
R. S. Peterson Chicago, Ill.
G. M. L. Sommerman Evanston, Ill.
Gordon Thompson New York, N. Y.
H. H. Watson Bridgeport, Conn.

Standards and Publications Subcommittee

L. E. Fogg, *Chairman;* Kennecott Wire and Cable Company, Phillipsdale, R. I
A. S. Brookes Newark, N. J.
M. H. McGrath New York, N. Y.
V. A. Sheals Schenectady, N. Y.
H. D. Short Toronto, Ontario, Canada
C. W. Zimmerer New York, N. Y.

Cable Characteristics Subcommittee

W. A. Del Mar, *Chairman;* Phelps Dodge Copper Products Company, Habirshaw Cable and Wire Division, Yonkers, N. Y.
E. D. Bent Montreal, Quebec, Canada
C. T. Hatcher New York, N. Y.
A. H. Kidder Philadelphia, Pa.
C. G. Mansfield Los Angeles, Calif.
M. H. McGrath New York, N. Y.
J. H. Neher Philadelphia, Pa.
G. B. Shanklin Schenectady, N. Y.
F. V. Smith Chicago, Ill.
E. R. Thomas New York, N. Y.
R. J. Wiseman Passaic, N. J.
F. O. Wollaston Vancouver, B. C., Canada
R. K. Woodson Kansas City, Mo.

Conductors Subcommittee

G. W. Acock, *Chairman;* J. A. Roebling's Sons, 640 South Broad Street, Trenton, N. J.
L. E. Fogg Phillipsdale, R. I.
R. C. Waldron Passaic, N. J.
G. W. Zink Yonkers, N. Y.

Insulations Subcommittee

G. M. L. Sommerman, *Chairman;* Department of Electrical Engineering, Northwestern Technological Institute, Evanston, Ill.
J. C. Balbaugh Cambridge, Mass.
C. E. Betzer Chicago, Ill.
F. M. Clark Pittsfield, Mass.
A. S. Dana Seymour, Conn.
E. W. Greenfield Hastings-on-Hudson, N. Y.
Thorstein Larsen Baltimore, Md.
E. L. Lotz Irvington, N. J.
R. B. McKinley Bridgeport, Conn.
J. D. Piper Detroit, Mich.
R. A. Schatzel Rome, N. Y.
E. G. Sturdevant Bristol, R. I.
A. J. Warner Nutley, N. J.
K. S. Wyatt Yonkers, N. Y.

Sheaths and Coverings Subcommittee

G. H. Fiedler, *Chairman;* Rochester Gas and Electric Company, Rochester, N. Y.
C. F. Avila Boston, Mass.
C. E. Betzer Chicago, Ill.
Andrew Bodicky St. Louis, Mo.
A. S. Brookes Newark, N. J.
A. H. Kidder Philadelphia, Pa.
F. E. Kulman New York, N. Y.
A. D. Pettee Perth Amboy, N. J.
V. A. Sheals Schenectady, N. Y.
R. C. Waldron Passaic, N. J.
G. W. Zink Yonkers, N. Y.

Cable Supply Systems Subcommittee

L. I. Komives, *Chairman;* Detroit Edison Company, 2000—2d Avenue, Detroit 26, Mich.
C. F. Avila Boston, Mass.
T. J. Brosnan Buffalo, N. Y.
W. R. Bullard New York, N. Y.
H. W. Clark Washington, D. C.
D. M. Farnham Montreal, Quebec, Canada
J. D. Frantz Portland, Oreg.
C. T. Hatcher New York, N. Y.
M. J. Lowenberg Boston, Mass.
A. D. Pettee Perth Amboy, N. J.
C. S. Schifreen Philadelphia, Pa.
G. B. Shanklin Schenectady, N. Y.
H. D. Short Toronto, Ontario, Canada
C. F. Titus Jacksonville, Fla.
R. J. Wiseman Passaic, N. J.
F. O. Wollaston Vancouver, B. C., Canada
K. S. Wyatt Yonkers, N. Y.

Utilization Wiring Systems Subcommittee

H. H. Watson, *Chairman;* General Electric Company, 1285 Boston Avenue, Bridgeport 2, Conn.
E. L. Bailey Detroit, Mich.
H. G. Barnett East Pittsburgh, Pa.
A. L. Barrett Franklin, Pa.
C. M. Boardman Pittsburgh, Pa.
T. P. Branch Washington, D. C.
C. A. Finkel Passaic, N. J.
R. W. Foster Canton, N. C.
F. S. Glass Freeport, Texas
Lester Goldsmith Philadelphia, Pa.
J. E. Huguelet Detroit, Mich.
M. J. Lowenberg Boston, Mass.
J. B. MacLean New York, N. Y.
S. J. Roach Hastings-on-Hudson, N. Y.
R. A. Schatzel Rome, N. Y.
J. S. Waddington Brockville, Ontario, Canada
C. W. Zimmerer New York, N. Y.

Special-Purpose Cable Subcommittee

W. T. Peirce, *Chairman;* American Steel and Wire Company, Worcester, Mass.
G. W. Acock Trenton, N. J.
J. F. Atkinson Washington, D. C.
A. L. Barrett Franklin, Pa.
E. D. Bent Montreal, Quebec, Canada
E. W. Davis Cambridge, Mass.
R. A. Hopkins Knoxville, Tenn.
J. E. Huguelet Detroit, Mich.
R. H. Kolks Cincinnati, Ohio
R. B. McKinley Bridgeport, Conn.
M. L. Perry Kansas City, Mo.
F. V. Smith Chicago, Ill.
E. G. Sturdevant Bristol, R. I.
C. F. Titus Jacksonville, Fla.
R. K. Woodson Kansas City, Mo.
W. N. Zippler New York, N. Y.
G. W. Zink Yonkers, N. Y.

Accessories Subcommittee

M. W. Ghen, *Chairman;* Duquesne Light Company, 1241 Reedsdale Street, N. S. Pittsburgh 33, Pa.
P. N. Borworth Pittsfield, Mass.
C. Christensen Melrose Park, Ill.
C. D. Eash Jackson, Mich.
J. D. Frantz Portland, Oreg.
G. G. Grissinger East Pittsburgh, Pa.
Fred Heller New York, N. Y.
J. E. Johnson Philadelphia, Pa.
R. H. Kolks Cincinnati, Ohio
L. E. Leinbach Detroit, Mich.
E. L. Lotz Irvington, N. J.
H. E. Martin Brooklyn, N. Y.
R. E. Morse New York, N. Y.
J. H. Nicholas Chicago, Ill.
Lawrence Palmer Seattle, Wash.
M. L. Perry, Jr. Kansas City, Mo.
F. P. West New York, N. Y.
D. S. Young Toronto, Ont., Canada
S. Zyak Schenectady, N. Y.

Structures Subcommittee

R. S. Peterson, *Chairman;* Commonwealth Edison Company, 72 West Adams Street, Chicago 90, Ill.
M. J. Andrews Los Angeles, Calif.

C. E. Baugh San Francisco, Calif.
Andrew Bodicky St. Louis, Mo.
T. J. Brennan Buffalo, N. Y.
H. W. Clark Washington, D. C.
C. D. Eash Jackson, Mich.
G. H. Fiedler Rochester, N. Y.
Lawrence Palmer Seattle, Wash.
L. G. Smith Baltimore, Md.
F. P. West New York, N. Y.
R. K. Woodson Kansas City, Mo.

TESTS AND MEASUREMENTS SUBCOMMITTEE

Gordon Thompson, *Chairman;* Electrical Testing Laboratories, Inc., 2 West End Avenue, New York 21, N. Y.
J. C. Balsbaugh Cambridge, Mass.
A. L. Brownlee Chicago, Ill.
A. S. Dana Seymour, Conn.
E. W. Davis Cambridge, Mass.
W. A. Del Mar Yonkers, N. Y.
E. W. Greenfield Hastings-on-Hudson, N. Y.
Thorstein Larsen Baltimore, Md.
J. C. Parker Memphis, Tenn.
G. M. L. Sommerman Evanston, Ill.
R. F. Tener Washington, D. C.
E. R. Thomas New York, N. Y.
R. C. Waldron Passaic, N. J.
C. W. Zimmerer New York, N. Y.

Power Generation

PRIME MOVERS SUBCOMMITTEE

B. G. A. Skrotzki, *Chairman;* Associate Editor, *Power*, 330 West 42d Street, New York 18, N. Y.
J. A. Brooks New York, N. Y.
E. P. Bryant Los Angeles, Calif.
A. D. Caskey Chicago, Ill.
Michael Pope New York, N. Y.
C. S. Randall Washington, D. C.
R. R. Wiener Boston, Mass.

SPEED GOVERNING SUBCOMMITTEE

J. B. McClure, *Chairman;* General Electric Company, Central Station Engineering Division, Schenectady 5, N. Y.
R. E. Appleyard Milwaukee, Wis.
C. P. Almon, Jr. Chattanooga, Tenn.
R. M. Beville Chicago, Ill.
A. P. Hayward Pittsburgh, Pa.
T. H. Mawson Birmingham, Ala.
G. H. McDaniel New York, N. Y.
F. L. Reinmann Michigan City, Ind.

EXCITATION SYSTEMS SUBCOMMITTEE

A. J. Krupy, *Chairman;* Commonwealth Edison Company, 72 West Adams Street, Chicago 90, Ill.
J. B. McClure, *Vice-Chairman*
Schenectady, N. Y.
J. E. Barkle, Jr. East Pittsburgh, Pa.
E. F. Dissmeyer Jackson, Mich.
Alex. Dovjikov Portland, Oreg.
C. B. Fontaine, Jr. Lynn, Mass.
L. A. Kilgore East Pittsburgh, Pa.
J. H. Kinghorn New York, N. Y.
H. A. P. Langstaff Pittsburgh, Pa.
T. B. Montgomery Milwaukee, Wis.
F. D. Troxel Chicago, Ill.
R. L. Witzke East Pittsburgh, Pa.

STATION DESIGN SUBCOMMITTEE

H. R. Harris, *Chairman;* The Detroit Edison Company, 2000—2d Avenue, Detroit 26, Mich.
H. E. Deardorff Dayton, Ohio
C. A. Harrington Cleveland, Ohio
D. R. Pattison Johnstown, Pa.
W. W. Perry Binghamton, N. Y.
R. R. Wiener Boston, Mass.

HYDROELECTRIC SYSTEMS SUBCOMMITTEE

F. L. Lawton, *Chairman;* Aluminum Laboratories, Ltd., 1800 Sun Life Building, Montreal, Quebec, Canada
S. M. Denton Denver, Colo.
J. T. Madill Arvida, Quebec, Canada
E. F. Maryatt San Francisco, Calif.
A. L. Pollard Seattle, Wash.
G. R. Woodman Los Angeles, Calif.

PACIFIC COAST SUBCOMMITTEE

E. P. Bryant, *Chairman;* Department of Water and Power, City of Los Angeles, 207 South Broadway, Los Angeles 12, Calif.
S. M. Denton Denver, Colo.
Alex Dovjikov Portland, Oreg.
F. F. Maryatt San Francisco, Calif.
A. L. Pollard Seattle, Wash.
G. R. Woodman Los Angeles, Calif.

Protective Devices

FAULT LIMITING DEVICES SUBCOMMITTEE

E. G. Norell, *Chairman;* Sargent and Lundy, 140 South Dearborn Street, Chicago 3, Ill.
J. P. Barron Dallas, Texas
V. J. Cisna Chattanooga, Tenn.
J. A. Coleman Boston, Mass.
G. B. Dodds Pittsburgh, Pa.
E. T. B. Gross Chicago, Ill.
W. D. Hardaway Denver, Colo.
H. W. Hartsell Jackson, Mich.
E. M. Hunter Schenectady, N. Y.
P. A. Jeanne New York, N. Y.
A. A. Johnson East Pittsburgh, Pa.
W. A. Lewis, Jr. Chicago, Ill.
F. R. Longley Springfield, Mass.
Cort Lowerison Los Angeles, Calif.
Corbett McLean Portland, Oreg.
H. D. Ruger Sparrows Point, Md.
O. L. Sidenfaden Los Angeles, Calif.
W. T. Smith Arlington, Va.
S. S. Watkins New York, N. Y.

Project 1: Application Guide on Methods of Grounding Transmission Systems
E. N. Hunter, *Chairman*
Schenectady, N. Y.
H. W. Hartsell Jackson, Mich.
A. A. Johnson East Pittsburgh, Pa.
R. E. Neidig Reading, Pa.

Project 2: Application Guide for the Grounding of Synchronous Generator Systems
A. A. Johnson, *Chairman*
East Pittsburgh, Pa.
E. M. Hunter Schenectady, N. Y.
D. M. MacGregor New York, N. Y.
W. E. Marter Pittsburgh, Pa.
E. G. Norell Chicago, Ill.
W. T. Smith Arlington, Va.

Project 3: Bibliography of Literature on Grounding
E. T. B. Gross, *Chairman* Chicago, Ill.
J. E. Clem Schenectady, N. Y.

Project 4: Guide for Application of Ground-Fault Neutralizers
J. E. Clem, *Chairman* Schenectady, N. Y.
H. H. Brown Cedar Rapids, Iowa
S. S. Cook Sharon, Pa.
N. E. Dillow Schenectady, N. Y.
W. D. Hardaway Denver, Colo.
R. E. Neidig Reading, Pa.
P. B. Speer Minneapolis, Minn.

Project 5: Power System Fault Control
F. R. Longley, *Chairman* Springfield, Mass.
J. O. Coleman Boston, Mass.
F. H. Kierstead Pittsfield, Mass.
L. B. LeVeneste Chicago, Ill.
H. F. Lindemuth New York, N. Y.
E. L. Michelson Chicago, Ill.
L. E. Sauer Sharon, Pa.

LIGHTNING PROTECTIVE DEVICES SUBCOMMITTEE

E. H. Yonkers, *Chairman;* Joslyn Manufacturing and Supply Company, 969 West 37th Place, Chicago 9, Ill.
J. E. Clem Schenectady, N. Y.
L. M. Connors Toronto, Ont., Canada
H. A. Cornelius Chicago, Ill.
F. M. Defandorf Washington, D. C.
G. K. Ditlow Washington, D. C.
J. R. Eaton Lafayette, Ind.
T. I. Eldridge Philadelphia, Pa.
I. W. Gross New York, N. Y.
E. H. Grosser Chicago, Ill.
H. W. Hartsell Jackson, Mich.
T. H. Mawson Birmingham, Ala.
W. A. McMorris Pittsfield, Mass.
A. M. Opsahl East Pittsburgh, Pa.
H. L. Rorden Portland, Oreg.
A. H. Schirmer New York, N. Y.
H. O. Stoelting So. Milwaukee, Wis.
J. M. Towner Baltimore, Md.

Project 1: Application Guide of Methods for Lightning Protection of Substations
H. A. Cornelius, *Chairman* Chicago, Ill.
Harris Barber Boston, Mass.
H. W. Hartsell Jackson, Mich.
S. B. Howard Pittsfield, Mass.
E. L. Jarrett Pittsburgh, Pa.
R. H. Mertz Detroit, Mich.
A. M. Opsahl East Pittsburgh Pa.
E. R. Whitehead Chicago, Ill.

Project 10: Recovery Voltage Characteristics of Distribution Systems
R. L. Witzke, *Chairman*
East Pittsburgh, Pa.
G. K. Ditlow Washington, D. C.
I. B. Johnson Schenectady, N. Y.
L. M. Olmstead Pittsburgh, Pa.
M. A. Pulster Baltimore, Md.

CO-ORDINATION OF INSULATION SUBCOMMITTEE

J. E. Clem, *Chairman;* Central Station Engineering Division, General Electric Company, Schenectady 5, N. Y.

Relays

PROJECT COMMITTEE ON BIBLIOGRAPHY OF RELAY LITERATURE

E. T. B. Gross, *Chairman* and *Sponsor;* Illinois Institute of Technology, 3300 Federal Street, Chicago 16, Ill.
S. Goldsmith Cincinnati, Ohio
C. E. Parks Indianapolis, Ind.
C. L. Smith Rochester, N. Y.

PROJECT COMMITTEE ON GENERATOR PROTECTION

H. R. Paxson, *Chairman* and *Sponsor;* Philadelphia Electric Company, 900 Sansom Street, Philadelphia 5, Pa.
L. L. Draper Los Angeles, Calif.
L. L. Fountain East Pittsburgh, Pa.
E. T. B. Gross Chicago, Ill.
B. C. Hicks Montreal, Quebec, Canada
L. F. Kennedy Schenectady, N. Y.
S. C. Leyland Newark, N. J.
H. F. Lindemuth New York, N. Y.
W. E. Marter Pittsburgh, Pa.
J. B. McClure Schenectady, N. Y.
A. J. McConnell Schenectady, N. Y.
C. E. Parks Indianapolis, Ind.
F. C. Poage New York, N. Y.
L. T. Rosenberg Milwaukee, Wis.
H. P. Sleeper Newark, N. J.
C. L. Smith Rochester, N. Y.

PROJECT COMMITTEE ON CO-ORDINATION OF CONSTRUCTION AND PROTECTION OF DISTRIBUTION CIRCUITS (JOINT WITH DISTRIBUTION SUBCOMMITTEE AND EDISON ELECTRIC INSTITUTE)

G. B. Dodds, AIEE *Chairman* and *Sponsor;* Duquesne Light Company, 435 Sixth Avenue, Pittsburgh 19, Pa.
R. O. Askey Chicago, Ill.
G. G. Auer Schenectady, N. Y.
T. J. Brennan Buffalo, N. Y.
Harold Cole Detroit, Mich.
W. B. Fisk, Jr. New York, N. Y.
C. L. Headley Baltimore, Md.
Cort Lowerison Los Angeles, Calif.
H. F. Ortman St. Louis, Mo.
C. L. Smith Rochester, N. Y.
C. J. Beller, EEI *Chairman* and *Sponsor;* Cleveland Electric Illuminating Company, 75 Public Square, Cleveland 1, Ohio
G. H. Fiedler Rochester, N. Y.
G. E. Dean Newark, N. J.
W. P. Holben Pittsburgh, Pa.
A. L. Malmstrom Detroit, Mich.

PROJECT COMMITTEE ON REVISION OF STANDARDS FOR POWER RELAYS

S. C. Leyland, *Chairman* and *Sponsor;* Westinghouse Electric Corporation, 95 Orange Street, Newark 2, N. J.
R. E. Cordray Philadelphia, Pa.
V. L. Cox Philadelphia, Pa.
L. L. Fountain East Pittsburgh, Pa.
W. A. Lewis Chicago, Ill.
J. R. Linders Cleveland, Ohio
E. L. Michelson Chicago, Ill.
W. A. Morgan Denver, Colo.
H. P. Sleeper Newark, N. J.
G. S. Steeb Buffalo, N. Y.

PROJECT COMMITTEE ON TRANSMISSION-LINE PROTECTION

J. H. Kinghorn, *Chairman* and *Sponsor;* American Gas and Electric Service Corporation, 30 Church Street, New York 7, N. Y.
L. J. Audlin Syracuse, N. Y.
J. E. Barkle, Jr. East Pittsburgh, Pa.
W. R. Brownlee Jackson, Mich.
B. C. Hicks Montreal, Quebec, Canada
W. A. Lewis Chicago, Ill.
W. E. Marter Pittsburgh, Pa.
A. J. McConnell Schenectady, N. Y.
M. S. Merritt Chattanooga, Tenn.
E. L. Michelson Chicago, Ill.
C. E. Parks Indianapolis, Ind.
K. N. Reardon Pittsburgh, Pa.

PROJECT COMMITTEE ON ELECTRONIC RELAY APPLICATIONS

A. J. McConnell, *Chairman* and *Sponsor;* General Electric Company, Schenectady 5, N. Y.
J. E. Barkle, Jr. East Pittsburgh, Pa.
R. J. Cooper Atlanta, Ga.
F. S. Fehr Reading, Pa.
L. F. Ferri Elyria, Ohio
E. L. Harder East Pittsburgh, Pa.
J. H. Kinghorn New York, N. Y.
D. M. MacGregor New York, N. Y.
E. L. Michelson Chicago, Ill.
E. G. Ratz Hamilton, Ontario, Canada

PROJECT COMMITTEE ON RELAYING OF INTERCONNECTIONS BETWEEN INDUSTRIAL AND UTILITY GENERATING SYSTEMS

K. N. Reardon, *Chairman* and *Sponsor;* West Penn Power Company, 14 Wood Street, Pittsburgh, Pa.
J. E. Barkle, Jr. East Pittsburgh, Pa.
G. E. Dana Binghamton, N. Y.
F. S. Fehr Reading, Pa.
T. R. Halman Detroit, Mich.
J. R. Linders Lakewood, Ohio

PROJECT COMMITTEE ON RELAYING PERFORMANCE OF CURRENT TRANSFORMERS (EMPHASIS ON HIGH IMPEDANCE SECONDARY TYPES)

W. E. Marter, *Chairman* and *Sponsor;* Duquesne Light Company, 435—6th Avenue, Pittsburgh 19, Pa.
J. E. Barkle East Pittsburgh, Pa.
J. E. Clem Schenectady, N. Y.
R. E. Cordray Philadelphia, Pa.
W. K. Dickinson Lynn, Mass.
T. R. Halman Detroit, Mich.
W. A. Lewis Chicago, Ill.
W. K. Sonnemann Newark, N. J.
E. C. Wentz Sharon, Pa.

PROJECT COMMITTEE ON REMOTE TRIPPING SCHEMES

H. P. Sleeper, *Chairman* and *Sponsor;* Public Service Gas and Electric Company, 80 Park Place, Newark 2, N. J.
J. L. Blackburn Newark, N. J.
M. A. Bostwick Portland, Oreg.
T. A. Cramer Schenectady, N. Y.
Sidney Goldsmith Cincinnati, Ohio
G. W. Hampe Chicago, Ill.
Y. J. Hayes Waterbury, Conn.
S. C. Leyland Newark, N. J.

PROJECT COMMITTEE ON PILOT WIRES

H. F. Lindemuth, *Chairman* and *Sponsor;* Consolidated Edison Company of New York, Inc., 4 Irving Place, New York 3, N. Y.
M. A. Bostwick Portland, Oreg.
J. L. Blackburn, Jr. Mineola, N. Y.
W. E. Marter Pittsburgh, Pa.
A. J. McConnell Schenectady, N. Y.
J. L. McKee New York, N. Y.
G. W. McKenna Philadelphia, Pa.
E. L. Michelson Chicago, Ill.
W. K. Sonnemann Newark N. J.

PROJECT COMMITTEE ON EFFECT OF SHOCK AND VIBRATION ON RELAYS

C. E. Asbury, *Chairman* and *Sponsor;* Commonwealth Services, Inc., 212 West Michigan Avenue, Jackson, Mich.
R. E. Cordray Philadelphia, Pa.
M. A. Faucett Urbana, Ill.
T. R. Halman Detroit, Mich.
H. F. Lindemuth New York, N. Y.
W. K. Sonnemann Newark, N. J.
G. S. Steeb Buffalo, N. Y.
R. I. Ward Chicago, Ill.

PROJECT COMMITTEE ON TEST METHODS

G. E. Dana, *Chairman* and *Sponsor;* New York State Electric and Gas Corporation, 62 Henry Street, Binghamton, N. Y.
R. E. Cordray Philadelphia, Pa.
L. F. Ferri Elyria, Ohio
T. R. Halman Detroit, Mich.
J. E. Lange Pittsburgh, Pa.
R. A. Larner Fort Worth, Texas

W. A. Morgan — Denver, Colo.
W. K. Sonnemann — Newark, N. J.

Rotating Machinery

Administrative Subcommittee

W. R. Heugh, *Chairman*, Reliance Electric and Engineering Company, 1068-1088 Ivanhoe Road, Cleveland 10, Ohio
C. G. Veinott, *Vice-Chairman* — Lima, Ohio
J. L. Fuller, *Secretary* — Cleveland, Ohio
R. E. Arnold — West Lynn, Mass.
B. H. Caldwell — Schenectady, N. Y.
James DeKiep — Minneapolis, Minn.
J. W. Jones — Philadelphia, Pa.
I. M. Levy — Dayton, Ohio
S. S. Wolff — St. Louis, Mo.

Synchronous Machinery Subcommittee

James DeKiep, *Chairman*; Electric Machinery Manufacturing Company, 1331 Tyler Street, Minneapolis 13, Minn.
Sterling Beckwith — Milwaukee, Wis.
J. F. Calvert — Evanston, Ill.
S. B. Crary — Schenectady, N. Y.
L. O. Dorfman — New York, N. Y.
E. L. Harder — East Pittsburgh, Pa.
J. W. Jones — Philadelphia, Pa.
C. E. Kilbourne — Schenectady, N. Y.
L. B. LeVesconte — Chicago, Ill.
M. R. Lory — East Pittsburgh, Pa.
J. G. Noest — New York, N. Y.
E. J. Pollard — Ridgway, Pa.
J. H. Vivian — Los Angeles, Calif.
S. S. Wolff — St. Louis, Mo.

Induction Machinery Subcommittee

S. S. Wolff, *Chairman*; Century Electric Company, 1806 Pine Street, St. Louis 3, Mo.
R. E. Arnold — West Lynn, Mass.
E. L. Bailey — Detroit, Mich.
E. C. Barnes — Cleveland, Ohio
C. F. Cameron — Stillwater, Okla.
S. F. Henderson — Buffalo, N. Y.
C. J. Koch — Schenectady, N. Y.
I. M. Levy — Dayton, Ohio
T. C. Lloyd — Springfield, Ohio
R. C. Moore — Milwaukee, Wis.
J. G. Noest — New York, N. Y.
C. P. Potter — St. Louis, Mo.
F. C. Rushing — Buffalo, N. Y.
F. H. Trickey — Finderne, N. J.
F. M. Winterhalter — Norwood, Ohio

D-C Machinery Subcommittee

B. H. Caldwell, *Chairman*; General Electric Company, 1 River Road, Schenectady 5, N. Y.
M. A. Baker — Fort Wayne, Ind.
C. F. Cobb — Cincinnati, Ohio
A. G. Darling — Schenectady, N. Y.
W. H. Fifer — Washington, D. C.
Lanier Greer — Cleveland, Ohio
C. B. Hathaway — Buffalo, N. Y.
L. H. Hildebrandt — Dayton, Ohio
H. E. Koenig — Urbana, Ill.
R. Lamborn — Erie, Pa.
Paul Lebenbaum, Jr. — Lynn, Mass.
Clarence Lynn — East Pittsburgh, Pa.
T. J. Martin — Seattle, Wash.
A. T. McClinton — Washington, D. C.
W. E. Meserve — Ithaca, N. Y.
J. G. Noest — New York, N. Y.
L. G. Opel — Buffalo, N. Y.
J. H. Schneider — Ridgway, Pa.
J. F. Sellers — Milwaukee, Wis.
F. H. Trickey — Finderne, N. J.
S. S. Wolff — St. Louis, Mo.

Single-Phase and Fractional-Horsepower Subcommittee

I. M. Levy, *Chairman*; Delco Products Division, General Motors Corporation, Dayton, Ohio
W. R. Appleman — Dayton, Ohio
C. F. Cameron — Stillwater, Okla.
J. S. Gault — Ann Arbor, Mich.
E. E. Kimberly — Columbus, Ohio
T. C. Lloyd — Springfield, Ohio
C. F. Miller — Baltimore, Md.
R. F. Munier — St. Louis, Mo.
C. P. Potter — St. Louis, Mo.
L. C. Schaefer — Lima, Ohio
M. L. Schmidt — Fort Wayne, Ind.
F. H. Trickey — Finderne, N. J.
C. G. Veinott — Lima, Ohio
S. S. Wolff — St. Louis, Mo.

Test Code Subcommittee

R. E. Arnold, *Chairman*; General Electric Company, 920 Western Avenue, West Lynn, Mass.
J. L. Fuller — Cleveland, Ohio
J. S. Gault — Ann Arbor, Mich.
Clarence Lynn — East Pittsburgh, Pa.
H. C. Marcroft — Lancaster, Pa.
R. F. Munier — St. Louis, Mo.
E. B. Paxton — Schenectady, N. Y.
E. I. Pollard — Ridgway, Pa.

Insulation Subcommittee

J. W. Jones, *Chairman*; Philadelphia Electric Company, Edison Building, Philadelphia 5, Pa.
L. J. Berberich — East Pittsburgh, Pa.
E. B. Curdts — Philadelphia, Pa.
E. F. Dissmeyer — Jackson, Mich.
Orville Fawcett — Pittsburgh, Pa.
D. D. Higgins — Chicago, Ill.
J. L. Kuehlthau — Milwaukee, Wis.
H. C. Marcroft — Lancaster, Pa.
G. L. Moses — East Pittsburgh, Pa.
E. I. Pollard — Ridgway, Pa.
R. H. Povey — Belmont, Mass.
V. E. Schloseberg — East Chicago, Ind.
J. B. Swering — Hartford, Conn.
H. R. Tomlinson — Boston, Mass.
A. L. Van Emden — Washington, D. C.
R. W. Wieseman — Schenectady, N. Y.

Substations

Executive Subcommittee

R. C. Ericson, *Chairman*; Northern Indiana Public Service Company, 5265 Hohman Avenue, Hammond, Ind.
M. V. Eardley — Los Angeles, Calif.
N. G. Larson — Chicago, Ill.
G. S. Lunge — Schenectady, N. Y.
M. E. Reagan — East Pittsburgh, Pa.
K. L. Wheeler — Cleveland, Ohio

Automatic and Supervisory Control Subcommittee

M. E. Reagan, *Chairman*; Switchboard Engineering Department, Westinghouse Electric Corporation, East Pittsburgh, Pa.
T. J. Allen — Atlanta, Ga.
Herman Bany — Philadelphia, Pa.
R. O. Bell — Milwaukee, Wis.
B. D. Dexter — San Francisco, Calif.
W. M. Larson — Minneapolis, Minn.
J. L. McKee — New York, N. Y.

Distribution and Conversion Substation Subcommittee

M. V. Eardley, *Chairman*; Department of Water and Power, City of Los Angeles, Los Angeles 54, Calif.
T. J. Allen — Atlanta, Ga.
Herman Bany — Philadelphia, Pa.
R. O. Bell — Milwaukee, Wis.
C. C. Crane — Madison, Wis.
G. P. Fallon — Baltimore, Md.
E. M. Hunter — Schenectady, N. Y.
I. S. Mendenhall — Detroit, Mich.

Transmission Substation Subcommittee

I. S. Mendenhall, *Chairman*; The Detroit Edison Company, 2000 Second Avenue, Detroit 26, Mich.
T. J. Allen — Atlanta, Ga.
Harris Barber — Boston, Mass.
F. J. Berger — Philadelphia, Pa.
H. P. Cadario — Toronto, Ontario, Canada
Marino Fraresso — Toronto, Ont., Canada
H. F. Gidlund — Denver, Colo.
E. M. Hunter — Schenectady, N. Y.
S. C. Killian — Chicago, Ill.
N. G. Larson — Chicago, Ill.
W. M. McCauley — Greenburg, Pa.
D. C. Millard — Denver, Colo.
J. H. Rixse, Jr. — Washington, D. C.
W. S. Scherring — Springfield, Mass.
R. F. Stevens — Portland Oreg.

Working Group on Device Function Numbers

Herman Bany, *Chairman*; General Electric Company, 6901 Elmwood Avenue, Philadelphia 42, Pa.
L. B. LeVesconte — Chicago, Ill.
M. E. Reagan — East Pittsburgh, Pa.
M. S. Schneider — Cincinnati, Ohio

Working Group on Substation Grounding Practice

H. F. Gidlund, *Chairman*; Public Service Company of Colorado, 810—15th Street, Denver 2, Colo.
F. J. Berger — Philadelphia, Pa.
M. K. Brown — Buffalo, N. Y.
F. R. Longley — Springfield, Mass.
J. M. Towner — Baltimore, Md.

Working Group on Rectifier Switchgear

M. E. Reagan, *Chairman*; Switchgear Engineering Department, Westinghouse Electric Corporation, East Pittsburgh, Pa.
D. C. Hoffman — Philadelphia, Pa.

Switchgear

Circuit Breaker Subcommittee

R. L. Webb, *Chairman*; Consolidated Edison Company of New York Inc., 4 Irving Place, New York 3, N. Y.
J. A. Elzi — Jackson, Mich.
R. M. Ferrill — Chattanooga, Tenn.
W. D. Hardaway — Denver, Colo.
A. W. Hill — East Pittsburgh, Pa.
M. H. Hobbs — East Pittsburgh, Pa.
C. L. Killgore — Denver, Colo.
F. A. Lane — New York, N. Y.
W. G. Lewis — Boston, Mass.
F. W. McCloska — Chicago, Ill.
W. J. McLachlan — Schenectady, N. Y.
A. Van Ryan — South Milwaukee, Wis.
J. H. Vivian — Los Angeles, Calif.
C. E. Winegartner — Cleveland, Ohio
J. D. Wood — Philadelphia, Pa.
J. C. Woods — Chicago, Ill.
B. W. Wyman — Philadelphia, Pa.

Working Groups:

(*1*). Automatic Circuit Reclosers

Anthony Van Ryan, *Chairman*; Line Material Company, Kyle Products Plant, 9th and Marion Avenues, South Milwaukee, Wis.
C. E. Asbury — Jackson, Mich.
L. L. Baird — Philadelphia, Pa.
Chase Hutchinson — New York, N. Y.
H. H. Rudd — Greensburg, Pa.
J. M. Wallace — East Pittsburgh, Pa.
C. E. Winegartner — Cleveland, Ohio

(*2*). Low-Voltage Air Circuit Breakers

J. D. Wood, *Chairman*; I.T.E. Circuit Breaker Company, 19th and Hamilton Streets, Philadelphia 30, Pa.
G. G. Grissinger — East Pittsburgh, Pa.
C. L. Killgore — Denver, Colo.
R. G. Meyerand — St. Louis, Mo.
V. E. Schloseberg — East Chicago, Ill.
J. W. Timmermaat, Jr. — Milwaukee, Wis.
J. C. Woods — Chicago, Ill.
B. W. Wyman — Philadelphia, Pa.
S. W. Zimmerman — Ithaca, N. Y.

(*3*). Power Circuit Breakers

A. W. Hill, *Chairman*; Westinghouse Electric Corporation, East Pittsburgh, Pa.
R. M. Bennett — Philadelphia, Pa.
J. A. Elzi — Jackson, Mich.
R. M. Ferrill — Chattanooga, Tenn.
S. B. Griscom — East Pittsburgh, Pa.
W. D. Hardaway — Denver, Colo.
C. L. Killgore — Denver, Colo.
W. G. Lewis — Boston, Mass.
J. H. Vivian — Los Angeles, Calif.
J. D. Wood — Philadelphia, Pa.
C. A. Woodrow — Schenectady, N. Y.

Switchgear Assemblies Subcommittee

C. P. West, *Chairman*; Westinghouse Electric Corporation, East Pittsburgh, Pa.
J. M. Geiger — Buffalo, N. Y.
C. L. Killgore — Denver, Colo.
M. G. Lewis — San Francisco, Calif.
F. W. McCloska — Chicago, Ill.
E. F. Miller — Davenport, Iowa
G. M. Reed — Philadelphia, Pa.
Garland Stamper — Dayton, Ohio
B. K. Sturgis — Philadelphia, Pa.
J. W. Timmerman, Jr. — Waukesha, Wis.
W. F. Wetmore — Detroit, Mich.

Switches, Fuses and Insulators Subcommittee

K. J. C. Falck, *Chairman*; Philadelphia Electric Company, 900 Sansom Street, Philadelphia 7, Pa.
T. E. Curtis — Hampton, Ga.
A. H. Powell — Philadelphia, Pa.
R. M. Smith — Greensburg, Pa.
J. M. Wallace — East Pittsburgh, Pa.
J. C. Woods — Chicago, Ill.

System Engineering

Administrative Subcommittee

Robert Brandt, *Chairman*; New England Power Company, 441 Stuart Street, Boston 16, Mass.
C. P. Almon, Jr. — Chattanooga, Tenn.
W. B. Fisk — New York, N. Y.
H. L. Harrington — Buffalo, N. Y.
C. B. Kelley — Des Moines, Iowa
H. A. Lott — Los Angeles, Calif.
O. W. Mans, Jr. — New York, N. Y.
G. B. Mayott — Hartford, Conn.
C. N. Metcalf — New York, N. Y.
C. W. Watchorn — Baltimore, Md.

System Planning Subcommittee

W. B. Fisk, *Chairman*; Consolidated Edison Company of New York, Inc., 4 Irving Place, New York 3, N. Y.
C. G. Adams — Schenectady, N. Y.
O. E. Charlton — Birmingham, Ala.
A. G. Dewars — Minneapolis, Minn.
A. P. Fugill — Detroit, Mich.
R. G. Hooke — Newark, N. J.
R. R. Jones — Chicago, Ill.
C. L. Killgore — Denver, Colo.
H. J. Klumb — Rochester, N. Y.
A. A. Kroseberg — Los Angeles, Calif.
R. F. Lawrence — East Pittsburgh, Pa.
W. H. Osterle — Pittsburgh, Pa.
H. P. St. Clair — New York, N. Y.
G. F. Switzer — Indianapolis, Ind.
J. J. Tesar — Cleveland, Ohio
D. C. Vaughan — Washington, D. C.
R. M. Walker — El Paso, Texas
Matthew Ward — Toronto, Ontario, Canada

System Operations Subcommittee

C. B. Kelley, *Chairman*; Interchange Power Service, P. O. Box 616, Des Moines, Iowa
F. A. Andrews — Baltimore, Md.
E. C. Brown — Hartford, Conn.
O. A. Demuth — Portland, Oreg.
G. D. Floyd — Toronto, Ontario, Canada
S. M. Hamill, Jr. — Cincinnati, Ohio
A. C. Hartranft — Philadelphia, Pa.
W. R. Johnson — San Francisco, Calif.
J. C. Jones — Portland, Oreg.
O. W. Mans, Jr. — New York, N. Y.
W. E. Montgomery — Los Angeles, Calif.
Noel Pike — Phoenix, Ariz.
G. M. Tatum — Richmond, Va.

System Economics Subcommittee

C. W. Watchorn, *Chairman*; Pennsylvania Water and Power Company, 1611 Lexington Building, Baltimore, Md.
E. C. Brown — Hartford, Conn.
E. E. George — New York, N. Y.
A. P. Hayward — Pittsburgh, Pa.
N. M. Lovell — Tucson, Ariz.
H. P. Peters — Atlanta, Ga.
H. W. Phillips — Philadelphia, Pa.
R. T. Purdy — Chicago, Ill.
J. A. Rose — Newark, N. J.
J. B. Ward — Lafayette, Ind.
A. L. Williams — Los Angeles, Calif.

System Controls Subcommittee

C. P. Almon, Jr., *Chairman*; Tennessee Valley Authority, Chattanooga 4, Tenn.
W. R. Brownlee — Jackson, Mich.
D. H. Cameron — Kansas City, Mo.
R. F. Lawrence — East Pittsburgh, Pa.
G. H. McDaniel — New York, N. Y.
C. N. Metcalf — New York, N. Y.
S. B. Morehouse — Philadelphia, Pa.
G. S. Whitlow — St. Louis, Mo.

Interconnection Contracts Subcommittee

C. W. Mayott, *Chairman*; Hartford Electric Light Company, 266 Pearl Street, Hartford, Conn.
Bradley Cozzens — Los Angeles, Calif.
E. D. Early — Birmingham, Ala.
E. E. George — New York, N. Y.
M. H. Lovelady — Corpus Christi, Tex.
G. H. McDaniel — New York, N. Y.

Transformers

Co-ordinated Study of Life of Transformer Insulation Subcommittee

J. L. Cantwell, *Chairman*; General Electric Company, 100 Woodlawn Avenue, Pittsfield, Mass.

C. E. Arntzen East Pittsburgh, Pa.
F. M. Clark Pittsfield, Mass.
J. F. Dexter Midland, Mich.
C. F. Hill East Pittsburgh, Pa.
Myron Kin Midland, Mich.
V. M. Montsinger Pittsfield, Mass.
T. D. Reimers New York, N. Y.
W. W. Satterlee Sharon, Pa.
W. M. Terry, Jr. Pittsburgh, Pa.
F. J. Vogel Chicago, Ill.
H. G. Zambell Pittsburgh, Pa.

INSTRUMENT TRANSFORMERS SUBCOMMITTEE

J. E. Clem, *Chairman;* Central Station Engineering Division, General Electric Company, Schenectady 5, N. Y.
Herman Bany Philadelphia, Pa.
J. H. Chiles Sharon, Pa.
R. E. Cordray Philadelphia, Pa.
F. E. Davis, Jr. Jackson, Mich.
K. J. C. Falck Philadelphia, Pa.
R. E. Franck Lynn, Mass.
J. M. Geiger Buffalo, N. Y.
T. R. Halman Detroit, Mich.
R. K. Huntington Rochester, N. Y.
L. F. Kennedy Schenectady, N. Y.
W. E. Marter Pittsburgh, Pa.
E. V. Sayles Jackson, Mich.
J. P. Scott St. Louis, Mo.
F. B. Silsbee Washington, D. C.
W. K. Sonnemann Newark, N. J.
W. M. Terry, Jr. Pittsburgh, Pa.
E. C. Wentz Sharon, Pa.
C. A. Woods East Pittsburgh, Pa.

AIEE PAPERS SUBCOMMITTEE

J. E. Clem, *Chairman;* Central Station Engineering Division, General Electric Company, Schenectady 5, N. Y.

MAGNETIZATION CHARACTERISTICS OF TRANSFORMERS SUBCOMMITTEE

J. E. Clem, *Chairman;* Central Station Engineering Divisions, General Electric Company, Schenectady 5, N. Y.
J. A. Elsi Jackson, Mich.
T. D. Gordy Pittsfield, Mass.
J. H. Kinghorn New York, N. Y.
W. E. Marter Pittsburgh, Pa.
A. J. Maslin Sharon, Pa.
A. H. Powell Philadelphia, Pa.
W. C. Sealey Milwaukee, Wis.
J. M. Wallace East Pittsburgh, Pa.

REVISION OF DIELECTRIC TESTS SUBCOMMITTEE

F. J. Vogel, *Chairman;* Illinois Institute of Technology, Chicago, Ill.
V. F. Christen St. Louis, Mo.
I. W. Gross New York, N. Y.
J. H. Hagenguth Pittsfield, Mass.
D. M. MacGregor New York, N. Y.
W. R. McCarty St. Louis, Mo.
J. R. Meador Pittsfield, Mass.
C. W. Miller Sharon, Pa.
V. M. Montsinger Pittsfield, Mass.
W. C. Sealey Milwaukee, Wis.
W. L. Teague Sharon, Pa.

GUIDES FOR OPERATION AND MAINTENANCE OF DRY-TYPE TRANSFORMERS WITH CLASS B INSULATION

J. A. Adams, *Chairman;* Philadelphia Electric Company, 900 Sansom Street, Philadelphia 5, Pa.
G. J. Johnston Pittsburgh, Pa.
T. D. Reimers New York, N. Y.
T. E. Rodhouse Pittsfield, Mass.
W. W. Satterlee Sharon, Pa.
H. H. Wagner Cannonsburg, Pa.
C. E. Winegartner Cleveland, Ohio

CO-ORDINATION OF INSULATION SUBCOMMITTEE

J. E. Clem, *Chairman;* Central Station Engineering Division, General Electric Company, Schenectady 5, N. Y.

ELECTRONIC POWER CONVERTERS SUBCOMMITTEE

W. C. Sealey, *Chairman;* Allis-Chalmers Manufacturing Company, Post Office Box 512, Milwaukee 1, Wis.

METHODS OF MAKING TEMPERATURE TESTS ON TRANSFORMERS SUBCOMMITTEE

J. E. Clem, *Chairman;* General Electric Company, Central Station Engineering Division, Schenectady 5, N. Y.
J. A. Adams Philadelphia, Pa.
M. F. Beavers Pittsfield, Mass.
M. K. Brown Buffalo, N. Y.
H. B. Keath St. Louis, Mo.
A. J. Maslin Sharon, Pa.
W. H. Mutschler Pittsburgh, Pa.

POWER FACTOR MEASUREMENTS SUBCOMMITTEE

J. B. Hodtum, *Chairman;* Allis-Chalmers Manufacturing Company, N. S. Station, Pittsburgh 33, Pa.

AUDIBLE NOISE IN TRANSFORMERS SUBCOMMITTEE

J. H. Chiles, *Chairman;* Westinghouse Electric Corporation, Transformer Engineering Department, Sharon, Pa.
J. E. Clem Schenectady, N. Y.
T. D. Gordy Pittsfield, Mass.
D. L. Levine Chicago, Ill.
A. J. Maslin Sharon, Pa.
T. D. Reimers New York, N. Y.
J. M. Towner Baltimore, Md.

HOT SPOT TEMPERATURE RISE OF CLASS B REACTORS SUBCOMMITTEE

D. L. Levine, *Chairman;* Commonwealth Edison Company, 72 West Adams Street, Chicago 90, Ill.
F. H. Kiersted Pittsfield, Mass.
L. E. Sauer Sharon, Pa.

PERMISSIBLE MAXIMUM OIL TEMPERATURE IN SERVICE SUBCOMMITTEE

M. H. Pratt, *Chairman;* Niagara Mohawk Power Corporation, 300 Erie Boulevard, Syracuse 2, N. Y.
J. G. Ford Sharon, Pa.
J. R. Meador Pittsfield, Mass.

THERMAL RATINGS AS AFFECTED BY ENCLOSURES SUBCOMMITTEE

A. A. Johnson, *Chairman;* Westinghouse Electric Corporation, East Pittsburgh, Pa.
J. E. Clem Schenectady, N. Y.
W. G. James Sharon, Pa.
E. K. Kane Pittsfield, Mass.
D. L. Levine Chicago, Ill.
W. C. Sealey Milwaukee, Wis.

A STUDY ON POSSIBLE SLIDING SCALE RELATION BETWEEN IMPEDANCE AND SHORT-CIRCUIT TIME FOR TRANSFORMERS AND REACTORS SUBCOMMITTEE
(Personnel to be selected)

Transmission and Distribution

CAPACITOR SUBCOMMITTEE

F. V. Smith, *Chairman;* Sargent and Lundy, 140 South Dearborn Street, Chicago 3, Ill.
Glen Appleman Allentown, Pa.
C. E. Baugh San Francisco, Calif.
P. L. Bellaschi Portland, Oreg.
H. V. Dryer So. Milwaukee, Wis.
K. B. Hapgood Chattanooga, Tenn.
E. R. Hendrickson Maywood, Ill.
R. E. Marbury East Pittsburgh, Pa.
D. B. Masters Jackson, Mich.
N. A. Miller Chicago, Ill.
R. B. Miller Davenport, Iowa
C. E. Parks Indianapolis, Ind.
Leon Podolsky North Adams, Mass.
F. F. Schaller, Jr. Boston, Mass.
M. E. Scoville Pittsfield, Mass.
E. C. Starr Corvallis, Oreg.

DISTRIBUTION SUBCOMMITTEE

T. J. Brosnan, *Chairman;* Niagara Mohawk Power Corporation, 300 Electric Building, Buffalo, N. Y.
C. E. Baugh San Francisco, Calif.
H. C. Bingham Cleveland, Ohio
D. K. Blake Schenectady, N. Y.
Bryce Brady Oklahoma City, Okla.
Harold Cole Detroit, Mich.
H. L. Davis Philadelphia, Pa.
E. R. Hendrickson Maywood, Ill.
J. B. Hodtum Pittsburgh, Pa.
E. K. Huntington Rochester, N. Y.
C. H. Kraft St. Louis, Mo.
J. E. O'Brien Washington, D. C.
E. W. Oesterreich Pittsburgh, Pa.
J. S. Parsons East Pittsburgh, Pa.
E. V. Sayles Jackson, Mich.

GENERAL SYSTEMS SUBCOMMITTEE

R. L. Witzke, *Chairman;* Industry Engineering Department, Westinghouse Electric Corporation, East Pittsburgh, Pa.
P. W. Blye New York, N. Y.
R. W. Caswell Chicago, Ill.
F. L. Code Toronto, Ontario, Canada
O. A. Demuth Portland, Oreg.
R. G. Hooke Newark, N. J.
E. K. Huntington Rochester, N. Y.
I. B. Johnson Schenectady, N. Y.
A. A. Kroneberg Los Angeles, Calif.
L. B. LeVesconte Chicago, Ill.
L. M. Robertson Denver, Colo.

LIGHTNING AND INSULATOR SUBCOMMITTEE

J. T. Lusignan, *Chairman;* Ohio Brass Company, Engineering Department, Mansfield, Ohio
L. V. Bewley Bethlehem, Pa.
H. N. Ekvall Philadelphia, Pa.
H. A. Frey Baltimore, Md.
I. W. Gross New York, N. Y.
J. H. Hagenguth Pittsfield, Mass.
K. J. Harder East Pittsburgh, Pa.
W. W. Lewis Schenectady, N. Y.
H. L. Rorden Portland, Oreg.
S. K. Waldorf Baltimore, Md.
E. R. Whitehead Chicago, Ill.

TOWERS, POLES, AND CONDUCTORS SUBCOMMITTEE

A. E. Davison, *Chairman;* Hydro-Electric Power Commission of Ontario, 620 University Ave., Toronto, Ontario, Canada
N. K. Barr Newark, Ohio
A. E. Beattie Beaumont, Texas
H. W. Bakeborn Newark, Ohio
A. A. Booker Boston, Mass.
P. J. Croft Toronto, Ontario, Canada
A. L. Duna Worcester, Mass.
K. E. Hapgood Chattanooga, Tenn.
E. L. Kanouse Los Angeles, Calif.
W. H. Knutz Hammond, Ind.
J. E. O'Brien Washington, D. C.
A. A. Osipovich Portland, Oreg.
F. W. Packer Allentown, Pa.
T. F. Peterson Cleveland, Ohio
J. A. Rawls Richmond, Va.
L. M. Robertson Denver, Colo.
A. S. Runciman Montreal, Quebec, Canada
A. N. Shealy Baltimore, Md.
E. J. Staubitz Pittsburgh, Pa.
Joel Tompkins Massena, N. Y.
F. Von Voigtlander Jackson, Mich.
R. G. Yerke Seward, Neb.

Science and Electronics Division

Basic Sciences

APPLIED MATHEMATICS SUBCOMMITTEE

M. G. Malti, *Chairman;* School of Electrical Engineering, Cornell University, Ithaca, N. Y.

Mathematicians

Garrett Birkhoff Cambridge, Mass.
D. G. Bourgin Urbana, Ill.
R. J. Duffin Pittsburgh, Pa.
A. E. Hines Pittsburgh, Pa.
Mark Kac Ithaca, N. Y.
John Von Neumann Princeton, N. J.
Harry Pollard Ithaca, N. Y.
J. J. Stoker New York, N. Y.
J. W. Tukey Princeton, N. J.
D. V. Widder Cambridge, Mass.
Norbert Wiener Cambridge, Mass.
Max Woodbury Princeton, N. J.

Electrical Engineers

P. L. Alger Schenectady, N. Y.
Murray Gardner Cambridge, Mass.
H. B. Hansteen New York, N. Y.
E. W. Kimbark Evanston, Ill.
Louis Pipes Los Angeles, Calif.
Joseph Slepian East Pittsburgh, Pa.
J. J. Smith Schenectady, N. Y.
Harry Sohon Philadelphia, Pa.

ELECTRIC CIRCUIT THEORY SUBCOMMITTEE

H. J. Carlin, *Chairman;* Microwave Research Institute, Polytechnic Institute of Brooklyn, Brooklyn, N. Y.
J. G. Brainerd Philadelphia, Pa.
R. L. Dietzold Murray Hill, N. J.
M. J. Di Toro Nutley, N. J.
A. B. Giordano Brooklyn, N. Y.
E. A. Guillemin Cambridge, Mass.
T. J. Higgins Madison, Wis.
F. F. Ordung New Haven, Conn.
W. O. Osbon East Pittsburgh, Pa.
M. B. Reed Urbana, Ill.
H. I. Tarpley State College, Pa.
Ernst Weber Brooklyn, N. Y.

ELECTRICAL PROPERTIES OF GASES SUBCOMMITTEE

T. B. Jones, *Chairman;* School of Electrical Engineering, Johns Hopkins University, Baltimore 18, Md.
J. D. Cobine Schenectady, N. Y.
L. H. Fisher New York, N. Y.
L. H. Germer Murray Hill, N. J.
Joseph Slepian East Pittsburgh, Pa.

ELECTRICAL PROPERTIES OF SOLIDS AND LIQUIDS SUBCOMMITTEE

C. Bradner Brown, *Chairman;* Naval Gun Factory, United States Naval Ordnance Laboratory, White Oak, Md.
J. A. Becker Murray Hill, N. J.
F. M. Clark Schenectady, N. Y.
W. C. Dunlap Schenectady, N. Y.
R. W. Engstrom Lancaster, Pa.
K. Lark-Horovitz Lafayette, Ind.
P. H. Miller, Jr. Philadelphia, Pa.
Fred Seitz Pittsburgh, Pa.
Lloyd Smith Ithaca, N. Y.
A. von Hippel Cambridge, Mass.
D. E. Wooldridge Culver City, Calif.

ENERGY SOURCES SUBCOMMITTEE

L. W. Matsch, *Chairman;* Illinois Institute of Technology, Department of Electrical Engineering, Chicago 16, Ill.
W. C. Brown Point Mugu, Calif.
M. A. Garstens Washington, D. C.
W. A. Lewis, Jr. Chicago, Ill.
Walther Richter Milwaukee, Wis.
J. J. Smith Schenectady, N. Y.
B. R. Teare Pittsburgh, Pa.
J. D. Tebo New York, N. Y.
Milton Tenzer Bradley Beach, N. J.

MAGNETICS SUBCOMMITTEE

R. M. Bozorth, *Chairman;* Bell Telephone Laboratories, Inc., Murray Hill, N. J.
R. A. Chegwidden, *Secretary* Murray Hill, N. J.
F. G. Brockman Irvington-on-Hudson, N. Y.
G. H. Cole Middletown, Ohio
E. A. Gaugler Silver Spring, Md.
J. E. Goldman Pittsburgh, Pa.
W. Morrill Pittsfield Pa.
W. E. Ruder Schenectady, N. Y.
C. W. Stoker Pittsburgh, Pa.

Computing Devices

ANALOG COMPUTERS SUBCOMMITTEE

E. L. Harder, *Chairman;* Industry Engineering Department 11-L, Westinghouse Electric Corporation, East Pittsburgh, Pa.
J. F. Calvert Evanston, Ill.
A. C. Hall Cambridge, Mass.
G. D. McCann Pasadena, Calif.
V. Paschkis New York, N. Y.
F. S. Rothe Schenectady, N. Y.
H. G. Tremblay Johnsville, Pa.

DIGITAL COMPUTERS SUBCOMMITTEE

S. N. Alexander, *Chairman;* National Bureau of Standards, Electronic Computers Section, Washington 25, D. C.
H. P. Kuehni Schenectady, N. Y.
J. W. Mauchly Philadelphia, Pa.
G. D. McCann Pasadena, Calif.
J. C. McPherson New York, N. Y.
P. L. Morton Berkeley, Calif.
R. L. Snyder Aberdeen Proving Ground, Md.

COMPUTER BIBLIOGRAPHY SUBCOMMITTEE

W. H. MacWilliams, Jr., *Chairman;* Bell Telephone Laboratories, Inc., Whippany, N. J.

Electronic Power Converters

ADMINISTRATIVE SUBCOMMITTEE

Main Committee Officers:
C. C. Herskind, *Chairman;* General Electric Company, Power Electronics Division, Schenectady 5, N. Y.

W. N. Farquhar, *Vice-Chairman* Pittsburgh, Pa.
C. R. Marcum, *Secretary* East Pittsburgh, Pa.
Harold Winograd, *Preceding Chairman* Milwaukee, Wis.

Subcommittee Chairmen:
I. K. Dortort Philadelphia, Pa.
R. A. Nelson Pittsfield, Mass.
Waldo Porter Vancouver, Wash.
August Schmidt, Jr. Schenectady, N. Y.
J. C. Walter Camden, N. J.

ELECTRONIC CONVERTER APPLICATION SUBCOMMITTEE

W. N. Farquhar, *Chairman;* Aluminum Company of America, 801 Gulf Building, Pittsburgh 19, Pa.
C. E. Buterbaugh
E. H. Cox, Jr. Baton Rouge, La.
F. W. Cramer Pittsburgh, Pa.
J. R. Donnelly Philadelphia, Pa.
N. W. Geist
W. E. Gutzwiller Milwaukee, Wis.
R. N. Hunter New York, N. Y.
Armin Leuthold Mt. Royal, Quebec, Canada
W. E. Bloecker New York, N. Y.
W. J. L. Rupprecht Midland, Mich.
S. L. Smith Philadelphia, Pa.
O. J. Swanson Gary, W. Va.
J. T. Thwaites Hamilton, Ontario, Canada
J. W. Ward Sylacauga, Ala.

ELECTRONIC CONVERTER CIRCUITS SUBCOMMITTEE

I. K. Dortort, *Chairman;* ITE Circuit Breaker Company, 19th & Hamilton Streets, Philadelphia 30, Pa.
W. F. Bonner Clifton, N. J.
J. L. Boyer East Pittsburgh, Pa.
G. N. Hughes Alcoa, Tenn.
Otto Jensen Philadelphia, Pa.
G. F. Jones East Pittsburgh, Pa.
W. E. Bloecker New York, N. Y.
A. H. Mittag Schenectady, N. Y.
R. A. Nelson Pittsfield, Mass.
M. E. Reagan East Pittsburgh, Pa.
August Schmidt, Jr. Schenectady, N. Y.
C. H. Willis Princeton, N. J.

Working Group:
Mechanical Rectifiers
Otto Jensen, *Chairman;* ITE Circuit Breaker Company, 19th & Hamilton Streets, Philadelphia 30, Pa.
I. K. Dortort Philadelphia, Pa.
D. H. Smith New York, N. Y.

PAPERS AND SPEAKERS SUBCOMMITTEE

August Schmidt, Jr., *Chairman;* General Electric Company, 1 River Road, Schenectady 5, N. Y.
J. B. Rice West Allis, Wis.
J. T. Thwaites Hamilton, Ontario, Canada
H. E. Zuvers Schenectady, N. Y.

RECTIFIER TRANSFORMERS SUBCOMMITTEE

R. A. Nelson, *Chairman;* General Electric Company, 100 Woodlawn Avenue, Pittsfield, Mass.
F. D. Kaiser Sharon, Pa.
A. J. Maslin Sharon, Pa.
W. C. Sealey Milwaukee, Wis.

RECTIFYING DEVICES SUBCOMMITTEE

Harold Winograd, *Chairman;* Allis-Chalmers Manufacturing Company, Electrical Department, Milwaukee 1, Wis.
D. V. Edwards Newark, N. J.
D. E. Marshall Bloomfield, N. J.
August Schmidt, Jr. Schenectady, N. Y.
H. C. Steiner Schenectady, N. Y.

WEST COAST SUBCOMMITTEE

Waldo Porter, *Chairman;* Aluminum Company of America, P. O. Box 120, Vancouver, Wash.
W. M. Allen Portland, Oreg.
E. D. Barens Los Angeles, Calif.
E. S. Benson San Francisco, Calif.
H. L. Burris Pittsburg, Calif.
R. J. Corfield Garfield, Utah
J. H. Cox Sunnyvale, Calif.
R. H. Denyer Portland, Oreg.
A. G. Dickinson Trail, British Columbia, Canada
E. F. Donatic Ontario, Calif.
Alex. Dovjikov Portland, Oreg.
R. H. Duguid Los Angeles, Calif.
S. R. Durand Milwaukee, Wis.
L. E. Dye Los Angeles, Calif.
T. F. Hadwin Vancouver, British Columbia, Canada
D. R. Hoopes Salt Lake City, Utah
J. V. Kresser San Francisco, Calif.
C. A. Langloid Portland, Oreg.
H. F. Lickey Pullman, Wash.
M. McCoy Portland, Oreg.
A. L. Munn San Leandro, Calif.
S. J. Pope Spokane, Wash.
H. H. Skilling Stanford, Calif.
E. C. Starr Corvallis, Oreg.
H. V. Strandberg Seattle, Wash.
J. R. Tenney Geneva, Utah

HOT-CATHODE POWER CONVERTER SUBCOMMITTEE

J. C. Walter, *Chairman;* Radio Corporation of America, Camden, N. J.
R. W. Barker Pittsfield, Mass.
W. H. Bixby Detroit, Mich.
H. R. Butler Newark, N. J.
F. W. Cramer Pittsburgh, Pa.
D. V. Edwards Newark, N. J.
C. E. Hamann Lynn, Mass.
J. F. Harris Newark, N. J.
E. W. Hutton Schenectady, N. Y.
W. E. Large East Pittsburgh, Pa.
F. G. Logan St. Louis, Mo.
E. J. Rathsack Milwaukee, Wis.
F. M. Rives Schenectady, N. Y.
W. C. Rudd Larchmont, N. Y.
J. W. Sanborn Camden, N. J.
D. H. Smith Schenectady, N. Y.
H. C. Steiner Schenectady, N. Y.
H. L. Thorson Schenectady, N. Y.
D. E. Trucksess New York, N. Y.

Electronics

ELECTRON TUBES SUBCOMMITTEE

H. C. Steiner, *Chairman;* Electronics Department, I. & T. Tube Division, General Electric Company, Schenectady 5, N. Y.
A. Y. Bentley Passaic, N. J.
W. R. Clark Philadelphia, Pa.
F. W. Cramer Pittsburgh, Pa.
D. V. Edwards Newark, N. J.
A. V. Glover Lancaster, Pa.
R. E. Graham Kew Gardens, N. Y.
William Happe, Jr. Clifton, N. J.
L. B. Headrick Lancaster, Pa.
Scott Helt Passaic, N. J.
J. H. Hutchings Geneva, Ill.
K. S. Koon Endicott, N. Y.
O. W. Livingston Schenectady, N. Y.
C. R. Marcum East Pittsburgh, Pa.
D. E. Marshall Bloomfield, N. J.
August Schmidt, Jr. Schenectady, N. Y.
Thomas Spooner East Pittsburgh, Pa.
J. T. Thwaites Hamilton, Ontario, Canada
Simeon Weston Brooklyn, N. Y.
W. C. White Schenectady, N. Y.
C. H. Willis Princeton, N. J.
Harold Winograd Milwaukee, Wis.

X-RAY TUBES, APPARATUS AND APPLICATIONS SUBCOMMITTEE

Scott W. Smith, *Chairman;* X-Ray Section, National Bureau of Standards, Washington 25, D. C.
Z. J. Atlee Chicago, Ill.
Arthur Klinckermann Chicago, Ill.
Joseph Lempert Bloomfield, N. J.
G. E. Maxim Cleveland, Ohio
T. H. Rogers Springdale, Conn.
David Susin Covington, Ky.
Robert F. Wilson Milwaukee, Wis.

ELECTROSTATIC PROCESSES SUBCOMMITTEE

G. W. Hewitt, *Chairman;* Research Laboratories, Westinghouse Electric Corporation, East Pittsburgh, Pa.
J. O. Amtus Troy, N. Y.
J. E. Coolidge, Jr. State College, Pa.
E. P. Miller Indianapolis, Ind.
H. V. Nelson Schenectady, N. Y.
S. R. Orens, Jr. Greenwich, Conn.
G. W. Penney Pittsburgh, Pa.
E. R. Thomas New York, N. Y.
J. B. Thomas Fort Worth, Texas
H. J. White Bound Brook, N. J.

HIGH FREQUENCY CONDUCTORS, CABLES, AND CONNECTORS SUBCOMMITTEE

G. J. Crowdes, *Chairman;* Simplex Wire and Cable Company, 79 Sidney Street, Cambridge 39, Mass.
W. R. Dohan Camden, N. J.
E. W. Greenfield Hastings-on-Hudson, N. Y.
J. D. Heibel Erie, Pa.
B. A. Jackson New York, N. Y.
W. J. King Murray Hill, N. J.
H. B. Slade Passaic, N. J.
W. R. Thurston Cambridge, Mass.

LIAISON WITH NUCLEONICS SUBCOMMITTEE

G. A. Morton, *Chairman;* R. C. A. Laboratories, Princeton, N. J.

ELECTRONIC AIDS TO NAVIGATION SUBCOMMITTEE

H. R. Mimno, *Chairman,* Cruft Laboratory, Harvard University, Cambridge 38, Mass.

ELECTRONIC AIDS TO GEOPHYSICS SUBCOMMITTEE

L. G. Cowles, *Chairman;* The Superior Oil Company, Houston, Texas

INFRARED APPLICATIONS SUBCOMMITTEE

A. H. Canada, *Chairman;* General Engineering and Consulting Laboratory, General Electric Company, Schenectady 5, N. Y.
A. R. Dennett Newport, R. I.
William A. Dynes Dayton, Ohio
W. G. Fastie Philadelphia, Pa.
B. J. Goldfarb Dayton, Ohio
E. D. Wilson East Pittsburgh, Pa.
C. S. Woodside Washington, D. C.

ELECTRONIC METHODS IN FOOD AND BIOLOGICAL PROCESSING SUBCOMMITTEE

T. H. Morris, *Chairman;* Department of Electrical Engineering, Stanford Research Institute, Stanford, Calif.

MAGNETIC AMPLIFIERS SUBCOMMITTEE

E. L. Harder, *Chairman;* Westinghouse Electric Corporation, East Pittsburgh, Pa.
E. V. Weir, *Secretary* Silver Spring, Md.
A. O. Black Butler, Pa.
L. W. Buechler St. Louis, Mo.
W. J. Dornhoefer St. Louis, Mo.
L. A. Finzi Pittsburgh, Pa.
A. S. Fitzgerald San Francisco, Calif.
W. A. Geyger Silver Spring, Md.
A. B. Haines Murray Hill, N. J.
J. E. Hart Washington, D. C.
A. D. Hitt, Jr. Washington, D. C.
W. C. Johnson Princeton, N. J.
R. E. Morgan Schenectady, N. Y.
H. B. Rex Washington, D. C.
P. L. Schmidt East Pittsburgh, Pa.
R. W. Wolke Schenectady, N. Y.
D. W. VerPlanck Pittsburgh, Pa.

Working Groups:

(1) Definitions
W. J. Dornhoefer, *Sponsor* St. Louis, Mo.
E. L. Harder East Pittsburgh, Pa.
L. A. Finzi Pittsburgh, Pa.
A. B. Haines Murray Hill, N. J.
E. B. McDowell Schenectady, N. Y.
E. V. Weir Silver Spring, Md.

(2) Speed of Response, Figure of Merit
L. A. Finzi, *Sponsor* Pittsburgh, Pa.
E. L. Harder East Pittsburgh, Pa.
W. J. Dornhoefer St. Louis, Mo.
W. C. Johnson Princeton, N. J.
R. E. Morgan Schenectady, N. Y.
H. B. Rex Washington, D. C.
D. W. VerPlanck Pittsburgh, Pa.
E. V. Weir Silver Spring, Md.

(3) Ratings
R. W. Wolke, *Sponsor* Schenectady, N. Y.
W. J. Dornhoefer St. Louis, Mo.
L. A. Finzi Pittsburgh, Pa.
E. L. Harder East Pittsburgh, Pa.
J. E. Hart Washington, D. C.
R. E. Morgan Schenectady, N. Y.

ELECTRONIC APPLICATIONS OF SEMICONDUCTOR DEVICES SUBCOMMITTEE

C. Bradner Brown, *Chairman;* Naval Ordnance Laboratory, White Oak, Md.
Harold Goldberg Washington, D. C.
J. R. Hyneman New York, N. Y.
G. D. O'Neill Kew Gardens, N. Y.

LIAISON WITH ELECTRONIC HEATING SUBCOMMITTEE

T. P. Kinn, *Chairman;* Electronics and X-Ray Division, Westinghouse Electric Corporation, 2519 Wilkens Avenue, Baltimore 3, Md.
R. M. Baker Baltimore, Md.
W. C. Rudd Larchmont, N. Y.

ELECTRONIC SYSTEMS ENGINEERING SUBCOMMITTEE

H. L. Flowers, *Chairman;* Aerophysics Department, Goodyear Aircraft Corporation, Akron 15, Ohio
(Personnel to be selected)

ELECTRONIC STANDARDS AND DEFINITIONS SUBCOMMITTEE

(Personnel to be selected)

LIAISON WITH IRE SUBCOMMITTEE

R. S. Burnap, *Chairman;* Radio Corporation of America, R. C. A. Victor Division, Harrison, N. J.

LIAISON WITH JETEC SUBCOMMITTEE

(Personnel to be selected)

EDUCATION IN ELECTRONICS SUBCOMMITTEE

J. D. Ryder, *Chairman;* University of Illinois, Urbana, Ill.
E. M. Boone Columbus, Ohio
M. A. Honnell Atlanta, Ga
R. K. Northrop Ithaca, N. Y.
A. J. Quigley Notre Dame, Ind
J. T. Thwaites Hamilton, Ont., Canada
D. G. Wilson Lawrence, Kansas

PAPERS REVIEW SUBCOMMITTEE

W. C. White, *Chairman;* General Electric Research Laboratory, The Knolls, Schenectady, N. Y.
G. M. K. Baker Princeton, N. J.
W. R. Clark Philadelphia, Pa.
H. F. Dart Bloomfield, N. J.
Rudolf Feldt Clifton, N. J.
R. E. Graham Kew Gardens, N. Y.
S. B. Ingram New York, N. Y.
L. A. Kilgore East Pittsburgh, Pa.
H. L. Palmer Schenectady, N. Y.
H. C. Steiner Schenectady, N. Y.
Dayton Ulrey Lancaster, Pa.
Harold Winograd Milwaukee, Wis.

Instruments and Measurements

ORGANIZATION SUBCOMMITTEE

T. S. Gray, *Chairman;* Massachusetts Institute of Technology, Cambridge 39, Mass.
C. F. Savage, *Secretary* Lynn, Mass.
E. I. Green Murray Hill, N. J.
H. C. Koenig New York, N. Y.
G. Reid, Jr. Washington, D. C.

DEFINITIONS SUBCOMMITTEE

C. L. Dawes, *Chairman;* Harvard University, Cambridge 39, Mass.
J. E. Clem Schenectady, N. Y.
A. B. Craig Boston, Mass.
H. C. Dickinson Lynn, Mass.
W. N. Goodwin, Jr. Newark, N. J.
Everett S. Lee Schenectady, N. Y.
R. E. Lenehan Newark, N. J.
F. B. Silsbee Washington, D. C.

ELECTRICAL TESTS ON DIELECTRICS IN THE FIELD SUBCOMMITTEE

F. C. Doble, *Chairman;* Doble Engineering Company, Box 544, Belmont 78, Mass.
W. G. Amey Philadelphia, Pa.
D. L. Brown Portland, Oreg.
A. L. Brownlee Chicago, Ill.
R. B. Curdts Philadelphia, Pa.
C. L. Dawes Cambridge, Mass.
W. F. Dunkle Hazleton, Pa.
I. G. Easton Cambridge, Mass.
W. N. Eddy Cambridge, Mass.
J. G. Ford Sharon, Pa.
I. W. Gross New York, N. Y.

Everett S. Lee Schenectady, N. Y.
W. N. Lindblad Emeryville, Calif.
G. M. L. Sommerman Evanston, Ill.
R. R. Thomas New York, N. Y.
L. Wetherill Pittsfield, Mass.

HIGH-FREQUENCY MEASUREMENTS SUBCOMMITTEE

Harold Lyons, *Chairman;* National Bureau of Standards, Microwave Measurement Laboratory, Washington, D. C.
S. L. Bailey Washington, D. C.
E. P. Felch, Jr. Murray Hill, N. J.
F. Hamburger, Jr. Baltimore, Md.
H. R. Meahl Schenectady, N. Y.
H. A. Wheeler Great Neck, N. Y.
A. J. Wing, Jr. Evanston, Ill.

INDUSTRIAL SPECTROSCOPY SUBCOMMITTEE

J. H. Enns, *Chairman;* Randall Laboratory, University of Michigan, Ann Arbor, Michigan
H. M. Bedell Cleveland, Ohio
G. D. Butler New York, N. Y.
D. K. Coles East Pittsburgh, Pa.
C. H. Corliss Washington, D. C.
H. M. Crosswhite Baltimore, Md.
W. G. Fastie Philadelphia, Pa.
W. D. Hershberger Berkeley, Calif.
E. K. Jaycox Murray Hill, N. J.
L. W. McNair Wood River, Ill.
John Sterner Cambridge, Mass.
J. Sherman Philadelphia, Pa.
Van Zandt Williams Glenbrook, Conn.

MARKING OF VARMETERS AND RELATED INSTRUMENTS SUBCOMMITTEE

A. B. Craig, *Chairman;* Boston Edison Company, 39 Boylston Street, Boston 12, Mass.
A. L. Brownlee Chicago, Ill.
A. L. Carvill Lynn, Mass
W. G. Knickerbocker Detroit, Mich.
A. E. Knowlton New York, N. Y.
F. A. Redding Los Angeles, Calif.
F. B. Silsbee Washington, D. C.
H. B. Smith Buffalo, N. Y.

MASTER TEST CODE FOR POWER MEASUREMENTS SUBCOMMITTEE

C. J. Zeller, *Chairman;* Consolidated Edison Company of New York, Inc., 708—1st Avenue, New York 17, N. Y.
W. G. Knickerbocker Detroit, Mich.
H. C. Koenig New York, N. Y.
B. E. Lenehan Newark, N. J.
L. W. Matsch Chicago, Ill.
J. H. Miller Newark, N. J.
C. F. Savage, Jr. West Lynn, Mass.
Harry Sohon Philadelphia, Pa.
L. N. Stone Corvallis, Oreg.

MASTER TEST CODE FOR TEMPERATURE MEASUREMENTS SUBCOMMITTEE

L. A. Burckmyer, Jr., *Chairman;* Cornell University, Ithaca, New York
P. A. Borden Waterbury, Conn.
E. D. Doyle Philadelphia, Pa.
J. L. Fuller Cleveland, Ohio
W. R. Hough Cleveland, Ohio
A. K. Joecks New York, N. Y.
S. S. Stack Schenectady, N. Y.

REVISION OF STANDARD NUMBER 4 (MEASUREMENT OF TEST VOLTAGE IN DIELECTRIC TESTS) SUBCOMMITTEE

J. T. Lusignan, Jr., *Chairman;* Engineering Department, Ohio Brass Company, Mansfield, Ohio
P. L. Bellaschi Portland, Oreg.
A. L. Brownlee Chicago, Ill.
J. S. Carroll Stanford University, Calif.
J. J. Clark East Pittsburgh, Pa.
E. W. Davis Cambridge, Mass.
C. M. Foust Schenectady, N. Y.
H. A. Frey Baltimore, Md.
I. W. Gross New York, N. Y.
J. H. Hagenguth Pittsfield, Mass.
W. B. Kouwenhoven Baltimore, Md.
R. L. Lapp LeRoy, N. Y.
W. W. Lewis Schenectady, N. Y.
M. Newman Minneapolis, Minn.
J. H. Park Washington, D. C.
W. C. Sealey Milwaukee, Wis.
W. T. Smith Arlington, Va.
R. W. Sorensen Pasadena, Calif.
W. L. Teague Sharon, Pa.
S. W. Zimmerman Ithaca, N. Y.

WATT-HOUR METERS SUBCOMMITTEE

C. F. Savage, Jr., *Chairman;* General Electric Company, 40 Federal Street, West Lynn, Mass.
H. A. Brown Rochester, N. Y.
G. N. Burkhart, Jr. Lafayette, Ind.
D. T. Canfield Lafayette, Ind.
A. B. Craig Boston, Mass.
F. C. Holtz Springfield, Ill.
W. G. Knickerbocker Detroit, Mich.
H. C. Koenig New York, N. Y.
B. E. Lenehan Newark, N. J.
W. N. Lindblad Emeryville, Calif.
F. H. Rogers Baltimore, Md.
K. M. Stevens Alhambra, Calif.
M. B. Stout Ann Arbor, Mich.
J. M. Vanderleck Toronto, Ontario, Canada

CO-OPERATION WITH INSTRUMENT SOCIETY OF AMERICA SUBCOMMITTEE

A. J. Hornfeck, *Chairman;* Bailey Meter Company, 1050 Ivanhoe Road, Cleveland 10, Ohio
J. J. Bowen Buffalo, N. Y.
C. J. Brumbaugh Hamburg, N. Y.
F. C. Rushing Buffalo, N. Y.

Metallic Rectifiers

TECHNICAL INFORMATION SUBCOMMITTEE

C. E. Hamann, *Chairman;* Rectifier Division, General Electric Company, 930 Western Avenue, Lynn 3, Mass.
M. E. Gamble Indianapolis, Ind.
L. K. Hedding Pittsburgh, Pa.
J. L. Wagner Endicott, N. Y.

MINIATURE RECTIFIERS SUBCOMMITTEE

P. G. Cobb, *Chairman;* Weston Electrical Instrument Corporation, 614 Frelinghuysen Avenue, Newark 5, N. J.

DEFINITIONS SUBCOMMITTEE

D. E. Truckess, *Chairman;* Bell Telephone Laboratories, Inc., 463 West Street, New York 14, N. Y.
W. F. Bonner Clifton, N. J.
C. W. Hansell Rocky Point, L. I., N. Y.

BIBLIOGRAPHY SUBCOMMITTEE

E. A. Harty, *Chairman;* Rectifier Engineering Division, General Electric Company, River Works, West Lynn 3, Mass.

TEST CODE SUBCOMMITTEE

W. F. Bonner, *Chairman;* Selenium-Intelin Division, Federal Telephone and Radio Corporation, 100 Kingsland Avenue, Clifton, N. J.
J. T. Cataldo Fort Monmouth, N. J.
K. S. Geiges New York, N. Y.

PATENTS SUBCOMMITTEE

Glen Ramsey, *Chairman;* Fansteel Metallurgical Corporation, Rectifier Division, North Chicago, Ill.

PAPERS AND MEETINGS SUBCOMMITTEE

L. W. Burton, *Chairman;* General Electric Company, River Works, 920 Western Avenue, Lynn, Mass.
E. A. Groeteke St. Louis, Mo.
Glen Ramsey North Chicago, Ill.

Nucleonics

ISOTOPIC TRACERS SUBCOMMITTEE

R. E. Watson, *Chairman;* Research Department, Leeds and Northrup Company, 4901 Stenton Avenue, Philadelphia 44, Pa.
(Personnel to be selected)

NUCLEAR THEORY SUBCOMMITTEE

P. N. Ross, *Chairman;* Atomic Power Division, Westinghouse Electric Corporation, Bettis Field, P. O. Box 1468, Pittsburgh 30, Pa.

NUCLEAR MACHINES SUBCOMMITTEE

J. G. Hutton, *Chairman;* General Engineering and Consulting Laboratory, General Electric Company, Schenectady 5, N. Y.
(Personnel to be selected)

Therapeutics

No subcommittees

Joint Subcommittees

JOINT SUBCOMMITTEE ON APPLICATIONS OF PROBABILITY METHODS TO POWER-SYSTEM PROBLEMS (JOINT WITH POWER GENERATION AND SYSTEM ENGINEERING COMMITTEES)

G. Calabrese, *Chairman;* Electrical Engineering Department, New York University, University Heights, New York 53, N. Y.
W. R. Blakely Toronto, Ontario, Canada
V. M. Cook New York, N. Y.
Howard Duryea Birmingham, Ala.
R. G. Hooke Newark, N. J.
H. A. Lott Los Angeles, Calif.
F. J. Leerburger New York, N. Y.
W. J. Lyman Pittsburgh, Pa.
Bela Mohr Oklahoma City, Okla.
H. W. Phillips Philadelphia, Pa.
H. B. Smith Buffalo, N. Y.
V. A. Thiemann New York, N. Y.
C. W. Watchorn Baltimore, Md.

JOINT SUBCOMMITTEE ON ELECTRICAL AIDS TO MEDICINE (JOINT WITH ELECTRONICS, INSTRUMENTS AND MEASUREMENTS, AND THERAPEUTICS COMMITTEES)

Kendrick Hare, *Chairman;* Childrens' Hospital, 219 Bryant Street, Buffalo 9, N. Y.
G. W. Dunlap Schenectady, N. Y.
W. A. Geohegan New York, N. Y.
Harry Grundfest New York, N. Y.
J. P. Hervey Baltimore, Md.
R. S. Mackay Berkeley, Calif.
G. A. Morton Princeton, N. J.
J. G. Reid, Jr. Washington, D. C.
S. W. Smith Washington, D. C.
C. A. Tobias Berkeley, Calif.
S. R. Warren, Jr. Philadelphia, Pa.
A. M. Zarem Los Angeles, Calif.

JOINT SUBCOMMITTEE ON ELECTRONIC INSTRUMENTS (JOINT WITH ELECTRONICS AND INSTRUMENTS AND MEASUREMENTS COMMITTEES)

Rudolf Feldt, *Chairman;* Allen B. DuMont Laboratories, Inc., 1000 Main Avenue, Clifton, N. J.
W. H. Tidd, *Vice-Chairman* New York, N. Y.
P. K. McElroy, *Secretary* Cambridge, Mass.
M. J. Ackerman Camden, N. J.
G. E. Beggs Philadelphia, Pa.
Cledo Brunetti Stanford, Calif.
C. C. Chambers Philadelphia, Pa.
H. F. Dart Bloomfield, N. J.
G. W. Downs Pasadena, Calif.
G. V. Eltgroth Philadelphia, Pa.
E. R. Haberland Silver Spring, Md.
C. E. Hastings Hampton, Va.
C. M. Hathaway Denver, Colo.
D. M. Hill Boonton, N. J.
G. B. Hoadley Raleigh, N. C.
E. J. Isbister Great Neck, N. Y.
W. J. Jones Belmar, N. J.
N. W. Matthews Washington, D. C.
H. R. Meahl Schenectady, N. Y.
Edmund Osterland Boonton, N. J.
David Packard Palo Alto, Calif.
T. B. Perkins Harrison, N. J.
J. G. Reid, Jr. Washington, D. C.
E. R. Thomas New York, N. Y.
J. T. Thwaites Hamilton, Ontario, Canada
Howard Vollum Portland, Oreg.
A. H. Waynick State College, Pa.
W. P. Wills Philadelphia, Pa.

JOINT SUBCOMMITTEE ON NUCLEONIC INSTRUMENTS (JOINT WITH NUCLEONICS AND INSTRUMENTS AND MEASUREMENTS COMMITTEES)

G. A. Morton, *Chairman;* Radio Corporation of America, R.C.A. Laboratories Division, Princeton, N. J.
(Personnel to be selected)

JOINT SUBCOMMITTEE ON STANDARD FREQUENCY BANDS AND DESIGNATIONS

G. B. Ransom, *Chairman;* American Telephone and Telegraph Company, 32 Avenue of the Americas, New York 13, N. Y.
I. G. Easton Cambridge, Mass.
T. P. Kinn Baltimore, Md.
J. E. McCormack New York, N. Y.
F. B. Silsbee Washington, D. C.

JOINT SUBCOMMITTEE ON TELEMETERING (JOINT WITH INSTRUMENTS AND MEASUREMENTS AND SUBSTATIONS COMMITTEES)

W. J. Mayo-Wells, *Chairman;* Applied Physics Laboratory, The Johns Hopkins University, 8621 Georgia Avenue, Silver Spring 18, Md.
J. L. McKee, *Secretary* New York, N. Y.
J. L. Blackburn Newark, N. J.
P. A. Borden Waterbury, Conn.
M. A. Bostwick Portland, Oreg.
J. F. Brinster Princeton, N. J.
E. C. Brown Hartford, Conn.
W. A. Derr East Pittsburgh, Pa.
C. K. Duff Toronto, Ontario, Canada
A. J. Hornfeck Cleveland, Ohio
G. S. Lunge Schenectady, N. Y.
E. E. Lynch West Lynn, Mass.
W. E. Phillips Philadelphia, Pa.
Merle Robison Toledo, Ohio
G. M. Thynell Waterbury, Conn.
J. H. Vivian Los Angeles, Calif.
B. G. Walker Minneapolis, Minn.
C. E. Wiesgartner Cleveland, Ohio

Working Group on Telemetering Terms:
W. J. Mayo-Wells, *Chairman* Silver Spring, Md.
G. R. Anderson North Hollywood, Calif.
J. L. Blackburn Newark, N. J.
A. T. Gruer Albuquerque, N. M.
M. V. Kiebert Philadelphia, Pa.
R. L. Harding South Bend, Ind.
F. Lehan Pasadena, Calif.
E. E. Lynch West Lynn, Mass.
M. G. Pawley Washington, D. C.
J. M. Pearce Baltimore, Md.
W. E. Phillips Philadelphia, Pa.
G. M. Thynell Waterbury, Conn.
F. L. Verwiebe Silver Spring, Md.
G. F. G. Weedon Toronto, Ontario, Canada
W. A. Wildhack Washington, D. C.

JOINT SUBCOMMITTEE ON CARBON BRUSHES (JOINT AIEE TECHNICAL COMMITTEES ON AIR TRANSPORTATION AND ROTATING MACHINERY, AND IN CO-OPERATION WITH NEMA ON CODES)

T. M. Linville, *Chairman;* General Electric Company, 1 River Road, Schenectady 5, N. Y.
W. H. Austry St. Marys, Pa.
R. J. Biais New York, N. Y.
H. R. Brown Seattle, Wash.
W. E. Clancy St. Marys, Pa.
J. V. Dobson St. Marys, Pa.
H. M. Elsey East Pittsburgh, Pa.
D. E. Fritz Cleveland, Ohio
L. A. Heath Long Island City, N. Y.
B. C. Henry Ironton, Ohio
C. J. Herman Fort Wayne, Ind.
V. P. Hessler Urbana, Ill.
L. H. Hildebrandt Dayton, Ohio
H. T. Hulbert St. Marys, Pa.
R. E. Klokow Lima, Ohio
E. A. Lapham Long Island City, N. Y.
K. Lugosch Johnsville, Pa.
C. Lynn East Pittsburgh, Pa.
I. H. Manfredo Brooklyn, N. Y.
M. S. May St. Marys, Pa.
H. F. Mitchel Saginaw, Mich.
L. C. Novak West Lynn, Mass.
H. R. Partridge Boonton, N. J.
D. Ramadanoff Cleveland, Ohio
O. C. Rutledge Schenectady, N. Y.
S. D. Summers Washington, D. C.
F. R. Terrant Cleveland, Ohio
A. L. VanEmden Washington, D. C.
W. W. Walker Yonkers, N. Y.